Journal of Pharmaceutical Sciences

JANUARY 1976

VOLUME 65 NUMBER 1

MARY H. FERGUSON
Editor

L. LUAN CORRIGAN
Assistant Editor

SHELLY ELLIOTT
Production Editor

JANET D. SHOFF
Copy Editor

EDWARD G. FELDMANN
Contributing Editor

SAMUEL W. GOLDSTEIN
Contributing Editor

LELAND J. ARNEY
Publications Director

EDITORIAL ADVISORY BOARD

JOHN AUTIAN	HARRY B. KOSTENBAUDER
LYNN R. BRADY	CARL J. LINTNER, JR.
WILLIAM O. FOYE	DAVID E. MANN, JR.
WILLIAM J. JUSKO	GERALD J. PAPARIELLO

The *Journal of Pharmaceutical Sciences* is published monthly by the American Pharmaceutical Association at 2215 Constitution Ave., N.W., Washington, DC 20037. Second-class postage paid at Washington, D.C., and at additional mailing office.

All expressions of opinion and statements of supposed fact appearing in articles or editorials carried in this journal are published on the authority of the writer over whose name they appear and are not to be regarded as necessarily expressing the policies or views of the American Pharmaceutical Association.

Offices—Editorial, Advertising, and Subscription Offices: 2215 Constitution Ave., N.W., Washington, DC 20037. Printing Offices: 20th & Northampton Streets, Easton, PA 18042

Annual Subscriptions—United States and foreign, industrial and government institutions $50, educational institutions $50, individuals *for personal use only* $30; single copies $5. All foreign subscriptions add $5 for postage. Subscription rates are subject to change without notice. Members of the American Pharmaceutical Association may elect to receive the *Journal of Pharmaceutical Sciences* as a part of their annual $60 (foreign $65) APhA membership dues.

Claims—Missing numbers will not be supplied if dues or subscriptions are in arrears for more than 60 days or if claims are received more than 60 days after the date of the issue, or if loss was due to failure to give notice of change of address. The Association cannot accept responsibility for foreign delivery when its records indicate shipment has been made.

Change of Address—Members and subscribers should notify at once both the Post Office and the American Pharmaceutical Association, 2215 Constitution Ave., N.W., Washington, DC 20037, of any change of address.

© Copyright 1976, American Pharmaceutical Association, 2215 Constitution Ave., N.W., Washington, DC 20037; all rights reserved.

AN "EQUAL OPPORTUNITY" JOURNAL

Fair treatment and equal opportunity are topics which have enjoyed considerable attention in recent years. Race, religion, sex, ethnic origin, and age are some of the areas in which prejudices have been challenged and barriers are being successfully removed.

In every aspect of its operation, this Journal has consistently strived to consider all things strictly on their merits and to exclude any element of bias. Quality and qualifications are what count in considering the acceptability of papers for publication, referees for reviewing manuscripts, authors for review articles, members to serve on the Editorial Advisory Board, and personnel for the editorial staff.

Unfortunately, however, the way in which things are perceived is often quite different from the way in which they actually exist. Erroneous conclusions are drawn from a situation largely because they have been based on false assumptions.

Specifically, indignant complaints have been received by the editors from time to time over the past fifteen years, alleging that the *Journal of Pharmaceutical Sciences* is prejudiced against pharmacy administration. Various groups and various individuals have heatedly charged that this Journal has a policy that denies equal access to its pages for publication purposes in the case of papers emanating from the field of pharmacy administration.

This simply is not true. The pages of this Journal are open to any research in the pharmaceutical sciences, providing that the resultant manuscript fulfills all prevailing Journal criteria for acceptance. Manuscripts in the field of pharmacy administration are required to meet the same standards as manuscripts from any other area of research. Among these standards, the most fundamental requisite is that the paper reports original, basic research.

Absence in the past of such papers from our pages has not been due to any limitation of Journal scope. Rather, it has been due to the unfortunate fact that the occasional manuscripts submitted from this field of science have reported upon poorly conceived studies or have been deficient in other respects so that they did not fulfill the quality standards established for the Journal. And lest there be any suspicion that this assessment reflected biased opinion on the part of the editors, it should be mentioned that the manuscripts were reviewed by competent, recognized experts in the field of pharmacy administration and that these peer referees recommended rejection on the basis of the quality of the manuscript—or more correctly, on the basis of the quality of the research study on which the manuscript reported.

On a somewhat related subject, many of our readers and authors have regarded as arbitrary and confusing the use of separate sections in the Journal for publication of reports dealing with "Pharmaceutical Analysis" and "Pharmaceutical Technology." In an effort to eliminate such segregation of these articles, this practice is being discontinued, effective with this month's issue. In the future, all articles in these subject areas will simply appear under the common heading of "Research Articles" or "Notes."

In conclusion, it has been and remains the policy of the *Journal of Pharmaceutical Sciences* to consider for publication papers reporting on any area of pharmacy-related research, provided that the editors and reviewers determine that: (*a*) the research study is well designed, (*b*) the research is adequately reported, and (*c*) the study and its results are of sufficient importance to warrant publication for the benefit of the scientific community.

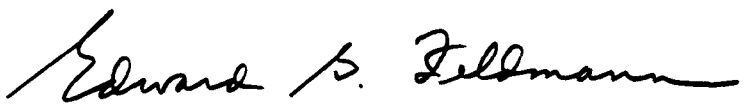

Journal of Pharmaceutical Sciences

JANUARY 1976
VOLUME 65 NUMBER 1

REVIEW ARTICLE

Mechanisms of Solid-State Reactions of Drugs

STEPHEN R. BYRN

Keyphrases □ Solid-state reactions—mechanisms, effect of crystal structure, drugs and related compounds, applications, review □ Solid dosage forms—solid-state reaction mechanisms, applications, review

During the past few years, substantial advances in the knowledge of the chemical and physical factors governing solid-state reactions of molecular crystals have occurred. Surprisingly, little of this knowledge has been applied to the study of the decompositions of drugs and related compounds.

The purposes of this review are to classify and discuss representative solid-state reactions of medicinal agents in terms of this knowledge and to support the idea that a thorough knowledge of the mechanism of solid-state reactions and the effect of crystal structure on solid-state reactions of drugs can suggest rational approaches to drug stabilization. This latter point is particularly important in the pharmaceutical industry, where a knowledge of solid-state chemistry could be used to develop methods of stabilizing drugs and solid dosage forms.

There have been recent reviews of solid-state photochemical (1), thermal (2), and solid–gas (3) reactions of organic compounds and the stability of solids and solid dosage forms (4), but none of these has treated the chemical and mechanistic aspects of solid-state reactions of pharmaceuticals. This review will emphasize the mechanistic and chemical aspects of solid-state reactions of drugs and will, in general, be restricted to solid-state reactions of pure compounds. It is divided into four general sections: (*a*) solid-state photochemical reactions, (*b*) solid-state thermal reactions, (*c*) solid–gas reactions, and (*d*) applications.

Before proceeding, it is important to attempt to define a solid-state reaction. The simplest definition of a solid-state reaction is one that proceeds below the eutectic melting point of the components of the system (2). However, such a definition automatically excludes all reactions that have a liquid as one of their products. For reactions of solids yielding both a solid and a liquid product, the criteria of Morawetz (5) may be more appropriate; *i.e.*, a reaction occurs in the solid state when: (*a*) pronounced differences are found in the reactivities of closely related compounds, (*b*) different reaction products are obtained from those formed when the reaction is carried out in the liquid state, or (*c*) different crystalline modifications of the compound have different reactivities or form different products.

SOLID-STATE PHOTOCHEMICAL REACTIONS

These reactions were reviewed recently (1, 6), and only selected studies related to solid-state reactions of biologically important compounds will be summarized here. Many solid-state photochemical reactions can be explained in terms of the topochemical postulate (1, 6), which states that solid-state reactions proceed with a minimum of atomic and molecular movement. Thus, the stereochemistry of the product depends upon the packing of the reactants in the crystal. The topochemical postulate permits prediction of the stereochemistry of many solid-state cycloaddition reactions including those of quinones, anthracenes,

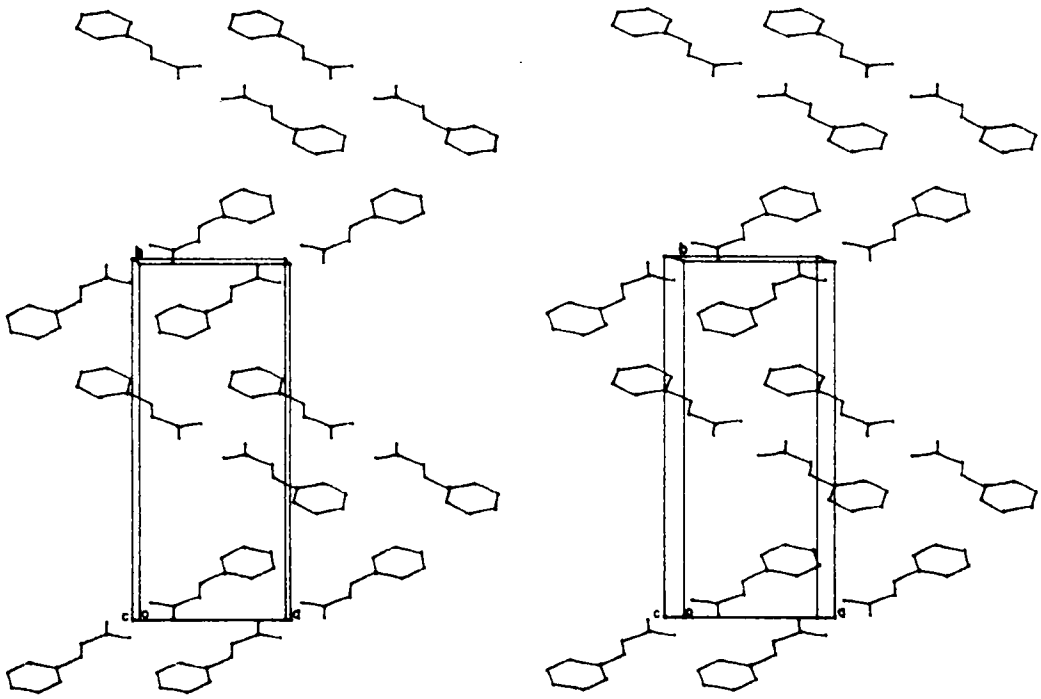

Figure 1—*Stereo pair view of the packing of the α-form of cinnamic acid.*

α,β-unsaturated ketones, chalcones, dienes, and cinnamic acids. The application of the topochemical postulate to these reactions will be illustrated using cinnamic acids.

However, several solid-state photochemical cycloaddition reactions do not obey the topochemical postulate. Careful study of these reactions has shown that they occur at defects, yielding products with stereochemistries different from those predicted from the crystal packing (7). Further discussion of this important topic is beyond the scope of this review.

Photodimerizations of Solid *trans*-Cinnamic Acids—The solid-state photochemistry of the *trans*-cinnamic acids can be generalized as follows. *trans*-Cinnamic acids solidify in three forms (polymorphs), α, β, and γ, which can be distinguished by their crystallographic cell dimensions. The shortest cell dimensions of 38 cinnamic acid polymorphs fall into three ranges: (*a*) >5.1 Å (α-type), (*b*) 3.9 ± 0.2 Å (β-type), and (*c*) 4.9 ± 0.2 Å (γ-type) (1, 6). Upon photolysis, each form yields characteristic cyclobutane products with the symmetries indicated in Table I. These products have been rationalized in terms of the relationship of the monomers in the crystal and the separation between neighboring double bonds.

In α-type crystals (Fig. 1[1]), the double bonds of the monomers are parallel, centrosymmetrically related, and 3.6–4.1 Å apart. The crystal packing of the α-form of cinnamic acid is shown in Fig. 1. The packing of molecules in the α-crystal is quite interesting, since there are pairs of molecules centrosymmetrically related.

In the β-type crystals, *e.g.*, *p*-chlorocinnamic acid (Fig. 2), the double bonds of the monomers are separated by about 4.0 Å and the molecules are arranged in stacks and are related only by translational symmetry. Both *trans*-α-bromocinnamic acid and *trans*-*m*-chlorocinnamic acid belong to the γ-type, with monomers related by translational symmetry but with their double bonds more than 5.1 Å apart. This correlation of the packing geometry and separation of the double bonds with the shortest cell dimension is surprising, since the choice of unit cell is somewhat arbitrary in many of the crystals studied. However, the significance of the correlation is underscored by the specificity of the solid-state photodimerizations.

Topochemical control of these solid-state photochemical reactions is illustrated by the dimerization of the two (α and β) polymorphic forms of *trans*-cinnamic acid whose crystal packing is shown in Figs. 1 and 2. The dimerization reaction is illustrated in Schemes I and II. Upon exposure to sunlight in cellophane-covered petri dishes or Pyrex cylinders, the centrosymmetric α-form (I) gives the centrosymmetric dimer α-truxillic acid (II) (74% yield). The unstable β-form (III) gives pure β-truxillic acid (IV) upon irradiation, provided care is taken to ensure that the photolysis is run below the α to β transition temperature.

It has been suggested that solid-state photodimeri-

Table I—*trans*-Cinnamic Acid Polymorphs and Cyclobutane Products

Crystal Type Packing	Shortest Cell Dimension, Å	Crystallographic Relationship of Monomers	Double Bond Separation, Å	Symmetry of Product
α	>5.1	$\bar{1}$ (centric)	3.6–4.1	$\bar{1}$ (centric)
β	3.9 ± 0.2	Translation	3.9–4.1	m (mirror)
γ	4.9 ± 0.2	Translation	4.2–5.1	No reaction

[1] The author thanks J. Ladell, Phillips Electronic Instruments, for making the atomic coordinates available through Dr. I. C. Paul. Glasses for viewing such drawings can be ordered from Hubbard Scientific Co., P.O. Box 105, Northbrook, Ill.

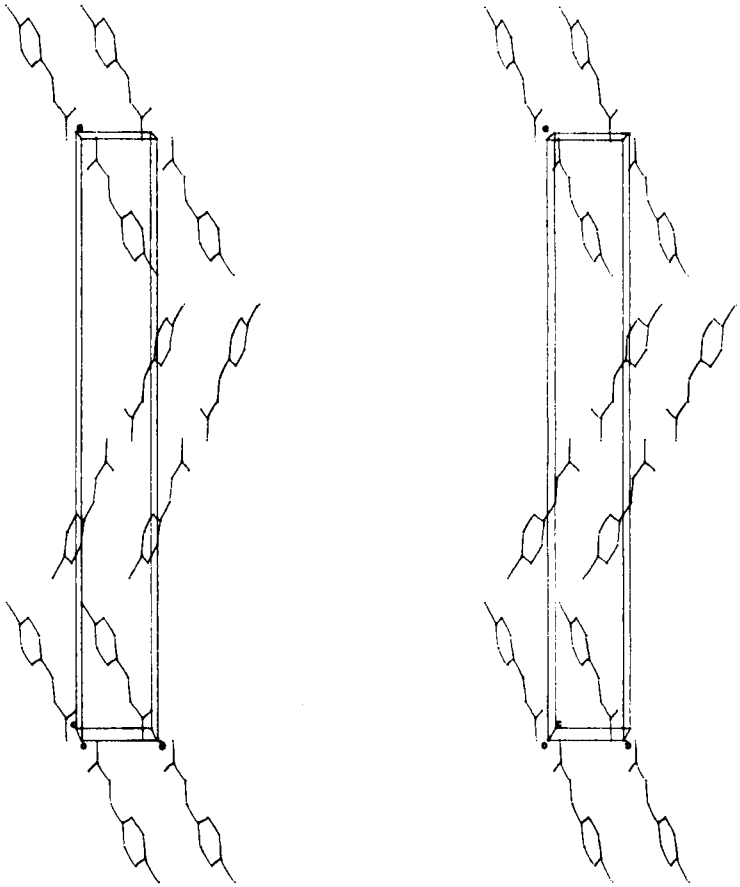

Figure 2—*Stereo pair view of the packing of the β-form of* p-*chlorocinnamic acid (8). This structure is isomorphous with the β-form of cinnamic acid.*

zation usually proceeds from the singlet state (6). This suggestion is based on experiments on solid solutions of cinnamides, for which the products indicate that the dimerization is faster than energy transfer, and on studies of thymine dimerization in frozen solution. However, none of these experiments rules out the possibility that the photodimerization of cinnamic acids proceeds through the triplet state.

The striking observation that the reacting double bonds of cinnamic acids must be not only within 4 Å but also aligned and parallel for cycloaddition to occur has been made (6). For example, *trans*-methyl *m*-bromocinnamate does not photodimerize over long periods of irradiation. This ester has its double bonds 3.93 Å from each other but nonparallel. (The double bonds are related by a glide plane.)

Recently, the concept of crystal engineering was introduced (6). The introduction of a dichlorophenyl group into unsaturated systems usually causes crystallization in a unit cell of the β-type with a 4-Å axis (Table I). Irradiation of such crystals yields a dimer with mirror symmetry. Thus, crystal engineering involves controlling the course of solid-state reactions by controlling crystal packing with appropriate functional groups.

Photodimerizations of Solid *cis*-Cinnamic Acids—The photochemistry of solid *cis*-cinnamic acids is complicated by the possibility of *cis–trans* isomerization (9). Many of the *cis*-acids studied by single-crystal X-ray techniques crystallized with their double bonds within 4 Å of each other and in position to yield *cis*-dimers; however, irradiation

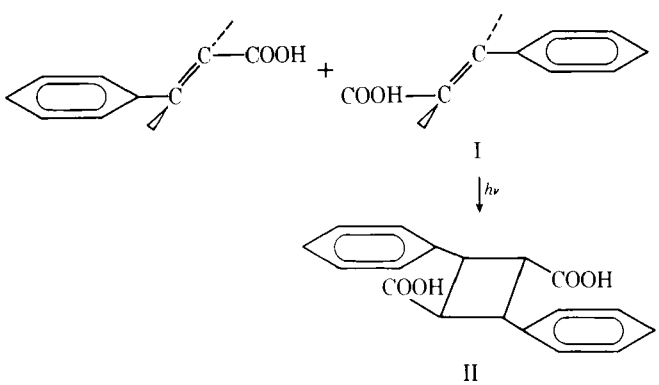

Scheme I

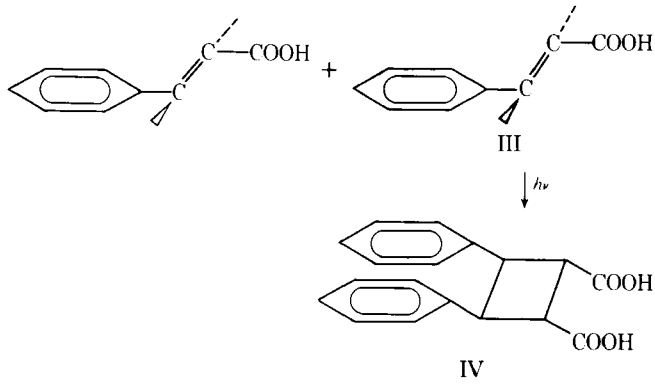

Scheme II

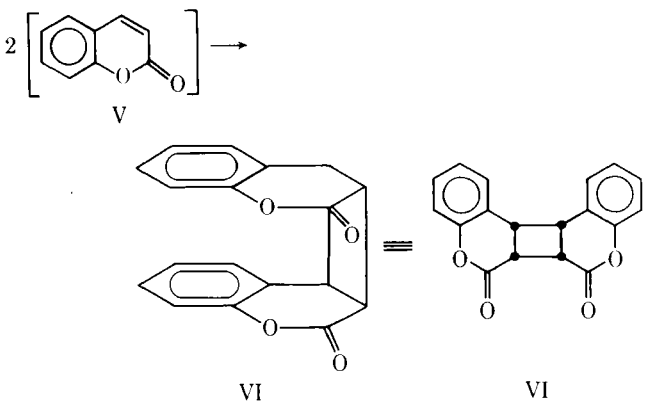

Scheme III

yielded either the *trans*-cinnamic acids or photoproducts derived from *trans*-acids. These products contained microcrystallites of the respective acids. Powder X-ray experiments indicated that the *cis*-acids isomerized to *trans*-acids, which then dimerized to give *trans*-type products (9). For the *trans*-acids that crystallized in several polymorphic forms, dimers expected from all of the polymorphs were often obtained. In contrast, coumarin (V), a *cis*-cinnamic acid derivative pinned in the *cis*-configuration, and the coumarin–mercuric chloride complex, crystallized with the double bonds 4 Å apart and gave upon irradiation the *cis–syn*-dimer (VI), as expected from the topochemical postulate (Scheme III).

Careful study of the solid-state photochemistry of *cis-o*-methoxycinnamic acid showed that mainly *o*-methoxy-α-truxillic acid (a derivative of II) was formed upon irradiation at room temperature while the *trans-o*-methoxycinnamic acid accumulated at low temperatures (between −80 and −180°) but no dimer was formed. Control experiments showed that the dimerization of *trans*-cinnamic acids was not temperature dependent (between 25 and −180°). On the basis of this evidence, the reaction of *cis*-cinnamic acids was explained as follows. Crystals of the *cis*-acid, upon irradiation, are transformed to a solid solution of *trans*-acid (formed by *cis* → *trans* photoisomerization) in the *cis*-host crystal. Then the *trans*-acid crystallizes out of the solid solution and these crystals dimerize to *trans*-products. At low temperatures, the crystallization of *trans*-crystals from the solid solution is slowed or stopped, allowing the *trans*-acid to accumulate.

In conclusion, solid-state photochemical reactions offer distinct synthetic advantages over the corresponding solution reactions since they allow control of the stereochemistry of the product (truxillic acids) and the course of the reaction. For example, *trans*-cinnamic acid yields 98% polymer when irradiated in solution.

Solid-State Photochemical Polymerizations—This area has been widely studied, and this brief discussion will only emphasize that these reactions also appear to obey the topochemical postulate.

Irradiation of crystals of 5-bromo-2-methoxy-*cis*-cinnamic acid yielded a polymer with a structure consistent with the topochemical postulate (10) along with other products. This cinnamic acid did not crys-

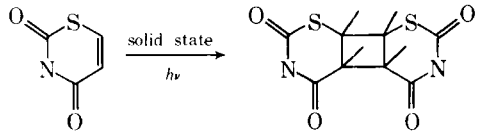

Scheme IV

tallize in either the α- or β-type (Table I) but had the double bonds related by both translation and screw-axis symmetry. Polymerization along the screw axis is consistent with the structure of the polymer obtained.

In several cases, topotaxy was observed in solid-state polymerizations. In the polymerization of trioxane (11, 12) induced by ionizing radiation and the photochemical polymerization of crystalline 2,5-distyrylpyrazines and 1,4-bis[β-pyridyl-2-vinyl]-benzene (13–17), chains of the polymer grew in the monomer crystal with the same orientation as the stacks of monomer (topotaxy).

SOLID-STATE PHOTOCHEMICAL REACTIONS OF BIOLOGICALLY IMPORTANT COMPOUNDS

Only unequivocal photochemical reactions are included in this section. The photochemical reactions of crystalline fumagillin, ergocalciferol (vitamin D_2), and vitamin A, which probably involve photochemical solid–gas reactions, are discussed later.

Nucleic Acids—The solution and frozen-state photochemical reactions of nucleotides, nucleosides, purines, and pyrimidines have been extensively reviewed (18–20) and will be briefly discussed here.

The solid-state photochemical reactions of pyrimidines obey the topochemical postulate. For example, irradiation of crystals of the thio analog of uracil (VII) yielded the *cis–syn*-dimer (VIII), as predicted from the crystal packing (21) (Scheme IV). Similarly, the irradiation of crystalline thymine, 1-methylthymine, 3-methylthymine, and 1,3-dimethylthymine gave the topochemically expected product (22, 23).

The irradiation of dinucleotides in the solid has not been extensively studied; however, irradiation of

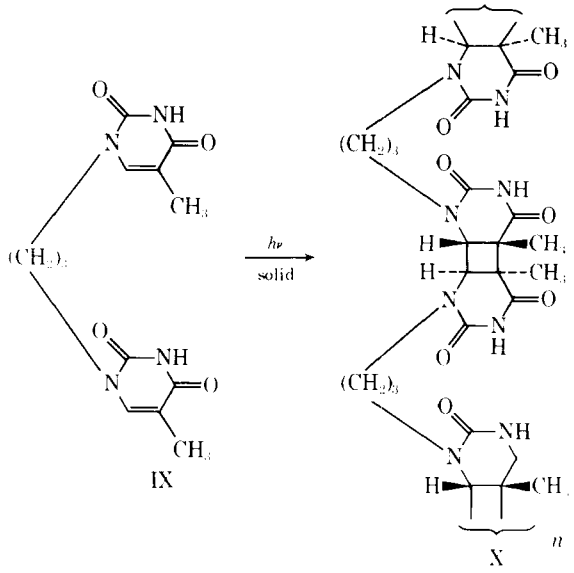

Scheme V

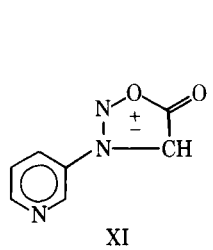

XI

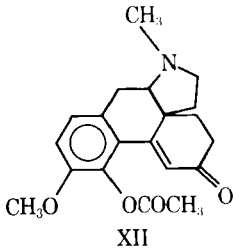

XII

crystals of the dinucleotide analog, trimethylene dithymine (IX), gave polymer X rather than the dimer which might have been expected from a casual glance at the crystal-packing arrangement (24, 25) (Scheme V). Closer examination of the molecular packing of IX shows that the double bonds are not perfectly aligned for intramolecular dimer formation; therefore, polymerization occurs. This observation, along with the observation that perfect double bond alignment is required before cinnamic acid dimerization will occur, indicates a surprisingly rigid requirement for π-bond overlap in these reactions. These observations are consistent with the idea that these reactions occur from the singlet state and are concerted, photochemically allowed [2 + 2] dimerizations.

Although none of these compounds is a medicinal agent, the principles discussed could be used to stabilize nucleic acid analogs that are anticancer agents. The fact that these reactions obey the topochemical postulate is also important in understanding the mechanisms of radiation damage of DNA.

Photochromic and Thermochromic Drugs—Photochromism and thermochromism, in general, involve light-induced or heat-induced color changes. They are not commonly observed phenomena in medicinal chemistry; however some sydnones are photochromic and at least one derivative of morphine has thermochromic properties. *N*-(3-Pyridyl)sydnone (XI) gives colorless crystals which almost instantly turn blue on exposure to sunlight. The blue crystals rapidly become colorless when heated to 80° and bleach more slowly at room temperature (26). The IR spectra of the blue and colorless crystals are identical.

The failure to observe different spectra and structures for the blue and colorless crystals is consistent with studies of the photochromic and thermochromic salicylideneanilines. No crystallographic differences between the colored and colorless forms of these anilines were observed (27, 28). Apparently, the color change in these crystals is due to a small concentration of a highly colored species. Recently, the blue sydnone color was suggested to be due to a small concentration of a charge-transfer complex of unknown structure (29). On the other hand, the photochromic properties of bicyclic ethylenimines were explained in terms of the formation of a structurally distinct, colored, azomethine ylide. These ylides had different IR spectra from the bicyclic ethylenimines (30).

The morphine derivative acetyl metathebainol (XII) is thermochromic in solution and near its melting point (31). A solution of acetyl metathebainol turns pink upon heating, and crystals turn pink at 143° before melting to a red liquid at 150°.

Since both photochromism and thermochromism are usually reversible phenomena, these color changes may cause substantial concern to the unaware observer, even though the drug is not degraded.

Other Biologically Important Molecules—Choline chloride (XIII) is a particularly interesting example of the effect of radiation on crystals of biologically important molecules. Choline chloride crystallizes in a stable α-form and an unstable β-form, which is present at temperatures greater than 78° (5, 32, 33). The α-form is the most ionizing-radiation-sensitive compound known (33). The G factor for radical formation (radicals produced per 100 ev) is about 2, while the G factor for radiolysis (molecules destroyed per 100 ev) is as high as 55,000.

In contrast, the high temperature β-form is not abnormally radiation sensitive. The difference in radiation sensitivity of these polymorphs is probably related to the crystal packing of the two forms. The choline molecules in the crystals of the α-form are apparently in a geometry favoring the propagation step in radiolysis (Scheme VI). This step involves the attack of an excited carbanion on a ground-state choline cation.

Examination of packing in the α-polymorph (Fig. 3) indicates that the abnormal radiation sensitivity of α-choline chloride may be due to the fact that the

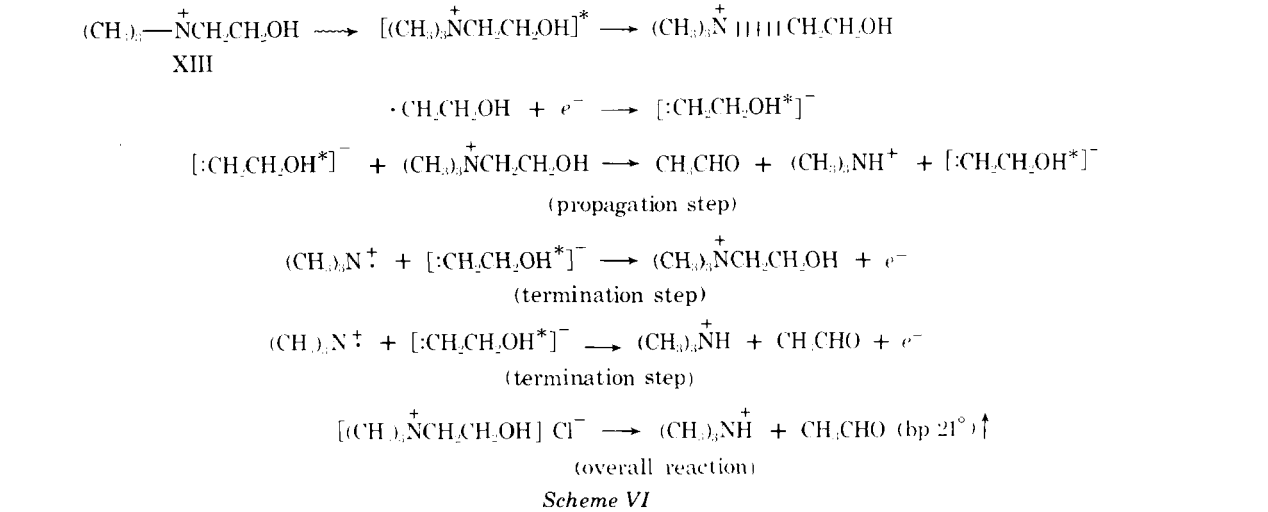

Scheme VI

Figure 3—*Stereo pair view of the packing of the α-form of choline chloride. The chloride ions are represented as dots, and the hydrogen atoms are not drawn. The atom coordinates were taken from the literature (34, 35).*

propagation step proceeds rapidly through the stacks of choline molecules, much like a topochemically controlled polymerization. A knowledge of the structure of the β-polymorph of choline chloride would be of interest, and a comparison of the packing in the two polymorphs might provide insight into this reaction.

Hirsutic acid (XIV) rearranges in the solid state upon exposure to X-rays (Scheme VII) (36). This sesquiterpenoid acid is an antibiotic isolated from *Stereun hirsutun,* and its *p*-bromophenacyl ester rearranges during crystallographic data collection. This reaction proceeded to the extent of 60% with the product dissolved in the crystal lattice of the starting material. Thus, the observed structure in the crystal is the weighted average of XIV and XV. The structure of the product was proved by chemical means, ruling out the possibility that disorder or some other crystallographic artifact was responsible for the observed structure in the crystal.

The observation of a solid solution containing nearly equal proportions of two materials is surprising when, in general, most solid solutions only exist for small amounts of guest molecule in the host lattice (2). The possibility of mixed crystal formation containing one molecule of XIV and one molecule of XV is also ruled out, since such mixed crystals would contain two molecules per asymmetric unit rather than one molecule as observed. Other hirsutic acid esters also rearrange on exposure to X-rays; however, unesterified hirsutic acid and other epoxy alcohols do not rearrange. For example, steroids containing either XVI or XVII epoxy alcohol groups are stable to X-irradiation. These observations suggest that rigid packing and structural requirements must be met before rearrangement will occur.

The solid-state photochemistry of 3-ketogibberellin (XVIII) is sensitive to packing influences (37). The methyl ester of 3-ketogibberellin (XVIII*a*) dimerizes to a cyclobutane (XIX) upon irradiation in the crystalline state (Scheme VIII), while the free acid, 3-ketogibberellic acid (XVIII*b*), photoaromatizes to XX (Scheme IX). Presumably, the acid functionality causes crystallization in a geometry unfavorable for dimerization.

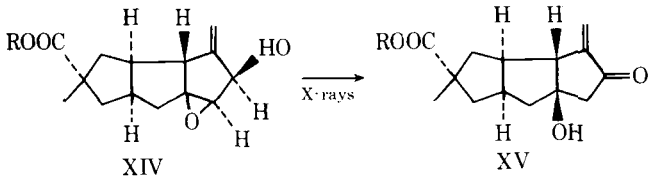

R = *p*-bromophenacyl

Scheme VII

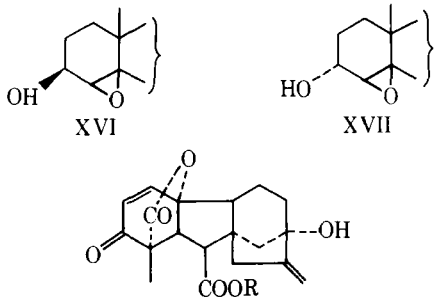

XVIII*a*: R = CH_3

XVIII*b*: R = H

The sodium salt of the antibiotic novobiocin (XXI) is light sensitive (38). It is possible that this light sensitivity is due to solid-state photodimerization of the coumarin functionality in novobiocin; however, air oxidation has not been ruled out.

In conclusion, it is clear that the packing of crystals can control their reactivity, and this control can potentially be used to advantage when one wishes to prepare a more stable form of a drug.

SOLID-STATE THERMAL REACTIONS

The scope of solid-state thermal reactions is broad, but several reviews are available (2, 5). One can expect that a reaction occurring in an inert solvent at a reasonable rate at 60–100° below the melting point of the substances present will occur in the solid (2), although this fact is not generally recognized.

A solid-state thermal reaction can be divided into four stages: (*a*) molecular loosening, (*b*) molecular change, (*c*) solid solution formation, and (*d*) separation of the product (2). Stages *b*, *c*, and *d* are very similar to the proposed steps of the photochemical reactions of *cis*-cinnamic acids (discussed previously). The first stage involves loosening or disordering of the reacting crystal at the reaction site. This step is required to allow the tightly packed reactant molecules sufficient space in which to react.

The second step involves conversion of the reactants to products. Few comparisons of the mecha-

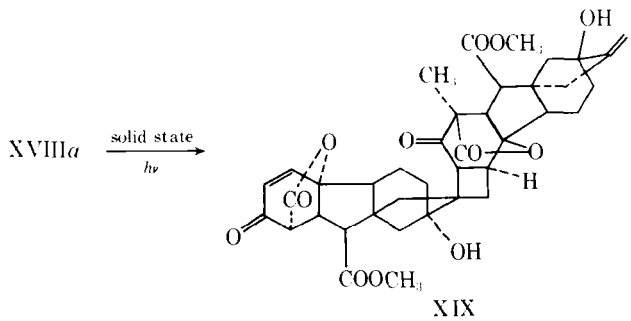

Scheme VIII

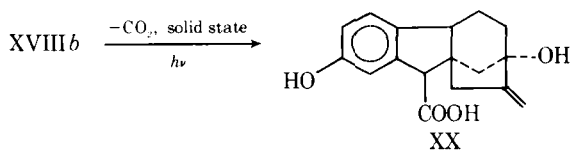

Scheme IX

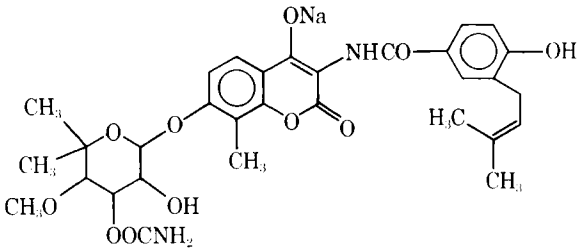

XXI

nisms of solid-state and solution thermal reactions have been made. However, the rates of solid-state thermal reactions apparently are two to 100 times slower than the corresponding solution reactions (2). Paul and Curtin (2) also pointed out that some solid-state thermal reactions proceed more cleanly than the corresponding solution reaction, just as do some solid-state photolyses (already discussed).

As the first molecules of product are formed, they probably appear as a solid solution of product molecules in the reactant crystals. Solid-solution formation has been studied (2), and it was noted that the range of solubility of one solid in another is surprisingly small, even when the two compounds have nearly the same shape. For example, the maximum solubility of acridine in anthracene is only 12%. The 60:40 solid solution of hirsutic acid (XIV) and its rearrangement product (XV) is an apparent exception to this generalization, although the solid solution is formed *in situ* by a chemical reaction. The existence of the 1:1 molecular complex of ergocalciferol and a thermal rearrangement product, pyrocalciferol, suggests that solid ergocalciferol could thermally rearrange to pyrocalciferol *via* this 1:1 complex.

After the solubility of the product in the reactant crystal is exceeded, it begins to crystallize out of the solid solution. Usually the crystalline product is highly disordered, since crystallization of this product occurs at many sites, each giving microcrystallites. However, several topotactic reactions are also known. In these reactions, single crystals of product are obtained from single crystals of starting material (39).

Almost all solid-state reactions begin at nucleation sites. The importance of defects in solid-state photochemical and thermal reactions has been discussed (1–3, 40). For example, the phase transition of the α-form of *p*-dichlorobenzene to the β-form begins at visually observable defects. Perfect crystals of the α-form are resistant to reaction. However, when these crystals are pricked with a pin, the reaction nucleates at this site (41, 42). In the phase transitions of the β-form of *p*-dichlorobenzene (41, 42) and the α-form of *p*-nitrophenol (43, 44), well-defined fronts between the starting phases and the product phases were observed.

Upon heating, the crystalline yellow isomer (Y-XXII) of dimethyl 3,6-dichloro-2,5-dihydroxyterephthalate is transformed to the white (W-XXII) isomer (Scheme X), nucleating at variable sites in the crystal (45). The formation of the white isomer proceeds through the crystal in a "front" moving along the long morphological axis. This highly anisotropic spread of the reaction can be explained in terms of

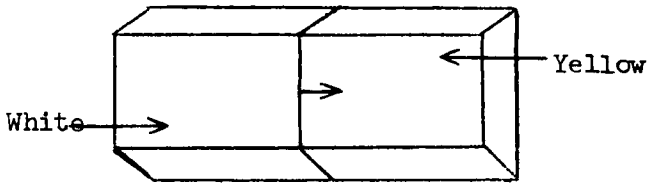

Figure 4—*Schematic drawing of the reaction spreading through the crystal.*

the packing and crystal structures of the yellow and white forms. Goniometric and crystal-packing studies showed that there were stacks of yellow molecules perpendicular to the plane of the paper in Fig. 4 and that each stack was associated with adjacent stacks in a direction perpendicular to the long morphological axis and relatively isolated from the stacks along the long morphological axis.

The relationship between the packing of crystals of Y-XXII and W-XXII showed that the white form could be obtained from the yellow form if every other molecule in a stack was "flipped" or rotated 180° about the Cl- - - Cl axis. The rapid spread of the reaction in both directions perpendicular to the long morphological axis is consistent with closer association of molecules in these directions and the relative isolation of molecules along the long morphological axis. One would expect that once the molecules in a stack are disrupted and loosened enough to allow one to flip, the rate of rearrangement would be rapid in that stack and would quickly spread to the closely associated adjacent stack. The rate of spread of the reaction to the relatively isolated adjacent stack would be slower.

The studies on dimethyl 3,6-dichloro-2,5-dihydroxyterephthalate emphasize the valuable information that can be obtained when data from crystallographic, photomicrographic, and goniometric experiments are combined to explain solid-state reactions (45).

SOLID-STATE THERMAL REACTIONS IN MEDICINAL CHEMISTRY

Phase Transitions of Drugs—Polymorphism of drugs is an important subject, much too large for detailed discussion in this review. A review of polymorphs in pharmacy has appeared (46). Here, studies of the transformations of polymorphs of medicinal agents will be briefly discussed as examples of the simplest solid-state thermal transformations. Although none of the polymorphic transformations discussed here has been studied using photomicrogra-

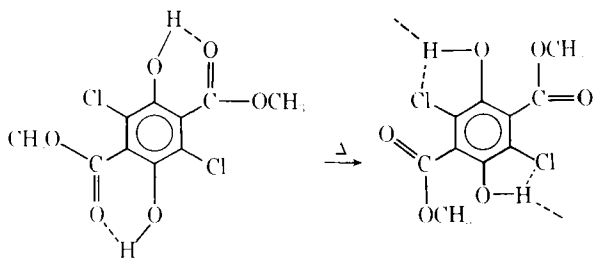

Y-XXII W-XXII

Scheme X

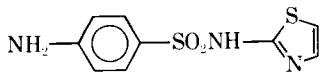

XXIII

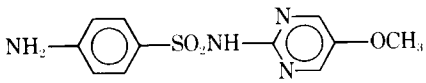

XXIV

phy, it is likely that these transformations nucleate at defects and proceed by a mechanism related to that for the phase transition of *p*-dichlorobenzene and *p*-nitrophenol (discussed previously).

Several studies of the crystal structures of polymorphs of drugs have been performed. One definitive series of studies concerned sulfathiazole (XXIII) (Table II) (47, 48). In these studies, the crystal structures of three polymorphs (I, II, and III) were determined. These polymorphs had different rates of dissolution; however, visual examination of the packing from the crystal structures revealed differences in hydrogen bonding but allowed no definite conclusions about the relative stability of the polymorphs. The densities of Polymorph I and either II or III could be correlated with their rates of solution; the denser polymorphs (II or III, mp 200–202°) had the slower rates of dissolution. Also, heating I yielded the more dense polymorphic forms. This correlation is consistent with Kitaigorodskii's (49) closest packing theory which states, in part, that the most dense crystal is the most stable, since it has the highest packing energy. On the other hand, the more stable polymorph of resorcinol has the lower density (1.33 *versus* 1.28 g/ml) (50).

Sulfameter (XXIV) exists in three polymorphs (I, II, and III), two solvates (IV and V), and an amorphous form (VI). All forms are transformed to Polymorph I upon heating. Grinding converts all forms to III. Forms IV and V were suggested to be solvates containing dioxane and chloroform, respectively (51). Powder patterns and IR spectra confirmed the crystallographic differences among all five forms. Studies of dissolution rates indicated that Form II had the fastest dissolution rate and yielded a solution, from which Form I slowly crystallized. However, the relative stabilities of these polymorphs are not known, although these experiments indicated that Form I is the most stable.

Table II—Polymorphs of Sulfathiazole

Polymorph	I[a]	II[a]	III[a]
Melting point	200–202°	200–202°	200–202°
Transition point (to I)	—	173–175°	173–175°
Habit	Rods	Prisms	Plates
Space group	$P2_1/c$	$P2_1/c$	$P2_1/c$
a, Å	10.554 (5)	8.235 (4)	17.570 (9)
b, Å	13.220 (7)	8.550 (4)	8.574 (4)
c, Å	17.050 (9)	15.558 (8)	15.583 (8)
β, °	108.06 (1)	93.67 (1)	112.93 (1)
Molecules per asymmetric unit	8	4	4
Observed density, g/ml	1.50	1.55	1.57
Calculated density, g/ml	1.499	1.550	1.567

[a] Numbers in parentheses designate the error in the least-significant digit.

A convenient method of determining the relative stabilities of polymorphs involves equilibration of crystals of two forms in a solvent in which these polymorphs are relatively insoluble (46). Under these conditions, the crystals of the more stable polymorph grow while those of the less stable one disappear. In an apparently related observation, the crystalline transformation of an unspecified antihypertensive drug was observed when crystals were bathed in 0.1 *N* HCl (52).

Since the polymorph present can affect the rate of dissolution and, to some extent, bioavailability, care must be taken during the manufacturing process to assure that no polymorphic transition occurs. A particularly disturbing transformation could occur when the solid is subjected to the relatively high pressures of tablet machines, which can range up to 2812 kg/cm^2 (4000 lb/sq in.) or 281 bar. These pressures might favor transformation to a denser polymorphic form. However, few, if any, documented cases showing that compression during tablet preparation can alter the polymorphic form have appeared (53).

A recent study of the effect of compressional force on the polymorphs of succinylsulfathiazole showed that compressional force did not cause a polymorphic transition (53). While this study involved pressures up to about 15 kbar, studies at much higher pressures, but of different compounds, resulted in chemical reactions (54, 55). Aromatic hydrocarbons such as pentacene condensed when subjected to pressures of 150–300 kbar (54, 55). It is rather unlikely that pressures in tableting machines could cause a large number of chemical reactions.

Aspirin Anhydride—Garrett *et al.* (56) reported an extremely interesting study of the solid-state decomposition of aspirin anhydride (XXV) (Scheme XI), which may be a superior form for the oral administration of aspirin.

Aspirin anhydride (mp 83–85°) decomposed in the solid state at temperatures ranging from 40 to 70°. At 70°, the starting crystals were completely liquefied after 24 hr and the rate of decomposition increased significantly after liquefaction. Even at the lower temperatures, liquefaction was noticeable after longer times. However, the rates of decomposition at 50° varied as much as 10 times from lot to lot of crystals. Samples containing moisture decomposed more rapidly than dried samples and, most important, crystals from ethyl acetate–hexane[2] were more stable than crystals from ethanol. It was suggested that the unstable crystals contain ethanol of solvation which, like moisture, accelerates the reaction. However, elemental analysis showed that crystals from ethanol do not contain solvent of crystallization[3]. This finding suggests that the reaction having the slower rate of decomposition might be a true solid-state reaction.

The solution thermal decomposition of aspirin anhydride has apparently not been studied. However,

[2] Skelly B.

[3] *Anal.*—Calc. for $C_{18}H_{14}O_7$: C, 63.16; H, 4.12. Found: C, 63.36; H, 4.35. These crystals belong to space group $P4_2\,2_12$ $a = b = 8.457$ (1), $c = 23.116$ (3) with four molecules per unit cell. S. R. Byrn, J. L. Killian, and P. Y. Siew, unpublished observations.

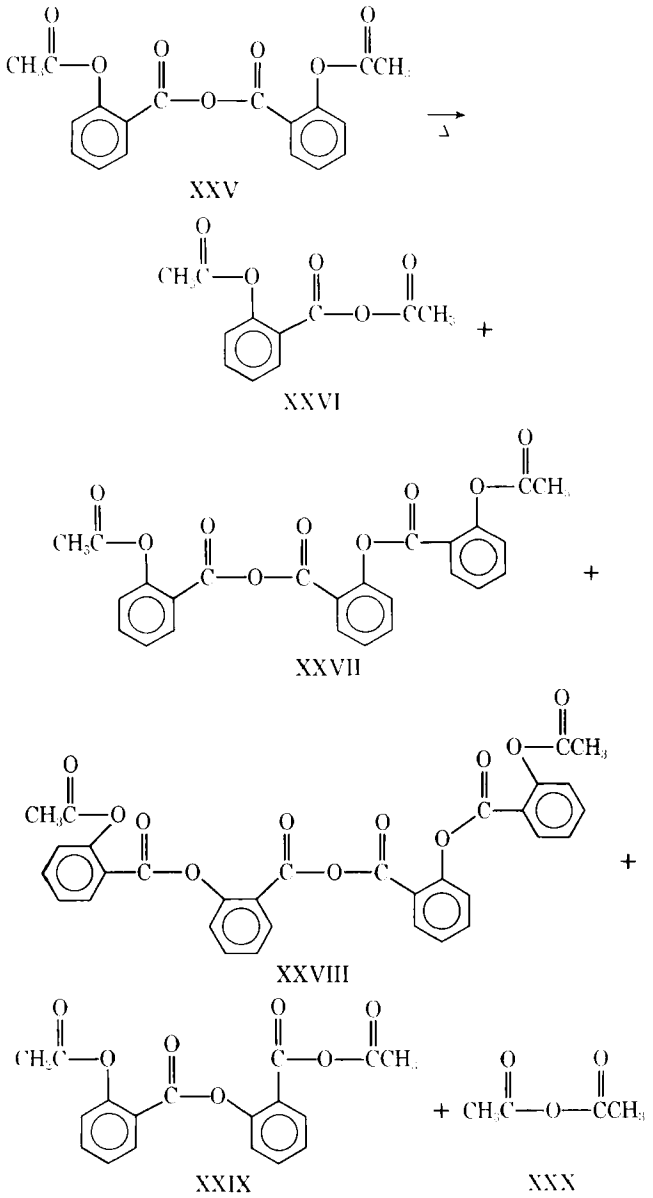

Scheme XI—Solid-state decomposition of aspirin anhydride. The products shown are those suggested by Garrett et al. *(56) and include all possible mixed anhydrides.*

the oxygen to oxygen acyl and benzoyl migrations observed are related to the reaction shown in Scheme XII (57) and solid-state nitrogen to oxygen benzoyl migrations of phenylazotribenzoylmethanes (58–60).

Studies of the crystal structures of the starting and product crystals of these azotribenzoylmethanes revealed that the benzoyl groups appeared to pack preferentially in a conformation that places the carbonyl oxygen of one group near the back side of the carbonyl carbon of an adjacent benzoyl group as shown in the hypothetical reaction in Scheme XIII. Such a packing arrangement in aspirin anhydride would be geometrically quite favorable to acyl and benzoyl migrations. Solid-state benzoyl migrations also have been found to yield different product ratios from the corresponding reaction in solution (58–60).

Solid-State Nucleophilic Cyclizations—Recently, two solid-state cyclization reactions of anticancer agents have been reported. These reactions render

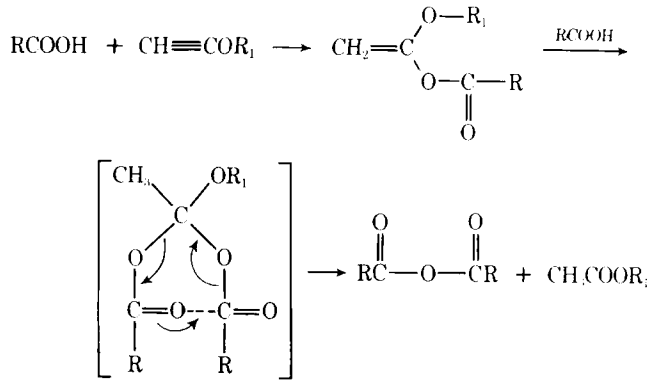

Scheme XII

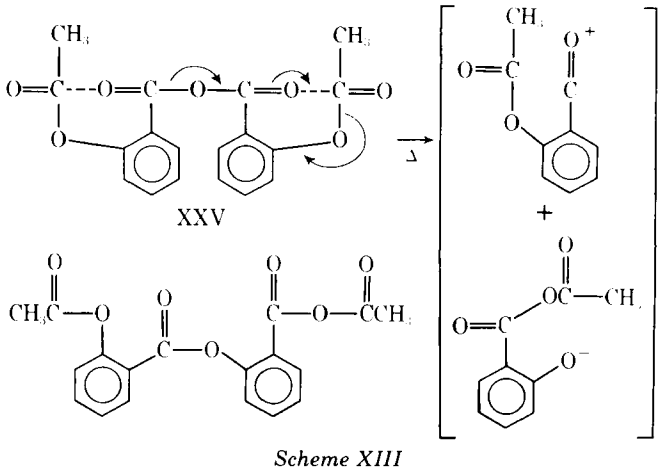

Scheme XIII

these compounds nearly useless as clinical agents because of the difficulty involved in stabilizing these materials during storage.

The nitrogen mustard 5(4)-[3,3-bis(2-chloroethyl)-1-triazeno]imidazole-4(5)-carboxamide (NSC-82196) (XXXI) is an antileukemic agent, which spontaneously cyclizes in the solid state at room temperature (Scheme XIV) (61–63). The structure of the product (XXXII) was unequivocally confirmed by crystal structure determination (64).

Similarly, 5-[3,3-bis(2-chloroethyl)-1-triazeno]pyrazole-4-carboxamide (XXXIII) spontaneously cyclizes (Scheme XV). The structure of the triazolium chloride (XXXIV) was determined by single-crystal X-ray techniques (65).

These reactions raise the question of whether the bis-2-chloroethyl-1-triazenes crystallize with one chloroethyl group in a conformation favorable to cyclization. Thus, the most important crystal structure in this series is that of the starting material rather

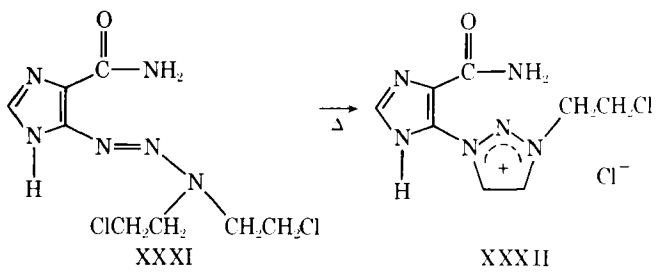

Scheme XIV

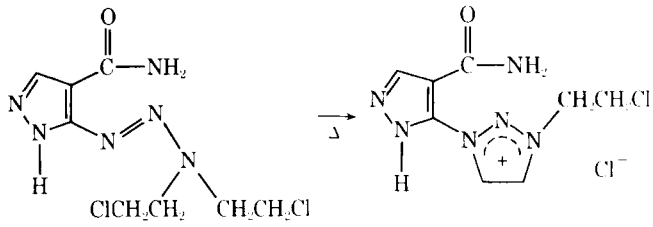

XXXIII XXXIV

Scheme XV

than the product. Of particular interest is the possibility that N····CH_2Cl atoms in the crystal are in a trigonal bipyrimidal geometry favorable to an S_N2 reaction. A packing arrangement favorable to this cyclization (XXXV) was recently proposed in connection with crystallographic studies of dacarbazine [5-(3,3-dimethyl- 1-triazeno)imidazole-4-carboxamide (NSC-45388)] (66). However, the geometry at the reaction center of XXXV is not perfectly trigonal bipyrimidal with the chloride anion leaving as the nitrogen attacks because of the proposed N—H- - -Cl hydrogen bond. Whether the solid-state geometry is that in XXXV or a trigonal bipyrimidal arrangement can only be resolved by the determination of the crystal structure of this compound.

Of practical importance are experiments directed toward crystallizing these bis-2-chloroethyltriazenes in unreactive solid-state conformations.

An interesting solid-state reaction involving nucleophilic addition of an amine to an amide (transamidation) was observed when crystals of cycloserine (XXXVI) were heated (Scheme XVI) (67). This reaction was studied in a humid atmosphere and may occur in solution. A similar dimerization was observed in concentrated solutions. Unfortunately, the crystal structure of cycloserine has not been determined. However, if a solid-state reaction is involved, the relationship of the crystal packing to dimerization would be of interest.

Decomposition of 3-Amino-4-hydroxybenzenearsonous Acid (XXXVII)—This acid, which was used to treat syphilis, quantitatively decomposed in the absence of oxygen at 100° (Scheme XVII) in 7 days (68–70). (After 5 years, essentially no decomposition was observed at room temperature.) In contrast, after 5 days at 100° under anaerobic conditions, the hydrochloride salt of the anhydride of 3-amino-4-hydroxybenzenearsonous acid (XXXVIII) decomposed only slightly and only 15% decomposition was observed under aerobic conditions. The pentahydrate of this anhydride (XXXVIII) liquefied

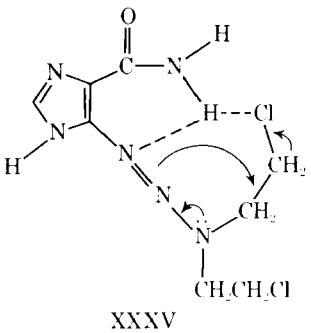

XXXV

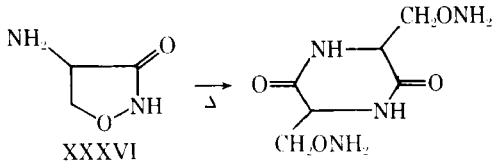

XXXVI

Scheme XVI

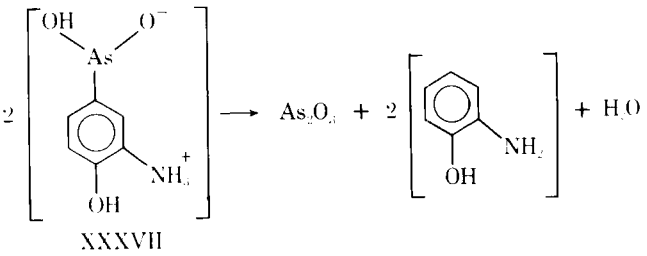

XXXVII

Scheme XVII

after only 24 hr at 100°, and after 48 hr an essentially quantitative yield of *m*-aminophenol was obtained. This pentahydrate, like other derivatives of 3-amino-4-hydroxybenzenearsonous acid, gave oxidation products (*e.g.*, XXXIX) of an aminophenol when heated in the air.

The lack of reactivity of the anhydride (XXXVIII) relative to the acid (XXXVII) may be related to packing in the crystal.

SOLID–GAS REACTIONS

A review of solid–gas reactions of molecular crystals recently appeared (3). Only some important points will be summarized here.

Sensitivity to Minor Structural Changes—One striking feature of solid–gas reactions is their sensitivity to minor changes in the structure of the solid. For example, solid tetramethylrubrene in the presence of light readily adds oxygen while the parent dye, rubrene, does not (71).

Similarly, hydrocortisone-21-*tert*-butylacetate (XL*a*) yielded, upon standing at room temperature for 1–2 years, 40% of the 11-one (XLI) (Scheme XVIII) (72, 73). In contrast, other esters, including the ethyl ester (XL*b*), were completely resistant to air oxidation even after 15 years at room temperature. The oxidation of XL*a* was accelerated by heat and greatly accelerated by free radical initiators and UV light. The reactivity of crystals of these esters was apparently related to the nonstoichiometric incorporation of solvent into the crystal lattice. The inert crystals were either stoichiometric solvates or unsolvated crystals. Unfortunately, the structure of these nonsolvated crystals was not studied further.

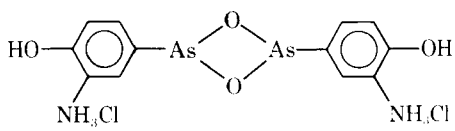

XXXVIII

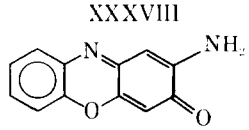

XXXIX

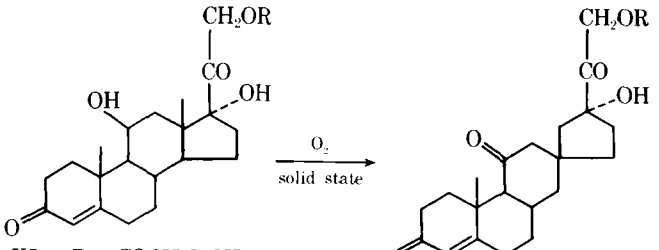

XL*a*: R = $COCH_2C(CH_3)_3$
XL*b*: R = COC_2H_5

XLI: R = $COCH_2C(CH_3)_3$

Scheme XVIII

A related but more dramatic observation was made during studies of the biological properties of dihydrophenylalanine (*l*-1,4-cyclohexadiene-1-alanine, XLII) (74, 75). Dihydrophenylalanine is an effective antagonist of phenylalanine and is obtained from a one-step Birch reduction of phenylalanine. Crystallization of XLII from a dilute 80% ethanol solution yielded stable prisms (mp 235–236°), while crystallization from a saturated 80% ethanol solution or methanol–ethyl acetate yielded unstable needles. After 10 min at 100°, these unstable needles contained 70% phenylalanine (XLIII) (Scheme XIX). In aqueous solution the dihydrophenylalanine was recovered unchanged after 5 hr at 100°. Elemental analysis and NMR studies showed that the unstable crystals were hydrates (three water molecules associated with four molecules of XLII). The stable prisms, however, contained no water of hydration. Furthermore, the rate of the solid-state dehydrogenation was obviously much faster than the rate in solution (70% decomposition in 10 min in the solid state at 100° and 0% decomposition in 300 min at 100° in solution).

A possible explanation of this observation is that the dehydrogenation is preceded by loss of the water of crystallization and that the dehydrated crystal form is very reactive, perhaps because of the large number of defects left after water evaporation. This explanation is inconsistent with studies of the loss of solvent from crystals of phenylazotribenzoylmethane hemietherate. While phenylazotribenzoylmethane (XLIV) rearranged in the solid state, the crystals formed after loss of ether of crystallization were no more reactive than unsolvated crystals (76). In fact, in this case, microcrystallites of the unsolvated crystalline form were obtained when ether was lost, as shown by X-ray diffraction studies[4].

Reactions of Acids and Anhydrides with Ammonia—Photomicrographic investigations of these reactions show that the penetration of ammonia into the crystal is highly anisotropic. The different reactivity of the crystal faces can be explained in terms of the crystal packing (3). For example, *p*-chlorobenzoic acid upon crystallization forms carboxylic acid dimers which pack, giving layers of nonpolar phenyl rings and polar carboxyl groups parallel to the (100)

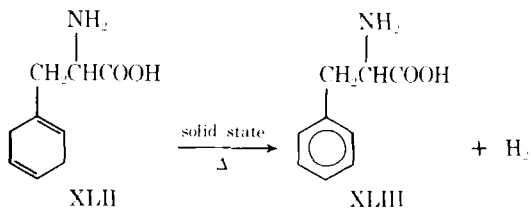

XLII XLIII

Scheme XIX

crystal face (the top or bottom face in Fig. 5). Ammonia can easily penetrate the faces of the crystal nearly perpendicular to the (100) face, since the polar NH_3 molecules can proceed down the polar stacks of carboxyl groups. However, ammonia molecules reacting with the (100) face encounter layers of polar and nonpolar material, which significantly retards the rate of reaction of gas with this face and leads to the observed anisotropy.

The anisotropic reactivity of crystals of at least six other acids and anhydrides was explained in terms of similar concepts related to the crystalline packing (3). Most of the reactions were ditropic (two pairs of faces were reactive); however, the crystals of the cyclopropane carboxylic acid (XLV) showed unitropic reactivity (one pair of faces was reactive). The unitropic reactivity of XLV may be related to the crystal packing. Crystals of XLV contained chains of carboxyl groups rather than dimers.

As for many solid-state photochemical and thermal reactions, defects appear to play an important role in the initiation of solid–gas reactions. These reactions often begin at a crystal edge and move inward in "fingers" toward the middle. All crystals retain their original shape for a substantial part of the reaction. In some cases, particularly the reaction of adipic acid with ammonia, the crystals were observed to crack and break apart (77). The reaction of ammonia with acenaphthylene-1-carboxylic acid was found to occur at relatively unreactive faces in the presence of certain slip defects (78).

SOLID-GAS REACTIONS OF MEDICINAL AGENTS

Solid–gas reactions are probably the most common solid-state reactions of medicinal agents, since solid-state hydrolysis with water vapor and solid-state oxidations by oxygen belong to this group. Solid–gas addition reactions and solid-state reactions involving elimination of a gas or elimination of a solvent from crystals are included in this section.

Photofading of Dyes Used in Coating Tablets—This area has been reviewed (79) and only selected examples will be treated.

Tablets were coated with the following dyes: FD&C Red No. 1, FD&C Red No. 3, FD&C Green No. 5, FD&C Green No. 3, FD&C Blue No. 2, FD&C

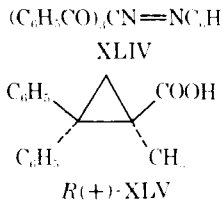

XLIV

R(+)-XLV

[4] *Added in proof:* Recently a second example of a solid-state reaction faster than the corresponding solution reaction was reported [C. N. Sukenik, J. A. P. Bonapace, N. S. Mandel, R. G. Bergman, P.-Y. Lau, and G. Wood, *J. Amer. Chem. Soc.*, **97**, 5290(1975). The X-ray crystallographic study of the reactive crystals showed that the crystal packing was particularly favorable to reaction.

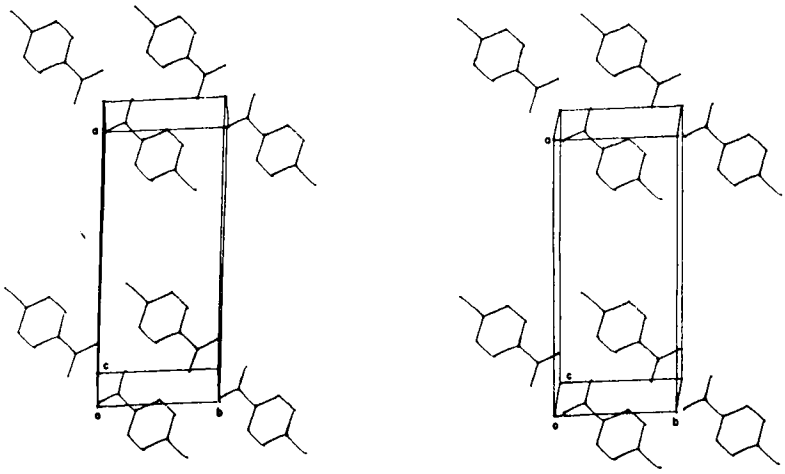

Figure 5—*Stereo pair view of the packing of* p-*chlorobenzoic acid (77).*

Blue No. 1, FD&C Yellow No. 5, FD&C Yellow No. 10, D&C Orange No. 3, and FD&C Violet No. 1. The dye erythrosine (XLVI) (FD&C Red No. 3) was the most reactive (80, 81). The decompositions of these dyes probably involve photochemical solid–oxygen reactions. Such an explanation is supported by the observation that erythrosine undergoes oxidative bleaching in solution (82). The triplet state of fluorescein also is reported to react with oxygen to yield a semioxidized dye (83).

The solid-state oxidation of these dyes may be mechanistically related to the photochemical oxidation of tetramethylrubrene and could involve addition of oxygen to an excited state of the dye. A plausible alternative explanation is that these reactions involve singlet oxygen addition to ground-state dye molecules. Rose bengal and eosin are fluorescein derivatives and are used as photosensitizers for the production of singlet oxygen in solution (84). As was the case for tetramethylrubrene and rubrene, different derivatives of fluorescein have different reactivities. A third mechanism involving free radical-initiated oxidation, similar to that postulated for β-carotene (discussed later), cannot be ruled out.

Indigo and triphenylmethane dyes are also oxidized in the solid state. Brilliant indigo 4B (XLVII) is oxidized and dehalogenated to give bromoisatin (XLVIII) (Scheme XX) (85), while FD&C Blue No. 2 (XLIX) decomposes in the presence of light and reducing agents to a leuco form (L) (86). In the presence of tablet excipients containing reducing sugars, this reaction is facile (86) and may proceed by a mechanism similar to the one shown in Scheme XXI. This mechanism was proposed for the corresponding solution reaction.

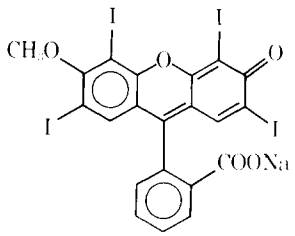

XLVI

Loss of Solvent of Crystallization—Whether the crystal form contains solvent of crystallization can affect the stability and bioavailability of a drug. The loss of solvent of crystallization, while not a chemical reaction, has several features in common with solid–gas reactions since considerable intermolecular interaction can be involved.

The loss of water of crystallization from theophylline monohydrate (LI) and ampicillin trihydrate (LII) was studied (87, 88). The kinetics of desolvation of theophylline monohydrate were followed using X-ray powder photography, since the powder patterns of the monohydrate and anhydrous forms are substantially different. The reaction obeyed zero-order kinetics from 38 to 54° and had an activation energy of 33 kcal/mole. Caffeine monohydrate also desolvated in the solid state and the hydrated and anhydrous forms had different powder patterns (87).

Similarly, ampicillin trihydrate (LII) lost water at temperatures ranging from 68 to 95°. This reaction was also followed using X-ray powder diffractometry. This reaction obeyed zero-order kinetics and had an energy of activation of about 23 kcal/mole. The zero-order kinetics of these reactions indicate that solvent loss proceeds from nuclei according to the diminishing-sphere model (87, 88).

In contrast to these studies, the powder patterns of the solvates and unsolvated crystal forms of cephaloglycin (LIII) and cephalexin (LIV) are virtually iden-

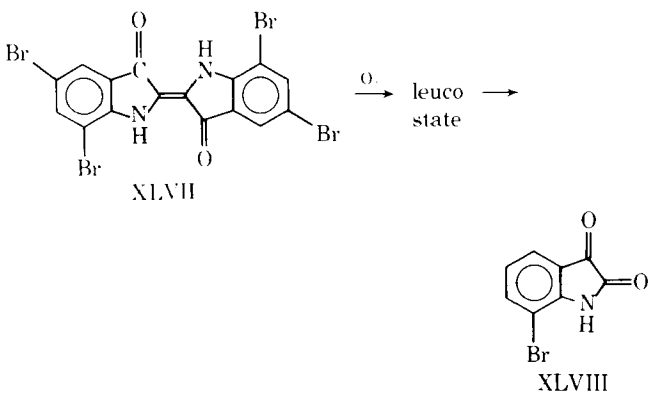

XLVII XLVIII

Scheme XX

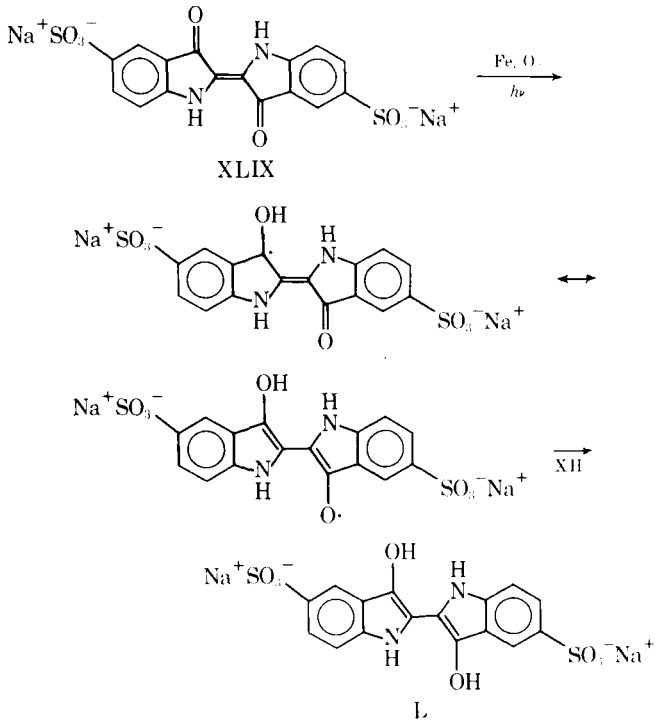

Scheme XXI

tical (89). Cephaloglycin forms solvates with water (1:2), formamide (1:1), methanol–water (1:1:1), acetonitrile–water (1:1:1), acetic acid–water (1:1:1), acetic acid (1:2), acetic acid–methanol (1:1:1), ethanol–water (1:1:1), and *N*-methylformamide (1:1). Cephalexin forms solvates with water (1:2 and 1:1), formamide (1:1), methanol (1:1), acetonitrile (1:2), acetonitrile–water (1:1:1), *N*-methylformamide (1:1), and *N*-ethylformamide (1:1). Drying of many of these solvates under normal conditions reportedly yielded a "desolvated" crystal with a powder pattern very similar to that of the solvated crystal form.

Although the powder patterns of the desolvated crystals were not identical to the patterns of the solvated forms, only minor differences such as a general loss of diffraction intensity and a change in the intensities at one or two reflections were reported. Exposure of the desolvated crystal to solvent vapor yielded the original solvate. This behavior has been termed crystal pseudopolymorphism and is perhaps related to the behavior of solvates of cyclodextrins, although no structural reasons for the presence of large cavities in the crystal are apparent. It would be interesting to determine the crystal structure of some of these solvates to find how the solvent molecules are packed in the lattice and to compare the theoretical powder pattern calculated from the atom positions in the single crystal to that observed.

Solid-State Hydrolysis of Aspirin (LV)—This

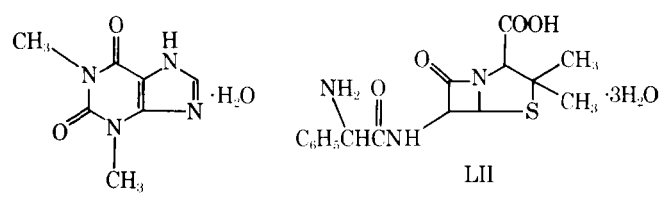

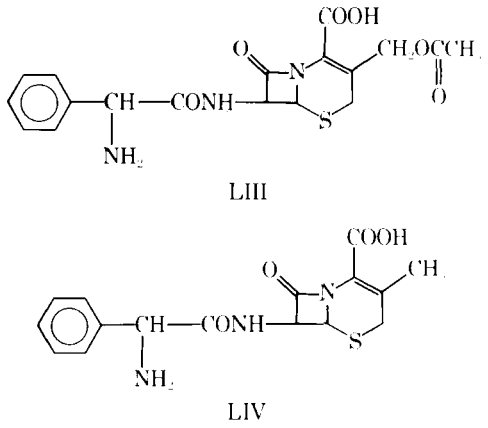

LIV

reaction (Scheme XXII) was studied in the presence and absence of moisture at 50–80° (90). As the humidity increased, the rate of reaction increased. The kinetics of this reaction were treated in terms of a solution reaction in which water was adsorbed onto the surface of the aspirin, with the amount of water adsorbed assumed to be proportional to the pressure of water. However, all experiments reported were run at a water pressure substantially below the vapor pressure (91); furthermore, aspirin is not hygroscopic. The reliability of these kinetic studies is probably poor, since a later study showed that sublimation of salicylic acid (LVI) from a cellulose-coated aspirin tablet caused appreciable errors in the measurement of the percent decomposition (92).

The observation of sublimed salicylic acid (LVI) on the surface of cellulose-coated aspirin tablets is also difficult to interpret in terms of a solution reaction on the surface of the solid, since it is unlikely that salicylic acid would sublime out of a water solution. However, it is quite likely that if the hydrolysis proceeds rapidly, the acetic acid produced will be unable to evaporate and the reaction will proceed in an acetic acid solution. The vapor pressure of acetic acid is 100 mm at 63°, indicating the substantial volatility of this acid. The eutectic point of mixtures of aspirin (mp 143–144°) and salicylic acid (mp 157–159°) has not been determined, but aspirin crystals containing 60.0, 23.9, 17.7, and 1.3% salicylic acid had melting points of 115, 115, 114, and 136.6°, respectively. These findings indicate that the eutectic point is probably much greater than 80° and rule out the possibility of reaction in a melt of these compounds in the absence of acetic acid.

Studies of aspirin crystals heated on a hot stage would perhaps provide a definitive solution to this problem. Our preliminary studies on aspirin crystals grown from benzene heated at 95, 87, and 68° on a hot stage in air showed that the crystal edges softened and liquid appeared after a few minutes, 24 hr, and 48 hr, respectively, although the crystals did not

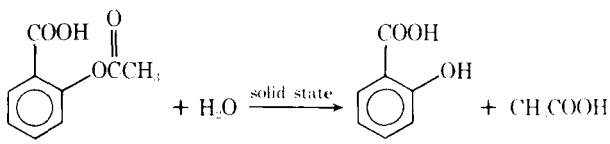

Scheme XXII

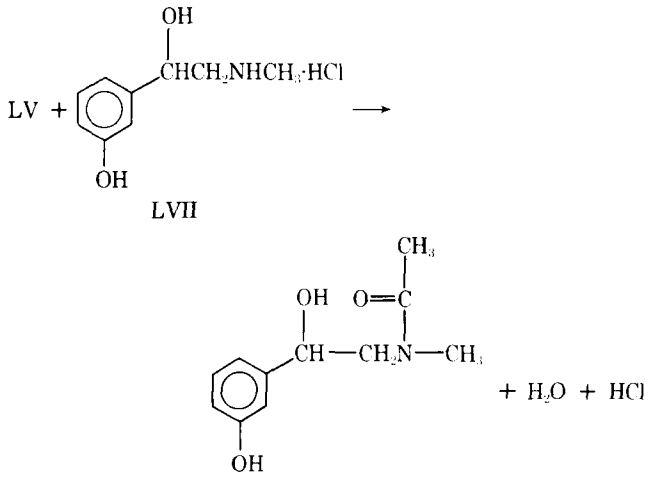

Scheme XXIII

melt. These observations substantiate the suggestion that this reaction proceeds in solution, at least at high temperatures. The solution may result because acetic acid does not evaporate rapidly enough.

Excipients and antacids accelerated the decomposition of aspirin. A study was made of the effect of antacids on the decomposition of aspirin after 1 year. In the presence of some antacids, such as calcium carbonate, aspirin was 4.4% decomposed; in the presence of others, such as sodium bicarbonate, there was complete decomposition in 44 weeks (93). Diluents also affected the stability of aspirin tablets, cellulose and calcium sulfate conferring substantially more stability than mannitol–starch or amylase (94). The decomposition of aspirin in the presence of these compounds was related to the amount of moisture sorption and to the tablet hardness (94).

A comparison of aspirin decomposition in suspensions and in tablets in the presence of diluents and antacids showed that the rates of decomposition were nearly the same (95). Of the compounds studied, hexanoic acid conferred the most stability to aspirin and magnesium trisilicate conferred the least.

Tablet mixtures containing aspirin and drugs with easily acylated functionalities react to give acyl compounds (LVIII) and salicylic acid (Scheme XXIII). For example, mixtures of phenylephrine hydrochloride (LVII) and aspirin (LV) contained 80% of acylated phenylephrine after 34 days at 70° (96). A mixture of starch and magnesium stearate slowed this acylation to only about 1% after 34 days, while magnesium stearate without starch caused complete decomposition after 16 days. Some diacylated product was also obtained. This reaction may proceed by direct acylation.

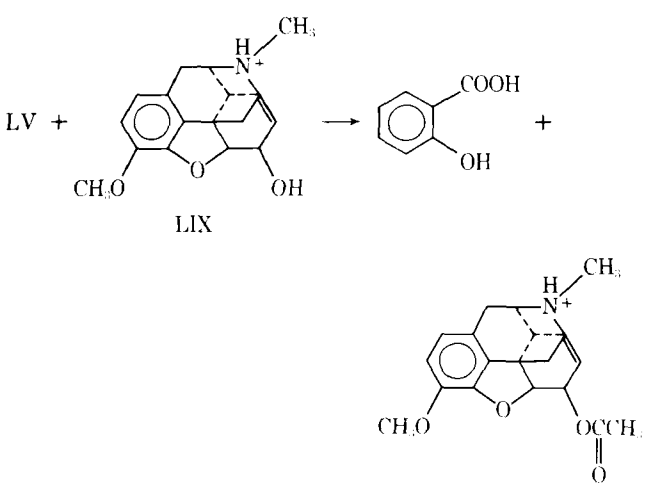

Scheme XXIV

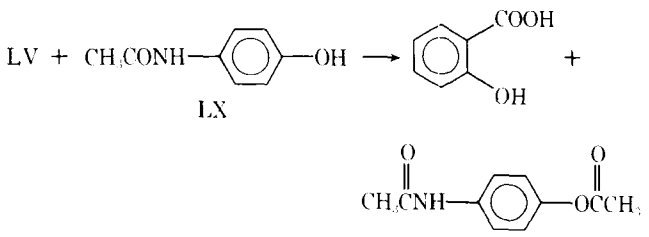

Scheme XXV

Similarly, tablets containing aspirin and codeine (LIX) (Scheme XXIV) and aspirin and acetaminophen (LX) (Scheme XXV) also yielded acylated drugs upon heating (97, 98).

Thermal Decarboxylation of *p*-Aminosalicylic Acid (LXI)—The solid-state and solution decarboxylations of the antituberculosis drug aminosalicylic acid have been carefully studied (99, 100). In buffered aqueous solution, the rate-determining step of the general-acid-catalyzed decarboxylation reaction apparently involves addition of a proton to the carboxylate anion (Scheme XXVI).

Crystals of aminosalicylic acid (mp 220° dec.) decarboxylated upon heating at 70, 75, or 80° to yield *m*-aminophenol (mp 122–123°). Photomicrographs showed that the crystals cracked and broke upon reaction (99). Kornblum and Sciarrone (99) also found that a carbon dioxide atmosphere did not retard the rate of solid-state decomposition, and the reaction was about 10 times as fast in moist atmospheres as in dry atmospheres. The rate of the reaction was apparently controlled by nucleus formation and was zero order. Recently, another study of the kinetics of decomposition of aminosalicylic acid in the solid state was reported (101). First-order kinetics were observed and interpreted in terms of competing solid-state and solution reactions (101). The solution reaction was suggested to occur in a sorbed moisture layer approximately 60 Å thick.

The decarboxylation of aminosalicylic acid was studied at 65, 68, and 72°[5,6]. Mixed melting-point studies showed that the eutectic point for a 1:1 mixture of aminosalicylic acid and *m*-aminophenol was

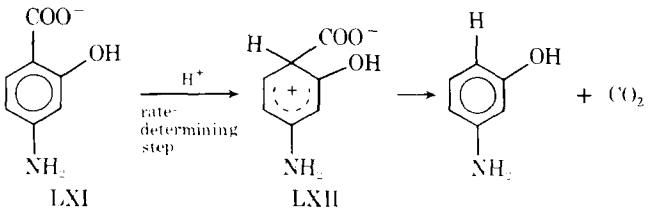

Scheme XXVI

[5] S. R. Byrn and J. L. Killian, unpublished observations.

[6] The atomic coordinates used for this drawing were recently determined by Dr. P. Y. Siew in our laboratories and correct those reported in the literature (102). Full details will be reported shortly.

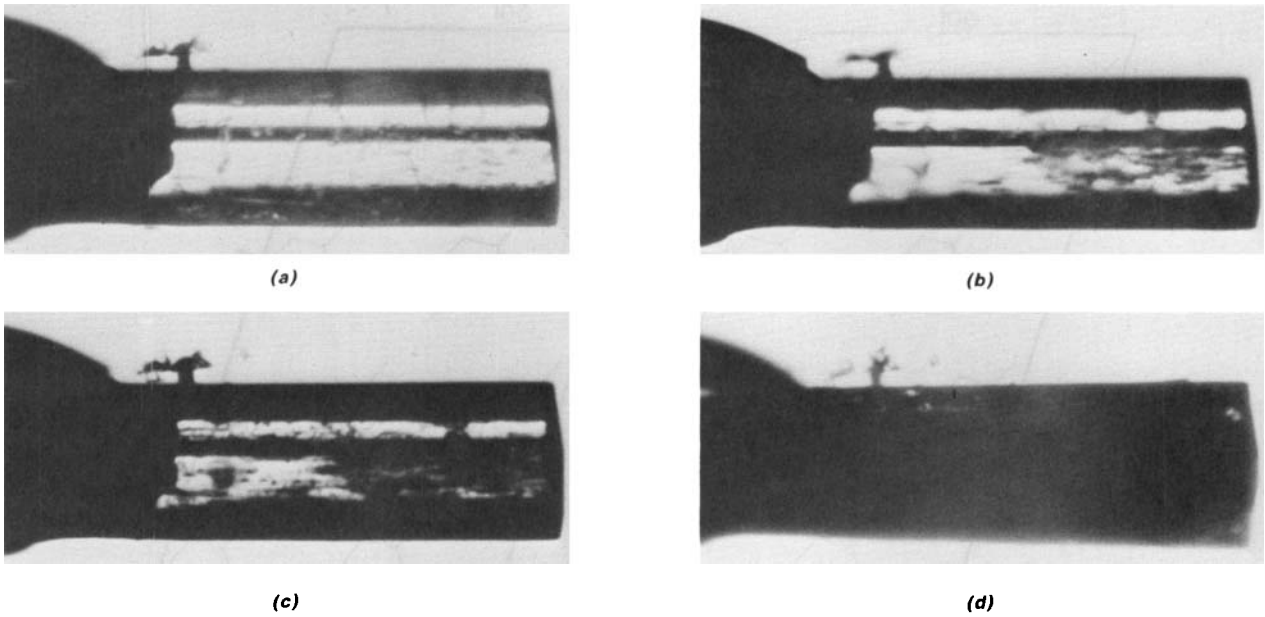

Figure 6—*View of a crystal of aminosalicylic acid after heating on a hot stage at 68° for* (a) *50 hr,* (b) *12 days,* (c) *21 days, and* (d) *33 days. The faces of the crystal were determined by optical goniometry and precession photography. The "crystal" shown in* (d) *was a mixture of pure* m*-aminophenol and aminosalicylic acid.*

about 110°. Figure 6 shows the behavior of a single crystal of aminosalicylic acid at 68° as photographed in air[7]. The decarboxylation reaction appears to occur on the 10$\bar{2}$ face, leaving the 001 face relatively unreacted.

The crystal packing of aminosalicylic acid is shown in Fig. 7[6]. An examination of these diagrams indicates that there are layers of polar carboxyl groups and nonpolar aromatic groups parallel to the 001 face and somewhat perpendicular to the 10$\bar{2}$ face. One possible explanation of the surface behavior of the crystal faces is that the carbon dioxide formed exits from the 10$\bar{2}$ face rather than passing through alternating planes of polar and nonpolar functionalities to exit from the 001 face. However, other explanations involving preferential sublimation of aminosalicylic acid or the more volatile *m*-aminophenol from the 10$\bar{2}$ face cannot be ruled out.

Furthermore, the relationship between the solid-state and solution reactions of aminosalicylic acid and the source of the proton for catalysis of the solid-state reaction (if the mechanisms of the solid-state and solution reactions are similar) is not known. Since the rate-determining step of the reaction is almost certainly not the exit of carbon dioxide from the crystal, the progress of the reaction through the crystal must be explained in terms of other processes. For example, the direction of migration of catalyzing protons through the crystal might be related to the progress of the reaction. We are presently studying this and other possible mechanisms as well as the surface behavior of the faces of these crystals.

[7] A Mettler FP-5 hot stage and a Zeiss microscope equipped with camera were used.

The reverse reaction also was reported to occur upon heating a mixture of *m*-aminophenol (mp 122–123°), potassium carbonate, and carbon dioxide at 175° in a ball mill (Scheme XXVII) (103). The melting point of *m*-aminophenol (122°) and the eutectic points of *m*-aminophenol and aminosalicylic acid (110°) indicate that this reaction probably occurs in the liquid state.

The decomposition reaction of solid benzoic acid derivatives to give carbon dioxide gas and a liquid product also was studied (104). The kinetics of these reactions were interpreted in terms of competing solid-state and liquid reactions. Interestingly, the rate of the solid-state reaction was inversely related to the melting point of the starting acid. (See section on vitamin A for a discussion of the effect of the melting point on reactivity.)

SOLID-STATE REACTIONS OF MEDICINAL AGENTS CONTAINING POLYENE FUNCTIONALITIES

These reactions are difficult to classify since polyene functionalities have been reported to undergo solid–gas reactions, thermal reactions, and photochemical reactions. Therefore, they have been placed in a section by themselves.

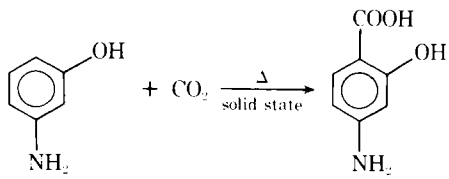

LXIII

Scheme XXVII

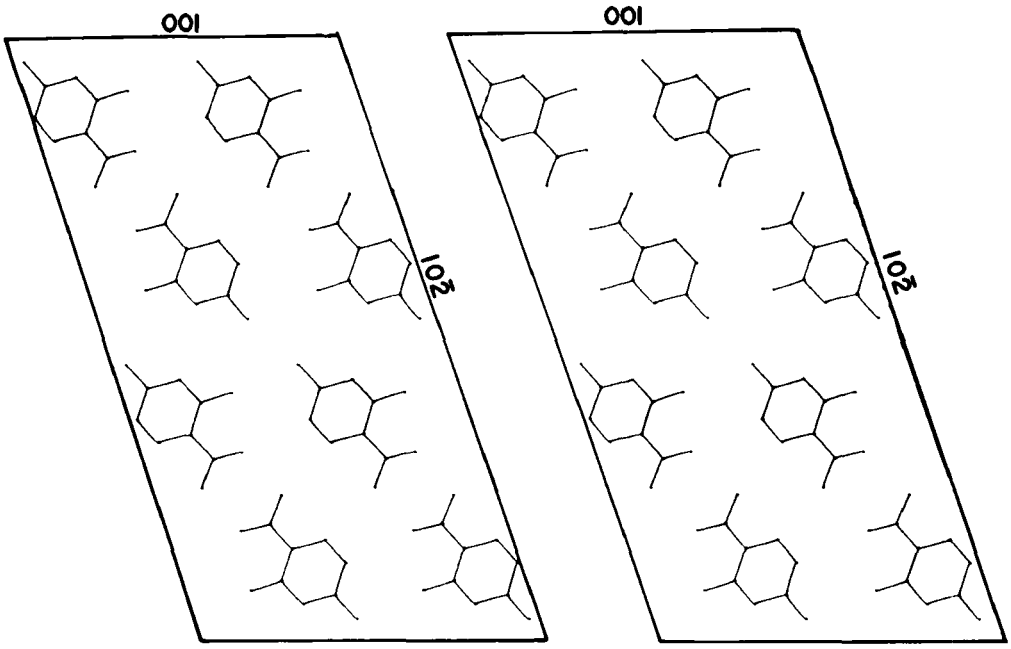

Figure 7—*Stereo pair view of the crystal packing of aminosalicylic acid as viewed from a direction parallel to the 001 and 10$\bar{2}$ planes.*

Thermal and Photochemical Degradation of Fumagillin—Fumagillin (LXIV) undergoes both solution and solid-state photochemical reactions, and the solid decomposes thermally (105–107). Irradiation of fumagillin with a fadeometer[8] (light about twice as intense as sunlight) in ethanol solution yielded neofumagillin (structure unknown). The rate and products of this reaction were the same whether the reaction was run in air or nitrogen. Experiments with filters indicated that the photoreaction of fumagillin (λ_{max} 351 and 366 nm, shoulder at 315 nm) required light of a wavelength greater than 280 nm.

Although Garrett and Eble (105) suggested that the polyene side chain of fumagillin might cyclize to yield the cyclohexadiene species neofumagillin (LXV), these workers also indicated that neofumagillin was photolabile and decomposed shortly after formation. It was also suggested that neofumagillin solvolytically rearranged, which hampered any further attempts to determine its structure.

The course of solid-state photolysis of fumagillin depends upon the atmosphere (106). In the presence of air, an oxidized product is obtained upon photolysis in a fadeometer; but in the absence of air, an oxygen-sensitive product is obtained. After the first 5 hr, the first-order rate constant of the solid-state photolysis in air is of the same order of magnitude as the solution photolysis (0.14 hr^{-1}). During the first 5 hr, the reaction is definitely not first order and it may involve a kinetically important intermediate (106). The relationship between the products of the solid-state and the solution reactions has not been studied, but some of the products are probably the same (106).

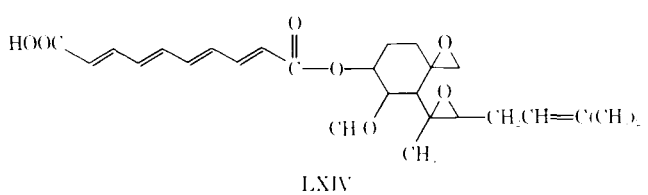

LXIV

The solid-state thermal reaction of fumagillin proceeds by different but unknown mechanisms in the presence and in the absence of air (107). The reaction in the presence of air was interpreted as a thermally induced oxidation. The solid-state thermal reaction is poorly understood but is slower than the photolytic reaction and should not interfere with photolytic studies. Fumagillin is thermally stable in ethanol solution. Further studies of the products and of the influence of crystal packing on this reaction are needed.

Thermal and Photochemical Degradation of Ergocalciferol (Vitamin D_2)—Ergocalciferol (LXVI) has an extensive series of solution, photochemical, and thermal reactions (Schemes XXVIII–XXX) [R = —$CH(CH_3)CH{=}CHCH(CH_3)CH(CH_3)_2$] (108, 109). Crystalline ergocalciferol is light, air, and heat sensitive and gives a number of products whose structures have not been determined (110, 111). Furthermore, although crystalline ergocalciferol is unstable and was deemed unsuitable for crystallographic studies, crystals of the 3,20-bisethylenedioxy (112) and the 4-iodo-5-nitrobenzoate (113) derivative are more stable and their crystal structures have been determined.

We found that crystalline ergocalciferol ($C_{28}H_{44}O$, mol. wt. 396.6; calc.: C, 84.8%; H, 11.2%) completely

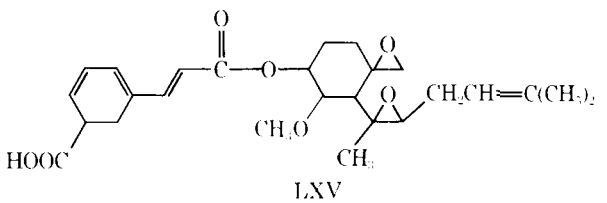

LXV

[8] Atlas.

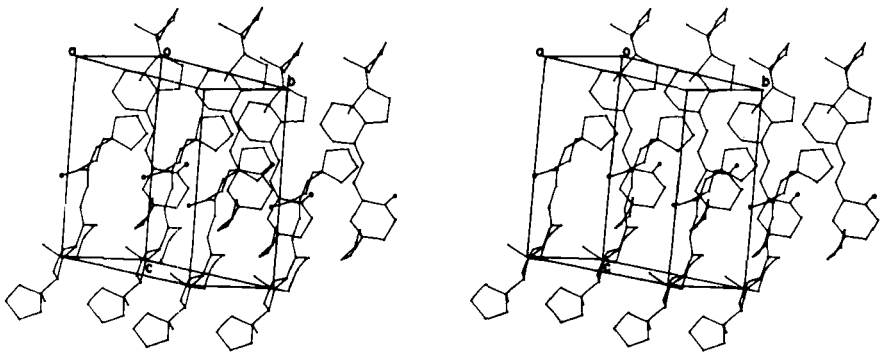

Figure 8—*Stereo pair packing drawing of 3,20-bisethylenedioxycalciferol (112). Contacts of less than 5.5 Å between the triene functionalities involved only C(19), which is designated by the heavy dot. These are: C(19)–C(5), 4.70 Å; C(19)–C(6), 4.24 Å; C(19)–C(7), 5.12 Å; and C(19)–C(8), 5.18 Å. (See Scheme XXVIII for numbering.)*

decomposed to a yellow powder (mp 58–100°) after 6 months at room temperature in air, although the "crystals" retained their original shape. TLC showed that at least five products were formed. Elemental analysis of this powder indicated extensive oxidation; observed: C, 66.0%; H, 7.7%; calc. for $C_{28}H_{44}O_8$: C, 66.12%; H, 8.72%[9]. Mass spectra indicated degradation since the highest molecular ion observed had a mass of 276. We also found that crystals of ergocalciferol decomposed and eventually melted when heated at 80° in air in the presence and absence of light. Elemental analysis of these melts indicated oxidation. Crystals were stable when heated for 1 week at 80° in the absence of oxygen[9].

These thermal and photochemical solid-state reactions in air apparently do not involve formation of cyclized ergocalciferol derivatives such as ergosterol (LXVIII), lumisterol (LXX), or suprasterols (LXXIII and LXXIV). Furthermore, the mass spectral data indicate that ergocalciferol does not undergo photochemical dimerization in the solid state. This finding is consistent with the packing (Fig. 8) of the bisethylenedioxy derivatives of ergocalciferol. No close contacts between double bonds are apparent in Fig. 8. In fact, the only intermolecular contacts less than 5.5 Å between atoms in the triene functionality involve only atom C(19). Topochemically controlled dimerization reactions do not seem possible. A topochemically controlled polymerization of bisethylenedioxy calciferol involving successive linkage of C(19) to C(6) is possible but is not consistent with the melting point and mass spectral studies discussed previously. An intramolecular photocyclization of ergocalciferol to suprasterol is possible; but if it is occurring, its rate must be substantially slower than the air oxidation.

Thus, the solid-state oxidation of ergocalciferol is much less specific than oxidations of the cortisone derivatives. However the ethylenedioxy and 4-iodo-5-nitrobenzoate derivatives are more stable than vitamin D itself. It is not known whether these compounds undergo any solid-state reactions.

The mechanism of the solid-state oxidation of ergocalciferol is unknown but may involve one or more of the following paths: (*a*) singlet-oxygen addition to the diene or triene group of ergocalciferol, (*b*) reaction of an excited state of ergocalciferol with ground-state oxygen (as in the rubrene reaction), and (*c*) free-radical reactions initiated by heat or light involving formation of hydroperoxides alpha to the double bond system. The singlet-oxygen path and the addition of ground-state oxygen to an excited state of ergocalciferol cannot be the only pathways, since oxidation was observed when ergocalciferol was heated in the dark.

Decomposition of Vitamin A and Derivatives—Crystalline esters of vitamin A (LXXV) (including the succinate half-ester, the nicotinate, and the 3,4,5-trimethoxybenzoate) decompose by both polymerization and oxidation pathways (114, 115). Vitamin A, exposed to air at room temperatures for several years or heated at 100° for 5 hr, gave at least five ketones on TLC plates treated with 2,4-dinitrophenylhydrazine (116).

β-Carotene (LXXVI) autooxidizes in the solid state at 25 and 35° (117). The rate of this oxidation depends on oxygen pressure and temperature, and a free radical mechanism was proposed for this reaction (Scheme XXXI) (117).

Diluents with antioxidant properties stabilize vitamin A palmitate in vitamin preparations (118). Aluminum salts of fatty acids such as stearic acid stabilize vitamin A, as does combination with gelatin and dextrin, which probably contain reducing sugars (119). In solution, vitamin A and its derivatives undergo several oxidation and isomerization reactions. For example, cobalt(II) stearate oxidized vitamin A to an epoxide with the postulated structure LXXVII. A hexane solution of vitamin A acetate was converted to peroxides in hexane in the presence of oxygen (120). Vitamin A gave 35% of the peroxide LXXVIII upon irradiation of a hexane solution (121) and a 50% yield of LXXVIII when irradiated in methanol in the presence of rose bengal (a singlet-oxygen sensitizer) (Scheme XXXII) (122).

It is impossible to predict the products of the solid-state oxidation on the basis of the solution studies discussed. These oxidation products probably can result from singlet-oxygen reactions, free-radical reactions, and perhaps even excited states of vitamin A. In this regard, the polymerization of vitamin A in the solid state could possibly be topochemically controlled. However, from the packing of vitamin A acetate in the solid state (Figs. 9 and 10), it is clear that there are no stacks of molecules that could undergo topochemically controlled polymerization. Two molecules have the C(11)–C(12) double bond parallel (di-

[9] S. R. Byrn and S. L. Midland, unpublished observations.

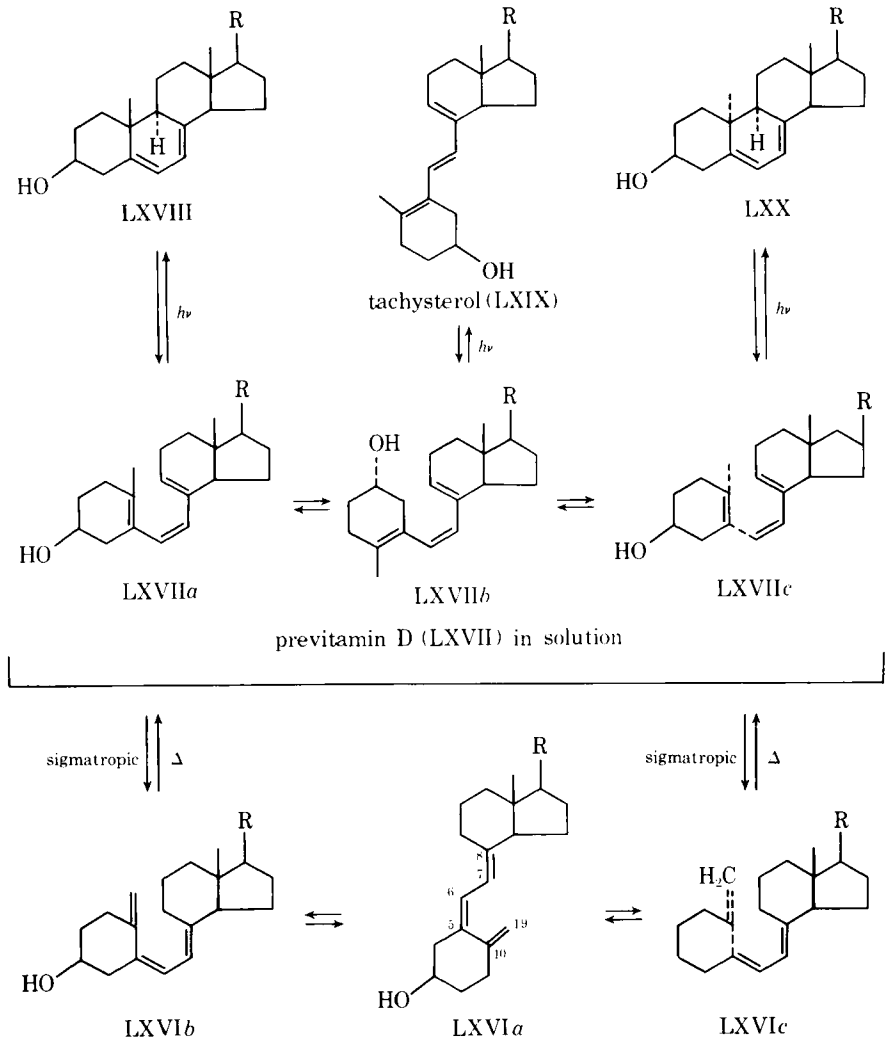

Scheme XXVIII

hedral angle = 0.0°) and related by a center of symmetry, but they are 5.41 Å apart, which is probably too far for dimerization, according to Schmidt's topochemical postulate (6).

An interesting correlation of the melting points of the vitamin A esters with their zero-order rate of solid-state decomposition was observed (114). The solution rates of decomposition of these esters were virtually identical. These results were interpreted in terms of crystal lattice energy. It was argued that the higher melting esters had more crystal lattice energy and thus were more stable to the solid–gas oxidation reaction. A much better measure of lattice energy in a series of compounds is the heat of sublimation (124). If the melting point is proportional to the heat of sublimation in this series, then the higher the melting point the more efficient is the packing and, conceivably, the less permeable is the crystal to reacting gas. The rates of reaction of acid crystals with ammonia do not correlate with the melting point of the acid (125). Whether this failure is due to the fact that the melting point does not correlate with the heat of sub-

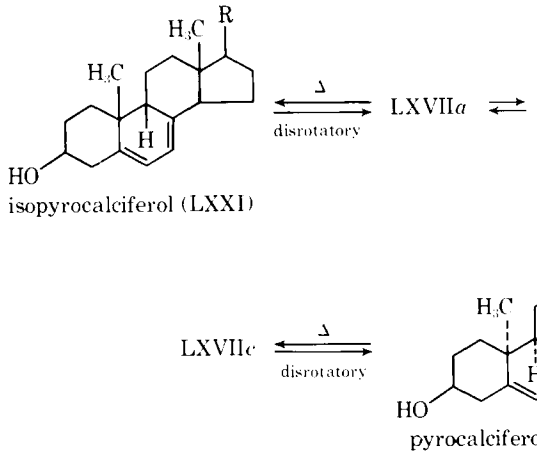

Scheme XXIX

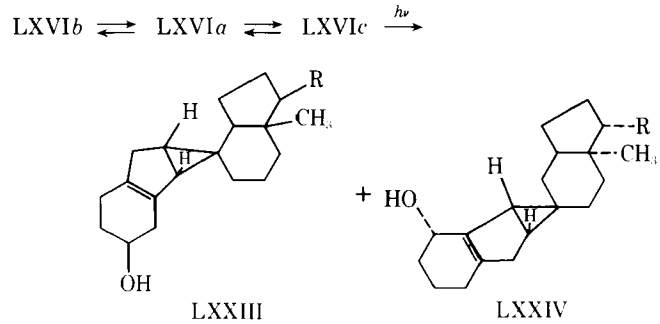

Scheme XXX

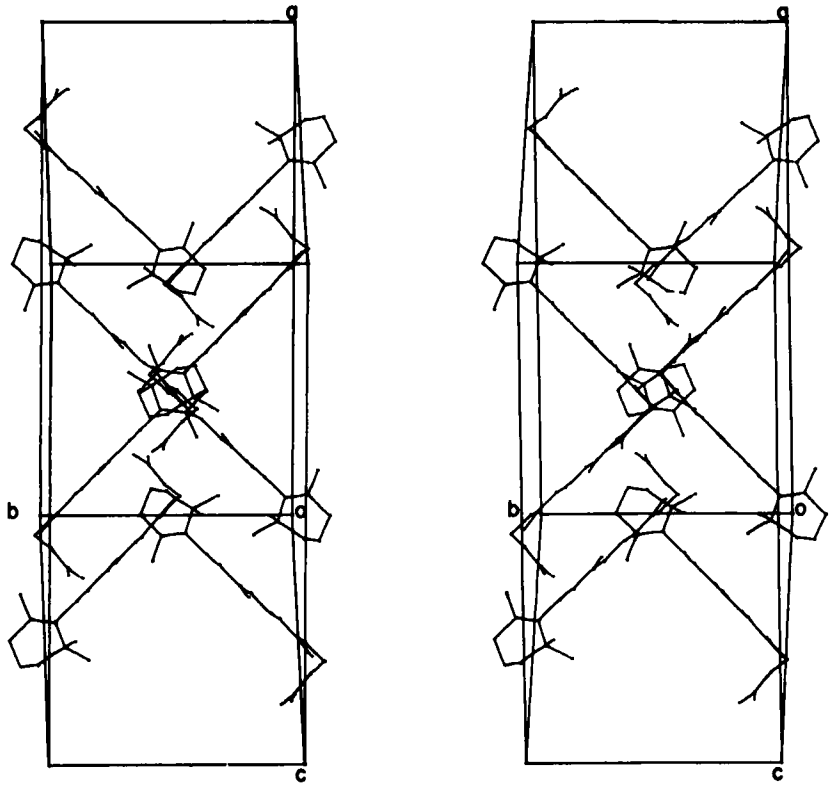

Figure 9—*Stereo pair drawing of the contents of the unit cell of vitamin A acetate, space group C2/c (123). A consideration of this drawing indicates that there are no stacks of molecules that could undergo topochemically controlled polymerization reactions.*

limation or other factors is not known.

In conclusion, it should be noted that the polyene antibiotics pimaricin (natamycin) (126) and filipin (127) are also oxidized in the solid state.

The degradation of solid polyenes apparently involves a complex series of reactions which can include: (*a*) polymerization, (*b*) oxidation by singlet oxygen, (*c*) free-radical-initiated oxidation, (*d*) reaction of oxygen with electronically excited drug molecules, and even (*e*) thermal rearrangement reactions.

APPLICATIONS: POTENTIAL FOR STABILIZATION OF DRUGS BY RATIONAL APPROACHES

In many of the solid-state reactions discussed, the derivative or crystal form present plays an important role in the reactivity. In the gibberellins, replacement of the ester by an acid changes the course of the photochemical reaction. Similarly, derivatives of ergocalciferol are more stable than the parent compound, and vitamin A esters with high melting points are more stable than those with lower melting points. Choline chloride crystallizes in two forms, one with unusually high radiation sensitivity and the other with normal radiation sensitivity. Cortisone derivatives containing nonstoichiometric quantities of solvent in the crystal are oxidized in air, while crystals containing stoichiometric amounts of solvent are unreactive as are unsolvated crystals. Crystals of the hydrate of dihydrophenylalanine dehydrogenate while the anhydrous crystals are thermally stable, and the crystalline hydrate of arsenous acid anhydride is more reactive than the anhydrous form.

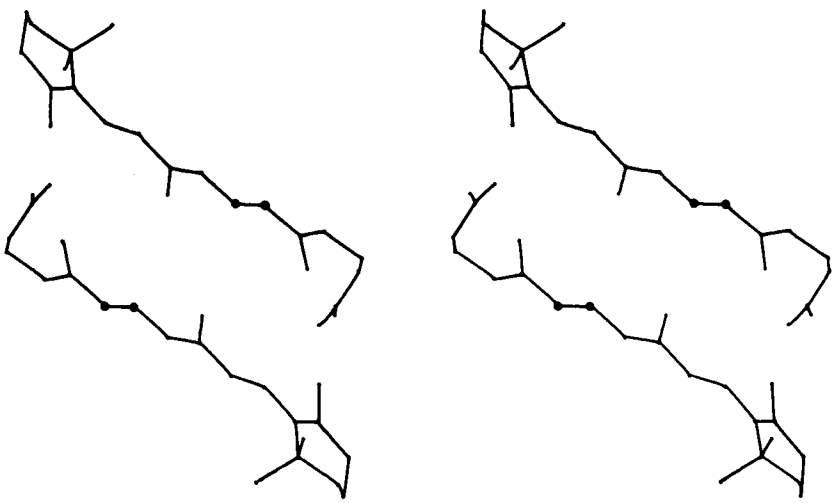

Figure 10—*Stereo pair view of two vitamin A acetate molecules. The atoms designated by heavy dots are C(11) and C(12), which are parallel and related by a center of symmetry. The C(11)–C(12) and C(12)–C(11) distance was 5.41 Å.*

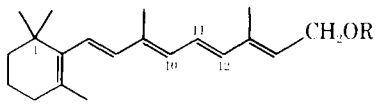

LXXV

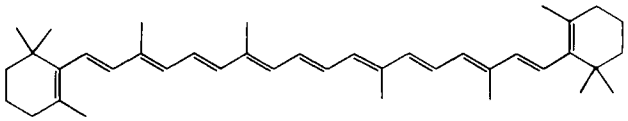

LXXVI

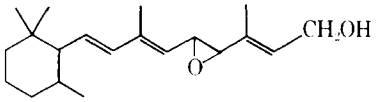

LXXVII

Recent studies on organic solid-state reactions have shown that a knowledge of crystal packing may explain the course of these reactions and the stereochemistry of the products. Furthermore, a knowledge of the factors influencing crystal packing is developing. In an example of the application of the concept called crystal engineering, Schmidt (6) was able to control the packing type of olefins using a 2,4-dichlorophenyl group. The presence of this group in a variety of olefins caused crystallization in the β-packing type. Irradiation of these crystals yielded the dimer with mirror symmetry, as expected from the topochemical postulate. Recently, Paul and Curtin (3) discussed the packing of carboxylic acids and showed the influence of this packing on solid–gas ammonia reactions.

Thus, many solid-state reactions can be explained in terms of crystal packing. An obvious corollary of this principle is that changing crystals packing can change the solid-state reactivity. The application of this idea to pharmaceutical problems will hopefully lead to more efficient and effective methods of drug stabilization.

In particular, once the mechanism of the decomposition process has been established, it is, in principle, possible to apply the concept of crystal engineering to the development of a more stable drug and dosage form. Attractive approaches involve the following:

1. Preparation of an equally active but more stable derivative of an unstable drug, in analogy with the attachment of a 2,4-dichlorophenyl group to olefins to control their packing. For example, esters of vitamin A have the same biological activity after correction for molecular weight differences but substantially different solid-state reactivity (115).

2. Crystallization of solvates or polymorphs with less solid-state reactivity, in analogy with the steroid and cinnamic acid reactions previously discussed.

These approaches will hopefully lead to more rational methods for stabilizing drugs in the solid state and the production of safer and more efficient products.

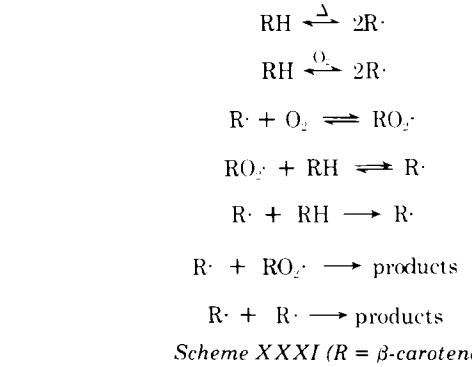

Scheme XXXI (R = β-carotene)

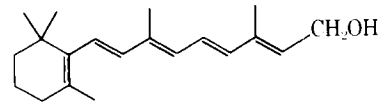

LXXV

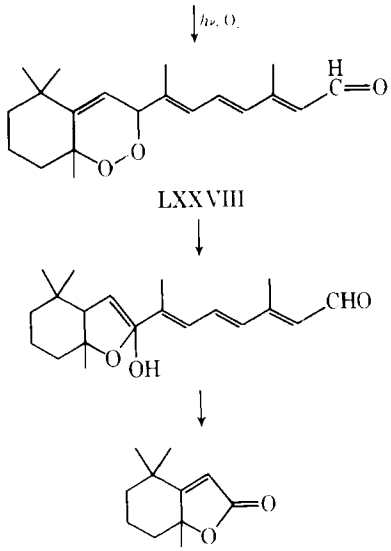

LXXVIII

LXXIX

Scheme XXXII

REFERENCES

(1) M. D. Cohen and B. S. Green, *Chem. Brit.*, **1973,** 490.

(2) I. C. Paul and D. Y. Curtin, *Acc. Chem. Res.*, **7,** 217(1973).

(3) I. C. Paul and D. Y. Curtin, *Science*, **187,** 19(1975).

(4) J. T. Carstensen, *J. Pharm. Sci.*, **63,** 1(1974).

(5) H. Morawetz, *Science*, **152,** 705(1966).

(6) G. M. J. Schmidt, *Pure Appl. Chem.*, **27,** 647(1971).

(7) J. P. Desvergne, J. M. Thomas, J. O. Williams, and H. Bouas-Laurent, *J. Chem. Soc., Perkin II*, **1974,** 363.

(8) J. P. Glusker, D. E. Zacharias, and H. L. Carrell, *ibid.*, **1975,** 68.

(9) J. Bregman, K. Osaki, G. M. J. Schmidt, and F. I. Sonntag, *J. Chem. Soc.*, 1961, 2021.

(10) F. L. Hirshfeld and G. M. J. Schmidt, *J. Polym. Sci., A,* **2,** 2181(1964).

(11) S. Okamura, K. Huyashi, and Y. Kitanishi, *J. Polym. Sci.*, **58,** 925(1962).

(12) S. Okamura, E. Kobayashi, M. Takeda, K. Tomikawa, and T. Hiyashimura, *J. Polym. Sci., C,* **4,** 827(1964).

(13) M. Hasegawa, Y. Suzuki, F. Suzuki, and H. Nakanishi, *J. Polym. Sci., A,* **7,** 743(1969).

(14) S. Fujishige and M. Hasegawa, *ibid.*, **7,** 2037(1969).

(15) H. Nakanishi, N. Nakano, and M. Hasegawa, *J. Polym. Sci., B,* **8,** 755(1970).

(16) Y. Sada, H. Shimanouchi, H. Nakanishi, and M. Hasegawa, *Bull. Chem. Soc. Jap.*, **44,** 1262(1971).

(17) H. Nakanishi, K. Ueno, M. Hasegawa, and Y. Sasada, *Chem. Lett.*, **1972,** 301.

(18) E. Fahr, *Angew. Chem. Int. Ed.*, **8,** 578(1969).

(19) R. E. Pincock, *Acc. Chem. Res.*, **2,** 97(1969).

(20) N. K. Kuchetkov and E. J. Budovskii, "Organic Chemis-

try of Nucleic Acids," Part B, Plenum, New York, N.Y., 1972, chap. 12.

(21) J. B. Bremaer, R. N. Warrener, E. Adman, and L. H. Jensen, *J. Amer. Chem. Soc.*, **93,** 4574(1971).

(22) R. Lisewski and K. L. Wierzchowski, *Photochem. Photobiol.*, **11,** 327(1970).

(23) R. F. Stewart, *Biochim. Biophys. Acta*, **75,** 129(1963).

(24) N. J. Leonard, R. S. McCredie, M. W. Logue, and R. L. Cundall, *J. Amer. Chem. Soc.*, **95,** 2320(1973).

(25) J. K. Frank and I. C. Paul, *ibid.*, **95,** 2324(1973).

(26) J. M. Tien and I. M. Hunsberger, *ibid.*, **77,** 6604(1955).

(27) M. D. Cohen and G. M. J. Schmidt, *J. Phys. Chem.*, **66,** 2442(1962).

(28) J. Bernstein and G. M. J. Schmidt, *J. Chem. Soc., Perkin II*, **1972,** 951, and references cited therein.

(29) S. Mitsil and N. Ebana, *Bull. Chem. Soc. Jap.*, **46,** 327(1973).

(30) T. Dominh and A. M. Trozzolo, *J. Amer. Chem. Soc.*, **94,** 4047(1972).

(31) L. F. Small and E. Meitzner, *ibid.*, **55,** 4602(1933).

(32) Y. Tomkiewicz, R. Agarwal, and R. M. Levason, *ibid.*, **95,** 3144(1973).

(33) A. Nater, R. Agarwal, L. Marton, V. Subramanyon, and R. M. Lemmon, *ibid.*, **93,** 2103(1971).

(34) J. Hjortes and H. Sorum, *Acta Crystallogr.*, **B27,** 1320(1971).

(35) M. E. Senko and D. H. Templeton, *ibid.*, **13,** 281(1960).

(36) F. W. Comer, F. McCapra, I. H. Qureshi, and A. I. Scott, *Tetrahedron*, **23,** 4761(1967), and references cited therein.

(37) G. Adam, *Tetrahedron Lett.*, **1971,** 1357, 4601.

(38) M. J. Busse, K. A. Lees, and V. J. Vergine, *J. Pharm. Pharmacol.*, **21,** 250T(1959).

(39) J. Z. Gougoutas, *Isr. J. Chem.*, **10,** 395(1972), and references cited therein.

(40) J. M. Thomas and J. O. Williams, *Progr. Solid State Chem.*, **6,** 119(1971), and references cited therein.

(41) A. I. Kitaigorodskii, Y. V. Mnyukh, and Y. G. Asadov, *J. Phys. Chem. Solids*, **26,** 463(1965).

(42) Y. V. Mnyukh, N. N. Petrotsavlov, and A. I. Kitaigorodskii, *Dokl. Akad. Nauk*, **166,** 80(1966).

(43) M. D. Cohen, P. Coppens, and G. M. J. Schmidt, *J. Phys. Chem. Solids*, **25,** 258(1964).

(44) P. Coppens and G. M. J. Schmidt, *Acta Crystallogr.*, **18,** 62, 654(1965).

(45) S. R. Byrn, D. Y. Curtin, and I. C. Paul, *J. Amer. Chem. Soc.*, **94,** 890(1972).

(46) J. Haleblian and W. McCrone, *J. Pharm. Sci.*, **58,** 911(1969).

(47) W. I. Higuchi, P. D. Bernardo, and S. C. Mehta, *ibid.*, **56,** 200(1967).

(48) G. J. Kruger and G. Gafner, *Acta Crystallogr.*, **27B,** 272(1971).

(49) A. I. Kitaigorodskii, "Organic Chemical Crystallography," Consultants Bureau, New York, N.Y., 1964.

(50) J. M. Robertson and A. R. Ubbelohde, *Proc. Roy. Soc.*, **167A,** 136(1936).

(51) M. A. Moustafa, A. R. Ebian, S. A. Khalil, and M. M. Motawi, *J. Pharm. Pharmacol.*, **23,** 868(1971).

(52) S.-L. Lin and L. Lachman, *J. Pharm. Sci.*, **58,** 377(1969).

(53) A. S. Rankell, Ph.D. thesis, University of Wisconsin, Madison, Wis., 1969.

(54) V. C. Bastron and H. G. Drickamer, *J. Solid State Chem.*, **3,** 550(1971).

(55) H. G. Drickamer, *Science*, **156,** 1183(1967).

(56) E. R. Garrett, E. L. Schumann, and M. F. Grostic, *J. Amer. Pharm. Ass., Sci. Ed.*, **48,** 684(1959).

(57) S. Patai, "The Chemistry of Carboxylic Acids and Esters," Interscience, New York, N.Y., 1969, p. 404.

(58) D. B. Pendergrass, Jr., D. Y. Curtin, and I. C. Paul, *J. Amer. Chem. Soc.*, **94,** 8722(1972).

(59) D. B. Pendergrass, Jr., I. C. Paul, and D. Y. Curtin, *ibid.*, **94,** 8730(1972).

(60) D. Y. Curtin and J. H. Englemann, *J. Org. Chem.*, **37,** 3439(1972), and references cited therein.

(61) Y. F. Shealy, C. A. Krauth, L. B. Holm, and W. E. Fitzgibbon, *J. Pharm. Sci.*, **57,** 83(1968).

(62) Y. F. Shealy and C. A. Krauth, *Nature*, **210,** 208(1966).

(63) W. H. James, P. D. Sternglanz, and Y. F. Shealy, *J. Pharm. Sci.*, **58,** 1193(1969).

(64) D. J. Abraham, J. S. Rutherford, and R. D. Rosenstein, *J. Med. Chem.*, **12,** 189(1969).

(65) J. E. Whinnery and W. H. Watson, *Acta Crystallogr.*, **B28,** 3635(1972).

(66) S. L. Edwards, J. S. Sherfinski, and R. E. Marsh, *J. Amer. Chem. Soc.*, **96,** 2593(1974).

(67) V. D. Kartseva, L. F. Yakhontova, N. L. Isaeva, and B. P. Burns, *Antibiotiki*, **12,** 772(1967).

(68) C. K. Banks, J. Controulis, D. F. Walker, and J. A. Sultzaberger, *J. Amer. Chem. Soc.*, **69,** 5(1947).

(69) C. K. Banks, J. Controulis, D. F. Walker, E. W. Tillitson, L. A. Sweet, and O. M. Gruhzit, *ibid.*, **70,** 1762(1948).

(70) C. K. Banks, *J. Amer. Pharm. Ass., Sci. Ed.*, **38,** 503, 509(1949).

(71) R. M. Hochstrasser, *Can. J. Chem.*, **36,** 1123(1959).

(72) M. L. Lewbart, *Nature*, **222,** 663(1969).

(73) G. Bremer, F. E. Roberts, A. Hoinowski, J. Budavari, B. Powell, D. Hinkley, and E. Schoenewaldt, *Angew. Chem. Int. Ed.*, **8,** 975(1969).

(74) M. L. Snow, C. Lauinger, and C. Ressler, *J. Org. Chem.*, **33,** 1774(1968).

(75) C. Ressler, *ibid.*, **37,** 2933(1972).

(76) J. D. McCullough, Jr., D. Y. Curtin, L. L. Miller, I. C. Paul, and D. B. Pendergrass, Jr., *Mol. Cryst. Liq. Cryst.*, **11,** 407(1970).

(77) R. S. Miller, D. Y. Curtin, and I. C. Paul, *J. Amer. Chem. Soc.*, **96,** 6334, 6340(1974).

(78) J. P. Desvergne and J. M. Thomas, *Chem. Phys. Lett.*, **23,** 343(1973).

(79) H. S. A. Gilmour, in "Physics and Chemistry of the Organic Solid State," D. Fox, M. M. Labes, and A. Weissberger, Eds., Wiley–Interscience, New York, N.Y., 1963, p. 329.

(80) L. Lachman, C. J. Swartz, T. Urbanyi, and J. Cooper, *J. Amer. Pharm. Ass., Sci. Ed.*, **49,** 165(1960).

(81) M. E. Everhard and F. W. Goodhart, *J. Pharm. Sci.*, **52,** 281(1963).

(82) Y. Usui, K. I. Toh, and M. Loizuma, *Bull. Chem. Soc. Jap.*, **38,** 1015(1965).

(83) V. Kasche and J. Lindquist, *J. Phys. Chem.*, **68,** 817(1964).

(84) H. O. House, "Modern Synthetic Reactions," 2nd ed., Benjamin, Menlo Park, Calif., 1972, pp. 338–352, and references cited therein.

(85) K. Iwamoto, *Bull. Chem. Soc. Jap.*, **10,** 420(1935).

(86) R. Kuramoto, L. Lachman, and J. Cooper, *J. Amer. Pharm. Ass., Sci. Ed.*, **47,** 175(1958).

(87) E. Shefter, H.-L. Fung, and O. Mok, *J. Pharm. Sci.*, **62,** 791(1973).

(88) E. Shefter and G. Mack, *ibid.*, **56,** 1028(1967).

(89) R. R. Pfeiffer, K. S. Yang, and M. A. Tucker, *ibid.*, **59,** 1809(1970).

(90) L. J. Leeson and A. M. Mattocks, *J. Amer. Pharm. Ass., Sci. Ed.*, **47,** 330(1958).

(91) "Handbook of Chemistry and Physics," 55th ed., CRC Press, Cleveland, Ohio, 1974, p. D-159.

(92) A. Y. Gore, K. B. Nacik, D. O. Kildsig, G. E. Peck, V. F. Smolen, and G. S. Banker, *J. Pharm. Sci.*, **57,** 1850(1968).

(93) F. J. Bandelin and W. Malesh, *J. Amer. Pharm. Ass., Pract. Ed.*, **19,** 152(1958).

(94) S. T. Lee, H. G. Dekay, and G. S. Banker, *J. Pharm. Sci.*, **54,** 1153(1965).

(95) H. V. Maulding, M. A. Zoglio, F. E. Pigois, and M. Wagner, *ibid.*, **58,** 1359(1969).

(96) A. E. Troup and H. Mitchner, *ibid.*, **53,** 375(1964).

(97) K. T. Koshy, A. E. Troup, R. N. Duvall, R. C. Conwell, and L. L. Shankle, *ibid.*, **56,** 1117(1967).

(98) A. L. Jacobs, A. E. Dilatush, S. Weinstein, and J. J. Windheuser, *ibid.*, **55,** 893(1966).

(99) S. S. Kornblum and B. J. Sciarrone, *ibid.*, **53,** 935(1964).

(100) A. V. Willi and P. Wilk, *Z. Phys. Chem.*, **59,** 189(1968).

(101) J. T. Carstensen and P. Pothisiri, *J. Pharm. Sci.*, **64,** 37(1975).

(102) F. Bertnotti, G. Giacumello, and A. M. Liqueri, *Acta Crystallogr.*, **7,** 808(1954).

(103) R. P. Parker and J. M. Smith, U.S. pat. 2,644,011(1953).

(104) J. T. Carstensen and M. N. Musa, *J. Pharm. Sci.*, **61**, 1112(1972).
(105) E. R. Garrett and T. E. Eble, *J. Amer. Pharm. Ass., Sci. Ed.*, **43**, 385(1954).
(106) E. R. Garrett, *ibid.*, **43**, 536(1954).
(107) T. E. Eble and E. R. Garrett, *ibid.*, **43**, 539(1954).
(108) K. Pfoertner and J. P. Weber, *Helv. Chim. Acta*, **55**, 921(1972).
(109) R. Hoffmann and R. B. Woodward, "The Conservation of Orbital Symmetry," Verlag Chemie, New York, N.Y., 1970, pp. 52, 80, and references cited therein.
(110) T. Kanzawa and S. Kotaku, *J. Pharm. Soc. Jap.*, **73**, 1357(1953).
(111) K. J. Keuning, *Pharm. Weekbl.*, **100**, 889(1965).
(112) C. Knobler, C. Romers, P. B. Braun, and J. Hornstra, *Acta Crystallogr.*, **28B**, 2097(1972).
(113) D. C. Hodgkin, M. S. Webster, and J. D. Dunitz, *Chem. Ind.*, **1957**, 1148.
(114) J. K. Guillory and T. Higuchi, *J. Pharm. Sci.*, **51**, 100(1962).
(115) J. G. Baxter and C. D. Robeson, *J. Amer. Chem. Soc.*, **64**, 2407(1942).
(116) R. Dobrucki, *Farm. Pol.*, **27**, 353(1971); through *Chem. Abstr.*, **75**, 80230(1971).
(117) E. I. Funkelstein, E. V. Alekseev, and E. I. Kozlov, *Zh. Org. Khim.*, **10**, 1027(1974).
(118) S. Bhattacharyen, *J. Inst. Chem. (India)*, **41**, 33(1969).
(119) B. Leszczynska, S. Halina, and H. Krowczynska, *Cesk. Farm.*, **19**, 109(1970).
(120) Y. Ogata, Y. Kosugi, and K. Tomizowa, *Tetrahedron*, **70**, 5939(1970).
(121) D. Lerner, J. C. Mani, and M. Mousseren-Canet, *Bull. Soc. Chem. Fr.*, **1970**, 1968.
(122) M. Mousseren-Canet, J. C. Mani, C. Farie, and D. Lerner, *C. R., Ser. C*, **262**, 153(1966).
(123) W. E. Oberhansli, H. P. Wagner, and O. Isler, *Acta Crystallogr.*, **B30**, 161(1974).
(124) A. I. Kitaigorodsky, "Molecular Crystals and Liquid Crystals," Academic, New York, N.Y., 1973, p. 168.
(125) R. S. Miller, D. Y. Curtin, and I. C. Paul, *J. Amer. Chem. Soc.*, **3**, 2784(1971).
(126) J. Dekher and P. A. Ark, *Antibiot. Chemother.*, **9**, 327(1949).
(127) J. E. Tingstad and E. R. Garrett, *J. Amer. Pharm. Ass., Sci. Ed.*, **49**, 352(1960).

ACKNOWLEDGMENTS AND ADDRESSES

Received from the *Department of Medicinal Chemistry and Pharmacognosy, School of Pharmacy and Pharmacal Sciences, Purdue University, West Lafayette, IN 47907*

Supported by National Institutes of Health Grant GM 21174.

The author is grateful to Professor D. Y. Curtin and Professor I. C. Paul, Chemistry Department, University of Illinois, Urbana, Ill., and to Professor K. N. Trueblood, Chemistry Department, University of California, Los Angeles, Calif., for carefully reviewing this paper and making many helpful comments. The able assistance of Warren Haws in preparation of the stereo pair drawings and Sharon Midland is also gratefully acknowledged.

RESEARCH ARTICLES

Glass for Parenteral Products: A Surface View Using the Scanning Electron Microscope

T. J. ROSEMAN *[x], J. A. BROWN [‡], and W. W. SCOTHORN *

Abstract □ The scanning electron microscope was utilized to explore the internal surface of glass ampuls and vials used in parenteral products. The surface topography of USP Type I borosilicate glass containers was viewed after exposure to "sulfur," ammonium bifluoride, and sulfuric acid treatments. The scanning electron micrographs showed startling differences in the appearance of the surface regions. "Sulfur treatment" of ampuls was associated with a pitting of the surface and the presence of sodium sulfate crystals. The sulfur treatment of vials altered the glass surface in a characteristically different manner. The dissimilarity between the surface appearances was attributed to the method of sulfur treatment. Ampuls exposed to sulfuric acid solutions at room temperature did not show the pitting associated with the sulfur treatment. Scanning electron micrographs of ammonium bifluoride-treated ampuls showed a relief effect, suggesting that the glass was affected by the bifluoride solution but that sufficient stripping of the surface layer did not occur to remove the pits associated with the sulfur treatment. Flakes emanating from the glass were identified with the aid of the electron microprobe. Scanning electron micrographs showed that these vitreous flakes resulted from a delamination of a thin layer of the glass surface. It is concluded that the scanning electron microscope, in conjunction with other analytical techniques, is a valuable tool in assessing the quality of glass used for parenteral products. The techniques studied should be of particular importance to the pharmaceutical industry where efforts are being made to reduce the levels of particulate matter in parenteral dosage forms.

Keyphrases □ Glass—ampuls and vials, internal surface, effect of sulfur, ammonium bifluoride, and sulfuric acid treatments, scanning electron micrographs □ Scanning electron microscopy—internal surface, glass ampuls and vials, effect of sulfur, ammonium bifluoride, and sulfuric acid treatments □ Parenteral containers—glass, scanning electron micrographs, surface view □ Containers, glass—surface, effects of sulfur, ammonium bifluoride, and sulfuric acid treatments, scanning electron micrographs

Glass vials and ampuls are the primary containers for parenteral products. The general inertness of glass has been the basis for its use since it is desirable for pharmaceutical products to have acceptable physical and chemical stability for extended periods, *i.e.*, up to 5 years. This report is concerned with the quali-

(104) J. T. Carstensen and M. N. Musa, *J. Pharm. Sci.*, **61**, 1112(1972).
(105) E. R. Garrett and T. E. Eble, *J. Amer. Pharm. Ass., Sci. Ed.*, **43**, 385(1954).
(106) E. R. Garrett, *ibid.*, **43**, 536(1954).
(107) T. E. Eble and E. R. Garrett, *ibid.*, **43**, 539(1954).
(108) K. Pfoertner and J. P. Weber, *Helv. Chim. Acta*, **55**, 921(1972).
(109) R. Hoffmann and R. B. Woodward, "The Conservation of Orbital Symmetry," Verlag Chemie, New York, N.Y., 1970, pp. 52, 80, and references cited therein.
(110) T. Kanzawa and S. Kotaku, *J. Pharm. Soc. Jap.*, **73**, 1357(1953).
(111) K. J. Keuning, *Pharm. Weekbl.*, **100**, 889(1965).
(112) C. Knobler, C. Romers, P. B. Braun, and J. Hornstra, *Acta Crystallogr.*, **28B**, 2097(1972).
(113) D. C. Hodgkin, M. S. Webster, and J. D. Dunitz, *Chem. Ind.*, **1957**, 1148.
(114) J. K. Guillory and T. Higuchi, *J. Pharm. Sci.*, **51**, 100(1962).
(115) J. G. Baxter and C. D. Robeson, *J. Amer. Chem. Soc.*, **64**, 2407(1942).
(116) R. Dobrucki, *Farm. Pol.*, **27**, 353(1971); through *Chem. Abstr.*, **75**, 80230(1971).
(117) E. I. Funkelstein, E. V. Alekseev, and E. I. Kozlov, *Zh. Org. Khim.*, **10**, 1027(1974).
(118) S. Bhattacharyen, *J. Inst. Chem. (India)*, **41**, 33(1969).
(119) B. Leszczynska, S. Halina, and H. Krowczynska, *Cesk. Farm.*, **19**, 109(1970).
(120) Y. Ogata, Y. Kosugi, and K. Tomizowa, *Tetrahedron*, **70**, 5939(1970).
(121) D. Lerner, J. C. Mani, and M. Mousseren-Canet, *Bull. Soc. Chem. Fr.*, **1970**, 1968.
(122) M. Mousseren-Canet, J. C. Mani, C. Farie, and D. Lerner, *C. R., Ser. C*, **262**, 153(1966).
(123) W. E. Oberhansli, H. P. Wagner, and O. Isler, *Acta Crystallogr.*, **B30**, 161(1974).
(124) A. I. Kitaigorodsky, "Molecular Crystals and Liquid Crystals," Academic, New York, N.Y., 1973, p. 168.
(125) R. S. Miller, D. Y. Curtin, and I. C. Paul, *J. Amer. Chem. Soc.*, **3**, 2784(1971).
(126) J. Dekher and P. A. Ark, *Antibiot. Chemother.*, **9**, 327(1949).
(127) J. E. Tingstad and E. R. Garrett, *J. Amer. Pharm. Ass., Sci. Ed.*, **49**, 352(1960).

ACKNOWLEDGMENTS AND ADDRESSES

Received from the *Department of Medicinal Chemistry and Pharmacognosy, School of Pharmacy and Pharmacal Sciences, Purdue University, West Lafayette, IN 47907*

Supported by National Institutes of Health Grant GM 21174.

The author is grateful to Professor D. Y. Curtin and Professor I. C. Paul, Chemistry Department, University of Illinois, Urbana, Ill., and to Professor K. N. Trueblood, Chemistry Department, University of California, Los Angeles, Calif., for carefully reviewing this paper and making many helpful comments. The able assistance of Warren Haws in preparation of the stereo pair drawings and Sharon Midland is also gratefully acknowledged.

RESEARCH ARTICLES

Glass for Parenteral Products: A Surface View Using the Scanning Electron Microscope

T. J. ROSEMAN *[x], J. A. BROWN [‡], and W. W. SCOTHORN *

Abstract □ The scanning electron microscope was utilized to explore the internal surface of glass ampuls and vials used in parenteral products. The surface topography of USP Type I borosilicate glass containers was viewed after exposure to "sulfur," ammonium bifluoride, and sulfuric acid treatments. The scanning electron micrographs showed startling differences in the appearance of the surface regions. "Sulfur treatment" of ampuls was associated with a pitting of the surface and the presence of sodium sulfate crystals. The sulfur treatment of vials altered the glass surface in a characteristically different manner. The dissimilarity between the surface appearances was attributed to the method of sulfur treatment. Ampuls exposed to sulfuric acid solutions at room temperature did not show the pitting associated with the sulfur treatment. Scanning electron micrographs of ammonium bifluoride-treated ampuls showed a relief effect, suggesting that the glass was affected by the bifluoride solution but that sufficient stripping of the surface layer did not occur to remove the pits associated with the sulfur treatment. Flakes emanating from the glass were identified with the aid of the electron microprobe. Scanning electron micrographs showed that these vitreous flakes resulted from a delamination of a thin layer of the glass surface. It is concluded that the scanning electron microscope, in conjunction with other analytical techniques, is a valuable tool in assessing the quality of glass used for parenteral products. The techniques studied should be of particular importance to the pharmaceutical industry where efforts are being made to reduce the levels of particulate matter in parenteral dosage forms.

Keyphrases □ Glass—ampuls and vials, internal surface, effect of sulfur, ammonium bifluoride, and sulfuric acid treatments, scanning electron micrographs □ Scanning electron microscopy—internal surface, glass ampuls and vials, effect of sulfur, ammonium bifluoride, and sulfuric acid treatments □ Parenteral containers—glass, scanning electron micrographs, surface view □ Containers, glass—surface, effects of sulfur, ammonium bifluoride, and sulfuric acid treatments, scanning electron micrographs

Glass vials and ampuls are the primary containers for parenteral products. The general inertness of glass has been the basis for its use since it is desirable for pharmaceutical products to have acceptable physical and chemical stability for extended periods, *i.e.*, up to 5 years. This report is concerned with the quali-

Table I—Electron Microprobe Analysis of Four Flakes

Element	Sample A, %	Sample B, %	Sample C, %	Sample D, %
Silicon	25—30	35—45	30—35	25—30
Aluminum	10—12	3—5	8—10	10—11
Potassium	4—6	Not detected	3—5	3—4
Calcium	1—2	Not detected	Not detected	1—2
Boron	3—8	2—6	3—8	Present
Sodium	1—3	1—2	1—3	1—2

ty of glass as viewed with the scanning electron microscope and its relationship to the formation of vitreous flakes in sterile solutions. The presence of particulates or foreign matter is undesirable in any product; but in the case of intravenously administered dosage forms, it must be avoided. Since the drug solution is administered directly into the vascular system, the presence of particulate matter is potentially harmful to the patient (1).

History demonstrates that glass has been an acceptable container for parenteral products. However, glass is not completely inert; it is attacked by different solution media (2–5) and its performance is affected by the method of manufacture of the final container (6). Specifications are set forth in the USP (7) for a water attack and a powdered-glass test. The USP test, however, does not guarantee that glass will withstand attack when in direct contact with a product. Physical inspections of the final dosage form are necessary to assure that no foreign material is present.

Three types of glass intended for parenteral products are set forth in the USP with corresponding test limits for titratable basicity. Type I is a highly resistant borosilicate glass, while Types II and III are "sulfur-treated" and "non-sulfur-treated" soda lime glass, respectively. The powdered-glass test is used to measure the overall degree of alkalinity, while the water attack test is used to measure surface alkalinity of sulfur-treated Type II glass. Since the inside surface of Type II glass is dealkalized by the sulfur treatment, the effectiveness of the treatment cannot be determined by powdering the glass and the water attack test is used (8).

Particulate matter can be derived from intrinsic sources other than glass such as stopper components, drug–stopper interactions, and bulk drug itself and from extrinsic sources such as unclean containers having lint or other contaminants attached to them. The constraints on parenteral dosage forms were reviewed recently (9), and an official standard for particulate matter in large-volume parenteral solutions is in the British Pharmacopoeia (10). Because the product is in intimate contact with the glass container, the quality of the glass can be an important factor in the formation of particulates. Glass of poor or variable quality can contribute particles that are seen with standard inspection techniques or even smaller particles, *i.e.*, less than 20 μm, which can be observed with more critical physical inspection systems.

The technology for quantitating (11–13) particulates and the automated detection (14–16) of them in containers appears to be advancing rapidly. It is believed that a greater understanding of the topography of the glass surface will be helpful in developing formulations to meet future standards. This paper explores the use of the scanning electron microscope to provide insight into the characteristics of the glass surface. Special emphasis is given to treatment processes such as "sulfuring" and ammonium bifluoride.

EXPERIMENTAL

All glass ampuls[1] and vials[1] employed were of Type I USP (7) borosilicate composition. The sulfur-treated containers were identical in composition, but they were exposed to the sulfuring process. Samples were obtained for scanning electron microscopic analysis by cutting approximately 1.27 × 1.27-cm sections with a circular saw. Unless otherwise specified, sections were cut approximately 0.8 cm above the bottom of the container.

Each sample was then washed several times with distilled water and analyzed. The washing procedure removed all traces of the sodium sulfate bloom present on the sulfur-treated containers. One sample was fractured and not washed so that the surface could be viewed in the presence of sodium sulfate.

A bifluoride wash of ampuls was performed with 5 and 20% aqueous ammonium bifluoride[2] solutions, prepared with distilled water. For non-sulfur-treated ampuls, the ammonium bifluoride solution was injected into inverted ampuls for 30 sec, followed by a 15–30-sec rinse with filtered deionized water. Bifluoride wash of the sulfur-treated ampuls was performed in a slightly different manner. Upright ampuls were filled completely with solution for 30 sec and then rinsed for 30 sec with distilled water. In each experiment, control ampuls were prepared by treatment with distilled water.

The samples for scanning electron microscope analysis were mounted on double-back tape[3] on the specimen stubs with the inside surface up. They were then placed in a vacuum evaporator and shadowed with gold to give surface conductivity. This procedure is necessary because the electron beam in the microscope[4] charges nonconducting materials, and the charge then repels the electron beam.

To examine the details of the surface properly, the samples were viewed at an oblique angle. The angle on all pictures was 70° unless otherwise noted. Some photographs were obtained at 45° for better detail. This angle is the angle of the specimen to the horizontal, with the electron beam impinging perpendicular to the horizontal. The net result is that the beam impinges on the specimen at 20° in the case of the angle designated 70° and at 45° in the case of the angle designated 45°. With the 70° angle, a shallow depth of field results in distorted shapes; *e.g.*, a circle appears as an ellipse.

The vitreous flakes were isolated from solution by the following procedure. A 5-ml ampul containing an aqueous parenteral solution was selected based upon the visual observance of flakes in the solution. The ampul was opened by melting off the ampul tip with an oxypropane flame. This procedure eliminated the shower of glass fragments commonly encountered when an impul is opened in the conventional manner, *i.e.*, breaking. The opening of the ampul, as well as the technique of isolating a single flake, was performed under U.S. Government Class 100 clean room conditions (17).

The open ampul was mounted in an upright fashion, with a strong beam of light[5] illuminating the ampul parallel to its longest axis. Under these conditions, the flakes appeared to twinkle or glitter as reflected light as they reached the observer's position, which was perpendicular to the axis of the light beam. By using a particulate-free capillary pipet, fitted with a dropper bulb, a single flake was aspirated into the pipet. The flake, with accompanying

[1] Kimble Products Division, Owens-Illinois Inc., Toledo, Ohio.
[2] Harshaw Chemical Co., Division of Kewanee Oil Co., Cleveland, OH 44106
[3] Scotch tape, Minnesota Mining and Manufacturing Co., St. Paul, MN 55101
[4] Cambridge Mark II Stereoscan, Kent Cambridge Scientific Inc., Morton Grove, IL 60053
[5] High intensity microscope illuminator, American Optical Corp., Buffalo, NY 14215

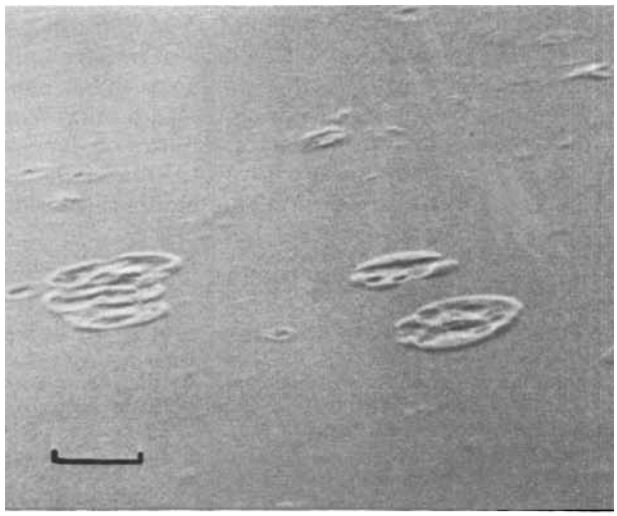

A

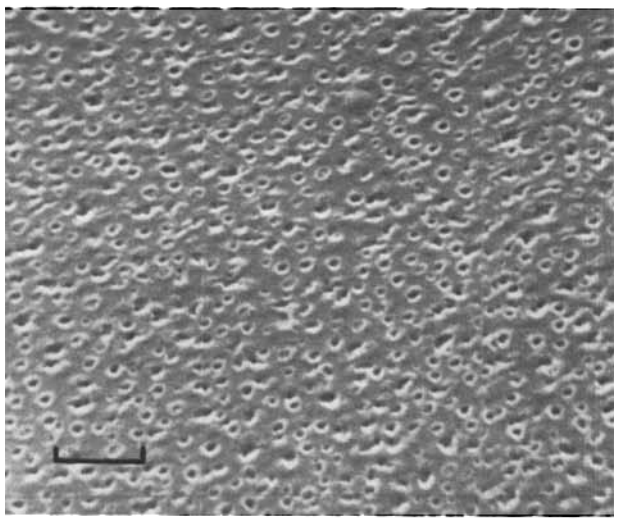

B

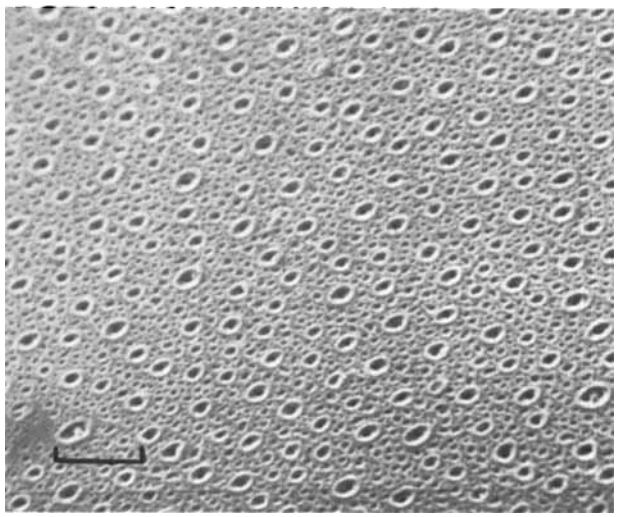

C

Figure 1—*Effect of sulfur treatment on the surface of glass ampuls (10,000× magnification; scale marker = 1 μm). Key: A, nonsulfur-treated 5-ml ampul; B, sulfur-treated 5-ml ampul (45° angle); and C, sulfur-treated 8-ml ampul (45° angle).*

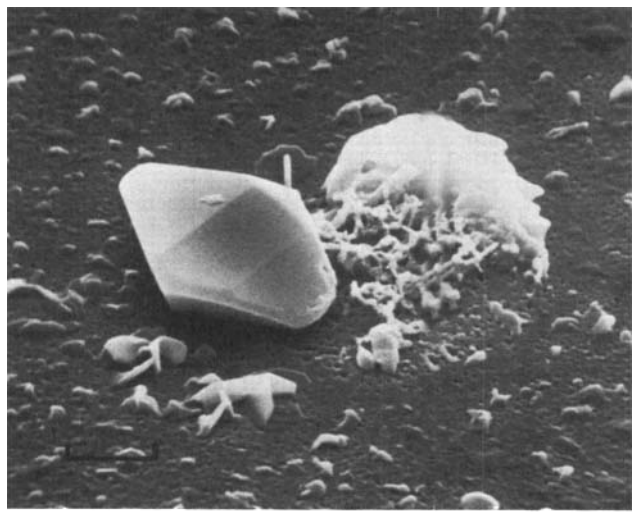

A

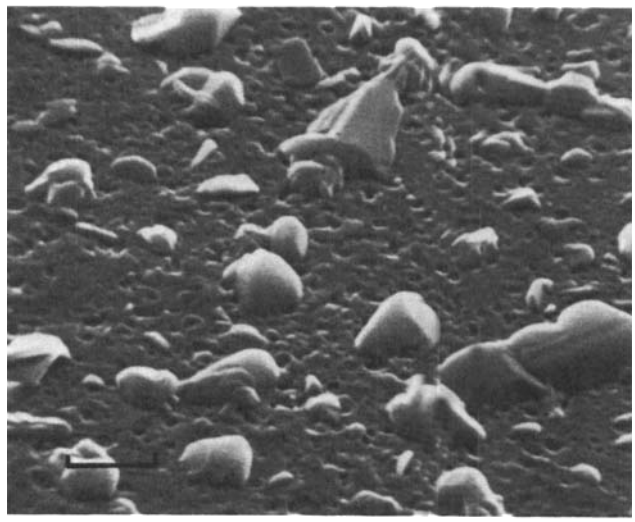

B

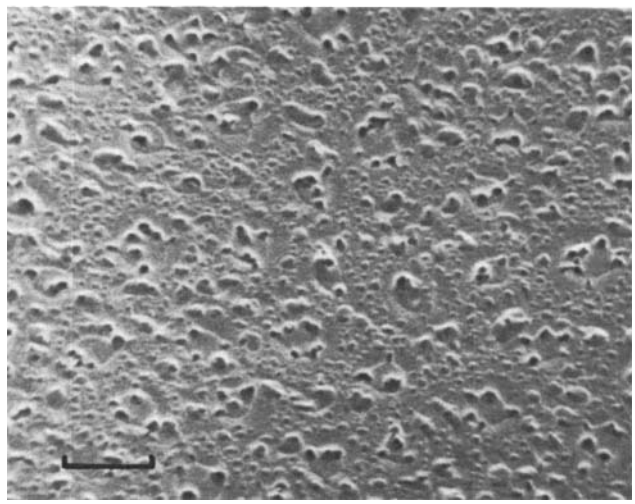

C

Figure 2—*Surface view of a sulfur-treated ampul which was not washed prior to obtaining the scanning electron micrographs. Key: A, 5000× magnification, scale marker = 2 μm; B, 10,000× magnification, scale marker = 1 μm; and C, control ampul which was washed (10,000× magnification; scale marker = 1 μm). Note the absence of sodium sulfate crystals on the surface of the control ampul.*

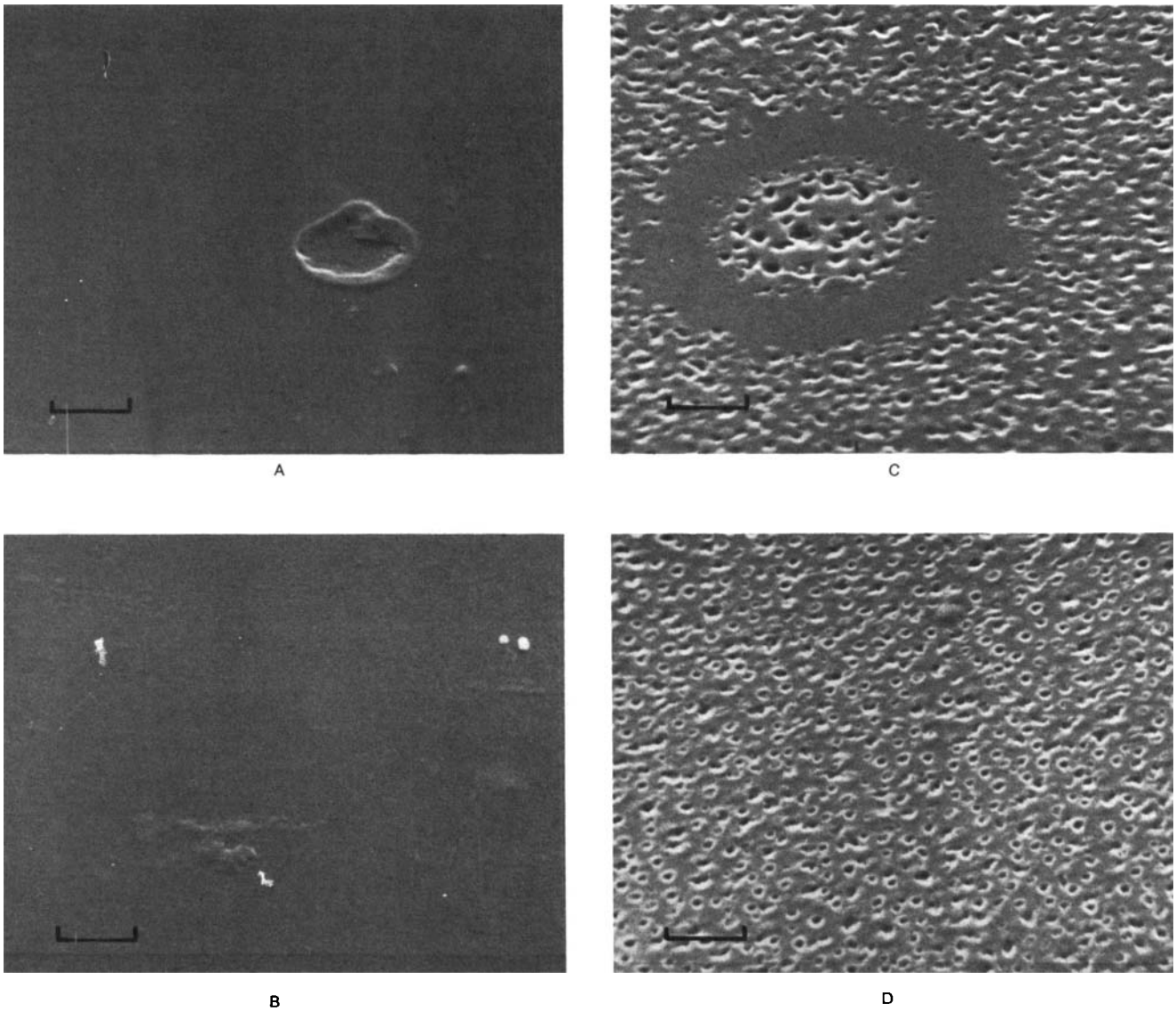

Figure 3—*Comparison of sulfuric acid soak with sulfur treatment of 5-ml ampuls (10,000× magnification; scale marker = 1 μm). Key: A, non-sulfur-treated control; B, non-sulfur treated but soaked in 50% (v/v) H_2SO_4 for 2 hr at room temperature; C, sulfur-treated control (45° angle); and D, sulfur treated and soaked in 50% (v/v) H_2SO_4 for 2 hr at room temperature.*

solution, was placed in the center of a scrupulously cleaned 2.54 × 7.62-cm glass microslide.

The preceding operations were performed with no supplemental magnification aiding the operator. The following operations were performed using a stereomicroscope[6] between 25 and 50 times magnification. By using moistened filters[7,8], the solution surrounding the flake was carefully wisked away from the flake. The procedure was repeated two times using a drop of filtered distilled water to wash the flake. After the flake was allowed to air dry in a stream of filtered air (high efficiency particulate air) (17), it was affixed to the glass microslide with a tiny drop of flexible collodion in isoamyl acetate. The collodion film provided a satisfactory bond.

The flakes for electron microprobe analysis were transferred to a beryllium plate with a tungsten needle. Since beryllium does not produce a detectable signal of its own when subjected to electron microprobe[9] analysis, the background is low. The flakes were glued to the beryllium with a thin film of collodion. Because boron is a difficult element to detect in low amounts, the accelerating voltage was dropped to 10 kv (from the usual 25 kv) and the specimen current was boosted from 200 namp (usually 10 namp). The light element spectrometer was then *manually turned,* using a boron nitride standard, and measurements were done. Standard and sample readings were repeated many times to minimize error.

RESULTS AND DISCUSSION

Ampuls—The effect of sulfur treatment on the inside surface of a glass ampul is shown in Fig. 1. After the sulfuring process was performed, many circular pits of uniform dimensions (<0.5 μm in diameter) were noted. The untreated ampul showed no pits, but some irregular areas were noted.

The sulfuring process was performed after the ampul was formed but before it entered the lehr. The procedure involves the injection of a small volume of a dilute solution of ammonium sulfate into the ampul. Vaporization of the ammonium sulfate occurs in the lehr, which is maintained at an elevated temperature [~593° (~1100° F)]. The *in situ* formed vapor reacts with the glass to neutralize its surface alkalinity, yielding sodium sulfate crystals which appear on the surface (18).

A literature survey indicates that the sulfur treatment of glass was mentioned as early as 1930 (19). In the case of soda lime glasses, this reaction has been well studied (20, 21). During the reaction, the surface composition of the glass is altered as hydrogen ions

[6] Wild M-5 stereomicroscope, Wild Heerbrugg Ltd., Heerbrugg, Switzerland.
[7] Millipore filters, Millipore Corp., Bedford, MA 07130
[8] Whatman, W & R Balston Ltd., England.
[9] EMX-SM electron microprobe, Applied Research Laboratories, Sunland, CA 91040

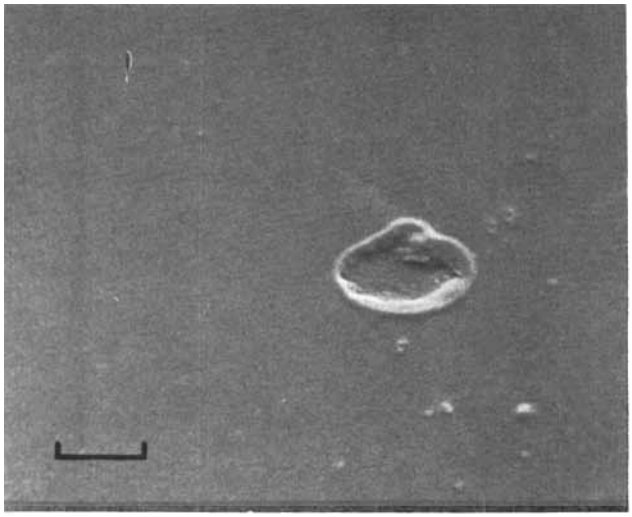

A

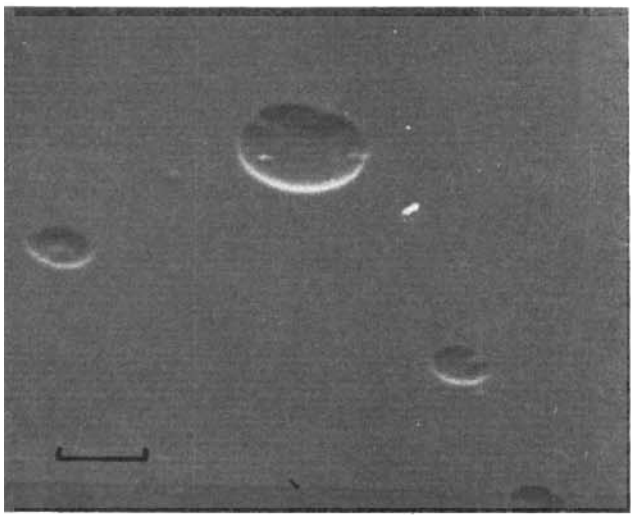

B

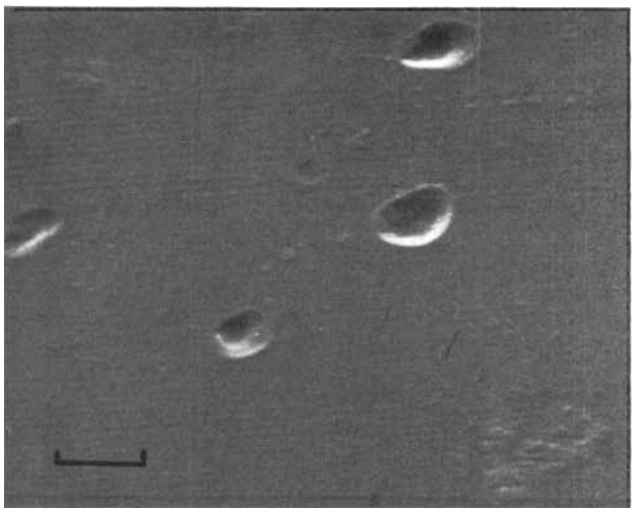

C

Figure 4—*Effect of bifluoride treatment on non-sulfur-treated 5-ml ampuls (10,000× magnification; scale marker = 1 μm). Key: A, nontreated control; B, 5% ammonium bifluoride; and C, 20% ammonium bifluoride.*

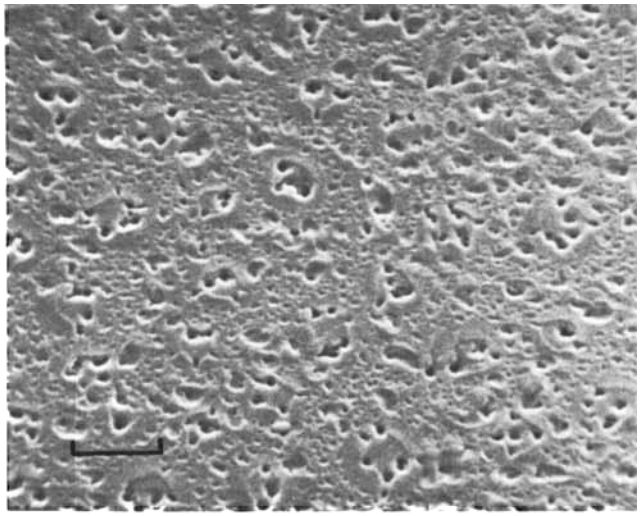

A

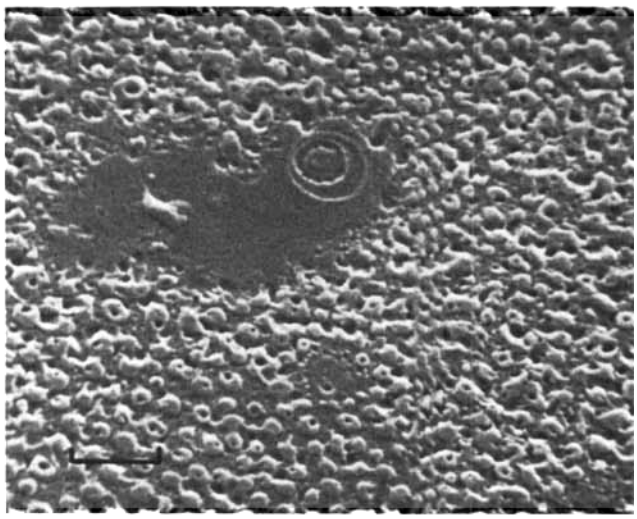

B

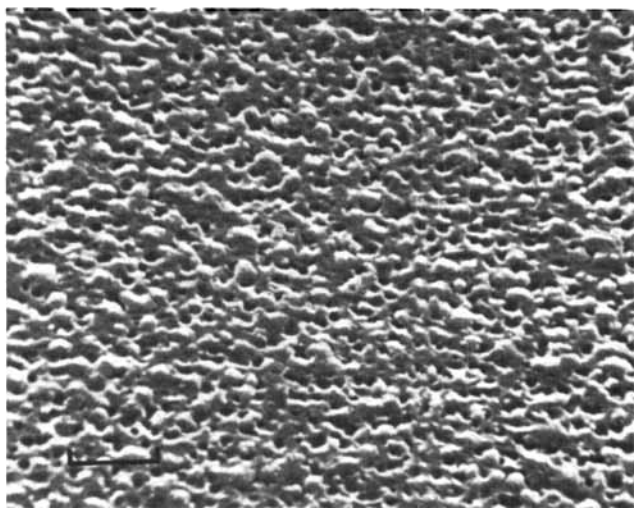

C

Figure 5—*Effect of bifluoride treatment on sulfur-treated 5-ml ampuls (10,000× magnification; scale marker = 1 μm). Key: A, sulfur-treated control; B, 5% ammonium bifluoride; and C, 20% ammonium bifluoride.*

from water exchange for the depleted sodium ion; it has been shown that this "hydrogen glass" can undergo a dehydration process (loss of water), yielding a compacted layer of glass on the surface. The rate of diffusion of sodium through this compacted layer is slower than through the parent glass, and sodium depletion rates have been analyzed according to Fick's law of diffusion (20). As a result of this process, attack by water is reduced and there is an improvement of the chemical durability of the glass toward neutral and acidic solutions and to weathering. In addition, it was reported that the mechanical strength of the glass can increase (21). Interestingly, these studies were performed with soda lime glass while sulfur-treated borosilicate glass received little attention.

In Fig. 1, the exact mechanism for the alteration of the surface topography with a sulfur treatment is not known. However, it may be a consequence of the formation of a crystalline material (*e.g.*, sodium sulfate) at elevated temperatures during the annealing step. If this is the case, treatment with an acidic gas such as hydrogen chloride should result in the formation of a sodium chloride bloom with a similar pitting pattern.

Figure 2 shows the surface of a sulfur-treated glass ampul before rinsing with distilled water. The presence of crystalline material on the surface is noted, with pits below the crystals. A similar pattern of pitting is seen in Fig. 1. Energy-dispersive X-ray analysis of these well-defined crystals indicated that they contained a high content of sodium and sulfur and probably were sodium sulfate, as noted with soda lime glass (18).

Figures 3–5 show the effect of different room temperature treatments. For the regions under consideration, the sulfuric acid soak (Fig. 3) had no apparent effect on either sulfur-treated or non-sulfur-treated ampuls. In contrast, ammonium bifluoride treatment of the glass resulted in a noticeable change. Figure 4 indicates that the bifluoride treatment of non-sulfur-treated ampuls relieves the appearance of the surface irregularities. Figure 5, however, shows this effect more dramatically, where the sulfur-treated ampuls were bifluoride treated. Here the pits, associated with the sulfur treatment, have a sharper appearance, which is not observed with sulfur-treated glass that is not bifluoride treated.

The action of the ammonium bifluoride seems to be consistent with the concept that a thin surface layer of the glass is removed; however, the bifluoride treatment did not penetrate to a sufficient depth to remove the pits associated with the sulfur treatment. Hinson (22) reported that an ammonium bifluoride wash of ampuls is superior to conventional wash methods. Based upon the results of the USP water attack test, it was concluded that bifluoride treatment is equivalent to a good sulfur treatment of USP Type I borosilicate glass. Although the chemical resistance as measured by the water attack test compared favorably, the mechanisms of action of the two treatments are dissimilar, with corresponding differences being observed with the scanning electron microscope.

Vials—Figure 6 presents a comparison of a non-sulfur-treated vial and treated vials. The surface of the nontreated vial was essentially smooth, as previously noted with ampuls (Fig. 1). The sulfur-treated vials, however, had pitting that was characteristically different than the pitting noted with ampuls (Fig. 7), and vial-to-vial variability was noted (Fig. 6). Scanning electron micrographs of numerous samples suggest that there is indeed a greater variability in the surface appearance of vials than ampuls.

This variability with vials and the difference between ampuls and vials are believed to be a consequence of the dissimilar treatment processes for the two containers. As mentioned previously, ampuls were treated with an aqueous solution of ammonium sulfate. Vials were treated with a mixture of sulfur dioxide and sulfur trioxide gases because the higher temperature of the glass in forming the vial is not conducive to treatment with an aqueous solution. Some variability in dissolved silica or titratable alkalinity has been reported with sulfur-treated soda lime bottles (18). It is possible that more variability occurs by injection of a gas because it is more difficult to confine in the container and moisture conditions are not as well controlled. The importance of gas composition, temperature, and time with respect to the sulfur treatment has been pointed out (21), and the influence of moisture on the sulfuring process was discussed previously (23).

Flake Formation—Glass is attacked by numerous reagents other than strong alkali or hydrofluoric acid. Among these substances are sodium citrate, sodium gluconate, and other salts of β-hydroxy acids (4) along with inorganic phosphate solutions (2). Attack on glass can be quantitated by various methods as outlined in

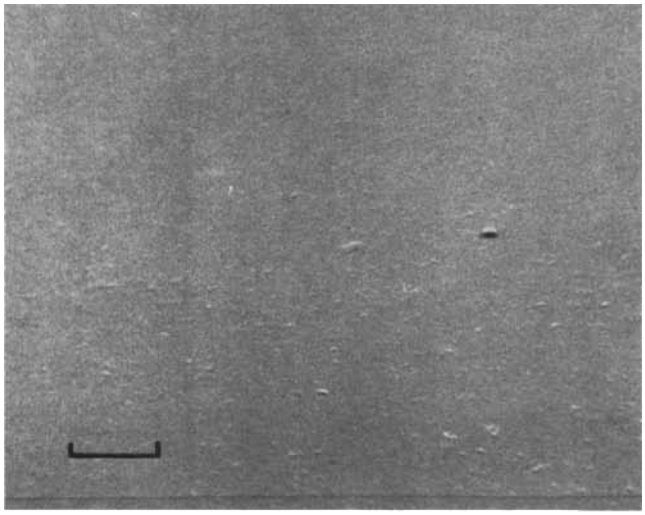

A

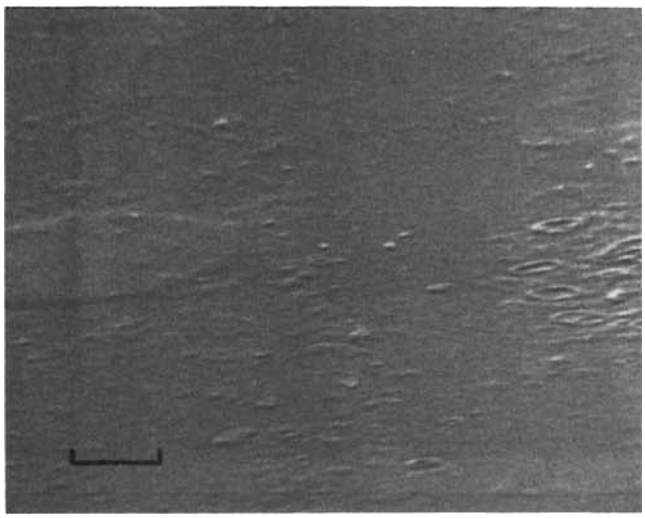

B

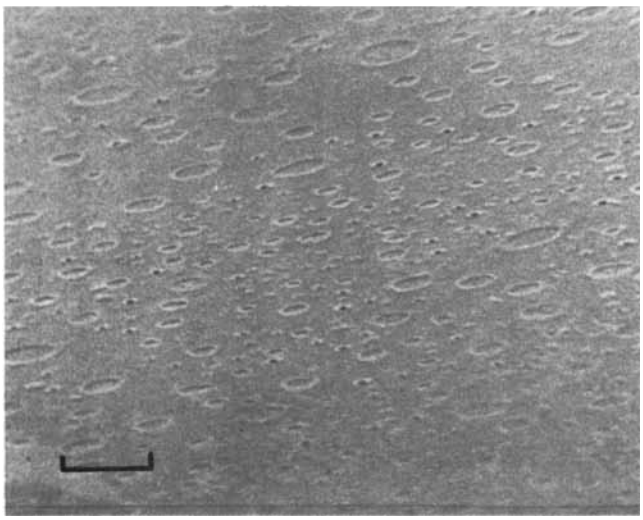

C

Figure 6—*Effect of sulfur treatment on the surface of 10-ml vials and vial-to-vial variability (10,000× magnification; scale marker = 1 μm). Key: A, untreated vial; B, treated Vial 1; and C, treated Vial 2.*

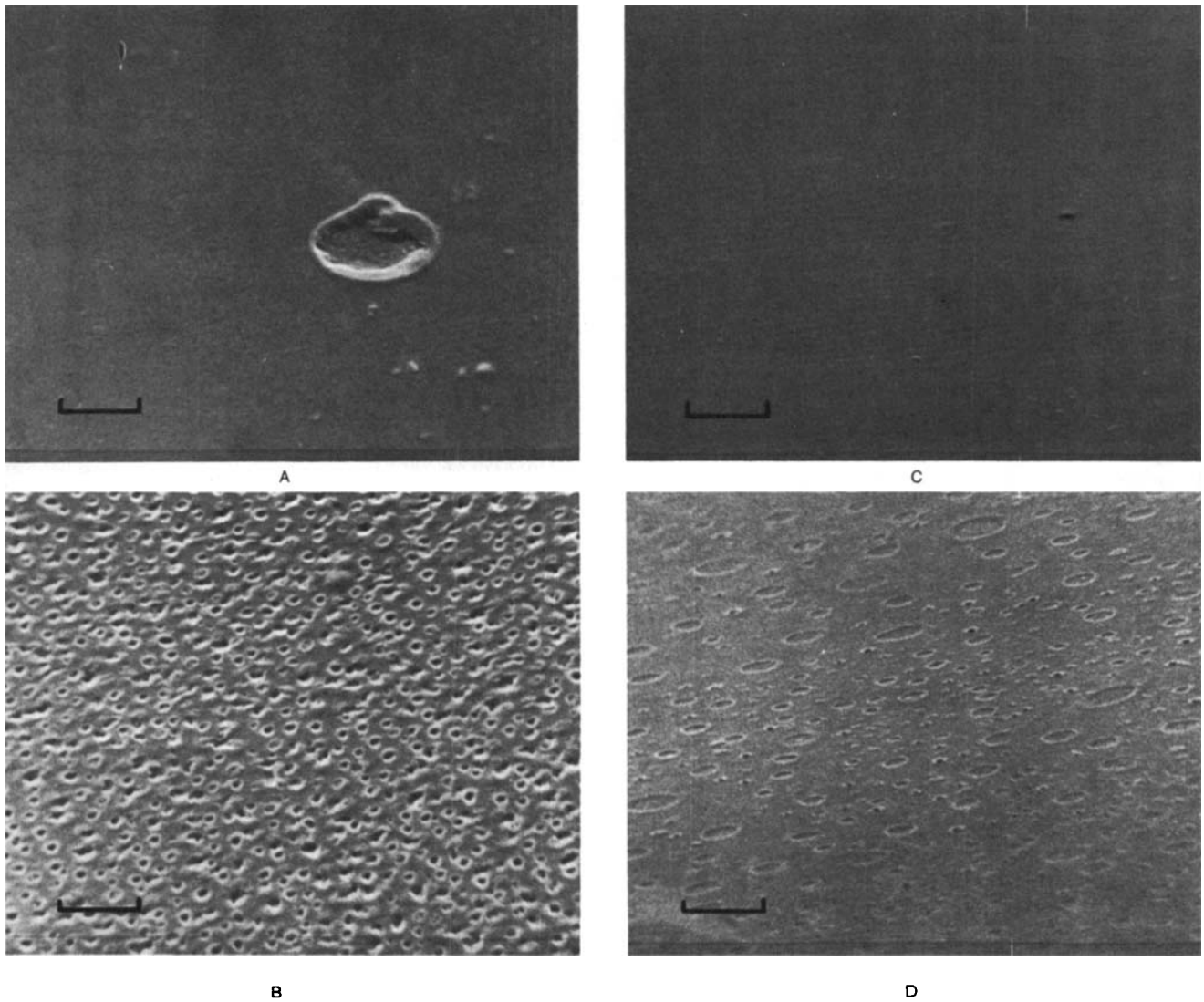

Figure 7—*Comparison of sulfur treatment on 5-ml ampuls and 10-ml vials (10,000× magnification; scale marker = 1 μm). Key: A, non-sulfur-treated ampul; B, sulfur-treated ampul (45° angle); C, non-sulfur-treated vial; and D, sulfur-treated vial.*

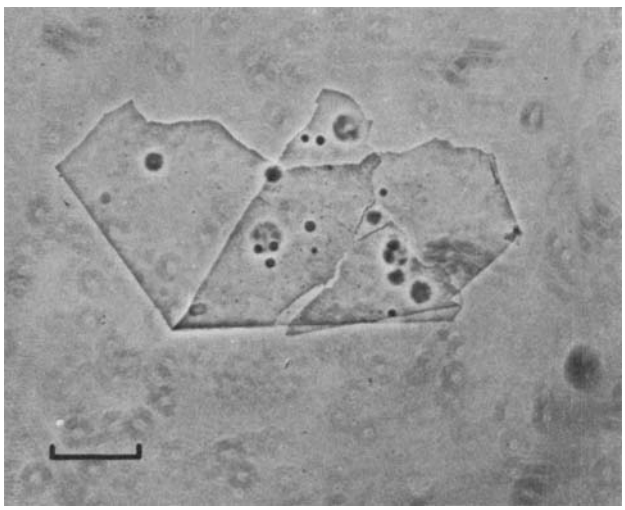

Figure 8—*Bright-field phase contrast photomicrograph of a vitreous flake (312.5× magnification; scale marker = 45 μm).*

a review article (3), where it was pointed out that the chemical resistance of glass is dependent upon its chemical composition, the temperature of the attacking agent, the length of contact, and the previous history of the glass (*i.e.*, method of production, annealing, special treatments, and storage).

Generally, there does not appear to be a direct correlation between the attack of glass as measured by the presence of dissolved silica and the formation of glass-related flakes in solution upon storage. The formation of these flakes after exposure to various solutions is documented (4, 24). The undesirability of foreign particulate matter in parenteral solutions was discussed earlier, but little information about the region of the glass from which these flakes emanate is available, and scanning electron microscope data are lacking. Products of disintegrated glass have been described as soft, hydrous, gel-like siliceous films (25) and have been reported to consist mainly of silicon dioxide (3). The composition of the flakes depends upon the type of glass employed and its history. Therefore, it is not possible to relate conclusively the following data with previous work, but flakes similar to the ones to be described have been noted under various conditions in this laboratory after storage of solutions in ampuls.

Figure 8 shows a photograph, taken through the optical microscope, of a flake after removal from a solution stored in an ampul. The flake is colorless and plate-like (<1 μm in thickness), does not melt below 300°, and exhibits a refractive index similar to glass. All flakes observed in the solution had similar characteristics, but their size ranged from a few micrometers to hundreds of micrometers in length. The electron microprobe analysis of four flakes is given in Table I.

Because the flake is composed of elements similar to those of the glass, an ampul was broken and a fragment was analyzed in an

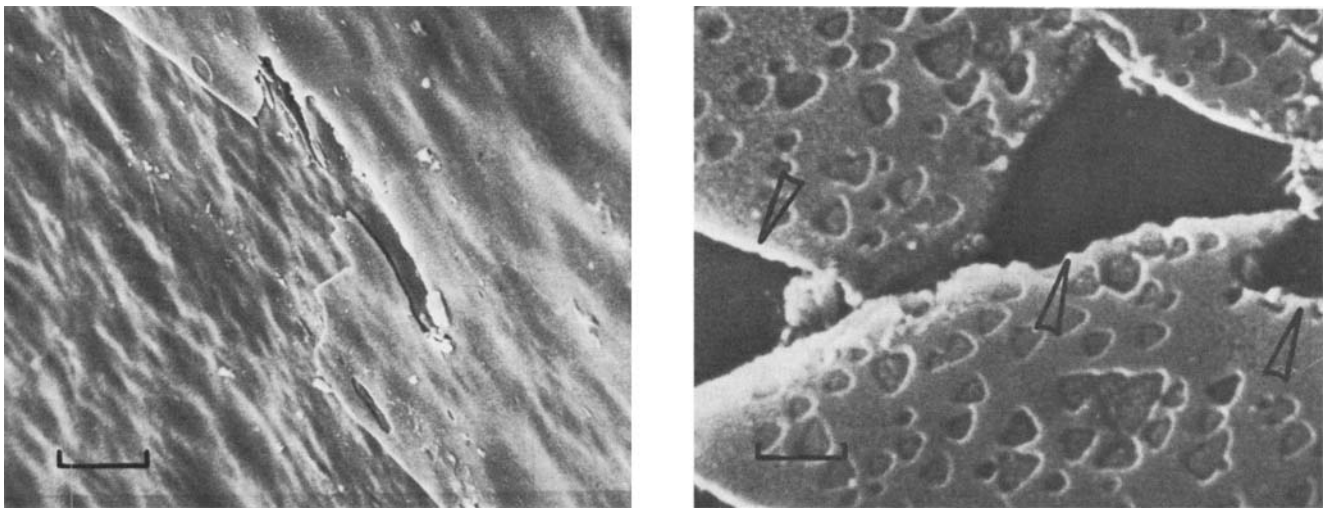

Figure 9—*Scanning electron micrographs of 5-ml ampuls which produced vitreous flakes. Left: delaminated region is on the left side of the micrograph while the intact glass surface appears on the right. Jagged edge separates the two regions (2000× magnification; scale marker = 5 μm). Right: delaminated region is at 20,000× magnification (scale marker = 0.5 μm). Arrows point to delaminated regions.*

identical manner as the flake. The following results were obtained from four replicate samples that yielded the same values: silicon, 30–40%; aluminum, 2–5%; potassium, not detected; calcium, not detected; boron, 4–10%; and sodium, 4–6%. (The elemental composition of the glass fragment agrees favorably with the values listed in Ref. 8, although the exact values differ.)

Since the composition of the flakes and glass fragments is similar, these flakes are believed to result directly from the glass ampul. The presence of boron was observed in all samples, further implicating the glass, since borosilicate glass was employed. Therefore, the scanning electron microscope was used to determine the region in the ampul from which the flakes came. Scanning electron micrographs about 0.8–2.0 cm up the side wall of the ampul did not show etched regions corresponding to the size of the flakes.

Further studies indicated that the area just above the bottom of the ampul showed distinct regions of delamination that were not noticed in control ampuls. Figure 9 shows this area quite vividly, where it appears as if a surface layer of the glass has peeled away. Careful examination of the delaminated area indicates that it extended at least halfway around the ampul. Triangular pits are also noted at high magnification in this photograph and may indicate that the glass had undergone a devitrification process during manufacture. This area of the glass represents a region where thermal stress could play an important role because intense heat is used to form the bottom of the container (6). It is not known, however, if a preferential chemical attack is a prerequisite for the removal of the flake. The sulfur treatment of the glass, however, did prevent this process from occurring.

Data in these laboratories indicate that the surface topography of ampuls can vary among manufacturers, even though the same treatment process is employed. Therefore, caution should be used when comparing sulfur treatments from different sources. In addition, the method of manufacture and thermal history of the glass can vary. In this work, a concerted effort was made to assure that the scanning electron micrographs were representative, recognizing that it was not possible to use the same ampul as its own control.

REFERENCES

(1) S. Turco and N. M. Davis, *Hosp. Pharm.*, **8**, 137(1973).

(2) J. B. Brown and A. S. Watts, *J. Amer. Ceram. Soc.*, **20**, 245(1937).

(3) V. Dimbleby, *J. Pharm. Pharmacol.*, **5**, 969(1953).

(4) F. R. Bacon and F. C. Raggon, *J. Amer. Ceram. Soc.*, **42**(4), 199(1959).

(5) F. R. Bacon, *Glass Ind.*, **49**, 438(1968).

(6) A. Peters, *Glastech. Ber.*, **46**(8), 161(1973).

(7) "The United States Pharmacopeia" 18th rev., Mack Publishing Co., Easton, Pa., 1970, p. 924.

(8) F. R. Bacon, "Specifications of Glass Containers for Pharmaceutical Use," Owens-Illinois Glass Co., Toledo, Ohio, 1970.

(9) W. E. Hamlin, "Parenteral Drug Delivery Systems," 16th Annual National Industrial Pharmaceutical Research Conference, Land O'Lakes, Wis., June 1974.

(10) "British Pharmacopoeia 1973," Her Majesty's Stationery Office, London, England, 1973, p. A123.

(11) J. Y. Masuda and J. H. Beckerman, *Amer. J. Hosp. Pharm.*, **30**, 72(1973).

(12) R. C. Hohmann, N. Conca, and K. P. Munnelly, *Bull. Parenteral Drug Ass.*, **27**, 96(1973).

(13) G. H. Hopkins and R. W. Young, *ibid.*, **28**, 15(1974).

(14) P. R. Rasanen and R. C. Louer, *ibid.*, **27**, 243(1973).

(15) A. B. McGinn, *ibid.*, **27**, 247(1973).

(16) R. J. Walsh and J. A. Monahan, *ibid.*, **27**, 250(1973).

(17) P. R. Austin, "Design and Operation of Clean Rooms," Business News Publishing, Birmingham, Mich., 1970.

(18) F. R. Bacon and S. W. Barber, "The Chemical Durability of Sulfur Treated Glass Bottles," Technical Bulletin, Owens-Illinois Glass Co., Toledo, Ohio, June 1948.

(19) K. Kamita, U.S. pat. 1,782,169.

(20) R. W. Douglas and J. O. Isard, *J. Soc. Glass Technol.*, **33**, T289(1949).

(21) E. L. Mochel, M. E. Nordberg, and T. H. Elmer, *J. Amer. Ceram. Soc.*, **49**, 585(1966).

(22) A. L. Hinson, *Bull. Parenteral Drug Ass.*, **25**, 266(1971).

(23) F. R. Bacon and G. L. Calcamuggio, *Amer. Ceram. Soc. Bull.*, **46**, 850(1967).

(24) J. P. Majeske, *Bull. Parenteral Drug Ass.*, **16**(4), 1(1962).

(25) G. A. Hudson and F. R. Bacon, *Amer. Ceram. Soc. Bull.*, **37**(4), 185(1958).

ACKNOWLEDGMENTS AND ADDRESSES

Received March 10, 1975, from the **Pharmacy Research Unit, The Upjohn Company, Kalamazoo, MI 49001,* and *‡Walter C. McCrone Associates Inc., Chicago, IL 60616*

Accepted for publication April 30, 1975.

The authors acknowledge the valuable discussions with Dr. T. O. Oesterling and the assistance of the Pharmacy Research Sterile Products Laboratory personnel. At the Walter C. McCrone Associates Inc. Laboratory, conversations with Mr. H. Humecki were appreciated; thanks are also expressed to Dr. J. Gavrilovic for performing the electron microprobe analysis. The assistance of Mrs. A. S. Teetsov was valued.

ˣ To whom inquiries should be directed.

Determination of Coumarin and Umbelliferone Mixtures in Whole Blood by Spectrophotofluorometry

HENRY S. I. TAN ˣ, WOLFGANG A. RITSCHEL, and PHYLLIS R. SANDERS *

Abstract □ A spectrophotofluorometric method is described for the quantitative analysis of coumarin, umbelliferone, and mixtures thereof in whole blood. The two drugs were selectively isolated from blood by solvent extraction. Analysis of the isolated coumarin was based on the measurement of the fluorophore at activation and emission wavelengths of 361 and 491 nm, respectively. The fluorophore was obtained by irradiating an alkaline methanolic solution of the drug with UV light. A linear relationship between fluorescence and concentration existed over the concentration range of 0.02–0.2 μg of coumarin/ml. A mean recovery value of 94.8% was obtained from whole blood. The isolated umbelliferone was determined according to established methods at activation and emission wavelengths of 370 and 450 nm, respectively, and the limit of detection was 10 times more sensitive than previously reported. A linearity response was obtained between 1 and 10 ng of umbelliferone/ml. Good recovery data for mixtures of coumarin and umbelliferone in whole blood were obtained.

Keyphrases □ Coumarin—spectrophotofluorometric analysis, alone and with umbelliferone, whole blood □ Umbelliferone—spectrophotofluorometric analysis, alone and with coumarin, whole blood □ Spectrophotofluorometry—analysis, coumarin and umbelliferone, alone and together, whole blood

Coumarin is the active principle in a number of European pharmaceutical preparations. It gains pharmaceutical importance due to its hemodynamic and lymphokinetic properties. Clinically, it has been used in postthrombotic syndromes, in varicose insufficiency, and in posttraumatic edema (1).

Recent pharmacokinetic studies on coumarin in this laboratory were hampered by the lack of suitable assay procedures for coumarin. Only one method has been reported for its determination in biological fluids. This method is based on an isotope dilution technique (2). Other published procedures (3–6) either dealt with coumarin in plant materials or involved methods that were not sufficiently sensitive for pharmacokinetic investigations, particularly since coumarin is administered in relatively low concentrations.

Coumarin is an acid–base fluorescence indicator. It fluoresces in alkaline solutions after UV irradiation, and this fluorescence behavior has been used for its detection (7). A fluorometric method for coumarin in clover was reported (8).

In test animals, the major metabolites of coumarin are 3-hydroxycoumarin and 7-hydroxycoumarin (umbelliferone) (2, 9). These hydroxycoumarins are known to fluoresce in alkaline solutions and are usually analyzed by fluorometry (9, 10).

Since current pharmacokinetic studies in this laboratory concern the evaluation of coumarin and free 7-hydroxycoumarin, an attempt was made to develop a sensitive assay procedure for coumarin, unconjugated umbelliferone, and mixtures thereof in whole blood. The methodology is based on the fluorescence characteristics of coumarin and umbelliferone.

EXPERIMENTAL

Apparatus—The following were used: a fluorescence spectrophotometer[1] with 1-cm cells and a fixed spectral bandwidth of 10 nm equipped with a 150-w, 7.5-amp, 20–75-v, dc xenon lamp[2] and a R212 photomultiplier tube; an analytical balance[3]; and a 250-w, 110–125 v, ac UV lamp[4]. The response of the fluorescence spectrophotometer was calibrated daily with a solution of quinine sulfate in dilute sulfuric acid (1 in 350) containing 0.25 μg/ml.

Materials and Reagents—The following were used: coumarin[5] (mp 69°); umbelliferone[6] (puriss. mp 231–233°); absolute methanol[7], containing 0.05% water; 2 *N* methanolic potassium hydroxide reagent, prepared by dissolving the required amount of the alkali in methanol, allowing the solution to settle for 24 hr in a closed container, and filtering rapidly the white precipitate of potassium carbonate through a glass wool filter; glycine[8] (ammonia free) buffer, pH 10.0, prepared according to Sørensen (11); and water, distilled from a glass distillation apparatus. All the other chemicals used were of analytical grade.

Preparation of Coumarin Standard Curve—A stock solution of coumarin was prepared by dissolving 25.0 mg of the drug in 250.0 ml of methanol. Further dilutions were made to obtain standard solutions containing 0.2–2.0 μg of coumarin/ml. One milliliter of each solution was transferred to a 10-ml volumetric flask for fluorophore development as described under *Assay Procedure for Coumarin in Whole Blood*, beginning with: "Add 5.0 ml of 2 *N* methanolic potassium hydroxide reagent . . . ." The stock and standard solutions should be freshly prepared.

Preparation of Umbelliferone Standard Curve—A stock solution of umbelliferone was prepared by dissolving 25.0 mg of the compound in 5.5 ml of methanol and diluting to 250.0 ml with water. Further dilutions were made to obtain standard solutions containing 0.01–2.0 μg of umbelliferone/ml. One milliliter of each solution was transferred to a 10-ml volumetric flask for fluorophore development as described under *Assay Procedure for Umbelliferone in Whole Blood*, beginning with: ". . . dilute to volume with pH 10.0 glycine buffer."

Assay Procedure for Coumarin in Whole Blood—Place 5.0 ml of normal saline solution and 0.1 ml of 15% (w/v) aqueous sodium citrate solution in a 50-ml glass-stoppered centrifuge tube. Swirl the contents of the tube, add 3.0 ml of the blood sample, and extract the blood two times with 5-ml portions of ether. Each time shake the mixture for 5 min and centrifuge for 5 min at 2000 rpm.

Transfer the ether layer to a beaker, and evaporate the combined ether fractions carefully at low heat to almost dryness with a gentle stream of nitrogen gas. Add approximately 1 ml of methanol and continue the evaporation until all ether is removed. Transfer quantitatively the remaining solution into a 10-ml volumetric flask with some methanol. Add 5.0 ml of 2 *N* methanolic potassium hydroxide reagent and dilute to volume with methanol.

Expose the flask to UV light, at a distance of 53.3 cm (21 in.) from the light source, for 40 min. Determine the fluorescence at activation and emission wavelengths of 361 and 491 nm, respectively, against a blank prepared similarly but without the coumarin. Read the concentration of coumarin present from a calibration curve.

Assay Procedure for Umbelliferone in Whole Blood—Place 5.0 ml of normal saline solution and 0.1 ml of 15% (w/v) aqueous sodium citrate solution in a 50-ml glass-stoppered centrifuge tube.

[1] Model 204, Perkin-Elmer Corp., Norwalk, Conn.
[2] Model XBO 150 W/1, Osram Gesellschaft, Berlin, Germany.
[3] Model H18, Mettler Instrument Corp., Princeton, N.J.
[4] General Electric Co., Cincinnati, Ohio.
[5] Schaper und Brümmer, Saltzgitter-Ringeheim, Germany.
[6] Fluka A. G., Buchs SG, Switzerland.
[7] Matheson, Coleman and Bell, Norwood, Ohio.
[8] Eastman Kodak Co., Rochester, N.Y.

Table I—Effect of Time on Fluorescence of Coumarin and Umbelliferone Fluorophores

Minutes	Coumarin[a], Relative Fluorescence	Umbelliferone[b], Relative Fluorescence
0	31.2	28.4
15	32.0	—
20	—	27.4
30	32.8	—
40	—	26.4
45	32.9	—
60	32.2	28.0
75	32.8	—
80	—	28.0
90	32.2	—
105	32.1	—

[a] Concentration, 0.08 μg/ml; selector, X 1; sensitivity 5 at λ_{act} 361 nm and $\lambda_{emission}$ 491 nm, after an irradiation time of 40 min with UV light. [b] Concentration, 0.08 μg/ml; selector, X 1/10; sensitivity 3 at λ_{act} 370 nm and $\lambda_{emission}$ 450 nm.

Swirl the contents of the tube and add 3.0 ml of the blood sample. Extract the blood two times with 5-ml portions of ether. Each time shake the mixture for 5 min and centrifuge for 5 min at 2000 rpm.

Transfer the ether layer into a clean glass-stoppered centrifuge tube. Extract the combined ether fraction two times with 3-ml portions of pH 10.0 glycine buffer. Each time shake the mixture vigorously for 5 min and centrifuge for 5 min at 2000 rpm. Transfer the glycine buffer fraction to a 10-ml volumetric flask and dilute to volume with pH 10.0 glycine buffer.

Measure the fluorescence at activation and emission wavelengths of 370 and 450 nm, respectively, against a blank prepared similarly but without the umbelliferone.

Assay Procedure for Mixtures of Coumarin and Umbelliferone in Whole Blood—Place 5.0 ml of normal saline solution and 0.1 ml of 15% (w/v) aqueous sodium citrate solution in a 50-ml glass-stoppered centrifuge tube. Swirl the contents and add 3.0 ml of the blood sample. Extract the blood two times with 5-ml portions of ether. Each time shake the mixture for 5 min and centrifuge for 5 min at 2000 rpm.

Transfer the ether fractions to a fresh glass-stoppered centrifuge tube and extract the ether two times with 3-ml portions of *cold* pH 10.0 glycine buffer. (*a*) Transfer the glycine buffer fractions to a fresh glass-stoppered centrifuge tube and extract once with 5 ml of ether. Combine the ether layer with the main ether solution in the beaker (see *b*). Transfer the glycine buffer solution to a 10-ml volumetric flask and proceed as described under *Assay Procedure for Umbelliferone in Whole Blood* beginning with: "... dilute to volume with pH 10.0 glycine buffer."

(*b*) Transfer the ether fractions to a beaker, evaporate the solvent cautiously at low heat with a gentle stream of nitrogen gas to almost dryness, and proceed as described under *Assay Procedure for Coumarin in Whole Blood* beginning with "Add approximately 1 ml of methanol...."

Table II—Recovery Data of Coumarin or Umbelliferone from Spiked Whole Blood Samples

Amount Added[a]	Analyzed at Concentration Level, ng/ml	Amount Found[a]	Recovery, %
Coumarin			
0.40	40	0.37	92.5
0.80	80	0.78	97.5
1.20	120	1.17	97.5
1.60	160	1.55	96.9
2.00	200	1.79	89.5
Overall percent recovery			94.8
SD			3.62
Standard error of the mean			1.62
Umbelliferone			
20.00	2	17.4	87.0
80.00	8	71.5	89.4
Overall percent recovery			88.2

[a] Coumarin: micrograms per 3 ml of blood; umbelliferone: nanograms per 3 ml of blood.

Table III—Reproducibility of Coumarin Determination from Replicate Whole Blood Samples Containing 0.4 μg of Coumarin/ml

Samples	Relative Fluorescence
1	37.9
2	38.6
3	43.0
4	41.0
5	37.0
Average	39.5
SD	2.46
Coefficient of variation, %	6.22

RESULTS AND DISCUSSION

Coumarin—Freshly prepared alkaline solutions of coumarin exhibit little fluorescence. However, when these solutions are irradiated with UV light, the solutions begin to fluoresce and the intensity increases to a maximum. It is assumed that when coumarin is dissolved in alkali, cleavage of the pyrone ring occurs whereby the anion of *cis*-coumaric acid is formed. Upon irradiation with UV light, the *cis*-form is converted to the *trans*-isomer (7). Apparently, in the *trans*-isomer the hydrogen atom of the phenol group forms a chelate with the sterically unhindered unsaturated carbon atom, giving rise to a six-membered ring which is the fluorophore.

The fluorophore showed excitation and emission wavelengths of 361 and 491 nm, respectively (Fig. 1). The fluorescence intensity depends upon the concentration of potassium hydroxide. Maximum fluorescence was obtained when the concentration of the potassium hydroxide was approximately 1 *N* in the final test solution. This finding is in agreement with previously reported data (8).

Since the fluorescence intensity increases to a maximum upon irradiation with UV light, the optimum exposure time was investigated. The distance of 53.3 cm (21 in.) between sample and light source was selected so that maximum irradiation could be achieved without heating the samples excessively. Figure 2 shows that maximum fluorescence was obtained in 20 min. However, for unknown reasons, samples irradiated for 20 min did not produce constant

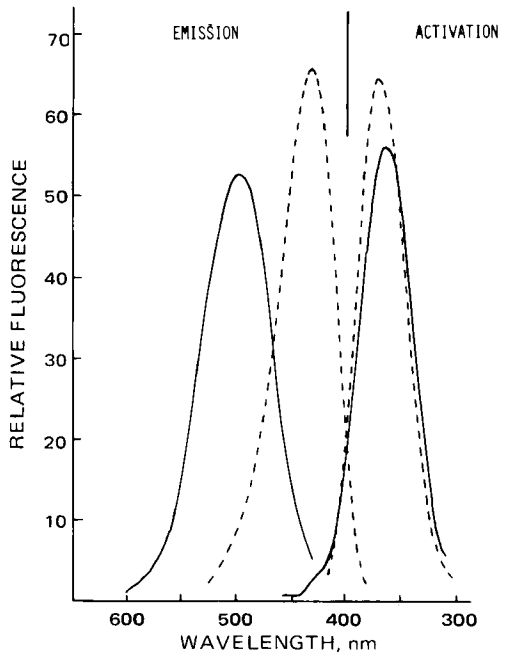

Figure 1—*Activation and emission spectra of coumarin* (——) *and umbelliferone* (- - -) *fluorophores.*

Table IV—Recovery Data of Mixtures of Coumarin and Umbelliferone from Whole Blood

Mixture	Amount Added, μg/3 ml of Blood		Amount Found, μg/3 ml of Blood		Recovery, %	
	Coumarin	Umbelliferone	Coumarin	Umbelliferone	Coumarin	Umbelliferone
A	0.400	0.020	0.361	0.0179	90.3	86.0
B	0.800	0.040	0.693	0.0339	86.6	84.8
C	1.600	0.060	1.36	0.0527	85.3	87.8
Overall percent recovery					87.4	86.2

fluorescence intensities, particularly if these samples were scanned repeatedly in the spectrophotofluorometer. An irradiation time of 40 min gave constant readings. The fluorescence intensities of samples so developed were stable for at least 90 min (Table I).

Under these experimental conditions, a linear relationship existed between fluorescence and concentration. A straight line was obtained over the concentration range of 0.02–0.2 μg of coumarin/ml. Statistical analysis shows a regression equation of $F_{361/491} = 292.21C + 1.37$ with a correlation coefficient of 0.9993, where F is expressed in relative fluorescence units and C in micrograms per milliliter[9]. The standard error of the estimate of F on C is 0.668.

Recovery experiments were performed by adding accurately known amounts of coumarin to freshly drawn whole blood. For best reproducibility, an anticoagulant must be present in the centrifuge tube into which the whole blood is transferred. In the absence of an anticoagulant, clotting commenced within a few minutes and the recovery of the drug was poor due to inclusion of the drug in the blood clot. For this purpose, sodium citrate was used at the concentration of 5 mg/ml of blood. The sodium citrate was mixed into the normal saline solution, which served as the diluting agent for the blood sample.

Care must be exercised upon evaporating the coumarin-containing ether extract. Because coumarin has a high vapor pressure and is steam distillable, the evaporation must be done at very low heat. Addition of methanol in the evaporation process greatly increased the recovery of drug. The results (Table II) indicated that recovery of coumarin from whole blood was essentially quantitative. The overall recovery was 94.8% with a standard deviation of 3.62% (n = 5).

The precision study on coumarin recovery from whole blood was performed by running replication studies on five samples. In each run the amount of coumarin added to whole blood was 0.4 μg/ml of blood. Each sample was analyzed by the proposed method. The relative standard deviation for the five replicate samples was 6.21% at this concentration level (Table III).

Umbelliferone—As mentioned previously, the major metabolites of coumarin are 3-hydroxycoumarin and 7-hydroxycoumarin (umbelliferone); these metabolities are conjugated mainly as sulfates and glucuronides. These conjugates are not isolated by the proposed extraction procedure, and they do not fluoresce (10). Umbelliferone does show the phenomenon of excited-state ionization, so its fluorescence behavior is completely different than that of the 3-isomer. The 3-isomer shows negligible fluorescence between pH 9 and 12 (9). Under the proposed experimental conditions, only free umbelliferone is measured. As shown in Fig. 1, umbelliferone showed an emission maximum of 450 nm when activated at 370 nm in pH 10.0 glycine buffer. The fluorescence was stable for at least 90 min (Table I).

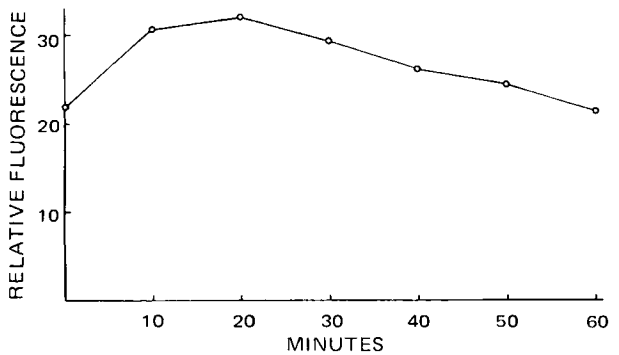

Figure 2—*Effect of time of light exposure on fluorescence development of coumarin.*

The concentration–fluorescence plot shows that the fluorescence response is linear with concentration in the investigated range of 1–10 ng/ml. Therefore, the proposed procedure is approximately 10 times more sensitive than the one previously reported by Mead *et al.* (10). The linear regression line is $F_{370/450} = 10.25C + 0.33$ with a correlation coefficient of 0.9998, where F is expressed in relative fluorescence units and C in nanograms per milliliter[9]. The standard error of the estimate of F on C is 0.382.

The recovery data of umbelliferone from whole blood are presented in Table II. The overall percent recovery for two samples was 88.2%. This value is in agreement with recovery data from liver homogenates reported by Creaven *et al.* (9).

Coumarin–Umbelliferone Mixtures—Results shown in Table IV indicate that the recovery of umbelliferone in the presence of coumarin was in agreement with its recovery when it alone was present in blood. However, the percent recoveries of coumarin were lower than expected. Presumably, a fraction of the coumarin undergoes hydrolysis during the extraction process with pH 10.0 glycine buffer to form the *o*-coumarinate anion which is insoluble in ether. Since the glycine fraction was not subjected to UV radiation, this solution showed no fluoresence at the coumarin activation and emission wavelengths. Thus, measurement of umbelliferone in this glycine buffer solution is not interfered with by coumarin. To keep the hydrolysis of coumarin to a minimum, *cold* glycine buffer must be used for the extraction.

SUMMARY

The developed fluorometric procedure was sensitive and specific for coumarin and umbelliferone and was adapted to drug level determination in whole blood. Among the advantages of the present procedure are its reproducibility, its sensitivity, and the relative lack of interference by constituents in blood. It also allows for measurement of free umbelliferone. In addition, both the umbelliferone conjugates and the other hydroxycoumarins do not interfere. Precipitation of proteins in blood with agents such as trichloroacetic acid is not necessary, as shown by the recovery studies.

This method is currently being applied to biopharmaceutical and pharmacokinetic studies of coumarin.

REFERENCES

(1) C. A. Scholten, *VASA*, **2**, 96(1973).

(2) M. Kaighen and R. T. Williams, *J. Med. Pharm. Chem.*, **3**, 25(1961).

(3) J. Duncan and R. Dustman, *Ind. Eng. Chem., Anal. Ed.*, **9**, 471(1937).

(4) M. Szymanska, *Acta Pol. Pharm.*, **29**, 511(1972); through *Chem. Abstr.*, **78**, 81717z(1973).

(5) J. R. Clopton, *J. Agr. Food Chem.*, **6**, 457(1958).

(6) V. Anger and H. E. Richter, *Mikrochim. Ichnoanal. Acta*, **1965**, 1025; through *Chem. Abstr.*, **64**, 14777b(1966).

(7) F. Feigle, H. E. Feigle, and D. Goldstein, *J. Amer. Chem. Soc.*, **77**, 4162(1955).

(8) K. Blyaim, *Biokhimiya*, **21**, 689(1956).

(9) P. J. Creaven, D. V. Parke, and R. T. Williams, *Biochem. J.*, **96**, 390(1965).

(10) J. A. R. Mead, J. N. Smith, and R. T. Williams, *ibid.*, **61**, 569(1955).

(11) "Scientific Tables," 7th ed., K. Diem and C. Lentner, Eds., Ciba-Geigy, Basle, Switzerland, 1971, p. 280.

[9] Olivetti Programma 101 minicomputer.

ACKNOWLEDGMENTS AND ADDRESSES

Received February 26, 1975, from the *College of Pharmacy, University of Cincinnati, Cincinnati, OH 45221*

Accepted for publication April 3, 1975.

Presented at the 22nd Canadian Conference on Pharmaceutical Research, Montreal, Canada, May 1975.

* Recipient of Research Fellowship from Schaper und Brümmer KG, Saltzgitter-Ringeheim, Germany.

ˣ To whom inquiries should be directed.

Binding of Salicylate and Sulfathiazole by Whole Blood Constituents

CHARLES A. CRUZE * and MARVIN C. MEYER ˣ

Abstract □ The binding of salicylic acid and sulfathiazole to bovine whole blood, plasma proteins, and purified albumin fraction was investigated using a dynamic dialysis system. The binding profiles for salicylic acid were quite similar in bovine plasma and 4% bovine serum albumin. In contrast, the binding of sulfathiazole was significantly greater in the plasma than in solutions of fraction V bovine serum albumin. Data from dynamic dialysis binding studies of the compounds, conducted in whole blood and suspended erythrocyte systems, did not lend themselves to analysis by classical methods. Hemolysis and alteration in the nature of the protein binding sites during the binding studies were shown to be factors that could explain the unusual binding observed in the whole blood system.

Keyphrases □ Salicylate—binding to bovine whole blood, plasma proteins, and purified albumin fractions compared □ Sulfathiazole—binding to bovine whole blood, plasma proteins, and purified albumin fractions compared □ Binding—salicylate and sulfathiazole to bovine whole blood, plasma proteins, and purified albumin fractions compared □ Plasma proteins—compared to bovine whole blood and purified albumin fraction binding of salicylate and sulfathiazole □ Albumin—purified fractions, compared to bovine whole blood and plasma protein binding of salicylate and sulfathiazole

Numerous drugs and endogenous substances are reported to be bound by serum proteins (1). Plasma albumin is generally thought to be the primary serum protein responsible for the binding of most drugs. Thus, drug binding studies aimed at determining the affinity of a drug for plasma proteins generally have employed albumin as the macromolecule.

In vitro studies with various protein fractions have shown that the summation of the binding to the individual fractions of the plasma may exceed the binding observed in the whole plasma (2). Therefore, binding studies employing purified protein fractions may not accurately reflect the binding that may occur *in vivo*. Several reports have dealt with the binding of drugs to plasma constituents (3–7). However, relatively little consideration has been given to the binding of drugs by erythrocytes (8, 9) or the binding in whole blood systems (10, 11).

The use of classical methods to study the binding of drugs to plasma and whole blood is difficult and subject to error. In equilibrium dialysis, the time necessary to establish equilibrium may be sufficient to permit significant denaturation of the blood and plasma components. The use of ultrafiltration methods for whole blood binding studies may result in separation of the blood components and blockage of the pores of conventional dialysis membranes. In view of these problems, the dynamic dialysis technique of Meyer and Guttman (12) seemed to hold promise for the quantitation of drug binding in whole blood. The time required for the determination of a complete binding profile is relatively short, temperature can be conveniently controlled, and no centrifugation, vacuum, or pressure is required.

Salicylic acid and sulfathiazole were selected as model compounds to test the applicability of the dynamic dialysis technique to the study of drug binding to bovine whole blood, erythrocytes, plasma, and purified serum albumin.

EXPERIMENTAL

Materials—Fraction V bovine serum albumin[1], sodium salicylate[2], and sulfathiazole sodium[3] were obtained from commercial sources. Regenerated cellulose dialysis tubing[4] was conditioned prior to use by rapidly running distilled water through the tubing for several hours, with the tubing immersed in distilled water. The tubing was then stored in distilled water at 4° until used.

Bovine blood was obtained from the jugular vein of freshly slaughtered cattle and was collected into large vessels containing either heparin[5], 50 units/ml of blood, or anticoagulant citrate dextrose solution A USP, 0.15 ml/ml of blood. The collected blood was divided into two portions. One portion was employed in the whole blood studies, and the other portion was centrifuged to separate the plasma and formed elements. The buffy coat was removed from the packed cells, and the erythrocytes were washed several times with pH 7.38, 0.128 *M*, isotonic phosphate buffer solution. The erythrocytes were then resuspended with the phosphate buffer to produce the same volume present before the plasma was removed.

Dynamic Dialysis Studies—The dynamic dialysis system of Meyer and Guttman (13) was employed with a few modifications. The dialysis behavior of the drug was first characterized with a control solution of the drug in pH 7.38, 0.128 *M* phosphate buffer. A 5-ml sample of the control drug solution was placed inside a 6.5-cm long dialysis sac, secured at one end with a knot and suspended in a jacketed beaker containing 175 ml of the phosphate

[1] Calbiochem, San Diego, Calif.
[2] J. T. Baker, Phillipsburg, N.J.
[3] Sigma Chemical Co., St. Louis, Mo.
[4] Union Carbide dialysis membrane.
[5] The Upjohn Co., Kalamazoo, Mich.

ACKNOWLEDGMENTS AND ADDRESSES

Received February 26, 1975, from the *College of Pharmacy, University of Cincinnati, Cincinnati, OH 45221*

Accepted for publication April 3, 1975.

Presented at the 22nd Canadian Conference on Pharmaceutical Research, Montreal, Canada, May 1975.

* Recipient of Research Fellowship from Schaper und Brümmer KG, Saltzgitter-Ringeheim, Germany.

ˣ To whom inquiries should be directed.

Binding of Salicylate and Sulfathiazole by Whole Blood Constituents

CHARLES A. CRUZE * and MARVIN C. MEYER ˣ

Abstract □ The binding of salicylic acid and sulfathiazole to bovine whole blood, plasma proteins, and purified albumin fraction was investigated using a dynamic dialysis system. The binding profiles for salicylic acid were quite similar in bovine plasma and 4% bovine serum albumin. In contrast, the binding of sulfathiazole was significantly greater in the plasma than in solutions of fraction V bovine serum albumin. Data from dynamic dialysis binding studies of the compounds, conducted in whole blood and suspended erythrocyte systems, did not lend themselves to analysis by classical methods. Hemolysis and alteration in the nature of the protein binding sites during the binding studies were shown to be factors that could explain the unusual binding observed in the whole blood system.

Keyphrases □ Salicylate—binding to bovine whole blood, plasma proteins, and purified albumin fractions compared □ Sulfathiazole—binding to bovine whole blood, plasma proteins, and purified albumin fractions compared □ Binding—salicylate and sulfathiazole to bovine whole blood, plasma proteins, and purified albumin fractions compared □ Plasma proteins—compared to bovine whole blood and purified albumin fraction binding of salicylate and sulfathiazole □ Albumin—purified fractions, compared to bovine whole blood and plasma protein binding of salicylate and sulfathiazole

Numerous drugs and endogenous substances are reported to be bound by serum proteins (1). Plasma albumin is generally thought to be the primary serum protein responsible for the binding of most drugs. Thus, drug binding studies aimed at determining the affinity of a drug for plasma proteins generally have employed albumin as the macromolecule.

In vitro studies with various protein fractions have shown that the summation of the binding to the individual fractions of the plasma may exceed the binding observed in the whole plasma (2). Therefore, binding studies employing purified protein fractions may not accurately reflect the binding that may occur *in vivo*. Several reports have dealt with the binding of drugs to plasma constituents (3–7). However, relatively little consideration has been given to the binding of drugs by erythrocytes (8, 9) or the binding in whole blood systems (10, 11).

The use of classical methods to study the binding of drugs to plasma and whole blood is difficult and subject to error. In equilibrium dialysis, the time necessary to establish equilibrium may be sufficient to permit significant denaturation of the blood and plasma components. The use of ultrafiltration methods for whole blood binding studies may result in separation of the blood components and blockage of the pores of conventional dialysis membranes. In view of these problems, the dynamic dialysis technique of Meyer and Guttman (12) seemed to hold promise for the quantitation of drug binding in whole blood. The time required for the determination of a complete binding profile is relatively short, temperature can be conveniently controlled, and no centrifugation, vacuum, or pressure is required.

Salicylic acid and sulfathiazole were selected as model compounds to test the applicability of the dynamic dialysis technique to the study of drug binding to bovine whole blood, erythrocytes, plasma, and purified serum albumin.

EXPERIMENTAL

Materials—Fraction V bovine serum albumin[1], sodium salicylate[2], and sulfathiazole sodium[3] were obtained from commercial sources. Regenerated cellulose dialysis tubing[4] was conditioned prior to use by rapidly running distilled water through the tubing for several hours, with the tubing immersed in distilled water. The tubing was then stored in distilled water at 4° until used.

Bovine blood was obtained from the jugular vein of freshly slaughtered cattle and was collected into large vessels containing either heparin[5], 50 units/ml of blood, or anticoagulant citrate dextrose solution A USP, 0.15 ml/ml of blood. The collected blood was divided into two portions. One portion was employed in the whole blood studies, and the other portion was centrifuged to separate the plasma and formed elements. The buffy coat was removed from the packed cells, and the erythrocytes were washed several times with pH 7.38, 0.128 *M*, isotonic phosphate buffer solution. The erythrocytes were then resuspended with the phosphate buffer to produce the same volume present before the plasma was removed.

Dynamic Dialysis Studies—The dynamic dialysis system of Meyer and Guttman (13) was employed with a few modifications. The dialysis behavior of the drug was first characterized with a control solution of the drug in pH 7.38, 0.128 *M* phosphate buffer. A 5-ml sample of the control drug solution was placed inside a 6.5-cm long dialysis sac, secured at one end with a knot and suspended in a jacketed beaker containing 175 ml of the phosphate

[1] Calbiochem, San Diego, Calif.
[2] J. T. Baker, Phillipsburg, N.J.
[3] Sigma Chemical Co., St. Louis, Mo.
[4] Union Carbide dialysis membrane.
[5] The Upjohn Co., Kalamazoo, Mich.

Table I—Binding of Salicylate by 4% Bovine Serum Albumin and Bovine Plasma Proteins

Protein	Buffer	pH	Binding Constants n_1	n_2	K_1, liters/mole	K_2, liters/mole	Temperature
4% bovine serum albumin[a]	Phosphate	7.38	1.04	6.27	5.00×10^4	2.98×10^2	37°
Bovine plasma[a]	Phosphate	7.38	1.01	7.85	6.54×10^4	2.50×10^2	37°
1.61% bovine serum albumin[b]	Phosphate	7.0	1	5	2.0×10^5	1.75×10^3	25°
0.69% bovine serum albumin[c]	Acetate	5.4	0.37	3.5	3.0×10^4	1.00×10^2	4°

[a] This study using pH 7.38, 0.128 *M* phosphate buffer, 37°. [b] Reference 18. [c] Reference 22.

buffer maintained at 37°. The contents of the sac were stirred with a twisted glass rod driven by a constant-speed motor[6], and the external buffer solution was agitated by a magnetic stirring bar.

At various time intervals, 50 ml of the external solution was withdrawn and immediately replaced with 50 ml of fresh buffer solution. The concentration of the small molecule in the external buffer solution was determined spectrophotometrically. The concentration of the small molecule inside the dialysis sac could then be calculated from a knowledge of the initial amount of drug inside the sac and the cumulative amount of drug that had exited the dialysis sac. The binding studies were conducted by replacing the control solution with drug in 5 ml of bovine blood, plasma, suspended erythrocytes, or 4% fraction V purified bovine serum albumin solution.

Binding in Presence of Hemolysis—To study the effects of hemolysis on drug binding, erythrocytes were suspended in an equal volume of 0.128 *M* phosphate buffer and were frozen for 72 hr to produce hemolysis. Upon thawing, 1-, 0.75-, or 0.5-ml aliquots of the resultant solution were added to 4 ml of fraction V bovine serum albumin solutions containing the drug. An appropriate volume of pH 7.38, 0.064 *M* phosphate buffer was added to each solution to maintain the final albumin concentration at 4%, the buffer concentration at 0.013 *M*, and the final volume at 5 ml. Dialysis studies of these solutions were then performed as previously described, using 0.128 *M* phosphate buffer as the external solution.

Analytical Methods—The salicylate and sulfathiazole phosphate buffer solutions were assayed spectrophotometrically for drug at 229 and 255 nm, respectively. Salicylate, in the presence of protein or whole blood, was determined by the method of Trinder (14). The Bratton and Marshall (15) procedure was utilized for the determination of sulfathiazole. Samples obtained from the hemolyzed material, plasma, or whole blood yielded identical blank values when employed in the salicylate or sulfathiazole assays.

The extent of hemolysis was determined spectrophotometrically. A 0.2-ml aliquot of the suspended erythrocytes was diluted to 25 ml with phosphate buffer and incubated for 1 hr in a water bath at 37°. For comparison, 100% hemolysis was achieved by dilution of the suspended erythrocyte samples with distilled water instead of the buffer solution (16).

Total protein and albumin concentrations of the whole blood and plasma were determined by the biuret reaction (17).

Data Treatment—The time course for the loss of drug from each system was analyzed as reported by Meyer and Guttman (18), or a fourth-degree polynomial regression analysis was utilized as described by Crooks and Brown (19). The binding data, computed as previously described from the dialytic rates (18), were employed in the generation of Scatchard plots (20) based on Eq. 1:

$$\bar{V} = \sum_{i=1}^{i=m} \frac{n_i K_i (D_f)}{1 + K_i (D_f)} \qquad \text{(Eq. 1)}$$

where $\bar{V}$ is the moles of small molecule bound divided by the total moles of protein; (D_f) is the free drug concentration; n_i and K_i are the number of binding sites and the corresponding association constant, respectively, for the ith class of binding sites; and m is the number of classes of binding sites.

The binding parameters were evaluated from Scatchard plots with the aid of a nonlinear regression digital computer program based on an algorithm by Marquardt (21). Two classes of binding sites were assumed if the experimentally determined Scatchard plots exhibited curvature.

RESULTS AND DISCUSSION

The binding of salicylate and sulfathiazole was studied to determine the contribution of albumin, plasma, erythrocytes, and whole blood to the binding of each drug *in vitro*.

Binding to Bovine Serum Albumin—Binding studies were ini-

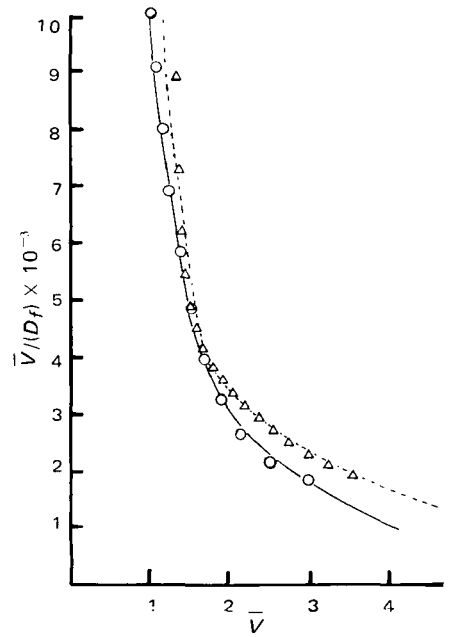

Figure 1—*Scatchard plot of salicylate binding in 4% bovine serum albumin (○) and bovine plasma (△) at 37°.*

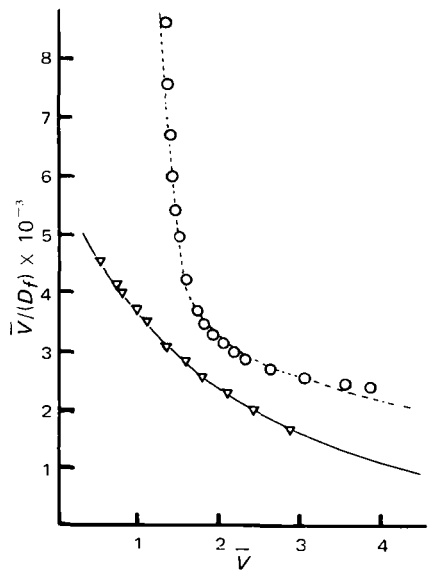

Figure 2—*Scatchard plot of sulfathiazole binding in 4% bovine serum albumin (▽) and bovine plasma (○) at 37°.*

[6] Cole-Parmer Instrument Co., Chicago, Ill.

Table II—Binding of Sulfathiazole to 4% Bovine Serum Albumin and Bovine Plasma Proteins[a]

Protein	Binding Constants			
	n_1	n_2	K_1, liters/mole	K_2, liters/mole
4% bovine serum albumin	1.98	9.77	2.96×10^3	1.21×10^2
Bovine plasma	1.03	8.93	6.51×10^4	2.21×10^2

[a] Using 7.38, 0.128 *M* phosphate buffer, 37°.

tiated with 4% bovine serum albumin solutions, based on the determination that the whole bovine plasma contained approximately 4.1% albumin. Figures 1 and 2 are the Scatchard plots for the binding of salicylic acid and sulfathiazole, respectively, to 4% bovine serum albumin and bovine plasma at 37°. The binding parameters (Tables I and II) were derived from the nonlinear regression analysis of the Scatchard plot.

Previously reported salicylate binding data are also given in Table I for comparison. The binding of the salicylate was somewhat weaker than that reported by Meyer and Guttman (18) but was stonger than found by Davison and Smith (22). The difference may be the result of buffer composition, protein source, degree of ionization, or temperature effects.

Binding to Bovine Plasma—It can be seen from Fig. 1 and Table I that the binding of salicylic acid was quite similar in both bovine plasma and 4% bovine serum albumin. The albumin concentration of the plasma was 4.1%, and the total protein concentration was 8.25%. In view of the comparable salicylate binding in the 4% bovine serum albumin and plasma, it appears that salicylic acid primarily interacts with the albumin.

In contrast, Fig. 2 and Table II illustrate a significant difference in the binding of sulfathiazole in bovine plasma and 4% bovine serum albumin, with a stronger interaction occurring in the plasma. It is apparent from these data that the use of purified fraction V bovine serum albumin may not adequately reflect the extent of binding that may occur for some drugs.

Binding to Whole Blood—As shown in Figs. 3 and 4, the decline of salicylate or sulfathiazole concentration within the dialysis sac with time, in the presence of 4% bovine serum albumin, followed the nonlinear behavior observed by Meyer and Guttman (13) for the dialysis of drugs bound by protein. The whole blood

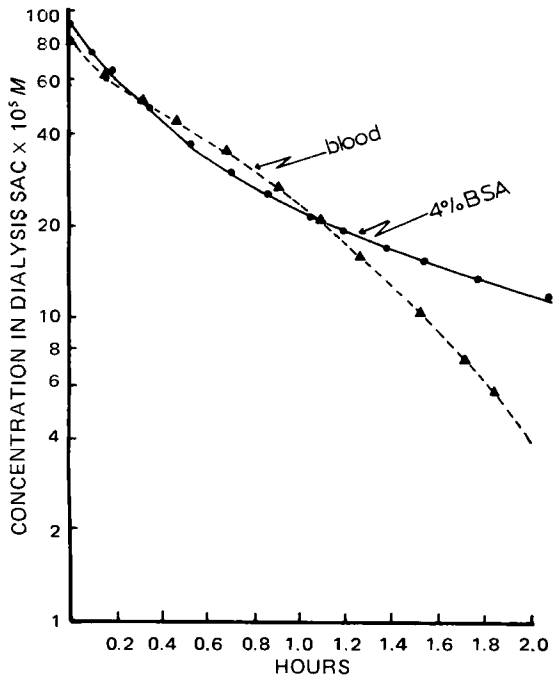

Figure 3—*Loss of salicylate from inside a dialysis sac in the presence of bovine whole blood (▲) and 4% bovine serum albumin (●) at 37°.*

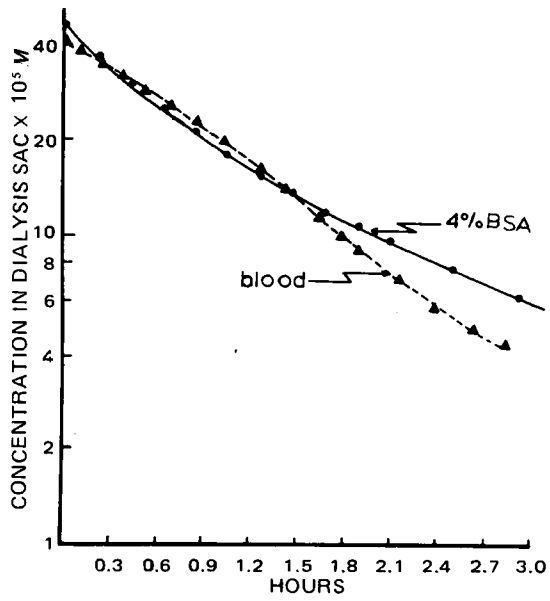

Figure 4—*Loss of sulfathiazole from inside the dialysis sac in the presence of bovine whole blood (▲) and 4% bovine serum albumin (●) at 37°.*

data, however, are most unusual. Instead of a constantly decreasing slope, as was observed for the 4% bovine serum albumin or plasma, the whole blood dialysis exhibited first a decreasing and then an increasing slope. This same phenomenon was observed when the drugs were dialyzed in the presence of suspended erythrocytes.

The dialysis data were fitted to a fourth-degree polynomial regression equation to permit the generation of Scatchard data from the dialytic rates (19). The Scatchard plots for the binding of salicylate in 4% bovine serum albumin, whole blood, and suspended erythrocytes are shown in Fig. 5. Similar profiles were obtained for the binding of sulfathiazole in these systems. In an attempt to rationalize the unusual appearance of the Scatchard plots, several possible explanations were explored. The Scatchard data treatment assumes that the various binding sites are mutually independent. If, in fact, the association of a small molecule with binding sites on the protein affects the binding of subsequent small mole-

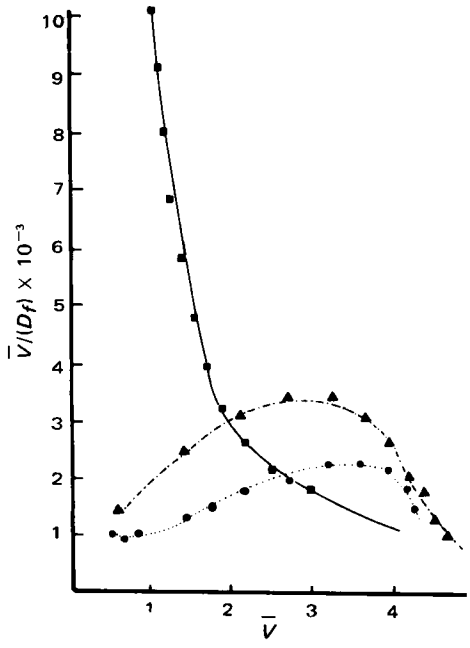

Figure 5—*Scatchard plot of salicylate binding in bovine whole blood (▲), suspended erythrocytes (●), and 4% bovine serum albumin (■) at 37°.*

Table III—Theoretical Scatchard Data for a Typical Drug[a]

$\bar{V}$	(D_f), moles/liter	$\bar{V}/(D_f)$, (liters/mole) × 10^{-5}
5.5	1.1×10^{-4}	0.5
5.0	5.0×10^{-5}	1.0
4.0	2.0×10^{-5}	2.0
3.0	1.0×10^{-5}	3.0
2.0	5.0×10^{-6}	4.0
1.0	2.0×10^{-6}	5.0
0.5	9.1×10^{-7}	5.5

[a] $n = 6$, and $K = 1.0 \times 10^5$ liters/mole.

Table IV—Effect on Binding of a Decreasing Number of Binding Sites[a]

$\bar{V}$	(D_f), (moles/liter) × 10^5	$\bar{V}/(D_f)$, (liters/mole) × 10^{-5}	n
5.0	5.0	1.0	6
4.5	3.0	1.5	6
4.0	2.0	2.0	6
3.5	1.4	2.5	6
3.0	1.5	2.0	5
2.5	1.7	1.5	4
2.0	2.0	1.0	3
1.5	3.0	0.5	2
0.5	1.0	0.5	1

[a] $K = 1.0 \times 10^5$ liters/mole.

cules, the classical mass balance data treatment is not applicable. Similar considerations apply if configurational alterations in the protein structure occur during the drug–protein interactions. For example, a rather complex computer analysis of Scatchard plots exhibiting both positive and negative slopes was described (23–25).

An alternative explanation for the unusual binding observed in the systems containing whole blood or suspended erythrocytes could be the presence of some agent competing with the small molecule for protein binding sites. If the competitor was dialyzed out of the dialysis sac at a different rate than the drug molecule, and/or if the competitor was being released in the dialysis sac during dialysis, the continually changing concentrations of drug and competitor could conceivably produce the observed phenomenon. One source of a potential competitor could be material released from the erythrocytes upon hemolysis. It has been shown, for example, that hemolysis alters the radioimmunoassay for insulin by competitive displacement mechanisms (26).

To test these possible explanations, theoretical data were computed in an attempt to simulate the experimental data. In addition, experiments were designed to study the influence of hemolysis on the binding of salicylate. Theoretical data were generated to simulate binding values that may be obtained if the number of binding sites or the affinity constant characterizing the sites varies over the time course of the dialysis. In addition, data were generated based on the hypothesis that a competitor could be present in increasing concentrations while the drug was continually decreasing in concentration within the dialysis sac.

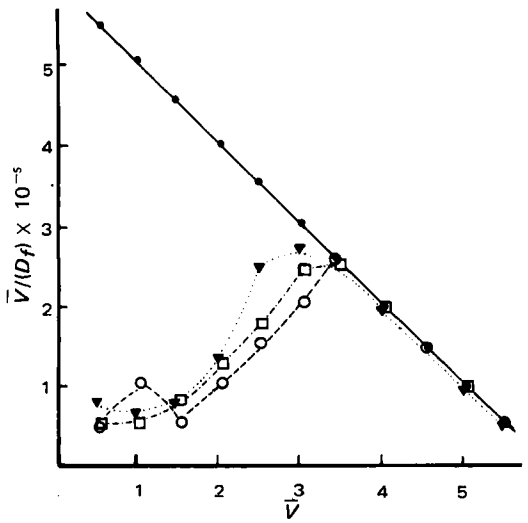

Figure 6—*Scatchard plot of theoretical drug binding data. Key: ●, normal (Table III); ○, decreasing number of sites (Table IV); □, decreasing association constant (Table V); and ▼, increasing competitor concentration (Table VI).*

Table V—Effect on Binding of a Decreasing Association Constant[a]

$\bar{V}$	(D_f), moles/liter	$\bar{V}/(D_f)$, (liters/mole) × 10^{-5}	K, (liters/mole) × 10^{-4}
5.0	5.00×10^{-5}	1.00	10.0
4.5	3.00×10^{-5}	1.50	10.0
4.0	2.00×10^{-5}	2.00	10.0
3.5	1.40×10^{-5}	2.50	10.0
3.0	1.25×10^{-5}	2.40	8.0
2.5	1.43×10^{-5}	1.75	5.0
2.0	1.67×10^{-5}	1.20	3.0
1.5	1.67×10^{-5}	0.90	2.0
1.0	2.00×10^{-4}	0.50	1.0
0.5	1.00×10^{-4}	0.49	0.9

[a] $n = 6$.

For simplicity, the theoretical data were derived assuming that a single class of binding sites was involved. Thus, free drug concentrations (D_f) could be computed, based on a rearrangement of Eq. 1:

$$(D_f) = \frac{\bar{V}}{nK - \bar{V}K} \qquad \text{(Eq. 2)}$$

The binding parameters were arbitrarily fixed at $n = 6$ and $K = 1 \times 10^5$ liters/mole. Table III gives the Scatchard data generated over a free drug concentration range of 10^{-4}–10^{-7} M, assuming constant values for n and K.

Table IV is based on the assumption that the number of available binding sites declines with a decrease in drug concentration. The data in Table V were obtained assuming that the affinity constant increases with decreasing drug concentration.

For the case where a competitor is present, Eq. 3 may be readily derived from the Scatchard equation, as presented by Meyer and Guttman (18):

$$(D_f) = \frac{\bar{V}_D + \bar{V}_D K_C (C_f)}{n_D K_D - \bar{V}_D K_D} \qquad \text{(Eq. 3)}$$

where K_D and K_C are the affinity constants for the drug and competitor, respectively; and (C_f) is the free competitor concentration. Table VI summarizes data generated with the use of Eq. 3, based on the assumption of an increasing competitor concentration occurring as drug concentration declines.

Figure 6 graphically summarizes the data presented in Tables III–VI. These data clearly illustrate that Scatchard plots exhibiting both positive and negative slopes can arise from the assumptions employed in the generation of these data. The similarity be-

Table VI—Effect on Binding of an Increasing Competitor Concentration[a]

$\bar{V}$	(D_f), moles/liter	(C_f), moles/liter	$\bar{V}/(D_f)$, liters/mole
5.5	1.10×10^{-4}	0.00	5.00×10^4
5.0	5.03×10^{-5}	5.00×10^{-9}	9.95×10^4
4.0	2.02×10^{-5}	1.00×10^{-8}	1.96×10^5
3.0	1.10×10^{-5}	1.00×10^{-7}	2.73×10^5
2.5	1.43×10^{-5}	1.00×10^{-6}	1.75×10^5
2.0	1.50×10^{-5}	2.00×10^{-6}	1.33×10^5
1.5	1.67×10^{-5}	4.00×10^{-6}	9.00×10^4
1.0	1.40×10^{-5}	6.00×10^{-6}	7.15×10^4
0.5	6.36×10^{-6}	6.00×10^{-6}	7.90×10^4

[a] $n_D = 6$, $K_D = 1.0 \times 10^5$ liters/mole, $n_C = 6$, and $K_C = 1.0 \times 10^6$ liters/mole.

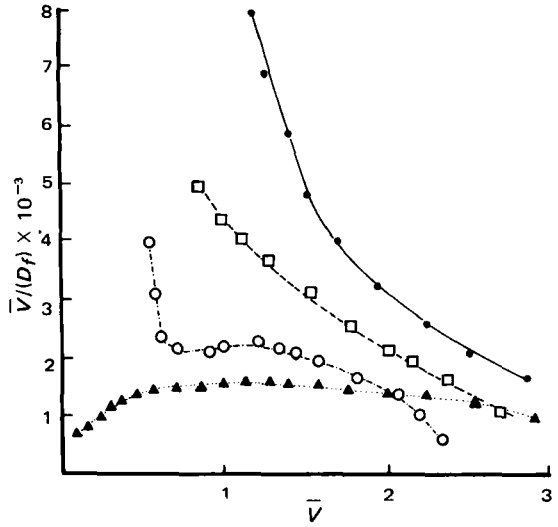

Figure 7—*Effect of hemolysis products on the binding of salicylate by 4% bovine serum albumin. Key: ●, no hemolysate; □, 0.5 ml of hemolysate; ○, 0.75 ml of hemolysate; and ▲, 1.0 ml of hemolysate.*

tween the profiles for these theoretical curves and the experimental data obtained for the binding of salicylate to whole blood and suspended erythrocyte systems is readily apparent. Thus, it appears that the unusual salicylate binding data could be attributed to an alteration in the binding parameters (n's and K's) during dialysis and/or the presence of a competitor species that interferes with the binding of salicylate.

In vitro binding studies were also initiated to investigate further the possibility that hemolysis was contributing to the observed effects. It was determined that between 2 and 10% erythrocyte hemolysis occurred during a dynamic dialysis study. Most hemolysis appeared to be due to the mechanical agitation of the stirring rod rotating within the dialysis sac. Various aliquots of hemolyzed cell constituents were added to solutions of salicylate in 4% bovine serum albumin. The pH of these samples was 7.38, and the phosphate concentration inside the dialysis sac was 0.013 M. The resulting decrease in salicylate binding with increasing amounts of hemolysis product is apparent from Fig. 7.

These results indicate that the characterization of drug binding in whole blood systems is difficult using common methodology and data treatment. The assumption of mutually independent binding sites apparently may not hold for the more complex whole blood systems, and/or hemolysis may produce products that may compete for drug binding sites.

The results of these studies suggest that plasma samples employed in drug binding studies should be obtained only from freshly drawn, nonhemolyzed blood specimens.

REFERENCES

(1) M. C. Meyer and D. E. Guttman, *J. Pharm. Sci.*, **57**, 895(1968).

(2) J. Judis, *ibid.*, **61**, 89(1972).

(3) E. M. Sellers and J. Koch-Weser, *Ann. N.Y. Acad. Sci.*, **226**, 319(1973).

(4) C. W. Bourne, R. M. Kudla, and A. M. Mattocks, *Invest. Urol.*, **3**, 557(1966).

(5) G. D. Potter and J. L. Guy, *Proc. Soc. Exp. Biol. Med.*, **116**, 658(1964).

(6) J. L. Kucera and F. J. Bullock, *J. Pharm. Pharmacol.*, **21**, 293(1969).

(7) E. E. Ohnhaus, P. Spring, and L. Dehli, *Eur. J. Clin. Pharmacol.*, **5**, 34(1972).

(8) R. C. Robbins, *J. Clin. Pharmacol.*, **13**, 401(1973).

(9) D. Bratlid, *Scand. J. Clin. Lab. Invest.*, **29**, 91(1972).

(10) B. G. Gazzard, A. W. Ford-Hutchinson, M. J. H. Smith, and R. Williams, *J. Pharm. Pharmacol.*, **25**, 964(1973).

(11) J. N. McArthur, P. D. Dawkins, and M. J. H. Smith, *ibid.*, **23**, 32(1971).

(12) M. C. Meyer and D. E. Guttman, *J. Pharm. Sci.*, **57**, 1627(1968).

(13) *Ibid.*, **59**, 33(1970).

(14) P. Trinder, *Biochem. J.*, **57**, 301(1954).

(15) A. C. Bratton and E. K. Marshall, *J. Biol. Chem.*, **128**, 537(1939).

(16) M. F. Coldman, M. Gent, and W. Wood, *Comp. Biochem. Physiol.*, **31**, 605(1969).

(17) A. G. Cornall, C. J. Bardawill, and M. M. David, *J. Biol. Chem.*, **177**, 751(1948).

(18) M. C. Meyer and D. E. Guttman, *J. Pharm. Sci.*, **59**, 39(1970).

(19) M. J. Crooks and K. F. Brown, *ibid.*, **62**, 1904(1973).

(20) G. Scatchard, *Ann. N.Y. Acad. Sci.*, **51**, 660(1949).

(21) D. W. Marquardt, *J. Soc. Ind. Appl. Math.*, **11**, 431(1963).

(22) C. Davison and P. K. Smith, *J. Pharmacol. Exp. Ther.*, **133**, 161(1949).

(23) A. A. Spector, E. C. Santos, J. D. Ashbrook, and J. E. Fletcher, *Ann. N.Y. Acad. Sci.*, **226**, 247(1973).

(24) J. E. Fletcher and A. A. Spector, *Comp. Biomed. Res.*, **2**, 164(1968).

(25) J. E. Fletcher, A. A. Spector, and J. D. Ashbrook, *Biochemistry*, **9**, 4580(1970).

(26) J. W. Cantrell, J. M. Hochholzer, and C. S. Frings, *Clin. Chem.*, **18**, 1423(1972).

ACKNOWLEDGMENTS AND ADDRESSES

Received February 8, 1975, from the *Division of Drug Metabolism and Biopharmaceutics, Department of Medicinal Chemistry, College of Pharmacy, University of Tennessee Center for the Health Sciences, Memphis, TN 38163*

Accepted for publication April 9, 1975.

Supported in part by U.S. Public Health Service Grant HL-09495.

Adapted in part from a dissertation to be submitted by C. A. Cruze to the Graduate School–Medical Sciences, University of Tennessee, in partial fulfillment of the Doctor of Philosophy degree requirements.

* Fellow of the American Foundation for Pharmaceutical Education.

ˣ To whom inquiries should be directed.

Comparison of Antimicrobial Activity of Nuclear-Substituted Aromatic Esters of 5-Dimethylamino-1-phenyl-3-pentanol and 3-Dimethylamino-1-phenyl-1-propanol with Related Cyclic Analogs

J. R. DIMMOCK *x, A. M. QURESHI *, L. M. NOBLE ‡, P. J. SMITH ‡, and H. A. BAKER §

Abstract □ A series of six aromatic esters of both 5-dimethylamino-1-phenyl-3-pentanol and 3-dimethylamino-1-(2-phenylcyclohexyl)-1-propanol was prepared. Antimicrobial evaluation showed that the cyclic analogs had approximately twice the activity of the open chain series; in particular, the *o*-chlorophenyl ester showed pronounced activity against three pathogenic fungi at approximately 10 ppm. Aromatic esters of 3-dimethylamino-1-phenyl-1-propanol were prepared and demonstrated lower activity than two esters of 2-dimethylamino-1-phenylcyclohexanol. The screening results showed that the best activity was found when a dimethylene chain was present between the phenyl ring and the carbon atom bearing the acyloxy function and that the cyclic derivatives were more active than their more flexible counterparts.

Keyphrases □ Esters, aromatic—nuclear substituted, preparation, IR, NMR, and mass spectra, comparison of antimicrobial activity with related cyclic analogs □ Antimicrobial evaluation—series of nuclear-substituted aromatic esters, compared with cyclic analogs

Various Mannich bases have antimicrobial activity (1–6), and reduction of the ketone group of Mannich bases has led to compounds with increased pharmacological activity (7). The activity of the alcohols possibly may be improved by esterification, thereby masking the polar hydroxyl group and facilitating transportation to a site of action. The hydrolysis of a series of benzoate esters derived from a precursor alcohol would be influenced by the Hammett and Taft values of the nuclear substituents, and a correlation between the rate of hydrolysis and the antimicrobial activity of the esters may emerge.

Recently, cyclic analogs of some pharmacologically active compounds, such as dopamine (8, 9), amphetamine (10), psychotropic drugs (11–13), antihistaminics (14), and acetylcholine (15–18) were prepared and screened. Some literature references described rigid analogs having enhanced potency over their more flexible counterparts (19, 20), while in other cases a comparison of flexible and rigid derivatives indicated higher bioactivity in the flexible compounds (21–23).

The preparation of the acyclic substituted pentanes (II–IV) (Scheme I) and the substituted propanes (IX and X), in addition to the corresponding rigid analogs [VI–VIII (Scheme II), XI, and XII], was planned so that their antimicrobial potency could be evaluated.

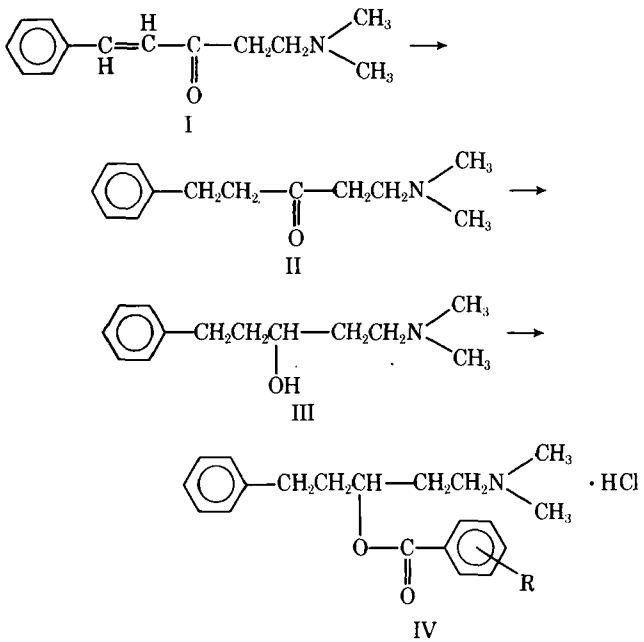

IV*a*: R = H IV*d*: R = 4-Cl
IV*b*: R = 2-Cl IV*e*: R = 4-CH_3
IV*c*: R = 3-Cl IV*f*: R = 4-NO_2

Scheme I

RESULTS AND DISCUSSION

The substituted pentane derivatives were prepared from the Mannich base (I) as shown in Scheme I. The cyclic series of derivatives shown in Scheme II required the synthesis of 1-acetyl-2-phenylcyclohexane (V). Reaction of butadiene with 1-phenyl-1-buten-3-one gave the required Diels–Alder adduct (22%) which, on reduction with Raney nickel, gave V in 92% yield; V was shown previously to have the *trans*-configuration (24).

A Mannich reaction between V, formaldehyde, and dimethylamine hydrochloride gave a product with the correct elemental analysis and molecular weight for VI. However, the possibility exists of a reaction occurring at the acetyl methyl or cyclohexyl methine group of V to give either VI or XIII (Scheme III). PMR evidence confirmed the identity of the product as VI. Furthermore, mass spectrometry of V showed a prominent M − 43 peak (26% relative abundance) due to the loss of the acetyl group, but no such loss was observed in the mass spectrum of the Mannich base obtained, supporting the structure assigned to VI. Reduction of VI gave the required alcohol (VII), acylation of which gave the corresponding esters in yields ranging from 30 to 50%.

Esterification of the acyclic alcohol (IX) gave the desired products (X) in 54–70% yields. The cyclic alcohol (XI), prepared by reaction between phenylmagnesium bromide and 2-dimethylaminomethylcyclohexanone, showed only one peak when examined by GLC, suggesting isomeric purity. Kinetic and thermodynamic consideration would predict that the product formed would have the

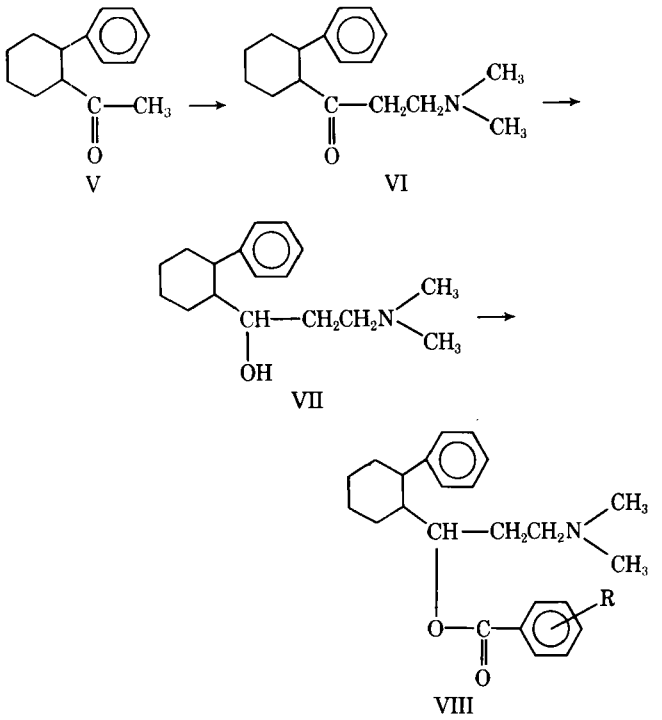

V VI VII VIII

VIII*a*: R = H VIII*d*: R = 4-Cl
VIII*b*: R = 2-Cl VIII*e*: R = 4-CH_3
VIII*c*: R = 3-Cl VIII*f*: R = 4-NO_2

Scheme II

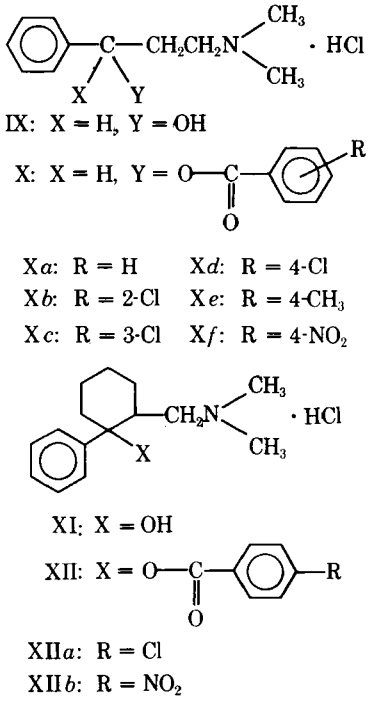

IX: X = H, Y = OH

X: X = H, Y = O—C(=O)—R

X*a*: R = H X*d*: R = 4-Cl
X*b*: R = 2-Cl X*e*: R = 4-CH_3
X*c*: R = 3-Cl X*f*: R = 4-NO_2

XI: X = OH

XII: X = O—C(=O)—R

XII*a*: R = Cl
XII*b*: R = NO_2

trans-N,N-dimethylbenzylamine configuration.

Attempted preparation of the esters under similar reaction conditions to those used with the previous series of compounds yielded only the *p*-chloro and *p*-nitro esters (XII*a* and XII*b*, respectively). In other cases, unreacted XI was obtained. More vigorous reaction conditions such as heating the reactants under reflux in ether or acetone for 6 hr or forming the lithium complex of X prior to treatment with an acyl chloride, followed by heating the mixture under reflux in ether for 8 hr, were unsuccessful in producing the desired esters.

After some compounds had been evaluated for antimicrobial activity (Table I), the screen became unavailable and the assessment of bioactivity was completed elsewhere (Table II). Since different microorganisms were used (Tables I and II), the average antimicrobial potency was evaluated for each compound so that activity correlations could be made.

Compound I is an α,β-unsaturated ketone, a class of compounds with demonstrated antibacterial effectiveness (25), but showed only marginal antimicrobial activity. If the alcohol III was an active antimicrobial agent, then the rate of hydrolysis to III would depend on the nuclear substituents on the ester aromatic ring in IV if base-catalyzed hydrolysis (ρ:2.460) took priority over acid-catalyzed hydrolysis (ρ:−0.144). The unsubstituted ester IV*a* showed a low level of activity. Use of the Hammett equation predicted that the base-catalyzed hydrolysis rate of IV*e* should be approximately half that of IV*a*, but IV*e* demonstrated approximately a threefold increase in antimicrobial potency. However, a predicted increase in hydrolysis of the esters in the case of the nuclear chlorinated derivatives (IV*b*–IV*d*) also brought about an increase in activity, suggesting that a correlation between the rate of hydrolysis of esters and antimicrobial activity did not exist.

In the case of the *p*-nitro ester, which would be expected to hydrolyze more quickly than the other esters, no activity at the highest dose level tested was observed. The nature of the substituents seemed more important than the rate of hydrolysis, and antimicrobial activity possibly was due to the ester *per se*.

Models suggest that the cyclic esters (VIII) would be less easily hydrolyzed than the acyclic compounds (IV) due to steric reasons. Thus, if hydrolysis to the precursor alcohol was responsible for biological activity, a decrease in activity would be predicted. The average antimicrobial activity was 190 in IV but 391 in the related cyclic esters. This twofold increase in activity further substantiated the view that the esters themselves are active. Furthermore, the general trend in activity was similar to that of the open chain analogs, *i.e.*, an increase in activity of the *p*-methyl and chlorinated esters (VIII*b*–VIII*e*) over the unsubstituted compound (VIII*a*), with the *p*-nitro ester showing the least activity. The high potency of VIII*b* against three pathogenic fungi is noteworthy.

While the acyclic alcohol (IX) was devoid of antimicrobial activity, esters X*a*–X*e* showed a low level of activity. In general, the results parallel those found with the previous series of esters, although these compounds were less active; *i.e.*, the average antimicrobial activity was 36, or less than one-fifth of the activity of the related *n*-pentane derivatives (IV). The cyclic alcohol (XI) was devoid of activity, like its acyclic relative IX, but the two esters obtained (XII*a* and XII*b*) had an antimicrobial activity of 73, higher than that for the open chain analogs (X*d* and X*f*).

The screening results may be summarized as follows. First, a dimethylene chain between the aromatic ring and the acyloxy function in the series of esters IV and VIII gave higher activity than esters X and XII, where the aromatic ring was attached to the same carbon atom as the acyloxy function. This result could be due to IV and VIII having preferred spatial arrangements at a possible re-

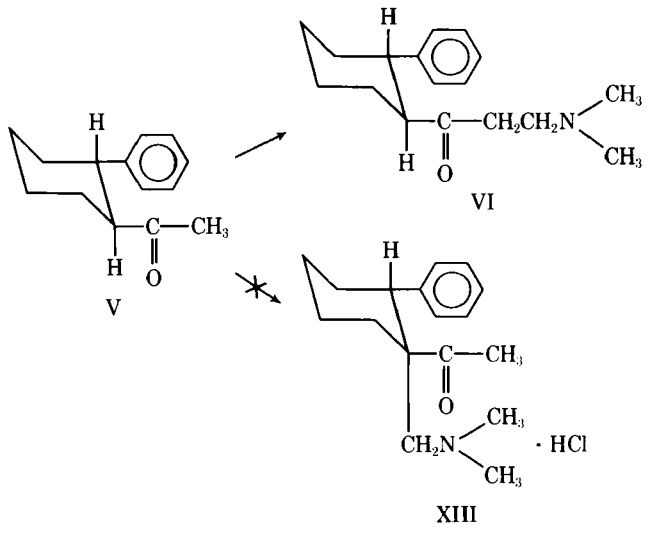

V VI XIII

Scheme III

Table I—Screening[a] of Esters of 1-Phenyl-5-dimethylamino-3-pentanols and 1-Phenyl-3-dimethylamino-1-propanols and Related Derivatives against Various Microorganisms[b]

Microorganism[c]	I	IVa	IVb	IVc	IVd	IVe	IVf	IX	Xb	Xc	Xd	Xe	Xf	XI	XIIa	XIIb
Streptococcus faecalis	> 200	200	200	50	50	200	> 200	> 200	> 200	> 200	> 200	> 200	> 200	> 200	200	200
Staphylococcus aureus (R)[d]	> 200	> 200	200	200	200	200	> 200	> 200	> 200	> 200	> 200	> 200	> 200	> 200	200	> 200
Staphylococcus aureus (S)[e]	> > 200	> > 200	200	200	200	200	> 200	> > 200	> > 200	> > 200	> > 200	> > 200	> > 200	> > 200	200	> > 200
Klebsiella pneumoniae	> 200	> 200	> 200	> 200	> 200	> 200	> 200	> 200	> 200	> 200	> 200	> 200	> 200	> 200	> 200	> 200
Pseudomonas aeruginosa	> 200	> > 200	> 200	> > 200	> > 200	> 200	> 200	> 200	> 200	> 200	> 200	> 200	> 200	> 200	> > 200	> > 200
Escherichia coli	> 200	> 200	> 200	> 200	> 200	> 200	> 200	> 200	> 200	> 200	> 200	> 200	> 200	> 200	> 200	> 200
Salmonella typhimurium	> 200	> 200	> 200	> 200	> 200	> 200	> 200	> 200	> > 200	> > 200	> > 200	> 200	> > 200	> > 200	> > 200	> > 200
Trichophyton mentagrophytes	50	200	200	50	50	200	200	> 200	> 200	200	200	> 200	> > 200	> > 200	50	200
Mycobacterium smegmatis	200	200	200	50	50	200	> 200	> 200	> 200	> 200	> 200	> 200	> > 200	> > 200	200	200
Candida albicans	> 200	200	200	50	50	50	> 200	> 200	> 200	200	200	> 200	> > 200	> > 200	200	> 200
Bacillus subtilis	200	200	200	50	50	50	200	> 200	> > 200	200	200	> 200	> > 200	> > 200	200	> 200
Fusarium oxysporum	200	200	200	50	50	50	200	> 200	> > 200	200	200	200	> > 200	> > 200	200	> > 200
Penicillium citrinum	200	200	200	50	50	50	200	> 200	> > 200	200	200	200	> > 200	> > 200	200	> > 200
Aspergillus niger	200	200	200	50	50	50	200	> 200	> > 200	200	200	200	> > 200	> > 200	200	> 200
Cryptococcus neoformans	200	200	200	50	50	50	200	> 200	> > 200	200	200	200	> > 200	> > 200	200	> 200
Blastomyces dermatitidis	200	200	200	50	50	200	200	> 200	> > 200	200	200	> 200	> > 200	> > 200	200	> > 200
Xanthomonas vesicatoria	200	200	200	50	50	200	> 200	> 200	> 200	> 200	> 200	> 200	> 200	> 200	50	200
Streptococcus pyogenes	> 200	50	50	< 12	50	50	200	> 200	200	200	200	200	> 200	> 200	200	200
Sarcina lutea	> 200	200	200	< 12	50	50	200	> 200	> 200	200	200	200	> 200	> 200	200	200
Average antimicrobial activity[f]	63	84	95	410	284	221	47	0	10	53	53	47	0	0	110	36

[a] Conducted by Dr. J. F. Pagono and staff, Smith Kline and French Laboratories, Philadelphia, Pa. [b] Figures in table are the minimum inhibitory concentrations of the compounds in micrograms per milliliter. [c] The strains of microorganisms in this table are identified by the following numbers: ATCC 9790, SK&F 24390, SK&F 23390, SK&F 4200, SK&F 11320, SK&F 12140, SK&F 11350, SK&F 17410, ATCC 101, SK&F 3470, ATCC 6633, ATCC 9848, ATCC 16040, SK&F 330, EK1, EK2, ATCC 11551, ATCC 8668, and ATCC 9341, respectively. [d] Strain resistant to penicillin G. [e] Strain sensitive to penicillin G. [f] Figures were evaluated from the following expression: (combined antimicrobial activity × 100)/number of microorganisms in screen. The combined antimicrobial activity was determined by giving the following scores at the highest potency of the compound against the microorganism: 200 μg = 1, 50 μg = 4, and 12.5 μg = 16.

ceptor site or be associated with lipoid solubility factors.

Second, in comparing the screening results of the cyclic with the analogous acyclic series, the cyclic compounds had higher antimicrobial potency. A degree of rigidity between functional groups favors activity.

Third, the evidence suggests that the esters are active and that hydrolysis to the corresponding alcohols is an insignificant factor in evaluating the activities of these compounds.

EXPERIMENTAL[1]

5-Dimethylamino-1-phenyl-1-penten-3-one Hydrochloride (I)—The literature method (26) was followed, except that the time of heating under reflux was 24 hr, to give I in 22% yield as colorless crystals from acetone, mp 157–157.5° [lit. (26) mp 157°]; IR (potassium bromide): 1675 (w) shoulder (C=O) and 1665 (s) (C=O) cm^{-1}; mass spectrum: *m/e* 203 (parent peak); NMR (deuterochloroform): δ 7.8 (d, 1, $J_{1,2}$ = 16.5 Hz, C_1H) and 6.8 (d, 1H, $J_{2,1}$ = 16.5 Hz, C_2H) ppm.

Anal.—Calc. for $C_{17}H_{18}ClNO$: C, 65.12; H, 7.56. Found: C, 64.60; H, 7.80.

5-Dimethylamino-1-phenylpentan-3-one (II)—5-Dimethylamino-1-phenyl-1-penten-3-one (23 g, 0.113 mole) in ethanol was hydrogenated in a Paar apparatus with Raney nickel [approximately 10% (w/v)]. The solution was filtered through diatomaceous earth[2], and removal of the ethanol afforded a very pale-yellow oil (19.5 g); IR (smear): 1715 (s) (C=O) cm^{-1}. Attempts to form a crystalline hydrochloride failed, but a small quantity of the oil was converted to a picrate, mp 90–91° [lit. (27) mp 90–92°].

5-Dimethylamino-1-phenylpentan-3-ol (III)—A solution of II (18.5 g, 0.090 mole) in dry ether (100 ml) was added dropwise to a stirred suspension of lithium aluminum hydride (1.63 g, 0.043 mole) in dry ether (100 ml). The reaction mixture was heated under reflux for 24 hr and, on cooling, was decomposed by the dropwise addition of water (8 ml). Removal of the solvent gave a colorless oil (16.0 g); IR (smear): 3400 (s) (OH) and 1715 (s) (C=O absent) cm^{-1}. Attempts to form a crystalline hydrochloride failed, and the structure of the alcohol was confirmed by conversion to various substituted benzoates.

Preparation of Benzoate Esters of 5-Dimethylamino-1-phenylpentan-3-ol Hydrochloride (IV)—The benzoate esters were prepared by the following general method. A solution of the acid chloride (0.0096 mole) in dry ether (30 ml) was added dropwise to a stirred solution of III (2 g, 0.0096 mole) in dry ether (30 ml). The temperature of the reaction was maintained at 0–10° during the addition process, and then the mixture was stirred at room temperature for 24 hr. Removal of the solvent afforded colorless to pale-yellow solids, which were recrystallized from ether–ethanol to give colorless crystals, except for the nitro ester which was pale yellow in color. The esters gave a parent ion corresponding to the molecular weight of the free base. The results are summarized in Table III.

3-Dimethylamino-1-(2-phenylcyclohexyl)-1-propanone Hydrochloride (VI)—A stirred mixture of *trans*-1-acetyl-2-phenylcyclohexane (3.4 g, 0.01 mole) (24), dimethylamine hydrochloride (1.4 g, 0.02 mole), paraformaldehyde (0.5 g, 0.01 mole), hydrochloric acid (0.5 ml), and isopentyl alcohol (15 ml) was heated under reflux for 48 hr. The reaction mixture was concentrated and, on scratching the side of the flask, a light-brown material deposited. On trituration with ether, a fawn solid (3.0 g) resulted. Recrystallization of the solid from ether–ethanol gave VI as colorless crystals

[1] Boiling points and melting points are uncorrected. IR spectra were determined on a Unicam SP200G spectrophotometer previously calibrated with polystyrene. Band intensities are designated as s (strong) and w (weak). Mass spectra were determined at 70 ev on an AE1 MS-12 single-focusing mass spectrometer, operated by Mr. D. Bain of the Department of Chemistry and Chemical Engineering, University of Saskatchewan. NMR spectra were determined using a Varian A60 instrument operating at 44°, with tetramethylsilane as the internal standard. Elemental analyses were carried out on a Coleman model 33 carbon–hydrogen analyzer by Mr. R. E. Teed of the Department of Chemistry and Chemical Engineering, University of Saskatchewan, and Mr. R. M. Smith of the College of Pharmacy, University of Saskatchewan. Hydrogenations were undertaken using a Paar series 3910 shaker apparatus at 27.2 kg (60 lb) of pressure. GLC was carried out using a MT model 220 gas chromatograph, equipped with flame-ionization detector and 1.8-m × 0.47-cm (6-ft × 0.18-in.) glass columns packed with 3% SE-52 adsorbed onto silanized Chromosorb W (70–80 mesh), and a Varian 90-P gas chromatograph employing different columns.

[2] Celite.

Table II—Screening[a] of 3-Dimethylamino-1-(2-phenylcyclohexyl)-1-propanone and Related Esters against Various Microorganisms[b]

Microorganism[c]	VI	VIIIa	VIIIb	VIIIc	VIIId	VIIIe	VIIIf	Xa
Staphylococcus pyogenes (S)[d]	100	100	50	25	25	50	100	>100
Staphylococcus pyogenes (R)[e]	100	100	50	25	25	50	100	>100
Streptococcus faecalis	100	100	50	25	25	50	100	>100
Escherichia coli	100	100	50	50	50	50	100	>100
Aerobacter aerogenes	100	50	100	100	100	100	100	>100
Salmonella pullorum	100	50	100	100	100	100	100	>100
Pseudomonas aeruginosa	100	50	100	100	100	100	100	>100
Proteus mirabilis	100	50	100	100	100	100	100	>100
Proteus vulgaris	100	100	100	100	50	100	100	>100
Klebsiella pneumoniae	100	50	100	12.5	25	50	100	100
Serratia marcescens	100	50	100	50	50	100	100	100
Candida albicans		100	12.5	100	100	100	100	100
Microsporum gypseum		50	6.25	50	50	50	50	>100
Trichophyton granulosum		100	12.5	50	100	100	100	>100
Trichomonas vaginalis		>100	50	50	50	50	100	
Trichomonas foetus	100							100
Average antimicrobial activity[f]	200	280	653	480	427	293	213	53

[a] Conducted by Ayerst Laboratories, Montreal, Quebec, Canada. [b] Figures in table are the minimum inhibitory concentrations of compounds in micrograms per milliliter. [c] The strains of microorganisms in this table are identified by the following numbers: AY-B-352, AY-B-353, AY-B-355, ATCC 11229, AY-B-357, AY-B-358, AY-B-359, AY-B-360, AY-B-361, ATCC 10081, ATCC 9103, AY-F-598, AY-F-605, AY-F-604, ATCC 30001, and ATCC 30003, respectively. [d] Strain sensitive to penicillin G potassium. [e] Strain resistant to penicillin G potassium. [f] Figures were evaluated from the following expression: (combined antimicrobial activity X 100)/number of microorganisms in screen. The combined antimicrobial activity was determined by giving the following scores at the highest potency of the compound against the microorganism: 100 μg = 2, 50 μg = 4, 25 μg = 8, 12.5 μg = 16, and 6.25 μg = 32.

Table III—Benzoate Esters of 5-Dimethylamino-1-phenylpentan-3-ol Hydrochloride (IV)

Compound	Yield, %	Melting Point	Molecular Formula	Analysis, % Calc.	Analysis, % Found	IR Spectra, cm^{-1} (C=O)
IV*a*	50	120–121°	$C_{20}H_{26}ClNO_2$	C 68.76 H 7.53	68.50 7.59	1710 (s)
IV*b*	43	101–101.5°	$C_{20}H_{25}Cl_2NO_2$	C 62.83 H 6.59	62.65 6.71	1710 (s)
IV*c*	45	103.5–105°	$C_{20}H_{25}Cl_2NO_2$	C 62.83 H 6.59	62.75 6.58	1710 (s)
IV*d*	36	122–123.5°	$C_{20}H_{25}Cl_2NO_2$	C 62.83 H 6.59	62.80 6.65	1710 (s)
IV*e*	60	133–134.5°	$C_{21}H_{28}ClNO_2$	C 69.69 H 7.78	70.10 8.18	1705 (s)
IV*f*	36	145–146°	$C_{20}H_{25}ClN_2O_4$	C 61.12 H 6.41	61.10 6.53	1720 (s)

(1.0 g, 20%), mp 177.5–178.0°; IR (mineral oil mull): 1710 (s) (C=O) cm^{-1}; mass spectrum: *m/e* 259 (M^+, 5), 91 (9), 73 (5), 72 (7), 59 (4), 58 (100), 57 (3), 45 (5), 44 (5), 42 (3), and 36 (8); NMR (deuterochloroform): δ 7.18 (m, 5H, C_6H_5), 3.0–1.2 (m, 14H, CH_2 and CH protons), 2.28, and 2.60 [m, 6H, $^+N(CH_3)_2$].

Anal.—Calc. for $C_{17}H_{26}ClNO$: C, 69.03; H, 8.76; N, 4.74. Found: C, 69.11; H, 9.17; N, 4.94.

From the mother liquors, a small quantity of a beige solid was obtained. This solid was recrystallized from ether–ethanol to give colorless crystals (0.3 g), mp 154–155°, considered to be VI contaminated with dimethylamine hydrochloride; IR (mineral oil mull): 1685 (s) and 1700 (s) (C=O) cm^{-1}; mass spectrum: *m/e* 259 (M^+, 4), 91 (9), 58 (75), 46 (18), 45 (58), 44 (100), 43 (38), 42 (45), 41 (35), 40 (37), 39 (14), 38 (76), 37 (30), 36 (78), 35 (86), 30 (37), and 27 (23); PMR (deuterochloroform): δ 7.3 (m, 5H, C_6H_5), 2.7 [s, 6H, $^+N(CH_3)_2$], and 2.2–1.0 (m, 22H, CH_3, CH_2, and CH protons).

Anal.—Found: C, 53.32; H, 9,69; N, 9.62.

The ether washings from the trituration were concentrated to give a fawn solid (3.0 g) which, on GLC analysis[3], had the same retention time as V.

In a previous experiment, 0.002-mole quantities of *trans*-1-acetyl-2-phenylcyclohexane, dimethylamine hydrochloride, and paraformaldehyde in ethanol (5 ml) containing hydrochloric acid (0.1 ml) were heated under reflux for 24 hr. On cooling and scratching the sides of the flask, a brown solid (0.3 g) deposited. Recrystallization from *n*-hexane showed this solid to be unreacted *trans*-1-acetyl-2-phenylcyclohexane (melting point and IR evidence).

3-Dimethylamino-1-(2-phenylcyclohexyl)propan-1-ol (VII)—A solution of VI (14.0 g, 0.054 mole) in dry ether (100 ml) was added dropwise to a stirred suspension of lithium aluminum hydride (1.02 g, 0.027 mole) in dry ether (100 ml). The reaction mixture was then heated under reflux for 24 hr and cooled, and water (6 ml) was added dropwise. Evaporation of the solvent gave a colorless oil[4] (11.5 g); IR (smear): 3400 (s) (OH) and 1710 (s) (C=O absent) cm^{-1}. All attempts to form a crystalline hydrochloride failed, and the alcohol was characterized by the formation of benzoate esters (Table IV).

Preparation of Benzoate Esters of 3-Dimethylamino-1-(2-phenylcyclohexyl)propan-1-ol Hydrochloride (VIII)—The method used was the same as for the preparation of IV, except that 0.0038-mole quantities of VII and the acid chloride were employed. The esters gave a parent ion corresponding to the molecular weight of the free base. The results are summarized in Table IV.

Preparation of 3-Dimethylamino-1-phenylpropan-1-ol Hydrochloride (IX)—3-Dimethylamino-1-phenylpropan-1-one, prepared in 50% yield according to a literature method (28), mp 155° [lit. (28) mp 155–156°], crystallized from acetone–ethanol (95% v/v) as colorless crystals. Reduction of the ketone with lithium aluminum hydride, using a published procedure (29), gave IX as a colorless oil in 70% yield, bp 90° (0.6 mm) [lit. (30) bp 70–72° (0.3 mm)]; IR (smear): 3400–3100 broad (OH) and 1670 (s) (C=O absent) cm^{-1}. The free base was converted to the hydrochloride salt, mp 131–133° [lit. (31) mp 132–133°]; mass spectrum: *m/e* 179 (parent peak).

[3] FFAP column, 3.66 m × 0.31 cm (12 ft × 0.125 in.), 218°, flow rate of 115 ml/min.

[4] Analyzed by GLC on SE-30 column, 1.8 m × 0.31 cm (6 ft × 0.125 in.), 175°, flow rate of 120 ml/min.

Table IV—Benzoate Esters of 3-Dimethylamino-1-(2-phenylcyclohexyl)propan-1-ol Hydrochloride (VIII)

Compound	Yield, %	Melting Point	Molecular Formula	Analysis, % Calc.	Analysis, % Found	IR Spectra, cm^{-1} (C=O)
VIII*a*	50	168–170°	$C_{24}H_{32}ClNO_2$	C 71.70 H 8.02	70.90 8.04	1715 (s)
VIII*b*	40	142–144°	$C_{24}H_{31}Cl_2NO_2$	C 66.04 H 7.15	65.40 7.18	1730 (s)
VIII*c*	30	152–154°	$C_{24}H_{31}Cl_2NO_2$	C 66.04 H 7.15	65.95 7.53	1725 (s)
VIII*d*	39	148–150°	$C_{24}H_{31}Cl_2NO_2$	C 66.04 H 7.15	65.15 7.32	1710 (s)
VIII*e*	40	128–130°	$C_{25}H_{34}ClNO_2$	C 72.17 H 8.23	70.90 8.64	1715 (s)
VIII*f*	40	108–110°	$C_{24}H_{31}ClN_2O_4$	C 64.58 H 6.95	64.85 7.52	1720 (s)

Table V—Benzoate Esters of 3-Dimethylamino-1-phenylpropan-1-ol Hydrochloride (X)

Compound	Yield, %	Melting Point	Molecular Formula	Analysis, % Calc.	Analysis, % Found	IR Spectra, cm^{-1} (C=O)
X*a*	55	166–167°	$C_{18}H_{22}ClNO_2$	C 67.59 H 6.93	66.75 6.76	1710 (s)
X*b*	54	126–127.5°	$C_{18}H_{21}Cl_2NO_2$	C 61.02 H 5.98	60.90 6.33	1730 (s)
X*c*	54	130.5–131°	$C_{18}H_{21}Cl_2NO_2$	C 61.02 H 5.98	61.13 6.15	1720 (s)
X*d*	68	148–149.5°	$C_{18}H_{21}Cl_2NO_2$	C 61.02 H 5.98	61.10 6.11	1710 (s)
X*e*	61	142–143°	$C_{19}H_{24}ClNO_2$	C 68.35 H 7.24	68.13 7.47	1715 (s)
X*f*	70	168–169°	$C_{18}H_{21}ClN_2O_4$	C 59.25 H 5.80	59.39 6.00	1730 (s)

Table VI—Reaction of 2-Dimethylaminomethyl-1-phenylcyclohexanol with Substituted Benzoyl Chlorides

Reactant: R = 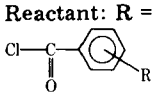	Product Isolated	Yield, %	Melting Point	Molecular Formula[a]	Analysis, % Calc.[a]	Analysis, % Found	IR Spectra, cm^{-1} (C=O)	Mass Spectrum P Calc.	Mass Spectrum P Found
H	XI	74[b]	162–164°	$C_{15}H_{24}ClNO$	C 70.66 H 7.54	66.63[c] 9.37[c]	Absent	337	233[d]
2-Cl	XI	71[b]	161–163°	$C_{15}H_{24}ClNO$	C 64.70 H 6.67	66.93[c] 9.19[c]	Absent	—	—
3-Cl	XI	71[b]	163–164°	$C_{15}H_{24}ClNO$	C 64.70 H 6.67	66.17[c] 9.21[c]	Absent	—	—
4-Cl	XII*a*	40[a]	190–192°	$C_{22}H_{27}Cl_2NO_2$	C 64.70 H 6.67	64.65 7.47	1725 (s)	371	371[d]
4-CH_3	XI	63[b]	163–164.5°	$C_{15}H_{24}ClNO$	C 71.21 H 7.79	65.82[c] 9.11[c]	Absent	—	—
4-NO_2	XII*b*	40[a]	189–191°	$C_{22}H_{27}ClN_2O_4$	C 63.07 H 6.50	62.85 6.39	1725 (s)	382	382[d]

[a] Calculated for benzoate esters. [b] This figure indicates the percentage recovery of unreacted alcohol. [c] Calculated analytical figures for 2-dimethylaminomethyl-1-phenylcyclohexanol hydrochloride: C, 66.72; H, 8.96. [d] Parent peak (P) represents the free base.

Anal.—Calc. for $C_{11}H_{18}ClNO$: C, 61.24; H, 8.40. Found: C, 61.30; H, 8.66.

Preparation of Benzoate Esters of IX (X)—A solution of the acyl chloride (0.0112 mole) in dry benzene (10 ml) was added slowly to a stirred solution of IX (2.0 g, 0.0112 mole) in dry benzene (10 ml) at 0–10°. The reaction mixture was stirred at room temperature for 2 hr, and evaporation of the solvent gave colorless to pale-yellow solids. Recrystallization of these solids from ether–ethanol gave colorless crystals, except in the case of the 4-nitro ester which was pale yellow in color. The esters gave a parent ion corresponding to the molecular weight of the free base. The results are summarized in Table V.

2-Dimethylaminomethyl-1-phenylcyclohexanol Hydrochloride (XI)—2-Dimethylaminomethylcyclohexanone was prepared in 17% yield using a literature procedure (32), bp 60–75° (1.0 mm) [lit. (33) bp 60° (1.0 mm)]; IR (smear): 1700 (s) (C=O) cm^{-1}. Reaction of XI with phenylmagnesium bromide, using a literature method (33), gave 2-dimethylaminomethyl-1-phenylcyclohexanol in 55% yield, bp 120–140° (1.0 mm) [lit. (33) bp 111–116° (0.20 mm)]. GLC[5] showed one component only; IR (smear): 3400–3020 (broad OH) and 1700 (s) (C=O absent) cm^{-1}. The alcohol was converted to the hydrochloride salt, mp 168.5–170°; mass spectrum: *m/e* 233 (parent peak).

Anal.—Calc. for $C_{15}H_{24}ClNO$: C, 66.72; H, 8.96. Found: C, 66.70; H, 9.26.

Attempted Preparation of Benzoate Esters of XI (XII)—The method employed was identical to that used in the preparation of the benzoate esters of IX, except that 0.0042-mole quantities of reactants were used and the reaction mixture was stirred at room temperature for 4 hr. The solids obtained were recrystallized from ether–ethanol to give colorless crystals, except in the case of the 4-nitro ester which was pale yellow in color. The results are given in Table VI.

[5] Microtek.

Screening of Compounds—The compounds in Table I were evaluated using an agar dilution method. In each case a stock solution of the compound was prepared by dissolving 20 mg of the sample in 1 ml of dimethyl sulfoxide, followed by the addition of 3 ml of water. Aliquots of the stock solution were pipetted into melted trypticase soy agar[6] to give final concentrations of the compound of 200, 50, 12.5, and 3.1 μg/ml. After hardening, the agar surface was inoculated with appropriately diluted suspensions of the test organisms using a Steers' multiple-inocula replicating device. The seeded plates were incubated (18 hr at 30° followed by 18 hr at 37°), and the plates were then observed for microbial growth.

The screening techniques for the compounds evaluated in Table II are as follows. In the antibacterial screen, 1 ml of stock solution (1000 μg/ml) was added to 9 ml of nutrient broth to give an initial concentration of 100 μg/ml; halving dilutions were then carried out in nutrient broth. All tubes were inoculated with 0.1 ml of a 1:10 dilution of an 18-hr culture of the test organism. All tubes were incubated for 24 hr at 37° and then examined for growth.

The antifungal screen involved the addition of 1 ml of the stock solution (1000 μg/ml), which was added to 9 ml of Sabouraud broth to give an initial concentration of 100 μg/ml; halving dilutions were carried out in Sabouraud broth. A spore suspension (0.1 ml) of *Trichophyton granulosum* and *Microsporum gypseum* and 0.1 ml of a 1:100 dilution of a broth culture of *Candida albicans* was added to the test tubes containing the various concentrations of the test substances. Tubes containing *C. albicans* were incubated at 37°, and tubes containing *M. gypseum* and *Tr. granulosum* were incubated at 28°. Tubes were examined for growth after 4 and 9 days of incubation.

In the antitrichomonal screen, 1 ml of the stock solution (1000 μg/ml) was added to 9 ml of Diamond medium to give an initial concentration of 100 μg/ml; halving dilutions were then carried out. Tubes were inoculated with approximately 2.5×10^5 organisms/ml and examined microscopically for growth after 48 hr of incubation.

[6] BBL.

REFERENCES

(1) J. R. Dimmock, W. A. Turner, and H. A. Baker, *J. Pharm. Sci.*, **64**, 995(1975).

(2) H. J. Florestano and M. E. Tahler, *J. Amer. Pharm. Ass., Sci. Ed.*, **45**, 320(1956).

(3) J. Sam and A. C. Thompson, *J. Pharm Sci.*, **53**, 535(1964).

(4) W. L. Nobles and B. B. Thompson, *ibid.*, **53**, 1554(1964).

(5) C. D. Blanton and W. L. Nobles, *ibid.*, **51**, 878(1962).

(6) R. S. Varma and W. L. Nobles, *ibid.*, **57**, 1801(1968).

(7) J. J. Denton, V. A. Lawson, W. B. Neier, and R. J. Turner, *J. Amer. Chem. Soc.*, **71**, 2052(1949).

(8) A. S. Horn, *J. Pharm. Pharmacol.*, **26**, 735(1974).

(9) G. N. Woodruff, A. O. Elkhawad, A. R. Crossman, and R. J. Walker, *ibid.*, **26**, 740(1974).

(10) W. L. Nelson and B. E. Sherwood, *J. Pharm. Sci.*, **63**, 1467(1974).

(11) R. J. Wolters, A. J. Bej, and N. S. Tanner, *ibid.*, **63**, 1379(1974).

(12) D. E. Nichols, C. F. Barfknecht, J. P. Long, R. T. Standridge, H. G. Howell, R. A. Partyka, and D. C. Dyer, *J. Med. Chem.*, **17**, 161(1974).

(13) R. T. Coutts and G. L. Malicky, *Can. J. Chem.*, **52**, 381(1974).

(14) P. E. Hanna, V. R. Grund, and M. W. Anders, *J. Med. Chem.*, **17**, 1020(1974).

(15) R. F. Borne, C. R. Clark, and I. W. Waters, *J. Pharm. Sci.*, **63**, 1559(1974).

(16) J. A. Hasbun, K. K. Barker, and M. P. Mertes, *J. Med. Chem.*, **16**, 847(1973), and references cited therein.

(17) N. J. Lewis, K. K. Barker, R. M. Fox, Jr., and M. P. Mertes, *ibid.*, **16**, 156(1973).

(18) E. E. Smissman and G. R. Parker, *ibid.*, **16**, 23(1973).

(19) A. F. Casy, N. J. Harper, and J. R. Dimmock, *J. Chem. Soc.*, **1964**, 3635.

(20) S. F. Friess and H. D. Baldridge, *J. Amer. Chem. Soc.*, **78**, 2482(1956).

(21) M. S. Atwal, L. Bauer, S. N. Dixit, J. E. Gearien, M. Megahy, R. Morris, and C. Pokorny, *J. Med. Chem.*, **12**, 994(1969).

(22) M. May and D. J. Triggle, *J. Pharm. Sci.*, **57**, 511(1968).

(23) M. R. Boots, *J. Med. Chem.*, **12**, 426(1969).

(24) H. E. Zimmerman, *J. Amer. Chem. Soc.*, **79**, 6554(1957).

(25) W. B. Geiger and J. E. Conn, *ibid.*, **67**, 112(1945).

(26) H. B. Nisbet, *J. Chem. Soc.*, **1938**, 1237.

(27) R. Jacquier, M. Mousseron, and S. Boyer, *Bull. Soc. Chim. Fr.*, **1956**, 1653; through *Chem. Abstr.*, **51**, 8022f(1957).

(28) C. E. Maxwell, "Organic Syntheses," coll. vol. III, Wiley, New York, N.Y., 1955, p. 305.

(29) Eli Lilly and Co., British pat. 777,758 (June 26, 1957); through *Chem. Abstr.*, **52**, 1276g(1958).

(30) E. A. Steck and P. Brundage, *J. Amer. Chem. Soc.*, **81**, 6511(1959).

(31) I. N. Nazarov and E. M. Cherkasova, *Zh. Obshchei Khim.*, **28**, 122(1958); through *Chem. Abstr.*, **52**, 12789c(1958).

(32) R. L. Frank and R. C. Pierle, *J. Amer. Chem. Soc.*, **73**, 724(1951).

(33) S. M. McElvain and R. B. Clampitt, *ibid.*, **81**, 5590(1959).

ACKNOWLEDGMENTS AND ADDRESSES

Received March 20, 1975, from the *College of Pharmacy and the ‡Department of Chemistry and Chemical Engineering, University of Saskatchewan, Saskatoon, Saskatchewan, Canada S7N 0W0, and §Ayerst Research Laboratories, Montreal, Quebec, Canada H4R 1J6.

Accepted for publication April 8, 1975.

A. M. Qureshi thanks the University of Saskatchewan for a Graduate Teaching Assistantship and the Canadian Foundation for the Advancement of Pharmacy for a Fellowship. Financial assistance for this project was also given by Smith Kline and French Laboratories of Philadelphia, Pa.

[x] To whom inquiries should be directed.

Spectrophotometric Determination of Sodium Nitroprusside and Its Photodegradation Products

M. J. FRANK, J. B. JOHNSON ˣ, and S. H. RUBIN

Abstract □ A specific spectrophotometric method of analysis for sodium nitroprusside was developed utilizing the molar absorptivity values at the maxima appearing in the electronic spectrum at 394 and 498 nm that may be attributed to metal $d \rightarrow \pi^*$ NO transitions. These measurements appear to be indicative of the unaltered nitroferricyanide complex. A reaction sequence is postulated for aqueous solutions of nitroprusside exposed to normal artificial light. Evidence suggests that one species in the sequence is nitroferricyanide in a higher energy state but with the nitrosyl moiety still present in the coordination sphere, which exhibits an increased molar absorptivity at 394 nm. The molar absorptivity at the 498-nm maximum remains unchanged. Corroborating polarographic data are presented.

Keyphrases □ Sodium nitroprusside—spectrophotometric determination, photodegradation products, compared to polarographic data □ Photoirradiation—spectrophotometric determination of sodium nitroprusside and degradation products, compared to polarographic data

Sodium nitroprusside (sodium nitroferricyanide), a potent, rapid acting hypotensive agent when administered intravenously, has been known for many years but has not been used extensively in clinical practice until recently. The chemical and physical properties of the nitroferricyanide ion, $[Fe(CN)_5NO]^{-2}$, have been investigated (1). The chemistry of the nitroferricyanide ion is dominated by the nitrosyl moiety; virtually all studies during the past 2 decades have centered on the reactivity and physicochemical properties of this ligand.

BACKGROUND

The crystal structure of sodium nitroprusside has been determined by X-ray diffraction; the nitroferricyanide ion possesses approximate C_{4v} symmetry (2). A complete interpretation of the electronic spectrum of nitroferricyanide was carried out (3) using extensive self-consistent charge and configuration molecular orbital calculations. Studies of the IR (4) and Mössbauer (5) spectra indicate a large amount of back-bonding between the metal and the nitrosyl ligand. There has been considerable controversy as to the formal charge of iron and nitrosyl in the complex; although no unambiguous assignment has been possible, the consensus is that iron and nitrosyl possess formal charges of +2 and +1, respectively (3, 6, 7).

The nitrosyl moiety can undergo numerous substitution and addition reactions with various reagents, and numerous transformations have been described (1). Polarographic studies also have been conducted (6, 8); three reduction waves, occurring at −0.4, −0.6, and −1.2 v *versus* a saturated calomel electrode, were observed. The first two waves involve one electron each, as calculated from the n in Ilkovic's equation, and are reversible; the third wave is irreversible and the value of n is 2.

In the presence of light, sodium nitroprusside undergoes numerous reactions, many of which are undefined. Most literature reports are vague and often contradictory when describing the characteristics and properties of its photodecomposition products. In direct sunlight, sodium nitroprusside ultimately yields Prussian blue, cyanic acid, and nitric oxide (9), while the immediate products of the photodecomposition in light of low energy are apparently nitric oxide and $[Fe(CN)_5(H_2O)]^{-3}$ (10). It has also been reported that nitroferricyanide is photoreduced in aqueous solution to yield nitroferrocyanide, $[Fe(CN)_5NO]^{-3}$ (11).

Table I—Microanalysis of Sodium Nitroprusside

Determination	Theory, %	Found, %
C	20.16	19.99
H	1.35	1.29
N	28.20	28.28
Fe	18.74	18.52

Photoirradiation of nitroferricyanide in dimethylformamide yields an electron spin resonance (ESR) spectrum, which is essentially identical to that obtained by electrolytic reduction of nitroferricyanide in dimethylformamide and is attributed to nitroferrocyanide (12–14). More recently (15), it has been argued that photoirradiation of nitroferricyanide facilitates the formation and stabilization of $[Fe(CN)_5NO_2H]^{-3}$, which has been postulated as an intermediate (Scheme I) (16).

This hypothesis is supported by the report that irradiation of a neutral solution of nitroferricyanide results in a pH decrease, which increases to nearly the original value when irradiation ceases (17). Depending on the intensity and energy of the incident light, aqueous solutions of nitroferricyanide eventually develop a blue color; no blue color is observed when nitroferricyanide is irradiated in water with light of moderate intensity over long periods.

Relatively few literature references describe analytical methods for the determination of sodium nitroprusside. It has been assayed colorimetrically as the isophorone complex (18), and the potentiometric titration with silver nitrate using a saturated calomel–silver-specific ion electrode system is well known. Although polarographic investigations (6, 8) have been conducted to evaluate equilibrium constants between the various reduced species in solution, polarography also can be applied to the quantitative determination of nitroprusside. Martin and Patel (19) analyzed aqueous solutions of sodium nitroprusside spectrophotometrically by determining the absorbance at 390 nm. Upon exposure to light and elevated temperatures, a pronounced increase in the absorbance was observed. However, no attempt was made to correlate the increase in absorbance to the amount of sodium nitroprusside degraded.

The introduction of sodium nitroprusside as a therapeutic agent for the treatment of hypertensive emergencies led to the present investigation to develop an analytical method for determining the purity and stability of crystalline and lyophilized powders of the material. Since the drug is often administered in 5% dextrose infusion solutions stored in clear glass or plastic containers, a study was initiated to determine its light stability when dissolved in an aqueous medium. The present investigation correlates absorbance changes upon photoirradiation with the amount of sodium nitroprusside degraded by utilizing the molar absorptivity values at the maxima appearing in the electronic spectrum at 394 and 498 nm that may be attributed to metal $d \rightarrow \pi^*$ NO transitions (3).

Since the nitrosyl moiety is the therapeutically active portion of the molecule (20), it was desirable to develop an analytical method that would be specific for the intact coordination sphere of iron and particularly for the nitrosyl substituent. The spectrophotometric method should provide this specificity, since the molar absorptivity values at 394 and 498 nm appear to be indicative of unaltered sodium nitroprusside.

$$[Fe(CN)_5NO]^{-2} + OH^- \rightleftharpoons [Fe(CN)_5NO_2H]^{-3}$$
$$[Fe(CN)_5NO_2H]^{-3} + OH^- \rightleftharpoons [Fe(CN)_5NO_2]^{-4} + H_2O$$

Scheme I

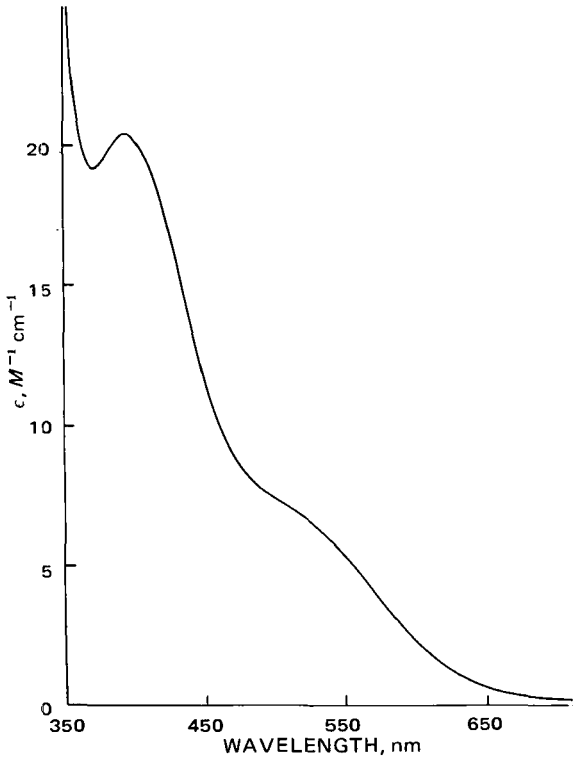

Figure 1—*Spectrum of sodium nitroprusside in aqueous solution.*

Polarographic studies also were conducted to compare the sensitivity and specificity of the polarographic and spectrophotometric techniques as applied to the photodegraded material. The thermal stability of aqueous solutions was investigated, and the rates of photodegradation *versus* thermal decomposition were determined.

EXPERIMENTAL

Spectrophotometry—Spectra and spectrophotometric assays were determined with a double-beam UV–visible recording spectrophotometer[1] using matched 1- or 10-cm quartz cells. All absorbance measurements were made at 25°.

Polarography—The polarographic studies were performed on a recording polarograph[2] at 25°. All potentials were measured *versus* a silver–silver chloride reference electrode in a saturated potassium chloride salt bridge containing 3% agar. The polarograms were run in pH 7.2 Britton–Robinson buffer prepared by combining 100 ml of a solution which is 0.04 *M* in phosphoric acid, acetic acid, or boric acid with 55 ml of 0.2 *N* sodium hydroxide. All test solutions were deoxygenated with nitrogen for at least 10 min and were maintained in a nitrogen atmosphere throughout the analysis. The polarographic cell was covered with aluminum foil to prevent exposure to light during the analysis.

Photoirradiation Studies—Solutions of sodium nitroprusside were photoirradiated in a Cooper–Lachman light chamber (21) or under normal laboratory fluorescent lighting. The solutions were stored in clear Pyrex flasks or in plastic containers[3] during the irradiation process.

Thermal Stability Studies—Solutions of sodium nitroprusside were sealed in 5-ml amber ampuls and stored in an oven thermostated at the desired temperature. Samples were withdrawn at appropriate time intervals and analyzed spectrophotometrically.

Reagents—The microanalysis of sodium nitroprusside[4] is presented in Table I. The microanalytical data indicate that the substance was essentially pure. The 5% dextrose injection USP solution was purchased in glass[5] or plastic[3] containers.

[1] Beckman Acta C III.
[2] Model EUW-401, Heath Co.
[3] Viaflex, Travenol Laboratories, Deerfield, Ill.
[4] Mallinckrodt reagent grade.
[5] Saftiflask, Cutter Laboratories, Berkeley, Calif.

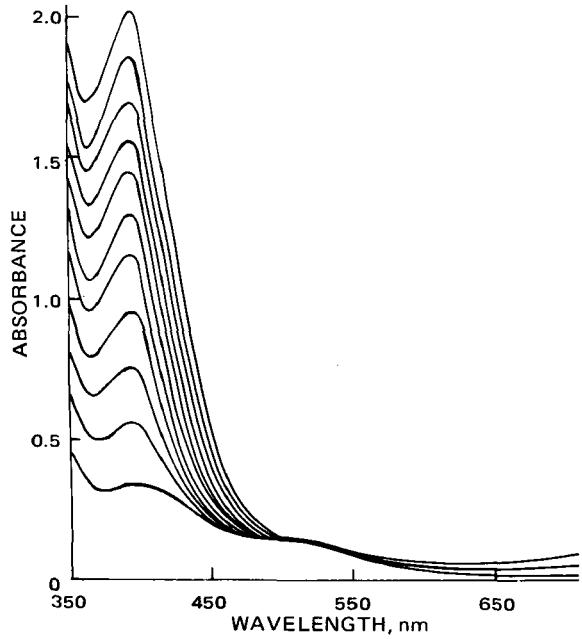

Figure 2—*Spectral changes observed on irradiation of a 0.5% aqueous solution of sodium nitroprusside in a Cooper–Lachman light chamber. Spectra were recorded at 1-hr time intervals.*

All other common reagents were ACS certified grade. Distilled, deionized water was used for the preparation and dilution of all solutions unless otherwise described.

RESULTS AND DISCUSSION

The spectrum of sodium nitroprusside in aqueous solution in the 350–700-nm region is shown in Fig. 1. There are two maxima in the spectrum at 394 and 498 nm, having molar absorptivity values of 20.4 and 7.4, respectively. These molar absorptivity values are in good agreement with those reported previously (3, 16).

Although the 498-nm transition appears only as a shoulder in the spectrum, its existence as a distinct absorption band was confirmed by the determination of the polarized crystal spectrum of a single crystal of sodium nitroprusside (3).

The molecular orbital energy level diagram for nitroferricyanide was derived previously (3). The two highest filled molecular orbitals in the ground state of the ion are designated $6e$ and $2b_2$; thus, the ground state is $(6e)^4(2b_2)^2$. The effective electronic configuration of iron is $3d^6$, and nitroferricyanide formally contains Fe (II) and NO^+, consistent with the observation that the ion is diamagnetic (22). The $6e$ level is mainly dxz and dyz but contains 24.8% π^* NO character, indicating substantial FE → NO back-bonding. The $2b_2$ level consists of 84.5% dxy, 13.9% π CN, and 1.6% π^* CN, suggesting that the degree of FE → NO back-bonding is relatively slight.

The lowest unfilled molecular orbital, represented by the symbol $7e$, contains 72.5% π^* NO and some contributions from $d\pi$, σ CN, π CN, and π^* CN. The low energy transitions appearing at 394 and 498 nm were given the following band assignments: 394 nm, $6e \rightarrow 7e$; and 498 nm, $2b_2 \rightarrow 7e$ (3). These long wavelength absorption bands involve transitions from essentially metal d orbitals to a molecular orbital containing primarily the antibonding π^* NO orbital on the nitrosyl moiety. Since the other absorption bands of nitroferricyanide appear in the UV region of the spectrum, irradiation of solutions of the ion with low energy light should have important consequences on the 394- and 498-nm transitions. Moreover, since there is no transmission through Pyrex below 360 nm, the course of the photochemical reactions should be intimately involved with the electronic transitions in the visible region of the electronic spectrum of nitroferricyanide.

The spectral changes observed on irradiation of a 0.5% aqueous solution of sodium nitroprusside in a Cooper–Lachman light chamber are illustrated in Fig. 2. The increase in absorbance at 394 nm as a function of irradiation time is shown in Fig. 3. The sam-

Table II—Light Stability Data (Absorbance) for Sodium Nitroprusside 0.01% Solutions

	Crystalline Powder in Dextrose Infusion Solution				Lyophilized Material							
					Water				Dextrose Infusion Solution			
Hours	394 nm	498 nm	700 nm	% Degraded	394 nm	498 nm	700 nm	% Degraded	394 nm	498 nm	700 nm	% Degraded
0	0.104	0.042	0.009	—	0.092	0.040	0.009	—	0.090	0.039	0.009	—
1	0.125	0.041	0.008	5.1	0.108	0.040	0.009	4.4	0.106	0.038	0.009	4.5
2	0.148	0.042	0.008	10.6	0.125	0.040	0.009	9.1	0.123	0.038	0.009	9.2
3	0.170	0.043	0.009	15.9	0.142	0.040	0.009	13.8	0.140	0.038	0.009	13.9
4	0.191	0.042	0.009	20.9	0.159	0.040	0.009	18.2	0.156	0.038	0.009	18.3
5	0.212	0.042	0.008	26.0	0.175	0.040	0.009	22.6	0.172	0.038	0.009	22.8
6	0.230	0.042	0.008	30.8	0.191	0.039	0.009	26.9	0.189	0.038	0.009	27.5
7	0.253	0.041	0.008	35.8	0.208	0.040	0.009	31.5	0.205	0.038	0.009	31.9
8	0.273	0.041	0.008	40.4	0.226	0.039	0.009	36.4	0.220	0.038	0.009	36.1
					Control Sample Stored in Dark							
0	0.104	0.042	0.009	—	0.092	0.040	0.009	—	0.090	0.039	0.009	—
24	0.105	0.042	0.008	None detected	0.094	0.041	0.008	None detected	0.091	0.039	0.009	None detected

ples were withdrawn at 1-hr intervals, and the spectrum was recorded. Irradiation for up to 8 hr produced an absorbance increase only at 394 nm while the absorbance at 498 nm remained constant. After 9 hr of exposure to light, an absorbance increase was observed not only at 394 but also at 498 and 700 nm, suggesting that another reaction was occurring subsequent to, or simultaneous with, the primary photodegradation reaction. That is, a process other than the one exhibiting an absorbance increase at only 394 nm became operative.

The literature (1) is ambiguous and inconclusive concerning the photochemical course of the reactions undergone by nitroferricyanide on photoirradiation. Photoaquation to yield nitric oxide and $[Fe(CN)_5(H_2O)]^{-3}$ (10) and photoreduction to produce nitroferrocyanide (11) have been described most frequently as the immediate photodecomposition products of nitroprusside. The difficulty in determining the reaction sequence of photochemical processes lies in the fact that usually a series of undefined, metastable intermediates are formed prior to the final product. Sometimes it is possible to detect these transitory intermediates by a variety of spectroscopic techniques such as electron spin resonance, NMR, and Mössbauer spectroscopy.

When the nature of electronic transitions is well understood, UV and visible spectrophotometry are applied routinely to elucidate the photochemical reactions. The two visible absorption bands of nitroferricyanide have been assigned on a theoretical basis (3), and these assignments receive substantial support from the measured spectra of a single crystal of sodium nitroprusside using polarized light. In the present study, absorption bands at 394 and 498 nm, attributed to metal $d \rightarrow \pi^*$ NO transitions, were followed to determine the course of the photodecomposition and the amount of sodium nitroprusside degraded on photoirradiation.

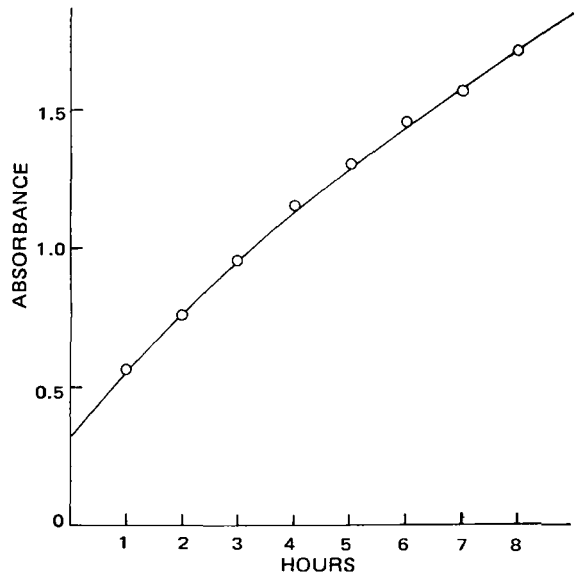

Figure 3—*Change in absorbance at 394 nm* versus *time on irradiation of a 0.5% sodium nitroprusside aqueous solution in a Cooper–Lachman light chamber.*

The fact that initially only the absorbance at 394 nm increased while no absorbance change was observed at 498 nm suggests that the nitrosyl moiety remains intact and that initial irradiation results in a photoexcited nitroferricyanide species accompanied by electronic rearrangement, most likely involving the π^* NO molecular orbital. If the effects of long wavelength irradiation of nitroferricyanide are essentially confined to the π^* NO molecular orbital, only the 394-nm band attributed to the $6e \rightarrow 7e$ transition is expected to reflect this transformation, since the $6e$ level contains approximately 24.8% π^* NO character. The 498-nm band assigned the $2b_2 \rightarrow 7e$ transition is not expected to be affected as markedly, since the $2b_2$ state possess no π^* NO character.

The facts that the energy of the absorption bands is constant and that no new bands appear in the visible region of the spectrum support the theory that initial irradiation chiefly involves the π^* NO molecular orbital. Irradiation apparently does not alter the relative energies of the $6e$, $2b_2$, and $7e$ levels, and photoexcitation results only in increased orbital overlap between the $6e$ and $7e$ orbitals, which is a powerful mechanism for enhancing absorbance.

The spectral data from the present study indicate that initial photoirradiation results in the formation of a relatively long-lived species, as evidenced by the constancy of the absorbance at 498 nm and the lack of any new absorption bands. This rationale is supported by the fact that a blue-green species and nitric oxide, whose distinct odor can easily be detected, are observed only on prolonged irradiation—greater than 8 hr in a Cooper–Lachman light chamber.

Although the course of the photochemical reaction has not been established conclusively, Scheme II is proposed. Species II is photoexcited nitroferricyanide, and III is the photoreduced aquation product. The transformation of II to III probably involves a series of complex intermediates whose identities are not well defined (1). Possible intermediates include $[Fe(CN)_5NO(OH^-)]^{-3}$, $[Fe(CN)_5NO_2]^{-4}$, and $[Fe(CN)_5NO]^{-3}$, but the true nature of these species cannot be ascertained.

If it is assumed that essentially all of I is converted to II prior to the appearance of spectral changes at 498 and 700 nm, a fivefold increase in the initial absorbance at 394 nm may be equated to a 100% conversion of I to II. Based on this assumption, the molar absorptivity of II may be approximated at 102 M^{-1} cm^{-1}. Since the molar absorptivity of sodium nitroprusside at 394 nm is 20.4, an increase of 0.8 in this value represents a 1% loss. The amount of

$$\underset{\text{I}}{[Fe(CN)_5NO]^{-2}} \xrightarrow[\text{fast}]{h\nu} \underset{\text{II}}{[Fe(CN)_5NO^*]^{-2}} \xrightarrow[\text{slow}]{h\nu} \underset{\text{III}}{[Fe(CN)_5(H_2O)]^{-3}} + NO$$

Scheme II

Table III—Spectrophotometric and Polarographic Changes Observed on Irradiation of Aqueous Sodium Nitroprusside Solution

Hours	Absorbance (10-cm Cell) 394 nm	498 nm	700 nm	Polarographic Response (Relative Units) Wave I	Wave II
0	0.214	0.079	0.006	46	91
1	0.608	0.080	0.007	43	85
2	0.925	0.080	0.007	41	82
4	1.410	0.085	0.008	40	80
6	1.761	0.093	0.010	40	80

degraded nitroprusside can be calculated from the following relationship:

$$\frac{\text{molar absorptivity} - 20.4}{0.8} = \%\ \text{degraded nitroprusside} \quad \text{(Eq. 1)}$$

The concentration of sodium nitroprusside in a dry filled vial can be determined spectrophotometrically by using the standard molar absorptivity value at 394 nm and inserting the appropriate dilutions into the equation relating absorbance and concentration:

$$\frac{\text{absorbance/cm} \times \text{dilution (ml)}}{\dfrac{1000\ \text{ml}}{297{,}970\ \text{mg}/M} \times \epsilon M^{-1}\ \text{cm}^{-1}} = \text{mg/vial} \quad \text{(Eq. 2)}$$

In the case of lyophilized material in the anhydrous form, a milliequivalent weight of 261,970 mg must be used in the calculation.

Since sodium nitroprusside is administered at concentrations of approximately 0.01%, the light stability of crystalline powder and lyophilized material in water and in 5% dextrose solution under normal laboratory fluorescent lighting conditions was investigated. All absorbances were determined with 10-cm quartz cells. The results (Table II) indicate that the rate of degradation is linear over the 8-hr period. The rate of degradation is lower than that encountered in a Cooper–Lachman light chamber because the light intensity is much less in the normal laboratory situation. Since sodium nitroprusside may also be dispensed in a 5% dextrose solution from polyvinyl chloride containers, the light stability of a 0.01% solution on exposure to laboratory fluorescent lighting also was determined. A comparison of the rate of photodecomposition of clear Pyrex and polyvinyl chloride containers is shown in Fig. 4. The increased rate of sodium nitroprusside degradation in the plastic

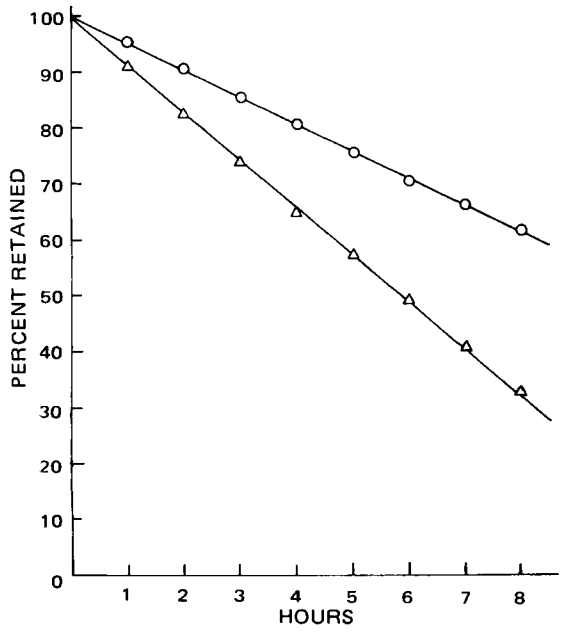

Figure 4—*Sodium nitroprusside stability in 5% dextrose infusion solution on photoirradiation. Key:* ○, *Pyrex container; and* △, *plastic container.*

Table IV—Effect of Temperature on the Molar Absorptivity of Sodium Nitroprusside Solutions

Hours	Molar Absorptivity 394 nm 25°	55°	65°	498 nm 25°	55°	65°	700 nm 25°	55°	65°
0	20.4	—	—	7.4	—	—	0.18	—	—
24	—	20.4	20.5	—	7.4	7.4	—	0.18	0.18
96	—	20.4	20.6	—	7.5	7.5	—	0.18	0.18
192	20.3	20.6	20.8	7.4	7.5	7.5	0.18	0.18	0.18
472	20.4	20.6	21.2	7.5	7.5	7.5	0.18	0.18	0.18

unit is due to the greater transparency of polyvinyl chloride to higher energy UV radiation as compared to glass.

Several reports (12, 14) indicate that electrolytic reduction and photoirradiation of nitroprusside in dimethylformamide yield the same species, $[Fe(CN)_5NO]^{-3}$. To establish a similar correlation in aqueous media, an investigation was conducted to determine the effect of photoirradiation on polarographic response, *i.e.*, wave height and half-wave potential. The solutions contained 0.3 mg/ml of sodium nitroprusside, and the absorbances and polarograms were determined initially and after irradiation in a Cooper–Lachman light chamber. The polarogram of the original solution showed two reduction waves of equal size at −0.31 and −0.58 v *versus* the silver–silver chloride reference electrode, and no new reduction waves appeared on photoirradiation. The results of the study are summarized in Table III.

The data show that the decrease in polarographic response levels off after 4 hr of light exposure, suggesting that photoreduction is not an initial primary photodegradation route of sodium nitroprusside. The results do indicate, however, that spectrophotometry is a much more sensitive method for detecting photodegradation than polarography. In addition, the fact that the polarographic response plateaued after approximately a fivefold increase in the absorbance at 394 nm supports the hypothesis that, on irradiation, nitroferricyanide is initially converted to III, which then slowly degrades to form IV.

A solution study of the thermal stability of sodium nitroprusside was reported previously (19). The stability relative to a sample stored at 25° was determined by measuring the increase in absorbance at 390 nm at selected time intervals. The data show that storage of a solution at 65° for 96 hr results in a threefold absorbance increase at 390 nm. Since preliminary results of experiments designed to ascertain the thermal stability of sodium nitroprusside solutions did not agree with the literature findings, a detailed study was conducted (Table IV).

The present results, as opposed to the earlier report (19), indicate that sodium nitroprusside solutions are stable for long periods even at elevated temperatures. The apparent discrepancies may arise from the previous study being carried out with sodium nitroprusside material containing impurities or with contaminated solutions, thereby accelerating the thermal degradation process.

The present results clearly demonstrate that sodium nitroprusside is extremely photosensitive. Although complex, the theory presented to explain photochemical phenomena provides a method for the simultaneous determination of the purity, stability, and concentration of sodium nitroprusside in the solid state and in solution.

REFERENCES

(1) J. H. Swinehart, *Coord. Chem. Rev.*, **2**, 385(1967).

(2) P. T. Manoharan and W. C. Hamilton, *Inorg. Chem.*, **2**, 1043(1963).

(3) P. T. Manoharan and H. J. Gray, *J. Amer. Chem. Soc.*, **87**, 3340(1965).

(4) W. Haberditzl, W. D. Schleinitz, and H. G. Bartel, *Naturforschung.*, **23b**, 891(1968).

(5) N. L. Costa, J. Danon, and R. M. Xavier, *J. Phys. Chem. Solids*, **23**, 1783(1962).

(6) J. Masek, *Inorg. Chim. Acta Rev.*, **3**, 101(1969).

(7) D. B. Brown, *ibid.*, **5**, 314(1971).

(8) I. M. Kolthoff and P. E. Toren, *J. Amer. Chem. Soc.*, **75**, 1197(1953).

(9) "Gmelin's Handbuch der Anorganischen Chemie, Iron 59B," Verlag Chemie, Gmbh, Berlin, Germany, 1938, p. 903.
(10) O. Baudisch, *Science*, **108**, 443(1948).
(11) W. P. Griffith, *Quart. Rev.*, **16**, 188(1962).
(12) E. F. Hockings and I. Bernal, *J. Chem. Soc.*, **1964**, 5029.
(13) J. D. W. VanVoorst and P. Hemmerich, *J. Chem. Phys.*, **45**, 3914(1966).
(14) J. B. Raynor, *Nature*, **201**, 1216(1964).
(15) J. Dempir and J. Masek, *Inorg. Chim. Acta*, **2**, 402(1968).
(16) J. H. Swinehart and P. A. Rock, *Inorg. Chem.*, **5**, 573(1966).
(17) P. P. Mitra, D. V. S. Juin, A. K. Banerjee, and K. V. R. Chari, *J. Inorg. Nucl. Chem.*, **25**, 1263(1963).
(18) B. Joselskis and J. C. Edwards, *Anal. Chem.*, **32**, 381(1960).
(19) T. Martin and J. A. Patel, *Amer. J. Hosp. Pharm.*, **26**, 51(1969).
(20) I. H. Page, *J. Amer. Med. Ass.*, **147**, 1311(1951).
(21) L. Lachman, C. J. Swartz, and J. Cooper, *J. Amer. Pharm. Ass., Sci. Ed.*, **49**, 213(1960).
(22) F. A. Cotton, R. R. Monchamp, R. J. M. Henry, and R. C. Young, *J. Inorg. Nucl. Chem.*, **7**, 32(1958).

ACKNOWLEDGMENTS AND ADDRESSES

Received December 23, 1974, from *Hoffmann-La Roche, Inc., Nutley, NJ 07110*

Accepted for publication April 1, 1975.

The authors are indebted to Mr. Vincent Rizzo for preparation of anhydrous, lyophilized sodium nitroprusside and to Ms. Mildred Sarli for drawing the figures.

[x] To whom inquiries should be directed.

Effect of Solvent Flow Reynolds Number on Dissolution Rate of a Nondisintegrating Solid (Potassium Chloride)

J. VALERIE FEE [x], D. J. W. GRANT [x], and J. M. NEWTON

Abstract □ An apparatus for measuring dissolution rates of solids in the form of disks was designed to possess the following features. The solvent flowed continuously and reproducibly past the disk at various rates associated with calculable Reynolds numbers, *Re*. The effluent solution was adequately mixed before analysis. The concentration of dissolved solute was much less than the solubility. The surface area of the disk in contact with the solvent was constant during measurements. The dissolution rate of the disk was reproducible, and the disk and its surface could be readily characterized. The apparatus was tested at 37° with compressed potassium chloride and water. The intrinsic dissolution rate, G, was a linear function of *Re* from *Re* = 360 to >6000. This relationship enabled one unknown constant in each dissolution theory to be expressed in terms of *Re*. For the diffusion layer model, the thickness of this layer, calculated from the experimental value of G, agreed well with that calculated from the various physical properties, provided that natural convection did not predominate. The dissolution of potassium chloride in this system was, therefore, controlled by diffusion.

Keyphrases □ Dissolution rates—solid nondisintegrating disk (potassium chloride), apparatus described, effect of solvent flow Reynolds number □ Solvent flow—Reynolds number, effect on dissolution rate of nondisintegrating solid disk (potassium chloride) □ Reynolds number—effect on dissolution rate of nondisintegrating potassium chloride solid disk, apparatus described and evaluated

The first major objective of this work was to design, construct, and test an apparatus with the following features for determining the dissolution rate of solids.

(*a*) The solvent flow in the apparatus should be controlled and characterized by a calculable value of the Reynolds number, *Re*.

(*b*) The effluent solution from the apparatus should be adequately mixed before analysis.

(*c*) The concentration, c, of dissolved solute must be much less than the solubility, c_s, *i.e.*, $(c_s - c) \approx c_s$, or, in other words, sink conditions must apply.

(*d*) The surface area of the solid disk in contact with the dissolution medium must be constant.

(*e*) The dissolution rate of the solid must be reproducible.

(*f*) The solid disk and its surface must have reproducible properties that can readily be characterized.

(*g*) The solid surface should be positioned in the solvent stream so that the flow over the solid is reproducible.

The second major objective was to study how the intrinsic dissolution rate, G, of a solid substrate depends on the flow rate of the solvent and, therefore, on *Re*. The third major objective was to deduce which dissolution theory or model best fits the results and describes the dissolution process.

EXPERIMENTAL

Materials—The potassium chloride was spectroscopic grade[1], and the solvent in the dissolution experiments was glass-distilled water of very low potassium content (<0.01 mg/liter).

Preparation of Solid Disks—Transparent disks, 13 mm in diameter, 2 mm thick, and encircled by a 21-mm external diameter Nimonic[2] creep-resistant alloy ring (disk holder K), were prepared by compressing 315 mg of finely powdered potassium chloride at 10 tons load for 5 min under vacuum in a die and punch assembly (Fig. 1). The upper surface of the finished disk to be exposed to the solvent was level with the rim of the holder while the lower surface was recessed to enable it to fit on the raised knob on stub D in dissolution chamber C (Fig. 2).

Petroleum jelly was used for adhesion and ensured that the sol-

[1] B.D.H. Chemicals Ltd., Poole, Dorset, BH12 4NN, England.
[2] Henry Wiggin and Co. Ltd., Wiggin Street, Birmingham, England.

(9) "Gmelin's Handbuch der Anorganischen Chemie, Iron 59B," Verlag Chemie, Gmbh, Berlin, Germany, 1938, p. 903.
(10) O. Baudisch, *Science*, **108**, 443(1948).
(11) W. P. Griffith, *Quart. Rev.*, **16**, 188(1962).
(12) E. F. Hockings and I. Bernal, *J. Chem. Soc.*, **1964**, 5029.
(13) J. D. W. VanVoorst and P. Hemmerich, *J. Chem. Phys.*, **45**, 3914(1966).
(14) J. B. Raynor, *Nature*, **201**, 1216(1964).
(15) J. Dempir and J. Masek, *Inorg. Chim. Acta*, **2**, 402(1968).
(16) J. H. Swinehart and P. A. Rock, *Inorg. Chem.*, **5**, 573(1966).
(17) P. P. Mitra, D. V. S. Juin, A. K. Banerjee, and K. V. R. Chari, *J. Inorg. Nucl. Chem.*, **25**, 1263(1963).
(18) B. Joselskis and J. C. Edwards, *Anal. Chem.*, **32**, 381(1960).
(19) T. Martin and J. A. Patel, *Amer. J. Hosp. Pharm.*, **26**, 51(1969).
(20) I. H. Page, *J. Amer. Med. Ass.*, **147**, 1311(1951).
(21) L. Lachman, C. J. Swartz, and J. Cooper, *J. Amer. Pharm. Ass., Sci. Ed.*, **49**, 213(1960).
(22) F. A. Cotton, R. R. Monchamp, R. J. M. Henry, and R. C. Young, *J. Inorg. Nucl. Chem.*, **7**, 32(1958).

ACKNOWLEDGMENTS AND ADDRESSES

Received December 23, 1974, from *Hoffmann-La Roche, Inc., Nutley, NJ 07110*

Accepted for publication April 1, 1975.

The authors are indebted to Mr. Vincent Rizzo for preparation of anhydrous, lyophilized sodium nitroprusside and to Ms. Mildred Sarli for drawing the figures.

[x] To whom inquiries should be directed.

Effect of Solvent Flow Reynolds Number on Dissolution Rate of a Nondisintegrating Solid (Potassium Chloride)

J. VALERIE FEE [x], D. J. W. GRANT [x], and J. M. NEWTON

Abstract □ An apparatus for measuring dissolution rates of solids in the form of disks was designed to possess the following features. The solvent flowed continuously and reproducibly past the disk at various rates associated with calculable Reynolds numbers, *Re*. The effluent solution was adequately mixed before analysis. The concentration of dissolved solute was much less than the solubility. The surface area of the disk in contact with the solvent was constant during measurements. The dissolution rate of the disk was reproducible, and the disk and its surface could be readily characterized. The apparatus was tested at 37° with compressed potassium chloride and water. The intrinsic dissolution rate, G, was a linear function of *Re* from *Re* = 360 to >6000. This relationship enabled one unknown constant in each dissolution theory to be expressed in terms of *Re*. For the diffusion layer model, the thickness of this layer, calculated from the experimental value of G, agreed well with that calculated from the various physical properties, provided that natural convection did not predominate. The dissolution of potassium chloride in this system was, therefore, controlled by diffusion.

Keyphrases □ Dissolution rates—solid nondisintegrating disk (potassium chloride), apparatus described, effect of solvent flow Reynolds number □ Solvent flow—Reynolds number, effect on dissolution rate of nondisintegrating solid disk (potassium chloride) □ Reynolds number—effect on dissolution rate of nondisintegrating potassium chloride solid disk, apparatus described and evaluated

The first major objective of this work was to design, construct, and test an apparatus with the following features for determining the dissolution rate of solids.

(*a*) The solvent flow in the apparatus should be controlled and characterized by a calculable value of the Reynolds number, *Re*.

(*b*) The effluent solution from the apparatus should be adequately mixed before analysis.

(*c*) The concentration, c, of dissolved solute must be much less than the solubility, c_s, *i.e.*, $(c_s - c) \approx c_s$, or, in other words, sink conditions must apply.

(*d*) The surface area of the solid disk in contact with the dissolution medium must be constant.

(*e*) The dissolution rate of the solid must be reproducible.

(*f*) The solid disk and its surface must have reproducible properties that can readily be characterized.

(*g*) The solid surface should be positioned in the solvent stream so that the flow over the solid is reproducible.

The second major objective was to study how the intrinsic dissolution rate, G, of a solid substrate depends on the flow rate of the solvent and, therefore, on *Re*. The third major objective was to deduce which dissolution theory or model best fits the results and describes the dissolution process.

EXPERIMENTAL

Materials—The potassium chloride was spectroscopic grade[1], and the solvent in the dissolution experiments was glass-distilled water of very low potassium content (<0.01 mg/liter).

Preparation of Solid Disks—Transparent disks, 13 mm in diameter, 2 mm thick, and encircled by a 21-mm external diameter Nimonic[2] creep-resistant alloy ring (disk holder K), were prepared by compressing 315 mg of finely powdered potassium chloride at 10 tons load for 5 min under vacuum in a die and punch assembly (Fig. 1). The upper surface of the finished disk to be exposed to the solvent was level with the rim of the holder while the lower surface was recessed to enable it to fit on the raised knob on stub D in dissolution chamber C (Fig. 2).

Petroleum jelly was used for adhesion and ensured that the sol-

[1] B.D.H. Chemicals Ltd., Poole, Dorset, BH12 4NN, England.
[2] Henry Wiggin and Co. Ltd., Wiggin Street, Birmingham, England.

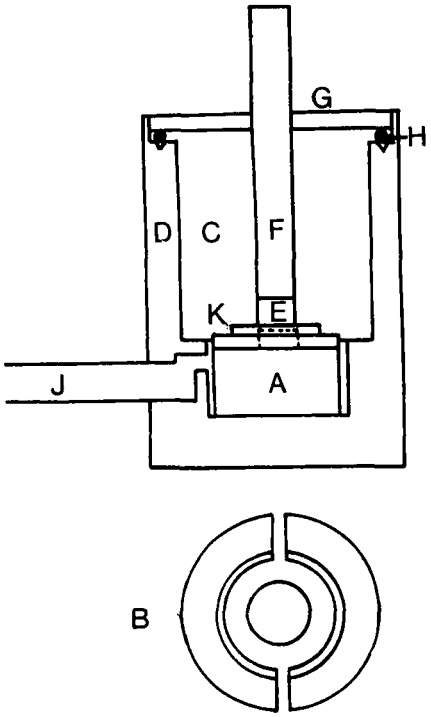

Figure 1—*Die and punch assembly for preparing compressed disks of potassium chloride (of mass 315 mg and diameter 13 mm) surrounded by a Nimonic alloy ring for dissolution experiments. Key: A, anvil; B, cylindrical recessed base of C; C, cylindrical barrel; D, die body; E, platen; F, plunger; G, die top; H, Neoprene O-ring seal; J, tube for connection to vacuum pump; and K, Nimonic alloy ring.*

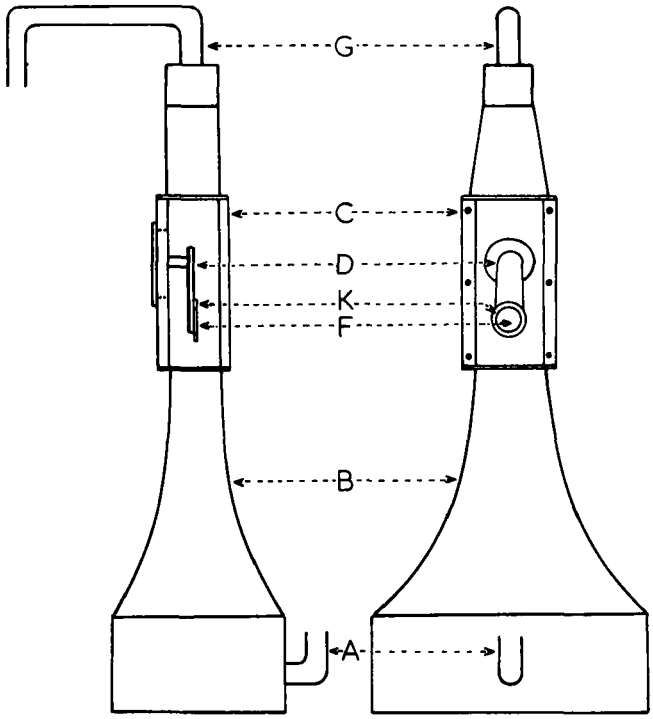

Figure 2—*Apparatus for determining the dissolution rate of a solid in a stream of flowing solvent (scale, approximately 0.23× actual size). Key: A, inlet tube from control valve and reservoirs; B, exponentially shaped horn; C, dissolution chamber; D, stub for fixing the disk holder; K, disk holder; F, solid disk of potassium chloride; and G, effluent tube.*

vent did not reach the hidden surface of the disk.

Dissolution Apparatus—The apparatus (Fig. 2) was constructed of stainless steel, except for one face of dissolution chamber C. This one face was of polymethyl methacrylate to enable the outer surface of the potassium chloride disk to be viewed. Stub D, carrying disk holder K, could be put into C and taken out of C through the back wall.

To produce uniform flow of solvent over the greatest possible cross-sectional area of dissolution chamber C, fluid was introduced through an exponentially shaped horn, B (Fig. 2). Such a system ensures a uniform flow velocity over the region beyond the hydrodynamic boundary layer adjacent to each wall (1) (Fig. 3). The thickness, h_0, of the hydrodynamic boundary layer can be calculated from:

$$h_0 \approx \frac{2.0x}{\sqrt{\frac{x\rho\bar{u}}{\eta}}} \qquad \text{(Eq. 1)}$$

where x is the length of the exponential horn (18 cm here); ρ and η are the density and dynamic viscosity, respectively, of the liquid [ρ= 0.99336 g/ml (2) and η = 0.006915 poise (3) for water at 37°]; and $\bar{u}$ is the mean linear flow velocity of the liquid.

At the minimum solvent flow rate used—*viz.*, $\bar{u}$ = 0.79 cm/sec, $h_0 \approx$ 8.0 mm. At the maximum possible flow rate for streamline (laminar) flow (Re = 3000)—*viz.*, $\bar{u}$ = 6.7 cm/sec, $h_0 \approx$ 2.7 mm. The dimensions of dissolution chamber C were such that the surface and lateral edges of the potassium chloride disk were in the middle of the flow stream and 13 mm (1 disk diameter) from each wall of C. Now, 13 mm > h_0 throughout the range of streamline flow rates used or, in other words, the whole surface of the dissolving solid was outside the hydrodynamic boundary layer of the chamber wall and, therefore, at a position of uniform approach velocity. Clearly, the presence of any object in the dissolution chamber will modify these otherwise ideal flow conditions.

The dissolving solid, F, was held at the center of dissolution chamber C in such a manner as to minimize the disturbance of the uniform flow pattern (Fig. 2). Accordingly, mounting stub D was oriented downstream from F and below the level of the solid surface; F was surrounded by ring K to protect its edges and to enable it to be mounted within an IR absorption spectrophotometer for future work. The thickness, annular area, and composition of ring K and the circular shape of dissolving solid F enabled F to be formed under pressure (Fig. 1) without distortion of the ring or fracture of F. The edges of ring K were rounded to give the least interference with the flow pattern within the dissolution chamber. All these factors contributed to reproducibility (feature *g*).

The solvent flowed from elevated reservoirs at the constant predetermined rate through an on–off valve and a fine control valve to inlet tube A (Fig. 2). The solvent then flowed upward through the apparatus. The dissolution apparatus and the solvent reservoirs were surrounded by thermostatically controlled water baths at 37.0 ± 0.1°. The water bath containing the dissolution apparatus had a glass front to permit observation of the disk.

Each dissolution run was begun with the solvent level just below the potassium chloride disk. The liquid from C passed through a cone of decreasing diameter to the narrow outlet tube, G. Samples were collected from G at 10-sec intervals in weighed flasks until part of the disk had been eroded (after 2–4 min). The flasks were reweighed and, from the mass of solution collected in each time interval, the mean volume flow rate, dV/dt, was calculated assuming that the density, ρ, of the solution, which was very dilute, was equal to that of pure water, *i.e.*, 0.99336 g/ml at 37° (2). The effluent solution was analyzed for dissolved potassium chloride. Samples taken from different regions of each effluent solution contained the same concentration of potassium chloride. This finding shows that mixing, which took place between C and G, was adequate (feature *b*).

Analysis—The concentration of potassium chloride dissolved in the effluent solution was determined as potassium ions by means of a flame photometer[3].

Calculation of Dissolution Rate—At a given instant in time t, let the volume of solution within the dissolution chamber be V, let this solution contain a mass, m, of solute dissolved from the solid disk, and let the mean concentration of solute within the dissolu-

[3] Evans Electroselenium Ltd., St. Andrews Works, Halstead, Essex, England.

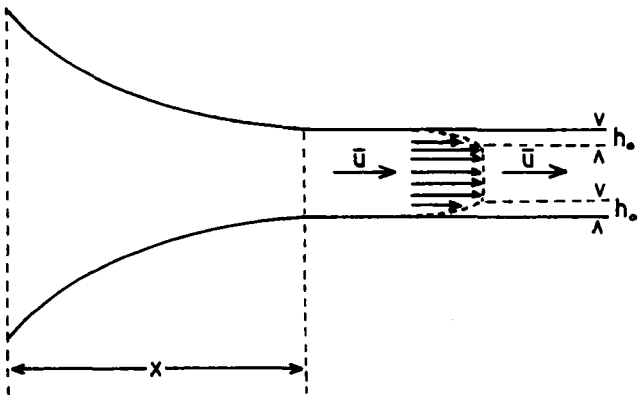

Figure 3—*Velocity distribution across a pipe (shown by horizontal arrows) when flow through the pipe is preceded by an exponentially shaped horn of length* x. *The mean linear velocity through the pipe is* ū, *and the thickness of the hydrodynamic boundary layer is* h_0.

tion chamber be c. In an infinitesimal interval of time, the solution in the chamber gains mass dm of solute from the dissolving solid and, in volume dV of effluent, it loses mass $c(dV)$ of solute.

In the present continuous-flow dissolution apparatus, there is no accumulation of solute within the dissolution chamber. Consequently, the gain in solute mass dm is exactly balanced by the loss in solute mass $c(dV)$, so that:

$$dm = c(dV) \qquad \text{(Eq. 2)}$$

and the concentration of solute in any sample of the effluent after thorough mixing gives a direct measure of c. If dt represents the infinitesimal time interval referred to:

$$\frac{dm}{dt} = c\frac{dV}{dt} \qquad \text{(Eq. 3)}$$

where dm/dt is the overall dissolution rate of the solid disk, and dV/dt is the overall solvent flow rate (*i.e.*, the rate of increase in effluent volume).

The intrinsic dissolution rate is defined as the dissolution rate per unit area. The dissolution rate may exhibit different values for each small element of surface of the dissolving solid. For practical purposes, the overall intrinsic dissolution rate, G, of the dissolving solid is taken to be:

$$G = \left(\frac{dm}{dt}\right)\left(\frac{1}{A}\right) \qquad \text{(Eq. 4)}$$

where dm/dt is the overall dissolution rate, and A is the total area of the dissolving solid exposed to the solvent (A = 1.3272 cm^2). Combining Eqs. 3 and 4 gives:

$$G = \left(\frac{c}{A}\right)\left(\frac{dV}{dt}\right) \qquad \text{(Eq. 5)}$$

from which G was calculated.

Calculation of Reynolds Number for Solvent Flow—The parameter used to represent solvent flow was the dimensionless grouping, Reynolds number, Re, which is given by:

$$Re = \frac{\rho\, du}{\eta} \qquad \text{(Eq. 6)}$$

where ρ is the density, and η is the dynamic viscosity of the solution. Since the solution was dilute, these values were taken to be the same as those for pure water, *i.e.*, ρ = 0.99336 g/ml (2) and η = 0.006915 poise (3) at 37°. The mean hydraulic diameter, d, of the rectangular chamber was given by four times the cross-sectional area divided by the wetted perimeter: $d = 4 \times 10.14$ cm^2/13 cm = 3.12 cm.

The linear flow rate, u, was given by dV/dt divided by the cross-sectional area of the dissolution chamber, 10.14 cm^2. Thus:

$$Re = 44.20\ (\text{sec/cm}^3) \times \frac{dV}{dt}\ (\text{in cm}^3/\text{sec}) \qquad \text{(Eq. 7)}$$

from which Re was calculated for each flow rate (feature *a*).

Visualization of Solvent Flow—Two methods of flow visualization were used. One was to pass aqueous 2 M $AgNO_3$ solution over a potassium chloride disk and to examine the resulting white colloidal solution of silver chloride. The other method was to incorporate 1 mg of gentian violet into a potassium chloride disk and to study the color pattern as the disk dissolved. The latter method was less satisfactory because initially very small particles of gentian violet tended to fall a few millimeters downward before being swept forward by the solvent.

RESULTS

Visualization of Solvent Flow—The white colloid silver chloride formed in the first method left the disk at right angles to the surface and changed direction a few millimeters from it. At Re < 360, the silver chloride flowed downward against the stream of flowing solvent, showing that back-convection was taking place. At Re > 360, the silver chloride flowed upward with the solvent stream. At Re < 3000, flow of silver chloride appeared laminar (or streamline). The second method of flow visualization using gentian violet gave similar results.

Effect of Reynolds Number for Water Flow on Intrinsic Dissolution Rate of Potassium Chloride—The concentration, c, of potassium chloride in the effluent (*e.g.*, in Fig. 4) was practically constant as long as the area, A, of the disk appeared constant (feature *d*). The coefficient of variation of the steady-state concentration during a run was about 6%. Initially, c was lower than the mean value, presumably because the steady state had not been attained. After about 120 sec, c decreased, since the disk began to be eroded and its area decreased thereafter. No matter what the flow rate, erosion commenced at the downstream edge of the disk, revealing the underlying metal stub.

The mean steady-state value of c decreased with increasing Re but fluctuated for Re > 3000. The highest recorded value of c (at Re = 367) was 0.153 g of potassium chloride/liter; this concentration was less than c_s by a factor of about 2000, where c_s is the solubility of potassium chloride in water at 37° (334 g/liter) (4). Thus, $c \ll c_s$, *i.e.*, $(c_s - c) \approx c_s$, as required (feature *c*).

At Re < 360, the system gave inconsistent results due to back-convection of the denser, concentrated solution formed in the immediate vicinity of the disk. This finding was proved by analysis of the liquid remaining in the base of the apparatus (B in Fig. 1) after a disk dissolved completely. At Re > 360, no back-convection was observed.

Figure 5 shows the effect of Re on G. At Re < 3000, *i.e.*, for streamline flow and in the transition region, G was a linear function of Re; thus:

$$G(\text{in g/m}^2\,\text{sec}) = 8.805 + 0.001414\,Re \qquad \text{(Eq. 8)}$$
$$r = 0.993 \qquad s^2 = 0.0235$$

where r is the correlation coefficient, and s^2 is the residual variance of the G values. In the region of definite turbulent flow, *i.e.*, at Re > 3000, values of G fluctuated about the mean regression line. This scatter was induced by turbulence. The linear regression line, calculated by giving equal weight to each result in the streamline, transition, and turbulent regions, was:

$$G(\text{in g/m}^2\,\text{sec}) = 8.820 + 0.001383\,Re \qquad \text{(Eq. 9)}$$
$$r = 0.981 \qquad s^2 = 2.46$$

Comparison of Eqs. 8 and 9 shows that inclusion of results at Re >

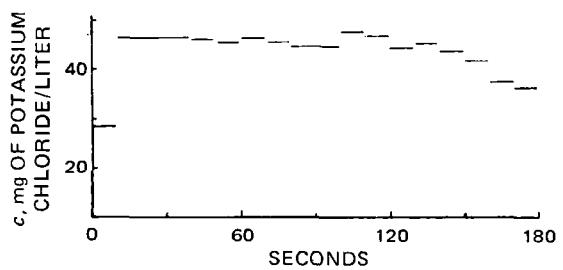

Figure 4—*Time dependence of the concentration of potassium chloride in the effluent of the dissolution apparatus from a disk of potassium chloride.*

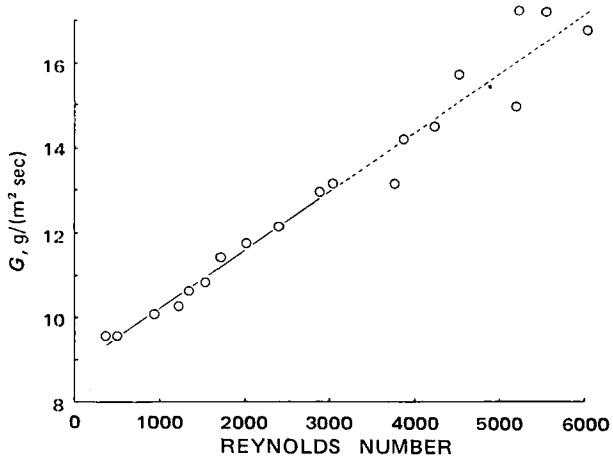

Figure 5—*Effect of Reynolds number for solvent flow on the intrinsic dissolution rate, G, of compressed disks of potassium chloride.*

3000 has little effect on the constants in the relationship between G and Re, but the greater fluctuation of points in the turbulent region is reflected in a much greater residual variance and in a slightly lower correlation coefficient.

When different potassium chloride disks were prepared and dissolved by the same or a different operator using the procedure described at Re = 1335, values of the mean steady-state concentration and G did not differ from disk to disk or from operator to operator by more than 2%. This finding indicates the high degree of reliability and reproducibility of the technique (feature *e*).

DISCUSSION

Dissolution Apparatus—The features required of the dissolution apparatus were achieved. The only limitation was back-convection of solute at $Re < 360$. The solvent flow rate under these conditions was insufficient to sweep forward all of the concentrated solution formed at the disk surface. In other respects, the apparatus and technique were satisfactory.

Disk Erosion—The upper (or downstream) segment of the disk was eroded preferentially. According to the theory of Levich (5) for a plate in a parallel stream of reactive liquid, the diffusional flux (*i.e.*, the intrinsic dissolution rate) at the upstream edge of the plate is greater than at the downstream edge. Thus, the asymmetric pattern of erosion of the solid in the present system differs from the theory. A possible reason for this difference may be that the metal ring surrounding the disk, although rounded, slightly disturbs the flow profile around the dissolving solid.

Reaction-Controlled Dissolution Models—These models are exemplified by the interfacial barrier model of Higuchi (6) and the theory of Szinai and Hunt (7). According to the former model:

$$G = k_i(c_s - c) \qquad \text{(Eq. 10)}$$

where k_i is known as the "effective interfacial transport rate constant." By introducing $(c_s - c) \approx c_s$ = 0.33414 g/ml (4) and expressing G in terms of Re (Eq. 9), k_i is found to be the following function of Re:

$$k_i(\text{in cm/sec}) = 0.00264 + (4.14 \times 10^{-7}\, Re) \qquad \text{(Eq. 11)}$$

Diffusion-Controlled Dissolution Models—According to the model of Danckwerts (8), which was originally developed for the dissolution of gases and has since been applied to the dissolution of solids (6), G is given by:

$$G = \sqrt{DS}\,(c_s - c) \qquad \text{(Eq. 12)}$$

where D is the integral diffusion coefficient of the solute from its saturated solution to pure water, and S is a constant known as the "mean rate of production of fresh surface." The term D was evaluated by extrapolating the integral diffusion coefficient of potassium chloride in water (9, 10) to c_s = 334.14 g/liter (4) at 37°. By introducing $D = 3.22 \times 10^{-5}$ cm²/sec so obtained and the value of c_s, assuming sink conditions, and expressing G in terms of Re (Eq. 9),

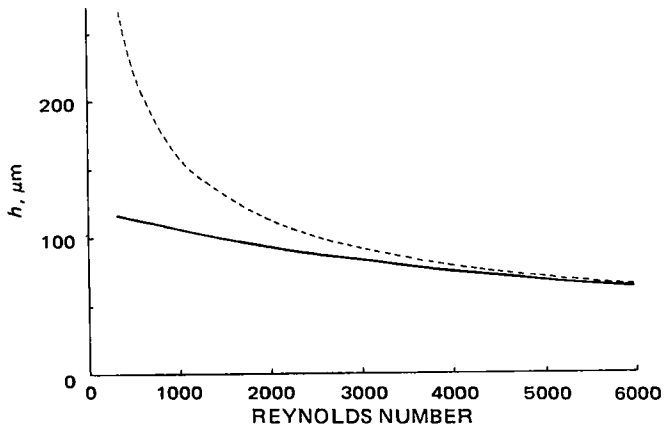

Figure 6—*Effect of Reynolds number for solvent flow on the thickness, h, of the diffusion layer for the dissolution of potassium chloride in water. Key: —, calculated from the experimental values of G by means of Eq. 14; and - - -, calculated from the physical constants of the system using Eq. 16.*

S is given as the following function of Re:

$$S(\text{in 1/sec}) = [0.465 + (7.30 \times 10^{-5}\, Re)]^2 \qquad \text{(Eq. 13)}$$

According to the diffusion layer model (11, 12):

$$G = \frac{D}{h}(c_s - c) \qquad \text{(Eq. 14)}$$

where h is the thickness of the diffusion layer. Introducing these values of D and c_s, assuming sink conditions, and expressing G in terms of Re (Eq. 9) give:

$$h = \frac{122.0\ \mu\text{m}}{1 + (1.568 \times 10^{-4}\, Re)} \qquad \text{(Eq. 15)}$$

This relationship between h and Re is expressed graphically as the lower curve in Fig. 6. Over the range of Reynolds numbers investigated, the thickness, h, of the diffusion layer was 60–110 μm, two to three times that found for other solid–liquid dissolution systems (12–14). The exceptionally high value of h may arise from the high solubility of potassium chloride, which would otherwise lead to very high concentration gradients near the solid surface.

Levich (5) derived the following equation for h in terms of fundamental physical quantities for nonturbulent (or laminar) flow along a flat disk, provided that the dimensions of the system are such that other wall and edge effects are negligible:

$$h = 3x^{1/2}D^{1/3}\nu^{1/6}u^{-1/2} \qquad \text{(Eq. 16)}$$

where D is the diffusion coefficient of the solute (3.22×10^{-5} cm²/sec, as before), ν is the kinematic viscosity of the solvent ($\eta/\rho = 6.961 \times 10^{-3}$ cm²/sec or stokes), x is the distance from the up-

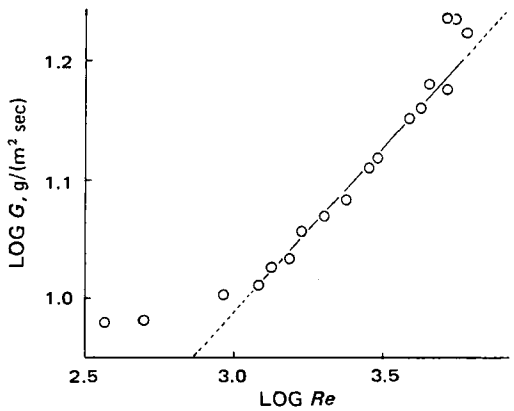

Figure 7—*Relationship between the logarithm of the intrinsic dissolution rate, G, of potassium chloride in water and the logarithm of the Reynolds number, Re, for solvent flow. This figure is a log–log plot of the data in Fig. 5.*

stream edge of the disk measured along an axis parallel to the direction of flow, and u is the characteristic linear flow velocity of the system (taken as the mean value), which is given by Eq. 6. By substituting the numerical values of η, ρ, and d previously quoted, the following expression for u is obtained:

$$u(\text{in cm/sec}) = 0.002231\,Re \qquad \text{(Eq. 17)}$$

The mean value of x along a line passing through the center is taken to be equal to the radius of the disk (0.650 cm), whereas it is zero at the extreme left-hand and right-hand sides of the disk. The mean value of x over the whole disk is probably close to the mean of these values, 0.325 cm. By substituting into Eq. 16 the numerical values previously quoted and the expression for u in terms of Re, the following expression for h in terms of Re is obtained:

$$h(\text{in } \mu\text{m}) = 5033\,Re^{-1/2} \qquad \text{(Eq. 18)}$$

The Levich equation (Eq. 16) was derived for a uniform plate that reacts with the solvent over its entire area, so that at its leading (or upstream) edge the thickness of the hydrodynamic boundary layer, h_0, and that of the diffusion boundary layer, h, are both zero. In the present work, the dissolving disk (F in Fig. 2) is surrounded by a chemically inert annular ring, K, such that the leading edge of the dissolving disk is 4 mm downstream from the hydrodynamic edge.

However, Eq. 16 is derived by considering the momentum balance on a control volume of fluid and assumes that the change of momentum within a given layer equals the retarding force due to the wall shear stress. This assumption is still valid for the present system in which the diffusion boundary layer, h, begins at a different point from the hydrodynamic boundary layer, h_0. Thus, Eq. 16 is not itself modified by the thickness of the ring.

The asymmetric pattern of erosion of the disk, previously discussed, suggests that the annular ring (K in Fig. 2) modifies the flow profile over the surface of disk F, even though the flow visualization experiments indicate that this disturbance is insufficient to create turbulence at $Re < 2000$. Therefore, the present system deviates markedly from the Levich theory as a result of the influence of the solid disk and its holder.

The fact that Eq. 16 and, by implication, Eq. 18 are not strictly valid for turbulent flow may not itself cause significant deviations from the Levich theory, because flow near the surface of a solid tends to be laminar even though the bulk of the liquid may be turbulent (15).

The theoretical relationship between h and Re (Eq. 18), involving only the physical constants of the system, is expressed graphically in Fig. 6 and compared with Eq. 15 derived from the experimental relationship between G and Re (Eq. 9). If the approximations made in deriving Eq. 16 are considered, there is good agreement between the theoretical and experimental h values at high Re. This finding strongly suggests that the diffusion layer model operates at the higher flow rates, where forced convection predominates over natural convection. That the experimental values of h become progressively smaller than the theoretical value as Re is reduced suggests that natural convection becomes increasingly important the lower the flow rate and reflects deviations from the Levich theory.

According to Nernst (11), an increase in the rate of agitation of the dissolution medium should reduce h and increase the dissolution rate. This effect has been amply confirmed by experiment (12, 16–18) and is usually expressed as a power law:

$$\frac{dm}{dt} = aR^b \qquad \text{(Eq. 19)}$$

where R is the rate of agitation or stirring, and a and b are constants such that $b \leq 1$. For the present continuous-flow apparatus, $G \propto dm/dt$ and $R \propto Re$, so the power law may be written:

$$G = a(Re)^b \qquad \text{(Eq. 20)}$$

or:

$$\log G = \log a + b \log Re \qquad \text{(Eq. 21)}$$

where a is a new constant.

If dissolution is reaction controlled, R or Re should exert little or no influence on the dissolution rate and b should be close to zero. If dissolution is diffusion controlled, b should be significant. Levich (5) calculated that b should be close to 0.5 when flow is laminar ($Re < 2000$) and close to 1.0 for turbulent flow ($Re > 3000$). These calculations were confirmed experimentally for the dissolution of benzoic acid and iodine in water (17).

Figure 7 shows a log–log plot of the data in Fig. 5 and is approximately linear, indicating that Eqs. 20 and 21 are obeyed except at $Re < 1000$. Linear regression analysis of the data, omitting the three deviant points for $Re < 1000$ and all those for definite turbulent flow ($Re > 3000$), gives $a = 1.546$ g/m^2 sec and $b = 0.2667$ as best fitting Eq. 21, with the correlation coefficient being 0.995 and the residual variance of log G being 0.000017. If only the three deviant points at $Re < 1000$ are omitted, the constants that best fit Eq. 21 are $a = 1.117$ g/m^2 sec and $b = 0.3096$, with the correlation coefficient being 0.972 and the residual variance of log G being 0.000328.

The increase in gradient, b, brought about by turbulence accords with Levich's (5) predictions for the diffusion layer theory, but the actual values (~0.3) are lower than those (0.4–1.0) found by other workers (13, 16–18) for the dissolution of solids and other diffusion-controlled chemical processes. Thus, the present dissolution system is less sensitive to solvent flow than other examples.

The form of the log G–log Re plot in Fig. 7 is similar to that for the dissolution of salicylic acid in water studied by Travers and Powdrill (19), who deduced that natural convection was an important feature in their experiments. The predominance of natural convection over forced convection at low solvent flow rates explains the constancy of log G at the lowest log Re values (Fig. 7) as well as the fact that the experimental values of h were less than those calculated theoretically for forced convection (Fig. 6).

Natural convection is unlikely to be caused by temperature gradients, since the system is thermostatically controlled to ±0.1°, but it could well arise from variations in density due to concentration changes within the liquid phase. The importance of the latter effect was shown by the convection of the dense solution formed on dissolution at $Re < 360$ in a downward direction against the rising solvent stream.

CONCLUSIONS

The present apparatus achieved our objectives. By enabling the intrinsic dissolution rate to be determined at various Reynolds numbers, the method enables the unknown constant in any dissolution model with only one such constant to be expressed in terms of Re. Comparison of the thickness of the diffusion layer so determined with that calculated from the physical constants of the system, using Eq. 16 (5), provides a simple means of testing the applicability of the diffusion layer model.

Indeed, the present work indicates that the dissolution of potassium chloride in water agrees with the diffusion layer model when forced convection predominates over natural convection. The effect of viscosity of the medium on the dissolution rate (20) supports this model. In the present system, natural convection becomes increasingly important as the solvent flow rate is reduced.

REFERENCES

(1) V. L. Streeter, "Fluid Mechanics," McGraw-Hill, New York, N.Y., 1966.

(2) "Handbook of Chemistry and Physics," 53rd ed., Chemical Rubber Co., Cleveland, Ohio, 1972.

(3) G. W. C. Kaye and T. H. Laby, "Tables of Physical Constants," 13th ed., Longmans, London, England, 1966.

(4) W. F. Linke, "Solubilities: Inorganic and Metal Organic Compounds," 4th ed., vol. II, American Chemical Society, Washington, D.C., 1965.

(5) V. G. Levich, "Physicochemical Hydrodynamics," Prentice-Hall, Englewood Cliffs, N.J., 1962.

(6) W. I. Higuchi, *J. Pharm. Sci.*, **56**, 315(1967).

(7) S. S. Szinai and A. C. Hunt, *Can. J. Pharm. Sci.*, **7**, 78(1972).

(8) P. V. Danckwerts, *Ind. Eng. Chem.*, **43**, 1460(1951).

(9) R. H. Stokes, *J. Amer. Chem. Soc.*, **72**, 2243(1950).

(10) H. S. Harned and R. L. Nuttall, *ibid.*, **71**, 1460(1949).

(11) W. Nernst, *Z. Phys. Chem.*, **47**, 52(1904).

(12) E. Brunner, *ibid.*, **47**, 56(1904).

(13) L. L. Bircumshaw and A. C. Riddiford, *Quart. Rev. Chem.*

Soc., 6, 157(1952).
(14) A. Hussain, *J. Pharm. Sci.*, 61, 811(1972).
(15) A. Fage and H. C. H. Townend, *Proc. Roy. Soc. A*, 135, 656(1932).
(16) W. Nernst and E. S. Merriam, *Z. Phys. Chem.*, 53, 235(1905).
(17) S. Bisaillon and R. Tawashi, *J. Pharm. Sci.*, 60, 1874(1971).
(18) J. H. Collett, J. A. Rees, and N. A. Dickinson, *J. Pharm. Pharmacol.*, 24, 724(1972).
(19) D. N. Travers and A. Powdrill, *J. Pharm. Pharmacol., Suppl.*, 24, 153P(1972).
(20) A. B. Zdanovskii, *Zh. Fiz. Khim.*, 25, 170(1951); through *Chem. Abstr.*, 48, 4291c(1954).

ACKNOWLEDGMENTS AND ADDRESSES

Received September 30, 1974, from the *Department of Pharmacy, University of Nottingham, University Park, Nottingham, NG7 2RD, England.*

Accepted for publication April 7, 1975.

The authors are grateful to Mr. John Trigg and Dr. R. K. Duggins for valuable discussions concerning the design of the apparatus and to the Sheffield Regional Hospital Board for financial support for Miss J. Valerie Fee.

* Present address: Royal Infirmary of Edinburgh, Lauriston Place, Edinburgh, EH3 9YW, Scotland.

ˣ To whom inquiries should be directed.

Fluorocarbon Aerosol Propellants VIII: Solubility of Trichloromonofluoromethane in Dog Blood and Tissue Homogenates

KUN CHANG and WIN L. CHIOU ˣ

Abstract □ The solubility of trichloromonofluoromethane in dog blood and tissue homogenates was measured indirectly using the head-space method at 37°. These values, except that in dog blood, were used to estimate the solubility in the whole tissues or organs. In most cases, the solubility so obtained was independent of equilibrium concentration. However, a considerable concentration dependence for the solubility was observed in dog heart and kidney. The highest solubility found was in dog fat *versus* air, *i.e.*, 45.6, which is almost 220 times higher than the solubility in water or normal saline. Fat solubilization and specific binding interactions appeared to be the two major factors in determining the solubility. The pharmacokinetic implications of such findings are discussed.

Keyphrases □ Fluorocarbon aerosol propellants—solubility of trichloromonofluoromethane in dog blood and tissue homogenates □ Aerosol propellants—solubility of trichloromonofluoromethane in dog blood and tissue homogenates □ Propellants—solubility of trichloromonofluoromethane in dog blood and tissue homogenates □ Trichloromonofluoromethane—solubility in dog blood and tissue homogenates

The wide use of fluorocarbon aerosol propellants in various household, cosmetic, and medicinal pressurized packages recently prompted extensive studies on their possible adverse effects on the cardiovascular system (1–10), enzyme activities (7, 11–13), mutation (14), and ozone concentrations in the stratosphere (15, 16). The high apparent volume of distribution in dogs (17–19) and the moderate to extensive binding with both bovine and human albumins (20–23) of the three most commonly used fluorocarbon propellants prompted the investigation of their solubilities in various tissues and organs. The information obtained from such an investigation is essential to the construction of a physiologically based pharmacokinetic model as reported for barbiturates (24) and methotrexate (25). The results of the solubility study of trichloromonofluoromethane in blood and tissue homogenates of dogs are reported in this article.

For a gaseous or volatile compound, the solubility is commonly defined as the ratio of its concentration in the liquid phase to its concentration in the gaseous phase at the equilibrium state (19, 26, 27). Such a definition is analogous to that of the partition coefficient, P, which has been conventionally used to describe the distribution of a nonvolatile compound between two immiscible liquid phases. These two terms are used interchangeably in this article.

EXPERIMENTAL

Preparation of Samples—Three male mongrel dogs, 17–20 kg, were sacrificed and their tissues were separated, individually wrapped, and kept in a freezer. Prior to the homogenization of the lean tissue, all conspicuous attached fatty tissues were removed and the "clean" tissue was weighed and chopped. Then for each gram of the prepared tissue, 4 ml of chilled sodium chloride injection USP[1] was added and the mixture was homogenized in a blender[2].

The stock bottle[3] of trichloromonofluoromethane[4] (bp 23.82°) was prepared within a month of the experiment to minimize the rate of loss due to storage (28). The bottle had a nominal volume of 500 ml and a fluorocarbon concentration in the 0.64–0.96-mg/ml range.

Procedure—For the study of the partition coefficient of the propellant in each tissue, four pairs of 60-ml serum bottles were prepared. Each pair consisted of an empty control and a sample bottle into which 40 ml of the tissue homogenate was introduced with a 50-ml glass syringe. All bottles were sealed with lacquer-coated stoppers[5] and aluminum caps. They were then immersed in a water bath preset at 37° and shaken mechanically for 15 min.

This step was followed immediately by releasing the extra pressure developed in the bottles by inserting a syringe needle for a moment. Then a calculated amount of air was withdrawn from these bottles, which were expected to show significant pressure

[1] Sodium chloride injection USP, McGaw Laboratories, Division of American Hospital Supply Corp., Glendale, CA 91201
[2] Waring blender, Scientific Products, McGaw Park, IL 60085
[3] Wheaton serum bottle, Wheaton Scientific, Division of Wheaton Industries, Millville, NJ 08332
[4] Freon 11, E. I. du Pont de Nemours and Co., Wilmington, Del.
[5] Lacquer-coated rubber stopper, West Co., Phoenixville, Pa.

Soc., 6, 157(1952).
(14) A. Hussain, *J. Pharm. Sci.*, 61, 811(1972).
(15) A. Fage and H. C. H. Townend, *Proc. Roy. Soc. A*, 135, 656(1932).
(16) W. Nernst and E. S. Merriam, *Z. Phys. Chem.*, 53, 235(1905).
(17) S. Bisaillon and R. Tawashi, *J. Pharm. Sci.*, 60, 1874(1971).
(18) J. H. Collett, J. A. Rees, and N. A. Dickinson, *J. Pharm. Pharmacol.*, 24, 724(1972).
(19) D. N. Travers and A. Powdrill, *J. Pharm. Pharmacol., Suppl.*, 24, 153P(1972).
(20) A. B. Zdanovskii, *Zh. Fiz. Khim.*, 25, 170(1951); through *Chem. Abstr.*, 48, 4291c(1954).

ACKNOWLEDGMENTS AND ADDRESSES

Received September 30, 1974, from the *Department of Pharmacy, University of Nottingham, University Park, Nottingham, NG7 2RD, England.*

Accepted for publication April 7, 1975.

The authors are grateful to Mr. John Trigg and Dr. R. K. Duggins for valuable discussions concerning the design of the apparatus and to the Sheffield Regional Hospital Board for financial support for Miss J. Valerie Fee.

* Present address: Royal Infirmary of Edinburgh, Lauriston Place, Edinburgh, EH3 9YW, Scotland.

ˣ To whom inquiries should be directed.

Fluorocarbon Aerosol Propellants VIII: Solubility of Trichloromonofluoromethane in Dog Blood and Tissue Homogenates

KUN CHANG and WIN L. CHIOU ˣ

Abstract □ The solubility of trichloromonofluoromethane in dog blood and tissue homogenates was measured indirectly using the head-space method at 37°. These values, except that in dog blood, were used to estimate the solubility in the whole tissues or organs. In most cases, the solubility so obtained was independent of equilibrium concentration. However, a considerable concentration dependence for the solubility was observed in dog heart and kidney. The highest solubility found was in dog fat *versus* air, *i.e.*, 45.6, which is almost 220 times higher than the solubility in water or normal saline. Fat solubilization and specific binding interactions appeared to be the two major factors in determining the solubility. The pharmacokinetic implications of such findings are discussed.

Keyphrases □ Fluorocarbon aerosol propellants—solubility of trichloromonofluoromethane in dog blood and tissue homogenates □ Aerosol propellants—solubility of trichloromonofluoromethane in dog blood and tissue homogenates □ Propellants—solubility of trichloromonofluoromethane in dog blood and tissue homogenates □ Trichloromonofluoromethane—solubility in dog blood and tissue homogenates

The wide use of fluorocarbon aerosol propellants in various household, cosmetic, and medicinal pressurized packages recently prompted extensive studies on their possible adverse effects on the cardiovascular system (1–10), enzyme activities (7, 11–13), mutation (14), and ozone concentrations in the stratosphere (15, 16). The high apparent volume of distribution in dogs (17–19) and the moderate to extensive binding with both bovine and human albumins (20–23) of the three most commonly used fluorocarbon propellants prompted the investigation of their solubilities in various tissues and organs. The information obtained from such an investigation is essential to the construction of a physiologically based pharmacokinetic model as reported for barbiturates (24) and methotrexate (25). The results of the solubility study of trichloromonofluoromethane in blood and tissue homogenates of dogs are reported in this article.

For a gaseous or volatile compound, the solubility is commonly defined as the ratio of its concentration in the liquid phase to its concentration in the gaseous phase at the equilibrium state (19, 26, 27). Such a definition is analogous to that of the partition coefficient, P, which has been conventionally used to describe the distribution of a nonvolatile compound between two immiscible liquid phases. These two terms are used interchangeably in this article.

EXPERIMENTAL

Preparation of Samples—Three male mongrel dogs, 17–20 kg, were sacrificed and their tissues were separated, individually wrapped, and kept in a freezer. Prior to the homogenization of the lean tissue, all conspicuous attached fatty tissues were removed and the "clean" tissue was weighed and chopped. Then for each gram of the prepared tissue, 4 ml of chilled sodium chloride injection USP[1] was added and the mixture was homogenized in a blender[2].

The stock bottle[3] of trichloromonofluoromethane[4] (bp 23.82°) was prepared within a month of the experiment to minimize the rate of loss due to storage (28). The bottle had a nominal volume of 500 ml and a fluorocarbon concentration in the 0.64–0.96-mg/ml range.

Procedure—For the study of the partition coefficient of the propellant in each tissue, four pairs of 60-ml serum bottles were prepared. Each pair consisted of an empty control and a sample bottle into which 40 ml of the tissue homogenate was introduced with a 50-ml glass syringe. All bottles were sealed with lacquer-coated stoppers[5] and aluminum caps. They were then immersed in a water bath preset at 37° and shaken mechanically for 15 min.

This step was followed immediately by releasing the extra pressure developed in the bottles by inserting a syringe needle for a moment. Then a calculated amount of air was withdrawn from these bottles, which were expected to show significant pressure

[1] Sodium chloride injection USP, McGaw Laboratories, Division of American Hospital Supply Corp., Glendale, CA 91201
[2] Waring blender, Scientific Products, McGaw Park, IL 60085
[3] Wheaton serum bottle, Wheaton Scientific, Division of Wheaton Industries, Millville, NJ 08332
[4] Freon 11, E. I. du Pont de Nemours and Co., Wilmington, Del.
[5] Lacquer-coated rubber stopper, West Co., Phoenixville, Pa.

change due to the later introduction of the stock propellant. Both 50-μl and 2.5-ml gastight syringes[6] were used in delivering the propellant into the bottles so that a wide range of concentrations could be effected with ease. Each pair of bottles (sample and control) received essentially the same amount of the stock propellant.

Equilibration of the propellant with the tissue homogenates was approached by shaking the bottles for 90 min. The propellant concentration in the head space was then measured by GC under the previously reported conditions (23, 29). Since the concentrations to be measured were mostly above the GC linear response, dilution of the propellant in the gas phase was routinely done using the following precautions. Preliminary GC analysis was made to predict the concentration to be measured within a few hundred percent. In the final analysis, the amount withdrawn from the head space was injected into a presealed clean serum bottle (either 5- or 60-ml size as required). A second clean syringe must be used to flush the propellant in this dilution bottle and to take a sample for GC analysis. This syringe must be reserved only for such use. If, by accident, this syringe was used with the same propellant at 10-fold or higher concentration, then the rate of desorbing the propellant from this syringe would be so slow that it would forbid its further use for GC injection with accuracy for a long period. This phenomenon of adsorption and desorption in the syringe was also observed for dichlorodifluoromethane and dichlorotetrafluoroethane.

The specific gravity for a given tissue was determined by its weight and the volume of deionized water it displaced from a stoppered serum bottle.

Calculations—The partition coefficient of a tissue homogenate *versus* the air ($P_{t.h.}$) is determined indirectly using the head-space method (29, 30). For convenience in the present study, the equation can be rewritten in the following form:

$$P_{t.h.} = \frac{C_0}{C_h}(V_r + 1) - V_r \qquad \text{(Eq. 1)}$$

where C_0 = concentration of the fluorocarbon in the control bottle, C_h = concentration of the fluorocarbon in the head space of the sample bottle, and V_r = ratio of the volume of the gas phase to that of the homogenate phase.

To estimate the partition coefficient of the propellant in tissue *versus* air, the interaction due to the dispersion and dissolution of the whole tissue is neglected. Accordingly, the conservation of the propellant in the bottle leads to the following equation:

$$W = C_h V_h + C_t V_t + C_s V_s \qquad \text{(Eq. 2)}$$

where W = total weight of the fluorocarbon in the bottle; and V_h, V_t, and V_s = volume of the head space, the tissue, and the normal saline, respectively.

By dividing Eq. 2 by C_h and substituting the term C_t/C_h by P and C_s/C_h by P_s, the following equation can be derived:

$$P = \frac{W - C_h(P_s V_s + V_h)}{C_h V_t} \qquad \text{(Eq. 3)}$$

where P and P_s are the partition coefficients in tissue and in normal saline, respectively. This equation is essentially the same as that given by Larson *et al.* (27), except that in their paper the corresponding term W was misinterpreted as the volume. Equation 3 can be reduced to:

$$P = \frac{P_{t.h.} - P_s f_s}{f_t} \qquad \text{(Eq. 4}a\text{)}$$

where:

$$f_s = \frac{V_s}{V_s + V_t} \qquad \text{(Eq. 4}b\text{)}$$

$$f_t = 1 - f_s \qquad \text{(Eq. 4}c\text{)}$$

The equilibrium concentration in the tissue was calculated, after P was determined, according to the definition of P, namely:

$$C_t = PC_h \qquad \text{(Eq. 5)}$$

In the calculation of the partition coefficient of the propellant in tissue *versus* air, Eq. 1 was used at first to calculate the partition coefficient of the propellant in the tissue homogenate ($P_{t.h.}$). Then P was calculated according to Eq. 4*a*, where P_s was derived in the same way as $P_{t.h.}$. The value of P_s was 0.208. The specific gravities listed in Table I were used to evaluate f_s and f_t in Eq. 4*a*. The partition coefficient of the propellant in tissue *versus* blood was calculated simply by dividing the solubility in tissue by the solubility in blood.

[6] Hamilton Co., Reno, Nev.

Table I—Partition Coefficients of Trichloromonofluoromethane in Dog Blood and Tissues and the Specific Gravities of the Tissues

Tissue	Equilibrium Concentration[a], C_t, μg/ml	Partition Coefficient, P, C_t/C_g	Partition Coefficient, Tissue / Blood	Specific Gravity
Liver	0.014–6.6	1.64	1.09	1.076
Heart	1–2[b]	1.02	0.68	1.051
Kidney	1–2[b]	1.20	0.80	1.033
Brain	1.72–82.6	1.75	1.17	1.040
Lung	0.77–34.2	0.54	0.36	0.823
Spleen	1.8–33.0	1.61	1.07	1.065
Muscle	1.3–47.9	0.81	0.54	1.028
Fat	6.0–212	45.6	30.4	0.947
Blood	1.2–6.6	1.50	—	—

[a] Including both bound and free form of the propellant. [b] Estimated from Figs. 1 and 2.

RESULTS AND DISCUSSION

The partition coefficients for trichloromonofluoromethane in dog blood and most tissue homogenates at 37° were approximately constant over a wide range of equilibrium concentrations (Table I). Each value is an average of three or four test results. For the dog heart and kidney, the partition coefficients were considerably concentration dependent over the similar range of concentrations, and the average results of three replicate studies from three dogs were plotted in Figs. 1 and 2, respectively.

Recently, the binding interactions of the propellant trichloromonofluoromethane with human and bovine albumin were studied along with two other propellants (20–23). The partition coefficients of the propellants in the aqueous 5% human and bovine albumin solutions were highly dependent on the propellant concentration, indicating that specific binding sites are available on these protein molecules. Similarly, such specific interactions appeared to exist in the tissue of dog heart and kidney, in which the partition coefficients of trichloromonofluoromethane are higher at lower equilibrium concentrations. The results obtained from the present study may not truly reflect the *in vivo* interactions between the propellant and tissues or organs due to the homogenization of the samples.

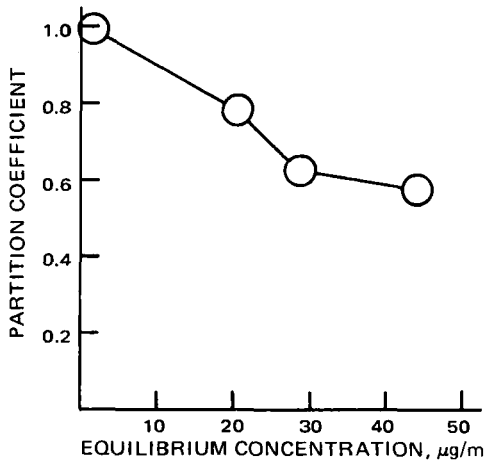

Figure 1—*Partition coefficient of trichloromonofluoromethane in dog heart* versus *air as a function of the equilibrium concentration in the heart tissue.*

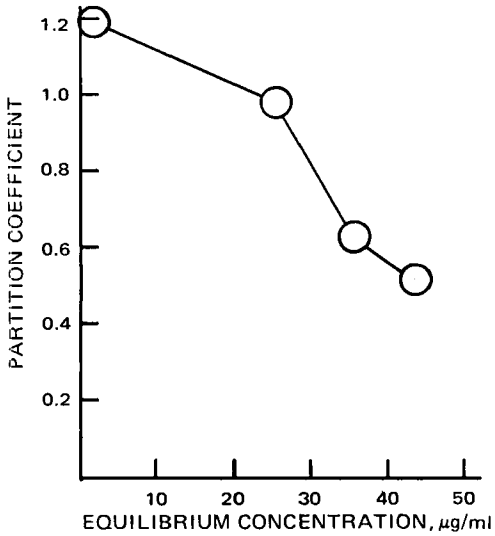

Figure 2—*Partition coefficient of trichloromonofluoromethane in dog kidney* versus *air as a function of the equilibrium concentration in the kidney tissue.*

In a study of arterial blood levels of fluorocarbons in asthmatic patients following use of pressurized aerosols (6), the dog heart muscle–human blood partition coefficient for trichloromonofluoromethane at 37° was determined to be 1.9. This value was derived at an equilibrium concentration in the heart probably slightly above 10 μg/ml. Accordingly, the solubility of this fluorocarbon in the dog heart is estimated to be 1.71 (*i.e.*, 1.9 × 0.9). No equilibrium concentration dependence was reported for such solubility. In the present study the solubility of trichloromonofluoromethane in dog heart was found to be concentration dependent (Fig. 1), and its value is 0.9 at the equilibrium concentration of 10 μg/ml. The discrepancy in the value of solubility may be attributed to the difference in dog species. Large variability of propellant solubility in blood and plasma among different animals was reported (18). In light of such differences, the simulation of the myocardial level of fluorocarbon in humans based on dog heart cannot be appropriate.

The partition coefficient of trichloromonofluoromethane in dog fat was calculated to be 45.6, the highest value obtained among all specimens studied. It is almost 220 times higher than that in normal saline or water, about 84 times higher than that in dog lung, and about 56 times greater than that in dog muscle. The relatively large solubility of the propellant in dog fat may be expected from its physical–chemical properties such as being nonionic, lipophilic, and highly soluble in cyclohexane (20, 23).

The partition coefficients of dog blood and tissues were greater than those in water or normal saline. This finding may be explained by the following two reasons:

1. The presence of a small amount of fat in the specimen can enhance the solubilization of the propellant. The fat contents of dog liver, lung, spleen, muscle, and heart were reported by Brodie *et al.* (31) and ranged from 1.6 to 3.0%. Thus, by solubilization in fat alone, the partition coefficients of the propellant in these tissues are expected to be at least from 0.73 to 1.37; these values are not too far from the values determined in this study in view of the possible biological variance.

2. The specific interaction (*e.g.*, protein binding and complexation) and other nonspecific interaction such as solubilization by surfactant also can increase the solubility of this propellant.

As mentioned, the specific interaction such as protein binding could explain the phenomenon of a concentration-dependent partition coefficient as observed in dog heart and kidney tissue. Such an effect of the specific interaction may also be observed from a complexation or hydrophobic interaction with other tissue components. When the binding sites are saturated or the binding capacity of a tissue is very small, the phenomenon of the concentration dependence of partition coefficient may not be easily observed.

The previous pharmacokinetic study (19) on the three dogs used in the present tissue solubility study showed that, on the average, the apparent volume of distribution of trichloromonofluoromethane in terms of blood concentration, estimated after the attainment of a pseudo-distribution equilibrium, was about six times their body weight. Since the partition coefficients of this propellant in all tissues studied except fat are fairly close to, or less than, that in blood, one can reasonably assume that the observed higher apparent volume of distribution is primarily due to its concentration or accumulation in fat tissues. The uptake by the fat tissues probably accounts for the existence of the second (deep) tissue compartment in the disposition of the propellant in dogs (19). Subjects with higher fat content also can conceivably accumulate more of this type of compound and have a longer biological half-life. The toxicological implications of this study remain to be explored.

REFERENCES

(1) *Consumer Rep.*, **May 1974**, 374.

(2) A Silverglade, *J. Amer. Med. Ass.*, **222**, 827(1972).

(3) W. S. Harris, *ibid.*, **223**, 1508(1973).

(4) T. Balazes, F. L. Earl, G. W. Bierbower, and M. A. Weinberger, *Toxicol. Appl. Pharmacol.*, **26**, 407(1973).

(5) D. M. Aviado and M. A. Belej, *Toxicology*, **2**, 31(1974).

(6) C. T. Dollery, W. M. Faith, G. H. Draffan, G. Wise, H. Sahgoun, J. W. Paterson, and S. R. Walker, *Clin. Pharmacol. Ther.*, **15**, 59(1974).

(7) G. Maier, H. MacFarland, G. S. Wiberg, H. Buchwald, and P. Dussault, *Can. Med. Ass. J.*, **111**, 39(1974).

(8) E. B. Thompson and W. S. Harris, *Toxicol. Appl. Pharmacol.*, **29**, 242(1974).

(9) W. L. Chiou, *J. Amer. Med. Ass.*, **227**, 658(1974).

(10) *Ibid.*, **229**, 1722(1974).

(11) D. B. Lund, *Arch. Biochem. Biophys.*, **129**, 181(1969).

(12) P. J. Cox, L. J. King, and D. V. Parke, *Biochem. J.*, **130**, 87p(1972).

(13) H. C. Warmkier, O. Fennema, and E. H. Marth, *J. Food Sci.*, **37**, 702(1972).

(14) V. C. Foltz and R. Fuerst, *Environ. Res.*, **7**, 275(1974).

(15) R. J. Cicerone, R. S. Stolarski, and S. Walters, *Science*, **185**, 1165(1974).

(16) *Chem. Eng. News*, **Sept. 23, 1974**, 6.

(17) W. L. Chiou, *Res. Commun. Chem. Pathol. Pharmacol.*, **7**, 679(1974).

(18) S. Niazi, Ph.D. thesis, University of Illinois at the Medical Center, Chicago, Ill., 1974.

(19) S. Niazi and W. L. Chiou, *J. Pharm. Sci.*, **64**, 763(1975).

(20) W. L. Chiou and J. H. Hsiao, *Res. Commun. Chem. Pathol. Pharmacol.*, **8**, 273(1974).

(21) J. H. Hsiao and W. L. Chiou, *Pharmacology*, **12**, 303(1974).

(22) W. L. Chiou and J. H. Hsiao, *J. Pharm. Sci.*, **64**, 1052(1975).

(23) W. L. Chiou and J. H. Hsiao, *Pharmacology*, **13**, 128(1975).

(24) K. B. Bischoff and R. L. Dedrick, *J. Pharm. Sci.*, **57**, 1346(1968).

(25) R. L. Dedrick, D. S. Zaharko, and R. J. Lutz, *ibid.*, **62**, 882(1973).

(26) N. C. Flowers and L. G. Horan, *J. Amer. Med. Ass.*, **219**, 33(1972).

(27) C. P. Larson, Jr., E. I. Eger, II, and J. W. Severinghaus, *Anesthesiology*, **23**, 349(1962).

(28) W. L. Chiou and J. H. Hsiao, *J. Pharm. Sci.*, **63**, 1614(1974).

(29) W. L. Chiou and S. Niazi, *Res. Commun. Chem. Pathol. Pharmacol.*, **6**, 481(1973).

(30) S. Niazi and W. L. Chiou, *J. Pharm. Sci.*, **63**, 532(1974).

(31) B. B. Brodie, E. Bernstein, and L. C. Mark, *J. Pharmacol. Exp. Ther.*, **105**, 421(1952).

ACKNOWLEDGMENTS AND ADDRESSES

Received January 20, 1975, from the *Department of Pharmacy, College of Pharmacy, University of Illinois at the Medical Center, Chicago, IL 60612*

Accepted for publication March 10, 1975.

Supported in part by Food and Drug Administration Grant 1 R01 FD-00574-02.

[x] To whom inquiries should be directed.

Fluorocarbon Aerosol Propellants IX: Adsorption on Activated Charcoal

KUN CHANG and WIN L. CHIOU ˣ

Abstract □ The adsorption of three commonly used fluorocarbons, trichloromonofluoromethane, dichlorodifluoromethane, and dichlorotetrafluoroethane, on activated charcoal was studied at 25°. The adsorption *versus* pressure plots are consistent with the Brunauer, Emmett, and Teller (BET) type II and type IV isotherms, which can be explained as the condensation of the gaseous molecules in a wide range of pores in the activated charcoal. The monolayer capacity derived from the BET equation is discussed and used to estimate the volume of micropores present in the activated charcoal. Below the relative pressure of 0.01, the adsorption deviated from the BET plot. The deviation revealed that the adsorption capacity and adsorption potential at these lower pressures are greater than the extrapolated values. It is concluded that activated charcoal can be used effectively to remove propellants from the air in pollution control.

Keyphrases □ Fluorocarbon aerosol propellants—adsorption on activated charcoal, Langmuir isotherm and Brunauer, Emmett, and Teller equation compared □ Trichloromonofluoromethane—adsorption on activated charcoal, isotherms compared □ Dichlorodifluoromethane—adsorption on activated charcoal, isotherms compared □ Dichlorotetrafluoroethane—adsorption on activated charcoal, isotherms compared □ Aerosol propellants, fluorocarbon—adsorption on activated charcoal, Langmuir isotherm and Brunauer, Emmett, and Teller equation compared

Activated charcoal, also called carbon black or activated carbon, may be derived from sucrose, lactose, starch, and various industrial wastes. It has been used in medicine as an adsorbent to reduce flatulence and as an antidote in many forms of poisoning. Possible acute and chronic toxicities, especially toward the heart, due to the inhalation of a large quantity of aerosol propellants have been widely investigated recently (1–12). In this paper, the adsorption of the three most commonly used propellants, trichloromonofluoromethane, dichlorodifluoromethane, and dichlorotetrafluoroethane, on activated charcoal is investigated.

The mechanism of adsorption was explored by plotting the adsorption data according to some commonly adopted models of the adsorption isotherm. The molecular cross-sectional areas of the three fluorocarbons were estimated with the formula of Emmett and Brunauer (13). From these data, the specific area of the activated charcoal was calculated. The significance of these findings, along with the potential of using the activated charcoal as a filtering medium to remove the fluorocarbon, is discussed.

EXPERIMENTAL

Materials—Activated charcoal[1], *n*-hexane[2], dichlorodifluoromethane[3] (bp −29.79°), dichlorotetrafluoroethane[3] (bp 3.77°), and trichloromonofluoromethane[3] (bp 23.82°) were used.

Adsorption Studies—For the study of each fluorocarbon, 11 60-ml serum bottles were dried at 120° for 1 hr and then cooled to room temperature in a desiccator. The activated charcoal was heated at 120° for 15 hr and then cooled in the same way. About 3% of the weight was lost after heating and may be accounted for by the loss of moisture content.

One teaspoonful (approximately 2 g) of such dried activated charcoal was transferred to each tared 60-ml bottle through a powder funnel and sealed immediately with a silicone-coated rubber stopper. The weight of the activated charcoal inside the bottle was determined by weighing to the nearest 0.1 mg. These bottles were then immersed in a water bath[4] maintained at 25 ± 0.5° to their bottle necks.

Dichlorodifluoromethane and dichlorotetrafluoroethane were transferred to the bottles by purging a preregulated aerosol propellant flow over the charcoal powder with no observable disturbance of the powder. The time period used for such purging process varied from 2 to 45 min. In the case of trichloromonofluoromethane, a precooled syringe was used to transfer the various amounts into each bottle. This transfer was followed by capping (aluminum caps) and releasing the excess pressure in the bottles properly over a short period.

After the transfer of each fluorocarbon, the bottles were weighed again to obtain the net weights of the fluorocarbon, which were in the range of approximately 0.1–1 g. When the process of releasing the excess pressure was carried out properly, a subsequent puncture, made a few hours later, in the cap with a syringe needle (27G) for several seconds resulted in no significant change in weight. If the punctures were made for longer than several seconds, they resulted in increased weights due to the adsorption of moisture from the air.

These bottles of the fluorocarbon and charcoal were then left to establish equilibrium in the constant-temperature water bath overnight (16–20 hr). Finally, the equilibrium concentration in the headspace of each bottle was analyzed by GC. The GC analysis was similar to those reported previously (12, 14, 15). However, the peak height-enhancing effect due to the presence of solvent was corrected for the detection of fluorocarbon in *n*-hexane. Preliminary experiments found that equilibration of the adsorption process could be accomplished within 7 hr and that the loss of propellants in highly concentrated bottles was negligible within a day.

THEORETICAL

Adsorption Isotherms—Both the Langmuir adsorption isotherm (16) and the Brunauer, Emmett, and Teller (BET) equation (17) have commonly been used to describe the phenomenon of adsorption. The former model is also called the monolayer adsorption isotherm. Its rearranged equation (18) can be written as shown here:

$$\frac{PX_s}{X} = \frac{P}{C_m} + \frac{1}{BC_m} \qquad \text{(Eq. 1)}$$

where P is the equilibrium pressure of the gaseous adsorbate, X_s is the weight of the solid adsorbent, X is the weight of a gas or vapor adsorbed, C_m is a constant called the monolayer capacity or the maximum adsorption capacity, and B is a constant.

In this study, the experimental procedure used differed from the conventional method (19) in measuring the value of P. Here the equilibrium pressure was substituted by the equilibrium partial pressure, which was calculated from the equilibrium concentration as discussed later. For each P value, the weight of a fluorocarbon adsorbed was calculated according to:

[1] Activated charcoal (Norit A) powder, CX655, I289, Matheson, Coleman and Bell, Norwood, Ohio.
[2] *n*-Hexane, 99 mole % pure, Fisher Scientific Co., Fair Lawn, N.J.
[3] E. I. du Pont de Nemours and Co., Wilmington, Del.
[4] Versa-bath, Fisher.

Table I—Some Physical Properties and Constants of Fluorocarbons

	Trichloromonofluoromethane	Dichlorodifluoromethane	Dichlorotetrafluoroethane
Molecular weight[a]	137.37	120.92	170.93
Boiling point[a], °K	296.9	243.3	269.3
Density in liquid state[a] at 25° (Q_l), g/ml	1.476	1.311	1.456
Density of saturated vapor pressure[a] at boiling point (Q_b), mg/ml	5.86	6.33	7.83
Saturated vapor pressure[a] at 25° (P_0), atm	1.003	6.38	2.13
Compressibility[b] at 1 atm and boiling point (Z_0)	0.962	0.957	0.988
Density[c] at 25° and 1 atm (Q_l), mg/ml	5.84	5.17	7.28
Molecular cross-sectional area[d] (A_m), Å^2	31.4	31.2	36.7

[a] See Ref. 20. [b] Calculated from Q_b according to Eq. 5. [c] Calculated with Eq. 5. [d] Calculated with Eq. 6.

$$X = W - Q\left(V - \frac{W_c}{d}\right)\left(1 - \frac{Q_a}{Q_f}\right) \qquad \text{(Eq. 2)}$$

where W is the weight gained by the serum bottle after the fluorocarbon is introduced and equilibrated with the activated charcoal; Q is the headspace equilibrium concentration (weight per unit volume) of the fluorocarbon over the activated charcoal; V is the volume of the serum bottle; W_c is the weight of the activated charcoal; d is the density of the activated charcoal; Q_a is the air density in the laboratory, which was approximately 1.19 mg/ml at 25° and 1 atm (20); and Q_f is the density of the fluorocarbon at 25° and 1 atm (Table I).

The factor Q_a/Q_f introduced in Eq. 2 was used to correct the weight of fluorocarbon in the headspace by subtracting the weight of air displaced from the bottle. The density of the activated charcoal was estimated by weighing the activated charcoal before and after it was immersed in a full bottle of deionized water. The density obtained was about 1.7 g/ml. With this information, the left-hand side term of Eq. 1 can be plotted with respect to P. A straight line can be expected to form for this type of adsorption isotherm, and the monolayer capacity can be calculated from the inverse of its slope.

The BET model is an extension of the Langmuir monolayer adsorption concept to a multilayer one. Theoretically, if an infinite number of adsorbed layers are allowed to form, the BET equation (18) can be written as:

$$\frac{X_s P}{X(P_0 - P)} = \frac{(C-1)P}{C_m C P_0} + \frac{1}{C_m C} \qquad \text{(Eq. 3)}$$

where X_s, X, and P are defined in the same way as in Eq. 1; P_0 is the saturated vapor pressure of the fluorocarbon at 25° (21) (Table I); C is a BET constant; and C_m is the BET monolayer capacity which is not the maximum adsorption capacity.

The plotting of the left-hand side term *versus* the relative pressure (P/P_0) should yield a straight line according to Eq. 3, where the values of the slope and the intersection can be used to calculate the BET constants C and C_m.

It is understood that both Eqs. 1 and 3 are special cases of a generalized equation called the modified BET equation (18). If the number of layers allowed to be adsorbed on the solid adsorbent is limited, then the generalized equation is expected to fit better the adsorption isotherm. However, due to the mathematical complexity involved in the generalized equation, this procedure is generally replaced by attempting to fit Eq. 3 because the generalized equation can be approximated by Eq. 3 at low relative pressures, so at least a portion of the curve is expected to be straight.

Estimation of Equilibrium Partial Pressure—The deviation of the fluorocarbon gas from the ideal gas behavior can be measured by a compressibility factor, Z, defined in the following equation (22):

$$PV = ZnRT \qquad \text{(Eq. 4)}$$

When Z is equal to 1, Eq. 4 is simply reduced to the ideal gas equation for n moles of gas. The Z values calculated for the fluorocarbons according to Eq. 4 based on the literature data (21) of vapor density at the boiling point and 1 atm, called Z_0, are given in Table I. These Z_0 values are at most about 4% smaller than 1. Under moderate pressures, the compressibility factor is known to be proportional to the gas temperature and inversely proportional to its pressure (22).

In this adsorption study, the equilibrium partial pressures were much less than 1 atm and the temperature was higher than any of the boiling points of the three fluorocarbons. Therefore, the Z values for the fluorocarbons under the present experimental conditions are expected to be larger than Z_0 but smaller than 1. In reality, air was also present in the serum bottles to make the total pressure near 1 atm. Thus, a good approximation for the estimation of the equilibrium partial pressure of the fluorocarbon in the headspace would be:

$$P = \frac{Z_0 Q R T}{M} \qquad \text{(Eq. 5)}$$

where M is the molecular weight of the fluorocarbon.

Molecular Cross-Sectional Area of Adsorbate (A_m) and Specific Surface of Adsorbent (S)—Emmett and Brunauer (23) proposed the following equation to estimate A_m for an ordinary adsorbate in the liquid form:

$$A_m\ (\text{cm}^2) = 1.091\left(\frac{M}{Q_l N}\right)^{2/3} \qquad \text{(Eq. 6)}$$

where M is the same as in Eq. 5, Q_l is the density of the fluorocarbon in liquid form at 25°, and N is Avogadro's number (6.02×10^{23}). Thus, the specific surface area of activated charcoal, defined as the total surface area per gram of adsorbent, can be estimated by:

$$S = \frac{A_m C_m N}{M} \qquad \text{(Eq. 7)}$$

RESULTS AND DISCUSSION

Some physical constants (21) and properties of the three fluorocarbons required for the analysis are listed in Table I. The adsorption (X/X_s) *versus* the relative pressure (P/P_0) was plotted for the three fluorocarbons (Fig. 1). The adsorption values, which may be called the adsorption capacities, for each fluorocarbon at $P = 0.5$ atm are indicated on each curve in Fig. 1. These values are 0.310, 0.351, and 0.450 for dichlorodifluoromethane, dichlorotetrafluoroethane, and trichloromonofluoromethane, respectively. The rank order of these adsorption capacities is in the same order as their

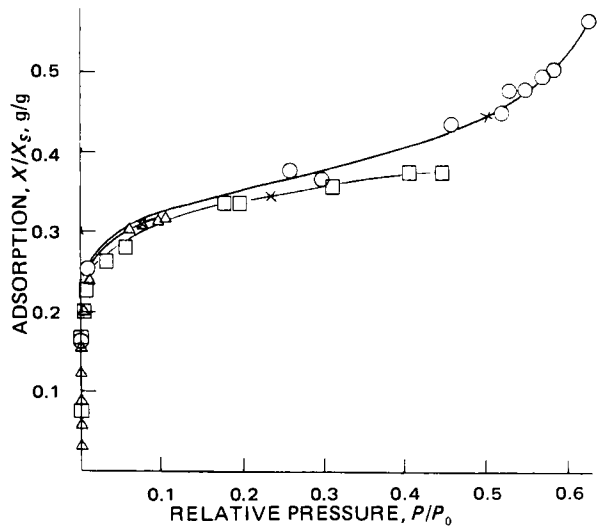

Figure 1—*Adsorption isotherms of three fluorocarbon aerosol propellants at 25°. Key: ○, trichloromonofluoromethane; △, dichlorodifluoromethane; and □, dichlorotetrafluoroethane; X, P = 0.5 atm.*

Table II—Adsorption and Related Values at Low Relative Pressures

Fluorocarbon	Q, mg/ml	P, atm	X/X_S, g/g	P/P_0	PX_S/X, atm
Trichloromonofluoromethane	3.17×10^{-3}	5.44×10^{-4}	0.1634	5.44×10^{-4}	3.33×10^{-3}
	5.36×10^{-2}	9.19×10^{-3}	0.2543	9.18×10^{-3}	3.62×10^{-2}
Dichlorotetrafluoroethane	6.77×10^{-4}	9.57×10^{-5}	0.0721	4.50×10^{-5}	1.33×10^{-3}
	1.20×10^{-2}	1.69×10^{-3}	0.1658	7.96×10^{-4}	1.02×10^{-2}
	6.14×10^{-2}	8.71×10^{-3}	0.1999	4.09×10^{-3}	4.34×10^{-2}
	0.107	1.51×10^{-2}	0.2290	7.09×10^{-3}	6.60×10^{-2}
Dichlorodifluoromethane	8.13×10^{-4}	1.57×10^{-4}	0.0302	2.46×10^{-5}	5.21×10^{-3}
	2.47×10^{-3}	4.78×10^{-4}	0.0554	7.49×10^{-5}	8.64×10^{-3}
	8.24×10^{-3}	1.59×10^{-3}	0.0884	2.49×10^{-4}	1.80×10^{-2}
	2.33×10^{-2}	4.51×10^{-3}	0.1219	7.07×10^{-4}	3.70×10^{-2}
	3.94×10^{-2}	7.63×10^{-3}	0.1546	1.20×10^{-3}	4.91×10^{-2}
	0.210	4.06×10^{-2}	0.201	6.36×10^{-3}	0.202

partition coefficients between *n*-hexane and air, which were determined in this laboratory to be 27, 60, and 213, respectively. Such correlation is in agreement with the predominantly lipophilic character of the adsorption surface existing in activated charcoal. For relative pressures below 0.01, the adsorption values along with some other functions are listed in Table II.

In attempting to investigate the mechanism of adsorption, the Langmuir adsorption isotherm was tested. This involved the plotting of PX_s/X *versus* P for the three fluorocarbons (Figs. 2–4). Between the relative pressures of about 0.01–0.3, the mechanism of adsorption apparently can be assumed to be of the monolayer type. For dichlorodifluoromethane, the highest relative pressure used in this experiment was only 0.105. Therefore, the extension of such a linear region to about 0.3 is only speculated. The limitation of the present experimental method confined this adsorption study to lower relative pressures for dichlorodifluoromethane due to its high saturated vapor pressure.

However, from the deviation observed in the Langmuir linear plots for dichlorotetrafluoroethane and trichloromonofluoromethane, one cannot explain the adsorption mechanism for these two propellants simply by the monolayer adsorption kinetics. To appreciate the nature of such deviation, it should be recalled that the slope of the Langmuir plot is equal to the reciprocal of the monolayer capacity. If the Langmuir plot is a curve, then the value of C_m is not a constant. In Figs. 3 and 4, the curves at the higher sides of their equilibrium partial pressures would yield higher C_m values. This phenomenon can be imagined as if more adsorption sites are created as more adsorption sites are occupied. Thus, the monolayer capacities evaluated from Figs. 2–4 do not represent their maximum adsorption capacities.

The failure to obtain a meaningful monolayer adsorption capacity from the Langmuir plot prompted the analysis of adsorption through the BET equation. The plots based on the BET equation are shown in Fig. 5; all three plots have a common linear range extending from the relative pressure of around 0.01 to about 0.25. Such a small linear section has been quite common in plotting the BET equation (18). Therefore, the mechanism of adsorption for these fluorocarbons on activated charcoal can be more satisfactorily described by the generalized BET model in which the possible number of adsorbed layers is greater than 1.

Based on this discussion and the characteristics of the adsorption isotherm shown in Fig. 1, these adsorption isotherms can be designated as the type II or type IV isotherm according to the BET classification (18). Under the same classification, the Langmuir adsorption isotherm belongs to the type I isotherm. Although the type I isotherm also follows the Langmuir equation, it is not restricted to the monolayer adsorption mechanism. The condensation of gas in the micropores of an adsorbent can also result in the type I isotherm (18).

The type IV isotherms are generally associated with the porous solid possessing a transitional range of pores (between micropores and macropores), *i.e.*, having diameters ranging from tens to hundreds of Angstrom units. The presence of micropores along with the transitional pores still leads to the type IV isotherm (18). Similarly, the general shape of the type II isotherm can also be found if the adsorbent is partially macroporous and partially microporous. In both cases, the effect of micropores can be felt at a lower range of relative pressures. That is, this branch of adsorption isotherm can be approximated by the type I isotherm if the amount of micropores present is quite large compared with the transitional pores or macropores. Apparently, such is the case with the present study. Therefore, the activated charcoal used in this analysis can be described as a porous solid possessing a wide range of pores including the smallest micropores, the transitional pores, and, possibly, the macropores.

The adsorption below the relative pressure of 0.01 is generally inexplicable by the Langmuir or BET method (18). To describe the adsorption phenomenon in this pressure region for the present study, it is convenient to call temporarily the expression $X/(QX_s)$ as the adsorption potential or simply as A. The physical meaning of A is the volume of adsorbate (X/Q) in concentration Q that can be condensed on a unit weight of adsorbent at the equilibrium concentration Q. At low relative pressures ($P/P_0 < 0.01$), the left-hand sides of both Eqs. 1 and 3 are inversely proportional to A as a good approximation. Therefore, both Eqs. 1 and 3 can be approximated

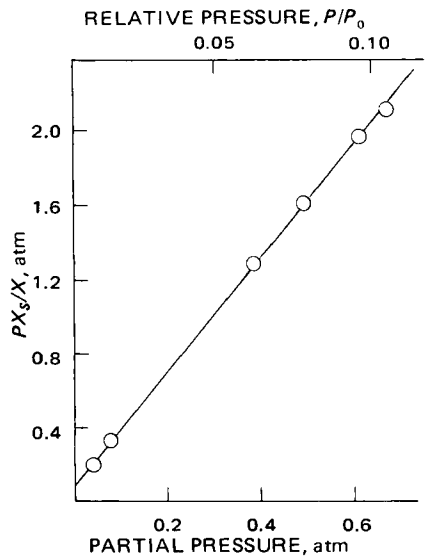

Figure 2—*Langmuir adsorption plot for dichlorodifluoromethane at 25°.*

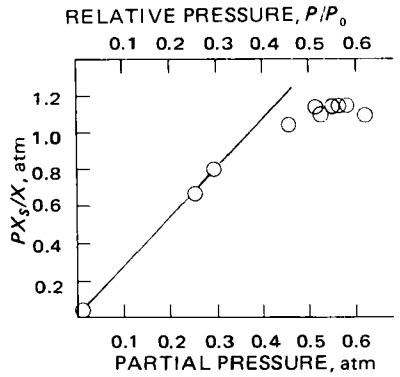

Figure 3—*Langmuir adsorption plot for trichloromonofluoromethane at 25°.*

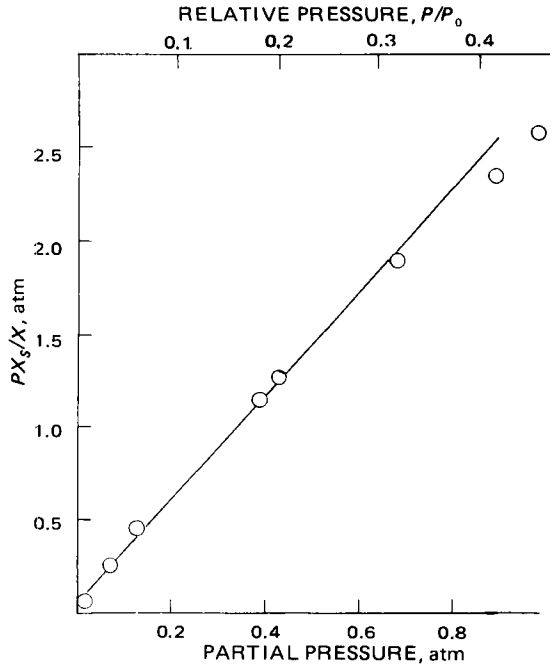

Figure 4—*Langmuir adsorption plot for dichlorotetrafluoroethane at 25°.*

by:

$$\frac{k}{A} = mP + d \qquad \text{for } P/P_0 < 0.01 \qquad \text{(Eq. 8)}$$

where k, m, and d are constants, and k/A is equal to PX_s/X.

The plotting of k/A *versus* P is essentially the Langmuir plot at low relative pressures. The data points required for the plot are shown in Table II. If such plots are made, it can be observed that the reciprocal of the adsorption potential does not increase linearly with the equilibrium pressure. On the contrary, it rises very sharply near the origin ($P \to 0$) and the slope of the curve decreases as P increases. In other words, both the adsorption potential and the adsorption capacity are greater near the origin than the prediction from either Eq. 1 or 3. A typical plot is shown in Fig. 6.

The monolayer capacities for the activated charcoal calculated from Fig. 5 vary only slightly with the fluorocarbons. The adsorbed weight of trichloromonofluoromethane or dichlorodifluoromethane by each gram of activated charcoal is about 0.292 g, and that of dichlorotetrafluoroethane is 0.278 g. The maximum adsorption capacity cannot be estimated for the type II or type IV isotherm without having the adsorption data near the relative pressure of 1. Therefore, the most that can be said here is that the maximum adsorption capacity must be considerably larger than the largest adsorption values in Fig. 1.

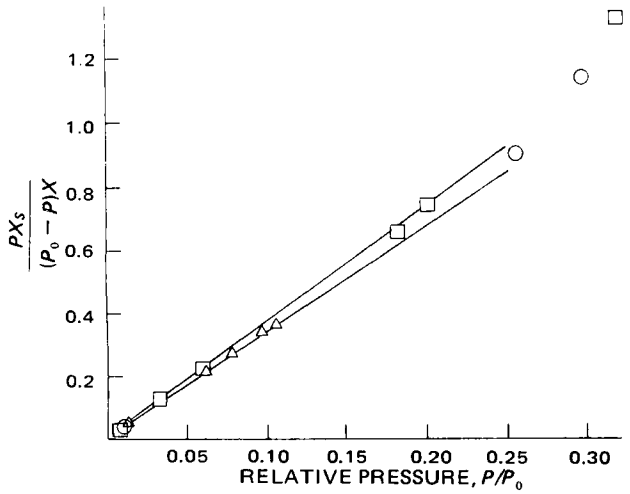

Figure 5—*BET adsorption plots for three fluorocarbon aerosol propellants at 25°. Key:* ○, *trichloromonofluoromethane;* △, *dichlorodifluoromethane; and* □, *dichlorotetrafluoroethane.*

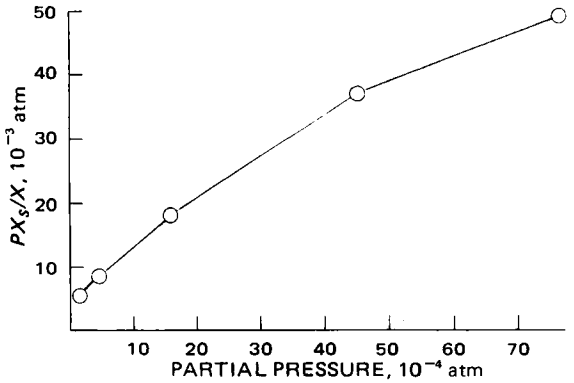

Figure 6—*Langmuir adsorption plot for dichlorodifluoromethane at relatively lower partial pressures.*

The estimated molecular cross-sectional areas (A_m) for the three fluorocarbons were calculated according to Eq. 6 (Table I). These values were used to calculate the specific surface area of activated charcoal using Eq. 7. The specific areas so calculated were 454, 402, and 359 m^2/g for dichlorodifluoromethane, trichloromonofluoromethane, and dichlorotetrafluoroethane, respectively. These values are in the same range as reported for sugar charcoal, *i.e.*, between 100 and 1000 m^2/g (19). However, the rather large variation occurring in this study suggests that the monolayer capacity may in fact represent the micropore capacity. Thus, by assuming that the mechanism of micropore condensation predominates over the monolayer adsorption at low pressures, the micropore volume may be estimated using the values of the liquid densities of fluorocarbons at 25° given in Table I, which leads to 0.223, 0.198, and 0.191 ml/g for the same order of fluorocarbons just mentioned. The somewhat larger value derived for dichlorodifluoromethane is not unusual because the micropore volume available for smaller molecules has been found to be larger (18).

In the preliminary trials of the adsorption study, 5-ml serum bottles were used. The equilibrium state of adsorption and desorption was found to establish almost immediately after the propellant was introduced over the activated charcoal. However, due to experimental difficulty in handling small quantities of activated charcoal in small bottles, the 60-ml serum bottles were used instead. Then the equilibrium was found to establish rather slowly, as mentioned before, although at least 90% of the propellant was estimated to be adsorbed in a few minutes. Thus, the rate of equilibration appeared to be dependent mainly on the rate of diffusion in both the headspace and the interspace of the adsorbent particles.

In conclusion, the adsorption of the three fluorocarbons on activated charcoal at 25° can be described by the BET type II or type IV isotherm. The adsorption mechanism can be assumed as primarily through the condensation of fluorocarbon gas in the pores of activated charcoal. The deviation of the adsorption isotherms at low relative pressures was in favor of adsorption, which is an advantage in using this adsorbent as a filtering medium to remove aerosol propellants from air.

REFERENCES

(1) *Consumer Rep.*, **May 1974**, 374.

(2) A. Silverglade, *J. Amer. Med. Ass.*, **222**, 827(1972).

(3) W. S. Harris, *ibid.*, **223**, 1508(1973).

(4) T. Balazes, F. L. Earl, G. W. Bierbower, and M. A. Weinberger, *Toxicol. Appl. Pharmacol.*, **26**, 407(1973).

(5) W. L. Chiou, *J. Amer. Med. Ass.*, **227**, 658(1974).

(6) D. M. Aviado and M. A. Belej, *Toxicology*, **2**, 31(1974).

(7) C. T. Dollery, W. M. Faith, G. H. Draffan, G. Wise, H. Sahgoun, J. W. Paterson, and S. R. Walker, *Clin. Pharmacol. Ther.*, **15**, 59(1974).

(8) S. Niazi and W. L. Chiou, *J. Pharm. Sci.*, **63**, 532(1974).

(9) W. L. Chiou, *Res. Commun. Chem. Pathol. Pharmacol.*, **6**, 481(1973).

(10) W. L. Chiou and J. H. Hsiao, *ibid.*, **8**, 273(1974).

(11) W. L. Chiou, *J. Amer. Med. Ass.*, **229**, 1722(1974).
(12) D. M. Aviado, *J. Clin. Pharmacol.*, **15**, 84(1975).
(13) P. H. Emmett and S. Brunauer, *J. Amer. Chem. Soc.*, **59**, 1553(1937).
(14) W. L. Chiou and J. H. Hsiao, *J. Pharm. Sci.*, **64**, 1052(1975).
(15) W. L. Chiou and S. Niazi, *Res. Commun. Chem. Pathol. Pharmacol.*, **6**, 481(1973).
(16) I. Langmuir, *J. Amer. Chem. Soc.*, **38**, 2221(1916).
(17) S. Brunauer, L. S. Deming, W. S. Deming, and E. Teller, *ibid.*, **62**, 1723(1940).
(18) S. J. Gregg and K. S. W. Sing, "Adsorption, Surface Area, and Porosity," Academic, New York, N.Y., 1967, pp. 41–44, 49–52, 96, 123, 199, 201–209.
(19) J. J. Bikerman, "Surface Chemistry," 2nd ed., Academic, New York, N.Y., 1958, pp. 197–200, 220.
(20) "Handbook of Chemistry and Physics," 48th ed., The Chemical Rubber Co., Cleveland, Ohio, 1967, p. F-10.
(21) "Freon Product Information," B-2, E. I. du Pont de Nemours and Co., Wilmington, Del.
(22) W. J. Moore, "Physical Chemistry," 3rd ed., Prentice-Hall, Englewood Cliffs, N.J., 1962, pp. 17, 19.
(23) P. H. Emmett and S. Brunauer, *J. Amer. Chem. Soc.*, **59**, 1553(1937).

ACKNOWLEDGMENTS AND ADDRESSES

Received January 20, 1975, from the *Department of Pharmacy, College of Pharmacy, University of Illinois at the Medical Center, Chicago, IL 60612*

Accepted for publication April 17, 1975.

Supported in part by Food and Drug Administration Grant 1 R01 FD-00574-02.

[x] To whom inquiries should be directed.

Fluorocarbon Aerosol Propellants X: Pharmacokinetics of Dichlorotetrafluoroethane in Dogs

SARFARAZ NIAZI and WIN L. CHIOU [x]

Abstract □ An intravenous dosage form of dichlorotetrafluoroethane, a common fluorocarbon aerosol propellant, was formulated in polyethylene glycol 400 for single dosing to unanesthetized dogs. A three-compartment open model was proposed for the disposition of this compound in dogs, with average half-lives of 1.3, 9.6, and 50.8 min for the three disposition phases. An analysis of tissue compartment distribution following a single dose showed that it took about 2 hr to achieve pseudo-distribution equilibration, following which more than 90% of the propellant remaining in the body was retained in the tissue compartments. Pulmonary clearance and volumes of distribution were calculated considering the first-pass effect through the lungs. The volume of distribution was approximately 10 times the body weight in terms of blood concentration, and about 84% of the propellant was cleared from the blood passing through the lungs in each cycle.

Keyphrases □ Fluorocarbon aerosol propellants—dichlorotetrafluoroethane, tissue compartment, distribution analysis, three-compartment open model, dogs □ Dichlorotetrafluoroethane—tissue compartment distribution analysis, three-compartment open model, dogs □ Aerosol propellants, fluorocarbon—dichlorotetrafluoroethane, tissue compartment distribution analysis, three-compartment open model, dogs □ Pharmacokinetics—dichlorotetrafluoroethane, tissue compartment distribution analysis, three-compartment open model, dogs

The wide use of fluorocarbon aerosol propellants in various household, cosmetic, and medicinal pressurized packages has recently prompted extensive studies on their possible adverse effects. These include effects on the cardiovascular system (1–4), enzyme activities (5), mutation (6), and ozone concentrations in the stratosphere (7). Arguments that have often been presented in favor of the low systemic toxicity of fluorocarbons is that these compounds are not absorbed to any significant extent when inhaled from commercial aerosol products and that the small fraction absorbed is eliminated rapidly from the body, decreasing the possibility of any toxic reaction (8–10).

Unfortunately, the conclusions drawn from most previous studies were not based on sound pharmacokinetic principles and do not reflect the true disposition pattern of these compounds (4, 11).

The objectives of this study were to demonstrate that dichlorotetrafluoroethane, one of the most commonly used fluorocarbon propellants, has a longer biological half-life than previously thought and undergoes extensive distribution in the body, an observation that might have an important bearing on its toxicity profile.

EXPERIMENTAL

Materials—A medical-grade silicone tubing[1] [0.3 cm (0.125 in.) i.d.] was used with 18–20-gauge cannulas[2] for venous cannulation. The infusion of the solution was performed using a constant-rate infusion pump[3].

Intravenous Dosage Form—Sterile solutions of dichlorotetrafluoroethane[4] were prepared by purging the fluorocarbon, which exists in gaseous form at room temperature, through a needle inserted deep into the sealed serum bottle containing a known volume of polyethylene glycol 400[5]. The gas was allowed to escape the bottle through a 27-gauge needle inserted just below the surface of the stopper. After purging for 15 min, the needles were removed and the solution was set aside for at least 30 min. Then the rubber stopper was pierced with another 27-gauge needle to release any excessive pressure.

[1] Dow Corning Corp., Midland, Mich.
[2] Medicut, Aloe Medical, St. Louis, Mo.
[3] Harvard Apparatus Co., Millis, Mass.
[4] Supplied by E. I. du Pont de Nemours & Co., Wilmington, Del.
[5] Union Carbide Chemical Co., New York, N.Y.

(11) W. L. Chiou, *J. Amer. Med. Ass.*, **229**, 1722(1974).
(12) D. M. Aviado, *J. Clin. Pharmacol.*, **15**, 84(1975).
(13) P. H. Emmett and S. Brunauer, *J. Amer. Chem. Soc.*, **59**, 1553(1937).
(14) W. L. Chiou and J. H. Hsiao, *J. Pharm. Sci.*, **64**, 1052(1975).
(15) W. L. Chiou and S. Niazi, *Res. Commun. Chem. Pathol. Pharmacol.*, **6**, 481(1973).
(16) I. Langmuir, *J. Amer. Chem. Soc.*, **38**, 2221(1916).
(17) S. Brunauer, L. S. Deming, W. S. Deming, and E. Teller, *ibid.*, **62**, 1723(1940).
(18) S. J. Gregg and K. S. W. Sing, "Adsorption, Surface Area, and Porosity," Academic, New York, N.Y., 1967, pp. 41–44, 49–52, 96, 123, 199, 201–209.
(19) J. J. Bikerman, "Surface Chemistry," 2nd ed., Academic, New York, N.Y., 1958, pp. 197–200, 220.
(20) "Handbook of Chemistry and Physics," 48th ed., The Chemical Rubber Co., Cleveland, Ohio, 1967, p. F-10.
(21) "Freon Product Information," B-2, E. I. du Pont de Nemours and Co., Wilmington, Del.
(22) W. J. Moore, "Physical Chemistry," 3rd ed., Prentice-Hall, Englewood Cliffs, N.J., 1962, pp. 17, 19.
(23) P. H. Emmett and S. Brunauer, *J. Amer. Chem. Soc.*, **59**, 1553(1937).

ACKNOWLEDGMENTS AND ADDRESSES

Received January 20, 1975, from the *Department of Pharmacy, College of Pharmacy, University of Illinois at the Medical Center, Chicago, IL 60612*

Accepted for publication April 17, 1975.

Supported in part by Food and Drug Administration Grant 1 R01 FD-00574-02.

[x] To whom inquiries should be directed.

Fluorocarbon Aerosol Propellants X: Pharmacokinetics of Dichlorotetrafluoroethane in Dogs

SARFARAZ NIAZI and WIN L. CHIOU [x]

Abstract □ An intravenous dosage form of dichlorotetrafluoroethane, a common fluorocarbon aerosol propellant, was formulated in polyethylene glycol 400 for single dosing to unanesthetized dogs. A three-compartment open model was proposed for the disposition of this compound in dogs, with average half-lives of 1.3, 9.6, and 50.8 min for the three disposition phases. An analysis of tissue compartment distribution following a single dose showed that it took about 2 hr to achieve pseudo-distribution equilibration, following which more than 90% of the propellant remaining in the body was retained in the tissue compartments. Pulmonary clearance and volumes of distribution were calculated considering the first-pass effect through the lungs. The volume of distribution was approximately 10 times the body weight in terms of blood concentration, and about 84% of the propellant was cleared from the blood passing through the lungs in each cycle.

Keyphrases □ Fluorocarbon aerosol propellants—dichlorotetrafluoroethane, tissue compartment, distribution analysis, three-compartment open model, dogs □ Dichlorotetrafluoroethane—tissue compartment distribution analysis, three-compartment open model, dogs □ Aerosol propellants, fluorocarbon—dichlorotetrafluoroethane, tissue compartment distribution analysis, three-compartment open model, dogs □ Pharmacokinetics—dichlorotetrafluoroethane, tissue compartment distribution analysis, three-compartment open model, dogs

The wide use of fluorocarbon aerosol propellants in various household, cosmetic, and medicinal pressurized packages has recently prompted extensive studies on their possible adverse effects. These include effects on the cardiovascular system (1–4), enzyme activities (5), mutation (6), and ozone concentrations in the stratosphere (7). Arguments that have often been presented in favor of the low systemic toxicity of fluorocarbons is that these compounds are not absorbed to any significant extent when inhaled from commercial aerosol products and that the small fraction absorbed is eliminated rapidly from the body, decreasing the possibility of any toxic reaction (8–10).

Unfortunately, the conclusions drawn from most previous studies were not based on sound pharmacokinetic principles and do not reflect the true disposition pattern of these compounds (4, 11).

The objectives of this study were to demonstrate that dichlorotetrafluoroethane, one of the most commonly used fluorocarbon propellants, has a longer biological half-life than previously thought and undergoes extensive distribution in the body, an observation that might have an important bearing on its toxicity profile.

EXPERIMENTAL

Materials—A medical-grade silicone tubing[1] [0.3 cm (0.125 in.) i.d.] was used with 18–20-gauge cannulas[2] for venous cannulation. The infusion of the solution was performed using a constant-rate infusion pump[3].

Intravenous Dosage Form—Sterile solutions of dichlorotetrafluoroethane[4] were prepared by purging the fluorocarbon, which exists in gaseous form at room temperature, through a needle inserted deep into the sealed serum bottle containing a known volume of polyethylene glycol 400[5]. The gas was allowed to escape the bottle through a 27-gauge needle inserted just below the surface of the stopper. After purging for 15 min, the needles were removed and the solution was set aside for at least 30 min. Then the rubber stopper was pierced with another 27-gauge needle to release any excessive pressure.

[1] Dow Corning Corp., Midland, Mich.
[2] Medicut, Aloe Medical, St. Louis, Mo.
[3] Harvard Apparatus Co., Millis, Mass.
[4] Supplied by E. I. du Pont de Nemours & Co., Wilmington, Del.
[5] Union Carbide Chemical Co., New York, N.Y.

The amount dissolved was determined by the mass difference before and after purging. The solutions were then analyzed to confirm the concentration using a headspace equilibration method. This method and the detailed procedure for the preparation of sterile solution in polyethylene glycol 400 were described earlier (11).

Animal Procedures—Four male, mongrel, unanesthetized conditioned dogs, 16.8–20 kg, were used. They were fasted for 16–18 hr prior to the experiments, and food and water were withheld during the experiments.

The cephalic veins of the forelegs were cannulated using an 18-gauge cannula to which a three-way stopcock was attached. The syringe containing the fluorocarbon solution was connected to the cannula through a silicone tubing. The solution was infused over 3 min at a constant rate of 2.2 ml/min. At the end of the infusion, the cannula was flushed with 5 ml of heparinized sterile normal saline.

Blood samples (0.5–3.0 ml) were collected following the end of administration from the other leg at 0, 1, 2, 3, 4, 6, 8, 10, 15, 20, 25, 30, 40, 50, 60, 70, 80, and 100 min and then up to 300 min at every 20 min. A blank blood sample was obtained before the solution was administered to study the partition coefficient. The cannula through which the solution was administered was removed immediately following the administration. Every time a blood sample was withdrawn, the cannula was flushed with heparinized normal saline to avoid clotting.

During all of the studies, adequate room ventilation was maintained. Care was taken not to excite the animal since the cardiac output and breathing rate can affect the results significantly. No study was performed when the animal got highly excited during the cannulation process.

Analysis of Dichlorotetrafluoroethane in Blood—The blood samples collected were transferred to sealed, preweighed, heparinized serum bottles of various capacities and allowed to equilibrate with the gaseous phase of the bottle. Appropriate volumes of the gaseous phase were then analyzed using a gas chromatograph equipped with an electron-capture detector. The concentration in the blood sample was arrived at indirectly through the partition coefficient value; this value was determined using the headspace equilibration method described earlier[6] (12, 13).

The analyses were performed as soon as possible within 1 hr after sampling to avoid any loss during storage. Duplicate analyses were performed on each sample, and a high degree of reproducibility was always achieved.

RESULTS AND DISCUSSION

Dosage Form and Route of Administration—An intravenous dosage form was chosen based on failures in the past to administer fluorocarbons quantitatively through the lungs (14, 15) and to avoid problems of biological availability in oral administration (16). The merits for the selection of polyethylene glycol 400 as the infusion solvent were discussed earlier (11).

Pharmacokinetic Model—For simplification in pharmacokinetic analyses of the blood level data, the zero time was assigned at the midpoint of infusion (17), *i.e.*, 1.5 min after the beginning of infusion. The blood level curves plotted on semilogarithmic paper were then subjected to the visual feathering method analysis (17, 18). A typical plot from one dog study is shown in Fig. 1. For clarity, the feathered data points in the faster biexponential phases are not shown in the figure. However, they all fell on or near the lines.

The triexponential blood level decay for all dogs studied indicates that the disposition kinetics for this propellant in dogs can be best described by a three-compartment open model (17–20) (Scheme I). The other two commonly used fluorocarbon propellants, trichloromonofluoromethane (11) and dichlorodifluoromethane (19), were also found to exhibit triexponential blood level decay patterns in dogs.

The two compartments besides the central compartment can be described as groups of tissues with distinct affinity and capacity (18) for dichlorotetrafluoroethane. The differences in affinity and capacity may be due to the solubility characteristics or to a specific interaction such as protein binding or other complexations. A compartment can also be distinguished based on the blood supply to the tissues such as a vessel-rich group or a vessel-poor group (18).

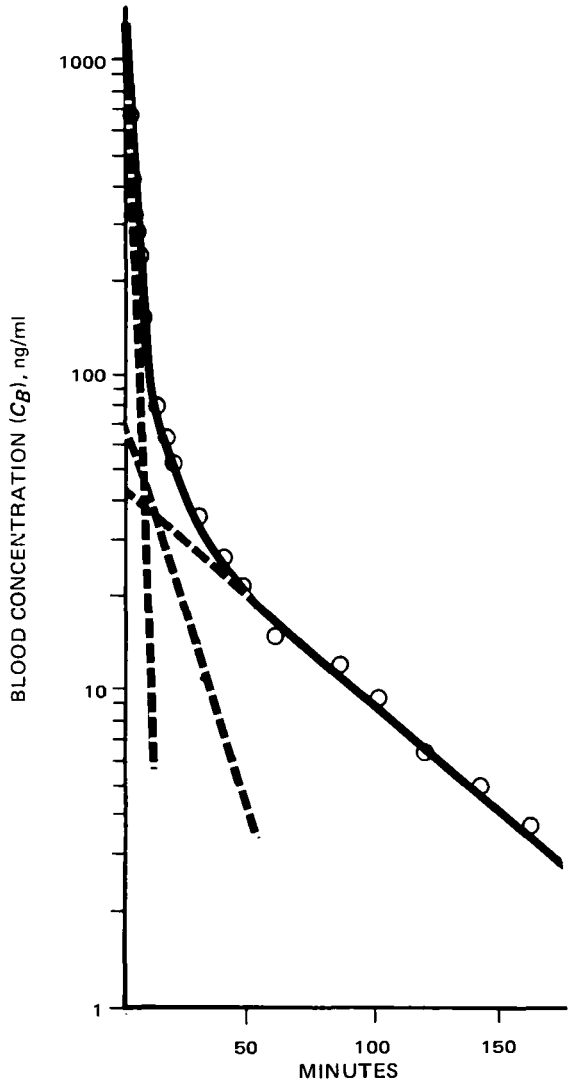

Figure 1—*Triexponential blood concentration decay following intravenous administration of 99 mg of dichlorotetrafluoroethane in 6.6 ml of polyethylene glycol 400 to a 19-kg dog:* $C_B = 1250e^{-0.375t} + 75e^{-0.0603t} + 42e^{-0.0161t}$.

The rate constants (Scheme I) were calculated using a digital computer[7], based on the differential equation solutions described by Rescigno and Segre (18).

The fraction of the dose remaining in various pharmacokinetic compartments can be described in terms of hybrid constants (18):

$$X_1/X_0 = C_1e^{-b_1t} + C_2e^{-b_2t} + C_3e^{-b_3t} \quad \text{(Eq. 1)}$$

$$X_2/X_0 = C_{12}e^{-b_1t} + C_{22}e^{-b_2t} + C_{32}e^{-b_3t} \quad \text{(Eq. 2)}$$

$$X_3/X_0 = C_{13}e^{-b_1t} + C_{23}e^{-b_2t} + C_{33}e^{-b_3t} \quad \text{(Eq. 3)}$$

where X_1, X_2, and X_3 are the amounts of the fluorocarbon present in different compartments; X_0 is the available dose, which in the model proposed will be the dose remaining in the body after the first pass through lungs.

The pharmacokinetic data reported here are based on the single-dose study (Table I). The previous study of trichloromonofluoromethane in dogs showed dose-independent pharmacokinetic disposition kinetics over a wide dose range (11).

Volume of Distribution and Pulmonary Clearance—The dose of fluorocarbon administered intravenously is not the same as the dose made available to the body, since the intravenously administered dose first passes through the lungs, where a significant

[6] References 11 and 13 should be consulted for a detailed description of the procedure.

[7] IBM 370.

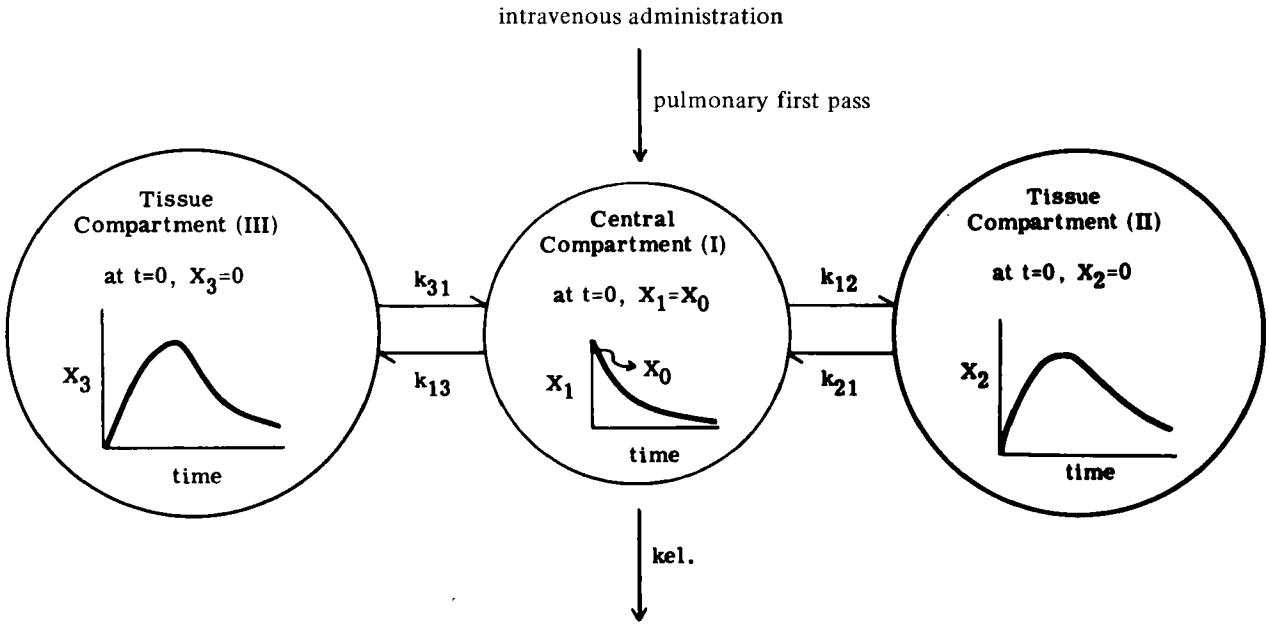

Scheme I—Three-compartment disposition model for dichlorotetrafluoroethane in dogs

fraction can be eliminated before it reaches the general body circulation. Therefore, the fraction eliminated in the first pass has to be accounted for in the calculation of the volume of distribution or pulmonary clearance.

The apparent volume of distribution, $(V_d)_{b_3}$, following pseudo-distribution equilibrium can be defined by the following equation (21), which takes into account the first-pass effect:

$$(V_d)_{b_3} = \frac{(PFR)(D^0)}{b_3[(AUC)(PFR + D^0)]} \qquad \text{(Eq. 4)}$$

where AUC is the area of the blood concentration–time curve from zero to infinity, b_3 is the first-order disposition constant in the terminal phase, D^0 is the dose administered, and PFR is the pulmonary blood flow rate (~cardiac output). Equation 4, however, assumes that the pulmonary clearance is the only route of elimination for the compound. The fluorocarbon studied in this investigation has been shown to be primarily eliminated intact from the lung (22). No volatile metabolite was detected in the GC assay in the present study. Therefore, Eq. 4 can be used as an approximation for the determination of the apparent volume of distribution and pulmonary clearance, PC:

$$PC = (V_d)_{b_3}(b_3) \qquad \text{(Eq. 5)}$$

The fraction eliminated in each pass through the lungs can be expressed as:

$$\text{fraction eliminated} = (1 - f) = \frac{PC}{PFR} \qquad \text{(Eq. 6)}$$

where f is the fraction of the administered dose retained in the body following the passage through the lung.

The volume of the central compartment, from where the elimination is assumed to take place, can be calculated easily since the clearance from the central compartment should equal the clearance from the body:

$$(V_d)_{b_3}(b_3) = V_c K_{el} \qquad \text{(Eq. 7)}$$

where K_{el} is the elimination rate constant from the central compartment.

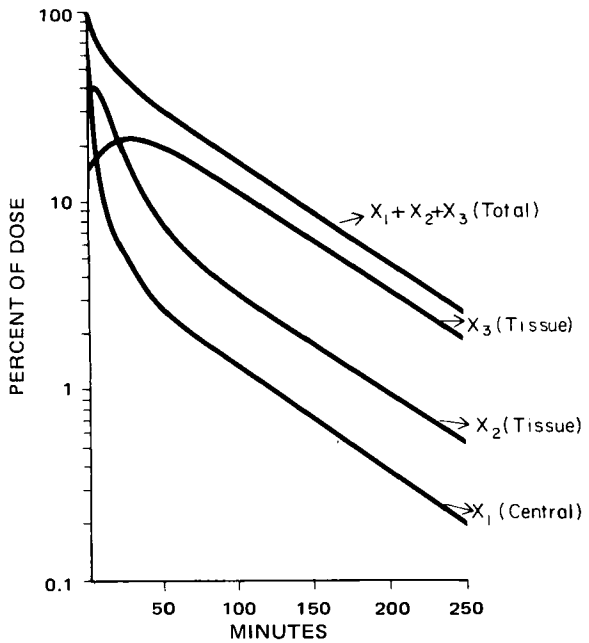

Figure 2—*Percent of available dose of dichlorotetrafluoroethane remaining in various body compartments based on a typical study (Dog 3287).*

Table II shows the values of the volumes of distribution, pulmonary clearance, and percent eliminated in each passage through the lungs. The average value of the volume of distribution, $(V_d)_{b_3}$, was approximately 10 times the average body weight (16.8–20 kg), indicating that this compound is indeed extensively distributed in the body tissues. Recent data (23, 24) have shown the possible contribution of tissue and plasma protein binding and partitioning in fat depots to the high volumes of distribution reported here.

The average pulmonary clearance volume of 2.53 liters/min was about 84% of the pulmonary blood flow rate (~3 liters) reported in the literature (25). This finding shows the magnitude of error that would have been involved if the correction for the first-pass effect had not been included.

Disposition Half-Lives—Table III shows the half-lives for the three disposition phases of dichlorotetrafluoroethane. The terminal disposition half-lives (~50 min) were much longer than previously reported or speculated (14, 26, 27) for two reasons. First, most studies were performed for very short periods within which the fluorocarbon was still in the distribution phase; and second, the analytical techniques were not sensitive enough to quantitate the low concentrations existing even after a short period following administration (Fig. 1).

The finding that dichlorotetrafluoroethane shows a multiexponential decay in the blood concentration can be utilized to study the true elimination rate from the body and to evaluate the degree of accumulation in the body following single or multiple exposures.

Table I—Pharmacokinetic Parameters of Dichlorotetrafluoroethane from Four Studies

Parameter[a]	Dog 3287	Dog 3288	Dog 3457	Dog 2976
b_1	0.737	0.375	0.577	0.591
b_2	0.0613	0.0603	0.107	0.0761
b_3	0.0120	0.0161	0.0157	0.0147
C_1	0.840	0.914	0.855	0.872
C_2	0.119	0.0548	0.137	0.101
C_3	0.0402	0.0307	0.00805	0.0263
C_{12}	−0.557	−0.265	−0.333	−0.409
C_{22}	0.454	0.224	0.325	0.363
C_{32}	0.103	0.0403	0.008	0.0454
C_{13}	−0.106	−0.185	−0.0687	−0.140
C_{23}	−0.271	−0.106	−0.0696	−0.172
C_{33}	0.377	0.292	0.138	0.313
K_{el}	0.156	0.190	0.305	0.217
K_{21}	0.162	0.0810	0.173	0.136
K_{31}	0.0217	0.0236	0.0183	0.0222
K_{13}	0.0900	0.0712	0.0449	0.0915
K_{12}	0.382	0.0850	0.158	0.213
D^0, mg[b]	297	99	281	160
X^0, mg[c]	38	17.7	51.6	22.3
$C_p{}^0$, mg/ml	2.26	1.37	6.43	1.88
AUC^∞, (mg/ml)/min[d]	14.5	7.18	21.1	8.63

[a] The units for all b and K values are minutes^{-1}. [b] Dose administered. [c] Available dose = fD^0, where f is the fraction retained in the first pass through lungs. [d] $AUC^\infty = C_p{}^0\left(\frac{C_1}{b_1} + \frac{C_2}{b_2} + \frac{C_3}{b_3}\right)$.

Table II—Volumes of Distribution and Clearance of Dichlorotetrafluoroethane

Dog	$(V_d)_{b_3}$, liters	V_c, liters	PC, liters/min	$(1-f)$, %
3287	217.10	16.81	2.62	87.20
3288	152.8	12.95	2.46	82.13
3457	155.5	8.02	2.45	81.64
2976	175.8	11.89	2.58	86.07
Mean ± *SEM*	175.31 ± 14.84	12.42 ± 1.81	1.53 ± 0.04	84.26 ± 1.39

The average half-life of the initial disposition phase was only 1.29 min. The actual value should be slightly smaller because this value was calculated after a 3-min infusion instead of an instantaneous administration.

Retention following Single Intravenous Administration—Following administration of dichlorotetrafluoroethane through intravenous infusion, the concentration in the blood dropped sharply. Such an observation was also reported for fluorocarbons following their inhalation (26, 27). However, such sharp declines in blood concentrations do not necessarily follow a parallel loss of the drug from the body (20). The amount of the drug remaining in the body as a function of time can also be calculated (20) using:

$$\text{fraction remaining in body} = \frac{(C_1/b_1)e^{-b_1t} + (C_2/b_2)e^{-b_2t} + (C_3/b_3)e^{-b_3t}}{(C_1/b_1) + (C_2/b_2) + (C_3/b_3)} \quad \text{(Eq. 8)}$$

Figure 2 shows a plot of amount of dichlorotetrafluoroethane remaining in the body and in various tissue compartments. For example, the amount of dichlorotetrafluoroethane in the central compartment dropped to about 5% of the available dose (dose after the first pulmonary pass) in 25 min, but about 45% of the available dose was still present in the body.

It is evident that a buildup of the fluorocarbon continues in the tissue compartments and that the maximum amount is reached at the steady state when the rate of change in the amount present in the tissue compartments equals zero; the amount present in the tissue compartments then declines. The ratio of the amount of the propellant in the tissue compartment over that in the central compartment, however, keeps increasing, since the rate of loss from the central compartment is greater than from the tissue compartments, until a pseudo-equilibration stage is reached; then the ratio of the amount in the tissue compartments to the amount in the

Table III—Disposition Half-Lives of Dichlorotetrafluoroethane

Disposition Phase	Half-Life (Mean + *SEM*), min
Initial	1.29[a] ± 0.19
Intermediate	9.60 ± 1.17
Final	50.8 ± 3.88

[a] This value may be slightly different from the true value because the experimental value would be influenced by the duration of the intravenous infusion.

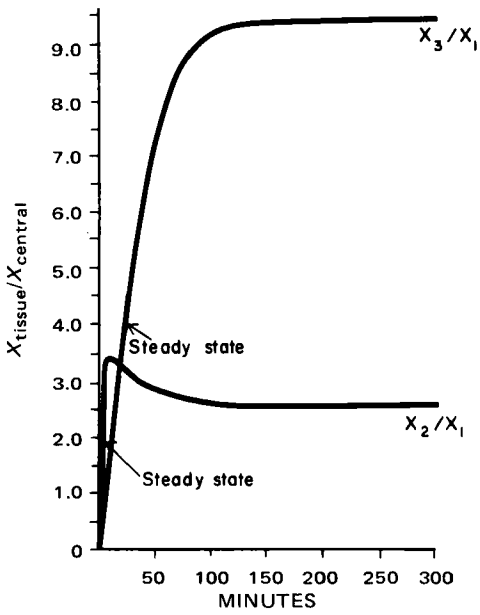

Figure 3—*Comparison of the relative amount of dichlorotetrafluoroethane remaining in the tissue and central compartments based on a typical study (Dog 3287).*

Table IV—Average Retention ± *SEM* of Dichlorotetrafluoroethane at 200 min following Pseudo-Distribution Equilibrium in Various Compartments

	$X_2 + X_3$ Compartments	X_1
Percent of available dose	1.74 ± 0.72	0.16 ± 0.01
Relative percent of total amount in the body	91.6 ± 37.9	8.4 ± 3.7

central compartment remains constant (28). To demonstrate this, a plot was made (Fig. 3) based on the data presented in Fig. 2. It took about 125 min to reach equilibration with the central compartment.

This finding is important since it shows that the claims made regarding the extremely fast elimination of the fluorocarbon from the body (14, 26, 27) may not be correct. Such a finding may have important implications in the evaluation of the toxicity of this compound.

In Compartment II (X_2), a peak was observed for the ratio of fluorocarbon in the tissue compartment over the amount in the central compartment. This kind of peak ratio was not observed for Compartment III (X_3) due to the slower accumulation in Compartment III. A constant ratio is obtained only when this compartment equilibrates with the central compartment.

The total amount of the available dose retained following pseudo-distribution equilibrium is an important parameter, especially when extrapolating the single-dose study to multiple-dose studies. Table IV shows the retention of dichlorotetrafluoroethane in the tissue and central compartments after pseudo-distribution equilibrium has been reached. The fraction of the fluorocarbon retained in the tissue compartments compared to the central compartment shows that more than 90% of the total amount present in the body is retained in tissue compartments. Thus, a sharp decline in the concentration in the central compartment does not necessarily parallel the decline in the amount in the body, an observation that was not well recognized in most studies reported earlier.

REFERENCES

(1) *Consumer Rep.*, **May 1974**, 374.

(2) A. Silverglade, *J. Amer. Med. Ass.*, **222**, 827(1972).

(3) W. S. Harris, *ibid.*, **223**, 1508(1973).

(4) W. L. Chiou, *ibid.*, **227**, 658(1974).

(5) D. B. Lund, *Arch. Biochem. Biophys.*, **129**, 181(1969).

(6) V. C. Foltz and R. Fuerst, *Environ. Res.*, **7**, 275(1974).

(7) R. J. Cicerone, R. S. Stolarski, and S. Walters, *Science*, **185**, 1165(1974).

(8) G. J. Taylor and W. S. Harris, *J. Clin. Invest.*, **50**, 1546(1971).

(9) G. J. Taylor and W. S. Harris, *J. Amer. Med. Ass.*, **214**, 81(1970).

(10) N. C. Flowers and L. G. Horan, *ibid.*, **219**, 33(1972).

(11) S. Niazi and W. L. Chiou, *J. Pharm. Sci.*, **64**, 763(1975).

(12) *Ibid.*, **63**, 532(1974).

(13) W. L. Chiou and S. Niazi, *Res. Commun. Chem. Pathol. Pharmacol.*, **6**, 481(1973).

(14) L. Shargel and R. Koss, *J. Pharm. Sci.*, **61**, 1445(1972).

(15) A. Azar, H. J. Trochimowicz, J. B. Terrill, and L. S. Mullin, *Amer. Ind. Hyg. Ass. J.*, **34**, 102(1973).

(16) J. B. Terrill, *ibid.*, **33**, 736(1972).

(17) W. L. Chiou and S. Riegelman, *J. Pharm. Sci.*, **58**, 1500(1969).

(18) A. Rescigno and G. Segre, "Drug and Tracer Kinetics," Blaisdell, New York, N.Y., 1966, pp. 57–137.

(19) S. Niazi, Ph.D. dissertation, University of Illinois, Chicago, Ill., 1974.

(20) W. L. Chiou, *J. Pharm. Pharmacol.*, **24**, 342(1972).

(21) W. L. Chiou, *Res. Commun. Chem. Pathol. Pharmacol.*, **7**, 679(1974).

(22) A. Morgan, A. Black, M. Walsh, and D. R. Belcher, *Int. J. Appl. Radiat. Isotop.*, **23**, 285(1972).

(23) W. L. Chiou and J. H. Hsiao, *Res. Commun. Chem. Pathol. Pharmacol.*, **8**, 273(1974).

(24) K. Chang and W. L. Chiou, *J. Pharm. Sci.*, **65**, 53(1976).

(25) W. S. Spector, "Handbook of Biological Data," Saunders, Philadelphia, Pa., 1956.

(26) J. W. Paterson, M. F. Sudlow, and S. R. Walker, *Lancet*, **2**, 565(1971).

(27) C. T. Dollery, G. H. Draffan, G. H. Daview, F. M. Williams, and M. E. Conolly, *ibid.*, **1**, 1164(1970).

(28) M. Gibaldi, R. Nagashima, and G. Levy, *J. Pharm. Sci.*, **58**, 193(1969).

ACKNOWLEDGMENTS AND ADDRESSES

Received December 30, 1974, from the *Department of Pharmacy, College of Pharmacy, University of Illinois at the Medical Center, Chicago, IL 60612*

Accepted for publication April 29, 1975.

Abstracted in part from a dissertation submitted by S. Niazi to the Graduate College, University of Illinois at the Medical Center, in partial fulfillment of the Doctor of Philosophy degree requirements.

Supported in part by Food and Drug Administration Grant 1 R01 FD-00574-01 and in part by Public Health Service GRSG Grant 1-501-RR05735-01.

[x] To whom inquiries should be directed.

Specific Colorimetric Determination of Niacinamide in Dosage Forms

N. SBARBATI NUDELMAN ˣ and O. NUDELMAN

Abstract □ A chemical method for determining the amount of niacinamide in multicomponent preparations was developed. Neither niacin resulting from the degradation of niacinamide nor vitamin A, thiamine hydrochloride, riboflavin, ascorbic acid, ergocalciferol, or calcium pantothenate interferes. The method is based on the reaction of niacinamide with 1-chloro-2,4-dinitrobenzene, followed by the spectrophotometric measurement of the colored solution obtained after treatment with sodium hydroxide. The proposed method is at least as accurate as the methods currently in use. A structure is proposed for the colored product, and its route of formation is outlined.

Keyphrases □ Niacinamide—colorimetric analysis, multicomponent vitamin preparations □ Colorimetry—analysis, niacinamide in multicomponent vitamin preparations □ Vitamins—colorimetric analysis of niacinamide in multicomponent preparations

Niacinamide (I) is a common ingredient in numerous multicomponent pharmaceutical preparations. Its degradation product, niacin, is undesirable in multivitamin preparations because it produces unpleasant physiological reactions in some patients. Most analytical methods give positive results with niacin, unless it is removed prior to the determination as in some recent chromatographic procedures (1, 2).

Most photometric methods are based on the Köenig reaction (3), including the method of the Association of Official Agricultural Chemists (4). A microbiological procedure using *Lactobacillus arabinosus* (5) was described for the determination of I plus niacin. When using *Leuconostoc mesenteroides* (6), it is possible to determine the amount of niacin alone. This method has the disadvantage of poor precision.

The purpose of the present research was to find a method for the accurate determination of I in the presence of niacin and other common components in multivitamin preparations. The proposed method is simple, specific, and at least as accurate as current methods. It has at least two advantages over the Köenig reaction: (*a*) it avoids the use of the toxic, unstable, cyanogen bromide; and (*b*) it does not give positive results with niacin, the principal degradation product of I.

EXPERIMENTAL[1]

Reagents—1-Chloro-2,4-dinitrobenzene (II) (p.a. grade) was crystallized from ethanol, mp 53°. 1-Fluoro-2,4-dinitrobenzene (p.a. grade) was distilled under reduced pressure, bp 122° (1 mm Hg). A niacinamide USP reference standard was used without further purification. Acetone (p.a. grade) was distilled. Pure methanol was made anhydrous by the Lund and Bjerrum method (7).

Benzene was stored over sodium strings for at least 3 days and then distilled over them. Chloroform was shaken with concentrated sulfuric acid, washed with water, dried over calcium chloride, and distilled. Pure chloroform was kept in the dark. All other reagents were ACS grade or equivalent and were used without further purification.

Sample Preparation—In the absence of ascorbic acid, weigh, powder, and mix 20 tablets or the contents of 20 capsules. Accurately weigh a portion of the sample equivalent to approximately 10 mg of I and extract it with 50 ml of acetone (using four portions of nearly 10 ml of acetone each time and washing the residue with the remainder of the acetone). Then filter, collecting the filtrate in a 100-ml round-bottom flask. Add 1.0 g of II to the solution and evaporate the solvent under reduced pressure.

When ascorbic acid is present, proceed in the same way but extract I with 100 ml of chloroform or benzene. Add 1.0 g of II, remove about one-half of the solvent under reduced pressure, transfer quantitatively to a 100-ml round-bottom flask, and evaporate to dryness.

Syrups and elixirs also were determined by this method, with a previous partial elimination of the solvent and extraction with chloroform or benzene. Niacinamide in one-drug injectables was determined by a previous complete elimination of the solvent under reduced pressure, addition of a small amount of acetone and of 1.0 g of II, and complete removal of the acetone under reduced pressure.

Color Development—Close the flask containing the solid residue with a ground-glass stopper and heat at 80° for 2 hr with constant stirring. The holder illustrated in Fig. 1 permits the processing of six samples at the same time[2]. The holder is attached to a suitable stirrer, and the flasks are immersed in a thermostated bath.

Remove the flasks from the bath, add 10 ml of benzene to each, shake to assure dissolution of the unreacted II, and extract with four portions of about 20 ml of distilled water, collecting the aqueous extracts in a 100-ml volumetric flask. Dilute to volume with water. Transfer a 2.0-ml aliquot to a 50-ml volumetric flask, add about 45 ml of 96% ethanol and then 2.0 ml of aqueous 1 *N* sodium hydroxide, and dilute to volume with ethanol.

Monitor the absorbance of the sample at 504 nm, using 96% eth-

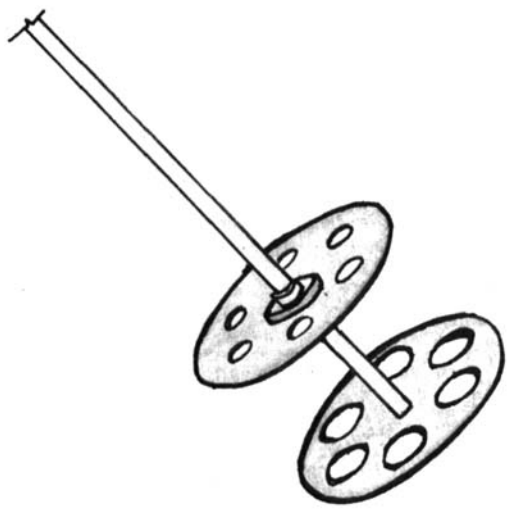

Figure 1—*Holder that allows six determinations of niacinamide at the same time (Scheme I).*

[1] A Beckman DU-2 spectrophotometer with 1-cm path length quartz cells was used for spectrophotometric measurements.

[2] Neoprene filter adapters, tapered collar type, are inserted in each hole of the plates to assure firm support of the flasks.

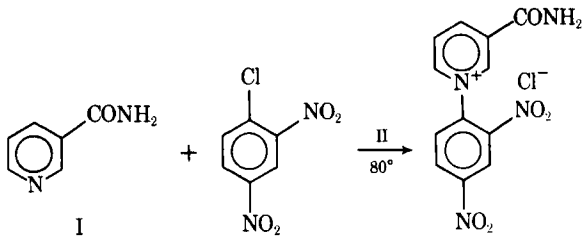

Scheme I

anol as a reference, until the highest absorption value is reached, *i.e.*, 5–6 min after the addition of the alkaline solution. The concentration of I present in the sample is calculated by comparison with the absorbance of a known amount of I treated in the same way. This value is then converted by the usual calculation to the basis of I declared in the sample and expressed as a percentage of the declared value.

RESULTS AND DISCUSSION

A procedure similar to the one described is given in NF XIII (8) as a qualitative assay for niacin but not for niacinamide (I). The NF procedure is more useful for the identification of I since it produces an unmistakable deep-violet color instead of the red one obtained in the assay with niacin. With the conditions described under *Experimental*, niacin does not give a measurable reaction.

Investigation of Parameters—Different experimental conditions were tested for the reaction of I with II (Scheme I) and for the reaction of the preceding reaction mixture with sodium hydroxide (Scheme II).

The influence of each of the following variables on the reaction shown in Scheme I was tested: solvent, temperature of the reaction, reagent (by using 1-fluoro-2,4-dinitrobenzene instead of II, no better results were obtained), time of reaction, and temperature and time of elimination of the solvent. The following solvents were used: anhydrous methanol, methanol–water (1:1), acetone, acetone–water (1:1), benzene, hexane, and dimethylformamide. No reaction was observed in any case, except for acetone in which about 5% of the reaction occurred. Acetone must be removed prior to the reaction in Scheme II to avoid the known reaction between II and acetone in alkaline media (9).

It is possible that most of the reaction in Scheme I occurred while the solvent was removed, and this may be also the reason that the temperature and the time of evaporation of the solvent seemed to influence the extent of the reaction. After several trials, it was concluded that fused II was by far the best solvent for the Scheme I reaction, since the reaction was less than 5% complete in all other media investigated.

For the Scheme II reaction, the following parameters were studied: solvent, sodium hydroxide concentration, ionic strength, time, and wavelength at which the maximum of absorbance is reached. Table I shows some solvents tested. Each increment of water in the ethanol–water mixture used as solvent had a hyperchromic effect accompanied by a small hypsochromic shift (Table I) and by an increase in the rate of the reaction. This effect became a disadvantage at over 12% of water because of the instability of the color. Changes in the concentration of sodium hydroxide from 0.02 to 0.2 *N* and of the ionic strength from 0.05 to 1 *N* did not modify the development of the color.

The linearity of the method was examined by performing the assay with different amounts of I, from 0.010 g (0.083 mmole) to 0.126 g (1 mmole). In all cases, 1.0–1.045 g of II was used (Table II). In addition, 12 determinations were performed with 10.0 mg of I and the standard deviation of the method was obtained; the mean value was 9.92 ± 0.06 mg.

It is possible to determine as little as 2 mg of I using the method described by extracting the Scheme I reaction mixture with 50 ml of water, taking a 4.0-ml aliquot, and using absolute ethanol for dilution prior to the Scheme II reaction.

Influence of Niacin (III)—Because niacin is the principal degradation product of I, the reaction of niacin under the same conditions used to determine I was performed. There was no develop-

Table I—Solvents for Reaction Shown in Scheme II

Solvent	λ_{max}, nm	t_{max}, min	Absorbance
Anhydrous methanol	510	70	—
96% ethanol–4% water	508	30	0.402
92% ethanol–8% water	507	20	0.438
88% ethanol–12% water	504	5	0.483
80% ethanol–20% water	502	~1	0.522
Water	490	≪1	

Table II—Determination of Niacinamide

Niacinamide Added, mg[a]	Absorbance	Niacinamide Found, mg
10.0	0.485	10.0
20.0	0.980	20.2
31.5	0.605	31.2
35.0	0.684	35.3
40.0	0.780	40.2
45.0	0.870	44.8
47.5	0.920	47.4
50.0	0.970	50.0
63.0	1.220	61.9
126.0[b]	1.235	127.3

[a] When the amount of niacinamide was ≥31.5 mg, the aqueous extracts were collected in a 250-ml volumetric flask. [b] An aliquot of 1.0 ml was used instead of 2.0 ml.

Table III—Influence of Niacin

Niacinamide Added, mg	Niacin Added, mg	Niacinamide Found, mg	Recovery Values, %
50.0	—	50.0	100
47.5	3.5	47.4	99.8
47.5	4.4	47.4	99.8
45.0	6.3	44.9	99.8
40.0	11.0	40.2	100.5
35.0	17.0	35.2	100.6
—	47.0	0.0	0.0
—	100.0	0.0	0.0

Table IV—Effects of Various Vitamins on Recovery of Niacinamide

Niacinamide Added, mg	Vitamin Added, mg	Niacinamide Found, mg
50.0	Niacin, 100	50.5
50.0	Vitamin A, 5000 IU	49.5
50.0	Thiamine hydrochloride, 59.0	49.8
50.0	Riboflavin, 20.0	51.0
50.0	Ascorbic acid, 50.0	17.5
50.0	Ergocalciferol, 5000 IU	51.0
50.0	Calcium pantothenate, 50.0	50.0

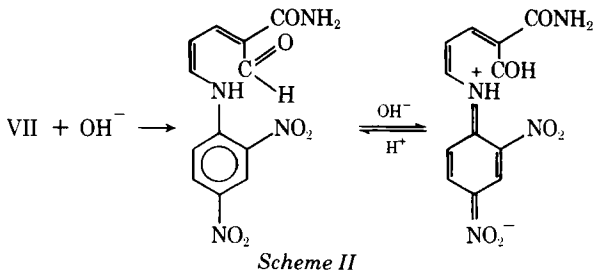

Scheme II

Table V—Recovery of Niacinamide from Synthetic Formulations

Mixture	Added Vitamins, mg							Niacinamide	
	Vitamin A	Thiamine Hydrochloride	Riboflavin	Pyridoxine	Ascorbic Acid	Ergocalciferol	Calcium Pantothenate	Added	Found
1	—	10	5	5	50	—	10	10.0	10.0
2	—	100	10	10	100	—	50	10.0	9.80
3	5000 IU	10	5	5	10	5000 IU	10	10.0	9.95
4	—	10	5	5	—	—	10	10.0	10.05

ment of color. To prove that this method could be used to follow hydrolytic degradation of I, mixtures containing it and small amounts of niacin in proportions slightly greater than expected from various degrees of deterioration of I were determined. Table III shows that the recovery of I was unaffected by the presence of niacin in the simulated degraded mixtures.

Other Interferences—Because I is usually formulated with other vitamins, the influence of vitamin A, thiamine hydrochloride (vitamin B_1), riboflavin (vitamin B_2), ascorbic acid (vitamin C), ergocalciferol (vitamin D_2), and calcium pantothenate (IV) was determined (Table IV). Only ascorbic acid (V) interfered. No exact correlation was observed between the content of ascorbic acid and the response. Ascorbic acid also interfered in the Scheme I reaction, because when it was added after the reaction was performed, the absorbances corresponded to the expected value in its absence. Oxidation to dehydroascorbic acid or neutralization with ammonia did not eliminate the interference. Extraction of I with chloroform or benzene, instead of acetone, gave satisfactory results since ascorbic acid was insoluble in these solvents. A 99.5% recovery was found using chloroform, and a 98.8% recovery was found using benzene.

Finally, Table V shows the amounts of I determined by the proposed method in synthetic mixtures. In the absence of ascorbic acid, extraction with acetone was performed; but when ascorbic acid was present, I was extracted with chloroform. The results shown are the averages of at least four determinations.

The proposed method was applied to authentic commercial multivitamin samples containing I with satisfactory results.

Mechanism—Niacinamide seems to be similar to pyridine in its reaction with II. When pyridine is added to an acetone solution of II, slightly colored crystals of 2,4-dinitrophenylpyridinium chloride, mp 195–195.5°, are formed (10). This compound, when treated with sodium hydroxide, develops a violet color which has a maximum absorbance at 540 nm (11) in 90% ethanol. The color is probably due to the anionic form of 5-(2′,4′-dinitrophenyl)amino-2,4-pentadienal (VI). Compound VI was prepared by an independent method (12), mp 179°, and its UV and visible spectra in the same media were identical with those obtained from the reaction of 2,4-dinitrophenylpyridinium chloride with sodium hydroxide.

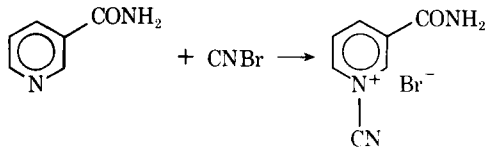

IX

Scheme III

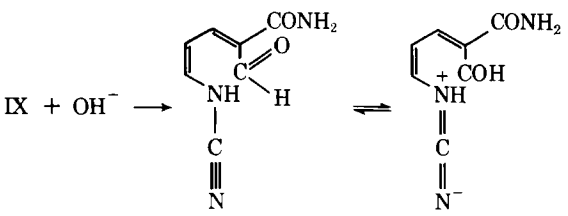

Scheme IV

In the case of I, the deactivation of the heterocyclic nucleus by the amido group is responsible for the more drastic conditions required to produce the pyridinium compound (VII), although it is not clear why it is formed more rapidly in the absence of solvent. When a carboxyl group is located at position 3, as in niacin, the nucleus is so deactivated that formation of the pyridinium complex is not possible under the conditions described.

The reaction in Scheme II probably occurs in the same way as that with the 2,4-dinitrophenylpyridinium chloride, since the complex formed has UV–visible spectra very similar to its pyridine analog, and its dependence on the ethanol–water ratio is also similar to that reported for the pyridine derivative (11).

Finally, it may be useful to point out that the parallelism between the reactions involved in this method and the mechanism accepted for the Köenig reaction (13) (Scheme III) can be postulated for the addition of cyanogen bromide (VIII), and it has been shown (14) that the condensation product (IX) of I with VIII has an open chain structure at pH 9 in water (Scheme IV) instead of the usual formulation as *N*-cyanopyridone.

REFERENCES

(1) M. T. Jeffus and C. T. Kenner, *J. Pharm. Sci.*, **58**, 749(1969).

(2) H. Brunink and E. J. Wessels, *Analyst*, **97**, 258(1972).

(3) R. Strohecker and H. M. Henning, "Vitamin Assay Tested Methods," Verlag Chemie GmB.H., Weinheim, Bergstr., Germany, 1965, p. 189.

(4) "Official Methods of Analysis," 10th ed., Association of Official Agricultural Chemists, Washington, D.C., 1965, p. 763.

(5) S. C. Barton-Wright, *Biochem. J.*, **38**, 314(1944).

(6) B. C. Johnson, *J. Biol. Chem.*, **159**, 227(1945).

(7) A. Vogel, "A Text-book of Practical Organic Chemistry," 3rd ed., Longman, New York, N.Y., 1964, p. 169.

(8) "The National Formulary," 13th ed., Mack Publishing Co., Easton, Pa., 1970, p. 475.

(9) R. J. Pollit and B. C. Saunders, *J. Chem. Soc.*, **1965**, 4615.

(10) A. F. Vompe and N. F. Turitsyna, *Zh. Obsch. Khim.*, **27**, 3282(1957).

(11) L. Légradi, *Acta Chim. Acad. Sci. Hung.*, **52**, 7(1967).

(12) N. E. Grigoreva and A. A. Pechka, *Zh. Obsch. Khim.*, **28**, 1677(1958).

(13) A. Mosher, *Heterocycl. Comp.*, **1**, 425(1950).

(14) S. Creyf and L. Roosens, *Meded. Vlaam. Chem. Ver.*, **19**, 1(1957); through *Chem. Abstr.*, **51**, 16303d(1957).

ACKNOWLEDGMENTS AND ADDRESSES

Received August 8, 1974, from the *Instituto Nacional de Farmacología y Bromatología and Facultad de Ciencias Exactas (Depto. Química Orgánica), Universidad de Buenos Aires, Argentina.*

Accepted for publication April 11, 1975.

[x] To whom inquiries should be directed (reprints are not available).

Mass Spectral and Pyrolytic Behavior of the Two Main Products of Phenylbutazone Degradation: Simulation of Unusual Mass Spectral Fragmentation

DENNIS V. C. AWANG ˣ **and A. VINCENT**

Abstract □ The two major routes of degradation of phenylbutazone (I) are oxidation and hydrolysis. Hydrolysis gives rise to *n*-butylmalonic acid mono-(*N,N'*-diphenyl)hydrazide (II). Oxidation at the C-4 position yields 1,2-diphenyl-4-*n*-butyl-4-hydroxypyrazolidine-3,5-dione (III), which is readily hydrolyzed to *n*-butyltartronic acid mono-(*N,N'*-diphenyl)hydrazide (IV). Whereas the mass spectra of I, III, and the methyl esters of carboxylic acids II and IV all demonstrate major peaks corresponding to their respective molecular ions, the mass spectrum of II is essentially identical with that of I, suggesting facile dehydration. In the mass spectrum of IV, the peak of highest mass is found at *m/e* 205; no peak could be perceived corresponding to the molecular ion or to loss of water, carbon dioxide, or both of these elements from the molecular ion. Under normal pyrolytic conditions, II is *decarboxylated* to *N*-caproylhydrazobenzene (V) and IV is readily *dehydrated* to yield III. The mass spectral fragmentation of IV was successfully simulated in the laboratory to give an excellent yield of aniline and α-keto-*N*-caproylaniline (VI) (mol. wt. 205). The probable course of this unusual transformation was elucidated from studies of the accelerated decomposition of IV and derivatives considered as possible intermediates in the degradation process.

Keyphrases □ Phenylbutazone—mass spectral and pyrolytic behavior of products of degradation by oxidation and hydrolysis □ Mass spectrometry—determination of products of phenylbutazone degradation by oxidation and hydrolysis □ Pyrolysis—behavior of products of phenylbutazone degradation by oxidation and hydrolysis

Qualitative and preparative TLC procedures were developed which allow unequivocal identification, as well as semiquantitative estimation, of the degradation products of phenylbutazone (I).

The utilization of mass spectrometry in the identification of material isolated by preparative TLC affords a considerable saving of time and effort in view of the small quantities of sample normally required for satisfactory analysis. However, while the mass spectrometric behavior of I and the majority of its derivatives is unexceptional, the fragmentations of the two carboxylic acids, the major products of phenylbutazone degradation, are unusual and essentially different.

Accordingly, to standardize identification procedures and to gain a better understanding of the chemical behavior of these two acids, a thorough examination of their thermal degradative and mass spectrometric behavior was undertaken.

RESULTS AND DISCUSSION

As illustrated in Scheme I, the two main routes of degradation of phenylbutazone (1,2-diphenyl-4-*n*-butylpyrazolidine-3,5-dione) (I) are oxidation and hydrolysis (1). Hydrolysis of I gives rise to *n*-butylmalonic acid mono-(*N,N'*-diphenyl)hydrazide (II). Oxidation at the C-4 position of I produces 1,2-diphenyl-4-*n*-butyl-4-hydroxypyrazolidine-3,5-dione (III), which is readily hydrolyzed to *n*-butyltartronic acid mono-(*N,N'*-diphenyl)hydrazide (IV).

Whereas hydrolysis of III to IV is a reaction that can be reversed

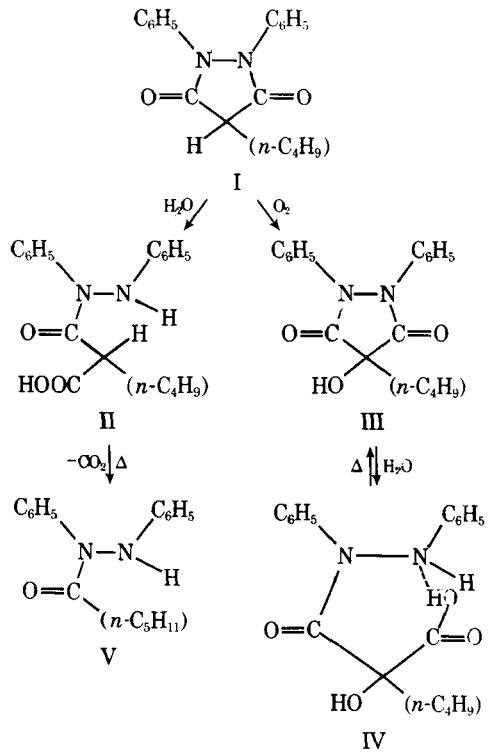

Scheme I—Some transformations of I

easily by heating the acid neat or in solution in most solvents, pyrolysis of II is an effective method of decarboxylation and yields *N*-caproylhydrazobenzene (V).

Since incorporation of electron-withdrawing substituents alpha to the carboxylic acid grouping normally facilitates decarboxylation of β-keto acids (2), the dramatic difference in the pyrolytic behavior of acids II and IV would seem to be attributable to a difference in the conformational disposition of the carboxylic acid group. The facile dehydration of IV could reflect a close proximity of the carboxylic acid grouping to the terminal nitrogen atom. Association between these two structural elements would also discourage the attainment of the cyclic transition state supported for decarboxylation of β-keto acids (3) (IV in Scheme II).

The mass spectra of I, III, and the methyl esters of II and IV all demonstrate major peaks corresponding to their respective molecular ions. The mass spectrum of II is essentially identical with that of I, indicating facile dehydration with ring closure under the mass spectral conditions employed. No peak corresponding to its molecular ion or to loss of water, carbon dioxide, or both of these elements from its parent molecule could be perceived in the mass spectrum of IV, the highest mass peak being found at *m/e* 205 (48%) and the base peak occurring at *m/e* 93. Scheme III illustrates the probable structures of the main fragments observed for I and its derivatives.

The preference of II for dehydration in the mass spectrometer, rather than decarboxylation as observed under normal pyrolytic conditions, can be rationalized on the basis that decomposition in the mass spectrometer occurs in the gaseous state which would favor the existence of unassociated molecules; the course of normal pyrolysis is directed by the conformation of intermolecularly associated molecules. An acceptable internal hydrogen bond can un-

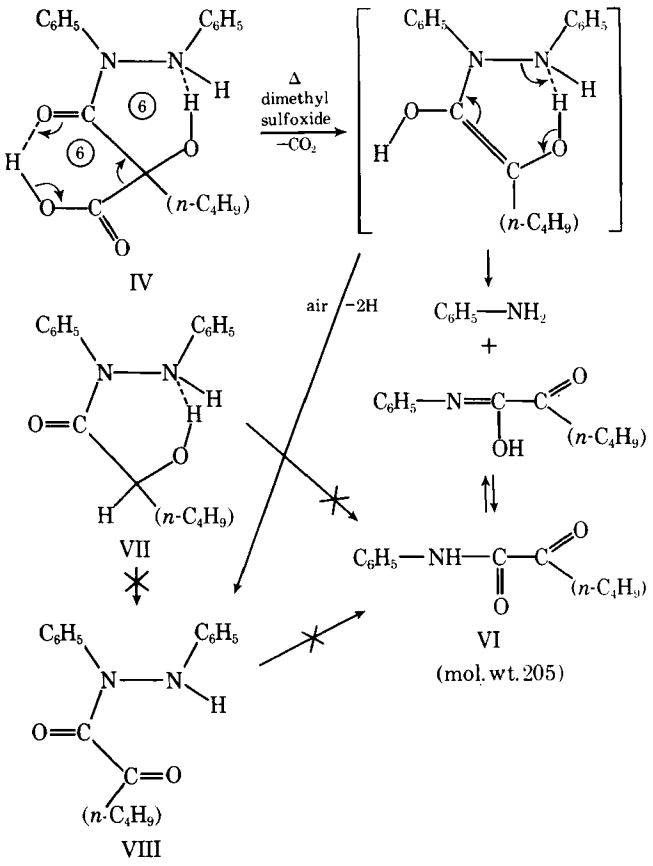

Scheme II—Degradation of IV

doubtedly be formed between the carboxylic hydroxyl group and the terminal nitrogen atom[1], as illustrated in Fig. 1.

The hydrogen-bonding arrangement suggested for unassociated IV would account for its failure to undergo dehydration in the mass spectrometer, yielding III which, as noted earlier, exhibits a molecular ion (*m/e* 324). In the solid state (and liquid melt), IV would then be extensively involved in intermolecular hydrogen bonding utilizing the 4-hydroxy and 3-keto functions, with the carboxylic hydroxyl group internally hydrogen bonded to the terminal nitrogen. In the solid state and in solution, II is probably not significantly involved in intramolecular hydrogen bonding[2].

It was felt that pyrolytic studies in a solvent possessing the ability to disrupt the hydrogen bonding proposed for IV in solid and molten state (as well as in solution in "inert" solvents) might test the preceding rationale. It was hoped that it would be possible to simulate the mass spectral fragmentation and to observe intermediates in this transformation. In particular, it was expected that disruption of the internal hydrogen bond involving the carboxylic acid group would make the decarboxylation step more favorable; it appeared to be the most likely initial phase of the fragmentation.

Accordingly, IV was pyrolyzed in dimethyl sulfoxide. Within 10 min at 160°, IV was totally decomposed and an excellent yield of α-keto-*N*-caproylaniline (VI) (mol. wt. 205) was realized. It was readily apparent that conversion to VI and aniline was close to quantitative, since a similar pyrolysis performed in dimethyl sulfoxide-d_6 yielded a product whose NMR spectrum was superimposable with that of an artificial mixture of authentic samples of the two compounds in equivalent proportions. The mass spectrum of IV was essentially a summation of the mass spectra of VI (*m/e* 205, 61%) and of aniline (*m/e* 93, 100%). The mass spectrum of deuterated IV showed peaks at *m/e* 206 and 95, corresponding to deuterated VI and dideuterated aniline, respectively.

[1] Spectroscopic data (4) and deuterium oxide solvent isotope effects (5) support the generalization that OH—NH bonds are stronger than NH—O bonds.

[2] Due to lack of solubility, a thorough IR investigation of the character of hydrogen bonding in II and IV could not be pursued. IR spectra of the solids also did not allow any meaningful conclusions to be drawn.

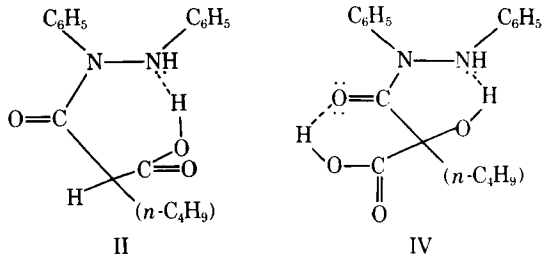

Figure 1—*Suggested hydrogen bond formation in unassociated molecules of II and IV.*

To gain evidence for the proposed mechanism of decomposition of IV, its pyrolysis under varying conditions was followed by TLC. Chromatography of the product of decomposition in dimethyl sulfoxide at 160° indicated the presence of two other compounds in addition to VI and aniline. Comparison of R_f values and reactions to spray reagents (1) indicated that the major product was VIII and the minor product was III, the product of dehydration of IV. The identity of VIII was confirmed by preparative TLC separation, followed by mass spectrometric and IR spectroscopic analysis; its spectra were identical to those of an authentic sample. Semiquantitative estimation (1) of the solid precipitated by aqueous dilution of the dimethyl sulfoxide solution indicated a ratio of 91:6:3 (VI:VIII:III). The aqueous filtrate contained aniline and only traces of the other compounds.

The detection of VIII supports the suggestion that the first step of the degradation is decarboxylation (Scheme II). However, formation of VIII requires an oxidation process in addition to loss of carbon dioxide. In the hope of observing the precursor of VIII, the hydroxy acid IV was heated at a reduced temperature (steam bath) under a nitrogen atmosphere. In a control experiment, as in the pyrolyses at 160°, no attempt was made to exclude oxygen. Under a nitrogen atmosphere, no trace of VIII was observed. GC and NMR analysis indicated formation of VIII and VI in a ratio of roughly 1:1, with III being produced in only minor quantity. Compounds VIII and VI were completely stable under all conditions of pyrolysis employed.

Compound VII, which was viewed as a possible precursor to VIII (and which is the acyloin that would be expected to be derived from ketonization of the suggested enediol product of decarboxylation of IV) (Scheme II), was resistant to oxidation under all conditions of pyrolysis utilized, an observation that precludes the intermediacy of VII in the formation of VIII.

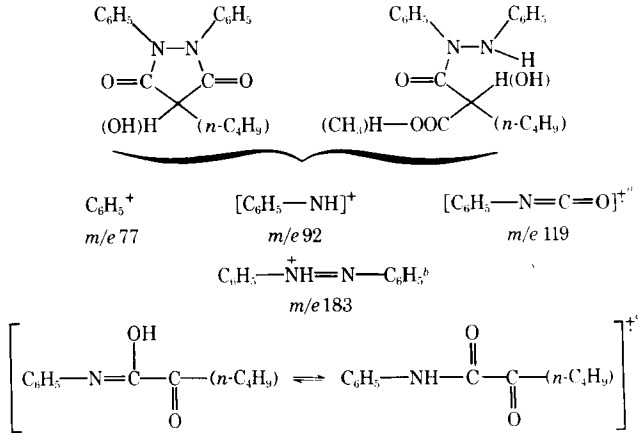

Scheme III—Postulated structures for salient mass spectral fragments of I and its derivatives. [a] *This fragment does not appear in the mass spectrum of V.* [b] *This ion is not observed for III, presumably because C-4 hydrogen is essential to its formation in the absence of NH hydrogen. Its abundance in the spectrum of IV is only 10% of that of the base peak, indicative of the ascendancy of N—N fracture.* [c] *Except for IV and VI, as discussed in the text, only III demonstrates significant abundance (26%) of this fragment; for VII and VIII, the only other compounds in which it is detected, its abundances are 11 and 6%, respectively.*

EXPERIMENTAL[3]

Materials—Reference samples of all compounds examined were used as obtained[4], and periodic checks by TLC[5] were made to ascertain their integrity. Additional quantities of IV were prepared by the method of Efimovsky (7).

Solvents were of analytical grade and were used as obtained commercially. Dimethyl sulfoxide was kept dry over molecular sieves.

Pyrolysis Procedures—*Neat*—Substrate (200 mg) was heated for 10 min in an oil bath preheated to 160°. The product was then subjected to TLC and spectroscopic analysis.

Dimethyl Sulfoxide—To 200 mg of substrate was added 2.0 ml of solvent, and the mixture was pyrolyzed in a preheated bath[6]. After cooling to room temperature, the reaction medium was diluted with approximately 8 ml of distilled water.

In the case of II, the cloudy aqueous dimethyl sulfoxide medium was extracted with 2 × 5-ml portions of chloroform, dried over anhydrous sodium sulfate, and then analyzed.

Aqueous dilution of the dimethyl sulfoxide solution of pyrolyzed IV resulted in precipitation of 0.9 g[7] of yellowish solid. This solid was purified by preparative TLC and identified as VI, mp[8] 84–85° (uncorrected); IR (mineral oil mull): 3322 (NH), 1720, and 1686 (C=O) cm^{-1}; UV (95% ethanol): λ_{max} 280 nm (ϵ 530); NMR (dimethyl sulfoxide-d_6): δ 10.40 (broad, 1H, amide proton), centered at 7.83 (pair of multiplets, 2H, phenyl protons *ortho* to amide grouping), centered at 7.32 (multiplet, 3H, phenyl protons *meta* and *para* to amide group), 2.92 (broadened triplet, J = 7 Hz, 2H, $-CH_2-$, α to carbonyl), centered at 1.45 (multiplet, 4H, $-CH_2-CH_2-$, β and γ to carbonyl), and 0.90 (triplet, J = 6 Hz, 3H, $-CH_3$).

Anal.[9]—Calc. for $C_{12}H_{15}NO_2$: C, 70.24; H, 7.31; N, 6.82. Found: C, 70.12; H, 7.46; N, 6.72.

Methylation of II and IV—To a magnetically stirred suspension of 500 mg of II or IV in 20 ml of anhydrous ether was added dropwise an ethereal alcoholic solution of diazomethane[10]. Immediate effervescence occurred in both cases, and addition was continued until the yellow color of diazomethane persisted. Stirring was continued for 15 min, and the solution was evaporated to dryness under reduced pressure.

For both reactions, TLC examination indicated complete consumption of II or IV. In the case of II, its methyl ester (IX) (R_f greater than that of II) was the exclusive product of the reaction; IR (film): 3330 (NH), 1750, and 1682 (C=O) cm^{-1}; NMR (deuterochloroform): δ centered at 7.08 (multiplet, 11H, NH and phenyl protons), 3.90 (broadened triplet, J = 7 Hz, 1H, α to ester grouping), 3.67 (singlet, 3H, $COOCH_3$), centered at 1.93 (multiplet, 2H, $-CH_2-$, β to carbonyl), centered at 1.28 (multiplet, 4H, $-CH_2-CH_2-$, γ and δ to carbonyl), and 0.87 [distorted triplet, J = 5 Hz, 3H, $CH_2-(CH_3)$].

The methyl ester (X) of IV was separated from traces of III[11] by preparative TLC; IR (potassium bromide): 3440 (OH), 3304 (NH), 1755, and 1690 (C=O) cm^{-1}; NMR (deuterochloroform): δ centered at 7.17 (multiplet, 10H, phenyl protons), 4.47 (broad, 1H, OH), 3.43 (singlet, 3H, $COOCH_3$), 2.07 (broadened triplet, J = 6 Hz, 2H, $-CH_2-$, β to carbonyl), 1.33 (broad multiplet, 4H, $-CH_2-CH_2-$, γ and δ to carbonyl), and 0.87 [distorted triplet, J = 5 Hz, 3H, $-CH_2-(CH_3)$].

SUMMARY AND CONCLUSIONS

The evidence suggests that the initial decomposition product of IV in dimethyl sulfoxide and in the mass spectrometer is a highly reactive product of decarboxylation and readily degrades to VI and aniline at elevated temperatures. However, at lower temperatures in the presence of atmospheric oxygen, IV undergoes decarboxylation plus oxidation to yield VIII; the latter reaction gains importance comparable with that of N—N cleavage under such conditions. Facile oxidation of the proposed intermediate 1,2-enediol would be consistent with the establishment of such species as intermediates to explain the ease of oxidation of acyloins (8).

In dimethyl sulfoxide and in the mass spectrometer, dehydration of IV is an insignificant mode of degradation.

REFERENCES

(1) D. V. C. Awang, A. Vincent, and F. Matsui, *J. Pharm. Sci.*, **62,** 1673(1973).

(2) J. Hine, "Physical Organic Chemistry," McGraw-Hill, New York, N.Y., 1962, chap. 13.

(3) D. B. Bigley and J. C. Thurman, *Tetrahedron Lett.*, **1967,** 2377.

(4) C. A. Coulson, *Research (London)*, **10,** 149(1957); H. H. Freedman, *J. Amer. Chem. Soc.*, **83,** 2900(1961).

(5) J. L. Halsam and E. M. Eyring, *J. Phys. Chem.*, **71,** 4470(1967).

(6) G. A. Neville and D. V. C. Awang, *Org. Mag. Res.*, **2,** 341(1970).

(7) O. Efimovsky, *J. Rech. C.N.R.S.*, **47,** 147(1959).

(8) W. A. Waters, "Mechanisms of Oxidation of Organic Compounds," Methuen and Co., London, England, 1964, p. 88.

ACKNOWLEDGMENTS AND ADDRESSES

Received November 15, 1974, from the *Drug Research Laboratories, Health Protection Branch, Health and Welfare Canada, Tunney's Pasture, Ottawa, Ontario, K1A 0L2, Canada.*

Accepted for publication April 11, 1975.

Presented in part at the 21st Canadian Conference on Pharmaceutical Research, Ottawa, Canada, May 1974.

The authors are grateful to Dr. A. By and Mr. J. C. Ethier for recording the mass spectra and to Dr. K. K. Midha and Dr. A. By for helpful discussions.

[x] To whom inquiries should be directed.

[3] NMR spectra were obtained with a Varian A-60A spectrometer, and chemical shifts are reported in parts per million downfield from tetramethylsilane as the internal standard. IR spectra were recorded on a Perkin-Elmer 621 spectrophotometer, and UV spectra were recorded on a Beckman Acta C-III spectrophotometer. Mass spectra were observed at 70-ev electron beam voltage with a Hitachi Perkin-Elmer RMU-6L spectrometer. IR and NMR spectra for all compounds but VI were previously reported and discussed (6).

[4] Ciba-Geigy, Basel, Switzerland.

[5] TLC procedures employed were as previously described (1).

[6] Pyrolyses were conducted at 160° in an oil bath and at 100° on a steam bath, with care being taken to exclude moisture from the reaction flask. For pyrolyses in a deoxygenated atmosphere, dry nitrogen was bubbled through the reaction medium for 2 hr prior to heating and during the pyrolysis, which was followed by TLC.

[7] TLC examination of the filtrate indicated only a trace amount of VIII in addition to VI and aniline.

[8] Kofler micro hot stage melting-point apparatus.

[9] H. Séguin, National Research Council of Canada Laboratories, Ottawa, Canada.

[10] Diazald procedure of Aldrich Chemical Co.

[11] After prolonged storage, even at 0° in ether solution, X gave rise to appreciable amounts (by TLC) of III. In a control experiment, it was determined that the parent hydroxy acid (IV) was not an intermediate in this conversion since the acid underwent no detectable dehydration under conditions leading to formation of III from X.

Spectrophotometric Determination of *p*-Aminophenol Alone or in the Presence of Acetaminophen

EVANGELOS KALATZIS ˣ **and IRENE ZARBI**

Abstract □ Small amounts of *p*-aminophenol were analyzed quantitatively by mixing with 4-nitro- or 2,4-dinitrobenzaldehyde in neutral alcoholic solution and then quantitatively forming the respective Schiff bases, 4′-nitro- and 2′,4′-dinitrobenzylidene-4-hydroxyaniline, by evaporating the alcoholic solutions to dryness. The Schiff bases thus formed were examined spectrophotometrically. This procedure was also used for the determination of *p*-aminophenol in the presence of its degradation products. It was necessary, however, to separate the respective Schiff bases by TLC from the degradation products and the reaction mixture prior to spectrophotometric examination. Small amounts of *p*-aminophenol present in acetaminophen were quantitatively determined by applying the procedure to a water–ethanol (95:5 v/v) extract of the samples of acetaminophen. TLC was used to separate the respective Schiff bases from the reaction mixture and acetaminophen prior to spectrophotometric examination.

Keyphrases □ *p*-Aminophenol—spectrophotometric analysis of Schiff base derivatives, alone or in presence of degradation products or acetaminophen, TLC separation □ Spectrophotometry—analysis, Schiff base derivatives of *p*-aminophenol, alone or in presence of degradation products or acetaminophen □ TLC—separation, Schiff base derivatives of *p*-aminophenol in presence of degradation products or acetaminophen

It was reported that *p*-aminophenol (I) liberated in mixtures containing acetaminophen (II) could be determined spectrophotometrically by using 4-nitrobenzaldehyde (1). A color test, with alkaline sodium nitroprusside solution, for small amounts of I in II was described in the British Pharmacopoeia (2), and another test with *p*-dimethylaminocinnamaldehyde was described in NF XIII (3).

Several methods for the determination of I are based on the formation of a colored reaction mixture (3–10), but the exact nature of the reaction products has not been established. A color reaction has also been reported (11). Other methods are based on titrating with perchloric acid (12) or carrying out a polarographic examination (13, 14), but these methods may prove difficult with samples containing small amounts of I.

This paper presents a method for the determination of I either alone or in the presence of its colored degradation products and/or II. This method is based on the reaction between I and 4-nitrobenzaldehyde (III) or 2,4-dinitrobenzaldehyde (IV) with the formation of the colored 4′-nitrobenzylidene-4-hydroxyaniline (V) or 2′,4′-dinitrobenzylidene-4-hydroxyaniline (VI), respectively (Schiff bases).

EXPERIMENTAL[1]

Materials—4-Nitro- and 2,4-dinitrobenzaldehydes[2], acetaminophen[3], petroleum ether[4] (bp 40–70°), and acetic acid[4] were used without further purification. *p*-Aminophenol[5] was purified by three sublimations at 110°/0.1 mm Hg (white crystals, mp 188°). Ethanol[6] and acetone[6] were purified by fractional distillation.

TLC—Separations by TLC were carried out on silica gel[7] layers of 0.50 mm or, when I was present in very small amounts, on silica gel[7] layers of 0.25 mm. The solvent system found suitable for separating V and VI from other interfering components was petroleum ether–acetone (70:30). TLC plates were usually eluted only once but, when necessary, were eluted twice for better separation.

TLC chromatograms were examined against the green fluorescence of the plate (Fig. 1) by viewing in short wavelength[8] (254 nm) UV light and clearly marking the boundaries of the areas containing the different components. It was thus easier to scrape off and then extract the component present in the silica gel in a particular area and determine its UV–visible spectrum. The fluorescence material had no effect on the analytical results.

Preparation of Reagent Solutions—Stock solutions of III and IV were freshly prepared by dissolving 15.1 and 20 mg of material, respectively, in 50 ml of ethanol (final solutions of 2×10^{-3} *M*). These solutions are not stable and must be freshly prepared, preferably, each day.

Standard Solution of I—A stock solution (2×10^{-3} *M*) was prepared by dissolving 10.9 mg of I in 50 ml of ethanol. This solution darkened on standing, but it could be used for 2–3 days. However, it was preferable to prepare it each day.

4′-Nitrobenzylidene-4-hydroxyaniline (V)—A mixture of 0.55 g of I and 0.80 g of III dissolved in 50 ml of ethanol was left standing for 0.5 hr. The alcohol was then evaporated under reduced pressure, and the solid mixture was dissolved in a small amount of ethanol which was again evaporated. The crude solid product obtained (mp 167–168°) was recrystallized from benzene (charcoal) three times, yielding 0.55 g (~60%) (dried at 70°/0.1 mm Hg for ~3 hr), mp 172°.

Anal.—Calc. for $C_{13}H_{10}N_2O_3$: C, 64.46; H, 4.16; N, 11.56. Found: C, 64.74; H, 4.00; N, 11.70.

2′,4′-Dinitrobenzylidene-4-hydroxyaniline (VI)—A mixture of 0.55 g of I and 0.99 g of IV was treated as described for V. The

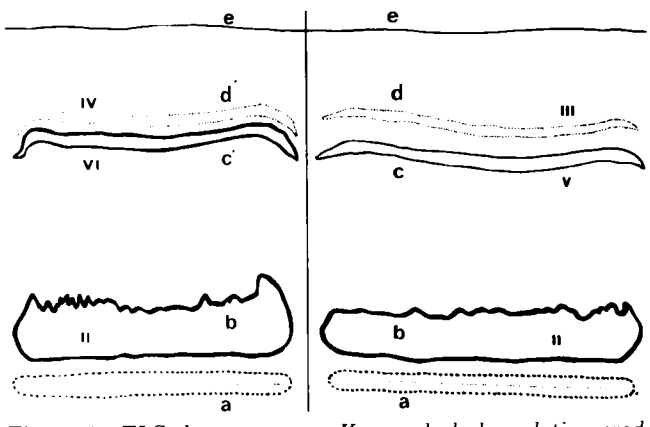

Figure 1—*TLC chromatograms. Key: a, dark degradation products remaining at starting point; and e, solvent front.*

[1] Spectra were determined using a Pye-Unicam SP 8000 recording spectrophotometer. Evaporations were carried out under reduced pressure, using a Büchi Rotavapor R/A, at temperatures not exceeding 40°.

[2] Fluka, puriss.

[3] Fluka, purum.

[4] Carlo Erba.

[5] Fluka, practical.

[6] Technical grade.

[7] GF_{254} Merck reagent.

[8] Chromato-Vue, Ultra-Violet Products, San Gabriel, Calif.

Table I—Deterioration of an Aqueous Solution of I (~8 × 10^{-4} *M*) as Determined by Method 2[a]

Days	Compound V Absorbance[b] at 380 nm	% Loss	Compound VI Absorbance[b] at 404 nm	% Loss
0	0.530	—	0.492	—
3	0.376	29.0	0.370	26.0
5	0.290	45.0	0.266	45.9
7	—	—	0.186	62.2
8	0.148	72.1	—	—

[a] Absorbances were read from full UV–visible spectra. [b] One-centimeter cells as described under Method 2.

yield after the first crystallization was 1 g (~70%). The product was further purified by three recrystallizations (dried at 70°/0.1 mm Hg for ~3 hr), mp 161°.

Anal.—Calc. for $C_{13}H_9N_3O_5$: C, 54.36; H, 3.16; N, 14.63. Found: C, 54.73; H, 3.33; N, 14.48.

Determination of I as V or VI—*Direct Measurement of V or VI (Method 1)*—An exact volume (*e.g.*, 5, 10, 15, or 20 ml) of a standard ethanolic solution of I (*e.g.*, 2 × 10^{-5} *M*), prepared by diluting a standard stock solution (*e.g.*, 2 × 10^{-3} *M*), is mixed with a volume of the reagent solution (III or IV) in ethanol 1.5 times larger than that of the I but of the same concentration (*i.e.*, 2 × 10^{-5} *M*). (Equal volumes may also be used, but the concentration of the reagent is then 1.5 times that of I.) The mixture is evaporated under reduced pressure, and the residue is redissolved in a small amount of ethanol and reevaporated. This process is repeated for a third time, after which the colored product is dissolved in 5.0 ml of ethanol.

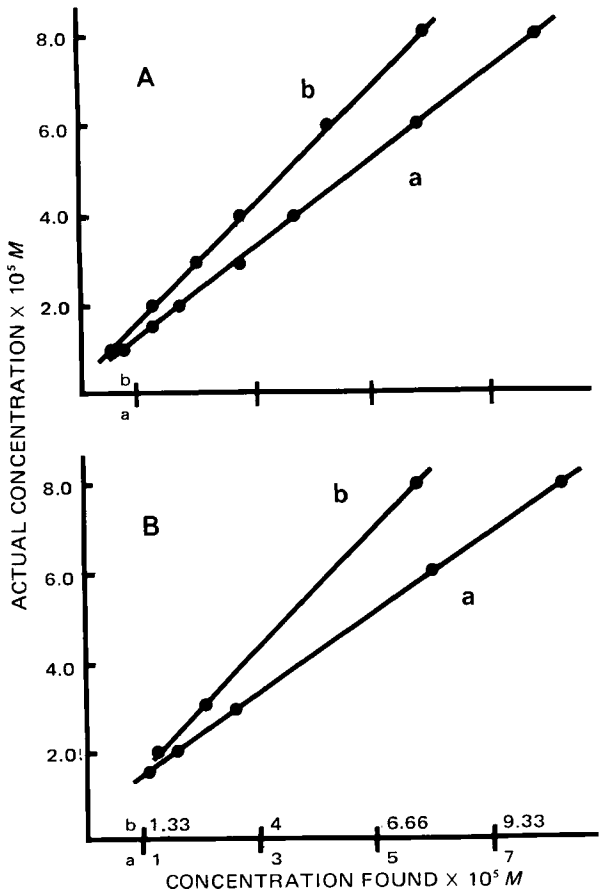

Figure 2—*Relationship between actual and determined (Method 3) I in excess of II. A: recovery of I calculated on the basis of the simultaneous analysis of reference samples of I. Key: a, I determined as V (slope = 0.97); and b, I determined as VI (slope = 0.98). B: recovery of I calculated on the basis of Beer–Lambert relationships using appropriate conversion factors. Key: a, I determined as V (slope = 0.91); and b, I determined as VI (slope = 1.02).*

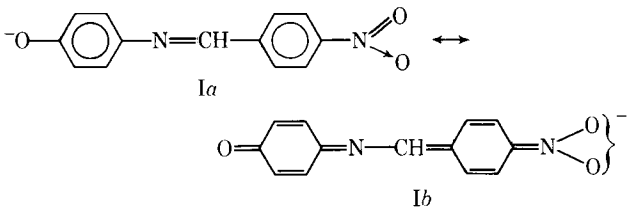

Scheme I

Two milliliters of this solution is pipetted into a 1.0-cm silica cell and its spectrum is recorded. Absorbances read at the λ_{max} of 380 nm for V and of 404 nm for VI are multiplied by the appropriate conversion factors (7.23 × 10^{-5} and 9.58 × 10^{-5} for V and VI, respectively) derived from the Beer–Lambert linear relationships to convert them to concentrations of I. Then 0.5 ml of 0.1 *M* sodium hydroxide ethanolic solution is added to the cell and the spectra are recorded again. Absorbances are read at the λ_{max} of 466 and 528 nm, respectively.

Measurement of V or VI after Recovery by TLC (Method 2)—This method is applicable when degradation products are present. The concentrations of I and reagent solutions used are 10 times greater than those used in Method 1 (2 × 10^{-4} *M*). The same procedure is then followed until the reaction product is dissolved in 5.0 ml of ethanol. Then 0.5 ml of this final solution is spotted as a band on a TLC plate.

After elution, the yellow band corresponding to V or VI is scraped off and extracted with ethanol until the silica gel is free from any yellow color (filtration under gentle suction). The filtrate and washings are then evaporated under reduced pressure, and the reaction product is dissolved in 5.0 ml of ethanol. The spectra are then examined as outlined in Method 1. (Appropriate conversion factors are 8.16 × 10^{-5} and 10.4 × 10^{-5} for V and VI, respectively.)

Determination of I Present in II—This method also is applicable when degradation products are present.

Preparation of Samples—To a known amount of II (*e.g.*, 0.05, 0.5, or 5.0 g), an exact volume (*e.g.*, 2.5 or 7.5 ml) of a standard ethanolic I solution (2 × 10^{-3} *M*) is added and the resultant mixture is evaporated under reduced pressure.

Analysis of V or VI after Separation and Recovery by TLC from II (Method 3)—The solid mixture of I and II obtained after evaporation is extracted with 25 ml of water–alcohol (95:5 v/v) by shaking the suspension for about 0.5 hr. The suspension is filtered under gentle suction. Then an exact volume (5, 10, 15, or 20 ml) from the filtrate, whose pH is checked to be ~6, is mixed with a known volume of ethanolic III or IV solution calculated to be 1.5 times that of the I solution[9]. The resultant solutions are then evaporated to dryness three times under reduced pressure, and the reaction product is dissolved in a known volume of ethanol (5 ml). After 0.5 ml of this solution is spotted on the TLC plate, the same procedure as that described for Method 2 is then followed.

RESULTS AND DISCUSSION

Compound IV in ethanolic solution deteriorated more rapidly than III (about 50 and 6% in 5 days at ambient temperature, respectively), and the determination of I with deteriorated reagent solution was unsatisfactory. For example, after a solution of IV in ethanol stood for 3 weeks, it gave unsatisfactory analytical results. An aqueous solution of I deteriorated rapidly due to oxidative degradation, as evidenced by the formation of a dark precipitate and the analytical results using Method 2 (Table I). An alcoholic solution of I was much more stable in spite of the apparent color deterioration; less than 5% of I, determined by Method 2, was degraded after 1 week.

The absorbances of the neutral ethanolic solutions of V and VI were determined at λ_{max} 380 and 404 nm, respectively. A bathochromic shift took place when the solutions were made alkaline,

[9] When analyzing unknown mixtures, duplicate determinations with varying amounts of reagent solutions may be needed to establish that the reagent is in excess.

Table II—Stability of Neutral Ethanolic Solutions of V and VI[a]

	Compound V				Compound VI					
	6×10^{-5} M[b]		5×10^{-4} M[c]		6×10^{-5} M[b]		5×10^{-4} M[b]		5×10^{-4} M[c]	
Days	A	% Loss	A	% Loss	A	% Loss	A	% Loss	A	% Loss
0	0.870	—	0.748	—	0.699	—	0.578	—	0.580	—
1	0.752	13.6	0.401	46.4	0.688	1.6	0.567	1.9	0.486	16.3
2	0.636	26.9	0.396	47.1	0.668	4.4	0.560	3.1	0.444	23.5
4	0.421	51.6	—	—	0.632	9.6	0.550	4.8	0.400	31.0
5	0.370	57.5	0.378	49.5	0.603	13.7	0.540	6.6	0.360	34.1

[a] Compound V measured at 380 nm, and Compound VI measured at 404 nm. Absorbance in 1.0-cm silica cell. Absorbances were read from full UV–visible spectra. [b] Measurement of the absorbance before recovery by TLC. [c] Measurement of the absorbance after recovery by TLC.

Table III—Absorbance of Solutions of V in Ethanol in the Absence and in the Presence of Excess III

	4×10^{-5} M V	6×10^{-5} M V	8×10^{-5} M V	Mean Value	4×10^{-5} M V	4×10^{-5} M V and 4×10^{-5} M III	4×10^{-5} M V and 8×10^{-5} M III	Mean Value
No TLC[a]								
A_1[b] at 380 nm	0.578	0.868	1.16	—	0.577	0.580	0.566	0.574
A_2 at 466 nm	0.710	1.07	1.42	—	0.720	0.721	0.696	0.712
Ratio A_2/A_1	1.23	1.23	1.22	1.23	1.24	1.24	1.23	1.24
TLC[c]								
A_1 at 380 nm	0.491	0.759	1.01	—	0.491	0.522	0.520	0.512
A_2 at 466 nm	0.606	0.934	1.25	—	0.606	0.658	0.658	0.641
Ratio A_2/A_1	1.24	1.23	1.24	1.24	1.23	1.26	1.26	1.25
Percent recovered at 380 nm	84.9	87.4	87.1	86.5	85.0	90.0	91.9	90.1
Percent recovered at 466 nm	85.3	87.5	87.9	86.9	84.2	91.3	94.5	91.3

[a] Measurement of absorbance before recovery by TLC. [b] Absorbance in 1.0-cm silica cell. [c] Measurement of absorbance after recovery by TLC.

Table IV—Absorbance of Solutions of VI in Ethanol in the Absence and in the Presence of Excess IV

	4×10^{-5} M VI	6×10^{-5} M VI	8×10^{-5} M VI	Mean Value	4×10^{-5} M VI	4×10^{-5} M VI and 4×10^{-5} M IV	4×10^{-5} M VI and 8×10^{-5} M IV	Mean Value
No TLC[a]								
A_1[b] at 404 nm	0.465	0.693	0.925	—	0.465	0.443	0.448	0.452
A_2 at 528 nm	0.710	1.08	1.42	—	0.720	0.687	0.685	0.697
Ratio A_2/A_1	1.53	1.56	1.54	1.54	1.55	1.55	1.53	1.54
TLC[c]								
A_1 at 404 nm	0.427	0.640	0.884	—	0.427	0.429	0.427	0.428
A_2 at 528 nm	0.649	0.934	1.27	—	0.649	0.652	0.653	0.651
Ratio A_2/A_1	1.52	1.46	1.44	1.46	1.52	1.52	1.53	1.52
Percent recovered at 404 nm	91.8	92.3	95.6	93.3	91.8	96.8	95.3	94.6
Percent recovered at 528 nm	91.4	87.8	89.8	89.4	90.1	94.9	95.2	93.4

[a] Measurement of absorbance before recovery by TLC. [b] Absorbance in 1.0-cm silica cell. [c] Measurement of absorbance after recovery by TLC.

and the absorbance could then be read at 466 and 528 nm, respectively. The bathochromic shift was due presumably to resonance between Ia and Ib and IIa and IIb (Schemes I and II). Not only the alkaline but the neutral solutions of V and VI were unstable. Recovery of these products by TLC from standing solutions also showed losses which increased with standing time (Table II).

Freshly prepared solutions, however, obeyed the Beer–Lambert relationship. After recovery by TLC (Tables III and IV), the results were lower by an average of 12% when I was determined as V and 8% when I was determined as VI, but they still gave a satisfactroy Beer–Lambert relationship. Excess reagent had no effect on the absorbance readings (Tables III and IV).

It is more accurate to construct a Beer–Lambert relationship by using standard ethanolic solutions of I (Tables V and VI). The direct reaction of I with the reagent solutions as described in Method 1 (not using TLC) gave results that were 3.3 or 9.5% lower than those obtained by measuring directly pure V or VI, respectively. The direct reaction of I with reagent solutions as described in Method 2 (using TLC) gave results that were 1.0 or 11.0% lower than those obtained for pure V or VI, respectively. These data suggest that the decrease in the results due to the direct reaction of I with the reagent solutions before and after recovery by TLC is rather constant. The average values for this decrease were 2.2 or 10.3% for V or VI, respectively. Moreover, a large excess of reagent was unnecessary for the reaction to go to completion (Tables V and VI).

It is also possible to calculate the decrease in the results due to losses occurring during the use of TLC. Thus, these losses for pure

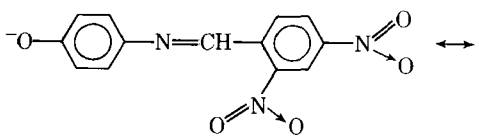

IIa

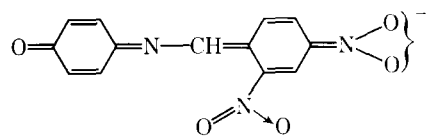

IIb

Scheme II

Table V—Absorbance of Ethanolic Reaction Solutions of I with III

	4×10^{-5} *M* I and 6×10^{-5} *M* III	6×10^{-5} *M* I and 9×10^{-5} *M* III	8×10^{-5} *M* I and 12×10^{-5} *M* III	Mean Value
No TLC[a]				
A_1[b] at 380 nm	0.552	0.840	1.10	—
A_2 at 466 nm	0.671	1.03	1.37	—
Ratio A_2/A_1	1.22	1.23	1.24	1.23
TLC[c]				
A_1 at 380 nm	0.477	0.740	0.985	—
A_2 at 466 nm	0.581	0.910	1.20	—
Ratio A_2/A_1	1.22	1.23	1.22	1.22
Percent recovered at 380 nm	86.4	88.1	89.5	88.1
Percent recovered at 466 nm	86.6	88.1	87.7	88.8

[a] Measurement of absorbance before recovery by TLC. [b] Absorbance in 1.0-cm silica cell. [c] Measurement of absorbance after recovery by TLC.

V and VI were 13.5 and 6.5%, respectively, while those for the direct reaction of I with the reagent solutions were 11.5 and 8.0%, respectively. The agreement between these figures is satisfactory when it is considered that the experimental error of the present method is about ±5%. Therefore, the average value for the losses due to TLC was 12.5 or 7.5% for the determination of I as V or VI, respectively.

A correction factor to account for losses due to TLC is not needed to convert absorbances to concentrations when the appropriate Beer–Lambert linear relationship is used. However, if a Beer–Lambert relationship is constructed using only pure V or VI as reference materials, correction factors are needed. The average factor calculated for this case is 1.17 or 1.21 for the determination of I as V or VI, respectively. On the other hand, if a Beer–Lambert relationship is constructed by the direct reaction of I with the reagent solutions of III or IV, then the average correction factor needed to correct for losses due to the recovery by TLC is 1.14 or 1.08 for the determination of I as V or VI, respectively. Nonetheless, it would be preferable to construct and use the appropriate Beer–Lambert linear relationship in each case.

The ratios of the absorbance of the alkaline solutions to that of the neutral solutions of V and VI were 1.24 and 1.52, respectively, when no TLC was used. After recovery by TLC, however, there was a small tendency for the ratios to decrease, especially for VI (Tables IV and VI). These ratios can be used as an additional check of the correct identification and accurate determination of V and VI. The percentage recovery figures were calculated from the readings obtained only at the λ_{max} of the neutral solutions, *i.e.*, 380 and 404 nm for V and VI, respectively.

A number of samples of II containing various amounts of I (0.05–4.2%) were analyzed by following Method 3, and the results were compared with those obtained with pure reference samples of I. These reference samples were analyzed under identical conditions and used as the basis for the percentage calculation of the recovery results (Table VII). These results were also compared with those obtained by a modification of Method 3, which seems satisfactory for an approximate determination of I in II, especially for samples not degraded. This procedure consisted of reading the absorbances after carrying out the appropriate dilutions and omitting the use of TLC for separating V or VI from the mixture. When TLC separation was used, the recovery was almost 100% for mixtures containing more than 0.3% of I; for mixtures containing less than 0.3%, the recovery figures decreased with a decrease in the I content, presumably due to some retention by the great excess of II.

The present method gave reproducible results (Tables VIII and IX) for mixtures also containing very small amounts of I and for

Table VI—Absorbance of Ethanolic Reaction Solutions of I with IV

	4×10^{-5} *M* I and 6 $\times 10^{-5}$ *M* IV	8×10^{-5} *M* I and 12 $\times 10^{-5}$ *M* IV	Mean Value	6×10^{-5} *M* I and 12 $\times 10^{-5}$ *M* IV	6×10^{-5} *M* I and 18 $\times 10^{-5}$ *M* IV	Mean Value
No TLC[a]						
A_1[b] at 404 nm	0.411	0.822	—	0.632	0.626	—
A_2 at 528 nm	0.625	1.25	—	0.971	0.971	—
Ratio A_2/A_1	1.52	1.52	1.52	1.54	1.55	1.55
TLC[c]						
A_1 at 404 nm	0.396	0.774	—	0.588	0.605	—
A_2 at 528 nm	0.575	1.15	—	0.853	0.859	—
Ratio A_2/A_1	1.45	1.49	1.47	1.45	1.42	1.44
Percent recovered at 404 nm	96.4	94.2	95.3	93.0	96.6	94.8
Percent recovered at 528 nm	92.0	92.0	92.0	87.8	88.6	88.2

[a] Measurement of absorbance before recovery by TLC. [b] Absorbance in 1.0-cm silica cell. [c] Measurement of absorbance after recovery by TLC.

Table VII—Recovery of I in Laboratory Prepared Samples of II Containing Known Amounts of I[a]

		Compound V			Compound VI		
I, mg	II, mg	% Recovery[b], CF[d]	% Recovery[b], RS[e]	% Recovery[c], RS[e]	% Recovery[b], CF[d]	% Recovery[b], RS[e]	% Recovery[c], RS[e]
0.275	500	—	75.3	82.5	—	76.9[f]	85.2[f]
0.410	500	75.6	82.7	92.4	—	—	—
0.545	500	78.8	84.6[g]	93.3[g]	84.2	81.8[g]	93.0[g]
0.820	500	86.2	89.3	93.4	93.9	88.3	95.2
1.090	500	—	92.0[h]	96.9[h]	91.3	91.5[h]	98.9[h]
1.635	500	100.4	96.5	97.2	—	94.9	—
2.180	500	102.4	98.3	98.9	94.6	99.3	—
0.545	50	95.8	99.6	98.3	97.2	105.0	—
1.090	50	97.3	100.0	100.0	104.3	98.3	—
1.635	50	95.5	96.8	101.2	105.7	101.2	—
2.180	50	102.4	99.6	98.6	105.9	102.5	—

[a] Compound V measured at 380 nm, and Compound VI measured at 404 nm. Absorbances were read from full UV–visible spectra. [b] Measurement of absorbance after recovery by TLC. [c] Measurement of absorbance before recovery by TLC. [d] Calculation of percent recovery using conversion factors 8.16×10^{-5} and 10.4 for V and VI, respectively. [e] Calculation of percent recovery on the basis of simultaneous analysis of reference samples of I. [f] Mean value of three determinations. [g] Mean value of two determinations. [h] Mean value of five determinations.

Table VIII—Reproducibility of Results[a]

I, mg	II, mg	Compound V		Compound VI	
		% Recovery, TLC	% Recovery, No TLC	% Recovery, TLC	% Recovery, No TLC
0.273	500	75.3		75.6	83.8
0.273	500	— } 75.3[b]		75.9 } 76.9	84.1 } 85.2
0.273	500	—		79.2	87.7
0.273	—			100.0	100.0
0.55	500	85.3 } 84.6	93.6 } 93.3	82.0 } 81.8	92.8 } 93.0
0.55	500	83.9	93.0	81.6	93.2
0.55	—	100.0	100.0	100.0	100.0
1.09	500	93.2	98.2	88.9	95.2
1.09	500	91.7	96.5	92.6	96.2
1.09	500	90.8 } 92.0	96.6 } 96.9	93.4 } 91.5	102.5 } 98.9
1.09	500	91.3	96.9	92.3	98.7
1.09	500	93.0	96.4	90.4	101.8
1.09	—	100.0	100.0	100.0	100.0

[a] Compound V measured at 380 nm, and Compound VI measured at 404 nm. Absorbances were read from full UV–visible spectra. [b] Mean value.

which the recovery figures were about 80%. These results suggest that laboratory samples of II containing a known amount of I also can be used as reference material for analyzing unknown mixtures.

The following solvent mixtures were unsatisfactory for the recovery of the Schiff bases by TLC, because V and VI hydrolyzed in these systems: (*a*) chloroform–acetone–acetic acid (80:18:2), (*b*) chloroform–petroleum ether–acetone (70:20:10), and (*c*) chloroform–petroleum ether (80:20). Hydrolysis was faster in Solvent System (*a*), especially for V (almost complete).

Dark degradation products of I do not interfere with the determination of I by Method 2 or 3 because the solvent system [petroleum ether–acetone (70:30 v/v)] separates V or VI from the reaction mixtures (Fig. 1 and Table IX). This finding was confirmed for all TLC separations when full UV–visible spectra of the components separated and then recovered by extraction of the silica gel with alcohol were recorded. These spectra were compared with those of pure samples of the various components to ascertain identity, as, for example, for samples of II, V, or VI. Incomplete separation can be established by such a comparison. Thus, when petroleum ether–acetone (20:80 v/v) was used as the solvent system for the TLC recovery during the analysis of a degraded sample of I, the spectrum of the yellow band corresponding to V was different from that of the authentic material; *i.e.*, in neutral solution the λ_{max} was 402 nm instead of 380 nm and in alkaline solution it was 510 nm instead of 466 nm. Proper TLC separation then confirmed that the yellow band was a mixture of more than one component.

In conclusion, it is recommended that samples of I can be analyzed as V or VI by using Method 1 or 3, depending on whether I is degraded or not. If I is present in II in amounts exceeding 0.3%, it is sufficient to use the appropriate conversion factors to calculate the concentration of I from the final absorbances. If the amount of I in II is less than 0.3%, it is possible to use a graphical relationship derived from the results of Table VII (Fig. 2) of the actual amount of I against the amount determined by Method 3 and calculated directly by using the appropriate conversion factors or by using the results of analysis of pure reference samples of I as the basis of comparison. However, for each analysis of an unknown sample, a reference sample of II containing a known amount of I should be analyzed also for comparison.

The use of an appropriate densitometer for the determination of all separated products directly on the same TLC plate could increase the speed and accuracy of the method and, perhaps, the detection limits.

Table IX—Recovery of I in Deteriorated Samples of II and Reproducibility of Results[a]

I, mg	II, mg	Percent Recovery of V, TLC	Percent Recovery of VI, TLC
1.09	500	95.8	92.2
1.09	500	94.3 } 95.7[b]	94.0 } 93.6
1.09	500	96.9	94.5
—	500	4.0	5.2
1.09	—	100.0	100.0

[a] Compound V measured at 380 nm, and Compound VI measured at 404 nm. Absorbances were read from full UV-visible spectra. [b] Mean value.

REFERENCES

(1) E. Kalatzis, *J. Pharm. Sci.*, **59**, 193(1970).

(2) "British Pharmacopoeia," Pharmaceutical Press, London, England, 1968, p. 707.

(3) "The National Formulary," 13th ed., Mack Publishing Co., Easton, Pa., 1970, p. 17.

(4) E. Klug, *Aerztl. Lab.*, **16** (a), 295(1970).

(5) M. Kuzelova, V. Kunor, and J. Merhaut, *Pract. Lek.*, **22**, 126(1970).

(6) M. Geldmacher-von Mallinckrodt and A. Herrmann, *Z. Klin. Chem. Klin. Biochem.*, **7**, 34(1969).

(7) G. Ropa, E. Radulescu-Jercan, and F. M. Albert, *Rev. Roum. Chim.*, **11**, 1449(1966).

(8) T. Yaichiro, S. Shigeru, K. Akemi, and S. Satomi, *Tokushima Daigaku Yakugaku Kenkyu Nempo*, **15**, 23(1966); through *Chem. Abstr.*, **68**, 5320c(1968).

(9) H. Thielemann, *Sci. Pharm.*, **40**, 206(1972).

(10) H. L. Gurtoo and B. M. Phillips, *J. Pharm. Sci.*, **62**, 383(1973).

(11) I. K. Shih, *ibid.*, **60**, 1853(1971).

(12) W. Jedrzejewsky and J. Badecka-Jedrzejewska, *Chem. Anal. (Warsaw)*, **14**, 73(1969).

(13) Y. I. Beilis, *Khim. Prom.*, **43**, 767(1967).

(14) R. D. Tiwari, J. P. Sharma, and I. C. Shukla, *Talanta*, **14**, 853(1967).

ACKNOWLEDGMENTS AND ADDRESSES

Received April 26, 1974, from the *National Hellenic Research Foundation, 48 Vassileos Konstantinou, Athens, Greece.*

Accepted for publication April 14, 1975.

The authors thank Miss T. Kouri for technical assistance. Microanalyses were carried out by Dr. C. Mantzos.

[x] To whom inquiries should be directed.

Electron Microscope Study of Effect of Benzalkonium Chloride and Edetate Disodium on Cell Envelope of *Pseudomonas aeruginosa*

R. M. E. RICHARDS *x and **R. H. CAVILL** ‡

Abstract □ Electron micrographs of *Pseudomonas aeruginosa* grown in nutrient broth or broth containing subinhibitory concentrations of benzalkonium chloride indicate that benzalkonium chloride at 50 and 100 μg/ml strips off the outer cell membrane. Cells grown in the presence of edetate disodium, 50–100 μg/ml, had convoluted surfaces (wavy in cross section). Cells damaged by growing on nutrient agar containing benzalkonium (200 μg/ml), when subsequently grown for 16 hr in nutrient broth, produced cells with apparently normal outer layers. Similar cells grown on nutrient agar plus benzalkonium (500 μg/ml) when grown for 16 hr in nutrient broth had normal resistance to edetate disodium lysis, but cells grown overnight in broth plus benzalkonium (500 μg/ml) showed increased sensitivity to edetate disodium lysis. Cells grown on nutrient agar in the presence of benzalkonium (800 μg/ml) grew in broth plus benzalkonium (10 μg/ml) without stripping of their external membrane, but replicate inocula into broth plus benzalkonium (10 μg/ml) and edetate disodium (50 μg/ml) produced cells with structural damage to the outer layers of the cell envelope.

Keyphrases □ *Pseudomonas aeruginosa*—cell envelope, effect of benzalkonium chloride and edetate disodium, electron microscope study □ Benzalkonium chloride—effect on cell envelope of *Pseudomonas aeruginosa*, electron microscope study □ Edetate disodium—effect on cell envelope of *Pseudomonas aeruginosa*, electron microscopy study □ Antibacterial agents—benzalkonium chloride, effect on cell envelope of *Pseudomonas aeruginosa*, electron microscope study □ Chelating agents—edetate disodium, effect on cell envelope of *Pseudomonas aeruginosa*, electron microscope study

Surprisingly little is known about the mode of antibacterial action of quaternary ammonium compounds, despite many publications concerning these substances since their introduction (1). The normal structure of bacteria and fungi appears to be unaffected by quaternary ammonium compounds and other surfactants (2). Several studies (3, 4) found that quaternary ammonium compounds caused a release of cellular constituents, so antibacterial activity was linked, at least in part, to this effect. Evidence was presented (5) of cytological damage induced by low doses (<100 μg/ml) of quaternary ammonium compounds, and this damage was related to cell death. A high dose (900 μg/ml) stripped off the cell walls of *Escherichia coli* and *Staphylococcus aureus*. Another suggested mode of action was the splitting of lipoprotein complexes with a resultant widespread action of autolytic enzymes throughout the cell (6). Other concepts relevant to the mode of action of quaternary compounds against microorganisms were reviewed (7).

Edetate disodium reversed the resistance of *Pseudomonas aeruginosa* cells which were resistant to a quaternary ammonium compound (8). It was postulated that the *P. aeruginosa* had become impermeable to the quaternary ammonium compounds due to an increased lipid content and that the edetate disodium enabled the quaternary compound to penetrate this barrier and then reach its site of antibacterial action.

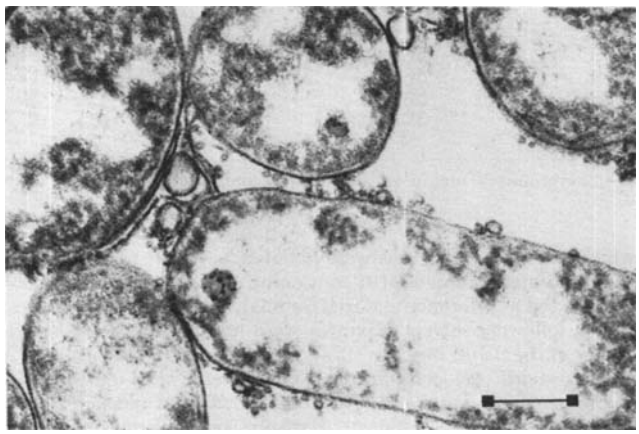

Figure 1—P. aeruginosa *cultured in broth containing benzalkonium chloride (50 μg/ml). (Bar represents 0.25 μm.)*

In another study (9), edetate disodium enhanced the activity of benzalkonium chloride, chlorhexidine acetate, and polymyxin B sulfate on growing cultures of *P. aeruginosa*. It also was demonstrated that quaternary ammonium–edetate disodium combinations were effective against *P. aeruginosa* sensitive and resistant to the quaternary ammonium compounds (10, 11).

The objective of this present investigation was to determine the usefulness of electron microscopy in evaluating the effect on cell morphology of benzalkonium chloride and edetate disodium alone and in combination. Cultures of *P. aeruginosa* growing in the presence of subinhibitory concentrations of the chemicals were used.

EXPERIMENTAL

Chemicals, Media, and Organism—Benzalkonium chloride[1] USP [alkyl (C_{14}, 50%; C_{12}, 40%; and C_{16}, 10%) dimethylbenzylammonium chlorides] and edetate disodium[2] BP (disodium ethylenediaminetetraacetate) were used. *P. aeruginosa*[3] was the test organism, nutrient broth[4] was the growth medium for liquid cultures, and nutrient agar[4] was the growth medium for solid cultures.

A spectrophotometer[5] was used to determine extinction measurements of cell suspensions at 660 nm.

Preparation of Cultures—Maintenance of stock cultures was described previously (12). One-milliliter quantities of an overnight culture of *P. aeruginosa* were used to inoculate 250-ml conical flasks containing 100 ml of nutrient broth and 100 ml of medium

[1] Rohm and Haas, New Germany, Natal, South Africa.
[2] May and Baker Ltd., Dagenham, England.
[3] NCTC 6750, National Collection of Type Cultures, Colindale, London, England.
[4] Oxoid, Oxo Ltd., London, England.
[5] Unicam SP 500, Pye Unicam Ltd., Cambridge, England.

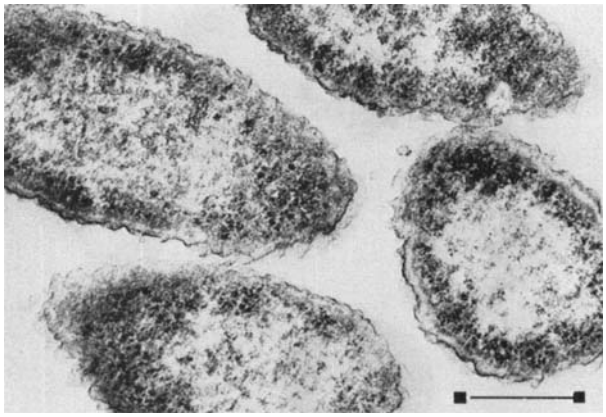

Figure 2—P. aeruginosa *cultured in broth containing edetate disodium (100 μg/ml). (Bar represents 0.25 μm.)*

containing various subinhibitory concentrations of benzalkonium chloride and/or edetate disodium. The cultures were incubated overnight (except for one set of benzalkonium-resistant cultures) at 37° in a shaking incubator[6] at 100 throws/min. Two different attempts were made to produce cultures having increased resistance to benzalkonium chloride.

On Agar—An overnight culture was spread on agar plates containing benzalkonium chloride at 100, 150, 200, and 400 μg/ml. The highest concentration showing growth was 150 μg/ml, which had three colonies. By using one of these colonies as the inoculum source, the procedure was repeated and then repeated again to obtain growth on agar containing 800 μg of benzalkonium chloride/ml.

In Broth—An overnight culture of *P. aeruginosa* was used to inoculate 100 ml of broth containing 50 μg of benzalkonium chloride/ml. The culture was incubated overnight in the shaking water bath and then used to inoculate a further 100 ml of broth containing benzalkonium (50 μg/ml). This procedure was followed six times.

The effect of low concentrations of benzalkonium (50 μg/ml or less) on cells having increased resistance to benzalkonium was investigated as follows:

1. A colony growing on nutrient agar containing benzalkonium chloride (200 μg/ml) was mixed with 2 ml of broth, and 0.4-ml quantities of this suspension were used to inoculate 100 ml of plain nutrient broth and 100 ml of broth containing benzalkonium (50 μg/ml).

2. Cells growing on nutrient agar containing benzalkonium (800 μg/ml) were mixed with 5 ml of nutrient broth, and 0.2-ml quantities were used to inoculate 100-ml quantities of plain nutrient broth, broth containing benzalkonium (10 μg/ml), and broth containing benzalkonium (10 μg/ml) and edetate disodium (50 μg/ml).

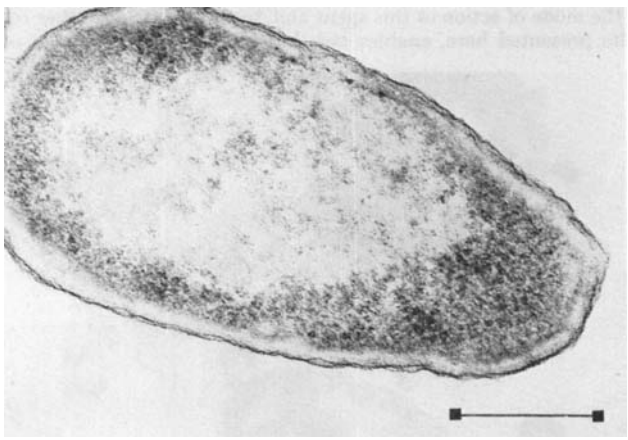

Figure 3—P. aeruginosa *cultured on agar containing benzalkonium (200 μg/ml) and then inoculated into nutrient broth and incubated for 16 hr. (Bar represents 0.25 μm.)*

[6] Baird and Tatlock, Chadwell Heath, Essex, England.

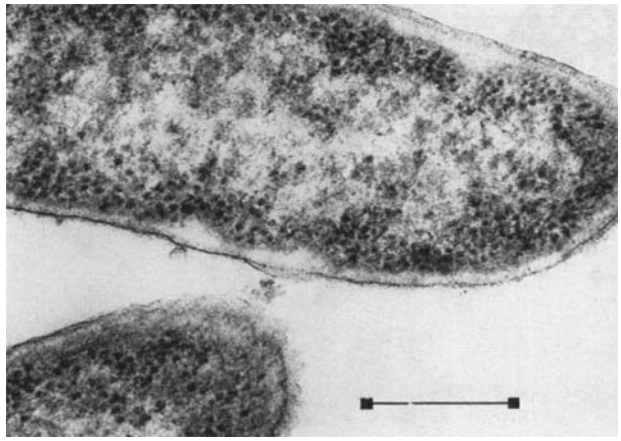

Figure 4—P. aeruginosa *cultured in nutrient broth. (Bar represents 0.25 μm.)*

These cultures were incubated for 42 hr.

Sensitivity to the lytic action of edetate disodium exhibited by normal cells and benzalkonium-treated cells was investigated as follows. Cells resistant to benzalkonium (500 μg/ml) were incubated overnight in broth with the same concentration of antibacterial and in broth without added benzalkonium. Normal cells were also used to prepare an overnight culture in nutrient broth. The resulting cultures were centrifuged and washed in an "inactivator" broth, as used by Riegelman *et al.* (13) but without the added agar. The cells were then washed in 0.5 *M* sodium chloride, suspended in 0.5 *M* sodium chloride at pH 8.2, and adjusted to a preselected extinction measurement. The lysis caused to these suspensions at 22° by adding edetate disodium (23 μg/ml) was followed at 1-min intervals up to 9 min after the addition of the chemical.

Electron Microscopy—Broth cultures were centrifuged, and the bulk of the supernate was removed. A volume of 8% (v/v) glutaraldehyde in 0.1 *M* Sørensen phosphate buffer (pH 7.2) equal to the volume of the remaining cultures was added, and the resulting suspensions were maintained at 4° for 1 hr. Then the suspensions were centrifuged, the supernates were removed, and 4% (v/v) glutaraldehyde in 0.1 *M* phosphate buffer was added. After 5 hr of fixation, the samples were washed overnight in three changes of phosphate buffer. This procedure was followed by postfixation for 1 hr in 1% osmium tetroxide in 0.1 *M* phosphate buffer. Samples were then dehydrated in methanol, embedded in araldite CY212, cut with glass knives on a microtome[7], stained with 5% aqueous vinyl acetate for 30 min followed by Reynold's lead citrate for 30 min, and examined on an electron microscope[8] at 50 kv.

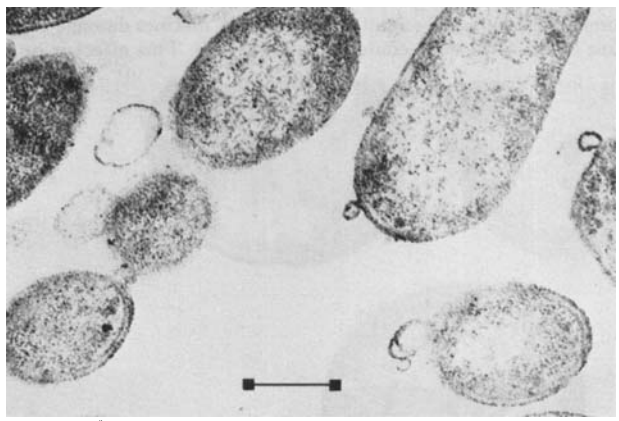

Figure 5—P. aeruginosa *cultured on agar containing benzalkonium chloride (200 μg/ml) and then inoculated into nutrient broth containing benzalkonium chloride (50 μg/ml). (Bar represents 0.25 μm.)*

[7] Reichert OMU2.
[8] Hitachi HU 11E.

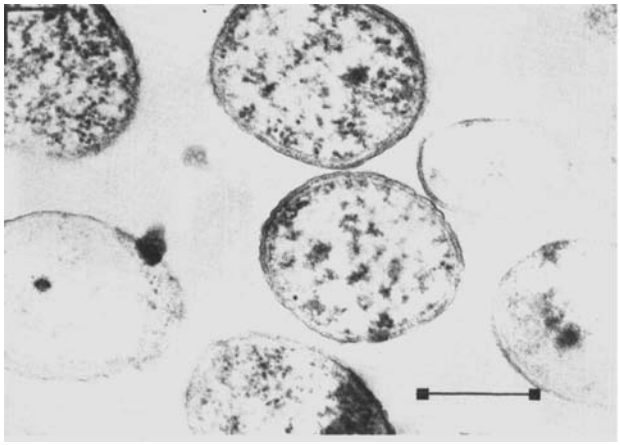

Figure 6—P. aeruginosa *cultured on agar containing benzalkonium chloride (800 μg/ml) and then inoculated into broth containing benzalkonium chloride (10 μg/ml). (Bar represents 0.25 μm.)*

Surface growth on agar was treated as follows. Small pieces of agar plus surface growth having a maximum dimension of 2 mm were immersed in 4% (v/v) glutaraldehyde in 0.1 *M* Sørensen buffer and fixed for 6 hr. After washing in buffer but before postfixation in 1% osmium tetroxide, the bulk of the agar was trimmed away and the resulting blocks were processed as already described for the suspensions.

RESULTS

P. aeruginosa cells grown in nutrient broth in the presence of benzalkonium chloride (50 and 100 μg/ml) or grown on solid medium in the presence of benzalkonium chloride (up to 400 μg/ml) showed widespread peeling of the outer cell membrane (Fig. 1). Cells grown in the presence of edetate disodium (50–200 μg/ml) had a distinctly wavy outer cell envelope (Fig. 2).

Cells with a resistance to benzalkonium chloride (200 μg/ml in agar), when subsequently grown in nutrient broth in the absence of benzalkonium, produced cells with apparently normal outer membranes (Fig. 3). This effect is seen when the cells in Fig. 3 are compared with the cells in Fig. 4, which were grown in nutrient broth. The cells grown in the presence of benzalkonium (50 μg/ml), however, showed peeling of their outer membranes (Fig. 5).

Cells grown on agar in the presence of benzalkonium (800 μg/ml) when grown in nutrient broth containing benzalkonium chloride (10 μg/ml) produced cells that showed no peeling of their outer membrane. [Compare Fig. 6 with cells grown in nutrient broth (Fig. 7).] When grown on agar containing 800 μg of benzalkonium chloride/ml and then grown in the presence of 10 μg of benzalkonium/ml plus 50 μg of edetate disodium/ml, distinct damage to the outer layer of the cells could be seen (Fig. 8). This effect is quite striking because these cells are able to grow in the presence of 80 times this concentration of benzalkonium. Figure 8 provides further evidence of the effectiveness of benzalkonium–edetate disodium combinations, which have been shown to be so effective against *P. aeruginosa* using different experimental techniques (8–10, 14, 15).

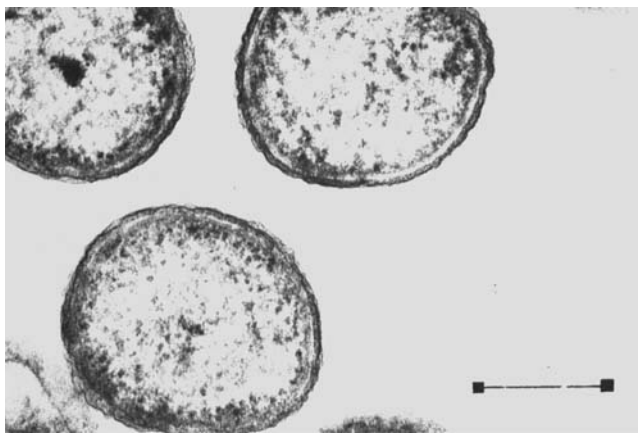

Figure 7—P. aeruginosa *cultured on agar containing benzalkonium chloride (800 μg/ml) and then inoculated into plain broth. (Bar represents 0.25 μm.)*

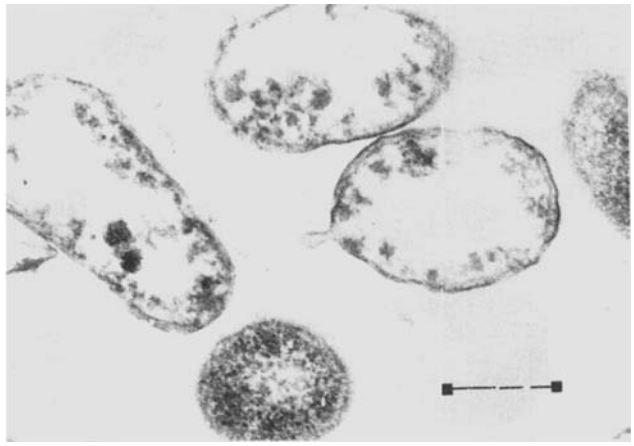

Figure 8—P. aeruginosa *cultured on agar containing benzalkonium chloride (800 μg/ml) and then inoculated into broth containing benzalkonium chloride (10 μg/ml) plus edetate disodium (50 μg/ml). (Bar represents 0.25 μm.)*

Repeated culturing in the presence of benzalkonium (50 μg/ml) did not produce cells resistant to the outer membrane damage caused by benzalkonium (Fig. 9).

The apparent variation in size of the cells is largely accounted for by the variation in the scale used in some of the figures. For example, the length of cells represented in all of the figures is within the 0.8–1.9-μm range.

The resistance of benzalkonium-damaged cells to the lytic action of edetate disodium was shown to be less than the resistance of normal cells (Table I).

DISCUSSION

The results indicate that electron micrographs of sections of *P. aeruginosa* cells cultured in the presence of subinhibitory concentrations of benzalkonium chloride and edetate disodium give valuable insights into the effect of these agents on the outer layers of the cell envelope. The ordinary light microscope reveals no change in cellular morphology after treating bacteria and fungi with quaternary ammonium compounds (2). (This finding was confirmed in this present study.) Therefore, the electron micrograph of the benzalkonium-affected cells that show pronounced stripping of the outer cell membrane (Fig. 1) gives a more detailed understanding of the mode of action of this agent and, together with the other results presented here, enables new interpretations to be made of

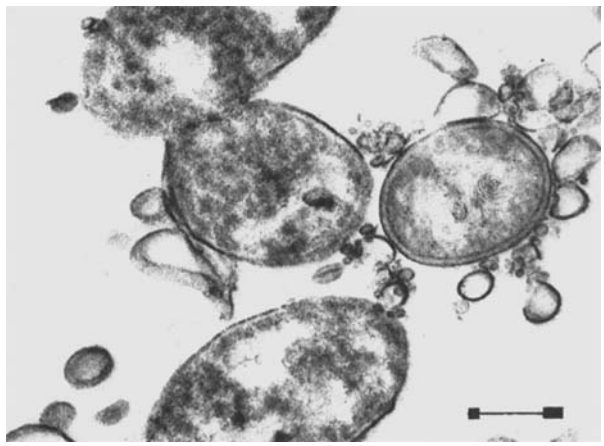

Figure 9—P. aeruginosa *cultured six times in broth containing benzalkonium chloride (50 μg/ml). (Bar represents 0.25 μm.)*

Table I—Effect of Benzalkonium Chloride on the Resistance of *P. aeruginosa* to the Lytic Action of Edetate Disodium[a]

Time after Addition of Edetate Disodium (23 μg/ml), min	Normal Cells Grown Overnight in Broth[b]	Cells Resistant to Benzalkonium (500 μg/ml)	
		Grown Overnight in Broth[c]	Grown Overnight in Broth plus Benzalkonium[d] (500 μg/ml)
0	0.290	0.288	0.288
1	0.270	0.269	0.268
2	0.270	0.269	0.262
3	0.269	0.269	0.252
4	0.269	0.263	0.245
5	0.269	0.263	0.240
6	0.264	0.263	0.231
7	0.264	0.261	0.228
8	0.261	0.259	0.219
9	0.260	0.259	0.215

[a] All cells were washed once in "inactivator" and once in 0.5 *M* sodium chloride before resuspending in 0.5 *M* sodium chloride at pH 8.2. Extinction was measured at 660 nm. [b] Reduction in extinction after 9 min = 10.3%. [c] Reduction in extinction after 9 min = 10.1%. [d] Reduction in extinction after 9 min = 25.4%.

some previous experimental findings with benzalkonium and edetate disodium. The fact that the cells retain their shape after the outer membrane is removed appears to indicate that the peptidoglycan layer remains intact. (Some results[9] with *P. aeruginosa* suspensions show that lysozyme causes considerable lysis to benzalkonium-treated cells.)

The average sterilization time for five separate duplicate determinations of benzalkonium chloride (100 μg/ml), inoculated with *P. aeruginosa* (10^7 cells/ml), was 15 min[9]. However, the same strain of *P. aeruginosa* grows in the presence of 200 μg of benzalkonium/ml in nutrient broth (10). It was thought that, in this latter situation, benzalkonium was having no effect because it was unable to penetrate the bacterial cell. In general, this concept has been held since MacGregor and Elliker (8) found that edetate disodium apparently enabled the quaternary ammonium compounds to penetrate to their sites of activity in *P. aeruginosa* cells having an increased resistance to quaternary ammonium compounds. This concept is seemingly supported by a similar situation with edetate disodium and lysozyme. Edetate disodium renders Gram-negative bacteria sensitive to the action of lysozyme, and it has been suggested that edetate disodium increases the permeability of the outer layers of the cell, allowing lysozyme to penetrate to its substrate (peptidoglycan) (16, 17).

The present study, however, indicates that, at the concentrations tested, the growing of cells in the presence of benzalkonium has a more drastic effect on the external layers of the cell than does growing in the presence of edetate disodium. Therefore, when edetate disodium is added to cultures of *P. aeruginosa* multiplying in the presence of benzalkonium, it appears that the edetate disodium is able to gain access to cell structures (possibly including the cytoplasmic membrane) on which it has a more potent effect than it has on the normal intact cell. This event would explain the results of Adair *et al.* (11), who found that, although a benzalkonium-sensitive strain of *P. aeruginosa* was able to grow in the presence of 10,000 μg of edetate disodium/ml, a benzalkonium-resistant strain did not show growth after 2 days in broth containing edetate disodium (10 μg/ml). However, after the benzalkonium-resistant strain was grown for 16 hr in the absence of benzalkonium, it regained the ability to grow in the presence of edetate disodium (10,000 μg/ml). Figure 3 shows that a culture of *P. aeruginosa* resistant to benzalkonium, when grown for 16 hr in the absence of the antibacterial, regained its outer membrane as per normal cells (Fig. 4).

Cells grown in the presence of benzalkonium (500 μg/ml) were more susceptible to the lytic action of 23 μg of edetate disodium/ml than were cells that had been grown in the presence of benzalkonium (500 μg/ml) and then grown overnight in the absence of the antibacterial (Table I). These latter cells showed the same level of resistance to 23 μg of edetate disodium/ml as normal cells grown for the same length of time.

The sensitivity of the cells grown in the presence of benzalkonium was not due to adsorption of the antibacterial on the cell surface, because the cells had been washed with inactivator medium to eliminate this possibility. Nor is it thought that cellular autolysis is induced by benzalkonium, which causes the outer membrane to peel off as a secondary effect, causing increased sensitivity to edetate disodium. This is not thought to be the case because cell suspensions of *P. aeruginosa* are immediately more susceptible to lysis by a benzalkonium–lysozyme combination than they are to benzalkonium alone[9].

Therefore, it appears that the outer membrane acts as a barrier to edetate disodium, and this would support the statement that "the outer membrane provides the basis of the barrier layer of the gram-negative cell wall" (18).

MacGregor and Elliker (8) also found that a strain of *P. aeruginosa* resistant to a quaternary ammonium compound was more sensitive to the action of edetate disodium (100 μg/ml) than normal cells, and other workers found that edetate disodium did not exhibit any pseudomonicidal activity against normal *P. aeruginosa* (15). Of relevance too are the findings of Brown (19) and Richards (10) that edetate disodium combined with either phenylmercuric nitrate or chlorobutanol did not exhibit greater antipseudomonal activity than phenylmercuric nitrate or chlorobutanol as single substances. This finding could result from the two antibacterials not requiring assistance in penetrating the outer membrane and not having an action on the outer membrane that would assist the penetration of edetate disodium to internal sites of activity. (Neither phenylmercuric nitrate nor chlorobutanol at concentrations of 5 and 1000 μg/ml, respectively, markedly strip the outer membrane of *P. aeruginosa*[9].)

None of the procedures used to develop cells having an increased resistance to benzalkonium appeared to result in cells with external membranes resistant to the stripping action of the antibacterial agent. Whether or not the *P. aeruginosa* survives such damage may depend on the tonicity and/or viscosity of the system. The results presented here, however, indicate that the resistance of *P. aeruginosa* to benzalkonium is at a location or locations internal to the external membrane, most likely at the cytoplasmic membrane.

Part of the study of Anderes *et al.* (20) compared the percentages of cell dry weight of total, free, and bound lipids from *P. aeruginosa* grown at 37° in the absence and presence of a quaternary ammonium compound. These investigators found no increase in the amount of lipids produced by the resistant cells grown at 25°. In fact, a reduction of lipids occurred in the resistant cells at 37°; this result appears to rule out the resistance to the quaternary ammonium being due to a nonspecific blanketing action of lipids, a phenomenon that has been implicated in certain situations (21).

It can be concluded that part of the mechanism of action of benzalkonium chloride in subinhibitory concentrations is to damage severely the external membrane of *P. aeruginosa*. Edetate disodium also damages the outer layers of the cell envelope and, when used in combination with benzalkonium chloride, appears to have a potent effect on sites internal to the external membrane of *P. aeruginosa* cells.

[9] R. M. E. Richards, unpublished results.

REFERENCES

(1) G. Domagk, *Deut. Med. Wochenschr.*, **61**, 829(1935); through Ref. 2.

(2) C. A. Lawrence, "Disinfection Sterilization and Preservation," Lea & Febiger, Philadelphia, Pa., 1971, p. 430.

(3) R. D. Hotchkiss, *Ann. N.Y. Acad. Sci.*, **46**, 479(1946).

(4) M. R. J. Salton, *J. Gen. Microbiol.*, **5**, 391(1951).

(5) M. R. J. Salton, R. W. Horne, and V. E. Cosslett, *ibid.*, **5**, 405(1951).

(6) I. M. Dawson, I. Lominski, and H. Stern, *J. Pathol. Bacteriol.*, **66**, 513(1953).

(7) C. A. Lawrence, *Ann. N.Y. Acad. Sci.*, **53**, 66(1950).

(8) D. R. MacGregor and P. R. Elliker, *Can. J. Microbiol.*, **4**, 499(1958).

(9) M. R. W. Brown and R. M. E. Richards, *Nature (London)*,

207, 1391(1965).
(10) R. M. E. Richards, *J. Pharm. Pharmacol., Suppl.*, **23**, 136S(1971).
(11) F. W. Adair, S. G. Geftic, and J. Gelzer, *Appl. Microbiol.*, **21**, 1058(1971).
(12) M. R. W. Brown and R. M. E. Richards, *J. Pharm. Pharmacol., Suppl.*, **16**, 41T(1964).
(13) S. Riegelman, D. G. Vaughan, and M. Okumoto, *J. Amer. Pharm. Ass., Sci. Ed.*, **45**, 93(1956).
(14) R. M. E. Richards and R. J. McBride, *J. Pharm. Pharmacol.*, **24**, 145(1972).
(15) D. C. Monkhouse and G. A. Groves, *Aust. J. Pharm.*, **48**, 570(1967).
(16) R. Repaske, *Biochim. Biophys. Acta*, **30**, 225(1958).
(17) J. W. Costerton, C. Forsberg, T. I. Matula, F. L. A. Buckmire, and R. A. MacLeod, *J. Bacteriol.*, **94**, 1764(1967).
(18) J. W. Costerton, R. J. Ingram, and K. J. Cheng, *Bacteriol. Rev.*, **38**, 87(1974).
(19) M. R. W. Brown, *J. Pharm. Sci.*, **57**, 389(1968).
(20) E. A. Anderes, W. E. Sandine, and P. R. Elliker, *Can. J. Microbiol.*, **17**, 1357(1971).
(21) W. B. Hugo, *J. Appl. Bacteriol.*, **30**, 17(1967).

ACKNOWLEDGMENTS AND ADDRESSES

Received February 10, 1975, from the **Department of Pharmacy and ‡Electron Microscope Unit, Medical Faculty, University of Rhodesia, Salisbury, Rhodesia.*

Accepted for publication April 8, 1975.

[x] To whom inquiries should be directed.

Oil–Water Distribution of *p*-Alkylpyridines

KUANG C. YEH * and WILLIAM I. HIGUCHI [x]

Abstract □ The distribution of a homologous series of *p*-alkylpyridines between water and six organic solvents with varying degrees of polarity was investigated. The distribution coefficients were considered as reflections of the strength of net interactions involved in the solvents. The order was chloroform > octanol > carbon tetrachloride > butyl ether > hexadecane > octane. The effect of the methylene group upon the distribution coefficients differed little among the six solvents. The relative constancy was attributed to the predominance of the dispersion forces in the incremental effect.

Keyphrases □ Alkylpyridines—distribution between water and six organic solvents, distribution and partition coefficients □ Distribution coefficients—*p*-alkylpyridines, water and six organic solvents, effect of methylene group □ Partition coefficients—*p*-alkylpyridines, water and six organic solvents □ Pyridines, *p*-alkyl—distribution and partition coefficients, water and six organic solvents

The distribution behavior of solutes between two immiscible phases is a phenomenon important to numerous pharmaceutical and biological situations. The partition principle has been utilized in various chromatographic and extraction techniques common to many analytical pharmaceutical chemistry procedures. In biopharmaceutics, the pH–partition principle is basic to the theories and concepts of drug absorption, tissue distribution, renal reabsorption, and other membrane transport situations important to bioavailability and therapeutics. The partitioning of organic compounds between water and various oil phases has been studied to correlate biological activities (1–10).

Earlier systematic investigations of partition coefficients employed several alcohols and ethyl ether as the oil phases (11, 12); in general, the partition coefficients of different solutes differed considerably less in the butanol–water system than in the ether–water system. Depending on the nature of the solute, the following linear relationship was observed between the partition coefficient obtained from the ether system and that obtained from the butanol system (11, 12):

$$\log (k_{\text{butanol}}) = A \log (k_{\text{ether}}) + B \qquad \text{(Eq. 1)}$$

where the k's are the partition coefficients, and A and B are constants. Later, this relationship was shown to hold between other solvent pairs (13, 14) when the partition coefficients of a number of barbiturates between water and various organic solvents were studied.

The partitioning of compounds in several alkyl homologous series between several organic solvents and semiaqueous solutions has been studied (15). A linear relationship was found between the logarithm of the partition coefficient and the number of carbons in the chain:

$$\log (k) = A + Bn \qquad \text{(Eq. 2)}$$

where A and B are constants, and n equals the number of carbons. The equation did not hold for the lower terms of the homologous series ($n < 3$ or 4). The deviation was ascribed to the inductive effect in which the interactions between the parent group and the adjacent CH_2 groups changed the physical properties of these groups.

Equation 2 implies that $\log (k)$ is additive; *i.e.*, $\log (k)$ is equal to the sums of the contribution from each group in the molecule. Using octanol and water as the partitioning phases, Hansch and Anderson (16, 17) defined a substituent constant (π) as follows:

$$\pi_x = \log (k_x) - \log (k_o) \qquad \text{(Eq. 3)}$$

where k_o is the partition coefficient of a parent compound between octanol and water, and k_x is that for a derivative. Tables of π values for various functional groups have been compiled (16–19). The π_x for the CH_2 group has a value of 0.5.

The primary purpose of this research was to con-

207, 1391(1965).
(10) R. M. E. Richards, *J. Pharm. Pharmacol., Suppl.*, **23**, 136S(1971).
(11) F. W. Adair, S. G. Geftic, and J. Gelzer, *Appl. Microbiol.*, **21**, 1058(1971).
(12) M. R. W. Brown and R. M. E. Richards, *J. Pharm. Pharmacol., Suppl.*, **16**, 41T(1964).
(13) S. Riegelman, D. G. Vaughan, and M. Okumoto, *J. Amer. Pharm. Ass., Sci. Ed.*, **45**, 93(1956).
(14) R. M. E. Richards and R. J. McBride, *J. Pharm. Pharmacol.*, **24**, 145(1972).
(15) D. C. Monkhouse and G. A. Groves, *Aust. J. Pharm.*, **48**, 570(1967).
(16) R. Repaske, *Biochim. Biophys. Acta*, **30**, 225(1958).
(17) J. W. Costerton, C. Forsberg, T. I. Matula, F. L. A. Buckmire, and R. A. MacLeod, *J. Bacteriol.*, **94**, 1764(1967).
(18) J. W. Costerton, R. J. Ingram, and K. J. Cheng, *Bacteriol. Rev.*, **38**, 87(1974).
(19) M. R. W. Brown, *J. Pharm. Sci.*, **57**, 389(1968).
(20) E. A. Anderes, W. E. Sandine, and P. R. Elliker, *Can. J. Microbiol.*, **17**, 1357(1971).
(21) W. B. Hugo, *J. Appl. Bacteriol.*, **30**, 17(1967).

ACKNOWLEDGMENTS AND ADDRESSES

Received February 10, 1975, from the **Department of Pharmacy and ‡Electron Microscope Unit, Medical Faculty, University of Rhodesia, Salisbury, Rhodesia.*

Accepted for publication April 8, 1975.

[x] To whom inquiries should be directed.

Oil–Water Distribution of *p*-Alkylpyridines

KUANG C. YEH * and WILLIAM I. HIGUCHI [x]

Abstract □ The distribution of a homologous series of *p*-alkylpyridines between water and six organic solvents with varying degrees of polarity was investigated. The distribution coefficients were considered as reflections of the strength of net interactions involved in the solvents. The order was chloroform > octanol > carbon tetrachloride > butyl ether > hexadecane > octane. The effect of the methylene group upon the distribution coefficients differed little among the six solvents. The relative constancy was attributed to the predominance of the dispersion forces in the incremental effect.

Keyphrases □ Alkylpyridines—distribution between water and six organic solvents, distribution and partition coefficients □ Distribution coefficients—*p*-alkylpyridines, water and six organic solvents, effect of methylene group □ Partition coefficients—*p*-alkylpyridines, water and six organic solvents □ Pyridines, *p*-alkyl—distribution and partition coefficients, water and six organic solvents

The distribution behavior of solutes between two immiscible phases is a phenomenon important to numerous pharmaceutical and biological situations. The partition principle has been utilized in various chromatographic and extraction techniques common to many analytical pharmaceutical chemistry procedures. In biopharmaceutics, the pH–partition principle is basic to the theories and concepts of drug absorption, tissue distribution, renal reabsorption, and other membrane transport situations important to bioavailability and therapeutics. The partitioning of organic compounds between water and various oil phases has been studied to correlate biological activities (1–10).

Earlier systematic investigations of partition coefficients employed several alcohols and ethyl ether as the oil phases (11, 12); in general, the partition coefficients of different solutes differed considerably less in the butanol–water system than in the ether–water system. Depending on the nature of the solute, the following linear relationship was observed between the partition coefficient obtained from the ether system and that obtained from the butanol system (11, 12):

$$\log (k_{\text{butanol}}) = A \log (k_{\text{ether}}) + B \qquad \text{(Eq. 1)}$$

where the k's are the partition coefficients, and A and B are constants. Later, this relationship was shown to hold between other solvent pairs (13, 14) when the partition coefficients of a number of barbiturates between water and various organic solvents were studied.

The partitioning of compounds in several alkyl homologous series between several organic solvents and semiaqueous solutions has been studied (15). A linear relationship was found between the logarithm of the partition coefficient and the number of carbons in the chain:

$$\log (k) = A + Bn \qquad \text{(Eq. 2)}$$

where A and B are constants, and n equals the number of carbons. The equation did not hold for the lower terms of the homologous series ($n < 3$ or 4). The deviation was ascribed to the inductive effect in which the interactions between the parent group and the adjacent CH_2 groups changed the physical properties of these groups.

Equation 2 implies that $\log (k)$ is additive; *i.e.*, $\log (k)$ is equal to the sums of the contribution from each group in the molecule. Using octanol and water as the partitioning phases, Hansch and Anderson (16, 17) defined a substituent constant (π) as follows:

$$\pi_x = \log (k_x) - \log (k_o) \qquad \text{(Eq. 3)}$$

where k_o is the partition coefficient of a parent compound between octanol and water, and k_x is that for a derivative. Tables of π values for various functional groups have been compiled (16–19). The π_x for the CH_2 group has a value of 0.5.

The primary purpose of this research was to con-

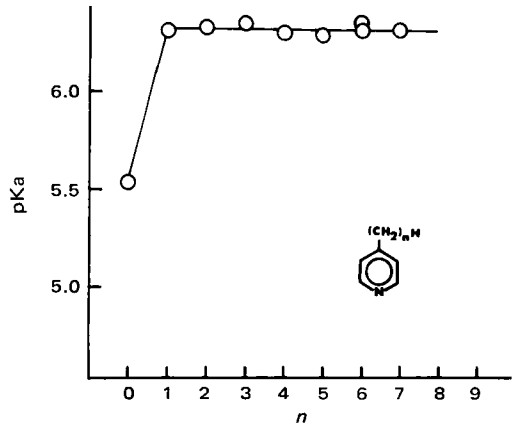

Figure 1—*Apparent pKa of 4-alkylpyridines in 1* M *NaCl at 25°.*

sider the oil–water partitioning of an organic alkyl series. Emphasis was to be placed upon developing useful theoretical concepts and methods jointly with meaningful and accurate experimental procedures. The basic objectives included obtaining experimental data of high accuracy and analyzing them by the appropriate concepts and theoretical relationships in terms of the different solute–solute, solvent–solvent, and solute–solvent interactions. Of special interest was the incremental effects of the CH_2 group upon the distribution coefficient as a function of the nature of the organic solvent.

For these purposes, the *p*-alkylpyridine homologous series ranging from pyridine to decylpyridine was chosen as solutes, and six organic solvents with varying degrees of complexity were selected: octane, hexadecane, butyl ether, carbon tetrachloride, chloroform, and octanol. The present article describes the experimental methods and the results obtained. The employment of Scatchard–Hildebrand-type theory (20) and some suggested modifications (21) will be reported[1].

EXPERIMENTAL

Materials—Reagent grade pyridine[2], 4-picoline[3], 4-ethylpyridine[3], and 4-propylpyridine[3] were obtained commercially. The higher homologs (4-butyl- to 4-decylpyridine) were synthesized according to the method of Wilbaut and Hey (22).

Pyridine and picoline were purified by recrystallizing the corresponding hydrochloride salts twice in absolute alcohol (23). Ethyl- and propylpyridines were purified by single distillation. The higher homologs were purified through partition chromatographic columns, using deactivated silica gel[4] (100–200 mesh) as the stationary phase. The silica gel was saturated with 0.6 *M* aqueous sodium citrate buffer (approximately 370 ml/kg of the powder). The pH of the buffer had been preadjusted to produce suitable R_f values. Normal heptane was used as the mobile phase.

The elutions were made on an automatic fraction collector[5], and the eluents were scanned in the range of 230–300 nm[6]. The impurities were detected by the shape of their UV spectra and were separated from the desired fraction (24).

Table I—Some Experimental Constants of Alkylpyridines

Chain Length	pKa[a]	CMC, m*M*[b]
Pyridine	5.539	—
C-1	6.323	—
C-2	6.338	—
C-3	6.357	—
C-4	6.314	—
C-5	6.304	—
C-6	6.345	—
C-7	6.331	50
C-8	—	17
C-9	—	5
C-10	—	1.5

[a] For alkylated derivatives, the average value was taken to be 6.332 in 1 *M* NaCl. [b] In 1 *M* NaCl.

Solvents—Six organic solvents were used as the nonaqueous phase in the partitioning measurements. The aqueous phase contained 1 *M* NaCl as the swamping electrolyte together with 0.01 *M* each of the citrate and phosphate buffers. The six solvents were *n*-hexadecane, *n*-octane, carbon tetrachloride, *n*-butyl ether, chloroform, and 1-octanol[7]. They were chosen because of their low mutual solubility with water. Octane and hexadecane were further purified by shaking with chromic–sulfuric acid solution[8] until the extract did not show any green color and then washing three times with double-distilled water. All other solvents were used without further treatment.

Determination of pKa—The apparent dissociation constant, K_a, for each alkylpyridine conjugate acid in 1 *M* NaCl was determined at 25° by a spectrophotometric method (25) (Table I and Fig. 1). Measurements of pH were made[9].

Critical Micelle Concentration (CMC) Determinations—In measuring the apparent partition coefficients, the solute concentrations in the aqueous phase were always kept below the CMC of the corresponding conjugate acid. The CMC of each protonated alkylpyridine in the aqueous phase was determined at room temperature using a modified drop volume method.

In the CMC determinations, a 2-ml pipet, graduated to 0.01 ml and with ground tip, was attached vertically to an automatic titrator[10]. The pipet was filled with the desired test solution, and the solution was delivered at a constant rate of 0.18 ml/min. At this slow speed, distinctive drops were formed at the tip. Results are shown in Table I.

Measurement of Partition Coefficients—Aliquots (about 0.01–0.1 ml) of alkylpyridine stock solutions (0.1 *M* as hydrochloride salt in 1 *M* NaCl) were added to 10-25-ml glass-stoppered

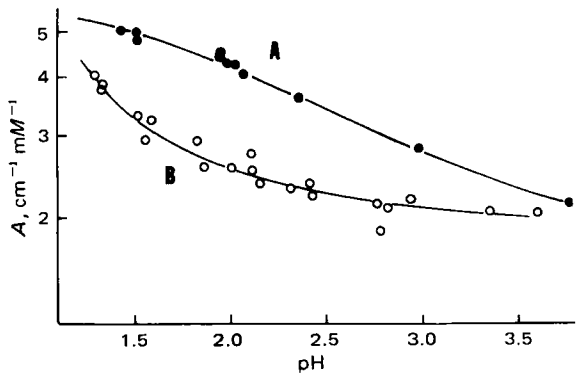

Figure 2—*Calibration curves for determining solute concentrations in the oil phase where significant amounts of ion-pairs are present. Key: A, chloroform phase; and B, octanol phase.*

[1] K. C. Yeh and W. I. Higuchi, *J. Pharm. Sci.*, in press.
[2] J. T. Baker Chemical Co., Phillipsburg, N.J.
[3] K & K Laboratories, Plainview, N.Y.
[4] Davison Chemical, Baltimore, Md.
[5] Gilson Medical Electronics, Middletown, Wis.
[6] Cary model 14 recording spectrophotometer, Cary Instruments, Monrovia, Calif.
[7] All from Matheson, Coleman & Bell, Norwood, Ohio. Hexadecane, carbon tetrachloride, and butyl ether were of spectrograde, octane was of chromatographic grade, and chloroform was of reagent grade.
[8] Fisher Scientific Co., Fair Lawn, N.J.
[9] Beckman model 1019 research pH meter, Beckman Instruments, Fullerton, Calif.
[10] Sargent-Welch Scientific Co., Skokie, Ill.

Table II—Mutual Solubilities between Water and Six Organic Solvents

Oil Phase	Mutual Solubility, moles/liter	
	Oil in Water	Water in Oil
Hexadecane	—	0.003[a]
Octane	—	0.0047[b]
Butyl ether	0.017[b]	0.0795
Octanol	0.0041[c]	0.758
Carbon tetrachloride	0.005[c]	0.0087[e]
Chloroform	0.069[d]	0.072[f]

[a] Reference 26. [b] Estimated. [c] Reference 27. [d] 20°, Ref. 27. [e] Reference 28. [f] Reference 29.

flasks containing 1–10 ml of the desired oil phase and 5–23 ml of the aqueous phase. The aqueous phase had been made alkaline or been preadjusted to the desired acid pH using the mixed buffers. The contents were shaken[11] for 24–48 hr at 25 ± 0.1°. For the octanol–aqueous system, the shaking speed was set at or below 100 rpm to avoid emulsion formation. The solute concentrations in both phases, usually in the range of 0.02–5 m*M*, were determined spectrophotometrically using diluted stock solutions as the reference.

When significant amounts of ion-pairs were present in the octanol or chloroform phase, solute concentrations in the nonaqueous layer were determined by a modified mass balance computation. This procedure was necessary because the UV spectrum of the ion-pair differed from that of the free base. In this case, the solute concentrations in the aqueous phase were determined as usual. By using the mass balance relationship, the solute concentrations in the oil phase were estimated. The spectra of the corresponding oil layers were taken, and the apparent absorptivities at λ_{max} were computed. These values were plotted against the aqueous pH on a semilog basis (λ_{max} varied with pH). A smooth curve was constructed, and it provided the Beer's law coefficients for determining the solute concentrations in the oil phase. As can be seen in Fig. 2, this procedure reduces random errors when a mass balance method is used to calculate the partition coefficient.

Solubility of Water—The solubility of water in octanol and in butyl ether was determined by the Karl Fischer method[12] after the solvents were saturated with double-distilled water by shaking[11]. The results are shown in Table II together with other solubility data.

Determination of Molar Volumes—Apparent densities of the solutes were determined by weighing a 1-ml sample of each alkylpyridine at room temperature. The values were then normalized and smoothed to the corresponding values at 25°, using pyridine as the reference (0.978 g/ml) (Fig. 3 and Table III).

RESULTS AND DISCUSSION

Apparent Partition Coefficients—Preliminary experiments showed that when the chain length of the alkyl group is greater than five or six, its intrinsic partition coefficient becomes so high that there will be significant error in measuring it directly. Instead, by determining the apparent partition coefficient (k') in the acid region, its intrinsic partition coefficient (k_t) may be estimated more accurately by extrapolating to a high pH. The two quantities are defined as:

$$k' = [B]_o/([B]_w + [HB^+]_w) \quad \text{(Eq. 4)}$$

$$k_t = [B]_o/[B]_w \quad \text{(Eq. 5)}$$

$$K_a = [B]_w[H^+]_w/[HB^+]_w \quad \text{(Eq. 6)}$$

where $[B]_o$ and $[B]_w$ are the concentrations of the free solute base in the oil phase and in the water phase, respectively; $[HB^+]_w$ is the concentration of the protonated conjugate acid; $[H^+]_w$ is the hydrogen-ion concentration, and K_a is the apparent dissociation constant of the conjugate acid in 1 *M* NaCl. All concentrations are expressed in units of moles per liter.

Table III—Densities and Molar Volumes of Alkylpyridines at 25°

Chain Length	Molecular Weight	Density, g/ml[a]	Molar Volume, ml/mole
Pyridine	79.10	0.978 (0.978)	80.88
C-1	93.13	0.961 (0.961)	96.91
C-2	107.15	0.949 (0.947)	113.15
C-3	121.18	0.936 (0.934)	129.74
C-4	135.21	0.923 (0.923)	146.49
C-5	149.23	0.909 (0.915)	163.09
C-6	163.26	0.908 (0.909)	179.60
C-7	179.29	0.907 (0.905)	195.90
C-8	191.32	0.902 (0.902)	212.11
C-9	205.34	— (0.900)	228.15
C-10	219.37	— (0.898)	244.29

[a] Values in parentheses were estimated from Fig. 3.

The apparent partition coefficient may also be expressed as:

$$k' = k_t K_a/(K_a + [H^+]_w) \quad \text{(Eq. 4a)}$$

When the pH of the aqueous phase is in the acid region and is much below the apparent pKa of 6.332, Eq. 4*a* may be simplified to:

$$\log (k') = \log (k_t) - \text{pKa} + \text{pH} \quad \text{(Eq. 4b)}$$

Since k_t and pKa are constant for any particular solute at constant temperature (25°), Eq. 4*b* predicts a linear relationship between log (k') and pH with a slope of 1.0.

On the other hand, in the alkaline region where the pH is much above the pKa, the experimentally measured k' is equal to the intrinsic k_t values since Eq. 4*a* is reduced to:

$$\log (k') = \log (k_t) \quad \text{(Eq. 7)}$$

Figure 4 compares the experimental data of log (k') in the carbon tetrachloride–aqueous phase pair and the theoretical curves generated from Eq. 4*a*.

One assumption in Eq. 4*a* is that the free base is always the only solute species in the oil phase throughout the pH range. Experimental results show that this is the case not only in carbon tetrachloride but also in hexadecane, octane, and butyl ether. By using

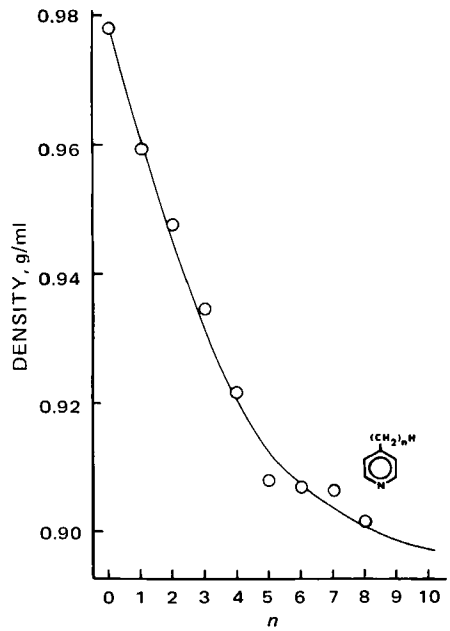

Figure 3—*Density of alkylpyridines as a function of the chain length at 25°.*

[11] Precision shaker bath, New Brunswick Scientific Co., New Brunswick, N.J.

[12] The determination was performed by Dr. Wenhai Hong, Pharmaceutical Development, Parke, Davis & Co., Detroit, MI 48232

Table IV—Logarithm of Partition Coefficients of Alkylpyridines between Various Organic Solvents and Aqueous 1 *M* NaCl at 25°

Chain Length	Hexadecane	Octane	Butyl Ether	Octanol	Chloroform	Carbon Tetrachloride
Pyridine	−0.305	−0.211	0.109	0.781	1.319	0.425
C-1	0.126	0.213	).530	1.327	1.821	0.839
C-2	0.741	0.829	—	—	—	—
C-3	—	—	—	—	—	—
C-4	—	—	2.373	3.128	3.737	2.812
C-5	2.641	2.810	—	3.750	4.380	3.433
C-6	3.274	3.448	3.617	4.348	5.006	4.114
C-7	3.919	4.105	—	5.008	5.653	—
C-8	4.569	4.794	4.894	5.542	6.331	—
C-9	5.208	5.445	5.543	6.109	—	6.046
C-10	5.839	—	—	—	—	—

this procedure, k_t values for the higher alkylpyridine homologs were calculated (Table IV).

Ion-Pair Effects—When octanol and chloroform were used as the nonaqueous phases, different log (k')–pH profiles were found. Figure 5 shows the results obtained in the octanol–water system. It differs from Fig. 4 in the low pH region where all curves are leveled off. This type of deviation from Eq. 4*b* has been attributed to the presence of ion-pairs in the oil phase (30).

Intrinsic Distribution Coefficients—The distribution coefficient k, defined as the ratio of the two mole fractions, is related to the experimentally determined partition coefficient k_t (Eq. 5) as follows:

$$k = [X]_i/[X]_w = g_i k_t \qquad \text{(Eq. 8}a\text{)}$$

or:

$$\log (k) = \log (g_i) + \log (k_t) \qquad \text{(Eq. 8}b\text{)}$$

where:

$$g_i = V_i(1000d + M_w - M)/1000M_w \qquad \text{(Eq. 9)}$$

$[X]_i$ and $[X]_w$ are the mole fractions of the solute free base in the oil phase i and in the aqueous phase w, respectively; g_i is the ratio of the mole numbers per liter needed to convert k_t into k; M is the molecular weight of sodium chloride (58.45); M_w is the molecular weight of water (18.01); d is the density of the aqueous 1 *M* NaCl at 25° (1.037 g/ml); and V_i is the molar volume of the organic phase. Values of V_i and g_i are shown in Table V.

Since k also may be expressed as the reciprocal of the two activity coefficients:

$$k = \gamma_w/\gamma_i \qquad \text{(Eq. 10)}$$

the ratio of the two activity coefficients remains constant only when both mixtures are in the Henry's law region. Analysis of the data showed a constant log (k) in all six cases. Figure 6 gives a typical plot for the octane–aqueous phase system.

Figure 7 illustrates the relationship between log (k) and the chain length for the hexadecane–aqueous phase system. An examination of the other systems (Table VI) revealed that they all shared the same characteristic features: a linear limiting relationship between log (k) and chain length n when n is greater than 3 and small positive deviations when n is less than 2.

Least-squares limiting slopes of each system are shown in the second column of Table VII. For convenience, these limiting slopes will be called the π values of the CH_2 groups. As can be seen in Table VII, these π values are all comparable. The constancy of the π values suggests that the effect of the CH_2 group on the net interaction energies in these different nonaqueous solvents is approximately the same. This finding probably reflects the predominance of the dispersion forces in the net interaction between the CH_2 group and the solvent.

The activity coefficient terms in Eq. 10 are actual values when the solvents are mutually saturated. The effect of the organic solvents dissolved in the aqueous phase is likely to be negligible due to their low water solubility (Table II). This assumption is based on the reasoning that the effect is small compared to the large primary interactions between the solute and the water molecules. In addition, the solubility would be further reduced in the presence of 1 *M* NaCl. Therefore, the γ_w may be taken as the value when there is no organic solvent in the aqueous phase.

Similarly, the solubility of water in these organic solvents, except octanol, is generally low. The effect of water in the organic solvent was studied by Johnson *et al.* (28). They found that, in the presence of water, pyridine may form a molecular complex with water whose equilibrium constant is in part a function of the intrinsic water solubility in that solvent.

The activity of water in 1 *M* NaCl at 25° is known to be 0.967 (33). If a linear relationship is assumed between its solubility and the activity, the hydration effect would not be significantly shifted by the small difference of 3.3% in the water solubility. A brief discussion of the hydration effect is presented in another paper[1].

The salt appears to have a strong effect on the distribution coefficient. Based on experimental data (28), the log (k) for pyridine in carbon tetrachloride–water has a value of 1.009. Our value of 1.155 represents an increase of 40% in the distribution coefficient or 0.146 on the log basis. The experimental log (k) for picoline in hexadecane–pure water was 1.158. A comparison with the corresponding value of 1.337 in 1 *M* NaCl shows an even greater change:

Table V—Conversion Factors and Molar Volumes of Six Organic Solvents

Organic Solvent (i)	log (g_i)	V_i, ml
Hexadecane	1.213	294.1
Octane	0.958	163.5
Butyl ether	0.974	170.3
Octanol	0.944	158.8
Chloroform	0.649	80.5
Carbon tetrachloride	0.730	96.8

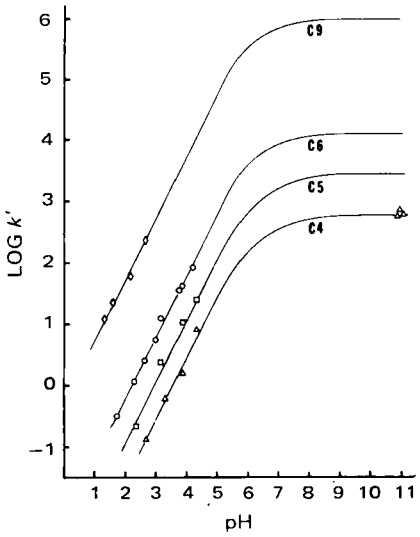

Figure 4—*Apparent partition coefficients of alkylpyridines between carbon tetrachloride and aqueous phase as a function of pH at 25°. Curves represent theory, and points represent experimental data.*

Table VI—Logarithm of Distribution Coefficients of Alkylpyridines between Six Organic Solvents and Aqueous 1 *M* NaCl[a]

Chain Length	Hexadecane	Octane	Butyl Ether	Octanol	Chloroform	Carbon Tetrachloride
Pyridine	0.906	0.745	1.083	1.724	1.975	1.155
C-1	1.337	1.169	1.504	2.263	2.471	1.569
C-2	1.940	1.792	(2.118)	(2.865)	(3.100)	(2.227)
C-3	(2.578)	(2.452)	(2.733)	(3.468)	(3.729)	(2.884)
C-4	(3.216)	(3.113)	3.347	4.071	4.357	3.542
C-5	3.854	3.773	(3.969)	4.693	5.029	4.163
C-6	4.487	4.414	4.591	5.291	5.655	4.844
C-7	5.132	5.071	(5.229)	5.952	6.302	(5.488)
C-8	5.782	5.752	5.868	6.485	6.980	(6.132)
C-9	6.421	6.411	6.517	7.052	—	6.776
C-10	7.052	—	—	—	—	—

[a] Values in parentheses were obtained by interpolation.

a 50% increase in k or 0.179 on the log basis.

Recently, Davis *et al.* (32) compiled various literature π values for the CH_2 group in a series of nonaqueous solvents. For comparison, some of their preferred values are reproduced in Table VII under the column headed "Water." The data from the present study are consistently higher, probably reflecting a significant effect of the electrolyte. Quantitative comparison of the salt effect may be made by using the empirical relation noted by Wilcox and Schrier (34). The effect of 1 *M* NaCl at 25° was found to increase the logarithm of the activity coefficient of ethanol by 0.1 unit. The corresponding value for 1-propanol was 0.15. If it is assumed that the salt effect is additive and composed of independent contributions from the constituent functional group, the difference of 0.05 may be regarded as the salting-out effect of 1 *M* NaCl on the CH_2 group. A comparison of this value with the differences in the data presented in Table VII indicates that these differences, although scattered and ranging from 0.03 to 0.11, are reasonable considering that they are taken from various studies.

The basis for the linear slope shown in Fig. 7 is well known. By definition:

$$RT \ln (\gamma_i) = \Delta G_i \qquad \text{(Eq. 11)}$$

where ΔG_i is the excess free energy of solution in the solvent i. That there are two steps in the dissolution of a solute molecule may be assumed. The first step is to remove the molecule from its own liquid. The second step is to place this molecule in the solvent after a cavity has been created in it. If the solute is increased by a CH_2 group, there is only a small difference in the two free energies of solution when the solvent is nonaqueous. However, there is a relatively large increase in the free energy of solution in the aqueous solution. This finding has been explained on the basis that, although the enthalpy of solution is favorably negative, it is more than counterbalanced by a very large negative entropy change on the immediately surrounding water molecules (35).

To compare the two activity coefficients shown in Eq. 10, it is only necessary to compare the free energy difference of the second step in the dissolution process. The difference in the two quantities is then equal to the free energy for the transfer of the CH_2 group from water to the organic solvent, $-\Delta G_{CH_2}$, and is related to the slope of Fig. 7 by the equation:

$$2.303RT\pi = -\Delta G_{CH_2} \qquad \text{(Eq. 12)}$$

While the π values in Table VII are roughly comparable to each other, the differences between them are still significant. The trend of these π values may be related to the relative magnitude of the net interactions between the solvent–solvent and the solvent–CH_2 group. However, the differences are so small that they are often neglected.

The small initial slopes observed in Fig. 7 when n is less than 2 or 3 may be attributed to the inductive effects of the alkyl groups. The decrease in acidity of the alkylated derivatives as compared to the parent pyridine suggests that the electron density on the nitrogen atom is higher when the ring is alkylated. This is consistent with the observation that 4-picoline has a higher dipole moment than pyridine (36). Furthermore, the polar cohesive energy of picoline, estimated from the homomorph plot of Weimer and Prausnitz (21), was 1.49 kcal/mole, which is somewhat higher than the corresponding value of 1.11 kcal/mole for pyridine. Thus, the higher ring polarity might produce a less favorable net interaction with the nonaqueous solvent and, hence, the solvent would be less likely to transfer into the oil phase. As a result, there is a partial energy cancellation in Eq. 12 and a smaller initial slope observed in the log (k)–chain-length plot.

On the other hand, it can be seen from Table VI that the absolute magnitudes of log (k) differ greatly from one solvent pair to

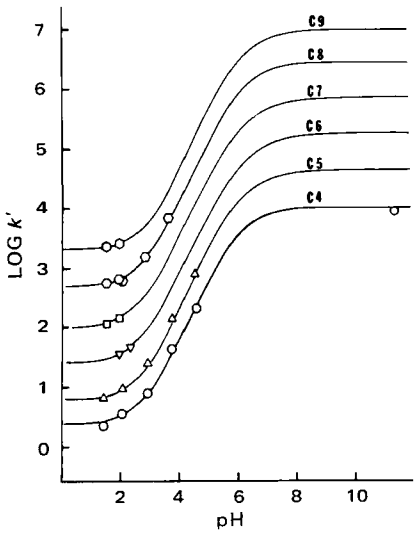

Figure 5—*Apparent partition coefficients of alkylpyridines between octanol and the aqueous phase as a function of pH at 25°. Curves represent theory, and points respresent experimental data.*

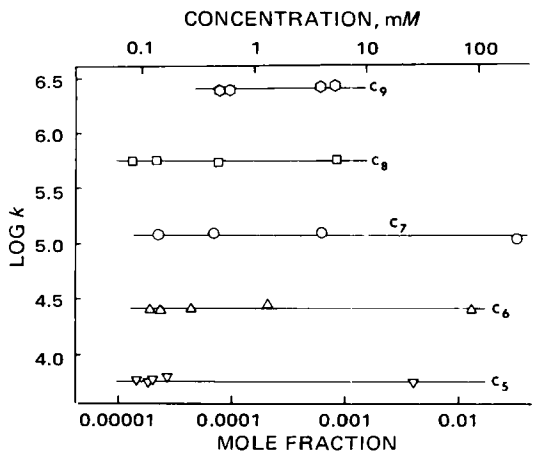

Figure 6—*Constancy of distribution coefficients as a function of concentration between octane and the aqueous phase.*

Table VII—Logarithmic Distribution Coefficients of the Methylene Group at 25°

Organic Phase	1 *M* NaCl	Water[a]
Hexadecane	0.64	0.57[b]
Octane	0.66	0.62
Butyl ether	0.63	—
Octanol	0.61[c]	0.50
Chloroform	0.65	0.6–0.64
Carbon tetrachloride	0.65	0.62

[a] Reference 32. [b] 20°, Ref. 31. [c] Average of 0.62 from ion-pair and 0.60 from free base (30).

another. In general, the octane system gave the lowest values while the chloroform system gave the highest. These values may be considered as a reflection of the relative net interactions between the polar head of the alkylpyridines and the solvent molecules. Based on these data, the strengths of these net interactions may be arranged as follows: chloroform > octanol > carbon tetrachloride > butyl ether > hexadecane > octane.

The weaker interactions in hexadecane and in octane may be attributed entirely to the nonpolar nature of the solvents. In these two cases, the London dispersion force and induction force are the only attractive ones involved. With butyl ether, there are additional forces involved; besides the dispersion forces and the induction forces due to the polarization of the solvent by the polar solute, the solute molecules are also polarized by the solvent, and there are dipole–dipole interactions. Therefore, the solvent–solute interactions might be expected to be more favorable for butyl ether than for the hydrocarbons.

With chloroform and octanol, hydrogen bonding (37, 38) between the pyridine ring and the solvent molecules produces rather strong solvent–solute interactions. These solvents consequently give the highest distribution coefficients with the alkylpyridines. The net solvent–solute interactions appear to be weaker in octanol than in chloroform, even though the strength of the alcohol–pyridine hydrogen bonding (37) is greater than that between chloroform and pyridine (39). The explanation probably resides in the higher polar cohesive energy density of octanol, because more energy is required to create a cavity for the solute molecule. Therefore, the net free energy gained in the second step of the dissolution process may be less in octanol than in chloroform.

Carbon tetrachloride is another interesting case. Its dispersive and inductive interactions with the solute would be expected to be similar to those in octane or hexadecane. Yet this solvent apparently is involved in stronger interactions with alkylpyridines than even butyl ether. This finding probably is in accord with the observations that pyridine has a higher dipole moment in carbon tetrachloride than in benzene (36) and that its heat of solution at infinite dilution in carbon tetrachloride is lower than in hexane (40).

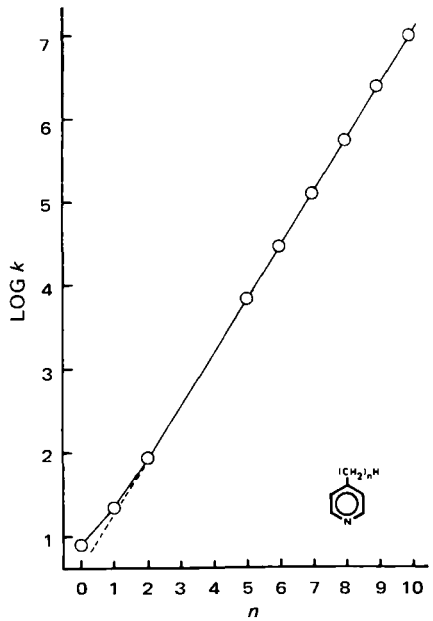

Figure 7—*Intrinsic distribution coefficients of alkylpyridines between hexadecane and the aqueous phase as a function of the chain length.*

REFERENCES

(1) J. Ferguson, *Proc. Roy. Soc. (London)*, **127B**, 387(1939).

(2) R. Collander, *Physiol. Plantarum*, **7**, 397(1954).

(3) M. D. Milne, H. B. Scriber, and M. A. Crawford, *Amer. J. Med.*, **24**, 709(1958).

(4) C. Hansch and W. J. Dunn, III, *J. Pharm. Sci.*, **61**, 1(1972).

(5) C. Hansch, R. M. Muir, T. Fujita, P. P. Maloney, F. Geiger, and M. Streich, *J. Amer. Chem. Soc.*, **85**, 2817(1963).

(6) C. Hansch, A. R. Steward, J. Iwasa, and E. W. Deutsch, *Mol. Pharmacol.*, **1**, 205(1965).

(7) E. W. Deutsch and C. Hansch, *Nature*, **211**, 75(1966).

(8) C. Hansch, *J. Med. Chem.*, **11**, 920(1968).

(9) E. J. Lien, C. Hansch, and S. M. Anderson, *ibid.*, **11**, 43(1968).

(10) C. Hansch, *ibid.*, **11**, 920(1968).

(11) R. Collander, *Acta Physiol. Scand.*, **13**, 363(1947).

(12) R. Collander, *Acta Chem. Scand.*, **4**, 1085(1950).

(13) D. J. Lamb and L. E. Harris, *J. Amer. Pharm. Ass., Sci. Ed.*, **49**, 583(1960).

(14) K. Kakemi, T. Arita, R. Hori, and R. Konishi, *Chem. Pharm. Bull.*, **15**, 1705(1967).

(15) L. Alders, *Appl. Sci. Res.*, **A4**, 171(1954).

(16) C. Hansch and S. M. Anderson, *J. Org. Chem.*, **32**, 2583(1967).

(17) C. Hansch and S. M. Anderson, *J. Amer. Chem. Soc.*, **86**, 1616(1964).

(18) T. Fujita, J. Iwasa, and C. Hansch, *ibid.*, **86**, 5175(1964).

(19) G. L. Flynn, *J. Pharm. Sci.*, **60**, 345(1971).

(20) J. H. Hildebrand, J. M. Prausnitz, and R. J. Scott, "Regular and Related Solutions," Van Nostrand Reinhold, New York, N.Y., 1970.

(21) R. F. Weimer and J. M. Prausnitz, *Hydrocarbon Process.*, **44**, 237(1965).

(22) J. P. Wilbaut and J. W. Hey, *Rec. Trav. Chem.*, **72**, 513(1953).

(23) B. E. Conway and L. H. Laliberte, in "Hydrogen-Bonded Solvent Systems," A. K. Covington and P. Jones, Eds., Taylor & Francis Ltd., London, England, 1968.

(24) K. C. Yeh, Ph.D. thesis, University of Michigan, Ann Arbor, Mich., 1972.

(25) L. J. Edward, *Trans. Faraday Soc.*, **46**, 723(1950).

(26) P. Schatzberg, *J. Phys. Chem.*, **67**, 976(1963).

(27) J. A. Riddick and E. E. Troops, Jr., "Technique of Organic Chemistry," vol. III, Interscience, New York, N.Y., 1955.

(28) J. R. Johnson, P. J. Kilpatrick, S. D. Christian, and H. E. Affsprung, *J. Phys. Chem.*, **72**, 3223(1968).

(29) W. L. Masterton and M. C. Gendrano, *ibid.*, **70**, 2895(1966).

(30) K. C. Yeh and W. I. Higuchi, *J. Pharm. Sci.*, **61**, 1648(1972).

(31) R. Aveyard and R. W. Mitchell, *Trans. Faraday Soc.*, **65**, 2645(1969).

(32) S. S. Davis, T. Higuchi, and J. H. Rytting, *J. Pharm. Pharmacol., Suppl.*, **24**, 30(1972).

(33) R. A. Robinson and R. M. Stokes, "Electrolyte Solutions," Academic, New York, N.Y., 1955.

(34) F. L. Wilcox and E. E. Schrier, *J. Phys. Chem.*, **75**, 3757(1971).

(35) G. Nemethy and H. A. Scheraga, *J. Chem. Phys.*, **36**, 3382, 3401(1962).

(36) A. N. Sharpe and S. Walker, *J. Chem. Soc.*, **1961**, 2974.

(37) T. J. V. Findlay and J. L. Copp, *Trans. Faraday Soc.*, **65**, 1463(1969).

(38) T. J. V. Findlay and R. S. Kenyon, *Aust. J. Chem.*, **22**, 865(1969).

(39) T. J. V. Findlay, J. S. Kenry, A. D. Kidman, and V. A. Pickles, *Trans. Faraday Soc.*, **63**, 846(1967).

(40) A. D. Sherry and K. F. Purcell, *J. Amer. Chem. Soc.*, **92**, 6386(1970).

ACKNOWLEDGMENTS AND ADDRESSES

Received June 27, 1974, from the *College of Pharmacy, University of Michigan, Ann Arbor, MI 48104*

Accepted for publication March 14, 1975.

Presented at the Basic Pharmaceutics Section, APhA Academy of Pharmaceutical Sciences, Houston meeting, April 1972.

Abstracted from a thesis submitted by K. C. Yeh to the University of Michigan in partial fulfillment of the Doctor of Philosophy degree requirements.

Supported in part by Training Grant 1T1-GM-1367 from the U.S. Public Health Service and in part by Grant GM-13368 from the National Institute of General Medical Sciences, U. S. Public Health Service, Bethesda, Md.

The authors thank Dr. W. Hong, Parke, Davis & Co., Detroit, Mich., for the determination of water solubilities.

* Present address: Merck Sharp & Dohme Research Laboratories, West Point, PA 19486

[x] To whom inquiries should be directed.

Fully Automated Analysis of Phenylbutazone in Plasma and Urine

GEORGE LUKAS [x], CATHERINE B. BORMAN, and SYLVIA B. ZAK

Abstract □ A rapid, automated method for the determination of phenylbutazone in plasma and urine was developed. The method offers distinct advantages over earlier procedures and is particularly suitable for large-scale bioavailability studies.

Keyphrases □ Phenylbutazone—analysis, automated method, human plasma and urine □ Automated methods—analysis of phenylbutazone in human plasma and urine □ Anti-inflammatory agents—phenylbutazone, analysis, automated method, human plasma and urine

Phenylbutazone (4-butyl-1,2-diphenyl-3,5-pyrazolidinedione) has been used extensively during the past 2 decades in the treatment of rheumatoid and other inflammatory conditions. Several methods have been developed for the analysis of the drug in body fluids in conjunction with investigations on its biological disposition.

The plasma levels of phenylbutazone were measured spectrophotometrically following its extraction (1), and several modifications were introduced (2, 3) to reduce the interference caused by oxyphenbutazone, the principal metabolite. The procedure also was modified for small samples (4). Another method based on hydrolysis of phenylbutazone to hydrazobenzene, with subsequent rearrangement to benzidine, was developed (5) and modified (6, 7). Also, phenylbutazone was oxidized to azobenzene, and the UV absorbance of the latter compound was measured (8, 9). Several workers (10–15) used GC for the assay of the drug in biological fluids or solid dosage forms. A method using liquid chromatography was reported recently (16).

Although most of these methods have merit in terms of specificity and/or sensitivity, they are rather time consuming. Ahuja *et al.* (17) developed an automated method capable of assaying solid dosage forms at the rate of 13 samples/hr. Unfortunately, their method lacks the sensitivity required for the analysis of phenylbutazone in biological fluids.

Analysis of plasma levels in conjunction with large-scale bioavailability assessments of phenylbutazone dosage forms after a therapeutic dose in humans requires speed, sensitivity, and specificity. The automated method presented here satisfies these criteria.

Table I—Standard Curve of Phenylbutazone from Aqueous Solutions[a]

Concentration, μg/ml	Peak Height[a]
0	0.0 ± 0.0
0.5	0.3 ± 0.1
1	0.6 ± 0.1
2	1.4 ± 0.2
3	2.5 ± 0.1
4	3.3 ± 0.2
5	4.1 ± 0.1
7	5.6 ± 0.3
10	8.0 ± 0.2
20	15.5 ± 0.4
30	25.4 ± 0.6
40	32.2 ± 0.5
50	38.5 ± 1.5
60	48.0 ± 2.7

[a] Each value represents the average ± *SD* of five determinations (arbitrary units).

EXPERIMENTAL

Reagents and Standards—All chemicals except heptane (chromatoquality) were reagent grade or of equivalent purity. The following were used: aminoacetic acid–hydrochloric acid buffer (pH 1.2), prepared by dissolving 25 g of aminoacetic acid and 50 ml of 6 *N* HCl in a final volume of 1000 ml of water; heptane–isopentyl alcohol (98.5:1.5); and 2.5 *N* NaOH.

The following standard solutions, preferably prepared daily, were used: (*a*) phenylbutazone, 1 or 10 mg/ml in 1.0 *N* NaOH; and (*b*) phenylbutazone, 2–80 μg/ml in plasma[1].

Procedure[2]—The flow diagram for the automated manifold is depicted in Fig. 1. At the beginning of the day's analyses, the re-

[1] Plasma was purchased from the American Red Cross and was mixed with varying amounts of phenylbutazone.

[2] The following equipment was used: Technicon sampler IV, Technicon proportioning pump III, Technicon continuous filter with hydrophobic filter paper (Product No. 518-3041), Beckman model DB-G grating spectrophotometer equipped with a 6-mm rectangular flowcell, and Technicon single-pen linearized recorder with linear-scale chart paper.

ACKNOWLEDGMENTS AND ADDRESSES

Received June 27, 1974, from the *College of Pharmacy, University of Michigan, Ann Arbor, MI 48104*

Accepted for publication March 14, 1975.

Presented at the Basic Pharmaceutics Section, APhA Academy of Pharmaceutical Sciences, Houston meeting, April 1972.

Abstracted from a thesis submitted by K. C. Yeh to the University of Michigan in partial fulfillment of the Doctor of Philosophy degree requirements.

Supported in part by Training Grant 1T1-GM-1367 from the U.S. Public Health Service and in part by Grant GM-13368 from the National Institute of General Medical Sciences, U. S. Public Health Service, Bethesda, Md.

The authors thank Dr. W. Hong, Parke, Davis & Co., Detroit, Mich., for the determination of water solubilities.

* Present address: Merck Sharp & Dohme Research Laboratories, West Point, PA 19486

[x] To whom inquiries should be directed.

Fully Automated Analysis of Phenylbutazone in Plasma and Urine

GEORGE LUKAS [x], CATHERINE B. BORMAN, and SYLVIA B. ZAK

Abstract □ A rapid, automated method for the determination of phenylbutazone in plasma and urine was developed. The method offers distinct advantages over earlier procedures and is particularly suitable for large-scale bioavailability studies.

Keyphrases □ Phenylbutazone—analysis, automated method, human plasma and urine □ Automated methods—analysis of phenylbutazone in human plasma and urine □ Anti-inflammatory agents—phenylbutazone, analysis, automated method, human plasma and urine

Phenylbutazone (4-butyl-1,2-diphenyl-3,5-pyrazolidinedione) has been used extensively during the past 2 decades in the treatment of rheumatoid and other inflammatory conditions. Several methods have been developed for the analysis of the drug in body fluids in conjunction with investigations on its biological disposition.

The plasma levels of phenylbutazone were measured spectrophotometrically following its extraction (1), and several modifications were introduced (2, 3) to reduce the interference caused by oxyphenbutazone, the principal metabolite. The procedure also was modified for small samples (4). Another method based on hydrolysis of phenylbutazone to hydrazobenzene, with subsequent rearrangement to benzidine, was developed (5) and modified (6, 7). Also, phenylbutazone was oxidized to azobenzene, and the UV absorbance of the latter compound was measured (8, 9). Several workers (10–15) used GC for the assay of the drug in biological fluids or solid dosage forms. A method using liquid chromatography was reported recently (16).

Although most of these methods have merit in terms of specificity and/or sensitivity, they are rather time consuming. Ahuja *et al.* (17) developed an automated method capable of assaying solid dosage forms at the rate of 13 samples/hr. Unfortunately, their method lacks the sensitivity required for the analysis of phenylbutazone in biological fluids.

Analysis of plasma levels in conjunction with large-scale bioavailability assessments of phenylbutazone dosage forms after a therapeutic dose in humans requires speed, sensitivity, and specificity. The automated method presented here satisfies these criteria.

Table I—Standard Curve of Phenylbutazone from Aqueous Solutions[a]

Concentration, μg/ml	Peak Height[a]
0	0.0 ± 0.0
0.5	0.3 ± 0.1
1	0.6 ± 0.1
2	1.4 ± 0.2
3	2.5 ± 0.1
4	3.3 ± 0.2
5	4.1 ± 0.1
7	5.6 ± 0.3
10	8.0 ± 0.2
20	15.5 ± 0.4
30	25.4 ± 0.6
40	32.2 ± 0.5
50	38.5 ± 1.5
60	48.0 ± 2.7

[a] Each value represents the average ± *SD* of five determinations (arbitrary units).

EXPERIMENTAL

Reagents and Standards—All chemicals except heptane (chromatoquality) were reagent grade or of equivalent purity. The following were used: aminoacetic acid–hydrochloric acid buffer (pH 1.2), prepared by dissolving 25 g of aminoacetic acid and 50 ml of 6 *N* HCl in a final volume of 1000 ml of water; heptane–isopentyl alcohol (98.5:1.5); and 2.5 *N* NaOH.

The following standard solutions, preferably prepared daily, were used: (*a*) phenylbutazone, 1 or 10 mg/ml in 1.0 *N* NaOH; and (*b*) phenylbutazone, 2–80 μg/ml in plasma[1].

Procedure[2]—The flow diagram for the automated manifold is depicted in Fig. 1. At the beginning of the day's analyses, the re-

[1] Plasma was purchased from the American Red Cross and was mixed with varying amounts of phenylbutazone.

[2] The following equipment was used: Technicon sampler IV, Technicon proportioning pump III, Technicon continuous filter with hydrophobic filter paper (Product No. 518-3041), Beckman model DB-G grating spectrophotometer equipped with a 6-mm rectangular flowcell, and Technicon single-pen linearized recorder with linear-scale chart paper.

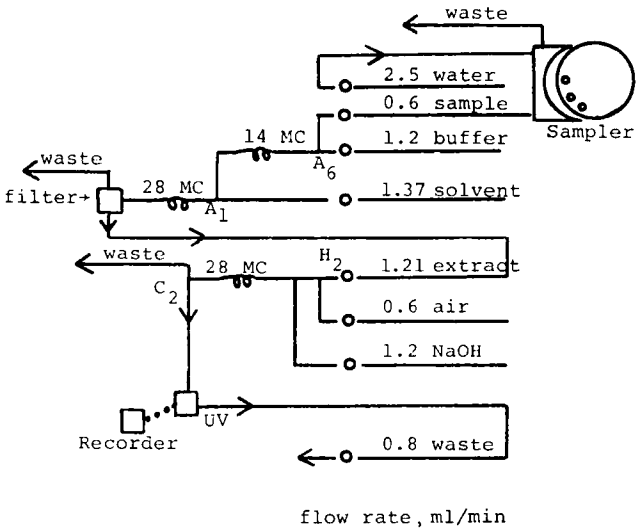

Figure 1—*Flow diagram of the automated analytical procedure for phenylbutazone. Key: 14 MC = 14-turn mixing coil; 28 MC = 28-turn mixing coil; and A_1, A_6, H_2, and C_2 = separators.*

agents were pumped through the system for at least 15 min and a reagent blank baseline was established.

Plasma samples containing phenylbutazone, normally in the range of 0–50 μg/ml, were analyzed, yielding the first standard curve of the day. The samples were aspirated with a proportioning pump from 2-ml plastic sample cups at the rate of 20/hr. Consecutive samples were separated by an aqueous wash, using a sample–wash ratio of 1:2. Under these conditions and with a sample flow rate of 0.6 ml/min, each assay required 0.6 ml of sample.

During these preliminary steps, the heparinized, frozen plasma samples containing unknown concentrations of phenylbutazone were allowed to stand at room temperature until thawing occurred. Particulate matter was removed by brief centrifugation, and the supernatant fluids were transferred to sample cups. The samples were aspirated into the flow system and analyzed at the rate of 20/hr. A detailed description of the method follows.

Samples and the pH 1.2 buffer were mixed in a 14-turn mixing coil. Subsequently, the buffered plasma and heptane–isopentyl alcohol (98.5:1.5) were mixed in a 28-turn mixing coil, where the extraction of phenylbutazone occurred. The stream of the mixed aqueous and organic phases was separated by being fed to the top side of a 2.5-cm (1-in.) wide strip of hydrophobic filter paper. Since this paper was moving at a rate of 2.5 cm (1 in.)/min, it was always providing a fresh surface for the separation. The organic phase was collected on the bottom side of the paper by aspiration, and it was fed once more through the pump. The flow was segmented with air and mixed with 2.5 *N* NaOH.

Mixing of the phases and extraction of phenylbutazone into the aqueous alkaline solution took place in a 28-turn mixing coil. The mixture was fed through a phase separator for the removal of air bubbles and the organic phase. Finally, the resulting aqueous solution containing the sodium salt of phenylbutazone was fed through a flowcell where the UV absorption of the solution at 265 nm was continuously monitored.

Polyethylene tubing was used between the first 28-turn coil and the continuous filter, as well as between the exit side of the continuous filter and the suction side of the pump. Solvent-resistant tubing[3] was used at all other points for streams containing organic solvent. Polyethylene tubing connected the phase separator with the flowcell. Tygon tubing was used at the remaining points of the system. Solvent-resistant sleevings[3] were used for all connections.

A series of plasma standards containing phenylbutazone (0–50 μg/ml) was assayed after every group of approximately 30 test samples. The values obtained with several standards at each concentration were averaged, and a calibration curve of peak height *versus* phenylbutazone concentration was prepared each day. The plasma blank samples gave average values of approximately 0.5 μg/ml. The blank values were subtracted from the standards before the latter data were tabulated.

The described method was applicable without modification to the analysis of phenylbutazone in urine.

[3] Acidflex, Technicon Inc., Tarrytown, N.Y.

Table II—Accuracy of Automated Analytical Procedure for Phenylbutazone

Concentration, μg/ml		Average Recovery, %	n[a]
Expected	Found (Average ± *SD*)		
2	1.6 ± 0.6	80	6
3	2.8 ± 0.4	93.3	6
4	4.0 ± 0.7	100	6
5	5.5 ± 0.6	110	6
7	7.0 ± 0.3	100	6
10	10.8 ± 0.5	108	6
20	21.9 ± 0.7	109.5	6
25	24.8 ± 1.9	99.2	10
40	38.0 ± 1.0	95	6
50	49.7 ± 2.0	99.4	11

[a] n = number of determinations.

RESULTS AND DISCUSSION

Standard Curves and Linearity—Aqueous solutions containing known amounts of phenylbutazone (0–60 μg/ml) were carried through the entire analysis. The blank samples, corresponding to the reagent blank, had a reading of zero. The data (Table I) gave a straight line for the entire range (r = 0.99). The smallest detectable concentration from aqueous solutions was 0.5 μg/ml.

Subsequently, standard curves in plasma were obtained. A typical curve was generated by analyzing phenylbutazone at concentrations of 0, 2, 3, 4, 5, 10, 20, 30, 40, 50, 60, 70, and 80 μg/ml. Five determinations were made at each concentration, except at 40 μg/ml (three measurements). The resulting curve of peak height readings *versus* concentrations had the following regression equation: $y = 0.672x - 0.361$, and demonstrated good linearity in the expected range of drug concentrations (r = 0.99). During the analyses of unknowns, similar standard curves were generated daily, using at least five concentrations, and were used for the calculation of the results obtained on that day.

Precision—The data generated for the standard curve of phenylbutazone in plasma gave a valid estimate of the precision of the methodology. At 2 μg/ml, a relative standard deviation of 20% was obtained. However, at each point between 3 and 80 μg/ml, the relative standard deviation was equal to or less than 7%, indicating good precision.

Sensitivity—A panel of 18 subjects had average predose plasma levels of apparent phenylbutazone of 0.3 μg/ml. Most subjects had nondetectable levels; three of the 18 individuals had values of 0.5 μg/ml, and another three had 1.5 μg/ml. Based on the variability of these data, it was estimated that the lowest value that could be assayed reliably (*i.e.*, quantitatively distinguished from the blank) would be approximately 3 μg/ml. This sensitivity is comparable to,

Table III—Specificity of Automated Analytical Procedure for Phenylbutazone[a]

Concentration of Oxyphenbutazone, μg/ml	Average Peak Height, % of control	n[b]
0	100	2
2	97.1	4
5	93.1	4
10	97.1	4
20	81.6	2
30	109.4	4
40	98.0	2

[a] Each sample contained 10 μg/ml of phenylbutazone. The samples containing no oxyphenbutazone served as controls. [b] n = number of determinations.

Table IV—Interference by Salicylic Acid with the Accuracy of Automated Analytical Procedure for Phenylbutazone

Concentration, μg/ml		Peak Height, Average ± SD, % of control	n^a
Phenylbutazone	Salicylic Acid		
20	0	100.0 ± 5.0	20
20	20	111.3 ± 7.8	8
20	40	116.3 ± 7.8	10
20	80	136.2 ± 9.9	10

[a] n = number of determinations.

or better than, the one obtainable with the manual method of Burns *et al.* (1). At the same time, the automated method is four to five times faster (100–120 analyses/8-hr day).

Accuracy—Solutions of phenylbutazone in plasma ranging from 2 to 50 μg/ml were prepared and then analyzed in a blind manner. The data (Table II) demonstrated that the analytical procedure gave reliable results in the 3–50-μg/ml range, with an average recovery of 101.3%. A relatively low recovery (80%) was obtained at 2 μg/ml.

Specificity—Varying concentrations (2–40 μg/ml) of oxyphenbutazone, the principal metabolite of phenylbutazone, were added to plasma samples containing 10 μg/ml of phenylbutazone. Results of the analyses (Table III) demonstrate that the presence of oxyphenbutazone did not affect appreciably the plasma level values obtained for phenylbutazone. Similarly, when each sample contained 25 μg/ml of phenylbutazone, the 20-fold increase in the concentration of oxyphenbutazone caused only a 13% increase in the values of apparent phenylbutazone.

A separate experiment showed that as much as 50 μg/ml of oxyphenbutazone did not interfere with the analysis of 5 μg/ml of phenylbutazone. Thus, the automated method is considerably more specific than the original method of Burns *et al.* (1), which suffers from appreciable interference by oxyphenbutazone.

Interference by salicylic acid was tested by analyzing plasma samples to which 20 μg/ml of phenylbutazone and 0, 20, 40, or 80 μg/ml of salicylic acid had been added. A 2-mg/ml stock solution of salicylic acid in 0.025 *N* NaOH was used. The data (Table IV) gave the regression line of $y = 14.1 + 0.063x$ (peak height *versus* concentration), indicating that each 10 μg/ml of the salicylic acid present in the plasma would be assayed as 0.63 μg/ml of apparent phenylbutazone. The magnitude of this interference depends on the relative proportions of the two drugs and, in practice, should not be troublesome.

In all likelihood, a single dose of a salicylate taken inadvertently during a bioavailability study would not interfere materially with the results of the phenylbutazone assay. On the other hand, steady-state salicylate levels, resulting from chronic intake prior to a phenylbutazone study, would appear as unusually high zero-time levels. Under these conditions, the subject would probably be eliminated from the study.

Human Plasma Level Studies—The described automated analytical method was used in several human studies. Plasma concentrations of phenylbutazone[4] were followed for up to 336 hr after a single oral dose. The data obtained in a representative study[5] were reported in preliminary form (18).

Analysis of Phenylbutazone in Urine—A standard curve was generated by analyzing phenylbutazone in urine at concentrations of 0, 2, 4, 6, 10, 20, 30, and 40 μg/ml. Ten determinations were made at each concentration between 4 and 40 μg/ml. The resulting curve of peak height readings *versus* concentrations showed good linearity ($r = 0.99$) with the following regression line: $y = 0.609x - 0.512$.

REFERENCES

(1) J. J. Burns, R. K. Rose, T. Chenkin, A. Goldman, A. Schulert, and B. B. Brodie, *J. Pharmacol. Exp. Ther.*, **109**, 346(1953).

(2) B. Herrmann, *Med. Exp.*, **1**, 170(1959).

(3) G. R. Van Petten, H. Feng, R. J. Withey, and H. F. Lettau, *J. Clin. Pharmacol.*, **11**, 177(1971).

(4) W. Fuchs, *Muench. Med. Wochenschr.*, **107**, 1267(1965).

(5) R. Pulver, *Schweiz. Med. Wochenschr.*, **80**, 308(1950).

(6) D. G. Moss, *J. Clin. Pathol.*, **1**, 344(1954).

(7) E. A. Tophøj, *Acta Med. Scand.*, **160**, 197(1958).

(8) J. E. Wallace, *J. Pharm. Sci.*, **57**, 2053(1968).

(9) E. Jähnchen and G. Levy, *Clin. Chem.*, **18**, 984(1972).

(10) R. Perego, E. Martinelli, and P. C. Vanoni, *J. Chromatogr.*, **54**, 280(1971).

(11) J. R. Watson, F. Matsui, R. C. Lawrence, and P. M. J. McConnell, *ibid.*, **76**, 141(1973).

(12) I. J. McGilveray, K. K. Midha, R. Brien, and L. Wilson, *ibid.*, **89**, 17(1974).

(13) R. B. Bruce, W. R. Maynard, and L. K. Dunning, *J. Pharm. Sci.*, **63**, 446(1974).

(14) K. K. Midha, I. J. McGilveray, and C. Charette, *ibid.*, **63**, 1234(1974).

(15) O. M. Bakke, G. H. Draffan, and D. S. Davies, *Xenobiotica*, **4**, 237(1974).

(16) N. J. Pound, I. J. McGilveray, and R. W. Sears, *J. Chromatogr.*, **89**, 23(1974).

(17) S. Ahuja, C. Spitzer, and F. R. Brofazi, in "Technicon Symposium, 1967, Automation in Analytical Chemistry," vol. 1, Medlad, White Plains, N.Y., 1968, p. 467.

(18) G. Lukas, M. B. Maggio-Cavaliere, C. B. Borman, and J. D. Arnold, *J. Clin. Pharmacol.*, **14**, 397(1974).

ACKNOWLEDGMENTS AND ADDRESSES

Received January 16, 1975, from the *Research Department, Pharmaceuticals Division, Ciba-Geigy Corporation, Ardsley, NY 10502*

Accepted for publication April 14, 1975.

[x] To whom inquiries should be directed.

[4] Butazolidin, Ciba-Geigy Corp., Ardsley, N.Y.

[5] G. Lukas, M. B. Maggio-Cavaliere, C. B. Borman, and J. D. Arnold, to be published.

Implant Pellets I: Effects of Compression Pressure on *In Vivo* Dissolution of Delmadinone Acetate Pellets

JOHN S. KENT

Abstract □ A formulation containing 95% delmadinone acetate was compressed at three different pressures. These pressures resulted in a pellet density difference of 19%. *In vivo* dissolution profiles were determined for five lots of pellets. The pellets were implanted subcutaneously in rats, removed periodically, and assayed chemically for remaining steroid. The resulting data were fit, using the computer program NONLIN, to a dissolution model. The dissolution rate for the lot with the lowest density made at the lowest compression was statistically ($p < 0.05$) different from the four other lots. A possible explanation for this increased dissolution rate could be that channeling occurs within the pellet, thereby increasing the effective dissolving surface. The results also indicate that equivalent dissolution rates between lots are reached at a certain compression and density.

Keyphrases □ Implants—delmadinone acetate pellets, effect of compression pressure on *in vivo* dissolution profile, rats □ Delmadinone acetate—pellet implants, *in vivo* dissolution profile, rats □ Dissolution—delmadinone acetate pellet implants, effect of compression pressure, rats

Steroid pellet implants were suggested many years ago (1) as a method for continuously delivering a steroid drug for a long period. This principle of drug delivery has been used frequently, and an excellent review of the subject has appeared (2).

In manufacturing a pellet implant, it is necessary to examine factors that may affect the *in vivo* dissolution of the pellet, including (*a*) the particle-size distribution of the steroid, (*b*) the pressure load used in pellet compression (hence, pellet density), (*c*) the granulation procedure, and (*d*) polymorphism.

Previous investigators (3, 4) demonstrated *in vivo* that the variation in compression (pellet density) had no effect on pellet dissolution. Cowie and Foley (4) examined a fivefold range in compression of hexosterol pellets, but only a 5% variation in pellet densities resulted. The *in vivo* dissolution result, not too surprisingly, demonstrated no difference in dissolution rate between groups. Other investigators (3) varied the compression pressure fourfold (a reported 15,000–60,000 psi) in making desoxycorticosterone acetate pellets (radius = 0.32 cm) and found no change in the pellet dissolution rate.

The compression or density effect on pellet dissolution was tested *in vitro* (5) over a 25% variation in pellet densities. The results indicated no difference in the *in vitro* dissolution rate over the density range and at the particular stirring rate studied.

The purpose of this preliminary investigation was to determine if varying the compression (or density) in the manufacturing of delmadinone acetate pellets would affect the *in vivo* pellet dissolution. The results of this study should be very helpful in setting production and quality control specifications for the pellets.

Delmadinone acetate (6-chloro-17-hydroxypregna-1,4,6-triene-3,20-dione acetate), the major component of the pellets studied, is a potent progestin with antiestrogenic and strong antiandrogenic properties (6, 7). Delmadinone acetate was studied for reproduction control in the cat (8), for which the pellet product would have application.

Table I—Delmadinone Acetate Pellet Implant Characteristics

Group	Compression Characteristic	Initial Pellet Weight, mg (*SD*)	Initial Pellet Height, cm	Density (ρ), g/ml
1	Low	29.48 (0.67)	0.393	0.944
2	Standard	27.55 (0.70)	0.298	1.16
3	High	28.38 (0.81)	0.307	1.16
4	Standard	27.36 (0.82)	0.295	1.17
5	Standard	26.52 (0.64)	0.286	1.17

EXPERIMENTAL

Pellet Formulation—The steroid pellets were composed of 95% delmadinone acetate and 5% inert ingredients. The pellet granulations were compressed on a single-punch tablet machine[1], using 0.318-cm (0.125-in.) flat-face beveled-edge punches and die.

The groups of pellets are identified in Table I. Groups 1–3 were manufactured from the same granulation. Each group, however, was compressed under a different compression load. The compression used is indicated as low, standard, or high. At the time of pellet manufacture, the tablet press was not instrumented so arbitrary terms were assigned. Since then the press has been instrumented with strain gauges so precise load values can be obtained. By using the results from pellet compression experiments with the instrumented press, approximate load values can be given to the arbitrary terms used here. Low compression corresponds to about 45.4–90.8-kg (100–200-lb) load, standard to about 227-kg (500-lb) load, and high to about 272.4-kg (600-lb) load.

Analytical Method—The pellets were analyzed for delmadinone acetate initially and after removal from implantation. The pellet was dissolved in chloroform, and the delmadinone acetate was isolated by TLC, using a silica gel plate with benzene–ethyl acetate (70:30) as the solvent. Final determination was by 4-aminoantipyrine hydrochloride color development, with absorbance measured at 420 nm.

Animals and Design—Twenty-four male Sprague–Dawley-derived albino rats, 200–220 g, were acclimatized to laboratory conditions for 1 week. The animals then were identified by a standard ear punch code, and six rats were randomly assigned to four groups.

On Day 0, each rat was implanted subcutaneously with six pellets, three in each flank. Each pellet was implanted separately so that each could be individually identified.

The animals were housed two to a standard rat cage with food and water *ad libitum*. One pellet from alternate sites was removed from each animal 28, 63, 119, 154, 182, and 238 days after subcutaneous implantation.

The implantation procedure for Group 5 was somewhat different than for Groups 1–4. Eighteen animals were implanted subcutaneously with two pellets, one in the right and one in the left flank areas. On Days 29, 59, 90, 120, 151, and 179 after implanta-

[1] Stokes model E.

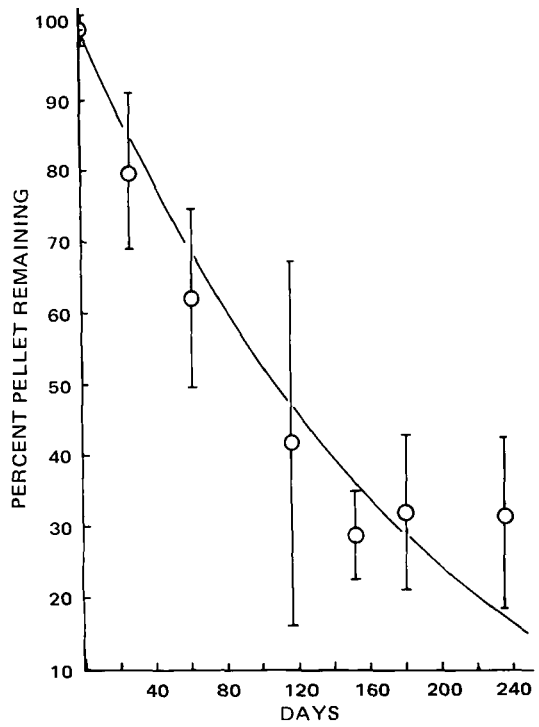

Figure 1—*Dissolution profile of delmadinone acetate pellets, Group 1, implanted subcutaneously in rats. Key: O, mean of observations with standard deviation as solid bar; curved solid line is computer fit of data to dissolution model.*

tion, groups of three rats were sacrificed and the pellets were removed for chemical analysis.

Data Treatment—The dissolution of a pellet implant is dependent on many factors, such as composition, surface area, and solubility. The weight of a dissolving pellet at any time, t, may be described as a function of the product of the pellet density and pellet volume (2). The dissolution equation assumes that the shape does not change during dissolution, nor does the dissolution rate per unit surface area change as the result of a change in diffusional distance or surface irregularities. The equations for a cylindrical pellet (2), such as the one under study, are:

$$W_t = (\pi)(\rho)(R_0 - kt)^2(H_0 - 2kt) \qquad \text{(Eq. 1)}$$

Table II—Percent of Delmadinone Acetate Pellet Remaining after Removal from Implantation at Specified Times[a]

	Days					
Group	28	63	119	154	182	238
1	79.6 (10.7), $n = 4$	62.4 (12.6), $n = 6$	41.3 (25.6), $n = 3$	28.5 (6.1), $n = 3$	32.2 (11.1), $n = 3$	30.1 (12.0), $n = 3$
2	87.7 (3.0), $n = 5$	74.2 (6.2), $n = 4$	64.4 (13.4), $n = 3$	51.6 (10.6), $n = 5$	58.6 (11.1), $n = 4$	35.1 (5.5), $n = 4$
3	87.1 (5.9), $n = 9$	75.6 (6.5), $n = 5$	69.5 (8.7), $n = 5$	61.1 (17.1), $n = 3$	65.4 (15.1), $n = 4$	35.9 (9.7), $n = 5$
4	90.6 (3.2), $n = 5$	76.5 (5.4), $n = 6$	66.6 (7.2), $n = 6$	45.3 (5.7), $n = 5$	47.5 (5.3), $n = 3$	37.5 (7.5), $n = 6$
	Days					
	28	59	90	120	151	179
5	88.2 (3.2), $n = 6$	80.7 (2.6), $n = 6$	67.5 (7.9), $n = 6$	76.4 (9.8), $n = 5$	54.7 (14.1), $n = 6$	50.8 (18.1), $n = 5$

[a] Numbers in parentheses are standard deviations; n = number of samples.

$$W_t = (\pi)(\rho)[-2k^3t^3 + R_0(4 + Q)k^2t^2 - 2R_0^2(1 + Q)kt + R_0^3Q] \qquad \text{(Eq. 2)}$$

where:

W_t = weight in milligrams of the pellet t days after initiation of dissolution
R_0 = initial radius of the pellet in centimeters
H_0 = initial height of the pellet in centimeters
$Q = H_0/R_0$
$\rho = W_0/\pi R_0^2 H_0$, pellet density
k = dissolution rate constant with units of centimeters per day

The constant k describes the rate at which the pellet radius decreases. The value for k was estimated using the NONLIN computer program (9). This program provides an estimate for k plus statistics such as the standard error about k, the 95% confidence limits, and the correlation coefficient. In addition, the program calculates the pellet weights from the equation, the pellet dissolution rate, the dissolution rate of active steroid, and the pellet surface area, all at each measured time point. The equations used follow:

$$\text{dissolution rate at time } t \text{ per pellet} = \frac{-dw}{dt} = 2\pi(\rho)k[(R_0 - kt)^2 + (R_0 - kt)(R_0Q - 2kt)] \qquad \text{(Eq. 3)}$$

$$\text{surface area at time } t \text{ per pellet} = 2\pi(R_0 - kt)^2 + 2\pi(R_0 - kt)(R_0Q - 2kt) \qquad \text{(Eq. 4)}$$

$$\text{dissolution rate per pellet} = \frac{-dw}{dt} = (\rho)(k)(\text{surface area}) \qquad \text{(Eq. 5)}$$

$$\text{active dissolution rate per pellet} = (\text{fraction active})(\text{pellet dissolution rate}) \qquad \text{(Eq. 6)}$$

RESULTS AND DISCUSSION

The results are presented in Table II and Figs. 1–5. The shape of the dissolution profiles conforms to the expected result, as indicated by the computer fit. The variation, as indicated by the standard deviation, was occasionally higher compared to earlier and later

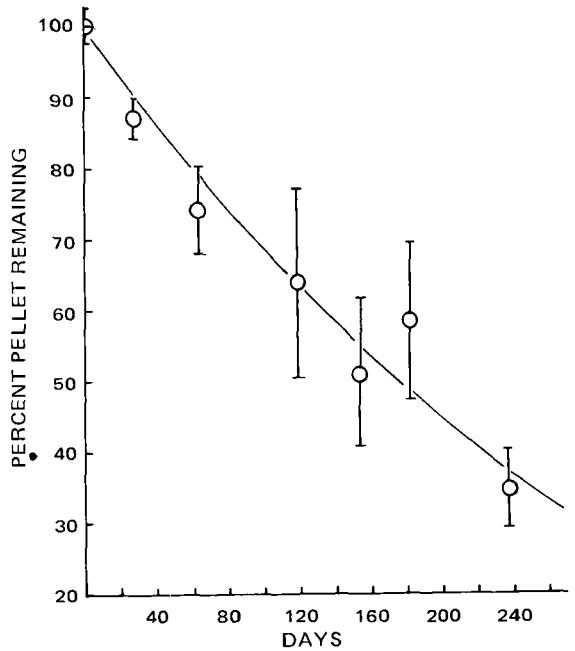

Figure 2—*Dissolution profile of delmadinone acetate pellets, Group 2, implanted subcutaneously in rats. Key: O, mean of observations with standard deviation as solid bar; curved solid line is computer fit of data to dissolution model.*

Table III—Summary of Output from Computer Fit of Dissolution Data

Group	Tablet Press Compression Setting	$k \times 10^4$ cm/day (*SE*)	95% Confidence Limits (Support Plane)	Correlation Coefficient	Dissolution Rate ($k \times \rho$), $\mu g/cm^2$ day: Mean (*SE*)	Dissolution Rate ($k \times \rho$), $\mu g/cm^2$ day: 95% Confidence Limits (Support Plane)
1	Low	3.24 (0.27)	2.31–4.17	0.972	306 (25.5)	218–394
2	Standard	1.80 (0.12)	1.39–2.21	0.974	209 (13.9)	161–256
3	High	1.59 (0.15)	1.09–2.09	0.948	184 (17.4)	126–242
4	Standard	1.94 (0.093)	1.62–2.26	0.987	227 (10.9)	190–264
5	Standard	1.69 (0.12)	1.26–2.11	0.961	198 (14.0)	147–247

experiments with this pellet formulation. This finding implies more variability in the present experiment

In the present experiment with Groups 1–4, it was discovered that the rat was difficult to keep alive through the duration of the experiment due to the stress produced with pellet removal. Therefore, the number of animals varies at each time point, and this fact may be in part the reason for some of the variability observed. Procedures similar to those for Group 5 were subsequently followed.

The use of a dissolution model provides a method to compare each set of data using parameters that have physical meaning. The NONLIN program coupled to the equations of the model provides an efficient and accurate method for determining the parameters of the model. The correlation coefficient of the mean data fit to the dissolution model is found in Table III; the data fit to the model is quite good.

The calculated k value for each group, with standard error and 95% confidence limits, is also found in Table III. If all pellet groups were of the same density, the k value could be used to compare the dissolution properties of each group. To make this comparison on an equivalent basis, density must be included. By derivation, the product of k and density is equivalent to the dissolution rate per unit surface area. The mean dissolution rates per unit surface area of the five groups, with standard error and 95% confidence limits, are found in Table III.

To compare the dissolution rates of each group with each other, a t test was performed. The mean dissolution rates of Groups 2–5 were not significantly different and that of Group 1 was significantly different ($p < 0.01$) compared to those of Groups 2–5.

There is a possible explanation for this significant increase in dissolution with the low density lot of pellets. For the observed dissolution rate to increase, one or combinations of the following need to occur:

1. An increase in drug solubility.
2. An increase in fluid dynamics around the pellet, thereby reducing diffusional distance.
3. An increase in diffusivity of the drug away from the pellet.
4. An increase in surface area due to channeling within the pellet and/or existence of a porous, uneven surface.

There is no reason to believe that items 1, 2, and 3 would be any different than the values for the other groups, since nothing changed in the experiment that would affect these factors. However, the decrease in density could affect the actual available surface, increasing it as mentioned and causing the observed increase in dissolution.

Possible reasons why previous investigators (3, 4) did not observe this effect were that the pellet densities were not as low as the one tested in this study and the pellets in the previous studies were 100% steroid.

The present results do not contradict those results observed earlier but suggest the importance of very low pellet densities which may result in increased surface areas after implantation. After a certain pellet density is achieved, however, the dissolution rate does not appear to change.

The *in vitro* dissolution situation is much different than the *in vivo*. Mainly, the hydrodynamics are increased, resulting in a decreased diffusional distance and, hence, an increased dissolution rate. Under these conditions, an increase in the dissolution rate due to an increase in surface due to channeling in a low density pellet would not be observed. This effect was observed in an *in vitro* dissolution study comparing Groups 1–4 where the dissolu-

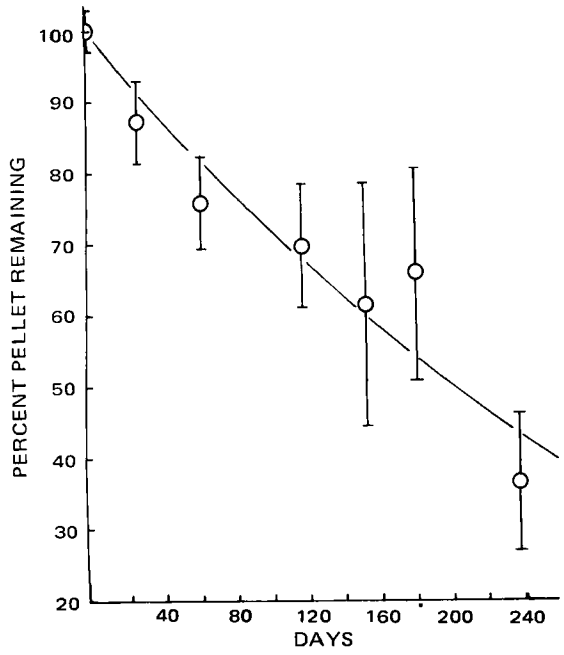

Figure 3—*Dissolution profile of delmadinone acetate pellets, Group 3, implanted subcutaneously in rats. Key: O, mean of observations with standard deviation as solid bar; curved solid line is computer fit of data to dissolution model.*

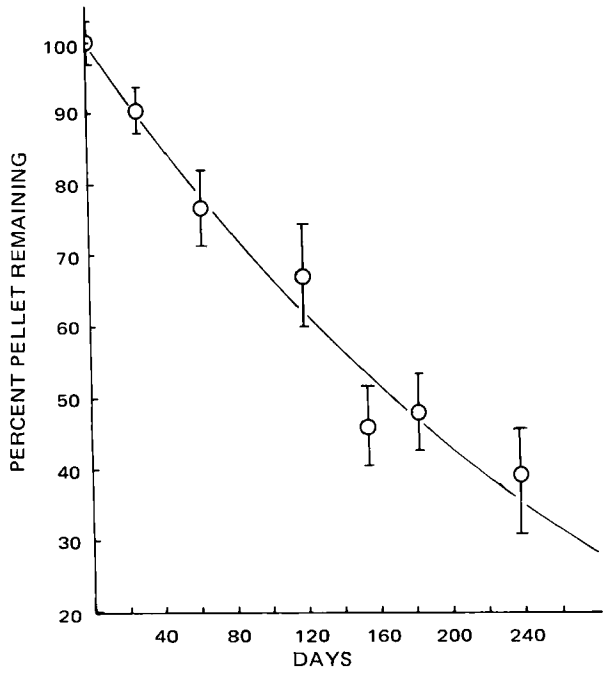

Figure 4—*Dissolution profile of delmadinone acetate pellets, Group 4, implanted subcutaneously in rats. Key: O, mean of observations with standard deviation as solid bar; curved solid line is computer fit of data to dissolution model.*

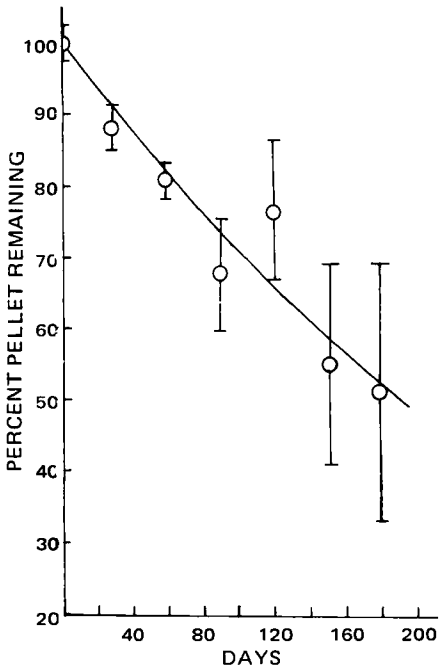

Figure 5—*Dissolution profile of delmadinone acetate pellets, Group 5, implanted subcutaneously in rats. Key: O, mean of observations with standard deviation as solid bar; curved solid line is computer fit of data to dissolution model.*

tion medium was ethanol–water (30:70). This test did not show significant differences between groups. A similar result was reported previously (5).

This finding indicates that an *in vivo* dissolution experiment is required to ascertain which physical parameters are important in pellet manufacture that cannot be immediately determined by an *in vitro* dissolution test. In the present study, the low compression group dissolved at a significantly greater rate than those pellets produced at a higher compression load. This result indicates that pellets with the desired dissolution rate could be produced by controlling the compression load (pellet density) without the necessity of an *in vitro* dissolution test.

Future studies will examine the *in vivo* dissolution rate of batches of pellets manufactured under known compression loads in the "standard compression" range and will examine the influence of steroid particle-size distribution on pellet manufacturability and *in vivo* dissolution.

REFERENCES

(1) D. Deanesly and A. S. Parkes, *Proc. Roy. Soc., Ser. B*, **124**, 279(1937).

(2) E. Ballard and E. Nelson, *J. Pharm. Sci.*, **51**, 915(1962).

(3) H. W. Hays, E. Oppenheimer, D. R. Mathieson, and J. Lein, *Fed. Proc.*, **4**, 123(1945).

(4) A. T. Cowie and S. J. Foley, *J. Endocrinol.*, **4**, 375(1944–46).

(5) E. L. Parrott, D. E. Wurster, and T. Higuchi, *J. Amer. Pharm. Ass., Sci. Ed.*, **44**, 269(1955).

(6) H. J. Ringold, E. Batres, A. Bowers, J. Edwards, and J. Zderic, *J. Amer. Chem. Soc.*, **81**, 3485(1959).

(7) "Report of Biological Activity of Delmadinone Acetate," Bioassay Department, Institute of Biological Sciences, Syntex Research, Palo Alto, Calif, 1968.

(8) H. A. Gerber, W. Jochle, and F. G. Sulman, *J. Small Anim. Pract.*, **14**, 151(1973).

(9) C. M. Metzler, "A User's Manual for NONLIN," Tech. Rep. 7297/69/7297/005, The Upjohn Co., Kalamazoo, Mich., 1969.

ACKNOWLEDGMENTS AND ADDRESSES

Received December 16, 1974, from the *Institute of Pharmaceutical Sciences, Syntex Research, Palo Alto, CA 94304*

Accepted for publication April 16, 1975.

The author thanks R. E. Jones for help with computer programs and D. Herriott and the staffs of the Department of Toxicology and the Department of Pharmaceutical Analysis, Syntex Research, for their technical assistance.

Neurogenic Influences of Bilateral Adrenalectomy on Monoamine Oxidase

DAVID E. CLARKE ˣ and SUMATHY S. SAMPATH *

Abstract □ Bilateral adrenalectomy (10 days) increased the monoamine oxidase activity of the rat heart, vas deferens, spleen, superior cervical ganglion, and hypothalamus but not that of the rest of the brain, kidney, and liver. Experiments were made to determine whether the increased activity was due to neurogenic influences and whether the enhanced activity of monoamine oxidase was intra- or extraneuronally located. Ganglionic blockade with chlorisondamine failed to alter the rise in cardiac monoamine oxidase. Likewise, superior cervical ganglion monoamine oxidase was unaffected by surgical denervation. 6-Hydroxydopamine abolished the increase in monoamine oxidase activity of the vas deferens, spleen, and superior cervical ganglion but failed to alter that of the kidney, hypothalamus, and the rest of the brain. Cardiac monoamine oxidase was reduced markedly by 6-hydroxydopamine, but the remaining activity was still significantly elevated over the respective control values. The data suggest that the increase in organ monoamine oxidase is predominantly of neuronal origin and that this increase is not due to transsynaptic induction.

Keyphrases □ Monoamine oxidase—activity, effect of bilateral adrenalectomy, 6-hydroxydopamine, chlorisondamine, rat organs □ 6-Hydroxydopamine—effect on monoamine oxidase activity after bilateral adrenalectomy, rat organs □ Chlorisondamine—effect on monoamine oxidase activity after bilateral adrenalectomy, rat organs □ Adrenalectomy, bilateral—effect on monoamine oxidase activity, rat organs

Bilateral adrenalectomy increases the monoamine oxidase [monoamine: oxygen oxidoreductase (deaminating) EC 1.4.3.4] activity of the rat heart (1–3) and of certain other organs (2). However, the mechanism(s) whereby steroids or steroid insufficiency influences monoamine oxidase remains speculative (4).

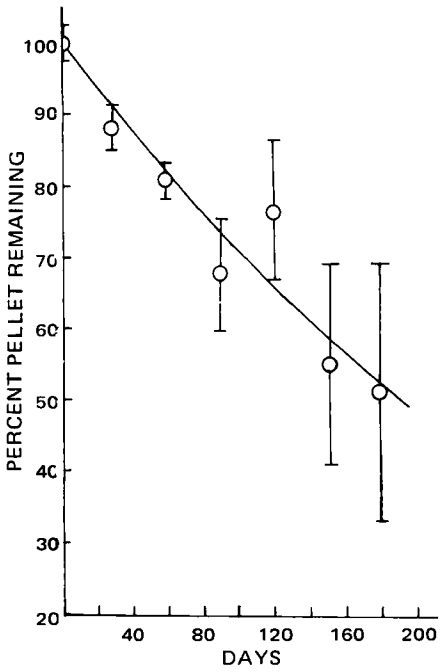

Figure 5—*Dissolution profile of delmadinone acetate pellets, Group 5, implanted subcutaneously in rats. Key: O, mean of observations with standard deviation as solid bar; curved solid line is computer fit of data to dissolution model.*

tion medium was ethanol–water (30:70). This test did not show significant differences between groups. A similar result was reported previously (5).

This finding indicates that an *in vivo* dissolution experiment is required to ascertain which physical parameters are important in pellet manufacture that cannot be immediately determined by an *in vitro* dissolution test. In the present study, the low compression group dissolved at a significantly greater rate than those pellets produced at a higher compression load. This result indicates that pellets with the desired dissolution rate could be produced by controlling the compression load (pellet density) without the necessity of an *in vitro* dissolution test.

Future studies will examine the *in vivo* dissolution rate of batches of pellets manufactured under known compression loads in the "standard compression" range and will examine the influence of steroid particle-size distribution on pellet manufacturability and *in vivo* dissolution.

REFERENCES

(1) D. Deanesly and A. S. Parkes, *Proc. Roy. Soc., Ser. B*, **124**, 279(1937).

(2) E. Ballard and E. Nelson, *J. Pharm. Sci.*, **51**, 915(1962).

(3) H. W. Hays, E. Oppenheimer, D. R. Mathieson, and J. Lein, *Fed. Proc.*, **4**, 123(1945).

(4) A. T. Cowie and S. J. Foley, *J. Endocrinol.*, **4**, 375(1944–46).

(5) E. L. Parrott, D. E. Wurster, and T. Higuchi, *J. Amer. Pharm. Ass., Sci. Ed.*, **44**, 269(1955).

(6) H. J. Ringold, E. Batres, A. Bowers, J. Edwards, and J. Zderic, *J. Amer. Chem. Soc.*, **81**, 3485(1959).

(7) "Report of Biological Activity of Delmadinone Acetate," Bioassay Department, Institute of Biological Sciences, Syntex Research, Palo Alto, Calif, 1968.

(8) H. A. Gerber, W. Jochle, and F. G. Sulman, *J. Small Anim. Pract.*, **14**, 151(1973).

(9) C. M. Metzler, "A User's Manual for NONLIN," Tech. Rep. 7297/69/7297/005, The Upjohn Co., Kalamazoo, Mich., 1969.

ACKNOWLEDGMENTS AND ADDRESSES

Received December 16, 1974, from the *Institute of Pharmaceutical Sciences, Syntex Research, Palo Alto, CA 94304*

Accepted for publication April 16, 1975.

The author thanks R. E. Jones for help with computer programs and D. Herriott and the staffs of the Department of Toxicology and the Department of Pharmaceutical Analysis, Syntex Research, for their technical assistance.

Neurogenic Influences of Bilateral Adrenalectomy on Monoamine Oxidase

DAVID E. CLARKE ˣ and SUMATHY S. SAMPATH *

Abstract □ Bilateral adrenalectomy (10 days) increased the monoamine oxidase activity of the rat heart, vas deferens, spleen, superior cervical ganglion, and hypothalamus but not that of the rest of the brain, kidney, and liver. Experiments were made to determine whether the increased activity was due to neurogenic influences and whether the enhanced activity of monoamine oxidase was intra- or extraneuronally located. Ganglionic blockade with chlorisondamine failed to alter the rise in cardiac monoamine oxidase. Likewise, superior cervical ganglion monoamine oxidase was unaffected by surgical denervation. 6-Hydroxydopamine abolished the increase in monoamine oxidase activity of the vas deferens, spleen, and superior cervical ganglion but failed to alter that of the kidney, hypothalamus, and the rest of the brain. Cardiac monoamine oxidase was reduced markedly by 6-hydroxydopamine, but the remaining activity was still significantly elevated over the respective control values. The data suggest that the increase in organ monoamine oxidase is predominantly of neuronal origin and that this increase is not due to transsynaptic induction.

Keyphrases □ Monoamine oxidase—activity, effect of bilateral adrenalectomy, 6-hydroxydopamine, chlorisondamine, rat organs □ 6-Hydroxydopamine—effect on monoamine oxidase activity after bilateral adrenalectomy, rat organs □ Chlorisondamine—effect on monoamine oxidase activity after bilateral adrenalectomy, rat organs □ Adrenalectomy, bilateral—effect on monoamine oxidase activity, rat organs

Bilateral adrenalectomy increases the monoamine oxidase [monoamine: oxygen oxidoreductase (deaminating) EC 1.4.3.4] activity of the rat heart (1–3) and of certain other organs (2). However, the mechanism(s) whereby steroids or steroid insufficiency influences monoamine oxidase remains speculative (4).

In the case of bilateral adrenalectomy, it has been suggested that reflexogenically induced activation of postganglionic sympathetic fibers may be involved (5). If so, a specific transsynaptic induction of intraneuronal monoamine oxidase might follow, assuming no trophic influence of the released transmitter upon the extraneuronal enzyme(s). Indeed, it was shown previously (6) that there is a selective increase in the activity of intraneuronal monoamine oxidase in the rat vas deferens 10 days after bilateral adrenalectomy. Alternatively, indirect evidence exists for an increase in the activity of extraneuronal monoamine oxidase. An enhanced deamination of levarterenol (norepinephrine) was reported during perfusion of isolated hearts taken from bilaterally adrenalectomized rats (1). Since the concentration of the perfused levarterenol was 5 μg/ml, deamination probably occurred primarily, if not entirely, at extraneuronal sites (7, 8).

The present study reports on experiments designed to distinguish between these two possibilities. Neurogenic influences were tested using ganglionic blockade and surgical denervation. In addition, 6-hydroxydopamine was used to assess relative changes in the activity of the intra- and extraneuronal enzymes.

METHODS

Male albino Wistar rats, 150–200 g, were used. The animal quarters were maintained at 22–24° on a circadian cycle of 12 hr (6:00 am to 6:00 pm, light; 6:00 pm to 6:00 am, dark). A 7–8 day acclimatization period was allowed prior to experimental procedures. Food and water were supplied *ad libitum*.

Bilateral Adrenalectomy—Surgical removal of the glands was performed under pentobarbital sodium anesthesia (60 mg/kg ip). Two bilateral incisions were made in the abdomen, and both adrenal glands, along with the periadrenal fat, were removed. The peritoneal cavity was closed with sterile surgical silk, and the skin incisions were closed with wound clips. Sham-operated rats differed only in that the glands were located but not removed. All animals were given tap water containing 0.9% (w/v) sodium chloride as the sole drinking fluid.

Denervation of Superior Cervical Ganglion—Surgical section of the preganglionic fibers to the superior cervical ganglion was made under pentobarbital sodium anesthesia, as already described. The trachea was exposed, and the vagus nerve was carefully dissected from the sympathetic fibers and the common carotid artery. A ligature was placed about 2 cm caudal to the ganglion, and the nerves were sectioned above the ligature. The contralateral ganglion was used as a control. A sham operation was carried out in which the nerves were located but not tied or severed. The muscle incision was closed with surgical silk and the skin with wound clips.

The denervated side was varied alternately, and the animals were sacrificed 10 days after the operation. The persistence of complete ptosis was used to verify the completeness of the operation. Bilateral adrenalectomy or sham adrenalectomy was conducted immediately following this procedure.

Monoamine Oxidase Determinations—Monoamine oxidase activity was assayed by determining the indoleacetic acid formed from tryptamine in the presence of excess aldehyde dehydrogenase, as described previously (3, 9). Whole tissue homogenates were prepared in 0.25 *M* sucrose, using a homogenizer[1]. A 50-mg/ml homogenate was prepared for all tissues except ganglia. The ganglia were either weighed on a microbalance and assayed individually or pooled and then assayed.

Tissues were checked for linearity with respect to both concentration and incubation time so as to be sure that the initial velocity rate of the reaction was being measured. The indoleacetic acid was measured spectrofluorometrically (excitation at 286 nm, emission at 365 nm, uncorrected), and the values were corrected for extraction losses by running a set of standards through the entire procedure.

Tissue Water Content—Wet to dry tissue weight ratios were determined by heating tissues to a constant weight at 85°.

Drugs—Chlorisondamine[2] and 6-hydroxydopamine[3] were used. 6-Hydroxydopamine was prepared just before use in 0.001 *N* HCl which had been previously gassed with nitrogen.

Statistics—The significance of the difference between means was calculated using the Student *t* test.

[1] Polytron.

Table I—Effect of Bilateral Adrenalectomy upon Monoamine Oxidase Activity of Various Rat Tissues

Tissue	Percent Increase[a]	*n*	Significance
Heart	151 ± 13.18	18	$p < 0.001$
Spleen	46 ± 6.30	12	$p < 0.001$
Superior cervical ganglion	41 ± 4.52	12	$p < 0.01$
Vas deferens	39 ± 6.80	16	$p < 0.01$
Hypothalamus	35 ± 8.78	12	$p < 0.01$
Rest of brain	6 ± 7.05	12	Not significant
Liver	4 ± 6.55	12	Not significant
Kidney	2 ± 8.00	12	Not significant

[a] Expressed as a percentage of sham-operated values 10 days after surgery. Shown are mean values ± *SE* for *n* animals.

RESULTS

The monoamine oxidase activity of various tissues was measured 10 days after bilateral adrenalectomy, and the results are expressed in Table I as a percentage of the respective sham-operated, control means. Heart monoamine oxidase activity was increased markedly. Also statistically significant but smaller elevations were found in the spleen, superior cervical ganglia, vas deferens, and hypothalamus. No changes were obtained in the rest of the brain, liver, and kidney.

Changes in heart monoamine oxidase were controlled using three separate groups of rats. Group I ($n = 6$) received water and no operation; Groups II ($n = 6$) and III ($n = 18$) were sham operated, but Group II was given water while Group III was given saline as the drinking fluid. The monoamine oxidase activity of the three groups was not significantly different, demonstrating that the anesthetic, surgery, or saline did not affect cardiac monoamine oxidase.

No change in the water content of the heart, spleen, or kidney was observed, but 2 and 6% increases over the sham-operated saline controls were obtained in the liver and vas deferens, respectively.

Thus, the results show that bilateral adrenalectomy specifically increased the monoamine oxidase activity of some organs but not others and that this effect was not due to enzyme concentration consequential to an increased tissue mass to water ratio.

An experiment was performed to study the effect of chronic ganglionic blockade upon the increase in cardiac monoamine oxidase activity following adrenalectomy. Sham-operated and bilaterally adrenalectomized rats were injected with chlorisondamine (5 mg/kg ip three times a day) for 10 days. The control groups received the vehicle only. Figure 1 shows that persistent ganglionic blockade, as judged by ptosis, failed to alter the rise in cardiac monoamine oxidase activity. Chlorisondamine also failed to affect the inherent activity of the enzyme in control, sham-operated rats.

A similar result was obtained following preganglionic nerve section to the superior cervical ganglion (Fig. 2). Denervated ganglia showed the same mean increase in monoamine oxidase activity as the intact contralateral controls. In addition, denervation failed to alter the monoamine oxidase activity in the sham-adrenalectomized group, indicating that normal physiological levels of presynaptic input did not affect cell body monoamine oxidase under the present experimental conditions.

[2] Ecolid, Ciba Pharmaceutical Co., Summit, N.J.
[3] Regis Chemical Co., Morton Grove, Ill.

In view of these data, it was important to establish whether bilateral adrenalectomy actually affected intraneuronal monoamine oxidase. Thus, experiments were conducted using 6-hydroxydopamine (100 mg/kg iv) given 9 days after bilateral adrenalectomy or the sham operation. Control groups received vehicle only. The rats were killed 31 hr later, and the results are shown in Table II. Bilateral adrenalectomy alone produced quantitatively similar results to those given in Table I.

The cardiac monoamine oxidase of sham-operated rats was not altered by 6-hydroxydopamine (compare Group III with Group I); but the elevated activity of monoamine oxidase, due to adrenalectomy, was decreased significantly (compare Group IV with Group II). However, the enzymatic activity remained significantly elevated compared with Group III (sham operated, 6-hydroxydopamine treated). In the spleen and superior cervical ganglion, 6-hydroxydopamine abolished completely the rise in monoamine oxidase activity following bilateral adrenalectomy; the activity of monoamine oxidase in spleens and ganglia of sham-operated rats remained unaffected. The vas deferens was most susceptible to 6-hydroxydopamine, and decreases in the monoamine oxidase activity of both the sham-operated and adrenalectomized groups (Groups III and IV) were obtained, with the adrenalectomized group being the most sensitive. The kidney, hypothalamus, and rest of the brain were unaffected by 6-hydroxydopamine.

The adrenalectomized, 6-hydroxydopamine-treated group (Group IV) originally contained seven rats. Subsequent to the administration of 6-hydroxydopamine, three animals died, presumably because of their inability to combat the considerable cardiovascular and general homeostatic changes induced by this compound.

DISCUSSION

In the present study, cardiac monoamine oxidase activity was increased markedly 10 days after bilateral adrenalectomy, but this increase was not affected by chlorisondamine. Chlorisondamine, a potent and long lasting ganglionic blocking agent, induced a persistent ptosis throughout the course of treatment. Thus, it may be concluded that a transsynaptic induction of monoamine oxidase is not the cause of the elevated activity of this enzyme in the heart. The same conclusion can be made for the superior cervical ganglion, since chronic denervation failed to curtail the rise in monoamine oxidase. In addition, neither chlorisondamine (heart) nor denervation (ganglia) changed the normal level of monoamine oxidase activity in sham-operated rats. Thus, using *in vitro* determinations, no evidence was obtained for any neurogenic influences on monoamine oxidase.

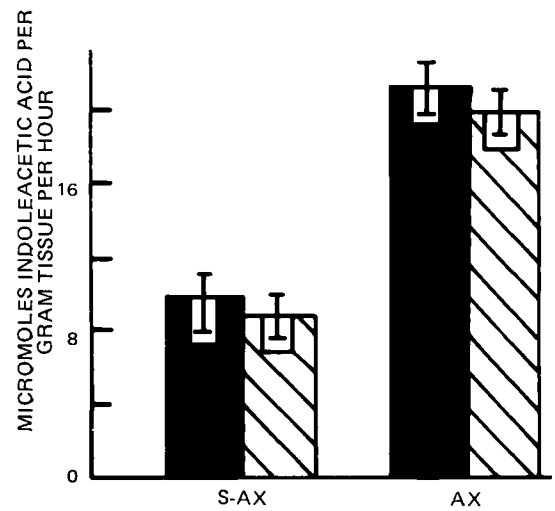

Figure 1—*Effect of chronic ganglionic blockade with chlorisondamine (5 mg/kg ip three times daily) for 10 days upon heart monoamine oxidase activity of bilaterally adrenalectomized and sham-adrenalectomized rats. Key: S-AX, sham adrenalectomized, mean values ± SE for five rats; AX, adrenalectomized, mean values ± SE for five rats; ■, without chlorisondamine; and ▨, with chlorisondamine. Significance of differences are: S-AX* versus *AX*, $p < 0.01$; *and S-AX plus chlorisondamine* versus *AX plus chlorisondamine*, $p < 0.01$.

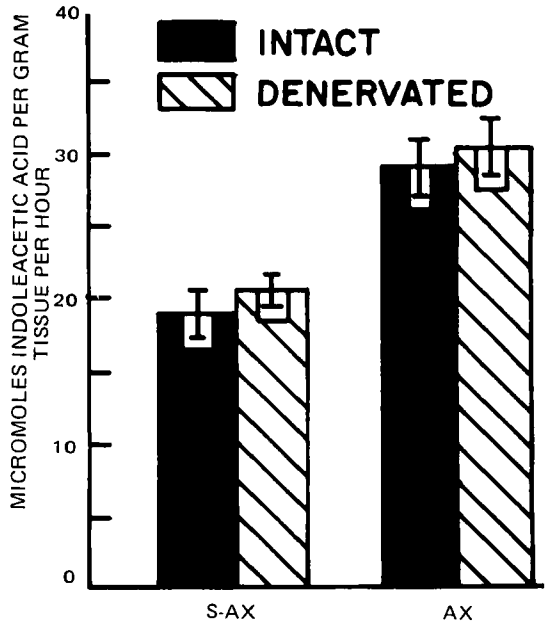

Figure 2—*Effect of chronic unilateral denervation for 10 days upon the monoamine oxidase activity of the superior cervical ganglion of bilaterally adrenalectomized and sham-adrenalectomized rats. Key: S-AX, sham adrenalectomized, mean values ± SE for six rats; and AX, adrenalectomized, mean values ± SE for six rats. Significance of differences are: intact S-AX* versus *intact AX*, $p < 0.05$; *and denervated S-AX* versus *denervated AX*, $p < 0.05$.

Sympathectomy, including that following 6-hydroxydopamine, has been used to assess the proportion of intraneuronal monoamine oxidase in sympathetically innervated tissues (10–12). In the present study, the fall in the monoamine oxidase activity of the vas deferens of sham-operated rats (about 30%) was short of the 50% decrease obtained in denervation studies (6, 10). This finding implies that the dose of 6-hydroxydopamine (100 mg/kg) failed to induce a complete sympathectomy. However, this conclusion cannot be extrapolated to all other tissues, since different sensitivities to 6-hydroxydopamine exist.

The heart is very sensitive to 6-hydroxydopamine compared with the vas deferens (13–15) and cardiac tyrosine hydroxylase activity (16), and both levarterenol levels and uptake (16, 17) are depressed markedly after a similar 6-hydroxydopamine dosage to that used in the present study. Thus, a more complete sympathectomy is likely in the heart than in the vas deferens. In fact, the data from sham-operated rats confirm the suggestion that heart (10, 12) and kidney (10) monoamine oxidase is located predominantly at extraneuronal sites, and the lack of any effect upon the brain enzyme is consistent with the inability of 6-hydroxydopamine to cross the blood–brain barrier.

Based upon these considerations, the results obtained with 6-hydroxydopamine in adrenalectomized rats (Table II) suggest that the increased activity of monoamine oxidase is largely of neuronal origin, but this contention is clouded by the unexpected fall in ganglionic monoamine oxidase and by the high mortality encountered. However, this latter phenomenon does not seem to represent a nonspecific cellular toxicity or generalized debilitating effect of 6-hydroxydopamine since brain, and more importantly, kidney monoamine oxidase remained unaffected.

Examination of the data for the vas deferens (Table II) reveals an increased sensitivity to 6-hydroxydopamine in adrenalectomized rats; a complete denervation seems to have been achieved. This finding might indicate that either the neurons or the monoamine oxidase itself is more susceptible to the damaging effects of this drug (6-hydroxydopamine is a substrate for monoamine oxidase). An increased neuronal accumulation of 6-hydroxydopamine is also likely. However, no evidence exists for an enhanced neuronal uptake in the hearts of adrenalectomized rats (1, 2), but differ-

Table II—Effect of 6-Hydroxydopamine on Monoamine Oxidase Activity of Bilaterally Adrenalectomized and Sham-Operated Rats[a]

Tissue	Monoamine Oxidase Activity, μmoles/g/hr[b]			
	Group I	Group II	Group III	Group IV
Vas deferens	7.42 ± 0.19[c,d]	11.09 ± 0.39[e,d]	5.31 ± 0.31[e,c]	3.50 ± 0.35[f,e,c]
Spleen	4.05 ± 0.36[c]	6.11 ± 0.19[e,d]	3.61 ± 0.30[c]	3.22 ± 0.08[e,c]
Superior cervical ganglion	9.11 ± 0.38[c]	13.72 ± 0.62[e]	9.22 ± 0.64[c]	8.95 ± 0.37[c]
Heart	8.61 ± 0.55[c]	19.72 ± 0.83[e,d]	8.18 ± 0.97[c]	11.94 ± 0.72[e,c,d]
Kidney	3.22 ± 0.11	3.39 ± 0.22	3.23 ± 0.09	3.39 ± 0.30
Hypothalamus	8.47 ± 0.49[c]	11.39 ± 0.37[e,d]	8.19 ± 0.76[c]	11.67 ± 0.53[e,d]
Rest of brain	5.08 ± 0.19	5.40 ± 0.27	5.00 ± 0.16	5.16 ± 0.26

[a] Group I = sham operated plus vehicle, Group II = adrenalectomy plus vehicle, Group III = sham operated plus 6-hydroxydopamine, and Group IV = adrenalectomy plus 6-hydroxydopamine. Surgical operations were made 9 days prior to the administration of 6-hydroxydopamine or the vehicle, and the rats were killed 31 hr later. [b] Mean values ± *SE* for six rats (Groups I and II), five rats (Group III), and four rats (Group IV). [c] Significantly different from Group II, $p < 0.05$. [d] Significantly different from Group III, $p < 0.05$. [e] Significantly different from Group I, $p < 0.05$. [f] Values expressed per pair × 10^2.

ences between organs cannot be excluded since uptake mechanisms in peripheral adrenergic neurons may vary (18, 19). Thus, although ganglionic damage with 6-hydroxydopamine is usually considered to be virtually nonexistent (13), similar changes to those proposed for the vas deferens could explain the observed fall in the monoamine oxidase activity of this structure.

It is worth noting that ganglia are not completely resistant to 6-hydroxydopamine (13), especially those of young animals (20–23) where extensive structural, histochemical, and biochemical changes have been observed. Thus, if adrenalectomy caused some reversal of the ganglionic "aging process," damage with 6-hydroxydopamine would be expected. In fact, steroids do appear to exert a marked cellular differentiating effect upon certain ganglionic cells of immature rats (24), but the effects of adrenalectomy on mature ganglia remain to be elucidated.

The data obtained with the heart suggest that both extra- and intraneuronal monoamine oxidase is increased by adrenalectomy. Thus, it is not surprising that Avakian and Callingham (1) found an enhanced deamination of levarterenol (5 μg/ml) during perfusion of isolated hearts taken from adrenalectomized rats. The surprising result is that the normally small proportion of intraneuronal monoamine oxidase is increased to such an extent as to alter significantly the total monoamine oxidase activity of the heart. A similar effect was also obtained in the spleen.

Tryptamine is a substrate for the two major types of monoamine oxidases, A and B (25). Thus, from the present study, no conclusions with regard to preferential influences of adrenalectomy on any particular type or molecular form of monoamine oxidase can be made. However, the intraneuronal enzyme(s) of the superior cervical ganglion and the vas deferens appear to be almost entirely of type A (25, 26).

In conclusion, this study has shown that bilateral adrenalectomy increases the monoamine oxidase activity of some organs but not others. No evidence was obtained for a transsynaptic mediation of this effect, but intraneuronal monoamine oxidase seems to be involved. Of the peripheral organs studied, only those with a fair to high content of endogenous norepinephrine were affected, suggesting that a relationship might exist (10). In addition, the increased monoamine oxidase activity of the superior cervical ganglion is, in itself, suggestive of an intraneuronal locus, since 90% of the monoamine oxidase in this structure is believed to be present within the cell bodies of the adrenergic fibers (26).

Overall, the results support previous findings where surgical denervation of the vas deferens inhibited the rise in monoamine oxidase activity due to bilateral adrenalectomy (6). However, the present results are rendered less conclusive due to the toxicity of 6-hydroxydopamine in adrenalectomized rats. Further investigations will be required to obtain more substantive evidence.

REFERENCES

(1) V. M. Avakian and B. A. Callingham, *Brit. J. Pharmacol.*, **33,** 211P(1968).

(2) P. M. Caesar, G. G. S. Collins, and M. Sandler, *Biochem. Pharmacol.*, **19,** 921(1970).

(3) D. E. Clarke and S. S. Sampath, *J. Pharmacol. Exp. Ther.*, **187,** 539(1973).

(4) M. B. H. Youdim, M. Holzbauer, and H. F. Woods, in "Neuropharmacology of Monoamines and Their Regulatory Enzymes," E. Usdin, Ed., Raven, New York, N.Y., 1974, p. 11.

(5) T. C. Westfall and H. Osada, *J. Pharmacol. Exp. Ther.*, **167,** 300(1969).

(6) S. S. Sampath and D. E. Clarke, *Life Sci.*, **11,** 1037(1972).

(7) L. L. Iversen, "The Uptake and Storage of Noradrenaline in Sympathetic Nerves," Cambridge University Press, Cambridge, Mass., 1967, p. 108.

(8) S. L. Lightman and L. L. Iversen, *Brit. J. Pharmacol.*, **37,** 638(1968).

(9) L. Lovenberg, R. J. Levine, and A. A. Sjoerdsma, *J. Pharmacol. Exp. Ther.*, **135,** 7(1962).

(10) B. Jarrott, *J. Neurochem.*, **18,** 7(1971).

(11) B. Jarrott and L. L. Iversen, *ibid.*, **18,** 1(1971).

(12) A. Horita and M. C. Lowe, in "Monoamine Oxidases—New Vistas," E. Costa and M. Sandler, Eds., Raven, New York, N.Y., 1972, p. 227.

(13) H. Thoenen and J. P. Tranzer, *Annu. Rev. Pharmacol.*, **13,** 169(1973).

(14) G. Jaim-Etcheverry and L. M. Zieher, *Eur. J. Pharmacol.*, **13,** 272(1971).

(15) G. Burnstock, B. Evans, B. J. Gannon, J. W. Heath, and V. James, *Brit. J. Pharmacol.*, **43,** 295(1971).

(16) J. De Champlain, *Can. J. Physiol. Pharmacol.*, **49,** 345(1971).

(17) H. Thoenen, in "6-Hydroxydopamine and Catecholamine Neurons," T. Malmfors and H. Thoenen, Eds., American Elsevier, New York, N.Y., 1971, p. 75.

(18) S. Spector, J. Tarver, and B. Berkowitz, *Pharmacol. Rev.*, **24,** 191(1972).

(19) D. E. Clarke, B. S. Jandhyala, I. Cavero, B. N. Dixit, and J. P. Buckley, *Can. J. Physiol. Pharmacol.*, **52,** 641(1974).

(20) P. U. Angeletti and R. Levi-Montalcini, *Proc. Nat. Acad. Sci. USA*, **65,** 114(1970).

(21) T. B. Cheah, L. B. Geffen, B. Jarrott, and A. Ostberg, *Brit. J. Pharmacol.*, **42,** 543(1971).

(22) T. Malmfors, in "6-Hydroxydopamine and Catecholamine Neurons," T. Malmfors and H. Thoenen, Eds., American Elsevier, New York, N.Y., 1971, p. 47.

(23) L. Eranko and O. Eranko, *Acta Physiol. Scand.*, **84,** 125(1972).

(24) *Ibid.*, **84,** 115(1972).

(25) N. H. Neff and H.-Y. T. Yang, *Life Sci.*, **14,** 2061(1974).

(26) G. Goridis and N. H. Neff, *Neuropharmacology*, **10,** 557(1971).

ACKNOWLEDGMENTS AND ADDRESSES

Received February 25, 1975, from the *Department of Pharmacology, College of Pharmacy, University of Houston, Houston, TX 77004*

Accepted for publication April 18, 1975.

* Present address: Department of Pharmacology, University of California Medical Center, San Francisco, CA 94143

ˣ To whom inquiries should be directed.

GLC Determination of Quinidines in Human Plasma

J. L. VALENTINE ˣ, PATRICIA DRISCOLL, ELLEN L. HAMBURG, and EVERETT D. THOMPSON

Abstract □ Human plasma was made alkaline and extracted with methylene chloride. To the extract was added the internal standard, cinchonine, followed by evaporation to dryness. The resultant residue was dissolved in a methanolic solution containing trimethylanilinium hydroxide. This solution was assayed by GLC for quinidines (quinidine and hydroquinidine). Evaluation of the method over a 0.5–10-μg/ml range in human plasma gave an overall precision and accuracy of ±4.5% (*RSD* and *RE*). Plasma of several patients was analyzed by the present method as well as by a fluorometric method for the level of quinidines. Results from the two methods were comparable.

Keyphrases □ Quinidine—GLC analysis in human plasma, compared to fluorometric analysis □ Hydroquinidine—GLC analysis in human plasma, compared to fluorometric analysis □ GLC—analysis, quinidine and hydroquinidine in human plasma, compared to fluorometric method □ Antiarrhythmic agents—quinidine and hydroquinidine, GLC analysis in human plasma, compared to fluorometric analysis

Quinidine (I*a*) is a clinically useful antiarrhythmic agent (1, 2). To achieve the proper therapeutic effect, the blood levels (3–8) and/or physiological responses (6) of quinidine must be closely monitored, especially in patients with impaired renal function (3, 9). Prior to the present work, blood levels of quinidine usually were determined by fluorometric (4, 5, 7–12) or colorimetric (13) assays.

The fluorometric assays offer extremely high sensitivity, with the lower limit of detection of blood reported to be 0.2 μg/ml (14). However, specificity may be lacking with certain fluorometric procedures since there is no prior chromatographic step and all resolution of interfering substances resides in the extraction method used. For example, Armand and Badinand (15) found that a benzene extraction of quinidine from alkaline plasma gave an interference when triamterene was present. Similarly, other investigators (8, 12, 16) showed that certain metabolites of quinidine or other substances interfere with the fluorometric assay unless specific protein precipitation and/or extraction methods are used.

A procedure using TLC to separate quinidine from its metabolites and other interfering substances, followed by fluorometric assay, was reported (17). Palmer *et al.* (18) used both TLC and GLC methods to study the metabolic fate of quinidine gluconate in humans. Their GLC method was based on precolumn derivatization to form appropriate silyl compounds.

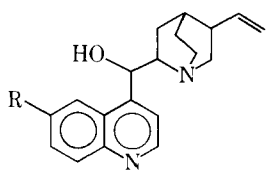

I*a*: R = OCH_3
I*b*: R = H

Recently, Smith *et al.* (19) reported a TLC and GLC method for separating quinidine from its pharmaceutical preparation. The GLC method was based on precolumn derivatization similar to that of Palmer *et al.* (18) but used a different stationary phase. The work of Smith *et al.* (19) also clearly showed that most pharmaceutical dosage forms of quinidine contain 5–9% hydroquinidine.

Two widely used fluorometric methods (8, 12) for evaluating therapeutic plasma levels of quinidine do not differentiate between quinidine and hydroquinidine (13) but give total quinidines. Thus, the range of quinidine plasma levels used to regulate dosage regimens (3, 20, 21) of patients is actually a combined determination of quinidine and its dosage form impurity, hydroquinidine. Therefore, one objective of the present work was to develop a rapid GLC procedure for the codetermination of quinidine and hydroquinidine as an adjunct to, or in place of, the established fluorometric methods for use in monitoring plasma levels in patients receiving quinidine. The use of such a method should be extremely important for verifying either subtherapeutic or toxic plasma levels of quinidine as determined by fluorometric analysis.

In the present method, a small volume of plasma is made alkaline and extracted. To the extract is added the internal standard (cinchonine, I*b*), followed by evaporating to dryness and reconstituting in a methanolic solution of trimethylanilinium hydroxide. A portion of this solution is analyzed by GLC *via* an on-column methylation reaction.

Previous literature reports (3, 20, 21) indicated that the therapeutic level of quinidine expected in plasma was 2–8 μg/ml. Thus, the present procedure was evaluated over the range of 0.5–10 μg/ml and gave excellent recovery values (Table I).

EXPERIMENTAL

Extraction Procedure—Whole blood was centrifuged at 2500 rpm for 10 min and the plasma was removed. To 1 ml of plasma was added 0.5 ml of 5% NaOH and 5 ml of methylene chloride. This solution was mixed thoroughly[1] for 10–15 sec and then allowed to stand for 1 min. The lower organic layer was removed, and the plasma layer was reextracted with 5 ml of methylene chloride. In general, this second extraction was centrifuged at 2500 rpm for 5 min to give separation of layers.

The lower layer was removed again and combined with the first extract, to which was added 0.5 ml of the cinchonine internal standard solution. This solution was evaporated to dryness under a stream of nitrogen at 50°. To the resultant residue was added 30 μl of 0.2 *M* trimethylanilinium hydroxide in methanol[2], followed by mixing[1]. Then 1 μl of this solution was analyzed by GLC.

GLC Determination—All experiments were performed using a gas chromatograph[3] equipped with a hydrogen flame-ionization

[1] Vortex.
[2] MethElute, Pierce Chemical Co.
[3] Packard 419.

Table I—Precision and Accuracy in Recovery of Quinidine Added to Human Plasma

Added, μg/ml	Found[a], μg/ml	±RSD, %	RE, %
0.5	0.50 (0.49–0.55)	5.42	0
1.0	1.01 (0.96–1.05)	3.61	+1.0
2.0	2.10 (2.0–2.25)	5.39	+5.0
4.0	4.11 (3.73–4.45)	3.74	+2.75
6.0	5.96 (5.50–6.30)	5.57	−0.67
8.0	7.82 (7.55–7.91)	2.24	−2.25
10.0	9.33 (9.25–9.48)	1.00	−6.7
Average percent recovered 99.9			

[a] Average of four different samples at each added concentration level (range).

detector. A 1.83-m × 2-mm glass coiled column was packed with 3% OV-17 on 80–100-mesh Chromosorb W-HP and conditioned at 340°. The column operating condition was programmed from 255 to 280° with an initial isothermal period of 4 min, a temperature rise of 5°/min, a final isothermal period of 5 min, and a nitrogen flow rate of 14.5 ml/min. The injector was operated at 220° and the detector was operated at 200° with 1.7 kg/cm^2 air and 1.0 kg/cm^2 hydrogen.

Chromatograms were recorded on a 1-mv recorder, and peak areas were determined using the method of triangulation. When using these conditions, the retention times of quinidine and cinchonine were 9.1 and 5.9 min, respectively.

Standards—Two stock solutions of quinidine and cinchonine were prepared in methanol. The quinidine standard solution contained 1 μg/ml of quinidine sulfate[4], and the cinchonine internal standard contained 4 μg/ml of cinchonine[5]. Aliquots of 0.5, 1, 2, 4, 6, 8, and 10 ml of the quinidine standard solution were added to suitable containers, each containing 0.5 ml of the cinchonine internal standard. These solutions were evaporated to dryness under a nitrogen stream at 50°.

To each residue was added 30 μl of 0.2 *M* trimethylanilinium hydroxide in methanol[2], and the resultant solution was mixed[1]. Then 1 μl of this solution was analyzed using the described GLC conditions, and peak areas were determined by triangulation. The area ratio of quinidine to cinchonine was plotted on the ordinate, and the micrograms of quinidine added was plotted on the abscissa to obtain the standard curve; this curve proved to be linear over the range evaluated.

Evaluation of Assay Method—Twenty-eight plasma samples with known amounts of quinidine added at seven different concentration levels were used in the method evaluation. The plasma used was obtained from pooled blood. A control sample of the plasma used gave no interferences with the determination of quinidine. Each plasma sample was extracted using the previously discussed extraction procedure and analyzed by the GLC determination method. The peak areas for quinidine and cinchonine were determined by triangulation, and an area ratio of quinidine to cinchonine was calculated. This area ratio was fitted to the standard curve to obtain the value for quinidine.

Table I gives the average micrograms of quinidine found, as well as precision and accuracy values.

Stability of Quinidine in Extraction Solvent—*Evaluation by GLC*—A quinidine[4] stock solution containing 5 μg/ml was prepared in methylene chloride. A 1-ml aliquot was placed in 24 different stoppered containers and stored at room temperature. Four samples were removed from storage each hour for 6 hr, and 0.5 ml of the stock cinchonine was added to each sample. This mixture was evaporated to dryness under a nitrogen stream at 50°.

To the resultant residue was added 30 μl of 0.2 *M* trimethylanilinium hydroxide in methanol[2] followed by mixing[1]. A 1-μl portion was analyzed by GLC, and peak areas were determined by triangulation. The amount of quinidine found was determined by fitting the area ratio of quinidine to cinchonine to the standard curve. At all time intervals, the average amount of quinidine found was 5 μg.

Evaluation by TLC—Two quinidine[4] stock solutions containing 5 μg/μl were prepared in methylene chloride and methanol, respectively. The alcoholic stock solution was used as the control, since the quinidine preparation was reported to be stable in alcohol (19). Both stock solutions were kept at room temperature.

By using the TLC methods of Smith *et al.* (19), three different plates were spotted at intervals of 0, 1, 2, 3, 4, 5, 6, and 12 hr with 20 μl of both stock solutions. When the previously described developing and visualization systems were used, no differences were noted between the two stock solutions during the first 6 hr. However, the 12-hr methylene chloride stock solution showed a small unknown spot at R_f 6.5 when developed in chloroform–acetone–methanol–ammonium hydroxide (60:20:20:1) and visualized by acid spraying and longwave UV light. In addition to quinidine and hydroquinidine, these TLC systems demonstrated that trace amounts of epiquinidine were also present in the quinidine[4] used in the method evaluation.

[4] Quinicardine, $(C_{20}H_{24}N_2O_2)_2H_2SO_4 \cdot 2H_2O$, USP grade, Merck. A weight corresponding to that needed to give 10 μg of quinidine free base/ml was used.

[5] USP grade, Fisher Scientific Co.

Table II—Assay Method Evaluation on Plasma of Male Patients Receiving Quinidine Gluconate[a] (206 mg po)

Patient Number	Postdose Blood Sample Taken, hr	Quinidine Found, μg/ml: GLC	Quinidine Found, μg/ml: Fluorometric
1	4.0	1.2	1.3
2[b]	5.5	1.9	1.7
3	6.0	3.0	2.7
4	6.0	2.9	2.8

[a] Expressed as milligrams of free base. [b] Also receiving allopurinol.

Clinical Utility of Assay Method—To evaluate the clinical utility of the present assay method, plasma from four patients receiving quinidine gluconate was assayed. These patients were being maintained on quinidine, and blood was drawn for analysis as indicated in Table II. The plasma of each patient was then assayed by the present method and by a commonly used fluorometric method (8). Results of this study are given in Table II.

RESULTS AND DISCUSSION

A GLC assay method for quinidines (quinidine and hydroquinidine) in human plasma was developed and evaluated over a concentration range of 0.5–10 μg/ml. The overall recovery of quinidines added to plasma was 99.9%. Control samples of the plasma used in the method evaluation were extracted and analyzed using the new procedure, thus demonstrating the lack of interfering components.

Plasma from four patients being maintained on quinidine was evaluated by the GLC assay method and by a commonly used fluorometric assay method. Results from the two different procedures were found to be comparable.

The present method does not distinguish between quinidine and hydroquinidine, a contaminant in commercial quinidine preparations (19); only one compound with the same retention time as an authentic sample of hydroquinidine was indicated by GLC analysis using the USP grade quinidine. Yet this same material was shown to contain hydroquinidine when examined by the TLC methods of Smith *et al.* (19). Hartel and Harjanne (13) pointed out that therapeutically it is desirable to codetermine quinidine and hydroquinidine since the antiarrhythmic properties are of the same magnitude.

Due to the unavailability of the metabolites of quinidine, these compounds were not evaluated by the present method. Earlier work (17) demonstrated that a benzene extract of urine gave the smallest amount of metabolites, apparently due to their low solubility (13). Thus, the authors recommended the use of the benzene extraction method of Cramer and Isaksson (8) due to its specificity and accuracy for codetermination of quinidine and hydroquinidine.

The proposed GLC method was evaluated clinically by comparing it to the Cramer and Isaksson method (Table II). Due to the excellent comparison between the two methods, the extraction of metabolites by the two methods is assumed to be aproximately the same. Indeed, no other components were noted on the chromatograms of patients receiving quinidine that were not on the chromatograms of plasma to which quinidine had been added.

A study was made of quinidine stability at room temperature in the extraction solvent methylene chloride by two chromatographic methods. This study was prompted by the report (19) that pharmaceutical dosage forms extracted with methylene chloride degrade rapidly to give several additional TLC spots. First, a stock solution of methylene chloride was evaluated by the proposed GLC method using multiple samples at 1-hr intervals for 6 hr. No decomposition of the quinidine was noted, as evidenced by complete recovery of the quinidine added. Second, a previously reported (19) TLC system was used to evaluate two stock solutions of quinidine in methylene chloride and methanol at 1-hr intervals for 6 hr, followed by a final 12-hr sample. A small unknown spot appeared in the 12-hr sample of the methylene chloride stock solution.

Thus, some decomposition of quinidines apparently can occur in methylene chloride, but it is not rapid at room temperature. Any potential decomposition of the quinidines can be avoided easily by immediately evaporating the extracting solvent and placing the enclosed residue under refrigeration until analysis.

REFERENCES

(1) S. S. Bloomfield, D. W. Romhilt, T. Chou, and N. O. Fowler, *Circulation*, **47**, 967(1973); *N. Engl. J. Med.*, **285**, 979(1971).

(2) J. Koch-Weser, *N. Engl. J. Med.*, **285**, 1024(1971).

(3) A. J. Atkinson, Jr., *Mod. Concepts Cardiovasc. Dis.*, **42**, 1(1973).

(4) H. E. Archer, D. Weitzman, and H. L. Kay, *Brit. Heart J.*, **17**, 534(1955).

(5) W. M. Goldberg and S. G. Chakrabarti, *Can. Med. Ass. J.*, **91**, 991(1964).

(6) M. Sokolow and R. E. Ball, *Circulation*, **14**, 568(1956).

(7) N. Gelfamn and D. Seligson, *Amer. J. Clin. Pathol.*, **36**, 390(1961).

(8) G. Cramer and B. Isaksson, *Scand. J. Clin. Lab. Invest.*, **15**, 553(1963).

(9) S. Bellet, L. R. Roman, and A. Boza, *Amer. J. Cardiol.*, **27**, 368(1971).

(10) B. B. Brodie and S. Udenfriend, *J. Pharmacol.*, **78**, 154(1943).

(11) A. J. Linenthal, S. Ulick, and L. A. Patterson, *J. Clin. Invest.*, **26**, 1188(1947).

(12) A. L. Edgar and M. Sokolow, *J. Lab. Clin. Invest.*, **36**, 478(1950).

(13) G. Hartel and A. Harjanne, *Clin. Chim. Acta*, **23**, 289(1969).

(14) M. Hasselmann, *C. R. Acad. Sci.*, **244**, 2860(1957).

(15) J. Armand and A. Badinand, *Anal. Biol. Clin.*, **30**, 599(1972); through *Chem. Abstr.*, **78**, 79529(1973).

(16) B. B. Brodie, S. Udenfriend, and J. E. Baer, *J. Biol. Chem.*, **168**, 299(1947).

(17) G. Hartel and A. Korhonen, *J. Chromatogr.*, **37**, 70(1968).

(18) K. H. Palmer, B. Martin, B. Baggett, and M. E. Wall, *Biochem. Pharmacol.*, **18**, 1845(1969).

(19) E. Smith, S. Barkan, B. Ross, M. Maienthal, and J. Levine, *J. Pharm. Sci.*, **62**, 1151(1973).

(20) J. E. Wallace and S. L. Ladd, *Ind. Med.*, **39**, 412(1970).

(21) E. S. Vesell and G. T. Passananti, *Clin. Chem.*, **17**, 855(1971).

ACKNOWLEDGMENTS AND ADDRESSES

Received August 16, 1974, from the *Bio-Analytics Laboratory, School of Pharmacy, University of Missouri–Kansas City, Kansas City, MO 64108*

Accepted for publication April 14, 1975.

The authors thank the School of Medicine, University of Missouri–Kansas City, for providing facilities for this work.

[x] To whom inquiries should be directed.

Synthesis of Histamine Analogs

CHARLES M. DARLING [x] and E. K. ROSE

Abstract □ Nineteen histamine analogs were synthesized, and their biological actions were compared to those of histamine in blood pressure, gastric secretion, and nasal decongestant screens. The analogs include *N*-substituted 4-aminoethylimidazoles, *N*-substituted 2-pyridylethylamines, 2-pyridylcyclohexylamines, and 2-pyridylcyclopropylcarbamates. None of the compounds showed appreciable histamine agonist or antagonist properties.

Keyphrases □ Histamine—19 analogs synthesized, biological actions compared, blood pressure, gastric secretion, and nasal decongestant screens □ Structure–activity relationships—19 histamine analogs □ Imidazole derivatives—synthesis of 19 histamine analogs, structure–activity relationships □ Pyridylethylamine derivatives—synthesis of 19 histamine analogs, structure–activity relationships

The biological properties of the naturally occurring autacoid, histamine, are well known. A molecule that selectively mimics or antagonizes a single action of histamine is a potentially useful agent in a broad range of pharmacological activities, including effects on vascular, bronchial, and intestinal musculature as well as inflammatory and secretory mechanisms. The classical antihistamines have only a narrow spectrum of histamine antagonism, blocking some histamine-stimulated secretions and intestinal smooth muscle contractions.

An excellent review of the actions of certain histamine analogs was reported (1), and the effect of structural modification on histamine agonist and antagonist actions was reviewed (2). A qualitative assessment suggests that the histamine molecule can be modified in many ways with retention of agonist activity so long as the length of the side chain remains unchanged. These modifications include replacement of the imidazole ring with other heterocyclic rings, alkyl substitutions on the side chain, and various substituents on the basic nitrogen of the side chain. The cyclopropyl derivative, 2-(4-imidazolyl)cyclopropylamine, was reported (3) to be almost devoid of activity.

The work reported here was designed to determine whether the selectivity of action could be increased by altering any of the three structural components of histamine: the ring, side chain, or *N*-substituent. The imidazole ring was substituted by a pyridine ring

A study was made of quinidine stability at room temperature in the extraction solvent methylene chloride by two chromatographic methods. This study was prompted by the report (19) that pharmaceutical dosage forms extracted with methylene chloride degrade rapidly to give several additional TLC spots. First, a stock solution of methylene chloride was evaluated by the proposed GLC method using multiple samples at 1-hr intervals for 6 hr. No decomposition of the quinidine was noted, as evidenced by complete recovery of the quinidine added. Second, a previously reported (19) TLC system was used to evaluate two stock solutions of quinidine in methylene chloride and methanol at 1-hr intervals for 6 hr, followed by a final 12-hr sample. A small unknown spot appeared in the 12-hr sample of the methylene chloride stock solution.

Thus, some decomposition of quinidines apparently can occur in methylene chloride, but it is not rapid at room temperature. Any potential decomposition of the quinidines can be avoided easily by immediately evaporating the extracting solvent and placing the enclosed residue under refrigeration until analysis.

REFERENCES

(1) S. S. Bloomfield, D. W. Romhilt, T. Chou, and N. O. Fowler, *Circulation*, **47**, 967(1973); *N. Engl. J. Med.*, **285**, 979(1971).

(2) J. Koch-Weser, *N. Engl. J. Med.*, **285**, 1024(1971).

(3) A. J. Atkinson, Jr., *Mod. Concepts Cardiovasc. Dis.*, **42**, 1(1973).

(4) H. E. Archer, D. Weitzman, and H. L. Kay, *Brit. Heart J.*, **17**, 534(1955).

(5) W. M. Goldberg and S. G. Chakrabarti, *Can. Med. Ass. J.*, **91**, 991(1964).

(6) M. Sokolow and R. E. Ball, *Circulation*, **14**, 568(1956).

(7) N. Gelfamn and D. Seligson, *Amer. J. Clin. Pathol.*, **36**, 390(1961).

(8) G. Cramer and B. Isaksson, *Scand. J. Clin. Lab. Invest.*, **15**, 553(1963).

(9) S. Bellet, L. R. Roman, and A. Boza, *Amer. J. Cardiol.*, **27**, 368(1971).

(10) B. B. Brodie and S. Udenfriend, *J. Pharmacol.*, **78**, 154(1943).

(11) A. J. Linenthal, S. Ulick, and L. A. Patterson, *J. Clin. Invest.*, **26**, 1188(1947).

(12) A. L. Edgar and M. Sokolow, *J. Lab. Clin. Invest.*, **36**, 478(1950).

(13) G. Hartel and A. Harjanne, *Clin. Chim. Acta*, **23**, 289(1969).

(14) M. Hasselmann, *C. R. Acad. Sci.*, **244**, 2860(1957).

(15) J. Armand and A. Badinand, *Anal. Biol. Clin.*, **30**, 599(1972); through *Chem. Abstr.*, **78**, 79529(1973).

(16) B. B. Brodie, S. Udenfriend, and J. E. Baer, *J. Biol. Chem.*, **168**, 299(1947).

(17) G. Hartel and A. Korhonen, *J. Chromatogr.*, **37**, 70(1968).

(18) K. H. Palmer, B. Martin, B. Baggett, and M. E. Wall, *Biochem. Pharmacol.*, **18**, 1845(1969).

(19) E. Smith, S. Barkan, B. Ross, M. Maienthal, and J. Levine, *J. Pharm. Sci.*, **62**, 1151(1973).

(20) J. E. Wallace and S. L. Ladd, *Ind. Med.*, **39**, 412(1970).

(21) E. S. Vesell and G. T. Passananti, *Clin. Chem.*, **17**, 855(1971).

ACKNOWLEDGMENTS AND ADDRESSES

Received August 16, 1974, from the *Bio-Analytics Laboratory, School of Pharmacy, University of Missouri–Kansas City, Kansas City, MO 64108*

Accepted for publication April 14, 1975.

The authors thank the School of Medicine, University of Missouri–Kansas City, for providing facilities for this work.

[x] To whom inquiries should be directed.

Synthesis of Histamine Analogs

CHARLES M. DARLING [x] and E. K. ROSE

Abstract □ Nineteen histamine analogs were synthesized, and their biological actions were compared to those of histamine in blood pressure, gastric secretion, and nasal decongestant screens. The analogs include *N*-substituted 4-aminoethylimidazoles, *N*-substituted 2-pyridylethylamines, 2-pyridylcyclohexylamines, and 2-pyridylcyclopropylcarbamates. None of the compounds showed appreciable histamine agonist or antagonist properties.

Keyphrases □ Histamine—19 analogs synthesized, biological actions compared, blood pressure, gastric secretion, and nasal decongestant screens □ Structure–activity relationships—19 histamine analogs □ Imidazole derivatives—synthesis of 19 histamine analogs, structure–activity relationships □ Pyridylethylamine derivatives—synthesis of 19 histamine analogs, structure–activity relationships

The biological properties of the naturally occurring autacoid, histamine, are well known. A molecule that selectively mimics or antagonizes a single action of histamine is a potentially useful agent in a broad range of pharmacological activities, including effects on vascular, bronchial, and intestinal musculature as well as inflammatory and secretory mechanisms. The classical antihistamines have only a narrow spectrum of histamine antagonism, blocking some histamine-stimulated secretions and intestinal smooth muscle contractions.

An excellent review of the actions of certain histamine analogs was reported (1), and the effect of structural modification on histamine agonist and antagonist actions was reviewed (2). A qualitative assessment suggests that the histamine molecule can be modified in many ways with retention of agonist activity so long as the length of the side chain remains unchanged. These modifications include replacement of the imidazole ring with other heterocyclic rings, alkyl substitutions on the side chain, and various substituents on the basic nitrogen of the side chain. The cyclopropyl derivative, 2-(4-imidazolyl)cyclopropylamine, was reported (3) to be almost devoid of activity.

The work reported here was designed to determine whether the selectivity of action could be increased by altering any of the three structural components of histamine: the ring, side chain, or *N*-substituent. The imidazole ring was substituted by a pyridine ring

Table I—Analytical Data for Pyridylethylamine Derivatives

Compound	R	Melting Point	Yield, %	Analysis, % Calc.	Found
XI	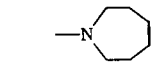	189–190.5°	47	C 56.31 H 7.99 N 10.11	56.56 7.90 10.15
XII	$-N(CH_3)-CH_2CH_2OH$	172–177°	31	C 47.44 H 7.17 N 11.06	47.50 7.21 10.94
XIII	$-N(CH_3)-CH_2CH_2Cl$	190–192°	51	C 44.22 H 6.31 N 10.31	44.43 6.30 10.20
XIV	$-N(CH_2CH_2OH)_2$	98–101[a]	24	C 53.12 H 6.29 N 7.29	53.29 6.35 7.20
XV	$-N(CH_2CH_2Cl)_2$	174–176.5°	59	C 41.28 H 5.67 N 8.75	41.47 5.70 8.65

[a] Sesquifumarate salt.

(Table I) in some compounds for comparison. The *N*-substituents were chosen because they appear in molecules that exhibit antagonist activity in other test systems. For example, an *N*-allyl appears in some narcotic antagonists, a 2-chloroethylamino group occurs in phenoxybenzamine (an adrenergic blocking agent), and bulky lipophilic groups are characteristic of some cholinergic blocking agents (Table II). The side-chain length was retained but placed in constrained three- and six-membered rings.

EXPERIMENTAL[1]

General Preparation—Compounds I–IV and VII were prepared by refluxing a solution of 4-(2-chloroethyl)imidazole hydrochloride (X) (4) (8.4 g, 0.050 mole) in an excess of the appropriate amine with no solvent. The solution was refluxed for from 15 min to 7 hr, and excess amine was removed by distillation *in vacuo*. The residue was treated with excess saturated sodium carbonate solution, and the mixture was reduced to dryness *in vacuo*. Then the residue was triturated with absolute ethanol and filtered. The filtrate was saturated with dry hydrogen chloride and filtered. The residue was recrystallized from a mixture of absolute ethanol and ethyl acetate with the aid of activated charcoal.

The respective yields, melting points, and elemental analyses are reported in Table II.

4-[2-(2-Chloroethylmethylamino)ethyl]imidazole Dihydrochloride (V)—A solution of III (1.6 g, 0.0066 mole) in thionyl chloride (25 ml) was refluxed for 1 hr. The mixture was concentrated *in vacuo*, and the residue was recrystallized from absolute ethanol with the aid of activated charcoal, 1.0 g (59%), mp 189.5–191°.

4-[2-(2-Phenylethyl)aminoethyl]imidazole Dihydrochloride (VI)—To a refluxing solution of phenethylamine (51.0 g, 0.420 mole) in 1-propanol (50 ml) was added X (15.4 g, 0.090 mole) in 1-propanol (50 ml) during 30 min. Reflux was continued for 70 min, and the solution was cooled and filtered. The filtrate was concentrated *in vacuo* to an oil, and about three volumes of dry ether was added.

The cooled solution was filtered, and the filtrate was concentrated *in vacuo*. Excess phenethylamine was removed by vacuum distillation, and the residue was dissolved in acetone (200 ml). After the addition of concentrated hydrochloric acid (10 ml), the product was removed by filtration and recrystallized from absolute ethanol with the aid of activated charcoal, 5.3 g (21%) mp 240–243°.

4-[2-(3-Azabicyclo[3.2.2]nonyl)ethyl]imidazole (VIII)—A stirred mixture of X (8.4 g, 0.050 mole), 3-azabicyclo[3.2.2]nonane (6.3 g, 0.050 mole), and triturated potassium carbonate (20.7 g, 0.15 mole) in 1-butanol (50 ml) was refluxed for 4 hr. The hot mixture was filtered, and the residue was washed twice with absolute ethanol. The combined filtrates were concentrated *in vacuo* and dissolved in dilute hydrochloric acid (100 ml).

The acidic solution was washed with ether and made basic with saturated sodium carbonate solution. Then the product was extracted into ether and crystallized from ether on cooling. The filtered product was recrystallized three times from toluene with the aid of activated charcoal and twice from isopropyl ether, 2.2 g (18%), mp 122–126°.

4-[2-Bis(2-hydroxyethylamino)ethyl]imidazole Dihydrochloride (IX)—A mixture of X (8.4 g, 0.050 mole) and diethanolamine (21.0 g, 0.20 mole) in 2-butanol (50 ml) was refluxed for 29 hr. The mixture was decanted, and the decantate was concentrated *in vacuo* and dissolved in a mixture of methyl ethyl ketone and methanol. The solution was saturated with hydrogen chloride gas, and most of the methanol was removed by boiling. The mixture was cooled and decanted, and the black oily residue was recrystallized from a mixture of absolute ethanol and ethyl acetate with the aid of activated charcoal, 1.0 g (8%), mp 122.5–124.5°.

1-[2-(2-Pyridyl)ethyl]perhydroazepine Dihydrochloride (XI)—A mixture of 2-vinylpyridine (5.3 g, 0.050 mole) and hexamethylenimine (10.0 g, 0.10 mole) was refluxed for 18 hr. The solution was concentrated *in vacuo*, and the residual oil was distilled, 8.1 g, bp 80–84°/0.07 mm. The free base was converted to the hydrochloride salt with ethereal hydrogen chloride. Then the product was recrystallized from isopropanol, 6.6 g (47%) mp 189–190.5°.

2-[2-(2-Hydroxyethylmethylamino)ethyl]pyridine Dihydrochloride (XII)—A mixture of 2-vinylpyridine (21.0 g, 0.20 mole) and 2-hydroxyethylmethylamine (15.0 g, 0.20 mole) was refluxed for 2.5 hr. The mixture was concentrated *in vacuo*, and the residue was distilled, 18.6 g, bp 111–115°/0.5 mm. Five grams of the distillate was treated with ethanolic hydrogen chloride, and the precipitate was recrystallized from absolute ethanol, 2.2 g (31%), mp 172–177°.

2-[2-(2-Chloroethylmethylamino)ethyl]pyridine Dihydrochloride (XIII)—To a solution of thionyl chloride (40 ml) in chloroform (50 ml) was added dropwise the free base of XII (9.0 g, 0.050 mole), followed by another portion of chloroform (50 ml). Refluxing conditions were continued for 1.5 hr, and then the solution was concentrated *in vacuo*. The residue was recrystallized from absolute ethanol with the aid of activated charcoal, 7.0 g (51%), mp 190–192°.

[1] Melting points are uncorrected. The NMR and IR data are consistent with the proposed structures. Analyses were performed by Analytical Research Laboratories, A. H. Robins Co., Richmond, Va.

Table II—Analytical Data for Imidazole Derivatives

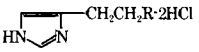

Compound	R	Melting Point	Yield, %	Analysis, % Calc.	Found
I	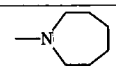	244–247°	26	C 49.63 H 7.95 N 15.78	49.54 8.20 15.54
II	$-NHCH_2CH{=}CH_2$	140.5–143°	40	C 42.87 H 6.74 N 18.75	42.82 6.80 18.80
III	$-N(CH_3)-CH_2CH_2OH$	164–167.5°	13	C 39.68 H 7.08 N 17.35	39.54 6.91 17.38
IV	$-NH-CH(CH_3)(CH_2)_4CH_3$	190–193°	14	C 51.06 H 8.93 N 14.89	50.39 8.77 15.08
V	$-N(CH_3)-CH_2CH_2Cl$	189.5–191°	59[a]	C 36.87 H 6.19 N 16.12	36.82 6.20 16.00
VI	$-NHCH_2CH_2C_6H_5$	240–243°	21	C 54.18 H 6.64 N 14.58	54.07 6.80 14.55
VII	$-N(CH_3)-CH_2CH{=}CH_2$	186–189°	15	C 45.39 H 7.19 N 17.64	45.26 7.13 17.52
VIII	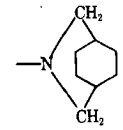	122–126°[b]	18	C 71.19 H 9.65 N 19.16	71.04 9.60 19.12
IX	$-N(CH_2CH_2OH)_2$	122.5–124.5°	8	C 39.72 H 7.04 N 15.44	39.69 7.25 15.36

[a] Yield calculated from Compound III. [b] Free base.

2-[2-Bis(2-hydroxyethyl)aminoethyl]pyridine Sesquifumarate (XIV)—A solution of 2-vinylpyridine (20.8 g, 0.198 mole) and diethanolamine (20.0 g, 0.190 mole) in 1-butanol (100 ml) was refluxed for 48 hr. The hot solution was poured into two volumes of cold water, and the separated organic layer was washed with water. The combined aqueous solutions were made basic with dilute sodium hydroxide solution and extracted with chloroform. The organic layer and chloroform extract were combined and concentrated *in vacuo*.

The residue was distilled, 9.7 g (24%), bp 155–170°/0.5 mm. Then 4.2 g of the free base in methyl isobutyl ketone was mixed with a hot solution of fumaric acid (2.4 g) in absolute ethanol (25 ml). After cooling, the product was filtered and recrystallized from absolute ethanol, 1.7 g, mp 98–101°. NMR data and elemental analysis suggest that the product is the sesquifumarate salt.

2-[2-Bis(2-chloroethyl)aminoethyl]pyridine Dihydrochloride (XV)—To a solution of XIV (5.6 g, 0.026 mole) in chloroform (30 ml) was added slowly thionyl chloride (30 ml), and the mixture was refluxed for 1 hr. The mixture was concentrated *in vacuo*, and the residue was recrystallized from absolute ethanol with the aid of activated charcoal, 5.0 g (59%), mp 174–176.5°.

2-(2-Aminocyclohexyl)pyridine Dihydrochloride (XVI)—A mixture of 2-(2-pyridyl)cyclohexanone (5) (17.5 g, 0.10 mole) and ammonium formate (25.2 g, 0.40 mole) was heated at 145–150° until distillation ceased and was then heated at 185–196° for 4 hr. The mixture was partitioned between water and benzene and the aqueous portion was extracted further with benzene. The combined benzene solutions were washed with water and concentrated *in vacuo*. Then the residue was distilled, retaining the *N*-formyl fraction, 4.0 g (20%), bp 143–155°/0.5 mm. This fraction was combined with the same fraction of another run and redistilled.

Of the redistilled *N*-formyl compound, 4.2 g (0.02 mole) was dissolved in concentrated hydrochloric acid and the solution was refluxed for 30 min. The cooled solution was made basic with dilute sodium hydroxide solution and extracted into chloroform which was concentrated *in vacuo*. The residue was distilled, 2.3 g, bp 100–101°/0.5 mm, and converted to the hydrochloride salt with ethereal hydrogen chloride. The product was recrystallized from absolute ethanol, 1.3 g (5% overall yield), mp 249–255°.

Anal.—Calc. for $C_{11}H_{16}N_2 \cdot 2HCl$: C, 53.02; H, 7.28; N, 11.24. Found: C, 52.83; H, 7.06; N, 11.19.

2-(2-Methylaminocyclohexyl)pyridine Dihydrochloride (XVII)—The redistilled *N*-formyl intermediate from the preparation of XVI was used without further purification. To a clear solution of lithium aluminum hydride (0.33 mole) in tetrahydrofuran was added ethyl acetate (29.1 g, 0.33 mole) under an atmosphere of nitrogen while a reaction temperature of 0–5° was maintained. The mixture was stirred for 10 min, and a solution of the *N*-formyl intermediate (16.3 g, 0.078 mole) in dry ether (70 ml) was added. The mixture was refluxed for 2 hr and stirred at ambient temperature overnight.

The mixture then was decomposed with magnesium sulfate solution, and the product was extracted into ether. The ethereal solu-

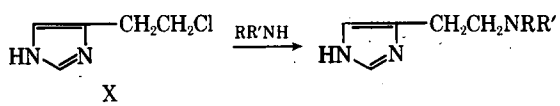

Scheme I

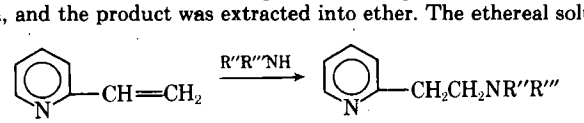

Scheme II

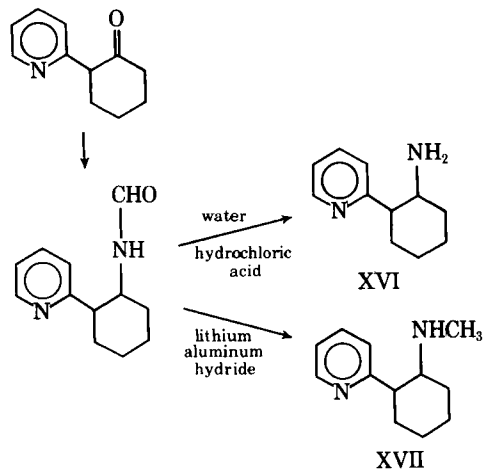

Scheme III

tion was concentrated *in vacuo*, and the residue was distilled, 10 g, bp 85–100°/0.1 mm. The distillate was converted to a salt with ethereal hydrogen chloride, and the product was recrystallized from isopropanol with the aid of activated charcoal. The hygroscopic crystals were dried *in vacuo*, 3.2 g (15.8%), mp 213–218°.

Anal.—Calc. for $C_{12}H_{18}N_2 \cdot 2HCl$: C, 54.76; H, 7.66; N, 10.64. Found: C, 54.48; H, 7.62; N, 10.48.

***trans*-2-(2-Pyridyl)cyclopropylcarboxyhydrazide (XXI)**—Ethyl *trans*-2-(2-pyridyl)cyclopropylcarboxylate (88.6 g, 0.5 mole), prepared by the method of Kaiser *et al.* (6), was added to a solution of anhydrous hydrazine (32.0 g, 1.0 mole) in absolute ethanol (200 ml), and the mixture was refluxed for 4 hr. The mixture then was concentrated *in vacuo*, and the residue was recrystallized twice from tetrahydrofuran, 71.6 g (80.8%), mp 116.5–118.5°.

Anal.—Calc. for $C_9H_{11}N_3O$: C, 61.00; H, 6.26; N, 23.71. Found: C, 60.93; H, 6.28; N, 23.88.

Ethyl *N*-*trans*-2-(2-Pyridyl)cyclopropylcarbamate Hydrochloride (XVIII)—To a cooled solution of *trans*-2-(2-pyridyl)cyclopropylcarboxyhydrazide (17.7 g, 0.10 mole) in a mixture of concentrated hydrochloric acid (50 ml) and water (100 ml) was added dropwise a solution of sodium nitrite (10.5 g, 0.15 mole) in water (30 ml) while the temperature of the reaction mixture was maintained below 0°. The cold mixture was made basic with sodium carbonate solution, and the azide was extracted into ether. The ether solution was dried over anhydrous magnesium sulfate.

The dried ether solution was added dropwise to refluxing absolute ethanol, allowing the ether vapors to escape. Then the mixture was refluxed for 18 hr and concentrated *in vacuo*. After acid and base washes, the residue was distilled, 10.1 g (49%), bp 130–155°/0.1 mm. For analysis, 2.5 g was converted to a hydrochloride salt, which was recrystallized from a mixture of absolute ethanol and ethyl acetate, mp 130–131.5°.

Anal.—Calc for $C_{11}H_{14}N_2O_2 \cdot HCl$: C, 54.44; H, 6.23; N, 11.54. Found: C, 54.43; H, 6.18; N, 11.47.

Benzyl *N*-*trans*-2-(2-Pyridyl)cyclopropylcarbamate (XIX)—The dry ether solution of the azide (0.187 mole), prepared as described for XVIII, was added rapidly to a solution of benzyl alcohol (40.5 g, 0.375 mole) in dry toluene (300 ml) at 85–90°, allowing the ether vapors to escape. The solution was heated at 90° for 30 min, and the mixture was concentrated *in vacuo*. The residue was eluted from a 1-kg column of magnesium silicate with 20% acetone in benzene (2.2 liters) and concentrated *in vacuo*. The residue was recrystallized from isopropyl ether, 22 g (44%), mp 85–85.5°.

Anal.—Calc. for $C_{16}H_{16}N_2O_2$: C, 71.62; H, 6.01; N, 10.44. Found: C, 71.47; H, 5.92; N, 10.42.

***tert*-Butyl *N*-*trans*-2-(2-Pyridyl)cyclopropylcarbamate (XX)**—The dry ether solution of azide (0.10 mole), prepared as described for XVIII, was added rapidly to refluxing *tert*-butyl alcohol (150 ml), allowing ether vapors to escape. The solution was refluxed for 4 hr and concentrated *in vacuo*. The residue was recrystallized from toluene and then isopropyl ether with the aid of activated charcoal, 3.1 g (13%), mp 77–79°.

Anal.—Calc. for $C_{13}H_{18}N_2O_2$: C, 66.64; H, 7.74; N, 11.96. Found: C, 66.89; H, 7.80; N, 12.07.

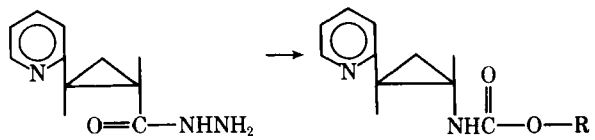

Scheme IV

Table III—Pharmacological Profile of Histamine Analogs[a]

Compound	Blood Pressure[b]	Gastric Secretion[c]	Nasal Congestion[d]
I	–	0	–
II	+	0	+
III	+	0	+
IV	+	0	0
V	+	0	+
VI	+	+	+
VII	+	0	+
VIII	+		–
IX	–	0	0
XI	+		
XII	–		0
XIII	+	0	0
XIV	0	0	–
XV	–	0	–
XVI	–	0	0
XVII	+	0	–
XVIII	+	0	0
XIX	+		0
XX	+		–

[a] The + denotes histamine-like action, – denotes action dissimilar to histamine, and 0 denotes no observable effect. [b] In anesthetized dogs. [c] In dogs and/or rats (9). [d] In dogs (see footnote 2).

RESULTS

Chemistry—The imidazole and pyridylethylamines were prepared by well-known methods of treating X (as the free base) and 2-vinylpyridine with appropriate amines, as shown in Schemes I and II, respectively.

A modification of the Leuckart reaction (7) was used for the preparation of the 2-(2-pyridyl)cyclohexylamines as outlined in Scheme III. The *N*-formyl intermediate was used in each reaction without further purification.

The cyclopropyl derivatives were prepared by a modification of the Curtius reaction (8), using the hydrazide shown in Scheme IV. Several unsuccessful attempts were made to hydrolyze and reduce the carbamates to the corresponding primary and secondary amines. However, only unresolvable mixtures resulted.

Pharmacology—Three pharmacological tests were used to assess the qualitative action of the compounds in relation to the action of histamine.

The effect of the compounds on blood pressure was determined in anesthetized adult mongrel dogs, 7.6–13.3 kg, of either sex. Anesthesia was induced and maintained with a combination of pentobarbital and phenobarbital. Conventional methods and equipment were employed for monitoring blood pressure. The compounds were administered intravenously in an initial dose of 1 mg/kg, with each subsequent dose doubled to the lethal dose or to a maximum of 32 mg/kg. A deviation of at least ±20% from the pretreatment mean arterial pressure was considered a blood pressure effect (Table III).

Gastric secretion experiments were performed in dogs and rats (9). The nasal decongestant studies were done in anesthetized dogs[2], using doses of 0.1–0.8 mg/kg iv (Table III).

DISCUSSION

Structural changes associated with changes in type of activity are not apparent. All compounds except VI exhibited no observ-

[2] The methodology will be published by C. A. Leonard, B. V. Franko, and J. W. Ward, Research Laboratories, A. H. Robins Co.

able effect on gastric secretion at 5 mg/kg sc in dogs; VI showed slight histamine-like activity. Compounds II–VII, XI, XIII, XVIII, and XIX exhibited histamine-like effect on blood pressure and histamine-like or no effect on nasal volume. Compounds IX, XII, and XVI caused an increase in blood pressure (dissimilar effect) and no effect on nasal volume, while XIV produced no effect on blood pressure and caused an increase in nasal volume (dissimilar effect). Compounds VIII, XVII, and XX lowered blood pressure (similar effect) and caused an increase in nasal volume (dissimilar effect). Compounds I and XV exhibited effects dissimilar to those of histamine by causing an increase in blood pressure and nasal volume.

While the data indicate that structural changes can selectively minimize certain pharmacological actions of histamine, no correlation of structural changes to selectivity of action was observed.

REFERENCES

(1) "Handbook of Experimental Pharmacology," vol. XVIII/1, M. Rocha e. Silva, Ed., Springer-Verlag, New York, N.Y., 1966.

(2) "Histamine and Antihistamines," M. Schachter, Pergamon, New York, N.Y., 1973.

(3) M. Bernabe and A. Burger, presented at the Southeastern Regional American Chemical Society Meeting, Richmond, Va., Nov. 1969.

(4) C. F. Huebner, *J. Amer. Chem. Soc.*, **73**, 4667(1951).

(5) M. Hamana and H. Noda, *Chem. Abstr.*, **63**, 13203(1965).

(6) C. Kaiser, B. M. Lester, C. L. Zirkle, A. Burger, C. S. Davis, T. J. Delia, and L. Zirngibl, *J. Med. Chem.*, **5**, 1243(1962).

(7) M. L. Moore, in "Organic Reactions," vol. 5, R. Adams, Ed., Wiley, New York, N.Y., 1949, p. 301.

(8) P. A. Smith, in "Organic Reactions," vol. 3, R. Adams, Ed., Wiley, New York, N.Y., 1946, p. 337.

(9) R. S. Alphin and J. S. Ward, *Arch. Int. Pharmacodyn. Ther.*, **168**, 82(1967).

ACKNOWLEDGMENTS AND ADDRESSES

Received October 7, 1974, from the *Research Laboratories, A. H. Robins Company, Inc., Richmond, VA 23220*

Accepted for publication April 16, 1975.

The authors thank Dr. B. V. Franko, Dr. R. S. Alphin, and Dr. C. A. Leonard of the Research Laboratories for directing the pharmacological studies.

[x] To whom inquiries should be directed. Present address: School of Pharmacy, Auburn University, Auburn, AL 36830

Multiliter Production and Immunochemical Cross-Reactivity of Plant Tissue Culture Antigens

W. L. WU [*§], E. J. STABA [x], and M. N. BLUMENTHAL [‡]**

Abstract □ Cells of short ragweed suspension culture were successfully propagated in a multiliter fermentor. Proteins were isolated from tissue cultures (short ragweed, cantaloupe, marigold, and Ammi) and plants (short ragweed pollen, cantaloupe fruit, and marigold flowers) by ammonium sulfate precipitation, cross-linked dextran gel filtration, and anion-exchange chromatography. Some fractions elicited allergenic responses in ragweed-sensitive patients but not in ragweed-nonsensitive control patients. Double-immunodiffusion analysis of these fractions showed their nonidentity with short ragweed antigen E.

Keyphrases □ Plant antigens—isolated from tissue cultures, allergenic activity screened □ Antigens—proteins isolated from plant tissue cultures, allergenic activity screened

Ragweed pollen is a major causative agent of allergic rhinitis. Active allergens were isolated from short ragweed pollen, and antigen E was found to be the most active (1–3). In one study, ragweed-sensitive patients reacted positively to intradermal injections of the allergens isolated from short ragweed tissue cultures (4). In the present study, short ragweed tissue cultures were grown in multiliter fermentors to determine their growth characteristics in such systems and to produce an adequate amount of cells for further clinical investigation.

The relationship between short ragweed allergic rhinitis and melon or banana sensitivity was studied (5). All patients with melon- or banana-induced oral pruritus were also sensitive to pollen. Therefore, other plant (melon and marigold flowers) and tissue culture (short ragweed, melon, marigold, and Ammi) sources were examined for their antigenic cross-reactivities with short ragweed pollen extract and antigen E.

EXPERIMENTAL

Plant Materials[1]—Short ragweed (*Ambrosia elatior* L.) pollen was purchased[2]. Cantaloupe[3] (*Cucumis melo* var. *cantalupensis* Naud.) and marigold[3] (*Tagetes patula* L.) seeds were germinated and grown in the medicinal garden of the University of Minnesota. Cantaloupe fruit and marigold flowers were harvested in August 1973.

Plant Tissue Cultures—Cantaloupe and marigold seeds were surface sterilized in 2.5% sodium hypochlorite solution for 20 min under reduced pressure and then rinsed three times with sterile distilled water. Germinated seeds were transferred into sterile 30-ml (1-oz.) square vials containing 18 ml of revised Murashige and Skoog tobacco medium (6) supplemented with 1% agar and 1.0 ppm of (2,4-dichlorophenoxy)acetic acid ($RT_{1.0}$). After incubation at 25° in the dark for 5–6 weeks, sufficient light-yellow cantaloupe callus and brownish-green marigold callus were obtained for transfer. They were designated seedling calli and were subcultured every 4 weeks.

The short ragweed and Ammi [*Ammi visnaga* (L.) Lam.] tissue cultures used were approximately 2 years old in June 1973. The short ragweed tissue culture was initiated from the leaves of short ragweed (4), and the Ammi callus culture was initiated from Ammi fruit. Both short ragweed and Ammi tussue cultures were maintained on $RT_{2.0}$ [2 ppm of (2,4-dichlorophenoxy)acetic acid] and $RT_{0.1}$ [0.1 ppm of (2,4-dichlorophenoxy)acetic acid] media, respectively.

Suspension cultures were initiated by aseptically transferring

[1] Short ragweed antigen E was provided by Dr. R. V. Pennington, National Institute of Allergy and Infectious Diseases, Bethesda, Md.

[2] Greer Labs, Lenoir, N.C. (1972 collection).

[3] George W. Park Seed Co., Greenwood, S.C.

able effect on gastric secretion at 5 mg/kg sc in dogs; VI showed slight histamine-like activity. Compounds II–VII, XI, XIII, XVIII, and XIX exhibited histamine-like effect on blood pressure and histamine-like or no effect on nasal volume. Compounds IX, XII, and XVI caused an increase in blood pressure (dissimilar effect) and no effect on nasal volume, while XIV produced no effect on blood pressure and caused an increase in nasal volume (dissimilar effect). Compounds VIII, XVII, and XX lowered blood pressure (similar effect) and caused an increase in nasal volume (dissimilar effect). Compounds I and XV exhibited effects dissimilar to those of histamine by causing an increase in blood pressure and nasal volume.

While the data indicate that structural changes can selectively minimize certain pharmacological actions of histamine, no correlation of structural changes to selectivity of action was observed.

REFERENCES

(1) "Handbook of Experimental Pharmacology," vol. XVIII/1, M. Rocha e. Silva, Ed., Springer-Verlag, New York, N.Y., 1966.

(2) "Histamine and Antihistamines," M. Schachter, Pergamon, New York, N.Y., 1973.

(3) M. Bernabe and A. Burger, presented at the Southeastern Regional American Chemical Society Meeting, Richmond, Va., Nov. 1969.

(4) C. F. Huebner, *J. Amer. Chem. Soc.*, **73**, 4667(1951).

(5) M. Hamana and H. Noda, *Chem. Abstr.*, **63**, 13203(1965).

(6) C. Kaiser, B. M. Lester, C. L. Zirkle, A. Burger, C. S. Davis, T. J. Delia, and L. Zirngibl, *J. Med. Chem.*, **5**, 1243(1962).

(7) M. L. Moore, in "Organic Reactions," vol. 5, R. Adams, Ed., Wiley, New York, N.Y., 1949, p. 301.

(8) P. A. Smith, in "Organic Reactions," vol. 3, R. Adams, Ed., Wiley, New York, N.Y., 1946, p. 337.

(9) R. S. Alphin and J. S. Ward, *Arch. Int. Pharmacodyn. Ther.*, **168**, 82(1967).

ACKNOWLEDGMENTS AND ADDRESSES

Received October 7, 1974, from the *Research Laboratories, A. H. Robins Company, Inc., Richmond, VA 23220*

Accepted for publication April 16, 1975.

The authors thank Dr. B. V. Franko, Dr. R. S. Alphin, and Dr. C. A. Leonard of the Research Laboratories for directing the pharmacological studies.

[x] To whom inquiries should be directed. Present address: School of Pharmacy, Auburn University, Auburn, AL 36830

Multiliter Production and Immunochemical Cross-Reactivity of Plant Tissue Culture Antigens

W. L. WU [*§], E. J. STABA [x], and M. N. BLUMENTHAL [‡]**

Abstract □ Cells of short ragweed suspension culture were successfully propagated in a multiliter fermentor. Proteins were isolated from tissue cultures (short ragweed, cantaloupe, marigold, and Ammi) and plants (short ragweed pollen, cantaloupe fruit, and marigold flowers) by ammonium sulfate precipitation, cross-linked dextran gel filtration, and anion-exchange chromatography. Some fractions elicited allergenic responses in ragweed-sensitive patients but not in ragweed-nonsensitive control patients. Double-immunodiffusion analysis of these fractions showed their nonidentity with short ragweed antigen E.

Keyphrases □ Plant antigens—isolated from tissue cultures, allergenic activity screened □ Antigens—proteins isolated from plant tissue cultures, allergenic activity screened

Ragweed pollen is a major causative agent of allergic rhinitis. Active allergens were isolated from short ragweed pollen, and antigen E was found to be the most active (1–3). In one study, ragweed-sensitive patients reacted positively to intradermal injections of the allergens isolated from short ragweed tissue cultures (4). In the present study, short ragweed tissue cultures were grown in multiliter fermentors to determine their growth characteristics in such systems and to produce an adequate amount of cells for further clinical investigation.

The relationship between short ragweed allergic rhinitis and melon or banana sensitivity was studied (5). All patients with melon- or banana-induced oral pruritus were also sensitive to pollen. Therefore, other plant (melon and marigold flowers) and tissue culture (short ragweed, melon, marigold, and Ammi) sources were examined for their antigenic cross-reactivities with short ragweed pollen extract and antigen E.

EXPERIMENTAL

Plant Materials[1]—Short ragweed (*Ambrosia elatior* L.) pollen was purchased[2]. Cantaloupe[3] (*Cucumis melo* var. *cantalupensis* Naud.) and marigold[3] (*Tagetes patula* L.) seeds were germinated and grown in the medicinal garden of the University of Minnesota. Cantaloupe fruit and marigold flowers were harvested in August 1973.

Plant Tissue Cultures—Cantaloupe and marigold seeds were surface sterilized in 2.5% sodium hypochlorite solution for 20 min under reduced pressure and then rinsed three times with sterile distilled water. Germinated seeds were transferred into sterile 30-ml (1-oz.) square vials containing 18 ml of revised Murashige and Skoog tobacco medium (6) supplemented with 1% agar and 1.0 ppm of (2,4-dichlorophenoxy)acetic acid ($RT_{1.0}$). After incubation at 25° in the dark for 5–6 weeks, sufficient light-yellow cantaloupe callus and brownish-green marigold callus were obtained for transfer. They were designated seedling calli and were subcultured every 4 weeks.

The short ragweed and Ammi [*Ammi visnaga* (L.) Lam.] tissue cultures used were approximately 2 years old in June 1973. The short ragweed tissue culture was initiated from the leaves of short ragweed (4), and the Ammi callus culture was initiated from Ammi fruit. Both short ragweed and Ammi tussue cultures were maintained on $RT_{2.0}$ [2 ppm of (2,4-dichlorophenoxy)acetic acid] and $RT_{0.1}$ [0.1 ppm of (2,4-dichlorophenoxy)acetic acid] media, respectively.

Suspension cultures were initiated by aseptically transferring

[1] Short ragweed antigen E was provided by Dr. R. V. Pennington, National Institute of Allergy and Infectious Diseases, Bethesda, Md.

[2] Greer Labs, Lenoir, N.C. (1972 collection).

[3] George W. Park Seed Co., Greenwood, S.C.

Table I—Growth Indexes of Plant Suspension Cultures[a]

Source	Sub-culture	Growth Period, days	Final Fresh Weight, g	Growth Index[b]	Growth Efficiency Index[c]
Short ragweed	19	18	29	4.8	2.7
Ammi	18	18	34	4.8	3.7
Cantaloupe	5	28	26	5.2	1.9
Marigold	4	18	28	5.6	3.1

[a] Conditions: Revised Murashige and Skoog tobacco medium (100 ml) in a 500-ml erlenmeyer flask at 22–23° and 80 rpm. [b] Growth index = final fresh weight of tissue/initial fresh weight of inoculum (average of five determinations). [c] Growth efficiency index = $\frac{\text{growth index at maximum growth}}{\text{volume of medium (liters)} \times \text{days required for growth}}$.

the calli from solid media to 500-ml flasks containing 100 ml of sterile liquid RT media. The flasks were placed on a rotary shaker[4] operating at 80 rpm at 25°. Preliminary studies showed that the cantaloupe suspension culture grew best in the $RT_{2.0}$ medium and that the marigold suspension culture grew best in the $RT_{0.1}$ medium. Once the suspension cultures were established, they were maintained by transferring about 5 g of inocula, with a stainless steel transfer spoon with perforations in its base, to flasks of fresh media every 2–3 weeks.

Short ragweed tissues from 14-day-old flask suspension cultures were used as inocula (~100 or 150 g in each fermentor) for three fermentors, each containing 2.5 liters of the sterilized $RT_{2.0}$ medium. The aeration was maintained at 500, 1000, or 1500 ml/min, with an agitation rate of 80 rpm, at 25–26° for 14 days. No antifoam was added to the fermentation system.

Allergen Isolation Procedure—The procedure of King *et al.* (2) and Shafiee and Staba (4) was slightly modified and used to isolate antigens from short ragweed pollen, plant tissues, and plant tissue cultures.

Short ragweed pollen (50 g) was defatted with peroxide-free anhydrous ether. The air-dried pollen was extracted with 0.005 *M* phosphate buffer (pH 7.4, 250 ml) on a gyrotory shaker[5] at 200 rpm for 24 hr at 22–23°. The buffer extract was filtered, and the filtrate pH was adjusted from 6.0 to 7.2 with 3 *N* ammonium hydroxide. The filtrate was brought to 90% saturation with ammonium sulfate at 4°. The resulting suspension was stirred overnight and centrifuged[6] at 14,350×*g* for 40 min at 4°.

The dark-brown gummy precipitate was dissolved in 0.1 *M* tromethamine–hydrochloric acid buffer (pH 7.9, 15 ml) and desalted and depigmented by passage through a cross-linked dextran gel column[7] (50 × 4 cm), previously equilibrated with 0.025 *M* tromethamine–hydrochloric acid buffer (pH 7.9). The cross-linked dextran gel column flow rate was adjusted to 60 ml/hr, and 10-ml fractions were collected at 22–23°. The presence of protein was determined by its UV absorption at 280 nm. The first peak, Fraction A, was concentrated[8], and the concentrate was exhaustively dialyzed against 0.025 *M* tromethamine–hydrochloric acid buffer (pH 7.9) and applied to a diethylaminoethylcellulose[9] column (26 × 2.7 cm), previously equilibrated with 0.025 *M* tromethamine–hydrochloric acid.

The second dextran gel column peak, Fraction B, contained yellow pigments and was discarded. The flow rate of 0.025 *M* tromethamine–hydrochloric acid buffer (pH 7.9) through the diethylaminoethylcellulose column was adjusted to 60 ml/hr, and 10-ml fractions were collected and monitored at 280 nm. The first diethylaminoethylcellulose peak, Fraction C, was collected. The column was then eluted with equal volumes of 0.05 *M* tromethamine–hydrochloric acid and 0.2 *M* sodium chloride buffer (pH 7.9) to obtain a second peak, Fraction D. Fraction D was concentrated to 30.5 ml and contained 5.0 mg of protein/ml. The protein content

[4] Model-53, New Brunswick Scientific Co., New Brunswick, N.J.
[5] Model-G-10, New Brunswick Scientific Co., New Brunswick, N.J.
[6] Sorvall SS-12, Newton, Conn.
[7] Sephadex G-25.
[8] Amicon ultrafiltration cell, model 402, Amicon Corp., Lexington, Mass., and UM-2 membrane.
[9] Exchange capacity of 0.88 mEq/g, medium mesh; Sigma Chemical Co., St. Louis, Mo.

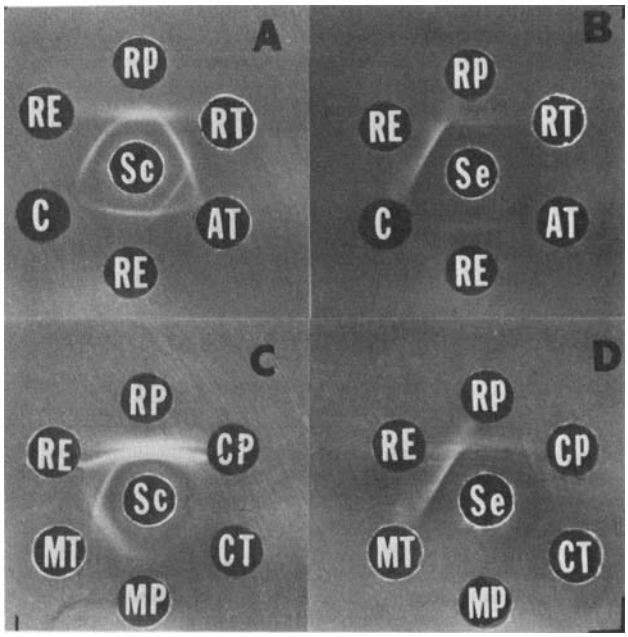

Figure 1—*Double-diffusion analysis of Fraction D tissue culture and plant extracts against short ragweed pollen serum (A and C) and antigen E serum (B and D). Key: AT, Ammi tissue culture; C, control (0.005 M phosphate buffer, pH 7.9); CP, cantaloupe plant (fruit); CT, cantaloupe tissue culture; MP, marigold plant (flower); MT, marigold tissue culture; RE, short ragweed antigen E; RP, short ragweed pollen; RT, short ragweed tissue culture; Sc, rabbit short ragweed pollen serum; and Se, rabbit antigen E serum. Plate wells were 3 mm in diameter and contained approximately 4 µl of suspension culture Fraction D (1 mg/ml) or antigen E (0.06 mg/ml).*

was determined by the method of Lowry *et al.* (7), with crystalline bovine albumin as the reference standard.

Suspension culture cells (1 kg fresh weight) of short ragweed, cantaloupe, marigold, and Ammi tissue cultures were in turn suspended in 0.005 *M* phosphate buffer (pH 7.5, 1.5 liters) and sonified at 90 w for 2 min. The sonified cell suspension was shaken overnight at 200 rpm at 22–23°, and the resulting suspension was centrifuged at 1230×*g* for 10 min. The pH of the collected supernate was adjusted to 7.0 with 3 *N* ammonium hydroxide. The supernate was concentrated by ultrafiltration[10] to about 500 ml and brought to 90% saturation with ammonium sulfate. The precipitated protein was further fractionated to Fraction D, as previously described for short ragweed pollen.

Peeled cantaloupe fruit and marigold flowers (1 kg fresh weight) were homogenized with an appropriate amount of 0.005 *M* phosphate buffer (pH 7.4) to prepare a slurry, and Fraction D was prepared as described for the tissue culture.

Skin Testing—Concentrated Fraction D proteins (anionic proteins) for skin testing were sterilized by passing through sterile filters[11] (0.22-µm pore size). The sterility of the filtered solutions was substantiated by plating on both blood agar and fluid thioglycolate medium and examining the plates for growth after 72 hr of incubation. The allergenic activity of the samples was determined by direct skin testing in ragweed-sensitive and ragweed-nonsensitive persons. A series of 10-fold sequential dilutions of sterile sample fractions in sterile buffered saline allergy diluent[12] was made approximately 12 hr before skin testing. Patients were injected intradermally on the forearm with a 0.02-ml volume of the diluted solutions, and the wheal and flare reactions were read within 20 min after injection. Ragweed-nonsensitive persons served as controls.

Immunodiffusion Analysis—The rabbit anti-short-ragweed-pollen serum and rabbit anti-antigen-E serum used were as pre-

[10] Diaflo.
[11] Millipore Corp., Bedford, Mass.
[12] Hollister-Stier Lab, Downers Grove, Ill.

Table II—Multiliter Growth of Short Ragweed Suspension Cultures

Experiment[a]	Inoculum, g	Aeration, ml/min	Final Weight, g	Growth Index[b]
Fermentor A				
1	100	500	263	2.6
2	100	500	205	2.1
3	100	500	250	2.5
Fermentor B				
1	100	1000	246	2.5
2	100	1000	260	2.6
3	100	1000	252	2.5
Fermentor C				
1	150	1500	640	4.3
2	150	1500	645	4.3
3	150	1500	600	4.0

[a] Experimental conditions: 2.5 liters of $RT_{2.0}$ medium in each fermentor for a 14-day growth period at 25–26° and 80 rpm agitation. [b] Growth index = final fresh weight of tissue/initial fresh weight of inoculum.

viously reported (8). Ouchterlony double-diffusion tests were carried out in 60-mm plastic petri dishes, each containing 5 ml of 1% Noble agar[13]/0.1% sodium azide (9). Antiserum was placed in the center well (3-mm diameter), and antigens were place in the outer wells. After 48–72 hr, precipitin lines were observed and photographed (10).

Disk Electrophoresis[14]—The electrophoretic system used was 7% acrylamide gel (pH 8.9) with a bromophenol blue tracking dye (11). The sample (0.1 ml containing about 0.05 mg of protein) was mixed with 0.1 ml of 20% sucrose, and the mixture was introduced into the gel tubes (7.7 × 0.7 cm). The gels were run at 4 mamp/tube at room temperature until the blue tracking dye had migrated from 2 to 5 mm from the bottom of the gel.

RESULTS AND DISCUSSION

Tissue Culture—Tissue cultures were successfully grown in both solid and liquid revised Murashige and Skoog tobacco medium. Experimental trials suggested that (2,4-dichlorophenoxy)acetic acid in the concentration of 1 ppm was most effective in promoting static culture growth; 0.1 ppm was best for the suspension culture growth of marigold and Ammi. Short ragweed and cantaloupe suspension cultures required 2.0 ppm of (2,4-dichlorophenoxy)acetic acid for growth. The suspension cultures were uniform in appearance, except for cantaloupe suspension culture which aggregated. Among the suspension cultures studied, Ammi had the highest growth efficiency index and cantaloupe the lowest, 3.7 and 1.9, respectively (Table I).

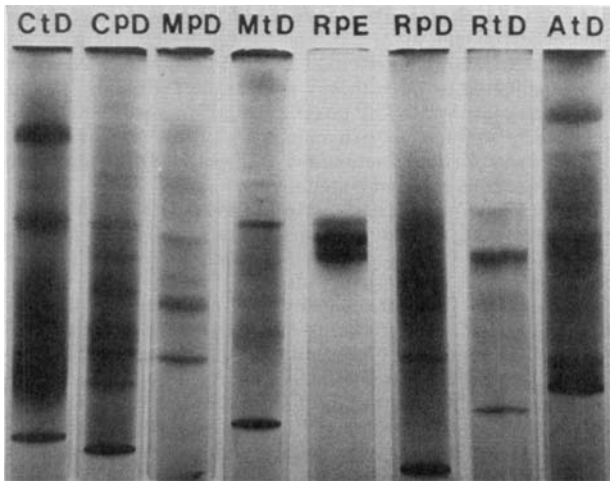

Figure 2—*Polyacrylamide disk electrophoretic patterns of Fraction D from tissue culture and plants. Tracking dye is shown at the top of each disk; disks are aligned from one electrophoretic determination. Key; ctD, cantaloupe tissue culture; CPD, cantaloupe fruit; MPD, marigold flower; MtD, marigold tissue culture; RPE, short ragweed antigen E; RPD, short ragweed pollen; RtD, short ragweed tissue culture; and AtD, Ammi tissue culture.*

[13] Difco Labs, Detroit, Mich.

[14] The reagents and apparatus were purchased from Canalco, Co., Rockville, Md.

Table III—Lowry Protein Content (Milligrams per Gram Fresh Weight) of Plant Tissue and Tissue Cultures

Material	Phosphate Buffer Extract	Dextran Gel Fraction A	Diethylaminoethylcellulose Fraction D
Plant tissue			
Short ragweed pollen	—[a]	—[b]	3.04
Cantaloupe fruit	4.23	0.63	0.21
Marigold flower	9.02	0.93	0.14
Tissue culture			
Short ragweed	2.19	0.57	0.06
Cantaloupe	1.99	0.86	0.07
Marigold	1.45	0.47	0.06
Ammi	2.05	0.21	0.05

[a] 10.53 g of extract/50 g of pollen. [b] 1.15 g of extract/50 g of pollen.

An important factor influencing the growth index is the amount of inoculum. A 50% increase in inoculum (Table II, Experiment C) resulted in a 2.5 increase in the harvested amount. The aeration rate at 500 and 1000 ml/min did not appear to change the growth rate significantly, but the 1500-ml/min rate may have. It is unknown if the growth increase observed resulted from the inoculum size or the aeration rate. The agitation rate was adjusted to a slow value (80 rpm) to avoid shearing the plant cells. Because low agitation and aeration rates were used, no serious foaming problem was encountered.

Short ragweed suspension culture was grown in multiliter fermentors for 14 days. The growth indexes ranged from 2.1 to 4.3 (Table II).

Isolation of Antigens and Skin Testing—The protein content of plant tissues and plant tissue culture fractions is shown in Table III. Fraction D portions of all tissue cultures contained approximately the same amount of protein. In general, the Fraction D protein content of tissue cultures was lower in quantity as compared to that of natural plant sources. Cantaloupe tissue culture had the highest soluble protein content among all tissue cultures examined, whereas marigold had the lowest.

Skin testing of ragweed pollen, plant, and tissue culture Fraction D was performed on three ragweed-sensitive and four ragweed-nonsensitive persons. The results, expressed in allergenic specific activities, are shown in Table IV. All fractions elicited sensitization reactions on two ragweed-sensitive persons (S.R. and T.M.). The third ragweed-sensitive person (K.S.) responded only

Table IV—Allergenic Activities of Tissue Culture and Plant Extracts, Fraction D, in Ragweed-Sensitive Persons

Material	Specific Activity[a], units/mg		
	Subject S.R.	Subject T.M.	Subject K.S.
Plant extracts			
Ragweed pollen	5×10^{10}	5×10^{7}	5×10^{4}
Marigold flower	5×10^{8}	5×10^{3}	(—)
Cantaloupe fruit	5×10^{9}	5×10^{4}	(—)
Tissue culture extracts			
Ragweed	5×10^{8}	5×10^{2}	(—)
Marigold	5×10^{6}	5×10^{2}	(—)
Cantaloupe	5×10^{8}	5×10^{3}	(—)
Ammi	5×10^{8}	5×10^{5}	5×10^{2}

[a] Specific activity is the reciprocal of the minimum quantity of intradermally injected protein fraction that elicits a minimum reaction in ragweed-sensitive persons (12). Four ragweed-nonsensitive individuals were tested and reacted negatively to both plant and tissue culture extracts.

to ragweed pollen and Ammi tissue culture. The response to the latter was low (5×10^2 units/mg of specific activity). Plant extract fractions generally elicited a stronger allergenic reaction than tissue culture fractions.

Of all of the fractions tested, the pollen extract consistently gave the highest allergenic activity. Ragweed-sensitive patients (S.R. and T.M.) reacted consistently to the plant materials and tissue cultures tested, whereas ragweed-nonsensitive individuals did not.

Immunodiffusion and Electrophoresis—Immunodiffusion analysis was performed to observe if Fraction D from plants and tissue cultures cross-reacted with short ragweed pollen and ragweed antigen E. No precipitin lines were observed between plant and tissue culture Fraction D and anti-antigen E serum (Fig. 1). None of the fractions tested, except ragweed pollen, contained allergens that have a total identity or partial identity with antigen E. Several fractions from short ragweed tissue cultures, Ammi tissue culture, marigold tissue culture, and marigold plant (weak) did have precipitin lines against anti-short-ragweed-pollen serum. It is possible that those fractions contained either other ragweed allergens, such as antigen K, Ra_3, or common proteins, *e.g.*, enzymes. It is presently unknown if the hypersensitivity reactions observed are specific reactions to Fraction D or a general hypersensitivity toward proteins that is peculiarly demonstrated by ragweed-sensitive patients. There also is some evidence that Fraction C from both plants and tissue cultures may contain allergens.

Polyacrylamide gel electrophoresis was used to determine if the plant and tissue culture allergenic fractions contained proteins with similar electrophoretic characteristics as antigen E. All plant and tissue culture fractions had a protein band in the antigen E region (Fig. 2). Ammi tissue culture, cantaloupe tisue culture, and short ragweed tissue culture had strong bands. The proteins in this region are responsible for the high allergenic activity in skin testing. However, further work is required to examine the proteins and allergenic properties of the protein band observed.

REFERENCES

(1) T. P. King and P. S. Norman, *Biochemistry*, **1**, 709(1962).

(2) T. P. King, P. S. Norman, and J. T. Connel, *ibid.*, **6**, 1992(1964).

(3) T. P. King, P. S. Norman, and L. M. Lichtenstein, *ibid.*, **3**, 458(1967).

(4) A. Shafiee and E. J. Staba, *In Vitro*, **9**, 19(1973).

(5) B. Anderson, E. M. Dreyfuss, J. Logan, D. E. Johnston, and J. Glaser, *J. Allergy*, **45**, 310(1970).

(6) E. J. Staba, in "Recent Advances in Phytochemistry," vol. 2, M. K. Seikel and V. C. Runeckles, Eds., Appleton-Century-Crofts, New York, N.Y., 1969, pp. 75–106.

(7) O. H. Lowry, N. J. Rosenberg, A. L. Farr, and R. J. Randall, *J. Biol. Chem.*, **193**, 265(1951).

(8) A. Shafiee, E. J. Staba, and Y. J. Abul-Hajj, *J. Pharm. Sci.*, **62**, 1654(1973).

(9) O. Ouchterlony, *Progr. Allergy*, **5**, 1(1958).

(10) C. A. Williams and M. W. Chase, in "Methods in Immunology and Immunochemistry," vol. 3, C. A. Williams and M. W. Chase, Eds., Academic, New York, N.Y., 1971, pp. 321–339.

(11) B. J. Davis and L. Ornstein, in "Methods in Immunology and Immunochemistry," vol. 2, C. A. Williams and M. W. Chase, Eds., Academic, New York, N.Y., 1968, pp. 38–47.

(12) L. Berrens, "The Chemistry of Atopic Allergens," S. Karger, New York, N.Y., 1971, pp. 6, 7.

ACKNOWLEDGMENTS AND ADDRESSES

Received July 22, 1974, from the *Department of Pharmacognosy, College of Pharmacy, and the [1]Department of Medicine, University of Minnesota, Minneapolis, MN 55455

Accepted for publication April 18, 1975.

The authors are grateful to R. V. Penington, National Institutes of Allergy and Infectious Diseases, Bethesda, Md., for providing purified antigen E. Financial support from the National Science Council of the Republic of China to W. L. Wu is gratefully acknowledged.

[§] Present address: Department of Biomorphics, National Defense Medical Centre, Taipei, Taiwan, Republic of China.

[x] To whom inquiries should be directed.

Single-Tablet Enantiomeric Purity Assay of Amphetamine by Rotation Enhancement

JOHN D. WEBER

Abstract □ Enhancement of the optical rotation of dextroamphetamine by production of an optically active chromophore through reaction with 1-fluoro-2,4-dinitrobenzene to give α-methyl-*N*-(2,4-dinitrophenyl)-β-phenylethylamine is reported. This reaction forms the basis of an assay for both the content and optical purity of dextroamphetamine sulfate at single-dose levels (5 mg). Results of assays of standard solutions and of commercial tablets demonstrate the suitability of the method for the determination of enantiomeric purity and amphetamine content.

Keyphrases □ Amphetamine—colorimetric analysis, optical purity assay, commercial tablets □ Colorimetry—analysis, amphetamine, commercial tablets

The USP XIX (1) isomeric purity[1] test for dextroamphetamine sulfate (I) requires separation of the amphetamine from dosage excipients and conversion to *N*-acetylamphetamine, followed by isolation, purification, and determination of the specific rotation of the derivative. This method suffers from low sensitivity; 130 mg of the drug is specified for the test, although amphetamine sulfate is commonly formulated in 5- or 10-mg dosage units. Some very sensitive tests (2, 3), which depend on physical examination of crystalline derivatives, readily distinguish *d*- from *dl*- and *l*-amphetamines at milligram levels, but they cannot be used for the determination of enantiomeric purity[1].

Although several NMR methods for the determination of enantiomeric composition were reported re-

[1] Isomeric purity, also called enantiomeric purity, is a measure of the percent of one enantiomer. Optical purity is the percent of the specific rotation of the pure enantiomer. The relationship between them is given in Eqs. 2 and 3.

to ragweed pollen and Ammi tissue culture. The response to the latter was low (5×10^2 units/mg of specific activity). Plant extract fractions generally elicited a stronger allergenic reaction than tissue culture fractions.

Of all of the fractions tested, the pollen extract consistently gave the highest allergenic activity. Ragweed-sensitive patients (S.R. and T.M.) reacted consistently to the plant materials and tissue cultures tested, whereas ragweed-nonsensitive individuals did not.

Immunodiffusion and Electrophoresis—Immunodiffusion analysis was performed to observe if Fraction D from plants and tissue cultures cross-reacted with short ragweed pollen and ragweed antigen E. No precipitin lines were observed between plant and tissue culture Fraction D and anti-antigen E serum (Fig. 1). None of the fractions tested, except ragweed pollen, contained allergens that have a total identity or partial identity with antigen E. Several fractions from short ragweed tissue cultures, Ammi tissue culture, marigold tissue culture, and marigold plant (weak) did have precipitin lines against anti-short-ragweed-pollen serum. It is possible that those fractions contained either other ragweed allergens, such as antigen K, Ra_3, or common proteins, *e.g.*, enzymes. It is presently unknown if the hypersensitivity reactions observed are specific reactions to Fraction D or a general hypersensitivity toward proteins that is peculiarly demonstrated by ragweed-sensitive patients. There also is some evidence that Fraction C from both plants and tissue cultures may contain allergens.

Polyacrylamide gel electrophoresis was used to determine if the plant and tissue culture allergenic fractions contained proteins with similar electrophoretic characteristics as antigen E. All plant and tissue culture fractions had a protein band in the antigen E region (Fig. 2). Ammi tissue culture, cantaloupe tisue culture, and short ragweed tissue culture had strong bands. The proteins in this region are responsible for the high allergenic activity in skin testing. However, further work is required to examine the proteins and allergenic properties of the protein band observed.

REFERENCES

(1) T. P. King and P. S. Norman, *Biochemistry*, **1**, 709(1962).

(2) T. P. King, P. S. Norman, and J. T. Connel, *ibid.*, **6**, 1992(1964).

(3) T. P. King, P. S. Norman, and L. M. Lichtenstein, *ibid.*, **3**, 458(1967).

(4) A. Shafiee and E. J. Staba, *In Vitro*, **9**, 19(1973).

(5) B. Anderson, E. M. Dreyfuss, J. Logan, D. E. Johnston, and J. Glaser, *J. Allergy*, **45**, 310(1970).

(6) E. J. Staba, in "Recent Advances in Phytochemistry," vol. 2, M. K. Seikel and V. C. Runeckles, Eds., Appleton-Century-Crofts, New York, N.Y., 1969, pp. 75–106.

(7) O. H. Lowry, N. J. Rosenberg, A. L. Farr, and R. J. Randall, *J. Biol. Chem.*, **193**, 265(1951).

(8) A. Shafiee, E. J. Staba, and Y. J. Abul-Hajj, *J. Pharm. Sci.*, **62**, 1654(1973).

(9) O. Ouchterlony, *Progr. Allergy*, **5**, 1(1958).

(10) C. A. Williams and M. W. Chase, in "Methods in Immunology and Immunochemistry," vol. 3, C. A. Williams and M. W. Chase, Eds., Academic, New York, N.Y., 1971, pp. 321–339.

(11) B. J. Davis and L. Ornstein, in "Methods in Immunology and Immunochemistry," vol. 2, C. A. Williams and M. W. Chase, Eds., Academic, New York, N.Y., 1968, pp. 38–47.

(12) L. Berrens, "The Chemistry of Atopic Allergens," S. Karger, New York, N.Y., 1971, pp. 6, 7.

ACKNOWLEDGMENTS AND ADDRESSES

Received July 22, 1974, from the *Department of Pharmacognosy, College of Pharmacy, and the [1]Department of Medicine, University of Minnesota, Minneapolis, MN 55455

Accepted for publication April 18, 1975.

The authors are grateful to R. V. Penington, National Institutes of Allergy and Infectious Diseases, Bethesda, Md., for providing purified antigen E. Financial support from the National Science Council of the Republic of China to W. L. Wu is gratefully acknowledged.

[§] Present address: Department of Biomorphics, National Defense Medical Centre, Taipei, Taiwan, Republic of China.

[x] To whom inquiries should be directed.

Single-Tablet Enantiomeric Purity Assay of Amphetamine by Rotation Enhancement

JOHN D. WEBER

Abstract □ Enhancement of the optical rotation of dextroamphetamine by production of an optically active chromophore through reaction with 1-fluoro-2,4-dinitrobenzene to give α-methyl-*N*-(2,4-dinitrophenyl)-β-phenylethylamine is reported. This reaction forms the basis of an assay for both the content and optical purity of dextroamphetamine sulfate at single-dose levels (5 mg). Results of assays of standard solutions and of commercial tablets demonstrate the suitability of the method for the determination of enantiomeric purity and amphetamine content.

Keyphrases □ Amphetamine—colorimetric analysis, optical purity assay, commercial tablets □ Colorimetry—analysis, amphetamine, commercial tablets

The USP XIX (1) isomeric purity[1] test for dextroamphetamine sulfate (I) requires separation of the amphetamine from dosage excipients and conversion to *N*-acetylamphetamine, followed by isolation, purification, and determination of the specific rotation of the derivative. This method suffers from low sensitivity; 130 mg of the drug is specified for the test, although amphetamine sulfate is commonly formulated in 5- or 10-mg dosage units. Some very sensitive tests (2, 3), which depend on physical examination of crystalline derivatives, readily distinguish *d*- from *dl*- and *l*-amphetamines at milligram levels, but they cannot be used for the determination of enantiomeric purity[1].

Although several NMR methods for the determination of enantiomeric composition were reported re-

[1] Isomeric purity, also called enantiomeric purity, is a measure of the percent of one enantiomer. Optical purity is the percent of the specific rotation of the pure enantiomer. The relationship between them is given in Eqs. 2 and 3.

Table I—NMR Data for Compound III

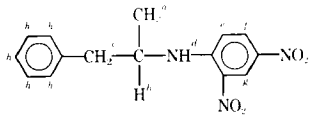

Proton	Chemical Shift[a], ppm δ	Coupling
a	1.38 (d)	J_{ab} = 7 Hz
b	4.05 (sext)	$J_{ab} = J_{bc}$ = 7 Hz
c	3.95 (d)	J_{bc} = 7 Hz
d	8.6 (s) broad	—
e	6.85 (d)	J_{ef} = 10 Hz
f	8.15 (d, d)	J_{ef} = 10 Hz, J_{fg} = 3 Hz
g	9.25 (d)	J_{fg} = 3 Hz
h	7.25 (s)	—

[a] (s) = singlet, (d) = doublet, (d, d) = doublet of doublets, (sext) = sextet.

cently (4–6), none of these has been developed into a working assay. A GLC method for the separation of enantiomers of amphetamine (7) has been developed into a working assay (8), collaboratively studied (9), and adopted as an official assay by the Association of Official Analytical Chemists (10). The method is sufficiently sensitive for a single-tablet assay but requires considerable manipulation; problems with instability of the reagent were also reported (7–9).

This report describes the reaction of I with 1-fluoro-2,4-dinitrobenzene (II) to form the 2,4-dinitrophenyl derivative, α-methyl-*N*-(2,4-dinitrophenyl)-β-phenylethylamine (III) (Scheme I). This derivative has an optical rotation at 546 nm, which is about 30 times greater than that of I itself. In acid solution, the absorptivity of III at 430 nm is linearly related to the concentration of I and is free from interferences from the reagent and by-products. This colorimetric reaction forms the basis for the determination of both the amphetamine content and apparent specific rotation[2] of III. These two measurements on separate dilutions of the same reaction mixture are used to calculate the amount of I and its optical purity[1].

No prior isolation is required, but the sample must be known to be free of primary or secondary amines. Reagents are added directly to the ground tablet; the

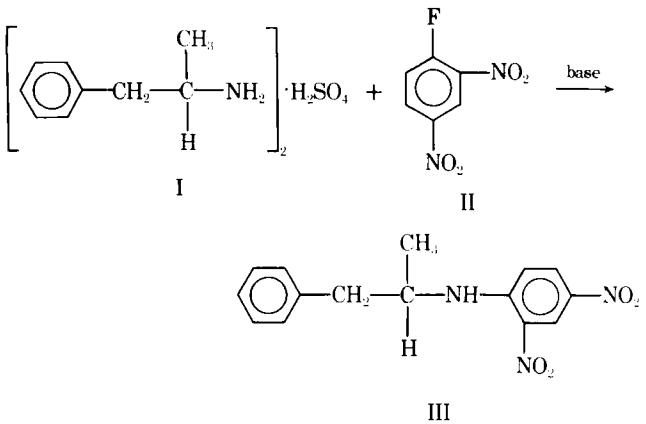

I II III

Scheme I

[2] Apparent specific rotation because the weight of I is used in the calculation, but rotation of III is measured.

Table II—Percent I Found *versus* Enantiomeric Composition of Amphetamine Sulfate

Composition Prepared as Percent I[a]	I Found, %	
100	99.1	98.9
89.9	91.2	91.2
79.9	78.9	79.1
69.9	71.4	74.8
59.9	60.7	—
50[b]	50.1	51.3
39.4	42.2	41.7

[a] Mixture was prepared by weighing samples of I and levoamphetamine sulfate into a volumetric flask; two aliquots were assayed. [b] Racemic amphetamine sulfate was used.

product, III, along with excess reagents, is separated from tablet excipients by column partition chromatography. The eluate is adjusted to a suitable concentration and measured polarimetrically and spectrophotometrically.

The use of reagent II for end-group analysis of proteins (11), gravimetric determination of phenols (12), and microanalysis of primary amines (13) is well known. However, its use in rotation enhancement appears to be novel.

EXPERIMENTAL

Instruments and Apparatus—An automatic polarimeter[3] capable of measuring rotations at 546 nm with a precision of ±0.005°, a spectrophotometer[4], a spectropolarimeter[5], and an NMR spectrometer[6] were used. Chromatographic tubes[7], 22 mm i.d. × 250 mm long, with a 6-mm i.d. tube affixed to the base, a tamping rod consisting of a metal disk about 21 mm in diameter on a rod about 600 mm long, and conventional glassware are required. A rotary evaporator[8] also was used.

Preparation of Compound III—Dextroamphetamine base[9] (2 ml), II (0.5 ml), and triethylamine (0.5 ml) were dissolved in 20 ml of dioxane, and the mixture was allowed to stand at room temperature. The reaction was monitored by TLC[10] until all II was consumed (about 2 hr). Dioxane and some excess amphetamine were removed under reduced pressure on a rotary evaporator.

The residue was dissolved in 100 ml of chloroform and passed over a chromatographic column packed with 10 ml of 4 *N* H_2SO_4 on 25 g of diatomaceous earth[11]. The column was eluted with an additional 100 ml of chloroform, and the combined chloroform eluate was evaporated on the rotary evaporator, leaving a residual yellow oil.

About 50 mg of the residue, Compound III, was dissolved in 0.5 ml of deuterated chloroform, dried with about 100 mg of anhydrous magnesium sulfate, and filtered into a 5-mm NMR tube; then the NMR spectrum was obtained (Table I). About 1 mg of III was dissolved in 10 ml of methanol, and the optical rotatory dispersion curve was determined in a 1-mm cell from 600 to about 380 nm, below which absorption became too great for further measurement of the rotation (Fig. 1).

[3] Perkin-Elmer model 141M automatic polarimeter.

[4] A Cary model 15 spectrophotometer was used in the time scan mode; thus, all measurements could be made without changing the monochromator settings since the absorption at 430 nm is on a slope.

[5] Model JASCO-ORD/CD-5, Japan Spectroscopic Co.

[6] Varian A-60 analytical spectrometer.

[7] Kontes Glass Catalog No. K 420300.

[8] Buchi Rotavapor-R rotary evaporator.

[9] Aldrich Chemical Co. ($[\alpha]_D$ + 34.0°, *c* = 10 in methanol, n_D^{20} 1.5170). It was used without further purification.

[10] Silica gel GF, 250 μm thick on 25 × 75-mm microscope slides, was spotted with 5 μl of reaction mixture, dried, and developed with chloroform. The product, III, was observed as a yellow spot under white light (R_f 0.75), and both III and II (R_f 0.50) were observed as dark spots under long wavelength UV. Excess I and triethylamine and their hydrofluorides were at the solvent front.

[11] Celite 545, acid washed, Johns-Manville Corp.

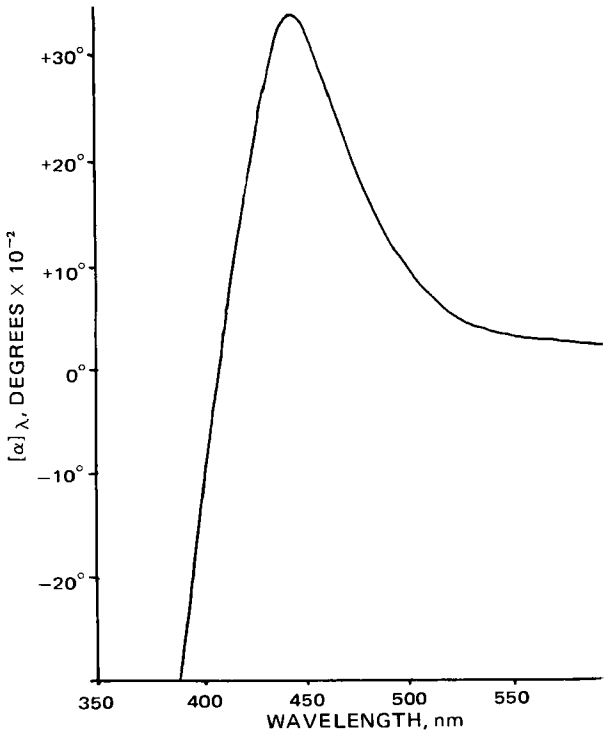

Figure 1—*Optical rotatory dispersion curve of III in methanol. Specific rotations are approximate, estimated from the known value at 546 nm.*

Reagents—The following were used: diatomaceous earth[11], acid-washed; 2% II in tetrahydrofuran; 10% sodium carbonate solution; 10% sodium citrate solution; diluted hydrochloric acid (1:3); water-saturated chloroform; dimethyl sulfoxide; and methanol.

Standard Solution—Dissolve sufficient USP dextroamphetamine sulfate reference standard, accurately weighed, in water to prepare a solution containing, in each 2 ml, an amount equivalent to the content of the tablet under analysis.

Procedure—Prepare separate columns for sample, standard, and blank. Thoroughly mix 3 g of diatomaceous earth and 1 ml of 10% sodium carbonate solution and transfer to chromatographic tubes, each of which has a wad of glass wool[12] in the base for support. Pack each column to a uniform mass with the tamping rod and position each column to elute into a 250-ml erlenmeyer flask.

Place single tablets or weighed amounts of composite equivalent to one tablet in individual 150-ml beakers. Add 2 ml of water to each beaker and to a separate beaker to serve as a blank. To another beaker, add 2.0 ml of standard solution. Gently agitate until the tablets completely disintegrate; then add 1 ml of dimethyl sulfoxide to each beaker. Mix by gentle agitation and add 5 ml of 2% II in tetrahydrofuran, followed by 1 ml of 10% sodium citrate solution. Let stand for 20 min with occasional gentle agitation, then add 5 g of diatomaceous earth to each beaker, and mix thoroughly. Add 50 ml of water-saturated chloroform, suspend the diatomaceous earth by stirring, and transfer to the column with the aid of 10 ml of chloroform, collecting the eluate in the 250-ml erlenmeyer flask. Add 1 g of diatomaceous earth and a few drops of water to the beaker and scrub the beaker, mixing the diatomaceous earth until it is uniform in texture and color.

After the column has drained, pack with the tamping rod, transfer the "dry wash" from the beaker, tamp, and top the column with a wad of glass wool. Elute the column with two 50-ml portions of water-saturated chloroform, collecting the combined eluates in the 250-ml flask. Evaporate the chloroform on a steam bath under a stream of air until only a viscous yellow liquid remains. Then dissolve the residue in 2 ml of methanol and, with the aid of a long-tip disposable pipet, transfer the solution to a 10-ml volumetric flask. Repeat with successive 2-ml portions of methanol, washing down the walls of the flask to effect quantitative transfer, and dilute to volume with methanol.

[12] Pyrex Filtering Fibre, Corning Glass Catalog No. 3959.

Table III—Standard Recoveries of I and Enantiomeric Purity of I

	Apparent[a] $[\alpha]_{546}$	Recovery[b], %	Enantiomeric Purity[c], %
	+788°	99.2	99.9
	+794°	97.5	100.3
	+792°[d]	99.7	100.2
	+779°[d]	98.1	99.4
	+786°[e]	100.5	99.8
	+790°[e]	99.7	100.0
	+794°	103.6	100.3
	+790°	102.5	100.0
	+792°	99.2	100.2
Average	+789°	100.0	100.0
SD	±5°	±1.96	±0.29
Coefficient of variation	±0.597	±1.96	±0.29

[a] See footnote 2 in text. [b] Percent of average value of absorptivity. [c] Average value of $[\alpha]_{546}$ was used as 100% reference. [d] One hundred milligrams of starch was added to an aliquot of the standard solution. [e] Three hundred milligrams of starch was added to an aliquot of the standard solution.

Transfer to a 1-dm cell and measure the rotation at 546 nm. Transfer 3.0 ml of the solution to the 100-ml volumetric flask containing 10 ml of diluted hydrochloric acid and adjust to volume with methanol. Measure the absorption of this solution in 1-cm cells at 430 nm *versus* the blank treated in the same manner. Similarly, measure the rotation at 546 nm and absorbance at 430 nm of the procedural standard.

From the absorbance of the sample and standard at 430 nm, calculate the concentration, c, of amphetamine sulfate in grams per 100 ml in the sample taken. Use this value in the calculation of specific rotation. From the absorbance of the sample and standard and the exact weight of the standard, calculate the apparent specific rotation, $[\alpha]_{546}$, of the standard and samples from:

$$[\alpha]_{546} = \frac{100\alpha}{lc} \qquad \text{(Eq. 1)}$$

where c is the concentration, in grams per 100 ml, of amphetamine sulfate calculated for the samples (or taken for the standard); α is the measured rotation in degrees; and l is the length of the polarimeter cell in decimeters (1 dm in this case).

Calculate the optical purity from the apparent specific rotations and:

$$\text{optical purity} = \frac{[\alpha_u]_{546}}{[\alpha_s]_{546}} \times 100 \qquad \text{(Eq. 2)}$$

where u and s refer to the sample and standard, respectively. The enantiomeric purity is calculated from:

$$\text{enantiomeric purity} = \frac{(\text{optical purity})}{2} + 50 \qquad \text{(Eq. 3)}$$

RESULTS AND DISCUSSION

The product of the reaction, III, was characterized by its NMR spectrum; the data given in Table I are consistent with the assigned structure. The optical rotatory dispersion curve shown in Fig. 1 has a large maximum at about 440 nm. The rotation is not measured at this wavelength, because the ratio of molar absorptivity to molar rotation of III is large at 440 nm and a solution sufficiently concentrated to give a measurable rotation is almost opaque even in a 0.01-dm cell. Because of instrumental limitations, rotations were measured at 546 nm, rather than the preferable wavelength at about 500 nm, where the apparent specific rotation is about 200% greater. The automatic polarimeter uses discharge lamps as its light source, and the intense mercury emission line nearest 440 nm at which the absorption of III will not interfere is at 546 nm.

The rotation of the reaction mixture showed a linear relationship to enantiomeric composition from 0 to 100% optical purity. The data for samples containing 40 to 100% of I (the balance was

Table IV—Enantiomeric Purity and Content of I in Commercial Tablets[a]

Milligrams per Tablet Found	Percent of Declared	$[\alpha]_{546}$[b]	Enantiomeric Purity, %
4.65	92.9	+656°	92.4
4.59	91.9	+662°	92.8
4.65	92.9	+677°	93.8
4.44	88.9	+674°	93.5
Average	91.6		93.1
SD	±1.89		±0.63
Coefficient of variation	±2.07		±0.68

[a] Content and enantiomeric purity were determined on the same sample as described in text. [b] The $[\alpha]_{546}$ of the standard was +773°.

levoamphetamine sulfate[13]) are given in Table II. The exact specific rotation of III was not determined and the apparent specific rotation, based on weight of I, varied slightly with reaction conditions. The problem of the variation of the apparent specific rotation was resolved by the use of a procedural standard run concomitantly with the samples.

The reaction between I and II takes place readily under a variety of conditions in a variety of solvents, particularly alcohols. The reaction conditions described were selected to provide for the facile separation of dyes and other tablet excipients that would interfere with the spectrophotometric measurement. Dimethyl sulfoxide was used to promote solubilization (14) because results were 2–5% low on tablet composites without it. The columns were wet-packed because tetrahydrofuran stripped the trap layer during elution when the diatomaceous earth–reaction mixture was packed on the column directly.

The results of the assay of standard solutions with 300, 100, and 0 mg of starch added are shown in Table III. Values of 100.0 ± 0.29% (*SD*) for enantiomeric purity and 100.0 ± 1.96% for percent amphetamine sulfate were obtained. The results with commercial tablet samples, 93.1 ± 0.63% for enantiomeric purity and 91.6 ± 1.87% for amphetamine sulfate content (Table IV), are in accord with a value of 93.5 ± 1.58% for amphetamine sulfate content obtained by an independent column chromatographic–spectrophotometric assay[14]. In every case, there was a distinct improvement in the precision of the enantiomeric purity calculated.

The marked improvement of the standard deviation for enantiomeric purity over that of amphetamine content was due in part to the method of calculation, but half of the improvement was real. The reason for the improvement is that the optical rotation and absorptivity were determined on the same sample in each case and were then used to calculate specific rotation. This method seems to eliminate a random, although unidentified, error which affects both optical rotation and amphetamine content. The improvement in precision of enantiomeric purity *vis-à-vis* specific rotation is only apparent, the result of the calculation.

[13] Levoamphetamine sulfate, K & K Laboratories ($[\alpha]_D$ − 21.0°, c = 10 in water). Free base was isolated, its (−)-tartrate was recrystallized three times from alcohol, and the recovered base was converted to the sulfate by an unpublished method of L. H. Welsh to give $[\alpha]_D$ − 23.4°, c = 10 in water.

[14] The assay used is an unpublished one, developed and validated by T. D. Doyle of this laboratory.

REFERENCES

(1) "The United States Pharmacopeia," 19th rev., Mack Publishing Co., Easton, Pa., 1975.

(2) J. H. Clark, *J. Ass. Offic. Anal. Chem.*, **56**, 1065(1973).

(3) J. A. Heagy, *Anal. Chem.*, **42**, 1459(1970).

(4) W. H. Pirkle, S. D. Beare, and T. G. Burlingame, *J. Org. Chem.*, **34**, 470(1969).

(5) J. A. Dale, D. L. Dull, and H. S. Mosher, *ibid.*, **34**, 2543(1969).

(6) G. M. Whiteside and D. W. Lewis, *J. Amer. Chem. Soc.*, **92**, 6979(1970).

(7) E. Gordis, *Biochem. Pharmacol.*, **15**, 2124(1966).

(8) C. E. Wells, *J. Ass. Offic. Anal. Chem.*, **53**, 113(1970).

(9) *Ibid.*, **55**, 146(1972).

(10) A. Romano, *J. Ass. Offic. Anal. Chem.*, **55**, 252(1972).

(11) F. Sanger, *Biochem. J.*, **39**, 507(1945), *et seq.*

(12) P. A. Lehmann, *Anal. Chim. Acta*, **54**, 321(1971).

(13) F. C. McIntire, L. M. Clements, and M. Sproull, *Anal. Chem.*, **25**, 1757(1953).

(14) J. Levine and T. D. Doyle, *J. Pharm. Sci.*, **56**, 619(1967).

ACKNOWLEDGMENTS AND ADDRESSES

Received February 3, 1975, from the *Division of Drug Chemistry, Food and Drug Administration, U.S. Department of Health, Education, and Welfare, Washington, DC 20204*

Accepted for publication April 28, 1975.

Presented at the 17th National Meeting of the APhA Academy of Pharmaceutical Sciences, New Orleans, November 10–14, 1974, under the title "Single Tablet Optical Purity Assay of Amphetamine by Rotation Enhancement."

Pharmacological Assessment of 3-*tert*-Butylsydnone

W. H. BULGER, P. R. WELLS *, and E. B. ROCHE ˣ

Abstract □ The pharmacological effects of the mesoionic derivative, 3-*tert*-butylsydnone, were investigated. Administration to rats caused clonic convulsions. The CD_{50} of 3-*tert*-butylsydnone was 0.471 ± 0.033 mmole/kg. Trimethadione, but not phenytoin sodium or proadifen hydrochloride, protected the rat from the effects of 3-*tert*-butylsydnone. After administration of this compound, pentobarbital sodium sleeping time was reduced in the rat, but blood pressure and ECG were unchanged in the dog. Pretreatment of the mouse with 3-*tert*-butylsydnone did not influence the LD_{50} of epinephrine hydrochloride. The action of methacholine chloride in the rat was not blocked, and the pupil of the rabbit eye was unaffected. Tests for analgesic and oxytocic activity were negative. Chronic administration of a small dose to the rat for 70 days had no effect on blood glucose, blood urea nitrogen, hemoglobin, or microhematocrit values.

Keyphrases □ 3-*tert*-Butylsydnone—pharmacological and toxicological evaluation □ Sydnones—pharmacological and toxicological evaluation of 3-*tert*-butylsydnone □ Pharmacology—screening of 3-*tert*-butylsydnone

The medicinal chemistry and pharmacology of mesoionic compounds, including the sydnones, have been reviewed (1). Mesoionic compounds generally consist of a five- or six-atom heterocyclic aromatic ring system. The ring has a partial positive charge, which is balanced by a corresponding negative charge on an exocyclic atom or group (2, 3). The sydnones are of interest to the pharmacologist because of their wide spectrum of biological activity, and their unique physical and chemical properties make the compounds potential tools in drug receptor studies. Other than the fact that 3-*tert*-butylsydnone (I) causes convulsions in the mouse, little is known about its actions (4). This study was undertaken to gain additional pharmacological data concerning I.

EXPERIMENTAL[1]

General Data and Criteria—All drugs and 3-*tert*-butylsydnone (I) were administered by the intraperitoneal route, maintaining a constant injection volume if possible. Suspensions of I were made in 0.5% (w/v) acacia. All control animals received equivalent volumes of the suspending agent.

Sprague–Dawley rats (175–200 g), New Zealand white rabbits (3.2–3.8 kg), Swiss Colony mice (16–26 g), and mongrel dogs (10–10.5 kg) were employed (all females). Animals were maintained on commercial laboratory feed[2] and water *ad libitum* but were fasted 12 hr before experimentation. Rats and mice were randomized according to weight.

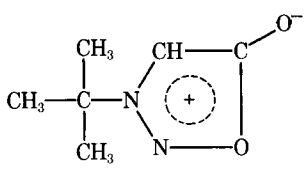

I

[1] An initial supply of I was generously provided by Dr. L. B. Kier, Massachusetts College of Pharmacy. Supplemental amounts were synthesized in this laboratory.

[2] Purina laboratory chows.

Table I—Effect of Pretreatment with Trimethadione, Phenytoin Sodium, and Proadifen Hydrochloride on 3-*tert*-Butylsydnone-Induced Convulsions and Death in the Rat[a]

Pretreatment	Protected from Convulsions	Deaths
Control (none)	0	4
Trimethadione (2.794 mmoles/kg)	8[b]	0
Phenytoin (0.091 mmole/kg)	0	3
Proadifen hydrochloride (0.077 mmole/kg)	0	7

[a] χ-Square test on each drug in comparison with untreated control. [b] $p < 0.005$ ($n = 8$); all other values are not significant.

Animals demonstrating clonic and/or tonic seizures of at least 5-sec duration within 1 hr of the administration of I or pentylenetetrazol were considered to have convulsed. However, animals demonstrating hyperflexia and tremors or fasciculations were not counted. The poor solubility of I precluded the use of isolated tissue techniques. Exceptions to this protocol are indicated.

CD_{50} Determination—The Reed–Muench (5) method was employed for the determination of the median convulsive dose (CD_{50}) of I for the rat and the median lethal dose (LD_{50}) of epinephrine hydrochloride[3] for the mouse. Five doses of I (0.211, 0.268, 0.345, 0.444, and 0.563 mmole/kg) were administered to 50 rats. Each dose was given to 10 rats. Two groups of 50 mice each were used to determine the effect of I upon the LD_{50} of epinephrine hydrochloride. The test group received 0.246 mmole/kg of I 15 min before epinephrine hydrochloride. The other group served as a control. Each group received five doses of epinephrine hydrochloride (0.009, 0.018, 0.032, 0.050, and 0.091 mmole/kg). The standard errors for the CD_{50} and LD_{50} values were computed by the method of Pizzi (6).

Convulsant Studies—Four groups of eight rats each were employed to determine the effects of two anticonvulsants and an inhibitor of drug metabolism on the convulsant action of I. One group served as a control, and each remaining group was pretreated with one of the following: phenytoin sodium[4], 0.091 mmole/kg; trimethadione[5], 2.794 mmoles/kg; and proadifen hydrochloride[6], 0.077 mmole/kg.

Sixty minutes after pretreatment with anticonvulsants or 30 min after proadifen hydrochloride, the animals were injected with 0.704 mmole/kg of I and the protection or lack of protection from convulsions and the frequency of death were observed. The results (Table I) were analyzed employing a 2×2 χ-square test.

Pentobarbital Sleeping Times—The effect of I on pentobarbital sodium[7] sleeping time in the rat was determined in the following manner. Two groups of 10 rats each were given 0.141 mmole/kg of pentobarbital sodium. Twenty minutes after the loss of the righting reflex, the animals in one group were injected with 0.704 mmole/kg of I. Control rats were sham injected. In place of I, pentylenetetrazol[8], 0.724 mmole/kg, was administered to a third group, and sleeping times were recorded. An animal was judged awake if righting of the anterior limbs could be demonstrated. The Student t test was employed to compare data from control and test animals (Table II).

Action on Anesthetized Dogs—The following procedure was

[3] Adrenalin hydrochloride, Parke-Davis.
[4] Dilantin sodium, Parke-Davis.
[5] Tridione, Abbott.
[6] SK&F 525-A.
[7] Nembutal sodium, Abbott.
[8] Sigma Chemical Co.

Table II—Effect of 3-*tert*-Butylsydnone on the Pentobarbital Sodium Sleeping Time of the Rat[a]

Treatment after Pentobarbital	Mean Sleeping Time, min	
	Test Group	Control
3-*tert*-Butylsydnone (0.704 mmole/kg)	89.40[b]	177.22
Pentylenetetrazol (0.724 mmole/kg)	34.56[b]	146.56

[a] Student *t* test in comparison with control sleeping times. [b] $p < 0.001$ ($n = 10$).

employed to determine the effect of I on the intact dog. One male and two female dogs were anesthetized with 0.141 mmole/kg of pentobarbital sodium, and the tracheas were cannulated. Blood pressure was measured directly off the left carotid artery. ECG recordings were from needle electrodes placed subcutaneously in the midthorax region. Transducers were connected to an amplifier and recorder[9].

Injections were *via* the femoral vein at least 5 min apart and were followed by a 0.9% saline wash. Acacia (0.5%) was injected as a control. One female dog received three doses of 0.070 and two doses of 0.176 mmole/kg of I; the other female received one dose of 0.007, three doses of 0.070, two doses of 0.176, three doses of 0.352, and two doses of 0.704 mmole/kg of I. After the final dose of I, epinephrine hydrochloride (0.046 nmole/kg), levarterenol bitartrate[8] (0.031 nmole/kg), and acetylcholine chloride[8] (0.006 nmole/kg) were injected.

Uterine Studies—Four rabbits, two multiparous and two pregnant, were employed to study the effect of I on the uterus. The animals were anesthetized with 19 mmoles of urethan[10]. A laparotomy was performed, and each uterine horn was attached to a separate myograph connected to a recorder. Throughout the experiment, the uterus and intestines were bathed with 37° isotonic saline. All injections were into the marginal ear vein with a minimum of 10 min between injections and were followed by a saline wash.

One multiparous animal received eight doses of I ranging between 0.070 and 0.352 mmole/kg. The other rabbit received 0.070, 0.141, and 0.211 mmole/kg of I. One pregnant rabbit was given two doses of 0.211 mmole/kg of I, and the second animal received two doses of 0.211 and one dose of 0.282 mmole/kg of I. Ergonovine maleate[11], 4.53×10^{-4} mmole/kg, was administered as a control to each rabbit.

Methacholine Studies—Forty rats were employed to study the effect of I on methacholine chloride[12]-induced salivation and bloody tears. The animals were divided equally into five groups and pretreated with I. Animals within each group received one of the following doses of I: 0.070, 0.092, 0.120, 0.162, and 0.211 mmole/kg 15 min prior to administration of 0.05 mmole/kg of methacholine chloride. Two additional groups were pretreated at 30 and 60 min with 0.162 mmole/kg of I.

Two control groups were employed: methacholine chloride alone and methacholine 15 min after 0.001 mmole/kg of atropine sulfate[10]. The presence or absence of bloody tears or salivation 15 min after methacholine was noted. This method was first described by Winbury *et al.* (7).

Ophthalmic Studies—Six rabbits were equally divided into two groups for the purpose of determining the effect of I on the eye. Into the left eyes of control animals, 0.2 ml of atropine sulfate (1.44×10^{-3} mmole/ml) was instilled. Into the left eyes of test rabbits, 0.2 ml of I (0.018 mmole/ml in a 1% aqueous solution of polysorbate 40)[13] was instilled. Right eyes served as controls.

The diameter of each pupil was measured at time 0, 30, 60, and 120 min and 24 hr after instillation. The pupil's response to light was noted. Constant room light was employed throughout. The procedure was repeated with polysorbate 40 alone (Table III). This method was previously described by Edwards *et al.* (8).

Analgesia—The analgesic screening technique of Marozzi and Malone (9), utilizing the tail flick response to a thermal stimulus from a conduction dolorimeter[14], was employed for the determination of possible analgesic activity. Tail flick responses were measured with an electrical timer equipped with a foot switch. For each rat, three successive reaction times in seconds were determined 1 min apart. The mean of the last two values was recorded.

After determination of control reaction times, the animals were treated with a test substance. Subsequent reaction times were determined at 15, 30, and 60 min after injection. A reaction time greater than 20 sec was considered equivalent to 100% analgesia. Each test group of five rats received one of the following doses of I: 0.070, 0.092, 0.120, 0.162, and 0.211 mmole/kg. There were two control groups; one was sham injected while the other received 0.013 mmole/kg of morphine sulfate[15] (Table IV).

Chronic Effects—To observe the chronic effects of I, 10 rats were injected daily with 0.035 mmole/kg of I for 70 days. Control animals were sham injected. Throughout the treatment period, cage droppings were observed for evidence of diarrhea and other changes. On the final day, 2 ml of blood was withdrawn under ether anesthesia from each animal by cardiac puncture. Blood glucose, blood urea nitrogen, and hemoglobin values were determined[16]. Microhematocrit values were also obtained. The mean values ±*SD* were determined (Table V).

Table III—Effect of 3-*tert*-Butylsydnone and Atropine Sulfate on the Mean Percent Change in the Diameter of the Pupil of the Rabbit Eye[a]

Time after Instillation into Eye	Mean Percent Change	
	0.2 ml 3-*tert*-Butylsydnone (0.018 mmole/ml)	0.2 ml Atropine Sulfate (1.44×10^{-3} mmole/ml)
0 min	0	0
30 min	0	+27
60 min	0	+26
24 hr	0	+9

[a] Percent change = $[(C_p - T_p)/C_p] \times 100$, where C_p = size of control pupil in millimeters, and T_p = size of test pupil in millimeters. Each value represents the mean percent change for three rabbits determined at a given time point.

RESULTS

The CD_{50} of I was 0.417 ± 0.033 mmole/kg. A dose of 0.704 mmole/kg was arbitrarily selected and always produced convulsions in the rat. Within 5 min after injection of I, asymmetric clonic convulsions were apparent in the animals and were indistinguishable from convulsions exhibited by rats poisoned with pentylenetetrazol. Subcutaneous and oral administration of I to rats also caused clonic convulsions.

The results shown in Table I demonstrate that trimethadione, but not phenytoin or proadifen hydrochloride, protected the rat from convulsions due to I. Although the frequency of death was greater in the proadifen hydrochloride group, the results were not significant.

Pentobarbital sodium sleeping time was decreased by convulsive doses of I without causing convulsions. Pentylenetetrazol reduced sleeping time in the control group (Table II).

Blood pressure and the ECG of the dog were unaffected by I. However, supplemental pentobarbital was required to maintain anesthesia after injection of greater than 0.176 mmole/kg of I. No convulsions were observed after the administration of I to the anesthetized dogs. Responses to epinephrine hydrochloride, levarterenol bitartrate, and acetylcholine chloride were all normal in the I-treated animals.

Pretreatment of the mouse with I did not influence the LD_{50} of epinephrine hydrochloride, which was determined to be 0.061 ±

[9] Narco Bio Systems.
[10] Merck Chemical Co.
[11] Ergotrate Maleate, Lilly.
[12] Mecholyl, Merck.
[13] Tween 40, Atlas Chemical Co.
[14] Metro Scientific Co.
[15] Mallinckrodt.
[16] Bio-Dynamics Unitest System.

Table IV—Effect of 3-*tert*-Butylsydnone and Morphine Sulfate on the Tail Flick Response to Thermal Stimulus in the Rat

Treatment	Mean Percent Analgesia[a]		
	15 min	30 min	60 min
3-*tert*-Butylsydnone (0.070, 0.092, 0.120, 0.162, and 0.211 nmole/kg)	0	0	0
Acacia, 0.5%	0	0	0
Morphine sulfate (0.013 mmole/kg)	35.81	52.86	21.35

[a] Percent analgesia = $[(Rx - C_0)/(20 - C_0)] \times 100$, where C_0 = control reaction time in seconds for each rat determined before treatment; Rx = reaction time in seconds for each rat determined 15, 30, or 60 min after treatment; and 20 = 20 sec (100% analgesia). Each value represents the mean percent analgesia of five rats.

0.013 nmole/kg in the control and 0.069 ± 0.010 nmole/kg in the test animals.

The administration of I had no effect on the rabbit uterus. Ergonovine maleate caused uterine contractions.

The production of bloody tears and salivation by methacholine chloride in the rat was not prevented by prior administration of I. However, atropine sulfate blocked the action of methacholine in the control animals.

As indicated in Table III, the instillation of a solution of I into the eye of the rabbit had no mydriatic or other observable effects. When treated with atropine sulfate, the eyes of control animals were dilated and unresponsive to light. Polysorbate 40 alone had no effect on the rabbit eye.

Morphine sulfate, but not I, produced analgesia in the rat (Table IV).

As indicated in Table V, blood glucose, blood urea nitrogen, hemoglobin, and microhematocrit values from control and I-treated rats were within the standard error of the mean of each other. There was no observable difference between the feces of the control and test animals in this study.

DISCUSSION

There is little question as to the convulsant action of 3-*tert*-butylsydnone (I). The physical similarities between the convulsions produced by I and pentylenetetrazol suggest that I may act primarily on the brain stem. Like pentylenetetrazol, convulsant doses of I decrease pentobarbital sleeping time without causing convulsions, indicating that hypnotic doses of pentobarbital sodium and convulsant doses of I antagonize the actions of each other. This finding is supported by the increase in the amount of pentobarbital sodium required to maintain anesthesia after injection of I into the dog.

The protection of the rat by trimethadione, but not by phenytoin, against seizures induced by I suggests that I could be employed in place of pentylenetetrazol as a screening agent for drugs effective against petit mal epilepsy. Furthermore, there may be some benefit to using activity against the convulsant effects of I as a criterion for hypnotic, antianxiety, or antiepileptic activity. However, the poor solubility of I may present a problem.

When compared on a millimolar basis, the doses of I are considerably larger than those of the control drugs. The highest dose of I was 623 times greater than the control dose of ergonovine maleate that caused uterine contractions. The concentration of I instilled into the eye of the rabbit was 12 times the control dose of atropine sulfate. In the methacholine experiment, the highest ineffective dose of I was 211 times in excess of the blocking dose of atropine sulfate. The analgesic dose of morphine sulfate was 16 times smaller than the maximum dose of I. In the experiments with the dog, the dosages of I were usually considerably greater than the doses of epinephrine, levarterenol, and acetylcholine administered as positive controls.

Table V—Blood Analysis of Rats Treated with 0.013 mmole/kg of 3-*tert*-Butylsydnone Daily for 70 Days[a]

	Test	Control
Blood glucose, mg %	115.5	104.45
SE	±5.69	±5.73
Blood urea nitrogen, mg %	12.22	12.05
SE	±0.67	±0.86
Hemoglobin, g %	16.98	16.27
SE	±0.29	±0.44
Microhematocrit, % rbc[b]	46.0	43.09
SE	±0.95	±1.63

[a] n = 10 for each group. [b] % rbc = percent red blood cells.

The comparatively high doses of I resulted in a predominance of negative results with respect to pharmacological activities other than convulsions. This finding suggests that these activities are absent or, if they do exist, that I is considerably weaker than the positive control drugs employed. Another possibility is that an additional pharmacological action of I is masked by the convulsions. However, the uneventful administration of doses of I greater than the CD_{50} (in rats) to anesthetized dogs appears to discount this argument.

It can be concluded from this study that the outstanding pharmacological activity of I was that of a convulsant and that future studies should be of a mechanistic neuropharmacological and neurochemical nature. Compound I is apparently devoid of other pharmacological–toxicological properties and associated problems. This information, coupled with the unique structural properties of sydnones, which lend themselves to the study of drug–receptor interactions, may be of value in determining the structural configuration requirement for convulsant activity and in mapping receptors to convulsant drugs.

REFERENCES

(1) L. B. Kier and E. B. Roche, *J. Pharm. Sci.*, **56**, 149(1967).

(2) W. Baker and W. D. Ollis, *Quart. Rev. (London)*, **15**, 11(1957).

(3) F. H. C. Steward, *Chem. Rev.*, **64**, 129(1964).

(4) L. B. Kier and D. Dhawan, *J. Pharm. Sci.*, **51**, 1058(1962).

(5) L. J. Reed and H. Muench, *Amer. J. Hyg.*, **27**, 493(1938).

(6) M. Pizzi, *Hum. Biol.*, **22**, 151(1950).

(7) M. M. Winbury, D. M. Schmalgemeier, and W. E. Hambourger, *J. Pharmacol. Exp. Ther.*, **95**, 53(1949).

(8) B. K. Edwards, A. A. Goldberg, and A. H. Wragg, *J. Pharm. Pharmacol.*, **12**, 179(1960).

(9) F. J. Marozzi and M. H. Malone, *J. Pharm. Sci.*, **57**, 989(1968).

ACKNOWLEDGMENTS AND ADDRESSES

Received May 21, 1974, from the *College of Pharmacy, University of Nebraska Medical Center, Lincoln, NB 68588*

Accepted for publication April 16, 1975.

Helpful suggestions by Dr. R. W. Piepho are gratefully acknowledged. W. H. Bulger acknowledges partial support from a University of Nebraska–NSF Summer Traineeship during a portion of this work.

* Present address: School of Pharmacy, Texas Southern University, Houston, TX 77004

ˣ To whom inquiries should be directed.

Determination of Nitroimidazoles in Biological Fluids by Differential Pulse Polarography

M. A. BROOKS ˣ, L. D'ARCONTE, and J. A. F. de SILVA

Abstract □ A sensitive differential pulse polarographic assay was developed for the determination of metronidazole, ornidazole, and 2-nitro-1*H*-imidazole-1-(3-methoxy-2-propanol) in plasma. The compounds are selectively extracted into ethyl acetate from a protein-free filtrate of plasma, buffered to pH 7.0 ± 0.2. The residue of the ethyl acetate extract is dissolved in 0.1 *N* NaOH and analyzed by differential pulse polarography for the reduction of the nitro group at approximately −0.600 v *versus* the saturated calomel electrode. The overall recovery from plasma was about 55 ± 3.0% (*SD*) for the three compounds investigated. A TLC step after the ethyl acetate extraction may also be included to ensure specificity. This step reduced the overall recovery to approximately 45%. The sensitivity limit of detection from plasma using a 2-ml sample is 0.1 μg/ml. The assay may also be employed for the analysis of urine. The urine is adjusted to pH 7.0 ± 0.2 and extracted with ethyl acetate, and the residue is analyzed as described for plasma. The assay was applied to the determination of ornidazole in blood and urine in the dog following 10 mg/kg po.

Keyphrases □ Nitroimidazoles—polarographic analysis, biological fluids □ Metronidazole—polarographic analysis, biological fluids □ Ornidazole—polarographic analysis, biological fluids □ Polarography—analysis, nitroimidazoles, biological fluids

The nitroimidazoles are antimicrobial agents and have been determined in biological fluids by various assay procedures.

These procedures include the spectrophotometric determinations of metronidazole (2-methyl-5-nitro-1*H*-imidazole-1-ethanol, I) (1), ornidazole [2-methyl-5-nitro-1*H*-imidazole-1-(3-chloro-2-propanol), II] (2), and 2-nitro-1*H*-imidazole-1-(3-methoxy-2-propanol) (III) (2); the polarographic determinations of I (3, 4), II (2), III (2), dimetridazole (1,2-dimethyl-5-nitroimidazole, IV) (5), and ipronidazole (2-isopropyl-1-methyl-5-nitroimidazole, V) (6); the spectrodensitometric determination of I and tinidazole [1-[2-(ethylsulfonyl)ethyl]-2-methyl-5-nitroimidazole, VI] (7); and the GC determination of I (8), II (2), and III (2).

The present work is a modification of the assay of de Silva *et al.* (2) and enables the polarographic assay to be performed on a routine basis with sensitivities as low as 0.1 μg/ml in biological fluids. The assay differs from the previous work (2) by the use of a protein-free filtrate of plasma, which yields extracts that can be assayed without further cleanup.

The assay was employed for the determination of I–III in plasma and urine; the compound of interest is selectively extracted into ethyl acetate either from a protein-free filtrate of plasma or from urine buffered to pH 7.0 ± 0.2. The residue of the ethyl acetate extract is dissolved in 0.1 *N* NaOH and analyzed by differential pulse polarography. A TLC separation step may be included to ensure specificity.

Blood levels of II and the urinary excretion of the unchanged drug were determined in the dog following a 10-mg/kg dose.

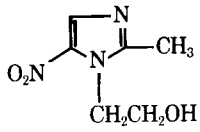

I

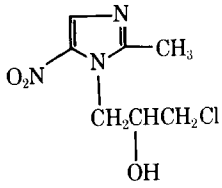

II

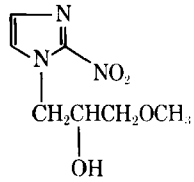

III

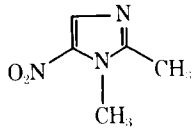

IV

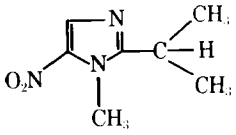

V

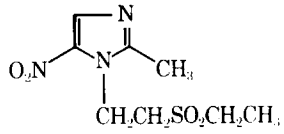

VI

EXPERIMENTAL

Conditions for Polarographic Analysis—A polarographic analyzer[1] equipped with a drop timer[2] was used in conjunction with a three-electrode polarographic cell comprised of a dropping mercury electrode, a saturated calomel electrode (SCE), and a platinum wire as the auxiliary electrode, as previously described (9). The drop time was 1.0 sec, and the drop mass was 2.32 mg/sec, where $(m^{2/3})(t^{1/6}) = 1.7525$. The current range was typically 0.5–5 μamp for a peak response of full-scale deflection, the scan range was 1.5 v, and the scan rate was 2 mv/sec.

The samples were scanned between −0.350 and −0.750 v *versus* the SCE, and the polarograms were recorded on an *X–Y* recorder[3].

[1] PAR model 174, Princeton Applied Research Corp., Princeton, N.J.
[2] PAR model 172A, Princeton Applied Research Corp., Princeton, N.J.
[3] Houston Omnigraph model 2200-3-3, Houston Instruments, Bellair, Tex.

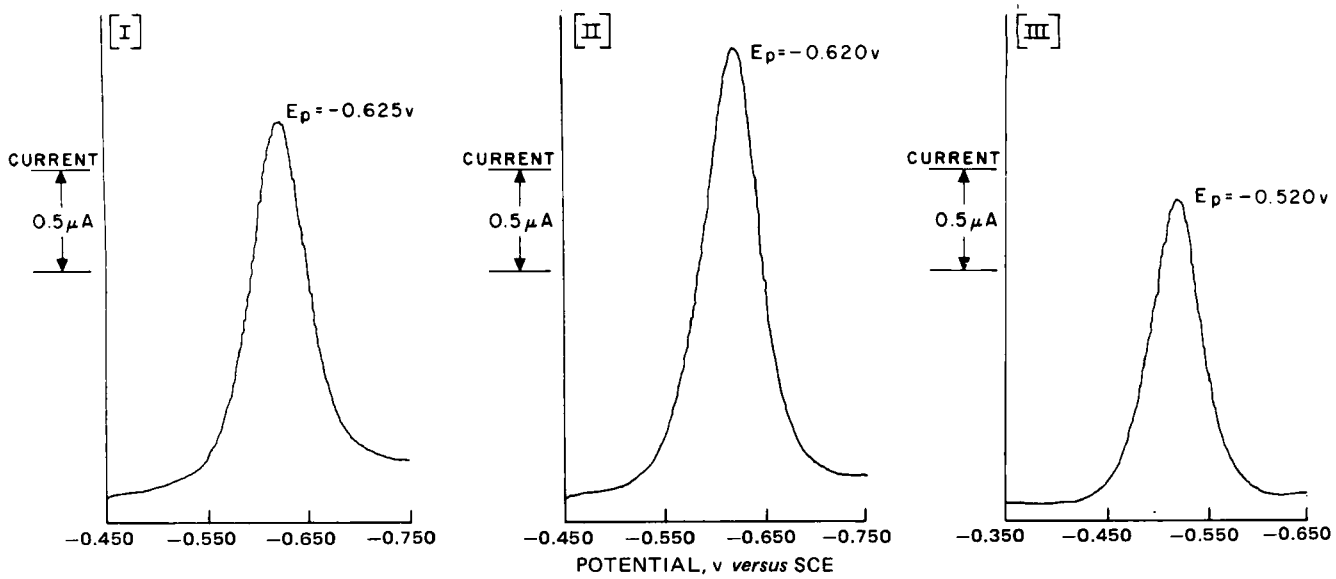

Figure 1—*Differential pulse polarograms of 5 μg of I–III in 3 ml of 0.1* N *NaOH.*

The peak potential, *Ep*, due to the reduction of the nitro group of I, II, and III occurred at −0.625, −0.620, and −0.520 v *versus* the SCE, respectively (Fig. 1).

Reagents—All reagents were analytical reagent grade and were used without further purification. All inorganic reagents were made up in double-distilled water. These included 10 *N* NaOH and 1.0 *M* phosphate buffer (pH 7), made by mixing 390 ml of 1 *M* KH_2PO_4 and 610 ml of 1 *M* K_2HPO_4. Ethyl acetate[4] (spectroquality), chloroform[5], methanol[6], ethanol[7], acetic acid[8], and hydrochloric acid[8] were the other reagents used.

Standard Solutions—Dissolve 10 mg of I, II, or III in 100 ml of absolute ethanol to give a stock solution containing 100 μg/ml. Dilute 1 ml of each stock solution to 10 ml with ethanol to give working solutions containing 10.0 μg/ml. Suitable aliquots of these solutions are added to blood as the internal standards.

Extraction from Plasma—Into a 50-ml glass-stoppered centrifuge tube, add 2 ml of the plasma sample, 6 ml of water, and 2 ml of concentrated hydrochloric acid. Along with the samples, process a 2-ml specimen of control plasma (taken from the same animal prior to medication) and separate 2-ml specimens of control plasma containing 0.5, 1.0, 2.0, 5.0, or 10.0 μg of the compound added as the internal standard. These latter specimens are prepared by evaporating 0.05, 0.1, 0.2, 0.5, and 1.0 ml of the working standards to dryness in a 65° water bath under a stream of nitrogen in 50-ml centrifuge tubes and then adding 2 ml of control plasma, 6 ml of water, and 2 ml of concentrated hydrochloric acid to the residue.

Stir the mixture well on a vortex mixer and place the solution in a water bath at 70° for about 15–20 min. Centrifuge for 10 min in a refrigerated centrifuge at 5° to obtain a clear supernate. If an emulsion is formed, repeat the centrifugation step.

Transfer an 8-ml aliquot into a clean 50-ml tube, and add 2 ml of 1.0 *M* phosphate buffer (pH 7) and sufficient 10 *N* NaOH dropwise to bring the pH of the solution to 7.0 ± 0.2. Extract twice with 10-ml portions of ethyl acetate and combine these extracts in a 15-ml tube by successive evaporation at 65° in a water bath.

TLC Separation—A TLC separation step may be included to ensure assay specificity. Dissolve the residue from the combined ethyl acetate extracts in 100 μl of ethyl acetate and transfer quantitatively onto a 20 × 20-cm silica gel chromatoplate[9]. Develop the plate in a vapor-saturated chamber, using chloroform–acetic acid–methanol (85:10:5), until the solvent front has ascended 15 cm. Examine the plate under shortwave UV light and identify the areas on the silica gel corresponding to I (R_f 0.34), II (R_f 0.55), or III (R_f 0.48) by the R_f values of 10 μg of authentic standards run alongside the sample extracts.

Scrape off these areas and transfer them to a 15-ml centrifuge tube. Add 5 ml of methanol, slurry the tubes on a vortex mixer for approximately 1 min, and centrifuge for 5 min at 2000 rpm to spin down the silica gel. Transfer the supernatant ethanol into another 15-ml conical centrifuge tube and evaporate to dryness in a water bath at 65° under a stream of nitrogen.

Polarographic Analysis—Dissolve the residue from the ethyl acetate extract or from the ethanol supernate in 3 ml of 0.1 *N* NaOH, deoxygenate the sample with nitrogen, and analyze by differential pulse polarography using the described parameters.

Extraction from Urine—Into a 50-ml glass-stoppered centrifuge tube, add 1 ml of urine, 4 ml of water, and 3 ml of 1.0 *M* phosphate buffer (pH 7.0). Adjust the pH to 7.0 ± 0.2 by the dropwise addition of 10 *N* NaOH and extract with ethyl acetate. Prepare internal standards and perform the assay exactly as described for plasma.

Table I—Blood and Urine Levels of Ornidazole (II) in the Dog following 10 mg/kg po[a]

	Plasma Level, μg of II/ml	
Sample Time	Without TLC Separation	With TLC Separation
10 min	11.3	10.5
20 min	10.2	10.3
30 min	9.3	9.7
60 min	10.1	9.2
1.5 hr	10.0	9.1
2.0 hr	8.3	8.5
3.0 hr	8.1	6.7
4.0 hr	7.1	6.2
6.0 hr	5.7	5.1
7.0 hr	3.4	3.5
11.25 hr	1.87	2.0
24 hr	0.55	0.33
30 hr	0.28	0.15
48 hr	0.10	n.m.

	Urine Levels (with TLC Separation)		
	II, μg/ml	Total, mg	Percent of Dose
0–24 hr	12.2	3.09	2.5
24–48 hr	1.35	0.135	0.11

[a] Dose: 122 mg of II in aqueous solution administered orally *via* gastric catheter.

[4] Catalog No. 5G 5212, Matheson, Coleman and Bell, Norwood, Ohio.
[5] Catalog No. C-298, Fisher Scientific Co., Fair Lawn, N.J.
[6] Catalog No. A-412, Fisher Scientific Co., Fair Lawn, N.J.
[7] Pharmaco, Publicker Industries Co., Linfield, Pa.
[8] J. T. Baker Co., Phillipsburg, N.J.
[9] Brinkmann F_{254} silica gel G chromatoplate.

Calculations—The current (microamperes) resulting from each peak and the overall recovery of each compound are determined as previously described (9), while the concentration of each component in the unknowns is determined from the respective internal standard curves.

RESULTS AND DISCUSSION

The polarographic activity of these compounds is attributed to the reduction of their nitro groups. The peaks are pH dependent in that they shift to more negative potential with decreased acidity. The polarographic behavior of the nitroimidazoles was reported previously (10–12).

The overall recovery of I, II, and III from plasma was 60.8 ± 5.4 (*SD*), 59.2 ± 2.6, and 52.7 ± 2.6%. The recovery of the compounds from the silica gel was approximately 90%; thus the overall recovery was approximately 10% lower when the TLC step was included. Extraction of the pure compounds from aqueous solutions under the same conditions as employed in the assay procedure yielded recoveries of 80–85%. Therefore, coprecipitation of the compounds in the formation of the protein-free filtrate from plasma is apparently the major factor resulting in recoveries that are as low as 50%.

The particular protein precipitation reagent and experimental conditions employed in the assay were selected because they yielded an extract for polarographic analysis that was free from interferences originating from the biological matrix. The overall recovery of the three compounds in the urine assay, including the TLC separation step, was approximately 70%. The sensitivity limit of detection was approximately 0.1 μg of I, II, or III/ml of plasma or urine when employing a 2-ml sample.

Specificity—The plasma assay that does not employ a TLC separation step is not specific for the parent drug and determines any extractable metabolite containing a nitro group. However, TLC inspection of the dog plasma extracts for II did not indicate the presence of any metabolite (Table I). This finding may be attributed to the poor extraction of these metabolites, which are probably very polar.

The TLC separation step can be employed effectively to resolve I–III from metabolites, thus establishing the required specificity of the plasma and urine assays. Chronic drug administration may reveal concentrations of metabolites that would require the TLC separation step.

Application to Biological Specimens—Plasma and urine levels were determined in a dog following oral administration of 10 mg/kg of II in aqueous solution *via* gastric catheter. Plasma levels of II employing the assay with and without the TLC separation are reported in Table I. The examination of the plasma extracts under shortwave UV light did not show the presence of any metabolites. The data from the two assays are in good agreement, indicating little interference from metabolites. The plasma levels are also in good agreement with those previously reported (2) for an identical oral dose of II.

The urinary excretion of II was also measured employing the assay with the TLC separation step to separate II from a metabolite noted upon TLC examination. Approximately 2.6% of the administered dose was excreted as unchanged II in the 0–48-hr collection period. This urinary level is lower than that previously reported (2) following an identical oral dose of II.

REFERENCES

(1) E. Lau, C. Yao, M. Lewis, and B. Senkowski, *J. Pharm. Sci.*, **58**, 55(1969).

(2) J. A. F. de Silva, N. Munno, and N. Strojny, *ibid.*, **59**, 201(1970).

(3) P. O. Kane, J. A. McFadzean, and S. Squires, *Brit. J. Vener. Dis.*, **37**, 276(1961).

(4) J. A. Taylor, J. R. Migliardi, and M. Schach von W. Henau, *Antimicrob. Ag. Chemother.*, **9**, 267(1969).

(5) P. C. Allen, *J. Ass. Offic. Anal. Chem.*, **55**, 743(1972).

(6) A. MacDonald, P. D. Duke, and G. Chen, presented at the 87th Annual Meeting of the Association of Official Analytical Chemists, Washington, D.C., Oct. 9–12, 1973.

(7) P. G. Welling and A. M. Monro, *Arzneim.-Forsch.*, **22**, 2128(1972).

(8) K. K. Midha, I. J. McGilveray, and J. K. Cooper, *J. Chromatogr.*, **87**, 491(1973).

(9) J. A. F. de Silva and M. R. Hackman, *Anal. Chem.*, **44**, 1145(1972).

(10) D. Dumanovic, J. Volke, and V. Vaygand, *J. Pharm. Pharmacol.*, **18**, 507(1966).

(11) D. Dumanovic and S. Perkucin, *Talanta*, **18**, 675(1971).

(12) D. Dumanovic and J. Ciric, *ibid.*, **20**, 525(1973).

ACKNOWLEDGMENTS AND ADDRESSES

Received February 24, 1975, from the *Department of Biochemistry and Drug Metabolism, Hoffmann-La Roche Inc., Nutley, NJ 07110*

Accepted for publication April 30, 1975.

[x] To whom inquiries should be directed.

Effect of Dioctyl Sodium Sulfosuccinate and Poloxamer 188 on Dissolution and Intestinal Absorption of Sulfadiazine and Sulfisoxazole in Rats

R. K. REDDY, SAID A. KHALIL *, and M. WAFIK GOUDA ˣ

Abstract □ The influence of two medicinal surfactants, poloxamer 188 and dioctyl sodium sulfosuccinate, on the dissolution of sulfisoxazole and sulfadiazine was investigated. A dramatic increase in the dissolution rate was observed at all surfactant concentrations. Drug absorption from the rat small intestine was also studied, and a significant but less dramatic increase was noted. Dissolution rate and absorption could be correlated only qualitatively. The two surfactants had no effect on the amount of sulfisoxazole excreted by the rat in 24 hr.

Keyphrases □ Absorption, intestinal—sulfadiazine and sulfisoxazole, effect of dioctyl sodium sulfosuccinate and poloxamer 188, rats □ Dissolution—sulfadiazine and sulfisoxazole, effect of dioctyl sodium sulfosuccinate and poloxamer 188 □ Sulfadiazine—dissolution and intestinal absorption, effect of dioctyl sodium sulfosuccinate and poloxamer 188, rats □ Sulfisoxazole—dissolution and intestinal absorption, effect of dioctyl sodium sulfosuccinate and poloxamer 188, rats □ Dioctyl sodium sulfosuccinate—effect on dissolution and intestinal absorption of sulfadiazine and sulfisoxazole, rats □ Poloxamer 188—effect on dissolution and intestinal absorption of sulfadiazine and sulfisoxazole, rats □ Surfactants—dioctyl sodium sulfosuccinate and poloxamer 188, effect on dissolution and intestinal absorption of sulfadiazine and sulfisoxazole, rats

Surfactants are common adjuvants in many pharmaceutical preparations. Certain surfactants also are used medicinally. Dioctyl sodium sulfosuccinate (I) and poloxamer 188 (II) are two such agents used internally as fecal softeners. The effect of these two surfactants on the absorption of readily absorbable and poorly absorbable drugs, from solution, in animals and humans was reported previously (1–4).

The influence of synthetic as well as physiological surfactants on the solubility of poorly soluble drugs has been widely investigated (5–9). The change in the dissolution rate of solid drugs also has been studied. Until recently, most dissolution studies were carried out in the presence of high concentrations [above the critical micelle concentration (CMC)] of surfactants. The increases in dissolution rates and solubilities were attributed to micellar effects (10–12).

Few investigators have studied the effect of premicellar concentrations of surfactants. Polyoxyethylene lauryl ether and lysolecithin, in premicellar concentrations, increased the dissolution rate of salicylic acid powder (13). The synthetic agent also increased the rate of dissolution of a commercial aspirin tablet dosage form at low concentrations and approached a stable value around its CMC. Low concentrations of polysorbate 80 increased the dissolution rate of phenacetin powder, and this finding was attributed to the lowering of interfacial tension between the drug and the dissolution medium (14). Increasing the concentration of the surfactant above 0.01% had little effect.

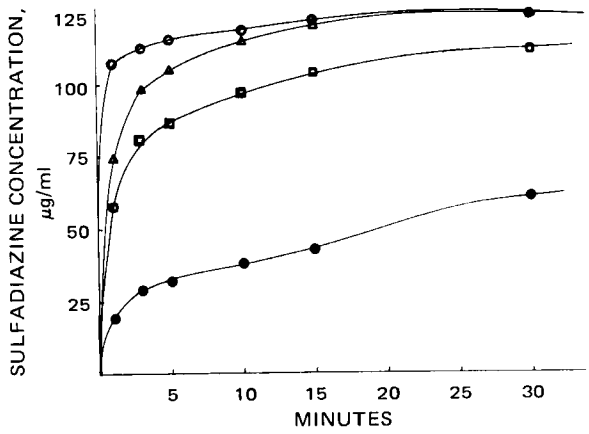

Figure 1—*Effect of poloxamer 188 on sulfadiazine dissolution. Key:* ●, *control;* □, *0.001%;* △, *0.01%, and* ○, *0.1%.*

Since both dioctyl sodium sulfosuccinate and poloxamer 188 are used in medicine primarily for their high wetting ability, the purpose of this study was to examine the influence of low concentrations of these two surfactants on the dissolution rate of drug powders. The effect of the same surfactant concentrations on absorption from the rat intestine was also examined. Sulfadiazine and sulfisoxazole were chosen as models because of their low solubility.

EXPERIMENTAL

Materials—Sulfadiazine[1] and sulfisoxazole[2] were pharmaceutical grade. Dioctyl sodium sulfosuccinate[3] and poloxamer 188[4] were used as received. All other chemicals were either reagent or analytical grade.

Absorption Studies from Rat *In Situ* Intestinal Loops—Male Sprague–Dawley[5] rats, 180–240 g, were fasted for 16–20 hr prior to the experiment, but water was allowed *ad libitum*. The procedure used was similar to the one reported by Nightingale *et al.* (15). Fifty milliliters of normal saline, warmed to 37°, was used to wash the intestinal loop, and a 10-min period was allowed for absorption of any residual solution prior to injection of the drug suspension. The abdominal cavity was closed with sutures, and the anesthetic was removed. At the end of 0.5 hr for sulfisoxazole and of 3 hr for sulfadiazine, the animal was sacrificed by placing it in an ether tank.

Analytical Procedure—After sacrifice of the animal, the intestinal loop was excised and homogenized with 10 ml of 0.1 *N* NaOH in a blender for 2 min. The blender was washed with water to yield 100 ml, and a fraction of the homogenate was centrifuged at 5000

[1] Matheson, Coleman and Bell, Norwood, Ohio.
[2] Supplied by Hoffmann-La Roche Inc., Nutley, N.J.
[3] Aerosol O. T. 100%, Sargent-Welch Scientific Co.
[4] Ethylene oxide–propylene oxide polymer of average molecular weight 8350, supplied as Pluronic F-68, by Wyandotte Chemicals Corp., Wyandotte, Mich.
[5] Horton Laboratories, Oakland, Calif.

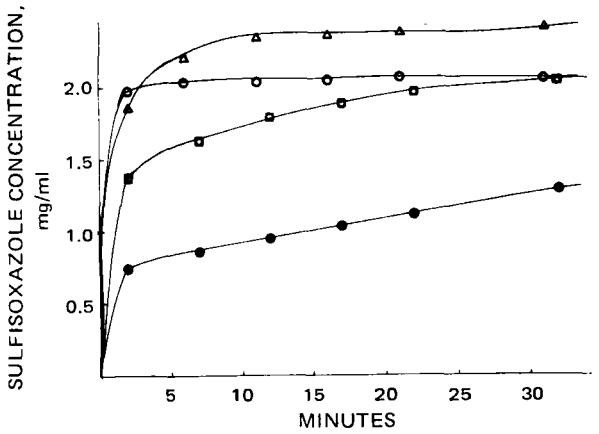

Figure 2—*Effect of poloxamer 188 on sulfisoxazole dissolution. Key: ●, control; □, 0.001%; △, 0.01%; and ○, 0.1%.*

rpm for 10 min. Ten milliliters of the supernate was pipetted into an equal volume of 30% trichloroacetic acid (w/v) and recentrifuged. The supernate was filtered, and an aliquot was assayed by the Bratton–Marshall method (16). All spectrophotometric[6] analyses were carried out at 533 nm for sulfisoxazole and at 530 nm for sulfadiazine. Tissue blanks were similarly analyzed, and no measurable absorbance was detected.

Absorption Studies in Intact Rats—The procedure used was similar to the one reported by Malik *et al.* (2). A 3.5-ml suspension of sulfisoxazole in water or a solution of the surfactants was administered by gastric intubation. Urine was collected for 24 hr, and the total sulfisoxazole was estimated by the Bratton–Marshall method.

Preparation of Drug Suspension—Drug suspensions for both *in situ* and intact rat studies were prepared in the same manner. The dosing volume was held constant at 3.5 ml. Eleven milligrams of the drug was weighed in a syringe, and the 3.5 ml of fluid was used in portions to inject or intubate the drug. The exact amount of drug administered was calculated by analyzing syringe washings and subtracting the amounts from the weighed value.

Drug Recovery—To see if the surfactants affected drug recovery, the following study was performed. After exposing the intestine and making a loop, the animal was sacrificed with ether and the drug suspension in water or surfactant solution was injected. After 0.5 hr (for sulfisoxazole) or 3 hr (for sulfadiazine), the loop was excised and analyzed for drug content. A mean recovery of 100% was obtained in the presence and absence of the surfactants.

Solubility Study—An excess of the drug was placed in 50-ml stoppered erlenmeyer flasks together with 25 ml of different concentrations of surfactant solutions in pH 6 phosphate buffer. The flasks were rotated in a constant-temperature water bath[7] at 37 ± 0.1° until equilibrium was attained (determined by repetitive sampling).

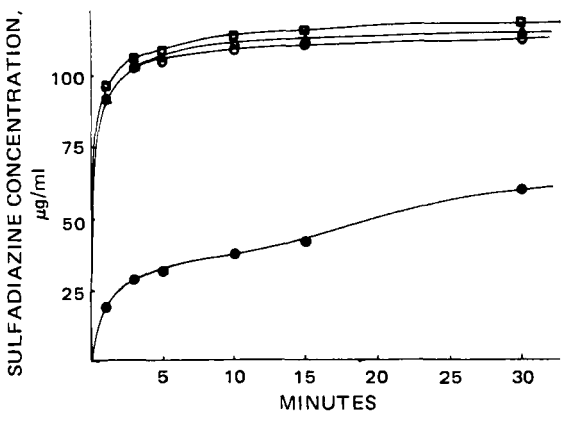

Figure 3—*Effect of dioctyl sodium sulfosuccinate on sulfadiazine dissolution. Key: ●, control; □, 0.001%; △, 0.01%; and ○, 0.1%.*

[6] Beckman ACTA CIII.
[7] Metabolyte water bath shaker, New Brunswick Scientific Co.

Table I—Effect of Poloxamer 188 and Dioctyl Sodium Sulfosuccinate on the Absorption of Sulfisoxazole from Rat Intestinal Loops[a]

Surfactant	Concentration, % w/v	Dose Absorbed, % ± *SD*
Control	—	45.3 ± 6.5
Poloxamer 188	0.01	56.1 ± 3.9
	0.10	57.3 ± 10.1
Dioctyl sodium sulfosuccinate	0.01	53.9 ± 9.4
	0.10	55.0 ± 8.4

[a] Values represent mean of six animals.

Dissolution Rate Studies—The dissolution rate was determined by the beaker method of Levy and Hayes (17) with slight modification. An 80–100-mesh powder was used. The dissolution medium consisted of 500 ml of 0.5 *M* phosphate buffer, pH 6, containing various concentrations of the surfactants. A 1-liter beaker was kept in a constant-temperature water bath at 37 ± 0.1°, and a three-blade, 4.4-cm (1.75-in.) diameter polyethylene stirrer[8] was centered and adjusted so that when the dissolution medium was added it would dip 3.5 cm into the liquid medium.

Sulfisoxazole (5 g) or sulfadiazine (2 g) was added to the beaker, and the fluid was poured along the walls of the beaker. Before the addition of the fluid, the stirrer was set to rotate at 60 rpm by means of a variable speed motor. At frequent time intervals, 2 ml of the dissolution medium was pipetted out and filtered through a membrane filter[9] (0.45-μm pore size) into a flask. The flask was kept at 37° to prevent possible crystallization of the drug. Two milliliters of fresh dissolution medium was immediately added to the beaker.

The amount of drug in solution at various time intervals was determined spectrophotometrically at 252 nm in a pH 7.5 phosphate buffer for sulfisoxazole and at 240 nm in 0.1 *N* HCl for sulfadiazine. Correction was made for the dilution effect (18). All dissolution rate experiments were performed at least in duplicate.

RESULTS AND DISCUSSION

Dissolution and Solubility Studies—Figures 1 and 2 illustrate the effect of poloxamer 188 on the dissolution behavior of sulfadiazine and sulfisoxazole, respectively. The presence of the surfactant in the dissolution medium significantly increased the dissolution rate of the two drugs. Figure 1 shows that increasing the concentration of poloxamer 188 from 0.001 to 0.1% increased the dissolution of the drug both initially and during the entire experiment. With sulfisoxazole (Fig. 2), an increase in the surfactant

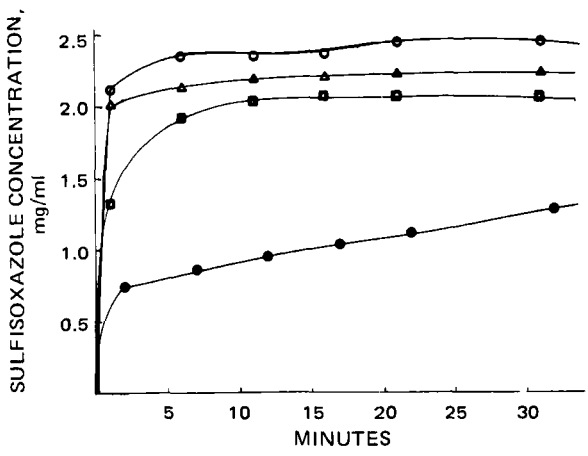

Figure 4—*Effect of dioctyl sodium sulfosuccinate on sulfisoxazole dissolution. Key: ●, control; □, 0.001%; △, 0.01%; and ○, 0.1%.*

[8] No. 6160, Nalge Co., Division of Sybron Corp.
[9] Millipore.

Table II—Effect of Poloxamer 188 and Dioctyl Sodium Sulfosuccinate on the Absorption of Sulfadiazine from Rat Intestinal Loops[a]

Surfactant	Concentration, % w/v	Dose Absorbed, % ± *SD*
Control	—	57.5 ± 5.0
Poloxamer 188	0.01	70.9 ± 4.3
	0.10	70.1 ± 3.2
Dioctyl sodium sulfosuccinate	0.01	66.9 ± 7.2
	0.10	71.3 ± 4.0

[a] Values represent mean of six animals.

concentration from 0.001 to 0.1% resulted in an initial increase in drug dissolution. However, there was less dissolution of sulfisoxazole in 0.1% poloxamer 188 than in 0.01% after 4 min. This slight decrease in dissolution at the higher surfactant concentration could be the result of particle aggregation or flocculation due to this specific concentration of the surfactant.

The dissolution behavior of sulfadiazine in the presence of dioctyl sodium sulfosuccinate is shown in Fig. 3. The dissolution rate of the drug increased in the presence of all surfactant concentrations studied. Increasing the concentration of the surfactant from 0.001 to 0.1% had no significant effect on the dissolution behavior of the drug.

Figure 4 shows the dissolution behavior of sulfisoxazole in the presence of various concentrations of dioctyl sodium sulfosuccinate. A concentration of 0.001% of the surfactant significantly increased the dissolution rate. Higher concentrations caused only a slight increase over that caused by 0.001%.

The solubility of sulfadiazine in the same pH 6 phosphate buffer, containing no surfactant, was 13.0 mg/100 ml. The solubility of the drug in 0.001, 0.01, and 0.1% of both surfactant solutions was 13.5 mg/100 ml. For sulfisoxazole, the solubility in the buffer solution and in all concentrations of the two surfactants was 242.4 mg/100 ml. The solubility studies indicate, in accordance with the reported CMC values of these two surfactants (19, 20), the lack of micellar solubilization. Therefore, the effect of these surfactants on the dissolution rate of the two sulfonamides studied is mainly caused by their ability to decrease the interfacial tension between the drug particles and the dissolution medium. Such lowering of interfacial tension is expected to increase the effective surface area of the drug exposed to the dissolution medium (14, 21, 22).

Absorption Studies—Results of the effect of both surfactants on the absorption of sulfisoxazole from *in situ* intestinal loops of rats are summarized in Table I. Except for 0.01% dioctyl sodium sulfosuccinate, the presence of the surfactants resulted in a small but significant ($p < 0.05$) increase in drug absorption. Table II shows the effect of these two surfactants on the absorption of sulfadiazine. A significant ($p < 0.001$; except for 0.01% of I, $p < 0.05$) increase in drug absorption was caused by all surfactant concentrations. A 10-fold increase in the surfactant concentration, from 0.01 to 0.1%, did not significantly increase drug absorption. This finding correlates well with what was observed in the dissolution studies (Figs. 1–4).

The observed effect of the two surfactants on the absorption of the two sulfonamides seems due primarily to the enhancement of the dissolution rate. Previous studies (2) indicated that poloxamer 188 does not have a direct effect on the permeability of the rat GI membrane. With dioctyl sodium sulfosuccinate, an additional effect on the intestinal membrane may also be operative (1–4). The extent of increase in drug absorption in the presence of the surfactants did not quantitatively correlate with the increase in dissolution rate. This finding could be due to the obvious difference in the intensity of agitation. In addition, the control experiments in the dissolution studies did not contain any surfactant whereas the controls in the absorption studies could have had residual bile and mucin in the intestinal loop. These physiological materials would probably lower the surface tension; therefore, the effect of the surfactants could be in addition to the effect of such materials.

Table III—Effect of Poloxamer 188 on the Total Urinary Excretion of Sulfisoxazole after Oral Administration to Rats[a]

Concentration, % w/v	Dose Absorbed, % ± *SD*
Control	76.7 ± 3.9
0.01	80.0 ± 6.0
Control	78.3 ± 5.5
0.10	80.0 ± 6.0

[a] Values represent mean of six animals.

Table IV—Effect of Dioctyl Sodium Sulfosuccinate on the Total Urinary Excretion of Sulfisoxazole after Oral Administration to Rats[a]

Concentration, % w/v	Dose Absorbed, % ± *SD*
Control	73.2 ± 9.0
0.01	77.9 ± 6.8
Control	75.5 ± 6.2
0.10	83.4 ± 10.4

[a] Values represent mean of six animals.

The amounts of sulfisoxazole excreted in 24 hr after oral administration of suspensions containing dioctyl sodium sulfosuccinate and poloxamer 188 are shown in Tables III and IV. The surfactants had no significant effect on the total drug absorbed in 24 hr. It seems that the effect of the surfactants on drug absorption is primarily on the initial rates—not on the total amount of drug absorbed. Fincher *et al.* (23) found that the same proportion of an oral dose of sulfisoxazole was absorbed when dogs were given suspensions of different particle sizes. Studies in humans indicated a difference in rate, but not in the extent, of urinary excretion of sulfisoxazole (24, 25). Solomon (26) found that although the dissolution rates of three commercial tablet dosage forms of sulfisoxazole were markedly different, the cumulative amount excreted in the urine at various times from 1 to 24 hr after administration did not differ significantly. In summary, the results of this study indicate that the dissolution rate of both sulfadiazine and sulfisoxazole increases dramatically in the presence of the two medicinal surfactants, poloxamer 188 and dioctyl sodium sulfosuccinate. A less dramatic but significant increase in the absorption rate of the two drugs was also observed.

REFERENCES

(1) M. W. Gouda, *Can. J. Pharm. Sci.*, **9**, 37(1974).

(2) S. N. Malik, D. H. Canaham, and M. W. Gouda, *J. Pharm. Sci.*, **64**, 987(1975).

(3) M. W. Gouda, S. N. Malik, and S. A. Khalil, *Can. J. Pharm. Sci.*, **10**, 24(1975).

(4) N. Khalafallah, M. W. Gouda, and S. A. Khalil, *J. Pharm. Sci.*, **64**, 991(1975).

(5) D. E. Wurster and J. A. Seitz, *J. Amer. Pharm. Ass., Sci. Ed.*, **49**, 335(1960).

(6) A. L. Thakkar and N. A. Hall, *J. Pharm. Sci.*, **58**, 68(1969).

(7) *Ibid.*, **57**, 1394(1968).

(8) T. R. Bates, S. Lin, and M. Gibaldi, *J. Pharm. Sci.*, **56**, 1492(1967).

(9) M. P. Short, P. Sharkey, and C. T. Rhodes, *ibid.*, **61**, 1732(1972).

(10) M. Gibaldi, S. Feldman, R. Wynn, and N. D. Weiner, *ibid.*, **57**, 787(1968).

(11) T. R. Bates, M. Gibaldi, and J. L. Kanig, *Nature*, **210**, 1331(1966).

(12) T. R. Bates, M. Gibaldi, and J. L. Kanig, *J. Pharm. Sci.*, **55**, 191(1966).

(13) H. Weintraub and M. Gibaldi, *ibid.*, **58**, 1368(1969).

(14) P. Finholt and S. Solvang, *ibid.*, **57**, 1322(1968).

(15) C. H. Nightingale, J. E. Axelson, and M. Gibaldi, *ibid.*, **60**, 145(1971).

(16) C. A. Bratton and E. K. Marshall, Jr., *J. Biol. Chem.*, **128**, 537(1939).

(17) G. Levy and B. A. Hayes, *N. Engl. J. Med.*, **262**, 1053(1960).

(18) D. E. Wurster and P. W. Taylor, *J. Pharm. Sci.*, **54**, 670(1965).

(19) E. F. Williams, N. T. Woodberry, and J. D. Dixon, *J. Colloid Sci.*, **12**, 452(1957).

(20) W. Saski and S. A. Shah, *J. Pharm. Sci.*, **54,** 17(1965).
(21) S. Lin, J. Menig, and L. Lachman, *ibid.*, **57,** 2143 (1968).
(22) G. Levy and R. H. Gumtow, *ibid.*, **52,** 1139(1963).
(23) J. H. Fincher, J. G. Adams, and H. M. Beal, *ibid.*, **54,** 704(1965).
(24) C. M. Martin, M. Rubin, W. E. O'Malley, V. F. Garagusi, and C. E. McCauley, *Pharmacologist,* **10,** 167(1968).
(25) *J. Amer. Med. Ass.*, **205,** 23, 24, 30(1968).
(26) H. Solomon, *Drug Inform. Bull.*, **Jan./June 1969,** 3, 75.

ACKNOWLEDGMENTS AND ADDRESSES

Received January 14, 1975, from the *School of Pharmacy, University of Montana, Missoula, MT 59801*

Accepted for publication April 29, 1975.

Supported in part by the U.S. National Science Foundation under the SFC, Grants GF 38851 and GF 39207.

* Faculty of Pharmacy, University of Alexandria, Alexandria, Egypt.

‡ To whom inquiries should be directed.

Polarographic Determination of Isosorbide Dinitrate

W. RICHARD TURNER * and ROBERT S. LENKIEWICZ ‡x

Abstract □ Isosorbide dinitrate and two isomeric isosorbide mononitrates are shown to be polarographically reducible in aqueous sodium perchlorate or potassium chloride solution. The current, measured at −1.6 v, *versus* the saturated calomel electrode is proportional to the concentration of organic nitrate in the 10–100-μg/ml range. Inorganic nitrate produces no interference. However, the mononitrate isomers produce an additive response to isosorbide dinitrate and cannot be determined individually. The polarographic method is applicable to single-tablet assay for content uniformity determination, with precision and accuracy comparable to automated colorimetric analysis. Comparison is made between replicate analyses obtained polarographically and by IR and automated colorimetric analysis for six different commercially available formulations. The polarographic determination is sensitive, specific for nitrate esters, precise, requires little sample preparation, and utilizes relatively inexpensive apparatus.

Keyphrases □ Isosorbide dinitrate—polarographic analysis, compared to IR and automated colorimetric methods, six commercial formulations □ Polarography—analysis, isosorbide dinitrate, compared to IR and automated colorimetric methods, six commercial formulations

Since the discovery that organic nitrate esters are reducible at the dropping mercury electrode, several polarographic methods have been developed for such pharmaceutically important compounds as nitroglycerin and pentaerythritol tetranitrate. Nitrate esters are reduced polarographically in a two-electron, pH-independent process to yield nitrite ion and the corresponding alcohol (1). The polarographic determination of nitroglycerin and other polynitrate esters, including pentaerythritol tetranitrate, was reported (2, 3).

Polarographic procedures have several advantages over other procedures for determining nitrate esters of pharmaceutical interest. The principal advantages are sensitivity, specificity, speed of analysis, and the moderate cost of the apparatus. Samples generally can be analyzed without prior separation or other sample preparation, since excipients usually do not interfere. This procedure results in a considerable saving in time, particularly when large numbers of single tablets must be analyzed to establish content uniformity.

For example, a procedure was developed for determining content uniformity for nitroglycerin sublingual tablets in which single tablets are introduced into the polarographic cell and are analyzed in the presence of tablet excipients such as lactose, mannitol, and corn starch (4). Lactose and mannitol had no effect on the polarographic reduction. Although corn starch produced a slight increase in the current–concentration ratio, this increase was negligible at concentrations normally found in sublingual tablets.

Table I—Current–Concentration Relationships for Isosorbide Dinitrate[a]

Concentration, μg/ml of Dinitrate	Current, μamp
10	0.92
20	1.66
30	2.46
40	3.44
50	4.26
60	4.94
70	5.80
80	6.82
90	7.53
100	8.33

[a] Micrograms per milliliter of dinitrate = 12.0 × μamp −0.41, and r = 0.9995.

There are several procedures for analyzing isosorbide dinitrate (I). A colorimetric procedure was described based on the hydrolysis of the nitrate ester and the determination of the nitrate ion produced using *vic-m*-xylenol (5). In a study of the dissolution rates of isosorbide dinitrate tablets, a UV absorption spectrophotometric method was utilized for assay

Table II—Current–Concentration Relationship for the Two Isosorbide Mononitrates

Micrograms per Milliliter of Mononitrate	Equivalent Concentration of Dinitrate, μg/ml	Current for *exo*-Mononitrate[a], μamp	Current for *endo*-Mononitrate[b], μamp
16.2	10	0.96	0.95
32.4	20	1.78	1.75
48.6	30	2.72	2.64
64.8	40	3.53	3.45
81.0	50	4.37	4.34

[a] Micrograms per milliliter of *exo*-mononitrate = 18.89 × μamp −1.88, and r = 0.9997. [b] Micrograms per milliliter of *endo*-mononitrate = 19.12 × μamp − 1.65, and r = 0.9999.

(20) W. Saski and S. A. Shah, *J. Pharm. Sci.*, **54,** 17(1965).
(21) S. Lin, J. Menig, and L. Lachman, *ibid.*, **57,** 2143 (1968).
(22) G. Levy and R. H. Gumtow, *ibid.*, **52,** 1139(1963).
(23) J. H. Fincher, J. G. Adams, and H. M. Beal, *ibid.*, **54,** 704(1965).
(24) C. M. Martin, M. Rubin, W. E. O'Malley, V. F. Garagusi, and C. E. McCauley, *Pharmacologist,* **10,** 167(1968).
(25) *J. Amer. Med. Ass.*, **205,** 23, 24, 30(1968).
(26) H. Solomon, *Drug Inform. Bull.*, **Jan./June 1969,** 3, 75.

ACKNOWLEDGMENTS AND ADDRESSES

Received January 14, 1975, from the *School of Pharmacy, University of Montana, Missoula, MT 59801*

Accepted for publication April 29, 1975.

Supported in part by the U.S. National Science Foundation under the SFC, Grants GF 38851 and GF 39207.

* Faculty of Pharmacy, University of Alexandria, Alexandria, Egypt.

‡ To whom inquiries should be directed.

Polarographic Determination of Isosorbide Dinitrate

W. RICHARD TURNER * and ROBERT S. LENKIEWICZ ‡x

Abstract □ Isosorbide dinitrate and two isomeric isosorbide mononitrates are shown to be polarographically reducible in aqueous sodium perchlorate or potassium chloride solution. The current, measured at −1.6 v, *versus* the saturated calomel electrode is proportional to the concentration of organic nitrate in the 10–100-μg/ml range. Inorganic nitrate produces no interference. However, the mononitrate isomers produce an additive response to isosorbide dinitrate and cannot be determined individually. The polarographic method is applicable to single-tablet assay for content uniformity determination, with precision and accuracy comparable to automated colorimetric analysis. Comparison is made between replicate analyses obtained polarographically and by IR and automated colorimetric analysis for six different commercially available formulations. The polarographic determination is sensitive, specific for nitrate esters, precise, requires little sample preparation, and utilizes relatively inexpensive apparatus.

Keyphrases □ Isosorbide dinitrate—polarographic analysis, compared to IR and automated colorimetric methods, six commercial formulations □ Polarography—analysis, isosorbide dinitrate, compared to IR and automated colorimetric methods, six commercial formulations

Since the discovery that organic nitrate esters are reducible at the dropping mercury electrode, several polarographic methods have been developed for such pharmaceutically important compounds as nitroglycerin and pentaerythritol tetranitrate. Nitrate esters are reduced polarographically in a two-electron, pH-independent process to yield nitrite ion and the corresponding alcohol (1). The polarographic determination of nitroglycerin and other polynitrate esters, including pentaerythritol tetranitrate, was reported (2, 3).

Polarographic procedures have several advantages over other procedures for determining nitrate esters of pharmaceutical interest. The principal advantages are sensitivity, specificity, speed of analysis, and the moderate cost of the apparatus. Samples generally can be analyzed without prior separation or other sample preparation, since excipients usually do not interfere. This procedure results in a considerable saving in time, particularly when large numbers of single tablets must be analyzed to establish content uniformity.

For example, a procedure was developed for determining content uniformity for nitroglycerin sublingual tablets in which single tablets are introduced into the polarographic cell and are analyzed in the presence of tablet excipients such as lactose, mannitol, and corn starch (4). Lactose and mannitol had no effect on the polarographic reduction. Although corn starch produced a slight increase in the current–concentration ratio, this increase was negligible at concentrations normally found in sublingual tablets.

Table I—Current–Concentration Relationships for Isosorbide Dinitrate[a]

Concentration, μg/ml of Dinitrate	Current, μamp
10	0.92
20	1.66
30	2.46
40	3.44
50	4.26
60	4.94
70	5.80
80	6.82
90	7.53
100	8.33

[a] Micrograms per milliliter of dinitrate = 12.0 × μamp −0.41, and r = 0.9995.

There are several procedures for analyzing isosorbide dinitrate (I). A colorimetric procedure was described based on the hydrolysis of the nitrate ester and the determination of the nitrate ion produced using *vic-m*-xylenol (5). In a study of the dissolution rates of isosorbide dinitrate tablets, a UV absorption spectrophotometric method was utilized for assay

Table II—Current–Concentration Relationship for the Two Isosorbide Mononitrates

Micrograms per Milliliter of Mononitrate	Equivalent Concentration of Dinitrate, μg/ml	Current for *exo*-Mononitrate[a], μamp	Current for *endo*-Mononitrate[b], μamp
16.2	10	0.96	0.95
32.4	20	1.78	1.75
48.6	30	2.72	2.64
64.8	40	3.53	3.45
81.0	50	4.37	4.34

[a] Micrograms per milliliter of *exo*-mononitrate = 18.89 × μamp −1.88, and r = 0.9997. [b] Micrograms per milliliter of *endo*-mononitrate = 19.12 × μamp − 1.65, and r = 0.9999.

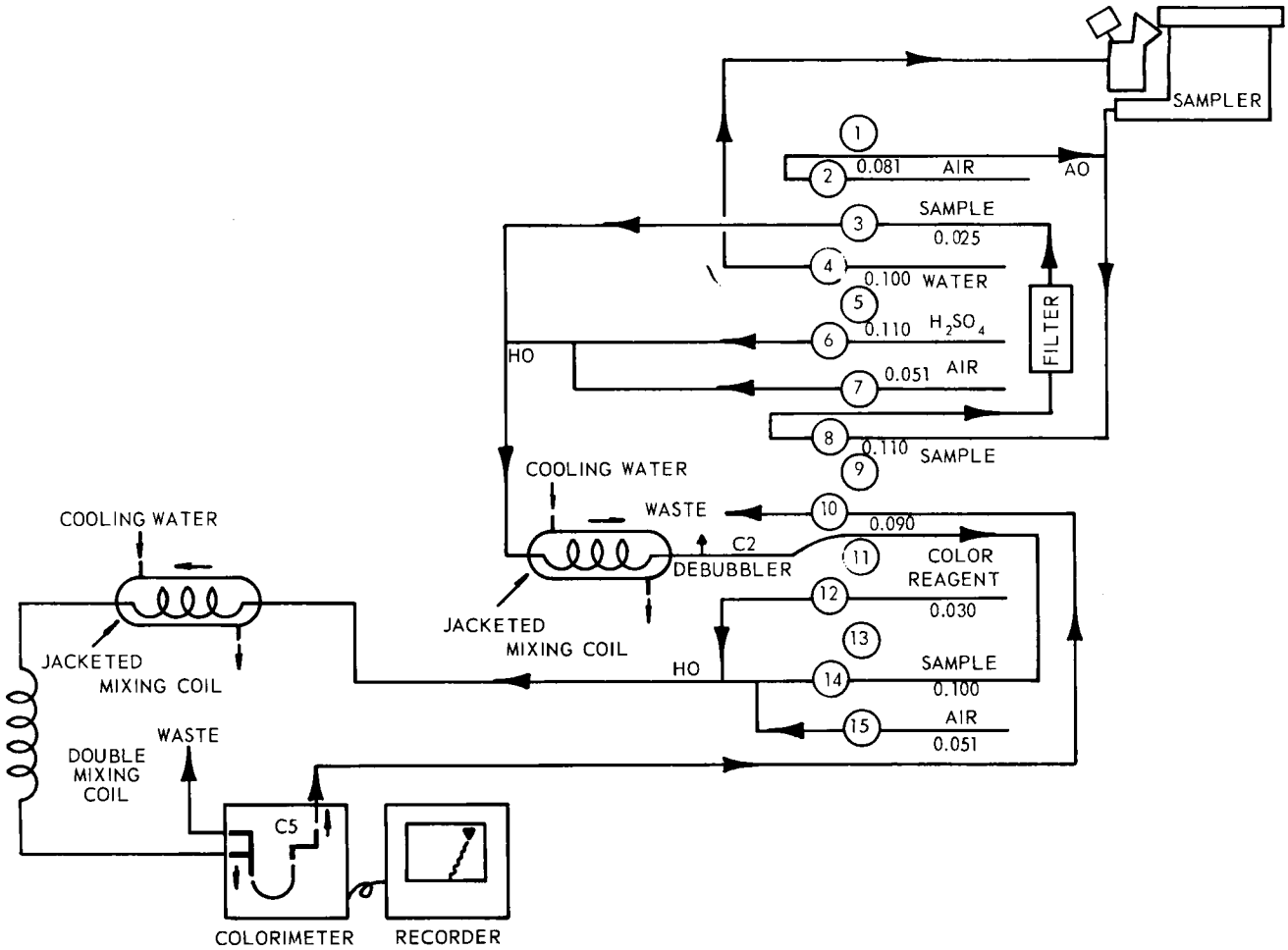

Figure 1—*Automated analyzer flow diagram for determining nitrate content of single tablets. The H_2SO_4 is 85% (v/v) sulfuric acid, and the color reagent is 4 g of* vic-m-*xylenol in 100 ml of acetic acid and 100 ml of sulfuric acid. Absorbance is measured at 498 nm with a 50-mm tubular flowcell. Tubing sizes and fittings are given.*

purposes (6). Excellent agreement was found between results obtained by IR analysis and colorimetric analysis for both synthetic mixtures and commercial 5- and 10-mg tablets (7). Several GLC procedures have been described for the analysis of nitrate esters (8–12) including isosorbide dinitrate. Recently, isosorbide dinitrate in tablets was analyzed using a polarographic procedure (13).

This article discusses the polarographic behavior of isosorbide dinitrate and the two isosorbide mononitrate esters. Isosorbide dinitrate can be determined polarographically in various dosage forms with comparable precision to that obtained by IR analysis and automated analysis methods, particularly in the single-tablet assays required for content uniformity.

EXPERIMENTAL

Polarographic Analysis—Analyses were performed using a polarograph[1] with jacketed cells maintained at 25 ± 0.1°. The supporting electrolyte consisted of 0.1 *M* $NaClO_4$[2], and 0.005% gelatin was used as a maximum suppressor. Sodium perchlorate was chosen for the initial polarographic studies because the wave for organic nitrates begins to form at around −0.1 v and by using perchlorate ion one can work at more positive potentials without interfering anodic waves. Dissolved oxygen was removed by vigorously bubbling nitrogen through the sample in the cell for approximately 5 min.

For bulk assays and single-tablet assays, potassium chloride was substituted for sodium perchlorate for reasons of convenience and economy. The whole tablet was dissolved (or dispersed) in approximately 100 ml of 0.1 *N* KCl using a blender, and the solution was diluted to 125 ml with the electrolyte solution. The current, measured at −1.6 v, *versus* the saturated calomel electrode (SCE) was proportional to the concentration of organic nitrate. The concentration was calculated from a calibration curve prepared using pure isosorbide dinitrate or by comparison with a single standard.

Automated Analysis—The flow diagram[3] for assaying single tablets is shown schematically in Fig. 1. The tablet was disintegrated in a solid sampler, with the water (70–80°) diluent delivered at a rate to give 0.05 mg/ml of organic nitrate. A water sample was required as a wash between standards and samples to reduce carryover. The aqueous suspension was then filtered, and the filtrate was reacted with 85% (v/v) sulfuric acid to hydrolyze the organic nitrate to inorganic nitrate.

Acid-resistant tubing was used for the delivery of sulfuric acid and the color reagent as well as for the sample stream after hydrolysis and color development. After about 16 hr of operation, the tubing had to be replaced. The inorganic nitrate was then reacted with *vic-m*-xylenol[4] reagent (4 g of *vic-m*-xylenol in 100 ml of acetic acid and 100 ml of sulfuric acid). After cooling and mixing, the yellow color was measured photometrically using a 498-nm filter.

IR Analysis—Because the IR analysis is not as sensitive as ei-

[1] Metrohm Polarecord E261, Brinkmann Instruments.
[2] Fisher Scientific Co., Pittsburgh, Pa.
[3] AutoAnalyzer, Technicon Instruments Corp.
[4] Eastman Organic Chemicals, Rochester, N.Y.

Table III—Analysis of Synthetic Mixtures of Isosorbide Dinitrate, the Two Mononitrates, and Potassium Nitrate by Polarographic Analyses

Isosorbide Dinitrate, mg	*exo*-Isosorbide Mononitrate, mg	*endo*-Isosorbide Mononitrate, mg	Potassium Nitrate, mg	Dinitrate Calculated, mg	Dinitrate Found, mg
10	—	—	8.57[a]	10	9.86
5	8.10[b]	—	—	10	10.1
5	—	8.10	—	10	10.2
—	8.10	8.10	—	10	10.4
5	8.10	8.10	4.28[b]	10	14.9

[a] Equivalent to 10 mg of dinitrate in nitrate content. [b] Equivalent to 5 mg of dinitrate in nitrate content.

Table IV—Comparison of Polarographic (POL) and IR Methods for Isosorbide Dinitrate Representative Portions of Powdered Tablets[a]

	2.5 mg Sublingual		5 mg Sublingual		5 mg Oral		10 mg Oral		10 mg Oral with Phenobarbital	
	POL	IR	POL	IR	POL	IR	POL	IR	POL	IR
	2.48	2.55	5.01	5.00	5.18	4.99	10.3	10.2	9.94	9.95
	2.57	2.53	4.87	4.83	5.01	5.08	10.3	10.3	10.1	9.90
	2.53	2.45	5.08	4.88	5.11	4.87	10.4	10.2	9.97	9.95
	2.51	2.51	4.93	4.95	5.08	4.91	10.2	10.2	10.1	10.1
	2.51	2.45	4.97	5.00	5.09	4.91	10.5	10.3	10.0	10.0
	2.46	2.46	4.93	4.97	5.11	4.99	10.2	10.4	9.95	9.90
	2.55	2.51	5.03	4.93	5.15	5.03	10.3	10.5	10.0	10.0
	2.51	2.51	5.00	4.82	5.03	5.00	10.3	10.3	10.1	9.95
	2.48	2.45	4.89	4.79	5.12	4.89	10.5	10.2	9.97	9.95
	2.51	2.47	5.01	4.93	5.08	4.99	10.3	10.4	9.95	10.1
Mean	2.51	2.49	4.97	4.91	5.10	4.97	10.3	10.3	10.0	9.98
SD	0.033	0.037	0.066	0.076	0.051	0.067	0.106	0.105	0.066	0.071
RSD, %	1.3	1.5	1.3	1.5	1.0	1.3	1.0	1.0	0.66	0.71

[a] Results expressed as milligrams per average tablet weight.

ther the polarographic or automated method, sufficient tablets to yield approximately 70 mg of isosorbide dinitrate were needed. The tablets were pulverized and extracted with chloroform. After filtering and concentrating, an IR spectrum[5] was run on the chloroform extract. The net absorbance at 1650 cm^{-1} is proportional to isosorbide dinitrate concentration and was compared with similarly prepared standards. Phenobarbital, if present, does not interfere with the analysis.

Standards—Isosorbide dinitrate[6], used for reference purposes and for the investigation of polarographic behavior, was purified by recrystallization from an aqueous ethanol solution. Its purity was established by elemental and TLC analyses.

Isosorbide mononitrates were prepared by the alkaline hydrolysis of the dinitrate. The two isomers were separated by either preparative liquid chromatography or countercurrent extraction and recrystallization from an ethanol–ethyl acetate solution. Isosorbide dinitrate and the 2- and 5-isosorbide mononitrates were well separated on silica gel G plates[7], using trichloroethylene–acetone (4:1), and were detected with diphenylamine–sulfuric acid spray reagent. This reagent produces an intense blue color with nitrates and other oxidizing substances.

The pharmaceutical dosage forms analyzed were actual production lots of commercially available formulations[6].

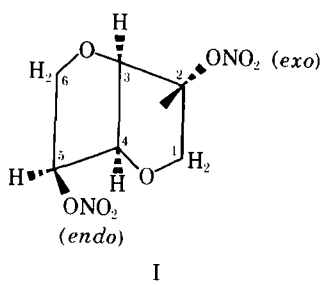

I

[5] Beckman IR-8 spectrophotometer.
[6] Stuart Pharmaceutical Division, ICI United States, Inc., Wilmington, Del.
[7] Analtech Inc., Newark, Del.

RESULTS AND DISCUSSION

As shown in Fig. 2, isosorbide dinitrate is reduced at the dropping mercury electrode, producing a rather broad polarogram with a half-wave potential of −0.45 v *versus* the SCE. Since isosorbide dinitrate contains two nonequivalent nitrate ester groups at the 2- (*exo*) and 5- (*endo*) positions, the broad shape of the wave is probably due to the overlap of two waves arising from the reduction of each of the two nonequivalent groups. The polarographic behavior of the 2- and 5-isosorbide mononitrate esters tends to confirm this theory since the former has a half-wave potential of −0.38 v and the latter has a half-wave potential of −0.46 v. It is consistent that the *exo*-isomer should be more easily reduced than the sterically hindered *endo*-isomer.

The current plateau in the region from −0.8 to −1.8 v provides a large potential range in which the current is independent of voltage and proportional to the concentration of isosorbide dinitrate. For analytical work, the current measurement was normally made at −1.6 v. The current–concentration relationship for isosorbide dinitrate in the range of 10–100 μg/ml is given in Table I. For comparison, similar data were obtained for the mononitrate esters, and one can see from Table II that the current values for the mononitrates correspond with those for equivalent amounts of the dinitrate ester. The equations given at the bottom of each table are calculated by the least-squares method. The correlation coeffi-

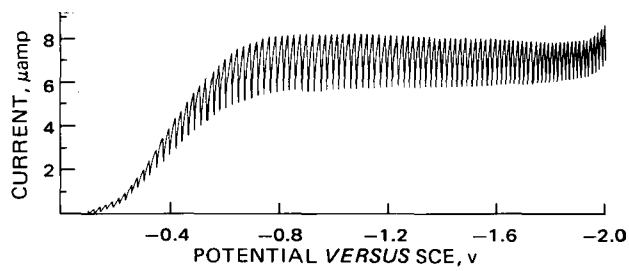

Figure 2—*Polarogram of 100 μg of isosorbide dinitrate/ml in 0.1 M $NaClO_4$ and 0.005% gelatin. The mononitrate esters produce polarograms similar in appearance.*

Table V—Comparison of Polarographic (POL) and Automated Analysis (AA) Methods for Isosorbide Dinitrate Content Uniformity Single-Tablet Assay[a]

	2.5 mg Sublingual		5.0 mg Chewable		5.0 mg Sublingual		5.0 mg Oral		10 mg Oral		10 mg Oral with Phenobarbital	
	POL	AA	POL	AA	POL	AA	POL	AA	POL	AA	POL	AA
	2.50	2.30	4.90	4.98	4.75	5.08	4.97	5.08	10.2	9.50	9.9	9.8
	2.51	2.30	4.96	4.85	4.83	4.84	5.18	4.74	10.4	9.71	10.5	9.6
	2.52	2.30	4.98	4.92	4.95	4.97	5.00	4.84	10.6	9.44	10.3	9.7
	2.56	2.25	4.92	4.85	5.14	4.62	4.86	5.00	10.3	9.71	11.1	9.3
	2.52	2.22	4.97	4.93	4.92	4.65	5.06	5.00	10.3	9.90	10.0	9.3
	2.46	2.25	5.12	4.88	4.87	4.80	4.90	5.08	10.0	10.1	10.0	8.9
	2.51	2.23	4.86	4.81	4.88	4.93	4.90	5.08	10.0	10.1	10.4	9.2
	2.62	2.25	4.87	4.79	5.14	4.90	5.05	5.13	10.0	10.2	10.2	8.8
	2.47	2.26	4.86	4.73	4.90	5.08	4.98	4.96	10.0	10.2	9.8	9.0
	2.47	2.27	4.92	4.78	4.90	4.81	5.08	5.10	9.8	10.1	10.2	8.8
Mean	2.51	2.26	4.94	4.85	4.93	4.87	5.00	5.00	10.2	9.90	10.2	9.2
SD	0.048	0.029	0.078	0.077	0.124	0.157	0.098	0.125	0.241	0.287	0.374	0.369
RSD, %	1.9	1.3	1.6	1.6	2.5	3.2	2.0	2.4	2.9	2.9	3.7	4.0

[a] Results expressed as milligrams per tablet.

cients in each case are better than 0.999, indicating a linear relationship between current and concentration.

Synthetic mixtures were prepared which included isosorbide dinitrate, the two isosorbide mononitrates, and potassium nitrate in various combinations and in equivalent amounts. The presence of inorganic nitrate in the form of potassium nitrate produced no interference. However, equivalent mixtures of the dinitrate and the two mononitrates yielded values proportional to the organic nitrate content. Although the mononitrates cannot be determined individually in the presence of the dinitrate, the total organic nitrate content, calculated as isosorbide dinitrate, can be determined (Table III).

Table IV gives 10 replicate analyses for each of five dosage forms of isosorbide dinitrate. Representative portions of powdered tablets were analyzed by both polarographic and IR methods. The agreement was excellent with respect to both accuracy and precision, with relative standard deviations in the range of 1.0–1.5%. The results are expressed as milligrams of isosorbide dinitrate per average tablet weight.

Table V shows a comparison of the polarographic analysis of single tablets compared with single-tablet assays using the automated analysis procedure. Ten individual tablets were assayed, representing actual production lots of six common dosage forms of isosorbide dinitrate: 2.5 mg sublingual, 5.0 mg sublingual, 5 mg chewable, 5 mg oral, 10 mg oral, and 10 mg oral with phenobarbital. The agreement between the polarographic method and the automated analysis method was generally good; however, the results appear not to be as precise as the previous results for the assay of representative portions of powdered tablets. This result is indicative of the tablet-to-tablet variations in isosorbide dinitrate content and is a measure of the content uniformity.

REFERENCES

(1) F. Kaufman, H. J. Cook, and S. M. Davis, *J. Amer. Chem. Soc.*, **74**, 4997(1952).

(2) G. C. Whitnack, J. M. Nielsen, and E. St. Clair Gantz, *ibid.*, **76**, 4711(1954).

(3) G. C. Whitnack, M. M. Mayfield, and E. St. Clair Gantz, *Anal. Chem.*, **27**, 899(1955).

(4) B. C. Flann, *J. Pharm. Sci.*, **58**, 122(1969).

(5) D. E. Reed, J. F. May, L. G. Hart, and D. H. McCurdy, *Arch. Int. Pharmacodyn. Ther.*, **191**, 318(1971).

(6) J. Tingstad, E. Gropper, L. Lachman, and E. Shami, *J. Pharm. Sci.*, **61**, 1985(1972).

(7) D. Woo, J. K. C. Yen, and P. Sofronas, *Anal. Chem.*, **45**, 2144(1973).

(8) D. A. Sherber, M. Marcus, and S. Kleinberg, *Biochem. Pharmacol.*, **19**, 607(1970).

(9) K. H. Gobbeler, *Pharm. Ztg.*, **27**, 961(1971).

(10) I. W. F. Davidson, F. J. DiCarlo, and E. I. Szabo, *J. Chromatogr.*, **57**, 345(1971).

(11) M. T. Rosseel and M. G. Bogaert, *ibid.*, **64**, 364(1972).

(12) M. T. Rosseel and M. G. Bogaert, *J. Pharm. Sci.*, **62**, 754(1973).

(13) A. B. Grigor'ev, L. T. Chistotinova, and M. K. Polievktov, *Khim. Farm. Zh.*, **7**, 50(1973).

ACKNOWLEDGMENTS AND ADDRESSES

Received November 22, 1974, from the *Chemical Research Department and the ‡Stuart Pharmaceutical Division, ICI United States Inc., Wilmington, DE 19897

Accepted for publication April 30, 1975.

Presented at the Pharmaceutical Analysis and Control Section, APhA Academy of Pharmaceutical Sciences, New Orleans meeting, November 1974.

The authors are grateful for the support provided by the Analytical Section of the Chemical Research Department and the Product Development Section of the Stuart Pharmaceutical Division of ICI United States Inc., particularly for the assistance provided by Mr. Paul H. Nason.

ˣ To whom inquiries should be directed.

Inhibition of Synaptosomal Accumulation of *l*-Norepinephrine II: *N*-Aryloxyalkylphentermines, Quaternary *d*-Amphetamines, and 3-Aryloxypropylamines

JAMES C. SCHAEFFER, ARTHUR K. CHO ˣ, and JOSEPH F. FISCHER

Abstract □ The inhibitory potencies of a series of *N*-substituted phentermines on the synaptosomal uptake of *l*-norepinephrine were found to be similar to those of the corresponding amphetamines. Quaternization of *N,N*-dimethyl-*d*-amphetamine diminished, but did not abolish, its inhibitory potency, indicating that a permanently charged cation is also effective. Since the addition of an aromatic moiety at the end of a four-atom chain originating at the nitrogen of amphetamine or phentermine significantly increased inhibitor strength, several 3-aryloxypropylamines and 4-phenylbutylamine were tested, but they were much weaker inhibitors than *dl*-amphetamine. Thus, the observed increase in inhibitor potency apparently was not simply the result of a specific interaction of the "nonmimic" portion of the *N*-substituted amphetamines or phentermines.

Keyphrases □ *l*-Norepinephrine—inhibition of synaptosomal accumulation by a series of *N*-substituted phentermines, corresponding amphetamines, and 3-substituted propylamines, compared □ Phentermines, *N*-substituted—inhibition of synaptosomal accumulation of *l*-norepinephrine □ Amphetamines, *N*-substituted—inhibition of synaptosomal accumulation of *l*-norepinephrine □ Propylamines, 3-substituted—inhibition of synaptosomal accumulation of *l*-norepinephrine □ Structure–activity relationships—inhibition of synaptosomal accumulation of *l*-norepinephrine by *N*-substituted phentermines, amphetamines, and 3-substituted propylamines

In a previous report from this laboratory, the relative inhibitory effects of a series of *N*-substituted amphetamines on the accumulation of ^{3}H-*l*-norepinephrine by a nonstriatal synaptosome preparation were described (1). The purpose of the study was to develop a specific inhibitor of the *l*-norepinephrine uptake mechanism by employing the "nonclassical inhibitor" principle (2, 3). This principle utilizes the concept that inhibitor specificity can result not only from the site of the substrate–receptor interaction but also through interactions with other regions remote from this center; these other regions depend on more distant physical and/or topographical features of both the oversized inhibitor and the macromolecules to which it binds.

In the previous study (1), *N*-substitution of a butyl group was found to reduce markedly inhibitory efficacy. However, through the introduction of a terminal, hydrophobic, aromatic moiety, a substantial portion of the lost inhibitor potency was regained. Furthermore, the addition of a second α-methyl group to *dl*-amphetamine, as in phentermine, did not alter inhibitor strength significantly (1).

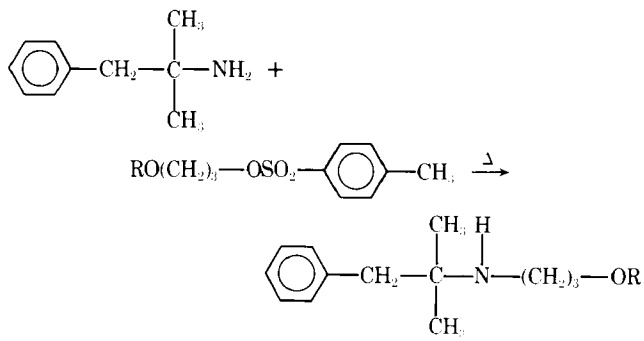

Scheme I—Method A

The present report describes additional studies on this general problem; three factors in the structural requirements for inhibition were examined. Initially, the effect of an additional α-methyl group on selectivity was explored through a series of *N*-substituted phentermine derivatives. The importance of the structural features surrounding the positively charged nitrogen then was investigated. Although the absolute requirement of a cationic species had been demonstrated (1), no evidence was presented concerning ligand toleration about a quaternized nitrogen. Finally, the relative inhibitory potencies of several primary amines representing the "nonmimic" portions of the corresponding nonclassical inhibitors were compared to see if the inhibitory enhancement observed was independent of the amphetamine moiety.

EXPERIMENTAL

Chemicals—Phentermine[1], *p*-hydroxyphentermine[1], tritiated *l*-norepinephrine[2] (4–10 Ci/mmole), and choline chloride[3] were obtained commercially. Trimethylethylammonium iodide and trimethylheptylammonium iodide were synthesized[4]. All other compounds used were prepared by methods described here.

Method A (Scheme I) was employed to synthesize III–VI (Table I). Compound VII was prepared from 4-phenoxybutyl bromide and phentermine, as indicated by Method B (Scheme II). These syntheses were carried out in the identical manner as those previously reported for the corresponding amphetamines (1). The Eschweiler–Clarke methylation of *S(d)*-amphetamine afforded *N,N*-dimethyl-*d*-amphetamine (XIX) (4). The quaternization of this compound with the appropriate alkyl halide provided VIII–X (Table II) (Method C, Scheme III). Azide replacement of toluenesulfonate followed by lithium aluminum hydride reduction (Method D, Scheme IV) gave the 3-aryloxypropylamines listed in Table III. Compound XVII was prepared by reacting equimolar amounts of toluenesulfonic acid hydrate and 4-phenylbutylamine[3] in acetone.

Synthetic Procedures[5]—*General Procedure (Method C)*—Fifty millimoles of *d*-amphetamine (6.75 g) was slowly added with cooling to 12.8 g of 88% formic acid. To this mixture was added 11.25 ml of formaldehyde (150 mmoles). After the vigorous evolution of gas had ceased, the mixture was heated at 90–100° for 8 hr.

[1] Pennwalt Corp., Rochester, N.Y.
[2] New England Nuclear Corp., Boston, Mass.
[3] Aldrich Chemical Co., Milwaukee, Wis.
[4] By Dr. D. J. Jenden, Department of Pharmacology, UCLA Center for the Health Sciences.
[5] Melting points were determined on a Mel-Temp apparatus and are not corrected. Either mulls or liquid films were used to obtain IR spectra on an Infracord instrument (Perkin-Elmer). Elemental analyses were performed by H. King, Department of Chemistry, UCLA Center for the Health Sciences.

Table I—Analytical Data for *N*-Alkyl- and 3-Aryloxypropylphentermine *p*-Toluenesulfonates[a]

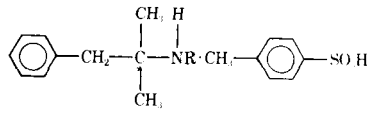

Compound	R	Method	Recrystallization Solvent	Yield[b], %	Melting Point	Analysis, %	Calc.	Found
III	$-(CH_2)_3CH_3$	A	Acetone	46	140–142°	C H	66.80 8.28	66.59 8.11
IV	$-(CH_2)_3O-C_6H_5$	A	Ethanol	55	209–212°	C H	68.53 7.30	68.50 7.27
V	$-(CH_2)_3O-C_{10}H_7$	A	Acetone	40	184–186°	C H	71.25 6.98	71.20 6.86
VI	$-(CH_2)_3O-C_{10}H_7$	A	Acetone–methanol (10:1)	35	196–199°	C H	71.25 6.98	71.23 6.86
VII	$-(CH_2)_4O-C_6H_5$	B	Acetone–ethanol (2:1)	34	176–178°	C H	69.05 7.51	68.96 7.52

[a] All compounds were uniform by TLC (free base, methanol) and exhibited spectra compatible with their proposed structures. [b] Minimum recrystallized yield from last step in synthetic sequence.

The reaction mixture then was allowed to cool to room temperature, and 25 ml of 4 *M* HCl was added.

The resulting basic mixture was extracted twice with 100-ml portions of benzene. The benzene extracts were combined, dried with magnesium sulfate, and spin evaporated to an oil, which was vacuum distilled. The fraction distilling between 111 and 113°/30 mm was collected (3.4 g). This material was dissolved in 100 ml of ether, and dry hydrogen chloride was bubbled through the solution. The precipitate that formed was filtered, recrystallized from acetone, and dried under high vacuum over phosphorus pentoxide at 100°. Two grams of *N,N*-dimethyl-*d*-amphetamine hydrochloride (20%), which melted[6] at 183–186°, was obtained. This material had a specific rotation[6] of +15.1°, exhibited no N–H bands in the IR spectrum, and gave the following analysis. Calc. for C, 66.14; H, 9.08. Found: C, 66.18; H, 8.99.

A mixture of 1.63 g of *N,N*-dimethyl-*d*-amphetamine (free base, 10 mmoles), 10 mmoles of the appropriate alkyl halide, and 25 ml of ether was allowed to stand for 7–10 days at 0–5°. The resulting precipitate was filtered, recrystallized from the appropriate solvent, and dried under high vacuum over phosphorus pentoxide at 60°. The physical properties of these compounds and the solvents of recrystallization are presented in Table II.

General Procedure (Method D)—A mixture of 2.5 mmoles of the appropriate 3-aryloxypropyl *p*-toluenesulfonate (1), 10 ml of dimethylformamide, 1 ml of water, and 195 mg of sodium azide (3 mmoles) was heated at 65–70° for 19 hr. After 100 ml of 1 *N* NaOH had been added to the mixture, it was extracted with two 25-ml portions of ether. The extract was backwashed with water, dried with magnesium sulfate, and spin evaporated to an oil; this oil exhibited a strong IR band at 2100 cm^{-1}, characteristic of azides.

To this material were added 25 ml of anhydrous ether and 190 mg of lithium aluminum hydride (5.0 mmoles). After this mixture was refluxed for 5 hr, 100 ml of 1 *N* NaOH was slowly added. The resulting mixture was extracted with two 50-ml portions of ether, which were combined and dried with magnesium sulfate, and the solvent was removed under vacuum. The residue was converted to the appropriate organic acid salt, recrystallized, and dried. The physical properties and solvents for recrystallization are given in Table III.

Filtration Assay—Male Sprague–Dawley rats, 180–200 g, were

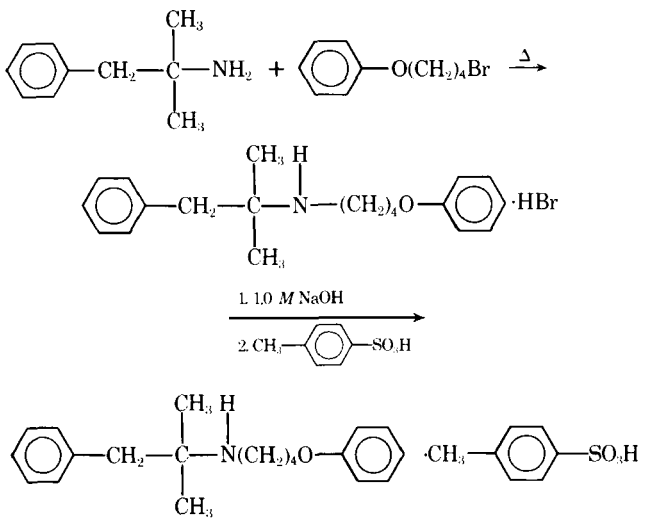

VII

Scheme II—Method B

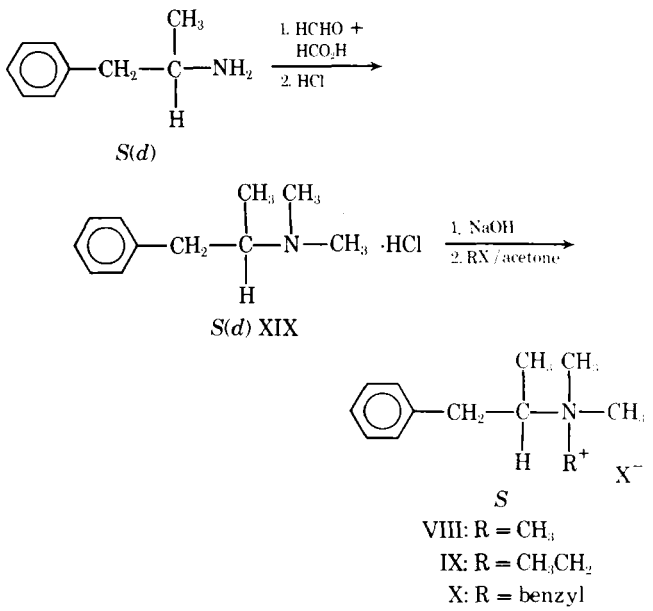

S(*d*) XIX

S

VIII: R = CH_3

IX: R = CH_3CH_2

X: R = benzyl

Scheme III—Method C

[6] Reference 4 reported mp 182–183° and [α] +13.1°.

Table II—Analytical Data for α-Methylphenethyldimethylammonium Halides

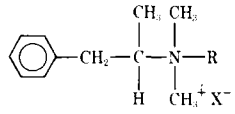

Compound[a]	R	X^-	Recrystallization Solvent	Yield[b], %	Melting Point	Analysis, %	Calc.	Found
VIII	CH_3—	I	Acetone	66	200–202°[c]	C	47.22	47.41
						H	6.60	6.64
IX	CH_3CH_2—	I	Ethanol	8	133–136°	C	48.91	49.02
						H	6.95	6.80
X	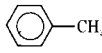	Br	Ether–methanol (2:1)	30	205–208°	C	64.67	64.53
						H	7.24	7.23

[a] Prepared using Method C. [b] Minimum recrystallized yield from last step in synthetic sequence. [c] This compound was prepared through a different route in Ref. 4, mp 197–198°.

Table III—Analytical Data for 3-Aryloxypropylamine Salts[a]

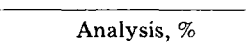

Compound[b]	R	X	Recrystallization Solvent	Yield[c], %	Melting Point	Analysis, %	Calc.	Found
XI[d]		Toluenesulfonic acid	Acetone	30	170–174°	C	59.42	59.31
						H	6.55	6.66
XII	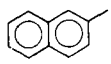	Toluenesulfonic acid	Acetone	23	164–167°	C	64.31	64.23
						H	6.20	6.15
XIII		Benzoic acid	Ether	36	136–137°	C	74.28	74.25
						H	6.55	6.62

[a] All compounds were uniform by TLC (free base, methanol). [b] Prepared using Method D. [c] Minimum recrystallized yield from azide formation step. [d] Previously prepared by treating 3-phenoxypropyl bromide with ammonia [J. V. Brahn *et al.*, *Ber.*, **70B**, 979(1937)].

killed by decapitation. The corpus striatum and cerebellum of each brain was rapidly removed by dissection. The remainder of the brain was homogenized, and a synaptosome-enriched tissue fraction was obtained (5). The test compounds were incubated with an aliquot of this preparation (protein concentration 15–20 mg/ml) in Krebs–Ringer phosphate containing nialamide for 5 min before addition of ^{3}H-*l*-norepinephrine (final concentration 1 μM).

Five minutes later, the uptake was quenched by addition of ice-cold 0.9% NaCl containing 100 μM of unlabeled substrate. The resulting mixture was filtered through a cellulose acetate filter assembly[7] (0.8-μm filter) (6). The net accumulation of ^{3}H-*l*-norepinephrine was determined by liquid scintillation counting. The details of these procedures were described previously (1).

RESULTS AND DISCUSSION

In Table IV the effects of the phentermine and analogous *dl*-amphetamine-derived inhibitors on the accumulation of *l*-norepinephrine are compared. With the exception of VI and VII, the two series appeared parallel. *para*-Hydroxylation (II) did not noticeably alter the potency of either compound (I, IA, II, and IIA). The addition of an *N*-butyl group (III) to phentermine resulted in a six- to sevenfold drop in inhibitor strength, while the same change in the amphetamine series caused a ninefold loss. In either series, the introduction of a phenyl (IV) or naphthyl (V and VI) ring at the end of a four-atom chain from the nitrogen brought about a two- to threefold increase in potency when compared to the simple *N*-butyl analogs. A five-atom chain (VII) was more favorable in the amphetamine case.

Overall, none of the compounds was more potent than the simple amines themselves. However, a properly placed aromatic moiety can partially overcome the initial unfavorable interactions associated with *N*-butylation. Although the amphetamine and phentermine derivatives exhibited similar inhibitory potencies for nonstriatal accumulation, greater differences may be expected in the striatal system, which has different stereochemical as well as structural requirements (7–10).

The monomethylation of *d*-amphetamine to *N*-methyl-*d*-amphetamine did not change inhibitor strength, but the introduction of a second methyl group caused a sevenfold decrease in inhibitory power (1). When the nitrogen was quaternized by the addition of a third methyl group (VIII, Table V), an additional threefold loss occurred. Since it is unlikely that VIII can penetrate membranes, at least part of the accumulative mechanism being blocked must involve interaction with the external synaptosomal membrane. Similar findings were reported for the methiodides of cocaine and imipramine (11). These compounds interfered with the accumulation of norepinephrine by cortex slices at concentrations of 1 and 0.2 μM, respectively.

The inactivity of XIV–XVI (Table V) points out that the inhibition of VIII is specific and not associated with a general ionic or detergent-like action. The addition of larger substituents, as in IX and X, did not alter inhibitor strength, so apparently only minimal steric factors are associated with the interaction of a fourth nitrogen ligand and the anionic carrier site. Choline (XIV) was shown to be accumulated by a similar preparation at micromolar concentrations (12, 13), and similar observations have been made in this laboratory (14) employing the same preparations used in this study. Therefore, there appears to be very little competition between

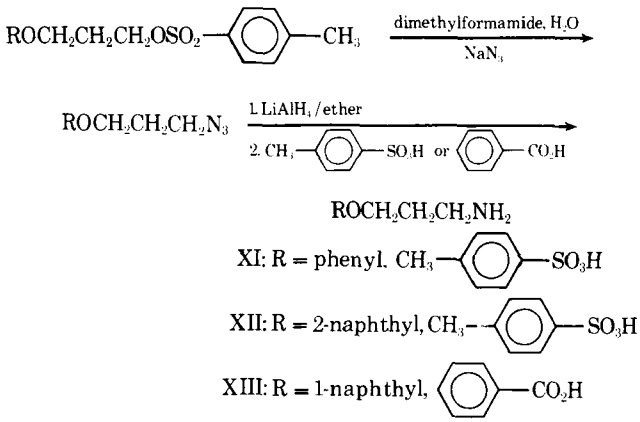

Scheme IV—Method D

[7] Millipore Corp., Bedford, Mass.

Table IV—Inhibition of Synaptosomal Uptake of *l*-Norepinephrine by *N*-Substituted Amphetamines and Phentermines[a]

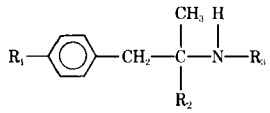

Compound	R_1	R_2	R_3	I_{50}, μM[b]
I	H	CH_3	H	1.6
IA[c]	H	H	H	1.3
II	OH	CH_3	H	2.4
IIA	OH	H	H	1.1
III	H	CH_3	$-(CH_2)_3CH_3$	10.8
IIIA	H	H	$-(CH_2)_3CH_3$	12.3
IV	H	CH_3	$-(CH_2)_3O-$	4.9
IVA	H	H	$-(CH_2)_3O-$	4.4
V	H	CH_3	$-(CH_2)_3O-$	7.2
VA	H	H	$-(CH_2)_3O-$	5.2
VI	H	CH_3	$-(CH_2)_3O-$	3.4
VIA	H	H	$-(CH_2)_3O-$	5.8
VII	H	CH_3	$-(CH_2)_4O-$	6.7
VIIA	H	H	$-(CH_2)_4O-$	2.1

[a] Substrate concentration was 1 μM *l*-norepinephrine. [b] The I_{50} values were determined as previously described (1). All values are the average of two or more independent measurements. The variation in each multiple determination was less than 25%. [c] Amphetamine analogs are represented in the A series.

these two compounds for the *l*-norepinephrine transport system.

The introduction of an aromatic moiety at the end of a four- or five-atom chain from the terminal nitrogen of amphetamine or phentermine caused a two- to fivefold increase in inhibitor strength when compared with the corresponding *N*-butyl derivative (Table IV). This increment in inhibitor potency could be the result of a nonspecific hydrophobic interaction, but it could also be the result of the nonmimic amine end of the molecule interacting with the transport system at a second site. If the latter were the case, the increase in inhibitor strength could be the result of two separate interactions.

In an attempt to resolve this question, XI–XIII and XVII were prepared and tested. As can be seen from Table VI, these compounds did inhibit *l*-norepinephrine accumulation but were much less effective than the corresponding amphetamine derivatives (A series). If a simple summation effect were involved, the stronger the nonmimic amine the more potent should be the combined nonclassical inhibitor. However, 3-phenoxypropylamine (XI) was two- to threefold more potent than 4-phenylbutylamine (XVII), and 3-(2-naphthyloxy)propylamine (XII) was two- to threefold stronger than 3-(1-naphthyloxy)propylamine (XIII), and the inhibitory potency of the substituted amphetamines had a different relative order so this apparently is not the case. Differences in I_{50} values of two to threefold are significant.

An alternative explanation might be that both the mimic and nonmimic moieties may compete for a common site on the carrier. Since all simple primary amines listed in Table VI are much less potent than *dl*-amphetamine (I_{50} = 1.3 μM), they may be considered competitive antagonists of the binding of the amphetamine moiety in this model. Thus, the I_{50} values of the corresponding

Table V—Inhibition of Synaptosomal Uptake of *l*-Norepinephrine by Quaternary Amines[a]

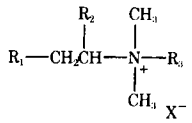

Compound	R_1	R_2	R_3	X^-	Optical Isomer	I_{50}, μM[b]
XIV	OH	H	CH_3	Cl	—	>100[c]
XV	H	H	CH_3	I	—	>100[c]
XVI	$CH_3(CH_2)_4-$	H	CH_3	I	—	294
VIII		CH_3	CH_3	I	*S(l)*	22.0
IX		CH_3	CH_3CH_2	I	*S*	21.6
X		CH_3	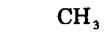	Br	*S*	22.2

[a] Substrate concentration was 1 μM *l*-norepinephrine. [b] The I_{50} values were determined as previously described (1). All values are the average of two or more independent measurements. The variation in each multiple determination was less than 25%. [c] No inhibition at 100 μM.

nonclassical inhibitor should be somewhere between the I_{50} values of its components. The stronger the nonmimic interaction, the closer the I_{50} of the nonclassical inhibitor should be to the value of its nonamphetamine part.

The data for the 3-phenoxypropyl (XI and IVA) and 4-phenylbutyl (XVII and XVIIA) compounds appear to qualitatively support this hypothesis. However, the results of the 2-naphthyl (XII and VIA) and 1-naphthyl (XIII and VA) studies do not, since the two- to threefold change in nonmimic strength has little effect on the potency of the corresponding nonclassical inhibitor. Furthermore, *N*-phenethyl-*dl*-amphetamine (I_{50} = 7.3 μM) is a weaker inhibitor than either of its parts; the I_{50} of phenethylamine is 6.0 μM (1). Therefore, unfavorable steric factors apparently are associated with the secondary amine structure of this nonclassical inhibitor and cannot be accounted for by this simple competition theory.

Another possibility is that the substituted amphetamines are inhibiting by a nonclassical mechanism but that the optimal configuration has not yet been reached. Thus, the binding of the amphetamine portion of the molecule to the normal substrate site could be perturbed by the interaction of the nonmimic moiety so that the affinity of the combined molecule is only comparable to the simple amphetamine moiety. If this is the nature of the inhibition, it should be possible to devise a nonclassical inhibitor whose interactions are more complementary. Because of its dependency on an adjacent area as well as the normal *l*-norepinephrine binding site,

Table VI—Inhibition of Synaptosomal Uptake of *l*-Norepinephrine[a] by R—X—$(CH_2)_3NH_2$

Compound	R	X	I_{50}, μM[b]
XI		O	10.8
IVA[c]			4.4
XVII		CH_2	23.9
XVIIA			2.7
XII	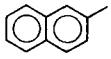	O	13.4
XIA			5.8
XIII		O	30.5
VA			5.2

[a] Substrate concentration was 1 μM *l*-norepinephrine. [b] The I_{50} values were determined as previously described (1). All values are the average of two or more independent measurements. The variation in each multiple determination was less than 25%. [c] Corresponding nonclassical inhibitor derived from *dl*-amphetamine.

this type of inhibitor is more likely to serve as a selective tool for studying the uptake of neurotransmitters by different tissues and brain regions.

REFERENCES

(1) J. C. Schaeffer, A. K. Cho, G. T. Nagami, and G. S. Takimoto, *J. Pharm. Sci.*, **64**, 1462(1975).

(2) B. R. Baker, *Cancer Chemother. Rep.*, **4**, 1(1959).

(3) B. R. Baker, "Design of Active-Site-Directed Irreversible Enzyme Inhibitors," Wiley, New York, N.Y., 1967.

(4) S. Senoh and I. Mita, *J. Pharm. Soc. Jap.*, **72**, 1096(1952).

(5) E. G. Gray and V. H. Whittaker, *J. Anat.*, **96**, 79(1962).

(6) R. Baldessarini and M. Vogt, *J. Neurochem.*, **18**, 951(1971).

(7) J. T. Coyle and S. H. Snyder, *J. Pharmacol. Exp. Ther.*, **170**, 221(1969).

(8) A. S. Horn, J. T. Coyle, and S. H. Snyder, *Mol. Pharmacol.*, **7**, 66(1971).

(9) J. E. Harris and R. J. Baldessarini, *Neuropharmacology*, **12**, 669(1973).

(10) R. M. Ferris, F. L. M. Tang, and R. A. Maxwell, *J. Pharmacol. Exp. Ther.*, **181**, 407(1972).

(11) S. B. Ross and A. L. Renyi, *Eur. J. Pharmacol.*, **2**, 181(1967).

(12) H. I. Yamamura and S. H. Snyder, *J. Neurochem.*, **21**, 1355(1973).

(13) P. Guyenet, P. Lefresne, J. Rossier, J. C. Beaujouan, and J. Glowinski, *Mol. Pharmacol.*, **9**, 630(1973).

(14) S. H. Butcher, A. K. Cho, and J. C. Schaeffer, *Fed. Proc.*, **33**, 505(1974).

ACKNOWLEDGMENTS AND ADDRESSES

Received January 20, 1975, from the *Department of Pharmacology, Center for the Health Sciences, University of California at Los Angeles, Los Angeles, CA 90024*

Accepted for publication April 29, 1975.

Supported in part by U.S. Public Health Service Grant MH-23839.

[x] To whom inquiries should be directed.

Synthesis and Biological Evaluation of Tetrakis(acetylsalicylato)-μ-dicopper(II)

DAVID A. WILLIAMS [*], DONALD T. WALZ [‡], and WILLIAM O. FOYE [*x]

Abstract □ The synthesis of a copper–aspirin chelate, previously reported to be a more active anti-inflammatory agent than aspirin itself, is given. Reaction of potassium acetylsalicylate with cupric sulfate gave a stable copper complex, which analysis and molecular weight determination showed to be a 4:2 chelate structure. Oil–water partition measurements showed the complex to be 10-fold more oil soluble than aspirin. Biological evaluation in rats showed the copper complex of aspirin to be approximately equal to aspirin in reducing carrageenan-induced inflammation, but it was 1.7 times more active than aspirin in reducing the primary lesion of adjuvant arthritis. Whereas aspirin produced a 50% or greater incidence of GI erosions at doses of 100–300 mg/kg in rats, the copper complex caused no erosions in doses up to 1200 mg/kg.

Keyphrases □ Tetrakis(acetylsalicylato)-μ-dicopper(II)— synthesis, biological evaluation, anti-inflammatory activity, physical properties □ Biological evaluation—tetrakis(acetylsalicylato)-μ-dicopper(II), anti-inflammatory activity, rats □ Aspirin–copper complex—synthesis, biological evaluation, anti-inflammatory activity, physical properties □ Copper–aspirin complex—synthesis, biological evaluation, physical properties □ Anti-inflammatory agents, potential—synthesis and biological evaluation of aspirin–copper complex

In 1956, Chenoweth (1) postulated that the salicylates may exert "some if not all" of their biological actions through their ability to bind metal ions, a property that isomers of salicylic acid lack. To test this postulate, a series of substituted salicylic acids and heterocyclic analogs was prepared; their metal-binding avidities were compared with several biological effects to determine possible parallels (2, 3). With hindered (3,5- and 3,6-disubstituted) salicylic acids, for instance, both metal-binding ability and anti-inflammatory activity were lowered (4).

Table I—Oil–Water Partition Coefficients

Compound	pH	K^a
Aspirin–copper complex	4.1	1.3
Salicylic acid	4.1	9.0
Aspirin	4.3	0.11

[a] $K = \frac{C_{\text{oleyl alcohol}}}{C_{\text{water}}}$

Table II—Anti-Inflammatory Activities

Compound	Dose, mg/kg po	Antiedema, Δ, ml (0 *versus* 3 hr)
Aspirin–copper complex	50	+0.40[a]
	100	+0.31[a]
	200	+0.26[a]
Aspirin	50	+0.34[a]
	100	+0.27[a]
	200	+0.20[a]
Controls		+0.55

[a] $p = 0.00$.

Sorenson (5) recently reported that copper chelates of some anti-inflammatory agents, including aspirin, gave marked increases in anti-inflammatory activity compared with the activities of the unchelated agents. Anti-inflammatory activity was also observed for copper chelates of some ligands having no anti-inflammatory properties at all in the nonchelated state. These findings indicate that the copper complexes may be active metabolites of many anti-inflammatory agents. Since the copper(II) complex of

this type of inhibitor is more likely to serve as a selective tool for studying the uptake of neurotransmitters by different tissues and brain regions.

REFERENCES

(1) J. C. Schaeffer, A. K. Cho, G. T. Nagami, and G. S. Takimoto, *J. Pharm. Sci.*, **64**, 1462(1975).

(2) B. R. Baker, *Cancer Chemother. Rep.*, **4**, 1(1959).

(3) B. R. Baker, "Design of Active-Site-Directed Irreversible Enzyme Inhibitors," Wiley, New York, N.Y., 1967.

(4) S. Senoh and I. Mita, *J. Pharm. Soc. Jap.*, **72**, 1096(1952).

(5) E. G. Gray and V. H. Whittaker, *J. Anat.*, **96**, 79(1962).

(6) R. Baldessarini and M. Vogt, *J. Neurochem.*, **18**, 951(1971).

(7) J. T. Coyle and S. H. Snyder, *J. Pharmacol. Exp. Ther.*, **170**, 221(1969).

(8) A. S. Horn, J. T. Coyle, and S. H. Snyder, *Mol. Pharmacol.*, **7**, 66(1971).

(9) J. E. Harris and R. J. Baldessarini, *Neuropharmacology*, **12**, 669(1973).

(10) R. M. Ferris, F. L. M. Tang, and R. A. Maxwell, *J. Pharmacol. Exp. Ther.*, **181**, 407(1972).

(11) S. B. Ross and A. L. Renyi, *Eur. J. Pharmacol.*, **2**, 181(1967).

(12) H. I. Yamamura and S. H. Snyder, *J. Neurochem.*, **21**, 1355(1973).

(13) P. Guyenet, P. Lefresne, J. Rossier, J. C. Beaujouan, and J. Glowinski, *Mol. Pharmacol.*, **9**, 630(1973).

(14) S. H. Butcher, A. K. Cho, and J. C. Schaeffer, *Fed. Proc.*, **33**, 505(1974).

ACKNOWLEDGMENTS AND ADDRESSES

Received January 20, 1975, from the *Department of Pharmacology, Center for the Health Sciences, University of California at Los Angeles, Los Angeles, CA 90024*

Accepted for publication April 29, 1975.

Supported in part by U.S. Public Health Service Grant MH-23839.

[x] To whom inquiries should be directed.

Synthesis and Biological Evaluation of Tetrakis(acetylsalicylato)-μ-dicopper(II)

DAVID A. WILLIAMS [*], DONALD T. WALZ [‡], and WILLIAM O. FOYE [*x]

Abstract □ The synthesis of a copper–aspirin chelate, previously reported to be a more active anti-inflammatory agent than aspirin itself, is given. Reaction of potassium acetylsalicylate with cupric sulfate gave a stable copper complex, which analysis and molecular weight determination showed to be a 4:2 chelate structure. Oil–water partition measurements showed the complex to be 10-fold more oil soluble than aspirin. Biological evaluation in rats showed the copper complex of aspirin to be approximately equal to aspirin in reducing carrageenan-induced inflammation, but it was 1.7 times more active than aspirin in reducing the primary lesion of adjuvant arthritis. Whereas aspirin produced a 50% or greater incidence of GI erosions at doses of 100–300 mg/kg in rats, the copper complex caused no erosions in doses up to 1200 mg/kg.

Keyphrases □ Tetrakis(acetylsalicylato)-μ-dicopper(II)— synthesis, biological evaluation, anti-inflammatory activity, physical properties □ Biological evaluation—tetrakis(acetylsalicylato)-μ-dicopper(II), anti-inflammatory activity, rats □ Aspirin–copper complex—synthesis, biological evaluation, anti-inflammatory activity, physical properties □ Copper–aspirin complex—synthesis, biological evaluation, physical properties □ Anti-inflammatory agents, potential—synthesis and biological evaluation of aspirin–copper complex

In 1956, Chenoweth (1) postulated that the salicylates may exert "some if not all" of their biological actions through their ability to bind metal ions, a property that isomers of salicylic acid lack. To test this postulate, a series of substituted salicylic acids and heterocyclic analogs was prepared; their metal-binding avidities were compared with several biological effects to determine possible parallels (2, 3). With hindered (3,5- and 3,6-disubstituted) salicylic acids, for instance, both metal-binding ability and anti-inflammatory activity were lowered (4).

Table I—Oil–Water Partition Coefficients

Compound	pH	K^a
Aspirin–copper complex	4.1	1.3
Salicylic acid	4.1	9.0
Aspirin	4.3	0.11

[a] $K = \frac{C_{\text{oleyl alcohol}}}{C_{\text{water}}}$

Table II—Anti-Inflammatory Activities

Compound	Dose, mg/kg po	Antiedema, Δ, ml (0 *versus* 3 hr)
Aspirin–copper complex	50	+0.40[a]
	100	+0.31[a]
	200	+0.26[a]
Aspirin	50	+0.34[a]
	100	+0.27[a]
	200	+0.20[a]
Controls		+0.55

[a] $p = 0.00$.

Sorenson (5) recently reported that copper chelates of some anti-inflammatory agents, including aspirin, gave marked increases in anti-inflammatory activity compared with the activities of the unchelated agents. Anti-inflammatory activity was also observed for copper chelates of some ligands having no anti-inflammatory properties at all in the nonchelated state. These findings indicate that the copper complexes may be active metabolites of many anti-inflammatory agents. Since the copper(II) complex of

Table III—Effects on Adjuvant-Induced Arthritis

Compound	Dose, mg/kg po	Decrease of Leg Volume[a], %			Body Weight Change[b]	
		Left Leg, Day 3	Left Leg, Day 16	Right Leg, Day 16	Day 3	Day 16
Aspirin	400	27	10 (NS)	25	−4	+2
	200	13	5 (NS)	2 (NS)	NS	NS
	100	8	0 (NS)	2 (NS)	NS	NS
	50	3 (NS)	0 (NS)	0 (NS)	NS	NS
	ED_{25} = 383 (250–748)					
Aspirin–copper complex	400	29	7 (NS)	22	−2	+1
	200	23	8 (NS)	5 (NS)	NS	+2
	100	9	0 (NS)	0 (NS)	NS	NS
	50	12	0 (NS)	13 (NS)	NS	NS
	ED_{25} = 256 (162–502)					
	Relative potency = 1.7 (1.2–2.7)					

[a] NS = nonsignificant. [b] 1, $p < 0.03$; 2, $p < 0.01$; 4, $t > 5.00 < 10.00$; + = increase; − = decrease.

aspirin was prepared in this laboratory previously (6), the synthesis, structure, and some physical and biological properties of this complex are now reported.

DISCUSSION

Chemistry—Reaction of the potassium salt of aspirin with cupric sulfate gave an immediate precipitate of an aquamarine complex. Elemental analysis showed it to be a 2:1 aspirin–copper complex without hydration or anions, indicating that four coordination bonds of the copper ion were filled by the organic ligand. Stability constants for the formation of the complex could not be determined because of the rapid hydrolysis of aspirin, which occurred during the attempted determination (by potentiometric titration). However, strong shifts in the IR spectra of the coordinating carbonyl groups indicated appreciable stability of the complex. The complex also has demonstrated remarkable stability in the dry state, remaining stable for years in a glass-stoppered bottle without precautions.

Oil–water partition coefficients, using oleyl alcohol, were determined for both aspirin and the copper(II) complex (Table I). It has been proposed that transport of organic ligands into the cells can be facilitated by the formation of metal complexes (7), and this concept recently was invoked to explain the transport and storage of catecholamines (8). The copper(II) complex of aspirin was found to be 10-fold more lipophilic than aspirin at a comparable pH (~4.0). This finding supports the idea that metal-ion complexation may be of importance for the transport of aspirin into cells.

Examination of the IR spectra of aspirin and its copper(II) complex revealed definite shifts in absorption for both the carboxyl and acetoxy groups (Figs. 1 and 2). The shifts occurred in the direction of longer wavelengths for both carbonyl groups, as expected for metal chelate formation involving covalent bonds. Donation of electrons to metal produces lower excited states and, therefore, shifts to longer wavelengths. Where ionic bonding is involved, these shifts also occur, but to a lesser degree (9). It may be concluded that both the carboxyl and acetoxy groups are involved in binding to the copper ion, which accounts for the stability of the product to the loss of acetic acid.

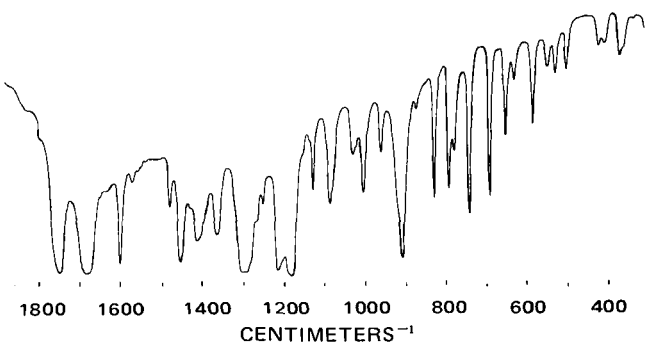

Figure 1—*IR absorption spectrum of aspirin (4.8 mg/g of potassium bromide).*

Previously, a structure was proposed for a copper(II) aspirinate (10) prepared at a higher temperature (50°) and described as "dark blue prisms insoluble in water and many common organic solvents." This structure included four units of acetylsalicylate and two copper ions; each copper ion resided in a distorted octahedral arrangement with five Cu–O bonds and one Cu–Cu linkage. The product reported here most likely has this structure, and a molecular weight determination confirmed the 4:2 ratio of ligand to copper.

Similar attempts to prepare aluminum and ferrous complexes of aspirin gave less satisfactory results. The isolated aluminum complex appeared to be quite stable but did not give suitable analytical results for either a 2:1 or 3:1 complex. The ferrous complex underwent immediate oxidation on exposure to air.

Biological Properties—The anti-inflammatory effect, antiarthritic effect, and ulcerogenic liability of the copper complex of aspirin were determined in rats and compared with the same effects from aspirin. The two agents were approximately equipotent in reducing carrageenan-induced inflammation (Table II). The copper complex, however, was 1.7 times more active than aspirin on the primary lesion (Day 3) of adjuvant arthritis (Table III). The compounds were administered orally.

Oral administration of aspirin to rats resulted in a 50% or greater incidence of GI erosions at doses of 100–300 mg/kg. The copper complex of aspirin caused no erosions in doses up to and including 1200 mg/kg on oral administration (Table IV). There was, however, evidence of hemorrhage caused by the copper complex at doses of 300, 600, and 1200 mg/kg.

EXPERIMENTAL[1]

Tetrakis(acetylsalicylato)-μ-dicopper(II)—Acetylsalicylic acid (3.60 g, 0.02 mole) was allowed to dissolve in a solution of potassium bicarbonate (2.02 g, 0.02 mole) in 30 ml of water. To this solution was added a solution of copper sulfate pentahydrate (2.50 g, 0.01 mole) in 20 ml of water, slowly and with constant stirring. An aquamarine precipitate formed, and the pH of the solution fell from 5.3 to 4.3. The precipitate was collected, washed with water, and dried (calcium chloride), giving a 79% yield; UV (water): 296 nm: IR (potassium bromide): 1755 (ester C=O), 1725 (carboxyl C=O), 1405 (C—O), 1240 (C—O), 1200 (C—O), and 500 (Cu—O) cm^{-1}; IR (potassium bromide) (aspirin): 1750 (ester C=O), 1680 (carboxyl C=O), 1300 (C—O), 1220 (C—O), and 1180 (C—O) cm^{-1}; mol. wt.: theoretical, 843.7, found (Rast, camphor), 854.5.

Anal.—Calc. for $C_{18}H_{14}CuO_8$: C, 51.21; H, 3.34; Cu, 15.07. Found: C, 51.19; H, 3.46; Cu, 15.27.

Oil–Water Partition Coefficients—Oil–water partition coeffi-

[1] The melting point was taken on a Mel-Temp apparatus and is uncorrected. Microanalyses for carbon and hydrogen were done by F. B. Strauss, Oxford, England. UV absorption spectra were determined with a Beckman model DU spectrometer, and IR absorption spectra were obtained with a Perkin-Elmer model 457 spectrometer in potassium bromide pellets. A copper analysis was performed by ashing the dried complex at 1000° and weighing the copper oxide formed.

Table IV—Ulcerogenic Liability

Compound	Dose, mg/kg po	Erosions	Average Number of Erosions
Aspirin	300	5/8	0.9
	200	7/8	4.1
	100	4/8	0.9
	50	2/8	0.4
Aspirin–copper complex	1200	0/8	0
	600	0/8	0
	300	0/8	0
	100	0/8	0

cients were determined by shaking 100 ml of a 0.002 *M* solution of acetylsalicylic acid or its copper complex with an equal volume of oleyl alcohol. After 4 hr of shaking, the aqueous layer was separated and heated at 70° for several hours to hydrolyze the complex. The hydrolyzed mixture was filtered, and the liberated salicylic acid was measured spectrophotometrically at 296 nm.

Anti-Inflammatory Activity—Groups of eight male Charles River Wistar rats were dosed orally with the respective drug or vehicle (tragacanth) and hydrated. One hour later, 0-hr (normal) paw measurements were made, and the animals were immediately injected with 0.05 ml of a 1% carrageenan (in 0.9% sodium chloride) suspension into the plantar surface of the right hindpaw. Paw measurements were made 3 hr after carrageenan injection, according to the procedure of Walz *et al.* (11). A statistically significant effect was determined by using the Student *t* test.

Adjuvant-Induced Arthritis Test—The procedure of Walz *et al.* (12) was followed. Eight groups of eight Charles River Wistar rats, 160–190 g, were given the following doses of drug orally in tragacanth (0.5%): aspirin—50, 100, 200, and 400 mg/kg; and copper complex of aspirin—50, 100, 200, and 400 mg/kg (aspirin as base). Sixteen rats were given 0.5% tragacanth as a vehicle control. On the afternoon of the same day, adjuvant arthritis was induced by the injection of 0.75 mg of *Mycobacterium butyricum*[2], suspended in white paraffin oil, into the left hind footpad of each rat.

Drug dosing was continued daily for 4 days (Day 0 through Day 3). On Day 3, the animal's left hindleg volume was determined plethysmographically. Leg volume was also determined on Day 16. Body weight changes with respect to Day 0 were calculated for Day 3 and Day 16. The ED_{25} (the dose giving a 25% decrease in leg volume) was calculated from a dose-response curve fitted by computer. All data were statistically analyzed for significant differences between drug-treated and control animals by the Student *t* test.

Ulcerogenic Liability Test—Groups of eight Charles River or Carworth Wistar rats, 210–240 g, were dosed orally with aspirin (50, 100, 200, or 300 mg/kg) and with the copper complex of aspirin (100, 300, 600, or 1200 mg/kg) (aspirin as base). After dosing, the animals were fasted for 18 hr. Then the animals were sacrificed, and the stomachs were removed, washed, cut along the greater curvature, and pinned to a cork sheet. The mucosal surface was examined under low magnification. Incidence of erosions and average number of erosions were recorded.

[2] Difco.

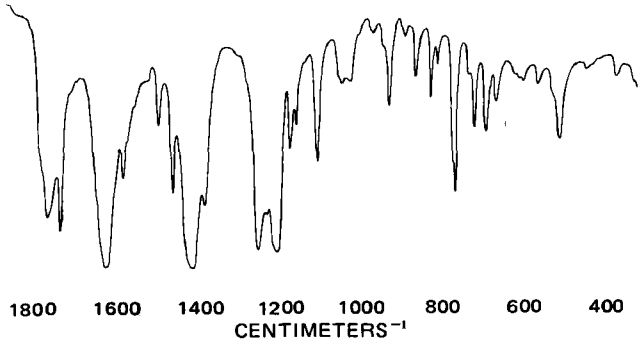

Figure 2—*IR absorption spectrum of the copper complex of aspirin (5.1 mg/g of potassium bromide).*

REFERENCES

(1) M. B. Chenoweth, *Pharmacol. Rev.*, **8**, 57(1956).

(2) W. O. Foye and J. G. Turcotte, *J. Pharm. Sci.*, **51**, 329(1962).

(3) W. O. Foye, M. D. Baum, and D. A. Williams, *ibid.*, **56**, 332(1967).

(4) W. O. Foye and J. M. Kauffman, *Chim. Ther.*, **1967**, 462.

(5) J. R. J. Sorenson, Abstracts, 167th National Meeting, American Chemical Society, Med. Chem. No. 73, 1974.

(6) D. A. Williams, M.S. thesis, Massachusetts College of Pharmacy, Boston, Mass., 1962.

(7) A. Albert, "Selective Toxicity," 4th ed., Methuen and Co., London, England, 1968, p. 328.

(8) K. S. Rajan, J. M. Davis, and R. W. Colburn, *J. Neurochem.*, **22**, 137(1974).

(9) A. E. Martell and M. Calvin, "Chemistry of the Metal Chelate Compounds," Prentice-Hall, New York, N.Y., 1952, pp. 219–224.

(10) L. Manojlović-Muir, *Chem. Commun.*, **1967**, 1057.

(11) D. T. Walz, M. J. DiMartino, C. L. Griffin, and A. Misher, *Arch. Int. Pharmacodyn. Ther.*, **185**, 337(1970).

(12) D. T. Walz, M. J. DiMartino, and A. Misher, *J. Pharmacol. Exp. Ther.*, **178**, 223(1971).

ACKNOWLEDGMENTS AND ADDRESSES

Received June 3, 1974, from the **Department of Chemistry, Massachusetts College of Pharmacy, Boston, MA 02115,* and [‡]*Smith Kline and French Laboratories, Philadelphia, PA 19101*

Accepted for publication April 28, 1975.

D. A. Williams and W. O. Foye express their appreciation to the Dow Chemical Co. for financial assistance.

[x] To whom inquiries should be directed.

Transfer of Alcohols and Ureas across the Oral Mucosa Measured Using Streaming Potentials and Radioisotopes

IVENS A. SIEGEL ˣ, KENNETH T. IZUTSU, and JOHN BURKHART

Abstract □ The permeability of the oral mucosa to an alcohol and a urea series was studied using radioisotope transfer and the measurement of streaming potentials. Both methods yielded similar quantitative estimates of permeability. The rate of transfer of the smallest member of both series (methanol and urea) was greater than the second member (ethanol and methylurea). In the alcohol series, permeability increased as the chain length increased from ethanol to butanol. In contrast, the permeability of the oral mucosa to ethylurea and propylurea was less than to methylurea. However, butylurea had a greater rate of transfer than either propylurea or ethylurea.

Keyphrases □ Permeability—oral mucosa to alcohol and urea series, radioisotope transfer, streaming potential, dogs □ Alcohol series—absorption through oral mucosa, radioisotope transfer, streaming potential, dogs □ Urea series—absorption through oral mucosa, radioisotope transfer, streaming potential, dogs □ Absorption—alcohol and urea series through dog oral mucosa, radioisotope transfer, streaming potential

A major function of the oral mucosa is to act as a protective barrier between substances present in the oral cavity and the underlying tissues. However, this barrier is not perfectly impermeable and many substances can cross it. For instance, the work of Brunton (1) established that nitroglycerin can be absorbed through the oral mucosa in sufficient quantities to cause pharmacological responses. Later, Walton (2) studied the sublingual absorption of several alkaloidal drugs. He pointed out that the oil-to-water distribution coefficient was the primary factor determining the extent of sublingual absorption of these drugs. More recently, buccal absorption was studied as an example of an *in vivo* model of passive transfer through a lipid membrane (3).

Despite the abundance of evidence suggesting that the oral mucosa acts as a passive semipermeable barrier, a recent review (4) pointed out that there is a paucity of quantitative data on the permeability of this barrier to specific compounds.

In this report, two methods were utilized to obtain quantitative estimates of the permeability of the lingual frenulum to selected compounds. The first method relies on the measurement of the streaming potential developed when water moves through a charged membrane in response to an osmotic gradient. This method has been extensively used in determining the permeability of the rabbit gallbladder to nonelectrolytes (5). The second method is the measurement of the rate of transfer of radioactively labeled compounds across the lingual frenulum of the dog. This method was used in earlier studies on transmucosal absorption of local anesthetics (6).

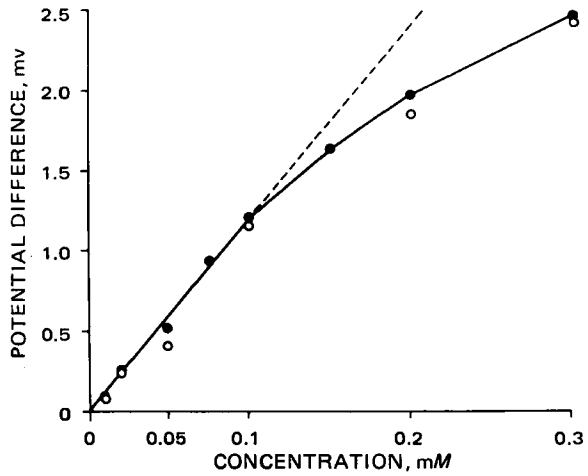

Figure 1—*Potential difference across the frenulum of the dog in response to osmotic gradients of sucrose (●) and mannitol (○). The dashed line is a continuation of the linear relationship that exists up to a concentration of 0.1 mM. Each point represents the mean value of at least three determinations on each of four separate pieces of tissue.*

EXPERIMENTAL

Streaming Potential Measurements—The lingual frenulum was removed from adult male mongrel dogs anesthetized with 30 mg/kg of pentobarbital sodium. The tissue was placed in oxygenated Krebs–Ringer phosphate solution and split along the cut edges, exposing an inner blood side surface as well as an outer oral side surface. The composition of the Krebs–Ringer phosphate solution was potassium (5 m*M*), sodium (148 m*M*), magnesium (1.33 m*M*), calcium (2.0 m*M*), chloride (154 m*M*), sulfate (1.33 m*M*), glucose (0.1%), and pH 7.4 phosphate buffer (8.6 m*M*).

The inner surface was carefully cleaned free of extraneous tissue, and the resulting thin membrane was placed in a modified Ussing (7) chamber. The methods described for determining streaming potentials in rat intestine (8) were adapted to this *in vitro* lingual frenulum preparation. Electric potential differences across the membrane were measured using polyethylene bridges filled with 4% agar in 150 m*M* sodium chloride. One bridge was placed in the solution facing the oral side of the membrane, and another bridge was placed in the solution facing the inner side. Each bridge led to a beaker of potassium chloride solution, which was connected through a potassium chloride–agar bridge to a second beaker of saturated potassium chloride; a calomel electrode was placed in the second beaker.

The potential difference between the electrodes was measured and recorded[1]. The asymmetry potential of the circuit was measured as the potential difference with both agar–sodium chloride bridges dipping into the solution bathing the same side of the tissue.

The solution bathing both sides of the membrane was identical (Krebs–Ringer phosphate), except that a known concentration (0.1

[1] Keithley model 602 electrometer and Keithley recorder.

Table I—Reflection Coefficients and Permeability Constants of Alcohols and Ureas on the Canine Oral Frenulum *In Vitro*

Compound	Molecular Weight	Partition Coefficient[a]	Permeability Constant, ($K_p \times 10^{-5}$ cm/sec)[b]	Reflection Coefficient[c]
Urea series				
Urea	60	0.00047	2.7 ± 0.83	0.17 ± 0.08 (39)
Methylurea	74	0.0012	1.4 ± 0.75	0.29 ± 0.12 (15)
Ethylurea	88	0.0041	—	0.76 ± 0.10 (15)
Propylurea	102	—	—	0.91 ± 0.03 (15)
Butylurea	116	—	—	0.43 ± 0.16 (18)
Alcohol series				
Methanol	32	0.14	9.7 ± 4.6	0.02 ± 0.02 (15)
Ethanol	46	0.26	3.7 ± 2.5	0.09 ± 0.01 (27)
Propanol	60	1.9	5.9 ± 3.6	0.02 ± 0.00 (19)
Butanol	74	7.7	10.1 ± 4.3	0.01 ± 0.01 (15)

[a] Ether to water; values are from Collander (13). [b] Mean permeability constant ± *SD* calculated from 12 pieces of tissue. [c] Mean reflection coefficient ± *SD*. The total number of determinations is given in parentheses.

M, unless otherwise mentioned) of substance to be tested was placed on one side. Sucrose was used as a nonpermeant substance. The potential developed by the test substance was compared to that developed in the presence of the same concentration of sucrose, as described by Wright and Diamond (5). Measurements of the potential difference developed by test substances were always bracketed by measurement with sucrose.

Radioactive Transfer Measurements—The lingual frenulum was removed from the animals, prepared, and placed in chambers as already described. Then 3 μCi of ^{14}C-labeled compound[2] plus sufficient nonradioactive compound to bring the total concentration to 1–10 m*M* (in Krebs–Ringer phosphate solution) was added to the half chamber facing one side of the membrane, and the other half chamber was filled with Krebs–Ringer phosphate solution.

Ten-microliter aliquots were removed from both half chambers at 30-min intervals. These samples were counted for a total of 5000 counts[3] using conventional techniques. All counts were corrected for quenching. Permeability constants were calculated from a knowledge of the area of exposed tissue, the volumes and concentrations present on both sides of the frenulum at each time interval, and the area of tissue exposed to the solutions using Fick's general law of diffusion:

$$\frac{Q}{At} = J_s = K_p \Delta C_s \qquad \text{(Eq. 1)}$$

where Q is the amount of solute that penetrates the membrane, A is the area of membrane exposed to solute, t is the time, J_s is the amount of solute that penetrates per unit area in unit time, K_p is the permeability constant, and ΔC_s is the difference in concentration on the two sides of the exposed membrane.

RESULTS

Potential Difference across Frenulum in Absence of Osmotic Gradients—In the absence of an osmotic gradient across the frenulum *in vitro*, there is essentially no potential difference between the outer (oral) and inner (blood) sides. The average value (±*SD*) for 42 preparations in which Krebs–Ringer phosphate solution was on both sides of the membrane was −0.0076 ± 0.031 mv (oral side negative). The range of recorded potential difference was from −0.06 to + 0.05 mv.

Potential Difference across Frenulum in Presence of Osmotic Gradient—Figure 1 shows the effect of adding either sucrose or mannitol to the bathing solution on the outside of the frenulum. The outside of the membrane went positive with respect to the inside. The amount by which the outside went positive depended on the concentration of sucrose or mannitol present in the bathing solution. The relationship between the concentration of sucrose present and the electrical response recorded was essentially linear when concentrations of 0.1 *M* or lower were used. At higher concentrations, the relationship was nonlinear.

If, after a steady potential had been reached, the sucrose-containing solution on the oral side of the frenulum was replaced with Krebs–Ringer phosphate solution, then the potential quickly returned to close to the original value. The potential difference that developed when sucrose was added to the outer side of the membrane could also be brought back to approximately zero by adding the identical concentration to the inside of the membrane (three experiments). Thus, at least two ways of eliminating the osmotic gradient resulted in abolition of the potential across the frenulum.

When a more permeant substance than sucrose was placed in the outside bathing solution, the potential difference across the preparation was less than when sucrose was used. Figure 2 shows the results of one experiment in which 0.1 *M* solutions of sucrose, urea, and ethylurea were compared. The potential differences developed to 0.1 *M* gradients of these three substances were 0.58, 0.11, and 0.45 mv, respectively. These data correspond to reflection coefficients of 0.19 for urea and 0.78 for ethylurea.

Table I gives the average reflection coefficients for each substance tested. The reflection coefficients for the second member of both the alcohol and urea series were higher (indicating a lower rate of penetration) than the first member of the series. In the alcohol series, the reflection coefficient then decreased with further increases in chain length. In contrast, the reflection coefficient continued to increase in the urea series until propylurea and then decreased when butylurea was tested.

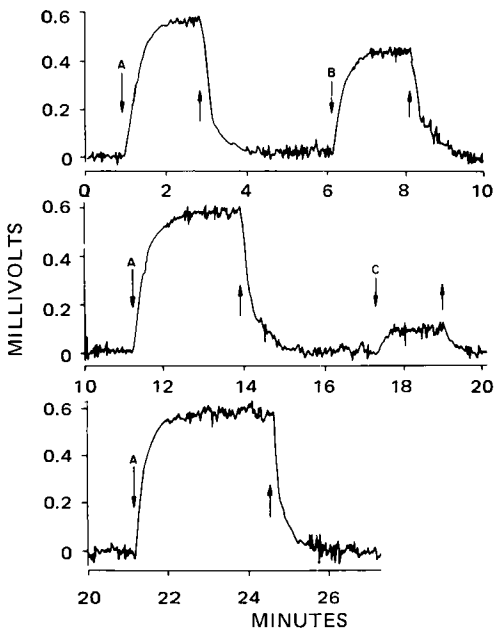

Figure 2—*Continuous record of the potential difference across the frenulum in response to 0.1* M *gradients of sucrose (A), ethylurea (B), and urea (C). Downward arrows indicate addition of the compound to the oral side of the preparation. Upward arrows indicate replacement of the compound-containing solution with Krebs–Ringer phosphate solution.*

[2] New England Nuclear Corp.
[3] Packard liquid scintillation counter.

Permeability Constant Measurements—The permeability of the frenulum to many compounds on which reflection coefficients were determined was measured by the rate of isotope penetration from the outside to the inside of the tissue. The permeability constants ranged from about 10^{-4} cm/sec for butanol to as low as 4×10^{-7} cm/sec for sucrose. The permeability for three of the compounds listed in Table I (ethylurea, propylurea, and butylurea) could not be determined because the labeled compounds were not commercially available.

Within both the alcohol and urea series, the permeability of the first member was higher than that of the second member of the series. This was true even though the ether-to-water distribution ratio is higher for the second member than the first. In the alcohol series, permeability then increased as chain length increased.

The electrical measurement of reflection coefficients is based on the principle that a flow of water across a charged membrane results in the development of an electrical potential difference across the membrane. The magnitude of these streaming potentials is directly proportional to the flow rate across the membrane (9). Since streaming potentials are set up rapidly, they offer a convenient means for determining osmotic flow. A fully impermeant molecule produces the greatest osmotic flow across a given membrane. The same concentration of a less permeant molecule results in a lower water flow and, consequently, a reduced potential across the membrane. Thus, as pointed out by Wright and Diamond (9), general agreement between direct chemical determination of permeability and results from the determination of reflection coefficients should be expected.

Collander (10, 11) made a detailed comparison of osmotic and chemical methods utilizing the alga *Nitella mucronata*. He measured the permeation of 17 nonionized compounds and demonstrated that similar permeability sequences were obtained by both methods. Our results using the dog frenulum also indicate that similar trends can be demonstrated by both methods.

Both methods have advantages and shortcomings. The primary advantage of the streaming potential technique is the rapidity of the measurement. Because each measurement takes only a few minutes, determinations of the streaming potential developed to a number of compounds can be performed on a single sample of tissue. An entire series of compounds can be run on the same tissue sample, thereby minimizing variations between tissue. Also, because of the short time of exposure to the test substances, there is less opportunity for damage to the tissue by a toxic compound.

However, higher concentrations of solute are required for the streaming potential measurement than for determinations using radioisotopes. Furthermore, the electrical signal generated under the conditions in this study was often less than 1 mv, particularly when very permeable compounds were tested. Thus, there are appreciable signal-to-noise ratio problems. These are particularly troublesome when either relatively highly permeable or impermeable compounds are compared.

The main advantage of the radioisotope method is that low concentrations of solute are used, which minimizes the opportunity for the test compound to injure the tissue. Also, when the isotope method is used, permeability constants rather than reflection coefficients can be calculated from the experimental results. These advantages are offset somewhat by the obvious disadvantages of the longer experimental time period and the necessity of making comparisons between tissues rather than on the same piece of frenulum.

Collander and Bärlund (12) concluded that lipid solubility is the most important factor determining the permeation of nonelectrolytes. However, they also pointed out that small molecules penetrate more rapidly than would be predicted from their lipid solubility. The current study of an alcohol series and a urea series suggests that a similar phenomenon exists for oral tissue. Both the reflection coefficient and the permeability constant data suggest that the smallest member of the series (one carbon) penetrates the frenulum more rapidly than some higher members of each series. This is true even though the ether-to-water partition coefficients are lower for the smaller compounds.

REFERENCES

(1) R. L. Brunton, "The Gaulstonian Lectures Delivered before the Royal College of Surgeons," Macmillan and Co., London, England, 1877.

(2) R. P. Walton, *Proc. Soc. Exp. Biol. Med.*, **32**, 1488(1935).

(3) A. H. Beckett and E. J. Triggs, *J. Pharm. Pharmacol.*, **19**, 31S(1967).

(4) I. A. Siegel, S. H. Hall, and V. V. Stambaugh, in "Histology of the Oral Mucosa," J. Meyer and C. Squires, Eds., Charles C Thomas, Springfield, Ill., 1971.

(5) E. M. Wright and J. M. Diamond, *Proc. Roy. Soc. B*, **172**, 227(1969).

(6) S. Bergman, D. Kane, I. A. Siegel, and S. Ciancio, *Arch. Oral Biol.*, **14**, 35(1969).

(7) H. Ussing, *Acta Physiol. Scand.*, **17**, 1(1949).

(8) D. H. Smyth and E. M. Wright, *J. Physiol.*, **182**, 591(1966).

(9) E. M. Wright and J. M. Diamond, *Proc. Roy. Soc. B*, **172**, 203(1969).

(10) R. Collander, *Physiol. Plant.*, **3**, 45(1950).

(11) *Ibid.*, **7**, 420(1954).

(12) R. Collander and H. Bärlund, *Acta Bot. Fenn.*, **11**, 1(1933).

(13) R. Collander, *Acta Chem. Scand.*, **3**, 717(1949).

ACKNOWLEDGMENTS AND ADDRESSES

Received September 23, 1974, from the *Departments of Oral Biology and Pharmacology and the Center for Research in Oral Biology, University of Washington, Seattle, WA 98195*

Accepted for publication March 31, 1975.

Supported by Grants DE-02600 and DE-00102 from the National Institutes of Health.

The authors express their gratitude to Ms. Elizabeth Toepfer for technical assistance.

[x] To whom inquiries should be directed.

Chemical Constituents of Fruit of *Cocculus carolinus* D.C. (Menispermaceae)

MAHMOUD A. ELSOHLY, JOSEPH E. KNAPP, PAUL L. SCHIFF, Jr., and DAVID J. SLATKIN ˣ

Abstract □ A phytochemical investigation of an ethanolic extract of the fruit of *Cocculus carolinus* resulted in the isolation and characterization of the alkaloids, cocculolidine and cocculine. The cyclitols (+)-quercitol and (−)-viburnitol and the alkaloids carococculine, magnoflorine, and palmatine, previously reported in the stems and leaves of this species, were also isolated and identified.

Keyphrases □ *Cocculus carolinus* fruit—isolation and characterization of alkaloids and cyclitols, IR, UV, NMR, and mass spectra, TLC □ Cyclitols—isolation and characterization from *Cocculus carolinus* fruit □ Alkaloids—isolated and characterized from *Cocculus carolinus* fruit, IR, UV, NMR, and mass spectra, TLC

Cocculus carolinus D.C. (Menispermaceae) is a species native to the southeastern United States. In previous phytochemical investigations (1, 2), the cyclitols (+)-quercitol and (−)-viburnitol, the lactone loliolide, and the alkaloids carocococculine, magnoflorine, palmatine, and sinoacutine were isolated and identified from the stems and leaves of the species. In this paper the chemical constituents of the fruit of this plant are reported.

An ethanolic extract of the fruit was fractionated into nonquaternary alkaloid, quaternary alkaloid, and acid–neutral fractions. Chromatography of the nonquaternary alkaloid fraction resulted in the isolation and identification of the *Erythrina* alkaloids cocculolidine (I) and cocculine (II). The insecticidal alkaloid cocculolidine (I) was first isolated in 1966 (3, 4) from the fresh leaves of *C. trilobus* D.C., while II was first found in 1950 (5–8) in *C. laurifolius* D.C.

EXPERIMENTAL[1]

Plant Material—The fruit of *C. carolinus* D.C. (Menispermaceae) was used[2].

Extraction—Air-dried ground fruits of *C. carolinus* (3.75 kg) were percolated at room temperature with 35 liters of ethanol. The extract was evaporated *in vacuo* at 40° to leave a dark-brown syrup (1.5 kg).

Isolation of Cyclitols—During the concentration of the ethanol extract, a white crystalline material precipitated (5.3 g). TLC on precoated cellulose plates[3], using a solvent system of acetone–water (4:1) and visualizing with potassium permanganate spray reagent (9), indicated the presence of two components, R_f 0.30 and 0.20. Fractional crystallization from ethanol–water afforded pure (+)-quercitol (350 mg), R_f 0.30, mp 229–230°, $[\alpha]_D^{25}$ + 20.8° (c 1.2, water), and (−)-viburnitol (50 mg), R_f 0.20, mp 177–178°, $[\alpha]_D^{25}$ − 55.0° (c 1.0, water). They were identical (melting point, mixed melting point, IR spectra, and $[\alpha]_D$) with authentic samples.

Fractionation—The fractionation of the concentrated ethanol extract was accomplished as previously reported (Scheme I, Ref. 1) and resulted in the following: acid–neutral fraction (Fraction A, 310.2 g), nonquaternary alkaloid fraction (Fraction B, 5.7 g), and quaternary alkaloid chloride fraction (Fraction C, 2.9 g).

Chromatography of Fraction B—The nonquaternary alkaloid fraction (Fraction B, 5.7 g) was chromatographed over silicic acid[4] (300 g) packed in petroleum ether (bp 60–90°). Elution with methanol–chloroform (8–20%) afforded a purified nonquaternary alkaloid fraction (4.3 g). This fraction was dissolved in chloroform (250 ml) and partitioned with 1% hydrochloric acid (3 × 250 ml). The aqueous acidic solution (750 ml) was made basic (pH 8) with concentrated ammonium hydroxide and extracted with chloroform (3 × 750 ml). The chloroform solutions were pooled, dried over anhydrous sodium sulfate, filtered, and evaporated *in vacuo* at 40° to leave a residue (3.0 g).[1]

A partition system of petroleum ether (bp 60–90°)–ethylene dichloride–methanol–water (12:3:2:0.4) was established as described previously (2). The purified fraction (3.0 g) was placed on the column (150 g, 3.0 × 60 cm), and alkaloidal bands were observed and collected accordingly.

Isolation of Carocococculine—After elution with 1 liter of mobile phase, an alkaloid band was collected (250 ml). Crystallization of this fraction from ethanol afforded carocococculine (15 mg), mp 218–220° dec.; $[\alpha]_D^{25}$ − 30° (c 0.5, chloroform); UV: λ_{max} (methanol) 214 (log ϵ 4.27) and 292 (3.68) nm; mass spectrometry: M^+ *m/e* 345 (100%). It was identical (melting point, mixed melting point, $[\alpha]_D$, and IR and mass spectra) with an authentic sample.

Isolation of Cocculolidine (I)—After elution with 250 ml of additional mobile phase, an alkaloidal band was collected (175 ml). Crystallization of this fraction from petroleum ether (bp 60–90°)–acetone afforded cocculolidine (200 mg), mp 140–141°; $[\alpha]_D^{20}$ + 258.0° (c 1.0, chloroform); UV: λ_{max} (methanol) 214 nm (log ϵ 4.15); IR: ν_{max} (potassium bromide) 1740, 1648, 1090, 1020, and 1005 cm^{-1}; NMR: δ 3.33 (3H) (OCH_3) and 5.65 (1H) (olefin); mass spectrometry: M^+ *m/e* 261 (15%), 230 (8), 203 (100), 174 (40), and 158 (13). This alkaloid was found to be identical (melting point, mixed melting point, $[\alpha]_D$, and UV, IR, and mass spectra) with an authentic sample of cocculolidine[5].

Isolation of Cocculine (II)—After elution with 150 ml of additional mobile phase, an alkaloidal band was collected (200 ml). Crystallization from methanol yielded II (35 mg), mp 207–208° [lit. (5) mp 217–218°]; $[\alpha]_D^{20}$ + 251.0° (c 1.0, chloroform) [lit. (5) $[\alpha]_D$ + 271.1°]; UV: λ_{max} (methanol) 211 (log ϵ 3.76), 223 (sh) (3.65), and 286 (3.19) nm; λ_{max} (0.1 *N* methanolic potassium hydroxide): 214 (log ϵ 3.84), 230 (sh) (3.62), 248 (sh) (3.44), 291 (3.18), and 307 (2.94) nm; IR: ν_{max} (potassium bromide) 3500, 2940, 2870, 1580, 1500, 1300, 1280, and 1090 cm^{-1}; NMR: δ 3.19 (3H) (OCH_3), 5.58 (1H) (olefin), and 6.50–7.00 (3H) (Ar); mass spectrometry: M^+ *m/e* 271 (19%), 256 (3), 240 (26), 213 (76), and 212 (100) [lit. (7) M^+ *m/e* 271 (15), 256 (3), 240 (20), 213 (100), and 212 (70)]. Repeated attempts to obtain a reference sample of this material failed.

Methylation of Cocculine (II)—The base (12 mg) was treated with ethereal diazomethane (20 ml) prepared from *p*-tolylsulfonylmethylnitrosamide[6] (2.14 g) (10) for 7 days. The solution was evaporated *in vacuo* to leave a residue which, following chromatogra-

[1] Melting points were determined on a Thomas-Hoover Uni-melt melting-point apparatus and are corrected. IR spectra were run in potassium bromide, using a Perkin-Elmer 257 spectrophotometer. Optical rotations were determined on a Perkin-Elmer 241 polarimeter. UV spectra were run on a Perkin-Elmer 202 spectrophotometer. NMR spectra were obtained in deuterated chloroform on a Hitachi Perkin-Elmer R-24 spectrometer, with tetramethylsilane as the internal standard. Mass spectra were recorded on an LKB-9000 spectrometer.

[2] Collected in Oxford, Miss., during the summer of 1973. Voucher specimens are deposited in the herbarium of the School of Pharmacy, University of Mississippi, University, MS 38677

[3] E. Merck, 0.10 mm.

[4] AR, 100 mesh, Mallinckrodt Chemical Works, St. Louis, MO 63160

[5] The authors thank Dr. Kojiro Wada, Nagoya University, Nagoya, Japan, for the reference sample.

[6] Diazald, Aldrich Chemical Co., Milwaukee, Wis.

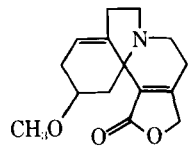

I

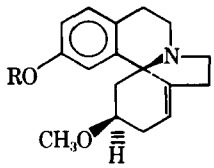

II: R = H
III: R = CH_3

phy over silicic acid[4] (5 g), elution with chloroform, and subsequent crystallization from petroleum ether (bp 60–90°), afforded *O*-methylcocculine (cocculidine) (III) (8 mg), mp 94–96° [lit. (5) mp 84–86°]; $[\alpha]_D^{17}$ + 199.0° (c 0.8, chloroform) [lit. (5) $[\alpha]_D$ + 250.9°]; UV: λ_{max} (methanol) 210 (log ϵ 4.09), 230 (sh) (3.91), 282 (3.37), and 288 (sh) (3.36) nm; IR: ν_{max} (potassium bromide) 2950, 2850, 1600, 1495, 1280, 1230, 1090, and 1040 cm^{-1}; NMR: δ 3.26 (3H) (OCH_3), 3.77 (3H) (OCH_3), 5.60 (1H) (olefin), and 6.65–7.11 (3H) (Ar); mass spectrometry: M^+ *m/e* 285 (10%), 270 (2), 254 (20), 227 (100), 226 (96), and 196 (30) [lit. (7) M^+ *m/e* 285 (15), 270 (3), 254 (17), 227 (100), 226 (55), and 196 (23)].

Chromatography of Quaternary Alkaloids—Fraction C (2.9 g) was chromatographed on silicic acid[4] (75 g) packed in chloroform.

Isolation of Palmatine—Elution with 8% methanol–chloroform afforded a fraction (39 mg) which, following rechromatography on polyamide[7] (25 g) and elution with concentrated ammonium hydroxide–ethanol (1:10), gave a fraction which was passed through a small ion-exchange column[8] (2 g). Evaporation and crystallization from methanol yielded palmatine iodide (5 mg), mp 219–221° dec.; UV: λ_{max} (methanol) 224 (log ϵ 4.65), 267 (4.20), 273 (4.20), 349 (4.22), and 432 (3.55) nm. It was identical (melting point, mixed melting point, and IR and UV spectra) with an authentic sample.

[7] M. Woelm, Waters Associates, Framingham, Mass.
[8] IRA-400 (iodide), Mallinckrodt Chemical Works, St. Louis, MO 63160

Isolation of Magnoflorine—Elution with 16% methanol–chloroform afforded a fraction (400 mg) which was dissolved in 1% hydrochloric acid and filtered. Mayer's (11) reagent was added, and the resulting precipitate was collected, washed with water, and dissolved in acetone–water (1:1) (100 ml). The solution was passed through a small ion-exchange column[8] (10 g). Evaporation and crystallization from methanol afforded magnoflorine iodide (55 mg), mp 251–253° dec.; $[\alpha]_D^{22}$ + 164.0° (c 0.25, methanol); UV: λ_{max} (methanol) 222 (log ϵ 4.67), 272 (4.03), and 311 (3.81) nm; λ_{max} (0.1 *N* methanolic potassium hydroxide) 224 (4.64), 280 (3.88), and 325 (3.91). It was identical (melting point, mixed melting point, and IR and UV spectra) with an authentic sample.

REFERENCES

(1) D. J. Slatkin, N. J. Doorenbos, J. E. Knapp, and P. L. Schiff, Jr., *J. Pharm. Sci.*, **61**, 1825(1972).

(2) D. J. Slatkin, N. J. Doorenbos, J. E. Knapp, and P. L. Schiff, Jr., *Lloydia*, **37**, 488(1974).

(3) K. Wada, S. Marumo, and K. Munakata, *Tetrahedron Lett.*, **42**, 5179(1966).

(4) K. Wada and K. Munakata, *Agr. Biol. Chem.*, **31**, 336(1967).

(5) S. Yunusov, *J. Gen. Chem.*, **20**, 391(1950).

(6) *Ibid.*, **20**, 1577(1951).

(7) S. Yunusov and R. Razakov, *Khim. Prir. Soedin.*, **6**, 74(1970).

(8) R. Rozakov, S. Yunusov, S. Nasyrov, A. Chekhlov, V. Andrianov, and Y. Struchkov, *J. Chem. Soc. (Chem. Commun.)*, **1974**, 150.

(9) E. Stahl, "Thin Layer Chromatography," Springer-Verlag, New York, N.Y., 1968.

(10) A. I. Vogel, "A Textbook of Practical Organic Chemistry," 3rd ed., Wiley, New York, N.Y., 1962.

(11) F. F. Mayer, *Amer. J. Pharm.*, **35**, 20(1863).

ACKNOWLEDGMENTS AND ADDRESSES

Received March 5, 1975, from the *Department of Pharmacognosy, School of Pharmacy, University of Pittsburgh, Pittsburgh, PA 15261*

Accepted for publication April 7, 1975.

The authors thank Dr. Soledad Campos Flor and Dr. James Flor for help in collection of plant material; and John Naworal, Graduate School of Public Health, University of Pittsburgh (NIH Grant RR00273), for mass spectra.

[x] To whom inquiries should be directed.

Mild and Safe Procedure for Hydrolyzing Oximes: Improved Synthesis of 1,2-Indandione

SURENDRA K. GUPTA and SURESH A. MARATHE ˣ

Abstract □ Four ketoximes were hydrolyzed to the corresponding ketones in 66–91% yields using 75% sulfuric acid and 37% formaldehyde at room temperature. An earlier procedure involving hydrochloric acid and 37% formaldehyde is extremely hazardous because it leads to the formation of bis(chloromethyl) ether, a potent carcinogen.

Keyphrases □ Oximes—hydrolysis, synthesis of 1,2-indandione and other ketones □ Hydrolysis—oximes to ketones, synthesis of 1,2-indandione □ 1,2-Indandione—synthesis by hydrolysis of 2-oximino-1-indanone

The hydrolysis of oximes can be accomplished using various reagents and conditions (1–4). Many procedures employ strong acids and elevated temperatures or long reaction times.

DISCUSSION

One of the mildest procedures used for hydrolyzing oximes was reported by Cava *et al.* (5). These investigators hydrolyzed 2-oximino-1-indanone using 36% formaldehyde and concentrated hydrochloric acid (Scheme I). The most serious drawback of this procedure is the formation of bis(chloromethyl) ether as a by-product.

According to Frankel *et al.* (6), formaldehyde and hydrochloric acid react at ambient temperatures in moist air, forming bis(chloromethyl) ether spontaneously in yields of about 0.01 mole %. Their studies showed that even formalin slurries containing Friedel–Crafts salts resulted in bis(chloromethyl) ether concentrations of 250–1500 ppb.

Bis(chloromethyl) ether has been shown (7, 8) to be an extremely potent carcinogen. For example, squamous cell carcinomas of the lung and esthesioneuroepitheliomas of the olfactory epithelium were produced in high incidence in rats following inhalation of 0.1 ppm of bis(chloromethyl) ether (7). A later report (8) indicated that repeated mouse skin application of bis(chloromethyl) ether produced papillomas and carcinomas, whereas subcutaneous injection in rats resulted in fibrosarcomas. As a result of these findings, the Occupational Safety and Health Administration (OSHA) included bis(chloromethyl) ether as one of the 14 carcinogens considered to be extremely hazardous to health (9).

The main purpose of this article is to emphasize the health hazards involved in the literature procedure (5) for preparing 1,2-indandione. In addition, a minor modification is described which offers a relatively safe and mild method for hydrolyzing oximes. The modified procedure consists of adding 75% sulfuric acid to a slurry or solution of the oxime in 37% formaldehyde at room temperature (Scheme II).

The hydrolysis of the oximes reported here was completed within 1 hr. When using this procedure, the hydrolysis of 2-oximino-1-indanone to 1,2-indandione was accomplished in 80% yield. The earlier conversion (5) of 2-oximino-1-indanone to 1,2-indandione was 55%. The general applicability of this procedure was demonstrated by hydrolyzing oximes from one heterocyclic and two commercially available ketones (Table I).

Table I—Hydrolysis of Oximes

Oxime	Hydrolysis Product	Workup Procedure	Yield, %
2-Oximino-1-indanone	1,2-Indandione	A	80
2-Piperidinoacetophenone oxime	2-Piperidinoacetophenone	B	91
p-Nitroacetophenone oxime	*p*-Nitroacetophenone	A	66
Benzophenone oxime	Benzophenone	A	80

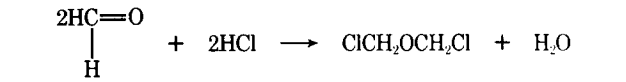

Scheme I

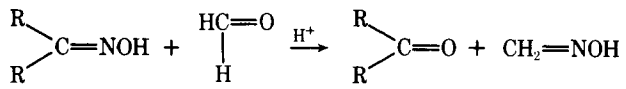

Scheme II

EXPERIMENTAL[1]

Starting Materials—2-Oximino-1-indanone was prepared from 1-indanone using *n*-butyl nitrite and concentrated hydrochloric acid according to the literature procedure (5). 2-Piperidinoacetophenone oxime was prepared by treating 2-piperidinoacetophenone (10) with hydroxylamine hydrochloride and potassium hydroxide using the procedure of Cromwell and Hoeksema (11). Benzophenone oxime and *p*-nitroacetophenone oxime were prepared by using the standard procedure (12).

General Procedure for Hydrolyzing Oximes—Sulfuric acid (200 ml, 75%) was added, cautiously, to a vigorously stirred solution or slurry of the oxime (0.31 mole) in formaldehyde (100 ml, 37%) at room temperature. The reaction became slightly exothermic. The suspension (or solution) was stirred for 45–60 min without any external heating or cooling. The mixture was poured over crushed ice (~1500 ml) with stirring, and the ketone was isolated by either of the following procedures.

Procedure A—This procedure is applicable for isolating ketones insoluble in aqueous mineral acids.

A precipitate was formed from which the desired ketone was isolated by filtration, washing with water, and drying. The following ketones were isolated from hydrolysis of the corresponding oximes.

1,2-Indandione was isolated in an 80% yield, mp 98–110°. The analytical sample was obtained by recrystallization from acetone, mp 105–118° [lit. (5) mp 95–115°]; IR: ν_{max} (mineral oil) 2930, 2899, 2825, 1761, 1701, 1661, 1600, 1585, 1570, 1460, 1380, 1320, 1300, 1250, 1200, 1180, 1150, 1110, 1080, 960, 940, 920, 770, 740, 710, and 630 cm^{-1}; UV: λ_{max} (ϵ) 248 (11,857), 290 (2763), and 300 (2482) nm.

Anal.—Calc. for $C_9H_6O_2$: C, 73.97; H, 4.14; O, 21.89. Found: C, 74.04; H, 4.10; O, 22.05.

Benzophenone was obtained in an 85% yield, mp 45–47° [lit. (13) mp 48°].

p-Nitroacetophenone was isolated in a 66% yield, mp 76–78° (after one recrystallization from ethanol) [lit. (13) mp 80–82°].

Procedure B—This procedure is applicable for isolating ketones soluble in aqueous mineral acids.

The solution was made alkaline (pH ≈ 10) by adding cold (0°) aqueous (10%) sodium hydroxide. The basic solution was extracted with ether, the ether extracts were washed with water and dried

[1] Melting points were determined using a Fischer-Johns melting-point apparatus and are corrected. Elemental analyses were performed by Enviro Analytical Laboratory, Knoxville, Tenn. Elemental analyses on commercially available materials were considered unnecessary. The purity and identity of the hydrolysis products were established by comparison with authentic samples. A Beckman IR-33 spectrophotometer was used for recording the IR spectra of the compounds. UV spectra were obtained using a Beckman ACTA CV spectrophotometer.

(magnesium sulfate), and the solvent was removed by evaporation under reduced pressure, giving the desired ketone.

This procedure was used to isolate 2-piperidinoacetophenone and gave a yield of 91%, bp 102–104° (0.2 mm Hg) [lit. (10) bp 180–181° (26 mm Hg)]; IR: ν_{max} (neat) 3050, 2925, 2840, 2790, 2747, 1684, 1672, 1590, 1570, 1440, 1374, 1290, 1274, 1250, 1230, 1210, 1190, 1168, 1150, 1120, 1100, 1069, 1030, 1012, 985, 955, 850, 740, 705, and 680 cm^{-1}; UV: λ_{max} 243 nm (ϵ 9670).

Anal.—Calc. for $C_{13}H_{17}NO$: C, 76.81; H, 8.43; N, 6.89. Found: C, 76.63; H, 8.40; N, 6.78.

REFERENCES

(1) C. H. Debury and B. W. Ponder, *J. Amer. Chem. Soc.*, **81**, 4629(1959).

(2) H. Alper and J. T. Edward, *J. Org. Chem.*, **32**, 2938(1967).

(3) S. G. Brooks, R. M. Evans, G. F. H. Green, J. S. Hunt, A. G. Long, B. Mooney, and L. J. Wyman, *J. Chem. Soc.*, **1958**, 4614.

(4) E. B. Hershberg, *J. Org. Chem.*, **13**, 542(1948).

(5) M. P. Cava, R. L. Little, and D. R. Napier, *J. Amer. Chem. Soc.*, **80**, 2257(1958).

(6) L. S. Frankel, K. S. McCallum, and L. Collier, *Environ. Sci. Technol.*, **8**, 356(1974).

(7) S. Laskin, M. Kuschner, R. T. Drew, V. P. Cappiello, and N. Nelson, *Arch. Environ. Health*, **23**, 135(1971).

(8) B. L. Van Duuren, "Proceedings of the Symposium on Chemical Carcinogens," Mellon Institute, Pittsburgh, Pa., June 28–29, 1973, pp. 25, 28.

(9) *Chem. Eng. News*, **Feb. 11, 1974**, 12, 13.

(10) P. Rahe and W. Schreiner, *Chem. Ber.*, **41**, 872(1908).

(11) N. H. Cromwell and H. Hoeksema, *J. Amer. Chem. Soc.*, **66**, 870(1944).

(12) A. I. Vogel, "A Textbook of Practical Organic Chemistry," 3rd ed., Wiley, New York, N.Y., 1956, pp. 721, 741.

(13) R. L. Shriner, R. C. Fuson, and D. Y. Curtis, "The Systematic Identification of Organic Compounds," Wiley, New York, N.Y., 1964, p. 344.

ACKNOWLEDGMENTS AND ADDRESSES

Received January 31, 1975, from *Starks Associates, Inc., Buffalo, NY 14213*

Accepted for publication April 1, 1975.

Supported by Contract NO1-CM-23203 from the Division of Cancer Treatment, National Cancer Institute, National Institutes of Health, Department of Health, Education, and Welfare, Bethesda, MD 20014

[x] To whom inquiries should be directed.

Synthesis of 5-Hydroxy-1-[[5-(*p*-nitrophenyl)furfurylidene]-amino]hydantoin, a Metabolite of Dantrolene

RALPH L. WHITE [x] and THOMAS J. SCHWAN

Abstract □ The synthesis and structural elucidation of 5-hydroxy-1-[[5-(*p*-nitrophenyl)furfurylidene]amino]hydantoin, a compound proposed as a metabolite of dantrolene sodium, are reported. In addition, a chromatographic comparison of the biological and synthesized materials is made.

Keyphrases □ Dantrolene metabolite—synthesis and structural elucidation of 5-hydroxy-1-[[5-(*p*-nitrophenyl)furfurylidene]amino]hydantoin □ 5-Hydroxy-1-[[5-(*p*-nitrophenyl)furfurylidene]-amino]hydantoin—dantrolene metabolite, synthesis and structural elucidation

Dantrolene sodium, 1-[[5-(*p*-nitrophenyl)furfurylidene]amino]hydantoin sodium salt hydrate[1], is a peripherally acting, novel, skeletal muscle relaxant (1–4). Metabolism of dantrolene sodium was reported to proceed through both reductive and nonreductive pathways (5). A polarographic method was developed for simultaneous determination of dantrolene (I) with its reduced and nonreduced metabolites (5).

Subsequently, a procedure was described for determining dantrolene alone and for estimating the amounts of two metabolites (6). One of these metabolites was referred to as Metabolite A (5, 6). Metabolite A now has been isolated, and evidence accumulated in these laboratories suggests that its structure is 5-hydroxy-1-[[5-(*p*-nitrophenyl)furfurylidene]amino]hydantoin (II) (Scheme I). This paper is concerned with the synthesis and structural elucidation of II and its subsequent chromatographic comparison with the isolated Metabolite A.

[1] Dantrium, Eaton Laboratories, Division of Morton-Norwich Products, Inc.

DISCUSSION

Cyclization of benzaldehyde semicarbazone (III) with oxalyl chloride (IV) allowed isolation of 1-(benzylideneamino)parabanic acid (V). By a combined catalytic hydrogenation and hydrogenolysis of V to 1-amino-5-hydroxyhydantoin (VI) and subsequent condensation of VI *in situ* with 5-(*p*-nitrophenyl)furfural (VII), II was prepared (Scheme II).

The NMR signal of the N_3—H proton (11.3 ppm) of II compared favorably with the N_3—H proton of dantrolene (11.3 ppm). In contrast, the N_1—H proton of the positional isomer 3-[[5-(*p*-nitrophenyl)furfurylidene]amino]hydantoin was observed at 8.3 ppm, close to the phenyl protons (7). Thus, the NMR spectrum of II supports catalytic reduction of the carbonyl of V in the 5-position rather than the 4-position; *i.e.*, II is a 1-amino-5-hydroxyhydantoin rather than a 3-amino-5-hydroxyhydantoin.

Compound II was unstable in the presence of base. When II was

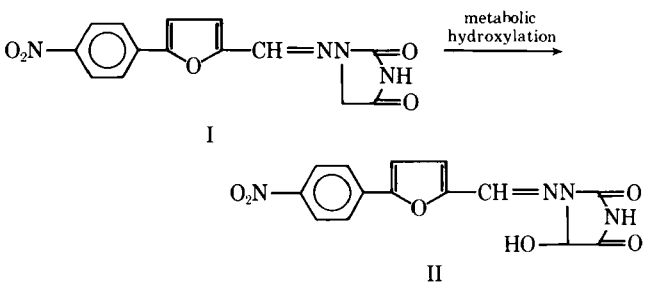

Scheme I

(magnesium sulfate), and the solvent was removed by evaporation under reduced pressure, giving the desired ketone.

This procedure was used to isolate 2-piperidinoacetophenone and gave a yield of 91%, bp 102–104° (0.2 mm Hg) [lit. (10) bp 180–181° (26 mm Hg)]; IR: ν_{max} (neat) 3050, 2925, 2840, 2790, 2747, 1684, 1672, 1590, 1570, 1440, 1374, 1290, 1274, 1250, 1230, 1210, 1190, 1168, 1150, 1120, 1100, 1069, 1030, 1012, 985, 955, 850, 740, 705, and 680 cm^{-1}; UV: λ_{max} 243 nm (ϵ 9670).

Anal.—Calc. for $C_{13}H_{17}NO$: C, 76.81; H, 8.43; N, 6.89. Found: C, 76.63; H, 8.40; N, 6.78.

REFERENCES

(1) C. H. Debury and B. W. Ponder, *J. Amer. Chem. Soc.*, **81**, 4629(1959).

(2) H. Alper and J. T. Edward, *J. Org. Chem.*, **32**, 2938(1967).

(3) S. G. Brooks, R. M. Evans, G. F. H. Green, J. S. Hunt, A. G. Long, B. Mooney, and L. J. Wyman, *J. Chem. Soc.*, **1958**, 4614.

(4) E. B. Hershberg, *J. Org. Chem.*, **13**, 542(1948).

(5) M. P. Cava, R. L. Little, and D. R. Napier, *J. Amer. Chem. Soc.*, **80**, 2257(1958).

(6) L. S. Frankel, K. S. McCallum, and L. Collier, *Environ. Sci. Technol.*, **8**, 356(1974).

(7) S. Laskin, M. Kuschner, R. T. Drew, V. P. Cappiello, and N. Nelson, *Arch. Environ. Health*, **23**, 135(1971).

(8) B. L. Van Duuren, "Proceedings of the Symposium on Chemical Carcinogens," Mellon Institute, Pittsburgh, Pa., June 28–29, 1973, pp. 25, 28.

(9) *Chem. Eng. News*, **Feb. 11, 1974**, 12, 13.

(10) P. Rahe and W. Schreiner, *Chem. Ber.*, **41**, 872(1908).

(11) N. H. Cromwell and H. Hoeksema, *J. Amer. Chem. Soc.*, **66**, 870(1944).

(12) A. I. Vogel, "A Textbook of Practical Organic Chemistry," 3rd ed., Wiley, New York, N.Y., 1956, pp. 721, 741.

(13) R. L. Shriner, R. C. Fuson, and D. Y. Curtis, "The Systematic Identification of Organic Compounds," Wiley, New York, N.Y., 1964, p. 344.

ACKNOWLEDGMENTS AND ADDRESSES

Received January 31, 1975, from *Starks Associates, Inc., Buffalo, NY 14213*

Accepted for publication April 1, 1975.

Supported by Contract NO1-CM-23203 from the Division of Cancer Treatment, National Cancer Institute, National Institutes of Health, Department of Health, Education, and Welfare, Bethesda, MD 20014

[x] To whom inquiries should be directed.

Synthesis of 5-Hydroxy-1-[[5-(*p*-nitrophenyl)furfurylidene]-amino]hydantoin, a Metabolite of Dantrolene

RALPH L. WHITE [x] and THOMAS J. SCHWAN

Abstract □ The synthesis and structural elucidation of 5-hydroxy-1-[[5-(*p*-nitrophenyl)furfurylidene]amino]hydantoin, a compound proposed as a metabolite of dantrolene sodium, are reported. In addition, a chromatographic comparison of the biological and synthesized materials is made.

Keyphrases □ Dantrolene metabolite—synthesis and structural elucidation of 5-hydroxy-1-[[5-(*p*-nitrophenyl)furfurylidene]amino]hydantoin □ 5-Hydroxy-1-[[5-(*p*-nitrophenyl)furfurylidene]-amino]hydantoin—dantrolene metabolite, synthesis and structural elucidation

Dantrolene sodium, 1-[[5-(*p*-nitrophenyl)furfurylidene]amino]hydantoin sodium salt hydrate[1], is a peripherally acting, novel, skeletal muscle relaxant (1–4). Metabolism of dantrolene sodium was reported to proceed through both reductive and nonreductive pathways (5). A polarographic method was developed for simultaneous determination of dantrolene (I) with its reduced and nonreduced metabolites (5).

Subsequently, a procedure was described for determining dantrolene alone and for estimating the amounts of two metabolites (6). One of these metabolites was referred to as Metabolite A (5, 6). Metabolite A now has been isolated, and evidence accumulated in these laboratories suggests that its structure is 5-hydroxy-1-[[5-(*p*-nitrophenyl)furfurylidene]amino]hydantoin (II) (Scheme I). This paper is concerned with the synthesis and structural elucidation of II and its subsequent chromatographic comparison with the isolated Metabolite A.

[1] Dantrium, Eaton Laboratories, Division of Morton-Norwich Products, Inc.

DISCUSSION

Cyclization of benzaldehyde semicarbazone (III) with oxalyl chloride (IV) allowed isolation of 1-(benzylideneamino)parabanic acid (V). By a combined catalytic hydrogenation and hydrogenolysis of V to 1-amino-5-hydroxyhydantoin (VI) and subsequent condensation of VI *in situ* with 5-(*p*-nitrophenyl)furfural (VII), II was prepared (Scheme II).

The NMR signal of the N_3—H proton (11.3 ppm) of II compared favorably with the N_3—H proton of dantrolene (11.3 ppm). In contrast, the N_1—H proton of the positional isomer 3-[[5-(*p*-nitrophenyl)furfurylidene]amino]hydantoin was observed at 8.3 ppm, close to the phenyl protons (7). Thus, the NMR spectrum of II supports catalytic reduction of the carbonyl of V in the 5-position rather than the 4-position; *i.e.*, II is a 1-amino-5-hydroxyhydantoin rather than a 3-amino-5-hydroxyhydantoin.

Compound II was unstable in the presence of base. When II was

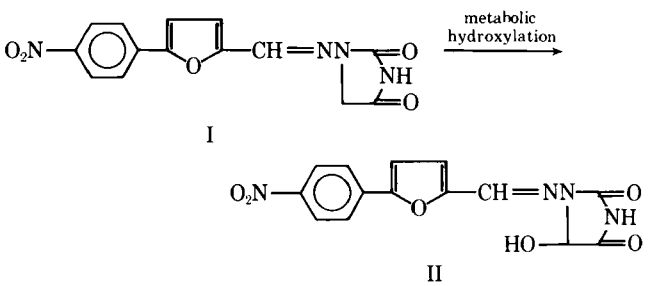

Scheme I

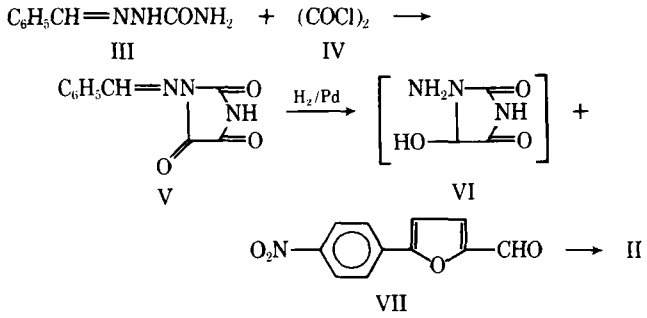

Scheme II

dissolved in dilute aqueous sodium hydroxide solution (Scheme III), an orange solid precipitated from the solution; it was shown to be the semicarbazone (VIII) by IR comparison with an authentic sample. The hydrolysis of 5-hydroxyhydantoin to urea was reported previously (8).

To assure the identity of Metabolite A with that of synthesized II, the two materials were cochromatographed on silica gel thin-layer plates in four solvent systems. There was no separation of the two components in any system.

In summary, the synthesis of II was accomplished, and the assignment of the structure of Metabolite A as II in these laboratories was shown to be correct by cochromatography of the biological and synthesized samples. The ring opening of synthetic Metabolite A in base to 5-(*p*-nitrophenyl)furfural semicarbazone also was found.

EXPERIMENTAL[2]

1-(Benzylideneamino)parabanic Acid (V)—In a 3-liter flask equipped with a condenser, drying tube, stirrer, and dropping funnel was placed 114 g (0.70 mole) of benzaldehyde semicarbazone in 1.0 liter of anhydrous ether. Oxalyl chloride (64 ml, 0.75 mole) was added dropwise during 0.5 hr rapidly enough to maintain a gentle reflux, and the solution then was stirred without heating for another 2.5 hr. The solid was collected by filtration and recrystallized from 3.5 liters of 2-propanol to yield 119 g (74%) of V, mp 205–207°.

Anal.—Calc. for $C_{10}H_7N_3O_3$: C, 55.30; H, 3.25; N, 19.35. Found: C, 55.19; H, 3.24; N, 19.30.

5-Hydroxy-1-[[5-(*p*-nitrophenyl)furfurylidene]amino]hydantoin (Metabolite A) (II)—In 500 ml of methanol were placed 87 g (0.40 mole) of V and 20 g of 5% palladium-on-carbon (50% moisture). Hydrogenation on a Parr apparatus gave uptake of two equivalents of hydrogen in 2 hr. An additional 20 g of catalyst was then added. Uptake of the third equivalent required 7 hr, with a total of 92% of the theoretical hydrogen uptake being observed.

The reduced solution was filtered, and the catalyst was washed with 500 ml of methanol. The combined methanolic filtrates were added to 87 g (0.40 mole) of VII (9), 2.0 liters of methanol, and 40 ml of concentrated hydrochloric acid. The mixture was refluxed for 2 hr and then filtered while hot. The collected solid was dried to give 20 g (15%) of II, mp 229–230°; NMR: δ 5.75 (d, 1H, CH, J = 9 Hz, exchange to s), 7.15 (d, 1H, furan CH, J = 3.5 Hz), 7.45 (d, 1H, OH, J = 9 Hz, exchange), 7.48 (d, 1H, furan CH, J = 3.5 Hz), 8.03 (d, 2H, phenyl CH, J = 9 Hz), 8.25 (s, 1H, azomethine CH), 8.36 (d, 2H, phenyl CH, J = 9 Hz), and 11.3 (broad s, 1H, NH, exchange); IR (potassium bromide): 3.1, 5.6, and 5.8 μm; mass spectrum M^+: *m/e* 330.

Anal.—Calc. for $C_{14}H_{10}N_4O_6$: C, 50.91; H, 3.05; N, 16.97. Found: C, 51.05; H, 3.10; N, 16.93.

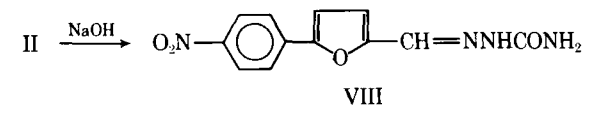

Scheme III

1-[[5-(*p*-Nitrophenyl)furfurylidene]amino]hydantoin (Dantrolene) (I)—The synthesis of this compound was reported previously (1); NMR: δ 4.40 (s, 2H, CH), 7.04 (d, 1H, furan CH, J = 4 Hz), 7.42 (d, 1H, furan CH, J = 4 Hz), 7.80 (s, 1H, azomethine CH), 7.98 and 8.32 (d of d, 4H, phenyl CH, J = 9 Hz), and 11.3 (broad s, 1H, NH, exchange).

5-(*p*-Nitrophenyl)furfural Semicarbazone (VIII) from II—To II (200 mg, 0.61 mmole) was added 100 ml of 0.5% sodium hydroxide, and the orange solution was shaken occasionally over 4 hr. Solid separated during that time. The mixture was filtered, and the collected solid was allowed to dry for 1 hr and washed with ether (20 ml). The IR spectrum of this product matched that of authentic 5-(*p*-nitrophenyl)furfural semicarbazone. The yield was 67 mg (32%), mp 223–226°. No depression was observed for a mixed melting point.

5-(*p*-Nitrophenyl)furfural Semicarbazone (VIII) from VII—To VII (9) (50 g, 0.25 mole) dissolved in warm dimethylformamide was added an aqueous solution of semicarbazide hydrochloride (30 g, 0.27 mole). The resulting solution was allowed to stand for 10 min and was then poured into a large volume of water. The resulting precipitate was recrystallized from acetic acid to give VIII (36%), mp 230–232°. A second recrystallization from acetic acid gave the analytical material, mp 236–237° [lit. (10) mp 193–194°[3]].

Anal.—Calc. for $C_{12}H_{10}N_4O_4$: C, 52.55; H, 3.68; N, 20.43. Found: C, 52.49; H, 3.57; N, 20.31.

REFERENCES

(1) H. R. Snyder, Jr., C. S. Davis, R. K. Bickerton, and R. P. Halliday, *J. Med. Chem.*, **10**, 807(1967).

(2) L. J. Honkomp, R. P. Halliday, and F. L. Wessels, *Pharmacologist*, **12**, 301(1970).

(3) K. O. Ellis and J. F. Carpenter, *Naunyn-Schmiedeberg's Arch. Pharmacol.*, **275**, 83(1972).

(4) K. O. Ellis and J. F. Carpenter, *Neuropharmacology*, **13**, 211(1974).

(5) P. L. Cox, J. P. Heotis, D. Polin, and G. M. Rose, *J. Pharm. Sci.*, **58**, 987(1969).

(6) R. D. Hollifield and J. D. Conklin, *ibid.*, **62**, 271(1973).

(7) T. J. Schwan and K. O. Ellis, *ibid.*, **64**, 1047(1975).

(8) C. T. Gray, M. S. Brooke, and J. C. Gerhart, *J. Bacteriol.*, **81**, 755(1961).

(9) H. Akashi and R. Oda, *Rep. Inst. Chem. Res., Kyoto Univ.*, **19**, 93(1949); through *Chem. Abstr.*, **45**, 7519h(1951).

(10) W. E. Hahn, F. Krajzewicz, and M. Nowaczyk, *Lodz. Tow. Nauk., Wydz.*, **3**(6), 15(1960); through *Chem. Abstr.*, **55**, 19891a(1961).

ACKNOWLEDGMENTS AND ADDRESSES

Received February 6, 1975, from the *Research and Development Department, Norwich Pharmacal Company, Division of Morton-Norwich Products, Inc., Norwich, NY 13815*

Accepted for publication March 25, 1975.

The authors thank Dr. H. R. Snyder, Jr., for synthesis of 5-(*p*-nitrophenyl)furfural semicarbazone. The cochromatography work under the direction of Dr. D. L. Pugh was much appreciated. Mrs. P. Curtis provided NMR spectra, and Mr. M. Tefft and Mr. G. Gustin supplied elemental analyses.

[x] To whom inquiries should be directed.

[2] Melting points were determined on a Mel-Temp apparatus and are corrected. A Varian Associates A-60A instrument was used for NMR spectra. All spectra were run in dimethyl sulfoxide-d_6 with tetramethylsilane as the internal standard. A Perkin-Elmer model 137B recording spectrophotometer was used for IR spectra. The mass spectrum was run on a Hitachi Perkin-Elmer RMV-7 mass spectrometer at Northern Illinois University, DeKalb, Ill.

[3] No reason for the difference in melting point is apparent.

Rapid TLC Determination of Methadyl Acetate and Some *In Vitro* Metabolites

MAN M. KOCHHAR ˣ, MAYNARD E. HAMRICK, and LALIT T. BAVDA

Abstract □ Methadyl acetate was metabolized by microsomal preparations of rat liver to yield nor-methadyl acetate and 6-(dimethylamino)-4,4-diphenyl-3-heptanol. The identification and separation of these three compounds was established by TLC, using iodoplatinate spray as a visualizing agent.

Keyphrases □ Methadyl acetate—TLC analysis, metabolism by rat liver microsomal preparations □ TLC—analysis and separation of methadyl acetate from metabolites, rat liver microsomes □ Analgesics—methadyl acetate, TLC analysis and separation from metabolites, rat liver microsomes

Methadyl acetate, a potent, long-acting, narcotic analgesic (1), is currently under clinical evaluation for the treatment of opiate addiction (2, 3). Its usefulness as a substitute for methadone prompted the development of a simple, accurate, and sensitive method for its identification using TLC.

Few methods to identify methadyl acetate and its metabolites have been reported (4, 5). Sung and Way (6) reported a colorimetric determination from tissue homogenates. Kaiko and Inturrisi (7, 8) reported the detection of methadyl acetate [6-(dimethylamino)-4,4-diphenyl-3-heptanol acetate], 6-(methylamino)-4,4-diphenyl-3-heptanol acetate (nor-methadyl acetate), 6-(dimethylamino)-4,4-diphenyl-3-heptanol, and 6-(methylamino)-4,4-diphenyl-3-heptanol by GLC using 3% SE-30 on Gas Chrom Q, 3.8% W-98 on Diatoport S, 5% OV-17 on Gas Chrom Q, 4% XF-1112 on Chromosorb W, 3% XE-60 on Gas Chrom Q, 3% 8BP on Gas Chrom Q, and 3% OV-225 on Gas Chrom Q. Billings and McMahon (1) identified the trichloroacetamide derivative of nor-methadyl acetate using GLC with an electron-capture detector.

This paper describes a highly sensitive TLC method for the detection of methadyl acetate, 6-(dimethylamino)-4,4-diphenyl-3-heptanol, and nor-methadyl acetate.

EXPERIMENTAL[1]

Male Sprague-Dawley rats were decapitated, and the livers were removed and immediately homogenized in two volumes of a cold tromethamine–hydrochloric acid–potassium chloride solution (0.05 *M* tromethamine buffer, pH 7.4, and 1.15% KCl) in a Teflon glass homogenizer. The homogenate was centrifuged for 20 min at 9000×*g* in a refrigerated centrifuge[2]. The supernate was then centrifuged for 1 hr at 78,000×*g* in a ultracentrifuge[3]. The microsomal pellet was resuspended in the same buffer to a volume of 10 ml.

Protein was determined by the biuret method described by Gornall *et al.* (9), and the microsomes were diluted to a concentration of 10 mg/ml. Metabolism of methadyl acetate was determined in a 3.0-ml incubation mixture consisting of 5 m*M* magnesium chloride, 12 m*M* glucose-6-phosphate dehydrogenase, 0.33 m*M* nicotinamide adenine dinucleotide phosphate (NADP), 50 m*M* tromethamine buffer (pH 7.4), 10 mg of microsomal protein, and 5 m*M* methadyl acetate. The mixture was incubated at 37° for 90 min. *N*-Demethylation of methadyl acetate was estimated by measuring the amount of formaldehyde formed by the method of Nash (10). After 90 min, the reaction was quenched by adding 1 *N* HCl. The mixture was centrifuged, and the supernate was removed.

The acidic supernate containing metabolites and unreacted methadyl acetate was adjusted to pH 11.5 with 1 *N* NaOH. The alkaline solution was extracted five times with 25-ml portions of ether. The ether layers were combined, dried over anhydrous magnesium sulfate, filtered, and evaporated under reduced pressure to 10 ml.

Three different types of precoated plates, instant thin-layer chromatography (ITLC) SG[4], LQD[5], and LQ6D[5], were used. The plate was spotted with approximately 5 μl of the ether solution concentrate previously prepared. The ITLC SG plates were then developed in a developing tank[4] containing ethyl acetate–cyclohexane–ammonia (50:40:0.1) (Solvent System A). The LQD and LQ6D plates were developed in ethyl acetate–methanol–water–ammonia (85:13:1:1) (Solvent System B).

The development requires 15 min for the ITLC plates and 45 min for the LQD and LQ6D plates. To visualize the spot, the LQD and LQ6D plates were dried and sprayed with iodoplatinate reagent (11) and the ITLC SG plates were dried and sprayed with iodine.

Table I—R_f Values and Color Reactions for Methadyl Acetate, Nor-methadyl Acetate, 6-(Dimethylamino)-4,4-diphenyl-3-heptanol, and Methadone Using ITLC SG Plates[a]

Compound	R_f	Color
Methadyl acetate	0.90	Brown
Nor-methadyl acetate	0.53	Light brown
6-(Dimethylamino)-4,4-diphenyl-3-heptanol	0.92	Dark brown
Methadone	0.72	Light yellowish brown

[a] Solvent System A was used, the spray reagent was iodine, and the sensitivity was 0.1 μg.

RESULTS AND DISCUSSION

In vitro metabolic studies indicated that approximately 0.05 μmole of formaldehyde was produced during the 90 min of incubation. A total of 15 μmoles of methadyl acetate was present, so approximately 0.3% was demethylated to form nor-methadyl acetate. However, three spots were observed on each of the three precoated plates (Tables I–III), indicating the presence of three compounds. These compounds were identified as nor-methadyl acetate, 6-(dimethylamino)-4,4-diphenyl-3-heptanol, and methadyl acetate by comparisons with authentic samples. These results were confirmed by GLC.

The R_f values and color reactions of each spot were compared with the pure compounds methadyl acetate, nor-methadyl acetate, 6-(dimethylamino)-4,4-diphenyl-3-heptanol, and methadone. The pure compounds were spotted on the same TLC plates along with *in vitro* metabolites. The nor-methadyl acetate and 6-(dimethyl-

[1] Methadyl acetate was obtained from the National Institute on Drug Abuse, Rockville, Md. Nor-methadyl acetate was supplied by Eli Lilly and Co., Indianapolis, Ind.

[2] Model RC-2, Ivan Sorvall Inc., Norfolk, CT 06470

[3] Model L3-50, Beckman Inc., Scientific Instrument Division, Fullerton, CA 92634

[4] Gelman Instrument Co., Ann Arbor, Mich.

[5] Quatum Assays Corp., Fairfield, NJ 07006

Table II—R_f Values and Color Reactions for Methadyl Acetate, Nor-methadyl Acetate, 6-(Dimethylamino)-4,4-diphenyl-3-heptanol, and Methadone Using LQD Plates[a]

Compound	R_f	Color
Methadyl acetate	0.75	Pinkish purple
Nor-methadyl acetate	0.64	Pinkish purple
6-(Dimethylamino)-4,4-diphenyl-3-heptanol	0.72	Purple
Methadone	0.68	Pinkish purple

[a] Solvent System B was used, the spray reagent was iodoplatinate, and the sensitivity was 0.1 μg.

Table III—R_f Values and Color Reactions for Methadyl Acetate, Nor-methadyl Acetate, 6-(Dimethylamino)-4,4-diphenyl-3-heptanol, and Methadone Using LQ6D Plates[a]

Compound	R_f	Color
Methadyl acetate	0.75	Pinkish purple
Nor-methadyl acetate	0.40	Pinkish purple
6-(Dimethylamino)-4,4-diphenyl-3-heptanol	0.68	Purple
Methadone	0.62	Pinkish purple[b]

[a] Solvent System B was used, the spray reagent was iodoplatinate, and the sensitivity was 0.1 μg. [b] Pinkish purple changed to brownish purple after a few minutes.

amino)-4,4-diphenyl-3-heptanol are the same metabolites found in human urine (12).

The identity of methadyl acetate, nor-methadyl acetate, and 6-(dimethylamino)-4,4-diphenyl-3-heptanol was confirmed by GLC, using 3% OV-1 on Shimalite W, 80–100 mesh[6]. The column temperature was 230°, and helium was the carrier gas (60-ml/min flow rate). The retention times for methadyl acetate, nor-methadyl acetate, 6-(dimethylamino)-4,4-diphenyl-3-heptanol, and methadone were 5.0, 4.8, 5.8, and 4.4 min, respectively. Methadone, a structurally related compound, was included for comparison because it is used along with methadyl acetate in opiate addicts.

Of the three different TLC plates used, LQ6D was the best in separating the methadyl acetate, nor-methadyl acetate, 6-(dimethylamino)-4,4-diphenyl-3-heptanol, and methadone. Iodoplatinate proved to be a better spraying reagent than iodine.

[6] American Instrument Co., Atlanta, Ga.

REFERENCES

(1) R. E. Billings and R. E. McMahon, *Fed. Proc., Abstr. 57 Annual meeting*, **32**, 764 Abstr.(1973).

(2) J. H. Jaffe and E. C. Senay, *J. Amer. Med. Ass.*, **216**, 1303(1971).

(3) A. Zaks, M. Fink, and A. M. Freedman, *ibid.*, **220**, 811(1972).

(4) R. E. Billings, R. Booher, S. Smits, A. Pohland, and R. E. McMahon, *J. Med. Chem.*, **16**, 305(1973).

(5) R. E. Billings, R. E. McMahon, and D. A. Blake, *Life Sci.*, **14**, 1437(1974).

(6) C. Y. Sung and E. L. Way, *J. Pharmacol. Exp. Ther.*, **110**, 260(1954).

(7) R. F. Kaiko and C. E. Inturrisi, *J. Chromatogr.*, **82**, 315(1973).

(8) R. F. Kaiko and C. E. Inturrisi, *Fed. Proc.*, **32**, 764 Abstr.(1973).

(9) A. G. Gornall, C. F. Bardawill, and M. M. David, *J. Biol. Chem.*, **177**, 751(1949).

(10) I. Nash, *Biochem. J.*, **55**, 416(1966).

(11) K. K. Kaistha and J. H. Jaffe, *J. Pharm. Sci.*, **61**, 679(1972).

(12) S. E. Smits and R. Booher, *Fed. Proc.*, **32**, 764 Abstr.(1973).

ACKNOWLEDGMENTS AND ADDRESSES

Received November 25, 1974, from the *School of Pharmacy, Auburn University, Auburn, AL 36830*

Accepted for publication April 7, 1975.

[x] To whom inquiries should be directed.

High-Speed Liquid Chromatographic Determination of Canrenone in Pharmaceutical Dosage Forms

DAVID E. WILLIAMSON

Abstract □ Canrenone can be determined by high-speed liquid chromatography in pharmaceutical dosage forms without interference from common excipients or degradation products. This stability-indicating assay, using *o*-nitroaniline as the internal standard, is rapid and accurate.

Keyphrases □ Canrenone—analysis, high-speed liquid chromatography, pharmaceutical dosage forms ■ High-speed liquid chromatography—analysis, canrenone, pharmaceutical dosage forms

Canrenone (I), 17-hydroxy-3-oxo-17α-pregna-4,6-diene-21-carboxylic acid γ-lactone, is a steroid that is an aldosterone antagonist and diuretic (1). Its synthesis was reported previously (2, 3).

Previous methods of analysis in biological fluids involved GC and fluorometric analyses (4–6). The fluorometric analysis involved the conversion of canrenone, a dienone, to a trienone using sulfuric acid (62% v/v). Since the major acid degradation product of canrenone is a trienone (II), this procedure could not be used as a stability-indicating assay for pharmaceutical dosage forms. Attempts by this author to use GC were not successful.

Recently, high-speed liquid chromatography

Table I—Standard Additions

Milligrams of Canrenone Added beyond 50 mg/25 μl	Found, mg/25 ml	Total Recovery, %
0.00	97.3	100.0
31.02	128.5	100.1
54.34	151.2	99.7

Table II—R_f Values and Color Reactions for Methadyl Acetate, Nor-methadyl Acetate, 6-(Dimethylamino)-4,4-diphenyl-3-heptanol, and Methadone Using LQD Plates[a]

Compound	R_f	Color
Methadyl acetate	0.75	Pinkish purple
Nor-methadyl acetate	0.64	Pinkish purple
6-(Dimethylamino)-4,4-diphenyl-3-heptanol	0.72	Purple
Methadone	0.68	Pinkish purple

[a] Solvent System B was used, the spray reagent was iodoplatinate, and the sensitivity was 0.1 μg.

Table III—R_f Values and Color Reactions for Methadyl Acetate, Nor-methadyl Acetate, 6-(Dimethylamino)-4,4-diphenyl-3-heptanol, and Methadone Using LQ6D Plates[a]

Compound	R_f	Color
Methadyl acetate	0.75	Pinkish purple
Nor-methadyl acetate	0.40	Pinkish purple
6-(Dimethylamino)-4,4-diphenyl-3-heptanol	0.68	Purple
Methadone	0.62	Pinkish purple[b]

[a] Solvent System B was used, the spray reagent was iodoplatinate, and the sensitivity was 0.1 μg. [b] Pinkish purple changed to brownish purple after a few minutes.

amino)-4,4-diphenyl-3-heptanol are the same metabolites found in human urine (12).

The identity of methadyl acetate, nor-methadyl acetate, and 6-(dimethylamino)-4,4-diphenyl-3-heptanol was confirmed by GLC, using 3% OV-1 on Shimalite W, 80–100 mesh[6]. The column temperature was 230°, and helium was the carrier gas (60-ml/min flow rate). The retention times for methadyl acetate, nor-methadyl acetate, 6-(dimethylamino)-4,4-diphenyl-3-heptanol, and methadone were 5.0, 4.8, 5.8, and 4.4 min, respectively. Methadone, a structurally related compound, was included for comparison because it is used along with methadyl acetate in opiate addicts.

Of the three different TLC plates used, LQ6D was the best in separating the methadyl acetate, nor-methadyl acetate, 6-(dimethylamino)-4,4-diphenyl-3-heptanol, and methadone. Iodoplatinate proved to be a better spraying reagent than iodine.

[6] American Instrument Co., Atlanta, Ga.

REFERENCES

(1) R. E. Billings and R. E. McMahon, *Fed. Proc., Abstr. 57 Annual meeting*, **32**, 764 Abstr.(1973).

(2) J. H. Jaffe and E. C. Senay, *J. Amer. Med. Ass.*, **216**, 1303(1971).

(3) A. Zaks, M. Fink, and A. M. Freedman, *ibid.*, **220**, 811(1972).

(4) R. E. Billings, R. Booher, S. Smits, A. Pohland, and R. E. McMahon, *J. Med. Chem.*, **16**, 305(1973).

(5) R. E. Billings, R. E. McMahon, and D. A. Blake, *Life Sci.*, **14**, 1437(1974).

(6) C. Y. Sung and E. L. Way, *J. Pharmacol. Exp. Ther.*, **110**, 260(1954).

(7) R. F. Kaiko and C. E. Inturrisi, *J. Chromatogr.*, **82**, 315(1973).

(8) R. F. Kaiko and C. E. Inturrisi, *Fed. Proc.*, **32**, 764 Abstr.(1973).

(9) A. G. Gornall, C. F. Bardawill, and M. M. David, *J. Biol. Chem.*, **177**, 751(1949).

(10) I. Nash, *Biochem. J.*, **55**, 416(1966).

(11) K. K. Kaistha and J. H. Jaffe, *J. Pharm. Sci.*, **61**, 679(1972).

(12) S. E. Smits and R. Booher, *Fed. Proc.*, **32**, 764 Abstr.(1973).

ACKNOWLEDGMENTS AND ADDRESSES

Received November 25, 1974, from the *School of Pharmacy, Auburn University, Auburn, AL 36830*

Accepted for publication April 7, 1975.

[x] To whom inquiries should be directed.

High-Speed Liquid Chromatographic Determination of Canrenone in Pharmaceutical Dosage Forms

DAVID E. WILLIAMSON

Abstract □ Canrenone can be determined by high-speed liquid chromatography in pharmaceutical dosage forms without interference from common excipients or degradation products. This stability-indicating assay, using *o*-nitroaniline as the internal standard, is rapid and accurate.

Keyphrases □ Canrenone—analysis, high-speed liquid chromatography, pharmaceutical dosage forms ■ High-speed liquid chromatography—analysis, canrenone, pharmaceutical dosage forms

Canrenone (I), 17-hydroxy-3-oxo-17α-pregna-4,6-diene-21-carboxylic acid γ-lactone, is a steroid that is an aldosterone antagonist and diuretic (1). Its synthesis was reported previously (2, 3).

Previous methods of analysis in biological fluids involved GC and fluorometric analyses (4–6). The fluorometric analysis involved the conversion of canrenone, a dienone, to a trienone using sulfuric acid (62% v/v). Since the major acid degradation product of canrenone is a trienone (II), this procedure could not be used as a stability-indicating assay for pharmaceutical dosage forms. Attempts by this author to use GC were not successful.

Recently, high-speed liquid chromatography

Table I—Standard Additions

Milligrams of Canrenone Added beyond 50 mg/25 μl	Found, mg/25 ml	Total Recovery, %
0.00	97.3	100.0
31.02	128.5	100.1
54.34	151.2	99.7

Table II—Precision and Accuracy

Trial	Canrenone Found, mg[a]	Percent Label Claim
1	49.1	98.2
2	48.9	97.8
3	49.5	99.0
4	49.5	99.0
5	49.1	98.2
6	48.9	97.8
7	49.3	98.7
8	49.4	98.7
9	49.1	98.2
10	49.0	98.1
	49.2 ± 0.23 mg/dose	98.4 ± 0.45%
Relative standard deviation	0.47%	0.46%

[a] Theory: 50 mg of canrenone.

(HSLC) has found wide usage in the analysis of steroids (7–12). This article describes the application of HSLC to the analysis of canrenone in pharmaceutical dosage forms.

EXPERIMENTAL

Apparatus—A high-pressure liquid chromatograph[1] equipped with a UV detector (254 nm) capable of operating at inlet pressures up to 1000 psig was used.

Column—The column was purchased from the instrument manufacturer[1] and was a 1-m × 2.1-mm i.d. × 0.6-cm o.d., precision bore, stainless steel tube, packed with Sil-X, an adsorption material[2].

Reagents—Heptane, 2-propanol, and methanol were reagent grade and required no further purification. *o*-Nitroaniline[3] and canrenone[4] were reference quality and were used without further purification.

2-Propanol in Heptane (4% v/v)—Dilute 20.0 ml of 2-propanol to 500 ml with heptane.

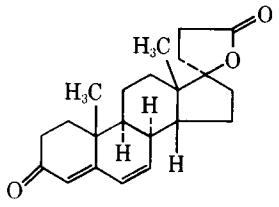

I

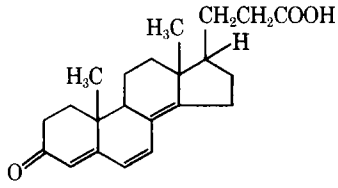

II

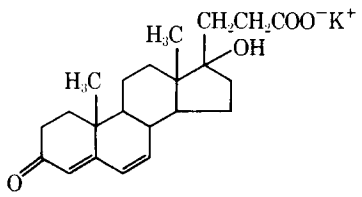

III

[1] DuPont 820, E. I. du Pont de Nemours and Co., Wilmington, Del.
[2] Perkin-Elmer, Norwalk, Conn.
[3] Highest Purity No. 646, Eastman Kodak Co., Rochester, N.Y.
[4] Abbott Laboratories, North Chicago, Ill., and Specia Paris, Paris, France.

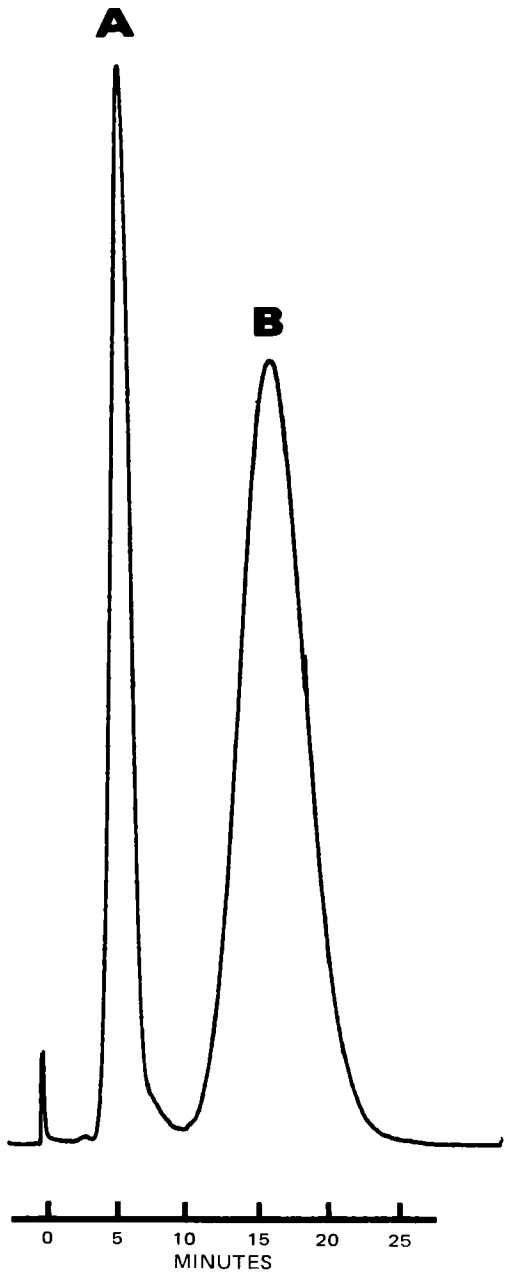

Figure 1—*High-speed liquid chromatogram of a sample preparation with internal standard. Key: A, o-nitroaniline, internal standard; and B, canrenone.*

Internal Standard Solution—Dissolve ~1.0 g of *o*-nitroaniline in 100 ml of methanol to yield a final concentration of ~10 mg/ml.

Standard Reference Solution—Accurately weigh about 125 mg of canrenone into a 25-ml volumetric flask containing ~10 ml of methanol and shake to dissolve. Pipet 5.0 ml of the internal standard solution into the flask and dilute to volume with methanol.

Sample Preparation—Weigh accurately an amount of powder equivalent to 125 mg of canrenone and transfer it to a 25-ml volumetric flask. Add about 10 ml of methanol, pipet in 5.0 ml of the internal standard solution, and shake for 15 min before diluting to volume with methanol. Withdraw about 10 ml of this suspension, using a 10-ml glass syringe equipped with a Teflon needle on a Kel-F-Hub. Filter the suspension through a filter holder[5] containing a silver membrane[6] filter and collect the filtrate in a 10-ml

[5] Swinnex-25 SX00-025-00, Millipore Corp., Bedford, Mass.
[6] FM-25 (0.45 μm), Selas Flotronic, Spring House, Pa.

ground-glass-stoppered flask. This solution is then ready to be chromatographed.

Chromatographic Procedure—The mobile phase was 4% 2-propanol in heptane, the temperature was ambient, and the solvent flow was ~1 ml/min (at an inlet pressure of 1000 psig). The precision photometer detector (254 nm) was set at an attenuation of ×16.

Samples and standards of 3 μl (~15 μg of canrenone) were injected with the flow stopped. A standard was injected for every five sample injections, and the peak heights of canrenone and the internal standard were measured.

Calculations—The concentration of canrenone in milligrams per dose is calculated using:

$$\text{mg/dose canrenone} = F \times \frac{H_1}{H_2} \times \frac{\text{average dose weight (mg)}}{\text{weight sample used (mg)}} \quad \text{(Eq. 1)}$$

$$\text{\% label claim} = \frac{\text{mg/dose found}}{\text{mg/dose theory}} \times 100 \quad \text{(Eq. 2)}$$

where H_1 and H_2 are the peak heights of canrenone and internal standard in the sample, respectively.

The response factor, F, is the ratio of the internal standard peak heights to the canrenone peak height in the standard reference solution multiplied by the weight of canrenone in the standard.

RESULTS AND DISCUSSION

Figure 1 shows the chromatogram of a typical sample containing the internal standard. The major degradation products, II and III, do not interfere with the analysis. Compound III does not elute but is retained on the column. Compound II elutes at ~32 min if present. Canrenone elutes at ~15 min, and the internal standard elutes at ~5 min. Methanol was chosen as the solvent for drug extraction due to the insolubility of common excipients.

The linearity of response has been shown for canrenone pharmaceutical formulations containing 40–60 mg/dose. Table I shows the results of standard addition experiments when the theory was 50 mg/dose.

The precision of the method was determined from 10 replicate determinations of canrenone in 50-mg/dose pharmaceutical formulations performed over 2 days (Table II). Peak height rather than peak area was found to yield better results on this analysis, because the pumping system on the chromatographic apparatus caused a recorder spike which interfered with digital integrator calculations.

This method is also applicable to single-tablet and capsule analysis if the attenuation of the UV detector and the internal standard concentrations are adjusted appropriately.

REFERENCES

(1) "Merck Index," 8th ed., Merck and Co., Rahway, N.J., 1968, p. 802.

(2) J. A. Cella and R. C. Twirt, *J. Org. Chem.*, **24**, 1109(1959).

(3) J. A. Cella (to G. D. Searle and Co.), U.S. pat. 2,900,383 (1959).

(4) W. Sadee, S. Riegelman, and S. C. Jones, *J. Pharm. Sci.*, **61**, 1129(1972).

(5) W. Sadee, M. Dagcioglu, and S. Riegelman, *ibid.*, **61**, 1126(1972).

(6) J. Chamberlain, *J. Chromatogr. Sci.*, **55**, 249(1971).

(7) S. Siggia and R. A. Dishman, *Anal. Chem.*, **42**, 1223(1970).

(8) K. Lotscher and H. Kern, *Chimia*, **27**, 348(1973).

(9) J. C. Touchsto and W. Wortmann, *J. Chromatogr.*, **76**, 244(1973).

(10) R. A. Henry, J. A. Schmit, and J. F. Dieckman, *J. Chromatogr. Sci.*, **9**, 513(1971).

(11) J. F. K. Huber, J. A. R. Hulsman, and C. A. M. Meyers, *J. Chromatogr.*, **62**, 79(1971).

(12) F. A. Fitzpatrick, S. Siggia, and J. Dingman, *Anal. Chem.*, **44**, 2211(1972).

ACKNOWLEDGMENTS AND ADDRESSES

Received January 30, 1975, from *Analytical Services & Methods Development, Hospital Products Division, Abbott Laboratories, North Chicago, IL 60064*

Accepted for publication April 15, 1975.

The author thanks James Raihle and Victor Papendick for assistance.

Time-Dependent Change in Renal Clearance of Bethanidine in Humans

A. N. CHREMOS *, D. SHEN ‡, M. GIBALDI ‡x, J. D. PROCTOR §, and J. H. NEWMAN §

Abstract □ Blood levels and urinary excretion rates of bethanidine were determined in three normal human subjects following oral administration of a single dose of the drug. The postabsorptive decline of blood concentration with time was noticeably slower than the corresponding decline in the urinary excretion rate. The discrepancy can be attributed to a continual decrease in the renal clearance of bethanidine throughout the study. Therefore, pharmacokinetic modeling of urinary excretion data alone would lead to erroneous conclusions concerning the persistence of drug in the blood.

Keyphrases □ Bethanidine—time-dependent change in renal clearance and blood levels, humans □ Excretion, urinary—rate of clearance of bethanidine, compared to blood levels, humans □ Antihypertensives—bethanidine, renal clearance compared to blood levels, humans

A previous study (1) on the pharmacokinetics of bethanidine in hypertensive patients found that the renal clearance of unchanged bethanidine fluctuated greatly in the initial 6 hr following a single 25-mg iv dose. The study also revealed that the elimination of bethanidine in humans occurs almost exclusively *via* renal excretion. Hence, a more extensive study on the renal clearance of the drug was undertaken.

EXPERIMENTAL

Three healthy male volunteers, 65–75 kg, were selected. Their

ground-glass-stoppered flask. This solution is then ready to be chromatographed.

Chromatographic Procedure—The mobile phase was 4% 2-propanol in heptane, the temperature was ambient, and the solvent flow was ~1 ml/min (at an inlet pressure of 1000 psig). The precision photometer detector (254 nm) was set at an attenuation of ×16.

Samples and standards of 3 μl (~15 μg of canrenone) were injected with the flow stopped. A standard was injected for every five sample injections, and the peak heights of canrenone and the internal standard were measured.

Calculations—The concentration of canrenone in milligrams per dose is calculated using:

$$\text{mg/dose canrenone} = F \times \frac{H_1}{H_2} \times \frac{\text{average dose weight (mg)}}{\text{weight sample used (mg)}} \quad \text{(Eq. 1)}$$

$$\text{\% label claim} = \frac{\text{mg/dose found}}{\text{mg/dose theory}} \times 100 \quad \text{(Eq. 2)}$$

where H_1 and H_2 are the peak heights of canrenone and internal standard in the sample, respectively.

The response factor, F, is the ratio of the internal standard peak heights to the canrenone peak height in the standard reference solution multiplied by the weight of canrenone in the standard.

RESULTS AND DISCUSSION

Figure 1 shows the chromatogram of a typical sample containing the internal standard. The major degradation products, II and III, do not interfere with the analysis. Compound III does not elute but is retained on the column. Compound II elutes at ~32 min if present. Canrenone elutes at ~15 min, and the internal standard elutes at ~5 min. Methanol was chosen as the solvent for drug extraction due to the insolubility of common excipients.

The linearity of response has been shown for canrenone pharmaceutical formulations containing 40–60 mg/dose. Table I shows the results of standard addition experiments when the theory was 50 mg/dose.

The precision of the method was determined from 10 replicate determinations of canrenone in 50-mg/dose pharmaceutical formulations performed over 2 days (Table II). Peak height rather than peak area was found to yield better results on this analysis, because the pumping system on the chromatographic apparatus caused a recorder spike which interfered with digital integrator calculations.

This method is also applicable to single-tablet and capsule analysis if the attenuation of the UV detector and the internal standard concentrations are adjusted appropriately.

REFERENCES

(1) "Merck Index," 8th ed., Merck and Co., Rahway, N.J., 1968, p. 802.

(2) J. A. Cella and R. C. Twirt, *J. Org. Chem.*, **24**, 1109(1959).

(3) J. A. Cella (to G. D. Searle and Co.), U.S. pat. 2,900,383 (1959).

(4) W. Sadee, S. Riegelman, and S. C. Jones, *J. Pharm. Sci.*, **61**, 1129(1972).

(5) W. Sadee, M. Dagcioglu, and S. Riegelman, *ibid.*, **61**, 1126(1972).

(6) J. Chamberlain, *J. Chromatogr. Sci.*, **55**, 249(1971).

(7) S. Siggia and R. A. Dishman, *Anal. Chem.*, **42**, 1223(1970).

(8) K. Lotscher and H. Kern, *Chimia*, **27**, 348(1973).

(9) J. C. Touchsto and W. Wortmann, *J. Chromatogr.*, **76**, 244(1973).

(10) R. A. Henry, J. A. Schmit, and J. F. Dieckman, *J. Chromatogr. Sci.*, **9**, 513(1971).

(11) J. F. K. Huber, J. A. R. Hulsman, and C. A. M. Meyers, *J. Chromatogr.*, **62**, 79(1971).

(12) F. A. Fitzpatrick, S. Siggia, and J. Dingman, *Anal. Chem.*, **44**, 2211(1972).

ACKNOWLEDGMENTS AND ADDRESSES

Received January 30, 1975, from *Analytical Services & Methods Development, Hospital Products Division, Abbott Laboratories, North Chicago, IL 60064*

Accepted for publication April 15, 1975.

The author thanks James Raihle and Victor Papendick for assistance.

Time-Dependent Change in Renal Clearance of Bethanidine in Humans

A. N. CHREMOS *, D. SHEN ‡, M. GIBALDI ‡x, J. D. PROCTOR §, and J. H. NEWMAN §

Abstract □ Blood levels and urinary excretion rates of bethanidine were determined in three normal human subjects following oral administration of a single dose of the drug. The postabsorptive decline of blood concentration with time was noticeably slower than the corresponding decline in the urinary excretion rate. The discrepancy can be attributed to a continual decrease in the renal clearance of bethanidine throughout the study. Therefore, pharmacokinetic modeling of urinary excretion data alone would lead to erroneous conclusions concerning the persistence of drug in the blood.

Keyphrases □ Bethanidine—time-dependent change in renal clearance and blood levels, humans □ Excretion, urinary—rate of clearance of bethanidine, compared to blood levels, humans □ Antihypertensives—bethanidine, renal clearance compared to blood levels, humans

A previous study (1) on the pharmacokinetics of bethanidine in hypertensive patients found that the renal clearance of unchanged bethanidine fluctuated greatly in the initial 6 hr following a single 25-mg iv dose. The study also revealed that the elimination of bethanidine in humans occurs almost exclusively *via* renal excretion. Hence, a more extensive study on the renal clearance of the drug was undertaken.

EXPERIMENTAL

Three healthy male volunteers, 65–75 kg, were selected. Their

Table I—Recovery of Radioactivity from Urine and Feces following a Single 10-mg Oral Dose of ^{14}C-Bethanidine Hemisulfate to Normal Subjects

Sample	Dose Recovered, %		
	Subject 1	Subject 2	Subject 3
Urine	84.6	82.4	70.7
Feces	13.46	3.39	18.28
Total	98.06	85.79	88.98

medical histories and the results of physical and laboratory examinations were unremarkable. Each subject gave signed, informed consent to participate.

Subjects were instructed to avoid the ingestion of any drug for at least 1 week before and during the study. Following an 8-hr fasting period, each subject received a 10-mg solution of ^{14}C-bethanidine hemisulfate containing approximately 100 μCi of radioactivity. Food was not allowed until 2 hr after drug administration.

The dose administered was approximately 50% of the usual pharmacologically effective dose (0.3 mg/kg). Arterial blood pressure was determined at 0, 2.5, 4.5, 6.5, 8.5, and 12 hr after drug administration with the subject in supine and standing positions. A clear pharmacological effect of the drug was not apparent.

Ten milliliters of blood was drawn in containers[1] containing potassium oxalate at 0.5, 1.5, 2, 3, 4, 5, 6, 8, 12, 24, and 48 hr after drug administration. The blood samples were immediately refrigerated pending assay. Urine was also collected at the following time intervals after drug administration: 0–2, 2–4, 4–6, 6–8, 8–12, 12–24, 24–36, 36–48, 48–72, and 72–96 hr. Stools were collected for 5–6 days. Both urine and stool samples were frozen until assay.

Aliquots of urine and fecal samples were prepared and assayed for total radioactivity by liquid scintillation counting. Urine and fecal samples were subjected to TLC and reverse isotope analysis as described previously (1). No significant amounts of metabolites (<5% of radioactive dose) were detected. Consequently, all total radioactivity measurements were assumed to represent unmetabolized bethanidine.

RESULTS AND DISCUSSION

The extent of urinary and fecal excretion of radioactivity following a single 10-mg oral dose of ^{14}C-bethanidine hemisulfate in three normal subjects is shown in Table I. The overall recovery of the radioactive dose was essentially complete in Subject 1 but was slightly less than complete in the other two subjects. Urinary excretion accounted for 71–85% of the administered dose.

Figure 1 illustrates both blood levels and urinary excretion rates in Subject 2 following a single 10-mg oral dose. Peak blood levels were observed 2–4 hr after administration, suggesting relatively rapid absorption.

When blood level and urinary excretion rate plots were compared for all three subjects, it became apparent that the postabsorptive decline of blood concentration with time was noticeably slower than the corresponding decline in urinary excretion rate. For example, in Subject 2 (Fig. 1) over the 12–48-hr period the blood concentrations of bethanidine declined from 0.09 to 0.02 μg/ml, a four- to-fivefold reduction. Over the same time interval, the average excretion rates fell by about 100-fold, from approximately 0.3 to 0.004 mg/hr.

The disparity in the rate of decline between blood concentration and urinary excretion rate suggested a lack of constancy in the renal clearance of bethanidine. Therefore, the renal clearance was calculated at various time intervals according to:

$$Cl_R = \frac{[X_u]^{t_1 \to t_2}}{AUC^{t_1 \to t_2}} \qquad \text{(Eq. 1)}$$

where X_u is the amount of drug excreted in the urine during $t_1 \to t_2$, and $AUC^{t_1 \to t_2}$ is the area under the blood curve between t_1 and t_2. The area under the blood curve was determined by the trapezoidal rule.

[1] Vacutainers.

Table II—Change in Renal Clearance of Bethanidine as a Function of Time following a Single 10-mg Oral Dose of ^{14}C-Bethanidine Hemisulfate to Normal Subjects

Time Interval, hr	Clearance[a], ml/min		
	Subject 1	Subject 2	Subject 3
0–2	880	1364	932
2–4	616	740	851
4–6	453	496	603
6–8	364	432	452
8–12	341	366	323
12–24	211	177	167
24–48	245	57.5	91.3

[a] Calculated based on whole blood concentrations.

Results for all three subjects are shown in Table II. The initial clearance values were higher than the normal glomerular filtration rate and of the order of normal renal blood flow, suggesting extensive active tubular secretion of bethanidine. In all three subjects, the renal clearance of bethanidine decreased progressively with time. By 48 hr, clearance values were reduced to about or below that of the normal glomerular filtration rate.

In pharmacokinetics, it is customarily assumed that there is a direct relationship between the urinary excretion rate and the blood or plasma level of intact drug or metabolites. At any instant of time, the relationship is expressed mathematically as:

$$\frac{dX_u}{dt} = Cl_R C_b \qquad \text{(Eq. 2)}$$

where dX_u/dt is the urinary excretion rate, and C_b is the blood concentration. Provided that renal clearance remains constant, any change in blood level will result in a parallel change in the excretion rate of the drug. In the present case, the renal clearance of bethanidine decreased with time. Consequently, the postabsorptive decline of the urinary excretion rate reflects not only the fall in blood concentration but also the diminishing capacity of the renal clearance mechanism, leading to a faster rate of decline in the excretion rate as compared to the blood level decline. A half-life determination from the urinary excretion of bethanidine, therefore, will not be a meaningful index of the persistence of drug in the blood.

The exact cause for the change in renal clearance of bethanidine is not known and requires further investigation. However, the

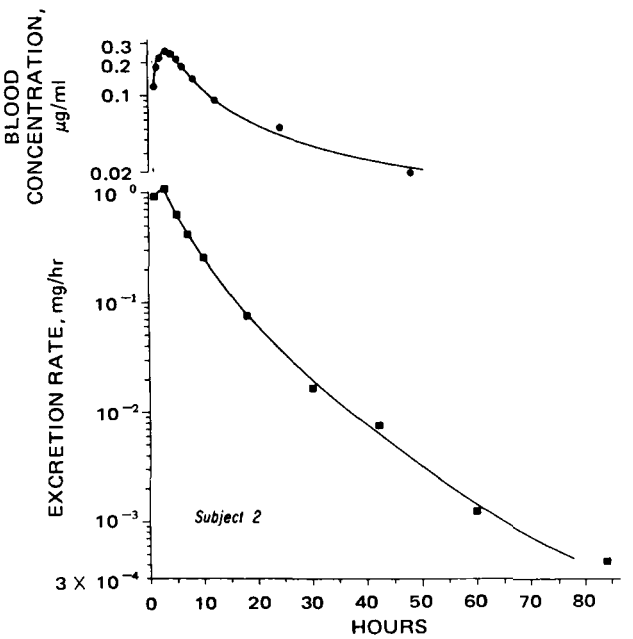

Figure 1—*Blood level (●) and urinary excretion rate (■) data from Subject 2 following administration of a single 10-mg oral dose of ^{14}C-bethanidine hemisulfate.*

renal clearance of bethanidine declined continually with time in the initial absorptive phase during which there were both a rise and a fall in blood concentration. Therefore, the change in renal clearance was not apparently related to the blood concentration of the drug. In addition, the reduction in renal clearance occurred in the absence of any noticeable hypotensive response.

In conclusion, this report clearly demonstrates the desirability of simultaneous measurements of drug levels in both blood and urine when studying the pharmacokinetics of drugs. If concomitant plasma or blood measurements are not available and if the constancy of renal clearance cannot be assured, information derived from urinary excretion data should be interpreted with caution.

REFERENCE

(1) D. Shen, M. Gibaldi, M. Throne, G. Bellward, R. Cunningham, Z. Israili, P. Dayton, and J. McNay, *Clin. Pharmacol. Ther.*, 17, 363(1975).

ACKNOWLEDGMENTS AND ADDRESSES

Received February 10, 1975, from the *Division of Research and Development, A. H. Robins Co., Richmond, VA 23220, the ‡Department of Pharmaceutics, School of Pharmacy, State University of New York at Buffalo, Buffalo, NY 14214, and the §Division of Clinical Pharmacology, Department of Medicine, Medical College of Virginia, Richmond, VA 23298

Accepted for publication April 4, 1975.

Supported in part by Grant GM-20852 from the National Institute of General Medical Sciences, National Institutes of Health.

x To whom inquiries should be directed.

Oxygen Solubilization by Lung Surfactant

WALTER F. STANASZEK *x, BERNARD ECANOW ‡, and ROBERT S. LEVINSON *

Abstract □ To illustrate the concept of solubilization as a possible mode of gas transport in biological systems, dog lung surfactants in varying concentrations were tested for their ability to solubilize oxygen. The degree of gas solubilization was determined by GC, using a modified tonometer as an absorption chamber. The concentration of surfactant was found to be an essential factor for gas solubilization. Surfactant concentration above the CMC yielded anomalously high gas absorption. Solubilization of the gas is thought to occur by a partitioning effect into the interior of surfactant micelles.

Keyphrases □ Surfactants, lung—oxygen solubilization at various surfactant concentrations □ Solubilization, oxygen—by various concentrations of dog lung surfactant

Throughout this study, the theory of gas uptake was developed from a reasonably well-established concept, *i.e.*, that of solubilization. Since solubilization is frequently applied to pharmaceutical systems, it is natural for this pharmaceutical background to allow correlation of many biological occurrences through similar mechanisms.

Solubilization is defined as the "spontaneous dissolution of normally water-insoluble substances by an aqueous solution of surfactant." The surfactant molecule is amphiphilic, possessing both a nonpolar (hydrophobic) portion and a polar (hydrophilic) portion which exist in solution as individual molecules in very dilute concentrations. With an increase in surfactant concentration above the critical micelle concentration (CMC), all surface-active agents have the ability to form micelles.

A micelle can be defined as an aggregate of surface-active agents acting as a unit. The basic physical characteristics of surface-active agents, which are present during and after the formation of micelles, are that they lower surface tension in dispersion, produce a wetting effect, are strongly adsorbed to hydrophobic surfaces, and can solubilize normally insoluble substances.

In this study, varying concentrations of dog lung surfactant were analyzed for oxygen-absorbing or solubilizing characteristics to illustrate the concept of solubilization as a possible mode of gas transport in biological systems, as proposed by Ecanow *et al.* (1–3). A great deal of information is available regarding the nature and composition of mammalian alveoli based on histochemical and extraction studies (4–11). Analyses of lung extracts have indicated that lecithin (phosphatidyl choline) depicts the characteristic surface-active properties of lung surfactant and that dipalmityl lecithin is the essential lung surfactant (12, 13).

EXPERIMENTAL

Gas solubilization was analyzed by GC. A modified tonometer, constructed of glass and fitted with rubber septums for the introduction and extraction of gas samples, was used as an absorption chamber (14, 15).

Gas syringes were used for transfer of the gas from the preparation tonometer to that containing the gas uptake sample. These syringes were fitted with 22-gauge, 6.35-cm (2.5-in.) needles. Gastight syringes[1] (100 and 250 μl), fitted with Teflon hub needles [24 gauge, 3.8 cm (1.5 in.)], were used for removal of gas analysis samples from the second tonometer and for injection of the samples into the gas chromatograph.

A gas chromatograph[2] equipped with a thermal conductivity detector was utilized to follow gas uptake. Helium, used as the carrier gas, was maintained at a flow rate of 40 ml/min. Operating temperatures were as follows: injection, 172°; column, 135°; internal detector, 137°; duct, 204°; outlet, 252°; and external oven, 232°. Stainless steel columns[3] used for analysis of gas uptake were 1.8 m × 0.64 cm (6 ft × 0.25 in.), packed with molecular sieves (5A).

Gas analysis samples were removed at intervals of approximately 1 min for 20 min; this time length had been determined as sufficient for data evaluation. The studies were conducted at ambient temperature and atmospheric pressure.

The lung surfactant solution was first warmed in a water bath at

[1] Hamilton.
[2] WCLID 1670, Warner-Chilcott Laboratories, Richmond, Calif.
[3] HCl Scientific Inc., Rockford, Ill.

renal clearance of bethanidine declined continually with time in the initial absorptive phase during which there were both a rise and a fall in blood concentration. Therefore, the change in renal clearance was not apparently related to the blood concentration of the drug. In addition, the reduction in renal clearance occurred in the absence of any noticeable hypotensive response.

In conclusion, this report clearly demonstrates the desirability of simultaneous measurements of drug levels in both blood and urine when studying the pharmacokinetics of drugs. If concomitant plasma or blood measurements are not available and if the constancy of renal clearance cannot be assured, information derived from urinary excretion data should be interpreted with caution.

REFERENCE

(1) D. Shen, M. Gibaldi, M. Throne, G. Bellward, R. Cunningham, Z. Israili, P. Dayton, and J. McNay, *Clin. Pharmacol. Ther.*, 17, 363(1975).

ACKNOWLEDGMENTS AND ADDRESSES

Received February 10, 1975, from the *Division of Research and Development, A. H. Robins Co., Richmond, VA 23220, the ‡Department of Pharmaceutics, School of Pharmacy, State University of New York at Buffalo, Buffalo, NY 14214, and the §Division of Clinical Pharmacology, Department of Medicine, Medical College of Virginia, Richmond, VA 23298

Accepted for publication April 4, 1975.

Supported in part by Grant GM-20852 from the National Institute of General Medical Sciences, National Institutes of Health.

x To whom inquiries should be directed.

Oxygen Solubilization by Lung Surfactant

WALTER F. STANASZEK *x, BERNARD ECANOW ‡, and ROBERT S. LEVINSON *

Abstract □ To illustrate the concept of solubilization as a possible mode of gas transport in biological systems, dog lung surfactants in varying concentrations were tested for their ability to solubilize oxygen. The degree of gas solubilization was determined by GC, using a modified tonometer as an absorption chamber. The concentration of surfactant was found to be an essential factor for gas solubilization. Surfactant concentration above the CMC yielded anomalously high gas absorption. Solubilization of the gas is thought to occur by a partitioning effect into the interior of surfactant micelles.

Keyphrases □ Surfactants, lung—oxygen solubilization at various surfactant concentrations □ Solubilization, oxygen—by various concentrations of dog lung surfactant

Throughout this study, the theory of gas uptake was developed from a reasonably well-established concept, *i.e.*, that of solubilization. Since solubilization is frequently applied to pharmaceutical systems, it is natural for this pharmaceutical background to allow correlation of many biological occurrences through similar mechanisms.

Solubilization is defined as the "spontaneous dissolution of normally water-insoluble substances by an aqueous solution of surfactant." The surfactant molecule is amphiphilic, possessing both a nonpolar (hydrophobic) portion and a polar (hydrophilic) portion which exist in solution as individual molecules in very dilute concentrations. With an increase in surfactant concentration above the critical micelle concentration (CMC), all surface-active agents have the ability to form micelles.

A micelle can be defined as an aggregate of surface-active agents acting as a unit. The basic physical characteristics of surface-active agents, which are present during and after the formation of micelles, are that they lower surface tension in dispersion, produce a wetting effect, are strongly adsorbed to hydrophobic surfaces, and can solubilize normally insoluble substances.

In this study, varying concentrations of dog lung surfactant were analyzed for oxygen-absorbing or solubilizing characteristics to illustrate the concept of solubilization as a possible mode of gas transport in biological systems, as proposed by Ecanow *et al.* (1–3). A great deal of information is available regarding the nature and composition of mammalian alveoli based on histochemical and extraction studies (4–11). Analyses of lung extracts have indicated that lecithin (phosphatidyl choline) depicts the characteristic surface-active properties of lung surfactant and that dipalmityl lecithin is the essential lung surfactant (12, 13).

EXPERIMENTAL

Gas solubilization was analyzed by GC. A modified tonometer, constructed of glass and fitted with rubber septums for the introduction and extraction of gas samples, was used as an absorption chamber (14, 15).

Gas syringes were used for transfer of the gas from the preparation tonometer to that containing the gas uptake sample. These syringes were fitted with 22-gauge, 6.35-cm (2.5-in.) needles. Gastight syringes[1] (100 and 250 μl), fitted with Teflon hub needles [24 gauge, 3.8 cm (1.5 in.)], were used for removal of gas analysis samples from the second tonometer and for injection of the samples into the gas chromatograph.

A gas chromatograph[2] equipped with a thermal conductivity detector was utilized to follow gas uptake. Helium, used as the carrier gas, was maintained at a flow rate of 40 ml/min. Operating temperatures were as follows: injection, 172°; column, 135°; internal detector, 137°; duct, 204°; outlet, 252°; and external oven, 232°. Stainless steel columns[3] used for analysis of gas uptake were 1.8 m × 0.64 cm (6 ft × 0.25 in.), packed with molecular sieves (5A).

Gas analysis samples were removed at intervals of approximately 1 min for 20 min; this time length had been determined as sufficient for data evaluation. The studies were conducted at ambient temperature and atmospheric pressure.

The lung surfactant solution was first warmed in a water bath at

[1] Hamilton.
[2] WCLID 1670, Warner-Chilcott Laboratories, Richmond, Calif.
[3] HCl Scientific Inc., Rockford, Ill.

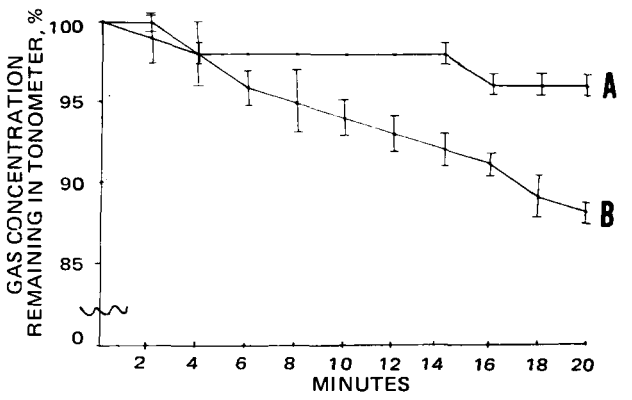

Figure 1—*Oxygen gas sorption by dog lung surfactant. Key: A, dilute lung surfactant in normal saline; and B, concentrated dog lung surfactant.*

40° to facilitate the escape of any dissolved gases, and the "degassed" lung surfactant solution was then placed in the sample tonometer. Helium was then passed through the tonometer to "clear" the atmosphere.

Oxygen was obtained in the form of oxygen USP. To allow for consistent transfer procedures, the oxygen was stored in a 300-ml tonometer at ambient temperature and atmospheric pressure. Since the columns used for oxygen detection in the chromatograph were also sensitive to nitrogen, tonometers were completely cleared with helium before being used for oxygen storage. This sensitivity to nitrogen was beneficial in that any leakage or contamination could be detected by the presence of a nitrogen peak.

Dogs were sacrificed by intravenous injection of pentobarbital sodium. Crude extracts of lung surfactant were prepared by the Bondurant–Miller (16) method, which produced a bulk liquid solution. A 0.9% sodium chloride solution, equivalent to 5–6 ml/g of lung, usually about 175 ml in total, was introduced through a tracheal cannula. From 70 to 80% of the volume was recovered from the tracheal (or bronchial) effluent. The liquid was retained in the lung for 10 min and then gently rinsed back and forth into a syringe five to 10 times. The solution became slightly turbid and, if allowed to stand, persisted in turbidity without formation of any significant precipitate except for a few mucoid strands. If centrifuged, however, the solution cleared and a distinctive precipitate was formed.

The lung extract was then divided into two equal parts. One portion was designated "dilute lung surfactant"; the remainder of the solution was concentrated to 20 ml by directing a jet of compressed air across the surface of the solution. This concentrate was then designated "concentrated dog lung surfactant."

RESULTS AND DISCUSSION

Figure 1 illustrates oxygen absorption obtained from studies on dilute lung surfactant in normal saline and concentrated dog lung surfactant. In original studies, the tonometer gas concentration (microliters per milliliter) in the vapor phase above the liquid sample *versus* the time (minutes) was followed graphically. For presentation purposes, graphic data were arranged to indicate the presence of the gas concentration remaining in the tonometer *versus* time (minutes). Results (Table I) indicate that oxygen absorption was negligible with distilled water and dilute surfactant in normal saline. The degree of oxygen solubilization with concentrated lung surfactant was significant, suggesting that solubilization of oxygen is mediated by micelle formation.

The oxygen gas absorption, found only in concentrated dog lung surfactant, indicates that micellar solubilization of oxygen may depend on the degree of micelle development in the surfactant solution. The dilute samples, ostensibly exhibiting little or no micelle development, showed insignificant gas absorption.

In previous studies (1, 2), a two-stage mechanism was proposed for molecular transport through an alveolar membrane across an aqueous barrier containing surfactants. The ability of the medium

Table I—Statistical Statement: *t* Values Based on Comparison between Degree of Oxygen Solubilization by Diluted Dog Lung Surfactant and Concentrated Dog Lung Surfactant Solutions

Minutes	$t_{[4]}$
0	0.00[a]
2	1.06[a]
4	0.32[a]
6	3.46[a]
8	3.00[a]
10	6.93[a]
12	8.66[b]
14	8.50[b]
16	12.72[b]
18	10.73[b]
20	16.97[b]

[a] Not significant. [b] $p < 0.001$.

interphase to concentrate the surfactant molecules to the aggregation point results in formation of micelles. A continued concentration increase unites the micelles to form large multicellular "films" at the alveolar membrane surface. These micellar films readily solubilize various nonpolar molecules.

In the second stage of the process, the interface is expanded to the point of micelle desegregation. The medium then consists of individual surfactant molecules with smaller micelles dispersed in the aqueous solution. The nonpolar gases are released to the interphase, and the essentially nonpolar molecules are readily soluble in portions of the alveolar membrane. The driving force for aggregation and dispersion of surfactant molecules in the lung lining is the expansion and contraction of the membrane surface during inhalation and exhalation (9).

Further ramifications of these findings are being studied.

REFERENCES

(1) B. Ecanow, R. Balagot, and V. Bandelin, *Amer. Rev. Respir. Dis.*, **99**, 106(1969).

(2) B. Ecanow, R. Balagot, and W. Stanaszek, *Presbyterian–St. Lukes Hospital Medical Bulletin*, **7**, No. 4 (Oct. 1968).

(3) B. Ecanow, B. Gold, S. Touquan, and W. Stanaszek, *Dis. Nerv. Syst.*, **28**, 240(1967).

(4) J. Bernstein, M. Wittner, and E. M. Scarpelli, *Amer. J. Pathol.*, **46**, 27a(1965).

(5) R. P. Bolande and M. H. Klaus, *ibid.*, **45**, 449(1964).

(6) W. H. Chase, *Exp. Cell Res.*, **18**, 15(1959).

(7) J. Groniowski and W. Biczyskowa, *Nature*, **204**, 745(1964).

(8) T. D. Hackney, C. R. Collier, and D. E. Rounds, *Med. Thorac.*, **22**, 77(1965).

(9) B. Ecanow, R. Balagot, and V. Santelices, *Nature*, **215**, 1400(1967).

(10) R. E. Pattle, *Physiol. Rev.*, **45**, 68(1965).

(11) R. E. Pattle, in "Advances in Respiratory Physiology," A. de Reuck and R. Porter, Eds., W. I. Churchill, London, England, 1966.

(12) T. R. Hill and T. N. Finley, *Physiologist*, **7**, 159(1964).

(13) E. S. Brown, *Amer. J. Physiol.*, **207**, 402(1964).

(14) W. Stanaszek and B. Ecanow, *J. Pharm. Sci.*, **61**, 860(1972).

(15) W. Stanaszek, R. Levinson, and B. Ecanow, *ibid.*, **63**, 1941(1974).

(16) S. Bondurant and D. A. Miller, *J. Appl. Physiol.*, **17**, 167(1962).

ACKNOWLEDGMENTS AND ADDRESSES

Received February 24, 1975, from the *College of Pharmacy, University of Oklahoma, Norman, OK 73069, and the ‡College of Pharmacy, University of Illinois, Chicago, IL 60612

Accepted for publication April 7, 1975.

Presented at the Basic Pharmaceutics Section, APhA Academy of Pharmaceutical Sciences, Chicago meeting, August 1974.

ˣ To whom inquiries should be directed.

Quantitative Determination of Resorcinol in Presence of Phenol

V. DAS GUPTA

Abstract □ A simple and accurate method for the quantitative determination of resorcinol in the presence of phenol is reported. The method is based on the formation of indophenol by reacting resorcinol with 2,6-dibromoquinone-4-chlorimide. The concentration of indophenol can be measured spectrophotometrically. This method is recommended for the determination of resorcinol in resorcinol–phenol–boric acid solution and carbol-fuchsin solution. The decomposition products of resorcinol and phenol, *e.g.*, colored quinones, do not interfere with the assay procedure.

Keyphrases □ Resorcinol—spectrophotometric analysis in presence of phenol, effect of pH, decomposition products □ Carbol-fuchsin solution—spectrophotometric analysis of resorcinol, effect of pH, decomposition products □ Spectrophotometry—analysis, resorcinol in presence of phenol, effect of pH, decomposition products

In most quantitative methods for the determination of resorcinol, phenol interferes (1). A combination of a bromometric technique and NMR spectroscopy was recommended for the analysis of resorcinol in the presence of phenol (1). However, the method lacks sensitivity and may not be adaptable by many laboratories due to the lack of an NMR spectrometer.

This paper reports a very simple, sensitive, and accurate colorimetric method for the quantitative analysis of resorcinol in the presence of phenol. The method is based on the formation of a pink-colored indophenol by reacting resorcinol with 2,6-dibromoquinone-4-chlorimide (I), as recommended by Gibbs (2). The decomposition products, *e.g.*, colored quinones, and phenol do not interfere with the assay procedure.

This method may be considered more sensitive than a reported GLC method (3) since the latter requires a concentration of 3 mg/ml for analysis. Due to the small injection volume (1–2 μl), the total resorcinol required is less in the GLC method. Nevertheless, the sensitivity of the developed method can be improved further (see *Discussion*). The developed method is more sensitive than the 4-dimethylaminobenzaldehyde method (4), since the latter requires about four times more resorcinol for the same absorbance value.

EXPERIMENTAL

Chemicals and Reagents—All chemicals and reagents were USP, NF, or ACS grade. Compound I[1] (97%), phenol[2] loose crystals, and resorcinol[3] were used without further purification.

Preparation of Solutions—*Resorcinol–Phenol–Boric Acid Solution*—This solution was prepared as reported earlier (1).

Carbol-fuchsin Solution—This solution was prepared according to NF X (5).

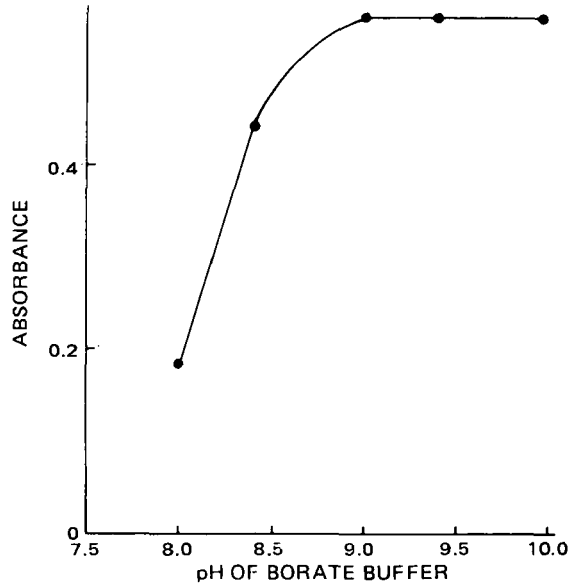

Figure 1—*Plot of pH* versus *absorbance.*

Compound I Solution—This solution was prepared fresh daily by dissolving 40.0 mg of I in 10.0 ml of methanol.

Sodium Borate Solution—A 1% aqueous solution was prepared fresh daily.

Borate Buffer Solution—The alkaline borate buffer solutions of various pH values (8.0, 8.4, 9.0, 9.4, and 10.0) were prepared according to USP XVIII (6).

Solutions of Potassium Ferricyanide—Four and 10% solutions in water were prepared fresh daily.

Standard Solutions of Resorcinol and Phenol for Colorimetric Analysis—The following were prepared in water every week: (*a*) a solution containing 10.0 μg of resorcinol/ml, (*b*) a solution containing 4.5 μg of phenol/ml, and (*c*) a solution containing 10.0 μg of resorcinol/ml and 4.5 μg of phenol/ml.

Wavelength of Maximum Absorption for Resorcinol—A 5.0-ml quantity of the standard aqueous solution of resorcinol was diluted to 10.0 ml with water. Then 2.0 ml of the borate buffer solution (pH 9.4) and 0.1 ml of the I solution were added and mixed. The solution was immediately scanned in the visible range. The maximum absorption was recorded at about 530 nm. This wavelength was selected for further investigations.

Effect of pH on Assay Sensitivity—The proposed procedure was followed to determine the absorbance values[4] at 530 nm using borate buffer solutions of various pH values (8.0, 8.4, 9.0, 9.4, and 10.0). A blank was prepared by substituting water for the resorcinol solution. All absorbance values were recorded after 90 sec of mixing (Fig. 1). For further investigations, a buffer solution of pH 9.4 was selected.

Calibration Curve—A 2.0-ml quantity of the borate buffer solution (pH 9.4) was mixed with 2.0, 3.0, 4.0, and 5.0 ml, respectively, of the standard aqueous resorcinol solution, and each mixture was brought to volume (12.0 ml) with water. Then 0.1 ml of the I solution was added, the solution was mixed, and the absorbance of each solution was measured within 50–120 sec against a reagent blank. Beer's law was followed.

[1] Aldrich Chemical Co., Milwaukee, Wis.
[2] Matheson, Coleman & Bell, Norwood, Ohio.
[3] Fisher Scientific Co., Fairlawn, N.J.

[4] A Bausch & Lomb Spectronic 20 was used.

Table I—Assay Results on Resorcinol

Product or Solution	Resorcinol Found, %
Standard aqueous solution of resorcinol and phenol	100.00
Standard aqueous solution of phenol	0.00
Resorcinol–phenol–boric acid solution	99.46
	99.65
	99.82
Average =	99.64
Average deviation =	±0.12
Carbol-fuchsin solution	100.25
	100.48
	100.25
Average =	100.33
Average deviation =	±0.10
All potassium ferricyanide-treated phenol solutions	0.00

Interference from Phenol—The procedure reported under *Calibration Curve* was repeated on a 5.0-ml sample of the standard aqueous solution of phenol and the standard solution containing both resorcinol and phenol. The results were calculated using a standard value (0.560) for resorcinol since Beer's law was followed (Table I).

Assay of Resorcinol–Phenol–Boric Acid Solution and Carbol-fuchsin Solution—Both solutions were diluted with water as follows: (*a*) 7.5 ml to 100.0 ml, (*b*) 5.0 ml of dilution (*a*) to 250.0 ml, and (*c*) 5.0 ml of dilution (*b*) to 250.0 ml.

To 10.0 ml of dilution (*c*), 2.0 ml of the borate buffer solution (pH 9.4) and 0.1 ml of the I solution were added and mixed. Within 50–120 sec, the absorbance values were recorded at 530 nm against a reagent blank made by substituting water for the assay solutions. The results for resorcinol were calculated using a standard value (0.336) since Beer's law was followed (Table I).

A minor interference from basic fuchsin was taken into consideration as follows. A 10.0-ml quantity of dilution (*c*) from the carbol-fuchsin solution was mixed with 2.0 ml of the borate buffer solution (pH 9.4). The absorbance of this solution was measured at 530 nm against a blank made by mixing 2.0 ml of the borate buffer solution with 10.0 ml of water. Before calculating the results on the carbol-fuchsin solution, this absorbance value (approximately 0.015) was subtracted from the absorbance value obtained in the assay procedure.

Interference from Decomposition Products of Resorcinol and Phenol—A 5.0-ml quantity of an aqueous solution of either resorcinol (0.5%) or phenol (0.225%) was transferred to a 50-ml volumetric flask. An appropriate quantity of potassium ferricyanide solution (1.0, 3.0, or 5.0 ml of 4% or 5.0 ml of 10% solution) was added and mixed. Then the mixture was brought to volume with 1% sodium borate solution. Then 5.0 ml of this mixture was diluted to 500 ml with water, and 10.0 ml of this mixture was mixed with 2.0 ml of the borate buffer solution (pH 9.4) and 0.1 ml of the I solution.

The absorbance of each solution (A_a) was measured after 50 sec at 530 nm against a blank made by substituting methanol for the I solution. The standard reading (A_s) for the resorcinol solution was determined similarly but without the addition of the potassium ferricyanide solution. The percent of resorcinol present in each solution was determined by:

$$\frac{A_a}{A_s} \times 100 = \% \text{ resorcinol} \qquad \text{(Eq. 1)}$$

The results on phenol solutions are presented in Table I. The results on resorcinol solutions are presented in Fig. 2. The percent of resorcinol oxidized was calculated by difference (100 − percent found).

DISCUSSION

The results (Table I) indicate that resorcinol can be assayed in the presence of phenol without any interference. Since phenol also reacts with I (2) to form a blue-colored indophenol, color must be measured within 50–120 sec of mixing the solutions. The full resorcinol color develops in about 50 sec, and phenol begins to react and cause interference after 120 sec. The method is simple and accurate. Beer's law is followed.

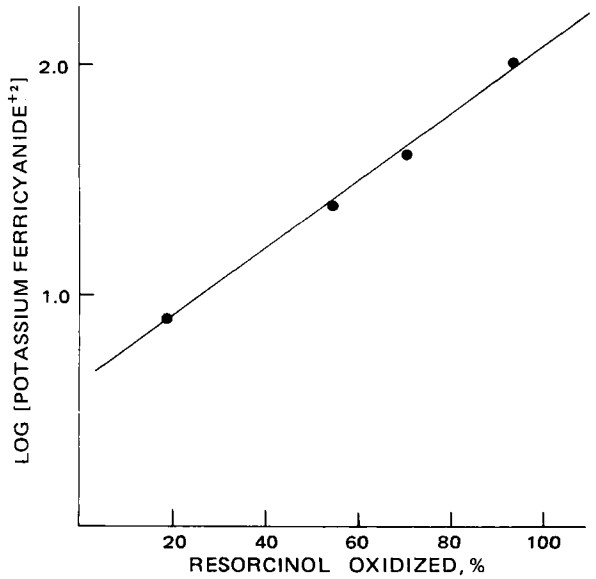

Figure 2—*Plot of percent resorcinol oxidized* versus *log of concentration (grams per 100 ml) of potassium ferricyanide.*

The effect of pH on the sensitivity of the assay method indicates (Fig. 1) that a buffer solution of pH 9–10 could be used. However, at pH 10 the phenol reaction proceeds faster, and at pH 9.0 the resorcinol reaction is slower; therefore, a pH value of 9.4 was preferred.

The decomposition products of resorcinol and phenol, *e.g.*, colored quinones, do not interfere with the assay method (Table I and Fig. 2), as was expected since two phenolic groups are required for this reaction. With one phenolic group, the reaction is delayed (2) and, therefore, does not interfere. If the benzene ring is ruptured, there is no reaction at all (2). When the resorcinol solution was treated with 5.0 ml of 10% solution of potassium ferricyanide in an alkaline sodium borate buffer solution, the decomposed solution was intensely colored (violet). On analysis with the method developed, the resorcinol contents were found to be only 6.5% of the original (Fig. 2).

By using smaller cells, such as a 1-cm cell of a spectrophotometer that requires approximately 3 ml of solution for measurement, the sensitivity of the method can be improved four times. Moreover, concentrations less than 3 μg/ml also can be easily measured since the absorbance value of a 3-μg/ml solution is fairly high (~0.336). This use will further improve the sensitivity of the developed method.

REFERENCES

(1) V. D. Gupta and L. A. Cates, *J. Pharm. Sci.*, **63**, 93(1974).

(2) H. D. Gibbs, *J. Biol. Chem.*, **72**, 649(1927).

(3) P. P. Karkhanis, D. O. Edlund, and J. R. Anfinsen, *J. Pharm. Sci.*, **62**, 804(1973).

(4) P. Rozsa, *Acta Pharm. Hung.*, **37**, 145(1967).

(5) "The National Formulary," 10th ed., Mack Publishing Co., Easton, Pa., 1955, p. 137.

(6) "The United States Pharmacopeia," 18th rev., Mack Publishing Co., Easton, Pa., 1970, p. 939.

ACKNOWLEDGMENTS AND ADDRESSES

Received October 10, 1974, from the *College of Pharmacy, University of Houston, Houston, TX 77004*

Accepted for publication April 11, 1975.

New Compounds: Synthesis of Carboxymethyl Carbodithioates

N. H. LEON

Abstract □ The synthesis and characterization of some new carboxymethyl carbodithioates are reported.

Keyphrases □ Carboxymethyl carbodithioates—synthesized from 1-thioacylpiperidines, NMR spectra, TLC separation □ 1-Thioacylpiperidines—used in synthesis of carboxymethyl carbodithioates

Carboxymethyl carbodithioates (III) are valuable thioacylating agents for amines, amino acids, hydrazines, and other related compounds. Some of the resulting products and the derived metal complexes and heterocycles exert many biological actions, ranging from hypnotic, analgesic, and anesthetic activities to fungicidal, bactericidal, and tuberculostatic activities (1).

Thioacylation of thiols with carboxymethyl carbodithioates is also rapid and has been used for preparing various new dithioesters (2). By the polycondensation of dicarboxymethyl dicarbodithioates with diamines and dithiols, novel polymers containing thiocarbonyl groups were prepared recently (3). Several new carboxymethyl carbodithioates (Table I) now have been prepared according to Scheme I.

A 1-thioacylpiperidine (I) (Table II) reacts with bromoacetic acid to give the *S*-carboxymethylthioacylpiperidinium bromide (II) (Table II), which, on thiohydrolysis with hydrogen sulfide, is converted into the carboxymethyl carbodithioate (III). The 1-thioacylpiperidines (I) are obtained by the Willgerodt–Kindler reaction from the corresponding aldehydes or by thionation with phosphorus pentasulfide of the corresponding 1-acylpiperidines. Neither the long chain aliphatic carboxymethyl carbodithioates (III*a*–III*f*) nor carboxymethyl 4-nitrobenzenecarbodithioate (III*g*) reported here could be prepared by previous investigators (4); but with certain modifications in the preparative procedure, they are readily obtainable, as indicated in the *Experimental* section for II*g* and III*c*.

The long chain aliphatic carboxymethyl carbodithioates are stable, readily purified, crystalline solids;

Table II—Analytical Data for *S*-Carboxymethylthioacylpiperidinium Bromides (II)

Compound	Yield, %	Melting Point	Formula[a]
I*a*	83	Oil[b]	$C_{13}H_{25}NS$
I*b*	65	Oil[b]	$C_{15}H_{29}NS$
I*c*	77	37.5–39.5°[c]	$C_{17}H_{33}NS$
I*d*	63	46–48°[c]	$C_{19}H_{37}NS$
I*e*	74	54–55.5°[c]	$C_{21}H_{41}NS$
I*f*	79	61–62.5°[c]	$C_{23}H_{45}NS$
I*h*	79	147.5–148°[d]	$C_{18}H_{19}NS$
I*i*	93	76–78°[e]	$C_{12}H_{14}FNS$
I*j*	57	168.5–170°[f]	$C_{12}H_{15}NOS$
II*g*	98	167–169°	$C_{14}H_{17}BrN_2O_4S$
II*h*	70	154–154.5° dec.	$C_{20}H_{22}BrN_3O_2S$
II*i*	98	125–127° dec.	$C_{14}H_{17}BrFNO_2S$
II*j*	88	165–167°	$C_{14}H_{18}BrNO_3S$

[a] Compounds I*a*–I*j* showed correct M^+ peaks in the mass spectra. [b] Decomposed on distillation (0.1 mm Hg). [c] Crystallized from methanol. [d] Crystallized from ethanol. [e] Crystallized from petroleum ether (bp 40–60°). [f] Crystallized from methanol–water.

Table III—Analytical Data for *S*-Carboxymethyl Carbothioates (IV)

Compound	Melting Point	Color[a]	PMR[b], δ SCH_2	Formula[c]
IV*g*	156–157.5°[d]	C	3.97	$C_9H_7NO_5S$
IV*h*	167.5–168°[e]	O	3.92	$C_{15}H_{12}N_2O_3S$
IV*i*	105–106°[e]	C	3.90	$C_9H_7FO_3S$
IV*j*	138–143°[e]	C	3.90	$C_9H_8O_3S$
IV*k*	128.5–130.5°[e]	C	3.90	$C_{10}H_{10}O_4S$

[a] C = colorless, and O = orange. [b] Measured in acetone-d_6, except IV*g* which was measured in dimethylformamide-d_6 and IV*i* which was measured in deuterochloroform; all other signals accounted for and in accord with the structure. [c] All compounds showed the correct M^+ in the mass spectra. [d] Crystallized from methanol. [e] Without recrystallization.

Table I—Analytical Data for Carboxymethyl Carbodithioates (III)

Compound	Yield, %	Melting Point	Color[a]	PMR[b], δ SCH_2	λ_{max}, nm (log ε)	Formula
III*a*	66[c]	55–56°[d]	Y	4.08		$C_{10}H_{18}O_2S_2$
III*b*	62[c]	58–59.5°[d]	Y	4.06		$C_{12}H_{22}O_2S_2$
III*c*	75[c]	64.5–66°[d]	Y	4.05	306 (3.90)[e]	$C_{14}H_{26}O_2S_2$
III*d*	65[c]	72–73°[d]	Y	4.07	450 (1.26)[f]	$C_{16}H_{30}O_2S_2$
III*e*	65[c]	77.5–78.5°[d]	Y	4.08		$C_{18}H_{34}O_2S_2$
III*f*	69[c]	80.5–81.5°[d]	Y	4.07		$C_{20}H_{38}O_2S_2$
III*g*	89	113–114°[g]	P-R	4.30	293 (4.27)[e] 495 (2.21)[h]	$C_9H_7NO_4S_2$
III*h*	71	158–158.5°[i]	R	4.36	343 (4.51)[e] 455 (3.06)[e]	$C_{15}H_{12}N_2O_2S_2$
III*i*	74	126–127°[j]	O	4.24		$C_9H_7FO_2S_2$

[a] Y = yellow, P = purple, R = red, and O = orange. [b] Measured in deuterochloroform, except III*h* which was measured in acetone-d_6; all other signals accounted for and in accord with the structure. [c] Based on 1-thioacylpiperidine. [d] Crystallized from methanol–water. [e] In methanol. [f] In 50% aqueous ethanol. [g] Crystallized from benzene. [h] In aqueous sodium hydroxide, pH 9.6. [i] Crystallized from ethanol. [j] Crystallized from benzene–petroleum ether (bp 40–60°).

Table IV—Elemental Analysis of New Compounds

Compound	Found, %				Required, %			
	C	H	N	S	C	H	N	S
III*a*	51.1	7.7	—	27.5	51.25	7.74	—	27.36
III*b*	55.2	8.4	—	24.8	54.92	8.45	—	24.44
III*c*	57.8	8.95	—	22.2	57.88	9.02	—	22.07
III*d*	59.9	9.4	—	20.4	60.33	9.49	—	20.13
III*e*	62.7	9.8	—	18.2	62.38	9.89	—	18.50
III*f*	63.85	10.1	—	16.7	64.12	10.22	—	17.12
III*g*	42.4	2.8	5.35	25.0	42.01	2.74	5.45	24.92
III*h*	56.9	3.9	9.0	19.8	56.94	3.82	8.86	20.27
III*i*	47.1	3.0	—	28.3	46.93	3.06	—	27.85
I*a*	68.4	11.0	6.1	14.25	68.66	11.08	6.16	14.10
I*b*	70.0	11.3	5.4	12.7	70.52	11.44	5.48	12.55
I*c*	72.1	11.7	4.95	11.2	72.02	11.73	4.94	11.31
I*d*	73.3	11.85	4.6	10.4	73.24	11.97	4.50	10.29
I*e*	74.2	12.2	4.2	9.3	74.27	12.17	4.13	9.44
I*f*	75.4	12.3	4.0	8.6	73.13	12.34	3.81	8.72
I*h*	69.95	6.2	13.5	10.3	69.87	6.19	13.58	10.36
I*i*	64.8	6.3	—	14.6	64.54	6.32	—	14.35
I*j*	65.1	6.8	6.3	14.5	65.12	6.83	6.33	14.49
II*g*	43.3	4.5	7.2	8.2	43.20	4.40	7.20	8.24
II*h*	53.7	5.0	9.3	7.1	53.57	4.95	9.37	7.15
II*i*	46.3	4.6	3.8	8.9	46.42	4.73	3.87	8.85
II*j*	46.4	5.0	3.8	8.9	46.67	5.03	3.89	8.90
IV*g*	44.5	3.1	5.8	13.5	44.81	2.93	5.81	13.29
IV*h*	59.8	4.1	9.4	10.6	59.98	4.03	9.33	10.67
IV*i*	50.6	3.1	—	14.7	50.47	3.30	—	14.96
IV*j*	50.65	3.9	—	15.2	50.95	3.80	—	15.11
IV*k*	52.7	4.4	—	14.25	53.09	4.46	—	14.17
—[a]	69.7	7.0	6.7	—	69.55	6.81	6.76	—

[a] 1-(4-Fluorobenzoyl)piperidine.

those with the alkyl chain shorter than tridecyl are soluble in dilute aqueous alkaline solutions. By virtue of the chromophoric group C=S, carboxymethyl carbodithioates are colored compounds; aliphatic derivatives are yellow, and aromatic ones are reddish.

Hydrolysis of II gives *S*-carboxymethyl carbothioate (IV) (Table III), which can be distinguished from III by an upfield shift of the methylene protons in the carboxymethyl group because the diamagnetic anisotropy of the C=S group is larger than that of the C=O group (2).

The stretching vibration of the C=S group in III is at 1223–1200 cm^{-1}, in agreement with the literature (5).

EXPERIMENTAL[1]

The following were prepared by the reaction of the acid chloride with piperidine in benzene: 1-lauroylpiperidine, bp 185°/2 mm [lit. (6) bp 185–187°/2–3 mm]; 1-myristoylpiperidine, bp 205–208°/2 mm [lit. (7) bp 206–209°/2 mm]; 1-palmitoylpiperidine, mp 35–37° (methanol) [lit. (8) mp 35–36°]; 1-stearylpiperidine, mp 43–44° [lit. (9) mp 44–44.5°]; and 1-(4-fluorobenzoyl)piperidine, mp 62–64° (petroleum ether, bp 40–60°). 1-(4-Nitrobenzoyl)piperidine (10) and 1-(4-phenylazobenzoyl)piperidine (11) were prepared by known methods.

1-Thiooctanoylpiperidine (Ia)—Caprylic aldehyde (19.2 g, 0.15 mole), piperidine (19.6 g, 0.23 mole), and sulfur (7.4 g, 0.23 mole) were mixed; the reaction mixture was refluxed for 3 hr, cooled slightly, and poured into water. The aqueous mixture was acidified with hydrochloric acid in the cold, and the orange oil was extracted with ether and dried (sodium sulfate). Evaporation of the solvent gave the crude product (28.3 g, 83%). Compound I*b* was obtained similarly.

1-Thiolauroylpiperidine (Ic)—Phosphorus pentasulfide (44.5 g, 0.2 mole) was added to a stirred solution of 1-lauroylpiperidine (107 g, 0.4 mole) in dry pyridine (200 ml), and the reaction mixture was refluxed for 3 hr with stirring. The hot solution was poured into a threefold volume of hot water with stirring. After 0.5 hr at room temperature, the mixture was cooled in ice with stirring. The precipitated oil soon solidified, and the brown solid was crystallized (methanol) and decolorized (charcoal) to give the product (87.3 g, 77%). Compounds I*d*–I*f*, I*g* [mp 179–180°; lit. (4) mp 176–178°], and I*h*–I*j* were similarly prepared. Compounds I*c*–I*j* were shown to be homogeneous (single spot on TLC, silica gel).

***S*-Carboxymethylthiolauroylpiperidinium Bromide (IIc)**—A solution of Ic (22.7 g, 70 mmoles) and bromoacetic acid (10.7 g, 77 mmoles) in dry ether (100 ml) was kept for 2 days at room temperature. The product, a pale-orange syrup, was separated by decanting the supernatant liquid, washed quickly (dry ether), and

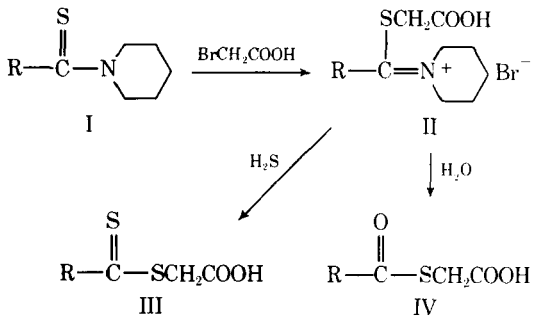

a: R = $CH_3(CH_2)_6$ — *g*: R = 4-$NO_2C_6H_4$
b: R = $CH_3(CH_2)_8$ — *h*: R = 4-$(C_6H_5N{=}N)C_6H_4$
c: R = $CH_3(CH_2)_{10}$ — *i*: R = 4-FC_6H_4
d: R = $CH_3(CH_2)_{12}$ — *j*: R = 4-HOC_6H_4
e: R = $CH_3(CH_2)_{14}$ — *k*: R = 4-$CH_3OC_6H_4$
f: R = $CH_3(CH_2)_{16}$

Scheme I

[1] Melting points are uncorrected. IR spectra of solids and liquids were determined in potassium bromide disks and as pressed-out films on sodium chloride disks, respectively, with a Perkin-Elmer 257 instrument. UV and visible spectra were measured with Perkin-Elmer 137 and Unicam SP 500 spectrophotometers. PMR spectra were recorded with a JEOL-PS-100 (100 MHz) spectrometer (tetramethylsilane). Mass spectra were obtained with an AEI MS-9 spectrometer at an ionizing energy of 70 ev. Elementary analyses were performed by the Ilse Beetz Microanalytical Laboratory, Kronach, Germany (Table IV).

used immediately in the next reaction. Compounds II*a*, II*b*, and II*d*–II*f* were prepared similarly. The crude products were not analyzed.

***S*-Carboxymethyl-(4-nitrothiobenzoyl)piperidinium Bromide (II*g*)**—Bromoacetic acid (20.8 g, 0.15 mole) was added to a warm solution of I*g* (25.0 g, 0.1 mole) in dry ethylene dichloride (200 ml). After 2 days at 40°, the crystalline solid was filtered off, washed (dry ether), and dried *in vacuo* over phosphorus pentoxide to give the product (37 g, 98%). With benzene as the solvent at room temperature, previous workers (4) failed to prepare this compound.

***S*-Carboxymethyl-(4-phenylazothiobenzoyl)piperidinium Bromide (II*h*)**—A solution of I*h* (30.9 g, 0.1 mole) and bromoacetic acid (20.9 g, 0.15 mole) in dry benzene (600 ml) was kept for 2 days at room temperature. Workup as described for II*g* gave the product (31.4 g, 70%). Compound II*i* was obtained similarly; II*j* was prepared in dry chloroform.

Carboxymethyl Undecanecarbodithioate (III*c*)—A slow stream of dry hydrogen sulfide was passed for 3–4 hr through a stirred solution of II*c*, freshly prepared from I*c* (22.7 g, 70 mmoles), in dry dimethylformamide (85 ml). After 16 hr at 0–5°, the reaction mixture was poured into a threefold volume of ice water with stirring to give a yellow precipitate (14.8 g, 73% based on I*c*), mp 64.5–66° (methanol–water); ν_{max} 3000–2500 and 1710 (COOH) and 1224 (C=S) cm^{-1}; δ 10.4 (1H, s, COOH), 4.05 (2H, s, SCH_2), 3.00 (2H, t, J = 7.8 Hz, CH_2CS), 1.8 (2H, m, CH_2CH_2CS), 1.25 [16H, distorted s, $CH_3(CH_2)_8$], and 0.86 (3H, distorted t, CH_3). Compounds III*a*, III*b*, and III*d*–III*f* were obtained similarly. Attempts by previous workers (4), using ethanol as the solvent, failed to produce these compounds. Compounds III*g*–III*i* were prepared in absolute ethanol. Compounds III*a*–III*i* were shown to be homogeneous (single spot on TLC, silica gel).

***S*-Carboxymethyl 4-Nitrobenzenecarbothioate (IV*g*)**—Compound II*g* in 10 parts of water, after 16 hr at room temperature, gave the product as colorless needles. Compounds IV*h*–IV*k* were obtained similarly. Compounds IV*g*–IV*k* were shown to be homogeneous (single spot on TLC, silica gel).

REFERENCES

(1) K. M. Doyle and F. Kurzer, *Chem. Ind. (London)*, **1974**, 803.

(2) N. H. Leon and R. S. Asquith, *Tetrahedron*, **26**, 1719(1970); N. H. Leon, *Org. Mass Spectrom.*, **6**, 407(1972).

(3) N. H. Leon and D. Broadbent, *J. Polym. Sci., B*, **12**, 963(1974).

(4) K. A. Jensen and C. Pedersen, *Acta Chem. Scand.*, **15**, 1087(1961).

(5) B. Bak, L. Hassen-Nygaard, and C. Pedersen, *ibid.*, **12**, 1451(1958).

(6) B. Wojcik and H. Adkins, *J. Amer. Chem. Soc.*, **56**, 2419(1934).

(7) M. Asano and T. Kanematsu, *J. Pharm. Soc. Jap.*, **No. 531**, 375(1926).

(8) H. Staudinger and H. Schneider, *Ber.*, **56B**, 699(1923).

(9) E. F. Jordan, Jr., and W. S. Port, *J. Amer. Oil Chem. Soc.*, **38**, 600(1961).

(10) C. Siebenmann and R. J. Schnitzer, *J. Amer. Chem. Soc.*, **65**, 2126(1943).

(11) E. O. Woolfolk and E. H. Roberts, *J. Org. Chem.*, **21**, 436(1956).

ACKNOWLEDGMENTS AND ADDRESSES

Received February 25, 1975, from *Unilever Research, Isleworth Laboratory, Isleworth, Middlesex, England.*

Accepted for publication April 17, 1975.

COMMUNICATIONS

Stereochemistry of Geometric Isomers of Clomiphene: A Correction of the Literature and a Reexamination of Structure–Activity Relationships

Keyphrases □ Clomiphene—stereochemistry of geometric isomers, structure–activity relationships □ Structure–activity relationships—clomiphene, geometric isomers

To the Editor:

The B-isomer of clomiphene[1] hydrochloride (I-HCl), 2-[*p*-(2-chloro-1,2-diphenylvinyl)phenoxy]triethylamine hydrochloride (IA-HCl, mp 156.5–158°; IB-HCl, mp 149–150.5°), was designated *cis* (Z) since it exhibits a UV λ_{max} attributed to a *trans*-*p*-alkoxystilbene chromophore at a higher wavelength than the A-isomer (1). A comparison of dipole moment, UV, IR, and PMR data of I geometric isomers, 2-[*p*-(2-bromo-1,2-diphenylvinyl)phenoxy]triethylamine (II) and *p*-(2-bromo-1,2-diphenylvinyl)anisole (III) (2), supported this conclusion. However, this conclusion rests on a tenuous stereochemical assignment for geometric isomers of III (3, 4).

In fact, based on a comparison of the dipole moments and spectra of isomers of I–III with those of isomers of 2-[*p*-(1,2-diphenyl-1-butenyl)phenoxy]-*N*,*N*-dimethylethylamine (IV), these assignments were inconsistent with the unequivocal crystallographic proof of stereochemistry for isomers of IV (5, 6). In addition, structure–activity relationships for these compounds were inconsistent since the *cis*-isomer of IV induces conventional estrogenic responses and is the more potent isomer in these respects (7–10), while IA, which had been assigned the *trans*-geometry, exhibits the conventional estrogenic responses and is the more potent isomer of I in these respects (11–21). Furthermore, while the *trans*-isomer of IV exhibits antiestrogenic actions (7–10), IB, previously designated *cis* (1, 2), is the antiestrogenic

[1] Clomid, Merrell-National Laboratories, Division of Richardson-Merrell Inc., Cincinnati, Ohio, is the citrate salt of an isomeric mixture.

used immediately in the next reaction. Compounds II*a*, II*b*, and II*d*–II*f* were prepared similarly. The crude products were not analyzed.

***S*-Carboxymethyl-(4-nitrothiobenzoyl)piperidinium Bromide (II*g*)**—Bromoacetic acid (20.8 g, 0.15 mole) was added to a warm solution of I*g* (25.0 g, 0.1 mole) in dry ethylene dichloride (200 ml). After 2 days at 40°, the crystalline solid was filtered off, washed (dry ether), and dried *in vacuo* over phosphorus pentoxide to give the product (37 g, 98%). With benzene as the solvent at room temperature, previous workers (4) failed to prepare this compound.

***S*-Carboxymethyl-(4-phenylazothiobenzoyl)piperidinium Bromide (II*h*)**—A solution of I*h* (30.9 g, 0.1 mole) and bromoacetic acid (20.9 g, 0.15 mole) in dry benzene (600 ml) was kept for 2 days at room temperature. Workup as described for II*g* gave the product (31.4 g, 70%). Compound II*i* was obtained similarly; II*j* was prepared in dry chloroform.

Carboxymethyl Undecanecarbodithioate (III*c*)—A slow stream of dry hydrogen sulfide was passed for 3–4 hr through a stirred solution of II*c*, freshly prepared from I*c* (22.7 g, 70 mmoles), in dry dimethylformamide (85 ml). After 16 hr at 0–5°, the reaction mixture was poured into a threefold volume of ice water with stirring to give a yellow precipitate (14.8 g, 73% based on I*c*), mp 64.5–66° (methanol–water); ν_{max} 3000–2500 and 1710 (COOH) and 1224 (C=S) cm^{-1}; δ 10.4 (1H, s, COOH), 4.05 (2H, s, SCH_2), 3.00 (2H, t, J = 7.8 Hz, CH_2CS), 1.8 (2H, m, CH_2CH_2CS), 1.25 [16H, distorted s, $CH_3(CH_2)_8$], and 0.86 (3H, distorted t, CH_3). Compounds III*a*, III*b*, and III*d*–III*f* were obtained similarly. Attempts by previous workers (4), using ethanol as the solvent, failed to produce these compounds. Compounds III*g*–III*i* were prepared in absolute ethanol. Compounds III*a*–III*i* were shown to be homogeneous (single spot on TLC, silica gel).

***S*-Carboxymethyl 4-Nitrobenzenecarbothioate (IV*g*)**—Compound II*g* in 10 parts of water, after 16 hr at room temperature, gave the product as colorless needles. Compounds IV*h*–IV*k* were obtained similarly. Compounds IV*g*–IV*k* were shown to be homogeneous (single spot on TLC, silica gel).

REFERENCES

(1) K. M. Doyle and F. Kurzer, *Chem. Ind. (London)*, **1974**, 803.

(2) N. H. Leon and R. S. Asquith, *Tetrahedron*, **26**, 1719(1970); N. H. Leon, *Org. Mass Spectrom.*, **6**, 407(1972).

(3) N. H. Leon and D. Broadbent, *J. Polym. Sci., B*, **12**, 963(1974).

(4) K. A. Jensen and C. Pedersen, *Acta Chem. Scand.*, **15**, 1087(1961).

(5) B. Bak, L. Hassen-Nygaard, and C. Pedersen, *ibid.*, **12**, 1451(1958).

(6) B. Wojcik and H. Adkins, *J. Amer. Chem. Soc.*, **56**, 2419(1934).

(7) M. Asano and T. Kanematsu, *J. Pharm. Soc. Jap.*, **No. 531**, 375(1926).

(8) H. Staudinger and H. Schneider, *Ber.*, **56B**, 699(1923).

(9) E. F. Jordan, Jr., and W. S. Port, *J. Amer. Oil Chem. Soc.*, **38**, 600(1961).

(10) C. Siebenmann and R. J. Schnitzer, *J. Amer. Chem. Soc.*, **65**, 2126(1943).

(11) E. O. Woolfolk and E. H. Roberts, *J. Org. Chem.*, **21**, 436(1956).

ACKNOWLEDGMENTS AND ADDRESSES

Received February 25, 1975, from *Unilever Research, Isleworth Laboratory, Isleworth, Middlesex, England.*

Accepted for publication April 17, 1975.

COMMUNICATIONS

Stereochemistry of Geometric Isomers of Clomiphene: A Correction of the Literature and a Reexamination of Structure–Activity Relationships

Keyphrases □ Clomiphene—stereochemistry of geometric isomers, structure–activity relationships □ Structure–activity relationships—clomiphene, geometric isomers

To the Editor:

The B-isomer of clomiphene[1] hydrochloride (I-HCl), 2-[*p*-(2-chloro-1,2-diphenylvinyl)phenoxy]triethylamine hydrochloride (IA-HCl, mp 156.5–158°; IB-HCl, mp 149–150.5°), was designated *cis* (Z) since it exhibits a UV λ_{max} attributed to a *trans*-*p*-alkoxystilbene chromophore at a higher wavelength than the A-isomer (1). A comparison of dipole moment, UV, IR, and PMR data of I geometric isomers, 2-[*p*-(2-bromo-1,2-diphenylvinyl)phenoxy]triethylamine (II) and *p*-(2-bromo-1,2-diphenylvinyl)anisole (III) (2), supported this conclusion. However, this conclusion rests on a tenuous stereochemical assignment for geometric isomers of III (3, 4).

In fact, based on a comparison of the dipole moments and spectra of isomers of I–III with those of isomers of 2-[*p*-(1,2-diphenyl-1-butenyl)phenoxy]-*N*,*N*-dimethylethylamine (IV), these assignments were inconsistent with the unequivocal crystallographic proof of stereochemistry for isomers of IV (5, 6). In addition, structure–activity relationships for these compounds were inconsistent since the *cis*-isomer of IV induces conventional estrogenic responses and is the more potent isomer in these respects (7–10), while IA, which had been assigned the *trans*-geometry, exhibits the conventional estrogenic responses and is the more potent isomer of I in these respects (11–21). Furthermore, while the *trans*-isomer of IV exhibits antiestrogenic actions (7–10), IB, previously designated *cis* (1, 2), is the antiestrogenic

[1] Clomid, Merrell-National Laboratories, Division of Richardson-Merrell Inc., Cincinnati, Ohio, is the citrate salt of an isomeric mixture.

isomer (11–21). For these reasons, an unequivocal determination of the stereochemistry of isomers of I was undertaken by X-ray diffraction of IB-HCl and IA-HI. The details of these crystal structures will be published elsewhere.

The space group of IB-HCl is $P2_1/c$. There are four formula weights per unit cell and one per asymmetric crystallographic unit. That is, all four molecules have the same conformation. The structure was solved by direct methods. Atomic, positional, and thermal parameters were refined by a full matrix procedure, which converged at a weighted reliability index of 4.0% for this structure. The torsion angle defining the orientation of the unsubstituted rings is 174.4°.

The space group for IA-HI is P1. There are four formula weights per unit cell, which is the asymmetric crystallographic unit. That is, all four molecules have different conformations. The structure was solved by direct methods. The atomic, positional, and thermal parameters for nonhydrogen atoms were refined by a full matrix procedure, which converged at a reliability index of 10% for this structure. The torsion angles defining the orientations of the unsubstituted rings are 10.3, 5.3, 5.1, and 12.7°.

The correct structures (IA and IB) are the reverse of those previously assigned to isomers of I. Thus, the physical data as well as the relationships between geometric isomerism and these biological actions are now consistent. It is the stereochemical assignment for isomers of III that is incorrect (3, 4) and that lent support (2) to the original incorrect assignment of stereochemistry to isomers of I (1).

A suitably oriented basic residue is a consistent feature of many antiestrogenic and estrogenic agents patterned on the triphenylethylene prototype (22). From the results described here, it now appears that a *trans*-disposition of "unsubstituted" benzene rings *favors* antiestrogenic action, although the *trans*-isomers of both I and IV exhibit estrogenic effects as well. While IB (*trans*) has three times the uterotropic (estrogenic) activity (ED_{50}) of IA, it is only 60% as effective (height of the dose–response curve) (12).

It has also been shown that the more estrogenic *cis*-isomers of I and IV have lower affinities than the antiestrogenic *trans*-isomers for the estrogenic receptor (70:1 and 20:4, respectively) (10). This finding is in accord with a lower intrinsic activity for the antiestrogenic *trans*-isomers (B) of I and IV. The antiestrogenic effect on the hypothalamus is primarily responsible for initiation of the ovulatory cycle (18, 23). This effect arises by antagonism of the effects of estrogen, which inhibits the release of follicle-stimulating hormone-releasing factor. Later phases in the development of an ovum are estrogen supported. The *unique* ovulation-inducing properties of IB (12, 23) would appear to be related more to tissue distribution patterns and/or metabolism than to the extent of the inhibition of binding of estrogen to its receptors (10, 24) since the association constant for IB is *only* 3.5 times larger than that for IVB (10). However, the reverse is more likely, as suggested by the magnitudes of the *trans–cis* ratios of the association constants of I and IV. These ascribe a higher degree

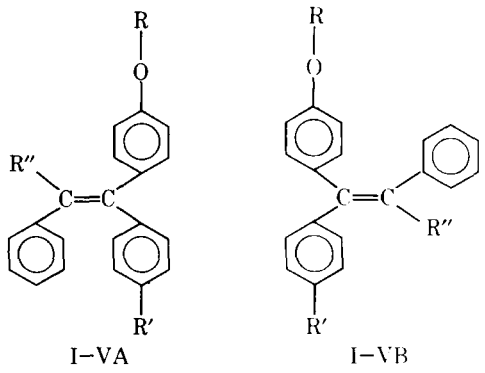

I: R = $CH_2CH_2N(CH_2CH_3)_2$, R′ = H, R″ = Cl
II: R = $CH_2CH_2N(CH_2CH_3)_2$, R′ = H, R″ = Br
III: R = CH_3, R′ = H, R″ = Br
IV: R = $CH_2CH_2N(CH_3)_2$, R′ = H, R″ = CH_2CH_3
V: R = $CH_2CH_2(NC_4H_8)$, R′ = *p*-CH_3O, R″ = NO_2

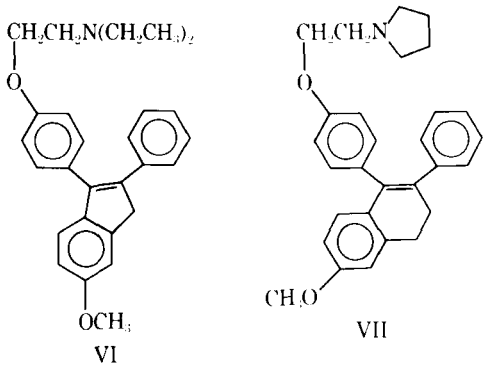

of biological selectivity to I. Furthermore, a mixture of IA and IB is apparently more effective than IB alone.

Thus, while the antiestrogenic effect is responsible for initiation of ovulation, the estrogenic effect is apparently desirable or necessary as well in a later estrogen-dependent phase of the ovulatory cycle. This suggests that the antiestrogenic–estrogenic ratio of the *trans*-isomer (or of the *cis–trans* mixture), as well as the actual magnitude of the antiestrogenic activity, is of paramount importance. Finally, while it may seem enigmatic that I induces ovulation as a result of both its antiestrogenic and estrogenic qualities, it may be pertinent that the estrogenic potency ratios for isomers of IV vary markedly, depending on the tissue used as the biological test system (7). This fact suggests that these tissues have differing sensitivities to antiestrogen as well. Accordingly, the unique ovulation-inducing effects of I perhaps may be ascribed to the unique balance of antiestrogenic and estrogenic effects.

These considerations may have a bearing on the biological effects of such analogs of I as 1-[2-[*p*-[1-(*p*-methoxyphenyl)-2-nitro-2-phenylvinyl]phenoxy]ethyl]pyrrolidine (V), 2-[*p*-(6-methoxy-2-phenylindene-3-yl)phenoxy]triethylamine (VI), and 1-[2-[*p*-(3,4-dihydro-6-methoxy-2-phenyl-1-naphthyl)phenoxy]ethyl]pyrrolidine (VII) (23). This suggests that desmethoxy analogs of these (and similar) prototypes, suitably functionalized in the alicyclic segment to provide optimal tissue distribution, may also exhibit

high affinity for the estrogenic receptor and a suitable balance of antiestrogenic and estrogenic effects associated with induction of ovulation by IB.

In summary, the establishment of the stereochemistry of isomers of I has corrected an error in the literature, permitted a consistent explanation of the biological and physical data available on isomers of I and IV, and provided insight into the molecular mechanisms of action and direction for additional studies in this area.

(1) F. P. Palopoli, V. L. Feil, R. E. Allen, D. E. Holtkamp, and A. Richardson, Jr., *J. Med. Chem.*, **10**, 84(1967).

(2) A. Richardson, Jr., and H. D. Benson, "Abstracts," 153rd National Meeting of the American Chemical Society, 1967, M4.

(3) C. F. Koelsch, *J. Amer. Chem. Soc.*, **54**, 2487(1932).

(4) D. Y. Curtin, E. E. Harris, and E. K. Meislich, *ibid.*, **74**, 2901(1952).

(5) G. R. Bedford and D. N. Richardson, *Nature*, **212**, 733(1966).

(6) B. T. Kilbourn and P. G. Owston, *J. Chem. Soc. B*, **1970**, 1.

(7) M. J. K. Harper and A. L. Walpole, *Nature*, **212**, 87(1966).

(8) M. J. K. Harper and A. L. Walpole, *J. Reprod. Fert.*, **13**, 101(1967).

(9) D. J. Collins, J. J. Hobbs, and C. W. Emmens, *J. Med. Chem.*, **14**, 952(1971).

(10) R. J. Skidmore, A. L. Walpole, and J. Woodburn, *J. Endocrinol.*, **52**, 289(1972).

(11) W. W. Leavitt and D. M. Meisner, *Nature*, **218**, 181(1968).

(12) L. W. Self, D. E. Holtkamp, and W. L. Kuhn, *Fed. Proc.*, **26**, 534(1967).

(13) M. S. Sankaran and M. R. N. Prasad, *J. Reprod. Fert.*, **35**, 203(1973).

(14) S. P. Singh, M. R. N. Prasad, and N. K. Uberoi, *Proc. Indian Nat. Sci. Acad., Part B*, **39**, 129(1973).

(15) J. F. Richards and D. R. Griffith, *Fert. Steril.*, **25**, 74(1974).

(16) L. Terenius, *Acta Endocrinol. (Copenhagen)*, **66**, 431(1971).

(17) S. Nagel, H. Baier, and H. D. Taubert, *Horm. Metab. Res.*, **344**, 2(1970).

(18) A. V. Schally, W. H. Carter, A. F. Perlow, M. Saito, A. Arimura, C. Y. Bowers, and D. E. Holtkamp, *Amer. J. Obstet. Gynecol.*, **107**, 1156(1970).

(19) T. R. Blohm, V. L. Stevens, T. Kariya, and H. N. Alig, *Biochem. Pharmacol.*, **19**, 2231(1970).

(20) P. L. DiPietro, F. L. Sanders, and D. A. Gross, *Endocrinology*, **84**, 1404(1969).

(21) S.-Y. Ying and R. K. Meyer, *Contraception*, **5**, 413(1972).

(22) D. Lednicer, S. C. Lyster, and G. W. Duncan, *J. Med. Chem.*, **10**, 78(1967).

(23) M. J. K. Harper, in "Progress in Drug Research," vol. 12, E. Jucker, Ed., Birkhauser Verlag, Basel, Switzerland, 1968, p. 47, and references cited therein.

(24) E. V. Jensen and E. R. DeSombre, *Science*, **182**, 126(1973).

S. Ernst
Department of Crystallography
University of Pittsburgh
Pittsburgh, PA 15260

G. Hite [x]
Division of Medicinal Chemistry and Pharmacognosy
School of Pharmacy
University of Connecticut
Storrs, CT 06268

J. S. Cantrell
Department of Chemistry
Miami University
Oxford, OH 45056

A. Richardson, Jr.
H. D. Benson
Merrell-National Laboratories
Division of Richardson-Merrell Inc.
Cincinnati, OH 45215

Received July 28, 1975.

Accepted for publication September 29, 1975.

Supported in part by the U.S. Public Health Service, Department of Health, Education, and Welfare, under Special Postdoctoral Fellowship GM-49037 (G. Hite) and Grant GM-01728 (S. Ernst) and in part by a grant from Merrell-National Laboratories, Division of Richardson-Merrell Inc. (J. S. Cantrell).

[x] To whom inquiries should be directed.

Corneal Drug Absorption: An Illustration of Parallel First-Order Absorption and Rapid Loss of Drug from Absorption Depot

Keyphrases □ Corneal drug absorption—pharmacokinetics, pilocarpine nitrate, rabbits □ Absorption, corneal—pharmacokinetics, pilocarpine nitrate, rabbits □ Pilocarpine nitrate—pharmacokinetics, corneal absorption, rabbits

To the Editor:

While studying corneal drug transport of pilocarpine nitrate, we encountered what at first appeared to be rapid permeation of drug into the cornea and aqueous humor but what, in fact, was a slow absorption process. The short time to achieve peak drug concentration in ocular tissues from an applied dose is caused by a rapid parallel elimination process from the absorption depot. This type of process was reported previously (1–3) but has not been reported as being applicable to the eye. The present communication presents evidence, using pilocarpine nitrate in rabbits, that corneal uptake of this drug and, presumably, other ocular drugs is not as rapid as the ocular tissue drug concentration *versus* time profile appears to indicate.

Ocular tissue drug level *versus* time profiles for most topically applied drugs have two common characteristics relative to the absorption phase: a low fraction of dose absorbed and a short time to achieve a peak drug level in either corneal tissue or aqueous humor (4, 5). The time of peak aqueous humor drug levels is generally in the range of 20–30 min postinstillation of drug, and the fraction of drug absorbed into the anterior chamber is usually less than 0.1 and often less than 0.01. The time of peak drug level in aqueous humor following instillation of an aqueous pilocarpine nitrate solution is around 20 min, and the fraction of dose absorbed is 0.002–0.003 (5). Figure 1 presents the corneal and aqueous humor drug levels *versus* time profiles for pilocarpine nitrate, illustrat-

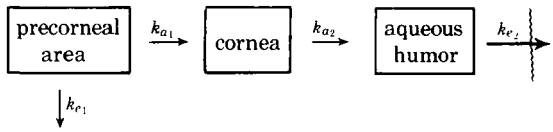

Scheme I

high affinity for the estrogenic receptor and a suitable balance of antiestrogenic and estrogenic effects associated with induction of ovulation by IB.

In summary, the establishment of the stereochemistry of isomers of I has corrected an error in the literature, permitted a consistent explanation of the biological and physical data available on isomers of I and IV, and provided insight into the molecular mechanisms of action and direction for additional studies in this area.

(1) F. P. Palopoli, V. L. Feil, R. E. Allen, D. E. Holtkamp, and A. Richardson, Jr., *J. Med. Chem.*, **10**, 84(1967).

(2) A. Richardson, Jr., and H. D. Benson, "Abstracts," 153rd National Meeting of the American Chemical Society, 1967, M4.

(3) C. F. Koelsch, *J. Amer. Chem. Soc.*, **54**, 2487(1932).

(4) D. Y. Curtin, E. E. Harris, and E. K. Meislich, *ibid.*, **74**, 2901(1952).

(5) G. R. Bedford and D. N. Richardson, *Nature*, **212**, 733(1966).

(6) B. T. Kilbourn and P. G. Owston, *J. Chem. Soc. B*, **1970**, 1.

(7) M. J. K. Harper and A. L. Walpole, *Nature*, **212**, 87(1966).

(8) M. J. K. Harper and A. L. Walpole, *J. Reprod. Fert.*, **13**, 101(1967).

(9) D. J. Collins, J. J. Hobbs, and C. W. Emmens, *J. Med. Chem.*, **14**, 952(1971).

(10) R. J. Skidmore, A. L. Walpole, and J. Woodburn, *J. Endocrinol.*, **52**, 289(1972).

(11) W. W. Leavitt and D. M. Meisner, *Nature*, **218**, 181(1968).

(12) L. W. Self, D. E. Holtkamp, and W. L. Kuhn, *Fed. Proc.*, **26**, 534(1967).

(13) M. S. Sankaran and M. R. N. Prasad, *J. Reprod. Fert.*, **35**, 203(1973).

(14) S. P. Singh, M. R. N. Prasad, and N. K. Uberoi, *Proc. Indian Nat. Sci. Acad., Part B*, **39**, 129(1973).

(15) J. F. Richards and D. R. Griffith, *Fert. Steril.*, **25**, 74(1974).

(16) L. Terenius, *Acta Endocrinol. (Copenhagen)*, **66**, 431(1971).

(17) S. Nagel, H. Baier, and H. D. Taubert, *Horm. Metab. Res.*, **344**, 2(1970).

(18) A. V. Schally, W. H. Carter, A. F. Perlow, M. Saito, A. Arimura, C. Y. Bowers, and D. E. Holtkamp, *Amer. J. Obstet. Gynecol.*, **107**, 1156(1970).

(19) T. R. Blohm, V. L. Stevens, T. Kariya, and H. N. Alig, *Biochem. Pharmacol.*, **19**, 2231(1970).

(20) P. L. DiPietro, F. L. Sanders, and D. A. Gross, *Endocrinology*, **84**, 1404(1969).

(21) S.-Y. Ying and R. K. Meyer, *Contraception*, **5**, 413(1972).

(22) D. Lednicer, S. C. Lyster, and G. W. Duncan, *J. Med. Chem.*, **10**, 78(1967).

(23) M. J. K. Harper, in "Progress in Drug Research," vol. 12, E. Jucker, Ed., Birkhauser Verlag, Basel, Switzerland, 1968, p. 47, and references cited therein.

(24) E. V. Jensen and E. R. DeSombre, *Science*, **182**, 126(1973).

S. Ernst
Department of Crystallography
University of Pittsburgh
Pittsburgh, PA 15260

G. Hite [x]
Division of Medicinal Chemistry and Pharmacognosy
School of Pharmacy
University of Connecticut
Storrs, CT 06268

J. S. Cantrell
Department of Chemistry
Miami University
Oxford, OH 45056

A. Richardson, Jr.
H. D. Benson
Merrell-National Laboratories
Division of Richardson-Merrell Inc.
Cincinnati, OH 45215

Received July 28, 1975.

Accepted for publication September 29, 1975.

Supported in part by the U.S. Public Health Service, Department of Health, Education, and Welfare, under Special Postdoctoral Fellowship GM-49037 (G. Hite) and Grant GM-01728 (S. Ernst) and in part by a grant from Merrell-National Laboratories, Division of Richardson-Merrell Inc. (J. S. Cantrell).

[x] To whom inquiries should be directed.

Corneal Drug Absorption: An Illustration of Parallel First-Order Absorption and Rapid Loss of Drug from Absorption Depot

Keyphrases □ Corneal drug absorption—pharmacokinetics, pilocarpine nitrate, rabbits □ Absorption, corneal—pharmacokinetics, pilocarpine nitrate, rabbits □ Pilocarpine nitrate—pharmacokinetics, corneal absorption, rabbits

To the Editor:

While studying corneal drug transport of pilocarpine nitrate, we encountered what at first appeared to be rapid permeation of drug into the cornea and aqueous humor but what, in fact, was a slow absorption process. The short time to achieve peak drug concentration in ocular tissues from an applied dose is caused by a rapid parallel elimination process from the absorption depot. This type of process was reported previously (1–3) but has not been reported as being applicable to the eye. The present communication presents evidence, using pilocarpine nitrate in rabbits, that corneal uptake of this drug and, presumably, other ocular drugs is not as rapid as the ocular tissue drug concentration *versus* time profile appears to indicate.

Ocular tissue drug level *versus* time profiles for most topically applied drugs have two common characteristics relative to the absorption phase: a low fraction of dose absorbed and a short time to achieve a peak drug level in either corneal tissue or aqueous humor (4, 5). The time of peak aqueous humor drug levels is generally in the range of 20–30 min postinstillation of drug, and the fraction of drug absorbed into the anterior chamber is usually less than 0.1 and often less than 0.01. The time of peak drug level in aqueous humor following instillation of an aqueous pilocarpine nitrate solution is around 20 min, and the fraction of dose absorbed is 0.002–0.003 (5). Figure 1 presents the corneal and aqueous humor drug levels *versus* time profiles for pilocarpine nitrate, illustrat-

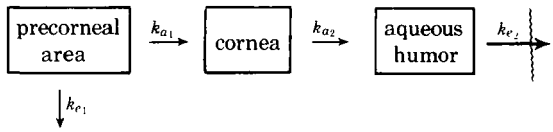

Scheme I

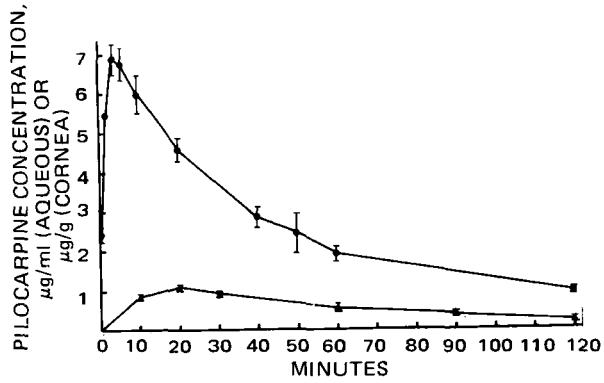

Figure 1—*Concentration of pilocarpine in rabbit aqueous humor (▲) and cornea (●) after dosing with 25 μl of 10^{-2} M pilocarpine in aqueous pH 6.24 buffer. Each point represents a minimum of six eyes, and the standard error of the mean is indicated as vertical bars.*

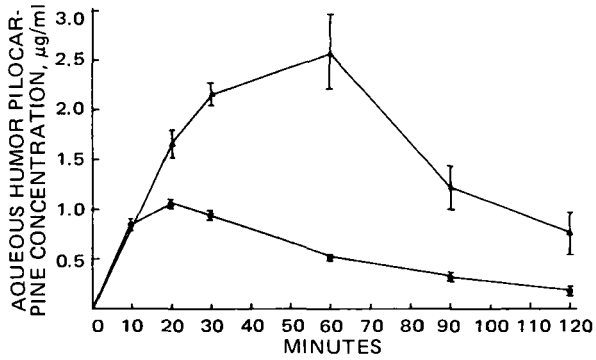

Figure 2—*Concentration of drug in rabbit aqueous humor after dosing with 25 μl of 10^{-2} M pilocarpine in aqueous pH 6.24 buffer. Key: ●, normal drainage; and ▲, drainage duct plugged (8). Each point represents a minimum of six eyes, and the standard error of the mean is indicated as vertical bars.*

ing the apparent rapid absorption.

Scheme I shows, in abbreviated form, the major pathways of disposition for pilocarpine following topical application, where k_{a_1} and k_{a_2} represent the apparent absorption constants into the cornea and aqueous humor, respectively; k_{e_1} represents elimination of drug from the precorneal area through drainage and nonproductive absorption; and k_{e_2} represents elimination of drug from the aqueous humor. This highly simplified scheme is not a complete representation for pilocarpine disposition in ocular tissues but is useful for describing limited data such as those presented in Fig. 1.

Graphical analysis of the corneal and aqueous humor drug data generates an apparent k_{a_1} of 0.8 min^{-1} and an apparent k_{a_2} of 0.08 min^{-1}. These rather large rate constants are considerably larger than published data from perfusion studies (6) and data generated from this laboratory[1] for small solute molecules.

Computer fitting the data in Fig. 1 to Scheme I generates a corneal absorption rate constant of approximately 0.006 min^{-1} for pilocarpine nitrate, which is considerably smaller than the 0.8-min^{-1} apparent rate constant that would be obtained by ignoring the parallel elimination step, *i.e.*, k_{e_1}. The parallel elimination step, consisting primarily of drainage and tear turnover, which has a first-order influence on drug concentration (7), and first-order nonproductive absorption (8) have been studied and demonstrate that loss of drug from the absorption depot is extensive with a large associated rate constant.

Evidence supporting this interpretation of the data is available from the following considerations:

1. Increasing the contact time of the drug with the cornea through the use of viscosity-inducing agents generates only nominal increases in aqueous humor drug levels in animals (9, 10) and almost none in humans (11). If the corneal absorption rate constant was indeed large, significantly higher levels would be expected. That only small increases are observed can be attributed to the large loss of drug to nonproductive absorption, *i.e.*, conjunctival absorption, as well as to the reduced, but appreciable, drainage loss of drug. Thus, long contact times are needed to overcome the small corneal uptake rate constant.

2. Pharmacokinetic equations predict that increasing the magnitude of the parallel elimination step rate constant, k_{e_1}, should shorten the time to achieve a maximum drug level with a corresponding reduction in peak height. Conversely, reducing the magnitude of k_{e_1} should prolong the peak time and increase the peak level. Patton (8) blocked the drainage ducts of rabbits prior to instilling drug solution and found that the time to achieve the maximum level of drug was lengthened from the normal 20 min to about 60 min. The shift in peak time is apparent in Fig. 2 and can only occur through a change in absorption mechanism or by fluctuating the magnitude of the parallel elimination rate constant.

Further aspects of corneal absorption, as well as the ramification of slow corneal absorption on drug delivery and vehicles, will be reported later. However, it is important to recognize, as one would intuitively expect for a sensitive tissue such as the cornea, that drug penetration is relatively slow and that the large apparent absorption rate constant, as evidenced by the short time to achieve a peak drug level, is caused by the appreciable parallel elimination step in the absorption depot.

[1] Perfusion studies with propionic and *n*-octanoic acid, where the cornea is bathed with drug solution, yield corneal uptake constants in the range of 0.001–0.002 min^{-1}.

(1) R. E. Notari, J. L. De Young, and R. H. Reuning, *J. Pharm. Sci.*, **61**, 135(1972).

(2) D. Perrier and M. Gibaldi, *ibid.*, **62**, 225(1973).

(3) L. Leeson and H. Weintraub, *ibid.*, **62**, 1936(1973).

(4) J. W. Sieg and J. R. Robinson, *ibid.*, **64**, 931(1975).

(5) S. S. Chrai and J. R. Robinson, *Amer. J. Ophthalmol.*, **77**, 735(1974).

(6) D. M. Maurice, in "The Eye," 2nd ed., vol. I, H. Davson, Ed., Academic, New York, N.Y., 1969, p. 549.

(7) S. Chrai, T. Patton, A. Mehta, and J. R. Robinson, *J. Pharm. Sci.*, **62**, 1112(1973).

(8) T. F. Patton, Ph.D. thesis, University of Wisconsin, Madison, Wis., 1975.

(9) S. S. Chrai and J. R. Robinson, *J. Pharm. Sci.*, **63**, 1218(1974).

(10) T. F. Patton and J. R. Robinson, *ibid.*, **64**, 1312(1975).

(11) C. A. Adler, D. M. Maurice, and M. E. Paterson, *Exp. Eye Res.*, **11**, 34(1971).

Michael C. Makoid *
James W. Sieg
Joseph R. Robinson ˣ
School of Pharmacy
University of Wisconsin
Madison, WI 53706

Received August 22, 1975.
Accepted for publication October 31, 1975.
Supported by a grant from Allergan Pharmaceuticals, Irvine, CA 92664, and by Grant EY-01332 from the National Institutes of Health.

* Present address: School of Pharmacy, University of Nebraska, Omaha, Neb.
ˣ To whom inquiries should be directed.

Elimination of Alcohol from Human Blood

Keyphrases □ Alcohol—kinetics of elimination from human blood, Michaelis–Menten equation □ Elimination kinetics—alcohol from human blood, Michaelis–Menten equation

To the Editor:

Traditionally, it has been assumed that the kinetics of elimination of alcohol from the blood of animals and humans can be described as zero order, *i.e.*, independent of the blood concentration (above about 2–3 m*M* or 0.09–0.14 mg/ml). Some investigators make this assumption simply because part of the alcohol concentration–time curve appears to be linear, while others believe that liver alcohol dehydrogenase is saturated at low concentrations of alcohol (1–5). Although some work (6–9) suggested non-zero-order elimination kinetics for alcohol in both animals and humans, the concept of zero-order kinetics persists (4, 5).

Newman *et al.* (6) gave various doses of alcohol to dogs, covering a wide range of concentration in blood, and found that there was a more rapid decrease in concentration at higher levels and doses than at the lower levels and doses. Eggleton (7) reported that Widmark's β value [the slope of the pseudolinear decline in blood alcohol concentration, expressed as milligrams of alcohol/(gram of blood × minutes)] in cats increased about 30% for every 1-mg/ml increase in alcohol concentration. If elimination kinetics were truly zero order, then the slope of the pseudolinear decline of blood alcohol concentration should be independent of dose or the C_0 value (the initial alcohol concentration at the beginning of the decline). Lundquist and Wolthers (8) showed that terminal serum alcohol concentrations in humans obeyed the integrated form of the Michaelis–Menten equation:

$$C_0 - C + K_m \ln C_0/C = V_m t \qquad \text{(Eq. 1)}$$

The corresponding Michaelis–Menten equation is:

$$-dC/dt = V_m C/(K_m + C) \qquad \text{(Eq. 2)}$$

In Eqs. 1 and 2, C_0 is the initial alcohol concentration, C is the alcohol concentration at time t, K_m is the Michaelis constant, V_m is the maximal velocity, and t is time. Studies in 10 normal subjects (8) gave an average K_m value of 2.03 m*M* (0.093 mg/ml) and an average V_m value of 0.22 mg of alcohol/ml of serum water/hr. Korsten *et al.* (10) reported a mean K_m value of 2.3 m*M* (0.11 mg/ml), estimated from terminal portions of alcohol disappearance curves derived from measurements of alcohol in whole blood from the arm veins of humans.

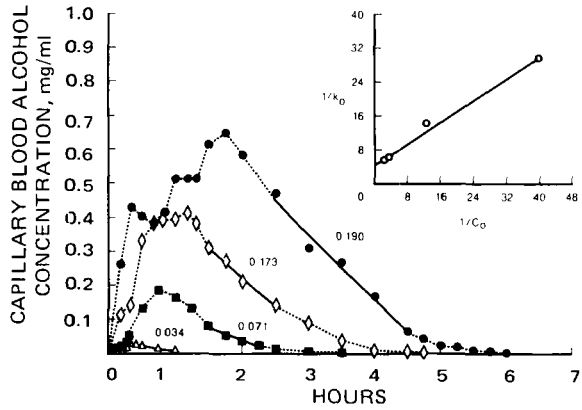

Figure 1—*Time courses of capillary blood alcohol concentrations in one of eight subjects following oral doses of 15, 30, 45, and 60 ml of 95% alcohol under fasting conditions. The absolute values of the slopes of the pseudolinear declines are shown above the declines (solid lines). Inset: double reciprocal plot of* $1/k_0$ *versus* $1/C_0$, *based on Eq. 3.*

As indicated previously, if elimination of alcohol from the blood of humans may be described by zero-order kinetics, then the absolute value of the slope of the linear decline of blood alcohol concentration, k_0, would be independent of dose or the C_0 value. If elimination kinetics are those of Michaelis and Menten, then the apparently linear segment of the alcohol concentration–time curve is actually slightly curved. Furthermore, evaluation as a linear component should disclose an increase in the absolute value of the slope with an increase in dose (or C_0) and a linear relationship between the reciprocal of the slope, $1/k_0$, and the reciprocal of the initial concentration, $1/C_0$ (11).

We followed the time course of alcohol concentrations in whole capillary blood of humans after administration of four different oral doses of alcohol in the fasting state. Capillary blood was used since: (*a*) the concentration of alcohol in capillary blood would be closer to the concentration in arterial blood than the concentration in venous blood, and the brain concentration would be determined by the concentration in arterial blood (12); (*b*) results with the Breathanalyzer are highly correlated with capillary blood alcohol concentrations (13); and (*c*) the large number of blood samples (20–40/subject/treatment) required to define adequately the entire time course makes use of capillary blood more desirable than venous blood, plasma, or serum. Alcohol was measured in 50-μl samples of capillary blood by a new head-space GLC method (14).

Eight normal male volunteers were given oral doses of 15, 30, 45, and 60 ml of 95% alcohol, made up to a volume of 150 ml with orange juice, in crossover fash-

Michael C. Makoid *
James W. Sieg
Joseph R. Robinson ˣ
School of Pharmacy
University of Wisconsin
Madison, WI 53706

Received August 22, 1975.
Accepted for publication October 31, 1975.
Supported by a grant from Allergan Pharmaceuticals, Irvine, CA 92664, and by Grant EY-01332 from the National Institutes of Health.

* Present address: School of Pharmacy, University of Nebraska, Omaha, Neb.
ˣ To whom inquiries should be directed.

Elimination of Alcohol from Human Blood

Keyphrases □ Alcohol—kinetics of elimination from human blood, Michaelis–Menten equation □ Elimination kinetics—alcohol from human blood, Michaelis–Menten equation

To the Editor:

Traditionally, it has been assumed that the kinetics of elimination of alcohol from the blood of animals and humans can be described as zero order, *i.e.*, independent of the blood concentration (above about 2–3 m*M* or 0.09–0.14 mg/ml). Some investigators make this assumption simply because part of the alcohol concentration–time curve appears to be linear, while others believe that liver alcohol dehydrogenase is saturated at low concentrations of alcohol (1–5). Although some work (6–9) suggested non-zero-order elimination kinetics for alcohol in both animals and humans, the concept of zero-order kinetics persists (4, 5).

Newman *et al.* (6) gave various doses of alcohol to dogs, covering a wide range of concentration in blood, and found that there was a more rapid decrease in concentration at higher levels and doses than at the lower levels and doses. Eggleton (7) reported that Widmark's β value [the slope of the pseudolinear decline in blood alcohol concentration, expressed as milligrams of alcohol/(gram of blood × minutes)] in cats increased about 30% for every 1-mg/ml increase in alcohol concentration. If elimination kinetics were truly zero order, then the slope of the pseudolinear decline of blood alcohol concentration should be independent of dose or the C_0 value (the initial alcohol concentration at the beginning of the decline). Lundquist and Wolthers (8) showed that terminal serum alcohol concentrations in humans obeyed the integrated form of the Michaelis–Menten equation:

$$C_0 - C + K_m \ln C_0/C = V_m t \qquad \text{(Eq. 1)}$$

The corresponding Michaelis–Menten equation is:

$$-dC/dt = V_m C/(K_m + C) \qquad \text{(Eq. 2)}$$

In Eqs. 1 and 2, C_0 is the initial alcohol concentration, C is the alcohol concentration at time t, K_m is the Michaelis constant, V_m is the maximal velocity, and t is time. Studies in 10 normal subjects (8) gave an average K_m value of 2.03 m*M* (0.093 mg/ml) and an average V_m value of 0.22 mg of alcohol/ml of serum water/hr. Korsten *et al.* (10) reported a mean K_m value of 2.3 m*M* (0.11 mg/ml), estimated from terminal portions of alcohol disappearance curves derived from measurements of alcohol in whole blood from the arm veins of humans.

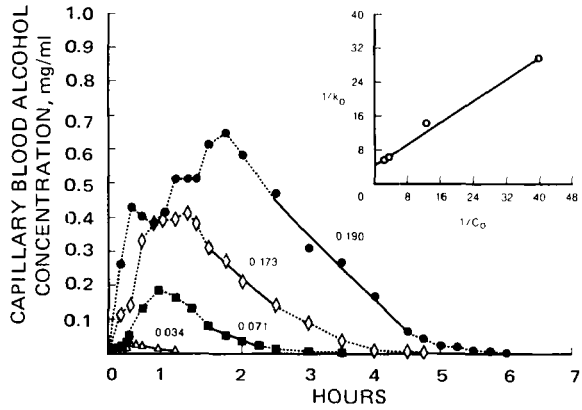

Figure 1—*Time courses of capillary blood alcohol concentrations in one of eight subjects following oral doses of 15, 30, 45, and 60 ml of 95% alcohol under fasting conditions. The absolute values of the slopes of the pseudolinear declines are shown above the declines (solid lines). Inset: double reciprocal plot of* $1/k_0$ *versus* $1/C_0$, *based on Eq. 3.*

As indicated previously, if elimination of alcohol from the blood of humans may be described by zero-order kinetics, then the absolute value of the slope of the linear decline of blood alcohol concentration, k_0, would be independent of dose or the C_0 value. If elimination kinetics are those of Michaelis and Menten, then the apparently linear segment of the alcohol concentration–time curve is actually slightly curved. Furthermore, evaluation as a linear component should disclose an increase in the absolute value of the slope with an increase in dose (or C_0) and a linear relationship between the reciprocal of the slope, $1/k_0$, and the reciprocal of the initial concentration, $1/C_0$ (11).

We followed the time course of alcohol concentrations in whole capillary blood of humans after administration of four different oral doses of alcohol in the fasting state. Capillary blood was used since: (*a*) the concentration of alcohol in capillary blood would be closer to the concentration in arterial blood than the concentration in venous blood, and the brain concentration would be determined by the concentration in arterial blood (12); (*b*) results with the Breathanalyzer are highly correlated with capillary blood alcohol concentrations (13); and (*c*) the large number of blood samples (20–40/subject/treatment) required to define adequately the entire time course makes use of capillary blood more desirable than venous blood, plasma, or serum. Alcohol was measured in 50-μl samples of capillary blood by a new head-space GLC method (14).

Eight normal male volunteers were given oral doses of 15, 30, 45, and 60 ml of 95% alcohol, made up to a volume of 150 ml with orange juice, in crossover fash-

ion, according to a Latin-square design. The subjects fasted overnight and for 3 hr after dosing. Blood sampling times were 0.067, 0.167, 0.333, 0.417, 0.5, 0.667, 0.833, 1, 1.167, 1.333, 1.5, 1.75, 2, 2.5, 3, 3.5, 4, 4.5, 4.75, 5, 5.25, 5.5, 5.75, 6, 6.25, 6.5, 6.75, and 7 hr. Blood sampling started at 0.067 hr and ceased at 3 hr after the 15-ml dose, started at 0.067 hr and ceased at 4.75 hr after the 30-ml dose, started at 0.167 hr and ceased at 6 hr after the 45-ml dose, and started at 0.167 hr and ceased at 7 hr after the 60-ml dose.

The results obtained with a typical subject are shown in Fig. 1. Each k_0 value was estimated by the method of least squares from points that appeared to be randomly distributed about a straight line. In Fig. 1, the estimated values of k_0 are shown on the graph. The averages (and ranges) of the k_0 values for the eight subjects were: 15-ml dose, 0.074 (0.034–0.119); 30-ml dose, 0.121 (0.071–0.144); 45-ml dose, 0.137 (0.104–0.173); and 60-ml dose, 0.147 (0.135–0.562). Hence, the slope increased with an increase in dose. The data were also evaluated by means of:

$$1/k_0 = 1/(k_0)_{max} + \left[\frac{K}{(k_0)_{max}}\right]\left[\frac{1}{C_0}\right] \qquad \text{(Eq. 3)}$$

which is a linear transformation of:

$$k_0 = \frac{(k_0)_{max}C_0}{K + C_0} \qquad \text{(Eq. 4)}$$

In Eqs. 3 and 4, k_0 is the absolute value of the slope of the pseudolinear decline of capillary blood alcohol concentration; $(k_0)_{max}$ is the apparent value of k_0 for an infinite dose of alcohol and is analogous to, but not the same as, V_m; and K is analogous to, but not the same as, K_m (due to Eqs. 2 and 4 having the same form on the right-hand sides).

An example of the application of Eq. 3 is shown in the inset in Fig. 1. For this subject, a $(k_0)_{max}$ value of 0.232 mg/(ml × hr) and a K value of 0.148 mg/ml were calculated from the intercept, $1/(k_0)_{max}$, and the slope, $K/(k_0)_{max}$, of the linear regression line. For all eight subjects, the average value of $(k_0)_{max}$ was 0.163 mg/(ml × hr) with a range of 0.128–0.232. The average value of K was 0.073 mg/ml with a range of 0.046–0.148.

If average terminal capillary blood alcohol concentrations obey Eq. 1, and if V_m and K_m are reasonably constant from subject to subject, then it should be possible to fit all terminal data, obtained after several doses, simultaneously to a modification to Eq. 1:

$$C_0 - C + K_m \ln C_0/C = V_m(t - t_1) \qquad \text{(Eq. 5)}$$

where t_1 is a lag time and the other symbols have the same meanings as given previously. The lag time is the time required to adjust for the duration of the absorption–distribution phase of alcohol following a given dose. The terminal average blood alcohol concentrations of the eight subjects given four different doses of alcohol were simultaneously fitted to Eq. 5 using a computer[1] and the NONLIN program (15). Concentrations were weighted according to their reciprocals (*i.e.*, $1/C_i$) during the fitting. The lag time for the 30-ml dose was taken as 2 hr, and the lag times for the other three doses became parameters to be estimated as well as V_m, K_m, and C_0.

Figure 2 shows the results of the simultaneous fitting; the solid line drawn through the points is the model-predicted concentrations based on Eq. 5 and the least-squares estimates of the parameters. The time scales are staggered to take into account the least-squares estimates of the lag times. The values of the parameters estimated were: V_m = 0.290 mg/(ml × hr), K_m = 0.138 mg/ml, C_0 = 0.194 mg/ml, t_1 (60-ml dose) = 4.92 hr, t_1 (45-ml dose) = 3.70 hr, and t_1 (15-ml dose) = 0.112 hr. These values of V_m and K_m agree reasonably well with those estimated previously (8, 10). This fitting strongly supports the applicability of Eqs. 1 and 5 to alcohol blood concentration data[2].

The percent saturation of an enzyme system, if Eq. 2 applies, is given by:

$$\text{percent saturation} = 100(-dC/dt)/V_m = 100C/(K_m + C) \qquad \text{(Eq. 6)}$$

Use of the *in vivo* K_m value of 0.138 mg/ml estimated in the simultaneous fitting and of various values for C in Eq. 6 yields values of percent saturation of 42.0, 78.4, 87.9, 93.6, 94.7, and 97.8 for blood alcohol concentrations of 0.1, 0.5, 1, 2, 3, and 6 mg/ml, corresponding to 2.2, 11, 22, 44, 65, and 130 mM, respectively. Thus, it is obvious that the alcohol "enzyme system" is never "saturated," even at alcohol levels lethal to humans.

The apparent linearity of part of the downslope of the blood alcohol concentration–time curve is just a consequence of Michaelis–Menten kinetics (11). The shapes of the curves derived from Eqs. 1 and 5 are always pseudolinear for about two-thirds of the concentration range, independent of the initial value. The collapsing of Eq. 2 into:

$$-dC/dt = V_m \qquad \text{(Eq. 7)}$$

as the zero-order concept implies, is not justified with alcohol. This follows from the change in k_0 values with a change in dose as already illustrated. Such changes would not be predicted from Eq. 7.

The product of the V_m value of 0.232 mg/(ml × hr) and the average volume of distribution of 0.535 liter/kg (which we obtained by fitting blood alcohol con-

[1] IBM 370/168 digital computer.

[2] In the simultaneous fitting of average blood alcohol concentrations (Fig. 2), the sum of squared observations was 7.57×10^{-2}, the sum of weighted squared deviations was 4.03×10^{-3}, the coefficient of determination was 0.996, and the correlation coefficient for the linear regression of $\hat{C}$ on C was 0.998. The standard deviations of the estimated parameters were 3.9, 5.4, 2.2, 0.5, 0.7, and 16% of the estimated parameters for V_m, K_m, C_0, t_1 for the 60-ml dose, t_1 for the 45-ml dose, and t_1 for the 15-ml dose, respectively. Hence, the fit was excellent by several criteria.

In the fitting of blood alcohol concentration data obtained following oral administration, only terminal data should be utilized to estimate V_m and K_m of Eq. 5, as in Fig. 2, since earlier concentration data are a function not only of elimination but also of absorption and/or distribution. However, there is no reason to believe that the same *elimination* parameters do not apply at earlier times in the time course. Also, if the two-compartment open model with Michaelis–Menten elimination kinetics applies, rather than the one-compartment open model, then the V_m of the former model would be $(1 + k_{12}/k_{21})$ times the V_m value estimated from terminal data as in this paper; k_{12} and k_{21} are first-order distribution rate constants between the two compartments of the two-compartment open model.

The fitting of average blood alcohol concentrations, as in this paper, circumvents the problem presented previously (9), where variations in estimated parameters were obtained when individual data sets from the same subject were fitted. However, the fitting of the averages (Fig. 2) illustrates the applicability of Michaelis–Melten kinetics to data obtained following four different doses of alcohol.

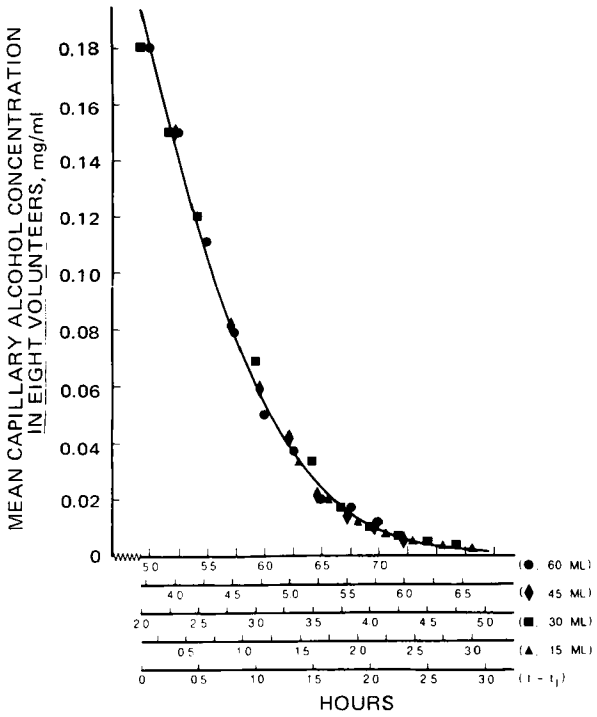

Figure 2—*Results of simultaneous nonlinear least-squares fitting to Eq. 5 of terminal average capillary blood alcohol concentrations of eight subjects given four different doses. The solid line gives the model-predicted concentrations.*

centration data obtained in six subjects given alcohol by constant-rate intravenous infusion) yields an estimate of 0.124 g of alcohol/kg/hr for the maximum elimination rate of alcohol in a normal male. For a 70-kg male, this is equivalent to 8.7 g of alcohol/hr.

In toxicology cases, where one wishes to estimate the future time course of blood alcohol concentrations, it is still valid to extrapolate an established pseudolinear decline in blood alcohol concentration down to about 0.2 mg/ml. However, this can only be done in individual patients who ingest a given dose of alcohol. It is invalid to predict the slope of the pseudolinear decline without a great deal of data and to compare slopes reported by two or more investigators who administer different doses of alcohol to different subjects. The slope of the pseudolinear decline is a function of C_0, V_m, and K_m, as indicated by Wagner (11) and the data in this report.

This work conclusively demonstrates that zero-order kinetics are inappropriate for describing the elimination of alcohol in humans. The slope of the pseudolinear decline should not be utilized as a measure of metabolism rate of alcohol as it has been used in the past (1, 2, 4–7). The rate of metabolism of alcohol is described more accurately by the V_m and K_m values and Eq. 2.

(1) E. M. P. Widmark, *Biochem. Z.*, **267**, 128(1933).

(2) H. Elbel and F. Schleyer, "Blutalkohal," 2nd ed., G. Thieme, Stuttgart, Germany, 1956.

(3) A. Goldstein, *N. Engl. J. Med.*, **283**, 875(1970).

(4) R. D. Hawkins and H. Kalant, *Pharmacol. Rev.*, **24**, 67(1972).

(5) N. H. Raskin, *N. Engl. J. Med.*, **292**, 422(1975).

(6) H. W. Newman, A. J. Lehman, and W. C. Cutting, *J. Pharmacol.*, **61**, 58(1937).

(7) M. G. Eggleton, *J. Physiol.*, **98**, 289(1940).

(8) F. Lundquist and H. Wolthers, *Acta Pharmacol. Toxicol.*, **14**, 265(1958).

(9) J. G. Wagner and J. A. Patel, *Res. Commun. Chem. Pathol. Pharmacol.*, **4**, 61(1972).

(10) M. A. Korsten, S. Matsuzaki, L. Feinman, and C. S. Lieber, *N. Engl. J. Med.*, **292**, 386(1975).

(11) J. G. Wagner, *J. Pharmacokinet. Biopharm.*, **1**, 103(1973).

(12) R. B. Forney, "General Pharmacology of Alcohol," Abstracts of Symposia and Contributed Papers Presented at APhA Academy of Pharmaceutical Sciences, San Francisco meeting, Vol. 1, No. 1, Mar. 1971, p. 28.

(13) R. W. Prouty and B. O'Neil, "An Evaluation of Some Qualitative Breath Screening Tests for Alcohol," Research Report, Insurance Institute for Highway Safety, Washington, DC 20037, May 1971, p. A-5.

(14) P. K. Wilkinson, J. G. Wagner, and A. J. Sedman, *Anal. Chem.*, **47**, 1506(1975).

(15) C. M. Metzler, "Biostatistics Technical Report 7292/69/7292/005," Upjohn Co., Kalamazoo, MI 49001, Nov. 25, 1969.

John G. Wagner [x]
Paul K. Wilkinson
Allen J. Sedman
Donald R. Kay
Donald J. Weidler
College of Pharmacy and
Upjohn Center for Clinical Pharmacology
University of Michigan
Ann Arbor, MI 48104

Received July 18, 1975.

Accepted for publication October 23, 1975.

Supported by Grant 1 R01 AA 00683-01A1 from the National Institute on Alcohol Abuse and Alcoholism, Alcohol, Drug Abuse, and Mental Health Administration, Rockville, Md. Three of us (J. G. Wagner, D. R. Kay, and D. J. Weidler) were partly supported by Public Health Service Grant 5-P11-GM-15559.

[x] To whom inquiries should be directed (at Upjohn Center for Clinical Pharmacology).

Analysis of Diffusion through Concentric Right Circular Cylinders and Concentric Spheres

Keyphrases □ Diffusion—concentric right circular cylinders and concentric spheres, models for drug release from tubular devices, cylindrical systems, and vaginal or GI lumen □ Drug release—tubular devices, cylindrical systems, and vaginal or GI lumen, concentric right circular cylinders and concentric spheres as models

To the Editor:

We recently have been modeling several diffusional systems involving diffusion through a series (two or more) of concentric right circular cylinders. The modeling encompasses (*a*) drug release from tubular devices, particularly in the presence of fluid boundary layers; (*b*) drug release from cylindrical systems containing drugs suspended in polymeric matrixes (1); (*c*) absorption of drugs from the vaginal lumen (2) or the lumen of the intestine (3), each of which, to a first approximation, may be considered a cylindrical membrane; and (*d*) combinations of *a*, *b*, and *c*.

A general phenomenon associated with all geometrical systems of this type, when diffusion is from the

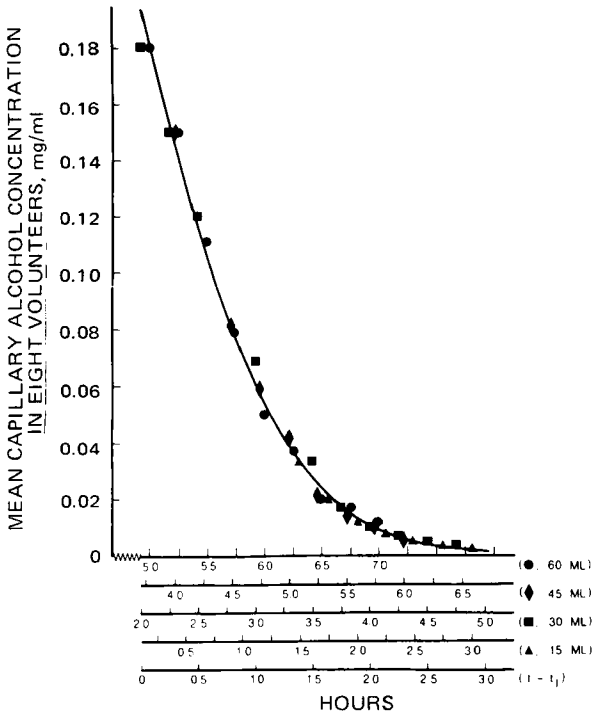

Figure 2—*Results of simultaneous nonlinear least-squares fitting to Eq. 5 of terminal average capillary blood alcohol concentrations of eight subjects given four different doses. The solid line gives the model-predicted concentrations.*

centration data obtained in six subjects given alcohol by constant-rate intravenous infusion) yields an estimate of 0.124 g of alcohol/kg/hr for the maximum elimination rate of alcohol in a normal male. For a 70-kg male, this is equivalent to 8.7 g of alcohol/hr.

In toxicology cases, where one wishes to estimate the future time course of blood alcohol concentrations, it is still valid to extrapolate an established pseudolinear decline in blood alcohol concentration down to about 0.2 mg/ml. However, this can only be done in individual patients who ingest a given dose of alcohol. It is invalid to predict the slope of the pseudolinear decline without a great deal of data and to compare slopes reported by two or more investigators who administer different doses of alcohol to different subjects. The slope of the pseudolinear decline is a function of C_0, V_m, and K_m, as indicated by Wagner (11) and the data in this report.

This work conclusively demonstrates that zero-order kinetics are inappropriate for describing the elimination of alcohol in humans. The slope of the pseudolinear decline should not be utilized as a measure of metabolism rate of alcohol as it has been used in the past (1, 2, 4–7). The rate of metabolism of alcohol is described more accurately by the V_m and K_m values and Eq. 2.

(1) E. M. P. Widmark, *Biochem. Z.*, **267**, 128(1933).

(2) H. Elbel and F. Schleyer, "Blutalkohal," 2nd ed., G. Thieme, Stuttgart, Germany, 1956.

(3) A. Goldstein, *N. Engl. J. Med.*, **283**, 875(1970).

(4) R. D. Hawkins and H. Kalant, *Pharmacol. Rev.*, **24**, 67(1972).

(5) N. H. Raskin, *N. Engl. J. Med.*, **292**, 422(1975).

(6) H. W. Newman, A. J. Lehman, and W. C. Cutting, *J. Pharmacol.*, **61**, 58(1937).

(7) M. G. Eggleton, *J. Physiol.*, **98**, 289(1940).

(8) F. Lundquist and H. Wolthers, *Acta Pharmacol. Toxicol.*, **14**, 265(1958).

(9) J. G. Wagner and J. A. Patel, *Res. Commun. Chem. Pathol. Pharmacol.*, **4**, 61(1972).

(10) M. A. Korsten, S. Matsuzaki, L. Feinman, and C. S. Lieber, *N. Engl. J. Med.*, **292**, 386(1975).

(11) J. G. Wagner, *J. Pharmacokinet. Biopharm.*, **1**, 103(1973).

(12) R. B. Forney, "General Pharmacology of Alcohol," Abstracts of Symposia and Contributed Papers Presented at APhA Academy of Pharmaceutical Sciences, San Francisco meeting, Vol. 1, No. 1, Mar. 1971, p. 28.

(13) R. W. Prouty and B. O'Neil, "An Evaluation of Some Qualitative Breath Screening Tests for Alcohol," Research Report, Insurance Institute for Highway Safety, Washington, DC 20037, May 1971, p. A-5.

(14) P. K. Wilkinson, J. G. Wagner, and A. J. Sedman, *Anal. Chem.*, **47**, 1506(1975).

(15) C. M. Metzler, "Biostatistics Technical Report 7292/69/7292/005," Upjohn Co., Kalamazoo, MI 49001, Nov. 25, 1969.

John G. Wagner [x]
Paul K. Wilkinson
Allen J. Sedman
Donald R. Kay
Donald J. Weidler
College of Pharmacy and
Upjohn Center for Clinical Pharmacology
University of Michigan
Ann Arbor, MI 48104

Received July 18, 1975.

Accepted for publication October 23, 1975.

Supported by Grant 1 R01 AA 00683-01A1 from the National Institute on Alcohol Abuse and Alcoholism, Alcohol, Drug Abuse, and Mental Health Administration, Rockville, Md. Three of us (J. G. Wagner, D. R. Kay, and D. J. Weidler) were partly supported by Public Health Service Grant 5-P11-GM-15559.

[x] To whom inquiries should be directed (at Upjohn Center for Clinical Pharmacology).

Analysis of Diffusion through Concentric Right Circular Cylinders and Concentric Spheres

Keyphrases □ Diffusion—concentric right circular cylinders and concentric spheres, models for drug release from tubular devices, cylindrical systems, and vaginal or GI lumen □ Drug release—tubular devices, cylindrical systems, and vaginal or GI lumen, concentric right circular cylinders and concentric spheres as models

To the Editor:

We recently have been modeling several diffusional systems involving diffusion through a series (two or more) of concentric right circular cylinders. The modeling encompasses (*a*) drug release from tubular devices, particularly in the presence of fluid boundary layers; (*b*) drug release from cylindrical systems containing drugs suspended in polymeric matrixes (1); (*c*) absorption of drugs from the vaginal lumen (2) or the lumen of the intestine (3), each of which, to a first approximation, may be considered a cylindrical membrane; and (*d*) combinations of *a*, *b*, and *c*.

A general phenomenon associated with all geometrical systems of this type, when diffusion is from the

core of the cylinder to some external surface, is dilution along the radial vector as the concentration gradient develops because, for each unit incremental increase in radius, Δr, a larger and larger differential volume, ΔV, is associated with the prescribed concentric tubular cylinder (ΔV lying between the hollow cylinder prescribed by r_i and $r_i + \Delta r$). In the steady state, the net flux through every concentric cylindrical plane is constant. However, since the incremental volume elements are growing to the third power of the radius as the radius is extended, the concentration gradient in the cylindrical case is nonlinear and effectively more severe than that generated in the planar case. Thus, the steady-state flux through a hollow tube of thickness Δr is greater than the steady-state flux of the same diffusant through a comparably thick planar slab of the same composition and area[1].

Yet, often, cylindrical geometrical influences are ignored and cylindrical membranes are "flattened" in our treatments. For example, intestinal absorption is often treated as a planar process rather than as absorption through a cylindrical or "tubular" tissue barrier. Intuitively, this approach seems reasonable because the involved tissue "thickness" is small relative to the radius of the GI lumen. The purpose of this communication, in addition to providing general equations for steady-state diffusion through concentric cylindrical barriers in series, is to quantitate the conditions where planarization of the diffusional process is mathematically appropriate.

A general approach to treating cylindrical barriers in series can be illustrated by considering the simplest such system, two concentric hollow cylindrical membranes. Figure 1 is an illustration of several such "membranes" in series. The situation specifically involves diffusion from a solution within the tubular lumen through the cylindrical membrane, determined by radii r_1 and r_2, and then through the contiguous and concentric tubular region, determined by radii r_2 and r_3. For the moment, we shall neglect diffusional resistance contributions of interfaces, although they could be treated as additional diffusional resistances in series.

For simplicity of treatment, it is assumed that there is a constant luminal concentration of the penetrant, C_0, at all times and that the diffusion is into an external sink (the outside concentration is zero at all times). Under these conditions, a true steady state develops in time and the flux is invariant through every concentric cylindrical plane. It also is assumed that the concentric cylinders are of length H and that there is no end diffusion.

Fick's first law states[2]:

$$J = -AD\left(\frac{dC}{dx}\right) \qquad \text{(Eq. 1)}$$

where J is the flux, A is the area, D is the diffusivity, and dC/dx is the concentration gradient. The lateral area of a right circular cylinder is given by:

$$A = 2\pi rH \qquad \text{(Eq. 2)}$$

where r is the radius, and H is the cylinder's length. Combining Eqs. 1 and 2 produces:

$$J = -2\pi rHD\left(\frac{dC}{dr}\right) \qquad \text{(Eq. 3)}$$

as the distance, x, is measured along a radial line. In the steady state, J is constant through every concentric cylindrical plane. In the first hollow cylindrical shell of a series of cylindrical shells:

$$J = -2\pi rHD_1\left(\frac{dC}{dr}\right) \qquad \text{(Eq. 4)}$$

and:

$$\frac{dr}{r} = -\frac{2\pi HD_1}{J}dC \qquad \text{(Eq. 5)}$$

which may be integrated from C_1' to C_2 and from r_1 to r_2 to yield[3]:

$$\ln\left(\frac{r_2}{r_1}\right) = \frac{2\pi HD_1}{J}(C_1' - C_2) \qquad \text{(Eq. 6)}$$

The second concentric cylindrical "membrane" may be similarly treated:

$$\ln\left(\frac{r_3}{r_2}\right) = \frac{2\pi HD_2}{J}(C_2' - C_3) \qquad \text{(Eq. 7)}$$

The assumption of a sink condition at the outer boundary leads to $C_3 = 0$ at all times and:

$$\ln\left(\frac{r_3}{r_2}\right) = \frac{2\pi HD_2}{J}C_2' \qquad \text{(Eq. 8)}$$

To combine Eqs. 6 and 8, one has to adopt a uniform, continuous "concentration" (activity) scale. This is most conveniently done with respect to C_0, the core concentration, using partition coefficients. Let $C_0/C_1' = K_I$ and $C_2/C_2' = K_{II}$. Then $C_1' = C_0/K_I$ and $C_2' = C_2/K_{II}$. The latter relationship, when incorporated in Eq. 8, yields for C_2:

$$C_2 = \frac{K_{II}J}{2\pi HD_2}\ln\left(\frac{r_3}{r_2}\right) \qquad \text{(Eq. 9)}$$

which, when substituted into Eq. 6 along with the other partitioning relationship, yields for the flux:

$$J = \frac{2\pi HD_1D_2C_0}{D_2K_I\ln\left(\frac{r_2}{r_1}\right) + D_1K_IK_{II}\ln\left(\frac{r_3}{r_2}\right)} \qquad \text{(Eq. 10)}$$

The product K_IK_{II} is itself a distribution coefficient and is $C_0C_2/C_1'C_2'$. If the system proceeds to a true equilibrium, this quantity, being the product of two constants, remains constant (to the extent that partitioning is concentration insensitive) and, at true equilibrium, $C_1' = C_2$ and $K_IK_{II} = K_2 = (C_0/C_2')$. But this is simply the equilibrium distribution coeffi-

[1] Radial diffusion in the opposite direction, to the center of the cylinder, is accompanied by a "concentration" relative to a planar system. For the comparison, one can take the inner cylindrical area, associated with r_i, as the severest test of the statement (see Table I).

[2] The flux here is defined in terms of total surface area rather than on a per unit area basis. This form is useful in characterizing the mass current from nonplanar geometrical barriers.

[3] A convention has been adopted here in which subscript numbers for concentrations at interfacial boundaries are numbered with respect to the order of the radii, the inner radius being r_1, the next longer radius being r_2, *etc.* There are, of course, two surface concentrations at each interface, one on each side. The inner surface concentration is simply designated by the radius subscript, while the surface concentration in the material on the outer side of the interface is designated by a prime superscript in addition to the radius subscript. Thus, C_1' is the outer surface concentration associated with the interface found at radius r_1.

cient of the permeant between the core phase and the material comprising the outer cylindrical membrane. Extending the relationship to additional cylindrical shells in series shows that only a singular partition coefficient need be considered as the diffusant enters a new phase, and this coefficient is the equilibrium partition coefficient between the core and that particular phase.

It is easy to show, by repetitively using these mathematical operations, that diffusion through multiple concentric cylindrical barriers in series in the steady state mathematically conforms to[4]:

$$J = \frac{2\pi H(D_1D_2\cdots D_n)C_0}{\frac{(D_1D_2\cdots D_n)}{D_1}K_1 \ln\left(\frac{r_2}{r_1}\right) + \frac{(D_1D_2\cdots D_n)}{D_2}K_2 \ln\left(\frac{r_3}{r_2}\right) + \cdots + \frac{(D_1D_2\cdots D_n)}{D_n}K_n \ln\left(\frac{r_{n+1}}{r_n}\right)} \quad \text{(Eq. 11)}$$

This form also can be applied to some quasi-steady-state problems upon substitution of $\Delta C = [C_0 - C_{n+1}]$ for C_0 (5).

We can now consider the conditions whereby a cylindrical system may be functionally planar. It can be seen from Eqs. 6 and 7 that, for any concentric tubular barrier, say the ith:

$$J = \frac{2\pi HD_i(C_i' - C_{i+1})}{\ln\left(\frac{r_{i+1}}{r_i}\right)} \quad \text{(Eq. 12)}$$

Furthermore, any r_{i+1} may be put in terms of r_i and a differential radius:

$$r_{i+1} = r_i + \Delta r \quad \text{(Eq. 13)}$$

and, thus:

$$J = \frac{2\pi HD_i(C_i' - C_{i+1})}{\ln\left(1 + \frac{\Delta r}{r_i}\right)} \quad \text{(Eq. 14)}$$

The terms C_i' and C_{i+1} are the inner and outer "membrane" surface concentrations, respectively[3].

The natural logarithmic term in Eq. 14 is in the general form ln $(1 + X)$, where X is obviously $\Delta r/r_i$. It can be shown that the function ln $(1 + X)$ expands to:

$$\ln(1 + X) = X - \frac{X^2}{2} + \int_0^x \left(\frac{X^2}{1 + X}\right) dx \quad \text{(Eq. 15)}$$

which, as X takes a value less than one, is first well approximated by $X - (X^2/2)$ and then, as X becomes sufficiently small, is simply approximated by X itself. Therefore, when using the simple but less exact approximation, in the limit that $\Delta r/r_i \ll 1$:

$$J = \frac{2\pi HD_i(C_i' - C_{i+1})}{\frac{\Delta r}{r_i}} \quad \text{(Eq. 16a)}$$

or:

$$J = \frac{2\pi Hr_iD_i(C_i' - C_{i+1})}{\Delta r} \quad \text{(Eq. 16b)}$$

which is a planar form of the flux equation where the area, A, is $2\pi r_iH$ and the laminate thickness is Δr.

[4] Barrer (4) presented a general derivation for concentric cylindrical barriers in series using a concise, alternative mathematical approach. The two forms, Barrer's and Eq. 11, appear different but can be shown to be interconvertable with proper manipulation and the use of a common set of symbols.

The applicability of Eq. 16 now can be quantitated. The exact solutions of the function ln $(1 + X)$ along with solutions using both of the function approximations are listed in Table I for several ratios of r_{i+1}/r_i. The table also gives the percentage deviations from the exact solution. It can be seen that the "long approximation" gives very satisfactory results (<1% deviation) at a radial ratio of 1.1 or a Δr 10% as large as r_i. The short approximation has an inherent 5% error at this ratio. When Δr is only 1% of r_i, the short approximation becomes quite satisfactory because the error is only 0.5%. In fact, the percentage error in using the short approximation converges to half the percentage increase of r_{i+1} over r_i. Thus, the planar form gives a 0.5% error when Δr is 1% of r_i, a 0.05% error when Δr is 0.1% of r_i, and so on. The long approximation provides virtually exact solutions as the radial ratio approaches one.

In vaginal and intestinal absorption, one is dealing with reasonably cylindrical cavities which have radii measured in whole centimeters and membranes and boundary layer barriers of estimated thicknesses ranging from fractional to whole millimeters. The upper limit on the radial ratio experienced in these circumstances seems to be about 1:1 and should be considerably less in most cases. Thus, planarization of the absorption processes through these tissues is

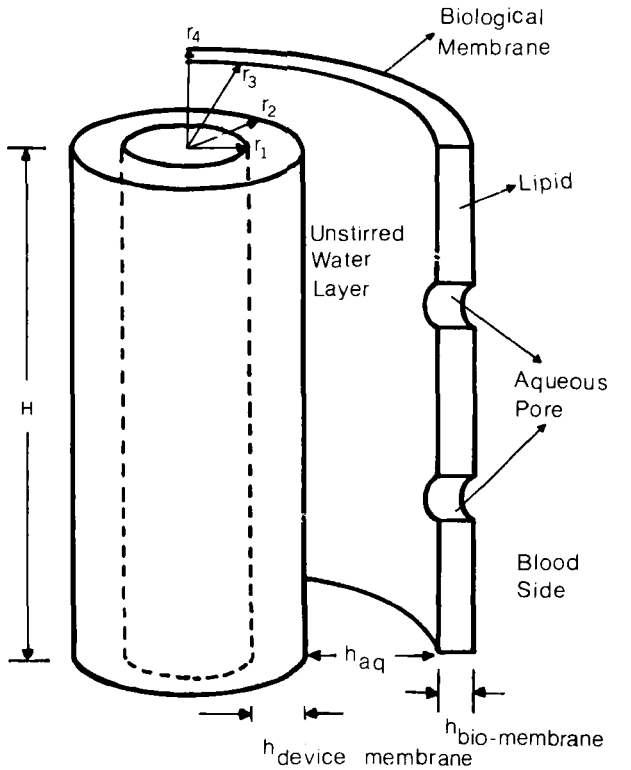

Figure 1—*Series of concentric cylinders as a drug delivery device in a biological setting. The "thicknesses" of the respective laminates are designated by* h *values. Each* h *can be described in terms of a differential radius,* Δr.

Table I—Comparison of Exact and Approximate Solutions of the Function $\ln\left(1+\frac{\Delta r}{r_i}\right)$

Radius[a] Ratio	Increase in r_{i+1} over r_i, %	$\ln\left(1+\frac{\Delta r}{r_i}\right)$	Solution by First Approximation $\frac{\Delta r}{r_i}-\left(\frac{\Delta r}{r_i}\right)^2/2$	Deviation[b], %	Solution by Second Approximation $\frac{\Delta r}{r_i}$	Deviation[b], %
1.5	50	0.40547	0.375	−7.51	0.5	23.3
1.1	10	0.095310	0.095	−0.325	0.1	4.93
1.05	5	0.048790	0.04875	−0.082	0.05	2.48
1.01	1	0.0099503	0.00995	−0.0030	0.01	0.50
1.005	0.5	0.00498754	0.0049875	−0.008	0.005	0.25
1.001	0.1	0.000999500	0.0009995	0	0.001	0.050

[a] This is the same as $1 + (\Delta r/r_i)$. [b] Percent deviation of approximate solution with respect to exact solution.

accompanied by a small and, in most cases, a negligible error.

However, in release of drugs through tubular membranes (drug delivery devices) where radii are in fractional centimeters (a 0.5-cm diameter could be considered typical) and tubing wall thicknesses approach whole millimeters (a Δr of 1 mm might be typical), planarization of the treatment introduces large errors in estimating diffusional parameters or in characterizing flux as a function of tubing thickness from known diffusivities and partition coefficients, *etc.* In these situations, the geometrical factor has to be accounted for in the mass transport characterization. Because of the remarkably simple relationship between the error of approximation and the radial ratio, it is easy to determine if one can employ the simplified form.

A similar analysis can be applied to concentric spheres. Barrer (4) gave a general form for the permeability coefficient of multiple concentric spherical barriers. Alternatively, the procedure illustrated here can be employed to develop a mathematical model (6, 7). In any case, one obtains for the ith spherical laminate:

$$J = \frac{4\pi D_i(C_i' - C_{i+1})}{\frac{1}{r_i} - \frac{1}{r_i + \Delta r}} \qquad \text{(Eq. 17)}$$

Table II—Comparison of Exact and Approximate Solutions for Concentric Spheres at a Constant Radial Ratio, 1.5

r_i	$r_i + \Delta r$	Δr	$\frac{1}{r_i} - \frac{1}{r_i + \Delta r}$	$\frac{\Delta r}{r_i^2}$	Deviation, %
1	1.5	0.5	0.02083	0.5	50
2	3	1	0.1667	0.25	50
4	6	2	0.0833	0.125	50
8	12	4	0.04167	0.0625	50
16	24	8	0.02083	0.0313	50

Table III—Comparison of Exact and Approximate Solutions for Concentric Spheres at Varying Radial Ratio for a Constant r_i Value of 1

$r_i + \Delta r$	Δr	$\frac{1}{r_i} - \frac{1}{r_i + \Delta r}$	$\frac{\Delta r}{r_i^2}$	Radius Increase, %	Deviation, %
1.5	0.5	0.3333	0.5	50	50
1.1	0.1	0.090909	0.1	10	10
1.05	0.05	0.047619	0.05	5	5
1.01	0.01	0.009901	0.01	1	1
1.005	0.005	0.0049752	0.005	0.5	0.5

where $r_i + \Delta r = r_{i+1}$. The denominator can also be written:

$$\frac{1}{r_i} - \frac{1}{r_i + \Delta r} = \frac{\Delta r}{r_i(r_i + \Delta r)} \qquad \text{(Eq. 18)}$$

and it can be seen by inspection that when Δr becomes very small, the function approaches $\Delta r/r_i^2$. When substituted into Eq. 17, this approximation gives a planar form of the flux equation of area $4\pi r_i^2$ and thickness Δr.

An analysis of the cylindrical case appears in Tables II and III. In Table II, the function $\Delta r/r_i^2$ is compared with the exact function $(1/r_i) - 1/(r_i + \Delta r)$ for varying r values but for a constant 50% increase in r_{i+1} over r_i. Unlike the cylindrical case, the absolute magnitude of r_i in addition to the ratio r_{i+1}/r_i is a determinant of the quantitative value of the function. However, the percentage error at a given ratio remains constant. Moreover, the percentage error is the same as the percentage increase of Δr over r_i (inspection of Eqs. 17 and 18 indicates that this is to be expected). The relationships are further illustrated in Table III, where the radial ratio has been varied but r_i has been held constant at 1.

These equations and their analysis indicate where one can simplify the characterization of absorption of drugs and nutrients by cultured cells and microorganisms, of uptake and release mechanisms of emulsion droplets in the presence of diffusion layers and interfacial barriers, and of release of drugs from spherical capsules and other spherical devices.

(1) T. J. Roseman and W. I. Higuchi, *J. Pharm. Sci.*, **59**, 353(1970).

(2) T. Yotsuyanagi, A. Molokhia, S. Hwang, N. F. H. Ho, G. L. Flynn, and W. I. Higuchi, *ibid.*, **64**, 71(1975).

(3) K. Desai, Ph.D. thesis, University of Michigan, Ann Arbor, Mich., 1975.

(4) R. M. Barrer, in "Diffusion in Polymers," J. Crank and G. S. Park, Eds., Academic, New York, N.Y., 1968, pp. 173, 174.

(5) G. L. Flynn, S. H. Yalkowsky, and T. J. Roseman, *J. Pharm. Sci.*, **63**, 479(1974).

(6) N. F. H. Ho, J. Turi, C. Shipman, and W. I. Higuchi, *J. Theoret. Biol.*, **34**, 451(1972).

(7) J. S. Turi, W. I. Higuchi, C. Shipman, Jr., and N. F. H. Ho, *J. Pharm. Sci.*, **61**, 1618(1972).

Gordon L. Flynn ˣ
Norman F. H. Ho
William I. Higuchi
College of Pharmacy
University of Michigan
Ann Arbor, MI 48104

John Kent
Institute of Pharmaceutical Sciences
Syntex Research
Palo Alto, Calif.

Received April 2, 1975.
Accepted for publication October 21, 1975.
Supported in part by Contract N01-HD-3-2740, National Institute of Child Health and Human Development, Bethesda, Md.
[x] To whom inquiries should be directed.

Consistency Relations in Solid Solution Melting-Point Diagrams

Keyphrases □ Solid solution systems—melting-point diagrams, consistency relations, thermodynamic analysis □ Melting-point diagrams—solid solution systems, consistency relations

To the Editor:

Solid solution systems have been of pharmaceutical interest in recent years (1–7). The thermodynamic basis for solid solution systems is given in standard texts on solid-state physics or chemistry; *e.g.*, Zhdanov (8) listed the expression for the free energy, F, at temperature T °K of a system containing x mole fraction A and $(1 - x)$ mole fraction B as:

$$F(x, T) = K(T) + 0.5NZ[x^2V_{AA} + (1-x)^2V_{BB} + 2x(1-x)V_{AB}] + RT[x \ln x + (1-x)\ln(1-x)] \quad \text{(Eq. 1)}$$

where:

N = Avogadro's number
Z = coordination number
V_{AA} = interaction energy between two A molecules
V_{BB} = interaction energy between two B molecules
V_{AB} = interaction energy between an A and a B molecule
$K(T) = \int_0^T c\,dT - T\int_0^T \frac{c}{T}\,dT$, where c = heat capacity

The assumptions made here are that: (*a*) only nearest neighbor interactions are considered, (*b*) Stirling's formula is applicable, and (*c*) the heat capacities for the two solids and for the solid solutions are identical. This last assumption is made in all published treatments [*e.g.*, Zhdanov (8) and Ashbee (9)] and is implicit in the use of the terminology $K(T)$ rather than $K(T, x)$. This assumption may not necessarily be a good one (as evidenced by a great deal of thermoanalytical work) but is, nevertheless, made here.

A typical plot of F as a function of composition x at temperatures $T_1 > T_2 > T_3 > T_4$, where T_2 is the eutectic temperature, is shown in Fig. 1. The curves in Fig. 1 are based on $2V_{AB} > V_{AA} + V_{BB}$ (9). The corresponding binary melting-point diagram is shown in Fig. 2.

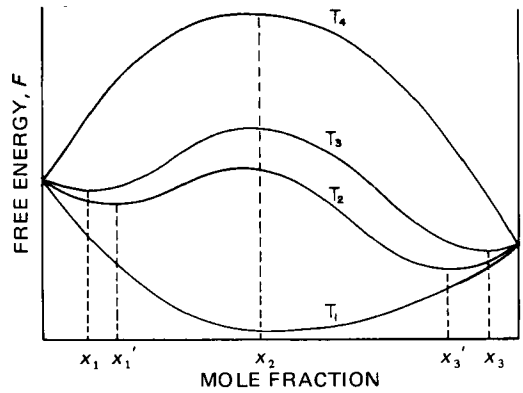

Figure 1—*Free energy* versus *mole fraction of a binary mixture forming a random solid solution. The indicated temperatures are of the rank* $T_1 > T_2 > T_3 > T_4$. *The minima correspond to solid solution compositions at the indicated temperatures (at which the mixture is solid). In this example,* T_2 *could be the eutectic temperature and* T_3 *could be room temperature.*

There are three extrema (at compositions x_1, x_2, and x_3) when solid solutions exist, the two minima (x_1 and x_3) being at the compositions of the solid solutions at the eutectic temperature, T_2. That the maximum coincides with the eutectic composition is, however, not thermodynamically obvious. The values for x_1, x_2, and x_3 satisfy the first derivative equation of Eq. 1 when equated to zero, *i.e.*:

$$\left.\frac{\partial F}{\partial x}\right|_T = NZ\{xV_{AA} - (1-x)V_{BB} + (1-2x)V_{AB}\} + NkT \ln\{x/(1-x)\} = 0 \quad \text{(Eq. 2)}$$

where k is Boltzmann's constant. Inserting $x = x_1$, x_2, and x_3 then yields three equations with three unknowns:

$$x_1V_{AA} + (x_1-1)V_{BB} + (1-2x_1)V_{AB} = -\frac{kT}{Z}\ln[x_1/(1-x_1)] \quad \text{(Eq. 3a)}$$

$$x_2V_{AA} + (x_2-1)V_{BB} + (1-2x_2)V_{AB} = -\frac{kT}{Z}\ln[x_2/(1-x_2)] \quad \text{(Eq. 3b)}$$

$$x_3V_{AA} + (x_3-1)V_{BB} + (1-2x_3)V_{AB} = -\frac{kT}{Z}\ln[x_3/(1-x_3)] \quad \text{(Eq. 3c)}$$

where V_{AA}, V_{BB}, and V_{AB} are the unknowns. There is no unique solution to these three equations, because the determinant $D = |x_i, (x_i - 1), (1 - 2x_i)|$ equals zero for all values of x_i; *i.e.*, there is a linear dependence among x_1, x_2, and x_3. If the coefficients of dependence are denoted α_1 and α_2, it follows from Eqs. 3*a*–3*c* that:

$$\alpha_1x_1 + \alpha_2x_2 = x_3 \quad \text{(Eq. 4a)}$$

$$\alpha_1(x_1-1) + \alpha_2(x_2-1) = (x_3-1) \quad \text{(Eq. 4b)}$$

$$\alpha_1(1-2x_1) + \alpha_2(1-2x_2) = 1-2x_3 \quad \text{(Eq. 4c)}$$

The solutions to Eqs. 4*a*–4*c* are:

$$\alpha_1 = (x_2 - x_3)/(x_2 - x_1) \quad \text{(Eq. 5)}$$

$$\alpha_2 = (x_3 - x_1)/(x_2 - x_1) \quad \text{(Eq. 6)}$$

John Kent
Institute of Pharmaceutical Sciences
Syntex Research
Palo Alto, Calif.

Received April 2, 1975.
Accepted for publication October 21, 1975.
Supported in part by Contract N01-HD-3-2740, National Institute of Child Health and Human Development, Bethesda, Md.
[x] To whom inquiries should be directed.

Consistency Relations in Solid Solution Melting-Point Diagrams

Keyphrases □ Solid solution systems—melting-point diagrams, consistency relations, thermodynamic analysis □ Melting-point diagrams—solid solution systems, consistency relations

To the Editor:

Solid solution systems have been of pharmaceutical interest in recent years (1–7). The thermodynamic basis for solid solution systems is given in standard texts on solid-state physics or chemistry; *e.g.*, Zhdanov (8) listed the expression for the free energy, F, at temperature T °K of a system containing x mole fraction A and $(1 - x)$ mole fraction B as:

$$F(x, T) = K(T) + 0.5NZ[x^2V_{AA} + (1-x)^2V_{BB} + 2x(1-x)V_{AB}] + RT[x \ln x + (1-x)\ln(1-x)] \quad \text{(Eq. 1)}$$

where:

N = Avogadro's number
Z = coordination number
V_{AA} = interaction energy between two A molecules
V_{BB} = interaction energy between two B molecules
V_{AB} = interaction energy between an A and a B molecule
$K(T) = \int_0^T c\,dT - T\int_0^T \frac{c}{T}\,dT$, where c = heat capacity

The assumptions made here are that: (*a*) only nearest neighbor interactions are considered, (*b*) Stirling's formula is applicable, and (*c*) the heat capacities for the two solids and for the solid solutions are identical. This last assumption is made in all published treatments [*e.g.*, Zhdanov (8) and Ashbee (9)] and is implicit in the use of the terminology $K(T)$ rather than $K(T, x)$. This assumption may not necessarily be a good one (as evidenced by a great deal of thermoanalytical work) but is, nevertheless, made here.

A typical plot of F as a function of composition x at temperatures $T_1 > T_2 > T_3 > T_4$, where T_2 is the eutectic temperature, is shown in Fig. 1. The curves in Fig. 1 are based on $2V_{AB} > V_{AA} + V_{BB}$ (9). The corresponding binary melting-point diagram is shown in Fig. 2.

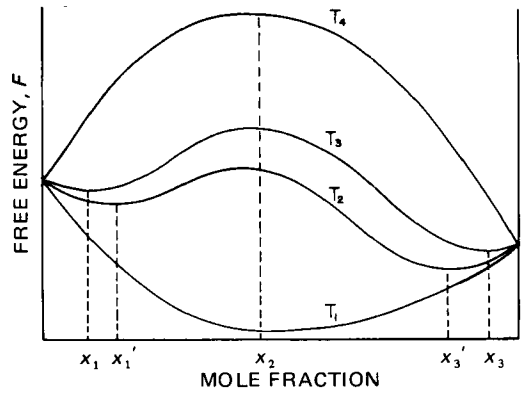

Figure 1—*Free energy* versus *mole fraction of a binary mixture forming a random solid solution. The indicated temperatures are of the rank* $T_1 > T_2 > T_3 > T_4$. *The minima correspond to solid solution compositions at the indicated temperatures (at which the mixture is solid). In this example,* T_2 *could be the eutectic temperature and* T_3 *could be room temperature.*

There are three extrema (at compositions x_1, x_2, and x_3) when solid solutions exist, the two minima (x_1 and x_3) being at the compositions of the solid solutions at the eutectic temperature, T_2. That the maximum coincides with the eutectic composition is, however, not thermodynamically obvious. The values for x_1, x_2, and x_3 satisfy the first derivative equation of Eq. 1 when equated to zero, *i.e.*:

$$\left.\frac{\partial F}{\partial x}\right|_T = NZ\{xV_{AA} - (1-x)V_{BB} + (1-2x)V_{AB}\} + NkT \ln\{x/(1-x)\} = 0 \quad \text{(Eq. 2)}$$

where k is Boltzmann's constant. Inserting $x = x_1$, x_2, and x_3 then yields three equations with three unknowns:

$$x_1V_{AA} + (x_1-1)V_{BB} + (1-2x_1)V_{AB} = -\frac{kT}{Z}\ln[x_1/(1-x_1)] \quad \text{(Eq. 3a)}$$

$$x_2V_{AA} + (x_2-1)V_{BB} + (1-2x_2)V_{AB} = -\frac{kT}{Z}\ln[x_2/(1-x_2)] \quad \text{(Eq. 3b)}$$

$$x_3V_{AA} + (x_3-1)V_{BB} + (1-2x_3)V_{AB} = -\frac{kT}{Z}\ln[x_3/(1-x_3)] \quad \text{(Eq. 3c)}$$

where V_{AA}, V_{BB}, and V_{AB} are the unknowns. There is no unique solution to these three equations, because the determinant $D = |x_i, (x_i - 1), (1 - 2x_i)|$ equals zero for all values of x_i; *i.e.*, there is a linear dependence among x_1, x_2, and x_3. If the coefficients of dependence are denoted α_1 and α_2, it follows from Eqs. 3*a*–3*c* that:

$$\alpha_1x_1 + \alpha_2x_2 = x_3 \quad \text{(Eq. 4a)}$$

$$\alpha_1(x_1-1) + \alpha_2(x_2-1) = (x_3-1) \quad \text{(Eq. 4b)}$$

$$\alpha_1(1-2x_1) + \alpha_2(1-2x_2) = 1-2x_3 \quad \text{(Eq. 4c)}$$

The solutions to Eqs. 4*a*–4*c* are:

$$\alpha_1 = (x_2 - x_3)/(x_2 - x_1) \quad \text{(Eq. 5)}$$

$$\alpha_2 = (x_3 - x_1)/(x_2 - x_1) \quad \text{(Eq. 6)}$$

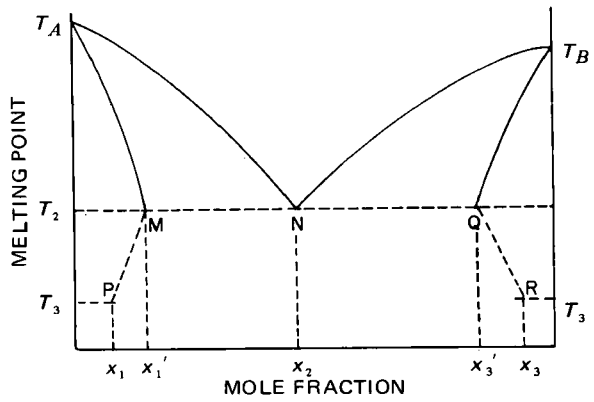

Figure 2—*Binary melting-point diagram corresponding to the free energy diagram in Fig. 1.* T_A-N *and* T_B-N *are liquidus lines and* T_A-M *and* T_B-Q *are solidus lines.*

For Eqs. 3*a*–3*c* to have solutions, the right-hand sides must also be subject to the linear dependence coefficients; *i.e.*:

$$\alpha_1 \ln [x_1/(1-x_1)] + \alpha_2 \ln [x_2/(1-x_2)] = \ln [x_3/(1-x_3)] \quad \text{(Eq. 7)}$$

Inserting Eqs. 5 and 6 into Eq. 7 and multiplying through by $(x_2 - x_1)$ then give:

$$(x_2 - x_3) \ln [x_1/(1-x_1)] + (x_3 - x_1) \ln [x_2/(1-x_2)] = (x_2 - x_1) \ln [x_3/(1-x_3)] \quad \text{(Eq. 8)}$$

Equation 8 is a consistency relation and should apply to the two minima and the maximum. Since the minima at the eutectic temperature are known and are at the solid solution compositions, x_2 can be found; in this fashion, it can be checked whether x_2 occurs on or about the eutectic composition.

Two examples will illustrate the utility of Eq. 8. If $x_2 = 0.5$, then Eq. 8 implies that:

$$(0.5 - x_3) \ln [x_1/(1-x_1)] + (x_3 - x_1) \ln (1.0) = (0.5 - x_1) \ln [x_3/(1-x_3)] \quad \text{(Eq. 9)}$$

The second term is zero, and the solution is $x_1 = (1 - x_3)$; *i.e.*, even when V_{AA} is different from V_{BB}, a maximum at $x_2 = 0.5$ implies symmetry.

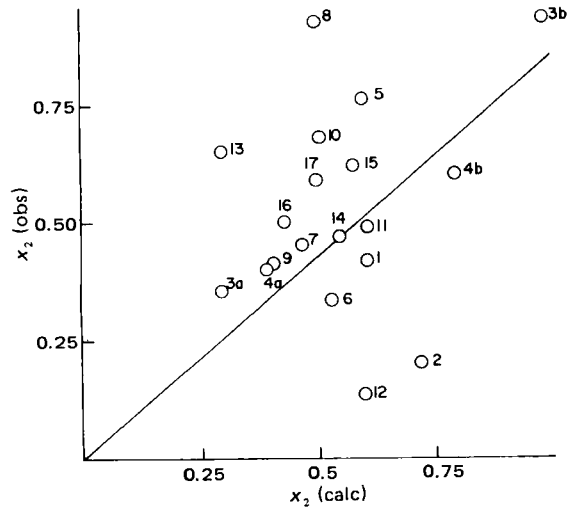

Figure 3—*Plot of the observed* versus *calculated eutectic composition in binary mixtures. The data are from Table I. Numbers correspond with systems shown in Table I.*

Table I—Referenced Binary Systems with Observed and Calculated Values of Eutectic Composition

Composition Number	System	Reference	x_2 (obs)	x_2 (calc)
1	Chloramphenicol–urea	5	0.37	0.62
2	Sulfathiazole–urea	7	0.20	0.73
3*a*	Deoxycholic acid–menadione	6	0.36	0.30
3*b*	Deoxycholic acid–menadione	6	0.94	0.98
4*a*	Quinine–phenobarbital	6	0.40	0.39
4*b*	Quinine–phenobarbital	6	0.60	0.79
5	Theophylline–phenobarbital	6	0.76	0.60
6	Phenacetin–phenobarbital	6	0.33	0.53
7	Acetaminophen–phenobarbital	6	0.45	0.47
8	Phenytoin–phenobarbital	6	0.93	0.50
9	Aspirin–phenobarbital	6	0.35	0.40
10	*p*-Nitroaniline–7-(2-hydroxyethyl)theophylline	2	0.68	0.51
11	*m*-Methoxybenzoic acid–7-(2-hydroxyethyl)theophylline	2	0.49	0.61
12	Aminopyrine–7-(2-hydroxyethyl)theophylline	2	0.13	0.65
13	Anthranilic acid–caffeine	2	0.65	0.30
14	Benzoic acid–7-(2-hydroxyethyl)theophylline	2	0.47	0.55
15	Benzidine–7-(2-hydroxyethyl)theophylline	2	0.62	0.58
16	Aminopyrine–allobarbital	2	0.50	0.38
17	*p*-Nitrophenol–7-(2-hydroxyethyl)theophylline	2	0.59	0.50

In the second example, it is assumed that x_2 does not occur at 0.5. The following figures are used: $x_1 = 0.2$ and $x_3 = 0.85$. These values inserted in Eq. 8 give the following equation in one unknown (x_2):

$$(x_2 - 0.85) \ln \{0.2/0.8\} + (0.85\text{-}0.2) \ln \{x_2/(1-x_2)\} = (x_2 - 0.2) \ln \{0.85/0.15\} \quad \text{(Eq. 10)}$$

The solution is found by trial and error and is $x_2 = 0.43$.

This method was used to determine x_2 from known values of x_1 and x_3 (solid solution compositions at the eutectic temperature); the values were taken from reported binary melting-point diagrams (2, 5–7). The calculated values of x_2, denoted x_2(calc), are tabulated *versus* the eutectic composition, denoted x_2(obs), in Table I and plotted in Fig. 3.

If x_2(obs) = x_2(calc), then a least-squares fit regression line of the data should be such that the 95% confidence limits of the intercept should include zero and the 95% confidence limits of the slope should include unity. This is the case since the least-squares fit equation is x_2(obs) = (0.37 ± 0.75)x_2(calc) + (0.27 ± 0.45). The data, as shown in Fig. 3, are scattered and the fit obviously is not excellent ($r = 0.22$, which is significant at the 75% level).

If x_2(obs) = x_2(calc) is plotted as a confined least-squares fit, then the 95% confidence limits on the slope should include unity, as indeed they do; the least-squares fit of the confined line is x_2(obs) = (0.85 ± 0.40)x_2(calc) (Fig. 3). Other tests fail to reject the hypothesis that x_2(obs) = x_2(calc). For instance, the differences x_2(obs) − x_2(calc) in Table I should be normally distributed about a mean of zero. A χ^2-test fails to show them to be nonnormal ($\chi^2 = 0.2 \ll \chi^2_{2,0.05} = 6$). Therefore, the data apparently are in-

dicative of the proposed theory and data treatment method.

(1) K. Sekiguchi and N. Obi, *Chem. Pharm. Bull.*, **9**, 866(1961).
(2) K. Sekiguchi, Y. Ueda, and Y. Nakamori, *ibid.*, **11**, 1108(1963).
(3) *Ibid.*, **11**, 1123(1963).
(4) K. Sekiguchi, N. Obi, and Y. Ueda, *Chem. Pharm. Bull.*, **12**, 134(1964).
(5) A. H. Goldberg, M. Gibaldi, and J. L. Kanig, *J. Pharm. Sci.*, **54**, 1145(1965).
(6) J. K. Guillory, S. Huang, and J. Lach, *ibid.*, **58**, 301(1969).
(7) W. L. Chiou and S. Niazi, *ibid.*, **60**, 1333(1971).
(8) G. S. Zhdanov, "Crystal Physics," Academic, New York, N.Y., 1965, pp. 335–338.
(9) K. H. G. Ashbee, in "Problems in Solid State Physics," H. J. Goldsmid, Ed., Academic, New York, N.Y., 1968, p. 191.

J. T. Carstensen [x]
Shabbir T. Anik
School of Pharmacy
University of Wisconsin
Madison, WI 53706

Received July 9, 1975.
Accepted for publication October 24, 1975.
[x] To whom inquiries should be directed.

Toxic Substances Produced by *Fusarium* I: Trichothecene Derivatives from Two Strains of *Fusarium oxysporum* f. sp. *carthami*

Keyphrases □ *Fusarium oxysporum*—cultured, trichothecenes isolated, phytotoxic and dermatitic properties evaluated □ Phytotoxins—trichothecenes isolated from *Fusarium oxysporum*, activity evaluated □ Fungi—*Fusarium oxysporum* cultured, trichothecenes isolated, phytotoxic and dermatitic properties evaluated

To the Editor:

Fusarium oxysporum Schlecht. f. *carthami* Klisiewicz & Houston is involved in the typical wilt disease of safflower (*Carthamus tinctorius* Linn.) (1, 2). However, the nature of the substance or substances responsible for the phytotoxic effects has not been evaluated previously. Since food materials infected with a species of *Fusarium* have often contained substances that produce high mammalian toxicity (3), the presence of *F. oxysporum* in safflower is thus cause for alarm.

Although previous investigations with other forms of *F. oxysporum* furnished biologically active 12,13-epoxytrichothecenes (3, 4), there is no report on this form of the fungus producing any toxic substance in artificial media or the host tissue. The present investigation was designed to isolate and study the substances produced by the fungus in artificial media that are responsible for the pathogenic property.

Two strains (weakly parasitic and virulent) were collected from Varanasi, India (2), and their identity was confirmed by the Commonwealth Mycological Institute, Kew, England [CMI (IMI-166917 and IMI-186539)]. These strains were separately grown in Richard's solution (200 ml) (5) in still culture flasks (1 liter) at 21° for 21 days.

When sprayed on safflower plants, the culture filtrates caused severe scorching of foliage accompanied by marked retardation of stem growth and frequently death of the plants. Even in high dilution (1:100), the culture filtrates inhibited root elongation of 2-day-old seedlings. There was no inhibition of germination of safflower seeds when sown in a medium containing the culture filtrates, but the seedlings showed the usual toxic symptoms.

The effects of the intracellular toxins (from the mycelium) were more severe than those of the extracellular ones (from the culture filtrates). For the extraction of the intracellular toxins, the mycelia were first washed and then macerated with water in a high-speed blender. The extract was passed through a bacteria-proof filter. The effect of the filtrate was tested on the host plant in the usual way.

The toxic substances were isolated from the culture filtrates by solvent extraction. In a typical experiment, the culture filtrate (5 liters) from the weakly parasitic strain at the natural pH (about 3.8) was successively extracted with chloroform (3 liters) and ethyl acetate (3 liters). The aqueous mother liquor was then concentrated to about 500 ml under reduced pressure and again extracted with hot ethyl acetate (3 liters). The three extracts were processed separately.

Evaporation of the solvent from the chloroform extract afforded a brown oil (0.88 g) which, in very low concentration (1–2 ppm), produced phytotoxic effects similar to those shown by the culture filtrates. It showed the presence of about six trichothecene derivatives by TLC (fluorescence under UV light, characteristic Ehrlich-reagent positive spots) (6).

A solution of the oil in ether–hexane (2:1, 50 ml) was filtered and set aside. Colorless crystals (58 mg) resulted, mp 158–160°; $[\alpha]_D^{22}$ +18° (c 0.52, ethyl alcohol); UV: λ_{max} (ethyl alcohol) only an end absorption; mass spectra: *m/e* 366 (M^+). The melting point, optical rotation, and spectral properties of this compound were indistinguishable from those of diacetoxyscirpenol (4β,15-diacetoxy-12,13-epoxytrichothec-9-en-3α-ol) (6).

The oily residue obtained from the ether–hexane mother liquor was dissolved in benzene (10 ml) and chromatographed over a magnesium silicate column (1.2 × 14 cm). Elution with chloroform and chloroform–methanol (98:2) yielded several 20-ml fractions containing a toxic material, as indicated by a rat skin bioassay (7). The residue from the concentrated eluates, when crystallized from hexane–benzene, gave colorless needles (33 mg), mp 148–150°; $[\alpha]_D^{22}$ +17.8° (c 0.48, ethyl alcohol), +16.5° (c 0.52); UV: λ_{max} (ethyl alcohol) only an end absorption; IR: ν_{max} (potassium bromide) 3400 (br), 1722, and 1245 cm^{-1}; mass spectra: *m/e* 466 (M^+, relative intensity 0.5%), 364 ($M^+ - C_5H_{10}O_2$, 22%), 322 (2.5), 305 (2), 304 (7), 291 (14), and 121 (100). The melting point, optical rotation, and spectral properties of this compound were indistinguishable from those of T-2 toxin (4β,15-diacetoxy-8-isovaleroxy-12,13-epoxytrichothec-9-en-3α-ol) (8).

dicative of the proposed theory and data treatment method.

(1) K. Sekiguchi and N. Obi, *Chem. Pharm. Bull.*, **9**, 866(1961).
(2) K. Sekiguchi, Y. Ueda, and Y. Nakamori, *ibid.*, **11**, 1108(1963).
(3) *Ibid.*, **11**, 1123(1963).
(4) K. Sekiguchi, N. Obi, and Y. Ueda, *Chem. Pharm. Bull.*, **12**, 134(1964).
(5) A. H. Goldberg, M. Gibaldi, and J. L. Kanig, *J. Pharm. Sci.*, **54**, 1145(1965).
(6) J. K. Guillory, S. Huang, and J. Lach, *ibid.*, **58**, 301(1969).
(7) W. L. Chiou and S. Niazi, *ibid.*, **60**, 1333(1971).
(8) G. S. Zhdanov, "Crystal Physics," Academic, New York, N.Y., 1965, pp. 335–338.
(9) K. H. G. Ashbee, in "Problems in Solid State Physics," H. J. Goldsmid, Ed., Academic, New York, N.Y., 1968, p. 191.

J. T. Carstensen [x]
Shabbir T. Anik
School of Pharmacy
University of Wisconsin
Madison, WI 53706

Received July 9, 1975.
Accepted for publication October 24, 1975.
[x] To whom inquiries should be directed.

Toxic Substances Produced by *Fusarium* I: Trichothecene Derivatives from Two Strains of *Fusarium oxysporum* f. sp. *carthami*

Keyphrases □ *Fusarium oxysporum*—cultured, trichothecenes isolated, phytotoxic and dermatitic properties evaluated □ Phytotoxins—trichothecenes isolated from *Fusarium oxysporum*, activity evaluated □ Fungi—*Fusarium oxysporum* cultured, trichothecenes isolated, phytotoxic and dermatitic properties evaluated

To the Editor:

Fusarium oxysporum Schlecht. f. *carthami* Klisiewicz & Houston is involved in the typical wilt disease of safflower (*Carthamus tinctorius* Linn.) (1, 2). However, the nature of the substance or substances responsible for the phytotoxic effects has not been evaluated previously. Since food materials infected with a species of *Fusarium* have often contained substances that produce high mammalian toxicity (3), the presence of *F. oxysporum* in safflower is thus cause for alarm.

Although previous investigations with other forms of *F. oxysporum* furnished biologically active 12,13-epoxytrichothecenes (3, 4), there is no report on this form of the fungus producing any toxic substance in artificial media or the host tissue. The present investigation was designed to isolate and study the substances produced by the fungus in artificial media that are responsible for the pathogenic property.

Two strains (weakly parasitic and virulent) were collected from Varanasi, India (2), and their identity was confirmed by the Commonwealth Mycological Institute, Kew, England [CMI (IMI-166917 and IMI-186539)]. These strains were separately grown in Richard's solution (200 ml) (5) in still culture flasks (1 liter) at 21° for 21 days.

When sprayed on safflower plants, the culture filtrates caused severe scorching of foliage accompanied by marked retardation of stem growth and frequently death of the plants. Even in high dilution (1:100), the culture filtrates inhibited root elongation of 2-day-old seedlings. There was no inhibition of germination of safflower seeds when sown in a medium containing the culture filtrates, but the seedlings showed the usual toxic symptoms.

The effects of the intracellular toxins (from the mycelium) were more severe than those of the extracellular ones (from the culture filtrates). For the extraction of the intracellular toxins, the mycelia were first washed and then macerated with water in a high-speed blender. The extract was passed through a bacteria-proof filter. The effect of the filtrate was tested on the host plant in the usual way.

The toxic substances were isolated from the culture filtrates by solvent extraction. In a typical experiment, the culture filtrate (5 liters) from the weakly parasitic strain at the natural pH (about 3.8) was successively extracted with chloroform (3 liters) and ethyl acetate (3 liters). The aqueous mother liquor was then concentrated to about 500 ml under reduced pressure and again extracted with hot ethyl acetate (3 liters). The three extracts were processed separately.

Evaporation of the solvent from the chloroform extract afforded a brown oil (0.88 g) which, in very low concentration (1–2 ppm), produced phytotoxic effects similar to those shown by the culture filtrates. It showed the presence of about six trichothecene derivatives by TLC (fluorescence under UV light, characteristic Ehrlich-reagent positive spots) (6).

A solution of the oil in ether–hexane (2:1, 50 ml) was filtered and set aside. Colorless crystals (58 mg) resulted, mp 158–160°; $[\alpha]_D^{22}$ +18° (c 0.52, ethyl alcohol); UV: λ_{max} (ethyl alcohol) only an end absorption; mass spectra: *m/e* 366 (M^+). The melting point, optical rotation, and spectral properties of this compound were indistinguishable from those of diacetoxyscirpenol (4β,15-diacetoxy-12,13-epoxytrichothec-9-en-3α-ol) (6).

The oily residue obtained from the ether–hexane mother liquor was dissolved in benzene (10 ml) and chromatographed over a magnesium silicate column (1.2 × 14 cm). Elution with chloroform and chloroform–methanol (98:2) yielded several 20-ml fractions containing a toxic material, as indicated by a rat skin bioassay (7). The residue from the concentrated eluates, when crystallized from hexane–benzene, gave colorless needles (33 mg), mp 148–150°; $[\alpha]_D^{22}$ +17.8° (c 0.48, ethyl alcohol), +16.5° (c 0.52); UV: λ_{max} (ethyl alcohol) only an end absorption; IR: ν_{max} (potassium bromide) 3400 (br), 1722, and 1245 cm^{-1}; mass spectra: *m/e* 466 (M^+, relative intensity 0.5%), 364 ($M^+ - C_5H_{10}O_2$, 22%), 322 (2.5), 305 (2), 304 (7), 291 (14), and 121 (100). The melting point, optical rotation, and spectral properties of this compound were indistinguishable from those of T-2 toxin (4β,15-diacetoxy-8-isovaleroxy-12,13-epoxytrichothec-9-en-3α-ol) (8).

No significant difference was observed in the amount of chloroform extractives or in the types of chemical constituents isolated from the culture filtrates of the virulent strain (IMI-186539) of the fungus.

The dermatitic properties of the trichothecene mycotoxins, diacetoxyscirpenol, T-2 and HT-2 toxins, nivalenol, and fusarenone, have been used as the basis for semiquantitative biological tests (7). Doses of 0.05, 0.1, and 0.2 mg of the residue from the chloroform extract were tested on albino rats (80–120 g, bred from CDRI strains) according to the method of Wei *et al.* (7). Two rats were used at each dose level. On the 2nd day, edema was noticed on all six rats. It became progressively severe, developing into a heavy scab and hemorrhaging by the 4th day. The animals that received 0.1 or 0.2 mg of the total toxins died within 6 days. Smaller doses (100–500 μg) of the chloroform extract left pinkish scars on the treated spots.

The chloroform extract of the culture filtrates of the fungus also showed prolonged emetic activity in pigeons at nonlethal concentrations on oral and intravenous administrations. The mean toxic values for this substance were 1.4 and 0.3 mg/kg, respectively.

The biological effects of the toxic substance from *F. oxysporum* are analogous to those reported for 12,13-epoxytrichothecenes (3, 9). The present study has additional significance because this is a seedborne disease of safflower. Furthermore, similar trichothecene derivatives, found in the culture filtrates of the fungus, also were detected in the infected safflower seeds. Work is now in progress to characterize and bioassay the remaining components in the chloroform and ethyl acetate extracts and in the infected seeds.

(1) I. M. Klisiewicz, *Phytopathology*, **53**, 1046(1963).
(2) A. K. Singh, D. K. Chakrabarti, and K. C. B. Chaudhary, *Curr. Sci.*, **44**, 397(1975).
(3) C. J. Mirocha and C. M. Christensen, *Ann. Rev. Phytopathol.*, **12**, 303(1974).
(4) Y. Ueno, H. Sato, K. Ishi, K. Sakai, H. Ysunoda, and M. Enomoto, *Appl. Microbiol.*, **25**, 699(1973).
(5) T. Fahmy, *Phytopathology*, **13**, 543(1923).
(6) P. W. Brian, A. W. Dawkins, J. F. Grove, H. G. Hemming, D. Lowe, and G. L. F. Norris, *J. Exp. Bot.*, **12**, 1(1961).
(7) R.-D. Wei, E. B. Smalley, and F. M. Strong, *Appl. Microbiol.*, **23**, 1029(1972).
(8) J. R. Bamburg, N. V. Riggs, and F. M. Strong, *Tetrahedron*, **24**, 3329(1968).
(9) J. R. Bamburg and F. M. Strong, in "Microbial Toxins," vol. VII, S. Kadis, A. Ciegler, and S. J. Ajl, Eds., Academic, New York, N.Y., 1971, p. 107.

S. Ghosal [x]
Pharmaceutical Chemistry Research Laboratory
Department of Pharmaceutics
Banaras Hindu University
Varanasi-5, India
D. K. Chakrabarti
K. C. Basu Chaudhary
Department of Plant Pathology
Faculty of Agriculture
Banaras Hindu University
Varanasi-5, India

Received July 3, 1975.
Accepted for publication October 7, 1975.
[x] To whom inquiries should be directed.

BOOKS

REVIEWS

Emulsions and Emulsion Technology, Part II (Surfactant Science Series, Vol. 6). Edited by KENNETH J. LISSANT. Dekker, 270 Madison Ave., New York, NY 10016, 1974. 971 pp. 16 × 23.5 cm. Price $48.50.

This text consists of five chapters covering *extensively* the various aspects of emulsion technology.

Chapter 9 dealing with emulsion polymerization is well organized, tracing the subject from its beginning with the technique of polymerizing liquid monomers in bulk and expanding the theory to include in detail the mechanism of polymerization of hydrophilic (in the presence and absence of surfactants) and hydrophobic monomers. The behavior of additives such as initiators, protective colloids, organic solvents, plasticizers, and the like including their role in emulsion polymerization is given careful attention.

Chapter 10 deals with emulsions in the paper-making industry, devoting special consideration to surface roughness and permeability of paper as well as emulsion stability. The role of emulsions in the process of making paper with a controlled sensitivity to water, referred to as sizing, is given thorough coverage. The extensive use of emulsions in coatings applied to paper is discussed in addition to other topics such as foam control, bubble, and encapsulated coatings.

Chapter 11 deals with emulsions in the graphic arts and points out the limited amount of research in this area. The first part of the chapter discusses prevention or remedy of emulsification that is deleterious to the production of a graphic arts product. The latter part of the chapter addresses itself to the creation of emulsification products or processes that facilitate or improve function or output in printing, duplication, copying, photography, or recording.

Chapter 12 moves on to discuss hydraulic fluid emulsions. The authors point out the advantages of the hydraulic system of power transmission and indicate requirements necessary for the successful operation of the hydraulic system. A good review of emulsion rheology is provided as well as general stability considerations for emulsion systems. A discussion of the basic components of any hydraulic system and methods for testing stability, viscosity, lubricity, *etc.*, concludes this section.

The final chapter is probably the most significant and relevant for the pharmaceutical scientist. It is very well organized, covering an initial section on emulsion theory, prediction of types of emulsions and their identification. The author does a very thorough job of discussing microemulsions. The HLB system and the selection, classification, and mechanism of emulsifying agents are covered in such detail that this section could serve as an excellent reference on the subject. Equipment generally used for emulsification and milling is covered to a lesser degree with some pictorial and di-

No significant difference was observed in the amount of chloroform extractives or in the types of chemical constituents isolated from the culture filtrates of the virulent strain (IMI-186539) of the fungus.

The dermatitic properties of the trichothecene mycotoxins, diacetoxyscirpenol, T-2 and HT-2 toxins, nivalenol, and fusarenone, have been used as the basis for semiquantitative biological tests (7). Doses of 0.05, 0.1, and 0.2 mg of the residue from the chloroform extract were tested on albino rats (80–120 g, bred from CDRI strains) according to the method of Wei *et al.* (7). Two rats were used at each dose level. On the 2nd day, edema was noticed on all six rats. It became progressively severe, developing into a heavy scab and hemorrhaging by the 4th day. The animals that received 0.1 or 0.2 mg of the total toxins died within 6 days. Smaller doses (100–500 μg) of the chloroform extract left pinkish scars on the treated spots.

The chloroform extract of the culture filtrates of the fungus also showed prolonged emetic activity in pigeons at nonlethal concentrations on oral and intravenous administrations. The mean toxic values for this substance were 1.4 and 0.3 mg/kg, respectively.

The biological effects of the toxic substance from *F. oxysporum* are analogous to those reported for 12,13-epoxytrichothecenes (3, 9). The present study has additional significance because this is a seedborne disease of safflower. Furthermore, similar trichothecene derivatives, found in the culture filtrates of the fungus, also were detected in the infected safflower seeds. Work is now in progress to characterize and bioassay the remaining components in the chloroform and ethyl acetate extracts and in the infected seeds.

(1) I. M. Klisiewicz, *Phytopathology*, **53**, 1046(1963).
(2) A. K. Singh, D. K. Chakrabarti, and K. C. B. Chaudhary, *Curr. Sci.*, **44**, 397(1975).
(3) C. J. Mirocha and C. M. Christensen, *Ann. Rev. Phytopathol.*, **12**, 303(1974).
(4) Y. Ueno, H. Sato, K. Ishi, K. Sakai, H. Ysunoda, and M. Enomoto, *Appl. Microbiol.*, **25**, 699(1973).
(5) T. Fahmy, *Phytopathology*, **13**, 543(1923).
(6) P. W. Brian, A. W. Dawkins, J. F. Grove, H. G. Hemming, D. Lowe, and G. L. F. Norris, *J. Exp. Bot.*, **12**, 1(1961).
(7) R.-D. Wei, E. B. Smalley, and F. M. Strong, *Appl. Microbiol.*, **23**, 1029(1972).
(8) J. R. Bamburg, N. V. Riggs, and F. M. Strong, *Tetrahedron*, **24**, 3329(1968).
(9) J. R. Bamburg and F. M. Strong, in "Microbial Toxins," vol. VII, S. Kadis, A. Ciegler, and S. J. Ajl, Eds., Academic, New York, N.Y., 1971, p. 107.

S. Ghosal [x]
Pharmaceutical Chemistry Research Laboratory
Department of Pharmaceutics
Banaras Hindu University
Varanasi-5, India
D. K. Chakrabarti
K. C. Basu Chaudhary
Department of Plant Pathology
Faculty of Agriculture
Banaras Hindu University
Varanasi-5, India

Received July 3, 1975.
Accepted for publication October 7, 1975.
[x] To whom inquiries should be directed.

BOOKS

REVIEWS

Emulsions and Emulsion Technology, Part II (Surfactant Science Series, Vol. 6). Edited by KENNETH J. LISSANT. Dekker, 270 Madison Ave., New York, NY 10016, 1974. 971 pp. 16 × 23.5 cm. Price $48.50.

This text consists of five chapters covering *extensively* the various aspects of emulsion technology.

Chapter 9 dealing with emulsion polymerization is well organized, tracing the subject from its beginning with the technique of polymerizing liquid monomers in bulk and expanding the theory to include in detail the mechanism of polymerization of hydrophilic (in the presence and absence of surfactants) and hydrophobic monomers. The behavior of additives such as initiators, protective colloids, organic solvents, plasticizers, and the like including their role in emulsion polymerization is given careful attention.

Chapter 10 deals with emulsions in the paper-making industry, devoting special consideration to surface roughness and permeability of paper as well as emulsion stability. The role of emulsions in the process of making paper with a controlled sensitivity to water, referred to as sizing, is given thorough coverage. The extensive use of emulsions in coatings applied to paper is discussed in addition to other topics such as foam control, bubble, and encapsulated coatings.

Chapter 11 deals with emulsions in the graphic arts and points out the limited amount of research in this area. The first part of the chapter discusses prevention or remedy of emulsification that is deleterious to the production of a graphic arts product. The latter part of the chapter addresses itself to the creation of emulsification products or processes that facilitate or improve function or output in printing, duplication, copying, photography, or recording.

Chapter 12 moves on to discuss hydraulic fluid emulsions. The authors point out the advantages of the hydraulic system of power transmission and indicate requirements necessary for the successful operation of the hydraulic system. A good review of emulsion rheology is provided as well as general stability considerations for emulsion systems. A discussion of the basic components of any hydraulic system and methods for testing stability, viscosity, lubricity, *etc.*, concludes this section.

The final chapter is probably the most significant and relevant for the pharmaceutical scientist. It is very well organized, covering an initial section on emulsion theory, prediction of types of emulsions and their identification. The author does a very thorough job of discussing microemulsions. The HLB system and the selection, classification, and mechanism of emulsifying agents are covered in such detail that this section could serve as an excellent reference on the subject. Equipment generally used for emulsification and milling is covered to a lesser degree with some pictorial and di-

agrammatic aid. The last section provides some 60 examples of every possible type of cosmetic emulsion with its specific formula and procedure for manufacture. This listing should prove particularly useful for academicians involved in teaching courses in cosmetic formulation.

In summary the text is well organized, and the pharmaceutical scientist will find chapters 9 and 13 of special interest.

Reviewed by Oscar E. Araujo
College of Pharmacy
University of Florida
Gainesville, FL 32610

Index Nominum 1975/76, 8th Ed. Edited by the Laboratory of the Swiss Pharmaceutical Society (Zurich), Swiss Pharmaceutical Society, Berne, Switzerland, 1975. xxvi + 1495 pp. 16 × 23 cm. Price $65.75 (U.S. Distributor: Drug Intelligence Publications, Inc., Hamilton, IL 62341)

"Index Nominum" is an alphabetic listing of generic and trade names of internationally available drug products containing one active substance. This newest edition includes about 3600 drug entities with more than 21,000 entries. Information is given on the International Nonproprietary Name (INN) and other generic names, trade names and manufacturers, chemical names and structures, pharmacopoeial monographs, and main therapeutic uses.

In this edition, the designations of the main therapeutic use have been completely revised according to a new systematic classification scheme. In addition, the English translation of the therapeutic use, which is given in French in the text, is now given in the front of the book.

This book is an accurate, reasonably complete, and easy-to-use reference source for international drug names and is recommended to those needing to locate and verify such information.

Staff Review

Official Methods of Analysis of the Association of Official Analytical Chemists, 12th Edition. Edited by WILLIAM HORWITZ. Association of Official Analytical Chemists, P.O. Box 540, Benjamin Franklin Station, Washington, DC 20044, 1975. 18.5 × 27 cm. 1094 pp. Price $40.00 (domestic); $41.00 (foreign).

"Official Methods of Analysis" compiles analytical methods developed and used by local, state, and federal regulatory officials. Collaborative studies are conducted to validate the methods which cover agricultural products, foods, beverages, drugs, cosmetics, and color additives.

Included in this 12th edition is a new forensic sciences chapter with methods for the examination of glass fragments and fingerprints. Five chapters provide methods for drug analysis: drugs, general; acidic drugs; alkaloid and related bases; neutral; and illicit. Two additional chapters detail the analysis of drugs in animal tissue and animal feed. Several automated methods are given for drugs.

Eight pesticide formulation methods included in this edition were approved by the Association of Official Analytical Chemists and the Collaborative International Pesticide Analytical Council Ltd. The approval of identical methods avoids unnecessary duplication and confusion.

Another important addition is the inclusion of collaboratively studied automated methods of analysis for phosphorus and potassium.

Staff Review

NOTICES

Angewandte Statistik. By LOTHAR SACHS. Springer-Verlag, Berlin, Germany, 1974. 545 pp. 16 × 24 cm. Price $23.70. *(German)*

Problemes Actuels de Biochimie Appliquee. Edited by MAURICE-LOUIS GIRARD and FRANCOIS ROUSSELET. Masson & Cie, 120 Boulevard Saint-Germain, Paris, France, 1974. 207 pp. 16 × 24 cm. Price 100 F. *(French)*

Problemes Actuels de Biochimie Appliquee. Edited by MAURICE-LOUIS GIRARD and FRANCOIS ROUSSELET. Masson & Cie, 120 Boulevard Saint-Germain, Paris, France, 1974. 281 pp. 16 × 24 cm. Price 140 F. *(French)*

Molecular Mechanisms of Gonadal Hormone Action: Advances in Sex Hormone Research, Vol. 1. By JOHN A. THOMAS and RADHEY L. SINGHAL. University Park Press, Chamber of Commerce Building, Baltimore, MD 21201, 1975. 399 pp. 16 × 24 cm. Price $32.50.

Problems of Drug Dependence 1975, Proceedings of the 37th Annual Scientific Meeting of the Committee on Problems of Drug Dependence. National Academy of Sciences Printing and Publishing Office, 2101 Constitution Ave., Washington, DC 20418, 1975. vii + 1212 pp. 22 × 28 cm. Price $22.50 (paper bound).

Contribution a la Determination de la Configuration et de la Conformation Moleculaires des Corticosteroides. By P. GENARD. Masson & Cie, 120 Boulevard Saint-Germain, Paris, France, 1974. 296 pp. 16 × 25 cm. Price 180 F. *(French)*

The Toxicology Newsletter, Vol. 1, No. 1. Edited by C. L. WINEK and W. D. COLLOM. Duquesne University, School of Pharmacy, Pittsburgh, Pa., August 1974. Published bimonthly, distributed without charge.

Drug and Chemical Blood Level Data. Chart prepared by C. L. WINEK. Duquesne University, School of Pharmacy, Pittsburgh, Pa. 2 pp.

Progress in Medicinal Chemistry, Vol. 11. Edited by G. P. ELLIS and G. B. WEST. North-Holland Publishing Co., distributed by American Elsevier, 52 Vanderbilt Ave., New York, NY 10017, 1975. 277 pp. 15.5 × 19 cm. Price $32.95.

Perfumes, Cosmetics and Soaps, Vol. 2. By W. A. POUCHER. Wiley, 605 Third Ave., New York, NY 10016, 1975. 379 pp. 16 × 24 cm. Price $24.00.

Proteinase Inhibitors, Proceedings of the 2nd International Research Conference, Bayer Symposium 5. Edited by H. FRITZ, H. TSCHESCHE, L. J. GREENE, and E. TRUSCHEIT. Springer-Verlag, 175 Fifth Ave., New York, NY 10010, 1974. 751 pp. 16 × 24 cm. Price $52.50.

Protein–Metal Interactions. Edited by MENDEL FRIEDMAN. Plenum, 227 West 17th St., New York, NY 10011, 1974. 692 pp. 16 × 24 cm. Price $39.50.

Advances in Drug Research, Vol. 8. Edited by N. J. HARPER and A. B. SIMMONDS. Academic, New York, N.Y., 1974. 338 pp. 15.5 × 22 cm. Price $26.00.

Advances in Drug Research, Vol. 9. Edited by N. J. HARPER and A. B. SIMMONDS. Academic, New York, N.Y., 1974. 142 pp. 15.5 × 22 cm. Price $12.25.

Notions de Pharmacie Galenique. By A. MANGEOT and M. POISSON. Masson & Cie, 120 Boulevard Saint-Germain, Paris, France, 1974. 236 pp. 16.5 × 21 cm. Price 48 F. *(French)*

Pharmacie. By YVAN TOUITOU. Masson & Cie, 120 Boulevard Saint-Germain, Paris, France, 1974. 14 × 18.5 cm. 288 pp. Price 34F. *(French)*

Drugs in Current Use and New Drugs 1975. Edited by WALTER MODELL. Springer Publishing Co., 200 Park Ave., New York, NY 10003, 1975. 179 pp. 14 × 18.5 cm. Price $5.25.

agrammatic aid. The last section provides some 60 examples of every possible type of cosmetic emulsion with its specific formula and procedure for manufacture. This listing should prove particularly useful for academicians involved in teaching courses in cosmetic formulation.

In summary the text is well organized, and the pharmaceutical scientist will find chapters 9 and 13 of special interest.

Reviewed by Oscar E. Araujo
College of Pharmacy
University of Florida
Gainesville, FL 32610

Index Nominum 1975/76, 8th Ed. Edited by the Laboratory of the Swiss Pharmaceutical Society (Zurich), Swiss Pharmaceutical Society, Berne, Switzerland, 1975. xxvi + 1495 pp. 16 × 23 cm. Price $65.75 (U.S. Distributor: Drug Intelligence Publications, Inc., Hamilton, IL 62341)

"Index Nominum" is an alphabetic listing of generic and trade names of internationally available drug products containing one active substance. This newest edition includes about 3600 drug entities with more than 21,000 entries. Information is given on the International Nonproprietary Name (INN) and other generic names, trade names and manufacturers, chemical names and structures, pharmacopoeial monographs, and main therapeutic uses.

In this edition, the designations of the main therapeutic use have been completely revised according to a new systematic classification scheme. In addition, the English translation of the therapeutic use, which is given in French in the text, is now given in the front of the book.

This book is an accurate, reasonably complete, and easy-to-use reference source for international drug names and is recommended to those needing to locate and verify such information.

Staff Review

Official Methods of Analysis of the Association of Official Analytical Chemists, 12th Edition. Edited by WILLIAM HORWITZ. Association of Official Analytical Chemists, P.O. Box 540, Benjamin Franklin Station, Washington, DC 20044, 1975. 18.5 × 27 cm. 1094 pp. Price $40.00 (domestic); $41.00 (foreign).

"Official Methods of Analysis" compiles analytical methods developed and used by local, state, and federal regulatory officials. Collaborative studies are conducted to validate the methods which cover agricultural products, foods, beverages, drugs, cosmetics, and color additives.

Included in this 12th edition is a new forensic sciences chapter with methods for the examination of glass fragments and fingerprints. Five chapters provide methods for drug analysis: drugs, general; acidic drugs; alkaloid and related bases; neutral; and illicit. Two additional chapters detail the analysis of drugs in animal tissue and animal feed. Several automated methods are given for drugs.

Eight pesticide formulation methods included in this edition were approved by the Association of Official Analytical Chemists and the Collaborative International Pesticide Analytical Council Ltd. The approval of identical methods avoids unnecessary duplication and confusion.

Another important addition is the inclusion of collaboratively studied automated methods of analysis for phosphorus and potassium.

Staff Review

NOTICES

Angewandte Statistik. By LOTHAR SACHS. Springer-Verlag, Berlin, Germany, 1974. 545 pp. 16 × 24 cm. Price $23.70. *(German)*

Problemes Actuels de Biochimie Appliquee. Edited by MAURICE-LOUIS GIRARD and FRANCOIS ROUSSELET. Masson & Cie, 120 Boulevard Saint-Germain, Paris, France, 1974. 207 pp. 16 × 24 cm. Price 100 F. *(French)*

Problemes Actuels de Biochimie Appliquee. Edited by MAURICE-LOUIS GIRARD and FRANCOIS ROUSSELET. Masson & Cie, 120 Boulevard Saint-Germain, Paris, France, 1974. 281 pp. 16 × 24 cm. Price 140 F. *(French)*

Molecular Mechanisms of Gonadal Hormone Action: Advances in Sex Hormone Research, Vol. 1. By JOHN A. THOMAS and RADHEY L. SINGHAL. University Park Press, Chamber of Commerce Building, Baltimore, MD 21201, 1975. 399 pp. 16 × 24 cm. Price $32.50.

Problems of Drug Dependence 1975, Proceedings of the 37th Annual Scientific Meeting of the Committee on Problems of Drug Dependence. National Academy of Sciences Printing and Publishing Office, 2101 Constitution Ave., Washington, DC 20418, 1975. vii + 1212 pp. 22 × 28 cm. Price $22.50 (paper bound).

Contribution a la Determination de la Configuration et de la Conformation Moleculaires des Corticosteroides. By P. GENARD. Masson & Cie, 120 Boulevard Saint-Germain, Paris, France, 1974. 296 pp. 16 × 25 cm. Price 180 F. *(French)*

The Toxicology Newsletter, Vol. 1, No. 1. Edited by C. L. WINEK and W. D. COLLOM. Duquesne University, School of Pharmacy, Pittsburgh, Pa., August 1974. Published bimonthly, distributed without charge.

Drug and Chemical Blood Level Data. Chart prepared by C. L. WINEK. Duquesne University, School of Pharmacy, Pittsburgh, Pa. 2 pp.

Progress in Medicinal Chemistry, Vol. 11. Edited by G. P. ELLIS and G. B. WEST. North-Holland Publishing Co., distributed by American Elsevier, 52 Vanderbilt Ave., New York, NY 10017, 1975. 277 pp. 15.5 × 19 cm. Price $32.95.

Perfumes, Cosmetics and Soaps, Vol. 2. By W. A. POUCHER. Wiley, 605 Third Ave., New York, NY 10016, 1975. 379 pp. 16 × 24 cm. Price $24.00.

Proteinase Inhibitors, Proceedings of the 2nd International Research Conference, Bayer Symposium 5. Edited by H. FRITZ, H. TSCHESCHE, L. J. GREENE, and E. TRUSCHEIT. Springer-Verlag, 175 Fifth Ave., New York, NY 10010, 1974. 751 pp. 16 × 24 cm. Price $52.50.

Protein–Metal Interactions. Edited by MENDEL FRIEDMAN. Plenum, 227 West 17th St., New York, NY 10011, 1974. 692 pp. 16 × 24 cm. Price $39.50.

Advances in Drug Research, Vol. 8. Edited by N. J. HARPER and A. B. SIMMONDS. Academic, New York, N.Y., 1974. 338 pp. 15.5 × 22 cm. Price $26.00.

Advances in Drug Research, Vol. 9. Edited by N. J. HARPER and A. B. SIMMONDS. Academic, New York, N.Y., 1974. 142 pp. 15.5 × 22 cm. Price $12.25.

Notions de Pharmacie Galenique. By A. MANGEOT and M. POISSON. Masson & Cie, 120 Boulevard Saint-Germain, Paris, France, 1974. 236 pp. 16.5 × 21 cm. Price 48 F. *(French)*

Pharmacie. By YVAN TOUITOU. Masson & Cie, 120 Boulevard Saint-Germain, Paris, France, 1974. 14 × 18.5 cm. 288 pp. Price 34F. *(French)*

Drugs in Current Use and New Drugs 1975. Edited by WALTER MODELL. Springer Publishing Co., 200 Park Ave., New York, NY 10003, 1975. 179 pp. 14 × 18.5 cm. Price $5.25.

agrammatic aid. The last section provides some 60 examples of every possible type of cosmetic emulsion with its specific formula and procedure for manufacture. This listing should prove particularly useful for academicians involved in teaching courses in cosmetic formulation.

In summary the text is well organized, and the pharmaceutical scientist will find chapters 9 and 13 of special interest.

Reviewed by Oscar E. Araujo
College of Pharmacy
University of Florida
Gainesville, FL 32610

Index Nominum 1975/76, 8th Ed. Edited by the Laboratory of the Swiss Pharmaceutical Society (Zurich), Swiss Pharmaceutical Society, Berne, Switzerland, 1975. xxvi + 1495 pp. 16 × 23 cm. Price $65.75 (U.S. Distributor: Drug Intelligence Publications, Inc., Hamilton, IL 62341)

"Index Nominum" is an alphabetic listing of generic and trade names of internationally available drug products containing one active substance. This newest edition includes about 3600 drug entities with more than 21,000 entries. Information is given on the International Nonproprietary Name (INN) and other generic names, trade names and manufacturers, chemical names and structures, pharmacopoeial monographs, and main therapeutic uses.

In this edition, the designations of the main therapeutic use have been completely revised according to a new systematic classification scheme. In addition, the English translation of the therapeutic use, which is given in French in the text, is now given in the front of the book.

This book is an accurate, reasonably complete, and easy-to-use reference source for international drug names and is recommended to those needing to locate and verify such information.

Staff Review

Official Methods of Analysis of the Association of Official Analytical Chemists, 12th Edition. Edited by WILLIAM HORWITZ. Association of Official Analytical Chemists, P.O. Box 540, Benjamin Franklin Station, Washington, DC 20044, 1975. 18.5 × 27 cm. 1094 pp. Price $40.00 (domestic); $41.00 (foreign).

"Official Methods of Analysis" compiles analytical methods developed and used by local, state, and federal regulatory officials. Collaborative studies are conducted to validate the methods which cover agricultural products, foods, beverages, drugs, cosmetics, and color additives.

Included in this 12th edition is a new forensic sciences chapter with methods for the examination of glass fragments and fingerprints. Five chapters provide methods for drug analysis: drugs, general; acidic drugs; alkaloid and related bases; neutral; and illicit. Two additional chapters detail the analysis of drugs in animal tissue and animal feed. Several automated methods are given for drugs.

Eight pesticide formulation methods included in this edition were approved by the Association of Official Analytical Chemists and the Collaborative International Pesticide Analytical Council Ltd. The approval of identical methods avoids unnecessary duplication and confusion.

Another important addition is the inclusion of collaboratively studied automated methods of analysis for phosphorus and potassium.

Staff Review

NOTICES

Angewandte Statistik. By LOTHAR SACHS. Springer-Verlag, Berlin, Germany, 1974. 545 pp. 16 × 24 cm. Price $23.70. *(German)*

Problemes Actuels de Biochimie Appliquee. Edited by MAURICE-LOUIS GIRARD and FRANCOIS ROUSSELET. Masson & Cie, 120 Boulevard Saint-Germain, Paris, France, 1974. 207 pp. 16 × 24 cm. Price 100 F. *(French)*

Problemes Actuels de Biochimie Appliquee. Edited by MAURICE-LOUIS GIRARD and FRANCOIS ROUSSELET. Masson & Cie, 120 Boulevard Saint-Germain, Paris, France, 1974. 281 pp. 16 × 24 cm. Price 140 F. *(French)*

Molecular Mechanisms of Gonadal Hormone Action: Advances in Sex Hormone Research, Vol. 1. By JOHN A. THOMAS and RADHEY L. SINGHAL. University Park Press, Chamber of Commerce Building, Baltimore, MD 21201, 1975. 399 pp. 16 × 24 cm. Price $32.50.

Problems of Drug Dependence 1975, Proceedings of the 37th Annual Scientific Meeting of the Committee on Problems of Drug Dependence. National Academy of Sciences Printing and Publishing Office, 2101 Constitution Ave., Washington, DC 20418, 1975. vii + 1212 pp. 22 × 28 cm. Price $22.50 (paper bound).

Contribution a la Determination de la Configuration et de la Conformation Moleculaires des Corticosteroides. By P. GENARD. Masson & Cie, 120 Boulevard Saint-Germain, Paris, France, 1974. 296 pp. 16 × 25 cm. Price 180 F. *(French)*

The Toxicology Newsletter, Vol. 1, No. 1. Edited by C. L. WINEK and W. D. COLLOM. Duquesne University, School of Pharmacy, Pittsburgh, Pa., August 1974. Published bimonthly, distributed without charge.

Drug and Chemical Blood Level Data. Chart prepared by C. L. WINEK. Duquesne University, School of Pharmacy, Pittsburgh, Pa. 2 pp.

Progress in Medicinal Chemistry, Vol. 11. Edited by G. P. ELLIS and G. B. WEST. North-Holland Publishing Co., distributed by American Elsevier, 52 Vanderbilt Ave., New York, NY 10017, 1975. 277 pp. 15.5 × 19 cm. Price $32.95.

Perfumes, Cosmetics and Soaps, Vol. 2. By W. A. POUCHER. Wiley, 605 Third Ave., New York, NY 10016, 1975. 379 pp. 16 × 24 cm. Price $24.00.

Proteinase Inhibitors, Proceedings of the 2nd International Research Conference, Bayer Symposium 5. Edited by H. FRITZ, H. TSCHESCHE, L. J. GREENE, and E. TRUSCHEIT. Springer-Verlag, 175 Fifth Ave., New York, NY 10010, 1974. 751 pp. 16 × 24 cm. Price $52.50.

Protein–Metal Interactions. Edited by MENDEL FRIEDMAN. Plenum, 227 West 17th St., New York, NY 10011, 1974. 692 pp. 16 × 24 cm. Price $39.50.

Advances in Drug Research, Vol. 8. Edited by N. J. HARPER and A. B. SIMMONDS. Academic, New York, N.Y., 1974. 338 pp. 15.5 × 22 cm. Price $26.00.

Advances in Drug Research, Vol. 9. Edited by N. J. HARPER and A. B. SIMMONDS. Academic, New York, N.Y., 1974. 142 pp. 15.5 × 22 cm. Price $12.25.

Notions de Pharmacie Galenique. By A. MANGEOT and M. POISSON. Masson & Cie, 120 Boulevard Saint-Germain, Paris, France, 1974. 236 pp. 16.5 × 21 cm. Price 48 F. *(French)*

Pharmacie. By YVAN TOUITOU. Masson & Cie, 120 Boulevard Saint-Germain, Paris, France, 1974. 14 × 18.5 cm. 288 pp. Price 34F. *(French)*

Drugs in Current Use and New Drugs 1975. Edited by WALTER MODELL. Springer Publishing Co., 200 Park Ave., New York, NY 10003, 1975. 179 pp. 14 × 18.5 cm. Price $5.25.

Journal of Pharmaceutical Sciences

FEBRUARY 1976

VOLUME 65 NUMBER 2

MARY H. FERGUSON
Editor

L. LUAN CORRIGAN
Assistant Editor

SHELLY ELLIOTT
Production Editor

JANET D. SHOFF
Copy Editor

EDWARD G. FELDMANN
Contributing Editor

SAMUEL W. GOLDSTEIN
Contributing Editor

LELAND J. ARNEY
Publications Director

EDITORIAL ADVISORY BOARD

JOHN AUTIAN — HARRY B. KOSTENBAUDER

LYNN R. BRADY — CARL J. LINTNER, JR.

WILLIAM O. FOYE — DAVID E. MANN, JR.

WILLIAM J. JUSKO — GERALD J. PAPARIELLO

The *Journal of Pharmaceutical Sciences* is published monthly by the American Pharmaceutical Association at 2215 Constitution Ave., N.W., Washington, DC 20037. Second-class postage paid at Washington, D.C., and at additional mailing office.

All expressions of opinion and statements of supposed fact appearing in articles or editorials carried in this journal are published on the authority of the writer over whose name they appear and are not to be regarded as necessarily expressing the policies or views of the American Pharmaceutical Association.

Offices—Editorial, Advertising, and Subscription Offices: 2215 Constitution Ave., N.W., Washington, DC 20037. Printing Offices: 20th & Northampton Streets, Easton, PA 18042

Annual Subscriptions—United States and foreign, industrial and government institutions $50, educational institutions $50, individuals *for personal use only* $30; single copies $5. All foreign subscriptions add $5 for postage. Subscription rates are subject to change without notice. Members of the American Pharmaceutical Association may elect to receive the *Journal of Pharmaceutical Sciences* as a part of their annual $60 (foreign $65) APhA membership dues.

Claims—Missing numbers will not be supplied if dues or subscriptions are in arrears for more than 60 days or if claims are received more than 60 days after the date of the issue, or if loss was due to failure to give notice of change of address. The Association cannot accept responsibility for foreign delivery when its records indicate shipment has been made.

Change of Address—Members and subscribers should notify at once both the Post Office and the American Pharmaceutical Association, 2215 Constitution Ave., N.W., Washington, DC 20037, of any change of address.

© Copyright 1976, American Pharmaceutical Association, 2215 Constitution Ave., N.W., Washington, DC 20037; all rights reserved.

THE LESSON FROM KEPONE

Let me begin by stating that I believe in pesticides. I believe they work; I believe their value outweighs their drawbacks; I believe they are needed if people are to live in reasonable comfort, enjoy health, and avoid a starvation diet. Indeed, I was one of those who felt that the action taken several years ago against DDT was too precipitous and too severe.

Moreover, as a weekend gardener of sorts, I have done my own full share of spraying, dusting, and otherwise bombarding the armies of insects that regularly invade the grounds surrounding my home from spring through fall each year. And for this purpose I maintain a veritable arsenal of bottles, bags, boxes, and tubes filled with a broad variety of chemicals that would have been the envy of the organic chemistry stockroom attendant back during my school days.

Having said all this, however, I am nonetheless appalled, dismayed, and, yes, even outraged over the so-called Kepone incident which first came to light several months ago in the town of Hopewell in southern Virginia. The manufacturing conditions under which this insecticide was produced were completely devoid of even the most elementary controls or care. Had the manufacturer set out purposely to poison his employees, destroy his town, and despoil the surrounding environment, a more effective job probably could not have been done.

Thriller fiction films depicting an enemy using biological warfare to sabotage a city's entire water supply pale by comparison with this real-life horror story. Air-borne contamination has spread to a radius of at least 60 miles; already, a major seafood-producing waterway system has been closed to fishing; and the extent of the damage is still in the early stages of assessment.

This did not come about through an accident or some natural disaster. Nor did it happen through simple carelessness such as that which would result from an undetected leak. It was due to gross, blatant disregard for the most obvious contamination. Kepone dust was so prevalent throughout the town and so thick in the plant that one observer is reported to have exclaimed that "if the plant had been producing water instead of Kepone, half the work force would have drowned in the mess of contamination!"

The plant producing the Kepone was reported to be a subsidiary operated by one of the giants in the American chemical industry. Consequently, the incident cannot be brushed off simply as the work of a single, greedy wayward, or even that of a small group of profit-hungry, irresponsible fly-by-nighters.

Simply stated, this firm failed to demonstrate the barest moral responsibility or the least concern for human welfare and quality of life. Such callous disregard will most surely be met by harsh restrictions and regulations. The full value that Kepone might have otherwise contributed to the general welfare, had it been employed judiciously and wisely, will probably be greatly diminished or even lost altogether as a result of current public indignation and forthcoming legislative reaction ensuing from this man-made disaster.

Sadly, as a result of this one company's deeds, the entire chemical industry will be tarred with the broad brush of distrust and a diminished public image. And who can blame the common citizen or the average legislator for reacting in this manner? There really is no basis for them to believe or expect that sister firms in the industry would not behave in the same manner if restrictions are not enacted to prevent such a reoccurrence.

Oftentimes, various observers have noted the close similarity between the chemical industry and the pharmaceutical industry. This similarity pervades many comparable features of the two industries, and one such aspect of commonality relates to public perception. Hence, the drug industry can learn a lesson—or actually a number of lessons—from the Kepone incident.

For our present purpose, it will be sufficient to focus attention on but one of the potential lessons derivable from this episode; namely, that the public image of the particular industry as a whole—or of a profession for that matter—will be no greater than the perceived performance of its weakest member. In turn, this standard of evaluation will also determine the breadth and depth of regulatory control that government will apply to monitor and control the operation of that industry or profession.

Hence, instead of creating doubts and suspicions regarding the quality of unnamed drug products and unnamed drug producers, the pharmaceutical industry would do a far greater service to everyone by quietly taking whatever constructive action is necessary to ensure that the level of performance of all manufacturers is sufficiently high so as to assure pharmacists, physicians, and patients that every drug product on the market will be safe, effective, and perform as expected.

—EGF

Journal of Pharmaceutical Sciences

FEBRUARY 1976

VOLUME 65 NUMBER 2

MARY H. FERGUSON
Editor

L. LUAN CORRIGAN
Assistant Editor

SHELLY ELLIOTT
Production Editor

JANET D. SHOFF
Copy Editor

EDWARD G. FELDMANN
Contributing Editor

SAMUEL W. GOLDSTEIN
Contributing Editor

LELAND J. ARNEY
Publications Director

EDITORIAL ADVISORY BOARD

JOHN AUTIAN — HARRY B. KOSTENBAUDER

LYNN R. BRADY — CARL J. LINTNER, JR.

WILLIAM O. FOYE — DAVID E. MANN, JR.

WILLIAM J. JUSKO — GERALD J. PAPARIELLO

The *Journal of Pharmaceutical Sciences* is published monthly by the American Pharmaceutical Association at 2215 Constitution Ave., N.W., Washington, DC 20037. Second-class postage paid at Washington, D.C., and at additional mailing office.

All expressions of opinion and statements of supposed fact appearing in articles or editorials carried in this journal are published on the authority of the writer over whose name they appear and are not to be regarded as necessarily expressing the policies or views of the American Pharmaceutical Association.

Offices—Editorial, Advertising, and Subscription Offices: 2215 Constitution Ave., N.W., Washington, DC 20037. Printing Offices: 20th & Northampton Streets, Easton, PA 18042

Annual Subscriptions—United States and foreign, industrial and government institutions $50, educational institutions $50, individuals *for personal use only* $30; single copies $5. All foreign subscriptions add $5 for postage. Subscription rates are subject to change without notice. Members of the American Pharmaceutical Association may elect to receive the *Journal of Pharmaceutical Sciences* as a part of their annual $60 (foreign $65) APhA membership dues.

Claims—Missing numbers will not be supplied if dues or subscriptions are in arrears for more than 60 days or if claims are received more than 60 days after the date of the issue, or if loss was due to failure to give notice of change of address. The Association cannot accept responsibility for foreign delivery when its records indicate shipment has been made.

Change of Address—Members and subscribers should notify at once both the Post Office and the American Pharmaceutical Association, 2215 Constitution Ave., N.W., Washington, DC 20037, of any change of address.

© Copyright 1976, American Pharmaceutical Association, 2215 Constitution Ave., N.W., Washington, DC 20037; all rights reserved.

THE LESSON FROM KEPONE

Let me begin by stating that I believe in pesticides. I believe they work; I believe their value outweighs their drawbacks; I believe they are needed if people are to live in reasonable comfort, enjoy health, and avoid a starvation diet. Indeed, I was one of those who felt that the action taken several years ago against DDT was too precipitous and too severe.

Moreover, as a weekend gardener of sorts, I have done my own full share of spraying, dusting, and otherwise bombarding the armies of insects that regularly invade the grounds surrounding my home from spring through fall each year. And for this purpose I maintain a veritable arsenal of bottles, bags, boxes, and tubes filled with a broad variety of chemicals that would have been the envy of the organic chemistry stockroom attendant back during my school days.

Having said all this, however, I am nonetheless appalled, dismayed, and, yes, even outraged over the so-called Kepone incident which first came to light several months ago in the town of Hopewell in southern Virginia. The manufacturing conditions under which this insecticide was produced were completely devoid of even the most elementary controls or care. Had the manufacturer set out purposely to poison his employees, destroy his town, and despoil the surrounding environment, a more effective job probably could not have been done.

Thriller fiction films depicting an enemy using biological warfare to sabotage a city's entire water supply pale by comparison with this real-life horror story. Air-borne contamination has spread to a radius of at least 60 miles; already, a major seafood-producing waterway system has been closed to fishing; and the extent of the damage is still in the early stages of assessment.

This did not come about through an accident or some natural disaster. Nor did it happen through simple carelessness such as that which would result from an undetected leak. It was due to gross, blatant disregard for the most obvious contamination. Kepone dust was so prevalent throughout the town and so thick in the plant that one observer is reported to have exclaimed that "if the plant had been producing water instead of Kepone, half the work force would have drowned in the mess of contamination!"

The plant producing the Kepone was reported to be a subsidiary operated by one of the giants in the American chemical industry. Consequently, the incident cannot be brushed off simply as the work of a single, greedy wayward, or even that of a small group of profit-hungry, irresponsible fly-by-nighters.

Simply stated, this firm failed to demonstrate the barest moral responsibility or the least concern for human welfare and quality of life. Such callous disregard will most surely be met by harsh restrictions and regulations. The full value that Kepone might have otherwise contributed to the general welfare, had it been employed judiciously and wisely, will probably be greatly diminished or even lost altogether as a result of current public indignation and forthcoming legislative reaction ensuing from this man-made disaster.

Sadly, as a result of this one company's deeds, the entire chemical industry will be tarred with the broad brush of distrust and a diminished public image. And who can blame the common citizen or the average legislator for reacting in this manner? There really is no basis for them to believe or expect that sister firms in the industry would not behave in the same manner if restrictions are not enacted to prevent such a reoccurrence.

Oftentimes, various observers have noted the close similarity between the chemical industry and the pharmaceutical industry. This similarity pervades many comparable features of the two industries, and one such aspect of commonality relates to public perception. Hence, the drug industry can learn a lesson—or actually a number of lessons—from the Kepone incident.

For our present purpose, it will be sufficient to focus attention on but one of the potential lessons derivable from this episode; namely, that the public image of the particular industry as a whole—or of a profession for that matter—will be no greater than the perceived performance of its weakest member. In turn, this standard of evaluation will also determine the breadth and depth of regulatory control that government will apply to monitor and control the operation of that industry or profession.

Hence, instead of creating doubts and suspicions regarding the quality of unnamed drug products and unnamed drug producers, the pharmaceutical industry would do a far greater service to everyone by quietly taking whatever constructive action is necessary to ensure that the level of performance of all manufacturers is sufficiently high so as to assure pharmacists, physicians, and patients that every drug product on the market will be safe, effective, and perform as expected.

—EGF

Journal of Pharmaceutical Sciences

FEBRUARY 1976

VOLUME 65 NUMBER 2

REVIEW ARTICLE

Derivatization in Gas Chromatography

S. AHUJA

Keyphrases □ GC—derivatization methodologies, applications in analysis of pharmaceutical compounds, review □ Derivatization—GC, methodologies, applications in analysis of pharmaceutical compounds, review □ Analysis—derivative formation in GC, review

GC is a valuable technique for analyzing compounds of pharmaceutical interest. The fact that a wide variety of compounds can be analyzed by GC has led to increased use of this technique. However, many pharmaceutical compounds cannot be gas chromatographed unmodified but must be converted into stable and volatile derivatives to achieve successful GC elution and separation. At times, derivatives are also prepared to achieve the desired sensitivity, selectivity, or specificity for a given separation.

GLC of pharmaceutical compounds is generally performed with the following objectives in mind: (*a*) determination of purity and stability of drugs, (*b*) determination of metabolic pathways and toxicology of drugs, (*c*) determination of pharmacokinetics of drugs, and (*d*) determination of drugs in tissues and fluids following overdosage in forensic situations.

All of these studies require that the methodology used should be sensitive and selective for the determination of the compound of interest. Since it is beyond the scope of this article to cover all approaches used for derivatization of pharmaceutical compounds, only those methods that meet the sensitivity and selectivity requirements are discussed. The reader may want to refer to some general references on the subject (1–10).

Pharmaceutical compounds cover a wide variety of different chemical classes and can be neutral, acidic, basic, or amphoteric in character. Furthermore, many of these compounds have high molecular weight and polyfunctional groups. Some functional groups make the compound very polar and reduce its volatility. Such a compound exhibits a long retention time or does not elute from a column. By derivatizing some or all of the functional groups, polarity is decreased, volatility is increased, and the compound can be eluted from the GLC column in a reasonable period.

Derivatization invariably involves a chemical reaction. Hence, it is important to remember that one can obtain an appropriate derivative by selecting suitable reaction conditions; however, the derivative should be sufficiently volatile for GC analysis. The compound must have a vapor pressure of 60 Torr to be carried through the column. The normal range of molecular weights for compounds resolved by GC is 2–500, although derivatives of carbohydrates with molecular weights up to 1800 have been chromatographed (11).

Table I shows the relationship between the structure and volatility or boiling points of different classes of compounds. Even though all of these compounds have essentially the same molecular weight, their boiling points differ. The high boiling points observed for alcohols are due to greater hydrogen bonding in alcohols than in ethers, aldehydes, and hydrocarbons. Furthermore, the hydroxyl group is often responsible for tailing of compounds. The carboxyl, amino, and imino groups also cause some tailing because of an interaction with the GLC column.

Table I—Relationship between Structure and Boiling Point

Compound	Structure	Molecular Weight	Boiling Point
n-Pentane	$CH_3CH_2CH_2CH_2CH_3$	72	36°
n-Butyraldehyde	$CH_3CH_2CH_2CHO$	72	76°
n-Butyl alcohol	$CH_3CH_2CH_2CH_2OH$	74	118°
Ether	$CH_3CH_2OCH_2CH_3$	74	35°

On the other hand, compounds with the carbonyl group show less tailing than those with the above-mentioned groups.

Derivatization can reduce the tailing and improve the separation of two closely related compounds or can make possible a separation that could not be accomplished otherwise. For example, estrone, estradiol, and estriol separate poorly on a nonpolar column, but good separation can be obtained with the silyl derivatives (10). Derivatization also can convert a heat-labile compound to a heat-stable compound or can convert compounds that are too volatile for GC analysis to derivatives that yield good separation.

Specific derivatives of a compound can be prepared to increase the sensitivity of the resultant compound for a given detector. The flame-ionization detector in GC can readily detect 10^{-11} g and the electron-capture detector can detect down to 10^{-12} g of many compounds. Halogen derivatives are often used with an electron-capture detector. Phosphorus- or nitrogen-containing compounds also can be employed for the phosphorus or nitrogen detectors, respectively.

Some common derivatization procedures for various functional groups are shown in Table II.

DERIVATIZATION METHODS

For the purpose of this review article, the derivatization procedures of interest fall into eight classes: on-column reactions, reactions with dialkyl acetals, silylation, esterification, acylation, hydrazone formation, ion-pair formation, and derivatization for electron-capture detection. The methodologies, including limitations, are briefly discussed to alert the reader to the pitfalls of these techniques when he/she is investigating new approaches of derivatization.

As mentioned earlier, it is frequently necessary to derivatize some or all of the functional groups in a polyfunctional compound to decrease the polarity and to increase the volatility. Similar results can be obtained by the use of innovative approaches which lead to relatively nonpolar cyclic compounds (12). For example, substituted *o*-amidophenylacetic acid was cyclized readily to yield relatively nonpolar oxindole (Scheme I), which was gas chromatographed

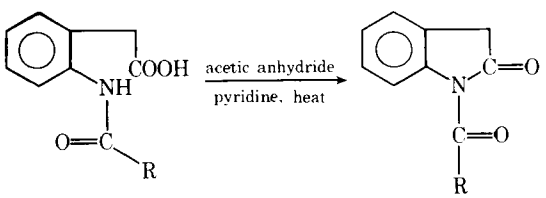

Scheme I

with ease. GC–mass spectrometry was used to confirm that the cyclized product was being chromatographed.

Examples of better known cyclization reactions can be found in some fundamental textbooks of organic chemistry. For example, biguanides undergo the formation of diamine-*s*-triazines when acylated with acid anhydrides (13). Recently, this reaction was used for cyclizing phenformin, buformin, and metformin by reacting them with monochlorodifluoroacetic anhydride (14). This reaction is of interest because it provided a convenient way of introducing a functionality in a group that imparts structural stability, volatility, and sensitivity of detection.

On-Column Reactions—Column interaction or incomplete partition of a compound on the GLC column can cause tailing of chromatographic peaks. Interactions with the solid support or incomplete partition on a GLC column can be eliminated by saturating the carrier gas with the sample vapors. This procedure then leads to negative peaks, when a thermal conductivity detector is used, which can be used to quantitate trace amounts of sample (15).

The addition of formic acid vapor to the carrier gas improved the analysis of fatty acids by GLC (16); similar results were also obtained with barbiturates (17, 18). This effect may be attributed to decreased adsorption of a test substance on the column support by formic acid. The column deactivation can result from the formation of a derivative of the barbiturate with formic acid or the interaction of the formic acid with the support material (19). These results indicate that on-column reactions can be used as a simple means of preventing column interactions.

On-column pyrolysis is another simple approach which can be used for quantitative analysis of pharmaceutical compounds such as menadione sodium bisulfite (20). Differential thermal analysis, mass spectrometry, and GLC retention data were used to prove conclusively the formation of menadione after on-column pyrolysis.

Flash heater methylation of barbiturates (21, 22), *Cannabis* metabolites (23), phenytoin (24), phenylureas (25), and fatty acids (26) with trimethylanilinium hydroxide improves the GLC characteristics of these compounds. The derivatization employing an alkylammonium salt is now accepted as a method of choice for routine urine and serum analyses of barbiturates and related drugs (27).

The formation of anisole, a heretofore unknown by-product, was reported in flash heater methylation experiments with trimethylanilinium hydroxide (28). A possible explanation for the formation of anisole is that the strongly alkaline trimethylanilinium hydroxide reagent is vulnerable to nucleophilic attack by the solvent in the injection heater. Since such a nucleophilic displacement should be enhanced by electronegative substituents in the *ortho*- or *para*-position of the aromatic ring, methanolic solutions of *N,N,N*-trimethylnitroanilinium hydroxide and *N,N,N*-trimethylchloroanilinium hydroxide were used for on-column methylation experiments. In these cases, nitroanisole (95%) and chloroanisole (8%) were the re-

Table II—Derivatives Commonly Employed in GC

Group(s)	Derivative
—OH	Alkyl ester Alkyl ether Silyl ether
—COOH	Alkyl ester Silyl ester
—NH_2	Acyl derivative Silyl derivative
=NH	Silyl derivative
—C(=O)—	Hydrazone Oxime
—C(=O)—H	Dimethyl acetal
—C(=O)—NH_2	Acyl derivative *O*-Methoxyl *N*-Alkyl Nitrile
—S(=O)—NH_2	Methyl derivative
—N^+—	Desmethyl derivative
—COOR	Methyl ester (transesterification) Derivative from reductive acylation
—SH	Thioether Silylthioether
—SO_2H	Sulfonyl chloride
—NH_2 and —OH	*n*-Butyl boronate
—NH_2 and —COOH	Acyl ester or amide *N*-Dimethylaminomethylene alkyl ester
—OH and —COOH	*n*-Butyl boronate Acyl ester Diester

action products. Preparations of *N,N,N*-trimethyl-*p*-chloroanilinium hydroxide in ethanol and propanol gave the corresponding ethers. The presence of the respective anisoles sometimes interferes with the GLC analysis of fatty and amino acids. The use of solutions of anilinium hydroxide and dimethylformamide was recommended in these cases (28).

Reactions with Dialkyl Acetals—Dimethylformamide dialkyl acetals are useful reagents because of the speed of derivatization. The reactions are generally complete as soon as solution is achieved. This one-step procedure can lead to the formation of methyl, ethyl, propyl, *n*-butyl, or *tert*-butyl derivatives. Some examples of the reactions of dimethylformamide dialkyl acetals are shown in Scheme II (29).

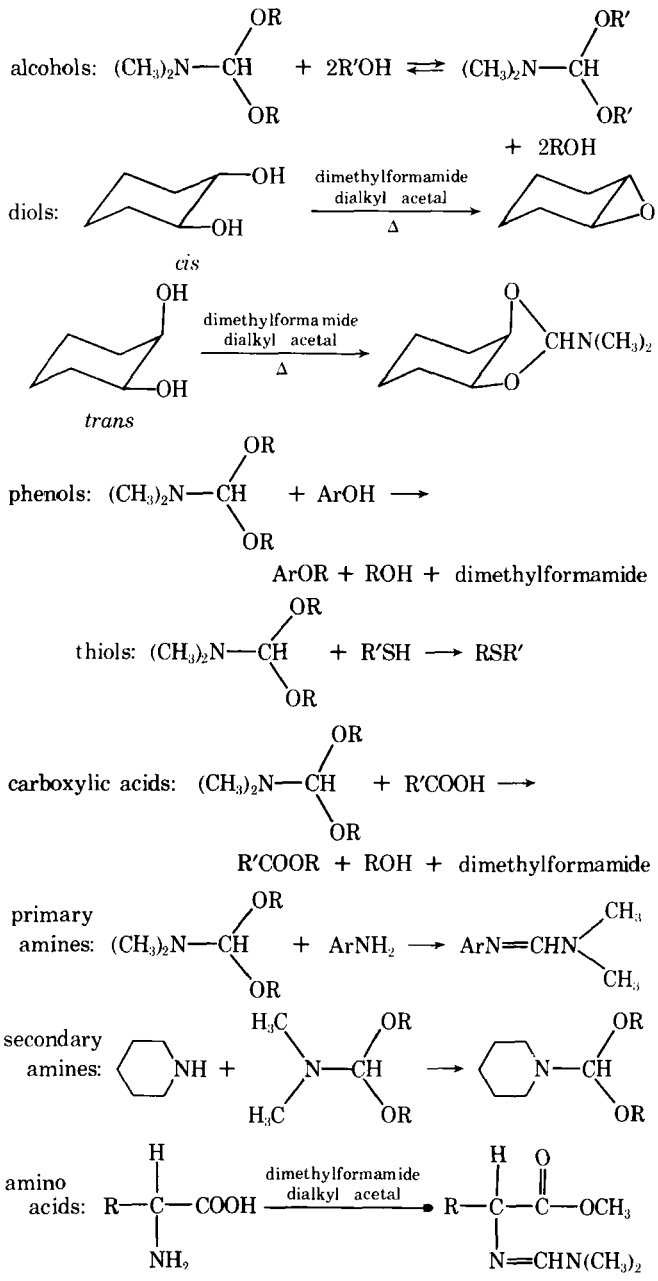

Scheme II

Silylation—A trimethylsilyl group can be readily introduced into a wide variety of organic compounds containing —OH, —COOH, —SH, —NH_2, and =NH groups. Thus, compounds amenable to silylation include alcohols, amides, amines, carbohydrates, carboxylic acids, phenols, steroids, sterols, and many other compounds with polyfunctional groups. It is important to remember that the general order of decreasing ease of silylation of the proton-active acceptor group is: alcohols (primary, secondary, and then tertiary), phenols, carboxylic acids, amines (primary, secondary, and then tertiary), and amides. The replacement of active hydrogen by the silyl group reduces the polarity of the compound and decreases the possibility of hydrogen bonding, with the resultant increase in volatility. Furthermore, stability is enhanced by reduction in the number of reactive sites.

The derivatives are simply and conveniently prepared in a few minutes by the following methods (30): trimethylchlorosilane-based methods, hexamethyldisilazane-based methods, silylimine methods, silylamide methods, and hexamethyldisilthiane or alkylthiotrimethylsilane methods. Some of the applications of silylation are illustrated in Scheme III.

Silylation is often looked upon with too much confidence as an unfailing means of improving GC separations. However, no technique is without hazards. Chambaz *et al.* (31) warned of the formation of enol trimethylsilyl ethers and oxysilylation products from steroidal ketones. When the same gas chromatograph is used for the analysis of phenols after the analysis of samples containing silylation reagent, both the phenol and its trimethylsilyl ether may be eluted (32). For example, when estrone is chromatographed

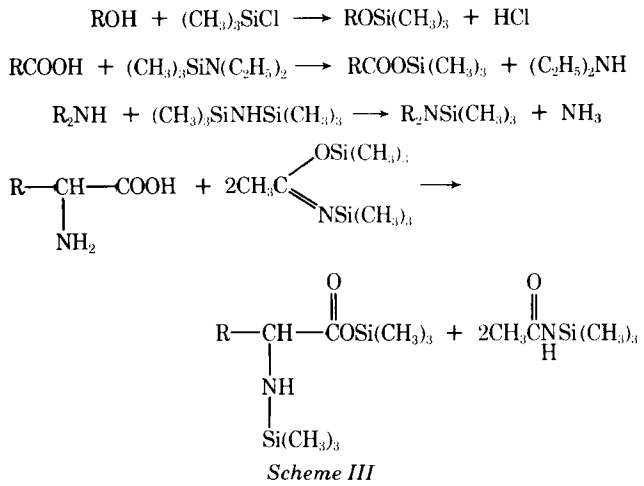

Scheme III

in a gas chromatograph–mass spectrometer 15 min after application of 10 μl of *N,O*-bis(trimethylsilyl)-acetamide to the column, mass spectral scans of the ascending, center, and descending portions of the resulting peaks demonstrate that it has two components: estrone (molecular ion *m/e* 270) and estrone trimethylsilyl derivative (molecular ion *m/e* 342).

Diethylstilbestrol has been commonly chromatographed as its trimethylsilyl derivative (33–36). Diethylstilbestrol occurs nearly exclusively in the *trans*-form. When a sample of *trans*-isomer is dissolved in organic solvent, such as ethyl acetate, and an aliquot is treated with *N,O*-bis(trimethylsilyl)-acetamide after removal of the solvent, GC of the reaction mixture indicates two components. Isomerization of *trans*-diethylstilbestrol to a mixture of the *cis*- and *trans*-isomers is known to occur in a number of common organic solvents (35, 36), and it has also been demonstrated that *cis*-diethylstilbestrol may be formed during trimethylsilylation (6).

Esterification—Esterification is an extremely valuable procedure for the alkylation of acidic compounds to increase volatility for GC analysis and to protect the acidic group during other reactions.

A mixture of a commercially available boron trifluoride etherate and an alcohol functions as an effective reagent in the direct esterification of some aromatic carboxylic acids bearing additional functions (*e.g.*, —OH, —NH_2, >C=O, —O—, and —S—). Unlike the Fischer esterification procedure where strongly acidic conditions prevail, the boron trifluoride etherate–alcohol reagent is unique in that it is both mild and effective. It esterifies the carboxyl group without affecting the other functionality in the molecule or the stability of the acid itself. Furthermore, it satisfactorily meets the esterification requirements of more different classes of carboxylic acids than does any other single reagent (37).

The amount of boron trifluoride etherate to be used has to be determined by the nature and number of functional groups present. Groups such as —OH, —NH_2, and >C=O each require an additional equivalent of boron trifluoride etherate for complex formation. Thus, for 1 mole of sodium *p*-aminosalicylate, 3 moles of boron trifluoride etherate should be employed for good results. When only 1 mole of the reagent is used, the yield of ester drops from 84 to 15%. However, in the case of *o*-aminobenzoic acid, 2 moles of the reagent seems to be sufficient (37).

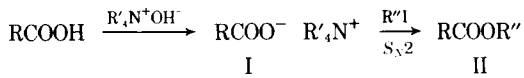

Scheme IV

A new method of esterification for stearic acid overcomes many problems common to traditional esterification reactions (38). The reaction utilizes extremely mild conditions and nonacidic reagents, is complete for analytical purposes in less than 10 min, and can be used to prepare a variety of esters for an acidic compound. In essence, the reaction employs an organic base such as tetramethylammonium hydroxide and a highly polar solvent system.

When the acidic compound is dissolved in the alkali–solvent system, a soluble salt (I) is immediately formed (Scheme IV). In the solvent system used (*N,N*-dimethylacetamide–methanol), the anion of the soluble salt and any primary alkyl iodide undergo a rapid S_N2 reaction to form the corresponding ester (II). Phenyltrimethylammonium hydroxide was found to be the best organic alkali for GLC derivatization, both because its salts have a high solubility in the organic solvent system and there is no precipitation of the corresponding iodide in the concentration ranges used. The generality of this reaction was demonstrated by reacting a number of alkyl iodides with steric acid salts of tetramethylammonium hydroxide and phenyltrimethylammonium hydroxide. A yield of greater than 98% was observed with each primary iodide, regardless of the alkali employed. This method circumvents the common difficulty of GLC analysis of bile acid methyl esters from a physiological system since interference is caused by massive amounts of cholesterol. Since the bile acid butyl esters prepared by this technique are eluted later than methyl esters, they are easily separated from cholesterol (38).

After comparing various esterification techniques for (2,4-dichlorophenoxy)acetic acid, it was concluded that the reagent of choice for producing a high yield of GLC pure ester is boron trifluoride–alcohol. The diazomethane-based method produces many impurities. Mineral acid catalysis generally produces some impurities. Silyl esters are unstable and are very sensitive to moisture (39).

A reagent mixture of heptafluorobutyric anhydride, pyridine, and ethanol was used to esterify carboxyl groups with the alcohol and to derivatize hydroxyl and amine groups with the anhydride. Diesterification of hydroxy acids was confirmed by mass spectrometry (40).

Acetylation—Direct acetylation is usually possible for drugs having an alcoholic or phenolic hydroxyl group and for drugs that are primary or secondary amines. The acetylating agent is acetic anhydride, and derivatization can be carried out either in final solvent or directly on the GLC column. Acetylation was found to be the technique of choice when analyzing specimens of blood for amphetamines in therapeutic or toxic ranges, since the parent compounds

may not be detectable at these levels. In urine specimens, however, where these drugs are usually more concentrated, both the parent drugs and their acetyl derivatives often can be chromatographed, thus providing the analyst with one more criterion for identification (41). However, care must be exercised in determining the nature of acetylation reactions since anomalous reactions can occur (42). This technique also is discussed under electron-capture detection.

Hydrazone Formation—Carbonyl compounds can be analyzed by GLC as free compounds, as oximes (43), as 2,4-dinitrophenylhydrazones (44, 45), or as phenylhydrazones (46). Korolczuk *et al.* (46) indicated that the determination of carbonyl compounds as their phenylhydrazones seems to be easier than the determination of their 2,4-dinitrophenylhydrazones because the preparation of derivatives is simpler and less time consuming and their separation from aqueous solution by extraction with ether is very easy, rapid, and quantitative. It is possible to calculate by interpolation the exact position of each peak on the chromatogram for *n*-aldehydes, 2-alkanones, and, probably, other carbonyl compounds such as cyclic ketones, branched ketones, and aldehydes.

Ion-Pair Formation—An interesting variation on derivatization was achieved by the use of ion-pair complexes in GC (47). Ion-pair complexes of the base–sulfonic acid type decomposed under GC conditions to give the base. The method was applied to the analysis of five basic drugs: tripelennamine, dimethindene, chlorpromazine, meperidine, and methylphenidate. The principle is also applicable to the extraction and determination of acidic substances.

Ion-pair chromatography also can be used to increase the sensitivity of the method. Chlorthalidone is selectively converted to its tetramethyl derivative by extractive alkylation on the basis of extraction of the ion-pair with the quaternary ammonium ion into methylene chloride in the presence of methyl iodide. The derivative thus formed is very sensitive to electron-capture detection and can be determined down to 2 ng/ml of plasma (48).

Derivatization for Electron-Capture Detection—Silylation in conjunction with a flame-ionization detector can yield detection levels of 2–5 ng for the neuroamines (49); however, the use of electron-capture detection and mass fragmentography has brought the possibility of quantitative evaluation down to the level of a few picograms (50–52). For this purpose, the amines and related products have been converted to trifluoroacetyl (50–52), heptafluorobutyryl (51–53), pentafluoropropionyl (51, 53, 54), and perfluorobenzyl (55) derivatives.

One study compared electron-capture sensitivity with various derivatives (*e.g.*, heptafluorobutyramide, pentafluorobenzamide, and pentafluorobenzylidine) of some clinically important primary and secondary amines (56). The sensitivity and selectivity of the analysis of amines were greatly enhanced by formation of an appropriately halogenated derivative. Generally, the order of electron-capture sensitivity for the derivatives of primary amines is: pentafluorobenzamide > pentafluorobenzylidine > heptafluorobutyramide. The electron-capture sensitivities of various derivatives of amphetamine are shown in Table III.

Heptafluorobutyramides have been prepared for a large number of amino drugs. The electron-capture responses of various heptafluorobutyramides are shown in Table IV.

N-Trifluoroacetyl-L-prolyl derivatives have been used to separate the enantiomeric mixtures of various chiral compounds by GLC. Westley and Halpern (57), who separated many enantiomers, rationalized their results in terms of a configuration rule predicting that *N*-trifluoroacetyl-L-prolyl derivatives of the *R* enantiomer usually have a shorter retention time than the corresponding diastereoisomer. A method for GLC separation of some ephedrines and pseudoephedrines by means of their *N*-trifluoroacetyl-L-prolyl derivatives was described (58), and the results confirmed and extended the correlation. The configuration of the carbons (carbon alpha to the reaction nitrogen atom) controls the relative retention time irrespective of the configuration of C-1.

Attempts have been made to improve the GC properties of tertiary amines by derivatization. Thus, amitriptyline was methylated and a Hoffman degradation to an olefin then was performed; better GC separations were obtained (59, 60). *N,N*-Dimethyldibenzo[*b,f*]thiepin-10-methylamine gave, with ethyl chloroformate, the corresponding chloromethylene derivative, which was determined by electron-capture GC (61). A third approach is illustrated in Scheme V (62, 63).

The tertiary amine is transformed to carbamate by reaction with alkyl chloroformate. By hydrolysis the carbamate gives a secondary amine, which is acylated. The resultant heptafluorobutyramide is determined by electron-capture GC with good precision in the nanogram range according to well-established methods (64).

In studies of the reaction of several alkyl chloroformates with tertiary amines, the carbamates were formed in about the same yield irrespective of the alkyl substituent. The carbamates did not exhibit the adsorptive properties of amines. This finding was the basis for determining nanogram amounts of amines (65). A comparison of three benzyl chloroformates—*viz.*, unsubstituted and *p*-nitro and pentafluoro substituted, revealed that pentafluorobenzyl chloroformate was the most useful reagent.

Some commonly employed derivatization procedures used for electron-capture detection are summarized in Table V.

APPLICATIONS

Derivatization GC has been used for analysis of many classes of pharmaceutical compounds. For the purpose of this review article, the pharmaceutical compounds are classified as follows: acids (including amino acids and miscellaneous carboxylic acids); alkaloids; amides, imides, and related compounds; amines; antibiotics; azepines; barbiturates and other

Table III—Electron-Capture Sensitivity of Various Amphetamine Derivatives (56)

Compound	Structure[a]	Response, coulombs x 10^3/mole
N-Pentafluorobenzamide	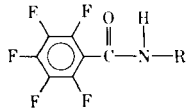	225
N-Pentafluorobenzylidine	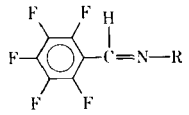	43
N-*p*-Nitrobenzamide	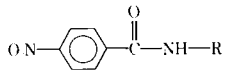	11
N-Pentafluorobenzylamine	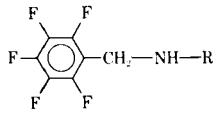	3.7
N-2,4-Dinitroaniline	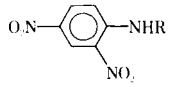	2.8
N-Heptafluorobutyramide	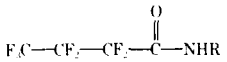	2.2
N-Heptafluorobutyrylidine	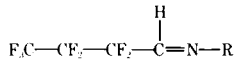	2.1
N-Heptafluorobutylamine		0.41

[a] R = $C_6H_5CH_2CH(CH_3)$.

urea derivatives; esters; hydroxy compounds and mercaptans; steroids; vitamins; and miscellaneous compounds. This classification will be helpful in understanding derivatization GC because derivatization is dependent not only on the number, nature, and stereochemical arrangement of the functional groups but also on the size and shape of the molecule (8).

Amino Acids—Derivatization and an analytical technique resembling GC was used in 1906 by Fischer for separation of amino acids as ethyl esters. Some other methods or reagents that have been used over the years with limited applications are (83): triketohydrindene oxidation with GLC of resultant aldehyde, α-chloroamino acid methyl esters, 2,4-dinitrophenylamino acid methyl esters, *N*,*N*-dimethylamino acid methyl esters, *N*-diethylphosphate amino acid methyl esters, alkylidine and alkylamino acid esters, and phenylthiohydantoin amino acids.

Silylation with several reagents has been used extensively for preparation of volatile derivatives of amino acids (83). *N*,*O*-Bis(trimethylsilyl)acetamide was found to be a useful reagent for quantitative analysis of methyldopa (III) and related amino acid impurities (84). This reagent was used earlier for silylating levodopa (IV) at ambient temperature (85). A silylation procedure has been used for the quantitative determination of liothyronine and thyroxine in dried thyroid (86).

Dual derivatization methods based on esterification of the carboxyl group and acylation of amino and other functional groups have been found to be useful in the analysis of amino acids. Some of these methods are summarized in Table VI.

The ease of reaction depends on the length of the alcohol chain, the amino acid being used, the amount of catalyst, temperature, and the quality of reagents. Methylation takes place in 30 min at room temperature, but increasing time and/or temperature are required through the methanol to pentanol series (91). Acylation reactions are generally carried out with acid anhydrides, often in the presence of pyridine. In addition to the primary amino (or imino) groups, hydroxyl, secondary amino, thiol, imidazole, guanidine, and indole groups can also be acylated.

Table IV—Electron-Capture Response of Various Heptafluorobutyramides (56)

Amine	Response, coulombs x 10^3/mole
β-Phenethylamine	2.0
Amphetamine	2.2
α-Methylbenzylamine	2.5
p-Methoxyphenethylamine	1.9
Mescaline	3.7
Phentermine	1.1
Phenmetrazine	8.8
Mephentermine	2.2
Methamphetamine	4.0
Methoxyphenamine	1.6

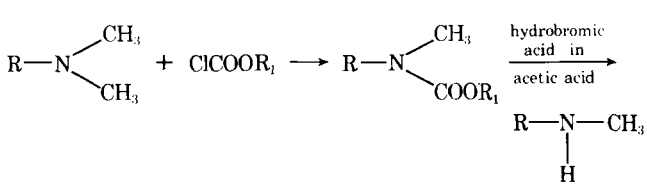

Scheme V

Table V—Derivatives Commonly Employed for Electron-Capture Detection (66)

Group	Derivative	Example	Reference
—OH	Heptafluorobutyrate	Perphenazine, digoxin	67, 68
	Trichloroacetate	Warfarin	69
	Trifluoroacetate	Warfarin, testosterone	69, 70
	Pentafluorobenzyl ether	Pentazocine	71
	Monochlorodifluoroacetate	Testosterone	70
$—NH_2$	Trifluoroacetamide	Amphetamine	72
	Pentafluoropropionamide	β-Phenethylamine	73
	Heptafluorobutyramide	Phentermine	56, 74
	Pentadecafluorooctanoate	β-Phenethylamine	73
	Pentafluorobenzylamine	Phenmetrazine	56
	Trichloroacetamide	Amphetamine	75
	Pentafluorobenzylcarbamate	Diphenhydramine	65
$—NH_2$, —OH (aliphatic)	Heptafluorobutyramide, heptafluorobutyrate	Pseudoephedrine	76
	Pentafluorobenzoyl ester	Tryptophol	73
$—NH_2$, —OH (aromatic)	Trifluoroacetamide, trifluoroacetate	Epinephrine	77, 78
	Pentafluorobenzylimine	Dopamine	79
—COOH	Trifluoroacetate	Bile acid	80
	Pentafluorobenzoyl ester	Aliphatic carboxylic acid	81
—C=O	Pentafluorophenyl hydrazone	Estrone	82

Dimethylformamide dialkyl acetals react with both carboxylic and amino groups of amino acids to form *N*-dimethylaminomethylene alkyl ester derivatives. The reaction is rapid and complete at 100°, and hydroxyl groups do not react under these conditions (92). Butler and Darbre (93) found that the relative molar response for the trifluoroacetyl ester of 14 amino acids with a nitrogen-sensitive thermionic detector was much greater than with a flame-ionization detector (Table VII).

In a weakly alkaline nonaqueous medium, a condensation reaction proceeds between dichlorotetrafluoroacetone and an α-amino acid. A low polarity cyclic derivative results and can be analyzed by GC (Scheme VI) (94). Substitution of X with —NH, —O, or —S resulted in 2,2-bis(chlorodifluoromethyl)-4-substituted 1,3-oxazolidine-5-one (V), -dioxolan-5-one (VI), or -oxathiolan-5-one (VII), respectively.

GC also was found to be the method of choice for analysis of mixtures of nonprotein amino acids (95). Sufficient volatility of the amino acids was obtained by a dual derivatization procedure—*viz.*, esterification of the carboxyl group and acylation of the amino group.

The inner esters of acylamino acids, azalactones, or oxazoline-5-ones provide useful derivatives for analysis. The analysis of α-methylamino acids as the corresponding 2-phenyloxazoline-5-ones, obtained by *N*-benzoylation of the amino groups followed by inner ester formation by dicyclohexylcarbodiimide (Scheme VII), was recently reported (96).

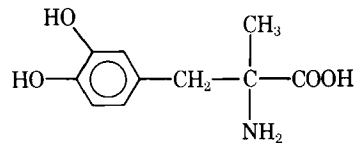

III

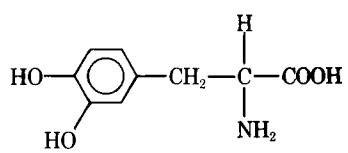

IV

Miscellaneous Carboxylic Acids—Free fatty acids can be determined directly on a phosphoric acid LAC-2R-446 column (97); however, they are most frequently determined as methyl esters. Methylation of carboxylic acids by thermal degradation of their quaternary ammonium salts in the injection port of a gas chromatograph was first accomplished by Robb and Westbrook (98); they injected tetramethylammonium hydroxide solutions of a number of acids and obtained chromatograms of methyl esters. Oakes and Willis (99) found trimethyl(α,α,α-trifluoro-*m*-tolyl)ammonium hydroxide useful for methylation of urinary carboxylic acids.

Ester formations using the ketal, 2,2-dimethoxypropane (100), anhydrous methanol–hydrogen chloride (101), and methanol–boron trifluoride (102) have been recommended. Methylation of fatty acids with diazomethane is hazardous (103). However, esterification with diazomethane has been reported by a technique that does not require esterification external to the chromatographic system (104). Thus, distilled diazomethane in ether appears promising as a reagent for esterification and analysis of fatty acids of moderate molecular weight using a precolumn reactor.

The methyl, ethyl, *n*-propyl, *n*-butyl, or *tert*-butyl esters of long chain fatty acids can be prepared quantitatively by reaction with dimethylformamide dialkyl acetals. A GC separation as soon as solution is achieved was reported (105). The mechanism of reaction is believed to involve the carboxylate ion and an alkoxy carbonium ion from the reagent (Scheme VIII) (106).

Table VI—Acyl Esters of Amino Acids

Ester	Acyl Derivative	Reference
Methyl	Acetyl/trifluoroacetyl	87
Ethyl	Acetyl/trifluoroacetyl	88
n-Propyl	Acetyl	88
n-Butyl	Acetyl	89
n-Butyl	Pentafluoropropionyl/ heptafluorobutyryl	90

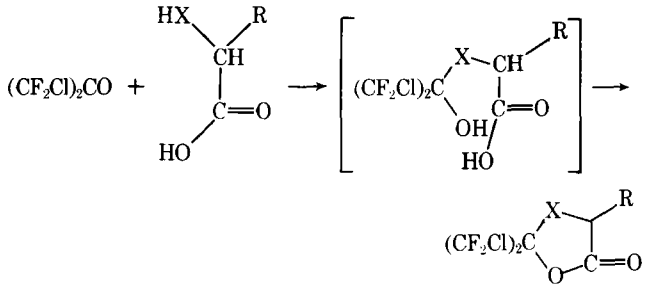

Scheme VI

The USP XVIII (107) method for analyzing aspirin tablets involves time-consuming column chromatography followed by separate spectrophotometric determination of aspirin and salicylic acid. GC methods that do not involve derivatization (108) show considerable tailing of the salicylic acid peak. Therefore, a method of analysis based on silylation with *N,O*-bis(trimethylsilyl)acetamide for aspirin, salicylic acid, and acetylsalicylsalicylic acid was proposed (109). The last compound was detected in varying amounts in tablets and granulations of different manufacturers.

Another method based on methylation was reported for the determination of traces of salicylic acid in aspirin tablets and other preparations containing phenacetin and caffeine (110). A method that utilizes esterification of salicylic acid with diazomethane was claimed to be precise for the estimation of salicylic acid in codeine and propoxyphene-type capsule and tablet analgesic formulations (111).

Aristolochic acid (VIII) can be analyzed by on-column methylation with trimethylanilinium hydroxide with a sensitivity limit of 1–5 μg/ml (112). β-Hydroxybutyric acid can be chromatographed as the methyl ester, and techniques for determining this compound in urine (113) and in blood and milk (114) were reported. Hydroxybutyric acids (α, β, and γ) were resolved after esterification with heptafluorobutyric anhydride on an OV-1 or Tabsorb column. The method is sensitive in the nanomole range (115).

1,1′-Carbonyldiimidazole is a useful reagent for facile esterification of free fatty acids. This reagent was used for almost instantaneous esterification of ibuprofen (IX) with sensitivity down to 0.5 μg/ml of plasma (116). The pentafluorobenzyl ester of flurbiprofen (X) yields a sensitivity of 0.05 μg/ml in plasma by electron-capture GC (117).

Flash heater methylation (118) was used for derivatizing bumetanide (XI) (Scheme IX). The GLC method was found to be accurate at concentrations as low as 0.1 μg/ml of human urine.

Probenecid (XII) was converted to the methyl ester for GLC analysis by reaction with diazomethane. The sensitivity of the method is 250 ng/ml of plasma (119). Ethylation with diazoethane (120) provided the basis for determination of indomethacin

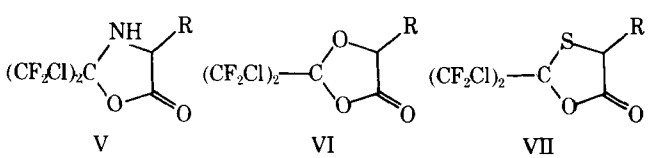

V VI VII

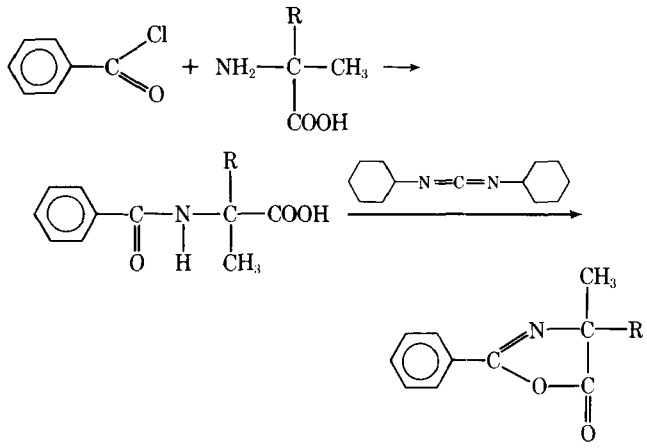

Scheme VII

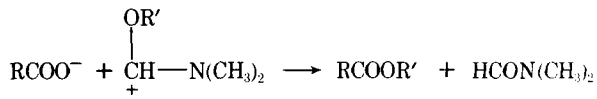

Scheme VIII

(XIII) by GC. The ethylation was essentially instantaneous and considerably improved the chromatographic response of indomethacin.

Alkaloids—Windheuser *et al.* (121) noted that the USP XVIII (107) method for the analysis of scopolamine (XIV) is not directly useful when all degradation products of scopolamine must be quantitatively determined. They reported a method based on trimethylsilylation. It can successfully separate and quantitatively determine the drug and its degradation products such as scopoline (XV), atropic acid (XVI), and tropic acid (XVII).

Silylation of the mandelic acid (XVIII) resulting from alkaline hydrolysis of homatropine methylbromide (XIX) was found to be suitable for the analysis of tablets and elixirs containing this compound (122).

A GC method was reported for opiates using trimethylsilyl derivatives (123). The narcotic analgesics were extracted with organic solvents from urine, blood, and bile and reacted with *N,O*-bis(trimethylsilyl)acetamide or bis(trimethylsilyl)trifluoroacetamide. The detectability of morphine from urine and blood was 0.1 μg/ml. Codeine, hydromorphone, methylhydromorphone, morphine, 3-monoacetylmor-

Table VII—Ratio of GLC Responses of Thermionic Detector (TD) to Flame-Ionization Detector (FID) for Trifluoroacetyl Amino Acid Methyl Esters (93)

Amino Acid	Ratio of Response, TD/FID
Alanine	16.6
Aspartic acid	9.1
Glutamic acid	5.9
Glycine	21.9
Hydroxyproline	8.3
Isoleucine	4.8
Leucine	5.7
Methionine	4.6
Norleucine	5.0
Phenylalanine	3.5
Proline	8.8
Serine	11.7
Threonine	7.9
Valine	3.5

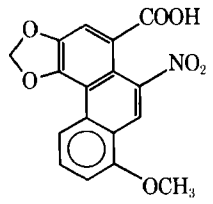

VIII

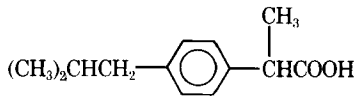

IX

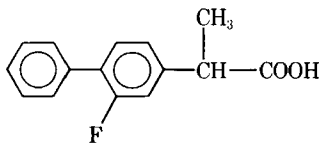

X

phine, 6-monoacetylmorphine, nalorphine, and oxycodone form trimethylsilyl derivatives.

The GC analysis of ergonovine maleate involves derivatization with *N*-trimethylsilyldiethylamine and *N*-trimethylsilylimidazole in pyridine followed by chromatography on a methyl silicone column (124). Ergonovinine, lumiergonovine I, and brucine can be resolved by this method. Procedures for analyzing and studying the biosynthesis of labile hop bitter compounds by means of GC have been developed (125). Derivatives of desoxyhumulones, humulones, and lupulones, obtained by reaction with hexamethyldisilazane in dimethylformamide, can be chromatographed in an all-glass system without any notable

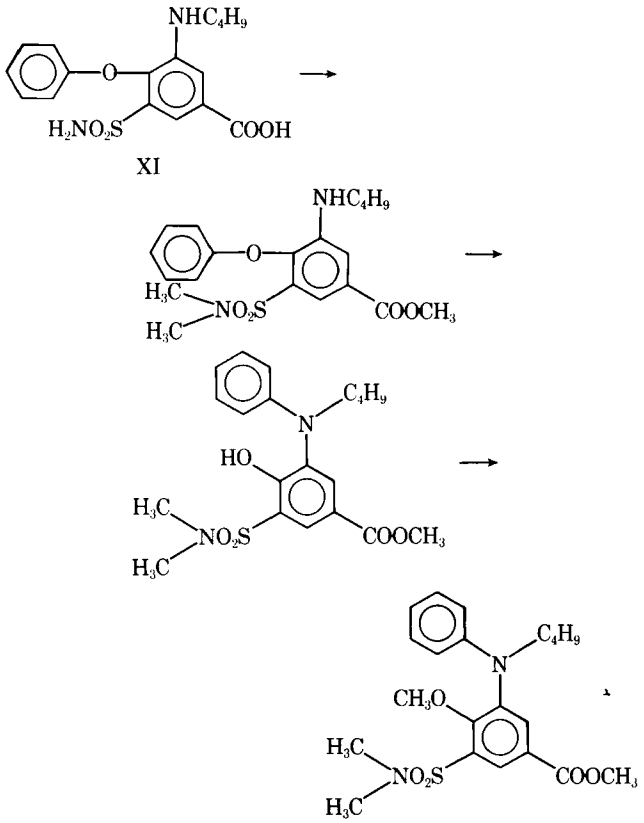

Scheme IX

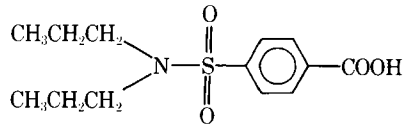

XII

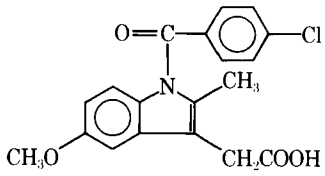

XIII

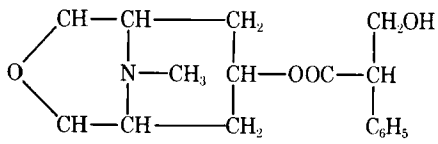

XIV

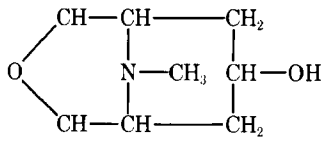

XV

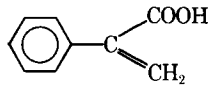

XVI

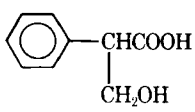

XVII

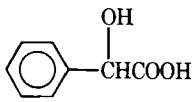

XVIII

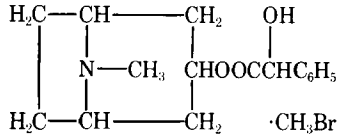

XIX

decomposition. A silylation procedure can be applied for the qualitative determination by GLC of active principles such as cannabichromene and cannabidiol in *Cannabis sativa* L. (126).

A method based on on-column methylation of quinidine with trimethylanilinium hydroxide was reported (127). Detection by flame ionization gives a linear response over the range of 0.2–12.0 μg of quini-

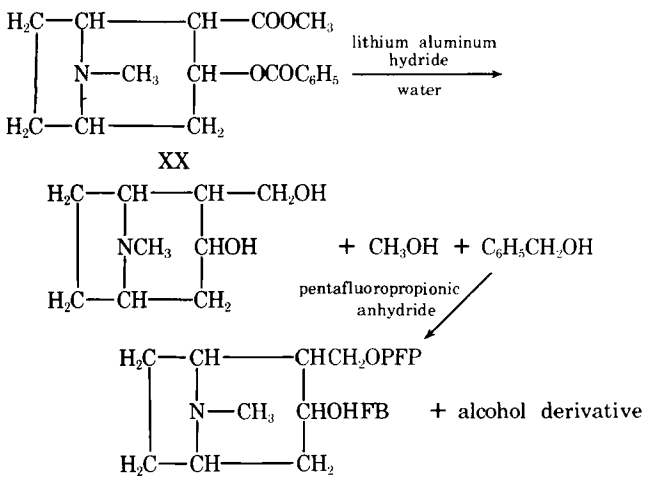

Scheme X

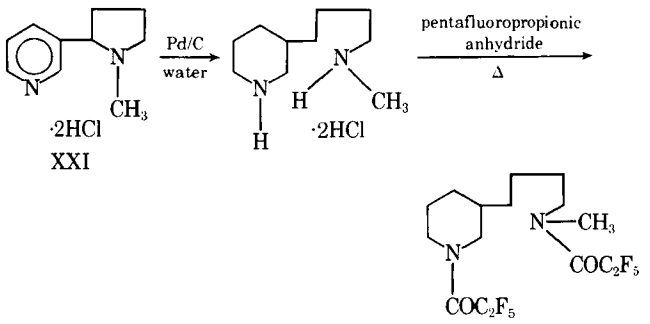

XXI

Scheme XI

dine/ml of plasma, with a 0.05-μg/ml limit of detectability. A method based on reduction and acylation of cocaine (XX) was proposed on the basis of Scheme X (128). With the pentafluoropropionic anhydride derivative, sensitivities of 20–30 ng/ml of sample could be achieved.

A unique determination method for nicotine in subpicomole quantities is based on catalytic hydrogenation of nicotine (XXI) to yield *N*-methyl-4-(3′-piperidyl)-*n*-butylamine (octahydronicotine). The two secondary amino functions then may be treated with a perfluoro acid anhydride to provide an electron-capture derivative. The dipentafluoropropionyl derivative can be readily quantitated in amounts corresponding to 0.03 pmole of nicotine as prepared by Scheme XI (129).

Amides, Imides, and Related Compounds—A GC method based on perfluoroacylation of amides was described (130). The method was found suitable for the analysis of *N*-decylacetamide, acetanilide (XXII), phenacetin (XXIII), and piperidione (XXIV). The minimum detectable quantity of the pentafluorobenzoyl derivative was 0.1 femtomole/sec by electron-capture detection.

Midha *et al.* (131) extended the GLC method for phenylbutazone (XXV) and its major metabolite, *p*-hydroxyphenylbutazone (oxyphenbutazone) (XXVI), to the estimation of the second major metabolite, γ-hydroxyphenylbutazone (XXVII). The method entails flash heater methylation and is sensitive down to 1.0 μg/ml. Flash heater methylation of γ-hydroxyphenylbutazone with trimethylanilinium hydroxide gives four peaks. Three of these peaks can be ascribed to the methylated breakdown products of γ-hydroxyphenylbutazone. Similarly, *p*-hydroxyphenylbutazone yields two peaks on flash heater methylation.

A GLC procedure based on on-column trimethylsilylation was described for chromatographing methsuximide (XXVIII) and its *N*-demethylated metabolite (132). The same silylation reagent was found useful for chromatographing saccharin (XXIX) in pharmaceutical products (133). Ingredients such as ascorbic acid, nicotinyl alcohol, aprobarbital, dextromethorphan hydrobromide, chlorpheniramine maleate, acetaminophen, and sulfamethoxazole do not interfere with the analysis.

Recently, Dusci *et al.* (134) reported an on-column methylation of theophylline (XXX) which matches the 1-μg/ml plasma sensitivity reported earlier (135). Theophylline was quantitatively converted to caffeine by on-column methylation. This technique was claimed to be more effective than the conventional techniques (136).

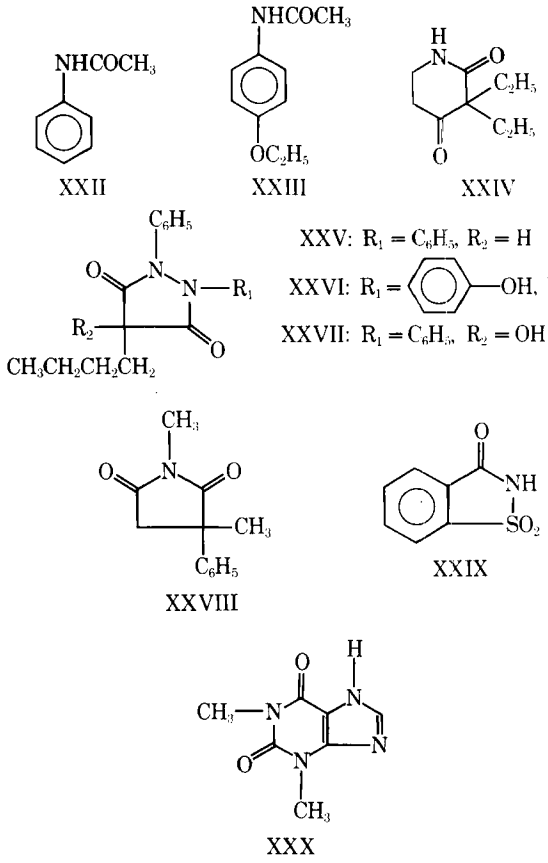

XXII XXIII XXIV

XXV: $R_1 = C_6H_5$, $R_2 = H$

XXVI: R_1 = p-hydroxyphenyl, $R_2 = H$

XXVII: $R_1 = C_6H_5$, $R_2 = OH$

XXVIII XXIX

XXX

Amines—Tailing, peak asymmetry, and decomposition are some of the problems encountered in the GLC analysis of amines. Pretreatment of the stationary phase with sodium hydroxide can overcome or eliminate some of them (137, 138). However, derivatization provides a valuable alternative, since both separation and sensitivity can be improved significantly. Specific and sensitive methods are necessary for the determination of biogenic amines of physiological importance. The most commonly used derivatization procedures are based on formation of trimethylsilyl (139, 140), acyl (141), isothiocyanate (142), 2,4-dinitrophenyl (143), and enamine (144) derivatives. With some of these methods, detection levels of 2–5 ng have been achieved (140) using a flame-ionization detector. The use of electron-capture detection and mass fragmentography permits quantitation down to a few picograms (144–146). For this purpose, amines and related products have been converted to trifluoroacetyl (144–146), heptafluorobutyryl (145, 147), pentafluoropropionyl (145, 147, 148), and perfluorobenzoyl (149) derivatives.

The conditions of formation and stability of pentafluorobenzyliminetrimethylsilyl derivatives have been optimized to permit quantitation of catecholamines in the picomole range (150). The highest sensitivity was obtained with a pulsed electron-capture detector, which allows quantitation down to 10 pg of the primary amine of biological interest. A sensitive and specific electron-capture GLC method based on

Table VIII—Detectability for Trifluoroacetyl Derivatives of β-Blocking Agents (151)

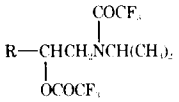

R	Compound	Detectable Amount, pg
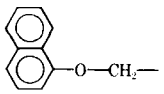	Propranolol	0.5
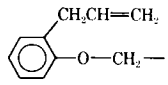	Alprenolol	0.7
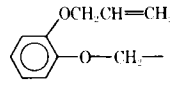	Oxprenolol	1.1
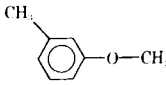	Toliprolol	0.9
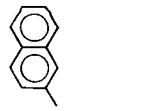	Pronethanol	0.6
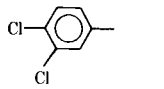	Dichloro-isoproterenol	0.1
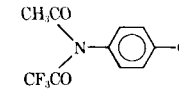	Practolol	0.7
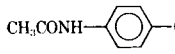	Practolol	0.7
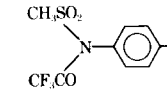	Sotalol	0.7

derivatization of both amino and alcoholic groups was reported for β-blocking agents including propranolol, oxprenolol, alprenolol, pronethalol, dichloroisoproterenol, practolol, sotalol, and several of their metabolites (151). The drugs were separated and detected as their trifluoroacetyl derivatives, and minimum detectable amounts ranged from 0.1 to 1.1 pg (Table VIII).

A method was reported involving the use of derivative reagents, such as trifluoroacetic anhydride and pentafluoropropionic anhydride, for the analysis of 1-(2,6-dimethylphenoxy)-2-propylamine (152). The flame-ionization detection of the derivative thus formed offered no advantages over electron-capture detection.

Derivatization of phenylephrine hydrochloride with trifluoroacetic anhydride combined with electron-capture detection permits sensitivities down to 12.5 ng/ml (153). A quantitative GC–mass spectrometry assay was used to determine the plasma and brain levels of amphetamine (XXXI) and phentermine (XXXII) as their *N*-trifluoroacetyl derivatives. The method was sensitive down to the 10-ng level (154).

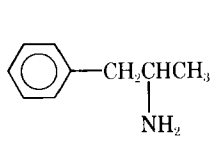

XXXI

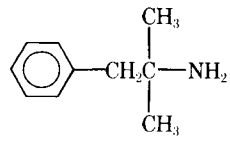

XXXII

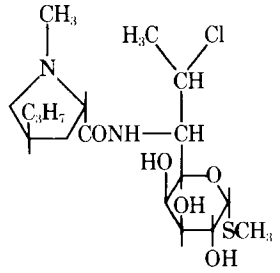

XXXIII

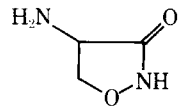

XXXIV

A GC method was described for the separation and identification of aliphatic amines in blood as their 2,4-dinitrophenyl derivatives (155). The secondary amines investigated (156) eluted more rapidly than the primary amines, even though they had higher molecular weights. This finding may be explained on the basis that the secondary amines have less tendency to form hydrogen bonds than the primary amines.

Antibiotics—GLC has been commonly used for the analysis of lincomycin, spectinomycin, and clindamycin and its esters and is potentially useful for other compounds (Table IX) (157).

Griseofulvin can be chromatographed directly; however, other antibiotics require derivatization. Thus, trimethylsilyl derivatives of lincomycin, spectinomycin, chloramphenicol, neomycins, erythromycins, penicillins, tetracycline, and cycloserine are made prior to analysis, whereas clindamycins are chromatographed as esters. Some derivatives that are frequently prepared for derivatization of antibiotics are summarized in Table IX.

GC–mass spectrometry of trifluoroacetylated clindamycin (XXXIII) indicates that it chromatographs intact as the derivatized free base containing three

Table IX—Derivatization of Antibiotics

Antibiotic	Derivatization Reagent	Reference
Clindamycin hydrochloride	Acetic anhydride	158
Clindamycin phosphate	Trifluoroacetic anhydride	158
Chloramphenicol	Hexamethyldisilazane	159
Cycloserine	*N,O*-Bis(trimethylsilyl)-acetamide, trimethylchlorosilane	160
Erythromycins	*N,O*-Bis(trimethylsilyl)-acetamide, trimethylchlorosilane, trimethylsilylimidazole	161
Kanamycin	Trimethylsilyldiethylamine	162
Lincomycin	Hexamethyldisilazane, trimethylchlorosilane	163, 164
Neomycin	Trimethylsilyldiethylamine	165, 166
Penicillins	Hexamethyldisilazane	167
Tetracyclines	*N,O*-Bis(trimethylsilyl)-acetamide, trimethylchlorosilane	168

Table X—Hydrolytic Products of Benzodiazepines

Benzodiazepine	Hydrolysis Product
Bromazepam	2-Amino-5-bromobenzoylpyridine
Chlordiazepoxide	2-Amino-5-chlorobenzophenone
Clonazepam	2-Amino-2′-chloro-5-nitrobenzophenone
Cloxazolam	2-Amino-7,2′-dichlorobenzophenone
Diazepam	2-Methylamino-5-chlorobenzophenone
Nitrazepam	2-Amino-5-nitrobenzophenone

trifluoroacetyl groups (169). The following four impurities were detected in a research lot of clindamycin hydrochloride: epilincomycin, lincomycin, clindamycin B, and epiclindamycin. Since derivatized clindamycin 2-phosphate could not be chromatographed satisfactorily, it was enzymatically hydrolyzed to clindamycin prior to derivatization and GLC.

The quantitative determination of cycloserine (XXXIV) in pharmaceutical preparations has been done by the nitroprusside method, titrimetry, UV spectrophotometry, and microbiology. The chemical treatment and solvents required for the assay can cause formation of degradation products which may interfere with the assay (170). The silylation procedure involving the use of *N,O*-bis(trimethylsilyl)-acetamide and trimethylchlorosilane was found to be more specific, because the cycloserine dimer does not chromatograph under these conditions.

Amphotericin B, nystatin, and several members of the aromatic group of heptene antibiotics have been degraded chemically by various methods. Some of the resulting products after derivatization were separated and compared by GC for structure confirmation (171, 172).

Azepines—Since the early 1960's, 1,4-benzodiazepine drugs have been established as widely used tranquilizers, sleep inducers, and muscle relaxants. With the extensive use of these compounds, there has been a parallel evolution of analytical methodology for their determination. Since they frequently have to be determined at low levels, chromatography is very widely used for determination of benzodiazepines (173). Many benzodiazepines are hydrolyzed by strong acids to give benzophenones, which are then used in chromatographic analysis. Some of the hydrolytic products of benzodiazepines (173) are summarized in Table X.

de Silva *et al.* (174) were the first to use hydrolysis products of diazepam (XXXV) for GC; these derivatives were found to be more volatile and their chromatography was easier than the parent compound. In 1968, Marcucci *et al.* (175) reported the chromatography of intact benzodiazepines; however, de Silva and Puglisi (176) found that incomplete resolution of various compounds in biological extracts was obtained. The formation of the trimethylsilyl derivative with a hexamethyldisilazane–trimethylchlorosilane reagent provided a 10-fold increase in sensitivity along with a shorter analysis time.

Oxazepam (XXXVI) rapidly loses a molecule of water on the GLC column to yield 6-chloro-4-phenylquinazoline-2-carboxyaldehyde (177, 178). Since the decomposition of oxazepam is rapid and almost quantitative, it can be used as a means of analyzing

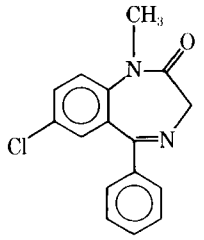

XXXV

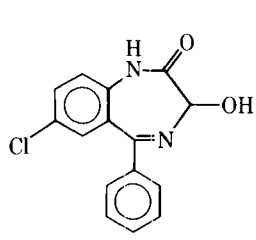

XXXVI

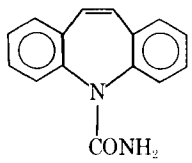

XXXVII

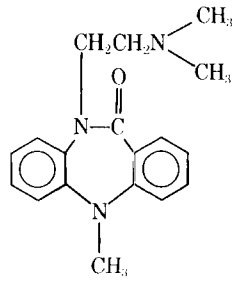

XXXVIII

oxazepam by GLC. Similar decomposition occurs for lorazepam, 3-hydroxynitrazepam, and 3-hydroxydesalkylflurazepam (173, 179).

A rapid method of analysis, based on the derivatization of carbamazepine (XXXVII) by dimethylformamide dimethyl acetal, was reported (180). Acetylation followed by GLC was used on a polar column for qualitative and quantitative determination of five *N*-demethylated metabolites of dibenzepin (XXXVIII) (181).

Barbiturates and Other Urea Derivatives—The analysis of barbiturates and related compounds requires derivatization to provide better resolution and peak symmetry than with the free drugs (182). Methylation of barbiturates has been accomplished by reacting them with dimethyl sulfate (183), diazomethane (184), and trimethylanilinium hydroxide for on-column methylation (185).

Venturella *et al.* (186) claimed that dimethylformamide dimethyl acetal is superior for methylation because of its rapid action. They proposed a method for simultaneous determination of amobarbital, secobarbital, hexobarbital, pentobarbital, phenobarbital, aprobarbital, and methyprylon. Scheme XII shows the mode of reaction. The mechanism of methylation using dimethylformamide dimethyl acetal depends on the presence of a rigid keto tautomer to prevent the slower rate reaction of the reagent with latent enols. For this reason, compounds such as amobarbital sodium and secobarbital sodium must be converted to their free acids and extracted prior to reaction.

GC provides a rapid and sensitive method for the determination of plasma urea as its trifluoroacetyl derivative using a gas chromatograph with a nitrogen detection system (187). Trifluoroacylation was also found useful for GLC of monosubstituted and symmetrically disubstituted ureas (188). Acylation was accomplished at room temperature in 2–3 min.

Silylation with *N,O*-bis(trimethylsilyl)trifluoroacetamide (189) has been used for GLC analysis of fluorouracil (XXXIX). However, Rao *et al.* (190) found it necessary to develop a flash methylation

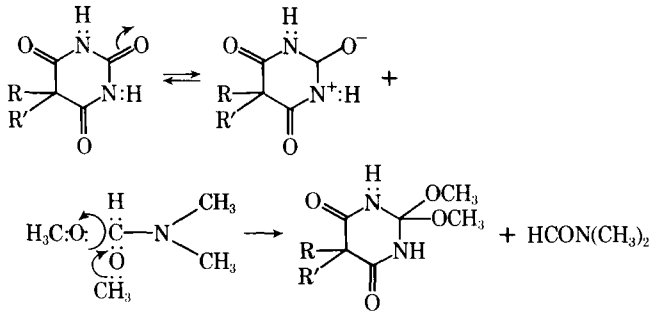

Scheme XII

technique, using trimethylanilinium hydroxide, for biopharmaceutical studies of fluorouracil.

Esters—Various esters can be chromatographed directly. Esterification is frequently used as a means of derivatization to increase the volatility and reduce the column interactions of a compound. However, some esters cannot be chromatographed directly. For example, direct GLC of meprobamate (XL) entails thermal decomposition at the injection port (191). A procedure was proposed for analyzing meprobamate based on the hydrolysis of meprobamate followed by silylation of the hydrolysis product to give the trimethylsilyl derivative for GLC (192).

Trimethylsilylation has also been used for the GLC analysis of chlorphenesin carbamate (XLI) in human serum (193) with sensitivities down to 0.5 μg/ml.

Drugs such as cocaine, atropine, and methylphenidate form sensitive derivatives when subjected to "reductive fragmentation" followed by acylation (194). The mode of reaction for derivatization of methylphenidate (XLII) is shown in Scheme XIII.

The technique of reductive fragmentation can be widely adapted for different drugs having reducible groups (195). Combined with the use of fluorinated derivatizing agents such as heptafluorobutyric anhydride and pentafluoropropionic anhydride, one can increase the sensitivity of the method significantly.

Hydroxy Compounds and Mercaptans—Sorbitol is a naturally occurring, straight-chain hexahydric alcohol commonly incorporated in pharmaceutical products as a humectant and sweetener. Silylation procedures reported in the 1960's (196–198) necessi-

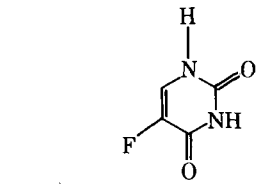

XXXIX

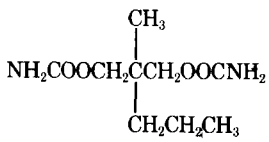

XL

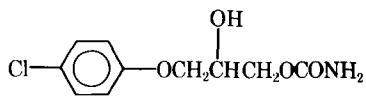

XLI

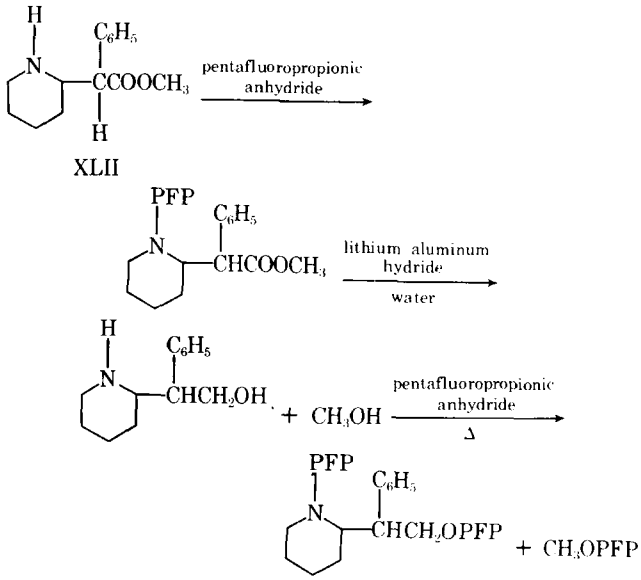

XLII

PFP = pentafluoropropionic group

Scheme XIII

tate complete removal of water from the sample before reaction, require extended reaction time, and do not completely separate sorbitol from mannitol and galactitol. Hexaacetate derivatives can be separated; however, this procedure also requires removal of water or residual solvent to assure no tailing of the peak (199, 200). Therefore, a GLC procedure was developed for analyzing sorbitol in solid and aqueous solution forms based on the ability of *n*-butylboronic acid to convert sorbitol quantitatively to the cyclic *n*-butylboronate ester (201). Baseline separations were reported for sorbitol, mannitol, and galactitol. Scheme XIV was proposed for this reaction.

Several GC methods have been reported for separating ethambutol (XLIII) and other antitubercular drugs; however, these methods are not entirely satisfactory because a complex derivatization procedure must be utilized along with a programmed temperature system. A single-step derivatization procedure was proposed followed by isothermal GC for analysis of ethambutol after an investigation of the following six drugs: ethionamide, pyrazinamide, cycloserine, isoniazid, pyridoxine, and ethambutol (202). *N*-Trimethylsilylimidazole derivatized ethambutol immediately and completely. Since *N*-trimethylsilylimidazole reacts only with hydroxyl groups (203, 204), only ethambutol and pyridoxine (XLIV) were derivatized.

Parabens are alkyl hydroxybenzoates. A silylation procedure is described in USP XVIII (107) for the analysis of methyl- and propylparabens (XLV) in various pharmaceutical preparations.

Sensitive methods are required for the toxicological analysis of phenolic compounds. Thiophosphoryl

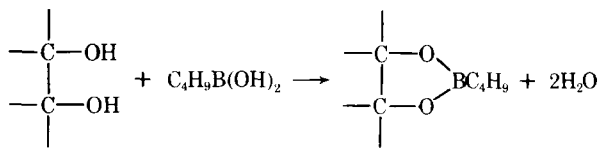

Scheme XIV

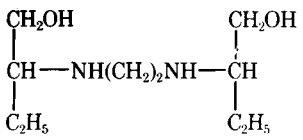

XLIII

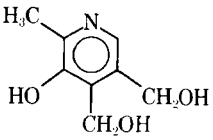

XLIV

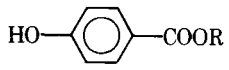

XLV

$R = CH_3$ or C_3H_7

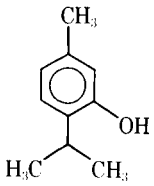

XLVI

phenolic derivatives and the use of flame photometric detection were found unsatisfactory for the determination of microgram amounts of phenols (205). A GC method based on formation of diethyl phosphate esters and flame photometric detection was proposed. The maximum sensitivity of detection of the analytically pure thymol (XLVI) phosphate ester was approximately 10 pg. A variety of other phenols such as isoeugenol, *p*-nitrophenol, *p*-chlorophenol, β-naphthol, and 2-methoxy-4-methylphenol were amenable to this method of analysis.

The speed of trimethylsilylation of sterically hindered phenols such as Δ^1-tetrahydrocannabinol can be increased by promoting the reaction with a small amount of trifluoroacetic acid. Trifluoroacetic acid may function as in Scheme XV (206). This reaction may also be of value in promoting silylation of other compounds that are difficult to silylate.

A GLC procedure involving acetylation was reported for the analysis of resorcinol monoacetate in dermatological products (207). The analysis of cream or lotion is performed by the addition of an internal standard, acetylation with acetic anhydride, extraction with benzene, and eventual chromatography of the chloroform solution on a 5% cyanosilicone column.

Gruber *et al.* (208) proposed a rapid GLC analysis based on formation of trimethylsilyl esters of 8-hydroxyquinoline and related halogenated 8-hydroxyquinoline with "significantly greater accuracy and precision" than the USP XVIII procedure. They were successful in resolving 5-chloro-7-iodo-8-hydroxyquinoline from impurities such as 8-hydroxyquinoline, 5-chloro-8-hydroxyquinoline, and 5,7-dichloro-8-hydroxyquinoline.

GC of the methyl derivative of warfarin (XLVII) was reported (209). The method was sufficiently sensitive to determine 0.25-μg/ml plasma levels in humans after single doses of 20 mg of warfarin. This sensitivity was extended down to 0.02 μg/ml by forming pentafluorobenzyl derivatives (210).

A method based on trifluoroacylation was developed for quantitative determinations of cyclazocine (XLVIII) and its *N*-dealkylated biotransformation

$$RSi(CH_3)_3 + CF_3COOH \rightleftharpoons RH + CF_3COOSi(CH_3)_3$$

$$ArOH + CF_3COOSi(CH_3)_3 \rightleftharpoons ArOSi(CH_3)_3 + CF_3COOH$$

Scheme XV

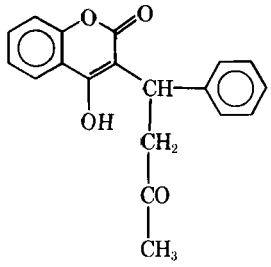

XLVII

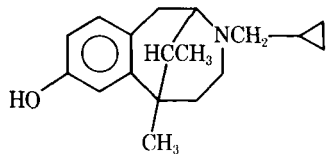

XLVIII

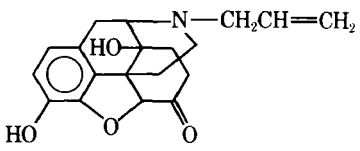

XLIX

product, norcyclazocine, in human urine (211). The method also can be used to estimate the levels of conjugated cyclazocine and norcyclazocine by measurement of these compounds released by acid hydrolysis. Heptafluorobutyric anhydride was used for derivatization of pentazocine and its metabolites followed by electron-capture detection (212). This method is claimed to be sensitive down to 0.1–0.2 μg/ml for pentazocine and its hydrolytic metabolites.

A silylation method was reported for determining naloxone (XLIX) in plasma (213). Enol ester derivatives of naloxone and naltrexate were prepared by reacting them with trifluoroacetic anhydride in the presence of pyridine (214) to achieve a sensitivity of 5 ng/ml in plasma or urine.

Normal and branched mercaptans containing up to eight carbon atoms and their 2,4- and 2,5-dinitrophenyl alkyl thioethers and thioalkylbenzoate derivatives were analyzed by GLC (215). The thioalkylbenzoate derivatives were suitable for resolving these mercaptans on an SE-30 column.

GC represents the most practical means to date for the analysis of phenothiazines and their derivatives. The normal methods of analysis of these drugs and their metabolites in biological media are nonspecific, insensitive, or time consuming in the cleanup and concentration steps. Phenothiazines containing a free primary alcohol group (acetophenazine, dixyrazine, fluphenazine, and perphenazine) cannot be eluted from the chromatographic column even at 280° but chromatograph easily as the acetates (216).

Similar derivatization is necessary for GLC of pericyazine (L) and dixyrazine (LI) (217). Phenothiazine sulfoxides can be readily separated and show chromatographic characteristics similar to those of corresponding free bases. Sulfoxides are prepared by oxidation of the free base in the presence of acetic acid (216).

Steroids—Steroids—natural and hormonal—possess a cyclopentanophenanthrene ring system with a variety of functional groups. The steroid hormones differ from other steroids in that they do not carry a long side chain. The state of oxygenation or dehydrogenation and the presence or absence of a side chain are the distinguishing factors of various hormones. Various derivatives may be used for GLC analysis of

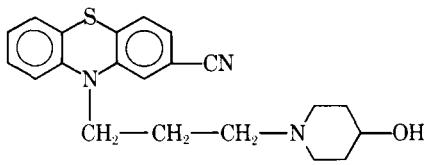

L

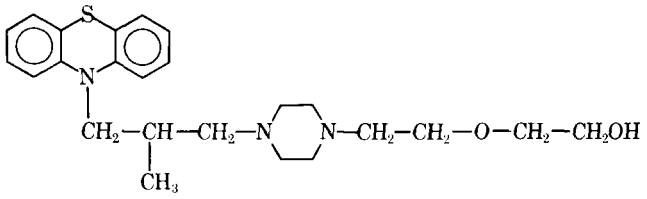

LI

steroids depending on the reactive group in the steroid molecule (8): trimethylsilyl ethers, acyl derivatives, phenolic ethers, and cyclic boronates for hydroxyl groups; methoximes and hydrazones for keto groups; and methyl esters for acid groups.

The retention indexes of various steroid derivatives such as acetates, trimethylsilyl ether, trifluoroacetate, heptafluorobutyrate, and chloromethyldimethylsilyl ether derivatives were reported (218).

Trimethylsilyl ethers are widely used in the analysis of steroids on the basis of etherification of the hydroxyl groups. With the presently available silyl reagents, it is possible to etherify selectively different types of steroid hydroxyl groups on the basis of differences in rates of reaction (219). Suitable reaction conditions have been established for the derivatization of even highly hindered and, therefore, normally unreactive groups such as the 14β-hydroxyl of cardenolides (220) and the 17α-hydroxyl of cortol (219).

Gleispach (221) showed that every hydroxyl group in a steroid can be transformed into its silyl ether, depending on the silylating mixture used. Oxo groups in the α-position to a hydroxyl group can react with formation of the enediol trimethylsilyl ether, whereas free oxo groups react under strong conditions with formation of the enol trimethylsilyl derivative. He concluded that hexamethyldisilazane or trimethylchlorosilane alone can be used for partial silylation of 3α-, 3β-, 21-, and 3-phenolic hydroxyl groups. Sterically nonhindered groups can be silylated with *N,O*-bis(trimethylsilyl)acetamide, *N,O*-bis(trimethylsilyl)trimethylsilyldiethylamine, or *N*-methyl-*N*-trimethylsilyltrifluoroacetamide. Silylation of the sterically hindered 17α-hydroxyl group can be carried out with trimethylsilylimidazole, whereas 11β-hydroxyl groups can be silylated with a mixture of trimethylsilyldiethylamine, *N,O*-bis(trimethylsilyl)acetamide, or *N*-methyl-*N*-trimethylsilyltrifluoroacetamide with trimethylchlorosilane. The use of *N*-methyl-*N*-trimethylsilyltrifluoroacetamide with an alkaline catalyst such as potassium acetate ensures the formation of the 20,21-enediol trimethylsilyl or 20,21-ene-17,20,21-triol trimethylsilyl derivatives of the glucocorticoids and also the formation of the enol trimethylsilyl ethers of oxo steroids.

Chambaz *et al.* (222) studied the conditions for an alkali-catalyzed silylation procedure using nucleophilic agents. This catalysis leads to preferential formation of enol trimethylsilyl derivatives from steroid keto groups without affecting the silylation rate of hindered hydroxyl groups. The most easily derivatized structures are the ketol and dihydroxyacetone side chains of the corticosteroid metabolites. Trimethylsilylation has also been found to be very useful for characterization of glucuronides and sulfate conjugates of hydroxysteroids (223, 224).

Trifluoropropyl, heptafluoropentyl, and pentafluorophenyl groups substituted into silyl ethers of steroids provide stable and volatile derivatives for GC of steroids. The first two show low sensitivity toward electron-capture detection, but the pentafluorophenyl group is more sensitive to electron-capture detection than the currently used chloromethyl group and is more thermally stable than the heptafluorobutyryl group (225).

A reported GC method (226) used high-resolution open-tubular glass capillary columns for simultaneous estimation of the following neutral steroids as trimethylsilyl ether derivatives: 11-oxoethiocholanolone, pregnanolone, 11β-hydroxyandrosterone, 11β-hydroxyetiocholanolone, allopregnanediol, pregnanediol, Δ^5-pregnanediol, pregnanetriol, and cholesterol.

Methoxime trimethylsilyl derivatives were prepared from several steroids isolated from urine (227). The retention indexes were measured for the methoxime trimethylsilyl derivatives of some corticosteroid metabolites at 250° on an SE-30 column using C_{28}–C_{30}, C_{30}–C_{32}, and C_{28}–C_{32} alkane mixtures as standards.

Steroids such as cortisone with a 17,21-dihydroxy side chain degrade when gas chromatographed unmodified. The cyclic boronates appear to offer advantages over the other derivatives in terms of ease of preparation and stability (228).

Some perfluorinated esters have been investigated to increase sensitivity by electron-capture detection. Heptafluorobutyrates are extremely volatile compounds and may be chromatographed at the picogram level (229). Esters of secondary alcohols are reasonably stable, but phenol esters are generally not stable. However, pentafluorobenzoates provide stable derivatives for phenols (230).

To study the absorption, metabolism, and excretion of medroxyprogesterone acetate (LII) in animals and humans, a method was developed for measurement of intact drug in plasma based on formation of a 3-enol heptafluorobutyrate ester and quantification with electron-capture detection. The assay was quantitative above 1 ng of medroxyprogesterone acetate/ml of plasma (231). The pentafluorobenzyl ester of dinoprost (LIII) was gas chromatographed as the tris(trimethylsilyl) ether (232). The derivative was stable during GLC, and the lower limit of detection by electron-capture detection was 12.5 pg of the ester injected on-column as the silylated product.

The estrone dimethylphosphinic esters prepared by derivatization of the monohydroxysteroid have good GC properties, and detectability of 10 pg can be achieved with the alkali flame-ionization detector (233). Some steroids that can be derivatized by this approach are: androsterone, dehydroepiandros-

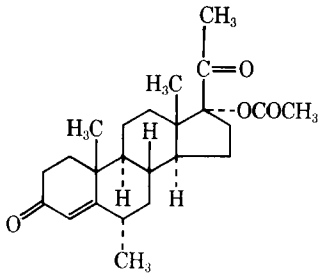

LII

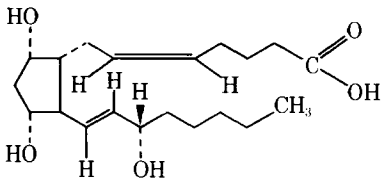

LIII

terone, stanolone, estrone, 3α-etiocholanolone, 3β-etiocholanolone, 3α-pregnanolone, 3α-pregnenolone, and testosterone.

Several methods have been recommended for GC of steroid hormones (Table XI) (234).

Vitamins—GC often has been used for the analysis of water-soluble and fat-soluble vitamins (235). Unmodified polyhydroxy and carboxylic organic compounds such as panthenol (LIV) and pantothenic acid (LV) and its salts are not sufficiently volatile for direct GLC. Furthermore, both LIV and LV tend to decompose at high temperatures. These problems can be easily overcome by converting the compounds to volatile derivatives such as acetates, trimethylsilyl ethers, or trifluoroacetates for GLC analysis.

The GLC determination of the acetate derivatives of pantothenic acid ethyl ester, pantothenol acid ethyl ester, and panthenol was described (236). The acetyl derivatives (acetates) were chosen because of their relatively high degree of volatility and stability and their ease of preparation and cleanup. Trimethylsilyl and trifluoroacetate derivatives of pantothenates and panthenol were also analyzed by GC.

A method based on silyl esterification of biotin (LVI) was reported (237); it uses the reaction of biotin with bis(trimethylsilyl)acetamide. The sodium salt of *d*-biotin did not yield a trimethylsilyl derivative. Therefore, Scheme XVI was proposed.

The interference of vitamin A in the determination of D vitamins by GLC is widely recognized. Removal of vitamin A generally necessitates lengthy pre-GLC workup. Tocopherols can also interfere, because they

Table XI—Derivatization GC of Steroid Hormones

Steroid	Sample	Derivative
Estrogens	Urine	Acetate
Estrogens	Blood	Heptafluorobutyrate
Pregnanediol	Urine	Acetate
Progesterone	Blood	Chloroacetate
Testosterone	Blood	Heptafluorobutyrate
17-Ketosteroids	Urine	Trimethylsilyl
Cortisol (hydrocortisone) metabolites	Urine	Trimethylsilyl
Tetrahydroaldosterone	Urine	Monochlorodifluoroacetate

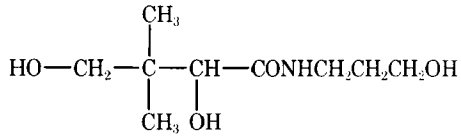

LIV

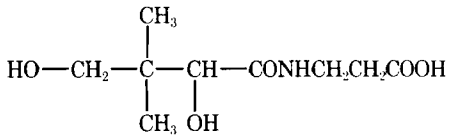

LV

have the same retention times as the D vitamins when the natural vitamins or their trimethylsilyl derivatives are chromatographed. A proposed improved procedure (238) consists of preliminary saponification and extraction steps to remove some interfering materials and then isolation and characterization of vitamins D (ergocalciferol, LVII), E (LVIII), and A (LIX) in their alcohol forms. The mixture so obtained is treated with propionic anhydride to esterify all alcohols to their corresponding propionates. The propionate esters of the following vitamins were prepared and chromatographed: α-tocopherol, β-tocopherol, γ-tocopherol, δ-tocopherol, pyrovitamin D_2, isopyrovitamin D_2, pyrovitamin D_3, and isopyrovitamin D_3. Acetic anhydride–pyridine reaction was utilized to determine whether α-tocopherol or α-tocopherol succinate was present in a sample, since the two analogs have similar retention times by GLC (239).

A method for the quantitative GLC determination of niacinamide (LX) is based on its conversion to nicotinonitrile. The dehydration reaction is mediated with trifluoroacetic anhydride and catalyzed by alkali (240).

Miscellaneous Compounds—Determination of diftalone (LXI) and its main metabolite, the 7-hydroxy derivative, is based on acid hydrolysis to isomeric carboxylic acid, followed by esterification with diazomethane for GC (241).

A general method for the analysis of guanidino drugs is based on hydrolysis and trifluoroacetylation of the resulting amines to obtain derivatives with excellent GC properties. Biological samples with levels of guanethidine (LXII) greater than 100 ng/ml can be analyzed easily by GLC with flame-ionization detection. Urine and plasma samples containing 1–100 ng/ml are readily amenable to analysis by GLC and

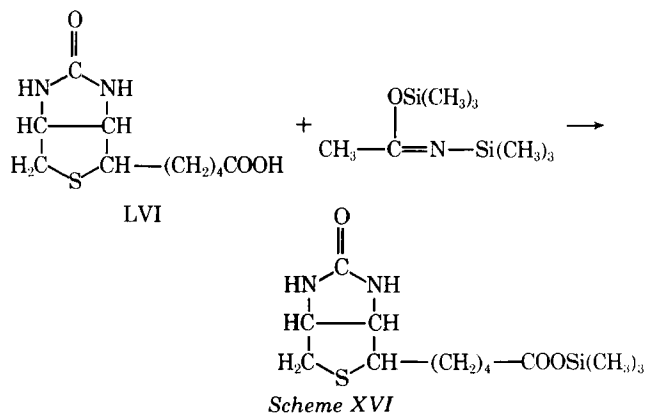

Scheme XVI

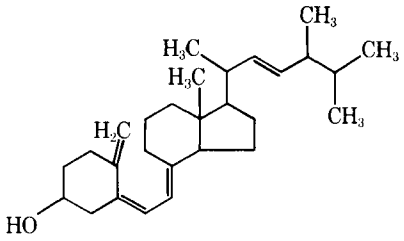

LVII

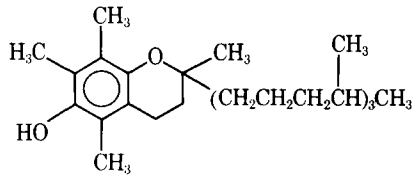

LVIII

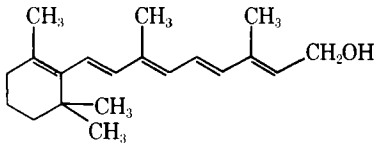

LIX

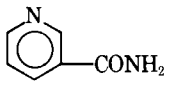

LX

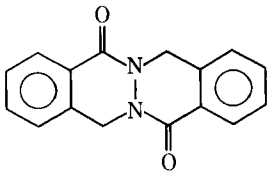

LXI

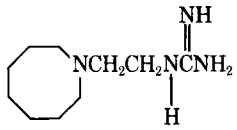

LXII

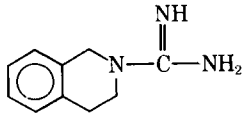

LXIII

multiple ion detection (242).

Recently, a hexafluoroacetylacetone derivatization procedure was used for the analysis of debrisoquin (LXIII), guanethidine, and 3,4-dihydro-1-methyl-2-(1*H*)-isoquinolinecarboxamidine (243).

CONCLUSIONS

Derivatization GC permits the analysis of pharmaceutical compounds with great selectivity and sensitivity down to the femtomole level. Furthermore, it is a valuable tool for structure determination, since derivatization GC–mass spectrometry surpasses either technique separately for structural information when only a small amount of sample is available. Anomalous reactions can occur in derivatization GC, and it is important that these reactions are considered in method development.

REFERENCES

(1) R. E. Heuttemann, M. L. Cotter, C. J. Shaw, C. A. Janicki, H. R. Almond, E. S. Moyer, A. P. Shroff, and F. Vestano, *Anal. Chem.*, **47**, 233(1975).

(2) *J. Chromatogr. Sci.*, **12**, 328(1974).

(3) S. Ahuja, in "Analysis of Drugs Containing Amino Group: Automated Analysis of Drugs," C. T. Rhodes and R. E. Hone, Eds., Butterworths, London, England, 1973.

(4) G. H. Wagman and M. J. Weinstein, "Chromatography of Antibiotics," Elsevier Scientific, New York, N.Y., 1973.

(5) R. C. Crippen, "Identification of Organic Compounds With the Aid of Gas Chromatography," McGraw-Hill, New York, N.Y., 1973.

(6) E. Heftman, "Modern Methods of Steroid Analysis," Academic, New York, N.Y., 1973.

(7) S. Siggia, "Instrumental Methods of Organic Functional Group Analysis," Wiley-Interscience, New York, N.Y., 1972.

(8) A. Niederweiser and G. Pataki, "New Techniques in Amino Acid, Peptide, and Protein Analysis," Ann Arbor Science Publishers, Ann Arbor, Mich., 1971.

(9) S. Ahuja, "Hormones: Encyclopedia of Industrial Analysis," vol. 14, Wiley, New York, N.Y., 1971, pp. 179–231.

(10) H. Kern, P. Schilling, and S. H. Miller, "Gas Chromatographic Analysis of Pharmaceuticals and Drugs," Varian Aerograph, Walnut Creek, Calif., 1968.

(11) H. M. McNair, *Chromatographia*, **7**, 161(1974).

(12) S. Ahuja, unpublished information, 1972.

(13) "The Chemistry of Heterocyclic Compounds: S-Triazines and Derivatives," A. Weissberger, Ed., Wiley-Interscience, New York, N. Y., 1959, p. 225.

(14) S. B. Matin, J. H. Karam, and P. H. Forsham, *Anal. Chem.*, **47**, 545(1975).

(15) S. Ahuja, G. D. Chase, and J. G. Nikelly, *ibid.*, **37**, 8406(1965).

(16) R. G. Ackman and R. D. Burgher, *ibid.*, **35**, 6(1963).

(17) B. Welton, *Chromatographia*, **3**, 211(1970).

(18) A. J. Williams, T. W. G. Jones, and J. D. H. Cooper, *Clin. Chem. Acta*, **43**, 327(1973).

(19) C. Ioanides, J. Chakraborty, and D. V. Parke, *Chromatographia*, **7**, 351(1974).

(20) V. Winkler, F. E. Regnier, J. M. Yoder, and L. R. Macy, *J. Pharm. Sci.*, **61**, 1462(1972).

(21) E. Brochmann-Hanssen and T. O. Oke, *ibid.*, **58**, 370(1969).

(22) H. V. Street, *Clin. Chim. Acta*, **34**, 357(1971).

(23) M. Widman, I. M. Nilsson, J. L. G. Nilsson, S. Agurell, and K. Leander, *Life Sci., Part II*, **10**, 157(1971).

(24) H. J. Kupferberg, *Clin. Chim. Acta*, **29**, 283(1970).

(25) F. S. Tanaka and R. G. Wien, *J. Chromatogr.*, **87**, 85(1973).

(26) B. S. Middleditch and D. M. Desiderio, *Anal. Lett.*, **5**, 605(1972).

(27) R. Osiewicz, V. Aggarwal, R. M. Young, and I. Sunshine, *J. Chromatogr.*, **88**, 157(1974).

(28) K. M. Williams and B. Halpern, *ibid.*, **97**, 267(1974).

(29) *Pierce Reviews*, Nov. 1972.

(30) A. E. Pierce, "Silylation of Organic Compounds," Pierce Chemical Co., Rockford, Ill., 1968.

(31) E. M. Chambaz, G. Maume, B. Maume, and E. C. Horning, *Anal. Lett.*, **1**, 748(1968).

(32) W. J. A. VandenHeuvel and G. W. Kuron, *J. Chromatogr.*, **38**, 532(1968).

(33) I. E. Smiley and E. D. Schall, *J. Ass. Offic. Anal. Chem.*, **52**, 107(1968).

(34) B. S. Rutherford, *ibid.*, **53**, 107(1968).

(35) V. W. Winkler, M. A. Nyman, and R. S. Egan, *Steroids*, **17**, 197(1971).

(36) W. A. White and N. H. Ludwig, *J. Agr. Food Chem.*, **19**, 388(1971).

(37) P. K. Kadaba, *J. Pharm. Sci.*, **63**, 1333(1974).

(38) R. H. Greeley, *J. Chromatogr.*, **88**, 229(1974).

(39) J. Horner, S. S. Que Hee, and R. G. Sutherland, *Anal. Chem.*, **46**, 110(1974).

(40) J. B. Brooks, C. C. Alley, and J. A. Liddle, *ibid.*, **46**, 1930(1974).

(41) G. Cimbura and J. Kofoed, *J. Chromatogr. Sci.*, **12**, 261(1974).

(42) R. Luders, P. O'Brien, and F. Tishler, *J. Pharm. Sci.*, **60**, 627(1971).

(43) J. W. Vogh, *Anal. Chem.*, **43,** 1618(1971).
(44) R. J. Soukup, R. J. Scarpellino, and E. Danielczik, *ibid.*, **36,** 2255(1964).
(45) H. Kallio, R. R. Linko, and J. Kaitoranta, *J. Chromatogr.*, **65,** 355(1972).
(46) J. Korolczuk, M. Daniewski, and Z. Mielniczuk, *ibid.*, **88,** 177(1974).
(47) P. F. G. Boon and A. F. Mace, *ibid.*, **41,** 105(1969).
(48) M. Ervik and K. Gustavi, *Anal. Chem.*, **46,** 139(1974).
(49) Y. Maruyamyama and A. E. Takemore, *Biochem. Pharmacol.*, **20,** 1833(1971).
(50) I. L. Martin and G. B. Ansell, *ibid.*, **22,** 521(1973).
(51) E. Anggard and G. Sedvall, *Anal. Chem.*, **41,** 1250(1969).
(52) L. J. Bertilsson, *J. Chromatogr.*, **87,** 147(1973).
(53) F. Karoum, F. Cattabeni, E. Costa, C. R. J. Ruthven, and M. Sandler, *Anal. Biochem.*, **47,** 550(1972).
(54) F. Cattabeni, S. H. Koslow, and E. Costa, *Science,* **178,** 166(1972).
(55) A. C. Moffat, E. C. Horning, S. B. Matin, and M. Rowland, *J. Chromatogr.*, **66,** 255(1972).
(56) S. B. Matin and M. Rowland, *J. Pharm. Sci.*, **61,** 1235(1972).
(57) J. W. Westley and B. Halpern, "Gas Chromatography," The Institute of Petroleum, London, England, 1969, pp. 119–128.
(58) A. H. Beckett and B. Testa, *J. Chromatogr.*, **69,** 285(1972).
(59) H. G. Hucker and J. K. Miller, *ibid.*, **32,** 408(1968).
(60) H. V. Street, *ibid.*, **73,** 73(1972).
(61) P. H. Degen and W. Riess, *ibid.*, **85,** 53(1973).
(62) J. Vessman, P. Hartvig, and M. Molander, *Anal. Lett.*, **6,** 699(1973).
(63) P. Hartvig and J. Vessman, *Acta Pharm. Suecica,* **11,** 115(1974).
(64) T. Walle and U. Ehrsson, *ibid.*, **7,** 389(1970).
(65) P. Hartvig and J. Vessman, *Anal. Lett.*, **47,** 223(1974).
(66) R. Sams, Ph.D. dissertation, Ohio State University, Columbus, Ohio, 1975.
(67) N. E. Larsen and J. Naestoft, *J. Med. Lab. Technol.*, **30,** 129(1973).
(68) E. Watson, P. Tramell, and S. M. Kalman, *J. Chromatogr.*, **69,** 157(1972).
(69) F. W. Deckart, *ibid.*, **69,** 201(1972).
(70) K. Nakagawa, N. L. McNiven, E. Forchielli, A. Vermeulen, and R. I. Dorfman, *Steroids,* **7,** 329(1966).
(71) H. Brötell, H. Ehrsson, and O. Gyllenhaal, *J. Chromatogr.*, **78,** 293(1973).
(72) J. E. O'Brien, W. Zazulak, V. Abbey, and O. Hinsvark, *J. Chromatogr. Sci.*, **10,** 336(1972).
(73) G. R. Wilkinson, *Anal. Lett.*, **3,** 289(1970).
(74) T. Walle and H. Ehrsson, *Acta Pharm. Suecica,* **7,** 389(1970).
(75) J. S. Noonan, P. W. Murdick, and R. S. Ray, *J. Pharmacol. Exp. Ther.*, **168,** 205(1969).
(76) L. M. Cummins and M. J. Fourier, *Anal. Lett.*, **2,** 403(1969).
(77) D. D. Clarke, S. Wilk, S. E. Gitlow, and M. J. Franklin, *J. Gas Chromatogr.*, **4,** 307(1967).
(78) D. D. Clarke, S. Wilk, and S. E. Gitlow, in "Biomedical Applications of Gas Chromatography," vol. 2, H. A. Szymanski, Ed., Plenum, New York, N.Y., 1968.
(79) J. C. Lhuguenot and B. F. Maume, *J. Chromatogr. Sci.*, **12,** 411(1974).
(80) T. Kanno, K. Tominaga, I. Fuji, and F. Funtani, *ibid.*, **9,** 53(1971).
(81) H. Ehrrson, *Acta Pharm. Suecica,* **8,** 113(1971).
(82) J. Attal, S. M. Hendeles, and K. B. Eik-Nes, *Biochemistry,* **20,** 394(1967).
(83) J. R. Coulter and C. S. Hann, in "New Techniques in Amino Acid, Peptide, and Protein Analysis," A. Niederweiser and G. Pataki, Eds., Ann Arbor Science Publishers, Ann Arbor, Mich., 1971, p. 75.
(84) J. R. Watson and R. C. Lawrence, *J. Chromatogr.*, **103,** 63(1975).
(85) J. R. Watson, *J. Pharm. Sci.*, **63,** 96(1974).
(86) R. Bilous and J. J. Windheuser, *ibid.*, **62,** 274(1973).
(87) A. Darbre and K. Blau, *J. Chromatogr.*, **17,** 31(1965).
(88) S. Makasumi, C. H. Nicholls, and H. Saroff, *ibid.*, **12,** 106(1963).
(89) W. M. Lamkin and C. W. Gehrke, *Anal. Chem.*, **37,** 383(1965).
(90) G. E. Pollock, *ibid.*, **39,** 1194(1967).
(91) D. L. Stalling, G. Gille, and C. W. Gehrke, *Anal. Biochem.*, **18,** 118(1967).
(92) J. P. Thenot and E. C. Horning, *Anal. Lett.*, **5,** 519(1972).
(93) M. Butler and A. Darbre, *J. Chromatogr.*, **101,** 51(1974).
(94) P. Husek, *ibid.*, **91,** 475(1974).
(95) O. Grahl-Nielsen and E. Solheim, *Chem. Commun.*, **1972,** 1093.
(96) O. Grahl-Nielsen and E. Solheim, *Anal. Chem.*, **47,** 333(1975).
(97) L. D. Metcalfe, *Nature,* **188,** 142(1960).
(98) E. W. Robb and J. J. Westbrook, III, *Anal. Chem.*, **35,** 1644(1963).
(99) T. R. Oakes and C. E. Willis, presented at the American Association of Clinical Chemists meeting, Aug. 1972.
(100) N. S. Radin, A. K. Hajra, and Y. Akahori, *J. Lipid Res.*, **1,** 250(1960).
(101) W. Stoffel, F. Chu, and E. H. Ahrens, Jr., *Anal. Chem.*, **31,** 307(1959).
(102) L. D. Metcalfe and A. A. Schmitz, *ibid.*, **33,** 363(1961).
(103) B. S. Middleditch and D. M. Desiderio, *Anal. Lett.*, **5,** 605(1972).
(104) D. B. deOlivera and W. E. Harris, *ibid.*, **6,** 1107(1973).
(105) J. MacGee and K. G. Allen, *J. Chromatogr.*, **100,** 35(1974).
(106) H. Brechbühler, H. Büchi, E. Hatz, J. Schreiber, and A. Eschenmoser, *Helv. Chim. Acta,* **48,** 1746(1965).
(107) "The United States Pharmacopeia," 18th rev., Mack Publishing Co., Easton, Pa., 1970.
(108) J. G. Nikelly, *Anal. Chem.*, **36,** 2248(1964).
(109) S. Patel, J. H. Perrin, and J. J. Windheuser, *J. Pharm. Sci.*, **61,** 1794(1972).
(110) S. Laik Ali, *Chromatographia,* **7,** 655(1974).
(111) J. R. Watson, F. Matsui, P. M. J. McConnell, and R. C. Lawrence, *J. Pharm. Sci.*, **61,** 929(1972).
(112) K. V. Rao, Y. Tarikut, and K. Killion, *ibid.*, **64,** 345(1975).
(113) L. Hagenfeldt and R. Blomstrand, *Acta Chem. Scand.*, **19,** 251(1965).
(114) J. M. L. Mee, *J. Chromatogr.*, **101,** 414(1974).
(115) J. B. Brooks and C. C. Alley, *Anal. Chem.*, **46,** 145(1974).
(116) D. G. Kaiser and G. J. VanGiessen, *J. Pharm. Sci.*, **63,** 219(1974).
(117) D. G. Kaiser, S. R. Shaw, and G. J. VanGiessen, *ibid.*, **63,** 567(1974).
(118) P. W. Feit, K. Roholt, and H. Sørensen, *ibid.*, **62,** 375(1973).
(119) A. G. Zacchei and L. Weidner, *ibid.*, **62,** 1972(1973).
(120) D. G. Ferry, D. M. Ferry, P. W. Moller, and E. G. McQueen, *J. Chromatogr.*, **89,** 110(1974).
(121) J. J. Windheuser, J. L. Sutter, and A. Sarrif, *J. Pharm. Sci.*, **61,** 1311(1972).
(122) B. F. Grabowski, B. J. Softly, B. L. Chang, and W. J. Haney, Jr., *ibid.*, **62,** 806(1973).
(123) K. D. Parker, J. A. Wright, A. F. Halpern, and C. H. Hine, *Forensic Sci. Soc. J.*, **10,** 17(1970).
(124) D. L. Sondak, *J. Pharm. Sci.*, **63,** 584(1974).
(125) F. Drawert and J. Beier, *Chromatographia,* **7,** 273(1974).
(126) C. E. Turner and K. W. Hadley, *J. Pharm. Sci.*, **62,** 1083(1973).
(127) K. K. Midha and C. C. Charette, *ibid.*, **63,** 1244(1974).
(128) J. W. Blake, R. S. Ray, J. S. Noonan, and P. W. Murdick, *Anal. Chem.*, **46,** 288(1974).
(129) L. Neelakantan and H. B. Kostenbauder, *ibid.*, **46,** 452(1974).
(130) H. Ehrsson and B. Mellstroem, *Acta Pharm. Suecica,* **9,** 107(1972).
(131) K. K. Midha, I. J. McGilveray, and C. Charette, *J. Pharm. Sci.*, **63,** 1751(1974).
(132) I. A. Muni, C. H. Altshuler, and J. C. Neicheril, *ibid.*, **62,** 1820(1973).
(133) E. M. Ratchik and V. Viswanathan, *ibid.*, **64,** 133(1975).
(134) L. J. Dusci, L. P. Hackett, and I. A. McDonald, *J. Chromatogr.*, **104,** 147(1975).
(135) P. A. Mitenko and R. I. Ogilive, *Clin. Pharmacol. Ther.*,

14, 509(1973).
(136) V. P. Shah and S. Riegelman, *J. Pharm. Sci.*, **63,** 1285(1974).
(137) J. R. L. Smith and D. J. Waddington, *Anal. Chem.*, **40,** 522(1968).
(138) J. F. O'Donnell and C. K. Mann, *ibid.*, **36,** 2097(1964).
(139) M. G. Horning, A. M. Moss, and E. C. Horning, *Biophys. Acta*, **148,** 597(1967).
(140) C. J. W. Brooks and E. C. Horning, *Anal. Chem.*, **36,** 1540(1964).
(141) N. Narasimhachari, *J. Chromatogr.*, **90,** 163(1974).
(142) D. J. Edwards and K. Blau, *Anal. Biochem.*, **45,** 387(1972).
(143) P. Capella and E. C. Horning, *Anal. Chem.*, **38,** 316(1966).
(144) I. L. Martin and G. B. Ansell, *Biochem. Pharmacol.*, **22,** 521(1973).
(145) E. Aggard and G. Sedvall, *Anal. Chem.*, **41,** 1250(1969).
(146) L. Bertilsson, *J. Chromatogr.*, **87,** 147(1973).
(147) F. Karoum, F. Cattabeni, E. Costa, C. R. J. Ruthven, and M. Sandler, *Anal. Biochem.*, **47,** 550(1972).
(148) F. Cattabeni, S. H. Koslow, and E. Costa, *Science*, **178,** 166(1972).
(149) A. C. Moffat, E. C. Horning, S. B. Matin, and M. Rowland, *J. Chromatogr.*, **66,** 255(1972).
(150) J. C. Lhugenolt and B. F. Maume, *J. Chromatogr. Sci.*, **12,** 411(1974).
(151) T. Walle, *J. Pharm. Sci.*, **63,** 1885(1974).
(152) R. J. Perchalski, B. J. Wilder, and R. H. Hammer, *ibid.*, **63,** 1489(1974).
(153) L. J. Dombrowski, P. N. Comi, and E. L. Pratt, *ibid.*, **62,** 1761(1973).
(154) A. K. Cho, B. J. Hodshon, B. Lindeke, and G. T. Miwa, *ibid.*, **62,** 1491(1973).
(155) Y. Ishitoya, S. Baba, and I. Hashimoto, *Clin. Chim. Acta*, **46,** 55(1973).
(156) S. Baba, I. Hashimoto, and Y. Ishitoya, *J. Chromatogr.*, **88,** 373(1974).
(157) M. Margosis, *J. Chromatogr. Sci.*, **12,** 549(1974).
(158) *Code of Federal Regulations*, Title 21, Parts 141 and 148 (1973).
(159) M. Margosis, *J. Chromatogr.*, **47,** 341(1970).
(160) M. Margosis, presented at the APhA annual meeting, Houston, Tex., 1972.
(161) K. Tsuji and J. H. Robertson, *Anal. Chem.*, **43,** 818(1971).
(162) *Ibid.*, **42,** 1661(1970).
(163) R. L. Houtman, D. G. Kaiser, and A. J. Taraszka, *J. Pharm. Sci.*, **57,** 693(1968).
(164) M. Margosis, *J. Chromatogr.*, **37,** 46(1968).
(165) K. Tsuji and J. H. Robertson, *Anal. Chem.*, **41,** 1332(1969).
(166) B. VanGiessen and K. Tsuji, *J. Pharm. Sci.*, **60,** 1069(1971).
(167) C. Hishta, D. L. Mays, and M. Garofalo, *Anal. Chem.*, **43,** 1530(1971).
(168) D. L. Sondack, F. E. Gainer, and H. J. Wesselman, *J. Pharm. Sci.*, **62,** 1344(1973).
(169) L. W. Brown, *ibid.*, **63,** 1597(1974).
(170) D. L. Sondack, F. E. Gainer, and H. J. Wesselman, *ibid.*, **62,** 1344(1973).
(171) H. J. Burrows and D. H. Calam, *J. Chromatogr.*, **53,** 566(1970).
(172) D. H. Calam, *J. Chromatogr. Sci.*, **12,** 614(1974).
(173) D. M. Hailey, *J. Chromatogr.*, **98,** 527(1974).
(174) J. A. F. de Silva, M. A. Schwartz, V. Stefanovic, J. Kaplan, and L. d'Arconte, *Anal. Chem.*, **36,** 2099(1964).
(175) F. Marcucci, R. Fanelli, and E. Mussini, *J. Chromatogr.*, **37,** 318(1968).
(176) J. A. F. de Silva and C. V. Puglisi, *Anal. Chem.*, **42,** 1725(1970).
(177) W. Sadee and E. vander Kleijn, *J. Pharm. Sci.*, **60,** 135(1971).
(178) A. Forgione, P. Martelli, F. Marcucci, R. Fanelli, E. Mussini, and G. C. Jommi, *J. Chromatogr.*, **59,** 163(1971).
(179) A. Frigerio, K. M. Baker, and G. Belvedere, *Anal. Chem.*, **45,** 1846(1973).
(180) R. J. Perchalski and B. J. Wilder, *Clin. Chem.*, **20,** 492(1974).
(181) A. De Leenheer and A. Heyndrickx, *J. Pharm. Sci.*, **62,** 31(1973).
(182) M. J. Barrett, *Clin. Chem. News Lett.*, **3,** 1(1971).
(183) H. F. Martin and J. L. Driscol, *Anal. Chem.*, **38,** 345(1966).
(184) J. G. H. Cook, C. Riley, R. F. Nunn, and D. E. Budgen, *J. Chromatogr.*, **6,** 182(1961).
(185) G. Kannen, R. Osciewicz, and I. J. Sunshine, *J. Chromatogr. Sci.*, **10,** 283(1972).
(186) V. S. Venturella, V. M. Gualario, and R. E. Lang, *J. Pharm. Sci.*, **62,** 662(1973).
(187) J. M. L. Mee, *J. Chromatogr.*, **94,** 302(1974).
(188) R. T. Evans, *ibid.*, **88,** 398(1974).
(189) J. L. Cohen and P. B. Brennan, *J. Pharm. Sci.*, **62,** 572(1973).
(190) K. V. Rao, K. Killion, and Y. Tanrikut, *ibid.*, **63,** 1328(1974).
(191) L. Martis and R. H. Levy, *ibid.*, **61,** 1341(1972).
(192) *Ibid.*, **63,** 834(1974).
(193) D. G. Kaiser and S. R. Shaw, *J. Pharm. Sci.*, **63,** 1094(1974).
(194) R. Huffman, J. W. Blake, R. Ray, J. Noonan, and P. W. Murdick, *J. Chromatogr. Sci.*, **12,** 382(1974).
(195) E. G. C. Clarke, "Isolation and Identification of Drugs," Pharmaceutical Press, London, England, 1969.
(196) E. P. Crowell and B. B. Burnett, *Anal. Chem.*, **39,** 121(1967).
(197) W. C. Ellis, *J. Chromatogr.*, **41,** 335(1969).
(198) J. A. House, J. A. Hubicki, and G. G. Hazen, *Anal. Chem.*, **34,** 1567(1967).
(199) P. F. Helgren, M. A. Thomas, and J. Q. Theivagt, *J. Pharm. Sci.*, **61,** 103(1972).
(200) G. Manius, F. P. Mahn, V. S. Venturella, and B. Z. Senkowski, *ibid.*, **61,** 1831(1972).
(201) M. P. Rabinowitz, P. Reisberg, and J. I. Bodin, *ibid.*, **63,** 1601(1974).
(202) B. M. Richard, J. E. Manno, and B. R. Manno, *J. Chromatogr.*, **89,** 80(1974).
(203) M. G. Horning, A. M. Moss, and E. C. Horning, *Biochim. Biophys. Acta*, **148,** 597(1967).
(204) M. G. Horning, A. M. Moss, E. A. Boucher, and E. C. Horning, *Anal. Lett.*, **1,** 311(1968).
(205) I. C. Cohen, J. Norcup, J. H. A. Ruzicka, and B. B. Wheals, *J. Chromatogr.*, **44,** 251(1969).
(206) N. E. Hoffman and K. A. Peteranetz, *Anal. Lett.*, **5,** 589(1972).
(207) P. O. Karkhanis, D. O. Edlund, and J. R. Afinsen, *J. Pharm. Sci.*, **62,** 804(1973).
(208) M. P. Gruber, R. W. Klein, M. E. Foxx, and J. Campisi, *ibid.*, **61,** 1147(1972).
(209) K. K. Midha, I. J. McGilveray, and J. K. Cooper, *ibid.*, **63,** 1725(1974).
(210) D. G. Kaiser and R. S. Martin, *ibid.*, **63,** 1579(1974).
(211) R. F. Kaiko and C. Inturriss, *J. Chromatogr.*, **100,** 63(1974).
(212) K. A. Pittman and C. Davidson, *J. Pharm. Sci.*, **62,** 765(1973).
(213) S. A. Weinstein, M. Pfeffer, J. M. Schor, L. Franklin, M. Mintz, and E. R. Tutko, *ibid.*, **62,** 1416(1973).
(214) R. Sams, personal communication, 1975.
(215) J. Korolezuk, M. Daniavski, and Z. Mielniczuk, *J. Chromatogr.*, **100,** 165(1974).
(216) A. DeLeenheer, *ibid.*, **77,** 339(1973).
(217) A. P. DeLeenheer, *J. Pharm. Sci.*, **63,** 389(1974).
(218) F. Berthou, L. Bardou, and H. H. Floch, *J. Chromatogr.*, **93,** 149(1974).
(219) E. M. Chambaz and E. C. Horning, *Anal. Biochem.*, **7,** 30(1969).
(220) B. Maume, W. E. Wilson, and E. C. Horning, *Anal. Lett.*, **1,** 401(1968).
(221) H. Gleispach, *J. Chromatogr.*, **91,** 407(1974).
(222) E. M. Chambaz, G. Defaye, and C. Madani, *Anal. Chem.*, **45,** 1090(1973).
(223) P. I. Jaakonmaki, K. A. Yarger, and E. C. Horning, *Biochim. Biophys. Acta*, **137,** 216(1967).
(224) W. J. A. VandenHeuvel, *J. Chromatogr.*, **28,** 406(1967).
(225) E. D. Morgan and C. F. Poole, *ibid.*, **89,** 225(1974).

(226) E. Bailey, M. Fenoughty, and J. R. Chapman, *ibid.*, **96,** 33(1974).
(227) J. A. Luyten and G. A. F. M. Rutten, *ibid.*, **91,** 393(1974).
(228) G. M. Anthony, C. J. W. Brooks, I. MacLean, and I. Sangster, *J. Chromatogr. Sci.*, **7,** 623(1969).
(229) D. Exley and J. Chamberlain, *Steroids*, **10,** 509(1967).
(230) A. Zmigrod, S. Ladany, and H. R. Lindner, *ibid.*, **15,** 535(1970).
(231) D. G. Kaiser, R. G. Carlson, and K. T. Kirton, *J. Pharm. Sci.*, **63,** 420(1974).
(232) J. A. F. Wickramsinghe, W. Morozowich, W. E. Hamlin, and S. R. Shaw, *ibid.*, **62,** 1428(1973).
(233) W. Vogt, K. Jacob, and M. Knedel, *J. Chromatogr. Sci.*, **12,** 658(1974).
(234) S. J. Clark and H. H. Wotiz, in "Modern Methods of Steroid Analysis," E. Heftman, Ed., Academic, New York, N.Y., 1973, p. 72.
(235) R. T. Nuttall and B. Bush, *Analyst*, **96,** 875(1971).
(236) A. R. Prosser and A. J. Sheppard, *J. Pharm. Sci.*, **58,** 718(1969).
(237) V. Viswanathan, F. P. Mahn, V. S. Venturella, and B. Z. Senkowski, *ibid.*, **59,** 400(1970).
(238) D. K. Feeter, M. F. Jacobs, and H. W. Rawlings, *ibid.*, **60,** 913(1971).
(239) A. J. Sheppard, W. D. Hubbard, and A. R. Prosser, *J. Ass. Offic. Anal. Chem.*, **52,** 442(1969).
(240) J. Vessman and S. Stromberg, *J. Pharm. Sci.*, **64,** 311(1975).
(241) G. G. Gallo, N. Rimorini, L. F. Zerilli, and P. Radaelli, *J. Chromatogr.*, **101,** 163(1974).
(242) J. H. Hengstman, F. C. Falkner, J. T. Watson, and J. Oates, *Anal. Chem.*, **46,** 34(1974).
(243) P. Erdtmansky and T. Goehl, *ibid.*, **47,** 750(1975).

ACKNOWLEDGMENTS AND ADDRESSES

Received from the *Research and Development Division, Ciba-Geigy Corp., Suffern, NY 10901*

RESEARCH ARTICLES

Influence of Hydrophobic Materials on Dissolution of a Nondisintegrating Hydrophilic Solid (Potassium Chloride)

J. VALERIE FEE *, D. J. W. GRANT ˣ, and J. M. NEWTON

Abstract □ A nondisintegrating hydrophilic solid was covered with coatings of hydrophobic materials as a model to study their influence on dissolution rates. Both solution and sublimation techniques were satisfactory for producing coatings of stearic acid. Only a sublimation method was applicable to magnesium stearate, but the resulting coating consisted mainly of a pyrolysis product, stearone. Reductions in dissolution rates in a continuous-flow system could best be interpreted by assuming that they reflected changes in the area of the hydrophilic solid exposed to the solvent. This concept is based on the assumptions that the intrinsic dissolution rate of uncoated potassium chloride did not change and that no dissolution occurred from coated areas. The most important factors controlling the dissolution rate were the strength of attachment of the hydrophobic coat to the surface of the hydrophilic substrate and the thickness of the coat.

Keyphrases □ Dissolution—potassium chloride, a nondisintegrating hydrophilic solid, effect of hydrophobic coating materials □ Potassium chloride disk—effect of hydrophobic coating materials on dissolution

The most common method of ensuring adequate lubrication of the interface between powders and metals during tablet and capsule manufacture is the addition of materials, such as stearic acid and magnesium stearate, in the form of powders. These materials, being hydrophobic in nature, inhibit the penetration of aqueous fluids into the final product (1, 2). This limitation of access results in retarded dissolution rates of tablets (3) and capsules (2–4).

The hydrophobic material, in addition to reducing the rate and extent of penetration of fluid into the preparation, can reduce the dissolution rate of individual particles by covering their surface. In formulated systems, it is difficult to decide which of these two effects is the rate-controlling step in the release of drugs from preparations. For example, liquid penetration of capsule formulations may or may not correlate with drug release (5). Moreover, because the spatial distribution of the lubricant in the final preparation is unknown, the extent and thickness of the hydrophobic covering of the drug particles are also unknown. It is, therefore, difficult to measure the effect of added hydrophobic materials on the dissolution rate of the individual particles within a preparation.

To investigate this problem, it is helpful to consider model systems. The present work describes a model in which the type, thickness, and area of cover

(226) E. Bailey, M. Fenoughty, and J. R. Chapman, *ibid.*, **96,** 33(1974).
(227) J. A. Luyten and G. A. F. M. Rutten, *ibid.*, **91,** 393(1974).
(228) G. M. Anthony, C. J. W. Brooks, I. MacLean, and I. Sangster, *J. Chromatogr. Sci.*, **7,** 623(1969).
(229) D. Exley and J. Chamberlain, *Steroids*, **10,** 509(1967).
(230) A. Zmigrod, S. Ladany, and H. R. Lindner, *ibid.*, **15,** 535(1970).
(231) D. G. Kaiser, R. G. Carlson, and K. T. Kirton, *J. Pharm. Sci.*, **63,** 420(1974).
(232) J. A. F. Wickramsinghe, W. Morozowich, W. E. Hamlin, and S. R. Shaw, *ibid.*, **62,** 1428(1973).
(233) W. Vogt, K. Jacob, and M. Knedel, *J. Chromatogr. Sci.*, **12,** 658(1974).
(234) S. J. Clark and H. H. Wotiz, in "Modern Methods of Steroid Analysis," E. Heftman, Ed., Academic, New York, N.Y., 1973, p. 72.
(235) R. T. Nuttall and B. Bush, *Analyst*, **96,** 875(1971).
(236) A. R. Prosser and A. J. Sheppard, *J. Pharm. Sci.*, **58,** 718(1969).
(237) V. Viswanathan, F. P. Mahn, V. S. Venturella, and B. Z. Senkowski, *ibid.*, **59,** 400(1970).
(238) D. K. Feeter, M. F. Jacobs, and H. W. Rawlings, *ibid.*, **60,** 913(1971).
(239) A. J. Sheppard, W. D. Hubbard, and A. R. Prosser, *J. Ass. Offic. Anal. Chem.*, **52,** 442(1969).
(240) J. Vessman and S. Stromberg, *J. Pharm. Sci.*, **64,** 311(1975).
(241) G. G. Gallo, N. Rimorini, L. F. Zerilli, and P. Radaelli, *J. Chromatogr.*, **101,** 163(1974).
(242) J. H. Hengstman, F. C. Falkner, J. T. Watson, and J. Oates, *Anal. Chem.*, **46,** 34(1974).
(243) P. Erdtmansky and T. Goehl, *ibid.*, **47,** 750(1975).

ACKNOWLEDGMENTS AND ADDRESSES

Received from the *Research and Development Division, Ciba-Geigy Corp., Suffern, NY 10901*

RESEARCH ARTICLES

Influence of Hydrophobic Materials on Dissolution of a Nondisintegrating Hydrophilic Solid (Potassium Chloride)

J. VALERIE FEE *, D. J. W. GRANT ˣ, and J. M. NEWTON

Abstract □ A nondisintegrating hydrophilic solid was covered with coatings of hydrophobic materials as a model to study their influence on dissolution rates. Both solution and sublimation techniques were satisfactory for producing coatings of stearic acid. Only a sublimation method was applicable to magnesium stearate, but the resulting coating consisted mainly of a pyrolysis product, stearone. Reductions in dissolution rates in a continuous-flow system could best be interpreted by assuming that they reflected changes in the area of the hydrophilic solid exposed to the solvent. This concept is based on the assumptions that the intrinsic dissolution rate of uncoated potassium chloride did not change and that no dissolution occurred from coated areas. The most important factors controlling the dissolution rate were the strength of attachment of the hydrophobic coat to the surface of the hydrophilic substrate and the thickness of the coat.

Keyphrases □ Dissolution—potassium chloride, a nondisintegrating hydrophilic solid, effect of hydrophobic coating materials □ Potassium chloride disk—effect of hydrophobic coating materials on dissolution

The most common method of ensuring adequate lubrication of the interface between powders and metals during tablet and capsule manufacture is the addition of materials, such as stearic acid and magnesium stearate, in the form of powders. These materials, being hydrophobic in nature, inhibit the penetration of aqueous fluids into the final product (1, 2). This limitation of access results in retarded dissolution rates of tablets (3) and capsules (2–4).

The hydrophobic material, in addition to reducing the rate and extent of penetration of fluid into the preparation, can reduce the dissolution rate of individual particles by covering their surface. In formulated systems, it is difficult to decide which of these two effects is the rate-controlling step in the release of drugs from preparations. For example, liquid penetration of capsule formulations may or may not correlate with drug release (5). Moreover, because the spatial distribution of the lubricant in the final preparation is unknown, the extent and thickness of the hydrophobic covering of the drug particles are also unknown. It is, therefore, difficult to measure the effect of added hydrophobic materials on the dissolution rate of the individual particles within a preparation.

To investigate this problem, it is helpful to consider model systems. The present work describes a model in which the type, thickness, and area of cover

of the hydrophobic layer and the method of applying it were each varied. The influence of these variables on the dissolution process of a hydrophilic substrate was studied, without interference from penetration problems, by means of the apparatus for determining dissolution rates described previously (6).

EXPERIMENTAL

Materials—The hydrophilic disk used as a model substrate was spectroscopic grade potassium chloride[1]. The hydrophobic coating materials were stearic acid, grade I[2], and magnesium stearate, superfine grade[3]. The solvents used in coating techniques were all analytical grade[4]. The dissolution medium was glass-distilled water.

Preparation of Potassium Chloride Disks—This procedure was carried out as described previously (6) to provide a transparent disk in a creep-resistant metal ring.

Coating Disks by Evaporation from Solvents—The hydrophobic material was dissolved in a solvent that had previously been shown not to interact with the disk surface. Solutions were applied in 0.1-ml volumes and allowed to evaporate under normal atmospheric conditions. By varying solute concentration and the number of applications of solution, the final quantity of coat on the surface could be controlled.

Coating Disks by Sublimation—The basic process was to allow vaporized hydrophobic material to condense onto one surface of a disk cooled at the end of a finger containing ice and water. The pressure of the vapor phase was maintained at 0.05 mm Hg. The rate of application of heat and the final temperature used to vaporize the hydrophobic material were varied to meet the requirements of the system and to provide different quantities of coat. When vaporization and condensation were complete, the heating source was removed and the system was slowly allowed to reach atmospheric conditions.

Determination of Quantity of Coating—The quantity of hydrophobic material covering the potassium chloride disk was determined by placing the disk and holder in the detection path of an IR spectrophotometer[5] and observing the extinction values of the carbonyl absorption peaks. Calibration curves were obtained by incorporating known quantities of coating material within the disk. Comparison of the extinction at different disk orientations provided a check on the uniformity of the coating.

Observation of Disk Surface—The surface of the coated disk was observed with an optical microscope and, after suitable pretreatment, with a scanning electron microscope[6].

Determination of Dissolution Rates—The rate at which potassium chloride dissolved in water was determined using the apparatus described previously (6). Measurements were carried out at flow rates that provided laminar flow but corresponded to the region in which forced convection of the solvent existed. The Reynolds number for solvent flow was close to 1300.

RESULTS

Coating with Stearic Acid—*Solution Coating*—A number of different organic liquids were examined for their suitability as coating solvents. Coated disks were examined by optical microscopy and by determining the IR spectra at different disk orientations. Light petroleum (bp 60–80°) gave the most complete coatings, which reduced the dissolution rate of the potassium chloride substrate. In no case, however, were the coatings even. They consisted of flakes of stearic acid about 100 μm long (Fig. 1). The coefficient of variation of the extinction values of coated disks at different disk orientations was about 8%.

Sublimation Coating—Vaporization at 126° for 6 min produced an even covering of the disk with no detectable change in IR extinction with different disk orientations. The covering was entirely different in nature from that produced by solution coating (*e.g.*, Figs. 1 and 2). Stearic acid deposited as globules approximately 2.5 μm in diameter.

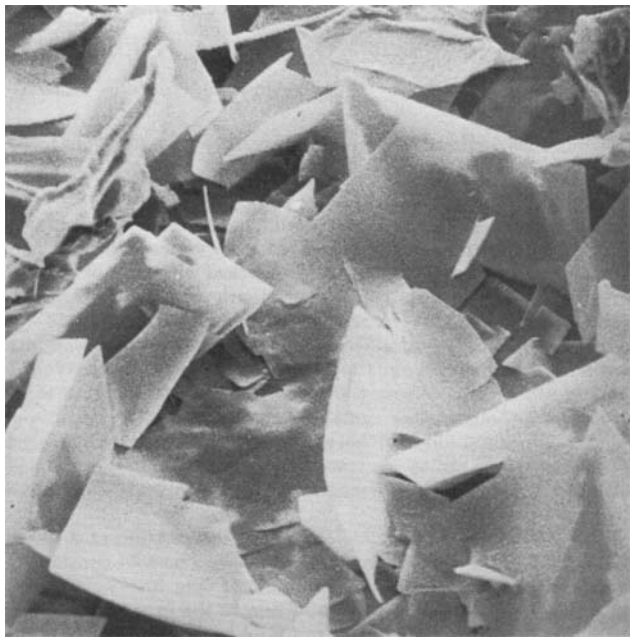

Figure 1—*Scanning electron micrograph of the coating of stearic acid formed on a potassium chloride disk by evaporation from a solution of stearic acid in light petroleum (bp 60–80°) (×208).*

Coating with Magnesium Stearate—*Solution Coating*—A solvent system that would provide an even cover without dissolving away the disk surface could not be found. Hence, no dissolution rate tests could be undertaken.

Sublimation Coating—To ensure vaporization of the magnesium stearate, it was necessary to heat the substance at 260° for 2 hr. The IR spectrum of the resulting coated disk did not correspond to that of magnesium stearate. It appeared that decomposition had occurred, probably the pyrolytic decarboxylation reaction

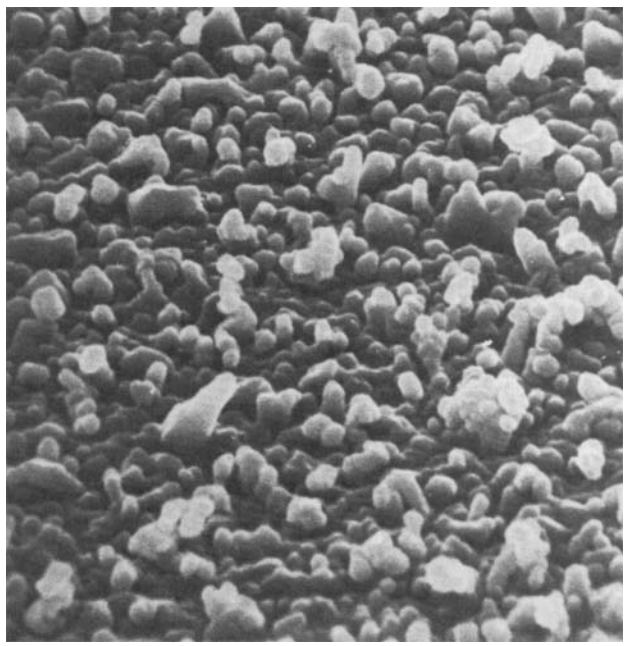

Figure 2—*Scanning electron micrograph of the coating of stearic acid formed on a potassium chloride disk by sublimation of stearic acid (×1900).*

[1] B.D.H. Chemicals Ltd., Poole, Dorset, BH12 4NN, England.
[2] Sigma London Chemical Co.
[3] Bush, Boake and Allen Ltd., London, N1, England.
[4] Koch-Light Laboratories Ltd., Colnbrook, Buckinghamshire, SL3 OBZ, England.
[5] Unicam SP200, Pye Unicam Ltd., Cambridge, CB1 2PX, England.
[6] Cambridge Stereoscan Mark 2A, Cambridge Instrument Co., Cambridge, England.

typical of Group II A salts of fatty acids (Scheme I).

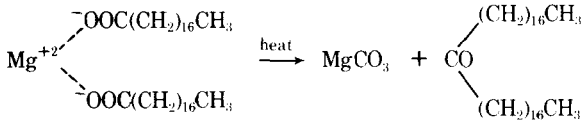

Scheme I

The product of this reaction would be stearone (diheptadecyl ketone or pentatriacontan-18-one). In accordance with this reaction, the IR spectrum was virtually identical with that of stearone prepared by the decarboxylation of stearic acid through heating with finely divided iron (7), removal of unchanged stearic acid with sodium hydroxide, decolorization with charcoal, and recrystallization from light petroleum (bp 100–120°). The mass spectrum of the material removed from the disk provided confirmation of the structure, although other materials also appeared to be present. These materials could have been stearic acid formed by hydrolysis of magnesium stearate by traces of moisture, other fatty acids present as impurities in the magnesium stearate, and ketones from their pyrolysis.

The coating itself was even, since the IR spectrum at different orientations showed no detectable variation. The coat consisted of closely packed globules, 1–4 μm in diameter (Fig. 3).

Coating with Stearone—In addition to the *in situ* production of stearone, the influence of this material by solution and sublimation coating was also studied.

Solution Coating—Due to the low solubility of stearone (about 1.5 g/liter) at 20° in light petroleum (bp 60–80°), several applications of 0.1 ml of such solutions were required to cover the disk adequately. The coatings were similar to solution coatings of stearic acid; they were uneven (with a coefficient of variation in IR extinction at different orientations of about 8%) and consisted of flakes about 10 μm long (Fig. 4).

Sublimation Coating—The quantity applied was varied by altering the conditions of application of heat and final temperature. As with other sublimed coatings, there was no detectable variation in the IR extinction at different disk orientations. The scanning electron micrographs (*e.g.*, Fig. 5) confirm the evenness of the coat but show that it consisted of loosely packed aggregates of globules and not of individual globules of the type produced by the sublimation of stearic acid or magnesium stearate. The diameter of the aggregates was about 10 μm; the diameter of the globules, of which they were composed, was about 1 μm.

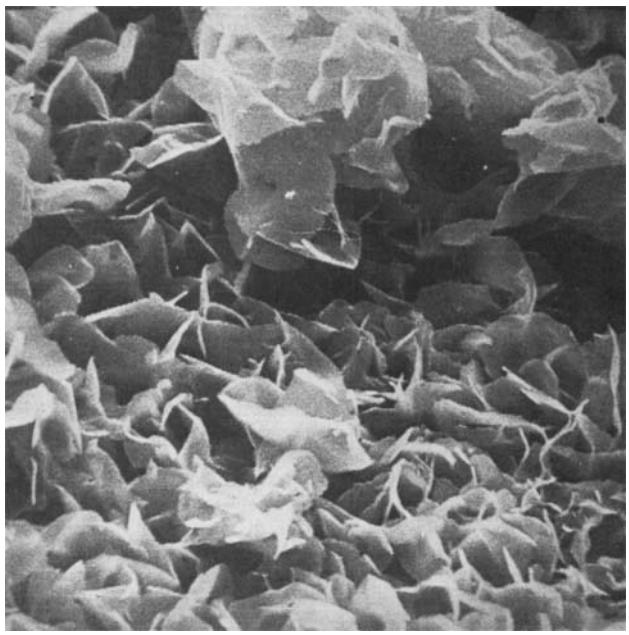

Figure 4—*Scanning electron micrograph of the coating of stearone formed on a potassium chloride disk by evaporation from a solution of stearone in light petroleum (bp 60–80°) (×2050).*

Influence of Hydrophobic Coatings on Dissolution of Potassium Chloride—Determinations of the dissolution rates of disks of potassium chloride that had been subjected to the solution or sublimation process, without hydrophobic material, established that these coating processes themselves in no way influenced the dissolution. Therefore, the effects produced were due to the presence of the hydrophobic coat and varied with the material and method of application.

In a flowthrough dissolution system such as that used here, a constant concentration, c, of dissolved material indicates a constant rate of dissolution, dm/dt, of the dissolving solid. Figure 4 in Ref. 6 illustrates this state for an uncoated disk of potassium chloride. Any change in concentration of dissolved material indicates a

Figure 3—*Scanning electron micrograph of the coating formed by the sublimation product of magnesium stearate on a potassium chloride disk (×1850).*

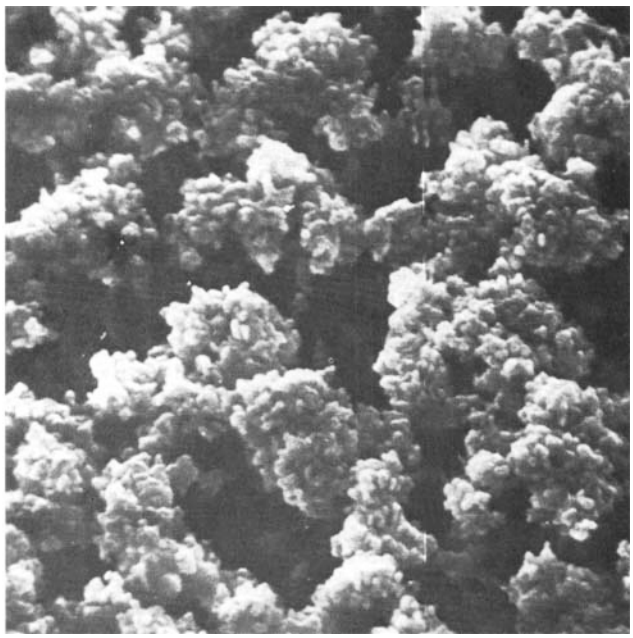

Figure 5—*Scanning electron micrograph of the coating of stearone formed on a potassium chloride disk by sublimation of stearone (×2080).*

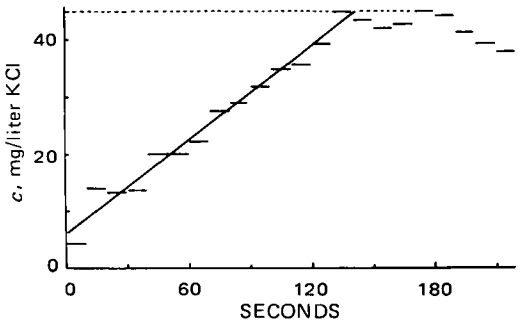

Figure 6—*Time dependence of the concentration of potassium chloride in the effluent of the dissolution apparatus from a potassium chloride disk covered with a solution coating of stearic acid (0.298 mg/cm²).*

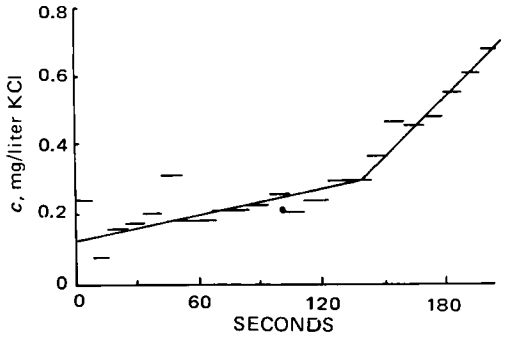

Figure 7—*Time dependence of the concentration of potassium chloride in the effluent of the dissolution apparatus from a potassium chloride disk covered with the sublimation product of magnesium stearate (0.594 mg/cm²).*

corresponding change in the dissolution rate, c being directly proportional to dm/dt (Eq. 3 in Ref. 6).

Influence of Stearic Acid—*Solution Coating*—For all quantities of stearic acid applied, c and dm/dt were considerably lower than those of the uncoated disk and increased with time until all coating was removed or until disk erosion brought about a decrease in area (Fig. 6). In general, the rate of increase in c (and dm/dt) decreased with an increasing quantity of stearic acid applied. Thus, the dissolution behavior of these coated disks differed in two fundamental ways from that of uncoated disks.

Sublimation Coating—In spite of the even coating, a covering corresponding to 0.269 mg/cm² produced no significant change in the release of potassium chloride. Therefore, either the coating did not retard the interfacial motion of the solvent and solute molecules or it was readily removed from the disk surface by the dissolution test procedure.

Influence of Magnesium Stearate—The covering resulting from the sublimation process produced a considerable reduction in c (and dm/dt). Again, there was an increase in c with time, but two linear sections were present in this case (Fig. 7), which is a further departure from the uncoated system.

Influence of Stearone—*Solution Coating*—A covering corresponding to 0.140 mg/cm² had little effect on potassium chloride dissolution (Table I); a steady level of c (and dm/dt) only slightly less than that for the uncoated disk was observed. Thicker coatings provided the linear increase in c (and dm/dt) observed with solution coatings of stearic acid.

Sublimation Coating—When the covering corresponded to 0.281 or 0.565 mg/cm², c (and dm/dt) increased with time until a constant level, slightly lower than that for the uncoated disk, was obtained (Fig. 8). A thicker coating, 1.2 mg/cm², gave, throughout a run, approximately constant values of c and dm/dt about 60% of those for the uncoated disk.

DISCUSSION

In the dissolution system (6) used here, relative motion between the fluid and solid phase is both controlled and defined. The method provides a system where penetration between particles is not involved; in addition to studying the dissolution process, an indication of the strength of attachment to the solid surface can be obtained.

If attachment to the surface is weak, the coating can be removed by the moving fluid. The dissolution process then corresponds to that for the uncoated disk. Alternatively, if attachment is strong and there is complete covering of the surface, total or partial inhibition of dissolution results, depending on whether the coating blocks or retards the movement of solvent and solute molecules to and from the surface. Between these two extremes, a range of possibilities exist.

For example, covering of the surface may be incomplete at a microscopic or macroscopic level, thus allowing varying areas of contact between the solvent and surface. If these areas remain constant because of firm attachment of the coating, the dissolution rate is constant but smaller and there is a reduced constant level of potassium chloride in the solution. If, however, attachment of the covering is not firm or dissolution of the coat takes place, an increase in dissolution rate and concentration occurs. Once a break in the coating is made, dissolution of the substrate can take place underneath it.

The results obtained provide examples of these effects. The total inhibition of the dissolution process was never obtained; it was impossible to provide complete cover with attachment sufficiently strong to exclude movement of solvent and solute molecules across the hydrophobic barrier. The alternative extreme of a coating that did not affect dissolution was obtained with sublimation coatings of stearic acid at 0.269 mg/cm² and solution coatings of stearone at 0.140 mg/cm² (Table I). The disappearance of the coat during the test supports the hypothesis that the moving fluid removes the coating and refutes the supposition that the coat retards solvent and solute movement across it. The former hypothesis is further supported by the fact that increasing the quantity of stearone sublimed onto the disk did reduce the final dissolution rate (Table I).

With all other coatings, there was a change in dissolution rate during the dissolution test. The observed dissolution rate, dm/dt, is given by:

$$\frac{dm}{dt} = GA \qquad \text{(Eq. 1)}$$

where m is the mass of dissolved material at time t, G is the intrinsic dissolution rate, and A is the area from which dissolution takes place. Any change in the dissolution rate implies a change in G and/or A. Visual observation of the disk suggests that a change in area is the most likely.

As a first approximation, it is postulated that: (*a*) the hydrophobic coating reduces to zero the rate of dissolution of the substrate directly beneath it, and (*b*) the intrinsic dissolution rate from the uncoated regions is equal to that from an uncoated disk. The observed dissolution rate, dm/dt, is then equal to the total rate of dissolution from the uncoated regions of the disk and, according to Eq. 1, is proportional to the exposed area, A, the constant of proportionality being the intrinsic dissolution rate, G. Thus, dm/dt provides a measure of the area that has lost its hydrophobic coating.

The rate of increase of the dissolution rate with respect to time, *i.e.*, d^2m/dt^2, reflects the rate of change in area with time, dA/dt.

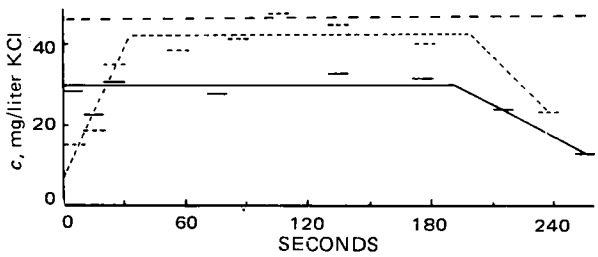

Figure 8—*Time dependence of the concentration of potassium chloride in the effluent of the dissolution apparatus from a potassium chloride disk covered with sublimation coatings of stearone. Key: – – –, uncoated disk; ——, 0.281 mg/cm² stearone; and - - -, 0.565 mg/cm² stearone.*

Table I—Influence of Hydrophobic Materials, when Applied as Coatings, on the Dissolution Properties of Potassium Chloride in Water at Reynolds Number 1300 for Solvent Flow

Coating System	Amount of Coat, mg/cm²	Values at Zero Time: Concentration of Potassium Chloride, c_0, µg/dm³	Values at Zero Time: Dissolution Rate $(dm/dt)_0$, µg/sec	Values at Zero Time: Area Exposed, A_0, mm²	Area Exposed, %	Rates of Change with: Change in Concentration, dc/dt, mg/dm³ sec	Rates of Change with: Change in Dissolution Rate, d^2m/dt^2, µg/sec²	Rates of Change with: Change in Area, dA/dt, mm²/sec	Time Taken to Remove Coat, sec: Calculated	Time Taken to Remove Coat, sec: Observed	After 120 sec: Dissolution Rate, µg/sec	After 120 sec: Surface Uncoated, %
None	0	28.6	871	819	61.7	Initial change rapid, then zero			0	0	1410	100
Stearic acid from solution	0.298	5.79	184	17.01	12.8	0.276	8.76	0.812	142	140	1242	86.7
	0.530	0.143	4.16	0.392	0.30	0.108	3.15	0.296	446		382	27.1
	0.632	1.25	32.2	3.09	2.33	0.121	3.10	0.298	435		404	29.3
	0.726	0.463	16.1	1.46	1.10	0.00794	0.275	0.0251	5,230		48.9	3.4
	0.821	0.929	24.4	2.34	1.76	0.0332	0.871	0.0836	1,560		129	9.3
	0.863	0.186	5.38	0.507	0.38	0.0534	1.55	0.146	907		190	13.5
	1.014	0.587	20.7	1.88	1.42	0.00342	0.121	0.0109	12,000		35.2	2.4
Stearic acid by sublimation	0.269	29.6	902	848	63.9	Initial change rapid, then zero			0	0	1410	100
Magnesium stearate	0.178	0.400	10.80	1.045	0.79	0.073[a]	2.10	0.198				
pyrolysis product	0.594	0.122	3.29	0.319	0.24	0.00111[b]	0.0291	0.0028				
by sublimation	0.667	0.098	2.65	0.256	0.19	0.00394[c]	0.100	0.0096				
	0.178					0.159[a]	4.58	0.432	354			
	0.594					0.0052[b]	0.138	0.0132	10,160			
	0.667					0.0170[c]	0.433	0.042	3,420			
Stearone from solution	0.140	—	—	—	—	Initial change rapid, then zero			0	0	1280	91.0
	0.473	0.752	21.3	2.015	1.52	0.0431	1.22	0.116	1,129		167	11.9
Stearone by sublimation	0.281	8.6	302	27.4	20.6	0.237	8.32	0.756	139	140	1299	89.0
	0.565	10.4	292	27.7	20.9	0.656	18.4	1.75	52	50	1202	85.9
	1.20	28.6	815	76.9	57.9	Very small values			—		875	62.2

[a] Change of slope at t = 90 sec, c = 7 mg/dm³. [b] Change of slope at t = 164 sec, c = 0.3 mg/dm³. [c] Change of slope at t = 345 sec, c = 1.45 mg/dm³.

This can be seen by differentiating Eq. 1 with respect to time:

$$\frac{d^2m}{dt^2} = G\frac{dA}{dt} \qquad \text{(Eq. 2)}$$

Also, as in Eq. 3 of Ref. 6, the rate of dissolution can be expressed in terms of the concentration, c, of dissolved potassium chloride and the volumetric flow rate, dV/dt:

$$\frac{dm}{dt} = c\frac{dV}{dt} \qquad \text{(Eq. 3)}$$

which, on differentiating with respect to time, t, at constant volumetric flow rate, dV/dt, gives:

$$\frac{d^2m}{dt^2} = \frac{dc}{dt}\frac{dV}{dt} \qquad \text{(Eq. 4)}$$

where dc/dt is the rate of change of potassium chloride concentration, c, with time. This equation enabled d^2m/dt^2 to be calculated in Table I. Comparison of Eqs. 2 and 4 gives:

$$G\frac{dA}{dt} = \frac{dc}{dt}\frac{dV}{dt} \qquad \text{(Eq. 5}a\text{)}$$

or:

$$\frac{dA}{dt} = \frac{1}{G}\frac{dc}{dt}\frac{dV}{dt} \qquad \text{(Eq. 5}b\text{)}$$

Values of dA/dt in Table I were calculated from this equation. The time, T, taken for the total surface area of the substrate to be exposed to the solvent by complete removal of the coating is obtained by integrating dt/dA over the total increase in exposed area:

$$T = \int_{A_0}^{A_T}\frac{dt}{dA}dA \qquad \text{(Eq. 6)}$$

where A_0 is the initial exposed area of the disk (when t = 0) and is usually very small[7], and A_T is the final exposed area of the disk. The A_T value was almost always the total area of the disk surface (132.73 mm²); but with a sublimed coating of stearone at 0.565 mg/cm², A_T was 85.9% of this value. If G, dc/dt, and dV/dt are constant, Eq. 5 indicates that dt/dA will be constant. The reciprocal, dA/dt, will also be constant, and Eq. 6 becomes:

$$T = \frac{dt}{dA}\int_{A_0}^{A_T}dA = \frac{dt}{dA}[A]_{A_0}^{A_T} \qquad \text{(Eq. 7)}$$

$$\therefore T = (A_T - A_0)/\frac{dA}{dt} \qquad \text{(Eq. 8)}$$

Thus, the time taken to remove the coating partially or completely can be calculated, as shown in Table I. This approach can be applied to the present results, since dA/dt calculated from Eq. 5 was constant. This is true because the flow rate, dV/dt, was constant, the intrinsic dissolution rate, G, was assumed to be constant, and dc/dt was found to be constant, since experiments indicated that c was a linear function of time.

Support for the hypothesis, expressed previously in postulates (a) and (b), is provided by the results for sublimed coatings of stearone (0.281 mg/cm² and 0.565 mg/cm²) and solution coatings of stearic acid (0.298 mg/cm²). In these cases, there was excellent agreement between the time taken to remove the coating, calculated by the described method, and the experimentally observed time to reach a constant level of potassium chloride release (Table I). The latter time for other coatings was too long to be experimentally accessible.

The thickest coating of sublimed stearone (Table I) resulted in a practically constant dissolution rate, which was lower than that for

[7] Values of A_0 can be obtained by applying Eqs. 1 and 3 at zero time:

$$A_0 = \frac{1}{G}\left(\frac{dm}{dt}\right)_0$$

where:

$$\left(\frac{dm}{dt}\right)_0 = c_0\frac{dV}{dt}$$

c_0 being the initial concentration of dissolved potassium chloride and $(dm/dt)_0$ being the initial dissolution rate (Table I).

the uncoated disk, suggesting the presence of a residual coating which was difficult to remove. Because of limitations of the duration of the experiment and differing loss of material, it may not always be possible to arrive at this simple result. The other types of results obtained were a continuous linear change, shown in Fig. 6 for solution coatings of stearic acid, and two distinct linear regions, shown in Fig. 7 for sublimation coatings of the pyrolysis product of magnesium stearate. The former result implies that the area available for dissolution increases in a linear manner with time.

The present experiments were unable to show whether the coating is removed by dissolution or erosion ("undermining" of the coating by the dissolution of the potassium chloride beneath it). The two distinct rates of dissolution (Fig. 7) suggest the removal of materials with differing affinities for the substrate. The rate of change of area, dA/dt, and the time, T, taken to remove the coating (Table I) were calculated for these different systems because they provide a means of comparing the relative effects of the coatings and methods of applying them.

Comparison of the results in Table I clearly shows that the sublimed coating of the pyrolysis product of magnesium stearate produced the greatest reduction in dissolution rate. Since this system is associated with the lowest rates of exposure of surface, it apparently exhibits the greatest attraction between surface and coating material. This finding could be attributed to the process of sublimation or to the formation of a mixed coating. Because other sublimed coatings are not always strongly attached, the latter suggestion seems to be more satisfactory.

In general, irrespective of the type of material or coating process (Table I), the thicker the coat the smaller was the initial exposed area, A_0, and the smaller was the rate of increase in exposed area with time (dA/dt), as expected. The major exception to this rule was provided by the differing thicknesses of sublimed coatings of stearone, where the thickest coat had the largest initial exposed area, A_0, and the intermediate coating had the greatest rate of exposure, dA/dt. The coatings were composed of aggregates of globules (Fig. 5). Increasing the amount deposited by sublimation increased the size of these aggregates and the number of individual globules attached to the surface. Thus, a thicker coating can provide a greater resistance to the flow; although thicker coatings of sublimed stearone had smaller initial effects on the dissolution processes than did thinner coatings, they had greater sustained effects.

Table I shows that, after 120 sec, during the later stages of the test, the thicker the coat the lower were the dissolution rate and the exposed area. Hence, a fraction of these sublimed coatings appears to be tenaciously held to the surface, this quantity increasing with the amount of coating applied. Consequently, the attachment of the hydrophobic layers to the ionic substrate is of fundamental importance in determining how the dissolution process is affected.

CONCLUSIONS

The reduction in the dissolution rate of nondisintegrating potassium chloride in a flowthrough system, brought about by hydrophobic coating, is controlled primarily by the force of attachment of the coating to the surface. The results can be explained by assuming that: (*a*) the intrinsic dissolution rate of potassium chloride, which is not coated, does not change; and (*b*) the hydrophobic material reduces to zero the dissolution rate of the hydrophilic material it covers. The changes in dissolution rate are, therefore, a measure of the changes in the surface area not coated.

REFERENCES

(1) D. Ganderton, *J. Pharm. Pharmacol.*, **21**, 219S(1969).

(2) J. C. Samyn and W. Y. Jung, *J. Pharm. Sci.*, **59**, 169(1970).

(3) G. Levy and R. Gumtow, *ibid.*, **52**, 1039(1963).

(4) H. C. Caldwell, *ibid.*, **63**, 770(1974).

(5) G. Rowley and J. M. Newton, *J. Pharm Pharmacol.*, **22**, 966(1971).

(6) J. V. Fee, D. J. W. Grant, and J. M. Newton, *J. Pharm. Sci.*, **65**, 48(1976).

(7) T. H. Easterfield and C. M. Taylor, *J. Chem. Soc.*, **99**, 2298(1911).

ACKNOWLEDGMENTS AND ADDRESSES

Received September 30, 1974, from the *Department of Pharmacy, University of Nottingham, University Park, Nottingham, NG7 2RD, England.*

Accepted for publication May 2, 1975.

The authors are grateful to Mr. L. Green and to the Wolfson Institute of Interfacial Technology, Nottingham University, for the preparation of the electron scanning photomicrographs and to the Sheffield Regional Hospital Board for providing financial support to Miss J. Valerie Fee.

* Present address: Royal Infirmary of Edinburgh, Lauriston Place, Edinburgh, EH3 9YW, Scotland.

[x] To whom inquiries should be directed.

GLC Identification and Determination of 3,4-Methylenedioxyamphetamine (MDA) from Plasma and Urine

K. K. MIDHA ˣ, I. J. McGILVERAY, S. P. BHATNAGAR, and J. K. COOPER

Abstract □ A GLC method for qualitative and quantitative determination of 3,4-methylenedioxyamphetamine in biological fluids is described. After extraction of the drug and the internal standard, 4-methoxyamphetamine, from plasma and urine, the solvent is evaporated and the residue is mixed with 20 μl of freshly distilled ether. Aliquots (1–2 μl) then are injected into the gas chromatograph. Both the drug and the internal standard give well-separated symmetrical peaks. Flame-ionization detection allows concentrations of 0.125 μg of 3,4-methylenedioxyamphetamine from plasma to be determined with a precision of 3.16%. The method is applicable to the estimation of 4-methoxyamphetamine, employing 3,4-methylenedioxyamphetamine as the internal standard. For identification purposes, various derivatives such as Schiff bases, isothiocyanates, trifluoroacetates, and heptafluorobutyrates of both compounds were formed following extraction from urine and their GLC behavior was investigated. Derivative formation was confirmed by GLC–mass spectrometry. Mass spectral data for these derivatives are presented.

Keyphrases □ 3,4-Methylenedioxyamphetamine—GLC analysis, mass spectrum, plasma and urine, human, dog □ 4-Methoxyamphetamine—GLC analysis, mass spectrum, plasma and urine, human, dog □ GLC—analysis, 3,4-methylenedioxyamphetamine and 4-methoxyamphetamine, plasma and urine, human, dog

3,4-Methylenedioxyamphetamine (MDA) (I) is chemically related to both mescaline and amphetamine. Some investigators found that the drug possesses stimulant and minor sympathomimetic activity; I inhibited monoamine oxidase (1) and increased muscular rigidity in a patient with Parkinson's disease (2). It was evaluated as an adjunct to psychotherapy (3), and another study (4) compared the subjective effects of I with those of amphetamine.

Because of the widespread abuse of I on the street (under such names as Mellow Drug of America, Love Drug, Love Pill, or MDA), it was felt that there was a need for its toxicological identification and quantitative estimation from biological fluids such as urine and plasma. A literature review on the analysis of this drug showed only one published method (5), which lacks details for quantitation from biological fluids. The present paper describes a GLC procedure for the positive identification and quantitation of I from plasma and urine.

Table I—Recovery of I and II from Plasma Determined by GLC Assay[a]

Micrograms Added to 1 ml of Plasma	Mean Micrograms Recovered	Mean Percent Recovery	*SD* of Percent Recovery
I			
1.04	1.00	99.72	2.19
4.00	4.04	100.86	0.96
Mean 100.29 ± 1.15%			
II			
1.0	1.01	100.24	1.23
4.0	4.02	100.42	1.36
Mean 100.30 ± 0.62%			

[a] $n = 4$.

Table II—Estimation of I Added to Plasma by GLC

I Added, μg	*n*	Mean Peak Height Ratio	*SD*	*CV*, %[a]
0.125	6	0.053	0.002	3.16
0.250	6	0.107	0.003	2.54
0.50	4	0.206	0.006	2.83
1.0	4	0.406	0.002	0.53
2.0	4	0.820	0.012	1.47
4.0	4	1.663	0.046	2.76

[a] Mean $CV = 2.22\%$, $y = mx$, where $m = 0.415 \pm 0.004$, $r^2 = 1$.

EXPERIMENTAL

Reagents—Acetone[1], ethyl acetate[1], carbon disulfide[2], and ether[3] were distilled in glass prior to use. Heptafluorobutyric anhydride[4] and trifluoroacetic anhydride[4] were refluxed on phosphorus pentoxide for 3 hr before glass distillation. The I[5], II[5], *dl*-amphetamine[5], methamphetamine[5], and *n*-propylamphetamine[5] were donated. Pyridine[4] was silylation grade, and all other chemicals employed were analytical grade.

Stock solutions of I (100 μg/ml) and the internal standard, 4-methoxyamphetamine (II) (100 μg/ml), were prepared fresh weekly by dissolving their hydrochloride salts in water. Appropriate dilutions of each were made fresh daily as required.

Plasma Level Study—3,4-Methylenedioxyamphetamine hydrochloride, 10 mg/kg, was administered to a male dog weighing 8.38 kg. Samples of blood (10 ml) were withdrawn from the femoral vein by means of heparinized tubes[6] at 12 appropriate time intervals. The blood samples were centrifuged, and the plasma was transferred to another tube before storing at −10°.

General Procedure for Extraction of I—To the sample [human or canine plasma (2 ml) or urine (5 ml) spiked with I or biological fluids from dosed animals], placed in screw-capped[7] cen-

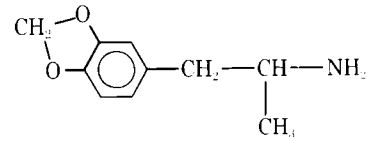

I

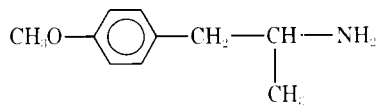

II

[1] Caledon Laboratories Ltd., Georgetown, Ontario, Canada.
[2] Fisher Scientific Co., Montréal, Québec, Canada.
[3] Mallinckrodt Chemical Works Ltd., Montréal, Québec, Canada.
[4] Pierce Chemical Co., Rockford, Ill.
[5] Dr. Keith Bailey, Pharmaceutical Chemistry Division, Drug Research Laboratories, Health Protection Branch, Ottawa, Canada.
[6] Vacutainers, Becton Dickinson and Co., Mississauga, Ontario, Canada.
[7] Lined with Teflon (du Pont).

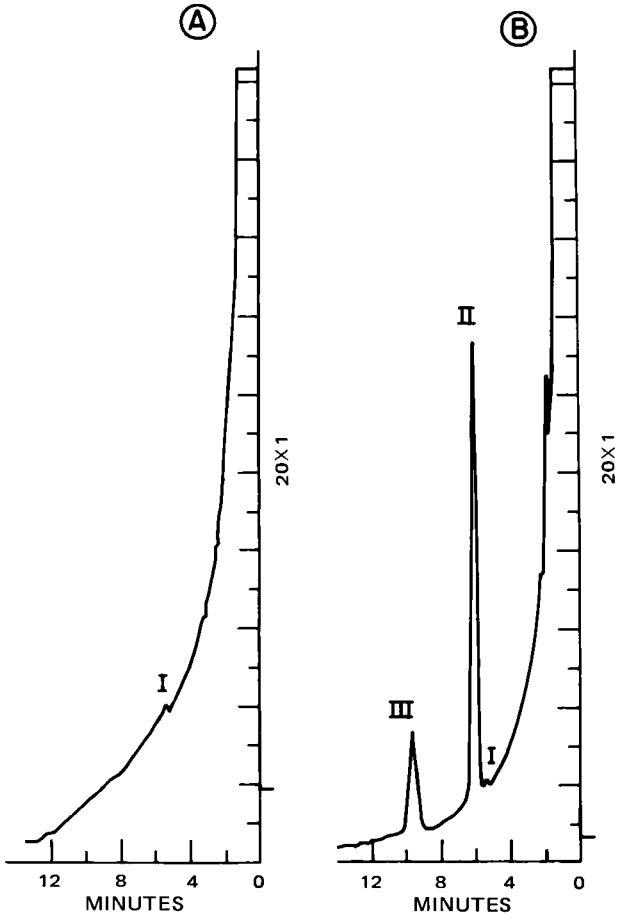

Figure 1—*Gas-liquid chromatogram of human plasma. Key: A, control plasma; B, plasma spiked with I (0.5 μg/ml) and II (3.0 μg/ml); peak I, endogenous material; peak II, II; and peak III, I.*

trifuge tubes (20 ml), are added 1 ml of II (3.0 μg/ml), 5 ml of 0.2 *M* phosphate buffer (pH 7.2), 1 ml of 1 *N* HCl, and 5 ml of ether. The sample is extracted by mixing[8] for 5 min at 40 rpm, followed by centrifugation at 3000 rpm for 5 min. The ethereal layer is removed by aspiration, and the extraction is repeated with another 5 ml of ether.

Following centrifugation, the ethereal layer is discarded and an aliquot of the aqueous layer is transferred (8 ml for plasma and 11 ml for urine) into another similar centrifuge tube containing 2 ml of 1 *N* NaOH. The sample is extracted with 6 ml of ether by mixing as before for 10 min at 40 rpm, followed by centrifugation at

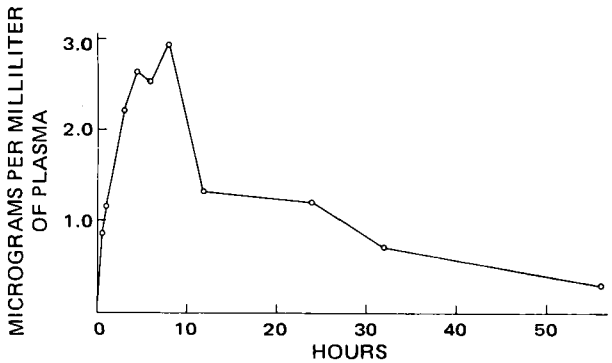

Figure 2—*Plasma concentration of I in a dog weighing 8.38 kg following a single oral dose of I-HCl (10 mg/kg).*

[8] Roto-Rack, Fisher Scientific Co., Montréal, Québec, Canada.

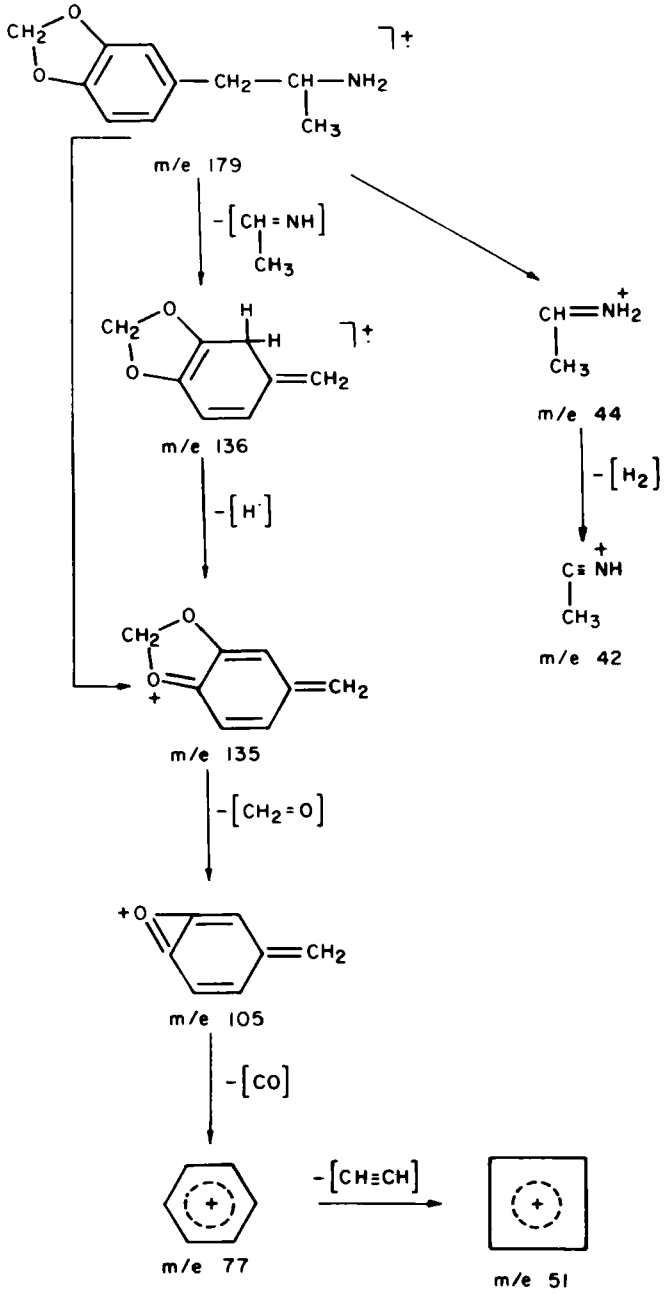

Scheme I—Postulated fragmentation of I

3000 rpm for 5 min. Five milliliters of the ethereal layer is transferred into a custom-made evaporating tube (6) containing a small antibumping granule[9].

The extraction is repeated as before with another 6 ml of ether. Six milliliters of the ethereal layer is removed and combined with the first extract. The combined extracts are concentrated[10] under a stream of dry nitrogen at 40° to a volume of approximately 20–30 μl. Aliquots (1–2 μl) then are injected into the gas chromatograph[11] equipped with a flame-ionization detector.

Derivatization—*Acetone Schiff Bases and Isothiocyanate Derivatives*—To the concentrated ethereal extracts from plasma or urine is added 0.5 ml of acetone (for Schiff base) or carbon disulfide (for isothiocyanate). The tubes are swirled on a mixer[12] for 30 sec and then concentrated to 50 μl at 60° under a stream of dry ni-

[9] British Drug House, Toronto, Ontario, Canada.
[10] Thermolyne Dri-Bath, Fisher Scientific Co., Montréal, Québec, Canada.
[11] Model F/11, Perkin-Elmer, Montréal, Québec, Canada.
[12] Vortex Genie, Fisher Scientific Co., Montréal, Québec, Canada.

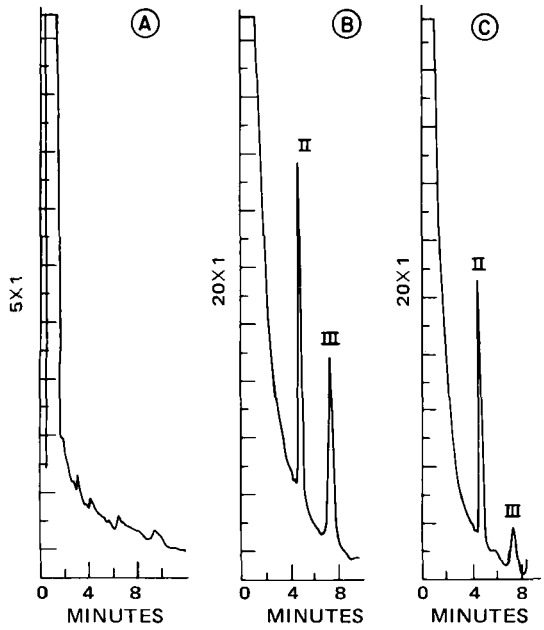

Figure 3—*Gas–liquid chromatogram of dog plasma. Key: A, control plasma; B, control plasma spiked with I (2.0 μg/ml) and II (5.0 μg/ml); C, plasma (12 hr) from a dog given 10 mg/kg po of I-HCl containing I (1.32 μg/ml) and II (5.0 μg/ml); peak II, II; and peak III, I.*

trogen. Aliquots (1–2 μl) are injected into the gas chromatograph[13].

Heptafluorobutyrate Derivatives—To dried ethereal extracts from plasma or urine are added 100 μl of freshly distilled ethyl acetate and 50 μl of heptafluorobutyric anhydride. The tubes are stoppered tightly, swirled on a mixer[12] for 30 sec, and then incubated at 60° for 1 hr. Concentrated ammonium hydroxide (0.5 ml) is added, and the mixture is extracted with 2.5 ml of glass-distilled benzene. The benzene extract is concentrated to 50 μl under a stream of dry nitrogen at 60°, and aliquots (1–2 μl) then are injected into the gas chromatograph[13].

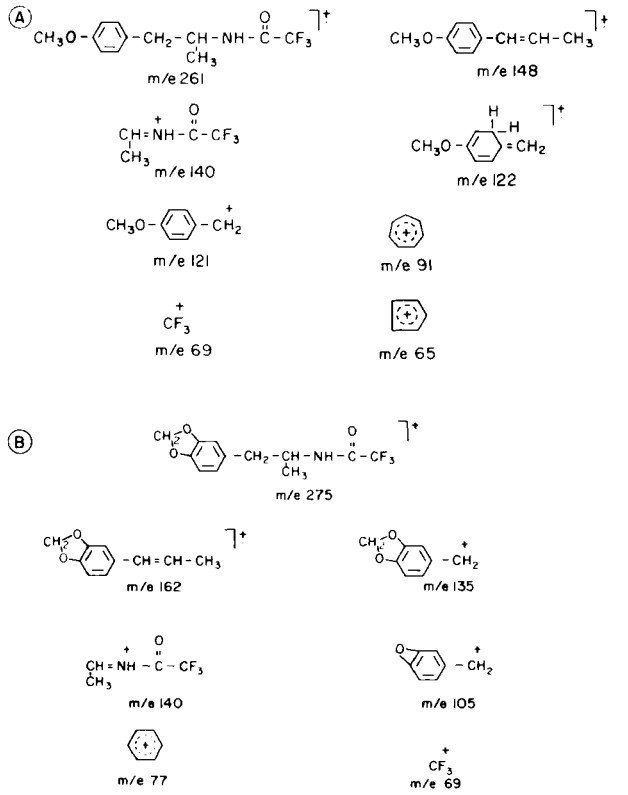

Scheme II—Postulated fragmentations of trifluoroacetyl derivatives of II (A) and I (B)

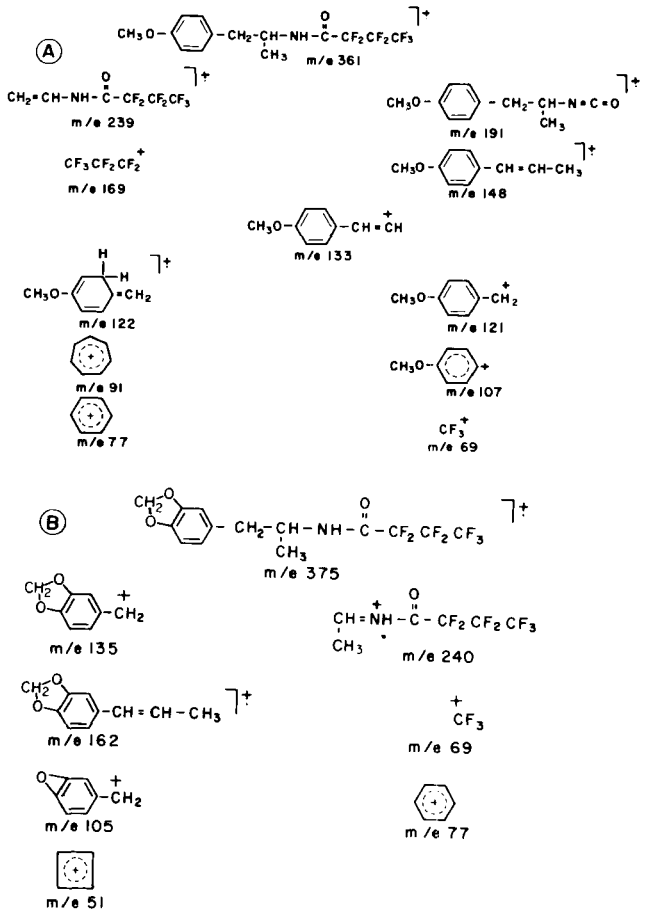

Scheme III—Postulated fragmentations of heptafluorobutyryl derivatives of II (A) and I (B)

Trifluoroacetyl Derivatives—Dried ethereal extracts were treated in the same manner as described for heptafluorobutyrate derivatives, except that trifluoroacetic anhydride was used instead of heptafluorobutyric anhydride.

GLC—GLC was effected on two gas chromatographs[11,13], both equipped with flame-ionization detectors. System I[11] consisted of a glass column, 1.8 m × 0.3 cm (6 ft × 0.125 in.) i.d. It was packed with saturated hydrocarbon lubricant[14] (20%) along with potassium hydroxide (10%) on acid-washed, dimethyldichlorosilane-treated, high performance flux-calcined diatomite support[15] (80–100 mesh).

The column was conditioned for 20 hr at 290° (oven) with a low nitrogen flow. The conditions of analysis for the assay were: column oven temperature, 190°; injection port temperature, 250°; and detector block temperature, 240°. The carrier gas was nitrogen at a flow rate of 60 ml/min. The hydrogen and compressed air were adjusted to give maximum response.

System II[13] consisted of a glass column, 1.8 m × 0.25 cm (6 ft × 0.10 in.) i.d., silanized with a 5.0% solution of trimethylchlorosilane[16] and hexamethyldisilazane[16] (1:1) in ether. It was packed with 5.0% phenylmethyldimethyl silicone[17] coated on acid-washed, dimethyldichlorosilane-treated, high performance flux-calcined diatomite support[15]. The column was conditioned by injecting a silylating mixture[18] (25 μl) and maintaining the column at 300° for 18 hr under low nitrogen flow. The injection port temperature and

[13] Model 3920, Perkin-Elmer, Montréal, Québec, Canada.

[14] Apiezon-L, Apiezon Products Ltd., 8 York Road, London, England.

[15] Chromosorb W, Chromatographic Specialties, Brockville, Ontario, Canada.

[16] Chromatographic Specialties, Brockville, Ontario, Canada.

[17] OV-7, Chromatographic Specialties, Brockville, Ontario, Canada.

[18] Silyl-8, Pierce Chemical Co., Rockford, Ill.

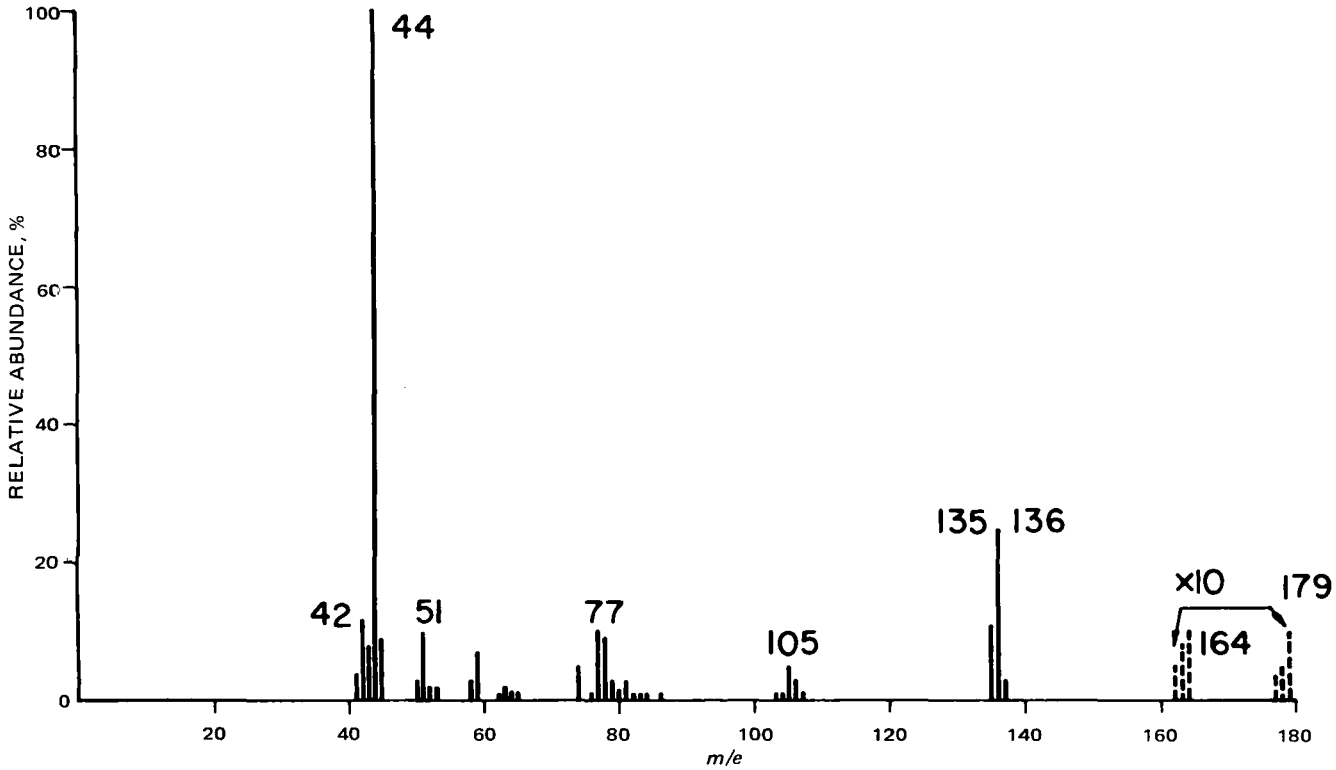

Figure 4—*GLC–mass spectra of I (peak III, Fig. 3C).*

detector block temperature were 240 and 230°, respectively. The oven temperatures employed ranged from 170 to 200°. Nitrogen was the carrier gas at a flow rate of 63 ml/min. Hydrogen and compressed air were adjusted to give maximum response.

Calculations—Peak height ratios were calculated by dividing the height of the peak due to I by the height of the peak due to II. Calibration curves were constructed from the results of spiked control plasma samples by plotting the concentration of I in micrograms per milliliter against the respective peak height ratios.

RESULTS AND DISCUSSION

Figure 1A shows a typical chromatogram obtained by processing control blank human plasma, as described in the general procedure, in which the internal standard II was omitted. The extraction procedure provided a relatively clean chromatogram, with only one extraneous peak from endogenous material in plasma with a retention time of 5.6 min (peak I, Fig. 1A). A chromatogram obtained when the method was applied to spiked human plasma containing 0.5 μg of I and 3.0 μg of II is shown in Fig. 1B; it is clear that the extraneous peak I did not interfere with the peak of II (6.04 min) or I (peak III, 9.6 min). An analysis time of 10 min was achieved.

The response of the flame-ionization detector was linear with concentrations in the 0.125–4.0-μg/ml range. The peak height ratio

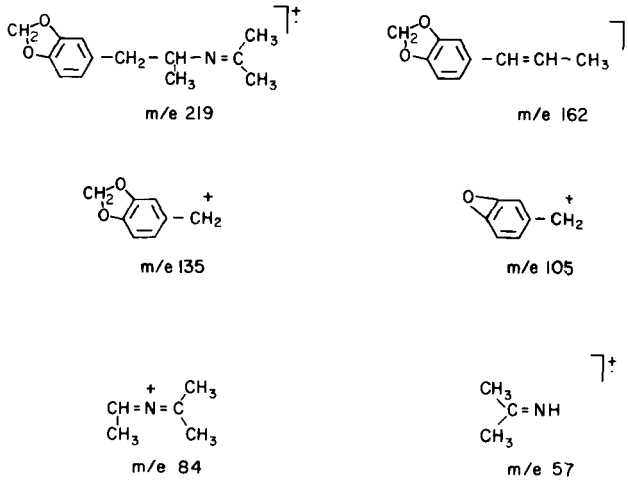

Scheme IV—Postulated fragmentations of Schiff base of I

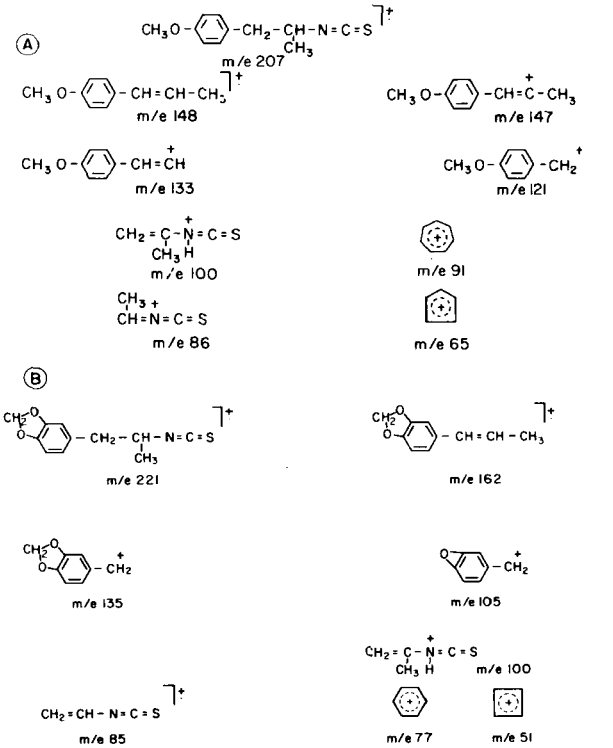

Scheme V—Postulated fragmentations of the isothiocyanate derivatives of II (A) and I (B)

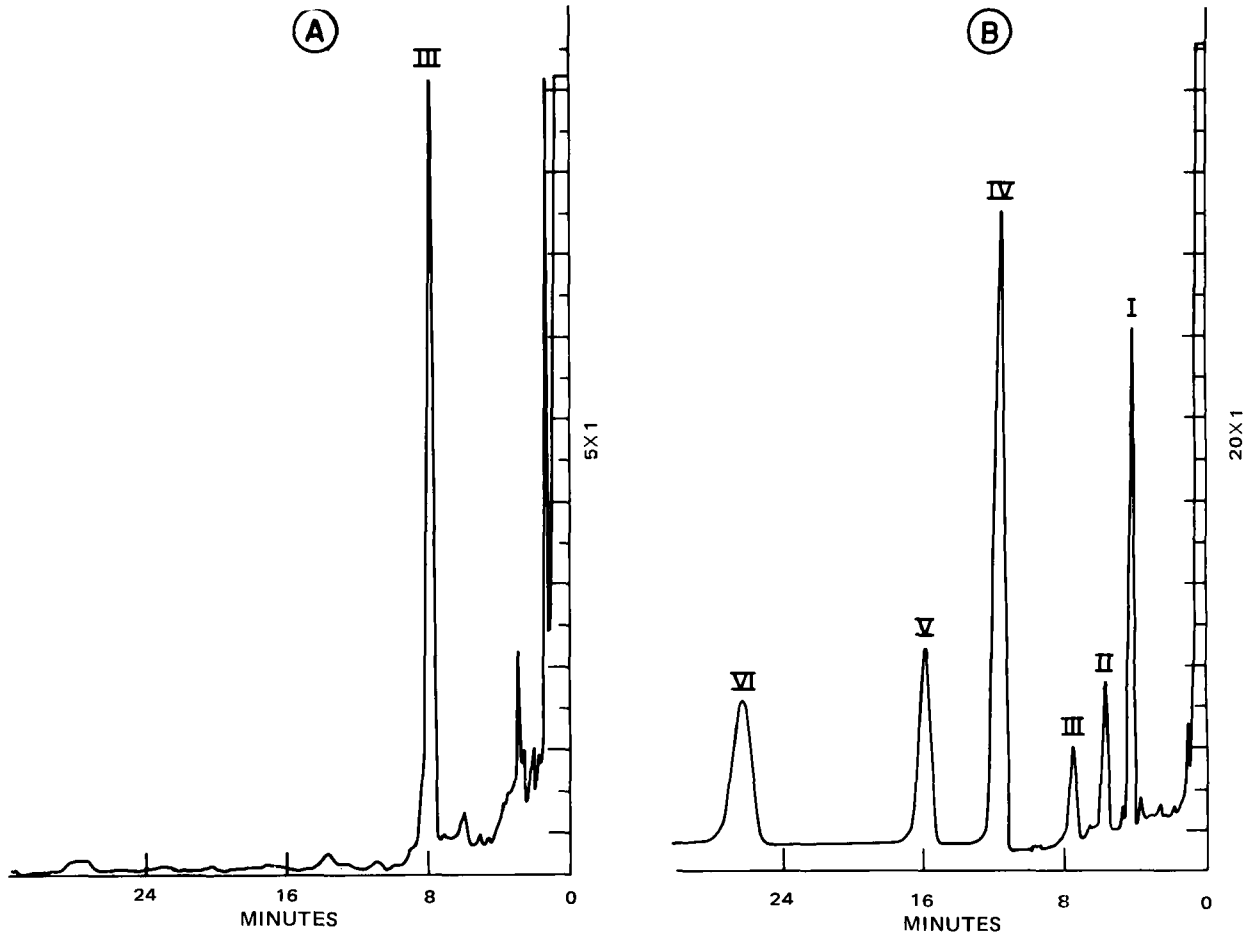

Figure 5—*Gas-liquid chromatograms of human urine extracts. Key: A, control urine; B, control urine spiked with* dl-*amphetamine, methamphetamine,* n-*propylamphetamine, II, and I; peak I,* dl-*amphetamine; peak II, methamphetamine; peak III, endogenous material; peak IV,* n-*propylamphetamine; peak V, II; and peak VI, I.*

of I and II was used as the index of the detector performance and overall efficiency of the analytical procedure. The overall recoveries of I and II from plasma were about 100.29 ± 1.15 and 100.30 ± 0.64%, respectively (Table I).

The accuracy and precision of the GLC assay for I are demonstrated in Table II. Results are based on at least four determinations of each I concentration, ranging from 0.125 to 4.0 μg/ml, which were treated as described in the general procedure. The overall coefficient of variation was 2.22%. The calibration curve obtained by plotting the peak height ratio of I–II *versus* the concentration of I was linear ($y = mx$) in the concentration range of 0.125–4 μg of I/ml of plasma and passed through the origin. A mean slope value of 0.415 ± 0.004 ($r^2 = 1$) was obtained.

Application of this method is demonstrated in Fig. 2. A 10-mg/kg dose of I-HCl was given orally to a dog (8.4 kg), and plasma was withdrawn at intervals over 56 hr and analyzed for I by the described GLC procedure. No interference was observed from the endogenous materials in dog plasma (Fig. 3). Retention times for I and II were slightly shorter due to a change in the carrier gas pressure.

To confirm that I and II were being measured in the dog study and not any endogenous materials from plasma, plasma extracts from the dog were pooled together and injected into the gas chromatograph. Mass spectra[19] were obtained for peaks III and II (Fig. 3C). The normalized mass spectrum of the compound giving rise to peak III is shown in Fig. 4. Structures for the molecular ion at *m/e* 179, the base peak at *m/e* 44, and other abundant ions at *m/e* 136, 135, 105, 77, 51, and 42 are postulated in Scheme I. The mass spectrum of the compound giving rise to peak II (Fig. 3C) was identical to that of synthetic II (7). These observations confirm that intact I

[19] Perkin-Elmer model 900 gas chromatograph attached to a Hitachi Perkin-Elmer model RMSU mass spectrometer through a jet-separator.

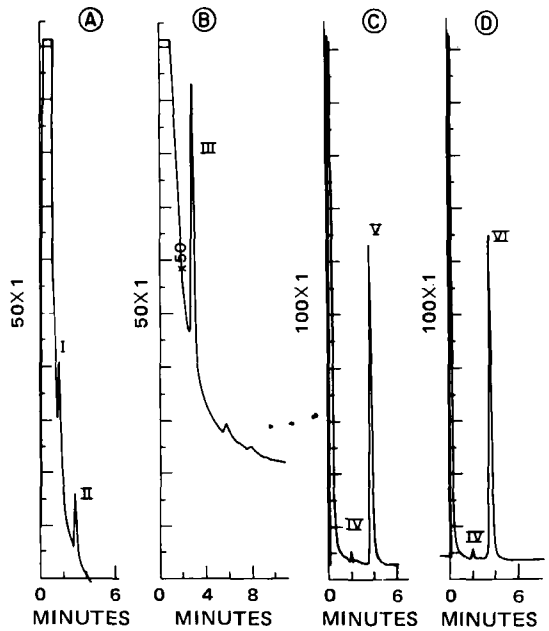

Figure 6—*Gas-liquid chromatograms of trifluoroacetyl and heptafluorobutyryl derivatives of I and II. Key: A, trifluoroacetyl derivative of I; B, heptafluorobutyryl derivative of I; C, trifluoroacetyl derivative of II; D, heptafluorobutyryl derivative of II; peak I, I; peak II, trifluoroacetyl derivative of I; peak III, heptafluorobutyryl derivative of I; peak IV, II; peak V, trifluoroacetyl derivative of II; and peak VI, heptafluorobutyryl derivative of II.*

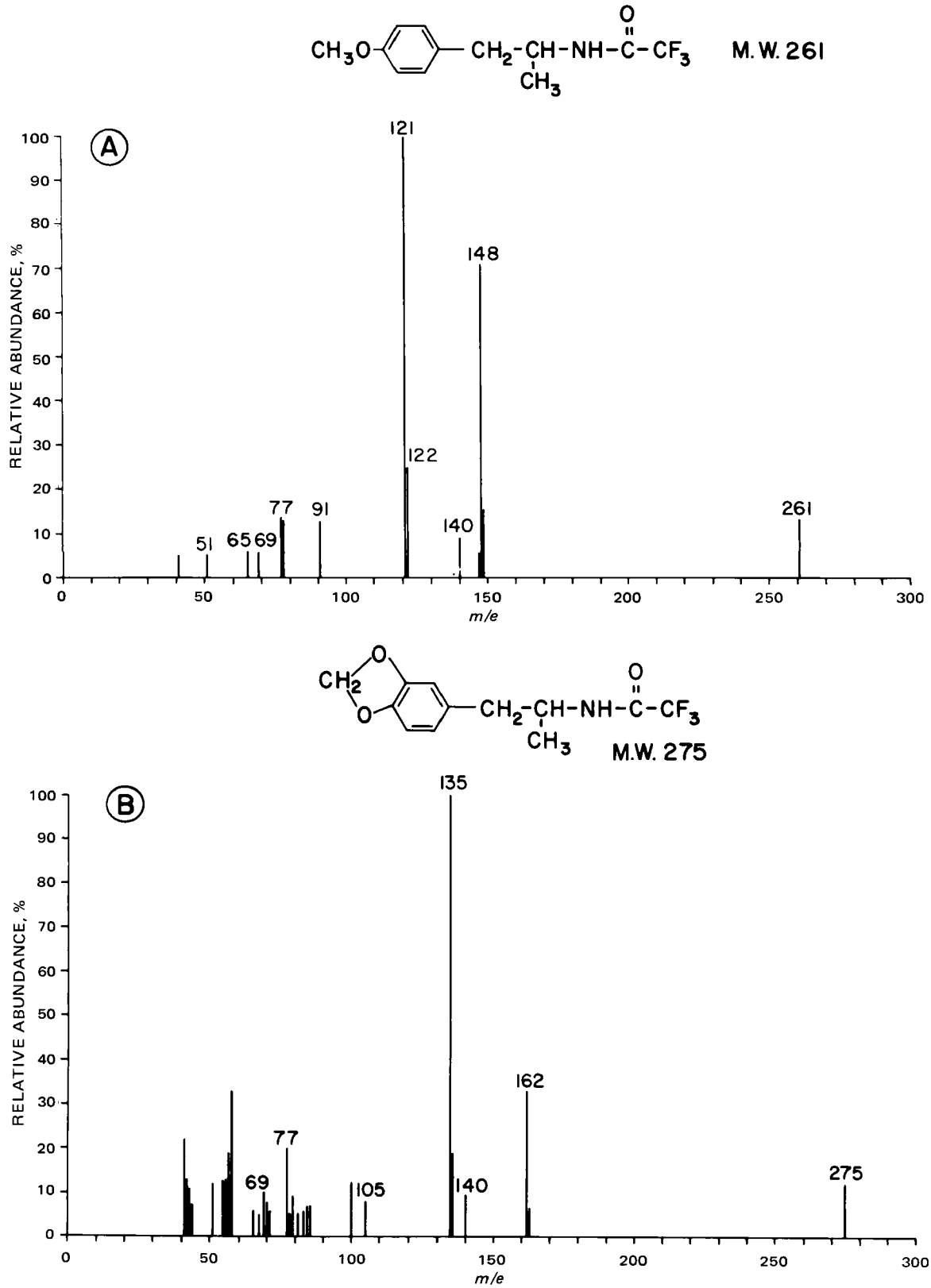

Figure 7—*GLC–mass spectra of trifluoroacetyl derivatives of II (A) and I (B).*

and II, devoid of any plasma interference, are measured in this assay.

The described GLC procedure is also applicable to the estimation and identification of *dl*-amphetamine[5], *N*-methylamphetamine[5], *n*-propylamphetamine[5], I, and II from human urine (Fig. 5). Blank control urine spiked with these compounds was processed according to the procedure given under *Experimental* and analyzed on chromatographic System I with a column oven temperature of 160°. The extraneous peak III (retention time 7.60 min, Fig. 5A) from urine did not interfere with the peaks due to *dl*-amphetamine, *N*-methylamphetamine, *n*-propylamphetamine, II, and I, *i.e.*, peaks I, II, IV, V, and VI, respectively (Fig. 5B). Any

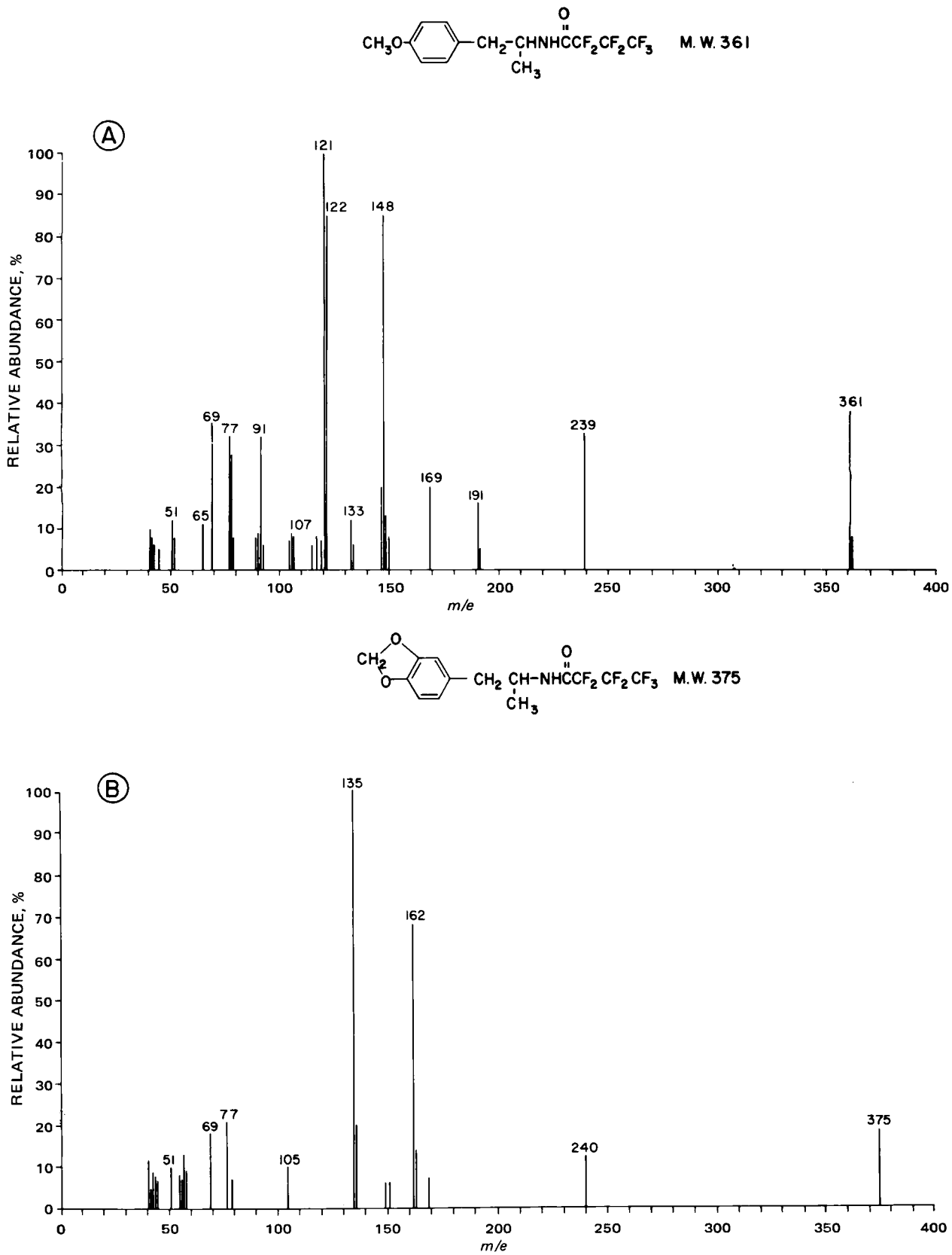

Figure 8—*GLC–mass spectra of heptafluorobutyryl derivatives of II (A) and I (B).*

of these compounds can be estimated in urine by choosing an internal standard. For quantitative analysis of I, II was chosen as the internal standard. The column oven temperature (System I) was raised to 190° to shorten analysis time to 10 min.

Fluoroacyl derivatives formed from trifluoroacetic and heptafluorobutyric anhydrides give good electron-capture response and have been used in the quantitative analysis of amphetamines and their metabolites in rat brain (8) and in biological fluids (9–11) at the nanogram level. However, use of these derivatives has not been explored in the qualitative or quantitative analysis of II and I. In

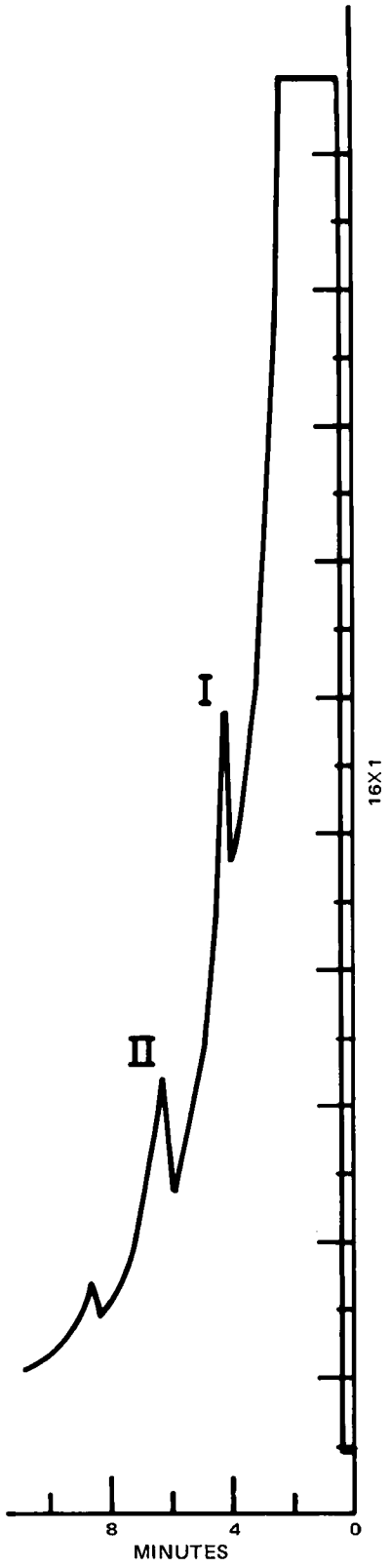

Figure 9—*Gas–liquid chromatogram of heptafluorobutyrates of II (2.5 ng/ml) and I (2.5 ng/ml) with electron-capture detector. Key: peak I, heptafluorobutyrate derivative of II; and peak II, heptafluorobutyrate derivative of I. The conditions were: glass column, 1.8 m × 2 mm i.d. packed with OV-7 on Chromosorb W (80–100 mesh); pulse, 3.5; nitrogen purge gas, 20 ml/min; electron-capture detector temperature, 310°; oven temperature, 165°; and injection port temperature, 220°.*

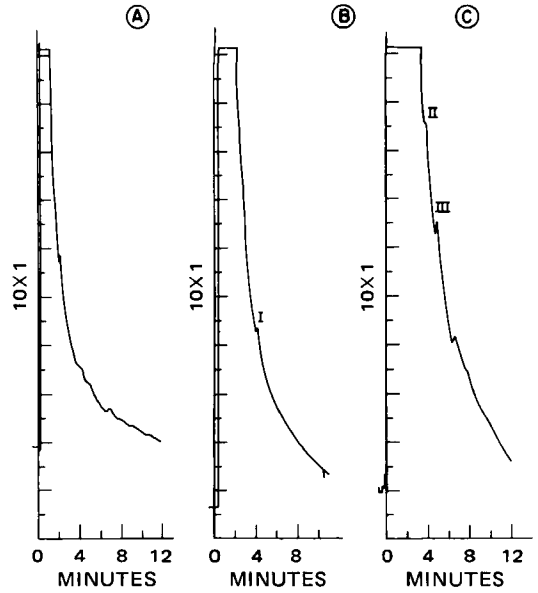

Figure 10—*Gas–liquid chromatograms of Schiff bases of II and I from human urine extract. Key: A, control urine; B, control urine spiked with II (0.25 μg/ml); C, control urine spiked with I (0.25 μg/ml); peak I, Schiff base of II; peak II, I; and peak III, Schiff base of I.*

the present study, these derivatives of II and I were formed and their GLC behavior was examined.

Figure 6 shows the trifluoroacetyl and heptafluorobutyryl derivatives of II and I on System II. The column oven temperature was 190°. The trifluoroacetate derivative of I (peak II, Fig. 6A) and the heptafluorobutyrate derivative of II (peak III, Fig. 6B) had retention times of 3.20 and 2.90 min, respectively. The trifluoroacetyl (peak V, Fig. 6C) and heptafluorobutyryl (peak VI, Fig. 6D) derivatives of II had retention times of 3.58 and 3.43 min, respectively, with a column oven temperature of 170° on System II. GLC–mass spectral[19] evidence of the formation of the trifluoroacetyl derivatives of II and I was obtained. Normalized mass spectra of trifluoroacetyl derivatives of II and I are shown in Figs. 7A and 7B. The molecular ion in each case is present, and other major ions are postulated for these derivatives in Scheme II. These ions indicate the formation of trifluoroacetyl derivatives of II and I.

Similarly, GLC–mass spectral[19] evidence for the formation of heptafluorobutyryl derivatives of II and I was obtained. Normalized mass spectra of these derivatives are shown in Fig. 8. The mass spectrum of the heptafluorobutyryl derivative of II (Fig. 8A) showed the molecular ion at *m/e* 361 and other major ions at *m/e* 239, 191, 169, 148, 122, 121, 107, 91, 77, 69, 65, and 51, indicative of

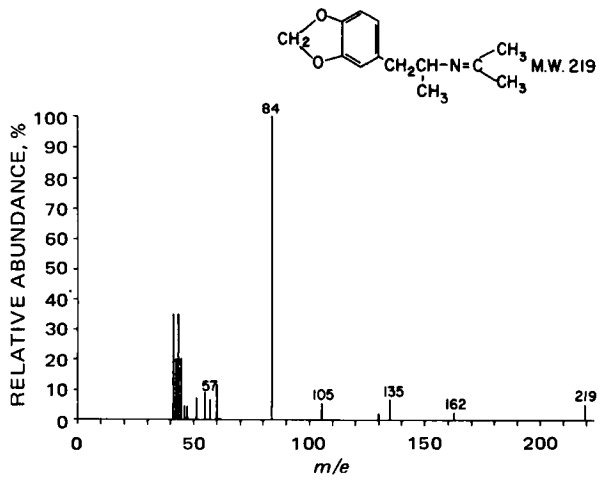

Figure 11—*GLC–mass spectra of Schiff base of I (peak III, Fig. 10C).*

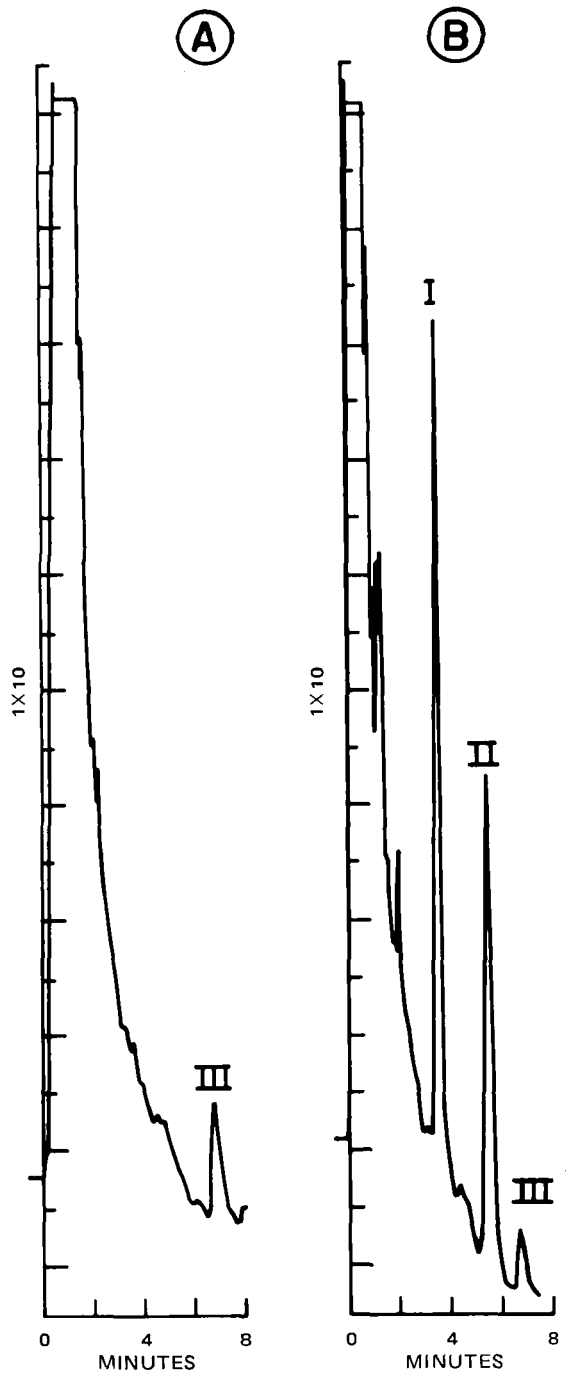

Figure 12—*Gas-liquid chromatograms of isothiocyanate derivatives of II and I from human urine extract. Key: A, control urine; B, control urine spiked with I and II (0.25 μg/ml of each); peak I, isothiocyanate derivative of II; peak II, isothiocyanate derivative of I; and peak III, endogenous material.*

the formation of the II derivative. Structures for these ions are postulated in Scheme IIIA. The heptafluorobutyryl derivative of I (Fig. 8B) also showed the molecular ion at *m/e* 375 and other diagnostic ions at *m/e* 240, 162, 135, 105, 77, 69, and 51. Postulated structures for these diagnostic ions are shown in Scheme IIIB, which confirm the formation of the heptafluorobutyryl derivative of I.

The heptafluorobutyryl derivatives showed tremendous electron-capture response. Levels as low as 1 ng can be detected and estimated. Figure 9 shows the chromatogram of 2.5 ng of I and II added to plasma, extracted according to the method of Walle and Ehrsson (11), and derivatized according to the details given under *Experimental*. By employing a ^{63}Ni-electron-capture detector in System II with a column oven temperature of 165°, 1–5 ng of II and I may be quantitated.

Qualitative identification of a substance in biological fluids by GLC is generally accompanied by comparison of its retention times after extraction from the fluids with those of the reference material on different columns. An alternative approach is to form derivatives of the unknown compound after extraction and to compare the retention times of similar derivatives of the reference material on the same column. For qualitative identification of II and I from urine, their Schiff bases and isothiocyanate derivatives were prepared after extraction from urine according to the method of Beckett *et al.* (12). Figure 10B shows urine spiked with II, and Fig. 10C shows urine spiked with I. No interference was observed from either I or II. System II was employed for chromatographic analysis with a column oven temperature of 180°. The Schiff bases for I and II had retention times of 6.65 (peak III, Fig. 10C) and 3.79 (peak I, Fig. 10B) min, again with System II with the oven at 180°. To confirm that the Schiff bases of I and II were formed (which would also afford conclusive proof of their presence in biological fluids), the mass spectrum of peak III (Fig. 10) was obtained[19]. The normalized mass spectrum of the compound giving rise to peak III is shown in Fig. 11. The molecular ion at *m/e* 221 and other major ions at *m/e* 185, 162, 105, 84, and 57 were present, consistent with formation of the Schiff base of I. Structures for these ions are postulated in Scheme IV. Similar confirmation of the formation of the Schiff base of 4-methoxyamphetamine was obtained.

Figure 12 shows the chromatograms of isothiocyanate derivatives of II (peak I, 3.38 min) and I (peak II, 5.43 min) along with that of blank control urine treated in the same manner as described under *Experimental*. Peak III (Fig. 12A) from endogenous material in blank control urine did not interfere with peaks due to isothiocyanate derivatives of II and I (peaks I and II) in System II with a column oven temperature of 200°. To confirm the formation of these isothiocyanate derivatives, eluates from the GLC column System II were fed directly into the mass spectrometer[19], and the mass spectra of compounds giving rise to peaks I and II were recorded (Fig. 13).

The mass spectrum of the isothiocyanate derivative of II (Fig. 13A) showed the molecular ion at *m/e* 207 and the base peak at *m/e* 121. Structures for other major ions at *m/e* 148, 147, 133, 100, 91, 86, and 65 are postulated in Scheme VA. The normalized mass spectrum of the isothiocyanate derivative of II is shown in Fig. 13B. Structures for the molecular ion at *m/e* 221, the base peak at *m/e* 135, and other major ions at *m/e* 162, 105, 100, 85, 77, and 51 are postulated in Scheme VB. These mass spectra indicate that isothiocyanate derivatives are formed and can aid in the identification of II and I from biological fluids.

The described GLC procedure is adequate for the qualitative as well as quantitative analysis of I from biological fluids. Formation of various derivatives of hallucinogenic amines, as well as the mass spectral behavior of these derivatives, aids in conclusive identification of these drugs of abuse. The procedure described gives high recoveries of these amines from biological fluids and is of sufficient sensitivity, using the conventional flame-ionization detector, to determine 0.125 μg of I/ml of plasma. The method is also applicable to quantitative estimation of II from biological fluids by using I as an internal standard. It can also be employed for estimating both I and II from biological fluids by using *n*-propylamphetamine as an internal standard. Analysis time with GLC is short (10 min), and multiple determinations can be performed on the same day.

REFERENCES

(1) P. J. G. Mann and J. H. Quastel, *Biochem. J.*, **34**, 414(1940).

(2) J. Loman, P. G. Myerson, and A. Myerson, *Trans. Amer. Neurol. Ass.*, **67**, 201(1941).

(3) C. Naranjo, A. T. Shulgin, and T. Sargent, *Med. Pharmacol. Exp.*, **17**, 359(1967).

(4) G. A. Alles, in "Neuropharmacology," H. A. Abramson, Ed., Josiah Macy, Jr. Foundation, New York, N.Y., 1959, pp. 181–268.

(5) G. Cimbura, *J. Forensic Sci.*, **17**, 329(1972).

(6) A. H. Beckett, *Dan. Tidsskr. Farm.*, **40**, 197(1966).

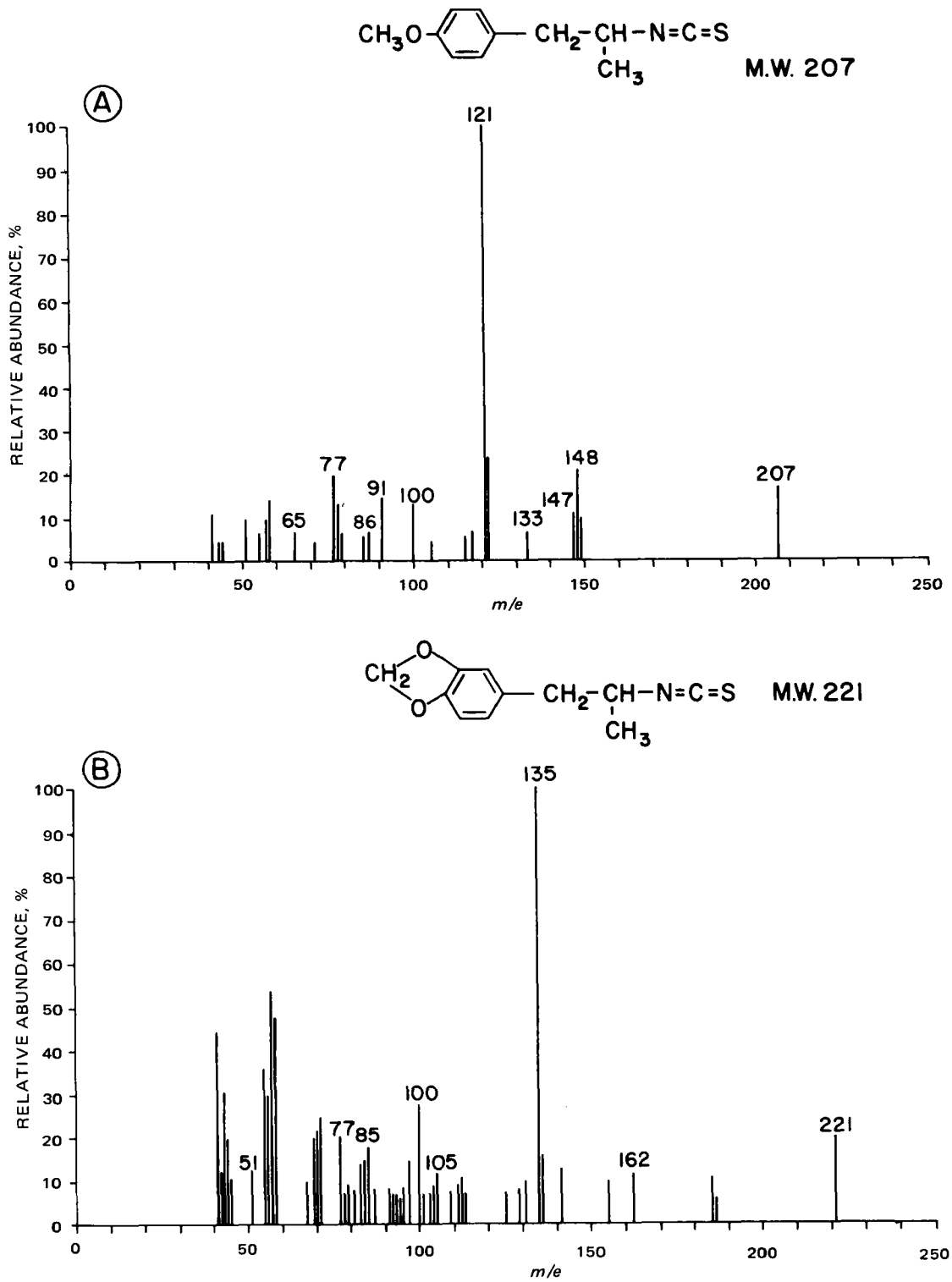

Figure 13—*GLC–mass spectra of isothiocyanate derivatives of II (A) and I (B).*

(7) A. H. Beckett and K. K. Midha, *Xenobiotica*, **4**, 297(1974).

(8) G. Belvedere, S. Caccia, A. Frigerio, and A. Jori, *J. Chromatogr.*, **84**, 355(1973).

(9) R. B. Bruce and W. R. Maynard, *Anal. Chem.*, **41**, 977(1969).

(10) E. Anggard, L.-M. Gunne, and F. Niklasson, *Scand. J. Clin. Lab. Invest.*, **26**, 137(1970).

(11) T. Walle and H. Ehrsson, *Acta Pharm. Suecica*, **8**, 27(1971).

(12) A. H. Beckett, G. T. Tucker, and A. C. Moffat, *J. Pharm. Pharmacol.*, **19**, 273(1967).

ACKNOWLEDGMENTS AND ADDRESSES

Received February 24, 1975, from the *Drug Research Laboratories, Health Protection Branch, Health and Welfare Canada, Ottawa, Ontario K1A OL2, Canada.*

Accepted for publication April 18, 1975.

Presented in part at the Drug Abuse Section, American Society for Pharmacology and Experimental Therapeutics, Montreal, 1974.

The authors acknowledge the excellent technical assistance of Miss I. Dupuis and thank Mr. Les Watts for veterinary help.

[x] To whom inquiries should be directed.

Quantitative Assessment of Factors Contributing to Mottling of Colored Tablets I: Manufacturing Variables

N. A. ARMSTRONG ˣ and G. A. MARCH *

Abstract □ By using a recently developed method for quantifying the degree of mottling of colored tablets, the effects of manufacturing variables such as the method and temperature of granule drying, granule size, and compaction pressure were investigated. Tablets of dibasic calcium phosphate colored with FD&C Blue No. 1 dye were used. Drying temperature had little effect, but the method of granule drying, granule size, and compaction pressure were major influences on mottling. Mechanisms to explain these results, based on the migration of dye during the drying process, are proposed.

Keyphrases □ Mottling—colored tablets, effects of method and temperature of granule drying, granule size, compaction pressure □ Calcium phosphate, dibasic—colored tablets, degree of mottling, effects of method and temperature of granule drying, granule size, compaction pressure □ Tablets, colored—degree of mottling, effects of method and temperature of granule drying, granule size, compaction pressure

Mottling, defined (1) as: "An unequal distribution of color on the surface of a tablet, with light or dark areas standing out in an otherwise uniform surface," has long constituted a problem to tablet manufacturers. It is now well established that mottling in tablets containing colored substrates is caused by the migration of dyes with the granulating fluid during drying. In the case of fluid-bed-dried granulations, this process results in the interior of the granule being deficient in coloring material while the dye is concentrated at the periphery. When, on subsequent comminution or compression, granule fragmentation occurs, the color deficiencies are exposed on the surface of the tablet.

King (2) surveyed the methods that have been suggested to reduce mottling. A critical review of these methods shows that many are vague in nature, with little or no experimental justification, and none is supported by quantitative evidence that mottling is reduced. However, a photographic method of quantitatively assessing mottling was published recently (3), and this technique has permitted a more critical approach to the problem of reducing mottling to an acceptable level.

EXPERIMENTAL

Tablet Preparation—Full details of the preparation of dibasic calcium phosphate tablets colored with FD&C Blue No. 1 were given elsewhere (3). Each tablet weighed 660 mg and, apart from tablets used in compaction pressure studies, each had a thickness of 4.00 mm.

The force exerted by the upper punch of the tablet press was measured with strain gauges using a technique similar to that described by Shotton and Ganderton (4).

Measurement of Tablet Mottling—Tablets were photographed under standard conditions, and the variation in optical density across the negative image of the tablet was measured using a microdensitometer[1]. Quantitation of this variation was made by the method of Armstrong and March (3), and the results are expressed in "mottling units."

RESULTS AND DISCUSSION

Effects of Granule Size and Method of Drying—At an early stage in the current investigation, it was noted that the size of the granules from which the tablets were prepared had an influence on the resultant color uniformity of the tablet. Furthermore, Scott *et al.* (5) drew attention to the fact that tablets prepared from granules dried in a fluid bed drier are less mottled than tablets prepared from granules of the same composition but subject to tray drying.

Figure 1 shows that for both methods of drying, the degree of tablet mottling was decreased as the granule size was reduced. In the case of fluid-bed-dried granules, tablets of acceptable color uniformity could be produced from granules of less than 0.48-mm diameter. In contrast, tablets prepared from tray-dried granules of the same size were severely mottled. [Visual correlation of these tablets with their mottling values was presented previously (3).]

During drying, migration of dye to the granule periphery leaves the granule interior color deficient, and the granule exterior contains an excess of colorant. The larger the granule, the greater is the volume to surface area ratio; therefore, the color density at the surface of large granules would be expected to be greater than that at smaller granules. Furthermore, in large granules, the color-deficient interior is larger in volume and more easily discernible after compaction.

The difference between the mottling of tray- and fluid-bed-dried granules can be attributed to two factors. First, during the fluid bed drying process, each granule is discrete and, although migration within each granule can occur, intergranular dye migration is not possible. However, severe intergranular migration can occur during tray drying, resulting in a high concentration of the colorant at the surface of the granule bed, with the bulk of material being devoid of colorant. This subsequently results in intensely colored specks on the tablet surface. Second, the interior of each fluid-bed-dried granule is completely covered by its peripheral layer of dye and, since the granules are not comminuted before compression, the dye-deficient material is only partially revealed when the granules are tableted. Chavkin (6) suggested that colorant migration in tray drying can be reduced by agitation of the granule bed, but only an intensity of agitation sufficient to prevent intergranular migration would produce the same level of mottling as is found in fluid-bed-dried granules.

The described tablets were made from relatively monosized systems, apart from the addition of lubricant. If tablets are made from granules exhibiting a range of sizes, mottling on the surface of the tablet compressed by the upper punch is greater than that on the other face. This result is attributed to granule segregation in the die (7), resulting in the lower portion of the tablet being composed of smaller granules than the upper. This result is especially noticeable at relatively low compaction pressures when granule integrity is largely retained.

Effect of Drying Temperature on Tablet Mottling—Both tray- and fluid-bed-dried granules were dried at 25 and 60°, followed by compression. The results (Table I) show the effect of drying temperature on the degree of mottling. It was reported that tablet mottling can be reduced by lowering the drying tempera-

[1] Joyce-Loebl microdensitometer Mark III C.S., Joyce Loebl and Co. Ltd., Gateshead, United Kingdom.

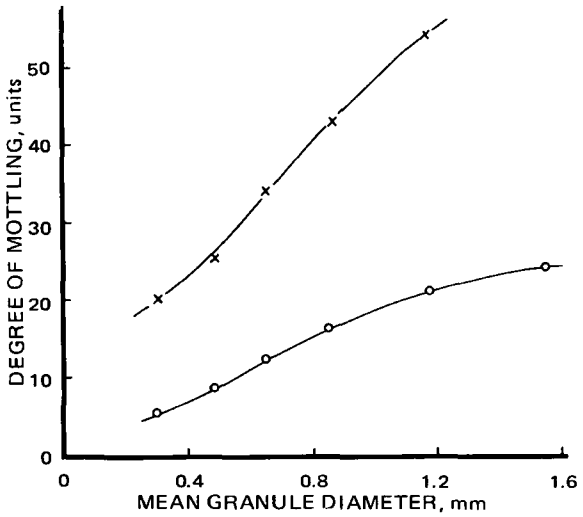

Figure 1—*Effect of drying process and granule diameter on the degree of mottling of calcium phosphate tablets colored with FD&C Blue No. 1 dye. Key: ×, tablets compressed from granules dried in a tray drier; and ○, tablets compressed from granules dried in a fluid bed drier.*

ture, but no experimental evidence for this statement was presented. This concept was also held by Scott *et al.* (5), who attributed the good color uniformity of tablets prepared from fluid-bed-dried granules to the "increased ability of a fluid bed drier to control product temperature during drying, thereby reducing color bleeding."

This concept is in contrast to that of other workers (8, 9) who postulated that solute migration on drying is reduced as the drying temperature is raised. They suggested that at high temperatures the flow of liquid through the granule cannot maintain the higher rate of drying at the periphery and evaporation takes place from progressively further inside the granule. This, in turn, reduces dye migration. From evidence presented here, it appears that drying temperature *per se* has a negligible effect on tablet mottling and the results noted by Scott *et al.* (5) are due to differences in the mode of dye migration in the two types of driers rather than to differences in the drying temperature itself.

Effect of Drying Technique—Since uniformly colored tablets could not be prepared from tray-dried granulations, further investigation was restricted to the more reproducible fluid bed drying technique. The extensive variation in the mottling values for tablets prepared from tray-dried granules probably was due to slight variations in the depth of the granule bed, since a difference of only 1 mm in a bed 1 cm thick produced a dye layer of 10% greater concentration and 10% more granules in which the dye concentration was low. The manner in which the resultant granule cake was fractured during comminution after drying was also unpredictable.

Effect of Compaction Pressure on Tablet Mottling—When the compressing force used to tablet a calcium phosphate granulation was increased, the degree of mottling exhibited by the resultant tablets increased sharply and then decreased by a small but reproducible amount (Fig. 2).

The increase in mottling is attributed to the disruption of the granules, thereby exposing their dye-deficient interiors. Shotton and Ganderton (4) showed similar effects using sugar pellets coated with dye. The decrease in mottling at higher pressures may possibly be due to the differing behavior, under compression, of the granule crust and the granule interior caused by migration of the granulating agent to the granule periphery (10). The soft granule interior would be compressed more on compaction than the exterior and thus would be reduced in size. Indirect evidence for this explanation is that the degree of color saturation (*i.e.*, the depth of the color) increases uniformly with compression pressure, tablets compressed at 49 MNm^{-2} being pale blue and tablets compressed at 65 MNm^{-2} being deep blue. Tablet porosity decreased linearly with an increase in pressure.

Table I—Effect of Granule Drying Technique and Drying Temperature on Tablet Mottling

Method of Drying	Tray-Dried Granules		Fluid-Bed-Dried Granules	
Temperature of drying air	25°	60°	25°	60°
Degree of tablet mottling, units	68.2	66.4	21.7	21.6
Limits of error $p = 0.95$	6.3	4.4	1.8	2.1

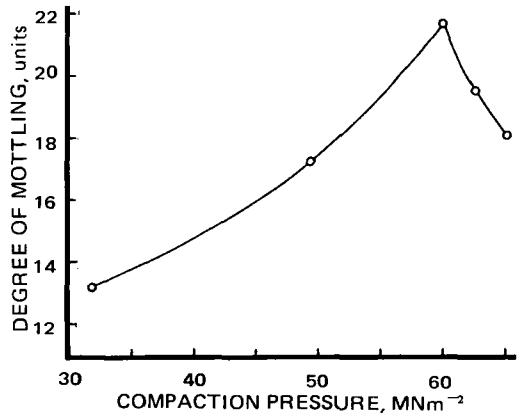

Figure 2—*Effect of compaction pressure on the degree of mottling shown by calcium phosphate tablets colored with FD&C Blue No. 1 dye.*

CONCLUSIONS

From the foregoing discussion, the following manufacturing principles can be proposed to minimize mottling, although the underlying cause of mottling, the migration of dye to the granule periphery, cannot be wholly prevented by these means.

1. The granules should be dried by a method that prevents intergranular migration of the dye, *e.g.*, by fluid bed drying as opposed to tray drying. Variation in drying temperature has little if any effect on the degree of mottling.
2. In contrast to usual manufacturing processes, the granules should not be subjected to a comminution process after drying; otherwise, the dye-deficient interior of the granule will be exposed.
3. As far as is commensurate with granule flow properties, the granule size should be as small as possible. In such granules, the amount of dye available for migration to the granule periphery is minimized and the color contrast between the periphery and the interior is reduced.
4. Tablet mottling and color saturation are both increased by an increase in compaction pressure.

REFERENCES

(1) W. C. Gunsel, C. J. Swartz, and J. L. Kanig, "The Theory and Practice of Industrial Pharmacy," Lea & Febiger, Philadelphia, Pa., 1970, p. 331.

(2) R. E. King, in "Remington's Pharmaceutical Sciences," Mack Publishing Co., Easton, Pa., 1970, p. 1653.

(3) N. A. Armstrong and G. A. March, *J. Pharm. Sci.*, **63,** 126(1974).

(4) E. Shotton and D. Ganderton, *J. Pharm. Pharmacol.*, **12,** 87T(1960).

(5) M. W. Scott, H. A. Lieberman, A. S. Rankell, F. S. Chow, and G. W. Johnston, *J. Pharm. Sci.*, **52,** 284(1963).

(6) L. Chavkin, *Drug. Cosmet. Ind.*, **75,** 466(1954).

(7) L. R. Lawrence and J. K. Beddow, *Powder Technol.*, **2,** 253(1969).

(8) D. M. Newitt and A. L. Papadopoulos, *Proc. Fert. Soc.*, **No. 55,** 3(1959).

(9) W. B. Pietsch and H. Rumpf, *Colloq. Int. C.N.R.S.*, **No. 160,** 213(1966).

(10) K. Ridgway and M. H. Rubinstein, *J. Pharm. Pharmacol.*, **23,** 11S(1971).

ACKNOWLEDGMENTS AND ADDRESSES

Received March 10, 1975, from the *Welsh School of Pharmacy, University of Wales Institute of Science and Technology, Cardiff, United Kingdom.*

Accepted for publication May 5, 1975.

The award to G. A. March of a research scholarship by the Pharmaceutical Society of Great Britain and the help of Merck Sharp & Dohme Research Laboratories are gratefully acknowledged.

* Present address: I.C.I. Pharmaceuticals Division, Macclesfield, United Kingdom.

[x] To whom inquiries should be directed.

Quantitative Assessment of Factors Contributing to Mottling of Colored Tablets II: Formulation Variables

N. A. ARMSTRONG [x] and G. A. MARCH *

Abstract □ The effects of several formulation variables were quantified with respect to factors affecting tablet mottling. Tablet mottling occurred with several commonly used binders and could not be prevented by using highly viscous binding solutions. However, mottling was reduced initially by increasing granule strength. Tablet diluents and dye–adsorbent materials had a profound effect on mottling, not by preventing dye migration but by affecting granule fragmentation on compression and the extent to which the dye-deficient material at the center of the granule was revealed. The lake form of FD&C Blue No. 1 was found to bleed in the presence of diluents that raised the pH of the granulating fluid above 6.4. Anionic impurities in the diluents also caused leaching of free dye and, consequently, increased tablet mottling. The conclusions from this study and previous papers were drawn together to give general principles for the production of uniformly colored tablets by aqueous granulation techniques.

Keyphrases □ Mottling—surface of colored tablets, effects of several formulation variables □ Tablets, colored—effects of several formulation variables on mottling

Recently, a method for measuring the amount of color variation on the surface of a tablet (mottling) was described (1), and this method enabled a study to be made of those factors that contribute to mottling in tablets. The manner in which some manufacturing variables can be controlled to minimize mottling was discussed earlier (2), but the underlying cause of mottling, the migration of dye to the periphery of the granule during drying, cannot be avoided simply by manipulation of manufacturing techniques.

King (3) reviewed some methods by which dye migration can be reduced, but the success of the techniques has been judged subjectively. By using the quantitative method for determining tablet mottling, the relative importance of formulation factors in the control of tablet color uniformity was assessed.

EXPERIMENTAL

General Method of Tablet Preparation—The solids to be tableted were colored with 0.0333% of FD&C Blue No. 1 dye or 0.2357% of FD&C Blue No. 1 lake (equivalent to the same dye concentration) dissolved in water. Each colored powder was massed with the appropriate quantity of granulating agent and sieved through a 2.8-mm mesh screen using an oscillating granulator[1]. The wet granulate was dried for 20 min in a fluid bed drier[2] (air inlet temperature 60°) and sieved on a vibratory sieve shaker[3]. Without further comminution, the 1000–1400-μm fraction was lubricated with magnesium stearate (1%) colored with the same concentration of dye. This size fraction was selected because previous work (1) had shown that such granules gave highly mottled tablets so any changes in mottling could be more readily detected. The lubricated granules were compressed by a single-stroke tablet machine fitted with flat-faced, 12.5-mm, stainless steel punches[4]. The tablet thickness was constant (4.00 mm), and the tablet weight for each diluent is shown in Table I.

Measurements of Tablet Mottling—Full details of this technique, using a microdensitometer[5], were published previously (1).

Measurement of Granule Crushing Strength (Fig. 1)—The apparatus consisted of two concentric cylinders, and their bases were separated by a washer of 1.0 mm thickness. A single granule was mounted centrally in the washer, and the inner cylinder was placed in position. Lead shot was poured into the inner cylinder until the granule fractured or deformed and the inner cylinder made contact with the washer. This contact completed an electric bell circuit, so granule fracture was signaled audibly.

Twenty-five granules of specified dimensions were assessed from each batch to give a mean value for granule crushing strength. A control on granule size was necessary since Capes (4) showed that granule strength is dependent on granule diameter. For this reason, a relatively narrow sieve fraction was selected (2.0–2.8 mm). An additional control on granule weight was also necessary to obtain reproducible results; the granule weight fraction for granules composed of different diluents varied according to the density of the granules (Table I).

The viscosity of starch mucilages used as binding agents was determined at 25° using a rotational viscometer[6].

RESULTS AND DISCUSSION

Role of Granulating Agent in Tablet Mottling—The granulating agent has been reported to inhibit solute migration in granules by means of imbibition (5) and complexation (6) and by its effect on the viscosity of the granulating fluid (4). Furthermore, since one fundamental cause of mottling is disruption of the granular structure on compression, thereby exposing the dye-deficient

[1] Type 143A, Apex Construction Co., London, United Kingdom.
[2] Type SSE65, Apex Construction Co., London, United Kingdom.
[3] Pascall Engineering Co. Ltd., Crawley, United Kingdom.
[4] Model E2, Manesty Machines Ltd., Liverpool, United Kingdom.
[5] Joyce-Loebl microdensitometer Mark IIIS, Joyce Loebl and Co. Ltd., Gateshead, United Kingdom.
[6] Epprecht Rheomat-30, Contraves A. G., Zurich, Switzerland.

ACKNOWLEDGMENTS AND ADDRESSES

Received March 10, 1975, from the *Welsh School of Pharmacy, University of Wales Institute of Science and Technology, Cardiff, United Kingdom.*

Accepted for publication May 5, 1975.

The award to G. A. March of a research scholarship by the Pharmaceutical Society of Great Britain and the help of Merck Sharp & Dohme Research Laboratories are gratefully acknowledged.

* Present address: I.C.I. Pharmaceuticals Division, Macclesfield, United Kingdom.

[x] To whom inquiries should be directed.

Quantitative Assessment of Factors Contributing to Mottling of Colored Tablets II: Formulation Variables

N. A. ARMSTRONG [x] and G. A. MARCH *

Abstract □ The effects of several formulation variables were quantified with respect to factors affecting tablet mottling. Tablet mottling occurred with several commonly used binders and could not be prevented by using highly viscous binding solutions. However, mottling was reduced initially by increasing granule strength. Tablet diluents and dye–adsorbent materials had a profound effect on mottling, not by preventing dye migration but by affecting granule fragmentation on compression and the extent to which the dye-deficient material at the center of the granule was revealed. The lake form of FD&C Blue No. 1 was found to bleed in the presence of diluents that raised the pH of the granulating fluid above 6.4. Anionic impurities in the diluents also caused leaching of free dye and, consequently, increased tablet mottling. The conclusions from this study and previous papers were drawn together to give general principles for the production of uniformly colored tablets by aqueous granulation techniques.

Keyphrases □ Mottling—surface of colored tablets, effects of several formulation variables □ Tablets, colored—effects of several formulation variables on mottling

Recently, a method for measuring the amount of color variation on the surface of a tablet (mottling) was described (1), and this method enabled a study to be made of those factors that contribute to mottling in tablets. The manner in which some manufacturing variables can be controlled to minimize mottling was discussed earlier (2), but the underlying cause of mottling, the migration of dye to the periphery of the granule during drying, cannot be avoided simply by manipulation of manufacturing techniques.

King (3) reviewed some methods by which dye migration can be reduced, but the success of the techniques has been judged subjectively. By using the quantitative method for determining tablet mottling, the relative importance of formulation factors in the control of tablet color uniformity was assessed.

EXPERIMENTAL

General Method of Tablet Preparation—The solids to be tableted were colored with 0.0333% of FD&C Blue No. 1 dye or 0.2357% of FD&C Blue No. 1 lake (equivalent to the same dye concentration) dissolved in water. Each colored powder was massed with the appropriate quantity of granulating agent and sieved through a 2.8-mm mesh screen using an oscillating granulator[1]. The wet granulate was dried for 20 min in a fluid bed drier[2] (air inlet temperature 60°) and sieved on a vibratory sieve shaker[3]. Without further comminution, the 1000–1400-μm fraction was lubricated with magnesium stearate (1%) colored with the same concentration of dye. This size fraction was selected because previous work (1) had shown that such granules gave highly mottled tablets so any changes in mottling could be more readily detected. The lubricated granules were compressed by a single-stroke tablet machine fitted with flat-faced, 12.5-mm, stainless steel punches[4]. The tablet thickness was constant (4.00 mm), and the tablet weight for each diluent is shown in Table I.

Measurements of Tablet Mottling—Full details of this technique, using a microdensitometer[5], were published previously (1).

Measurement of Granule Crushing Strength (Fig. 1)—The apparatus consisted of two concentric cylinders, and their bases were separated by a washer of 1.0 mm thickness. A single granule was mounted centrally in the washer, and the inner cylinder was placed in position. Lead shot was poured into the inner cylinder until the granule fractured or deformed and the inner cylinder made contact with the washer. This contact completed an electric bell circuit, so granule fracture was signaled audibly.

Twenty-five granules of specified dimensions were assessed from each batch to give a mean value for granule crushing strength. A control on granule size was necessary since Capes (4) showed that granule strength is dependent on granule diameter. For this reason, a relatively narrow sieve fraction was selected (2.0–2.8 mm). An additional control on granule weight was also necessary to obtain reproducible results; the granule weight fraction for granules composed of different diluents varied according to the density of the granules (Table I).

The viscosity of starch mucilages used as binding agents was determined at 25° using a rotational viscometer[6].

RESULTS AND DISCUSSION

Role of Granulating Agent in Tablet Mottling—The granulating agent has been reported to inhibit solute migration in granules by means of imbibition (5) and complexation (6) and by its effect on the viscosity of the granulating fluid (4). Furthermore, since one fundamental cause of mottling is disruption of the granular structure on compression, thereby exposing the dye-deficient

[1] Type 143A, Apex Construction Co., London, United Kingdom.
[2] Type SSE65, Apex Construction Co., London, United Kingdom.
[3] Pascall Engineering Co. Ltd., Crawley, United Kingdom.
[4] Model E2, Manesty Machines Ltd., Liverpool, United Kingdom.
[5] Joyce-Loebl microdensitometer Mark IIIS, Joyce Loebl and Co. Ltd., Gateshead, United Kingdom.
[6] Epprecht Rheomat-30, Contraves A. G., Zurich, Switzerland.

Table I—Experimental Data for Tablets of 4.0 mm Thickness and Granules Prepared from Various Tablet Diluents and Used for Crushing Strength Tests

Tablet Diluent	Density of Diluent, g/ml	Tablet Weight, mg	Tablet Porosity	Density of Granule, g/ml	Weight of One Granule, mg
Dibasic calcium phosphate	2.18	660	0.39	2.26	11–13
Lactose	1.53	485	0.35	1.50	6.5–8.5
Mannitol	1.49	480	0.34	1.42	7.0–8.0
Mannitol (65%) and dibasic calcium phosphate (35%)	1.73	540	0.37	1.60	8.0–9.0
Mannitol (35%) and dibasic calcium phosphate (65%)	1.94	590	0.38	1.81	9.0–10.5
Wheat starch (20%) and dibasic calcium phosphate (80%)	2.08	620	0.39	1.92	9.5–11.0
Potato starch (20%) and dibasic calcium phosphate (80%)	2.09	624	0.39	1.90	9.5–11.0
Wheat starch (20%) and lactose (80%)	1.55	490	0.35	1.49	7.0–8.5
Potato starch (20%) and lactose (80%)	1.56	495	0.36	1.49	7.0–8.5

granule interior, the granulating agent probably plays an important role in mottling by virtue of its effect on granule strength.

Dibasic calcium phosphate was granulated with several commonly used binding agents at a range of concentrations. Calcium phosphate was selected as the basis for the tablets because of its low solubility in water. Interparticulate bridges, therefore, made no contribution to granule strength, and dissolution of the solid could not significantly alter the viscosity of the granulating fluid.

The relationship between binder type and concentration and the crushing strength of the granules so formed is shown in Fig. 2. As expected, granule strength increased almost linearly with binder concentration. However, the relationship between granule strength and mottling was more complex (Fig. 3). In general, at low concentrations of the binding agent, mottling decreased as the constituent granules became more resistant to fragmentation, although migration of the dye to the granule periphery occurred in all cases. However, in the case of gelatin and povidone, as binder concentration and granule strength increased still further, mottling also increased. This finding resulted because, at high granule strengths, a few of the hardest granules remained intact after compression and appeared as dark blue patches on the tablet surface.

Dibasic calcium phosphate tablets prepared with acacia showed considerably reduced mottling compared with tablets prepared with other binding agents. This result is thought to be related to the observation that these tablets were pale blue-gray in color; consequently, the contrast between white and colored regions on the tablet surface was diminished. In the presence of acacia, an aqueous solution of FD&C Blue No. 1 showed a hypsochromic shift in its visible spectrum. Bornstein *et al.* (7) showed that acacia and FD&C Blue No. 1 form a complex, and it is concluded that the reduction in mottling is primarily due to a reduction in the overall degree of color saturation of the tablet surface rather than any effect of the acacia on the granule properties.

Prescott (6) claimed, although without apparent experimental

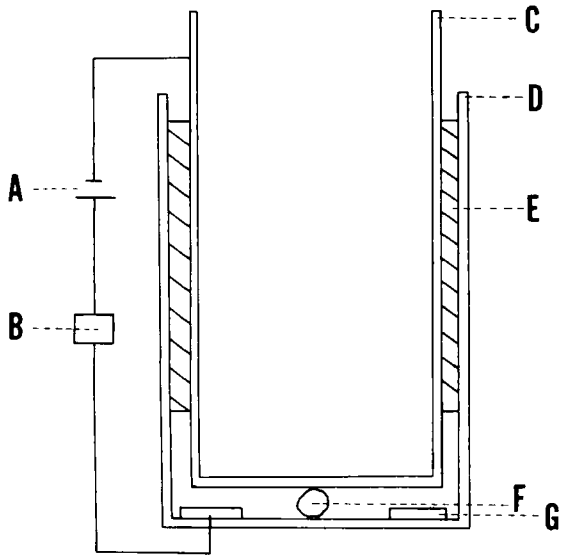

Figure 1—*Apparatus for the determination of granule crushing strength. Key: A, 4.5-v battery; B, buzzer; C, inner cylinder; D, outer cylinder; E, guide coated with Teflon; F, granule; and G, washer.*

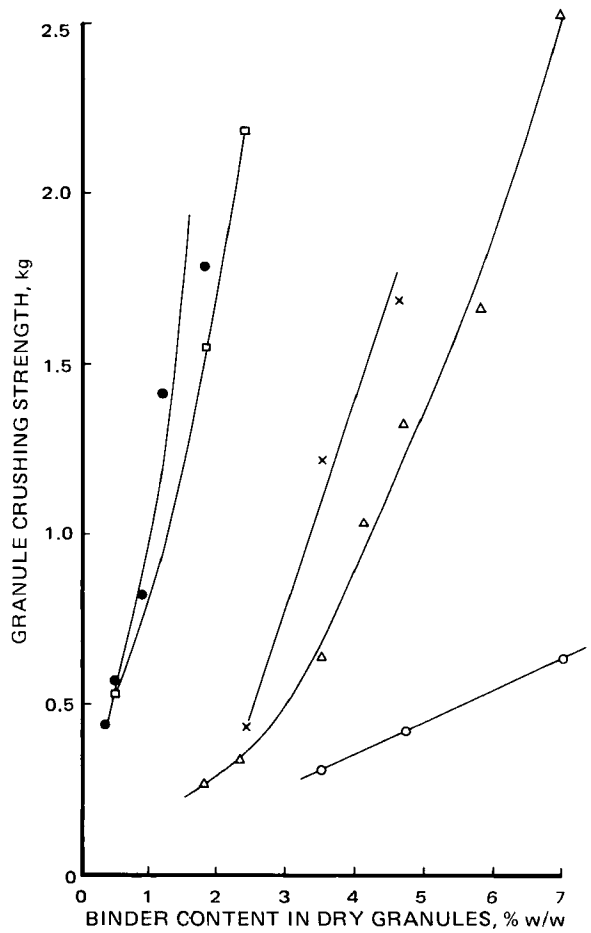

Figure 2—*Crushing strength of dibasic calcium phosphate granules prepared with various binding agents. Key: ●, gelatin; □, potato starch mucilage; ×, acacia; △, povidone; and ○, polyethylene glycol 4000.*

Table II—Influence of Binding Solution Viscosity on the Degree of Mottling of Dibasic Calcium Phosphate Tablets Prepared with Potato Starch Mucilage

Starch Mucilage		Starch Concentration in Dried Granules, % w/w	Degree of Mottling	
Concentration, % w/w	Viscosity at 25°, poises		Mean of 10 Tablets, units	Limits of Error (p = 0.95)
2.0	217	0.47	22.5	2.2
7.5	38,200	1.75	20.7	1.3
10.0	97,600	2.33	21.3	3.4

justification, that povidone solves the problem of tablet mottling because it "actually anchors the color evenly throughout the granulation," implying the formation of a povidone–dye complex which does not migrate to the granule surface on drying. Povidone does form complexes in aqueous solution of some dyes (8, 9), although the existence of such complexes in tableted systems has not been established. In the present study, tablets prepared with povidone were severely mottled, there was no evidence that dye migration was reduced, and the spectral absorbance of FD&C Blue No. 1 was not changed significantly by the presence of povidone. Furthermore, Ridgway and Rubinstein (10) found that on drying, povidone migrated to the granule periphery. Therefore, even if a povidone–dye complex does form, the complex also probably migrates to the surface of the granule, so mottling would not be visibly affected.

The migration of sodium chloride through a granulate of sand and water was reduced by a factor of five by the incorporation of a highly viscous binding agent; the tendency of the liquid to move to the granule surface by capillarity probably was reduced (4). Consequently, evaporation would take place within the granule, and dye migration would be reduced. The effect of the binding agent viscosity on the mottling of dibasic calcium phosphate tablets is shown in Table II. Migration of dye to the granule periphery occurred in each case, and the degree of mottling was not affected by the viscosity of the granulating agent.

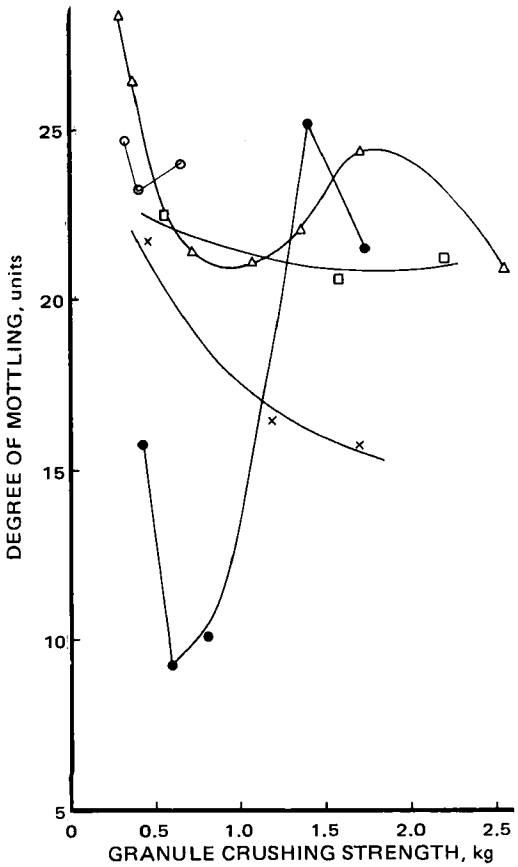

Figure 3—*Effect of granule crushing strength on the degree of mottling of dibasic calcium phosphate tablets colored with FD&C Blue No. 1 dye. Key: ●, gelatin; □, potato starch mucilage; ×, acacia; △, povidone; and ○, polyethylene glycol 4000.*

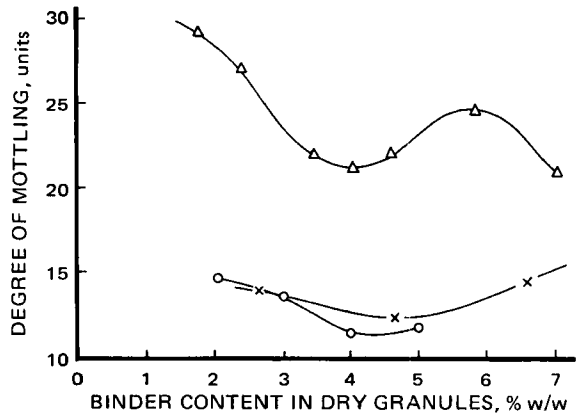

Figure 4—*Degree of mottling of tablets prepared with various diluents colored with FD&C Blue No. 1 dye. Key: △, dibasic calcium phosphate; ×, mannitol; and ○, lactose.*

Some of the binding agent may have been adsorbed by the dibasic calcium phosphate, leaving a less viscous fluid to move by capillarity. In support of this suggestion, it was found that the interior of granules prepared with starch mucilage was stained black by iodine.

Effect of Diluents on Degree of Mottling—*In a study on the properties of tablets colored with FD&C Red No. 3, Goodhart et al.* (11) noted that tablets prepared from calcium sulfate were

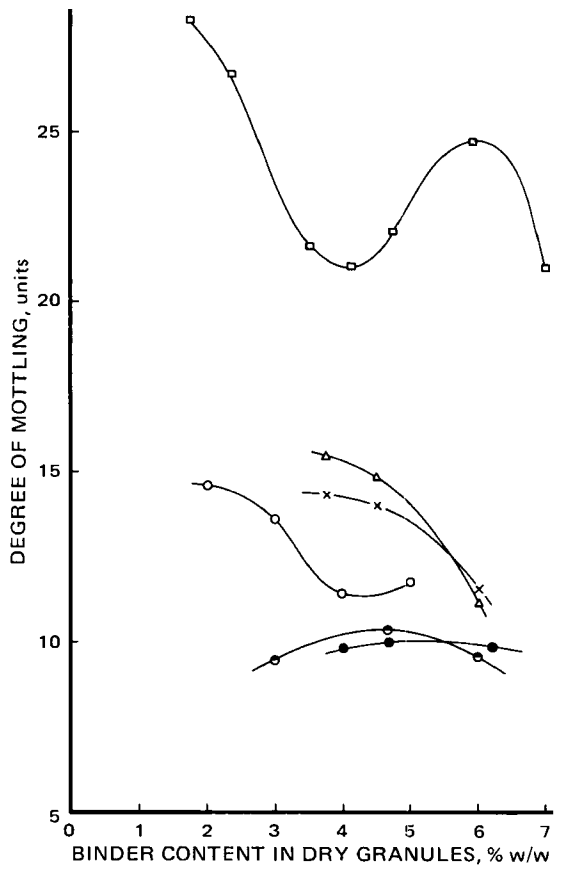

Figure 5—*Effect of potato and wheat starches on the degree of mottling shown by lactose and dibasic calcium phosphate tablets. All tablets were colored with FD&C Blue No. 1 dye and contained povidone as the binding agent. Key: □, dibasic calcium phosphate; △, dibasic calcium phosphate–wheat starch (80:20); ×, dibasic calcium phosphate–potato starch (80:20); ○, lactose; ⊖, lactose–wheat starch (80:20); and ●, lactose–potato starch (80:20).*

Table III—Effect of Tablet Diluents on Elution of Dye from Granules Colored with FD&C Blue No. 1 Lake and on Tablet Mottling

Diluent	Colorant	Degree of Mottling, units: Mean of 10 Tablets	Degree of Mottling, units: Limits of Error (p = 0.95)	pH of Supernatant Dye Solution	Percent Dye Eluted from Granules Containing FD&C Blue No. 1 Lake
Dibasic calcium phosphate	Dye	21.6	2.1	—	—
	Lake	21.8	2.3	7.1	100
Lactose	Dye	13.6	1.2	—	—
	Lake	8.9	1.1	5.9	68.8

more mottled than those produced from calcium phosphate and lactose.

In the present investigation, tablets were prepared from dibasic calcium phosphate, lactose, and mannitol. They were colored with FD&C Blue No. 1 and always granulated with povidone, thereby ensuring that changes in mottling were attributable only to the characteristics of the diluents employed. Figure 4 shows that tablets containing dibasic calcium phosphate were more mottled than those containing mannitol or lactose. However, there was no evidence that any of the substances adsorbed the dye to a significant extent, and examination of cross sections of the granules showed that dye had migrated to the periphery of the granule in all cases. Hence, it must be concluded that the more uniformly colored tablets of lactose and mannitol result from modification of the granule behavior on compression, which reduces granule fracture and the exposure of uncolored material.

Use of Adsorbents to Prevent Mottling—Zografi and Mattocks (12) showed that some anionic dyes are strongly adsorbed by several types of starch but not by potato starch. They concluded that the presence of an adsorbent starch should improve tablet color uniformity by prevention of dye migration. A similar conclusion was reached by Jaffe and Lippmann (5), who found that attapulgite prevented migration of FD&C Blue No. 1 dye in lactose columns. Unfortunately, neither of these studies was supported by the manufacture of uniformly colored tablets.

In the present study, tablets were prepared with a range of concentrations of povidone as the granulating agent. Twenty percent of the calcium phosphate was replaced by either wheat starch, which adsorbs FD&C Blue No. 1, or potato starch, which does not. A similar range of tablets made from lactose with these starches was also prepared. The results (Fig. 5) show that while the addition of an adsorbent starch reduced mottling, an almost identical reduction in mottling was obtained with a nonadsorbing starch.

Fuchs (13) showed that starch grains remain intact after tablet compaction. In the present study, it was noted that whereas calcium phosphate granules fragmented during determinations of granule crushing strength, those containing starch remained largely intact. It is thought, therefore, that starch can accommodate compressive forces by elastic deformation and thereby reduce the tendency of granules to fracture on compression. Thus, the present investigation confirmed the suggestion made by Zografi and Mattocks (12) that color uniformity can be improved by incorporating starch in the wet granulation. However, the mechanism by which mottling is reduced is not due to adsorption of the dye.

Effects of Dyes and Their Lakes on Mottling—Since dye migration is the primary cause of mottling, it may be expected that if the dye is bound to an insoluble substrate, *e.g.*, aluminum hydroxide, thereby giving the lake of the dye, migration and mottling should be reduced significantly.

Table III shows that, in the case of lactose granulated with povidone, mottling was reduced, although not abolished, when the dye lake was used. However, the lake had no effect on tablets made from calcium phosphate. This finding supports that of Goodhart *et al.* (11), who found that while lactose tablets colored with FD&C Red No. 3 lake exhibited uniform color, a high degree of mottling was observed with calcium phosphate and calcium sulfate.

It is well known that a dye can be leached from its lake by extremes of pH or by the presence of anions. It was found that FD&C Blue No. 1 was rapidly eluted from its lake at pH values greater than 6.4. Thus, while the elution in the presence of calcium phosphate can be accounted for by the pH of the medium, the elution in the presence of lactose was probably due to traces of anionic impurities such as chloride. Although chloride ions were found to be present in lactose only as trace impurities, the small amount of water present during the drying process resulted in relatively concentrated electrolyte solutions.

Hence, although in some circumstances the use of a lake will give a less mottled product than will the parent dye, the extent of the reduction is dependent on the pH of the system and the anions present.

CONCLUSIONS

The basic cause of mottling is dye migration in the granules on drying. None of the techniques reported in this paper successfully overcomes this problem. Nevertheless, in spite of the coarse granule size used, relatively uniformly colored tablets were prepared. The improvement in color uniformity was due to the effect of excipients on granule behavior on compression.

Tablet mottling occurred with each binding agent investigated, but was less apparent with acacia because that excipient reduced the overall tablet color. Mottling was also reduced initially by an increase in granule strength, but tablet mottling increased at high values due to the presence of a small number of extremely hard granules which did not fracture and appeared as dark patches on the tablet surface. The use of highly viscous binding solutions had no beneficial effect on tablet mottling.

Tablets prepared from lactose and mannitol granules, which deformed plastically and retained their integrity after compression, were relatively uniformly colored. In contrast, corresponding tablets prepared from dibasic calcium phosphate granules, which were brittle and dispersed into fragments on compression, were severely mottled. Incorporation of starch (20%) with dibasic calcium phosphate or lactose before wet granulation reduced the extent of granule fracture on compression and the degree of mottling. The starch grains are thought to reduce mottling by accommodating the compressive forces by deformation and, hence, resisting granule fracture.

Lactose tablets colored with FD&C Blue No. 1 lake were less mottled than corresponding tablets colored with an equivalent quantity of dye. However, dibasic calcium phosphate tablets colored with the lake were equally as mottled as those colored with the dye. The slight mottling observed in lactose tablets prepared with the lake is attributed to elution of dye from the lake, which may have been caused by chloride ions present as impurities in the tablet diluents. Severe elution of dye from FD&C Blue No. 1 lake also occurred in aqueous solutions with a pH in excess of 6.4. Hence, dye elution will also occur in the presence of those tablet excipients that raise the pH of the granulating fluid above 6.4.

As a result of the present investigation, the following general principles for the preparation of uniformly colored tablets are suggested:

1. Granules should be dried in such a manner (*e.g.*, with a fluid bed dryer) as to prevent intergranular solute migration.
2. No dye-deficient material should be visible before compression. Irrespective of the method of drying and the formulation used, the dye will migrate to the granule periphery, leaving the interior of the granule deficient of dye. Thus, compression should not be preceded, as is the custom, by a comminutive process; such a process exposes colorant-free zones of the granule interior.
3. As far as is commensurate with granule flow properties, the granule size used during compression should be as small as possible, so that the visible contrast between the granule interior and periphery is minimized.

REFERENCES

(1) N. A. Armstrong and G. A. March, *J. Pharm. Sci.*, **63**, 126(1974).

(2) *Ibid.*, **65**, 198(1976).

(3) R. E. King, in "Remington's Pharmaceutical Sciences," Mack Publishing Co., Easton, Pa., 1970, p. 1653.

(4) C. E. Capes, *Powder Technol.*, **4**, 77(1971).

(5) J. Jaffe and I. Lippmann, *J. Pharm. Sci.*, **53**, 441(1964).

(6) F. Prescott, *Drug Cosmet. Ind.*, **97**, 497(1965).

(7) M. Bornstein, J. P. Walsh, W. J. Munden, and J. L. Lach, *J. Pharm. Sci.*, **56**, 1410(1967).

(8) H. P. Frank, S. Barkin, and F. R. Eirich, *J. Phys. Chem.*, **61**, 1375(1957).

(9) R. E. Phares, *J. Pharm. Sci.*, **57**, 53(1968).

(10) K. Ridgway and M. H. Rubinstein, *J. Pharm. Pharmacol.*, **23**, 11S(1971).

(11) F. W. Goodhart, M. E. Everhard, and D. A. Dickcius, *J. Pharm. Sci.*, **53**, 338(1964).

(12) G. Zografi and A. M. Mattocks, *ibid.*, **52**, 1103(1963).

(13) P. Fuchs, *Arch. Pharm.*, **303**, 471(1970).

ACKNOWLEDGMENTS AND ADDRESSES

Received March 10, 1975, from the *Welsh School of Pharmacy, University of Wales Institute of Science and Technology, Cardiff, United Kingdom.*

Accepted for publication May 5, 1975.

The award to G. A. March of a research scholarship by the Pharmaceutical Society of Great Britain and the help of Merck Sharp & Dohme Research Laboratories are gratefully acknowledged.

* Present address: I.C.I. Pharmaceuticals Division, Macclesfield, United Kingdom.

[x] To whom inquiries should be directed.

Constant Returns to Scale for Prescription Dispensing in U.S. Community Pharmacy

DAVID LOHRISCH *, S. CABELL SHULL [‡], and MICKEY C. SMITH *[x]

Abstract □ By using data from a sample of 1767 community pharmacies, a total cost function was estimated by a polynomial regression of total cost on output. The Cobb–Douglas production function was estimated by a multiple linear regression of natural logarithmic transformations of output on natural logarithmic transformation of labor and capital. No economies of scale were found in prescription departments. Cost data led to a conclusion of constant marginal costs.

Keyphrases □ Prescription dispensing—community pharmacies, total cost function in relation to size, Cobb–Douglas production function □ Cobb–Douglas production function—community pharmacies, prescription dispensing, total cost in relation to size □ Pharmacies—total cost function in relation to size, prescription dispensing, Cobb–Douglas production function

The pervasive economic influence of the 1970's is inflation with an associated recession. The news media daily report on the state of the economy and profusely illustrate their conclusions by examples from agriculture and industry. These two sectors of the economy at least have the advantage of being well studied and somewhat understood.

The service industries are not so fortunate. Only one cost and scale study (of the U.S. Postal Service) was published in recent years (1). The health service industries have been subjected to some indepth studies. Most of these have concentrated on output specifications (2) and cost functions (3), resulting in seven hospital investigations reporting increasing returns to scale and three with constant returns. A production function was calculated (4) for medical office practice, but no economies of scale were calculated.

Many studies have concerned pharmacy and prescription costs (5–8). But there has been a dearth of studies concerning economies of scale in the health services and pharmacy practice generally. The purpose of this study was to find what, if any, economies of scale exist in the prescription dispensing operations of U.S. community pharmacies.

THEORETICAL

Economies of scale, or increasing returns to scale, may be defined as the proportional increase in output greater than the proportional increase in each input. If the proportional increase in output is less than the proportional increase in inputs, or equal to them, then the firm is experiencing decreasing returns to scale or constant returns to scale, respectively.

These economies of scale are due to the following factors (9):

1. Bulk transactions of materials—the ease of dealing with large quantities of materials reduces unit costs.
2. Pooled reserves—operating on a large scale reduces the cost of uncertainty through a spreading of the risk.
3. Multiples—the costs of personnel and machines fall with increasing size due to their indivisibilities.

The neoclassical theorists thought that diseconomies of scale would be manifest in the form of managerial inefficiencies with increasing size (10). In addition, the increasing division of labor might be taken so far that employees would become bored and inefficient with their highly specialized and repetitive tasks. On the other hand, it has been suggested that with the increasing usage of computers in large industry, the expected inefficiencies have not occurred, resulting in constant rather than decreasing returns to scale.

Economies of scale are closely related to both cost and production functions. Depending on the design of the study, economies of scale may be investigated by an examination of the shape of the marginal cost function or an examination of the parameters of the Cobb–Douglas production function.

The marginal cost is, mathematically, the derivative with re-

REFERENCES

(1) N. A. Armstrong and G. A. March, *J. Pharm. Sci.*, **63**, 126(1974).

(2) *Ibid.*, **65**, 198(1976).

(3) R. E. King, in "Remington's Pharmaceutical Sciences," Mack Publishing Co., Easton, Pa., 1970, p. 1653.

(4) C. E. Capes, *Powder Technol.*, **4**, 77(1971).

(5) J. Jaffe and I. Lippmann, *J. Pharm. Sci.*, **53**, 441(1964).

(6) F. Prescott, *Drug Cosmet. Ind.*, **97**, 497(1965).

(7) M. Bornstein, J. P. Walsh, W. J. Munden, and J. L. Lach, *J. Pharm. Sci.*, **56**, 1410(1967).

(8) H. P. Frank, S. Barkin, and F. R. Eirich, *J. Phys. Chem.*, **61**, 1375(1957).

(9) R. E. Phares, *J. Pharm. Sci.*, **57**, 53(1968).

(10) K. Ridgway and M. H. Rubinstein, *J. Pharm. Pharmacol.*, **23**, 11S(1971).

(11) F. W. Goodhart, M. E. Everhard, and D. A. Dickcius, *J. Pharm. Sci.*, **53**, 338(1964).

(12) G. Zografi and A. M. Mattocks, *ibid.*, **52**, 1103(1963).

(13) P. Fuchs, *Arch. Pharm.*, **303**, 471(1970).

ACKNOWLEDGMENTS AND ADDRESSES

Received March 10, 1975, from the *Welsh School of Pharmacy, University of Wales Institute of Science and Technology, Cardiff, United Kingdom.*

Accepted for publication May 5, 1975.

The award to G. A. March of a research scholarship by the Pharmaceutical Society of Great Britain and the help of Merck Sharp & Dohme Research Laboratories are gratefully acknowledged.

* Present address: I.C.I. Pharmaceuticals Division, Macclesfield, United Kingdom.

[x] To whom inquiries should be directed.

Constant Returns to Scale for Prescription Dispensing in U.S. Community Pharmacy

DAVID LOHRISCH *, S. CABELL SHULL [‡], and MICKEY C. SMITH *[x]

Abstract □ By using data from a sample of 1767 community pharmacies, a total cost function was estimated by a polynomial regression of total cost on output. The Cobb–Douglas production function was estimated by a multiple linear regression of natural logarithmic transformations of output on natural logarithmic transformation of labor and capital. No economies of scale were found in prescription departments. Cost data led to a conclusion of constant marginal costs.

Keyphrases □ Prescription dispensing—community pharmacies, total cost function in relation to size, Cobb–Douglas production function □ Cobb–Douglas production function—community pharmacies, prescription dispensing, total cost in relation to size □ Pharmacies—total cost function in relation to size, prescription dispensing, Cobb–Douglas production function

The pervasive economic influence of the 1970's is inflation with an associated recession. The news media daily report on the state of the economy and profusely illustrate their conclusions by examples from agriculture and industry. These two sectors of the economy at least have the advantage of being well studied and somewhat understood.

The service industries are not so fortunate. Only one cost and scale study (of the U.S. Postal Service) was published in recent years (1). The health service industries have been subjected to some indepth studies. Most of these have concentrated on output specifications (2) and cost functions (3), resulting in seven hospital investigations reporting increasing returns to scale and three with constant returns. A production function was calculated (4) for medical office practice, but no economies of scale were calculated.

Many studies have concerned pharmacy and prescription costs (5–8). But there has been a dearth of studies concerning economies of scale in the health services and pharmacy practice generally. The purpose of this study was to find what, if any, economies of scale exist in the prescription dispensing operations of U.S. community pharmacies.

THEORETICAL

Economies of scale, or increasing returns to scale, may be defined as the proportional increase in output greater than the proportional increase in each input. If the proportional increase in output is less than the proportional increase in inputs, or equal to them, then the firm is experiencing decreasing returns to scale or constant returns to scale, respectively.

These economies of scale are due to the following factors (9):

1. Bulk transactions of materials—the ease of dealing with large quantities of materials reduces unit costs.
2. Pooled reserves—operating on a large scale reduces the cost of uncertainty through a spreading of the risk.
3. Multiples—the costs of personnel and machines fall with increasing size due to their indivisibilities.

The neoclassical theorists thought that diseconomies of scale would be manifest in the form of managerial inefficiencies with increasing size (10). In addition, the increasing division of labor might be taken so far that employees would become bored and inefficient with their highly specialized and repetitive tasks. On the other hand, it has been suggested that with the increasing usage of computers in large industry, the expected inefficiencies have not occurred, resulting in constant rather than decreasing returns to scale.

Economies of scale are closely related to both cost and production functions. Depending on the design of the study, economies of scale may be investigated by an examination of the shape of the marginal cost function or an examination of the parameters of the Cobb–Douglas production function.

The marginal cost is, mathematically, the derivative with re-

Table I—Analysis of Variance for the Polynomial Regression

Source of Variance	Mean Square Regression	*df* Regression	Mean Square Error	*df* Error	*F* Calculated	Variance Explained
Linear	3501.011	1	1.08364	1372	1109.88[a]	0.7019
Quadratic	24.191	1	1.06678	1371	22.68[a]	0.7068
Cubic	8.569	1	1.06131	1370	8.07[a]	0.7084
Quartic	5.972	1	1.05772	1369	5.64[a]	0.7096
Quintic	10.545	1	1.05079	1368	10.04[a]	0.7118
Sextic	7.905	1	1.04577	1367	7.56[a]	0.7134
Seventh order	1.174	1	1.04568	1366	1.12	—

[a] Significant *F* values.

spect to the output of the total cost function. Total cost is a relationship between total costs and output, the most common form being quadratic or linear:

$$TC = A + BY + CY^2 + E \quad \text{(Eq. 1)}$$

$$TC = A + BY + E \quad \text{(Eq. 2)}$$

where TC = total costs and Y = output.

With these two forms, the derivative (marginal cost) may be constant or a function of output, with marginal cost either increasing or decreasing with increasing outputs: (*a*) increasing returns to scale, Eq. 1 with C negative; (*b*) constant returns to scale, Eq. 2; and (*c*) decreasing returns to scale, Eq. 1 with C positive.

A production function may be defined as a physical technical relationship between the output of a well-defined good or service and the various inputs used in its production, within the existing state of technology (11). Production functions may be determined by cross-sectional or time series analysis of the data. A time series analysis follows the behavior of one firm over time, while a cross-sectional analysis studies the behavior of a sample of firms at one point in time.

A production function may be of an aggregate form, which aggregates data from all firms in an industry to obtain an industry production function, or a micro form, in which the data are obtained from individual operating units to describe the (average) operation of the units.

The Cobb–Douglas production function is a popular log–linear estimator of production. Factor inputs of labor and capital are exponentially related to output. This type of analysis results in a three-dimensional production surface, a statistical estimate of the maximum production point of each producing unit (12):

$$Y = AL^{\alpha}C^{\beta} \quad \text{(Eq. 3)}$$

where Y = output, L = units of labor input, C = units of capital input, α = elasticity of production with respect to labor, β = elasticity of production with respect to capital, and A = constant. With increasing returns to scale, $\alpha + \beta > 1$; with constant returns to scale, $\alpha + \beta = 1$; and with decreasing returns to scale, $\alpha + \beta < 1$.

This function may be linearized by taking natural logarithms of both sides:

$$\ln Y = \ln A + \alpha \ln L + \beta \ln C \quad \text{(Eq. 4)}$$

The Cobb–Douglas production function only describes firms that have undergone the same economies of scale throughout the whole range of outputs. It is not applicable in cases where economies of scale change from increasing returns to scale to constant returns to scale. For the different regions of production, different production functions must be used.

EXPERIMENTAL

Study Population—Cost and operational data[1] on 1767 community pharmacies for the calendar year 1972 were available. Due to incomplete data from some pharmacies, only 1374 pharmacies were used in the study. The items supplied were:

1. Prescription sales (1972)
2. Total store sales (1972)
3. Cost of advertising (1972)
4. Depreciation allowance (1972)
5. Delivery costs (1972)
6. Rent (1972)
7. Heat and light (1972)
8. Total expenses (1972)
9. Prescription department inventory
10. Proportion of prescription sales to total sales
11. Proportion of prescription department area to total area
12. Number of prescriptions dispensed (1972)
13. Number of hours worked each week by the manager
14. Number of hours worked each week by professional employees

Means tests were performed to determine if there were any statistical differences between the pharmacies used and those rejected. No differences were found on any of the variables used at the 0.05 level.

Variables—All variables were adjusted to reflect only the prescription department.

The output of community pharmacy may be expressed as an aggregation, *i.e.*, some weighting of separate outputs in a common unit of measure such as dollar value (the value added approach), or in a disaggregated manner using innumerable units. In this study the latter route was taken. The output of community pharmacy was defined as the prescription service associated with the dispensing of a prescription. As the output measure, the number of prescriptions dispensed for the year was used.

The change in quality of this service during the study (1 year) was considered negligible.

The total cost was found by allocating total expenses for the pharmacy to the prescription department. The best method of cost allocation is direct separation of expenses of various departments. Unfortunately, the nature of the data was such that no expense items could be separated for the prescription area directly.

As a compromise, rent, heat, and light were allocated in proportion to the space utilized, since the cost of these items is dependent on area. Depreciation is a function of investment in capital. Since investment figures were unavailable, it was decided that equipment (fixtures and office machines) was better allocated on the basis of area rather than the alternative method of relative sales.

The remaining costs were allocated on the basis of the proportion of prescription sales to the total sales (13).

Cobb–Douglas production functions were originally applied to manufacturing industries, and measures of capital were tailored to fit these industries. Capital was taken as the value of plant, buildings, tools, and machinery (14). The annual rent paid by a pharmacy is a measure of the total value of the buildings. Similarly, the value of fixtures and equipment is expressed in the depreciation figure allowed for this item in the accounts of the firm.

Working capital in a retail establishment is an important part of the capital requirements. The value of the prescription department inventory was used as a substitute for this working capital since no other measure was available. Capital was obtained by summing allocated rent, depreciation, and inventory.

Table II—Statistics on Coefficients of Multiple Regression

Variable	Regression Coefficient	Standard Error of Regression Coefficient	*t* Value
Capital	0.66761	0.02473	26.996
Labor	0.34889	0.02148	16.244

[1] Data taken from Lilly Digest compilations, supplied by Eli Lilly & Co.

Labor was defined as the number of hours worked in the prescription department by professionals. No data were available for the time spent by nonprofessionals in prescription-related work. Employee pharmacists were considered as spending 100% of their time in the prescription department, while the pharmacist/manager divided his or her time in production to the relative sales of the prescription department and the remainder of the store. The measure of labor input was then equal to the sum of these two values for the year.

Functions—The total cost function was estimated by a polynomial regression of total cost on output.

The Cobb–Douglas production function was estimated by a multiple linear regression of natural logarithmic transformations of output on natural logarithmic transformations of labor and capital.

RESULTS AND DISCUSSION

Total Cost Function—The large sample size made the use of available polynomial regression programs impossible. The source program of BMD05R (15) was obtained, and its capacity was altered so that a seventh-order polynomial regression could be performed on the sample of 1374. Table I shows the analysis of variance for the regression. The table F value used to test significance of regression was $F_{1,1000,0.05} = 3.85$ (16).

The coefficients of regression were tested for difference from zero by the following t test (17):

$$t_{N-2} = \frac{bi - 0}{SeRC} \qquad \text{(Eq. 5)}$$

where bi = regression coefficients, N = sample size, and $SeRC$ = standard error of regression coefficient using the t value (18):

$$t_{1000,0.05} = 1.96 \qquad \text{(Eq. 6)}$$

For the purpose of this study, only first- and second-order terms were of value (19). Even so, all of the nonlinear terms together only explain an additional variance of 1.15% above the linear term.

Of the two relevant equations:

$$Y = 1921 + 1.13346X - 0.02263X^2 \qquad \text{(Eq. 7)}$$

$$Y = 4768 + 1.14793X \qquad \text{(Eq. 8)}$$

where Y = predicted total cost, and X = output. Equation 7 has a maximum value of 25 prescriptions; between 50 and 51 prescriptions, the total cost becomes less than the intercept. This curve clearly does not explain the real world and was rejected in favor of Eq. 8.

With a linear total cost function, marginal cost is constant at 1.14793. This finding leads to the conclusion that costs do not change with increasing size of the pharmacy.

Production Functions—A Cobb–Douglas production function was estimated using the multiple regression program BMD03R (20). An F-test ($F_{2,1371,0.05}$) was performed on the regression, and the value of 1060.0 was found to be significant. Table II shows the coefficients of labor and capital and the t-values associated with them. Both values of t were significant at the 0.05 level.

The sum of the coefficients was equal to 1.01650, which was not significantly different from one at the 0.05 level. This value was determined by a t test given by Murphy (21).

CONCLUSIONS

In this study, two different approaches were used to arrive at the same conclusion. No economies of scale were found in U.S. community pharmacy prescription departments. Constant marginal costs were found, based on cost data. The sum of the coefficients of the Cobb–Douglas production function coefficients was found to be unitary, pointing to constant returns to scale based on production data.

These results show that there is no difference between the economies of operation of the prescription departments of small pharmacies and larger ones. Apart from factors not considered in this study such as differences in cost of goods sold, a small pharmacy should be able to compete with a larger one in the prescription area but not necessarily in other areas such as nonprescription products or health and beauty aids.

REFERENCES

(1) L. Merewitz, *J. Amer. Statist. Ass.*, **66**, 504(1970).

(2) S. E. Berki, "Hospital Economics," D.C. Heath, Lexington, Mass., 1972, p. 51.

(3) J. R. Lave, *Inquiry*, **3**, 57(May 1966).

(4) R. M. Bailey, in "Empirical Studies in Health Economies," H. E. Klarman, Ed., Johns Hopkins Press, Baltimore, Md., 1970, p. 255.

(5) R. A. Gosselin and Co., "Pharmacy Charges for Prescription Drugs under Third Party Programs," report prepared for N.A.R.D./N.A.C.D.S., May 5, 1971.

(6) M. D. Jacoff, Ph.D. dissertation, Purdue University, Lafayette, Ind., 1961.

(7) S. E. Berki, J. W. Richards, and A. Weeks, "Prescription Dispensing in Twenty Pharmacies: Characteristics, Utilizers, Service, and Costs," report of a study conducted for the Social Security Administration, 1971.

(8) M. J. Myers, presented at the Economics and Administrative Sciences Section, APhA Academy of Pharmaceutical Sciences, Montreal, Canada, May 19, 1969.

(9) J. Johnston, "Statistical Cost Analysis," McGraw-Hill, New York, N.Y., 1960, p. 21.

(10) R. H. Leftwich, "The Price System and Resource Allocation," 4th ed., Dryden Press, Hinsdale, Ill., 1970, p. 164.

(11) A. A. Walters, *Econometrica*, **31**, 1(1963).

(12) P. H. Douglas, *Amer. Econ. Rev.*, **38**, 1(1948).

(13) M. D. Jacoff, Ph.D. dissertation, Purdue University, Lafayette, Ind., 1961, p. 8.

(14) P. H. Douglas, *Amer. Econ. Rev.*, **38**, 12(1948).

(15) "Biomedical Computer Programs," W. J. Dixon, Ed., University of California Press, Berkeley, Calif., 1971, p. 289.

(16) "Scientific Tables," K. Diem and C. Lentner, Eds., Ciba-Geigy Ltd., Basle, Switzerland, 1970, p. 40.

(17) J. L. Murphy, "Introductory Econometrics," Richard D. Irwin, Homewood, Ill., 1973, p. 212.

(18) "Scientific Tables," K. Diem and C. Lentner, Eds., Ciba-Geigy Ltd., Basle, Switzerland, 1970, p. 35.

(19) A. A. Walter, *Econometrica*, **31**, 45(1963).

(20) "Biomedical Computer Programs," W. J. Dixon, Ed., University of California Press, Berkeley, Calif., 1971, p. 258.

(21) J. L. Murphy, "Introductory Econometrics," Richard D. Irwin, Homewood, Ill., 1973, p. 228.

ACKNOWLEDGMENTS AND ADDRESSES

Received November 29, 1974, from the **Department of Health Care Administration and the ‡Department of Economics and Finance, University of Mississippi, University, MS 38677*

Accepted for publication March 10, 1975.

Presented at the APhA Academy of Pharmaceutical Sciences, New Orleans meeting, November 1974.

Supported in part by the Research Institute of Pharmaceutical Sciences, University of Mississippi. Assistance of Eli Lilly and Company, through the office of Mr. William Turenne, is gratefully acknowledged.

ˣ To whom inquiries should be directed.

Drug Permeation through Membranes V: Interaction of Diazepam with Common Excipients

E. G. LOVERING ˣ, C. A. MAINVILLE, and M. L. ROWE

Abstract □ The effects of common tablet excipients on the permeation of diazepam through polydimethylsiloxane membranes and on the turnover time of goldfish were studied. The permeability coefficient decreased and the turnover time increased in the presence of talc, polysorbate 80, and, possibly, fumed silicon dioxide, but these parameters were unaffected by lactose, microcrystalline cellulose, and starch.

Keyphrases □ Permeation—diazepam through polydimethylsiloxane membranes, effect of excipients □ Diazepam—permeation through polydimethylsiloxane membranes, effect of excipients □ Polydimethylsiloxane—membranes, permeation of diazepam, effect of excipients □ Membrane permeation—diazepam through polydimethylsiloxane, effect of excipients

Tablet and capsule excipients are known to influence the absorption of drugs from the GI tract. For example, low blood levels of phenytoin in epileptic patients were associated with a formulation containing calcium sulfate (1), and significant differences in the plasma level of dicumarol in dogs were reported with six of 10 excipients investigated (2).

Drug–excipient interactions can sometimes be detected by experiments *in vitro*. Thus, the dialysis rate of prednisolone was found to depend upon the drug formulation (3). The effect of excipients and other materials on the permeation of amobarbital (4), phenylbutazone (5), chlordiazepoxide (6), and chlorpromazine (7) through polydimethylsiloxane also was reported.

There is little direct evidence relating drug–excipient interactions observed *in vitro* to pharmacological effects observed *in vivo*. Therefore, the effects of excipients on the permeation of diazepam through polydimethylsiloxane membranes and on the turnover time of goldfish in a diazepam solution was examined.

EXPERIMENTAL

Permeation—Cells similar to those employed by Garrett and Chemburkar (8) were used, except that the 5-mil polydimethylsiloxane membranes were attached with silicone adhesive. The cells were placed in a beaker containing a solution of the drug buffered at pH 7 (phosphate buffer) and thermostated at 37.0°. The desorbing fluid within the permeation cells was dilute hydrochloric acid, pH 1.2.

The solutions were pumped continuously through the sample cells of a spectrophotometer set at 284 nm, and the absorbance was read at appropriate time intervals. Beer's law calibration curve, made with NF diazepam reference standard, yielded a molar absorptivity of 13,260. Permeation rates were obtained from the steady-state slope of graphs of moles of drug in the desorbing solution plotted against time.

Turnover Time—Diazepam solutions, about 2.1×10^{-4} mole/liter, were prepared for turnover time experiments by dissolving the drug in 25 ml of 0.5 *N* hydrochloric acid, neutralizing with 0.5 *N* sodium hydroxide, diluting to 2 liters, and adjusting the pH to 7.0. Excipients were added before the final pH adjustment.

Turnover time experiments were carried out by placing each fish in 250 ml of the diazepam solution at 25°. Each fish and each solution were used only once. The end-point was taken as that time when the fish failed to right itself within 1–2 sec after being turned over with a glass rod.

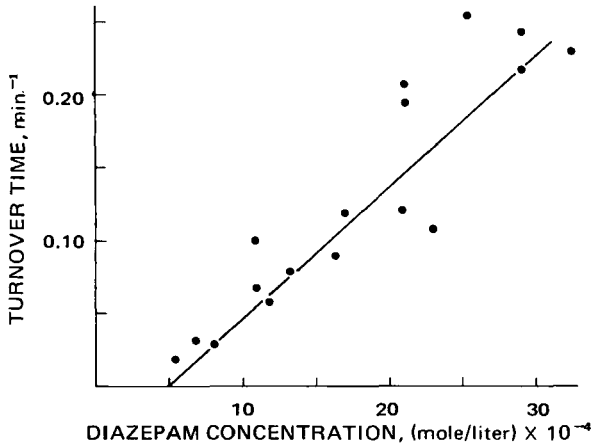

Figure 1—*Reciprocal turnover time of goldfish* versus *diazepam concentration.*

Some experiments were carried out using pairs of fish, one member of the pair being placed in a solution of the drug without excipient and the other being placed in the drug–excipient solution under test. The results were expressed as a ratio of drug–excipient turnover time to drug turnover time. This procedure reduced variations due to interbatch differences in the fish and in operator judgment of the turnover time.

The excipients were tested for toxicity by immersing fish in solutions or suspensions containing only the excipient at concentrations higher than those encountered under test conditions. After several hours the fish were removed to distilled water and observed for 24 hr. No adverse effects were noted.

Materials—Diazepam was used as received[1]. Other materials used were talc USP[2], starch USP[2], polysorbate 80[2], lactose USP[3], fumed silicon dioxide[4], and microcrystalline cellulose[5]. Goldfish (*Carassius auratus*), 3–6 cm in length, were obtained locally in batches of 50 or 100 fish.

RESULTS AND DISCUSSION

Characteristics of *In Vitro* System—The permeability coefficient, *P*, was calculated from:

$$P = \frac{(dq/dt)l}{AC} \qquad \text{(Eq. 1)}$$

where (dq/dt) is the rate at which drug permeates the cell membrane under steady-state conditions, l is the membrane thickness, A is its surface area, and C is the drug concentration outside the permeation cell. Steady-state conditions were achieved by an excess of drug outside the cell and a low pH within the cell. At low pH, diazepam is in the ionic state and the concentration of unionized drug is virtually zero. Ionized drug molecules are unlikely to permeate polydimethylsiloxane membranes.

Permeability coefficients were calculated from data obtained over a diazepam concentration range from 0.98×10^{-5} to $6.08 \times$

[1] Courtesy of Hoffmann–La Roche Ltd., Montreal, Quebec, Canada.
[2] Fisher Scientific Co., Montreal, Quebec, Canada.
[3] Courtesy of Peebles Products Ltd., Cornwall, Ontario, Canada.
[4] Courtesy of Cabot Carbon Corp., Boston, Mass.
[5] PH101, courtesy of FMC Corp., Marcus Hook, Pa.

Table I—Apparent Permeability Coefficients in Talc Slurry

Concentration of Talc, g/liter	Concentration, C_0, of Drug, moles/liter $\times 10^5$	Apparent Permeability[a] Coefficient, $(cm^2/sec) \times 10^6$	Equilibrium Concentration of Drug, mg/100 ml
1.5	5.303	1.58 ± 0.09	1.181
4.0	5.794	1.25 ± 0.06	1.021
6.0	5.303	1.06 ± 0.03	0.792
10.0	6.005	0.85 ± 0.04	0.720
20.0	5.478	0.62 ± 0.02	0.479

[a] Mean of three determinations ± *SD*.

10^{-5} mole/liter. The permeability coefficient was independent of concentration over this range, the mean being $(2.02 \pm 0.12) \times 10^{-6}$ cm^2/sec for 20 individual experiments. The permeability coefficient was independent of the pH of the drug solution over the 4.8–7.6 range.

Excipient interactions were investigated by adding excipient, either in solution or as a slurry, to the drug solution and calculating the permeability coefficient from the experimental permeation rate, dq/dt. If a drug–excipient interaction occurs, the concentration of free drug decreases and the permeability coefficient also appears to decrease. All excipient experiments were carried out at pH 7, and no pH correction was made as in previous studies (5, 6).

Characteristics of *In Vivo* System—To ensure that the behavior of goldfish toward diazepam was consistent with that observed toward other drugs (9, 10), the effect of changes in drug concentration on the time to the loss of the righting reflex was determined. The results were plotted as mean reciprocal turnover time *versus* concentration (Fig. 1). Each point represents the mean of experiments on four, six, or eight fish. In agreement with theoretical predictions and previous observations (11, 12), the results fall on a straight line. The minimum concentration for pharmacological effect was about 5×10^{-4} mole/liter of diazepam.

Lactose—The permeability coefficients of diazepam at lactose concentrations of 7.5, 40, and 80 g/liter were $(1.97 \pm 0.21) \times 10^{-6}$, $(1.94 \pm 0.04) \times 10^{-6}$, and $(1.87 \pm 0.06) \times 10^{-6}$ cm^2/sec, respectively (means of three experiments). These values were not significantly different from the permeability coefficient of the drug alone.

The turnover time of goldfish was not affected by lactose concentrations up to 40 g/liter. Turnover times were 5.61 ± 0.96, 6.08 ± 1.71, and 5.58 ± 1.18 min (means of eight fish) for lactose concentrations of 4, 8, and 40 g/liter, respectively, and a drug concentration of 2.111×10^{-5} mole/liter.

Lactose, at the concentrations investigated, appears to have no effect on the permeability coefficient of diazepam or on the turnover time of goldfish.

Microcrystalline Cellulose—Permeability coefficients calculated from measurements made in the presence of 2.5, 10.0, and 20.0 g/liter of microcrystalline cellulose were $(1.92 \pm 0.22) \times 10^{-6}$, $(1.98 \pm 0.07) \times 10^{-6}$, and $(1.87 \pm 0.12) \times 10^{-6}$ cm^2/sec, respectively (means of three experiments). These values were not significantly different from the permeability coefficient of diazepam alone.

Turnover times due to 2.111×10^{-5} mole/liter of diazepam in microcrystalline cellulose slurries of 5, 10, and 20 g/liter were 5.52 ± 1.15, 5.28 ± 0.83, and 5.65 ± 0.84 min, respectively (means of eight goldfish). There was no significant difference among these means at the 95% confidence level. Paired experiments, in which one fish was placed in a solution containing 20 g/liter of microcrystalline cellulose and drug and the other was placed in a solution of drug, showed no significant difference in turnover times: 7.31 ± 1.3 and 7.17 ± 1.3 min, respectively (means of four fish).

The permeability coefficient and the turnover time were not detectably influenced by microcrystalline cellulose.

Starch—Permeability coefficients of diazepam in the presence of 0.75, 3.75, 7.00, and 15.00 g/liter of starch were $(2.00 \pm 0.09) \times 10^{-6}$, $(1.88 \pm 0.11) \times 10^{-6}$, $(1.83 \pm 0.10) \times 10^{-6}$, and $(1.85 \pm 0.10) \times 10^{-6}$ cm^2/sec, respectively (means of three experiments). The values were not significantly different from the permeability of drug alone.

Talc—The permeability coefficient of diazepam appears to decrease if talc is slurried into the diazepam solution (Table I), prob-

Table II—Paired Turnover Times Using Talc

Concentration of Talc, g/liter	Number of Pairs of Fish	Mean Turnover Time, min: Drug	Mean Turnover Time, min: Drug and Excipient	Ratio of Turnover Time
2	4	6.10 ± 1.10	6.15 ± 1.43	1.01
4	8	6.21 ± 1.28	10.02 ± 3.02	1.61[a]
6	8	6.21 ± 1.28	8.56 ± 1.97	1.38[a]
6	4	8.02 ± 0.87	13.93 ± 1.16	1.75
8	8	6.21 ± 1.28	13.55 ± 3.13	2.18[a]
10	4	5.50 ± 0.82	14.42 ± 1.23	2.36
10	8	6.21 ± 1.28	15.05 ± 1.89	2.42[a]

[a] Experiments done on the same batch of fish but not using the paired technique.

Table III—Apparent Permeability Coefficients in Fumed Silicon Dioxide

Concentration of Fumed Silicon Dioxide, g/liter	Concentration, C_0, of Drug, moles/liter $\times 10^5$	Apparent Permeability Coefficient[a], $(cm^2/sec) \times 10^6$	Equilibrium Concentration of Drug, moles/liter $\times 10^5$
0.5	5.443	1.98 ± 0.07	5.335
2.0	6.040	1.81 ± 0.04	5.412
3.5	5.724	1.80 ± 0.10	5.101
8.0	5.338	1.24 ± 0.04	3.277

[a] Mean of three determinations ± *SD*.

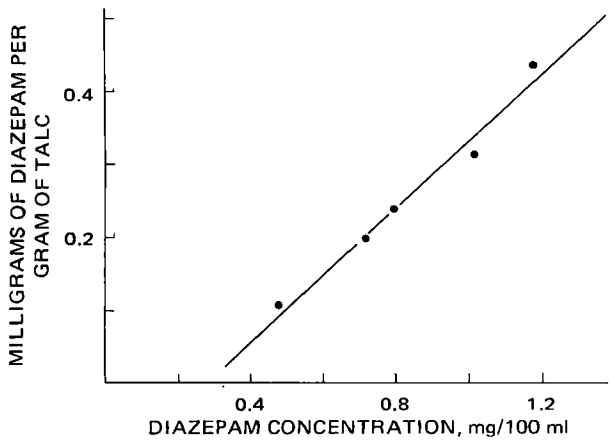

Figure 2—*Equilibrium ratio of drug to talc plotted against the concentration of drug.*

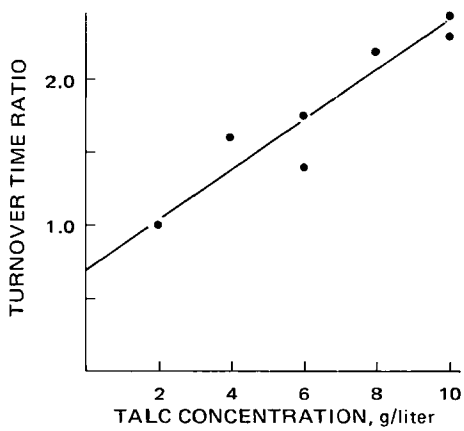

Figure 3—*Ratio of turnover times, drug in talc slurry to drug, plotted against the concentration of talc.*

Table IV—Paired Turnover Times Using Fumed Silicon Dioxide

Concentration of Fumed Silicon Dioxide, g/liter	Number of Pairs of Fish	Mean Turnover Time, min		Ratio of Turnover Times
		Drug	Drug and Excipient	
2	4	5.77 ± 1.28	6.39 ± 0.98	1.14 (NS)[a]
5	4	5.10 ± 0.71	7.75 ± 1.69	1.50
7	4	7.99 ± 2.02	10.14 ± 4.98	1.14 (NS)
7	4	6.56 ± 0.78	10.73 ± 0.98	1.66
10	4	6.17 ± 0.76	10.29 ± 1.51	1.65
10	4	8.88 ± 2.20	10.43 ± 1.42	1.22 (NS)

[a] NS = not significant.

ably due to drug adsorption on the talc surface. The apparent decrease in the permeability coefficient can be used to calculate the equilibrium concentration of drug in solution, C, from:

$$C = C_0 \frac{P_a}{P} \qquad \text{(Eq. 2)}$$

where C_0 is the initial drug concentration prior to the addition of talc, P_a is the permeability coefficient measured in the presence of talc, and P is the permeability coefficient uninfluenced by the excipient. A plot of drug adsorbed per gram of talc *versus* the equilibrium concentration of drug in solution (Fig. 2) indicates that the amount of drug adsorbed increases linearly with the equilibrium concentration of drug.

The results of *in vivo* experiments using the paired fish technique were expressed as the ratio of the turnover times with and without talc slurried into the drug solution. The initial drug concentration was held constant (Fig. 3). The experimental data are given in Table II.

Talc is usually present in formulations only to the extent of a few percent, although amounts over 40% have been observed. The data suggest that the interaction between talc and diazepam would be important in cases where formulations high in talc content were taken under conditions of low fluid content in the GI tract. Such conditions occur, and prudence suggests that excessive amounts of talc should not be used in formulating diazepam.

Fumed Silicon Dioxide—A modest reduction in the permeability coefficient was observed with the addition of increased quantities of fumed silicon dioxide to the diazepam solution (Table III).

Table V—Apparent Permeability Coefficients in Polysorbate 80 Solution

Concentration of Polysorbate 80, g/liter	Apparent Permeability Coefficient[a], $(cm^2/sec) \times 10^6$	Concentration, C_0, of Drug, moles/liter $\times 10^5$	Equilibrium Concentration of Drug, moles/liter $\times 10^5$
1.00	1.51 ± 0.07	5.092	3.806
1.75	1.25 ± 0.03	5.689	3.520
4.00	0.92 ± 0.04	4.916	2.239
10.00	0.62 ± 0.10	5.549	1.703

[a] Mean of three determinations ± *SD*.

Table VI—Mean Turnover Times Using Polysorbate 80

Concentration of Polysorbate 80, g/liter	Turnover Time[a], min	Significant Difference[b] (95% Confidence)
0.0000	6.21 ± 1.28	
0.0056	4.74 ± 0.51	S
0.0127	3.90 ± 0.91	S
0.0283	4.19 ± 0.70	S
0.0444	4.51 ± 0.95	S
0.0573	4.52 ± 0.60	S
0.0828	6.23 ± 1.23	NS
0.1081	7.08 ± 2.07	NS
0.2017	4.72 ± 1.77	NS

[a] Mean of eight fish ± *SD*. [b] Between turnover time at zero concentration of polysorbate 80. S = significant, and NS = not significant.

Experiments carried out using the paired goldfish technique suggest the possibility of a weak effect at concentrations over 5.0 g/liter of fumed silicon dioxide (Table IV). Unpaired experiments at 1.0, 2.0, 5.0, and 10 g/liter of fumed silicon dioxide yielded turnover times of 5.61 ± 0.81, 7.26 ± 1.01, 6.64 ± 0.46, and 7.15 ± 2.19 min, respectively (means of eight fish). The differences between the effects of 1.0 g and of 2.0 and 5.0 g were significant at the 95% level, but the difference between 1.0 and 10 g was not.

There may be a slight interaction between diazepam and fumed silicon dioxide. However, at the concentrations used in formulation manufacture, usually less than 1%, the interaction is unlikely to affect absorption adversely.

Polysorbate 80—The permeation rate of diazepam through polydimethylsiloxane membranes declined as the concentration of polysorbate 80 was increased up to 10 g/liter (Table V). The effect was probably due to partitioning of the drug between the aqueous phase and the micelles of the surfactant. The partition coefficient was calculated to be about 60, using a method described previously (4).

Polysorbate 80 at concentrations in the region of the critical micelle concentration (CMC) is known to increase the absorption of certain drugs by goldfish and to retard absorption at higher concentrations (13, 14). The results (Table VI) with diazepam are in general agreement with these findings. In the concentration range straddling the CMC of 0.014 g/liter (15), there was a significant decrease in the turnover time; but at a concentration above 0.0573 g/liter and up to at least 0.2017 g/liter of surfactant, there was no significant difference at the 95% level of confidence. The concentration ranges of the *in vitro* and *in vivo* experiments do not overlap because of the toxic effect of higher surfactant concentrations on the fish. The results suggest that low concentrations of polysorbate 80 may increase the rate of diazepam absorption.

REFERENCES

(1) J. H. Tyrer, M. J. Eadie, J. M. Sutherland, and W. D. Hooper, *Brit. Med. J.*, **4**, 271(1970).

(2) M. J. Abers, J. L. Lach, and L. J. Fischer, *J. Pharm. Sci.*, **62**, 391(1973).

(3) R. E. Northern, J. L. Lach, and J. H. Fincher, *Amer. J. Hosp. Pharm.*, **30**, 622(1973).

(4) E. G. Lovering and D. B. Black, *J. Pharm. Sci.*, **62**, 602(1973).

(5) *Ibid.*, **63**, 671(1974).

(6) E. G. Lovering, D. B. Black, and M. L. Rowe, *J. Pharm. Sci.*, **63**, 1224(1974).

(7) M. Nakano, *ibid.*, **60**, 571(1971).

(8) E. R. Garrett and P. B. Chemburkar, *ibid.*, **57**, 944(1968).

(9) G. Levy and S. P. Gucinski, *J. Pharmacol. Exp. Ther.*, **146**, 80(1964).

(10) M. Gibaldi and C. H. Nightingale, *J. Pharm. Sci.*, **57**, 226(1968).

(11) C. H. Nightingale and M. Gibaldi, *ibid.*, **60**, 1360(1971).

(12) S. H. Yalkowsky, O. S. Carpenter, G. L. Flynn, and T. G. Slunick, *ibid.*, **62**, 1949(1973).

(13) A. Kaneda, K. Nishimura, S. Muranishi, and H. Sezaki, *Chem. Pharm. Bull.*, **22**, 523(1974).

(14) J. A. Anello and G. Levy, *J. Pharm. Sci.*, **58**, 721(1969).

(15) L. S. C. Wan and P. F. S. Lee, *ibid.*, **63**, 136(1974).

ACKNOWLEDGMENTS AND ADDRESSES

Received February 6, 1975, from the *Drug Research Laborato-*

ries, Health Protection Branch, Health and Welfare Canada, Ottawa, Ontario K1A OL2, Canada.

Accepted for publication April 30, 1975.
[x] To whom inquiries should be directed.

Effect of Dimethyl Sulfoxide on Permeability of Human Skin *In Vitro*

J. P. ASTLEY and M. LEVINE [x]

Abstract □ A diffusion flow cell is described for the continuous monitoring of skin permeability. The technique was used to study the permeability behavior of human skin subsequent to treatment with dimethyl sulfoxide. Such treatment produced an increased penetration rate of tritiated water, which was dependent upon the time of exposure and the concentration of dimethyl sulfoxide applied. Removal of the solvent resulted in partial recovery of barrier capacity. Skin, incubated *in vitro* in growth medium containing dimethyl sulfoxide, survived only at very low concentrations. Degeneration occurred after a few days in 4.5% dimethyl sulfoxide and much sooner at higher concentrations.

Keyphrases □ Dimethyl sulfoxide—effect on growth and permeability of human skin *in vitro*, diffusion flow monitoring cell described □ Permeability—human skin *in vitro*, effect of dimethyl sulfoxide □ Diffusion flow cell—description, continuous monitoring of skin permeability *in vitro* □ Skin, human—effect of dimethyl sulfoxide on growth and permeability *in vitro*

There are numerous reports concerning the enhancement of skin permeability by dimethyl sulfoxide (I) but very little agreement regarding the extent or degree of reversibility of this effect. High concentrations of I *in vivo* caused striking increases in permeability, which were almost completely reversible upon removal (1). Measurement of *in vivo* water vapor loss found an 11- to 17-fold permeability increase subsequent to contact with I, and the effect was partially reversible (2); other results (3) indicated a 25-fold increase in penetration of hexapyronium bromide *in vivo* after exposure to 50% I, with no mention of reversibility.

In vitro work has yielded more quantitative data. A maximum of a 66-fold permeability increase was found upon exposure to I, but the degree of reversibility was variable (4). With I–water mixtures, there was no effect until 60–70% I was applied (5). A 90-fold increase observed with 100% I was not reversible. Concentrations in excess of 70% I were necessary to produce appreciable enhancement of picrate-ion penetration, and such concentrations reduced the lag time from 5 to 2 hr (6). Subsequently it was demonstrated that the effect was not reversible (7).

In the present study, the effect of varying exposure times and concentrations of I on the permeability to tritiated water was investigated. Preliminary experiments revealed a rapid recovery of a fraction of the initial barrier capacity upon removal of I. Therefore, a continuous diffusion flow cell was developed to follow the permeability behavior in a more quantitative manner.

An *in vitro* system (8) was used to study the effect of I on the growth and maturation of human epidermis and thus to relate toxicity levels to the concentrations that enhance penetration.

Table I—Permeability of Human Skin to Tritiated Water Subsequent to Storage[a] at −20°

Sample	Storage Time at −20°			
	Zero	1 Month	3 Months	6 Months
1	3.2 ± 0.1[b]	2.3 ± 0.7	4.3 ± 0.2	3.4 ± 0.4
2	3.8 ± 0.1	3.4 ± 1.0	4.3 ± 0.3	3.2 ± 0.9
3	4.1 ± 0.2	1.8 ± 0.5	4.5 ± 0.4	3.4 ± 0.9
4	3.5 ± 0.3	2.4 ± 0.6	5.9 ± 3.0	2.6 ± 0.6

[a] Permeability coefficients × 10^7 (cm/sec). [b] Errors are quoted as ±95% confidence limits.

EXPERIMENTAL

Skin Samples—Excised thigh or lower leg skin (nominally 0.38 mm thickness) was obtained from amputated limbs using a battery-operated dermatome[1]. Before excision, the skin was cleaned by swabbing with 0.5% chlorhexidine in 70% ethanol, followed by 50% ethanol.

Strips of skin were rolled in sterile gauze, moistened with Hank's balanced salt solution, and stored in screw-capped containers at −20° until required for use. Such storage did not significantly affect the permeability of the skin (Table I).

Skin for growth studies was stored at 4° until required for use. This storage was without effect upon subsequent behavior (9).

Organ Culture—Explants were incubated by the method described by Levine (8) and harvested at 2, 4, 8, 11, 17, and 22 days after 24 hr in medium labeled with thymidine-6-T[2], 1 μCi/ml.

Dimethyl sulfoxide in growth medium[3] was tested at concentrations of 0, 0.9, 4.5, and 9% I.

Histology and Autoradiography—The methods used were described previously (8).

Diffusion Cells—*Glass Diffusion Cell*—The design and use of this type of cell were described previously (9). The "initial" permeability of the skin specimen is determined by filling the dermal compartment with a phosphate buffer medium (pH 7.0) and applying to the epidermal side a known volume of the same medium containing tritiated water[4] at a concentration of 80 μCi/ml.

[1] Davol Ltd., Providence, R.I.
[2] Radiochemical Centre, Amersham, Bucks, England.
[3] Eagle's Minimal Essential Medium plus 10% fetal bovine serum.
[4] Radiochemical Centre, Amersham, Bucks, England.

ries, Health Protection Branch, Health and Welfare Canada, Ottawa, Ontario K1A OL2, Canada.

Accepted for publication April 30, 1975.
[x] To whom inquiries should be directed.

Effect of Dimethyl Sulfoxide on Permeability of Human Skin *In Vitro*

J. P. ASTLEY and M. LEVINE [x]

Abstract □ A diffusion flow cell is described for the continuous monitoring of skin permeability. The technique was used to study the permeability behavior of human skin subsequent to treatment with dimethyl sulfoxide. Such treatment produced an increased penetration rate of tritiated water, which was dependent upon the time of exposure and the concentration of dimethyl sulfoxide applied. Removal of the solvent resulted in partial recovery of barrier capacity. Skin, incubated *in vitro* in growth medium containing dimethyl sulfoxide, survived only at very low concentrations. Degeneration occurred after a few days in 4.5% dimethyl sulfoxide and much sooner at higher concentrations.

Keyphrases □ Dimethyl sulfoxide—effect on growth and permeability of human skin *in vitro*, diffusion flow monitoring cell described □ Permeability—human skin *in vitro*, effect of dimethyl sulfoxide □ Diffusion flow cell—description, continuous monitoring of skin permeability *in vitro* □ Skin, human—effect of dimethyl sulfoxide on growth and permeability *in vitro*

There are numerous reports concerning the enhancement of skin permeability by dimethyl sulfoxide (I) but very little agreement regarding the extent or degree of reversibility of this effect. High concentrations of I *in vivo* caused striking increases in permeability, which were almost completely reversible upon removal (1). Measurement of *in vivo* water vapor loss found an 11- to 17-fold permeability increase subsequent to contact with I, and the effect was partially reversible (2); other results (3) indicated a 25-fold increase in penetration of hexapyronium bromide *in vivo* after exposure to 50% I, with no mention of reversibility.

In vitro work has yielded more quantitative data. A maximum of a 66-fold permeability increase was found upon exposure to I, but the degree of reversibility was variable (4). With I–water mixtures, there was no effect until 60–70% I was applied (5). A 90-fold increase observed with 100% I was not reversible. Concentrations in excess of 70% I were necessary to produce appreciable enhancement of picrate-ion penetration, and such concentrations reduced the lag time from 5 to 2 hr (6). Subsequently it was demonstrated that the effect was not reversible (7).

In the present study, the effect of varying exposure times and concentrations of I on the permeability to tritiated water was investigated. Preliminary experiments revealed a rapid recovery of a fraction of the initial barrier capacity upon removal of I. Therefore, a continuous diffusion flow cell was developed to follow the permeability behavior in a more quantitative manner.

An *in vitro* system (8) was used to study the effect of I on the growth and maturation of human epidermis and thus to relate toxicity levels to the concentrations that enhance penetration.

Table I—Permeability of Human Skin to Tritiated Water Subsequent to Storage[a] at −20°

Sample	Storage Time at −20°			
	Zero	1 Month	3 Months	6 Months
1	3.2 ± 0.1[b]	2.3 ± 0.7	4.3 ± 0.2	3.4 ± 0.4
2	3.8 ± 0.1	3.4 ± 1.0	4.3 ± 0.3	3.2 ± 0.9
3	4.1 ± 0.2	1.8 ± 0.5	4.5 ± 0.4	3.4 ± 0.9
4	3.5 ± 0.3	2.4 ± 0.6	5.9 ± 3.0	2.6 ± 0.6

[a] Permeability coefficients × 10^7 (cm/sec). [b] Errors are quoted as ±95% confidence limits.

EXPERIMENTAL

Skin Samples—Excised thigh or lower leg skin (nominally 0.38 mm thickness) was obtained from amputated limbs using a battery-operated dermatome[1]. Before excision, the skin was cleaned by swabbing with 0.5% chlorhexidine in 70% ethanol, followed by 50% ethanol.

Strips of skin were rolled in sterile gauze, moistened with Hank's balanced salt solution, and stored in screw-capped containers at −20° until required for use. Such storage did not significantly affect the permeability of the skin (Table I).

Skin for growth studies was stored at 4° until required for use. This storage was without effect upon subsequent behavior (9).

Organ Culture—Explants were incubated by the method described by Levine (8) and harvested at 2, 4, 8, 11, 17, and 22 days after 24 hr in medium labeled with thymidine-6-T[2], 1 μCi/ml.

Dimethyl sulfoxide in growth medium[3] was tested at concentrations of 0, 0.9, 4.5, and 9% I.

Histology and Autoradiography—The methods used were described previously (8).

Diffusion Cells—*Glass Diffusion Cell*—The design and use of this type of cell were described previously (9). The "initial" permeability of the skin specimen is determined by filling the dermal compartment with a phosphate buffer medium (pH 7.0) and applying to the epidermal side a known volume of the same medium containing tritiated water[4] at a concentration of 80 μCi/ml.

[1] Davol Ltd., Providence, R.I.
[2] Radiochemical Centre, Amersham, Bucks, England.
[3] Eagle's Minimal Essential Medium plus 10% fetal bovine serum.
[4] Radiochemical Centre, Amersham, Bucks, England.

Table II—Effect of Exposure to Dimethyl Sulfoxide upon Subsequent Permeability of Skin to Tritiated Water[a]

		Exposure Time, min					
		0	5	15	30	60	120
Initial (least squares)		2.56 ± 0.27	1.89 ± 0.45	2.08 ± 0.17	2.47 ± 0.72	2.24 ± 0.13	2.52 ± 0.69
Test	75 min	2.28	9.23	29.2	36.1	47.3	62.9
(individual	135 min	1.96	7.85	20.5	27.9	33.1	32.0
values)[b]	210 min	2.19	6.94	17.6	24.3	34.2	43.7
	300 min	2.18	7.13	13.4	21.1	28.3	34.0
	405 min	2.22	5.84	14.2	16.1	26.3	29.1
	525 min	2.37	5.80	10.2	15.8	22.8	32.5
Recovery (least squares)		2.55 ± 0.31	4.20 ± 0.56	9.4 ± 0.9	15.2 ± 4.3	20.2 ± 1.85	20.2 ± 2.1

[a] Permeability coefficients × 10^7 (cm/sec) ±95% confidence limits. [b] Individual values refer to calculation of an individual permeability coefficient for each sample taken during the measurement by substitution of the relevant values into the rate equation.

Samples are removed from the dermal compartment at required time intervals and replaced by buffer. The activity of the samples and a suitably diluted standard is determined in ethanolic scintillator[5] using a liquid scintillation spectrometer[6].

The cell is emptied, and all radioactivity is washed from the skin by soaking in several changes of buffer. The skin is then dried and exposed to I for the required time interval. After the solvent is removed, the "test" permeability is determined in the same way as described for initial permeability. Twenty-four hours later, "recovery" is determined, giving the skin permeability subsequent to recovery of barrier capacity. Permeability coefficients are calculated as described previously (9).

Diffusion Flow Cell—The Perspex cell is shown in Fig. 1 with a specimen of skin inserted between the two blocks and clamped into position using three nylon screws. Tubing is stainless steel (18 gauge).

The assembled apparatus is shown in Fig. 2. Buffered medium containing tritiated water (80 μCi/ml) is placed in the donor compartment and stirred. Buffered medium flows from the reservoir through the acceptor compartment in the direction shown by arrows; the geometry of this compartment ensures efficient elution of penetrant from the whole surface of the skin. The eluent passes *via* a small prefilter to a scintillation flow cell assembly[7].

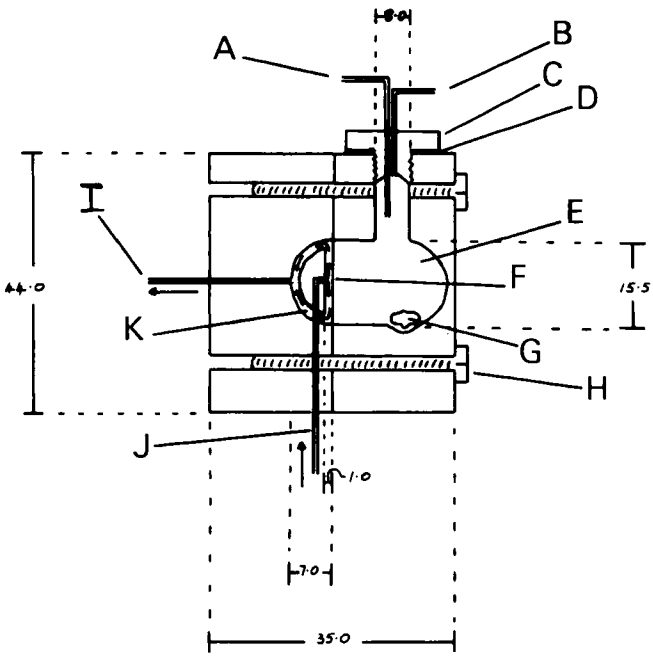

Figure 1—*Diffusion flow cell. Key: A, application tube; B, removal tube; C, donor compartment stopper; D, Neoprene rubber washer; E, donor compartment; F, skin specimen clamped between Perspex blocks; G, stirrer; H, clamping screw; I, inlet tube; J, acceptor compartment; and K, outlet tube.*

The prefilter, a glass tube packed with anthracene and plugged with glass wool at each end, removes any contaminants in the eluent which might otherwise adsorb onto the anthracene in the scintillation flow cell and affect the counting efficiency. It also prevents any air bubbles in the system from reaching the scintillation flow cell. A constant flow rate is maintained using a peristaltic pump[8].

The procedure is as follows. The apparatus is assembled as shown in Fig. 2 but omitting the diffusion flow cell. Background is determined by passing buffered medium through for long periods, so background subtraction can be carried out automatically. The activity of the donor solution is now determined by passing a suitably diluted solution through the scintillation cell. Measurement of donor activity is repeated at the end of the determinations to ensure that there has been no change in counting efficiency over the test period.

The skin is now clamped between the two Perspex blocks of the diffusion cell, using a small amount of vacuum grease around the edge of the skin to maintain an efficient seal. The acceptor compartment is filled by means of a syringe, and its volume is adjusted so that the skin is planar. The inlet and outlet are clamped until the donor compartment is filled and sealed, the fixed volume maintaining planarity of the skin when flow begins.

The donor compartment volume (V_0) is determined by weighing. The diffusion cell is then inserted into the system, and stirring of the donor compartment and flow through the acceptor compartment are commenced. The flow rate is determined by weighing the eluent collected in a known time interval. The counting interval is chosen to suit the rate of permeability change observed. Permeability values for any time interval may then be calculated from Eq. A8 (*Appendix*).

RESULTS AND DISCUSSION

Glass Diffusion Cell—Permeability was measured before exposure (initial), immediately after exposure (test), and 24 hr later (recovery). Two milliliters of I was applied to the epidermal surface of the skin, and the same time interval elapsed between removal of the solvent and the beginning of the test determination

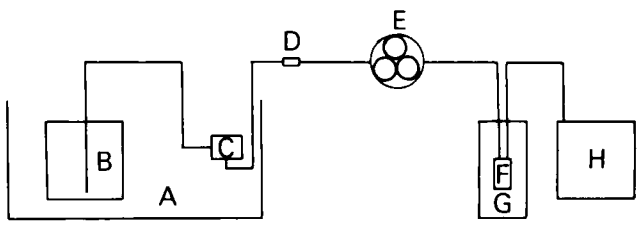

Figure 2—*Block diagram of flow cell apparatus. Key: A, thermostated water bath; B, reservoir; C, diffusion flow cell; D, anthracene prefilter; E, peristaltic pump; F, flow cell; G, scintillation counter; and H, collector.*

[5] Composed of 0.4% 2,5-diphenyloxazole and 0.04% 1,4-bis[2-(4-methyl-5-phenyloxazolyl]benzene in xylene–ethanol (68:30, v:v).
[6] Packard Tri-Carb model 3320.
[7] Packard Ltd.
[8] L.K.B. Varioperpex model 12000.

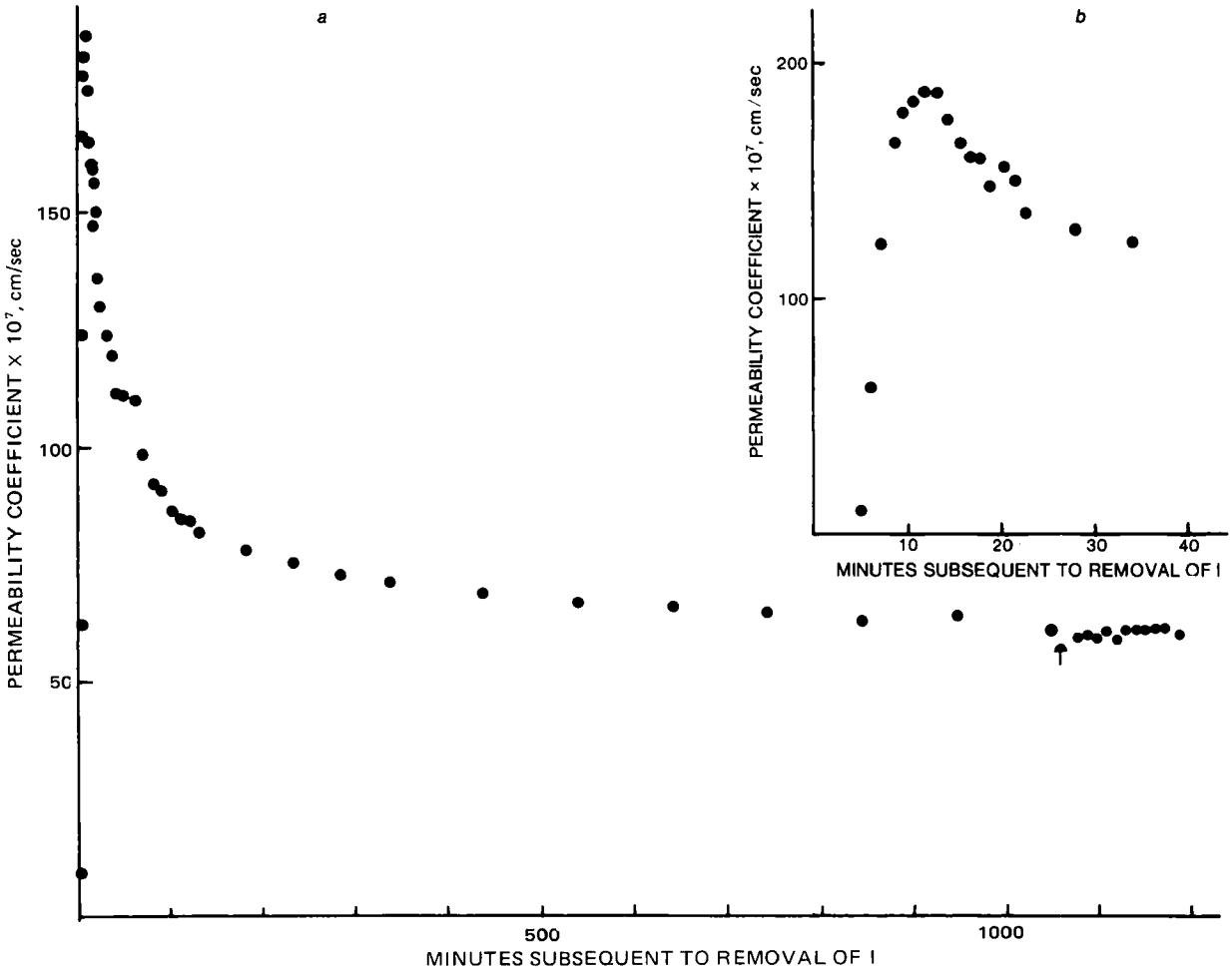

Figure 3—(a) *Permeability of human skin to tritiated water subsequent to dimethyl sulfoxide (I) treatment. Arrow refers to the replenishment of the donor solution. The final permeability value is obtained subsequent to the replenishment.* (b-*insert*) *Permeability of human skin to tritiated water subsequent to dimethyl sulfoxide treatment (early part of Fig. 3a plotted on an expanded time scale). The apparent rise in permeability to a peak value at 12 min is due to a lag phase inherent in the method of measurement. The peak permeability is given by the maximum in the plot.*

for each skin specimen. During exposure to I, no solution was in contact with the dermal surface of the skin. The results of one of two similar experiments are given in Table II.

Permeability values are usually calculated from the slope of the straight line obtained by least squares from a plot between ($t_n - t_{n-1}$) and the left side of the equation (see Eq. 14 in Ref. 9):

$$-\ln\left[\frac{C_T - (\chi/V_0)\sum_1^{n-1} C_i - C_{i(n)}(V_T/V_0)}{C_T - (\chi/V_0)\sum_1^{n-1} C_i - C_{i(n-1)}(V_T/V_0)\{1 - [\chi/(V_T - V_0)]\}}\right] = PA(t_{(n)} - t_{(n-1)})\frac{V_T}{V_0(V_T - V_0)} \quad \text{(Eq. 1)}$$

Once the steady state is established, such a plot is linear and the intercept on the ordinate (left side of Eq. 1) is close to zero.

A steady state was observed for initial and recovery permeability determinations, and the values calculated are given in Table II. But during the test determination, the steady state was not maintained, resulting in a marked curvature when counts of radioactivity were plotted against time. The linear plot according to Eq. 1 had an intercept significantly greater than that observed for initial or recovery data. This result could be due either to an initial high permeability decreasing over the test period or to the presence of residual radioactivity in the acceptor compartment of the diffusion cell at the start of the test determination. The possibility of residual radioactivity was eliminated by another experiment in which the initial permeability determination was omitted.

Results (Table III) from specimens exposed to I exhibited the large negative intercept on the ordinate of the linear plot. The individual test permeability values calculated for specimens exposed to I (Tables II and III) showed a decrease during the measurement period. An estimate of the reversibility can be obtained, since the first sample gives an approximation to the maximum value and the recovery gives the final effect, indicating approximately 50% recovery of barrier capacity subsequent to removal of the solvent. Another noticeable feature was the increase in both temporary and permanent effects with an increase in exposure time.

Diffusion Flow Cell—Skin specimens were mounted on the flow cell and exposed to the required treatment. Then the solvent was removed, and the permeability of the skin was monitored con-

Table III—Permeability Coefficients x 10^7 (cm/sec) Subsequent to Dimethyl Sulfoxide Exposure

		Exposure Time, hr			
		16	16	0	0
Test (individual values)[a]	70 min	130	133	1.49	2.88
	120 min	104	122	1.82	2.66
	180 min	103	93	1.81	3.30
	250 min	91	83	1.92	3.02
	330 min	69	111	2.00	2.76
	420 min	71	84	2.19	4.11
Intercept x 10^4		−757.4	−484.1	+8.0	+16.1

[a] Individual values refer to calculation of an individual permeability coefficient for each sample taken during the measurement by substitution of the relevant values into the rate equation.

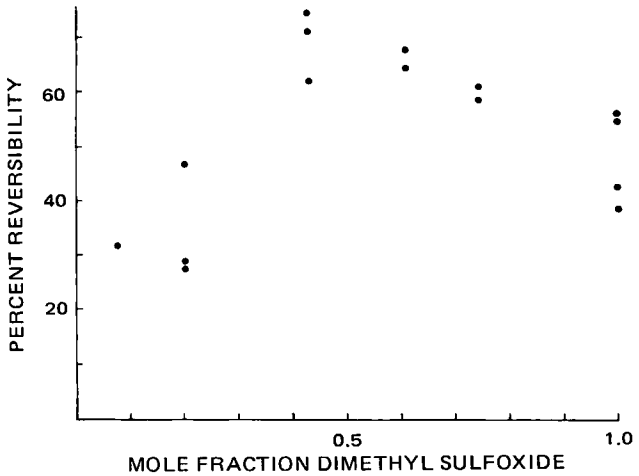

Figure 4—*Effect of dimethyl sulfoxide concentration upon reversibility of permeability enhancement (calculated from data in Table V).*

tinuously for 16–20 hr, *i.e.*, until a constant value was observed. The type of behavior exhibited is shown in Fig. 3*a*. Figure 3*b* (insert) shows the first portion of Fig. 3*a* plotted on an expanded time scale. The maximum permeability observed is shown by the peak in the plot of permeability coefficient against time. Permeability then decreased to a final steady value.

Replacement of the donor solution was carried out (indicated by the arrow in Fig. 3*a*) to avoid any possibility of its depletion. Final permeability values were obtained subsequent to the replacement. To ensure that the behavior observed for treated skin specimens was due to barrier recovery, a measurement was carried out using dialysis tubing. A steady permeability, fivefold greater than that observed for treated skin specimens, was obtained, thus confirming the validity of the technique.

The "maximum" and "final" permeability values for a series of pretreatment times are given in Table IV. A significant increase in permeability was observed after 30 min of exposure, the maximum change being attained after 24 hr.

By using exposure conditions of 24 hr in contact with stirred solvent at room temperature, the effect of a range of concentrations was studied. The results obtained using skin from two different individuals are given in Table V. The concentration of dimethyl sulfoxide is expressed as mole fraction. The generally used "volume percent" artificially introduces a nonlinear element, since water is 55.5 *M* and I is only 14 *M*. The relationship between the final permeability coefficient and the mole fraction of dimethyl sulfoxide is nonlinear and possibly correlates with removal of one or more components of the stratum corneum[9]. The relationship between maximum permeability coefficient and concentration of I, although much less curved, is again nonlinear.

The permeability increase subsequent to treatment of the skin was consistently partially reversible upon removal of the solvent. The extent of reversibility varied with the concentration of I applied (Fig. 4). The curve in Fig. 4 passes through a maximum at mole fraction = 0.5, *i.e.*, a 1:1 molar ratio of dimethyl sulfoxide to water. The reduced reversibility observed at higher concentrations of I may have been due to more efficient extraction of barrier components.

The results suggest possible reasons for the widely varying reports concerning the effect of dimethyl sulfoxide upon skin.

1. The 24-hr period required to produce the maximum effect is considerably greater than that employed by most investigators, and the conditions vary.

2. Since the recovery of barrier is an extremely rapid process, conventional permeability measurement techniques may not detect a considerable portion of the effect.

3. Since water is 55.5 *M* and dimethyl sulfoxide is 14 *M*, contamination of the applied solvent by water may result in an appreciable reduction in the mole fraction of I present and hence a reduced effect upon permeability. This factor is particularly relevant if aqueous medium is in contact with the dermal surface of the skin when the dimethyl sulfoxide is applied to the epidermis.

[9] Unpublished data.

Table IV—Effect of Exposure Time

Time of Exposure to Dimethyl Sulfoxide[a]	Peak Permeability Coefficient[b], (cm/sec) × 10^7	Final Permeability Coefficient, (cm/sec) × 10^7
30 min	55	28.0
60 min	71	35.0
60 min	67	45.0
12 hr	143.5	75.0
12 hr	121.5	63.0
12 hr	135.0	65.0
24 hr (stirred)	250	183.0
12 hr (stirred)[c]	247	180.5

[a] Concentration of I applied was 100%. [b] Calculated from peak value observed on graph of permeability *versus* time subsequent to exposure. [c] Reapplication of I to same skin specimen that was used to study 24-hr effect.

Table V—Effect of Dimethyl Sulfoxide (I) Concentration

Mole Fraction of I in Treatment Solution	Peak Permeability Coefficient, (cm/sec) × 10^7		Final Permeability Coefficient, (cm/sec) × 10^7	
	(a)[a]	(b)[a]	(a)	(b)
0.0	—	—	7.3	—
0.076	(i)[b] 14.3	15.8	9.8	10.2
	(ii)[b]	14.8	—	9.95
0.202	(i) 19.1	39.3	13.6	11.0
	(ii) 25.0	39.4	13.3	14.1
	(iii) 28.6	—	20.8	—
0.431	(i) 84	91.0	32.0	25.2
	(ii) 136	—	35.0	—
	(iii) 120.5	—	35.5	—
0.608	(i) 185.0	91.0	60.0	33.7
	(ii) 182.0	—	65.5	—
0.744	(i) 205.0	200	86.0	70.0
	(ii) 241.0	193	94.0	73.0
1.00	(i) 312.0	248	143.0	180
	(ii) 332.0	—	205.0	—
	(iii) 252.0	—	155.0	—
	(iv) 312.0	—	137.0	—
	(v) 295.0	—	170.0	—

[a] (a) and (b) refer to experiments with skin from different individuals. [b] (i), (ii), *etc.*, refer to experiments using skin specimens from the same limb.

Scheuplein and Ross (4) reported enhancement of reversibility when the tissue was rinsed with 1-butanol between exposure to I and water contact. The exact role of the butanol was, however, uncertain. A decrease in permeability subsequent to exposure of human skin to 1-butanol was observed[9], and it was associated with extensive dehydration of the epidermis.

Claims of complete reversibility also have been made. These claims usually stem from *in vivo* work; the situation is complicated by active regeneration of the barrier, which has been shown to progress rapidly *in vivo* subsequent to injury.

The relationship between maximum permeability and dimethyl sulfoxide concentration was considerably less curved than data reported previously. A similar type of relationship was observed by Elfbaum and Laden (10) while studying the effect of I concentration upon swelling of hair fibers. The solvent also produced a swelling of globular proteins. In both cases, the swelling was reversible upon removal of the solvent, and a similar mechanism could possibly account for the barrier recovery observed in human stratum corneum.

Growth of Human Skin *In Vitro*—After 4 days of incubation in the absence of I, control explants of skin showed some thickening and vacuolization (Fig. 5*a*). By 17 days (Fig. 5*b*), further alteration of the normal growth pattern was observed. At this stage, there were two parakeratotic layers and below them were rapidly proliferating cells. This pattern of growth is generally found in organ culture of skin (8). Autoradiograms of the regenerating tis-

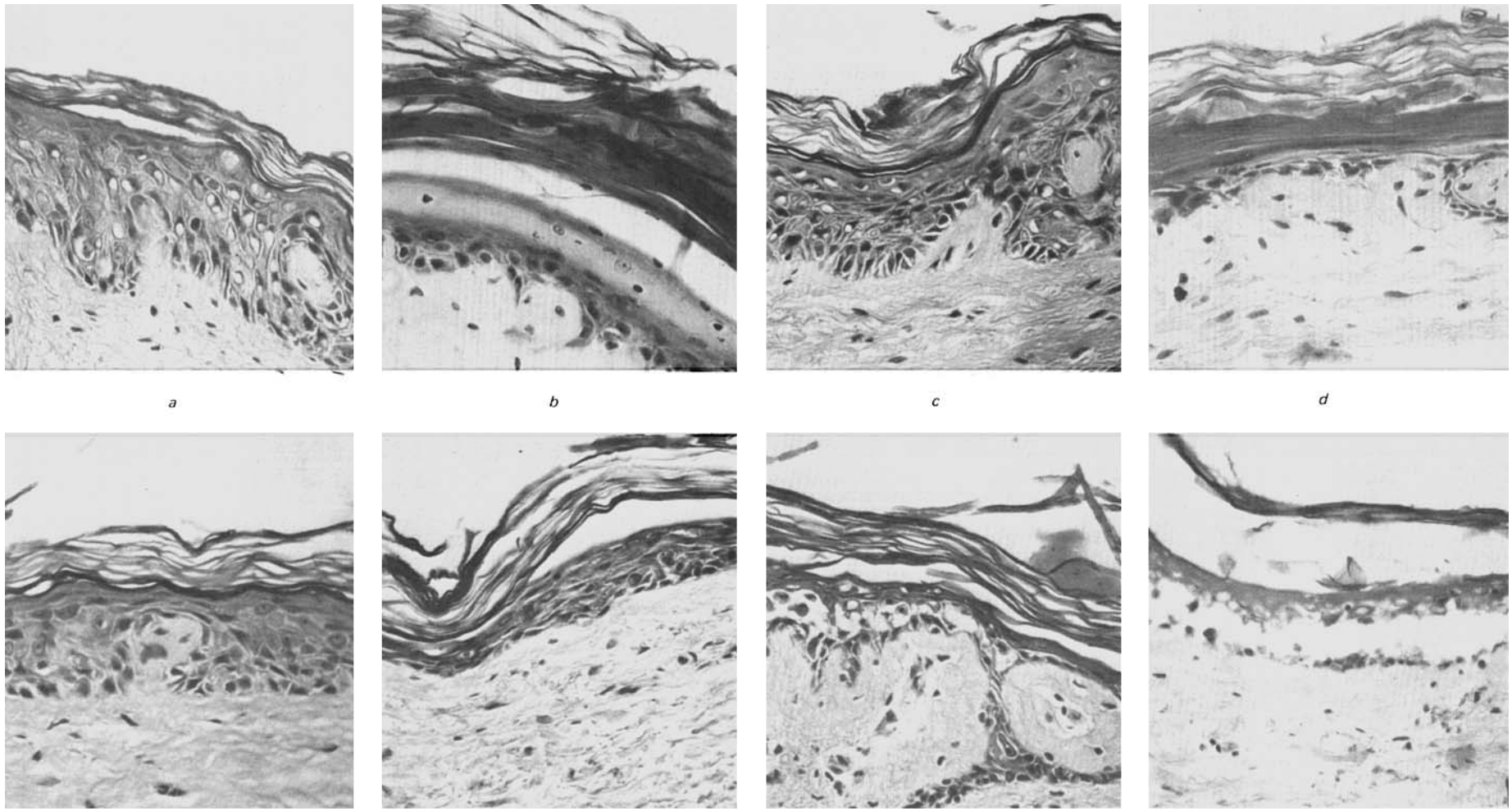

Figure 5—*Photographs of sections of skin showing the effect of dimethyl sulfoxide (I) on* in vitro *growth (×250, stained with hematoxylin and eosin).* (a) *and* (b)*: No I in the growth medium. Time of incubation was 4 days in* (a) *and 17 days in* (b)*. Vacuolization and the thickening of the epidermis can be observed in* (a)*. In* (b)*, parakeratotic layers have appeared and below them are proliferating cells.* (c) *and* (d)*: 0.9% I. Time of incubation was 4 days in* (c) *and 17 days in* (d)*. Growth of skin was similar to the control.* (e) *and* (f)*: 4.5% I. Time of incubation was 4 days in* (e) *and 11 days in* (f)*. There was no thickening at 4 days. Some flattening of the cells existed at 11 days, but no maturation was observed.* (g) *and* (h)*: 9% I. Time of incubation was 4 days in* (g) *and 17 days in* (h)*. Degeneration of the tissue was seen at 4 days, and complete disintegration was observed at 17 days.*

sue showed highly labeled cells subsequent to incubation in medium containing radioactively-labeled thymidine.

In the presence of 0.9% I, growth *in vitro* proceeded in a similar fashion to that in its absence. At 4 days, the organization of the malpighian layers was better in the presence of I (Fig. 5*c*) than in the control. At 17 days (Fig. 5*d*), the thick, parakeratotic layers indicated that growth and maturation had occurred.

Specimens in 0.9% I showed less epiboly (migration of cells around the explant) than the controls without I. In the first few days of cultivation, the stratum corneum of skin in 0.9% I appeared looser in structure, but this difference was not noticeable at longer incubation times.

DNA synthesis was evident throughout the incubation period in 0.9% I. At 11 and 17 days, autoradiograms showed more labeled cells than in the controls without I. The increase may have been due to an effect on the cell membranes resulting in an enhanced diffusion of thymidine. In addition, the thicker epiboly present in the control explants could have reduced the rate of diffusion. Both factors probably contributed to the difference observed in the degree of labeling. Another interpretation is that the presence of I resulted in alteration of the cell cycle.

In contrast, higher concentrations of I (4.5%) resulted in an absence of thickening of the epidermis at 4 days (Fig. 5*e*) and no subsequent maturation (Fig. 5*f*). In growth medium containing 9% I, the epidermis showed considerable degeneration at 4 days (Fig. 5*g*) and complete disintegration at 17 days (Fig. 5*h*).

In either 4.5 or 9% I, there was no epiboly at any time during 22 days of incubation. Malpighian cells began to degenerate after 2 days, and disintegration was more noticeable in 9% I. No maturation into a parakeratotic layer was observed; after 4 days, no DNA synthesis could be detected by autoradiography.

It would thus appear that 0.9% I in a growth medium did not prevent growth and maturation of epidermis *in vitro* over the 22-day period of the culture studies. Higher concentrations, however, of 4.5 and 9% I cannot support *in vitro* growth, as judged by histology and DNA synthesis.

APPENDIX

The derivation of the rate equation applied to flow cell data was as follows:

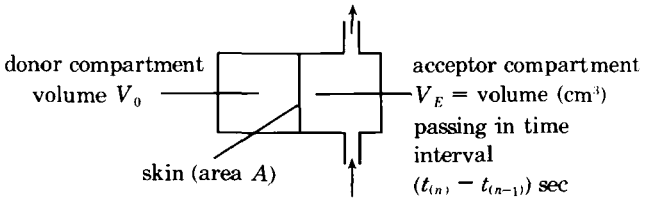

From Fick's law:

$$\frac{d}{dt} V_E C_E = PAC_0(t) \qquad \text{(Eq. A1)}$$

where P is the permeability coefficient, C_E is the concentration of penetrant in the eluent (cpm), and $C_0(t)$ is the concentration of donor solution at time t (cpm).

Application of the law of mass conservation gives:

$$C_0(t) = C_0(0) - \frac{V_E}{V_0} C_E(t) \qquad \text{(Eq. A2)}$$

where $C_0(0)$ is the concentration of penetrant in donor solution at time 0, and $C_E(t)$ is the concentration of penetrant in eluent at time t. Substituting from Eq. A2 into Eq. A1 gives:

$$\frac{d}{dt} V_E C_E = PA \left[C_0(0) - \frac{V_E}{V_0} C_E(t) \right] \qquad \text{(Eq. A3)}$$

Integrating from $C_{E(n-1)}$ to $C_{E(n)}$ and from $t_{(n-1)}$ to $t_{(n)}$ gives:

$$-\ln \left[\frac{C_0(0) - \frac{1}{V_0}\left(\sum_1^{n-1} V_E C_E\right) - \frac{1}{V_0}[(V_E C_E)_n]}{C_0(0) - \frac{1}{V_0}\left(\sum_1^{n-1} V_E C_E\right)} \right] = \frac{P_{(n)} A [t_{(n)} - t_{(n-1)}]}{V_0} \qquad \text{(Eq. A4)}$$

The left side is of the form $-\ln(1 - x)$ where:

$$x = \frac{\frac{1}{V_0}(V_E C_E)_{(n)}}{C_0(0) - \frac{1}{V_0}\left(\sum_1^{n-1} V_E C_E\right)} \qquad \text{(Eq. A5)}$$

Then, provided $x \ll 1$[10], Eq. A4 becomes:

$$\frac{(V_E C_E)_{(n)}}{C_0(0) - \frac{1}{V_0}\left(\sum_1^{n-1} V_E C_E\right)} = P_{(n)} A [t_{(n)} - t_{(n-1)}] \qquad \text{(Eq. A6)}$$

Hence:

$$P_{(n)} = \frac{(V_E C_E)_{(n)}}{\left[C_0(0) - \frac{1}{V_0}\left(\sum_1^{n-1} V_E C_E\right) \right] A [t_{(n)} - t_{(n-1)}]} \qquad \text{(Eq. A7)}$$

As written in Eq. A7, V_E represents the volume flowing through the flow cell in time period $(t_{(n)} - t_{(n-1)})$. The instrument has a noncounting interval of 10.5 sec between counting periods, and the volume flowing in this time interval must be included in the summation term. Thus, if $(t_{(n)} - t_{(n-1)})$ is expressed in seconds, Eq. A7 becomes:

$$P_{(n)} = \frac{(V_E C_E)_{(n)}}{\left[C_0(0) - \frac{1}{V_0} \sum_1^{n-1} \left(\frac{(t_{(n)} - t_{(n-1)} + 10.5)}{t_{(n)} - t_{(n-1)}} \right) V_E C_E \right] A [t_{(n)} - t_{(n-1)}]} \qquad \text{(Eq. A8)}$$

REFERENCES

(1) A. M. Kligman, *J. Amer. Med. Ass.*, **193**, 10, 796(1965).

(2) H. Baker, *J. Invest. Dermatol.*, **50**, 4, 283(1968).

(3) R. B. Stoughton and W. Fritsch, *Arch. Dermatol.*, **90**, 512(1964).

(4) R. J. Scheuplein and L. Ross, *J. Soc. Cosmet. Chem.*, **21**, 853(1970).

(5) T. M. Sweeney, A. M. Downes, and A. G. Matoltsy, *J. Invest. Dermatol.*, **46**, 3, 300(1966).

(6) S. G. Elfbaum and K. Laden, *J. Soc. Cosmet. Chem.*, **19**, 119(1968).

(7) *Ibid.*, **19**, 841(1968).

(8) M. Levine, *Brit. J. Dermatol.*, **86**, 481(1972).

(9) J. P. Astley and M. Levine, *ibid.*, **90**, 53(1974).

(10) S. G. Elfbaum and K. Laden, *J. Soc. Cosmet. Chem.*, **19**, 163(1968).

ACKNOWLEDGMENTS AND ADDRESSES

Received July 5, 1974, from the *Department of Biochemistry, University of Manchester, Manchester, M13 9PL, England.*

Accepted for publication May 6, 1975.

Supported by Unilever Ltd., Port Sunlight Cheshire, England.

[x] To whom inquiries should be directed.

[10] In view of this approximation, it is necessary to ensure that the donor solution does not become excessively depleted and periodic replacement of the donor solution is carried out during the experiment.

Evaluation of Emulsion Stability by Diffuse Reflectance Spectroscopy

MICHAEL J. AKERS ˣ and JOHN L. LACH

Abstract □ A new method is described for evaluating the stability of emulsion bases and active components contained within such emulsions. Diffuse reflectance spectroscopy (DRS) is a technique that has the capability of detecting changes in particle size, surface properties, or drug quality of emulsions as a function of time without disturbance of the system. Such physical or chemical changes are monitored by changes in the visible and UV wavelength spectral characteristics of the emulsified systems. Four basic emulsion systems were prepared and analyzed for physical stability for 6 months by three techniques: visible coalescence, particle counting measurement, and DRS. Two drugs, aspirin and ascorbic acid, were then incorporated within stable emulsion bases, and the chemical stability of these drugs was monitored by DRS for 6 months. Results were compared with concomitant quantitative drug assay procedures. Good agreement was observed when data from DRS and analytical measurements were compared. The DRS technique may be used as a supportive method, offering simplicity and expedience, with other methods of evaluating emulsion stability and drug stability within emulsified systems.

Keyphrases □ Emulsions—system stability and stability of incorporated drugs, evaluated by diffuse reflectance spectroscopy, compared to visible coalescence and particle counter techniques □ Spectroscopy, diffuse reflectance—evaluation of stability of emulsions and active components in emulsions, compared to visible coalescence and particle counter techniques □ Aspirin—stability in emulsions, evaluated by diffuse reflectance spectroscopy □ Ascorbic acid—stability in emulsions, evaluated by diffuse reflectance spectroscopy

The stabilization of a thermodynamically unstable emulsified system presents a challenging proposition to the developmental pharmacist. The intimate dispersal of two immiscible liquids is prone to instability due to the natural tendency of like molecules to coalesce.

A literature survey shows that various techniques have been employed to evaluate emulsion stability. Most of these methods were reviewed previously (1). Size–distribution analysis of the emulsion as a function of time is the physical property most commonly measured, but other emulsion physical properties evaluated include particle charge, viscosity, creaming rate, and interfacial tension.

Lloyd (2) reported that optical methods to evaluate emulsion stability had received minimal attention and showed that the following relationship exists for oil-in-water emulsions:

$$R = \frac{c}{D^k} \qquad \text{(Eq. 1)}$$

where R is the reflectance at the wavelength at which the colored internal phase partially absorbs the incident light, D is the surface mean particle diameter:

$$D = \frac{\Sigma n_i d_i^3}{\Sigma n_i d_i^2}$$

and c and k are constants characteristic of the emulsion system. It was demonstrated that reflectance techniques can be applied to evaluate different emulsion stabilizers and to study the kinetics of emulsion coalescence.

Although Lloyd's reflectance technique has been utilized (3), few published papers relate to this subject. The reflectance technique known as diffuse reflectance spectroscopy (DRS) was utilized to study solid–solid interactions between drugs and formulation ingredients (4–7). DRS was sensitive to changes occurring at the surfaces of solid drug molecules due to interactions with other solid molecules. It was assumed that DRS might also detect surface changes due to the coalescence of particles in emulsions. In addition, since DRS gives spectra that closely resemble transmittance spectra, it should be possible to monitor the stability of an active ingredient formulated within an emulsified system.

Four 50% oil-in-water emulsions were prepared, each containing a different stabilizer, and analyzed for physical stability as a function of time using this DRS technique. Subsequently, aspirin and ascorbic acid were incorporated into the emulsion bases shown to be stable, and DRS was applied to ascertain the chemical stability of these drugs as a function of time. Thus, the intent of this investigation was to show the application of DRS as a sensitive tool for evaluating emulsion stability and drug stability in an emulsified formulation.

EXPERIMENTAL

Reagents—The stabilizers used were gum arabic[1] USP, polyoxyethylene sorbitan monooleate[2], sorbitan monopalmitate[2], sorbitan monolaurate[2], and sodium lauryl sulfate[3] USP. The two drugs used were aspirin[4], mp 133–135°, and L-ascorbic acid[5], reagent grade, mp 190–193°.

Preparation of Emulsions—All oil-soluble components were dissolved in the oil phase; heat was used if necessary, but precaution was taken not to use excessive temperatures. Water-soluble components were dissolved in the aqueous phase. Equal volumes of oil and aqueous phase were combined and triturated by a mortar and pestle to form a coarse emulsion. The emulsion was then emulsified for 2 min[6].

Composition of Emulsions—All emulsions were 50% oil-in-water emulsions except for emulsions containing gum arabic, which were 40% (Table I). Heavy mineral oil[7] was used as the oil phase. The percentage of stabilizer in these oil-in-water emulsions is given in Table I.

For the drug-containing emulsions, 6% (w/v) aspirin was formulated into Emulsion 1. The drug was dissolved in the oil phase. L-Ascorbic acid was incorporated into two different emulsion formulations: (*a*) 11.7% ascorbic acid in Emulsion 1, and (*b*) 9.33% ascorbic acid in Emulsion 2.

[1] S. B. Penick & Co., New York, N.Y.
[2] Atlas Chemical Industries, Wilmington, Del.
[3] E. I. du Pont de Nemours and Co., Wilmington, Del.
[4] Mallinckrodt Chemical Works, St. Louis, Mo.
[5] Fisher Scientific Co., Fair Lawn, N.J.
[6] Eppenbach colloid mill, Gifford-Wood Co., New York, N.Y.
[7] Paraffin oil, heavy, Fisher Scientific Co., Fair Lawn, N.J.

Table I—Composition of Emulsion Bases Used in This Study

Emulsion 1	40% mineral oil in water 10% (w/v) gum arabic 0.02% sorbic acid
Emulsion 2	50% mineral oil in water 4% (v/v) sorbitan monopalmitate and polyoxyethylene sorbitan monooleate, HLB = 10.85
Emulsion 3	50% mineral oil in water 4% (w/v) sorbitan monolaurate
Emulsion 4	50% mineral oil in water 4% (w/v) sodium lauryl sulfate

Reflectance Measurement—Diffuse reflectance spectra were measured using a spectrophotometer with a reflectance attachment[8]. Special Plexiglas cells (Fig. 1) were manufactured to contain the emulsion sample to be analyzed.

The emulsion sample was introduced into the cell through a hole on top with a disposable pipet until the entire shaded area was filled with sample. All cells were leakproof. The reflectance of emulsions was measured relative to a white standard such as magnesium oxide, while reflectances of drug-containing emulsions were measured relative to an identical emulsion base containing no drug. The instrument was zeroed in at 400 nm using two white standards, and the reflectance spectrum was measured from 700 to 200 nm. Precision of the technique was 0.1% R.

Measurement of Particle-Size Distribution of Emulsions—The particle counter[9], calibrated periodically with monosized ragweed pollen particles, was used to determine average particle size (d_m) of emulsions as a function of time. The emulsions were gently shaken prior to the withdrawal of a 2-ml sample, which was then diluted to 1 liter with distilled water. The 1-liter solution was vigorously shaken for 2 min, and then another 2-ml sample was withdrawn and diluted to 200 ml with 0.9% sodium chloride solution. Since the emulsion sample was diluted 50,000-fold, it was assumed that droplet sizes would not be affected significantly by using the saline vehicle rather than the appropriate surfactant vehicle.

To test this assumption and to check the reproducibility of the particle-size determination, Emulsions 1 and 2, triplicates and duplicates, respectively (Table I), were treated in this manner. The results are shown in Table II. The low standard error and percent error indicate that use of the saline vehicle did not cause irreproducible results.

Measurement of Coalescence—The same procedure as described by Rowe (8) was used immediately after preparation. A 50-ml emulsion sample was poured into a 50-ml graduated cylinder and stoppered. The volume ratio of the two phases was ascertained at room temperature as a function of time.

Methods of Drug Analysis—The aspirin emulsion was analyzed by determining the percent of salicylic acid formed as a result of aspirin partitioning from the oil to the aqueous phase and immediately hydrolyzed. A modification of the spectrophotometric method of Clayton and Thiers (9) was used for the assay of salicylic acid in the emulsion aqueous phase. A 20-ml emulsion sample was taken at the appropriate time intervals and centrifuged[10] for 15 min to separate the aqueous and oil phases. Aliquots of the aqueous phase were diluted with 2 N NaOH, filtered, and analyzed at 301 nm for salicylic acid[11].

Identical emulsions without drug were treated by the same procedure and used as reference blanks. A standard curve was obtained by dissolving known quantities of salicylic acid in the aqueous phase of the emulsion and using the same procedure.

The USP iodometric titration method was used to measure the degradation of ascorbic acid in emulsions. An emulsion sample equivalent to 400 mg of ascorbic acid was dissolved in a mixture of 100 ml of carbon dioxide-free water and 25 ml of dilute sulfuric acid. The solution was titrated at once with 0.1 N iodine solution

[8] Beckman model DB-G.
[9] Coulter counter, model B, Coulter Electronics Industrial Division.
[10] International centrifuge, No. 6404914.
[11] Gilford spectrophotometer model 240.

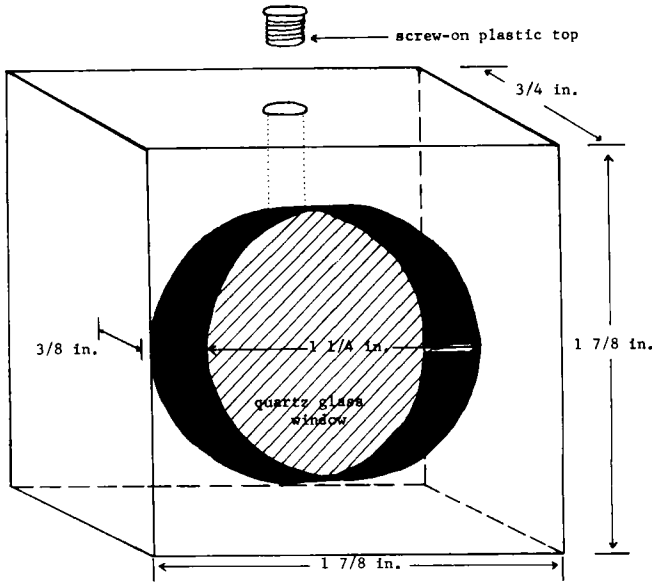

Figure 1—*Design of special Plexiglas cell used for diffuse reflectance measurement of emulsions.*

standardized with arsenious oxide; as the end-point was approached, a few drops of starch TS were added as an indicator. Each milliliter of 0.1 N iodine was equivalent to 8.8 mg of ascorbic acid.

Experimental Design—After preparation, the emulsions were allowed to stand for 1 day before initial measurements were taken. This period allowed the emulsion components to reach a pseudo-equilibrium state. Emulsions were subjected to coalescence measurement, particle-size analysis, reflectance measurement, and analysis of the active ingredient once each month for 6 months. The aspirin emulsions were subjected to these studies each week for the 1st month and then treated like the other emulsions for the remaining 5 months.

THEORY

When radiation is directed onto the surface of a solid or semisolid, two types of reflectance from that surface can result. The first type, called regular reflectance or "mirror reflection," is governed by the Fresnel equations. The second type, called diffuse reflectance, is interpreted by the Kubelka–Munk equation (10):

$$f(r_\infty) = \frac{(1 - r_\infty)^2}{2r_\infty} = \frac{k}{s} \qquad \text{(Eq. 2)}$$

where $f(r_\infty)$ is the remission function, r_∞ is the relative reflectance, k is the absorption coefficient, and s is the scattering coefficient. A portion of the radiant flux penetrates into the interior of a sample, and part of this radiation returns to the sample surface. The remaining part of the incident flux is absorbed and scattered at the boundaries of the individual particles comprising the sample.

Taking the logarithm of the remission function gives:

$$\log f(r_\infty) = \log k - \log s \qquad \text{(Eq. 3)}$$

Table II—Data Verifying the Reproducibility of Particle Counting Measurements Using Emulsion 1 (Triplicates) and Emulsion 2 (Duplicates)

	Emulsion 1		Emulsion 2	
Months	Mean d_m (n = 3)	Standard Error	Mean d_m (n = 2)	Percent Error
0	2.916	0.108	2.601	1.920
1	3.146	0.181	2.816	1.060
2	3.055	0.195	2.976	3.020
3	3.320	0.125	2.850	1.750
4	3.276	0.176	2.805	2.862
5	3.386	0.162	2.850	4.387
6	3.586	0.185	2.904	4.141

Table III—Stability Evaluation of Oil-in-Water Emulsion Bases Indicated by Changes[a] in Percent Coalescence ($\Delta\%C$), Changes[a] in Percent Mean Particle Diameter ($\Delta\%d_m$), and Changes[a] in Percent Reflectance Intensity at Selected Wavelengths ($\Delta\%R\lambda$) as a Function of Time

	Emulsion 1				Emulsion 2				Emulsion 3				Emulsion 4			
Months	$\Delta\%C$	$\Delta\%d_m$	$\Delta\%R$, 500 nm	$\Delta\%R$, 320 nm	$\Delta\%C$	$\Delta\%d_m$	$\Delta\%R$, 500 nm	$\Delta\%R$, 300 nm	$\Delta\%C$	$\Delta\%d_m$	$\Delta\%R$, 500 nm	$\Delta\%R$, 300 nm	$\Delta\%C$	$\Delta\%d_m$	$\Delta\%R$, 500 nm	$\Delta\%R$, 300 nm
1	0	11.8	−3	−2	0	11.7	0	0	25	16.4	−4	−1	31	38.6	−4	+2
2	1	3.8	−3	0	0	20.4	−2	+3	31	34.0	−5	−4	31	52.7	−5	0
3	3	9.2	−4	0	0	9.8	−2	+3	36	51.3	−10	−6	31	42.6	−10	−5
4	9	16.0	−4	−2	0	6.6	−2	+3	37	41.0	−17	−11	31	54.0	−18	−18
5	10	18.5	−6	−2	0	6.6	−2	+5	38	61.9	−17	−13	31	71.1	−22	−17
6	10	20.2	−8	−7	0	9.0	−2	+4	38	68.8	−18	−16	31	76.2	−29	−24

[a] Changes relative to measurements taken at zero time.

Table IV—Correlation Coefficients (r) between Any Two of Three Dependent Variables Used to Evaluate Stability of the Four Basic Emulsions Monthly for 6 Months

Months	$\Delta\%d_m$ *versus* $\Delta\%R_{300}$	$\Delta\%d_m$ *versus* $\Delta\%C$	$\Delta\%C$ *versus* $\Delta\%R_{300}$
1	0.864	0.806	0.609
2	0.264	0.863	0.713
3	0.952	0.985	0.974
4	0.997	0.927	0.900
5	0.990	0.958	0.946
6	0.971	0.960	0.894

Thus, a plot of $\log f(r_\infty)$ *versus* wavelength results in a curve corresponding to the real absorption spectrum of the compound determined by $\%T$, except for a displacement of $-\log s$ in the ordinate direction. The value of s is a very complicated function of the ratio of the particle size to the wavelength used (11). In the experiments described in this paper, one or two representative wavelengths were selected and comparisons with time were made at these two wavelengths only. However, $\log s$ may not remain constant if the ratio of drop size to wavelength changes appreciably with time.

The intensity of reflectance at a selected wavelength can be related directly to the concentration of the absorbing species in the sample because of the following relationship (12):

$$f(r_\infty) = \frac{\epsilon c}{s} \qquad \text{(Eq. 4)}$$

where ϵ is the molar extinction coefficient, and c is the molar concentration.

The application of reflectance measurements to emulsion stability studies was first investigated by Langlois *et al.* (13). They found a direct relationship between the specific interfacial area of emulsions composed of nonabsorbing components and the transmission of light by emulsions relative to the continuous phase. The relative light transmission, I_0/I, was related to the interfacial area, A, by the following equation:

$$\frac{I_0}{I} = 1 + \beta A \qquad \text{(Eq. 5)}$$

The term β was a constant found to be a function of the ratio N_d/N_c, the refractive indexes of the disperse and continuous phases, respectively.

Lloyd (2) demonstrated the existence of an inverse relationship between the reflectances, r, of colored oil-in-water emulsions and the surface-average particle diameter, d, of their dispersed phases:

$$\log R = -k \log D + \log c \qquad \text{(Eq. 6)}$$

where k and c are constants characteristic of the emulsion system. The surface average particle diameter is inversely related to the specific interfacial area, A, of a given emulsion by:

$$D = \frac{6f}{A} \qquad \text{(Eq. 7)}$$

where f is the volume fraction of the dispersed phase. This equation is based on the implicit assumption that all drops are the same size. Thus, reflectance is proportional to the specific interfacial area of the emulsion raised to the k power:

$$R = C^1 A^k \qquad \text{(Eq. 8)}$$

where $C^1 = c/(6f)^k$.

Table V—Areas under the Percent Reflectance *versus* Wavelength Curves (AUC)[a]

Emulsion	Emulsifying Agent	AUC Zero Time, cm²	AUC 6 Months, cm²	Difference
1	Gum arabic	106	100	−6
2	Sorbitan monopalmitate/polyoxyethylene sorbitan monooleate	156	164	+8
3	Sorbitan monolaurate	144	116	−28
4	Sodium lauryl sulfate	158	112	−46

[a] AUC determined by the $K + E$ polar planimeter No. 62 0005 between 550 and 200 nm.

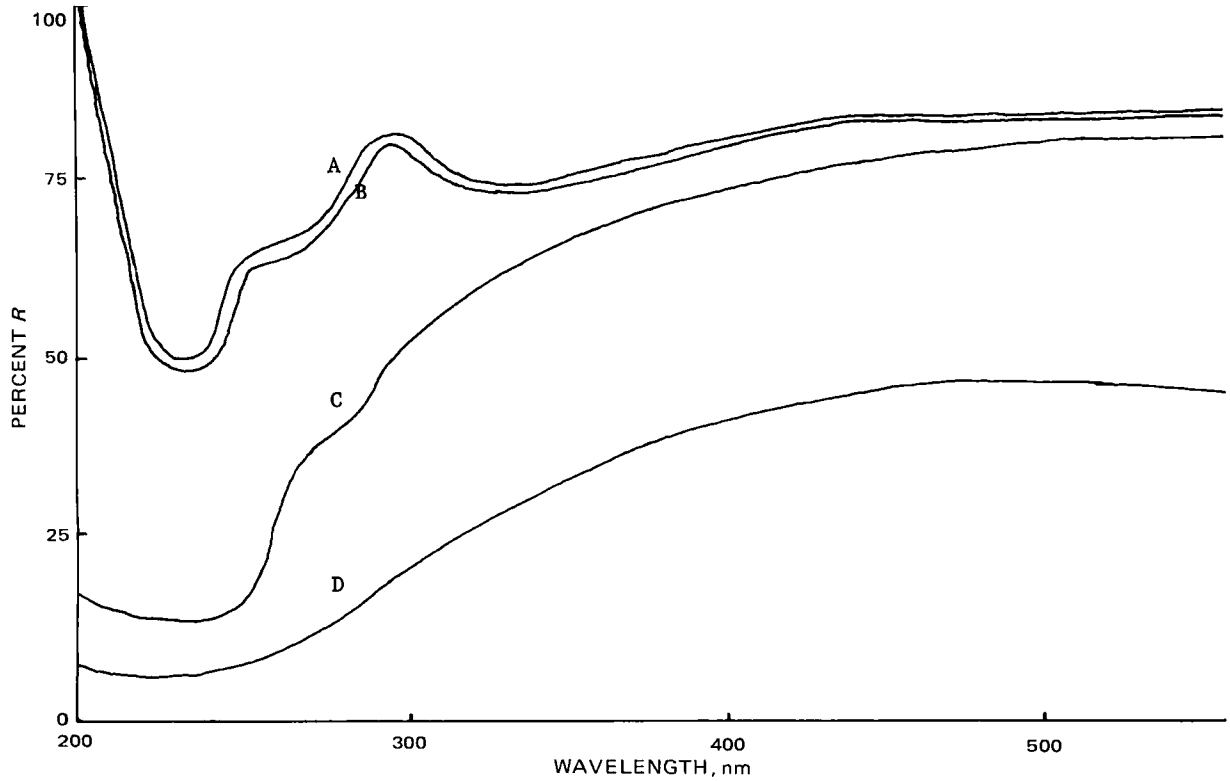

Figure 2—*Reflectance spectra of a stable 50% oil-in-water emulsion initially (curve A) and 1 month after preparation (curve B) and of an unstable 50% oil-in-water emulsion initially (curve C) and 1 month after preparation (curve D).*

Giovanelli (14) studied the influence of particle aggregation on the reflectance of nonhomogeneous media. In a uniform medium, R depends only on k/s (Eq. 2), which represents the fraction of light lost by scattering. In aggregated systems, represented by unstable emulsions, R depends on the attenuation coefficient K:

$$K = k + s \qquad \text{(Eq. 9)}$$

which represents all radiation lost by both absorption, k, and scattering, s. Although k/s may still be constant, R may be decreased by 30% if large aggregates are present. Previously, it was stated that the diffusely reflected component must be scattered by individual particles for reflectance to occur. As Giovanelli (14) indirectly showed, if aggregation of these individual particles occurs, the concentration of scattering centers and, consequently, the diffuse reflectance is reduced.

Interpretations based on light scattering of dispersed systems may be complex. Additional confusion may be introduced by realizing that reflectance can be influenced by factors other than particle size, *e.g.*, wavelength, refractive index, and particle shape (10). However, to simplify the interpretations, the following things were done:

1. Simple emulsion compositions were used.
2. All emulsions were prepared in exactly the same manner, which initially provided nearly a constant particle size of all emulsions.
3. By using the Plexiglas cell (Fig. 1), equal emulsion volumes were measured, with distances and angles between radiation source and sample being identical.
4. Only one wavelength was monitored per emulsion, except for the determination of areas under the reflectance curves.
5. The experiments were duplicated.

RESULTS AND DISCUSSION

Emulsions are dynamic systems in which changes in the physical properties and/or phase composition of the components of the system are constantly occurring. In this paper, the mere separation of the two phases into a cream layer and aqueous phase is defined as an instability. With most analytical techniques, it is necessary to sample the emulsion and thus disturb the pseudoequilibrium state of that system. This disturbance possibly could affect the reproducibility of later analyses.

DRS offers the advantage that the stability of an emulsion can be evaluated without disturbance of the system. Once the freshly prepared emulsion sample is placed in the specially designed DRS Plexiglas cell, the cell is sealed and the emulsion is left undisturbed for the duration of the experiment. Theoretically, DRS should detect changes occurring in the microenvironment within the surfaces of emulsion systems which cannot be seen visually.

Figure 2 shows general characteristics of DRS curves. Wavelength regions in the visible and UV spectra are scanned, and reflectance intensities from 0 (100% absorbance) to 100 (0% absorbance) are recorded as a function of wavelength. As certain physical and chemical changes occur in particle size, shape, color, or chemical structure, the DRS technique manifests the changes in the reflectance intensities or shifts in the spectral peaks (15). The curves in Fig. 2 indicate that minimal changes in DRS spectra occur if the emulsion system remains stable (curves A and B, Fig. 2). However, unstable emulsions result in marked differences in reflectance curves after a period of time (compare curves C and D).

Four simple oil-in-water (o/w) emulsion bases were prepared, each differing in the type of emulsifying agent used (Table I). Table III presents the data obtained on these four emulsions after being evaluated for 6 months by three techniques. Generally, as the emulsions coalesced, indicated by an increase in percent C, the mean particle diameter of the emulsions also increased; this increase was accompanied by a decrease in the percent reflectance at the measured wavelength (300 nm).

Correlation coefficients among the measured parameters are presented in Table IV. The data indicate that good correlations were obtained among the three techniques at 3 months or later. The poor correlations during the first 2 months probably reflected both unfamiliarity with the particle counting technique and the very rapid coalescence of two of the four emulsions. This coalescence, measured in volumetric cylinders, was not so readily apparent in the small Plexiglas DRS cells. The good correlation seen in Table IV indicates that, despite the use of different methods to evaluate stability, which, admittedly, are probing different characteristics of the system, the results may be favorably compared and utilized to support one another.

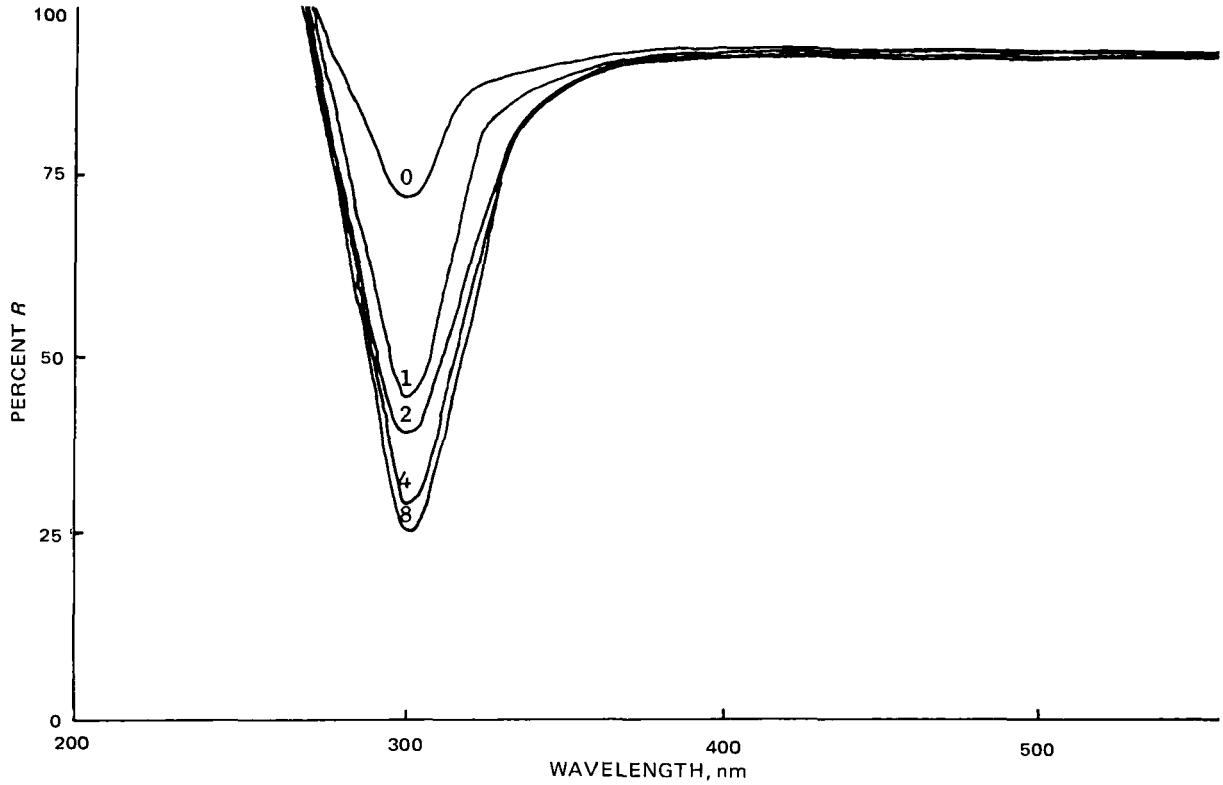

Figure 3—*Reflectance spectra of a 6% aspirin oil-in-water emulsion. The numbers on the curves correspond to the week after preparation.*

Vold and Mittal (16) discussed why confusion exists concerning the stability of emulsions. Reasons include: (*a*) different definitions of the term emulsion stability, particularly in the failure to distinguish clearly between creaming and coalescence; (*b*) insensitivity of some methods to detect subtle changes occurring in the emulsions; and (*c*) different methods of characterization that measure different properties of the emulsion, or emulsions that may be in different physical states in the various experiments.

In light of these reasons, it was realized that correlating reflectance with particle count and volume ratio data could generate serious arguments and confusion. However, Lloyd (2) showed the correlation of reflectance and particle size, and Rowe (8) showed the correlation of particle-size and coalescence measurements. It has been attempted here only to show some credibility for using the DRS technique for evaluating emulsion stability; accordingly, some older or more conventional technique must be employed to verify this credibility.

Another method of interpreting DRS evaluation of emulsion stability is to measure the area under the percent reflectance *versus* wavelength curves (*AUC*) as a function of time. The relative difference of the *AUC*, measured between the same two wavelengths, could further substantiate the application of DRS in evaluating emulsion stability.

Areas under the percent *R versus* wavelength curves for each of the four basic emulsions were measured at zero time and again 6 months later (Table V). The difference in the *AUC* after a certain

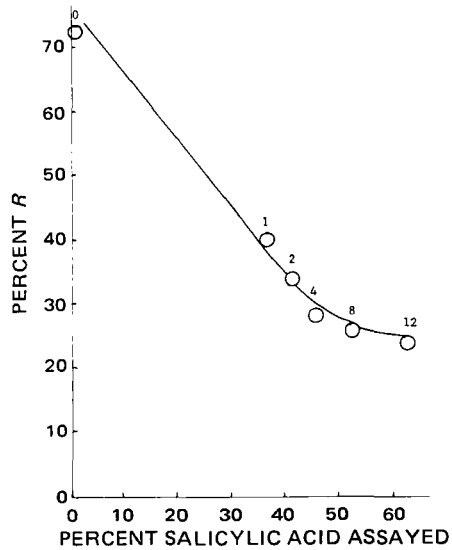

Figure 4—*Plot of percent reflectance* versus *percent salicylic acid assayed as a function of time. The percent reflectance was determined at 310 nm. The numbers correspond to the week after preparation of the drug-containing emulsion.*

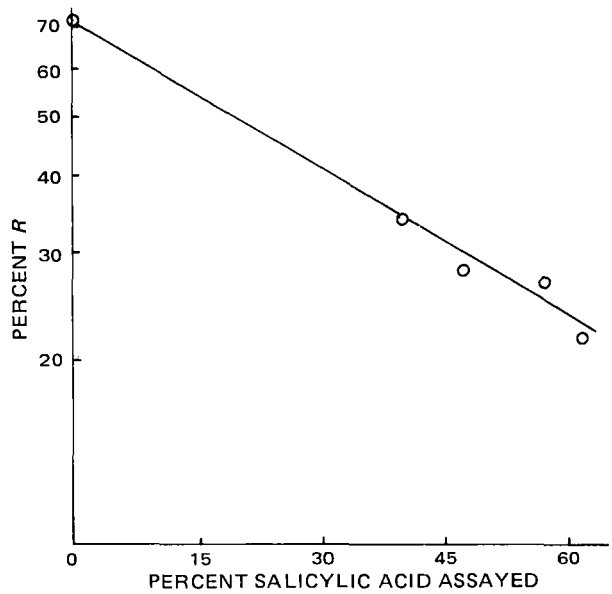

Figure 5—*Semilogarithmic plot of percent reflectance* versus *percent salicylic acid assayed using the points shown in Fig. 4.*

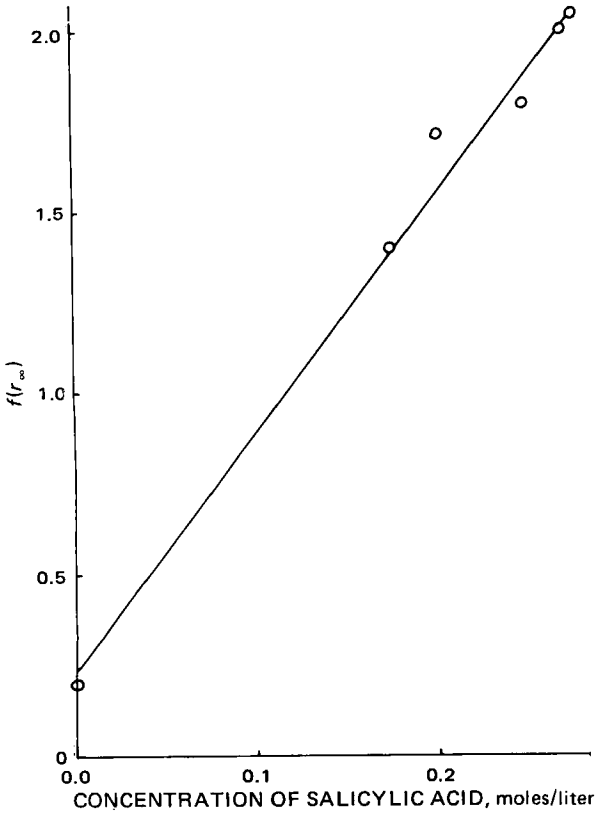

Figure 6—*Plot of remission coefficient* versus *molar concentration of salicylic acid in Emulsion 1.*

time can be a useful indicator for comparing the relative effectiveness of different emulsifying agents on producing stable emulsions. According to the data in Table V, the rank order of effective emulsifying agents would be sorbitan monopalmitate/polyoxyethylene sorbitan monooleate > gum arabic ≫ sorbitan monolaurate > sodium lauryl sulfate.

Since DRS compared favorably with the more established methods for emulsion stability evaluation, it was decided to study the ability of DRS to evaluate the chemical stability of an active ingredient incorporated into a stable emulsion formulation. The emulsion base was used as the reference material in the DRS measurements with the same emulsion base containing the drug as the sample. The two emulsions, with and without drug, were monitored simultaneously by coalescence, particle-size, and reflectance measurements to determine whether the emulsion base or the drug or both were causing the observed changes in the measured parameters. Since some drugs possess surface activity, the possibility does exist that a surface-active drug could affect the stability of the base emulsion.

Aspirin (6%) was dissolved in the oil phase of Emulsion 1. This emulsion was shown previously to be stable (Table III). Figure 3 shows the DRS results in analyzing the stability of aspirin in Emulsion 1.

Changes in the reflectance spectra occurred at the wavelength region where salicylic acid molecules are known to absorb light (approximately 310 nm). In Fig. 3, this change can be observed by the continual decrease in percent R at 310 nm. As salicylic acid formed, light was absorbed by the molecules, resulting in a decrease in the quantity of light reflected. Over a period of time, aspirin gradually degraded to salicylic acid; this change was monitored by a gradual decrease in percent R.

Figure 4 shows a plot of percent R at 310 nm *versus* the percent salicylic acid recovered in quantitative assay work over 12 weeks. A logarithmic relationship apparently existed between percent R and percent salicylic acid for this system (Fig. 5).

According to theory, the remission coefficient, $f(r_\infty)$, is directly proportional to the molar concentration of the absorbing species (Eq. 4). For the appearance of salicylic acid as a direct result of aspirin degradation, this proportionality appears to hold, as evidenced by the linearity seen in Fig. 6.

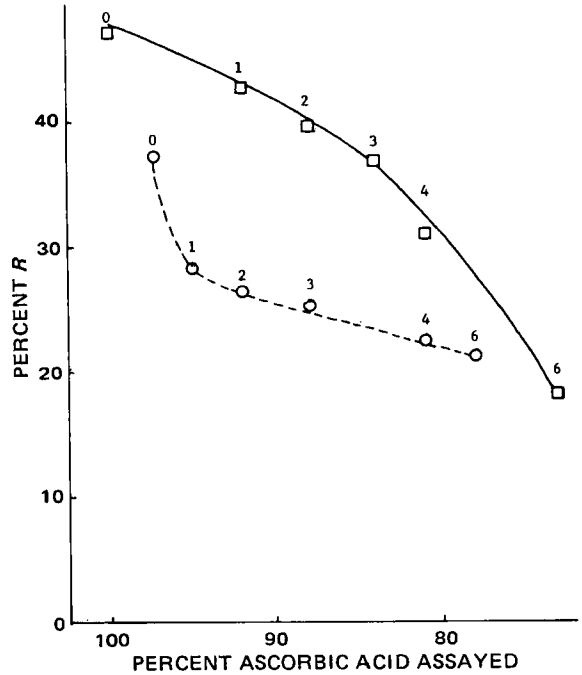

Figure 7—*Plot of percent reflectance* versus *percent ascorbic acid assayed as a function of time. The numbers correspond to the month after preparation of the drug-containing emulsion. Key:* □, *Emulsion 1, percent reflectance measured at 350 nm; and* ○, *Emulsion 2, percent reflectance measured at 320 nm.*

Aspirin was chosen as the drug for monitoring stability in emulsions by DRS because its hydrolytic degradation is well known, and it was felt that aspirin would be an ideal drug with which to test the DRS method. Since good correlation between reflectance and drug assay results indeed were seen, it seemed necessary to use a different drug that is formulated as an emulsion dosage form. Ascorbic acid was chosen, and its stability in two different stable emulsion systems (Emulsions 1 and 2) was analyzed.

In Fig. 7, percent R is plotted *versus* percent ascorbic acid found

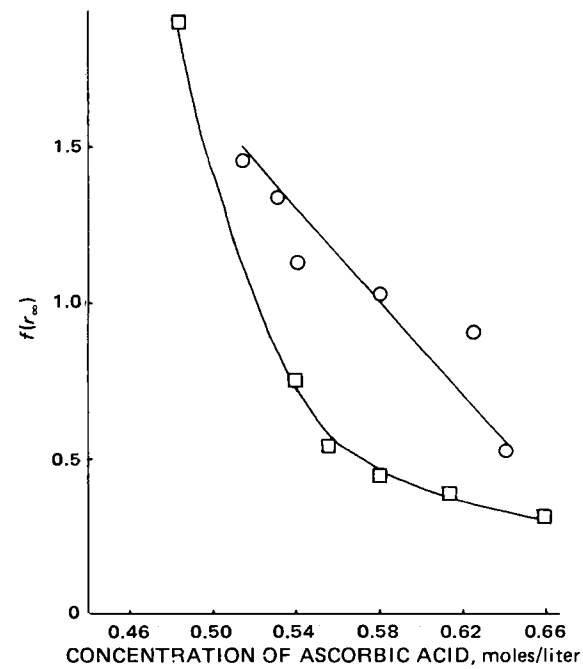

Figure 8—*Plot of remission coefficient* versus *molar concentration of ascorbic acid in two different emulsion bases. Key:* □, *Emulsion 1; and* ○, *Emulsion 2.*

when using a quantitative assay procedure. Ascorbic acid appeared to degrade to a greater extent in Emulsion 1 than in Emulsion 2. This finding agreed with the results of Bandelin and Tuschhoff (17), who found that vegetable gums added to produce liquids of greater viscosity seemed to accelerate the degradation of ascorbic acid. However, the main point to be emphasized once again is that drug degradation within a stable emulsion can be monitored at least semiquantitatively by DRS. Using DRS alone with no quantitative assay, one could conclude with little trepidation that ascorbic acid was unstable in these emulsion systems.

Figure 8 is shown to test the Kubelka–Munk hypothesis relating $f(r_\infty)$ directly to the concentration of the absorbing species. A linear relationship was evident for the drug in Emulsion 2 but not for the drug in Emulsion 1. Unfortunately for this drug emulsion system, no other wavelength could be used as an indicator of ascorbic acid degradation. However, the evidence indicates that ascorbic acid degradation in an emulsified formulation was monitored adequately by DRS.

SUMMARY AND CONCLUSIONS

DRS is a simple method and can be used in combination with other methods for evaluating emulsion stability. The method is sensitive and can detect subtle changes in the emulsion microenvironment, but it does not demand sampling or manipulation of the system. Should a semiquantitative estimate of an active component within an emulsion be desired, then the DRS method offers the unique advantage of estimating drug stability without disturbing the system.

Additional research is recommended to improve or define exactly the interpretation of the data obtained from reflectance measurements. These studies only show the application of DRS as a corroborative tool for the monitoring and evaluation of emulsion stability and drug stability within an emulsified system.

REFERENCES

(1) E. R. Garrett, *J. Pharm. Sci.*, **54**, 1557(1965).

(2) N. E. Lloyd, *J. Colloid Sci.*, **14**, 441(1959).

(3) "The Theory and Practice of Industrial Pharmacy," L. Lachman, H. Liebermann, and J. Kanig, Eds., Lea & Febiger, Philadelphia, Pa., 1970, pp. 698, 699.

(4) J. L. Lach and M. Bornstein, *J. Pharm. Sci.*, **54**, 1730(1965).

(5) M. Bornstein, J. L. Lach, and B. J. Munden, *ibid.*, **57**, 1653(1968).

(6) J. L. Lach and L. D. Bighley, *ibid.*, **59**, 1261(1970).

(7) J. D. McCallister, T. F. Chin, and J. L. Lach, *ibid.*, **59**, 1286(1970).

(8) E. L. Rowe, *ibid.*, **54**, 260(1965).

(9) A. W. Clayton and R. E. Thiers, *ibid.*, **55**, 404(1966).

(10) P. Kubelka, *J. Opt. Soc. Amer.*, **38**, 448(1948); *ibid.*, **38**, 1067(1948).

(11) M. Kerker, "The Scattering of Light and Other Electromagnetic Radiation," Academic, New York, N.Y., 1969, chap. 7.

(12) G. Kortum and G. Schreyer, *Angew. Chem.*, **67**, 694(1955).

(13) G. E. Langlois, J. E. Gulberg, and T. Vermeulen, *Rev. Sci. Instrum.*, **25**, 360(1954).

(14) R. G. Giovanelli, *Aust. J. Phys.*, **10**, 227(1957); *ibid.*, **12**, 164(1959).

(15) R. W. Frei and J. D. MacNeil, "Diffuse Reflectance Spectroscopy in Environmental Problem Solving," CRC Press, Cleveland, Ohio, 1973.

(16) R. D. Vold and K. L. Mittal, *J. Soc. Cosmet. Chem.*, **23**, 171(1972).

(17) F. J. Bandelin and J. V. Tuschhoff, *J. Amer. Pharm. Ass., Sci. Ed.*, **44**, 241(1955).

ACKNOWLEDGMENTS AND ADDRESSES

Received November 22, 1974, from the *College of Pharmacy, University of Iowa, Iowa City, IA 52240*

Accepted for publication May 14, 1975.

Presented at the Industrial Pharmaceutical Technology Section, APhA Academy of Pharmaceutical Sciences, New Orleans meeting, November 1974.

[x] To whom inquiries should be directed. Present address: Alcon Laboratories, Fort Worth, TX 76101

Retardation of Dissolution and Growth of Calcium Oxalate Monohydrate

S. BISAILLON and R. TAWASHI [x]

Abstract □ The kinetics of dissolution and growth of calcium oxalate monohydrate were examined in the presence of small concentrations of pyrophosphate, chlorophyll, and other agents. Data presented show that the retardation in mass transport in both processes is controlled by the nature of the additive, its concentration, and the way the additives are combined in the dissolution medium. Dissolution was studied using a particle counter method, and growth was conducted in a gel system under the slow diffusion of the reacting ions. Results obtained show that chlorophyll is more active than other inhibitors studied and suggest a higher surface adsorption intensity on the primary sources of the crystal surface.

Keyphrases □ Calcium oxalate monohydrate—kinetics of dissolution and crystal growth, effects of various additives alone and in combination □ Dissolution—calcium oxalate monohydrate, kinetics, effects of various additives alone and in combination □ Crystal growth—calcium oxalate monohydrate, kinetics, effects of various additives alone and in combination □ Renal stone formation—calcium oxalate monohydrate, kinetics of dissolution and crystal growth, effects of various additives alone and in combination

Genesis and growth of calcium oxalate calculi are still unclear (1). To explain the ability of urine to remain supersaturated without precipitation, crystallization inhibitors should be studied. Equally important are the factors influencing the kinetics of dissolution of the stone components.

The complexity of urine in stone formation is certainly responsible for the slow progress in the area. The interaction of one compound with the others [*e.g.*, the action of magnesium on the solubility of calcium oxalate (2)] and the presence of material with a high epitaxial activity [such as organic material (3–

when using a quantitative assay procedure. Ascorbic acid appeared to degrade to a greater extent in Emulsion 1 than in Emulsion 2. This finding agreed with the results of Bandelin and Tuschhoff (17), who found that vegetable gums added to produce liquids of greater viscosity seemed to accelerate the degradation of ascorbic acid. However, the main point to be emphasized once again is that drug degradation within a stable emulsion can be monitored at least semiquantitatively by DRS. Using DRS alone with no quantitative assay, one could conclude with little trepidation that ascorbic acid was unstable in these emulsion systems.

Figure 8 is shown to test the Kubelka–Munk hypothesis relating $f(r_\infty)$ directly to the concentration of the absorbing species. A linear relationship was evident for the drug in Emulsion 2 but not for the drug in Emulsion 1. Unfortunately for this drug emulsion system, no other wavelength could be used as an indicator of ascorbic acid degradation. However, the evidence indicates that ascorbic acid degradation in an emulsified formulation was monitored adequately by DRS.

SUMMARY AND CONCLUSIONS

DRS is a simple method and can be used in combination with other methods for evaluating emulsion stability. The method is sensitive and can detect subtle changes in the emulsion microenvironment, but it does not demand sampling or manipulation of the system. Should a semiquantitative estimate of an active component within an emulsion be desired, then the DRS method offers the unique advantage of estimating drug stability without disturbing the system.

Additional research is recommended to improve or define exactly the interpretation of the data obtained from reflectance measurements. These studies only show the application of DRS as a corroborative tool for the monitoring and evaluation of emulsion stability and drug stability within an emulsified system.

REFERENCES

(1) E. R. Garrett, *J. Pharm. Sci.*, **54**, 1557(1965).

(2) N. E. Lloyd, *J. Colloid Sci.*, **14**, 441(1959).

(3) "The Theory and Practice of Industrial Pharmacy," L. Lachman, H. Liebermann, and J. Kanig, Eds., Lea & Febiger, Philadelphia, Pa., 1970, pp. 698, 699.

(4) J. L. Lach and M. Bornstein, *J. Pharm. Sci.*, **54**, 1730(1965).

(5) M. Bornstein, J. L. Lach, and B. J. Munden, *ibid.*, **57**, 1653(1968).

(6) J. L. Lach and L. D. Bighley, *ibid.*, **59**, 1261(1970).

(7) J. D. McCallister, T. F. Chin, and J. L. Lach, *ibid.*, **59**, 1286(1970).

(8) E. L. Rowe, *ibid.*, **54**, 260(1965).

(9) A. W. Clayton and R. E. Thiers, *ibid.*, **55**, 404(1966).

(10) P. Kubelka, *J. Opt. Soc. Amer.*, **38**, 448(1948); *ibid.*, **38**, 1067(1948).

(11) M. Kerker, "The Scattering of Light and Other Electromagnetic Radiation," Academic, New York, N.Y., 1969, chap. 7.

(12) G. Kortum and G. Schreyer, *Angew. Chem.*, **67**, 694(1955).

(13) G. E. Langlois, J. E. Gulberg, and T. Vermeulen, *Rev. Sci. Instrum.*, **25**, 360(1954).

(14) R. G. Giovanelli, *Aust. J. Phys.*, **10**, 227(1957); *ibid.*, **12**, 164(1959).

(15) R. W. Frei and J. D. MacNeil, "Diffuse Reflectance Spectroscopy in Environmental Problem Solving," CRC Press, Cleveland, Ohio, 1973.

(16) R. D. Vold and K. L. Mittal, *J. Soc. Cosmet. Chem.*, **23**, 171(1972).

(17) F. J. Bandelin and J. V. Tuschhoff, *J. Amer. Pharm. Ass., Sci. Ed.*, **44**, 241(1955).

ACKNOWLEDGMENTS AND ADDRESSES

Received November 22, 1974, from the *College of Pharmacy, University of Iowa, Iowa City, IA 52240*

Accepted for publication May 14, 1975.

Presented at the Industrial Pharmaceutical Technology Section, APhA Academy of Pharmaceutical Sciences, New Orleans meeting, November 1974.

[x] To whom inquiries should be directed. Present address: Alcon Laboratories, Fort Worth, TX 76101

Retardation of Dissolution and Growth of Calcium Oxalate Monohydrate

S. BISAILLON and R. TAWASHI [x]

Abstract □ The kinetics of dissolution and growth of calcium oxalate monohydrate were examined in the presence of small concentrations of pyrophosphate, chlorophyll, and other agents. Data presented show that the retardation in mass transport in both processes is controlled by the nature of the additive, its concentration, and the way the additives are combined in the dissolution medium. Dissolution was studied using a particle counter method, and growth was conducted in a gel system under the slow diffusion of the reacting ions. Results obtained show that chlorophyll is more active than other inhibitors studied and suggest a higher surface adsorption intensity on the primary sources of the crystal surface.

Keyphrases □ Calcium oxalate monohydrate—kinetics of dissolution and crystal growth, effects of various additives alone and in combination □ Dissolution—calcium oxalate monohydrate, kinetics, effects of various additives alone and in combination □ Crystal growth—calcium oxalate monohydrate, kinetics, effects of various additives alone and in combination □ Renal stone formation—calcium oxalate monohydrate, kinetics of dissolution and crystal growth, effects of various additives alone and in combination

Genesis and growth of calcium oxalate calculi are still unclear (1). To explain the ability of urine to remain supersaturated without precipitation, crystallization inhibitors should be studied. Equally important are the factors influencing the kinetics of dissolution of the stone components.

The complexity of urine in stone formation is certainly responsible for the slow progress in the area. The interaction of one compound with the others [*e.g.*, the action of magnesium on the solubility of calcium oxalate (2)] and the presence of material with a high epitaxial activity [such as organic material (3–

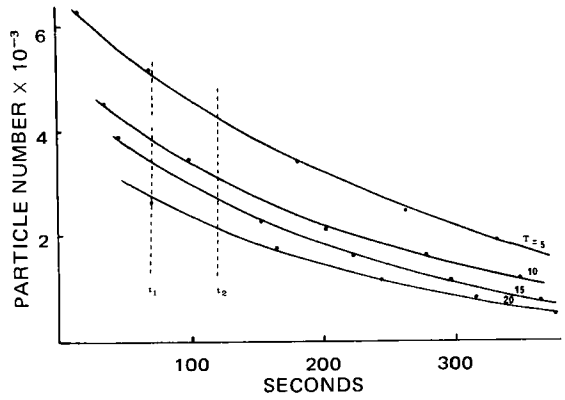

Figure 1—*Dissolution rate determination method showing the counts of particles as a function of time for different threshold settings* (T).

5)] make the clinical picture an undesirable approach in understanding basically renal stone formation.

A previous report from this laboratory, dealing with the influence of pH and magnesium on dissolution and growth rates of calcium oxalate monohydrate, demonstrated the effect of these parameters on the kinetics of these processes (6). Intensive and controversial studies were reported on the effect of pyrophosphate as a potential inhibitor of calcium oxalate growth (7–9), and no data are available on the dissolution process. Recent work demonstrated the possibility of using a gel technique to grow artificial concretions of calcium oxalate (10) and calcium carbonate (11).

The present work examines the effect of pyrophosphate, chlorophyll, and other agents on both processes. Quantitative data on the influence of these additives, alone and in combination, are presented, and the mechanism of action on the crystal surface is discussed.

EXPERIMENTAL

Materials—The following materials were used: calcium chloride dihydrate, oxalic acid dihydrate, sodium pyrophosphate decahydrate, potassium chloride, potassium carbonate, sodium orthophosphate, magnesium chloride, hydrochloric acid, and methylene blue (all reagent grade). Tromethamine[1], gelatin[2], chlorophyll[3], povidone[4], and normal saline[5] also were used.

Dissolution Rate Studies—The dissolution rate determinations were carried out using the particle counter[6] technique described previously (6). A suspension of calcium oxalate monohydrate was added to saline solution buffered at pH 6.2. A series of counts was taken, and cumulative size distribution curves were plotted. From the change in diameter for a fixed number of particles, the rate of dissolution was determined for a selected time period (t_1 and t_2) (Fig. 1).

The data were manipulated as previously described, and the dissolution rates were determined in centimeters per second in the absence and presence of additives at different levels of concentration. The estimated error by this method was approximately 5%.

Growth Studies—Growth studies were carried out using a gel technique (12). Figure 2 illustrates the U-tube system used for growing calcium oxalate crystals. In the U-shaped tube, each ion diffused from each branch of the tube; crystallization occurred at a front determined by the diffusion speed of each ion species. Figure 2 also illustrates the concentration variation as a function of distance in the tube for both reacting ions. The critical concentration of the precipitating components obeys Fick's second law of diffusion, as demonstrated by Pučar *et al.* (13).

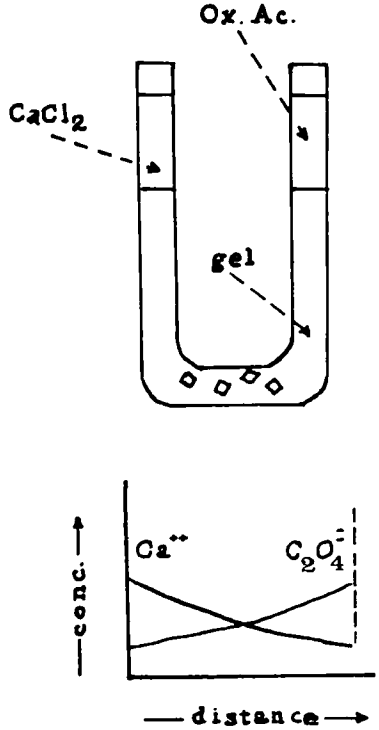

Figure 2—(*Top*) *U-tube system used for growing calcium oxalate crystals.* (*Bottom*) *Concentration variation as a function of distance for both ions.*

The growth support medium used was a gelatin gel in which the additive was incorporated. The gelatin was preferred to silica for its high purity regarding the presence of other ions (14). It also has a high optical clarity for crystal observations, and quantitative recovery does not present any difficulty. Gelatin also has the advantage of being an organic material and close to collagen in its structure, properties that can lead to interesting conclusions.

A 5% aqueous gelatin solution was prepared by gentle heating (below 50°) for 1 hr. Formaldehyde solution was added to prevent mold growth at a concentration of 0.1%. The solution was buffered to pH 6.2 using tromethamine. Then 25 ml of the solution was poured into the U-tubes and allowed to gel for 24 hr in a controlled-temperature room (22°). When additives were studied, 1 ml of the additive in aqueous solution was added prior to gelling to obtain the desired concentration.

After 24 hr, 10 ml of calcium chloride (0.5 *M*) and oxalic acid (0.5 *M*) solutions were layered carefully on top of the gel on each

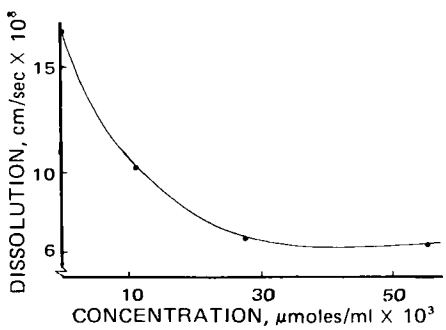

Figure 3—*Dissolution rate of calcium oxalate monohydrate in the presence of small concentrations of chlorophyll.*

[1] THAM, Fisher Scientific Co., Montreal, Canada.
[2] Purified calfskin, Eastman Kodak Co., Rochester, N.Y.
[3] Chlorophyllin copper complex sodium salt, E. Merck Chemicals; distributed by Brinkmann Instruments, Rexdale, Canada.
[4] Kollidon 17, B.A.S.F. Chemicals, Canada Ltd., Montreal, Canada.
[5] Sodium chloride injection USP, Abbott Laboratories, Montreal, Canada.
[6] Coulter.

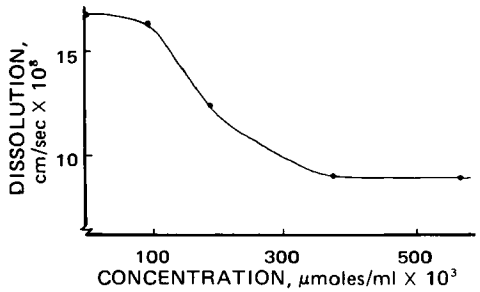

Figure 4—*Dissolution rate of calcium oxalate monohydrate in the presence of small concentrations of pyrophosphate.*

side of the tubes. After incubation at 22° for a fixed period, the crystals were examined in polarized light and recovered quantitatively. The recovery was achieved by centrifugation of the melted section containing the crystallization front and separation of the supernate.

Several washings were needed to discard gelatin or the other foreign additives from the calcium oxalate crystals. Maximum crystal yield was obtained after 6 days. In these experiments, the estimated error was approximately 8%.

RESULTS AND DISCUSSION

The dissolution rate dependence on additive concentration was systematically determined. Figure 3 shows the rate of dissolution of calcium oxalate monohydrate as a function of chlorophyll concentration at pH 6.2. This plot demonstrates the remarkable effect of chlorophyll as a powerful inhibitor of dissolution. A 2.5-fold decrease in the dissolution rate was reached with a concentration as low as 27.55×10^{-3} μmole/ml. Pyrophosphate demonstrated a lower activity than chlorophyll (Fig. 4), and the dissolution rate tended to stabilize at 37.59×10^{-2} μmole/ml. Methylene blue showed dissolution inhibition approximately similar to pyrophosphate for about the same concentration (20.06×10^{-2} μmole/ml).

It was interesting to observe that povidone acted differently on the dissolution rate of calcium oxalate monohydrate. An increase in the dissolution rate (25%) was noticed at a concentration of 29.41×10^{-4} μmole/ml. Further study is needed to explain the mechanism behind the increase in the mass transport of calcium oxalate in the presence of povidone. Other tested substances like potassium chloride, potassium carbonate, and sodium orthophosphate gave less significant inhibition even at higher concentrations. Table I summarizes the data obtained for other additives.

The remarkable inhibiting activity observed with chlorophyll and pyrophosphate at low concentration encouraged the examination of the effect of these additives in combination with other anions and cations with the aim of potentiating their inhibitory effect. Chlorophyll, at a concentration of 0.01 μmole/ml, was combined with small concentrations of potassium, orthophosphate, and magnesium [the latter demonstrated no effect on the dissolution rate as reported previously (6)] and with another active substance, pyrophosphate. Combining two additives improved the dissolution inhibition activity (Fig. 5). In Fig. 5, for example, the second diagram shows the combination effect of chlorophyll and potassium on the dissolution rate. The first column represents the action of chlorophyll alone, the second represents the action of potassium alone, and the third represents the effect of a combination of chlorophyll and potassium.

Table I—Dissolution Rate Values for Calcium Oxalate Monohydrate in the Absence or Presence of Different Additives

	Concentration, μmoles/ml	Dissolution Rate, cm/sec × 10^8
No additive	—	16.8
Methylene blue	0.134	10.0
Povidone	0.003	21.0
Chlorophyll	0.055	6.5
Pyrophosphate	0.188	12.4
Orthophosphate	3.0	8.5
Potassium		
As chloride	3.0	12.5
As carbonate	3.0	16.5

Table II—Yield of Calcium Oxalate Crystallites Grown in Gelatin Gel in the Absence or Presence of Different Additives after 3 Days of Incubation

Additive	Quantities Recovered from the Gel, mg
None	24.3
Chlorophyll	10.0
Pyrophosphate	8.4
Magnesium	7.4

Again, the combination of the two most active inhibitors in this study, chlorophyll and pyrophosphate, with an ionic substance gave a more pronounced effect on the dissolution rate (Fig. 6). The dissolution rate of calcium oxalate was reduced six fold in the presence of chlorophyll–pyrophosphate–magnesium in the dissolution medium.

The growth rate studies using the gelatin gel medium resulted in a significant reduction of the yield of calcium oxalate crystallites (Table II). The addition of chlorophyll, pyrophosphate, and magnesium lowered the quantity of crystals separated from the gel growth front by 2.5–3-fold after 3 days of incubation. The results obtained with magnesium are in agreement with previous data using the particle counter method (6). Other tested additives are presently being evaluated.

The present findings show that chlorophyll and pyrophosphate exert a remarkable inhibition on the dissolution and growth of calcium oxalate crystals. This inhibition, as far as the dissolution is concerned, is much more pronounced when pyrophosphate and/or chlorophyll are combined with an ionic substance. The effect observed cannot be attributed to a change in ionic strength, since the concentrations added (3.0 μmoles/ml) in the dissolution medium would not change this parameter significantly (the dissolution medium being 0.9% saline solution).

The inhibition produced by pyrophosphate, chlorophyll, and methylene blue can be examined in the light of the Langmuir ad-

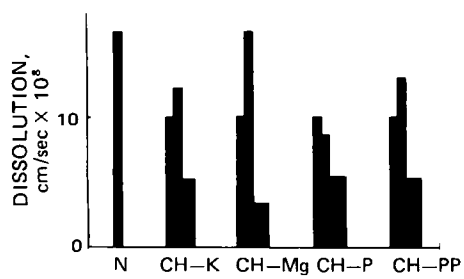

Figure 5—*Histogram showing the effect of combining chlorophyll (CH, 0.01 μmole/ml) with other additives. Key: N, no additive; PP, pyrophosphate (0.11 μmole/ml); K, potassium (3.0 μmoles/ml); Mg, magnesium (3.0 μmoles/ml); and P, orthophosphate (3.0 μmoles/ml). (See text.)*

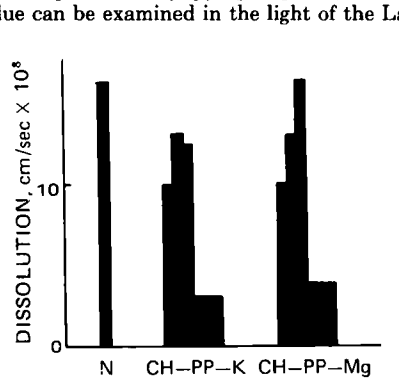

Figure 6—*Histogram showing the effect of combining chlorophyll (CH, 0.01 μmole/ml) and pyrophosphate (PP, 0.11 μmole/ml) with other additives. Key: N, no additive; Mg, magnesium (3.0 μmoles/ml); and K, potassium (3.0 μmoles/ml).*

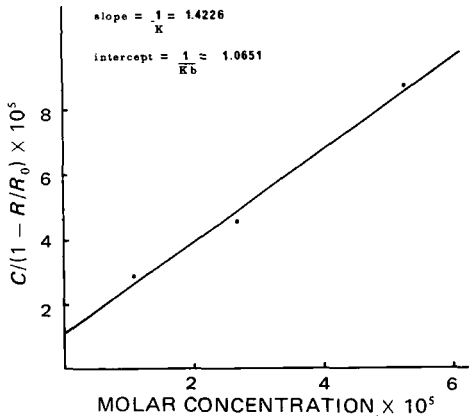

Figure 7—*Determination of adsorption constant for calcium oxalate monohydrate in the presence of chlorophyll according to Langmuir adsorption.*

sorption isotherm. If it is assumed that: (*a*) the fractional rate reduction caused by the additive is proportional to the fraction of the surface covered by the inhibitor, and (*b*) the adsorption of the substance can be represented by the simple Langmuir adsorption isotherm, the dissolution rate of calcium oxalate can be expressed as a simple function of the inhibitor concentration in solution as:

$$R = R_0\left[1 - \frac{KbC}{1 + bC}\right] \qquad \text{(Eq. 1)}$$

where R = dissolution rate of calcium oxalate monohydrate with one inhibitor, R_0 = dissolution rate of calcium oxalate monohydrate without additive, C = concentration of the inhibitor in the bulk solution, K = fraction of the surface covered when the surface is saturated with the inhibitor, and b = Langmuir adsorption constant reflecting the affinity of the substance for the binding sites on the crystal surface.

Equation 1 was rearranged and $C/(1 - R/R_0)$ was plotted against C, using a linear regression program for each substance studied. An example of the plots obtained can be seen in Fig. 7 for chlorophyll. From these data, a correlation with the Langmuir adsorption isotherm can be established. The values of the constants K and b were determined from the slopes and intercepts, respectively (Table III).

The K value, a measure of the saturation capacity, is approximately the same for pyrophosphate and chlorophyll; however, the b value, illustrating the affinity of the bound substance on the crystal surface, is 30 times greater for chlorophyll than for pyrophosphate. This finding explains the higher dissolution inhibition obtained with chlorophyll than with pyrophosphate. For methylene blue, which exerts an inhibition activity approximately the same as pyrophosphate, the surface coverage (K value) is smaller than for pyrophosphate; but its surface adsorption intensity on the crystal, as represented by the b value, is much more pronounced.

Table III—Values of the Constants K and b for the Langmuir Adsorption Isotherm Correlation[a]

	K	b
Chlorophyll	0.7029	1.3357
Pyrophosphate	0.7505	0.0457
Methylene blue	0.4189	0.7492

[a] K represents the fraction of the surface covered when the surface is saturated with the inhibitor, and b represents the Langmuir adsorption constant related with the affinity of the substance (strength of the bonds) for the surface.

The growth retardation in the presence of chlorophyll, pyrophosphate, and magnesium in the gel system can be explained in the same manner; more studies are necessary for complete characterization of the effect of these additives on crystal morphology.

The present observations and results show that very small changes in the levels of these factors in the biological system, for a relatively short period, can change the whole pattern of deposition and dissolution of calcium oxalate.

REFERENCES

(1) G. Kallistratos, *Urol. Int.*, **29**, 93(1974).

(2) J. S. Elliot and M. E. Ribeiro, *Invest. Urol.*, **10**, 295(1973).

(3) F.-H. C. Chow, D. W. Hamar, and R. H. Udall, *Proc. Soc. Exp. Biol. Med.*, **144**, 912(1973).

(4) M. Gebhardt, *J. Cryst. Growth*, **20**, 6(1973).

(5) H. G. Hanley, *J. Urol.*, **111**, 305(1974).

(6) J. F. Desmars and R. Tawashi, *Biochim. Biophys. Acta*, **313**, 256(1973).

(7) H. Fleisch, *Experientia*, **20**, 276(1964).

(8) R. G. G. Russell, R. C. Mühlbauer, S. Bisaz, D. A. Williams, and H. Fleisch, *Calcif. Tissue Res.*, **6**, 183(1970).

(9) R. Z. LeGeros and P. Morales, *Invest. Urol.*, **11**, 12(1973).

(10) S. Bisaillon and R. Tawashi, *J. Pharm. Sci.*, **64**, 458(1975).

(11) R. Tawashi, S. Bisaillon, and K. Wolter, *Experientia*, **30**, 1153(1974).

(12) H. K. Henisch, "Crystal Growth in Gels," Pennsylvania State University Press, University Park, Pa., 1970.

(13) Z. Pučar, B. Pokrić, and A. Graovac, *Anal. Chem.*, **46**, 403(1974).

(14) E. Banks, R. Chianelli, and F. Pintchovsky, *J. Cryst. Growth*, **18**, 185(1973).

ACKNOWLEDGMENTS AND ADDRESSES

Received November 18, 1974, from the *Faculty of Pharmacy, University of Montreal, Montreal 101, Quebec, Canada.*

Accepted for publication May 13, 1975.

Supported by the Medical Research Council of Canada.

[x] To whom inquiries should be directed.

Binding Study of Tetracyclines to Human Serum Albumin Using Difference Spectrophotometry

H. ZIA *§ **and J. C. PRICE** ‡×

Abstract □ The binding of several tetracyclines to human serum albumin was studied using difference spectrophotometry and a spectrophotometric probe, 2-(4′-hydroxybenzeneazo)benzoic acid. Difference spectra observed for the interaction between the probe and human serum albumin were similar to probe–bovine serum albumin spectra but were less intense for a given concentration of probe and did not reach saturation as quickly. Difference spectra for the tetracyclines were dependent on the characteristics of the ring substituents. More hydrophobic substituents on the D and C rings tended to give more intense difference spectra, but charge-transfer complexing may also have been involved since methacycline with a methylene group in the 6-position showed the most intense spectra of the compounds studied. Solvent perturbation, pH, and urea studies tended to confirm that something other than hydrophobic binding of the tetracyclines was involved. Drug–probe displacement studies showed that methacycline gave the greatest probe displacement followed by doxycycline, chlortetracycline, oxytetracycline, and tetracycline. This order of displacement of the anionic probe indicates that both hydrophobic and charge-transfer binding are involved. Experiments with calcium ion and ethylenediaminetetraacetic acid showed that the difference spectra obtained with the tetracyclines and human serum albumin were not the result of metallic bridge–chelate formation.

Keyphrases □ Tetracyclines—binding to human serum albumin, related to ring substituents, difference spectrophotometry, spectrophotometric probe □ Albumin, human serum—binding to tetracyclines, related to ring substituents, difference spectrophotometry, spectrophotometric probe □ Difference spectrophotometry—study of binding of tetracyclines to human serum albumin □ Spectrophotometric probe—2-(4′-hydroxybenzeneazo)benzoic acid, study of binding of tetracyclines to human serum albumin

The interaction of drugs with plasma proteins has been the subject of many investigations (1). The antibiotics have received considerable attention because of the involvement of binding in events of pharmacological importance. Various mechanisms such as chelation, adsorption, and ionic and hydrophobic binding have been proposed for the binding of tetracyclines to serum albumins (2–5).

Recent studies established difference spectrophotometry as a powerful tool for detecting small changes in the environment of a chromophore (6) and for elucidating conformational changes of globular proteins in solutions (7). In a preceding article, the binding of sulfonylureas and phenothiazines to bovine serum albumin, using difference spectrophotometry and 2-(4′-hydroxybenzeneazo)benzoic acid as a probe, was reported (8). The purpose of the present study was to use 2-(4′-hydroxybenzeneazo)benzoic acid as a spectrophotometric probe with difference spectrophotometry to study the binding of selected tetracyclines to human serum albumin.

EXPERIMENTAL

Materials—Human serum albumin[1] (crystalline, 4×), 2-(4′-hydroxybenzeneazo)benzoic acid[2], oxytetracycline hydrochloride[3], doxycycline hyclate[3], methacycline hydrochloride[3], chlortetracycline hydrochloride[4], and tetracycline hydrochloride[5] were used as obtained without further purification. Solvents were spectral grade, and all other chemicals were reagent grade.

Apparatus—Absorption spectra and difference absorbance measurements were made with a double-beam spectrophotometer[6] equipped with tandem cell holders.

Absorbance Difference Titrations—The absorbance difference titrations in the presence and absence of tetracyclines were carried out manually with microsyringes[7]. The 2-(4′-hydroxybenzeneazo)benzoic acid probe was dissolved in methanol at a concentration of 1×10^{-2} *M*. The human serum albumin solutions were prepared in 0.05 *M* tromethamine buffer (pH 7.4). Concentrations of the albumin solutions were estimated by measuring the absorbance at 280 nm (9) and using $E^{1\%}_{1\,cm} = 5.30$; the molecular weight of 69,000 was used to calculate the molar concentrations.

Two 300-ml quantities of albumin solution were pipetted into two other cells and were placed in the reference and sample beams in such a manner that a buffer and a protein solution cell were in tandem in each beam. After running a baseline, the contents of the buffer solution cell in the reference beam and the protein solution cell in the sample beam were titrated with successive additions of 6 μl of probe solution. Absorbance differences then were measured.

All difference spectra were obtained by using a pair of split-compartment tandem cells of 4-mm light path except where otherwise noted. All absorbance difference measurements were made at ambient temperature.

Data Treatment for Probe Studies—The absorbance difference observed upon addition of the probe to human serum albumin was measured for each successive addition of the probe in the absence and presence of the competitive drugs at 484 nm. These data were used to calculate the fraction of bound probe, *X*, in a manner similar to that reported previously (8) using the following equation:

$$X = \frac{\Delta A_l}{\Delta A_h} \qquad \text{(Eq. 1)}$$

where ΔA_l and ΔA_h refer to the absorbance difference of a given concentration of probe in solutions of low and high protein concentration or to the absorbance difference in the absence and presence of excess sites, respectively.

To determine the value of ΔA_h for a given concentration of probe, absorbance difference titrations were carried out at several different protein concentrations and the values of ΔA_h were taken to be values extrapolated to the intercepts of plots of $1/\Delta A$ *versus* $1/[P]$, where $[P]$ represents the total concentration of protein.

After values of *X* were found for all points along the titration curve, the data were treated according to the Scatchard (10) equation:

$$\bar{V}/[D] = nK_a - \bar{V}K_a \qquad \text{(Eq. 2)}$$

where $\bar{V}$ is the number of moles of bound probe per mole of protein, $[D]$ is the concentration of free probe, *n* is the number of binding sites on the protein, and K_a is the intrinsic association constant of the complex.

The competitive binding of tetracyclines was studied using 2-(4′-hydroxybenzeneazo)benzoic acid as an indicating probe. The binding of probe to albumin was determined in the presence and

[1] Nutritional Biochemicals Corp., Cleveland, Ohio.

[2] Aldrich, Milwaukee, Wis.
[3] Pfizer, Brooklyn, N.Y.
[4] American Cyanamid Co., Pearl River, N.Y.
[5] Bristol Laboratories, Syracuse, N.Y.
[6] Cary 118c, Varian Associates, Palo Alto, Calif.
[7] Hamilton Co., Reno, Nev.

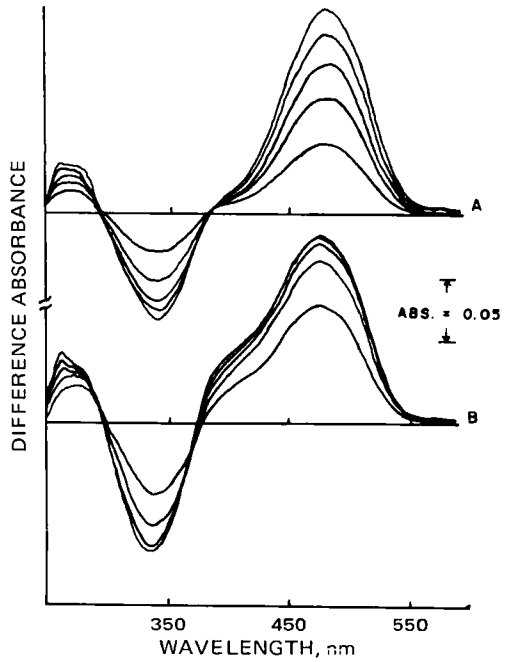

Figure 1—*Difference spectra of serum albumin solutions (1.38×10^{-5} M) with successive (2×10^{-5} M) increments of 2-(4'-hydroxybenzeneazo)benzoic acid in 0.05 M tromethamine buffer, pH 7.4. Absorbance difference increased with increasing probe concentration. (Tandem 10-mm light path cells were used.) Key: A, human serum albumin–probe system; and B, bovine serum albumin–probe system.*

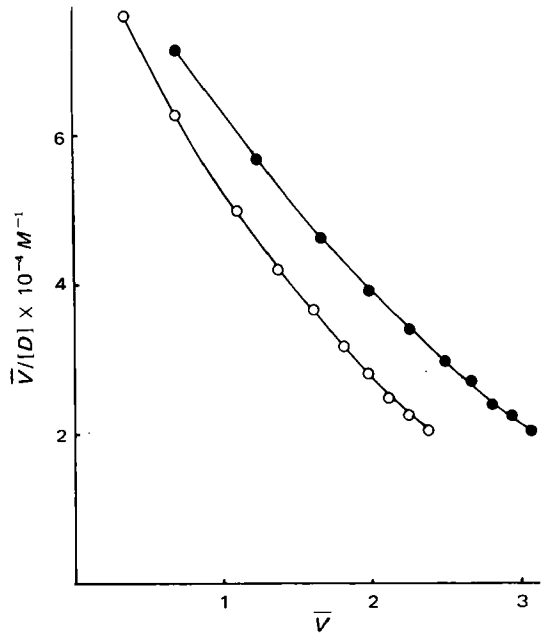

Figure 2—*Scatchard plots of 2-(4'-hydroxybenzeneazo)benzoic acid binding to human serum albumin in 0.05 M tromethamine buffer, pH 7.4. $\bar{V}$ = number of moles bound probe per mole of protein, and [D] = concentration of free probe. Key: ●, 1.36×10^{-5} M human serum albumin; and ○, 3.45×10^{-5} M human serum albumin.*

absence of competitive drugs by varying the concentration of probe at constant albumin and tetracycline concentrations. The binding constants of competitive drugs were calculated by using the Klotz *et al.* (11) equation:

$$K_b = \frac{n[P_t]K_a[D] - K_a[D][PD] - [PD]}{[B_t]K_a[D] - n[P_t]K_a[D] + K_a[D][PD] + [PD]} \times \frac{K_a[D]}{[PD]} \quad \text{(Eq. 3)}$$

where K_b is the association constant for the competitor, K_a is the association constant for the probe, $[D]$ is the concentration of free probe, n is the number of binding sites, $[P_t]$ is the total concentration of protein, $[B_t]$ is the total concentration of competitor, and $[PD]$ is the concentration of bound probe.

RESULTS AND DISCUSSION

The difference absorption spectra for the interaction of several concentrations of probe and human serum albumin in 0.05 *M* tromethamine buffer at pH 7.4 are presented and compared to the difference spectra of probe–bovine serum albumin in Fig. 1. The spectra were characterized by two positive peaks (484 and 262 nm) and one negative peak (345 nm) in the wavelength range of 250–600 nm. The difference spectra obtained for the interaction between human serum albumin and probe were similar to the difference spectra obtained for bovine serum albumin. However, difference spectra of the human serum albumin–probe system were less intense than the bovine serum albumin system and did not reach saturation as easily upon the increase in concentration of the probe.

Difference absorbance data, measured at 484 nm for human serum albumin–probe system and treated according to the method outlined under *Experimental*, are shown as Scatchard plots for two concentrations of albumin in Fig. 2. The Scatchard plots deviate from linearity. Such deviation has been considered to be due to the heterogeneity of the albumin with respect to its binding properties and was discussed elsewhere (8). It is sufficient to note here that binding parameters for the interaction between the probe and human serum albumin were concentration dependent. The greater probe binding capacity at low albumin concentrations may be due to a conformational change in the protein. Similar ob-

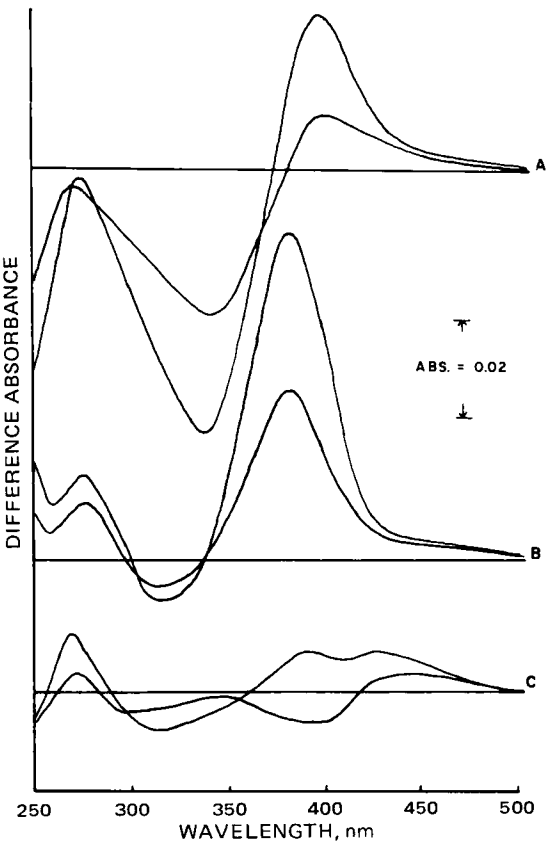

Figure 3—*Difference spectra of oxytetracyclines (1.25×10^{-4} and 2.5×10^{-4} M) and human serum albumin (1.38×10^{-5} M) in 0.05 M tromethamine buffer, pH 7.4. Absorbance difference increased with the higher drug concentration. Key: A, methacycline; B, doxycycline; and C, oxytetracycline.*

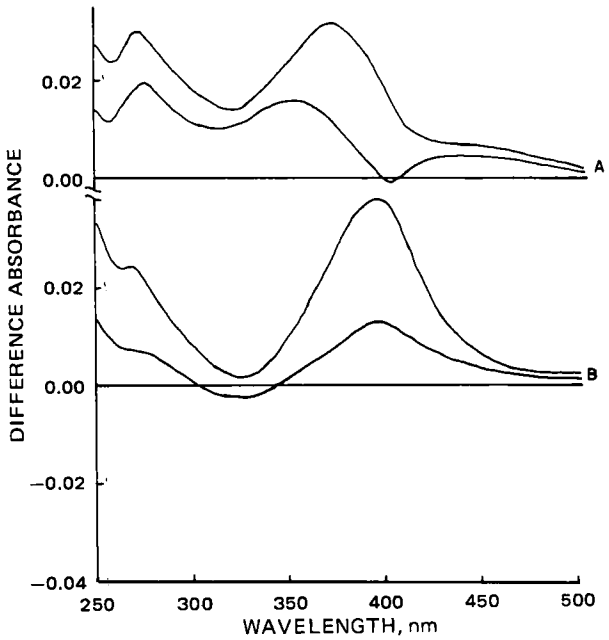

Figure 4—*Difference spectra of tetracyclines (1.25×10^{-4} and 2.5×10^{-4} M) and human serum albumin (1.38×10^{-5} M) in 0.05 M tromethamine buffer, pH 7.4. Absorbance difference increased with higher drug concentration. Key: A, tetracycline; and B, chlortetracycline.*

servations and interpretations were made for the interaction between methyl red and albumin (12).

Figures 3 and 4 show the difference absorption spectra for the binding of tetracyclines and oxytetracyclines, respectively, to human serum albumin in tromethamine buffer at pH 7.4. The interactions between both groups (tetracyclines and oxytetracyclines) with human serum albumin consistently revealed at least

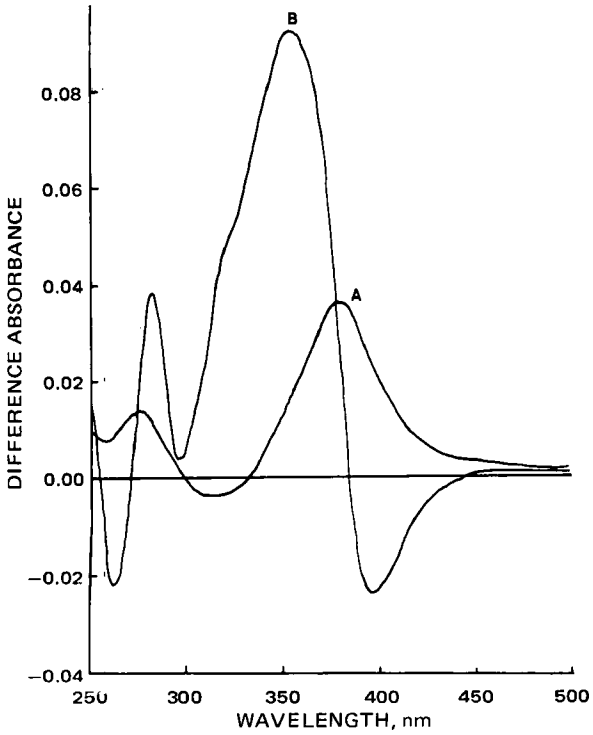

Figure 5—*Difference spectrum of doxycycline–human serum albumin and solvent perturbation spectrum of doxycycline in 20% dioxane. Key: A, doxycycline (1.25×10^{-4} M) and human serum albumin (1.38×10^{-5} M) in buffer* versus *buffer; and B, doxycycline (1.25×10^{-4} M) and 20% dioxane in buffer* versus *buffer.*

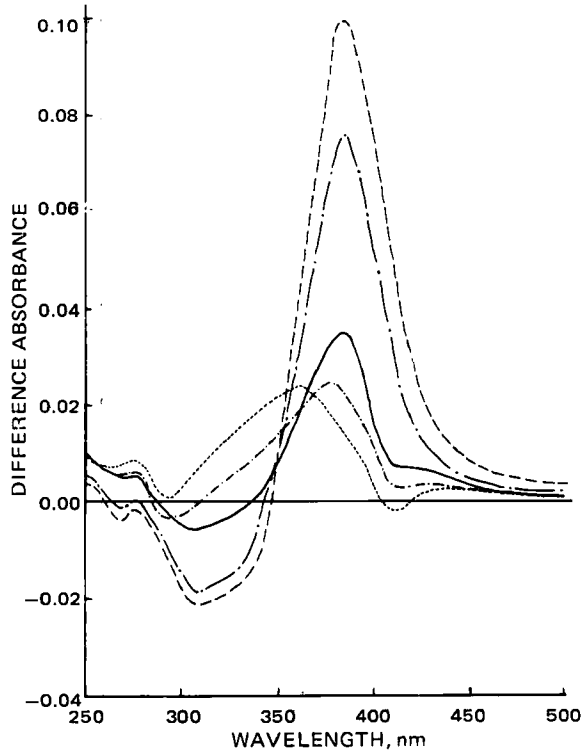

Figure 6—*Effect of pH on the difference spectrum of doxycycline (8.33×10^{-5} M) and human serum albumin (1.38×10^{-5} M). (Tandem 10-mm light path cells were used.) Key: – – –, pH 7.95; —·—, pH 7.70; ——, pH 7.40; —··—, pH 7.25; and ····, pH 7.05.*

two positive absorption peaks and one negative peak. The positions of the peaks were concentration dependent.

The increase in the intensity of the difference spectra for the interaction of drugs with human serum albumin depended on the characteristics of the ring substituent groups at various positions of the 2-naphthacenecarboxamide moiety, especially at the 4-, 5-, 6-, and 7- positions. The 7-chloro- and/or 6-deoxytetracyclines induced more intense difference spectra than other tetracyclines. Although this result was consistent with the hydrophobic nature of the interaction as suggested by Ma *et al.* (13) based on fluorescence studies, additional factors such as charge-transfer-type complexing also seem to have been involved. Such indications were the large red shift in the absorption maxima and/or the presence of a new absorption band at about 374–393 nm. Further support of the charge-transfer-type complexing was shown with methacycline with a methylene group at the 6-position. This compound had the most intense difference spectra of any of the compounds studied.

Solvent Perturbation Spectra—The generation of the difference spectra in the presence of protein may be attributed either to the perturbation of the drug's chromophores by a different environment at the protein binding sites or to the perturbation of the protein as the result of the binding or to a combination of both. In an attempt to characterize the nature of the difference spectra observed, a study of drugs in buffered 20% dioxane against buffer was performed. Figure 5 shows the interaction difference spectrum of doxycycline and human serum albumin as opposed to solvent perturbation spectra in 20% dioxane and buffer. Comparison of these difference spectra indicates some similarities in their patterns, which may indicate the existence of a nonpolar environment around the albumin binding sites. However, since deviations in the positions of the absorption bands existed between the spectra, the additional contribution from mechanisms other than the nonpolar environment and/or the perturbation of the protein *via* binding with drugs must also be involved.

Effect of pH on Difference Spectra—Figure 6 shows the effect of pH on difference spectra of the interaction between doxycycline and human serum albumin. As pH decreased (from 8 to 7), a slight blue shift along with a marked decrease of the intensity of the spectra was seen. The effect of pH on the difference spectra indicates that, although hydrophobic binding has some role, the

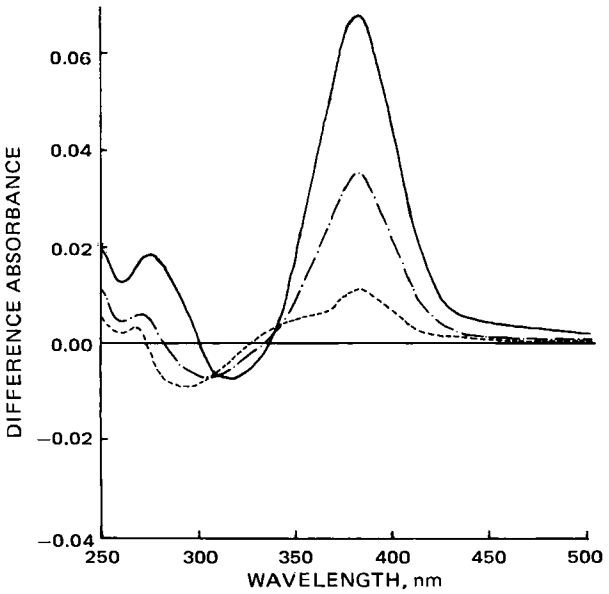

Figure 7—*Effect of urea on the difference spectrum of doxycycline (2.5 × 10^{-4} M) and human serum albumin (1.38 × 10^{-5} M). Key: ——, in the absence of urea; —·—·, in the presence of 2 M urea; and ----, in the presence of 4 M urea.*

ionic interaction cannot be ignored.

The ability of acidic groups on the doxycycline molecule to donate hydrogen was in order of tricarbonylmethane (pKa = 3.4), phenol diketone (pKa = 7.7), and the dimethylammonium group (pKa = 9.7) (14). Thus, neither the dimethylammonium group nor the tricarbonylmethane group underwent significant changes in the pH 7–8 range, and changes in the difference spectra in this range can be attributed to changes in the degree of ionization of the phenol diketone moiety.

As the pH was decreased from 7.95 to 7.7, good correlation was shown between the absorbance difference decrease (21% decrease) and the decrease in calculated amount of ionized phenol diketone

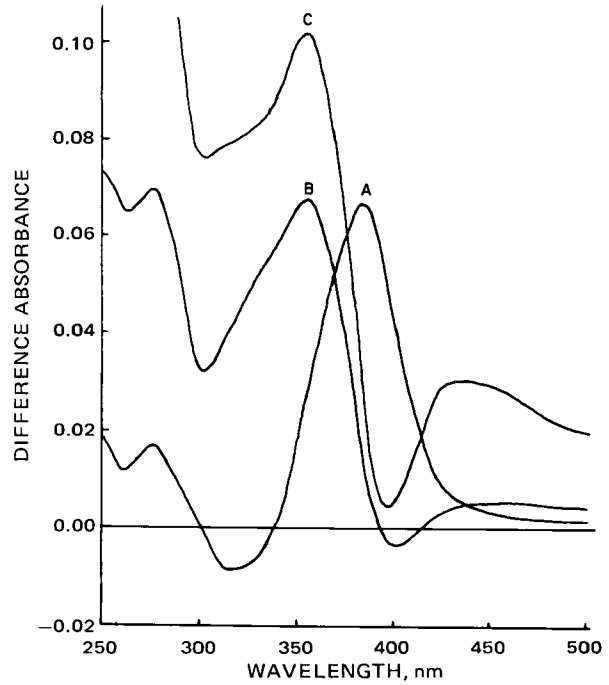

Figure 8—*Effect of calcium ion on difference spectrum of doxycycline (2.5 × 10^{-4} M) and human serum albumin (1.38 × 10^{-5} M). Key: A, in the absence of calcium ion; B, in the presence of 1.25 × 10^{-4} M $CaCl_2$; and C, in the presence of 2.5 × 10^{-4} M $CaCl_2$.*

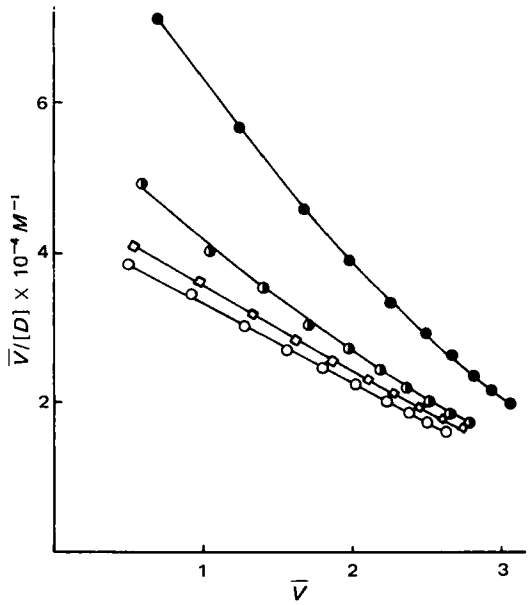

Figure 9—*Scatchard plots of 2-(4′-hydroxybenzeneazo)benzoic acid binding to human serum albumin in 0.05 M tromethamine buffer, pH 7.4. $\bar{V}$ = number of moles bound probe per mole of protein, and [D] = concentration of free probe. Key: ●, in the absence of drug; ◑, in the presence of 1.5 × 10^{-4} M oxytetracycline; □, in the presence of 1.5 × 10^{-4} M doxycycline; and ○, in the presence of 1.5 × 10^{-4} M methacycline.*

(22% calculated decrease). As the pH was further decreased to 7.25, a blue shift was observed in the spectrum and the correlation between absorbance difference change and ionized group concentration correlation was lessened, indicating that the proportion of unionized phenol diketone had increased sufficiently to contribute to the spectrum through hydrophobic interaction with the protein. A further decrease in pH to 7.05 caused little change in absorbance difference but resulted in a rather marked blue shift in the spectrum from increased hydrophobic bonding.

Effect of Urea on Difference Spectra—The effect of urea on the difference spectrum of the interaction between doxycycline

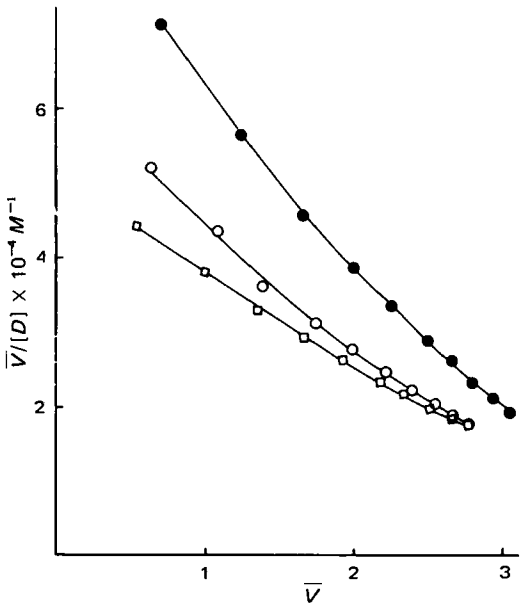

Figure 10—*Scatchard plots of 2-(4′-hydroxybenzeneazo)benzoic acid binding to human serum albumin in 0.05 M tromethamine buffer, pH 7.4. $\bar{V}$ = number of moles bound probe per mole of protein, and [D] = concentration of free probe. Key: ●, in the absence of drug; ○, in the presence of 1.5 × 10^{-4} M tetracycline; and □, in the presence of 1.5 × 10^{-4} M chlortetracycline.*

Table I—Association Constants of Selected Tetracyclines to Human Serum Albumin

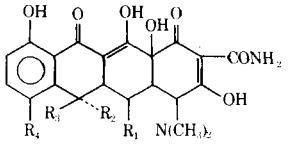

Generic Name	R_1	R_2	R_3	R_4	Association Constant × 10^{-4} M^{-1}
Oxytetracycline	OH	CH_3	OH	H	3.53
Doxycycline	OH	CH_3	H	H	5.32
Methacycline	OH	$=CH_2$	—	H	6.28
Tetracycline	H	CH_3	OH	H	3.15[a]
Chlortetracycline	H	CH_3	OH	Cl	4.03

[a] Powis (17) reported two classes of binding sites for tetracycline on human serum albumin and calculated a binding constant of 4.38 × 10^4 for the first class of sites (dialysis method).

and human serum albumin is shown in Fig. 7. Use of 2 *M* urea markedly decreased the absorption intensity of positive bands and caused a blue shift on the negative band. The fact that the difference spectrum for doxycycline–albumin interaction decreased significantly in the 2 *M* or higher urea-treated albumin strongly indicates that hydrophobic binding is not the only mode of the interaction and, as was concluded earlier, that additional factors must be involved. However, since many aspects of the action of urea on small molecule–protein interaction are still obscure, the conclusion that such observed change in the difference spectrum is due to: (*a*) conformational change of albumin (conversion of the N form to the F form and/or increase of levorotation) (15), (*b*) breakage of hydrogen bonds of the tetracycline–albumin complex (16), (*c*) true competition between tetracycline and urea for the same sites (11), or (*d*) a combination of these factors may be made only with ambiguity.

Effect of Calcium Ion and Ethylenediaminetetraacetic Acid on Difference Spectra—It is known that tetracycline–divalent ion complexes are capable of forming metal–bridge chelates with albumins (2). To examine whether such chelates are the cause of the observed difference spectra, ethylenediaminetetraacetic acid, calcium ion, and ethylenediaminetetraacetic acid plus calcium ion were added to the solutions of doxycycline and human serum albumin.

It was found that the addition of either chelating agent alone or an equilvalent amount of chelating agent and calcium ion had no effect on the difference spectra. However, the addition of calcium ion alone changed difference spectra considerably (Fig. 8). The difference spectra generated from solutions of tetracycline–human serum albumin obviously were not the result of a metal–bridge chelate formation. Similar results were reported for fluorescence spectra (5).

Displacement of 2-(4′-Hydroxybenzeneazo)benzoic Acid by Tetracycline—To have a better understanding of the functional groups and the nature of the binding force, the displacement of tetracyclines by the spectrophotometric probe was examined. The binding of probe to human serum albumin was determined in the presence and absence of tetracyclines by varying the probe concentration from 2 × 10^{-5} to 2 × 10^{-4} *M* at constant albumin (1.38 × 10^{-5} *M*) and tetracycline (1.5 × 10^{-4} *M*) concentrations.

The results of difference absorbance measurements at 484 nm in the presence and absence of each tetracycline are shown as Scatchard plots in Figs. 9 and 10. The binding constants calculated using the Klotz equation (11), with $n = 4$ and probe $K_a = 1.95 \times 10^{-4}\ M^{-1}$, are shown in Table I. Methacycline showed the greatest displacement of the probe followed by doxycycline, chlortetracycline, oxytetracycline, and tetracycline. The increased displacement ability of chlortetracycline compared to tetracycline and/or deoxytetracyclines (methacycline and doxycycline) compared to oxytetracycline may be attributed to the increased hydrophobicity of the molecules in the D and C ring region. The fact that tetracycline had a lesser affinity in comparison to the oxytetracyclines, along with the observed displacement of the anionic probe by these drugs, reinforces the earlier conclusion that hydrophobic binding is not the only mode of the interaction of tetracyclines with human serum albumin.

REFERENCES

(1) M. C. Meyer and D. E. Guttman, *J. Pharm. Sci.*, **57**, 895(1968).

(2) K. W. Kohn, *Nature*, **191**, 1156(1961).

(3) G. Kivman and N. M. Smolnikova, *Antibiotiki*, **10**, 229(1965).

(4) L. J. Bononi, G. Pagnini, C. Scioli, and E. Genazzani, *Antibiotica*, **4**, 105(1966).

(5) P. G. Popov, K. I. Vaptzarova, G. P. Kossekova, and T. K. Nikolov, *Biochem. Pharmacol.*, **21**, 2363(1972).

(6) L. R. Goldbaum, *Anal. Chem.*, **24**, 1604(1952).

(7) T. T. Herskovits, "Methods in Enzymology," vol. 11, Academic, New York, N.Y., 1967, p. 748.

(8) H. Zia and J. C. Price, *J. Pharm. Sci.*, **64**, 1177(1975).

(9) P. Clark, M. R. Rachinsky, and J. F. Foster, *J. Biol. Chem.*, **237**, 2509(1962).

(10) G. Scatchard, *Ann. N.Y. Acad. Sci.*, **51**, 660(1949).

(11) I. M. Klotz, H. Triwush, and F. M. Walker, *J. Amer. Chem. Soc.*, **70**, 2935(1948).

(12) B. Breyer and H. H. Bauer, *Aust. J. Chem.*, **6**, 332(1953).

(13) J. K. H. Ma, H. W. Jun, and L. A. Luzzi, *J. Pharm. Sci.*, **62** 1260(1973).

(14) C. R. Stephens, J. J. Beereboom, H. H. Rennhard, P. N. Gordon, K. Murai, R. K. Blackwood, and M. S. von Wittenau, *J. Amer. Chem. Soc.*, **85**, 2643(1963).

(15) N. A. Attalah and G. F. Lata, *Biochim. Biophys. Acta*, **168**, 321(1968).

(16) H. S. Frank and F. Franks, *J. Chem. Phys.*, **48**, 4746(1968).

(17) G. Powis, *J. Pharm. Pharmacol.*, **26**, 113(1974).

ACKNOWLEDGMENTS AND ADDRESSES

Received August 22, 1974, from the *School of Pharmacy, University of Isfahan, Isfahan, Iran, and the ‡School of Pharmacy, University of Georgia, Athens, GA 30602

Accepted for publication May 13, 1975.

§ Senior Fulbright–Hays Scholar from University of Isfahan, Isfahan, Iran.

x To whom inquiries should be directed.

IR Studies of Development of Order in Aluminum Hydroxide Gels

STEVEN L. NAIL *, JOE L. WHITE ‡, and STANLEY L. HEM *x

Abstract □ The usefulness of deuteration in detecting the development of order in aluminum hydroxide gel by IR spectra is demonstrated. By treatment of gel samples with deuterium oxide vapor at room temperature, the relative ease with which deuteroxyl–hydroxyl exchange takes place is determined as a function of the age of the gel. The use of scale expansion in conjunction with deuteration allows detection of IR absorbance characteristic of gibbsitic material long before such detection is possible by conventional IR analysis or X-ray diffraction.

Keyphrases □ IR spectroscopy—detection of development of order in deuterated aluminum hydroxide gels □ Aluminum hydroxide gels—deuteration, IR detection of development of order □ Deuteration—aluminum hydroxide gels, related to age of gel

IR spectral analysis of aluminum hydroxide gel detects well-defined absorption bands in the hydroxyl bending and hydroxyl deformation regions of the spectrum as the gel ages (1). These bands represent structural hydroxyls that are part of an ordered structure (2–4). Since each structural unit absorbs IR radiation independently, the detection of order does not depend on the regular successive stacking required to give X-ray diffraction (2). Structural information on amorphous alumina systems was obtained using a generalized Fourier synthesis (5); however, conventional X-ray diffraction was shown to be less sensitive than IR spectral analysis in detecting the early development of order in aluminum hydroxide gel (1).

Treatment of minerals with deuterium oxide vapor leads to conversion of some or all of the hydroxyl groups to deuteroxyl groups (4, 6, 7). Since the deuteroxyl stretching vibration occurs in the 2700–2200-cm^{-1} region of the IR spectrum, as opposed to 3700–2900 cm^{-1} for the hydroxyl stretching frequency, this exchange is readily detected.

The comparative ease with which hydrogen–deuterium exchange takes place in hydroxyl groups of layer silicates yields information about the accessibility of the hydroxyl groups. In studying the IR spectra of synthetic hydroxyl interlayers in expanding clays, Ahlrichs (7) observed that flushing with deuterium oxide vapor at room temperature removes water and that heating at 100° in deuterium oxide vapor exchanges interlayer hydroxyl but not the clay crystal hydroxyl. Complete replacement of lattice hydroxyl by deuteroxyl in beidellite, montmorillonite, saponite, and hectorite is only achieved after repeated treatment at temperatures of 350° or higher (6).

This report demonstrates the usefulness of deuteration in detecting the development of order in aluminum hydroxide gel. By treatment of the gel sample with deuterium oxide vapor at room temperature, the relative ease with which deuteration takes place is determined as a function of the age of the gel. Use of the scale expansion feature of the spectrophotometer enhances sensitivity in studying spectral changes.

EXPERIMENTAL

Materials—All chemicals used were either official or reagent grade.

Preparation of Aluminum Hydroxide Gel—Aluminum hydroxide gel was prepared by the neutralization of 8.5% aluminum chloride hexahydrate solution with 13% ammonium hydroxide to a final pH of 7.0 (8).

Analytical Procedures—The acid-consuming capacity test (9) was modified by titrating to pH 3.5 rather than using bromophenol blue TS, as given in the USP. Duplicate determinations were made for each sample. The antacid property of each gel is given as the percentage of the theoretical acid-consuming capacity.

For X-ray analysis, a gel sample was air dried at room temperature and ground to a fine powder with an agate mortar and pestle. Powder mounts were prepared using aluminum McCreery mounts. The diffraction pattern[1] was recorded from 14 to 27° 2θ under the following conditions: Cu K_α radiation, 40 kv, 20 mamp, 500 Hz full scale, and 1°/min scan speed.

IR spectra of the gel samples were obtained[2] by air drying a 0.10-ml gel sample on a silver chloride window[3]. The concentration on the window was 0.3 mg of aluminum oxide/cm^2.

For deuterium oxide treatment, two matched quartz vacuum cells of square cross-section were used (Fig. 1). One cell was used for the sample, and the other was used for the reference beam of the spectrophotometer. The vacuum cells were fitted with a quartz rod with a ring at the bottom to hold a silver chloride window. A three-way stopcock at the top of the cell was connected by rubber vacuum tubing to the vacuum pump[4] and to a glass Thunberg tube[5] containing deuterium oxide.

The silver chloride window with the gel film was placed in the quartz holder and inserted into the vacuum cell. The cell was then evacuated, and the spectrum was recorded from 4000 to 2100 cm^{-1} by aligning the vacuum cell containing the sample in the sample beam of the spectrophotometer. The matching cell was placed in the reference beam.

After the spectrum of the untreated sample was recorded, the sample cell was connected to the deuterium oxide source. The evacuated cell was then filled with deuterium oxide vapor and allowed to stand for 5 min at room temperature. The cell was evacuated again, and the procedure was repeated. After two flushings with deuterium oxide, the spectrum was again recorded.

The IR spectrum was also recorded in the hydroxyl deformation region (1100–800 cm^{-1}) using both regular (1×) scale and 5× scale expansion. By using scale expansion, the signal to noise ratio is enhanced by widening the slits to increase the signal while slowing the attenuator response to decrease noise (10).

RESULTS

Figure 2 shows the IR spectra of the fresh gel and of the same gel following deuteration. The broad, diffuse peak in the hydroxyl stretching region of the gel indicates a highly unordered structure (2). The absence of hydroxyl stretching absorbance in the spec-

[1] Norelco, Phillips Electronic Instruments, Mount Vernon, N.Y.
[2] Harshaw Chemical Co., Cleveland, Ohio
[3] Model 421, Perkin-Elmer Corp., Norwalk, Conn.
[4] "Duo-Seal" vacuum pump, M. W. Welch Manufacturing Co., Chicago, Ill.
[5] Lab Glass, Inc., Vineland, N.J.

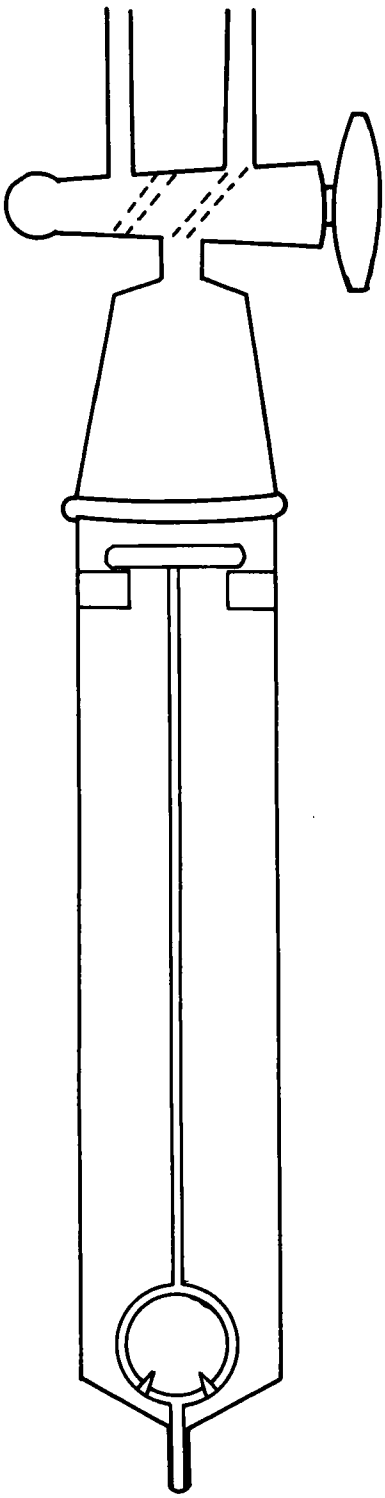

Figure 1—*Vacuum IR cell for deuteration studies.*

trum of the deuterated gel indicates that all of the water and structural hydroxyl have been exchanged.

Figure 3 shows the IR spectra of the same gel in the 3700–3100-cm^{-1} region for the untreated gel *versus* the deuterated gel at various times during aging. After 42 days (Fig. 3B), the weak absorbance in the hydroxyl stretching region for the deuterated sample indicates that not all of the hydroxyl groups have been exchanged. The increasing absorbance of the deuterated sample in this region indicates an increase in the relative number of unexchanged hydroxyl groups.

After 74 days of aging (Fig. 3D), the maximum hydroxyl absorbance of the deuterated sample occurs from 3450 to 3515 cm^{-1}.

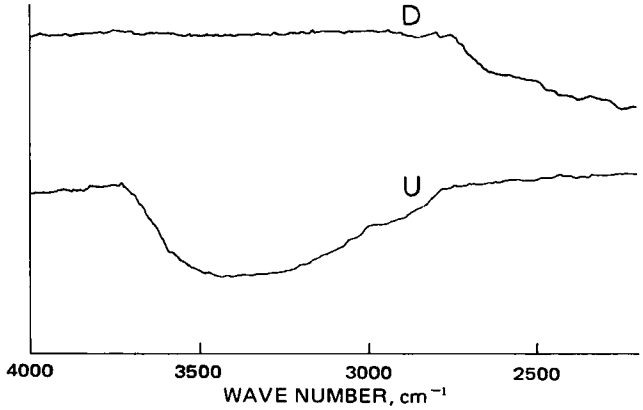

Figure 2—*IR spectrum of freshly prepared gel. Key: U, untreated; and D, deuterated.*

After 81 days (Fig. 3E), a well-defined peak is seen at 3520 cm^{-1} for the deuterated sample. This peak becomes more intense with continued aging. After 97 days (Fig. 3F), shoulders are seen in the deuterated sample at 3470 and at about 3600 cm^{-1} in addition to the peak at 3520 cm^{-1}. Further aging (Fig. 3G) results in a well-defined band at 3612 cm^{-1} along with the sharp peak at 3520 cm^{-1} and the shoulder at 3470 cm^{-1}.

In the spectra of the untreated gels, the first indication of the 3520-cm^{-1} band is barely perceptible as an inflection point at 3520 cm^{-1} after 81 days (Fig. 3E). After 147 days (Fig. 3G), a sharp peak is seen at 3520 along with shoulders at 3612 and 3470 cm^{-1}.

The use of scale expansion is illustrated in Fig. 4, where the spectra of the untreated and deuterated gels are shown at 5× scale expansion. Figure 4A shows the gel after 59 days of aging. The 5× spectrum of the deuterated gel shows a maximum absorbance band from 3470 to 3525 cm^{-1}. This band is not discernible in the 1× spectrum of the deuterated gel. After 65 days (Fig. 4B), the maximum absorbance band in the expanded scale spectrum of the deuterated gel occurs from 3480 to 3515 cm^{-1}. Finally, after 74 days (Fig. 4C), a sharp peak is seen at 3520 cm^{-1} in the 5× spectrum of the deuterated sample. This peak is not resolved in the 1×

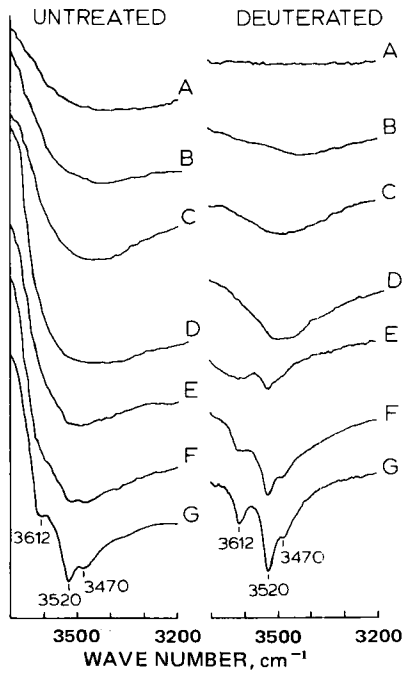

Figure 3—*Change in hydroxyl stretching frequency region of IR spectrum of aluminum hydroxide gel for untreated and deuterated samples during aging at 25°. Key: A, fresh precipitate; B, 42 days; C, 59 days; D, 74 days; E, 81 days; F, 97 days; and G, 147 days.*

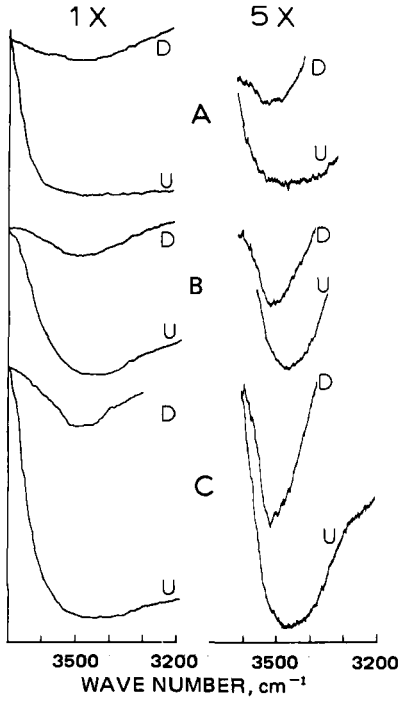

Figure 4—*Change in hydroxyl stretching frequency region during aging by regular (1X) scale and 5X scale expansion for both untreated (U) and deuterated (D) samples. Key: A, 59 days; B, 65 days; and C, 74 days.*

spectrum of the deuterated sample.

Scale expansion also is useful in examining the hydroxyl deformation region of the spectrum (Fig. 5). When using the 1X scale, the hydroxyl deformation absorbance appears as a broad band centered at about 900 cm^{-1} for a fresh gel (1). The better resolution of scale expansion shows a peak at 880 cm^{-1} (Fig. 5A). Continued aging leads to the disappearance of the 880 cm^{-1} band and the appearance of another band at 970 cm^{-1}. After 74 days, another sharp peak appears at 1020 cm^{-1} (Fig. 5E). By this time there is no evidence of a peak at 880 cm^{-1}. With further aging, the intensity of the 1020-cm^{-1} peak increases relative to the peak at 970 cm^{-1} (Fig. 5F). After 80 days, the 1020-cm^{-1} peak is easily identifiable by the 1X scale.

The X-ray diffraction pattern of the gel at various aging times is seen in Fig. 6. The first evidence of crystallinity is seen after 94 days of aging (Fig. 5C), at which time a broad peak is seen from 18.4 to 19.6° 2θ (4.82–4.52 Å) and a sharper peak is seen at 20.35° 2θ (4.36 Å). Even after 189 days of aging, the peak at 18.5° 2θ (4.80 Å) remains relatively diffuse and of low intensity. While the 4.80- and 4.36-Å spacings correspond to the interplanar spacings for gibbsite, the relative intensities are reversed from those of highly crystalline gibbsite (11).

A plot of the log of the acid-consuming capacity of the gel *versus* time at room temperature is shown in Fig. 7. As previously reported (1, 8), the loss in acid reactivity follows apparent first-order kinetics (slope = -3.10×10^{-3}/day, $r = 0.99$). Although the gel used in this study was prepared under the same conditions of pH of precipitation, rate of addition of base, and washing and contained the same amount of chloride (0.35% w/v) as the earlier gel (1), the rate constant for loss of reactivity was 7.13×10^{-3}/day in contrast to a rate constant for the previous gel of 13.65×10^{-3}/day. The reason for the observed difference in behavior is not known.

DISCUSSION

The initial precipitate resulting from the reaction of a soluble aluminum salt with base is probably a highly random structure. With aging, structural rearrangement occurs to form a more stable system. For example, a polymerization-like process may occur to produce a more highly ordered system which is resistant to attack by acid (12–15). The end-product of this process is a crystalline

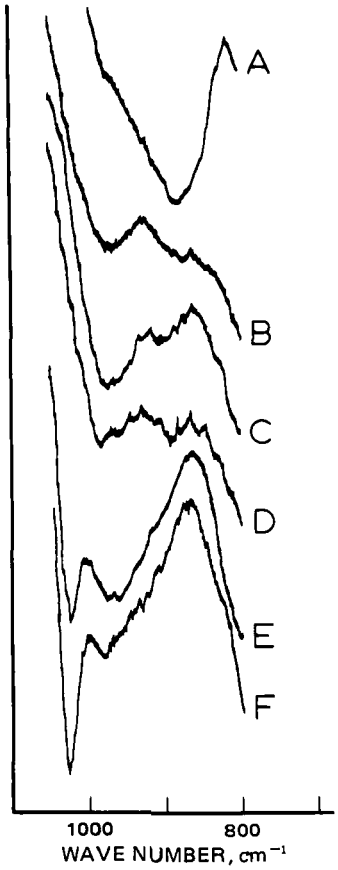

Figure 5—*Change in hydroxyl deformation frequency of IR spectrum during aging at 25° by 5X scale expansion. Key: A, fresh precipitate; B, 45 days; C, 52 days; D, 65 days; E, 74 days; and F, 81 days.*

form of aluminum hydroxide (16–20). Under the conditions used in preparing the gel for this study, it was determined that gibbsite is the primary crystalline phase that develops on aging (1). Highly crystalline gibbsite has bands in the hydroxyl stretching region of the IR spectrum at 3612, 3520, 3440, and 3395 cm^{-1} and bands in the hydroxyl deformation region at 1030 and 970 cm^{-1} (21).

Treatment of aluminum hydroxide gel with deuterium oxide

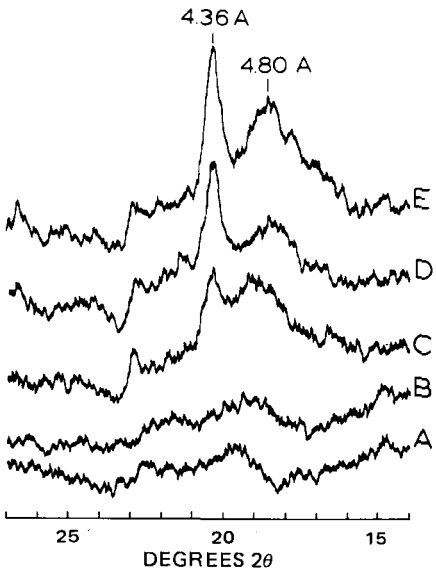

Figure 6—*Change in X-ray diffraction pattern of aluminum hydroxide gel during aging at 25°. Key: A, 56 days; B, 78 days; C, 94 days; D, 115 days; and E, 189 days.*

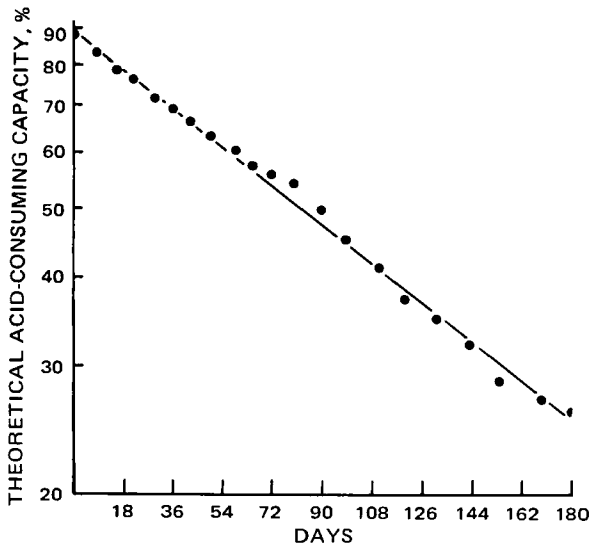

Figure 7—*Change in acid-consuming capacity of aluminum hydroxide gel during aging at 25°.*

vapor at room temperature enhances the sensitivity of IR spectral analysis in observing the development of order in the gel. In the freshly precipitated gel, which is fully reactive by the USP acid-consuming capacity test, all structural hydroxyl groups are exchanged. This condition indicates ready accessibility of the hydroxyl groups to deuterium oxide vapor. The residual hydroxyl stretching absorbance following deuteration of aged samples indicates that the accessibility of the structural hydroxyl groups is diminished. The magnitude of this residual absorbance increases with age, and the maximum absorbance occurs within a narrower frequency range with age. The observation of the narrowing of the range of maximum absorbance of deuteration-resistant hydroxyl is facilitated by use of scale expansion. The deuteration-resistant hydroxyl absorbance becomes more specific until a sharp band is seen at 3520 cm^{-1}, corresponding to a major gibbsite peak.

The development of distinct bands resistant to deuterium oxide exchange indicates that the chemical environment of the hydroxyl groups is becoming more uniform; *i.e.*, the structure is more highly ordered. The first indication of the development of order in the gel by IR analysis is seen after 43 days of aging by the residual hydroxyl stretching absorbance following deuteration. At this time, the acid-consuming capacity is 67% of the theoretical capacity. A distinct peak at 3520 cm^{-1} following deuteration is seen by 5× scale expansion after 74 days, when the gel is 54% reactive. The first evidence of crystallinity by conventional X-ray diffraction is seen after 94 days, corresponding to 44% reactivity. Thus, while the acid-consuming capacity is the most sensitive indicator of developing order, the application of deuteration is of considerable value in relating structural changes on aging to decreased acid reactivity.

Spectral changes in the hydroxyl deformation region also show the gradual development of a gibbsite structure. Three different peaks are seen during the aging process. The first is at 880 cm^{-1} and is subsequently replaced by a band at 970 cm^{-1} and later by a sharp peak at 1020 cm^{-1}. The 1020- and 970-cm^{-1} peaks are associated with the gibbsite structure. The structural significance of the early peak at 880 cm^{-1} is not known.

The reversal in the relative intensities of the 4.80- and 4.36-Å peaks in the X-ray diffractogram of the gel studied in comparison to highly crystalline gibbsite may also yield information on the structure of the gel. According to Schoen and Roberson (22), diffraction from the (002) or basal planes gives rise to the 4.80-Å peak. The width of this peak indicates that the crystallites are relatively small in the basal or *c*-axis direction. The 4.35-Å peak is caused by reflection from the (100) plane. The relatively intense nature of this reflection indicates preferential growth in the *ab* plane. Thus, a thin platelet structure is suggested.

REFERENCES

(1) S. L. Nail, J. L. White, and S. L. Hem, *J. Pharm. Sci.*, **64**, 1166(1975).

(2) V. C. Farmer, *Clay Miner.*, **7**, 373(1968).

(3) V. C. Farmer and J. D. Russell, *Clays Clay Miner.*, **15**, 121(1972).

(4) V. C. Farmer, J. D. Russell, and J. L. Ahlrichs, *Trans. Int. Congr. Soil Sci., 9th*, **3**, 101(1968).

(5) A. J. Leonard, F. Van Cauwelaert, and J. J. Fripiat, *J. Phys. Chem.*, **71**, 695(1967).

(6) J. D. Russell, V. C. Farmer, and B. Velde, *Min. Mag.*, **37**, 869(1970).

(7) J. L. Ahlrichs, *Clays Clay Miner.*, **16**, 63(1968).

(8) S. L. Hem, E. J. Russo, S. M. Bahal, and R. S. Levi, *J. Pharm. Sci.*, **59**, 317(1970).

(9) "The United States Pharmacopeia," 17th rev., Mack Publishing Co., Easton, Pa., 1965, p. 27.

(10) "Instruction Manual, Perkin-Elmer Model 421 Spectrophotometer," Instruments Division, Perkin-Elmer Corp., Norwalk, Conn.

(11) K. Wefers and G. M. Bell, Technical Paper No. 19, Alcoa Research Laboratories, 1972.

(12) R. W. Smith and J. D. Hem, Geological Survey Water-Supply Paper 1827-D, U.S. Government Printing Office, Washington, D.C., 1971.

(13) J. D. Hem and C. E. Roberson, Geological Survey Water-Supply Paper 1827-A, U.S. Government Printing Office, Washington, D.C., 1967.

(14) P. H. Hsu and T. F. Bates, *Min. Mag.*, **33**, 749(1964).

(15) P. H. Hsu, *Soil Sci. Soc. Amer. Proc.*, **30**, 173(1966).

(16) E. C. Marboe and S. Bentor, *Silic. Ind.*, **26**, 389(1961).

(17) R. C. Turner and G. J. Ross, *Can. J. Chem.*, **48**, 723(1970).

(18) R. J. Barnhisel and C. I. Rich, *Soil Sci. Soc. Amer. Proc.*, **29**, 531(1965).

(19) P. H. Hsu, International Committee for the Study of Bauxites and Aluminum Oxides-Hydroxides, 3 Congres, Nice, France, 613(1973).

(20) G. J. Ross and R. C. Turner, *Soil Sci. Soc. Amer. Proc.*, **35**, 389(1971).

(21) J. L. White, *Soil Sci.*, **112**, 22(1971).

(22) R. Schoen and C. E. Roberson, *Amer. Mineral.*, **55**, 43(1970).

ACKNOWLEDGMENTS AND ADDRESSES

Received March 17, 1975, from the *[*]Industrial and Physical Pharmacy Department, School of Pharmacy and Pharmacal Sciences, and the [‡]Department of Agronomy, Purdue University, West Lafayette, IN 47907*

Accepted for publication May 6, 1975.

Supported in part by an American Foundation for Pharmaceutical Education Fellowship to S. L. Nail.

This report is Journal Paper 5834, Purdue University Agricultural Experiment Station, West Lafayette, IN 47907

[x] To whom inquiries should be directed.

NMR Analysis of Pharmaceuticals XIV: Determination of Amyl Nitrite in Its Inhalant Dosage Form

JOHN W. TURCZAN ˣ and THOMAS MEDWICK *

Abstract □ An NMR procedure is described for the analysis of amyl nitrite as a drug entity and in inhalant dosage forms. The choices of solvent (carbon tetrachloride) and internal standards (biphenyl or benzyl benzoate) were made with respect to stability problems and the presence of stabilizers in the formulation. The method is precise, with a standard deviation of ±0.5. The NMR results of synthetic solutions and commercial preparations were compared with those obtained by a published relative NMR procedure and a compendial titrimetric method. The results were generally satisfactory.

Keyphrases □ NMR spectroscopy—analysis, amyl nitrite, drug entity and inhalant dosage form □ Amyl nitrite—NMR analysis, drug entity and inhalant dosage form

Analytical procedures for amyl nitrite (I) have been complicated because of the instability of the material; a number of different decomposition products result. The various analytical approaches were summarized recently in a paper (1) describing the use of NMR in the analysis of I. The reported NMR procedure is a relative one and permits the specific measurement of I in terms of the resonance of the methylene protons alpha to the nitrite. The resonance of the two methyl groups is used as the reference area against which the α-methylene proton area is compared. Since the latter group is affected by instability whereas the former is not, this analysis yields stability information in a relative sense but does not provide absolute measurement.

The present study extends the use of NMR for the analysis of I to yield absolute results. The choices of solvent and internal standards were made with the stability problems and the presence of stabilizers in the formulation clearly in mind. Results from the NMR measurements were compared with an independent procedure and were generally satisfactory. The NMR procedure described in this study is rapid, simple, and specific.

EXPERIMENTAL

Apparatus and Chemicals—An NMR spectrometer[1] equipped with a variable temperature probe[2], having a six-turn insert, was used.

Amyl nitrite[3] (USP XVI) (stored at −2° when not in use), internal standards of benzyl benzoate[4] USP and biphenyl[5], and 0.18- and 0.30-ml commercial dosage units of amyl nitrite inhalant were used.

All chemical shifts reported are in reference to tetramethylsilane at 0 ppm.

Preparation of I Standard Solution—Transfer an accurately weighed quantity of approximately 5 mEq of internal standard [biphenyl (II) or benzyl benzoate (III)] into a "microflex tube"[6] and add 2–3 ml of carbon tetrachloride. Screw on the "microflex valve"[6] and the septum seal[6], thereby sealing the contents of the tube, and determine the weight of the sealed vessel.

Open the valve, introduce about 0.5 ml of I using a syringe, close the valve, and weigh the vessel when it has attained constant weight. Shake the vessel, transfer about 0.5 ml of the solution into a precision NMR tube, cap the tube, and proceed as directed under *Instrumental Measurement and Calculation.*

Preparation of I Ampul Sample Solution—Remove the gauze jacket and then clean, dry, and weigh an ampul containing 0.30 ml of I. (If the declared amount per ampul is 0.18 ml of I, use two ampuls.)

Place the weighed ampul into a freezer for at least 15 min[7]. When chilled, place the ampul into a 25-ml glass-stoppered erlenmeyer flask containing 4–5 mEq of accurately weighed internal standard in 1–2 ml of carbon tetrachloride.

With a glass rod, carefully break the ampul; then wash the rod with an additional 1 ml of carbon tetrachloride and immediately stopper the flask and shake. Transfer about 0.5 ml of the solution into a precision NMR tube, cap the tube, and proceed as directed under *Instrumental Measurement and Calculation.* Accurately weigh the glass fragments of the broken ampul to determine the tare weight.

Instrumental Measurement and Calculation—Place the tube containing the solution in an NMR spectrometer and obtain the spectrum. Integrate the triplet at 4.6 ppm (I) and the signal from the internal standard, the multiplet at 7.0–7.8 ppm (II), or the singlet at 5.3 ppm (III) (Fig. 1) at least five times and determine the average integral.

The amount of I may then be calculated as follows:

$$\% \text{ of I} = \frac{A_{\text{I}}}{A_{\text{II or III}}} \frac{E.W._{\text{I}}}{E.W._{\text{II or III}}} \frac{\text{mg of II or III}}{\text{mg of sample}} \times 100 \quad \text{(Eq. 1)}$$

where:

A_{I} = integral value of the signal representing I
A_{II} or $_{\text{III}}$ = integral value of the signal representing II or III
$E.W._{\text{I}}$ = formula weight of I/2 = 58.57
$E.W._{\text{II}}$ or $_{\text{III}}$ = formula weight of II/10 = 15.42 or III/2 = 106.12
mg of sample = sample weight in milligrams corrected for the stabilizer added

RESULTS AND DISCUSSION

The choice of a particular organic solvent as an analytical medium is complicated by the instability of I. Although several decomposition products of I are possible (1), work in this laboratory indicated the presence of isoamyl alcohol (IV) only in some ampul dosage forms. As shown in Fig. 1, IV is manifest by a triplet at 3.6 ppm, identified as *e*, ascribable to the methylene protons alpha to the hydroxyl group. Even though I is very soluble in almost every organic solvent, carbon tetrachloride was the only solvent tested in which there was no noticeable decomposition of I into IV. Thus, carbon tetrachloride was used in all studies.

Generally, an internal standard is chosen on the basis of the available regions of the spectrum of the compound undergoing analysis. In this case, the choice is complicated by the need to incorporate stabilizers in the commercial ampuls; an epoxidized oil[8] and diphenylamine (V) are the compounds used today. The epoxidized oil exhibits an NMR spectrum with multiplets whose centers are at 5.2, 4.2, 3.0, 2.3, 1.5, and 1.1 ppm (with respect to tetramethylsilane). The resonance multiplet at 1.5 ppm is most intense and

[1] Varian A-60.
[2] V-6031.
[3] Matheson, Coleman and Bell, Norwood, OH 45212
[4] Merck & Co., Rahway, NJ 07065
[5] Eastman Organic Chemicals, White label.
[6] Described in Kontes New Product Bulletin No. 471, Kontes, Vineland, NJ 08360

[7] *Caution:* Although this chilling step is included partly to reduce the volatility of I, the primary reason is to guard against possible explosions when ampuls containing degraded I are broken as directed.
[8] Epoxol 9-5, Swift Chemical Co., Chicago, IL 60604

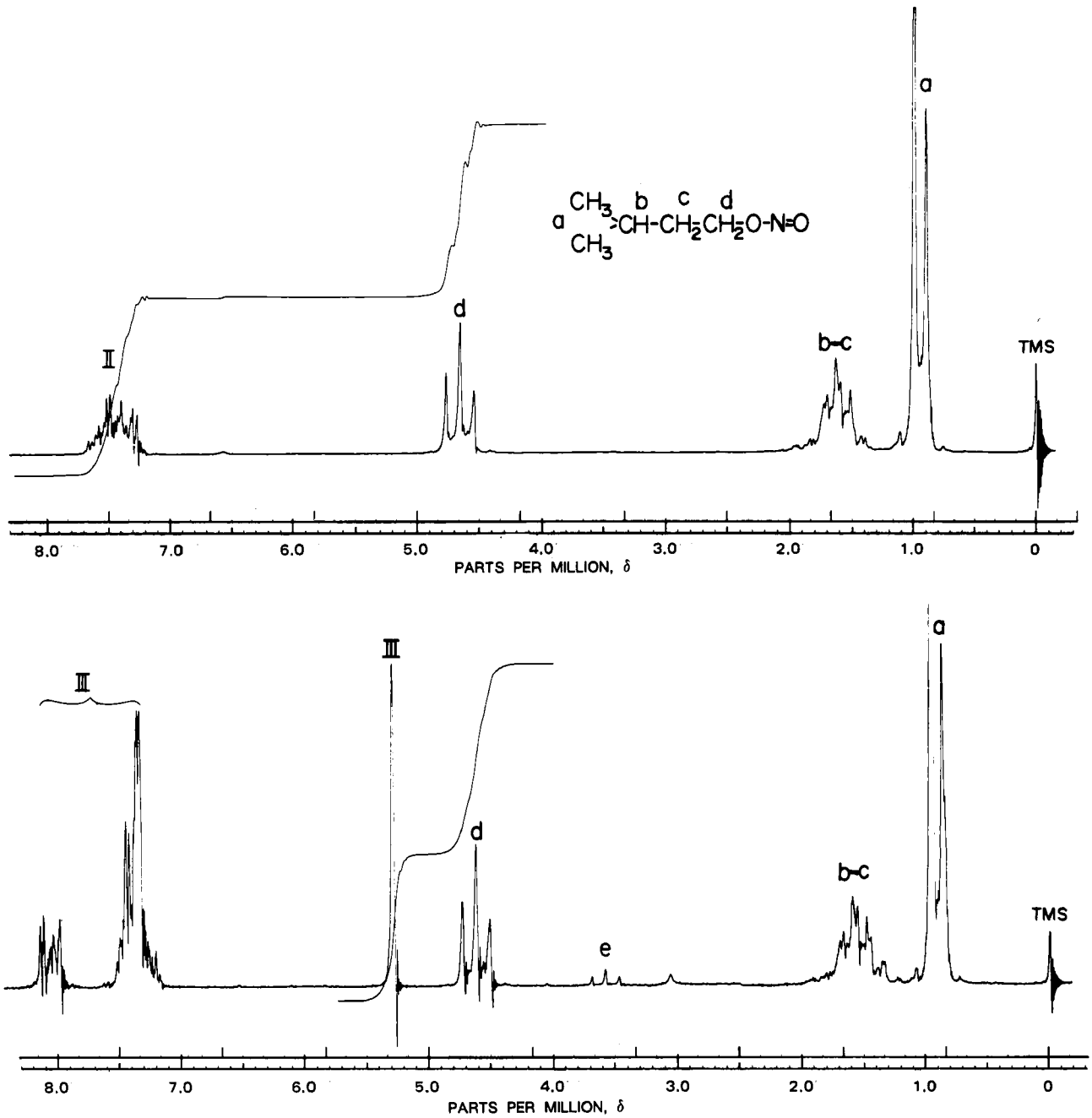

Figure 1—*NMR spectrum of amyl nitrite in carbon tetrachloride. Key: II, biphenyl; III, benzyl benzoate; and TMS, tetramethylsilane.*

is the only NMR signal seen when the spectrum of the sample is taken at a concentration level (2%) equivalent to that when it is used as a stabilizer in amyl nitrite. Compound V exhibits a multiplet ranging from 6.7 to 7.6 ppm, signals ascribable to aromatic protons. These data dictated the choice of internal standards.

Two internal standards, biphenyl (II) and benzyl benzoate (III), were found to be satisfactory and useful under particular circumstances. Compound II can be used whenever the nonaromatic stabilizer is present and is manifest as a multiplet in the 7.0–7.8-ppm range, ascribable to all 10 aromatic protons. Clearly, II is unsuitable when the stabilizer is V owing to the latter's NMR resonance in the aromatic region.

For all formulations, no matter what the stabilizer, a singlet at 5.3 ppm due to the two methylene protons of III is a good choice. Compound III also is manifest as a multiplet over the 7.0–8.3-ppm region, activity ascribable to the resonance of the 10 aromatic protons of the ester. The $\Delta\nu$ between the α-methylene proton triplet of I and the methylene singlet of III is about 40 Hz. Since this finding raises some question concerning interference with the integration owing to spinning side bands, it is advisable to integrate such samples with no spinning.

Thus, to summarize, III is a standard useful in the analysis of all samples whereas II is a compound that cannot be used if an aromatic stabilizer is present in the formulation. From the *Experimental* section, it is noted that the equivalent weight advantage lies with II, which means that more intense NMR absorption will be achievable per unit mass of II than per unit mass of III. Clearly, either standard may be used if the sample is a pure amyl nitrite. Fortunately, the analyst has a choice of standards. If the stabilizer is a compound other than the two discussed here, it might be necessary to choose an internal standard different from II and III.

At this point it seems appropriate to comment briefly about initial studies involving the selection of an internal standard and solvent. The NMR singlet of maleic acid (VI) at 6.3 ppm, ascribable to the resonance of the two methylene hydrogens, seemed a good choice. However, when I was analyzed with VI as the internal stan-

Table I—Comparative Analysis of Amyl Nitrite and Its Dosage Form Using Various Spectral Areas

Nature of Sample	Relative Analysis $3 \times \frac{d}{a} \times 100$	Absolute Analysis (Benzyl Benzoate Internal Standard) For Amyl Nitrite, % w/w			For Isoamyl Alcohol, % w/w
		a	*b–c*	*d*	*e*
Amyl nitrite standard	95.7	99.7	98.9	95.5	—
with no stabilizer	96.1	99.5	—	95.6	—
	95.0	100.5	100.1	95.5	—
Average	95.6	99.9	99.5	95.5	—
SD	±0.6	±0.5	±0.9	±0.06	—
Sample with 2% (w/v)	94.7	100.2	101.5	94.9	—
epoxidized oil[a],	94.4	99.7	102.1	94.2	1.5
specific gravity 0.874	94.4	99.4	102.1	93.9	2.2
Average	94.5	99.8	101.9	94.3	—
SD	±0.2	±0.4	±0.3	±0.5	—
Sample with 2%	92.9	100.1	100.0	93.0	2.9
(w/v) diphenylamine,	93.1	99.6	100.2	92.8	3.7
specific gravity 0.875	92.4	99.8	100.5	92.2	4.1
Average	92.8	99.8	100.2	92.7	—
SD	±0.4	±0.3	±0.3	±0.5	—

[a] Epoxol 9-5, Swift Chemical Co., Chicago, IL 60604

dard in deuterochloroform, definite evidence of hydrolysis of I was manifest, making rapid manipulations necessary to achieve satisfactory analytical results. Therefore, it was desirable to search for other standards and solvents.

The NMR spectrum of I offers three separate resonance signals (*a*, *b–c*, and *d* in Fig. 1) for integration and possible quantitative analysis. The assignments for the origins of the multiplets noted in Fig. 1 follow the work of Schirmer *et al.* (1). The doublet labeled *a* is ascribable to the methyl groups present in I as well as each decomposition product arising from I. This area is a good index of total I included in the original dosage form but gives no indication of intact I present at the time of analysis.

The multiplet labeled *b–c*, assigned to the β-methylene and methine protons, occurs in I and its decomposition products and has the same restricted use as doublet *a*. However, the triplet labeled *d* is ascribable to the α-methylene of I with the possible interference from overlap with a triplet ascribable to amyl nitrate, an impurity sometimes present in I at insignificant levels (1). Thus, this area presents the possibility of differential measurement of I. The work of Schirmer *et al.* (1) was based on resonance signals *a* and *d* and resulted in a relative analysis; the findings reported in this paper are absolute in nature.

In a study involving the quantitative NMR analysis of a substance such as I, which offers more than a single resonance structure as an analytical peak, the suitability of a particular peak for analytical use must be established. The data in Table I are results of studies with regions *a*, *b–c*, *d*, and *e* and with III as an internal standard. Values are reported after correction for the stabilizer present in the original sample weight. When the doublet *a* was used, the analyses were all very close to 100%, indicating that only I or compounds related to I were present. The values based on multiplet *b–c* also were close to 100%, with the exception of higher results for one sample where the stated stabilizer would be expected to contribute to the integrated area. The results derived from triplet *d* were lower than those observed with *a* and *b–c*, indicating some decomposition.

In the case of the ampul samples, manifestation of IV in terms of the triplet *e* permitted its measurement. The results (Table I) were much more variable than those obtained for the parent I. Two potential sources of variation may be cited. First, levels of decomposition differ in individual dosage units. And second, since *e* is manifest by an integral height of about 1–4 mm, measurement errors of these small heights contribute to the observed large variations. From these studies, the triplet designated as *d* was chosen as the analytical index of I and was used in subsequent measurements.

Table II—Determination of Amyl Nitrite in Standard Solutions by NMR

Standard Solution	Internal Standard, mg	Amyl Nitrite Added, mg	Found, mg	Recovery, % w/w
	Biphenyl			
1	72.4	206.6	196.5	95.1
2	68.1	200.9	190.5	94.8
3	64.9	213.8	203.5	95.2
4	69.6	475.4	453.1	95.3
5	72.1	395.1	374.2	94.7
6	70.5	300.2	285.2	95.0
			Average	95.0
			SD	±0.2
	Benzyl benzoate			
1	410.9	386.4	365.2	94.5
2	489.7	311.0	295.5	95.0
3	495.1	170.2	162.5	95.5
4	500.3	165.5	157.1	94.9
5	450.9	275.3	262.6	95.4
6	505.1	295.7	278.8	94.3
7	450.6	261.5	249.2	95.3
			Average	95.0
			SD	±0.5
		By alternative procedure (2)		92.5[a]

[a] Average of three determinations.

Table III—Comparison of NMR and Titrimetric Analysis of Amyl Nitrite in Ampuls

Sample with Internal Standard[a]	By NMR Procedure		By Titrimetric Procedure	
Biphenyl				
1[b]	332.9	94.2	320.0	91.0
2[b]	331.2	94.7	318.8	90.6
3[b]	330.3	93.9	314.2	89.8
4[b]	334.5	94.7	318.7	90.5
5[b]	332.7	94.6	—	—
Average	—	94.4	—	90.5
SD	—	±0.4	—	±0.6
Benzyl benzoate				
1[b]	252.4	91.9	246.8	89.5
2[b]	251.7	92.6	253.2	90.4
3[b]	260.4	92.3	—	—
4[c]	147.2	91.8	141.9	88.8
5[c]	150.3	93.2	142.7	88.9
6[c]	150.2	91.5	—	—
Average	—	92.2	—	89.4
SD	—	±0.7	—	±0.8

[a] Sample numbers represent separate lots, and the corresponding results are obtained for an individual ampul from each lot. Results are for individual ampuls, milligrams per ampul (% w/w). The sample weight was corrected for the stabilizer. [b] 0.30 ml/ampul declared. [c] 0.18 ml/ampul declared.

The analysis of a series of I standard solutions containing either II or III as an internal standard is presented in Table II. Where both internal standards were used, the results were the same, indicating that both standards were satisfactory. Furthermore, the results show that the overall procedure is very reproducible.

Table III presents the analytical results, corrected for the weight of stabilizer present, obtained when I ampul dosage forms were analyzed by the proposed NMR method. When the epoxidized oil was the stabilizer, II was used as the internal standard; when V was the stabilizer, III was the internal standard. The analytical values indicate good reproducibility for each of the two series of samples. Comparison of the NMR method with the titrimetric procedure (2), involving reaction of all nitrites with chlorate ion followed by the determination of the chloride formed, indicates that the classical titration method yields lower results. It is not possible to reproduce by calculation comparable results for the same lot from the data in Table III since each analytical result represents the analysis of a different ampul (with its own sample weight) from the indicated lot.

The problems involved in the analysis of I in ampuls have been evident from the standpoint of specificity. The NMR procedure described here uses a property that allows the absolute measurement of I in the presence of decomposition products. Furthermore, this specificity is achieved without any evidence of decomposition during the measurement. The analytical results indicate that this NMR method is precise.

REFERENCES

(1) R. E. Schirmer, R. E. Zemer, and G. G. Cooke, *J. Pharm. Sci.*, **61**, 428(1972).

(2) "Specifications for the Quality Control of Pharmaceutical Preparations (Second Edition of the International Pharmacopoeia)," World Health Organization, Geneva, Switzerland, 1967, pp. 43, 44.

ACKNOWLEDGMENTS AND ADDRESSES

Received October 4, 1974, from the *Food and Drug Administration, Department of Health, Education, and Welfare, Brooklyn, NY 11232*

Accepted for publication May 7, 1975.

For the previous article in this series, see J. W. Turczan, *J. Ass. Offic. Anal. Chem.*, **57**, 893(1974).

* Present address: College of Pharmacy, Rutgers University, New Brunswick, NJ 08903

[x] To whom inquiries should be directed.

Utilization of an Enantiomer as a Solution to a Pharmaceutical Problem: Application to Solubilization of 1,2-Di(4-piperazine-2,6-dione)propane

A. J. REPTA [x], M. J. BALTEZOR, and P. C. BANSAL

Abstract □ An enantiomer of the cytotoxic agent (±)-1,2-di(4-piperazine-2,6-dione)propane [(±)-I] (ICRF 159) was utilized to overcome a solubility problem in the preparation of a solution suitable for intravenous use. The enantiomers were about five times more soluble and melted at about 40° lower than the racemic compound. This study appears to be the first reported instance in which the difference in the physical properties of a racemic compound and its enantiomers was utilized to improve a pharmaceutical formulation. The expected differences in the physical properties of racemic solids and their corresponding enantiomers are discussed briefly in relation to the three racemic modifications known to exist.

Keyphrases □ Enantiomers—physical properties compared to racemic substance, potential use in pharmaceutical formulations □ 1,2-Di(4-piperazine-2,6-dione)propane—solubilization of enantiomers compared to racemate, potential use in intravenous formulations □ Solubilization—enantiomers compared to racemates, pharmaceutical formulations

Some advantages of using various crystalline modifications such as polymorphs, hydrates, and other solvates in improving pharmaceutical formulations of drugs are well documented (1–5). An additional type of crystalline modification may be encountered when the drug molecules possess an asymmetric or optically active center. Although the employment of optically active compounds in pharmaceutical formulations is not new, their past and present usage has been due largely to one enantiomer exhibiting a quantitatively or qualitatively different biological activity than the corresponding racemic compound (6, 7). Examples of such drugs include epinephrine, ephedrine, hyoscyamine, and dextropropoxyphene (8).

The chemical and physical properties such as melting behavior, IR spectra, and solubility of crystalline racemic substances and their enantiomeric components have been well studied (9–15). The combination of these different physical properties with the stereochemical requirements of biological systems is an approach that has been largely overlooked as a means of formulation improvement.

BACKGROUND

In the case of solid crystalline compounds, the intercrystalline forces between molecules may be greatly affected by only a minor change in the crystal geometry (11, 13, 16). The intercrystalline forces between the two like (+ and + or − and −) enantiomer molecules are the same (16). Therefore, the physical properties of a pair of pure crystalline enantiomers are identical except for the direction in which they rotate plane polarized light. However, the intercrystalline forces between opposite (+ and −) enantiomer molecules are usually very different than those between like enantiomer molecules. Such differences may give rise to different solid-state physical properties, and the nature and magnitude of these differences between enantiomers and the corresponding racemic material are dependent upon the relative strength of the intermolecular forces in the crystal. Enantiomeric systems may fall into one of three possible types (11, 16), and the solubility behavior as a function of the composition for each of the three cases is shown in Fig. 1.

The analysis of a series of I standard solutions containing either II or III as an internal standard is presented in Table II. Where both internal standards were used, the results were the same, indicating that both standards were satisfactory. Furthermore, the results show that the overall procedure is very reproducible.

Table III presents the analytical results, corrected for the weight of stabilizer present, obtained when I ampul dosage forms were analyzed by the proposed NMR method. When the epoxidized oil was the stabilizer, II was used as the internal standard; when V was the stabilizer, III was the internal standard. The analytical values indicate good reproducibility for each of the two series of samples. Comparison of the NMR method with the titrimetric procedure (2), involving reaction of all nitrites with chlorate ion followed by the determination of the chloride formed, indicates that the classical titration method yields lower results. It is not possible to reproduce by calculation comparable results for the same lot from the data in Table III since each analytical result represents the analysis of a different ampul (with its own sample weight) from the indicated lot.

The problems involved in the analysis of I in ampuls have been evident from the standpoint of specificity. The NMR procedure described here uses a property that allows the absolute measurement of I in the presence of decomposition products. Furthermore, this specificity is achieved without any evidence of decomposition during the measurement. The analytical results indicate that this NMR method is precise.

REFERENCES

(1) R. E. Schirmer, R. E. Zemer, and G. G. Cooke, *J. Pharm. Sci.*, **61**, 428(1972).

(2) "Specifications for the Quality Control of Pharmaceutical Preparations (Second Edition of the International Pharmacopoeia)," World Health Organization, Geneva, Switzerland, 1967, pp. 43, 44.

ACKNOWLEDGMENTS AND ADDRESSES

Received October 4, 1974, from the *Food and Drug Administration, Department of Health, Education, and Welfare, Brooklyn, NY 11232*

Accepted for publication May 7, 1975.

For the previous article in this series, see J. W. Turczan, *J. Ass. Offic. Anal. Chem.*, **57**, 893(1974).

* Present address: College of Pharmacy, Rutgers University, New Brunswick, NJ 08903

[x] To whom inquiries should be directed.

Utilization of an Enantiomer as a Solution to a Pharmaceutical Problem: Application to Solubilization of 1,2-Di(4-piperazine-2,6-dione)propane

A. J. REPTA [x], M. J. BALTEZOR, and P. C. BANSAL

Abstract □ An enantiomer of the cytotoxic agent (±)-1,2-di(4-piperazine-2,6-dione)propane [(±)-I] (ICRF 159) was utilized to overcome a solubility problem in the preparation of a solution suitable for intravenous use. The enantiomers were about five times more soluble and melted at about 40° lower than the racemic compound. This study appears to be the first reported instance in which the difference in the physical properties of a racemic compound and its enantiomers was utilized to improve a pharmaceutical formulation. The expected differences in the physical properties of racemic solids and their corresponding enantiomers are discussed briefly in relation to the three racemic modifications known to exist.

Keyphrases □ Enantiomers—physical properties compared to racemic substance, potential use in pharmaceutical formulations □ 1,2-Di(4-piperazine-2,6-dione)propane—solubilization of enantiomers compared to racemate, potential use in intravenous formulations □ Solubilization—enantiomers compared to racemates, pharmaceutical formulations

Some advantages of using various crystalline modifications such as polymorphs, hydrates, and other solvates in improving pharmaceutical formulations of drugs are well documented (1–5). An additional type of crystalline modification may be encountered when the drug molecules possess an asymmetric or optically active center. Although the employment of optically active compounds in pharmaceutical formulations is not new, their past and present usage has been due largely to one enantiomer exhibiting a quantitatively or qualitatively different biological activity than the corresponding racemic compound (6, 7). Examples of such drugs include epinephrine, ephedrine, hyoscyamine, and dextropropoxyphene (8).

The chemical and physical properties such as melting behavior, IR spectra, and solubility of crystalline racemic substances and their enantiomeric components have been well studied (9–15). The combination of these different physical properties with the stereochemical requirements of biological systems is an approach that has been largely overlooked as a means of formulation improvement.

BACKGROUND

In the case of solid crystalline compounds, the intercrystalline forces between molecules may be greatly affected by only a minor change in the crystal geometry (11, 13, 16). The intercrystalline forces between the two like (+ and + or − and −) enantiomer molecules are the same (16). Therefore, the physical properties of a pair of pure crystalline enantiomers are identical except for the direction in which they rotate plane polarized light. However, the intercrystalline forces between opposite (+ and −) enantiomer molecules are usually very different than those between like enantiomer molecules. Such differences may give rise to different solid-state physical properties, and the nature and magnitude of these differences between enantiomers and the corresponding racemic material are dependent upon the relative strength of the intermolecular forces in the crystal. Enantiomeric systems may fall into one of three possible types (11, 16), and the solubility behavior as a function of the composition for each of the three cases is shown in Fig. 1.

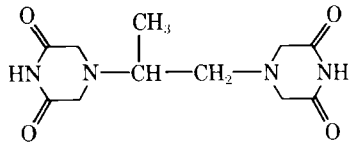

I

The first type, a racemic solid solution, occurs when there is little difference in the affinity between like and unlike enantiomeric molecules in the crystal. For compounds of this category, such as camphor oxime (9, 16), the physical properties (such as solubility) of the pure enantiomers, the racemic material, or any combination of the enantiomers vary only slightly and such variation is continuous (Fig. 1*a*).

The second situation, called a racemic mixture or conglomerate (16), occurs when there is a greater affinity between the molecules of like enantiomers than between opposite enantiomers. This type of system results in a gross mixture of the crystals of the two enantiomers, which in some cases may be physically separable (17). As is often the case in a normal binary mixture of solids, this type of system forms a eutectic with the eutectic composition identical to the racemic composition, which causes the minimum melting point and maximum solubility also to occur at the racemic composition. Figure 1*b* illustrates this type of system. Compounds showing this behavior include the dimethyl ester of *O,O*-diacetyltartaric acid (9, 10), β-benzoylhydratropic acid (14), and sodium ammonium tartrate (16).

The third and apparently most common situation (9, 10, 14, 16) occurs when opposite enantiomer molecules have a greater affinity for each other than do like enantiomer molecules. Such systems constitute true racemic compounds and normally exhibit solubility and melting-point behavior grossly different than those of the pure enantiomers. The racemic compound usually exhibits a higher melting point and lower solubility than either enantiomer. The solubility diagram of such systems exhibits a minimum at the racemic composition and two maxima symmetrically located at some composition between those of the pure enantiomers and the racemic compound (Fig. 1*c*). Tartaric acid (10), the dimethyl ester of tartaric acid (9, 10), and leucine (18) exhibit this behavior.

In some systems, the temperature at which the crystallization of a racemic substance occurs may determine the nature of the crystalline solid obtained. For instance, depending upon the conditions of crystallization, a compound might be obtained as either a racemic mixture or a racemic compound. Compounds exhibiting this behavior are sodium ammonium tartrate (16) and rubidium tartrate (16).

The fact that crystalline enantiomers often exhibit different physical properties than the corresponding racemic drug may be pharmaceutically useful in the formulation of some racemic drugs. The applicability of this approach depends upon the desired physical properties of the drug in the formulation[1] and the enantomeric system to which the drug belongs.

The remainder of this paper deals with the use of the observed differences in the physical–chemical properties of a racemic compound and its enantiomers in overcoming a problem encountered in the pharmaceutical formulation of a cytotoxic substance. The problem confronted stemmed from a request from the National Cancer Institute to develop an intravenous formulation of the racemic cytotoxic compound 1,2-di(4-piperazine-2,6-dione)propane[2] [(±)-I] (ICRF 159) suitable for clinical testing. A concentration of 25 mg of (±)-I/ml of solution was desired, and the adult dose was estimated to be about 1 g[3].

The solubility of (±)-I was only ~3 mg/ml in water at 25°. The use of cosolvents to overcome the low solubility problem was not a viable approach due to the low solubility of (±)-I in most solvents. Several alternative approaches were considered, including complexation, chemically derived prodrugs (19), and crystalline modifications of the drug. For reasons that will not be explored here, none of these approaches appeared very promising except the one involving physical crystalline modifications.

[1] In some cases, a decrease in solubility may be desired while in others an increase may be sought.

[2] This substance is also commonly referred to in the literature as NSC 129943.

[3] J. P. Davignon, National Cancer Institute, personal communication.

Table I—Effect of pH on the Optical Rotation of (−)-(*R*)-I[a]

pH	$[\alpha]_D^{25}$
1	−63.47°
2	−58.92°
3	−44.32°
4	−40.92°
5	−40.80°

[a] The sample used in this study contained ~97.4% (−)-(*R*)-I.

Table II—Some Properties of (±)-I and the Enantiomer (−)-(*R*)-I

Property	(−)-(*R*)-I	(±)-I
Melting point	~192° dec.	~233° dec.
Solubility (water at 25°), mg/ml	~15	~3
Absolute rotation, $[\alpha]_D^{25}$ (c 0.5, water)	−43°	0

The low solubility of (±)-I in most solvents together with its high melting point (~233° dec.) indicated the existence of strong intercrystalline forces. Therefore, an approach aimed at decreasing the intercrystalline forces of (±)-I, thereby altering the physical properties of the solid so as to increase solubility, appeared to offer the greatest chance of success. A review of available data gave no evidence for the existence of polymorphs, hydrates, or other solvates of (±)-I that could be useful in overcoming the solubility problem. Consequently, an investigation of the properties of the crystalline enantiomers of (±)-I was undertaken.

Although the potential for success of such an approach was not quantitatively predictable, a number of features enhanced its probability and attractiveness. First of all, as previously mentioned, in a racemic modification the most common situation appears to be one where the enantiomers are more soluble than the racemic drug (9, 10, 14, 16) (Fig. 1*c*).

Second, one enantiomer may possess a greater biological activity than the other (8). If this were found to be the situation with either enantiomer, a lower dose would be required and the severity of the original problem would be decreased. It had already been shown that both enantiomers (20) of (±)-I exhibited the same qualitative biological activity (21), but no quantitative data for the relative activity of the enantiomers with respect to each other were available.

Third, since the use of an enantiomer would require no change in the molecular structure, there probably would be no change in the *in vitro* chemical stability such as might be encountered when using other solubilizing techniques such as preparing water-soluble prodrug derivatives (22).

EXPERIMENTAL

Chemicals—The (±)-I was used as obtained from the National Cancer Institute. Formamide was purified by vacuum distillation (75°/5 mm Hg) prior to use. All other chemicals used were of reagent grade. The water used was triple distilled, with the last distillation being from acid permanganate solution in an all-glass apparatus.

Synthesis and Characterization of (+)-(*S*)-I[4] and (−)-(*R*)-I—The synthesis of (+)-(*S*)-I was carried out asymmetrically as follows. (±)-1,2-Diaminopropane[5] (27 g) was resolved using (−)-*l*-tartaric acid[5] (80 g) according to the method of Dwyer *et al.* (24). The precipitate obtained was recrystallized five times from water to yield 27 g of (+)-(*S*)-1,2-diaminopropane bis(*l*-tartrate), mp 141.5° [lit (25) mp 142°].

The bitartrate salt (27 g) was suspended in methanol (135 ml). Hydrogen chloride was bubbled through the suspension for about 30 min, during which time the solid initially present completely dissolved (after about 5 min). After about 7 min, another white crystalline solid appeared. Excess hydrogen chloride was removed

[4] The assignment of (*R*)- and (*S*)-configurations is based on the configuration of the enantiomers of 1,2-diaminopropane (23).

[5] Aldrich Chemical Co.

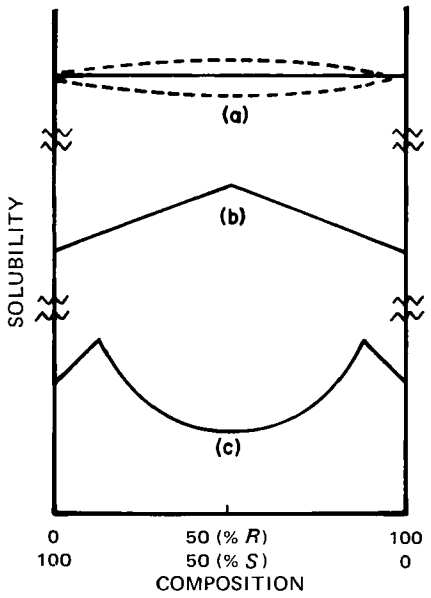

Figure 1—*Effect of enantiomer composition on solubility for the three racemic modifications:* (a) *solid solution,* (b) *racemic mixture, and* (c) *racemic compound.*

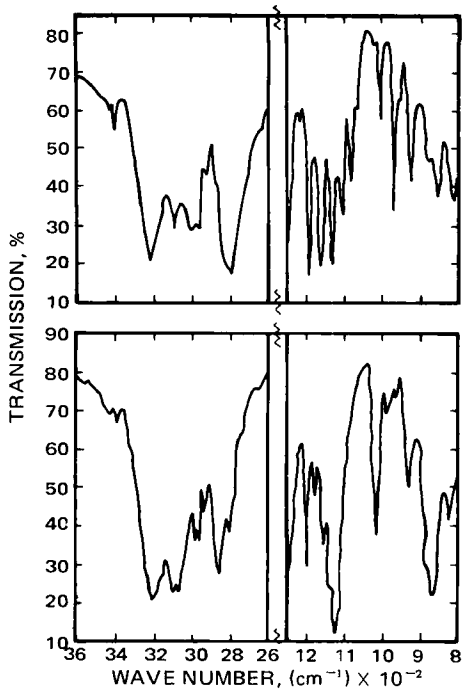

Figure 2—*Partial IR spectra of* (±)-*I (top) and* (−)-(R)-*I (bottom) as a 2% dispersion in a potassium bromide pellet.*

by passing dry nitrogen gas through the suspension for about 20 min. The precipitate was separated by filtration to yield 9.3 g of (−)-(*S*)-1,2-diaminopropane dihydrochloride, mp 238.5°; $[\alpha]_D^{25}$ −4.12° (c 4.0, water) [lit. (26) mp 240°; lit. (25) $[\alpha]_D^{25}$ −4.08° (c 1.7 − 10.4, water)].

The optically active acid, (+)-(*S*)-1,2-propylene dinitrilotetraacetic acid, was synthesized using the (−)-(*S*)-1,2-diaminopropane dihydrochloride (9 g) according to the method of Wing and Callahan (27). After 7 days, the reaction solution was concentrated to about 50 ml and filtered. The isolation of the product from the filtrate was accomplished using a cation-exchange resin[6] (800-ml wet volume in a glass column, 5 cm i.d.). Elution of the column consisted of 2 liters of cold water (~50 ml/min) followed by 12 liters of hot (90°) water (~80 ml/min). The temperature of the column was maintained at 90° with a heating tape wrapped around the column.

The portion of the eluate containing the bulk of the optical activity (as determined by measuring the α_D of the eluate) was concentrated by heating. The crystalline material that formed on standing was separated by filtration, dried (120 hr at 110°/~10 mm Hg), and found to be (+)-(*S*)-1,2-propylene dinitrilotetraacetic acid (12.5 g), mp 199–200°; $[\alpha]_D^{25}$ +49.3° (water) [lit. (27) mp 198°; lit. (28) $[\alpha]_D^{25}$ +50° (water)].

The (+)-(*S*)-1,2-propylene dinitrilotetraacetic acid (12 g) was heated with formamide[7] (30 ml), according to the method of Creighton (20), to yield 4.9 g of a white crystalline powder, mp 193–194°; $[\alpha]_D^{25}$ +41.0° (c 0.5, water) [lit. (20) mp 193°]. This powder was shown to be (+)-(*S*)-1,2-di(4-piperazine-2,6-dione)propane [(+)-(*S*)-I] by NMR[8], elemental, IR[9], and polar rotation analyses; $[\alpha]_D^{25}$ +11.50° (5%, dimethylformamide) [lit. (20) $[\alpha]_D^{25}$ +11.35° (5%, dimethylformamide)].

The asymmetric synthesis of (−)-(*R*)-I [(−)-(*R*)-1,2-di(4-piperazine-2,6-dione)propane] was carried out by a procedure identical to that used for synthesizing (+)-(*S*)-I, with the exception that (+)-*d*-tartaric acid[10] was used to obtain the (−)-(*R*)-1,2-diaminopropane bis(*d*-tartrate) salt.

The characterization of (−)-(*R*)-I was based on the same types of physical and chemical information as were used for the characterization of (+)-(*S*)-I (as already described). NMR spectra (d_6-dimethyl sulfoxide), melting point, elemental analysis, and IR spectra (2% KBr pellet) for (−)-(*R*)-I were all essentially identical to those for (+)-(*S*)-I.

Solubility Determination—Due to the instability of (±)-I and both of its enantiomers in aqueous solution, equilibrium solubility values could not be determined. The approximate solubilities for each enantiomer and for (±)-I were obtained by the addition of increasing amounts of the solid into vials containing 5 ml of water. The closed vials were vigorously agitated at 25° for 1 hr.

With the enantiomers, the quantity of drug was increased by increments of 0.2 mg/ml in the range of 14–16 mg/ml of water. Similarly, the quantity of (±)-I was increased by 0.2-mg/ml increments from 2 to 4 mg/ml of water. Visual observation of these samples indicated a solubility of approximately 15 mg/ml for each enantiomer and of 3 mg/ml for (±)-I.

The apparent solubility of I as a function of the enantiomer–racemate composition was determined using physical mixtures of two optically active samples. One sample exhibited a specific rotation of +39.4° (c 0.5, water), corresponding to a composition of 95.8% (+)-(*S*)-I and 4.2% (−)-(*R*)-I. The specific rotation of the other sample was −42.0° (c 0.5, water), corresponding to 98.85% (−)-(*R*)-I and 1.15% (+)-(*S*)-I. The composition of these samples was calculated on the basis of an absolute rotation of ±43° for a pure enantiomer sample as discussed later.

The mixtures of (+)-(*S*)-I and (−)-(*R*)-I were agitated with 5-ml portions of water at 25° for 2 hr and filtered. A weighed aliquot of the filtrate was placed in a small, tared evaporating dish, and the sample was slowly evaporated (35°/130 mm Hg) to apparent dryness. The samples were dried to a constant weight at 95° for 72 hr, and the weight of dissolved solid per milliliter of water was calculated.

Purity Analysis—Samples of (±)-I, (+)-(*S*)-I, and (−)-(*R*)-I appeared to be homogeneous when analyzed by TLC on silica gel plates[11], using chloroform–methanol–formic acid [(9:3:1) R_f 0.50, (7:2.5:2) R_f 0.37, and (6:3:3) R_f 0.45]. Spots were visualized using iodine vapor; no other spots were visible by UV or after development with ninhydrin. NMR spectra (10% in d_6-dimethyl sulfoxide) showed no extraneous peaks.

An estimation of the absolute rotation of the enantiomers was obtained by purification of an optically active sample with a high content of (−)-(*R*)-I, $[\alpha]_D^{25}$ −40.28° (c 0.5, water). A sample (one part) was partially dissolved (~90%) in methanol (300 parts) at

[6] Bio-Rad AG 50W-X8, 50–100 mesh, hydrogen form.
[7] Eastman Chemicals.
[8] Varian model T-60 NMR spectrophotometer (10% in d_6-dimethyl sulfoxide).
[9] Beckman model IR-33 IR spectrophotometer (2% KBr pellet).
[10] J. T. Baker.
[11] Macherey-Nagel Polygram Sil G/UV_{254}.

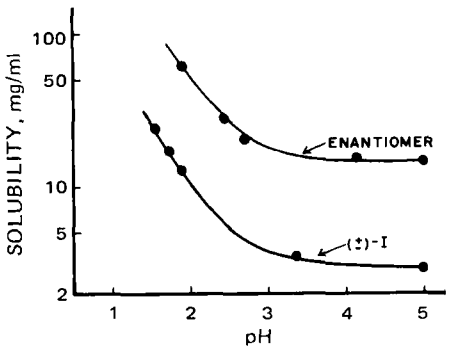

Figure 3—*Plot of solubility of (±)-I and an enantiomer as a function of pH. Solid lines were calculated on the basis of pKa 2.4, solubility of (±)-I = 3 mg/ml, and solubility of enantiomer = 15 mg/ml.*

25°, filtered, and then cooled (10°). The filtrate was slowly evaporated (150 mm Hg) to about 90% of its original volume, and the precipitate was removed by filtration and discarded.

The filtrate was then evaporated to dryness under reduced pressure (50 mm Hg) at room temperature, and the specific rotation of the solid obtained was determined[12] in water at a concentration of 0.5%. This procedure was repeated until the specific rotation obtained for three such successive treatments remained constant at a value of $[\alpha]_D^{25}$ −43.0° (c 0.5, water). This value was taken to be the value of the absolute rotation.

By comparison of specific rotations determined for other optically active samples of I with the value of the absolute rotation, the optical purity of less pure samples was calculated (16).

Lyophilization of Formulations—An initial solution containing 25 mg of (−)-(*R*)-I and 1.7 mg of hydrogen chloride/ml of solution was prepared [0.5 mEq of hydrogen chloride/mEq of (−)-(*R*)-I]. Optical rotation, pH, and TLC determinations were performed on this solution. Approximately 5 ml of this solution was placed into each of nine preweighed vials, and the total weight was determined. These vials were then placed into a dry ice–acetone bath and frozen. The samples were lyophilized[13] for 48 hr with an initial shelf temperature of −40°. The shelf temperature rose to about −20° during the first 24 hr, and then heat was applied to maintain a shelf temperature of 25° during the last 24 hr.

After lyophilization, the vials were weighed and found to contain about 2.4% more mass than expected if all water had been removed. This excess weight was attributed to residual water. Several vials were reconstituted to their original weights by the addition of water, and the optical rotation and pH of the solutions were measured. The solutions were also assayed by TLC as described previously.

Due to a slight increase in the pH of the reconstituted samples, the effect of pH on the optical rotation of aqueous solutions of the enantiomers at pH < 5 was determined in aqueous hydrochloric acid solutions. The results obtained for an optically active sample in the 1–5 pH range are shown in Table I.

RESULTS AND DISCUSSION

The enantiomers of (±)-I were prepared by asymmetric synthesis, and samples of (−)-(*R*)-I[14] and (+)-(*S*)-I[15] were sent to the National Cancer Institute for biological testing for relative activity. Data from these tests indicated that the antitumor activity for each enantiomer was equivalent to that of the (±)-I. Therefore, any pharmaceutical advantage to be realized from the use of an enantiomer could only arise from its significantly greater solubility relative to (±)-I.

The physical properties of (−)-(*R*)-I and (±)-I were studied[16] (Table II). The melting point and solubility data indicated that

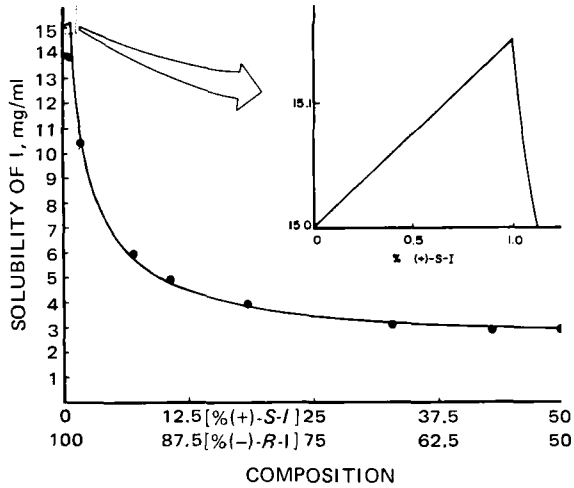

Figure 4—*Aqueous solubility of I at 25° as a function of the enantiomeric composition of the sample. The solid line was calculated (30) using solubility values of 15 mg/ml for (−)-(R)-I and 3 mg/ml for (±)-I.*

the naturally occurring racemic modification of (±)-I is that of a true racemic compound (Fig. 1c). This finding was demonstrated by the 40° decrease in the melting point and the fivefold increase in the solubility of (−)-(*R*)-I as compared with (±)-I.

Portions of the IR spectra of (−)-(*R*)-I and (±)-I (as 2% KBr pellets) are shown in Fig. 2. As expected (15), there were significant differences in the two spectra, and these differences were attributable to the differences in crystal structure (as evidenced by data in Table II). However, the IR spectra for (−)-(*R*)-I and (+)-(*S*)-I were identical. The NMR spectra (in d_6-dimethyl sulfoxide) and the values of pKa (~2.4) were identical for both enantiomers and (±)-I. Again these results were expected since the chemical properties in dilute solution would not be expected to be related to the enantiomeric composition of the sample.

A comparison of expected solubility as a function of pH based on solubility values of 3 and 15 mg/ml for (±)-I and (−)-(*R*)-I, respectively, is shown in Fig. 3. The experimental values obtained in a limited study are also shown and agree quite well with the calculated lines. From this figure, it is apparent that the desired concentration of 25 mg of I/ml of solution can be obtained using an enantiomer at pH ~2.5. To achieve a similar concentration using (±)-I, a pH of ~1.5 would be required.

The increased solubility of the individual enantiomers relative to the racemate also may be useful from the standpoint of formulating an oral dosage form, since the increased solubility should result in an increased absorption rate and, thus, improve bioavailability by that route.

An inherent drawback in the use of an enantiomer is the greater difficulty and expense of preparation relative to the racemic material. Generally, it is not particularly difficult to attain an optical purity greater than 90%. However, the preparation of essentially 100% optically pure material is extremely difficult and expensive. Therefore, it must be realized that it is not necessary to strive for 100% optically pure samples to obtain greatly increased solubility.

The solubility of a sample is dependent upon its composition with respect to each enantiomer. Since the solubility in such systems is governed by a solubility product relationship, it is possible to predict solubility as a function of the enantiomeric composition of the solute sample[17]. Figure 4 shows a theoretical plot of the total solubility of I (sum of both enantiomers) as a function of solute composition. The data points shown demonstrate the excellent agreement of the predicted values and the solubility actually obtained with the samples of various compositions.

The theoretical plot (30) is based on a solubility of 3 mg/ml for (±)-I and of 15 mg/ml for the pure enantiomer at 25° in water. From the calculated curve in Fig. 4, it is clear that the maximum solubility corresponds to a composition containing about 2% race-

[12] Perkin-Elmer model 141 polarimeter with 1-dm cell (3.5-ml volume).
[13] Virtis model 10-800 freeze dryer.
[14] NSC 169779; also ICRF 186.
[15] NSC 169780; also ICRF 187.
[16] Subsequent to completion of this study, it was discovered that A. M. Creighton had also noted enhanced solubility for the enantiomers relative to the racemic material (29).

[17] A rather complete and concise discussion of the effects of enantiomeric composition on solubility was provided by Mader (30).

Table III—Comparison of Some Properties of the Formulated Solution of (−)-(*R*)-I prior to Lyophilization and following Reconstitution at Different Times following Lyophilization[a]

Sample History	Properties of Solutions		
	$[\alpha]_D^{25}$	pH	TLC[b] (R_f Values)
Freshly prepared solution prior to lyophilization	−51.8°	2.37	0.50
Solution reconstituted immediately after completion of lyophilization	−51.0°	2.41	0.51
Solution reconstituted 5 days after lyophilization	−51.0°	2.42	0.50
Solution reconstituted 35 days after lyophilization	−48.3°[c]	2.58[c]	0.51

[a] Samples were stored in closed vials at room temperature. [b] All exhibited only one spot. [c] The higher pH value of this solution apparently caused the lower specific rotation. When using the data in Table I, at pH 2.4 the corrected value is $[\alpha]_D^{25}$ −51.0°.

mic material. Furthermore, the solubility is relatively independent of composition at higher optical purity. Thus, it would be unnecessary to strive for a completely optically pure product when a sample containing 2% or less racemic material would be essentially equally soluble and more readily attainable than a more optically pure sample.

The equations used in calculating the theoretical curve in Fig. 4 were discussed by Mader (30). It may be shown that the closer the values of the solubilities are for the racemic compound and the enantiomers, the less optically pure the solute need be to achieve maximum solubility. However, if the solubilities of the enantiomers and the racemate are similar, little advantage would be realized by their use in the formulation.

As a test of the usefulness of an enantiomer in solving the problem of formulating I, a prospective formulation was developed and evaluated. Due to the instability of I in aqueous solutions[18], a lyophilized formulation to be reconstituted just prior to use appeared to be most suitable. An aqueous solution of (−)-(*R*)-I at a concentration of 25 mg/ml at pH 2.5 was prepared, and aliquots were freeze dried in serum bottles. The resulting lyophilized samples were stored in a desiccator at 25° and reconstituted at various time intervals. Reconstitution to a concentration of 25 mg of (−)-(*R*)-I/ml was rapid (less than 2 min) and complete.

Some properties of the solutions prior to lyophilization and after reconstitution at various times were measured (Table III). These data indicate that no significant degradation of (−)-(*R*)-I occurred during lyophilization or after storage for more than 1 month. The slight decreases in the absolute rotation may be attributed to the fact that some hydrochloric acid was probably lost during the lyophilization process and the observed rotation decreased with increasing pH (Table I).

CONCLUSION

On the basis of this study, it is apparent that the utilization of an enantiomer of I resulted in improved solubility properties which, in turn, permitted the development of a formulation suitable for parenteral use without requiring modification of the basic molecular structure of the drug and without other pharmaceutical additives. This study appears to be the first reported instance in which the differences in the physical properties of a racemic compound and an enantiomeric component were used explicitly to overcome a problem in pharmaceutical formulation.

REFERENCES

(1) M. A. Miyamoto, T. Kiyotaki, N. A. Kisoh, T. Mitsunaga, and T. Maeda, *Chem. Pharm. Bull.*, **21**, 1857(1973).

(2) J. S. G. Cox, G. D. Woodard, and W. C. McCrone, *J. Pharm. Sci.*, **60**, 1458(1971).

(3) L. Borka, P. R. Kirstiansen, and K. Bache-Hansen, *Acta Pharm. Suecica*, **9**, 573(1972).

(4) E. Shefter and T. Higuchi, *J. Pharm. Sci.*, **52**, 781(1963).

(5) J. K. Haleblian, R. T. Koda, and J. A. Biles, *ibid.*, **60**, 1485(1971).

(6) A. F. Casy, in "Medicinal Chemistry," 3rd ed., vol. I, A. Burger, Ed., Wiley–Interscience, New York, N.Y., 1970, pp. 81–87.

(7) P. Friberger and G. Aberg, *Acta Pharm. Suecica*, **8**, 361(1971).

(8) T. C. Daniels and E. C. Jorgensen, in "Textbook of Organic, Medicinal and Pharmaceutical Chemistry," 6th ed., C. O. Wilson, O. Gisvold, and R. F. Doerge, Eds., Lippincott, Philadelphia, Pa., 1971, pp. 31–33.

(9) J. H. Adriani, *Z. Phys. Chem.*, **33**, 453(1900).

(10) A. Findlay and A. N. Campbell, *J. Chem. Soc.*, **1928**, 1768.

(11) H. W. B. Roozeboom, *Z. Phys. Chem.*, **28**, 494(1899).

(12) H. Mauser, *Chem. Ber.*, **90**, 299(1957).

(13) *Ibid.*, **90**, 307(1957).

(14) C. L. Bickel and A. T. Peaslee, Jr., *J. Amer. Chem. Soc.*, **70**, 1790(1948).

(15) E. L. Eliel and J. T. Kofron, *ibid.*, **75**, 4585(1953).

(16) E. L. Eliel, "Stereochemistry of Carbon Compounds," McGraw-Hill, New York, N.Y., 1962, pp. 43–47.

(17) L. Pasteur, *Ann. Chim. Phys.*, **24**, 442(1848).

(18) "Handbook of Chemistry and Physics," 42nd ed., Chemical Rubber Publishing Co., Cleveland, Ohio, 1960, p. 1768.

(19) V. Stella and T. Higuchi, *J. Pharm. Sci.*, **62**, 968(1973).

(20) A. M. Creighton, British pat. 1,234,935 (June 1971).

(21) A. M. Creighton, I. Hellmann, and S. Whitecross, *Nature*, **222**, 382(1969).

(22) A. J. Repta, B. J. Rawson, R. D. Shaffer, K. B. Sloan, N. Bodor, and T. Higuchi, *J. Pharm. Sci.*, **64**, 392(1975).

(23) H. Reihlen, E. Weinbrenner, and G. v. Hessling, *Ann. Chem.*, **494**, 143(1932).

(24) F. Dwyer, F. Garvan, and A. Schulman, *J. Amer. Chem. Soc.*, **81**, 290(1959).

(25) T. O'Brien and R. Toole, *ibid.*, **76**, 6009(1954).

(26) "Dictionary of Organic Compounds," 4th ed., vol. 5, Oxford University Press, New York, N.Y., 1965, p. 2781.

(27) R. Wing and K. Callahan, *Inorg. Chem.*, **8**, 2303(1969).

(28) F. Dwyer and F. Garvan, *J. Amer. Chem. Soc.*, **81**, 2955(1959).

(29) A. M. Creighton, Canadian pat. 941,378 (1974).

(30) W. J. Mader, in "Organic Analysis," vol. II, J. Mitchell, Jr., *et al.*, Eds., Interscience, New York, N.Y., 1954, pp. 253–276.

[18] Five percent decomposition appears to occur in less than 5 hr at pH 2–5; unpublished data from this laboratory.

ACKNOWLEDGMENTS AND ADDRESSES

Received March 24, 1975, from the *Department of Pharmaceutical Chemistry, School of Pharmacy, University of Kansas, Lawrence, KS 66044*

Accepted for publication May 8, 1975.

Presented in part at the Basic Pharmaceutics Section, APhA Academy of Pharmaceutical Sciences, New Orleans meeting, November 1974.

Supported in part by Contract N01-CM-23217 from the Division of Cancer Treatment, National Cancer Institute, National Institutes of Health, Department of Health, Education, and Welfare.

[x] To whom inquiries should be directed.

Limitations in Interpretation of Digoxin Absorption Using Averaged Pharmacological Response Intensities

J. H. GUSTAFSON [x], R. D. SCHOENWALD [*], and L. Z. BENET

Abstract □ In this paper, the interpretation of averaged pharmacological effect data for the cardiac glycoside digoxin is reconsidered through a comparison with theoretically simulated data. Four parameters, with their standard deviations calculated from the best-fit biexponential equation for the experimentally derived transformed pharmacological response intensity, were the basis for the random development of a series of 17 individual sets of data with average parameters and standard deviations identical to the values found experimentally. Parameters from these 17 data sets were averaged and randomly altered as a function of the standard deviations for each average. Loo–Riegelman analyses, modified for application to the peripheral compartment, and fraction remaining to be absorbed plots were made. Results of this comparison of experimental pharmacological simulated data indicate that the presence or absence of enterohepatic recycling may not be unambiguously determined here.

Keyphrases □ Digoxin—absorption, different methods of data interpretation, averaged pharmacological response data compared to simulated data with averaged parameters □ Analysis—*in vivo* experimental data, different methods of interpretation compared

When several identical studies are run on a series of individuals, each of whom may serve as his or her own control, the analysis may include: (*a*) determining the appropriate pharmacokinetic parameters for each subject from the data obtained for that subject, averaging parameters for all subjects, and treating the average of those parameters as descriptive of the group of subjects as a whole; or (*b*) averaging the experimental data for all individuals and treating this average to produce the parameters descriptive of the group as a whole.

Recently, both methods were utilized in a methaqualone study, and no significant differences were found between the values resulting from both methods of analysis (1). Still, in the analysis of parameters determined from averaged grouped data, the standard deviations around the individual averaged data points need to be considered when defining how specific an interpretation can be placed on the data (*i.e.*, averaged data with greater standard deviations may lead to a more uncertain interpretation than averaged data with smaller standard deviations due solely to the variation among the data points treated collectively). One recent study (2) utilized the method of treatment of averaged data in interpretating averaged pharmacological effect data for the cardiac glycoside digoxin.

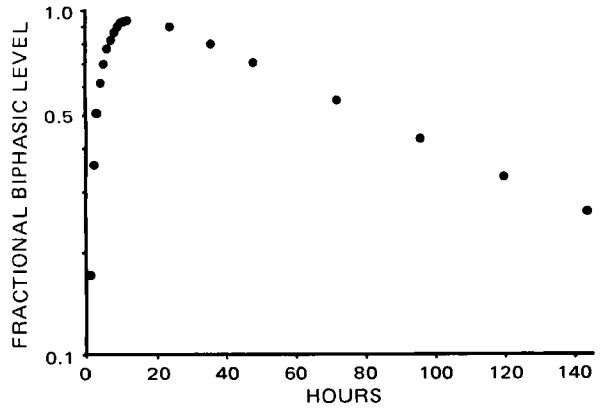

Figure 1—*Logarithm of the average of 17 individual ideal fractional biphasic levels as a function of time.*

Digoxin, a drug with a very low therapeutic ratio, recently was critically studied with respect to its possible varied bioavailability (3–6). Schoenwald (2) analyzed digoxin solely from averaged pharmacological effect data and suggested that his findings indicated enterohepatic recycling. Since the suggestion was totally based on averaged data, the intent of the present study was to evaluate the validity of the interpretation as to the prevalence of biliary recycling.

EXPERIMENTAL

Schoenwald's (2) method of treating the published pharmacological response data of Gold *et al.* (7) was followed. Gold *et al.* (7) studied the decrease in ventricular heart rate for 17 selected patients after administration of 1.2 mg of digoxin by either the oral or the intravenous route. The 17 subjects for the pharmacological effect study were selected from approximately 1000 adult patients. The patients selected had various common heart diseases, but "with few exceptions only those with a rapid ventricular rate during the period without digitalis" (7) were included. This restriction was intended to minimize the variation in heart rate sensitivity to digoxin.

From the individual data of their studies, Gold *et al.* (7) presented a graph of the average decrease in ventricular rate as a function of time. These averaged data are treated by Eqs. 1 and 2 to calculate the transformed pharmacological response intensity, f':

$$F_I = \frac{I}{I_{max}} \qquad \text{(Eq. 1)}$$

$$f' = \frac{F_I}{1 - F_I} \qquad \text{(Eq. 2)}$$

where I = intensity of effect, I_{max} = maximum possible intensity of effect, and F_I is the fraction of maximum intensity attainable. The maximum intensity attainable for the dose given is 59.97 beats/min[1].

Following Schoenwald's procedure, treatment of the data was carried out on the normalized pharmacological response intensity, f, as given in:

$$f = f'/f'_{max} \qquad \text{(Eq. 3)}$$

where f'_{max} is the maximum value of the f' observed within a collected study. The normalized averaged pharmacological response intensity following a single intravenous injection to the 17 patients described by Gold *et al.* (7) was fit to equations containing both bi- and triexponential terms by Schoenwald (2). Reciprocal weighting was used to provide a biexponential and a triexponential least-squares fit of the data as a function of time, and the following

[1] Due to a misprint in Ref. 2, a value of 51.3 beats/min was designated as I_{max}. However, 59.97 was, in fact, the value used in the calculation.

expressions with accompanying mean sum of squares (SS) were obtained:

$$f = 2.842e^{-0.0144t} - 3.134e^{-1.200t} \qquad SS = 1.25 \times 10^{-2} \quad \text{(Eq. 4)}$$

$$f = 1.708e^{-0.0086t} + 2.138e^{-0.073t} - 3.478e^{-0.500t} \qquad SS = 1.03 \times 10^{-2} \quad \text{(Eq. 5)}$$

Schoenwald (2) pointed out that the triexponential fit (Eq. 5) only slightly improves the fit compared to the biexponential fit (Eq. 4), as judged by the similar sum of squares values. In fact, if the error mean squares (EMS) of the two fits were calculated, where the sum of squares is corrected for the number of degrees of freedom in each fit as given in Eq. 6, the fits are almost equivalent ($EMS = 9.62 \times 10^{-4}$ and 9.36×10^{-4} for the bi- and triexponential fits, respectively):

$$EMS = \frac{\sum_{i=1}^{n} w_i(f_i - \hat{f}_i)^2}{(n - p)} \quad \text{(Eq. 6)}$$

where:

f_i = experimentally determined transformed pharmacological effect at time t_i
$\hat{f}_i$ = computer estimated value for f_i
w_i = weighting factor for each value of f_i
n = number of data points to be fit, in this case 17
p = number of parameters to be estimated by the equation (*i.e.*, four and six in the bi- and triexponential equations, respectively)

The minimal model consistent with the intravenous results was chosen, and the values calculated by Schoenwald were used in Eq. 4. An attempt was made to computer fit the normalized pharmacological response intensity data observed following oral administration of digoxin to the 17 patients in the study of Gold *et al.* (7). The normalized oral data were fit to both bi- and triexponential equations, using the value of 59.97 for I_{max} as already discussed. The corresponding value of f_{max} calculated for the oral data from Eqs. 1 and 2 is 1.232, since the largest decrease in ventricular heart rate noted by Gold *et al.* (7) following oral dosing was 33.1 beats/min.

The best fit for the oral data is given in Eq. 7 for the biexponential fit and in Eq. 8 for a triexponential fit:

$$f_{oral} = -1.26e^{-0.227t} + 1.18e^{-0.0107t} \qquad EMS = 1.15 \times 10^{-2} \quad \text{(Eq. 7)}$$

$$f_{oral} = -1.41e^{-0.188t} + 1.16e^{-0.0189t} + 0.207e^{-(2.32 \times 10^{-10})t} \qquad EMS = 1.20 \times 10^{-2} \quad \text{(Eq. 8)}$$

Note here that the comparison of EMS values again indicates that the bi- and triexponential fits are almost equivalent, although here the biexponential fit has a slightly lower value for the EMS than the triexponential fit. In addition, as would be expected, the biexponential parameters have smaller coefficients of variation than the triexponential parameters.

The third exponential term in Eq. 8 is so small that it may be considered negligible for all data points except those seen extremely early in the experiment. Thus, it seems appropriate to use the biexponential equations and the values given in Eq. 7 to simulate the oral data that would be randomly varied. This approach is consistent with the idea of using the minimal pharmacokinetic model as stated by Garrett (8): "The general operating rule in such pharmacokinetic analysis is to postulate the minimum number of compartments consistent with physiological reality."

One may question whether an appropriate oral fit of the data to a biexponential equation is valid when it is known that the intravenous data also are best described by a biexponential equation. The usually expected triexponential form for the oral data may degenerate to a biexponential equation when the absorption rate constant approaches a value equal to the sum of the exit rate constants from the peripheral compartment[2]. This may be the case with respect to the present data; however, irregularities in the apparent absorption profile preclude validation of this point without additional experiments.

The following discussion will be presented with respect to data manipulation using the parameters given in Eq. 7 for $I_{max} = 59.97$. The parameters are designated as Case I in Table I.

The constants in Case I were treated by random number multiplication of their standard deviations until a series of 17 individual constants were calculated having averages and standard deviations with values very close to the original constants and their standard deviations. Generally, this process was accomplished by multiplying a random number[3] by one- or twofold values of the given standard deviation values and adding that product to the given average value. Minor adjustments were made in selected randomly calculated constants to make the averages and standard deviations of the calculated constants equal to the values given in Table I, Case I.

Once 17 such sets of individual values for each parameter in Case I were developed, the parameters were randomly combined into 17 sets of A_1, A_2, r_1, and r_2, the constants in the biexponential equation, $f = A_1e^{-r_1t} + A_2e^{-r_2t}$. Each set of constants was then used to calculate f_i for this set of constants at 19 different time points utilized by Schoenwald (2), thereby providing ideal f values at 19 different times for 17 ideal individuals. The 17 ideal f values for each time point were then averaged, and individual standard deviations were calculated for each average.

To put the averaged ideal f values into a more "real" setting, the standard deviation for each averaged f multiplied by a random number was added to its averaged ideal f value. Three random number series were utilized: (*a*) $\mu = 0$, $\sigma = 0.5$; (*b*) $\mu = 0$, $\sigma = 1.0$; and (*c*) $\mu = 0$, $\sigma = 2.0$; μ is the mean and σ is the standard deviation. Thus, three new sets of averaged values were obtained; one series of values varied by $\sigma = 0.5$, one series of values varied by $\sigma = 1.0$, and one series of values varied by $\sigma = 2.0$. These series will be referred to as sigma 0.5, sigma 1, and sigma 2.

Calculations of intensity of effect for the series of averaged ideal f values and the three sigma series of f values were compared. For sigma 0.5, sigma 1, and the averaged ideal series, the differences between intensities at each time point from 1 to 48 hr inclusive ranged from 0.5 to 6.0 (average = 3) beats/min, with one "outlier"[4] variation of 11 beats/min.

A Loo–Riegelman (10) treatment, modified for application to the peripheral compartment (2), was then applied to the ideal data and the data from sigma 0.5, sigma 1, sigma 2, and Schoenwald's f values calculated from averaged data of Gold *et al.* (7). The values calculated by the Loo–Riegelman modification for the four series of f values were analyzed by plotting both the log fraction of the dose remaining to be absorbed *versus* time and the log absorption rate *versus* the midpoint of the time interval. A parallel treatment of parameters derived from the treatment of pharmacological response data (7) was also carried out utilizing $I_{max} = 51.3$ beats/min [the value reported by Schoenwald (2)] instead of the actual value, 59.97 beats/min, to test whether the results reported here may only have been due to the specific combination of random numbers used in the computer simulations.

RESULTS AND DISCUSSION

Figure 1 is a semilog plot of the average for each time point of the 17 individual ideal f values calculated from the randomly deviated biexponential parameters. Figure 2 is the same type of semilog plot for the following situations: (*a*) the f values for the Gold *et al.* (7) original averaged data, (*b*) the f values for sigma 0.5, (*c*) the f values for sigma 1, and (*d*) the f values for sigma 2. Corresponding plots of fraction remaining to be absorbed data are presented in Fig. 3.

All four calculations included negative values which could not be plotted on the logarithmic scale. The negative values are indicated by arrows on the abscissas of the plots in Fig. 3. A plot of the original data in this series as treated by Schoenwald (2) also demonstrated negative values, as did plots when $I_{max} = 51.3$ beats/min was used. Semilog plots of the absorption rate *versus* the midpoint time were too erratic to permit interpretation. Table I collates the

[2] R. A. Ronfeld and L. Z. Benet, to be published.

[3] All random numbers were from random number tables in the Appendix of Ref. 9.

[4] As defined by Table A-8e (Criteria for Testing for Extreme Mean) in Ref. 9, 11 beats/min is an outlier for hours 1–48 inclusive with P_{90}, and it is an outlier for hours 1–144 inclusive with P_{95}.

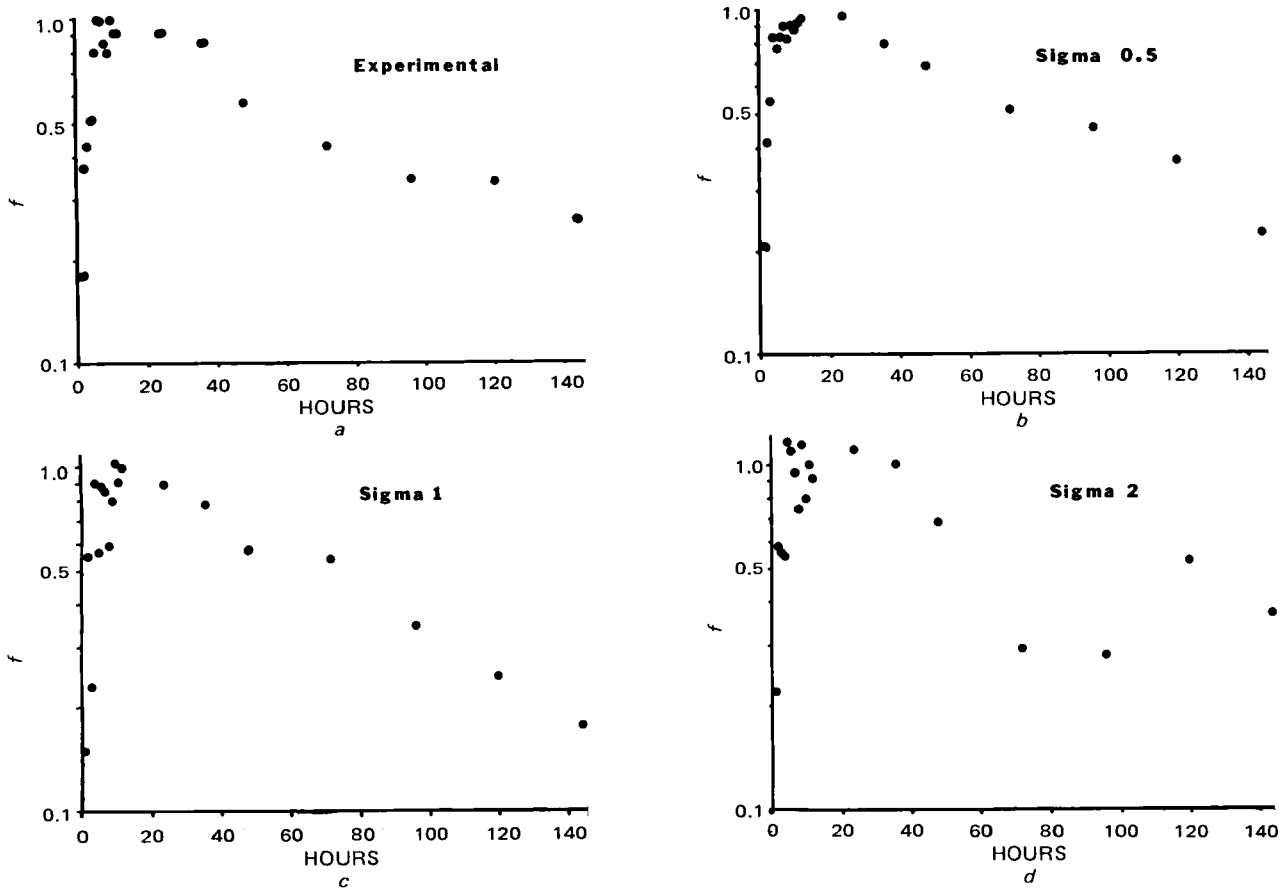

Figure 2—*Logarithm of fractional biphasic levels as a function of time for:* (a) *experimental data of Gold* et al. *(7),* (b) *sigma 0.5,* (c) *sigma 1, and* (d) *sigma 2.*

least-squares best-fit biexponential parameters with their corresponding standard deviations for the five semilog plots of pharmacological effect as a function of time presented in Figs. 1 and 2.

The graphs of the computer-generated data and the graph of the Gold *et al.* (7) data in Fig. 3 have similar general appearances. For example, all graphs have the increases and decreases of fraction remaining to be absorbed, which could be identified as enterohepatic recycling. The recycling aspect, however, was not included in the computer generation of data. For the computer-generated data, the increases and decreases in the fraction remaining to be absorbed are solely a function of the treatment of the ideal data. The treatment of ideal data here included only two factors: the averaging of individual ideal values and the random alteration of an average as a function of the standard deviation of that average. Thus, enterohepatic recycling is not a necessary interpretation of any of the data presented in Fig. 2.

No variations in the intravenous parameters used, *i.e.*, the parameters given in Eq. 4, were carried out since fraction remaining to be absorbed plots for oral ideal data did not show erratic changes in slope, even though these oral data were generated using values already different than the intravenous best-fit values. Further variance of the intravenous parameters should not markedly affect the plots seen in Fig. 3.

Perrier and Gibaldi (11) noted that fraction remaining to be absorbed plots can present a good estimate of the absorption rate when there is no lag time, there is some uniformity in absorption (*i.e.*, zero order, first order), and there is no parallel nonabsorptive loss of drug from the absorption site. The erratic plots of the fraction remaining to be absorbed for the Gold *et al.* (7) data, sigma 0.5, sigma 1, and sigma 2 demonstrate that the necessary underlying assumptions were not met by the data in any of these studies.

Negative fractions remaining to be absorbed were seen in three of the four sigma plots for I_{max} = 59.97 and also in the plot of the Gold *et al.* (7) data. A greater number of negative values were seen in three of the four sigma plots for the incorrect I_{max} = 51.3. Thus, negative values were considered to reflect the sensitivity of the fraction remaining to be absorbed function to nonideal variations in the data.

The protocol of this study included an *ab initio* correlation of the standard deviation of the least-squares-fitted grouped experimental data with the standard deviation of the arithmetic averages of groups of individual parameters. The data in Table I show this assumption to be realistic. Here, the range of values determined for the coefficients of the exponentials (*i.e.*, A_1 and A_2) from Case II to Case V is actually less than the range of values for the standard deviations of the parameters. With the exception of Case IV, the range of the values for the rate constant r_2 is less than the range of values for the respective standard deviations. With the exception of Case IV, the range of values for r_1 is within 14% of the range of values for the respective standard deviations. The comparison of the five cases presented in Table I is actually a comparison of their standard deviations.

Case II, the averaged ideal data, has very small standard deviations for all parameters; this should be so in the ideal situation. Case I, based on the Gold *et al.* (7) data, is true experimental pharmacological effect data. Cases III, IV, and V are based on random

Table I—Parameters with Standard Deviations for the Least-Squares Exponential Fit of: Case I, Data of Gold *et al.* (7); Case II, Averaged Values of 17 Ideal Data Sets; Case III, Sigma 0.5; Case IV, Sigma 1; and Case V, Sigma 2

Case	A_1 (*SD*)	r_1 (*SD*)	A_2 (*SD*)	r_2 (*SD*)
I	−1.26	0.227	1.18	0.0107
	(0.10)	(0.048)	(0.10)	(0.0013)
II	−1.22	0.212	1.18	0.0107
	(0.01)	(0.004)	(0.01)	(0.0014)
III	−1.18	0.286	1.12	0.0101
	(0.04)	(0.029)	(0.04)	(0.0007)
IV	−1.30	0.155	1.31	0.0139
	(0.26)	(0.051)	(0.27)	(0.0031)
V	−1.27	0.354	1.11	0.0108
	(0.13)	(0.128)	(0.15)	(0.0026)

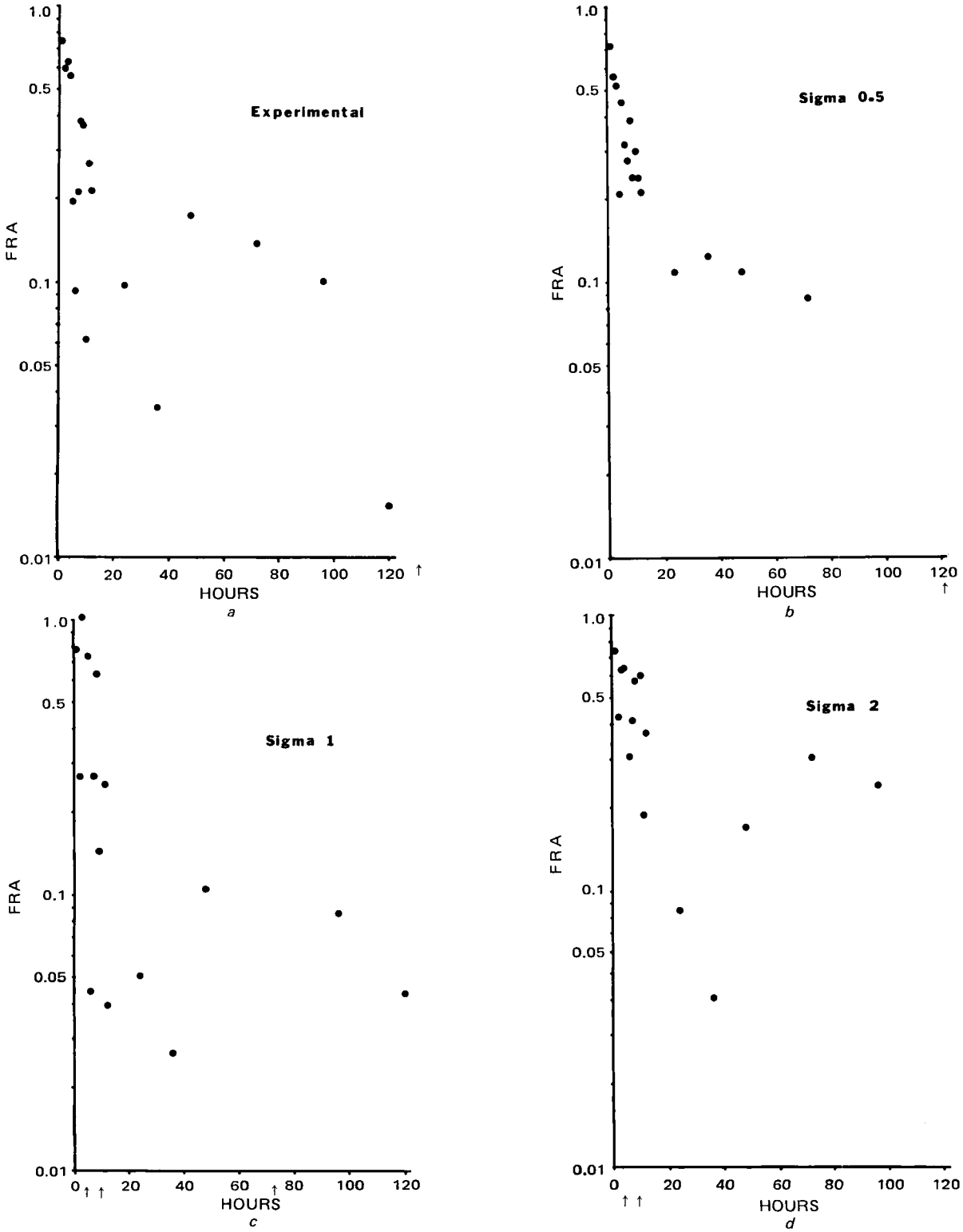

Figure 3—*Logarithm of fraction remaining to be absorbed (FRA) as a function of time for:* (a) *experimental data of Gold* et al. *(7),* (b) *sigma 0.5,* (c) *sigma 1, and* (d) *sigma 2. Arrows along the abscissa indicate negative values.*

alterations of Case II data as described under *Experimental.* The standard deviations in Case V are much greater than those in Case I, and the standard deviations in Case III are all smaller than the values for Case I. The standard deviations in Case IV are all greater than the standard deviations in Case I, although they are closer in value to the values for Case I than are the values for Case V. For the theoretical development cited here, the data from these five cases demonstrate that a sigma between 0.5 and 1.0 would give similar standard deviations as are given for the true experimental data of Case I. It is the similarity of standard deviations of similar parameters that permits this comparison of the theoretically determined data with the experimentally determined data.

Mathematical models, whether they be empirically or theoretically derived, may be misleading when obtained from averaged data since they represent averaged data and not necessarily any of the individual data. An example of this type was reported (12) in which two subjects were found to absorb drug according to a single first-order process; however, first-order rate constants differed considerably, *i.e.*, 0.0693 and 0.00866 min^{-1}. The averaged data for these two subjects could best be fit by a biexponential relationship.

This finding would artifactually lead one into concluding that absorption was occurring by two consecutive first-order processes. It should not be concluded that averaging of individual data is inappropriate, but its primary function should be to reduce the variance so that an accurate theoretical interpretation becomes more feasible.

CONCLUSION

Minor random deviations from averages of ideal data have been shown to be capable of producing results similar to those expected from enterohepatic recycling when the ideal data exclude that phenomenon. Thus, the definition of enterohepatic recycling from real pharmacological data probably requires an experimental study before confirmation can be made.

REFERENCES

(1) R. K. Nayak, R. D. Smyth, J. H. Chamberlain, A. Polk, A. F. DeLong, T. Herczog, P. B. Chemburkar, R. S. Joslin, and N. H. Reavey-Cantwell, *J. Pharmacokinet. Biopharm.*, **2**, 107(1974).

(2) R. D. Schoenwald, *J. Pharm. Sci.*, **63**, 411(1974).

(3) A. G. Hibble, P. Isaac, and D. G. Grahame-Smith, *Lancet*, **2**, 90(1972).

(4) J. Lindenbaum, M. H. Mellow, M. O. Blackstone, and V. P. Butler, Jr., *N. Engl. J. Med.*, **285**, 1344(1971).

(5) T. R. D. Shaw, M. R. Howard, and J. Hamer, *Lancet*, **2**, 303(1972).

(6) J. G. Wagner, M. Christensen, E. Sakmar, D. Blair, J. D. Yates, P. W. Willis, III, A. J. Sedman, and R. G. Stoll, *J. Amer. Med. Ass.*, **224**, 199(1973).

(7) H. Gold, M. Cattell, T. Greiner, L. W. Hanlon, N. T. Kwit, W. Modell, E. Cotlove, J. Benton, and H. L. Otto, *J. Pharmacol. Exp. Ther.*, **109**, 45(1953).

(8) E. R. Garrett, *J. Pharmacokinet. Biopharm.*, **1**, 341(1973).

(9) W. J. Dixon and F. J. Massey, Jr., "Introduction to Statistical Analysis," 2nd ed., McGraw-Hill, New York, N.Y., 1957, pp. 366–380, 457–461.

(10) J. C. K. Loo and S. Riegelman, *J. Pharm. Sci.*, **57**, 918(1968).

(11) D. Perrier and M. Gibaldi, *ibid.*, **62**, 225(1973).

(12) G. Levy and L. E. Hollister, *ibid.*, **53**, 1446(1964).

ACKNOWLEDGMENTS AND ADDRESSES

Received December 16, 1974, from the *Department of Pharmacy, School of Pharmacy, University of California, San Francisco, CA 94143*

Accepted for publication May 7, 1975.

Presented in part at the Basic Pharmaceutics Section, APhA Academy of Pharmaceutical Sciences, New Orleans meeting, November 1974.

Supported in part by Project Grant GM 16496 from the Institute of General Medical Sciences, National Institutes of Health. Ms. Gustafson received support from Training Grant in Pharmaceutical Chemistry GM 00728 from the National Institutes of Health. Ms. Gustafson also received support as a Fellow of the American Foundation for Pharmaceutical Education during 1974–1975.

* Present address: Alcon Laboratories, Fort Worth, TX 76101

ˣ To whom inquiries should be directed.

Anaerobic Photodecomposition of an Acridan Drug through Energy Transfer

GEORGE A. DIGENIS ˣ, SHUKRI SHAKHSHIR *, M. A. MIYAMOTO ‡, and H. B. KOSTENBAUDER

Abstract □ Anaerobic irradiation of 2-chloro-9-(3-dimethylaminopropyl)acridan phosphate (1:1) (III*a*) with filtered visible light (300–400 nm) resulted in its quantitative conversion to its acridine derivative IV. Photoproduct IV exerted significant product catalysis on the reaction rate at concentrations of 5×10^{-6} *M*. The anaerobic photodecomposition of III*a* to IV was catalyzed by the monosodium salt of riboflavin 5-phosphate (I*a*). Loss of I*a* was insignificant relative to that of III*a*, and reagents known to serve as quenchers of the triplet state of I*a* retarded the reaction. Fluorescence spectra of I*a* in the presence of III*a* and 1×10^{-4} *M* KI indicated no quenching of the I*a* singlet excited state. No deuterium isotope effect was noticed when III*a* and its deuterated derivative III*b* were subjected to anaerobic photodecomposition in the presence of I*a*. It is suggested that the anaerobic photodecomposition of III*a* by visible light in the presence of I*a* proceeds *via* a triplet–triplet energy transfer from I*a* to III*a*.

Keyphrases □ Photodecomposition, anaerobic—acridan derivative converted to acridine derivative in visible light through energy transfer, riboflavin 5-phosphate as catalyst □ Acridans—2-chloro-9-(3-dimethylaminopropyl)acridan phosphate converted to acridine derivative in visible light through energy transfer □ 2-Chloro-9-(3-dimethylaminopropyl)acridan phosphate—anaerobic photodecomposition to acridine derivative

Flavin coenzymes participate in various enzymatic dehydrogenation reactions. The overall dehydrogenation can be represented by Scheme I, where I*a* and A are the oxidized forms of riboflavin and substrate, respectively, and I*b* and AH_2 represent the reduced forms of the coenzyme and substrate, respectively (R = ribityl group).

Several classes of such reactions are known including: (*a*) alcohol dehydrogenation (glucose oxidase and lactate dehydrogenase); (*b*) amine dehydrogenation, commonly referred to as oxidative deamination (amino acid oxidases); (*c*) dehydrogenation alpha and beta to a carbonyl (succinate dehydrogenase); and (*d*) dihydronicotinamide dehydrogenation (NADH dehydrogenase).

BACKGROUND

Based on model studies, a mechanism was proposed for amine and alcohol dehydrogenations. This mechanism involves the formation of a carbanion-like intermediate (II, Scheme II) formed after the addition of an alcohol or amine at the C_{4a}-position of the flavin (1).

This finding would artifactually lead one into concluding that absorption was occurring by two consecutive first-order processes. It should not be concluded that averaging of individual data is inappropriate, but its primary function should be to reduce the variance so that an accurate theoretical interpretation becomes more feasible.

CONCLUSION

Minor random deviations from averages of ideal data have been shown to be capable of producing results similar to those expected from enterohepatic recycling when the ideal data exclude that phenomenon. Thus, the definition of enterohepatic recycling from real pharmacological data probably requires an experimental study before confirmation can be made.

REFERENCES

(1) R. K. Nayak, R. D. Smyth, J. H. Chamberlain, A. Polk, A. F. DeLong, T. Herczog, P. B. Chemburkar, R. S. Joslin, and N. H. Reavey-Cantwell, *J. Pharmacokinet. Biopharm.*, **2**, 107(1974).

(2) R. D. Schoenwald, *J. Pharm. Sci.*, **63**, 411(1974).

(3) A. G. Hibble, P. Isaac, and D. G. Grahame-Smith, *Lancet*, **2**, 90(1972).

(4) J. Lindenbaum, M. H. Mellow, M. O. Blackstone, and V. P. Butler, Jr., *N. Engl. J. Med.*, **285**, 1344(1971).

(5) T. R. D. Shaw, M. R. Howard, and J. Hamer, *Lancet*, **2**, 303(1972).

(6) J. G. Wagner, M. Christensen, E. Sakmar, D. Blair, J. D. Yates, P. W. Willis, III, A. J. Sedman, and R. G. Stoll, *J. Amer. Med. Ass.*, **224**, 199(1973).

(7) H. Gold, M. Cattell, T. Greiner, L. W. Hanlon, N. T. Kwit, W. Modell, E. Cotlove, J. Benton, and H. L. Otto, *J. Pharmacol. Exp. Ther.*, **109**, 45(1953).

(8) E. R. Garrett, *J. Pharmacokinet. Biopharm.*, **1**, 341(1973).

(9) W. J. Dixon and F. J. Massey, Jr., "Introduction to Statistical Analysis," 2nd ed., McGraw-Hill, New York, N.Y., 1957, pp. 366–380, 457–461.

(10) J. C. K. Loo and S. Riegelman, *J. Pharm. Sci.*, **57**, 918(1968).

(11) D. Perrier and M. Gibaldi, *ibid.*, **62**, 225(1973).

(12) G. Levy and L. E. Hollister, *ibid.*, **53**, 1446(1964).

ACKNOWLEDGMENTS AND ADDRESSES

Received December 16, 1974, from the *Department of Pharmacy, School of Pharmacy, University of California, San Francisco, CA 94143*

Accepted for publication May 7, 1975.

Presented in part at the Basic Pharmaceutics Section, APhA Academy of Pharmaceutical Sciences, New Orleans meeting, November 1974.

Supported in part by Project Grant GM 16496 from the Institute of General Medical Sciences, National Institutes of Health. Ms. Gustafson received support from Training Grant in Pharmaceutical Chemistry GM 00728 from the National Institutes of Health. Ms. Gustafson also received support as a Fellow of the American Foundation for Pharmaceutical Education during 1974–1975.

* Present address: Alcon Laboratories, Fort Worth, TX 76101

ˣ To whom inquiries should be directed.

Anaerobic Photodecomposition of an Acridan Drug through Energy Transfer

GEORGE A. DIGENIS ˣ, SHUKRI SHAKHSHIR *, M. A. MIYAMOTO ‡, and H. B. KOSTENBAUDER

Abstract □ Anaerobic irradiation of 2-chloro-9-(3-dimethylaminopropyl)acridan phosphate (1:1) (III*a*) with filtered visible light (300–400 nm) resulted in its quantitative conversion to its acridine derivative IV. Photoproduct IV exerted significant product catalysis on the reaction rate at concentrations of 5×10^{-6} *M*. The anaerobic photodecomposition of III*a* to IV was catalyzed by the monosodium salt of riboflavin 5-phosphate (I*a*). Loss of I*a* was insignificant relative to that of III*a*, and reagents known to serve as quenchers of the triplet state of I*a* retarded the reaction. Fluorescence spectra of I*a* in the presence of III*a* and 1×10^{-4} *M* KI indicated no quenching of the I*a* singlet excited state. No deuterium isotope effect was noticed when III*a* and its deuterated derivative III*b* were subjected to anaerobic photodecomposition in the presence of I*a*. It is suggested that the anaerobic photodecomposition of III*a* by visible light in the presence of I*a* proceeds *via* a triplet–triplet energy transfer from I*a* to III*a*.

Keyphrases □ Photodecomposition, anaerobic—acridan derivative converted to acridine derivative in visible light through energy transfer, riboflavin 5-phosphate as catalyst □ Acridans—2-chloro-9-(3-dimethylaminopropyl)acridan phosphate converted to acridine derivative in visible light through energy transfer □ 2-Chloro-9-(3-dimethylaminopropyl)acridan phosphate—anaerobic photodecomposition to acridine derivative

Flavin coenzymes participate in various enzymatic dehydrogenation reactions. The overall dehydrogenation can be represented by Scheme I, where I*a* and A are the oxidized forms of riboflavin and substrate, respectively, and I*b* and AH_2 represent the reduced forms of the coenzyme and substrate, respectively (R = ribityl group).

Several classes of such reactions are known including: (*a*) alcohol dehydrogenation (glucose oxidase and lactate dehydrogenase); (*b*) amine dehydrogenation, commonly referred to as oxidative deamination (amino acid oxidases); (*c*) dehydrogenation alpha and beta to a carbonyl (succinate dehydrogenase); and (*d*) dihydronicotinamide dehydrogenation (NADH dehydrogenase).

BACKGROUND

Based on model studies, a mechanism was proposed for amine and alcohol dehydrogenations. This mechanism involves the formation of a carbanion-like intermediate (II, Scheme II) formed after the addition of an alcohol or amine at the C_{4a}-position of the flavin (1).

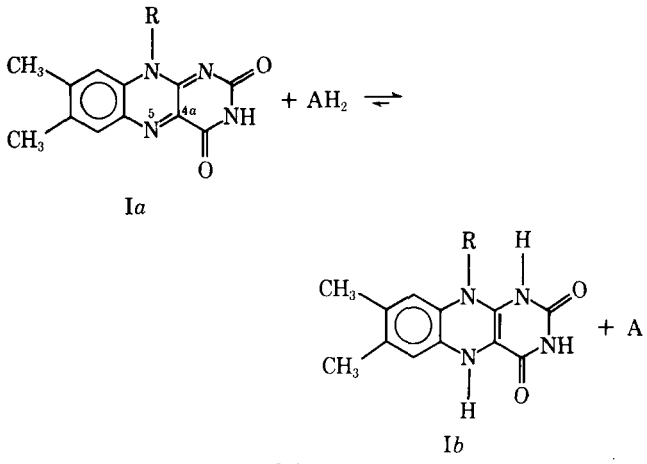

Scheme I

The partial reaction sequence depicted in Scheme II is an example of covalent catalysis (2). This type of catalysis involves an intermediate, such as II, in which substrate and coenzyme become covalently bonded. The isoalloxazine moiety of flavins has been implicated in the formation of covalent intermediates. The existence of such intermediates is substantiated by several examples including the photoinduced decarboxylation of phenylacetate (3), the photocatalyzed formation of 3-benzyl-5-(2-thiolyl)-1,5-dihydroflavin from 3-benzyllumiflavin and tetrahydrothiophene (4), the nucleophilic addition of sulfite ion at the N-5 position of the flavin coenzyme in D- and L-amino acid oxidases (5), and the oxidation of β-chloroalanine to chloropyruvate by D-amino acid oxidase (6).

It was previously reported that, in UV light, the antipsychotic drug 2-chloro-9-(3-dimethylaminopropyl)acridan (III*a*) is photooxidized to an acridine (IV) as the initial photoproduct (Scheme III). Compound III*a* is relatively stable to visible light (>400 nm); but in the presence of riboflavin phosphate, exposure to visible light results in rapid photooxidation of III*a* without comparable destruction of riboflavin (7). The present article presents evidence to show that the riboflavin-mediated photooxidation of III*a* in visible light occurs *via* energy transfer involving a flavin triplet excited state.

The participation of drugs such as III*a* in energy transfer reactions in aqueous solution has obvious implications with respect to the stability of the drug when it is combined with an agent that absorbs visible light and that has a triplet state favorable to energy transfer. Also, the ability of III*a* to quench the flavin triplet excited state suggests that the drug might also intercept biological electron transport *in vivo* at the NADH dehydrogenase (flavoprotein) level by quenching a flavin excited state. Published data from these laboratories indicate that III*a* interferes with electron transfer in the NADH dehydrogenase segment of the respiratory chain in *Pseudomonas saccharophila*, a facultative autotrophic bacterium (8).

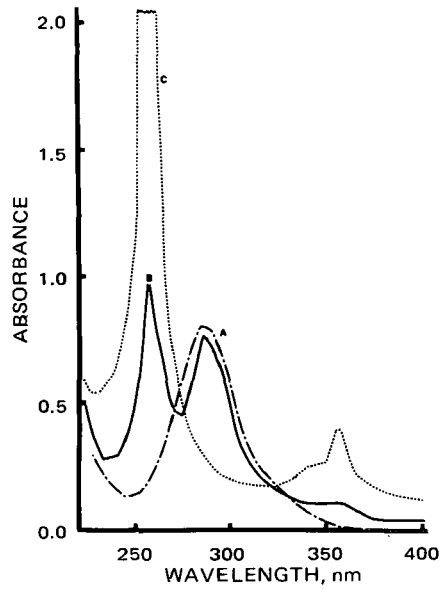

Figure 1—*Progressive loss of III*a *(282 nm) upon irradiation with filtered sunlamp light source (300–400 nm) and appearance of the acridine photoproduct (IV). Key: A, 5 × 10⁻⁵ M of III*a *prior to irradiation; and B and C, appearance of IV.*

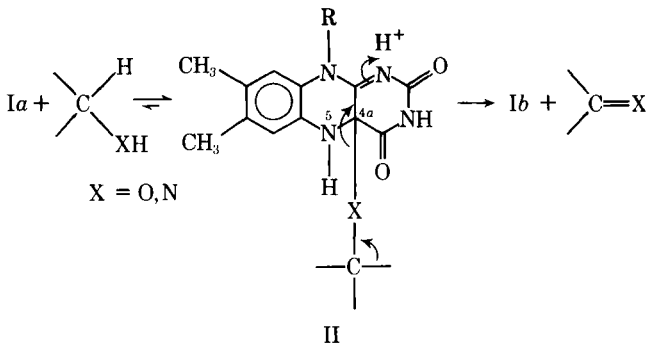

Scheme II

EXPERIMENTAL

Reagents—Compound III*a*[1] [2-chloro-9-(3-dimethylaminopropyl)acridan phosphate (1:1)] and its acridine derivative[1] [2-chloro-9-(3-dimethylaminopropyl)acridine dihydrochloride] (oxidized form, IV) were used as supplied. Riboflavin 5-phosphate monosodium salt[2] (I*a*) was recrystallized from 95% ethanol. Potassium iodide, USP grade, was recrystallized from methanol.

Spectroscopy[3]—The disappearance of III in the presence of riboflavin phosphate (I*a*) was determined by following the decrease in absorbance at 292 nm near the 282-nm maximum for III. Measurement at 292 nm, an isosbestic point for riboflavin (I*a*) and its photoproducts (9), facilitated correction for contribution of flavin mononucleotide to the total absorbance.

Riboflavin Photooxidation of III*a* and III*b*—Unless otherwise specified, solutions were prepared daily in degassed double-distilled water and reactions were run in a 1-cm quartz Thunberg cell, equipped with a bulb (2 ml) and a side arm fitted to a stopcock. The Thunberg cell was put under nitrogen by repeated (at least seven times) evacuation and introduction of nitrogen. Immediately prior to irradiation, the riboflavin phosphate (I*a*) was introduced anaerobically into the cell, from the bulb, by tilting the Thunberg cell.

The light source for the photocatalyzed oxidation of III*a* by I*a* was the unfiltered light from a 500-w projection lamp. The cell was placed in a water bath (27°) 155 cm from the center of the light source. The thickness of the glass wall of the water bath was 0.31 cm. For the photooxidation of III*b* by I*a*, filtered visible light[4] (300–400 nm) was utilized. The cell was placed 6.5 and 155 cm

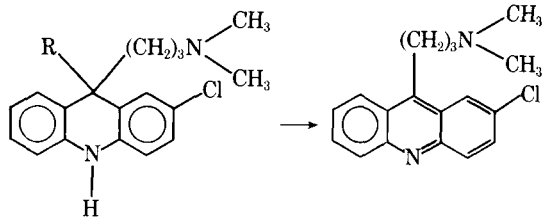

III*a*: R = H
III*b*: R = D

IV

Scheme III

[1] Smith Kline and French Laboratories, Philadelphia, PA 19101
[2] Mann Research, Orangeburg, NY 10962
[3] Absorbance was measured with a Cary 15 recording spectrophotometer in the 220–500-nm region. Kinetic studies were performed with a Gilford spectrophotometer (model 240).
[4] General Electric 275-w sunlamp.

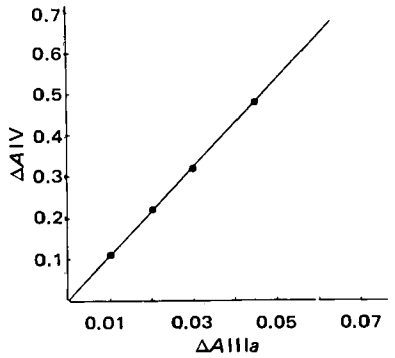

Figure 2—*Plot of increase in absorbance of photoproduct (IV) (ΔA IV) at 255 nm* versus *loss of IIIa (ΔA IIIa) at 282 nm, resulting from the anaerobic irradiation of IIIa with filtered sunlamp light.*

from the filter and light source, respectively.

Photolysis of IIIa Alone or in Presence of IV by Filtered Visible Light—Photolytic studies in the presence of filtered light[4] (300–400 nm, filter placed 6.25 cm from cell) were performed in double-distilled water in a Thunberg cell under anaerobic conditions and at 25°. The Thunberg cell was placed 155 cm from the light source.

Isolation and Identification of Acridine (IV) from Anaerobic Photodecomposition of IIIa and Ia—One gram (2.5 mmoles) of IIIa and 2.7 g (5.25 mmoles) of riboflavin 5-phosphate monosodium salt (Ia), dissolved in 600 ml of a methanol–water (1:1) mixture, was introduced into a flask fitted through a glass joint to a nitrogen inlet. The reaction mixture was put under nitrogen by repeated (at least seven times) evacuation and introduction of nitrogen. After 23 hr of irradiation under a sunlamp, the reaction mixture was flash evaporated to remove its methanol content.

The remaining aqueous mixture was first adjusted to pH 8 by adding 10% NH_4OH and then extracted twice with 2 liters of chloroform. The chloroform extracts were then dried and evaporated to dryness with reduced pressure, and the residue was chromatographed on fine silica gel G TLC plates (0.5 mm) with chloroform–methanol (9:1) as the eluent. A large band was visualized (UV lamp) at the same level (R_f 0.45) as that from an authentic solution of acridine (IV), obtained by neutralizing the solution with

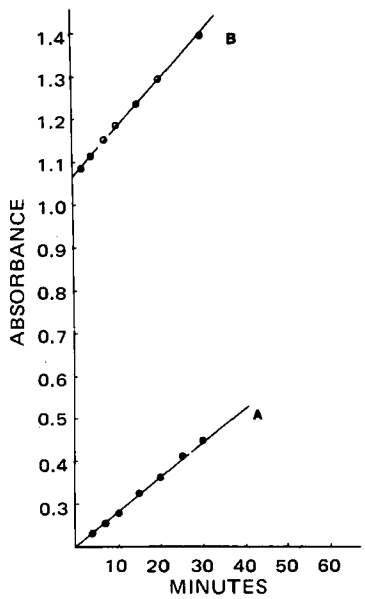

Figure 3—*Rate of appearance of photoproduct IV (at 252 nm) upon anaerobic irradiation of IIIa with filtered sunlamp light. Key: A, 5 × 10⁻⁵ M IIIa (slope 0.008); and B, 5 × 10⁻⁵ M IIIa and 5 × 10⁻⁶ M IV (slope 0.0115).*

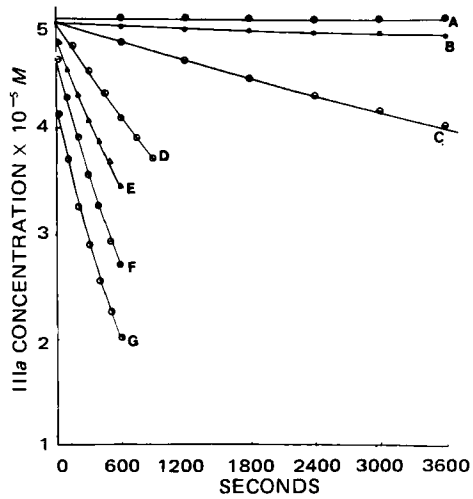

Figure 4—*Riboflavin- (Ia) photocatalyzed decomposition of IIIa with visible light (anaerobic conditions). Key: A, 5 × 10⁻⁵ M IIIa; B, 5 × 10⁻⁵ M IIIa and 5 × 10⁻⁷ M Ia; C, 5 × 10⁻⁵ M IIIa and 5 × 10⁻⁶ M Ia; D, 5 × 10⁻⁵ M IIIa and 5 × 10⁻⁵ M Ia; E, 5 × 10⁻⁵ M IIIa and 1 × 10⁻⁴ M Ia; F, 5 × 10⁻⁵ M IIIa and 1.5 × 10⁻⁴ M Ia; and G, 5 × 10⁻⁵ M IIIa and 5 × 10⁻⁴ M Ia.*

10% NH_4OH. Elution of the band (R_f 0.45) with chloroform and subsequent evaporation of the solvent yielded 0.76 g (2.5 mmoles, quantitative yield) of a thick orange-brown liquid. The latter exhibited identical IR and UV spectra with an authentic sample of IV, obtained in its free amine form by neutralization of its aqueous solution with 10% NH_4OH and subsequent extraction with chloroform.

Preparation of 9-D-IIIb—Two grams of IV was dissolved in water and extracted with ether after it was made alkaline with 10% NH_4OH. The ether extracts were reduced to 250 ml under reduced pressure. The ethereal solution was added slowly into a previously stirred (for 1.5 hr) mixture of 3–4 g of lithium aluminum deuteride[5] ($LiAlD_4$) and 450 ml of ether. The mixture was heated under reflux with stirring under nitrogen for 24 hr. At the end of this time, the excess hydride was decomposed by adding a 50% aqueous solution of sodium potassium tartrate with cooling (5°). The mix-

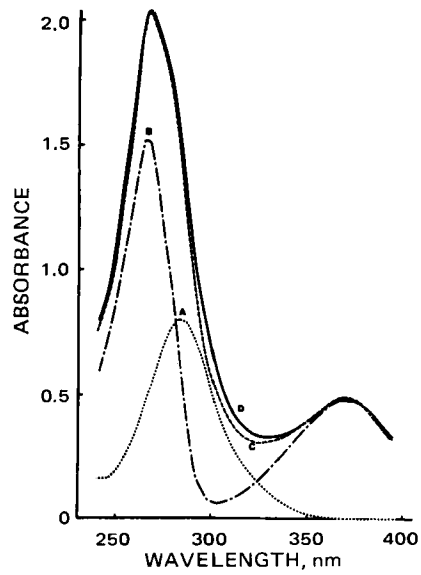

Figure 5—*UV spectra of IIIa and Ia. Key: A, 5 × 10⁻⁵ M IIIa; B, 5 × 10⁻⁵ M Ia; C, theoretical summation spectra of A and B; and D, spectrum of a mixture of 5 × 10⁻⁵ M IIIa and 5 × 10⁻⁵ M Ia.*

[5] International Chemical and Nuclear Corp., Irvine, CA 92664

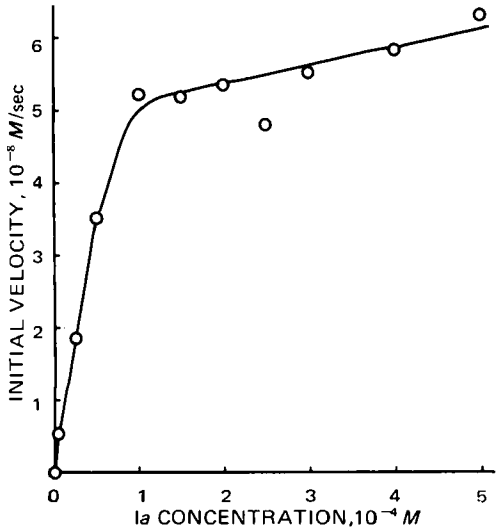

Figure 6—*Influence of riboflavin phosphate Ia concentration on the rate of anaerobic photodecomposition (visible light) of IIIa (5×10^{-5} M).*

ture was filtered, and the aqueous layer was extracted with ether.

Distillation of the solvent under reduced pressure at 25° yielded a yellowish-brown oil. The mass spectrum of this product exhibited major fragments at *m/e* 301 (m), 257, 256, and 254; the free amine base of IIIa exhibited fragments at *m/e* 300 (m), 256, 255, and 254. The NMR spectrum of the deuterated product showed the absence of the 9-H proton and the presence of the 10-H(—NH) proton, which was found to undergo a facile exchange with deuterium oxide in accordance with other acridans (10). Treatment of the yellowish-brown oil with aqueous phosphoric acid led to the production of 9-D-IIIb, mp[6] 205–208°, in 70% yield.

RESULTS AND DISCUSSION

The progressive loss of absorbance at 282 nm and the increase in absorbance at 255 and 360 nm when IIIa is irradiated with light of predominantly 300–400 nm are shown in Fig. 1. It is clear that the loss of IIIa can be measured in the presence of its acridine photoproduct IV. Figure 2 shows that a plot of the increase in absorbance at 255 nm *versus* the loss of absorbance at 282 nm is linear

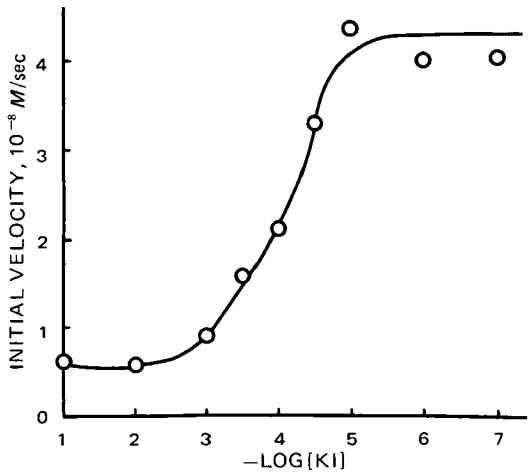

Figure 7—*Effect of potassium iodide on the riboflavin-catalyzed (5×10^{-5} M Ia) anaerobic photodecomposition (visible light) of IIIa (5×10^{-5} M).*

[6] Melting points were taken in a Fisher-Johns apparatus and are uncorrected. Compound IIIa exhibited a melting point at 203–206°.

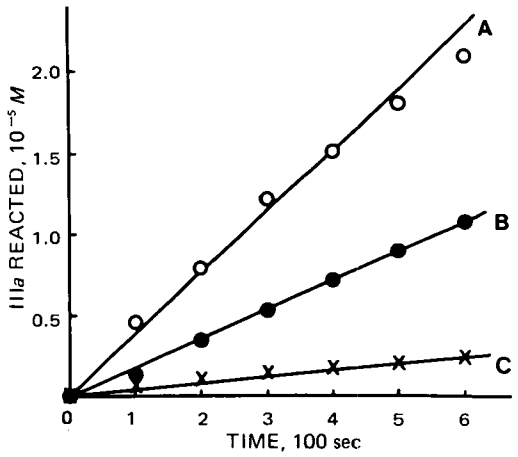

Figure 8—*Effect of quenchers of riboflavin phosphate (Ia, 5×10^{-5} M) photodecomposition (visible light) of IIIa (5×10^{-5} M). Key: A, IIIa and Ia, anaerobic; B, IIIa and Ia, aerobic; and C, IIIa, Ia, and 10^{-2} M KI, anaerobic.*

and that the slope (10:1) corresponds to the ratio of the molar absorptivity of IV (1.7×10^5) at 255 to the molar absorptivity of IIIa (1.6×10^4) at 282. The isolated photoproduct (IV) was shown through comparison of UV and IR spectra and TLC to be identical with an authentic sample of IV.

As seen from Fig. 3, the presence of the acridine photoproduct catalyzes the photodecomposition of IIIa in the absence of oxygen. To avoid the complication of product catalysis of the reaction, all rate data were obtained during the first 6.4% of decomposition of IIIa, where concentration of the photoproduct was such that it did not influence the reaction rate.

Compound IIIa was stable to visible light in the absence of riboflavin. However, in the presence of riboflavin, there was photodecomposition of IIIa as indicated by a loss of absorbance at 292 nm, an isosbestic point for riboflavin and reduced riboflavin (9) (Fig. 4). Although riboflavin is notoriously light sensitive (11–13), the photodecomposition of riboflavin was markedly inhibited by IIIa. Riboflavin loss due to photoreduction was insignificant relative to loss of IIIa, and the photolysis of IIIa proceeded to completion with IIIa concentrations 100 times those of riboflavin. Therefore, the riboflavin-catalyzed photooxidation of IIIa is not a coupled oxidation–reduction involving production of reduced flavin. There also was no spectral evidence for complex formation between riboflavin and IIIa, since spectra for mixtures of riboflavin and IIIa exhibit the expected additivity (Fig. 5).

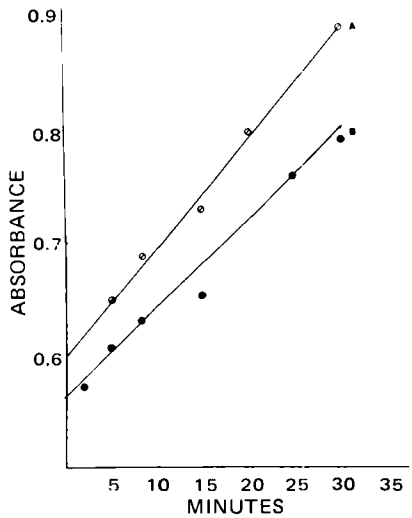

Figure 9—*Rate of appearance of photoproduct IV (at 252 nm) upon anaerobic irradiation of III with filtered sunlamp light. Key: A, 1×10^{-4} M IIIa; and B, 1×10^{-4} M IIIb.*

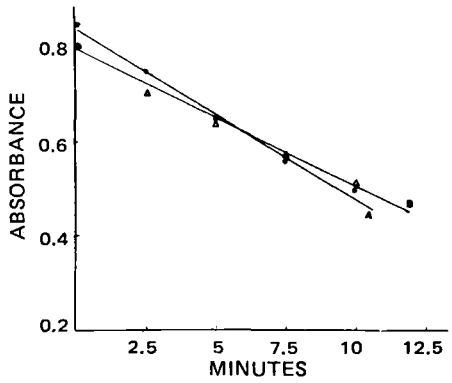

Figure 10—*Rate of disappearance of III (at 292 nm) in presence of Ia upon anaerobic irradiation with filtered sunlamp light. Key: A, 5 × 10⁻⁵ M IIIa and 5 × 10⁻⁵ M Ia; and B, 5 × 10⁻⁵ M IIIb and 5 × 10⁻⁵ M Ia.*

The rate of anaerobic photodecomposition of IIIa, at an initial concentration of 1×10^{-5} *M*, was directly proportional to riboflavin concentration up to about 1.0×10^{-4} *M* flavin (Fig. 6). At flavin concentrations above 1×10^{-4} *M*, concentration quenching of a flavin excited state (14) led to less efficient catalysis.

Fluorescence spectra of 5×10^{-5} *M* riboflavin in the presence of up to 1×10^{-4} *M* IIIa show no evidence of quenching of the riboflavin singlet state by IIIa. Figure 7 illustrates the inhibition of the riboflavin-catalyzed anaerobic photooxidation by 10^{-4} *M* iodide ion, a concentration of iodide recognized as effective in quenching riboflavin triplet species, but not shorter-lived riboflavin singlet species, in a 10^{-4}–10^{-5} *M* riboflavin solution (15). Inhibition of the photooxidation by oxygen, as shown in Fig. 8, also is explicable as oxygen quenching of a triplet excited state of riboflavin.

On the basis of these observations, the following mechanism is proposed to account for the influence of riboflavin on IIIa photodecomposition. Ground-state riboflavin (Ia^0) absorbs visible light and is promoted to a singlet excited state (Ia) (Scheme IV). Riboflavin triplet (Ia^3) species are generated *via* radiationless transition from the singlet (Scheme IV); energy transfer occurs between the riboflavin triplet and ground state of $IIIa^0$ with generation of the $IIIa^3$ triplet and ground-state riboflavin (Scheme V). The $IIIa^3$ triplet may then undergo decomposition to its oxidized form IV (Scheme VI).

Compound IIIa and its deuterated derivative IIIb (deuterium atom at 9-position of the acridan nucleus) were exposed to filtered visible light under anaerobic conditions. The rate of production of IV from both isomers was nearly identical; *i.e.*, it failed to exhibit a kinetic isotope effect (Fig. 9). Similarly, no kinetic isotope effect was noticed when IIIa and IIIb were exposed to anaerobic irradiation with filtered visible light in the presence of 5×10^{-5} *M* Ia (Fig. 10). These results show that the elimination of hydrogen from III, which results in its conversion to photoproduct IV (Scheme VI) in the presence and absence of Ia is a kinetically fast step.

Walsh *et al.* (6) found that in the D-amino acid oxidase-catalyzed conversion of β-chloroalanine to β-chloropyruvate, substitution of the α-hydrogen of the former by deuterium or tritium results in kinetic isotope effects which slow down its conversion to pyruvate. The work of these investigators suggests that the conversion of chloroalanine to pyruvate by D-amino acid oxidase, a riboflavin-dependent enzyme, involves an intermediate similar to II in which the α-hydrogen of the substrate is removed as a proton. Furthermore, this step is rate determining in the formation of the intermediate. The absence of the deuterium isotope effect in the photocatalyzed conversion of IIIa and IIIb to IV indicates that an intermediate such as V is not involved in the rate-determining step of the reaction.

Furthermore, the results indicate that the photooxidation does not involve a covalent bond catalysis with Ia in the manner represented by Structure II.

$$Ia^0 \underset{\text{fluorescence}}{\overset{h\nu}{\rightleftharpoons}} Ia^1 \rightarrow Ia^3$$

Scheme IV

$$Ia^3 + IIIa^0 \rightarrow Ia^0 + IIIa^3$$

Scheme V

$$IIIa^3 \rightarrow IV + H_2$$

Scheme VI

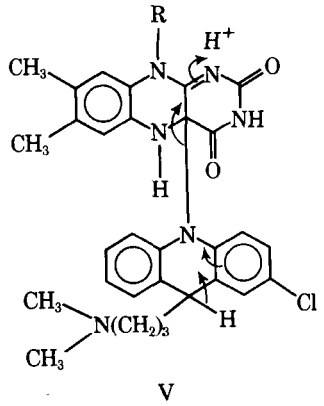

V

REFERENCES

(1) L. E. Brown and G. A. Hamilton, *J. Amer. Chem. Soc.*, **92**, 7225(1970).

(2) W. P. Jencks, "Catalysis in Chemistry and Enzymology," McGraw-Hill, New York, N.Y., 1969, p. 42.

(3) P. Hemmerich, V. Massey, and G. Weber, *Nature*, **213**, 728(1967).

(4) W. R. Knappe and P. Hemmerich, *FEBS Lett.*, **13**, 293(1971).

(5) V. Massey, F. Muller, R. Feldberg, M. Schuman, P. A. Sullivan, L. G. Howell, S. G. Mayhen, R. G. Matthews, and G. P. Foust, *J. Biol. Chem.*, **244**, 3999(1969).

(6) C. T. Walsh, A. Schonbrunn, and R. H. Abeles, *J. Biol. Chem.*, **246**, 6855(1971).

(7) M. A. Miyamoto, H. B. Kostenbauder, D. Walstad, and G. A. Digenis, *FEBS Lett.*, **7**, 101(1970).

(8) G. A. Digenis, D. L. Walstad, M. Ishaque, and M. I. H. Aleem, *Biochem. Pharmacol.*, **20**, 919(1971).

(9) H. Beinert, in "The Enzymes," vol. II, part A, 2nd ed., P. D. Boyer, H. Lardy, and K. Myrback, Eds., Academic, New York, N.Y., 1960, p. 379.

(10) G. A. Digenis, *J. Pharm. Sci.*, **58**, 335(1969).

(11) O. Warburg and W. Christian, *Naturwissenschaften*, **20**, 980(1932).

(12) G. Oster, J. S. Bellin, and B. Holmstrom, *Experientia*, **18**, 249(1962).

(13) H. Beinert, in "The Enzymes," vol. II, part A, 2nd ed., P. D. Boyer, H. Lardy, and K. Myrback, Eds., Academic, New York, N.Y., 1960, p. 356.

(14) Q. H. Gibson, V. Massey, and N. M. Atherton, *Biochem. J.*, **85**, 369(1962).

(15) J. Posthuma and W. Berends, *Biochim. Biophys. Acta*, **122**, 422(1966).

ACKNOWLEDGMENTS AND ADDRESSES

Received March 12, 1975, from the *College of Pharmacy, University of Kentucky, Lexington, KY 40506*

Accepted for publication May 13, 1975.

* Present address: Arab Pharmaceutical Manufacturing Co., Salt, Jordan.

‡ Present address: Sumitomo Chemical Co., Ltd., Osaka, Japan.

ˣ To whom inquiries should be directed.

Solution Thermodynamics of Alkyl *p*-Aminobenzoates

PETER A. SCHWARTZ and ANTHONY N. PARUTA ˣ

Abstract □ Equilibrium solubilities of the first four homologous alkyl *p*-aminobenzoate esters were determined in methanol, ethanol, and 1-propanol at 25, 33, and 40°; the esters and the alcohols comprise separate homologous series. The solution process of a solute may be considered to be the summation of two sequential steps, melting and mixing, and the magnitude of solubility depends upon temperature and the extent of interactions between solute and solvent molecules. Quantitative solute concentrations, obtained from spectrophotometric analysis, were converted to mole fractions. Statistical analysis of the logarithmic mole fraction solubilities of the aminobenzoates, which were linear with respect to both reciprocal absolute temperature and the logarithm of absolute temperature, generated enthalpies and entropies of solution, respectively. The heats of fusion and the melting points of these aminobenzoates were determined to calculate their ideal solubilities. Excess free energies and partial molal free energies of each solution were calculated from the activity coefficients of the solutes; the thermodynamic elements for these systems are discussed.

Keyphrases □ *p*-Aminobenzoates—equilibrium solubilities of four alkyl esters in alcohols, solution thermodynamics □ Thermodynamics, solution—four alkyl *p*-aminobenzoate esters, equilibrium solubilities in alcohols

Solubility results principally from interactions between solute and solvent molecules (1). The extent of these interactions, *i.e.*, the magnitude of solubility, depends partially upon the polarity and the hydrogen bonding characteristics of the solution components with respect to each other and to themselves; it depends also on the temperature of the system.

Solutes studied included four normal alkyl *p*-aminobenzoate esters (methyl, ethyl, propyl, and butyl), chosen because these esters comprise a series differing in structure from each other by one methylene (CH_2) group. The solvents were methanol, ethanol, and 1-propanol; this homologous series was chosen because it would provide a range of solvent polarity. The equilibrium solubilities of each solute in these solvents were determined at several temperatures to provide enthalpies and entropies of solution with respect to fundamental thermodynamic relationships.

BACKGROUND

The solubility of nonelectrolytes has often been interpreted on the basis of polarity differences between solutes and solvents (2–9). An incremental increase in the length of a hydrocarbon side chain effects a polarity difference between consecutive members of a homologous series. These structural differences result in altered physical properties such as boiling-point elevation, increased partition coefficient (lipid solubility), decreased aqueous solubility, and increased surface tension.

Since many properties of a homologous series change according to a geometric progression (10), the plot of the logarithm of these properties against the carbon number of the nonpolar hydrocarbon chain is linear. Solubility studies (11) on the first four homologs of the alkyl *p*-aminobenzoate esters demonstrated such linearity for semilogarithmic plots of solubility in silicone oil and hexane, two nonpolar solvents, as well as of their partition coefficients with water against alkyl carbon numbers. The solubility increased with alkyl carbon number equal to four and decreased thereafter. The heats of fusion, melting points, and solubility parameters were used to generate expected values for molar solubility, all of which agreed well with the experimental values for hexane. However, poor agreement was found with experimental data for water, a polar, hydrogen-bonding solvent.

The similar series of homologous esters, alkyl *p*-hydroxybenzoates, was studied (3, 4) in several alcohols, *i.e.*, polar, hydrogen-bonding solvents. The Hildebrand and Scott (5) solubility parameter theory was used to predict the points of maximum solubility in each solvent. However, the magnitude of solubility depends upon specific solute–solvent interactions (6) and is not always predictable.

Solubility is a colligative property and is related to the temperature-dependent thermodynamic equation for freezing-point depression (12). At any temperature, the concentration of pure solid solute is constant and is in equilibrium with the liquid state. The solution process is considered to occur in two steps as shown in Scheme I:

$$\text{solid solute} \xrightarrow{\text{melting}} \text{liquid solute} \xrightarrow{\text{mixing}} \text{solute in solution } (X_2)$$

Scheme I

where X_2 is the solute mole fraction. The enthalpy change for melting is the heat of fusion, ΔH^F, and the enthalpy for the second step is the heat of mixing, ΔH^M (12). For ideal solutions, the enthalpy of the second step is zero, since, by definition, no heat is evolved or absorbed (13).

The equation for the ideal mole fraction solubility of a solute, X_2^i, at a temperature below its melting point, T_m, is given in terms of the natural logarithm of the solubility, *i.e.*:

$$\ln X_2^i = \frac{-\Delta H^F}{R}\left(\frac{1}{T} - \frac{1}{T_m}\right) \qquad \text{(Eq. 1)}$$

when it is assumed that the heat of fusion is constant with respect to temperature, and the gas constant, R, equals 1.987 cal/degree. The solubility at any given temperature should be the same for all solvents with which it forms an ideal solution. From Eq. 1, it is apparent that a solute with a low heat of fusion and a low melting point will have a high ideal solubility, that the solubility of a solute increases as the melting point decreases, and that solubility appears to be independent of the nature of the solvent.

Hildebrand and Scott (14) equated the activity of a solute, a_2, with X_2^i for ideal solutions. The activity is a relative quantity and represents the deviation from a designated reference state. The most useful standard state for solubility is one in which the pure liquid solute, extrapolated below the melting point as a supercooled liquid (15), has a value of unity when its mole fraction is unity. The ratio of the activity to the mole fraction is the activity coefficient, γ, *i.e.*:

$$\gamma = a/x \qquad \text{(Eq. 2)}$$

Because the activity varies with composition, the activity coefficients, which remain relatively constant, are more suitable parameters for expressing deviations from ideal solutions.

Equation 1 is valid only when the heat of fusion is constant with respect to temperature. From the heat of fusion at the melting point, $\Delta H_m{}^F$, and the change in molal heat capacity between liquid and solid solute, ΔC_P, also extrapolated below the melting point, the heat of fusion at any temperature can be derived (16):

$$\Delta H^F = \Delta H_m{}^F - \Delta C_P(T_m - T) \qquad \text{(Eq. 3)}$$

Substitution of this heat expression in Eq. 1 gives the following for ideal mole fraction solubility:

$$\ln X_2^i = [\Delta H_m{}^F/R(T_m - T/T_m T)] + [\Delta C_P/R(T_m - T/T)]\,[\Delta C_P/R(\ln T_m/T)] \qquad \text{(Eq. 4)}$$

For the ideal solution, the plot of the natural logarithm of the mole fraction solubility, $\ln X_2$, *versus* the reciprocal of the abso-

Table I—Structure and Thermal Properties of Alkyl *p*-Aminobenzoate Esters

Ester[a]	Melting Point: Literature	Melting Point: Capillary Tube	Melting Point: Differential Scanning Calorimetry	Heats of Fusion, cal/mole	Entropy of Fusion, cal/mole deg
Methyl	112°[b], 114°[c]	110.5–111°	112.5°	5180	13.5
Ethyl	89°[d], 90°[c], 92°[b]	88–90°	89.7°	5030	13.9
n-Propyl	73°[d], 73–74°[b], 75°[c]	73–74°	73.0°	5000	14.5
n-Butyl	57°[d], 58°[b,c]	56–58°	55.8°	5290	16.1

[a] C. O. Wilson, O. Gisvold, and R. F. Doerge, "Textbook of Organic, Medicinal and Pharmaceutical Chemistry," 5th ed., Lippincott, Philadelphia, Pa., 1966, p. 602. [b] "Dictionary of Organic Compounds," 4th rev., Oxford University Press, New York, N.Y., 1065. [c] "Handbook of Chemistry and Physics," 51st ed., Chemical Rubber Co., Cleveland, Ohio, 1970. [d] R. Adams, E. K. Rideal, W. B. Burnett, R. L. Jenkins, and E. E. Dreger, *J. Amer. Chem. Soc.*, 48, 1758 (1926).

lute temperature, $1/T$, has a slope proportional to the heat of fusion at the melting point and an intercept proportional to the entropy of fusion, *i.e.*, $\Delta H_m^F/T_m$. Data from nonideal solutions plotted in this manner have slopes and intercepts proportional to the differential heats and entropy of solution, respectively (12).

Hildebrand and Scott (17) showed that the heat capacity is not negligible and can be approximated by the entropy of fusion. Substitution of ΔS_m^F for ΔC_P in Eq. 4 cancels out the first two terms on the right side and leaves the ideal mole fraction solubility equation as:

$$\ln X_2^i = (\Delta S_m^F/R)(\ln T/T_m) \qquad \text{(Eq. 5)}$$

Accordingly, a plot of $\ln X_2$ *versus* the natural logarithm of the absolute temperature, $\ln T$, is linear with a slope proportional to the entropy of fusion. For nonideal data, the entropy of solution can be obtained from the slope of this line (18).

Since orienting and chemical effects, such as hydrogen bonding, solvation, and association, are absent in regular solutions (19) and molecules are randomly distributed as in ideal solutions, the two types of solutions have equal entropies. The deviation from ideality for a regular solution represents the magnitude of the enthalpy of mixing, since no heat is evolved in the formation of an ideal solution.

The free energy, F, represents the maximum of work that can be obtained from a process and applied to useful purposes (20). At equilibrium, the total free energy is at a minimum (21) with no separation of enthalpic and entropic components (22). Nonideal solutions have an excess free energy of mixing, which can be regarded as "the excess of the nonideal free energy of mixing over the ideal free energy of mixing" (23); *i.e.*, in terms of free energy:

$$\bar{F}^E = RT \ln \gamma_2 \qquad \text{(Eq. 6)}$$

A partial molal quantity is defined as "the rate of increase in the content of the system in that particular quantity while the component is being added to the system" (24). However, Hildebrand and Scott (25) warned that the physical property of partial molal quantities cannot be attributed to molecules of one species alone and that it is a property of the solution as a whole—not of the particular component.

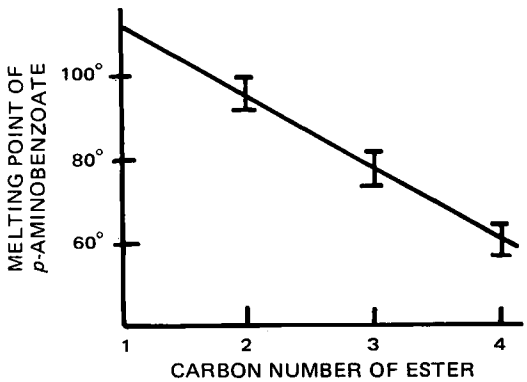

Figure 1—*Plot of the range of melting points for the alkyl* p-*aminobenzoate esters as a function of the alkyl carbon number of the ester.*

The log γ_2 term for the excess free energy of regular solutions is due to the intermolecular forces of the solute and solvent that are not present in ideal solutions. These forces can be characterized by considering the solubility parameters of the solute and solvent, the volume fraction of the solvent, ϕ_1, and the molar volume of the solute, V_2, so that the deviation from the ideal is:

$$\ln \gamma_2 = (\delta_1 - \delta_2)^2 V_2 \phi_1^2/RT \qquad \text{(Eq. 7)}$$

Since the solubility parameter is a measure of polarity, the greater the differences in polarity between solute and solvent, the greater is the deviational term of the activity coefficient.

Entropy is related to structure (12) and indicates the probability of a combination between solute and solvent. An increased entropy of solution denotes a more probable state for such a system than do the separate pure solute and solvent. As the degree of randomness and disorder for a system increases, the entropy increases, but the free energy decreases. For example, at increased temperatures there is more randomness, *i.e.*, increased entropy, while the amount of useful work or free energy is diminished. For alcohols in solution with nonpolar components, there is a decreased entropy due to specific interactions, *i.e.*, ordering due to hydrogen bonding, and large positive deviations from ideality are expected (26).

Highly nonideal solubility with such large entropy terms cannot be calculated from Eqs. 1–7 and are best calculated in terms of free

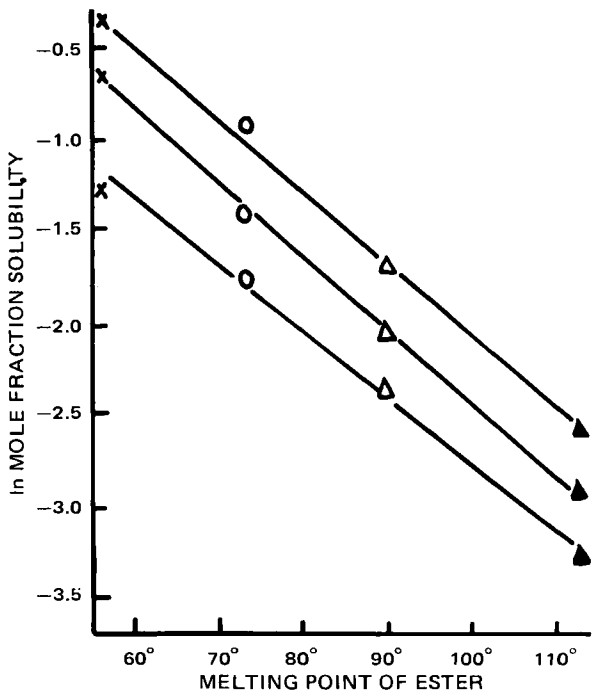

Figure 2—*Plot of the ln mole fraction solubility in methanol versus the melting point of the aminobenzoate ester at the three temperatures noted. Key:* ▲, *methyl* p-*aminobenzoate;* △, *ethyl* p-*aminobenzoate;* O, *propyl* p-*aminobenzoate; and* ×, *butyl* p-*aminobenzoate.*

Table II—Average Mole Fraction Solubilities of Alkyl *p*-Aminobenzoate Esters in Each Solvent at 25, 33, and 40°

Ester	Temperature	Solvent			Ideal A[a]	Ideal B[b]
		Methanol	Ethanol	1-Propanol		
Methyl	25°	0.0367	0.0419	0.0306	0.1369	0.1752
	33°	0.0524	0.0545	0.0428	0.1722	0.2096
	40°	0.0730	0.0740	0.0586	0.2084	0.2442
Ethyl	25°	0.0945	0.0895	0.0836	0.2195	0.2539
	33°	0.1256	0.1276	0.0953	0.2741	0.3054
	40°	0.1811	0.1843	0.1455	0.3299	0.3576
n-Propyl	25°	0.1709	0.1634	0.1826	0.3100	0.3376
	33°	0.2402	0.2177	0.2485	0.3866	0.4093
	40°	0.4016	0.4018	0.3680	0.4648	0.4825
n-Butyl	25°	0.2779	0.2212	0.2544	0.4319	0.4507
	33°	0.5247	0.4319	0.3705	0.5457	0.5586
	40°	0.7030	0.6220	0.6205	0.6632	0.6709

[a] Calculated from Eq. 1. [b] Calculated from Eq. 5.

Table III—Enthalpies and Entropies of Alkyl *p*-Aminobenzoates in Alcohols

Ester	Solvent	Enthalpy, cal/mole			Entropy, cal/mole deg				
		ΔH_s	$\Delta H_m{}^F$	ΔH^{Ma}	$\Delta S_s{}^b$	$\Delta S_m{}^F$	ΔS^{Mc}	$S_s{}^d$	$S_s{}^d/S_s{}^b$
Methyl	Methanol	8,470	5180	3280	21.9	13.5	8.4	27.7	1.27
	Ethanol	7,000	5180	1810	17.2	13.5	3.7	22.9	1.34
	1-Propanol	7,990	5180	2800	19.9	13.5	6.4	26.2	1.34
Ethyl	Methanol	7,990	5030	2960	22.1	13.9	8.2	26.2	1.19
	Ethanol	8,900	5030	3870	25.1	13.9	11.2	29.2	1.16
	1-Propanol	6,710	5030	1680	17.5	13.9	3.6	22.1	1.26
n-Propyl	Methanol	10,460	5000	5460	31.5	14.5	17.0	34.3	1.09
	Ethanol	10,970	5000	5970	33.1	14.5	18.6	36.0	1.09
	1-Propanol	8,610	5000	3610	25.5	14.5	11.0	28.2	1.15
n-Butyl	Methanol	11,570	5290	6280	36.3	16.1	20.2	37.8	1.04
	Ethanol	12,850	5290	7560	40.2	16.1	24.1	42.1	1.01
	1-Propanol	10,940	5290	5650	33.9	16.1	17.8	35.9	1.06

[a] $H^M = H_S - H_m{}^F$. [b] R times intercept of $\ln X_2$ *versus* $1/T$. [c] $S^M = S_S - S_m{}^F$. [d] R times intercept of $\ln X_2$ *versus* $\ln T$.

energies. This approach avoids serious errors of oversimplification and does not separate enthalpic and entropic effects (22).

EXPERIMENTAL[1]

Chemicals—The following chemicals were used: methyl *p*-aminobenzoate[2]; ethyl *p*-aminobenzoate[3]; propyl *p*-aminobenzoate[4]; butyl *p*-aminobenzoate[5]; methanol, anhydrous, spectrophotometric grade solvent[6]; absolute alcohol USP, reagent quality[7]; 1-propanol[8]; ethanol[9] 95%, USP grade; stearic acid[10], 99.8% pure; and water, distilled and deionized.

Calorimeter Calibration—The calorimeter cell of a differential scanning calorimeter, used to determine heats of fusion, was calibrated with stearic acid, 99.8% pure. Three samples of the acid, in amounts empirically chosen to produce endothermic fusion peaks of maximum area, were accurately weighed (±0.002 mg) on an electrobalance into tared aluminum pans. The pans were subsequently sealed to prevent volatilization.

The samples were heated in a nitrogen atmosphere in the calorimeter cell over a temperature range of 60–75° at a heating rate of 5°/min and at a chart recording speed of 304.8 cm (120 in.)/min. Each sample was melted twice, and calibration constants were calculated from only those curves having essentially straight baselines for both pre- and postfusion.

The value of $H_m{}^F$, the heat absorbed by a sample during fusion, is proportional to the area under the curve defined by the endothermic peak and by a line drawn between the point of departure from the baseline (onset of fusion) to the point of baseline return after fusion (27). The thermograms generated by the samples were reproduced on paper of a uniform thickness, and each area was carefully cut out and weighed (28). The stearic acid calibration coefficient, 0.0641969 (0.0642), is the average of the determinations from each sample calculated according to the following equation:

$$K = \frac{H_{sa}{}^F M}{Wr} \qquad \text{(Eq. 8)}$$

where:

K = calibration coefficient, millicalories per milligram of paper
$H_{sa}{}^F$ = heat of fusion for stearic acid, −47.54 mcal/mg
M = weight of stearic acid sample, milligrams
W = weight of stearic acid sample, milligrams of paper
r = power coefficient of the instrument

Because the instrument does not provide readings in Celsius degrees, the fusion endotherms of stearic acid were used to determine a calibration constant for temperature correction. The melting point for a solid is best represented by the extrapolation to the prefusion baseline of its endotherm (28). The known melting point of 68.82° was subtracted from the average value of the instrument readings for the onset of fusion for stearic acid to produce a correction constant of 378.4°.

Melting-Point Determinations—The average of the two calorimeter melting points for each aminobenzoate ester was converted to Celsius melting points by subtracting the temperature correction constant. Since there was a close agreement in melting points

[1] The following equipment was used: Thomas-Hoover capillary melting-point apparatus, No. 6404, A. H. Thomas Co., Philadelphia, Pa.; Cary model 16 spectrophotometer, Cary Instruments, Monrovia, Calif.; Precision-Porta-Temp unit, Precision Scientific Co., Chicago, Ill.; Mettler balance, type H6T, Mettler Instrument Corp., Princeton, N.J.; rotating sample holder with small motor, Department of Pharmacy, University of Rhode Island; Pyrex Corning glass wool, Corning Glass Works, Corning, N.Y.; Cahn gram electrobalance, model 18, Cahn Instruments, Paramount, Calif.; and Perkin-Elmer differential scanning calorimeter, DSC-18, Perkin-Elmer Corp., Instrument Division, Norwalk, Conn.

[2] Lot 3403, Eastman Chemical Co., Rochester, N.Y.

[3] Lot EX 305, Matheson, Coleman and Bell, Norwood, Ohio.

[4] Lot 3, City Chemical Co., supplied through the courtesy of Astra Pharmaceutical Products, Worcester, Mass.

[5] Lot 7, Matheson, Coleman and Bell, Norwood, Ohio.

[6] Lot VNM, Mallinckrodt Chemical Works, St. Louis, Mo.

[7] U.S. Industrial Chemicals Co., New York, N.Y.

[8] Analyzed reagent, Lot 39420, J.T. Baker Chemical Co., Phillipsburg, N.J.

[9] Lot TM 288671, Industrial Chemicals Co., Littleton, Mass.

[10] Applied Sciences, State College, Pa.

Table IV—Ideal, Actual, and Excess Free Energy of Alkyl *p*-Aminobenzoates in Alcohols

Ester	Solvent	Free Energy, cal/mole ΔF^A	ΔF^I	ΔF^E
Methyl	Methanol	1790	1063	+727
	Ethanol	1754	1063	+691
	1-Propanol	1920	1063	+863
Ethyl	Methanol	1250	790	+460
	Ethanol	1244	790	+454
	1-Propanol	1372	790	+582
n-Propyl	Methanol	852	577	+275
	Ethanol	874	577	+297
	1-Propanol	832	577	+255
n-Butyl	Methanol	498	379	+119
	Ethanol	587	379	+210
	1-Propanol	600	379	+221

between experimental and literature values for the esters, these compounds were used directly and without further purification. The purity of the solutes was accepted from the label claiming greater than 99.8% in all cases, since the melting point of these materials did not differ from ethanolic recrystallized samples of these solutes.

Heats of Fusion—Samples of the four aminobenzoate esters were carefully weighed into aluminum volatile sample pans, and thermograms of a 10° prefusion baseline and a fusion endotherm were recorded. Because direct remelts of the same sample indicated an apparent formation of liquid crystals after fusion, each fused sample was cooled to 0° for 30 min prior to remelting. Recordings were analyzed for melting points and endothermic areas in the same manner as for stearic acid.

Solubility Determinations—The solubility of the four aminobenzoate esters in several alcohols and water was determined by the following procedure. Each solute, in an amount in excess of its solubility, was placed in screw-capped glass vials[11] with each solvent. The vials were sealed with adhesive tape. Vials were rotated at 28 rpm in a large constant-temperature (±0.2°) water bath maintained successively at 25, 33, and 40°.

After an equilibrium solubility was attained by at least 24 hr of continuous rotation[12], each of six[13] sample vials was removed in succession for assay. The exterior of the vial was quickly dried, the sealing tape was removed, and the cap was carefully unscrewed to prevent water contamination. A filtered aliquot of the saturated solution was pipetted into tared containers, weighed, and appropriately diluted for spectrophotometric assay with 95% ethanol to give a final concentration of solute in the range of 1–5 μg/ml. All pipets were prewarmed to prevent thermal precipitation, and each had a pledget of fiber glass wrapped around its tip to act as a filter. The variation in solubility values was about 5% for the methyl derivatives and fell to about 3% for the butyl derivative.

Spectrophotometric Determination—The spectrophotometer was calibrated for each aminobenzoate ester at its wavelength of maximum absorbance, at concentrations up to 15 μg/ml in 95% ethanol, in matched silica cells. A least-squares method was used to determine the statistical significance ($\alpha = 0.0001$) of the linear relationship between absorbance and concentration, *i.e.*, the Beer's law equation.

The molar absorptivities for the esters were very close in value, varying from 2.05 for the methyl, ethyl, and propyl esters to 2.07 for the butyl ester.

RESULTS AND DISCUSSION

The chemical structures of the alkyl *p*-aminobenzoate esters and their thermal properties are shown in Table I. Experimentally determined differential scanning calorimetric and capillary tube melting points in Table I agree well with literature values shown there and are the same as those recently reported (11). The heats of fusion show the same trend as do the Yalkowsky *et al.* (11) data; *i.e.*, enthalpies for the methyl and butyl esters are higher than for the ethyl and propyl esters.

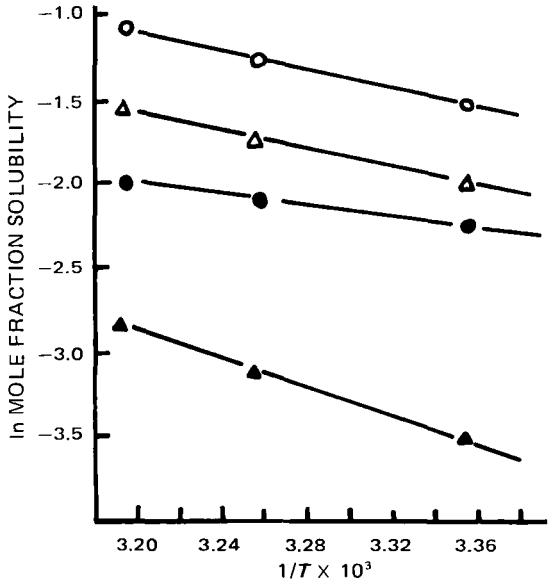

Figure 3—*Plot of the ln mole fraction solubility in 1-propanol versus the reciprocal temperature, °K. The ideal curves are from heat of fusion data, and the actual curves are from experimental data. Key: ○, ethyl p-aminobenzoate, ideal; ●, ethyl p-aminobenzoate, actual; △, methyl p-aminobenzoate, ideal; and ▲, methyl p-aminobenzoate, actual.*

The average mole fraction solubilities of these esters in methanol, ethanol, and 1-propanol and the ideal solubilities predicted by both Eqs. 3 and 7 at 25, 33, and 40° are summarized in Table II and show an expected direct relationship between the magnitude of solubility and the temperature for each solvent.

In Fig. 1, the melting-point range for the alkyl *p*-aminobenzoates is plotted *versus* the alkyl carbon number. This relationship is approximately linear and reflects a regularity on the structural differences between homologs.

Figure 2 shows a plot of the $\log_e$ mole fraction solubility in methanol at the three temperatures studied *versus* the melting points of the solutes. The decrease in solubility at any temperature is linear with increasing melting point for carbon numbers less than or equal to four. The parallelism observed for the three temperatures indicates similar solute–solvent interactions and a constant dissolution mechanism for these solutes.

In Fig. 3, the ln X_2 in 1-propanol for each solute is plotted *versus* the ln T at the temperatures studied. The heats of fusion, heats of solution, and heats of mixing were obtained from the slopes of the lines generated from observed and calculated data as shown in Fig. 3. The entropy of fusion, entropy of solution, and entropy of mixing were obtained as intercepts of Figs. 3 and 4.

The entropies of solution in Table III were determined from a least-squares analysis of the mole fraction data in Table II. The value of $S_s{}^b$ was obtained from the intercepts of ln X_2 *versus* the reciprocal absolute temperature shown graphically in Fig. 3 for 1-propanol solutions. The Hildebrand entropy of solution, $S_s{}^d$, was obtained from the slopes of ln X_2 *versus* the natural logarithm of the absolute temperature, shown graphically in Fig. 4 for 1-propanol solutions. These graphs are similar to the graphs of the other alcohol solutions and were chosen as representative examples of the solute behavior.

Hildebrand's entropy of solution for the solid solutes, $S_s{}^d$, which includes the heat of fusion of the solute, has values several entropy units (calories per mole degree) higher than the corresponding values of entropy of solutions, $S_s{}^b$ (Table III). However, Hildebrand applied a correction factor to his experimental data from solutions with mole fractions greater than 0.1, *i.e.*, good solvents (29). The "Henry's law" factor (the change in solute activity per change in solute mole fraction) could not be calculated for the aminobenzoates because the solutions were not considered dilute systems. Thus, the Hildebrand entropy of solution values are uncor-

[11] Lined with Teflon.

[12] Previous studies showed that this time was sufficient to obtain saturated solutions at 25°.

[13] Only three samples of propyl *p*-aminobenzoate were used because of its scarcity.

Table V—Activity Coefficients for Alkyl *p*-Aminobenzoates Based upon the Ideal Solubilities from Eq. 3

Ester	Temperature	Solvent: Methanol	Ethanol	1-Propanol
Methyl	25°	3.7	3.3	4.5
	33°	3.3	3.2	4.0
	40°	2.8	2.8	3.6
Ethyl	25°	2.3	2.5	2.6
	33°	2.2	2.2	2.9
	40°	1.8	1.8	2.3
n-Propyl	25°	1.8	1.9	1.7
	33°	1.6	1.8	1.6
	40°	1.2	1.2	1.3
n-Butyl	25°	1.6	2.0	1.7
	33°	1.0	1.3	1.5
	40°	1.0	1.1	1.1

Table VI—Partial Molal Excess Free Energies Calculated from the Activity Coefficients of Alkyl *p*-Aminobenzoates

Ester	Temperature	Solvent: Methanol	Ethanol	1-Propanol
Methyl	25°	−34	−30	−40
	33°	−40	−38	−48
	40°	−44	−43	−55
Ethyl	25°	−33	−36	−40
	33°	−39	−38	−60
	40°	−35	−33	−55
n-Propyl	25°	−30	−34	−25
	33°	−29	−39	−26
	40°	−5	−5	−12
n-Butyl	25°	−30	−58	−41
	33°	−1	−16	−38
	40°	−2	−2	−3

rected, and actual values of the entropy of solution, S_s^d, would be less than those given in Table III.

The diminishing difference between the two values for entropy of solution as the alkyl chain length increases is shown by the decrease in the ratio S_s^d/S_s^b in Table III. Since the two values of the ideal solubilities from Eqs. 1 and 5 in Table II are reasonably close, the ideal values from Eq. 1 were chosen as a basis for comparison in the activity coefficient determinations. The choice of the entropy of solution obtained from plots of Eq. 1, ln X_2 *versus* $1/T$, was due to its conventional and generally accepted use.

The maximum entropy of solution within a group of solvents denotes the best solvent for that solute, and comparison between groups illustrates the effect of the alcohols upon the solubility of each ester. As the solute alkyl chain length increases, the molecules become less polar and the entropy of solution increases. Although the methyl ester, the most polar of these solutes (11), has a maximum entropy in methanol, the most polar alcohol, all other esters have their entropic maxima in ethanol, a less polar solvent.

The heats of solution in Table III can be compared with the heats of fusion in Table I to show that a positive heat of mixing, ΔH_{mix}, was generated for all solutions in the alcohols and that the magnitudes of these heats increased as the alkyl chain length increased. This excess heat above ideal also showed the most increase in methanol for the methyl ester and in ethanol for all other esters, *i.e.*, the same result observed for the entropy of solution data.

Since values for the entropy and heat of solution are determined as averages over a narrow temperature range, they do not reflect the temperature change upon the solubility parameters or the dielectric constant of the solutes. This objection limits the usefulness of separate entropic or enthalpic interpretations of solubility (22).

From the values presented in Table III, various free energy values can be calculated. Table IV presents the ideal, actual, and excess free energies for each solute in each solvent. As expected from the solubility data, the excess free energies decrease with increasing size. The closer the ideal and actual free energies, the smaller are the excess free energy terms and the actual mole fraction solubility approaches the ideal mole fraction solubility.

The activity coefficients in Table V are based upon the ideal mole fraction solubilities of Eq. 1 and were used to calculate the partial molal excess free energy of the solutes (Table VI). Since the activity coefficients are high for the methyl ester (2.82–4.47) and decrease progressively to near unity for the butyl ester (1.96–0.95), the excess free energies also decrease proportionally. Although free energies near zero were obtained for several butyl solutions at high temperatures, the high entropy of solution values indicate increased molecular disorder and prevent these from being classed as regular solutions.

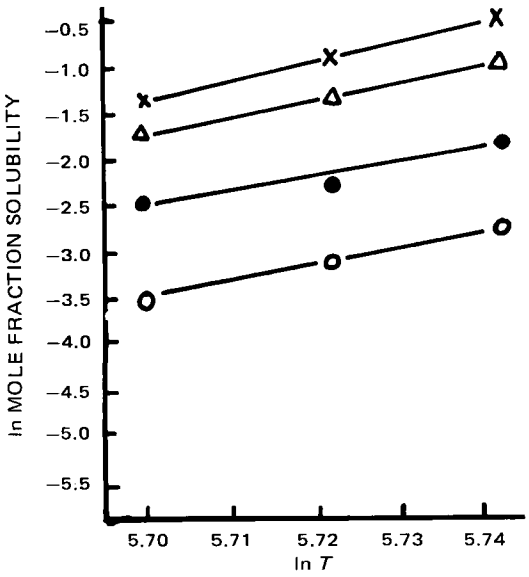

Figure 4—*Plot of the ln mole fraction solubility in 1-propanol for each solute as a function of the ln temperature, °K. Key:* ×, *butyl* p-*aminobenzoate;* △, *propyl* p-*aminobenzoate;* ●, *ethyl* p-*aminobenzoate; and* ○, *methyl* p-*aminobenzoate.*

SUMMARY

The magnitudes of the solubility of these esters dissolved in the normal alcohols increased with increased temperatures, indicative of an endothermic dissolution process. The conventional relationship between the natural log mole fraction data and the reciprocal temperature was linear for all solutions and produced values for the enthalpy and entropy of solution. The Hildebrand entropy of solution values were obtained from the linear relationship between the natural log mole fraction solubility and the log of the absolute temperature. The Hildebrand entropy values include the heat capacity of the solute.

Thermodynamic data for the aminobenzoates dissolved in the normal alcohols indicate increased entropy of solution as the alkyl chain length increases. There was no significant difference between the conventional entropy of solution values and the Hildebrand entropy of solution values.

The butyl ester was highly soluble in the alcohols. From the heat of fusion and the melting-point data determined for these solutes, their ideal mole fraction solubilities were calculated. Activity coefficients of the solutes compare ideal to actual solubilities and were used to calculate partial molal excess free energies. These free energies were near zero in some cases, but the high entropy of solution values for these solutions do not indicate regular solutions.

REFERENCES

(1) T. Higuchi, in "Pharmaceutical Compounding and Dispensing," R. Layman, Ed., Lippincott, Philadelphia, Pa., 1949, chap. 7.

(2) M. Sax and J. Pletcher, *Science*, **166**, 1546(1969).

(3) F. A. Restaino and A. N. Martin, *J. Pharm. Sci.*, **53**, 636(1964).

(4) A. N. Paruta, *ibid.*, **58**, 216(1969).

(5) J. H. Hildebrand and R. L. Scott, "The Solubility of Nonelectrolytes," 3rd ed., Reinhold, New York, N.Y., 1949.
(6) A. N. Paruta, B. J. Sciarrone, and N. G. Lordi, *J. Pharm. Sci.*, **53**, 1349(1964).
(7) M. J. Chortkoff and A. N. Martin, *J. Amer. Pharm. Ass., Sci. Ed.*, **49**, 444(1960).
(8) W. G. Gorman and G. D. Hall, *J. Pharm. Sci.*, **53**, 1017(1964).
(9) J. H. Hildebrand, J. M. Prausnitz, and R. L. Scott, "Regular and Related Solutions," Van Nostrand Reinhold, New York, N.Y., 1970.
(10) J. Ferguson, *J. Proc. Roy. Soc. (Ser. B)*, **127**, 397(1939).
(11) S. H. Yalkowsky, G. L. Flynn, and T. G. Slunick, *J. Pharm. Sci.*, **61**, 853(1972).
(12) B. H. Mahan, "Elementary Chemical Thermodynamics," W. A. Benjamin, New York, N.Y., 1963, chap. 4.
(13) J. H. Hildebrand and R. L. Scott, "The Solubility of Nonelectrolytes," 3rd ed., Reinhold, New York, N.Y., 1949, p. 47.
(14) J. H. Hildebrand and R. L. Scott, "Regular Solutions," Prentice Hall, Englewood Cliffs, N.J., 1962, p. 132.
(15) *Ibid.*, p. 13.
(16) *Ibid.*, p. 270.
(17) *Ibid.*, p. 20.
(18) J. H. Hildebrand, J. M. Prausnitz, and R. L. Scott, "Regular and Related Solutions," Van Nostrand Reinhold, New York, N.Y., 1970, p. 144.
(19) J. H. Hildebrand, *J. Amer. Chem. Soc.*, **51**, 66(1929).
(20) G. N. Lewis and M. Randall, "Thermodynamics," McGraw-Hill, New York, N.Y., 1923, p. 158.
(21) J. H. Hildebrand and R. L. Scott, "The Solubility of Nonelectrolytes," 3rd ed., Reinhold, New York, N.Y., 1949, p. 44.
(22) *Ibid.*, p. 136.
(23) J. H. Hildebrand, J. M. Prausnitz, and R. L. Scott, "Regular and Related Solutions," Van Nostrand Reinhold, New York, N.Y., 1970, p. 17.
(24) J. H. Hildebrand and R. L. Scott, "The Solubility of Nonelectrolytes," 3rd ed., Reinhold, New York, N.Y., 1949, p. 5.
(25) *Ibid.*, p. 14.
(26) *Ibid.*, p. 218.
(27) J. K. Guillery, *J. Pharm. Sci.*, **56**, 72(1967).
(28) R. Reubke and J. A. Mollica, *J. Pharm. Sci.*, **56**, 822(1967).
(29) A. E. Lewis, "Biostatistics," Reinhold, New York, N.Y., 1966, p. 76.

ACKNOWLEDGMENTS AND ADDRESSES

Received March 20, 1974, from the *College of Pharmacy, University of Rhode Island, Kingston, RI 02881*

Accepted for publication May 9, 1975.

Abstracted in part from a dissertation submitted by P. A. Schwartz to the Graduate School, University of Rhode Island, in partial fulfillment of the Master of Science degree requirements.

[x] To whom inquiries should be directed.

Simultaneous Determination of Pilocarpine and Isopilocarpine in Pharmaceutical Preparations by Liquid Chromatography

T. URBÁNYI [x], A. PIEDMONT, E. WILLIS, and G. MANNING

Abstract □ A liquid chromatographic assay method is described for the simultaneous determination of pilocarpine and isopilocarpine in pharmaceutical preparations. The method involves separation of the isomers on a high-resolution ion-exchange column, followed by detection of pilocarpine and isopilocarpine by UV absorption in the 217-nm region. The specificity of the method is such that pilocarpine and isopilocarpine can be assayed separately in the presence of one another and in the presence of the excipients commonly found in commercial pilocarpine solutions. Its sensitivity for isopilocarpine is at least 25 ppm (independent of the concentration of pilocarpine). In contrast, USP methods lack both specificity and sensitivity. It is concluded that this method is applicable to the routine analysis of commercial pilocarpine preparations and is an improvement over the official methods.

Keyphrases □ Pilocarpine—chromatographic separation and UV analysis, pharmaceutical preparations, in presence of isopilocarpine, compared to USP methods □ Isopilocarpine—chromatographic separation and UV analysis, pharmaceutical preparations, in presence of pilocarpine, compared to USP methods □ Chromatography—separation of pilocarpine and isopilocarpine in pharmaceutical preparations □ UV analysis—pilocarpine and isopilocarpine in pharmaceutical preparations

It is almost a century since the pilocarpine alkaloid was isolated from the plant *Pilocarpus microphyllus* Stapf (1), and its highly effective therapeutic application for glaucoma (2) treatment was soon realized. After the isolation of pilocarpine, its structure was well defined. However, the isolated alkaloid contains an inactive stereoisomer, which is not purely an artifact formed during the isolation process but occurs in the natural plant (3).

The common isomer is isopilocarpine, differing from pilocarpine only in the position of the ethyl substitution at the α-carbon on the lactone ring. Isopilocarpine has been reported to be therapeutically inactive (4). A literature review revealed only one paper reporting the determination of isopilocarpine (5). Isopilocarpine is thermodynamically more stable than pilocarpine in most environments (5) and readily forms from pilocarpine upon heating or in neutral or alkaline solutions (4, 6).

DISCUSSION

The lactone ring in pilocarpine is very labile (7); even under mild conditions, it can be opened, forming another inactive product, pilocarpic acid. While pilocarpic acid can be detected by the official methods (8–10), neither isomerization to isopilocarpine nor differentiation from pilocarpine in pharmaceutical preparations has been reported until now.

(5) J. H. Hildebrand and R. L. Scott, "The Solubility of Nonelectrolytes," 3rd ed., Reinhold, New York, N.Y., 1949.
(6) A. N. Paruta, B. J. Sciarrone, and N. G. Lordi, *J. Pharm. Sci.*, **53**, 1349(1964).
(7) M. J. Chortkoff and A. N. Martin, *J. Amer. Pharm. Ass., Sci. Ed.*, **49**, 444(1960).
(8) W. G. Gorman and G. D. Hall, *J. Pharm. Sci.*, **53**, 1017(1964).
(9) J. H. Hildebrand, J. M. Prausnitz, and R. L. Scott, "Regular and Related Solutions," Van Nostrand Reinhold, New York, N.Y., 1970.
(10) J. Ferguson, *J. Proc. Roy. Soc. (Ser. B)*, **127**, 397(1939).
(11) S. H. Yalkowsky, G. L. Flynn, and T. G. Slunick, *J. Pharm. Sci.*, **61**, 853(1972).
(12) B. H. Mahan, "Elementary Chemical Thermodynamics," W. A. Benjamin, New York, N.Y., 1963, chap. 4.
(13) J. H. Hildebrand and R. L. Scott, "The Solubility of Nonelectrolytes," 3rd ed., Reinhold, New York, N.Y., 1949, p. 47.
(14) J. H. Hildebrand and R. L. Scott, "Regular Solutions," Prentice Hall, Englewood Cliffs, N.J., 1962, p. 132.
(15) *Ibid.*, p. 13.
(16) *Ibid.*, p. 270.
(17) *Ibid.*, p. 20.
(18) J. H. Hildebrand, J. M. Prausnitz, and R. L. Scott, "Regular and Related Solutions," Van Nostrand Reinhold, New York, N.Y., 1970, p. 144.
(19) J. H. Hildebrand, *J. Amer. Chem. Soc.*, **51**, 66(1929).
(20) G. N. Lewis and M. Randall, "Thermodynamics," McGraw-Hill, New York, N.Y., 1923, p. 158.
(21) J. H. Hildebrand and R. L. Scott, "The Solubility of Nonelectrolytes," 3rd ed., Reinhold, New York, N.Y., 1949, p. 44.
(22) *Ibid.*, p. 136.
(23) J. H. Hildebrand, J. M. Prausnitz, and R. L. Scott, "Regular and Related Solutions," Van Nostrand Reinhold, New York, N.Y., 1970, p. 17.
(24) J. H. Hildebrand and R. L. Scott, "The Solubility of Nonelectrolytes," 3rd ed., Reinhold, New York, N.Y., 1949, p. 5.
(25) *Ibid.*, p. 14.
(26) *Ibid.*, p. 218.
(27) J. K. Guillery, *J. Pharm. Sci.*, **56**, 72(1967).
(28) R. Reubke and J. A. Mollica, *J. Pharm. Sci.*, **56**, 822(1967).
(29) A. E. Lewis, "Biostatistics," Reinhold, New York, N.Y., 1966, p. 76.

ACKNOWLEDGMENTS AND ADDRESSES

Received March 20, 1974, from the *College of Pharmacy, University of Rhode Island, Kingston, RI 02881*

Accepted for publication May 9, 1975.

Abstracted in part from a dissertation submitted by P. A. Schwartz to the Graduate School, University of Rhode Island, in partial fulfillment of the Master of Science degree requirements.

[x] To whom inquiries should be directed.

Simultaneous Determination of Pilocarpine and Isopilocarpine in Pharmaceutical Preparations by Liquid Chromatography

T. URBÁNYI [x], A. PIEDMONT, E. WILLIS, and G. MANNING

Abstract □ A liquid chromatographic assay method is described for the simultaneous determination of pilocarpine and isopilocarpine in pharmaceutical preparations. The method involves separation of the isomers on a high-resolution ion-exchange column, followed by detection of pilocarpine and isopilocarpine by UV absorption in the 217-nm region. The specificity of the method is such that pilocarpine and isopilocarpine can be assayed separately in the presence of one another and in the presence of the excipients commonly found in commercial pilocarpine solutions. Its sensitivity for isopilocarpine is at least 25 ppm (independent of the concentration of pilocarpine). In contrast, USP methods lack both specificity and sensitivity. It is concluded that this method is applicable to the routine analysis of commercial pilocarpine preparations and is an improvement over the official methods.

Keyphrases □ Pilocarpine—chromatographic separation and UV analysis, pharmaceutical preparations, in presence of isopilocarpine, compared to USP methods □ Isopilocarpine—chromatographic separation and UV analysis, pharmaceutical preparations, in presence of pilocarpine, compared to USP methods □ Chromatography—separation of pilocarpine and isopilocarpine in pharmaceutical preparations □ UV analysis—pilocarpine and isopilocarpine in pharmaceutical preparations

It is almost a century since the pilocarpine alkaloid was isolated from the plant *Pilocarpus microphyllus* Stapf (1), and its highly effective therapeutic application for glaucoma (2) treatment was soon realized. After the isolation of pilocarpine, its structure was well defined. However, the isolated alkaloid contains an inactive stereoisomer, which is not purely an artifact formed during the isolation process but occurs in the natural plant (3).

The common isomer is isopilocarpine, differing from pilocarpine only in the position of the ethyl substitution at the α-carbon on the lactone ring. Isopilocarpine has been reported to be therapeutically inactive (4). A literature review revealed only one paper reporting the determination of isopilocarpine (5). Isopilocarpine is thermodynamically more stable than pilocarpine in most environments (5) and readily forms from pilocarpine upon heating or in neutral or alkaline solutions (4, 6).

DISCUSSION

The lactone ring in pilocarpine is very labile (7); even under mild conditions, it can be opened, forming another inactive product, pilocarpic acid. While pilocarpic acid can be detected by the official methods (8–10), neither isomerization to isopilocarpine nor differentiation from pilocarpine in pharmaceutical preparations has been reported until now.

The official methods—optical rotation for the drug substance and colorimetric methods (9) for pharmaceutical preparations—lack selectivity and specificity. These methods do not discriminate isopilocarpine. Although formulations containing isopilocarpine have a lower optical rotation than those with pure pilocarpine, this method is not sensitive enough for isopilocarpine determination and is not applicable to pharmaceutical formulations. Additionally, a decrease in the optical rotation does not show which degradation products are formed. The colorimetric test is specific for pilocarpine so long as the lactone ring is intact; it differentiates pilocarpine from pilocarpic acid, its decomposition product.

It was observed in this study that the primary degradation product of pilocarpine was not pilocarpic acid but its isomer, isopilocarpine. The experiments showed that isomerization occurred fairly easily at elevated temperatures. Isomerization is known to proceed with increasing pH as well as with buffer effect (11, 12). Since the commercially available ophthalmic solutions analyzed were mostly in buffered solution and had variable pH values, some isomerization probably occurred.

The goal of this study was to develop a suitable, sensitive method that would improve the specificity of the official method. The proposed method is based on chromatographic separation of isopilocarpine and pilocarpine in the presence of various commonly used excipients in aqueous solutions. Isopilocarpine and pilocarpine are detected by their UV absorption at about 217 nm where their absorbances are identical. The method can be adopted for pilocarpine and isopilocarpine determination in commercial ophthalmic formulations, even where extremely high sensitivities are desired. In routine analysis, the proposed method has a sensitivity of 25 ppm for either pilocarpine or isopilocarpine in pharmaceutical formulations.

EXPERIMENTAL

Reagents and Solutions—The following were used: pilocarpine nitrate USP, isopilocarpine nitrate[1] (reagent grade), tromethamine[2] (ultrapure grade), cation-exchange resin[3], and reagent grade isopropanol, sulfuric acid, hydrochloric acid, methylene chloride, and ether.

Chromatography—For the elution method, the resin was placed in a glass column[4] (6 mm i.d. × 10 cm) packed by the slurry technique; the mobile phase was used to prepare the slurry. The column was washed thoroughly with the mobile phase until an optimum stable baseline was obtained.

A 0.2 *M* tromethamine buffer solution was prepared in distilled water. Then 5% isopropanol was added, and the pH was adjusted to 9 with sulfuric acid.

The flow rate during the elution was adjusted to 0.4 ml/min, and a pressure of 200 ± 100 psi was maintained. As conditioning proceeds, a slight increase in pressure and resolution may be observed.

A liquid chromatograph equipped with a suitable high or low pressure pump[5], a detector[6], and a recorder[7] were used. The detector was a variable wavelength spectrophotometer equipped with 8-μl flowcells of 1-cm pathlength. A pH meter[8] was used also.

Other column materials, sizes, and flow rates may be used so long as adequate resolution is obtained; a column "bed volume" of 2.8–3.0 cm^3 is normally required for separation. The assay time can be reduced by utilizing a larger bore or a shorter column or by changing the flow rates and the pressure.

Standard Preparation—USP pilocarpine nitrate reference standard and isopilocarpine nitrate (reagent grade) were accurately weighed into separate volumetric flasks and then dissolved and diluted to volume with water to obtain solutions containing 3–4 mg/ml of pilocarpine. To prepare a standard calibration curve, the two solutions were mixed accurately and proportionally, thus providing various concentrations of isopilocarpine. Fifty microliters was then injected by means of an injection loop on the column, and the chromatogram was recorded.

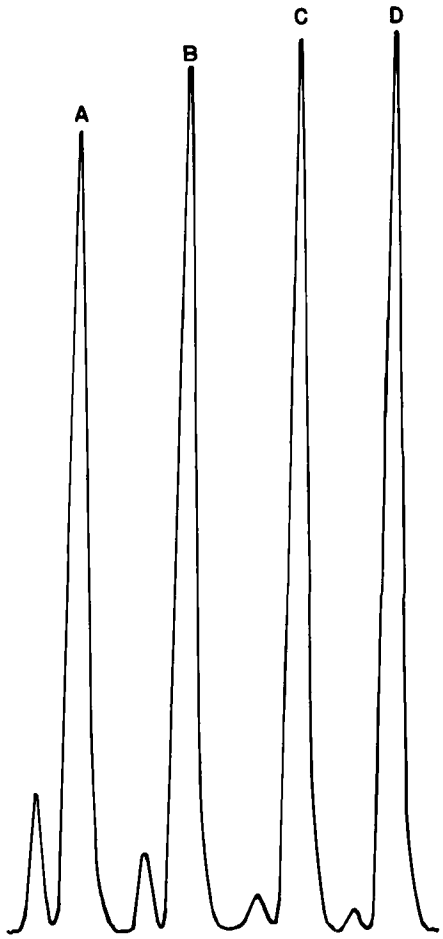

Figure 1—*Synthetic mixtures of pilocarpine adulterated with (A) 10, (B) 5, (C) 2, and (D) 1% isopilocarpine. Retention times are 45 and 38 min, respectively.*

Preparation of Commercial Products—Aliquots of commercially used ophthalmic solutions were accurately pipetted into separate containers and diluted with water to obtain about 3–4 mg of pilocarpine/ml. These solutions (50 μl) were injected in the same manner as the standard preparation, and the chromatograms were recorded.

Ocular Therapeutic Systems Containing Pilocarpine—In an ocular therapeutic system[9], pilocarpine is surrounded by a rate-controlling polymer membrane. Therefore, an extraction procedure was employed to liberate the pilocarpine. One or two systems were placed in a small centrifuge tube in 1 ml of methylene chloride to dissolve the polymer membrane. Then 3.0 ml of 0.1 *N* sulfuric acid was added, and the pilocarpine was extracted for a few minutes. Fifty microliters from the aqueous phase was withdrawn and injected on the column, and the chromatogram was recorded.

RESULTS

A suitable method that shows specificity and sensitivity for the determination of a pure substance and/or pharmaceutical preparation has always been a primary requirement of analytical chemistry. The various pilocarpine methods in the literature all lack specificity. Under certain mild conditions, pilocarpine undergoes isomerization. The existing methods are unable to detect the isomerized product, which is a main degradation product not only of the drug substance but of commercial products as well. Therefore, an attempt was made to develop a technique that would allow the determination of pilocarpine in the presence of isopilocarpine and vice versa.

[1] Aldrich Chemical Co.
[2] Tris buffer solution, Aldrich Chemical Co.
[3] Aminex A-7, sulfonated styrene divinylbenzene copolymer with 8% divinyl benzene cross-linking, particle size of 7–11 μm, Bio-Rad Laboratories.
[4] Chromatronic.
[5] Water Associates model M-6000.
[6] Schoeffel model 770.
[7] Texas Instrument Inc.
[8] Radiometer model 26.
[9] Ocusert, Alza Corp.

Table I—Determination of Total Pilocarpine and Isopilocarpine in a Mixture by USP Colorimetric Method[a]

Isopilocarpine–Pilocarpine Ratio	Total Isopilocarpine and Pilocarpine Weight, mg	Total Pilocarpine Found, mg	Recovery, %
Pure isopilocarpine	2.26	1.82 ± 0.02	80.5
1:4	2.05	1.99 ± 0.02	97.1
1:1	2.07	1.81 ± 0.02	87.5

[a] All tests were performed in duplicate.

Various concentrations of pilocarpine and isopilocarpine standard solutions were chromatographed using the recommended column and buffer solution. Figure 1 shows a fairly good resolution and linear relation between the two compounds.

To illustrate the validity of the proposed method, Fig. 2 demonstrates the separation of isopilocarpine from pilocarpine in a sample and the absence of isopilocarpine in USP pilocarpine nitrate reference standard. It is evident from these curves that sufficient resolution is obtained with the specified conditions; the method is adequate for the quantitative determination of pilocarpine in the presence of isopilocarpine.

To demonstrate that the official method is not specific enough for the determination of isopilocarpine, pure isopilocarpine and isopilocarpine in a mixture with pilocarpine were analyzed by the official colorimetric method. The reaction rate of hydroxylamine hydrochloride with isopilocarpine was slower than with pilocarpine. When using the official method, only 80% of the isopilocarpine was recovered. The recovery was not improved with an increased reaction time; but when the concentration of the reagent was doubled, the isopilocarpine was fully recovered. The data obtained on pure isopilocarpine and on mixtures with pilocarpine by the official method are summarized in Table I. One can see from this table that the total recovery of pilocarpines increased significantly with the increase of pilocarpine.

The data collected in Table II clearly show that the official method does not differentiate between the pilocarpine isomers and that the liquid chromatographic method shows significant differences in pilocarpine and isopilocarpine content. To prove the efficacy of the proposed method, several commercial ophthalmic solutions with the manufacturer's information (such as the name, formulation, and content) were analyzed for pilocarpine by the official colorimetric method and simultaneously for pilocarpine and isopilocarpine by the chromatographic method (Table III). The pH of these solutions was determined using a combination glass electrode.

It was observed that some ophthalmic formulations (C and D) could not be analyzed by the official method and gave very high assays; no significant interferences were observed with the chromatographic method. When the USP method was modified so that the extraction solvent was changed from ether to methylene chloride, normal results were obtained, indicating that the interfering substances were removed by methylene chloride but not by ether.

To date, no substance including pilocarpic acid has been found to interfere with the new method. Furthermore, since the ophthal-

Table II—Determination of Pilocarpine Content in Synthetic Mixtures with Isopilocarpine by the Official and Liquid Chromatographic Methods

	Pilocarpine and Isopilocarpine Assay[a]		
		Chromatographic	
Solution	USP	Pilocarpine	Isopilocarpine
49.7% pilocarpine and 50.3% isopilocarpine	90.0% ± 1.0	49.4% ± 0.4	50.6% ± 0.4
74.7% pilocarpine and 25.3% isopilocarpine	95.2% ± 0.9	74.8% ± 0.3	25.2% ± 0.4

[a] Average from duplicate determinations.

Table III—Comparison of USP and Liquid Chromatographic Methods for the Determination of Pilocarpine and Isopilocarpine in Commercial Products

					USP Method			Liquid Chromatographic Method			
Manufacturer	Salt	Pilocarpine Declared, mg/ml	pH	Expiration Date	Extracting Solvent	Total Pilocarpine Found, mg/ml	Recovery, %	Isopilocarpine, mg/ml	Pilocarpine, mg/ml	Recovery, %	Isopilocarpine in Total Pilocarpine, %
A	HNO_3	20	5.3	—	Ether	13.6	68.0	3.6	10.7	71.5	25.2
B	HCl	20	4.2	2/78	Ether	20.3	101.5	0.5	19.7	101.0	2.5
C	HNO_3	10	4.8	7/77	Ether	20.3	203.0	0.1	11.3	114.0	0.9
C		10	4.8		Methylene chloride	10.3	103.0				
D	HNO_3	40	4.6	6/77	Ether	49.7	124.3	0.5	43.8	110.0	1.1
D		40	4.6		Methylene chloride	44.3	110.8				
E	HCl	5	4.5	—	Ether	4.9	98.0	0.1	4.7	96.0	2.1
F	HCl	10	4.4	—	Ether	10.1	101.0	0.4	10.1	105.0	3.8
G	HCl	40	4.5	5/78	Ether	39.7	99.3	0.9	39.0	99.8	2.3
Ocular system[a]	Base	5.0	—	5/76	Methylene chloride	4.86	97.2	0.05	4.84	97.8	1.0

[a] Milligrams per system.

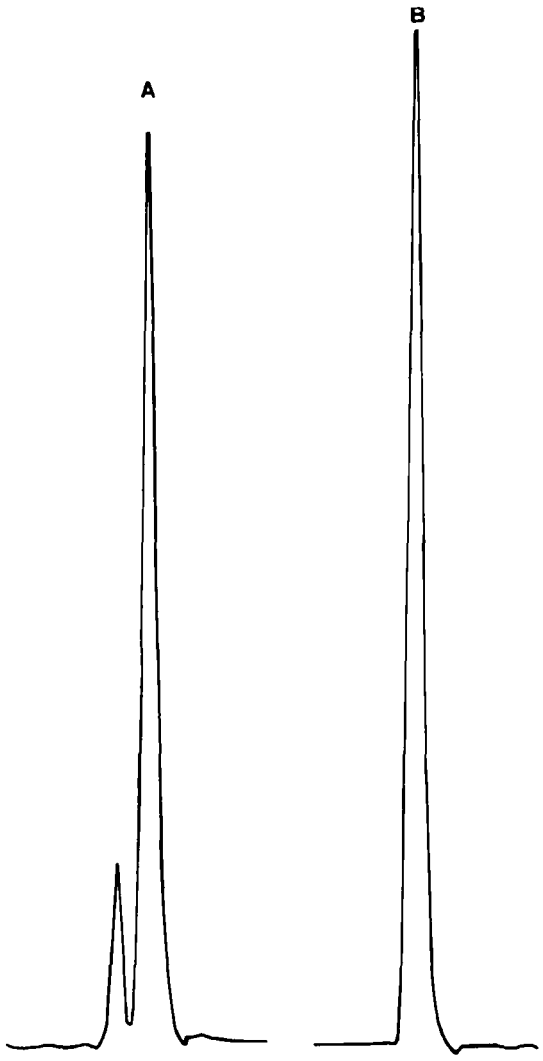

Figure 2—*Comparison of a commercial sample containing isopilocarpine (A) to USP pilocarpine nitrate reference standard (B).*

mic solutions can be injected directly onto the column, the analysis is simpler than with the USP method, a great advantage in everyday routine assay. Table III clearly indicates that the proportion of isomer tends to be higher when pH values are higher.

From Tables I–III, it is obvious that the official method does not discriminate between pilocarpine and isopilocarpine content. It is also evident that the official method is not suitable for total isopilocarpine and pilocarpine determination because of reaction rate differences between the two compounds.

A further study was carried out to fill the gap caused by the official method and to separate the two compounds quantitatively. The official method was compared with the liquid chromatographic method for the analysis of mixtures where the ratio of pilocarpine and isopilocarpine varied. These observations have already been mentioned. However, the official method was unable to differentiate between the two pilocarpine isomers and, unfortunately, its values depended on isopilocarpine concentration. The liquid chromatographic method distinguished the pilocarpine from the isopilocarpine with true and accurate results.

The pilocarpine and isopilocarpine values presented so far in this paper were based on ophthalmic solutions where the buffer effect and the storage conditions greatly affected the isomerization. Data are now presented for an ocular therapeutic system where the alkaloid was not in aqueous buffered solutions but in a semisolid form, enclosed by rate-controlling polymeric membranes. Accelerated stability studies showed that isomerization took place in this system with increasing temperature and time. Since the rate of delivery of the active drug was in the microgram range and this amount regulated the effectiveness of the product, the determination of its inactive degradation product was a critical problem from the analytical standpoint. The linearity and stability of pilocarpine and isopilocarpine were demonstrated in the figures. A plot of these values showed that concentrations of pilocarpine in the 0–100-μg range resulted in a straight line that followed Beer's law. A similar plot was obtained for isopilocarpine in the region of 0–6 μg. The extraction procedure was necessary to eliminate the excess polymer which ruins the column in continuous assays, consequently increasing the pressure and diminishing the resolution.

The method described in this paper was applied to ophthalmic solutions and ocular therapeutic systems. However, with a slight modification, this method can be applied to other pilocarpine formulations. The method has been used in these laboratories as a routine test with great success and accuracy.

SUMMARY AND CONCLUSION

A novel and specific method for the simultaneous determination of pilocarpine and isopilocarpine in various pharmaceutical formulations is presented. The procedure is based on a liquid chromatographic separation, followed by spectrophotometric analysis. The chromophoric groups of pilocarpine and isopilocarpine are the same; the absorbances of the two compounds in the range of measurement are similar. This similarity makes possible the quantitative determination of pilocarpine relative to isopilocarpine. The measurement can be performed by peak areas or by peak heights from the same chromatogram.

The proposed method is applicable for pure substances and/or pharmaceutical preparations containing various excipients. The method is sensitive at the microgram level required for low dose formulations. The specificity of the proposed method provides great improvement over the official and other published methods for pilocarpine analysis and is convenient for routine use. The limits of detection are approximately 0.1 μg of isopilocarpine in the presence of 100 μg of pilocarpine or vice versa.

REFERENCES

(1) "The Merck Index," 7th ed., Merck & Co., Inc., Rahway, N.J., 1960, p. 818.

(2) W. H. Havener, "Ocular Pharmacology," 3rd ed., C. V. Mosby, New York, N.Y., 1964, p. 262.

(3) R. A. Anderson and F. B. Cowle, *Brit. J. Ophthalmol.*, **52**, 607(1965).

(4) R. K. Hill and S. Barcza, *Tetrahedron*, **22**, 2889(1966).

(5) A. Mathews, A. Nunes, and E. Brochmann-Hanssen, *J. Pharm. Sci.*, **63**, 716(1974).

(6) W. Dopke and G. d'Heureuse, *Tetrahedron Lett.*, **1968**, 1807.

(7) P. H. Chung, T. F. Chin, and J. L. Lach, *J. Pharm. Sci.*, **59**, 1300(1970).

(8) T. Higuchi and E. Brochmann-Hanssen, "Pharmaceutical Analysis," Interscience, New York, N.Y., 1961, chap. 18.

(9) "The United States Pharmacopeia," 18th rev., Mack Publishing Co., Easton, Pa., 1970, pp. 505–507.

(10) I. S. Gibbs and M. M. Tuckerman, *J. Pharm. Sci.*, **59**, 395(1970).

(11) C. J. Blok, *Pharm. J.*, **155**, 282(1945).

(12) R. A. Anderson and S. D. Fitzgerald, *Australas. J. Pharm.*, **48**, S108(1967).

ACKNOWLEDGMENTS AND ADDRESSES

Received March 19, 1975, from the *Analytical Research and Development Department, Alza Research, Division of Alza Corporation, Palo Alto, CA 94304*

Accepted for publication May 15, 1975.

[x] To whom inquiries should be directed.

Electron Beam Ionization Mass Fragmentographic Analysis of Tricyclic Antidepressants in Human Plasma

JOHN T. BIGGS ˣ, WILLIAM H. HOLLAND, SIDNEY CHANG, PAUL P. HIPPS, and WILLIAM R. SHERMAN

Abstract □ A method for the measurement, in human plasma, of all tertiary and secondary tricyclic antidepressants prescribed in the United States is described. The method uses electron beam ionization GLC–mass spectrometry, employing a computer-controlled multiple-ion detector. This method, mass fragmentography, is used with internal standards for each drug. Plasma levels to as low as 10 ng/ml of the following drugs can be measured: amitriptyline, nortriptyline, doxepin, desmethyldoxepin, imipramine, desipramine, and protriptyline. Deuterium-labeled amitriptyline and imipramine are used as internal standards for those two drugs; for the other drugs, deuterated amitriptyline, nortriptyline, desmethyldoxepin, or desipramine is used. The method can measure up to 15 samples/hr, making it practical for large-scale studies of these drugs in patients. Spectra of each drug and examples of their analysis are given.

Keyphrases □ Antidepressants, tricyclic—analysis, GLC–mass spectrometry (mass fragmentography), plasma □ GLC–mass spectrometry—analysis, tricyclic antidepressants, plasma □ Mass fragmentography—analysis, tricyclic antidepressants, plasma

One aspect of the rational treatment of depression with tricyclic antidepressants is a knowledge of the plasma level attained by the patient with a given dose. While methods for the measurement of the secondary tricyclic amines (*e.g.*, desipramine and nortriptyline) have been utilized for several years, the tricyclic antidepressants bearing tertiary amine groups on the side chain are more difficult to analyze. This paper describes studies using electron beam ionization mass fragmentography that have resulted in a rapid and general method for the measurement of all tertiary amine tricyclic antidepressants and their demethylated active metabolites used in the United States.

The use of individual mass spectral ions, selected because of their specificity for a molecule, as detectors for the gas chromatograph has become one of the most powerful modern analytical techniques. The essentials of the method were introduced in 1966 (1), and the power of the technique in the study of drugs was first demonstrated in 1968 through the identification of chlorpromazine and its metabolites in human plasma (2).

The ease of acquiring data by this method has been greatly enhanced by computer methods (3–6). The improvement of the signal by computer processing has extended the sensitivity of the method (3). In this system, the signal is sampled up to 400 times/sec, the findings are averaged to improve the signal to noise ratio, and the resulting data are stored and displayed. Finally, the increased accuracy of focusing on ions by computer control and the ability to monitor the ions sampled using the computer display have made it possible to make measurements using baseline resolution, with minimal contribution from adjacent interfering ions.

By the judicious choice of ions, selected for their intensity (sensitivity), their uniqueness to the drug being measured (selectivity), and their absence from plasma during the elution of the particular drug, the simultaneous measurement of each tricyclic drug and its internal standard is possible at the rate of 15 samples/hr. All data are stored on-line on magnetic tape and can be recalled for graphic or alphanumeric output at any time (7).

EXPERIMENTAL

GLC–Mass Spectrometry—All analyses were carried out on a gas chromatograph–mass spectrometer[1] computer[2] system, which was described previously (3). The mass spectrometric conditions were: ionizing energy, 70 ev; trap current, 60 μamp; source temperature, 270°; separator temperature, 250°; and helium carrier flow, 30 ml/min. Resolution was set to 0% valley at the masses monitored.

Silanized glass columns, 50 cm × 6 mm o.d., were packed with either 3% OV-17 or 1% SE-30 on 100–120-mesh Gas Chrom Q[3]. An injection port temperature of 230° was maintained, and column oven temperatures were varied from 180 to 220° to attain a retention time for the drugs analyzed of 2–3.5 min. The analysis of desipramine and protriptyline was carried out on SE-30, and the other drugs were chromatographed on OV-17. The electron multiplier preamplifier used in the mass fragmentography mode was modified to give approximately 30-fold greater amplification by substitution of a 10,000-Mohm resistor[4] for the standard input resistor of the preamplifier.

Reagents and Standards—Pure samples of each drug were provided by their manufacturers: amitriptyline[5], *N,N*-di-C^2H_3-amitriptyline[5], clomipramine[6], desipramine[7], desmethyldoxepin[8], doxepin[8], imipramine[6], nortriptyline[9], and protriptyline[5]. Solvents and reagents used were: nanograde petroleum ether[10], spectranalyzed carbon disulfide[11], analyzed reagent grade chloroform[12], and trifluoroacetic anhydride[13].

Derivatization of the secondary tricyclic amines (desipramine, desmethyldoxepin, nortriptyline, and protriptyline) was carried out by dissolving the drug in chloroform containing 10% trifluoroacetic anhydride. The reaction was complete in 30 min and was immediately subjected to GLC–mass spectrometry. Both desipramine and protriptyline underwent decomposition after standing in the 10% trifluoroacetic anhydride overnight. Tertiary tricyclic antidepressants were analyzed without derivatization.

Determination of Tricyclic Antidepressant Levels in Plasma—To 4 ml of heparinized plasma is added the appropriate internal standard (Table I) followed by 1 ml of 0.5 *M* NaOH. The plasma is then extracted with 10 ml of petroleum ether by shaking

[1] LKB-9000, LKB Produkter AB, Stockholm-Bromma 1, Sweden.
[2] PDP-12, Digital Equipment Corp., Maynard, Mass.
[3] Applied Science Laboratories, State College, Pa.
[4] Victoreen.
[5] Merck Sharp and Dohme, West Point, Pa.
[6] Ciba-Geigy Corp., Summit, N.J.
[7] Lakeside Laboratories, Milwaukee, Wis.
[8] Chas. Pfizer & Co., Brooklyn, N.Y.
[9] Eli Lilly and Co., Indianapolis, Ind.
[10] Mallinckrodt Chemical Co., St. Louis, Mo.
[11] Fisher Scientific Co., Fair Lawn, N.J.
[12] Baker Chemical Co., Philadelphia, Pa.
[13] Pierce Chemical Co., Rockford, Ill.

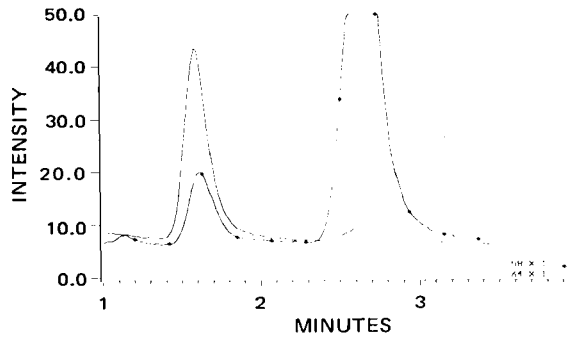

Figure 1—*Mass fragmentogram from patient plasma showing the ion intensities of amitriptyline,* m/e *58, and* N,N-*di*-C^2H_3-*amitriptyline,* m/e *64,* versus *elution time (4 ng of amitriptyline injected). The electron multiplier was operated at 2.7 kv. See text for other conditions.*

for 10 min in a shaker[14]. Occasional emulsions result, which are broken by sonication or freezing in dry ice–acetone. After centrifugation at 850×*g*, 8 ml of the organic phase is transferred to a 5-ml centrifuge tube, in two steps, and taken to dryness under a stream of nitrogen in a 60° water bath. The tubes are cooled to room temperature and rinsed down with 3 ml of petroleum ether. In the measurement of secondary amines, 0.1 ml of trifluoroacetic anhydride is added and the samples are allowed to stand for 30 min. The tubes are then rinsed down an additional three times with 0.1–0.25 ml of petroleum ether and are taken to dryness as before.

Samples are stable when stored at −20° for at least 1 week prior to analysis. At the time of analysis, the dry residue is taken up in 80 μl of carbon disulfide or chloroform and placed on ice to minimize evaporation prior to injection into the GLC–mass spectrometer. Depending on the plasma concentration of the drugs, 0.5–10 μl of the solution is chromatographed.

Dilution curves for each drug to be measured are prepared by adding various amounts of the test drug and a constant amount of the internal standard (Table I). Dilutions of 10, 50, 100, 200, and 300 ng/ml are made, in triplicate, of the free base form of the drug in 4 ml of pooled, non-drug-treated human plasma. Patient samples are similarly prepared by adding the same amount of internal standard. For overdose studies, a 1500-ng/ml sample is also prepared.

As an example, a patient treated with amitriptyline would have both that drug and its demethylated metabolite nortriptyline measured. To the patient's plasma would be added 50 ng/ml of deuterated amitriptyline and 100 ng/ml of desmethyldoxepin (Table I). After extraction and evaporation partially to dryness, trifluoroacetic anhydride would be added to derivatize the nortriptyline and desmethyldoxepin. Mass fragmentography would be carried out in two separate analyses, one for the amitriptyline–deuterated

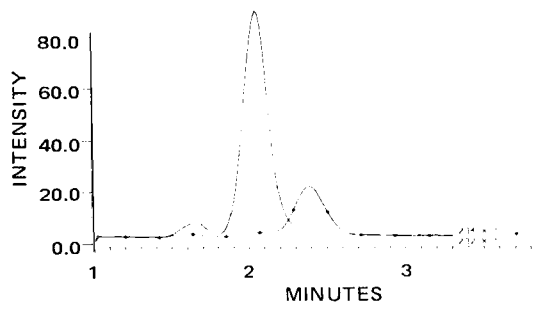

Figure 2—*Mass fragmentogram from patient plasma showing the ion intensities of* N-*trifluoroacetyl derivatives of nortriptyline,* m/e *232, and desmethyldoxepin,* m/e *234, the internal standard,* versus *elution time (8 ng of the nortriptyline derivative injected). The electron multiplier was operated at 2.5 kv. See text for other conditions.*

[14] Equipoise.

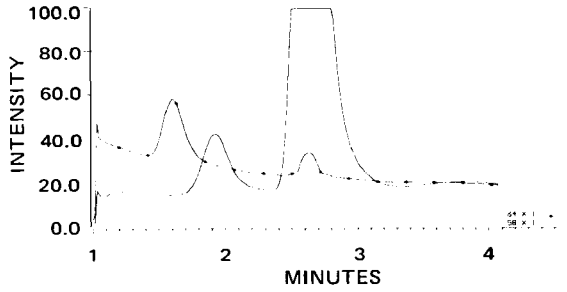

Figure 3—*Mass fragmentogram from patient plasma showing the ion intensities of doxepin,* m/e *58, and* N,N-*di*-C^2H_3-*amitriptyline,* m/e *64, the internal standard,* versus *elution time (4 ng of doxepin injected). The electron multiplier was operated at 3.5 kv. See text for other conditions.*

amitriptyline (Fig. 1) and the other for the desmethyl drugs (Fig. 2).

The determination of the concentration of each drug is made by reference to the internal standard, using the ratio of peak heights of the mass fragmentograms of the drug and internal standard. The use of area measurements did not improve the precision. Examples of these mass fragmentograms are given in Figs. 1–6. When this ratio of ion intensities is related to a dilution curve prepared as already described, the drug concentration in plasma is obtained directly. A typical standard dilution curve is illustrated in Fig. 7.

Whenever patients are on combinations of tricyclic antidepressants, internal standards for the desmethyl drugs cannot be used since the patient may be ingesting the compound used as an internal standard. In such cases, all injection and sample volumes must be carefully controlled throughout the procedure and the measurement must be made using the dilution curve and the measurement of mass fragmentographic peak heights instead of ratios to an internal standard.

RESULTS

GLC Retention Times—Table II shows the relative retention times on 3% OV-17 of the tricyclic antidepressants measured in this study. All tertiary tricyclic amines have shorter retention times than their *N*-trifluoroacetylmonomethyl counterparts, with the exception of clomipramine. For practical reasons, the *N*-trifluoroacetyl derivatives of desipramine and protriptyline are measured in patient samples using a 1% SE-30 column, resulting in better separation from plasma contaminants. Although retention times on SE-30 are shorter than on OV-17, the relative retention of these two drugs remains the same on the two columns.

Mass Spectra—*Amitriptyline (I)*—Under electron beam ionization, this drug gives one major fragment ion, *m/e* 58 (Fig. 8). In the spectrum of the *N,N*-di-C^2H_3-analog of amitriptyline, *m/e* 58 shifts to *m/e* 64. Thus, this ion results from chain fragmentation and has the structure $[CH_2{=}N(CH_3)_2]^+$ (I).

Doxepin (II)—Doxepin fragments similarly, giving even less abundant species at higher *m/e* values than amitriptyline.

Nortriptyline—As the *N*-trifluoroacetate (III), nortriptyline

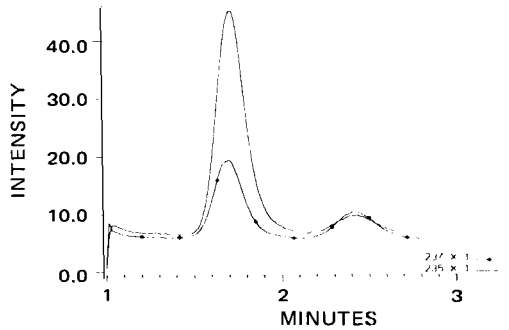

Figure 4—*Mass fragmentogram from patient plasma of imipramine,* m/e *235, and 10,10-di-*$^2H_2$-*imipramine,* m/e *237,* versus *elution time (4 ng of imipramine injected). The electron multiplier was operated at 3.5 kv. See text for other conditions.*

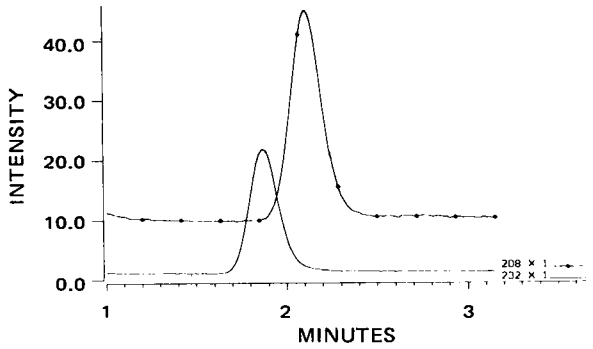

Figure 5—*Mass fragmentogram from patient plasma showing the ion intensities of the* N-*trifluoroacetyl derivatives of desipramine,* m/e *208, and nortriptyline,* m/e *232, the internal standard,* versus *elution time from the SE-30 column (4 ng of the desipramine derivative injected). The electron multiplier was operated at 2.5 kv. See text for other conditions.*

gives *m/e* 232 as the base peak (Fig. 9), which results from the loss of *N*-trifluoroacetylmethylamine from the molecular ion observed to a small extent at *m/e* 359.

Desmethyldoxepin (IV)—As the *N*-trifluoroacetyl derivative, desmethyldoxepin fragments in the same way as the nortriptyline derivative, losing *N*-trifluoroacetylmethylamine to give the base peak ion *m/e* 234 (Fig. 10).

Imipramine (V) and N-*Trifluoroacetyldesipramine (VI)*—These compounds fragment in a similar manner, as a result of the tertiary nitrogen in the tricyclic nucleus. Imipramine eliminates dimethylamine to give *m/e* 235, again the base peak. The molecular ion (*m/e* 280) is present in an abundance of 25% (Fig. 11). The spectrum of *N*-trifluoroacetyldesipramine (Fig. 12) also shows an abundant molecular ion (*m/e* 362). The ion used for analysis, *m/e* 208, results from α–β chain cleavage with charge retention, again by the tricyclic nucleus. In the spectrum of 10,10-$^2H_2$-imipramine, *m/e* 235 is shifted to *m/e* 237 as expected.

Protriptyline—As the *N*-trifluoroacetyl derivative (VII), protriptyline cleaves principally at the ring–chain juncture to give *m/e* 191, the dibenzocycloheptene ion, not surprising in its abundance (Fig. 13).

In experiments performed with the mass spectrometer source, the separator, and the chromatographic system at 180°, no noteworthy changes were seen in the spectra of amitriptyline or imipramine or of their trifluoroacetylated desmethyl counterparts. Thus, thermal effects on fragmentation, if present, are not abated at 180°.

Plasma Analysis of Tricyclic Antidepressants—*Amitriptyline*—This compound is measured by mass fragmentography monitoring *m/e* 58, and the deuterium-labeled internal standard is measured using *m/e* 64. Figure 1 shows an example of the analysis of a patient sample. The early (1.65 min) peaks are the drug and standard; the following peaks are from a plasma contaminant, well resolved chromatographically from the drug. The reliability of this analysis is surprising considering the possible substances that might have fragment ions at *m/e* 58–64. However, as the dilution curve (Fig. 7) shows from its linearity and extrapolation to zero concentration, no interfering substances are present. Typically, the standard curve has a slope of 0.011 and intercepts the ordinate at −0.072, with a correlation coefficient of 0.998. That this analysis, using electron beam ionization with its apparently unfavorable

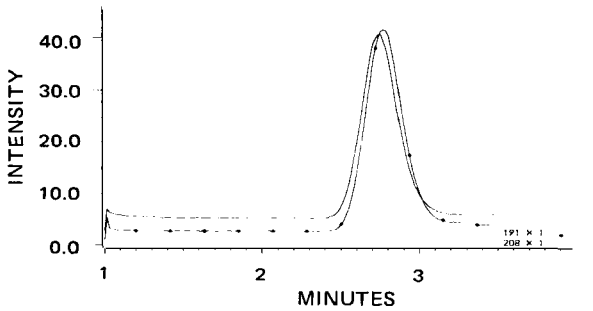

Figure 6—*Mass fragmentogram from patient plasma showing the ion intensities of the* N-*trifluoroacetyl derivatives of protriptyline,* m/e *191, and desipramine,* m/e *208, the internal standard,* versus *elution time (4 ng of the protriptyline derivative injected). The electron multiplier was operated at 2.5 kv. See text for other conditions.*

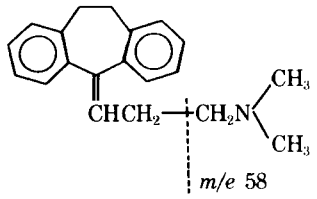

I: amitriptyline

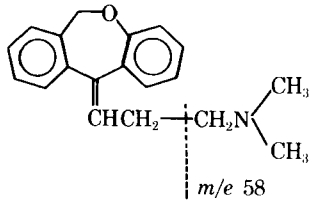

II: doxepin (*cis*-form)

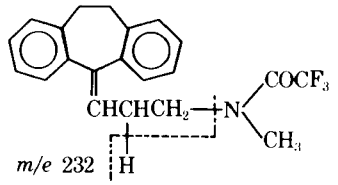

III: *N*-trifluoroacetylnortriptyline

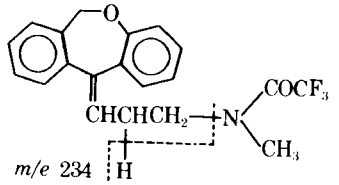

IV: *N*-trifluoroacetyldesmethyldoxepin (*cis*-form)

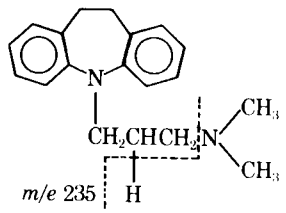

V: imipramine

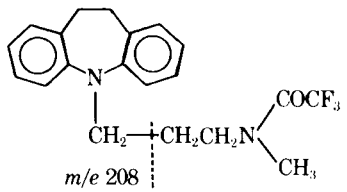

VI: *N*-trifluoroacetyldesipramine

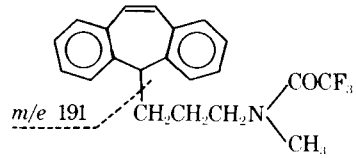

VII: *N*-trifluoroacetylprotriptyline

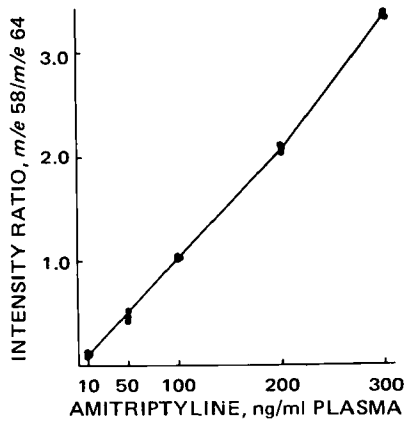

Figure 7—*Amitriptyline standard curve from pooled human plasma.*

fragmentation mode, is practical has been shown many times in this laboratory (*e.g.*, Fig. 14).

These analyses would not be possible without the use of the deuterium-labeled internal standard. Amitriptyline, as is true of imipramine and doxepin, is a difficult substance to analyze by GLC. All columns and phases tested in this laboratory show variable adsorption of these amines. This problem is overcome by making eight to 10 injections of 100 ng of the amine to prime the chromatographic column. The priming is seen as an increase in the peak height of the drug on sequential injections.

Even after the tertiary amines achieve a maximal chromatographic peak height, they show much greater variability in analysis than do the trifluoroacetyl secondary amines. However, the deuterated internal standards undergo the same vagaries in the analytical process as do the drugs themselves; thus, the ratio of the two is a very precise measure of the drug, as can be seen by the agreement of triplicate analyses in Fig. 7. Surprisingly, even immediately following the priming procedure, the injection of volumes of carbon disulfide or chloroform comparable to those used in the analysis does not displace the tricyclic amines from the column as a ghost peak. Nevertheless, the column does not remain saturated with the drug over extended periods and must be primed on each day of use.

Table I—Mass Fragmentography Internal Standards

Compound	*m/e*	Internal Standard	*m/e*	Amount of Internal Standard, ng/ml of Plasma
Amitriptyline	58	*N,N*-Di-C^2H_3-amitriptyline	64	50
Nortriptyline	232[a]	Desmethyldoxepin	234[a]	100
Doxepin	58	*N,N*-Di-C^2H_3-amitriptyline	64	50
Desmethyldoxepin	234[a]	Nortriptyline	232[a]	100
Imipramine	235	10,10-Di-$^2H_2$-imipramine	237	50
Desipramine	208[a]	Nortriptyline	232[a]	100
Protriptyline	191[a]	Desipramine	208[a]	100

[a] Measured as *N*-trifluoroacetyl derivatives.

Nortriptyline—Nortriptyline is measured with desmethyldoxepin as an internal standard, both as the *N*-trifluoroacetyl derivatives. Ions *m/e* 232 and 234 are measured, respectively. Figure 2 shows a mass fragmentogram of these two drugs from patient plasma, with *N*-trifluoroacetylnortriptyline having a retention time of 2 min and trifluoroacetyldoxepin eluting at 2.4 min. A small plasma contaminant frequently precedes the nortriptyline peak. A five-point standard dilution curve of nortriptyline, using desmethyldoxepin as the internal standard, typically has a slope of 0.02, an ordinate intercept of −0.035, and a correlation coefficient of 0.999. As is typical of the other secondary amine tricyclics, *N*-trifluoroacetylnortriptyline can be analyzed by GLC without priming effects or other complications.

Doxepin—This compound has been analyzed successfully by mass fragmentography using *N,N*-di-C^2H_3-amitriptyline as the internal standard. The analysis is much the same as that of amitriptyline. Again a plasma contaminant is detected by *m/e* 58 (Fig. 3), but the chromatographic separation is sufficient for the analysis. The standard curve follows the equation for a straight line be-

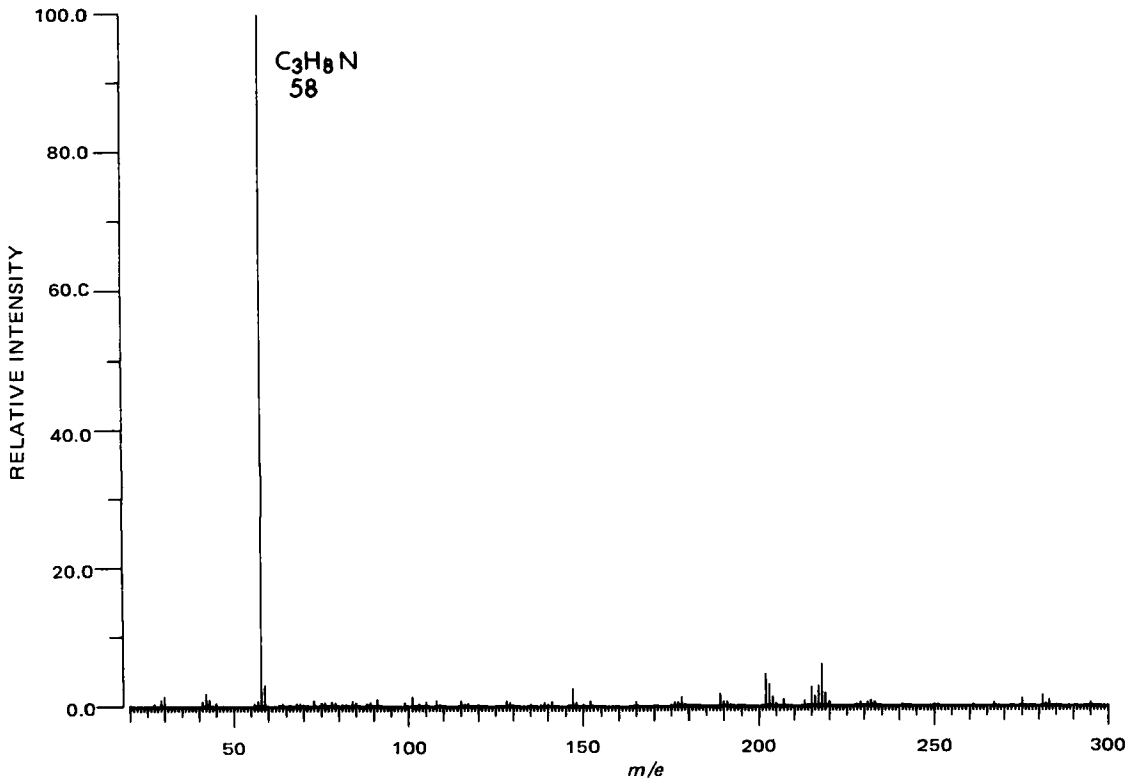

Figure 8—*The 70-ev mass spectrum of amitriptyline.*

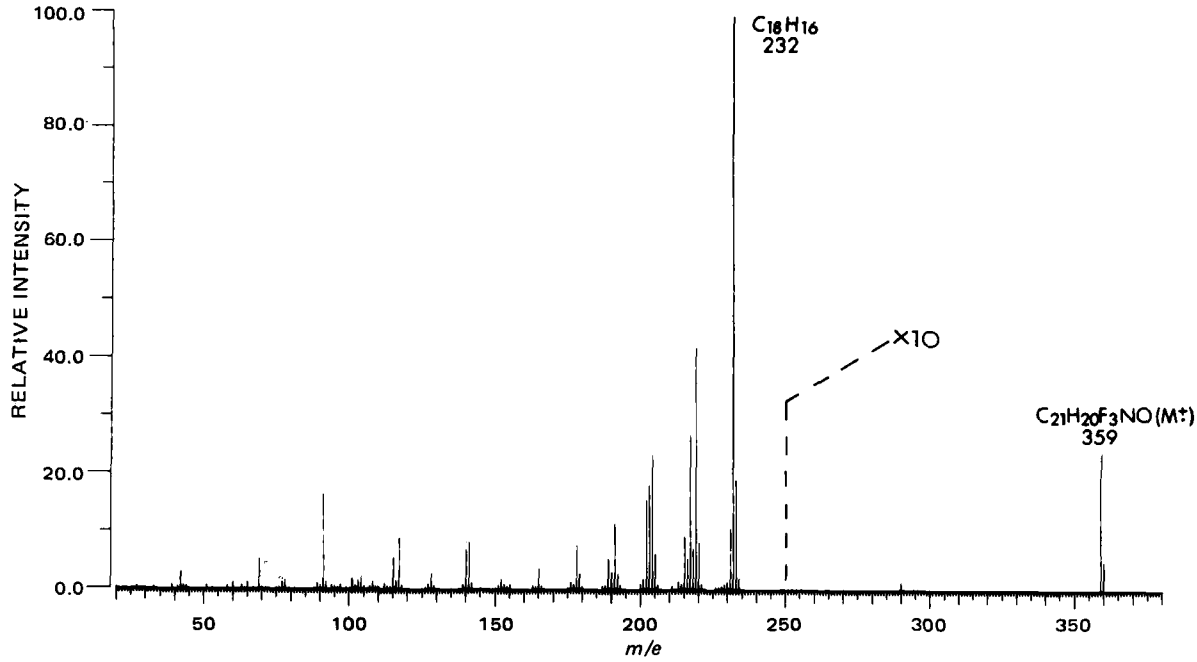

Figure 9—*The 70-ev mass spectrum of* N-*trifluoroacetylnortriptyline.*

tween 10 and 300 ng/ml, with a slope of 0.008, an ordinate intercept at 0.078, and a correlation coefficient of 0.989. As with amitriptyline, doxepin usually requires priming of the GLC column prior to a series of analyses.

Desmethyldoxepin—This derivative is measured using nortriptyline as an internal standard (Fig. 2). A typical five-point standard dilution curve for this procedure follows the equation for a straight line between 10 and 300 ng/ml, with a slope of 0.004, an ordinate intercept of 0.001, and a correlation coefficient of 0.997.

Imipramine—This drug, analyzed using 10,10-$^2H_2$-imipramine as the internal standard, presents problems similar to amitriptyline and doxepin chromatographically. However, following priming, a symmetrical chromatographic peak is obtained, resolved from a small plasma contaminant (Fig. 4). As with each of the other drugs studied, analyses can be carried out to levels of 10 ng/ml of plasma. The standard curve is linear to 1500 ng/ml, with a slope of 0.026, an ordinate intercept of 0.385, and a correlation coefficient of 0.995.

Desipramine—Desipramine can be measured conveniently using nortriptyline as the internal standard (Fig. 5). When analyzed on a 1% SE-30 column, the drug is separated better from the plasma contaminants, which precede the trifluoroacetyldesipramine peak (a trace may be seen eluting at 1 min in Fig. 5). A typical six-point standard curve for this procedure is linear between 10 and 1500 ng/ml, with a slope of 0.016, an ordinate intercept of 0.016, and a correlation coefficient of 0.998.

With proper attention to solvent volumes and chromatographic injection size, the desipramine analyses can be carried out readily without an internal standard. This procedure is necessary when a patient is being treated with amitriptyline or nortriptyline as well as desipramine. A significant peak in the spectrum of *N*-trifluoroacetyldesipramine, *m/e* 193 (Fig. 12), is unreliable for quantitative

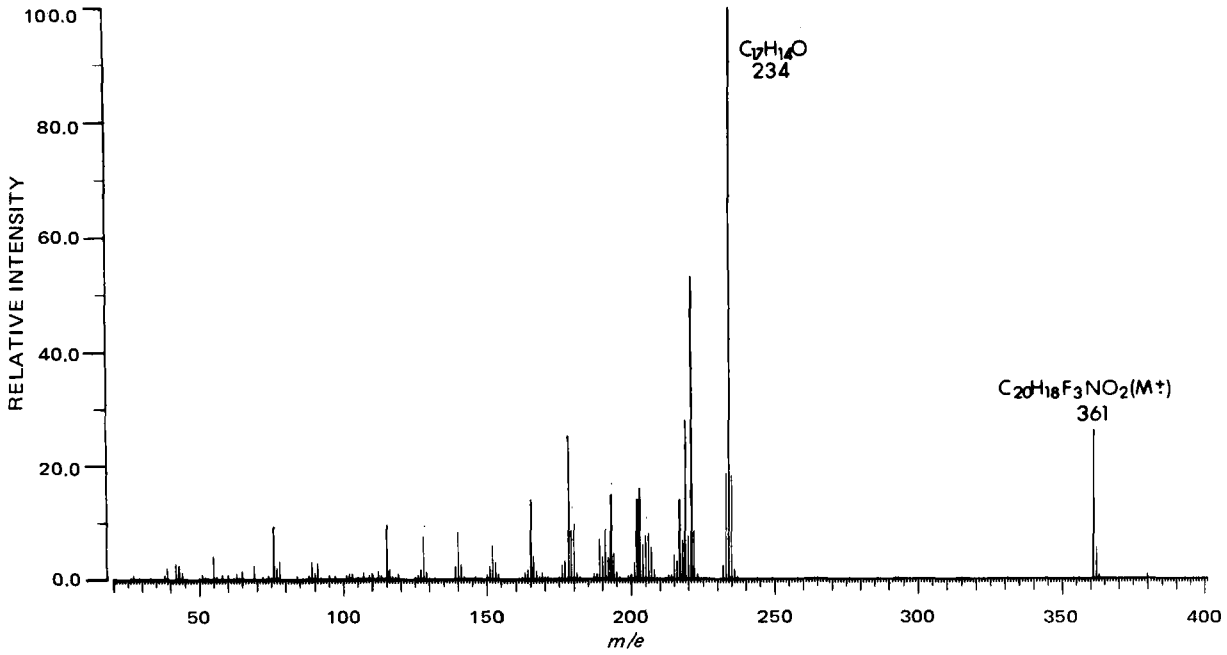

Figure 10—*The 70-ev mass spectrum of* N-*trifluoroacetyldesmethyldoxepin.*

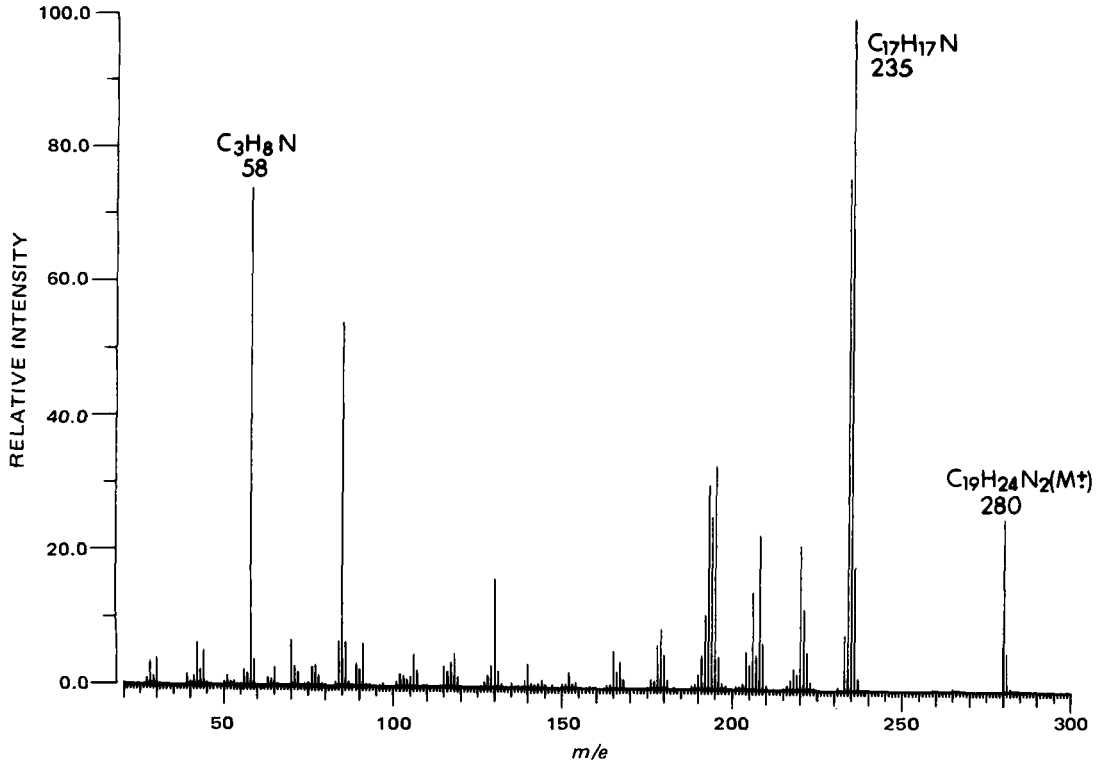

Figure 11—*The 70-ev mass spectrum of imipramine.*

measurements, probably due to plasma contaminants.

Protriptyline—This compound is similar to desipramine in that chromatography of the *N*-trifluoroacetyl derivative is best carried out on SE-30. Figure 6 shows a mass fragmentogram of the protriptyline derivative measured with trifluoroacetyldesipramine as the internal standard. Occasionally, plasma contaminants elute following the protriptyline derivative, but they are well resolved from it. A five-point standard dilution curve for this procedure is linear between 10 and 300 ng/ml in plasma, with a slope of 0.011, an ordinate intercept of −0.027, and a correlation coefficient of 0.996.

DISCUSSION

The measurement of plasma tricyclic antidepressant levels in patients is becoming generally accepted as a desirable component of treatment. However, major difficulties still exist in the measurement of the tertiary tricyclic amines, amitriptyline, doxepin, and imipramine, although these drugs are the most widely used clinically to treat depression. One fluorometric method (8) has not gained widespread use, nor have other indirect methods, due to a lack of sensitivity and/or specificity (9, 10).

GLC analysis of amitriptyline in this laboratory by the method of Braithwaite and Widdop (11) was complicated by variable chromatographic recovery as measured by inconsistent detector response for repetitive analysis of a standard. In addition, the column liquid phase described by these workers had a short useful life, necessitating frequent replacement. Even this column, which uses an amine liquid phase, required priming before it could be

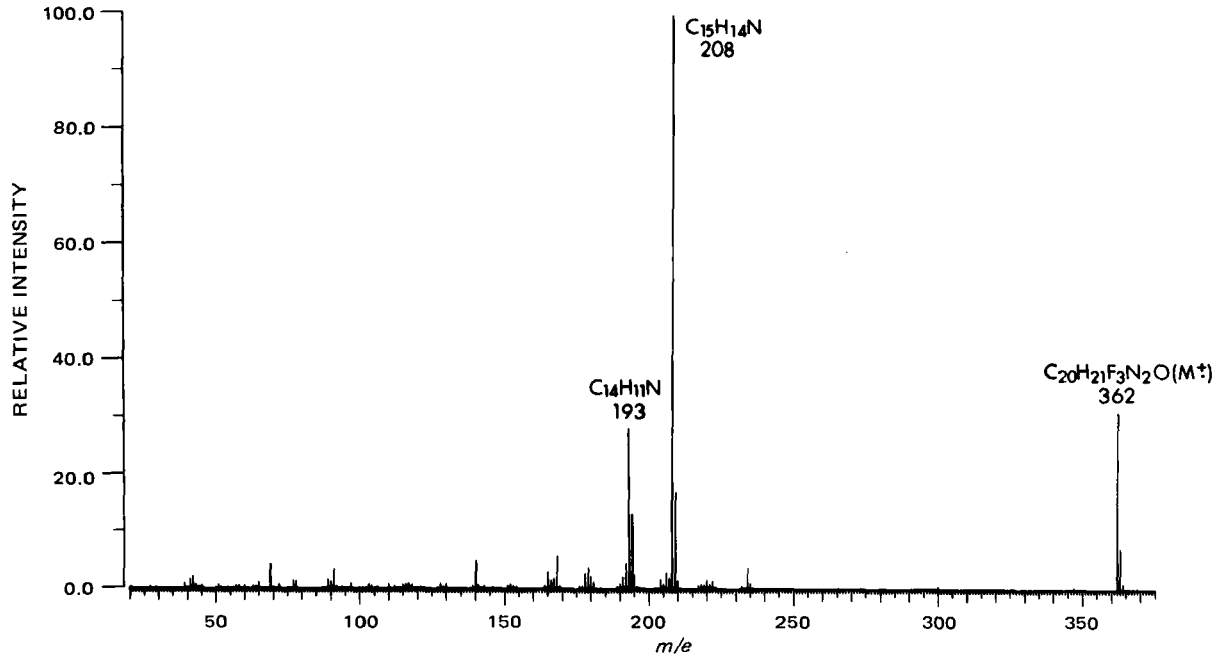

Figure 12—*The 70-ev mass spectrum of* N-*trifluoroacetyldesipramine.*

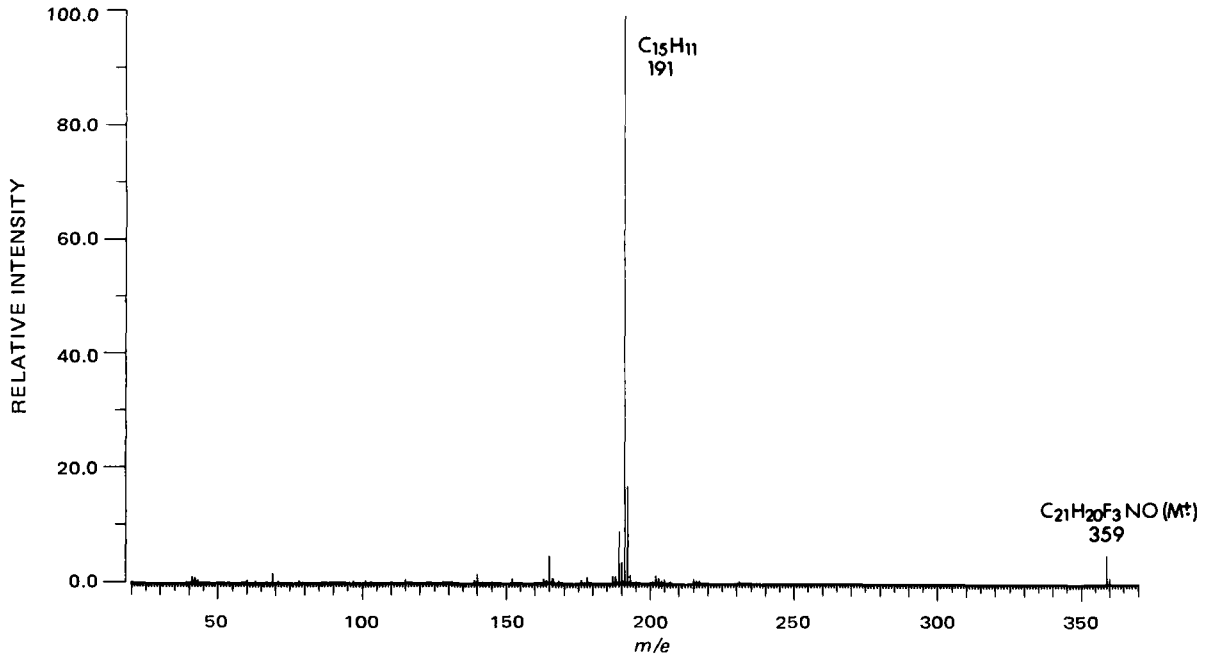

Figure 13—*The 70-ev mass spectrum of* N-*trifluoroacetylprotriptyline.*

used. And at best, only one or two analyses per hour could be carried out because of interference by late-eluting plasma substances which had to be cleared from the column prior to another analysis. It was also found, as reported by Hucker and Stauffer (12), that OV-17 columns served as well as the Braithwaite and Widdop column but without rapid degradation. However, the slowness of the GLC method using flame-ionization detection makes it impractical for clinical studies where many samples must be examined.

The most successful method for the measurement of the tertiary tricyclic amines has been mass fragmentography. Frigerio *et al.* (13), using promazine as an internal standard, measured imipramine in human plasma by this method. In this study, deuterium-labeled internal standards were employed wherever possible. They appear to be the ideal internal standards in that they most closely mimic the parent drugs with respect to plasma protein binding as well as analytical variables such as the partition coefficient in the extraction procedure and adsorption to glassware and chromatographic columns.

The secondary tricyclic amines (*e.g.*, nortriptyline, desipramine, desmethyldoxepin, and protriptyline) are much more readily measured in plasma, a consequence of having an available functional group for derivatization. The original method of Hammer and Brodie (14), wherein ^{3}H-acetic anhydride is reacted with the secondary amine to form a radioactive derivative, has been most widely used but is not applicable to the measurement of the tertiary amines. Borgå and Garle (15) showed that the heptafluorobutyryl derivative could be chromatographed as readily as the trifluoroacetate (11). Hucker and Stauffer (12) showed that the secondary amines can be analyzed by GLC without derivatization.

By using mass fragmentography, *N*-trifluoroacetylnortriptyline was measured in cerebrospinal fluid, plasma, and urine (16). The metabolism of nortriptyline was studied in humans using nortriptyline and deuterium-labeled nortriptyline (17). By this means the metabolites of the drug are easily discerned in chromatograms by their mass spectra, which show a "signature," seen as doublet spectra separated by three mass units whenever a GLC peak contains a metabolite.

Only one clinical study has been published in which a plasma tertiary tricyclic antidepressant level was compared with the therapeutic effect (18). This study involved the measurement of amitriptyline in 15 patients. Several studies of the relationship between nortriptyline plasma levels and antidepressant effect have been carried out with conflicting results (19–22). This correlation remains controversial (23); before the question can be resolved, much larger studies must be conducted and the tertiary tricyclic antidepressants must be included. Furthermore, in this center the availability of routine tricyclic plasma assays for the clinic service has, in many cases, improved patient care, from the trivial, but essential, case of ensuring patient compliance with ingesting the pre-

Table II—GLC Retention Times of Tricyclic Antidepressants[a]

Compound	Retention Time Relative to *N*-Trifluoroacetylnortriptyline
Amitriptyline	0.47
N,N-Di-C^2H_3-amitriptyline	0.46
N-Trifluoroacetylnortriptyline	1.00 (5.75 min)
Doxepin	0.56[b]
N-Trifluoroacetyldesmethyldoxepin	1.26[b]
Imipramine	0.51
10,10-Di-$^2H_2$-imipramine	0.50
Clomipramine	1.01
N-Trifluoroacetyldesipramine	1.21
N-Trifluoroacetylprotriptyline	1.20

[a] Obtained on an F&M model 810 gas chromatograph using 50-cm × 6-mm o.d. silanized glass columns packed with 3% OV-17 on Gas Chrom Q, with a helium flow of 100 ml/min and an oven temperature of 195°. [b] Doxepin was obtained as a mixture containing 15% of the *cis*-isomer and 85% of the *trans*-isomer, which did not separate under the chromatographic conditions used. Desmethyldoxepin was obtained as the *trans*-isomer.

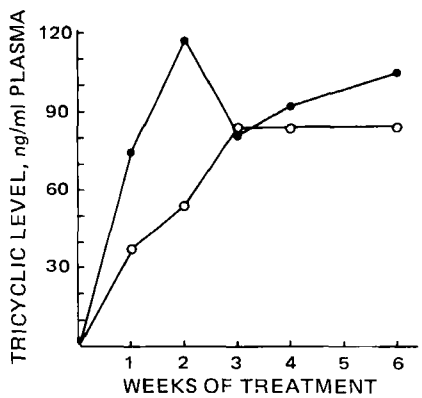

Figure 14—*Weekly measurement of amitriptyline* (●) *and nortriptyline* (○) *in plasma from a patient ingesting amitriptyline (50 mg three times daily).*

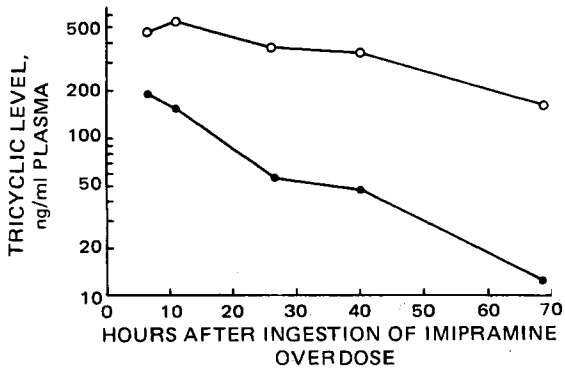

Figure 15—*Disappearance curve of imipramine (●) and desipramine (○) from patient plasma following an imipramine overdose.*

scribed drug to the question of attaining an "adequate" plasma tricyclic level. In addition to such applications, in which several hundred patient samples have been analyzed during the past year, plasma levels in overdose patients have also been studied.

Figure 14 illustrates the measurement of amitriptyline and nortriptyline in a patient treated with 50 mg of amitriptyline three times daily. Samples were collected weekly at 8 am prior to the morning dose. This patient essentially reached a steady-state plasma level in 3 weeks. Figure 16 illustrates the disappearance of doxepin and desmethyldoxepin from a patient who, after several weeks of treatment with doxepin, discontinued the medication. As can be seen, both drugs were measured over 50 hr. The last two data points in this figure were obtained by extrapolation of the standard curve.

Figure 15 illustrates the measurement of imipramine and desipramine in patients who ingested an imipramine overdose of an unknown amount. In this case, plasma samples were collected for up to 70 hr following the overdose. The data from patients presented in Figs. 14–16 were assayed in duplicate, with differences in all cases being less than 10%. Data involving patients treated with protriptyline were presented elsewhere (24).

In conclusion, a method has been developed that can be applied to the rapid and accurate measurement of all tricyclic antidepressants currently available in the United States. The use of internal standards and of computerized mass fragmentography has given the analysis unsurpassed precision and speed.

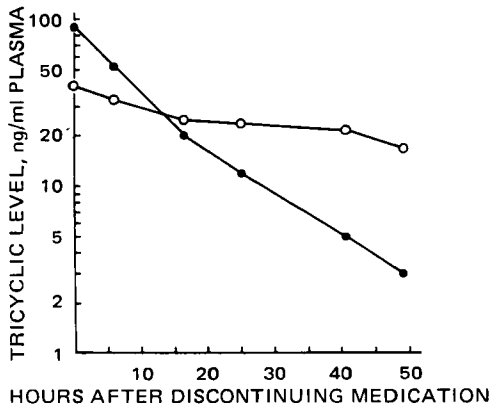

Figure 16—*Multiple analysis of doxepin (●) and desmethyldoxepin (○) after a subject discontinued doxepin (100 mg three times daily).*

REFERENCES

(1) C. C. Sweeley, W. H. Elliot, I. Fries, and R. Ryhage, *Anal. Chem.*, **38**, 1549(1966).

(2) C.-G. Hammar, B. Holmstedt, and R. Ryhage, *Anal. Biochem.*, **25**, 532(1968).

(3) W. F. Holmes, W. H. Holland, B. L. Shore, D. M. Bier, and W. R. Sherman, *Anal. Chem.*, **45**, 2063(1973).

(4) J. T. Watson, D. R. Pelster, B. J. Sweetman, J. C. Frolich, and J. A. Oates, *ibid.*, **45**, 2071(1973).

(5) J. F. Holland, C. C. Sweeley, R. E. Thrush, R. E. Teets, and M. A. Bieber, *ibid.*, **45**, 308(1973).

(6) K. Elkin, I. Pierrou, U. G. Ahlborg, B. Holmstedt, and J.-E. Lindgren, *J. Chromatogr.*, **81**, 47(1973).

(7) W. F. Holmes, W. H. Holland, and J. A. Parker, *Anal. Chem.*, **43**, 1806(1971).

(8) J. P. Moody, A. C. Tait, and A. Todrick, *Brit. J. Psychiat.*, **113**, 183(1967).

(9) S. R. Harris, L. E. Gaudette, D. H. Efron, and A. Manian, *Life Sci.*, **9**, 781(1970).

(10) T. P. Michaels, W. W. Holl, and V. J. Greely, *Ann. N.Y. Acad. Sci.*, **153**, 493(1968).

(11) R. A. Braithwaite and B. Widdop, *Clin. Chim. Acta*, **35**, 461(1971).

(12) H. B. Hucker and S. C. Stauffer, *J. Pharm. Sci.*, **63**, 296(1974).

(13) A. Frigerio, G. Belvedere, F. DeNadai, R. Fanelli, C. Pantarotto, E. Riva, and P. L. Morselli, *J. Chromatogr.*, **74**, 201(1972).

(14) W. M. Hammer and B. B. Brodie, *J. Pharmacol. Exp. Ther.*, **157**, 503(1967).

(15) O. Borga and M. Garle, *J. Chromatogr.*, **68**, 77(1972).

(16) C.-G. Hammar, B. Alexanderson, B. Holmstedt, and F. Sjöqvist, *Clin. Pharmacol. Ther.*, **12**, 496(1971).

(17) D. R. Knapp, T. E. Gaffney, R. E. McMahon, and G. Kiplinger, *J. Pharmacol. Exp. Ther.*, **180**, 784(1972).

(18) R. A. Braithwaite, R. Goulding, G. Theano, J. Bailey, and A. Coppen, *Lancet*, **1**, 1297(1972).

(19) M. Åsberg, B. Crönholm, F. Sjöqvist, and D. Tuck, *Brit. Med. J.*, **3**, 331(1971).

(20) P. Kragh-Sørensen, M. Åsberg, and C. Eggert-Hansen, *Lancet*, **1**, 113(1973).

(21) G. Burrows, B. A. Scoggins, L. R. Turecek, and B. Davies, *Clin. Pharmacol. Ther.*, **16**, 639(1974).

(22) P. Kragh-Sørensen, C. Eggert-Hansen, N.-E. Larsen, J. Naestoft, and E. F. Hvidberg, *Psychol. Med.*, **4**, 174(1974).

(23) M. Åsberg, *Clin. Pharmacol. Ther.*, **16**, 215(1974).

(24) J. T. Biggs and W. R. Sherman, *Pharmacologist*, **16**, 219(1974).

ACKNOWLEDGMENTS AND ADDRESSES

Received February 26, 1975, from the *Department of Psychiatry, School of Medicine, Washington University, St. Louis, MO 63110*

Accepted for publication May 12, 1975.

Supported in part by Public Health Service Grants MH-13002, MH-07081, DA-00259, and DA-4RG008 from the National Institute of Mental Health.

The authors acknowledge the technical assistance of Ms. Deborah Bolton. They also thank Merck Sharp and Dohme for the special preparation of N,N-di-C^2H_3-amitriptyline and Ciba-Giegy Corp. for the 10,10-di-$^2H_2$-imipramine.

[x] To whom inquiries should be directed.

Isomeric Inversion of Ibuprofen (*R*)-Enantiomer in Humans

D. G. KAISER ˣ, G. J. VANGIESSEN, R. J. REISCHER, and W. J. WECHTER

Abstract □ Enantiomeric compositions of the major urinary metabolites of ibuprofen [(*RS*)-2-(4-isobutylphenyl)propionic acid] were characterized after oral administration of the racemic mixture and oral administration of the individual enantiomers to normal human volunteers. Resolution of the diastereomeric amides, formed by reaction of the urinary metabolites with (*S*)-(−)-α-methylbenzylamine, was achieved by GLC. Only the (*R*)-(−)-enantiomer of the intact drug was inverted to its optical antipode, (*S*)-(+), in humans. However, both (*S*)-(+)- and (*R*)-(−)-enantiomers of the intact drug were transformed independently *in vivo* to the major metabolites, *i.e.*, 2,4′-(2-hydroxy-2-methylpropyl)phenylpropionic acid and 2,4′-(2-carboxypropyl)phenylpropionic acid. *In vivo* metabolism of ibuprofen to its carboxy metabolite was not stereoselective.

Keyphrases □ Ibuprofen—isomeric inversion of enantiomers, determined by characterization of major urinary metabolites □ Isomeric inversion—ibuprofen enantiomers, determined by characterization of major urinary metabolites □ Enantiomers—ibuprofen, isomeric inversion determined by characterization of major urinary metabolites

Extensive pharmacological, toxicological, and biochemical studies of ibuprofen[1] [(*RS*)-2-(4-isobutylphenyl)propionic acid] (I) (1, 2), a potent orally active anti-inflammatory agent in animals (3–6) and humans (7–9), have been reported. Interest in the stereochemistry of the metabolism of I was stimulated by the early report (1) that: (*a*) after oral administration of the racemic drug, the major metabolites excreted in human urine (IV and VII) were optically active; and (*b*) the *in vivo* biological activities of the individual enantiomers of the intact drug were equivalent.

Subsequently, it was shown that, after oral administration of the individual enantiomers of I, the major metabolites isolated from human urine were dextrorotatory (5). Utilizing GLC methods for measuring the individual enantiomers (10–12), the facile epimerization of the (*R*)-(−)-isomer of I to its optical antipode, *i.e.*, II, was observed *in vivo* prior to oxidative metabolism (13, 14).

With the availability of suitable analytical methodology for separating the enantiomers of the major metabolites excreted in human urine (10, 12), studies were designed to further characterize the epimerization of the (*R*)-(−)-isomer and metabolism of I in humans.

EXPERIMENTAL

Reagents and Materials—The I used in this study was synthesized[2], and the (*S*)-(+)- and (*R*)-(−)-isomers were resolved (*vide infra*). Compounds IV and VII, used for initial metabolite characterization, were isolated and purified from human urine[3]. The partially resolved (*R*)-(−)-isomer of IV (*i.e.*, VI) was synthesized[4] (15). Tridecanoic acid[5], isophthalic acid[6], (*R*)-(+)-α-methylbenzylamine[7], (*S*)-(−)-α-methylbenzylamine[7], and hydrocarbon-stabilized chloroform[8] were used as supplied. Stock solutions of 1,1′-carbonyldiimidazole (65 mg/ml) in hydrocarbon-stabilized chloroform were prepared fresh daily. All other solvents were analytical grade.

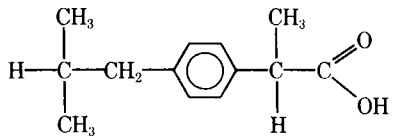

ibuprofen
I: racemate
II: (*S*)-(+)
III: (*R*)-(−)

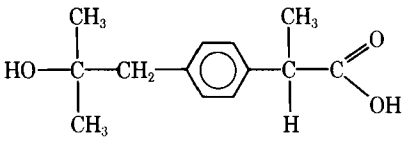

hydroxy metabolite
IV: isomeric mixture
V: (*S*)-(+)
VI: (*R*)-(−)

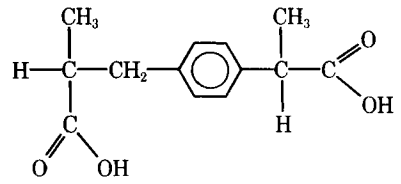

carboxy metabolite
VII: isomeric mixture
VIII: (*S*)-(+)/(*S*)-(+)
IX: (*R*)-(−)/(*S*)-(+)
X: (*S*)-(+)/(*R*)-(−)
XI: (*R*)-(−)/(*R*)-(−)

Diethylene glycol succinate on 80–100-mesh Diatoport-S[9], phenyl methyl silicone fluid (OV-17) on 60–80-mesh Gas Chrom Q[5], chromatography plates coated with thin layers (250 μm) of silica gel F-254[10], and silica gel for preparative chromatography[10] (0.05–0.2 mm) were used as supplied. Amberlite XAD-2 resin[11] was washed successively with two bed volumes each of water, acetone, methanol, and water prior to utilization for chromatography.

Resolution of Ibuprofen—(*S*)-(−)-α-Methylbenzylamine (0.291 mole) was added dropwise, with stirring, to an ice-cooled solution of I (0.291 mole) in 600 ml of ether. The resulting solid, *i.e.*,

[1] Motrin, The Upjohn Co., and Brufen, The Boots Co., Ltd.
[2] The Boots Co., Ltd., Nottingham, England.
[3] Supplied by R. Cobb, The Boots Co., Ltd., Nottingham, England.
[4] By The Upjohn Co.
[5] Applied Science Labs., State College, Pa.
[6] Eastman Organic Chemicals, Rochester, N.Y.
[7] Aldrich Chemical Co., Milwaukee, Wis.
[8] Matheson, Coleman and Bell, Milwaukee, Wis.
[9] LAC-728, Hewlett-Packard Co., Avondale, Pa.
[10] Brinkmann Instruments, Westbury, N.Y.
[11] Rohm and Haas, Philadelphia, Pa.

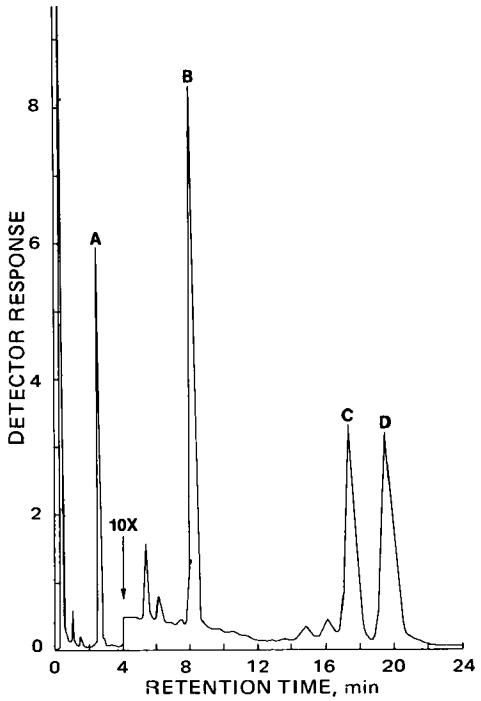

Figure 1—*Gas–liquid chromatogram of methyl esters of ibuprofen, its major urinary metabolites, and isophthalic acid. Key: A, ibuprofen; B, isophthalic acid standard; C, hydroxy metabolite; and D, carboxy metabolite.*

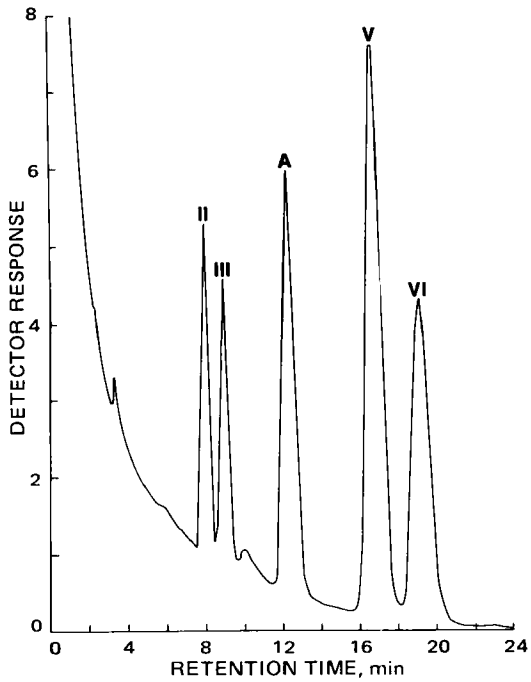

Figure 2—*Gas–liquid chromatogram of* (S)-(−)-*α-methylbenzylamide derivatives of ibuprofen enantiomers and enantiomers of hydroxy metabolite. Key: II,* (S)-(+)-*enantiomer of ibuprofen; III,* (R)-(−)-*enantiomer of ibuprofen; A,* n-*tridecanoic acid standard; V,* (S)-(+)-*enantiomer of hydroxy metabolite; and VI,* (R)-(−)-*enantiomer of hydroxy metabolite.*

the more insoluble (*S*)-(−)-α-methylbenzylamine salt of II (mp 155–170°), was filtered and recrystallized from 300 ml of isopropanol. Two additional recrystallizations, from 200 and 150 ml of absolute ethanol, afforded 12.9 g of white crystals (mp 179–185°). The material was acidified with 3 *N* aqueous sulfuric acid and extracted into ether.

After washing with water and saline, the ether extract was evaporated to dryness. The resulting white solid (mp 49–51°) was recrystallized twice from absolute ethanol to afford 4.5 g of II (mp 50–52°, $[\alpha]_D$ + 57°). GLC analysis, as the (*S*)-(−)-α-methylbenzylamide derivative (*vide infra*), showed an optical purity of 95%.

Anal.—Calc. for $C_{13}H_{18}O_2$: C, 75.69; H, 8.79. Found: C, 75.88; H, 8.92.

The procedure was repeated using (*R*)-(+)-α-methylbenzylamine as the resolving agent. The (*R*)-(+)-α-methylbenzylamine salt of III (mp 153–172°) was filtered and recrystallized from isopropanol. Two additional recrystallizations from absolute ethanol afforded 15.5 g of white crystals (mp 181–185°). The material was acidified with 3 *N* aqueous sulfuric acid and extracted into ether.

After washing with water and saline, the ether extract was evaporated to dryness. The resulting white solid (mp 49–52°) was recrystallized twice from absolute ethanol to afford 6.3 g of III (mp 50–52°, $[\alpha]_D$ −57°). GLC analysis, as the (*S*)-(−)-α-methylbenzylamide derivative (*vide infra*), showed an optical purity of 96%.

Anal.—Calc. for $C_{13}H_{18}O_2$: C, 75.69; H, 8.79. Found: C, 75.86; H, 9.09.

Instrumentation—All GLC measurements were made with a gas chromatograph[12] equipped with dual hydrogen flame-ionization detectors and a −0.2–1.0-mv dual-pen recorder[13]. All gas cylinders used for chromatography (*i.e.*, helium, hydrogen, and oxygen) were fitted with filters containing molecular sieve 4A. All mass spectrometric measurements were made with a combined GLC–mass spectrometer interfaced to a computer (16). Optical rotation measurements, $[\alpha]_D$ in 95% ethanol, were made with a polarimeter[14] at 25° in a 1-dm tube.

TLC—Analytical chromatography was conducted on thin layers of silica gel F-254, ascendingly developed in a solvent system of 10% (v/v) acetic acid in toluene. The separated materials were visualized by irradiation of the plates with a short wavelength (254 nm) UV lamp. Under these chromatographic conditions, I, IV, and VII had R_f values of 0.42, 0.20, and 0.29, respectively.

GLC—The GLC procedure described for the determination of I in plasma (17) as the methyl ester was modified to measure the intact drug and its major metabolites excreted in human urine. Reaction time for the free carboxylic acids with 1,1′-carbonyldiimidazole was increased from 1 to 5 min, and isophthalic acid was selected as an internal standard to replace naphthalene.

During analysis, the column [*i.e.*, 6% (w/w) diethylene glycol succinate on 80–100-mesh Diatoport-S], injection port, and detector block were maintained isothermally at 180, 220, and 240°, respectively. Helium, hydrogen, and oxygen flow rates were 60, 40, and 400 ml/min, respectively. Under these conditions, the methyl esters of I, isophthalic acid, IV, and VII had retention times of 2.6, 8.1, 17.3, and 19.6 min, respectively (Fig. 1).

The individual enantiomers of I, IV, and VII excreted in human urine were measured as the (*S*)-(−)-α-methylbenzylamide derivatives *via* GLC on a column of 3% (w/w) OV-17 (10, 12). With the column temperature maintained isothermally at 220°, the retention times for the derivatives of II, III, V, and VI were 8.0, 9.0, 16.9, and 19.1 min, respectively (Fig. 2). To measure the enantiomers of VII, the column temperature was maintained isothermally at 285°. Three partially resolved peaks, designated VIII, IX–X, and XI, were observed with retention times of 25.2, 28.4, and 30.8 min, respectively (Fig. 3).

For all measurements utilizing combined GLC–mass spectrometry, the temperatures of the ion source and separator were maintained isothermally at 280°. The electron-impact energy was maintained at 70 ev, and helium was used as carrier gas. Columns of 6% (w/w) diethylene glycol succinate and 3% (w/w) OV-17 were maintained isothermally at 180 and 250°, respectively. Mass spectra and tabular presentations of ion intensities were obtained *via* computer data reduction (16).

Column Chromatography—Aliquots (1500 ml) of pooled 24-hr urine speciments were adjusted to pH 3 with acetic acid and applied to columns[11] (65 × 3 cm i.d.). The columns were eluted successively with 600 ml of water, 600 ml of 50% (v/v) ethanol in water, 1100 ml of 95% (v/v) ethanol in water, and 500 ml of acetone. The effluent was monitored by TLC of the free carboxylic

[12] HP model 402, Hewlett-Packard Co., Avondale, Pa.
[13] HP model 7128A, Hewlett-Packard Co., Avondale, Pa.
[14] PE model 141, Perkin-Elmer Corp., Norwalk, Conn.

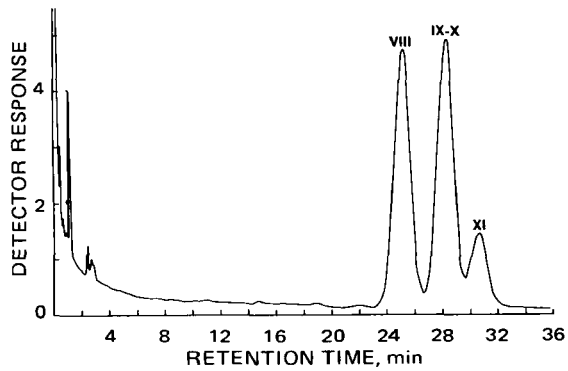

Figure 3—*Gas–liquid chromatogram of* (S)-(−)-α-*methylbenzylamide derivatives of enantiomers of carboxy metabolite. Key: VIII,* (S)-(+)/(S)-(+)-*enantiomer of carboxy metabolite; IX–X, mixture of* (R)-(−)/(S)-(+)- *and* (S)-(+)/(R)-(−)-*enantiomers of carboxy metabolite; and XI,* (R)-(−)/(R)-(−)-*enantiomer of carboxy metabolite.*

acids and GLC of the methyl esters of the carboxylic acids.

Fractions containing I, IV, and VII were pooled and concentrated to 300 ml under reduced pressure (15 mm) at 50°. The concentrate was adjusted to pH 3 with acetic acid and extracted three times with 300 ml of benzene. Then the extracts were pooled and concentrated under reduced pressure (15 mm) at 50°. The resulting residue was reconstituted in 10 ml of 10% (v/v) acetic acid in toluene and applied to a silica gel column (50 × 3 cm i.d.) packed in the same solvent mixture.

The column was developed with 10% (v/v) acetic acid in toluene, and the effluent was monitored by TLC. Fractions containing I, IV, and VII were pooled separately and evaporated to dryness under reduced pressure (15 mm) at 50°. The viscous oil, obtained from I fractions, was too small to crystallize. Residues from IV and VII fractions were recrystallized separately from benzene and hexane. Purification was monitored by TLC and optical rotation measurements of the free carboxylic acids as well as GLC–mass spectrometric analysis of the methyl esters and α-methylbenzylamide derivatives of the acids.

Drug Administration to Humans—Informed written consent was obtained from each of three normal human male volunteers prior to participation. All subjects were between the ages of 27 and 44 years; they ranged in body weight from 70.9 to 93.2 kg and in height from 1.74 to 1.85 m. All subjects were fasted for 12 hr prior to, and 4 hr after, drug administration.

On Days 1, 8, and 15, each subject received a single 800-mg dose of II, III, and I, respectively, in hard-filled gelatin capsules. All doses were taken with 240 ml of water. Total urine specimens were collected for 12 hr prior to drug ingestion and at predetermined time intervals from 0 to 72 hr postadministration. All specimens were stored at −18° until assayed.

RESULTS AND DISCUSSION

Synthesis and Characterization of Methyl Esters—Earlier investigations (17) showed that 1,1′-carbonyldiimidazole was a useful reagent for the facile esterification of I. A series of samples containing known amounts of IV, VII, and isophthalic acid were prepared to determine the optimal reaction conditions for (*a*) imidazolide formation and (*b*) methyl ester formation from the imidazolide and triethylamine in methanol. In studies with IV and VII, known amounts of dimethyl isophthalate were added as the internal standard. The results indicated that imidazolide formation was completed within 1 min for IV and within 5 min for VII and isophthalic acid. Methyl ester formation was completed within 5 min for all compounds.

GLC, in conjunction with mass spectrometry, showed that the methyl ester of IV had a very weak molecular ion of mass 236 (Fig. 4). Major fragmentation peaks were observed at *m/e* 178, 119, 118, 91, and 59. The mass spectrum of VII dimethyl ester showed a molecular ion of mass 264 and major fragmentation peaks at *m/e* 205, 177, 145, 117, and 91 (Fig. 4). The combined results for the methyl esters of IV and VII showed excellent agreement with reported studies (11) using diazomethane in ether for esterification.

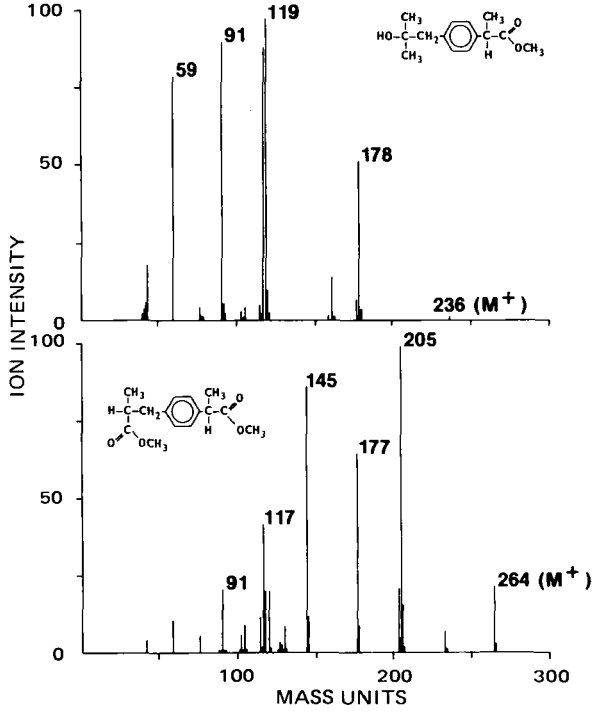

Figure 4—*Mass spectra of methyl esters of major urinary metabolites of ibuprofen. Upper panel: hydroxy metabolite. Lower panel: carboxy metabolite.*

Synthesis and Characterization of (*S*)-(−)-α-Methylbenzylamide Derivatives—Pilot studies using thionyl chloride as an acylating reagent showed that, although I and VII were easily acylated, IV was readily dehydrated and hydrohalogenated. Subsequent reaction of the intermediate(s) of IV with (*S*)-(−)-α-methylbenzylamine produced undesirable side products. Utilization of 1,1′-carbonyldiimidazole, analogous to studies reported for I (10, 12), produced the desired amides of all three compounds.

A series of samples containing known amounts of IV, VII, and *n*-tridecanoic acid was prepared to determine the optimal reaction times for (*a*) imidazolide formation and (*b*) amide formation from the imidazolides and (*S*)-(−)-α-methylbenzylamine. The results

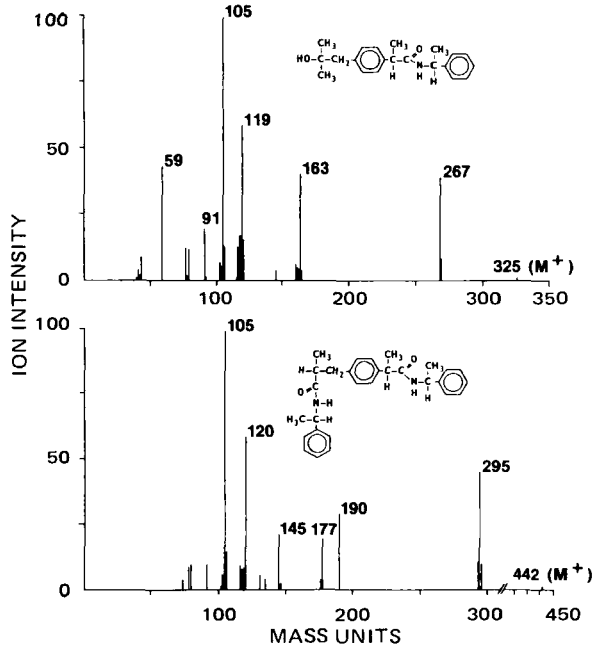

Figure 5—*Mass spectra of* (S)-(−)-α-*methylbenzylamide derivatives of major urinary metabolites of ibuprofen. Upper panel: hydroxy metabolite. Lower panel: carboxy metabolite.*

Table I—Enantiomeric Composition of Drug-Related Materials Excreted in Human Urine after Single-Dose Oral Administration (800 mg) of Ibuprofen or Its Individual Enantiomers

Drug Administered			Drug-Related Materials Excreted in Human Urine					
			Intact Drug		Hydroxy Metabolite		Carboxy Metabolite	
Enantiomer	Optical Rotation	GLC Ratio[a]	Optical Rotation[b]	GLC Ratio[a]	Optical Rotation	GLC Ratio[a]	Optical Rotation	GLC Ratio[c]
II	+57	95:5	+42	95:5	+48 (+35.4)[d]	97:3	+49 (+47.2)[d]	51 (*S*)-(+)/(*S*)-(+) 47 (*R*)-(−)/(*S*)-(+); (*S*)-(+)/(*R*)-(−) 2 (*R*)-(−)/(*R*)-(−)
III	−57	6:94	+24	80:20	+2 (+2.8)[d]	54:46	+6 (+7.2)[d]	33 (*S*)-(+)/(*S*)-(+) 42 (*R*)-(−)/(*S*)-(+); (*S*)-(+)/(*R*)-(−) 25 (*R*)-(−)/(*R*)-(−)
I	0	50:50	+13	71:29	+21 (+29.7)[d]	71:29	+28	43 (*S*)-(+)/(*S*)-(+) 44 (*R*)-(−)/(*S*)-(+); (*S*)-(+)/(*R*)-(−) 13 (*R*)-(−)/(*R*)-(−)

[a] Ratio of (*S*)-(+)- and *R*-( )-enantiomers, as measured by GLC of the *S*-(−)-α-methylbenzylamide derivatives. [b] Chemical purity of isolated materials estimated to be 60–80%. [c] Ratio of (*S*)-(+)/(*S*)-(+)-, (*R*)-( )/(*S*)-(+)-, (*S*)-(+)/(*R*)-(−)-, and (*R*)-(−)/(*R*)-( )-enantiomers, as measured by GLC of the (*S*)-(−)-α-methylbenzylamide derivatives. [d] Optical rotation as reported in Ref. 5.

showed that imidazolide formation from IV, VII, and *n*-tridecanoic acid was completed in 5 min. Amide formation from the imidazolide was completed in 20 min. GLC, in conjunction with mass spectrometry, showed that the amides of V and VI were well resolved on a 1.5-m column of 3% (w/w) OV-17 (Fig. 2) and had extremely weak molecular ions of mass 325 (Fig. 5). Major fragmentation peaks were observed at *m/e* 267, 163, 119, 105, 91, and 59. The mass spectra for the three peaks, designated VIII, IX–X, and XI (Fig. 3), had nearly identical fragmentation patterns. The molecular ions of mass 442 were very weak. Intense fragmentation peaks were observed at *m/e* 295, 190, 120, and 105 (Fig. 5).

Enantiomeric Composition of Drug-Related Materials Excreted in Human Urine—Results from GLC measurement of the major metabolites of I, as the methyl esters, showed that urinary excretion of the unconjugated compounds was greater than 95% complete within 24 hr. Thus, the 0–24-hr urine specimens, from three subjects receiving the individual enantiomers of I, were pooled for determining the enantiomeric compositions of the intact drug and its major metabolites. The results from these studies are summarized in Table I.

The (*S*)-(−)-α-methylbenzylamides of II and III were well resolved on a 1.5-m column of 3% (w/w) OV-17 (Fig. 2). GLC–mass spectrometric analyses established that the materials responding to the assay were identical to known (*S*)-(−)-α-methylbenzylamide derivatives of II and III (10, 12). The enantiomeric composition of the intact drug excreted in urine after oral administration of II was identical to the drug ingested (Table I). However, after oral administration of III and I, 80 and 71% of the intact drugs excreted in urine, respectively, were of the (*S*)-(+)-configuration.

In vitro studies established that known I, II, and III were optically stable between pH 1 and 10 for at least 24 hr. Furthermore, isolation and characterization of known amounts of III added to urine showed that the (*R*)-(−)-configuration was retained. Optical rotation measurements, in combination with GLC, showed a linear relationship between optical rotation, $[\alpha]_D$, and isomeric composition. Optical rotation analyses of the small amounts of intact drug excreted and isolated from human urine indicated that the chemical purities ranged from 60 to 80% (Table I).

As shown in Fig. 2, the (*S*)-(−)-α-methylbenzylamides of V and VI were well resolved on the 3% (w/w) OV-17 column. Measurement of the enantiomeric composition of the major hydroxy metabolite excreted in urine after oral administration of II showed that essentially all of the material was of the (*S*)-(+)-configuration (Fig. 6). Results from the GLC measurement of the enantiomeric composition of VI (Fig. 6), partially synthesized *via* microbial oxygenation, were in excellent agreement with the reported optical rotation (15). After oral administration of III and I, 54 and 71% of the free hydroxy metabolites excreted in urine, respectively, were of the (*S*)-(+)-configuration (Table I). Results from measurement of optical rotations showed good agreement with reported values (5) and were consistent with enantiomeric composition as measured by GLC.

Measurement of the enantiomeric composition of the carboxy metabolite excreted in urine after oral administration of II showed that 51% of the material was associated with the GLC peak designated as VIII [(*S*)-(+)/(*S*)-(+)-configuration] and 47% of the material was associated with the peak designated as IX–X [combination of (*R*)-(−)/(*S*)-(+)- and (*S*)-(+)/(*R*)-(−)-configuration] (Fig. 7). A trace amount (2%) of the material was contained in the peak designated XI [(*R*)-(−)/(*R*)-(−)-configuration], consistent with metabolism of the small amount of III present in the administered drug.

After oral administration of III, 33, 42, and 25% of the carboxy

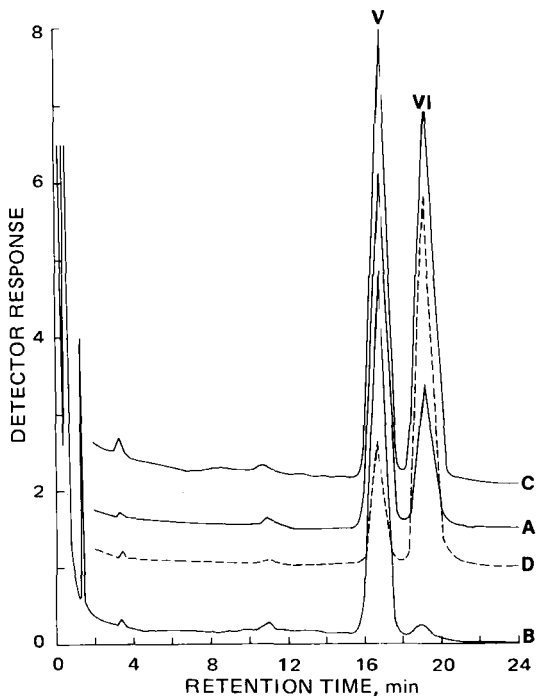

Figure 6—*Gas–liquid chromatograms of* (S)-(−)-α-*methylbenzylamide derivatives of hydroxy metabolites isolated from human urine after single-dose oral administration of 800 mg of ibuprofen (scan A),* (S)-(+)-*enantiomer (scan B), or* (R)-(−)-*enantiomer (scan C). The* (R)-(−)-*enantiomer was partially synthesized via microbial oxygenation (scan D).*

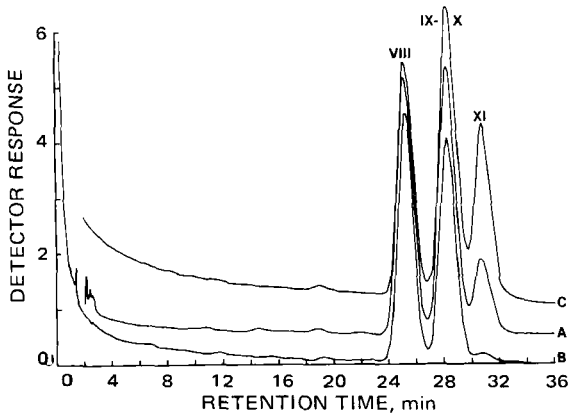

Figure 7—*Gas–liquid chromatograms of* (S)-(−)-α-*methylbenzylamide derivatives of carboxy metabolites isolated from human urine after single-dose oral administration of 800 mg of ibuprofen (scan A),* (S)-(+)-*enantiomer (scan B), or* (R)-(−)-*enantiomer (scan C).*

metabolite were associated with the peaks designated VIII, IX–X, and XI, respectively. Similarly, after oral administration of I, 43, 44, and 13% of the carboxy metabolite were associated with peaks VIII, IX–X, and XI, respectively (Fig. 7).

During oxidative metabolism of II to the carboxy metabolite, a second chiral center is introduced into the molecule. Since the chiral center in the propionic acid side chain retained its (*S*)-(+)-configuration, as observed in the intact drug and hydroxy metabolite, and with the assumption of an equal probability for oxidative metabolism of the isobutyl side chain to result in an (*S*)-(+)- or (*R*)-(−)-configuration in the second carboxyl moiety, two diastereomeric carboxy metabolites could be formed with (*S*)-(+)/(*S*)-(+)- and (*R*)-(−)/(*S*)-(+)-configurations. Two major components were found when the carboxy metabolite, isolated from urine after oral administration of II, was chromatographed as the disubstituted (*S*)-(−)-α-methylbenzylamide derivative. Repetitive mass spectrometric scanning showed that the individual chromatographic peaks were homogeneous and the mass fragmentation patterns were identical. Consistent with GLC behavior of the individual enantiomers of I and IV as well as results from optical rotation measurements, the components with retention times of 25.2 and 28.4 min were designated as VIII and IX, respectively (Fig. 7).

After administration of I or III, potentially four diastereomeric carboxy metabolites could be formed. GLC of the carboxy metabolites as the (*S*)-(−)-α-methylbenzylamide derivatives showed only three components. Results from mass spectral analyses showed that all components were homogeneous and had identical fragmentation patterns. Considering the spatial configuration of the amide derivatives used for GLC separation, it was highly likely that the component with a retention time of 28.4 min was a mixture of IX and X. Thus, the components with retention times of 25.2, 28.4, and 30.8 min were designated VIII, IX–X, and XI, respectively. Metabolic studies are in progress, using tetradeuterated I, to confirm the present assignments and to define the epimerization mechanism.

From these results, it is concluded that only the (*R*)-(−)-enantiomer of I is inverted to its optical antipode, (*S*)-(+), in humans. Both (*S*)-(+)- and (*R*)-(−)-enantiomers are transformed *in vivo* to the hydroxy and carboxy metabolites. *In vivo* oxidation of the isobutyl group of I to the corresponding 2-carboxypropyl moiety is not stereoselective.

REFERENCES

(1) S. S. Adams, E. E. Cliffe, B. Lessel, and J. S. Nicholson, *J. Pharm. Sci.*, **56**, 1687(1967).

(2) S. S. Adams, K. F. McCullough, and J. S. Nicholson, *Arch. Int. Pharmacodyn. Ther.*, **178**, 115(1969).

(3) S. S. Adams, R. G. Bough, E. E. Cliffe, B. Lessel, and R. F. N. Mills, *Toxicol. Appl. Pharmacol.*, **15**, 310(1969).

(4) S. S. Adams, R. G. Bough, E. E. Cliffe, W. Dickinson, B. Lessel, K. F. McCullough, R. F. N. Mills, J. S. Nicholson, and G. A. H. Williams, *Rheumatol. Phys. Med. Suppl.*, **1970**, 9.

(5) R. F. N. Mills, S. S. Adams, E. E. Cliffe, W. Dickinson, and J. S. Nicholson, *Xenobiotica*, **3**, 589(1973).

(6) S. Masumoto, K. Takase, Y. Maruyama, and M. Okumura, *Pharmacometrics*, **6**, 77(1972).

(7) C. D. Brooks, F. R. Schmid, J. Biundo, S. Blau, R. Gonzalez-Alcover, J. D. C. Gowans, E. Hurd, R. E. H. Partridge, and E. L. Tarpley, *Rheumatol. Phys. Med. Suppl.*, **1970**, 48.

(8) E. F. Davies and G. S. Avery, *Drugs*, **2**, 416(1971).

(9) C. D. Brooks, C. A. Schlagel, N. C. Sekhar, and J. T. Sobota, *Curr. Ther. Res.*, **15**, 180(1973).

(10) D. G. Kaiser and G. J. VanGiessen, *Pharmacologist*, **16**, 221(1974).

(11) C. J. W. Brooks and M. T. Gilbert, *J. Chromatogr.*, **99**, 541(1974).

(12) G. J. VanGiessen and D. G. Kaiser, *J. Pharm. Sci.*, **64**, 798(1975).

(13) W. J. Wechter, D. G. Loughhead, R. J. Reischer, G. J. VanGiessen, and D. G. Kaiser, "Abstracts, 14th National Medicinal Chemistry Symposium," American Chemical Society, Durham, N.H., 1974, pp. 91–98.

(14) W. J. Wechter, D. G. Loughhead, R. J. Reischer, G. J. VanGiessen, and D. G. Kaiser, *Biochem. Biophys. Res. Commun.*, **61**, 833(1974).

(15) R. A. Johnson, C. M. Hall, W. C. Krueger, and H. C. Murray, *Bioorg. Chem.*, **2**, 99(1973).

(16) L. Baczynskyj, D. J. DuChamp, J. F. Zieserl, Jr., and U. F. Axen, *Anal. Chem.*, **45**, 479(1973).

(17) D. G. Kaiser and G. J. VanGiessen, *J. Pharm. Sci.*, **63**, 219(1974).

ACKNOWLEDGMENTS AND ADDRESSES

Received April 4, 1975, from the *Research Laboratories, The Upjohn Company, Kalamazoo, MI 49001*

Accepted for publication May 12, 1975.

The authors thank Dr. C. D. Brooks for conducting the clinical portion of the study.

[x] To whom inquiries should be directed.

Fluorescence of Hydralazine in Concentrated Sulfuric Acid

DATTA V. NAIK, BRIEN R. DAVIS, KATHLEEN M. MINNET, and STEPHEN G. SCHULMAN ˣ

Abstract □ Hydralazine shows intense fluorescence at 353 nm in concentrated sulfuric acid when excited at 320 nm. This fluorescence can be utilized for the quantitative analysis of the drug in dosage forms.

Keyphrases □ Hydralazine—fluorometric analysis, dosage forms □ Fluorometry—analysis, hydralazine in dosage forms

Hydralazine (1-hydrazinophthalazine) has been used in the treatment of hypertension for many years. It apparently lowers blood pressure by inhibiting the enzymes responsible for the decarboxylation of amino acids to pressor amines and exerts a peripheral vasodilating effect through a direct relaxation of vascular smooth muscle.

Most methods for hydralazine analysis are spectrophotometric and are based on (*a*) its UV absorption in the 260–270-nm region (1), (*b*) condensation of carbonyl compounds with the reactive hydrazino group to yield hydrazone derivatives (2–8), or (*c*) the complexing and reducing property of hydralazine (9–11). The spectrophotometric method of analysis based on the reaction of hydralazine with ninhydrin (5) gave incomplete recovery and variable results (6), so an alternative method was developed based on the condensation of hydralazine with *p*-hydroxybenzaldehyde. This procedure was modified later to obtain reproducible results (7).

Recently, Zak *et al.* (8) found that neither the original (6) nor the modified (7) method afforded satisfactory reproducible results. They developed a new spectrophotometric method based on the reaction of hydralazine with *p*-methoxybenzaldehyde. In this procedure, the absorbance values were proportional to the concentration of hydralazine in the 0.1–5.0-μg/ml range, but the derivatization reaction required 30 min at elevated temperature for completion.

To date, no fluorometric method for hydralazine analysis has been reported. Because of the usual sensitivity and simplicity of fluorescence methods, the present study was undertaken to develop such a method for hydralazine.

EXPERIMENTAL

Reagents and Equipment—The pH measurements were made on a pH meter[1] with a combination silver–silver chloride glass electrode. Electronic absorption spectra were taken in 1-cm silica cells on a grating-type spectrophotometer[2]. Fluorescence spectra and intensity measurements were taken on a fluorescence spectrophotometer[3] whose monochromators were calibrated against the xenon line emission spectrum and whose output was corrected for instrumental response by means of a rhodamine-B quantum counter.

Hydralazine hydrochloride[4] was purified by recrystallization from 95% ethanol. Sulfuric acid (18 *M*) and sodium hydroxide were of analytical grade[5], and anhydrous methanol[5] was of spectroscopic quality. Formaldehyde solution[6], acetaldehyde[7], and benzaldehyde[6] were used as supplied. Sulfuric acid solutions were prepared by dilution with distilled deionized water, and the corrected Hammett acidity scale of Jorgenson and Hartter (12) was employed to calibrate these solutions. Solutions in the 0–3 pH region were prepared by appropriate dilution of 1 *N* sulfuric acid. Trace amounts of the acid or sodium hydroxide were used to adjust the pH of solutions in the pH 4–10 region. Solutions with higher pH were obtained by appropriate dilution of 1 *N* NaOH.

Standard Curves—A 1.0×10^{-2} *M* stock solution of pure hydralazine hydrochloride was prepared in 50% methanol. Appropriate dilutions of the stock solution were made with 50% methanol to give a range of concentrations. For the fluorescence standard curve, 0.1 ml of hydralazine hydrochloride solution of the appropriate concentration (concentration = 100 times the final desired concentration) was delivered to a 10-ml glass-stoppered volumetric flask, which was then filled to the mark with concentrated sulfuric acid.

The acid solution was shaken and transferred to a stoppered 1-cm² silica cell, and its fluorescence intensity was measured at 353 nm with the excitation monochromator set at 320 nm. The background intensity due to concentrated sulfuric acid alone was also measured and subtracted from the intensity obtained for the drug solution. The corrected intensities for different concentrations were plotted against the respective concentrations.

For the absorption (UV) standard curve, 0.1 ml of hydralazine hydrochloride solution of the appropriate concentration (concentration = 100 times the final desired concentration) was delivered to a 10-ml glass-stoppered volumetric flask. The flask was then filled to the mark with 50% methanol. The absorption of this solution at 270 nm was measured with 50% methanol as a reference. The absorption of several standard solutions were measured and plotted against their respective concentrations.

Tablet Extraction and Analysis—For individual tablet analysis, a tablet of hydralazine[8] was crushed in a glassine paper and the powder was quantitatively transferred to a 250-ml erlenmeyer flask. Exactly 100 ml of 50% methanol then was added, and the flask was shaken in an ultrasonic bath for 20 min to effect the dissolution of hydralazine hydrochloride. The solution was filtered through a sintered-glass funnel, and the first 5 ml of the filtrate was discarded. The filtrate thus obtained for a tablet whose labeled content is 50 mg of the drug would be 0.5 mg/ml.

For fluorometric analysis, 0.1 ml of the tablet extract was transferred to a 10-ml glass-stoppered volumetric flask, which was then filled to volume with concentrated sulfuric acid. The fluorescence intensity of the acid solution was measured in the same way as for the standard solutions. For absorptiometric analysis, 0.5 ml of the tablet extract was transferred to a 25-ml glass-stoppered volumetric flask, which was then filled to volume with 50% methanol. The absorption of this solution at 270 nm was measured with 50% methanol as a reference.

Analysis of Hydralazine Hydrochloride Injection—Exactly 0.5 ml of hydrazine hydrochloride injection[8] with a labeled content of 20 mg was transferred to a 25-ml volumetric flask and diluted to

[1] Research model 12-B, Corning Scientific Instruments, Corning, N.Y.
[2] Model DB-GT, Beckman Instruments, Fullerton, Calif.
[3] Model MPF-2A, Perkin-Elmer Corp., Norwalk, Conn.
[4] Pfaltz & Bauer, Flushing, N.Y.
[5] Mallinckrodt Chemical Works, St. Louis, Mo.
[6] J. T. Baker Chemical Co., Phillipsburg, N.J.
[7] Matheson, Coleman & Bell, East Rutherford, N.J.
[8] Apresoline, 50 mg, Ciba-Geigy Corp.

volume with 50% methanol. The expected concentration of this solution would be 0.4 mg/ml. For fluorometric analysis, 0.1 ml of the solution was added to a 10-ml glass-stoppered volumetric flask, which was then filled to the mark with concentrated sulfuric acid. The intensity measurements on the acid solution were carried out in the same way as for the acid solution of the tablet extract. For absorptiometric analysis, 0.5 ml of the solution of the injection was transferred to a 25-ml glass-stoppered volumetric flask, which was then filled to volume with 50% methanol. The absorption of this solution was measured at 270 nm with 50% methanol as a reference.

The background fluorescence intensity near 350 nm largely depends on the concentration of sulfuric acid because of a fluorescing impurity in the latter. This impurity is present in the analytical reagent grade sulfuric acid from essentially all commercial suppliers. Moreover, the sulfuric acid concentration affects the amount of fluorophore produced (Fig. 2); therefore, to avoid absorption of atmospheric moisture by the acid, it should be kept tightly stoppered in a dry place. When a fresh bottle of sulfuric acid is used or if the concentration of sulfuric acid is suspected to have changed, a new standard curve should be prepared. It is desirable to carry out the intensity measurement on at least one standard solution (preferably having a final concentration close to that of the unknown solution) of the drug at the same time that the unknowns are measured, so as to check any variation in the concentration of sulfuric acid.

RESULTS AND DISCUSSION

Since hydralazine does not fluoresce in aqueous solution in the pH 0–14 range, an attempt was made to make a fluorescent derivative of hydralazine. First, the benzaldehyde hydrazone of hydralazine was prepared by condensation of hydralazine with benzaldehyde in water. The product obtained had fluorescence at 358 nm when excited at 296 nm. However, the reaction was very slow, was dependent on the initial concentration of hydralazine in the reaction mixture, and required the use of heat for completion in a short time. Therefore, it was unsatisfactory for analytical use.

Next, the acetaldehyde hydrazone was prepared by condensation of hydralazine with acetaldehyde using a 1% aqueous solution of the latter. The product obtained *in situ* had fluorescence at 410 nm when excited at 320 nm. The reaction could be taken to completion with concentrations of hydralazine as low as 2 μg/ml by heating at 70° for 20 min. The fluorophore obtained was stable for 24 hr. Fluorescence intensity varied linearly with the concentration of hydralazine over the 2–10-μg/ml range. However, the main disadvantage of this procedure was the instability of the aqueous acetaldehyde solution, whose concentration was found to affect the sensitivity of the analysis.

An attempt was made to prepare the formaldehyde hydrazone of hydralazine. When hydralazine was directly reacted with a 10% aqueous solution of formaldehyde at room temperature, no fluorescence resulted. On heating the reaction mixture, the hydrazone was generated and showed a broad fluorescence band at 345 nm when excited at 275 nm. However, the reaction did not go to completion even after heating at 80° for 40 min. The fluorescence intensity kept increasing with the amount of heat, which made it unsuitable for analytical use.

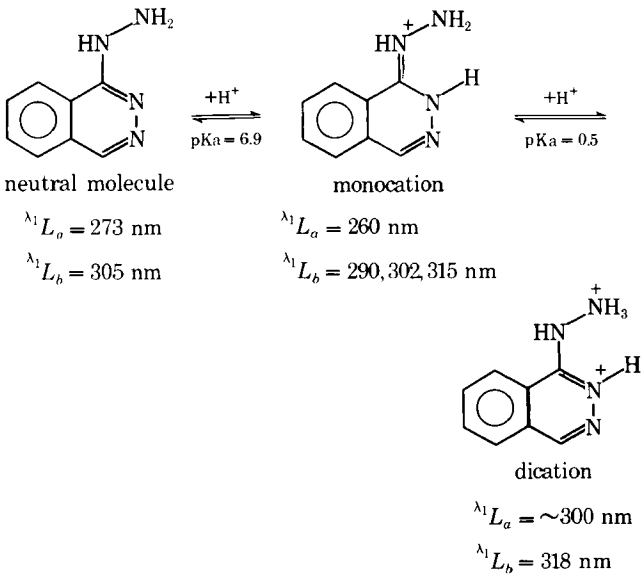

Scheme I

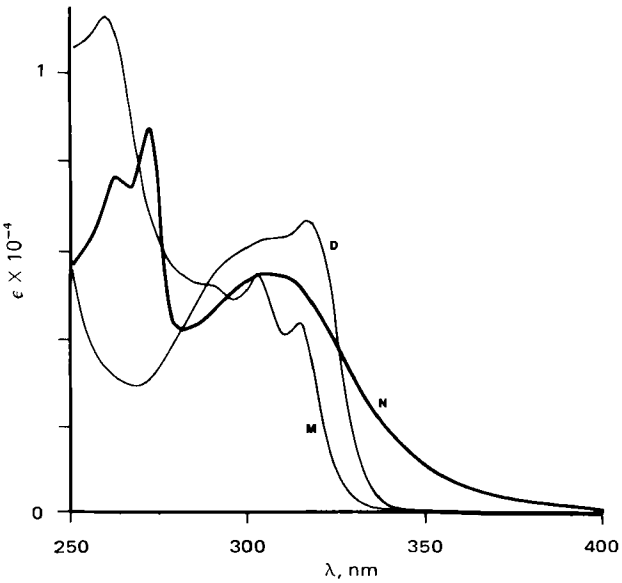

Figure 1—*Absorption spectra of hydralazine (1 × 10⁻⁴ M). Key: N, neutral; M, monocation; and D, dication.*

Hydralazine has four basic nitrogen atoms. However, only two of them show protolytic equilibria, involving three distinct species, in the acidity range of −10–10. These species, along with their ^1L_a and ^1L_b absorption bands, and the pKa values corresponding to their interconversion are presented in Scheme I. The absorption spectra of the neutral molecule, monocation, and dication are shown in Fig. 1.

The neutral molecule and doubly protonated cation yield broad long wavelength absorption bands with blurred vibrational structure. The spectral features of these species, given in the scheme, correspond to the band maxima. The monocation, however, exhibits some vibrational structure in the absorption band, but the most distinct and intense vibrational features of the absorption bands are given. The ground-state pKa's were determined absorptiometrically.

The ^1L_b band in hydralazine is broad and occurs in the same spectral region as in phthalazine (13). However, the ^1L_a band moves from 260 nm in the latter to 273 nm in the former. This difference indicates that the substitution of the hydrazino group in the 1-position does not affect the ^1L_b band of phthalazine but, as expected, shifts the ^1L_a band to a longer wavelength due to the charge transfer from the hydrazino group to the ring.

In the first protonation, the proton undoubtedly goes on the more basic ring nitrogen. In the case of 1-hydroxy- and 1-mercaptophthalazine, Albert and Barlin (14) showed that the first proton goes on the ring nitrogen in the 2-position of phthalazine. In hydralazine, however, the positive charge can be located at the protonated ring nitrogen (I) or at the imino nitrogen of the hydrazino group (II).

If the positive charge was on the ring nitrogen, a red shift in both the ^1L_b and ^1L_a bands would be expected. Alternatively, if the positive charge resided on the amino nitrogen of the hydrazino

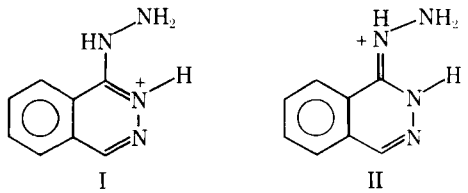

I II

Table I—Results of Analysis of Commercial Hydralazine Hydrochloride Preparations

	Labeled Contents, mg	Fluorometric Method		UV Absorption Method (NF XIII)	
		Average Found[a], mg	%	Average Found[a], mg	%
Hydralazine hydrochloride[b] tablet	50	49.2 ± 2	98.2 ± 4	48.8 ± 2	97.6 ± 4
Hydralazine hydrochloride[c] injection (0.5 ml analyzed)	20	20.0 ± 0.5	100 ± 2.5	20.2 ± 0.5	101 ± 2.5

[a] Based on five samples from a 10-tablet or a 10-injection batch. [b] Apresoline, Lot 10064. [c] Apresoline, Lot 37022-402.

group, the ^1L_a band should show a blue shift because the conjugation of the hydrazino group with the ring is less extensive in the excited state than in the ground state of the monocation. The observed blue shift of 13 nm in the ^1L_a on the first protonation of hydralazine indicates that II is the more plausible representation of the monocation. A similar amidine-type structure was also suggested for 2-aminoquinoline (15).

In the second protonation, which would be the protonation of the terminal nitrogen of the hydrazino group, there is no ambiguity about the location of the two positive charges, and the dication can be represented as shown in Scheme I. Just as in the case of the protonation of quinoline, the second protonation of hydralazine causes the ^1L_a band to red shift and overlap the ^1L_b band (Fig. 1). The red shift, which is anomalous for the protonation of the hydrazino group (16), is caused by the restoration of the aromaticity of the heterocyclic ring by partial withdrawal of the lone pair of the hydrazino group due to attraction by the positive charge on the terminal nitrogen of the same group.

No fluorescence could be detected from the neutral molecule or the singly protonated species. However, a slight fluorescence was detected in the hydralazine solution of Hammett acidity of −5. Therefore, a fluorometric titration in the Hammett region was carried out, and the titration curve is shown in Fig. 2. Since the absorption spectra showed no change in very concentrated sulfuric acid, the fluorescence must occur as a result of an excited-state protolytic process. The fluorescence band at 353 nm is thus due to either the doubly protonated hydralazine, which is more acidic in the excited state, or a triply protonated hydralazine, which is more basic in the excited state. Which one of the two species is responsible for fluorescence at 353 nm cannot be ascertained at this time.

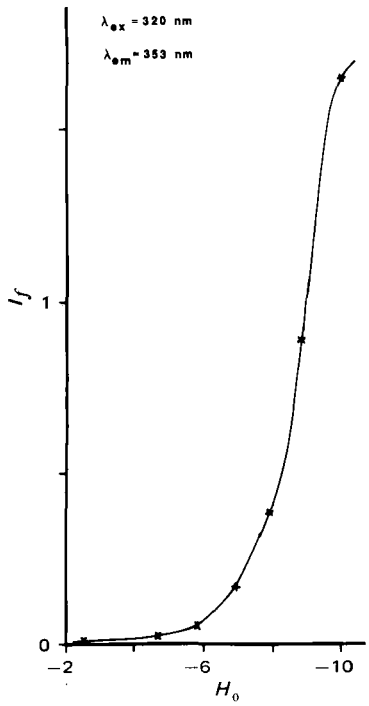

Figure 2—*Relative fluorescence intensity,* I_f, versus *the Hammett acidity of the hydralazine solutions* (1×10^{-4} M).

The fluorophore can be generated instantly in concentrated sulfuric acid; the amount of the fluorophore produced and, hence, the fluorescence intensity at 353 nm directly depend on the concentration of sulfuric acid (Fig. 2). The fluorescence is quite strong at Hammett acidity of −10, and the intensity remains unchanged at least for 24 hr. Heating the acid solution of hydralazine followed by cooling at room temperature did not alter the fluorescence intensity. Strict temperature control of the sample compartment was not necessary because of the insensitivity of the fluorescence intensity to small changes in the temperature of the solution.

The relative fluorescence intensity of the acid solutions varied linearly with the concentration of hydralazine hydrochloride in the 2–8-μg/ml range. The limit of detection, based on the amount of hydralazine hydrochloride required to yield a fluorescent intensity greater than twice that of the background, was 0.15 μg/ml.

Table I shows the results of analysis of hydralazine hydrochloride tablets and injections. The method is very reproducible, and the agreement between the analyses of several tablets and injections is excellent. To confirm the results, the same tablets or injections were analyzed by the UV absorption method similar to that recommended in NF XIII (1) (Table I). The agreement between the fluorometric method and the UV method is excellent.

This method of analysis is very simple and is the first reported method using a fluorescence technique. It is relatively fast and involves only one easily available reagent. This fluorometric method should be useful for doing fast assays on small quantities of hydralazine.

REFERENCES

(1) "The National Formulary," 13th ed., Mack Publishing Co., Easton, Pa., 1970, p. 349.

(2) R. Ruggieri, *Farmaco, Ed. Prat.*, **11**, 571(1956).

(3) B. Wesley-Hadzija and F. Abaffy, *Croat. Chem. Acta*, **30**, 15(1958).

(4) G. I. Luk'yanchikova, *Byul. Izobret., No. 14*, **1962**, 44.

(5) H. M. Perry, H. A. Schroeder, and J. D. Morrow, *Amer. J. Med. Sci.*, **228**, 405(1954).

(6) A. R. Schulert, *Arch. Int. Pharmacodyn. Ther.*, **13**, 420(1972).

(7) R. Zacest and J. Koch-Weser, *Clin. Pharmacol. Ther.*, **13**, 420(1972).

(8) S. B. Zak, M. F. Bartlett, W. E. Wagner, T. G. Gilleran, and G. Lukas, *J. Pharm. Sci.*, **63**, 225(1974).

(9) S. Fallab and H. Erlenmeyer, *Helv. Chim. Acta*, **45**, 1957(1962).

(10) P. Cooper, *Pharm. J.*, **177**, 495(1956).

(11) T. Urbanyi and A. O'Connell, *Anal. Chem.*, **44**, 565(1972).

(12) M. J. Jorgenson and D. R. Hartter, *J. Amer. Chem. Soc.*, **85**, 878(1963).

(13) S. F. Mason, *J. Chem. Soc.*, **1962**, 493.

(14) A. Albert and G. B. Barlin, *ibid.*, **1962**, 3129.

(15) P. J. Kovi. A. C. Capomacchia, and S. G. Schulman, *Anal. Chem.*, **44**, 1611(1972).

(16) A. Albert and G. Catterall, *J. Chem. Soc., C*, **1967**, 1533.

ACKNOWLEDGMENTS AND ADDRESSES

Received September 30, 1974, from the *College of Pharmacy, University of Florida, Gainesville, FL 32610*

Accepted for publication May 28, 1975.

[x] To whom inquiries should be directed.

Solubility of Straight-Chain and Branched Alkyl Barbiturates in Straight-Chain Alcohols

BERTRAND LAPRADE, JOHN W. MAUGER, HAROLD PETERSEN, Jr., KENNETH S. ALEXANDER, and ANTHONY N. PARUTA ˣ

Abstract □ The solubilities of a series of chemically related barbiturates, including some medically useful ones as well as phenobarbital, were determined at 25° in the straight-chain alcohols methanol through butanol. The solubility values are given in both milligrams per milliliter and the mole fraction notation. The solubility in methanol was the highest and decreased nonlinearly for the solubility in 1-butanol. In several cases, mole fraction solubility gave shouldering or peaking as a function of the carbon number of the solvent. This series of barbiturates was broken down into two subsets of straight-chain and branched alkyl barbiturates, and solubility ratios in these subsets were considered.

Keyphrases □ Barbiturates—straight-chain and branched alkyl substituents, solubility in straight-chain alcohols □ Alcohols, straight chain—solubility of 5,5-disubstituted barbiturates □ Solubility—5,5-disubstituted barbiturates in straight-chain alcohols

This study involved a basic approach to physical–chemical behavior. The approach utilized the experimental measurement of the solubility of a chemically related series of compounds in a chemically related series of solvents. This type of investigation allows for a delineation of the relationship between the magnitude of solubility and chemical differences.

The solubility of an important pharmacological class of sedative compounds—the 5,5-disubstituted barbituric acids with varying substituent groups—was studied. The compounds have both a straight-chain and branched series, allowing for a possible relationship for both the chain size and positional variations (1). Phenobarbital, a 5,5-disubstituted barbituric acid containing one phenyl ring in the 5-position, was included to observe the effect of an aromatic system on solubility as compared to the alkyl substituents of the other barbiturates. The magnitude of solubility was determined in straight-chain alcohols from methanol through butanol to allow for some definitive relationship for a particular solute in these related solvents.

EXPERIMENTAL

Materials—The following materials were used: 5,5-diethylbarbituric acid[1]; 5-ethyl-5-propylbarbituric acid[2]; 5-ethyl-5-isopropylbarbituric acid[3]; 5-butyl-5-ethylbarbituric acid[4]; 5-ethyl-5-pentylbarbituric acid[5]; 5-ethyl-5-(2-methylpropyl)barbituric acid[6]; 5-ethyl-5-(3-methylbutyl)barbituric acid[7]; 5-ethyl-5-(1-methylbutyl)barbituric acid[8]; 5-ethyl-5-(1-methylpropyl)barbituric acid[9]; 5-ethyl-5-phenylbarbituric acid[10]; methanol, anhydrous, spectrophotometric grade solvent[11]; ethanol (absolute alcohol), USP reagent quality[12]; 1-propanol[13]; 1-butanol, analytical reagent[14]; certified acetone, 99 mole % pure[15]; certified benzene, 99 mole % pure (thiophene free)[16]; sodium phosphate dibasic heptahydrate, analytical reagent[17]; sodium metal[18]; sodium hydroxide[19]; diethyl ethyl-*n*-propylmalonate[20]; diethyl ethyl-*n*-amylmalonate[21]; diethyl isobutylmalonate[22]; ethyl iodide certified[23]; sulfuric acid[24]; urea[25] USP; magnesium metal turnings[26]; and iodine crystals[27].

The purity of the alcohols was determined by measurements of physical constants. The refractive index[28] was determined at 25° using a standard with a known refractive index to check the accuracy of the instrument.

An oscillometer[29] was used in the measurements of dielectric constant values. Agreement with values in the literature was obtained.

For the synthesized barbiturates (II, IX, and X), purity and identification were evidenced by carbon, hydrogen, and nitrogen analysis and IR spectra. For all compounds studied, both IR and NMR spectra were determined. All solutes were recrystallized from ethanol and dried to constant weight, and their melting points[30] were determined. These values are shown in Table I, and there is excellent agreement between determined and literature values (3, 4). Table I also lists the chemical nomenclature, the chemical structure, and the common name of the barbiturate, if one exists.

Procedure—The solubilities of the various barbiturates in the various alcohols were determined by a procedure given previously (5). Screw-capped[31] bottles with an excess of a barbiturate in each solvent were rotated for 24 hr in a constant-temperature bath set at 25 ± 0.1°. Samples were withdrawn through a pledget of glass wool into a pipet, which was wiped clean and allowed to drain into a tared volumetric flask. The flasks were reweighed to determine the weight of the sample.

A pH 10.9 buffer solution was prepared by dissolving 134 g of sodium phosphate dibasic heptahydrate in 2 liters of distilled water and adjusting to pH 10.9 with 1 *M* sodium hydroxide. Suitable dilutions were made with this buffer, and the concentration of the solute was determined spectrophotometrically. Each solubility determination represents the average values for at least four runs of the 10 barbiturates in each solvent. The variation in the results of the solubility study was 2–4%.

Assay Procedure—A spectrophotometric assay[32] was used for the quantitative determination of each barbiturate. UV spectra of each compound were obtained to determine the wavelength at which maximum absorbance occurred. The maxima for all these barbiturates were between 239 and 240 nm. A linear relationship

[1] Lot 5115, Merck and Co.
[2] Compound II; synthesized in this laboratory (2).
[3] Lot SQ3540, E. R. Squibb and Sons.
[4] Lot 20-4441-01, Abbott Laboratories.
[5] Compound IX; synthesized in this laboratory.
[6] Compound X; synthesized in this laboratory.
[7] Lot 3180, Ruger Chemical Co.
[8] Lot 776-7548, Abbott Laboratories.
[9] Lot 5086, McNeil Laboratories.
[10] Lot MPY, Mallinckrodt Chemical Works.
[11] Lot VMN, Mallinckrodt Chemical Works.
[12] U.S. Industrial Chemical Co.
[13] Lot 35592, Baker Analyzed, J. T. Baker Chemical Co.
[14] Lot +DY, Mallinckrodt Chemical Works.
[15] Lot 792702, Fisher Scientific Co.
[16] Lot 793859, Fisher Scientific Co.
[17] Lot WTKL, Mallinckrodt Chemical Works.
[18] Lot 71046, J. T. Baker Chemical Co.
[19] Lot W183J, Allied Chemical.
[20] Lot 26294, K & K Laboratories.
[21] Lot 20929, K & K Laboratories.
[22] Lot 11008, K & K Laboratories.
[23] Lot 794939, Fisher Scientific Co.
[24] Lot D610153, Allied Chemical.
[25] Lot 701909, Fisher Scientific Co.
[26] Lot 55053, Fisher Scientific Co.
[27] Lot 772803, Fisher Scientific Co.
[28] Abbe-3L refractometer.
[29] Model V Sargent Chemical oscillometer.
[30] Hoover melting-point apparatus.
[31] Lined with Teflon.
[32] Beckman DU model spectrophotometer.

Table I—Summary of the Compound Number, Chemical Name, Alkyl Substituent Group Structure, and Melting Point of Solutes Used in This Study

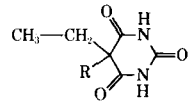

Compound	Chemical Name	R Group	Common Name	Melting Point	
				Determined	Literature (Refs. 3 and 6)
I	5,5-Diethylbarbituric acid	CH_3CH_2—	Barbital	188–190°	188–192°
II	5-Ethyl-5-propylbarbituric acid	$CH_3CH_2CH_2$—	—	146–147°	146–147°
III	5-Butyl-5-ethylbarbituric acid	$CH_3CH_2CH_2CH_2$—	Butethal	126–128°	124–127°
IV	5-Ethyl-5-pentylbarbituric acid	$CH_3CH_2CH_2CH_2CH_2$—	—	135–136°	135–136°
V	5-Ethyl-5-phenylbarbituric acid		Phenobarbital	156–157°	156–157°
VI	5-Ethyl-5-isopropylbarbituric acid	$(CH_3)_2CH$—	Probarbital	202–203°	203°
VII	5-Ethyl-5-(1-methylpropyl)-barbituric acid	$CH_3CH_2(CH_3)CH$—	Butabarbital	165–166°	165–168°
VIII	5-Ethyl-5-(2-methylpropyl)-barbituric acid	$(CH_3)_2CHCH_2$—	—	174–175°	174–176°
IX	5-Ethyl-5-(1-methylbutyl)-barbituric acid	$CH_3CH_2CH_2(CH_3)CH$—	Pentobarbital	129–130°	130°
X	5-Ethyl-5-(3-methylbutyl)-barbituric acid	$(CH_3)_2CHCH_2CH_2$—	Amobarbital	156–158°	156–158°

existed in all cases, indicating that the Beer–Lambert relationship was operative within the concentration ranges studied.

RESULTS AND DISCUSSION

All compounds studied were 5,5-disubstituted barbituric acid derivatives where one substituent was an ethyl group. The chemical variation in these compounds was the other group at the 5-position; differences in physicochemical behavior were due to the differences in the functional group at this position. Thus, the solubility of 5-ethyl-5-butylbarbituric acid when compared with the solubility of 5-ethyl-5-amylbarbituric acid was due to the relative influences of the amyl and butyl groups. The effect of positional changes in branching also could be deduced by comparing 5-ethyl-5-(1-methylbutyl)barbituric acid and 5-ethyl-5-(3-methylbutyl)-barbituric acid.

From the compounds listed in Table I, two subsets of derivatives can be considered, those possessing a linear arrangement of a carbon chain and those with a branched carbon chain. Phenobarbital, the only aromatic substituted barbiturate, was grouped with the *n*-alkyl set since a phenyl group is considered to correspond in effect to an *n*-propyl group. The ensuing discussion is based on a comparative effect for the particular substituent in a set or series of compounds.

The magnitudes of solubilities were experimentally determined for a series of barbituric acid derivatives at 25°. The solubility values for these compounds in straight-chain alcohols are given in Table II, where solubilities are expressed as milligrams per milliliter and mole fraction. Previous studies (1, 4, 6–9) of barbiturate solubility dealt with solubility maxima, solubility parameters, and dielectric constant relationships.

In Fig. 1, the solubilities of the barbiturates noted are plotted in milligrams per milliliter at 25° *versus* the carbon number of the alcohols. Nonlinear solubility curves were evidenced for all barbiturates studied; they were plotted as two derivative subsets including linear derivatives (and aromatic phenyl) and branched derivatives.

From inspection of Table II, the following rank-order solubilities were noted regardless of solvent for the linear substituted

Table II—Barbiturate Solubilities at 25° in Straight-Chain Alcohols

Compound	Melting Point	Solubility[a], mg/ml			
		Methanol	Ethanol	1-Propanol	1-Butanol
I	189°	166 (4.1)	95 (3.2)	58 (2.4)	41 (2.1)
II	147°	325 (8.3)	195 (6.4)	123 (4.2)	78 (3.8)
III	127°	530 (17.1)	392 (14.3)	341 (14.3)	278 (13.4)
IV	136°	553 (20.6)	444 (16.9)	377 (17.1)	324 (16.6)
V	157°	252 (5.8)	127 (3.7)	71 (2.9)	54 (2.4)
VI	203°	129 (3.1)	65 (2.1)	21 (0.8)	13 (0.6)
VII	166°	132 (2.8)	80 (2.3)	42 (1.5)	28 (1.2)
VIII	175°	123 (2.6)	72 (2.1)	35 (1.3)	28 (1.3)
IX	130°	313 (7.5)	235 (7.4)	201 (7.7)	151 (6.8)
X	157°	293 (7.4)	215 (6.2)	177 (6.5)	134 (6.0)

[a] Mole fraction solubilities × 10^2 are given in parentheses.

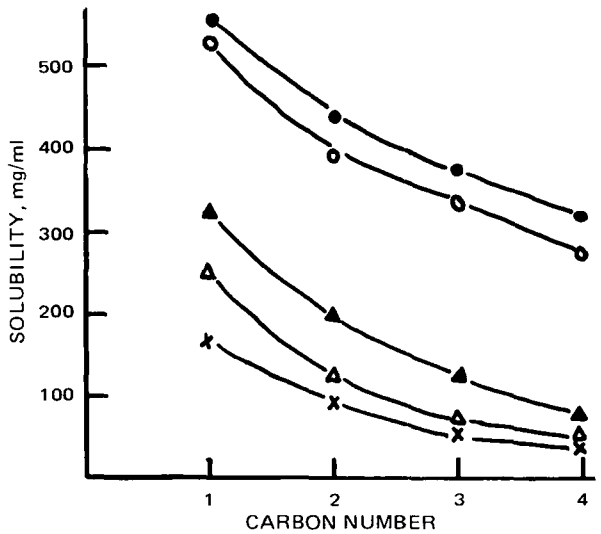

Figure 1—*Solubility at 25° of various* n*-alkyl barbiturates as a function of the carbon number of the alcohol solvents. Key:* ●, *IV;* ○, *III;* ▲, *II;* △, *V; and* ×, *I. See Table I.*

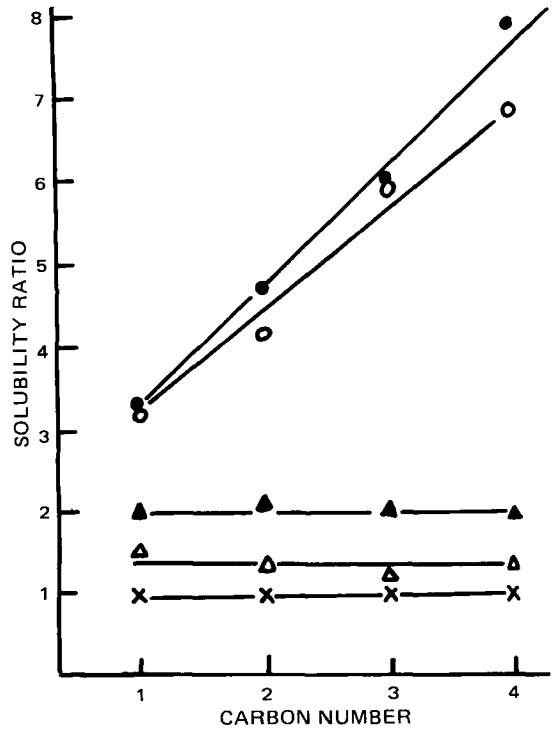

Figure 2—*Ratio of solubility of the various* n*-alkyl barbiturates to that of ethyl barbiturate as a function of the carbon number of the alcohol solvents: Key:* ●, *IV;* ○, *III;* ▲, *II;* △, *V; and* ×, *I. See Table I.*

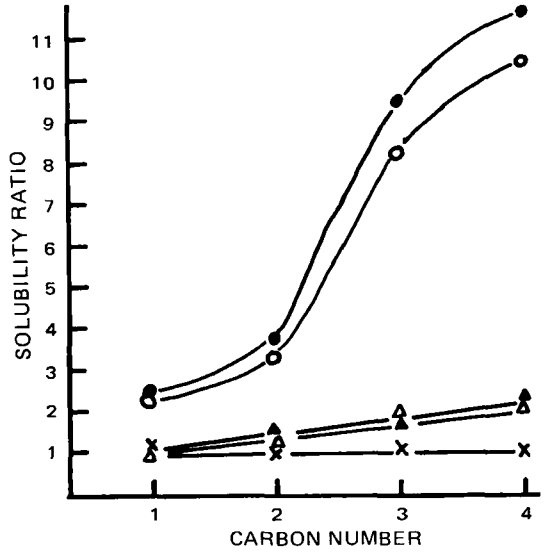

Figure 3—*Ratio of solubility of the various branched-chain barbiturates to that of 1-propyl barbiturate as a function of the carbon number of the alcohol solvents. Key:* ●, *IX;* ○, *X;* △, *VIII;* ▲, *VII; and* ×, *VI. See Table I.*

groups (I–V): amyl > butyl > propyl > ethyl; the effect of the phenyl group on solubility was intermediate between the ethyl and propyl groups. Moreover, solubilities expressed in milligrams per milliliter decreased for each solute as the alkyl chain length of the solvent was increased from one to four. When the data were expressed in the mole fraction notation, however, IV (amyl) and III (butyl) gave solubility profiles that showed shouldering or peaking effects in ethanol and 1-propanol.

For the branched solutes (VI–X), the rank-order solubilities were 1-methylbutyl > 3-methylbutyl > 1-methylpropyl > 2-methylpropyl > isopropyl. The solubilities of the last three compounds were quite similar to one another. For these solutes, the melting points, as expected from preferred configurational interactions, would at best be approximately correlatable with solubilities and this was found to be the case. Compounds VI–VIII, possessing similar solubilities, had high melting points whereas the lower melting compounds possessed significantly higher solubilities. In the mole fraction notation given in Table II, it can be discerned that VI and VII produced shouldering in methanol, whereas IX and X produced peaks in 1-propanol in the solubility profiles as a function of the carbon number of the alcohol solvent.

Inspection of the data reveals the following relationships among the derivatives studied. Solubility expressed in the pharmaceutical notation showed that each derivative had the highest solubility in methanol and decreased nonlinearly in each successive alcohol up to and including 1-butanol. The solubility increased with increasing chain length in both the linear and branched subsets of 5,5-disubstituted barbituric acids studied. The solubility isotherm of phenobarbital resided between the two and three linear carbon chain of the alkyl barbiturate. In all cases, the linear three, four, and five carbon chains (II–V) were more soluble in the alcohols than the branched three, four, and five carbon chains (VI–X).

Positional variations such as the 5-ethyl-5-(1-methylpropyl)barbituric acid and 5-ethyl-5-(2-methylpropyl)barbituric acid (VII and VIII) and the 5-ethyl-5-(1-methylbutyl)barbituric acid and the 5-ethyl-5-(3-methylbutyl)barbituric acid (IX and X) did not cause very large shifts in the magnitude of solubility of the solutes. However, these solubility shifts were greater for the larger branched chains (IX and X) than for the smaller branched chains (VII and VIII).

Another parameter of interest would be the relative magnitudes of solubility in the alcohol solvent series as the variable groups changed. Thus, the magnitudes could be compared between 5,5-diethylbarbituric acid and 5-ethyl-5-propylbarbituric acid or any other set of compounds. If the ratios of solubility were similar for the alcohol series, then the solubility profiles would be parallel, indicating that the solubility increased proportionately and invariantly in the linear alcohol series. If the ratios were not parallel (or/and linear), this finding would indicate a disproportionate relative effect in the alcohol series. In Figs. 2 and 3, the ratios of the solubilities in straight-chain alcohols are plotted for both the *n*-alkyl and branched alkyl barbiturate series utilizing 5,5-diethylbarbituric acid and 5-ethyl-5-isopropylbarbituric acid as unity, respectively.

The solubility ratios are given in Tables III and IV, and the data are plotted in Fig. 2 as a function of carbon number. There was a direct proportionality between 5-ethyl-5-propyl- and 5,5-diethylbarbituric acid such that the effect of the propyl group compared to the ethyl group was constant. Furthermore, the solubility of 5-ethyl-5-propylbarbituric acid was about twice as large in all alcohols studied. The other *n*-alkyl groups, butyl (III) and amyl (IV), showed ratios of about threefold in methanol rising to seven- or eightfold in 1-butanol. This finding indicates that the solubility of 5,5-diethylbarbituric acid in these alcohols decreased at a more rapid rate than the solubility of 5-ethyl-5-butyl- or 5-ethyl-5-amylbarbituric acids.

Table III—Ratios of Barbiturate Solubilities to Ethyl Barbiturate Solubility

Compound	Methanol	Ethanol	1-Propanol	1-Butanol
I	1.0	1.0	1.0	1.0
II	2.0	2.1	2.0	1.9
III	3.2	4.1	5.9	6.8
IV	3.3	4.7	6.5	7.9
V	1.5	1.3	1.2	1.3

Table IV—Ratios of Barbiturate Solubilities to 5-Ethyl-5-isopropylbarbituric Acid Solubility

Compound	Methanol	Ethanol	1-Propanol	1-Butanol
VI	1.0	1.0	1.0	1.0
VII	1.0	1.2	2.0	2.2
VIII	1.0	1.1	1.7	2.2
IX	2.4	3.7	9.5	11.6
X	2.3	3.2	8.2	10.3

REFERENCES

(1) A. N. Paruta and T. L. Breon, *J. Pharm. Sci.*, **59**, 1306(1970).

(2) E. Fisher and F. Dilthey, *Ann.*, **335**, 334(1904).

(3) "The Merck Index," 7th ed., Merck & Co., Rahway, N.J., 1960, pp. 71, 119, 794.

(4) A. N. Paruta, B. J. Sciarrone, and N. G. Lordi, *J. Pharm. Sci.*, **51**, 705(1962).

(5) A. N. Paruta, *ibid.*, **58**, 204(1969).

(6) S. A. Khalil and A. N. Martin, *ibid.*, **56**, 1225(1967).

(7) N. G. Lordi, B. J. Sciarrone, T. J. Ambrosio, and A. N. Paruta, *ibid.*, **53**, 463(1964).

(8) *Ibid.*, **53**, 1349(1964).

(9) L. Reber and C. Pathamanon, *Amer. J. Pharm.*, **139**, 234(1967).

ACKNOWLEDGMENTS AND ADDRESSES

Received February 19, 1974, from the *College of Pharmacy, University of Rhode Island, Kingston, RI 02881*

Accepted for publication May 21, 1975.

Abstracted in part from a dissertation submitted by B. Laprade to the Graduate School, University of Rhode Island, in partial fulfillment of the Doctor of Philosophy degree requirements.

[x] To whom inquiries should be directed.

Determination of Methyl Methacrylate in Surgical Acrylic Cement

ERIC B. SHEININ, WALTER R. BENSON [x], and WILSON L. BRANNON

Abstract □ A methyl methacrylate cement used in hip surgery as well as in dentistry was identified and quantitatively analyzed for its monomer content in starting materials and in the finished cement by proton magnetic resonance spectroscopy. IR data indicated that the monomer continued to escape from the product after it had hardened. The presence of 21% methyl methacrylate monomer relative to the polymer was demonstrated at the time the cement normally would be inserted into the body.

Keyphrases □ Methyl methacrylate—PMR analysis, ratio of monomer to polymer content, surgical acrylic cement □ Cement, surgical—PMR analysis of methyl methacrylate monomer relative to polymer content □ PMR spectroscopy—analysis, methyl methacrylate in surgical acrylic cement

The biomedical applications of polymers have increased rapidly in recent years (1, 2). One of the more widely used polymeric materials is methyl methacrylate bone cement. This polymer has been used extensively in dentistry and was approved for use in the United States for hip replacement and knee replacement operations. It is also used in skull surgery. Some deaths reported in 1971 during surgery prompted the examination of the material.

BACKGROUND

The methyl methacrylate cement is supplied as a kit made up of a sterile ampul of liquid and a sterile package of powder. The liquid consists of methyl methacrylate monomer, *N,N*-dimethyl-*p*-toluidine (polymerization initiator), and hydroquinone (polymerization inhibitor). The powder consists of polymethyl methacrylate–styrene copolymer (83.3%) and polymethyl methacrylate (16.7%) with benzoyl peroxide added as an initiator; preparations are available with or without barium sulfate (10%).

In the surgical application of the product, the liquid is mixed intimately with the powder until a putty is formed. This soft, workable putty is generally made into a ball and kept until just before being placed around the metal prosthesis. In this form, the prosthesis is placed in the body of the patient where the putty continues to harden.

Under normal surgical procedures, some monomer can diffuse out of the cement and into the body. It has been detected in the breath of patients undergoing this type of surgery. The high lipid solubility of the monomer aids its distribution throughout the body and makes hepatotoxicity a real possibility. This toxicity has been demonstrated in mice (3). In addition, extensive studies on dogs have shown large drops in blood pressure, decreases in heart rate, increased respiration, and changes in the ECG (4).

Sensitization to the monomer in humans has been reported (5–8); some investigators also suggested that it is responsible for, or a contributory factor in, observed cases of hypotensive states and cardiac arrest (4). In 1970, the British literature reported nine cases of cardiac arrest following the use of methyl methacrylate cement, and at least one fatality was reported in 1971 in this country (9).

There have been no definitive reports on the concentration of the potentially toxic monomer in the putty stage of the cement during the 4–5-min period after mixing when the putty is placed into the body of the patient. It was estimated that there may be up to 10% residual monomer in the curing mass after 1 hr (10). In a related study using a GLC method, Bechtel *et al.* (11), using the same product as that analyzed in the authors' laboratories, determined the amount of monomer leaching out of acrylic bone cements into tissues during polymerization. At 2 min after mixing, the monomer killed varying amounts of the surrounding tissue cells. However, the putty was placed in contact with the tissues earlier than the instructions indicated for the material used in that work. The monomer concentration in the putty at any time was unknown.

In 1971, Smith (12) reported the approximate composition of very similar acrylic cements used for dental applications, using an assay method based on the bromination of the double bond (13), and obtained 1.9 and 3.5% monomer content in acrylic cements used in hip replacement surgery. In these cases, the earliest reported analysis was obtained 1 hr after the kit contents were mixed. Methods based on IR spectrophotometry (14) and on polarography (15) have been used to determine the monomer content in bone cements sampled 1 hr or more after mixing.

The purpose of this investigation was to determine the amount of monomer, relative to the polymer, present in the putty at the recommended time of insertion into the body. Proton magnetic resonance (PMR) spectroscopy was used; this method requires no internal standard nor weighing of the sample, since the ratio of monomer to polymer is determined from the ratio of the vinyl to methoxyl signals.

REFERENCES

(1) A. N. Paruta and T. L. Breon, *J. Pharm. Sci.*, **59**, 1306(1970).

(2) E. Fisher and F. Dilthey, *Ann.*, **335**, 334(1904).

(3) "The Merck Index," 7th ed., Merck & Co., Rahway, N.J., 1960, pp. 71, 119, 794.

(4) A. N. Paruta, B. J. Sciarrone, and N. G. Lordi, *J. Pharm. Sci.*, **51**, 705(1962).

(5) A. N. Paruta, *ibid.*, **58**, 204(1969).

(6) S. A. Khalil and A. N. Martin, *ibid.*, **56**, 1225(1967).

(7) N. G. Lordi, B. J. Sciarrone, T. J. Ambrosio, and A. N. Paruta, *ibid.*, **53**, 463(1964).

(8) *Ibid.*, **53**, 1349(1964).

(9) L. Reber and C. Pathamanon, *Amer. J. Pharm.*, **139**, 234(1967).

ACKNOWLEDGMENTS AND ADDRESSES

Received February 19, 1974, from the *College of Pharmacy, University of Rhode Island, Kingston, RI 02881*

Accepted for publication May 21, 1975.

Abstracted in part from a dissertation submitted by B. Laprade to the Graduate School, University of Rhode Island, in partial fulfillment of the Doctor of Philosophy degree requirements.

[x] To whom inquiries should be directed.

Determination of Methyl Methacrylate in Surgical Acrylic Cement

ERIC B. SHEININ, WALTER R. BENSON [x], and WILSON L. BRANNON

Abstract □ A methyl methacrylate cement used in hip surgery as well as in dentistry was identified and quantitatively analyzed for its monomer content in starting materials and in the finished cement by proton magnetic resonance spectroscopy. IR data indicated that the monomer continued to escape from the product after it had hardened. The presence of 21% methyl methacrylate monomer relative to the polymer was demonstrated at the time the cement normally would be inserted into the body.

Keyphrases □ Methyl methacrylate—PMR analysis, ratio of monomer to polymer content, surgical acrylic cement □ Cement, surgical—PMR analysis of methyl methacrylate monomer relative to polymer content □ PMR spectroscopy—analysis, methyl methacrylate in surgical acrylic cement

The biomedical applications of polymers have increased rapidly in recent years (1, 2). One of the more widely used polymeric materials is methyl methacrylate bone cement. This polymer has been used extensively in dentistry and was approved for use in the United States for hip replacement and knee replacement operations. It is also used in skull surgery. Some deaths reported in 1971 during surgery prompted the examination of the material.

BACKGROUND

The methyl methacrylate cement is supplied as a kit made up of a sterile ampul of liquid and a sterile package of powder. The liquid consists of methyl methacrylate monomer, *N,N*-dimethyl-*p*-toluidine (polymerization initiator), and hydroquinone (polymerization inhibitor). The powder consists of polymethyl methacrylate–styrene copolymer (83.3%) and polymethyl methacrylate (16.7%) with benzoyl peroxide added as an initiator; preparations are available with or without barium sulfate (10%).

In the surgical application of the product, the liquid is mixed intimately with the powder until a putty is formed. This soft, workable putty is generally made into a ball and kept until just before being placed around the metal prosthesis. In this form, the prosthesis is placed in the body of the patient where the putty continues to harden.

Under normal surgical procedures, some monomer can diffuse out of the cement and into the body. It has been detected in the breath of patients undergoing this type of surgery. The high lipid solubility of the monomer aids its distribution throughout the body and makes hepatotoxicity a real possibility. This toxicity has been demonstrated in mice (3). In addition, extensive studies on dogs have shown large drops in blood pressure, decreases in heart rate, increased respiration, and changes in the ECG (4).

Sensitization to the monomer in humans has been reported (5–8); some investigators also suggested that it is responsible for, or a contributory factor in, observed cases of hypotensive states and cardiac arrest (4). In 1970, the British literature reported nine cases of cardiac arrest following the use of methyl methacrylate cement, and at least one fatality was reported in 1971 in this country (9).

There have been no definitive reports on the concentration of the potentially toxic monomer in the putty stage of the cement during the 4–5-min period after mixing when the putty is placed into the body of the patient. It was estimated that there may be up to 10% residual monomer in the curing mass after 1 hr (10). In a related study using a GLC method, Bechtel *et al.* (11), using the same product as that analyzed in the authors' laboratories, determined the amount of monomer leaching out of acrylic bone cements into tissues during polymerization. At 2 min after mixing, the monomer killed varying amounts of the surrounding tissue cells. However, the putty was placed in contact with the tissues earlier than the instructions indicated for the material used in that work. The monomer concentration in the putty at any time was unknown.

In 1971, Smith (12) reported the approximate composition of very similar acrylic cements used for dental applications, using an assay method based on the bromination of the double bond (13), and obtained 1.9 and 3.5% monomer content in acrylic cements used in hip replacement surgery. In these cases, the earliest reported analysis was obtained 1 hr after the kit contents were mixed. Methods based on IR spectrophotometry (14) and on polarography (15) have been used to determine the monomer content in bone cements sampled 1 hr or more after mixing.

The purpose of this investigation was to determine the amount of monomer, relative to the polymer, present in the putty at the recommended time of insertion into the body. Proton magnetic resonance (PMR) spectroscopy was used; this method requires no internal standard nor weighing of the sample, since the ratio of monomer to polymer is determined from the ratio of the vinyl to methoxyl signals.

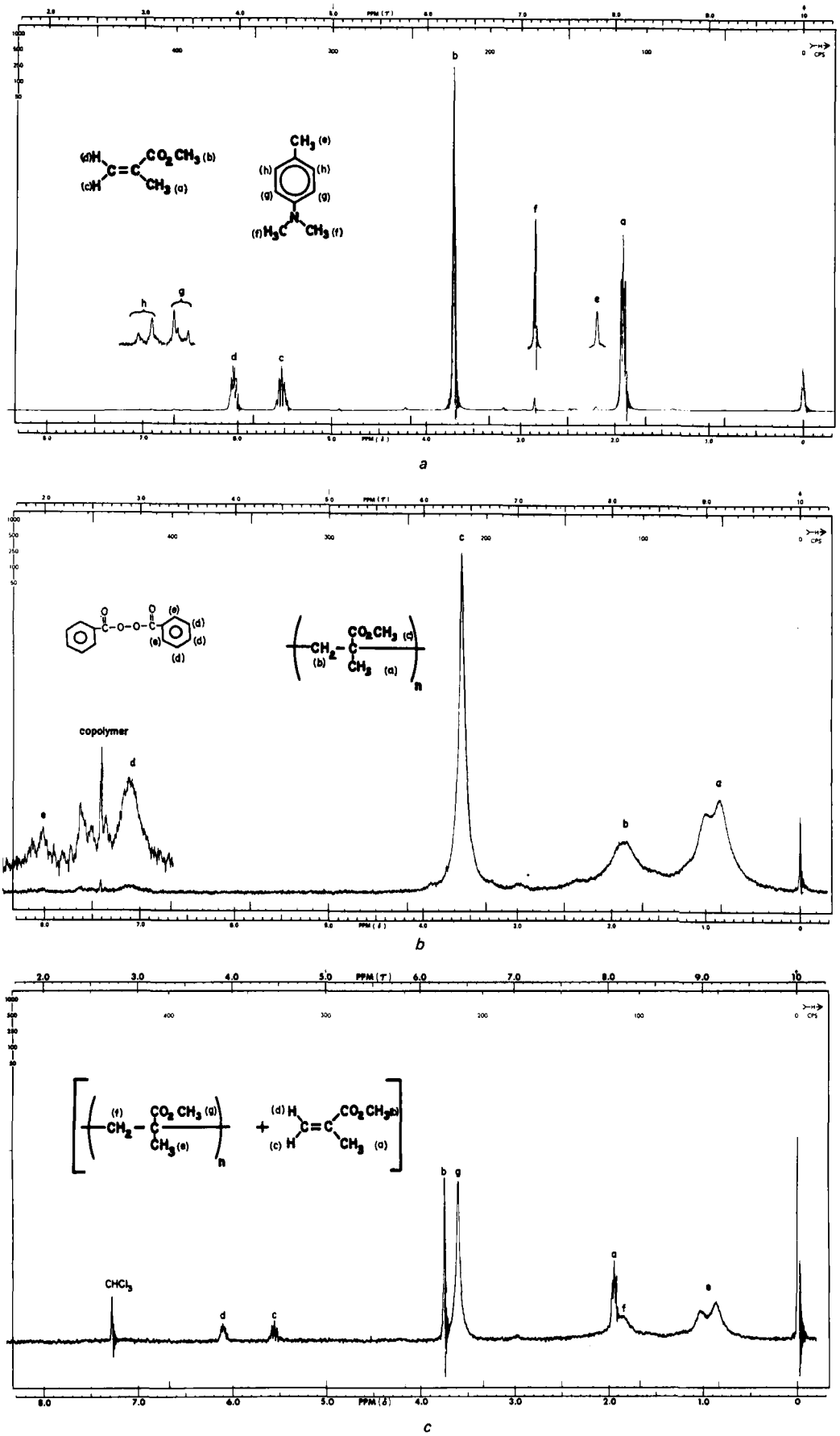

Figure 1—*PMR spectra of:* (a) *starting liquid (neat) consisting of methyl methacrylate and* N,N-*dimethyl*-p-*toluidine;* (b) *starting powder (in deuterated chloroform) consisting of polymethyl methacrylate, methyl methacrylate–styrene copolymer, and benzoyl peroxide; and* (c) *sample of the polymerizing mixture (in deuterated chloroform).*

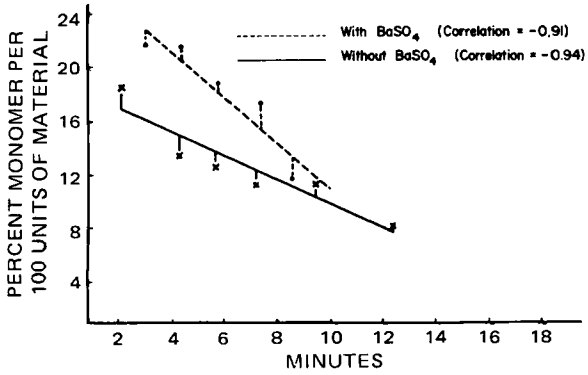

Figure 2—*Plot of the concentration of monomer found by PMR relative to the total amount of material* versus *time.*

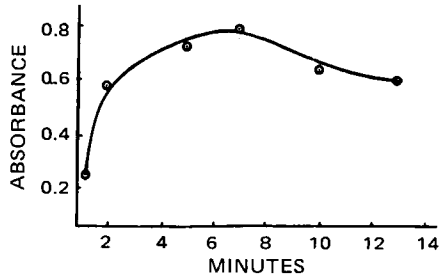

Figure 3—*Plot of the IR absorbance of a sample of the polymerizing mixture at 940.7 cm^{-1}* versus *time.*

EXPERIMENTAL

Instrumentation—A PMR spectrometer[1], having a six-turn insert, was used. Integrals were recorded by means of an automatic digital voltmeter[2]. An IR spectrophotometer[3] equipped with a small volume gas cell[4] was used for IR measurements.

PMR Analysis—Typically, the powder from one packet, 40 g (polymethyl methacrylate, 16.7%; methyl methacrylate–styrene copolymer, 83.3%; and a small amount of benzoyl peroxide), was placed in a mortar, and the contents from one vial, 20 ml (methyl methacrylate, *N,N*-dimethyl-*p*-toluidine, and hydroquinone) was added (this work was carried out in a well-ventilated hood). The resulting mixture was mulled with a pestle, with care to ensure that the liquid came in contact with all of the powder and that the mixture appeared to be homogeneous. When the material could be handled without sticking to rubber gloves, it was shaped into a ball and placed in a petri dish.

At intervals during a 2–11-min period after the initial mixing, small, thin samples (approximately 10 × 10 × 2 mm) were taken from the surface and placed into an erlenmeyer flask containing 2 ml of deuterated chloroform[5]. The flask was immediately stoppered, with care to ensure that the sample was in contact with the deuterated chloroform. Generally, five or six samples were used per experiment for the PMR determinations. After the sample had dissolved, the PMR spectrum was recorded and the integrals of the vinyl (δ 5.50–6.20)[6] and the methoxyl (δ 3.38–3.87) regions were determined in quintuplicate. (Figure 1*c* shows a representative spectrum.)

The percent of the monomer present in the total sample was calculated using:

$$\% \text{ monomer} = \frac{1.5 \times A_V}{A_M} \times 100 \qquad \text{(Eq. 1)}$$

where A_M = average of five determinations of the methoxyl integral, A_V = average of five determinations of the vinyl integral, and 1.5 = a conversion factor relating the number of protons in the vinyl region (two) to those in the methoxyl group (three).

Quenching of Polymerization by Solvent—To determine the effect of chloroform on the polymerization, 80.0 mg of the powder from a kit was dissolved in 0.5 ml of deuterated chloroform in an NMR tube[7]; 43.6 mg of the liquid was then added and the tube was stoppered and shaken. Twenty minutes later, the PMR spectrum was recorded and the integrals of the vinyl and the methoxyl regions were determined.

IR Analysis—At approximately 3 min after mixing, a small piece of putty was placed in the gas cell and the IR spectrum of the escaping vapor was recorded from 980 to 880 cm^{-1} every 1.5–2 min. In a separate experiment, another piece of putty was placed in the gas cell and the peak at 940.7 cm^{-1} was recorded at various intervals.

RESULTS AND DISCUSSION

Results at 4 min showed an average of 20.5 ± 2.25% of the monomer present in the putty for four determinations (range of 16–23%) using kits containing barium sulfate and an average of 14.6 ± 1.3% in the putty for five determinations (range of 13–17%) using kits containing no barium sulfate. These percentages decreased regularly until the surface of the mix was too hard to sample (10–12 min from the time of mixing) (Fig. 2). According to the package label, the putty is normally placed into the body 4–5 min after mixing is begun. The PMR spectroscopic procedure was equally applicable to either preparation.

Deuterated chloroform was chosen as the solvent for the PMR determinations because it quenched the polymerization reaction. Solutions of the polymeric powder and the monomeric liquid in deuterated chloroform were mixed together, as described under *Experimental,* to give a concentration of the monomer of 34.7%. After standing for 20 min, the monomer content was determined by the PMR procedure to be 34.6%, virtually identical to the known concentration within the limits of the measurement. This finding shows that polymerization of the monomer was effectively inhibited in chloroform, even in the presence of a catalyst. Since the dissolution of the polymerized product takes several hours, some further polymerization conceivably might take place within the sample mass during the dissolution period. Then the actual monomer content would be higher than the values reported here (Fig. 2).

The possibility was considered that depolymerization may take place in the deuterated chloroform solution, but it did not occur. When a sample of hardened material (approximately 2 weeks old) was dissolved in deuterated chloroform, the PMR spectrum did not show any changes over 1 week.

The integration accuracy of the instrument was shown by recording the spectrum of methyl methacrylate in deuterated chloroform and integrating the vinyl and methoxyl regions five times. The average value of the vinyl region was 102.1% of the average methoxyl integral after correcting for the number of protons in each region. This value agreed well with the original instrument specification of ±2%.

Several components in the starting materials can be identified by the PMR procedure. In the case of the liquid, the identification of both methyl methacrylate and *N,N*-dimethyl-*p*-toluidine is straightforward (Fig. 1*a*). The low level of hydroquinone used in the preparation could not be detected. When the powder was examined, the presence of benzoyl peroxide was detected (Fig. 1*b*). Quantitative analysis of the starting materials was not attempted during this investigation.

The starting materials from a similar preparation used in skull surgery were examined for comparison. The concentration of *N,N*-dimethyl-*p*-toluidine in the liquid of the second preparation appeared to be approximately half the amount observed relative to monomeric methyl methacrylate in the preparation used in hip surgery. The PMR spectra of the powder of the two preparations differed in the upfield region, indicating different tacticities of the polymers (16–18). These analyses indicate that PMR will distinguish between two starting polymers and show the relative amounts of starting materials in both liquid and solid.

[1] Varian A-60, Varian Associates, Palo Alto, Calif.
[2] Model 405BR, Hewlett-Packard Co., Palo Alto, Calif.
[3] Model 621, Perkin-Elmer Corp., Norwalk, Conn.
[4] A 7.5-cm path length; Perkin-Elmer Corp., Norwalk, Conn.
[5] Containing 99.8% deuterium, Stohler Isotope Chemicals, Rutherford, N.J.
[6] Chemical shifts are reported in parts per million downfield from tetramethylsilane.
[7] Catalog No. K-897205, Kontes Glass Co., Vineland, N.J.

The amount of the monomer present at the time of insertion is dependent on the mode of mixing. Even when the same operator mixed the putty every time, variations in the data were observed, both in the actual monomer content and in the slope of the resultant monomer *versus* time plot. (Figure 2 shows the plot of a representative experiment.) The slope varied from −1.5 to −1.7 for the preparation with barium sulfate and from −0.8 to −1.1 for the preparation without barium sulfate. Additionally, the length of time before the putty was completely set varied from 8 to 15 min.

The temperature of the bolus during polymerization reached 96° about 14 min after mixing, as determined by placing a thermometer in the bolus and recording the temperature at intervals. It has been reported (2) that this temperature is never approached in a surgical procedure because of the larger surface area of the mass used.

The authors have established that the monomer escapes at a rapid rate from the polymer bolus long after the bolus is too hard to take samples from it. The intent was to follow the rate of release of the vapor by gas phase IR spectrophotometry. However, when a piece of the putty was examined by IR beginning at approximately 3 min after mixing, the concentration of monomer in the gas cell increased for approximately 7 min and then began to drop slightly (Fig. 3). This drop was attributed to leakage of the monomer out of the cell or adsorption by the inner surfaces of the cell.

To distinguish between these processes, 4 μl of the monomer was placed in the cell; the intensity of the peak decreased with time and leveled off after 40 min. At this point, the sample was removed by purging the monomer vapor with dry nitrogen. Upon standing, the characteristics IR bands of the monomer reappeared and grew in intensity, indicating that the adsorbed monomer was coming from the walls and/or gaskets.

Polymerization of methyl methacrylate is initiated by the reaction between *N,N*-dimethyl-*p*-toluidine and benzoyl peroxide. No report was found that showed the fate of these catalysts. Because of their low concentrations in the finished product, the reaction of 10% solution[8,9] in deuterated benzene-d_6[10] was examined by PMR. Preliminary results indicated the possible presence of benzoic acid and 2,2′-(*N,N*-dimethylamino)-5,5′-dimethylbiphenyl[11]. Further work is needed to confirm these assignments and to identify other reaction products.

CONCLUSIONS

The high content (21%) of monomer in the putty about 4 min after the time of mixing was considerably higher than the previously published value (10) for the monomer content of the hardened cement after 60 min (1.9–3.5%). Since the recommended time of insertion into the human body is about 4 min and not 1 hr, any evaluation of the toxicity of the putty should be related to the 21% monomer value rather than the concentration after 1 hr. This conclusion suggests that further consideration be given to the effect of concentration of monomer in all commercial cement products upon the health of the exposed patients. This suggestion is based on the implication of the monomer in hepatotoxicity (9, 11) and on the reported deaths due to cardiac arrest attributed to the monomer (9).

[8] *N,N*-Dimethyl-*p*-toluidine was purchased from Eastman Organic Chemicals Division, Rochester, N.Y.

[9] Benzoyl peroxide was purchased from Fisher Scientific Co., Pittsburgh, Pa.

[10] Norell Chemical Co., Landisville, N.J.

[11] G. M. Brauer, National Bureau of Standards, Gaithersburg, Md., personal communication.

REFERENCES

(1) K. Kammermeyer, *Chem. Tech.*, **1**, 719(1971).

(2) J. Charnley, "Acrylic Cement in Orthopaedic Surgery," E. and S. Livingstone, London, England, 1970.

(3) *J. Amer. Med. Ass.*, **219**, 1143(1972).

(4) G. N. Mir, W. H. Lawrence, and J. Autian, *J. Pharm. Sci.*, **63**, 376(1974), and references therein.

(5) A. A. Fisher, *Cutis*, **12**, 333(1973).

(6) E. R. Kepes, P. S. Underwood, and L. Pecsey, *J. Amer. Med. Ass.*, **222**, 574(1972).

(7) B. Bentley-Phillips, *S. Afr. Med. J.*, **1970**, 1293.

(8) J. S. Pegum and F. A. Midhurst, *Brit. Med. J.*, **1971**, 141.

(9) C. A. Cohen and T. C. Smith, *Anesthesiology*, **35**, 547(1971).

(10) J. Wickstrom, Chairman, Committee on Biomedical Engineering, "What's Methyl Methacrylate?," American Academy of Orthopaedic Surgeons, exhibit by R. D. Keagy, J. Galante, and P. W. Mayer.

(11) A. Bechtel, H.-G. Willert, and H.-A. Frech, *Chromatographia*, **6**, 226(1973).

(12) D. C. Smith, *J. Biomed. Mater. Res.*, **1**, 189(1971).

(13) D. C. Smith and M. E. D. Bains, *J. Dent. Res.*, **35**, 16(1956).

(14) H. J. Caul, L. A. Wall, and N. Acquista, *J. Amer. Dent. Ass.*, **53**, 56(1956).

(15) R. J. Lacoste, I. Rosenthal, and C. H. Schmittinger, *Anal. Chem.*, **28**, 983(1956).

(16) P.-Q.-Tho, J. Mordini, and A. Guyot, *C. R., Ser. C*, **271**, 1294(1970).

(17) P.-Q.-Tho and J. Guillot, *J. Polym. Sci., A-1*, **8**, 2893(1970).

(18) I. R. Peat and W. F. Reynolds, *Tetrahedron Lett.*, **1972**, 1359.

ACKNOWLEDGMENTS AND ADDRESSES

Received April 15, 1975, from the *Division of Drug Chemistry (HFD-420), Food and Drug Administration, U.S. Department of Health, Education, and Welfare, Washington, DC 20204*

Accepted for publication May 27, 1975.

[x] To whom inquiries should be directed.

Tumor Inhibitors II: Constituents and Antitumor Activity of *Sarracenia flava*

D. HOWARD MILES[x] and UDOM KOKPOL

Abstract □ The chloroform extracts of the roots and leaves of *Sarracenia flava* showed antitumor activity against lymphocytic leukemia P-388. Lupeol was identified as one constituent responsible for this activity. β-Sitosterol and α-amyrin were isolated from the hexane extract of the roots.

Keyphrases □ *Sarracenia flava*—constituents isolated, identified, and screened for antitumor activity □ Lupeol—isolated from *Sarracenia flava*, screened for antitumor activity □ β-Sitosterol—isolated from *Sarracenia flava*, screened for antitumor activity □ α-Amyrin—isolated from *Sarracenia flava*, screened for antitumor activity □ Antitumor activity—constituents isolated from *Sarracenia flava* screened

The chloroform and aqueous extracts of the insectivorous (1, 2) plant *Sarracenia flava* (golden trumpet) were reported (3) to possess antitumor activity against human epidermoid carcinoma of the nasopharynx (KB). Betulin was identified as one constituent responsible for this activity.

The antitumor activity of *S. flava*[1,2] in the lymphocytic leukemia P-388 test system is now discussed, and the isolation of several constituents from the roots of this plant is reported.

RESULTS AND DISCUSSION

Preliminary screening[3] data of the activity of the roots of *S. flava* against lymphocytic leukemia P-388 indicated that the crude hexane and ethanol extracts were inactive (T/C < 125%). However, further fractionation of the roots yielded the alkaline-soluble Fraction H, as previously described (1). Removal of betulinic acid *via* crystallization yielded a fraction giving a T/C value of 138% at a dose level of 400 mg/kg against lymphocytic leukemia in BDF_1 mice. Sequential extraction of the pitchers of *S. flava* with hexane and benzene resulted in a fraction (benzene extract from which betulinic acid was removed by crystallization) with a T/C value of 150% at a dose level of 50 mg/kg. Thus, significant activity has been demonstrated against lymphocytic leukemia. Further purification of the benzene extract of the leaves is expected to result in enrichment of activity, since the active components (betulin and lupeol) present in the roots occur in this active extract in only trace quantities.

Utilization of the previously reported (3) procedure resulted in the isolation of the sterol β-sitosterol (M^+ = 414) and the triterpene α-amyrin (M^+ = 426) from the hexane fraction. α-Amyrin and α-amyrin acetate were identical with authentic samples based on NMR, mass, and IR spectra and melting points. The melting points and IR, mass, and NMR spectra of β-sitosterol and its acetate were also identical with authentic samples. The Cancer Chemotherapy National Service Center[3] indicated that β-sitosterol and α-amyrin possess only marginal activity in the SWA 16 tumor systems.

Repetitive chromatography of chloroform-soluble Fraction B (3), after removal of betulinic acid by fractional crystallization, resulted in the isolation of the known tumor (3, 4) inhibitor lupeol in addition to betulin, which was reported (3) previously. The mass spectrum of lupeol showed an M^+ peak at 426 with major fragments at *m/e* 218, 207, and 189, indicative of the lupene skeleton. Identification was confirmed by a comparison of the mixed melting point and IR spectrum with those of an authentic sample. Lupeol is a known antitumor agent (4) and has shown activity in Sprague rats against the Walker 256 intramuscular tumor system (T/C = 39% at doses of 200 mg/kg).

EXPERIMENTAL

Column Chromatography Separation of Fraction A (3)—The crude hexane extract (Fraction A) (41 g) was dissolved in petroleum ether (100 ml) and placed on the chromatography column (4.5 cm diameter) with 600 g of alumina (neutral, activity I) as an adsorbent. The column was eluted with, in order, petroleum ether, 10% ether–petroleum ether, 20% ether–petroleum ether, 50% ether–petroleum ether, and methanol. After the collection of 1-liter fractions, the solvent was removed *in vacuo*. The separations were monitored by TLC, using acetone–benzene–chloroform (1:2:17) as the eluting system.

Isolation and Identification of α-Amyrin—The waxy compound from the petroleum ether eluate was dissolved in hexane (50 ml) and passed through a chromatography column (2 cm diameter, neutral alumina, activity I, 100 g). The column was eluted with hexane (1300 ml) and 5% ether–hexane (1700 ml). The eluate was collected in 100-ml fractions. Combined fractions 24–31, which were eluted with 5% ether–hexane, contained mainly one spot on TLC (R_f 0.153 in 10% ether–petroleum ether). Crystallization from ether–petroleum ether gave white leaflet crystalline α-amyrin, mp 171–175°, 2.45 g (0.06%). Recrystallization of α-amyrin from ethanol yielded needle crystals, mp 185–186° [lit. (5) mp 186°].

The melting point of lupeol was undepressed on admixture with an authentic sample of α-amyrin[4]. The IR, NMR, and mass spectra were in complete agreement with those of an authentic sample of α-amyrin. The IR, NMR, and mass spectra of α-amyrin acetate were also in complete agreement with those of an authentic sample of α-amyrin acetate prepared by standard procedures (3).

Isolation and Identification of β-Sitosterol—When the 20% ether–petroleum ether eluate was concentrated to about 20 ml and filtered and the residue was recrystallized from hot chloroform–methanol (1:2), 220 mg (0.005%) of white needle crystalline β-sitosterol, mp 135–136° [lit. (6) mp 137°], was obtained. The melting point of β-sitosterol was undepressed on admixture with an authentic sample[5]. The IR, NMR, and mass spectra of β-sitosterol were identical with those of the authentic sample. The IR, NMR, and mass spectra of β-sitosterol acetate were also in complete agreement with those of an authentic sample. Standard procedures (3) were employed in the preparation of β-sitosterol acetate.

Isolation of Lupeol—Fifty grams of Fraction E (3) was extract-

[1] The plant material used in this investigation was identified as *Sarracenia flava* L. (Sarraceniaceae) by Dr. Sidney McDaniel, Department of Botany, Mississippi State University. A voucher (preserved) specimen (SM-16,702) representing material collected for this investigation is available for inspection at the Herbarium of the Department of Botany, Mississippi State University.

[2] Collected 14 miles west of Panama City, Fla., in June 1973.

[3] Cancer Chemotherapy National Service Center, Bethesda, MD 20014, 1970.

[4] Pfaltz and Bauer.

[5] Aldrich Chemical Co.

ed seven times with 250 ml of 20% benzene–petroleum ether. The solvent was removed *in vacuo* from the combined extracts to yield 11.2 g of material. The crude extract was dissolved in 50 ml of benzene and placed on a chromatography column (2.5 cm diameter × 55 cm long, neutral alumina, activity I). The column was eluted with, in order, petroleum ether, 20% benzene–petroleum ether, 40% benzene–petroleum ether, and pure benzene (200 ml/fraction).

Fractions 1–7 of the 40% benzene–petroleum ether elution were purified by preparative TLC [9.75 mm thickness, silica gel GF-254, acetone–benzene–chloroform (1:2:17) as the solvent, and chloroform as the extracting solvent]. Lupeol was obtained as a white crystalline solid (11 mg), mp 206–208° [lit. (7) mp 215–216°]. The IR and mass spectra of lupeol were completely in agreement with those of authentic lupeol.

REFERENCES

(1) G. L. Plummer and J. B. Kethley, *Bot. Gaz.*, **125**, 245(1964).

(2) R. M. Harper, *J. Elisha Mitchell Sci. Soc.*, **34**, 110(1918).

(3) D. H. Miles, U. Kokpol, L. H. Zalkow, S. J. Steindel, and J. B. Nabors, *J. Pharm. Sci.*, **63**, 613(1974).

(4) K. Sheth, E. Bianchi, R. Wiedhopf, and J. R. Cole, *ibid.*, **62**, 139(1973).

(5) "Dictionary of Organic Compounds," vol. 1, Oxford University Press, New York, N.Y., 1965, p. 2028.

(6) "Dictionary of Organic Compounds," vol. 5, Oxford University Press, New York, N.Y., 1965, p. 2902.

(7) "Dictionary of Organic Compounds," vol. 4, Oxford University Press, New York, N.Y., 1965, p. 2028.

ACKNOWLEDGMENTS AND ADDRESSES

Received January 20, 1975, from the *Department of Chemistry, Mississippi State University, Mississippi State, MS 39762*

Accepted for publication April 18, 1975.

Presented in part at the Southeastern Regional Meeting, American Chemical Society, Norfolk, Va., October 1975.

Supported by Grant 3-ROI-CA-13268, National Cancer Institute, National Institutes of Health, Bethesda, MD 20014

The authors thank Dr. Sidney McDaniel for invaluable help in the location and collection of plant material.

[x] To whom inquiries should be directed.

Potential Organ or Tumor Imaging Agents XV: Radioiodinated Phenytoin Derivatives

RAYMOND E. COUNSELL [x], VASANT V. RANADE, WILLIAM KLINE, BONG H. HONG, and ANTHONY A. BUSWINK

Abstract □ Three radioiodinated phenytoin analogs were synthesized, and tissue distribution studies were conducted in rats. Except for a greater retention of radioactivity following administration of the radioiodinated derivatives, the tissue distribution patterns were qualitatively similar to those found for ^{14}C phenytoin. In nearly all cases, the adrenals, heart, kidneys, and liver displayed the greatest capacity to retain radioactivity. The high uptake of radioactivity observed for the thyroid was attributed to *in vivo* metabolic deiodination of the radioiodinated derivatives.

Keyphrases □ Phenytoin—radioiodinated derivatives, potential tumor imaging agents, tissue distribution studies, rats □ Radiopharmaceuticals—radioiodinated phenytoin derivatives, potential tumor imaging agents, tissue distribution studies, rats □ Tissue distribution—radioiodinated phenytoin derivatives, potential tumor imaging agents, rats □ Tumor imaging agents—radioiodinated phenytoin derivatives, tissue distribution studies, rats

In the search for radiopharmaceuticals that will selectively concentrate in various tumors and organs, several reports concerning the tissue distribution of phenytoin were of interest. Although early studies with this drug focused on only a few tissues, the concentration of phenytoin in the liver, kidneys, skeletal muscle, and brain was found to exceed plasma levels (1–3). Moreover, higher concentrations of phenytoin were reported in human primary brain tumors than in normal brain tissue (4).

More recently, autoradiographic studies (5) revealed that the concentration of phenytoin in the brain of cats was one to three times greater than in plasma at 0.5–6 hr following an intravenous dose. Similar studies in pregnant mice (6) revealed an intense and persistent concentration of phenytoin in the heart. This finding suggested that the antiarrhythmic action of phenytoin may be related to its affinity for myocardial tissue.

Several ^{11}C-hydantoins were synthesized (7), and an accumulation of radioactivity in the liver and, to a lesser extent, heart was noted within 5–10 min following intravenous administration to dogs. The uptake was not specific for cardiac muscle, however, since skeletal muscle contained a comparable concentration of radioactivity. Radioactivity was also high in the pancreas and mesenteric fat.

The purposes of the present study were to synthesize several radioiodinated analogs of phenytoin and to evaluate their potential utility as brain or myocardial scanning agents. Although several radiopharmaceuticals are currently employed in nuclear medicine for localization of brain tumors, these agents do not concentrate selectively in brain tissue or tumors. Instead, their selective localization arises from their passive diffusion from the bloodstream to the tumor as a result of a breakdown in the blood–brain barrier (8). As a result, positive uptake of radiopharmaceuticals is shown by hematomas, abscesses, and infarcts as well as tumors. A more tumor-specific agent is needed. Moreover, no radiopharmaceutical is currently available for imaging the myocardium, but several are undergoing evaluation for this purpose.

Since none of the elements of phenytoin has a useful γ-emitting nuclide, it was thus necessary to intro-

ed seven times with 250 ml of 20% benzene–petroleum ether. The solvent was removed *in vacuo* from the combined extracts to yield 11.2 g of material. The crude extract was dissolved in 50 ml of benzene and placed on a chromatography column (2.5 cm diameter × 55 cm long, neutral alumina, activity I). The column was eluted with, in order, petroleum ether, 20% benzene–petroleum ether, 40% benzene–petroleum ether, and pure benzene (200 ml/fraction).

Fractions 1–7 of the 40% benzene–petroleum ether elution were purified by preparative TLC [9.75 mm thickness, silica gel GF-254, acetone–benzene–chloroform (1:2:17) as the solvent, and chloroform as the extracting solvent]. Lupeol was obtained as a white crystalline solid (11 mg), mp 206–208° [lit. (7) mp 215–216°]. The IR and mass spectra of lupeol were completely in agreement with those of authentic lupeol.

REFERENCES

(1) G. L. Plummer and J. B. Kethley, *Bot. Gaz.*, **125**, 245(1964).

(2) R. M. Harper, *J. Elisha Mitchell Sci. Soc.*, **34**, 110(1918).

(3) D. H. Miles, U. Kokpol, L. H. Zalkow, S. J. Steindel, and J. B. Nabors, *J. Pharm. Sci.*, **63**, 613(1974).

(4) K. Sheth, E. Bianchi, R. Wiedhopf, and J. R. Cole, *ibid.*, **62**, 139(1973).

(5) "Dictionary of Organic Compounds," vol. 1, Oxford University Press, New York, N.Y., 1965, p. 2028.

(6) "Dictionary of Organic Compounds," vol. 5, Oxford University Press, New York, N.Y., 1965, p. 2902.

(7) "Dictionary of Organic Compounds," vol. 4, Oxford University Press, New York, N.Y., 1965, p. 2028.

ACKNOWLEDGMENTS AND ADDRESSES

Received January 20, 1975, from the *Department of Chemistry, Mississippi State University, Mississippi State, MS 39762*

Accepted for publication April 18, 1975.

Presented in part at the Southeastern Regional Meeting, American Chemical Society, Norfolk, Va., October 1975.

Supported by Grant 3-ROI-CA-13268, National Cancer Institute, National Institutes of Health, Bethesda, MD 20014

The authors thank Dr. Sidney McDaniel for invaluable help in the location and collection of plant material.

[x] To whom inquiries should be directed.

Potential Organ or Tumor Imaging Agents XV: Radioiodinated Phenytoin Derivatives

RAYMOND E. COUNSELL [x], VASANT V. RANADE, WILLIAM KLINE, BONG H. HONG, and ANTHONY A. BUSWINK

Abstract □ Three radioiodinated phenytoin analogs were synthesized, and tissue distribution studies were conducted in rats. Except for a greater retention of radioactivity following administration of the radioiodinated derivatives, the tissue distribution patterns were qualitatively similar to those found for ^{14}C phenytoin. In nearly all cases, the adrenals, heart, kidneys, and liver displayed the greatest capacity to retain radioactivity. The high uptake of radioactivity observed for the thyroid was attributed to *in vivo* metabolic deiodination of the radioiodinated derivatives.

Keyphrases □ Phenytoin—radioiodinated derivatives, potential tumor imaging agents, tissue distribution studies, rats □ Radiopharmaceuticals—radioiodinated phenytoin derivatives, potential tumor imaging agents, tissue distribution studies, rats □ Tissue distribution—radioiodinated phenytoin derivatives, potential tumor imaging agents, rats □ Tumor imaging agents—radioiodinated phenytoin derivatives, tissue distribution studies, rats

In the search for radiopharmaceuticals that will selectively concentrate in various tumors and organs, several reports concerning the tissue distribution of phenytoin were of interest. Although early studies with this drug focused on only a few tissues, the concentration of phenytoin in the liver, kidneys, skeletal muscle, and brain was found to exceed plasma levels (1–3). Moreover, higher concentrations of phenytoin were reported in human primary brain tumors than in normal brain tissue (4).

More recently, autoradiographic studies (5) revealed that the concentration of phenytoin in the brain of cats was one to three times greater than in plasma at 0.5–6 hr following an intravenous dose. Similar studies in pregnant mice (6) revealed an intense and persistent concentration of phenytoin in the heart. This finding suggested that the antiarrhythmic action of phenytoin may be related to its affinity for myocardial tissue.

Several ^{11}C-hydantoins were synthesized (7), and an accumulation of radioactivity in the liver and, to a lesser extent, heart was noted within 5–10 min following intravenous administration to dogs. The uptake was not specific for cardiac muscle, however, since skeletal muscle contained a comparable concentration of radioactivity. Radioactivity was also high in the pancreas and mesenteric fat.

The purposes of the present study were to synthesize several radioiodinated analogs of phenytoin and to evaluate their potential utility as brain or myocardial scanning agents. Although several radiopharmaceuticals are currently employed in nuclear medicine for localization of brain tumors, these agents do not concentrate selectively in brain tissue or tumors. Instead, their selective localization arises from their passive diffusion from the bloodstream to the tumor as a result of a breakdown in the blood–brain barrier (8). As a result, positive uptake of radiopharmaceuticals is shown by hematomas, abscesses, and infarcts as well as tumors. A more tumor-specific agent is needed. Moreover, no radiopharmaceutical is currently available for imaging the myocardium, but several are undergoing evaluation for this purpose.

Since none of the elements of phenytoin has a useful γ-emitting nuclide, it was thus necessary to intro-

Table I—Distribution of Radioactivity in Rats at 2 hr following Subcutaneous Administration of ^{14}C-Phenytoin and ^{125}I-Phenytoin Analogs[a]

Tissue	^{14}C-Phenytoin	^{125}I-III*a*	^{125}I-III*b*	^{125}I-III*c*
Adrenal	0.39 ± 0.02	1.52 ± 0.10	0.35 ± 0.06	1.20 ± 0.16
Brain	0.14 ± 0.01	0.36 ± 0.04	0.05 ± <0.01	0.55 ± 0.10
Blood	0.15 ± 0.01	0.40 ± 0.05	0.08 ± 0.01	0.36 ± 0.07
Heart	0.26 ± 0.01	1.02 ± 0.09	0.43 ± 0.04	0.76 ± 0.13
Kidney	0.37 ± 0.02	0.88 ± 0.05	0.23 ± 0.02	0.77 ± 0.10
Liver	0.48 ± 0.03	1.66 ± 0.14	0.33 ± 0.01	1.08 ± 0.16
Lung	—	0.81 ± 0.09	0.18 ± 0.01	0.78 ± 0.13
Ovary	0.21 ± 0.01	0.88 ± 0.05	0.19 ± 0.02	0.69 ± 0.13
Pancreas	0.29 ± 0.01	0.74 ± 0.07	—	—
Pituitary	0.26 ± 0.02	0.70 ± 0.07	0.16 ± 0.01	0.72 ± 0.14
Thyroid	—	1.40 ± 0.12	0.87 ± 0.04	4.74 ± 0.31

[a] Values are expressed as the mean percentage of administered dose per gram of tissue ± *SEM* from three rats. The percent dose per gram was calculated as follows:

$$\frac{\text{dpm/mg} \times 1000 \times 100}{2.22 \times 10^6 \times \mu\text{Ci administered dose}}$$

duce this feature into the molecule. Three iodinated analogs of phenytoin were synthesized for radiolabeling (Scheme I). Compounds III*a* and III*b* were prepared by standard methods for the synthesis of hydantoins, and III*c* had been synthesized previously in this laboratory (9).

Iodine-125 was selected as the radiolabel for preliminary studies because its half-life (60 days) and low radiation energy (35 kev) simplified synthesis and storage. Radioiodine was incorporated at the final synthetic step by heating the iodinated analogs with ^{125}I-sodium iodide in ethylene glycol at temperatures above 165°. Each radioiodinated analog was purified by recrystallization and gave a single peak of radioactivity when analyzed radiochromatographically.

EXPERIMENTAL

Preparation of 3,3′-Diiodobenzil (II)—A solution of *m*-iodobenzaldehyde (2.3 g, 0.01 *M*) and potassium cyanide (0.2 g) in ethanol–water (1:1, 25 ml) was refluxed for 1.5 hr. The mixture was cooled, water (25 ml) was added, and the solution was extracted with ether. The ether extract was dried (sodium sulfate) and evaporated. The residual crude oil was dissolved in pyridine (20 ml) and water (10 ml), and cupric sulfate pentahydrate (2.0 g) was added.

The mixture was refluxed for 2 hr, allowed to cool, and poured into water. Ether extraction and workup as already described afforded II (0.5 g, 11%). Recrystallization from ethanol gave the purified compound, mp 133–134°. The IR and NMR spectra were as expected.

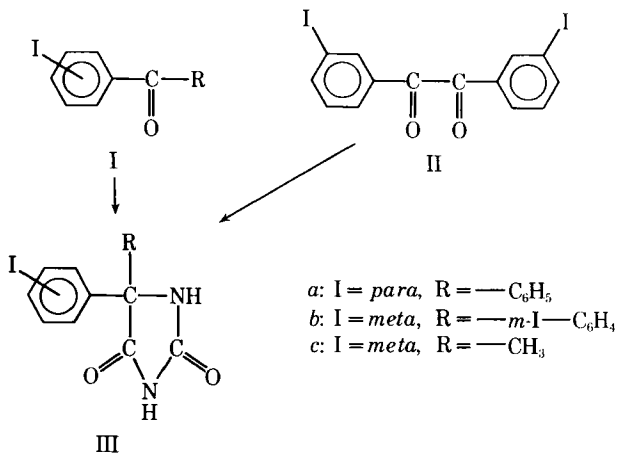

Scheme I—Synthesis of iodinated analogs of phenytoin

Anal.—Calc. for $C_{14}H_8I_2O_2$: C, 36.36; H, 1.73. Found: C, 36.55; H, 1.93.

Preparation of 5-Phenyl-5-(*p*-iodophenyl)hydantoin (III*a*)—A mixture of 50% ethanol (10 ml), *p*-iodobenzophenone[1] (250 mg), sodium cyanide (50 mg), acetamide (93 mg), and ammonium carbonate (250 mg) was placed in an ampul. The ampul was sealed and kept in an autoclave at 140–150° for 7 days. Then the ampul was broken, and the contents were extracted with 10% NaOH solution. The clear alkaline solution was made slightly acidic with 10% H_2SO_4. The solid which separated was collected, washed with water, and recrystallized from methanol–water to give pure III*a* (60 mg, 28%), mp 235–237° dec. The IR and NMR spectra were as expected.

Anal.—Calc. for $C_{15}H_{11}IN_2O_2$: C, 47.60; H, 2.91. Found: C, 47.75; H, 3.03.

Preparation of 5,5-Di(*m*-iodophenyl)hydantoin (III*b*)—Sodium (0.2 g) was dissolved in ethanol (15 ml), and urea (0.1 g) was added to the boiling solution. Small portions of II (0.2 g) were added, and the mixture was refluxed for 50 min. Ethanol was removed by distillation, water (5 ml) was added, and the solution was refrigerated. Acidification of the solution afforded a white precipitate which, after collection and recrystallization from methanol, gave pure III*b* (0.11 g, 30%), mp 245–248°. The IR and NMR spectra were as expected.

Anal.—Calc. for $C_{15}H_{10}I_2N_2O_2$: C, 35.71; H, 1.98. Found: C, 35.99; H, 2.25.

Preparation of Radioiodinated Hydantoins—A solution of ^{125}I-sodium iodide (4 mCi) in water (0.3 ml) was added to a solution of III*a* (50 mg) in ethylene glycol (2.0 ml). The solution was heated with stirring at 165° for 28 hr under a nitrogen atmosphere. Then the solution was allowed to cool, water (20 ml) was added, and the mixture was extracted with ether. The ether extract was carefully washed with water to remove ^{125}I and dried (sodium sulfate). Removal of the solvent *in vacuo* and trituration of the resulting residue with a small amount of water gave essentially pure ^{125}I-III*a* in crystalline form.

Further purification was achieved by recrystallization from ethanol–water to give 30 mg with a specific activity[2] of 20 μCi/mg. TLC using two solvent systems, benzene–ethyl acetate (2:1) and benzene–ethanol (4:1), displayed a single radioactive peak on scanning (R_f 0.34 and 0.40, respectively). The peak was coincident with the single spot observed visually. Treatment of III*b* (100 mg) with ^{125}I-sodium iodide (3 mCi) in a similar manner gave 60 mg of ^{125}I-III*b* with a specific activity of 13.3 μCi/mg, R_f 0.73 and 0.85 in benzene–ethyl acetate (2:1) and benzene–ethanol (4:1), respectively.

Similarly, treatment of III*c* (9) (80 mg) with ^{125}I-sodium iodide (6 mCi) gave 27 mg of ^{125}I-III*c* with a specific activity of 5.5 μCi/mg, R_f 0.52 and 0.60 in benzene–ethyl acetate (2:1) and benzene–ethanol (4:1), respectively.

[1] Prepared according to the method of Koopal (10).

[2] Determined using Picker isotope calibrator, Picker Nuclear, White Plains, N.Y.

Table II—Tissue to Blood Ratios 2 hr Postinjection of ^{14}C-Phenytoin and ^{125}I-Phenytoin Analogs

Tissue	^{14}C-Phenytoin	^{125}I-III*a*	^{125}I-III*b*	^{125}I-III*c*
Adrenal	2.8 ± 0.11	3.94 ± 0.60	4.42 ± 0.53	3.39 ± 0.26
Brain	0.98 ± 0.03	0.92 ± 0.09	0.59 ± 0.08	1.51 ± 0.05
Heart	1.83 ± 0.02	2.59 ± 0.21	5.48 ± 0.86	2.12 ± 0.08
Ovary	1.51 ± 0.06	2.24 ± 0.14	2.38 ± 0.15	1.90 ± 0.15
Pancreas	2.03 ± 0.03	1.89 ± 0.24	—	—

Tissue Distribution Studies—All subjects were Spartan Sprague–Dawley female rats, 190–275 g. The animals were housed in air-conditioned quarters under normal lighting conditions. Tap water and food[3] were available *ad libitum*.

The hydantoins were dissolved in dimethyl sulfoxide and administered subcutaneously into the nape of the neck using a 1-ml tuberculin syringe and a 23-gauge 2.54-cm (1-in.) hypodermic needle. Three rats were used for each evaluation, and the doses were as follows: ^{14}C-phenytoin[4], 7 μCi/0.23-ml injection, specific activity 19.3 μCi/mg; III*a*, 30 μCi/0.30-ml injection, specific activity 20 μCi/mg; III*b*, 26 μCi/0.20-ml injection, specific activity 13.3 μCi/mg; and III*c*, 20 μCi/0.30-ml injection, specific activity 5.5 μCi/mg.

The subjects were anesthetized with ether in a desiccator jar and sacrificed by exsanguination from the heart ventricle at 0.25, 2, and 24 hr postinjection. The major organs such as brain, heart, kidneys, liver, lungs, pancreas, spleen, and stomach were excised, washed thoroughly with isotonic saline to remove blood, and minced with surgical scissors to a paste-like consistency. Smaller organs such as adrenals, ovaries, pituitary, and thyroid were weighed intact.

Several weighed samples of minces, heparinized blood, and the smaller organs were placed in microfuge tubes and radioassayed[5] using a tetrabutyltin liquid scintillation cocktail (11). Counts were accumulated to attain a 3% counting error with 95% confidence intervals. All counts were corrected for system efficiency using calibrated ^{125}I-sodium iodide solution[6] or liquid scintillation ^{14}C quenched standards[7].

RESULTS AND DISCUSSION

The tissue distribution of radioactivity at 2 hr after administration of radioiodinated hydantoins is compared with that shown for ^{14}C-phenytoin (Table I). In all cases, high levels of radioactivity were found in the liver, kidneys, and heart, as expected from previous studies.

Although not previously noted by other investigators, the adrenal gland also demonstrated high levels of radioactivity. No attempt was made to ascertain whether the radioactivity resided mainly in the cortex or the medulla. However, it is believed to be the former on the basis that other polycyclic aromatic compounds such as 1,1-dichloro-2-(*o*-chlorophenyl)-2-(*p*-chlorophenyl)ethane are taken up well by the adrenal cortex (12, 13). Despite the known hyperglycemic action of phenytoin and its ability to impair secretion of insulin from pancreatic β-cells (14, 15), there appeared to be no extraordinary uptake of radioactivity by the pancreas following administration of ^{14}C-phenytoin or the radioiodinated derivative of III*a*.

While there were quantitative differences among all compounds, the adrenal to blood ratios for the radioiodinated hydantoins were very close to one another and ranged between 3.4 and 4.4. These values were slightly higher than those shown for phenytoin itself. The tissue to blood ratios at 2 hr for the adrenal and other organs of interest appear in Table II. Except for minor differences, all radiolabeled phenytoin derivatives displayed a similar tissue distribution pattern.

The tissue distribution of only ^{14}C-phenytoin was examined at 15 min following administration. In contrast to previous studies in cats (5), no selective uptake of radioactivity was noted for the brain. Moreover, the general distribution pattern was similar to that noted in the 2-hr experiments.

Distribution analysis at 24 hr demonstrated that radioactivity associated with ^{14}C-phenytoin had essentially cleared from most tissues by this time. Similar analysis of the radioiodinated hydantoins, however, revealed only a modest decrease in radioactivity associated with the tissues. The increase in lipid solubility caused by introduction of iodine could account for the apparent increase in retention for the radioiodinated hydantoins.

Despite the ability of the radioiodinated hydantoins to concentrate in the heart, the heart to blood ratio was not sufficiently encouraging to pursue these agents as potential myocardial scanning agents, particularly in light of recent studies showing the selective localization of certain radioiodinated bretylium analogs in myocardial tissue (16, 17).

REFERENCES

(1) C. H. Hine and F. L. Kozelka, *J. Pharmacol. Exp. Ther.*, **72**, 280(1941).

(2) W. A. Dill, A. Kazenko, L. M. Wolf, and A. J. Glazko, *ibid.*, **118**, 270(1956).

(3) E. L. Noach, D. M. Woodbury, and L. S. Goodman, *ibid.*, **122**, 301(1958).

(4) I. Rosenblum and A. A. Stern, *Biochem. Pharmacol.*, **12**, 1453(1963).

(5) H. Firemark, C. F. Barlow, and L. J. Roth, *Int. J. Neuropharmacol.*, **2**, 25(1963).

(6) W. J. Waddell and B. L. Mirkin, *Biochem. Pharmacol.*, **21**, 547(1972).

(7) W. B. Winstead, S. Parr, T. H. Lin, A. Khentigan, J. Lamb, and H. S. Winchell, *J. Nucl. Med.*, **13**, 479(1972).

(8) R. G. Long, J. G. McAfee, and J. Winkelman, *Cancer Res.*, **23**, 98(1963).

(9) R. E. Counsell, P. Desai, T. D. Smith, P. S. Chan, P. A. Weinhold, V. B. Rethy, and D. Burke, *J. Med. Chem.*, **13**, 1040(1970).

(10) S. A. Koopal, *Rec. Trav. Chim.*, **34**, 115(1915).

(11) J. Ashcroft, *Anal. Biochem.*, **37**, 268(1970).

(12) W. DiGuilio and W. H. Beierwaltes, *J. Nucl. Med.*, **9**, 634(1968).

(13) R. E. Counsell, R. E. Willette, and W. DiGuilio, *J. Med. Chem.*, **10**, 975(1967).

(14) J. G. Millichap, *N. Engl. J. Med.*, **281**, 447(1969).

(15) S. R. Levin, G. M. Grodsky, R. Hagura, and D. Smith, *Diabetes*, **21**, 856 (1972).

(16) R. E. Counsell, T. Yu, V. V. Ranade, and A. Buswink, *J. Med. Chem.*, **16**, 1038(1973).

(17) R. E. Counsell, T. Yu, V. V. Ranade, A. A. Buswink, E. A. Carr, Jr., and M. Carroll, *J. Nucl. Med.*, **15**, 991(1974).

ACKNOWLEDGMENTS AND ADDRESSES

Received January 23, 1975, from the *Laboratory of Medicinal Chemistry, College of Pharmacy, University of Michigan, Ann Arbor, MI 48104*

Accepted for publication May 2, 1975.

Supported by Grant CA-08349 from the National Cancer Institute, National Institutes of Health.

[x] To whom inquiries should be directed.

[3] Purina Laboratory Rat and Dog Chow.

[4] New England Nuclear, Boston, Mass.

[5] Beckman LS-150 liquid scintillation spectrometer.

[6] Phoenix Memorial Laboratory, University of Michigan, Ann Arbor, Mich.

[7] Beckman Instruments, Inc., Fullerton, Calif.

Permethylation of Barbiturates: Variation in Product Ratios with Varying Methylsulfinylmethide Carbanion

RICHARD M. THOMPSON

Abstract □ Permethylation of a barbiturate with the methylsulfinylmethide carbanion and methyl iodide gave three products clearly separable by GLC. Alteration of the reaction conditions by varying the barbiturate to carbanion ratio or the barbiturate to carbanion exposure time resulted in a single product for only one examined barbiturate, secobarbital. This derivatization technique is useful for the GLC analysis of polar barbiturate metabolites, such as glucuronides, in biological fluids but is of limited value for the analysis of the parent compounds.

Keyphrases □ Permethylation—barbiturates with methylsulfinylmethide carbanion and methyl iodide, GLC separation □ Barbiturates—permethylation with methylsulfinylmethide carbanion and methyl iodide, GLC separation □ GLC—determination, permethylation, barbiturate derivatives

A previous publication (1) noted that barbituric acid derivatives (I*a*–I*c*) were not stable under the conditions employed for the permethylation of peptides (2), sugars (3), and polar drug metabolites (4); the substrate in dimethyl sulfoxide was exposed to the methylsulfinylmethide carbanion (1 *M*) for a short period, after which methyl iodide or deuterated methyl iodide was added to complete the reaction. The reaction mixture contained three products, II, III, and IV, whose relative amounts were thought to be dependent only upon the nature of the alkyl groups at the 5-position of the parent compound (I) and upon *N*-substitution [*e.g.*, hexobarbital (I*a*) and mephobarbital]. Compounds II–IV were well-characterized by GLC–mass spectrometry for a series of six barbiturates, and their mass spectral fragmentation patterns were elucidated (1). Permethylation was shown not to be a practical technique for the quantitative analysis of barbiturates in biological extracts. However, it was considered a useful derivatization method for the GLC–mass spectrometry analysis of polar metabolites, especially glucuronides, in nonextracted biological fluids, such as rat bile, even though the structure of the barbiturate nucleus was altered (4).

The current study was an attempt to establish reaction conditions under which a single product could be formed. Two parameters were examined: the bar-

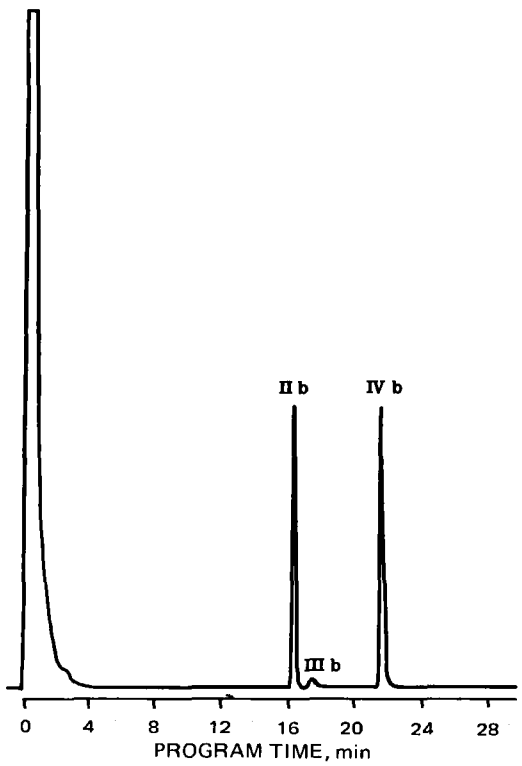

Figure 1—*GLC separation of a product mixture obtained from the permethylation of phenobarbital (I*b*). Reaction conditions were: 100 μg of phenobarbital (B), 5 μl of methylsulfinylmethide carbanion (C) (B/C = 0.09), 25 μl of methyl iodide, 15-min B to C exposure time, and 1-hour total reaction time. GLC conditions were as described in* Experimental *(using SE-30).*

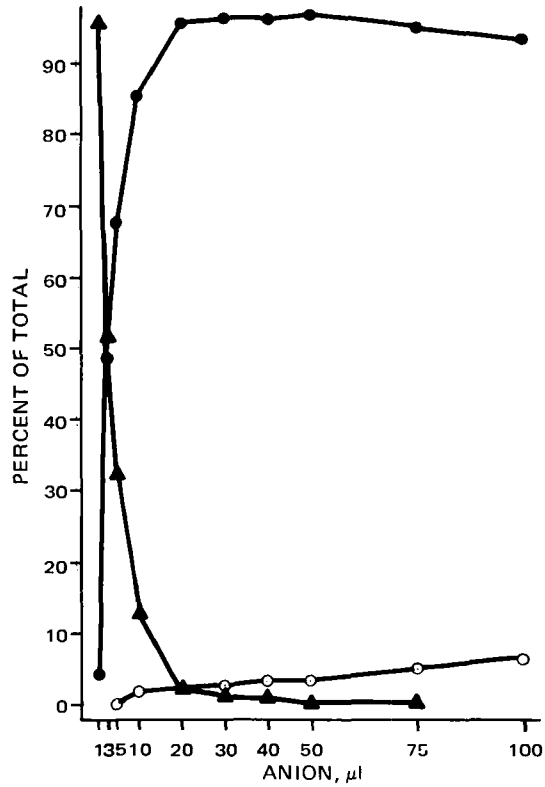

Figure 2—*Relative proportions of the products obtained from the permethylation of 100 μg of hexobarbital (I*a*) with varying amounts of methylsulfinylmethide carbanion. Key:* ▲, *II*a; ○, *III*a; *and* ●, *IV*a.

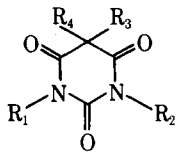

I

Ia: $R_1 = H$, $R_2 = CH_3$, $R_3 = CH_3$, R_4 = 1-cyclo-C_6H_9

Ib: $R_1 = H$, $R_2 = H$, $R_3 = C_2H_5$, $R_4 = C_6H_5$

Ic: $R_1 = H$, $R_2 = H$, $R_3 = CH_2{=}CHCH_2$, $R_4 = CH_3(CH_2)_2CH(CH_3)$

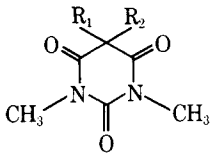

II

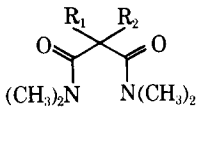

III

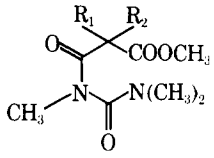

IV

IIa, IIIa, IVa: $R_1 = CH_3$, R_2 = 1-cyclo-C_6H_9

IIb, IIIb, IVb: $R_1 = C_2H_5$, $R_2 = C_6H_5$

IIc, IIIc, IVc: $R_1 = CH_2{=}CHCH_2$, $R_2 = CH_3(CH_2)_2CH(CH_3)$

biturate to carbanion ratio and the length of barbiturate to carbanion exposure time prior to the addition of methyl iodide.

EXPERIMENTAL

Hexobarbital (Ia), phenobarbital (Ib), and secobarbital (Ic) analytical standards[1] were each dissolved in dimethyl sulfoxide[2] (2 μg/μl). Aliquots then were permethylated with the methylsulfinylmethide carbanion, prepared as previously described (2), and methyl iodide (always added in excess). The barbiturate to carbanion ratio was adjusted by varying either the barbiturate (micrograms) or the carbanion (microliters).

The exposure time prior to the addition of methyl iodide was usually 15 min, but it was the variable (0–30 min) in one experiment. The total reaction time was 1 hr. The reactions were stopped by the addition of water, the products were extracted into chloroform and washed three times with water, and the product mixture was obtained by evaporation of the chloroform under a gentle stream of nitrogen. The residue was redissolved in an amount of chloroform equal to the original amount of barbiturate for GLC and GLC–mass spectrometry analysis.

The separations were carried out using 1.8-m (6-ft) × 4-mm coiled columns[3] packed with 3% SE-30 on Gas Chrom Q (100–120 mesh) or 10% OV-17 on Gas Chrom Q (80–100 mesh)[4]. Operating parameters included: injector temperature, 250°; flame-ionization detector temperature, 300°; nitrogen flow rate, 30 ml/min; and temperature programming, from 125° at 4°/min. Quantification was by means of an automatic digital integrator[5].

All chromatographic peaks were identified with a combination gas chromatograph–mass spectrometer[6], with a 1.8-m (6-ft) × 4-mm coiled glass column packed with 1% SE-30 on Gas Chrom Q (100–120 mesh) as the inlet. The ionizing and accelerating potentials were 70 ev and 3.5 kv, respectively. The trap current was 60 μamp, the source temperature was 270°, the flash heater and separator temperatures were 250°, and the column oven temperature was programmed from 125° at 4°/min.

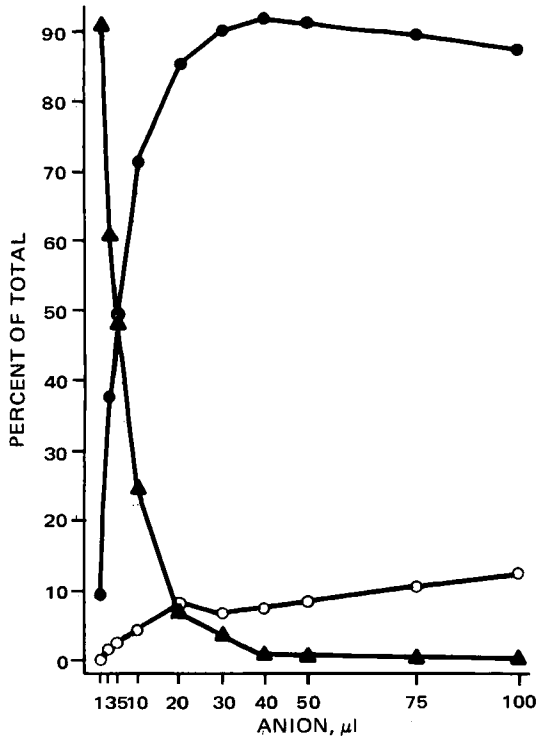

Figure 3—*Relative proportions of the products obtained from the permethylation of 100 μg of phenobarbital (Ib) with varying amounts of methylsulfinylmethide carbanion. Key:* ▲, *IIb;* ○, *IIIb; and* ●, *IVb.*

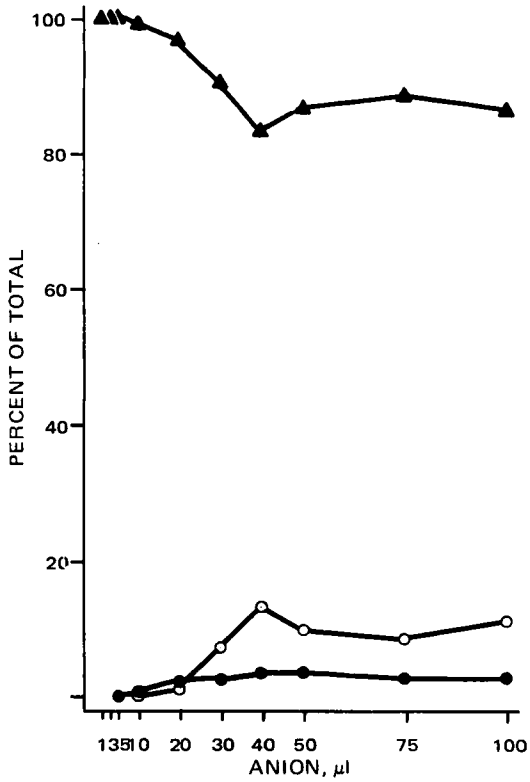

Figure 4—*Relative proportions of the products obtained from the permethylation of 100 μg of secobarbital (Ic) with varying amounts of methylsulfinylmethide carbanion. Key:* ▲, *IIc;* ○, *IIIc; and* ●, *IVc.*

RESULTS AND DISCUSSION

The three products (II, III, and IV) formed by permethylation of a barbiturate (I) were all clearly separated by GLC analysis on ei-

[1] Gifts from Mrs. Elizabeth Solow, Department of Neurological Surgery, Indiana University School of Medicine.

[2] Eastman Chemical Co., Spectro-grade; distilled over calcium hydride.

[3] Tracor model 550 dual-column gas chromatograph.

[4] Applied Science Laboratories, State College, Pa.

[5] Infotronics model CRS-204.

[6] LKB-9000-S.

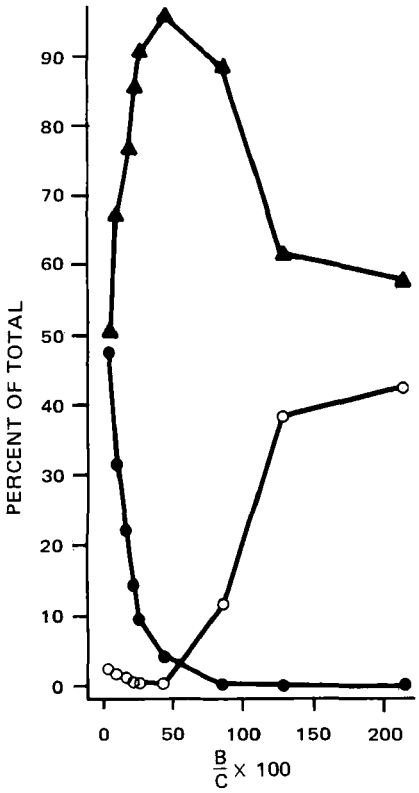

Figure 5—*Relative proportions of the three products obtained from the permethylation of phenobarbital (Ib) at varying barbiturate (B) to carbanion (C) ratios. Key:* ▲, *IIb;* ○, *IIIb; and* ●, *IVb.*

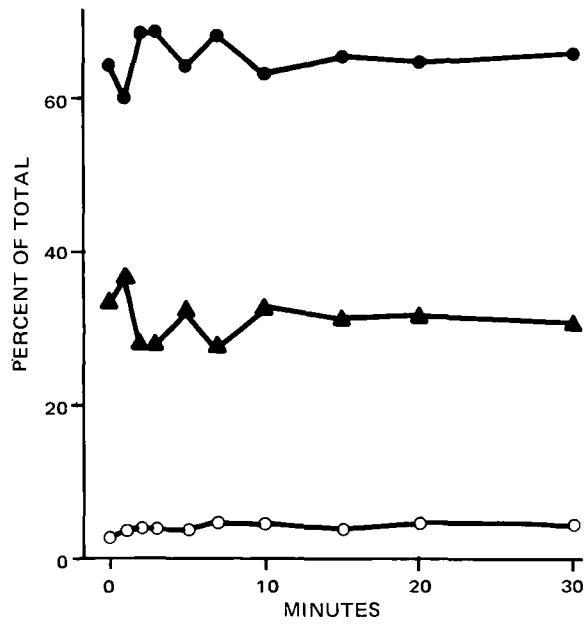

Figure 6—*Relative proportions of three products obtained from the permethylation of phenobarbital (Ib) at varying barbiturate to methylsulfinylmethide carbanion exposure times. Key:* ▲, *IIb;* ○, *IIIb; and* ●, *IVb.*

ther SE-30 or OV-17 columns (*e.g.*, *Ib* in Fig. 1). If the barbiturate to carbanion ratio was less than unity, the conversion to II–IV was complete. At a ratio >2, the total conversion to products was less than 50%. All detector responses were assumed to be essentially identical, because only relative yields are important to this discussion.

Figures 2–4 show the relative proportions of II, III, and IV obtained by varying the amount of methylsulfinylmethide carbanion used during the permethylation of a constant amount of *Ia* (0.45 μmole), *Ib* (0.43 μmole), and Ic (0.42 μmole), respectively. The lowest amount of carbanion used, 1 μmole, was a slight excess, assuming that the only product formed was the *N,N'*-dimethyl derivative, II. In two cases, *Ia* (Fig. 2) and *Ib* (Fig. 3), II (*a* or *b*) made up over 90% of the total product mixture when 1 μmole of carbanion was used, but this proportion rapidly decreased to zero above 50 μmoles (~60-fold excess). However, the relative proportion of IV (*a* or *b*) increased from <10% with 1 μmole of carbanion to >90% with 20–30 μmoles. The proportion of IV decreased slightly above 50 μmoles of carbanion with a concomitant rise in the proportion of III to between 5 and 10%.

The third case, Ic, was completely different from the previous two (Fig. 4). A quantitative yield of IIc was obtained with 1–5 μmoles of carbanion, and the relative proportion was never less than 83%. The relative proportion of IVc was always <5%. Compound IIIc leveled off between 8 and 13% at higher carbanion levels (≥40 μmoles). Therefore, Ic was the only barbiturate examined that formed a single derivative at any barbiturate to carbanion ratio. It is unlikely that any steric effect of the substituents at C-5 is the only factor governing the observation that Ic is much more stable to permethylation than either *Ia* or *Ib*, since all three barbiturates have bulky C-5 substituents. Electronic factors, such as the relative stabilities of the polyanions formed prior to the addition of methyl iodide, probably are more important.

An attempt was made to obtain a single product from *Ib* by using less than a 1:1 molar ratio of carbanion to barbiturate (Fig. 5). In Fig. 5, the values along the abscissa that are <50 reflect an excess of carbanion, again assuming that only the dimethyl derivative (*IIb*) forms. It is obvious that no single product could be formed, even when the barbiturate was in a greater than twofold excess. The relative proportion of IV*b* decreased to zero when the barbiturate to carbanion ratio was >0.85. After reaching a maximum of 96% at a ratio of 0.43, the proportion of II*b* also decreased surprisingly, accompanied by a very significant increase in III*b*. The total product yield began to decrease at barbiturate to carbanion ratios >1 and was finally <50% when this ratio was >2.

Another variable, which was considered to be of potential importance in studying the permethylation of barbiturates, was the length of time the barbiturate was exposed to the methylsulfinylmethide carbanion prior to the addition of methyl iodide. In an experiment in which exposure time was the variable (Fig. 6), there were slight fluctuations in the relative proportions of II*b*, III*b*, and IV*b* (from 0 to 10 min), but the overall result was that the proportions were constant enough to show that the barbiturate to carbanion exposure time is not a variable for this reaction.

In conclusion, methylating reagents such as diazomethane, trimethylanilinium hydroxide, or tetramethylammonium hydroxide are still to be preferred for derivatizing barbiturates prior to GLC and GLC–mass spectrometry analysis, although permethylation is most useful for polar metabolites such as glucuronides.

REFERENCES

(1) R. M. Thompson and D. M. Desiderio, *Org. Mass Spectrom.*, **7**, 989(1973).

(2) P. A. Leclercq and D. M. Desiderio, *Anal. Lett.*, **4**, 305(1971).

(3) H. Bjorndal, C. G. Hellerqvist, B. Lindberg, and S. Svensson, *Angew. Chem. Int. Ed. Engl.*, **9**, 610(1970).

(4) R. M. Thompson, N. Gerber, R. A. Seibert, and D. M. Desiderio, *Drug Metab. Dispos.*, **1**, 489(1973).

ACKNOWLEDGMENTS AND ADDRESSES

Received March 14, 1975, from the *Department of Pediatrics, Indiana University School of Medicine, Indianapolis, IN 46202*

Accepted for publication May 2, 1975.

The author is grateful for financial support from the James Whitcomb Riley Memorial Association.

Synthesis of 2′-Acetoxybiphenyl-2-carboxylic Acid and Its Derivatives as Potential Anti-Inflammatory and Analgesic Agents

ALEX GRINGAUZ

Abstract □ 2′-Acetoxybiphenyl-2-carboxylic acid and a series of derivatives were synthesized. The title compound and its unsubstituted amide had both anti-inflammatory and analgesic properties. Its aminoethyl esters exhibited only analgesia. None of the compounds showed any significant antimicrobial activity.

Keyphrases □ 2′-Acetoxybiphenyl-2-carboxylic acid and derivatives—synthesized and evaluated for anti-inflammatory and analgesic properties and antimicrobial activity □ Anti-inflammatory agents—2′-acetoxybiphenyl-2-carboxylic acid and derivatives synthesized and evaluated □ Analgesic agents—2′-acetoxybiphenyl-2-carboxylic acid and derivatives synthesized and evaluated □ Antipyretic agents—2′-acetoxybiphenyl-2-carboxylic acid and derivatives synthesized and evaluated

The search for effective nonsteroidal anti-inflammatory agents with or without analgesic and antipyretic properties is a continuous one. Indomethacin (1, 2), phenylbutazone (3), mefenamic acid (4), and flufenamic acid (5) are relatively recent examples. Each, however, has disadvantages—some serious—in clinical use.

Salicylic acid and its acetyl derivative, aspirin (I), are probably the oldest and most extensively exploited leads for research in this area. One text (6) gives data on 27 aspirin derivatives and analogs that have been marketed over the years.

Homologs and vinylogs also have been synthesized and evaluated recently (7, 8), and numerous salicylic acid derivatives have been prepared and tested for their anti-inflammatory effects (9). In spite of the extensive work over the last 75 years, many innovative approaches to modify the structure are still possible. The latest apparently successful derivative is flufenisal (4′-fluoro-4-hydroxy-3-biphenylcarboxylic acid acetate) (II) (10, 11).

When the *ortho* relationship of the hydroxy or acetoxy functions to the carboxyl group of aspirin-like compounds is altered, products devoid of analgesic and anti-inflammatory properties invariably result. Therefore, it was of interest to determine the effect of "spreading out" the carboxyl and acetoxy groups as they are in aspirin by placing them on different rings of the biphenyl system. Examination of molecular models indicates that the distance between the two groups in I and the high energy conformation 2′-acetoxybiphenyl-2-carboxylic acid (III) are not significantly different.

The normally favored conformation of *ortho*-substituted biphenyls would place the aromatic rings in planes approximately perpendicular to each other. In aspirin the functional groups project from a single plane. Since the title compound exhibits both pharmacological properites of aspirin, it is interesting to speculate on the requirements of the anti-inflammatory–analgesic receptors. The possibility of an interaction with a relatively planar conformation of III should not be ruled out.

RESULTS AND DISCUSSION

Chemistry—Compound III was prepared by the reactions in Scheme I. 9-Fluorenone was oxidized by a modified Baeyer–Villig-

Table I—Pharmacological Properties of 2′-Acetoxybiphenyl-2-carboxylic Acid and Derivatives

Compound	Carrageenan Edema Single Dose, 0.324 mmole/kg po[a], % Inhibition	Adjuvant Arthritis 6-Day Test, 0.324 mmole/kg po[a], % Inhibition	Acetylcholine Writhing, % Inhibition		Antimicrobial Activity
			Oral[b]	Subcutaneous[c]	MIC, g/ml[d]
III	52[e]	45	40	53	125
IV	50 (at 0.648 mmole/kg)	20	Inactive	Inactive	62.5[f]
V	53	62	53	27	—
VI	37 (at 1.11 mmoles/kg)	—	Inactive	Inactive	125
VII	Inactive	—	Inactive	Inactive	125
VIII	49 (at 1.11 mmoles/kg)	—	Inactive	Inactive	125
IX	Inactive	—	Inactive	Inactive	125
X	Inactive	—	Inactive	Inactive	—
XI	34 (at 1.11 mmoles/kg)	—	Inactive	Inactive	—
XII	Toxic[g]	—	—	—	—
XIII	Inactive	Inactive	—	—	—
XIV	Inactive	Inactive	53[h]	87	500
XV	36	Inactive	33	67	—
XVI	13	Inactive	53	87	—
Aspirin	40[i]	51[h]	71[j]	39[j]	—
Phenylbutazone	55	86	100[j]	—	—
Indomethacin	34[k]	80[l]	—	—	—

[a] 0.324 mmole = 100 mg of phenylbutazone. [b] Oral dose = 200 mg/kg. [c] 100 mg/kg. [d] Minimum inhibitory concentration on synthetic Staphylococcus medium against the following organisms: *Saureus, Pseudomonas aeruginosa, Klebsiella pneumoniae* (39645), *Escherichia coli* (198), and *Proteus vulgaris* (9920). [e] Asbestos granuloma 7-day test showed 27% inhibition. [f] Nalidixic acid is active at 5–10 μg/ml. [g] Seven of eight animals died at 100 mg/kg. [h] At 300 mg/kg (1.67 mmoles). [i] At 150 mg/kg (0.833 mmole). [j] ED_{50}. [k] At 3 mg/kg. [l] At 2 mg/kg.

Table II—Physical Properties of 2′-Acetoxybiphenyl-2-carboxylic Acid and Derivatives

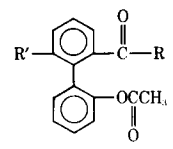

Compound	R	R′	Formula	Melting Point	Analysis, % Calc.	Found
III	—OH	H	$C_{15}H_{12}O_4$	147.5–148.5°	C 70.37 H 4.72	70.27 4.74
V	—NH_2	H	$C_{15}H_{13}NO_3$	162.5–163°	C 70.58 H 5.13 N 5.49	70.42 5.17 5.44
VI	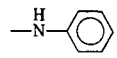	H	$C_{21}H_{17}NO_3$	108–108.5°	C 76.12 H 5.17 N 4.23	75.71 5.21 4.05
VII	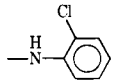	H	$C_{21}H_{16}ClNO_3$	139–139.5°	C 68.95 H 4.41 Cl 9.69 N 3.83	68.96 4.33 9.89 3.80
VIII	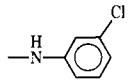	H	$C_{21}H_{16}ClNO_3$	104–104.5°	C 68.95 H 4.41 Cl 9.69 N 3.83	69.17 4.31 9.84 3.76
IX	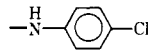	H	$C_{21}H_{16}ClNO_3$	148–149°	C 68.95 H 4.41 Cl 9.69 N 3.83	69.02 4.40 9.66 3.74
X	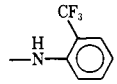	H	$C_{22}H_{16}F_3NO_3$	130–131°	C 66.17 H 4.08 F 14.27 N 3.51	66.31 4.02 14.40 3.35
XI	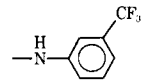	H	$C_{22}H_{16}F_3NO_3$	109–110.5°	C 66.17 H 4.08 F 14.27 N 3.51	66.30 4.10 14.21 3.51
XII	$-N(C_2H_5)_2$	H	$C_{19}H_{22}NO_3$	93–93.5°[a]	C 73.05 H 7.10 N 4.48	73.26 6.87 4.46
XIII	$-N[CH(CH_3)_2]_2$	H	$C_{21}H_{25}NO_3$	112–113°[a]	C 74.31 H 7.42 N 4.13	74.70 7.53 4.07
XIV	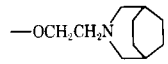	H	$C_{25}H_{29}NO_4 \cdot HCl$	152.5–154°	C 67.63 H 6.81 Cl 7.99 N 3.15	68.13 6.89 8.28 3.17
XV	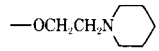	H	$C_{22}H_{25}NO_4 \cdot HCl$	114.5–115°	C 65.42 H 6.49 N 3.47	64.76[b] 6.70 3.25
XVI	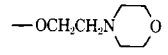	H	$C_{21}H_{23}NO_5 \cdot HCl$[c]	128.5–130°	C 62.14 H 5.96 Cl 8.73 N 3.45	62.35 5.94 8.83 3.40
XVIII	—OH	COOH	$C_{16}H_{12}O_6$	215–216°	C 62.50 H 4.20	62.86[d] 4.09

[a] Recrystallized from absolute ethanol four times. [b] TLC detected no impurities; NMR was consistent. [c] Extremely hygroscopic. [d] NMR spectrum was consistent with assigned structure, showing seven aromatic H, two acidic H, and three methyl H; mass spectrum showed a parent peak at *m/e* 300 (mol. wt. 300.3) and *m/e* 256 ($-CO_2$).

er reaction to 2′-hydroxybiphenyl-2-carboxylic acid lactone (3,4-benzocoumarin) (IV) in good yield. Hydrolysis of IV with 2 moles of ethanolic sodium hydroxide, followed by acetylation and careful acidification of the sodium salt of III, afforded the product in satisfactory yield. The acid chloride III*a*, readily prepared with thionyl chloride, was utilized to synthesize the anilides VI–XI as well as the amides V, XII, and XIII. The aminoester hydrochlorides XV and XVI were similarly derived from III*a*.

Compound XIV was prepared by direct reaction of III with 3-(2-chloroethyl)-3-azabicyclo[3.3.2]nonane. The treatment of diphenic acid with hot sulfuric acid afforded 9-fluorenone-4-carboxylic acid (12), which, when reacted as per Scheme I, afforded XVIII. Attempts to oxidize 2,7-dibromo-9-fluorenone to the corresponding lactone failed due to very poor solubility, even in 98% H_2SO_4. Hawthorne and Mihelic (13) reported the facile conversion of diphenic acid to IV by lengthy refluxing with hydrogen peroxide in aqueous sodium bicarbonate or calcium hydroxide. All attempted modifications of this reaction with 4,4′-dichloro- and 6,6′-dimethyldiphenic acids failed to give the desired lactones.

Biology—The anti-inflammatory activity of the compounds was

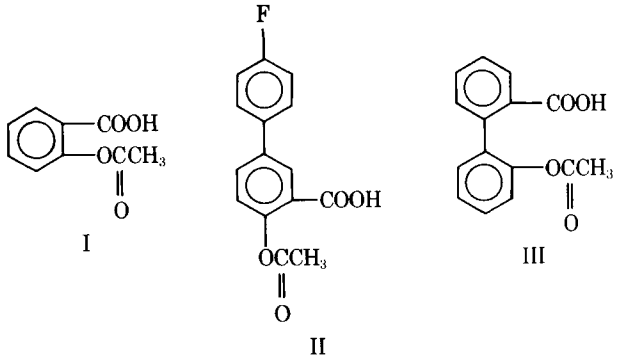

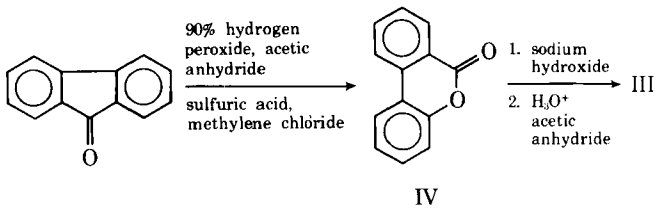

Scheme I

assessed by their ability to inhibit rat hindpaw carrageenan edema (14), by the adjuvant arthritis test (15, 16), and by the asbestos granuloma test (17). Analgesic activity was determined by the acetylcholine writhing method (18). Antimicrobial activity was ascertained by the tube dilution test, determining the minimum inhibitory concentration (MIC) in micrograms per milliliter (Table I).

As can be seen from Table I, III and V showed significant anti-inflammatory activity in at least two test systems. The analgesic potency of III is probably less than one-fourth that of aspirin. However, the compound is highly hypothermic. The latter property might be expected to prevent it from exhibiting clinically useful antirheumatic activity. The diacid XVIII showed no anti-inflammatory properties. This result might be expected since additional acid functions, such as carboxyl, tend to lower biological activity sharply (19). The three aminoethyl esters XIV, XV, and XVI exhibited analgesic activity but insignificant anti-inflammatory properties.

The data suggest that III and some of its derivatives show interesting and potentially useful activity in the anti-inflammatory–analgesic area. Expansion of this series may lead to more useful compounds and help clarify the structure–activity relationships.

EXPERIMENTAL[1]

2′-Hydroxybiphenyl-2-carboxylic Acid Lactone (IV)—This compound was prepared by an improved Baeyer–Villiger oxidation of 9-fluorenone (20) in 80–85% yield, mp 93–94° (21).

2′-Acetoxybiphenyl-2-carboxylic Acid (III)—To a solution of 80 g (2 moles) of sodium hydroxide in 50% ethanol was added 196 g (1 mole) of IV. The mixture was heated on a water bath until a syrup was obtained. After cooling (ice–salt), 110 g (1.08 moles) of acetic anhydride was added in portions while stirring was continued for 1 hr. A thick paste resulted. Treatment with cold water, rapid filtration (recovering unreacted IV), and acidification (congo red) of filtrate with hydrochloric acid afforded a light-brown semisolid which solidified on trituration. The crude product was air dried and crystallized from benzene, yielding 200.6 g (78%) of product.

Two additional recrystallizations gave a melting point of 147.5–148.5°; IR: 3.2–3.75 (continuous series, bonded OH), 5.65 (C=O, acetoxy), and 5.90 (C=O, carboxyl) μm; NMR: δ 1.96 (3H, acetoxy CH_3), 7.0–8.0 (8H, aromatic), and 12.5 (1H, carboxyl).

Anal.—Calc. for $C_{15}H_{12}O_4$: C, 70.37; H, 4.72. Found: C, 70.27; H, 4.74. Neutralization equivalent: Calc. 256.3. Found 252.7.

2′-Acetoxybiphenyl-2-carboxylic Acid Chloride (IIIa)—A solution of III in benzene was refluxed with excess thionyl chloride 2 hr. The solvent was removed *in vacuo*, and the residue was washed two times with benzene, giving a quantitative yield. Recrystallization from cyclohexane gave a melting point of 86–88°.

2′-Acetoxybiphenyl-2-carboxamide (V)—To a well-chilled solution of 12.4 g (0.4 mole) of anhydrous ammonia in 100 ml of ether was added a benzene solution of 27.5 g (0.1 mole) of IIIa over 2 hr while a temperature of 5° was maintained. The formed solid was filtered and washed with water. The residual product was recrystallized three times from 2-propanol, yielding 19.1 g (75%), mp 162.5–163°; IR: 2.96, 3.20 (N—H), 5.87 (C=O, acetoxy), and 6.02 (C=O, amide) μm; NMR: δ 1.98 (3H, acetoxy CH_3), 5.5–6.5 (2H, NH_2), and 7–8 (8H, aromatic).

Anal.—Calc. for $C_{15}H_{13}NO_3$: C, 70.58; H, 5.17; N, 5.49. Found: C, 70.42; H, 5.13; N, 5.44.

Compounds XII and XIII were prepared similarly (Table II).

2′-Acetoxybiphenyl-2-carboxanilide (VI)—A benzene solution of 5.36 g (0.0195 mole) of IIIa was added to 3.63 g (0.039 mole) of aniline, and the mixture was refluxed for 2 hr. Filtration of aniline hydrochloride and removal of the solvent *in vacuo* gave a product which solidified on trituration with ether. Recrystallization four times from 2-propanol afforded 3.6 g (56%), mp 108–108.5°; IR: 3.02 (NH), 5.63 (C=O, acetoxy), 5.77, and 5.92 (C=O, amide) μm; NMR: δ 2.0 (3H, acetoxy CH_3), 6.8–7.9 (13H, aromatic), and 8.44 (1H, NH).

Anal.—Calc. for $C_{21}H_{17}NO_3$: C, 76.12; H, 5.17; N, 4.23. Found: C, 75.71; H, 5.21; N, 4.05.

Compounds VII–XI were analogously prepared in similar yields (Table II).

2-(Morpholino)ethyl-2′-acetoxy-2-biphenylcarboxylate Hydrochloride (XVI)—A benzene solution of 16.75 g (0.061 mole) of IIIa and 8.7 g (0.061 mole) of 2-morpholinoethanol was refluxed 2 hr, cooled, and treated with absolute ether. The solid obtained, 19.3 g (78%), was crystallized [ethyl acetate–2-propanol (9:1)] to a constant melting point of 128.5–130°; IR: 3.02 (NH), 5.68 (C=O, acetoxy), and 5.74 (C=O, amino ester) μm.

Anal.—Calc. for $C_{21}H_{23}NO_5 \cdot HCl$: C, 62.14; H, 5.96; Cl, 8.73; N, 3.45. Found: C, 62.35; H, 5.94; Cl, 8.83; N, 3.40.

Compound XV was prepared similarly. Compound XIV was synthesized by reacting 27.9 g (0.15 mole) of 3-(2-chloroethyl)-3-azabicyclo[3.2.2]nonane with 25.6 g (0.1 mole) of III in 2-propanol under reflux (10 hr). Workup and recrystallization from 2-propanol afforded 23.5 g (53%) of product. Attempts to react IIIa with 2-diisopropylaminoethanol gave an oil, which only partially crystallized after 3 months at −5°.

2′-Hydroxy-2,6-biphenyldicarboxylic Acid 2′,6-Lactone (XVII)—Diphenic acid, 44.4 g (0.1 mole), was dissolved in 200 g of concentrated sulfuric acid and maintained for 2 hr at 120°. The solution of 9-fluorene-4-carboxylic acid thus obtained (12) was then oxidized under modified Baeyer–Villiger conditions, omitting methylene chloride as the cosolvent. The 13.9 g (58%) of yellow product was recrystallized from ethanol–petroleum ether (bp 30–60°) (9:1), mp 264–266° dec.; IR: 3.27 (OH) and 5.95 (C=O) μm; NMR: δ 5.5–6.9 (7H, aromatic) and 11.0 (1H, COOH).

Anal.—Calc. for $C_{14}H_8O_4$: C, 70.00; H, 3.36. Found: C, 69.73; H, 3.47.

2′-Acetoxy-2,6-biphenyldicarboxylic Acid (XVIII)—This compound was obtained in 64% yield by alkaline hydrolysis of XVII, followed by acetylation as described for III.

[1] Melting points were determined on a Thomas-Hoover Uni-Melt and are uncorrected. IR spectra were obtained, using KBr pellets, with a Perkin-Elmer 337; UV spectra were obtained on a Coleman-Hitachi 124. NMR spectra were carried out on a Varian A60 in $CDCl_3$, CF_3COOD, or dimethyl sulfoxide-d_6 using tetramethylsilane as the internal reference. Elemental analyses were performed by Galbraith Laboratories, Inc., Knoxville, Tenn., and by Dr. F. B. Strauss, Oxford, England.

REFERENCES

(1) T. Y. Shen, T. B. Windholz, A. Rosegay, B. E. Witzel, A. N. Wilson, J. D. Willett, W. J. Holtz, R. L. Ellis, A. R. Matzuk, S. Lucas, C. H. Stammer, F. W. Holly, L. H. Sarett, E. A. Risley, G. W. Nuss, and C. A. Winter, *J. Amer. Chem. Soc.*, **85**, 488(1963).

(2) C. A. Winter, E. A. Risley, and G. Nuss, *J. Pharmacol. Exp. Ther.*, **141**, 369(1963).

(3) M. W. Whitehouse, *Progr. Drug Res.*, **8**, 321(1965).

(4) C. V. Winder, J. Wax, L. Scotti, R. A. Scherrer, E. M. Jones, and F. W. Short, *J. Pharmacol. Exp. Ther.*, **138**, 405(1962).

(5) C. V. Winder, J. Wax, B. Serrano, E. M. Jones, and M. L. McPhee, *Arthritis Rheum.*, **6**, 36(1963).

(6) "Mays Chemistry of Synthetic Drugs," 5th ed., G. M. Dyson, Ed., Wiley, New York, N.Y., 1959, pp. 132, 133.
(7) C. W. Bauer and E. F. Lasala, *J. Amer. Pharm. Ass., Sci. Ed.*, **49**, 48(1960).
(8) A. Gringauz, *J. Med. Chem.*, **11**, 611(1968).
(9) M. W. Whitehouse, *Biochem. Pharmacol.*, **13**, 319(1964).
(10) S. Bloomfield, T. Barden, and R. Hille, *Clin. Pharmacol. Ther.*, **11**, 747(1970).
(11) S. Bloomfield, T. Barden, and R. Hille, *Fed. Proc., Fed. Amer. Soc. Exp. Biol.*, **29**, 686(1970).
(12) L. F. Fieser and M. Fieser, "Organic Chemistry," 3rd ed., Heath, Boston, Mass., 1956, p. 667.
(13) J. O. Hawthorne and E. L. Mihelic, Sr., U.S. pat. 3,106,567 (1963).
(14) C. A. Winter, E. A. Risley, and G. W. Nuss, *Proc. Soc. Exp. Biol. Med.*, **111**, 544(1962).
(15) C. M. Pearson, *J. Chronic Dis.*, **16**, 863(1963).
(16) E. M. Glenn and J. Gay, *Amer. J. Vet. Res.*, **26**, 1180(1965).
(17) R. Meier, W. Schuler, and P. Desaulles, *Experientia*, **6**, 469(1950).
(18) H. O. J. Collier, L. C. Dinneen, C. A. Johnson, and C. Schneider, *Brit. J. Pharmacol. Chemother.*, **32**, 295(1968).
(19) "Medicinal Chemistry," 2nd ed., A. Burger, Ed., Interscience, New York, N.Y., 1960, p. 43.
(20) A. Gringauz and E. Tosk, *Org. Prep. Proc.*, **2**, 185(1970).
(21) C. Grabe and P. Schestakow, *Ann.*, **284**, 306(1895).

ACKNOWLEDGMENTS AND ADDRESSES

Received March 22, 1974, from the *Department of Chemistry, Brooklyn College of Pharmacy, Long Island University, Brooklyn, NY 11216*

Accepted for publication April 15, 1975.

Presented at the APhA Academy of Pharmaceutical Sciences, Chicago meeting, August 1974.

Supported by the Sterling-Winthrop Research Institute.

The author thanks Dr. F. C. Nachod for personal interest in the project, Mr. Eugene Tosk for technical assistance, and Dr. S. I. Mauer, Mrs. A. K. Pierson, Dr. W. A. Goss, and Mr. E. B. Cimijotti from Sterling-Winthrop Research Institute for the pharmacological and bacteriological data.

Isolation and Chemistry of Alkaloids from Plants of the Family Papaveraceae LXVII: *Corydalis cava* (L.) Sch. et K. (*C. tuberosa* DC)

V. PREININGER, R. S. THAKUR *, and F. ŠANTAVÝ ˣ

Abstract □ From *Corydalis cava* (L.) Sch. et K. (*C. tuberosa* DC) (Papaveraceae: genus *Corydalis* Med.), a mixture of alkaloids (0.53%) was isolated. The main alkaloid was (+)-bulbocapnine, and the minor alkaloids were coptisine, (+)-domestine, adlumidiceine, (+)-predicentrine, protopine, (−)-capnoidine, (+)-stylopine, (+)-isoboldine, 8-oxocoptisine, 1,2-methylenedioxy-6a,7-dehydroaporphine-10,11-quinone, and corysamine. In addition, fumaric acid was obtained. Coptisine, adlumidiceine, predicentrine, 8-oxocoptisine, corysamine, 1,2-methylenedioxy-6a,7-dehydroaporphine-10,11-quinone, and isoboldine were found in *C. cava* for the first time, but rhoeadine and papaverrubine alkaloids were not detected. Predicentrine and isoboldine were identified on the basis of the UV, IR, mass, and PMR spectra.

Keyphrases □ *Corydalis cava*—alkaloids isolated, UV, IR, PMR, and mass spectra □ Alkaloids—isolated from *Corydalis cava*, UV, IR, PMR, and mass spectra

During the Middle Ages, the tubers of *Corydalis cava* (L.) Sch. et K. (*C. tuberosa* DC) (Papaveraceae: genus *Corydalis* Med.) (1) were used for headache, neuroses, tremor, pain, and paralysis of the extremities (2). So far, 20 alkaloids have been isolated (3, 4), and Trabert and Schneidewind (5) isolated bulbocapnine as the main alkaloid (97%). The other alkaloids were (+)-stylopine, corydaline, an alkaloid of the formula $C_{18}H_{19}NO_5$, mp 230°, $[\alpha]_D^{20}$ −112.5° (chloroform), and an alkaloid with a melting point of 225–226°. Manske (6) isolated capnoidine, domestine (nantenine), and narcotine, and Blaschke *et al.* (7) detected sinoacutine.

DISCUSSION

As part of a systematic investigation of the alkaloids of the genus *Papaver* and *Corydalis*, *C. cava*, which flowers in abundance in the meadows and woods, was studied using chromatographic methods. In addition to the alkaloids isolated earlier, *i.e.*, (+)-bulbocapnine (53.1%) (3–7), (+)-domestine, protopine, (+)-stylopine, and (−)-capnoidine, the alkaloids coptisine (according to quantity the second main alkaloid), adlumidiceine (8), (+)-predicentrine, (+)-isoboldine, corysamine, 8-oxocoptisine, and 1,2-methylenedioxy-6a,7-dehydroaporphine-10,11-quinone were isolated. The last two substances are new alkaloids which have not been isolated previously.

In the material studied, it was not possible to detect corydine, corytuberine, glaucine, hydrohydrastinine, (+)-canadine, corybulbine, sinoacutine, isocorybulbine, corydaline, dehydrocorydaline, (+)-corypalmine, scoulerine, (+)-isocorypalmine, thalictricavine, corycavamine, corycavidine, corycavine, and narcotine, which had been found previously (3, 4). Neither was it possible to detect the rhoeadine or papaverrubine alkaloids, which are characteristic for the genus *Papaver* (4). An attempt was made to identify some of the earlier isolated alkaloids by comparison of their physical constants. Thus, it was found that the previously isolated (5, 9, 10) alkaloid with a melting point of 230° might be capnoidine (237°), and the previously isolated (9) alkaloid with a melting point of 137° might be domestine (138°).

The structure of the alkaloid called predicentrine (I) (1,9,10-trimethoxy-2-hydroxyaporphine) (11, 12), whose methylation with

(6) "Mays Chemistry of Synthetic Drugs," 5th ed., G. M. Dyson, Ed., Wiley, New York, N.Y., 1959, pp. 132, 133.
(7) C. W. Bauer and E. F. Lasala, *J. Amer. Pharm. Ass., Sci. Ed.*, **49**, 48(1960).
(8) A. Gringauz, *J. Med. Chem.*, **11**, 611(1968).
(9) M. W. Whitehouse, *Biochem. Pharmacol.*, **13**, 319(1964).
(10) S. Bloomfield, T. Barden, and R. Hille, *Clin. Pharmacol. Ther.*, **11**, 747(1970).
(11) S. Bloomfield, T. Barden, and R. Hille, *Fed. Proc., Fed. Amer. Soc. Exp. Biol.*, **29**, 686(1970).
(12) L. F. Fieser and M. Fieser, "Organic Chemistry," 3rd ed., Heath, Boston, Mass., 1956, p. 667.
(13) J. O. Hawthorne and E. L. Mihelic, Sr., U.S. pat. 3,106,567 (1963).
(14) C. A. Winter, E. A. Risley, and G. W. Nuss, *Proc. Soc. Exp. Biol. Med.*, **111**, 544(1962).
(15) C. M. Pearson, *J. Chronic Dis.*, **16**, 863(1963).
(16) E. M. Glenn and J. Gay, *Amer. J. Vet. Res.*, **26**, 1180(1965).
(17) R. Meier, W. Schuler, and P. Desaulles, *Experientia*, **6**, 469(1950).
(18) H. O. J. Collier, L. C. Dinneen, C. A. Johnson, and C. Schneider, *Brit. J. Pharmacol. Chemother.*, **32**, 295(1968).
(19) "Medicinal Chemistry," 2nd ed., A. Burger, Ed., Interscience, New York, N.Y., 1960, p. 43.
(20) A. Gringauz and E. Tosk, *Org. Prep. Proc.*, **2**, 185(1970).
(21) C. Grabe and P. Schestakow, *Ann.*, **284**, 306(1895).

ACKNOWLEDGMENTS AND ADDRESSES

Received March 22, 1974, from the *Department of Chemistry, Brooklyn College of Pharmacy, Long Island University, Brooklyn, NY 11216*

Accepted for publication April 15, 1975.

Presented at the APhA Academy of Pharmaceutical Sciences, Chicago meeting, August 1974.

Supported by the Sterling-Winthrop Research Institute.

The author thanks Dr. F. C. Nachod for personal interest in the project, Mr. Eugene Tosk for technical assistance, and Dr. S. I. Mauer, Mrs. A. K. Pierson, Dr. W. A. Goss, and Mr. E. B. Cimijotti from Sterling-Winthrop Research Institute for the pharmacological and bacteriological data.

Isolation and Chemistry of Alkaloids from Plants of the Family Papaveraceae LXVII: *Corydalis cava* (L.) Sch. et K. (*C. tuberosa* DC)

V. PREININGER, R. S. THAKUR *, and F. ŠANTAVÝ ˣ

Abstract □ From *Corydalis cava* (L.) Sch. et K. (*C. tuberosa* DC) (Papaveraceae: genus *Corydalis* Med.), a mixture of alkaloids (0.53%) was isolated. The main alkaloid was (+)-bulbocapnine, and the minor alkaloids were coptisine, (+)-domestine, adlumidiceine, (+)-predicentrine, protopine, (−)-capnoidine, (+)-stylopine, (+)-isoboldine, 8-oxocoptisine, 1,2-methylenedioxy-6a,7-dehydroaporphine-10,11-quinone, and corysamine. In addition, fumaric acid was obtained. Coptisine, adlumidiceine, predicentrine, 8-oxocoptisine, corysamine, 1,2-methylenedioxy-6a,7-dehydroaporphine-10,11-quinone, and isoboldine were found in *C. cava* for the first time, but rhoeadine and papaverrubine alkaloids were not detected. Predicentrine and isoboldine were identified on the basis of the UV, IR, mass, and PMR spectra.

Keyphrases □ *Corydalis cava*—alkaloids isolated, UV, IR, PMR, and mass spectra □ Alkaloids—isolated from *Corydalis cava*, UV, IR, PMR, and mass spectra

During the Middle Ages, the tubers of *Corydalis cava* (L.) Sch. et K. (*C. tuberosa* DC) (Papaveraceae: genus *Corydalis* Med.) (1) were used for headache, neuroses, tremor, pain, and paralysis of the extremities (2). So far, 20 alkaloids have been isolated (3, 4), and Trabert and Schneidewind (5) isolated bulbocapnine as the main alkaloid (97%). The other alkaloids were (+)-stylopine, corydaline, an alkaloid of the formula $C_{18}H_{19}NO_5$, mp 230°, $[\alpha]_D^{20}$ −112.5° (chloroform), and an alkaloid with a melting point of 225–226°. Manske (6) isolated capnoidine, domestine (nantenine), and narcotine, and Blaschke *et al.* (7) detected sinoacutine.

DISCUSSION

As part of a systematic investigation of the alkaloids of the genus *Papaver* and *Corydalis*, *C. cava*, which flowers in abundance in the meadows and woods, was studied using chromatographic methods. In addition to the alkaloids isolated earlier, *i.e.*, (+)-bulbocapnine (53.1%) (3–7), (+)-domestine, protopine, (+)-stylopine, and (−)-capnoidine, the alkaloids coptisine (according to quantity the second main alkaloid), adlumidiceine (8), (+)-predicentrine, (+)-isoboldine, corysamine, 8-oxocoptisine, and 1,2-methylenedioxy-6a,7-dehydroaporphine-10,11-quinone were isolated. The last two substances are new alkaloids which have not been isolated previously.

In the material studied, it was not possible to detect corydine, corytuberine, glaucine, hydrohydrastinine, (+)-canadine, corybulbine, sinoacutine, isocorybulbine, corydaline, dehydrocorydaline, (+)-corypalmine, scoulerine, (+)-isocorypalmine, thalictricavine, corycavamine, corycavidine, corycavine, and narcotine, which had been found previously (3, 4). Neither was it possible to detect the rhoeadine or papaverrubine alkaloids, which are characteristic for the genus *Papaver* (4). An attempt was made to identify some of the earlier isolated alkaloids by comparison of their physical constants. Thus, it was found that the previously isolated (5, 9, 10) alkaloid with a melting point of 230° might be capnoidine (237°), and the previously isolated (9) alkaloid with a melting point of 137° might be domestine (138°).

The structure of the alkaloid called predicentrine (I) (1,9,10-trimethoxy-2-hydroxyaporphine) (11, 12), whose methylation with

diazomethane afforded glaucine (II) (Scheme I), was elucidated by UV, IR, mass, and PMR spectra; λ_{max} (ethanol) (log ϵ): 218 (4.58), 236 (sh), (4.36), 273 (sh) (4.09), 282 (4.16), 304 (4.14), and 314 (sh) (4.09) nm. Those values are characteristic of the 1,2,9,10-tetrasubstituted aporphine alkaloid (13); the presence of the phenolic hydroxyl was confirmed by the bathochromic shift of the two long wavelength bands due to ionization of the molecule (sodium hydroxide) [λ_{max} (ethanolic sodium hydroxide) (log ϵ): 233 (4.11), 305 (sh) (4.08), and 330 (4.23) nm].

The IR spectrum in chloroform showed a hydroxyl band at 3530 cm^{-1} and aromatic double bond peaks at 1605 and 1585 cm^{-1}. The substitution at C-9 and C-10 also was confirmed by the mass spectrum, where the ion (M − 1) represents a base peak (14). The molecular peak of mass M^+ 341 corresponds to the formula $C_{20}H_{23}NO_4$. In the PMR spectrum of predicentrine (deuterochloroform), the singlet at 2.55 ppm (3H) is attributable to the N—CH_3 group, the singlet at 3.63 (3H) is attributable to the OCH_3 group of ring A, and the singlet at 3.87 (6H) is attributable to two OCH_3 groups at C-9 and C-10 on ring D. The singlets at 6.55 (1H), 6.80 (1H), and 8.03 (1H) correspond to the aromatic protons at C-3, C-8, and C-11, respectively. The broad singlet at 5.65 is attributable to the proton of the hydroxyl group.

The methoxyl bands were separated by using benzene as a solvent. The signals of the methoxyl groups with a free *ortho*-position (at C-9 and C-10) shifted to higher fields (3.42 and 3.45 ppm), whereas the position of the signal of the methoxyl group in ring A practically did not change (3.55). This finding is confirmatory evidence for its position at C-1 and the position of the phenolic hydroxyl group at C-2.

Besides predicentrine (I), another aporphine alkaloid of a phenolic nature was isolated. Its methylation with diazomethane gave glaucine (II). Its UV spectrum [λ_{max} (ethanol) (log ϵ): 219 (4.54), 273 (sh) (4.03), 281 (4.11), 305 (4.16), and 311 (sh) (4.14) nm] was characteristic of a 1,2,9,10-tetrasubstituted aporphine alkaloid. The presence of phenolic hydroxyls was confirmed by the bathochromic shift of both long wavelength bands due to ionization of the molecule (sodium hydroxide) [λ_{max} (ethanolic sodium hydroxide) (log ϵ): 232 (4.20), 299 (sh) (3.95), and 326 (4.07) nm].

The IR spectrum in chloroform showed a hydroxyl frequency at 3530 cm^{-1}. The molecular peak of mass M^+ 327 corresponds to the formula $C_{19}H_{21}NO_4$. The PMR spectrum (deuterochloroform) exhibited the signals of the N—CH_3 group and of two OCH_3 groups. The spectral data showed that this alkaloid is isoboldine (III). Its identity was confirmed by a comparison of its melting point and IR spectrum with those of the authentic sample.

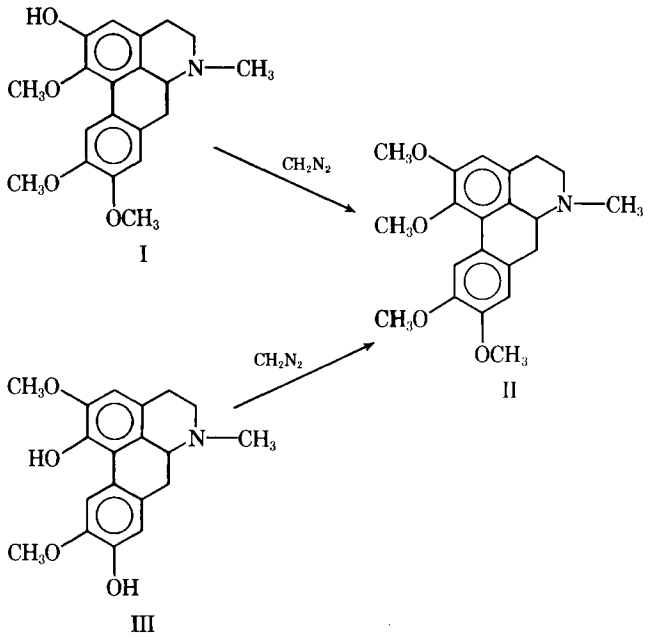

Scheme I

EXPERIMENTAL[1]

Plant Material—The plant material was collected around Hynkov (district of Olomouc, Czechoslovakia) in June 1973. Voucher specimens were identified and authenticated[2].

Extraction, Separation, and Purification of Alkaloids—The dried ground drug (5.8 kg) was extracted (16) with 50 liters of methanol, concentrated *in vacuo* at 36° to ~1.0 liter, diluted with equal volumes of 5% acetic acid, and taken up into light petroleum and then into ether. The acidic aqueous residue was made alkaline with sodium carbonate to pH ~8 and then extracted with ether (Portion A, 27.7 g).

The aqueous residue was made alkaline with sodium hydroxide to pH ~12 and extracted with ether (Portion B, 4.29 g) and then with chloroform (Portion C, 6.0 g). The aqueous phase was acidified with hydrochloric acid to pH ~3, and a saturated solution of potassium iodide was added. After extraction with chloroform, Portion D (2.5 g) was obtained (17), which did not contain any alkaloids.

Workup of Acidic Light Petroleum Extract—The extract was dissolved in 5% acetic acid, refiltered, and taken up into ether to afford fumaric acid (1.25 g), mp 285–287° (in a sealed capillary). Its identity was confirmed with IR spectroscopy. No alkaloids could be detected in the extract.

Workup of Acidic Ether Extract—The extract was dissolved in 5% acetic acid, refiltered, and taken up into ether to give 3.43 g more of fumaric acid. Even in this extract, the alkaloids could not be detected.

Workup of Portion A—Portion A yielded directly 15.14 g of bulbocapnine, mp 197–199° (ethyl acetate and ether), $[\alpha]_D^{25}$ +235 ± 3° (c 0.462, chloroform). After separation of bulbocapnine, the mother liquors were concentrated *in vacuo*, and the residue was dissolved in 500 ml of 1% sulfuric acid. An attempt was made to isolate the benzophenanthridine alkaloids in the form of pseudocyanides (18), but these alkaloids could be neither isolated nor detected. The extract was then made alkaline with ammonium hydroxide and taken up into ether to afford 12.57 g of a mixture of alkaloids. This mixture was chromatographed on a column of aluminum oxide (300 g); 750-ml fractions were collected.

Fraction 1 [ether–light petroleum (50:50)] gave (+)-stylopine (0.09 g), mp 201–203° (ethyl acetate and ether), $[\alpha]_D^{25}$ +313 ± 3° (c 0.984, chloroform), hR_f 63 (Solvent System 1). Fraction 2 [ether–light petroleum (50:50)] yielded domestine (1.08 g), mp 137–139° (ethyl acetate and ether), hR_F 54 (Solvent System 1). Fraction 4 [ether–light petroleum (50:50)] gave capnoidine (0.11 g), mp 235–237°, $[\alpha]_D^{25}$ −115 ± 2° (c 0.652, chloroform), hR_F 28 (Solvent System 1). Fractions 5–14 (ether) gave bulbocapnine (1.86 g), mp 197–199° (ethyl acetate and ether), $[\alpha]_D^{25}$ +235 ± 3° (c 0.832, chloroform), hR_F 33 (Solvent System 1). The mother liquors, after isolation of bulbocapnine from fraction 6, yielded protopine (0.17 g), mp 205–207° (acetone and ether), $[\alpha]_D^{25}$ ± 0° (c 0.902, chloroform).

Fraction 15 [ether–chloroform (90:10)] gave an alkaloid (0.006 g) which formed blue-green crystals, mp 218–220° (acetone and methanol). On the basis of the melting point and the UV and IR spectra, this alkaloid was identical with 1,2-methylenedioxy-6a,7-dehydroaporphine-10,11-quinone[3]; λ_{max} (log ϵ): 229 (4.35), 286 (4.01), 346 (4.20), 405 (3.81), and 639 (3.69) nm. The IR spectrum showed bands in the carbonyl region at 1685, 1650, 1590, and 1580 cm^{-1}. Fractions 16–22 [ether–chloroform (90:10–50:50)] yielded an alkaloid (0.37 g), mp 156–158° (benzene); hydrobromide, mp 200–

[1] Melting points were determined on a Kofler block and are uncorrected. For the measurements, the substances were dried for 1 hr at 100°/Torr. The optical rotation was measured on a polarimeter (Hilger), the UV spectra were measured on a Unicam SP 700, the IR spectra were measured on an Infrascan H-900 (Hilger), the PMR spectra were measured on a Varian T-60 (tetramethylsilane as the internal standard), and the mass spectra were measured on an AEI MS 902 instrument. Preparative column chromatography was carried out on aluminum oxide W 200 neutral (Woelm, Germany) or on aluminum oxide neutral (Reanal, Hungary). TLC was performed on silica gel G plates (Merck, Germany) using cyclohexane–diethylamine (80:20) (Solvent System 1) or methanol–diethylamine (80:20) (Solvent System 2). The alkaloids were detected with Dragendorff reagent or under UV light (protoberberine alkaloids); for the detection of the papaverrubines, hydrochloric acid and heating were used (15).

[2] By Dr. B. Šula, botanist of the Museum in Olomouc. Voucher specimens were deposited at Palacký University.

[3] This substance was prepared by Cava *et al.* (19) by oxidation of bulbocapnine with mercuric chloride.

210° dec. (methanol), $[\alpha]_D^{25}$ +105 ± 3° (c 0.800, chloroform), hR_F 16 (Solvent System 1), which was assigned the structure of predicentrine (I).

Fraction 26 [chloroform–methanol (98:2)] gave the alkaloid isoboldine (III) (0.03 g), mp 122–124° (acetone, no depression with authentic sample), $[\alpha]_D^{25}$ +70 ± 3° (c 0.700, chloroform), hR_F 9 (Solvent System 1). In the presence of air, crystalline isoboldine readily gave a red oxidation product. The mother liquors yielded still another Dragendorff-positive substance of hR_F 3 (Solvent System 1), which could be neither isolated nor identified. Finally, fractions 29–31 [chloroform–methanol (92:8–84:16)] gave adlumidiceine (0.33 g), mp 244–246° (methanol and ether), $[\alpha]_D^{25}$ ±0° (c 0.576, methanol).

Workup of Portion B—Portion B was worked up in the usual manner (20) to afford 4.72 g of coptisine chloride, hR_F 71 (Solvent System 2) and 0.01 g of corysamine chloride, hR_F 29 (Solvent System 2), the identity of which was confirmed by IR.

Workup of Portion C—Portion C (6.0 g) was subjected to column chromatography on aluminum oxide (180 g); 600-ml fractions were collected. Fractions 1 and 2 [ether–light petroleum (50:50)] gave an alkaloid (in traces) which, after transformation into a chloride, was identified by IR as corysamine. Fraction 3 [ether–light petroleum (50:50)] yielded domestine (in traces), and fraction 5 [ether–light petroleum (50:50)] yielded capnoidine. Fractions 6–14 [ether and ether–chloroform (90:10)] gave bulbocapnine (0.04 g).

Fractions 15 and 16 [ether–chloroform (90:10)] yielded an alkaloid (0.01 g), mp 284–286°, which was identified as 8-oxocoptisine [λ_{max} (log ϵ): 228 (4.58), 257 (sh) (4.04), 272 (sh) (3.91), 290 (3.80), 317 (sh) (4.01), 341 (sh) (4.25), 349 (4.28), 377 (4.13), and 398 (sh) (4.01) nm]. In the IR spectrum, the band at 1647 cm^{-1} (potassium bromide) indicated the presence of a carbonyl group. Fraction 28 [chloroform–methanol (92:8)] gave the alkaloid (0.12 g) of hR_F 71 (Solvent System 2) which, after transformation into a chloride, was identified by IR as coptisine.

Acetylation of Predicentrine (I)—Predicentrine (25 mg) was dissolved in 2 ml of anhydrous pyridine, 2 ml of acetic anhydride was added, and the mixture was left standing at room temperature for 24 hr. After removal of the solvent by distillation, the product could not be crystallized from common solvents. In the PMR spectra (deuterochloroform), the singlet at 2.28 ppm (3H) corresponded to the CH_3COO group; the chemical shifts of the signals of the N—CH_3 group (2.47, 3H), OCH_3 groups on ring A (3.62, 3H) and ring D (3.83, 6H), and aromatic protons (6.57, C-3; 6.87, C-8; and 8.10, C-11) were practically consistent with the chemical shifts in the spectrum of predicentrine.

Methylation of Predicentrine (I)—Predicentrine (30 mg) was dissolved in a mixture of methanol and ether (3 ml), an ether solution of diazomethane was added, and the product was left standing for 24 hr at room temperature. After removal of the solvents by distillation, a substance with melting point of 118–120° (ethyl acetate and ether), hR_F 28 (Solvent System 1), was obtained. On the basis of the IR spectrum (chloroform), it was identical with glaucine (II).

Methylation of Isoboldine (III)—Isoboldine (20 mg) was dissolved in a mixture of methanol and ether (3 ml), an ether solution of diazomethane was added, and the mixture was left standing for 24 hr at room temperature. After removal of the solvents by distillation, a substance with a melting point of 118–120° (ethyl acetate and ether), hR_F 28 (Solvent System 1), was obtained. On the basis of the IR spectrum (chloroform), it was identical with glaucine.

REFERENCES

(1) H. Melchior, in "Syllabus der Pflanzenfamilien," 12th ed., part II, A. Engler, Ed., Borntraeger, Berlin, Germany, 1964, p. 179.

(2) P. A. Matthioli, "Kräuterbuch," Prag, 1568.

(3) R. H. F. Manske, in "The Alkaloids," vol. 4, R. H. F. Manske and H. C. Holmes, Eds., Academic, New York, N.Y., 1954, p. 81.

(4) F. Šantavý, in "The Alkaloids," vol. 12, R. H. F. Manske, Ed., Academic, New York, N.Y., 1970, p. 335.

(5) C. H. Trabert and U. Schneidewind, *Pharm. Zentrallh.*, **98,** 447(1959).

(6) R. H. F. Manske, *Can. J. Chem.*, **47,** 1103(1969).

(7) G. Blaschke, G. Waldheim, M. v. Scahntz, and P. Peura, *Arch. Pharm.*, **307,** 122(1974).

(8) V. Preininger, V. Šimánek, O. Gašić, L. Dolejš, and F. Šantavý, *Phytochemistry*, **12,** 2513(1973).

(9) O. Haars, *Arch. Pharm.*, **243,** 154(1905).

(10) C. Wachsmuth, Dissertation, Marburg, Germany, 1924.

(11) M. P. Cava, Y. Watanabe, J. Kunitomo, K. Bessho, M. J. Mitchell, A. I. daRocha, B. Hwang, J. A. Weisbach, and B. Douglas, "Abstracts of Papers," Second Natural Products Symposium, Mona, Kingston, Jamaica, Jan. 1968, p. 3; through M. P. Cava and A. Vekateswarlu, "Annual Reports in Medicinal Chemistry," Academic, New York, N.Y., 1969, p. 331.

(12) M. P. Cava and A. Venkateswarlu, *Tetrahedron*, **27,** 2639(1971).

(13) M. Shamma, *Experientia*, **16,** 484(1960).

(14) A. H. Jackson and J. A. Martin, *J. Chem. Soc. (C)*, **1966,** 2181.

(15) D. Walterová and F. Šantavý, *Collect. Czech. Chem. Commun.*, **33,** 1623(1968).

(16) V. Preininger, J. Appelt, L. Slavíková, and J. Slavík, *ibid.*, **32,** 2682(1967).

(17) L. Slavíková and J. Slavík, *ibid.*, **31,** 3362(1966).

(18) J. Slavík and L. Slavíková, *ibid.*, **20,** 21(1955).

(19) M. P. Cava, A. Venkateswarlu, M. Srinivasan, and D. L. Edie, *Tetrahedron*, **28,** 4299(1972).

(20) J. Slavík and L. Slavíková, *Collect. Czech. Chem. Commun.*, **26,** 1839(1961).

ACKNOWLEDGMENTS AND ADDRESSES

Received January 16, 1975, from the *Chemical Institute, Medical Faculty, Palacký University, Olomouc, Czechoslovakia.*

Accepted for publication April 18, 1975.

Presented in part at the American Society of Pharmacognosy–Academy of Pharmaceutical Sciences Joint Meeting in Chicago, August 6, 1974.

The authors thank Dr. V. Šimánek (from this Institute) for the PMR spectra, Mrs. S. Dvořáčková (from this Institute) for the UV and IR spectra, and Dr. L. Dolejš (Institute of Organic Chemistry and Biochemistry, Czechoslovak Academy of Sciences, Prague) for the mass spectra.

For a previous paper in this series, see *Collect. Czech. Chem. Commun.*, **40,** 705(1975).

* Present address: Regional Research Laboratory, Canal Road, Jammu-Tawi, India.

ˣ To whom inquiries should be directed.

Synthesis of Site-Directed Chelating Agents II: 2-Formyl-3-hydroxy-4,5-bis(hydroxymethyl)pyridine Thiosemicarbazone

KRISHNA C. AGRAWAL [x], STANLEY CLAYMAN, and ALAN C. SARTORELLI

Abstract □ 2-Formyl-3-hydroxy-4,5-bis(hydroxymethyl)pyridine thiosemicarbazone was synthesized in an attempt to direct the chelating potential of this agent to the active site of the zinc-requiring enzyme pyridoxal phosphokinase. Evaluation of the antineoplastic activity of this agent in the sarcoma 180 and L-1210 leukemia systems in mice showed potent activity. The presence or absence of pyridoxine hydrochloride in the diet did not influence the degree of inhibition of the growth of sarcoma 180 ascites cells. In addition, 2-formyl-3-hydroxy-4,5-bis(hydroxymethyl)pyridine thiosemicarbazone was inactive against a subline of sarcoma 180 resistant to 1-formylisoquinoline thiosemicarbazone, suggesting that the former agent may have a biochemical mechanism of action similar to that of the latter. In keeping with this expectation, 2-formyl-3-hydroxy-4,5-bis(hydroxymethyl)pyridine thiosemicarbazone inhibited the synthesis of DNA but not of RNA or protein in sarcoma 180 ascites cells *in vitro*.

Keyphrases □ Chelating agents, site directed—synthesis of 2-formyl-3-hydroxy-4,5-bis(hydroxymethyl)pyridine thiosemicarbazone, potential antineoplastic agent □ 2-Formyl-3-hydroxy-4,5-bis(hydroxymethyl)pyridine thiosemicarbazone—synthesized, screened for antineoplastic activity □ Antineoplastic agents, potential—2-formyl-3-hydroxy-4,5-bis(hydroxymethyl)pyridine thiosemicarbazone synthesized and screened

Numerous heterocyclic carboxaldehyde thiosemicarbazones with the side chain alpha to a heteroaromatic ring nitrogen possess both antineoplastic and antiviral activities in various experimental systems (1). Furthermore, one agent of this series, 5-hydroxy-2-formylpyridine thiosemicarbazone, demonstrated weak carcinostatic potency in humans (2, 3). The antineoplastic activity of this class of agents, as elucidated with 5-hydroxy-2-formylpyridine thiosemicarbazone and the related compound, 1-formylisoquinoline thiosemicarbazone, requires metal-binding potential and the capacity to inhibit the synthesis of DNA (4). These related phenomena result from inhibition of the enzyme ribonucleoside diphosphate reductase, an iron-requiring biocatalyst.

BACKGROUND

It is conceivable that the chelating potential of the formyl thiosemicarbazone side chain, positioned alpha to a heteroaromatic ring nitrogen atom, might be directed toward other metal-containing enzymes by modification of the heterocyclic ring system such that it resembles the natural substrate of the targeted metalloenzyme. An earlier report (5), based in part upon this concept, involved the synthesis of pteridine carboxaldehyde thiosemicarbazones directed against the enzyme dihydrofolate reductase. Since heterocyclic carboxaldehyde thiosemicarbazones have been shown to form coordination complexes with various transition metals (4, 6), pyridoxal phosphokinase, a zinc-requiring enzyme (7) that catalyzes the phosphorylation of pyridoxine hydrochloride at position 5 to form the active coenzyme form, was chosen as a likely candidate for such direct metabolic assault.

The idea that interference with the function of pyridoxine hydrochloride can lead to impairment of neoplastic growth gains support from the findings (8) that the incidence of complete regression of sarcoma 180 brought about by administration of methylglyoxal bis(N^4-methylthiosemicarbazone) was markedly enhanced in animals fed a pyridoxine-deficient diet from the day of initial tumor transplantation, although this relatively mild degree of pyridoxine hydrochloride deficiency alone did not impair the growth of the tumor significantly. Although clinical studies in patients on diets low in pyridoxine and as well as on pyridoxine antimetabolites did not show definite antitumor effects (9, 10), observations were reported in which tumor growth in model systems was depressed by creation of a pyridoxine hydrochloride deficiency (11, 12). Thus, blockade of pyridoxal phosphokinase activity by chelation of the zinc cofactor could conceivably yield a useful cancer chemotherapeutic agent.

Since the 2-formyl thiosemicarbazone derivative of pyridoxine

Table I—Antitumor Effect of 2-Formyl-3-hydroxy-4,5-bis(hydroxymethyl)pyridine Thiosemicarbazone against Murine Neoplasms Sarcoma 180, Leukemia L-1210, and Sarcoma 180/IQ-1

	Sarcoma 180							
	Complete Diet		Pyridoxine-Deficient Diet		L-1210 Leukemia		Sarcoma 180/IQ-1	
Daily Dose, mg/kg[a]	Average Weight Change, %[b]	Average Survival Time, days	Average Weight Change, %[b]	Average Survival Time, days	Average Weight Change, %[b]	Average Survival Time, days	Average Weight Change, %[b]	Average Survival Time, days
Control	+11.0	12.2	+6.0	12.0	+7.1	8.0	+18.5	13.0
20	+7.0	16.2	+6.9	19.3	—	—	+3.0	16.2
40	+5.6	21.8	+8.1	17.7	—	—	+3.5	16.2
60	+6.2	16.0	+4.1	19.8	—	—	—	—
80	+0.0	16.4	+2.3	15.4	—	—	—	—
20 × 2	−4.6	19.8	—	—	−2.8	12.7	—	—
40 × 2	−5.7	29.8	—	—	−2.7	14.4	—	—
60 × 2	—	—	—	—	+1.5	16.2	—	—
IQ-1[c] (40)	−10.8	39.7	—	—	+2.4	16.6	−0.6	13.8

[a] Administered once or twice daily at 12-hr intervals, as indicated, for 6 consecutive days beginning 24 hr after tumor implantation. [b] Average change in body weight from onset to termination of drug therapy. [c] IQ-1 = 1-formylisoquinoline thiosemicarbazone.

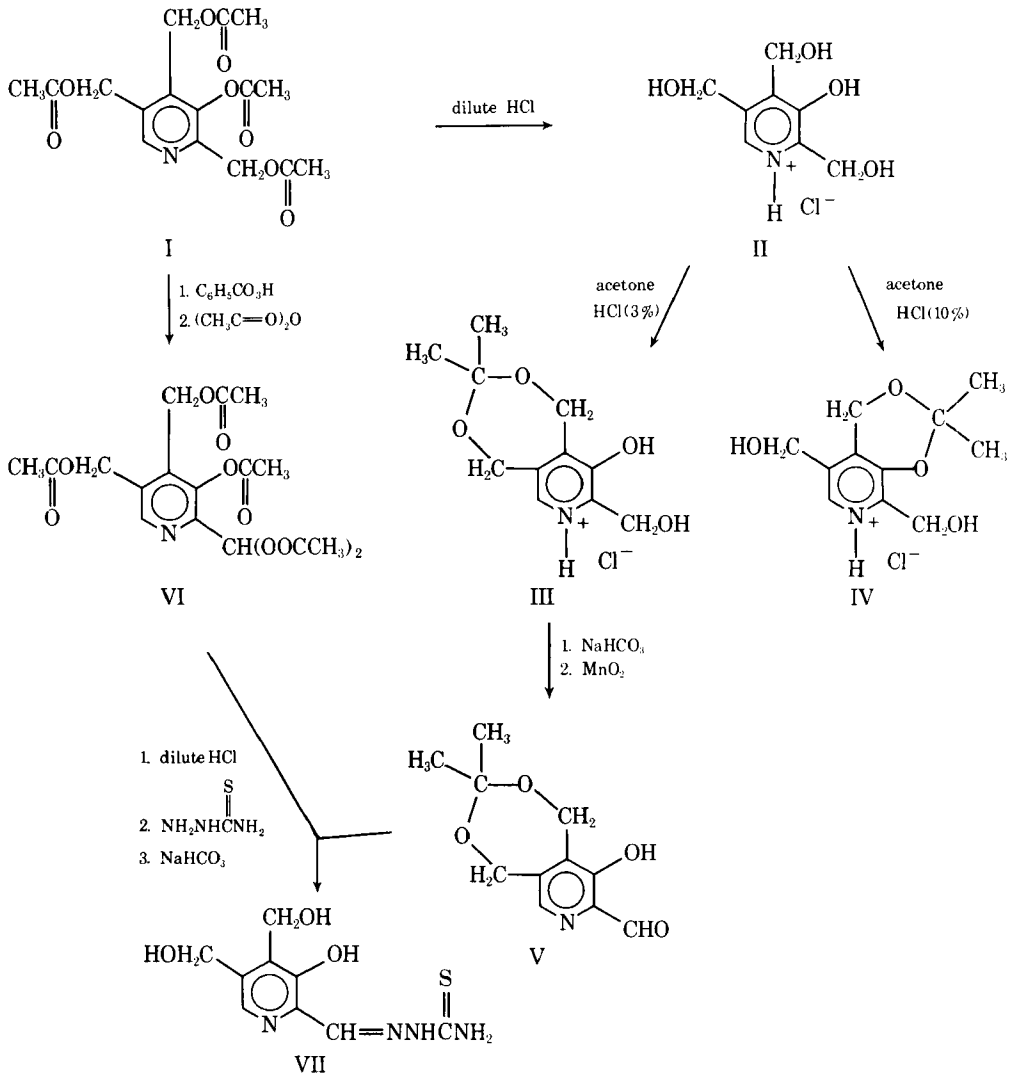

Scheme I

has structural features similar to those deemed necessary for inhibition of the ribonucleoside diphosphate reductase enzyme (13), it is probable that this compound would exert blockade of two metabolic processes *in vivo*. This paper describes the synthesis of 2-formyl-3-hydroxy-4,5-bis(hydroxymethyl)pyridine thiosemicarbazone (VII) as well as several biological and biochemical effects of this compound; a preliminary report of this work was presented earlier in abstract form (14).

RESULTS AND DISCUSSION

The synthesis of VII was accomplished by two different procedures (Scheme I). The common intermediate, 3-acetoxy-2,4,5-tris(acetoxymethyl)pyridine (I), was synthesized according to the procedure of Bedford *et al.* (15). Acid hydrolysis of I afforded 3-hydroxy-2,4,5-tris(hydroxymethyl)pyridine hydrochloride (II), which was treated with hydrogen chloride as a suspension in acetone according to the procedure of Korytnyk (16). The amount of hydrogen chloride taken up by the suspension is a critical factor, and, accordingly, yields are variable.

If the quantity of hydrogen chloride utilized was about 10%, only a six-membered ring ketal (IV) was formed; 3% hydrogen chloride afforded the seven-membered ketal (III) and unreacted compound II. Recently, Korytnyk *et al.* (17) reported that acetonation of II in the presence of *p*-toluenesulfonic acid yielded primarily III in 65% yield. Compound III as the free base was then oxidized with manganese dioxide to yield the corresponding aldehyde (V). Compound V, after hydrolysis with dilute hydrochloric acid and subsequent reaction with thiosemicarbazide and neutralization with sodium bicarbonate, produced the desired compound, VII.

An alternative route produced a better yield of VII. This procedure required the initial formation of the *N*-oxide of I which, upon rearrangement with acetic anhydride, yielded the pentaacetate VI (15). After acid hydrolysis of the pentaacetate, the solution was reacted with thiosemicarbazide, which yielded the desired compound VII upon neutralization with sodium bicarbonate.

The antitumor effects of VII in three different murine neoplastic test systems are shown in Table I. Although preliminary experiments showed that relatively high levels of VII (about 10^{-4} *M*) caused slight inhibition of pyridoxal phosphokinase from *Escherichia coli*, the effects of this agent on sarcoma 180, as measured by the average survival time of mice bearing this ascites cell neoplasm, were similar in tumor-bearing animals fed a complete diet or a pyridoxine hydrochloride-deficient diet. Thus, in each group, a single daily dose of VII exhibited slight, but significant, antitumor activity as compared to a dose of 1-formylisoquinoline thiosemicarbazone in the same range, which was employed as a standard control. However, when VII was administered twice daily at 12-hr intervals, a level of 40 mg/kg/dose increased the average survival time of tumor-bearing mice to 29.8 days as compared to 12.2 days for untreated control animals bearing this tumor.

In the L-1210 lymphoma system, however, VII showed antineoplastic activity equivalent to 1-formylisoquinoline thiosemicarbazone, which essentially doubled the lifespan of lymphoma-bearing animals. In a strain of sarcoma 180 ascites tumor, selected for resistance to 1-formylisoquinoline thiosemicarbazone, VII was essentially inactive, suggesting a similar biochemical mechanism of action for these two compounds. To gain evidence for this possibility, the effect of VII on the synthesis of DNA, RNA, and protein was measured *in vitro*.

The results indicated that the synthesis of DNA, as measured by the incorporation of ^{3}H-thymidine into acid-insoluble material, was significantly inhibited by this compound at a concentration of 4×10^{-5} *M* (Table II). RNA synthesis, as measured by ^{3}H-uridine incorporation, was unaffected by VII, while a 33% inhibition of protein synthesis was obtained at the relatively high concentration of 4×10^{-4} *M*. The inhibition of the formation of DNA, with little or no effect on the syntheses of RNA and protein, is similar to that found for 1-formylisoquinoline thiosemicarbazone (18) and 5-hydroxy-2-formylpyridine thiosemicarbazone (19) under these conditions. Thus, the findings suggest that the antineoplastic activity of VII in these systems is primarily due to its inhibition of the replication of DNA in a manner similar to that of other α-*N*-heterocyclic carboxaldehyde thiosemicarbazones.

Table II—Effect of 2-Formyl-3-hydroxy-4,5-bis(hydroxymethyl)pyridine Thiosemicarbazone on Incorporation of ^{3}H-Thymidine, ^{3}H-Uridine, and ^{14}C-Leucine into DNA, RNA, and Protein, Respectively[a]

Concentration, *M*	Inhibition, %		
	DNA	RNA	Protein
4×10^{-6}	12	0	0
4×10^{-5}	49	5	0
4×10^{-4}	66	0	33

[a] All data are average values of duplicate flasks from each of two experiments. Control specific activities were: ^{3}H-thymidine into DNA = 2.9×10^5 cpm/μmole, ^{3}H-uridine into RNA = 4.0×10^6 cpm/μmole, and ^{14}C-leucine into protein = 2.1×10^5 cpm/μmole. Results are expressed as the percent change in radioactivity present in nucleic acids or protein from controls containing 2% dimethyl sulfoxide.

EXPERIMENTAL[1]

Antitumor Activity—Antitumor activity was determined in mice bearing the ascites cell forms of either sarcoma 180, sarcoma 180 resistant to 1-formylisoquinoline thiosemicarbazone (sarcoma 180/IQ-1), or L-1210 leukemia. The experimental details of such tests were described previously (20).

Transplantation of the neoplasms was accomplished by inoculating mice intraperitoneally with approximately 6×10^6 ascites cells. The drug was administered by intraperitoneal injection beginning 24 hr later, and such therapy was continued once or twice daily at 12-hr intervals for 6 consecutive days in mice bearing sarcoma 180 or sarcoma 180/IQ-1 ascites cells. Mice bearing the L-1210 leukemia were treated twice daily at 12-hr intervals for 4 consecutive days.

Animals were weighed throughout the experiments, and the percent change in body weight from onset to termination of therapy was used as an indication of drug toxicity. Determination of the sensitivity of the tumors toward this agent was based upon the prolongation of survival time afforded by the drug treatments.

Biochemical Studies—The effects of VII on the incorporation of ^{3}H-thymidine, ^{3}H-uridine, and ^{14}C-leucine into DNA, RNA, and protein, respectively, were determined by previously described methodology (18, 19) (Table II). The experiments were carried out in duplicate on pooled 6-day growths of sarcoma 180 ascites cells. Approximately 1.5×10^8 cells were incubated for 30 min at 37° in 10 ml of Fischer's medium minus horse serum, with the inhibitor dissolved in dimethyl sulfoxide and diluted to yield a final concentration of dimethyl sulfoxide no greater than 2%.

^{3}H-Thymidine (200 μg/flask, 2.1×10^4 cpm/μg) and ^{3}H-uridine (200 μg/flask, 1.3×10^4 cpm/μg) were utilized to monitor nucleic acid biosynthetic pathways. 1-^{14}C-D,L-Leucine (125 μg/flask, 5.3×10^4 cpm/μg) was used to measure the rate of protein synthesis.

Acetonation of 3-Hydroxy-2,4,5-tris(hydroxymethyl)pyridine Hydrochloride (II)—Compound II (1.11 g, 0.005 mole) was suspended in 50 ml of dry acetone and cooled to −10°. Hydrogen chloride was bubbled through the suspension slowly until 1.2 g (3% w/v) was utilized. The mixture was then stirred at 0° for 2 hr and kept at −15° for an additional 48 hr. The product was filtered and washed with acetone and then with ether. The yield was 1.1 g, consisting of unreacted II and the cyclic ketal with a seven-membered ring (III).

The mixture was dissolved in 5 ml of water and neutralized with 5% $NaHCO_3$. Compound III, as the free base, was isolated by extraction with ether. The ether extracts were dried (magnesium sulfate), the solvent was removed, and the residue was crystallized from benzene to yield 0.27 g (24%) of white crystals, mp 145–147° [lit. (13) mp 149–151°].

Anal.—Calc. for $C_{11}H_{15}NO_4$: C, 58.66; H, 6.66; N, 6.22. Found: C, 58.41; H, 6.72; N, 6.02.

In another experiment, hydrogen chloride was passed into a suspension of 1.11 g of II in 50 ml of dry acetone at −10° until 5.0 g (10% w/v) was gained. The mixture was stirred at room temperature for 30 min and kept in a freezer overnight. Ether was added to the acetone solution, and the obtained precipitate was filtered and washed with ether to give 1.0 g (76%) of IV. The hydrochloride salt was dissolved in 5 ml of water, neutralized with 10% Na_2CO_3, and evaporated under vacuum to dryness. Then IV, as the free base, was extracted with hot benzene, which, upon cooling, gave 0.7 g of white crystals, mp 116° [lit. (13) mp 110°].

Anal.—Calc. for $C_{11}H_{15}NO_4$: C, 58.66; H, 6.66; N, 6.22. Found: C, 58.54; H, 6.80; N, 6.08.

Oxidation—Compound III (225 mg, 0.001 mole) as the free base was dissolved in 50 ml of chloroform, and the solution was stirred with 500 mg of active manganese dioxide[2] at room temperature for 48 hr. The mixture was then filtered through diatomaceous earth[3], the filtrate was evaporated under vacuum, and the residue was crystallized from petroleum ether to yield 100 mg (45%) of V as white needles, mp 93–94°; NMR (deuterochloroform): δ 1.53 [$(CH_3)_2C$], 4.9, 4.97 (two CH_2), 8.07 (C_6-H), and 10.03 (CHO) ppm.

Anal.—Calc. for $C_{11}H_{13}NO_4$: C, 59.19; H, 5.83; N, 6.28. Found: C, 58.91; H, 5.74; N, 6.24.

2-Formyl-3-hydroxy-4,5-bis(hydroxymethyl)pyridine Thiosemicarbazone (VII)—Compound V (111.5 mg, 0.5 mmole) or VI (11) (206 mg, 0.5 mmole) was heated at 100° for 1 hr in 5 ml of 10% HCl. Thiosemicarbazide (46 mg) was then added, and heating was continued for 5 min. The solution was neutralized with 10% $NaHCO_3$, and the resulting precipitate of VII was filtered, washed with water, and dried to yield 95 mg of yellow solid (74%), mp 200–202°; IR: λ_{max} (potassium bromide) 3170 (NH), 1615 (CH=N), and 1117 (C=S) cm^{-1}.

Anal.—Calc. for $C_9H_{12}N_4O_3S$: C, 42.19; H, 4.69; N, 21.87. Found: C, 42.31; H, 4.52; N, 21.62.

REFERENCES

(1) K. C. Agrawal and A. C. Sartorelli, in "Handbook of Experimental Pharmacology," vol. 38, part II, A. C. Sartorelli and D. G. Johns, Eds., Springer-Verlag, Berlin, Germany, 1975, pp. 793–807.

(2) R. C. DeConti, B. R. Toftness, K. C. Agrawal, R. Tomchick, J. A. R. Mead, J. R. Bertino, A. C. Sartorelli, and W. A. Creasey, *Cancer Res.*, **32**, 1455(1972).

(3) I. H. Krakoff, E. Etcubanas, C. Tau, K. Meyer, V. Bethune, and J. Burchenal, *Cancer Chemother. Rep., Part D*, **58**, 207(1974).

(4) K. C. Agrawal, B. A. Booth, R. L. Michaud, A. C. Sartorelli, and E. C. Moore, *Biochem. Pharmacol.*, **23**, 2421(1974).

(5) H. I. Hochman, K. C. Agrawal, C. W. Shansky, and A. C. Sartorelli, *J. Pharm. Sci.*, **62**, 150(1973).

(6) F. A. French and E. J. Blanz, Jr., *J. Med. Chem.*, **9**, 585(1966).

(7) D. B. McCormick, M. E. Gregory, and E. E. Snell, *J. Biol. Chem.*, **236**, 2076(1961).

(8) E. Mihich and C. A. Nichol, *Cancer Res.*, **25**, 794(1965).

(9) F. Rosen, E. Mihich, and C. A. Nichol, *Vitam. Horm.*, **22**, 609(1964).

[1] Melting points were determined using a Thomas-Hoover capillary melting-point apparatus and are uncorrected. The IR absorption spectra were obtained with a Perkin-Elmer model 257 spectrophotometer. NMR spectra were determined with a Varian A-60A spectrometer. The spectral data were as expected; important chemical shifts (δ) are given in parts per million downfield from tetramethylsilane, which was used as an internal standard. Elemental analyses were performed by the Baron Consulting Co., Orange, Conn.

[2] Winthrop Laboratories.

[3] Celite.

(10) S. D. Graila, J. F. Holland, A. Nussbaum, and K. B. Olson, *Cancer*, **21**, 975(1968).
(11) C. A. Nichol, *Cancer Res.*, **29**, 2422(1969).
(12) G. P. Tryfiates and H. P. Morris, *J. Nat. Cancer Inst.*, **52**, 1259(1974).
(13) A. C. Sartorelli, K. C. Agrawal, and E. C. Moore, *Biochem. Pharmacol.*, **20**, 3119(1971).
(14) S. Clayman, K. C. Agrawal, and A. C. Sartorelli, "Abstracts of Papers," MEDI-77, 158th American Chemical Society National Meeting, New York, N.Y., Sept. 1969.
(15) G. R. Bedford, A. R. Katritzky, and H. M. Wuest, *J. Chem. Soc.*, **1963**, 4600.
(16) W. Korytnyk, *J. Org. Chem.*, **27**, 3724(1962).
(17) W. Korytnyk, S. C. Srivastava, N. Angelino, P. G. G. Potti, and B. Paul, *J. Med. Chem.*, **16**, 1096(1973).
(18) E. C. Moore, M. S. Zedeck, K. C. Agrawal, and A. C. Sartorelli, *Biochemistry*, **9**, 4492(1970).
(19) B. A. Booth, E. C. Moore, and A. C. Sartorelli, *Cancer Res.*, **31**, 228(1971).
(20) K. C. Agrawal, B. A. Booth, and A. C. Sartorelli, *J. Med. Chem.*, **11**, 700(1968).

ACKNOWLEDGMENTS AND ADDRESSES

Received March 27, 1975, from the *Department of Pharmacology, Yale University School of Medicine, New Haven, CT 06510*

Accepted for publication May 7, 1975.

Supported by U.S. Public Health Service Research Grant CA-02817 from the National Cancer Institute.

[x] To whom inquiries should be directed.

N-Bromosuccinimide Assay of Penicillins and Cephalosporins

JOSEPH F. ALICINO

Abstract □ All penicillins and cephalosporins known to possess biological activity respond to an *N*-bromosuccinimide assay. The developed method is not yet usable for determining stability, but it is useful as a bulk or batching assay.

Keyphrases □ *N*-Bromosuccinimide—reagent for iodometric analysis of penicillins and cephalosporins □ Penicillins—analysis, using *N*-bromosuccinimide, iodometric titration □ Cephalosporins—analysis, using *N*-bromosuccinimide, iodometric titration □ Titrimetry, iodometric—analysis of penicillins and cephalosporins

The iodometric assay for penicillin has been used successfully for almost 30 years (1), and it also has been used for cephalosporins (2). Recently, the results of some iodometric assays of synthetic cephalosporins proved difficult to interpret because of the complexity of the side chains. For such cases, another simple and rapid method was sought that might permit easier interpretation of the assays of complicated structures and that might supplement the iodometric assay.

A bromometric method, reported for penicillin O (3), differed from the iodometric method in that no inactivation of penicillin with alkali was required prior to the measurement. In this laboratory, the reaction of *N*-bromosuccinimide with penicillin was found to require no inactivation of the antibiotic with alkali or penicillinase. An attempt to use a direct assay procedure with this reagent, which had been used for several years by a host of investigators (4–12), led to the realization that the reaction between the penicillins and *N*-bromosuccinimide was time dependent. Moreover, the reagent was found to be somewhat light sensitive and subject to oxidation in air when used as a direct titrant for penicillins, in spite of its prior use in the determination of such simple compounds as sulfides, thiocyanates, cysteine, thiourea, mercaptans, phenols, and sulfur-containing amino acids (4–12). Technical grade *N*-bromosuccinimide deteriorated rapidly in solution.

To offset these difficulties, a different approach was used. In experiments involving the reaction of penicillin with an excess of *N*-bromosuccinimide, a rapid rise in the consumption of *N*-bromosuccinimide was evident from time zero to 1 hr, after which consumption increased at a slower rate. The most reproducible results were obtained when the reaction time was limited to 2.0 hr; it is suggested that this period be used. Results on samples shielded from light or assayed at a lower temperature did not differ significantly from those obtained under the described assay conditions.

EXPERIMENTAL

Reagents—*0.02* N *N-Bromosuccinimide*[1]—Dissolve 1.9 g of *N*-bromosuccinimide in about 5 ml of reagent grade dimethylformamide. Pour into a 1-liter volumetric flask containing about 500 ml of distilled water. Stir or shake and then dilute to volume with distilled water. Transfer to a dark, amber bottle and store immediately in the refrigerator.

Despite reports of the instability of *N*-bromosuccinimide, this solution will maintain its titer for several weeks under proper storage conditions, with a loss of less than 5% of its original value.

0.01 N *Sodium Thiosulfate*—Dissolve 2.5 g of sodium thiosulfate pentahydrate in cooled, freshly boiled distilled water and add 2–3 ml of toluene (preservative). Then dilute to 1 liter with water.

Buffer Solution—To 40 g of anhydrous sodium acetate dissolved in about 500 ml of distilled water, add 1.93 ml of concentrated sulfuric acid. Dilute to 1 liter with distilled water.

Starch Solution—Prepare a 1% solution of starch in saturated saline.

Dimethylformamide (reagent grade), potassium iodide (reagent grade), and acetic acid were used also.

[1] Aldrich analyzed reagent grade, Aldrich Co., Milwaukee, WI 53233

(10) S. D. Graila, J. F. Holland, A. Nussbaum, and K. B. Olson, *Cancer*, **21**, 975(1968).
(11) C. A. Nichol, *Cancer Res.*, **29**, 2422(1969).
(12) G. P. Tryfiates and H. P. Morris, *J. Nat. Cancer Inst.*, **52**, 1259(1974).
(13) A. C. Sartorelli, K. C. Agrawal, and E. C. Moore, *Biochem. Pharmacol.*, **20**, 3119(1971).
(14) S. Clayman, K. C. Agrawal, and A. C. Sartorelli, "Abstracts of Papers," MEDI-77, 158th American Chemical Society National Meeting, New York, N.Y., Sept. 1969.
(15) G. R. Bedford, A. R. Katritzky, and H. M. Wuest, *J. Chem. Soc.*, **1963**, 4600.
(16) W. Korytnyk, *J. Org. Chem.*, **27**, 3724(1962).
(17) W. Korytnyk, S. C. Srivastava, N. Angelino, P. G. G. Potti, and B. Paul, *J. Med. Chem.*, **16**, 1096(1973).
(18) E. C. Moore, M. S. Zedeck, K. C. Agrawal, and A. C. Sartorelli, *Biochemistry*, **9**, 4492(1970).
(19) B. A. Booth, E. C. Moore, and A. C. Sartorelli, *Cancer Res.*, **31**, 228(1971).
(20) K. C. Agrawal, B. A. Booth, and A. C. Sartorelli, *J. Med. Chem.*, **11**, 700(1968).

ACKNOWLEDGMENTS AND ADDRESSES

Received March 27, 1975, from the *Department of Pharmacology, Yale University School of Medicine, New Haven, CT 06510*

Accepted for publication May 7, 1975.

Supported by U.S. Public Health Service Research Grant CA-02817 from the National Cancer Institute.

[x] To whom inquiries should be directed.

N-Bromosuccinimide Assay of Penicillins and Cephalosporins

JOSEPH F. ALICINO

Abstract □ All penicillins and cephalosporins known to possess biological activity respond to an *N*-bromosuccinimide assay. The developed method is not yet usable for determining stability, but it is useful as a bulk or batching assay.

Keyphrases □ *N*-Bromosuccinimide—reagent for iodometric analysis of penicillins and cephalosporins □ Penicillins—analysis, using *N*-bromosuccinimide, iodometric titration □ Cephalosporins—analysis, using *N*-bromosuccinimide, iodometric titration □ Titrimetry, iodometric—analysis of penicillins and cephalosporins

The iodometric assay for penicillin has been used successfully for almost 30 years (1), and it also has been used for cephalosporins (2). Recently, the results of some iodometric assays of synthetic cephalosporins proved difficult to interpret because of the complexity of the side chains. For such cases, another simple and rapid method was sought that might permit easier interpretation of the assays of complicated structures and that might supplement the iodometric assay.

A bromometric method, reported for penicillin O (3), differed from the iodometric method in that no inactivation of penicillin with alkali was required prior to the measurement. In this laboratory, the reaction of *N*-bromosuccinimide with penicillin was found to require no inactivation of the antibiotic with alkali or penicillinase. An attempt to use a direct assay procedure with this reagent, which had been used for several years by a host of investigators (4–12), led to the realization that the reaction between the penicillins and *N*-bromosuccinimide was time dependent. Moreover, the reagent was found to be somewhat light sensitive and subject to oxidation in air when used as a direct titrant for penicillins, in spite of its prior use in the determination of such simple compounds as sulfides, thiocyanates, cysteine, thiourea, mercaptans, phenols, and sulfur-containing amino acids (4–12). Technical grade *N*-bromosuccinimide deteriorated rapidly in solution.

To offset these difficulties, a different approach was used. In experiments involving the reaction of penicillin with an excess of *N*-bromosuccinimide, a rapid rise in the consumption of *N*-bromosuccinimide was evident from time zero to 1 hr, after which consumption increased at a slower rate. The most reproducible results were obtained when the reaction time was limited to 2.0 hr; it is suggested that this period be used. Results on samples shielded from light or assayed at a lower temperature did not differ significantly from those obtained under the described assay conditions.

EXPERIMENTAL

Reagents—*0.02* N *N-Bromosuccinimide*[1]—Dissolve 1.9 g of *N*-bromosuccinimide in about 5 ml of reagent grade dimethylformamide. Pour into a 1-liter volumetric flask containing about 500 ml of distilled water. Stir or shake and then dilute to volume with distilled water. Transfer to a dark, amber bottle and store immediately in the refrigerator.

Despite reports of the instability of *N*-bromosuccinimide, this solution will maintain its titer for several weeks under proper storage conditions, with a loss of less than 5% of its original value.

0.01 N *Sodium Thiosulfate*—Dissolve 2.5 g of sodium thiosulfate pentahydrate in cooled, freshly boiled distilled water and add 2–3 ml of toluene (preservative). Then dilute to 1 liter with water.

Buffer Solution—To 40 g of anhydrous sodium acetate dissolved in about 500 ml of distilled water, add 1.93 ml of concentrated sulfuric acid. Dilute to 1 liter with distilled water.

Starch Solution—Prepare a 1% solution of starch in saturated saline.

Dimethylformamide (reagent grade), potassium iodide (reagent grade), and acetic acid were used also.

[1] Aldrich analyzed reagent grade, Aldrich Co., Milwaukee, WI 53233

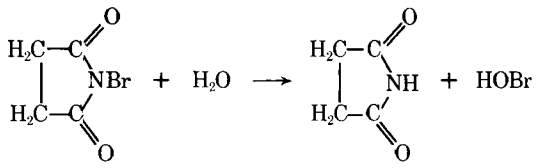

Scheme I

Standardization of *N*-Bromosuccinimide Reagent—Pipet exactly 5 ml of *N*-bromosuccinimide solution into a 125-ml flask. Add 5 ml of the buffer solution to simulate the conditions used in the actual analysis. Add 1 ml of acetic acid and then 100–200 mg of solid potassium iodide, and let the solution stand for 3–5 min. Titrate the liberated iodine with 0.01 *N* sodium thiosulfate solution, using starch when approaching the end-point (indicated by the paleness of the iodine color).

This *N*-bromosuccinimide solution is 0.2 *N* with respect to the thiosulfate solution and is actually 0.01 *M*. The *N*-bromosuccinimide solution is twice the strength of the thiosulfate solution (to maintain the excess needed for the assay) and should result in a titer of about 10 ml of sodium thiosulfate solution; the titer is determined *daily*. This value, called R_4, can be referred to as *the blank*.

Assay—Prepare an aqueous solution of the test sample so that it contains approximately 0.2–0.3 mg/ml. If the material to be determined is insoluble in water, dissolve it in a few milliliters of dimethylformamide and add water to attain the desired volume. Pipet two 5.0-ml aliquots into two 125-ml flasks, R_1 and R_2, and add 5 ml of buffer solution to each. To a third flask, R_3, add about the same amount of reference standard and buffer. The fourth flask, R_4, is the blank.

To each flask, add exactly 5.0 ml of the *N*-bromosuccinimide solution and set a timer for a preselected interval (usually 1 or 2 hr). At the end of this time, add 1 ml of acetic acid and 100–200 mg of potassium iodide. Then titrate the liberated iodine in each flask as directed in the standardization procedure.

Calculations—Since this method can be used for the assay of all penicillins and cephalosporins, the calculation factor (C.F.) will vary for each species to be determined. The generic formula is:

$$\frac{\text{ml of thiosulfate} \times \text{C.F.} \times 1000}{\text{mg of sample}} = \mu\text{g} \qquad \text{(Eq. 1)}$$

where:

ml of thiosulfate = difference in milliliters between the amount required for titration of the blank and of the sample

C.F. = the ratio of the weight of the reference standard for the particular compound to milliliters of thiosulfate, determined as expressed in Eq. 2:

$$\text{C.F.} = \frac{\text{mg of reference standard}}{\text{ml of 0.01 } N \text{ } Na_2S_2O_3 \text{ } (R_3)} \qquad \text{(Eq. 2)}$$

The complete calculation may, therefore, be represented as:

$$R_4 - \left(\frac{R_1 + R_2}{2}\right) \times \frac{\text{mg of standard}}{R_3} \times 1000 = \mu\text{g/mg} \qquad \text{(Eq. 3)}$$

RESULTS AND DISCUSSION

The penicillins assayed included penicillin G potassium, ampicillin, penicillin V, epicillin, cloxacillin, cloxacillin benzathine, and oxacillin. The cephalosporins assayed were cephradine, cephalexin, cephalothin, cephaloridine, cephaloglycin, and numerous cephalosporin candidates. All gave responses with *N*-bromosuccinimide. Notably, sulfoxides did not react. Essentially, the reaction (11) involves the formation of hypobromous acid (Scheme I).

The hypobromous acid attacks the ring system and, because of its great oxidizing capacity, yields a large number of equivalents of iodine. A study showed that 10–17 equivalents of iodine were consumed when cephradine was allowed to react with *N*-bromosuccinimide for 0.5–6 hr. Therefore, the reaction time must be controlled. More consistent results were obtained at about 2 hr when the reaction curve started to flatten. Experiments with cephradine indicated that approximately 14 equivalents of iodine were used for a reaction time of 2 hr. Because the reagents used in routine analysis of penicillins and cephalosporins are standardized against pure reference standards, that practice was continued here. Nevertheless, in experimental work, one can determine the number of equivalents of iodine from the following:

$$\frac{\text{mg of reference material}}{\text{ml of sodium thiosulfate} \times \text{normality}} = \text{equivalent wt.} \qquad \text{(Eq. 4)}$$

$$\frac{\text{mol. wt. of reference material}}{\text{equivalent wt.}} = \text{number of } I_2 \text{ equivalents} \qquad \text{(Eq. 5)}$$

Experiments on formulated products showed some interferences that would prevent the direct application of this method; some separation step must be included in the analysis of such products. On purified materials, the results corresponded to those obtained by the iodometric method, but the method, unlike the iodometric assay, does not provide an indication of stability. For samples of cephalosporins with a complicated structure, the results obtained by this method were in better agreement with the results of the biological assay than were those obtained by the iodometric assay.

In contrast to the iodometric method, which shows a twofold difference between cephalosporins and penicillins in uptake of iodine (2), the *N*-bromosuccinimide assay shows very little difference in this respect. This contrast prompts some speculation about the relative ease of oxidation of the two classes of compounds. As mentioned earlier, penicillanic acid, 7-aminodesacetylcephalosporanic acid, and penicillamine react with *N*-bromosuccinimide, but the sulfoxides of penicillins and cephalosporins do not.

REFERENCES

(1) J. F. Alicino, *Ind. Eng. Chem., Anal. Ed.*, **18**, 619(1946).

(2) J. F. Alicino, *Anal. Chem.*, **33**, 648(1961).

(3) P. J. Weiss and W. W. Wright, *Antibiot. Chemother.*, **3**, 1154(1953).

(4) M. Sarwar, M. Elahi, M. Anwar, and M. Hanif, *Mikrochim. Acta*, **1970**, 846.

(5) M. Sarwar, S. P. Hamdani, I. Ahmad, and R. J. Thibert, *ibid.*, **1971**, 573.

(6) M. Sarwar and K. U. Butt, *ibid.*, **1973**, 679.

(7) M. Sarwar, H. A. Waheed, M. A. Chowdhri, and R. J. Thibert, *ibid.*, **1973**, 683.

(8) M. Sarwar, A. K. Rana, and S. P. Hamdani, *Microchem. J.*, **16**, 184(1971).

(9) M. Sarwar and R. J. Thibert, *Anal. Lett.*, **1**, 381(1968).

(10) R. J. Thibert and M. Sarwar, *Mikrochim. Acta*, **1969**, 259.

(11) R. J. Thibert, M. Sarwar, and J. E. Carroll, *ibid.*, **1969**, 615.

(12) M. Z. Barekat and S. K. Shebab, *Analyst*, **90**, 50(1965).

ACKNOWLEDGMENTS AND ADDRESSES

Received February 24, 1975, from *The Squibb Institute for Medical Research, Princeton, NJ 08540*

Accepted for publication May 8, 1975.

Effect of Polyethylene Glycol 4000 on Dissolution Properties of Sulfathiazole Polymorphs

SARFARAZ NIAZI

Abstract □ The dissolution rates of the two polymorphic forms of sulfathiazole containing polyethylene glycol 4000 were significantly different in water. The effect of agitation on the dissolution rates also was studied. At higher stirring speeds, the dissolution rates of the stable form were affected more than the metastable form. A high concentration of polyethylene glycol 4000 seemed to affect the dissolution properties of the metastable polymorph more than the stable polymorph.

Keyphrases □ Polyethylene glycol 4000—effect on dissolution properties of two sulfathiazole polymorphs □ Sulfathiazole—polymorphs, effect of polyethylene glycol 4000 on dissolution properties □ Dissolution—sulfathiazole polymorphs, effect of polyethylene glycol 4000

The pharmaceutical and biological aspects of polymorphism have been elaborated in detail (1). Generally, the high energy or metastable polymorphs show higher dissolution rates than the stable form, except in instances where the conversion of metastable to stable forms is extremely rapid in the solvent medium (2, 3). This conversion was reported for sulfathiazole, which exists in at least two polymorphic forms (3).

The purpose of this paper is to demonstrate significant differences in the dissolution rates of sulfathiazole polymorphs in water when combined with polyethylene glycol 4000. The effects of agitation and the percent composition of polyethylene glycol 4000 are also discussed.

EXPERIMENTAL

Material—Sulfathiazole[1] and polyethylene glycol 4000[2] were obtained commercially.

Preparation and Identification of Polymorphs—The commercially supplied sulfathiazole was form I. Form II was prepared by a thermal method (4, 5) by heating form I in an oven at 175° for 20 min. The polymorphic forms were confirmed using a differential thermal analyzer[3]. The use of thermal analysis was shown to correspond well with the X-ray diffraction spectrum (5). Figure 1 shows the thermograms for both forms I and II.

Preparation of Physical Mixtures—Both sulfathiazole and polyethylene glycol 4000 were passed through a 200-mesh sieve and mixed to give 2, 5, and 10% (w/w) composition of polyethylene glycol 4000. These physical mixtures were then mixed in a drum-type mixer, using 30-ml (1-oz) plastic vials mounted at a 45° angle to a variable speed motor. Each sample was mixed for 30 min at 30 rpm, with occasional tapping of the vial with a spatula to avoid any aggregation on the vial wall.

Dissolution Rate Studies—Dissolution rates were determined using constant-surface tablets made by compressing 300 mg of physical mixture in a press[4] at 3178 kg (7000 lb) of pressure. These tablets were then mounted with a commercial cement[5] in a tablet holder to expose a surface area of 1.327 cm^2, and the tablet holders were attached to a variable speed motor. The dissolution studies were performed in 500 ml of distilled water thermostatically controlled at 25 ± 0.1°.

The absorbance of the solution was monitored using a continuous-flow assembly at 283 nm through a spectrophotometer[6]. The dissolution of each tablet was determined at 42, 96, 126, and 216 rpm in the order of both increasing and decreasing speed. In all instances, at least duplicate measurements were made and a high degree of reproducibility was achieved.

RESULTS AND DISCUSSION

The dissolution rates of the two polymorphs of sulfathiazole were obtained from constant-surface tablets, containing 2, 5, or 10% polyethylene glycol 4000, by linear regression of the amount dissolved *versus* time data from the linear parts of the plots. In all instances, the r^2 value was greater than 0.99. The differences between the dissolution rates of the two polymorphs and of each polymorph at different polyethylene glycol 4000 compositions were always significant at the 95% confidence level.

Effect of Polyethylene Glycol 4000—It has been shown (6) that the addition of high molecular weight, water-soluble polymers can increase the dissolution rates of poorly water-soluble drugs. Figure 2 shows the dissolution rates of sulfathiazole form I containing different proportions of polyethylene glycol 4000.

The addition of polyethylene glycol 4000 as a physical mixture clearly increased the dissolution rate of sulfathiazole. Comparisons with the dissolution rates of pure sulfathiazole were not made, however, since the pure compound offered great resistance to compression in a tablet form at the low compression pressures used to avoid any complexities due to polymorphic transition or glass formation (5–7) at high compression pressures. The tablets made at 3178 kg (7000 lb) of pressure showed no polymorphic transition or glass formation, as indicated by differential thermal analysis of compressed samples.

Effect of Stirring Speed—The dissolution rates were deter-

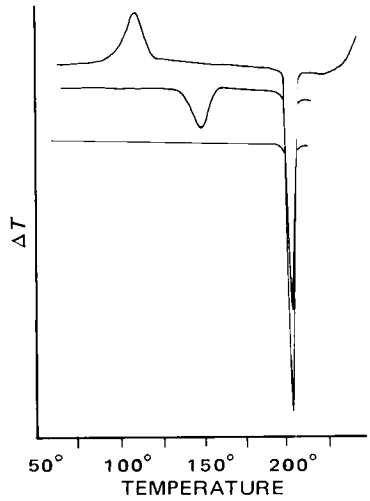

Figure 1—*Differential thermal analysis thermograms of sulfathiazole. Key: bottom, sulfathiazole form II; middle, sulfathiazole form I; and top, rerun of sulfathiazole form I sample heated to 215° and cooled to ambient temperature. The exothermic peak indicates the conversion of amorphous to crystalline form. All runs were obtained at a heating rate of 10°/min.*

[1] Eli Lilly & Co., Indianapolis, Ind.
[2] Pluracol E-4000, BASF Wyandotte Corp., Wyandotte, Mich.
[3] DuPont 990, E. I. du Pont de Nemours & Co., Wilmington, Del.
[4] Loomis Engineering & Manufacturing Co., Caldwell, N.J.
[5] Duco Cement, E. I. du Pont de Nemours & Co., Wilmington, Del.
[6] Beckman DB-G, Beckman Instrument Co., Fullerton, Calif.

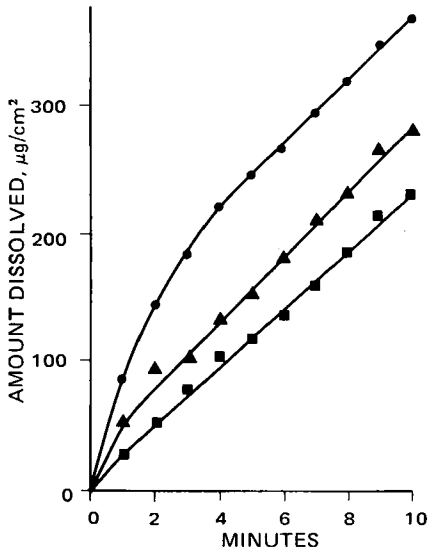

Figure 2—*Dissolution rates of sulfathiazole form I–polyethylene glycol 4000 physical mixtures. Key (polyethylene glycol 4000): ●, 10%; ▲, 5%; and ■, 2%.*

mined at 42, 96, 126, and 216 rpm to study the effect of diffusion layer thickness around the constant-surface tablets. As shown in Fig. 3, the dissolution rates invariably increased with the stirring speed. The slopes in Fig. 3 representing the change of dissolution rate with respect to the stirring speed are much steeper at low stirring speeds, indicating that the diffusion layer thickness indeed is a rate-limiting step. At high stirring speeds, the slopes decreased, indicating a smaller contribution of the diffusion layer thickness in determining the dissolution rates.

Effect of Polymorphism—The dissolution rates of the two polymorphs of sulfathiazole were reported to be indistinguishable in water and in water–ethanol mixtures containing up to 25% (v/v) ethanol (3). It was suggested that this result was due to the extremely rapid conversion of form II to form I in these solvents. In the present study, a highly significant difference was observed between the dissolution rates of the two polymorphs when polyethylene glycol 4000 was added to the formulation.

Figure 3 shows the dissolution rates of the two polymorphs from formulations containing different proportions of polyethylene glycol 4000 at different stirring speeds. In all instances, sulfathiazole form II showed a higher dissolution in water than did form I. The data presented here allow some interesting observations. For example, the ratio of the dissolution rates of forms II and I changed with the stirring speed (Fig. 4). At speeds above 96 rpm, the increase in the dissolution rate of form II was invariably less than that of form I. This finding can be explained on the basis of the

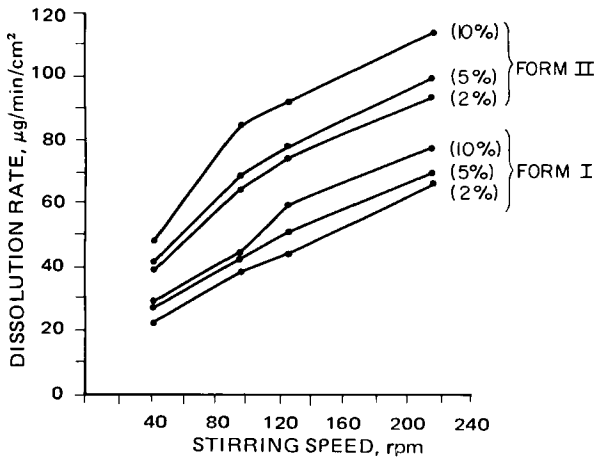

Figure 3—*Dissolution rates of sulfathiazole polymorphs containing different proportions of polyethylene glycol 4000 as a function of stirring speed.*

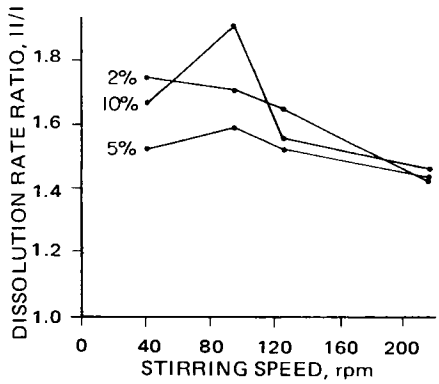

Figure 4—*Relationship between the dissolution rate ratios of the two sulfathiazole polymorphs and the stirring speed at different percentage compositions of polyethylene glycol 4000.*

diffusion layer thickness and the chemical potential of the two polymorphic forms. Since form I has lower solubility than form II (7), a decrease in the diffusion layer thickness will result in a greater increase in the dissolution rate of form I compared to form II (6).

At low stirring speeds where the diffusion layer thickness was large, the relationships were more complicated. The addition of polyethylene glycol 4000 significantly affected the surface properties; but at low percentage composition of polyethylene glycol 4000, *e.g.*, 2%, the effect on the surface property was minimal. As shown in Fig. 4, the ratio of the dissolution rates at the lowest stirring speed (42 rpm) was 1.75, which is in agreement with the solubility ratios of these polymorphs (3, 8). The high percentage compositions of polyethylene glycol 4000 showed a lower dissolution rate ratio at 42 rpm.

A similar argument as already presented can be developed here: that the dissolution rate of sulfathiazole form I having lower solubility is affected more due to the inclusion of the hydrophilic polyethylene glycol 4000 than is form II. As the stirring speed increased from 42 to 96 rpm, a dramatic increase in the dissolution rate ratio was observed, the magnitude of which was proportional to the percentage composition of polyethylene glycol 4000. The 10% compositon showed a much larger increase than the 5% composition, and the 2% composition showed a decrease in the ratio. These observations are difficult to explain, but some speculation can be made.

At the intermediate diffusion layer thickness, as the speed increased from 42 to 96 rpm, the effect of the polyethylene glycol 4000 interaction became more significant, possibly by increasing the diffusion of the solute molecules through the diffusion layer or by increasing the solubility in this layer. This aspect was further reflected in higher ratios of dissolution for the two polymorphs with 10% polyethylene glycol 4000 compared to 5% at all stirring speeds.

Therefore, the presence of polyethylene glycol 4000 significantly

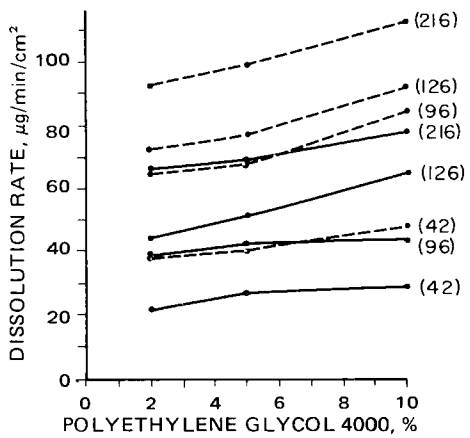

Figure 5—*Dissolution rates of sulfathiazole as a function of polyethylene glycol composition at different stirring speeds. Key: —, form I; and - - -, form II.*

affects the dissolution rate relationship as a function of diffusion layer thickness. Figure 5 shows the dissolution rates plotted as a function of the polyethylene glycol 4000 percentage composition. An interesting observation that can be made from this plot is that as the percentage of polyethylene glycol 4000 increased from 2 to 5%, the increase in the dissolution rates of form I was higher compared to form II for all stirring speeds except the highest speed of 216 rpm. However, as the percentage increased from 5 to 10%, the relationship was inversed, showing a greater increase in the dissolution rate of form II compared to form I at all stirring speeds.

This analysis further strengthens the postulate that at low percentage composition of polyethylene glycol 4000, the surface property changes affect the dissolution rates of form I more than of form II, but the dissolution rates of form II are affected more than those of form I at high percentage compositions.

These observations clearly show that the dissolution rates of the two sulfathiazole polymorphs can differ significantly even if small amounts of additive such as polyethylene glycol 4000 are added. Furthermore, the comparisons of dissolution rates should be made in conjunction with reference to the diffusion layer thickness since the mechanism of dissolution appears to be highly dependent on this factor.

The study presented here also shows that there is no significant conversion of form II to form I in water in the presence of polyethylene glycol 4000. The bioavailability aspects of these findings will be reported later.

REFERENCES

(1) J. Haleblian and W. McCrone, *J. Pharm. Sci.*, **58**, 911(1969).

(2) W. I. Higuchi, P. K. Lau, T. Higuchi, and J. W. Shell, *ibid.*, **52**, 150(1963).

(3) W. I. Higuchi, P. D. Bernardo, and S. C. Mehta, *ibid.*, **56**, 200(1967).

(4) W. L. Chiou and S. Niazi, *ibid.*, **60**, 1333(1971).

(5) S. Niazi, M.S. thesis, Washington State University, Pullman, Wash., 1971.

(6) "Dissolution Technology", L. J. Leeson and J. T. Carstensen, Eds., American Pharmaceutical Association, Washington, D.C., 1974.

(7) W. L. Chiou and S. Riegelman, *J. Pharm. Sci.*, **60**, 1281(1971).

(8) G. Milosovich, *ibid.*, **53**, 484(1964).

ACKNOWLEDGMENTS AND ADDRESSES

Received March 31, 1975, from the *Department of Pharmacy, College of Pharmacy, University of Illinois at the Medical Center, Chicago, IL 60612*

Accepted for publication May 7, 1975.

The author thanks W. Kolling for technical assistance.

Selenium Heterocycles XVIII: Synthesis and Antibacterial Activity of 4-Substituted (1,2,3-Selenadiazol-5-yl)carbamic Acid Esters and Their Sulfur Analogs

A. SHAFIEE ˣ, I. LALEZARI, S. YAZDANI, F. M. SHAHBAZIAN, and T. PARTOVI

Abstract □ 4-Substituted (1,2,3-selenadiazol-5-yl)carbamic acid esters and their sulfur analogs were prepared from the Curtius rearrangement of the corresponding carboxazides. None of the compounds showed significant antibacterial activity.

Keyphrases □ Selenium heterocycles—synthesis and antibacterial activity of 4-substituted (1,2,3-selenadiazol-5-yl)carbamic acid esters and sulfur analogs □ Sulfur heterocycles—synthesis and antibacterial activity of 4-substituted (1,2,3-thiadiazol-5-yl)carbamic acid esters and selenium analogs □ Antibacterial agents, potential—4-substituted (1,2,3-selenadiazol-5-yl)carbamic acid esters and sulfur analogs

It has been reported that 1,3,4-thiadiazolylcarbamic acid esters have significant antiviral activity (1). These compounds and 1,3,4-selenadiazolylcarbamic acid esters showed antibacterial efficacy (2, 3). 1,2,3-Thiadiazole derivatives of benzimidazole, benzoxazole, and benzothiazole were reported as anthelmintics (4). Some phosphorus compounds having the 1,2,3-thiadiazole ring system showed insecticide activity (5), and 4-amino-1,2,3-thiadiazolesulfonamides exhibited antibacterial properties (6). In a continuing effort to find antiviral and antimicrobial agents, 4-substituted (1,2,3-selenadiazol-5-yl)carbamic acid esters and their sulfur analogs were prepared and their efficacy was determined.

DISCUSSION

Chemistry—4-Substituted 1,2,3-thiadiazole-5-carboxylic acid ethyl esters were prepared by an oxidative cyclization of methyl or methylene ketone semicarbazones with thionyl chloride (7).

4-Substituted 1,2,3-selenadiazole-5-carboxylic acid ethyl esters were prepared following the general method reported previously (8) (Scheme I).

1,2,3-Thiadiazole-5-carboxazides and their selenium analogs were prepared by two independent methods. In Method A, the appropriate ester was hydrolyzed to the carboxylic acid and the carboxazide was prepared with thionyl chloride and sodium azide (Scheme II). In Method B, the ester was reacted with hydrazine hydrate and the corresponding hydrazide was then transformed to the carboxazide by reaction with sodium nitrite in acetic acid (9) (Scheme III).

Curtius rearrangement of the azides was readily achieved in alcohols (Schemes II and III). Although 1,2,3-selenadiazole is unstable at 170–180° and decomposes to give acetylene (8), it is quite stable under the conditions used in this work for the Curtius rearrangement.

The physical data for the prepared compounds are summarized in Table I.

Microbiological Evaluation—All compounds listed in Table I were tested against *Bacillus subtilis* (NCTC 3610), *Staphylococ-*

affects the dissolution rate relationship as a function of diffusion layer thickness. Figure 5 shows the dissolution rates plotted as a function of the polyethylene glycol 4000 percentage composition. An interesting observation that can be made from this plot is that as the percentage of polyethylene glycol 4000 increased from 2 to 5%, the increase in the dissolution rates of form I was higher compared to form II for all stirring speeds except the highest speed of 216 rpm. However, as the percentage increased from 5 to 10%, the relationship was inversed, showing a greater increase in the dissolution rate of form II compared to form I at all stirring speeds.

This analysis further strengthens the postulate that at low percentage composition of polyethylene glycol 4000, the surface property changes affect the dissolution rates of form I more than of form II, but the dissolution rates of form II are affected more than those of form I at high percentage compositions.

These observations clearly show that the dissolution rates of the two sulfathiazole polymorphs can differ significantly even if small amounts of additive such as polyethylene glycol 4000 are added. Furthermore, the comparisons of dissolution rates should be made in conjunction with reference to the diffusion layer thickness since the mechanism of dissolution appears to be highly dependent on this factor.

The study presented here also shows that there is no significant conversion of form II to form I in water in the presence of polyethylene glycol 4000. The bioavailability aspects of these findings will be reported later.

REFERENCES

(1) J. Haleblian and W. McCrone, *J. Pharm. Sci.*, **58**, 911(1969).

(2) W. I. Higuchi, P. K. Lau, T. Higuchi, and J. W. Shell, *ibid.*, **52**, 150(1963).

(3) W. I. Higuchi, P. D. Bernardo, and S. C. Mehta, *ibid.*, **56**, 200(1967).

(4) W. L. Chiou and S. Niazi, *ibid.*, **60**, 1333(1971).

(5) S. Niazi, M.S. thesis, Washington State University, Pullman, Wash., 1971.

(6) "Dissolution Technology", L. J. Leeson and J. T. Carstensen, Eds., American Pharmaceutical Association, Washington, D.C., 1974.

(7) W. L. Chiou and S. Riegelman, *J. Pharm. Sci.*, **60**, 1281(1971).

(8) G. Milosovich, *ibid.*, **53**, 484(1964).

ACKNOWLEDGMENTS AND ADDRESSES

Received March 31, 1975, from the *Department of Pharmacy, College of Pharmacy, University of Illinois at the Medical Center, Chicago, IL 60612*

Accepted for publication May 7, 1975.

The author thanks W. Kolling for technical assistance.

Selenium Heterocycles XVIII: Synthesis and Antibacterial Activity of 4-Substituted (1,2,3-Selenadiazol-5-yl)carbamic Acid Esters and Their Sulfur Analogs

A. SHAFIEE ˣ, I. LALEZARI, S. YAZDANI, F. M. SHAHBAZIAN, and T. PARTOVI

Abstract □ 4-Substituted (1,2,3-selenadiazol-5-yl)carbamic acid esters and their sulfur analogs were prepared from the Curtius rearrangement of the corresponding carboxazides. None of the compounds showed significant antibacterial activity.

Keyphrases □ Selenium heterocycles—synthesis and antibacterial activity of 4-substituted (1,2,3-selenadiazol-5-yl)carbamic acid esters and sulfur analogs □ Sulfur heterocycles—synthesis and antibacterial activity of 4-substituted (1,2,3-thiadiazol-5-yl)carbamic acid esters and selenium analogs □ Antibacterial agents, potential—4-substituted (1,2,3-selenadiazol-5-yl)carbamic acid esters and sulfur analogs

It has been reported that 1,3,4-thiadiazolylcarbamic acid esters have significant antiviral activity (1). These compounds and 1,3,4-selenadiazolylcarbamic acid esters showed antibacterial efficacy (2, 3). 1,2,3-Thiadiazole derivatives of benzimidazole, benzoxazole, and benzothiazole were reported as anthelmintics (4). Some phosphorus compounds having the 1,2,3-thiadiazole ring system showed insecticide activity (5), and 4-amino-1,2,3-thiadiazolesulfonamides exhibited antibacterial properties (6). In a continuing effort to find antiviral and antimicrobial agents, 4-substituted (1,2,3-selenadiazol-5-yl)carbamic acid esters and their sulfur analogs were prepared and their efficacy was determined.

DISCUSSION

Chemistry—4-Substituted 1,2,3-thiadiazole-5-carboxylic acid ethyl esters were prepared by an oxidative cyclization of methyl or methylene ketone semicarbazones with thionyl chloride (7).

4-Substituted 1,2,3-selenadiazole-5-carboxylic acid ethyl esters were prepared following the general method reported previously (8) (Scheme I).

1,2,3-Thiadiazole-5-carboxazides and their selenium analogs were prepared by two independent methods. In Method A, the appropriate ester was hydrolyzed to the carboxylic acid and the carboxazide was prepared with thionyl chloride and sodium azide (Scheme II). In Method B, the ester was reacted with hydrazine hydrate and the corresponding hydrazide was then transformed to the carboxazide by reaction with sodium nitrite in acetic acid (9) (Scheme III).

Curtius rearrangement of the azides was readily achieved in alcohols (Schemes II and III). Although 1,2,3-selenadiazole is unstable at 170–180° and decomposes to give acetylene (8), it is quite stable under the conditions used in this work for the Curtius rearrangement.

The physical data for the prepared compounds are summarized in Table I.

Microbiological Evaluation—All compounds listed in Table I were tested against *Bacillus subtilis* (NCTC 3610), *Staphylococ-*

Table I—4-Substituted (1,2,3-Selenadiazol-5-yl)carbamic Acid Esters and Their Sulfur Analogs

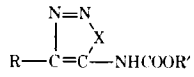

Compound	R	R′	X	Yield, %	Melting Point[a]	Formula[b]	Analysis, % Calc.	Found
Ia	H	CH_3	S	35	205–206°	$C_4H_5N_3O_2S$	C 30.19	30.28
							H 3.14	3.26
							N 26.42	26.33
Ib	CH_3	CH_3	S	46	193–195°	$C_5H_7N_3O_2S$	C 34.68	34.85
							H 4.05	4.01
							N 24.28	24.17
Ic	C_6H_5	CH_3	S	30	207–208°	$C_{10}H_9N_3O_2S$	C 51.05	51.27
							H 3.83	3.95
							N 17.87	17.99
Id	H	C_2H_5	S	95	210–212°[c]	$C_5H_7N_3O_2S$	C 34.68	34.47
							H 4.05	4.02
							N 24.28	24.35
Ie	CH_3	C_2H_5	S	96	121–124°	$C_6H_9N_3O_2S$	C 38.50	38.35
							H 4.81	4.89
							N 22.46	22.55
If	C_6H_5	C_2H_5	S	88	105–107°	$C_{11}H_{11}N_3O_2S$	C 53.01	53.18
							H 4.42	4.37
							N 16.87	16.93
Ig	H	n-C_3H_7	S	60	194–195°	$C_6H_9N_3O_2S$	C 38.50	38.65
							H 4.81	4.85
							N 22.46	22.34
Ih	CH_3	n-C_3H_7	S	32	105–107°	$C_7H_{11}N_3O_2S$	C 41.79	41.55
							H 5.47	5.62
							N 20.90	20.75
Ii	C_6H_5	n-C_3H_7	S	47	83–85°	$C_{12}H_{13}N_3O_2S$	C 54.75	54.89
							H 4.94	5.12
							N 15.97	15.85
Ij	H	iso-C_3H_7	S	42	205–209°	$C_6H_9N_3O_2S$	C 38.50	38.63
							H 4.81	4.92
							N 22.46	22.62
Ik	CH_3	iso-C_3H_7	S	46	145–148°	$C_7H_{11}N_3O_2S$	C 41.79	41.64
							H 5.47	5.55
							N 20.90	20.83
Il	C_6H_5	iso-C_3H_7	S	42	83–85°	$C_{12}H_{13}N_3O_2S$	C 54.75	54.82
							H 4.94	5.12
							N 15.97	16.15
Im	H	n-C_4H_9	S	60	125–127°	$C_7H_{11}N_3O_2S$	C 41.79	41.83
							H 5.47	5.62
							N 20.90	20.82
In	CH_3	n-C_4H_9	S	28	113–116°	$C_8H_{13}N_3O_2S$	C 44.65	44.71
							H 6.05	6.17
							N 19.53	19.75
Io	C_6H_5	n-C_4H_9	S	43	81–83°	$C_{13}H_{15}N_3O_2S$	C 56.32	56.43
							H 5.42	5.35
							N 15.16	15.19
Ip	H	iso-C_4H_9	S	63	160–163°	$C_7H_{11}N_3O_2S$	C 41.79	41.85
							H 5.47	5.32
							N 20.90	20.98
Iq	CH_3	iso-C_4H_9	S	30	126–129°	$C_8H_{13}N_3O_2S$	C 44.65	44.47
							H 6.05	6.15
							N 19.53	19.62
Ir	C_6H_5	iso-C_4H_9	S	20	129–132°	$C_{13}H_{15}N_3O_2S$	C 56.32	56.28
							H 5.42	5.56
							N 15.16	15.06
Is	H	$CH_2C_6H_5$	S	44	148–151°	$C_{10}H_9N_3O_2S$	C 51.06	51.22
							H 3.83	3.65
							N 17.87	17.63
It	CH_3	$CH_2C_6H_5$	S	60	132–134°	$C_{11}H_{11}N_3O_2S$	C 53.01	53.18
							H 4.42	4.27
							N 16.87	16.69
Iu	C_6H_5	$CH_2C_6H_5$	S	42	146–149°	$C_{16}H_{13}N_3O_2S$	C 61.74	61.85
							H 4.18	4.14
							N 13.50	13.65
IIa	CH_3	CH_3	Se	65	172–173°	$C_5H_7N_3O_2Se$	C 27.27	27.14
							H 3.18	3.21
							N 19.09	19.17
IIb	C_6H_5	CH_3	Se	35	198–200°	$C_{10}H_9N_3O_2Se$	C 42.55	42.63
							H 3.19	3.25
							N 14.89	14.95
IIc	CH_3	C_2H_5	Se	75	160–162°	$C_6H_9N_3O_2Se$	C 30.77	30.82
							H 3.85	3.76
							N 17.95	17.63
IId	C_6H_5	C_2H_5	Se	80	178–181°	$C_{11}H_{11}N_3O_2Se$	C 44.59	44.71
							H 3.72	3.85
							N 14.19	14.25

(continued)

Table I—*(Continued)*

Compound	R	R'	X	Yield, %	Melting Point[a]	Formula[b]	Analysis, % Calc.	Found
IIe	CH_3	n-C_3H_7	Se	50	115–118°	$C_7H_{11}N_3O_2Se$	C 33.87 H 4.44 N 16.94	33.92 4.14 16.72
IIf	C_6H_5	n-C_3H_7	Se	46	140–142°	$C_{12}H_{13}N_3O_2Se$	C 46.45 H 4.19 N 13.55	46.53 4.21 13.67
IIg	CH_3	iso-C_3H_7	Se	40	120–122°	$C_7H_{11}N_3O_2Se$	C 33.87 H 4.44 N 16.94	33.92 4.25 16.99
IIh	C_6H_5	iso-C_3H_7	Se	48	138–140°	$C_{12}H_{13}N_3O_2Se$	C 46.45 H 4.19 N 13.55	46.32 4.25 13.75
IIi	CH_3	n-C_4H_9	Se	40	115–118°	$C_8H_{13}N_3O_2Se$	C 36.64 H 4.96 N 16.03	36.71 4.83 16.22
IIj	C_6H_5	n-C_4H_9	Se	45	95–97°	$C_{13}H_{15}N_3O_2Se$	C 48.15 H 4.63 N 12.96	48.22 4.52 12.79
IIk	CH_3	$tert$-C_4H_9	Se	50	198–200°	$C_8H_{13}N_3O_2Se$	C 36.64 H 4.96 N 16.03	36.73 4.79 16.17
IIl	C_6H_5	$tert$-C_4H_9	Se	45	180–181°	$C_{13}H_{15}N_3O_2Se$	C 48.15 H 4.63 N 12.96	48.24 4.72 12.99

[a] Unless otherwise indicated, the recrystallization solvent was ethyl acetate. [b] IR, NMR, and mass spectra of all compounds were as expected. [c] Reference 10, mp 217°.

cus aureus (ATCC 6538), *Klebsiella pneumoniae* (ATCC 10031), and *Sarcina lutea* (ATCC 9341).

The compounds were dissolved in sterile distilled water and diluted to a 0.5% (w/v) concentration. Standard paper disks, 6 mm diameter, were immersed in the solution and placed on an inoculated assay medium surface[1]. None of the compounds of Table I showed significant antibacterial activity.

EXPERIMENTAL[2]

Ethyl 4-Phenyl-1,2,3-thiadiazole-5-carboxylate (III)—Thionyl chloride (50 ml) was gradually added to ethyl benzoylacetate semicarbazone (24 g, 0.1 mole) at ice bath temperature, and the mixture was kept 30 min at this temperature. Chloroform (200 ml) was then added, and the mixture was decomposed with an ice-cold saturated sodium bicarbonate solution, separated, and filtered. The organic layer was washed with water and dried. After evaporation of the solvent, the residue was distilled to give 13.5 g (58%) of the desired compound, bp 185–190° (25 mm); *m/e* 234.

Anal.—Calc. for $C_{11}H_{10}N_2O_2S$: C, 56.41; H, 4.27; N, 11.97. Found: C, 56.52; H, 4.38; N, 11.73.

4-Phenyl-1,2,3-thiadiazole-5-carboxyhydrazide (IV) (Method A)—A solution of 23.4 g (0.1 mole) of the ester III in 50 ml of ethanol was added dropwise to a stirred solution of 25 g (0.5 mole) of hydrazine hydrate in 150 ml of ethanol. After 30 min, the solvent was evaporated and the residue was crystallized from ethanol to give 15 g (68%) of the desired compound, mp 130°; *m/e* 220.

Anal.—Calc. for $C_9H_8N_4OS$: C, 49.09; H, 3.64; N, 25.45. Found: C, 49.25; H, 3.55; N, 25.27.

4-Phenyl-1,2,3-thiadiazole-5-carboxazide (V) (Method A)—To a stirred solution of the carboxyhydrazide IV (22 g, 0.1 mole) in 200 ml of 50% acetic acid at 50° was added dropwise a solution of sodium nitrite (6.9 g, 0.1 mole) in 100 ml of water. The reaction mixture was stirred for 30 min, and the precipitate was filtered, washed with water, and dried under reduced pressure at room temperature, mp 102–103° dec.; *m/e* 231; IR (potassium bromide): 2190 and 2155 cm^{-1} (azide).

4-Phenyl-(1,2,3-thiadiazol-5-yl)carbamic Acid Methyl Ester (Ic) (Method A)—A solution of the azide V (2.31 g, 0.01 mole) in 50 ml of absolute methanol was refluxed for 5 hr. The solvent was evaporated, and the residue was crystallized from ethyl acetate to give 0.84 g (40%) of Ic, mp 207–208°; *m/e* 235; NMR (deuterochloroform): δ 7.1 (broad s, 1H, NH), 7.17 (s, 5H, aromatic), and 3.52 (s, 3H, OCH_3) ppm.

Anal.—Calc. for $C_{10}H_9N_3O_2S$: C, 51.05; H, 3.83; N, 17.87. Found: C, 51.23; H, 3.95; N, 17.79.

Other 4-phenyl-(1,2,3-thiadiazol-5-yl)carbamic acid esters were prepared similarly from 4-phenyl-1,2,3-thiadiazole-5-carboxazide and appropriate alcohols (Table I).

4-Methyl-1,2,3-selenadiazole-5-carboxyhydrazide (VI) (Method A)—A solution of 21.9 g (0.1 mole) of ethyl 4-methyl-1,2,3-selenadiazole-5-carboxylate (8) in 50 ml of methanol was added dropwise to a stirred solution of 25 g (0.5 mole) of hydrazine hydrate in 100 ml of ethanol. The mixture was allowed to stand at room temperature to complete the precipitation. The crystals were filtered and recrystallized from ethanol to give 12.3 g (60%) of the desired compound, mp 151–153°.

Anal.—Calc. for $C_4H_6N_4OSe$: C, 23.41; H, 2.93; N, 27.32. Found: C, 23.57; H, 2.85; N, 27.14.

4-Phenyl-1,2,3-selenadiazole-5-carboxyhydrazide was prepared similarly, mp 115–117°.

Anal.—Calc. for $C_9H_8N_4O_2Se$: C, 38.16; H, 2.83; N, 19.79. Found: C, 38.28; H, 2.73; N, 19.63.

4-Methyl-1,2,3-selenadiazole-5-carboxazide (VII) (Method A)—A solution of sodium nitrite (6.9 g, 0.1 mole) in 100 ml of water was added dropwise to a stirred solution of the carboxyhydrazide VI (20.5 g, 0.1 mole) in 200 ml of 50% acetic acid at 0–5°. After the addition was complete, the reaction mixture was stirred for 30 min. The precipitate was filtered, washed with water, and dried under reduced pressure at room temperature, mp 30–32°.

4-Phenyl-1,2,3-selenadiazole-5-carboxazide was prepared simi-

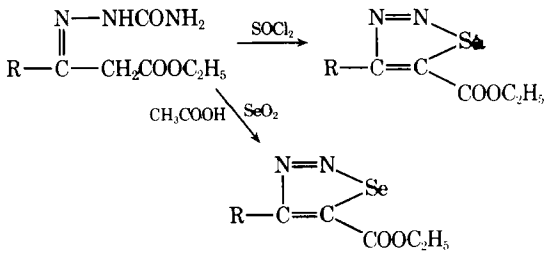

Scheme I

[1] AAM, antibiotic assay medium, The British Pharmacopoeia, 1968.

[2] Melting points were taken on a Kofler hot-stage microscope and are uncorrected. IR spectra were recorded using a Leitz model III spectrophotometer. Mass spectra were recorded on a Varian Mat 111 instrument. NMR spectra were determined with a Varian A-60A instrument.

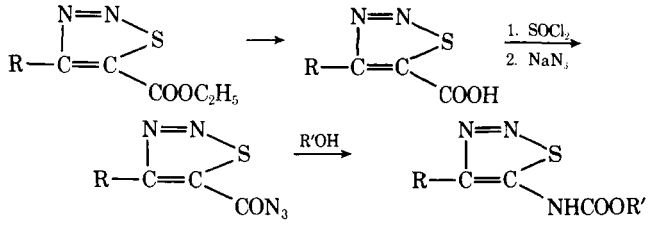

Scheme II

larly, mp 86–88°; IR (potassium bromide): 2165 and 2137 cm^{-1} (azide).

4-Methyl-(1,2,3-selenadiazol-5-yl)carbamic Acid Methyl Ester (IIa) (Method A)—A solution of the azide VII (2.16 g, 0.01 mole) in 50 ml of absolute methanol was refluxed for 4 hr. Then the mixture was filtered and evaporated. The residue was crystallized from ethanol–ethyl acetate to give a 1.1 g (50%) of the desired compound, mp 172–173°; NMR (trifluoroacetic acid): δ 4.06 (s, 3H, OCH_3) and 2.40 (s, 3H, CH_3) ppm.

Other 4-substituted (1,2,3-selenadiazol-5-yl)carbamic acid esters were prepared similarly from the azide and appropriate alcohols.

1,2,3-Thiadiazole-5-carboxylic Acid Ethyl Ester (VIII) (Method B)—Ethyl formylacetate semicarbazone (70 g, 0.4 mole), cooled in an ice bath, was treated slowly with 84 ml of thionyl chloride. The mixture was allowed to stand at room temperature for 30 min, and then chloroform (300 ml) was added. The mixture was decomposed with ice-cold saturated sodium bicarbonate solution and filtered. The organic layer was washed with water, separated, and filtered. The solvent was evaporated and the residue was distilled to give 26.6 g (38%) of the product, bp 115° (25 mm) [lit. (6) bp 103–105° (14 mm)].

1,2,3-Thiadiazole-5-carboxylic Acid (IX) (Method B)—To a solution of VIII (15.8 g, 0.1 mole) in 30 ml of ethanol–water (1:1) was added a solution of sodium hydroxide (4 g, 0.1 mole) in 10 ml of water, and the mixture was heated on a steam bath for 30 min. The solution was acidified (hydrochloric acid) and evaporated to dryness. Then the acid was extracted with ether (soxhlet) to give 12.35 g (95%) of the desired compound, mp 105–108° [lit. (6) mp 104–106°].

1,2,3-Thiadiazol-5-carboxyl Chloride (X) (Method B)—A mixture of the acid IX (13 g, 0.1 mole) and thionyl chloride (30 ml) was refluxed for 4 hr. Excess thionyl chloride was removed under reduced pressure, and the residue was fractionated to give 12.6 g (85%) of the desired compound, bp 80–81° (25 mm).

1,2,3-Thiadiazole-5-carboxazide (XI) (Method B)—A stirred solution of sodium azide (7.15 g, 0.11 mole) in 15 ml of water, chilled in an ice bath, was treated with the acid chloride (X) (14.85 g, 0.1 mole) in 30 ml of acetone. After the addition of the chloride, the reaction mixture was stirred for 30 min. Then 50 ml of water was added, and the azide was extracted with chloroform. The organic layer was dried (sodium sulfate) and filtered. The solvent

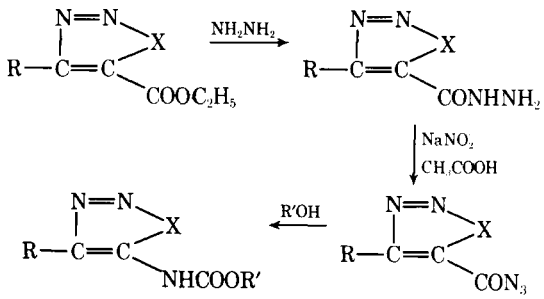

Scheme III

was evaporated to give an oil, 10.85 g (70%); IR (potassium bromide): 2190 and 2155 cm^{-1} (azide).

(1,2,3-Thiadiazol-5-yl)carbamic Acid Ethyl Ester (Id) (Method B)—A solution of the azide XI (15.5 g, 0.1 mole) in 100 ml of absolute ethanol was refluxed for 6 hr. The solvent was evaporated and the residue was crystallized from ethyl acetate to give 15.6 g (90%) of Id, mp 210–212° [lit. (10) mp 217° dec.]; NMR (deuterochloroform): δ 8.87 (s, 1H, H_4), 4.10 (q, 2H, OCH_2), and 1.17 (t, 3H, CH_3) ppm; *m/e* 173.

Other (1,2,3-thiadiazol-5-yl)carbamic acid esters and 4-methyl-(1,2,3-thiadiazol-5-yl)carbamic acid esters were prepared similarly.

REFERENCES

(1) H. Mirshmsi, I. Lalezari, M. Kamali, G. Nilofari, and N. Rezvani, *Arch. Virusforsch.*, **29**, 267(1970).

(2) I. Lalezari and A. Vahdat, *J. Med. Chem.*, **14**, 59(1971).

(3) A. Shafiee, I. Lalezari, S. Yazdany, and A. Pournorouz, *J. Pharm. Sci.*, **62**, 839(1973).

(4) L. H. Sarett and H. D. Brown, U.S. pat. 3,017,415 (1962), 3,357,884 (1967), and 3,478,046 (1969) and French pat. M 4234 (1966).

(5) R. L. McConnell and H. W. Coover, U.S. pat. 3,072,669.

(6) D. L. Pain and R. Slack, *J. Chem. Soc.*, **1965**, 5166.

(7) I. Lalezari, A. Shafiee, and S. Yazdany, *J. Pharm. Sci.*, **63**, 628(1974).

(8) I. Lalezari, A. Shafiee, and M. Yalpani, *J. Org. Chem.*, **36**, 2836(1971).

(9) J. H. Looker and L. W. Wilson, Jr., *J. Heterocycl. Chem.*, **2**, 348(1965).

(10) D. Martin and W. Mucke, *Annalen*, **682**, 90(1965).

ACKNOWLEDGMENTS AND ADDRESSES

Received March 19, 1975, from the *Department of Chemistry, College of Pharmacy, Tehran University, Tehran, Iran.*

Accepted for publication May 7, 1975.

[x] To whom inquiries should be directed.

Orthostatic Influences on Cardiovascular Responses to Nitroglycerin in Conscious Dogs

BERNARD KOROL *x, LYNN J. McLAUGHLIN ‡, and LOWELL D. MILLER §

Abstract □ The influence of body position change on the arterial pressure and heart rate responses produced by acute short-acting and sustained-release dosage forms of nitroglycerin was evaluated in a series of chronically prepared, conscious beagle dogs. The upright repositioning of the dog to 60° from horizontal markedly enhanced the hypotensive and bradycardic responses produced by both dosage forms. Since it has been suggested that the lowering of arterial pressure is an essential component resulting in the therapeutic usefulness of nitroglycerin in angina pectoris, the experimental orthostatic model could be a sensitive procedure for the laboratory assessment of drugs of this class.

Keyphrases □ Nitroglycerin—effect of body position on cardiovascular response, short-acting and sustained-release dosage forms, dogs □ Cardiovascular response—nitroglycerin, influence of body position, short-acting and sustained-release dosage forms, dogs □ Vasodilators—nitroglycerin, effect of body position on cardiovascular response, short-acting and sustained-release dosage forms, dogs

In pentobarbital-anesthetized dogs, sublingual nitroglycerin doses as high as 1.95 mg (3/100 gr) were devoid of apparent coronary flow effects, although they lowered the mean arterial pressure significantly (1). However, the intravenous administration of 0.65 mg of nitroglycerin to the anesthetized dog did produce a significant, although short-duration, coronary dilatation associated with a hypotensive and tachycardic response. These findings supported postulates (2) regarding the therapeutic effectiveness of nitroglycerin against anginal pain in humans. Based upon these experimental results with pentobarbital-anesthetized dogs (2), the three important aspects of the pharmacological action of nitroglycerin were: (*a*) a reduction of cardiac work secondary to a lowering of arterial pressure, (*b*) a concurrent dilatation of the coronary vessels, and (*c*) an indirect reduction in myocardial oxygen consumption due to decreased cardiac work.

According to Bernstein *et al.* (3), the therapeutic usefulness of nitroglycerin in angina pectoris is due to its ability to increase coronary blood flow and simultaneously to decrease the cardiac work. However, they did not demonstrate a statistically significant change in myocardial blood flow following sublingual nitroglycerin. Similarly, the therapeutic effects of nitroglycerin were suggested to be due to its coronary flow and blood pressure effects, although sublingual administration failed to demonstrate a significant coronary flow effect in 14 of 15 anesthetized dogs examined (4).

Large intravenous doses (0.22–1.3 mg) of nitroglycerin increased coronary vasodilatation, which endured for longer than 16 min in conscious, trained dogs (5). However, according to Melville (6), the coronary vasodilatation afforded by nitroglycerin is a minor factor in its antianginal action. The results of a subsequent study (1) supported this speculation, since the sublingual nitroglycerin dosage form failed to alter significantly the coronary flow of anesthetized dogs while consistently depressing the arterial blood pressure.

An accurate, reliable, and convenient method was needed for the assessment of both acute and sustained-release coronary dilators of the nitroglycerin type. In view of the apparent and more selective effect of this agent upon blood pressure levels of anesthetized dogs, use of the conscious dog preparation while upright (orthostatic) should fulfill this methodological requirement. A series of experiments was performed to examine the ability of oral nitroglycerin, in sublingual and sustained-release dosage forms, to alter the systolic and diastolic arterial pressures and heart rates in conscious beagle dogs while in the horizontal and upright (60° from horizontal) body positions. This report describes the experimental method and the results obtained with these two dosage forms of nitroglycerin.

EXPERIMENTAL

Six male and female beagle dogs, 8.1–12.2 kg, were used. These dogs had not been previously treated with nitroglycerin or other vasodilators of this class, although they had been used repeatedly over the years for behavioral and psychopharmacological evaluations (7, 8).

Each dog previously had been surgically prepared (9) with externalized bilateral carotid artery loops to allow for the direct measurement of systolic and diastolic arterial pressure while conscious. Direct arterial pressure measurements were obtained by cannulation of one externalized carotid artery and subsequent connections of the cannula[1] supplying input into an arterial pressure coupler[2] of the recorder. Patency of the cannula was maintained with an infusion pump producing a slow volume, retrograde intraarterial infusion of physiological saline through the pressure transducer into the dwelling arterial cannula.

Beat-to-beat heart rate level was determined concomitantly through bipolar silver–silver chloride electrodes positioned and affixed to the skin surface over the sternum. These electrodes were suitably connected to a cardiotachometer coupler[3] of the recorder and supplied a lead I electrode[4] selection to drive the cardiotachometer. Respiration was monitored indirectly through a pneumotachograph belt placed around the thoracico-abdominal region of the dog's body. This pneumotachograph belt was connected to a low level pressure transducer[5], supplying input into a pressure coupler[6] of the recorder. All recording was performed by a dynograph[7] using a paper speed of 2.5 mm/sec.

Two dosage forms of nitroglycerin were evaluated: a sublingual

[1] Type P-23AA Statham pressure transducer.
[2] Type 9872.
[3] Type 9853.
[4] Wilson.
[5] Statham type P-32BB.
[6] Type 9872.
[7] Beckman type R.

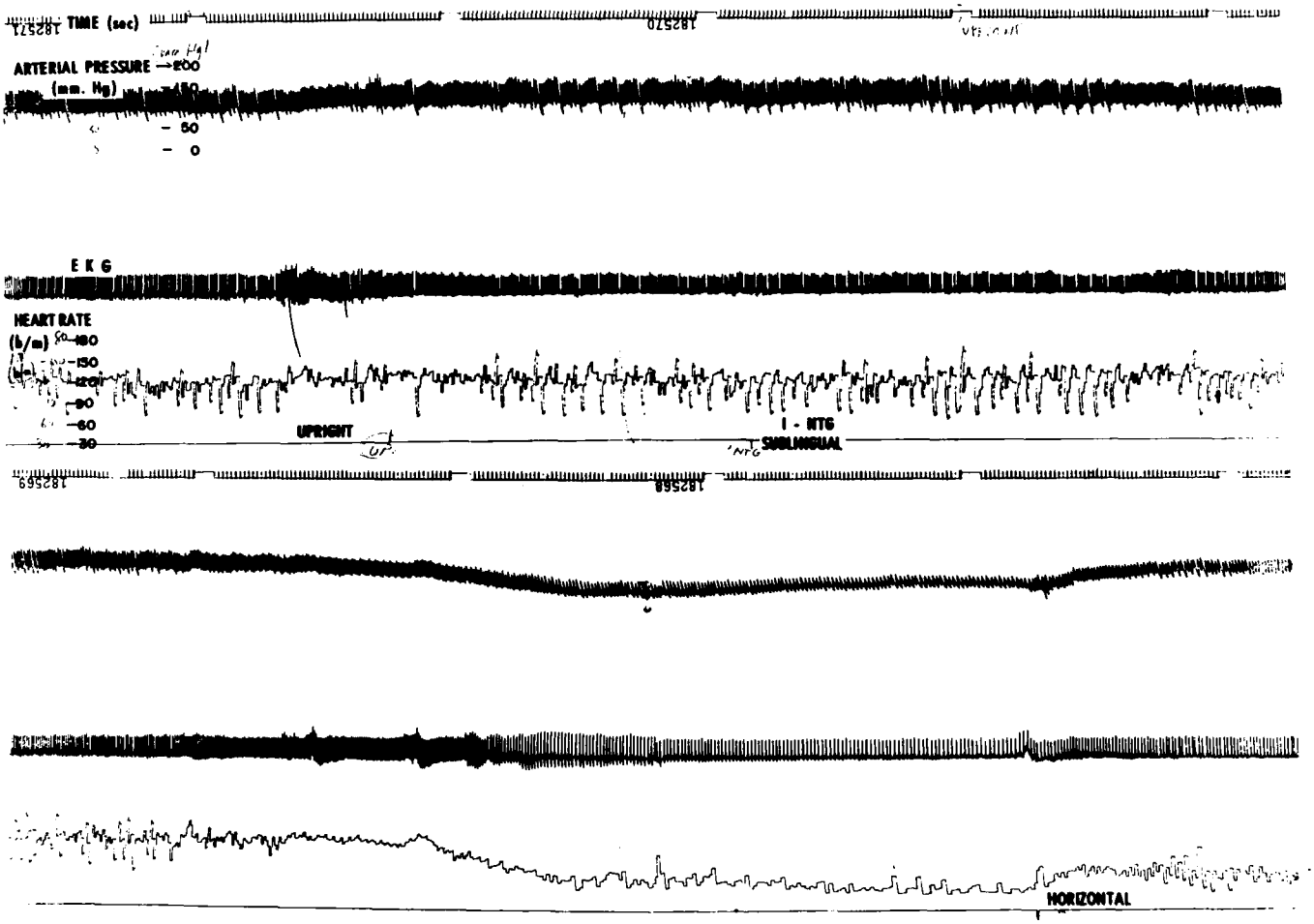

Figure 1—*Arterial pressure (mm Hg) and heart rate (beats per minute) effects of acute sublingual nitroglycerin (0.65 mg) to conscious beagle dogs while upright. Upper and lower records are continuous.*

form containing 0.6 mg (1/100 gr)/tablet and a sustained-released form[8] containing 6.5 mg (1/10 gr)/capsule. Single or multiple amounts of each dosage form were employed and evaluated for their cardiovascular effects.

Because of the minimal response induced by sublingual nitroglycerin in the normotensive dogs while horizontal, four dogs were trained to remain in an upright position (approximately 60° from horizontal) with the aid of a chest sling. This procedure enhanced the amplitude of the hypotensive response to the sublingually administered nitroglycerin and was also the method used to evaluate the effectiveness of the sustained-release form.

Simply, the procedure was to raise-tilt (upright) the dog for 5-min intervals at fixed times of −10, +5, +20, +35, +50, +65, +85, +105, +125, +155, and +185 min after administration of the sustained-release oral capsule. In experiments with the sublingual dosage form, the animal was upright when the tablet was placed in the lip-sac and remained upright for 5 min thereafter. For control purposes, 0.25-gr saccharin tablets, which approximated the size of the sublingual form of nitroglycerin, were similarly placed in the lip-sac while identical manipulations (*e.g.*, body position change) were applied.

The data were analyzed for statistical significance using the matched-pair *t* test (10), with each animal serving as its own control.

RESULTS AND DISCUSSION

The influence of sublingual nitroglycerin on systolic/diastolic arterial pressure and heart rate in two conscious dogs maintained in a horizontal body position was evaluated. The data indicated that the low sublingual dose of one nitroglycerin tablet (0.65 mg) did not produce an apparent lowering of the normotensive arterial pressure nor have an appreciable effect upon the heart rate. The pretreatment systolic/diastolic arterial pressure and heart rate were 150/80 mm Hg and 150 beats/min, respectively, and changed randomly.

The sublingual placement of three nitroglycerin tablets (1.95 mg) in two dogs maintained in a normotensive horizontal position did produce a discernible lowering of arterial pressure level, with an apparently greater effect on the systolic phase than on the diastolic phase of the hypotensive response. A tachycardic response was associated with the blood pressure lowering response. Four minutes after placing the three nitroglycerin tablets in the lip-sac of the dog's mouth, there was a 20-mm Hg lowering of systolic arterial pressure, a 10-mm Hg depression of the diastolic pressure, and an associated 18-beats/min increase in heart rate.

The effects of sublingual nitroglycerin on systolic/diastolic arterial pressure and heart rate in two conscious beagle dogs with orthostatic hypertension maintained by upright body position also was examined. The enhanced arterial pressure lowering effects produced by one nitroglycerin tablet (0.65 mg), sublingually, while the dog was maintained in an upright body position is illustrated on Fig. 1. Within 2 min postadministration, the upright systolic/diastolic pressures were reduced from a control of 160/90 to 140/85 mm Hg with no apparent associated effect upon heart rate. Both the systolic and diastolic arterial pressures continued to decrease over the next 3 min (5 min after nitroglycerin lip-sac placement), at which time maximum depression to 60/30 mm Hg was reached. Heart rate was decreased by this nitroglycerin treatment from a control of 105 beats/min to a 5-min posttreatment level of 60 beats/min. Both the depressed arterial pressure and heart rates returned toward normal when the animal was returned to the normal horizontal body position.

[8] Nitrobid, Marion Laboratories, Kansas City, Mo.

Table I—Arterial Pressure (mm Hg) and Heart Rate (Beats per Minute) Effects of Extended Duration Form of Nitroglycerin in Six Conscious Beagle Dogs while in an Upright Body Position

Minutes after Treatment	Treatment: Control Systolic	Control Diastolic	Control Heart Rate	19.5 mg Sustained-Release Nitroglycerin Systolic	19.5 mg Sustained-Release Nitroglycerin Diastolic	19.5 mg Sustained-Release Nitroglycerin Heart Rate
0	135	75	105	160	90	90
20	140	85	99	140	85	87
35	135	85	99	115[a]	70[b]	78
50	145	90[b]	96	120[b]	80	102
65	135	85	96	120[b]	85	87
80	140	85	84[b]	115[a]	80	75[b]
100	140	85	99	110[a]	80	84
120	150	90[b]	90	120[b]	90	99
140	145	90	90	115[b]	80	78[b]
160	155[b]	95[b]	87[b]	120	90	96
180	160[b]	95[b]	90	130	95	93

[a] $p \leq 0.01$. [b] $p \leq 0.05$.

The placement of a saccharin tablet into the lip-sac area of the dog did not produce a discernible blood pressure or heart rate response when the dog was in either the upright or horizontal body position.

Furthermore, the effects of oral administration of a sustained-release preparation of nitroglycerin on the systolic/diastolic arterial pressure and heart rate in two conscious beagle dogs in an upright body position were investigated. The oral administration of a 6.5-mg sustained-release capsule was devoid of an apparant effect upon systolic/diastolic arterial pressure and heart rate over the 180-min observation period.

The oral administration of three sustained-release capsules (total nitroglycerin dose of 19.5 mg) resulted in a systolic depressor response when the animal was in either body position, although the response was enhanced when the dog was upright. These data, summarized in Table I, reveal that there was a discernible lowering of systolic arterial pressure within 20–30 min after drug administration; a peak effect of −40 mm Hg was reached at 115 min when the dog was in the upright position, and a peak effect of −20 mm Hg appeared at 35 min when the dog was in the normal horizontal body position. The diastolic pressures obtained when the animals were in either body position were not appreciably altered by the drug treatment.

Table I also contains data of the influence on systolic/diastolic pressures of repeated body position changes with no drug treatment in accordance with the schedule used when nitroglycerin was administered. Examination of these data reveals that repeated positional change from horizontal to upright was not associated with a reduction in arterial pressure over time but, in fact, demonstrated a 25-mm Hg increase in the systolic component of the orthostatic pressor response.

The findings from this study support the speculation that an essential component of the pharmacological action of nitroglycerin is a lowering of the arterial pressure. In many studies, any observed coronary dilatation was always associated with a lowering of existing arterial pressure (1, 4). The corollary that the lowering of arterial pressure by nitroglycerin is always associated with a coronary vasodilatation is, however, not true.

In this study, the ability of nitroglycerin in an acute sublingual dosage form, or in a sustained-release form, to lower the arterial pressure in conscious beagle dogs was markedly accentuated when the dog was maintained in an upright body position. The procedure of repositioning the dog to an upright body position for 5-min intervals was performed at a frequency not exceeding one episode every 15 min. The dog was maintained upright with the use of a chest sling which fit under the forearms, over the sternum, and suspended from the top beams of the Pavlov stand. There was no response fatigue when the dogs were challenged with body repositioning every 15 min over 3 hr.

The enhanced arterial pressure lowering response to the vasodilator, nitroglycerin, accomplished by placing the conscious dog in an upright body position could be a useful technique not only for the evaluation of vasodilators of this drug class but also for the study of the physiological mechanisms in orthostatic hypotension or hypertension.

REFERENCES

(1) R. A. Gillis and K. I. Melville, *Amer. J. Cardiol.*, **28,** 38(1971).

(2) G. V. Marchetti, L. Merlo, and R. M. Antognetti, *ibid.*, **13,** 51(1964).

(3) L. Bernstein, G. C. Friesinger, P. R. Lichtten, and R. S. Ross, *Circulation*, **33,** 107(1966).

(4) J. K. Vyden, M. Carvalho, E. Boszormenyi, T. Lang, H. Bernstein, and E. Corday, *Amer. J. Cardiol.*, **25,** 53(1970).

(5) R. Wegria, *Pharmacol. Rev.*, **3,** 197(1951).

(6) K. I. Melville, *Pharmacol. Physicians*, **4,** 1(1970).

(7) B. Korol, W. J. Lang, M. L. Brown, and S. Gershon, *Nature*, **209,** 1249(1966).

(8) B. Korol and M. L. Brown, *Pharmacology*, **1,** 115(1968).

(9) M. L. Brown and B. Korol, *Physiol. Behav.*, **3,** 207(1967).

(10) G. W. Snedecor, "Statistical Methods," 5th ed., Iowa State Press, Ames, Iowa, 1956, pp. 87–92.

ACKNOWLEDGMENTS AND ADDRESSES

Received January 15, 1975, from the *Veterans Administration Hospital, St. Louis, MO 63125, and the ‡Department of Psychiatry, St. Louis University School of Medicine, St. Louis, Mo.

Accepted for publication May 6, 1975.

The authors thank Lonnie Plunk for technical assistance.

§ Present address: Marion Laboratories, Kansas City, MO 64137

ˣ To whom inquiries should be directed (Medical Research Information System No. 4675-01).

Terminology Regarding Labeled and Contained Amounts in Dosage Forms

Keyphrases □ Dosage forms—terminology regarding labeled and contained amounts, definitions suggested for the terms shelflife, outdate, expiration date, label date □ Terminology—regarding labeled and contained amounts in dosage forms, definitions suggested for the terms shelflife, outdate, expiration date, label date

To the Editor:

Dating of pharmaceutical preparations has become standard practice in this country. To this end, an acceptable nomenclature for various phases of the decay cycle of a product is of essence; we should like to suggest definitions for the terms "shelflife," "outdate," "expiration date," and "label date."

As pointed out by Crout (1), concise definitions of terms are necessary for the sake of rational debate. The difficulties encountered without such definitions are, for instance, evident in Canadian Regulations C.01.004[7]. Here, such statements are used as: "Where evidence indicates that . . . a drug[1] . . . does not maintain its potency, purity, or physical characteristics for at least three years from the date of manufacture . . . ." If definition of the pertinent terms existed, the wording could be much simpler.

Of the mentioned terms, only label date is a defined quantity at present; it is simply the date appearing on the label. The following discussion does not suggest that more than the label date should appear on the label. However, certain definitions for the other three terms would make scientific and technological dialog more precise, particularly in light of the proposed new Current Good Manufacturing Practices, paragraph 133.14.

In general, the stability of a drug is followed by storing it at constant temperature and assaying it from time to time. The points plotted are the assays, which are estimates of the true contents. The decay curve may be of many types [zero order, first order, with or without lag times, downward parabolic (autocatalytic), and any of these types with or without equilibrium levels (2, 3)]. Although an uncomplicated zero-order decomposition is used as an example here, this usage in no way places any restriction on the definitions to follow. That the statistics of drug decomposition in a dosage form generally may not be this simple is granted; the work by Fusari (4) is an example.

If all dosage units of all batches of a product were of identical content and stability, a decay plot such as the one shown in bold in Fig. 1, the stability line ($y = -ax + b$), would result. The ordinate is percent label claim but could be any scale that linearizes the decay. The initial content is 100% label claim plus excess. In the example in Fig. 1, the excess is $(10 - e)$%; *i.e.*, the initial content is $(100 - e)$% label claim[2]. The point where the stability line reaches 100% is denoted shelflife in our definition. In reality, the stability line will not be an "exact" line but will be subject to variation. The stability line then is the least-squares fit line, and the shelflife is defined as the point where this line cuts the 100% label claim line; it is a function of the excess used.

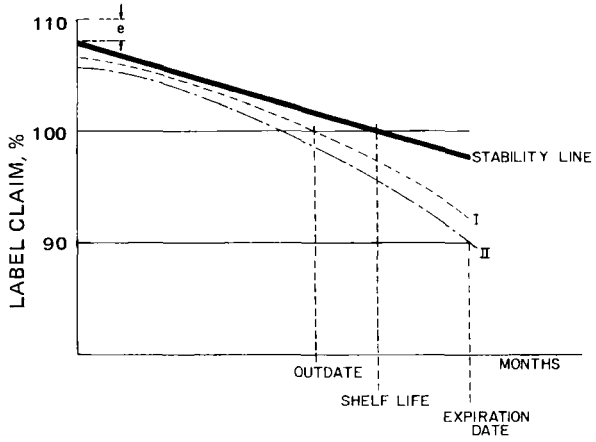

Figure 1—*Plot of stability of product, starting at (110 − e)% label claim.*

To define the pertinent quantities, let us assume that the study involves q batches. A sample of size p dosage units[3] is taken at time x and assayed *in toto*[4]; the assay of the sample divided by p is the y value, which is plotted on the stability line. In the uncomplicated case with which the definitions are illustrated, the variance of the y values is assumed not to change with time. This assumption, as shown by Fusari (4), is an oversimplification but poses no restrictions on the definitions.

At the time a stability report is prepared, there are n assays, the times involved being $x_0, x_1, \ldots, x_k$, where k and n may (or may not) be identical (since several samples may be assayed at one storage time). The true mean of the assays of all possible samples at time x_i lies in the interval (5):

$$\{[b - ax_i - f(x_i)]\|[b - ax_i + f(x_i)]\}$$

where:

$$f(x_i) = t_{0.10,n-2} s_{yx} \sqrt{\frac{1}{n} + \frac{(x_i - \bar{x})^2}{\sum (x_j - \bar{x})^2}} \qquad \text{(Eq. 1)}$$

where the summation is from $j = 1$ to $j = n$ and the statement is made with 90% confidence (since $t_{0.10}$ is

[1] The word "drug" in regulations encompasses (among other factors) the dosage form as well.

[2] It is assumed here that the process and assay variances, with 95% confidence, contribute $\pm e$% to the initial assay (which is an average of p units). The specification limits are assumed to be the conventional 90–110% label claim, so initial assays lie between $(110 - 2e)$% and 110% label claim with a frequency of 0.95.

[3] Alternatively, a subsample of p units from a sample of P units could be used.

[4] This, for instance, could be obtained by grinding up p units and either assaying the total sample or performing k chemical determinations on $(1/k)$ segments of a uniformly blended mix of the ground-up sample. In the latter case, information regarding assay variance can be inferred.

being used). Hence, it may be stated with 95% confidence that the true mean of all assays will be above $b - ax_i - f(x_i)$. Here n is the number of assays, t is the Student t value, $\bar{x}$ is the mean of the x values, and s_{yx}^2 is the mean square about the regression (6).

The line marked I in Fig. 1 is denoted the lower (one-tailed) 95% confidence line about the least-squares fit line[5], *i.e.*, $\bar{y} - f(x)$; we should like to define the outdate as the point where this line cuts the 100% label claim line.

An individual assay (average of p units) will, with 90% confidence *at time* x_i, lie in the interval (7):

$$\{[b - ax_i - g(x)][b - ax_i + g(x)]\}$$

where now:

$$g(x) = t_{0.10,n-2}s_{yx}\sqrt{\frac{n+1}{n} + \frac{(x_i - \bar{x})^2}{\sum(x_i - \bar{x})^2}} \qquad \text{(Eq. 2)}$$

The line marked II in Fig. 1 is the 95% confidence line[5] for individual assays by the same argument as already given, *i.e.*, $y - g(x)$. As stated previously, it is assumed that the lower specification limit is 90%; the point where line II cuts the horizontal 90% line. we should like to denote the expiration date. The January or July immediately preceding this date should be denoted the label date and is the date appearing on the label. The other three defined terms do not appear on the label but may occur in documents (regulations, New Drug Application, *etc.*).

In using the nomenclature, it would (except in the case of the label date, which simply is the date that appears on the label) be advisable to indicate the excess (xs) and confidence limits (CL) in parentheses. The number of batches (N), the number of assays (n), the sample size (P), and the subsample size (p) are also pertinent. Thus, the suggested mode of writing would be shelflife s months (xs = 8%, CL = 95%, N = 5, n = 20, P = 100, and p = 10) to denote an 8% excess, 95% confidence, five batches, 20 points, a sample size of 100 dosage units, and a subsample size of 10 units assayed.

A similar statement would apply to the outdate, and the difference between the shelflife and the outdate would show the goodness of fit. For expiration dates, the lower specification limit (SL) would have to be added, *e.g.*, expiration date July 1975 (xs = 8%, CL = 95%, N = 5, n = 20, P = 100, p = 10, and SL = 90%). It is suggested that omission of the last figure implies a 90% lower limit.

These definitions do not help solve all dilemmas of stability testing. For instance, a good product with a high assay variance may still require a higher excess than a product with poorer stability and smaller assay variance. In assays with notoriously high variance (*e.g.*, microbiological assays), an increase in n or a decrease in SL is usually the means used if the assay method cannot be improved.

The 95% confidence limits can be replaced by other confidence limits provided the proper t value is used. The excess used is based on the considerations in Footnote 2 and on stability considerations and will, of course, vary from product to product; it should be calculated by a systematic method, such as an overage chart (8). The excess used also depends on the lower specification limit, which, of course, depends on the product (*e.g.*, *via* compendial standards) and particular company policies.

[5] A single-tailed test is employed since one is interested in the assay falling above a lower limit. It is already known that it will fall below 110% label claim (Footnote 2). It is possible to conceive situations where the potency increases with time (*e.g.*, when an assay is not stability indicating and a degradation product contributes more to the assay than the parent compound or in the case of improper closures), but the study is always invalid in such cases.

(1) J. R. Crout, conference on "Bioavailability—Scientific and Legal Implications for IND/NDA Submissions," Extension Services in Pharmacy, University of Wisconsin, Madison, Wis., Oct. 21–28, 1974.

(2) J. T. Carstensen, "Pharmaceutics of Solids," Badger-Freund Inc., Fond Du Lac, Wis., 1974, pp. 156–158.

(3) J. T. Carstensen, "Theory of Pharmaceutical Systems," vol. II, Academic, New York, N.Y., 1973, pp. 329–341.

(4) S. Fusari, *J. Pharm. Sci.*, **62**, 2012(1973).

(5) N. R. Draper and H. Smith, "Applied Regression Analysis," Wiley, New York, N.Y., 1966, p. 23.

(6) *Ibid.*, p. 19.

(7) *Ibid.*, p. 24.

(8) J. Haynes, J. T. Carstensen, J. C. Callahan, and R. Card, "Third Stevens Symposium on Statistical Methods in the Chemical Industry," Hoboken, N.J., Jan. 24, 1959, p. 1.

J. T. Carstensen [x]
School of Pharmacy
University of Wisconsin
Madison, WI 53706

Elwynn Nelson
Miles Laboratories Inc.
Elkhart, IN 46518

Received July 15, 1974.

Accepted for publication November 10, 1975

Presented at the Industrial Pharmaceutical Technology Section, APhA Academy of Pharmaceutical Sciences, Eastern Regional Meeting, Cherry Hill, N.J., 1974.

[x] To whom inquiries should be directed.

Sample Size Changes in USP XIX and NF XIV

Keyphrases □ Sampling—effect of sample size, USP and NF tests for content uniformity, dissolution, disintegration, and weight variation, changes from previous editions □ Test specifications—USP and NF tests for content uniformity, dissolution, disintegration, and weight variation, sample size changes from previous editions □ Compendial tests—changes in sample size, effects

To the Editor:

Changes in USP XIX and NF XIV regarding sample size introduce an inconsistency into the tests for content uniformity, dissolution, disintegration, and weight variation. In USP XVIII and NF XIII, the sample size for the final stage of the sequential tests for content uniformity, dissolution time, and disintegration time and for the nonsequential test for weight variation was uniquely determined by the description of the test. However, in the General Notices of USP XIX (1) and NF XIV (2), the following sentences have been inserted under the heading "Procedures":

> *"In the performance of assay or test procedures, not less than the specified number of dosage units should be taken for analysis."*

being used). Hence, it may be stated with 95% confidence that the true mean of all assays will be above $b - ax_i - f(x_i)$. Here n is the number of assays, t is the Student t value, $\bar{x}$ is the mean of the x values, and s_{yx}^2 is the mean square about the regression (6).

The line marked I in Fig. 1 is denoted the lower (one-tailed) 95% confidence line about the least-squares fit line[5], *i.e.*, $\bar{y} - f(x)$; we should like to define the outdate as the point where this line cuts the 100% label claim line.

An individual assay (average of p units) will, with 90% confidence *at time* x_i, lie in the interval (7):

$$\{[b - ax_i - g(x)][b - ax_i + g(x)]\}$$

where now:

$$g(x) = t_{0.10,n-2}s_{yx}\sqrt{\frac{n+1}{n} + \frac{(x_i - \bar{x})^2}{\sum(x_i - \bar{x})^2}} \qquad \text{(Eq. 2)}$$

The line marked II in Fig. 1 is the 95% confidence line[5] for individual assays by the same argument as already given, *i.e.*, $y - g(x)$. As stated previously, it is assumed that the lower specification limit is 90%; the point where line II cuts the horizontal 90% line. we should like to denote the expiration date. The January or July immediately preceding this date should be denoted the label date and is the date appearing on the label. The other three defined terms do not appear on the label but may occur in documents (regulations, New Drug Application, *etc.*).

In using the nomenclature, it would (except in the case of the label date, which simply is the date that appears on the label) be advisable to indicate the excess (xs) and confidence limits (CL) in parentheses. The number of batches (N), the number of assays (n), the sample size (P), and the subsample size (p) are also pertinent. Thus, the suggested mode of writing would be shelflife s months (xs = 8%, CL = 95%, N = 5, n = 20, P = 100, and p = 10) to denote an 8% excess, 95% confidence, five batches, 20 points, a sample size of 100 dosage units, and a subsample size of 10 units assayed.

A similar statement would apply to the outdate, and the difference between the shelflife and the outdate would show the goodness of fit. For expiration dates, the lower specification limit (SL) would have to be added, *e.g.*, expiration date July 1975 (xs = 8%, CL = 95%, N = 5, n = 20, P = 100, p = 10, and SL = 90%). It is suggested that omission of the last figure implies a 90% lower limit.

These definitions do not help solve all dilemmas of stability testing. For instance, a good product with a high assay variance may still require a higher excess than a product with poorer stability and smaller assay variance. In assays with notoriously high variance (*e.g.*, microbiological assays), an increase in n or a decrease in SL is usually the means used if the assay method cannot be improved.

The 95% confidence limits can be replaced by other confidence limits provided the proper t value is used. The excess used is based on the considerations in Footnote 2 and on stability considerations and will, of course, vary from product to product; it should be calculated by a systematic method, such as an overage chart (8). The excess used also depends on the lower specification limit, which, of course, depends on the product (*e.g.*, *via* compendial standards) and particular company policies.

[5] A single-tailed test is employed since one is interested in the assay falling above a lower limit. It is already known that it will fall below 110% label claim (Footnote 2). It is possible to conceive situations where the potency increases with time (*e.g.*, when an assay is not stability indicating and a degradation product contributes more to the assay than the parent compound or in the case of improper closures), but the study is always invalid in such cases.

(1) J. R. Crout, conference on "Bioavailability—Scientific and Legal Implications for IND/NDA Submissions," Extension Services in Pharmacy, University of Wisconsin, Madison, Wis., Oct. 21–28, 1974.

(2) J. T. Carstensen, "Pharmaceutics of Solids," Badger-Freund Inc., Fond Du Lac, Wis., 1974, pp. 156–158.

(3) J. T. Carstensen, "Theory of Pharmaceutical Systems," vol. II, Academic, New York, N.Y., 1973, pp. 329–341.

(4) S. Fusari, *J. Pharm. Sci.*, **62**, 2012(1973).

(5) N. R. Draper and H. Smith, "Applied Regression Analysis," Wiley, New York, N.Y., 1966, p. 23.

(6) *Ibid.*, p. 19.

(7) *Ibid.*, p. 24.

(8) J. Haynes, J. T. Carstensen, J. C. Callahan, and R. Card, "Third Stevens Symposium on Statistical Methods in the Chemical Industry," Hoboken, N.J., Jan. 24, 1959, p. 1.

J. T. Carstensen [x]
School of Pharmacy
University of Wisconsin
Madison, WI 53706

Elwynn Nelson
Miles Laboratories Inc.
Elkhart, IN 46518

Received July 15, 1974.

Accepted for publication November 10, 1975

Presented at the Industrial Pharmaceutical Technology Section, APhA Academy of Pharmaceutical Sciences, Eastern Regional Meeting, Cherry Hill, N.J., 1974.

[x] To whom inquiries should be directed.

Sample Size Changes in USP XIX and NF XIV

Keyphrases □ Sampling—effect of sample size, USP and NF tests for content uniformity, dissolution, disintegration, and weight variation, changes from previous editions □ Test specifications—USP and NF tests for content uniformity, dissolution, disintegration, and weight variation, sample size changes from previous editions □ Compendial tests—changes in sample size, effects

To the Editor:

Changes in USP XIX and NF XIV regarding sample size introduce an inconsistency into the tests for content uniformity, dissolution, disintegration, and weight variation. In USP XVIII and NF XIII, the sample size for the final stage of the sequential tests for content uniformity, dissolution time, and disintegration time and for the nonsequential test for weight variation was uniquely determined by the description of the test. However, in the General Notices of USP XIX (1) and NF XIV (2), the following sentences have been inserted under the heading "Procedures":

> *"In the performance of assay or test procedures, not less than the specified number of dosage units should be taken for analysis."*

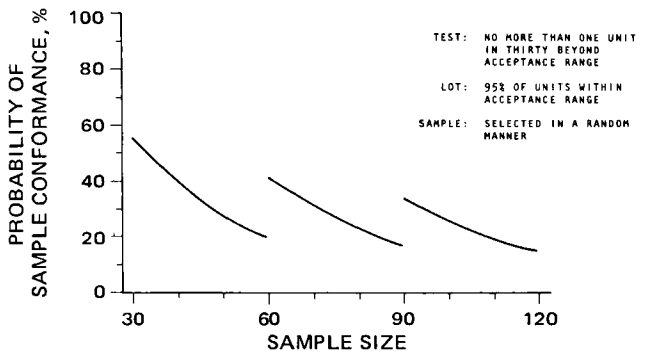

Figure 1—*Example of the effect of sample size on the content uniformity test.*

and:

> *"Where it is directed in an assay or a test that a counted number of dosage units is to be examined, the specified number is a minimal figure chosen only for convenience of analytical manipulation; it is not intended to restrict the total number of units that may be subjected to the assay or test. Regardless of the number of units so examined, the article meets the requirements if the same proportion of units conforms as is stated in the assay or single-stage test, or at the conclusion of a multiple-stage test."*

The employment of sample sizes greater than those stipulated in the monograph increases the discriminatory ability of the acceptance tests and provides a "cushion" in the event that some unit assays are not completed. However, the probability of drawing an unsatisfactory sample is a function of sample size. For example, consider the application of the compendial test for content uniformity to a randomly mixed lot with 5% of the units beyond the acceptance range.

The probability of sample conformance is 0.55, 0.42, 0.34, and 0.28 for samples of 30, 60, 90, and 120 units, respectively (Fig. 1). The lower probability of conformance of a sample of, for example, 59 units as compared to one of 60 units is due to the discrete nature of the dosage units. Only one nonconforming unit in a sample of 59 is acceptable, whereas two are acceptable in a sample of 60. Different, but similar, saw-toothed curves would be obtained for other percentages of units beyond the acceptance range. (For values less than 3.33%, the probability of sample conformance approaches 100% for increasing sample size, whereas the probability approaches 0% for values greater than 3.33%.) A similar situation exists for the other three tests.

(1) "The United States Pharmacopeia," 19th rev., Mack Publishing Co., Easton, Pa., 1975, p. 4.

(2) "The National Formulary," 14th ed., Mack Publishing Co., Easton, Pa., 1975, p. 11.

Bruce Flann

Drug Research Laboratories
Health Protection Branch
Health and Welfare Canada
Ottawa, Canada K1A 0L2

Received October 2, 1975.
Accepted for publication November 5, 1975.

Starch Paste Granulations: Binder Dilution Effects on Granulations and Tablets

Keyphrases □ Starch paste granulations—effect of gelatin binder solution concentrations, tableting characteristics □ Granulations, starch paste—effect of gelatin binder solution concentrations, tableting characteristics □ Dosage forms—tablets, effect of gelatin binder solution concentrations on starch paste granulations and tableting characteristics

To the Editor:

It was reported previously that the dilution factor of a gelatin binder solution used in a fluidized-bed granulating process influenced the friability of the granules (1). Specifically, the more dilute binder solutions resulted in less friable granules. The present communication reports similar results with aqueous dilutions of starch paste and a conventional granulating process.

Starch paste has long been used as a tablet binder in the pharmaceutical industry, but the literature contains few references to studies of this use. Starch paste granulations usually result in faster disintegrating tablets than do many other binders (especially the gum type) and may be preferred for this reason. Despite its wide usage, the effect of starch paste preparation variables on granulation or tablet quality has received little attention. One variable is the viscosity or thickness of the paste. In some cases, starch paste may be made with the maximum amount of water that can be used without overwetting the granulation. In other cases, less water is used and additional water is added to the granulation after some massing, based on the operator's judgment.

The formulations shown in Table I were manufactured in a small planetary-type mixer to find whether dilution of the starch paste affects granulation or tableting characteristics.

The lactose and starch were dry mixed in the mixer bowl for 5 min. The amount of water used to make the paste was varied from a 4:1 to a 6:1 water to starch ratio. The total amount of water used in each experiment was kept constant by varying the amount of water added to the mass after the starch paste had been mixed with the lactose–starch mixture for 1 min. The starch paste was cooked to a temperature of 72 ± 1°, and the total massing time was kept at 5 min

Table I—Starch Paste Dilutions

	Experiment A	Experiment B	Experiment C
Lactose, g	860	860	860
Starch (in dry mix), g	47	47	47
Starch (in paste), g	26	26	26
Water (for paste), ml	100	130	160
Water (used to *qs*), ml	100	70	40

Table II—Percent Fines Formed by Attrition

Experiment	500 Revolutions	1000 Revolutions
A	8.4	11.0
B	5.6	7.1
C	3.4	4.5

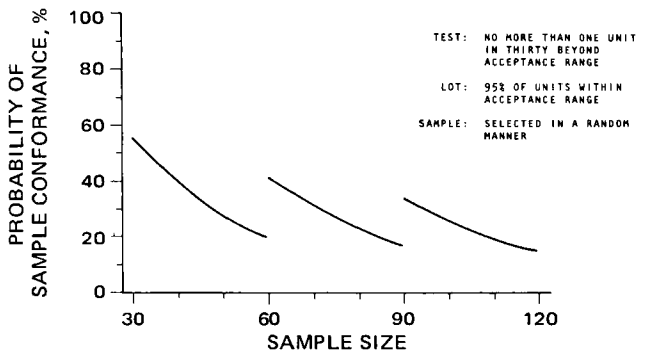

Figure 1—*Example of the effect of sample size on the content uniformity test.*

and:

> *"Where it is directed in an assay or a test that a counted number of dosage units is to be examined, the specified number is a minimal figure chosen only for convenience of analytical manipulation; it is not intended to restrict the total number of units that may be subjected to the assay or test. Regardless of the number of units so examined, the article meets the requirements if the same proportion of units conforms as is stated in the assay or single-stage test, or at the conclusion of a multiple-stage test."*

The employment of sample sizes greater than those stipulated in the monograph increases the discriminatory ability of the acceptance tests and provides a "cushion" in the event that some unit assays are not completed. However, the probability of drawing an unsatisfactory sample is a function of sample size. For example, consider the application of the compendial test for content uniformity to a randomly mixed lot with 5% of the units beyond the acceptance range.

The probability of sample conformance is 0.55, 0.42, 0.34, and 0.28 for samples of 30, 60, 90, and 120 units, respectively (Fig. 1). The lower probability of conformance of a sample of, for example, 59 units as compared to one of 60 units is due to the discrete nature of the dosage units. Only one nonconforming unit in a sample of 59 is acceptable, whereas two are acceptable in a sample of 60. Different, but similar, saw-toothed curves would be obtained for other percentages of units beyond the acceptance range. (For values less than 3.33%, the probability of sample conformance approaches 100% for increasing sample size, whereas the probability approaches 0% for values greater than 3.33%.) A similar situation exists for the other three tests.

(1) "The United States Pharmacopeia," 19th rev., Mack Publishing Co., Easton, Pa., 1975, p. 4.

(2) "The National Formulary," 14th ed., Mack Publishing Co., Easton, Pa., 1975, p. 11.

Bruce Flann

Drug Research Laboratories
Health Protection Branch
Health and Welfare Canada
Ottawa, Canada K1A 0L2

Received October 2, 1975.
Accepted for publication November 5, 1975.

Starch Paste Granulations: Binder Dilution Effects on Granulations and Tablets

Keyphrases □ Starch paste granulations—effect of gelatin binder solution concentrations, tableting characteristics □ Granulations, starch paste—effect of gelatin binder solution concentrations, tableting characteristics □ Dosage forms—tablets, effect of gelatin binder solution concentrations on starch paste granulations and tableting characteristics

To the Editor:

It was reported previously that the dilution factor of a gelatin binder solution used in a fluidized-bed granulating process influenced the friability of the granules (1). Specifically, the more dilute binder solutions resulted in less friable granules. The present communication reports similar results with aqueous dilutions of starch paste and a conventional granulating process.

Starch paste has long been used as a tablet binder in the pharmaceutical industry, but the literature contains few references to studies of this use. Starch paste granulations usually result in faster disintegrating tablets than do many other binders (especially the gum type) and may be preferred for this reason. Despite its wide usage, the effect of starch paste preparation variables on granulation or tablet quality has received little attention. One variable is the viscosity or thickness of the paste. In some cases, starch paste may be made with the maximum amount of water that can be used without overwetting the granulation. In other cases, less water is used and additional water is added to the granulation after some massing, based on the operator's judgment.

The formulations shown in Table I were manufactured in a small planetary-type mixer to find whether dilution of the starch paste affects granulation or tableting characteristics.

The lactose and starch were dry mixed in the mixer bowl for 5 min. The amount of water used to make the paste was varied from a 4:1 to a 6:1 water to starch ratio. The total amount of water used in each experiment was kept constant by varying the amount of water added to the mass after the starch paste had been mixed with the lactose–starch mixture for 1 min. The starch paste was cooked to a temperature of 72 ± 1°, and the total massing time was kept at 5 min

Table I—Starch Paste Dilutions

	Experiment A	Experiment B	Experiment C
Lactose, g	860	860	860
Starch (in dry mix), g	47	47	47
Starch (in paste), g	26	26	26
Water (for paste), ml	100	130	160
Water (used to *qs*), ml	100	70	40

Table II—Percent Fines Formed by Attrition

Experiment	500 Revolutions	1000 Revolutions
A	8.4	11.0
B	5.6	7.1
C	3.4	4.5

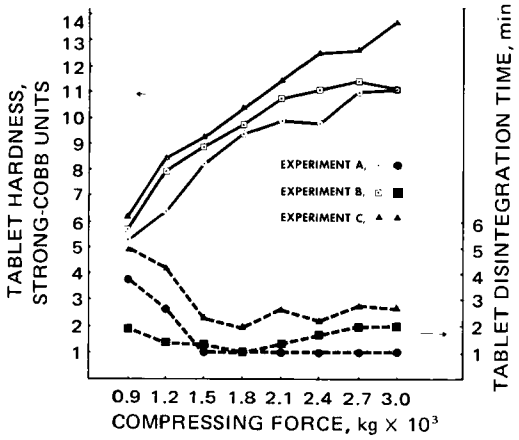

Figure 1—*Tablet hardness–pressure profile and corresponding disintegration times. Key: ⊙—⊙, tablet hardness; and ● - - ●, disintegration time.*

in each experiment to eliminate these variables. The wet mass was put through a 6-mesh screen, dried at 50° to a moisture content of 1%, and then passed through a 16-mesh screen.

Granulation friability was chosen as a measure of granulation quality. Friability was measured by tumbling 25 g of granulation larger than 150 mesh end over end in a Plexiglas cylinder, 3.81 cm in diameter and 30.48 cm long. The powder finer than 150 mesh generated by the tumbling was sifted off and weighed after 500 and 1000 revolutions and is shown in Table II as the percent of fines formed. The thinnest starch paste (C) yielded the strongest granulation and the thickest paste (A) yielded the most friable granulation, even though the same total amount of water was used in all three experiments. A sieve analysis showed that the percentage of particles coarser than 20 mesh also increased as the starch paste was made more dilute (Table III). This finding agrees with that of Marks and Sciarra (2) who concluded that the degree of granule friability decreased as the size of the granule increased.

Table III—Sieve Analyses

Experiment	Percent Remaining on 20 Mesh	40 Mesh	60 Mesh	100 Mesh	150 Mesh	Pan
A	21.3	40.6	17.3	9.6	10.7	0.5
B	28.9	41.6	13.2	7.1	6.6	2.5
C	30.7	40.7	12.1	7.0	5.5	4.0

The three granulations were lubricated with talc and magnesium stearate and compressed on an instrumented rotary tablet machine[1] at eight different compressing forces to obtain a pressure–hardness profile. This experiment showed that granulation compressibility improved with increasing starch paste dilution (Fig. 1). Tablet disintegration time was determined in the USP tablet disintegration apparatus using 37° water without disks (Fig. 1). The average disintegration time of six tablets was used. Disintegration time increased slightly with each dilution of the starch paste.

These data illuminate the influence of a seemingly inconsequential detail, the dilution factor of starch paste binder. Changes in starch paste thickness ordinarily may not have an adverse effect on tablet production, except for certain products that have rigid hardness or disintegration time specifications.

(1) W. L. Davies and W. T. Gloor, Jr., *J. Pharm. Sci.*, **62**, 170(1973).

(2) A. M. Marks and J. J. Sciarra, *ibid.*, **57**, 497(1968).

Philip M. Hill

Tablet Products Research and Development
Pharmaceutical Products Division
Abbott Laboratories
North Chicago, IL 60064

Received August 18, 1975.
Accepted for publication November 19, 1975.

[1] Stokes model B-2.

Journal of Pharmaceutical Sciences

MARCH 1976

VOLUME 65 NUMBER 3

MARY H. FERGUSON
Editor

L. LUAN CORRIGAN
Assistant Editor

SHELLY ELLIOTT
Production Editor

JANET D. SHOFF
Copy Editor

EDWARD G. FELDMANN
Contributing Editor

SAMUEL W. GOLDSTEIN
Contributing Editor

LELAND J. ARNEY
Publications Director

EDITORIAL ADVISORY BOARD

JOHN AUTIAN	HARRY B. KOSTENBAUDER
LYNN R. BRADY	CARL J. LINTNER, JR.
WILLIAM O. FOYE	DAVID E. MANN, JR.
WILLIAM J. JUSKO	GERALD J. PAPARIELLO

The *Journal of Pharmaceutical Sciences* is published monthly by the American Pharmaceutical Association at 2215 Constitution Ave., N.W., Washington, DC 20037. Second-class postage paid at Washington, D.C., and at additional mailing office.

All expressions of opinion and statements of supposed fact appearing in articles or editorials carried in this journal are published on the authority of the writer over whose name they appear and are not to be regarded as necessarily expressing the policies or views of the American Pharmaceutical Association.

Offices—Editorial, Advertising, and Subscription Offices: 2215 Constitution Ave., N.W., Washington, DC 20037. Printing Offices: 20th & Northampton Streets, Easton, PA 18042

Annual Subscriptions—United States and foreign, industrial and government institutions $50, educational institutions $50, individuals *for personal use only* $30; single copies $5. All foreign subscriptions add $5 for postage. Subscription rates are subject to change without notice. Members of the American Pharmaceutical Association may elect to receive the *Journal of Pharmaceutical Sciences* as a part of their annual $60 (foreign $65) APhA membership dues.

Claims—Missing numbers will not be supplied if dues or subscriptions are in arrears for more than 60 days or if claims are received more than 60 days after the date of the issue, or if loss was due to failure to give notice of change of address. The Association cannot accept responsibility for foreign delivery when its records indicate shipment has been made.

Change of Address—Members and subscribers should notify at once both the Post Office and the American Pharmaceutical Association, 2215 Constitution Ave., N.W., Washington, DC 20037, of any change of address.

© Copyright 1976, American Pharmaceutical Association, 2215 Constitution Ave., N.W., Washington, DC 20037; all rights reserved.

THE SUM OF ITS PARTS

Mitosis, or cell division to form two daughter cells, constitutes one of the most basic and elementary of life processes. From time to time a comparable phenomenon is encountered in other aspects of life and society, including that peculiar organizational structure called "government" that man has established for the purpose of providing an orderly system for the operation of society.

A primary feature of legislation recently introduced in the U.S. Senate under the co-sponsorship of Senators Kennedy and Javits would have the net effect of mitosis on what is now the federal Food and Drug Administration. The pertinent bills would create a Drug and Devices Administration and a Food and Cosmetic Administration. Each would be staffed, budgeted, operated, and administered completely independently of the other, in contrast to the present arrangement whereby all of these functions and responsibility fall within the purview of the FDA under the sole direction of the Commissioner of Food and Drugs.

Much can be said in favor of such a split:

(*a*) Smaller specialized agencies are more responsive and can be mobilized faster and more effectively;
(*b*) Narrowed responsibilities would enable greater concentration of attention and enhance the focusing of available resources;
(*c*) Foods and drugs are quite different commodities, having entirely different purposes and presenting basically different problems;
(*d*) The technical and scientific programs for surveillance of foods and of drugs have very little in common so that testing facilities and personnel have limited interchangeability; and
(*e*) Separate allocation of budget, manpower, and other resources would clarify the commitment actually made to each area, thereby facilitating administrative review and congressional oversight in terms of expended costs *versus* achieved results.

But by the same token, much also can be said in favor of a single unified agency:

(*a*) A single large agency has more visibility and political clout than several fragmented smaller ones;
(*b*) Internal communications are more simple, direct, and prompt within a single agency than between dual agencies;
(*c*) Despite their obvious differences, foods and drugs do have definite areas of overlap, calling for a unified, comprehensive approach—for example, drugs in animal feeds and vitamin products of various potencies;
(*d*) In the event of major emergencies, such as the botulism incident, even specialized inspectors can contribute valuable, alternate duty in a relatively unfamiliar area of activity; and
(*e*) Destructive interagency rivalries and competition for limited funds are eliminated while flexibility of resource allocation is at least possible, even though applicable opportunities may be relatively limited.

Hence, the proposal that FDA undergo karyokinesis is a complex matter requiring considerable analysis before a judgment can be rendered to the effect that it would be either beneficial or detrimental. Basically, the determination must come down to an assessment of whether in this case the whole is greater than, or less than, the sum of its component parts.

In announcing their joint bill, Senators Kennedy and Javits stated that they would be soliciting advice, recommendations, and opinions from a wide variety of sources before proceeding further with their proposal. They are to be commended for this attitude because it is evident that not only is the preferred route not yet clear but also that the decision eventually made will have a major impact on the public health and welfare. We add our sincere hope that the ultimate outcome will prove both successful and beneficial to all concerned.

—EGF

Journal of Pharmaceutical Sciences

MARCH 1976

VOLUME 65 NUMBER 3

MARY H. FERGUSON
Editor

L. LUAN CORRIGAN
Assistant Editor

SHELLY ELLIOTT
Production Editor

JANET D. SHOFF
Copy Editor

EDWARD G. FELDMANN
Contributing Editor

SAMUEL W. GOLDSTEIN
Contributing Editor

LELAND J. ARNEY
Publications Director

EDITORIAL ADVISORY BOARD

JOHN AUTIAN	HARRY B. KOSTENBAUDER
LYNN R. BRADY	CARL J. LINTNER, JR.
WILLIAM O. FOYE	DAVID E. MANN, JR.
WILLIAM J. JUSKO	GERALD J. PAPARIELLO

The *Journal of Pharmaceutical Sciences* is published monthly by the American Pharmaceutical Association at 2215 Constitution Ave., N.W., Washington, DC 20037. Second-class postage paid at Washington, D.C., and at additional mailing office.

All expressions of opinion and statements of supposed fact appearing in articles or editorials carried in this journal are published on the authority of the writer over whose name they appear and are not to be regarded as necessarily expressing the policies or views of the American Pharmaceutical Association.

Offices—Editorial, Advertising, and Subscription Offices: 2215 Constitution Ave., N.W., Washington, DC 20037. Printing Offices: 20th & Northampton Streets, Easton, PA 18042

Annual Subscriptions—United States and foreign, industrial and government institutions $50, educational institutions $50, individuals *for personal use only* $30; single copies $5. All foreign subscriptions add $5 for postage. Subscription rates are subject to change without notice. Members of the American Pharmaceutical Association may elect to receive the *Journal of Pharmaceutical Sciences* as a part of their annual $60 (foreign $65) APhA membership dues.

Claims—Missing numbers will not be supplied if dues or subscriptions are in arrears for more than 60 days or if claims are received more than 60 days after the date of the issue, or if loss was due to failure to give notice of change of address. The Association cannot accept responsibility for foreign delivery when its records indicate shipment has been made.

Change of Address—Members and subscribers should notify at once both the Post Office and the American Pharmaceutical Association, 2215 Constitution Ave., N.W., Washington, DC 20037, of any change of address.

© Copyright 1976, American Pharmaceutical Association, 2215 Constitution Ave., N.W., Washington, DC 20037; all rights reserved.

THE SUM OF ITS PARTS

Mitosis, or cell division to form two daughter cells, constitutes one of the most basic and elementary of life processes. From time to time a comparable phenomenon is encountered in other aspects of life and society, including that peculiar organizational structure called "government" that man has established for the purpose of providing an orderly system for the operation of society.

A primary feature of legislation recently introduced in the U.S. Senate under the co-sponsorship of Senators Kennedy and Javits would have the net effect of mitosis on what is now the federal Food and Drug Administration. The pertinent bills would create a Drug and Devices Administration and a Food and Cosmetic Administration. Each would be staffed, budgeted, operated, and administered completely independently of the other, in contrast to the present arrangement whereby all of these functions and responsibility fall within the purview of the FDA under the sole direction of the Commissioner of Food and Drugs.

Much can be said in favor of such a split:

(*a*) Smaller specialized agencies are more responsive and can be mobilized faster and more effectively;
(*b*) Narrowed responsibilities would enable greater concentration of attention and enhance the focusing of available resources;
(*c*) Foods and drugs are quite different commodities, having entirely different purposes and presenting basically different problems;
(*d*) The technical and scientific programs for surveillance of foods and of drugs have very little in common so that testing facilities and personnel have limited interchangeability; and
(*e*) Separate allocation of budget, manpower, and other resources would clarify the commitment actually made to each area, thereby facilitating administrative review and congressional oversight in terms of expended costs *versus* achieved results.

But by the same token, much also can be said in favor of a single unified agency:

(*a*) A single large agency has more visibility and political clout than several fragmented smaller ones;
(*b*) Internal communications are more simple, direct, and prompt within a single agency than between dual agencies;
(*c*) Despite their obvious differences, foods and drugs do have definite areas of overlap, calling for a unified, comprehensive approach—for example, drugs in animal feeds and vitamin products of various potencies;
(*d*) In the event of major emergencies, such as the botulism incident, even specialized inspectors can contribute valuable, alternate duty in a relatively unfamiliar area of activity; and
(*e*) Destructive interagency rivalries and competition for limited funds are eliminated while flexibility of resource allocation is at least possible, even though applicable opportunities may be relatively limited.

Hence, the proposal that FDA undergo karyokinesis is a complex matter requiring considerable analysis before a judgment can be rendered to the effect that it would be either beneficial or detrimental. Basically, the determination must come down to an assessment of whether in this case the whole is greater than, or less than, the sum of its component parts.

In announcing their joint bill, Senators Kennedy and Javits stated that they would be soliciting advice, recommendations, and opinions from a wide variety of sources before proceeding further with their proposal. They are to be commended for this attitude because it is evident that not only is the preferred route not yet clear but also that the decision eventually made will have a major impact on the public health and welfare. We add our sincere hope that the ultimate outcome will prove both successful and beneficial to all concerned.

—EGF

Journal of Pharmaceutical Sciences

MARCH 1976
VOLUME 65 NUMBER 3

REVIEW ARTICLE

Platinum Complexes: A New Class of Antineoplastic Agents

FRANCIS K. V. LEH and WALTER WOLF ˣ

Keyphrases □ Platinum complexes—antineoplastic activity related to chemical structure, biological and toxicological effects, methods of preparation, mechanism of action, pharmacokinetics, review □ Complexes, platinum—antineoplastic activity related to chemical structure, biological and toxicological effects, methods of preparation, mechanism of action, pharmacokinetics, review □ Antineoplastic agents—platinum complexes, activity related to chemical structure, review □ Structure-activity relationships—platinum complexes, antineoplastic activity, review □ Pharmacokinetics—platinum complexes, distribution, retention, and excretion, review □ Toxicity—platinum complexes, effects in various animals, review □ Radioplatinum compounds—labeling, distribution, use, review

The potential of platinum compounds as a new class of antitumor agents was discussed in 1965 (1). Their antineoplastic activity has been demonstrated in many animal tumor-screening systems. Sarcoma 180, L-1210 leukemia, Dunning ascitic leukemia, Walker 256 carcinosarcoma, dimethylbenzanthracine (DMBA)-mammary tumors, and ascitic B-16 melanosarcoma are inhibited by these compounds. *cis*-Dichlorodiammineplatinum(II) (I) is the agent that has been studied most; as NSC-119875, it has been tested clinically in patients (2, 3). The preliminary results of a Phase I clinical trial of the National Cancer Institute (2, 4–8) are encouraging and indicate that tumor growth is inhibited in humans. These preliminary studies intensified the search for related platinum(II) compounds with better antitumor activity.

A large number of platinum complexes have been prepared and tested for their ability to cause regression of tumor cells. Their activities depend on the chemical structures of the complexes. As most such agents at chemotherapeutic dose, they are quite toxic. Therefore, assessments of their biological and toxicological effects are important. This paper reviews our present knowledge of these antineoplastic platinum compounds.

NATURE OF ANTITUMOR PLATINUM COMPOUNDS

The ability of certain platinum coordination compounds to cause regression of tumor cells depends on the chemical structures of the complexes. These active complexes can be represented as:

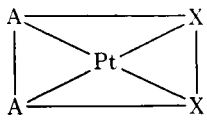

where A is the carrier ligand(s) [usually amines, either monodentate (NH_3) or bidentate ($NH_2CH_2CH_2NH_2$)], and X is the anionic leaving group(s) [either monodentate (Cl^-) or bidentate ($-OOCCH_2COO^-$)]. Among these complexes, certain common features appear to be required for antitumor activity.

Nature of Metal Ion—The central metal cation must be at a low oxidation state. Such a restriction is apparent in the system of platinum coordination compounds, since most active platinum compounds are square planar platinum(II). In bivalent platinum compounds, the special inertness of the platinum–ligand bond may be the key to the unique activity of platinum(II) complexes as antitumor drugs (9).

Geometry—The platinum(II) complexes have two isomers according to their geometric arrangement.

Table I—Activity of *cis*- and *trans*-$[PtA_2X_2]$

Complex	Solvent[a]	Dose Range[b], mg/kg	Dose Response[c]	Toxic Level[d], mg/kg	T/C[e]	Dose, mg/kg	Reference
cis-$[Pt(NH_3)_2Cl_2]$	S	0.5–20	+	9	1	8	11, 14, 48, 50, 92
trans-$[Pt(NH_3)_2Cl_2]$	S	2.5–40	—	740	83	2.5–40	11, 14, 48, 50, 87
cis-$[Pt(NH_3)_2Br_2]$	B	5–20	+	15	30	14	11
trans-$[Pt(NH_3)_2Br_2]$	B	10–40	—	740	110	10–40	11
cis-$[Pt(CH_3NH_2)_2Cl_2]$	S	10–30	+	10–20	25	15	11, 14
trans-$[Pt(CH_3NH_2)_2Cl_2]$	S	5–100	—	25	101	5–20	11
cis-$[Pt(C_2H_5NH_2)_2Cl_2]$	S	5–50	+	45	14	40	11
trans-$[Pt(C_2H_5NH_2)_2Cl_2]$	SS	5–20	—	720	106	5–20	11
cis-$[Pt(C_6H_5N)_2Cl_2]$	SS	5–200	—	7200	91	50–200	11
trans-$[Pt(C_6H_5N)_2Cl_2]$	SS	5–40	—	740	116	5–40	11
cis-$[Pt(NH_3)_2(SCN)_2]$	S	5–100	—	250	70	20–35	11
trans-$[Pt(NH_3)_2(SCN)_2]$	SS	20–80	—	780	73	20–80	11
trans-$[Pt(CH_2)_2NH]_2Cl_2]$			—				14, 87
trans-$[Pt(NH_2C_2H_4OH)_2Cl_2]$			—				87
trans-$[Pt(C_4H_9N)_2Cl_2]$			—				87
trans-$[Pt[(CH_3)_2SO]_2Cl_2]$			—				87
trans-$[Pt(C_6H_{11}NH_2)_2Cl_2]$			—				87

[a] S = saline, B = 0.04 *M* sodium bromide solution, and SS = slurry. [b] The dose range indicates the maximum and minimum doses administered. [c] The dose response is termed positive (+) for cases where a consistent decrease in tumor size is observed. [d] The toxic level is the highest dose at which survivors are equal to 90%. [e] The ratio of tumor weights of treated and control animals (T/C), expressed as a percentage, is a measure of the potency of the antitumor effect. The T/C values that are less than 50 are generally considered significant.

The *trans*-isomers are always inactive, whereas all active complexes found so far have the *cis*-configuration (Table I).

Nature of Leaving Group—The correlation between the nature of the leaving groups and their antitumor activity can be established from their rates of substitution. Kinetic studies (10) on the reaction $[Pt[H_2NCH_2CH(NH)CH_2NH_2]X]^+ + C_6H_5N \rightarrow [Pt[H_2NCH_2CH(NH)CH_2NH_2]C_6H_5N]^{+2} + X^-$ shows that the order of their rate of leaving for a series of X^- ligands is:

$$NO_3^- > H_2O > Cl^- > Br^- > I^- > N_3^- > SCN^- > NO_2^- > CN^-$$

highly toxic | active | inactive relatively nontoxic

This order reflects the change of activity in the animal test results (10) (Table II).

The complexes consisting of labile ligands such as nitrate ion hydrolyze rapidly, thus preventing a sufficient amount of the complex from reaching the site(s) responsible for antitumor activity (8). The hydrolysis produces the highly toxic diaquo species. On the other hand, ligands (*e.g.*, cyanide ion) that form strong bonds with platinum tend not to interact either rapidly enough or to a sufficient degree to elicit the antitumor response; complexes containing such ligands thus are expected to be inactive (11–13). The most active complexes contain either chloride, bromide, oxalate, or malonate ligands (11) (Tables III–V).

Nature of Carrier Ligand—The carrier ligand A may affect the activity of the complexes due to their difference in basicities and steric and electronic properties. In general, chemotherapeutic activity of *N*-donor atom ligands (Tables I–IV, VI, and VII) decreases along the series: $NH_3 < RNH_2 > R_2NH > R_3N$. The increase in the size of R and the substitution of the hydrogen atom by alkyl or other functional groups similarly decrease activity. As R becomes larger and more hydrophobic, the complex may become less soluble and so less effective (10).

The hydrogen bonding interactions between the amine ligands and biological receptors is believed to be important in stabilizing the receptor–drug complex. A decrease in the strength of hydrogen bonding could be related to the decrease in the activity of alkyl substitution in ammonia and ethylenediamine complexes (11). It has also been noted that toxicity is unrelated to antitumor action; substitution of the hydrogen atom by an alkyl group decreases activity but has virtually no effect in toxicity (11, 14).

The carrier ligands A found so far that are capable of producing active complexes are ammonia (I–III), ethyleneimine (IV), pyrrolidine (V), alicyclic amines (VI), cyclohexane-*trans*-1,2-diamine (VII), and *o*-phenylenediamine (VIII).

A group of pyrimidines and substituted pyrimidines constitute another series of active complexes (Table VIII). They exhibit a deep-blue color and are called generically "platinum blues," but their structures are unknown (15, 16).

Little work has been reported on carrier ligands with phosphorus, oxygen, and sulfur donor atoms

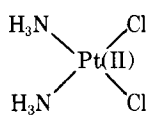

$[Pt(NH_3)_2Cl_2]$

cis-dichlorodiammine-platinum(II)
I

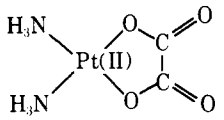

$[Pt(NH_3)_2(C_2O_4)]$

cis-oxalatodiammine-platinum(II)
II

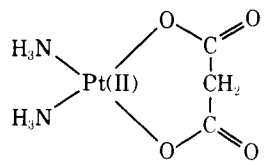

$[Pt(NH_3)_2(H_2C_3O_4)]$

cis-malonatodiammine-platinum(II)
III

Table II—Changes in Activity on Varying X in *cis*-[PtA_2X_2]

A	X	Solvent[a]	Dose Range[b], mg/kg	Dose Response[c]	Toxic Level[d], mg/kg	T/C[e]	Dose, mg/kg	Reference
NH_3	NO_3^-	W	6–12	—	7[f]	54	6	11
NH_3	NO_3^-	S	2.5–12	+	11	8	10	11
NH_3	H_2O	W	2–20	—	5[f]			11
NH_3	Cl^-	S	0.5–20	+	9	1	8	11, 87
NH_3	Br^-	B	5–20	+	15	30	14	11
NH_3	Br^-	S	10–25	+	15	30	15	11
NH_3	Br^-	S	2–6	+	5–6	13	5	11
NH_3	I^-	WS	10–25	—	725	110	10–25	11
NH_3	SCN^-	S	5–100	—	~50	70	20–85	11
NH_3	NO	SS	5–100	—	>100	99	5–100	11
CH_3NH_2	Br^-	B	5–40	±	20–40	60	~20	11
	I^-	W	10–80	—	780	~87	10–40	11
$(CH_3)_2NH$	Br^-	BS	10–120	+	>120	~65	10–80	11
	I^-	WS	5–30	±	30	~77	5–30	11
$(CH_3)_2NH$	Br^-	BS	10–120	+	>120	~65	10–80	11
$(CH_3)_2NH$	I^-	WS	5–30	±	>30	~77	5–30	11
$C_2H_5NH_2$	Br^-	BS	20–80	—	>80	~75	20–80	11
$HOC_2H_4NH_2$	I^-	W	5–150	+	~125	~40	60–100	11
$(C_2H_5)_2NH$	Cl^-	SS	15–60	—	>60	75	60	88
					ID_{90}	LD_{50}	TI	
Ethyleneimine	Cl	Oil	2.5–10	+	2.6	56.6[g]	21.7	14, 87
Cyclopropylamine	Cl	Oil	1.25–80	+	2.8	56.6	24.6	
Cyclohexylamine	Cl	Oil	10–1250	—	12.0		>267	14, 87
Cyclohexylmethylamine	Cl			+			2.6	88
Cyclopentylamine	Cl	Oil	12.5–400	+	2.4	565.5	235.7	14, 87
2-Aminomethyl-1-cyclopentylamine	Cl			+			40.7	88
Cyclobutylamine	Cl	Oil	0.25–128	+	2.9	90[g]	31.0	14, 87
Cycloheptylamine	Cl	Oil	5–625	—	18	625[g]	34.7	87
Isopropylamine	Cl	Oil	40	+	0.9	33.5	37.2	87
Isoamylamine	Cl	Oil	12–1500	—	>12	7125	>1500	87
2-Aminohexane	Cl	Oil	12–1500	—	>12	670	55	87
Acetonitrile	Cl			—	>27.0	>1.0	27.0	87
Benzonitrile	Cl			—	>90.0	>90.0	1.0	87
1-Aziridinoethanol	Cl			—				87
Di(ethylaminoethylchloro)	Cl			—				87
Methylamine	Cl			—				87
Hexamethyleneimine	Cl			—				87
2,2′-Dichloro-*N*-methyldiethylamine	Cl			—				87
Piperidine	Cl			—				87
Cyclooctylamine	Cl			—				87
Pyridine	Cl			+	10.8	131	14.1	14, 87
N-Ethylaminopyrrolidine	Cl			+	10.8	131	14.1	14, 87
N-Ethylaminopyrrolidine	Cl			+			11.1	88
N-(2-Hydroxyethyl)-ethyleneimine	Cl			—	>90	90	1.0	14

[a] W = water, S = saline, B = 0.4 *M* sodium bromide solution, WS = water slurry, SS = slurry, and BS = sodium bromide slurry. [b–e] See footnotes in Table I. [f] Highly toxic—convulsions. [g] Only 50% survivors.

(9–11, 17). The data for these complexes are listed in Table IX, with only the triphenylphosphine complex showing a marginal response. Other complexes have not shown any significant activity as antitumor agents.

Electronic Charge—Only neutral platinum(II) complexes are known to possess antitumor activity. The charged complexes have shown no antitumor activity (18, 19) (Table X). This phenomenon may be connected with the problem of drug transport through cell membranes. The neutral species pass through the cell membranes more easily than do

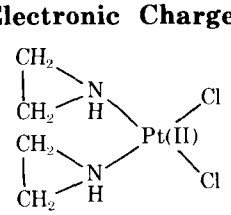

$[Pt((CH_2)_2NH)_2Cl_2]$
cis-dichlorobis(ethyleneimine)-platinum(II)
IV

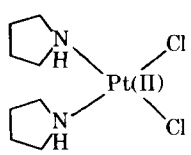

$[Pt((CH_2)_4NH)_2Cl_2]$
cis-dichlorobis(pyrrolidine)-platinum(II)
V

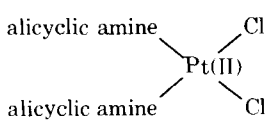

alicyclic amines=
cyclopropylamine, cyclobutylamine, cyclopentylamine, and cyclohexylamine

[Pt(alicyclic amine)$_2$Cl$_2$]
cis-dichlorobis(alicyclic amine)platinum(II)
VI

Table III—Changes in Activity on Varying X in *cis*-[$PtAX_2$]

A	X	Solvent[a]	Dose Range[b], mg/kg	Dose Response[c]	ID	TI	LD	Reference
DL-Cyclohexane-*trans*-1,2-diamine	Cl	Oil	0.3–40	+	2.1	6.9	14.1	14, 81, 89
4,5-Dimethyl-*o*-phenylenediamine	Cl	Oil		±				
2-Aminomethyl-1-cyclopentylamine	Cl	Oil	20	+	0.59	40.7	24	87
Ethionine	Cl			—	>41.0	>1.0	41.0	14, 87
Methionine	Cl			—	>300	>1.0	>300	14, 87
Cysteamine	Cl			—				87
2-Thia-4-aminobutane	I			—				87
2-Thia-4-aminobutane	Cl			—				87
Proline	Cl			—				87
2-Chloroethylamine	Cl			±	17.5	2.6	45.0	87
Edetic acid	Cl			—				87
2-Pipecoline	Cl			—				87
4-Pipecoline	Cl			—				87
Morpholine	Cl			—	>18.0	>1.0	18.0[f]	14, 87
Ethylenediamine-*N,N'*-diacetic acid	Cl			—				87
Benzimidazole	Cl			—	>9.0	>1.0	9.0[f]	14, 87
N-Ethylaminomorpholine	Cl			—				87
2-Aminoethylpyridine	Cl			—				87
1,4-Diazocyclo[2.2.2]octane	Cl			—				87
L-*N*-β-Diethylaminoethylaziridine	Cl			—				87
o-Phenylenediamine	Cl			+	2.35	20.4	48	87
					Toxic Level[d], mg/kg	T/C[e]	Dose, mg/kg	
N,N'-Dimethylethylenediamine	Br^-	BS	25–100	—	>100	83	25–100	11
	I^-	WS	25–100	—	>100	128	25–100	11
N,N-Dimethylethylenediamine	Br^-	B	20–120	±	100	49	80–90	11
N,N'-Diethylethylenediamine	Br^-	B	5–100	—	>100	75	10–100	11
N,N,N',N'-Tetramethylethylenediamine	Br^-	BS	10–80	—	>80	65	10–80	11
	I^-	WS	10–80	—	>80	100	10–80	11
	H_2O	W	2–16	±	5	25	4	11
	Cl^-	S	2.5–32	+	14	27	12	11
	Cl^-	S	1–10[g]	+	6	4	5	11
	Br^-	S	8–16	+	>16	71	16	11
	I^-	SS	5–40	—	>40	82	5–40	11
	SCN^-	W	10–40	—	>40	83	10–40	11
	NO_2	SS	14–100	—	>100	71	75–100	11

[a] BS = sodium bromide slurry, WS = water slurry, B = 0.04 *M* sodium bromide solution, W = water, S = saline, and SS = slurry. [b–e] See footnotes in Table I. [f] Only 50% survivors. [g] Daily injection for 9 days.

charged species. However, no definitive data on rate of membrane transfer are available.

In summary, to synthesize platinum complexes possessing antitumor activity, the following requirements are important: (*a*) the complexes must be neutral, (*b*) the central metal atom should be at the platinum(II) oxidation state, (*c*) the complex should contain a pair of *cis*-leaving groups of intermediate lability, (*d*) the complex should contain relatively inert carrier ligands, and (*e*) the complex should have good solubility and excretion rates to meet pharmacological and pharmacokinetic requirements.

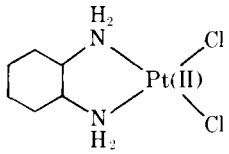

[$Pt(C_6H_{10}(NH_2)_2)Cl_2$]
cis-dichloro(cyclohexane-*trans*-1,2-diamine)-platinum(II)

VII

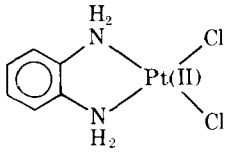

[$Pt(C_6H_4(NH_2)_2)Cl_2$]
cis-dichloro(*o*-phenylenediamine)platinum(II)

VIII

METHODS OF PREPARATION

The general methods for preparation of platinum compounds of the type *cis*-[PtA_2X_2] can be summarized in four classes:

1. Direct reaction of dipotassiumtetrachloroplatinum(II) with carrier ligand A. Because platinum belongs to a class of metals that are soft acceptors, whereas chloride ion is a fairly hard donor, this constitutes a weak metal–ligand bond (10). The chloride ion can be easily replaced by soft donors A to form new complexes (11, 14). This reaction may lead to the formation of either *cis*- or *trans*-products, depending on the *trans*-effect of the ligands. The approximate order of the decreasing *trans*-effect has been estimated as:

$$CO, CN^-, C_2H_4 > PR_3, H > CH_3, SC(NH_2)_2 > C_6H_5^-$$
$$NO_2^-, I^-, SCN^- > Br^-, Cl^- > Py, NH_3, OH^-, H_2O$$

If the *trans*-directing influence of the chloride ion is greater than that of A, *e.g.*, amines, then ligand A will enter the *trans*-position to chloride to give a *cis*-isomer (Scheme I).

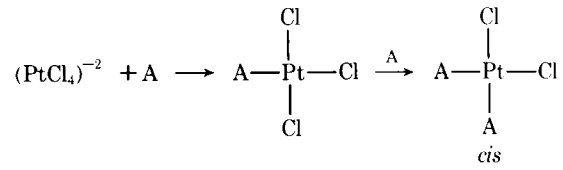

Scheme I

More often, the tetraiodoplatinumate ion is used in the synthesis of the desired *cis*-platinum(II) complexes because the iodide ion has a greater *trans*-effect than the chloride ion.

2. Indirect reaction, *via* the intermediate dipotassiumtetraiodoplatinum(II), which can be prepared quantitatively by the reaction of dipotassiumtetrachloroplatinum(II) with potassium iodide (Scheme II). The iodo derivative is then converted to *cis*-(PtA_2I_2) when treated with ligand A (Scheme III). If a chloro derivative is desired, the iodo derivative can be converted to the diaquo complex by silver nitrate treatment (Scheme IV), from which the chloro product can be obtained readily with potassium chloride (Scheme V).

$$K_2(PtCl_4) + 4KI \longrightarrow K_2(PtI_4) + 4KCl$$

Scheme II

$$K_2(PtI_4) + 2A \longrightarrow cis\text{-}(PtA_2I_2) + 2KCl$$

Scheme III

$$cis\text{-}(PtA_2I_2) + 2AgNO_3 + 2H_2O \longrightarrow cis\text{-}[PtA_2(H_2O)_2]^{+2} + 2AgI + 2NO_3^-$$

Scheme IV

$$[PtA_2(H_2O)_2]^{+2} + 2KCl \longrightarrow cis\text{-}(PtA_2Cl_2) + 2K^+ + 2H_2O$$

Scheme V

This method has more general application due to its high yield and low ratio in the formation of by-products.

3. Reactions of *cis*-(PtA_2X_2) (X = Cl, I) with monodentate or bidentate anionic ligands Y to give the complexes of the type *cis*-(PtA_2Y_2) (Scheme VI).

$$cis\text{-}(PtA_2X_2) + 2Y^- \longrightarrow cis\text{-}(PtA_2Y_2) + 2X^-$$

Scheme VI

4. Exchange of ligand X in *cis*-(PtA_2X_2) *via* the diaquo species, which is formed when *cis*-(PtA_2Cl_2) is treated with silver nitrate (Scheme IV). The new complexes *cis*-(PtA_2X_2) are produced by addition of the appropriate anion X to the diaquo complex (Scheme VII).

$$cis\text{-}[PtA_2(H_2O)_2]^{+2} + 2X^- \longrightarrow cis\text{-}(PtA_2X_2) + 2H_2O$$

Scheme VII

Table V—Activity of Neutral Complexes of the Type [PtA_2]

Complex	Dose Response[a]	Reference
cis-[Pt(glycinate)$_2$]	—	87
trans-[Pt(glycinate)$_2$]	±	87
cis-[Pt(NH_3)$_2$(malonate)]	+	14
Pt(*N*-oxyethylethylene-*N,N,N*-triacetic acid)Cl	—	87

[a] The dose response is positive (+) for cases where a consistent decrease in tumor size is observed.

MECHANISM OF ACTION

The discovery of the action of platinum compounds on biological systems was first noted by observing their disruptive effect on growth processes in bacterial systems (1); cells did not divide but produced filamentous masses where individual cells of

Table IV—Changes in Activity on Varying X in *cis*-[PtA_2X]

A	X	Solvent[a]	Dose Range[b], mg/kg	Dose Response[c]	Toxic Level[d], mg/kg	T/C[e]	Dose, mg/kg	Reference
NH_3	Oxalate^{-2}	Dimethyl sulfoxide (slurry)	5–20	+	16–20	9	15	11
		WS	12–18	+	17	24	14–16	11
		W	10–20	+	~10	0	20	11
		W	0.5–6	+	3–4	25	25	11
NH_3	Malonate^{-2}	WS	10–60	+	~35	7	30	11, 87
		W	5–24	+	20–24	28	20–24	11
NH_3	Methylmalonate^{-2}	W	10–80	+	65	7	60	11
	Ethylmalonate^{-2}	W	30–80	+	>80	17	70–80	11
	1,1-Cyclobutanedicarboxylic acid^{-2}	W	20–160	+	~150	18	120	11
	Hydroxymalonate^{-2}	WS	10–40	±	>40	52	30–40	11
NH_3	Pyrophosphate^{-4}	WS	5–160	±	>160	70	5–160	11
CH_3NH_2	Oxalate^{-2}	W	5–80	+	20–30	21	30	11
	Malonate^{-2}	W	80–180	+	>180	~21	120–180	11
	Pyrophosphate^{-4}	W	20–80	—	40	68	40	11
C_2H_5NH	Oxalate^{-2}	W	10–80	±	~20–40	21	10	11
$CH_2(NH_2)CH(NH_2)CH_3$	Malonate^{-2}	W	45–90	+	65	9	60	11
$CH_2(NH_2)CH_2CH_2(NH)$	Malonate^{-2}	W	20–80	+	~90	28	60–80	11
1,2-$C_6H_{10}(NH_2)_2$	Malonate^{-2}	WS	50–200	±	~100	41	100	11
	Oxalate^{-2}	W	0.25–16	—	35	73	0.23–2	11
	Malonate^{-2}	W	5–80	+	45–60	18	40	11, 87
	Malonate^{-2}	S	45–60	±	>60	41	50–60	11
	Malonate^{-2}	S	5–20[f]	+	6–10	24	5	11
	Methylmalonate^{-2}	W	30–90	+	>90	4	90	11
	Ethylmalonate^{-2}	WS	40–120	±	>120	51	90–120	11

[a] WS = water slurry, W = water, and S = saline. [b–e] See footnotes in Table I. [f] Daily injection for 9 days.

Table VI—Changes in Activity on Varying A in *cis*-[PtA_2Cl_2] (A = Monodentate and N = Donor Atom)

A	Solvent[a]	Dose Range[b], mg/kg	Dose Response[c]	Toxic Level[d], mg/kg	T/C[e]	Dose, mg/kg	Reference
NH_3	S	4–10	+	9	3	8	11
ND_3	S	4–10	+	~9	17	~9	11
CH_3NH_2	S	10–30	+	12–20	14	14[f]	11, 14
$(CH_3)_2NH$	S	30–150	+	~100	25	80	11
$C_2H_5NH_2$	S	5–50	+	~40	14	40	11
	S	3–9	+	5–7	13	5	11
$(C_2H_5)_2NH$	SS	15–60	—	>60	75	60	11
$HOC_2H_4NH_2$	S	20–225	+	~125	22	125	11
$(CH_3)_2CHNH_2$	SS	20–50	±	>50	33	30	11
C_5H_5N	WS	5–40	—	>40	94	5	11, 18
3-HO_2C—C_5H_5N	W	4–80	±	>80	51	40–60	11
$C_6H_5NH_2$	SS	10–50	+	>50	33	10–20	11

[a] S = saline, SS = slurry, WS = water slurry, and W = water. [b–e] See footnotes in Table I. [f] Only 66% survivors.

Escherichia coli attained lengths up to 300 times those of normal cells. Subsequently, studies conducted using ^{191}Pt (20) to determine the distribution of some platinum complexes in *E. coli* after the induction of filaments suggested that there were two different modes of action. In the filamentous cells induced by action of *cis*-dichlorodiammineplatinum(II), the platinum(II) is associated with nucleic acid and cytoplasmic proteins (20). In cells inhibited by the tetrachloroplatinumate ion, the platinum(II) is associated only with the cytoplasmic protein. Furthermore, Gram-positive cells of *Bacillus cereus* and *Staphylococcus aureus* show no filamentous growth in the presence of *cis*-dichlorodiammineplatinum(II). This finding led Renshaw and Thomson (20) to suggest that after the metal complex penetrates the cell wall of these bacteria, it is metabolized (hydrolyzed?) to intermediates such as B, $[Pt(NH_3)_2Cl]^+$, and C, $[Pt(NH_3)_2]^{+2}$, where the starting material A, $[Pt(NH_3)_2Cl_2]$, is suggested as being substantially devoid of activity *per se* against the test system. Intermediate B inhibits synthesis of DNA, RNA, and protein; and C is highly selective toward inhibition of DNA synthesis and is devoid of activity against RNA and protein synthesis. This hypothesis attempts to correlate the antitumor action of *cis*-dichlorodiammineplatinum(II) with the rate of synthesis of DNA, RNA, and protein (2, 21). At 12–24 hr postinjection, both RNA and protein syntheses are gradually restored; they return to normal rates after 72–96 hr. The inhibition of DNA synthesis is persistent for several days after injection of *cis*-dichlorodiammineplatinum(II) (12).

Other hypotheses that could account for the delayed onset of inhibitory action are: (*a*) a slow rate of diffusion into the cell of these lipid-insoluble complexes through membrane pores, and (*b*) a platinum–membrane interaction, which is time dependent and which gradually increases the rate of diffusion of the compound into the cell (12).

Gale *et al.* (22) studied the inhibition of the syntheses of DNA, RNA, and protein by *cis*-dichloro(4,5-dimethyl-*o*-phenylenediamine-*N,N'*)platinum(II). Cellular DNA, RNA, and protein became more acid soluble upon incubation *in vitro* with this agent, leading Morris and Gale (23) to suggest that the most probable point of platinum–DNA association would be at the derepressed area of DNA undergoing RNA synthesis.

The rate of loss of viability of all suspensions incubated with *cis*-dichloro(4,5-dimethyl-*o*-phenylenediamine-*N,N'*)platinum(II) was considerably greater than the rate obtained upon incubation of cells with an equivalent concentration of *cis*-dichlorodiammineplatinum(II). More direct correlations are needed to verify if this proposed mechanism is really op-

Table VII—Changes in Activity on Varying A in *cis*-[$PtACl_2$] (A = Bidentate and N = Donor Atom)

A	Solvent[a]	Dose Range[b], mg/kg	Dose Response[c]	Toxic Level[d] mg/kg	T/C[e]	Dose, mg/kg	Reference
Ethylenediamine	S	2–32	+	16	27	12	11
N-Methylethylenediamine	S	7.5–20	±	10–15	51	15[f]	11
N,N-Dimethylethylenediamine	S	20–80	±	25–35	26	30	11
N,N-Dimethylethylenediamine	SS	25–100	—	75–100	60	25–75	11
N,N,N',N'-Tetramethylethylenediamine	SS	10–40	—	>40	64	20–40	11
N,N-Dimethyl-*N'*-ethylethylenediamine	SS	50–125	±	~120	62	100	11
N,N'-Diethylethylenediamine	SS	75–225	—	>225	96	75–225	11
N,N-Diethylethylenediamine	S	10–100	±	>100	54	75–100	11
1,2-Propylenediamine	SS	5–20	±	8–12	62	12[f]	11
1,3-Propylenediamine	SS	8–30	±	10–15	58	12[f]	11
1,2-Cyclohexanediamine	SS	10–30	±	20–35	62	15–30	11
1,2-Phenylenediamine	SS	20–80	—	>80	119	20–80	11, 14
1,2-Phenylenediamine	Oil	5–40	+				87
1,10-Phenanthroline	SS	10–30	—	~15	60	10	11, 87
1,10-Phenanthroline	SS	10–30	+	2.4	69	48.0	11, 87
Adenosine	SS	20–220	+	>220	32	160–220	11

[a] S = saline, and SS = slurry. [b–e] See footnotes in Table I. [f] Only 66% survivors.

Table VIII—Activity of "Platinum Blue" Complexes against Ascites Sarcoma 180 in Swiss Mice[a]

Compound	Solvent[b]	Dose Range[c], mg/kg	Toxic Level[d], mg/kg	Best Percent ILS[e]	Dose of Best Percent ILS[e], mg/kg	Physical State[f]	Number of Cures	Reference
cis-$[Pt(NH_3)_2(H_2O)_2]$ + "Amide" → Class IA and Class IB Complexes								
Class IAπ								
Uracil	W	50–400	400	91	200	S	5	90
Uracil	S	50–400	400	80	100	S	1	90
5,6-Dihydrouracil	W	20–800	400	92	200	S	4	90
Thymine	W	150–600	45	72	300	S	2	90
Thymine	S	50–200	>200	67	150	S	1	90
5,6-Dihydro-6-methyluracil	W	50–400	200	89	50	S	2	90
6-Methyluracil	S	200–800	>800	87	600	S	3	90
5,6-Dimethyluracil	W	50–400	>400	100	400	S	5	90
5,6-Dihydrothymine	S	50–400	400	87	200	S	2	90
1-Methyluracil	S	50–400	>400	85	400	S	3	90
1-Methylthymine	S	50–400	400	94	100	S	3	90
1-Ethyluracil	S	50–400	200	38	50	S	0	90
5-Fluorouracil	W	50–400	200	90	100	S	4	90
5-Chlorouracil	W	50–400	200	67	50	S	3	90
6-Chlorouracil	S	25–200	>200	88	200	S	3	90
5-Bromo-1-methyluracil	S	50–400	>400	88	200	S	1	90
5-Iodouracil	PO	25–600	500	8	250	S1	0	90
5-Hydroxymethyluracil	S	50–400	200	98	100	S	2	90
5-Carbethoxyuracil	S	25–200	200	56	200	S	0	90
6-Carbomethoxyuracil	S	25–200	>200	38	25	S	0	90
Uridine deoxyribose	S	25–200	>200	46	200	S	0	90
Thymidine	S	50–400	200	46	50	S	1	90
5-Iodouridine deoxyribose	PO	50–200	>200	23	200	S1	0	90
2′,3′,5′-Triacetyluridine	S	50–1000	800	79	600	S	2	90
2′,3′,5′-Tribenzoyluridine	S	50–400	>400	19	100, 200	S	0	90
2′,3′-Isopropylidine-uridine	S	50–400	400	61	50	S	2	90
Acetamide	S	25–200	25	−94	25	S	0	90
Trimethylacetamide	S	3.1–25	12.5	10	6	S	0	90
3-Chloropropionamide	S	3.1–25	>25	61	25	S	2	90
Benzamide	S	50–400	23	23	400	S1	0	90
Class IB								
Uracil	W	25–675	500	95	340	S	4	90
Thymine	S	50–400	>400	60	200	S	0	90
1-Methylthymine (yellow)	S	50–400	400	−14	100	S	0	90
1-Ethyluracil	S	50–400	100	15	50	S1	0	90
5-Fluorouracil	S	25–200	>200	37	200	S	0	90
Hydantoin	S	25–200	>200	60	50	S1	1	90
Benzamide	S	3.1–25	25	14	3.1, 6.2	S	0	90
Trimethylacetamide	S	3.1–25	3.1	−55	3.1	S	0	90
$[Pt(R-CN)_2Cl_2 + 2AgNO_3]$ or [Class III Complex + $2AgNO_3$] → Class IIA and Class IIB Complexes								
Class IIA								
Acetamide	W	100–400	>400	93	200	S	1	15
Fluoroacetamide	S	50–400	>400	94	400	S	0	15
Chloroacetamide	S	50–400	>400	96	400	S	1	15
Propionamide	2% C_2H_5OH	50–400	>400	89	200	S	2	15
n-Butyramide	S	50–400	>400	23	100	S1	0	15
Benzamide	S	50–400	>400	14	100	S1	0	15
Class IIB								
Acetamide	S	50–400	400	14	100	S1	0	15
$Pt(CH_3CN)_2Cl_2 + R-CO-NH_2$ → Class III Complexes								
Class III								
Acetamide (purple)	S	50–400	400	31	400	S	1	15
Acetamide (blue)[g]	S	50–200	200	76	150	S1	0	15
Acetamide (blue)	S	25–200	200	39	100	S	0	15
Fluoroacetamide	S	50–400	400	66	400	S1	0	15
Chloroacetamide	S	50–400	400	53	200	S	0	15
Trimethylacetamide	S	50–400	400	67	50	S	0	15
Acetamide (red)	S	6.3–400	100	91	25	S	2	15
Miscellaneous								
Dichlorobis(acetonitrile)-platinum(II)	S	6.3–50	50	83	25	S	1	15

[a] Average day of death, untreated controls = 17.5 (*SD* ± 2.16). Six animals per test; cures are considered as having *no* distention of abdominal cavity but do include formation of solid tumors at site of injection in some cases. Single injections given intraperitoneally on Day 1 only. [b] W = water, S = saline, and PO = peanut oil. [c] The dose range indicates the maximum and minimum doses administered. [d] The toxic level is the highest dose at which survivors are equal to 90%. [e] Percent ILS = percent increase in lifespan, with the maximum being 100%. [f] S = solution, and S1 = slurry. [g] Prepared by hydrolysis of dichlorobis(acetonitrile)platinum(II).

Table IX—Activity of Complexes of Type *cis*-$[PtL_2Cl_2]$[a]

L	Solvent	Dose Range[b], mg/kg	Dose Response[c]	Toxic Level[d], mg/kg	T/C[e]	Dose, mg/kg
Triphenylphosphine	Saline	25–100	±	100	53	25–100
	Saline–dimethyl sulfoxide	40–160	±	160	78	40–160
Dimethyl sulfoxide	Saline	6–12	—	12	86	6–12
Diethyl sulfide	Dimethyl sulfoxide	5–40	—	40	67	5–20
Glycinate	Saline	10–200	—	125–150	79	40–100

[a] Reference 11. [b–c] See footnotes in Table I.

erative.

The suppression of DNA synthesis in the rat kidney has also been suggested to proceed *via* direct interaction of platinum compounds with renal cell nucleic acid. By using ^{14}C-labeled dichloroethylenediamineplatinum(II), the effect of this drug upon DNA appeared to be mediated *via* the guanine, cytosine, and adenine bases (24–26). The change in UV absorption was measured, and a hyperchromic change was observed. This change was proposed to be due to a direct interaction of *cis*-dichlorodiammineplatinum(II) with some of the DNA bases (27). The binding of *cis*-dichlorodiammineplatinum(II) to DNA is markedly lowered when the concentration of chloride ion is increased.

Further studies on nucleosides showed that guanosine, adenosine, and cytidine interact with *cis*-dichlorodiammineplatinum(II), whereas uridine and thymidine show very little interaction (28, 29). Since the formation constants of platinum–guanosine complexes are the largest in magnitude (Table XI), guanosine in DNA may be the primary target for complexation. It was speculated that such a complex might result in partial denaturation of the DNA helix, which would open other sites on cytidine and adenosine for further interactions with *cis*-dichlorodiammineplatinum(II).

In the case of DNA-containing bacteriophage T, the inactiviation by *cis*-dichlorodiammineplatinum(II) is correlated to the interstrand cross-linking of neighboring bases on the same nucleic acid chain as well as to intrastrand cross-linking of nucleic acid (30) with platinum. The binding of *cis*-dichlorodiammineplatinum(II) to DNA can be estimated from the changes of buoyant density and sedimentation rates, which parallel the change in the conformation of the DNA molecule. An increase in sedimentation efficiency follows an increase in molecular weight and a decrease of partial specific volume (31).

The ready formation of platinum–nucleic acid bonds is probably the determinant in the inhibitory actions of platinum compounds on tumor growth and DNA synthesis. *cis*-Dichlorodipyridineplatinum(II) forms an acid-resistant bond when incubated with intact cells and DNA but does not bind appreciably with proteins, polysaccharides, or erythrocyte membranes. The last interaction with DNA is inhibited by sodium chloride and nitrogen mustard complexation (32), and this finding may indicate that the antitumor and antimitotic action of the square-planar platinum complex depends on the dissociation of one or both chlorine atoms from the central platinum atom.

cis-Dichlorodiammineplatinum(II) has two neighboring leaving chlorine groups and may act as a bifunctional agent, whereas *trans*-dichlorodiammineplatinum(II) probably behaves as a monofunctional agent. The study on the interaction of *cis*- and *trans*-dichlorodiammineplatinum(II) with purines, substituted purines, pyrimidines, and substituted pyrimidines shows that the *cis*-isomer forms a bidentate chelate with either 6-NH_2 and N-7 or 6-NH_2 and N-1 of adenosine and 4-NH and N-3 of cytidine. The

Table X—Activity of Miscellaneous Charged Complexes

Complex	Solvent[a]	Dose Range[b], mg/kg	Dose Response[c]	Toxic Level[d], mg/kg	T/C[e]	Dose, mg/kg	Reference
$K_2[PtCl_4]$	S	10–100	—	40–50	127	25	11
$K_2[PtBr_4]$	S	3.5–60	±	~45	73	15–30	11
$K_2[Pt(C_2O_4)_2]\cdot 2H_2O$	W	5–160	—	~40	91	10–40	11
$K_2[Pt(C_3H_2O_4)_2]\cdot 2H_2O$	W	20–250	±	>250	60	20–250	11
$K[Pt(C_2H_4)Cl_3]$	S	5–40	—	>40	122	5–40	11
$K[Pt(H_2NCH_2CO_2)Cl_2]$	S	10–200	—	125–150	79	40–100	11
$[Pt(NH_3)_4][Pt(NH_3)Cl_2]_2$	SS	20–80	+	~50	35	40	11
$K_2[Pt(NO_2)Cl_3]$	S	5–200	—	~75	81	50	11
$[Pt(NH_3)_4]Cl_2$	S	5–200	—	>200	100	5–200	11
$[Pt(H_2NCH_2CH_2NH_2)_2]Cl_2$	S	5–40	—	>40	90	5–40	11
$[Pt(H_2NCH_2CH(NH)CH_2NH_2)Cl]Cl$	S	10–100	—	>100	71	10–100	11
$[Pt(H_2NCH_2CH(NH)CH_2NH_2)Br]Br$	S	10–80	—	>80	93	10–80	11
$K[Pt(C_{12}H_8N_2\cdot H_2O\text{-}5\text{-}SO_3)Cl_2]$	S	5–40	—	>40	58	5–40	9
$[Pt[CH_3S(CH_2)_2CH(NH_2)CO_2H]_2]Cl_2$			—				87
$[Pt(CH_3SCH_2CH_2NH_2)_2][PtCl_4]$			—				87
$[Pt[H_2NCH_2CH_2NH(C_2H_4OH)]Ce]Cl$			—				87
$[Pt((CH_2)_2NH)_4][PtCl_4]$			—				87

[a] S = saline, W = water, and SS = slurry. [b–e] See footnotes in Table I.

Table XI—Formation Constant of the Stoichiometry of $[Pt(NH_3)_2Cl_2]$–Nucleoside Complexes[a]

Ligand L	$K_f(cis)$	$K_f(trans)$	Type of Complexes
Adenosine	0.24×10^5	0.64×10^5	PtL
Cytidine	0.66×10^5	—	$Pt^{II}L$
Guanosine	1.06×10^9	1.06×10^9	$Pt^{II}L_2$

[a] Reference 27.

trans-isomer interacts monofunctionally at either N-7 or N-1 of adenosine and at N-3 of cytidine; it does not bind to the free amino groups (33, 34). Both isomers bind monofunctionally to N-7 of guanosine and inosine but do not bind to uridine or thymidine.

In DNA, both adenosine and cytidine bases are the probable sites available for binding with *cis*-dichlorodiammineplatinum(II) (35). In the latter, the spacing between the two chlorine atoms is 3.3 Å (36), which is very close to the 3.4 Å of the stacking spacing of the bases in the Watson–Aich model (IX). It appears, therefore, that such platinum complexes could act like bifunctional alkylating agents to form interstrand and intrastrand cross-links (37). This assumption is supported by recent evidence that the platinum complexes inhibit a single-stranded bacteriophage as well as the double-stranded bacteriophage (38). Other evidence supporting interstrand cross-links are obtained from circular dichroism measurements (39) and from isolation of hybrid cross-link species of DNA and *cis*-dichlorodiammineplatinum(II) (40).

A different hypothesis relates the antitumor effect of platinum compounds with the stimulation of immune processes (41), since immunity plays an important role in the arrest of malignant diseases (42). In mice, studies on antibody formation (43), graft *versus* host reaction (44), and phytohemoagglutinin-induced lymphocyte blastogenesis (45) show that *cis*-dichlorodiammineplatinum(II) has strong immunosuppressive effect. This effect is more prominent when the drug is administered at the time of sensitization and is also effective within 2 days either before or after the sensitization and will last for 3 days after a single injection.

cis-Dichlorodiammineplatinum(II) suppresses antibody formation in cells after they have been exposed to the antigen. The diminished weight of spleen and suppression of antibody plaque-forming cells indicate that this drug has definite effects on the normal lymphoid tissue (43). *cis*-Dichlorodiammineplatinum(II) suppresses the graft *versus* host reaction but prolongs the survival of skin graft against the host's histocompatibility barrier during the initial phase of graft injection. A delay in the administration of the drug leads to abolition of the effect (46).

cis-Dichlorodiammineplatinum(II) not only affects the tumor cell but also affects the normal lymphocytes during their blastic transformation (45). In patients being treated with *cis*-dichlorodiammineplatinum(II), an immediate effect on the lymphocytes was observed, as evidenced by inhibition of blastogenesis 15 min following the administration of the drug in dose ranges from 1 to 4 mg/kg (47). The immunosuppressive effect lasted for 18–72 hr, a relatively short period compared to other immunosuppressive drugs. The short-lived immunosuppressive effect of *cis*-dichlorodiammineplatinum(II) may prove to be advantageous, because a rapid recovery of the immune system may help in the control of the malignant disease.

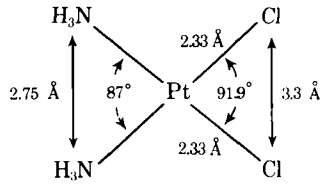

spacial structure of *cis*-dichlorodiammineplatinum(II)
IX

ANTITUMOR ACTIVITY

The platinum complexes studied have been shown to have activity against a wide range of animal tumors. Rosenberg *et al.* (48) first reported the inhibition of sarcoma 180 and L-1210 leukemia in mice by *cis*-dichlorodiammineplatinum(II). Some treated mice appeared normal and healthy and remained in remission for 10 months (37). The initial tumor transplant disappeared. *cis*-Dichlorodiammineplatinum(II) was also active in inhibiting and causing regression of large solid sarcoma 180 tumors in 63–100% of the animals with no apparent irreversible damage to the host (41). This compound is the first chemotherapeutic agent able to accomplish such complete regression and is superior to other agents, such as mercaptopurine, that have been used with sarcoma 180 tumors with approximately 50% recovery (49).

In the rat, *cis*-dichlorodiammineplatinum(II) had strong antileukemic effects on myeloid and lymphatic leukemias but no detectable effect on the normal cells of the marrow, gonads, and intestine (50). The effectiveness of *cis*-dichlorodiammineplatinum(II) against Dunning ascitic leukemia and intramuscular Walker 256 carcinosarcoma was reported (51). A single treatment with *cis*-dichlorodiammineplatinum-(II) on Day 1 inhibited the development of Dunning ascitic leukemia in Fisher 344 rats. Delayed treatment even on Day 7 can cause significant regression of tumor development and extend the survival time. *cis*-Dichloro(4,5 -dimethyl-*o*- phenylenediamine -*N*,-*N'*)platinum(II) exhibited the same effect as *cis*-dichlorodiammineplatinum(II). It extended up to 175% the survival time of mice bearing the Ehrlich ascitic tumor and up to 74% the survival time of mice bearing the L-1210 leukemia (22).

Two other types of tumors that are more relevant to the cancers occurring in humans are those caused by chemical agents (carcinogens) and by viruses. The platinum compounds are also capable of exhibiting antitumor activity against carcinogenically or virally induced tumor systems. The effectiveness of *cis*-dichlorodiammineplatinum(II) was reported in treating a virus-induced reticulum cell sarcoma and in pro-

Table XII—Effectiveness of Chemotherapeutic Agents in Mice with L-1210 Leukemia (93)

Tumor Site[a]	Drug	Treatment Schedule[b], days	Percent ILS[c]
ip	Doxorubicin (Adriamycin)	q3h/1	60
ip	Daunorubicin	1, 5, 9	20
ip	Camptothecin	1, 5, 9	112
sc	*cis*-Dichlorodiammine-platinum(II)	q3h/5, 9, 13	67
sc	Cytosine arabinoside	5, 7, 9, 11, 13	100
ip	Harringtonine	1–9	40
sc	5-Azacytidine	1, 5, 9	117
sc	Methotrexate	5, 9, 13	83
sc	Cyclophosphamide	5, 9, 13	279
sc	Isophosphamide	5, 13, 21	144

[a] ip = 10^5 L-1210 ascites cells inoculated intraperitoneally; sc = 10^6 L-1210 ascites cells inoculated subcutaneously. [b] Days of treatment after tumor inoculation; q3h = injections every 3 hr for 24 hr on 1 day only or on every 4th day. [c] Percent ILS = percent increase in lifespan.

moting regression of carcinogen-induced rat mammary tumors (52) and *cis*-dichlorodiammineplatinum(II) was studied against the dimethylbenzanthracene-induced mammary tumor (53). In the latter study, complete regression of a large number of extensively developed mammary tumors was observed in the rats, with three out of 14 animals completely "cured" of all tumors. The same compound was tested against the Rous sarcoma virus-induced tumor in the chicken (54). Again, regression of this tumor in 95% of the animals was seen after the treatment with *cis*-dichlorodiammineplatinum(II). The platinum compounds have one of the broadest spectra of action of any class of antitumor agents yet discovered. They cause regression of large tumors and rescue animals even injected a few days prior to their death.

The data in Table XII summarize the effectiveness of *cis*-dichlorodiammineplatinum(II) in mice with L-1210 leukemia in comparison with other drugs tested in this model system. This comparison only provides limited indication, since the percent increase of lifespan varies greatly with the test model chosen and the treatment schedule. To date, there is no precise way to compare the effectiveness of drugs by a single animal test system. It would be desirable to compare *cis*-dichlorodiammineplatinum(II) with chemotherapeutic agents in various tumor models.

Clinical trials on *cis*-dichlorodiammineplatinum(II) have been conducted in hospitals. Phase I studies on clinical toxicology (7, 13, 55) showed that renal toxicity was the most serious side effect, and damage was noted in the bone marrow and GI tract. Ototoxicity (initially high tone hearing loss and eventually deafness) also was described.

Phase II trials for antitumor activity of *cis*-dichlorodiammineplatinum(II) were performed by many investigators to assess its effectiveness toward different types of malignancies (Table XIII). Very good results were reported with *cis*-dichlorodiammineplatinum(II) in nine of 11 (56) and seven of 16 (57) patients with testicular tumors. Good responses in carcinoma of the bladder, breast, and thyroid also were noted. Talley *et al.* (58) observed objective remission in neuroblastoma, malignant thymoma, and three out of five lymphomas. *cis*-Dichlorodiammineplatinum(II) was inferior to fluorouracil for colon carcinoma (59). The toxicity of *cis*-dichlorodiammineplatinum(II) does limit its use in cancer chemotherapy as a single agent, but very promising developments were observed when this agent was used in combination therapy with fluorouracil (60), doxorubicin (adriamycin) (61), and other agents (62).

Thus, by using combination therapy of flurouracil and *cis*-dichlorodiammineplatinum(II), over 50% tumor regression was obtained in nine of 25 patients (63, 64). Four of nine patients with colon carcinomas showed 50% tumor regression, and one of these patients had previously failed on fluorouracil treatment as a single agent. Of the 50% or better responders, mammary, jejunal, and tonsillary adenocarcinoma were included. Encouraging response was found in patients treated with combined *cis*-dichlorodiammineplatinum(II) and doxorubicin (61). In two patients with embryonal carcinoma of the testis, one had complete regression of a large retroperitoneal mass and another had partial regression of an abdominal mass. Other responses were seen in anaplastic carcinoma of the lung, squamous cell carcinoma of the lung, and adenocarcinoma of the sigmoid colon. The promising antitumor activity of *cis*-dichlorodiammineplatinum(II) in the treatment of squamous cell carcinoma, lymphosarcoma, adenocarcinoma of the pancreas, testicular carcinoma, and endometrial carcinoma was also found in 201 patients (62).

BIOLOGICAL DISTRIBUTION

Both biological activity and side effects of drugs have some relation to their distribution, retention, and excretion in the various organs of animals and humans as well as to the rate of distribution (pharmacokinetics). The use of radioplatinum has proven most useful for such studies.

Table XIII—Responses to *cis*-Dichlorodiammineplatinum(II) in Various Malignant Diseases

Malignant Disease	Number of Patients	Number of Complete Responses	Number of Partial Responses[a]	Number of Improvements[b]	Total Response Rate, %	Reference
Testicular carcinoma	16	7	3	3	81	57, 91
	11	9			81	56
Lymphoma	16	2	7	1	63	4, 8, 57, 97
	5	3			60	58
Squamous cell carcinoma of the head and neck	17	0	1	6	41	13, 91
Ovarian carcinoma	20	0	5	3	40	91

[a] Greater than or equal to 50% tumor reduction. [b] Less than 50% tumor reduction and significant subjective improvement.

Platinum possesses 28 radioactive isotopes and six stable nuclides. Of the radionuclides, a few possess physical characteristics that are desirable for biological and/or clinical studies. Table XIV summarizes the main radionuclides of platinum. Most of these are γ-emitters and are amenable to external detection. Their half-lives are also suitable for *in vivo* studies.

The distribution of *cis*-dichlorodiammineplatinum(II) labeled with ^{193m}Pt and ^{195m}Pt was evaluated in mice, rabbits, and humans (65, 66). The tumor to blood ratio of radioactivity varied from 1:3 to 2:0 (4 hr to 5 days after injection) in mice bearing sarcoma 180. In rats bearing the Walker 256 carcinosarcoma, the tumor did not exhibit selective uptake of the drug inasmuch as the tumor to blood ratio was near unity (67, 68). However, the rate of clearance in tumor animals was significantly higher than in control animals, an effect observed within the first few minutes postinjection. This result suggests that, in the tumor animals, the renal clearance mechanism has been altered, a possible paraneoplastic effect, or that the blood contains (or lacks) a protein with unique and specific binding characteristics to *cis*-dichlorodiammineplatinum(II). This effect was dependent on tumor size and may be of potential interest in objective assessment of remission status of a tumor. Otherwise, the organ distribution in mice, rats, and rabbits with tumors was similar to the control animals. The kidneys and the liver are the principal targets of localization of platinum compounds (15, 37). Renal retention appears to involve irreversible binding of the platinum complex to the renal cell and is cleared slowly.

The distribution of the labeled *cis*-dichlorodiammineplatinum(II) has been studied in patients (66, 69). Early concentration is in the kidneys and in the head regions, but the brain area is relatively devoid of activity. Plasma disappearance reveals an initial rapid fall in radioactivity following intravenous injection and then a slow phase. About 60–70% of the radioactivity injected is retained for 2 days and excreted in the urine. After 40 hr, organs containing most of the radioactivity are the kidney, liver, and the intestine. The pattern of clearance of *cis*-dichlorodiammineplatinum(II) from the plasma, kidney, liver, and whole body is similar to that observed in animals. The half-lives of retention in humans are in the order of 8–10 days.

The subcellular distribution of ^{195m}Pt- and ^{14}C-ethylenediamine-labeled *cis*-dichloroethylenediammineplatinum(II) was studied in the liver, kidneys, and two transplanted tumors (70). This drug shows a distribution pattern similar to that for *cis*-dichlorodiammineplatinum(II) in normal and tumor tissues. Among nuclear cell debris, mitochondria, lysosomes, microsomes, and cytosol, *cis*-dichloroethylenediammineplatinum(II) is localized mainly in the cytosol in the form of low molecular weight complex. Similar results (71) were noted in the subcellular distribution studies of ^{195m}Pt-*cis*-dichlorodiammineplatinum(II) and other platinum complexes.

The study of the distribution of *cis*-dichloro-bis-(cyclopentylamine)platinum(II) in Walker 256 and in control rats illustrated that such a highly insoluble complex not only diffused very slowly out of the site of injection but was also retained at the kidney to an inordinate amount (15). Thus, animals injected at 100 mg/kg retained over 50% of the injected dose at the kidney even after 8 days.

It has been recommended that kidney function be closely monitored and correlated to platinum compounds to prevent severe renal toxicity, the main undesirable side effect of these complexes.

Table XIV—Potentially Useful Radionuclides of Platinum-99[a]

Nuclide	$t_{1/2}$	Nature of Radiation[b]	Main Energies	Production
188	10.2 days	EC	140 kev, 190 kev	^{191}Ir (p, 4n)
189	10.9 hr	EC	Complex	^{191}Ir (p, 3n)
191	3 days	EC	129 kev, 360 kev	^{191}Ir (d, 2n)
^{m}193	4.3 days	IT	Pt X-rays: 66 kev, 77 kev	^{193}I (d, 2n) ^{192}Pt (n, γ)
^{m}195	4.0 days	IT	99 kev, 129 kev, Pt X-rays	^{194}Pt (n, γ)
197	17 hr	β^-	0.670 Mev	^{196}Pt (n, γ)

[a] Reference 93. [b] EC = electron capture, and IT = internal transition.

TOXICITY AND DOSAGE

In animals, treatment with high doses of platinum compound elicits severe acute toxicity such that death or severe morbidity occurs within 3–4 days after termination of treatment. The nontoxic dose range of *cis*-dichlorodiammineplatinum(II) established for dogs is 0.625 mg/kg as a single dose or 0.185 mg/kg/day for 5 days. Monkeys can tolerate 0.156 mg/kg/day for 5 days without ill effects (72). The minimum lethal dose for the dog is a single injection of 2.5 mg/kg or five daily consecutive injections of 0.75 mg/kg. For the monkey, the minimum lethal dose is five daily doses of 2.5 mg/kg. The LD_{50} for Swiss mice is 13.4 mg/kg for males and 12.32 mg/kg for females (73). Animals receiving maximally tolerated doses recover from the toxic effects within 14–124 days. Toxic signs include damage to the GI tract, bone marrow, lymph nodes, liver, and kidneys. The renal lesions are the most severe toxic changes and are characterized by increasing excretion of urinary lactic dehydrogenase. Thus, the urinary lactic dehydrogenase excretion can be used as a monitor of *cis*-dichlorodiammineplatinum(II)-induced renal toxicity (74).

In rats, a single intraperitoneal injection of a toxic dose of *cis*-dichlorodiammineplatinum(II) (12.2 mg/kg) causes leukopenia, the decrease of both neutrophiles and lymphocytes, and the depression of the number of circulating platelets, but it does not produce significant alteration for circulating erythrocytes, packed cell volumes, and hemoglobin. At such dosage, blood urea nitrogen values, serum glucose levels, and serum albumin levels are elevated, whereas total protein levels are depressed. Serum levels of uric acid, calcium, and inorganic phosphorus are not altered (75).

The histological alterations in rats are most pronounced in tissues having cellular constituents. Thymic atrophy, splenic depletion of lymphoid elements, intestinal epithelial denudation, and bone marrow problems are most severe. Renal tubular sloughing also occurs. Rats surviving the intoxication regenerate the cellular constituents in those tissues affected (75).

The histological, hematological, and serum alterations observed in animals after a toxic dose may indicate that platinum compounds possess antitumor properties as a result of their general cytoinhibitory effects.

In humans, single doses of 1.95 mg/kg of *cis*-dichlorodiammineplatinum(II) are likely to produce renal impairment and may result in severe morbidity (76). Thus, human tolerance for the platinum compound is quite similar to that of dogs and monkeys. Patients receiving doses of more than 0.75 mg/kg experience nausea and vomiting within several hours; these effects are more intense at the higher dose levels (2). At doses above 2.0 mg/kg, toxic effects are hematological, renal, and neural (eighth nerve) (13, 76). Reversible leukopenia and thrombopenia also occur. Nephrotoxicity manifested by azotemia, rise in serum creatinine and uric acid, fall in creatinine and uric acid clearances, and concentration defects happen in some patients (13, 77). Partially reversible, high frequency nerve deafness is usually the earliest sign of toxicity. A minimal decrease in lymphodenopathy is observed in patients with undifferentiated carcinoma or with advanced lymphosarcoma (4). For patients with advanced unsusceptible cancer who have failed to respond to conventional therapy, dose levels have been used in increments up to a total cumulative dose of 8.5 mg/kg. In such high doses, renal toxicity increases (7, 13).

CONCLUSION

This review has discussed the design of platinum compounds that would show antitumor activity. The compounds should be neutral and contain a pair of *cis*-leaving groups. The carrier groups also play an important role in the determination of activity. They should be inert and neutral. The new derivatives should be synthesized with high tumor affinity and low renal toxicity—problems yet to be overcome.

Although the platinum compounds have shown a broad spectrum of action on various tumors, their immunosuppressive effect, prolonged retention, slow urinary elimination, and severe renal toxicity pose a possible clinical danger. Drug treatments scheduled at too close intervals may lead to accumulation of a toxic body load of platinum. Therefore, the choices of dose level and time schedule are important factors in the treatment. Based on the preclinical studies of tumor inhibition (41, 51) and pharmacological data (2, 76), a widely spaced treatment schedule is desired. Fiserova *et al.* (78) reported that no apparent and serious manifestation of toxicity was observed during the treatment of patients with *cis*-dichlorodiammineplatinum(II) at weekly intervals and a low dose.

In view of the toxicity and suppression of the immune response of platinum compounds, the combination of platinum compounds with certain other antitumor agents proves to be more practical than using them as single agents (79). Enhanced therapeutic effects of *cis*-dichlorodiammineplatinum(II) were observed against L-1210 leukemia in mice when it was combined with cyclophosphamide, isophosphamide, 1,2-bis(3,5-dioxopiperazine-1-yl)propane, thioguanine, 5-thiouracil, methotrexate, daunomycin, or other antitumor agents (79–83). The treatment of neoplastic disease with this combination gave greater survival than the maximum survival obtainable after treatment with either drug alone.

Conran and Rosenberg (84) studied the combination of immune therapy with *cis*-dichlorodiammineplatinum(II) chemotherapy against sarcoma 180 tumors in mice. They found that an immunodepressant, *e.g.*, hydrocortisone, reduced the antitumor activity of the platinum compound, whereas a nonspecific immune stimulant produced less effect on the drug activity. Alternatively, the usage of cysteine and other nucleophiles with the platinum compound affords protection against the toxicity of these drugs (85). In a search of platinum compounds with the promising antitumor activity and a low toxic side effect, Leh and Wolf (86) recently reported a new type of platinum–bleomycin compound. These compounds show higher tumor affinity and reduced kidney retention than *cis*-dichlorodiammineplatinum(II). It is hoped that some new platinum compounds will be synthesized and regarded as a new class of drugs to be added to the medical armamentarium.

REFERENCES

(1) B. Rosenberg, L. VanCamp, and T. Krigas, *Nature (London)*, **205**, 698(1965).

(2) R. C. DeConti, B. R. Toftness, R. C. Lange, and W. A. Creasey, *Cancer Res.*, **33**, 1310(1973).

(3) R. W. Talley, R. M. O'Bryan, R. W. Brownlee, and R. A. Gastesi, *Proc. Amer. Ass. Cancer Res.*, **13**, 81(1972).

(4) R. W. Talley, R. M. O'Bryan, J. Gutterman, R. W. Brownlee, and K. B. McCredie, in "Platinum Coordination Complexes in Cancer Chemotherapy," T. A. Connors and J. J. Roberts, Eds., Springer-Verlag, Berlin, Germany, 1974, p. 160.

(5) J. M. Hill, E. Loeb, R. J. Speer, A. MacLellan, and N. O. Hill, *Proc. Amer. Ass. Cancer Res.*, **13**, 20(1972).

(6) A. H. Rossof, R. E. Slayton, and C. P. Perlia, VIII Annual Meeting of the American Society of Clinical Oncology, Boston, Mass., May 1972, Abstract 55.

(7) D. J. Higby, H. J. Wallace, Jr., and J. F. Holland, *Cancer Chemother. Rep.*, **57**, 459(1973).

(8) R. W. Talley, R. M. O'Bryan, J. U. Gutterman, R. W. Brownlee, and K. B. McCredie, *ibid.*, **57**, 465(1973).

(9) F. Basolo, H. B. Gray, and R. G. Pearson, *J. Amer. Chem. Soc.*, **82**, 4200(1960).

(10) F. Basolo and R. G. Pearson, "Mechanisms of Inorganic Reactions," 2nd ed., Wiley, New York, N.Y., 1967, pp. 23, 355.

(11) M. J. Cleare and J. D. Hoeschele, *Bioinorg. Chem.*, **2**, 187 (1973).

(12) J. A. Howle and G. R. Gale, *Biochem. Pharmacol.*, **19**, 2757 (1970).

(13) A. T. Lippmann, C. Helson, L. Helson, and I. H. Krakoff, *Cancer Chemother. Rep., Part 1*, **57**, 191(1973).

(14) T. A. Connors, M. Jones, W. C. J. Ross, P. D. Braddock, A. R. Khokhar, and M. L. Tobe, *Chem.-Biol. Interact.*, **5**, 415(1972).

(15) W. Wolf, J. A. Berman, F. K. V. Leh, and K. Poggenburg, "1st World Congress in Nuclear Medicine," Tokyo, Japan, Sept. 1974, p. 944.

(16) B. Rosenberg, *Cancer Chemother. Rep.*, **59**, 589(1975).

(17) S. C. Dhara, *Indiana J. Chem.*, **8**, 143(1970).
(18) M. J. Cleare and J. D. Hoeschele, "Proceedings of the VII International Congress on Chemotherapy, Prague," Avicenum, Prague, Czechoslovakia, 1970, p. 193.
(19) M. A. Tucker, C. B. Colvin, and D. S. Martin, Jr., *Inorg. Chem.*, **3**, 1373(1964).
(20) E. Renshaw and A. J. Thomson, *J. Bacteriol.*, **94**, 1915 (1967).
(21) H. C. Harden and B. Rosenberg, *Int. J. Cancer*, **6**, 207(1970).
(22) G. R. Gale, L. M. Atkins, E. M. Walker, Jr., A. B. Smith, and S. J. Meischen, *Proc. Soc. Exp. Biol. Med.*, **142**, 1349(1973).
(23) C. R. Morris and G. R. Gale, *Chem.-Biol. Interact.*, **7**, 305 (1973).
(24) A. B. Robin, "Advances in Antimicrobial and Antineoplastic Chemotherapy," VII International Congress on Chemotherapy, Prague, Aug. 1971, University Park Press, Baltimore, Md., 1972, p. 213.
(25) A. B. Robins, *Chem.-Biol. Interact.*, **6**, 35(1973).
(26) *Ibid.*, **7**, 11(1973).
(27) P. Horacek and J. Drobnik, *Biochim. Biophys. Acta*, **254**, 341(1971).
(28) S. Mansy and B. Rosenberg, "Advances in Antimicrobial and Antineoplastic Chemotherapy," VII International Congress on Chemotherapy, Prague, Aug. 1971, University Park Press, Baltimore, Md., 1972, p. 191.
(29) I. A. G. Roos, A. J. Thomson, and J. Eagles, *Chem.-Biol. Interact.*, **8**, 421(1974).
(30) K. V. Shooter, R. Howse, R. K. Merrifield, and A. B. Robins, *ibid.*, **5**, 289(1972).
(31) K. V. Shooter and R. K. Merrifield, *Biochim. Biophys. Acta*, **287**, 16(1972).
(32) J. A. Howle, G. R. Gale, and A. B. Smith, *Biochem. Pharmacol.*, **21**, 1465(1972).
(33) P. C. Kong and T. Theophanides, *Inorg. Chem.*, **13**, 1167 (1974).
(34) *Ibid.*, **13**, 1981(1974).
(35) S. Mansy, B. Rosenberg, and A. J. Thomson, *J. Amer. Chem. Soc.*, **95**, 1633(1973).
(36) C. W. Milburn and M. R. Truter, *J. Chem. Soc.*, **1966**, 1609.
(37) B. Rosenberg, *Platinum Met. Rev.*, **15**, 42(1971).
(38) J. J. Roberts, in "Platinum Coordination Complexes in Cancer Chemotherapy," T. A. Connors and J. J. Roberts, Eds., Springer-Verlag, Berlin, Germany, 1974, p. 79.
(39) A. J. Thomson and S. Mansy, "Advances in Antimicrobial and Antineoplastic Chemotherapy," VII International Congress on Chemotherapy, Prague, Aug. 1971, University Park Press, Baltimore, Md., 1972, p. 189.
(40) J. J. Roberts and J. M. Pascol, *ibid.*, p. 249.
(41) B. Rosenberg and L. VanCamp, *Cancer Res.*, **30**, 1799 (1970).
(42) A. Khan, *Wadley Med. Bull.*, **2**, 33(1972).
(43) A. Khan and J. M. Hill, *Infec. Immun.*, **4**, 320(1971).
(44) A. Khan and J. M. Hill, *Transplantation*, **13**, 56(1972).
(45) A. Khan and J. M. Hill, *J. Surg. Ontol.*, **3**, 565(1971).
(46) A. Khan, A. Albayrak, and J. M. Hill, *Proc. Soc. Exp. Biol. Med.*, **141**, 7(1972).
(47) A. Khan and J. M. Hill, *ibid.*, **142**, 324(1973).
(48) B. Rosenberg, L. VanCamp, J. E. Trosko, and V. H. Mansour, *Nature*, **222**, 385(1969).
(49) D. A. Clarke, F. S. Phillip, S. S. Sternberg, and C. C. Stock, *Ann. N.Y. Acad. Sci.*, **60**, 235(1954).
(50) B. J. Leonard, E. Eccleston, D. Jones, P. Todd, and A. Walpole, *Nature*, **234**, 43(1971).
(51) R. T. Kociba, S. D. Sleight, and B. Rosenberg, *Cancer Chemother. Rep., Part 1*, **54**, 325(1970).
(52) R. W. Talley, *Proc. Amer. Ass. Cancer Res.*, **11**, 78(1970).
(53) C. Welsch, International Symposium on Bacterial, Viral and Antitumor Activities of Platinum Compounds, Michigan State University, Lansing, Mich., Sept. 1970.
(54) R. Hinz, *ibid.*
(55) S. K. Carter and M. Goldsmith, in "Platinum Coordination Complexes in Cancer Chemotherapy," T. A. Connors and J. J. Roberts, Eds., Springer-Verlag, Berlin, Germany, 1974, p. 140.
(56) D. J. Higby, H. J. Wallace, D. Albert, and J. F. Holland, *J. Urol.*, **112**, 100(1974).
(57) A. H. Rossof, R. E. Slayton, and C. P. Perlia, *Cancer*, **30**, 1451(1972).
(58) R. W. Talley, R. M. O'Bryan, J. Gutterman, R. W. Brownlee, and K. B. McCredie, in "Platinum Coordination Complexes in Cancer Chemotherapy," T. A. Connors and J. J. Roberts, Eds., Springer-Verlag, Berlin, Germany, 1974, p. 160.
(59) J. S. Kovach, C. G. Moertel, A. J. Schutt, R. G. Reitemeier, and R. G. Hahn, *Cancer Chemother. Rep., Part 1*, **57**, 3(1973).
(60) R. A. Ellerby, F. J. Ansfield, and H. L. Davis, in "Platinum Coordination Complexes in Cancer Chemotherapy," T. A. Connors and J. J. Roberts, Eds., Springer-Verlag, Berlin, Germany, 1974, p. 153.
(61) H. J. Wallace, Jr., and D. J. Higby, in *ibid.*, p. 167.
(62) E. Loeb, J. M. Hill, A. MacLellan, N. O. Hill, A. Khan, J. J. King, R. Speer, and H. Ridgway, *Wadley Med. Bull.*, **5**, 281(1975).
(63) R. A. Ellerby, H. L. Davis, F. J. Ansfield, and G. Ramirez, *Cancer*, in press.
(64) R. A. Ellerby, H. L. Davis, and F. J. Ansfield, in "Platinum Coordination Complexes in Cancer Chemotherapy," T. A. Connors and J. J. Roberts, Eds., Springer-Verlag, Berlin, Germany, 1974, p. 151.
(65) R. C. Lange, R. P. Spencer, and H. C. Harder, *J. Nucl. Med.*, **13**, 328(1972).
(66) *Ibid.*, **14**, 191(1973).
(67) W. Wolf and R. B. Ingalls, *J. Nucl. Med.*, **13**, 790(1972).
(68) W. Wolf and R. C. Manaka, Second International Symposium on Platinum Coordination Complexes in Cancer Chemotherapy, Oxford, England, 1973.
(69) P. H. S. Smith and D. M. Taylor, *J. Nucl. Med.*, **15**, 349(1974).
(70) D. M. Taylor, J. D. Jones, and A. B. Robins, *Biochem. Pharmacol.*, **22**, 833(1973).
(71) C. Karahalios, W. Wolf, and F. K. V. Leh, unpublished.
(72) R. L. Dixon, D. A. Cooney, R. D. Davis, I. Heyman, U. H. Schaeppi, and R. W. Fleischman, "Advances in Antimicrobial and Antineoplastic Chemotherapy," VII International Congress on Chemotherapy, Prague, Aug. 1971, vol. 2, University Park Press, Baltimore, Md., 1972, p. 243.
(73) U. H. Schaeppi, I. A. Heyman, R. W. Fleischman, H. Rosenkrantz, V. Ilievski, R. Phelan, D. A. Cooney, and R. D. Davis, *Toxicol. Appl. Pharmacol.*, **25**, 230(1973).
(74) U. H. Schaeppi, I. A. Heyman, R. W. Fleischman, H. Rosenkrantz, V. Ilievski, R. Phelan, D. A. Cooney, and R. D. Davis, U.S. Government Research Report MRI-CC02-71-19-1971 and MRI-CC05-71-45.
(75) R. J. Kociba and S. D. Sleight, *Cancer Chemother. Rep., Part 1*, **55**, 1(1971).
(76) A. Lippmann, C. Helson, L. Helson, R. Kaufman, and I. H. Krakoff, *Cancer Chemother. Rep.*, **13**, 40(1972).
(77) R. C. DeConti, R. C. Lange, H. C. Harder, and W. A. Creasey, *ibid.*, **13**, 96(1972).
(78) J. Fiserova, O. Dostalova, J. Drobnik, J. Oohnalova, and F. Holik, *Neoplasma*, **20**, 2(1973).
(79) R. J. Woodman, A. E. Sinica, M. Gang, I. Kline, and J. M. Vendetti, *Chemotherapy*, **18**, 169(1973).
(80) R. J. Woodman, *Cancer Chemother. Rep.*, **4**, 45(1974).
(81) G. R. Gale, E. M. Walker, Jr., L. M. Atkins, A. B. Smith, and S. J. Meischen, *Res. Commun. Chem. Pathol. Pharmacol.*, **7**, 529(1974).
(82) E. M. Walker, Jr., and G. R. Gale, *ibid.*, **6**, 419(1973).
(83) J. M. Hill, E. Loeb, R. J. Speer, A. MacLellan, and N. O. Hill, *Cancer Chemother. Rep.*, **13**, 20(1972).
(84) P. B. Conran and B. Rosenberg, "Advances in Antimicrobial and Antineoplastic Chemotherapy," VII International Congress on Chemotherapy, Prague, Aug. 1971, University Park Press, Baltimore, Md., 1972.
(85) T. A. Connors, in *ibid.*, p. 237.
(86) F. K. V. Leh and W. Wolf, Northern and Southern California Society of Nuclear Medicine, 6th Annual Meeting, San Francisco, Calif., Oct. 25–26, 1974.
(87) M. L. Tobe, personal communication, 1973.
(88) M. J. Clear, in "Platinum Coordination Complexes in Cancer Chemotherapy," T. A. Connors and J. J. Roberts, Eds., Springer-Verlag, Berlin, Germany, 1974, p. 18.
(89) M. J. Cleare and J. D. Hoeschele, *Platinum Met. Rev.*, **17**, 2(1973).

(90) J. P. Davidson, P. J. Faber, R. G. Fischer, Jr., S. Mansy, H. J. Peresie, B. Rosenberg, and L. VanCamp, *Cancer Chemother. Rep.*, **59**, 287(1975).

(91) J. A. Gottlieb and B. Drewinko, *ibid.*, **59**, 621(1975).

(92) A. J. Thomson, R. J. P. Williams, and S. Reslova, *Struct. Bonding (Berlin)*, **11**, 1(1972).

(93) I. Kline, *Cancer Chemother. Rep.*, **4**, 33(1974).

(94) C. M. Lederer, T. M. Hollander, and I. Perlman, "Table of Isotopes," 6th ed., Wiley, New York, N.Y., 1967, p. 195.

ACKNOWLEDGMENTS AND ADDRESSES

Received from the *Radiopharmacy Program, School of Pharmacy and Cancer Hospital and Research Institute, University of Southern California, Los Angeles, CA 90033*

Supported in part by Cancer Center Grant 5-PO1-CA-14089.

The authors thank Dr. B. Rosenberg, Dr. E. Lien, Mr. J. Berman, and other individuals for helpful discussion.

* To whom inquiries should be directed.

RESEARCH ARTICLES

Effects of Lipids on Bioavailability of Sulfisoxazole Acetyl, Dicumarol, and Griseofulvin in Rats

DUANE C. BLOEDOW * and WILLIAM L. HAYTON *

Abstract □ The effects of hexadecane, oleyl alcohol, polysorbate 80, trioctanoin, and triolein on the bioavailability of sulfisoxazole N^1-acetyl, dicumarol, and griseofulvin were investigated. Compared to administration of the drugs in water, the rate of absorption of the drugs was either decreased or not changed by the lipids. The extent of absorption of sulfisoxazole acetyl and dicumarol was significantly increased by polysorbate 80 and triolein and not affected by hexadecane or oleyl alcohol. Trioctanoin increased the extent of absorption of sulfisoxazole acetyl but had no effect on the absorption of dicumarol. Compared to the aqueous vehicle, the extent of absorption of griseofulvin was decreased by hexadecane, oleyl alcohol, and triolein, increased by polysorbate 80, and not affected by trioctanoin. The extent of absorption of sulfisoxazole acetyl was not affected by the amount of triolein in which it was administered nor by emulsification of triolein prior to administration.

Keyphrases □ Bioavailability—sulfisoxazole acetyl, dicumarol, griseofulvin, effect of lipids, rats □ Sulfisoxazole acetyl—effect of lipids on bioavailability, rats □ Dicumarol—effect of lipids on bioavailability, rats □ Griseofulvin—effect of lipids on bioavailability, rats □ Lipids—effect on bioavailability of sulfisoxazole acetyl, dicumarol, and griseofulvin, rats

The bioavailability of orally administered drugs having low aqueous solubility may be incomplete due primarily to slow dissolution in the lumen of the GI tract. Several reports indicate that the bioavailability of poorly water-soluble drugs, particularly drugs that are also lipophilic, can be improved by coadministration of a lipid, which apparently increases the rate of dissolution of such drugs. For example, the bioavailability of indoxole in humans is increased following oral administration of the drug in a lipid emulsion compared to administration as an aqueous suspension (1). Similar results in rats were reported following the oral administration of indoxole dissolved or suspended in cottonseed oil or dissolved in polysorbate 80 (2).

The bioavailability of griseofulvin in humans increases with the amount of lipid in the diet (3) and is greater following oral administration with corn oil (4) or corn oil emulsion (5) than with water. The therapeutic effect of N^1-acyl derivatives of sulfanilamide in mice is increased following oral administration of suspensions of the drugs in olive oil compared to administration in water (6). In rats and humans, the bioavailability of sulfisoxazole N^1-acetyl is greater following oral administration of the drug in a vegetable oil-in-water emulsion than it is when administered in water (7).

While bioavailability may be improved by lipids, there are also examples of lipids decreasing the bioavailability of lipophilic substances. The absorption of chlorophenothane (DDT), as reflected by LD_{50} values, is increased when it is administered in corn oil or olive oil but decreased when given in mineral oil compared to its administration in an aqueous vehicle (8). And ingestion of potato chips containing small amounts of methyl polysiloxane, a lipid-like agent that enhances crispness, apparently significantly reduced the absorption of warfarin and phenindione in patients taking these drugs (9).

The purpose of this study was to examine physicochemical and physiological properties of lipids that may alter the bioavailability of lipophilic, poorly water-soluble drugs. The drugs used and their aqueous solubilities in milligrams per liter were: sulfisoxazole acetyl, 70 (10); dicumarol, 0.5 at low pH (11); and griseofulvin, 8.8 (12). The bioavailabilities of the drugs were determined following their oral administration in selected lipid vehicles and water.

The lipid vehicles (Table I) were selected on the basis of their diverse physicochemical and physiological properties. Because the environment of the GI lumen is aqueous, the primary physicochemical prop-

(90) J. P. Davidson, P. J. Faber, R. G. Fischer, Jr., S. Mansy, H. J. Peresie, B. Rosenberg, and L. VanCamp, *Cancer Chemother. Rep.*, **59**, 287(1975).

(91) J. A. Gottlieb and B. Drewinko, *ibid.*, **59**, 621(1975).

(92) A. J. Thomson, R. J. P. Williams, and S. Reslova, *Struct. Bonding (Berlin)*, **11**, 1(1972).

(93) I. Kline, *Cancer Chemother. Rep.*, **4**, 33(1974).

(94) C. M. Lederer, T. M. Hollander, and I. Perlman, "Table of Isotopes," 6th ed., Wiley, New York, N.Y., 1967, p. 195.

ACKNOWLEDGMENTS AND ADDRESSES

Received from the *Radiopharmacy Program, School of Pharmacy and Cancer Hospital and Research Institute, University of Southern California, Los Angeles, CA 90033*

Supported in part by Cancer Center Grant 5-PO1-CA-14089.

The authors thank Dr. B. Rosenberg, Dr. E. Lien, Mr. J. Berman, and other individuals for helpful discussion.

* To whom inquiries should be directed.

RESEARCH ARTICLES

Effects of Lipids on Bioavailability of Sulfisoxazole Acetyl, Dicumarol, and Griseofulvin in Rats

DUANE C. BLOEDOW * and WILLIAM L. HAYTON *

Abstract □ The effects of hexadecane, oleyl alcohol, polysorbate 80, trioctanoin, and triolein on the bioavailability of sulfisoxazole N^1-acetyl, dicumarol, and griseofulvin were investigated. Compared to administration of the drugs in water, the rate of absorption of the drugs was either decreased or not changed by the lipids. The extent of absorption of sulfisoxazole acetyl and dicumarol was significantly increased by polysorbate 80 and triolein and not affected by hexadecane or oleyl alcohol. Trioctanoin increased the extent of absorption of sulfisoxazole acetyl but had no effect on the absorption of dicumarol. Compared to the aqueous vehicle, the extent of absorption of griseofulvin was decreased by hexadecane, oleyl alcohol, and triolein, increased by polysorbate 80, and not affected by trioctanoin. The extent of absorption of sulfisoxazole acetyl was not affected by the amount of triolein in which it was administered nor by emulsification of triolein prior to administration.

Keyphrases □ Bioavailability—sulfisoxazole acetyl, dicumarol, griseofulvin, effect of lipids, rats □ Sulfisoxazole acetyl—effect of lipids on bioavailability, rats □ Dicumarol—effect of lipids on bioavailability, rats □ Griseofulvin—effect of lipids on bioavailability, rats □ Lipids—effect on bioavailability of sulfisoxazole acetyl, dicumarol, and griseofulvin, rats

The bioavailability of orally administered drugs having low aqueous solubility may be incomplete due primarily to slow dissolution in the lumen of the GI tract. Several reports indicate that the bioavailability of poorly water-soluble drugs, particularly drugs that are also lipophilic, can be improved by coadministration of a lipid, which apparently increases the rate of dissolution of such drugs. For example, the bioavailability of indoxole in humans is increased following oral administration of the drug in a lipid emulsion compared to administration as an aqueous suspension (1). Similar results in rats were reported following the oral administration of indoxole dissolved or suspended in cottonseed oil or dissolved in polysorbate 80 (2).

The bioavailability of griseofulvin in humans increases with the amount of lipid in the diet (3) and is greater following oral administration with corn oil (4) or corn oil emulsion (5) than with water. The therapeutic effect of N^1-acyl derivatives of sulfanilamide in mice is increased following oral administration of suspensions of the drugs in olive oil compared to administration in water (6). In rats and humans, the bioavailability of sulfisoxazole N^1-acetyl is greater following oral administration of the drug in a vegetable oil-in-water emulsion than it is when administered in water (7).

While bioavailability may be improved by lipids, there are also examples of lipids decreasing the bioavailability of lipophilic substances. The absorption of chlorophenothane (DDT), as reflected by LD_{50} values, is increased when it is administered in corn oil or olive oil but decreased when given in mineral oil compared to its administration in an aqueous vehicle (8). And ingestion of potato chips containing small amounts of methyl polysiloxane, a lipid-like agent that enhances crispness, apparently significantly reduced the absorption of warfarin and phenindione in patients taking these drugs (9).

The purpose of this study was to examine physicochemical and physiological properties of lipids that may alter the bioavailability of lipophilic, poorly water-soluble drugs. The drugs used and their aqueous solubilities in milligrams per liter were: sulfisoxazole acetyl, 70 (10); dicumarol, 0.5 at low pH (11); and griseofulvin, 8.8 (12). The bioavailabilities of the drugs were determined following their oral administration in selected lipid vehicles and water.

The lipid vehicles (Table I) were selected on the basis of their diverse physicochemical and physiological properties. Because the environment of the GI lumen is aqueous, the primary physicochemical prop-

Table I—Lipids Used in This Investigation

Lipid	Characteristics
Hexadecane	Nonpolar, nondigestible
Oleyl alcohol	Polar, Class I, nondigestible
Polysorbate 80	Polar, Class III, digestible[a]
Trioctanoin	Polar, Class I, digestible
Triolein	Polar, Class I, digestible; forms chylomicrons

[a] Following hydrolysis in the gut, the oleic acid moiety is absorbed and the polyoxyethylene sorbitan portion is eliminated in the feces (33).

erty considered was polarity as it relates to the interaction of lipids with water (13). Thus, lipids are classified as *nonpolar* (no interaction with water) or *polar*. Polar lipids interact with water and, depending on the interaction, are placed in one of three groups: Class I, spread on water to form a stable monolayer; Class II, form a stable monolayer on water and water dissolves in them; or Class III, form no stable monolayer but dissolve in water and form micelles. The physiological properties considered in selecting the lipids are digestibility and, for digestible lipids, chylomicron formation.

EXPERIMENTAL

Materials—Sulfisoxazole N^1-acetyl[1] (mp 192°), dicumarol[2] (mp 260°), and griseofulvin[3] (mp 222°) were used as received. Dicumarol-^{14}C-methylene[4] was mixed with unlabeled dicumarol, and the radiochemical purity was determined by TLC on silica gel G developed with 1-propanol–ammonium hydroxide (7:3). Dicumarol was visualized with UV light, consecutive 1-cm^2 scrapings of silica gel were removed from the chromatogram, and the radioactivity in each scraping was determined by liquid scintillation counting[5]. Dicumarol and radioactivity moved as a single spot, with 97% of the radioactivity associated with the visualized spot.

Hexadecane[6], oleyl alcohol[6], polysorbate 80[7], polyethylene glycol 400 USP[8], trioctanoin[9], triolein[2], and methylcellulose 4000[8] were used as received. Anhydrous analytical reagent grade ether[10] was distilled immediately prior to use.

Solubility—A sufficient quantity of sulfisoxazole acetyl, dicumarol, or griseofulvin was placed in each of a series of 10-ml glass ampuls to assure saturation of the solvent with the drug. Approximately 5 ml of lipid was added to each ampul, which was sealed by flame. The ampuls were rotated for 72 hr in a 37 ± 0.5° water bath and then placed upright for several hours to allow suspended particles to settle. A sample of the supernate was removed and filtered[11], and the concentration of the drug was determined. Preliminary experiments showed that the lipids were saturated with drug prior to 72 hr.

Bioavailability—Male Sprague–Dawley rats[12], 225–350 g, were fasted 16 hr prior to and 12 hr following drug administration. Access to water was allowed *ad libitum* throughout the experiments, and all studies were initiated at the same time of day to eliminate the effects of circadian variation.

Sulfisoxazole acetyl (100 mg/kg), dicumarol (10 mg/kg), and griseofulvin (50 mg/kg) were administered orally as suspensions in 5 ml/kg of each lipid and 0.5% aqueous methylcellulose. The animals were anesthetized lightly with ether to facilitate drug administration. The particle-size distributions of the drugs, determined from scanning electron micrographs of the powders (14), were log normal. The geometric mean diameter and standard deviation in micrometers were: sulfisoxazole acetyl, 1.8 (2.3); dicumarol, 1.3 (2.5); and griseofulvin, 0.43 (1.5).

Table II—Percent of Drug Dissolved in the Suspension Dosage Forms

Vehicle	Percent Dissolved[a]		
	Sulfisoxazole Acetyl	Dicumarol	Griseofulvin
Hexadecane	<0.01	1.4	<0.01
Oleyl alcohol	1.7	12	3.6
Polysorbate 80	100[b]	100[b]	94
Trioctanoin	6.8	19	13
Triolein	3.1	13	3.4

[a] Calculated from solubilities. [b] Solutions.

All suspensions were agitated at room temperature for 72 hr before administration to ensure that the vehicles were saturated with drug. The amount of drug dissolved in the suspensions is shown in Table II. Dicumarol was also administered in solution at a dose of 1.0 mg/kg in all vehicles except hexadecane, where the dose was 0.1 mg/kg due to low solubility. The specific activity of ^{14}C-dicumarol in all solutions and suspensions was approximately 1 × 10^6 dpm/ml.

The drugs were administered orally with a 2- or 5-ml syringe attached to a No. 8 French rubber catheter having a blunt tip and a hole in the side 5 mm from the tip. Each syringe and catheter was calibrated to determine the amount of drug delivered to the stomach of each animal. Solutions of the drugs in polyethylene glycol 400 containing 10% water were administered intravenously *via* the dorsal penile vein. The dose of drug was the same as that given orally, and the volume injected was 2–3 ml/kg.

Following the administration of sulfisoxazole acetyl and dicumarol, the animals were placed in individual metabolism cages[13]. Urine was collected at 12 and 24 hr and at 24-hr intervals until drug was no longer excreted. All urine samples were frozen and stored at −20° until assayed. After administration of griseofulvin, each animal was placed in a separate cage and 0.4-ml samples of blood were collected from the tail into heparinized micro blood collecting tubes (15).

Blood was collected at approximately 1, 2, 4, 6, 8, and 12 hr postadministration, except for the oleyl alcohol vehicle where the times of collection were 2, 4, 6, 8, 11, and 14 hr. Blood samples were obtained at 24 hr by cardiac puncture. Plasma was separated from the blood samples and stored frozen in 10-ml centrifuge tubes with screw caps[14] until assayed for griseofulvin.

The bioavailability of dicumarol was based on the urinary excretion of radioactivity following administration of ^{14}C-dicumarol. Since dicumarol and its metabolites were measured together, bioavailability refers to the rate and extent of absorption of dicumarol, provided the drug is not altered in the lumen of the GI tract. The bioavailabilities of sulfisoxazole acetyl and griseofulvin were based on urinary excretion and blood plasma concentration of intact drug and, therefore, reflect the relative amount of drug that reached the general circulation.

Analytical Methods—In the solubility studies, sulfisoxazole acetyl, dicumarol, and griseofulvin were determined by UV spectrophotometry[15] after dilution with chloroform. The appropriate lipid containing no drug was diluted with chloroform, and its absorbance was used for the blank. A colorimetric method (16) was used to determine free (non-N^4-conjugated) sulfisoxazole in urine samples. No sulfisoxazole acetyl was detected on thin-layer chromatograms of the 0–96-hr urine collected following oral or intravenous administration of 100 mg/kg of sulfisoxazole acetyl.

[1] Donated by Hoffmann-La Roche, Nutley, N.J.
[2] Pfaltz and Bauer, Flushing, N.Y.
[3] Sigma Chemical Co., St. Louis, Mo.
[4] Activity of 8.4 mCi/mmole, New England Nuclear, Boston, Mass.
[5] Packard Tri-Carb model 3320, Packard Instrument Co., Downers Grove, Ill.
[6] Eastman Organic Chemicals, Rochester, N.Y.
[7] Atlas Chemical Industries, Wilmington, Del.
[8] Ruger Chemical Co., Irvington, N.J.
[9] J. T. Baker, Phillipsburg, N.J.
[10] Mallinckrodt Chemical Works, St. Louis, Mo.
[11] Millipore filter, type UG, 0.25-μm pore size, Millipore Corp., Bedford, Mass.
[12] Hilltop Lab Animals, Chatsworth, Calif.
[13] Model HB-11M with HB-66 food tunnel, Hoeltge, Inc., Cincinnati, Ohio.
[14] Lined with Teflon.
[15] Beckman DU, Beckman Instruments, Inc., Fullerton, Calif., with Gilford model 2000 multiple sample absorbance recorder, Gilford Instrument Laboratories, Oberlin, Ohio.

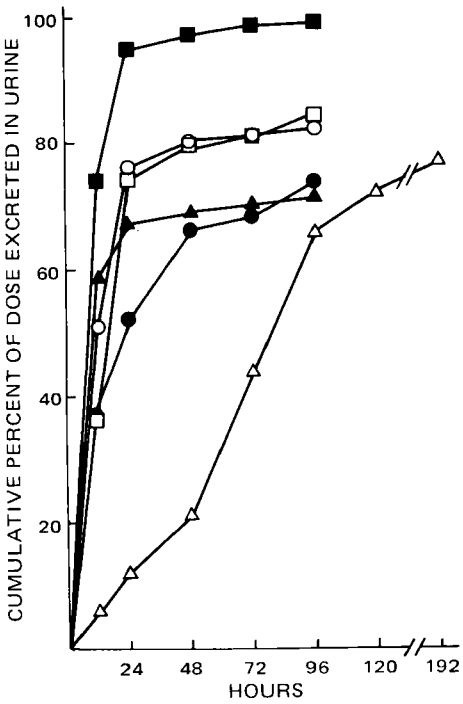

Figure 1—*Cumulative urinary excretion of free sulfisoxazole (expressed as a percent of the administered dose on a molar basis) following oral administration of 100 mg/kg of sulfisoxazole acetyl suspended in lipid vehicles and water. Each point represents the mean of six animals. Key: ●, hexadecane; △, oleyl alcohol; ■, polysorbate 80 (solution); □, trioctanoin; ○, triolein; and ▲, water (with 0.5% methylcellulose).*

Chromatograms were prepared by extracting the urine, diluted to 500 ml and adjusted to pH 5, with chloroform, reducing the volume of the extract by evaporation, and spotting the concentrated extract on silica gel-coated plates. The chromatograms were developed with chloroform–methanol (95:5) and visualized with *p*-dimethylaminobenzaldehyde (17). When using this method, less than 1% of the administered dose could be detected. These results agree with other reports indicating that sulfisoxazole acetyl is not present in the urine following its oral administration (18, 19).

The amounts of sulfisoxazole determined in the urine were converted on a molar basis to sulfisoxazole acetyl for comparison with the amount of sulfisoxazole acetyl administered. The mean assay blank, determined for each animal from urine collected for 24 hr prior to drug administration, was equivalent to 0.86 mg/24 hr of apparent sulfisoxazole acetyl. The oral administration of 5.0 ml/kg of the vehicles without drug did not affect the assay blank. In addition, oral administration of the vehicles did not affect the urinary excretion kinetics of sulfisoxazole following the simultaneous intravenous administration of 100 mg/kg of sulfisoxazole acetyl (20).

Table III—Plasma Concentration–Time Parameters[a] following Oral Administration of 50 mg/kg of Griseofulvin in Various Vehicles

Vehicle	Peak Plasma Concentration, μg/ml	t_{max}[b], min	Area under Plasma Concentration–Time Curve[c], μg hr/ml
Water (with 0.5% methylcellulose)	0.95 ± 0.60	281 ± 64	9.43 ± 4.61
Oleyl alcohol	0.36 ± 0.17[d]	576 ± 97[d]	3.16 ± 1.06[d]
Triolein	0.33 ± 0.04[d]	269 ± 83	3.36 ± 1.38[d]
Hexadecane	0.46 ± 0.15	317 ± 166	4.50 ± 0.92[d]
Trioctanoin	0.42 ± 0.16	277 ± 101	5.11 ± 1.55
Polysorbate 80	1.53 ± 0.28	422 ± 96[d]	15.77 ± 3.34[d]

[a] Average of six animals ± *SD* for each vehicle. [b] Time of occurrence of peak plasma concentration. [c] Determined by using Simpson's method (34). [d] Significantly different from water as determined by the Student *t* test ($p < 0.05$).

Table IV—Bioavailability of Orally Administered Sulfisoxazole Acetyl, Dicumarol, and Griseofulvin in Various Lipids and Water

Vehicle	Bioavailability, %			
	Sulfisoxazole Acetyl[a] Suspension (100 mg/kg)	Dicumarol[b]		Griseofulvin[c] Suspension (50 mg/kg)
		Solution (1 mg/kg)	Suspension (10 mg/kg)	
Hexadecane	78	114	102	6
Oleyl alcohol	81	105	115	4
Polysorbate 80	104	157	121	19
Trioctanoin	90	112	90	6
Triolein	87	125	111	4
Water[d]	77	105	95	12

[a] Bioavailability determined by comparing cumulative urinary recovery of free drug at 96 hr (for oleyl alcohol, 192 hr) following oral administration with that following intravenous administration. [b] Bioavailability determined by comparing cumulative urinary recovery of radioactivity at 288 hr following oral administration of ^{14}C-dicumarol with that following intravenous administration. [c] Bioavailability determined by comparing area under the plasma concentration–time curve following oral administration with that following intravenous administration. [d] Water with 0.5% methylcellulose for all suspensions and 0.01 *M* pH 8 tromethamine buffer for the dicumarol solution.

Radioactivity, representing dicumarol and its metabolites, in urine was determined by liquid scintillation counting[5]. Urine samples of 0.5–2.0 ml were mixed with 15 ml of scintillation fluid[16]. The efficiency of the counting system was approximately 80%; quench corrections were made for each sample, using ^{14}C-toluene as an internal standard. Griseofulvin was determined in blood plasma samples by a modification (5) of a fluorometric[17] procedure (21).

RESULTS AND DISCUSSION

The effects of the lipids on the absorption of sulfisoxazole acetyl, dicumarol, and griseofulvin are apparent in the urinary excretion and plasma concentration–time data in Figs. 1–4 and Table III. The effects of the lipids on the bioavailabilities of the drugs relative to a standard administered intravenously are shown in Table IV; changes induced by the lipids in the rate and extent of absorption of the drugs with reference to an aqueous vehicle are shown in Tables V and VI.

Absorption Rate—Compared to the aqueous vehicle, the lipids either reduced or did not change the rate of absorption of the drugs (Table V). The digestible lipids polysorbate 80, trioctanoin, and triolein generally had no detectable effect on absorption rate while hexadecane and oleyl alcohol tended to reduce the rate of absorption of the drugs.

To measure the rate of drug release from the lipids, suspensions of the drugs in the lipids were added to a 4-liter bottle, 15-cm diameter by 25 cm, containing 1 liter of water. The bottle was rotated horizontally around the long axis at 1 rpm at room temperature, and the concentration of drug in filtered samples of the aqueous phase was measured periodically. In all cases except polysorbate 80, the solid drug remained in the lipid phase, which floated as a lens on the surface of the aqueous phase. The results for all drugs were similar to those obtained for griseofulvin (Fig. 5).

The relatively slow release of drug from oleyl alcohol *in vitro* (Fig. 5) suggests that this lipid reduces the absorption rate of the drugs *in vivo* by reducing the rate of drug release to the fluids of the GI tract. However, in addition to slowing the rate of release of the drugs, oleyl alcohol also appears to reduce markedly GI motility. For example, the absorption of sulfisoxazole acetyl appears to continue for 2–3 days following its administration in oleyl alcohol (Fig. 1); this period is well beyond the normal GI transit time of

[16] PCS Solubilizer, Amersham/Searle Corp., Arlington Heights, Ill.
[17] Aminco-Bowman spectrofluorometer, American Instrument Co., Silver Spring, Md.

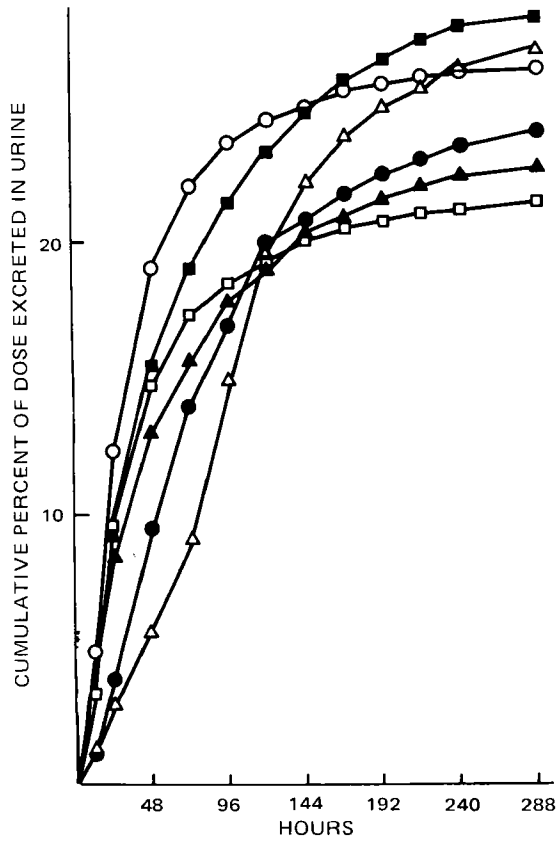

Figure 2—*Cumulative urinary excretion of radioactivity (expressed as a percent of the administered dose) following oral administration of 10 mg/kg of ^{14}C-dicumarol suspended in lipid vehicles and water. Each point represents the mean of six animals. Key: see Fig. 1.*

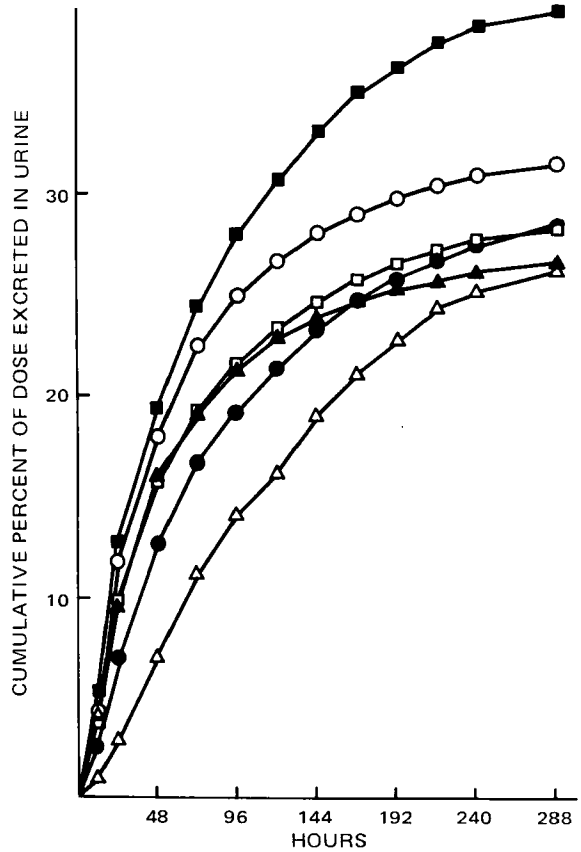

Figure 3—*Cumulative urinary excretion of radioactivity (expressed as a percent of the administered dose) following oral administration of 1 mg/kg (0.1 mg/kg for hexadecane) of ^{14}C-dicumarol dissolved in lipid vehicles and 0.01 M pH 8 aqueous tromethamine buffer. Each point represents the mean of six animals. Key: see Fig. 1.*

16–24 hr in the rat (22). Thus, the rate of gastric emptying, an important determinant of the rate of absorption of many drugs (23), may be slowed by oleyl alcohol.

Since hexadecane does not appear to slow significantly the rate of drug release *in vitro*, its effect *in vivo* may also be to reduce the rate of gastric emptying. Although the digestible lipids are also known inhibitors of gastric emptying, they apparently did not slow emptying enough to reduce significantly the rate of drug absorption in this study.

A statistically significant ($p < 0.05$) correlation was found between the rate of release of griseofulvin *in vitro* and both its bioavailability (Fig. 6) and peak plasma concentration (not shown). Such correlations indicate that the absorption of griseofulvin was dissolution rate limited, in agreement with results reported previously (24, 25). No significant correlation was established between the *in vitro* rate of release of sulfisoxazole acetyl and dicumarol and their *in vivo* rates of absorption. When considering the low aqueous solubilities of dicumarol and sulfisoxazole acetyl, it is likely that their absorption is limited by their rate of release from the lipids *in vivo*. The lack of *in vitro–in vivo* correlation indicates that drug release *in vitro* did not simulate drug release in the complex digestion mixture present in the intestinal lumen following administration of the digestible lipids (26).

More sophisticated *in vitro* release rate studies will be required to identify factors that control the rate of drug release from lipids *in vivo*. Examples of factors that may be important are the lipid

Table V—Comparison[a] between the Effects of Lipids and Water on the Apparent Rate of Absorption of Sulfisoxazole Acetyl, Dicumarol, and Griseofulvin

Vehicle	Sulfisoxazole Acetyl[b]	Dicumarol[c]		Griseofulvin[d]
		Solution	Suspension	
Hexadecane	—	0	—	0
Oleyl alcohol	—	—	—	—
Polysorbate 80	0	0	0	—
Trioctanoin	—	0	0	0
Triolein	0	0	0	0

[a] The (–) indicates a statistically significant ($p < 0.05$, Student t test) negative effect on the rate of absorption of the drug from the lipid vehicle as compared to the water vehicle, and the (0) indicates no significant difference. [b] Rate of absorption based on amounts of sulfisoxazole excreted in the urine at 12 hr after dosing. [c] Rate of absorption based on amounts of radioactivity excreted in the urine at 12 hr after dosing. [d] Rate of absorption based on time of occurrence of peak plasma concentrations of griseofulvin.

Table VI—Comparison[a] between the Effects of Lipid and Water on the Bioavailability of Sulfisoxazole Acetyl, Dicumarol, and Griseofulvin

Vehicle	Sulfisoxazole Acetyl[b]	Dicumarol[c]		Griseofulvin[d]
		Solution	Suspension	
Hexadecane	0	0	0	—
Oleyl alcohol	0	0	0	—
Polysorbate 80	+	+	+	+
Trioctanoin	+	0	0	0
Triolein	+	+	+	–

[a] The (+) and ( ) indicate a significant ($p < 0.05$) increase or decrease, respectively, in bioavailability compared to the aqueous vehicle; the (0) indicates no significant difference. [b] Based on amounts of sulfisoxazole excreted in urine at 96 hr (192 hr for oleyl alcohol). [c] Based on amounts of radioactivity excreted in urine at 288 hr. [d] Based on area under the plasma concentration–time curve from 0–24 hr.

Table VII—Urinary Recovery[a] of Radioactivity following Intravenous Administration of ^{14}C-Dicumarol

Dose, mg/kg	Cumulative Percent of Dose Recovered at 288 hr
1	25.3 ± 0.91
10	23.8 ± 1.62

[a] Average of six animals ± *SD* for each dose.

viscosity, the lipid–water partition coefficient of the drug, the micellar phase–lipid partition coefficient of the drug (27), and the possible wetting of the solid drug by the aqueous phase. The latter factor is determined by the relative interfacial tensions between lipid and water, lipid and drug, and water and drug (28) and could be very sensitive to the presence of surface-active agents.

Bioavailability—Compared to the aqueous vehicle, the lipids either increased or did not change the bioavailability of sulfisoxazole acetyl or dicumarol (Table VI). The bioavailability of griseofulvin was decreased by hexadecane, oleyl alcohol, and triolein and increased only by polysorbate 80. The negative effect of triolein on the bioavailability of griseofulvin does not agree with the positive effects of digestible triglycerides on griseofulvin absorption reported previously (4, 5). Differences in the strain of rat (4), use of corn oil rather than triolein (4, 5), volume of lipid administered (4, 5), and particle size of the drug (5) may explain the different effects observed.

In general, the extent of drug absorption from the lipids increased with the polarity of the lipid. There is a perfect rank-order correlation between the bioavailability of sulfisoxazole acetyl and lipid polarity and, while not correlated perfectly, there is a tendency for the bioavailability of griseofulvin and dicumarol to increase with the polarity of the lipid. The solubility of the drugs in the lipids also increases with the polarity of the lipids (Table II), and the correlation between bioavailability and polarity may simply reflect the fraction of the dose in solution at the time of administration. However, when dicumarol was administered as a solution, the lipids affected its rate of absorption and bioavailability the same as when the drug was given as a suspension (Tables V and VI), indicating that the extent of dissolution of the drugs at the time of administration was not an important factor in this study.

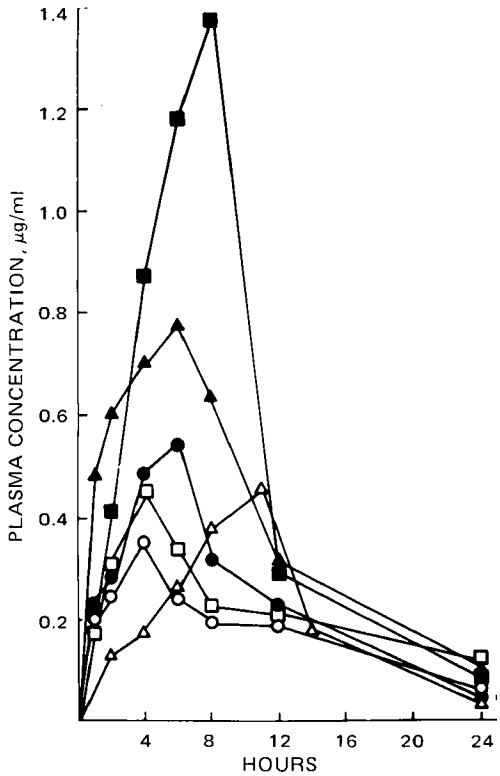

Figure 4—*Representative plasma concentrations of griseofulvin following oral administration of 50 mg/kg of griseofulvin suspended in lipid vehicles and water. Each curve, representing data from one animal, has a peak plasma concentration and t_{max} closest to the mean values for each group as reported in Table III. Key: see Fig. 1.*

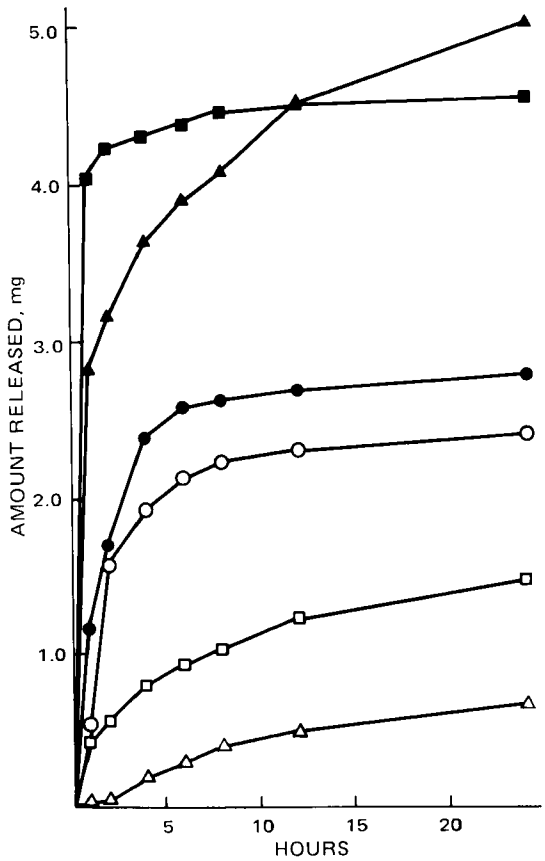

Figure 5—*Release of griseofulvin into water from suspensions containing 5 mg of drug in lipid and water. Each point represents the mean of three experiments. Key: see Fig. 1.*

In several instances, the bioavailability of dicumarol was significantly greater than 100% (Table IV), particularly with the 1-mg/kg dose. When 1 and 10 mg/kg of the drug were given intravenously, the same fraction of the administered radioactivity was excreted in the urine (Table VII). Differences in the mode of metabolism of dicumarol following intravenous and oral administration to rats have been reported (29), and the abnormally high bioavailability of orally administered dicumarol compared to the intravenously ad-

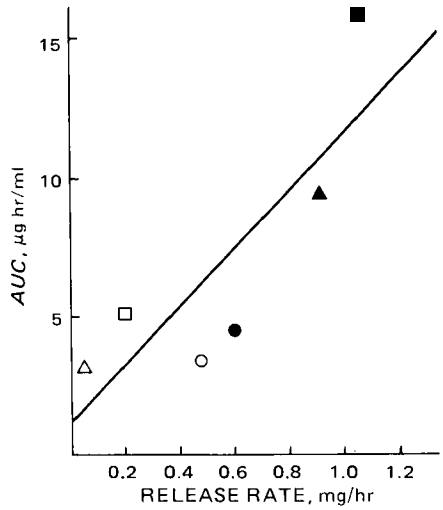

Figure 6—*Correlation of the area under the plasma concentration–time curve* (AUC) *with the average 0–4-hr rate of release of griseofulvin* in vitro. *Key: see Fig. 1.*

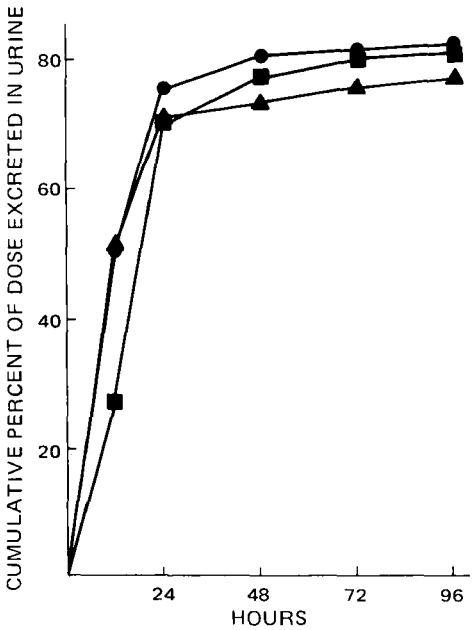

Figure 7—*Effect of the volume of triolein administered on the cumulative urinary excretion of free sulfisoxazole (expressed as a percent of the administered dose on a molar basis) following oral administration of 100 mg/kg of sulfisoxazole acetyl. Each point represents the mean of six animals. Key: ▲, 2.0 ml/kg; ●, 5.0 ml/kg; and ■, 10.0 ml/kg.*

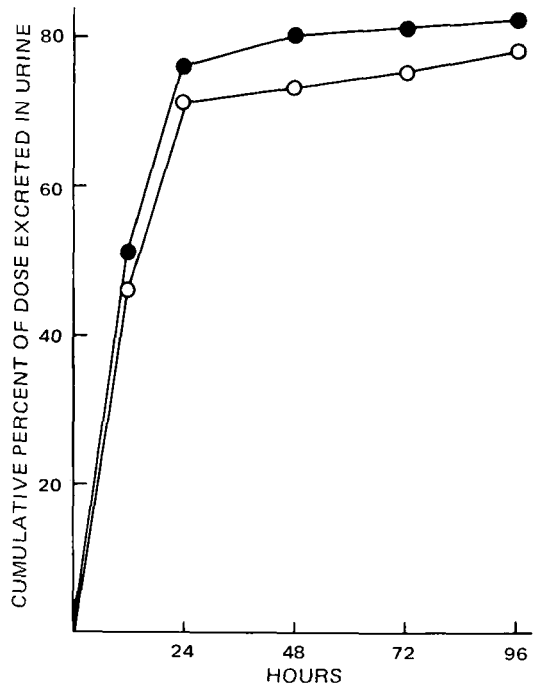

Figure 8—*Effect of emulsification of triolein on the cumulative urinary excretion of free sulfisoxazole (expressed as a percent of the administered dose on a molar basis) following oral administration of 100 mg/kg of sulfisoxazole acetyl. Each point represents the mean of six animals. Key: ○, emulsion; and ●, suspension.*

ministered standard may be due to such differences. Polysorbate 80, trioctanoin, and triolein were the only lipids that promoted bioavailability (Table VI); therefore, digestibility may be an important characteristic of lipids for enhancement of bioavailability. Since the digestible lipids were also the most polar, it is not possible to establish the relative importance of polarity and digestibility.

Chylomicrons are important for the transport of some lipophilic substances, such as cholesterol (30) and octadecanol (31), from the intestinal mucosa, and it might be anticipated that chylomicron generation would be an important characteristic of lipids for enhancing the bioavailability of lipophilic drugs. The bioavailability of sulfisoxazole acetyl and griseofulvin was not increased when the drugs were administered in triolein compared to trioctanoin (Table IV), indicating that chylomicrons are not important for absorption of these drugs. However, the bioavailability of dicumarol is greater from triolein than from trioctanoin and the generation of chylomicrons by triolein may explain the increased bioavailability.

The effect on bioavailability of the amount of triolein administered with sulfisoxazole acetyl was investigated. The results (Fig. 7) indicate that over the range studied the extent of absorption of the drug is not affected by the amount of lipid administered. However, the highest dose of lipid reduced the initial rate of absorption of sulfisoxazole acetyl, probably by reducing the rate of drug emptying from the stomach.

To investigate the effect of emulsification of the lipid vehicle on the bioavailability of sulfisoxazole acetyl, an oil-in-water emulsion containing 0.5 ml of triolein, 125 mg of acacia, and 10 mg of sulfisoxazole acetyl/ml was prepared. The emulsion was mixed by the dry-gum method (32), passed three times through a hand homogenizer[18], and agitated for 72 hr prior to administration of 10 ml/kg. The particle-size distribution of the triolein was determined by a photomicrographic method to be log normal (14). The geometric mean diameter and standard deviation were 1.5 and 2.2 μm, respectively. Neither the rate nor the extent of bioavailability of sulfisoxazole acetyl was affected significantly by emulsifying the triolein (Fig. 8).

The results of this study indicate that polar, digestible lipids increase the bioavailability of lipophilic, poorly water-soluble drugs without increasing their rate of absorption. The nonpolar, nondigestible lipids generally do not affect the bioavailability of lipophilic, poorly water-soluble drugs, but they do appear to reduce the rate of absorption of such drugs. Neither the amount of lipid administered nor emulsification of the lipid affected bioavailability significantly.

[18] Aloe Scientific Division, St. Louis, Mo.

REFERENCES

(1) J. G. Wagner, E. S. Gerard, and D. G. Kaiser, *Clin. Pharmacol. Ther.*, **7**, 610(1966).

(2) D. G. Kaiser, E. M. Glenn, R. H. Johnson, and R. L. Johnson, *J. Pharmacol. Exp. Ther.*, **155**, 174(1967).

(3) R. G. Crounse, *J. Invest. Dermatol.*, **37**, 529(1961).

(4) M. Kraml, J. Dubuc, and D. Beall, *Can. J. Biochem. Physiol.*, **40**, 1449(1962).

(5) P. J. Carrigan and T. R. Bates, *J. Pharm. Sci.*, **62**, 1476(1973).

(6) W. H. Feinstone, R. Wolff, and R. D. Williams, *J. Bacteriol.*, **39**, 47(1940).

(7) S. E. Svenson, W. L. Delorenzo, R. Engelberg, M. Spooner, and L. O. Randall, *Antibiot. Med.*, **2**, 148(1956).

(8) R. T. Williams, "Detoxication Mechanisms," Wiley, New York, N.Y., 1959, p. 267.

(9) J. M. Talbot and B. W. Meade, *Lancet*, **1**, 1292(1971).

(10) M. Hoffer, *Chem. Abstr.*, **50**, 10333(1956).

(11) M. J. Cho, A. G. Mitchell, and M. Pernarowski, *J. Pharm. Sci.*, **60**, 196(1971).

(12) S. H. Crowdy, J. F. Grove, and P. McCloskey, *Biochem. J.*, **72**, 241(1959).

(13) D. M. Small, *J. Amer. Oil Chem. Soc.*, **45**, 108(1968).

(14) A. N. Martin, J. Swarbrick, and A. Cammarata, "Physical Pharmacy," 2nd ed., Lea & Febiger, Philadelphia, Pa., 1969, p. 474.

(15) A. Hurwitz, *J. Lab. Clin. Med.*, **78**, 172(1971).

(16) A. C. Bratton and E. K. Marshall, Jr., *J. Biol. Chem.*, **128**, 537(1939).

(17) H. R. Klein and W. J. Mader, *J. Pharm. Sci.*, **60**, 448(1971).

(18) L. Randall, R. Engelberg, V. Iliev, M. Roe, H. Haar, and T. H. McGavack, *Antibiot. Chemother.*, **4**, 877(1954).

(19) E. R. Flake, J. Griffin, E. Townsend, and E. M. Yow, *J.*

Lab. Clin. Med., **44**, 582(1954).
(20) D. C. Bloedow and W. L. Hayton, *J. Pharm. Sci.*, **65**, 334(1976).
(21) V. P. Shah, S. Riegelman, and W. L. Epstein, *ibid.*, **61**, 635(1972).
(22) Y. Yamatani and S. Ishikawa, *Agr. Biol. Chem.*, **32**, 474(1968).
(23) L. Z. Benet, in "Drug Design," vol. 4, E. J. Ariens, Ed., Academic, New York, N.Y., 1973, pp. 29–32.
(24) B. Katchen and S. Symchowicz, *J. Pharm. Sci.*, **56**, 1108 (1967).
(25) S. Symchowicz and B. Katchen, *ibid.*, **57**, 1383(1968).
(26) J. M. Johnston, in "Handbook of Physiology: Alimentary Canal," W. Heidel, Ed., American Physiological Society, Washington, D.C., 1968, p. 1353.
(27) B. Borgstrom, *J. Clin. Invest.*, **39**, 309(1960).
(28) P. Becher, "Emulsions: Theory and Practice," Reinhold, New York, N.Y., 1957, p. 127.
(29) E. P. Hausner, C. L. Shafer, M. Corson, O. Johnson, T. Trujillo, and W. Langham, *Circulation*, **3**, 171(1951).
(30) B. Borgstrom, S. Radner, and B. Werner, *Scand. J. Clin. Lab. Invest.*, **26**, 227(1970).
(31) V. H. Cohn and S. Sieber, *Pharmacologist*, **12**, 292(1972).
(32) "Remington's Pharmaceutical Sciences," 14th ed., J. E. Hoover, Ed., Mack Publishing Co., Easton, Pa., 1970, p. 346.
(33) P. J. Culver, C. S. Wilcox, C. M. Jones, and R. S. Rose, Jr., *J. Pharmacol. Exp. Ther.*, **103**, 377(1951).
(34) G. B. Thomas, Jr., "Calculus," Addison-Wesley, Reading, Mass., 1969, p. 308.

ACKNOWLEDGMENTS AND ADDRESSES

Received August 26, 1974, from the *College of Pharmacy, Washington State University, Pullman, WA 99163*

Accepted for publication June 3, 1975.

Presented at the APhA Academy of Pharmaceutical Sciences, San Francisco meeting, April 1975.

Supported in part by funds provided for biological and medical research by the State of Washington Initiative Measure 171.

The authors express their appreciation to Dr. W. E. Scott, Research Division, Hoffmann–La Roche Inc., for providing the sulfisoxazole acetyl used.

* AFPE Robert Lincoln McNeil Memorial Fellow. Present address: College of Pharmacy, South Dakota State University, Brookings, SD 57006

ˣ To whom inquiries should be directed.

Saturable First-Pass Metabolism of Sulfisoxazole N^1-Acetyl in Rats

DUANE C. BLOEDOW * and WILLIAM L. HAYTON ˣ

Abstract □ Saturable metabolism of sulfisoxazole N^1-acetyl in the rat during the initial pass of the drug from the intestinal lumen through the liver following oral administration of the drug (saturable first-pass metabolism) was investigated. The fraction of the total amount of drug recovered from the urine as the N^4-conjugate decreased as the dose of orally administered sulfisoxazole acetyl was increased. No dose dependency of the N^4-conjugated fraction was apparent following the intravenous administration of sulfisoxazole acetyl or the oral administration of sulfisoxazole at the same dose levels.

Keyphrases □ Sulfisoxazole acetyl—saturable first-pass metabolism, rats □ Metabolism, saturable first pass—sulfisoxazole acetyl, rats

Evidence of saturable metabolism of drugs in humans during the initial pass of the drug from the intestinal lumen through the liver following oral administration (saturable first-pass metabolism) has been reported for various drugs including propranolol (1), levodopa (2), lidocaine (3), and aspirin (4). Recent studies indicate that the aromatic amino group of certain drugs may undergo first-pass conjugation. For example, aminosalicylic acid is more extensively acetylated following oral administration than following intravenous administration, and the extent of acetylation following oral administration is dose dependent (5, 6).

This type of dose dependency may have great clinical implications, since small changes in the dose given, or in the rate or extent of absorption, may result in large, unexpected changes in the systemic availability of the drug. This study investigated the saturable first-pass conjugation of the aromatic amino group of sulfisoxazole N^1-acetyl (sulfisoxazole acetyl) and sulfisoxazole over a dose range where the extent of conjugation following intravenous administration of sulfisoxazole acetyl is constant.

EXPERIMENTAL

Materials—Sulfisoxazole N^1-acetyl[1], sulfisoxazole[2], propantheline bromide[3], polysorbate 80[4], polyethylene glycol 400 USP[5], ammonium sulfamate[6], reagent grade sodium nitrite[7], and N-(1-naphthyl)ethylenediamine dihydrochloride[8] were used as received. All other reagents were reagent grade.

Dosage Forms—Solutions for oral administration contained 2, 5, or 20 mg of sulfisoxazole acetyl or sulfisoxazole/ml of polysorbate 80. Solutions for intravenous administration contained 5, 12.5, or 50 mg of sulfisoxazole acetyl/ml of polyethylene glycol 400 containing 10% water. A solution of propantheline bromide for intraperitoneal administration contained 2.5 mg of the drug/ml of water.

***In Vivo* Urinary Excretion**—Male Sprague–Dawley rats[9], 200–350 g, were fasted 16 hr prior to and 12 hr following the initia-

[1] Donated by Hoffmann–La Roche, Nutley, N.J.
[2] Sigma Chemical Co., St. Louis, Mo.
[3] Pfaltz and Bauer, Flushing, N.Y.
[4] Atlas Chemical Industries, Wilmington, Del.
[5] Ruger Chemical Co., Irvington, N.J.
[6] MCB Manufacturing Chemists, Norwood, Ohio.
[7] J. T. Baker, Phillipsburg, N.J.
[8] Eastman Organic Chemicals, Rochester, N.Y.
[9] Hilltop Lab Animals, Chatsworth, Calif.

Lab. Clin. Med., **44**, 582(1954).
(20) D. C. Bloedow and W. L. Hayton, *J. Pharm. Sci.*, **65**, 334(1976).
(21) V. P. Shah, S. Riegelman, and W. L. Epstein, *ibid.*, **61**, 635(1972).
(22) Y. Yamatani and S. Ishikawa, *Agr. Biol. Chem.*, **32**, 474(1968).
(23) L. Z. Benet, in "Drug Design," vol. 4, E. J. Ariens, Ed., Academic, New York, N.Y., 1973, pp. 29–32.
(24) B. Katchen and S. Symchowicz, *J. Pharm. Sci.*, **56**, 1108 (1967).
(25) S. Symchowicz and B. Katchen, *ibid.*, **57**, 1383(1968).
(26) J. M. Johnston, in "Handbook of Physiology: Alimentary Canal," W. Heidel, Ed., American Physiological Society, Washington, D.C., 1968, p. 1353.
(27) B. Borgstrom, *J. Clin. Invest.*, **39**, 309(1960).
(28) P. Becher, "Emulsions: Theory and Practice," Reinhold, New York, N.Y., 1957, p. 127.
(29) E. P. Hausner, C. L. Shafer, M. Corson, O. Johnson, T. Trujillo, and W. Langham, *Circulation*, **3**, 171(1951).
(30) B. Borgstrom, S. Radner, and B. Werner, *Scand. J. Clin. Lab. Invest.*, **26**, 227(1970).
(31) V. H. Cohn and S. Sieber, *Pharmacologist*, **12**, 292(1972).
(32) "Remington's Pharmaceutical Sciences," 14th ed., J. E. Hoover, Ed., Mack Publishing Co., Easton, Pa., 1970, p. 346.
(33) P. J. Culver, C. S. Wilcox, C. M. Jones, and R. S. Rose, Jr., *J. Pharmacol. Exp. Ther.*, **103**, 377(1951).
(34) G. B. Thomas, Jr., "Calculus," Addison-Wesley, Reading, Mass., 1969, p. 308.

ACKNOWLEDGMENTS AND ADDRESSES

Received August 26, 1974, from the *College of Pharmacy, Washington State University, Pullman, WA 99163*

Accepted for publication June 3, 1975.

Presented at the APhA Academy of Pharmaceutical Sciences, San Francisco meeting, April 1975.

Supported in part by funds provided for biological and medical research by the State of Washington Initiative Measure 171.

The authors express their appreciation to Dr. W. E. Scott, Research Division, Hoffmann–La Roche Inc., for providing the sulfisoxazole acetyl used.

* AFPE Robert Lincoln McNeil Memorial Fellow. Present address: College of Pharmacy, South Dakota State University, Brookings, SD 57006

ˣ To whom inquiries should be directed.

Saturable First-Pass Metabolism of Sulfisoxazole N^1-Acetyl in Rats

DUANE C. BLOEDOW * and WILLIAM L. HAYTON ˣ

Abstract □ Saturable metabolism of sulfisoxazole N^1-acetyl in the rat during the initial pass of the drug from the intestinal lumen through the liver following oral administration of the drug (saturable first-pass metabolism) was investigated. The fraction of the total amount of drug recovered from the urine as the N^4-conjugate decreased as the dose of orally administered sulfisoxazole acetyl was increased. No dose dependency of the N^4-conjugated fraction was apparent following the intravenous administration of sulfisoxazole acetyl or the oral administration of sulfisoxazole at the same dose levels.

Keyphrases □ Sulfisoxazole acetyl—saturable first-pass metabolism, rats □ Metabolism, saturable first pass—sulfisoxazole acetyl, rats

Evidence of saturable metabolism of drugs in humans during the initial pass of the drug from the intestinal lumen through the liver following oral administration (saturable first-pass metabolism) has been reported for various drugs including propranolol (1), levodopa (2), lidocaine (3), and aspirin (4). Recent studies indicate that the aromatic amino group of certain drugs may undergo first-pass conjugation. For example, aminosalicylic acid is more extensively acetylated following oral administration than following intravenous administration, and the extent of acetylation following oral administration is dose dependent (5, 6).

This type of dose dependency may have great clinical implications, since small changes in the dose given, or in the rate or extent of absorption, may result in large, unexpected changes in the systemic availability of the drug. This study investigated the saturable first-pass conjugation of the aromatic amino group of sulfisoxazole N^1-acetyl (sulfisoxazole acetyl) and sulfisoxazole over a dose range where the extent of conjugation following intravenous administration of sulfisoxazole acetyl is constant.

EXPERIMENTAL

Materials—Sulfisoxazole N^1-acetyl[1], sulfisoxazole[2], propantheline bromide[3], polysorbate 80[4], polyethylene glycol 400 USP[5], ammonium sulfamate[6], reagent grade sodium nitrite[7], and N-(1-naphthyl)ethylenediamine dihydrochloride[8] were used as received. All other reagents were reagent grade.

Dosage Forms—Solutions for oral administration contained 2, 5, or 20 mg of sulfisoxazole acetyl or sulfisoxazole/ml of polysorbate 80. Solutions for intravenous administration contained 5, 12.5, or 50 mg of sulfisoxazole acetyl/ml of polyethylene glycol 400 containing 10% water. A solution of propantheline bromide for intraperitoneal administration contained 2.5 mg of the drug/ml of water.

***In Vivo* Urinary Excretion**—Male Sprague–Dawley rats[9], 200–350 g, were fasted 16 hr prior to and 12 hr following the initia-

[1] Donated by Hoffmann–La Roche, Nutley, N.J.
[2] Sigma Chemical Co., St. Louis, Mo.
[3] Pfaltz and Bauer, Flushing, N.Y.
[4] Atlas Chemical Industries, Wilmington, Del.
[5] Ruger Chemical Co., Irvington, N.J.
[6] MCB Manufacturing Chemists, Norwood, Ohio.
[7] J. T. Baker, Phillipsburg, N.J.
[8] Eastman Organic Chemicals, Rochester, N.Y.
[9] Hilltop Lab Animals, Chatsworth, Calif.

Table I—Urinary Recovery of Sulfisoxazole following Oral Administration of 100 mg/kg of Sulfisoxazole Acetyl Suspended in Various Lipids and Water

Vehicle	Cumulative Percent[a] of Dose Recovered at 96 hr			Fraction[c] Conjugated
	Free Drug	N^4-Conjugate[b]	Total	
Water (with 0.5% methylcellulose)	72.72 ± 7.90	5.21	77.93 ± 18.00	0.067
Polysorbate 80[d]	99.27 ± 14.54[e]	12.52	111.79 ± 22.08[e]	0.112
Hexadecane	73.85 ± 3.55	11.25	85.10 ± 9.66	0.132
Triolein	82.29 ± 6.69[e]	13.62	95.91 ± 14.94	0.142
Trioctanoin	84.54 ± 2.22[e]	15.90	100.44 ± 4.95[e]	0.158
Oleyl alcohol[f]	77.14 ± 5.51	25.11	104.56 ± 2.93[e]	0.262

[a] On a molar basis; average of six animals ± *SD* for each vehicle. [b] Difference between total and free drug. [c] Ratio of N^4-conjugate to total. [d] Solution. [e] Significantly different from the water vehicle as determined by the Student *t* test ($p < 0.05$). [f] Urinary recovery at 192 hr to achieve complete drug recovery.

tion of each absorption experiment. Free access to water was allowed throughout the experiments. All studies were initiated at the same time of the day to eliminate circadian variation.

All animals were lightly anesthetized with ether during the administration of oral and intravenous doses. Each oral sulfisoxazole acetyl or sulfisoxazole dosage form was administered *via* gastric tube at dose levels of 10, 25, and 100 mg/kg. The oral dose volume employed was 5.0 ml/kg. Each intravenous dosage form of sulfisoxazole acetyl was administered *via* the dorsal penile vein at dose levels of 10, 25, and 100 mg/kg. The dose volume for all intravenous dosage forms was 2.0 ml/kg.

As in previous studies (7), the amount of sulfisoxazole acetyl and sulfisoxazole delivered by the oral dosage form delivery system[10] was assayed in triplicate by UV spectroscopy (278 and 268 nm, respectively) to calculate the actual dose of drug administered. When it was used, propantheline bromide was injected at a dose of 5 mg/kg ip 1 hr before the administration of 100 mg/kg po of sulfisoxazole acetyl in polysorbate 80.

The animals were subsequently placed in individual metabolism cages[11] in a room with a timed light exposure of 9 hr of light alternated with 15 hr of darkness. Urine was collected at 12, 24, 48, 72, and 96 hr. All urine samples were immediately frozen and stored at −20° until assayed.

Analytical Methods—The colorimetric method of Bratton and Marshall (8) was used to assay for both free (non-N^4-conjugated) and total (N^4-conjugated and non-N^4-conjugated) sulfisoxazole in the urine. As reported previously (7), sulfisoxazole N^1-acetyl was not detected by TLC of urine following oral or intravenous administration of sulfisoxazole acetyl. The amounts of sulfisoxazole recovered from the urine following administration of sulfisoxazole acetyl were converted on a molar basis to apparent milligrams of

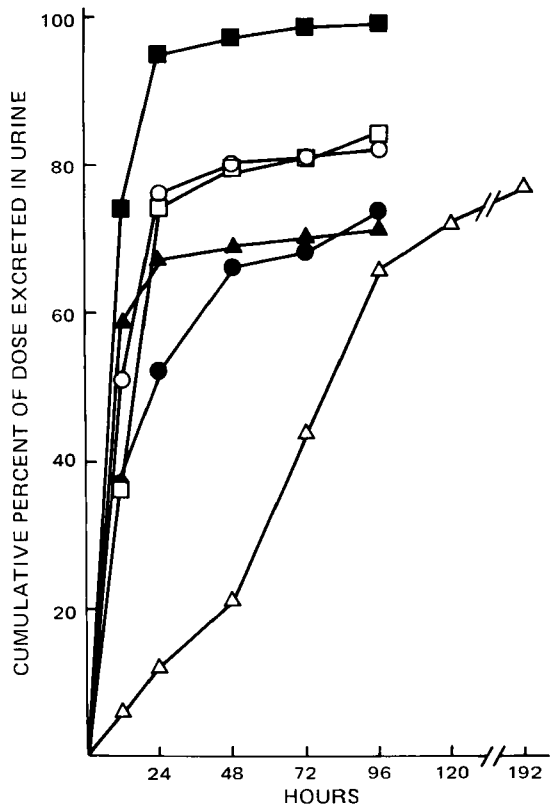

Figure 1—*Cumulative urinary excretion of free sulfisoxazole (expressed as a percent of the administered dose on a molar basis) following oral administration of a 100-mg/kg dose of sulfisoxazole acetyl in lipid vehicles and water. Each point represents the average of six animals. Key: ●, hexadecane; △, oleyl alcohol; ■, polysorbate 80 (solution); □, trioctanoin; ○, triolein; and ▲, water (with 0.5% methylcellulose).*

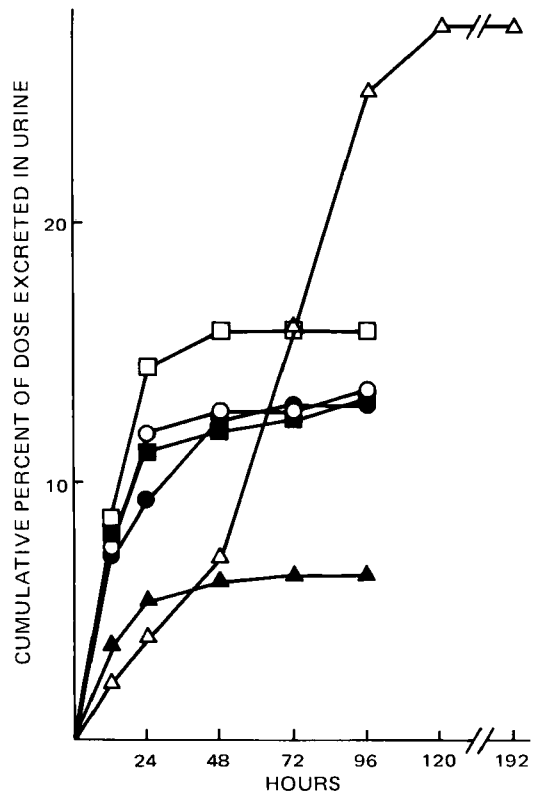

Figure 2—*Cumulative urinary excretion of N^4-conjugated sulfisoxazole (expressed as a percent of the administered dose on a molar basis) following oral administration of a 100-mg/kg dose of sulfisoxazole acetyl in lipid vehicles and water. Each point represents the average of six animals. Key: see Fig. 1.*

[10] Two-milliliter syringe with attached No. 8 French rubber catheter having a blunt tip and a hole in the side 5 mm from the tip.

[11] Model HB-11M with HB-66 food tunnel, Hoeltge, Inc., Cincinnati, Ohio.

Table II—Urinary Recovery of Free[a] Sulfisoxazole following Oral Administration of 100 mg/kg of Sulfisoxazole Acetyl Suspended in Various Lipids and Water

Vehicle	Cumulative Percent[b] of Dose Recovered at 12 hr
Water (with 0.5% methylcellulose)	58.07 ± 8.63
Polysorbate 80[c]	74.09 ± 17.02
Hexadecane	36.96 ± 14.91[d]
Triolein	50.91 ± 6.33
Trioctanoin	35.50 ± 10.71[d]
Oleyl alcohol	6.46 ± 2.49[d]

[a] Non-N^4-conjugated. [b] On a molar basis; average of six animals ± *SD* for each vehicle. [c] Solution. [d] Significantly different from water vehicle as determined by the Student *t* test ($p < 0.05$).

sulfisoxazole acetyl excreted for comparison to the dose of the drug administered to the animal.

Urine was collected from each animal for 24 hr prior to sulfisoxazole acetyl or sulfisoxazole administration and used to determine the assay blank. The assay blank of approximately 0.80 apparent mg of sulfisoxazole acetyl excreted/24 hr was not affected when polysorbate 80 was administered orally (5.0 ml/kg) or when polyethylene glycol 400 containing 10% water was administered intravenously (2.0 ml/kg) without the drug.

RESULTS AND DISCUSSION

The cumulative urinary recoveries of free (non-N^4-conjugated), N^4-conjugated, and total (N^4-conjugated and non-N^4-conjugated) sulfisoxazole following oral administration of sulfisoxazole acetyl (100 mg/kg) in various lipid vehicles and water (7) are plotted against time in Figs. 1, 2, and 3, respectively. The percent of the dose of sulfisoxazole acetyl excreted in the urine as the N^4-conjugate (Fig. 2) is the difference between the percent of the dose excreted in the urine as total sulfisoxazole following oral administration of sulfisoxazole acetyl (Fig. 3) and the percent of the dose excreted in the urine as free sulfisoxazole (Fig. 1) following oral administration of sulfisoxazole acetyl.

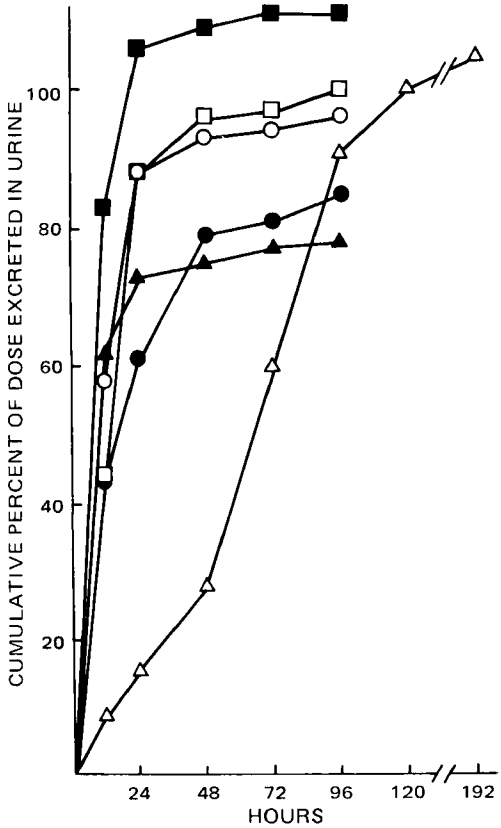

Figure 3—*Cumulative urinary excretion of total (free and N⁴-conjugated) sulfisoxazole (expressed as a percent of the administered dose on a molar basis) following oral administration of a 100-mg/kg dose of sulfisoxazole acetyl in lipid vehicles and water. Each point represents the average of six animals. Key: see Fig. 1.*

Table III—Urinary Recovery of Sulfisoxazole following Intravenous Administration of 100 mg/kg of Sulfisoxazole Acetyl and Simultaneous Oral Administration of the Indicated Vehicle

Vehicle	Cumulative Percent[a] of Dose Recovered at 96 hr: Free Drug	N^4-Conjugate[b]	Total	Fraction[c] Conjugated
Water (with 0.5% methylcellulose)	96.29	12.62	108.91	0.116
Polysorbate 80	94.49	12.93	107.42	0.120
Hexadecane	100.41	14.21	114.62	0.124
Triolein	99.59	12.53	112.12	0.112
Trioctanoin	99.19	11.81	111.00	0.106
Oleyl alcohol	100.61	12.66	113.27	0.112

[a] On a molar basis; average of two animals for each vehicle. [b] Difference between total and free drug. [c] Ratio of N^4-conjugate to total.

The cumulative urinary recoveries of free, N^4-conjugated, and total sulfisoxazole through 96 hr and the fraction conjugated following oral administration of sulfisoxazole acetyl (100 mg/kg) in various lipid vehicles and water (7) are listed in Table I. The fraction conjugated is the ratio of N^4-conjugated sulfisoxazole to total sulfisoxazole recovered from the urine through 96 hr following oral administration of sulfisoxazole acetyl. This fraction apparently varies with the vehicle in which the sulfisoxazole acetyl is administered. The rates of bioavailability, as indicated by the urinary recoveries of free sulfisoxazole at 12 hr (Table II), also have been shown to be affected by the vehicles (7).

Comparison of the fractions conjugated with the rates of bioavailability as indicated by the urinary recoveries of free sulfisoxazole acetyl at 12 hr results in a statistically significant ($p < 0.05$) negative linear correlation (Fig. 4). A similar correlation is ob-

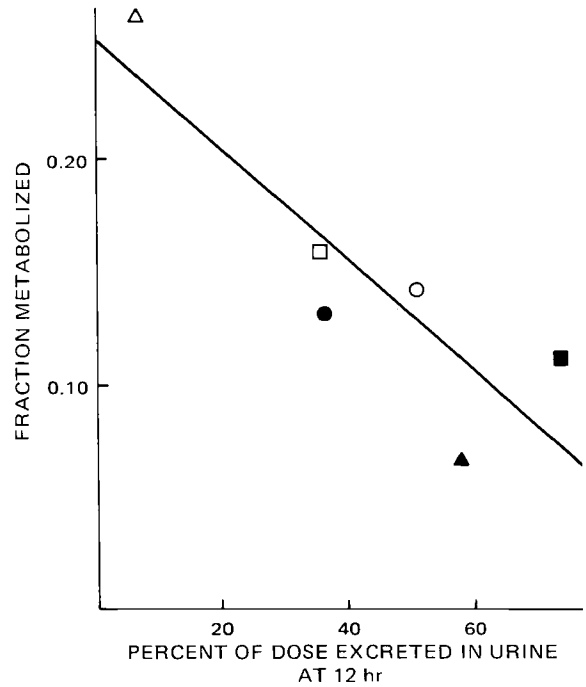

Figure 4—*Correlation of the rate of bioavailability of free sulfisoxazole (expressed as a percent of the administered dose on a molar basis excreted in the urine at 12 hr) with the total N⁴-conjugated metabolite excreted in the urine (expressed as a fraction of the total dose recovered from the urine). Each point represents the average of six animals. Key: see Fig. 1.*

Table IV—Urinary Recovery of Sulfisoxazole following Oral and Intravenous Administration of 10, 25, and 100 mg/kg of Sulfisoxazole Acetyl

Dose, mg/kg	Cumulative Percent[a] of Dose Recovered at 96 hr: Free Drug	N^4-Conjugate[b]	Total	Fraction[c] Conjugated
Oral Administration as Solution in Polysorbate 80				
10	88.68 ± 2.34	26.15	114.83 ± 5.06	0.228
25	85.75 ± 3.67	18.97	104.72 ± 2.79	0.181
100	99.27 ± 14.54	12.52	111.79 ± 22.08	0.112
Intravenous Administration as Solution in Polyethylene Glycol 400 Containing 10% Water				
10	101.15 ± 5.91	9.32	110.49 ± 4.94	0.085
25	99.81 ± 2.89	10.36	110.67 ± 3.29	0.098
100	95.02 ± 8.70	8.42	103.44 ± 9.13	0.081

[a] On a molar basis; average of six animals ± *SD* for each dose. [b] Difference between total and free drug. [c] Ratio of N^4-conjugate to total.

tained when the rate of absorption based on urinary recovery of total sulfisoxazole is used. These correlations suggest saturable first-pass conjugation of the aromatic amino group of sulfisoxazole acetyl during the initial pass of the drug from the GI lumen through the liver following oral administration. The correlation is not attributed to a direct effect of the vehicles, since the fraction conjugated following the intravenous administration of sulfisoxazole acetyl apparently is not affected when the vehicles without sulfisoxazole acetyl are administered orally (Table III).

The cumulative urinary recoveries of free, N^4-conjugated, and total sulfisoxazole and the fraction conjugated following oral and intravenous administration of sulfisoxazole acetyl at dose levels of 10, 25, and 100 mg/kg are listed in Table IV. The fractions conjugated following oral and intravenous administration of sulfisoxazole acetyl at the three dose levels are plotted in Fig. 5. From these data, it is apparent that the extent of conjugation of the drug increased with decreasing dose following oral administration. This behavior is consistent with the hypothesis of saturable first-pass conjugation.

Table V—Urinary Recovery of Sulfisoxazole following Oral Administration of 10, 25, and 100 mg/kg of Sulfisoxazole

Dose, mg/kg	Cumulative Percent[a] of Dose Recovered at 96 hr: Free Drug	N^4-Conjugate[b]	Total	Fraction[c] Conjugated
10	87.01 ± 7.46	12.77	99.78 ± 6.76	0.128
25	81.70 ± 3.48	12.86	94.56 ± 2.79	0.136
100	79.88 ± 4.24	11.41	91.29 ± 5.72	0.125

[a] Average of five animals ± *SD* for each dose. [b] Difference between total and free drug. [c] Ratio of N^4-conjugate to total.

Dose-dependent conjugation of sulfisoxazole acetyl was not observed when the drug was administered intravenously, indicating that the dose-dependent conjugation occurs before the drug reaches the systemic circulation. The extent of conjugation was greater when the drug was administered orally than when it was administered intravenously, giving additional evidence for a first-pass effect. The extent of drug absorption was complete following oral administration of sulfisoxazole acetyl dissolved in polysorbate 80 (Table IV).

To confirm further that the extent of conjugation is related to the rate of bioavailability or the absorption rate of sulfisoxazole acetyl, the effect of reducing the absorption rate by pretreating the animals with propantheline bromide was investigated. Propantheline bromide inhibits the motor activity of the stomach and small intestine and slows the absorption of drugs (9, 10). The extent of conjugation was increased in animals pretreated with propantheline bromide (5 mg/kg) 1 hr prior to the oral administration of sulfisoxazole acetyl in polysorbate 80 compared to the untreated con-

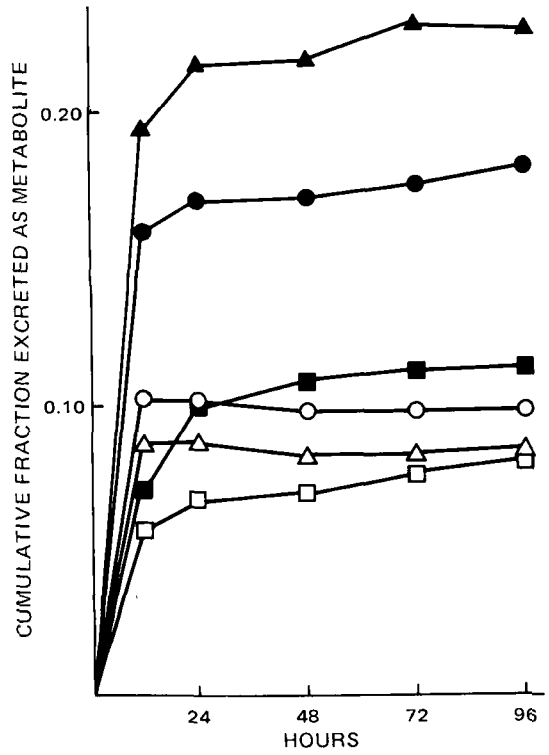

Figure 5—*Effect of the route of administration and dose on the cumulative* N^4*-conjugated metabolite excreted in the urine (expressed as a fraction of the total dose recovered from the urine) following administration of sulfisoxazole acetyl. Each point represents the average of six animals. Key:* △, *10 mg/kg iv;* ○, *25 mg/kg iv;* □, *100 mg/kg iv;* ▲, *10 mg/kg po;* ●, *25 mg/kg po; and* ■, *100 mg/kg po.*

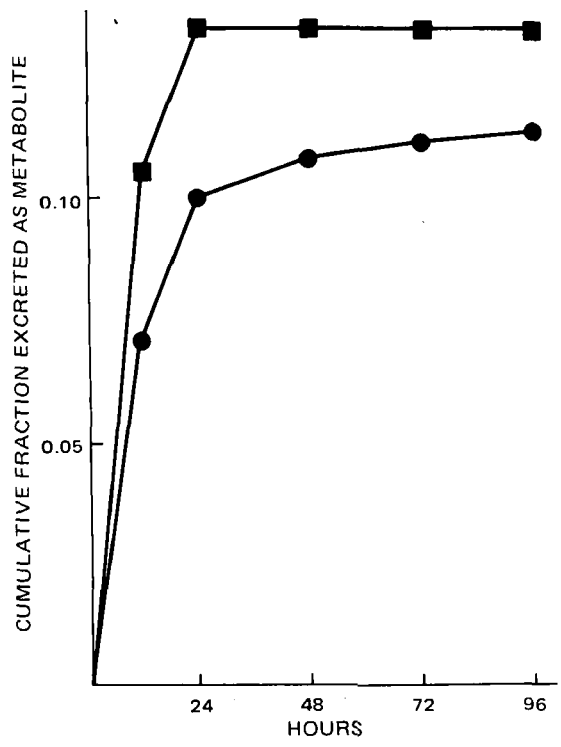

Figure 6—*Effect of propantheline bromide on the cumulative* N^4*-conjugated metabolite excreted in the urine (expressed as a fraction of total dose recovered from the urine) following oral administration of a 100-mg/kg dose of sulfisoxazole acetyl dissolved in polysorbate 80. Each point represents the average of six animals. Key:* ●, *no propantheline pretreatment; and* ■, *5-mg/kg propantheline pretreatment.*

trol group (Fig. 6). However, there was no significant difference between the conjugated fractions of the propantheline bromide-pretreated group and the untreated group.

The cumulative urinary recoveries of free, N^4-conjugated, and total sulfisoxazole and the fraction conjugated following oral administration of sulfisoxazole at dose levels of 10, 25, and 100 mg/kg dissolved in polysorbate 80 are listed in Table V. No difference exists among the total recoveries of sulfisoxazole. In addition, the fraction of sulfisoxazole metabolized following oral administration does not appear to be dose dependent.

This study shows the existence of saturable first-pass metabolism for orally administered sulfisoxazole acetyl in rats at dose levels equivalent to therapeutic maintenance dose levels used in humans (15 mg/kg every 4–6 hr). However, the results also indicate that saturable first-pass metabolism does not occur following the oral administration of similar doses of sulfisoxazole in rats.

Sulfisoxazole acetyl was originally synthesized to obtain an active preparation of sulfisoxazole without a bitter taste, which could be administered as an oral suspension to children (11, 12). Early reports indicate that the poorly water-soluble, lipophilic, sulfisoxazole acetyl is converted to sulfisoxazole in the GI tract, presumably by digestive enzymes (11, 12). The data in this study indicate that sulfisoxazole acetyl may be absorbed intact and presented to the site of N^4-conjugation at a concentration exceeding that of the less lipophilic sulfisoxazole. Thus, following oral administration, sulfisoxazole acetyl saturates the enzymes responsible for N^4-conjugation whereas sulfisoxazole does not.

This theory is supported by the decrease in the fraction metabolized (N^4-conjugated) as the dose of orally administered sulfisoxazole acetyl is increased from 10 to 100 mg/kg, whereas no dose dependency in the fraction metabolized (N^4-conjugated) is apparent following the oral administration of sulfisoxazole over this dose range. Approximately 85% of sulfisoxazole is protein bound in the blood of humans (13). Sulfisoxazole acetyl may be protein bound to a lesser extent than sulfisoxazole at the pH of the blood due to the ionization of sulfisoxazole but not sulfisoxazole acetyl. In general, the degree of protein binding is greater for charged sulfonamides than for uncharged sulfonamides (14).

The rate of uptake of the drug by the liver or another site of metabolism may depend upon its lipophilicity and the concentration of nonprotein-bound drug in the portal blood during the initial pass of the drug from the intestinal lumen through the liver following oral administration. Thus, protein binding of sulfisoxazole may spare it from first-pass metabolism over the dose range studied.

REFERENCES

(1) D. G. Shand, E. M. Nuckolls, and J. A. Oates, *Clin. Pharmacol. Ther.*, **11**, 112(1970).

(2) W. B. Abrams, C. B. Coutinho, A. S. Leon, and H. E. Spiegel, *J. Amer. Med. Ass.*, **218**, 1912(1971).

(3) R. N. Boyes, H. J. Adams, and B. R. Duce, *J. Pharmacol. Exp. Ther.*, **174**, 1(1970).

(4) P. A. Harris and S. Riegelman, *J. Pharm. Sci.*, **58**, 71(1969).

(5) J. G. Wagner, P. D. Holmes, P. K. Wilkinson, D. C. Blair, and R. Ç. Stoll, *Amer. Rev. Respir. Dis.*, **108**, 536(1973).

(6) P. Pentikainen, S. H. Wan, and D. L. Azarnoff, *ibid.*, **108**, 1340(1973).

(7) D. C. Bloedow and W. L. Hayton, *J. Pharm. Sci.*, **65**, 328(1976).

(8) A. C. Bratton and E. K. Marshall, Jr., *J. Biol. Chem.*, **128**, 537(1939).

(9) G. Levy, M. Gibaldi, and J. A. Procknal, *J. Pharm. Sci.*, **61**, 798(1972).

(10) J. Nimmo, R. C. Heading, P. Tothill, and L. F. Prescott, *Brit. Med. J.*, **1**, 587(1973).

(11) L. O. Randall, R. Engelberg, V. Iliev, M. Roe, H. Haar, and T. H. McGavack, *Antibiot. Chemother.*, **4**, 877(1954).

(12) R. E. Flake, J. Griffin, E. Townsend, and E. M. Yow, *J. Lab. Clin. Med.*, **44**, 582(1954).

(13) T. Struller, *Antibiot. Chemother.*, **14**, 179(1968).

(14) Å. Agren, R. Elofsson, and S. O. Nilsson, *Acta Pharmacol. Toxicol.*, **29**, 48(1971).

ACKNOWLEDGMENTS AND ADDRESSES

Received August 9, 1974, from the *College of Pharmacy, Washington State University, Pullman, WA 99163*

Accepted for publication January 10, 1975.

Presented in part at the APhA Academy of Pharmaceutical Sciences, Chicago meeting, August 1974.

Supported in part by funds provided for biological and medical research by the State of Washington Initiative Measure 171.

The authors express their appreciation to Dr. W. E. Scott, Research Division, Hoffmann–La Roche Inc., for providing the sulfisoxazole acetyl used.

* AFPE Robert Lincoln McNeil Memorial Fellow. Present address: College of Pharmacy, South Dakota State University, Brookings, SD 57006

ˣ To whom inquiries should be directed.

Mechanism of Action of BCG Vaccine on Neoplastic Proliferation and Host Immune Responses

ANWAR A. HAKIM [x] and NICHOLAS G. GRAND

Abstract □ BCG (Bacillus Calmette–Guerin) vaccine, Tice strain, caused a threefold increase in spleen weight of normal animals and a fourfold increase in spleen weight of sarcoma-bearing mice. In the latter group, the BCG vaccine caused infiltration of the sarcoma cells into the peritoneum and tumor metastasis in the spleen. Spleen lymphocytes from mice immunized with neuraminidase-treated sarcoma or from mice that had overcome an inoculum (100 cells) and a challenge (10^4 cells) of sarcoma P-1798 were cytotoxic against ^{51}Cr- or ^{14}C-2-thymidine-labeled sarcoma cells. The serum of these mice enhanced the cytotoxic activity and inhibited the migration of the syngeneic lymphocytes. These serums also inhibited the migration of peritoneal macrophages from guinea pigs immunized with the sarcoma cells. BCG vaccine enhanced the development and growth of sarcoma P-1798; *i.e.*, 50–100 viable sarcoma cells produced solid tumors in 8% of the untreated animals but in 100% of the BCG-treated animals. The serum of BCG-treated sarcoma-bearing animals inhibited the spleen lymphocyte-mediated cytotoxic action. The spleen lymphocytes from the BCG-treated sarcoma-bearing animals had no effect against ^{51}Cr- or ^{14}C-2-thymidine-labeled sarcoma cells. The data indicate that the serum from BCG-treated sarcoma-bearing animals blocks the spleen lymphocyte-mediated cytotoxic activities directed against proliferation and growth of the sarcoma.

Keyphrases □ Bacillus Calmette–Guerin vaccine—mechanism of action, effect on spleen weight, neoplastic proliferation, mice □ Neoplastic proliferation—effect of BCG vaccine, mice □ Spleen weight—effect of BCG vaccine, mice □ BCG vaccine—mechanism of action, effect on spleen weight, neoplastic proliferation, mice

BCG (Bacillus Calmette–Guerin) vaccine is an attenuated microorganism derived from the bovine tubercle bacillus. Some strains of this mycobacterium act as potent nonspecific stimulators of the reticuloendothelial system. They interfere with the growth of some experimental transplantable neoplasms in laboratory animals and cause regression of established cancers in selected experimental tumor models (1). This form of tumor response occurs in steps which require participation of host immune response (2–4).

Immunological defenses are important in malignant diseases as well as in tuberculosis. The acquired cellular immunity to tuberculosis, whether induced by vaccination or by actual infection, consists of an increased capability of the reticuloendothelial system to prevent intracellular multiplication and both lymphatic and hematogenous spread. Several reports concern the difference between the Tice strain and other Phipps or H 37 Ra strains of the mycobacterium. The Tice strain enhances rather than inhibits tumor growth (5), and more tuberculosis developed among children vaccinated with Tice strain than among the controls (6).

This article reports on the stimulating effect of the BCG Tice strain on tumor growth, namely a transplantable sarcoma P-1798 in BALB/c mice. It also presents *in vitro* evidence of the inhibition of spleen cell- or lymphocyte-mediated response with serum from BCG-treated sarcoma-bearing mice.

EXPERIMENTAL

Cells—Mouse sarcoma P-1798 that had been continuously carried in male BALB/c mice (16–20 g) and lyophilized BCG vaccine, Tice strain[1], were used.

Neuraminidase Treatment—*Vibrio cholera* neuraminidase, 500 units of enzyme/ml, was used. One unit of enzyme activity is equivalent to the release of 1 μg of *N*-acetylneuraminic acid from a glycoprotein substrate at pH 5.5 at 37°. The enzyme itself is not cytolytic (7, 8) and can release sialic acid from both normal and malignant cell surfaces at physiological pH values (9).

The sarcoma cells were incubated with neuraminidase (25 units/5×10^7 cells) at 37° for 1 hr. After incubation, the cells were washed three times in an excess of supplemented Eagle's medium and finally suspended in the same medium.

Effect of BCG Vaccine Dose on Tumor Growth—Various doses of sarcoma cells, from 22 to 2.2×10^7, were inoculated subcutaneously into groups (20 mice/group) of male BALB/c mice (16–20 g). At contralateral sites of the same animal, 4.5 mg of the lyophilized vaccine in 0.1 ml of sterile water was administered by subcutaneous injections. Animals were checked every day to detect appearance of the tumor nodule, and the survival of the animals from the date of appearance of the tumor nodule was noted (Tables I and II).

On the day the mouse expired, the spleens were removed and weighed. When the mouse was observed to be dying, it was sacrificed; the spleen was removed and was used to prepare the lymphocytes and to assess lymphocyte-mediated cytotoxicity. Spleen lymphocytes from normal mice were always prepared fresh and run as controls.

Effect of Various Doses of BCG Vaccine in Tumor Growth by Sarcoma Cells—Inocula of 1.4×10^2 and 1.4×10^4 sarcoma cells were inoculated subcutaneously in groups (20 mice/group) of male BALB/c mice (16–20 g). At contralateral sites of the same animal, the indicated dose of the BCG vaccine in 0.1 ml of sterile water was administered by subcutaneous injections. The animals were checked as described previously.

Preparation of Target Cells—The tumor tissue was cut into 1-mm pieces, gently teased through sieve No. 80 into Eagle's minimum essential medium containing 100 units/ml of both streptomycin and penicillin, and then centrifuged at 100 rpm. The cells were resuspended and washed three times in the Eagle's medium supplemented with 10% heat-inactivated calf serum. Two million sarcoma cells were suspended in 1 ml of the supplemented Eagle's medium, and 0.2 ml of ^{14}C-2-thymidine (specific activity 59 mCi/mole) or 150 μCi ^{51}Cr-sodium chromate (specific activity 200 mCi/mg) was added. After incubation at 37° for 180 min, the mixture was centrifuged at 100 rpm for 5 min. Then the cell pellet was washed with aliquots of the supplemented Eagle's medium until the washings became free of radioactivity.

Lymphoid-Cell Suspension—Lymphoid cell suspensions were prepared from spleens of normal, sarcoma-bearing, and BCG-treated sarcoma-bearing adult BALB/c mice. The spleens were removed aseptically, cut into small pieces, and gently teased through sieve No. 80 into supplemented Eagle's medium. The cell suspension was centrifuged at 1500 rpm for 5 min, and the supernates

[1] Manufactured by the Tuberculosis Research Institute, BCG Laboratories, University of Illinois.

Table I—Effect of Single Dose of BCG Vaccine on Tumor Growth and Spleen Weight by Various Doses of Sarcoma Cells

Inoculum in 0.1 ml Live Cells/ml	Survival[a], days	Average Spleen Weight, mg	Difference, mg (E − C)
2.26×10^7	C: 12–26	C: 324 (280–399)[b]	285
	E: 12–18	E: 619 (387–1124)	
2.26×10^5	C: 18–27	C: 371 (302–424)	326
	E: 18–24	E: 697 (566–1169)	
2.26×10^3	C: 21–25	C: 367 (313–389)	532
	E: 20–25	E: 899 (686–1084)	
22	C: 28–32	C: 359 (308–402)	579
	E: 22–28	E: 938 (755–1399)	
Tumor free[c]		366 (234–673)	

[a] C is the control without BCG treatment, and E is the experimental group that received BCG with tumor cell inoculum. [b] Numbers in parentheses are the range of weights. [c] Group that received only BCG without tumor cell inoculum.

were discarded. Then the cell pellet was resuspended in the Eagle's medium and repelleted at 900 rpm for 60 sec.

The cells in the supernate were recentrifuged at 1500 rpm for 5 min. The resulting cell pellet was washed three times with Eagle's medium, and the cell suspension was evaluated for viability by the trypan blue exclusion reaction. The lymphocytes present in the cell suspension (10^7 cells/spleen) were 90% viable. Morphologically, about 80% of the mononuclear cells present in these suspensions were lymphocytes; the remaining cells were principally macrophages.

Cytolytic Assay—The cytolytic assay used was described by Brunner *et al.* (10). Adult BALB/c mice were injected subcutaneously in the right hindleg with 10^6 sarcoma cells. Twenty-one days later, these animals were sacrificed, the spleens were removed, and a lymphocyte suspension was prepared. This lymphocyte suspension was compared to a lymphocyte suspension of identical cell concentration but obtained from animals (20 mice) inoculated with neuraminidase-treated sarcoma cells.

Ten million viable lymphocytes from these two groups of mice and from normal mice (control) were mixed with 10^5 ^{14}C-2-thymidine- (or ^{51}Cr-) labeled sarcoma cells in a reaction volume of 1.5 ml of the supplemented Eagle's medium. The interaction between the lymphocytes and the sarcoma cells was allowed to proceed at 37°. After 69 min of incubation, 0.5 ml of tromethamine buffer at pH 8.2, containing 1000 units of trypsin, was added. The cells were centrifuged at 1500 rpm for 5 min, 0.5-ml aliquots of the cell-free supernates were taken, and their radioactivity was assessed.

The percentage cytolysis of the target cells was calculated by subtracting from the radioactivity released in the presence of lymphocytes from sarcoma-treated mice that percentage of radioactivity released in the presence of the same number of normal lymphoid cells.

Cell Migration—Using 10^7 cells/ml suspended in the supplemented Eagle's medium, heparin-coated capillary tubes were filled with the washed spleen cells, lymphocytes, or the washed sarcoma P-1798 cells and placed on the bottom coverslip of a Mackanese-type chamber. The cells were incubated at 37° for 24 hr in the supplemented Eagle's medium in the presence and absence of the factors or serums studied. The area of cell migration was calculated as described previously (11).

Table II—Effect of Various Doses of BCG Vaccine and Sarcoma Cells on Spleen Weight[a]

BCG Vaccine, mg	Tumor Inoculum, viable cells/ml	Viability, days	Average Spleen Weight, mg
4.5	1.4×10^4	26–33	709 (534–993)[b]
	1.4×10^2	27–40	834 (602–1356)
4.5×10^{-2}	1.4×10^4	28–33	338 (273–367)
	1.4×10^2	33–47	453 (130–577)
4.5×10^{-4}	1.4×10^4	29–33	341 (263–445)
	1.4×10^2	41–48	379 (304–444)
4.5×10^{-6}	1.4×10^2	37–41	580 (522–624)
	1.4×10^4	31–32	424 (343–499)
None	1.4×10^4	28–33	445 (210–726)
	1.4×10^2	33–50	200 (180–238)

[a] Groups of 20 mice were used. [b] Numbers in parentheses are the range of weights.

Table III—Spleen Lymphocyte-Mediated Cytotoxicity from Animal Immunized against Sarcoma P-1798 Cells

Spleen Lymphocytes from Animals Treated with	Percent of Radioactivity Released into Cell-Free Supernate	
	^{51}Cr-Sarcoma Cells	^{14}C-Sarcoma Cells
Buffered saline	19.0 ± 1.2[a]	0.86 ± 0.03[a]
Buffered saline, but sarcoma bearing[b]	21.6 ± 1.1	1.14 ± 0.04
Neuraminidase-treated sarcoma cells (10^6)[b]	86.2 ± 4.9	58.17 ± 2.5
100 Sarcoma and then challenged with 10^6 cells[b]	85.8 ± 4.6	57.28 ± 2.4

[a] The data are the averages from 10 experiments ± *SE*. [b] The animals were sacrificed and spleen lymphocytes were obtained 21 days after the last treatment or 21 days after inoculation of the tumor cells.

RESULTS

Effect of BCG Vaccine and Inoculum Size on Tumor Growth—When inoculated subcutaneously in the right hindleg, sarcoma P-1798 grew readily and the animals died between 15 and 20 days, depending on the number of cells inoculated. The sarcoma inoculum varied between 10^6 and 10^2 viable cells/mouse. In over 1000 mice inoculated with the sarcoma, there were no spontaneous regressions.

The spleen wet weight of normal BALB/c mice (16–20 g) varied between 64 and 161 mg (average ± *SE* = 120 ± 10.5 mg). Sarcoma-bearing mice had a spleen wet weight of 150–225 mg (average ± *SE* = 190 ± 36.5 mg). Inoculation of the BCG vaccine into normal mice caused an approximately threefold increase in the spleen wet weight (range, 312–647 mg; average ± *SE*, 462 ± 35 mg). If inoculated into sarcoma-bearing mice, the BCG vaccine produced an approximately fourfold increase in the spleen wet weight (range, 491–993 mg; average ± *SE*, 709 ± 53 mg). A greater increase in the spleen wet weight was produced with the smaller initial sarcoma

Table IV—Lysis of ^{51}Cr- or ^{14}C-Labeled Sarcoma Cells: Spleen Cell-Mediated Cytotoxic Activity

Spleen Cell Source	Percent of Radioactivity Released into Cell-Free Supernate	
	^{51}Cr-Sarcoma Cells	^{14}C-Sarcoma Cells
Normal mice	27 ± 2.6	0.66 ± 0.02
Sarcoma-bearing mice		
1st week	37.5 ± 1.7	62.9 ± 1.9
2nd week	30.6 ± 1.3	29.5 ± 1.1
3rd week	21.3 ± 1.06	0.93 ± 0.04
BCG vaccine-treated[a] sarcoma-bearing mice		
1st week	30.4 ± 1.6	10.06 ± 0.94
2nd week	11.5 ± 1.5	6.06 ± 2.35
3rd week	9.6 ± 0.67	5.88 ± 0.09
BCG vaccine-treated[b] sarcoma-bearing mice		
1st week	68.5 ± 2.4	94.33 ± 4.7
2nd week	47.7 ± 2.9	65.60 ± 3.7
3rd week	32.3 ± 1.2	41.16 ± 2.1
Immune mice[c]	85.9 ± 4.7	96.23 ± 2.4

[a] Mice were treated with 4.5 mg/mouse of the lyophilized BCG vaccine. The data are the averages of 10 experiments ± *SE*. [b] Mice were treated with 4.5×10^{-6} mg/mouse of lyophilized BCG vaccine. [c] Mice were immunized with the neuraminidase-treated sarcoma cells. The data are the averages of 10 experiments ± *SE*.

Table V—Effect of Serum on Spleen Cell-Mediated Cytoxic Activities

Serum	Spleen Cells: Normal Mice	Sarcoma-Bearing Mice	Immune Mice	BCG Vaccine-Treated Sarcoma-Bearing Mice
Normal mice	32 ± 3[a]	2278 ± 132[a]	2260 ± 113[a]	184 ± 12[a]
Sarcoma-bearing mice				
1st week	572 ± 39	4125 ± 179	4067 ± 169	4265 ± 183
2nd week	109 ± 8	3397 ± 116	3845 ± 145	1983 ± 74
3rd week	47 ± 3	3918 ± 137	4257 ± 173	49 ± 4
Immune mice[b]	73 ± 4	4689 ± 192	4985 ± 207	76 ± 5
BCG vaccine-treated sarcoma-bearing mice[c]				
1st week	986 ± 97	3671 ± 167	3578 ± 143	4329 ± 191
2nd week	95 ± 8	732 ± 67	895 ± 83	3194 ± 157
3rd week	75 ± 6	77 ± 36	236 ± 36	531 ± 72
O Inactivated	37 ± 3	2530 ± 143	4124 ± 173	92 ± 7
BCG vaccine-treated sarcoma-bearing mice[d]				
1st week	375 ± 27	4123 ± 180	4429 ± 213	4135 ± 185
2nd week	125 ± 8	3915 ± 162	4215 ± 198	3876 ± 157
3rd week	115 ± 6	3761 ± 153	4198 ± 180	3625 ± 132

[a] The data are in disintegrations per minute, the average of 10 experiments ± *SE*. [b] Immune mice are the mice immunized with neuraminidase-treated sarcoma cells. [c] Mice were treated with 4.5 mg/mouse of the lyophilized Tice BCG. [d] Mice were treated with 4.5 × 10^{-6} mg/mouse of the lyophilized Tice BCG.

inoculum of less than 10^2 viable cells. In this experiment, 20 mice/group were used.

The data summarized in Table I suggest that, if administered subcutaneously to mice inoculated simultaneously with sarcoma cells and 4.5 mg of the lyophilized BCG vaccine, the vaccine increased the spleen wet weight in a magnitude that varied inversely with the number of the sarcoma cells in the inoculum.

Effect of BCG Dose on Tumor Growth Induced by Sarcoma Cells—Table II summarizes the results obtained from the effect of various doses of the BCG vaccine administered to mice inoculated with 1.4 × 10^2 and 1.4 × 10^4 sarcoma cells. All groups treated with the vaccine showed hyperplasia of the spleen. The greatest increase in the spleen wet weight was obtained with the highest dose of the BCG vaccine in mice inoculated with 10^2 viable sarcoma cells.

Spleen Lymphocyte-Mediated Cytotoxic Activity of Animals Immunized against Sarcoma P-1798—Mice that were immunized with three successive doses of nonviable sarcoma cells or with neuraminidase-treated viable sarcoma cells successfully overcame a tumor inoculum of 100 viable cells/mouse and survived a second challenging dose, 10^4 viable sarcoma cells, given a month later. During this time, mice from each of these groups (initially 40 mice/group) were sacrificed at various periods to establish the general pattern of the development of cellular immunity.

Four days after the second challenge, six spleens from each group were removed and examined for lymphocyte-mediated cytotoxic activity using the ^{51}Cr- and the ^{14}C-2-thymidine-labeled sarcoma cells. The data summarized in Table III show that low levels of cytotoxic activity against the ^{51}Cr-labeled sarcoma cells were found in the spleen lymphocytes of normal mice. High levels of cytolytic activity against the labeled cells were found in the spleens of mice that were immunized with either nonviable sarcoma cells or neuraminidase-treated sarcoma cells and survived the challenging doses of viable sarcoma cells.

Spleen Lymphocyte-Mediated Cytotoxic Activity of Animals Treated with BCG Vaccine—The same techniques were used to compare the properties of the spleen cells derived from immune mice [*i.e.*, mice inoculated with a low number (60–100) of viable sarcoma cells but tumors failed to grow], sarcoma-bearing, and BCG-treated sarcoma-bearing mice. One group of mice was treated with 0.1 ml of 4.5 mg/ml of BCG vaccine, and a second group was treated with 0.1 ml of 4.5 × 10^{-6} mg/ml. Seven days later, the mice were challenged with 10^4 viable sarcoma cells. In this experiment, 20 BALB/c mice were used per group. The results (Table IV) indicate that pretreatment with BCG vaccine (0.45 mg/ml) suppresses the cellular immune response against the sarcoma challenge. In spite of their depressed cytolytic potentials, the spleens from BCG-treated animals were hyperplastic and histological examination revealed viable sarcoma cells.

Effect of Serum on Spleen Cell-Mediated Cytolytic Activities—The cytolytic activities of spleen cells mixed with serums of normal, sarcoma-bearing, immunized, and BCG-treated sarcoma-bearing mice are presented in Table V. The data indicate that the spleen cell-mediated cytolytic activity against the ^{14}C-2-thymidine-labeled sarcoma cells in the sarcoma-bearing mice decreased as the tumor progressively grew. Similarly, the spleen cell-mediated cytolytic activity against ^{14}C-2-thymidine-labeled sarcoma cells in the BCG-treated tumor-bearing mice also decreased as the tumor grew. The magnitude of the spleen cell-mediated cytolytic activity varied with the dose of BCG vaccine administered. Ani-

Table VI—Cytotoxic Activities of Spleen Cells and Serum

	Spleen Cells: Disintegrations per Minute	Spleen Cells: Disintegrations per Minute Released, %	Serum: Disintegrations per Minute	Serum: Disintegrations per Minute Released, %
None	4501 ± 124	0	4501 ± 124	0
Normal mice	30 ± 6	0.66	35 ± 7	0.78
Sarcoma-bearing mice				
1st week	2837 ± 74	62.9	1218 ± 32	27.1
2nd week	1327 ± 37	29.5	539 ± 17	12.8
3rd week	42 ± 5	0.93	32 ± 5	0.93
BCG vaccine-treated sarcoma-bearing mice[b]				
1st week	453 ± 11	10.1	2347 ± 71	52.14
2nd week	273 ± 8	6.06	2167 ± 63	48.14
3rd week	265 ± 7	5.88	658 ± 21	14.62
Immune mice	2531 ± 82	56.23[c]	1656 ± 47	36.79
BCG vaccine-treated sarcoma-bearing mice[d]				
1st week	4249 ± 120	94.33	3785 ± 103	84.09
2nd week	2953 ± 80	65.60	3156 ± 95	70.11
3rd week	1873 ± 57	41.61	275 ± 80	60.98

[a] The data are in disintegrations per minute, the average of 10 experiments ± *SE*. [b] Mice were treated with 4.5 mg/mouse of the lyophilized Tice BCG. [c] Immune mice are the mice immunized with neuraminidase-treated sarcoma cells. [d] Mice were treated with 4.5 × 10^{-6} mg/mouse of the lyophilized Tice BCG.

Table VII—Migration Inhibition or Enhancing Factor

Cells	Serum[a] from Mice			
	Normal Mice	Immune Mice	BCG-Treated Sarcoma-Bearing Mice	Sarcoma-Bearing Mice
Spleen cells from mice				
Normal	100 ± 4.5[b]	99 ± 4.4[b]	100 ± 5.2[b]	98 ± 4.3[b]
Sarcoma bearing	96 ± 4.3	65 ± 3.1	153 ± 6.4	71 ± 3.7
BCG-treated sarcoma bearing	115 ± 5.3	87 ± 3.9	92 ± 4.1	95 ± 4.2
BCG-treated normal	99 ± 4.4	98 ± 4.4	69 ± 3.2	99 ± 4.4
Immune[c]	98 ± 4.3	8 ± 0.8	141 ± 6.0	56 ± 3.2
Macrophages from guinea pigs				
Normal	93 ± 4.1	94 ± 4.2	105 ± 5.1	98 ± 4.3
Immune	95 ± 4.3	6 ± 0.7	93 ± 4.1	51 ± 3.1
BCG-treated normal	92 ± 4.0	98 ± 4.5	73 ± 3.3	101 ± 4.7
BCG-treated sarcoma-cell inoculated	97 ± 4.5	143 ± 6.5	154 ± 7.1	99 ± 4.4
Sarcoma cells	100 ± 4.6	2 ± 0.0	127 ± 6.0	85 ± 4.2

[a] The serum was drawn from animals 7 days after appearance of the tumor. [b] The data are in percent of the control and represent the average of four separate experiments ± *SE*. [c] Immune animals are mice immunized with three subcutaneous injections of neuraminidase-treated sarcoma cells.

mals receiving higher doses of the vaccine had lower spleen cell-mediated cytotoxic activity.

These experiments suggest that higher doses of the vaccine cause the release of "blocking factors" which block the cytolytic effects of the spleen cells. Serum was drawn from normal, sarcoma-bearing, BCG-treated sarcoma-bearing, and immune mice. Each serum was mixed with a fixed number of viable cytotoxic lymphocytes from immune mice, *i.e.*, from mice that had survived at least one challenge of viable sarcoma cells. The lymphocyte-mediated cytolytic activities were then assessed. The data in Table V indicate that the serum from normal mice had no effect but that the serum from the BCG-treated (4.5 mg/mouse) sarcoma-bearing mice inhibited the spleen lymphocyte-mediated cytotoxic activity of spleens from sarcoma-bearing and immune mice; it had no effect on spleen lymphocytes from normal or BCG-treated sarcoma-bearing mice.

The data in Table VI summarize the cytotoxic activity of spleen cells and of serum from the various groups, each examined separately. The data indicate differences in the cytotoxic activities of spleen cells and serum from BCG-treated sarcoma-bearing mice. In mice treated with 4.5×10^{-6} mg of BCG, the cytotoxic activity of both spleen cells and the serum was enhanced. Higher doses of BCG vaccine inhibited the cytotoxic activity of the spleen cells and of the serum.

Migration of Spleen Cells, Guinea Pig Macrophages, and Sarcoma Cells—In absence of mouse serum and in Eagle's essential medium, migration of spleen cells from capillaries results in three zones: dense, medium, and light. The data in Table VII indicate that if 0.05 ml of serum from normal mice was incorporated into the 1.0 ml of the medium, normal spleen cells migrated in dense and medium zones. The migration pattern indicates that the serum from tumor-bearing mice had no apparent inhibiting effect on the migration of spleen cells from normal mice. On the other hand, the serum from tumor-bearing mice inhibited the migration of spleen cells from tumor-bearing animals. The serum from BCG vaccine-treated tumor-bearing mice enhanced the migration of spleen cells from the tumor-bearing and immune mice but had no effect on the migration of spleen cells from normal mice. Therefore, these observations suggest that the effect of the serum from tumor-bearing mice is specific or related to the tumor. This effect disappeared if the tumor-bearing animals were treated with BCG vaccine, Tice strain. If migration inhibition is caused by the release of a "migration inhibition factor," the serum from the BCG-treated sarcoma-bearing mice causes the release of a "migration enhancing factor."

Migration of sarcoma cells was inhibited by serum from immune and sarcoma-bearing mice, but it was enhanced by serum from BCG-treated sarcoma-bearing mice.

DISCUSSION

The observed changes in the wet weight of the spleens could be the result of several reactions. One of the earliest events in the initiation of humoral immune response is the recruitment of peripheral lymphocytes (12–17), and Zatz and Lance (14,15) showed that lymphocyte "trapping" exhibits immunological specificity and demonstrated the retention of circulating lymphocytes in lymph nodes and spleen after challenge with conventional antigens and skin grafts (15, 18). This effect is thought to lead to the recruitment of increased numbers of antigen-sensitive cells during initiation of an immune response (19). Aberration in lymphocyte circulation patterns also occurs in response to tumor growth (20). More recently, Zatz *et al.* (21) demonstrated the trapping of ^{51}Cr-labeled Moloney sarcoma in the lymph nodes and spleens of tumor-bearing mice.

Freund's adjuvant, complete or incomplete, modified the immune response of mice to an immunizing dose of tumor antigen, and the tumor was able to grow and kill the animals. Pretreatment with complete Freund's adjuvant alone also led to enhanced tumor growth (22).

Animals immunized with normal or neoplastic tissues and individuals bearing spontaneous tumors carry humoral antibodies and cytotoxic lymphocytes which compete for the same antigens on the target cell surface (10, 23–27). Lymphocyte-mediated cytolysis is a complex multistage phenomenon separable into binding followed by a lytic phase (28–32). Therefore, the present studies represent an attempt to expose the mechanisms allowing enhanced tumor growth in mice treated with BCG vaccine, Tice strain. Two phenomena were investigated.

The cytotoxic activities of the spleen cells from tumor-bearing animals are in line with the results of other investigators using a variety of tumor systems. Individuals carrying progressively growing neoplasms have lymphoid cells with a specific cytotoxic effect on cultured tumor cells from the same individual (33–36). The magnitude of the spleen cells cytotoxic effect varied from one group to another and from one period to another. These variations are to be expected since the serums of tumor-bearing individuals have been shown to prevent tumor cell destruction by immune lymphocytes of the spleen cells *in vitro* (34, 37–39) and since this serum blocking activity appears early in primary tumor development (37, 39).

Differences are to be expected in the magnitude of the blocking or enhancing activities of the serum on the spleen cell cytotoxic potency. At any time, a serum may show complete blocking by one method but only partial by another and even a reverse effect against some target cells (40). Even with the same tumor system, the level of blocking detectable may vary under different experimental conditions. For example, by adding serum and lymphocytes to mammary tumor target cells at the same time, Heppner (41) detected only partial blocking whereas Blair and Lane (40) observed complete blocking.

An alternative possibility is that animals with progressively growing tumors have depressed immunological systems. Studies have demonstrated the immunosuppressive properties of various carcinogens (42–52). Based on these observations, the enhancing growth by the BCG vaccine, Tice strain, could be associated with a

BCG-mediated immunosuppression. Thus the vaccine might be acting similarly to a carcinogen.

CONCLUSIONS

Aberrations in lymphocyte circulation patterns cause infiltration of the sarcoma cells into the lymphatic system and their trapping in lymphoid tissue. Catalysis of these aberrations by BCG vaccine, Tice strain, resulted in the hyperplasia of the spleen and metastasis of the tumor in the spleen and the peritoneum.

BCG vaccine also modified the immune response of mice to an immunizing dose of neoplastic cells, so as to enable the tumor to grow and kill the animals. The significance of this effect is complicated by its dependence on several factors: the dose of the mycobacterium and the immune status of the host. At doses higher than 4.5×10^{-6} mg of the lyophilized vaccine, BCG caused suppression of the host cellular immunity.

The serum of progressively growing sarcoma-bearing or BCG-treated sarcoma-bearing mice contains inhibitor(s) of lymphocyte-mediated cytotoxic activities. Since there is no reason to assume that immune responses in any tumor system are directed against a single antigen and since a serum of a tumor donor may contain not only different levels of free antigen, antigen–antibody complexes, and free antibody but also antigens and antibodies of different specificities at different times in the development and growth of the tumor, BCG vaccine, Tice strain, must have catalyzed the formation of humoral complexes that blocked the cellular immunity directed against neoplasms, in this case sarcoma P-1798.

REFERENCES

(1) B. Zbar, H. T. Wepsig, and T. Borsos, *J. Nat. Cancer Inst.*, **44,** 473(1970).

(2) B. Zbar, I. D. Bernstein, and H. J. Rapp, *ibid.*, **46,** 831(1971).

(3) G. L. Bartlett, B. Zbar, and H. J. Rapp, *ibid.*, **48,** 245(1972).

(4) E. B. Chung, B. Zbar, and R. J. Rapp, *ibid.*, **51,** 241(1973).

(5) I. Millman, H. C. Maquire, Jr., J. P. Youmans, and A. S. Youmans, *Proc. Soc. Exp. Biol. Med.*, **147,** 765(1974).

(6) G. W. Comstock, V. T. Livesay, and S. F. Woolpert, *Amer. J. Pub. Health*, **64,** 283(1974); **65,** 309(1975).

(7) P. K. Ray, H. Gewurz, and R. L. Simmons, *Clin. Exp. Immunol.*, **11,** 441(1972).

(8) P. K. Ray and R. L. Simmons, *ibid.*, **10,** 139(1972).

(9) P. K. Ray and R. L. Simmons, *Cancer Res.*, **38,** 936(1973).

(10) K. T. Brunner, J. Mauel, J. C. Cerottini, and B. Chapuis, *Immunology*, **14,** 181(1968).

(11) A. A. Hakim, *Experientia*, **29,** 865(1973).

(12) O. Sprent, J. F. A. P. Miller, and G. F. Mitchell, *Cell Immunol.*, **2,** 171(1971).

(13) E. E. Emerson and D. R. Thursh, *J. Immunol.*, **106,** 635(1971).

(14) M. M. Zatz and E. M. Lance, *Fed. Proc.*, **30,** 409(1971).

(15) M. M. Zatz and E. M. Lance, *J. Exp. Med.*, **134,** 224(1971).

(16) R. N. Taub and R. K. Gershon, *Fed. Proc.*, **30,** 509(1971).

(17) D. W. Dresser, R. N. Taub, and A. R. Krantz, *Immunology*, **18,** 663(1970).

(18) M. M. Zatz and E. M. Lance, *Nature New Biol.*, **234,** 253(1971).

(19) W. L. Ford, *Cell Tissue Kinet.*, **2,** 171(1969).

(20) R. K. Gershorn and R. S. Fightlin, International Symposium on Chemotherapy of Cancer Dissemination and Metastasis, 1972.

(21) M. M. Zatz, A. White, and A. L. Goldstein, *J. Immunol.*, **111,** 706(1973).

(22) H. Zola, *Clin. Exp. Immunol.*, **11,** 585(1972).

(23) I. Hellstrom, K. E. Hellstrom, C. A. Evans, G. H. Heppner, G. E. Pierce, and J. P. S. Yang, *Proc. Nat. Acad. Sci. USA*, **62,** 362(1969).

(24) I. Hellstrom, H. O. Sjogren, G. Warner, and K. E. Hellstrom, *Int. J. Cancer*, **7,** 226(1971).

(25) J. Mauel, H. Rudolf, B. Chapuis, and K. T. Brujner, *Immunology*, **18,** 517(1970).

(26) E. Moller, *J. Exp. Med.*, **122,** 11(1965).

(27) G. Berke and D. B. Amos, *Transplant. Rev.*, **17,** 27(1974).

(28) G. Berke and K. A. Sullivan, *Transplant. Proc.*, **5,** 421(1973).

(29) G. Berke, K. A. Sullivan, and B. Amos, *J. Exp. Med.*, **136,** 1594(1972).

(30) R. D. Stulting and G. Berke, *ibid.*, **137,** 932(1973).

(31) A. A. Hakim, *Naturwissenschaften*, **60,** 53(1973).

(32) R. T. Todd, II, R. D. Stulting, and G. Berke, *Cancer Res.*, **33,** 3203(1973).

(33) I. Hellstrom, K. E. Hellstrom, and G. E. Pierce, *Int. J. Cancer*, **3,** 467(1968).

(34) I. Hellstrom and K. E. Hellstrom, *ibid.*, **4,** 587(1969).

(35) I. Hellstrom, K. E. Hellstrom, H. O. Sjogren, and G. A. Warner, *ibid.*, **7,** 1(1971).

(36) K. E. Hellstrom and I. Hellstrom, *Advan. Cancer Res.*, **12,** 167(1969).

(37) H. O. Sjogren and K. Borum, *Cancer Res.*, **31,** 890(1971).

(38) I. Hellstrom, H. O. Sjogren, G. A. Warner, and K. E. Hellstrom, *Int. J. Cancer*, **7,** 226(1971).

(39) K. E. Hellstrom and I. Hellstrom, *Ann. Rev. Microbiol.*, **24,** 373(1970).

(40) P. B. Blair and M. A. Lane, *J. Immunol.*, **112,** 439(1974).

(41) G. H. Heppner, *Int. J. Cancer*, **4,** 608(1969).

(42) J. K. Ball, *J. Nat. Cancer Inst.*, **44,** 1(1970).

(43) I. Davidson, K. Stern, and I. Sabet, *Proc. Amer. Soc. Cancer Res.*, **2,** 102(1956).

(44) R. G. Doel, St. Cyr. C. DeVaux, and P. Grabner, *Int. J. Cancer*, **2,** 103(1967).

(45) H. W. Fox and F. G. Bock, *J. Nat. Cancer Inst.*, **38,** 789(1967).

(46) M. I. Kipke and D. W. Weiss, *Int. J. Cancer*, **6,** 422(1970).

(47) R. A. Malmgren, B. E. Bennison, and T. W. Mckinley, Jr., *Proc. Soc. Exp. Biol. Med.*, **79,** 484(1952).

(48) G. Parmiani, *Int. J. Cancer*, **3,** 260(1970).

(49) R. T. Prehn, *J. Nat. Cancer Inst.*, **31,** 791(1963).

(50) B. A. Rubin, *Proc. Amer. Ass. Cancer Res.*, **3,** 146(1960).

(51) J. Stjernsward, *Antibiot. Chemother.*, **15,** 213(1969).

(52) B. J. Wetson, *Nature*, **215,** 1497(1967).

ACKNOWLEDGMENTS AND ADDRESSES

Received January 6, 1975, from the *Departments of Surgery and Physiology, College of Medicine, University of Illinois at the Medical Center, Chicago, IL 60680*

Accepted for publication May 15, 1975.

Presented at the Annual Meeting of the Federation of the American Societies for Experimental Biology, Atlantic City, N.J., April 13–18, 1975.

[x] To whom inquiries should by directed.

Effect of Alpha Tocopherol (Vitamin E) Deficiency on Intestinal Transport of Passively Absorbed Drugs

MAHASEN M. MESHALI * and CHARLES H. NIGHTINGALE ˣ

Abstract □ Alpha tocopherol (vitamin E) deficiency has been shown to cause changes in membrane structure. The present study relates alpha tocopherol deficiency with increased rates of transport and absorption of passively absorbed drugs. The pharmacokinetics of barbital in alpha tocopherol-deficient and control rats was studied. The barbital absorption rate constant in deficient animals increased compared to control values. This finding indicates that alpha tocopherol deficiency affects the intestinal membrane structure. This finding was confirmed by studying the intestinal transport of phenolsulfonphthalein, barbital, and salicylate using the everted gut technique. Phenolsulfonphthalein was transported more rapidly through the alpha tocopherol-deficient gut, but this difference was not significant after 30 min, probably due to membrane decomposition. Barbital, which is more lipid soluble and less dependent on changes in pore volume and size, was transported more rapidly through the deficient gut during the entire experiment. The transport rate of salicylate was not altered by the deficiency state. This result was expected since the drug is normally rapidly transported; therefore, comparatively small changes in permeability such as those induced by alpha tocopherol deficiency would be masked. After the oral administration of phenolsulfonphthalein to intact animals, a significantly higher amount of drug was recovered in the urine of the deficient group.

Keyphrases □ Vitamin E—deficiency, effect on intestinal transport and absorption of barbital, phenolsulfonphthalein, and salicylate, rats □ Barbital—absorption and intestinal transport, alpha tocopherol-deficient rats □ Phenolsulfonphthalein—absorption and intestinal transport, alpha tocopherol-deficient rats □ Salicylate—absorption and intestinal transport, alpha tocopherol-deficient rats □ Absorption, GI—effect of alpha tocopherol deficiency, rats □ Transport rates, GI—effect of alpha tocopherol deficiency, rats □ Alpha tocopherol—effect of deficiency on intestinal transport and absorption of barbital, phenolsulfonphthalein, and salicylate, rats

Alpha tocopherol (vitamin E) is believed to play an important role in the maintenance of normal membrane structure and function. The relationship between alpha tocopherol body levels and membrane structure is not clear. It has been proposed (1) that alpha tocopherol may form a stable "complex" with membrane phospholipids in that the methyl groups at positions 4′ and 8′ of alpha tocopherol fit into pockets created by the *cis* double bonds of the fatty acid. An alpha tocopherol deficiency, therefore, would cause inefficient packing of the polyunsaturated fatty acids and alter membrane structure. An alternative postulation for the mechanism of action of alpha tocopherol in maintaining membrane structure is based upon its antioxidant properties (2–6). Since membrane lipids decompose *via* a free radical peroxidation reaction, a lack of the antioxidant alpha tocopherol would allow random free radical membrane damage to occur.

Regardless of the mechanism involved, alpha tocopherol deficiency has been shown to affect membrane structure. Examples are the increased tendency of red cells to hemolyze (7, 8) and membrane damage to subcellular structure such as mitochondria and ribosomes (6). Changes in the GI membrane structure in humans as well as Peking ducklings deficient in alpha tocopherol were demonstrated (9). Normal membrane structure was observed after treatment with alpha tocopherol. A decrease in the active transport of valine in alpha tocopherol-deficient animals was reported (10).

Since alpha tocopherol deficiency generally occurs in cases of malabsorption or malnutrition, the absorption of nutrients or drugs might be affected by the deficiency state. It is not known whether the general changes observed in membrane structure lead to changes in the transport or absorption rates of drugs. The purpose of this study was to determine the effect of alpha tocopherol deficiency on the passive transport of several drugs through the intestinal membrane.

EXPERIMENTAL

Sprague–Dawley albino male rats[1], 156 ± 10 g, were divided into two groups. The animals were fed either an alpha tocopherol-deficient diet (deficient group) or the deficient diet supplemented with alpha tocopherol (control group). The dietary composition, food consumption, and growth patterns of these animals were described previously (11). The animals were found to be alpha tocopherol deficient 4–6 weeks after being placed on the diets (11), and the experiment was started after that time.

Intestinal Transport Rate Measurements—Rats from each group were fasted 20–24 hr prior to the experiment but were allowed free access to water. The animals were anesthetized with ether, and a midline abdominal incision was made. About 40 cm of the intestine was removed, prepared, and everted as described by Mayersohn and Gibaldi (12). After removal of the intestine, the animals were sacrificed by etherization. The intestine, after discarding the first 10 cm, was divided into two segments and placed into 100 ml of pregassed Kreb's bicarbonate buffer. The pH of the gassed buffer was 7.4 and remained constant throughout the experiment. The buffer contained either sodium salicylate[2] (1 mg/ml), barbital sodium[3] (0.25 mg/ml), or phenolsulfonphthalein[4] (reagent grade) (0.1 mg/ml). One milliliter of the buffer was placed into, and completely filled, the serosal portion of the sac. The entire preparation was maintained at 37° and continuously gassed with oxygen containing 5% (v/v) carbon dioxide. The serosal solution was sampled every 15 min and assayed for drug content.

The amount of drug transported by each segment was calculated and statistically compared within each group. Since differences in drug transport between the segments of each group were not observed, the data were combined and transport rates, expressed as clearance, were compared between groups. Clearance was calculated by dividing the combined amount of drug transported every 15 min by the mucosal concentration.

Salicylate was determined colorimetrically by the method of Trinder (13). Barbital was assayed spectrophotometrically by a modification of the method described by Brodie *et al.* (14) for pentobarbital. Two milliliters of serosal solution (1 ml of sample and 1 ml of washings) was mixed in a 50-ml glass-stoppered tube with 1

[1] Blue Spruce Farms, Altamont, N.Y.
[2] Allied Chemical Corp., New York, N.Y.
[3] Merck and Co., Rahway, N.J.
[4] Fisher Chemical Co., Pittsburgh, Pa.

ml of 0.1 *N* HCl, 1 g of sodium chloride, and 12 ml of chloroform. The mixture was shaken mechanically at high speed for 1 hr and then centrifuged at 3000 rpm for 10 min. Ten milliliters of the chloroform layer was accurately measured and filtered through filter paper[5] into a glass-stoppered centrifuge tube containing 4 ml of pH 11 phosphate buffer. The filter paper was washed with 1 ml of chloroform, and the washing was added to the original filtrate.

The mixture was shaken mechanically for 20 min and then centrifuged. The absorption of the aqueous phase was determined at 240 nm against a similarly prepared blank. Phenolsulfonphthalein was assayed by mixing 2 ml of serosal solution (1 ml of sample and 1 ml of washings) with 1 ml of sodium hydroxide and 2 ml of Kreb's bicarbonate buffer. The mixture was centrifuged at 3500 rpm for 10 min, and the supernate was read spectrophotometrically at 560 nm against a similarly prepared reagent blank.

Urinary Excretion of Phenolsulfonphthalein after Oral Administration—Five rats from each group were fasted for 20 hr prior to drug dosing but allowed free access to water. The rats were lightly anesthetized with ether, and 1.5 ml of Kreb's bicarbonate buffer containing 1 mg/ml of phenolsulfonphthalein was administered directly into the stomach by oral intubation. Each animal was then placed into individual metabolic cages for urine collection and allowed free access to water. The cumulative amounts of urine excreted during the first 9 hr after dosing and then during the subsequent 15 hr were collected quantitatively.

The volume of each sample was measured, and phenolsulfonphthalein was assayed as described previously except that the supernate was filtered through a 0.22-μm cellulose filter. The solution was read spectrophotometrically against a similarly prepared 24-hr urine blank for each rat.

Pharmacokinetic Study of Barbital in Rats—*Oral Dosing*—Eight rats from each group, deficient and supplemented, weighing 350–400 g, were fasted for 20–24 hr prior to drug dosing but were allowed free access to water. Barbital sodium was dissolved in pH 6.8 phosphate buffer to produce a final concentration (pH 8.9) of 100 mg of drug/ml of buffer. The solution was administered to the animals by oral intubation at a constant dosage level of 200 mg/kg.

Blood samples were collected from the tail artery 5 min after administration of the drug and then at 15-min intervals for the 1st hr. Samples were also taken every hour for the next 3 hr and then every 12 hr for a total of 3 days. Each blood sample was centrifuged, and a 0.2-ml aliquot of the plasma was accurately transferred into a 50-ml glass-stoppered extraction tube. The plasma sample was frozen until assayed for drug content.

Intracardiac Dosing—The experiment was essentially the same as that described for the oral dosing, except that barbital sodium was injected intracardially. Blood samples were collected from the tail artery into heparinized tubes at 5-min intervals for 20 min, every 15 min for the subsequent 30 min, and then every 12 hr for a total of 3 days.

Determination of Barbital in Plasma—Plasma samples (0.2 ml) were mixed with 1 ml of pH 5.5 phosphate buffer, 1 g of sodium chloride, and 18 ml of chloroform. The process was then completed following essentially the same procedure used for determining barbital in the serosal solution of the everted gut, except for measuring and filtering 15 ml of the chloroform extract instead of 10 ml.

To determine the percent recovery of barbital from plasma, five samples of plasma, 0.2 ml each, were collected from rats not receiving the barbiturate for at least 2 weeks. Different concentrations of barbital, ranging from 2 to 12 μg/ml, were added to the plasma samples. This assay procedure was carried through using a plasma blank. Recovery of the drug was 98 ± 2.0%.

RESULTS AND DISCUSSION

Barbiturates are usually classified as short or long acting, according to the duration of their effects. It is assumed that the short-acting barbiturates are readily destroyed in the liver while the long-acting compounds are either eliminated through the kidneys or partly destroyed and partly eliminated (15). Barbital, the longest-acting barbiturate, is subjected to very slight, if any, metabolic breakdown. The drug is quantitatively excreted unmetabolized in dogs (16), 93% in mice (17), 95% or more in rats (18), 98% in guinea pigs (19), and 75–95% in humans after oral administration (20).

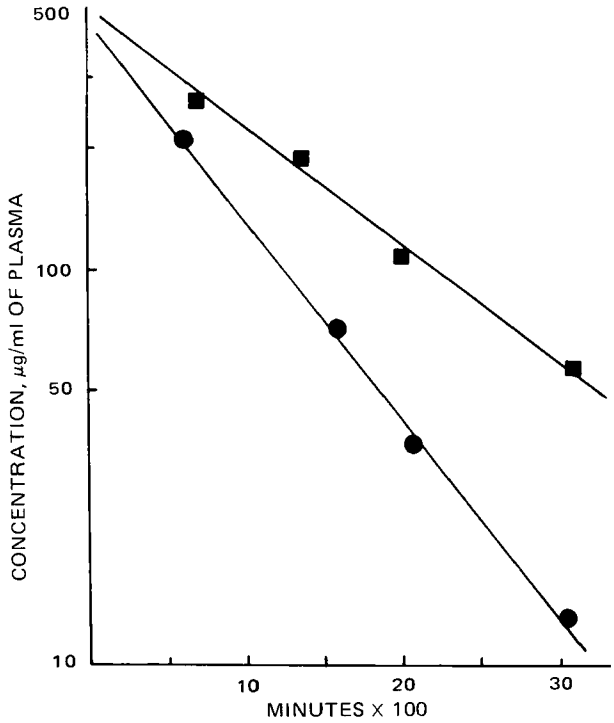

Figure 1—*Plasma concentration of barbital as a function of time following intracardiac administration of 200 mg/kg to rats. Key:* ●, *control; and* ■, *alpha tocopherol deficient.*

Barbital is also excreted very slowly; *i.e.*, 7–10 days is required for the complete excretion of a single dose by some mammals (21). This slow elimination rate, coupled with a zero value protein-binding capacity (22), implies that the drug is filtered through the kidney and is largely reabsorbed. Giotti and Maynert (21), by comparing barbital renal clearance to creatinine clearance, showed that barbital was excreted by glomerular filtration in dogs. By comparing barbital concentration in both the plasma and urine, these investigators proved that the drug was reabsorbed in the renal tubules as the free acid by a process of back-diffusion.

Being excreted almost unmetabolized, barbital was found to be the most suitable barbiturate for studying the effect of alpha tocopherol deficiency on drug absorption, distribution, and elimination, since it was reported that alpha tocopherol interferes with barbiturate metabolism (23).

A plot of the logarithm of plasma concentration *versus* time after intracardiac dosing of barbital to both the deficient and control groups (200 mg/kg) is presented in Fig. 1. The drug was distributed rapidly, and an equilibrium between blood and body tissues was achieved within 10 min after administration. The plasma level of barbital then declined slowly in a monoexponential fashion over 3–4 days. These data suggested that the pharmacokinetics of barbital in the rat can be adequately described by a one-compartment open model (Scheme I):

$$D_B \xrightarrow{K_E} D_C$$

Scheme I

where D_B is the amount of barbital in the body at any time t, D_C is the amount of barbital eliminated from the body at any time t, and K_E is the apparent first-order overall elimination rate constant. Since barbital is eliminated only by excretion in the urine, K_E is the first-order excretion rate constant of barbital through the kidney.

By definition, $D_B = (V_d)(c)$, where V_d is the apparent volume of distribution of barbital, and c is the plasma concentration of the drug at any time t.

The apparent elimination rate constant in each rat was calculated from the slope of the least-squares fit of log plasma concentration *versus* time plots. The apparent volume of distribution of bar-

[5] Whatman No. 1.

Table I—Calculated Pharmacokinetic Parameters for Barbital after Intracardiac Administration[a]

Parameter	Control Group	Alpha Tocopherol-Deficient Group	Significance Level of Difference between Groups[b]
K_E, min^{-1}	0.0010 (0.0001)	0.0006 (0.0001)	S ($p < 0.05$)
V_d, ml	214.10 (34.8)	214.40 (39.0)	NS ($p > 0.05$)
Clearance, ml/min	0.227 (0.060)	0.127 (0.031)	S ($p < 0.05$)

[a] Standard deviation in parentheses. [b] The Student t test. S = significant, and NS = not significant.

bital was calculated by dividing the intracardiac dose (D) by c_0, the plasma concentration extrapolated to time zero:

$$V_d = D/c_0 \qquad \text{(Eq. 1)}$$

Total body clearance was obtained from the relationship:

$$\text{clearance} = V_d K_E \qquad \text{(Eq. 2)}$$

The values of K_E, V_d, and clearance for each group of rats were analyzed statistically (Table I). Although the mean volume of distribution was not statistically different between the two groups, there existed a significant difference in the overall elimination rate constant. In the alpha tocopherol-deficient animals, barbital elimination was at a slower rate than with the control animals. Since the kidney is the main route of elimination for barbital, any change in the elimination rate constant could be attributed to changes in the kidney function as a consequence of alpha tocopherol deficiency. Alpha tocopherol deficiency caused degenerative changes in the kidney tubules of rats (24–28). Such a decrease in the elimination rate constant can then be explained by a decrease in glomerular filtration and/or an increase in the drug's tubular reabsorption. The renal tubular epithelium, like the GI epithelium, is lipoid in nature; it is possible that the barrier membrane responsible for glomerular filtration and tubular reabsorption might be influenced by alpha tocopherol deficiency.

The absence of any difference in the volume of distribution between the deficient and the supplemented animals indicated that barbital was distributed throughout the body to the same extent in both groups. However, a difference in the rate of penetration to various tissues might exist.

Since the value of K_E was different between the groups while the V_d was unchanged, the clearance was significantly different between the groups (Table I). The plasma of alpha tocopherol-deficient animals was cleared of drug at a slower rate than that of the control animals. This result underlines the role of alpha tocopherol deficiency in drug clearance through the kidney, a parameter that could influence the duration of the pharmacological effect.

To determine the effect of alpha tocopherol deficiency on the absorption of barbital, a 200-mg/kg dose was administered orally.

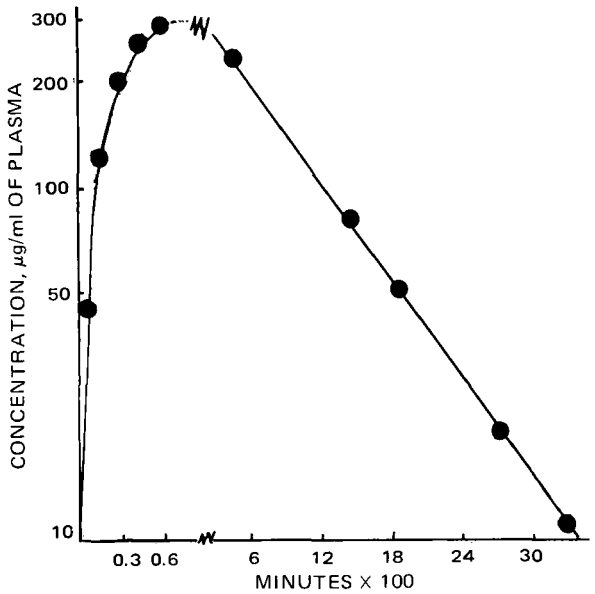

Figure 2—*Plasma concentration of barbital as a function of time following oral administration of 200 mg/kg to control rats.*

The overall elimination rate constant and the volume of distribution were determined and compared to those calculated after intracardiac administration. Two other important parameters that reflect the efficiency of the GI absorption of barbital were also considered. One parameter, the plasma drug concentration peak height (C_{max}), reflects the intensity as well as the duration of pharmacological effect. The other parameter, the time of occurrence of the peak height concentration (T_{max}), reflects the onset of occurrence of the drug's pharmacological effect.

After oral administration, the plasma barbital concentration–time data were plotted semilogarithmically (Fig. 2). The drug entered the plasma rapidly, reaching a maximum level and then exhibiting a slow exponential decline. The shape of the curve indicated that the pharmacokinetics of barbital could be described, as in the case of the intracardiac dosing, by a one-compartment open model (Scheme II):

$$D_A \xrightarrow{K_a} D_B \xrightarrow{K_E} D_C$$

Scheme II

where D_A is the amount of barbital in the GI fluid at any time t, and K_a is the first-order absorption rate constant of the drug from the GI fluids. All other parameters were as previously described. The plasma barbital concentration, c, at time t is determined by integrating the equation resulting from Scheme II, which gives:

$$c = \left(\frac{FD}{V_d}\right)\left(\frac{K_a}{K_a - K_E}\right)\{\exp[-K_E(t)] - \exp[-K_a(t)]\} \qquad \text{(Eq. 3)}$$

where F is the fraction of the oral dose (D) absorbed, and all other parameters are as previously defined. The absorption rate constant, K_a, was graphically determined for each individual rat by the method of feathering. The elimination rate constant, K_E, was calculated from the slope of the terminal elimination phase. The data were then fitted with the aid of a digital computer, nonlinear regression analysis program (NONLIN). Excellent computer fits to the experimental data were obtained using Eq. 3 for a one-compartment open model (Fig. 2).

The time of occurrence of the peak height and peak concentration for both groups is found using Eqs. 4 and 5, respectively:

$$T_{max} = \frac{\ln(K_a/K_E)}{K_a - K_E} \qquad \text{(Eq. 4)}$$

$$C_{max} = \frac{FD\, e^{-K_E T_{max}}}{V_d} \qquad \text{(Eq. 5)}$$

Table II represents the mean value of the computer-generated nonlinear least-squares regression estimates of K_a, K_E, and V_d/F for each group of animals. The calculated mean values of T_{max} and C_{max} and the statistical analysis of all parameters obtained for both groups of animals are included in the table. An examination of the mean absorption rate constants revealed a significant difference between the alpha tocopherol-deficient and control animals. The deficient group absorbed barbital at a rate twice that of the control animals. In addition, the deficient animals eliminated the drug at a slower rate.

No statistical difference was observed between the groups with respect to V_d/F. A comparison of the elimination rate constant, K_E, obtained after intracardiac (Table I) and oral dosing revealed no difference in this parameter. The value of V_d/F obtained from the computer-generated nonlinear least-squares regression after oral administration was not statistically different from the value of V_d calculated from the least-squares fit of log plasma concentration *versus* time after intracardiac dosing. This finding can be true only if F is equal to one, since the volume of distribution of a drug is constant and independent of the route of administration. To prove that F in Eq. 2 is unity, the area under the plasma concen-

Table II—Calculated Pharmacokinetic Parameters for Barbital after Oral Administration[a]

Parameter	Control Group	Alpha Tocopherol-Deficient Group	Significance Level of Difference between Groups[b]
K_a, min^{-1}	0.017 (0.004)	0.037 (0.014)	S ($p < 0.05$)
K_E, min^{-1}	0.0011 (0.0001)	0.0008 (0.00015)	S ($p < 0.05$)
V_d/F, ml	223.5 (26.0)	213.8 (28.5)	NS ($p > 0.05$)
T_{max}, min	179.96 (42.46)	116.0 (42.42)	S ($p < 0.05$)
C_{max}, μg/ml	287.64 (52.36)	331.22 (51.54)	S ($p < 0.05$)

[a] Standard deviation in parentheses. [b] The Student t test. S = significant, and NS = not significant.

tration–time curve for a representative number of orally dosed amounts was calculated using Simpson's rule. The fraction of the dose absorbed, F, was calculated using:

$$\text{area under the curve} = \frac{FD}{V_d K_E} \qquad \text{(Eq. 6)}$$

The fraction of the dose absorbed, F, was equal to unity, indicating that while the rate of absorption was faster in the deficient compared to the control group, the extent of absorption was the same. This result also indicated that barbital was not subjected to any metabolic process in the GI tract or in its first or subsequent passes through the liver.

Table II shows that T_{max} for the deficient group was significantly shorter than that of the control group, obviously due to the higher rate of absorption in the deficient animals. It was found that C_{max} was significantly higher in the deficient group. This finding implies that the pharmacological effect of barbital would be of a higher intensity and longer duration in the deficient than in the supplemented animals.

When unmetabolized drugs, like barbital and phenolsulfonphthalein, are administered orally, their plasma levels are a function of three factors: (*a*) the rate of absorption from the GI tract, (*b*) the rate of diffusion from the blood to other tissues, and (*c*) the rate of excretion from the blood out of the body, mainly in the urine. The present study showed that alpha tocopherol deficiency caused an increase in the absorption rate of barbital (Table II). A reasonable explanation is that a change in the structural integrity and stability of the GI epithelium resulted as a consequence of alpha tocopherol deficiency. This assumption is supported by the barbital everted gut transport study, where increased barbital permeability was observed in the alpha tocopherol-deficient animals.

To confirm the effect of alpha tocopherol deficiency on drug absorption and transport, phenolsulfonphthalein was used as a marker compound. Phenolsulfonphthalein was chosen because it is absorbed mainly from the small intestine by a simple diffusion process. It is a highly charged molecule and, as such, is poorly absorbed. Therefore, the rate of phenolsulfonphthalein absorption would be sensitive to changes in membrane structure. In addition, it is easily assayed in biological fluids and has been used to test the effect of several compounds, such as edetic acid (29, 30) and bile salt (31, 32), on GI permeability in rats. Since it is eliminated essentially unmetabolized in the urine, the amount excreted depends on the amount of phenolsulfonphthalein absorbed. A measure of the rate of phenolsulfonphthalein excreted in the urine would then reflect its rate of absorption.

The amount of phenolsulfonphthalein excreted in the urine after oral dosing to both groups, control and deficient, is presented in Table III. In the first 9 hr after dosing, the amount of phenolsulfonphthalein excreted by the deficient group was more than double that excreted by the control group. However, there was no significant difference in the amount of drug excreted by both groups in the subsequent 15-hr period. The total amount excreted in 24 hr after dosing was 62% more in the deficient group than in the control group.

Table III—Urinary Excretion of Phenolsulfonphthalein in Alpha Tocopherol-Deficient and Control Groups after Oral Administration[a]

Hours	Deficient Group	Control Group	Significance Level of Difference between Groups[b]
0–9	48.18 ± 9.77	24.76 ± 7.49	S ($p < 0.005$)
9–24	9.19 ± 1.78	10.53 ± 2.34	NS ($p > 0.05$)
Total in 24	57.38 ± 8.38	35.29 ± 7.81	S ($p < 0.05$)

[a] Average of five rats in micrograms ± *SD*. [b] The Student t test. S = significant, and NS = not significant.

Passive absorption occurs mostly in the small intestine, where the surface area is large, and gradually decreases in the more distal portion of the intestine, where the surface area decreases and the viscosity of the intestinal contents increases. Therefore, phenolsulfonphthalein absorption is expected to occur mainly in the small intestine during the first 9 hr after administration. The larger amount of phenolsulfonphthalein excreted in the urine of the deficient group in that period reflected the greater extent of absorption of this compound. In the subsequent 15-hr period, some phenolsulfonphthalein was absorbed while the unabsorbed drug passed through the GI tract. This additional amount absorbed was small compared to that absorbed during the first 9 hr.

It is clear from the data in Table III that the amount of phenolsulfonphthalein excreted in the urine during the subsequent 15-hr period was not significantly different between both groups. One possible explanation for this observation is that other factors, such as diffusion through the viscous medium present in the large intestine, might interfere with the absorption process. Examination of the intestinal contents of rats fasted for 24 hr revealed appreciable amounts of semisolid and solid material in the more distal segments of the intestine. Since the rate of passive absorption is a function of the diffusion coefficient which, in turn, is inversely proportional to viscosity, one would expect that unabsorbed drug incorporated in this semisolid viscous mass would diffuse to the absorption site at a slower rate compared to that found in the proximal portion of the intestine.

In addition, the surface area for absorption found in the distal segments of the intestine is much smaller than that of the proximal segments. Due to the smaller absorptive surface, factors affecting membrane structure would not be expected to have as dramatic an effect on absorption through the distal as compared to the proximal segments of the intestine. These facts allow one to speculate that the phenolsulfonphthalein absorption differences between the control and deficient animals during the period when

Table IV—Phenolsulfonphthalein Transport as a Function of Time through the Everted Gut[a]

Minutes	Amount Transported[b], μg	Clearance, ml/15 min
	Alpha Tocopherol-Deficient Group	
15	3.09 (0.45)[c]	0.03
30	6.57 (0.65)	0.07
45	10.84 (1.74)	0.11
60	16.51 (2.59)	0.17
75	19.37 (3.08)	0.19
90	21.96 (2.65)	0.22
	Control Group	
15	2.26 (0.26)	0.02
30	5.38 (0.60)	0.05
45	11.25 (1.77)	0.11
60	14.56 (1.15)	0.15
75	17.83 (2.03)	0.18
90	20.21 (3.38)	0.20

[a] Average of six rats in each group; mucosal concentration of phenolsulfonphthalein was 0.1 mg/ml of Kreb's bicarbonate buffer. [b] Values are significantly different only at 15 and 30 min ($p < 0.05$). [c] Standard deviation in parentheses.

Table V—Barbital Transport as a Function of Time through the Everted Gut[a]

Minutes	Amount Transported[b], μg	Clearance, ml/15 min
	Alpha Tocopherol-Deficient Group	
15	55.24 (5.18)[c]	0.22
30	59.89 (6.27)	0.24
45	58.88 (7.39)	0.24
60	66.37 (8.83)	0.27
75	64.88 (10.47)	0.26
90	67.28 (5.72)	0.27
		Mean = 0.25 (0.02)
	Control Group	
15	46.35 (10.02)	0.19
30	53.37 (4.79)	0.21
45	53.54 (7.16)	0.21
60	57.95 (8.39)	0.23
75	55.88 (8.50)	0.22
90	58.24 (7.48)	0.23
		Mean = 0.22 (0.02)

[a] Average of five rats in each group; mucosal concentration of barbital sodium was 250 μg/ml of Kreb's bicarbonate buffer. [b] Significant difference between both groups at all 15-min intervals ($p < 0.05$) except the 45-min period. [c] Standard deviation in parentheses.

unabsorbed drug should be in the more distal portions of the intestine (9–24 hr) are probably masked by a decreased rate of diffusion to the absorptive site.

Table III shows that the cumulative amount of phenolsulfonphthalein excreted in the urine in the 24-hr period was higher in the deficient group than in the supplemented animals. Feldman *et al.* (31) reported that phenolsulfonphthalein absorption, as evidenced by urinary excretion studies, occurs within 24 hr and that the urine is completely free of the compound after 24 hr. In this study, the cumulative amount of phenolsulfonphthalein excreted in the urine by the control animals was within the range reported by these investigators and the extent of absorption was significantly greater in the deficient than in the control animals.

Although the results suggest that the observed increase in passive GI absorption of phenolsulfonphthalein in the alpha tocopherol-deficient animals is due to changes in membrane permeability, other factors may partially account for the results. These factors include altered stomach emptying, GI secretion, bile or blood flow, and kidney function. It was, therefore, decided to measure the intestinal transport of this compound in the absence of these variables, *i.e.*, *via* the *in vitro* everted gut preparation. The results (Table IV) show that phenolsulfonphthalein was transported significantly faster through the everted gut of the deficient animals as compared to the controls during the first 30 min of the experiment. Thereafter, differences in transport could not be detected.

Table VI—Salicylate Transport as a Function of Time through the Everted Gut[a]

Minutes	Amount Transported[b], mg	Clearance, ml/15 min
	Alpha Tocopherol-Deficient Group	
15	0.234 (0.03)[c]	0.23
30	0.270 (0.01)	0.27
45	0.290 (0.01)	0.29
60	0.296 (0.02)	0.30
75	0.315 (0.02)	0.32
90	0.340 (0.04)	0.34
		Mean = 0.29 (0.03)
	Control Group	
15	0.235 (0.02)[c]	0.24
30	0.285 (0.02)	0.29
45	0.278 (0.02)	0.28
60	0.307 (0.01)	0.31
75	0.314 (0.02)	0.31
90	0.344 (0.03)	0.34
		Mean = 0.29 (0.03)

[a] Average of five rats in each group; mucosal concentration of salicylate was 1 mg/ml of Kreb's bicarbonate buffer. [b] No significant difference between groups. [c] Standard deviation in parentheses.

Table VII—Comparative Data for Clearance of Salicylate, Barbital, and Phenolsulfonphthalein in Alpha Tocopherol-Deficient and Control Animals

Drug	pKa	Partition[a] Coefficient	Group	Clearance 0–30 min
Salicylate	3.0	2.9	Deficient	0.50
			Control	0.52
Barbital	7.2	0.7	Deficient	0.46[b]
			Control	0.40
Phenol-sulfonphthalein	2 7.9	0.0001	Deficient	0.10[b]
			Control	0.08

[a] Partition coefficient of the undissociated compound between chloroform–water (36, 38). [b] Significantly different from control group; the Student *t* test ($p < 0.05$).

One criterion for adequate characterization of the transfer of compounds across the everted gut is that the viability of the epithelium must be known throughout the entire experiment. In a histological evaluation of the everted gut technique for studying drug transport, the intestinal sacs of rats were morphologically intact after eversion but progressively lost their structural integrity (32). The effect of such structure changes on the transport of drugs through the everted gut was evaluated (33); the clearance of poorly lipid-soluble compounds such as methyl orange showed a continual increase in clearance over a 2-hr period. This finding is supported in the present study.

Phenolsulfonphthalein is a lipid-insoluble compound and is transported very slowly, mainly through pores or aqueous channels present in the GI membrane (34–36). Therefore, progressive decomposition changes in the everted gut preparation would reflect a progressive increase in the normally low transport rate of phenolsulfonphthalein. Biochemical changes in membrane structure due to alpha tocopherol deficiency might also produce significant changes in the transport. The differences in phenolsulfonphthalein transport observed during the first 30 min between the deficient and control groups apparently can be attributed to differences in membrane integrity due to the vitamin deficiency. After 30 min, the everted gut degenerates such that differences in membrane permeability, induced by the deficiency, are masked.

Drugs that have a somewhat greater lipid solubility were transported across the everted gut at a constant rate for at least 2 hr (33). Since these compounds are transported *via* a partitioning process involving the lipid components of the membrane, changes in aqueous pore volumes or diameters should not appreciably affect the overall absorption processes as compared to substances such as phenolsulfonphthalein. Barbital, a drug classified (37) as moderately transported, passed through the everted gut at a constant rate for the entire 90-min experimental period (Table V). During each time period (except the 45-min period), the transport of barbital through the everted gut of the alpha tocopherol-deficient animals was greater than that of the control group, indicating a definite effect of alpha tocopherol deficiency on GI membrane permeability.

Rapidly transported drugs such as salicylate (33, 37) would not be expected to be sensitive to changes in membrane structure due to alpha tocopherol deficiency. Slight changes in permeability of the everted gut preparation would cause comparatively slight increases in the normally high transport rate of salicylate. The data in Table VI show that salicylate transport, like barbital, did not change during the experiment.

A comparison of the *in vitro* transport characteristics of the compounds studied showed the following rank order: salicylate > barbital > phenolsulfonphthalein. Table VII represents the comparative data for clearance of the three compounds during the first 30 min of the experiment, as well as their pKa and partition coefficients. The clearance data for these substances seem to correlate with their partition coefficients.

The *in vitro* data also suggest that the changes in membrane structure induced by the deficiency state are different from that observed after *in vitro* membrane decomposition. The transport of rapidly absorbed drugs appears to be the least affected by alpha tocopherol deficiency. This finding seems reasonable intuitively

since it is difficult to see increases in the rate of transport of substances for which the GI membrane ordinarily offers little resistance.

Based upon the increased rate of barbital absorption *in vivo*, the increased rate of barbital transport *in vitro*, the increased *in vitro* transport observed for phenolsulfonphthalein through the everted gut of alpha tocopherol-deficient animals, and the enhanced excretion of phenolsulfonphthalein after oral administration in the same animals, it appears that morphological changes in membrane structure previously observed with alpha tocopherol-deficient animals and humans result in increased membrane permeability, at least to the drugs used in this study. The significance of these changes in terms of pharmacological effect is currently under study.

REFERENCES

(1) J. A. Lucy, *Ann. N.Y. Acad. Sci.*, **203**, 4(1972).

(2) A. L. Tappel, *Vitam. Horm.*, **20**, 493(1962).

(3) L. A. Witling, *Progr. Chem. Fats Lipids*, **9**, 519(1970).

(4) M. K. Horwitt, *Fed. Proc.*, **24**, 68(1965).

(5) A. L. Tappel, in "The Fat Soluble Vitamins," H. F. DeLuca and J. W. Suttie, Eds., University of Wisconsin Press, Madison, Wis., 1969, pp. 369–373.

(6) A. L. Tappel, *Ann. N.Y. Acad. Sci.*, **203**, 12(1972).

(7) R. E. Heikkila, J. A. Mezick, and D. G. Cornwell, *Physiol. Chem. Phys.*, **3**, 93(1971).

(8) S. Gross and D. K. Melhorn, *Ann. N.Y. Acad. Sci.*, **203**, 141(1972).

(9) I. Molenaar, F. A. Hommes, W. G. Braams, and H. A. Polman, *Proc. Nat. Acad. Sci. USA*, **61**, 982(1968).

(10) R. H. Imami, S. Reiser, and P. A. Christiansen, *J. Nutr.*, **100**, 101(1970).

(11) M. M. Meshali and C. H. Nightingale, *J. Pharm. Sci.*, **63**, 1084(1974).

(12) M. Mayersohn and M. Gibaldi, *ibid.*, **60**, 225(1971).

(13) P. Trinder, *Biochem. J.*, **57**, 301(1954).

(14) B. B. Brodie, J. J. Burns, L. C. Mark, P. A. Lief, E. Bernstein, and E. M. Papper, *J. Pharmacol. Exp. Ther.*, **108**, 26(1953).

(15) "The Pharmacological Basis of Therapeutics," 4th ed., L. S. Goodman and A. Gilman, Eds., Macmillan, New York, N.Y., 1970, pp. 98–120.

(16) E. W. Maynert and H. B. Van Dyke, *J. Pharmacol. Exp. Ther.*, **98**, 184(1950).

(17) A. Dorfman and L. R. Goldbaum, *ibid.*, **90**, 330(1947).

(18) A. G. Ebert, G. K. W. Yim, and T. S. Miya, *Biochem. Pharmacol.*, **13**, 1267(1964).

(19) J. J. Burns, C. Evans, and N. Trousof, *J. Biol. Chem.*, **227**, 785(1957).

(20) P. Lous, *Acta Pharmacol. Toxicol.*, **10**, 147(1954).

(21) A. Giotti and E. W. Maynert, *J. Pharmacol. Exp. Ther.*, **101**, 296(1951).

(22) A. Goldstein, L. Aronow, and S. M. Kalman, "Principles of Drug Action," Harper and Row, New York, N.Y., 1969, pp. 106–205.

(23) N. J. Giarman, G. N. Bowers, P. G. Quie, and L. J. Hampton, *Arch. Int. Pharmacodyn. Ther.*, **97**, 473(1954).

(24) A. J. P. Martin and T. Moore, *Chem. Ind.*, **57**, 973(1938).

(25) A. J. P. Martin and T. Moore, *J. Hyg.*, **39**, 643(1939).

(26) T. Moore, *Chem. Ind.*, **58**, 651(1939).

(27) V. M. Emmel, *J. Nutr.*, **61**, 51(1957).

(28) V. M. Emmel and P. L. LaCelle, *ibid.*, **75**, 335(1961).

(29) C. S. Tidball, *Amer. J. Physiol.*, **206**, 243(1964).

(30) M. M. Cassidy and C. S. Tidball, *J. Cell Biol.*, **32**, 685(1967).

(31) S. Feldman, M. Salvino, and M. Gibaldi, *J. Pharm. Sci.*, **59**, 705(1970).

(32) R. R. Levine, W. F. McNary, P. J. Kornguth, and R. LeBlanc, *Eur. J. Pharmacol.*, **9**, 211(1970).

(33) M. Gibaldi and B. Grundhofer, *J. Pharm. Sci.*, **61**, 116(1972).

(34) H. Kunze and W. Vogt, *Naunyn-Schmiedebergs Arch. Pharmakol. Exp. Pathol.*, **256**, 139(1967).

(35) H. Kunze, *ibid.*, **259**, 260(1968).

(36) C. S. Tidball, *Amer. J. Physiol.*, **206**, 239(1964).

(37) C. A. M. Hogben, D. J. Tocco, B. B. Brodie, and L. S. Schanker, *J. Pharmacol. Exp. Ther.*, **125**, 275(1959).

(38) L. S. Schanker, P. A. Shore, B. B. Brodie, and C. A. M. Hogben, *ibid.*, **120**, 528(1957).

ACKNOWLEDGMENTS AND ADDRESSES

Received July 5, 1974, from the *School of Pharmacy, University of Connecticut, Storrs, CT 06268*

Accepted for publication May 7, 1975.

Supported by Grant 107 from the University of Connecticut Research Foundation and by a grant from Lederle Laboratories, Pearl River, N.Y.

* Present address: University of Assiut, Assiut, Egypt.

ˣ To whom inquiries should be directed.

Automated *In Vitro* Dissolution Rate Analysis of Potassium in Plastic Matrix Slow Release Tablets

ALF ENGDAHL *, BO KARLBERG ˣ, and SIDSEL THELANDER

Abstract □ A fully automated system for dissolution rate analysis of potassium in slow release tablets is described. Aliquots are removed after 1, 2, and 4 hr from six samples, and potassium is analyzed in a flame photometer at 768 nm. A complete study of six samples takes 5.5 hr. The system may be run overnight. During the time intervals between the removal of aliquots, the system can be used for the determination of the total assay of tablets.

Keyphrases □ Potassium chloride—slow release tablets, dissolution rate analysis by automated system □ Dissolution rate analysis—potassium chloride slow release tablets, automated system □ Automated analysis—dissolution rate of potassium chloride slow release tablets

Potassium chloride tablets are often administered in the form of sustained-release preparations (1, 2). The dissolution rates of 12 different potassium chloride tablets were measured using a potassium selective glass electrode (2). The selectivity for potassium ions over other ions is poor; sodium and hydrogen ions in particular interfere strongly (3). Fortunately, sodium ions are not present; in the *in vitro* methods

since it is difficult to see increases in the rate of transport of substances for which the GI membrane ordinarily offers little resistance.

Based upon the increased rate of barbital absorption *in vivo*, the increased rate of barbital transport *in vitro*, the increased *in vitro* transport observed for phenolsulfonphthalein through the everted gut of alpha tocopherol-deficient animals, and the enhanced excretion of phenolsulfonphthalein after oral administration in the same animals, it appears that morphological changes in membrane structure previously observed with alpha tocopherol-deficient animals and humans result in increased membrane permeability, at least to the drugs used in this study. The significance of these changes in terms of pharmacological effect is currently under study.

REFERENCES

(1) J. A. Lucy, *Ann. N.Y. Acad. Sci.*, **203**, 4(1972).

(2) A. L. Tappel, *Vitam. Horm.*, **20**, 493(1962).

(3) L. A. Witling, *Progr. Chem. Fats Lipids*, **9**, 519(1970).

(4) M. K. Horwitt, *Fed. Proc.*, **24**, 68(1965).

(5) A. L. Tappel, in "The Fat Soluble Vitamins," H. F. DeLuca and J. W. Suttie, Eds., University of Wisconsin Press, Madison, Wis., 1969, pp. 369–373.

(6) A. L. Tappel, *Ann. N.Y. Acad. Sci.*, **203**, 12(1972).

(7) R. E. Heikkila, J. A. Mezick, and D. G. Cornwell, *Physiol. Chem. Phys.*, **3**, 93(1971).

(8) S. Gross and D. K. Melhorn, *Ann. N.Y. Acad. Sci.*, **203**, 141(1972).

(9) I. Molenaar, F. A. Hommes, W. G. Braams, and H. A. Polman, *Proc. Nat. Acad. Sci. USA*, **61**, 982(1968).

(10) R. H. Imami, S. Reiser, and P. A. Christiansen, *J. Nutr.*, **100**, 101(1970).

(11) M. M. Meshali and C. H. Nightingale, *J. Pharm. Sci.*, **63**, 1084(1974).

(12) M. Mayersohn and M. Gibaldi, *ibid.*, **60**, 225(1971).

(13) P. Trinder, *Biochem. J.*, **57**, 301(1954).

(14) B. B. Brodie, J. J. Burns, L. C. Mark, P. A. Lief, E. Bernstein, and E. M. Papper, *J. Pharmacol. Exp. Ther.*, **108**, 26(1953).

(15) "The Pharmacological Basis of Therapeutics," 4th ed., L. S. Goodman and A. Gilman, Eds., Macmillan, New York, N.Y., 1970, pp. 98–120.

(16) E. W. Maynert and H. B. Van Dyke, *J. Pharmacol. Exp. Ther.*, **98**, 184(1950).

(17) A. Dorfman and L. R. Goldbaum, *ibid.*, **90**, 330(1947).

(18) A. G. Ebert, G. K. W. Yim, and T. S. Miya, *Biochem. Pharmacol.*, **13**, 1267(1964).

(19) J. J. Burns, C. Evans, and N. Trousof, *J. Biol. Chem.*, **227**, 785(1957).

(20) P. Lous, *Acta Pharmacol. Toxicol.*, **10**, 147(1954).

(21) A. Giotti and E. W. Maynert, *J. Pharmacol. Exp. Ther.*, **101**, 296(1951).

(22) A. Goldstein, L. Aronow, and S. M. Kalman, "Principles of Drug Action," Harper and Row, New York, N.Y., 1969, pp. 106–205.

(23) N. J. Giarman, G. N. Bowers, P. G. Quie, and L. J. Hampton, *Arch. Int. Pharmacodyn. Ther.*, **97**, 473(1954).

(24) A. J. P. Martin and T. Moore, *Chem. Ind.*, **57**, 973(1938).

(25) A. J. P. Martin and T. Moore, *J. Hyg.*, **39**, 643(1939).

(26) T. Moore, *Chem. Ind.*, **58**, 651(1939).

(27) V. M. Emmel, *J. Nutr.*, **61**, 51(1957).

(28) V. M. Emmel and P. L. LaCelle, *ibid.*, **75**, 335(1961).

(29) C. S. Tidball, *Amer. J. Physiol.*, **206**, 243(1964).

(30) M. M. Cassidy and C. S. Tidball, *J. Cell Biol.*, **32**, 685(1967).

(31) S. Feldman, M. Salvino, and M. Gibaldi, *J. Pharm. Sci.*, **59**, 705(1970).

(32) R. R. Levine, W. F. McNary, P. J. Kornguth, and R. LeBlanc, *Eur. J. Pharmacol.*, **9**, 211(1970).

(33) M. Gibaldi and B. Grundhofer, *J. Pharm. Sci.*, **61**, 116(1972).

(34) H. Kunze and W. Vogt, *Naunyn-Schmiedebergs Arch. Pharmakol. Exp. Pathol.*, **256**, 139(1967).

(35) H. Kunze, *ibid.*, **259**, 260(1968).

(36) C. S. Tidball, *Amer. J. Physiol.*, **206**, 239(1964).

(37) C. A. M. Hogben, D. J. Tocco, B. B. Brodie, and L. S. Schanker, *J. Pharmacol. Exp. Ther.*, **125**, 275(1959).

(38) L. S. Schanker, P. A. Shore, B. B. Brodie, and C. A. M. Hogben, *ibid.*, **120**, 528(1957).

ACKNOWLEDGMENTS AND ADDRESSES

Received July 5, 1974, from the *School of Pharmacy, University of Connecticut, Storrs, CT 06268*

Accepted for publication May 7, 1975.

Supported by Grant 107 from the University of Connecticut Research Foundation and by a grant from Lederle Laboratories, Pearl River, N.Y.

* Present address: University of Assiut, Assiut, Egypt.

ˣ To whom inquiries should be directed.

Automated *In Vitro* Dissolution Rate Analysis of Potassium in Plastic Matrix Slow Release Tablets

ALF ENGDAHL *, BO KARLBERG ˣ, and SIDSEL THELANDER

Abstract □ A fully automated system for dissolution rate analysis of potassium in slow release tablets is described. Aliquots are removed after 1, 2, and 4 hr from six samples, and potassium is analyzed in a flame photometer at 768 nm. A complete study of six samples takes 5.5 hr. The system may be run overnight. During the time intervals between the removal of aliquots, the system can be used for the determination of the total assay of tablets.

Keyphrases □ Potassium chloride—slow release tablets, dissolution rate analysis by automated system □ Dissolution rate analysis—potassium chloride slow release tablets, automated system □ Automated analysis—dissolution rate of potassium chloride slow release tablets

Potassium chloride tablets are often administered in the form of sustained-release preparations (1, 2). The dissolution rates of 12 different potassium chloride tablets were measured using a potassium selective glass electrode (2). The selectivity for potassium ions over other ions is poor; sodium and hydrogen ions in particular interfere strongly (3). Fortunately, sodium ions are not present; in the *in vitro* methods

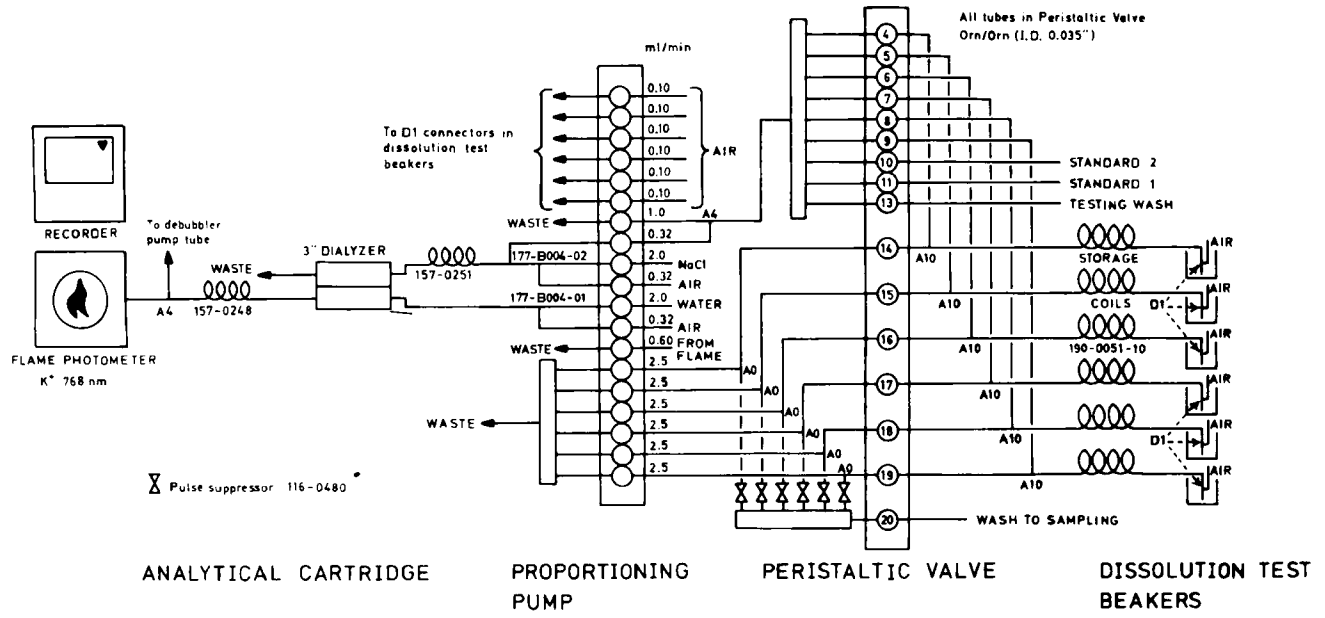

Figure 1—*Hydraulic flow diagram for determination of potassium in slow release tablets.*

applied, pure water was used as the dissolution medium. Sink conditions may be applied for the dissolution of potassium chloride into water at 37° (4).

The absorption of potassium in humans has been studied (1). Tablets of the insoluble plastic matrix type (5–7) were compared with three other sustained-release tablets. The *in vitro* method used was a modification of the beaker method of Levy and Hayes (8). The modified method has been approved for quality control in this laboratory. Manually, this method is time consuming and tedious. Therefore, automation was desirable since potassium chloride tablets frequently occur in the quality control schedule.

Several automated apparatus for dissolution studies have been developed (9–12).

EXPERIMENTAL

Reagents—Sodium chloride, reagent grade (1.0 g/liter in distilled water containing 1.5 ml of a wetting agent[1]), and distilled water containing 1.0 ml of a wetting agent[1]/liter were used.

Apparatus—The automated system for programmed sampling consists of the following: six 600-ml dissolution test beakers with stirrers placed in a thermostatically controlled water bath at 37°

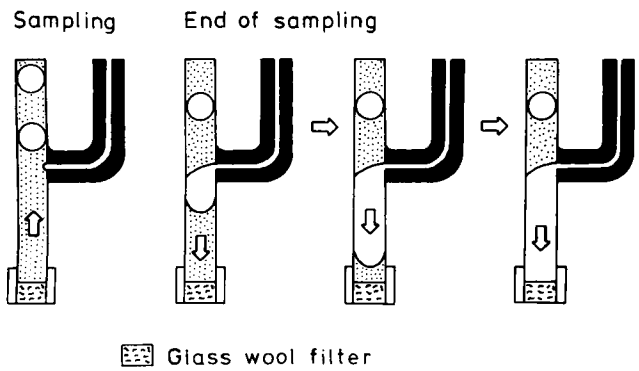

Figure 2—*Function of sampling probe with filter device.*

and a sample acquisition system for dissolution rate analysis consisting of a peristaltic valve[2], a programmer[2], and a proportioning pump III[2] with manifold.

The analytical system connected to the sample acquisition system consisted of an analytical cartridge for determination of potassium including a 7.6-cm (3-in.) dialyzer, a flame photometer IV[2], and a one-channel strip-chart recorder[2].

Standard Preparation—Standards of potassium chloride corresponding to 25, 50, and 75% of tablet specification were prepared. For dissolution rate analysis, six tablets were taken and 500 ml of distilled water was added. The tablet specification was 0.75 g in this case. The 50% standard thus contained 4.5 g of potassium chloride/liter. When 1.0 g of potassium chloride was specified, five tablets were taken for each run. When using the same standards, conversion of the percentages gave 22.5, 45, and 67.5, respectively.

Sample Preparation—Representative tablets from each batch were placed on a wire net of stainless steel 1.5 cm above the bottom of a 600-ml beaker. A total of six tablets was taken if the specification was 0.75 g, and five tablets were used if the specification was 1.0 g. A volume of 500 ml of distilled water at 37° was added to each beaker, and the temperature was kept at this value by keeping the beakers in a thermostatically controlled bath. Stirring was carried out with a steel blade (45 × 15 mm) at a rate of 40 rpm. If three batches or less were to be investigated, duplicate analyses were readily performed.

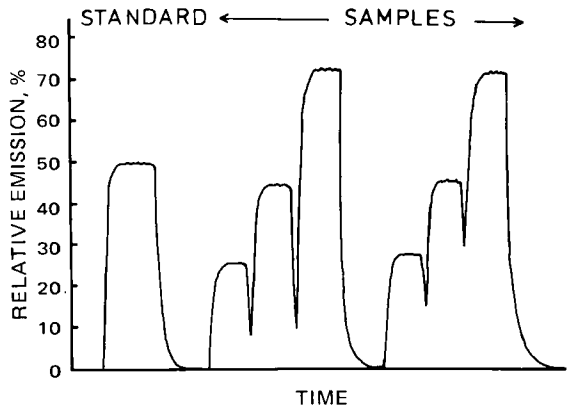

Figure 3—*Typical curves for potassium standard (50% of tablet specification) and dissolution rate analyses of two samples.*

[1] Brij 35, Atlas Chemical Industries.

[2] Technicon Corp., Tarrytown, N.Y.

Table I—Tape Program and Corresponding Activities of the System

Roller	Roller Time, min	Total Time, min	Activity of System
1	58.5	58.5	Wash to testing
2	1.5	60.0	First sampling
3	58.5	118.5	Introduction of Standard 1
2	1.5	120.0	Second sampling
3	118.5	238.5	Introduction of Standard 1
4	1.5	240.0	Third sampling
5	12.0	252.0	Emptying of coil 1
6	12.0	264.0	Emptying of coil 2
7	12.0	276.0	Emptying of coil 3
8	12.0	288.0	Emptying of coil 4
9	12.0	300.0	Emptying of coil 5
10	12.0	312.0	Emptying of coil 6
11	5.0	317.0	Introduction of Standard 2
12	5.0	322.0	Wash to testing

To determine the total assay, 15–20 tablets were pulverized in an electrical mill. An amount corresponding to exactly 1.5 times the average tablet weight was taken, dissolved in water, diluted to a volume of 250 ml, and filtered. The solution was introduced in the flame photometer alternately with the 50% standard solution. A total assay of 100% of tablet specification corresponded exactly to this standard for the 0.75-g tablets. A conversion factor was used for the 1.0-g tablets.

Procedure—A schematic diagram of the automated system is shown in Fig. 1. The system controls both the sampling and testing cycles of the dissolution study according to the tape program (Table I). Forward and reverse indexing of the peristaltic valve is achieved by means of signals from the programmer. One sampling cycle consists of three 3.6-ml aliquots taken simultaneously after 1, 2, and 4 hr from the six dissolution vessels.

The aliquots are filtered through a glass wool filter and immediately air segmented in the dissolution vessel by a connector (Fig. 2). Air also is used to prevent contamination by the solution in the vessel between the sampling periods. At the conclusion of the sampling cycle, each storage coil thus contains aliquots taken at three different times. The total volume of each coil is 14 ml.

The contents of the storage coils are then introduced in turn into the analytical system for quantitation. The sample is diluted with an air-segmented stream of sodium chloride solution and dialyzed into distilled water (Fig. 1). The emission of potassium is measured in the flame photometer; the sodium serves as an internal standard. The system is calibrated by a standard solution of potassium chloride, which is introduced when rollers 3 and 11 are in position, *i.e.*, before and after the test cycle.

When roller 3 is in position between the second and third samplings, 2 hr is available for determining total assays of potassium tablets. This is done by connecting line 11 (Standard 1 in Fig. 1) to a sampler or by direct immersion into the test solutions.

Table II—Correlation between Manual and Automated Sampling Techniques

Lot	Hours	Manual Method, % Specification	Automated Method, % Specification
1	1	27	26
	2	46	46
	4	74	73
2	1	34	33
	2	54	54
	4	80	80
3	1	35	33
	2	53	53
	4	77	77
4	1	29	28
	2	47	47
	4	73	73

Table III—Dissolution Rate Analysis of Six Batches of Potassium Chloride Plastic Matrix Tablets

Batch	Hours	Manual Method, % Specification	Automated Method, % Specification	
			Run 1	Run 2
1	1	29	31	29
	2	47	50	49
	4	73	74	75
2	1	33	32	31
	2	53	53	51
	4	79	79	77
3	1	31	28	31
	2	50	50	51
	4	78	77	77
4	1	29	28	28
	2	48	46	47
	4	74	72	72
5	1	28	28	29
	2	47	45	46
	4	73	69	71
6	1	30	29	32
	2	50	50	52
	4	78	77	78

RESULTS AND DISCUSSION

Typical curves from dissolution rate analyses of two batches of potassium chloride tablets are given in Fig. 3. A standard corresponding to 50% dissolved potassium chloride of the tablet specification was run prior to the analyses to calibrate the readings. This arrangement allows a direct reading on the chart paper of the amount dissolved as a percentage of the tablet specification.

In Table II, analytical results are presented from manual and automated sample removal carried out simultaneously. Samples taken manually were analyzed on an atomic absorption spectrophotometer[3]. The values after 1 hr were slightly higher for the manual method than for the automated one. This difference may be due to a certain time delay in the manual process, since it is almost impossible to synchronize both processes fully. Furthermore, the initial part of the dissolution curve was steep in this range, making the time parameter critical.

Results from two different automated runs on six batches are shown in Table III together with results from one manually performed test. The discrepancies obtained reflect tablet variations rather than variations in the method, since removal of aliquots from *one* beaker into two separate coils gave identical analytical results.

During the development of the automated system, some minor difficulties appeared.

1. Initially, a 0.5-g/liter sodium chloride solution was used as the diluent. This concentration gave too weak a reference signal compared with the sample signal, resulting in a nonlinear calibration curve. This problem was overcome by increasing the concentration of the sodium chloride to 1.0 g/liter.

2. A source of extra peaks was detected. When the coils were emptied for analysis one by one, simultaneous filling of the sample solution occurred if the sample probes were not removed from the beakers. If the entire system was not rinsed after an analysis, potassium-containing solution thus remained in the sample coils and tubings. Therefore, a special "rinsing program" was developed so that the system could be completely washed automatically.

3. The mechanical tenacity of the tape to the programmer decreased considerably after punching. Cracks and other damages caused disturbances and wrong indexing of the peristaltic valve. This malfunction was avoided by punching the tape at the midpoint between two sprocket holes throughout. Furthermore, reverse indexing of the peristaltic valve failed if the punch holes were too small.

The system is capable of carrying out 12 complete dissolution rate studies of the type described in 24 hr. Each run with the automated system requires approximately 5 hr less work than with the manually performed tests, corresponding to a timesaving of about 60%.

[3] Perkin-Elmer 403.

REFERENCES

(1) C. Graffner and J. Sjögren, *Acta Pharm. Suecica*, **8**, 13(1971).

(2) W. H. Thomas, *J. Pharm. Pharmacol.*, **25**, 27(1973).

(3) G. Eisenman, "Glass Electrodes for Hydrogen and other Cations," Dekker, New York, N.Y., 1967.

(4) J. V. Fee, D. J. W. Grant, and J. M. Newton, *J. Pharm. Pharmacol., Suppl.*, **25**, 148P(1973).

(5) L. E. Fryklöf, E. Sandell, and I. Östholm, British pat. 808,014 (1959).

(6) J. Sjögren and L. E. Fryklöf, *Farm. Revy*, **59**, 171(1960).

(7) J. Sjögren, *Acta Pharm. Suecica*, **8**, 153(1971).

(8) G. Levy and B. A. Hayes, *N. Engl. J. Med.*, **262**, 1053(1960).

(9) A. Richter, B. Myhre, and S. C. Khanna, *J. Pharm. Pharmacol.*, **21**, 409(1969).

(10) R. Fatton, D. Fielding, S. C. Khanna, and A. Richter, *Pharm. Acta Helv.*, **47**, 487(1972).

(11) A. C. Shah, C. B. Peot, and J. F. Ochs, *J. Pharm. Sci.*, **62**, 671(1973).

(12) J. B. Johnson, P. G. Kennedy, and S. H. Rubin, *ibid.*, **63**, 1931(1974).

ACKNOWLEDGMENTS AND ADDRESSES

Received February 13, 1975, from *Analytical Control, Astra Pharmaceuticals AB, S-151 85 Södertälje, Sweden.*

Accepted for publication May 22, 1975.

* Present address: Technicon Scandinavia, Application Laboratory, S-171 48 Solna, Sweden.

ˣ To whom inquiries should be directed.

Structure and Toxicity of Alkaloids and Amino Acids of *Sophora secundiflora*

MOHAMED IZADDOOST *, BEN G. HARRIS, and R. W. GRACY ˣ

Abstract □ Seeds from *Sophora secundiflora* were extracted into three major fractions: lipids, alkaloids, and amino acids. Most of the lipid material was composed of steroid esters. These esters were hydrolyzed, and the fatty acid compositions were determined. The major alkaloid component was cytisine, with *N*-methylcytisine, anagyrine, and termopsine in lower concentration. The major free ninhydrin-positive compound was γ-glutamyltyrosine. In addition to several common amino acids, pipecolic acid and 4-hydroxypipecolic acid were identified. Both the amino acid fraction and the alkaloid fractions caused minor pharmacological disorder when injected into rats. However, when both fractions were simultaneously administered, they were lethal.

Keyphrases □ *Sophora secundiflora*—seeds, alkaloids and amino acids isolated and identified, toxicity investigated in rats □ Alkaloids—isolated and identified, *Sophora secundiflora* seeds, toxicity, rats □ Amino acids—isolated and identified, *Sophora secundiflora* seeds, toxicity, rats

The toxicity of *Sophora secundiflora* (Ort.) DC to humans and domestic animals has been recognized for some time (1–3). The ingestion of the leaves was reported to lead to the production of poisonous milk (1), and *S. secundiflora* seeds (mescal beans) are known for their hallucinogenic effects among Indian tribes in the Southwestern United States and Mexico (4). Although the hallucinogenic effects of these seeds have been attributed to the presence of a high concentration of the alkaloid cytisine (4, 5), several species of *Laburnum, Ulex, Cytisus,* and *Sophora* containing this alkaloid are not hallucinogenic (6).

The presence of toxic amino acids in various plants has been documented (7, 8), and the toxic and/or hallucinogenic effects of *S. secundiflora* possibly may be due to nonalkaloid materials. Furthermore, atypical fatty acids and steroids are known to cause some neuropathies (9). Therefore, it was of interest to isolate and characterize these constituents and to determine which component(s) are responsible for the toxicity of these seeds.

EXPERIMENTAL

Extraction of Seeds—Mature seeds of *S. secundiflora*[1] were obtained from Mt. Bonnell, Austin, Tex. The hulled seeds (200 g) were machine ground and extracted with 500 ml of petroleum ether (lipid fraction). The residue was then extracted (soxhlet) with 800 ml of chloroform containing 0.5 ml of ammonium hydroxide (alkaloid fraction), and this residue was then extracted with 1000 ml of 50% ethanol (amino acid fraction). In some cases, the ground seeds were directly extracted with acidic chloroform from a methanolic extraction (soxhlet) of the ground seeds.

Fractionation and Analysis of Amino Acids—The amino acid fraction was reduced to 100 ml and applied to a 3.8 × 45-cm column of ion-exchange resin[2] (ammonium form). After washing with water, the column was eluted with 0.5 *N* ammonium hydroxide, and the ninhydrin-positive fractions were combined and reduced to dryness *in vacuo* to yield 3.8 g of solids. This mixture was then applied to a 2.8 × 45-cm column of ion-exchange resin[3] (acetate form) and washed with water to elute the neutral and basic amino acids. Subsequent elution with 0.5 *N* acetic acid resulted in the isolation of aspartic and glutamic acids and 350 mg of the unknown dipeptide.

The mixture of neutral and basic amino acids was then applied to a 2.2 × 100-cm column of ion-exchange resin[4] (hydrogen form), and the neutral amino acids were eluted with water. This fraction was applied to a 5.2 × 75-cm column of ion-exchange resin[3] (hydrogen form) and washed with water. Subsequent elution with 0.2 *N* HCl led to the isolation of 4-hydroxypipecolic acid and pipecolic acid.

[1] The plant material was identified as *Sophora secundiflora* L. by Dr. M. Aboul-Ela, Department of Biology, Texas Women's University. A voucher specimen (5-175) is available for inspection at the Herbarium of the Department of Biological Sciences, North Texas State University.

[2] Amberlite CG 120.

[3] Amberlite CG 400.

[4] Amberlite IR 50.

REFERENCES

(1) C. Graffner and J. Sjögren, *Acta Pharm. Suecica*, **8**, 13(1971).

(2) W. H. Thomas, *J. Pharm. Pharmacol.*, **25**, 27(1973).

(3) G. Eisenman, "Glass Electrodes for Hydrogen and other Cations," Dekker, New York, N.Y., 1967.

(4) J. V. Fee, D. J. W. Grant, and J. M. Newton, *J. Pharm. Pharmacol., Suppl.*, **25**, 148P(1973).

(5) L. E. Fryklöf, E. Sandell, and I. Östholm, British pat. 808,014 (1959).

(6) J. Sjögren and L. E. Fryklöf, *Farm. Revy*, **59**, 171(1960).

(7) J. Sjögren, *Acta Pharm. Suecica*, **8**, 153(1971).

(8) G. Levy and B. A. Hayes, *N. Engl. J. Med.*, **262**, 1053(1960).

(9) A. Richter, B. Myhre, and S. C. Khanna, *J. Pharm. Pharmacol.*, **21**, 409(1969).

(10) R. Fatton, D. Fielding, S. C. Khanna, and A. Richter, *Pharm. Acta Helv.*, **47**, 487(1972).

(11) A. C. Shah, C. B. Peot, and J. F. Ochs, *J. Pharm. Sci.*, **62**, 671(1973).

(12) J. B. Johnson, P. G. Kennedy, and S. H. Rubin, *ibid.*, **63**, 1931(1974).

ACKNOWLEDGMENTS AND ADDRESSES

Received February 13, 1975, from *Analytical Control, Astra Pharmaceuticals AB, S-151 85 Södertälje, Sweden.*

Accepted for publication May 22, 1975.

* Present address: Technicon Scandinavia, Application Laboratory, S-171 48 Solna, Sweden.

ˣ To whom inquiries should be directed.

Structure and Toxicity of Alkaloids and Amino Acids of *Sophora secundiflora*

MOHAMED IZADDOOST *, BEN G. HARRIS, and R. W. GRACY ˣ

Abstract □ Seeds from *Sophora secundiflora* were extracted into three major fractions: lipids, alkaloids, and amino acids. Most of the lipid material was composed of steroid esters. These esters were hydrolyzed, and the fatty acid compositions were determined. The major alkaloid component was cytisine, with *N*-methylcytisine, anagyrine, and termopsine in lower concentration. The major free ninhydrin-positive compound was γ-glutamyltyrosine. In addition to several common amino acids, pipecolic acid and 4-hydroxypipecolic acid were identified. Both the amino acid fraction and the alkaloid fractions caused minor pharmacological disorder when injected into rats. However, when both fractions were simultaneously administered, they were lethal.

Keyphrases □ *Sophora secundiflora*—seeds, alkaloids and amino acids isolated and identified, toxicity investigated in rats □ Alkaloids—isolated and identified, *Sophora secundiflora* seeds, toxicity, rats □ Amino acids—isolated and identified, *Sophora secundiflora* seeds, toxicity, rats

The toxicity of *Sophora secundiflora* (Ort.) DC to humans and domestic animals has been recognized for some time (1–3). The ingestion of the leaves was reported to lead to the production of poisonous milk (1), and *S. secundiflora* seeds (mescal beans) are known for their hallucinogenic effects among Indian tribes in the Southwestern United States and Mexico (4). Although the hallucinogenic effects of these seeds have been attributed to the presence of a high concentration of the alkaloid cytisine (4, 5), several species of *Laburnum, Ulex, Cytisus,* and *Sophora* containing this alkaloid are not hallucinogenic (6).

The presence of toxic amino acids in various plants has been documented (7, 8), and the toxic and/or hallucinogenic effects of *S. secundiflora* possibly may be due to nonalkaloid materials. Furthermore, atypical fatty acids and steroids are known to cause some neuropathies (9). Therefore, it was of interest to isolate and characterize these constituents and to determine which component(s) are responsible for the toxicity of these seeds.

EXPERIMENTAL

Extraction of Seeds—Mature seeds of *S. secundiflora*[1] were obtained from Mt. Bonnell, Austin, Tex. The hulled seeds (200 g) were machine ground and extracted with 500 ml of petroleum ether (lipid fraction). The residue was then extracted (soxhlet) with 800 ml of chloroform containing 0.5 ml of ammonium hydroxide (alkaloid fraction), and this residue was then extracted with 1000 ml of 50% ethanol (amino acid fraction). In some cases, the ground seeds were directly extracted with acidic chloroform from a methanolic extraction (soxhlet) of the ground seeds.

Fractionation and Analysis of Amino Acids—The amino acid fraction was reduced to 100 ml and applied to a 3.8 × 45-cm column of ion-exchange resin[2] (ammonium form). After washing with water, the column was eluted with 0.5 *N* ammonium hydroxide, and the ninhydrin-positive fractions were combined and reduced to dryness *in vacuo* to yield 3.8 g of solids. This mixture was then applied to a 2.8 × 45-cm column of ion-exchange resin[3] (acetate form) and washed with water to elute the neutral and basic amino acids. Subsequent elution with 0.5 *N* acetic acid resulted in the isolation of aspartic and glutamic acids and 350 mg of the unknown dipeptide.

The mixture of neutral and basic amino acids was then applied to a 2.2 × 100-cm column of ion-exchange resin[4] (hydrogen form), and the neutral amino acids were eluted with water. This fraction was applied to a 5.2 × 75-cm column of ion-exchange resin[3] (hydrogen form) and washed with water. Subsequent elution with 0.2 *N* HCl led to the isolation of 4-hydroxypipecolic acid and pipecolic acid.

[1] The plant material was identified as *Sophora secundiflora* L. by Dr. M. Aboul-Ela, Department of Biology, Texas Women's University. A voucher specimen (5-175) is available for inspection at the Herbarium of the Department of Biological Sciences, North Texas State University.

[2] Amberlite CG 120.

[3] Amberlite CG 400.

[4] Amberlite IR 50.

Table I—Amino Acid Analysis of *S. secundiflora* Seeds

Amino Acid	Elution Time, min	Macromoles of Amino Acid per Gram of Seeds	
		Unhydrolyzed	Hydrolyzed
Aspartic acid	75	5.0	12.5
Asparagine	85	Trace[a]	0
Serine	102	Trace	3.0
4-Hydroxypipecolic acid	110	32.0	26.0
Glutamic acid	122	31.0	80.0
Proline	132	3.5	3.0
Glycine	168	3.0	17.0
Alanine	176	6.0	7.0
Pipecolic acid	220	Trace	Trace
Unknown	225	90.0	Trace
Valine	231	Trace	Trace
Isoleucine	260	Trace	Trace
Leucine	272	Trace	Trace
Tyrosine	315	11.0	46.0
Phenylalanine	324	0	1.0
Cadaverine	14	Trace	0
Tryptophan	18	Trace	0
Lysine	24	Trace	Trace
Histidine	28	Trace	Trace
Arginine	48	Trace	Trace

[a] "Trace" indicates less than 0.5 μmole/g of seeds.

Amino acid analysis was carried out on an automatic amino acid analyzer[5], employing a buffer change from pH 3.28 to 4.25 at 150 min (flow rate = 80 ml/hr, temperature = 55°). Basic amino acids were analyzed by the standard procedure (10).

Fractionation and Analysis of Alkaloids—Samples of the alkaloid fraction were applied to thin-layer plates[6] (250 μm) and chromatographed in chloroform–methanol (75:25). Spots were visualized with the Dragendorff reagent, and the R_f values of the alkaloids were compared with those of authentic standards. The cytisine alkaloids were also identified by a modification of the specific color reaction of White (11). Upon spraying with a 1% (w/v) solution of ferric chloride in chloroform–acetone (3:1), the cytisine alkaloids developed an orange-red color. Subsequent spraying with a 3% solution of hydrogen peroxide caused the color to change to a light blue.

Cytisine was extracted and crystallized from acetone by the addition of ether; *N*-methylcytisine (caulophylline) was synthesized from cytisine according to the method of Cocklurn and Marion (12) for *N*-ethylcytisine. The physical and chemical properties of all these alkaloids were verified by comparison with published values (11–13).

Fractionation and Analysis of Lipids—The lipid extract was chromatographed on thin-layer plates[6] containing 1% ammonium sulfate. Chromatograms were developed in ether–benzene–ethanol–acetic acid (40:50:2:0.2) and visualized by charring at 200° (14). The steroid esters were isolated by preparative chromatography of 100 mg of the lipid extract on thin-layer plates, using a solvent of petroleum ether–ethanol (95:5). Under these conditions, most lipids remained at the origin, while the steroid esters migrated ($R_f \sim 0.45$).

The appropriate areas were scraped and eluted with chloroform–methanol (2:1). After solvent removal, the steroid esters were hydrolyzed under nitrogen by refluxing in methanol–benzene–sulfuric acid (90:5:5) for 3 hr. The methyl esters of the fatty acids were extracted with ether and subjected to GC at 250° on 15% ethylene glycol succinate[7] (80–120 mesh).

Pharmacology—Male Sprague–Dawley rats, 150–200 g, were used. Samples to be injected were taken to dryness and redissolved in physiological saline. Injections of 0.5 ml were performed subcutaneously, and controls received 0.5 ml of saline. For each experiment, five animals were used and received identical injections.

Spectral Studies—Proton NMR spectra were obtained on a 60 MHz spectrometer[8]. Deuterium oxide was used as the solvent, and all spectra are expressed relative to sodium 3-(trimethylsilyl)propinate-2,2,3,3-d_4. IR spectra were obtained using either potassium bromide or sodium chloride disks[9].

[5] Beckman 120C, using Aminex 4A resin (BioRad).
[6] Adsorbosil-5.
[7] Gas Chrom P.
[8] Varian Mini-Mar.

Table II—Identification of the Unknown Peptide and 4-Hydroxypipecolic Acid

Method	Unknown Peptide	γ-Glutamyltyrosine[a]	4-Hydroxypipecolic Acid[b]
Paper chromatography			
Solvent 1[c]	0.29	0.29	0.25
Solvent 2	0.21	0.21	0.83
TLC			
Solvent 3	0.59	0.59	0.61
Solvent 4	0.03	0.03	0.27
Elemental analysis			
Carbon	54.35	(54.19)[d]	49.98 (50.00)
Hydrogen	5.88	(5.89)	7.96 (7.58)
Nitrogen	9.04	(9.07)	9.90 (9.72)
Amino terminal analysis [reaction with 1-fluoro-2,4-dinitrobenzene (12)]	Glutamic acid	Glutamic acid	—
Mass spectrum of trifluoroacetylated sample (13), daltons	310	310	—

[a] From Morris and Thompson (19). [b] Component that eluted at 100 min in amino acid analysis. [c] Solvent 1 = butanol–acetic acid–water (4:1:1 v/v); Solvent 2 = phenol–water (4:1) in the presence of ammonia vapor; Solvent 3 = 2-propanol–butanone–1 *N* HCl (60:15:25 v/v); Solvent 4 = 2-methylpropanol–butanone–methanol–propanone–water with 0.88% ammonia (40:20:1:20:14 v/v). [d] Calculated theoretical values are shown in parenthesis.

RESULTS

Amino Acids and Peptides—The results of amino acid analysis of the 50% ethanol-soluble extract of *S. secundiflora* seeds are presented in Table I. In addition to several L-α-amino acids, three unusual ninhydrin-positive compounds were resolved. 4-Hydroxypipecolic acid eluted at 100 min between serine and glutamic acid and comprised a major free amino acid. Acid hydrolysis of the extract resulted in a slight decrease in the concentration of 4-hydroxypipecolic acid, while its oxidation products, aspartic acid and glycine (aminoacetic acid), increased. Its proton NMR spectrum was found to be identical to that reported for authentic 4-hydroxypipecolic acid (15, 16). The structure of the compound was verified further by chromatography in several solvent systems and by carbon, hydrogen, and nitrogen analysis (Table II). A trace of ninhydrin-positive material eluted at 220 min coincident with standard pipecolic acid.

The major ninhydrin-positive material of the seeds eluted at 225 min. Upon acid hydrolysis, this component was destroyed with the stoichiometric formation of glutamic acid and tyrosine. These data suggested that the material was probably a peptide composed of tyrosine and glutamic acid or glutamine. This unknown peptide was isolated as described under *Experimental* and subjected to further analysis. Chromatographic properties in four solvent systems, carbon, hydrogen, and nitrogen analysis, amino terminal analysis, and mass and IR spectra were all consistent with an authentic sample of γ-glutamyltyrosine (Table II) (17–20).

The proton NMR spectrum of the isolated dipeptide was as follows: δ 6.8–7.4 (quartet, 4H, J = 8 Hz, aromatic H), ~4.7 (partially hidden by water peak, ~ triplet, tyrosine CH), 4.06 (quartet, 1H, J = 6 Hz, glutamic acid CH), 2.9–3.2 (~two doublets, 2H, tyrosine CH_2), and 1.9–2.8 (multiplet, 4H, glutamic acid CH_2CH_2).

The γ-linkage of the dipeptide was determined by quantitating the carbon dioxide released upon reaction with ninhydrin (21, 22) (Table III). Controls of the aspartic acid and glycine with one free

[9] Perkin-Elmer model 237.

Table III—Titration Results from Van Slyke Ninhydrin Determination

	0.013 g of Aspartic Acid	0.007 g of Glycine	0.013 g of Glycylglycine	0.019 g of Glycylaspartic Acid	0.031 g of γ-Glutamyltyrosine
Control (without sample)	7.5[a]	7.15	7.3	7.5	6.9
Experiment (with sample)	5.10	5.15	7.1	7.4	4.7
Difference	2.40	2.00	0.20	0.10	2.2

[a] Volume of 0.1 *N* HCl in milliliters used to titrate the carbon dioxide evolved from 100 μmoles of amino acid or dipeptide upon reaction with ninhydrin.

α-amino-α-carboxylic acid showed evolution of 1 mole of carbon dioxide/mole of amino acid upon reaction with ninhydrin. Control dipeptides (glycylglycine and glycylaspartic acid) containing no free α-amino-α-carboxylic group showed essentially no carbon dioxide evolution. The unknown dipeptide, upon reaction with ninhydrin, evolved 1 mole equivalent of carbon dioxide/mole of peptide, thus confirming the presence of an α-amino-α-carboxylic group. These data are only consistent with the γ-glutamyltyrosine linkage.

Alkaloids—Cytisine was isolated in crystalline form from the alkaloid fraction. *N*-Methylcytisine was synthesized from cytisine according to the literature (11) and used as a reference to confirm the presence of this alkaloid in the plant. Anagyrine and termopsine were also isolated but in lower quantities. The IR and UV spectra and the chromatographic behavior of these alkaloids corresponded to reported values (11–13).

Lipids—The lipid fraction comprised 20% of the dry weight of the seeds of *S. secundiflora*. When this lipid fraction was analyzed by TLC, only small amounts of phospholipids, free fatty acids, and *mono-, di-, and triglycerides were observed.* Most of the lipid materials migrated at the solvent front and thus were presumed to be steroid esters (14). After hydrolysis of these esters, the fatty acid components were determined by GC. The number of carbons, degree of unsaturation, and relative amounts of each fatty acid were determined as follows: 16:0 (13.1%), 16:1 (0.7%), 18:0 (3.6%), 18:1 (47.0%), 18:2 (34.5%), 18:3 (0.5%), 20:0 (0.5%), and 20:1 (0.1%).

Toxicity—To assess the toxic nature of the various fractions, a series of pharmacological experiments was conducted. When the 50% ethanol-soluble extracts from 250 mg of seeds (containing both amino acid and alkaloid fractions) were injected simultaneously into rats, death occurred within 10 min. But if the alkaloids were first removed from this extract by alkaline chloroform, the alkaloid-free material (amino acid fraction) was no longer lethal to the animals. However, the animals displayed an obvious hypersensitivity to sound for at least 1 hr following the injection.

When the alkaloids alone (from 250 mg of seeds) were injected, the animals exhibited drowsiness and complete closure of the eyes. However, the alkaloid extract alone was not lethal, and complete recovery was apparent by 2 hr postinjection. When mixtures of the alkaloid extract and the alkaloid-free amino acid fraction were injected together at the same concentration as before, death resulted to all animals within 10 min.

Lipid extracts from 250 mg of seeds administered either as the crude extract or the isolated steroid esters caused no observable effects on the animals. Mixtures of either the lipid extract and alkaloid fraction or the lipid extract plus the amino acid fraction gave the same response as the extracts without the added lipid fractions.

DISCUSSION

Although the presence of pipecolic acid, 4-hydroxypipecolic acid, and γ-glutamyltyrosine was observed previously in plants, this study is the first demonstration of a combination of these amino acids and the dipeptide in a single plant. While the physiological function of γ-glutamyltyrosine remains obscure, high concentrations of this peptide were reported in other plants (19, 20, 23).

The described pharmacological studies demonstrate that a 50% ethanolic extract of 250 mg of the seeds containing both amino acid and alkaloid fractions is lethal to animals. However, neither the alkaloid nor amino acid fractions alone are lethal; therefore, both classes of compounds apparently are involved in the toxicity of these seeds. While it is known that homologs of proline (such as pipecolic acid and 4-hydroxypipecolic acid) can be incorporated into peptides leading to nonfunctional proteins (24), the rapid death of the animals does not seem to be consistent with the synthesis of such nonfunctional proteins.

Although a variety of possible explanations could be proposed to account for the synergistic toxicity of the alkaloids and amino acid fractions, more detailed studies are required to establish the precise mechanisms involved.

REFERENCES

(1) R. J. Garner, "Veterinary Toxicology," Williams & Wilkins, Baltimore, Md., 1967, p. 350.

(2) P. C. Plugge and A. Vauverda, *Arch. Pharm.*, **234**, 685(1869).

(3) R. D. Redeleff, "Veterinary Toxicology," Lea & Febiger, Philadelphia, Pa., 1964, p. 374.

(4) R. C. Troike, *Amer. Anthropol.*, **64**, 946(1962).

(5) J. W. Hardin and B. M. Arena, "Human Poisoning from Native and Cultivated Plants," Duke University Press, Durham, N.C., 1969.

(6) S. Moeschlin, "Poisoning," Grune and Stratton, New York, N.Y., 1969, p. 524.

(7) E. A. Bell, *Nature*, **230**, 378(1964).

(8) L. Fowden, *Ann. Rev. Plant Physiol.*, **18**, 173(1964).

(9) W. Wahlke, "Lipids and Lipidosis," G. Schlettler, Ed., Springer-Verlag, New York, N.Y., 1967, p. 370.

(10) D. H. Spackman, S. Moore, and W. H. Stein, *Anal. Chem.*, **30**, 1190(1959).

(11) E. P. White, *N. Z. J. Sci. Technol.*, **B38**, 707(1957).

(12) W. F. Cocklurn and L. Marion, *Can. J. Chem.*, **30**, 92(1952).

(13) R. C. Cambie, *N.Z. J. Sci. Technol.*, **4**, 13(1960).

(14) C. P. Freeman and D. West, *J. Lipid Res.*, **7**, 324(1966).

(15) A. I. Virtanen and S. Kari, *Acta Chem. Scand.*, **8**, 1290(1954).

(16) J. N. Schoolery and A. I. Virtanen, *ibid.*, **16**, 2457(1962).

(17) F. Sanger and E. O. P. Thompson, *Biochem. J.*, **53**, 366(1953).

(18) B. L. Brian, R. W. Gracy, and V. E. Scholes, *J. Chromatogr.*, **63**, 386(1971).

(19) C. J. Morris and J. F. Thompson, *Biochem. J.*, **1**, 706(1962).

(20) P. O. Larsen and H. Sorensen, *Acta Chem. Scand.*, **21**, 2908(1967).

(21) R. F. Lloyd, C. G. Skinner, W. Shive, and R. J. Sledmans, *Med. Chem.*, **8**, 398(1965).

(22) D. D. Van Slyke, D. A. Macfayden, and P. Hamilton, *J. Biol. Chem.*, **141**, 671(1941).

(23) G. A. Darden and P. H. Thonart, *Phytochemistry*, **12**, 473(1973).

(24) L. Fawden, P. Lewis, and H. Tristram, *Advan. Enzymol.*, **29**, 89(1967).

ACKNOWLEDGMENTS AND ADDRESSES

Received February 24, 1975, from the *Departments of Chemistry, Biological Sciences, and Basic Health Sciences, North Texas State University, Denton, TX 76203*

Accepted for publication May 8, 1975.

Supported in part by grants from the National Institutes of Health (AM14638, AI10263, and AI12331), the Robert A. Welch Foundation (B-502), the National Science Foundation (BMS 74-14637), and North Texas State University Faculty Research Funds. R. W. Gracy is the recipient of a National Institutes of Health Research Career Development Award (KO4 AM70198).

* Present address: Department of Pharmacology, University of Tehran, Tehran, Iran 00014.

[x] To whom inquiries should be directed.

Dissolution Rates of High Energy Sulfathiazole–Povidone Coprecipitates II: Characterization of Form of Drug Controlling Its Dissolution Rate *via* Solubility Studies

A. P. SIMONELLI [x], S. C. MEHTA *, and W. I. HIGUCHI

Abstract □ Solubility studies were made to characterize the form of sulfathiazole controlling the rate of dissolution exhibited in previously reported dissolution rate studies of sulfathiazole coprecipitated with povidone. The aqueous solubility of the high energy form of sulfathiazole obtained using sulfathiazole–povidone coprecipitates was determined in the presence of polymer in solution. Its aqueous solubility in the absence of polymer was determined by extrapolation. The solubility value was much greater than either the supercooled melt or the crystalline forms of sulfathiazole. Stabilization of these sulfathiazole solutions supersaturated with respect to the more stable crystalline form was achieved by the addition of sufficient polymer to the solution to prevent nucleation of the crystalline form. The concentration of polymer required to prevent nucleation of the crystalline forms was much higher than the previously reported concentrations required to inhibit crystal growth of sulfathiazole. The ratio of the solubility value obtained for the coprecipitated sulfathiazole as compared with its crystalline form I was in agreement with the ratio of their dissolution rates obtained in the plateau regions of the dissolution rate experiments reported previously. The extrapolated aqueous solubility values in the absence of povidone were obtained as a function of temperature and were utilized to obtain thermodynamic parameters. The difference in the heat of solution of the two forms of sulfathiazole from the slope of the van't Hoff plots of the extrapolated solubility values was 1618 cal/mole, in excellent agreement with the literature value. The free energy, enthalpy, and entropy at 27° for the coprecipitated drug relative to its crystalline form I were 1125 cal/mole, 8439 cal/mole, and 24 eu, respectively, indicating the high degree of molecular randomness and lack of structure in these high energy systems. These results provide strong evidence for the presence of an amorphous state of sulfathiazole as the controlling phase of both the solubility and dissolution rate experiments involving the high energy form of sulfathiazole obtained by coprecipitation with povidone.

Keyphrases □ Sulfathiazole–povidone coprecipitates—dissolution rates, solubility studies, compared to supercooled melt and crystalline forms of sulfathiazole, thermodynamic parameters □ Dissolution rates—sulfathiazole–povidone coprecipitates, compared to supercooled melt and crystalline forms of sulfathiazole, thermodynamic parameters □ Solubility studies—sulfathiazole–povidone coprecipitates, dissolution rates, compared to supercooled melt and crystalline forms of sulfathiazole, thermodynamic parameters

A previous article (1) showed that the dissolution rates of sulfathiazole could be significantly increased by coprecipitating the drug with povidone. As suggested in that report and subsequently shown (2), these results are generally applicable to other drugs and coprecipitating agents. Other workers also have reported (3–8) increased dissolution rates of drugs by the method of coprecipitation.

Numerous reasons have been presented to explain these observed increases in dissolution rates including glass solutions (6), solid solutions (8), decreased particle size (9), eutectic mixtures (10), and colloidal dispersions (11). Although the previous study (1) led to the postulation of a model that was consistent with all of the results obtained, the specific form of the drug in the solid sulfathiazole–povidone coprecipitate responsible for increasing its dissolution rate was not determined. This study was initiated primarily to investigate this aspect of these coprecipitates. Obviously, this information is essential for a complete understanding of the mechanism operative in these systems.

The importance of increasing the dissolution rates of poorly soluble drugs to obtain better therapeutic results cannot be overestimated. Furthermore, a proper understanding of these systems may also permit the formulator to increase the apparent solubility of a given drug as well as its dissolution rate. Although the dissolution rate of a drug in a solvent will increase if its apparent solubility in that solvent is increased, the reverse is very often not true. For example, if a more soluble form of the drug readily reverts to a less soluble form, the dissolution rate of the drug can still be increased by utilizing the more soluble form if the reversion rate is not too rapid, but a stable apparent solubility can be achieved only if the reversion can be completely prevented.

EXPERIMENTAL

Materials—Sulfathiazole[1] was recrystallized from 95% ethanol prior to use. Povidone[2] (average molecular weight of 10,000) was used as received.

Preparation of Different Forms of Sulfathiazole—Crystalline forms I and II of sulfathiazole were obtained by crystallization from 95% ethanol and 1-propanol, respectively (12). The glassy state (supercooled melt) of sulfathiazole was prepared by heating crystalline sulfathiazole on a hot plate[3] at a controlled temperature to prevent any charring, followed by rapid cooling of the melt.

The povidone coprecipitates of sulfathiazole, used in the solubility determination, were prepared by the alcohol evaporation method described previously (1).

The different forms of sulfathiazole were characterized by obtaining their X-ray diffraction[4] patterns (12) using the nickel filter and copper K alpha I radiation.

Solubility Determinations—A weighed excess quantity of the drug or coprecipitate was placed in a 5-ml test tube for each system studied, and 3 ml of the solvent (distilled water or povidone solution) was added at zero time. The test tube was sealed by using a screw cap[5] and placed on a rotating device[6] immersed in a constant-temperature water bath. Duplicate samples were withdrawn and filtered through a Swinney adapter syringe assembly as a function of time, and the filtrate was analyzed for both sulfathiazole and povidone.

[1] Merck and Co., Rahway, N.J.
[2] PVP K-15, GAF Corp., Easton, Pa.
[3] Kofler, Reichert Co., Austria.
[4] Siemens Crystaloflex IV counter-tube X-ray diffractometer.
[5] Lined with Teflon.
[6] Ernest B. Menold Co., Lester, Pa.

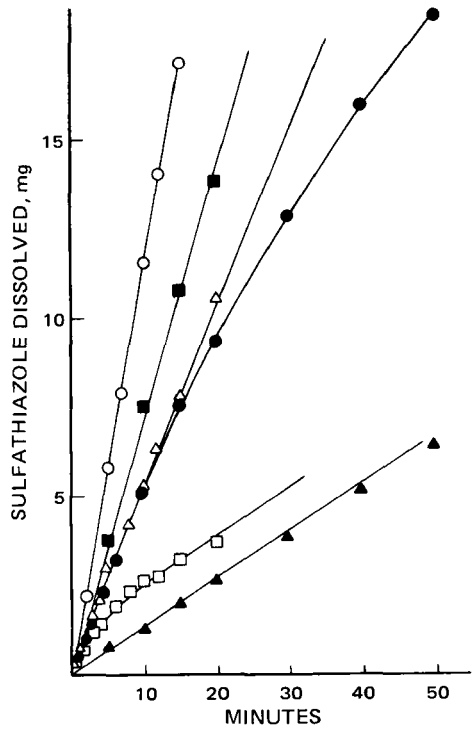

Figure 1—*Effect of sulfathiazole crystalline Form I to povidone ratio on the release profile of sulfathiazole from tablets made from 95% alcohol coprecipitated mixture. Key: ○, 1:3 ratio; ■, 1:2 ratio; △, 1:1.5 ratio; ●, 1:1 ratio; □, 1.5:1 ratio; and ▲, 1:0 ratio.*

Sulfathiazole was analyzed using its UV absorption peak at 282 nm[7]. The polymer was analyzed by means of the refractive index difference[8] between the solution and its solvent after subtracting the contribution due to the sulfathiazole present. The contribution of sulfathiazole was calculated by multiplying its concentration (determined from its UV absorbance) by its refractive index parameter (1). The concentration of the polymer was then obtained from its calibration curve of the refractive index difference *versus* povidone concentration.

RESULTS AND DISCUSSION

Previous work on dissolution rates of sulfathiazole as a function of the povidone weight fraction of the coprecipitate showed that the concentration of drug as a function of time was linear for coprecipitates containing high polymer weight fractions (1). The coprecipitates containing low polymer weight fractions, however, showed a continual decrease in slope, which then became linear as a function of time (Fig. 1). For these coprecipitates in which curvature appeared, both the initial and limiting slopes were determined. The relative rates of dissolution of tablets containing coprecipitates as compared to those containing pure crystalline drug were plotted *versus* the povidone weight fraction in the solid coprecipitate (Fig. 2).

At low polymer weight fractions, there were two plateaus. One plateau, obtained from the limiting slopes of the concentration *versus* time plot, was designated as the limiting rate of dissolution for that system (solid line in Fig. 2). It was reasoned that the drug at the surface of the coprecipitate tablet in this region had to be that of the crystalline form I, since the limiting rate of solution was equal to that exhibited by a pure tablet of the crystalline form I of the drug.

At that time, it was also postulated that the initial rate of dissolution exhibited at the higher plateau (dashed line in Fig. 2) in this region also could be represented by the dissolution rate of a tablet composed of a pure drug but in a higher energy form. This higher energy form, however, could not be crystalline because all known crystalline forms of sulfathiazole would have yielded much lower

[7] Cary 14 UV–visible recording spectrophotometer.
[8] Brice-Phoenix differential refractometer (model BP-2000V).

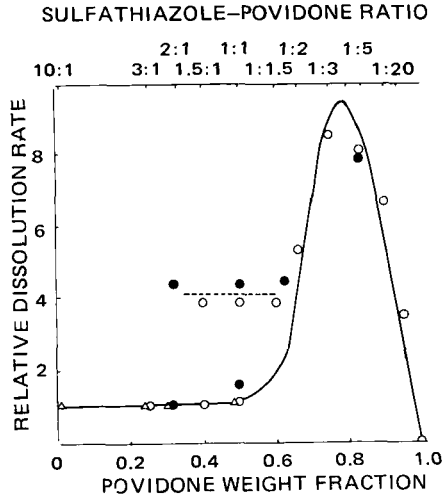

Figure 2—*Comparison of theoretical and experimental relative release rates of sulfathiazole compared to a 1:0 crystalline form I as a function of the povidone weight fraction in tablet. Key: ●, 95% alcohol coprecipitated mixtures; ○, aqueous coprecipitated mixtures; △, mechanical mixtures; - - -, rates calculated from initial slopes (Fig. 1); and —, rates calculated from final slopes (Fig. 1). The curves were empirically drawn. For the theoretical curves, the reader is referred to Fig. 20 of Ref. 1.*

dissolution rates. As a result, it was hypothesized that at initial times the surface of the tablet was composed of a high energy form of the drug, which reverted in solution to the crystalline form I with the passage of time. This hypothesis explained why the initial and limiting rates of drug dissolution yielded a release rate that was independent of the polymer weight fraction in this region (less than a 3:2 ratio of povidone to drug).

An equally compatible explanation would be that both forms were initially present. However, due to its higher dissolution rate, the higher energy form was rapidly depleted from the surface, leaving only the crystalline form on the surface. This process resulted in the composition of the outer layer being effectively transformed to one containing only the crystalline drug. It should be emphasized that this reversion only occurred at the lower povidone weight fractions; for this reason, coprecipitates in this region should not be expected to yield useful dosage forms. This region, however, due to its invariant reproducible release rates, is excellent for study to develop a better understanding of the system.

Solubility of Different Forms—It was of interest to define the physical state of the drug, whether it was another polymorph, a complex, or some other form. The first experiments utilized solubility determinations of each different known form in the presence of povidone. The concentration of drug in solution of the various forms of sulfathiazole was measured as a function of time rather than simply at equilibrium, because important information not otherwise available is often obtained in this way.

Figure 3 shows the concentration of drug in 7% povidone solution in the presence of excess solid drug as a function of time at 37°. The lower curve shows that the concentration of drug rapidly

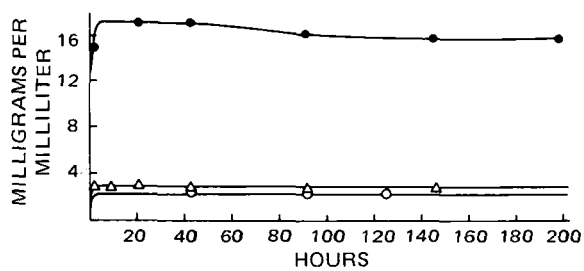

Figure 3—*Concentrations of different forms of sulfathiazole in 7% povidone solutions in the presence of excess solid (drug) as a function of time at 37°. Key: ○, sulfathiazole form I; △, sulfathiazole form II; and ●, sulfathiazole–povidone coprecipitate (1:2).*

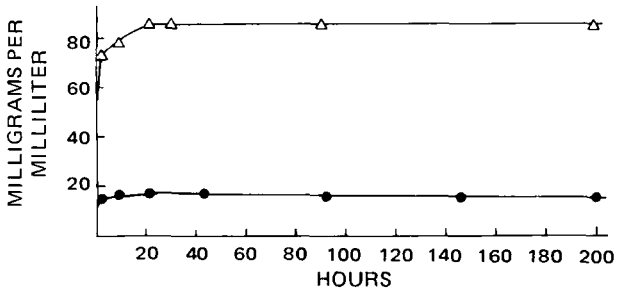

Figure 4—*Release of sulfathiazole and povidone in solution from a sulfathiazole–povidone coprecipitate (1:2) as a function of time at 37°. Key: ●, sulfathiazole; and △, povidone.*

reached a plateau level in the presence of excess crystalline form I of the drug. The same type of behavior was exhibited by the crystalline form II of sulfathiazole, except that the plateau was higher. This finding is interesting, because sulfathiazole crystalline form II has been shown to revert very rapidly in water (12). The higher apparent solubility exhibited by the crystalline form II indicated that the polymer must inhibit its reversion in water to a more stable form and strongly suggested that the solubility of the crystalline form II might be measurable in aqueous solutions under these conditions. Povidone inhibition of sulfathiazole crystal growth was reported previously (13) and, therefore, supported this possibility.

Since povidone solutions were apparently necessary to prevent the reversion of crystalline form II, studies with crystalline form I also were made in solutions of the polymer for a comparison of their activities in solution (Fig. 3). The uppermost curve in Fig. 3 shows the results obtained using the povidone coprecipitate of sulfathiazole. In this case, the concentration of drug rapidly increased, reached a peak, and then decreased slightly to a plateau. Since povidone has a high aqueous solubility, all of the polymer incorporated in the coprecipitate should have dissolved in these solubility experiments. If this expectation was true, the solid that was in apparent equilibrium with the drug solution must have been composed of only drug.

To investigate this aspect, it was decided that the solubility experiments should include measurements of the concentration of the polymer as well as drug in solution as a function of time (Fig. 4). As shown in Fig. 4, the sulfathiazole in solution again reached a plateau. The polymer also behaved in a similar manner, since its concentration in solution increased rapidly as a function of time and reached a plateau value.

The quantity of polymer in solution was calculated using the plateau concentration in solution, and this procedure confirmed the expectation that all of the polymer incorporated in the coprecipitate was indeed in solution. This finding indicated that, within experimental error, only drug and no povidone was present in the apparently equilibrated solid phase. Therefore, it would appear that the drug solution was indeed in apparent equilibrium with pure solid drug, eliminating the possibility, at least in these solubility experiments, that a polymer complex of the drug was the controlling solid phase causing the apparent increased solubility.

Effect of Polymer on Solubility—It was decided to study the solubility of sulfathiazole as a function of the povidone concentration in solution. In this way, the contribution of polymer complexation to the apparent drug solubility can be separated from that due to the free drug. The two lower curves of Fig. 5 show the solubilities of crystalline forms I and II as a function of the polymer concentration in solution at 37°. The apparent solubility of both forms exhibited a linear relationship as a function of the polymer concentrations in solution over the polymer concentration range studied. This finding strongly suggests that extrapolation of the data to 0% polymer should yield the solubility of the respective form of the drug in water in the absence of povidone. To check this possibility, the crystalline form I data were extrapolated to 0% polymer. A value for its solubility of 0.81 mg/ml was obtained, in excellent agreement with the experimentally determined value in water (Fig. 5).

It seemed reasonable to assume at this point that the crystalline form II data also could be extrapolated to obtain its correct solubility in water. This value cannot be obtained by any direct methods due to the rapid transformation to its more stable form (crystalline form I). This extrapolation yielded a solubility of 1.22 mg/ml, 1.5 times higher than the value for the crystalline form I at 37°. It was reported previously (12, 14) that the relative dissolution rate of the crystalline form II as compared to the crystalline form I was 1.7 times higher at 30° in nonaqueous solvents. If one considers the effect of temperature, the latter two ratios are within extrapolation and experimental error.

The dissolution rate technique assumes that the chemical potentials are dependent only on the activity of the respective solids; that is, the diffusion layer, diffusion coefficient, and degree of solvation in solution are constant for both systems. Interestingly, the solubility ratios of form II to form I obtained by these different methods yielded a ratio that showed excellent agreement with the values obtained by direct measurements (1) of the relative dissolution rates in povidone solutions. The measurement of solubility by extrapolation involves fewer assumptions and should provide more reliable value than the other methods; this technique should be used when applicable.

These results indicated that it would be worthwhile to use this approach to study the sulfathiazole–povidone coprecipitate system. Therefore, the apparent solubility of coprecipitated drug as a function of povidone in water was determined by measuring both the drug and polymer concentrations in the presence of excess solid when the system reached an apparent equilibrium. For this purpose, coprecipitates containing different ratios of drug to polymer were used. The final concentration of polymer in solution was only a function of the polymer weight fraction in the solid coprecipitates and the amount of solid coprecipitate added to the solvent, since all of the polymer in solution was provided by the coprecipitate and no attempt was made to control the polymer concentration in solution by the addition of exogenous povidone.

The ratios of drug to polymer in the solid coprecipitate used were 1:1.5, 1:2, 1:3, and 1:4. The data plotted in Fig. 6 show the results of such a study made at 37°. As expected, the solubility using coprecipitated drug was substantially higher than with either crystalline drug and increased with increasing polymer concentration in solution. These data were obtained using a wide range of drug to

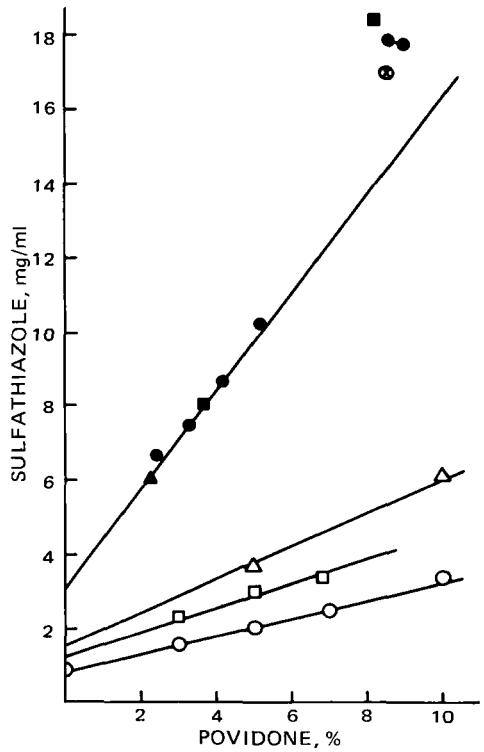

Figure 5—*Solubilities of different forms of sulfathiazole as a function of povidone concentrations in solution at 37°. Key: ○, sulfathiazole form I; □, sulfathiazole form II; △, supercooled melt of sulfathiazole; ▲, 1:1.5 sulfathiazole–povidone coprecipitate; ●, 1:2 sulfathiazole–povidone coprecipitate; ■, 1:3 sulfathiazole–povidone coprecipitate; and ⊕, 1:4 sulfathiazole–povidone coprecipitate.*

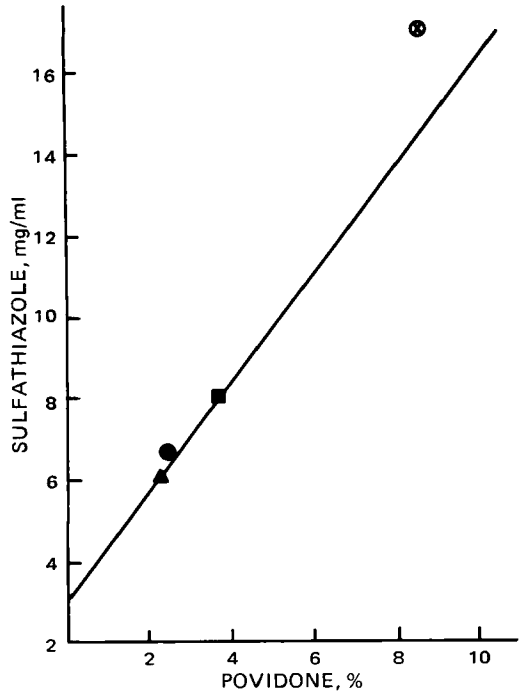

Figure 6—*Apparent solubility of sulfathiazole coprecipitated with different povidone weight ratios as a function of povidone concentrations in solution at 37°. Key: ▲, 1:1.5 sulfathiazole–povidone coprecipitate; ●, 1:2 sulfathiazole–povidone coprecipitate; ■, 1:3 sulfathiazole–povidone coprecipitate; and ⊕, 1:4 sulfathiazole–povidone coprecipitate.*

polymer weight ratios in the coprecipitate, and the final povidone concentration in the solution varied from 2.3 to 8.5%.

If the apparent relationship shown in Fig. 6 for the coprecipitated sulfathiazole is valid, the same curve should be obtained if the drug to polymer weight ratio in the coprecipitate is kept constant and the apparent solubility of the drug is determined in solutions containing varying initial concentrations of povidone. The studies were made using a 1:2 drug to povidone coprecipitate; as expected, the data points showed excellent agreement with those obtained using different coprecipitates. The results of all solubility experiments using coprecipitates were plotted in Fig. 5 to facilitate comparison of the data.

To verify further that the results were independent of the drug to polymer weight ratio of the coprecipitate used, a coprecipitate containing a 1:3 drug to polymer weight ratio was used to determine the apparent drug solubility at the higher polymer concentration in solution. Figure 5 shows that the same results were obtained regardless of the weight ratio of drug to polymer used in the coprecipitate. These latter results also could have been obtained by using the same coprecipitate but controlling the final povidone concentration in solution by simply varying the solid to solvent (water) ratio. Although there appear to be higher orders of interactions between drug and polymer at the higher polymer concentrations in solution contributing to the overall drug solubility, the data points at the lower povidone concentrations strongly suggest that a linear relationship would be applicable in this range of polymer concentrations.

Solubility of Unstable Forms in Absence of Polymer—Having established the validity of the solubility profile of the high energy form of the coprecipitated drug, it seemed reasonable to assume that if the linear portion of these data is extrapolated to 0% povidone, the aqueous solubility of the high energy form of the drug in the coprecipitate can be obtained. This extrapolation (Fig. 5) yielded a solubility of 3.06 mg/ml for the high energy form of sulfathiazole, about 3.8 times greater than that of its crystalline form I.

The solubility of the high energy form in water in the absence of povidone could not be obtained directly for two reasons. First, the high energy form would revert too rapidly to a crystalline form. Second, the coprecipitate itself contains povidone which, of course, would be released simultaneously with the drug when the coprecipitate is added to water. Furthermore, the extrapolation method utilized here allows one to use equilibrium solubility rather than dissolution rate data to obtain this solubility. This fact is very important because the extrapolated solubilities of the different solid forms of sulfathiazole then can be used as a measure of their relative activities.

Correlation to Dissolution Rate Data—This factor of 3.8 is equal to the ratio of the limiting and initial rate plateaus seen in Fig. 2. This evidence strongly supports the hypothesis that pure drug during dissolution is on the surface of the tablet containing the lower polymer weight ratios. This excellent agreement between the solubility and dissolution rate experiments also provides strong evidence that the high energy form of the drug dictating the solubility value exhibited in these solubility experiments is identical to the form controlling the initial dissolution rates of tablets compressed from coprecipitated sulfathiazole at the lower polymer weight fractions (Fig. 2).

These conclusions infer that the amount of polymer at tablet surfaces (containing lower povidone weight fractions) is negligible during the dissolution rate experiments. This implication also can be justified by an alternative approach. Since these experiments showed that the presence of increasing concentration of polymer significantly increased the solubility of sulfathiazole, it would be reasonable to state that increasing the concentration of povidone at the tablet surface would also increase the apparent dissolution rate of the drug. Therefore, increasing the amount of povidone compressed in the tablet would be expected to increase the polymer concentration at the surface and thereby increase the apparent dissolution rate of the drug.

It is seen in Fig. 2, however, that the rates of solution of tablets containing low polymer weight fractions show the same rate of dissolution, despite an increasing weight fraction of povidone incorporated in the tablet. This finding strongly suggests that at low polymer weight fractions the concentration of polymer at the surface is indeed insignificant and that the drug is not present as, or interacting with polymer to form, a polymer complex, dispersion, *etc.*, at the tablet surface in these experiments. This reasoning lends further support to the concept of a pure drug layer existing during dissolution at the surface of tablets containing low povidone weight fractions.

Studies with Supercooled Melts—To investigate this possibility further, a supercooled melt of sulfathiazole was prepared. Sulfathiazole was melted on a hot stage at a controlled temperature to prevent charring, and then the melt was quickly frozen. This process produced a transparent solid which appeared to be in the "glassy state." This material was powdered, and an X-ray diffractogram of the powder was obtained. The diffraction pattern showed no evidence of crystallinity and suggested that the drug may be amorphous and may correspond to the high energy form of the drug present in the coprecipitate. Therefore, the apparent solubility of this form of sulfathiazole was determined as a function of the povidone concentration in solution (Fig. 5).

Although the resultant solubilities were higher than those obtained for the crystalline form I or form II, they were significantly lower than those obtained for the coprecipitate. This finding indicated that the specific form of the drug obtained in this way did not correspond to any of the previous forms encountered, including the high energy form found in the coprecipitate. Since the amorphous state is generally defined in terms of a lack of crystalline structure, it is possible to produce amorphous states containing varying degrees of structuring that are not crystalline. The lower solubility of the powder obtained by supercooling as compared with that of the coprecipitated drug implied that it contained a higher degree of structuring than the high energy form of the drug present in coprecipitates. Therefore, sulfathiazole may be highly structured in the molten state.

Mathematical Analysis of Solubility *versus* Polymer Concentration Curves—The solubility curves of the different forms found in Figs. 5–7 can be analyzed since they should all follow the following relationship:

$$S_t = \sum_{i=1}^{i=n} \sum_{j=0}^{j=m} K_{i,j} S_x^i \%_p^j \qquad \text{(Eq. 1)}$$

where S_t is the total apparent solubility of drug; S_x is the concentration of the free drug at equilibrium in the presence of excess solid for each form X of the drug; $\%_p$ is the percent povidone in so-

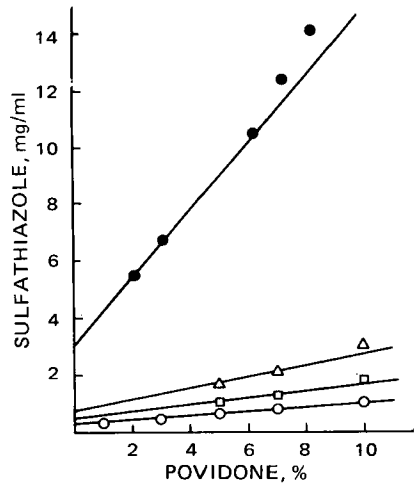

Figure 7—*Solubilities of different forms of sulfathiazole as a function of povidone concentrations in solution at 17°. Key:* ○, *sulfathiazole form I;* □, *sulfathiazole form II;* △, *supercooled melt of sulfathiazole; and* ●, *sulfathiazole–povidone coprecipitate.*

lution; i and j are the stoichiometry of the drug and polymer, respectively, in the complex; and K_{ij} is the corresponding stability constant. For a system limited to a 1:1 complex, Eq. 1 becomes:

$$S_t = S_x + K_{1,1}S_x\%_p \qquad \text{(Eq. 2)}$$

Equation 2 predicts that a straight line relationship will be obtained with an intercept of S_x and a slope of $K_{1,1}S_x$. Thus, the ratios of the intercepts obtained with two forms of sulfathiazole will be equal to the ratio of their respective slopes. Within experimental error, one sees that the curves for the different forms in Figs. 5 and 7 follow this relationship reasonably well and provide further evidence in support of the proposed relationships.

Dissolution Plots—Even though its magnitude is small (≈7%), it is worthwhile commenting on the possible reasons for the overshoot peak in the solubility curve for the high energy form shown in Fig. 3. There are a number of possible explanations but no definitive evidence. One explanation which may be applicable is the nonhomogeneity of the amorphous phase of sulfathiazole. Evidence presented in this report indicates that it is possible for an amorphous solid to have a varying degree of structure. It would not be unreasonable, therefore, to assume that a fraction of the coprecipitated drug may have less structure than the bulk of the amorphous solid. If this assumption is true, the less structured fractions would be expected to exhibit a higher solubility and dissolution rate. As a result, the less structured fractions would preferentially dissolve.

If the fraction of the less structured components initially present was sufficiently large and its dissolution rate sufficiently rapid relative to the more structured components, a slight oversaturation of the solution would result with respect to the more structured amorphous components remaining in the solid phase. This would cause the concentration in solution to overshoot the final controlling solubility. Needless to say, if this explanation is applicable, the range of degree of structuring initially present in the solid would only need to be small since the overshoot is very small.

It is also possible that the peak in the sulfathiazole concentration is due to different rates of solution of the polymer and drug. Figure 4 shows that the polymer exhibits a slower rate of equilibrium than the drug. If so, the polymer concentration at the surface of the solid particles would initially decrease at a slower rate than that of the drug. During this initial period, the higher polymer concentration at the surface of the solid would permit the drug, because of complexation, to continue dissolving despite the concentration of the bulk of the solution being at or above the saturation point. After this initial period, however, the polymer concentration at the surface would decrease to its bulk solution concentration, requiring that the excess drug return to the solid phase. If this explanation is true, the drug supersaturation is not sufficient for nucleation of new particles in the bulk. Since the overshoot shown in Fig. 3 is only of the order of 7%, one should not expect nucleation to occur in the presence of solid drug particles.

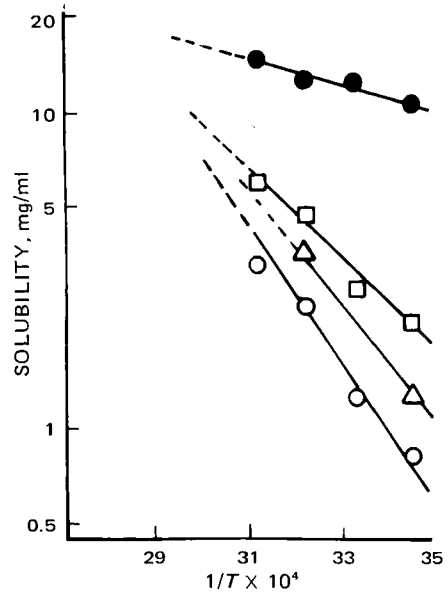

Figure 8—*Van't Hoff plots of the solubilities of the different forms of sulfathiazole in 7% povidone solution. Key:* ○, *sulfathiazole form I;* △, *sulfathiazole form II;* □, *supercooled melt of sulfathiazole; and* ●, *sulfathiazole–povidone coprecipitate.*

Thermodynamic Parameters—The reproducibility of these experiments suggests that further evidence regarding the form of the drug in the coprecipitate could be obtained by obtaining the thermodynamic parameters of the various forms. Therefore, the apparent solubility of the various forms of the drug as a function of the povidone in solution was determined as a function of the temperature. Figure 7 shows the results obtained at 17°. Plots similar to Figs. 5 and 7 were also obtained at 27 and 47°.

A van't Hoff plot of the sulfathiazole solubility was made for each percent povidone solution utilized. A typical plot is shown in Fig. 8. Although the plots yield apparently linear curves, permitting enthalpies to be calculated from their slopes, the enthalpies so obtained are difficult to interpret due to the large number of possible species involved. For this reason, it is difficult to extract from these data the enthalpy of the individual processes. Nevertheless, the linearity of all van't Hoff plots of the different forms of sulfathiazole in the different percent polymer solutions strongly indicates that these solubilities are not due to a chemical kinetic barrier existing between the solid and solution phases but are due to a balance of their chemical potentials.

Since all plots of solubility *versus* povidone concentrations were

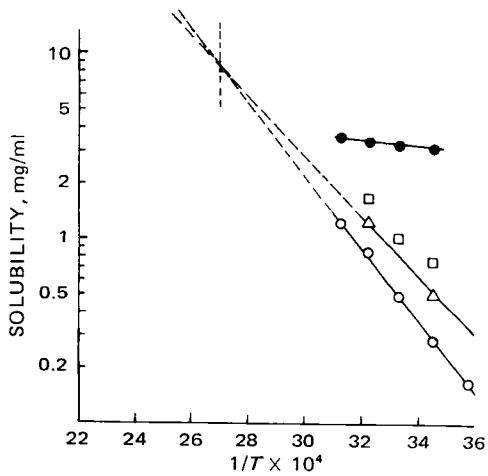

Figure 9—*Van't Hoff plots of the aqueous solubilities of the different forms of sulfathiazole obtained by extrapolation of solubility* versus *povidone concentration plots. Key:* ○, *sulfathiazole form I;* △, *sulfathiazole form II;* □, *supercooled melt of sulfathiazole; and* ●, *sulfathiazole–povidone coprecipitate.*

Table I—Free Energy Values Calculated for the Different Forms of Sulfathiazole Relative to the Crystalline Form I at 27°

Solid Form	S°_X/S°_I	$\Delta F^{27^{\circ}}_{I,X}$, cal/mole
Crystalline form II	1.70	316
Glassy state form	2.06	431
Coprecipitated form	6.60	1125

reasonably linear (*e.g.*, Figs. 5 and 7), one should be able to extrapolate the curves of 0% polymer to obtain the apparent solubility of the respective form of the drug in water at a particular temperature. These solubilities would then permit the thermodynamic parameters for each form of the drug to be obtained in the absence of polymer, without the complications due to the presence of complexes.

The equations needed to calculate the thermodynamic parameters can be obtained (15) by considering the following processes, $S_{\text{solid } I} \rightleftarrows S_{\text{solution}}$, and $S_{\text{solid } X} \rightleftarrows S_{\text{solution}}$. One can utilize the thermodynamic parameters obtained from solubility experiments to calculate the corresponding parameters for the two solids.

Free Energy—Since the ratio of the activities[9] of the solids are equal to the ratios of their respective solubilities (assuming that the activity coefficient in solution remains constant) at a given temperature, one can calculate the free energy for the different forms of sulfathiazole relative to the crystalline form I from:

$$\Delta F^{T}_{I,X} = RT \ln \frac{S^{\circ}_X}{S^{\circ}_I} \qquad \text{(Eq. 3)}$$

The calculated free energies for 27° are listed in Table I. The free energy of the coprecipitated drug is more than three times higher than that of the crystalline form I and justifies the term "high energy form" used previously to describe the form of the coprecipitated drug.

Enthalpy—The van't Hoff plot using the solubilities obtained by extrapolation to 0% polymer is shown in Fig. 9. As previously stated, the heat of solution for each form is calculable from this plot because only one species of sulfathiazole is involved in the solution phase. The enthalpies calculated from these slopes are given in Table II.

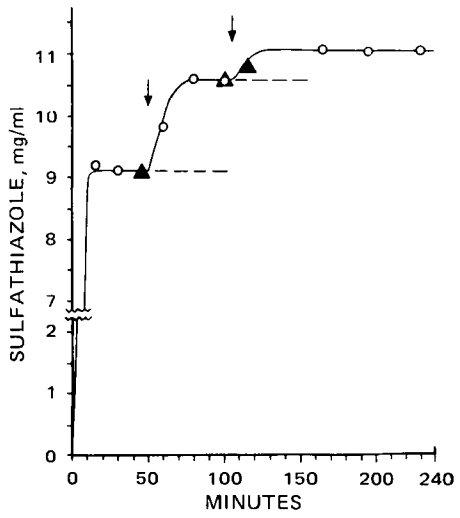

Figure 10—*Effect of incremental additions of 1% povidone to apparently equilibrated drug solutions in two different vials in the presence of excess coprecipitated drug. The time of each incremental addition of 1% polymer is indicated by an arrow. The concentration of povidone was initially 4%; it was increased to 5% after the first addition of polymer and finally was increased to 6% with the second addition. Key: —, observed sulfathiazole concentration as a function of time; - - -, expected curve if subsequent addition of povidone was not made;* ○, *vial A; and* ▲, *vial B.*

[9] If one follows the generally accepted convention for solids, this ratio should be referred to as the ratio of the fugacities rather than the activities. The authors, however, preferred the term activities in this context due to the more obvious extension of the relative properties of the solids to that of their saturated solutions such as rates of solutions and absorption.

Table II—Heats of Solution of the Various Forms of Sulfathiazole

Solid Form	Heat of Solution, cal/mole	Heat of Transition, cal/mole
Crystalline form I	9244	—
Crystalline form II	7626	1618
Glassy state form	5632	3612
Coprecipitated form	805	8439

Theoretically, the curves of the crystalline forms I and II should intersect at their transition temperature. For this reason, the curves in Fig. 9 were arbitrarily drawn through the experimental points so that the curves of forms I and II intersected at the transition temperature, which was previously reported (14) in the literature as 94.5°. Figure 9 shows that, despite this restriction, the agreement of the slopes of the drawn curves with the data points was excellent.

This result strongly indicates that the solubilities obtained by extrapolation are, in fact, thermodynamic values of the solubility in water for both forms. This viewpoint was supported by the fact that the solubility of the crystalline form I obtained by extrapolation to 0% polymer corresponds, as expected, to that obtained by direct measurement. The validity of the extrapolated solubility values of the crystalline form II cannot be tested directly due to its rapid reversion in the absence of povidone. It can be confirmed, however, by an indirect approach using the difference of the heat of solution of the two forms and comparing this value with the literature value determined by a different method.

The value of this difference was calculated from the heat of solution of the two forms determined from the slopes of their respective van't Hoff plots and found to be 1618 cal/mole, in excellent agreement with the previously reported value of 1744 cal/mole (14) obtained from dissolution rates in 95% alcohol. Surprisingly, the data obtained using the supercooled melt was relatively high and yielded 5632 cal/mole as the heat of solution. This relatively high enthalpy confirms the earlier postulation that the supercooled melt was highly structured. On the other hand, the heat of solution for the coprecipitated drug was unexpectedly small, only about 805 cal/mole. This finding indicates that the enthalpy of the coprecipitated drug is approximately 8 kcal/mole higher than that of the crystalline form I and is a clear indication of the lack of structure in the coprecipitated sulfathiazole.

These results are summarized in Table II. The large enthalpic differences between the crystalline and high energy forms shown in Table II strongly suggest that the higher solubility and dissolution rates of the high energy form may be due to the relatively small cohesive and adhesive forces present in the coprecipitated drug.

Entropy—The previous discussion suggests that the molecules of the coprecipitated sulfathiazole in the solid state are more random than those of the glassy state since it has less structure. Since entropy is a measure of the randomness of a system, the entropy difference between the crystalline form I and the other forms of sulfathiazole were calculated (Table III) using:

$$\Delta S_{I,X} = \frac{\Delta H_{I,X} - \Delta F_{I,X}}{T} \qquad \text{(Eq. 4)}$$

Table III confirms that the greater degree of randomness existing in the coprecipitated sulfathiazole (expressed as its entropy) relative to the other forms is indeed very high.

Reversibility of Coprecipitate Solubility System—The data

Table III—Entropy Values Calculated for the Different Forms of Sulfathiazole Relative to the Crystalline Form I at 27°

Solid Form	$\Delta S_{I,X}$, eu
Crystalline form II	4.3
Glassy state form	10.6
Coprecipitated form	24.4

strongly support the postulation that the solubilities reported in this article are equilibrium values. Nevertheless, the importance of future experiments dictated that this postulation should be put on as firm a base as possible. If these solubilities were the result of a kinetic barrier between phases, they would not be reversible. Not only would the opposite be true for two phases in equilibrium, but one of the best tests for equilibrium is to demonstrate the reversibility of the system.

Since the previous solubilities were determined from a solution in which the drug was previously at a higher concentration, it was only necessary to test the approach to the same equilibrium value from a lower concentration of drug in solution to establish reversibility. The solubility experiment shown in Fig. 3 was repeated. After apparent equilibration, more povidone was added. If a kinetic barrier was maintaining a supersaturated solution of drug, no effect on the apparent solubility of the drug should be observed due to the addition of more polymer. If, however, the concentration of drug in solution was due to an equilibrium process, the apparent solubility of the drug should increase with additional povidone as predicted by the previous data shown in Fig. 5.

The results of this experiment are shown in Fig. 10. The concentration of drug in solution did increase, and the coprecipitated drug dissolved rapidly until it reached a plateau. At this point, all of the polymer of the coprecipitate had dissolved, but part of the drug remained undissolved as a suspended solid. After the plateau was clearly established, a sufficient amount of pure povidone (*i.e.*, containing no drug) was added to increase its concentration from 4 to 5% polymer. As expected, the solubility of the drug was increased. After a plateau was established for a second time, 1% more povidone was again added. The concentration of sulfathiazole again increased until all of it dissolved to produce a crystal clear solution.

This result clearly demonstrated that the solubility value previously obtained was controlled by an equilibrium process and was not influenced by any kinetic factors. As expected, the values of the drug concentrations at the new equilibria after each addition of povidone corresponded closely to the solubility predicted by the solubility curve of the high energy form (Fig. 5) at the corresponding polymer concentration in solution.

CONCLUSIONS

A number of important points and conclusions should be emphasized regarding the results of this study involving high energy drug coprecipitates. The evidence presented strongly confirms the original postulate that the dissolution rate of tablets containing high energy drug coprecipitates at lower povidone weight fractions is controlled by a layer of solid drug on the tablet surface. It also adds credence to the postulate that when reversion occurs, the layer of high energy drug solid is replaced by a layer of the crystalline form of the drug.

These studies showed that a solution of an unstable form of a drug that is supersaturated with respect to a more stable form of the drug can be stabilized by the addition of a sufficient concentration of another agent. For sulfathiazole, this result was successfully accomplished by adding a sufficient concentration of povidone. In addition, these studies showed that higher concentrations of povidone were required to prevent nucleation as compared to the concentration of polymer required to inhibit crystal growth (13).

The applicability of high energy forms could be severely limited unless reliable methods are available for their identification and analysis. Melting points, IR absorption, differential thermal analysis, thermal gravimetric analysis, differential scanning calorimetry, and X-ray diffractograms often can be useful for this purpose.

If one is to utilize fully the potential of higher energy forms, however, one needs to characterize their solution behavior as well. The solubility and thermodynamic parameters can be useful for this purpose but often are not available due to instability of the solid phase. This study illustrated the use of a third component, povidone, which stabilized the higher energy forms of sulfathiazole in order to determine the solubility of the otherwise physically unstable higher energy forms of the drug. The effect of the stabilizing agent was eliminated by determining the solubility of the higher energy form as a function of the concentration of the stabilizing agent in solution. Extrapolation of the resultant curve to zero concentration of the stabilizing agent yields the desired solubility.

This study also provided strong evidence for the presence of an amorphous state of sulfathiazole as the controlling phase of both the solubility and dissolution rate experiments involving the high energy form which was obtained by coprecipitation with povidone. Other possibilities such as drug–polymer complexes, molecular or colloidal dispersions, and solid solutions are not controlling in these systems.

Although previous studies utilizing coprecipitates showed that higher dissolution rates could be obtained, it had not been shown that a higher solubility measured by the equilibrium method could be obtained. This study clearly demonstrated that high energy forms of a drug made by the coprecipitation technique can be used to provide metastable solutions of a drug which are significantly supersaturated with respect to the stable crystalline form. For sulfathiazole, this supersaturation ratio was approximately 3.8 at 37°.

Although higher dissolution rates are due to a higher solubility of the high energy forms involved, the implication that higher solubilities can also be achieved is not necessarily true. It can be easily shown that rapidly reverting systems of high energy forms can be successfully utilized to obtain faster dissolution rates, particularly from dissolving powders, but they may not show higher solubility values due to rapid reversion during equilibrium solubility studies. Needless to say, rapidly dissolving systems that revert can be used to obtain higher blood levels of poorly soluble drugs only if administered as a solid dosage form. Very often, a solid dosage form cannot be used. For this reason, effectively increasing the apparent solubility of many drugs could significantly increase their usefulness in therapeutic situations as compared to increasing only their dissolution rates.

REFERENCES

(1) A. P. Simonelli, S. C. Mehta, and W. I. Higuchi, *J. Pharm. Sci.*, **58**, 538(1969).

(2) A. P. Simonelli, S. C. Mehta, and W. I. Higuchi, presented at the APhA Academy of Pharmaceutical Sciences, Montreal meeting, May 1969.

(3) I. M. Stone, U.S. pat. 3,089,818 (1963).

(4) T. Suyama, Japanese pat. 8476 (1963).

(5) M. Mayersohn and M. Gibaldi, *J. Pharm. Sci.*, **55**, 1323(1966).

(6) W. L. Chiou and S. Riegelman, *ibid.*, **58**, 1505(1969).

(7) T. R. Bates, *J. Pharm. Pharmacol.*, **21**, 710(1969).

(8) A. H. Goldberg, M. Gibaldi, and J. L. Kanig, *J. Pharm. Sci.*, **54**, 1145(1965).

(9) M. Gibaldi, S. Feldman, and T. R. Bates, *ibid.*, **57**, 708(1968).

(10) K. Sekiguchi and N. Obi, *Chem. Pharm. Bull.*, **9**, 866(1961).

(11) T. Tachibana and A. Nakamura, *Kolloid-Z. Polym.*, **203**, 130(1965).

(12) W. I. Higuchi, P. D. Bernardo, and S. C. Mehta, *J. Pharm. Sci.*, **56**, 200(1967).

(13) A. P. Simonelli, S. C. Mehta, and W. I. Higuchi, *ibid.*, **59**, 633(1970).

(14) G. Milosovich, *ibid.*, **53**, 484(1964).

(15) E. Shefter and T. Higuchi, *ibid.*, **52**, 781(1963).

ACKNOWLEDGMENTS AND ADDRESSES

Received March 14, 1972, from the *College of Pharmacy, University of Michigan, Ann Arbor, MI 48104*

Accepted for publication May 15, 1975.

Presented at the Basic Pharmaceutics Section, APhA Academy of Pharmaceutical Sciences, Montreal meeting, May 1969.

Supported in part by Contract PH 43-68-1284 with Chemotherapy, National Cancer Institute, National Institutes of Health.

* Present address: Parke-Davis & Co., Detroit, MI 48232

x To whom inquiries should be directed. Present address: School of Pharmacy, Institute of Materials Science, University of Connecticut, Storrs, CT 06268

Biosynthesis of Deuterated Riboflavin: Structure Determination by NMR and Mass Spectrometry

PAUL L. PLUTA *, HENRY L. CRESPI ˣ, MICHAEL KLEIN ‡, MARTIN I. BLAKE §, MARTIN H. STUDIER, and JOSEPH J. KATZ

Abstract □ The riboflavin-producing fungus *Eremothecium ashbyii* was cultured in various growth media containing high concentrations of deuterium, and the product was isolated. The structures of highly deuterated riboflavin, in which at least 13 of 15 nonexchangeable hydrogens were replaced by deuterium, and fully deuterated riboflavin, in which all 15 nonexchangeable sites contained deuterium, were established by NMR and mass spectrometry. The aromatic protons (C-5 and C-8) were partially substituted in the highly deuterated molecule. Information regarding three areas of the biosynthetic pathway within the microorganism was obtained as a result of the formation of these compounds. Extensive solvent interaction, possibly due to passage of sugar through the transaldolase–transketolase pathway, occurs during formation of the ribityl chain. Limited solvent participation takes place during formation of 6,7-dimethyl-8-ribityllumazine, the immediate precursor of riboflavin. Deuteration of the riboflavin C-6 and C-7 methyl groups indicates significant solvent exchange during the final step of the biosynthetic process.

Keyphrases □ Riboflavin—deuterated, biosynthesis by fungus *Eremothecium ashbyii*, isolation, structure determination by NMR and mass spectrometry □ Biosynthesis—deuterated riboflavin by fungus *Eremothecium ashbyii* □ NMR—structure elucidation of biosynthesized deuterated riboflavin □ Mass spectrometry—structure elucidation of biosynthesized deuterated riboflavin

Deuterated drugs have proven useful in the study and measurement of isotope effects (1, 2), the elucidation of metabolic and biosynthetic pathways (3, 4), the determination of pharmacological mechanisms of drug action (5, 6), and other experimental investigations (7).

The biochemical reactions within various microorganisms that lead to the production of riboflavin have been the subject of extensive research for many years. The pathway has been almost completely determined and was reviewed (8–12). The final reaction of the biosynthetic process also was explained recently (13–16).

The production and isolation of deuterated riboflavin are reported in this study. Proof of deuterium incorporation at specific molecular sites by means of NMR and mass spectrometry is presented, and the implications of these results on the biosynthetic pathway of riboflavin are considered.

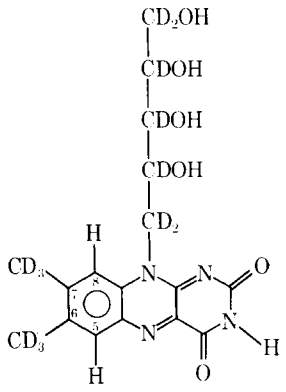

I

EXPERIMENTAL

Production and Isolation of Deuterated Riboflavin—The medium used for the *Eremothecium ashbyii*[1] culture in deuterium oxide is listed in Table I. Production cultures contained 1 liter of medium in cotton-plugged 2-liter flasks. All cultures were grown on a rotary shaker[2] at 120 rpm under subdued light at 30°.

Maximum riboflavin production with this organism was obtained in 30 days under these conditions. According to Mohammed *et al.* (17), atmospheric dilution of medium deuterium is less than 10% during this period. Riboflavin was measured[3] by the USP method (18).

The preparative method used here is a combination of methods reported earlier (19–21). Column chromatography was followed by solvent extraction. The purification procedure was monitored by optical spectrometry. Purity of the final product was established by TLC (22), NMR, and mass spectrometry.

NMR Spectroscopy (^{1}HMR)—^{1}HMR spectra were obtained by use of a spectrometer[4] modified for pulse operation. A 5-mg sample was dissolved in 1 ml of solution containing equal parts of deuterated trifluoroacetic acid and trifluoroacetic acid anhydride. Hexamethyldisiloxane was added for internal standardization. Chemical shifts are reported in delta, δ, parts per million downfield from hexamethyldisiloxane.

Mass Spectrometry[5]—Samples were dissolved in ethanol for application to a platinum ribbon, which was placed directly into the ionization source and heated electrically.

RESULTS AND DISCUSSION

Structure Determination—Evidence of deuterium participation during biosynthesis was obtained by a spectral comparison of isolated biosynthesized deuterated riboflavin with known riboflavin. The inability of deuterium to produce a ^{1}HMR signal makes this technique ideal for the determination of deuterium incorporation. The capability of making multiple comparisons of parent and fragment masses makes mass spectrometry equally valuable, especially when high sensitivity is required.

Consideration of deuterium participation will be limited to nonexchangeable (carbon-bound) hydrogen sites only. Of the 20 hydrogen sites in the molecular structure of riboflavin, 15 are of this type. The other five sites are bound to oxygen or nitrogen and are, therefore, exchangeable. Since the last solvent contact was with large volumes of water during purification, these sites contained ^{1}H at the conclusion of the isolation procedure. All further references to the hydrogen sites of riboflavin are to nonexchangeable sites.

Figure 1 shows the ^{1}HMR spectrum of riboflavin. The use of tri-

[1] *Eremothecium ashbyii* (NRRL Y 136) was obtained from the U.S. Department of Agriculture, Northern Regional Research Laboratory, Peoria, Ill.

[2] Eberbach Corp., Ann Arbor, Mich.

[3] Hitachi Perkin-Elmer model MPF 2A fluorescence spectrometer.

[4] Varian HR 220 spectrometer.

[5] Mass spectra were obtained with a modified Bendix Time-of-Flight model 12 mass spectrometer (23).

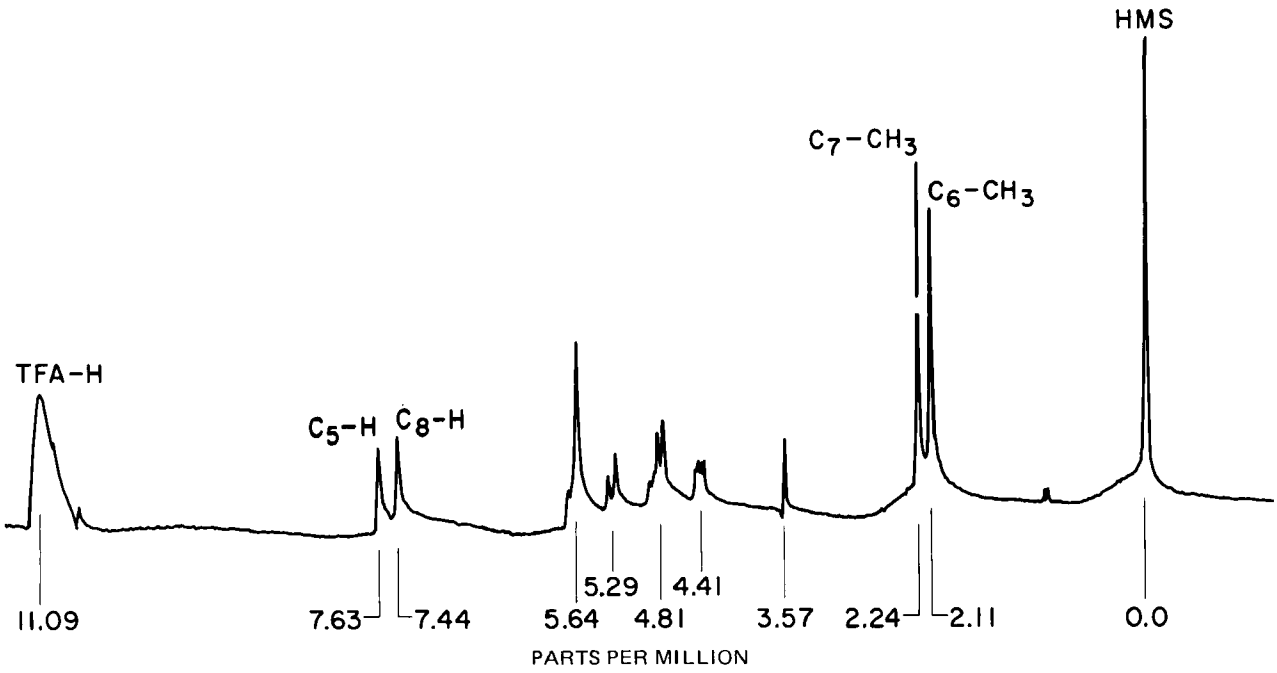

Figure 1—*^{1}HMR spectrum of riboflavin.*

fluoroacetic acid anhydride along with deuterated trifluoroacetic acid as the solvent enabled the aromatic protons of riboflavin to be resolved completely. Proton assignments are analogous to those of other investigators for riboflavin (13) and riboflavin phosphate (24–26). The high sensitivity of the instrument used, attained by operating in pulse mode with computer assistance, enabled procurement of spectra with a minimum of material.

Table II lists the respective masses and relative abundances of fragments in the first reported mass spectrum of riboflavin. The decomposition properties of this compound, which heretofore prevented obtaining its mass spectrum, were overcome by the inlet system of the instrument. A solution of the sample was applied to a thin metal ribbon, which was inserted directly into the ionizing region of the spectrometer. Passage of a variable electric current through this filament enabled heating to be controlled exactly. As the temperature was increased slowly, vaporized samples were ionized by electron impact prior to major decomposition; mass spectra of components of the sample were obtained sequentially.

Highly Deuterated Riboflavin—The product isolated from cultures grown in the medium listed in Table I was composed of a mixture of compounds containing a minimum of 13 nonexchangeable deuterium atoms and a maximum of two nonexchangeable aromatic hydrogen atoms at C-5 and C-8. The ^{1}HMR spectrum of this compound showed only a singlet peak at 7.50 ppm, indicating the presence of hydrogen in the aromatic region of the molecule and the presence of deuterium in both methyl and ribityl regions.

The chemical shift of this peak was between those of the known aromatic peaks of riboflavin, and the peak height suggests the presence of two protons. However, without a quantitative proton reference within the molecule, a more specific determination of the extent of deuterium incorporation was not possible. Resolution of this peak was not realized, apparently due to the isotope effect related to deuteration in the methyl groups (27). The congruence of spectra of known riboflavin in protio and deuterated solvent systems showed that exchange of protons with deuterium did not occur while the ^{1}HMR spectra were being obtained.

Comparison of the mass spectrum of highly deuterated riboflavin with that of riboflavin USP (Fig. 2) substantiates the ^{1}HMR findings by indicating that at least 13 deuterium atoms participated in biosynthesis, the only remaining hydrogens being located in the isoalloxazine ring. The conclusions are based on the following major peak analyses:

1. 389 (*versus* 376), parent peak: difference of 13 amu indicates 13 of 15 possible deuterium atoms in the molecule.
2. 370 (*versus* 358), loss of HDO (*versus* loss of H_2O): 12 of 14 possible D in fragment.
3. 356 (*versus* 345), loss of CD_2OH (*versus* loss of CH_2OH): 11 of 13 possible D in fragment.
4. 325 (*versus* 315), loss of CDOH—CD_2OH (*versus* loss of CHOH—CH_2OH): 10 of 12 possible D in fragment.
5. 294 (*versus* 285), loss of $(CDOH)_2$—CD_2OH [*versus* loss of $(CHOH)_2$—CH_2OH]: nine of 11 possible D in fragment.
6. 262 (*versus* 256), loss of $(CDOH)_3$—CD_2OH and H/D transfer [*versus* loss of $(CHOH)_3$—CH_2OH and H transfer]: eight of 10 possible D in fragment.
7. 249 (*versus* 243), loss of CD_2—$(CDOH)_3$—CD_2OH and H/D transfer [*versus* loss of CH_2—$(CHOH)_3$—CH_2OH and H transfer]: six of eight possible D in fragment.
8. 219 (*versus* 213), loss of CD_2—$(CDOH)_3$—CD_2OH and CO [*versus* loss of CH_2—$(CHOH)_3$—CH_2OH and CO]: six of eight possible D in fragment.
9. 191 (*versus* 185), loss of CD_2—$(CDOH)_3$—CD_2OH and N—CO—NH and H transfer [*versus* loss of CH_2—$(CHOH)_3$—CH_2OH and N—CO—NH and H transfer]: six of eight possible D in fragment.
10. 177 (*versus* 171), loss of CD_2—$(CDOH)_3$—CD_2OH and CO—NH—CO and H transfer [*versus* loss of CH_2—$(CHOH)_3$—CH_2OH and CO—NH—CO and H transfer]: six of eight possible D in fragment.

Table I—Deuterated Riboflavin Production Medium

Ingredient		Amount, g
Sucrose[a]		25.0
Potassium phosphate, dibasic		1.0
Potassium phosphate, monobasic		1.0
Sodium chloride		1.0
Magnesium sulfate heptahydrate		0.7
Ferrous sulfate heptahydrate		0.005
Inositol		0.03
Thiamine hydrochloride		0.0015
Biotin		0.7 μg
Boric acid		0.02
Manganese chloride tetrahydrate		0.02
Calcium chloride		0.5
Yeast extract		0.7
Casein (vitamin free)		0.5
Deuterium oxide	Dilute to	1000.0 ml

[a] Algal deuterated sugars were used for the production of fully deuterated riboflavin (33).

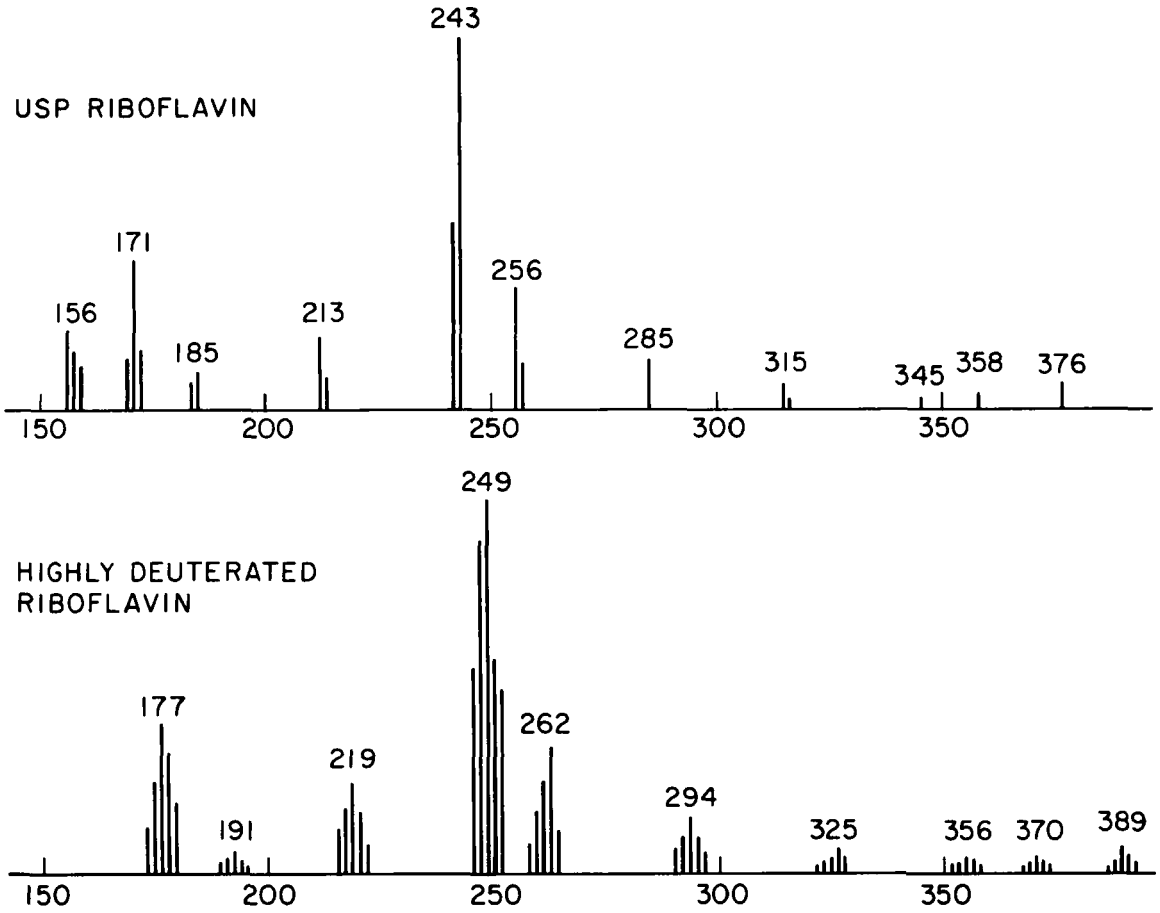

Figure 2—*Comparison of mass spectra of riboflavin USP and highly deuterated riboflavin.*

The range of fragments existing at each highly deuterated riboflavin mass number indicates the presence of minor amounts of compounds containing more than 13 deuterium atoms. This range may also exist due to hydrogen/deuterium transfer to double bonds in the isoalloxazine ring or to hydrogen/deuterium loss from carbon or nitrogen, two processes known to occur under the operating conditions of the spectrometer. The presence of compounds containing less than 13 deuterium atoms was shown not to occur by the previously reported ^{1}HMR data. Therefore, on the basis of data obtained from both spectral techniques, the major compound present appears to be one containing 13 nonexchangeable deuterium atoms in the methyl and ribityl regions and two nonexchangeable aromatic hydrogen atoms at C-5 and C-8 (I).

Fully Deuterated Riboflavin—The compound isolated from cultures grown on medium containing deuterium oxide and deuterated sugars was found to be deuterated in all 15 possible nonexchangeable molecular positions. A mass spectral comparison of major peaks at *m/e* 179, 221, 251, and 264 in this compound with corresponding fragments in ordinary and highly deuterated riboflavin indicates that, in contrast to highly deuterated riboflavin, all hydrogen sites in the isoalloxazine portion of the molecule have been replaced by deuterium and all seven nonexchangeable sites in the ribityl chain have been completely deuterium substituted.

Biosynthetic Implications—As previously mentioned, the biosynthetic pathway of riboflavin has been studied extensively. Most work involved the use of radioactive compounds, which traced the movement of carbon into the vitamin. The method applied in the present study focused on the movement of hydrogen and represents a new approach to the study of riboflavin biosynthesis. Reaction mechanisms in three areas of this pathway were considered in explaining the results.

Synthesis of Ribityl Chain—The exact biosynthetic mode of attachment of the ribityl chain to the riboflavin molecule is unknown, although it is known that the five-carbon moiety is attached by the time 6,7-dimethyl-8-ribityllumazine has been formed (9). Early studies showed that carbon dioxide, formate, glycine, and serine are not incorporated into the ribityl chain (28, 29). Plaut (30) and Plaut and Broberg (29) concluded that at least two carbohydrate pathways, the hexose monophosphate shunt and the transaldolase–transketolase pathway, are involved in the formation of the chain. The results of Ali and Al-Khalidi (31) corroborated this conclusion.

The results of the present study using protiosugars and solvent deuterium oxide, in which substitution occurred in all positions of the chain, suggest that under these experimental conditions the transaldolase–transketolase pathway is of major importance in the synthesis of this moiety. The presence of deuterium at all carbon–hydrogen positions indicates a significant interaction occurring with the solvent. No carbon–hydrogen bond was protected from exchange, as would occur if the hexose monophosphate shunt were involved without further reaction.

For example, if glucose 6-phosphate were metabolized to ribose 5-phosphate *via* this pathway and condensed with the purine, the protons of C-4, C-5, and C-6 of glucose would not be able to exchange with solvent deuterium. Consequently, their presence would be reflected by signals in the corresponding ^{1}HMR spectrum. Extensive interaction with solvent, as is possible in the transaldolase–transketolase pathway, must occur for deuterium to enter all seven nonexchangeable positions.

Synthesis of 6,7-Dimethyl-8-ribityllumazine—This compound, the immediate precursor of riboflavin, is synthesized by condensation of 4-ribitylamino-5-aminouracil with a four-carbon donor molecule. Although various compounds, including acetoin, butanedione, pyruvate, and glucose, have been suggested as the source of the four-carbon fragment, the true identity of this compound remains uncertain (12). The methyl protons of 6,7-dimethyl-8-ribityllumazine are supplied by the four-carbon donor; thereafter, they become the C-5 and C-8 aromatic protons or the C-6 and C-7 methyl protons of riboflavin.

Since the C-5 and C-8 aromatic protons of fully deuterated riboflavin are deuterium substituted when riboflavin is formed in a medium containing deuterium oxide and deuterated sugars and

Table II—Mass Spectrum of Riboflavin

m/e	Percent
55	10.2
56	11.0
57	10.1
60	6.1
61	7.4
69	5.1
70	6.5
71	4.8
74	8.2
77	10.2
78	6.3
91	7.6
116	8.1
117	4.9
130	7.3
131	5.8
143	16.5
144	15.0
145	14.1
156	20.6
157	13.3
158	10.7
170	14.4
171	41.6
172	16.1
184	6.2
185	7.9
213	18.8
214	8.3
242	50.0
243	100.0
256	33.9
257	9.9
285	12.1
315	5.7
316	2.8
345	3.4
358	4.4
376	6.3

are not extensively deuterated in a medium containing only deuterium oxide, it is concluded that these protons must arise directly from the sugar contained in the growth medium. Ali and Al-Khalidi (31) also indicated the likelihood of the sugar being the true four-carbon donor in studies using glucose and ^{14}C-acetate.

Furthermore, since the mass spectral data of the present study indicated the presence of only minor amounts of deuterium at C-5 and C-8 in highly deuterated riboflavin, it is concluded that the pathway from sugar to the lumazine is one in which these positions are protected from extensive solvent interaction. This lack of solvent interaction is a contrast to that observed in the synthesis of the ribityl chain. The conclusion (32) that the four-carbon unit arising from sugar does not pass through an acetate pool is thus confirmed, since the occurrence of pooling would have caused greater deuterium substitution than was actually observed.

Synthesis of Riboflavin—The mechanism in which two molecules of 6,7-dimethyl-8-ribityllumazine are condensed to form riboflavin was explained recently (13–16). In this reaction, the C-6 and C-7 methyl groups of one lumazine molecule (acceptor lumazine) condense with C-7 and C-6, respectively, of a second lumazine molecule (donor lumazine). Lumazine methyl protons thus become the C-5 and C-8 aromatic protons (from acceptor lumazine) and the C-6 and C-7 methyl protons (from donor lumazine) of riboflavin.

In highly deuterated riboflavin (I), the C-5 and C-8 aromatic protons are present as hydrogen and the C-6 and C-7 methyl hydrogens are present as deuterium. Thus, despite a common molecular origin, the hydrogens in these areas of highly deuterated riboflavin may be distinguished. In applying the known reaction mechanism to the formation of highly deuterated riboflavin, it is apparent that this molecule could only have been formed if the following reaction sequence had occurred. Initially, two protiolumazines interacted and the riboflavin C-7 to C-8 (donor lumazine C-6 to acceptor lumazine C-7 methyl) bond formed without extensive solvent interaction. After this bond formed, complete exchange of the riboflavin C-6 and C-7 methyl groups (donor lumazine C-6 and C-7 methyl groups) took place. The biosynthesis of riboflavin was then completed by the formation of the riboflavin C-5 to C-6 (donor lumazine C-7 to acceptor lumazine C-6 methyl) bond, the solvent again being excluded from any significant interaction.

The exclusion of solvent interaction during formation of the riboflavin C-5 to C-6 bond and the C-7 to C-8 bond is necessary to retain the presence of hydrogen at C-5 and C-8. The possibility that exchange of the riboflavin C-6 and C-7 methyl groups occurred after riboflavin synthesis was complete was also considered. An attempted exchange of known riboflavin at pH 5, the pH maintained in the production culture, was performed by treating riboflavin with deuterium oxide at sterilization conditions of 15 psig for 15 min, followed by five repeated additions and evaporations of deuterium oxide. ^{1}HMR data showed that no exchange occurred as a result of this treatment, thereby establishing that once riboflavin was fully synthesized in the culture medium, exchange of both methyl or ribityl groups with solvent deuterium oxide did not occur.

The following summarizes the proposed synthetic sequence. The presence of hydrogen at C-5 and C-8 of highly deuterated riboflavin indicated that this reaction sequence arose from two ^{1}H-lumazine molecules. The congruence of ^{1}HMR spectra of known and deuterium oxide-treated riboflavin indicated that deuterium exchange did not occur after the synthesis was completed. Therefore, it is concluded that incorporation of deuterium into the riboflavin C-6 and C-7 methyl groups occurred at an intermediate stage before total riboflavin synthesis was complete.

REFERENCES

(1) D. A. Nona, M. I. Blake, H. L. Crespi, and J. J. Katz, *J. Pharm. Sci.*, **57**, 1993(1968).

(2) R. G. Mrtek, H. L. Crespi, M. I. Blake, and J. J. Katz, *ibid.*, **56**, 1234(1967).

(3) R. L. Foreman, F. P. Siegel, and R. G. Mrtek, *ibid.*, **58**, 189(1969).

(4) B. C. Carlstedt, H. L. Crespi, M. I. Blake, and J. J. Katz, *ibid.*, **62**, 856(1973).

(5) C. Hansch, E. Kutter, and A. Lee, *J. Med. Chem.*, **12**, 746(1969).

(6) E. Kutter and H. Machleidt, *ibid.*, **14**, 931(1971).

(7) M. I. Blake, H. L. Crespi, and J. J. Katz, *J. Pharm. Sci.*, **64**, 367(1975).

(8) G. W. E. Plaut, *Ann. Rev. Biochem.*, **30**, 409(1961).

(9) T. W. Goodwin, "The Biosynthesis of Vitamins and Related Compounds," Academic, New York, N.Y., 1963, pp. 24–68.

(10) V. H. Cheldelin and A. Baich, in "Biogenesis of Natural Compounds," P. Bernfeld, Ed., Pergamon, New York, N.Y., 1967, pp. 699–742.

(11) F. A. Robinson, "The Vitamin Co-Factors of Enzyme Systems," Pergamon, New York, N.Y., 1966, pp. 143–233.

(12) A. L. Demain, *Ann. Rev. Microbiol.*, **26**, 369(1972).

(13) R. L. Beach and G. W. E. Plaut, *J. Amer. Chem. Soc.*, **92**, 2913(1970).

(14) G. W. E. Plaut, R. L. Beach, and T. Aogaichi, *Biochemistry*, **9**, 771(1970).

(15) T. Paterson and H. C. S. Wood, *Chem. Commun.*, **1969**, 290.

(16) T. Paterson and H. C. S. Wood, *J. Chem. Soc., Perkin*, **1**, 1052(1972).

(17) K. Mohammed, D. A. Nona, and M. I. Blake, *J. Pharm. Sci.*, **57**, 2049(1968).

(18) "The United States Pharmacopeia," 17th rev., Mack Publishing Co., Easton, Pa., 1965, p. 886.

(19) C. R. Brewington and D. P. Schwartz, *J. Dairy Sci.*, **55**, 263(1972).

(20) R. D. Greene and D. Black, *J. Amer. Chem. Soc.*, **59**, 1820(1937).

(21) J. C. Keresztesy and E. Rickes, U.S. pat. 2,355,220 (1944).

(22) K. Maslowski, *J. Chromatogr.*, **18**, 609(1965).

(23) M. H. Studier and R. Hayatsu, *Anal. Chem.*, **40**, 1011(1968).

(24) F. J. Bullock and O. Jardetzky, *J. Org. Chem.*, **30**, 2056(1956).

(25) M. Kainosho and Y. Kyogoku, *Biochemistry*, **11**, 741(1972).

(26) R. H. Sarma, P. Dannies, and N. O. Kaplan, *ibid.*, **7**, 4359(1968).

(27) H. Batiz-Hernandez and R. A. Bernheim, *Progr. Nucl. Magn. Reson. Spectros.*, **3**, 63(1967).
(28) T. W. Goodwin and O. T. G. Jones, *Biochem. J.*, **64**, 9(1956).
(29) G. W. E. Plaut and P. L. Broberg, *J. Biol. Chem.*, **219**, 131(1956).
(30) G. W. E. Plaut, *ibid.*, **211**, 111(1954).
(31) S. N. Ali and U. A. S. Al-Khalidi, *Biochem. J.*, **98**, 182(1966).
(32) T. W. Goodwin and D. McEvoy, *ibid.*, **71**, 742(1959).
(33) M. I. Blake, H. L. Crespi, V. Mohan, and J. J. Katz, *J. Pharm. Sci.*, **50**, 425(1961).

ACKNOWLEDGMENTS AND ADDRESSES

Received November 6, 1974, from the *Chemistry Division, Argonne National Laboratory, Argonne, IL 60439*

Accepted for publication May 23, 1975.

Presented at the Pharmacognosy and Natural Products Section, APhA Academy of Pharmaceutical Sciences, Chicago meeting, August 1974.

Performed under the auspices of the U.S. Atomic Energy Commission.

The authors acknowledge the contribution of Mr. Leon P. Moore in obtaining the mass spectra and Mr. Arthur G. Kostka in obtaining the ^{1}HMR spectra.

* Argonne Universities Association–Argonne National Laboratory Fellowship appointee. Present address: Abbott Laboratories, North Chicago, Ill.

‡ Present address: U.S. Department of Justice, Drug Enforcement Administration Special Training and Research Laboratory, McLean, VA 22101

§ Present address: Department of Pharmacy, College of Pharmacy, University of Illinois at the Medical Center, Chicago, IL 60612

x To whom inquiries should be directed.

Catharanthus Alkaloids XXXII: Isolation of Alkaloids from *Catharanthus trichophyllus* Roots and Structure Elucidation of Cathaphylline

G. A. CORDELL and N. R. FARNSWORTH x

Abstract □ Further examination of the cytotoxic alkaloid fractions of *Catharanthus trichophyllus* roots afforded nine alkaloids. Two of these alkaloids, lochnericine and horhammericine, are responsible for part of the cytotoxic activity. The structure elucidation of cathaphylline, a new β-anilino acrylate derivative, is described.

Keyphrases □ *Catharanthus* alkaloids—isolation of nine alkaloids from *Catharanthus trichophyllus* roots, cytotoxic activity screened, structure elucidation of cathaphylline □ Alkaloids—isolated from *Catharanthus trichophyllus*, screened for cytotoxic activity □ Cathaphylline—isolated from *Catharanthus trichophyllus*, structure elucidated, cytotoxic activity screened □ Cytotoxicity—nine alkaloids isolated from *Catharanthus trichophyllus* screened

The cytotoxic and antitumor activities of the alkaloid fraction of *Catharanthus trichophyllus* were described previously (1, 2). However, the alkaloids isolated from this plant in those studies were devoid of antitumor and/or cytotoxic activity. The present phytochemical study dealt with the isolation of the two known alkaloids, lochnericine (I) and horhammericine (II), which were found to be cytotoxic. In addition, the isolation of several other bases from *C. trichophyllus* is reported, including a new indole alkaloid, cathaphylline, for which Structure X is proposed.

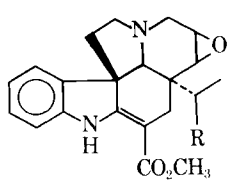

I: R = H
II: R = OH

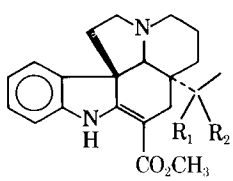

III: R_1R_2 = O
IV: R_1 = H, R_2 = $OCOCH_3$
V: R_1 = H, R_2 = OH
IX: R_1 = H, R_2 = H

EXPERIMENTAL[1]

Plant Material—The coarsely milled, air-dried roots[2] of *C. trichophyllus* (Bak.) Pich. (Apocynaceae) used were collected in Madagascar during 1969.

Preparation of pH Gradient Fractions—Fractionation of the crude alkaloids from this plant and the pH gradient separation of the Extract N alkaloids were described previously (2).

Chromatographic Separation of N-3.0 Alkaloids—Fraction

[1] Melting points were determined using an American Optical Instrument Co. model 569 instrument and are uncorrected. Specific rotations were measured using a Carl Zeiss optical polarimeter (Merz Optical Instruments, Chicago, Ill.). UV spectra were recorded in ethanol using a Beckman model DB-G grating spectrophotometer. IR spectra were measured as potassium bromide pellets *versus* air with a Beckman model IR-18A spectrophotometer. Low-resolution mass spectra were recorded at 70 ev using a Hitachi Perkin-Elmer model RMU-6D mass spectrometer. High-resolution mass spectra were recorded using a double-focusing mass spectrometer, model 110 (Consolidated Electro Dynamics Co.), operating at 70 ev. NMR spectra were determined in deuterochloroform, with tetramethylsilane as the internal standard, using a Varian model T-60A spectrometer. Column chromatography was carried out using silica gel PF_{254} (E. Merck, Darmstadt, West Germany). Routine analytical TLC was carried out using silica gel PF_{254} on 0.25-mm layers (E. Merck), and preparative TLC was performed using silica gel PF_{254} on 2-mm layers. Resolved components were detected by quenching under 254-nm UV light and visualized with ceric ammonium sulfate reagent. Appropriate zones were removed from the plates and the components were purified by filtered elution with methanol and evaporation of the solvent *in vacuo*. The residue was taken up in chloroform or ethyl acetate and filtered, and the filtrate was evaporated *in vacuo*. Solvent systems used in this study were: A, 1-butanol–acetic acid–water (4:4:1); B, 1-butanol–acetic acid–water (10:1:1); C, benzene–triethylamine (9:1); D, ethyl acetate–absolute ethanol (3:1); and E, 1-butanol–acetic acid–water (10:10:1).

[2] Obtained from the Curran Corp., South Hackensack, N.J. Voucher specimens representing the collection are deposited in the Herbarium of the Department of Pharmacognosy and Pharmacology, College of Pharmacy, University of Illinois at the Medical Center, Chicago, Ill. The identification was confirmed by N. R. Farnsworth.

(27) H. Batiz-Hernandez and R. A. Bernheim, *Progr. Nucl. Magn. Reson. Spectros.*, **3**, 63(1967).
(28) T. W. Goodwin and O. T. G. Jones, *Biochem. J.*, **64**, 9(1956).
(29) G. W. E. Plaut and P. L. Broberg, *J. Biol. Chem.*, **219**, 131(1956).
(30) G. W. E. Plaut, *ibid.*, **211**, 111(1954).
(31) S. N. Ali and U. A. S. Al-Khalidi, *Biochem. J.*, **98**, 182(1966).
(32) T. W. Goodwin and D. McEvoy, *ibid.*, **71**, 742(1959).
(33) M. I. Blake, H. L. Crespi, V. Mohan, and J. J. Katz, *J. Pharm. Sci.*, **50**, 425(1961).

ACKNOWLEDGMENTS AND ADDRESSES

Received November 6, 1974, from the *Chemistry Division, Argonne National Laboratory, Argonne, IL 60439*

Accepted for publication May 23, 1975.

Presented at the Pharmacognosy and Natural Products Section, APhA Academy of Pharmaceutical Sciences, Chicago meeting, August 1974.

Performed under the auspices of the U.S. Atomic Energy Commission.

The authors acknowledge the contribution of Mr. Leon P. Moore in obtaining the mass spectra and Mr. Arthur G. Kostka in obtaining the ^{1}HMR spectra.

* Argonne Universities Association–Argonne National Laboratory Fellowship appointee. Present address: Abbott Laboratories, North Chicago, Ill.

‡ Present address: U.S. Department of Justice, Drug Enforcement Administration Special Training and Research Laboratory, McLean, VA 22101

§ Present address: Department of Pharmacy, College of Pharmacy, University of Illinois at the Medical Center, Chicago, IL 60612

x To whom inquiries should be directed.

Catharanthus Alkaloids XXXII: Isolation of Alkaloids from *Catharanthus trichophyllus* Roots and Structure Elucidation of Cathaphylline

G. A. CORDELL and N. R. FARNSWORTH x

Abstract □ Further examination of the cytotoxic alkaloid fractions of *Catharanthus trichophyllus* roots afforded nine alkaloids. Two of these alkaloids, lochnericine and horhammericine, are responsible for part of the cytotoxic activity. The structure elucidation of cathaphylline, a new β-anilino acrylate derivative, is described.

Keyphrases □ *Catharanthus* alkaloids—isolation of nine alkaloids from *Catharanthus trichophyllus* roots, cytotoxic activity screened, structure elucidation of cathaphylline □ Alkaloids—isolated from *Catharanthus trichophyllus*, screened for cytotoxic activity □ Cathaphylline—isolated from *Catharanthus trichophyllus*, structure elucidated, cytotoxic activity screened □ Cytotoxicity—nine alkaloids isolated from *Catharanthus trichophyllus* screened

The cytotoxic and antitumor activities of the alkaloid fraction of *Catharanthus trichophyllus* were described previously (1, 2). However, the alkaloids isolated from this plant in those studies were devoid of antitumor and/or cytotoxic activity. The present phytochemical study dealt with the isolation of the two known alkaloids, lochnericine (I) and horhammericine (II), which were found to be cytotoxic. In addition, the isolation of several other bases from *C. trichophyllus* is reported, including a new indole alkaloid, cathaphylline, for which Structure X is proposed.

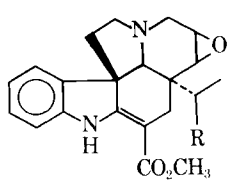

I: R = H
II: R = OH

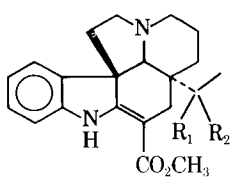

III: R_1R_2 = O
IV: R_1 = H, R_2 = $OCOCH_3$
V: R_1 = H, R_2 = OH
IX: R_1 = H, R_2 = H

EXPERIMENTAL[1]

Plant Material—The coarsely milled, air-dried roots[2] of *C. trichophyllus* (Bak.) Pich. (Apocynaceae) used were collected in Madagascar during 1969.

Preparation of pH Gradient Fractions—Fractionation of the crude alkaloids from this plant and the pH gradient separation of the Extract N alkaloids were described previously (2).

Chromatographic Separation of N-3.0 Alkaloids—Fraction

[1] Melting points were determined using an American Optical Instrument Co. model 569 instrument and are uncorrected. Specific rotations were measured using a Carl Zeiss optical polarimeter (Merz Optical Instruments, Chicago, Ill.). UV spectra were recorded in ethanol using a Beckman model DB-G grating spectrophotometer. IR spectra were measured as potassium bromide pellets *versus* air with a Beckman model IR-18A spectrophotometer. Low-resolution mass spectra were recorded at 70 ev using a Hitachi Perkin-Elmer model RMU-6D mass spectrometer. High-resolution mass spectra were recorded using a double-focusing mass spectrometer, model 110 (Consolidated Electro Dynamics Co.), operating at 70 ev. NMR spectra were determined in deuterochloroform, with tetramethylsilane as the internal standard, using a Varian model T-60A spectrometer. Column chromatography was carried out using silica gel PF_{254} (E. Merck, Darmstadt, West Germany). Routine analytical TLC was carried out using silica gel PF_{254} on 0.25-mm layers (E. Merck), and preparative TLC was performed using silica gel PF_{254} on 2-mm layers. Resolved components were detected by quenching under 254-nm UV light and visualized with ceric ammonium sulfate reagent. Appropriate zones were removed from the plates and the components were purified by filtered elution with methanol and evaporation of the solvent *in vacuo*. The residue was taken up in chloroform or ethyl acetate and filtered, and the filtrate was evaporated *in vacuo*. Solvent systems used in this study were: A, 1-butanol–acetic acid–water (4:4:1); B, 1-butanol–acetic acid–water (10:1:1); C, benzene–triethylamine (9:1); D, ethyl acetate–absolute ethanol (3:1); and E, 1-butanol–acetic acid–water (10:10:1).

[2] Obtained from the Curran Corp., South Hackensack, N.J. Voucher specimens representing the collection are deposited in the Herbarium of the Department of Pharmacognosy and Pharmacology, College of Pharmacy, University of Illinois at the Medical Center, Chicago, Ill. The identification was confirmed by N. R. Farnsworth.

N-3.0 (8.7 g) from the pH gradient fractionation of Extract N was intimately mixed with silica–diatomaceous earth[3] (3:1)(8.7 g) and placed at the top of a chromatographic column slurry packed with 500 g of silica and petroleum ether. Elution was carried out with petroleum ether; 2100 fractions (10 ml each) were collected, analyzed by TLC, and combined on the basis of similarities or differences in the separation patterns.

Isolation and Identification of (−)-Minovincine (III), (−)-Echitovenine (IV), and Lochnericine (I)—Fractions 818–1125 from the chromatographic separation of N-3.0 were combined and taken to dryness *in vacuo*. The combined total fraction (2.5 g) was chromatographed over a silica (175 g) column slurry packed with a chloroform–benzene (1:1) mixture. Elution with the same eluent afforded 580 fractions (10 ml each), which were combined on the basis of TLC patterns.

Fractions 11–20 from the column were combined, taken to dryness *in vacuo* (0.065 g), and further separated by preparative TLC, eluting with 1-butanol–acetic acid–water (10:1:1). A band at R_f 0.75 was removed, purified, and subjected to preparative TLC, eluting with benzene–triethylamine (9:1). The band at R_f 0.47 was removed and purified to afford (−)-lochnericine (I), which was recrystallized from ethanol to afford 38.2 mg of white needles, mp 190–192°, $[\alpha]_D^{23}$ −510° (c 0.1, chloroform).

The alkaloid was homogeneous by TLC using Solvent Systems A–D. It exhibited R_f values of 0.52, 0.75, 0.48, and 0.68, respectively, and a strong dark-blue chromogenic response with the ceric ammonium sulfate reagent. The UV spectrum showed λ_{max} (ethanol) at 299 (log ϵ 4.12) and 328 (4.30) nm. A mass spectrum of the alkaloid (3, 4) gave ions at *m/e* 352 (M^+, 90%), 323 (17), 214 (45), 138 (100), and 108 (60). An IR spectrum (potassium bromide) exhibited principal absorptions at ν_{max} 3380, 1675, and 1615 cm^{-1}. NMR data were identical with those obtained for lochnericine (3).

Fractions 21–30 from the column were combined and taken to dryness *in vacuo* (0.241 g), and the fraction was subjected to preparative TLC, eluting with 1-butanol–acetic acid–water (10:1:1). Four bands were removed. One, at R_f 0.75, was further purified and shown to be lochnericine (39 mg), identical with the previously isolated material. A second band at R_f 0.25 was purified to afford (−)-minovincine (III) as an amorphous powder (0.49 g), $[\alpha]_D^{23}$ −480° (c 0.1, chloroform).

This alkaloid was homogeneous by TLC using Solvent Systems B, C, and D; it exhibited R_f values of 0.22, 0.51, and 0.66, respectively, as well as an initial strong dark-blue chromogenic response with ceric ammonium sulfate reagent. A UV spectrum showed λ_{max} (ethanol) at 298 (log ϵ 4.09) and 328 (4.28) nm. The mass spectrum exhibited ions at *m/e* 352 (M^+, 41%), 309 (23), 214 (26), and 138 (100). An IR spectrum (potassium bromide) showed principal absorptions at ν_{max} 3390, 1715, 1672, and 1610 cm^{-1}. The NMR spectrum revealed two strong singlets: for the C-18 methyl group at δ 1.87 ppm and for the carbomethoxyl group at δ 3.76 ppm. These data correspond to those previously reported for minovincine (4).

A third band at R_f 0.6 was separated by preparative TLC, eluting with chloroform. A band at R_f 0.55 was removed and purified to afford (−)-echitovenine (IV), which was crystallized from aqueous ethanol to give white needles (13 mg), mp 170–172°, $[\alpha]_D^{23}$ −436° (c 0.1, chloroform). This isolate was homogeneous by TLC using Solvent Systems B, C, and D; it exhibited R_f values of 0.53, 0.50, and 0.68, respectively, and an initial dark-blue chromogenic response with the ceric ammonium sulfate reagent.

A UV spectrum of the isolate exhibited λ_{max} (ethanol) at 298 (log ϵ 4.09) and 328 (4.28) nm.

The mass spectrum of the isolate displayed ions at *m/e* 396 (M^+, 18%), 337 (12), 309 (8), and 182 (100). The IR spectrum showed principal absorptions at ν_{max} 3390, 1715, 1680, 1615, and 1245 cm^{-1}. An NMR spectrum showed a doublet, J = 7 Hz, for the C-18 protons at δ 1.00 ppm and a quartet, J = 7 Hz, for the C-19 proton at δ 4.76 ppm. The protons of the carbomethoxyl and acetyl groups were observed at δ 3.80 and 2.16 ppm, respectively. The compound exhibited identical spectral data with an authentic sample of (+)-echitovenine (5). This study is the first reported isolation of the (−)-isomer of echitovenine.

Chromatographic Separation of N-3.5 Alkaloids—Fraction N-3.5 (5.55 g) from the pH gradient fractionation of Extract N was chromatographed over a column containing silica (400 g) packed in ethyl acetate–95% ethanol (3:1). A total of 266 fractions (10 ml each) was collected from the column and combined on the basis of their TLC patterns.

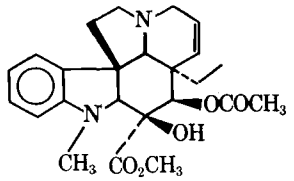

VI

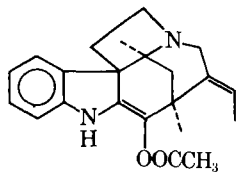

VII

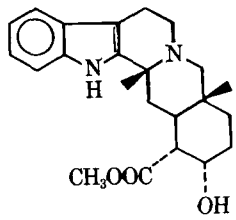

VIII

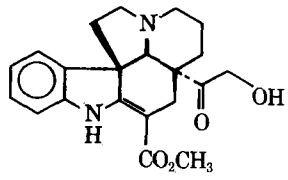

X

Isolation of Minovincinine (V) and Horhammericine (II)—Fractions 1–30 from the chromatographic separation of N-3.5 were combined, and the total fraction (1.5 g) was chromatographed over a column of silica (150 g) packed in chloroform–benzene (1:1). Elution with the same solvent mixture afforded 480 fractions (10 ml each), which were combined on the basis of their TLC patterns. Combined fractions 268–282 (0.128 g) were subjected to preparative TLC, eluting with 1-butanol–acetic acid–water (10:1:1). Two bands at R_f 0.55 and 0.35 were removed and purified. Material from the less polar band was crystallized from benzene to afford white needles (58 mg) of horhammericine (II), mp 138–140°, $[\alpha]_D^{23}$ −395° (c 0.1, chloroform).

The compound was homogeneous by TLC using Solvent Systems B, C, and D; it exhibited R_f values of 0.55, 0.35, and 0.58, respectively, and a strong dark-blue chromogenic response with the ceric ammonium sulfate reagent. A UV spectrum showed λ_{max} (ethanol) at 299 (log ϵ 4.14) and 328 (4.32) nm. The mass spectrum displayed ions at *m/e* 368 (M, 40%), 350 (53), 323 (12), 214 (54), and 154 (100). An IR spectrum (potassium bromide) showed principal absorptions at ν_{max} 3350, 1675, and 1610 cm^{-1}. The NMR spectrum of the isolate showed a doublet, J = 7 Hz, for the C-18 protons at δ 1.10 ppm as well as a quartet, J = 7 Hz, for the C-19 proton at δ 3.80 ppm. A mixed melting-point determination with authentic horhammericine showed no depression. Acetylation (acetic anhydride in pyridine at room temperature for 12 hr) afforded acetylhorhammericine as fine needles, mp 176–178°, whose mass spectrum exhibited ions at *m/e* 410 (M^+, 82%), 351 (100), 350 (80), 214 (80), and 196 (90).

Attempts to crystallize the material from the more polar band were unsuccessful. The white, amorphous minovincinine (V) (0.35 g), $[\alpha]_D^{23}$ −412° (c 0.1, chloroform), was homogeneous by TLC in Solvent Systems B, C, and D; it exhibited R_f values of 0.35, 0.38, and 0.60, respectively, and a dark-blue response with the ceric ammonium sulfate reagent. The UV spectrum showed λ_{max} (ethanol) at 299 (log ϵ 4.07) and 329 (4.26) nm.

A mass spectrum of the isolate exhibited ions at *m/e* 352 (M^+, 18%), 309 (2.6), and 140 (100). An IR spectrum (potassium bromide) displayed principal absorptions at ν_{max} 3460, 3380, 1680, and 1612 cm^{-1}. The NMR spectrum showed a doublet, J = 7 Hz, for the C-18 protons at δ 0.94 ppm and a quartet, J = 7 Hz, for the C-19 proton at δ 3.45 ppm. Acetylation (acetic anhydride in pyridine at room temperature for 12 hr) afforded (−)-echitovenine

[3] Celite.

Table I—Mass Spectral Comparison of β-Anilino Acrylate Derivatives

Compound	Parent Ion	Ion A	Ion B	Ion C	Ion D
			m/e		
IX	338	214	124	29	309
I	352	214	138	29	323
II	368	214	154	45	323
III	352	214	138	43	309
IV	396	—	182	87	309
V	354	—	140	45	309
Cathaphylline	368	214	154	59	309

(IV), which exhibited identical melting point, mixed melting-point, TLC, mass spectral, UV, IR, and NMR properties as the material isolated from Fraction N-3.0.

Isolation and Identification of Vindorosine (VI)—Fractions 31–51 from the chromatographic separation of N-3.5 were combined and taken to dryness *in vacuo*, and the total fraction (3.2 g) was chromatographed over a column of silica (350 g) packed in chloroform–benzene (3:1). Elution of the column with the same solvent mixture afforded 500 fractions (10 ml each), which were combined on the basis of TLC patterns. Combined fractions 241–310 (0.330 g) were subjected to preparative TLC on silica gel plates (2 mm), eluting with 1-butanol–acetic acid–water (10:1:1).

One band at R_f 0.25 was removed, purified, and rechromatographed on silica, eluting twice with benzene–triethylamine (19:1). Two bands at R_f 0.35 and 0.25 were removed and purified. The less polar band was crystallized from benzene–petroleum ether to afford vindorosine (VI) (0.181 g), mp 165–166°. This isolate was essentially homogeneous by TLC, displaying a highly characteristic orange-yellow chromogenic response with the ceric ammonium sulfate reagent and giving R_f values of 0.40, 0.25, 0.38, and 0.22 in Solvent Systems A, B, C, and E, respectively. Trace contamination with vindoline was observed (6). The IR, UV, NMR, and mass spectral data were identical with those of an authentic sample of vindorosine. A mixed melting-point determination showed no depression.

The more polar band was rechromatographed on silica, eluting three times with benzene–triethylamine (98:2). One major band at R_f 0.28 was removed and purified. Attempts to crystallize this material (23.6 mg) were unsuccessful. It exhibited a high negative rotation, $[\alpha]_D^{23}$ −438° (c 0.1, chloroform). The compound was homogeneous by TLC, using Solvent Systems A, B, C, and E; it exhibited R_f values of 0.35, 0.25, 0.44, and 0.32, respectively, and an initial strong dark-blue response with the ceric ammonium sulfate reagent.

The UV spectrum of the isolate showed λ_{max} (ethanol) 299 (log ε 4.14) and 328 (4.31) nm. The mass spectrum showed ions at *m/e* 368 (M^+, 65%), 337 (82), 309 (31), 214 (45), and 154 (100). An IR spectrum showed principal absorptions at ν_{max} 3450, 3350, 1710, 1675, and 1615 cm^{-1}. The NMR spectrum showed a complex multiplet in the δ 6.70–7.40-ppm region corresponding to four aromatic protons. The carbomethoxyl group gave rise to a singlet at δ 3.75 ppm, and the *N* proton was observed at δ 8.81 ppm; a two-proton broad doublet was found at δ 4.13 ppm. The structure elucidation of this new alkaloid, which has been given the trivial name cathaphylline, will be described (*vide infra*).

Isolation of Akuammicine (VII)—Fractions 150–260 from the chromatography of N-3.5 were combined, and a portion of this fraction (0.020 g) was subjected to preparative TLC, eluting with benzene–triethylamine (9:1). One band at R_f 0.36 was removed, purified, and chromatographed on silica gel, eluting with ethyl acetate–methanol (3:1). The band at R_f 0.20 was removed, purified, and chromatographed on silica gel, eluting with 1-butanol–acetic acid–water (8:1:1). A second major band at R_f 0.26 was removed and purified to a white amorphous powder (1.2 mg). This product was homogeneous by TLC, having R_f values of 0.62, 0.18, and 0.25 using Solvent Systems A, B, and D, respectively. The mass spectrum gave *m/e* 322 (M^+, 100), 263 (77), and 121 (33). The mass spectral and TLC data were identical with those of authentic akuammicine (VII).

Table II—High-Resolution Mass Spectral Analysis of Cathaphylline and Acetylcathaphylline

Cathaphylline			Acetylcathaphylline		
m/e	Percent	Molecular Formula	*m/e*	Percent	Molecular Formula
368	65	$C_{21}H_{24}N_2O_4$	410	54	$C_{23}H_{26}N_2O_5$
337	82	$C_{20}H_{21}N_2O_3$	337	15	$C_{20}H_{21}N_2O_3$
309	31	$C_{19}H_{21}N_2O_2$	309	36	$C_{19}H_{21}N_2O_2$
214	45	$C_{13}H_{12}NO_2$	214	41	$C_{13}H_{12}NO_2$
154	100	$C_8H_{12}NO_2$	196	100	$C_{10}H_{14}NO_3$

Chromatographic Separation of N-6.5 and N-7.0 Alkaloids—Fractions N-6.5 and N-7.0 were combined, and the total fraction (2.92 g) was chromatographed over a column of silica (220 g) packed in ethyl acetate–95% ethanol (3:1). A total of 290 fractions (10 ml each) was collected and combined on the basis of TLC patterns.

Isolation of Pseudoyohimbine (VIII)—Fractions 70–88 from the chromatography of N-6.5 and N-7.0 were combined, and the total fraction (0.16 g) was chromatographed on silica, eluting with 1-butanol–acetic acid–water (10:1:1). Four bands were removed from the plate and purified. A compound obtained from the band at R_f 0.42, *m/e* 296 (M^+), was new but thus far has resisted structure elucidation.

A second purified band crystallized on standing to afford pseudoyohimbine (VIII) (0.014 g), mp 266–267°. The compound was homogeneous by TLC, using Solvent Systems B, C, and D; it exhibited R_f values of 0.25, 0.05, and 0.15, respectively, and a yellow chromogenic response with the ceric ammonium sulfate reagent. The UV, IR, NMR, mass spectral, and specific rotation data were identical with those of authentic pseudoyohimbine. A mixed melting-point determination showed no depression.

Cytotoxic Activities—Echitovenine, (−)-minovincine, cathaphylline, lochnericine, and horhammericine were examined for their activity against Eagle's 9KB carcinoma of the nasopharynx in cell culture using established protocols (7). Lochnericine and horhammericine were found to be active (ED_{50} 1.1 μg/ml).

DISCUSSION

The retro Diels–Alder fragmentation pathway, which is characteristic for the mass spectra of many aspidosperma-type alkaloids, proved to be of considerable diagnostic value. For the purposes of discussing the elucidation of the structure of cathaphylline, four ions were considered important in in the fragmentation patterns of the β-anilino acrylate alkaloids isolated in this study. Ions A and B arise from the retro Diels–Alder fragmentation of ring C and fission of the 5,6-bond. Ions C and D arise by loss of the two-carbon side chain.

A comparison of the *m/e* values for these ions is shown in Table I for the compounds isolated [and vincadifformine (IX) for comparison]. Substitution in the indole portion leads to a change in the mass of A, whereas substitution in the piperidine ring leads to an increase in the mass of B and D. Substitution solely in the side chain affords an increase in mass for B and C from the "standard" values of 124 and 29 mass units (mu), respectively.

On this basis, examination of these four fragments in the case of

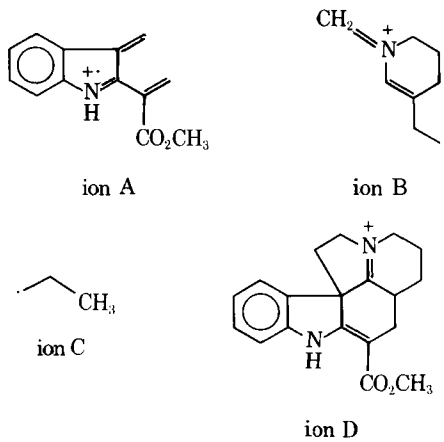

cathaphylline indicates: (*a*) no substitution in the indole ring, (*b*) no substitution in the piperidine ring, and (*c*) an addition of 30 mu in the two-carbon side chain.

The high-resolution mass spectral data for cathaphylline (Table II) indicate that four oxygen atoms are present: two in the carbomethoxyl group and two in the side chain. The side chain was shown to have a molecular formula of $C_2H_3O_2$ (M^+ – ion D).

Treatment of cathaphylline with acetic anhydride and pyridine afforded a monoacetate, showing three-proton singlets at δ 3.78 and 1.99 ppm in the NMR spectrum. The mass spectrum shows *m/e* 410 (M^+), in which ion B is shifted by 42 mu to *m/e* 196, indicating the presence of a hydroxyl group in the side chain. Confirmation of this point is found in the IR spectrum of cathaphylline, which shows a band at 3450 cm^{-1}. Two distinct possibilities exist for the functionality of the two-carbon side chain, a hydroxyaldehyde or a hydroxyketone. In the NMR spectrum of cathaphylline, no signal was observed which could be assigned to an aldehyde function. In the mass spectra of cathaphylline and acetylcathaphylline, a fragment ion was observed at *m/e* 337, corresponding to initial losses of CH_3O and $C_3H_5O_2$, respectively. Therefore, the acetylated functional group is at the terminal carbon of the side chain, *i.e.*, C-18.

In support of this assignment of a hydroxyketone to the side chain, the ion at *m/e* 337 loses CO to give *m/e* 309 (ion D); in the NMR spectrum, a two-proton broadened doublet was observed at δ 4.13 ppm, corresponding with the C-18 protons of the hydroxymethyl group. This signal became two doublets, δ 4.84 and 4.34 ppm (J = 16.5 Hz), in the NMR spectrum of acetylcathaphylline. The high negative specific rotation is characteristic of α-methylene indole alkaloids having the absolute stereochemistry shown. Therefore, Structure X is suggested for cathaphylline.

Akuammicine, an alkaloid originally isolated from *Picralima nitida* (8, 9), has also been isolated from *Vinca erecta* (10), *V. minor* (11), and *C. roseus* (12, 13). Vindorosine (VI) is apparently characteristic of the genus *Catharanthus*, rather than *Vinca*, having been isolated from *C. pusillus* (14), *C. roseus* (6), and *C. trichophyllus* (1). Lochnericine has been obtained from *Amsonia angustifolia* (15), *A. tabernaemontana* (16), and *C. roseus* (17–19). (+)-Echitovenine was reported previously only from *Alstonia venenata* (5). Horhammericine was isolated previously from *C. lanceus* (20, 21). (−)-Minovincinine was isolated previously from *V. minor* (22) and *V. erecta* (4), and the (+)-isomer was obtained from *A. venenata* (5). Minovincine was previously obtained only from *V. erecta* (4). Pseudoyohimbine was not reported previously from *Catharanthus* or *Vinca* species.

REFERENCES

(1) H. K. Kim, R. N. Blomster, H. H. S. Fong, and N. R. Farnsworth, *Econ. Bot.*, **24,** 42(1970).

(2) A. B. Segelman and N. R. Farnsworth, *J. Pharm. Sci.*, **63,** 1419(1974).

(3) B. K. Moza and J. Trojánek, *Tetrahedron Lett.*, **1964,** 2561.

(4) M. Plat, J. LeMen, M.-M. Janot, H. Budzikiewicz, J. M. Wilson, L. J. Durham, and C. Djerassi, *Bull. Soc. Chim. Fr.*, **1962,** 2237.

(5) B. Das, K. Biemann, A. Chatterjee, A. B. Ray, and P. L. Majumder, *Tetrahedron Lett.*, **1966,** 2483.

(6) B. K. Moza and J. Trojánek, *Collect. Czech. Chem. Commun.*, **28,** 1419(1963).

(7) R. I. Geran, N. H. Greenberg, M. M. MacDonald, A. M. Schumacher, and B. J. Abbott, *Cancer Chemother. Rep.*, **3,** 1(1972).

(8) J. Levy, J. LeMen, and M.-M. Janot, *Bull. Soc. Chim. Fr.*, **1960,** 979.

(9) G. F. Smith and J. T. Wrobel, *J. Chem. Soc.*, **1960,** 793.

(10) M. A. Kuchenkova, P. K. Yuldashev, and S. Y. Yunusov, *Dokl. Akad. Nauk Uzek SSR*, **21,** 42(1964).

(11) T. H. van der Meulen and G. J. M. van der Kerk, *Rec. Trav. Chim. Pays-Bas*, **83,** 141(1964).

(12) G. H. Svoboda, A. T. Oliver, and D. R. Bedwell, *Lloydia*, **26,** 141(1963).

(13) A. I. Scott, P. B. Reichardt, M. B. Slaytor, and J. G. Sweeny, *Bioorg. Chem.*, **1,** 157(1971).

(14) W. M. Fylypiw, N. R. Farnsworth, R. N. Blomster, J. P. Buckley, and D. J. Abraham, *Lloydia*, **28,** 254(1965).

(15) O. Clauder, A. Kocsis, K. Bojthe-Horvath, I. Mathe, and J. Tamas, *Acta Chim. Acad. Sci. Hung.*, **75,** 423(1973).

(16) B. Zsadon, J. Tamas, and M. Szilasi, *Magy. Kem. Foly.*, **79,** 341(1973).

(17) G. H. Svoboda, N. Neuss, and M. Gorman, *J. Amer. Pharm. Ass., Sci. Ed.*, **48,** 659(1959).

(18) C. P. N. Nair and P. P. Pillay, *Tetrahedron*, **6,** 89(1959).

(19) B. K. Moza and J. Trojánek, *Chem. Ind.*, **1962,** 1425.

(20) R. N. Blomster, N. R. Farnsworth, and D. J. Abraham, *Naturwissenschaften*, **55,** 298(1968).

(21) D. J. Abraham, N. R. Farnsworth, W. D. Loub, and R. N. Blomster, *J. Org. Chem.*, **34,** 1575(1969).

(22) W. Döpke and H. Meisel, *Tetrahedron Lett.*, **1970,** 749.

ACKNOWLEDGMENTS AND ADDRESSES

Received April 14, 1975, from the *Department of Pharmacognosy and Pharmacology, College of Pharmacy, University of Illinois at the Medical Center, Chicago, IL 60612*

Accepted for publication May 30, 1975.

Presented in part at the 9th IUPAC Meeting, Ottawa, Canada, June 1974 (Abstract 11F) and at the American Pharmaceutical Association, Chicago meeting, August 1974 (Abstract p. 158).

Supported in part by Research Grant CA-12230, National Institutes of Health, U.S. Department of Health, Education, and Welfare, Bethesda, MD 20014

The authors are grateful to Professor Mrs. A. Chatterjee for a sample of (+)-echitovenine, to Dr. M. Gorman, Lilly Research Laboratories, Indianapolis, Ind., for providing high-resolution mass spectra, and to Mr. Richard Dvorak for providing low-resolution mass spectral data.

[x] To whom inquiries should be directed.

GLC Determination of Griseofulvin in Human Plasma

H. J. SCHWARZ ˣ, B. A. WALDMAN, and V. MADRID

Abstract □ A specific and quantitative GLC method for the determination of griseofulvin in human plasma is described. The method involves extraction with ether, evaporation, addition of the internal standard dissolved in benzene, and GLC analysis using an electron-capture detector. The sensitivity of the method is 0.05 μg/ml of plasma. The results obtained with this specific GLC method were compared with the results obtained with the more frequently used spectrofluorometric method by analyzing duplicate plasma samples obtained from 12 subjects following a single dose of griseofulvin. It was deduced that the 30% higher plasma levels obtained spectrofluorometrically were due to the coextraction and presence of the metabolite 6-demethylgriseofulvin in the assay solutions.

Keyphrases □ Griseofulvin—GLC analysis in plasma, compared to spectrofluorometric method □ GLC analysis—griseofulvin in plasma, compared to spectrofluorometric method □ Antifungal agents—griseofulvin, GLC analysis in plasma

Griseofulvin is an orally active antifungal agent widely used in the treatment of fungal infections in animals and humans (1).

Several spectrofluorometric methods for the determination of griseofulvin in plasma (2–7) have been described. Most of them are modifications of the original method (2). The latest modification (7), which was to be preferred because of its high sensitivity and low blank values, was also very time consuming.

A GLC method for the determination of griseofulvin in skin was described (7), and a determination in plasma was mentioned (8). These investigators used an electron-capture detection method.

The purpose of the present study was to develop a specific, highly sensitive method which was simple enough to permit the assay of a large number of samples. Work progressed along two lines, simplification of the spectrofluorometric method and adaptation of the previously reported (7) GLC method to plasma samples.

EXPERIMENTAL

Reagents and Chemicals—The following reagents and chemicals were used: sodium chloride[1], anhydrous ether[2], methanol[3], and sulfuric acid[1], all analyzed reagents; benzene[4], glass distilled; OV-17[5]; Chromosorb W[5]; diazepam[6]; and griseofulvin[7]. 6-Demethylgriseofulvin was isolated from human urine (9).

Instrumentation—The gas chromatograph[8] was equipped with a ^{63}Ni electron-capture detector and a 152.4-cm (5-ft) long, 4-mm (0.157-in.) i.d. glass column, packed with 3% OV-17 on 80–100 mesh Chromosorb W. The following conditions were used: column temperature, 270°; injection port temperature, 310°; detector block temperature, 330°; carrier gas (10% methane–90% argon) flow, 150 ml/min; and range, 10 with attenuation factor of 16×. Chromatograms were recorded on a 1-mv recorder[8].

Table I—GLC Analyses of Griseofulvin after *In Vitro* Addition to Human Plasma

Griseofulvin Added, μg/ml	Griseofulvin Recovered[a]	
	μg/ml ± *SD*	%
0.1	0.100 ± 0.013	100.0
0.5	0.483 ± 0.037	96.6
1.0	1.068 ± 0.073	106.8
1.5	1.464 ± 0.120	97.6
2.0	1.942 ± 0.154	97.1
Average recovery		99.6

[a] Average of eight determinations.

Method—A 1-ml aliquot of plasma was pipetted into a glass-stoppered test tube, and 1 ml of saturated sodium chloride solution and 10 ml of anhydrous ether were added. The tube was shaken for 1 min, and a 5-ml aliquot of the ether phase was transferred to a pear-shaped flask and evaporated to dryness *in vacuo*. The residue was dissolved in 1 ml of benzene containing 0.25 μg/ml of diazepam as the internal standard. About 5 μl of this solution was injected.

The heights of the peaks corresponding to griseofulvin and the internal standard were measured, and the ratio of the peak heights, griseofulvin–internal standard, was converted into micrograms of griseofulvin per milliliter of assay solution by means of a standard curve. The plasma concentration was obtained after correction for dilution (concentration); the recovery was assumed to be quantitative.

Standard curves were prepared by injecting standard solutions of griseofulvin in benzene in the 0.1–1.5-μg/ml range, each containing 0.25 μg/ml of internal standard, under the same analysis conditions as the samples. The peak height ratios of griseofulvin–internal standard were plotted against the concentration of griseofulvin in the assay solution.

Fluorometric Determination—The spectrofluorometric method described previously (7) was simplified and modified in the following manner.

To 1.0 ml of plasma in a stoppered test tube was added 1.0 ml of saturated sodium chloride solution followed by 10.0 ml of anhydrous ether. The test tube was shaken for 1 min. A 9-ml aliquot of the ether layer was transferred to a 50-ml pear-shaped flask and evaporated to dryness *in vacuo*. The residue was dissolved in 5.0 ml of 80% methanol (v/v). The fluorescence was read in a spectrophotofluorometer[9] with the following settings: excitation wavelength, 300 nm; detection wavelength, 420 nm; sensitivity, 70; and slits, 4, 5, 4, 2, 2, and 5.

The samples were read a second time after the addition of three drops of concentrated sulfuric acid, the second reading being used as a blank reading.

Standard solutions of griseofulvin were made up in 80% methanol (v/v) in the 0.05–0.5-μg/ml range. The solutions were read under the identical instrument settings. Linearity was obtained between 0 and 0.5 μg/ml of assay solution (corresponding to 0–2.5 μg/ml of plasma). The lowest measurable plasma concentration was 0.1 μg/ml.

The recovery was determined by adding known amounts of griseofulvin to human plasma in the 0.1–1.5-μg/ml range and ana-

[1] Fisher Scientific Co.
[2] Mallinckrodt, Inc.
[3] Lehigh Valley Chemical Co.
[4] Burdick and Jackson Laboratories.
[5] Supelco Inc.
[6] Roche Laboratories.
[7] Schering Corp.
[8] Hewlett-Packard.
[9] Aminco-Bowman.

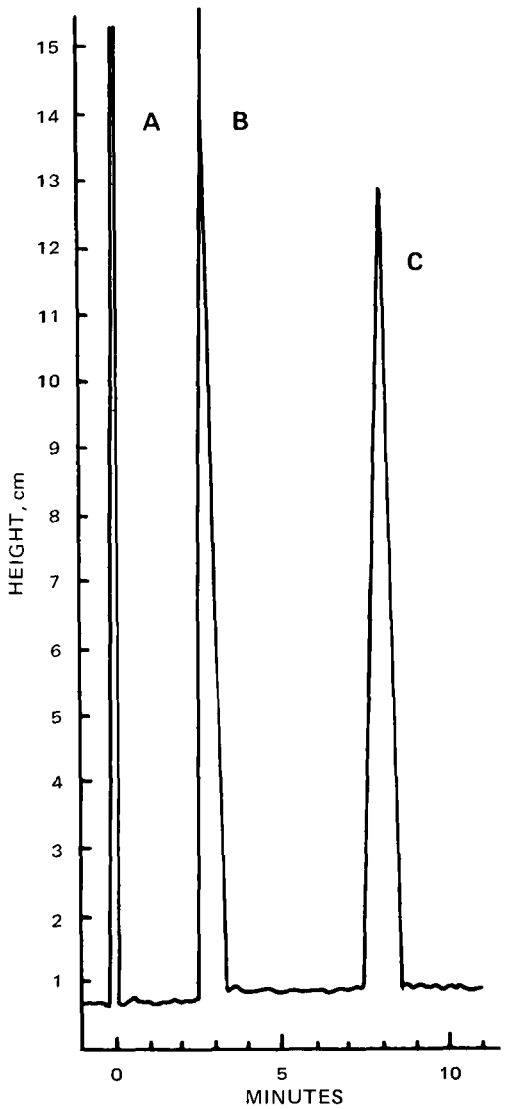

Figure 1—*Gas chromatogram showing a 5-μl injection of a standard solution. Key: A, solvent front; B, internal standard; and C, griseofulvin.*

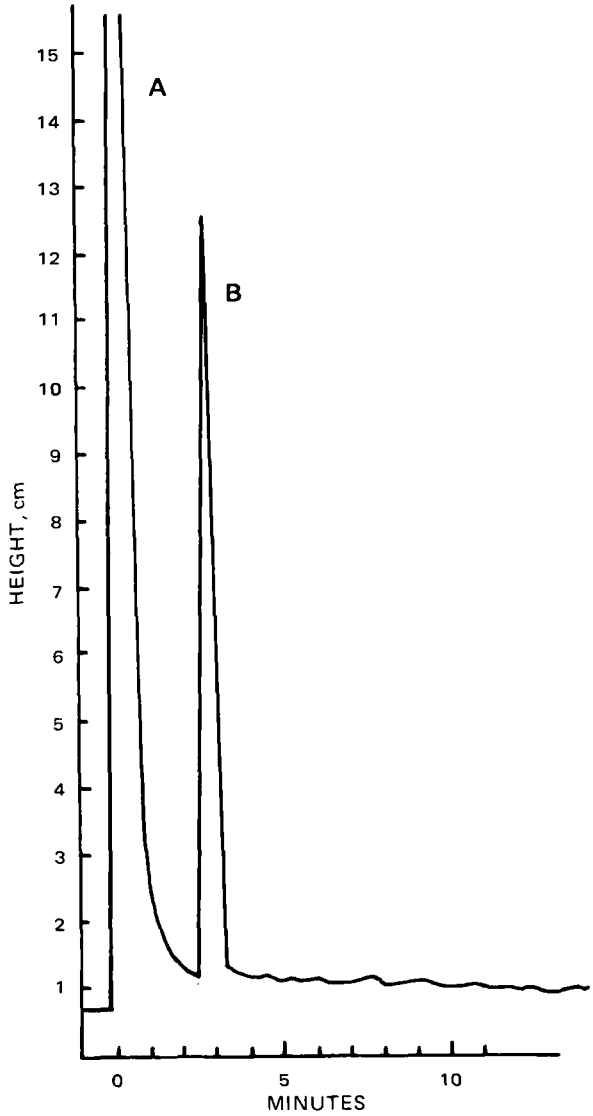

Figure 2—*Gas chromatogram showing a 5-μl injection of blank plasma extract. Key: A, solvent front; and B, internal standard.*

lyzing the samples as already described. The recovery varied from 88 to 102% (average of 93%) and seemed to be independent of the griseofulvin concentration within this range.

Plasma Samples—Twelve normal adult males, 21–50 years of age, received on a fasting stomach one 500-mg tablet of micronized griseofulvin with 120–180 ml (4–6 oz.) of water. Duplicate 10-ml blood samples were obtained by venipuncture at 0, 0.5, 1, 2, 4, 6, 8, 12, and 24 hr after dosing. The plasma was isolated by centrifugation and stored in the frozen state until analyzed.

RESULTS AND DISCUSSION

Standard Curve—A typical recorder tracing of a standard mixture is shown in Fig. 1. A complete separation of the peaks was obtained. The retention times were: internal standard, 3.0 min; and griseofulvin, 8.0 min.

A typical standard curve was smooth but nonlinear in the range of 0–1.5 μg of griseofulvin/ml of assay solution. This nonlinearity was probably due to the nonlinear response characteristics of the electron-capture detector.

Sensitivity—The detection limit (two to three times the noise level) for griseofulvin was 30 pg, corresponding to 6 ng/ml of assay solution, under the conditions of the assay method. Four times this concentration (10 times the noise level) or 0.025 μg/ml of assay solution (peak height ratio = 0.06) was found to be the lowest measurable concentration. This assay sensitivity, corresponding to 0.050 μg/ml of plasma, was sufficient to follow the plasma level after a single dose of 250–500 mg of griseofulvin for 72 hr.

Due to the flattening of the standard curve, the method also has a practical upper limit of usefulness of about 1.5 μg of griseofulvin/ml of plasma. Higher concentrations can be measured by decreasing the volume of plasma or increasing the amount of benzene used in making up the assay solution.

Specificity—The combination of extraction, GLC retention

Table II—Plasma Concentrations of Griseofulvin following a Single Oral Dose of 500 mg of Micronized Griseofulvin in 12 Human Volunteers (Parallel Determinations by the GLC Method and the Spectrofluorometric Method)

Hours	Fluorometric, μg/ml ± *SD*[a]	GLC, μg/ml ± *SD*[a]	Ratio
0.5	0.08 ± 0.10	0.06 ± 0.09	1.33
1	0.29 ± 0.25	0.21 ± 0.21	1.38
2	0.56 ± 0.31	0.48 ± 0.35	1.17
4	0.73 ± 0.21	0.60 ± 0.29	1.22
6	0.73 ± 0.22	0.54 ± 0.26	1.35
8	0.66 ± 0.20	0.48 ± 0.24	1.38
10	0.57 ± 0.16	0.46 ± 0.20	1.24
12	0.56 ± 0.17	0.44 ± 0.18	1.27
24	0.41 ± 0.12	0.28 ± 0.12	1.46

[a] Mean of 12 subjects.

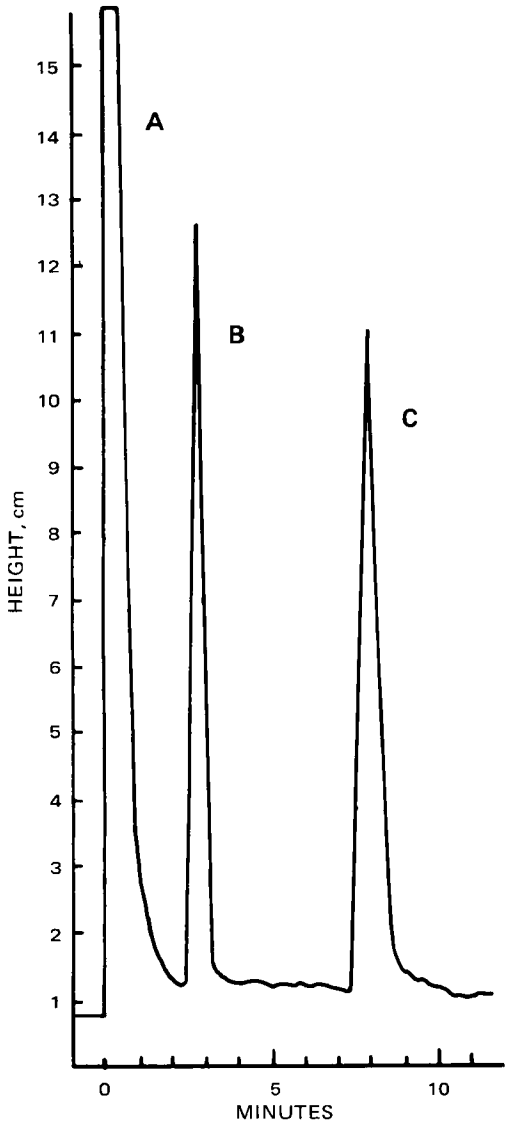

Figure 3—*Gas chromatogram showing a 5-μl injection of plasma extract spiked with griseofulvin. Key: A, solvent front; B, internal standard; and C, griseofulvin.*

time, and sensitivity to electron capture makes this method very specific. The only major plasma metabolite of griseofulvin (8), 6-demethylgriseofulvin, has a much longer retention time and elutes as a very flat, almost indistinguishable band at corresponding concentrations.

Determination in Plasma—The GLC tracing of an extract of a blank plasma sample (Fig. 2) was compared with an extract of a plasma sample containing griseofulvin (Fig. 3). The blank plasma extract showed no interfering peak in the area of the griseofulvin peak. Zero blank values were obtained throughout. Because of variations in the response of the electron-capture detector, standard curves were run daily when plasma samples were analyzed.

Recovery—The validity of the method was verified and the recovery was determined by adding various known amounts of griseofulvin to human plasma. Each plasma standard as well as blank plasma was analyzed eight times according to the described procedure (Table I).

The mean recoveries varied from 97 to 107% of the added amount with an average of 100%, and no correlation with the concentration of griseofulvin was observed.

Comparison of GLC and Spectrofluorometric Results—The duplicate plasma samples obtained from 12 subjects after a single dose of 500 mg of griseofulvin were analyzed by both the GLC and the simplified spectrofluorometric methods (Table II).

The fluorometrically obtained plasma concentrations were consistently higher than the corresponding GLC results. This observation indicated that while the GLC method was specific for griseofulvin, one or several metabolites contributed to the fluorescence. Table II also shows that the ratio of the results obtained by the two methods was constant over the whole time course. From this finding it can be inferred that the ratio of griseofulvin to contributing metabolite(s) is constant at all times, that the disappearance of griseofulvin or fluorescence from plasma would yield the same half-life, and that, therefore, the half-life of disappearance is determined by the metabolism of griseofulvin. In addition, Table II shows that the standard deviation was of the same order for both determinations, indicating that the intersubject variation was the same for both methods.

These results and conclusions are in good agreement with the data obtained (8) with ^{14}C-labeled griseofulvin. Blood contained about equal amounts of griseofulvin and 6-demethylgriseofulvin, the two compounds accounting for 86% of the radioactivity in blood (8). In addition, the disappearance curves of griseofulvin and radioactivity were parallel and yielded the same half-life, indicating that demethylation of griseofulvin was the rate-limiting step in the elimination process.

To tie the two sets of findings together, the fluorescence of 6-demethylgriseofulvin and mixtures of equal amounts of 6-demethylgriseofulvin and griseofulvin was determined at the instrument settings used for the griseofulvin assay. 6-Demethylgriseofulvin did give fluorescence readings, albeit less than griseofulvin, and indeed the 6-demethylgriseofulvin added about 30% to the fluorescence yield of griseofulvin when present at an equal concentration. Thus, the 1.3 times higher plasma levels obtained with the spectrofluorometric method were most likely due to the coextracted 6-demethylgriseofulvin. How far this was the case in other modifications of the spectrophotofluorometric determination method (2–7) cannot be ascertained; however, it is probable that 6-demethylgriseofulvin contributed to the plasma level readings in some or all of them.

SUMMARY AND CONCLUSIONS

The time requirement per sample is about the same for both methods described in this paper if manual injection of the gas chromatograph is employed. However, by using an automatic GLC injector, the output can be doubled or even tripled.

Based on equal sensitivity, better specificity, and the capacity for greater output, it was concluded that the GLC method as described here is the preferred method of assay for griseofulvin in human plasma. Because of its simplicity, it is well suited for the routine analysis of a large number of samples. The method was successfully used in this laboratory in several bioequivalency studies.

REFERENCES

(1) *Arch. Dermatol.*, **81**, 650(1960).

(2) C. Bedford, K. J. Child, and E. G. Tomich, *Nature*, **184**, 364(1959).

(3) G. D. Weinstein and H. Blank, *Arch. Dermatol.*, **81**, 746(1960).

(4) M. Kraml, J. Dubuc, and D. Dvornik, *J. Pharm. Sci.*, **54**, 655(1965).

(5) L. J. Fisher and S. Riegelman, *ibid.*, **54**, 1571(1965).

(6) M. Rowland, S. Riegelman, and W. L. Epstein, *ibid.*, **57**, 984(1968).

(7) V. P. Shah, S. Riegelman, and W. L. Epstein, *ibid.*, **61**, 634(1972).

(8) C.-C. Lin, J. Magat, R. Chang, J. McGlotten, and S. Symchowicz, *J. Pharmacol. Exp. Ther.*, **187**, 415(1973).

(9) M. J. Barnes and B. Boothroyd, *Biochem. J.*, **78**, 41(1961).

ACKNOWLEDGMENTS AND ADDRESSES

Received April 15, 1975, from the *Drug Metabolism Section, Sandoz Pharmaceuticals, East Hanover, NJ 07936*

Accepted for publication May 27, 1975.

The authors thank Ms. Carolyn Tanner for technical assistance and Mr. E. Papp for technical consultations.

[x] To whom inquiries should be directed.

Adsorption Sites of Kaolin

N. A. ARMSTRONG [x] and C. D. CLARKE *

Abstract □ The electrophoretic mobility and adsorptive properties of kaolin and kaolin pretreated with anionic and cationic materials were examined over a range of pH values. Pretreatment with anionic compounds had little effect on mobility, while adsorption of cationic species markedly reduced mobility. These results are explained by reference to the structure of kaolin, and the interdependence of adsorption properties and electrophoretic mobility are discussed.

Keyphrases □ Kaolin—electrophoretic mobility and adsorptive properties, effect of pretreatment with anionic and cationic materials, various pH values □ Adsorptive properties—kaolin, effect of pretreatment with anionic and cationic materials, various pH values □ Electrophoretic mobility—kaolin, effect of pretreatment with anionic and cationic materials, various pH values

Kaolin and other clays have long been used for medicinal purposes, their therapeutic action being attributed to their adsorptive capacity. Recently, the uptake of benzoic acid and gentian violet by kaolin has been extensively studied (1–3), and the mechanism of adsorption of anionic and cationic materials has been discussed in relation to the structure of the clay and the likely adsorption sites on the surface of the kaolin particle.

The primary adsorptive mechanism is believed to be electrostatic charges on the kaolin surface. Furthermore, the adsorptive sites of certain substances have been established fairly definitely. Therefore, if kaolin is subjected to preliminary treatment with substances whose site of adsorption is known, and this kaolin is subsequently used to study the adsorptive properties and electrophoretic mobility of the clay, information may be obtained on the location and properties of the electrostatic charges on the kaolin surface.

EXPERIMENTAL

Light kaolin, BP quality, was dried at 100° (3 hr), blended thoroughly, and stored in tightly closed containers. The weight mean diameter of the kaolin was 3.3 μm (sedimentation balance[1]), and the surface area was 11.2 m^2/g (nitrogen adsorption, using 0.163 nm^2 as the cross-sectional area of a nitrogen molecule[2]). Sodium hexadecyl sulfate[3] and other reagents were used without further purification.

Microelectrophoretic Techniques—A water-jacketed microelectrophoresis cell mounted on a binocular microscope was used (4). In all experiments, a 0.004% (w/v) suspension of kaolin in 0.004 *M* potassium chloride containing varying quantities of 0.02 *N* HCl or NaOH was used to give the required pH within the 3.0–10.0 range. The addition of such small quantities of acid or alkali had a negligible effect on the current flowing through the cell. After preparation, the suspensions were shaken in a water bath for 30 min; individual flasks were then removed, and the pH of the system was measured. The remainder of the suspension was used for flushing through and subsequently filling the electrophoresis cell.

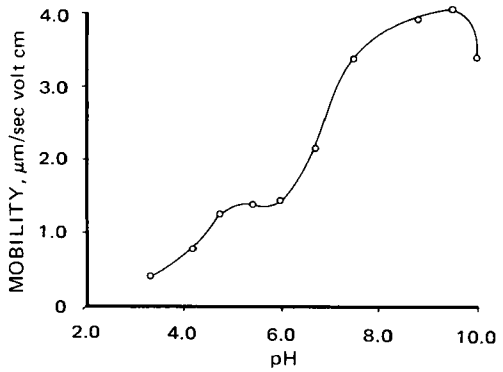

Figure 1—*Variation with pH of the electrophoretic mobility of kaolin in 0.004* M *potassium chloride.*

The time for 10 particles to traverse the calibrated distance in both directions was measured at the upper stationary layer, and the electrophoretic mobility of the kaolin at each pH value was calculated from the mean transit time. The mobility of samples of kaolin that had been equilibrated with solutions of sodium hexadecyl sulfate, gentian violet, cetrimide[4], benzoic acid, alizarin red S, sodium pyrogallol, or sodium pyrophosphate was determined over a similar pH range. All measurements were carried out at 24 ± 0.1°.

Zero Point of Charge—The clay suspensions used in the electrophoresis studies were not sufficiently concentrated to permit ready visual determination of the edge zero point of charge by flocculation–deflocculation transitions. However, the edge zero point of charge of these suspensions could be satisfactorily determined by placing the suspensions in standard cells and examining them photoelectrically after standing for 24 hr.

Electron Microscopy—An electron microscope[5] was used, and samples were examined by pipetting one drop of a 1% dispersion of kaolin in water onto the carbon film of the specimen holder. To investigate the ratio between the edge and face areas of the kaolin platelets, a kaolin specimen was shadowed with gold–palladium at a 30° angle.

Adsorption Studies—Kaolin (100 g) was added to a 1% cetrimide solution (400 ml), and the suspension was shaken for 16 hr. The sediment was removed by centrifugation, washed with water, and centrifuged again. The moist sediment cake was dried (vacuum oven, 50° for 8 hr), passed through a 0.25-mm sieve, and blended to ensure homogeneity. Further kaolin samples were treated identically with sodium lauryl sulfate solution (1%) and with water to constitute a control sample.

The effect of this treatment on the surface area of the kaolin was negligible. The uptake of gentian violet onto these treated samples of kaolin was determined as follows. Kaolin (2 g) was added to flasks containing gentian violet (50 mg), ethylenediaminetetraacetic acid (100 mg), and Teorell and Stenhagen buffer (2.5 ml), together with sufficient 0.1 *N* HCl or NaOH to give the required pH; purified water was added to a total volume of 100 ml. The flasks were agitated at 24° for precise periods of time from 7 to 70 min, the solid was removed by centrifugation, and the gentian violet in the supernate was determined spectrophotometrically at 590 nm. The magnesium content of the supernate was measured by atomic absorption spectroscopy[6].

RESULTS AND DISCUSSION

Electron microscopy showed that the kaolin exists as character-

[1] Model PC 650, Gallenkamp Ltd., London, United Kingdom.
[2] Model 212D sorptometer, Perkin-Elmer Ltd., Beaconsfield, United Kingdom.
[3] Proctor and Gamble Ltd., Newcastle on Tyne, United Kingdom.
[4] Cetrimide BP, Glovers Ltd., Leeds, United Kingdom.
[5] JEM 7, Japan Electronic Optics Laboratory Co. Ltd., Tokyo, Japan.
[6] Model 290B, Perkin-Elmer Ltd., Beaconsfield, United Kingdom.

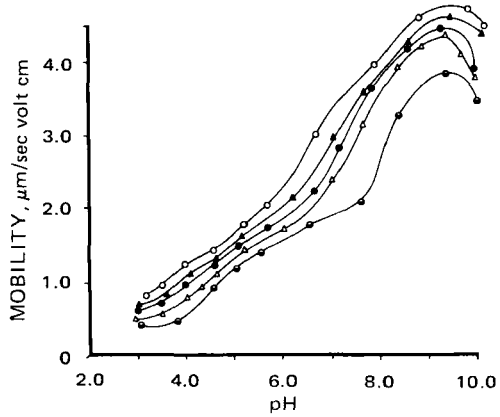

Figure 2—*Variation with pH of the electrophoretic mobility of kaolin treated with anionic material. Key: ●, kaolin plus sodium hexadecyl sulfate; △, kaolin plus sodium pyrophosphate; ○, kaolin plus sodium pyrogallol; ▲, kaolin plus alizarin red S; and ⊖, kaolin plus benzoic acid.*

istic hexagonal platelets, as described by Woodward and Lyons (5). The average thickness–diameter ratio was 1:20, giving an edge–cleavage surface area of 1:9. This figure is in good agreement with reported findings (6, 7), although a ratio of 44% edge area and 56% cleavage surface area was reported (8) for kaolin from the same source as used in this study. Therefore, the kaolin is considered to be characterized by a particle cleavage layer surface area that is considerably greater than that of the edge surface.

Effect of pH on Electrophoretic Mobility of Kaolin—The hydrogen-ion concentration markedly affected the mobility of kaolin (Fig. 1). The increase in mobility with pH to a maximum value at about pH 9.5 was only modified by the near plateau in the pH 5.0–6.0 region. The decrease in mobility at pH values above 9.5 confirms an earlier report (9) and is attributed to erosion of the kaolin structure. Dissolution of lattice aluminum occurs at pH values above 9.5 (1).

Below pH 4.3, a few clay particles reversed their direction of travel, as previously noted (10). Schofield (11) postulated the existence of clays that exhibit an isoelectric point and are positively charged below a particular pH. Since, irrespective of pH, the negative charge on the face of the kaolin platelet is greater than the positive edge charge, the kaolin used is unlikely to exhibit an isoelectric point. However, Woodward and Lyons (5) described platelet aggregations that show a greater edge surface area and that could conceivably exhibit an overall zero point of charge.

The photoelectrically determined edge zero point of charge of the kaolin suspensions in 0.004 *M* potassium chloride occurred at pH 6.0, which is in good agreement with the value obtained from ion-exchange studies (12).

This value for the zero point of charge of kaolin corresponds to the plateau region of Fig. 1. With a negative edge and cleavage face charge, the mobility rose rapidly with an increase in pH to a maximum at about pH 9.5. This result was probably due to the exchange of the sodium (added as sodium hydroxide to adjust pH) for divalent clay counterions, resulting in an increase in negative charge. The magnitude of the edge negative charge may also be increased by increased adsorption of hydroxyl ions on the edge surface (13).

Electrophoretic Mobility of Pretreated Kaolin—Since the

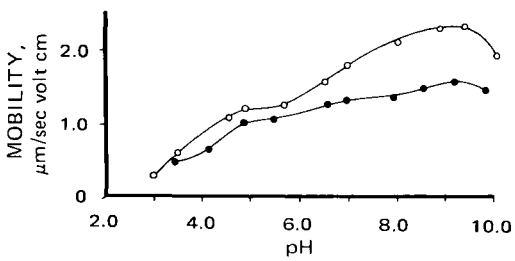

Figure 3—*Variation with pH of the electrophoretic mobility of kaolin treated with cationic material. Key: ○, kaolin plus gentian violet; and ●, kaolin plus cetrimide.*

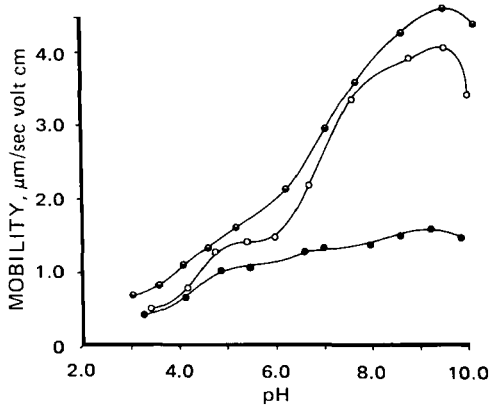

Figure 4—*Variation with pH of the electrophoretic mobility of natural kaolin and of kaolin treated with anionic and cationic material. Key: ○, kaolin; ⊖, kaolin plus alizarin red S; and ●, kaolin plus cetrimide.*

negative charge of kaolin is situated on the cleavage surface and the edge surface can bear a positive charge in acid conditions, adsorption of a cationic material on the cleavage layer should permit the contribution of the edge charge to the overall mobility to become apparent. Conversely, following adsorption of an edge-adsorbed species, the role of the cleavage surface charge in electrophoresis should be more readily discernible.

Several workers claimed that anionic materials are adsorbed onto the edges of clay minerals, *e.g.*, sodium hexadecyl sulfate (8), sodium pyrophosphate (14), sodium pyrogallol (15), and alizarin red S (13). When samples of kaolin were treated with these materials, a higher maximum electrophoretic mobility was obtained compared to untreated kaolin (Fig. 2). The shape of the mobility curve of kaolin treated with benzoic acid also suggests that this substance is edge adsorbed (3).

Conversely, the cationic substance cetrimide is claimed to be adsorbed onto the cleavage surface of kaolin (16), and this view is supported by the fact that the mobility curve of kaolin pretreated with cetrimide and also gentian violet showed much reduced mobility compared to that of untreated kaolin or kaolin bearing adsorbed anionic substances (Fig. 3). A leveling of the mobility curve was still evident between pH 5.0 and 6.0, suggesting that this near plateau reflects the character of the particle edge surface, which is relatively free of adsorbed cetrimide.

To facilitate comparison, Fig. 4 shows the variation in mobility with pH of kaolin, kaolin plus anionic material (alizarin red S), and kaolin plus cationic material (cetrimide). The adsorption of cationic material on the cleavage surface caused this large area to have its negative charge partly or wholly neutralized, thus decreasing the negativity of the particle and thereby reducing mobility. On the other hand, adsorption of anionic material on the positively charged edge increased the total negative charge and therefore in-

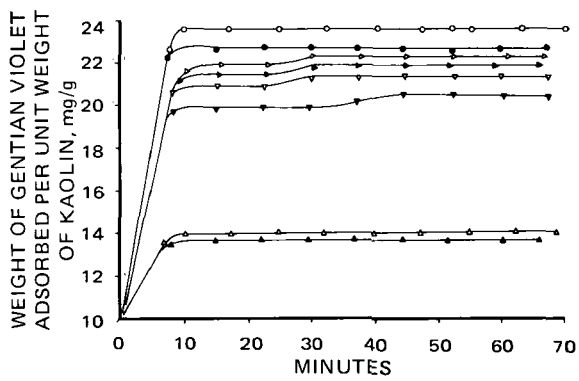

Figure 5—*Variation with pH of the uptake of a 0.05% (w/v) solution of gentian violet on natural kaolin and on kaolin treated with anionic and cationic materials. Key: kaolin, pH 7.4 (▷) and 5.7 (▶); washed kaolin, pH 7.4 (▽) and 5.4 (▼); kaolin plus sodium hexadecyl sulfate, pH 7.5 (○) and 5.6 (●); and kaolin plus cetrimide, pH 7.6 (△) and 5.4 (▲).*

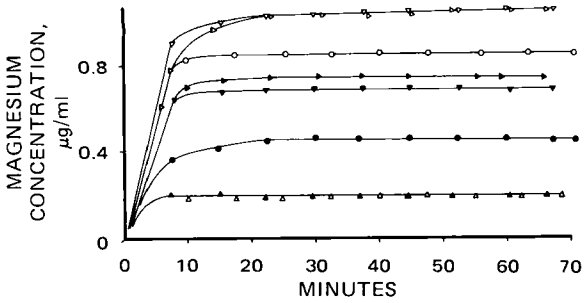

Figure 6—*Variation in magnesium exchange with pH of natural kaolin and of kaolin treated with anionic and cationic material. Key: kaolin, pH 7.4 (▷) and 5.7 (◗); washed kaolin, pH 7.4 (▽) and 5.4 (▼); kaolin plus sodium hexadecyl sulfate, pH 7.5 (○) and 5.6 (●); and kaolin plus cetrimide, pH 7.6 (△) and 5.4 (▲).*

creased mobility. The pH at which maximum mobility was reached was identical for all three forms of kaolin.

Adsorptive Properties of Pretreated Kaolin—Previously, it was suggested that the exchange of monovalent ions in the suspension medium for clay counterions, *e.g.*, magnesium, plays an important role in cation adsorption (1).

Figure 5 shows the rate of uptake of gentian violet onto kaolin and kaolin pretreated with anionic material (sodium lauryl sulfate) and cationic material (cetrimide). Uptake was studied at two pH values, 5.7 and 7.4, both being in the range where a 0.05% gentian violet solution does not fade significantly during the period of experimental observation, thus permitting spectrophotometric determination (1). Compared to untreated kaolin, kaolin pretreated with cetrimide showed a marked decrease in its adsorptive capacity toward gentian violet, although a small increase in uptake was obtained with increases in pH. In monitoring the increase of magnesium ions in the supernate (as being indicative of variations in the ion-exchange process), no difference was seen in the amount of cation exchange at these two pH levels (Fig. 6).

In contrast, kaolin treated with sodium lauryl sulfate showed differences both in dye uptake (Fig. 5) and magnesium exchanged (Fig. 6) at the two pH values. The differences were of comparable magnitude to those exhibited by the standard and control clays; *i.e.*, the saturation of the edge adsorption sites of kaolin has no effect on total dye uptake or on the levels of magnesium involved in cation exchange.

Both the adsorptive and electrophoretic data presented here confirm that the characteristic charge on kaolin and hence the site of cation exchange are situated on the cleavage layer surface of the clay and are not, as has been suggested, an edge effect.

The picture of kaolin that emerges is of a clay bearing a negative charge on the cleavage faces due to lattice defects, the edge charge being reflective of the exposed atoms. While the cleavage plane negative charge is unaffected by pH, the sign and magnitude of the charges on the edge faces are strongly dependent on pH. The base-exchange capacity of kaolin in acidic or neutral solution is due to isomorphous replacement within the lattice in a similar manner to that proposed for montmorillonite and other clays. In alkaline solutions, however, the edge faces of the kaolin become negatively charged and can participate in exchange reactions. Thus, the fact that kaolin has never been shown to exhibit a positive potential by decreasing the pH is due to the negative charge of the greater area of the cleavage surface outweighing the positive charge on the smaller edge face area.

REFERENCES

(1) N. A. Armstrong and C. D. Clarke, *J. Pharm. Pharmacol., Suppl.*, **23**, 95S(1971).

(2) N. A. Armstrong and C. D. Clarke, *J. Pharm. Sci.*, **62**, 379(1973).

(3) C. D. Clarke and N. A. Armstrong, *Pharm. J.*, **209**, 44(1972).

(4) C. D. Clarke and G. Williams, *Lab. Pract.*, **20**, 656(1971).

(5) L. A. Woodward and S. C. Lyons, *Tappi*, **34**, 438(1951).

(6) A. L. Johnson, *J. Amer. Ceram. Soc.*, **32**, 210(1949).

(7) W. H. East, *ibid.*, **33**, 211(1950).

(8) A. W. Flegmann and R. H. Ottewill, *Proc. Int. Congr. Chem. Phys. Surface-Active Substances, 4th*, **2**, 1271(1964).

(9) N. Street and A. S. Buchanan, *Aust. J. Chem.*, **9**, 450(1956).

(10) S. Mattson, *J. Phys. Chem.*, **37**, 223(1933).

(11) R. K. Schofield, *Soils Fert.*, **2**, 1(1939).

(12) A. W. Flegmann, J. W. Goodwin, and R. H. Ottewill, *Proc. Brit. Ceram. Soc.*, **13**, 31(1969).

(13) H. van Olphen, "An Introduction to Clay Colloid Chemistry," Interscience, New York, N.Y., 1963.

(14) J. R. van Wazer and E. Besmertnuk, *J. Phys. Colloid Chem.*, **54**, 89(1950).

(15) P. E. Watkins and T. White, "Proceedings of the 2nd International Conference on Surface Activity," Butterworths, London, England, 1958.

(16) J. P. Law and G. W. Kunze, *Proc. Soil Sci. Soc. Amer.*, **30**, 321(1966).

ACKNOWLEDGMENTS AND ADDRESSES

Received March 10, 1975, from the *Welsh School of Pharmacy, University of Wales Institute of Science & Technology, Cardiff, United Kingdom.*

Accepted for publication May 29, 1975.

* Present address: Southlands Hospital, Shoreham-by-Sea, United Kingdom.

[x] To whom inquiries should be directed.

Granule Consolidation during Compaction

MICHAEL H. RUBINSTEIN

Abstract □ The deformation of small cylindrical aggregates of dibasic calcium phosphate was measured during compaction. An analogy between these aggregates and cylindrical granules was proposed. No change in the original shape of the aggregates occurred; the cylindrical shape was maintained even at high compaction pressures. Relaxation of the aggregates occurred at pressures higher than 420 MNm^{-2} (60.9×10^3 lb $in.^{-2}$) when removed from the compacts, but no relaxation took place at pressures below this value. In addition, the aggregates relaxed by an increase in thickness only; there was no corresponding change in diameter. Up to a pressure of 200 MNm^{-2} (29.0×10^3 lb $in.^{-2}$), an increase in aggregate diameter occurred, which was accompanied by a reduction in thickness. This change produced only a small reduction in volume, which was attributable to interparticulate slippage resulting in a closer packed arrangement. At a pressure of 200 MNm^{-2}, the aggregate diameter no longer increased because solid bridges were formed between the particles and the die wall, preventing further spreading. From 200 to 420 MNm^{-2}, failure of the material occurred by plastic deformation, which produced only a decrease in aggregate thickness. From 420 to 800 MNm^{-2} (116.0×10^3 lb $in.^{-2}$), a structure was formed that could support the applied load without further reduction of thickness, and this structure was shown to behave elastically.

Keyphrases □ Granules—consolidation during compaction, dibasic calcium phosphate aggregate deformation measured, effect of pressure, granule thickness □ Calcium phosphate, dibasic—deformation of aggregates measured during compaction, effect of pressure, granule thickness

The mechanism by which a mass of powder is compressed into a coherent tablet has been studied (1–4). By measuring the exposed punch length during static compression of heavy magnesium carbonate, Train (5) evaluated the relationship between the relative volume of the compact and the applied pressure. Using a modification of Train's method, Kristoffersson and Krogerus (6) measured the deformation of whole tablets containing polyethylene glycols; they recorded the changes in height at various compaction pressures.

Various theoretical attempts have been made to quantify the consolidation of powders as compression proceeds (7, 8). All of these treatments have involved measurements of the external dimensions of the finished tablet. Train (5), however, emphasized that evidence obtained from measurements of the external dimensions of compacts may not truly reflect the internal situation.

The present study was carried out to examine the deformation of granules during compaction and then the three-dimensional changes that occur with individual granules within the compacting mass.

EXPERIMENTAL

The powder used was dibasic calcium phosphate[1] because it is a common tablet excipient and produces hard tablets at low compaction pressures. The mean particle size was 48 μm with 100% by weight less than 90 μm (sieve analysis). The dibasic calcium phosphate powder was intimately mixed with 10% by weight of radiographic barium sulfate[1]. The barium sulfate was ground so that the powder was of an identical particle size. The powder mix was granulated in a coating pan with 4% mucilage of methylhydroxyethylcellulose[2] to produce spherical granules. The objectives of producing these round granules were to eliminate the shape factor that may influence the deformation process and to standardize, as far as possible, the surface roughness of the granules.

The resultant granules were carefully dried to maintain uniformity of composition, and the 387–500-μm fraction was selected for experimentation. The moisture content of this fraction was found by drying a sample to constant weight (0.5% w/w), and the uniformity of granule strength was checked by measuring the load applied at a constant rate to produce failure of individual granules. The apparatus used for testing granule strength was a modified version of a reported instrument (9). The belt-driven pulley of this apparatus was reversed so that the lower jaw was driven upward rather than downward. An individual granule was placed between the two jaws of the instrument. Movement of the lower jaw upward at a constant velocity of 6.6×10^{-5} m/sec applied a diametrical crushing load. The granule strength was read from the chart record as the maximum load applied before failure occurred. Thirty determinations were made.

The granules were then mixed with 1% (w/w) dried magnesium stearate, and consolidation was performed at 15 MNm^{-2} (2.175×10^3 lb $in.^{-2}$) between 3.20-mm diameter, new flat-faced punches. The die was filled by hand; a collection of small cylindrical aggregates were produced which were identical in weight, thickness, and diameter. The 15 MNm^{-2} was just enough pressure to aggregate the spherical granules, and the granule structure could be readily observed by eye.

The diameter and thickness of each cylindrical aggregate were individually measured with a traveling microscope to 0.01 mm, and the aggregate volume was calculated from these data. Each measured aggregate was numbered for subsequent identification and each was considered to be one "granule," which could be subsequently compacted at much higher pressures. It can be argued that there might be significant differences in particle to particle bond strength and void space between materials making up these aggregates and true granules. However, for the purposes of this work, the analogy between the two was close enough for the aggregates to be assumed to be cylindrical granules.

Sucrose was granulated similarly to the dibasic calcium phosphate except that 7.5% (w/v) povidone[3] in industrial methylated spirits was used as the granulating agent. The sucrose[1] was milled so that this material possessed the same particle size as the dibasic calcium phosphate. A 1-g quantity of the dried sucrose granules was introduced into a specially hardened die[4], 2.54 cm in diameter. After leveling, three aggregates were positioned diametrically upon the surface of the sucrose granules: one in the center and one each 5 mm from the die wall. A further 1-g quantity of sucrose granules was poured into the die, and the mass was compacted at 30 MNm^{-2} (43.5×10^3 lb $in.^{-2}$) on a stationary precision press[5]. This arrangement ensured, as far as possible, that the dibasic calcium phosphate aggregates were compressed to the same compaction pressure within the larger diameter compacts.

Fifteen additional compacts were produced at increasing pressures up to 800 MNm^{-2}. At each compaction pressure, three compacts were produced. Then X-rays, in two directions at right angles, were taken of the large compacts. From the radiographs, diameter and thickness measurements of the dibasic calcium phosphate aggregates were again determined with the traveling microscope and the volumes were calculated. The aggregates were recov-

[1] British Drug Houses.

[2] Tylose MH50, Hoechst A.G.
[3] Plasdone K29-32, GAF Corp.
[4] EN26 chrome molybdenum steel.
[5] Dennison, grade A.

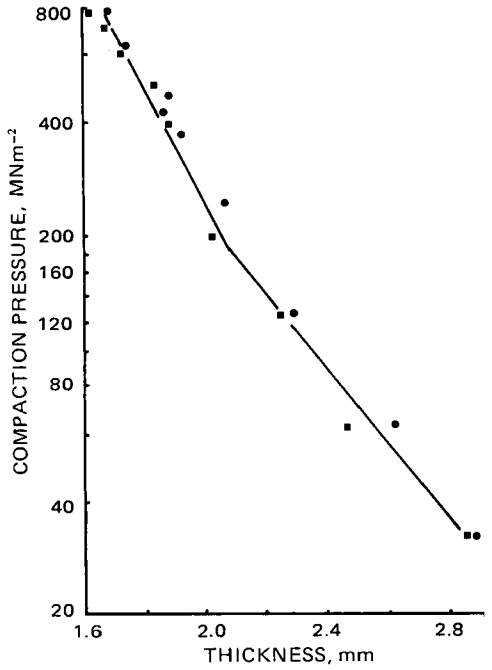

Figure 1—*Variation of compact thickness with compaction pressure. Key: ●, sucrose; and ■, dibasic calcium phosphate (90% w/w) and barium sulfate (10% w/w).*

ered from the large compacts by dissolving out the sucrose with water. An inspection confirmed that no damage was done to the aggregates by this process.

The recovered, intact, identifiable dibasic calcium phosphate aggregates were again measured with the traveling microscope, and the volumes were calculated. Confirmation of the volume values was carried out by water-displacement measurements in a specific gravity bottle. Finally, the crushing strength of the recovered aggregates was determined in the granule strength apparatus by measuring the load applied at a constant rate of 6.6×10^{-5} m/sec to produce failure.

To confirm that the compaction characteristics of sucrose and dibasic calcium phosphate and barium sulfate were similar, thickness measurements were recorded for 2-g compacts composed of only sucrose and of only dibasic calcium phosphate and barium sulfate.

RESULTS AND DISCUSSION

Figure 1 shows the results obtained when compact thickness was plotted against compaction pressure for the sucrose and dibasic calcium phosphate granulations. In all figures, each point represents the mean values of nine determinations; the range of the measured values for the various properties was not more than 10% of the plotted means. Identical graphs were obtained in Fig. 1, indicating that both materials consolidated in a similar manner to produce compacts of identical dimensions.

Table I shows the volumes of the aggregates calculated from dimensional measurements after removal from the large compacts and the corresponding values obtained by water-displacement measurements. There was a negligible difference between the values, indicating that no change in the cylindrical shape of the aggregates had occurred over the whole pressure range studied. This finding was also confirmed by a close inspection of the radiographs. Apparently, the initial shape of the aggregates is maintained inside the compacts and granule shape may be an important factor in the compaction process.

Figure 2 shows the amount the volume of the dibasic calcium phosphate aggregates was reduced at increasing compaction pressures. Inside the compacts up to about 200 MNm^{-2}, the volume of the aggregates was not greatly reduced (about 0.8×10^{-3} ml). From 200 to 420 MNm^{-2}, there was a much greater reduction in volume, ranging from 0.8×10^{-3} ml at 200 MNm^{-2} to a maximum value of 4.6×10^{-3} ml at 420 MNm^{-2}. Over this compaction range, a linear relationship existed between aggregate volume reduction

Table I—Volumes of the Aggregates Removed from the Compacts Calculated from Dimensional and Water-Displacement Measurements

Compaction Pressure, MNm^{-2}	Volume Calculated from Water-Displacement Measurements, ml	Volume Calculated from Dimensional Measurements, ml
32	0.0079	0.0081
32	0.0084	0.0082
32	0.0076	0.0082
360	0.0102	0.0104
360	0.0096	0.0111
360	0.0094	0.0101
540	0.0092	0.0104
540	0.0098	0.0092
540	0.0105	0.0096
660	0.0114	0.0103
660	0.0103	0.0101
660	0.0098	0.0112

and compaction pressure. Beyond 420 MNm^{-2}, no further volume reduction occurred and a constant value of 4.6×10^{-3} ml over the pressure range of 420–800 MNm^{-2} was recorded.

The graphs obtained when the aggregates were removed from the large compacts were the same up to about 380 MNm^{-2} (55.1×10^3 lb $in.^{-2}$), indicating no relaxation of the aggregates. After 380 MNm^{-2}, the aggregates relaxed and increased in volume by a constant amount, 0.9×10^{-3} ml. Therefore, capping probably would be more liable to occur at compaction pressures higher than 380 MNm^{-2} and there probably would be no tendency to cap below 380 MNm^{-2}. This transition point, at which elasticity is first exhibited, could provide a useful index for measuring the capping tendencies of different granular systems.

The relationship between aggregate thickness and compaction pressure is shown in Fig. 3. Again, similar graphs were obtained inside the compacts and removed from the compacts up to 420 MNm^{-2}. At pressures higher than 420 MNm^{-2}, an increase in thickness was observed when the aggregates were removed from the compacts. This increase in thickness accounted for the relaxa-

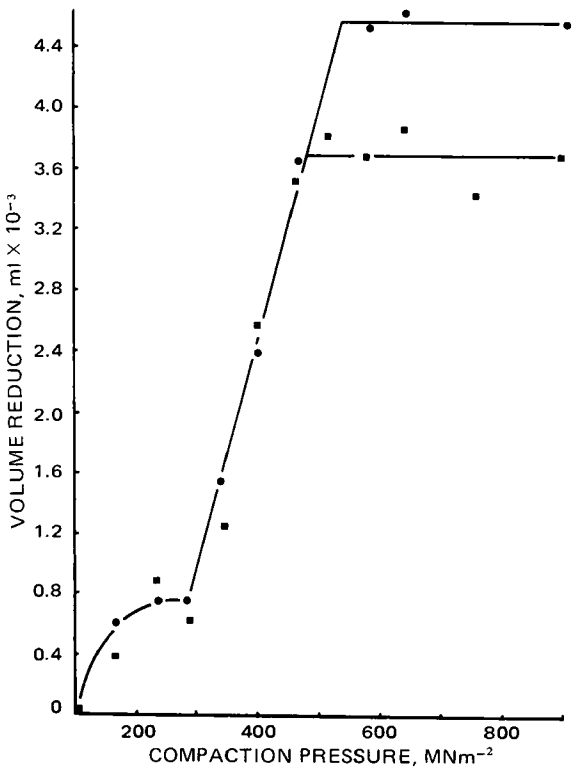

Figure 2—*Reduction of aggregate volume with compaction pressure. Key: ●, inside compacts; and ■, removed from compacts.*

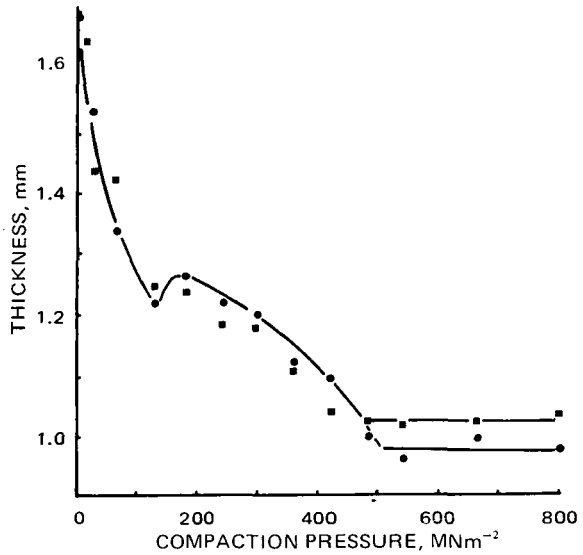

Figure 3—*Change in aggregate thickness with compaction pressure. Key: ●, inside compacts; and ■, removed from compacts.*

tion of the aggregates at high compaction pressures and demonstrated that the structure was then behaving elastically.

The change in aggregate diameter with compaction pressure inside the compacts and removed from the compacts is shown in Fig. 4. Both graphs are identical, indicating that no change in diameter occurred when the aggregates were removed from the compacts over the whole pressure range. Therefore, it can be concluded that relaxation of the aggregates occurred only in a direction perpendicular to the compact faces; that is, the aggregates relaxed in thickness only at pressures higher than 420 MNn^{-2} and no elasticity was exhibited at lower pressures.

By combining Figs. 2–4, a picture can be built of what happens during compaction. Up to 200 MNm^{-2}, there is an increase in aggregate diameter accompanied by a corresponding reduction in thickness. The result is that there is only a relatively small reduction in aggregate volume. This phase may be attributable to interparticulate slippage, which leads to a closer packed arrangement. The increase in diameter is the result of granules being squeezed outward by the descending upper punch. At about 200 MNm^{-2}, the aggregate diameter no longer increases because solid bridges

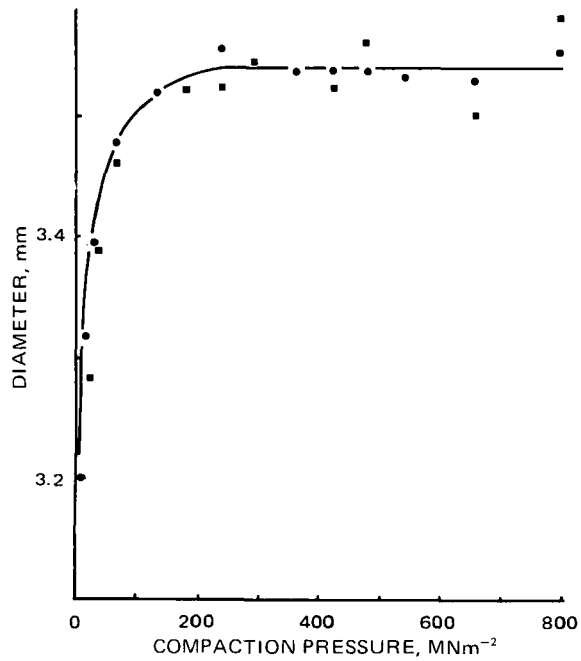

Figure 4—*Change in aggregate diameter with compaction pressure. Key: ●, inside compacts; and ■, removed from compacts.*

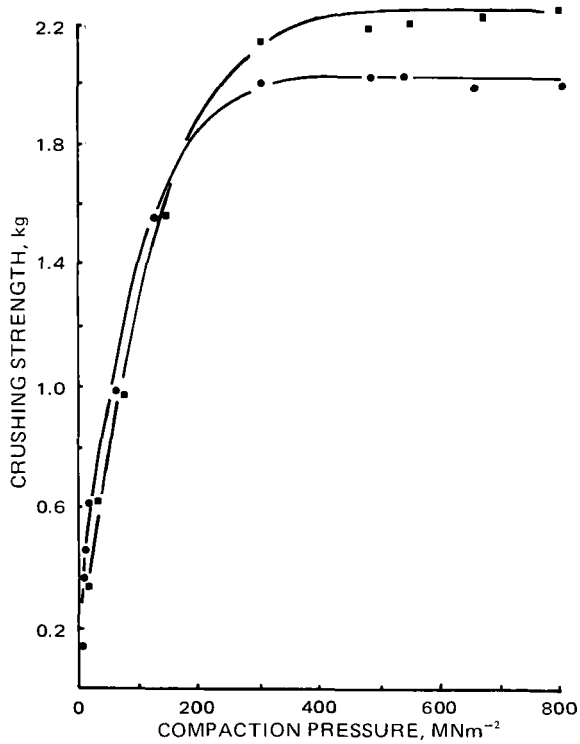

Figure 5—*Variation of aggregate crushing strength with compaction pressure. Key: ●, aggregates removed from compacts; and ■, aggregates compressed directly.*

are formed between the particles making up the granules and the die walls, preventing any further squeezing out of the granules. From 200 to 420 MNm^{-2}, failure of the granular material occurs by plastic deformation and a consolidation occurs by a reduction in aggregate thickness only. Finally, from 420 to 800 MNm^{-2}, a structure is formed that can support the applied load without further consolidation. This structure behaves elastically, since the aggregates increase in size when removed from the compacts.

This theory is supported by Fig. 5. This figure shows the crushing strength of dibasic calcium phosphate aggregates after removal from the compacts and of similar aggregates, compressed at varying pressures, that had not been inside the sucrose compacts. Similar shaped curves were obtained in each case. The aggregates that had been inside the compacts were weaker at pressures above 200 MNm^{-2} than were similar aggregates that had been directly compressed. The water used to dissolve the sucrose probably had modified the crushing strength characteristics of the aggregates. However, it can still be seen from both graphs that a constant value of crushing strength existed when the final elastic structure had been formed at pressures above 420 MNm^{-2} while increasingly weaker structures were found at pressures below 240 MNm^{-2} (34.8×10^3 lb $in.^{-2}$).

It was not possible to extend the scope of the present work to spherical aggregates due to the difficulty in producing aggregates of a perfectly round shape. Spherical aggregates might behave in a different manner than cylindrical aggregates because the compressional forces would probably be distributed differently. However, small short cylinders are likely to be the usual shape produced by a wet massing and screening granulation process. Thus, the results should be applicable to granules produced in this way.

CONCLUSIONS

The results indicate that cylindrical granules of dibasic calcium phosphate do not change their shape when compacted. Deformation occurs by a change in granule thickness and diameter at low compaction pressures and by only a reduction in thickness at intermediate pressures. High pressures produce no further consolidation. Only after being compacted at high pressures do granules exhibit relaxation when the applied pressure is removed. No granule relaxation occurs at low or intermediate pressures.

REFERENCES

(1) C. Fuehrer, *Chem.-Ing.-Tech.*, **43**, 849(1971).

(2) J. A. Hersey and J. E. Rees, Particle Size Analysis Conference, Bradford, England, 1970.

(3) D. Train, *Trans. Inst. Chem. Eng.*, **35**, 258(1957).

(4) D. Train and J. A. Hersey, *Powder Metall.*, **6**, 20(1960).

(5) D. Train, *J. Pharm. Pharmacol.*, **8**, 745(1956).

(6) E. Kristoffersson and V. E. Krogerus, *Farm. Aikak.*, **79**, 1(1970).

(7) K. Kawakita and Y. Tsutsumi, *Bull. Chem. Soc.*, **39**, 1364(1966).

(8) R. W. Heckel, *Trans. Metall. Soc.*, **221**, 671(1961).

(9) J. N. C. Healey, M. H. Rubinstein, and V. Walters, *J. Pharm. Pharmacol.*, **26**, 41p(1974).

ACKNOWLEDGMENTS AND ADDRESSES

Received November 5, 1974, from the *School of Pharmacy, Liverpool Polytechnic, Byrom Street, Liverpool L3 3AF, England.*

Accepted for publication June 3, 1975.

The author thanks Dr. R. W. Galloway for preparing the radiographs.

Effect of Cycloamyloses on Apparent Dissociation Constants of Carboxylic Acids and Phenols: Equilibrium Analytical Selectivity Induced by Complex Formation

KENNETH A. CONNORS ˣ **and JOHN M. LIPARI**

Abstract □ Apparent dissociation constants of organic acids were determined by potentiometric titration in the presence of cyclohexaamylose or cycloheptaamylose. The quantity $\Delta pKa' = pKa'$ (cycloamylose) − pKa (water) was positive or zero for all carboxylic acids studied and negative or zero for all phenols. The term $\Delta pKa'$ can be related to the cycloamylose concentration, K_{11a}, and K_{11b}, where K_{11a} and K_{11b} are 1:1 stability constants for complexes of the acid and the anion, respectively. From the dependence of $\Delta pKa'$ on cycloamylose concentration, estimates of K_{11a} and K_{11b} can be obtained. If $\Delta pKa' \neq 0$, then $K_{11a} \neq K_{11b}$; for carboxylic acids, $K_{11a} \geq K_{11b}$; for phenols, $K_{11b} \geq K_{11a}$. Because of variable pKa′ shifts, it is possible to carry out differentiating titrations of some acid mixtures in cycloamylose solutions, whereas the same acids cannot be differentiated in water. If an acid is weakened by cycloamylose, its conjugate base is strengthened, and some carboxylate salts can be readily titrated in the presence of a cycloamylose.

Keyphrases □ Cycloamyloses—effect on apparent dissociation constants of carboxylic acids and phenols, stability constants for complex formation □ Dissociation constants, apparent—carboxylic acids and phenols, effect of cycloamyloses, complex formation □ Carboxylic acids—apparent dissociation constants, effect of cycloamyloses □ Phenols—apparent dissociation constants, effect of cycloamyloses

Cycloamyloses (also called cyclodextrins or Schardinger dextrins) are cyclic oligomers containing six or more D-glucose units linked 1 → 4; they are produced by the action of *Bacillus macerans* amylase on starch. The six-unit and seven-unit substances are called cyclohexaamylose (α-cyclodextrin) and cycloheptaamylose (β-cyclodextrin), respectively. These molecules are doughnut shaped, and their possession of a cavity of fixed size and shape has led to considerable interest in their chemical properties. The production, purification, and chemistry of the cycloamyloses have been reviewed (1, 2). The catalytic properties of cycloamyloses, which have been widely studied as enzyme models, also have been discussed (3).

Any molecule smaller than the cavity of a cycloamylose molecule can enter the cavity and there undergo noncovalent interaction with the atoms lining and rimming the cavity. The resulting association product is called an inclusion compound or complex. The cycloamylose is thus a "host" for the smaller "guest" molecule. A 1:1 stoichiometry is typical, although other ratios have been observed and interpreted as the result of another guest molecule lying across the cavity opening. The dimensions of the cavity are such that many mono- and disubstituted benzene derivatives can fit into the cyclohexaamylose cavity, but polysubstituted benzenes may be excluded.

By forming an inclusion complex with a guest molecule, a cycloamylose is capable of altering some physical and chemical properties of the guest substance; it is by such changes that the complex formation is recognized and studied. Among the solution properties that can be modified are solubility, chemical reactivity, vapor pressure, and the electronic absorption spectrum. This capability for changing the chemical and physical behavior of solutes through complex formation may have analytical potential, and the present study examines the effects of cyclodextrins on the apparent dissociation constants of organic acids in aqueous solution.

It has been well established that many organic acids interact with the cycloamyloses (4–10), although little is known about the effects of complexing on acid dissociation equilibria. The potentiometric titration curve of monophenylphosphoric acid in the presence of cycloamylose reveals changes in pKa values, and even in the stoichiometric consumption of base, that require specific intermolecular interactions for their interpretation (2, 11). The pKa of

REFERENCES

(1) C. Fuehrer, *Chem.-Ing.-Tech.*, **43**, 849(1971).

(2) J. A. Hersey and J. E. Rees, Particle Size Analysis Conference, Bradford, England, 1970.

(3) D. Train, *Trans. Inst. Chem. Eng.*, **35**, 258(1957).

(4) D. Train and J. A. Hersey, *Powder Metall.*, **6**, 20(1960).

(5) D. Train, *J. Pharm. Pharmacol.*, **8**, 745(1956).

(6) E. Kristoffersson and V. E. Krogerus, *Farm. Aikak.*, **79**, 1(1970).

(7) K. Kawakita and Y. Tsutsumi, *Bull. Chem. Soc.*, **39**, 1364(1966).

(8) R. W. Heckel, *Trans. Metall. Soc.*, **221**, 671(1961).

(9) J. N. C. Healey, M. H. Rubinstein, and V. Walters, *J. Pharm. Pharmacol.*, **26**, 41p(1974).

ACKNOWLEDGMENTS AND ADDRESSES

Received November 5, 1974, from the *School of Pharmacy, Liverpool Polytechnic, Byrom Street, Liverpool L3 3AF, England.*

Accepted for publication June 3, 1975.

The author thanks Dr. R. W. Galloway for preparing the radiographs.

Effect of Cycloamyloses on Apparent Dissociation Constants of Carboxylic Acids and Phenols: Equilibrium Analytical Selectivity Induced by Complex Formation

KENNETH A. CONNORS ˣ **and JOHN M. LIPARI**

Abstract □ Apparent dissociation constants of organic acids were determined by potentiometric titration in the presence of cyclohexaamylose or cycloheptaamylose. The quantity $\Delta pKa' = pKa'$ (cycloamylose) − pKa (water) was positive or zero for all carboxylic acids studied and negative or zero for all phenols. The term $\Delta pKa'$ can be related to the cycloamylose concentration, K_{11a}, and K_{11b}, where K_{11a} and K_{11b} are 1:1 stability constants for complexes of the acid and the anion, respectively. From the dependence of $\Delta pKa'$ on cycloamylose concentration, estimates of K_{11a} and K_{11b} can be obtained. If $\Delta pKa' \neq 0$, then $K_{11a} \neq K_{11b}$; for carboxylic acids, $K_{11a} \geq K_{11b}$; for phenols, $K_{11b} \geq K_{11a}$. Because of variable pKa′ shifts, it is possible to carry out differentiating titrations of some acid mixtures in cycloamylose solutions, whereas the same acids cannot be differentiated in water. If an acid is weakened by cycloamylose, its conjugate base is strengthened, and some carboxylate salts can be readily titrated in the presence of a cycloamylose.

Keyphrases □ Cycloamyloses—effect on apparent dissociation constants of carboxylic acids and phenols, stability constants for complex formation □ Dissociation constants, apparent—carboxylic acids and phenols, effect of cycloamyloses, complex formation □ Carboxylic acids—apparent dissociation constants, effect of cycloamyloses □ Phenols—apparent dissociation constants, effect of cycloamyloses

Cycloamyloses (also called cyclodextrins or Schardinger dextrins) are cyclic oligomers containing six or more D-glucose units linked 1 → 4; they are produced by the action of *Bacillus macerans* amylase on starch. The six-unit and seven-unit substances are called cyclohexaamylose (α-cyclodextrin) and cycloheptaamylose (β-cyclodextrin), respectively. These molecules are doughnut shaped, and their possession of a cavity of fixed size and shape has led to considerable interest in their chemical properties. The production, purification, and chemistry of the cycloamyloses have been reviewed (1, 2). The catalytic properties of cycloamyloses, which have been widely studied as enzyme models, also have been discussed (3).

Any molecule smaller than the cavity of a cycloamylose molecule can enter the cavity and there undergo noncovalent interaction with the atoms lining and rimming the cavity. The resulting association product is called an inclusion compound or complex. The cycloamylose is thus a "host" for the smaller "guest" molecule. A 1:1 stoichiometry is typical, although other ratios have been observed and interpreted as the result of another guest molecule lying across the cavity opening. The dimensions of the cavity are such that many mono- and disubstituted benzene derivatives can fit into the cyclohexaamylose cavity, but polysubstituted benzenes may be excluded.

By forming an inclusion complex with a guest molecule, a cycloamylose is capable of altering some physical and chemical properties of the guest substance; it is by such changes that the complex formation is recognized and studied. Among the solution properties that can be modified are solubility, chemical reactivity, vapor pressure, and the electronic absorption spectrum. This capability for changing the chemical and physical behavior of solutes through complex formation may have analytical potential, and the present study examines the effects of cyclodextrins on the apparent dissociation constants of organic acids in aqueous solution.

It has been well established that many organic acids interact with the cycloamyloses (4–10), although little is known about the effects of complexing on acid dissociation equilibria. The potentiometric titration curve of monophenylphosphoric acid in the presence of cycloamylose reveals changes in pKa values, and even in the stoichiometric consumption of base, that require specific intermolecular interactions for their interpretation (2, 11). The pKa of

Table I—Apparent Dissociation Constants of Carboxylic Acids and Phenols in the Presence of 0.02 *M* Cyclohexaamylose[a]

Compound	pKa'	pKa	ΔpKa'
Acetic acid	4.83	4.76	+0.07
Propionic acid	5.16	4.97	+0.19
Monochloroacetic acid	3.30	3.20	+0.10
Maleic acid	3.40, 6.38	3.32, 6.23	+0.08, +0.15
Malonic acid	3.69, 5.92	3.60, 5.70	+0.09, +0.22
Benzoic acid	5.20	4.11	+1.09
Salicylic acid	3.63	3.40	+0.23
m-Hydroxybenzoic acid	4.95	4.10	+0.85
p-Hydroxybenzoic acid	5.83	4.58	+1.25
o-Methoxybenzoic acid	4.20	4.15	+0.05
m-Methoxybenzoic acid	5.13	4.18	+0.95
o-Nitrobenzoic acid	3.20	3.19	+0.01
m-Nitrobenzoic acid	3.83	3.60	+0.23
p-Nitrobenzoic acid	4.53	3.74	+0.79
p-Fluorobenzoic acid	4.98	4.18	+0.80
o-Phthalic acid	3.50, 5.34	3.40, 5.20	+0.10, +0.14
Nicotinic acid	4.85	4.85	0.00
Picolinic acid	5.33	5.31	+0.02
Gallic acid	4.53	4.20	+0.33
Cinnamic acid	5.80	4.43	+1.37
o-Hydroxycinnamic acid	5.82	4.69	+1.13
m-Hydroxycinnamic acid	5.64	4.49	+1.15
p-Hydroxycinnamic acid	5.88	4.40	+1.48
o-Methoxycinnamic acid	5.20	4.70	+0.50
m-Methoxycinnamic acid	5.76	4.47	+1.29
p-Methoxycinnamic acid	6.24	4.90	+1.34
Phenol	9.81	9.81	0.00
o-Nitrophenol	7.21	7.21	0.00
m-Nitrophenol	8.00	8.29	−0.29
p-Nitrophenol	6.15	7.09	−0.94
p-Bromophenol	9.20	9.20	0.00
1-Naphthol	9.20	9.20	0.00
2-Naphthol	9.30	9.40	−0.10

[a] At 25.0° in aqueous solution.

p-nitrophenol decreases by one unit upon its complexation with cyclohexaamylose (12).

In this study, the apparent dissociation constants of carboxylic acids and phenols in the presence of cycloamyloses were determined by potentiometric titration. This experimental approach has been elaborated into a systematic technique for studying molecular complexes of acids and bases.

EXPERIMENTAL

Materials—Organic acids were from commercial sources and were used directly or were recrystallized before use until a satisfactory melting point was obtained. Purities were established by potentiometric titration. α-Cyclodextrin[1] and β-cyclodextrin[2] were used directly. All water was freshly boiled, deionized, and distilled. Cyclodextrin concentrations are expressed on the anhydrous basis.

Potentiometric Titration—An aqueous solution was prepared to contain appropriate concentrations of the sample acid and cyclohexaamylose or cycloheptaamylose. A 25.0- or 50.0-ml portion of this solution was transferred to the titration vessel, a glass-jacketed beaker thermostated at 25°. Through a stopper on the beaker were passed an inlet tube for flushing the system with nitrogen, a combination glass–saturated calomel electrode[3], and a 5-ml buret graduated to 0.01 ml. Stirring was accomplished by magnetic stirrer.

Titration was with 0.07 or 0.1 *N* sodium hydroxide. The initial concentration of acid in the sample solution was in the 0.001–0.01 *N* range.

[1] Eastman Lot No. A4X (mp 262–265°) or Aldrich Lot No. 011747 (mp 260–264°).
[2] Lot No. 5022, Nutritional Biochemical Corp.
[3] Corning 476051; the pH meter was a Radiometer model 25SE.

Table II—Apparent Dissociation Constants of Acids in the Presence of 0.014 *M* Cycloheptaamylose[a]

Compound	pKa'	ΔpKa'
Benzoic acid	4.95	+0.84
o-Nitrobenzoic acid	3.33	+0.13
p-Nitrobenzoic acid	4.02	+0.28
o-Methoxybenzoic acid	4.48	+0.28
Salicylic acid	3.68	+0.28
Cinnamic acid	5.08	+0.65
o-Hydroxycinnamic acid	5.33	+0.58
o-Methoxycinnamic acid	5.48	+0.78
m-Methoxycinnamic acid	4.88	+0.41
p-Methoxycinnamic acid	5.29	+0.39
Potassium hydrogen phthalate	5.55	+0.17
p-Nitrophenol	6.70	−0.39
2-Naphthol	9.05	−0.35

[a] At 25.0° in aqueous solution.

pKa' Determination—The apparent acid dissociation constant, K_a', was determined using:

$$pKa' = pH - \log \frac{V}{V_{ep} - V} \quad \text{(Eq. 1)}$$

where V is the volume of titrant added, pH is the corresponding value of pH, and V_{ep} is the volume of titrant required to reach the end-point. Alternatively, pKa' was determined as the pH corresponding to the midpoint of the titration. The ionic strength changed during the titration but was never greater than 0.005 *M* at the titration midpoint.

RESULTS

Dissociation Constants—Equation 2 defines ΔpKa', the change in pKa value caused by incorporating a cycloamylose in the aqueous solution of the acid:

$$\Delta pKa' = pKa' - pKa \quad \text{(Eq. 2)}$$

where pKa' is the value observed in the presence of cycloamylose, and pKa is the corresponding value in the absence of cycloamylose. (Although pKa is itself an apparent constant rather than the thermodynamic constant in water, pKa' and pKa were determined under identical conditions except for the presence or absence of the cycloamylose.)

According to Eq. 2, positive and negative values of ΔpKa' correspond to a weakening or strengthening, respectively, of the acid by the cycloamylose. The term ΔpKa' is a function of cyclodextrin concentration; but for purposes of screening a large number of acids, ΔpKa' was measured at a fixed cycloamylose concentration. Table I shows these results for cyclohexaamylose. Several polyprotic acids with dissociation constants too similar to be readily resolved were not included in Table I; for these acids (citric, oxalic, 3-nitrophthalic, succinic, and terephthalic), the pH at half-neutralization indicated very small acid-weakening effects by cyclohexaamylose. This same quantity was about +0.5 for fumaric acid; 0.12 *M* dextrose had no effect on the pKa of cinnamic acid.

Table II shows some data for cycloheptaamylose.

The dependence of ΔpKa' on cycloamylose concentration was studied, and Fig. 1 shows the results for benzoic acid and *p*-nitrophenol. A quantitative interpretation of these curves is given in the *Discussion* section.

Potentiometric Titrations—Essentially no alkali was consumed by the cycloamyloses, and the accuracy and precision of potentiometric titration in the presence of a cycloamylose were comparable with those observed in its absence. For example, nine titrations of 0.115 mEq of benzoic acid in the presence of cyclohexaamylose gave a mean recovery of 99.9% with a standard deviation of 0.23%.

One interesting feature of the data in Tables I and II is the wide variation in ΔpKa' values, which do not seem to be simply related to pKa. This behavior suggested the possibility of carrying out certain differentiating titrations in the presence of cycloamylose, titrations that would be impossible or difficult in its absence. Although it is generally recognized that successful differentiating titrations of two acids can be made if the ratio of acid dissociation constants is at least 10^4 (13, 14), useful titrations are possible with

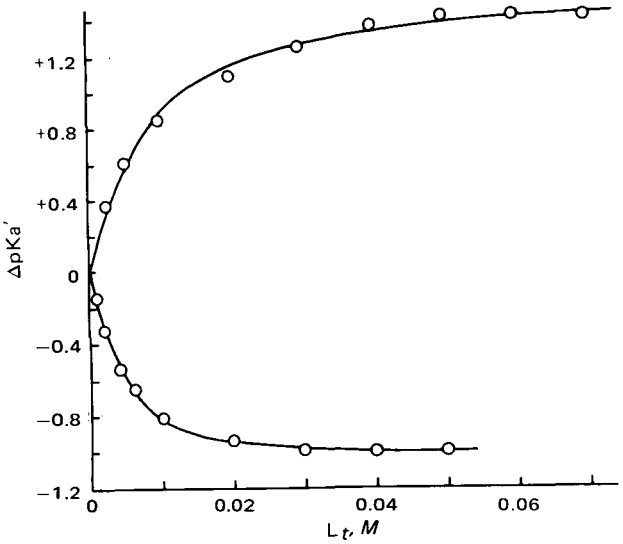

Figure 1—*Dependence of ΔpKa' on total cyclohexaamylose concentration (L_t) for benzoic acid (upper curve) and* p*-nitrophenol (lower curve). The lines were drawn with Eq. 10 as described under* Discussion. *The experimental points are at 25° and ionic strength 0.002* M.

much smaller ratios. The accuracy and precision depend upon the quality of the data and their treatment.

Many pairs of the acids included in Table I cannot be differentiated in aqueous solution; but in the presence of cyclohexaamylose, the resulting selective shifts of acid strength generate ratios of dissociation constants adequate for differentiating potentiometric titration. Table III shows some of these pairs of acids, none of which can be differentiated in water. In 0.02 *M* cyclohexaamylose, however, these pairs of acids can be quantitatively analyzed for both components by potentiometric titration. Figures 2 and 3 show some of these titrations.

These data suggest that effective differentiating titrations can be performed if the ratio of dissociation constants is about 10^2 (accuracy is also dependent upon the ratio of concentrations and individual strengths—the titration in Fig. 3 exemplifies a borderline case), and they demonstrate that this condition sometimes can be met simply by incorporating a cycloamylose in the titration mixture. From the data in Table I it is easy to predict which acids can be successfully differentiated by this means. Percent recoveries of the acids in Table III were within 1% of theory, except for mixtures of benzoic and salicylic acids in a 1:5 ratio. The precision is also satisfactory; five titrations of a mixture of 0.114 mEq of salicylic acid and 0.119 mEq of *p*-hydroxybenzoic acid gave standard deviations of 0.27% (salicylic) and 0.45% (*p*-hydroxybenzoic).

If the strength of an acid is decreased by treatment with cycloamylose, then the strength of its conjugate base should be increased since pKb = pKw − pKa. Therefore, the salts of some carboxylic acids were titrated potentiometrically with standard acid in the presence of cyclohexaamylose (Fig. 4). Evidently, the cyclohexaamylose treatment gives a simple and accurate analytical method for some carboxylate salts in aqueous solution. The pKa' values obtained by titration of the salt with hydrochloric acid were in agreement with those found from titration of the acid with sodium hydroxide.

DISCUSSION

ΔpKa and Complex Stability—The magnitudes and variability of pKa' shifts given in Tables I and II rule out a nonspecific medium effect, and it is instead assumed that molecular complex formation takes place between the substrate (acid) and ligand (cycloamylose). Let HA represent the unionized substrate and L the ligand. Suppose only 1:1 stoichiometry occurs; then the solution may contain the unionized and ionized forms of the substrate, and both of these species may be complexed with the ligand. Schemes I and II show the acid dissociation equilibria for the uncomplexed and complexed forms of HA, respectively, and Eqs. 3 and 4 give the corresponding dissociation constants:

Table III—Pairs of Acids Differentiated by Potentiometric Titration in 0.02 *M* Cyclohexaamylose

Acids	pKa Difference: In Water	pKa Difference: In 0.02 *M* Cyclohexaamylose
Cinnamic–chloroacetic	1.23	2.20
Benzoic–*o*-nitrobenzoic	0.92	2.00
Benzoic–salicylic	0.71	1.57
Salicylic–*p*-hydroxybenzoic	1.18	2.20
Cinnamic–*o*-nitrobenzoic	1.24	2.60
p-Nitrophenol–*m*-nitrophenol	1.20	1.85

$$HA \rightleftharpoons H^+ + A^-$$

Scheme I

$$HAL \rightleftharpoons H^+ + AL^-$$

Scheme II

$$K_a = \frac{[H^+][A^-]}{[HA]} \qquad \text{(Eq. 3)}$$

$$K_a{}^c = \frac{[H^+][AL^-]}{[HAL]} \qquad \text{(Eq. 4)}$$

The complexation equilibria and complex stability constants (K_{11a} and K_{11b} are 1:1 stability constants for the acid and anion, respectively) are as follows:

$$HA + L \rightleftharpoons HAL$$

Scheme III

$$K_{11a} = \frac{[HAL]}{[HA][L]} \qquad \text{(Eq. 5)}$$

$$A^- + L \rightleftharpoons AL^-$$

Scheme IV

$$K_{11b} = \frac{[AL^-]}{[A^-][L]} \qquad \text{(Eq. 6)}$$

These equations are easily combined to give:

$$\frac{K_a}{K_a{}^c} = \frac{K_{11a}}{K_{11b}} \qquad \text{(Eq. 7)}$$

which shows that only three of the four constants can be independent. Cramer *et al.* (12) verified Eq. 7 for the *p*-nitrophenol–cyclohexaamylose system.

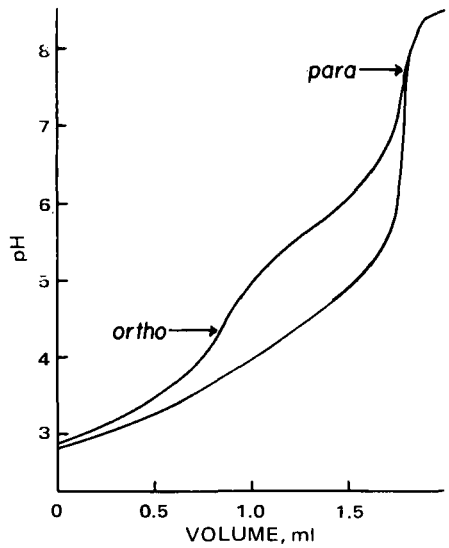

Figure 2—*Potentiometric titration of a mixture of 14.0 mg of salicylic acid and 13.8 mg of* p*-hydroxybenzoic acid with 0.1131* N *NaOH. Key: lower line, in water; and upper line, in 0.02* M *cyclohexaamylose. Arrows indicate end-points in the differentiating titration.*

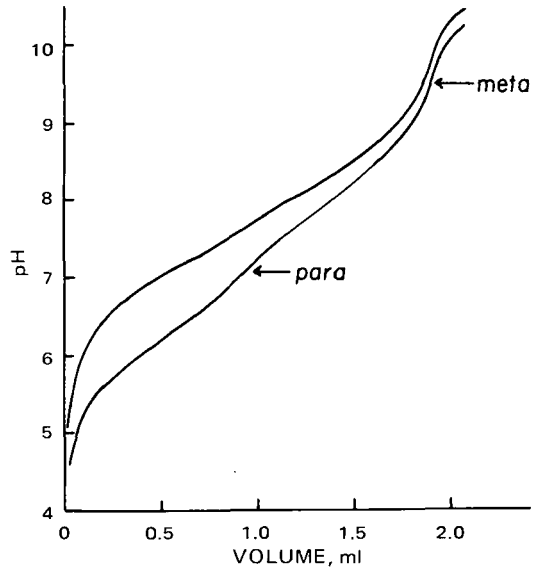

Figure 3—*Potentiometric titration of 15.2 mg of* p-*nitrophenol and 14.5 mg of* m-*nitrophenol with 0.1131* N *NaOH. Key: upper line, in water; and lower line, in 0.02* M *cyclohexaamylose. Arrows indicate end-points in the differentiating titration.*

In the present study, an apparent constant K_a' was measured. This constant is not identical with K_a^c, since in the potentiometric measurements the substrate is present in both the free and complexed forms. It is necessary to find the relationship between K_a' and the ligand concentration. The apparent acid dissociation constant can be defined by:

$$K_a' = \frac{[H^+]([A^-] + [AL^-])}{[HA] + [HAL]} \quad \text{(Eq. 8)}$$

Then, substitution from Eqs. 3, 5, and 6 gives:

$$K_a' = K_a \frac{(1 + K_{11b}[L])}{(1 + K_{11a}[L])} \quad \text{(Eq. 9)}$$

which may also be written:

$$\Delta pKa' = \log \frac{(1 + K_{11a}[L])}{(1 + K_{11b}[L])} \quad \text{(Eq. 10)}$$

In the limit as the ligand concentration becomes very large, Eq. 9 approaches Eq. 7. The observation of a ΔpKa' value significantly different from zero implies that $K_{11a} \neq K_{11b}$.

To estimate stability constants with the aid of Eq. 10, it is necessary to know [L], the free ligand concentration. Let L_t and A_t be the total (formal) molar concentrations of ligand and acid, respectively; then these mass balance equations can be written:

$$L_t = [L] + [HAL] + [AL^-] \quad \text{(Eq. 11)}$$

$$A_t = [HA] + [A^-] + [HAL] + [AL^-] \quad \text{(Eq. 12)}$$

If $L_t >>> A_t$, as in many complexing studies, it may be acceptable to set $[L] \approx L_t$. This was not possible in the present study, however, since A_t was in the 0.001–0.01 *M* range and L_t was 0.001–0.07 *M*. Expanding Eqs. 11 and 12 with the aid of the equilibrium constants defined earlier gives:

$$L_t = [L] + K_{11a}[HA][L] + K_aK_{11b}[HA][L]/[H^+] \quad \text{(Eq. 13)}$$

$$A_t = [HA] + K_a[HA]/[H^+] + K_{11a}[HA][L] + K_aK_{11b}[HA][L]/[H^+] \quad \text{(Eq. 14)}$$

Since $K_{11a} \neq K_{11b}$ and an increasing fraction of the substrate is in the anion form as titration proceeds, the effective stability constant[4] varies throughout the titration and [L] varies according to these equations. Therefore, from Eq. 9, pKa' must vary.

Experimentally, it is found that pKa', evaluated with Eq. 1 in the buffer region of the titration, does vary but not markedly (0.05 unit or less while the pH changes more than 0.5 unit; part of this variation is an activity coefficient effect). Therefore, it is necessary

[4] The effective stability constant can be defined as $K_{11a}f_a + K_{11b}f_b$, where f_a and f_b are the fractions of uncomplexed substrate in the acid and anion forms, respectively.

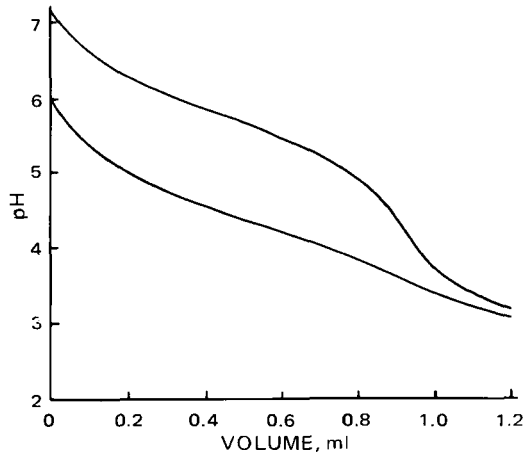

Figure 4—*Potentiometric titration of 0.0675 mEq of sodium cinnamate with 0.0722* N *HCl. Key: lower line, in water; and upper line, in 0.02* M *cyclohexaamylose.*

to choose a value of $[H^+]$ for the solution of Eqs. 13 and 14; the reasonable value of $[H^+] = K_a'$ was selected. The experimental observations were made at this condition, *i.e.*, the titration midpoint. With this condition, Eqs. 9, 13, and 14 are combined to yield:

$$L_t = [L]\left\{1 + \frac{K_{11}A_t}{1 + C + K_{11}[L]}\right\} \quad \text{(Eq. 15)}$$

where:

$$K_{11} = K_{11a} + K_{11b}C \quad \text{(Eq. 16)}$$

and:

$$C = \frac{1 + K_{11a}[L]}{1 + K_{11b}[L]} \quad \text{(Eq. 17)}$$

The procedure is to assign a reasonable value to [L] and, with preliminary estimates of K_{11a} and K_{11b}, to calculate L_t using Eq. 15. The corresponding value of ΔpKa' is then calculated with the relation $\Delta pKa' = \log C$. This procedure is repeated with additional values of [L] until the entire experimental range of L_t is covered. The experimental data points then can be compared with the calculated curve. The constants K_{11a} and K_{11b} are treated as adjustable parameters, and the calculation is continued until a reasonable agreement is achieved.

Preliminary estimates of K_{11a} and K_{11b} can be obtained from the data. From Eq. 10, the limiting value of ΔpKa' at large L_t is log (K_{11a}/K_{11b}); the ratio K_{11a}/K_{11b} estimated in this way is a minimum value (if $K_{11a} > K_{11b}$) or a maximum value (if $K_{11b} > K_{11a}$). Estimates of the individual constants can be made as follows. Equation 9 can be written:

$$\frac{K_a'}{K_a} = 1 + \frac{(K_{11b} - K_{11a})[L]}{1 + K_{11a}[L]} \quad \text{(Eq. 18)}$$

which can be rearranged into several forms suitable for linear plotting. Equation 19 shows the common "double reciprocal" (Benesi–Hildebrand or Lineweaver–Burk) form:

$$\frac{K_a}{K_a' - K_a} = \frac{1}{[L](K_{11b} - K_{11a})} + \frac{K_{11a}}{(K_{11b} - K_{11a})} \quad \text{(Eq. 19)}$$

The free concentration [L] is not known but may be approximated by $(L_t - A_t)$. From a plot of $K_a/(K_a' - K_a)$ against $1/(L_t - A_t)$, the constants are evaluated for use in the calculation as described. (If $K_{11a} > K_{11b}$, a similar form of Eq. 19 is used.)

Figure 1 shows the dependence of ΔpKa' on cyclohexaamylose concentration for benzoic acid and *p*-nitrophenol. The solid curves were calculated as already described. Evidently, Eq. 10 gives a quantitative description of the *p*-nitrophenol system. Agreement between the calculated curve and the experimental points is fair for the benzoic acid system. For the *p*-nitrophenol–cyclohexaamylose system, these constants are found: $K_{11a} = 200\ M^{-1}$ and $K_{11b} = 2200\ M^{-1}$ at 25°. These values can be compared with the values $K_{11a} = 290\ M^{-1}$ and $K_{11b} = 2230\ M^{-1}$ found spectrophotometrically by Cramer *et al.* (12) (calculated for 25° from the data of Cramer *et al.*, these are at ionic strength 0.5 *M*). The benzoic acid curve yields the constants $K_{11a} = 1400\ M^{-1}$ and $K_{11b} = 38\ M^{-1}$.

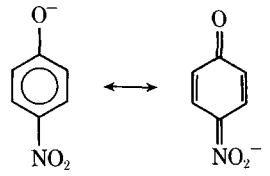

Scheme V

Casu and Rava (9) found $K_{11a} = 1050\ M^{-1}$ for benzoic acid in 0.08 *N* HCl using a spectrophotometric technique.

The potentiometric method described here appears to be a valuable technique that has not heretofore been applied to the study of organic molecular complexes. It is, of course, equivalent to the classical potentiometric method for studying complexes of metal ions with weak bases (15, 16). The data treatment suggested here, in terms of apparent dissociation constants, is different from, and rather simpler than, a treatment using the conventional Bjerrum formation function. The extension of this method to systems containing complexes of higher orders is easy in principle, but much more experimental work will be necessary to establish the practical value of the technique to these complicated systems.

Complex Stability and Interactant Structure—One striking feature of the data in Tables I and II is the relationship of ΔpKa′ to molecular structure. For several aromatic acids, ΔpKa′ seems to be determined mainly by the location of a substituent group rather than by its identity. Such effects are often observed with cycloamyloses, and they have been widely interpreted in terms of inclusion complex formation, with the stability of the complex being determined in part by the spatial compatibility of the guest molecule and the cycloamylose cavity. Of course, ΔpKa′ is not a simple measure of complex stability (see Eq. 10), and its dependence upon both K_{11a} and K_{11b} introduces another possibility for dispersion within a series.

Another notable characteristic of these data is that, for substances showing a nonzero value of ΔpKa′, carboxylic acids have positive ΔpKa′ values and phenols have negative values. That is, for carboxylic acids, $K_{11a} > K_{11b}$ (the acid complexes more strongly than does the anion); for phenols, $K_{11b} > K_{11a}$. Even if this generalization should be found to have exceptions, the observation is sufficiently arresting in individual examples to invite discussion.

For example, *p*-nitrobenzoic acid (ΔpKa′ = +0.79 at 0.02 *M* cyclohexaamylose) can be compared with *p*-nitrophenol (ΔpKa′ = −0.94). The result for the phenol is the unexpected one; it is unusual for an anion to complex (with a common neutral ligand in aqueous solution) more strongly than the uncharged species. Viewed another way, the *p*-nitrophenolate ion "partitions" into the cycloamylose cavity to a greater extent than does *p*-nitrophenol, in contrast with the reverse situation for the benzoic acid. The extensive charge delocalization in the *p*-nitrophenol anion possibly is responsible for this behavior (Scheme V).

The carboxylic acid anion is incapable of this type of charge distribution and may be more strongly solvated than is the phenolate. *p*-Nitrophenol itself is a good hydrogen-bond donor, and its affinity for the solvent may destabilize its complex with the cycloamylose.

If ΔpKa′ at a fixed ligand concentration is taken as a rough measure of complex stability, the comparative data of Tables I and II for cycloheptaamylose and cyclohexaamylose seem qualitatively reasonable. The cavity of cycloheptaamylose has a larger diameter than that of cyclohexaamylose, which will lead to stronger complexes with substrates (such as some 1,2-disubstituted aromatics and naphthols) too large to fit the cyclohexaamylose cavity and to weaker complexes with substrates (monosubstituted, 1,3- and 1,4-disubstituted aromatics) that fit snugly into the cyclohexaamylose cavity.

Analytical Applications—These applications fall into two classes:

1. Potentiometric titration of aqueous solutions of substances whose apparent acid or base strength is increased by the addition of a cycloamylose. Some phenols show an increase in acidity, and some carboxylate salts become stronger bases. These applications may be quite practical, because the analysis of dilute aqueous solutions of these substances can be difficult. A sample concentration range of 0.001–0.01 *M* is suitable, and the substances for which useful effects can be expected are shown or suggested by the data in Tables I and II.

2. Differentiating potentiometric titration of mixtures of acids, with the addition of a cycloamylose being the means of "tuning" the pKa′ values of the mixture to optimize the selectivity. The equilibrium selectivity of a process can be defined as log (K_2/K_1) or $pK_1 - pK_2$ (17). This value should be 2 or greater for titrations of acids in aqueous solution, and addition of a cycloamylose has been shown capable of producing this selectivity.

Other uses can be expected for these effects. For example, the effective buffer ranges of acids are shifted in the presence of cycloamyloses. The pKa′ shifts could be useful for separating acids in aqueous chromatographic systems, as in ion exchange.

REFERENCES

(1) D. French, *Advan. Carbohyd. Chem.*, **12**, 189(1957).

(2) J. A. Thoma and L. Stewart, in "Starch: Chemistry and Technology," vol. I, R. L. Whistler and E. F. Paschall, Eds., Academic, New York, N.Y., 1965, p. 209.

(3) D. W. Griffiths and M. L. Bender, *Advan. Catal. Relat. Subj.*, **23**, 209(1973).

(4) H. Schlenk and D. M. Sand, *J. Amer. Chem. Soc.*, **83**, 2312(1961).

(5) J. Cohen and J. L. Lach, *J. Pharm. Sci.*, **52**, 132(1963).

(6) J. L. Lach and J. Cohen, *ibid.*, **52**, 137(1963).

(7) J. L. Lach and T.-F. Chin, *ibid.*, **53**, 69(1964).

(8) W. A. Pauli and J. L. Lach, *ibid.*, **54**, 1745(1965).

(9) B. Casu and L. Rava, *Ric. Sci.*, **36**, 733(1966).

(10) S. Takenaka, N. Matsuura, and N. Tokura, *Tetrahedron Lett.*, **1974**, 2325.

(11) F. Cramer, *Angew. Chem.*, **73**, 49(1961).

(12) F. Cramer, W. Saenger, and H.-C. Spatz, *J. Amer. Chem. Soc.*, **89**, 14(1967).

(13) S. Bruckenstein and I. M. Kolthoff, in "Treatise on Analytical Chemistry," part I, vol. I, I. M. Kolthoff and P. J. Elving, Eds., Interscience, New York, N.Y., 1959, p. 470.

(14) J. S. Fritz and G. H. Schenk, Jr., "Quantitative Analytical Chemistry," 2nd ed., Allyn and Bacon, Boston, Mass., 1969, p. 174.

(15) M. M. Jones, "Elementary Coordination Chemistry," Prentice-Hall, Englewood Cliffs, N.J., 1964, chap. 8.

(16) M. T. Beck, "Chemistry of Complex Equilibria," Van Nostrand Reinhold, London, England, 1970.

(17) K. A. Connors, "Reaction Mechanisms in Organic Analytical Chemistry," Wiley–Interscience, New York, N.Y., 1973, p. 178.

ACKNOWLEDGMENTS AND ADDRESSES

Received February 24, 1975, from the *School of Pharmacy, University of Wisconsin, Madison, WI 53706*

Accepted for publication June 3, 1975.

Supported by National Science Foundation Grant GP-36567.

[x] To whom inquiries should be directed.

5′-Nucleotide Phosphodiesterase Activity of Floxuridine-Resistant Mouse Glioma

ELIZABETH E. MILLER ˣ, STEPHEN L. LEDIS, K. W. LO, and K. C. TSOU

Abstract □ In tissue culture experiments, cells derived from glioma 26, a transplantable tumor of C57B1/6 mice, were sensitive to both floxuridine (5-fluorodeoxyuridine) and 5-fluorodeoxyuridine-5′-(5-iodo-3-indolyl) phosphate, an enzyme-mediated drug activated by 5′-nucleotide phosphodiesterase. When these compounds were tested on the tumor in the animals at a level of 5 mg/kg for 5 days, tumor growth was inhibited approximately 20% by both compounds. When higher levels of 5-fluorodeoxyuridine, 100 mg/kg four times weekly throughout the lifespan of the mouse, were given, the tumor, although inhibited at first, developed resistance and continued to grow until it killed the animal. Phosphodiesterase levels in the tumor rose as the tumor grew. On the other hand, thymidine kinase levels dropped, as anticipated from the known 5-fluorodeoxyuridine-resistant hepatoma tissue culture data. This enzyme pattern was maintained in transplantable mouse glioma lines established from the resistant tumors. One of these lines, tested at a level of 5 mg/kg for 5 days, showed no response to 5-fluorodeoxyuridine but was still sensitive to 5-fluorodeoxyuridine-5′-(5-iodo-3-indolyl) phosphate. These experiments, therefore, offer a model system and a rationale for the design and study of more compounds that could be activated by the enzyme phosphodiesterase. Such compounds might be used alternatively when resistance to 5-fluorodeoxyuridine develops, a common clinical experience in the use of this anticancer drug.

Keyphrases □ 5′-Nucleotide phosphodiesterase—activation of antitumor compounds, mice □ 5-Fluorodeoxyuridine-5′-(5-iodo-3-indolyl) phosphate—role of 5′-nucleotide phosphodiesterase in antitumor activity, mice □ Floxuridine—role of 5′-nucleotide phosphodiesterase in antitumor activity, mice □ Antitumor drugs—floxuridine and 5-fluorodeoxyuridine-5′-(5-iodo-3-indolyl) phosphate, role of 5′-nucleotide phosphodiesterase in antitumor activity, mice

An interest in the 5′-(5-iodo-3-indolyl) phosphodiester of floxuridine (5-fluorodeoxyuridine) (1, 2) as an enzyme-mediated drug led to the investigation of the 5′-nucleotide phosphodiesterase level of glioma 26, a tumor that showed sensitivity to this compound as well as 5-fluorodeoxyuridine[1]. In addition, the enzyme changes in the same tumor as it became resistant to treatment with 5-fluorodeoxyuridine were investigated.

Umeda and Heidelberger (3) found that Novikoff hepatoma cells, grown in tissue culture, that are resistant to 5-fluorodeoxyuridine have a low thymidine kinase activity. This finding suggested that if the 5′-nucleotide phosphodiesterase level could be maintained in such resistant tumors, the use of phosphodiesters of 5-fluorodeoxyuridine would provide a biochemical rationale for cancer chemotherapy of 5-fluorodeoxyuridine-resistant tumors. In other words, 5-fluorodeoxyuridine 5′-phosphate, the active intermediate (4), could be obtained through a different enzyme activation process.

The present work describes the phosphodiesterase and thymidine kinase activities of the mouse glioma tissue before, during, and after treatment with high levels of 5-fluorodeoxyuridine.

EXPERIMENTAL

Tumors and Animals—The mouse tumor, glioma 26, was originally obtained in the frozen state from the National Cancer Institute tumor bank. It is now maintained in C57B1/6 mice by sterile trocar transplant.

Tissue Cultures—A tissue culture line from glioma 26 was adapted to grow from minced tumor fragments in Eagles Minimal Essential Medium with Hanks base and 10% calf serum. Calf serum was heat inactivated 2–24 hr at 56° if phosphodiesterase was found to be present. When the cell line was established, the comparative cytotoxicity of the drugs on the glioma cells was tested by the method of Umeda and Heidelberger (3).

Due to clumping of the cells, growth was determined by protein determinations instead of cell counts. The assays were carried out in Leighton tubes initially seeded with approximately 60,000 cells/ml of the medium. After incubation for 24 hr at 37° to allow cells to attach to the glass, drug dilutions were added and incubation was continued for 3 days. Cells were then prepared for protein determination by the Lowry *et al.* (5) method by pouring off the growth medium and rinsing the cells three times with 4.0 ml of 0.9% NaCl while they were still attached to the glass surface of the Leighton tube.

The cells were dissolved by adding 5.0 ml of the alkaline reagent used in the protein determination and allowing them to stand for 20–40 min. One milliliter of 0.9% NaCl was added to adjust the volume to that of the protein standard, and the color was developed by adding the phenol reagent directly to the Leighton tubes. In periods of maximum growth, when the amount of color developed exceeded the range of the colorimeter, aliquots were removed and treated like those used for the protein standard. In this way, the effect of clumping was minimized since the entire sample or a large portion of it was represented in the assay, rather than only the small drop from it used on the counting chamber.

The protein value for Day 0 was determined by centrifuging the cells from 4.0 ml of the cell suspension used for preparing the Leighton tubes, washing three times with 0.9% NaCl, dissolving the cell pellet, and making the protein determination as already described. Analyses were always carried out in duplicate, and the reliability of the method is indicated by the high reproducibility obtained for analyses on the duplicate Leighton culture tubes. The average deviation from the mean calculated from 19 pairs of control cultures (untreated with drug) was only 4%. In drug-treated culture tubes when cell growth was inhibited 0–60% by the drug, the average deviation also was only 4%. But when growth inhibition was greater than 60%, the average deviation was 10% (calculated from 132 pairs of drug-treated culture tubes).

Compounds and Methods of Administration—The synthesis of 5-fluorodeoxyuridine-5′-(5-iodo-3-indolyl) phosphate (I) and 5-fluorodeoxyuridine-3′-(5-iodo-3-indolyl) phosphate (II) was reported previously (1, 2). The effect of these drugs was tested on the tumor in the mice according to the following procedure. Twenty-seven mice were injected intraperitoneally with 20 mg/kg of 5-fluorodeoxyuridine, I, II, or 0.9% NaCl, starting on the day after tumor transplantation. Tumor size was calculated from measurements of the length, width, and depth of each tumor at weekly intervals made with centimeter calipers.

In efforts to produce a 5-fluorodeoxyuridine-resistant glioma line, preliminary experiments were carried out to find how much drug could be given without obtaining toxic deaths. Based on these experiments, a level of 100 mg/kg given four times weekly through-

[1] FUdR, Hoffmann-La Roche, Inc., Nutley, N.J.

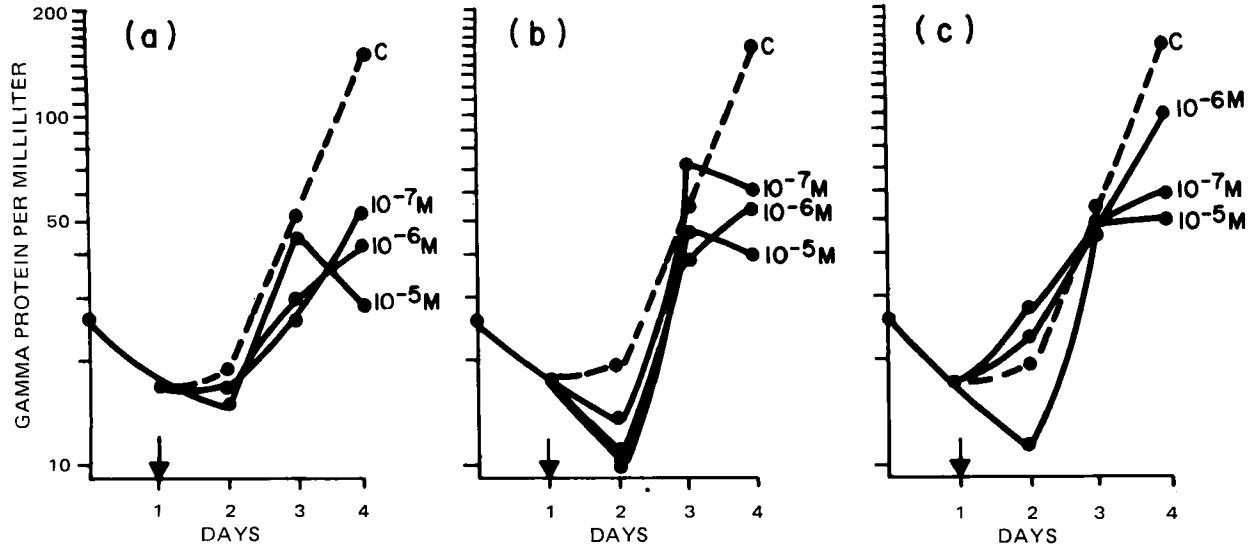

Figure 1—*Effect of 5-fluorodeoxyuridine* (a), *I* (b), *and II* (c) *at* 10^{-5}, 10^{-6}, *and* 10^{-7} M *concentrations on the growth of tissue-cultured mouse glioma cells compared with control cell growth* (*C*). *Compounds were added on Day 1* (↓).

out the tumor growth period was chosen. To study tumor enzyme levels, 37 glioma-bearing mice were treated in this manner. Mice were sacrificed at appropriate intervals to obtain tumor tissue for enzyme assays.

Extraction—The excised tumor tissue was minced, weighed, and frozen immediately in dry ice and alcohol and stored in the frozen state. Extracts from the thawed tissue were made in 0.25 *M* sucrose with a glass homogenizer in an ice bath. Samples of tissue weighing 0.5–1.0 g were extracted with 2 volumes of 0.25 *M* sucrose solution and centrifuged for 10 min at 2000 rpm. The protein concentration was determined by the Lowry *et al.* (5) method.

Enzyme Assays—5′-Nucleotide phosphodiesterase determinations were made by a previously reported method (6) using the fluorogenic substrate thymidine-5′-(4-methylumbelliferyl) phosphate[2].

Thymidine kinase was measured by a paper chromatographic method using the incubation conditions described by Breitman (7). The reaction mixture consisted of 2.0 μmoles of adenosine triphosphate, 2.0 μmoles of magnesium chloride, 0.04 μmole of thymidine, 2.5 μmoles of 3-phosphoglycerate, 33.75 μmoles of tromethamine buffer (pH 8.0), and 50.0 μl of tumor tissue extract in a total volume of 0.25 ml. Reactions were carried out in 2.0-ml screw-capped vials at 37° and were quenched at regular time intervals by placing the vials in a boiling water bath for 2 min.

Each entire reaction mixture was applied to Whatman No. 1 paper in a horizontal band 4.0 cm long and developed with ethanol–1 *M* CH_3COONH_4 (7:3, v/v). This solvent is commonly used in nucleoside and nucleotide separations (8). Several reactions could be chromatographed on each paper sheet. The thymidine bands were cleanly separated from the thymidylate bands by this method. The thymidine bands (higher R_f) were visualized by a short wavelength UV illumination and outlined in pencil. A blank solution consisted of the reaction mixture without the cell extract. The thymidine bands were cut out and quantitatively eluted with 2.0 ml of water.

The absorbances of the eluates were measured[3] at 267 nm (A_{267}). To correct for the small amount of UV-absorbing material in the paper, the absorbances at 300 nm (A_{300}) were also measured. Thus, the true absorbance due to thymidine is $A_{267} - A_{300}$ and the percent conversion can easily be calculated from:

$$\%\ \text{conversion at 10 min} = \left[1 - \frac{(A_{267} - A_{300})}{(A_{267} - A_{300})_{\text{blank}}}\right] \times 100 \quad \text{(Eq. 1)}$$

Because of interference by other enzymes, such as alkaline phosphatase and 5′-nucleotidase, the percent conversion deviated from linearity at about 20 min after incubation. Accordingly, the percent conversion at 10 min per milligram of protein in the extract was taken as the apparent activity of thymidine kinase. This useful and practical method can be done without radioactive thymidine, and it gives a comparative value of the activity of the different extracts.

[2] Fluorescence was measured in a Turner model 111 fluorometer.
[3] Beckman DB-G spectrophotometer.

RESULTS AND DISCUSSION

As shown in Fig. 1, when tested in the tissue culture system, the 5′-(5-iodo-3-indolyl) phosphodiester (I) was found to be more cytotoxic than the 3′-phosphodiester (II) and its activity was comparable to that of 5-fluorodeoxyuridine. In addition, the activity of I on the glioma cells was higher than in other tissue culture systems previously tested (1, 2).

Results obtained with the glioma cells in tissue culture indicated that it would be interesting to test these compounds in mice bearing the glioma. Again, the growth inhibitory effects of I and 5-fluorodeoxyuridine were comparable, a maximum of 20% of control tumor size, and II had little effect. The average survival time was 55 days for 5-fluorodeoxyuridine-treated mice and 58 days for I-treated mice, compared to 44 days for controls. Since clinically 5-fluorodeoxyuridine had been of limited use for human glioma, the mouse data indicated that further study was necessary.

In preliminary efforts to produce a resistant glioma line, low levels of 5-fluorodeoxyuridine were not effective. In studying the toxic effects of higher doses, it was found that 100 mg/kg could be given to normal mice for long periods if administered intermittently. In glioma-bearing mice treated with 100 mg/kg four times weekly, tumor growth was markedly inhibited at first. Under continued treatment, however, the tumor grew progressively until it killed the animals, presumably due to the development of drug resistance.

The phosphodiesterase and thymidine kinase concentrations of tumor tissue during treatment of the glioma with 5-fluorodeoxyuridine are shown in Fig. 2. The drug was administered as indicated by the arrows at the bottom of the chart, 100 mg/kg four times

Table I—Thymidine Kinase Activity of 5-Fluorodeoxyuridine-Resistant Mouse Glioma Tumor Lines

Tumor Line	Thymidine Kinase Activity[a] Experiment 1	Experiment 2
Resistant A	31	26
Resistant B	36	10
Resistant C	21	26
Original	110	97

[a] Percent conversion at 10 min per milligram of protein.

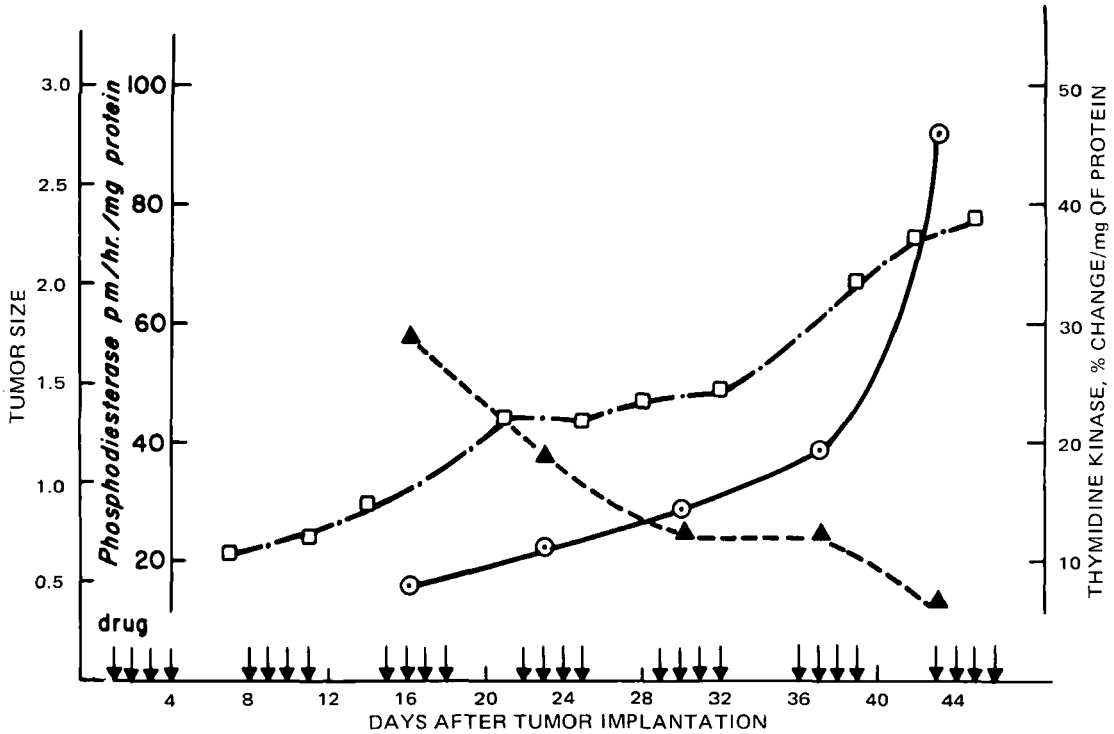

Figure 2—*Phosphodiesterase and thymidine kinase concentrations of glioma tumor tissue from mice during treatment with 5-fluorodeoxyuridine. Key: ⊙, phosphodiesterase; ▲, thymidine kinase; □, tumor growth; and ↓, drug administered intraperitoneally at 100 mg/kg/day.*

weekly. Phosphodiesterase activities and thymidine kinase activities were calculated in terms of milligrams of protein in the extracts. The progressive growth of the tumor is shown by the increase in tumor size plotted against time in days. The phosphodiesterase concentration in the tumor tissue rose as the tumor grew, while the thymidine kinase activity decreased on continued treatment with 5-fluorodeoxyuridine. The decrease in thymidine kinase is an indication of development of resistance to 5-fluorodeoxyuridine, while the maintenance of high levels of phosphodiesterase activity suggests that compounds whose action is mediated by this enzyme would still be effective in these resistant tumors.

In some of these mice receiving high levels of 5-fluorodeoxyuridine, the tumor tended to become very fluid. The fluid accumulated under the skin, and the head became very puffy. This fluid contained tumor cells and produced tumors when injected into mice. Histologically, the original and 5-fluorodeoxyuridine-resistant tumors looked different, the latter tumors tending to have more mitotic figures and a slightly more malignant appearance.

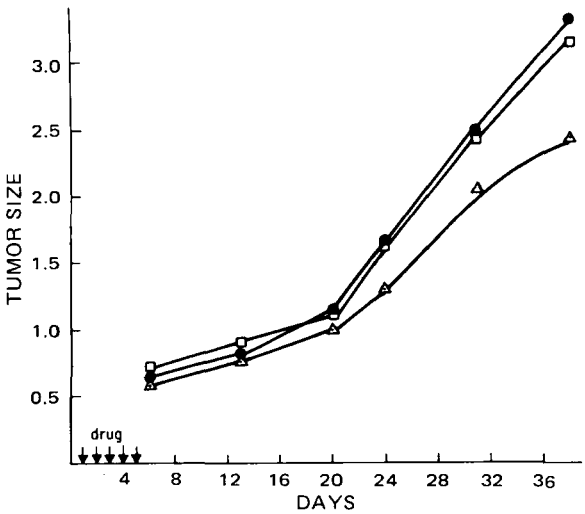

Figure 3—*Effect of 5-fluorodeoxyuridine and I on the 5-fluorodeoxyuridine-resistant glioma tumor line C in mice. Key: ●, control mice injected with 0.9% NaCl; □, mice injected with 5-fluorodeoxyuridine; △, mice injected with I; and ↓, drug administered intraperitoneally at 20 mg/kg or molar equivalent per day. Each point on the curves represents the average measurement of tumor size in six or seven mice.*

Several times during this experiment, animals were killed to obtain tissue for enzyme analysis. New transplants were made in other mice, and three of these tumor lines (A, B, and C) are now carried by transplanting from mouse to mouse at 3–4-week intervals. These lines are maintained with 5-fluorodeoxyuridine; after the tumor is transplanted, each mouse receives three or four weekly injections of 5-fluorodeoxyuridine, 100 mg/kg ip.

After the tumors had been transplanted several times, the enzyme determinations were again made on the tumor tissue taken from mice killed 20–30 days after tumor transplantation, corresponding in time to the midarea in Fig. 2. Table I shows values for thymidine kinase made on the three lines taken from two different transplant generations. Again, low values were obtained compared to those of the original tumors. Table II shows phosphodiesterase values obtained from the same tumor tissue extracts, indicating that the phosphodiesterase concentration was maintained at a level corresponding to that in the original tumor and did not drop under continued influence of high levels of 5-fluorodeoxyuridine.

One resistant glioma line was tested under the conditions used previously with the sensitive glioma line; the compounds were in-

Table II—Phosphodiesterase Activity of 5-Fluorodeoxyuridine-Resistant Mouse Glioma Lines

Tumor Line	Phosphodiesterase Activity[a] Experiment 1	Experiment 2
Resistant A	28.4	28.3
Resistant B	24.2	34.1
Resistant C	22.2	58.1
Original	34.0	28.6

[a] Picomoles per hour per milligram of protein.

jected intraperitoneally for 5 days, starting on the 1st day after tumor transplantation (Fig. 3). On this resistant line, 5-fluorodeoxyuridine had no effect at this level while I still inhibited tumor growth. Obviously, the effects of other nucleoside phosphodiesters whose action also would be aided by high levels of phosphodiesterase in these resistant tumors should be studied.

REFERENCES

(1) K. C. Tsou, S. Aoyagi, and E. E. Miller, *J. Med. Chem.*, **13**, 765(1970).

(2) K. C. Tsou, K. W. Lo, S. L. Ledis, and E. E. Miller, *ibid.*, **15**, 1221(1972).

(3) M. Umeda and C. Heidelberger, *Cancer Res.*, **28**, 2529(1968).

(4) S. S. Cohen, J. G. Flaks, H. D. Barner, M. R. Loeb, and J. Lichtenstein, *Proc. Nat. Acad. Sci. USA*, **44**, 1004(1958).

(5) O. H. Lowry, N. J. Rosebrough, A. L. Farr, and R. J. Randall, *J. Biol. Chem.*, **193**, 265(1951).

(6) K. W. Lo, W. Ferrar, W. Fineman, and K. C. Tsou, *Anal. Biochem.*, **47**, 609(1972).

(7) T. R. Breitman, *Biochim. Biophys. Acta*, **67**, 153(1963).

(8) A. C. Palidini and L. F. Leloir, *Biochem. J.*, **51**, 426(1952).

ACKNOWLEDGMENTS AND ADDRESSES

Received May 4, 1973, from the *Harrison Department of Surgical Research, School of Medicine, University of Pennsylvania, Philadelphia, PA 19174*

Accepted for publication June 3, 1975.

Supported by American Cancer Society Grant CI-91A and National Institutes of Health Grant Ca 07339 (to K. C. Tsou).

The authors thank Mr. W. Ferrar for assistance with this work.

[x] To whom inquiries should be directed.

GLC Determination of Plasma Concentrations of Phenprocoumon

K. K. MIDHA [*x], J. W. HUBBARD [‡], J. K. COOPER [*], and I. J. McGILVERAY [*]

Abstract □ A GLC method for the quantitative estimation of phenprocoumon from plasma is described. Plasma containing phenprocoumon, to which a known amount of phenytoin is added as the internal standard, is acidified and extracted with ethylene dichloride. The drug and the internal standard are then back-extracted into alkali, which is acidified and reextracted with ethylene dichloride. The organic extract is evaporated, and the evaporated residue is mixed with 50 μl of trimethylanilinium hydroxide in methanol. Aliquots (1–2 μl) are injected into a gas chromatograph equipped with a flame-ionization detector in which the injection port is held at 325°. The methyl derivatives of phenprocoumon and the internal standard give sharp, well-separated, symmetrical peaks. The method is of sufficient sensitivity to determine 0.125 μg/ml of the drug in plasma with a coefficient of variation of 7%.

Keyphrases □ Phenprocoumon—GLC determination from human plasma, phenytoin as internal standard □ GLC—analysis, phenprocoumon in plasma, phenytoin as internal standard

Phenprocoumon (I) is an orally administered anticoagulant with action and uses similar to those of phenindione (1). Phenprocoumon is structurally related to warfarin; both are oral coumarin anticoagulants. Several analytical procedures (2–8) were described for the estimation of warfarin and its metabolites from biological fluids, but only one fluorometric method (9) was reported for phenprocoumon. The latter is subject to interference from plasma constituents at low values and from any metabolites present.

The GLC behavior of several coumarin anticoagulants including phenprocoumon, as well as their trimethylsilyl ethers, acetates, trichloroacetates, and trifluoroacetates, was reported (10, 11). These results suggest that derivatization of coumarin drugs might be useful for measuring their concentrations in biological fluids. To facilitate study of the pharmacokinetics and potential interactions with other drugs

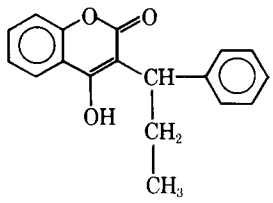

I

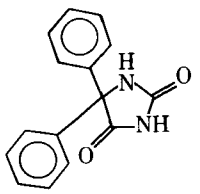

II

after single- and multiple-dose oral administration of phenprocoumon, a sensitive and specific GLC procedure was developed for the measurement of intact drug in plasma.

EXPERIMENTAL

Reagents—Ethylene dichloride[1] and ether[2] were glass distilled prior to use. Stock solutions containing 100 μg/ml of phenprocoumon[3] were prepared daily in 0.1 *N* NaOH and stored in the dark in a refrigerator. Appropriate dilutions (0.125–4.00 μg/ml) were made immediately before use. Aqueous solutions containing 100 μg/ml of the internal standard, phenytoin[4] (II), were prepared weekly by

[1] Caledon Laboratories Ltd., Georgetown, Ontario, Canada.
[2] Mallinckrodt Chemical Works Ltd., Montréal, Québec, Canada.
[3] Hoffmann-La Roche Ltd., Vaudreuil, Québec, Canada.
[4] USP reference standard.

jected intraperitoneally for 5 days, starting on the 1st day after tumor transplantation (Fig. 3). On this resistant line, 5-fluorodeoxyuridine had no effect at this level while I still inhibited tumor growth. Obviously, the effects of other nucleoside phosphodiesters whose action also would be aided by high levels of phosphodiesterase in these resistant tumors should be studied.

REFERENCES

(1) K. C. Tsou, S. Aoyagi, and E. E. Miller, *J. Med. Chem.*, **13**, 765(1970).

(2) K. C. Tsou, K. W. Lo, S. L. Ledis, and E. E. Miller, *ibid.*, **15**, 1221(1972).

(3) M. Umeda and C. Heidelberger, *Cancer Res.*, **28**, 2529(1968).

(4) S. S. Cohen, J. G. Flaks, H. D. Barner, M. R. Loeb, and J. Lichtenstein, *Proc. Nat. Acad. Sci. USA*, **44**, 1004(1958).

(5) O. H. Lowry, N. J. Rosebrough, A. L. Farr, and R. J. Randall, *J. Biol. Chem.*, **193**, 265(1951).

(6) K. W. Lo, W. Ferrar, W. Fineman, and K. C. Tsou, *Anal. Biochem.*, **47**, 609(1972).

(7) T. R. Breitman, *Biochim. Biophys. Acta*, **67**, 153(1963).

(8) A. C. Palidini and L. F. Leloir, *Biochem. J.*, **51**, 426(1952).

ACKNOWLEDGMENTS AND ADDRESSES

Received May 4, 1973, from the *Harrison Department of Surgical Research, School of Medicine, University of Pennsylvania, Philadelphia, PA 19174*

Accepted for publication June 3, 1975.

Supported by American Cancer Society Grant CI-91A and National Institutes of Health Grant Ca 07339 (to K. C. Tsou).

The authors thank Mr. W. Ferrar for assistance with this work.

[x] To whom inquiries should be directed.

GLC Determination of Plasma Concentrations of Phenprocoumon

K. K. MIDHA [*x], J. W. HUBBARD [‡], J. K. COOPER [*], and I. J. McGILVERAY [*]

Abstract □ A GLC method for the quantitative estimation of phenprocoumon from plasma is described. Plasma containing phenprocoumon, to which a known amount of phenytoin is added as the internal standard, is acidified and extracted with ethylene dichloride. The drug and the internal standard are then back-extracted into alkali, which is acidified and reextracted with ethylene dichloride. The organic extract is evaporated, and the evaporated residue is mixed with 50 μl of trimethylanilinium hydroxide in methanol. Aliquots (1–2 μl) are injected into a gas chromatograph equipped with a flame-ionization detector in which the injection port is held at 325°. The methyl derivatives of phenprocoumon and the internal standard give sharp, well-separated, symmetrical peaks. The method is of sufficient sensitivity to determine 0.125 μg/ml of the drug in plasma with a coefficient of variation of 7%.

Keyphrases □ Phenprocoumon—GLC determination from human plasma, phenytoin as internal standard □ GLC—analysis, phenprocoumon in plasma, phenytoin as internal standard

Phenprocoumon (I) is an orally administered anticoagulant with action and uses similar to those of phenindione (1). Phenprocoumon is structurally related to warfarin; both are oral coumarin anticoagulants. Several analytical procedures (2–8) were described for the estimation of warfarin and its metabolites from biological fluids, but only one fluorometric method (9) was reported for phenprocoumon. The latter is subject to interference from plasma constituents at low values and from any metabolites present.

The GLC behavior of several coumarin anticoagulants including phenprocoumon, as well as their trimethylsilyl ethers, acetates, trichloroacetates, and trifluoroacetates, was reported (10, 11). These results suggest that derivatization of coumarin drugs might be useful for measuring their concentrations in biological fluids. To facilitate study of the pharmacokinetics and potential interactions with other drugs

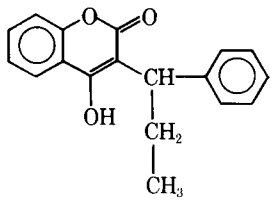

I

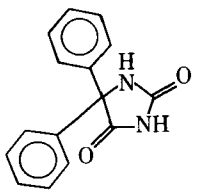

II

after single- and multiple-dose oral administration of phenprocoumon, a sensitive and specific GLC procedure was developed for the measurement of intact drug in plasma.

EXPERIMENTAL

Reagents—Ethylene dichloride[1] and ether[2] were glass distilled prior to use. Stock solutions containing 100 μg/ml of phenprocoumon[3] were prepared daily in 0.1 *N* NaOH and stored in the dark in a refrigerator. Appropriate dilutions (0.125–4.00 μg/ml) were made immediately before use. Aqueous solutions containing 100 μg/ml of the internal standard, phenytoin[4] (II), were prepared weekly by

[1] Caledon Laboratories Ltd., Georgetown, Ontario, Canada.
[2] Mallinckrodt Chemical Works Ltd., Montréal, Québec, Canada.
[3] Hoffmann-La Roche Ltd., Vaudreuil, Québec, Canada.
[4] USP reference standard.

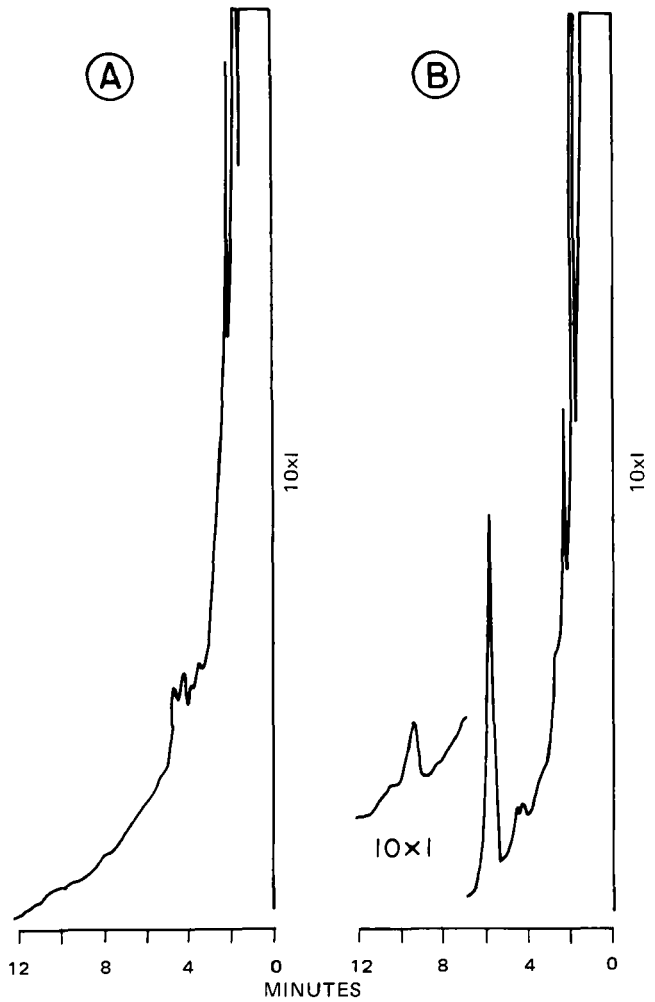

Figure 1—*Gas-liquid chromatograms of human plasma extracts. Key: A, control plasma; and B, plasma spiked with 0.5 μg/ml of phenprocoumon and 2.0 μg/ml of phenytoin.*

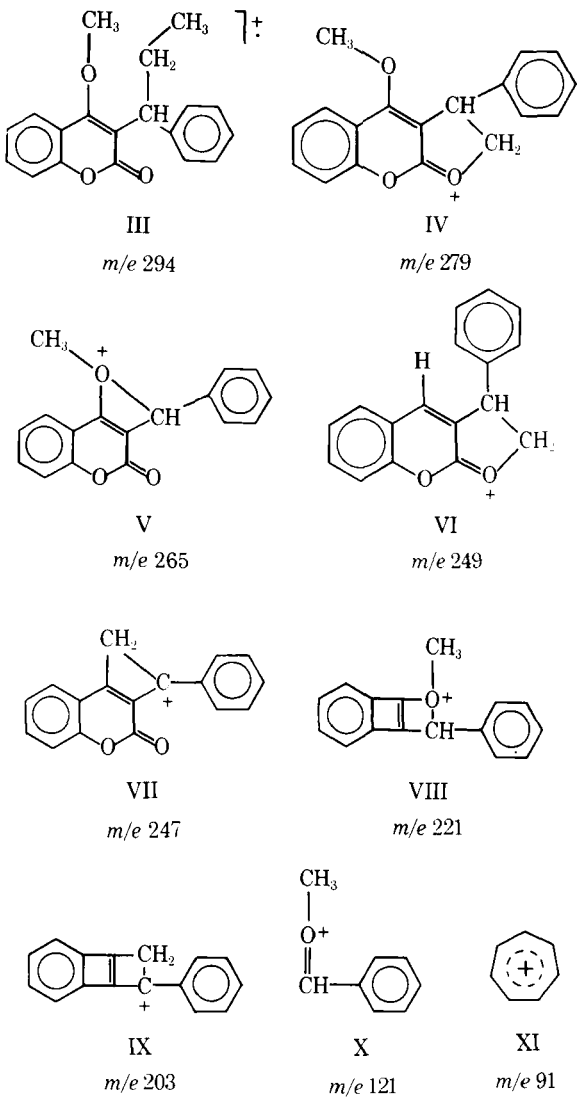

dissolving appropriate amounts of the sodium salt of phenytoin and diluted daily to 2 μg/ml with distilled water.

Methanolic trimethylanilinium hydroxide was synthesized according to the method of Barret (12). All other chemicals were analytical grade.

Plasma Level Study—Phenprocoumon (5 mg) was administered separately to two dogs weighing 17.2 and 21.5 kg. Ten-milliliter blood samples were withdrawn from the cephalic vein, using heparinized evacuated tubes[5], at 22 appropriate time intervals over 18 days following dosing. The blood samples were centrifuged, and the plasma was transferred to another tube before storage at −10°.

Extraction of Phenprocoumon—To a 2-ml human or canine plasma sample (spiked or from dosed animals) in a glass-stoppered centrifuge tube[6] (50 ml) were added 1 ml of phenytoin (2.0 μg/ml), 2 ml of 3 *N* HCl, and 20 ml of ethylene dichloride. The samples were stoppered and extracted by shaking at a 30° angle for 10 min at 180 cpm on a flat bed shaker[7]. After centrifugation at 3000 rpm for 10 min, the aqueous layer was removed by aspiration and 18 ml of the ethylene dichloride layer was transferred into another glass-stoppered centrifuge tube[6] (50 ml) containing 10 ml of 1 *N* NaOH.

The extraction was repeated (shaking for 15 min and centrifuging for 10 min), and 9 ml of the sodium hydroxide was transferred to another glass-stoppered tube[6] (50 ml) containing 3 ml of 5 *N* HCl. The tube was swirled gently and the extraction was carried out with another 20 ml of ethylene dichloride for 20 min. The aqueous layer was removed by aspiration, and 18 ml of ethylene dichloride was transferred to a glass-stoppered centrifuge tube[6] (50 ml). The ethylene dichloride was evaporated[8] at 85° under a stream of dry nitrogen to a volume of approximately 4 ml. A crystal of anhydrous calcium chloride[6] was added and the tube was swirled gently. Then the extract was transferred quantitatively into a custom-made evaporation tube (13) containing a small antibumping granule[9] and evaporated as before to dryness.

The tube was allowed to cool to room temperature and the residue was dissolved in 50 μl of methanolic trimethylanilinium hydroxide (0.4 *M*) by mixing[10]. Aliquots (1–2 μl) were injected into the gas chromatograph. The retention times of flash-methylated phenprocoumon and phenytoin were 9.36 and 5.70 min, respectively.

Reference Samples for Recovery—Reference samples were prepared by dissolving appropriate amounts of phenprocoumon and phenytoin in methanol to obtain solutions containing final concentrations of 2 and 4 μg/ml of each drug. One milliliter of methanol solution (2 and 4 μg/ml) of phenprocoumon was pipetted into an evaporating tube containing 1 ml of methanolic solution of phenytoin (2 and 4 μg/ml). The mixture was evaporated to dryness at 85° under a stream of dry nitrogen, and the dried residue was dissolved in 50 μl of methanolic trimethylanilinium hydroxide (0.4 *M*) by means of a vibrating mixer. Aliquots (1–2 μl) were injected into the gas chromatograph, and the peak height ratios thus obtained were designated the 100% value.

[5] Vacutainers, Becton Dickinson and Co., Mississauga, Ontario, Canada.
[6] Fisher Scientific Co. Ltd., Montréal, Québec, Canada.
[7] Eberbach Corp., Ann Arbor, Mich.
[8] Thermolyne Dri-Bath, Fisher Scientific Co. Ltd., Montréal, Québec, Canada.
[9] British Drug House, Toronto, Ontario, Canada.
[10] Vortex Genie, Fisher Scientific Co. Ltd., Montréal, Québec, Canada.

Table I—Recovery of Phenprocoumon and Phenytoin from Plasma[a]

Micrograms Added to 1 ml of Plasma	Mean Micrograms Recovered	Mean Percent Recovery ± *SD*
	Recovery of Phenprocoumon	
2.0	1.72	85.97 ± 1.33
4.0	3.50	87.43 ± 1.10
	Mean = 86.70 ± 1.38%	
	Recovery of Phenytoin	
2.0	1.80	90.18 ± 1.52
4.0	3.61	90.28 ± 0.89
	Mean = 90.23 ± 1.16%	

[a] $n = 4$.

For the recovery experiments of phenprocoumon, drug (2 or 4 μg/ml) was added to plasma and extracted as already described. To the final extract, a methanolic solution of phenytoin (2 μg/ml) was added and the described procedure was followed. The recovery of phenprocoumon was calculated from the peak height ratios thus obtained. Phenprocoumon was used as an external standard in a similar fashion for the recovery experiment with phenytoin.

GLC—A gas chromatograph[11] equipped with a flame-ionization detector was employed. The column was a coil of stainless steel tubing[12], 1.8 m long × 0.3 cm o.d., packed with 5.0% methyl phenyl silicone containing about 75% phenyl silicone[13] coated on acid-washed, dimethylchlorosilane-treated, 80–100-mesh, high performance flux-calcined diatomite support[14].

The column was conditioned by maintaining it at 290° for 18 hr with low nitrogen flow. The injection port, detector, and oven temperatures were 325, 300, and 260°, respectively. Nitrogen, as a carrier gas, was maintained at a flow rate of 60 ml/min. Hydrogen and compressed air flow rates were adjusted to give maximum response.

Calculations—Peak height ratios were calculated by dividing the height of the peak due to methylated phenprocoumon (9.36 min) by that of methylated phenytoin (5.70 min). Calibration curves were constructed from the results of spiked control plasma samples by plotting the peak height ratios against the concentrations of phenprocoumon (micrograms per milliliter of plasma).

RESULTS AND DISCUSSION

Flash-heater methylation of phenprocoumon with trimethylanilinium hydroxide gave a sharp peak with a retention time of 9.36 min (Fig. 1B) under the conditions described under *Experimental*. Flash-heater methylation of phenytoin was reported previously (14, 15). Under the described conditions, the flash-heater methylated derivative of phenytoin gave a sharp symmetrical peak with a retention time of 5.70 min (Fig. 1B); this peak was well resolved from the peak of methylated phenprocoumon.

To establish the structure of the compound giving rise to the peak with a retention time of 9.36 min (Fig. 1) from flash-heater methylation of phenprocoumon, eluates from the GLC column were fed directly into the mass spectrometer[15] and the mass spectrum of the compound giving rise to the peak was recorded. The mass spectrum (Fig. 2) showed a molecular ion of *m/e* 294 and a base peak at *m/e* 265 (V). Other abundant ions were observed at *m/e* 279, 249, 247, 221, 203, 121, and 91. Structures III–XI have been postulated for these ions.

These fragmentations suggest that the flash-heater methylated derivative of phenprocoumon has the structure 3-(α-ethylbenzyl)-4-methoxycoumarin. These observations also confirmed that the intact drug was being measured. The combined GLC–mass spectral evidence obtained for the peak with a retention time of 5.70 min (Fig. 1) derived from flash-heater methylation of the internal standard in the present study was consistent (molecular ion at *m/e* 280 and other diagnostic ions at *m/e* 251, 223, 203, 194, 165, 118, and 77) with the mass spectrum of the dimethylated derivative of phenytoin (14).

Table II—GLC Estimation of Phenprocoumon Added to Plasma

Phenprocoumon Added, μg	*n*	Mean Peak Height Ratio	*SD*	*CV*[a], %
0.125	5	0.033	0.002	6.35
0.250	6	0.058	0.004	7.03
0.5	5	0.122	0.005	3.66
1.0	5	0.238	0.005	1.88
2.0	5	0.468	0.013	2.79
4.0	5	0.946	0.024	2.55

[a] Mean $CV = 4.04\%$; $y = mx$, where $m = 0.236 \pm 0.003$; and $r^2 = 1$.

The use of trimethylanilinium hydroxide as a convenient methylating agent was reported previously (14–17). It offers the advantage that purified plasma extracts do not need to be completely moisture free—a factor that saves time. The reagent is stable over a long period and is easily prepared. The methylation reaction is instantaneous in the injection port at temperatures above 300° (14–17). During the transfer of the final ethylene dichloride extract separated from the acidic solution, it is important to avoid transfer of trace amounts of acid because it was found that in such circumstances methylation with trimethylanilinium hydroxide was not quantitative.

Attempts to prepare trimethylsilyl ethers of phenprocoumon with silylating reagents such as hexamethyldisilazane[16], bis(trimethylsilyl)*trifluoroacetamide*[16], *a mixture of* trimethylsilylimidazole[16], bis(trimethylsilyl)acetamide[16], and trimethylchlorosilane[16], and a mixture of hexamethyldisilazane and trimethylchlorosilane in solvents such as pyridine[16] and acetonitrile[16] were successful, but interference from plasma constituents discouraged this approach.

Various drugs such as phenylbutazone[17], oxyphenbutazone[18], and several barbiturates were investigated as possible internal standards. On flash-heater methylation with trimethylanilinium hydroxide, phenylbutazone gave two peaks as reported earlier (16). The minor peak of methylated phenylbutazone interfered with that of flash-heater methylated phenprocoumon, thereby precluding its use as an internal standard.

Oxyphenbutazone was discarded as a possible internal standard in the assay of phenprocoumon since its flash-heater methylated products (16) had much greater retention times than that of phenprocoumon, thereby increasing the time of analysis. Various barbiturates such as phenobarbital[19], amobarbital[20], and secobarbital[21] could not be employed since the retention times of their flash-heater methylated derivatives were too short. However, since flash-heater methylated phenytoin gave a GLC peak with the desired retention time and had partition characteristics similar to those of phenprocoumon, this compound adequately satisfied the requirements of an internal standard.

Several other liquid phases such as saturated hydrocarbon lubricant[22], *methyl silicone*[23], *phenyl methyl dimethyl silicone*[24], and phenyl methyl (50:50) silicone[25] were tested, but a peak from endogenous material in the plasma interfered with the peak of flash-heater methylated phenprocoumon.

Refrigerated plasma samples containing phenprocoumon were observed to be stable for several weeks. However, evaporated extracts to which trimethylanilinium hydroxide had been added were unstable over 12 hr. The tubes containing evaporated extracts, when stored overnight at −15°, showed lesser amounts (4–5%) of

[11] Model F/11, Perkin-Elmer, Montréal, Québec, Canada.
[12] Chromatographic Specialties, Brockville, Ontario, Canada.
[13] OV-25, Chromatographic Specialties, Brockville, Ontario, Canada.
[14] Chromasorb W, Chromatographic Specialties, Brockville, Ontario, Canada.
[15] Perkin-Elmer model 900 gas chromatograph attached to a Hitachi Perkin-Elmer model RMSU mass spectrometer through a jet-separator.
[16] Pierce Chemical Co., Rockford, Ill.
[17] Butazolidin, Geigy Pharmaceuticals, Montréal, Québec, Canada.
[18] Ciba-Geigy, Dorval, Québec, Canada.
[19] Jules R. Gilbert Ltd., Toronto, Ontario, Canada.
[20] Eli Lilly and Co. Ltd., Toronto, Ontario, Canada.
[21] May & Baker Co. Ltd., Dagenham, Essex, England.
[22] Apiezon-L, Apiezon Products Ltd., London, England.
[23] OV-1, Chromatographic Specialties, Brockville, Ontario, Canada
[24] OV-7, Chromatographic Specialties, Brockville, Ontario, Canada.
[25] OV-17, Chromatographic Specialties, Brockville, Ontario, Canada.

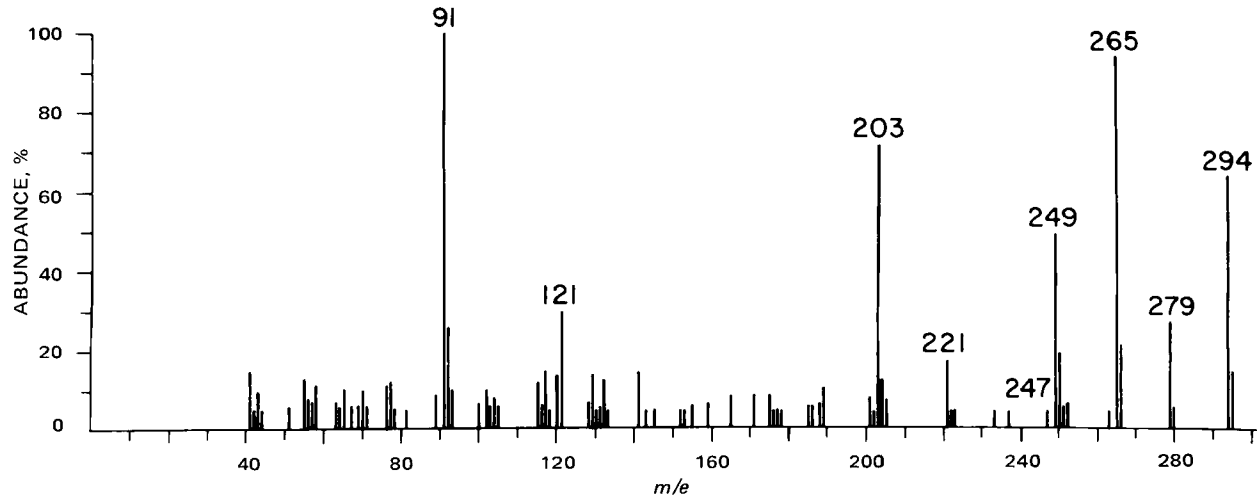

Figure 2—*GLC–mass spectrum (normalized) of flash-methylated phenprocoumon.*

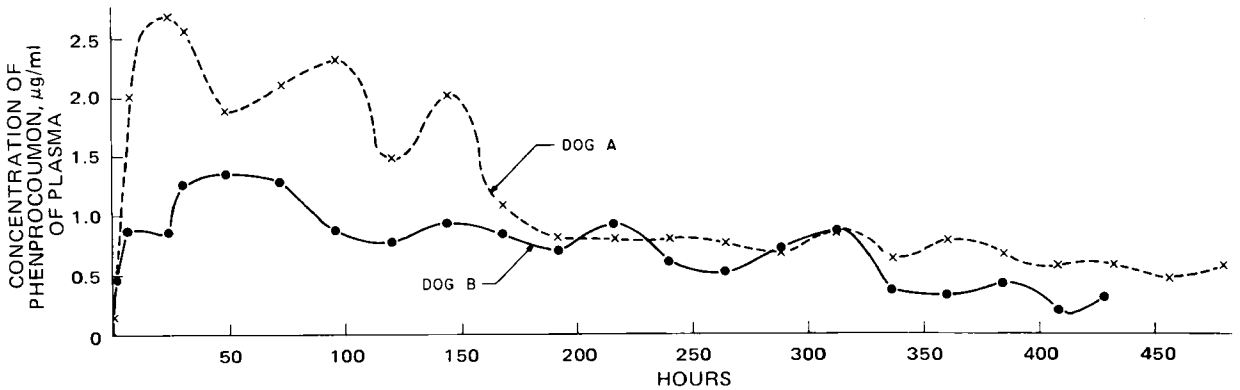

Figure 3—*Plasma profiles of phenprocoumon. Dog A (17.2 kg) and Dog B (21.5 kg) each received 5 mg of phenprocoumon orally in a capsule.*

phenprocoumon. Thus, extraction and GLC analysis of phenprocoumon should be completed on the same day.

Figure 1A shows a typical chromatogram obtained by processing fresh blank plasma as described under *Experimental.* The extraneous peaks near the solvent front were observed in chromatograms of all human plasma samples but not in those of dog plasma samples. A chromatogram obtained when the method was applied to spiked plasma containing 0.5 μg/ml of phenprocoumon and 2.0 μg/ml of phenytoin is shown in Fig. 1B. The extraneous peaks close to the solvent front clearly do not interfere with the peak from the internal standard (retention time of 5.70 min) or phenprocoumon (retention time of 9.36 min).

The response of the flame-ionization detector to flash-heater methylated phenprocoumon was linear with concentration in the 0.125–4.00-μg/ml range. The peak height ratio of the drug and internal standard was used as the index of detector performance and overall efficiency of the analytical procedure. The overall recoveries of phenprocoumon and phenytoin from plasma were in the order of 86.70 ± 1.38 and 90.23 ± 1.16%, respectively (Table I).

The accuracy and precision of the GLC assay are demonstrated in Table II. Results are based on at least five determinations of each phenprocoumon concentration, ranging from 0.125 to 4.00 μg/ml, which were treated as described under *Experimental.* The overall coefficient of variation was 4.04%. The calibration curve obtained by plotting the peak height ratio of flash-heater methylated phenprocoumon/phenytoin *versus* the concentration of phenprocoumon was linear ($y = mx$) over the concentration range of 0.125–4.00 μg of phenprocoumon/ml of plasma. A mean slope value of 0.236 ± 0.002 ($p = 0.05$, $r = 0.9997$) was obtained. When the equation $y = mx + b$ was used for calculations, the slope value was 0.2356 ± 0.0025 ($r = 0.9994$) while the intercept ($b = 0.001457$) obtained was not significant ($p = 0.05$).

Application of the method to plasma level determinations in dogs is demonstrated in Fig. 3. Dogs A and B, 17.2 and 21.5 kg, respectively, each received 5 mg of phenprocoumon orally in an extemporaneously prepared capsule[26]. The many peaks and valleys in the plasma profile remain unexplained and investigations continue. The data provided by Seiler and Duckert (9, 18) for humans do not allow full evaluation, although some scatter is evident from the profiles given.

The described GLC procedure is sensitive for the determination of phenprocoumon, and the plasma samples required are not large. The procedure also offers the advantage that the methyl derivative of the intact drug is measured. It should be suitable for single- or multiple-dose pharmacokinetic studies.

REFERENCES

(1) "Martindale—The Extra Pharmacopoeia," 26th ed., The Pharmaceutical Press, London, England, 1974, p. 874.

(2) R. A. O'Reilly, P. M. Aggeler, M. S. Hoag, and L. Leong, *Thromb. Diath. Haemorrh.*, **8**, 82(1962).

(3) R. A. O'Reilly, P. M. Aggeler, and L. S. Leong, *J. Clin. Invest.*, **42**, 1542(1963).

(4) R. J. Lewis and L. P. Ilnicki, *Clin. Res.*, **17**, 332(1969).

(5) P. G. Welling, K. P. Lee, U. Khanna, and J. G. Wagner, *J. Pharm. Sci.*, **59**, 1621(1970).

(6) E. S. Vessel and C. A. Shively, *Science*, **184**, 466(1974).

(7) D. G. Kaiser and R. S. Martin, *J. Pharm. Sci.*, **63**, 1579(1974).

(8) K. K. Midha, I. J. McGilveray, and J. K. Cooper, *ibid.*, **63**, 1725(1974).

(9) K. Seiler and F. Duckert, *Thromb. Diath. Haemorrh.*, **19**, 389(1968).

[26] Gelatin capsules No. 2, Eli Lilly & Co., Indianapolis, Ind. No excipients were added.

(10) F. W. Deckert, *J. Chromatogr.*, **64**, 201(1972).
(11) *Ibid.*, **64**, 355(1972).
(12) M. J. Barret, *Clin. Chem. Newslett.*, **3**, 16(1971).
(13) A. H. Beckett, *Dan. Tidssk. Farm.*, **40**, 197(1966).
(14) R. H. Hammer, B. J. Wilder, R. R. Streiff, and A. Mayersdorf, *J. Pharm. Sci.*, **60**, 327(1971).
(15) J. MacGee, *Anal. Chem.*, **42**, 421(1970).
(16) K. K. Midha, I. J. McGilveray, and C. Charette, *J. Pharm. Sci.*, **63**, 1234(1974).
(17) *Ibid.*, **63**, 1244(1974).
(18) K. Seiler and F. Duckert, *Thromb. Diath. Haemorrh.*, **21**, 320(1969).

ACKNOWLEDGMENTS AND ADDRESSES

Received February 11, 1975, from the *Drug Research Laboratories, Health Protection Branch, Health and Welfare Canada, Ottawa, Ontario K1A OL2, Canada, and the ‡Faculty of Pharmacy, University of Manitoba, Winnipeg 2, Manitoba, Canada.

Accepted for publication May 31, 1975.

The authors thank Dr. A. By and Mr. J.-C. Ethier for determining the mass spectra and Mr. J. Evans and Mr. L. Martin for veterinary assistance.

ˣ To whom inquiries should be directed.

Anticonvulsant Activity and Selective Inhibition of Nicotinamide Adenine Dinucleotide-Dependent Oxidations by 10-(2-Arylimino-3-acetylamino-4-thiazolidonyl)phenothiazines

SHIVA P. SINGH *§, BASHEER ALI *, THEODORE K. AUYONG ‡, SURENDRA S. PARMAR *‡ˣ, and BENJAMIN De BOER ‡

Abstract □ Several 10-(1-acetyl-4-arylthiosemicarbazido)phenothiazines and their corresponding cyclized 10-(2-arylimino-3-acetylamino-4-thiazolidonyl)phenothiazines were synthesized and characterized by their sharp melting points and elemental analyses. All compounds inhibited nicotinamide adenine dinucleotide (NAD)-dependent oxidation of pyruvate and α-ketoglutarate selectively, whereas NAD-independent oxidation of succinate remained unaltered. All phenothiazine derivatives exhibited anticonvulsant activity, which was reflected by the 20–60% protection observed against pentylenetetrazol-induced convulsions in mice. The ability of substituted thiosemicarbazidophenothiazines to inhibit cellular respiratory activity was reduced considerably by cyclization to the corresponding substituted thiazolidinophenothiazines. On the other hand, cyclization generally resulted in increased anticonvulsant activity. Thus, the anticonvulsant activity possessed by these substituted phenothiazines bore no relationship with their ability to inhibit selectively the NAD-dependent oxidations. Selective inhibition of NAD-dependent oxidation of pyruvate and α-ketoglutarate in isolated rat brain mitochondria by some 10-(1-acetyl-4-arylthiosemicarbazido)phenothiazines was concentration dependent and competitive in nature.

Keyphrases □ Phenothiazines—synthesis, effects on NAD-dependent oxidations, anticonvulsant activity screened, mice □ Oxidation, NAD dependent—pyruvate and α-ketoglutarate, effect of phenothiazines □ Anticonvulsant activity—phenothiazines, synthesized, screened, mice □ Structure–activity relationships—substituted phenothiazines, anticonvulsant activity

The striking clinical success of chlorpromazine as an antipsychotic agent led to the synthesis of numerous phenothiazine derivatives. Chlorpromazine has been shown to diminish convulsant effects of nicotine and cocaine, whereas no protection was provided by chlorpromazine against convulsions induced by the administration of strychnine, caffeine, and pentylenetetrazol (1, 2). Earlier studies indicated that small differences in the chemical structure of the phenothiazine compounds produce significant changes in their pharmacological properties (3).

Furthermore, the ability of thiazolidone derivatives to afford protection against pentylenetetrazol-induced convulsions (4, 5) and of phenothiazines and thiazolidones to inhibit cellular respiratory activity of brain homogenates (4, 6) prompted synthesis of phenothiazine derivatives possessing the thiazolidone moiety at position 10 of the phenothiazine portion of their molecular structure. Anticonvulsant activity of these substituted thiazolidonylphenothiazines and their precursor thiosemicarbazidophenothiazines was determined against pentylenetetrazol-induced convulsions in an attempt to show the effect of cyclization on the anticonvulsant activity of these phenothiazines.

The ability of these substituted phenothiazines to inhibit cellular respiratory activity of brain homogenates was also investigated with a view to study the biochemical mechanism of action of these compounds. The various 10-(2-arylimino-3-acetylamino-4-thiazolidonyl)phenothiazines were synthesized as outlined in Scheme I.

EXPERIMENTAL[1]

10-Chloroacetylphenothiazine—Following the method of Ekstrand (7), a mixture of phenothiazine (0.3 mole) and chloroacetyl chloride (0.45 mole) in 100 ml of dry benzene was refluxed on a steam bath for 4 hr. Excess benzene was removed by distillation.

[1] All compounds were analyzed for their carbon, hydrogen, and nitrogen content. Melting points were taken in open capillary tubes and are corrected. IR spectra were obtained with Perkin-Elmer Infracord spectrophotometer model 137 equipped with sodium chloride optics in potassium bromide films in the 700–3500-cm^{-1} range.

(10) F. W. Deckert, *J. Chromatogr.*, **64**, 201(1972).
(11) *Ibid.*, **64**, 355(1972).
(12) M. J. Barret, *Clin. Chem. Newslett.*, **3**, 16(1971).
(13) A. H. Beckett, *Dan. Tidssk. Farm.*, **40**, 197(1966).
(14) R. H. Hammer, B. J. Wilder, R. R. Streiff, and A. Mayersdorf, *J. Pharm. Sci.*, **60**, 327(1971).
(15) J. MacGee, *Anal. Chem.*, **42**, 421(1970).
(16) K. K. Midha, I. J. McGilveray, and C. Charette, *J. Pharm. Sci.*, **63**, 1234(1974).
(17) *Ibid.*, **63**, 1244(1974).
(18) K. Seiler and F. Duckert, *Thromb. Diath. Haemorrh.*, **21**, 320(1969).

ACKNOWLEDGMENTS AND ADDRESSES

Received February 11, 1975, from the *Drug Research Laboratories, Health Protection Branch, Health and Welfare Canada, Ottawa, Ontario K1A OL2, Canada, and the ‡Faculty of Pharmacy, University of Manitoba, Winnipeg 2, Manitoba, Canada.

Accepted for publication May 31, 1975.

The authors thank Dr. A. By and Mr. J.-C. Ethier for determining the mass spectra and Mr. J. Evans and Mr. L. Martin for veterinary assistance.

ˣ To whom inquiries should be directed.

Anticonvulsant Activity and Selective Inhibition of Nicotinamide Adenine Dinucleotide-Dependent Oxidations by 10-(2-Arylimino-3-acetylamino-4-thiazolidonyl)phenothiazines

SHIVA P. SINGH *§, BASHEER ALI *, THEODORE K. AUYONG ‡, SURENDRA S. PARMAR *‡ˣ, and BENJAMIN De BOER ‡

Abstract □ Several 10-(1-acetyl-4-arylthiosemicarbazido)phenothiazines and their corresponding cyclized 10-(2-arylimino-3-acetylamino-4-thiazolidonyl)phenothiazines were synthesized and characterized by their sharp melting points and elemental analyses. All compounds inhibited nicotinamide adenine dinucleotide (NAD)-dependent oxidation of pyruvate and α-ketoglutarate selectively, whereas NAD-independent oxidation of succinate remained unaltered. All phenothiazine derivatives exhibited anticonvulsant activity, which was reflected by the 20–60% protection observed against pentylenetetrazol-induced convulsions in mice. The ability of substituted thiosemicarbazidophenothiazines to inhibit cellular respiratory activity was reduced considerably by cyclization to the corresponding substituted thiazolidinophenothiazines. On the other hand, cyclization generally resulted in increased anticonvulsant activity. Thus, the anticonvulsant activity possessed by these substituted phenothiazines bore no relationship with their ability to inhibit selectively the NAD-dependent oxidations. Selective inhibition of NAD-dependent oxidation of pyruvate and α-ketoglutarate in isolated rat brain mitochondria by some 10-(1-acetyl-4-arylthiosemicarbazido)phenothiazines was concentration dependent and competitive in nature.

Keyphrases □ Phenothiazines—synthesis, effects on NAD-dependent oxidations, anticonvulsant activity screened, mice □ Oxidation, NAD dependent—pyruvate and α-ketoglutarate, effect of phenothiazines □ Anticonvulsant activity—phenothiazines, synthesized, screened, mice □ Structure–activity relationships—substituted phenothiazines, anticonvulsant activity

The striking clinical success of chlorpromazine as an antipsychotic agent led to the synthesis of numerous phenothiazine derivatives. Chlorpromazine has been shown to diminish convulsant effects of nicotine and cocaine, whereas no protection was provided by chlorpromazine against convulsions induced by the administration of strychnine, caffeine, and pentylenetetrazol (1, 2). Earlier studies indicated that small differences in the chemical structure of the phenothiazine compounds produce significant changes in their pharmacological properties (3).

Furthermore, the ability of thiazolidone derivatives to afford protection against pentylenetetrazol-induced convulsions (4, 5) and of phenothiazines and thiazolidones to inhibit cellular respiratory activity of brain homogenates (4, 6) prompted synthesis of phenothiazine derivatives possessing the thiazolidone moiety at position 10 of the phenothiazine portion of their molecular structure. Anticonvulsant activity of these substituted thiazolidonylphenothiazines and their precursor thiosemicarbazidophenothiazines was determined against pentylenetetrazol-induced convulsions in an attempt to show the effect of cyclization on the anticonvulsant activity of these phenothiazines.

The ability of these substituted phenothiazines to inhibit cellular respiratory activity of brain homogenates was also investigated with a view to study the biochemical mechanism of action of these compounds. The various 10-(2-arylimino-3-acetylamino-4-thiazolidonyl)phenothiazines were synthesized as outlined in Scheme I.

EXPERIMENTAL[1]

10-Chloroacetylphenothiazine—Following the method of Ekstrand (7), a mixture of phenothiazine (0.3 mole) and chloroacetyl chloride (0.45 mole) in 100 ml of dry benzene was refluxed on a steam bath for 4 hr. Excess benzene was removed by distillation.

[1] All compounds were analyzed for their carbon, hydrogen, and nitrogen content. Melting points were taken in open capillary tubes and are corrected. IR spectra were obtained with Perkin-Elmer Infracord spectrophotometer model 137 equipped with sodium chloride optics in potassium bromide films in the 700–3500-cm^{-1} range.

Table I—Physical Constants of 10-(1-Acetyl-4-arylthiosemicarbazido)phenothiazines

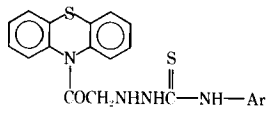

Compound	Ar	Melting Point[a]	Yield, %	Molecular Formula	Analysis, % Calc.	Found
I	C_6H_5	130°	79	$C_{21}H_{18}N_4OS_2$	C 62.07	61.68
					H 4.43	4.35
					N 13.79	13.72
II	2-$CH_3C_6H_4$	164°	68	$C_{22}H_{20}N_4OS_2$	C 62.86	62.38
					H 4.76	4.57
					N 13.33	13.19
III	3-$CH_3C_6H_4$	155°	76	$C_{22}H_{20}N_4OS_2$	C 62.86	62.54
					H 4.76	4.48
					N 13.33	13.46
IV	4-$CH_3C_6H_4$	170°	88	$C_{22}H_{20}N_4OS_2$	C 62.86	62.72
					H 4.76	4.69
					N 13.33	13.40
V	2-$OCH_3C_6H_4$	175°	63	$C_{22}H_{20}N_4O_2S_2$	C 60.55	60.58
					H 4.59	4.55
					N 12.84	12.72
VI	4-$OCH_3C_6H_4$	182°	85	$C_{22}H_{20}N_4O_2S_2$	C 60.55	60.23
					H 4.59	4.29
					N 12.84	12.93
VII	4-ClC_6H_4	174°	82	$C_{21}H_{17}ClN_4OS_2$	C 57.20	57.55
					H 3.86	3.66
					N 12.71	12.53
VIII	4-BrC_6H_4	210°	95	$C_{21}H_{17}BrN_4OS_2$	C 51.96	51.87
					H 3.50	3.48
					N 11.55	11.59
IX	4-IC_8H_4	144°	90	$C_{21}H_{17}IN_4OS_2$	C 47.37	47.17
					H 3.19	3.22
					N 10.53	10.67
X	1-$C_{10}H_7$ (α-Naphthyl)	162°	83	$C_{25}H_{20}N_4OS_2$	C 65.79	65.51
					H 4.39	4.33
					N 12.28	12.47

[a] Melting points were taken in an open capillary tube with an immersion thermometer and are corrected.

The solid mass which separated on cooling was collected by filtration, washed with water to remove chloroacetyl chloride, dried, and recrystallized from benzene (yield, 75%), mp 114° [lit. (7) mp 115–116°].

10-Hydrazinoacetylphenothiazine—A mixture of 10-chloroacetylphenothiazine (0.3 mole) and hydrazine hydrate (99%, 0.45 mole) in 100 ml of absolute ethanol was refluxed on a steam bath for 18 hr. Excess ethanol was removed by distillation under reduced pressure. The crude product which separated on cooling was collected by filtration, dried, and recrystallized from ethanol (yield, 54%), mp 180°.

Anal.—Calc. for $C_{14}H_{13}N_3OS$: C, 61.99; H, 4.79; N, 15.49. Found: C, 62,24; H, 4.68; N, 15.38.

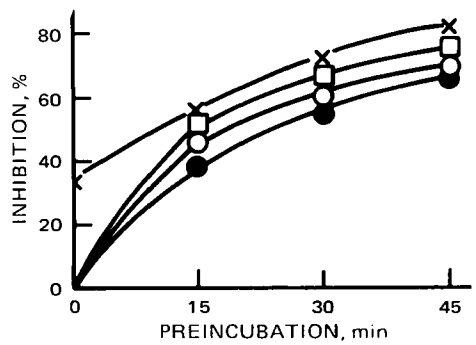

Figure 1—*Effect of preincubation of substituted phenothiazines (III, VIII, and X) and chlorpromazine with isolated rat brain mitochondrial preparations for various times prior to the addition of pyruvate. Zero-time experiments represent those where both the test compound and pyruvate were added simultaneously to the mitochondrial preparations. Assay procedures and the contents of the reaction vessels are described in the text. Key:* ○, *III (0.4 mM);* □, *VIII (0.4 mM);* ●, *X (0.4 mM); and* ×, *chlorpromazine (1 mM).*

10-(1-Acetyl-4-arylthiosemicarbazido)phenothiazines—A mixture of 10-hydrazinoacetylphenothiazine (0.01 mole) and the appropriate aryl isothiocyanates (0.01 mole) in 25 ml of absolute ethanol was refluxed on a steam bath for 6 hr. Excess ethanol was removed by distillation, and the solid mass which separated on cooling was collected by filtration, washed with ether and dilute hydrochloric acid, dried, and recrystallized from ethanol (Table I).

10-(2-Arylimino-3-acetylamino-4-thiazolidonyl)phenothiazines—Following the method reported earlier (5, 8), a mixture of 10-(1-acetyl-4-arylthiosemicarbazido)phenothiazine (0.01 mole), chloroacetic acid (0.01 mole), and fused anhydrous sodium acetate (0.015 mole) was dissolved in 25 ml of acetic acid. Then the mixture was refluxed on a free flame for 4–5 hr. The reaction mixture was poured over ice-cold water and kept in a refrigerator for 24 hr. The crude products which separated were collected by filtration, washed several times with water, dried, and recrystallized from ethanol (Table II).

Determination of Respiratory Activity of Rat Brain Homogenates and Isolated Mitochondria[2]—Male albino rats, kept on an *ad libitum* diet, were used in all experiments. Rats, 100–150 g, were sacrificed by decapitation. The brains were removed immediately and homogenized[3] in ice-cold 0.25 *M* sucrose solution in a ratio of 1:9 (w/v). Brain mitochondria were isolated by using differential centrifugation techniques (9). Rat brain homogenate was centrifuged[4] at 600×*g* for 10 min to sediment nuclei and cell debris.

The mitochondria were separated by centrifugation of the supernatant fraction at 10,000×*g* for 15 min. The isolated mitochondria were washed and recentrifuged twice and then suspended in a known volume of 0.25 *M* cold sucrose. All incubations were carried out at 37° in the conventional Warburg manometric apparatus,

[2] Commercial chemicals were used for the determination of cellular respiratory activity of rat brain homogenates and isolated mitochondria. Sodium pyruvate, sodium α-ketoglutarate, adenosine monophosphate (sodium salt), nicotinamide adenine dinucleotide, and cytochrome c were obtained from Sigma Chemical Co., St. Louis, Mo.

[3] Potter–Elvehjem.

[4] International refrigerated centrifuge model B-20.

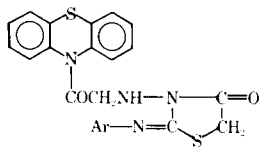

Table II—Physical Constants of 10-(2-Arylimino-3-acetylamino-4-thiazolidonyl)phenothiazines

Compound	Ar	Melting Point[a]	Yield, %	Molecular Formula	Analysis, % Calc.	Found
XI	C_6H_5	122°	56	$C_{23}H_{18}N_4O_2S_2$	C 61.88	61.46
					H 4.04	3.82
					N 12.56	12.22
XII	2-$CH_3C_6H_4$	177°	54	$C_{24}H_{20}N_4O_2S_2$	C 62.60	62.44
					H 4.35	4.17
					N 12.17	12.08
XIII	3-$CH_3C_6H_4$	148°	55	$C_{24}H_{20}N_4O_2S_2$	C 62.60	62.35
					H 4.35	4.21
					N 12.17	11.88
XIV	4-$CH_3C_6H_4$	180°	62	$C_{24}H_{20}N_4O_2S_2$	C 62.60	62.68
					H 4.35	4.28
					N 12.17	11.78
XV	2-$OCH_3C_6H_4$	169°	58	$C_{24}H_{20}N_4O_3S_2$	C 60.50	60.48
					H 4.20	4.22
					N 11.76	11.57
XVI	4-$OCH_3C_6H_4$	185°	60	$C_{24}H_{20}N_4O_3S_2$	C 60.50	60.63
					H 4.20	3.87
					N 11.76	11.35
XVII	4-ClC_6H_4	179°	61	$C_{23}H_{17}ClN_4O_2S_2$	C 57.46	57.33
					H 3.54	3.29
					N 11.65	11.68
XVIII	4-BrC_6H_4	145°	64	$C_{23}H_{17}BrN_4O_2S_2$	C 52.57	52.59
					H 3.24	3.28
					N 10.67	10.53
XIX	4-IC_6H_4	132°	58	$C_{23}H_{17}IN_4O_2S_2$	C 48.25	48.00
					H 2.97	2.75
					N 9.79	9.66
XX	1-$C_{10}H_7$ (α-Naphthyl)	128°	56	$C_{27}H_{20}N_4O_2S_2$	C 65.32	65.38
					H 4.03	4.20
					N 11.29	11.31

[a]Melting points were taken in an open capillary tube with an immersion thermometer and are corrected.

using air as the gas phase (10). The oxygen uptake was measured at 10-min intervals.

Fresh rat brain homogenate (1 ml) or mitochondrial preparation (0.5 ml), equivalent to 100 mg wet brain weight, was added to the chilled Warburg vessels containing 6.7 m*M* magnesium sulfate, 20 m*M* sodium hydrogen phosphate buffer solution (pH 7.4), 1 m*M* adenosine monophosphate (sodium salt), 33 m*M* potassium chloride, and 500 μg of cytochrome c in a final volume of 3 ml unless otherwise stated. The central well contained 0.2 ml of 20% KOH solution. Pyruvate, α-ketoglutarate, and succinate were used at a final concentration of 10 m*M*. It was presumed that the endogenous nicotinamide adenine dinucleotide (NAD) present in brain homogenates was sufficient for the cellular respiratory activity. In mitochondrial preparations, NAD was added to the reaction mixture in a final concentration of 0.5 m*M*.

All 10-(1-acetyl-4-arylthiosemicarbazido)phenothiazines and the corresponding cyclized 10-(2-arylimino-3-acetylamino-4-thiazolidonyl)phenothiazines were dissolved in propylene glycol (100%) and used at a final concentration of 2 m*M*. An equal volume of propylene glycol was added to the control vessels.

In preincubation studies, isolated rat brain mitochondrial preparations in the incubation mixture were incubated with or without some 10-(1-acetyl-4-arylthiosemicarbazido)phenothiazines at 37° for 15, 30, and 45 min prior to the addition of pyruvate or α-ketoglutarate. The zero-time experiments represent those in which the substituted phenothiazines and pyruvate or α-ketoglutarate were added simultaneously to the reaction mixture containing appropriate rat brain mitochondrial preparations. These preincubation studies were also carried out with chlorpromazine, which was used as the reference drug for comparative evaluation.

The I_{50} values (concentration producing 50% inhibition) were determined graphically for some 10-(1-acetyl-4-arylthiosemicarbazido)phenothiazines from the values obtained for the inhibition of the cellular respiratory activity of rat brain mitochondria during oxidation of pyruvate and α-ketoglutarate by the use of different concentrations of these substituted phenothiazines.

In the present study, the nature of inhibition of cellular respiratory activity of isolated rat brain mitochondria during oxidation of pyruvate was evaluated by following the graphic method of Lineweaver and Burk (11) as modified by Dixon (12).

Determination of Anticonvulsant Activity—Anticonvulsant activity was determined in albino mice of either sex, 25–30 g, against pentylenetetrazol-induced convulsions. The mice were divided in groups of 10, keeping the group weights as near the same as possible. All 10-(1-acetyl-4-arylthiosemicarbazido)phenothiazines and 10-(2-arylimino-3-acetylamino-4-thiazolidonyl)phenothiazines were suspended in 5% aqueous gum acacia to give a concentration of 1% (w/v). These test compounds were administered in a dose of 100 mg/kg ip to a group of 10 mice.

Four hours after the administration of the test compounds, the

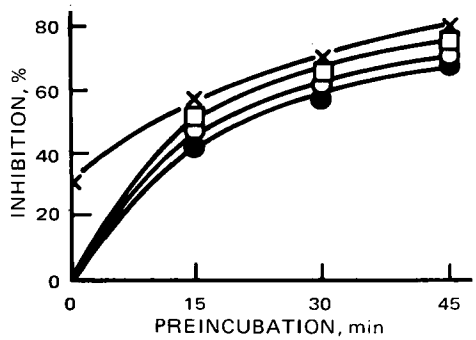

Figure 2—*Effect of preincubation of substituted phenothiazines (III, VIII, and X) and chlorpromazine with isolated rat brain mitochondrial preparations for various times prior to the addition of α-ketoglutarate. Zero-time experiments represent those where both the test compound and α-ketoglutarate were added simultaneously to the mitochondrial preparations. Assay procedures and the contents of the reaction vessels are described in the text. Key:* ○, *III (0.4 mM);* □, *VIII (0.4 mM);* ●, *X (0.4 mM); and* ×, *chlorpromazine (1 mM).*

Table III—Inhibition of Cellular Respiratory Activity of Rat Brain Homogenates by 10-(1-Acetyl-4-arylthiosemicarbazido)phenothiazines and Their Anticonvulsant Activity

Compound	Inhibition of Respiratory Activity[a], %		Anticonvulsant Activity[b], % Protection	Pentylenetetrazol Mortality[c], %
	Pyruvate	α-Ketoglutarate		
I	54.8 ± 1.2	61.2 ± 1.3	20	40
II	45.7 ± 1.0	54.4 ± 0.9	40	10
III	76.4 ± 1.4	79.4 ± 1.3	60	10
IV	15.3 ± 0.5	30.0 ± 0.6	30	30
V	15.0 ± 0.4	14.3 ± 0.5	30	40
VI	50.0 ± 0.9	48.2 ± 0.9	60	Nil
VII	54.0 ± 0.9	51.2 ± 1.0	20	50
VIII	81.8 ± 1.2	88.2 ± 1.3	40	50
IX	87.0 ± 1.3	74.1 ± 1.1	50	30
X	94.3 ± 1.3	83.4 ± 1.3	50	50

[a] Assay procedures are as indicated in the text. Each experiment was done in duplicate, and the values represent mean values of percent inhibition with ± *SE* of the mean calculated from three separate experiments. Inhibition was determined by the decrease in the oxygen uptake/100 mg wet tissue weight/hr. All substituted phenothiazines were used at a final concentration of 2 m*M*. Pyruvate and α-ketoglutarate were used at a concentration of 10 m*M*. The percent inhibition with succinate was nil. [b] Screening procedures are as indicated in the text. Each compound was used at a dose of 100 mg/kg ip. In the present study, administration of an equivalent amount of 5% gum acacia solution was found to possess no anticonvulsant activity. [c] Represents mortality during 24 hr in each group of animals administered 90 mg/kg sc of pentylenetetrazol.

mice were injected with pentylenetetrazol (90 mg/kg sc). This dose of pentylenetetrazol was shown to produce convulsions in almost all untreated mice, and the mice exhibited 100% mortality during 24 hr (5). No mortality was observed during 24 hr in mice treated with 100 mg/kg ip of the substituted phenothiazines.

The mice were observed for 60 min for the occurrence of seizures. An episode of clonic spasm persisting for at least 5 sec was considered a threshold convulsion. Transient intermittent jerks and tremulousness were not counted. Animals devoid of threshold convulsions during the 60 min were considered protected. The number of animals protected in each group was recorded, and the anticonvulsant activity of substituted phenothiazines was represented as the percent protection. The mice were then observed for 24 hr, and their mortality was recorded.

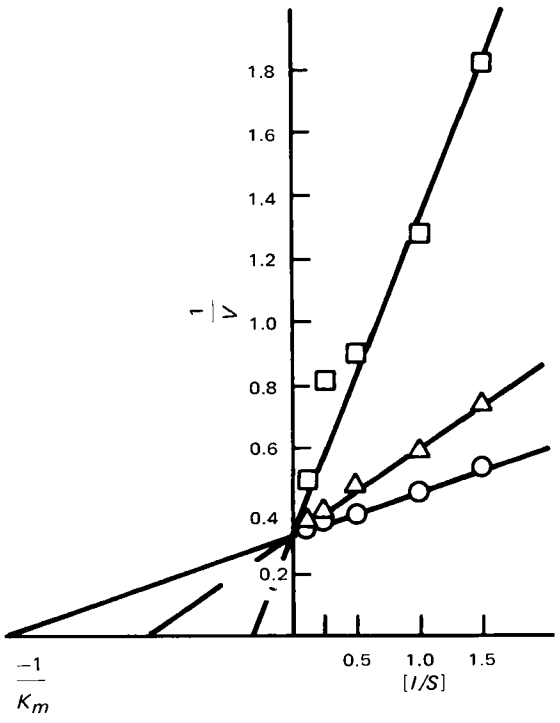

Figure 3—*Competitive inhibition of the cellular respiratory activity of isolated rat brain mitochondria by X during pyruvate oxidation. Assay procedures and the contents of the reaction vessels are described in the text.* [S] *denotes the molar concentration of pyruvate, and 1/V represents the reciprocal of the units of oxygen uptake equivalent to 100 mg of wet brain weight for mitochondrial preparations/30 min. Each experiment was done in duplicate, and the values are the means of three separate experiments. Key:* ○, *pyruvate control;* △, *0.4 m*M *X; and* □, *1 m*M *X. The* K_m *value for pyruvate was 0.4 m*M.

RESULTS AND DISCUSSION

In the present study, various 10-(1-acetyl-4-arylthiosemicarbazido)phenothiazines (Table I) were synthesized and converted into their corresponding cyclized 10-(2-arylimino-3-acetylamino-4-thiazolidonyl)phenothiazines (Table II). The presence of the characteristic bands of C=O (1640 cm^{-1}), NH (3400 cm^{-1}) and C=S (1050 cm^{-1}) groups in the IR spectra of 10-(1-acetyl-4-phenylthiosemicarbazido)phenothiazine (I) and C=O (1630 cm^{-1}), NH (3400 cm^{-1}), and C=N (1690 cm^{-1}) groups in the IR spectra of 10-(2-phenylimino-3-acetylamino-4-thiazolidonyl)phenothiazine (XI) provided further support for the molecular structure of substituted phenothiazines. All of these compounds were evalu-

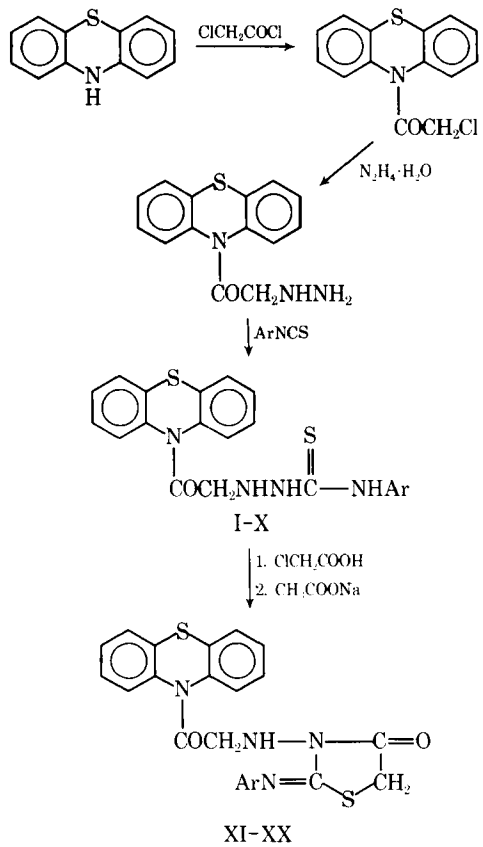

Scheme I

Table IV—Inhibition of Cellular Respiratory Activity of Rat Brain Homogenates by 10-(2-Arylimino-3-acetylamino-4-thiazolidonyl)phenothiazines and Their Anticonvulsant Activity

Compound	Inhibition of Respiratory Activity[a], %		Anticonvulsant Activity[a], % Protection	Pentylenetetrazol Mortality[a], %
	Pyruvate	α-Ketoglutarate		
XI	29.0 ± 0.7	22.1 ± 0.4	40	50
XII	30.2 ± 0.6	32.1 ± 0.5	60	20
XIII	47.2 ± 0.7	36.9 ± 0.6	30	50
XIV	12.9 ± 0.4	23.1 ± 0.5	40	40
XV	5.2 ± 0.4	8.1 ± 0.4	60	20
XVI	15.7 ± 0.5	27.5 ± 0.5	60	30
XVII	22.5 ± 0.5	16.3 ± 0.4	60	20
XVIII	44.8 ± 0.7	46.8 ± 0.6	40	50
XIX	34.1 ± 0.7	45.2 ± 0.6	60	30
XX	49.9 ± 0.6	57.7 ± 0.8	50	40

[a] Details of the experimental methods for the determination of the cellular respiratory activity of rat brain homogenates, screening of the anticonvulsant activity, and pentylenetetrazol mortality are as described in Table III. The percent inhibition with succinate was nil.

ated for anticonvulsant activity and their ability to inhibit the cellular respiratory activity of rat brain homogenates.

As is evident from Table III, all 10-(1-acetyl-4-arylthiosemicarbazido)phenothiazines (I–X) inhibited selectively the NAD-dependent oxidation of pyruvate and α-ketoglutarate; NAD-independent oxidation of succinate remained unaltered. Cyclization of these compounds into corresponding 10-(2-arylimino-3-acetylamino-4-thiazolidonyl)phenothiazines (XI–XX) retained their selective inhibitory effectiveness (Table IV), but the degree of inhibition was significantly lowered by cyclization during oxidation of both pyruvate and α-ketoglutarate.

In both series of substituted phenothiazines, α-naphthyl-substituted compounds (X and XX) exhibited maximum inhibitory activity. The presence of the substituents in the phenyl nucleus of these substituted phenothiazines significantly altered the ability of these compounds to inhibit selectively the oxidation of pyruvate and α-ketoglutarate. Moreover, in both series of substituted phenothiazines, the presence of bromo (VIII and XVIII) or iodo (IX and XIX) at the *para*-position of the phenyl nucleus resulted in a significantly greater degree of inhibition of the cellular respiratory activity as compared to phenothiazines possessing an unsubstituted phenyl nucleus in their structure (I and XI). The degree of inhibition, in general, was found to bear no relationship with the electronegativity of these halogen substituents on the phenyl nucleus.

Introduction of methyl (II–IV and XII–XIV) and methoxy (V, VI and XV, XVI) substituents on the phenyl nucleus caused decreased inhibition, with the exception of *m*-tolyl-substituted phenothiazines (III and XIII) which produced greater inhibition of the oxidation of pyruvate and α-ketoglutarate by rat brain homogenates as compared to compounds devoid of substituents in their phenyl nucleus (I and XI). The selective inhibitory effects of 10-(1-acetyl-4-arylthiosemicarbazido)phenothiazines and 10-(2-arylimino-3-acetylamino-4-thiazolidonyl)phenothiazines were not found to be related with their chemical structure, so a definite structure–activity relationship was not exhibited.

The inhibitory effects of some of the more potent 10-(1-acetyl-4-arylthiosemicarbazido)phenothiazines were investigated on the respiratory activity of isolated rat brain mitochondria. As is evident from Table V, increase in the concentration of 3-methylphenyl- (III), 4-bromophenyl- (VIII), and α-naphthyl- (X) substituted phenothiazines caused greater inhibition of the oxidation of pyruvate and α-ketoglutarate. The comparative inhibitory effectiveness of these compounds was also reflected by their I_{50} values. The low I_{50} values of 0.6 and 0.56 m*M* observed for 10-[1-acetyl-4-(4-bromophenyl)thiosemicarbazido]phenothiazine (VIII) corresponded well with its maximum inhibitory effectiveness during oxidation of pyruvate and α-ketoglutarate, respectively.

In the present study, preincubation effects of three 10-(1-acetyl-4-arylthiosemicarbazido)phenothiazines (III, VII, and X) were investigated on the respiratory activity of isolated rat brain mitochondria at a concentration of 0.4 m*M*. Chlorpromazine, used as a standard drug for comparative evaluation, was used at a higher concentration of 1 m*M*. All substituted phenothiazines exhibited greater inhibitory activity as compared to the inhibitory activity of chlorpromazine during oxidation of pyruvate (Fig. 1) and α-ketoglutarate (Fig. 2).

Preincubation of these substituted phenothiazines as well as chlorpromazine with the mitochondrial preparations for a varying length of time prior to the addition of pyruvate or α-ketoglutarate resulted in progressive increases in their degree of inhibition. Maximum inhibition was observed when preincubation with appropriate mitochondrial preparations was carried out for 45 min before the addition of the substrate. On the other hand, simultaneous addition of the substituted phenothiazines and the substrate (zero-time experiments) to the reaction vessel containing brain mitochondrial preparation produced no inhibition of the oxidation of pyruvate and α-ketoglutarate.

These results, indicating the irreversible nature of inhibition by substituted phenothiazines, prompted kinetic studies using 10-[1-acetyl-4-(α-naphthyl)thiosemicarbazido]phenothiazine (X) to determine the nature of its inhibition during oxidation of pyruvate by isolated rat brain mitochondrial preparations. These kinetic studies (Fig. 3) revealed the competitive nature of inhibition by this compound. The intercept at the $1/S$ axis was taken as $-1/K_m$ (Fig. 3), and the value of 0.4 m*M* was obtained as the Michaelis

Table V—Inhibition of Cellular Respiratory Activity of Isolated Rat Brain Mitochondria by 10-(1-Acetyl-4-arylthiosemicarbazido)phenothiazines

Compound	Substrate	Inhibition by Substituted Phenothiazines[a], %				
		0.6 m*M*	0.8 m*M*	1.2 m*M*	1.5 m*M*	I_{50}, m*M*[b]
II	Pyruvate	30.0 ± 0.8	42.4 ± 0.6	91.8 ± 1.2	100	0.86
VIII	Pyruvate	50.5 ± 0.9	85.4 ± 1.0	94.6 ± 1.2	100	0.60
X	Pyruvate	20.5 ± 0.9	29.1 ± 0.8	94.0 ± 1.0	96.2 ± 1.1	0.90
II	α-Ketoglutarate	32.4 ± 0.8	62.4 ± 0.9	71.5 ± 0.6	98.2 ± 0.7	0.72
VIII	α-Ketoglutarate	55.4 ± 1.2	80.0 ± 0.9	88.4 ± 0.6	100	0.56
X	α-Ketoglutarate	32.4 ± 0.4	52.0 ± 0.7	66.6 ± 0.8	90.4 ± 0.8	0.79

[a] Assay procedures and the contents of the reaction mixture are as indicated in the text. Each experiment was done in duplicate, and the values represent mean values of percent inhibition with ± *SE* of the mean calculated from three separate experiments. Inhibition was determined by the decrease in the oxygen uptake/100 mg wet weight of the tissue equivalent to mitochondrial preparation/hr. Pyruvate and α-ketoglutarate were used at a concentration of 10 m*M*. [b] Calculated graphically.

constant (K_m) in these experiments with pyruvate as the substrate. The irreversible nature of inhibition by these substituted phenothiazines, as indicated by preincubation studies, and the competitive nature of inhibition observed with kinetic studies indicated that these substituted phenothiazines react relatively irreversibly with rat brain mitochondrial preparation to produce "nonequilibrium antagonism," as reported earlier for monoamine oxidase inhibitors (13, 14).

The anticonvulsant activity possessed by these substituted phenothiazines was reflected by their ability to afford protection against pentylenetetrazol-induced convulsions in mice. The degree of protection ranged from 20 to 60% with 10-(1-acetyl-4-arylthiosemicarbazido)phenothiazines (Table III) and from 30 to 60% with their corresponding cyclized 10-(2-arylimino-3-acetylamino-4-thiazolidonyl)phenothiazines. Contrary to the decrease in the degree of selective inhibition of NAD-dependent oxidations, the anticonvulsant activity, in general, increased on cyclization. Such an increase in the anticonvulsant activity, however, remained constant on cyclization with three compounds (XVI, XVIII, and XX), and less protection was observed with one cyclized phenothiazine (XIII) as compared to its precursor (III). These results do not provide evidence for the structural requirements in the molecular makeup of these substituted phenothiazines responsible for their anticonvulsant activity.

The results presented in this study have failed to provide a correlation between the anticonvulsant activity of these substituted phenothiazines and their ability to inhibit selectively the NAD-dependent oxidations of pyruvate and α-ketoglutarate by rat brain homogenates and isolated mitochondria. Detailed pharmacological and toxicological studies and further study of the effects of these substituted phenothiazines on other enzyme systems possibly may reflect a biochemical basis for the anticonvulsant activity of 10-(1-acetyl-4-arylthiosemicarbazido)phenothiazines and their cyclized 10-(2-arylimino-3-acetylamino-4-thiazolidonyl)phenothiazines.

REFERENCES

(1) S. Courvoisier, J. Fournel, R. Durcot, M. Kolsky, and P. Koetschet, *Arch. Int. Pharmacodyn. Ther.*, **92,** 305(1953).

(2) F. Meidinger, *C. R. Soc. Biol.*, **150,** 1340(1956).

(3) M. Gordon, L. Cook, D. H. Tedeschi, and R. E. Tedeschi, *Arzneim.-Forsch.*, **13,** 318(1963).

(4) S. S. Parmar, C. Dwivedi, A. Chaudhari, and T. K. Gupta, *J. Med. Chem.*, **15,** 99(1972).

(5) C. Dwivedi, T. K. Gupta, and S. S. Parmar, *ibid.*, **15,** 553(1972).

(6) T. K. Auyong, S. P. Singh, S. S. Parmar, and B. DeBoer, *Pharmacologist*, **15,** 196(1973).

(7) T. Ekstrand, *Acta Chem. Scand.*, **3,** 302(1949).

(8) N. P. Buu-Hoi, N. D. Xuong, and F. Binon, *J. Chem. Soc.*, **1956,** 713.

(9) S. S. Parmar, M. Sutter, and M. Nickerson, *Can. J. Biochem. Physiol.*, **39,** 1335(1961).

(10) P. K. Seth and S. S. Parmar, *Can. J. Physiol. Pharmacol.*, **43,** 1019(1965).

(11) H. Lineweaver and D. Burk, *J. Amer. Chem. Soc.*, **56,** 658(1934).

(12) M. Dixon, *Biochem. J.*, **55,** 170(1953).

(13) M. Nickerson and S. S. Parmar, *Fed. Proc.*, **20,** 165(1961).

(14) S. S. Parmar, in "International Symposium on CNS Drugs," Council of Scientific and Industrial Research, New Delhi, India, Publication, Hyderabad, India, 1966, p. 198.

ACKNOWLEDGMENTS AND ADDRESSES

Received April 16, 1975, from the **Department of Pharmacology and Therapeutics, King George's Medical College, Lucknow University, Lucknow 226003, India,* and the ‡*Department of Physiology and Pharmacology, School of Medicine, University of North Dakota, Grand Forks, ND 58202*

Accepted for publication June 5, 1975.

Supported in part by the Department of Atomic Energy, Government of India, Bombay, India, the Council of Scientific and Industrial Research, New Delhi, India, and the U.S. Public Health Service, National Institutes of Health Grants 1 T01 HL 05939 and 1 R01 DA00996-01.

The authors thank Professor Virgil I. Stenberg and Professor Stanley J. Brumleve for their advice and encouragement. Grateful acknowledgment is made to the Department of Atomic Energy, Bombay, India, and the Council of Scientific and Industrial Research, New Delhi, India, for providing Research Fellowships to S. P. Singh and B. Ali, respectively.

§ Present address: Department of Chemistry, University of North Dakota, Grand Forks, ND 58202

ˣ To whom inquiries should be directed (at the University of North Dakota).

Fragmentation of 3-Oximino-4-chromanone

H. C. WORMSER ˣ **and SU-YA LIEU**

Abstract □ Heating either the methanesulfonate ester of 3-oximino-4-chromanone or 3-oximino-4-chromanone and an alternative acylating agent such as *p*-toluenesulfonyl chloride or acetic anhydride in the presence of aqueous base afforded two major fragments: salicylic acid and 2-carboxyphenoxyacetonitrile. These compounds are derived from two separate cleavage pathways involving the acylated oxime. In one pathway, fragmentation appears to be assisted by the ether ring oxygen; in the other, it is assisted by the α-carbonyl group of the oxime ester.

Keyphrases □ 3-Oximino-4-chromanone—Beckmann fragmentation study after acylating □ Fragmentation—Beckmann rearrangement of 3-oximino-4-chromanone after acylating

Although the Beckmann rearrangement is principally concerned with the conversion of an oxime to an amide, products other than amides are frequently isolated from the attempted oxime rearrangement. In particular, many oximes take an alternative course of reaction, cleaving into a nitrile, especially when an electron-deficient intermediate can be ejected from the oxime carbon. Consequently, substituents on the α-carbon that stabilize carbonium ions favor this process. Thus, fragmentation reactions are seen with α-trisubstituted ketoximes (1–6), α-disubstituted ketoximes (7–9), α-oximino ketones (10, 11), γ-oximino ketones (12–15), α-oximino acids (16, 17), α-amino oximes (18–23), α-imino oximes (24), α-hydroxy oximes (25–28), β-keto ether oximes (29–32), and β-keto thioether oximes (33, 34). In these cases, rearrangement to amides does not take place. Whereas the fragmentation of an α-oximino ketone is facilitated by the formation of a stable acylium ion, the fragmentation reaction of an α-amino ketoxime or a β-keto ether oxime is assisted by the lone pair electrons of the neighboring nitrogen or oxygen.

DISCUSSION

Oximes containing two of these functionalities (an α-carbonyl group and a β-oxygen) in the same ring system have not been thoroughly studied. Rodina *et al.* (35) reported on the abnormal Beckmann rearrangement of the monoketoxime of 2,2,5,5-tetramethyltetrahydrofuran-3-one-4-oxime (I), which gave the nitrile II when treated with *p*-toluenesulfonyl chloride in base or when simply heated (Scheme I).

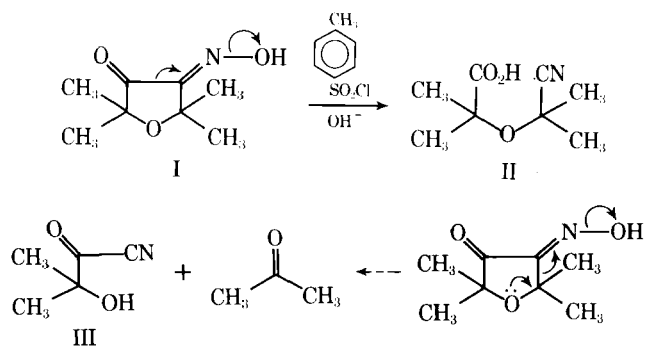

Scheme I

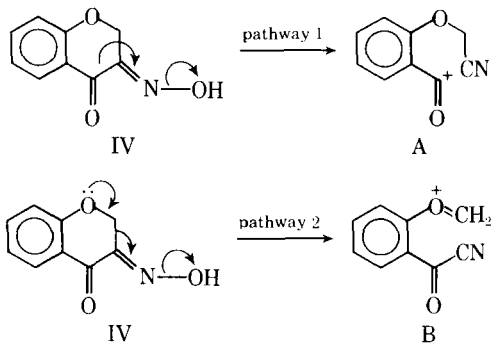

Scheme II

In principle, an additional cleavage pathway induced by the ether oxygen is possible. The latter should lead to product III and acetone; this was not reported previously (35).

The objective of this research was to examine the Beckmann fragmentation of a compound capable of a twofold fragmentation process. The model compound chosen was 3-oximino-4-chromanone (IV), which in theory should be capable of cleaving to either of two resonance-stabilized cations, A or B (Scheme II).

Workup of the reaction mixture resulting from the fragmentation of IV could afford two products: 2-carboxyphenoxyacetonitrile and 2-hydroxybenzoyl cyanide, derived from cations A and B, respectively.

When the methanesulfonate of IV was subjected to one equivalent of sodium hydroxide in dilute solution, three products were obtained, VI, VII, and VIII (Scheme III). Product VI was readily identified as salicylic acid and presumably arises from cation B. It is not clear at this point how this product is actually formed, but several tentative explanations can be put forth:

1. Following hydrolysis to 2-hydroxybenzoyl cyanide, primary fragment B undergoes decarbonylation to 2-hydroxybenzonitrile, which is then hydrolyzed to salicylic acid.
2. Hydrolysis of B gives 2-hydroxybenzoylformic acid, and this compound is subsequently decarbonylated to salicylic acid.
3. 2-Hydroxybenzoylformic acid undergoes decarboxylation rather than decarbonylation, and the resultant aldehyde undergoes a Cannizzaro reaction, affording both salicylic acid and salicyl alcohol.

Needless to say, none of the intermediates mentioned under 1–3 was detected in the crude reaction mixture. Product VII (mp 145–147°) did not give a purple color when treated with ferric chloride solution, but it did dissolve in 5% sodium bicarbonate with the evolution of carbon dioxide. It proved extremely unstable to dilute aqueous base. When dissolved in 5% sodium hydroxide at room temperature and acidified immediately thereafter, a different product (mp 227–229°) was obtained. The latter compound proved identical to VIII and was subsequently identified as 2-carboxyphenoxyacetamide. The IR spectrum of VII showed carboxyl stretching but no absorption in the 4.24–4.55-μm region (nitrile) as anticipated from pathway 1 (Scheme II).

To establish firmly the structures of VII and VIII as postulated from their chemical behavior, spectra, and elemental analyses, these compounds were synthesized independently from methyl salicylate (IX) as shown in Scheme III.

The IR spectra of both ester X and its corresponding acid VII failed to reveal nitrile stretching even in concentrated solutions. Kitson and Griffith (36) observed that in nitriles possessing an α-oxy group, the nitrile band becomes weak or is completely absent. This quenching effect was reported by other investigators (37–40). Substituents such as halogens and methyl groups on the benzene ring do not significantly affect the occurrence or absence of the nitrile band (37–40). However, if the oxygen in these deriva-

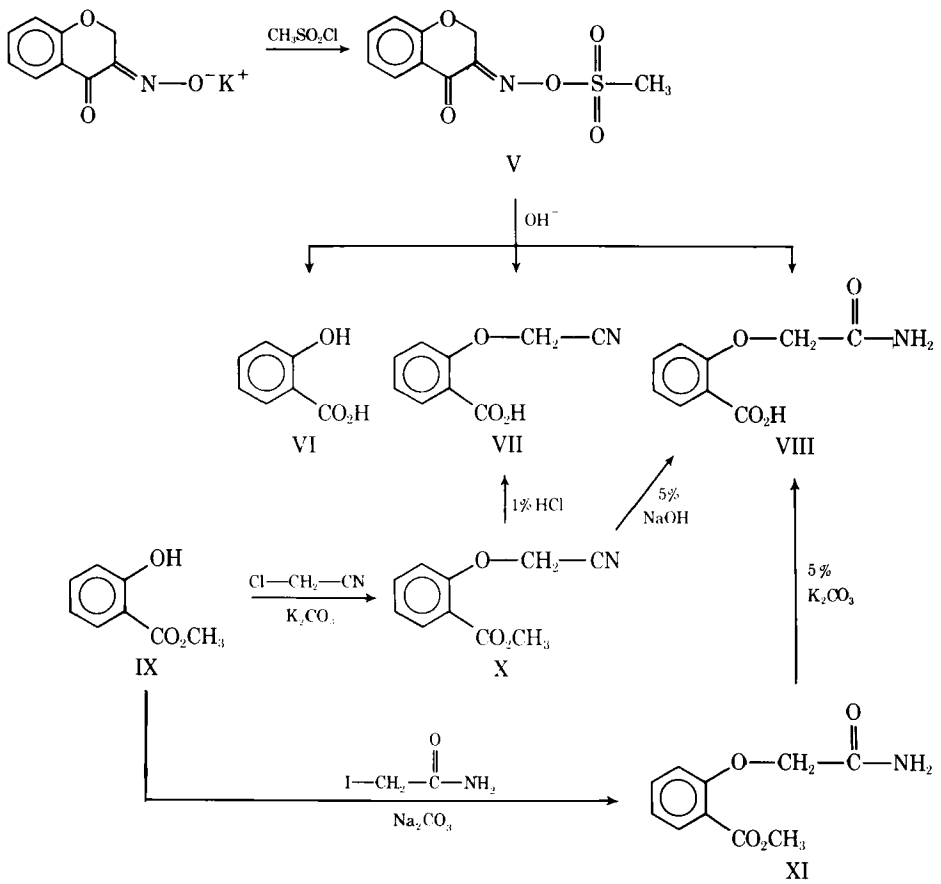

Scheme III

tives is replaced by sulfur, selenium, or amino groups or if the oxygen atom is separated from the nitrile group by two or more methylene groups, then the stretching band of nitrile occurs as predicted.

The extreme sensitivity toward base-catalyzed hydrolysis of VII might lend support to some theories postulated previously to explain the formation of VI. More than likely, the *o*-carboxyl group serves as an intramolecular catalyst for the facilitated hydrolytic reaction. Such intramolecularly assisted hydrolyses of esters and amide derivatives have been well documented (41–45).

The Beckmann fragmentation of IV was also examined with additional leaving groups such as *p*-toluenesulfonate and acetate (Scheme IV). Similar results were obtained. In the case where IV was treated with *p*-toluenesulfonyl chloride in 10% base, salicylic acid and 2-carboxyphenoxyacetic acid (XII) were the only products isolated; when acetic anhydride and 5% sodium hydroxide were used, VI, VII, and VIII were identified as the products from the fragmentation reaction.

This degradation pathway is a potentially applicable method for the structural determination of natural products containing the 4-chromanone ring system. Such chromanone-containing substances are found among the flavanones and flavanone glycosides such as pinocembrin, naringin, and hesperidin.

EXPERIMENTAL[1]

3-Oximino-4-chromanone Methanesulfonate (V)—To a stirred suspension of 0.8 g (4.0 mmoles) of the potassium salt of 3-oximino-4-chromanone (IV) (46) in 20 ml of ice-cold anhydrous ether was added dropwise freshly distilled methanesulfonyl chloride (0.5 g, 0.44 mole). The reaction mixture was then stirred for 20 min in an ice bath, during which time the brown suspension gradually turned yellow. The yellow precipitate was filtered, washed with several portions of ice-cold water until free of chloride, and air dried (0.7 g, 75%), mp 121–122°.

TLC on silica gel G (4% methanol in chloroform) showed a major spot with R_f 0.7; UV: λ_{max} (ethanol) 277 nm; IR: λ_{max} (mineral oil) 5.85, 7.30, and 8.46 μm; NMR (deuterochloroform): δ 3.34 (s, 3H, CH_3), 5.44 (s, 2H, OCH_2), and 7.00–8.13 (m, 4H, aromatic H). Attempts to recrystallize the compound failed due to its instability, so an analytical sample could not be obtained. When V was dissolved in 80% ethanol at 75° for 50 min, TLC on silica gel G (5% methanol in chloroform) showed several new spots in addition to V.

Fragmentation of V—An equimolar quantity (4 ml) of 1% sodium hydroxide was added to 0.5 g (2.0 mmoles) of V, and the mixture was heated on the steam bath until solution was complete. The neutral solution was filtered and cooled. A pale-yellow precipitate formed slowly, and an additional quantity was obtained by adding two to three drops of 10% hydrochloric acid. The precipitate was filtered and dried (0.20 g). TLC on silica gel G [benzene–methanol–acetic acid (45:8:4)] showed one major and two minor spots with R_f 0.6, 0.5, and 0.3, respectively.

Extraction of the aqueous, acidified filtrate with chloroform afforded a crystalline residue (0.03 g), mp 160–161°. TLC of this compound using the same solvent system showed correspondence to the R_f 0.6 spot of the mixture. This compound gave a purple reaction with ferric chloride and was soluble in 5% sodium bicarbonate (effervescence); IR: λ_{max} (chloroform) 3.35 and 5.92 μm; NMR (acetone-d_6): δ 6.80–7.98 (m, 4H, aromatic protons) and 11.03 (s, 2H, OH and COOH). This substance was characterized as salicylic acid (VI) on the basis of superimposable spectral data and undepressed mixed melting point with an authentic sample. Preparative TLC on silica gel $PF_{254+366}$ of the initially obtained solid precipitate [benzene–methanol–acetic acid (45:8:4)] afforded the three substances as crystalline residues: VI (0.094 g, mp 159–161°), VII (0.031 g, mp 142–145°), and VIII (0.024 g, mp 220–223°).

Compound VII was recrystallized from chloroform, yielding colorless plates, mp 145–147°; IR: λ_{max} (mineral oil) 5.90 μm; NMR

[1] Melting points were taken on a Fisher-Johns melting-point stage and a Thomas-Hoover melting-point apparatus and are uncorrected. UV absorption spectra were determined in 95% ethanol on a Beckman (model DK2A) recording spectrophotometer. IR absorption spectra were recorded on Beckman (models 8 and 33) recording spectrophotometers. NMR spectra were determined on a Varian EM 360 spectrometer. Microanalyses were carried out by Spang Microanalytical Laboratory, Ann Arbor, Mich. TLC was carried out with silica gel G, silica gel $HF_{254+366}$, and silica gel $PF_{254+366}$.

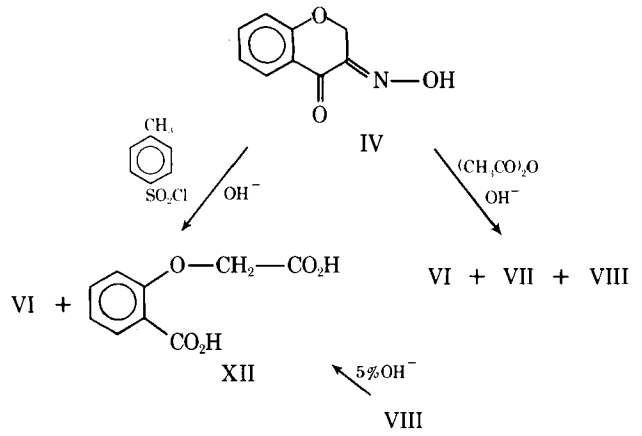

Scheme IV

(dimethyl sulfoxide-d_6): δ 5.26 (s, 2H, OCH_2) and 7.00–8.00 (m, 4H, aromatic H).

Anal.—Calc. for $C_9H_7NO_3$: C, 61.02; H, 3.98; N, 7.91. Found: C, 60.90; H, 3.99; N, 7.86.

On the basis of the data obtained, VII was characterized as 2-carboxyphenoxyacetonitrile.

Compound VIII (corresponding to R_f 0.3) was recrystallized from methanol, mp 227–229°; IR: λ_{max} (mineral oil) 2.93, 3.09, 5.90, and 6.00 μm; UV: λ_{max} (ethanol) 231 and 289 nm; NMR (deuterium oxide-sodium deuteroxide): δ 4.65 (s, 2H, OCH_2) and 6.80–7.55 (m, 4H, aromatic H).

Anal.—Calc. for $C_9H_9NO_4$: C, 55.37; H, 4.65; N, 7.18. Found: C, 55.40; H, 4.73; N, 7.20.

On the basis of the data obtained, VIII was identified as 2-carboxyphenoxyacetamide.

2-Carbomethoxyphenoxyacetonitrile (X)—A mixture of methyl salicylate (IX) (15.2 g, 0.10 mole), chloroacetonitrile (8.0 g, 0.11 mole), and anhydrous potassium carbonate (14.0 g, 0.10 mole) in 200 ml of acetone was refluxed overnight. The solvent was removed under reduced pressure, and the remaining slurry was partitioned between chloroform and water. The organic phase was washed with several portions of 2% sodium hydroxide and dried over anhydrous sodium sulfate. Following filtration and evaporation to dryness, a light-yellow oil was obtained (12.5 g, 65%). Upon standing, the oil crystallized, mp 52–53°. Recrystallization from petroleum ether gave colorless needles, mp 53–54°; IR: λ_{max} (chloroform) 5.81 μm; NMR (deuterochloroform): δ 3.92 (s, 3H, CH_3), 4.88 (s, 2H, OCH_2), and 6.98–8.03 (m, 4H, aromatic H).

Anal.—Calc. for $C_{10}H_9NO_3$: C, 62.82; H, 4.74; N, 7.33. Found: C, 62.86; H, 4.78; N, 7.29.

2-Carboxyphenoxyacetonitrile (VII)—A suspension of 0.20 g (1.0 mmole) of X in 10 ml of 1% hydrochloric acid was heated to reflux for 2 hr. The oily reaction mixture became clear during this time and was then allowed to cool. The crystalline product that had formed was filtered and dried (0.17 g, 97%), mp 141–145°. Recrystallization from chloroform gave shiny, colorless plates, mp 145–147°. The mixed melting point with VII obtained from the fragmentation of V was undepressed, and their IR and NMR spectra were superimposable.

2-Carbomethoxyphenoxyacetamide (XI)—A mixture of IX (7.6 g, 0.05 mole), iodoacetamide (9.3 g, 0.05 mole), and anhydrous sodium carbonate (6.9 g, 0.05 mole) in 125 ml of acetone was refluxed for 6 hr. The solvent was removed under reduced pressure, and the crystalline residue was washed with several portions of water and dried (5.4 g, 52%), mp 140–145°. Recrystallization from acetone gave shiny needles, mp 147–148°; IR: λ_{max} (mineral oil) 2.93, 3.10, 5.80, and 5.90 μm; NMR (dimethyl sulfoxide-d_6): δ 3.87 (s, 3H, OCH_3), 4.60 (s, 2H, OCH_2), and 6.83–8.16 (m, 4H, aromatic H).

Anal.—Calc. for $C_{10}H_{11}NO_4$: C, 57.41; H, 5.30; N, 6.70. Found: C, 57.33; H, 5.28; N, 6.65.

2-Carboxyphenoxyacetamide (VIII)—*Method A*—A suspension of 0.20 g (1.0 mmole) of XI in 10 ml of 5% potassium carbonate was stirred for 12 hr at room temperature. The reaction mixture was cooled, filtered, and acidified with concentrated hydrochloric acid to congo red. The precipitate was filtered and dried (0.084 g, 45%), mp 210–220°. Two recrystallizations from methanol gave fine colorless needles, mp 227–229°. The mixed melting point with VIII obtained from the fragmentation of V was undepressed, and their IR and NMR spectra were superimposable.

Method B—2-Carboxyphenoxyacetonitrile (0.20 g, 1.0 mmole) was dissolved in 10 ml of 5% sodium hydroxide, and as soon as all of the nitrile had gone into solution, the mixture was acidified with 10% hydrochloric acid to congo red. The white precipitate was filtered and dried (0.13 g, 59%), mp 220–222°. Recrystallization from methanol afforded colorless needles, mp 226–228°. The mixed melting point with the product obtained by Method A was undepressed.

Reaction of 3-Oximino-4-chromanone (IV)—*With p-Toluenesulfonyl Chloride in Presence of Aqueous Base*—A solution of IV (0.20 g, 1.0 mmole) in 10 ml of 10% aqueous sodium hydroxide was treated with 0.8 g (4.0 mmoles) of *p*-toluenesulfonyl chloride. The mixture was heated on the steam bath for 20 min, cooled, and filtered. The clear filtrate was acidified with 10% hydrochloric acid, and the turbid mixture was extracted with chloroform. The chloroform extract was dried over anhydrous sodium sulfate and, following filtration, concentrated to dryness. TLC of the solid residue on silica gel G [benzene–methanol–acetic acid (45:8:4)] showed two spots of roughly equal intensity with R_f 0.2 and 0.6.

Sublimation of the solid mixture at atmospheric pressure (75–80°) gave a shiny, colorless sublimate, mp 159–160°. TLC analysis and ferric chloride color reaction indicated that this product was salicylic acid. The residue remaining after the sublimation contained primarily the compound with the lower R_f (0.2). Recrystallization from methanol–chloroform–petroleum ether gave a crystalline product, mp 191–193°; IR: λ_{max} (mineral oil) 3.16, 5.75, and 5.90 μm; NMR (dimethyl sulfoxide-d_6): δ 4.84 (s, 2H, OCH_2) and 7.00–7.90 (m, 4H, aromatic H). This product was identified as 2-carboxyphenoxyacetic acid (XII) [lit. (47) mp 186° and (48) mp 190–193°].

With Acetic Anhydride in Presence of Aqueous Base—To a solution of IV (0.40 g, 2.0 mmoles) in 20 ml of 5% aqueous sodium hydroxide was added 4.3 g (0.042 mole) of acetic anhydride dropwise over 10 min. After the exothermal reaction ceased, the mixture was acidified with 10% hydrochloric acid and extracted with several portions of chloroform. The combined chloroform extracts were dried over anhydrous sodium sulfate, and the solvent was removed under reduced pressure. TLC of the solid residue on silica gel G [benzene–methanol–acetic acid (45:8:4)] showed two major and one minor spots with R_f 0.6, 0.5, and 0.3, respectively.

The compound with R_f 0.6, giving a violet color with ferric chloride solution, was identified as salicylic acid by comparison of the TLC mobility of an authentic sample. The compound with R_f 0.5 was identical with VII, while the minor component with R_f 0.3 was found to be identical with VIII by comparison of thin-layer chromatograms.

2-Carboxyphenoxyacetic Acid (XII)—A suspension of VIII (1.0 g, 5 mmoles) in 10 ml of 5% sodium hydroxide was refluxed overnight. As soon as the reaction began to reflux, a strong evolution of ammonia was detected at the mouth of the reflux condenser. The pink solution was cooled and acidified with concentrated hydrochloric acid, and the crystalline precipitate was filtered and dried (0.10 g, mp 191–193°). Recrystallization from methanol–chloroform–petroleum ether gave shiny, colorless crystals, mp 192–193°. A mixed melting point with the product obtained from the fragmentation of IV (*p*-toluenesulfonyl chloride and base) was undepressed, and their IR and NMR spectra were superimposable.

REFERENCES

(1) H. Goldschmidt, *Ber.*, **20,** 483(1887).

(2) F. Tiemann, *ibid.*, **28,** 1079(1895).

(3) T. Sato and H. Obase, *Tetrahedron Lett.*, **1967,** 1633.

(4) R. K. Hill and R. T. Conley, *J. Amer. Chem. Soc.*, **82,** 645 (1960).

(5) R. T. Conley and B. E. Nowak, *J. Org. Chem.*, **27,** 3196 (1962).

(6) R. T. Conley and R. J. Lange, *ibid.*, **28,** 210(1963).

(7) O. Wallach, *Ann.*, **309,** 1(1889).

(8) W. A. Lazier and G. W. Rigby, U.S. pat. 353,650 and 2,234,566 (1941).

(9) V. Davydov, *Chem. Tech.*, **7,** 645(1955); through *Chem. Abstr.*, **50,** 10678d(1956).

(10) S. N. Chakravarti and M. Swaminathan, *J. Indian Chem.*

Soc., **11**, 101(1934).
(11) A. Hassner, W. A. Wentworth, and I. H. Pomerantz, *J. Org. Chem.*, **28**, 304(1963).
(12) W. Eisele, C. A. Grob, and E. Renk, *Tetrahedron Lett.*, **1963**, 75.
(13) W. Eisele, C. A. Grob, E. Renk, and H. Tschammer, *Helv. Chim. Acta*, **51**, 816(1968).
(14) E. S. Olson and J. H. Richards, *J. Org. Chem.*, **33**, 434 (1968).
(15) W. Dieckmann, *Ber.*, **33**, 579(1900).
(16) A. Ahmad and I. D. Spencer, *Can. J. Chem.*, **38**, 1625 (1960).
(17) M. F. Bartlett, D. F. Dickel, and W. I. Taylor, *J. Amer. Chem. Soc.*, **80**, 126(1958).
(18) M. V. Rubtsov, E. E. Mikhlina, V. Y. Vorobéva, and A. D. Yanina, *Zh. Obsch. Khim.*, **34**, 2222(1964).
(19) H. P. Fischer, C. A. Grob, and E. Renk, *Helv. Chim. Acta*, **42**, 872(1959).
(20) *Ibid.*, **45**, 2539(1962).
(21) H. P. Fischer and C. A. Grob, *Helv. Chim. Acta*, **46**, 936 (1963).
(22) C. A. Grob, H. P. Fischer, H. Link, and E. Renk, *ibid.*, **46**, 1190(1963).
(23) C. A. Grob and A. Sieber, *ibid.*, **50**, 2520, 2531(1967).
(24) E. C. Taylor, C. W. Jefford, and C. C. Cheng, *J. Amer. Chem. Soc.*, **83**, 1261(1961).
(25) A. Werner and T. Deutscheff, *Ber.*, **38**, 69(1905).
(26) J. S. Buck and W. S. Ide, *J. Amer. Chem. Soc.*, **53**, 1912 (1931).
(27) A. H. Blatt and R. P. Barnes, *ibid.*, **56**, 1148(1934).
(28) C. W. Shoppee and S. K. Roy, *J. Chem. Soc.*, **1963**, 3774.
(29) C. Schöpf, *Ann.*, **452**, 211(1927).
(30) C. F. Hennion and J. L. O'Brien, *J. Amer. Chem. Soc.*, **71**, 2933(1947).
(31) R. K. Hill, *J. Org. Chem.*, **27**, 29(1962).
(32) M. Ohno and I. Terasawa, *J. Amer. Chem. Soc.*, **88**, 5683(1966).
(33) R. L. Autrey and P. W. Scullard, *ibid.*, **87**, 3284(1965).
(34) *Ibid.*, **90**, 4924(1968).
(35) L. L. Rodina, L. V. Koroleva, and I. K. Korobitsyna, *Zh. Org. Khim.*, **6**, 2336(1970).
(36) R. E. Kitson and N. E. Griffith, *Anal. Chem.*, **23**, 334(1952).
(37) L. J. Bellamy, "The Infrared Spectra of Complex Molecules," Methuen and Co., London, England, 1958, p. 225.
(38) R. G. Janes and W. J. Orville-Thomas, *Spectrochim. Acta*, **20**, 291(1964).
(39) H. Sterk and H. Junck, *Monatsh.*, **99**, 810(1968).
(40) Z. Ejmocki and A. Eckstein, *Rocz. Chem.*, **45**, 345(1971).
(41) M. L. Bender, Y. L. Chow, and F. Chloupek, *J. Amer. Chem. Soc.*, **80**, 5380(1958).
(42) H. Morawetz and I. Oreskes, *ibid.*, **80**, 2591(1958).
(43) M. L. Bender, F. Chloupek, and M. C. Neveu, *ibid.*, **80**, 5384(1958).
(44) L. Eberson, *Acta Chem. Scand.*, **16**, 2245(1962).
(45) *Ibid.*, **18**, 2015(1964).
(46) H. H. Auf dem Keller and F. Zymalkowski, *Arch. Pharm.*, **304**, 543(1971).
(47) R. Rossing, *Ber.*, **17**, 2995(1884).
(48) R. Meyer and C. Duczmal, *ibid.*, **46**, 3371(1913).

ACKNOWLEDGMENTS AND ADDRESSES

Received February 27, 1975, from the *College of Pharmacy and Allied Health Professions, Wayne State University, Detroit, MI 48202*

Accepted for publication June 11, 1975.

Abstracted in part from a thesis submitted by S. Y. Lieu to Wayne State University in partial fulfillment of the Master of Science degree requirements.

[x] To whom inquiries should be directed.

Analysis of Tetracycline in Pharmaceutical Preparations by Improved High-Performance Liquid Chromatographic Method

KIYOSHI TSUJI [x] and JOHN H. ROBERTSON

Abstract □ The analysis of tetracycline in pharmaceutical preparations by an improved high-performance liquid chromatographic (HPLC) method is described. The improved method uses a 30-cm long stainless steel column packed with octadecylsilane bonded on 10-μm silica gel, with a linear gradient from 10 to 60% acetonitrile in pH 2.5, 0.02 *M* phosphate buffer in 11 min at a flow rate of 1.0 ml/min (68 atm). The resolution functions obtained between 4-epitetracycline and tetracycline and between 4-epianhydrotetracycline and anhydrotetracycline were improved 150 and 250%, respectively. The analysis of a tetracycline sample takes approximately 16 min; the original method required more than 25 min. The relative standard deviation for the analysis of tetracycline powder was 0.66%, and the recovery of 4-epianhydrotetracycline added in tetracycline was linear over the 0.3–100% range. Recovery of tetracycline from products was better than 99.6% at label concentration. The drug content of products as calculated from the HPLC data agreed well with those of the microbiological assay methods.

Keyphrases □ Tetracycline—analysis, high-performance liquid chromatography, pharmaceutical preparations □ High-performance liquid chromatography—analysis, tetracycline in pharmaceutical preparations □ Antibiotics—tetracycline, analysis, high-performance liquid chromatography, pharmaceutical preparations

On March 4, 1974, the Food and Drug Administration (FDA) established the limit for 4-epianhydrotetracycline in tetracycline pharmaceutical dosage forms marketed in the United States (1). However, the limit is higher than that outlined in the European Pharmacopoeia (2).

Prior to the development of high-performance liquid chromatographic (HPLC) assay methods for tetracycline (3–6), the methods used for the detection and quantitation of tetracycline impurities (7, 8) were very tedious, and none has been accepted by FDA as an alternative method for potency determination. There is also some indication that degradation compounds may be forming on-column during

Soc., **11**, 101(1934).
(11) A. Hassner, W. A. Wentworth, and I. H. Pomerantz, *J. Org. Chem.*, **28**, 304(1963).
(12) W. Eisele, C. A. Grob, and E. Renk, *Tetrahedron Lett.*, **1963**, 75.
(13) W. Eisele, C. A. Grob, E. Renk, and H. Tschammer, *Helv. Chim. Acta*, **51**, 816(1968).
(14) E. S. Olson and J. H. Richards, *J. Org. Chem.*, **33**, 434 (1968).
(15) W. Dieckmann, *Ber.*, **33**, 579(1900).
(16) A. Ahmad and I. D. Spencer, *Can. J. Chem.*, **38**, 1625 (1960).
(17) M. F. Bartlett, D. F. Dickel, and W. I. Taylor, *J. Amer. Chem. Soc.*, **80**, 126(1958).
(18) M. V. Rubtsov, E. E. Mikhlina, V. Y. Vorobéva, and A. D. Yanina, *Zh. Obsch. Khim.*, **34**, 2222(1964).
(19) H. P. Fischer, C. A. Grob, and E. Renk, *Helv. Chim. Acta*, **42**, 872(1959).
(20) *Ibid.*, **45**, 2539(1962).
(21) H. P. Fischer and C. A. Grob, *Helv. Chim. Acta*, **46**, 936 (1963).
(22) C. A. Grob, H. P. Fischer, H. Link, and E. Renk, *ibid.*, **46**, 1190(1963).
(23) C. A. Grob and A. Sieber, *ibid.*, **50**, 2520, 2531(1967).
(24) E. C. Taylor, C. W. Jefford, and C. C. Cheng, *J. Amer. Chem. Soc.*, **83**, 1261(1961).
(25) A. Werner and T. Deutscheff, *Ber.*, **38**, 69(1905).
(26) J. S. Buck and W. S. Ide, *J. Amer. Chem. Soc.*, **53**, 1912 (1931).
(27) A. H. Blatt and R. P. Barnes, *ibid.*, **56**, 1148(1934).
(28) C. W. Shoppee and S. K. Roy, *J. Chem. Soc.*, **1963**, 3774.
(29) C. Schöpf, *Ann.*, **452**, 211(1927).
(30) C. F. Hennion and J. L. O'Brien, *J. Amer. Chem. Soc.*, **71**, 2933(1947).
(31) R. K. Hill, *J. Org. Chem.*, **27**, 29(1962).
(32) M. Ohno and I. Terasawa, *J. Amer. Chem. Soc.*, **88**, 5683(1966).
(33) R. L. Autrey and P. W. Scullard, *ibid.*, **87**, 3284(1965).
(34) *Ibid.*, **90**, 4924(1968).
(35) L. L. Rodina, L. V. Koroleva, and I. K. Korobitsyna, *Zh. Org. Khim.*, **6**, 2336(1970).
(36) R. E. Kitson and N. E. Griffith, *Anal. Chem.*, **23**, 334(1952).
(37) L. J. Bellamy, "The Infrared Spectra of Complex Molecules," Methuen and Co., London, England, 1958, p. 225.
(38) R. G. Janes and W. J. Orville-Thomas, *Spectrochim. Acta*, **20**, 291(1964).
(39) H. Sterk and H. Junck, *Monatsh.*, **99**, 810(1968).
(40) Z. Ejmocki and A. Eckstein, *Rocz. Chem.*, **45**, 345(1971).
(41) M. L. Bender, Y. L. Chow, and F. Chloupek, *J. Amer. Chem. Soc.*, **80**, 5380(1958).
(42) H. Morawetz and I. Oreskes, *ibid.*, **80**, 2591(1958).
(43) M. L. Bender, F. Chloupek, and M. C. Neveu, *ibid.*, **80**, 5384(1958).
(44) L. Eberson, *Acta Chem. Scand.*, **16**, 2245(1962).
(45) *Ibid.*, **18**, 2015(1964).
(46) H. H. Auf dem Keller and F. Zymalkowski, *Arch. Pharm.*, **304**, 543(1971).
(47) R. Rossing, *Ber.*, **17**, 2995(1884).
(48) R. Meyer and C. Duczmal, *ibid.*, **46**, 3371(1913).

ACKNOWLEDGMENTS AND ADDRESSES

Received February 27, 1975, from the *College of Pharmacy and Allied Health Professions, Wayne State University, Detroit, MI 48202*

Accepted for publication June 11, 1975.

Abstracted in part from a thesis submitted by S. Y. Lieu to Wayne State University in partial fulfillment of the Master of Science degree requirements.

[x] To whom inquiries should be directed.

Analysis of Tetracycline in Pharmaceutical Preparations by Improved High-Performance Liquid Chromatographic Method

KIYOSHI TSUJI [x] and JOHN H. ROBERTSON

Abstract □ The analysis of tetracycline in pharmaceutical preparations by an improved high-performance liquid chromatographic (HPLC) method is described. The improved method uses a 30-cm long stainless steel column packed with octadecylsilane bonded on 10-μm silica gel, with a linear gradient from 10 to 60% acetonitrile in pH 2.5, 0.02 *M* phosphate buffer in 11 min at a flow rate of 1.0 ml/min (68 atm). The resolution functions obtained between 4-epitetracycline and tetracycline and between 4-epianhydrotetracycline and anhydrotetracycline were improved 150 and 250%, respectively. The analysis of a tetracycline sample takes approximately 16 min; the original method required more than 25 min. The relative standard deviation for the analysis of tetracycline powder was 0.66%, and the recovery of 4-epianhydrotetracycline added in tetracycline was linear over the 0.3–100% range. Recovery of tetracycline from products was better than 99.6% at label concentration. The drug content of products as calculated from the HPLC data agreed well with those of the microbiological assay methods.

Keyphrases □ Tetracycline—analysis, high-performance liquid chromatography, pharmaceutical preparations □ High-performance liquid chromatography—analysis, tetracycline in pharmaceutical preparations □ Antibiotics—tetracycline, analysis, high-performance liquid chromatography, pharmaceutical preparations

On March 4, 1974, the Food and Drug Administration (FDA) established the limit for 4-epianhydrotetracycline in tetracycline pharmaceutical dosage forms marketed in the United States (1). However, the limit is higher than that outlined in the European Pharmacopoeia (2).

Prior to the development of high-performance liquid chromatographic (HPLC) assay methods for tetracycline (3–6), the methods used for the detection and quantitation of tetracycline impurities (7, 8) were very tedious, and none has been accepted by FDA as an alternative method for potency determination. There is also some indication that degradation compounds may be forming on-column during

chromatography (3) when the method outlined in the "Federal Register" is used (1).

The original HPLC method (3, 4) reported for the analysis of tetracycline took a minimum of 25 min of chromatographic time. Also, the resolution between tetracycline and 4-epitetracycline and between anhydrotetracycline and 4-epianhydrotetracycline peaks was not optimum. The new improved HPLC method for tetracycline has many advantages over other methods of analysis, including high speed of analysis, precise quantitation, and improved resolution between tetracycline and its degradation products. The method eliminates the need to perform separate analyses for identity, potency, and stability.

The purpose of this paper is to describe the improved methodology and its application to the analysis of tetracycline in pharmaceutical preparations.

EXPERIMENTAL

Apparatus—A modular liquid chromatograph[1] equipped with a 280-nm UV monitor was used, along with a high-pressure reciprocating positive displacement pump (maximum of 340 atm) equipped with a pulse dampener.

The column, 4.6 × 300 mm packed with octadecylsilane bonded on 10-μm silica gel[2], was attached to a septumless injector valve[3] and the sample side of the 280-nm UV monitor.

Reagents—*Mobile Phases*—

A. One hundred milliliters of acetonitrile and 800 ml of water were placed into a 1000-ml graduated cylinder. One hundred milliliters of 0.2 *M*, pH 2.5 phosphate buffer was then added and mixed.

B. Six hundred milliliters of acetonitrile and 300 ml of water were placed into a 1000-ml graduated cylinder. One hundred milliliters of 0.2 *M*, pH 2.5 phosphate buffer was then added and mixed.

The 0.2 *M*, pH 2.5 phosphate buffer was prepared as follows. A solution containing a suitable quantity of dibasic sodium phosphate was prepared, and the pH of the solution was adjusted to pH 2.5 with phosphoric acid. Water was then added to the volume for a phosphate concentration of 0.2 *M*.

Column Rinse Solution—An aqueous solution containing 80% methanol was prepared and used for rinsing the column after the end of each assay day to prolong column life. This column packing material is unstable when kept at pH < 2.5 for extended periods.

Gradient Elution—A gradient mixer[4] with a 0.25-ml mixing chamber was used. A programmed linear gradient elution, from Mobile Phase A to B in 15 min, was used.

Chromatographic Conditions—The column temperature was ambient with a recorder chart speed of 6.4 mm/min. The electrometer range setting was 0.16 full scale. The column pressure was 68 atm (1000 psi) with a flow rate of 1.0 ml/min. The standard and sample volume injected on-column was 2 μl.

Sample Injection—Immediately after final dilution of the tetracycline reference standards and samples, they were quantitatively injected on-column with the septumless valve injector.

Preparation of Tetracycline Standard—USP tetracycline hydrochloride reference standard, Issue H, was dried at 60° under less than 5 mm Hg pressure for 3 hr. After drying, approximately 4 mg of the reference standard was accurately weighed using an electromagnetic balance[5] and placed into a 10-ml volumetric flask.

Just prior to analysis, each standard was dissolved with 1 ml of absolute methanol and then diluted to volume with 0.01 *M*, pH 4.5 phosphate buffer. When tetracycline was dissolved in 0.01 *M*, pH 4.5 phosphate buffer, no detectable epimerization took place in 6 hr, as determined by the HPLC method.

[1] Laboratory Data Control, Riviera Beach, Fla.
[2] Waters Associates, Framingham, Mass.
[3] Micromeritics, Inc., Norcross, Ga.
[4] Ultragrad, LKB, Stockholm, Sweden.
[5] Cahn Instrument Corp., Paramount, Calif.

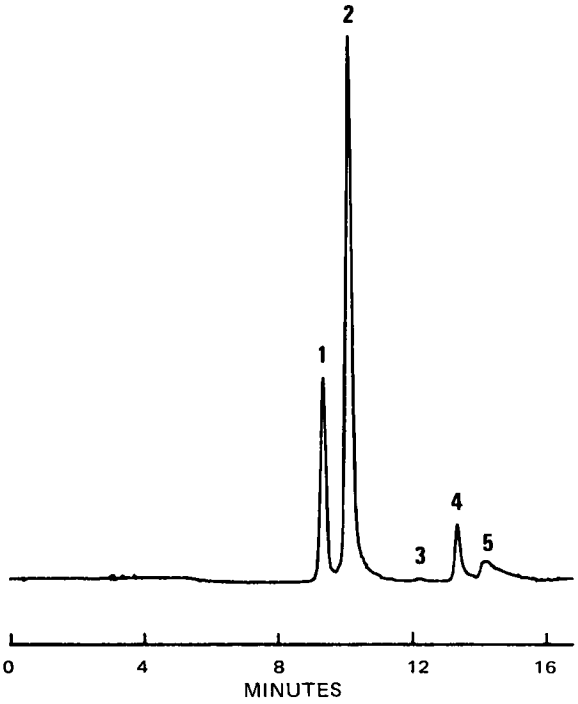

Figure 1—*HPLC of an expired lot of tetracycline phosphate powder indicating improved separation of tetracycline, its epimer, and degradation compounds. A 30-cm column packed with octadecylsilane bonded on 10-μm silica gel was used with 15-min linear gradient elution from 10 to 60% acetonitrile in pH 2.5, 0.02 M phosphate buffer at a 1.0-ml/min flow rate. Key: 1, 4-epitetracycline; 2, tetracycline; 3, chlortetracycline; 4, 4-epianhydrotetracycline; and 5, anhydrotetracycline.*

Sample Preparation—*Tetracycline Bulk Powder*—Approximately 4 mg of the tetracycline sample was accurately weighed into a 10-ml volumetric flask. Just prior to analysis, each sample was diluted with 1 ml of absolute methanol and brought to volume with 0.01 *M*, pH 4.5 phosphate buffer.

Hard Filled Capsules Containing 250 mg of Tetracycline Hydrochloride—Ten capsules were carefully emptied, and their contents were accurately weighed. From this material, the equivalent of two capsules was then weighed and placed in a 50-ml round-bottom, glass-stoppered, centrifuge tube. Twenty-five milliliters of absolute methanol was added, and the contents were shaken for 5 min. The tubes were then centrifuged for 10 min at 1800 rpm. After centrifuging, 2 ml was removed and placed in a 100-ml volumetric flask. Immediately prior to the analysis of each sample, the flask was diluted to volume with 0.01 *M*, pH 4.5 phosphate buffer.

Hard Filled Capsules Containing 250 mg of Tetracycline Phosphate Complex with Nystatin—With one modification, the same extraction procedure for hard filled capsules containing tetracycline hydrochloride was used. Acidified methanol (2% concentrated hydrochloric acid in absolute methanol) was substituted for absolute methanol. This modification was to convert the tetracycline phosphate complex to the hydrochloride form in order to solubilize the tetracycline in methanol.

Hard Filled Capsules Containing Tetracycline Phosphate Complex with Novobiocin—Ten capsules were weighed for content uniformity. The equivalent weight of three capsules was then weighed and placed in a 50-ml ground-glass-stoppered, round-bottom centrifuge tube. Twenty-five milliliters of acidified methanol (2% concentrated hydrochloric acid in absolute methanol) was volumetrically added, and the contents were shaken for 5 min on a reciprocating shaker. After shaking, the samples were centrifuged for 5 min at 1800 rpm.

Four milliliters of acidified methanol extract was then volumetrically transferred to a 100-ml volumetric flask and diluted to volume with 15% methanol in 0.02 *M*, pH 7.0 phosphate buffer. The pH 7.0 buffer was needed to solubilize novobiocin in an alco-

Table I—Precision of the Tetracycline Determination by HPLC

Weight of Tetracycline, mg/ml	Area of Tetracycline, mm^2	Area–Weight Ratio
0.3896	180.5	463.3
0.4000	182.1	455.3
0.3931	181.1	460.7
0.3948	181.7	460.2
0.3980	181.5	456.0
0.3946	181.9	461.0
0.3942	180.0	456.6
	RSD	0.66%

holic solution. Recovery of tetracycline was reduced when novobiocin was allowed to precipitate.

Film-Coated Tablets Containing 250 or 500 mg of Tetracycline Hydrochloride—To minimize tablet weight variation, 10 film-coated tablets were weighed accurately and then finely ground using a Wiley mill with a 60-mesh screen. A portion of the powder equivalent to the weight of two tablets for the 250-mg tablets and of one tablet for the 500-mg formulation was weighed accurately and placed in a 50-ml ground-glass-stoppered, round-bottom centrifuge tube.

Twenty-five milliliters of methanol was added, and the tube was tightly stoppered and then shaken vigorously on a reciprocating shaker for 5 min. The samples were then centrifuged at 1800 rpm for 10 min. Two milliliters of the methanol extract was then pipetted into a 100-ml volumetric flask. Immediately prior to analysis, the volumetric flask was diluted to volume with 0.01 *M*, pH 4.5 phosphate buffer.

Syrup Containing 125 mg of Tetracycline Base/5 ml—Three milliliters of thoroughly mixed syrup was volumetrically transferred to a 200-ml volumetric flask and diluted to volume with absolute methanol. The contents were thoroughly shaken, and then about 30 ml was decanted into a 50-ml glass-stoppered, round-bottom centrifuge tube and centrifuged at 1800 rpm for 5 min.

Oral Suspension Containing 100 mg of Tetracycline Base/ml and Saccharin—One milliliter of the product was volumetrically pipetted into a 50-ml volumetric flask. One milliliter of 0.2 *M*, pH 2.5 phosphoric acid buffer was added, and the contents were diluted to volume with dimethylformamide. Approximately 30 ml of this solution was transferred into a 50-ml glass-stoppered, round-bottom centrifuge tube. The tube was centrifuged at 2500 rpm for 5 min. This procedure was necessary to remove saccharin, which interferes with the chromatography. After centrifugation, 2 ml of the supernate was pipetted into a 10-ml volumetric flask and diluted to volume with Mobile Phase A.

Calculations—The areas under the peaks of tetracycline, its degradation compounds, and chlortetracycline were measured. The percent composition of these compounds was calculated using the following formula:

$$(A_1 + A_2 + A_3 + A_4 + A_5)/A_s \times W_s/W \times 100 \qquad \text{(Eq. 1)}$$

where:

A_1 = area of tetracycline peak in sample
A_2 = area of 4-epitetracycline peak in sample
A_3 = area of chlortetracycline peak in sample
A_4 = (area of 4-epianhydrotetracycline peak in sample) × 0.76
A_5 = (area of anhydrotetracycline in sample) × 0.76
W_s = weight of tetracycline reference standard in milligrams
W = weight of tetracycline sample in milligrams
0.76 = response factor (The response factor was calculated from the molar absorptivity at 280 nm in the mobile phase, chromatographic peak area, and purity of each component preparation)

Microbiological Assay Method—The methods described in the "Code of Federal Regulations" (9) were used. The pharmaceutical preparations containing tetracycline phosphate complex were analyzed by an agar diffusion cylinder cup method using *Bacillus cereus* (ATCC 11778), and the remaining preparations were analyzed by a turbidimetric method using *Staphylococcus aureus* (ATCC 6538P) as the test microorganism.

Table II—Recovery of 4-Epianhydrotetracycline Added in Tetracycline by HPLC

Weight of Tetracycline, mg/ml	Weight of 4-Epianhydrotetracycline (Corrected), mg/ml	4-Epianhydrotetracycline Added, %	4-Epianhydrotetracycline Recovered, %
0.4000	0	0	0
0.3942	0.00145	0.368	0.34
0.3946	0.00364	0.914	0.98
0.3980	0.01456	3.53	3.5
0.3948	0.02913	6.88	6.2
0.3931	0.05826	12.9	12.3
0	0.07282	100	99.0

RESULTS AND DISCUSSION

The major modifications made to the original HPLC method for tetracyclines (3) were the use of a different reverse-phase column packing material, which necessitated a change in the composition of the mobile phases, and incorporation of a gradient elution system. The column packing material selected was octadecylsilane bonded on 10 μm of silica gel, which was successfully applied for the analysis of bacitracin (10). This packing material is far more stable and efficient than the originally used hydrocarbon polymer. The gradient elution system was used to shorten the chromatographic time and to make the detection of trace quantities of degradation compounds easier. The addition of ethylenediaminetetraacetic acid in the mobile phase was not essential for the analysis of tetracycline with this new system.

Separation of Tetracyclines—As may be seen in Fig. 1, tetracycline, its epimer, and degradation compounds were well separated. The resolution function (R_s) between 4-epitetracycline and tetracycline was improved from 0.93, the original method (3), to 2.29. Between 4-epianhydrotetracycline and anhydrotetracycline, it was improved from 0.43 to 1.50. The R_s was calculated using the formula: $R_s = 2(t_2 - t_1)/(W_1 + W_2)$, where $t_2 - t_1$ equals the difference in retention time of the two adjacent peaks, and $(W_1 + W_2)/2$ equals the average baseline peak width.

The chromatography of a tetracycline sample was shortened to approximately 16 min from the 25 min required by the original method (3).

Quantitative Determination of Tetracycline—The precision of the improved HPLC method was determined by comparing several replicate preparations of the USP reference standard. Table I indicates that the relative standard deviation of the HPLC method

Table III—Recovery of Tetracycline from Pharmaceutical Preparations

Percent of Label Dosage	Tetracycline Added, mg[a]	Tetracycline Recovered, mg[a]	Recovery, %
Hard Filled Capsules Containing Tetracycline Hydrochloride, 250 mg/Capsule			
80 (200 mg/capsule)	401.68	396.14	98.6
100 (250 mg/capsule)	500.62	499.98	99.9
120 (300 mg/capsule)	600.84	584.57	97.3
Syrup Containing Tetracycline Base, 125 mg/5 ml			
90 (112.5 mg/5 ml)	115.17	113.77	98.8
100 (125 mg/5 ml)	128.10	127.54	99.6
120 (150 mg/5 ml)	153.83	152.93	99.4

[a] Weight equivalent to two capsules.

Table IV—Relative Standard Deviation Using a Lot of Hard Filled Capsules Containing 250 mg of Tetracycline Hydrochloride

Weight of Capsules, mg	Area, mm^2	Area–Weight Ratio	Tetracycline/ Capsule Recovered, mg
947.67	166.5	0.17669	265.3
944.92	164.3	0.17388	262.5
950.46	164.0	0.17255	260.6
946.87	164.0	0.17322	261.6
946.82	160.0	0.16989	256.5
947.00	160.7	0.17141	258.8
948.03	163.0	0.17351	262.0
		$\bar{x}$ =	261.0
		RSD =	1.07%

for tetracycline was 0.66%. Thus, good quantitation can be obtained without the use of an internal standard with a valve injector system. However, when an internal standard is preferred, tryptophan at 0.7 mg/ml may be used. Tryptophan elutes earlier, is well separated from 4-epitetracycline, and is not interfered with by incipients in pharmaceutical dosage forms.

To correlate the HPLC data with the microbiological potencies, the microbiological responses of tetracycline, 4-epitetracycline, chlortetracycline, anhydrotetracycline, and 4-epianhydrotetracycline were determined. Five concentrations of each component were prepared and assayed against *B. cereus* (ATCC 11778) and *S. aureus* (ATCC 6538P) using the cylinder cup agar diffusion assay method and the turbidimetric assay method, respectively (9).

The HPLC data indicated that the USP tetracycline hydrochloride reference standard, Issue H, contained 0.25% 4-epitetracycline; 4-epitetracycline powder contained 3.0% tetracycline and 0.34% 4-epianhydrotetracycline; chlortetracycline powder contained 0.98% tetracycline; 4-epianhydrotetracycline powder contained 0.5% chlortetracycline and 8.0% anhydrotetracycline; and anhydrotetracycline powder contained 2.2% 4-epianhydrotetracycline. Therefore, the microbiological responses of these compounds were corrected to compensate for these impurities. The corrected microbiological response factors for 4-epitetracycline, chlortetracycline, 4-epianhydrotetracycline, and anhydrotetracycline are 0.29, 5.92, 0.22, and 0.03 for *B. cereus* and 0.10, 3.26, 0.09, and 0.04 for *S. aureus*, respectively. Therefore, the following equation was devised to make the HPLC data comparable with that of the microbiological assay data:

$$\text{HPLC calculated biopotency } (\mu g/mg) = (A_1 + \alpha A_2 + \beta A_3 + \gamma A_4 + \delta A_5)/A_s \times (W_s/W) \times F_1 \times F_2 \quad \text{(Eq. 2)}$$

where:

F_1 = assigned value of the tetracycline reference standard
F_2 = dilution factor
$\alpha, \beta, \gamma, \delta$ = microbiological response factors for 4-epitetracycline, chlortetracycline, 4-epianhydrotetracycline, and anhydrotetracycline

The sensitivity of the HPLC method to tetracycline remained at approximately 10 ng/sample injected. The method was successfully applied to the determination of tetracycline in clinical samples and in fermentation broth with a minimum of sample preparation.

Determination and Quantitation of 4-Epianhydrotetracycline in Tetracycline—To examine the detection limit and quantitation of 4-epianhydrotetracycline in a tetracycline sample by the HPLC method, USP reference standard solutions containing 0, 0.37, 0.91, 3.5, 6.9, 13, and 100% of 4-epianhydrotetracycline were prepared and analyzed. The purity of 4-epianhydrotetracycline was determined by molar absorptivity (20.08) at 438 nm using the method outlined in the "Federal Register" (1) and the HPLC method. The purity thus determined (71.9%) was used to correct the weight of 4-epianhydrotetracycline added in tetracycline samples.

Table V—Analysis of Pharmaceutical Preparations Containing Tetracycline Base and Tetracycline Hydrochloride by HPLC

Lot	Microbiological Potency	Calculated HPLC Potency	Percent Composition by HPLC[a] I	II	III	IV	V
Hard filled capsules:							
A	254	237.8	95.8	2.7	<0.3	<0.3	<0.3
B	251	253.7	96.8	2.4	<0.3	<0.3	<0.3
C	247	246.6	95.4	2.7	<0.3	<0.3	<0.3
D	255	246.3	94.7	4.3	<0.3	<0.3	<0.3
E	251	254.2	96.1	2.8	<0.3	<0.3	<0.3
F	246	252.3	94.7	3.8	<0.3	<0.3	<0.3
G	250	255.4	92.8	5.1	<0.3	<0.3	<0.3
H	249	260.6	98.9	1.1	<0.3	<0.3	<0.3
I	253	261.0	95.0	2.0	<0.3	<0.3	<0.3
Film-coated tablets:							
A	274	273.5	98.1	1.9	<0.3	<0.3	<0.3
B	259	253.1	97.1	2.2	<0.3	<0.3	<0.3
C	252	258.5	97.4	2.6	<0.3	<0.3	<0.3
D	248	256.8	96.7	3.2	<0.3	<0.3	<0.3
E	252	267.1	97.9	2.1	<0.3	<0.3	<0.3
F	253	258.5	97.6	2.3	<0.3	<0.3	<0.3
G	253	249.5	97.3	2.7	<0.3	<0.3	<0.3
Film-coated tablets:							
A	521	531.5	97.6	2.4	<0.3	<0.3	<0.3
B	490	522.6	97.5	2.5	<0.3	<0.3	<0.3
C	493	509.6	97.5	2.5	<0.3	<0.3	<0.3
Syrup:							
A	137	135.9	93.1	3.9	<0.3	<0.3	<0.3
B	138	136.6	92.8	4.5	<0.3	<0.3	<0.3
C	139	134.9	93.3	4.4	<0.3	<0.3	<0.3
D	131	138.3	92.8	5.3	<0.3	<0.3	<0.3
E	133	135.1	93.6	3.9	<0.3	<0.3	<0.3
F	129	129.9	92.2	4.2	<0.3	<0.3	<0.3
G	133	123.2	92.9	3.4	<0.3	<0.3	<0.3
Oral suspension:							
A	109	108.7	95.6	4.4	<0.3	<0.3	<0.3
B	102	102.7	96.5	3.5	<0.3	<0.3	<0.3
C	112	103.1	96.5	3.5	<0.3	<0.3	<0.3
D	112	104.6	96.8	3.2	<0.3	<0.3	<0.3
E	102	103.1	96.5	3.5	<0.3	<0.3	<0.3

[a] I = tetracycline, II = 4-epitetracycline, III = chlortetracycline, IV = 4-epianhydrotetracycline, and V = anhydrotetracycline.

Table VI—Analysis of Expired Lots of Pharmaceutical Preparations Containing Tetracycline Phosphate Complex by HPLC

Lot	Microbiological Potency	Calculated HPLC Potency	Percent Composition by HPLC[a] I	II	III	IV	V
Hard-filled capsule[b]:							
A	61.6	64.0	76.2	19.9	<0.3	1.9	2.0
B	56.3	58.3	72.3	21.8	<0.3	3.2	2.7
Hard-filled capsule[c]:							
A	241	220	78.3	16.5	<0.3	1.6	3.5
B	219	240	78.3	17.2	<0.3	2.4	2.2
C	226	203	75.5	19.2	<0.3	2.9	2.4
D	226	196	71.1	24.3	<0.3	2.8	1.8

[a] I = tetracycline, II = 4-epitetracycline, III = chlortetracycline, IV = 4-epianhydrotetracycline, and V = anhydrotetracycline. [b] Containing tetracycline phosphate complex with novobiocin. [c] Containing tetracycline phosphate complex with nystatin.

The results shown in Table II indicate that the recovery of 4-epianhydrotetracycline was linear (r = 1.000) over the 0.3–100% range with a linear regression of $y = x - 0.201$. The relative standard deviation of the 4-epianhydrotetracycline determination, performed using a tetracycline sample containing approximately 3% 4-epianhydrotetracycline, was approximately 6%.

Analysis of Pharmaceutical Preparations—Since tetracycline base and tetracycline hydrochloride are readily soluble in methanol, this solvent has been used for extraction of tetracycline from pharmaceutical formulations. The methanol extraction procedure has a distinct advantage over aqueous systems since tetracycline hydrochloride is unstable and the base form is insoluble in water. Both of these tetracycline forms, however, are soluble and stable in methanol for at least 8 hr, with no increase in 4-epitetracycline (3). Also, many of the incipient formulation components are insoluble in methanol and are separated from the tetracycline with a simple centrifuging procedure.

Tetracycline recovery studies were performed using hard filled capsules containing tetracycline hydrochloride and a syrup containing tetracycline base. Recovery was 99.9% for the capsules and 99.6% for the syrup, both at label concentration (Table III). Recovery studies were performed on these two products, since the composition of most formulations is similar.

The relative standard deviation of the method was determined by using eight separate weighings and extractions on one lot of hard filled capsules containing 250 mg of tetracycline hydrochloride. The relative standard deviation of the method was 1.1% (Table IV).

Excellent agreement was obtained between the HPLC calculated biological equivalence and the data obtained by the microbiological method using *S. aureus* (9) for products containing tetracycline base and tetracycline hydrochloride (Table V).

Two products containing tetracycline phosphate complex were then assayed; expired lots were used (Table VI). These expired lots contained less than 3% 4-epianhydrotetracycline, with the exception of one lot containing 3.2%. The limit of 4-epianhydrotetracycline in capsule products is 3% (1). Thus, the HPLC method would be of value as a stability-indicating assay method. The agreement between the HPLC calculated values and values obtained by the agar diffusion assay method using *B. cereus* (9) were satisfactory, although considerable variations in assay values were noted. The variation may be due to the agar diffusion assay method using *B. cereus*, since the method is infrequently performed in our laboratory. We are converting the agar diffusion assay method to the more reliable turbidimetric assay method using *S. aureus* (9).

The high speed of analysis, the precision, and the good sensitivity to minor quantities of degradation compounds make the improved HPLC method ideal for the analysis of pharmaceutical preparations containing tetracycline to determine compliance with the requirements of the FDA (1) and the European Pharmacopoeia (2).

REFERENCES

(1) *Fed. Regist.*, **39** (22), part III, 3935(1974).

(2) "European Pharmacopoeia," amendments to vol. II, **39,** 1973.

(3) K. Tsuji, J. H. Robertson, and W. F. Beyer, *Anal. Chem.*, **46,** 539(1974).

(4) A. G. Butterfield, D. W. Hughes, N. J. Pound, and W. L. Wilson, *Antimicrob. Ag. Chemother.*, **4,** 11(1973).

(5) A. G. Butterfield, D. W. Hughes, W. L. Wilson, and N. J. Pound, *J. Pharm. Sci.*, **64,** 316(1975).

(6) E. R. White, M. A. Carroll, J. E. Zarembo, and A. D. Bender, *J. Antibiot.*, **28,** 205(1975).

(7) B. G. Kelly, *J. Pharm. Sci.*, **53,** 1551(1964).

(8) P. P. Ascione, J. B. Zagar, and G. P. Chrekian, *ibid.*, **56,** 1393(1967).

(9) "Code of Federal Regulations," Title 21, 1974.

(10) K. Tsuji, J. H. Robertson, and J. A. Bach, *J. Chromatogr.*, **99,** 597(1974).

ACKNOWLEDGMENTS AND ADDRESSES

Received December 19, 1974, from *Control Analytical Research and Development, The Upjohn Company, Kalamazoo, MI 49001*

Accepted for publication June 11, 1975.

A. R. Lewis is thanked for his statistical evaluation of these data. T. L. Branch is acknowledged for arranging the microbiological analysis.

[x] To whom inquiries should be directed.

Synthesis of Substituted Thiobenzoxazoles/Benzothiazoles: Inhibition of Cellular Respiratory and Monoamine Oxidase Activities and Anticonvulsant Property

RADHEY S. MISRA *§, JAYANTI P. BARTHWAL *, SURENDRA S. PARMAR *x, SHIVA P. SINGH ‡, and VIRGIL I. STENBERG ‡

Abstract □ Several 2-(substituted alkoxy/hydrazinocarbonyl acetanilidothio)benzoxazoles/benzothiazoles were synthesized and characterized by their sharp melting points, elemental analyses, and IR spectra. All thiobenzoxazoles/benzothiazoles possessed low anticonvulsant activity, which was reflected by the 10–40% protection afforded by these compounds against pentylenetetrazol-induced convulsions. All thiobenzoxazoles/benzothiazoles inhibited selectively the nicotinamide adenine dinucleotide (NAD)-dependent oxidation of pyruvate, DL-isocitrate, and α-ketoglutarate by rat brain homogenates. NAD-independent oxidation of succinate remained unaltered. All 2-(substituted hydrazinocarbonyl acetanilidothio)benzoxazoles/benzothiazoles inhibited monoamine oxidase activity of rat brain homogenates. Greater monoamine oxidase inhibition was observed with thiobenzothiazoles than with the corresponding thiobenzoxazoles. The low anticonvulsant activity possessed by these thiobenzoxazoles/benzothiazoles was found to be unrelated with their ability to inhibit cellular respiratory and monoamine oxidase activities of rat brain homogenates.

Keyphrases □ Thiobenzoxazoles, substituted—synthesis and characterization, anticonvulsant activity, effect on NAD-dependent oxidation, monoamine oxidase activity □ Thiobenzothiazoles, substituted—synthesis and characterization, anticonvulsant activity, effect on NAD-dependent oxidation, monoamine oxidase activity □ Anticonvulsant activity—screened in substituted thiobenzoxazoles and thiobenzothiazoles □ Oxidation, NAD dependent—screened in substituted thiobenzoxazoles and thiobenzothiazoles □ Monoamine oxidase activity—screened in substituted thiobenzoxazoles and thiobenzothiazoles

Depressant effects of benzimidazole (1) and anticonvulsant properties of benzimidazoles and benzothiazoles (2) led to the development of zoxazolamine (3) and chlorozoxazone (4) as centrally acting muscle relaxants. Benzimidazole (5, 6) and benzoxazole (5, 7) derivatives have been reported to raise the threshold of electroshock convulsions. Earlier studies also indicated the anticonvulsant activity of benzothiazole, an isoester of benzoxazole and benzimidazole, which, in the form of a methyl derivative, raised the electroshock threshold in cats (5). Furthermore, diverse psychopharmacological properties exhibited by benzoxazoles (8) and benzothiazoles (2, 9) prompted synthesis of 2-(substituted alkoxy/hydrazinocarbonyl acetanilidothio)benzoxazoles/benzothiazoles.

In the present study, thiobenzoxazoles/benzothiazoles were evaluated for their anticonvulsant activity and ability to inhibit cellular respiratory and monoamine oxidase activities of rat brain homogenates.

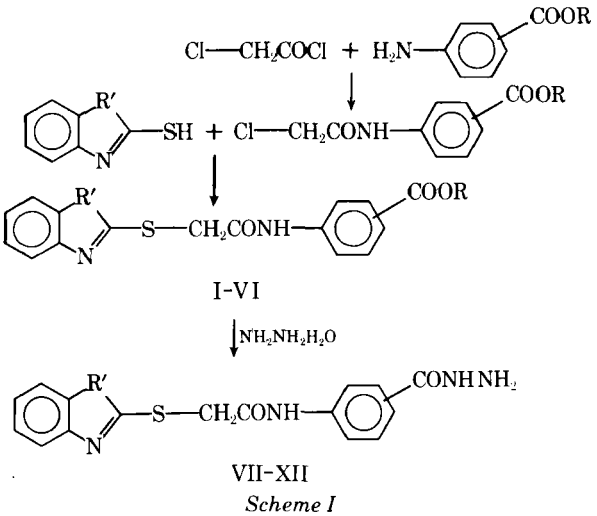

Scheme I

EXPERIMENTAL[1]

Chemistry—The various 2-(substituted alkoxy/hydrazinocarbonyl acetanilidothio)benzoxazoles/benzothiazoles were synthesized by following the methods outlined in Scheme I (R′ = O or S). 2-Mercaptobenzoxazole or 2-mercaptobenzothiazole, on condensation with *N*-chloroacetylamino esters, resulted in the formation of 2-(substituted alkoxycarbonyl acetanilidothio)benzoxazoles/benzothiazoles. These compounds were treated with hydrazine hydrate to form the corresponding 2-(substituted hydrazinocarbonyl acetanilidothio)benzoxazoles/benzothiazoles.

Alkylamino Benzoates—These alkylamino benzoates were prepared by treating aminobenzoic acids with the appropriate alcohol according to the method reported earlier (10).

***N*-Chloroacetylaminoalkyl Esters**—To a solution of an appropriate aminoalkyl benzoate (0.04 mole) in 20 ml of dry benzene was gradually added chloroacetyl chloride (0.022 mole), and the mixture was refluxed on a steam bath for 2–4 hr. Excess benzene was distilled, and the resulting mixture was poured over ice-cold water. The desired *N*-chloroacetylaminoalkyl esters, which separated out, were reported earlier (11).

2-(Substituted Alkoxycarbonyl Acetanilidothio)benzoxazoles/benzothiazoles—A mixture of the appropriate 2-mercaptobenzoxazole or 2-mercaptobenzothiazole (0.01 mole) in 20 ml of dry acetone, anhydrous potassium carbonate (0.011 mole), and the suitable chloroacetylaminoalkyl ester (0.01 mole) was refluxed on a steam bath for 16–18 hr. The mixture was filtered to remove potassium chloride. Excess acetone from the filtrate was distilled; the crude products, which separated on cooling, were collected by filtration, washed with water, and recrystallized from ethanol.

The various 2-(substituted alkoxycarbonyl acetanilidothio)benzoxazoles/benzothiazoles were characterized by their sharp melting points and elemental analyses (Table I). The presence of characteristic bands for —C(=O)O (1735 cm^{-1}), CH_2 (2800 cm^{-1}), and CONH (1690 cm^{-1}) in the IR spectra of these compounds provided further confirmation of their molecular structure.

2-(Substituted Hydrazinocarbonyl Acetanilidothio)benzoxazoles/benzothiazoles—To a solution of the appropriate 2-(sub-

[1] All compounds were analyzed for their carbon, hydrogen, and nitrogen content. Melting points were taken in open capillary tubes with a partial immersion thermometer and are corrected. IR spectra were obtained with Perkin-Elmer Infracord spectrophotometer model 137 equipped with sodium chloride optics in potassium bromide films in the 700–3500-cm^{-1} range.

Table I—Physical Constants of 2-(Substituted Alkoxycarbonyl Acetanilidothio)-benzoxazoles/benzothiazoles

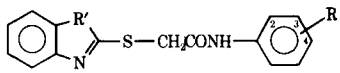

Compound	R′	R	Melting Point[a]	Yield, %	Molecular Formula	Analysis, % Calc.	Found
I	O	2-$COOCH_3$	116°	58	$C_{17}H_{14}N_2O_4S$	C 59.64 H 4.09 N 8.19	59.86 3.90 7.93
II	O	3-$COOC_2H_5$	90°	63	$C_{18}H_{16}N_2O_4S$	C 60.67 H 4.49 N 7.86	60.98 4.29 7.70
III	O	4-$COOC_2H_5$	140°	72	$C_{18}H_{16}N_2O_4S$	C 60.67 H 4.49 N 7.86	60.89 4.30 7.74
IV	S	2-$COOCH_3$	109°	60	$C_{17}H_{14}N_2O_3S_2$	C 56.98 H 3.91 N 7.82	56.66 4.10 7.64
V	S	3-$COOC_2H_5$	147°	66	$C_{18}H_{16}N_2O_3S_2$	C 58.06 H 4.30 N 7.52	58.28 4.16 7.40
VI	S	4-$COOC_2H_5$	135°	70	$C_{18}H_{16}N_2O_3S_2$	C 58.06 H 4.30 N 7.52	57.84 4.42 7.38

[a] Melting points were taken in open capillary tubes with a partial immersion thermometer and are corrected.

stituted alkoxycarbonyl acetanilidothio)benzoxazole/benzothiazole (0.01 mole) in 20 ml of absolute ethanol was added hydrazine hydrate (99–100%; 0.02 mole), and the mixture was refluxed on a steam bath for 10–12 hr. Excess ethanol was distilled; the crude products, which separated, were collected by filtration, dried, and recrystallized from ethanol.

The various 2-(substituted hydrazinocarbonyl acetanilidothio)-benzoxazoles/benzothiazoles were characterized by their sharp melting points and elemental analyses (Table II). The molecular structure of these compounds was further characterized by the presence of the characteristic bands for CONH (1660 cm^{-1}), CH_2 (2850 cm^{-1}), and NH_2 (3350 cm^{-1}) groups in their IR spectra.

Determination of Respiratory Activity of Rat Brain Homogenates[2]—Male albino rats, kept on an *ad libitum* diet, were used in all experiments. Rats, 100–150 g, were sacrificed by decapitation. The brains were removed immediately and homogenized[3] in ice-cold 0.25 *M* sucrose in a ratio of 1:9 (w/v). All incubations were carried out at 37° in the conventional Warburg manometric apparatus, using air as the gas phase (12). The oxygen uptake was measured at 10-min intervals.

Fresh brain homogenate (1 ml) equivalent to 100 mg of wet brain weight was added to the chilled Warburg vessels containing 6.7 m*M* magnesium sulfate, 20 m*M* sodium hydrogen phosphate buffer solution (pH 7.4), 1 m*M* adenosine monophosphate (sodium salt), 33 m*M* potassium chloride, and 500 μg of cytochrome c in a final volume of 3 ml unless otherwise stated. The central well contained 0.2 ml of 20% potassium hydroxide solution. Pyruvate, DL-isocitrate, α-ketoglutarate, and succinate were used at a final concentration of 10 m*M*. It was assumed that the endogenous NAD, present in brain homogenates, was sufficient for the cellular respiratory activity of rat brain homogenates.

All 2-(substituted alkoxy/hydrazinocarbonyl acetanilidothio)-benzoxazoles/benzothiazoles were dissolved in propylene glycol (100%) and were used at a final concentration of 2 m*M*. An equal volume of propylene glycol was added to the control vessels.

Determination of Anticonvulsant Activity—Anticonvulsant activity was determined in mice of either sex, 25–30 g, against pentylenetetrazol-induced convulsions. The mice were divided in groups of 10, keeping the group weights as near the same as possible. All 2-(substituted alkoxy/hydrazinocarbonyl acetanilidothio)benzoxazoles/benzothiazoles were suspended in 5% aqueous gum acacia to give a concentration of 1% (w/v). The test compounds were administered intraperitoneally in a dose of 100 mg/kg to a group of 10 mice.

Four hours after the administration of the test compounds, the mice were injected with pentylenetetrazol (90 mg/kg sc). This dose was shown to produce convulsions in almost all untreated mice, and the mice exhibited 100% mortality during 24 hr (12). No mortality was observed during 24 hr in mice treated with 100 mg/kg of thiobenzoxazoles/benzothiazoles alone.

The mice were observed for 60 min for the occurrence of seizures. An episode of clonic spasm persisting for at least 5 sec was considered a threshold convulsion. Transient intermittent jerks and tremulousness were not counted. Animals devoid of threshold convulsions during the 60-min period were considered protected. The number of animals protected in each group was recorded, and the anticonvulsant activity of 2-(substituted alkoxy/hydrazinocarbonyl acetanilidothio)benzoxazoles/benzothiazoles was represented as percent protection. The mice were then observed for 24 hr, and their mortality was recorded.

Determination of Monoamine Oxidase Activity—Monoamine oxidase activity of rat brain homogenates was determined spectrophotofluorometrically, using kynuramine as the substrate (10). Male albino rats, 100–150 g, were allowed food and water *ad libitum* and were sacrificed by decapitation. The brains were removed immediately and homogenized[3] in the ratio of 1:9 (w/v) in ice-cold 0.25 *M* sucrose. The monoamine oxidase activity of rat brain homogenates was determined by incubation at 37° in air for 30 min. The reaction mixture in a total volume of 3 ml consisted of 0.5 ml of phosphate buffer (0.02 *M*, pH 7.5), 0.01 m*M* kynuramine, and 0.5 ml of brain homogenates equivalent to 10 mg of wet weight of the tissue.

The various 2-(substituted hydrazinocarbonyl acetanilidothio)-benzoxazoles/benzothiazoles were dissolved in propylene glycol (100%) and added to the brain homogenates to produce a final concentration of 0.1 m*M*. An equivalent amount of propylene glycol was added to the control tubes, and the mixture was incubated for 10 min before the addition of kynuramine. The reaction mixture, after addition of kynuramine, was further incubated for 30 min. The reaction was stopped by the addition of 1 ml of 10% trichloroacetic acid (w/v), and the precipitated proteins were removed by centrifugation.

Suitable 1-ml aliquots of the supernatant solution were taken in 2 ml of 1 *N* NaOH solution and were assayed for 4-hydroxyquinoline, formed during oxidative deamination of kynuramine by rat brain homogenates. The 4-hydroxyquinoline formed was measured fluorometrically in a spectrophotofluorometer[4], using activating light of 315 nm and measuring fluorescence at the maximum of 380 nm. An increase in absorbance provided a direct measurement of 4-hydroxyquinoline formation, which was taken as an index of the monoamine oxidase activity. The percentage inhibition was calcu-

[2] Commercial chemicals were used. Sodium pyruvate, trisodium DL-isocitrate, sodium α-ketoglutarate, adenosine monophosphate (sodium salt), and cytochrome c were obtained from Sigma Chemical Co., St. Louis, Mo. Other common chemicals were obtained from British Drug House, Bombay, India.

[3] Potter-Elvehjem.

[4] Aminco Bowman.

Table II—Physical Constants of 2-(Substituted Hydrazinocarbonyl Acetanilidothio)-benzoxazoles/benzothiazoles

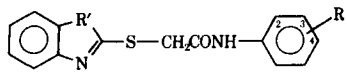

Compound	R′	R	Melting Point[a]	Yield, %	Molecular Formula	Analysis, %	
						Calc.	Found
VII	O	2-CONHNH$_2$	160°	45	$C_{16}H_{14}N_4O_3S$	C 56.14	56.02
						H 4.09	4.20
						N 16.37	16.18
VIII	O	3-CONHNH$_2$	270°	50	$C_{16}H_{14}N_4O_3S$	C 56.14	56.32
						H 4.09	3.90
						N 16.37	16.24
IX	O	4-CONHNH$_2$	188°	56	$C_{16}H_{14}N_4O_3S$	C 56.14	55.90
						H 4.09	4.20
						N 16.37	16.18
X	S	2-CONHNH$_2$	185°	48	$C_{16}H_{14}N_4O_2S_2$	C 53.63	53.90
						H 3.91	3.76
						N 15.64	15.52
XI	S	3-CONHNH$_2$	230°	52	$C_{16}H_{14}N_4O_2S_2$	C 53.63	53.34
						H 3.91	3.98
						N 15.64	15.40
XII	S	4-CONHNH$_2$	195°	58	$C_{16}H_{14}N_4O_2S_2$	C 53.63	53.80
						H 3.91	3.82
						N 15.64	15.46

[a] Melting points were taken in open capillary tubes with a partial immersion thermometer and are corrected.

Table III—Effects of 2-(Substituted Alkoxycarbonyl Acetanilidothio)benzoxazoles/benzothiazoles on the Oxidation of Pyruvate, DL-Isocitrate, α-Ketoglutarate, and Succinate by Rat Brain Homogenates and Their Anticonvulsant Activity

Compound	Inhibition[a], %			Anti-convulsant Activity[b], % Protection	Pentylene-tetrazol Mortality[b], %
	Pyruvate	DL-Isocitrate	α-Keto-glutarate		
I	30.0 ± 0.4	26.2 ± 0.3	23.7 ± 0.5	20	40
II	52.6 ± 0.8	51.0 ± 0.8	51.0 ± 0.7	10	50
III	71.5 ± 1.1	58.8 ± 1.0	55.3 ± 0.8	20	40
IV	23.4 ± 0.3	21.3 ± 0.3	20.3 ± 0.3	40	30
V	35.9 ± 0.4	42.5 ± 0.5	24.6 ± 0.4	20	40
VI	59.3 ± 0.9	50.8 ± 0.8	34.2 ± 0.5	30	30

[a] Assay procedures and the contents of the reaction mixture are as indicated in the text. Each experiment was done in duplicate, and the values represent mean values of percent inhibition with ± *SE* of the mean calculated from three separate experiments. Inhibition was determined by the decrease in the oxygen uptake/100 mg wet brain weight/hr. All substrates and the test compounds were used at a final concentration of 10 and 2 m*M*, respectively. The oxygen uptake in the control experiments, in the absence of added test compounds, was 96.4 ± 5.8, 116.2 ± 6.3, 102.5 ± 6.7, and 171.8 ± 10.6 μl/100 mg wet tissue weight/hr using pyruvate, DL-isocitrate, α-ketoglutarate, and succinate, respectively, as substrates. The percent inhibition by succinate was nil. [b] Screening procedures are as described in the text. The test compounds were administered (100 mg/kg ip) 4 hr prior to the administration of pentylenetetrazol (90 mg/kg sc). Mortality in pentylenetetrazol-treated animals was observed for 24 hr.

lated from the decrease observed in absorbance, and this value provided an index of the monoamine oxidase inhibitory property of these 2-(substituted hydrazinocarbonyl acetanilidothio)benzoxazoles/benzothiazoles.

RESULTS AND DISCUSSION

The effects of 2-(substituted alkoxycarbonyl acetanilidothio)-benzoxazoles/benzothiazoles on the cellular respiratory activity of rat brain homogenates are recorded in Table III. All compounds selectively inhibited the *in vitro* NAD-dependent oxidations of pyruvate, DL-isocitrate, and α-ketoglutarate by rat brain homogenates. However, NAD-independent or flavine-dependent oxidation of succinate remained unaltered.

As is evident from Table III, substituted thiobenzoxazoles (I–III) possessed greater inhibitory effectiveness than the corresponding thiobenzothiazoles (IV–VI) during oxidation of all substrates. These 2-(substituted alkoxycarbonyl acetanilidothio)benzoxazoles/benzothiazoles possessed low anticonvulsant activity, and the protection afforded by these compounds against pentylenetetrazol-induced convulsions ranged from 10 to 40%. Data on anticonvulsant activity and 24-hr pentylenetetrazol mortality provided evidence for some association between increased protection from convulsions and decreased pentylenetetrazol-induced mortality by these compounds in experimental animals.

The selective inhibitory effects of 2-(substituted hydrazinocarbonyl acetanilidothio)benzoxazoles/benzothiazoles during NAD-dependent oxidations of pyruvate, DL-isocitrate, and α-ketoglutarate by rat brain homogenates are recorded in Table IV. Contrary to such a selective inhibition of NAD-dependent oxidations by the precursors, 2-(substituted alkoxycarbonyl acetanilidothio)benzoxazoles/benzothiazoles, the 2-(substituted hydrazinocarbonyl acetanilidothio)benzothiazoles possessed greater inhibitory effectiveness than the corresponding 2-(substituted hydrazinocarbonyl acetanilidothio)benzoxazoles only during oxidation of pyruvate and DL-isocitrate. The inhibition of the oxidation of α-ketoglutarate by X and XI was an exception to such an increased effectiveness of 2-(substituted hydrazinocarbonyl acetanilidothio)benzothiazoles, since these compounds possessed lower inhibitory activity as compared to their corresponding 2-(substituted hydrazinocarbonyl acetanilidothio)benzoxazoles (VII and VIII). The oxidation of succinate, as was observed with their precursors (I–VI), was not inhibited by these compounds (VII–XII).

The various 2-(substituted hydrazinocarbonyl acetanilidothio)-benzoxazoles/benzothiazoles also provided low protection against pentylenetetrazol-induced convulsions. The low anticonvulsant activity possessed by these compounds ranged from 10 to 40%. These results indicated that, in general, the compounds possessing higher anticonvulsant activity also provided greater protection against pentylenetetrazol mortality in experimental mice.

The monoamine oxidase inhibitory activity of 2-(substituted hydrazinocarbonyl acetanilidothio)benzoxazoles/benzothiazoles is recorded in Table V. The inhibition of rat brain monoamine oxidase was found to be higher with 2-(substituted hydrazinocarbonyl ac-

Table IV—Effects of 2-(Substituted Hydrazinocarbonyl Acetanilidothio)benzoxazoles/benzothiazoles on the Oxidation of Pyruvate, DL Isocitrate, α-Ketoglutarate, and Succinate by Rat Brain Homogenates and Their Anticonvulsant Activity

Compound	Inhibition[a], %			Anticonvulsant Activity[a], % Protection	Pentylenetetrazol Mortality[a], %
	Pyruvate	DL-Isocitrate	α-Ketoglutarate		
VII	52.5 ± 0.7	46.3 ± 0.7	69.5 ± 1.1	30	60
VIII	43.9 ± 0.4	33.2 ± 0.5	65.3 ± 1.0	30	50
IX	56.9 ± 0.6	31.4 ± 0.5	53.1 ± 0.8	30	60
X	72.1 ± 1.1	51.3 ± 0.9	31.7 ± 0.4	40	10
XI	65.8 ± 0.9	36.6 ± 0.4	51.7 ± 0.5	10	80
XII	74.2 ± 1.6	65.8 ± 1.0	56.4 ± 0.7	20	70

[a] Assay procedures for the cellular respiratory activity of rat brain homogenates and screening procedures for the determination of anticonvulsant activity are as described in Table III. The percent inhibition by succinate was nil.

etanilidothio)benzothiazoles (X–XII) than with the corresponding 2-(substituted hydrazinocarbonyl acetanilidothio)benzoxazoles (VII–IX). The monoamine oxidase inhibitory effectiveness of these compounds was similar to their ability to inhibit the cellular respiratory activity during NAD-dependent oxidations of pyruvate and DL-isocitrate by rat brain homogenates.

These results indicated that the conversion of 2-(substituted alkoxycarbonyl acetanilidothio)benzoxazoles/benzothiazoles (I–VI) into 2-(substituted hydrazinocarbonyl acetanilidothio)benzoxazoles/benzothiazoles (VII–XII) in no way altered the low anticonvulsant activity against pentylenetetrazol-induced convulsions. However, opposite effects were observed by such a conversion with respect to their ability to inhibit the cellular respiratory activity of rat brain homogenates. In the present study, 2-(substituted hydrazinocarbonyl acetanilidothio)benzothiazoles (X–XII) exhibited greater inhibition of the NAD-dependent oxidations of pyruvate and DL-isocitrate as compared to 2-(substituted hydrazinocarbonyl acetanilidothio)benzoxazoles (VII–IX).

On the other hand, such an inhibition of NAD-dependent oxidations was greater with 2-(substituted alkoxycarbonyl acetanilidothio)benzoxazoles (I–III) than with the corresponding 2-(substituted alkoxycarbonyl acetanilidothio)benzothiazoles (IV–VI). These results indicated an altered inhibition of cellular respiratory activity by the conversion of the COOR (I–VI) to $CONHNH_2$ (VII–XII) group during oxidation of pyruvate and DL-isocitrate by brain homogenates. The increased basicity of 2-(substituted hydrazinocarbonyl acetanilidothio)benzoxazoles/benzothiazoles (VII–XII) compared to the corresponding precursors, 2-(substituted alkoxycarbonyl acetanilidothio)benzoxazoles/benzothiazoles (I–VI), may presumably account for the generally greater selective inhibitory effectiveness of 2-(substituted hydrazinocarbonyl acetanilidothio)benzoxazoles/benzothiazoles.

Table V—Monoamine Oxidase Inhibitory Activity of 2-(Substituted Hydrazinocarbonyl Acetanilidothio)benzoxazoles/benzothiazoles

Compound	Monoamine Oxidase Inhibition[a], %
VII	33.4 ± 0.5
VIII	46.0 ± 0.7
IX	52.3 ± 0.5
X	35.3 ± 0.3
XI	57.8 ± 0.6
XII	64.1 ± 0.9

[a] Assay procedure and the contents of the reaction mixture are as indicated in the text. Each experiment was done in triplicate, and the values are the mean values with ± *SE* of the mean calculated from three separate experiments. Kynuramine and the test compounds were used at a final concentration of 0.1 m*M*. The enzyme activity observed in the absence of the test compounds ranged from 21.3 to 24.9% change in transmission/10 mg wet brain weight/30 min.

These results failed to provide any correlation between the *in vitro* selective inhibition of NAD-dependent oxidations and monoamine oxidase inhibition and the low anticonvulsant activity of these thiobenzoxazoles/benzothiazoles. Further studies dealing with detailed pharmacological and toxicological properties may account for the enzyme inhibitory effectiveness of 2-(substituted alkoxy/hydrazinocarbonyl acetanilidothio)benzoxazoles/benzothiazoles.

REFERENCES

(1) L. S. Goodman, *Bull. N. Engl. Med. Centre*, **5**, 97(1943).

(2) E. F. Domino, R. J. Peterson, and K. R. Unna, *J. Pharmacol. Exp. Ther.*, **103**, 342(1951).

(3) D. F. Marsh, *Fed. Proc.*, **14**, 1183(1955).

(4) A. P. Roszkowski, *J. Pharmacol. Exp. Ther.*, **129**, 75(1960).

(5) W. G. Bywater, W. R. Coleman, O. Kamm, and H. H. Merrit, *J. Amer. Chem. Soc.*, **67**, 905(1945).

(6) L. S. Goodman and J. E. P. Toman, *Fed. Proc.*, **4**, 120(1945).

(7) T. R. J. Putnam and H. H. Merrit, *Arch. Neurol. Psychiat.*, **45**, 505(1941).

(8) S. Joseph, C. W. Richmond, and J. L. Valentine, *J. Med. Chem.*, **10**, 408(1952).

(9) E. F. Domino, K. R. Unna, and J. Kerwin, *J. Pharmacol. Exp. Ther.*, **105**, 486(1952).

(10) R. S. Misra, J. P. Barthwal, S. S. Parmar, and S. J. Brumleve, *J. Pharm. Sci.*, **63**, 401(1974).

(11) G. Z. Sanna and M. Granta, *Chem. Zentralbl.*, **11**, 3313(1937); *Rend. Semin. Fac. Sci. Univ. Cagliari*, **5**, 88(1935).

(12) A. K. Chaturvedi, J. P. Barthwal, S. S. Parmar, and V. I. Stenberg, *J. Pharm. Sci.*, **64**, 454(1975).

ACKNOWLEDGMENTS AND ADDRESSES

Received March 31, 1975, from the *Department of Pharmacology and Therapeutics, King George's Medical College, Lucknow University, Lucknow 226003, India, and the ‡Department of Chemistry, University of North Dakota, Grand Forks, ND 58202

Accepted for publication June 11, 1975.

Supported in part by U.S. Public Health Service National Institutes of Health Grants 1 T01 HL-05939, 1 R01 DA-00996-01 (Department of Physiology and Pharmacology, School of Medicine, University of North Dakota), GM-21590, and Career Development Award 1-K4-GM-09888 to V. I. Stenberg.

The authors thank Professor K. P. Bhargava and Professor R. G. Severson for their advice and encouragement. Grateful acknowledgment is made to the Council of Scientific and Industrial Research, New Delhi, India, for providing a Research Fellowship to R. S. Misra.

§ Present address: Bio-Organic Laboratory, Michigan Cancer Foundation, Meyer L. Prentis Cancer Center, Detroit, MI 48201

x To whom inquiries should be directed. Present address: Department of Physiology and Pharmacology, School of Medicine, University of North Dakota, Grand Forks, ND 58202

Synthesis of *N,N'*-Bis(3-substituted Benzylideneaminopropyl)-piperazines and Their Anti-Inflammatory, Antiproteolytic, and Anticonvulsant Properties

ARVIND K. CHATURVEDI *‡, B. V. RAMA SASTRY *, ANSHUMALI CHAUDHARI ‡, and SURENDRA S. PARMAR ‡x

Abstract □ Some *N,N'*-bis(3-substituted benzylideneaminopropyl)piperazines were synthesized and characterized by their sharp melting points and elemental analyses. These substituted piperazines possessed anti-inflammatory activity, and the protection afforded by these compounds against carrageenan-induced edema ranged from 23 to 67%. The antiproteolytic activity of these piperazines was reflected by their ability to inhibit *in vitro* hydrolysis of bovine serum albumin and casein by trypsin. The inhibition of trypsin-induced hydrolysis was concentration dependent and competitive in nature.

Keyphrases □ Piperazines—*N,N'*-substituted, synthesis, anti-inflammatory, antiproteolytic, and anticonvulsant properties screened □ Anti-inflammatory activity—*N,N'*-substituted piperazines synthesized and screened □ Antiproteolytic activity—*N,N'*-substituted piperazines synthesized and screened □ Anticonvulsant activity—*N,N'*-substituted piperazines synthesized and screened □ Structure–activity relationships—*N,N'*-substituted piperazines, anti-inflammatory, antiproteolytic, and anticonvulsant properties

Search for effective antiphlogistics necessitated the evaluation of a wide variety of chemical structures (1, 2). Among these compounds, general piperazine derivatives have been reported to possess significant anti-inflammatory activity (3–7). This observation prompted the synthesis of some piperazine derivatives, which were evaluated for their effectiveness as antiphlogistics.

Furthermore, the role of proteolytic enzymes in the inflammatory processes and the well-known pharmacological effects of piperazine derivatives (8, 9) prompted the investigation of the *in vitro* effects of these new piperazines on protein catabolism and an evaluation of their anticonvulsant effects. In the present study, attempts were made to correlate the anti-inflammatory activity of these substituted piperazines with their antiproteolytic activity for elucidation of their biochemical mechanism of action.

EXPERIMENTAL[1]

***N,N'*-Bis(3-substituted Benzylideneaminopropyl)piperazines**—To a solution of the appropriate aromatic aldehyde (0.02 mole) in 20 ml of absolute ethanol was added 2.0 g of *N,N'*-bis(3-aminopropyl)piperazine (0.01 mole), and the mixture was refluxed on a steam bath for 2 hr. The reaction mixture was allowed to stand for 24 hr in a refrigerator, and the excess ethanol was removed under reduced pressure. The solid mass which separated was collected, dried, and recrystallized from ethanol or isopropyl alcohol. The substituted piperazines were characterized by their sharp melting points and elemental analyses (Table I).

[1] All compounds were analyzed for their carbon, hydrogen, and nitrogen content. Melting points were taken in open capillary tubes with a partial immersion thermometer and are uncorrected.

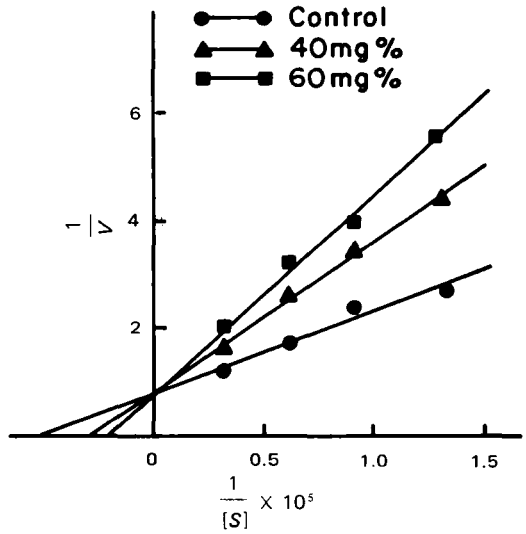

Figure 1—*Inhibition of the trypsin-induced hydrolysis of bovine serum albumin by IV. The* V *represents the change in percent absorbance/0.075 mg of crystalline trypsin/5 min, and* [S] *denotes molar concentration of bovine serum albumin. Key:* ●, *control with no inhibitor;* ▲, *40 mg % of piperazine; and* ■, *60 mg % of piperazine. The* K_m *value for bovine serum albumin is* 2×10^{-5} M; *the* K_i *value for IV is* 0.96×10^{-3} M.

Determination of Anti-Inflammatory Activity—Albino rats, 80–100 g, were allowed food and water *ad libitum;* they were used for the evaluation of the anti-inflammatory activity of these substituted piperazines. The rats were divided into groups of six animals each. A suspension of carrageenan (1.0%) in 0.9% NaCl was prepared fresh 1 hr before use, and 0.5 ml was injected into the plantar side of the right hindpaw (10).

The substituted piperazines (100 mg/kg) were administered intraperitoneally to a group of six rats 1 hr before carrageenan injection, while six control rats received 0.5 ml of 0.9% NaCl solution. Sodium salicylate (100 mg/kg ip) was used as a standard anti-inflammatory agent. The mean increase in paw volume due to carrageenan-induced edema was measured by the micropipet method (11) before and 3 hr after carrageenan treatment.

Assay of Proteolytic Activity[2]—The antiproteolytic activity of substituted piperazines was determined by studying their ability to inhibit *in vitro* trypsin-induced hydrolysis of bovine serum albumin and casein. The reaction mixture consisted of 0.05 *M* tromethamine buffer at pH 8.2, 0.075 mg of crystalline trypsin (1 g sufficient to hydrolyze 250 g of casein), 3.3×10^{-5} *M* of bovine serum albumin (substrate) or casein (substrate), and water in a total volume of 1 ml.

All substituted piperazines were dissolved in dimethylformamide and were used at a final concentration of 40 and 60 mg %. An

[2] Commercial chemicals were used. Bovine serum albumin and casein were obtained from Sigma Chemical Co., St. Louis, Mo. Trypsin was obtained from Serva Chemical Co., Heidelberg, Germany. Sodium salicylate and other common chemicals were obtained from British Drug House, Bombay, India.

Table I—Physical Constants of *N,N'*-Bis(3-substituted Benzylideneaminopropyl)piperazines

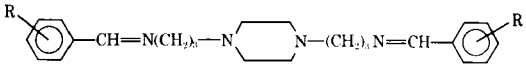

Compound	R	Recrystallization Solvent	Melting Point[a]	Yield, %	Formula	Analysis, % Calc.	Analysis, % Found
I	*m*-NO_2	Ethanol	125°	55	$C_{24}H_{30}N_6O_4$	C 61.80 H 6.43 N 18.02	61.47 6.78 17.94
II	*p*-Cl	Isopropyl alcohol	100°	67	$C_{24}H_{30}Cl_2N_4$	C 64.71 H 6.74 N 12.58	64.52 6.92 12.88
III	*p*-OCH_3	Ethanol	110°	62	$C_{26}H_{36}N_4O_2$	C 71.55 H 8.25 N 12.72	71.38 7.89 13.12
IV	*p*-$N(CH_3)_2$	Ethanol	167°	64	$C_{28}H_{42}N_6$	C 72.72 H 9.09 N 18.18	72.51 9.22 18.45

[a] Melting points were taken in open capillary tubes with a partial immersion thermometer.

equivalent amount of dimethylformamide was added to the control tubes. All piperazines were preincubated with trypsin for 10 min prior to the addition of bovine serum albumin or casein, unless otherwise stated, and the reaction mixture was incubated for another 5 min after the addition of bovine serum albumin or casein.

The reaction was stopped by the addition of 5 ml of 15% trichloroacetic acid solution. The acid-soluble products of protein breakdown, obtained after centrifugation, were determined by the method of Lowry *et al.* (12) as an index of the proteolytic activity of trypsin. A decrease in the degree of trypsin-induced hydrolysis of bovine serum albumin or casein in experiments with the test compound reflected the antiproteolytic activity of these substituted piperazines.

In preincubation studies, trypsin was incubated with or without the substituted piperazines at 37° for 10, 20, and 30 min prior to the addition of bovine serum albumin or casein. The zero-time experiments represent those in which substituted piperazines and bovine serum albumin or casein were added simultaneously to the reaction mixture containing trypsin. In the present study, the nature of the enzyme inhibition by IV was evaluated by the graphic method of Lineweaver and Burk (13) as modified by Dixon (14), using bovine serum albumin and casein as the substrates.

Determination of Anticonvulsant Activity—Anticonvulsant activity was determined against pentylenetetrazol-induced convulsions in mice of either sex weighing between 25 and 30 g. The mice were divided into groups of 10, keeping the group weights as nearly the same as possible. All compounds were suspended in 5% aqueous gum acacia to give a concentration of 0.25% (w/v). The test compounds were administered in a dose of 100 mg/kg ip to a group of 10 animals.

Four hours after the administration of the substituted piperazines, the mice were injected with pentylenetetrazol (90 mg/kg sc). This dose of pentylenetetrazol produced convulsions in almost all untreated mice, which died within 24 hr. No mortality was observed during 24 hr in animals treated with 100 mg/kg of the substituted piperazine alone.

The mice were observed 60 min for the occurrence of seizures. An episode of clonic spasm persisting for at least 5 sec was considered a threshold convulsion. Transient intermittent jerks and tremulousness were not counted. Animals devoid of threshold convulsions during the 60-min period were considered protected. The number of animals protected in each group was recorded, and the anticonvulsant activity of the substituted piperazines was represented as percent protection. The animals were then observed for 24 hr, and their mortality was recorded.

Table II—Anti-Inflammatory Activity of *N,N'*-Bis(3-substituted Benzylideneaminopropyl)piperazines

Compound	Mean Volume of Edema[a], ml ± *SE*	Anti-Inflammatory Activity, % Protection	*p*
Saline control	0.48 ± 0.04	—	—
I	0.18 ± 0.04	62.5	<0.001
II	0.29 ± 0.06	49.5	0.05–0.02
III	0.37 ± 0.03	23.0	0.02
IV	0.16 ± 0.03	66.6	0.01–0.001
Sodium salicylate	0.32 ± 0.01	33.3	0.01–0.001

[a] The experimental procedures are as indicated in the text. All substituted piperazines and sodium salicylate were administered in a dose of 100 mg/kg ip. The decrease in the volume of carrageenan-induced edema was used to calculate the anti-inflammatory activity of substituted piperazines. Statistical tables of Fisher and Yates (15) were used to determine *p* values.

Table III—Anticonvulsant Activity of *N,N'*-Bis(3-substituted Benzylideneaminopropyl)piperazines

Compound	Anticonvulsant Activity[a], % Protection	Pentylenetetrazol Mortality[a], % Protection after 24 hr
I	20	70
II	30	50
III	20	40
IV	30	50

[a] Screening procedures for the determination of anticonvulsant activity are as described in the text. Mortality in pentylenetetrazol-treated animals was observed during 24 hr.

RESULTS AND DISCUSSION

All substituted piperazines were evaluated for anti-inflammatory activity against carrageenan-induced edema in albino rats in a dose of 100 mg/kg (Table II). All piperazines possessed anti-inflammatory activity, and their degree of protection against carrageenan-induced edema ranged from 23 to 67%. Maximum protec-

Table IV—Effect of *N,N'*-Bis(3-substituted Benzylideneaminopropyl)piperazines on the Proteolytic Activity of Trypsin

Compound	Bovine Serum Albumin: Piperazine Concentration 40 mg %	Bovine Serum Albumin: Piperazine Concentration 60 mg %	Casein: Piperazine Concentration 40 mg %	Casein: Piperazine Concentration 60 mg %
	Inhibition[a], %			
I	33.9 ± 1.0	51.6 ± 0.4	14.0 ± 0.9	25.4 ± 0.7
II	28.0 ± 0.8	43.4 ± 0.9	13.3 ± 0.4	23.4 ± 0.8
III	16.8 ± 0.4	34.4 ± 0.7	11.6 ± 0.7	17.3 ± 0.8
IV	40.2 ± 0.7	63.5 ± 0.4	26.0 ± 0.9	31.1 ± 0.7
Sodium salicylate	65.5 ± 0.9	74.5 ± 0.6	28.7 ± 2.0	32.8 ± 0.9

[a] Assay procedures are as indicated in the text. Each experiment was done in triplicate, and the values are the mean values of three separate experiments with ± standard error of the mean.

Table V—Preincubation Studies with *N,N'*-Bis(3-substituted Benzylideneaminopropyl)piperazines to Study Trypsin-Induced Hydrolysis of Bovine Serum Albumin and Casein

Compound	Bovine Serum Albumin, Preincubation Time, min				Casein, Preincubation Time, min			
	0	10	20	30	0	10	20	30
	Inhibition[a], %							
I	32.7 ± 0.7	32.9 ± 0.8	33.8 ± 0.9	34.1 ± 1.0	14.0 ± 1.2	14.0 ± 0.9	13.9 ± 1.0	14.3 ± 0.7
II	28.4 ± 1.0	27.5 ± 0.7	28.9 ± 0.4	27.9 ± 0.7	13.2 ± 1.2	13.2 ± 1.1	13.9 ± 1.0	12.9 ± 0.8
III	16.7 ± 0.5	17.2 ± 0.4	17.0 ± 0.8	16.5 ± 0.6	10.7 ± 1.0	12.0 ± 0.5	11.9 ± 0.7	12.2 ± 0.8
IV	41.1 ± 1.0	39.0 ± 1.2	40.0 ± 0.9	40.9 ± 0.7	26.0 ± 0.9	25.7 ± 0.9	25.8 ± 0.4	26.2 ± 1.5

[a] Contents of the reaction mixture and the assay procedures are as indicated in Table IV. Trypsin was incubated with substituted piperazines for varying times before the addition of the substrate (bovine serum albumin or casein). Zero-time experiments indicate that both the substrate and the piperazines were added to the reaction mixture containing trypsin simultaneously. Each experiment was done in triplicate, and the values are the mean values of three separate experiments with ± standard error of the mean. The various substituted piperazines were used at a final concentration of 40 mg %.

tion of about 67% was observed with IV, having a p-$N(CH_3)_2$ group as the substituent on the phenyl nucleus of this piperazine.

The compound possessing the p-OCH_3 substituent on the phenyl nucleus (III) showed minimum protection against carrageenan-induced edema. In the present study, I, II, and IV possessed greater anti-inflammatory activity than sodium salicylate, which produced about 33% protection of carrageenan-induced edema under similar experimental conditions.

All piperazines possessed low anticonvulsant activity (Table III). The protection offered by these compounds in a dose of 100 mg/kg against pentylenetetrazol-induced convulsions ranged from 20 to 30%. Data on the anticonvulsant activity of these piperazines indicate that there is no relationship between the increased protection from convulsions and the decreased mortality in experimental animals.

All piperazines exhibited antiproteolytic activity (Table IV). These results indicated that, with the exception of IV during casein hydrolysis, sodium salicylate exhibited a higher degree of inhibition of the hydrolysis of bovine serum albumin and casein by trypsin than the substituted piperazines. Among the new compounds, IV exhibited the highest degree of inhibition against trypsin. All of the new compounds as well as sodium salicylate were better inhibitors of trypsin with bovine serum albumin as the substrate than with casein as the substrate.

The results of preincubation studied to evaluate the nature of the inhibition by substituted piperazines are recorded in Table V. Preincubation of trypsin with the piperazines for varying times (0, 10, 20, and 30 min) before the addition of bovine serum albumin or casein *in vitro* did not alter the degree of hydrolysis. Therefore,

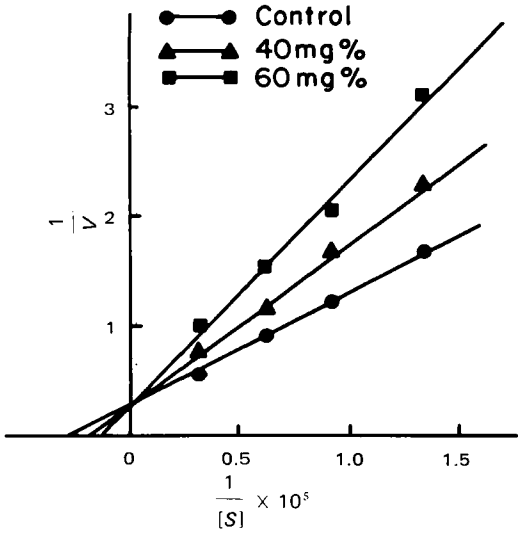

Figure 2—*Inhibition of trypsin-induced hydrolysis of casein by IV. The* [S] *denotes the molar concentration of casein, and* V *represents the change in percent absorbance/0.075 mg of crystalline casein/5 min. Key:* ●, *control with no inhibitor;* ▲, *40 mg % of piperazine; and* ■, *60 mg % of piperazine. The* K_m *value for casein is* 3.6×10^{-5} M; *the* K_i *value for IV is* 1.06×10^{-3} M.

these studies indicated the reversible and/or competitive nature of inhibition of trypsin-induced hydrolysis by substituted piperazines. These findings were further supported by kinetic studies with IV, where the nature of its inhibition of trypsin was evaluated. Compound IV was a competitive inhibitor of the hydrolysis of bovine serum albumin (Fig. 1) and casein (Fig. 2) by trypsin.

In the present series of piperazines, there is a direct relationship between the inhibition of trypsin-induced hydrolysis and anti-inflammatory activity. A similar relationship was reported between the anti-inflammatory and antiproteolytic activities of amyrin acetates (16–18).

REFERENCES

(1) W. C. Kuzell, *Ann. Rev. Pharmacol.*, **8**, 357(1968).

(2) T. Y. Shen, in "Topics in Medicinal Chemistry," vol. 1, J. L. Rabinowitz and R. M. Meyerson, Eds., Wiley, New York, N.Y., 1967, pp. 45–64.

(3) Warner-Lambert Pharmaceutical Co., British pat. 1,089,811 (C1.C07d) (Nov. 8, 1967); through *Chem. Abstr.*, **68**, 105241m(1968).

(4) G. de Stevens and R. P. Mull, Ciba Ltd., Swiss pat. 436,309 (C1.C07d) (Nov. 15, 1967); through *Chem. Abstr.*, **69**, 19206t(1968).

(5) *Ibid.*, Swiss pat. 434,268 (C1.C07d) (Oct. 14, 1967); through *Chem Abstr.*, **69**, 10468x(1968).

(6) W. D. Vigelius, Warner-Lambert Pharmaceutical Co., U.S. pat. 3,378,553 (C1.260-240) (Apr. 16, 1968); through *Chem. Abstr.*, **69**, 59278z(1968).

(7) G. L. Regnier, R. J. Canevari, M. J. Laubie, and J. C. Le Douarec, *J. Med. Chem.*, **11**, 1151(1968).

(8) M. I. Barnhart, C. Quintana, H. L. Lenon, G. B. Bluhm, and J. M. Riddle, *Ann. N.Y. Acad. Sci.*, **146**, 527(1968).

(9) A. Bertelli, *Biochem. Pharmacol. Suppl.*, **1968**, 229.

(10) C. A. Winter, E. A. Risley, and G. W. Nuss, *Proc. Soc. Exp. Biol. Med.*, **111**, 544(1962).

(11) C. A. H. Buttle, P. F. D'Arcy, E. M. Howard, and D. N. Kellet, *Nature (London)*, **179**, 629(1957).

(12) O. H. Lowry, N. J. Rosebrough, A. L. Farr, and R. J. Randall, *J. Biol. Chem.*, **193**, 265(1951).

(13) H. Lineweaver and D. Burk, *J. Amer. Chem. Soc.*, **56**, 658(1934).

(14) M. Dixon, *Biochem. J.*, **55**, 170(1953).

(15) R. A. Fisher and F. Yates, "Statistical Tables," Oliver and Boyd, London, England, 1953.

(16) M. B. Gupta, T. N. Bhalla, G. P. Gupta, C. R. Mitra, and K. P. Bhargava, *Eur. J. Pharmacol.*, **6**, 67(1969).

(17) M. B. Gupta, T. N. Bhalla, K. K. Tangri, and K. P. Bhargava, *Biochem. Pharmacol.*, **20**, 401(1971).

(18) A. Chaudhari, A. K. Chaturvedi, S. S. Parmar, and S. J. Brumleve, *Res. Commun. Chem. Pathol. Pharmacol.*, **7**, 205(1974).

ACKNOWLEDGMENTS AND ADDRESSES

Received April 14, 1975, from the *Department of Pharmacology, Vanderbilt University School of Medicine, Nashville, TN 37232, and the [1]Department of Pharmacology and Therapeutics, King George's Medical College, Lucknow University, Lucknow 226003, India.

Accepted for publication June 11, 1975.

Supported in part by U.S. Public Health Service Grants RR-05424 and NS-04699 and the Council of Scientific and Industrial Research, New Delhi, India.

The authors thank Professor K. P. Bhargava and Dr. J. P. Barthwal for their advice and encouragement. Grateful acknowledgment is made to the Council of Scientific and Industrial Research, New Delhi, India, and the Indian National Science Academy, New Delhi, India, for providing Senior Research Fellowships to A. K. Chaturvedi and A. Chaudhari, respectively.

[x] To whom inquiries should be directed. Present address: Department of Physiology and Pharmacology, School of Medicine, University of North Dakota, Grank Forks, ND 58202

NMR Study of Amphetamines Using Europium Shift Reagents

ROBERT V. SMITH [*x], PAUL W. ERHARDT [*], DAVID B. RUSTERHOLZ [‡], and CHARLES F. BARFKNECHT [‡]

Abstract □ Amphetamine and certain of its methoxylated derivatives show a high degree of interaction with NMR shift reagents of the type tris(1,1,1,2,2,3,3-heptafluoro-7,7-dimethyl-4,6-octanedione)europium(III). The shifts are not accompanied by appreciable line broadening, and both the aliphatic and aromatic protons can be resolved. The strong interaction between amine and shift reagent diminishes rapidly as the amine function is alkylated. For derivatives containing *ortho*-methoxyl groups, a weaker interaction with this functionality also becomes evident as the amine is alkylated. The stereospecificity of the shifting process was investigated by employing tris[3-(trifluoroacetyl)-*d*-camphorato]europium(III), a chiral shift reagent, with stereochemically pure enantiomers and known enantiomeric mixtures. Although certain (*R*)-enantiomers showed greater downfield C-methyl group shifts, these shift differences from the corresponding (*S*)-enantiomers were small and not well resolved.

Keyphrases □ Amphetamine and methoxylated derivatives—interaction with NMR europium shift reagents, stereospecificity of shifting process □ NMR spectroscopy—study of amphetamines and methoxylated derivatives, interaction with europium shift reagents, stereospecificity of shifting process □ Europium—NMR shift reagents, interaction with amphetamines and methoxylated derivatives

Methods for the use of lanthanide NMR shift reagents in spectral simplification and interpretation of molecules possessing a single functional group are well established (1–3). Their use with polyfunctional compounds and the techniques employing chiral shift reagents, however, are not as well characterized (4–6). Korver and Van Gorkom (7) referred to the scarcity of data defining the scope of application of chiral reagents in determining enantiomeric purity, while Armitage *et al.* (8) referred to the highly neglected problem of employing shift reagents in the determination of molecular configuration.

An interest in these analytical tools and a desire for an efficient assay of enantiomeric composition in certain amphetamine derivatives (9) were the bases for this investigation. The NMR spectra of amphetamine (I) and the derivatives II–VII were examined in the presence of increasing amounts of tris-(1,1,1,2,2,3,3-heptafluoro-7,7-dimethyl-4,6-octanedione)europium(III) (VIII). Certain enantiomers and enantiomeric mixtures of amphetamine, *p*-methoxyamphetamine, and 2,5-dimethoxyamphetamine were also studied with the chiral reagent tris[3-(trifluoroacetyl)-*d*-camphorato]europium(III) (IX).

EXPERIMENTAL

Chemistry—The enantiomers of I–V were prepared by a modification of the method of Weinges and Graab (10) as described previously (9). The optical purity of these compounds is in the 96–99% range (9). Racemic samples were prepared by reaction of the appropriate benzaldehyde with nitroethane (11), followed by lithium aluminum hydride reduction of the resulting 1-phenyl-2-nitropropenes (12). Racemates were purified by distillation or by recrystallization of the hydrochloride salts.

NMR Studies—Free amines were generated by first dissolving 100-μmole quantities of hydrochloride salts in 7 ml of water. These solutions were placed in separators, 5-ml portions of ether were added, and the aqueous phases were made basic with 0.5 ml of 3 *N* sodium hydroxide. After separation of the ether layers, the aqueous phases were extracted with a second 5-ml portion of ether. The

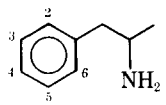

I: amphetamine

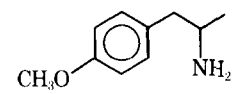

II: *p*-methoxyamphetamine

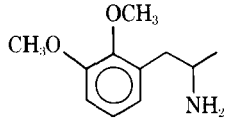

III: 2,3-dimethoxyamphetamine

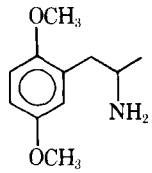

IV: 2,5-dimethoxyamphetamine

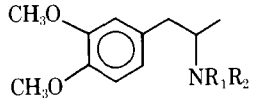

V: 3,4-dimethoxyamphetamine, $R_1 = R_2 = H$

VI: 3,4-dimethoxy-*N*-methylamphetamine, $R_1 = CH_3$, $R_2 = H$

VII: 3,4-dimethoxy-*N*,*N*-dimethylamphetamine, $R_1 = R_2 = CH_3$

Supported in part by U.S. Public Health Service Grants RR-05424 and NS-04699 and the Council of Scientific and Industrial Research, New Delhi, India.

The authors thank Professor K. P. Bhargava and Dr. J. P. Barthwal for their advice and encouragement. Grateful acknowledgment is made to the Council of Scientific and Industrial Research, New Delhi, India, and the Indian National Science Academy, New Delhi, India, for providing Senior Research Fellowships to A. K. Chaturvedi and A. Chaudhari, respectively.

[x] To whom inquiries should be directed. Present address: Department of Physiology and Pharmacology, School of Medicine, University of North Dakota, Grank Forks, ND 58202

NMR Study of Amphetamines Using Europium Shift Reagents

ROBERT V. SMITH [*x], PAUL W. ERHARDT [*], DAVID B. RUSTERHOLZ [‡], and CHARLES F. BARFKNECHT [‡]

Abstract □ Amphetamine and certain of its methoxylated derivatives show a high degree of interaction with NMR shift reagents of the type tris(1,1,1,2,2,3,3-heptafluoro-7,7-dimethyl-4,6-octanedione)europium(III). The shifts are not accompanied by appreciable line broadening, and both the aliphatic and aromatic protons can be resolved. The strong interaction between amine and shift reagent diminishes rapidly as the amine function is alkylated. For derivatives containing *ortho*-methoxyl groups, a weaker interaction with this functionality also becomes evident as the amine is alkylated. The stereospecificity of the shifting process was investigated by employing tris[3-(trifluoroacetyl)-*d*-camphorato]europium(III), a chiral shift reagent, with stereochemically pure enantiomers and known enantiomeric mixtures. Although certain (*R*)-enantiomers showed greater downfield C-methyl group shifts, these shift differences from the corresponding (*S*)-enantiomers were small and not well resolved.

Keyphrases □ Amphetamine and methoxylated derivatives—interaction with NMR europium shift reagents, stereospecificity of shifting process □ NMR spectroscopy—study of amphetamines and methoxylated derivatives, interaction with europium shift reagents, stereospecificity of shifting process □ Europium—NMR shift reagents, interaction with amphetamines and methoxylated derivatives

Methods for the use of lanthanide NMR shift reagents in spectral simplification and interpretation of molecules possessing a single functional group are well established (1–3). Their use with polyfunctional compounds and the techniques employing chiral shift reagents, however, are not as well characterized (4–6). Korver and Van Gorkom (7) referred to the scarcity of data defining the scope of application of chiral reagents in determining enantiomeric purity, while Armitage *et al.* (8) referred to the highly neglected problem of employing shift reagents in the determination of molecular configuration.

An interest in these analytical tools and a desire for an efficient assay of enantiomeric composition in certain amphetamine derivatives (9) were the bases for this investigation. The NMR spectra of amphetamine (I) and the derivatives II–VII were examined in the presence of increasing amounts of tris-(1,1,1,2,2,3,3-heptafluoro-7,7-dimethyl-4,6-octanedione)europium(III) (VIII). Certain enantiomers and enantiomeric mixtures of amphetamine, *p*-methoxyamphetamine, and 2,5-dimethoxyamphetamine were also studied with the chiral reagent tris[3-(trifluoroacetyl)-*d*-camphorato]europium(III) (IX).

EXPERIMENTAL

Chemistry—The enantiomers of I–V were prepared by a modification of the method of Weinges and Graab (10) as described previously (9). The optical purity of these compounds is in the 96–99% range (9). Racemic samples were prepared by reaction of the appropriate benzaldehyde with nitroethane (11), followed by lithium aluminum hydride reduction of the resulting 1-phenyl-2-nitropropenes (12). Racemates were purified by distillation or by recrystallization of the hydrochloride salts.

NMR Studies—Free amines were generated by first dissolving 100-μmole quantities of hydrochloride salts in 7 ml of water. These solutions were placed in separators, 5-ml portions of ether were added, and the aqueous phases were made basic with 0.5 ml of 3 *N* sodium hydroxide. After separation of the ether layers, the aqueous phases were extracted with a second 5-ml portion of ether. The

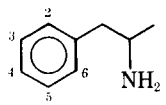

I: amphetamine

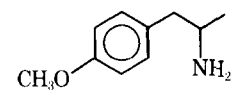

II: *p*-methoxyamphetamine

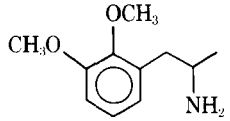

III: 2,3-dimethoxyamphetamine

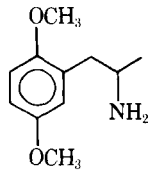

IV: 2,5-dimethoxyamphetamine

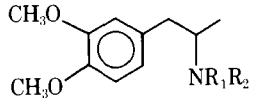

V: 3,4-dimethoxyamphetamine, $R_1 = R_2 = H$

VI: 3,4-dimethoxy-*N*-methylamphetamine, $R_1 = CH_3$, $R_2 = H$

VII: 3,4-dimethoxy-*N*,*N*-dimethylamphetamine, $R_1 = R_2 = CH_3$

Table I—Lanthanide-Induced Shifts of Amphetamines[a]

Compound	—$NH_{2,1}$	—CH—	—CH_2—	—CH_3	Ar—$H_{2,6}$	Ar—$H_{3,4,5}$	2-O—CH_3	3-O—CH_3	4-O—CH_3	5-O—CH_3	NH—CH_3	N—$(CH_3)_2$
I	19.4	5.4	5.7	4.8	1.4	0.5	—	—	—	—	—	—
II	16.5	4.5	2.5	4.0	1.0	0.4	—	—	0.1	—	—	—
III	10.7	2.3	1.9	2.4	0.8	0.3	0.8	0.1	—	—	—	—
IV	13.4	3.2	2.0	3.7	1.0	0.3	0.5	—	—	0.2	—	—
V	14.1	4.1	2.3	3.6	1.0	0.4	—	0.2	0.1	—	—	—
VI	—	1.2	1.2	0.9	0.7	0.6	—	0.5	0.5	—	1.4	—
VII	—	0.2	0.2	0.1	0.2	0.2	—	0.2	0.2	—	—	0.2

[a] Data represent $\Delta\delta$ values for R/S = 0.2. Values increased in a linear fashion up to and including R/S = 0.5 for all compounds except I, where deviation from linearity was observed for R/S values >0.3.

Table II—IX-Induced Shifts of Racemic Amphetamines[a]

Compound	—NH_2	—CH—	—CH_2	—CH_3	Ar—$H_{2,6}$	Ar—$H_{3,4,5}$	2-O—CH_3	4-O—CH_3	5-O—CH_3
I[b]	12.3	2.5	1.7	1.9 2.0[c]	0.7	0.2	—	—	—
II[b]	8.5	1.7	1.3	1.4	0.5	0.2	—	0.1	—
IV[b]	9.4	2.1	1.4	1.5 1.6[c]	0.5	0.2	0.3	—	0.1

[a] Data represent $\Delta\delta$ for R/S = 0.2. Values increased in a linear fashion up to and including R/S = 0.5. [b] Both pure enantiomers and their racemic mixtures were examined. Data reported are for the racemic mixtures. In all cases, the pure enantiomer spectra were identical to those of their corresponding racemic mixtures, except that in the latter spectra separation of the —CH_3 resonances for each enantiomer of I and IV occurred, as indicated. Compound II did not exhibit such resolution even at R/S = 0.5. [c] (*R*)-Enantiomer.

ethereal extracts then were combined and evaporated *in vacuo*, and the residues were dissolved in 2.0 ml of benzene–ethanol (4:1) and again evaporated to dryness *in vacuo*. Each residue was dissolved in 0.5 ml of deuterochloroform (1% tetramethylsilane)[1].

Shift reagent solutions were prepared by dissolving 100 μmoles of VIII[2] or IX[3] in 5.0 ml of deuterochloroform (1% tetramethylsilane). Solutions were prepared immediately before use, and a new solution was prepared for each series of spectra obtained for a single amphetamine sample. NMR spectra were recorded on a 60-MHz spectrometer[4].

After an initial NMR spectrum was obtained without shift reagent, the deuterochloroform solutions were evaporated *in vacuo*, the residues were dissolved in 0.5 ml of the shift reagent solution, and the NMR spectra were recorded. This process was repeated with increasing increments of shift reagent. Alternatively, in instances where substrate volatility appeared to be a problem (*i.e.*, leading to losses of amphetamine), larger quantities of the free amine were isolated and separately weighed for admixture with shift reagent solutions.

RESULTS AND DISCUSSION

The NMR spectral shifts of each proton signal accompanying incremental rises in shift reagent concentration were followed by plotting the proton signal location *versus* the molar ratio of shift reagent, R, to compound, S, at each increment (4). An R/S range of 0.0–0.5 was studied at four or more increments. Figure 1 illustrates the linear nature of the plots generated by this treatment.

Selected spectra from the amphetamine study are presented in Fig. 2 and are illustrative of the spectra for the methoxylated derivatives II–V as well. The utility of this method is demonstrated by the marked enhancement of resolution in the aliphatic spectral region and in the resolution of certain aromatic regions. Furthermore, in most instances, lanthanide-induced shifts were not accompanied by significant signal broadening up to R/S ratios of 0.5. With the secondary amine, VI, however, severe line broadening was inexplicably observed at R/S values above 0.17.

Table I presents the lanthanide-induced shift data for each compound obtained at similar R/S values and permits comparisons between compounds. Tabulation of the lanthanide-induced shifts data as their Demarco slopes (13–15) was not chosen because the polyfunctionality in many of these molecules offers different sites of interaction with the shift reagent (Scheme I), and a linearity beyond the actual R/S range studied should not be implied (4, 16–19). Similarly, tabulation as the Armitage bound chemical shifts seemed inappropriate (8, 20, 21).

From the decreasing —CH—C*H*$_3$ lanthanide-induced shifts in V–VII, it is apparent that the strong interaction between shift reagent and the amine function diminished rapidly as the amine was methylated (converted from primary to tertiary). This effect has

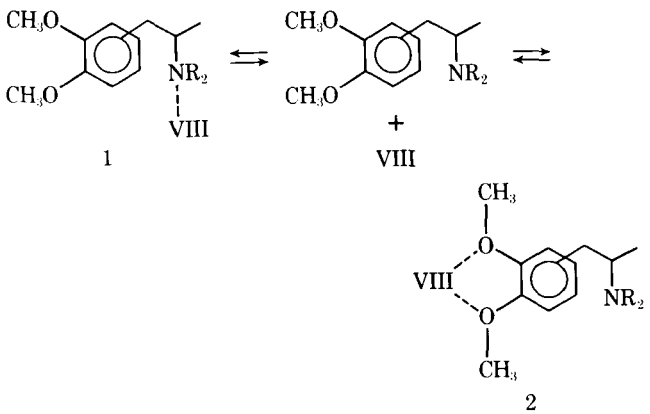

Scheme I—Possible sites of interaction between shift reagent and polyfunctional amphetamine derivatives

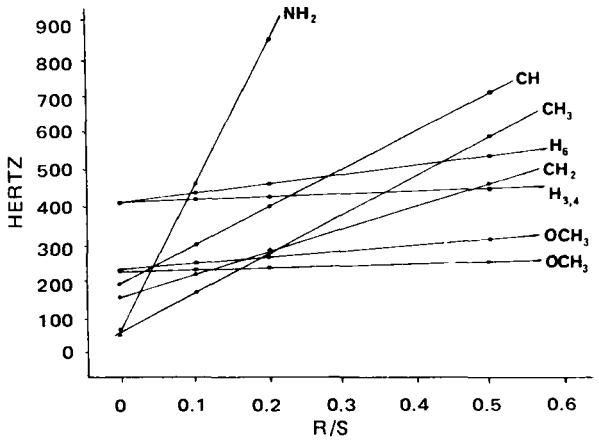

Figure 1—*Typical linear relationship observed between proton signal location (hertz) and R/S (actual data for IV).*

[1] Silanor-C, Merck Sharp & Dohme.
[2] Eu(fod)$_3$, Aldrich Chemical Co.
[3] Eu-OPT, Ventron Alfa Products.
[4] Varian T-60.

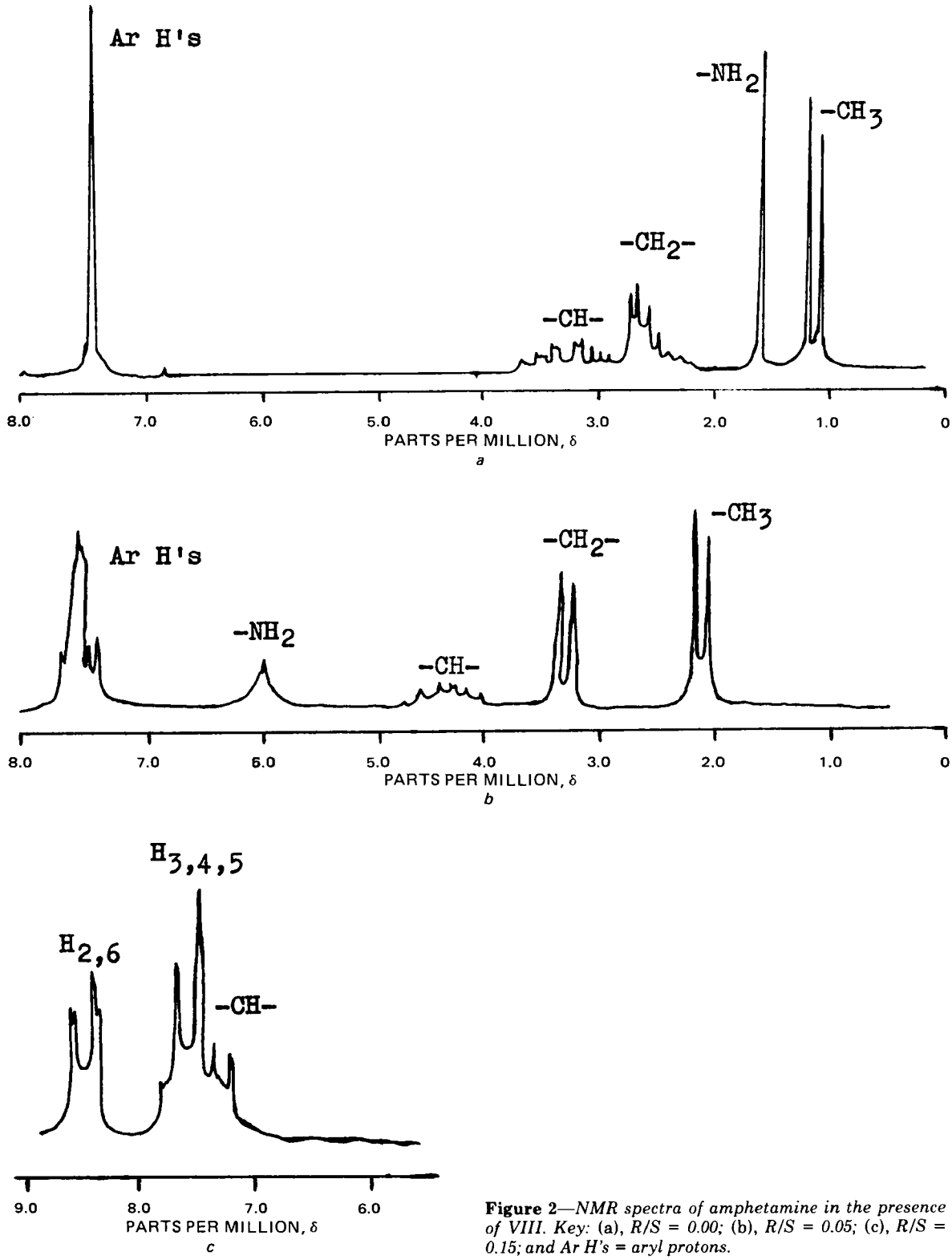

Figure 2—*NMR spectra of amphetamine in the presence of VIII. Key:* (a), *R/S = 0.00;* (b), *R/S = 0.05;* (c), *R/S = 0.15; and Ar H's = aryl protons.*

been attributed to an increase in steric hindrance for interaction with the nitrogen as it is alkylated (22). When comparing compounds V (primary amine) and VI (secondary amine), an increase in lanthanide-induced shifts of the methoxyl protons was observed, due perhaps to a shifting in equilibria (Scheme I) toward Structure 2 (or its equivalent). This phenomenon was somewhat curiously reversed with respect to the lanthanide-induced shifts of the methoxyl protons in Compounds VI and VII (tertiary amine). However, the lanthanide-induced shift of the *N*-methyl protons of VII was definitely decreased compared to that of V; and if shift reagent interaction occurred solely with the amine, then the lanthanide-induced shifts for the methoxyl protons in VII also should have been dramatically reduced compared to those in V.

This implies, in general, that a second point of interaction in this region of the molecule (2 in Scheme I) is enhanced by a shifting in equilibria as the interaction with the amine (1 in Scheme I) decreases. Similar preferential shift reagent interactions between two functionalities on opposite ends of molecules were reported previously (23). Taylor and Walters (24) found that when the primary amine of a phosphorus-containing compound was methylated (primary to secondary), interaction with shift reagent switched from the amine to the phosphorus atom.

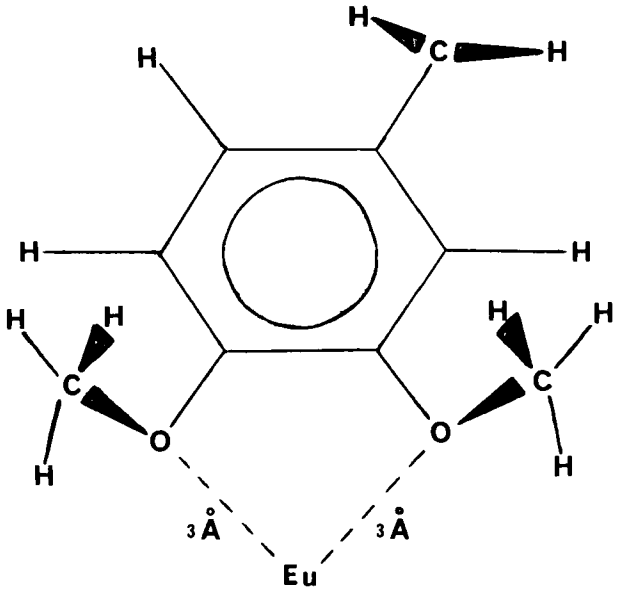

Figure 3—*Conformationally semirigid portion of the VII–europium bidentate complex model as it was positioned on the dipolar map of Wing* et al. (38).

Shift reagents have been found to interact with aromatic methoxyl groups in preference to aliphatic ethers (25), carbonyl groups (26), and pyrimidine nitrogens (27), but this interaction is generally regarded as being rather weak. However, when two methoxyl groups are present in an *ortho* relationship, it has been suggested that a bidentate interaction of the shift reagent can occur and that this type of interaction is considerably stronger (28). Lanthanide ions can show coordination numbers of three to 10 or 12 (29), and octavalent coordination, required for bidentate interaction, is reminiscent of the europium shift reagent form originally employed by Hinckley (30). The following structural types also have been implicated in bidentate interactions with NMR shift reagents: alicyclic diamines (31), furanone aliphatic ethers (32), aliphatic polyethers (33–35), and a tridentate interaction with alditols (36).

To define the nature of the shift reagent interaction occurring in VII, attempts were made to determine the geometry of the VIII–VII complex. Application of the McConnel–Robertson (37) equation and its logarithmic form (18) were attempted first. As is commonly done (38), the angular dependency term was ignored. In addition, only the molecular fragment embodying the methoxyl, aromatic, and methylene protons was examined. This portion of the molecule (Fig. 3) can be considered conformationally semirigid in each europium complex and should most readily lend itself to analysis.

The assumption that a europium atom location, midway between two functional groups, indicates a bidentate interaction may be erroneous for two reasons. First, a monodentate interaction, to an equal extent (through competitive equilibria) with each functional group, could also give an average McConnel–Robertson location midway between the two functionalities. An averaged europium atom location between two hydroxyl groups was demonstrated by Cockerill and Rackham (39). Second, bidentate interaction does not require that the europium atom be symmetrically located between the two functions, because the extent of interaction with each function will be determined by the unique electronic and steric properties of that function.

The results of these initial studies gave poor fits in both cases. This finding can be attributed either to contact contributions to the shifting process (40) or, more likely, to a neglect of the angular dependency term (41). The latter possibility is particularly appealing since a bidentate complex would restrict the rotational freedom about the europium–substrate single bonds. This effect of a bidentate interaction is extremely important, because such rotation about the symmetry axis in solution (42) gives effective axial symmetry. Such solution symmetry has been offered as one explanation for the success of the McConnel–Robertson equation in light of the growing X-ray evidence that implies that it should not work due to the lack of axial symmetry in many solid-state complexes (43–46).

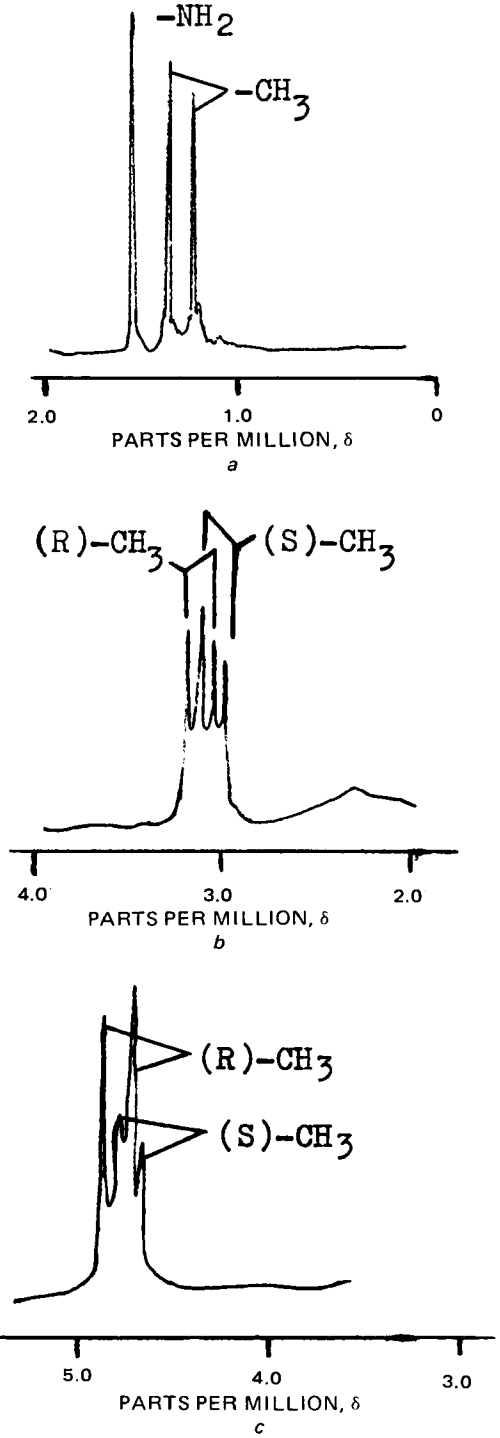

Figure 4—*NMR selectivity of the diastereotopic interaction of IX with enantiomeric mixtures of amphetamine. Key:* (a), (±)-*I, R/S = 0;* (b), (±)-*I, R/S = 0.25; and* (c), (±)-*I spiked with* (R)-*enantiomer.*

The graphical approach described by Wing *et al.* (38) was also employed to determine the europium atom location. This method accounts for the angular dependency term in the shifting process. Figure 3 illustrates the graphical positioning[5] of the semirigid por-

[5] The molecular fragment shown in Fig. 3 was superimposed on the dipolar map supplied by Wing *et al.* (38). Proper alignment of the europium and ligand oxygen atoms permitted assignment of coordinates, which predicted the relative lanthanide-induced shifts of the depicted protons.

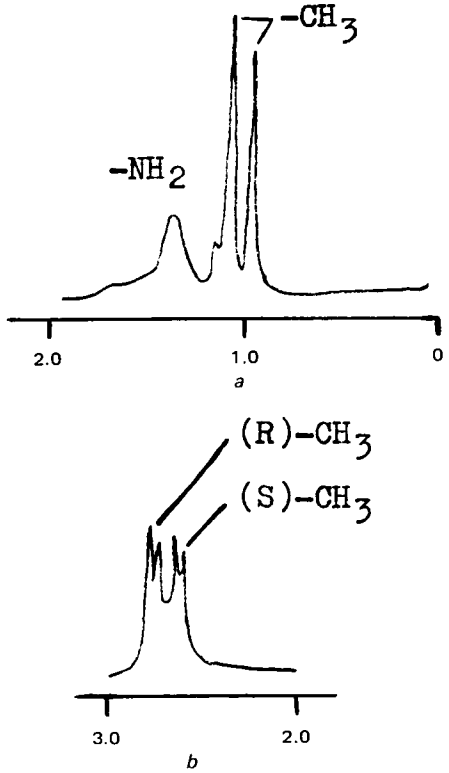

Figure 5—*NMR selectivity of the diastereotopic interaction of IX with enantiomeric mixtures of IV. Key:* (a), (±)-*IV, R/S = 0; and* (b), (±)-*IV, R/S = 0.22.*

tion of VII, which successfully predicted the observed lanthanide-induced shifts for the methoxyl, aromatic, and methylene protons. The europium atom–oxygen distance of 3 Å is in accord with the literature (4). However, the bonding picture implied by the graphical method indicates that interaction of the europium with the two methoxyl groups occurs *via* a single *d*-orbital of the europium atom. Such an event is questionable, and this method probably is subject to the same limitations as the mathematical approach when dealing with polyfunctional molecules capable of interacting with a shift reagent through various functional groups and/or in a bidentate fashion.

The interactions of IX with racemates and resolved enantiomers of I, II, and IV also were investigated. As indicated in Table II, these interactions are similar in magnitude to those observed with the VIII reagent (Table I). There were no dramatic spectral differences between enantiomers, but subtle lanthanide-induced shift preferences for the (*R*)-enantiomer methyl groups of I and IV were seen (Figs. 4 and 5). This assignment was based on (*R*)-spiked racemic samples in which the correspondingly larger peak moved the farthest downfield. Preferential shifts of (*R*)-enantiomers have been observed for related structures (47, 48), and this study indicates that the technique can be successfully applied to certain amphetamines.

However, a lack of enantiomeric discrimination obtained with (*R*)-*p*-methoxyamphetamine indicates that the method may not be useful for all compounds within this class. It was originally thought that IX might be useful in optical purity studies with amphetamines and/or similar systems. Results from these investigations indicate that its utility may be limited to only certain structures, although work with higher resolution spectrometers (100 MHz or greater) might provide sufficient separation of component C-methyl signals to study enantiomeric enrichment.

REFERENCES

(1) B. C. Mayo, *Chem. Soc. Rev.*, **2**, 49(1973).

(2) A. F. Cockerill, G. L. Davies, R. C. Harden, and D. M. Rackham, *Chem. Rev.*, **73**, 553(1973).

(3) J. R. Wasson and D. K. Johnson, *Anal. Chem.*, **46**, 314 (1974).

(4) R. Von Ammon and R. D. Fischer, *Angew. Chem., Int. Ed.*, **11**, 675(1972).

(5) M. D. McCreary, D. W. Lewis, D. L. Wernick, and G. M. Whitesides, *J. Amer. Chem. Soc.*, **96**, 1038(1974).

(6) H. L. Goering, J. N. Eikenberry, G. S. Koermer, and C. J. Lattimer, *ibid.*, **96**, 1493(1974).

(7) O. Korver and M. Van Gorkom, *Tetrahedron*, **30**, 4041(1974).

(8) I. M. Armitage, L. D. Hall, A. G. Marshall, and L. G. Werbelow, *J. Amer. Chem. Soc.*, **95**, 1437(1973).

(9) D. E. Nichols, C. F. Barfknecht, D. B. Rusterholz, F. Benington, and R. D. Morin, *J. Med. Chem.*, **16**, 480(1973).

(10) F. Weinges and G. Graab, *Chem. Ztg., Chem. Appar.*, **94**, 728(1970).

(11) C. B. Gairaud and G. R. Lappin, *J. Org. Chem.*, **18**, 1(1953).

(12) B. T. Ho, W. M. McIssac, R. An, L. W. Tansey, K. E. Walker, L. F. Englert, Jr., and M. B. Noel, *J. Med. Chem.*, **13**, 26(1970).

(13) H. Hart and G. M. Love, *Tetrahedron Lett.*, **1971**, 625.

(14) P. V. Demarco, T. K. Elzey, R. B. Lewis, and E. Wenkert, *J. Amer. Chem. Soc.*, **92**, 5734(1970).

(15) H. Yanagawa, F. Kato, and Y. Kitahara, *Tetrahedron Lett.*, **1973**, 2137.

(16) G. N. LaMar and D. L. Budd, *J. Amer. Chem. Soc.*, **96**, 7317(1974).

(17) I. Fleming, S. W. Hanson, and J. K. M. Sanders, *Tetrahedron Lett.*, **1971**, 3733.

(18) C. C. Hinckley, M. R. Klotz, and F. Patil, *J. Amer. Chem. Soc.*, **93**, 2417(1971).

(19) G. E. Wright, *Tetrahedron Lett.*, **1973**, 1097.

(20) D. A. Deranleau, *J. Amer. Chem. Soc.*, **91**, 4044(1969).

(21) I. M. Armitage, G. Dunsmore, L. D. Hall, and A. D. Marshall, *Can. J. Chem.*, **50**, 2119(1972).

(22) L. Ernst and A. Mannschreck, *Tetrahedron Lett.*, **1971**, 3023.

(23) T. H. Ward, I. L. Allcox, and G. H. Wahl, Jr., *ibid.*, **1971**, 4421.

(24) R. C. Taylor and D. B. Walters, *ibid.*, **1972**, 63.

(25) C. Nishino and T. Mitsui, *ibid.*, **1973**, 335.

(26) G. A. Neville, *Org. Mag. Res.*, **4**, 633(1972).

(27) G. A. Neville, *Can. J. Chem.*, **50**, 1253(1972).

(28) G. E. Wright and T. Y. Tang Wei, *Tetrahedron*, **29**, 3775(1973).

(29) D. C. Bradley, J. S. Ghorta, F. A. Hart, M. B. Hursthouse, and P. R. Raithby, *Chem. Commun.*, **1974**, 40.

(30) C. C. Hinckley, *J. Amer. Chem. Soc.*, **91**, 5160(1969).

(31) H. van Brederode and W. G. B. Huysmans, *Tetrahedron Lett.*, **1971**, 1695.

(32) S. B. Tjan and F. R. Visser, *ibid.*, **1971**, 2833.

(33) A. M. Grotens and J. Smid, *ibid.*, **1971**, 4863.

(34) A. M. Grotens, *ibid.*, **1972**, 2067.

(35) A. M. Grotens, E. deBoer, and J. Smid, *ibid.*, **1973**, 1471.

(36) T. Spoormaker, A. P. G. Kieboom, A. Sinnema, J. M. van der Toorn, and H. van Bekkum, *ibid.*, **1974**, 3713.

(37) H. M. McConnel and R. E. Robertson, *J. Chem. Phys.*, **29**, 1361(1958).

(38) R. M. Wing, T. A. Early, and J. J. Uebel, *Tetrahedron Lett.*, **1972**, 4153.

(39) A. F. Cockerill and D. M. Rackham, *ibid.*, **1970**, 5153.

(40) K. Tori, Y. Yoshimura, M. Kainosho, and K. Ajisaka, *ibid.*, **1973**, 3127.

(41) P. H. Mazzochi, H. L. Ammon, and C. W. Jameson, *ibid.*, **1973**, 573.

(42) J. H. Briggs, G. P. Moss, E. W. Randall, and K. D. Sales, *Chem. Commun.*, **1972**, 1180.

(43) W. D. Horrocks, Jr., J. P. Sipe, III, and D. Sudnick, in "Nuclear Magnetic Resonance Shift Reagents," R. E. Sievers, Ed., Academic, New York, N.Y., 1973, pp. 53–86.

(44) D. S. Dyer, J. A. Cunningham, J. J. Brooks, R. E. Sievers, and R. E. Rondeau, in *ibid.*, pp. 21–51.

(45) J. J. Uebel and R. M. Wing, *J. Amer. Chem. Soc.*, **94**, 8910(1972).

(46) R. E. Cramer and K. Seff, *Chem. Commun.*, **1972**, 400.

(47) G. M. Whitesides and D. W. Lewis, *J. Amer. Chem. Soc.*, **92**, 6979(1970).

(48) *Ibid.*, **93**, 3914(1971).

ACKNOWLEDGMENTS AND ADDRESSES

Received March 27, 1975, from the *Drug Dynamics Institute, College of Pharmacy, University of Texas at Austin, Austin, TX 78712, and the ‡Division of Medicinal Chemistry and Natural Products, College of Pharmacy, University of Iowa, Iowa City, IA 52242

Accepted for publication June 11, 1975.

Presented at the Pharmaceutical Analysis and Control Section, APhA Academy of Pharmaceutical Sciences, San Francisco meeting, April 1975.

Supported in part by Grant NS-12259, National Institute of Neurological Diseases and Stroke, National Institutes of Health.

The authors are grateful to Dr. Robert J. Borgman, School of Pharmacy, West Virginia University, Morgantown, W.Va., for providing the *N*-methyl-3,4-dimethoxyamphetamine and *N,N*-dimethyl-3,4-dimethoxyamphetamine samples.

ˣ To whom inquiries should be directed.

Intestinal Secretion of Erythromycin Base

D. R. HOLLAND ˣ and J. F. QUAY

Abstract □ Erythromycin fluxes into rabbit midjejunal segments were studied. When erythromycin was infused into the jugular vein of anesthetized rabbits, the antibiotic was secreted into the segments at a rate of 0.0136 ± 0.0023 mg/min. Preloading of the segments with five and 20 times the plasma concentration did not diminish this secretion. Protein binding of the antibiotic within the lumen could not explain this secretion, since both ultrafiltration and chromatography of luminal solutions indicated that the biological activity was free erythromycin. Moreover, the transmural potential across the intestinal mucosa is not likely to be the principal driving force, since greater than 80 mv would be required to sustain the observed secretion against an imposed 20-fold concentration difference between blood and lumen. The best explanation for the intestinal secretion of erythromycin appears to be an active transport pathway capable of concentrating erythromycin in the lumen. It is not clear what endogenous substances are transported by this pathway.

Keyphrases □ Erythromycin—intestinal secretion, rabbit midjejunal segments □ Intestinal secretion—erythromycin, rabbit midjejunal segments □ Antibiotics—erythromycin, intestinal secretion, rabbits

In humans, oral administration of erythromycin free base produces low blood levels of antibiotic. For example, a 250-mg tablet of erythromycin free base produces average peak blood levels of 0.12–0.54 μg/ml (1, 2). In comparison, similarly administered propionyl erythromycin produces peak blood levels of 1.11–1.92 μg/ml.

The lower blood levels of erythromycin base have been attributed to a number of factors including: (*a*) a deleterious effect of ingested food on absorption of the base (3), (*b*) acid degradation in the stomach (4), (*c*) the volume of distribution following absorption (5), (*d*) biliary secretion (6–8), and (*e*) a combination of low absorption rate with high renal excretion rate (9).

Preliminary studies in this laboratory confirmed the observation (10) that a fraction of intravenously administered erythromycin base appeared in the intestinal lumens of rats with extracorporal bile fistulas. Since biliary excretion was clearly eliminated as a source of intestinal secretion, these studies suggested the direct secretion of erythromycin across the intestinal mucosa. Such a pathway of secretion might be important not only as a new route of elimination but also as an influence on the oral administration of erythromycin.

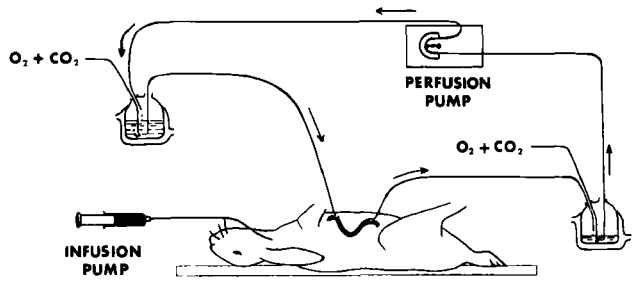

Figure 1—*Schematic representation of perfusion circuit through rabbit midjejunum.*

EXPERIMENTAL

Surgical Preparation—Male New Zealand white rabbits, 3.2–3.7 kg, were anesthetized with 50 mg/kg iv of secobarbital[1]. A 50-cm segment of midjejunum, measured 75 cm proximal to the ileocecal valve, was cannulated both proximally and distally. The segment did not include the bile duct. Krebs–Ringer bicarbonate buffer, saturated with 95% oxygen–5% carbon dioxide at 40°, was initially washed through the segment. This buffer had the following composition: Na^+, 0.143 *M*; K^+, 0.006 *M*; Ca^{+2}, 0.003 *M*; Mg^{+2}, 0.001 *M*; Cl^-, 0.128 *M*; PO_4^{-2}, 0.001 *M*; SO_4^{-2}, 0.001 *M*; and HCO_3^-, 0.025 *M*.

After rinsing with buffer, air was injected to displace excess solution. One hundred milliliters of buffer was then circulated through the segment between two water-jacketed reservoirs maintained at 40° (Fig. 1). Inflow pressure was maintained below 20 cm of water to prevent damage to the mucosa. Both reservoirs were initially bubbled with 95% oxygen–5% carbon dioxide. As the experiment progressed, the pH of the perfusate tended to increase but was maintained at a constant value of 7.4 by increasing the proportion of carbon dioxide in the gas mixture.

A polyethylene cannula in the left external jugular vein allowed vascular infusion of erythromycin. Blood samples were withdrawn through a second cannula placed in the left common carotid artery.

Perfusion Experiments—A constant concentration of erythromycin in the plasma (1 μg/ml) was maintained by a bolus injection of 3 mg into the jugular cannula followed by infusion at a rate of 5 mg/hr. The appearance of erythromycin in the intestinal segment was then followed by sampling at 20-min intervals. Carotid blood samples were taken concomitantly. The perfusate and carotid plasma were assayed by the disk-plate microbiological assay tech-

[1] Seconal, Eli Lilly and Co.

ACKNOWLEDGMENTS AND ADDRESSES

Received March 27, 1975, from the *Drug Dynamics Institute, College of Pharmacy, University of Texas at Austin, Austin, TX 78712, and the ‡Division of Medicinal Chemistry and Natural Products, College of Pharmacy, University of Iowa, Iowa City, IA 52242

Accepted for publication June 11, 1975.

Presented at the Pharmaceutical Analysis and Control Section, APhA Academy of Pharmaceutical Sciences, San Francisco meeting, April 1975.

Supported in part by Grant NS-12259, National Institute of Neurological Diseases and Stroke, National Institutes of Health.

The authors are grateful to Dr. Robert J. Borgman, School of Pharmacy, West Virginia University, Morgantown, W.Va., for providing the *N*-methyl-3,4-dimethoxyamphetamine and *N,N*-dimethyl-3,4-dimethoxyamphetamine samples.

ˣ To whom inquiries should be directed.

Intestinal Secretion of Erythromycin Base

D. R. HOLLAND ˣ and J. F. QUAY

Abstract □ Erythromycin fluxes into rabbit midjejunal segments were studied. When erythromycin was infused into the jugular vein of anesthetized rabbits, the antibiotic was secreted into the segments at a rate of 0.0136 ± 0.0023 mg/min. Preloading of the segments with five and 20 times the plasma concentration did not diminish this secretion. Protein binding of the antibiotic within the lumen could not explain this secretion, since both ultrafiltration and chromatography of luminal solutions indicated that the biological activity was free erythromycin. Moreover, the transmural potential across the intestinal mucosa is not likely to be the principal driving force, since greater than 80 mv would be required to sustain the observed secretion against an imposed 20-fold concentration difference between blood and lumen. The best explanation for the intestinal secretion of erythromycin appears to be an active transport pathway capable of concentrating erythromycin in the lumen. It is not clear what endogenous substances are transported by this pathway.

Keyphrases □ Erythromycin—intestinal secretion, rabbit midjejunal segments □ Intestinal secretion—erythromycin, rabbit midjejunal segments □ Antibiotics—erythromycin, intestinal secretion, rabbits

In humans, oral administration of erythromycin free base produces low blood levels of antibiotic. For example, a 250-mg tablet of erythromycin free base produces average peak blood levels of 0.12–0.54 μg/ml (1, 2). In comparison, similarly administered propionyl erythromycin produces peak blood levels of 1.11–1.92 μg/ml.

The lower blood levels of erythromycin base have been attributed to a number of factors including: (*a*) a deleterious effect of ingested food on absorption of the base (3), (*b*) acid degradation in the stomach (4), (*c*) the volume of distribution following absorption (5), (*d*) biliary secretion (6–8), and (*e*) a combination of low absorption rate with high renal excretion rate (9).

Preliminary studies in this laboratory confirmed the observation (10) that a fraction of intravenously administered erythromycin base appeared in the intestinal lumens of rats with extracorporal bile fistulas. Since biliary excretion was clearly eliminated as a source of intestinal secretion, these studies suggested the direct secretion of erythromycin across the intestinal mucosa. Such a pathway of secretion might be important not only as a new route of elimination but also as an influence on the oral administration of erythromycin.

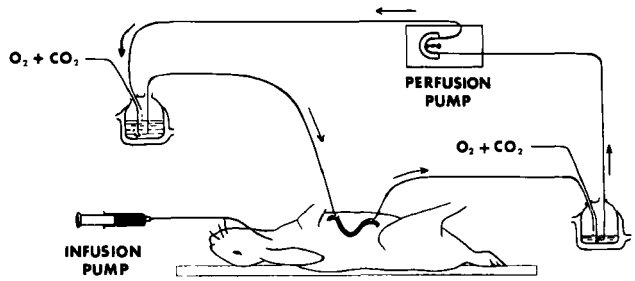

Figure 1—*Schematic representation of perfusion circuit through rabbit midjejunum.*

EXPERIMENTAL

Surgical Preparation—Male New Zealand white rabbits, 3.2–3.7 kg, were anesthetized with 50 mg/kg iv of secobarbital[1]. A 50-cm segment of midjejunum, measured 75 cm proximal to the ileocecal valve, was cannulated both proximally and distally. The segment did not include the bile duct. Krebs–Ringer bicarbonate buffer, saturated with 95% oxygen–5% carbon dioxide at 40°, was initially washed through the segment. This buffer had the following composition: Na^+, 0.143 *M*; K^+, 0.006 *M*; Ca^{+2}, 0.003 *M*; Mg^{+2}, 0.001 *M*; Cl^-, 0.128 *M*; PO_4^{-2}, 0.001 *M*; SO_4^{-2}, 0.001 *M*; and HCO_3^-, 0.025 *M*.

After rinsing with buffer, air was injected to displace excess solution. One hundred milliliters of buffer was then circulated through the segment between two water-jacketed reservoirs maintained at 40° (Fig. 1). Inflow pressure was maintained below 20 cm of water to prevent damage to the mucosa. Both reservoirs were initially bubbled with 95% oxygen–5% carbon dioxide. As the experiment progressed, the pH of the perfusate tended to increase but was maintained at a constant value of 7.4 by increasing the proportion of carbon dioxide in the gas mixture.

A polyethylene cannula in the left external jugular vein allowed vascular infusion of erythromycin. Blood samples were withdrawn through a second cannula placed in the left common carotid artery.

Perfusion Experiments—A constant concentration of erythromycin in the plasma (1 μg/ml) was maintained by a bolus injection of 3 mg into the jugular cannula followed by infusion at a rate of 5 mg/hr. The appearance of erythromycin in the intestinal segment was then followed by sampling at 20-min intervals. Carotid blood samples were taken concomitantly. The perfusate and carotid plasma were assayed by the disk-plate microbiological assay tech-

[1] Seconal, Eli Lilly and Co.

Table I—Erythromycin Flux into Intestinal Segments Preloaded with the Antibiotic

Initial Concentration in Lumen, μg/ml	n^a	Flux[b], mg/min	p^c
0	5	0.0136 ± 0.0023	<0.002
5	4	0.0138 ± 0.0036	<0.02
20	7	0.0299 ± 0.0144	<0.05

[a] Number of animal preparations used to determine flux. [b] Mean ± *SE* of the mean. [c] Probability that fluxes did not differ from zero were determined by the Student *t* test.

nique of Davis and Stout (11). The ratio of lumen to plasma concentrations (*L/P*) was calculated to facilitate statistical analysis. The Student *t* test was used to determine if *L/P* exceeded 1, indicating net movement into the lumen.

To determine if secretion proceeded against a concentration gradient, luminal solutions were initially loaded with 5 or 20 μg/ml of erythromycin. Fluxes into the lumen with different levels of preloading were then compared. The method of calculation of fluxes was as follows. The volume of solution in the segment at each sampling time was determined by four experiments using the nonabsorbable marker ^{14}C-inulin. The product of this volume and the concentration of erythromycin in perfused buffer was the total amount of erythromycin in the lumen. The change in total luminal erythromycin with time, as determined by linear regression analysis, was taken as the flux into the lumen.

Assay differences for erythromycin in plasma and perfused buffer were evaluated by loading samples of antibiotic-free plasma and perfused buffer with 1 μg/ml of erythromycin. The *L/P* ratios for these inoculated controls did not differ significantly from 1.

Ultrafiltration—The binding of erythromycin to macromolecules within the intestine was studied by ultrafiltration of a sample of luminal buffer preloaded with erythromycin. The ultrafilter membrane[2] had a cutoff at a molecular weight of 30,000 with an apparent pore radius of 29 Å. The filter was saturated with *N*-methyl-^{14}C-erythromycin by passing 20 ml of 0.9% NaCl containing 3 mg/ml of radiolabeled erythromycin through the filter.

Ultrafiltrate samples (1 ml) were collected sequentially. After addition of 15 ml of scintillation cocktail[3], these samples were counted in a scintillation detector. Saturation of binding sites on the filter was judged to be complete when the erythromycin concentration in the ultrafiltrate reached a plateau of radioactivity equivalent to 3 μg/ml. The saline solution in the ultrafiltration chamber was then replaced with a 2-hr luminal solution preloaded with 3 μg/ml of radiolabeled erythromycin. This solution was then passed through the same filter, and the ultrafiltrate was collected for counting.

Chromatography—Chromatographic analyses were made of luminal perfusate in two systems to confirm the identity of the biologically active component concentrated in the lumen. The first system consisted of TLC on silica gel plates[4] with the following solvent mixture: methylene chloride–methanol–benzene–formamide (20:5:5:1).

The second system was descending paper chromatography with Whatman No. 1 paper, using a mixture of ammonium hydroxide–methyl isobutyl ketone–water (0.5:1:98.5). In the second system, three chromatographic analyses were done on samples from two animal preparations. Samples from a third animal were chromatographed in the first system.

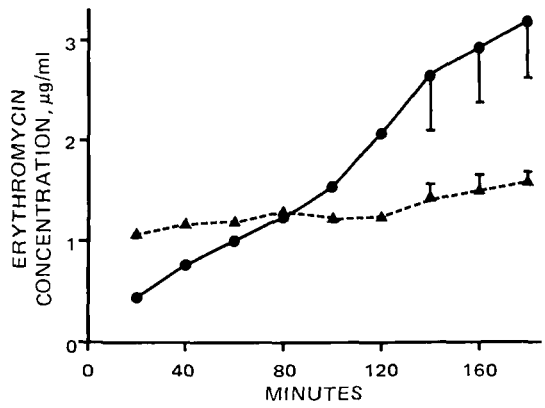

Figure 2—*Erythromycin concentration in plasma (▲) and lumen of jejunal segment (●) following vascular infusion in six animals. Standard errors of the mean are represented by vertical bars.*

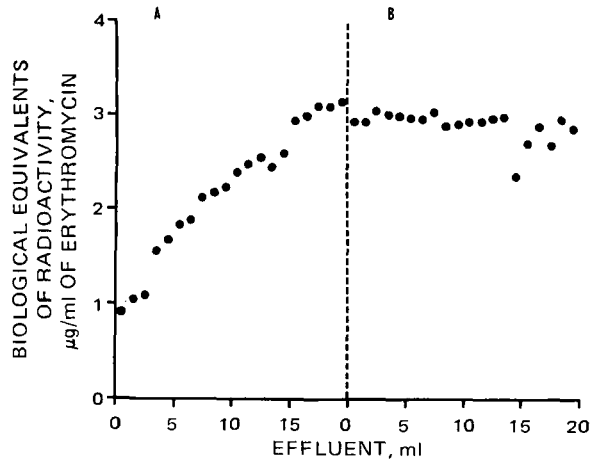

Figure 3—*Radioactivity in ultrafiltrate during saturation of filter with erythromycin (3 μg/ml) in saline (A) and following filtration of luminal buffer containing erythromycin (3 μg/ml) through saturated filter (B). See text for details of technique.*

RESULTS AND DISCUSSION

When erythromycin was infused into the jugular vein, the antibiotic concentration in the intestinal segment progressively rose and exceeded plasma concentration after 80 min (Fig. 2). The *L/P* ratios were significantly greater than 1 at 120 min and thereafter ($p < 0.025$), indicating a concentrative secretion of erythromycin. Preloading the luminal perfusate with five and 20 times the plasma concentration did not diminish the flux of erythromycin into the lumen (Table I). Net secretion of erythromycin into the lumen was significantly greater than zero ($p < 0.05$) at all levels of preloading.

Since the movement of erythromycin into the lumen of the intestine proceeds against a concentration gradient, passive fluxes alone are not sufficient to explain the data. At least three possible mechanisms might be responsible for this secretion: luminal trapping of erythromycin, diffusion down the transmural electrical gradient of the intestinal mucosa, and active transport.

Luminal trapping of erythromycin would involve, conceptually, diffusion into the lumen, followed by binding to some macromolecule to form a nondiffusable soluble complex. Alternatively, erythromycin in the lumen of the intestine might form an insoluble salt that could not be reabsorbed. The results of three types of experiments decrease the likelihood that luminal trapping is the mechanism of erythromycin secretion:

1. In the set of assay controls, the luminal perfusate was loaded to 1 μg/ml of erythromycin and assayed against a standard curve of erythromycin in Krebs–Ringer bicarbonate buffer solution. Zones of inhibition were of comparable size in both diluents. Any complex or insoluble precipitate would be expected to diffuse more slowly on an agar plate than would molecularly dispersed erythromycin. Therefore, the lack of assay difference between luminal perfusate and buffer solution suggests that erythromycin is freely dispersed in the luminal solution.

2. The ultrafiltration in Fig. 3 suggests that erythromycin in the luminal perfusate was not bound to large molecular weight proteins. When erythromycin in luminal buffer was filtered, 97% (2.9 μg/ml) appeared in the ultrafiltrate. Thus, erythromycin in the lu-

[2] PM30 Diaflow filter, Amacon Corp.
[3] Aquasol, New England Nuclear.
[4] Plate 5765, E. M. Laboratories, Inc.

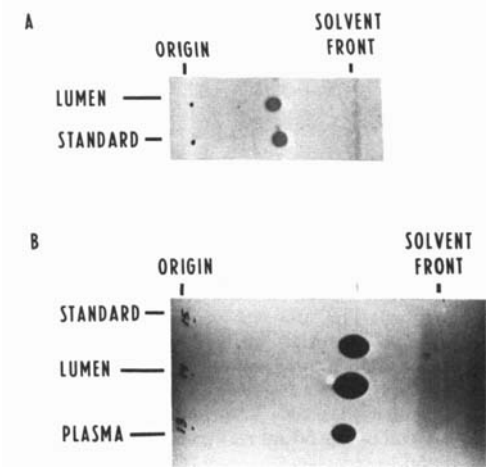

Figure 4—*Chromatography of erythromycin in luminal buffer and plasma on silica gel (A) and on Whatman No. 1 paper in a descending system (B). See text for solvent systems. Both chromatograms were developed on agar plates using* Sarcina lutea.

minal buffer is not bound in a complex with a radius larger than 29 Å.

There are two qualifications, however, to ultrafiltration data: (*a*) erythromycin was readily taken up by the ultrafiltration membrane itself, and presaturation of the membrane with erythromycin may not have fully compensated for this effect; and (*b*) binding of erythromycin to complexes smaller than 29 Å in radius would not be detected by this technique.

3. Chromatographic studies further suggested that erythromycin in luminal buffer was not complexed. In all chromatograms, only one spot of biological activity was found in the lumen as well as plasma, and this spot corresponded to erythromycin (Fig. 4). These data suggest that erythromycin in the lumen was molecularly dispersed, since an erythromycin complex would be expected to have a lower mobility than the free compound.

In view of the results of these three independent experiments, luminal trapping does not appear to be responsible for the concentrative intestinal secretion of erythromycin.

The transmural electrical potential across the intestinal mucosa must also be considered as a possible driving force for the secretion of erythromycin. In rabbit intestine *in vivo*, the transmural potential is 5.6 mv with the mucosal side negative (12).

When the flux of an ion across a semipermeable membrane is the result of simple diffusion driven by an electrical asymmetry across the membrane, the steady state of the concentration distribution can be determined from the following relationship (13):

$$\ln \frac{Ci'}{Ci''} = \frac{ZiF\,\Delta\gamma}{RT} \qquad \text{(Eq. 1)}$$

where Ci' and Ci'' are the respective concentrations on each side of the membrane, $\Delta\gamma$ is the potential difference across the membrane, Zi is the charge on the ion, F is Faraday's constant, R is the gas constant, and T is the absolute temperature.

Substituting 5.6 mv into this equation reveals that a steady-state L/P concentration ratio of only 1.23 would be expected if erythromycin were passively distributed across the intestinal mucosa due to the transmural potential alone. This predicted asymmetry is far less than the fivefold and 20-fold concentration ratios seen in tests with luminal preloading of erythromycin. Conversely, a transmural potential of 80 mv would be required to produce a 20-fold concentration asymmetry. The transmural potential, therefore, cannot be the primary energy source for erythromycin secretion.

A third possible mechanism for intestinal secretion of erythromycin is active, energy-dependent, transport into the lumen of the gut. Lee *et al.* (7, 8) found that erythromycin is actively secreted in the liver. The data in the present article strongly suggest that an active transport pathway for erythromycin is also present in the rabbit intestine. This report constitutes the first evidence for a pathway of intestinal secretion that transports erythromycin. It is not known what endogenous substances are served by this transport pathway nor what physiological function it fulfills.

REFERENCES

(1) R. S. Griffith, *Antibiot. Annu.*, **1959**, 364.

(2) S. Salitsky, J. K. Geiger, W. J. Mellman, and E. L. Foltz, *ibid.*, **1960**, 893.

(3) R. S. Griffith and H. R. Black, *Amer. J. Med. Sci.*, **247**, 69(1964).

(4) H. A. Blough, W. H. Hall, and L. Hong, *ibid.*, **239**, 539(1960).

(5) B. Lake and S. M. Bell, *Med. J. Aust.*, **1**, 449(1969).

(6) F. R. Heilman, W. E. Herrell, W. E. Wellman, and J. E. Geraci, *Proc. Staff Meet., Mayo Clin.*, **27**, 285(1952).

(7) C. Lee, R. C. Anderson, and K. K. Chen, *Antibiot. Annu.*, **1954**, 485.

(8) C. Lee, R. C. Anderson, H. L. Bird, Jr., and K. K. Chen, *ibid.*, **1954**, 493.

(9) B. A. Shidlovsky, A. Prigot, and W. R. Dickens, *Antimicrob. Ag. Annu.*, **1960**, 178.

(10) C. Lee, R. C. Anderson, and K. K. Chen, *J. Pharmacol. Exp. Ther.*, **117**, 265(1956).

(11) W. W. Davis and T. R. Stout, *Appl. Microbiol.*, **22**, 666(1971).

(12) J. Hajjar, R. Nassar, H. Kurkjian, and R. N. Khuri, *Comp. Biochem. Physiol.*, **28**, 717(1969).

(13) P. F. Curran and S. G. Schultz, in "Handbook of Physiology," vol. 3, sec. 6, C. F. Code, Ed., American Physiologic Society, Washington, D.C., 1968, p. 1236.

ACKNOWLEDGMENTS AND ADDRESSES

Received May 8, 1975, from the *Division of Pharmacological Research, Lilly Research Laboratories, Eli Lilly and Company, Indianapolis, IN 46206*

Accepted for publication June 12, 1975.

The authors thank Dr. W. E. Wright for his helpful suggestions in the preparation of the manuscript.

[x] To whom inquiries should be directed

Filtration Rates of Pharmaceutical Suspension Systems

A. DAKKURI * and B. ECANOW ‡x

Abstract □ This study was undertaken to find if a correlation exists between the filtration rate and the H_u/H_0 ratio. For this purpose, flocculated and coagulated structures of sulfamerazine were used. Suspension settling profiles and filtration rates, using additives and additive-free sulfamerazine suspensions, were studied. A straight-line correlation was found. Effects of filter bed parameters on refiltration rates were studied, and a relationship was found by the use of the Kozeny–Carman equation. A straight-line relationship existed between the H_u/H_0 ratio and the filtration rate exhibited by the different suspension aggregates.

Keyphrases □ Suspensions—settling profiles and filtration rates, flocculated and coagulated structures of sulfamerazine, effects of filter bed parameters on refiltration rates □ Filtration rate—pharmaceutical suspensions, sulfamerazine, correlation with ratio of final to initial suspension settling height □ Sulfamerazine—flocculated and coagulated suspension structures, settling profiles and filtration rates

There are several parameters for following the aggregation and deaggregation of suspended particles: (*a*) rate of settling, (*b*) sediment height ratio, (*c*) filtration of the suspension and refiltration of the filtrate through the formed filter bed, (*d*) height of the consolidated filter bed, and (*e*) turbidity of the supernate (1, 2). Each method has its advantages and disadvantages. Few, if any, pharmaceutical suspensions have been studied utilizing the filtration or refiltration rate. The structures of these suspensions have been determined employing electrokinetic measurements, the H_u/H_0 ratio, and other empirical procedures (3, 4).

The present study was undertaken to find if a correlation exists between the filtration rate and the H_u/H_0 ratio. Flocculated and coagulated structures of sulfamerazine were used. A flocculated system is considered to consist of an open network structure formed by aggregated particles. At the other extreme is the dense structure, consisting of closely packed particles that exist in a coagulated system.

EXPERIMENTAL

Materials—Sulfamerazine USP, Calcomites grade[1], was used. Dioctyl sodium sulfosuccinate[2] (I) was obtained commercially. Aluminum chloride hexahydrate and sodium chloride were reagent grade.

General Procedure—Sulfamerazine was mixed with 50 ml of distilled water for 10 min using a magnetic stirrer. The agitation intensity was then decreased, and 25 ml of I solution was added. Stirring was continued for 15 more min; then 20 ml of aluminum chloride solution was added together with sufficient water to yield a final volume of 100 ml, and the suspension was stirred for another 2.5 min. The latter interval and the lower agitation intensity were chosen to minimize disruption of flocs, which may occur at high shear rates.

The final concentrations of the additives in the suspensions are indicated in the text. The volumes of the solutions were replaced by equivalent volumes of water when settling profiles and filtration rates of additive-free suspensions were studied. Sodium chloride was used in lieu of aluminum chloride to determine its effect on sulfamerazine particles coated with I.

Filtration Process—Each suspension was transferred into a sulfur adsorption tube of 130-ml capacity with a fritted-glass disk (30 mm in diameter). The tube was described previously (5). The intervals required to collect 10, 40, and 50 ml of filtrate were recorded. The 50-ml filtrate was then immediately poured back into the funnel, and the intervals required to collect the same volumes of refiltrate were also observed. The time, in seconds, required to collect the last 40 ml of the 50-ml refiltrate was designated as refiltration time 10–50.

Subsidence Rate and Sediment Height—In another series of experiments, the suspension was transferred into a 100-ml glass-stoppered graduated cylinder. The sediment height (volume) was determined every minute, or more frequently, for the first 15 min, and then the time lapse between readings was increased.

RESULTS AND DISCUSSION

Settling Profiles and Filtration Rates of Additive-Free Sulfamerazine Suspensions—The ultimate height, H_u, to which a suspension settles without agitation is a function of the concentration of the solid phase, C (6). The sediment volume is reported in terms of the H_u/H_0 ratio, where H_0 is the initial height of the suspension (7). The rate of settling of sulfa suspensions in concentrations of 1, 2, 3, 4, and 5% is observed. Plotting the sediment height *versus* time shows that these suspensions behave in accordance with the Type I curve (8). They show a coarse appearance when set aside to settle, and the coarseness decreases as C increases. Such an appearance is ascribed to aggregation affected by van der Waals' forces and hydrophobic bonds.

The calculated porosity of the sediment (9) is shown in Table I, and the high values indicate the presence of a loose structure. The percent difference between the extreme values is about half that calculated using data reported by Steinour (10, 11). A straight line is obtained when H_u/H_0 is plotted *versus* C on log–log paper. A similar relationship is also exhibited by sulfamerazine–trichlorotrifluoroethane suspensions where flotation rather than settling occurs (12).

Filtration of the suspension and, in particular, refiltration of the filtrate through an already formed sediment or filter bed have proved to be accurate and readily reproducible measures of the state of aggregation (2). However, the suspension must be prepared under controlled conditions to minimize disruption of the

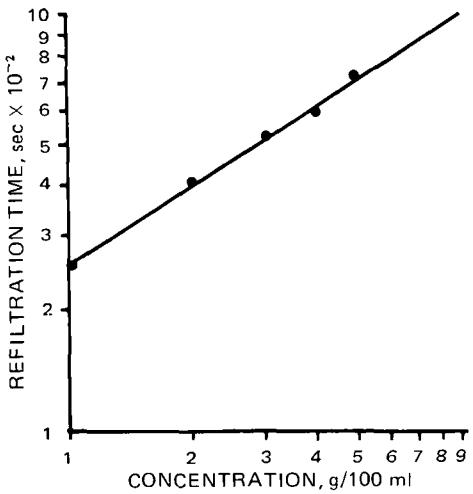

Figure 1—*Refiltration time 10–50, time required to collect the last 40 ml of the first 50 ml of refiltrate, of sulfamerazine suspensions.*

[1] American Cyanamid Co., Pearl River, N.Y.
[2] Aerosol OT 100% solid, Fisher Scientific Co., Fair Lawn, N.J.

Table I—Parameters of Sulfamerazine Suspensions

Sulfamerazine Concentration, % w/v	Sediment Volume, ml	Sediment Porosity	Refiltration Time 10–50[a], sec
1	20	0.964	247
2	33	0.956	415
3	45	0.952	523
4	54	0.947	589
5	66	0.946	722

[a] Time required to collect the last 40 ml of the first 50 ml of refiltrate.

structure and, consequently, to obtain reproducible results.

In Table I, refiltration time 10–50 is given for sulfa suspensions with no additives. This parameter is preferred to the time required to collect the first 50 ml of refiltrate because it allows sufficient time for the filter bed to reform if it is disturbed by the addition of the filtrate. A straight line is also obtained when refiltration time 10–50 is plotted against C on log–log paper; the slope of the line is 0.666 (Fig. 1). When H_u/H_0 is plotted *versus* C on log–log paper, the slope is 0.723.

The two slopes, that for t_{ref} *versus* C and H_u/H_0 *versus* C on a log–log grid, are of nearly similar magnitude. This similarity may lead to the conclusion that the factors controlling the structures of both the filter bed and the sediment are the same. Thus, this similarity suggests the close relationship between the two methods, *i.e.*, refiltration and settling, for studying the suspension structure.

Relationship between Initial Settling Rate and Initial Filtration Time—The initial settling rate is the slope of the straight-line component (constant-rate zone) of a settling curve obtained by plotting subsidence level *versus* time; it represents the maximum subsidence rate. Initial filtration time 0–10 is the interval required to collect the first 10 ml of filtrate. Since the suspension structures in the initial stages of the two processes are comparable, it was of interest to find if a correlation exists between these parameters.

Steinour (10) described the dependence of the subsidence rate, S, on the velocity of sedimentation of isolated spheres, V_s, and the volume fractions occupied by the liquid, E, and solid phase, $1 - E$, as:

$$S \propto \frac{E^3}{1-E} V_s \qquad \text{(Eq. 1)}$$

However, since hindered settling (2, 3) is absent in suspensions of low concentrations, as in the present suspensions, V_s may be assumed to be constant. Furthermore, $1 - E$ is proportional to C. Consequently, $(E^3/s) \propto C$.

Figure 2 shows that filtration time 0–10 is a linear function of C. Thus, $t_{fil} \propto (E^3/S)$. When t_{fil} is plotted against E^3/S (Fig. 3), a straight line is obtained in conformity with this relationship.

Effect of Filter Bed Parameters on Refiltration Rate—The refiltration rate is more indicative of the type of structure of the filter bed than is the filtration rate. During refiltration time 40–50, the compression rate in the filter bed is negligible. Therefore, if it is assumed that all parameters, except e and L, of the Kozeny–Carman equation (13–16) are constant, it can be reduced to:

$$Q = \frac{1}{k}\frac{e^3}{L} \qquad \text{(Eq. 2)}$$

where Q is the refiltration rate in milliliters per second, e is porosity, and L is the thickness of the filter bed in centimeters; k is a constant that includes all other parameters in the original equation.

A linear relationship is obtained when refiltration rate 40–50 is plotted against e^3/L (Fig. 4). Thus, it appears that Eq. 2 expresses the dependence of the refiltration rate on the bed parameters in the studied suspensions.

Effect of I on Settling and Filtration Rates—Table II lists the refiltration time 10–50 of 5% sulfa suspensions treated with I. The variation among the determinations within concentration groups is 3–5%. Being a surfactant, I disperses the hydrophobic sulfa into smaller aggregates and/or primary particles. As the concentration of I increases, the hydrophobicity decreases and a finer dispersion of particles is produced. The extent to which secondary particles are broken into primary entities influences the packing

Table II—Effect of I on Refiltration Time 10–50, Thickness of Filter Bed, and H_u/H_0 Ratio of 5% Sulfamerazine Suspension

I Concentration, % w/v	Refiltration Time 10–50		Thickness of Filter Bed, cm	H_u/H_0 Ratio
	min	sec		
0.00	14	12	4.0	0.66
0.025×10^{-2}	13	55	4.0	0.65
0.25×10^{-2}	18	50	4.0	0.59
2.5×10^{-2}	23	35	3.3	0.52
7.5×10^{-2}	42	15	2.7	0.36
12.5×10^{-2}	59	5	2.2	0.215
17.5×10^{-2}	77	—	2.1	0.212
25×10^{-2}	82	40	2.1	0.207
32.5×10^{-2}	85	40	1.9	0.190

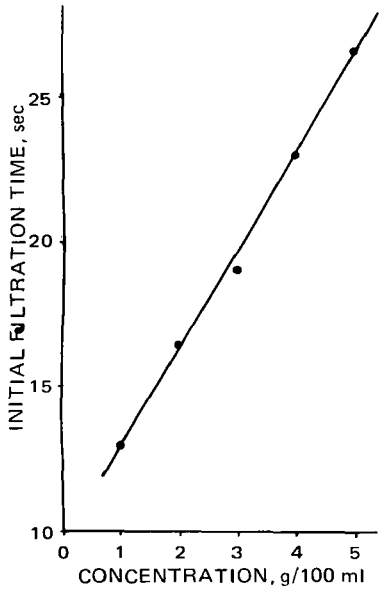

Figure 2—*Initial filtration time, time required to collect the first 10 ml of filtrate, of sulfamerazine suspension at various concentrations.*

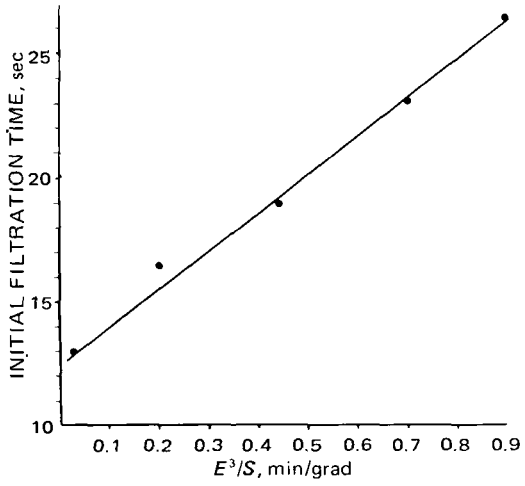

Figure 3—*Relationship between initial filtration time (time required to collect the first 10 ml of filtrate) and* E^3/S *of sulfamerazine suspensions, where* E *is the volume fraction of suspension occupied by the liquid phase and* S *is the rate of subsidence as determined from the slope of the straight-line component of a settling curve obtained by plotting subsidence level* versus *time.*

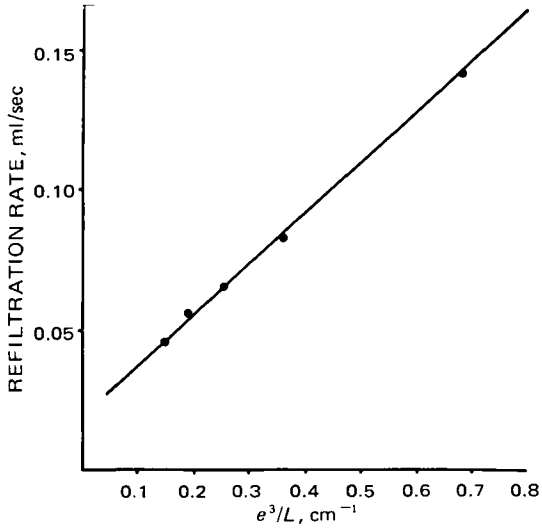

Figure 4—*Relationship between porosity of the filter bed, e, its thickness, L, in centimeters, and the refiltration rate of sulfamerazine suspensions. The refiltration rate is calculated using the refiltration time required to collect the last 10 ml of the first 50 ml of refiltrate.*

characteristics of the filter bed, and this effect is reflected on the refiltration rate.

As the particles settle, geometrical rearrangements take place and the interparticle pores are occupied by smaller particles. Therefore, the liquid has to travel through a closely packed sediment. In addition, the coalescence of the hydrated adsorbed layers covering the particles results in a denser bed (17, 18). These effects increase with an increasing surfactant concentration. Figure 5 shows a linear relationship between the refiltration time and the I concentration up to 17.5×10^{-2}%; a plateau is then approached. It is possible that a monolayer is formed at this particular concentration, whereas at higher concentrations a multilayer may start forming.

Table II also shows the thickness of the filter bed and H_u/H_0 ratio for the same suspensions. Both parameters apparently decrease with an increasing concentration of I up to 12.5×10^{-2}%. No significant change is observed at higher concentrations. The decrease is accompanied by an increased tendency to form a dense and smooth bed, which may be attributed to an increase in the availability of I for adsorption at the interface.

Effect of Aluminum Chloride on Filtration Behavior of I-Coated Sulfamerazine Suspensions—A flocculated structure is formed, due to interaction of Al^{+3} with the negatively charged particles, when aluminum chloride is added to suspended sulfa particles coated with I (19). Flocculation takes place instantaneously. But the coagulation process affected by indifferent salts acting on the diffuse double layer of colloidal particles may take a prolonged time to become manifest (20, 21). Due to the open network structure present in a flocculated system, the filtration rate is expected to be higher than that obtained with a coagulated sediment.

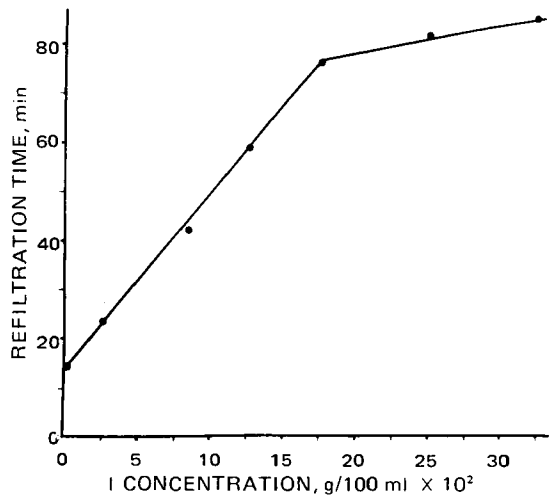

Figure 5—*Effect of I on refiltration time 10–50 of 5% sulfamerazine suspension.*

Table III—Effect of Aluminum Chloride on Refiltration Time 10–50 of 5% Sulfamerazine Suspensions Containing I

I Concentration, % w/v	Aluminum Chloride Concentration, % w/v	Refiltration Time 10–50	
		min	sec
0.025×10^{-2}	0.00	13	55
	0.02	14	15
	0.04	14	2
	0.10	14	20
0.25×10^{-2}	0.00	18	50
	0.02	18	35
	0.04	18	28
	0.10	18	24
25×10^{-2}	0.00	82	40
	0.10	49	38
	0.20	50	43

Table III shows the effect of various concentrations of aluminum chloride on the refiltration time of suspensions containing different amounts of I. It is apparent that the salt does not exert a noticeable effect on the refiltration time at very low surfactant concentrations ($<0.25 \times 10^{-2}$%). At these concentrations, the amount adsorbed is rather small, causing few, if any, bridges to be formed between particles. However, at 0.25% I, the addition of 0.1 or 0.2% aluminum chloride results in about a 40% decrease in the refiltration time. The refiltration time of surfactant-free suspensions at 0.1 and 0.2% aluminum chloride does not differ from that obtained in the absence of the aluminum salt. This result indicates that the flocculated structure, obtained in the presence of both dioctyl sulfosuccinate and Al^{+3} ions, is due to chemical bridging through interaction between the two ions.

The H_u/H_0 ratio of 5% sulfa suspensions coated with 0.25% I to which various concentrations of aluminum chloride are added is reported in Table IV. The increase in the ratio for the last two systems in the table corresponds to the decrease in refiltration time. This finding is a further indication of the correlation existing between the two parameters.

Effect of Sodium Chloride on Sulfamerazine Suspensions Containing I—Filtration times 10–50 and 40–50 of suspensions

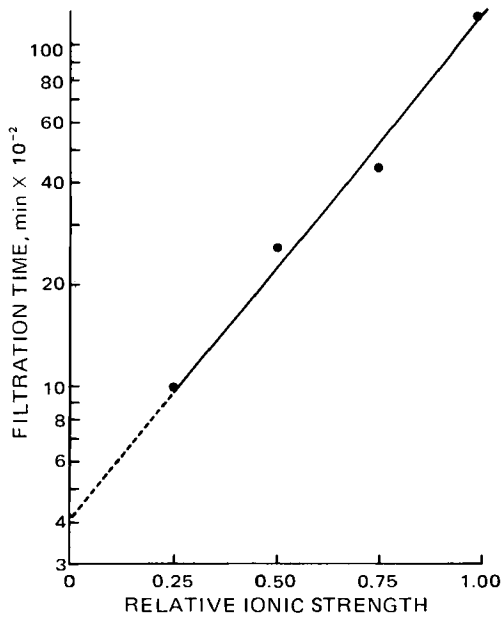

Figure 6—*Effect of relative ionic strength contributed by sodium chloride on filtration time 10–50 of 5% sulfamerazine suspensions in the presence of 0.25% I.*

Table IV—Effect of Aluminum Chloride on the Sediment Height Ratio of 5% Sulfamerazine Suspensions Containing 0.25% I

Aluminum Chloride Concentration, % w/v	H_u/H_o Ratio
0.00	0.20
0.02	0.19
0.04	0.35
0.06	0.40
0.08	0.40
0.10	0.40
0.20	0.40

Table V—Effect of Sodium Chloride on the Filtration Time of 5% Sulfamerazine Suspensions Containing 0.25% I

Relative Ionic Strength[a]	Filtration Time 10–50, min	Filtration Time 40–50, min
1.00[b]	1274	832
0.75	432	220
0.50	270	131
0.25	100	39
0.00	41	15

[a] Contributed by sodium chloride only. [b] At 0.29% NaCl.

containing 0.25% I and various concentrations of sodium chloride are shown in Table V. The highest concentration used (0.29%) corresponds to 0.2% $AlCl_3 \cdot 6H_2O$ with respect to ionic strength. The data show that the filtration rate decreases as sodium chloride concentration increases. Probably, I is partially salted out of solution as sodium chloride is added, and an excess amount of the surfactant is then available for adsorption onto the sulfa particles. Consequently, the sediment is expected to become denser as the amount adsorbed increases and a lower filtration rate is observed.

Increased filtration time with increased availability of surfactant has already been demonstrated (Fig. 5). In contrast, formation of an open network structure consisting of large clusters of particles is anticipated if the electrolyte is acting on the diffuse double layer of the negatively charged particles, and the filtration rate is expected to increase with an increasing salt concentration. However, the data indicate the opposite effect. Figure 6 shows that there is a steady increase in filtration time 10–50 as the ionic strength is increased.

REFERENCES

(1) R. W. Slater and J. A. Kitchener, *Discuss. Faraday Soc.*, **42**, 267(1966).

(2) V. K. La Mer, R. H. Smellie, Jr., and L. Pui-Kum, *J. Colloid Sci.*, **12**, 230(1957).

(3) A. N. Martin, *J. Pharm. Sci.*, **50**, 513(1961).

(4) A. Felmeister, G. M. Kuchtyak, S. Koziol, and C. J. Felmeister, *ibid.*, **62**, 2026(1973).

(5) G. Edgar and G. Calingaert, *Ind. Eng. Chem., Anal. Ed.*, **22**, 104(1930).

(6) H. T. Ward and K. Kammermeyer, *ibid.*, **32**, 622(1940).

(7) C. S. Robinson, *ibid.*, **18**, 869(1926).

(8) C. B. Egolf and W. L. McCabe, *Trans. Amer. Inst. Chem. Eng.*, **33**, 620(1937).

(9) American Society for Testing and Materials, C 204-55, adopted 1951, revised 1955.

(10) H. H. Steinour, *Ind. Eng. Chem.*, **56**, 618(1944).

(11) *Ibid.*, **56**, 840(1944).

(12) A. Dakkuri and B. Ecanow, *Amer. Perfum. Cosmet.*, **81**, 33(1966).

(13) P. C. Carman, *J. Soc. Chem. Ind., London, Trans. Commun.*, **57**, 225(1938).

(14) *Ibid.*, **58**, 1(1939).

(15) P. C. Carman and P. le R. Malherbe, *J. Soc. Chem. Ind., London, Trans. Commun.*, **69**, 134(1950).

(16) P. C. Carman and P. le R. Malherbe, *J. Appl. Chem.*, **1**, 105(1951).

(17) B. Ecanow, B. Gold, and C. Ecanow, *Amer. Perfum. Cosmet.*, **84**, 27(1969).

(18) B. Ecanow and H. Takruri, *J. Pharm. Sci.*, **59**, 1848(1970).

(19) R. G. Wilson and B. Ecanow, *ibid.*, **52**, 757(1963).

(20) H. A. Abramson, "Electrokinetic Phenomena and Their Application to Medicine," Chemical Catalog Co., New York, N.Y., 1934, p. 64.

(21) E. F. Burton, "The Physical Properties of Colloidal Solutions," 2nd ed., Longmans, Green and Co., London, England, 1921, chap. VIII.

ACKNOWLEDGMENTS AND ADDRESSES

Received January 31, 1972, from the *Department of Pharmacy, School of Pharmacy, American University of Beirut, Beirut, Lebanon, and the ‡Department of Pharmacy, College of Pharmacy, University of Illinois at the Medical Center, Chicago, IL 60680

Accepted for publication June 11, 1975.

ˣ To whom inquiries should be directed.

Nonaqueous Titration of Sulfates of Quinine and Quinidine Using Barium Acetate

SOBHI A. SOLIMAN ˣ, HASSAN ABDINE, and NASHAAT A. ZAKHARI

Abstract □ A nonaqueous titrimetric method is proposed for determining the diastereomeric sulfates of quinine and quinidine. The sulfuric acid content of the alkaloid salts is precipitated, in the form of barium sulfate, with acetous barium acetate solution before the liberated alkaloid is titrated; the necessary calculations are provided. A favorable characteristic of the proposed procedure is the accuracy, speed, and ease of performance. The mean percent recoveries ($p = 0.05$) obtained with the proposed method for the sulfates of quinine and quinidine were 98.84 ± 1.00 and 99.74 ± 1.27, respectively, compared with 100.73 ± 1.44 and 100.82 ± 1.16, respectively, when the BP 1968 procedure was applied.

Keyphrases □ Quinine sulfate—nonaqueous titrimetric analysis of base after barium acetate precipitation of sulfate, pure compound and synthetic tablets □ Quinidine sulfate—nonaqueous titrimetric analysis of base after barium acetate precipitation of sulfate, pure compound and synthetic tablets □ Titrimetry—analysis, quinine sulfate and quinidine sulfate, pure compound and synthetic tablets

Sulfates of nitrogenous bases were determined by several nonaqueous titration methods. The free alkaloid may be extracted in chloroform or carbon tetrachloride from its sulfate salt and then titrated against standard *p*-toluenesulfonic acid (1). When sulfates of nitrogenous bases were titrated directly against perchloric acid, only one equivalent of the base was titrated (2); the other equivalent, being bound in the form of bisulfate, was not titratable.

BACKGROUND

The benzidine method for the determination of sulfates of nitrogenous bases (3) is based on the precipitation of the sulfuric acid content in the form of benzidine sulfate. Since any free benzidine will also be titrated, the investigators suggested that only 95% of the equivalent quantity of sulfate ions should be bound in the form of benzidine sulfate. In this method, however, a previous knowledge of the content of the base sulfate in the sample is essential for a successful determination. Almost at the same time the sulfates of streptomycin, dihydrostreptomycin, and neomycin were determined (4) by essentially the same benzidine method.

Because of the poor solubility of most alkaloid sulfates in glacial acetic acid, it was suggested (5) that titration should be performed in a mixture of phenol, chloroform, and acetone against standard perchloric acid solution in dioxane. This method was used for the determination of some alkaloid sulfates, and the end-point was determined either potentiometrically or visually using methyl red indicator. Several alkaloid sulfates were titrated (6) to the bisulfate stage in an acetic anhydride medium. Gentian violet proved to be a suitable indicator. Some alkaloid sulfates were determined (7) in the same manner with bromophenol blue as the indicator. It was reported (8) that there was a drawnout color change of Fettblau B[1] indicator in the titration of the sulfates of quinine, quinidine, atropine, and strychnine in glacial acetic acid solvent and that these alkaloids could not be satisfactorily determined.

Quinine sulfate was titrated (9) in glacial acetic acid against standard perchloric acid. The consumption of the latter was 3.00 and 2.87 equivalents/mole of quinine sulfate when α-naphtholbenzein and quinaldine red were used as indicators, respectively. Photometric titration of quinine sulfate was performed in glacial acetic acid against standard perchloric acid solution (10).

Selective determination of quinine in compound pharmaceutical preparations was carried out (11) by preliminary isolation and transformation to quinine picrate. Then the picrate was titrated visually with gentian violet indicator against standard perchloric acid solution. The acidic components of alkaloid sulfates were determined (12) in an anhydrous pyridine medium against standard sodium methoxide solution.

A method was described for the indirect determination of inorganic sulfates (13) in solutions of reactor fuels. However, this method is best suited for the determination of inorganic sulfates in liquid samples when the components are generally known.

The objective of this study was to develop a nonaqueous titration method for the determination of the sulfates of quinine and quinidine by precipitating the sulfuric acid content of the alkaloid salt with barium acetate and titrating the liberated nitrogenous base.

EXPERIMENTAL

Apparatus and Materials—The following were used: a suitable titrimeter[2] equipped with a combination electrode[3], a magnetic stirrer, and a microburet with a 10-ml capacity (graduated to 0.02 ml).

Solutions—The following were used: 0.1 *N* perchloric acid solution in glacial acetic acid, 0.3 *N* barium acetate solution in glacial acetic acid, and 0.2% (w/v) solution of gentian violet indicator in glacial acetic acid.

Acetous perchloric acid solution was standardized against potassium biphthalate[4], previously dried at 110° for 2 hr, in glacial acetic acid, and the end-point was determined potentiometrically.

Acetous barium acetate solution was prepared by dissolving 29.604 g of barium carbonate[5], accurately weighed, in about 500 ml of glacial acetic acid. The solution was boiled on a hot plate for 3 min and cooled, and sufficient glacial acetic acid was added to produce 1000 ml. Five milliliters of this solution, accurately measured, was diluted with 30 ml of glacial acetic acid, 2 drops of gentian violet indicator solution were added, and the solution was titrated potentiometrically against 0.1 *N* acetous perchloric acid solution. Titrations were also carried out in different solvent systems, and titration curves are illustrated in Fig. 1.

Determination of Sulfates of Quinine and Quinidine by Proposed Method—An accurately weighed amount (50–300 mg) of the alkaloid sulfate was transferred into a 100-ml titration beaker and dissolved in about 30 ml of glacial acetic acid. To the magnetically stirred solution was added slowly an accurately measured volume (2–4 ml) of 0.3 *N* barium acetate solution; then 2 drops of

[1] Ciba.

[2] Pye model 79.

[3] Pye Catalog No. 401 E07, Series 546022.

[4] Rhone-Poulenc, France.

[5] General Chemical and Pharmaceutical Co., Sudbury, Middlesex, England.

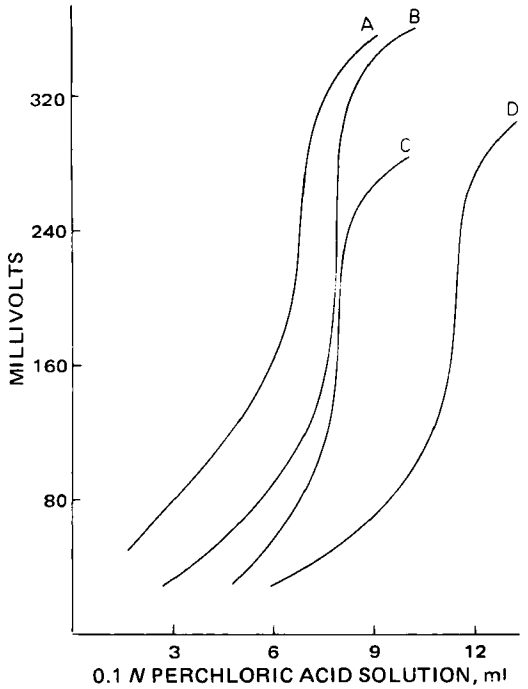

Figure 1—*Potentiometric titration curves of acetous barium acetate solution in different solvent systems. Key: A, glacial acetic acid–dioxane (1:4); B, glacial acetic acid–dioxane (1:1); C, glacial acetic acid; and D, glacial acetic acid–acetic anhydride (2:1).*

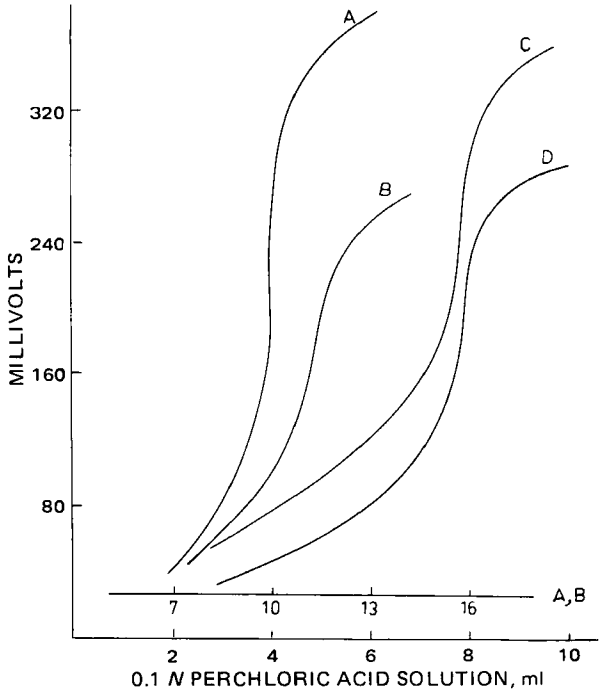

Figure 2—*Potentiometric titration curves in different solvent systems. Key: A, quinidine sulfate and barium acetate, glacial acetic acid–dioxane (1:1); B, quinidine sulfate and barium acetate, glacial acetic acid; C, quinine sulfate and barium acetate, glacial acetic acid–dioxane (1:1); and D, quinine sulfate and barium acetate, glacial acetic acid.*

gentian violet indicator solution were added, and the solution was titrated potentiometrically with 0.1 *N* acetous perchloric acid solution.

A blank determination was performed in the same manner using the same volume of barium acetate solution. The proper color change of the indicator at the point of maximum inflection in the titration curves, obtained by plotting the volume of titrant in milliliters against the millivolt readings, was noted. Potentiometric titrations were also performed in a glacial acetic acid–dioxane solvent system.

Analysis of Tablets—Twenty tablets of quinine sulfate or quinidine sulfate were weighed and reduced to a fine powder. An amount of powdered tablets equivalent to about 200 mg of alkaloid sulfate was accurately weighed and placed in a 100-ml titration beaker containing 30 ml of glacial acetic acid. The solution was heated gently for a few minutes, and 4.0 ml, accurately measured, of 0.3 *N* barium acetate solution was added slowly with continuous stirring. Two drops of gentian violet solution were added, and the solution was titrated with 0.1 *N* acetous perchloric acid solution to a pure blue color change. A blank experiment was carried out using the same volume of barium acetate solution.

RESULTS AND DISCUSSION

In glacial acetic acid and glacial acetic acid–dioxane solvent systems, barium acetate behaves as a moderately strong base. Therefore, when it is titrated with acetous perchloric acid solution, the consumption of the latter is 2 moles/mole of barium acetate (Scheme I).

$$(CH_3COO)_2Ba + 2HClO_4 \rightarrow Ba(ClO_4)_2 + 2CH_3COOH$$

Scheme I

Because of its basic properties in nonaqueous media, barium acetate has not been used to liberate nitrogenous bases from their sulfate salts, in a manner similar to the use of mercuric acetate reagent which binds halide ions (2) and prevents their interference in the nonaqueous titration of halides of nitrogenous bases, since the liberated base and excess barium acetate will consume perchloric acid. However, in the determination of sulfates of quinine and quinidine by the proposed method, the sulfuric acid content of the alkaloid is precipitated in the nonaqueous solvent in the form of barium sulfate by the addition of excess barium acetate solution; 2 moles of quinine or quinidine is liberated for each mole of barium acetate consumed (Scheme II).

$$(C_{20}H_{24}N_2O_2)_2H_2SO_4 + (CH_3COO)_2Ba \rightarrow 2C_{20}H_{24}N_2O_2 + \text{excess } (CH_3COO)_2Ba + BaSO_4 + 2CH_3COOH$$

Scheme II

The liberated alkaloid and the unconsumed barium acetate, being moderately strong bases in glacial acetic acid and glacial acetic acid–dioxane solvent systems, cannot be differentiated when potentiometrically titrated with perchloric acid solution, and only one inflection can be observed in the titration curve of the mixture. Consequently, this single inflection makes the assignment of an equivalent volume of standard perchloric acid to the liberated alkaloid or the remaining excess of barium acetate impossible, so the concentration of alkaloid sulfate in the sample cannot be calculated. However, since 1 mole of barium acetate is equivalent to 2 moles of perchloric acid (Scheme I), as in the blank titration, and since 2 moles of quinine or quinidine is produced in the precipitation reaction (Scheme II) and then consumes 4 moles of perchloric acid (Scheme III), there is a quantitative double increase in the consumption of the titrant for each mole of barium acetate reacting in the precipitation reaction.

$$2C_{20}H_{24}N_2O_2 + 4HClO_4 \rightarrow 2C_{20}H_{24}N_2O_2 \cdot 2H^+ + 4ClO_4^-$$

Scheme III

Advantage was taken of this quantitative increase in the consumption of titrant, as a result of the precipitation reaction, to calculate the percent recovery of quinine sulfate or quinidine sulfate as follows. If $HClO_{4(1)}$ and $HClO_{4(2)}$ are the milliequivalents of perchloric acid utilized in blank and experimental titrations, respectively, then:

$$HClO_{4(1)} = \text{mEq } (CH_3COO)_2Ba \qquad \text{(Eq. 1)}$$

and:

$$HClO_{4(2)} = \text{mEq alkaloid sulfate} + \text{mEq excess } (CH_3COO)_2Ba \qquad \text{(Eq. 2)}$$

Table I—Nonaqueous Titration of Diastereomeric Sulfates of Quinine and Quinidine by Proposed Method

Sample	Quinine Sulfate			Quinidine Sulfate		
	Weight, mg	Weight Found, mg	Recovery, %	Weight, mg	Weight Found, mg	Recovery, %
			Pure Compound			
1	285.0	281.6	98.89	204.2	203.3	99.56
2	255.3	256.2	100.35	198.0	196.7	99.34
3	228.0	222.5	97.59	132.2	132.3	100.07
4	205.7	205.6	99.95	102.3	101.7	99.41
5	146.0	146.5	100.34	102.2	101.8	99.61
6	102.1	103.6	101.47	101.0	100.9	99.99
7	99.3	97.8	98.49	99.9	99.5	99.60
8	94.0	92.1	97.98	70.3	69.7	99.15
9	57.3	57.5	100.35	57.4	57.9	100.90
	Mean percent recovery (p = 0.05)		98.84 ± 1.00	Mean percent recovery (p = 0.05)		99.74 ± 1.27
			Synthetic Tablets			
1	200.2	199.5	99.65	200.2	203.3	101.55
2	200.1	198.8	99.35	200.2	199.5	99.65
3	200.0	197.9	98.95	200.2	199.5	99.65
4	200.0	195.6	97.80	200.0	201.4	100.70
5	199.8	195.4	97.79	200.0	199.4	99.70
	Mean percent recovery (p = 0.05)		98.71 ± 1.08	Mean percent recovery (p = 0.05)		100.25 ± 0.38

Table II—Determination of Quinine Sulfate and Quinidine Sulfate by BP 1968 Procedure

Sample	Quinine Sulfate			Quinidine Sulfate		
	Weight, mg	Weight Found, mg	Recovery, %	Weight, mg	Weight Found, mg	Recovery, %
1	502.7	510.0	101.45	501.9	509.0	101.41
2	500.0	504.0	100.80	500.5	508.0	101.49
3	500.0	498.0	99.60	500.0	501.6	100.32
4	501.0	499.2	99.64	500.0	500.4	100.08
	Mean percent recovery (p = 0.05)		100.37 ± 1.44	Mean percent recovery (p = 0.05)		100.82 ± 1.16

Also, according to the stoichiometries expressed by reactions shown in Schemes I–III, it can be stated that:

$$\text{mEq alkaloid sulfate} = 2\{[\text{mEq } (CH_3COO)_2Ba] - [\text{mEq excess } (CH_3COO)_2Ba]\} \quad \text{(Eq. 3)}$$

Substituting Eq. 1 into Eq. 3 and dividing by 2 yield:

$$\tfrac{1}{2}\text{mEq alkaloid sulfate} = HClO_{4(1)} - \text{mEq excess } (CH_3COO)_2Ba \quad \text{(Eq. 4)}$$

On rearranging, Eq. 4 becomes:

$$\text{mEq excess } (CH_3COO)_2Ba = HClO_{4(1)} - \tfrac{1}{2}\text{mEq alkaloid sulfate} \quad \text{(Eq. 5)}$$

Then substituting Eq. 5 into Eq. 2 and rearranging give:

$$\text{mEq alkaloid sulfate} = 2(HClO_{4(2)} - HClO_{4(1)}) \quad \text{(Eq. 6)}$$

Therefore, the percent recovery of quinine sulfate or quinidine sulfate is:

$$\% \text{ recovery} = \frac{2(HClO_{4(2)} - HClO_{4(1)}) \times 195.74 \times 10^2}{W} \quad \text{(Eq. 7)}$$

which simplifies to:

$$\% \text{ recovery} = \frac{2(E - B) \times N \times 195.74 \times 10^2}{W} \quad \text{(Eq. 8)}$$

where E = milliliters of perchloric acid equivalent to total basicity in the experimental titration, B = milliliters of perchloric acid equivalent to barium acetate in the blank titration, N = normality of perchloric acid, W = weight of sample (milligrams), and 195.74 = equivalent weight of quinine or quinidine sulfate dihydrate.

Potentiometric titration curves for barium acetate alone and mixed with either quinine or quinidine sulfate in different solvent systems are shown in Figs. 1 and 2, respectively. In all solvent systems studied, the appearance of the blue color of gentian violet indicator signaled the potentiometric end-point. Glacial acetic acid–dioxane (1:1) mixture was the solvent of choice, since a greater break in the titration curve and a more satisfactory indicator color change were obtained.

Recovery data for quinine sulfate and quinidine sulfate, in pure form and in synthetic tablets, using the proposed method are listed in Table I. The results were quantitative and reproducible. The overall mean percent recoveries (p = 0.05) for the assay of samples of quinine sulfate and synthetic tablets, prepared to contain 150 mg of the drug, were 98.84 ± 1.00 and 98.71 ± 1.08, respectively. Recoveries (p = 0.05) for quinidine sulfate and its synthetic 200-mg tablets were 99.74 ± 1.27 and 100.25 ± 0.38, respectively. Starch and talc, the common excipients of tablets, do not interfere with the proposed method; however, titratable lubricants such as magnesium stearate do interfere.

In comparison, the mean percent recoveries (p = 0.05) for the determination of the diastereomers, quinine and quinidine sulfate, by the gravimetric method of BP 1968 (14) were 100.37 ± 1.44 and 100.82 ± 1.16, respectively (Table II). Statistical analysis of the two sets of results obtained by applying the proposed and BP 1968 procedures indicated that the difference between the two mean percent recoveries obtained for each compound was statistically insignificant and that the results obtained by the two methods were almost equally accurate and precise.

REFERENCES

(1) I. Gyenes, *Magy. Kem. Foly.*, **56,** 383(1950).

(2) C. W. Pifer and E. G. Wollish, *Anal. Chem.*, **24,** 300(1952).

(3) J. A. Gautier and F. Pellerin, *Ann. Pharm. Fr.*, **12,** 505(1954); through *Anal. Abstr.*, **2,** 1320(1955).

(4) H. Penau, E. Saias, and J. Ferdet, *ibid.*, **12,** 505(1954); through *Chem. Abstr.*, **48,** 14118(1954).

(5) L. G. Chatten, *J. Pharm. Pharmacol.*, **7,** 586(1955).

(6) B. Salvesen, *Medd. Norsk Farm. Selskap*, **23,** 141(1961); through *Chem. Abstr.*, **56,** 14397(1962).

(7) H. Feltkamp, *Deut. Apoth.-Ztg.*, **101,** 207(1961); through *Anal. Abstr.*, **8,** 4811(1961).

(8) M. Rink, R. Lux, and E. Franken, *ibid.*, **98**, 660(1958); through *Anal. Abstr.*, **6**, 1885(1959).
(9) T. Higuchi and J. Concha, *J. Amer. Pharm. Ass., Sci. Ed.*, **40**, 173(1951).
(10) H. Ellert, T. Jasinski, and K. Marcinkowska, *Acta Pol. Pharm.*, **17**, 29(1960); through *Chem. Abstr.*, **54**, 11806(1960).
(11) M. Hadicke and K. Howorka, *Pharm. Zentralhalle*, **99**, 312(1960); through *Anal. Abstr.*, **8**, 773(1961).
(12) J. Vacek and J. Kracmar, *Cesk. Farm.*, **5**, 80(1956).
(13) G. Goldstein, O. Menis, and D. L. Manning, *Anal. Chem.*, **33**, 266(1961).
(14) "The British Pharmacopoeia," The Pharmaceutical Press, London, England, 1968, pp. 858, 865.

ACKNOWLEDGMENTS AND ADDRESSES

Received November 25, 1974, from the *Pharmaceutical Analytical Chemistry Department, College of Pharmacy, University of Alexandria, Alexandria, Egypt.*

Accepted for publication May 5, 1975.

[x] To whom inquiries should be directed.

Quantitative GLC Determination of Codeine in Plasma

RUTH A. ZWEIDINGER [x], F. M. WEINBERG [*], and R. W. HANDY

Abstract □ A sensitive and accurate GLC method for quantitating codeine in plasma at levels of 50 ng/ml, with limits of detection as low as 5 ng/ml, is described.

Keyphrases □ Codeine—GLC analysis, *n*-butyl chloride extraction, plasma □ GLC—analysis, codeine in plasma

Codeine has long been used as an analgesic in pharmaceutical preparations. Because of the recent interest in drug efficacy and bioavailability, a sensitive method for determining low nanogram quantities in plasma is needed. Several methods for the analysis of codeine in urine have been developed for the study of its metabolism and for forensic purposes (1–3). However, the levels found in urine are many times greater than those found in plasma, so these methods are generally not applicable in plasma analysis.

Schmerzler *et al.* (4) reported a GLC method for codeine in serum (and urine) of adequate sensitivity. This method has two serious drawbacks: the tendency for chloroform to form emulsions, especially with serum or plasma, and a variable recovery of codeine in the extraction procedure.

In this study, *n*-butyl chloride, which does not readily form emulsions with plasma, was used in place of chloroform. Dihydrocodeinone was added to the plasma to serve as an internal standard for both the extraction procedure and GLC quantitation.

EXPERIMENTAL

Apparatus—A gas chromatograph[1] with a flame-ionization detector was used.

Reagents—*n*-Butyl chloride[2] saturated with water was used for all extractions. Dihydrocodeinone was synthesized in this laboratory from thebaine by a two-step procedure (5). The water used to prepare aqueous reagents was checked to ensure low GLC background; all other solvents and chemicals were reagent grade.

Glassware was oven cleaned at 400° (6), silanized with 5% dimethyldichlorosilane in toluene, and rinsed with toluene and methanol. Immediately before use, the glassware was rinsed with chloroform to maintain a low GLC background. Chromatographic grade carbon disulfide[3] was used for GLC.

Procedure—To 2.0 ml of plasma was added 1 μg of dihydrocodeinone internal standard in aqueous solution. The plasma was made alkaline with 0.10 ml of 1 *N* NaOH and extracted twice with 2 ml of butyl chloride on a reciprocal shaker at 60 cpm for 20 min. The organic fractions were combined, a 0.5-ml aliquot of 0.05 *N* H_2SO_4 was added, and the solution was shaken for 20 min. Then the organic layer was discarded, and the aqueous phase was washed with an additional 1 ml of butyl chloride. The aqueous layer then was made alkaline with 0.05 ml of 1 *N* NaOH and extracted twice with 1 ml of butyl chloride.

The organic layers were combined in a conical vial, and the solvent was evaporated immediately before GLC analysis. The residue was taken up in 10 μl of carbon disulfide, and 2 μl was injected for GLC analyses. The column used was a 1.8-m (6-ft), 2.5-mm i.d., silanized glass column with 2% (w/w) XE-60 on acid-washed Anakrom A (90–100 mesh).

The temperatures were: injector, 250°; column, 230°; and detector, 250°. The nitrogen carrier gas flow rate was 20 ml/min. The ratio of the codeine to dihydrocodeine peak areas was compared to a standard curve; peak areas were measured by peak height times width at half-height.

Table I—Recoveries of Codeine Added to Plasma

Codeine Added to Plasma, ng/ml	Codeine Found[a], ng/ml
0	ND[b]
50	48 ± 2 (n = 2)
100	105 ± 7 (n = 3)

[a] Corrected for the calculated extraction recovery. [b] Not detected.

RESULTS AND DISCUSSION

The objective of this study was to devise a method that was accurate and precise without requiring inordinate amounts of time for evaluation of recoveries. Several codeine analogs were considered as possible internal standards. Of these, morphine and norcodeine could not be used since they are major metabolites of codeine (7). Dihydrocodeine and codeine were unresolved by GLC on OV-17 or XE-60. Since dihydrocodeinone was well resolved on both columns and had a relative retention time of 1.67 (codeine = 1.0) on the XE-60 column, it was the choice as an internal standard. With the use of dihydrocodeinone, this procedure is nearly

[1] Fisher Victoreen series 4400.
[2] Burdick and Jackson.
[3] Fisher.

(8) M. Rink, R. Lux, and E. Franken, *ibid.*, **98**, 660(1958); through *Anal. Abstr.*, **6**, 1885(1959).
(9) T. Higuchi and J. Concha, *J. Amer. Pharm. Ass., Sci. Ed.*, **40**, 173(1951).
(10) H. Ellert, T. Jasinski, and K. Marcinkowska, *Acta Pol. Pharm.*, **17**, 29(1960); through *Chem. Abstr.*, **54**, 11806(1960).
(11) M. Hadicke and K. Howorka, *Pharm. Zentralhalle*, **99**, 312(1960); through *Anal. Abstr.*, **8**, 773(1961).
(12) J. Vacek and J. Kracmar, *Cesk. Farm.*, **5**, 80(1956).
(13) G. Goldstein, O. Menis, and D. L. Manning, *Anal. Chem.*, **33**, 266(1961).
(14) "The British Pharmacopoeia," The Pharmaceutical Press, London, England, 1968, pp. 858, 865.

ACKNOWLEDGMENTS AND ADDRESSES

Received November 25, 1974, from the *Pharmaceutical Analytical Chemistry Department, College of Pharmacy, University of Alexandria, Alexandria, Egypt.*

Accepted for publication May 5, 1975.

[x] To whom inquiries should be directed.

Quantitative GLC Determination of Codeine in Plasma

RUTH A. ZWEIDINGER [x], F. M. WEINBERG [*], and R. W. HANDY

Abstract □ A sensitive and accurate GLC method for quantitating codeine in plasma at levels of 50 ng/ml, with limits of detection as low as 5 ng/ml, is described.

Keyphrases □ Codeine—GLC analysis, *n*-butyl chloride extraction, plasma □ GLC—analysis, codeine in plasma

Codeine has long been used as an analgesic in pharmaceutical preparations. Because of the recent interest in drug efficacy and bioavailability, a sensitive method for determining low nanogram quantities in plasma is needed. Several methods for the analysis of codeine in urine have been developed for the study of its metabolism and for forensic purposes (1–3). However, the levels found in urine are many times greater than those found in plasma, so these methods are generally not applicable in plasma analysis.

Schmerzler *et al.* (4) reported a GLC method for codeine in serum (and urine) of adequate sensitivity. This method has two serious drawbacks: the tendency for chloroform to form emulsions, especially with serum or plasma, and a variable recovery of codeine in the extraction procedure.

In this study, *n*-butyl chloride, which does not readily form emulsions with plasma, was used in place of chloroform. Dihydrocodeinone was added to the plasma to serve as an internal standard for both the extraction procedure and GLC quantitation.

EXPERIMENTAL

Apparatus—A gas chromatograph[1] with a flame-ionization detector was used.

Reagents—*n*-Butyl chloride[2] saturated with water was used for all extractions. Dihydrocodeinone was synthesized in this laboratory from thebaine by a two-step procedure (5). The water used to prepare aqueous reagents was checked to ensure low GLC background; all other solvents and chemicals were reagent grade.

Glassware was oven cleaned at 400° (6), silanized with 5% dimethyldichlorosilane in toluene, and rinsed with toluene and methanol. Immediately before use, the glassware was rinsed with chloroform to maintain a low GLC background. Chromatographic grade carbon disulfide[3] was used for GLC.

Procedure—To 2.0 ml of plasma was added 1 μg of dihydrocodeinone internal standard in aqueous solution. The plasma was made alkaline with 0.10 ml of 1 *N* NaOH and extracted twice with 2 ml of butyl chloride on a reciprocal shaker at 60 cpm for 20 min. The organic fractions were combined, a 0.5-ml aliquot of 0.05 *N* H_2SO_4 was added, and the solution was shaken for 20 min. Then the organic layer was discarded, and the aqueous phase was washed with an additional 1 ml of butyl chloride. The aqueous layer then was made alkaline with 0.05 ml of 1 *N* NaOH and extracted twice with 1 ml of butyl chloride.

The organic layers were combined in a conical vial, and the solvent was evaporated immediately before GLC analysis. The residue was taken up in 10 μl of carbon disulfide, and 2 μl was injected for GLC analyses. The column used was a 1.8-m (6-ft), 2.5-mm i.d., silanized glass column with 2% (w/w) XE-60 on acid-washed Anakrom A (90–100 mesh).

The temperatures were: injector, 250°; column, 230°; and detector, 250°. The nitrogen carrier gas flow rate was 20 ml/min. The ratio of the codeine to dihydrocodeine peak areas was compared to a standard curve; peak areas were measured by peak height times width at half-height.

Table I—Recoveries of Codeine Added to Plasma

Codeine Added to Plasma, ng/ml	Codeine Found[a], ng/ml
0	ND[b]
50	48 ± 2 (n = 2)
100	105 ± 7 (n = 3)

[a] Corrected for the calculated extraction recovery. [b] Not detected.

RESULTS AND DISCUSSION

The objective of this study was to devise a method that was accurate and precise without requiring inordinate amounts of time for evaluation of recoveries. Several codeine analogs were considered as possible internal standards. Of these, morphine and norcodeine could not be used since they are major metabolites of codeine (7). Dihydrocodeine and codeine were unresolved by GLC on OV-17 or XE-60. Since dihydrocodeinone was well resolved on both columns and had a relative retention time of 1.67 (codeine = 1.0) on the XE-60 column, it was the choice as an internal standard. With the use of dihydrocodeinone, this procedure is nearly

[1] Fisher Victoreen series 4400.
[2] Burdick and Jackson.
[3] Fisher.

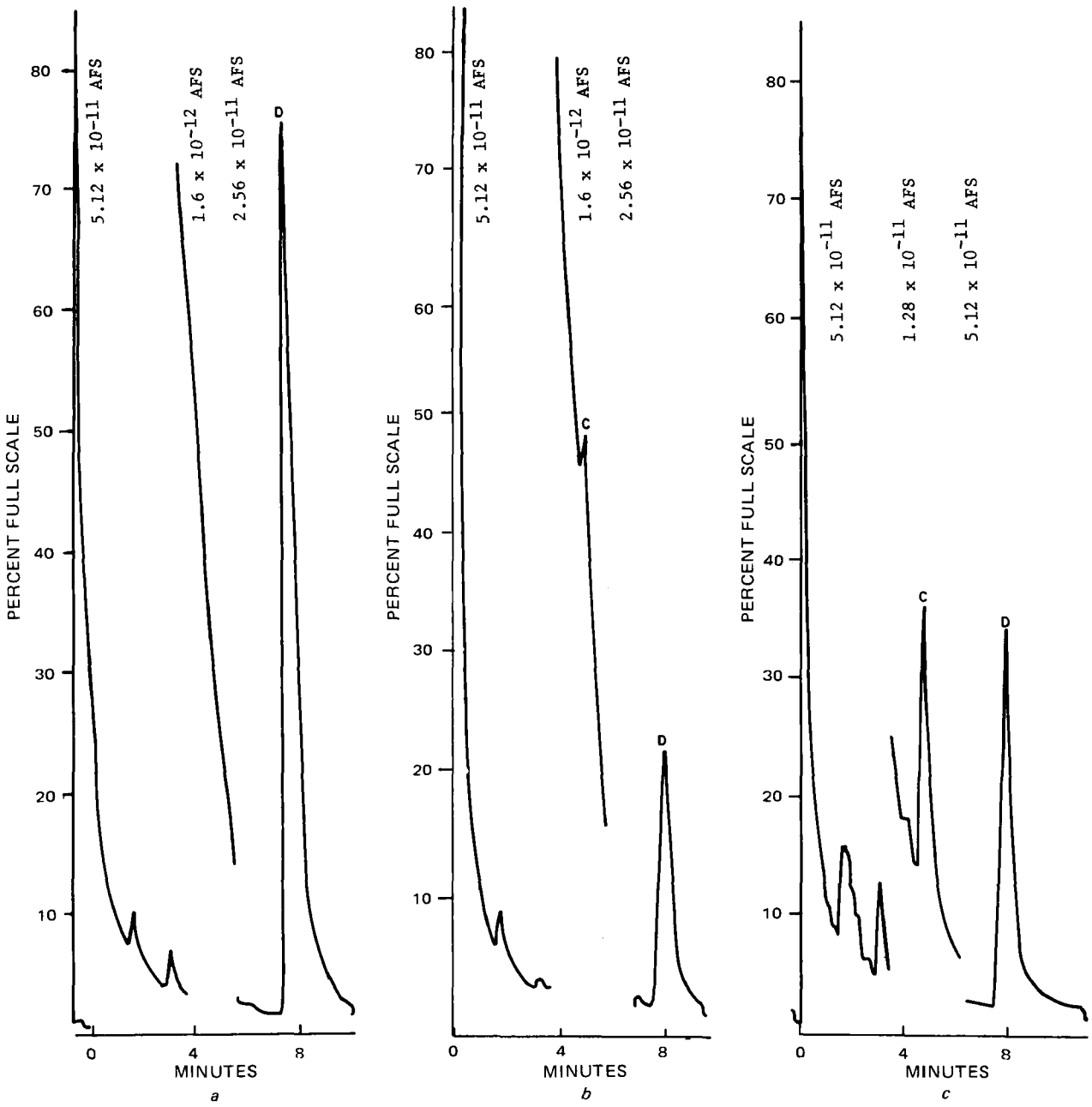

Figure 1—*Gas–liquid chromatograms of plasma extract. Key:* a, *blank;* b, *10 min after oral dose of codeine (14 ng/ml codeine);* c, *40 min after oral dose of codeine (181 ng/ml codeine); C, codeine; and D, dihydrocodeinone.*

independent of recovery so long as sufficient material is available for GLC detection.

The distribution coefficient for codeine between *n*-butyl chloride and aqueous base was found to be 2. On this basis, a theoretical maximum recovery of 85% would be predicted from the described extraction procedure. In a similar manner, a 99.5% recovery would be predicted for dihydrocodeinone (partition coefficient = 14). Recoveries of codeine relative to the internal standard are calculated to be 86% based on the partition coefficients; this value correlates well with the observed recoveries (averaging 87.6 ± 7.8%) obtained by GLC analysis (Table I). Quantitation was possible at the 50-ng/ml level as indicated, but limits of detection as low as 5 ng/ml were obtained when detector noise was optimal.

Although the amount of internal standard used is larger than the amounts of codeine encountered in plasma samples, the validity of this approach was demonstrated by the linearity of the calibration curve obtained from standard mixtures of codeine and dihydrocodeinone (r = 0.99997). An intercept for the calibration curve at 5 ng/ml correlated well with the observed limit of detection. Over the concentration range from 50 to 250 ng/ml plasma, the slope of the calibration curve including the factor for the calculated recovery was 0.000815 (peak area ratio *versus* nanograms of codeine per milliliter of plasma). This standard curve was used for the determination of the samples. Standard deviations for duplicate injections averaged 3% for eight standard mixtures in the codeine concentration range between 50 and 250 ng/ml. Standards chromatographed over 8 days gave standard deviations between days of not greater than 3.1%. Table I lists the results of the analysis of codeine added to plasma.

Figure 1 shows GLC tracings of codeine in the plasma of a subject 10 and 40 min after an oral dose of two tablets containing 65 mg of codeine as well as the plasma blank. The plasma codeine levels as a function of time for this subject are shown in Fig. 2. The standard deviations indicated are for duplicate injections of the same sample.

Some practical benefits are obtained using *n*-butyl chloride as the extraction solvent, including lower background, greatly reduced tendency to form emulsions, cleaner solvent–water interfaces, and the fact that only the upper phase must be transferred. This added convenience permits a set of 20 samples to be prepared

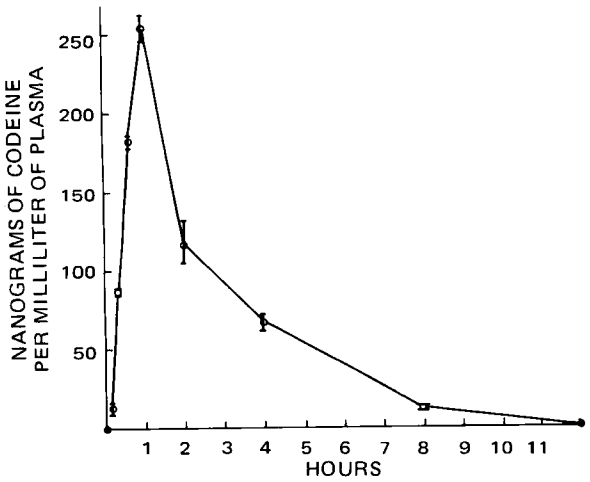

Figure 2—*Plasma codeine levels after an oral dose of two tablets containing 65 mg of codeine.*

for GLC analysis in an 8-hr day. The chromatography of the samples requires approximately the same time. Precision for codeine determination was 7% for levels of 50 ng/ml or greater.

REFERENCES

(1) D. W. Cornish, D. M. Grossman, A. L. Jacobs, A. F. Michaelis, and B. Salsitz, *Anal. Chem.*, **45**, 221R(1973).

(2) J. W. Sutherland, D. E. Williamson, and J. G. Theivagt, *ibid.*, **43**, 206(1971).

(3) B. S. Finkle, *ibid.*, **44**, 18A(1972).

(4) E. Schmerzler, W. Uy, M. I. Hewitt, and I. J. Greenblatt, *J. Pharm. Sci.*, **55**, 155(1966).

(5) K. W. Bentley, "The Chemistry of the Morphine Alkaloids," Oxford University Press (Claverdon), Oxford, England, 1954.

(6) S. Kushinsky and W. Paul, *Anal. Biochem.*, **30**, 465(1969).

(7) H. Yoshimura, M. A. Mori, K. Oguri, and H. Tsuhamoto, *Biochem. Pharmacol.*, **19**, 2353(1970).

ACKNOWLEDGMENTS AND ADDRESSES

Received January 17, 1975, from *Research Triangle Institute, Research Triangle Park, NC 27709*

Accepted for publication May 19, 1975.

Supported by the Wellcome Research Laboratories, Burroughs Wellcome Co., Research Triangle Park, N.C.

The authors are indebted to Dr. George A. Brine for synthesizing the dihydrocodeinone.

* Present address: 34 Winoka Drive, Huntington Station, NY 11746

ˣ To whom inquiries should be directed.

Aqueous Solubility of ^{14}C-Triamcinolone Acetonide

CHARANJIT RAI BEHL, LAWRENCE H. BLOCK ˣ, and MITCHELL L. BORKE

Abstract □ The blue tetrazolium colorimetric assay has often been employed in the analysis of corticosteroids. However, the reaction between blue tetrazolium and corticosteroids partly depends on the apparent pH of the system. In an earlier study of the temperature dependence of the solubility and dissolution of triamcinolone acetonide in aqueous dissolution media (distilled water and 0.2–1.0 *M* potassium chloride solutions), pH was not considered. To determine the reliability of the data previously reported, the solubility of ^{14}C-triamcinolone acetonide was determined by a radioisotopic method. The results of the analyses, using a liquid scintillation counting system, indicate that the steroid solubility is generally about 20% lower than that reported previously.

Keyphrases □ Triamcinolone acetonide, ^{14}C-labeled—synthesized, aqueous solubility determined, radioisotopic method □ Radioisotopic methods—determination of aqueous solubility of ^{14}C-triamcinolone acetonide □ Glucocorticoids—^{14}C-triamcinolone acetonide, synthesis, aqueous solubility determined, radioisotopic method □ Solubility, aqueous—^{14}C-triamcinolone acetonide, radioisotopic method

In a previous report from these laboratories (1), data were presented for the dissolution and solubility of triamcinolone acetonide in aqueous media. The data were obtained from the colorimetric determination of steroid concentration. The pH of the aqueous dissolution systems employed was not considered.

Graham and Kenner (2) studied the parameters affecting the chemical reaction involved in the colorimetric assay of triamcinolone acetonide and indicated a dependence of absorbance on the apparent pH of the system. Thus, the colorimetric process employed might have involved some error, particularly when the measured absorbance was relatively low. To define more precisely the solubility of the steroid in aqueous media, ^{14}C-labeled triamcinolone acetonide was synthesized and its aqueous solubility was determined by measuring the associated radioactivity.

EXPERIMENTAL

Materials—The following were used as received: concentrated perchloric acid (70%)[1], spectrophotometric grade acetone[2], anisole[2], ethanol[2], ether[2], dioxane[2], 1,4-bis[2-(5-phenyloxazolyl)]-benzene[2], potassium chloride[2], 2,5-diphenyloxazole[2], sodium bicarbonate[2], 1,3-^{14}C-acetone[3], ^{14}C-benzoic acid[4], triamcinolone acetonide[5], triamcinolone alcohol[5], 1,2-dimethoxane[6], recrystallized blue tetrazolium[2], chloroform[2], toluene[2], sodium hydroxide[2], and methanol[2].

Solutions—A stock solution of 1,3-^{14}C-acetone was diluted with acetone to yield a solution with a specific activity of 3.02×10^7 dpm/ml. A liquid scintillation solution was prepared by dissolving 12 g of 2,5-diphenyloxazole and 0.5 g of 1,4-bis[2-(5-phenyloxazolyl)]benzene in 750 ml of dioxane, along with 125 ml of anisole and 125 ml of 1,2-dimethoxane. A standard solution of ^{14}C-benzoic acid was prepared to provide suitable specific activity.

[1] Allied Chemicals, General Chemical Division, Morristown, N.J.
[2] Fisher Scientific Co., Fair Lawn, N.J.
[3] ICN Chemical and Radioisotope Division, Irvine, Calif.
[4] New England Nuclear Corp., Boston, Mass.
[5] Squibb Institute for Medical Research, E.R. Squibb and Sons, New Brunswick, N.J.
[6] Eastman Organic Chemicals, Rochester, N.Y.

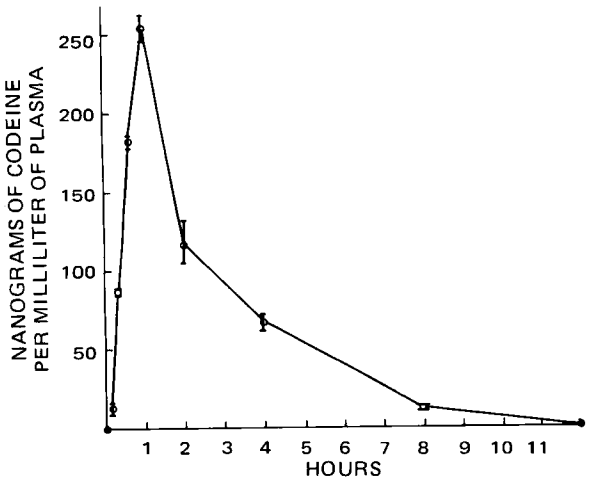

Figure 2—*Plasma codeine levels after an oral dose of two tablets containing 65 mg of codeine.*

for GLC analysis in an 8-hr day. The chromatography of the samples requires approximately the same time. Precision for codeine determination was 7% for levels of 50 ng/ml or greater.

REFERENCES

(1) D. W. Cornish, D. M. Grossman, A. L. Jacobs, A. F. Michaelis, and B. Salsitz, *Anal. Chem.*, **45**, 221R(1973).

(2) J. W. Sutherland, D. E. Williamson, and J. G. Theivagt, *ibid.*, **43**, 206(1971).

(3) B. S. Finkle, *ibid.*, **44**, 18A(1972).

(4) E. Schmerzler, W. Uy, M. I. Hewitt, and I. J. Greenblatt, *J. Pharm. Sci.*, **55**, 155(1966).

(5) K. W. Bentley, "The Chemistry of the Morphine Alkaloids," Oxford University Press (Claverdon), Oxford, England, 1954.

(6) S. Kushinsky and W. Paul, *Anal. Biochem.*, **30**, 465(1969).

(7) H. Yoshimura, M. A. Mori, K. Oguri, and H. Tsuhamoto, *Biochem. Pharmacol.*, **19**, 2353(1970).

ACKNOWLEDGMENTS AND ADDRESSES

Received January 17, 1975, from *Research Triangle Institute, Research Triangle Park, NC 27709*

Accepted for publication May 19, 1975.

Supported by the Wellcome Research Laboratories, Burroughs Wellcome Co., Research Triangle Park, N.C.

The authors are indebted to Dr. George A. Brine for synthesizing the dihydrocodeinone.

* Present address: 34 Winoka Drive, Huntington Station, NY 11746

ˣ To whom inquiries should be directed.

Aqueous Solubility of ^{14}C-Triamcinolone Acetonide

CHARANJIT RAI BEHL, LAWRENCE H. BLOCK ˣ, and MITCHELL L. BORKE

Abstract □ The blue tetrazolium colorimetric assay has often been employed in the analysis of corticosteroids. However, the reaction between blue tetrazolium and corticosteroids partly depends on the apparent pH of the system. In an earlier study of the temperature dependence of the solubility and dissolution of triamcinolone acetonide in aqueous dissolution media (distilled water and 0.2–1.0 *M* potassium chloride solutions), pH was not considered. To determine the reliability of the data previously reported, the solubility of ^{14}C-triamcinolone acetonide was determined by a radioisotopic method. The results of the analyses, using a liquid scintillation counting system, indicate that the steroid solubility is generally about 20% lower than that reported previously.

Keyphrases □ Triamcinolone acetonide, ^{14}C-labeled—synthesized, aqueous solubility determined, radioisotopic method □ Radioisotopic methods—determination of aqueous solubility of ^{14}C-triamcinolone acetonide □ Glucocorticoids—^{14}C-triamcinolone acetonide, synthesis, aqueous solubility determined, radioisotopic method □ Solubility, aqueous—^{14}C-triamcinolone acetonide, radioisotopic method

In a previous report from these laboratories (1), data were presented for the dissolution and solubility of triamcinolone acetonide in aqueous media. The data were obtained from the colorimetric determination of steroid concentration. The pH of the aqueous dissolution systems employed was not considered.

Graham and Kenner (2) studied the parameters affecting the chemical reaction involved in the colorimetric assay of triamcinolone acetonide and indicated a dependence of absorbance on the apparent pH of the system. Thus, the colorimetric process employed might have involved some error, particularly when the measured absorbance was relatively low. To define more precisely the solubility of the steroid in aqueous media, ^{14}C-labeled triamcinolone acetonide was synthesized and its aqueous solubility was determined by measuring the associated radioactivity.

EXPERIMENTAL

Materials—The following were used as received: concentrated perchloric acid (70%)[1], spectrophotometric grade acetone[2], anisole[2], ethanol[2], ether[2], dioxane[2], 1,4-bis[2-(5-phenyloxazolyl)]-benzene[2], potassium chloride[2], 2,5-diphenyloxazole[2], sodium bicarbonate[2], 1,3-^{14}C-acetone[3], ^{14}C-benzoic acid[4], triamcinolone acetonide[5], triamcinolone alcohol[5], 1,2-dimethoxane[6], recrystallized blue tetrazolium[2], chloroform[2], toluene[2], sodium hydroxide[2], and methanol[2].

Solutions—A stock solution of 1,3-^{14}C-acetone was diluted with acetone to yield a solution with a specific activity of 3.02×10^7 dpm/ml. A liquid scintillation solution was prepared by dissolving 12 g of 2,5-diphenyloxazole and 0.5 g of 1,4-bis[2-(5-phenyloxazolyl)]benzene in 750 ml of dioxane, along with 125 ml of anisole and 125 ml of 1,2-dimethoxane. A standard solution of ^{14}C-benzoic acid was prepared to provide suitable specific activity.

[1] Allied Chemicals, General Chemical Division, Morristown, N.J.
[2] Fisher Scientific Co., Fair Lawn, N.J.
[3] ICN Chemical and Radioisotope Division, Irvine, Calif.
[4] New England Nuclear Corp., Boston, Mass.
[5] Squibb Institute for Medical Research, E.R. Squibb and Sons, New Brunswick, N.J.
[6] Eastman Organic Chemicals, Rochester, N.Y.

Table I—Solubility of ^{14}C-Triamcinolone Acetonide in Dissolution Media[a]

Temperature	Distilled Water	Potassium Chloride Solution		
		0.2 *M*	0.5 *M*	1.0 *M*
28°	17.5 (±0.05)	9.8 (±0.05)	6.6 (±0.03)	2.5 (±0.05)
37°	20.7 (±0.13)	13.0 (±0.08)	9.6 (±0.05)	4.2 (±0.06)
50°	26.5 (±0.17)	21.0 (±0.01)	15.9 (±0.01)	8.4 (±0.05)

[a] Results (in micrograms per milliliter) are the averages of eight determinations (±1 *SD*).

Table II—Setschenow Equation Data for Triamcinolone Acetonide (Setschenow Ratios[a])

Temperature	0.2 *M* KCl	0.5 *M* KCl	1.0 *M* KCl	*k*[b]
28°	1.77	2.66	6.88	0.746
37°	1.59	2.15	4.90	0.622
50°	1.34	1.67	3.16	0.475

[a] The Setschenow ratio, S_0/S, represents the solubility of the steroid in pure solvent to its solubility in electrolyte solution of a given molar concentration. [b] "Salting-out" constant.

Table III—Differential Heats of Solution of Triamcinolone Acetonide in Dissolution Media

Dissolution Media	$\Delta H_{solution}$ Values, cal/mole	
	This Study	Previously Reported
Distilled water	3,736	4207
0.2 *M* KCl	6,760	8340
0.5 *M* KCl	7,840	8722
1.0 *M* KCl	10,549	9855

Synthesis of ^{14}C-Triamcinolone Acetonide—The method reported by Heller *et al.* (3) was modified, and the following procedure was employed. Eight hundred milligrams of triamcinolone alcohol was suspended in approximately 15 ml of the stock solution of 1,3-^{14}C-acetone, and enough concentrated perchloric acid (about 2 ml) was added to the suspension to dissolve the steroid. The solution was maintained at 25° for 30 min; then 200 ml of distilled water was added, followed by sufficient saturated sodium bicarbonate solution (approximately 250 ml) to make the solution alkaline.

The acetone was allowed to evaporate at ambient temperature, and a white crystalline solid precipitated. The solid, washed with distilled water, was dried at 35° to yield 750 mg of ^{14}C-triamcinolone acetonide, mp 272–276°. Its melting point, chromatographic behavior[7], and UV and IR spectra were identical to those of an authentic sample of triamcinolone acetonide[5]. The molar absorptivities in absolute alcohol of the ^{14}C-triamcinolone acetonide and of the authentic sample of the steroid were 14,690 and 14,714, respectively. Bernstein *et al.* (4) reported a molar absorptivity for the steroid of 14,600. The steroid's specific activity, in comparison with standard ^{14}C-benzoic acid, was 6.53×10^3 dpm/ml.

Assay of Aqueous Triamcinolone Acetonide Solutions—One milliliter of the steroid-containing solution was transferred to a polyethylene vial[8] and was followed by the addition of 10 ml of the liquid scintillation solution. The mixture was shaken well. A blank was prepared by adding 1.0 ml of the dissolution medium and 10 ml of the liquid scintillation solution. The activity of the steroid-containing solution relative to the background was measured in a liquid scintillation analyzer[9] over 20 min. Counting efficiency was determined with standard samples of ^{14}C-benzoic acid.

Solubility Determination—The solubility of ^{14}C-triamcinolone acetonide in distilled water and in 0.2, 0.5, and 1.0 *M* potassium chloride solutions was determined as a function of temperature, as in the previous study (1).

RESULTS AND DISCUSSION

Although concentration plateaus were reached within 4–6 days, as in the previous study (1), investigations were continued for 3–4 additional days to confirm the development of saturation equilibria. The increased sensitivity of the radioisotopic method, compared to the colorimetric method previously employed (1), leads us to accept the lower triamcinolone acetonide solubility values reported in Table I. A minimum of eight determinations of triamcinolone acetonide concentration was made after equilibrium had been achieved.

This procedure had, in fact, been followed in the earlier study (1). The "two determinations" evaluated by Block and Patel were actually two separate experimental runs, each of which involved the collection and analysis of at least four samples postequilibrium. It was possible, therefore, to subject the data to statistical analysis (5). A three-way analysis of variance indicated that the results of the two studies were distinctly different ($p \ll 0.01$).

The recalculated values of the Setschenow ratios and the "salting-out" constants are listed in Table II. The differential heats of solution are listed in Table III. The constants tabulated in Tables II and III, based on the more reliable data presented in this study, can thus be considered to reflect more accurately the solubility of triamcinolone acetonide in water and in electrolyte solutions.

REFERENCES

(1) L. H. Block and R. N. Patel, *J. Pharm. Sci.*, **62**, 617(1973).

(2) R. E. Graham and C. T. Kenner, *ibid.*, **62**, 103(1973).

(3) M. Heller, S. M. Stolar, and S. Bernstein, *J. Org. Chem.*, **26**, 5044(1961).

(4) S. Bernstein, R. H. Lenhard, W. S. Allen, M. Heller, R. Littel, S. M. Stolar, L. I. Feldman, and R. H. Blank, *J. Amer. Chem. Soc.*, **81**, 1689(1959).

(5) P. Barthakur, "700 A/B-720 A/B-701: Analysis of Variance and Regression Analysis (Conversational Mode)," Wang Laboratories, Tewksbury, Mass., 1971.

ACKNOWLEDGMENTS AND ADDRESSES

Received January 15, 1975, from the *Department of Pharmaceutical Chemistry and Pharmaceutics, School of Pharmacy, Duquesne University, Pittsburgh, PA 15219*

Accepted for publication May 6, 1975.

The authors express their gratitude to E. R. Squibb and Sons, Inc., New Brunswick, N.J., for their generous supply of triamcinolone acetonide and triamcinolone alcohol.

[x] To whom inquiries should be directed.

[7] The steroids were chromatographed on Eastman Chromagram sheets (cellulose, without fluorescent indicator, No. 6064), using chloroform–toluene (1:3) as the solvent system. The plates were sprayed with 0.1% blue tetrazolium in methanol–16% sodium hydroxide in methanol (1:1).

[8] Polyethylene Prima Vials, No. 40-227, Nuclear Associates.

[9] Uniflux II liquid scintillation system, Nulcear Chicago Corp., Chicago, Ill.

Fluorometric Assay of Verapamil in Biological Fluids and Tissues

R. G. McALLISTER ˣ **and S. M. HOWELL**

Abstract □ Verapamil concentrations in blood, urine, or tissue homogenates may be measured fluorometrically in the 0.1–10-μg/ml range after extraction into heptane and back-extraction into acid; recovery rates are above 87%. The drug apparently is eliminated rapidly in guinea pigs, with a plasma half-life of 45 min.

Keyphrases □ Verapamil—fluorometric analysis, biological fluids and tissues □ Fluorometry—analysis, verapamil, biological fluids and tissues □ Antiarrhythmic agents—verapamil, fluorometric analysis, biological fluids and tissues

Verapamil, 5-[(3,4-dimethoxyphenethyl)methylamino]-2-(3,4-dimethoxyphenyl)-2-isopropylvaleronitrile (I), has been widely used outside the United States as an antianginal (1, 2) and antiarrhythmic (3–5) agent. Although not available for clinical use in this country, verapamil is being intensively studied because of its ability to suppress inward calcium currents in cardiac and other excitable tissues (6–8). Such "slow" calcium currents may be involved in fatal arrhythmias occurring during myocardial ischemia or infarction and associated with sudden cardiac death (9).

Although the mechanism of verapamil's action at the cellular level in terms of excitation–contraction coupling and competitive antagonism of calcium-induced effects has been studied *in vitro* (5, 9, 10), little information is available regarding the pharmacological disposition of the drug, either in animal species or in humans. McIlhenny (11) studied ^{14}C-verapamil in rats and dogs and reported that it was rapidly metabolized to *O*- and *N*-dealkylated forms and eliminated primarily in feces.

Slow channel depolarization phenomena may be studied by determining the effects of different antiarrhythmic agents on calcium-dependent currents (12). There is, therefore, considerable interest in correlating tissue concentrations of verapamil with the electrophysiological effects observed. Present studies in these laboratories involve the use of guinea pigs pretreated with verapamil and studied at varying times after drug administration. To determine the kinetics of verapamil in experimental animals and to correlate tissue drug levels with measured effects, a spectrophotofluorometric assay procedure that permits determination of verapamil levels in the 0.1–10-μg/ml range was developed and is reported here.

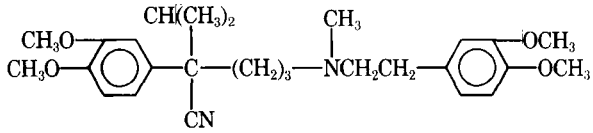

I

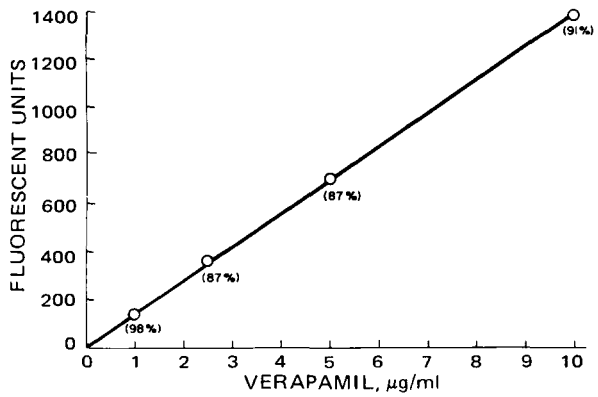

Figure 1—*Standard curve obtained by assay of control guinea pig liver homogenate to which known quantities of verapamil had been added. Similar results were obtained in plasma, serum, urine, and heart homogenates.*

EXPERIMENTAL

The assay procedure for verapamil is identical for plasma, serum, urine, or tissue homogenates. To prepare tissue homogenates, the liver and heart were removed from guinea pigs and mice immediately after sacrifice. Then a sufficient volume of 0.1 *N* HCl was added to give an approximate concentration of 75 mg/ml for liver and 500 mg/ml for heart. The tissues were then homogenized in hydrochloric acid by a motor-driven pestle[1] within a prefitted glass container.

An external standard solution of verapamil was prepared at a concentration of 100 μg of base/ml in 0.1 *N* HCl. To prepare internal standards, blank samples of body fluids or tissue homogenate aliquots of 4.75 ml were combined with 0.25 ml of the standard solution. Both external and internal standards showed a linear correlation between fluorescence and drug concentration in the 1.0–10-μg/ml range (Fig. 1).

To 5 ml of homogenate or body fluid in a 45-ml centrifuge tube were added 1.0 ml of 1 *N* NaOH and 10 ml of heptane (analytical

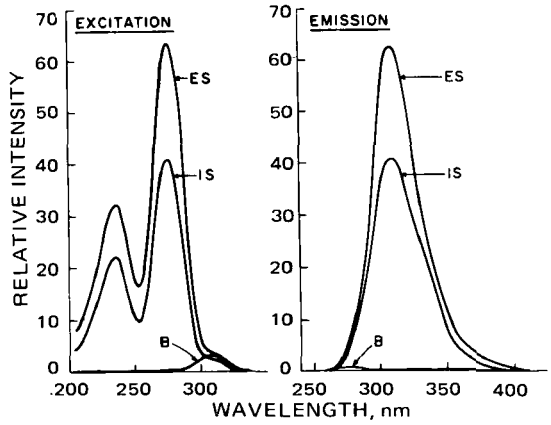

Figure 2—*Excitation and emission spectra of verapamil in external (ES) and internal (IS) standards at concentrations of 5 and 3.5 μg/ml, respectively. Fluorescence of the internal blank (B) was negligible.*

[1] Coated with Teflon.

Table I—Fluorescent Verapamil Concentrations in Guinea Pig Plasma and Tissue (Mean ± *SE*) after 30-mg/kg Injection

Minutes after Injection	n^a	Plasma Verapamil, μg/ml	Micrograms of Verapamil per Milligram of Tissue	
			Heart ($\times 10^{-3}$)	Liver ($\times 10^{-2}$)
30	5	1.98 ± 0.29	7.78 ± 1.27	4.27 ± 0.87
60	3	1.96 ± 0.41	7.73 ± 1.22	4.67 ± 1.22
90	3	1.18 ± 0.22	5.63 ± 1.74	2.40 ± 0.46
120	3	0.71 ± 0.14	1.53 ± 0.28	2.27 ± 0.33

[a] Number of different guinea pigs studied. From each animal, samples of plasma and tissue homogenate were assayed in triplicate.

grade). Each sample was shaken vigorously for 15 min in the upright position and then centrifuged for 10 min at 1800 rpm. Prior to shaking liver homogenates, a sufficient quantity of sodium chloride was added to make a saturated solution to assist in emulsifying the supernatant fatty layer.

After centrifugation, 7 ml of the heptane layer was transferred to a clean 45-ml centrifuge tube containing 5 ml of 0.1 *N* HCl. Each tube was vigorously shaken for 15 min and centrifuged at 1800 rpm for 10 min. The supernatant organic phase was aspirated and discarded. Two milliliters of the aqueous phase was used for spectrophotofluorometric[2] analysis at an excitation wavelength of 275 nm and an emission wavelength of 310 nm (Fig. 2).

The true final concentration of internal standards was calculated, and the spectrophotofluorometer reading was related to that of the corresponding external standard to find the percent recovery. Values ranged from 87 to 98%. Concentrations of unknown samples were calculated by comparison to the readings obtained for internal standards.

In the present series of experiments, guinea pigs were pretreated with intraperitoneal injections of verapamil hydrochloride, 30 mg of base/kg. They were sacrificed at varying periods after injection, and verapamil concentrations in plasma and tissue homogenates were measured (Table I).

RESULTS AND DISCUSSION

Consistently reproducible readings were obtained on multiple samples of control homogenates of the liver and heart, as well as plasma, to which known quantities of verapamil had been added (Fig. 1). Six replicate determinations at each concentration showed a standard deviation no greater than 2% at any point. Subsequent work demonstrated a continuing linear relationship between fluorescence and drug concentration to a lower limit of 0.1 μg/ml.

Verapamil was administered to guinea pigs, and drug concentrations were determined in the plasma, heart, and liver. The fluorescence spectra obtained after extraction were identical with that found for pure verapamil (Fig. 2). This finding does not eliminate the possibility of a metabolite containing the fluorophore being extracted and measured with the parent drug. Therefore, the quantity measured in these *in vivo* experiments is termed "fluorescent verapamil."

In the 200–300-g guinea pigs given verapamil, 30 mg/kg ip, fluorescent plasma verapamil levels demonstrated a first-order decline with an apparent half-life of 45 min (Table I). The drug was concentrated in both heart and liver, with a similar rate of elimination. Disappearance rates of fluorescent verapamil were studied in other groups of guinea pigs given 50- and 20-mg/kg injections. At the former dosage, half of the animals died within 30 min, at the latter dosage, elimination rates similar to those already noted were seen.

These preliminary studies demonstrated a rapid and reproducible assay for fluorescent verapamil in tissue homogenates and plasma; the drug appears to follow first-order kinetics at the dose level used, and it is rapidly eliminated from both plasma and tissues.

Preliminary tissue concentration–electrophysiological effect studies indicate that the ability of verapamil to block calcium-dependent membrane phenomena is apparent when measurable quantities of the drug have vanished[3]. Thus, concentrations of physiologically active material may be below the level of detection of this assay, or much of the drug's effects may be attributable to active metabolites not measured in the procedure reported here. Both possibilities are currently being investigated.

REFERENCES

(1) G. Sandler, *Bruxelles-Med.*, **50,** 669(1970).

(2) B. Tschirdewahn and H. Klepzig, *Deut. Med. Wochenschr.*, **88,** 1702(1963).

(3) J. Vohra, D. Hunt, J. Stuckey, and G. Sloman, *Brit. Heart J.*, **36,** 570(1974).

(4) L. Schamroth, *Cardiovasc. Res.*, **5,** 419(1971).

(5) B. N. Singh and O. Hauswirth, *Amer. Heart J.*, **3,** 367(1974).

(6) M. R. Rosen, J. P. Ilvento, H. Gelband, and C. Merker, *J. Pharmacol. Exp. Ther.*, **189,** 414(1974).

(7) A. L. Wit and P. F. Cranefield, *Circulation (Suppl. III)*, **49–50,** 146(1974).

(8) K. Shigenobu, J. A. Schneider, and N. Sperelakis, *J. Pharmacol. Exp. Ther.*, **190,** 280(1974).

(9) B. Surawicz, *Amer. J. Cardiol.*, **33,** 689(1974).

(10) G. Haeusler, *J. Pharmacol. Exp. Ther.*, **180,** 672(1972).

(11) H. M. McIlhenny, *J. Med. Chem.*, **14,** 1178(1971).

(12) B. Surawicz and S. Imanishi, *Circulation (Suppl. III)*, **49–50,** 84(1974).

ACKNOWLEDGMENTS AND ADDRESSES

Received February 13, 1975, from the *Medical Service, Lexington Veterans Administration Hospital,* and the *Department of Medicine, University of Kentucky Medical Center, Lexington, KY 40506*

Accepted for publication May 12, 1975.

The authors are grateful for the advice and encouragement of Dr. H. B. Kostenbauder.

[x] To whom inquiries should be directed.

[2] Aminco-Bowman spectrophotofluorometer, American Instrument Co.

[3] B. Surawicz, S. Imanishi, and R. G. McAllister, unpublished observations.

Homogeneity of *Pasteurella avicida* Bacterin

JOEL KIRSCHBAUM ˣ **and JOHN M. DUNHAM**

Abstract □ A simple rapid procedure is described for determining whether an emulsified bacterin is homogeneous by measuring the UV absorbances of chloroform-washed centrifugates. These absorbances appear to depend on nucleic acid content.

Keyphrases □ *Pasteurella avicida*—determination of homogeneity of emulsified suspension, UV measurement of extracted cell contents □ Bacterial vaccine (bacterin)—determination of homogeneity of emulsified suspension of *Pasteurella avicida*, UV measurement of extracted cell contents □ Vaccine, bacterial—determination of homogeneity of emulsified suspension of *Pasteurella avicida*, UV measurement of extracted cell contents

Methods are available for determining either the number of microorganisms or the amount of cellular material in a suspension (1–4). However, a simple method is needed to determine the homogeneity of a bacterin (5), which is typically an inactivated aqueous suspension of bacterial cells emulsified with mineral oil. The bacterin is administered to chickens or turkeys from a multiple-dose container without shaking during the dosing period. Settling in the opaque emulsion during this time could change the bacterin concentration without visual detection, leading to the administration of different doses.

The procedure of Chalenko *et al.* (6) for quantitating all organic constituents in a typhus vaccine involves adsorption on aluminum hydroxide, oxidation with dichromate in sulfuric acid, and colorimetry at 580 nm; the reproducibility is ±7%. The method proposed here permits a simple, rapid determination of the homogeneity of a bacterial vaccine (bacterin) by measuring the UV absorbance of the washed extracted contents of cells.

EXPERIMENTAL

Shake thoroughly a 500-ml bottle of *Pasteurella avicida* bacterin[1] 30 times and then open the bottle. With a Cornwall syringe adjusted to deliver 1 ml, remove gently two 1-ml aliquots from approximately 1 cm below the surface. The syringe is fitted with a 12.7-cm (5-in.),, 14-gauge cannula[2] to which is attached a 5-cm length of tubing[3]. Transfer each aliquot to a different 60-ml separator.

Gently take two aliquots from the middle (half-full mark, 250 ml) of the bottle and discard them into a waste container. Then take two more aliquots from the middle of the bottle and transfer each aliquot to one of two additional separators. Gently remove two aliquots from within 1 cm of the bottom and discard them. Then remove two more aliquots and transfer each to a fifth and sixth separator.

Wipe both the needle and the extension after drawing each aliquot. Do not disturb the bottle during the period in which the homogeneity of the emulsion is being determined, except for the removal of samples at 1, 2, and 4 hr after the shaking. The sampling period was deliberately made longer than the time needed for a veterinarian to administer the contents from the container.

Add 15 ml of 6.7% sodium chloride solution to each funnel and shake the funnels intermittently for 15 min. Wash the aqueous suspension three times with 15-ml portions of chloroform to remove the oil and such inactivating agents as phenol and β-propiolactone. Discard the lower chloroform layer each time.

Transfer the aqueous layer from each separator through a narrow stem funnel into a different 25-ml wide mouth, screw-capped volumetric flask. Rinse each separator with water and use the washings to fill the appropriate flask to the mark. Cover the opening of each flask with aluminum foil, cap, shake each flask vigorously, and allow it to stand for 10 min. Then transfer approximately 5 ml from the flask with a pasteur pipet into a centrifuge tube and centrifuge for 30 min. Measure the absorbance[4] at the 257-nm maximum of the clear aqueous solution in 1-cm cells against water. Figure 1 shows the UV absorbance for the spectrum of a washed centrifuged extract between 230 and 350 nm.

RESULTS

Table I summarizes the UV absorbances of chloroform-washed, centrifuged 1-ml aliquots taken in duplicate from three regions of the container during a typical analysis. The data indicate that the emulsified suspension remains homogeneous for at least 4 hr after being shaken, allowing the administration of uniform doses during this period. The absorbances did not vary by more than the 5% expected to occur by chance. The coefficient of variation was 3%.

Four other lots from the same manufacturer were homogeneous, with coefficients of variation ranging from 1.9 to 3%. The average absorbance for different batches varied from 0.32 to 0.60, indicating variation in either cell number or cell contents.

DISCUSSION

This method appears to measure the UV absorbance of nucleic acids in the aqueous centrifugate, since there is a peak in the spectrum at 257 nm (Fig. 1) and the absorbance at 260 nm, when divided by the absorbance at 280 nm, yields a ratio of 1.95. This ratio is 1.94 for deoxyribonucleic acid (7) and 2.0 for ribonucleic acid (8), with peak absorbances at approximately 259 (9) and 258 (10) nm, respectively. The absorbance maximum depends greatly on nucleic acid composition (11).

Saline solution denatures some proteins and solubilizes nucleic acids (8). Chloroform, in addition to removing the oil and such inactivating agents as phenol and β-propiolactone from the bacterin, washes out some low molecular weight compounds, lipids, and proteins (4). Saline solution also helps to prevent the formation of an emulsion when the oil is extracted into chloroform.

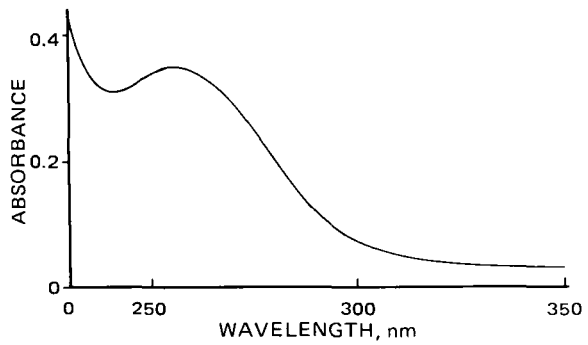

Figure 1—*UV spectrum of chloroform-washed centrifugate of* P. avicida *bacterin between 230 and 350 nm. Absorbance was determined against water. For details, see* Experimental.

[1] E. R. Squibb and Sons.
[2] Becton, Dickinson and Co.
[3] Teflon.

[4] Cary model 15 or other suitable spectrophotometer.

Table I—Absorbance of Chloroform-Washed Centrifugates from *P. avicida* Bacterin[a]

Hours after Shaking Bacterin	Region of Bottle	Peak Absorbance	
		Sample	Average
0	Top	0.329	0.327
	Top	0.324	
	Middle	0.324	0.330
	Middle	0.336	
	Bottom	0.330	0.328
	Bottom	0.326	
1	Top	0.320	0.318
	Top	0.315	
	Middle	0.303	0.315
	Middle	0.326	
	Bottom	0.331	0.318
	Bottom	0.305	
2	Top	0.323	0.329
	Top	0.335	
	Middle	0.315	0.322
	Middle	0.328	
	Bottom	0.318	0.322
	Bottom	0.325	
4	Top	0.316	0.319
	Top	0.321	
	Middle	0.320	0.326
	Middle	0.332	
	Bottom	0.316	0.321
	Bottom	0.326	

[a] See *Experimental* for details of sampling and handling.

Additional experiments demonstrated that only bacterial cell contents contribute significantly to the UV absorbance. A placebo mixture of oil, emulsifying agent, and water carried through the recommended procedure had an absorbance of 0.003 at 257 nm. Batches of the bacterin were allowed to stand undisturbed at 4° for about 10 days to allow the cellular material to settle approximately 2 cm below the surface. One-milliliter samples of clear liquid were removed from bottles of these batches within 1 cm of the surface and were carried through the analytical procedure. Samples of clear liquid taken from five batches obtained from four different vendors all gave final solutions with absorbances at 257 nm of less than 0.010. Neither 1% phenol nor 0.15% β-propiolactone (used as bacterial inactivating agents) interfered in the assay. In separate experiments, they were added to mineral oil which was carried through the procedure. The final absorbance at 257 nm in each case was 0.006. The preservative thimerosal used in some bacterins at a concentration of 1:10,000 does interfere. The absorbance at 257 nm for this concentration of thimerosal in water is 0.046. When this amount of thimerosal was added to mineral oil and carried through the procedure, the final absorbance at 257 nm was 0.027. Should thimerosal be present in a formulation, this slight increase in absorbance would be the same for samples from each time period. This would not change the conclusions about the homogeneity of the samples.

Weight variance of six 1-ml samples of cell suspension obtained with the Cornwall syringe was 3 mg, and the standard deviation was 2.4 mg. Other variables investigated that had no effect on absorbance were the concentration of saline solution (5–8%), the time of contact of the bacterin with chloroform (10–120 min), the number of chloroform washes (three to five), the time before centrifugation (10–50 min), and the duration of centrifugation (10–30 min). Higher absorbances may be obtained by using 2 or 3 ml of bacterin and extracting five times with chloroform.

Four samples of *P. avicida* bacterin from other vendors gave spectra similar to Fig. 1, with peak absorbances between 256 and 258 nm.

REFERENCES

(1) M. F. Mallette, in "Methods in Microbiology," vol. 1, J. R. Norris and D. W. Ribbons, Eds., Academic, New York, N.Y., 1969, p. 521.

(2) H. E. Kubitschek, in *ibid.*, p. 593.

(3) D. Herbert, P. J. Phipps, and R. E. Strange, in "Methods in Microbiology," vol. 5B, J. R. Norris and D. W. Ribbons, Eds., Academic, New York, N.Y., 1971, p. 209.

(4) I. W. Sutherland and J. F. Wilkinson, in *ibid.*, p. 345.

(5) J. Heji, in "Proceedings of the Veterinary Biological Licenses Committee of the Animal Health Institute," Denver, Colo., Nov. 9, 1971, p. 24.

(6) V. G. Chalenko, S. N. Rumyantsev, I. K. Volodina, and G. V. Belova, *Zh. Mikrobiol. Epidemiol. Immunobiol.*, **49**, 62(1972).

(7) J. Marmur, *J. Mol. Biol.*, **3**, 208(1961).

(8) G. von Ehrenstein, in "Methods in Enzymology," vol. XIIA, L. Grossman and K. Moldave, Eds., Academic, New York, N.Y., 1970, p. 596.

(9) T. T. Herskovits, *Biochemistry*, **2** 335(1963).

(10) G. Zubay, in "Procedures in Nucleic Acid Research," G. L. Cantoni and D. R. Davies, Eds., Harper and Row, New York, N.Y., 1966, p. 455.

(11) "Handbook of Biochemistry," 2nd ed., H. A. Sober, Ed., Chemical Rubber Co., Cleveland, Ohio, 1971, p. G-219.

ACKNOWLEDGMENTS AND ADDRESSES

Received February 27, 1975, from the *Squibb Institute for Medical Research, New Brunswick, NJ 08903*

Accepted for publication May 14, 1975.

The authors thank Mr. H. Lerner for assistance, Mr. R. Lanza for statistical evaluations, Dr. J. Stoner for advice, Dr. G. Mueller for bacterin samples, Mrs. Sandra Willis for the spectra, Mr. E. Ivashkiv for translating Ref. 6, and Dr. D. Frost for editorial comments.

[x] To whom inquiries should be directed.

Electrode Sensitive to Sulfa Drugs

NORIO HAZEMOTO, NAOKI KAMO ˣ, and YONOSUKE KOBATAKE

Abstract □ An electrode sensitive to sulfa drugs was constructed by using the iron(II)–bathophenanthroline chelate embedded in a liquid membrane. Rapid and Nernstian responses were exhibited against solutions of sulfamerazine and sulfisomidine ranging between 10^{-3} and 10^{-1} *M* in concentration. High selectivity was observed in the presence of urea, glycine, aminopyrine, or *p*-aminobenzoic acid. These chemicals are known to interfere in the usual colorimetric analysis of sulfa drugs.

Keyphrases □ Sulfamerazine—potentiometric analysis, liquid membrane electrode sensitive to sulfa drugs □ Sulfisomidine—potentiometric analysis, liquid membrane electrode sensitive to sulfa drugs □ Potentiometry—analysis, sulfamerazine and sulfisomidine, liquid membrane electrode sensitive to sulfa drugs □ Iron(II)–bathophenanthroline chelate—ion associations with sulfa drugs, used in preparation of electrodes for potentiometric analysis of sulfa drugs

Various ion-selective electrodes have been developed as electrochemical sensors in the last decade (1–8). These electrodes are able to respond to activity (or concentration) of specific ions rapidly and selectively in a complicated mixed solution. The attractive advantages of an analysis with an ion-selective electrode are the continuous determination of the concentration of respective ion species and the shortening of the analysis period.

It was desired to develop ion-selective electrodes for drugs in the field of pharmaceutical analysis. In the present study, liquid membrane electrodes sensitive to sulfisomidine and sulfamerazine were made by dissolving ion associations formed between an iron(II)–bathophenanthroline chelate and the sulfa drugs in nitrobenzene. The presence of a tenfold molar excess of urea, glycine, aminopyrine, or *p*-aminobenzoic acid, agents known to interfere in the usual colorimetric analysis of sulfa drugs, did not cause interference in the observed electromotive force (emf).

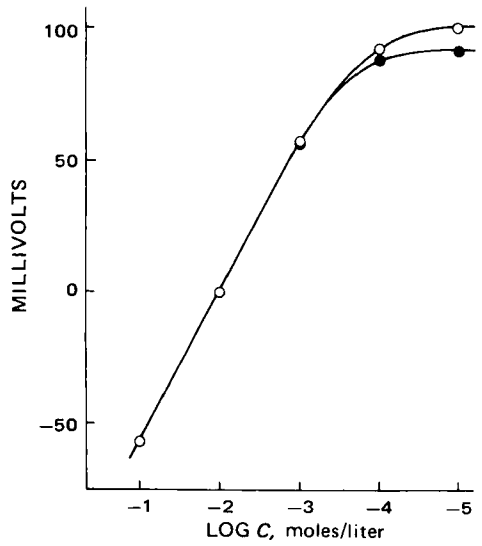

Figure 1—*Plots of the membrane potential against the concentration of sulfa drugs. The concentration of the ion association in the membrane was 5 × 10^{-5} M. Key: ○, sulfisomidine; and ●, sulfamerazine.*

Table I—Selectivity Coefficients of Various Substances for Sulfisomidine Selective Electrode

Substance	K_i
Urea	10^{-2}
Glutamic acid	3×10^{-2}
Glycine	2×10^{-2}
p-Aminobenzoic acid	10^{-1}
Aminopyrine	10^{-2}
Aspirin	5
Sodium chloride	10^{-2}
Sulfamerazine	4×10^{-1}
Sulfanilic acid	8×10^{-2}
Citric acid	4×10^{-3}
Sodium Trichloroacetate	17
Sodium borate	5×10^{-1}
Boric acid	10^{-2}

EXPERIMENTAL

The ion association existing between iron(II)–bathophenanthroline chelate and the sulfa drugs was determined by the same procedure as that employed previously (9). Bathophenanthroline (6×10^{-5} mole) was dissolved in 100 ml of nitrobenzene, into which 50 ml of ferrous sulfate aqueous solution (8×10^{-4} *M*) was added and shaken. Then 200 ml of aqueous sulfa drug (1×10^{-2} *M*), a large excess compared with the amount of iron chelate, was added and the mixture was shaken vigorously for 10 min. The nitrobenzene solution of the ion association was separated from the aqueous phase. The solution thus prepared was diluted to a desired concentration with nitrobenzene and was used as the liquid membrane.

The following cell was used for measuring the electromotive force (emf) across the liquid membrane:

SCE|reference solution|liquid membrane|sample solution|SCE

where SCE stands for the saturated calomel electrode. The electromotive force was measured at a room temperature (20 ± 2°) with an electrometer[1] connected to a penwriting recorder[2]. The sample and the reference solutions were separated by the liquid membrane, which was located in the bottom of a U-shaped glass tube. An aqueous solution (10^{-2} *M*) of sodium salt of the sulfa drug was used as the reference solution.

RESULTS AND DISCUSSION

The electrodes for sulfisomidine and sulfamerazine were used as the representatives of sulfa drugs. Steady potential was achieved within a few seconds and was reproducible to ±1 mv. The ion association used as the ion exchanger was positively charged and dissociated in the nitrobenzene. Then, the electrode could respond only to negative ions.

Since sulfa drugs are amphoteric, the effects of pH in the solution on the membrane potential were examined by adding sulfuric acid and sodium hydroxide to a sample containing 10^{-3} *M* sulfisomidine or sulfamerazine. The electromotive force observed was not affected by a pH variation in the media between 8.5 and 11 for sulfisomidine and between 8.3 and 10.0 for sulfamerazine. The electromotive force was not stable outside these pH ranges. In the

[1] Type TR-8651, Takeda Riken Co., Tokyo, Japan.
[2] Type VP-625 A, National Electric Co., Yokohama, Japan.

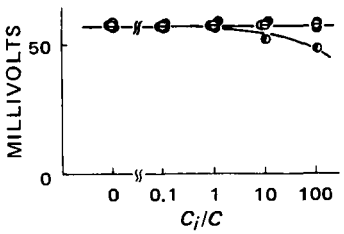

Figure 2—*Observed potential of the sulfisomidine electrode in various organic ions as a function of the relative concentration of added ions* (C_i) *against sulfisomidine* (C). *Key:* ◐, *glycine;* ⊖, *p-aminobenzoic acid;* ●, *aminopyrine; and* ○, *urea. These reagents interfere with the colorimetric method. The concentration of sulfisomidine in the test solution was fixed at* 10^{-3} M.

practical use of the electrode, the measurements should be made with solutions with these pH values. In the experiments described here, the pH value of the sample solution was adjusted at 9.0 by tromethamine and sulfuric acid buffer.

The electrodes were tested in solutions of sulfa drugs over a range of 10^{-1} and 10^{-5} M. As shown in Fig. 1, the response of the electrode was linear with a slope of 57 mv when the observed potential was plotted against the logarithm of the concentration of sulfa drug until the concentration decreased to 10^{-3} M. Although the electromotive force was not linear against log C in a dilute solution lower than 10^{-3} M, the electrode could be used down to about 10^{-4} M, since the potential response was stable and reversible.

The electrode responded to certain specific substances other than the sulfa drugs. When the sample solution contained both a sulfa drug and other interfering substances, i, the electromotive force observed was analyzed by the following equation (10):

$$E = E_0 - (RT/F) \ln (C + K_i C_i) \qquad \text{(Eq. 1)}$$

where E, C, C_i, and K_i are the membrane potential observed, the concentrations of sulfa drugs and of interfering substances i, and the selectivity coefficient, respectively, and E_0 is a constant dependent only on the concentration of the reference solution. For the sake of illustration, the selectivity coefficient, K_i, is determined for the sulfisomidine-selective electrode in the subsequent analysis. When the potential observed in a solution containing no interfering reagent is denoted by E', Eq. 1 is transformed to give:

$$K_i C_i = C \exp [F(E' - E)/RT] - C \qquad \text{(Eq. 2)}$$

If the right-hand side of Eq. 2 is plotted against C_i, the slope should give the value of K_i. The values of K_i thus obtained are listed in Table I. For some interfering substances (*e.g.*, glycine, sulfanilic acid, and sodium borate), the value of K_i depended on the concentration of the substance. In such case, the largest value of K_i is given in the table. As shown in Fig. 2, the potential was not affected noticeably by the presence of urea, glycine, aminopyrine and *p*-aminobenzoic acid. These chemicals are known to interfere considerably in the usual colorimetric analysis of sulfa drugs (11, 12). In contrast to these reagents, a small amount of sodium trichloroacetate and aspirin produced an appreciable effect in the measured potential. In spite of this restriction, the electrode developed here may be useful in the analysis of sulfa drugs.

REFERENCES

(1) E. Pungor, K. Toth, and J. Havas, *Acta Chim. Acad. Sci. Hung.*, **48**, 17(1966).

(2) J. W. Ross, *Science*, **156**, 1378(1967).

(3) G. A. Rechnitz, M. R. Kresz, and S. B. Zamochnick, *Anal. Chem.*, **38**, 973(1966).

(4) J. Ruzicka, C. G. Lamm, and J. C. Tjell, *Anal. Chim. Acta*, **62**, 15(1972).

(5) G. Baum and F. B. Ward, *Anal. Chem.*, **43**, 947(1971).

(6) K. Kina, N. Maekawa, and N. Ishibashi, *Bull. Chem. Soc. Jap.*, **46**, 2772(1973).

(7) C. J. Coetzee and H. Freiser, *Anal. Chem.*, **40**, 2071(1968).

(8) R. P. Buck, *ibid.*, **46**, 28R(1974).

(9) N. Hazemoto, N. Kamo, and Y. Kobatake, *J. Ass. Offic. Anal. Chem.*, **57**, 1205(1974).

(10) K. Srinivasan and G. A. Rechinitz, *Anal. Chem.*, **41**, 1203(1969).

(11) A. E. A. Werner, *Lancet*, **236**, 18(1939).

(12) A. T. Fuller, *ibid.*, **232**, 194(1937).

ACKNOWLEDGMENTS AND ADDRESSES

Received March 17, 1975, from the *Faculty of Pharmaceutical Sciences, Hokkaido University, Sapporo, Japan.*

Accepted for publication May 13, 1975.

[x] To whom inquiries should be directed.

Binding of Sulfisoxazole to Protein Fractions of Tears

SUKHBIR S. CHRAI * and JOSEPH R. ROBINSON ˣ

Abstract □ By using equilibrium dialysis experiments, it is shown that sulfisoxazole binds extensively with albumin and α-globulin and to a lesser extent with γ-globulin and lysozyme, all of which are normal components of tears. The binding of sulfisoxazole to the various protein fractions quantitatively accounts for the overall binding of this drug to human tears. It is suggested that to predict the binding of drugs to proteins in lacrimal fluid, both in normal and pathological conditions, it is necessary to conduct binding studies of the drug with the major protein fractions of tears. Moreover, it is essential to know the composition of the major protein fractions of tears in both normal and various pathological conditions to conduct the necessary *in vitro* binding studies.

Keyphrases □ Sulfisoxazole—binding to protein fractions of human tears, normal and irritant induced □ Protein binding—sulfisoxazole to protein fractions of human tears, normal and irritant induced □ Lacrimal fluids—human, normal and irritant induced, binding of sulfisoxazole to protein fractions

It is well established that binding of drugs to proteins can substantially influence the bioavailability and biological activity of drugs in the body (1, 2). Recently, the problem of drug binding to proteins in ocular fluids and tissues was examined (2–4); it was shown that this interaction can significantly affect the bioavailability of drugs in the eye. This effect is perhaps more important in the eye than in other areas of the body because of the great rates of drainage and fluid turnover, *e.g.*, tear and aqueous humor turnover and instilled solution drainage.

All *in vitro* binding work thus far relative to the eye has been conducted using albumin as the protein. While albumin is the principal protein in tear fluid and aqueous humor, it is by no means the only protein. The purpose of the present study was to examine the drug binding potential of several proteins, which are known to be components of tears, in an attempt to gain a more quantitative picture of the drug binding capabilities of proteins in tears.

A significant feature of tear composition is the presence of relatively high concentrations of proteins. The total protein present varies qualitatively and quantitatively, depending upon the method of analysis, the method of collecting tear samples, the species of animal involved, and the pathological state of the eye. A relatively conservative estimate (5) lists the albumin content of tears to be 0.4% for humans with a total protein content of approximately 0.7%; for rabbits, the estimate is 0.3% albumin with a total protein content of 0.5% (6). Emotional stress, irritation, disease, and other factors greatly influence the protein content (7). Table I lists the reported (7) major protein components of both normal tears and irritant-induced tears.

Detailed studies (8–11) have been conducted on tear proteins and immunoglobulins in both normal and pathological cases in humans and animals. Sapse *et al.* (12, 13) identified serum albumin, ceruloplasmin, transferrin, immunoglobulins A and G, lysozyme, globulins, and specific tear albumin in human tears. Other proteins reported are plasmin (14) and tear lactoferrin (15). Pathological processes in the eye cause significant qualitative and quantitative changes in the protein pattern and a significant increase in the total proteins. None of the pathological conditions reported brought about the total disappearance of any of the major protein fractions. Therefore, changes in protein composition in pathological conditions would be expected to change the extent of drug–protein interaction for drugs that are susceptible to drug–protein binding.

EXPERIMENTAL[1]

Materials—Water was distilled from alkaline permanganate in an all-glass apparatus. Cellulose dialysis tubing[2] was purified according to the procedures described by Mikkelson (2). Crystalline rabbit serum albumin[3], α- and γ-globulins[3], lysozyme[3] (specific activity of 11,800 units[4]/mg), and sulfisoxazole[5] were used as received. All other chemicals were either reagent or analytical grade.

Sulfisoxazole Assay—Quantitative determination of sulfisoxazole was accomplished by utilizing the primary aromatic amine character of the drug molecule. Diazotization of the primary aromatic amine followed by coupling with the Bratton–Marshall reagent [*N*-(1-naphthyl)ethylenediamine] yields a product that displays an absorbance maximum in the visible region. The procedure described by Connors (16) was followed, except that the final dilution was taken to 25 ml rather than to 50 ml. Sulfisoxazole exhibited an absorbance maximum at 546 nm with a molar absorptivity of $2.85 \times 10^{-3}\ M^{-1}\ cm^{-1}$ at this wavelength. Beer's law was obeyed in the concentration range studied.

Solution Preparation—Sulfisoxazole solutions were prepared by the addition of the drug to pH 6.24 Sørensen phosphate buffer. Protein solutions were prepared fresh by addition of an appropriate weight of protein to pH 6.24 Sørensen phosphate buffer solution.

Equilibrium Dialysis Studies—The methods used and dialysis cell descriptions were reported previously (3).

RESULTS

For reference purposes, the binding of sulfisoxazole to human lacrimal "overflow" tears is shown (3) in Fig. 1. The lacrimal fluid employed was obtained from healthy human eyes. Overflow tears were collected in the form of drops rolling from the eyelids during late hours of the day or as an accompanying phenomenon to yawning. It is clear from Fig. 1 that sulfisoxazole is extensively bound at the concentrations tested.

For therapy, a 4% solution of this drug is generally used. This concentration is well above the concentration range studied, although with tear turnover the concentration of drug is quickly reduced to encompass the range studied here. Thus, although protein binding of sulfisoxazole in ocular therapy would not appear to have a very significant influence on drug activity, the drug is a useful experimental probe for ocular drugs in general. Other ocular drugs, *e.g.*, steroids, are influenced much more by drug binding to proteins. It is important to recognize that the tears used in this

[1] All spectral measurements were carried out on either a Cary 14 or Cary 16 spectrophotometer.
[2] Union Carbide Corp., Chicago, Ill.
[3] Schwarz/Mann, Orangeburg, N.Y.
[4] A unit is defined as a decrease in absorbance at 450 nm of 0.001/min at pH 7.0 and 25°.
[5] Donated by Hoffmann-La Roche Inc., Nutley, N.J.

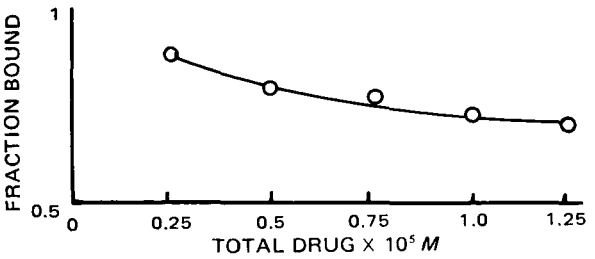

Figure 1—*Extent of protein binding of sulfisoxazole to human overflow tears. The data points are mean values from three separate determinations, and standard errors of the mean are within ±7% of the mean values (3).*

study (Fig. 1) were obtained from healthy eyes and hence were presumably low in protein content as compared with tears obtained from inflamed or diseased eyes.

As mentioned earlier, there are several protein fractions in human tears, estimated by some to be as many as 14 (12). Since it was not possible to obtain all of the different fractions of tear proteins, drug binding studies were conducted on serum albumin, lysozyme, and α- and γ-globulins. Binding of sulfisoxazole to these different protein components is shown in Fig. 2. The data are presented as a plot of fraction of drug bound *versus* the amount of drug present in the system.

The total amount of protein present in tears and the values reported (7, 12, 17, 18) for the different fractions are conflicting. To assess the binding capacity of each protein component at a fixed concentration of sulfisoxazole and its contribution to the total binding of drug in tears, it is assumed that the values reported by Brunish (7) are closest to the actual values. It is assumed that the binding capacity of a particular class of proteins is similar for a given drug irrespective of source; *i.e.*, specific tear prealbumin has the same binding properties as serum albumin in tears. The second assumption reduces the seven major components of tear proteins into three classes. These assumptions are necessary to reduce the complexity of the problem.

According to Brunish (7), protein concentration for normal tears is 0.6% with 0.23% albumin, 0.27% globulin, and 0.1% lysozyme. Upon instillation of drug solution, due to mixing of 7.5 μl of resident tears with 25 μl of instilled drug solution, these concentrations of albumin, globulin, and lysozyme in tears decrease by 4.3-fold to 0.053, 0.062, and 0.023%, respectively. If it is assumed that the fraction of drug bound is directly proportional to the concentration of the protein fractions (2, 3), it appears from Fig. 2 that the fraction of drug bound to albumin, globulin, and lysozyme at their diluted concentrations should be 0.2, 0.05, and 0.004, respectively, for 1×10^{-5} *M* sulfisoxazole. Thus, the fraction of 1×10^{-5}

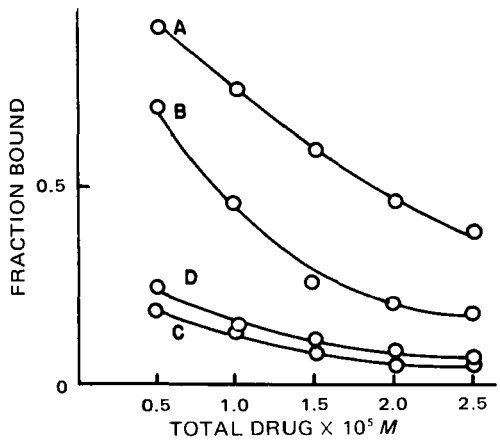

Figure 2—*Equilibrium dialysis experiments on the extent of sulfisoxazole binding to different protein components of human tears. Key: A, binding with 0.2% albumin; B, binding with 1.0% α-globulin; C, binding with 0.5% γ-globulin; and D, binding with 1.0% lysozyme. The data points are mean values from three separate determinations, and standard errors of the mean are within ±10% of the mean values.*

Table I—Protein Composition of Human Tears (7)

Type of Tear	Number of Subjects	Albumin, %	Globulin, %	Lysozyme, %
Normal	21	38.8	44.8	16.4
Irritant induced	12	19.3	54.0	26.7

M sulfisoxazole bound to normal tears upon instillation of 25 μl is calculated to be 0.254.

It appears from Fig. 1 that the fraction of drug bound to total proteins in tears for 1×10^{-5} *M* sulfisoxazole is 0.7. This high binding value with total tears is due to the fact that the concentration of protein is 4.3-fold higher than the concentration of protein fractions assumed for reaching the calculated value of 0.254. After the necessary correction is made for the change of protein concentration of tears due to dilution with instilled drug solution, the experimental binding fraction value of 0.7 reduces to 0.161.

The difference in the experimental value of 0.161 and the calculated value of 0.254 is due to the fact that the tears used for the original study were obtained by stimulation and were thus low in protein content. Correction in the experimental value for the difference in protein content of normal tears and irritant tears yields an experimental value of 0.242—in excellent agreement with the calculated value of 0.254.

DISCUSSION

It is clear from the equilibrium dialysis studies that not only albumin but also other fractions of proteins do bind with drugs. According to Goldstein (1), γ-globulins appear almost exclusively to be highly involved in specific protein–protein interactions for immune reactions. Very few drugs have been shown to interact with α- and γ-globulins and those that do are poorly soluble in water. Based on the results from the present study, it appears that all of the protein fractions, including α- and γ-globulins, interact with the drug to some extent and the degree of binding varies from protein to protein, with albumin having the greatest binding for sulfisoxazole.

It is now apparent that the use of albumin to study the binding of a particular drug to a specific ocular tissue or fluid *in vitro* is not correct unless other proteins are included. However, for tears, using three fractions of protein, namely, lysozyme, albumin, and globulin, does apparently allow for the approximate quantitation of binding of drugs to the proteins in tears. Specifically with sulfisoxazole, the important components of tears are albumin and α-globulin insofar as binding is concerned.

As mentioned earlier, the values of the different fractions of tear proteins reported are conflicting. Newell (17) claimed that human lacrimal fluid contains 1–2% protein composed of 30% albumin, 40% globulins, and 30% lysozyme. Because of the different ratios of albumin to globulin and albumin to lysozyme, the different overall binding of drugs to human tear fluid will be different than the one reported here using the values of Brunish (7). Ridley (18) and Bonavida *et al.* (19) reported the total protein content to be about 0.7%. The former reported the albumin and globulin to be approximately 0.4 and 0.3%, respectively, with no lysozyme; the latter reported that 20–40% of the total protein is lysozyme. The calculation for the contribution made by each fraction to the overall protein binding by tears will be different if the calculations are done with the values of each fraction as reported by Ridley (18) and Sapse *et al.* (12).

The importance of the results of the present study will be more significant in pathological conditions. In most diseases of the human eye, the lysozyme content is reported to decrease tremendously (20). Even if the total protein content is kept constant in pathological conditions, the decrease of lysozyme (20) and the increase in serum albumin (8) increase the overall binding of the drug to lacrimal fluid. Serum albumin is a relatively minor component of nonstimulated tears whose level rises after mechanical stimulation in certain disease states (8). In rabbits, tear lysozyme comprises only 1% of the total tear protein, which is reported as 1.3% (20). Since the total protein is greater in rabbit tears than in human tears and the lysozyme content is greater in human tears

than in rabbit tears, the change in binding capacity in disease states for rabbit tears is expected to be greater than in human tears.

Thus, based on the results of the present study, it is clear that to study the influence of drug–protein interaction on drug bioavailability in the eye, it is important to know: (*a*) the binding capacity of each major fraction of tear protein, and (*b*) the changes that occur in the major fractions during the disease state. This information will be of great help in predicting the loss of drug in pathological conditions due to drug–protein interaction.

REFERENCES

(1) A. Goldstein, *Pharmacol. Rev.*, **1**, 102(1949).

(2) T. J. Mikkelson, Ph.D. thesis, University of Wisconsin, Madison, Wis., 1970.

(3) T. J. Mikkelson, S. S. Chrai, and J. R. Robinson, *J. Pharm. Sci.*, **62**, 1648(1973).

(4) *Ibid.*, **62**, 1942(1973).

(5) F. H. Adler, "Physiology of the Eye," 4th ed., C. V. Mosby, St. Louis, Mo., 1968.

(6) "System of Ophthalmology," vol. 4, S. Duke-Elder, Ed., C. V. Mosby, St. Louis, Mo., 1968.

(7) R. Brunish, *Arch. Ophthalmol.*, **57**, 554(1957).

(8) U. Krause, *Acta Ophthalmol. Suppl.*, **1959**, 53.

(9) A. S. Josephson and D. W. Hockwood, *J. Immunol.*, **93**, 532(1964).

(10) W. Kuhl, *Albrecht von Graefes Arch. Klin. Exp. Ophthalmol.*, **182**, 76(1971).

(11) W. Kuhl, *ibid.*, **183**, 163(1971).

(12) A. T. Sapse, B. Bonavida, W. Stone, Jr., and E. E. Sercarz, *Arch. Ophthalmol.*, **81**, 815(1969).

(13) A. T. Sapse, B. Bonavida, W. Stone, Jr., and E. E. Sercarz, *Amer. J. Ophthalmol.*, **66**, 76(1968).

(14) O. Storm, *Scand. J. Clin. Lab. Invest.*, **7**, 55(1955).

(15) R. M. Broekhuyse, *Invest. Ophthalmol.*, **13**, 550(1974).

(16) K. A. Connors, "A Textbook of Pharmaceutical Analysis," Wiley, New York, N.Y., 1967, p. 198.

(17) F. W. Newell, "Ophthalmology, Principles and Concepts," C. V. Mosby, St. Louis, Mo., 1965, p. 78.

(18) F. Ridley, *Brit. J. Exp. Pathol.*, **11**, 217(1930).

(19) B. Bonavida, A. T. Sapse, and E. E. Sercarz, *Invest. Ophthalmol.*, **7**, 435(1968).

(20) E. Regan, *Amer. J. Ophthalmol.*, **33**, 600(1950).

ACKNOWLEDGMENTS AND ADDRESSES

Received April 4, 1975, from the *School of Pharmacy, University of Wisconsin, Madison, WI 53706*

Accepted for publication June 3, 1975.

Supported by Allergan Pharmaceuticals, Irvine, CA 92664, and a grant from the Graduate School, University of Wisconsin, Madison, WI 53706

* Present address: Schering Corp., Bloomfield, NJ 07003

ˣ To whom inquiries should be directed.

Phosphorus–Nitrogen Compounds XIX: Distribution of ^{32}P and Effect of an Active Oncolytic on Intracerebral Leukemia in Rodents

L. A. CATES ˣ and M. B. CRAMER

Abstract □ *P,P*-Bis(1-aziridinyl)-*N*-1-adamantylphosphinic amide displayed oncolytic activity against intracerebral and intraperitoneal L-1210 leukemia. Administration of the isotope-labeled compound to rats shows ^{32}P distribution to the brain.

Keyphrases □ Organophosphorus compounds—adamantyl substituted, synthesis, oncolytic activity and tissue distribution screened □ Distribution, tissue—studied, adamantyl-substituted organophosphorus compounds □ Oncolytic activity—adamantyl-substituted organophosphorus compounds screened

Of 19 adamantyl-substituted organophosphorus compounds synthesized and tested for anticancer activity (1, 2), only *P,P*-bis(1-aziridinyl)-*N*-1-adamantylphosphinic amide (NSC 166199, I) displayed oncolytic properties. Closely related to triethylenephosphoramide, I possesses a 1-adamantylamino moiety in lieu of one aziridinyl group. This modification produces a marked change in physical properties, with I having very low water solubility compared to triethylenephosphoramide, which is extremely soluble in water. The lipophilic nature of I suggests it may have the ability to overcome the blood–brain barrier and produce anticancer effect in the central nervous system (CNS). The eradication of leukemic cells in the CNS is a major goal of modern cancer chemotherapy.

To ascertain the ability of I to affect intracerebral leukemia, this agent was administered intraperitoneally to mice injected intracerebrally and intraperitoneally with L-1210 leukemia cells for survival time determination. The ^{32}P compound (II) of I was synthesized and administered intraperitoneally to rats to estimate its distribution to certain tissues and organs, including the brain.

EXPERIMENTAL

Chemistry—A mixture of 0.14 g (0.9 mmole) of ^{32}P-phosphorus oxychloride (4.47 mCi) and 10.3 g (67 mmoles) of phosphorus oxychloride in 50 ml of ether was added dropwise with stirring and cooling (0–5°) to a solution of 22.0 g (146 mmoles) of 1-aminoadamantane in 250 ml of ether. After standing for 24 hr, the reaction mixture was filtered and the filtrate containing *N*-1-adamantylphosphoramidic dichloride (3) was used for the *in situ* preparation of II.

The ethereal solution was added dropwise with stirring to a solution of 18 g (420 mmoles) of aziridine in 50 ml of ether, with a re-

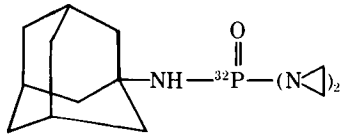

II

than in rabbit tears, the change in binding capacity in disease states for rabbit tears is expected to be greater than in human tears.

Thus, based on the results of the present study, it is clear that to study the influence of drug–protein interaction on drug bioavailability in the eye, it is important to know: (*a*) the binding capacity of each major fraction of tear protein, and (*b*) the changes that occur in the major fractions during the disease state. This information will be of great help in predicting the loss of drug in pathological conditions due to drug–protein interaction.

REFERENCES

(1) A. Goldstein, *Pharmacol. Rev.*, **1**, 102(1949).

(2) T. J. Mikkelson, Ph.D. thesis, University of Wisconsin, Madison, Wis., 1970.

(3) T. J. Mikkelson, S. S. Chrai, and J. R. Robinson, *J. Pharm. Sci.*, **62**, 1648(1973).

(4) *Ibid.*, **62**, 1942(1973).

(5) F. H. Adler, "Physiology of the Eye," 4th ed., C. V. Mosby, St. Louis, Mo., 1968.

(6) "System of Ophthalmology," vol. 4, S. Duke-Elder, Ed., C. V. Mosby, St. Louis, Mo., 1968.

(7) R. Brunish, *Arch. Ophthalmol.*, **57**, 554(1957).

(8) U. Krause, *Acta Ophthalmol. Suppl.*, **1959**, 53.

(9) A. S. Josephson and D. W. Hockwood, *J. Immunol.*, **93**, 532(1964).

(10) W. Kuhl, *Albrecht von Graefes Arch. Klin. Exp. Ophthalmol.*, **182**, 76(1971).

(11) W. Kuhl, *ibid.*, **183**, 163(1971).

(12) A. T. Sapse, B. Bonavida, W. Stone, Jr., and E. E. Sercarz, *Arch. Ophthalmol.*, **81**, 815(1969).

(13) A. T. Sapse, B. Bonavida, W. Stone, Jr., and E. E. Sercarz, *Amer. J. Ophthalmol.*, **66**, 76(1968).

(14) O. Storm, *Scand. J. Clin. Lab. Invest.*, **7**, 55(1955).

(15) R. M. Broekhuyse, *Invest. Ophthalmol.*, **13**, 550(1974).

(16) K. A. Connors, "A Textbook of Pharmaceutical Analysis," Wiley, New York, N.Y., 1967, p. 198.

(17) F. W. Newell, "Ophthalmology, Principles and Concepts," C. V. Mosby, St. Louis, Mo., 1965, p. 78.

(18) F. Ridley, *Brit. J. Exp. Pathol.*, **11**, 217(1930).

(19) B. Bonavida, A. T. Sapse, and E. E. Sercarz, *Invest. Ophthalmol.*, **7**, 435(1968).

(20) E. Regan, *Amer. J. Ophthalmol.*, **33**, 600(1950).

ACKNOWLEDGMENTS AND ADDRESSES

Received April 4, 1975, from the *School of Pharmacy, University of Wisconsin, Madison, WI 53706*

Accepted for publication June 3, 1975.

Supported by Allergan Pharmaceuticals, Irvine, CA 92664, and a grant from the Graduate School, University of Wisconsin, Madison, WI 53706

* Present address: Schering Corp., Bloomfield, NJ 07003

ˣ To whom inquiries should be directed.

Phosphorus–Nitrogen Compounds XIX: Distribution of ^{32}P and Effect of an Active Oncolytic on Intracerebral Leukemia in Rodents

L. A. CATES ˣ and M. B. CRAMER

Abstract □ *P,P*-Bis(1-aziridinyl)-*N*-1-adamantylphosphinic amide displayed oncolytic activity against intracerebral and intraperitoneal L-1210 leukemia. Administration of the isotope-labeled compound to rats shows ^{32}P distribution to the brain.

Keyphrases □ Organophosphorus compounds—adamantyl substituted, synthesis, oncolytic activity and tissue distribution screened □ Distribution, tissue—studied, adamantyl-substituted organophosphorus compounds □ Oncolytic activity—adamantyl-substituted organophosphorus compounds screened

Of 19 adamantyl-substituted organophosphorus compounds synthesized and tested for anticancer activity (1, 2), only *P,P*-bis(1-aziridinyl)-*N*-1-adamantylphosphinic amide (NSC 166199, I) displayed oncolytic properties. Closely related to triethylenephosphoramide, I possesses a 1-adamantylamino moiety in lieu of one aziridinyl group. This modification produces a marked change in physical properties, with I having very low water solubility compared to triethylenephosphoramide, which is extremely soluble in water. The lipophilic nature of I suggests it may have the ability to overcome the blood–brain barrier and produce anticancer effect in the central nervous system (CNS). The eradication of leukemic cells in the CNS is a major goal of modern cancer chemotherapy.

To ascertain the ability of I to affect intracerebral leukemia, this agent was administered intraperitoneally to mice injected intracerebrally and intraperitoneally with L-1210 leukemia cells for survival time determination. The ^{32}P compound (II) of I was synthesized and administered intraperitoneally to rats to estimate its distribution to certain tissues and organs, including the brain.

EXPERIMENTAL

Chemistry—A mixture of 0.14 g (0.9 mmole) of ^{32}P-phosphorus oxychloride (4.47 mCi) and 10.3 g (67 mmoles) of phosphorus oxychloride in 50 ml of ether was added dropwise with stirring and cooling (0–5°) to a solution of 22.0 g (146 mmoles) of 1-aminoadamantane in 250 ml of ether. After standing for 24 hr, the reaction mixture was filtered and the filtrate containing *N*-1-adamantylphosphoramidic dichloride (3) was used for the *in situ* preparation of II.

The ethereal solution was added dropwise with stirring to a solution of 18 g (420 mmoles) of aziridine in 50 ml of ether, with a re-

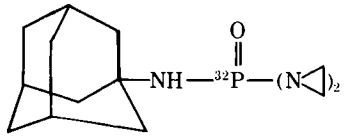

II

sultant rise in temperature of 5° and formation of a white precipitate. After standing for 24 hr, the reaction mixture was filtered and the precipitate was washed with water until the washings no longer gave a positive test for chloride ion when treated with silver nitrate solution. When a hot acetone solution of the residue was cooled, white crystals of II, mp 177–178°, formed.

To test the radiochemical purity of II, an acetone solution was spotted on TLC plates, developed with ethanol–chloroform (1:9), and exposed to film[1] for 17 hr. The film showed a single spot at R_f ~ 0.21.

Tissue Distribution—Nine female Sprague–Dawley rats, 90–120 g, were administered 2.5 μCi of II (approximately 200 mg/kg) by intraperitoneal injection of a carboxymethylcellulose suspension of II. Each animal was then placed in a plastic metabolism cage for separation and collection of urine and feces.

Three animals were decapitated at each of three time periods: 3, 6, and 12 hr after injection of II. Blood was collected, and the spleen and brain were dissected from the carcass. The spleen was weighed, and a portion (100–200 mg) was placed in a counting vial containing 1 ml of a tissue solubilizer[2]. The remainder of the carcass was homogenized[3], and portions were prepared for counting in a similar manner.

Urine was diluted with water to 10 ml, and an aliquot was taken. Feces were suspended in water prior to sampling. All vials containing tissue or feces were placed in a 50° water bath until dissolution was complete and then decolorized with benzoyl peroxide. Radioactivity in each sample was determined by liquid scintillation counting[4].

An aliquot of each urine sample was spotted on a silica gel plate and developed in the same manner as that previously described for II.

Antileukemia Testing—L-1210 leukemia cells were injected intraperitoneally (10^5 cells) or intracerebrally (10^4 cells) to groups of 10 mice. Each mouse was given various doses of I by intraperitoneal injection on Day 1 only or on Days 1, 5, and 9, and survival times were determined.

RESULTS AND DISCUSSION

The literature reports few examples of *in vivo* distribution studies involving radioisotopic organophosphorus antitumor agents. Crossley *et al.* (4) followed the distribution of ^{32}P-triethylenephosphoramide (III) and found a greater concentration of radioactivity in testes and less in the bone than with ^{32}P-dibasic sodium phosphate. Craig and Jackson (5), using III and rats implanted with Walker carcinosarcoma or Jensen sarcoma, showed that only a small part of the administered radioactivity was retained after 24 hr. Other investigators studied the distribution of the oncolytic agent ^{32}P-oxapentamethylenediethylenethiophosphoramide in the rat (6) and human (7) and found no evidence of selective uptake in any tissues, including the tumors, by any mode of administration. A degree of success at selective uptake by a phosphorus isotopic-labeled agent was reported by Fletcher *et al.* (8) who found that ^{32}P-diethylstilbestrol was taken up by breast tumors to an extent twice that of ^{32}P-dibasic sodium phosphate. None of these investigations involved determination of radioactivity in the brain.

In this present study, approximately one-third of the recovered activity appeared in the urine and one-half was found in the feces 12 hr after intraperitoneal injection of II. Thus, 80% of the activity was excreted within 12 hr. TLC of the urine resulted in the appearance of two radioactive spots, one with the same R_f value as II and a second that remained at the origin.

Levels of ^{32}P in all tissues sampled and in plasma were highest at the 3-hr time period and declined thereafter. A comparison of these results with those of Craig and Jackson (5), who also used a single intraperitoneal injection, shows that relatively more ^{32}P from III (0.18 and 0.08% after 3.5 and 12 hr, respectively) than from II (0.09 and 0.006% after 3 and 12 hr, respectively) was present in plasma. Spleen values, however, were essentially the same after the first time period (0.23% for III and 0.25% for II) and higher in the case of III (0.12%) compared to II (0.02%) after 12 hr.

The brain level of ^{32}P from the administration of II was about half that in the plasma after 3 hr compared to values reported for III (0.04 *versus* 0.09%) and one-third after 6 hr (0.01 *versus* 0.03%). This latter determination indicates a degree of penetration of II, or a metabolite, into the CNS, which may correlate with the activity found in intracerebral L-1210 testing.

Against intraperitoneal L-1210 cells, II administered on Day 1 only gave one 45-day survivor and a 50% increase in lifespan at 40 mg/kg. When this dose was given on Days 1, 5, and 9, the percent increase in lifespan was 75. The same dosage regimen against intracerebral leukemia cells gave 40 and 30% increases in lifespan for the single and triple injections, respectively.

As expected, II had better activity against intraperitoneal than intracerebral L-1210, but the margin was surprisingly narrow, at least for the single treatment. Although the activity of II is considered minimal compared to such oncolytics as 1-(2-chloroethyl)-3-cyclohexyl-1-nitrosourea, the ability of this agent to pass the blood–brain barrier in a cytotoxic form is encouraging; these data may prove helpful in the design of future compounds. The water solubility of II is possibly too low (less than 1 mg/liter) to provide the correct hydrophilic–lipophilic balance for optimum absorption and/or distribution.

[1] Type 57 Polaroid film.
[2] NCS.
[3] Waring blender.
[4] Packard Tri-Carb liquid scintillation spectrometer.

REFERENCES

(1) L. A. Cates and R. L. Gallio, *J. Pharm. Sci.*, **63**, 1480(1974).

(2) L. A. Cates, *Phosphorus*, **5**, 1(1974).

(3) L. A. Cates, R. L. Gallio, and M. B. Cramer, *J. Pharm. Sci.*, **62**, 1719(1973).

(4) M. L. Crossley, J. B. Allison, R. Wannemacher, J. Migliarese, R. P. Parker, E. Kuh, D. R. Seeger, and R. Partridge, *Proc. Soc. Exp. Biol. Med.*, **83**, 398(1953).

(5) A. W. Craig and H. Jackson, *Brit. J. Pharmacol.*, **10**, 321(1955).

(6) R. K. Maller and C. Heidelberger, *Cancer Res.*, **17**, 284(1956).

(7) R. K. Maller, F. A. McIver, and C. Heidelberger, *ibid.*, **17**, 291(1956).

(8) W. S. Fletcher, E. D. McSweeney, and J. E. Dunphy, *J. Amer. Med. Ass.*, **191**, 116((1965).

ACKNOWLEDGMENTS AND ADDRESSES

Received April 21, 1975, from the *College of Pharmacy, University of Houston, Houston, TX 77004*

Accepted for publication June 3, 1975.

Presented at the Medicinal Chemistry Section, APhA Adacemy of Pharmaceutical Sciences, New Orleans meeting, November 1974.

Supported in part by Grant CA-13123 from the National Cancer Institute, U.S. Public Health Service, Bethesda, MD 20014

[x] To whom inquiries should be directed.

Liquid–Solid Chromatographic Determination of 6-Demethylgriseofulvin in Urine

E. PAPP [x], K. MAGYAR, and H. J. SCHWARZ

Abstract □ A specific and quantitative liquid–solid chromatographic method for the determination of 6-demethylgriseofulvin in human urine is reported. The method consists of extraction into an organic solvent, addition of internal standard, and analysis by liquid–solid chromatography using a UV detector. Griseofulvin, if present, can be determined simultaneously. The sensitivity of the method is 6 μg/ml of urine. Total 6-demethylgriseofulvin is determined after hydrolysis of the glucuronide conjugate with glucuronidase–sulfatase enzyme solution. The method is well suited for the analysis of a large number of samples.

Keyphrases □ 6-Demethylgriseofulvin—griseofulvin metabolite, liquid–solid chromatographic analysis, urine □ Griseofulvin metabolite—6-demethylgriseofulvin, liquid–solid chromatographic analysis, urine □ Liquid–solid chromatography—analysis, 6-demethylgriseofulvin, urine

6-Demethylgriseofulvin was found to be present in human urine after the administration of the antifungal agent griseofulvin. At the same time, only traces of griseofulvin were found (1). 6-Demethylgriseofulvin and its glucuronide were later shown to be the major urinary metabolites of griseofulvin in humans (2, 3), accounting for 65% of an intravenous dose (4) and 35–64% of an oral dose (2, 4).

The rate of excretion of free or total 6-demethylgriseofulvin was found to be directly proportional to the plasma concentration of griseofulvin (4), and the cumulative amount excreted was a direct measure of the amount absorbed (4, 5). Since less than 0.2% of the dose was excreted as griseofulvin (2), the measurement of 6-demethylgriseofulvin in urine provides a convenient estimation of the absorption and bioavailability of griseofulvin.

Analytical methods for the determination of 6-demethylgriseofulvin in urine by GLC as the trimethylsilyl derivative (5) or by UV spectrophotometry (3) were published previously. The method described in this report is both simple (avoids derivatization) and specific and shows good reproducibility.

EXPERIMENTAL

Reagents and Chemicals—The following reagents and chemicals were used: sodium hydroxide[1], methanol[2], isopropanol[2], acetic acid[2], 1-butanol[2], and griseofulvin[3] (all analyzed reagents); benzene[4], glass distilled; heptane[5], spectrograde; high-speed pellicular column packing[6]; and glucuronidase–sulfatase enzyme solution[7]. 6-Demethylgriseofulvin was isolated from human urine (1), and 4-(*m*-hydroxyphenyl)-1-isopropyl-7-methyl-2(1*H*)-quinazolinone was synthesized.

Instrumentation—A high-pressure liquid chromatograph[8] equipped with a 254-nm UV detector, using a 31.4-cm (3-ft) long and 2-mm i.d. [0.0984-cm (0.25-in.) o.d.] stainless steel column[6], was employed. The following conditions were used: column temperature, ambient; air pressure, 900 psi; gradient rate, 1%/min; function, concave 3; mode, operation and gradient; flow rate, 1.5–2.0 ml/min; initial composition, 0.0% secondary solvent; final composition, 6.0% secondary solvent; attenuation, 16; solvent in primary reservoir, 100% heptane; and solvent in secondary reservoir, methanol–isopropanol (1:1). Chromatograms were recorded on a 1-mv recorder[9].

Method—The pH of 3 ml of urine was adjusted to 5.35 with acetic acid and/or 2 *N* sodium hydroxide, and 0.2 ml of glucuronidase–sulfatase enzyme solution was added. The solution was incubated overnight at 37.5°. The incubated urine was extracted with 10 ml of 20% 1-butanol in benzene (v/v). An 8.0-ml aliquot of the extract was transferred to a pear-shaped flask and evaporated to dryness *in vacuo* on a rotary evaporator. The residue was dissolved in 0.4 ml of methanol containing 0.25 mg/ml of 4-(*m*-hydroxyphenyl)-1-isopropyl-7-methyl-2(1*H*)-quinazolinone as the internal standard. About 5 μl of this solution was injected into the chromatograph.

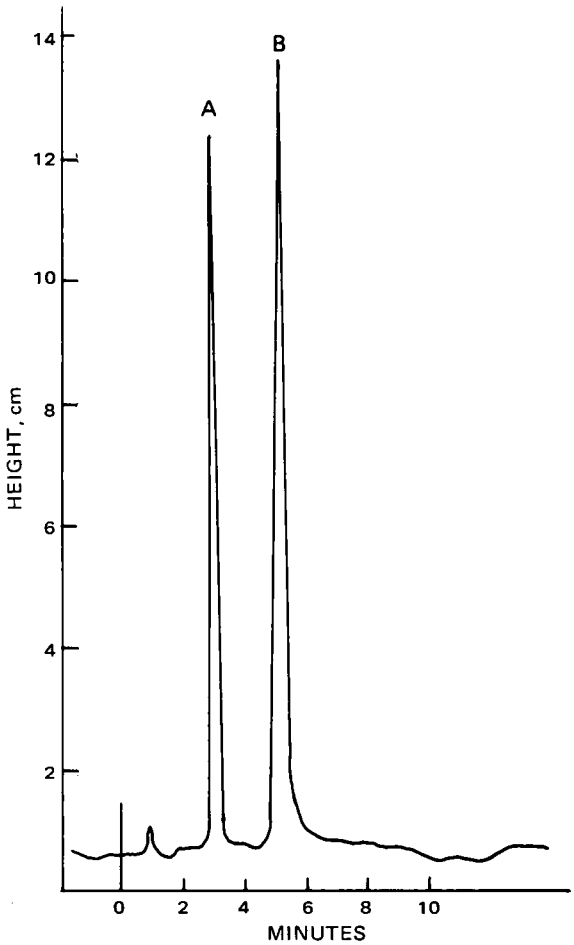

Figure 1—*Liquid chromatogram of a standard solution (5 μl). Key: A, internal standard; and B, 6-demethylgriseofulvin.*

[1] Mallinckrodt, Inc.
[2] Fisher Scientific Co.
[3] Schering Corp.
[4] Burdick and Jackson Laboratories, Inc.
[5] Matheson, Coleman and Bell.
[6] High Speed Pellosil, Reeve Angel.
[7] Glusulase, Endo Laboratories, Inc.
[8] DuPont model 830.
[9] Honeywell.

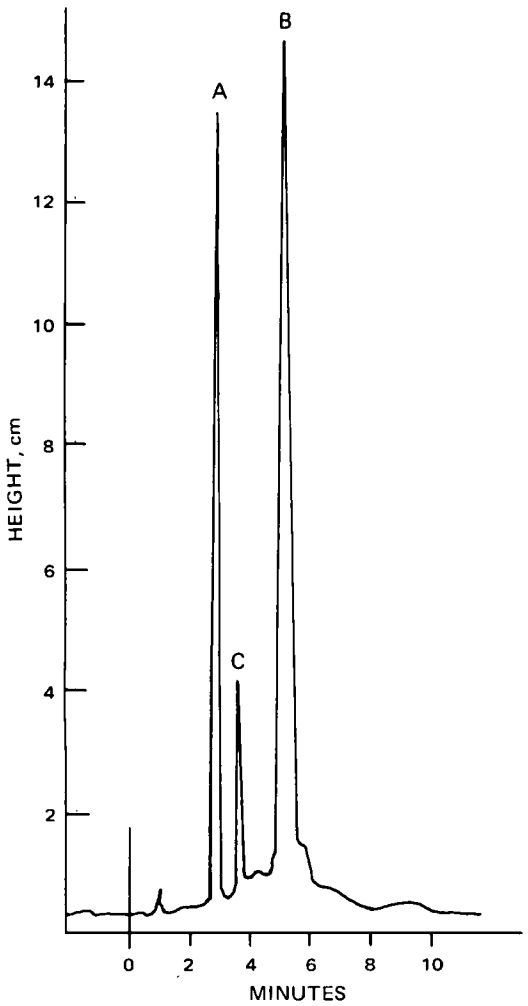

Figure 2—*Liquid chromatogram of a urine extract containing griseofulvin and 6-demethylgriseofulvin. Key: A, internal standard; B, 6-demethylgriseofulvin; and C, griseofulvin.*

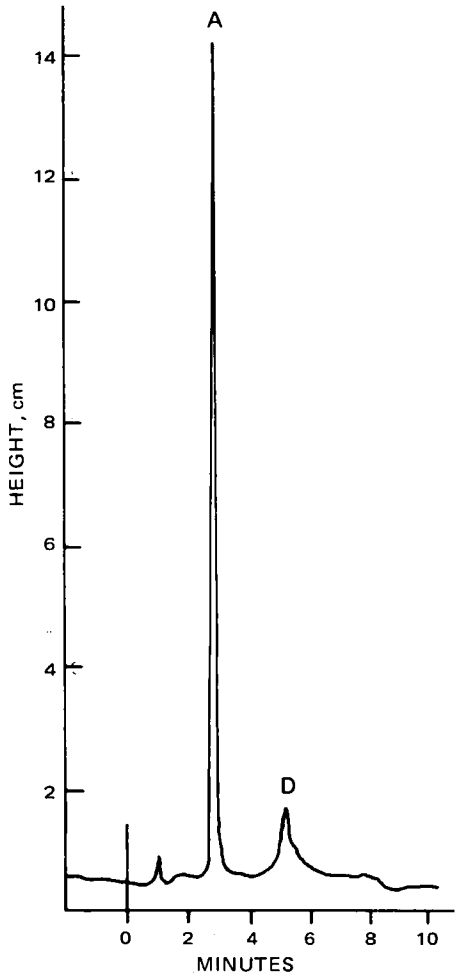

Figure 3—*Liquid chromatogram of a blank urine extract. Key: A, internal standard; and D, interfering blank value.*

The heights of the peaks corresponding to 6-demethylgriseofulvin and internal standard were then measured, and the ratio of the peak heights was converted into milligrams of 6-demethylgriseofulvin per milliliter of assay solution using the slope of the standard curve. The urinary concentration was obtained after correction for blank values, dilution (concentration), and recovery.

Standard curves were prepared by injecting standard solutions of 6-demethylgriseofulvin in methanol in the range of 0.05–1.00 mg/ml, each containing 0.25 mg/ml of internal standard, under the same analysis conditions as the samples. The peak height ratios of 6-demethylgriseofulvin–internal standard were then plotted against the concentration of 6-demethylgriseofulvin in the assay solution.

RESULTS AND DISCUSSION

Standard Curve—A typical recorder tracing of a standard mixture is shown in Fig. 1. A complete separation of the peaks was obtained. The retention times were: internal standard, 3.0 min; 6-demethylgriseofulvin, 5.2 min; and griseofulvin (Fig. 2), 3.6 min. Linearity between peak height ratio and concentration of 6-demethylgriseofulvin was obtained between 0 and 1.00 mg/ml. The slope of the standard curve changed very little from day to day.

Sensitivity—Under the described conditions, the lowest measurable concentration of 6-demethylgriseofulvin was 0.05 mg/ml of assay solution (peak height ratio = 0.1), which corresponds to a lower limit of 6 μg/ml of urine. This sensitivity was sufficient to follow the excretion of a single dose of 250–500 mg of griseofulvin for 72 hr. The instrument had practically no noise level. Therefore, the detection limit (two to three times signal to noise ratio) could not be determined.

Specificity—The combination of extraction, liquid–solid chromatographic retention time, and low blank values imparts good specificity to this method. However, it is not known whether 4-demethylgriseofulvin, the minor metabolite of griseofulvin in humans (2), has a different retention time from 6-demethylgriseofulvin.

Determination in Urine—The liquid–solid chromagtographic tracing of an extract of a blank urine sample (Fig. 3) was compared with an extract of a urine sample containing griseofulvin and 6-demethylgriseofulvin (Fig. 2). Some blank extracts showed an interfering peak with about the same retention time as 6-demethylgriseofulvin. In such a case, the peak height ratio of the interfering peak to the internal standard was deducted as a blank value in the calculation of the peak height ratios of 6-demethylgriseofulvin–

Table I—Recovery of 6-Demethylgriseofulvin after *In Vitro* Addition to Human Urine

6-Demethylgriseofulvin Added, mg/3 ml	6-Demethylgriseofulvin Recovered[a]	
	mg/3 ml ± *SD*	%
0.10	0.103 ± 0.023	103
0.20	0.224 ± 0.024	112
0.50	0.435 ± 0.044	87
1.00	0.939 ± 0.092	94
1.50	1.47 ± 0.08	98
2.00	1.91 ± 0.13	96
Average recovery		98

[a] Average of eight determinations.

internal standard in the drug-containing samples of the same urine (recovery) or subject.

Recovery—The validity of the method was verified and the recovery was determined by adding various known amounts of 6-demethylgriseofulvin to human urine. Each urine standard, as well as the blank urine, was analyzed eight times according to the method described (Table I).

The mean recoveries varied from 87 to 112% of the added amount. Recovery was independent of the concentration of 6-demethylgriseofulvin and averaged 98%.

Because of its simplicity, this method is well suited for the routine analysis of a large number of samples. It measures total, free, and conjugated 6-demethylgriseofulvin. Free metabolite can be determined by omitting the initial hydrolysis step. The method also allows griseofulvin, if present, to be determined simultaneously.

The method was used successfully in several bioavailability studies, and the results will be reported elsewhere.

REFERENCES

(1) M. J. Barnes and B. Boothroyd, *Biochem. J.*, **78**, 41(1961).

(2) C.-C. Lin, J. Margat, R. Chang, J. McGlotten, and S. Symchowicz, *J. Pharmacol. Exp. Ther.*, **187**, 415(1973).

(3) M. Rowland and S. Riegelman, *J. Pharm. Sci.*, **62**, 2030(1973).

(4) W. L. Chiou and S. Riegelman, *ibid.*, **60**, 1376(1971).

(5) P. Kabasakalian, M. Katz, B. Rosenkrantz, and E. Townley, *ibid.*, **59**, 595(1970).

ACKNOWLEDGMENTS AND ADDRESSES

Received April 15, 1975, from the *Drug Metabolism Section, Sandoz Pharmaceuticals, East Hanover, NJ 07936*

Accepted for publication May 27, 1975.

The authors thank Ms. Monica Tuttle for technical assistance.

[x] To whom inquiries should be directed.

CNS Depressant Activity of Pyrimidylthiazolidones and Their Selective Inhibition of NAD-Dependent Pyruvate Oxidation

MAHIMA CHAUDHARY [*], SURENDRA S. PARMAR [*x], SUNIL K. CHAUDHARY [*], ARVIND K. CHATURVEDI [*‡], and B. V. RAMA SASTRY [‡]

Abstract □ Several 1-aryl-3-(2-pyrimidyl)thiocarbamides and their corresponding cyclized 2-arylimino-3-(2-pyrimidyl)thiazolid-4-ones were synthesized and characterized by their sharp melting points and elemental analyses. These thiocarbamides and thiazolidones possessed anticonvulsant activity against pentylenetetrazol-induced convulsions and potentiated pentobarbital-induced hypnosis in mice. Most of these thiocarbamides and thiazolidones selectively inhibited nicotinamide adenine dinucleotide (NAD)-dependent oxidation of pyruvate, where the use of added NAD decreased the degree of inhibition. The NAD-independent oxidation of succinate, on the other hand, remained unaltered. The anticonvulsant activity of thiocarbamides and thiazolidones was unrelated to their ability to inhibit the respiratory activity of rat brain homogenates during oxidation of sodium pyruvate. Cyclization of thiocarbamides to the corresponding thiazolidones in general enhanced their CNS depressant and enzyme inhibitory effectiveness.

Keyphrases □ Thiazolidones—synthesis, evaluation of CNS activity, effect on NAD-dependent oxidation □ Thiocarbamides—synthesis, evaluation of CNS activity, effect on NAD-dependent oxidation □ CNS activity—synthesis and evaluation of several thiocarbamides and thiazolidones □ Enzyme activity—effect of thiocarbamides and thiazolidones on NAD-dependent oxidation □ Anticonvulsants—synthesis and evaluation of several thiocarbamides and thiazolidones

Considerable interest recently has been focused in this laboratory on substituted thiazolidones that have been shown to possess anticonvulsant (1–3), hypnotic (4), and local anesthetic (5) properties. Earlier studies indicated diverse pharmacological profiles of pyrimidine derivatives, including diuretic (5), local anesthetic (6), and anticonvulsant (7, 8) properties. Piperazinothiocarbamides also have been shown to possess effects on the central nervous system (CNS) activity (9, 10). These observations prompted synthesis of substituted thiocarbamides, which were cyclized into the corresponding 2-arylimino-3-(2-pyrimidyl)thiazolid-4-ones.

In the present study, these thiocarbamides and thiazolidones were evaluated for their anticonvulsant activity and their ability to potentiate pentobarbital-induced hypnosis and to inhibit cellular respiratory activity of rat brain homogenates, with a view to studying their biochemical mechanism of action. The various thiazolidones were synthesized by following the methods outlined in Scheme I (3).

EXPERIMENTAL [1]

The various 1,3-disubstituted thiocarbamides (Table I) were prepared by refluxing equimolar quantities of 2-aminopyrimidine and the appropriate arylisothiocyanate in dry benzene. These substituted thiocarbamides were cyclized into the corresponding 2-arylimino-3-(2-pyrimidyl)thiazolid-4-ones by refluxing with chloroacetic acid and anhydrous sodium acetate in acetic acid by the following method.

1-Aryl-3-(2-pyrimidyl)thiocarbamides (I–VIII)—2-Aminopyrimidine (0.01 *M*) was mixed with a suitable arylisothiocyanate (0.01 *M*) in 15 ml of dry benzene, and the mixture was refluxed on a steam bath for 4 hr. The reaction mixture was concentrated by distilling the excess benzene under reduced pressure. The solid mass which separated on cooling was filtered, washed with ether and dilute hydrochloric acid, dried, and recrystallized from ethanol. All thiocarbamides, characterized by their sharp melting points and elemental analyses, are recorded in Table I.

2-Arylimino-3-(2-pyrimidyl)thiazolid-4-ones (IX–XVI)—A

[1] All compounds were analyzed for their carbon, hydrogen, and nitrogen content. Melting points were taken in open capillary tubes with a partial immersion thermometer and are corrected.

internal standard in the drug-containing samples of the same urine (recovery) or subject.

Recovery—The validity of the method was verified and the recovery was determined by adding various known amounts of 6-demethylgriseofulvin to human urine. Each urine standard, as well as the blank urine, was analyzed eight times according to the method described (Table I).

The mean recoveries varied from 87 to 112% of the added amount. Recovery was independent of the concentration of 6-demethylgriseofulvin and averaged 98%.

Because of its simplicity, this method is well suited for the routine analysis of a large number of samples. It measures total, free, and conjugated 6-demethylgriseofulvin. Free metabolite can be determined by omitting the initial hydrolysis step. The method also allows griseofulvin, if present, to be determined simultaneously.

The method was used successfully in several bioavailability studies, and the results will be reported elsewhere.

REFERENCES

(1) M. J. Barnes and B. Boothroyd, *Biochem. J.*, **78**, 41(1961).

(2) C.-C. Lin, J. Margat, R. Chang, J. McGlotten, and S. Symchowicz, *J. Pharmacol. Exp. Ther.*, **187**, 415(1973).

(3) M. Rowland and S. Riegelman, *J. Pharm. Sci.*, **62**, 2030(1973).

(4) W. L. Chiou and S. Riegelman, *ibid.*, **60**, 1376(1971).

(5) P. Kabasakalian, M. Katz, B. Rosenkrantz, and E. Townley, *ibid.*, **59**, 595(1970).

ACKNOWLEDGMENTS AND ADDRESSES

Received April 15, 1975, from the *Drug Metabolism Section, Sandoz Pharmaceuticals, East Hanover, NJ 07936*

Accepted for publication May 27, 1975.

The authors thank Ms. Monica Tuttle for technical assistance.

[x] To whom inquiries should be directed.

CNS Depressant Activity of Pyrimidylthiazolidones and Their Selective Inhibition of NAD-Dependent Pyruvate Oxidation

MAHIMA CHAUDHARY [*], SURENDRA S. PARMAR [*x], SUNIL K. CHAUDHARY [*], ARVIND K. CHATURVEDI [*‡], and B. V. RAMA SASTRY [‡]

Abstract □ Several 1-aryl-3-(2-pyrimidyl)thiocarbamides and their corresponding cyclized 2-arylimino-3-(2-pyrimidyl)thiazolid-4-ones were synthesized and characterized by their sharp melting points and elemental analyses. These thiocarbamides and thiazolidones possessed anticonvulsant activity against pentylenetetrazol-induced convulsions and potentiated pentobarbital-induced hypnosis in mice. Most of these thiocarbamides and thiazolidones selectively inhibited nicotinamide adenine dinucleotide (NAD)-dependent oxidation of pyruvate, where the use of added NAD decreased the degree of inhibition. The NAD-independent oxidation of succinate, on the other hand, remained unaltered. The anticonvulsant activity of thiocarbamides and thiazolidones was unrelated to their ability to inhibit the respiratory activity of rat brain homogenates during oxidation of sodium pyruvate. Cyclization of thiocarbamides to the corresponding thiazolidones in general enhanced their CNS depressant and enzyme inhibitory effectiveness.

Keyphrases □ Thiazolidones—synthesis, evaluation of CNS activity, effect on NAD-dependent oxidation □ Thiocarbamides—synthesis, evaluation of CNS activity, effect on NAD-dependent oxidation □ CNS activity—synthesis and evaluation of several thiocarbamides and thiazolidones □ Enzyme activity—effect of thiocarbamides and thiazolidones on NAD-dependent oxidation □ Anticonvulsants—synthesis and evaluation of several thiocarbamides and thiazolidones

Considerable interest recently has been focused in this laboratory on substituted thiazolidones that have been shown to possess anticonvulsant (1–3), hypnotic (4), and local anesthetic (5) properties. Earlier studies indicated diverse pharmacological profiles of pyrimidine derivatives, including diuretic (5), local anesthetic (6), and anticonvulsant (7, 8) properties. Piperazinothiocarbamides also have been shown to possess effects on the central nervous system (CNS) activity (9, 10). These observations prompted synthesis of substituted thiocarbamides, which were cyclized into the corresponding 2-arylimino-3-(2-pyrimidyl)thiazolid-4-ones.

In the present study, these thiocarbamides and thiazolidones were evaluated for their anticonvulsant activity and their ability to potentiate pentobarbital-induced hypnosis and to inhibit cellular respiratory activity of rat brain homogenates, with a view to studying their biochemical mechanism of action. The various thiazolidones were synthesized by following the methods outlined in Scheme I (3).

EXPERIMENTAL [1]

The various 1,3-disubstituted thiocarbamides (Table I) were prepared by refluxing equimolar quantities of 2-aminopyrimidine and the appropriate arylisothiocyanate in dry benzene. These substituted thiocarbamides were cyclized into the corresponding 2-arylimino-3-(2-pyrimidyl)thiazolid-4-ones by refluxing with chloroacetic acid and anhydrous sodium acetate in acetic acid by the following method.

1-Aryl-3-(2-pyrimidyl)thiocarbamides (I–VIII)—2-Aminopyrimidine (0.01 *M*) was mixed with a suitable arylisothiocyanate (0.01 *M*) in 15 ml of dry benzene, and the mixture was refluxed on a steam bath for 4 hr. The reaction mixture was concentrated by distilling the excess benzene under reduced pressure. The solid mass which separated on cooling was filtered, washed with ether and dilute hydrochloric acid, dried, and recrystallized from ethanol. All thiocarbamides, characterized by their sharp melting points and elemental analyses, are recorded in Table I.

2-Arylimino-3-(2-pyrimidyl)thiazolid-4-ones (IX–XVI)—A

[1] All compounds were analyzed for their carbon, hydrogen, and nitrogen content. Melting points were taken in open capillary tubes with a partial immersion thermometer and are corrected.

Table I—Physical Constants of 1-Aryl-3-(2-pyrimidyl)thiocarbamides

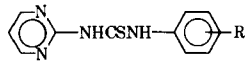

Compound	R	Melting Point[a]	Yield, %	Molecular Formula	Analysis, %	Calc.	Found
I	H	199°	85	$C_{11}H_{10}N_4S$	C	57.39	57.54
					H	4.34	4.39
					N	24.34	24.76
II	2-CH_3	214°	90	$C_{12}H_{12}N_4S$	C	59.01	59.34
					H	4.91	4.82
					N	22.95	22.95
III	4-CH_3	212°	84	$C_{12}H_{12}N_4S$	C	59.01	58.79
					H	4.91	5.02
					N	22.95	23.26
IV	2,4-$(CH_3)_2$	218°	65	$C_{13}H_{14}N_4S$	C	60.46	60.72
					H	5.42	5.34
					N	21.70	21.56
V	2,6-$(CH_3)_2$	228°	73	$C_{13}H_{14}N_4S$	C	60.49	60.29
					H	5.42	5.38
					N	21.70	21.84
VI	4-OCH_3	215°	75	$C_{12}H_{12}N_4OS$	C	55.38	55.72
					H	4.61	4.69
					N	21.53	21.75
VII	4-Br	220°	80	$C_{11}H_9BrN_4S$	C	42.71	42.92
					H	2.91	2.86
					N	18.12	18.18
VIII	4-Cl	225°	72	$C_{11}H_9ClN_4S$	C	49.90	50.21
					H	3.40	3.57
					N	21.17	21.42

[a] Melting points were taken in open capillary tubes with a partial immersion thermometer and are corrected.

mixture of 1-aryl-3-(2-pyrimidyl)thiocarbamide (0.01 *M*), chloroacetic acid (0.01 *M*), and anhydrous sodium acetate (0.015 *M*) in 15 ml of acetic acid was refluxed on a free flame for 5–6 hr. The reaction mixture was poured into water, and the contents were allowed to stand overnight in a refrigerator. The crude thiazolidones which separated were filtered, washed several times with water, and recrystallized from ethanol (Table II).

Determination of Anticonvulsant Activity—Anticonvulsant activity was determined in albino mice of either sex weighing 25–30 g. The mice were divided into groups of 10, keeping the group weights as nearly the same as possible. All thiocarbamides and thiazolidones were suspended in 5% aqueous gum acacia to give a concentration of 0.25% (w/v).

The test compounds were injected at a dose of 100 mg/kg ip. Four hours later, the mice were injected with pentylenetetrazol (90 mg/kg sc). This dose of pentylenetetrazol produced convulsions in all untreated mice and caused 100% mortality within 24 hr.

The mice were observed for 60 min for the occurrence of seizures. An episode of clonic spasm that persisted for a minimum of 5 sec was considered a threshold convulsion (11). Transient intermittent jerks and tremulousness were not counted. Animals devoid of threshold convulsions during the 60-min period were considered protected. The number of animals protected in each group was recorded, and the anticonvulsant activity of the compounds was represented as percent protection. The mice were then observed for 24 hr and mortality was recorded.

Potentiation of Pentobarbital (Sodium) Sleeping Time—The method of Winter (12) was followed to investigate the ability

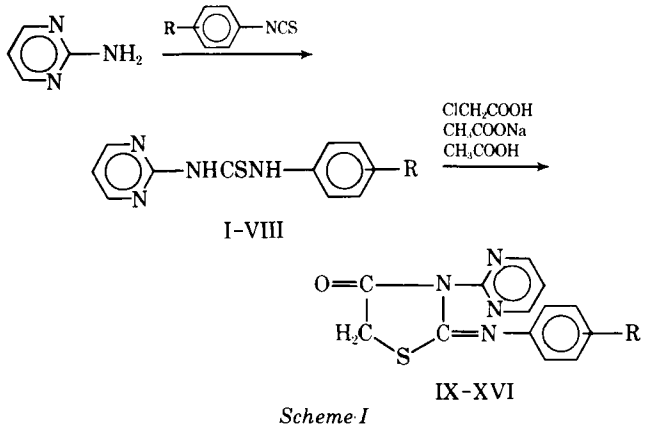

Scheme I

of thiocarbamides and thiazolidones to potentiate pentobarbital-induced hypnoses. Albino mice, 20–25 g, were divided into groups of six animals. One group was used for each compound, while another group served as the control. Pentobarbital, when administered in a dose of 40 mg/kg ip to the control group, produced ataxia and no sleep. Increasing the dose of pentobarbital produced sleep in the mice. All thiocarbamides and thiazolidones were suspended in 5% aqueous gum acacia to give a concentration of 0.25% (w/v) and were injected at a dose of 100 mg/kg ip 1 hr prior to the administration of pentobarbital (40 mg/kg).

The animals were observed for sleep as evidenced by the loss of the righting reflex. The degree of potentiation produced by these compounds was calculated by the mean average time of sleep observed in experimental animals.

Determination of Respiratory Activity of Rat Brain Homogenate[2]—Male albino rats[3], kept on an *ad libitum* diet, were used. Rat brains, isolated from decapitated animals, were immediately homogenized in ice-cold 0.25 *M* sucrose in a homogenizer[4] in a ratio of 1:9 (w/v). All incubations were carried out at 37°, and the oxygen uptake was measured using air as the gas phase (13). Fresh rat brain homogenate (1 ml), equivalent to 100 mg wet weight, was added to chilled Warburg vessels containing 6.7 m*M* magnesium sulfate, 20 m*M* sodium hydrogen phosphate buffer solution (pH 7.4), 1 m*M* adenosine monophosphate (sodium salt), 33 m*M* potassium chloride, and 500 μg of cytochrome *c* in a final volume of 3 ml unless otherwise stated.

The central well contained 0.2 ml of 20% KOH solution. Pyruvate and succinate were used at a final concentration of 10 m*M*. NAD was used at a final concentration of 0.5 m*M*. It was presumed that the endogenous NAD, present in this homogenate, was sufficient for these oxidative processes. All compounds (final concentration of 2 m*M*) under assay were dissolved in propylene glycol (100%), and an equal volume of the solvent was added to the control vessels.

RESULTS AND DISCUSSION

In the present study, 1-aryl-3-(2-pyrimidyl)thiocarbamides and their corresponding cyclized 2-arylimino-3-(2-pyrimidyl)thiazolid-

[2] Commercial chemicals were used in this study. Adenosine monophosphate (sodium salt), nicotinamide adenine dinucleotide, pyruvate, succinate, and cytochrome c were obtained from Sigma Chemical Co., St. Louis, Mo. Other common chemicals were obtained from British Drug House, Bombay, India.

[3] Animal Supply House, Lucknow, India.

[4] Potter-Elvehjem homogenizer.

Table II—Physical Constants of 2-Arylimino-3-(2-pyrimidyl)thiazolid-4-ones

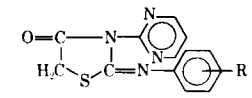

Compound	R	Melting Point[a]	Yield, %	Molecular Formula	Analysis, %	
					Calc.	Found
IX	H	260° dec.	64	$C_{13}H_{10}N_4OS$	C 57.77	57.60
					H 3.70	3.59
					N 20.74	20.82
X	2-CH_3	209°	58	$C_{14}H_{12}N_4OS$	C 59.15	59.26
					H 4.22	4.42
					N 19.71	19.60
XI	4-CH_3	140°	52	$C_{14}H_{12}N_4OS$	C 59.15	59.25
					H 4.22	4.18
					N 19.71	19.35
XII	2,4-$(CH_3)_2$	175°	54	$C_{15}H_{14}N_4OS$	C 60.40	60.72
					H 4.69	4.50
					N 18.79	18.92
XIII	2,6-$(CH_3)_2$	199°	62	$C_{15}H_{14}N_4OS$	C 60.40	60.50
					H 4.69	4.43
					N 18.79	18.49
XIV	4-OCH_3	264°	67	$C_{14}H_{12}N_4O_2S$	C 56.00	56.21
					H 4.00	3.96
					N 18.66	18.72
XV	4-Br	234°	70	$C_{13}H_9BrN_4OS$	C 44.69	44.52
					H 2.57	2.60
					N 16.04	16.13
XVI	4-Cl	250°	55	$C_{13}H_9ClN_4OS$	C 51.23	51.27
					H 2.95	3.04
					N 18.39	18.45

[a] Melting points were taken in open capillary tubes with a partial immersion thermometer and are corrected.

4-ones were synthesized and evaluated for their CNS depressant activity. Anticonvulsant activity was determined against pentylenetetrazol-induced convulsions. The degree of protection afforded by thiocarbamides (100 mg/kg) ranged from 20 to 50% (Table III). The data in general indicate a trend of more protection from convulsions with less mortality. These thiocarbamides, in a dose of 100 mg/kg, potentiated pentobarbital sleeping time in mice, which was of a low order and ranged from 10 to 24 min. With the exception of II, IV, and VIII, these thiocarbamides showed low inhibition of the oxidation of pyruvate by rat brain homogenates. On the other hand, oxidation of succinate remained unaltered.

As is evident from Table IV, cyclization of thiocarbamides to their corresponding thiazolidones resulted in increased anticonvulsant activity with the exception of X, XI, and XVI. The anticonvulsant activity of substituted thiazolidones in doses of 100 mg/kg ranged from 20 to 80%, while XI failed to provide any protection against pentylenetetrazol-induced convulsions. The data seem to indicate a definite trend of more protection from convulsions with less mortality with the exception of XV, where 30% anticonvulsant activity was associated with low pentylenetetrazol-induced mortality of only 20%.

The cyclization of thiocarbamides to thiazolidones exhibited a significant increase in the ability of thiazolidones to potentiate pentobarbital-induced sleeping time in mice. Such an increase was two- to fivefold with thiazolidones as compared to substituted thiocarbamides. All thiazolidones inhibited the oxidation of pyruvic acid by rat brain homogenate, while the oxidation of succinate remained unaltered.

The results recorded in Table IV clearly show the increased inhibition of cellular respiratory activity by thiazolidones as compared to their precursor thiocarbamides. The presence of added NAD not only increased the cellular respiratory activity of rat brain homogenates during oxidation of pyruvate but also decreased the inhibitory effectiveness of substituted thiazolidones. These results, which are in good agreement with earlier reports (14, 15), thus provide evidence for a possible competition between the thiazolidones and NAD for the active site(s) on the enzyme molecule. Therefore, these results have indicated the selective inhibition of NAD-dependent oxidation of pyruvate by thiocarbamides (Table III) and thiazolidones (Table IV).

There was no definite relationship between the chemical structure of thiocarbamides and thiazolidones and their anticonvulsant effects or the inhibition of oxidation of pyruvate. Inhibition of certain metabolic processes in the brain has been proposed as a biochemical basis for the mechanism of action of various CNS depressants (16, 17), where a parallelism was observed between greater *in*

Table III—Pharmacological and Biochemical Properties of 1-Aryl-3-(2-pyrimidyl)thiocarbamides

Compound	Anticonvulsant Activity[a], % Protection	Pentylenetetrazol Mortality in 24 hr[a], %	Potentiation of Pentobarbital Sleeping Time[b], min	Inhibition[c], %	
				Pyruvate	Succinate
I	50	30	18 ± 2	20.1 ± 1.6	Nil
II	40	70	10 ± 3	Nil	Nil
III	20	80	24 ± 6	24.9 ± 1.4	Nil
IV	30	70	17 ± 4	Nil	Nil
V	40	70	17 ± 2	15.6 ± 1.3	Nil
VI	30	50	22 ± 7	13.9 ± 1.2	Nil
VII	20	100	12 ± 2	22.1 ± 1.2	Nil
VIII	50	20	Nil	Nil	Nil

[a] Substituted thiocarbamides were administered (100 mg/kg ip) 4 hr before the administration of pentylenetetrazol (90 mg/kg sc). [b] Pentobarbital (40 mg/kg ip) produced ataxia and no sleep. Substituted thiocarbamides were administered (100 mg/kg ip) 1 hr prior to the administration of pentobarbital. The values represent the mean ± standard error from six mice. [c] Each experiment was done in duplicate. All values represent mean ± standard error from three experiments. The oxygen uptake was measured at 5-min intervals during 1 hr of incubation. The percent inhibition was calculated from the decrease in oxygen uptake per 100 mg wet brain weight.

Table IV—Pharmacological and Biochemical Properties of 2-Arylimino-3-(2-pyrimidyl)thiazolid-4-ones

Compound	Anticonvulsant Activity[a], % Protection	Pentylenetetrazol Mortality in 24 hr[a], %	Potentiation of Pentobarbital Sleeping Time[a], min	Inhibition[a], %		
				Pyruvate		Succinate
				Without Added NAD	With Added NAD[b]	
IX	80	30	51 ± 6	25.6 ± 0.8	15.3 ± 1.4	Nil
X	30	60	50 ± 9	48.8 ± 1.2	37.3 ± 1.5	Nil
XI	Nil	100	70 ± 8	35.5 ± 1.7	29.6 ± 1.7	Nil
XII	70	50	51 ± 5	40.3 ± 1.4	35.8 ± 1.3	Nil
XIII	50	50	54 ± 7	39.3 ± 1.7	32.4 ± 1.1	Nil
XIV	60	40	60 ± 4	38.9 ± 0.7	30.7 ± 1.7	Nil
XV	30	20	46 ± 10	27.9 ± 1.6	21.3 ± 1.8	Nil
XVI	20	70	27 ± 6	16.9 ± 1.2	11.8 ± 1.5	Nil

[a]Details of the experiments are as described in Table III. The various substituted thiazolidones were administered in a dose of 100 mg/kg ip for studying pharmacological properties and were used at a final concentration of 2 m*M* for biochemical studies. [b]The final concentration of the added NAD in the incubation mixture was 0.5 m*M*.

vivo hypnotic activity of some compounds and their ability to cause greater *in vitro* inhibition of cellular respiratory activity (18, 19).

The present study has failed to provide any definite correlation between anticonvulsant activities of thiocarbamides and thiazolidones and their abilities to potentiate pentobarbital-induced hypnosis and inhibit selectively NAD-dependent oxidation of pyruvate. Similar results were reported earlier with 3,4,5-trimethoxybenzamides (20). However, the results have indicated that cyclization of thiocarbamides to the corresponding thiazolidones in general resulted in increased CNS depressant activity, which correlated well with the increased ability of thiazolidones to inhibit selectively cellular respiratory activity of rat brain homogenates as compared to their precursor thiocarbamides.

REFERENCES

(1) R. Kumar, T. K. Gupta, and S. S. Parmar, *J. Prakt. Chem.*, **312,** 201(1970).

(2) S. S. Parmar, C. Dwivedi, A. Chaudhari, and T. K. Gupta, *J. Med. Chem.*, **15,** 99(1972).

(3) C. Dwivedi, T. K. Gupta, and S. S. Parmar, *ibid.*, **15,** 553(1972).

(4) W. J. Doran and H. A. Shoule, *J. Org. Chem.*, **3,** 193 (1938).

(5) L. M. Hofmann, H. A. Wagner, and R. S. Jacobs, *Arch. Int. Pharmacodyn. Ther.*, **165,** 476(1967).

(6) A. Quevanvillen, B. Mazieve, and M. Mazieve, *Anesth. Analg. Reanim.*, **25,** 53(1968).

(7) B. Mazieve and M. Mazieve, *Chim. Ther.*, **2,** 336(1967).

(8) P. G. Dashputra, M. L. Sharma, M. K. Jagtap, M. D. Khapre, and M. V. Rajapurkar, *Arch. Int. Pharmacodyn. Ther.*, **160,** 106(1966).

(9) A. K. Chaturvedi and S. S. Parmar, *Biochem. Pharmacol.*, **22,** 2355(1973).

(10) A. K. Chaturvedi and S. S. Parmar, *Curr. Sci.*, **41,** 253(1973).

(11) R. P. Kohli, T. K. Gupta, S. S. Parmar, and R. C. Arora, *Jap. J. Pharmacol.*, **17,** 409(1967).

(12) C. A. Winter, *J. Pharmacol. Exp. Ther.*, **94,** 1(1948).

(13) P. K. Seth and S. S. Parmar, *Can. J. Physiol. Pharmacol.*, **43,** 1019(1965).

(14) S. S. Parmar, A. K. Chaturvedi, and B. Ali, *J. Prakt. Chem.*, **312,** 950(1970).

(15) S. S. Parmar, A. K. Chaturvedi, A. Chaudhari, and S. J. Brumleve, *J. Pharm. Sci.*, **63,** 356(1974).

(16) J. H. Quastel, *Physiol. Rev.*, **19,** 135(1939).

(17) J. H. Quastel, *Trans. Faraday. Soc.*, **39,** 348(1943).

(18) J. H. Quastel and A. H. M. Wheatley, *Proc. Roy. Soc. London*, **112,** 60(1932).

(19) F. A. Furnam and J. Field, *J. Pharmacol. Exp. Ther.*, **77,** 392(1943).

(20) A. K. Chaturvedi, A. Chaudhari, and S. S. Parmar, *J. Pharm. Sci.*, **61,** 1157(1972).

ACKNOWLEDGMENTS AND ADDRESSES

Received April 3, 1975, from the *Department of Pharmacology and Therapeutics, King George's Medical College, Lucknow University, Lucknow, 226003, India, and the ‡Department of Pharmacology, Vanderbilt University School of Medicine, Nashville, TN 37232

Accepted for publication May 22, 1975.

Supported in part by the Department of Atomic Energy, Government of India, Bombay, India, Council of Scientific and Industrial Research, New Delhi, India. A. K. Chaturvedi and B. V. R. Sastry were supported by U.S. Public Health Service Research Grant NS-04699 and General Research Support Grant RR-05424.

The authors thank Professor K. P. Bhargava and Dr. J. P. Barthwal for their advice and encouragement. Grateful acknowledgment is made to the Department of Atomic Energy, Government of India, Bombay, India, for providing a Research Fellowship to S. K. Chaudhary.

ˣ To whom inquiries should be directed. Present address: Department of Physiology and Pharmacology, University of North Dakota School of Medicine, Grand Forks, ND 58201

Influence of Aspirin Formulation and Dose on Concentration of Total Salicylate in Rat Kidney

JERRY L. LEELING ˣ, BARRIE M. PHILLIPS, TONI L. KOWALSKI, and ROBERT L. KOWALSKI

Abstract □ Rats received the equivalent of 100, 250, 500, or 700 mg/kg of ^{14}C-aspirin orally as a suspension or as a solution of a buffered, effervescent, aspirin-containing product. Animals in each dose group were sacrificed at time intervals ranging from 0.5 to 24 hr after dosing. The ^{14}C content of whole blood, plasma, and homogenized whole kidney (after perfusion) was determined. The concentration of total salicylate proved to be dose dependent and was lower in tissues from rats receiving the buffered, effervescent product, especially at the higher doses. The results suggest that salicylate-induced renal toxicity should be less likely to occur after administration of the buffered, effervescent formulation.

Keyphrases □ Aspirin—effect of formulation and dose on total salicylate concentration in rat kidney □ Salicylate—concentration in rat kidney, effect of formulation and dose □ Renal excretion—salicylates, effect of formulation and dose, rats

Chronic, oral administration of high (500 mg/kg) single daily doses of aspirin was reported (1) to produce renal papillary necrosis in rats. The incidence of nephropathy was enhanced if the rats were dehydrated for 16 hr each day and reduced by measures that alkalinized the urine.

The latter observation is interesting in view of the demonstration (2) that the renal excretion of salicylates is profoundly influenced by urinary pH and is much more rapid in alkaline than in acid urine. The increased rate of salicylate excretion observed when the urine is alkaline is generally accepted to reflect a reduction in the filtered salicylate reabsorbed from tubular urine (3). Therefore, salicylate levels in renal tissue (defined as renal tubular epithelial cells and the interstitial spaces between these cells and renal blood vessels, excluding renal blood and tubular urine) would arise largely as a consequence of the passive reabsorption processes involved in excretion. Thus, renal tissue salicylate levels would be maximal when tubular urine is acidic and minimal when tubular urine is alkaline. This condition has important toxicological implications since, as Prescott (4) stated, "the pharmacological and toxic effects of most therapeutic agents are thought to be related to the concentration of free drug at the receptors of the target cells."

This report describes experiments in which kidney tissue levels of total radioactive salicylate were determined, after perfusion, in rats receiving various equivalent single doses of aspirin or an effervescent aspirin product[1]. The latter formulation, when dissolved in water as intended, becomes essentially sodium acetylsalicylate in sodium citrate buffer, a medium well known to alkalinize urine (5). The results produced by the two formulations were compared to support the contention that aspirin administered as a buffered formulation should be less likely to produce renal toxicity.

EXPERIMENTAL

^{14}C-Aspirin[2] was added to pure unlabeled aspirin[3] or to powdered, buffered, effervescent aspirin. Each dose contained 12.4 μCi of ^{14}C/kg. Aspirin was administered by gavage as single doses of 0.5, 1.25, 2.5, or 3.5% aqueous suspensions (4 ml/200 g of body weight, providing 100, 250, 500, or 700 mg/kg, respectively). The other formulation was similarly administered as an aqueous solution (doses contained equivalent amounts of aspirin as the sodium salt).

Animals—One hundred and sixty-eight male Charles River COBS-CD rats, 130–182 g, were randomly assigned to eight groups of 21 rats each. The animals were fasted overnight prior to drug administration but were fed thereafter. Drinking water was available *ad libitum*.

Experimental Design—At time zero, rats in four of the eight groups received the aspirin suspension at the doses described and the remaining animals received the buffered, effervescent formulation equivalent in aspirin to the suspension. After dosing, all of the animals were immediately placed in individual metabolism cages.

Three rats from each dose group were killed using chloroform at each of the following intervals: 0.5, 1, 2, 4, 8, 16, and 24 hr. Immediately after death, each rat was opened by ventral midline incision; a sample of whole blood was obtained by cardiac puncture and chilled in an ice bath. Incisions were made in both ventricles, and a 16-gauge perfusion needle then was inserted through the left ventricle into the aorta. Helium was perfused for 5 min at a flow rate of about 2 liters/min. Preliminary experiments indicated that this technique expelled a significant portion of the blood and urine from the kidneys. After perfusion, the kidneys were excised and kept on ice.

Analytical Methods—One kidney from each rat was stripped of fat, weighed to the nearest 0.1 mg, and homogenized[4] in 5 ml of distilled water. A 50-μl sample of each homogenate was transferred to counting vials (low potassium glass) to which were added 1 ml of 2 *M* NaOH, 3.5 ml of a solubilizer[5], and 10 ml of a liquid scintillator[6].

A 100-μl aliquot of whole blood from each rat was placed in counting vials, followed by 1 ml of 2 *M* NaOH and two drops of 30% H_2O_2. The vials were left at room temperature overnight and then were capped and heated at 80° for 30 min. After the solutions returned to room temperature, 3.5 ml of the solubilizer[5] and 10 ml of the liquid scintillator[6] were added to each.

Plasma samples derived from each blood sample (except the 500-mg/kg dose group) were prepared for liquid scintillation counting by transferring 100-μl aliquots to counting vials containing a solution of 8 ml of scintillator[6] and 2 ml of a plasma solubilizer[7].

All samples were counted[8] for a period of time sufficient to guarantee less than 2% counting error. Counting efficiency was deter-

[1] Alka-Seltzer, Miles Laboratories, Elkhart, Ind.

[2] New England Nuclear Corp., Boston, Mass.

[3] Dow Chemical Co., Midland, Mich.

[4] Potter-Elvehjem homogenizer with a Teflon pestle.

[5] Bio-Solv BBS-2, Beckman Instruments, Fullerton, Calif.

[6] A solution containing 4 g of 2,5-diphenyloxazole and 0.1 g of 1,4-bis[2-(4-methyl-5-phenyloxazolyl)]benzene/liter of toluene.

[7] Bio-Solv BBS-3, Beckman Instruments, Fullerton, Calif.

[8] Model 3375 liquid scintillation counter, Packard Instrument Co., Downers Grove, Ill.

Table I—Levels of Total Salicylates in Kidney Tissue following the Oral Administration of Aspirin

Dose, mg/kg[a], and Product	Kidney Tissue Total Salicylate Concentration, mg/g[b]						
	0.5 hr	1.0 hr	2.0 hr	4.0 hr	8.0 hr	16.0 hr	24.0 hr
100							
Aspirin suspension	0.071 ±0.042	0.167 ±0.024	0.137 ±0.018	0.200 ±0.035	0.105 ±0.011	0.062 ±0.008	0.020 ±0.006
Buffered, effervescent aspirin	0.170 ±0.003	0.187 ±0.006	0.147 ±0.002	0.126 ±0.011	0.081 ±0.002	0.023 ±0.003	0.016 ±0.006
250							
Aspirin suspension	0.252 ±0.027	0.269 ±0.017	0.289 ±0.017	0.216 ±0.011	0.186 ±0.024	0.062 ±0.031	0.060 ±0.013
Buffered, effervescent aspirin	0.236 ±0.036	0.262 ±0.024	0.225 ±0.020	0.165 ±0.024	0.110 ±0.001	0.043 ±0.015	0.027 ±0.010
500							
Aspirin suspension	0.390 ±0.038	0.529 ±0.069	0.570 ±0.058	0.415 ±0.070	0.363 ±0.041	0.248 ±0.070	0.131 ±0.040
Buffered, effervescent aspirin	0.192 ±0.009	0.293 ±0.004	0.376 ±0.082	0.216 ±0.061	0.205 ±0.069	0.115 ±0.016	0.077 ±0.019
700							
Aspirin suspension	0.277 ±0.015	0.473 ±0.110	0.642 ±0.030	0.435 ±0.030	0.353 ±0.021	0.437 ±0.093	0.225 ±0.029
Buffered, effervescent aspirin	0.216 ±0.043	0.412 ±0.072	0.492 ±0.064	0.367 ±0.067	0.234 ±0.015	0.107 ±0.036	0.140 ±0.090

[a] Aspirin equivalent. [b] Mean ± *SE* (n = 3).

mined by internal standardization, and all count rates were converted first to absolute disintegration rates and then to milligrams of salicylate.

Average kidney total salicylate values were calculated by estimating the area under tissue concentration *versus* time curves using the trapezoidal technique.

RESULTS

The concentration levels of total salicylate in renal tissue of rats after 100-, 250-, 500-, or 700-mg/kg oral doses of aspirin as either the suspension or a buffered, effervescent, aspirin-containing formulation are summarized in Table I. At doses of 100 or 250 mg/kg, no difference in salicylate concentration was observed before 4 hr. However, after the higher doses, the suspension produced higher kidney levels of total salicylate throughout the 24-hr period.

The average concentrations of total salicylate in rat renal tissue following the various doses of each preparation are summarized in Table II. The aspirin suspension produced average concentrations that were 40, 45, 85, or 83% higher than those produced by the buffered, effervescent aspirin when the equivalent doses of aspirin were 100, 250, 500, or 700 mg/kg, respectively. The effect of dose of each product on the average concentration of total salicylate in the kidney is illustrated in Fig. 1.

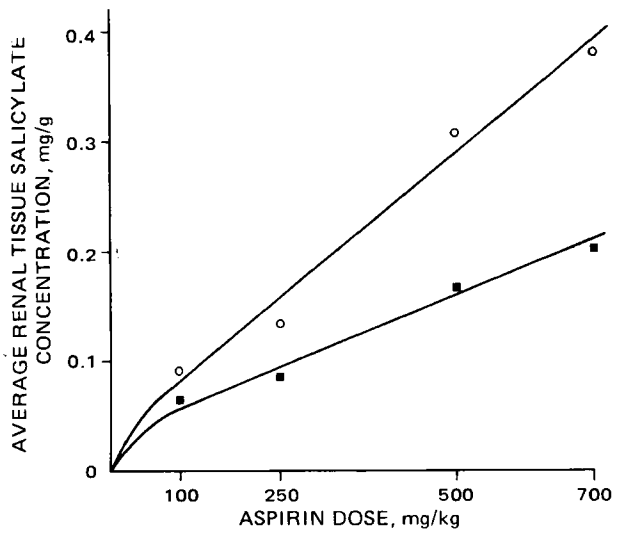

Figure 1—*Average salicylate concentrations in rat kidney after the oral administration of aspirin suspension* (○) *or a buffered, effervescent aspirin-containing formulation* (■).

Total salicylate concentrations in whole blood and plasma are summarized in Tables III and IV, respectively. The estimated average total salicylate concentrations in whole blood and plasma are summarized in Table V. The results of the blood studies agree with the analyses of kidney homogenates and show that higher levels of salicylate are present after these high doses of the aspirin suspension than after similar doses of the buffered, effervescent aspirin.

DISCUSSION

The results of this study show unequivocally that levels of total salicylate in rat kidney tissue are significantly lower when aspirin is administered as the buffered, effervescent formulation than when the aspirin suspension is administered. Since the former preparation produces an alkaline urine and since salicylate excretion is enhanced when the urine is alkaline (2), it is concluded that the lower renal tissue levels are the result of decreased tubular reabsorption of salicylic acid and increased excretion.

At the 700-mg/kg aspirin dose, the buffered, effervescent formulation approached its acute LD_{50} in the rat; indeed, three of the 21 rats died at that dose. Thus, for practical purposes, renal tissue total salicylate levels obtained at 700 mg/kg are maximal for that formulation. Similar aspirin doses as the suspension produced higher renal tissue salicylate levels (Fig. 1). Inasmuch as the acute oral LD_{50} of aspirin in the rat is about 1500 mg/kg (6), much higher kidney salicylate concentrations than those demonstrated are possible after the administration of single doses of the aspirin suspension.

The dose–tissue level relationship indicates that even lethal doses of the buffered, effervescent formulation produce kidney salicylate levels equivalent to about a 350-mg/kg dose of the suspension. This finding, in turn, indicates that it would be impossible to produce, with a single dose of the buffered, effervescent formulation, kidney tissue salicylate levels equivalent to those produced

Table II—Estimated Average Renal Tissue Total Salicylate Concentrations

Dose, mg/kg[a]	Average Renal Tissue Total Salicylate Concentrations, mg/g	
	Aspirin Suspension	Buffered, Effervescent Aspirin
100	0.091	0.065
250	0.136	0.094
500	0.308	0.165
700	0.387	0.212

[a] Aspirin equivalent.

Table III—Levels of Total Salicylates in Whole Blood following the Oral Administration of Aspirin

Dose, mg/kg[a], and Product	Whole Blood Total Salicylate Concentration, mg/ml[b]						
	0.5 hr	1.0 hr	2.0 hr	4.0 hr	8.0 hr	16.0 hr	24.0 hr
100							
Aspirin suspension	0.085 ±0.018	0.105 ±0.028	0.136 ±0.018	0.134 ±0.026	0.047 ±0.003	0.015 ±0.007	0.002 ±0.001
Buffered, effervescent aspirin	0.094 ±0.028	0.108 ±0.013	0.083 ±0.002	0.072 ±0.004	0.039 ±0.002	0.001 ±0.001	0.000 ±0.000
250							
Aspirin suspension	0.239 ±0.017	0.253 ±0.025	0.288 ±0.012	0.244 ±0.011	0.157 ±0.043	0.081 ±0.010	0.040 ±0.009
Buffered, effervescent aspirin	0.198 ±0.012	0.228 ±0.023	0.235 ±0.013	0.187 ±0.003	0.106 ±0.005	0.040 ±0.011	0.003 ±0.001
500							
Aspirin suspension	0.475 ±0.030	0.476 ±0.080	0.521 ±0.095	0.399 ±0.058	0.398 ±0.027	0.282 ±0.075	0.154 ±0.021
Buffered, effervescent aspirin	0.160 ±0.017	0.263 ±0.018	0.362 ±0.067	0.181 ±0.034	0.209 ±0.088	0.129 ±0.014	0.071 ±0.016
700							
Aspirin suspension	0.220 ±0.039	0.365 ±0.040	0.481 ±0.022	0.306 ±0.047	0.374 ±0.037	0.274 ±0.058	0.170 ±0.042
Buffered, effervescent aspirin	0.213 ±0.021	0.277 ±0.042	0.270 ±0.014	0.215 ±0.006	0.185 ±0.046	0.103 ±0.036	0.056 ±0.002

[a] Aspirin equivalent. [b] Mean ± *SE* (n = 3).

Table IV—Levels of Total Salicylates in Plasma following the Oral Administration of Aspirin

Dose, mg/kg[a], and Product	Plasma Total Salicylate Concentration, mg/ml[b]						
	0.5 hr	1.0 hr	2.0 hr	4.0 hr	8.0 hr	16.0 hr	24.0 hr
100							
Aspirin suspension	0.261 ±0.022	0.242 ±0.031	0.282 ±0.006	0.264 ±0.003	0.159 ±0.006	0.054 ±0.021	0.006 ±0.002
Buffered, effervescent aspirin	0.268 ±0.009	0.258 ±0.013	0.219 ±0.005	0.189 ±0.015	0.129 ±0.009	0.005 ±0.002	0.000 ±0.000
250							
Aspirin suspension	0.325 ±0.055	0.475 ±0.053	0.476 ±0.013	0.422 ±0.015	0.284 ±0.065	0.170 ±0.022	0.068 ±0.009
Buffered, effervescent aspirin	0.373 ±0.019	0.410 ±0.005	0.420 ±0.016	0.342 ±0.006	0.249 ±0.015	0.092 ±0.024	0.009 ±0.001
700							
Aspirin suspension	0.489 ±0.017	0.820 ±0.146	1.008 ±0.037	0.726 ±0.041	0.622 ±0.043	0.615 ±0.091	0.411 ±0.075
Buffered, effervescent aspirin	0.496 ±0.028	0.763 ±0.106	0.732 ±0.084	0.548 ±0.012	0.443 ±0.040	0.113 ±0.075	0.208 ±0.042

[a] Aspirin equivalent. [b] Mean ± *SE* (n = 3).

by a single aspirin dose of 500 mg/kg, *i.e.*, the dose reported to produce renal papillary necrosis in rats (1).

While it is generally difficult to extrapolate the results of acute experiments into a prediction of what might occur on a chronic basis, there is some justification for doing so in this instance. It was reported (1) that chronic coadministration of 500 mg/kg of aspirin and 50 mg/kg of sodium bicarbonate reduces the incidence of analgesic nephropathy by about one-half. The buffered, effervescent formulation, containing about 2.94 g/kg of sodium bicarbonate at a 500-mg/kg aspirin-equivalent dose, would have a more profound effect on urine pH and concomitantly should enhance the urinary excretion of salicylate. This condition should result in lower levels of salicylate in tissues and should, thereby, reduce or eliminate the potential for tissue toxicity.

Table V—Estimated Average Whole Blood and Plasma Total Salicylate Concentrations

Tissue	Dose, mg/kg[a]	Average Total Salicylate Concentration, mg/100 ml	
		Aspirin Suspension	Buffered, Effervescent Aspirin
Whole blood	100	4.7	3.0
	250	13.4	9.0
	500	29.3	13.2[b]
	700	29.0	15.1
Plasma	100	12.2	8.5
	250	24.7	18.4
	500	45.1	25.8[b]
	700	43.0	32.9

[a] Aspirin equivalent. [b] Calculated from values obtained by interpolation.

The results of the blood studies, which showed higher levels of total salicylates after various single doses of the aspirin suspension, substantiate the findings in kidney homogenates. The observation that salicylate concentrations are higher in plasma than in whole blood may be accounted for by the fact that salicylate is bound to plasma protein (7).

REFERENCES

(1) R. Nanra and P. Kincaid-Smith, *Brit. Med. J.*, **3**, 559 (1970).

(2) P. K. Smith, H. L. Gleason, C. G. Stoll, and S. Ogorzalek, *J. Pharmacol. Exp. Ther.*, **87**, 237(1946).

(3) M. Bjornboe and S. Dalgaard-Mikkelsen, *Scand. J. Clin. Invest.*, **1**, 287(1949).

(4) L. F. Prescott, *Lancet*, **2**, 1939(1969).

(5) G. Cronheim and C. F. Bullock, *J. Amer. Pharm. Ass., Pract. Pharm. Ed.*, **8**, 263(1947).

(6) E. Eagle and A. J. Carlson, *J. Pharmacol. Exp. Ther.*, **99**, 450(1950).

(7) J. A. Sturman and M. J. H. Smith, *J. Pharm. Pharmacol.*, **19**, 621(1967).

ACKNOWLEDGMENTS AND ADDRESSES

Received September 21, 1973, from the *Toxicology Department, Miles Research Division, Miles Laboratories, Inc., Elkhart, IN 46514*

Accepted for publication May 28, 1975.

The authors are grateful to Ms. Linda Went for technical assistance and to Dr. George A. Foster, Jr., for assistance in preparation of this manuscript.

[x] To whom inquiries should be directed.

Measurement of Sulfamethizole Clearance Rate by Nonthrombogenic Constant Blood-Withdrawal System

C. R. KOWARSKI [*x], C. GIANCATARINO [*], R. KREAMER [*], D. BRECHT [*], and A. KOWARSKI [‡]

Abstract □ A method for the measurement of the total body clearance rate (*CR*) of drugs is described. It involves a single intravenous injection of a known quantity of the drug (*D*) and automatic integration of the plasma concentration curve, using a portable, nonthrombogenic, constant blood-withdrawal system. When blood withdrawal is carried out until the concentration of the drug in the plasma approaches zero, the concentration of the drug in the collected pool, the integrated concentration (IC_T) multiplied by the time of collection (*T*) yields the integral of the concentration curve: $\int_0^\infty X'\,dt = IC_T \times T$ and $CR = (D/\int_0^\infty X'\,dt)$. The method was tested by measuring the clearance rate of sulfamethizole in five dogs by the established constant infusion method. At three plasma levels (25, 75, and 200 mg/liter), the plasma concentration had no significant effect on the clearance rate. The clearance rate of sulfamethizole was subsequently measured in the same dogs by the new single-injection constant withdrawal method. Multiple blood samples were collected at 15-min intervals simultaneously with the constant withdrawal of blood. There was no significant difference between the clearance rate of sulfamethizole measured by the two methods. The initial peak mean concentration of the drug from the time of injection ($t = 0$) to the time of the first blood sampling ($t = 15$ min) was calculated from the difference between $\int_0^\infty X'\,dt$ obtained by the constant withdrawal method and that obtained from the results of the multiple blood withdrawals by the trapezoidal rule. The integrated concentration IC_{15} was significantly higher than its estimation by the semilogarithmic linear regression method.

Keyphrases □ Sulfamethizole—measurement of total body clearance rate, nonthrombogenic constant blood-withdrawal system, dogs □ Clearance rate, total body—sulfamethizole, measured using nonthrombogenic constant blood-withdrawal system, dogs □ Blood-withdrawal system—nonthrombogenic, use in measurement of total body clearance rate of sulfamethizole, dogs

The total body clearance rate of drugs (*CR*) is defined as the volume of blood containing the amount of the drug under study that is irreversibly removed in a unit of time. Two established methods for measuring the clearance rate are currently in use (1–5): (*a*) a steady-state constant infusion method, in which the clearance rate is derived from the infusion rate at a situation where both reach equilibrium; and (*b*) a single-pulse injection method, in which the value $\int_0^\infty X'\,dt$ of the disappearance curve is calculated from multiple determinations of X'.

A new method for the measurement of $\int_0^\infty X'\,dt$ is proposed. The new method became possible by the development of a nonthrombogenic, constant blood-withdrawal system (6). A single determination of the integrated concentration of the drug in the pool obtained by constant withdrawal yields the $\int_0^\infty X'\,dt$. This method is not dependent on an assumed knowledge of the equation of the disappearance curve. The purposes of this work were to demonstrate the use of this new method and to test its accuracy in comparison with the established method.

EXPERIMENTAL

Apparatus—A constant infusion pump[1] was used for the constant infusion method. Nonthrombogenic, presterilized, disposable Kowarski sets and withdrawal pump[2] were used for the withdrawal method.

The method of Bratton and Marshall (7) was used to assay sulfamethizole[3] spectrophotometrically[4] in plasma and in saline solutions.

Clearance Rate Measurement by Constant Infusion Method—An intravenous catheter was placed in a jugular vein and another in a hindleg cephalic vein. The jugular catheter was then connected to a 100-ml syringe containing a sterile solution of sulfamethizole in saline. Three experiments were carried out on each dog. In each experiment, the concentration of sulfamethizole was maintained at 15, 35, or 100 mg/ml.

The syringe was then placed in a constant infusion pump. The pump was set to infuse at a rate of 4 ml/hr and continued without interruption for at least 5.5 hr. While the sulfamethizole solution was infused through the jugular vein, blood samples were drawn every 15 min from the cephalic vein into a heparinized syringe. Each blood sample was centrifuged and the plasma was stored at 4°.

At the end of 5.5 hr of infusion, the syringe was disconnected from the catheter in the jugular vein, without stopping the pump. The pump effluent was delivered into a measuring cylinder for an additional hour, and the rate of delivery was noted. The concentration of sulfamethizole in both the plasma sample and in the infusion solution was measured.

Since there was no detectable fluctuation in the plasma level of sulfamethizole during the final 2 hr of infusion, the mean of these results was considered the concentration at equilibrium (X^c). The infusion rate (*IR*) was calculated from the measured concentration in the infusion solution and the volume actually delivered into the measuring cylinder during the final hour. The total body clearance rate was then calculated:

$$CR = \frac{IR}{X^c} \qquad \text{(Eq. 1)}$$

[1] Model 352, Sage Co., Oriane Research, Cambridge, Mass.
[2] Sigmamotor Inc., Middleport, N.Y.
[3] Ayerst Laboratories, New York, N.Y.
[4] Beckman DU.

ACKNOWLEDGMENTS AND ADDRESSES

Received September 21, 1973, from the *Toxicology Department, Miles Research Division, Miles Laboratories, Inc., Elkhart, IN 46514*

Accepted for publication May 28, 1975.

The authors are grateful to Ms. Linda Went for technical assistance and to Dr. George A. Foster, Jr., for assistance in preparation of this manuscript.

[x] To whom inquiries should be directed.

Measurement of Sulfamethizole Clearance Rate by Nonthrombogenic Constant Blood-Withdrawal System

C. R. KOWARSKI [*x], C. GIANCATARINO [*], R. KREAMER [*], D. BRECHT [*], and A. KOWARSKI [‡]

Abstract □ A method for the measurement of the total body clearance rate (*CR*) of drugs is described. It involves a single intravenous injection of a known quantity of the drug (*D*) and automatic integration of the plasma concentration curve, using a portable, nonthrombogenic, constant blood-withdrawal system. When blood withdrawal is carried out until the concentration of the drug in the plasma approaches zero, the concentration of the drug in the collected pool, the integrated concentration (IC_T) multiplied by the time of collection (*T*) yields the integral of the concentration curve: $\int_0^\infty X'\,dt = IC_T \times T$ and $CR = (D/\int_0^\infty X'\,dt)$. The method was tested by measuring the clearance rate of sulfamethizole in five dogs by the established constant infusion method. At three plasma levels (25, 75, and 200 mg/liter), the plasma concentration had no significant effect on the clearance rate. The clearance rate of sulfamethizole was subsequently measured in the same dogs by the new single-injection constant withdrawal method. Multiple blood samples were collected at 15-min intervals simultaneously with the constant withdrawal of blood. There was no significant difference between the clearance rate of sulfamethizole measured by the two methods. The initial peak mean concentration of the drug from the time of injection ($t = 0$) to the time of the first blood sampling ($t = 15$ min) was calculated from the difference between $\int_0^\infty X'\,dt$ obtained by the constant withdrawal method and that obtained from the results of the multiple blood withdrawals by the trapezoidal rule. The integrated concentration IC_{15} was significantly higher than its estimation by the semilogarithmic linear regression method.

Keyphrases □ Sulfamethizole—measurement of total body clearance rate, nonthrombogenic constant blood-withdrawal system, dogs □ Clearance rate, total body—sulfamethizole, measured using nonthrombogenic constant blood-withdrawal system, dogs □ Blood-withdrawal system—nonthrombogenic, use in measurement of total body clearance rate of sulfamethizole, dogs

The total body clearance rate of drugs (*CR*) is defined as the volume of blood containing the amount of the drug under study that is irreversibly removed in a unit of time. Two established methods for measuring the clearance rate are currently in use (1–5): (*a*) a steady-state constant infusion method, in which the clearance rate is derived from the infusion rate at a situation where both reach equilibrium; and (*b*) a single-pulse injection method, in which the value $\int_0^\infty X'\,dt$ of the disappearance curve is calculated from multiple determinations of X'.

A new method for the measurement of $\int_0^\infty X'\,dt$ is proposed. The new method became possible by the development of a nonthrombogenic, constant blood-withdrawal system (6). A single determination of the integrated concentration of the drug in the pool obtained by constant withdrawal yields the $\int_0^\infty X'\,dt$. This method is not dependent on an assumed knowledge of the equation of the disappearance curve. The purposes of this work were to demonstrate the use of this new method and to test its accuracy in comparison with the established method.

EXPERIMENTAL

Apparatus—A constant infusion pump[1] was used for the constant infusion method. Nonthrombogenic, presterilized, disposable Kowarski sets and withdrawal pump[2] were used for the withdrawal method.

The method of Bratton and Marshall (7) was used to assay sulfamethizole[3] spectrophotometrically[4] in plasma and in saline solutions.

Clearance Rate Measurement by Constant Infusion Method—An intravenous catheter was placed in a jugular vein and another in a hindleg cephalic vein. The jugular catheter was then connected to a 100-ml syringe containing a sterile solution of sulfamethizole in saline. Three experiments were carried out on each dog. In each experiment, the concentration of sulfamethizole was maintained at 15, 35, or 100 mg/ml.

The syringe was then placed in a constant infusion pump. The pump was set to infuse at a rate of 4 ml/hr and continued without interruption for at least 5.5 hr. While the sulfamethizole solution was infused through the jugular vein, blood samples were drawn every 15 min from the cephalic vein into a heparinized syringe. Each blood sample was centrifuged and the plasma was stored at 4°.

At the end of 5.5 hr of infusion, the syringe was disconnected from the catheter in the jugular vein, without stopping the pump. The pump effluent was delivered into a measuring cylinder for an additional hour, and the rate of delivery was noted. The concentration of sulfamethizole in both the plasma sample and in the infusion solution was measured.

Since there was no detectable fluctuation in the plasma level of sulfamethizole during the final 2 hr of infusion, the mean of these results was considered the concentration at equilibrium (X^c). The infusion rate (*IR*) was calculated from the measured concentration in the infusion solution and the volume actually delivered into the measuring cylinder during the final hour. The total body clearance rate was then calculated:

$$CR = \frac{IR}{X^c} \qquad \text{(Eq. 1)}$$

[1] Model 352, Sage Co., Oriane Research, Cambridge, Mass.
[2] Sigmamotor Inc., Middleport, N.Y.
[3] Ayerst Laboratories, New York, N.Y.
[4] Beckman DU.

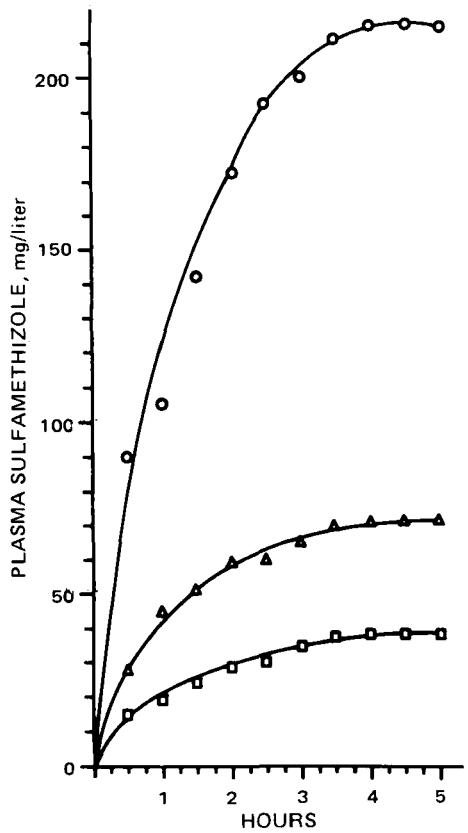

Figure 1—*Plasma concentrations of sulfamethizole in Dog 3 during 5 hr of constant intravenous infusion at 68 (□), 141 (△), and 385 (○) mg/hr.*

The experiment on each dog was repeated at three different infusion rates to demonstrate that the clearance rate of sulfamethizole remained constant over a wide range of blood concentrations.

Clearance Rate Measurement by New Constant Withdrawal Method—The same five dogs used in the constant infusion method were restudied. Five milliliters of a 40-mg/ml sterile solution of sulfamethizole was injected as a single pulse through an intravenous catheter. The catheter was left in place and flushed by a slow drip of saline. A constant withdrawal of blood from a vein in another limb was initiated at the moment of the pulse injection, using a nonthrombogenic, presterilized, disposable Kowarski set and withdrawal pump. The use and function of this system were described previously (6). The rate of withdrawal was set at 6 ml/hr and was continued for 5 hr.

In addition to the constant withdrawal, 2-ml blood samples were withdrawn from another vein every 15 min. The concentration of sulfamethizole in the plasma samples obtained every 15 min, as well as in the plasma from the pool of blood collected by constant withdrawal, was measured (6). The concentration of sulfamethizole in the constant withdrawal pool was the integrated concentration (IC_{5hr}).

Calculations—The integral of the concentration curve was calculated as follows: $\int_0^\infty X'\,dt = IC_{5hr} \times 5$; the clearance rate was calculated from this integral and the amount of injected sulfamethizole (D) using:

$$CR = \frac{D}{\int_0^\infty X'\,dt} \qquad \text{(Eq. 2)}$$

The integral of the concentration curve from the time the first blood sample was taken (t = 15 min) was calculated from the results of the multiple blood withdrawals by the trapezoidal rule:

$$\int_0^\infty X'\,dt = 7.5\,(X_{15} + 2X_{30} + 2X_{45} + \cdots + 2X_{285} + X_{300}) \qquad \text{(Eq. 3)}$$

Table I—Sulfamethizole Clearance Rate at Various Plasma Levels

Dog	Infusion Rate, mg/hr	Plasma Concentration at Equilibrium, mg/liter	Clearance Rate, liters/hr
1	56.8	28.2	2.0
	137.6	64.8	2.1
	420.0	196.0	2.1
2	70.0	25.6	2.8
	143.0	49.3	2.9
	415.0	143.0	2.9
3	68.0	36.2	1.9
	140.8	72.8	1.9
	385.0	214.0	1.8
4	65.6	45.0	1.5
	138.0	92.0	1.5
	375.0	251.0	1.5
5	60.8	31.5	1.9
	163.0	76.0	2.1
	343.0	156.0	2.2

The initial peak, IC_{15}, was then calculated using:

$$IC_{15} = \frac{\left(\int_0^\infty X'\,dt\right) - \left(\int_{15}^\infty X'\,dt\right)}{15} \qquad \text{(Eq. 4)}$$

The result was compared to an estimated peak concentration of sulfamethizole obtained by the extrapolation to t = 0 of the semilogarithmic linear regression of $X_{15}\cdots C_{300}$.

RESULTS AND DISCUSSION

In the present study, the clearance rate of sulfamethizole was first measured by the constant infusion method. The study was repeated three times on each dog. A different infusion rate was used each time, leading to a different level at which the equilibrium concentration was reached.

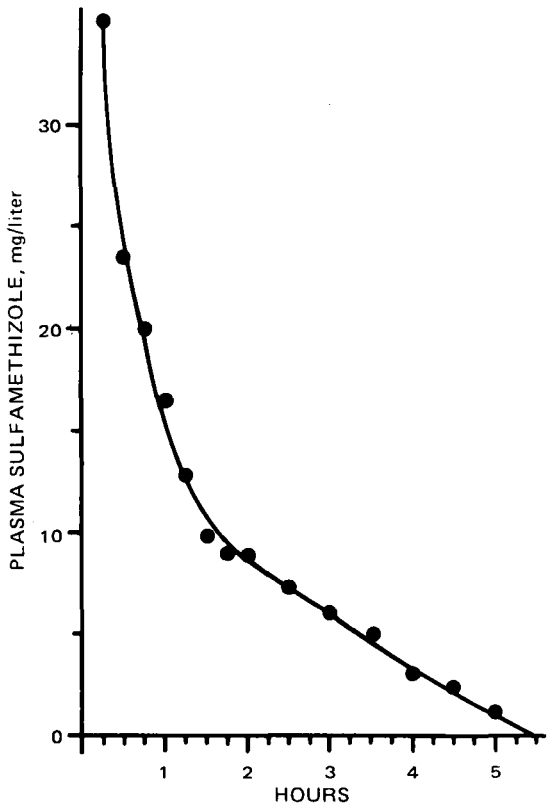

Figure 2—*Disappearance curve of plasma sulfamethizole in a dog after a single intravenous injection.*

Table II—Sulfamethizole Clearance Rate (liters/24 hr)

Dog	Constant Infusion Method	Constant Withdrawal Method
1	2.0	2.1
2	2.9	2.9
3	1.9	1.8
4	1.5	1.5
5	2.1	2.5

The plasma concentrations of sulfamethizole that were registered during these three tests in one dog are shown in Fig. 1. Although the plateau level of sulfamethizole was different in each experiment, the calculated clearance rates were essentially equal. The results in all of the dogs are given in Table I. As can be seen, the clearance rate remained unaffected by changes in the sulfamethizole concentration.

After the clearance rate of sulfamethizole was measured by the constant infusion method, each dog was restudied by the single intravenous injection method. After a pulse injection of sulfamethizole, the level of sulfamethizole in the blood was followed by multiple blood withdrawals from one limb and a continuous constant withdrawal from another limb. A representation of the disappearance curve for one dog is given in Fig. 2.

The results obtained by the two methods are given in Table II. There was no significant difference between the clearance rates obtained ($p < 0.001$ by the paired t test).

The initial peak concentration of the drug, which occurs a short time after the pulse intravenous injection, has a major effect on the final integral, but there is no way to predict the initial integral from the instant of injection to the first blood sampling. This problem is solved by the continuous constant withdrawal, since $\Delta t \rightarrow 0$ in this method. The integral of the concentration curve from the first moment of sampling (t = 15 min) was calculated by the trapezoidal rule. The difference between the two integrals allows the calculation of the initial integral ($\int_0^{15} X' dt$) and the initial IC_{15}.

In the five described experiments, IC_{15} was always higher than the extrapolated concentration at $t = 0$ calculated by the semilogarithmic linear regression (Table III). The accuracy of the constant blood-withdrawal method was demonstrated by the similarity between the clearance rate obtained by the two methods.

Table III—Calculated Initial Concentration of Sulfamethizole

Dog	Extrapolation to $t = 0$, mg/liter	IC_{15}, mg/liter
1	37.8	278.6
2	31.2	161.9
3	56.7	250
4	60.3	365.1
5	37.0	232.6

REFERENCES

(1) J. F. Tait and S. Burstein, in "The Hormones," vol. 5, G. Pincus, K. V. Thimann, and E. B. Astwood, Eds., Academic, New York, N.Y., 1964, pp. 41, 550.

(2) J. F. Tait, *J. Clin. Endocrinol. Metab.*, **23**, 1285(1963).

(3) J. C. K. Loo and S. Riegelman, *J. Pharm. Sci.*, **57**, 918(1968).

(4) M. Rowland, S. Riegelman, and W. L. Epstein, *ibid.*, **57**, 984(1968).

(5) S. Riegelman and W. Sadee, in "Clinical Pharmacokinetics," G. Levy, Ed., American Pharmaceutical Association, Washington, D.C., 1974, p. 169.

(6) A. Kowarski, R. G. Thompson, C. J. Migeon, and R. M. Blizzard, *J. Clin. Endocrinol. Metab.*, **32**, 356(1971).

(7) A. C. Bratton and E. K. Marshall, *J. Biol. Chem.*, **128**, 537(1939).

ACKNOWLEDGMENTS AND ADDRESSES

Received October 16, 1974, from the *Department of Pharmacy, School of Pharmacy, Temple University, Philadelphia, PA 19140, and the ‡Department of Pediatrics, School of Medicine, Johns Hopkins University, Baltimore, Md.

Accepted for publication June 3, 1975.

Presented at the American Pharmaceutical Association, Chicago meeting, 1974.

Supported by National Institutes of Health Grant R01-HD-06284 and Grant in Aid of Temple University 750-020-40; 405-063-68.

* To whom inquiries should be directed.

Volume of Distribution as a Function of Time

SARFARAZ NIAZI

Abstract □ A single definition for all volume terms in pharmacokinetic modeling is proposed; this parameter is considered as a function of time. This definition will represent the kinetic nature of pharmacokinetic models and will provide a highly sensitive parameter for correlation with pharmacological responses.

Keyphrases □ Volume—terms in pharmacokinetic modeling, single definition proposed as a function of time □ Pharmacokinetic modeling—single definition for all volume terms proposed as a function of time □ Distribution volume—volume terms in pharmacokinetic modeling, single definition proposed as a function of time

In the pharmacokinetic modeling of the absorption, distribution, metabolism, and excretion of drugs, various volume terms have been defined, such as the volumes of central (V_c) and tissue (V_T) compartments, the steady-state volume of distribution ($V_{d_{ss}}$), and the volume of distribution following pseudo-distribution equilibrium (V_{d_β} or $V_{d_{area}}$) (1–9).

The purpose of this paper is to propose a single definition for volume terms that can be used regardless of the complexity of the pharmacokinetic model. If this term is considered as a variable rather than a constant, this parameter will be more meaningful and add a new dimension to the characterization of drug response through pharmacokinetic studies.

THEORETICAL

When a drug is introduced in the body such as by intravenous injection, it starts to eliminate and to distribute to other parts of the body instantaneously (Scheme I). The measured concentra-

Table II—Sulfamethizole Clearance Rate (liters/24 hr)

Dog	Constant Infusion Method	Constant Withdrawal Method
1	2.0	2.1
2	2.9	2.9
3	1.9	1.8
4	1.5	1.5
5	2.1	2.5

The plasma concentrations of sulfamethizole that were registered during these three tests in one dog are shown in Fig. 1. Although the plateau level of sulfamethizole was different in each experiment, the calculated clearance rates were essentially equal. The results in all of the dogs are given in Table I. As can be seen, the clearance rate remained unaffected by changes in the sulfamethizole concentration.

After the clearance rate of sulfamethizole was measured by the constant infusion method, each dog was restudied by the single intravenous injection method. After a pulse injection of sulfamethizole, the level of sulfamethizole in the blood was followed by multiple blood withdrawals from one limb and a continuous constant withdrawal from another limb. A representation of the disappearance curve for one dog is given in Fig. 2.

The results obtained by the two methods are given in Table II. There was no significant difference between the clearance rates obtained ($p < 0.001$ by the paired t test).

The initial peak concentration of the drug, which occurs a short time after the pulse intravenous injection, has a major effect on the final integral, but there is no way to predict the initial integral from the instant of injection to the first blood sampling. This problem is solved by the continuous constant withdrawal, since $\Delta t \rightarrow 0$ in this method. The integral of the concentration curve from the first moment of sampling (t = 15 min) was calculated by the trapezoidal rule. The difference between the two integrals allows the calculation of the initial integral ($\int_0^{15} X' dt$) and the initial IC_{15}.

In the five described experiments, IC_{15} was always higher than the extrapolated concentration at $t = 0$ calculated by the semilogarithmic linear regression (Table III). The accuracy of the constant blood-withdrawal method was demonstrated by the similarity between the clearance rate obtained by the two methods.

Table III—Calculated Initial Concentration of Sulfamethizole

Dog	Extrapolation to $t = 0$, mg/liter	IC_{15}, mg/liter
1	37.8	278.6
2	31.2	161.9
3	56.7	250
4	60.3	365.1
5	37.0	232.6

REFERENCES

(1) J. F. Tait and S. Burstein, in "The Hormones," vol. 5, G. Pincus, K. V. Thimann, and E. B. Astwood, Eds., Academic, New York, N.Y., 1964, pp. 41, 550.

(2) J. F. Tait, *J. Clin. Endocrinol. Metab.*, **23**, 1285(1963).

(3) J. C. K. Loo and S. Riegelman, *J. Pharm. Sci.*, **57**, 918(1968).

(4) M. Rowland, S. Riegelman, and W. L. Epstein, *ibid.*, **57**, 984(1968).

(5) S. Riegelman and W. Sadee, in "Clinical Pharmacokinetics," G. Levy, Ed., American Pharmaceutical Association, Washington, D.C., 1974, p. 169.

(6) A. Kowarski, R. G. Thompson, C. J. Migeon, and R. M. Blizzard, *J. Clin. Endocrinol. Metab.*, **32**, 356(1971).

(7) A. C. Bratton and E. K. Marshall, *J. Biol. Chem.*, **128**, 537(1939).

ACKNOWLEDGMENTS AND ADDRESSES

Received October 16, 1974, from the *Department of Pharmacy, School of Pharmacy, Temple University, Philadelphia, PA 19140, and the ‡Department of Pediatrics, School of Medicine, Johns Hopkins University, Baltimore, Md.

Accepted for publication June 3, 1975.

Presented at the American Pharmaceutical Association, Chicago meeting, 1974.

Supported by National Institutes of Health Grant R01-HD-06284 and Grant in Aid of Temple University 750-020-40; 405-063-68.

* To whom inquiries should be directed.

Volume of Distribution as a Function of Time

SARFARAZ NIAZI

Abstract □ A single definition for all volume terms in pharmacokinetic modeling is proposed; this parameter is considered as a function of time. This definition will represent the kinetic nature of pharmacokinetic models and will provide a highly sensitive parameter for correlation with pharmacological responses.

Keyphrases □ Volume—terms in pharmacokinetic modeling, single definition proposed as a function of time □ Pharmacokinetic modeling—single definition for all volume terms proposed as a function of time □ Distribution volume—volume terms in pharmacokinetic modeling, single definition proposed as a function of time

In the pharmacokinetic modeling of the absorption, distribution, metabolism, and excretion of drugs, various volume terms have been defined, such as the volumes of central (V_c) and tissue (V_T) compartments, the steady-state volume of distribution ($V_{d_{ss}}$), and the volume of distribution following pseudo-distribution equilibrium (V_{d_β} or $V_{d_{area}}$) (1–9).

The purpose of this paper is to propose a single definition for volume terms that can be used regardless of the complexity of the pharmacokinetic model. If this term is considered as a variable rather than a constant, this parameter will be more meaningful and add a new dimension to the characterization of drug response through pharmacokinetic studies.

THEORETICAL

When a drug is introduced in the body such as by intravenous injection, it starts to eliminate and to distribute to other parts of the body instantaneously (Scheme I). The measured concentra-

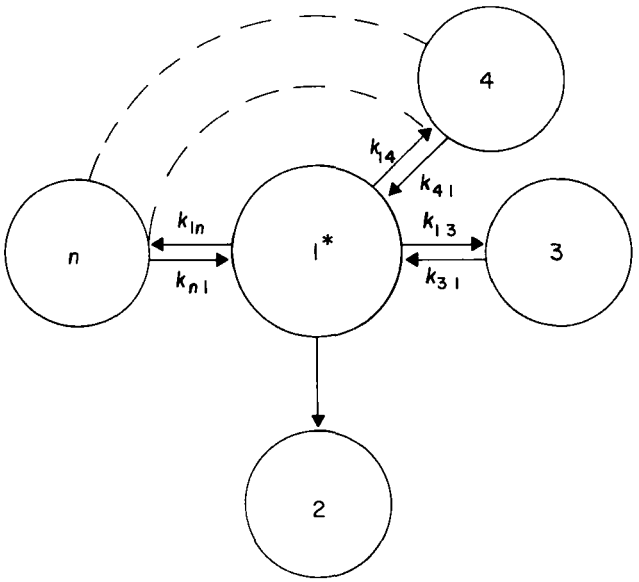

Scheme I—Mammalian system with n *compartments. The* (*) = *central, sampled compartment.*

tion, C_1, can be expressed as:

$$C_1 = \sum_{i=1}^{n} A_i e^{-a_i t} \qquad \text{(Eq. 1)}$$

where A_i is the intercept on the C_1 *versus* time plot, and a_i is the hybrid rate constant.

The total area under the C_1 *versus* time plot (AUC_∞) is proportional to the dose made available to the body (D_A) regardless of the route of administration (6):

$$D_A \alpha AUC_\infty = \int_0^\infty \sum_{i=1}^{n} A_i e^{-a_i t} = \sum_{i=1}^{n} \frac{A_i}{a_i} \qquad \text{(Eq. 2)}$$

In a multicompartment model where the drug is eliminated only from the central compartment, the amount of drug remaining in the body (D_B) as a function of time can be expressed in terms of fractional area (10):

$$D_B = \frac{D_A \int_t^\infty \sum_{i=1}^{n} A_i e^{-a_i t}}{\sum_{i=1}^{n} \frac{A_i}{a_i}} = \frac{D_A \sum_{i=1}^{n} \frac{A_i e^{-a_i t}}{a_i}}{\sum_{i=1}^{n} \frac{A_i}{a_i}} \qquad \text{(Eq. 3)}$$

The term volume of distribution is expressed as the ratio of the amount of drug in body and the measured concentration:

$$V_d = \frac{D_B}{C_1} = \frac{D_A \sum_{i=1}^{n} \frac{A_i e^{-a_i t}}{a_i}}{\sum_{i=1}^{n} \frac{A_i}{a_i} \sum_{i=1}^{n} A_i e^{-a_i t}} \qquad \text{(Eq. 4)}$$

This equation can be used for all compartmental models, linear or nonlinear, and provides one definition of volume of distribution as a function of time. At time $t = 0$, the volume of distribution becomes:

$$V_{d_0} = \frac{D_A}{\sum_{i=1}^{n} A_i} \qquad \text{(Eq. 5)}$$

This is analogous to the volume of the central compartment. Similarly, as time exceeds some value, t^* (*i.e.*, attainment of pseudo-distribution equilibrium):

$$\sum_{i=1}^{n} A_i e^{-a_i t^*} \simeq A_n e^{-a_n t^*} \qquad \text{(Eq. 6)}$$

the volume of distribution becomes constant and is referred to as the volume of distribution following pseudo-distribution equilibrium:

$$V_{d_{eq}} = \frac{D_A}{a_n \sum_{i=1}^{n} \frac{A_i}{a_i}} \qquad \text{(Eq. 7)}$$

This equation is the same as was described by Perrier and Gibaldi (9) except for the term D_A, which is the available dose compared to the intravenously administered dose. In some instances, these two may not be the same. For example, compounds mainly eliminated through the lungs undergo a first-pass effect if the compound is administered intravenously (11, 12).

The rate at which the volume of distribution V_{d_0} approaches $V_{d_{eq}}$ represents the distribution nature of the drug. Differentiation of Eq. 4 leads to:

$$\frac{dV_d}{dt} \simeq \frac{D_A \left[\sum_{i=1}^{n} \frac{A_i e^{-a_i t}}{a_i} \sum_{i=1}^{n} a_i A_i e^{-a_i t} - \left(\sum_{i=1}^{n} A_i e^{-a_i t} \right)^2 \right]}{\left[\left(\sum_{i=1}^{n} A_i e^{-a_i t} \right)^2 \sum_{i=1}^{n} \frac{A_i}{a_i} \right]} \qquad \text{(Eq. 8)}$$

An important parameter can be the rate of volume of distribution change at $t = 0$, RV_{d_0}, and from Eq. 8:

$$RV_{d_0} = \frac{dV_d}{dt} \text{ (at } t = 0) = \frac{D_A \sum_{i=1}^{n} a_i A_i}{\left(\sum_{i=1}^{n} A_i \right)^2} - \frac{D_A}{\sum_{i=1}^{n} \frac{A_i}{a_i}} \qquad \text{(Eq. 9)}$$

This parameter will most characteristically describe the distributional behavior of drugs in the body since it is not only the function of $V_{d_{eq}}$ but also of the rate at which it is achieved. It will be shown later that this is a highly sensitive index to intersubject and intrasubject variations in the distributional properties of a drug and an important parameter for correlation between the drug responses based on the rate at which the site of action is saturated.

DISCUSSION

The pharmacokinetic parameter of volume has several connotations (7) and is generally used to describe an actual size of the body region (8), such as the volume of body fluid dissolving the substance at the same concentration as the plasma (13), or the volume of a particular compartment assuming that all of the substance or drug concentration within the compartment is actually distributed at a uniform concentration equal to the concentration measured in a particular reference region (2). The confusion in defining and expressing the volume terms often has resulted due to the misrepresentation of the essential characteristics of compartmental modeling.

First, the compartment model for the disposition of a drug is a kinetic representation characterizing the absorption, distribution, and elimination properties. Consequently, these interpretations should be limited to the rate processes expressed as compartments, which may have little physical meaning as discrete units. Therefore, it is not justified to categorize a group of tissues as representing a compartment (6). For example, a drug acting on the myocardium often is erroneously classified as having its site of action in the central compartment whereas it may actually be a part of another compartment, depending on the rate at which it undergoes equilibration.

Second, the equilibration between the site of administration and other parts of the body is a function of the thermodynamic activity

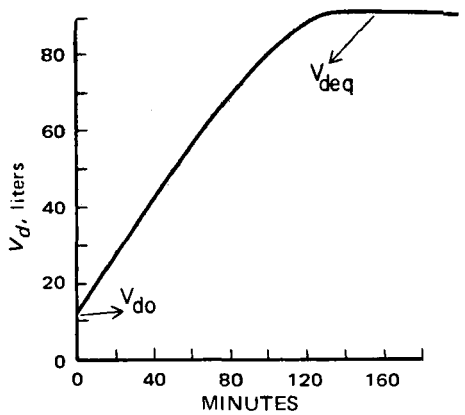

Figure 1—*Volume of distribution of trichloromonofluoromethane as a function of time following intravenous administration in a dog.*

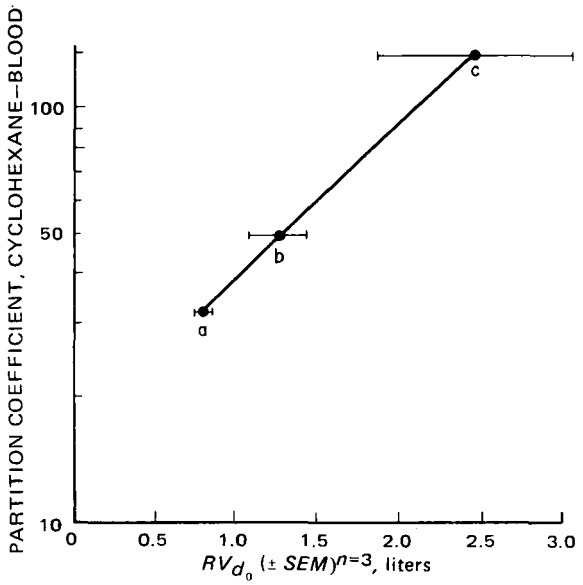

Figure 2—*Initial rate of volume of distribution change as a function of partition coefficient. Key: a, trichloromonofluoromethane; b, dichlorodifluoromethane; and c, dichlorotetrafluoroethane.*

of the drug. Therefore, such terms as volume and concentration of tissue compartments have little meaning. Briefly, the kinetics of absorption, distribution, and elimination of drugs should be viewed as continuous rate processes represented by compartments that undergo equilibration to yield uniform thermodynamic activity in the body.

In terms of continuous rate processes, when a drug is introduced in an easily accessible fluid or tissue of the body, the processes of distribution and elimination begin simultaneously, resulting in a nonproportional relationship between the amount of drug in the body and the concentration measured in any specific part of the body. This proportionality can be expressed by the term volume which, as a function of time, should characterize the distributional nature of the drug in the body.

This new perspective in the definition of the volume of distribution will make this parameter more useful in the characterization of drug response and drug properties in general. For example, drugs having low solubility in the blood should be expected to show a greater RV_{d_0}, rate of volume change at $t = 0$, compared to highly soluble compounds simply because of their higher chemical potential if the nonprotein bound or, more appropriately, the activity is measured in the blood. A higher value of RV_{d_0} may be expected if the drug molecules have higher affinity for the tissues with which they are equilibrating. Since RV_{d_0} is also proportional to $V_{d_{eq}}$, it not only represents the affinity for distribution but also the capacity.

It has been suggested that the biological activity of many drugs depends on the rate at which they interact with the receptor site (14), and this can be characterized easily by comparing RV_{d_0} for a series of drugs and their potency. Therefore, this term can be employed in the characterization of the drug–receptor interaction.

The concept of the volume of distribution as a function of time is depicted in Fig. 1, which illustrates the data for trichloromonofluoromethane calculated from pharmacokinetic parameters reported recently (11, 12). A further evaluation of these data shows that the term RV_{d_0} for three fluorocarbon aerosol propellants can be correlated to several *in vitro* properties (11, 12).

For example, Fig. 2 shows the relationship between RV_{d_0} and the partition coefficient between cyclohexane and blood. A log–linear relationship shows that dichlorotetrafluoroethane equilibrates much faster with tissues that are lipoidal in nature since cyclohexane often has been shown to mimic the fatty tissue properties (15).

However, this comparison of RV_{d_0} and partition coefficients is made based on whole blood concentration measurements, and this relationship might change if due consideration is given to thermodynamic activity in the blood rather than concentration.

The term RV_{d_0} thus provides more information than can be obtained from the consideration of the volume of distribution itself. For example, if the following blood concentration profiles are obtained for a drug in two subjects:

$$C_1 = 80e^{-0.0693t} + 20e^{-0.01386t} \text{ (Subject 1)} \qquad \text{(Eq. 10)}$$

$$C_1 = 85e^{-0.0561t} + 15e^{-0.01386t} \text{ (Subject 2)} \qquad \text{(Eq. 11)}$$

they give identical values for the volume of distribution at equilibrium (13.88 liters), the volume of distribution at $t = 0$ (5 liters), the terminal disposition half-life (50 min), and AUC_∞ (2597.40 μg min/ml). However, the RV_{d_0} values differ by 75% (Subject 1 = 98.56 ml/min; Subject 2 = 56.32 ml/min). Such a difference may be important for drugs whose action depends on the rate of equilibration. Thus, the RV_{d_0} can be better correlated with various pharmacological, physiological, and toxicological parameters.

REFERENCES

(1) R. Nagashima, G. Levy, and R. A. O'Reilly, *J. Pharm. Sci.*, **57**, 1888(1968).

(2) D. S. Riggs, "The Mathematical Approach to Physiological Problems," M.I.T. Press, Cambridge, Mass., 1970, pp. 193–217.

(3) J. G. Wagner and J. I. Northam, *J. Pharm. Sci.*, **56**, 529(1967).

(4) J. G. Wagner, E. Novak, L. G. Leslie, and C. M. Metzler, *Int. J. Clin. Pharmacol.*, **1**, 261(1968).

(5) S. Riegelman, J. Loo, and M. Rowland, *J. Pharm. Sci.*, **57**, 128(1968).

(6) M. Gibaldi, R. Nagashima, and G. Levy, *ibid.*, **58**, 193(1969).

(7) L. Z. Benet and R. A. Ronfeld, *ibid.*, **58**, 639(1969).

(8) R. Dominguez, *Proc. Soc. Exp. Biol. Med.*, **3**, 1146(1934).

(9) D. Perrier and M. Gibaldi, *J. Pharmacokinet. Biopharm.*, **1**, 17(1973).

(10) W. L. Chiou, *J. Pharm. Pharmacol.*, **34**, 342(1972).

(11) S. Niazi and W. L. Chiou, *J. Pharm. Sci.*, **64**, 1538(1975).

(12) S. Niazi, Ph. D. dissertation, University of Illinois, Chicago, Ill., 1974.

(13) S. A. Cucinell and W. Perl, *J. Pharm. Sci.*, **59**, 1423(1970).

(14) W. D. M. Patton and D. R. Wand, *Arch. Exp. Pathol. Pharmacol.*, **248**, 124(1964).

(15) T. Higuchi and S. S. Davis, *J. Pharm. Sci.*, **59**, 1376(1970).

ACKNOWLEDGMENTS AND ADDRESSES

Received February 26, 1975, from the *Department of Pharmacy, College of Pharmacy, University of Illinois at the Medical Center, Chicago, IL 60612*

Accepted for publication June 3, 1975.

Bioavailability of Flufenamic Acid in Hard and Soft Gelatin Capsules

L. ANGELUCCI *x, B. PETRANGELI ‡, P. CELLETTI ‡, and S. FAVILLI §

Abstract □ The biological availability of flufenamic acid after oral administration of the drug in both hard and soft gelatin capsules was studied in dogs and humans. The soft gelatin capsules produced consistently higher plasma concentration–time curves.

Keyphrases □ Flufenamic acid—bioavailability, hard and soft gelatin capsules, dogs, humans □ Bioavailability—flufenamic acid, hard and soft gelatin capsules, dogs, humans □ Gelatin capsules—hard and soft, effect on bioavailability of flufenamic acid, dogs, humans □ Anti-inflammatory agents—flufenamic acid, bioavailability in hard and soft gelatin capsules, dogs, humans

Pharmaceutical technology is able to produce a variety of preparations for oral administration to ensure palatable qualities, constancy of dosage, and stability of the active ingredients. However, these preparations may have different degrees of biological availability. It has been demonstrated that depending on the type of capsule—hard (microprecipitated drug) or soft (polysorbate 80, dissolved drug) gelatin—remarkable differences in absorption of a drug may occur (1). These differences, in turn, may be followed by important differences in plasma drug concentrations and, consequently, in therapeutic efficacy. Such factors may play an important role when drugs are administered in one or very few doses, from which amelioration or relief is expected in the shortest time possible, *e.g.*, analgesics, antipyretics, and antiallergics.

This paper reports on a study of plasma concentrations of flufenamic acid, an analgesic–anti-inflammatory agent, after administration to dogs and humans in the form of hard gelatin capsules in comparison with soft gelatin capsules. Some important changes in biological availability were observed.

EXPERIMENTAL

Subjects—*Dogs*—For the study of plasma levels, 10 mongrel dogs, 10–28 kg, were housed in individual kennels and fed on canteen surplus food. Flufenamic acid, 200 mg, in one of the two capsule forms was administered to each animal after fasting for 10 hr.

Table II—Areas (Micrograms per Milliliter times Minutes) under Plasma Concentration–Time Curves of Flufenamic Acid (200 mg) Administered in Hard or Soft Capsule to Dogs

Dog	Hard	Soft	Percent[a]
1	46.62	60.25	29.22
2	99.25	128.50	29.5
3	93.00	118.50	27.4
4	34.00	73.75	116.9
5	92.75	141.75	52.8
6	98.50	133.00	35.0
7	55.00	82.75	50.4
8	96.00	108.00	12.5
9	55.25	64.25	16.3
10	52.50	61.25	16.7
Mean	72.29	97.20	34.5
SE	±8.12	±10.18	
Student's *t* test	5.685 ($p = 0.001$)		
Wilcoxon's signed rank test	T+ = 55.0 ($p = 0.01$) T− = 0		

[a] Soft compared with hard.

This dose was followed using the alternative capsule form 15 days later. The order of drug administration was randomized in the sense that five dogs received one soft capsule each and five were given hard capsules on the same day. Blood samples were drawn at 30, 90, 150, and 210 min after administration.

Humans—Nine healthy male volunteers, 60–78 kg, received flufenamic acid, 200 mg, in the same two capsule forms after fasting for 10 hr. A 15-day interval was allowed between treatments, and the order of drug administration was randomized as in the dog study. Blood samples were drawn at 90, 180, and 360 min after administration.

Treatments—The hard capsule contained 200 mg of flufenamic acid and 20 mg of magnesium stearate. The soft capsule contained 200 mg of flufenamic acid, 100 mg of vegetable oil, 40 mg of hydrogenated vegetable oils, 8 mg of beeswax, and 5 mg of soya lecithin.

Dissolution time of capsules in simulated gastric fluid was studied in accordance with the USP XVIII method (120 rpm, 150 ml, one capsule); the quantity of the drug released in the dissolution medium was determined. The values ($n = 6$) were 65 ± 1.4 (*SEM*) and 60 ± 1.4% at 15 min and 93 ± 1.4 and 98 ± 0.7% at 30 min of the total present in the soft and hard capsules, respectively. The determination of flufenamic acid was carried out spectrophotofluorometrically (2) on plasma from venous blood drawn with a heparinized syringe.

Table I—Flufenamic Acid Plasma Levels (Micrograms per Milliliter) in 10 Dogs at Various Times after the Administration of 200 mg in Hard or Soft Gelatin Capsules

Minutes	Mean ± *SE*		Percent[a]	Student's *t* Test[b]	Wilcoxon's Signed Rank Test[b]
	Hard	Soft			
30	24.05 ± 3.84	30.80 ± 5.03	28.1	2.188 (NS)	T+ = 45.5 (NS) T− = 9.5
90	25.90 ± 3.23	35.70 ± 3.68	37.8	5.580 ($p = 0.001$)	T+ = 55.0 ($p = 0.01$) T− = 0
150	21.75 ± 2.06	28.70 ± 3.89	32.0	2.286 ($p = 0.05$)	T+ = 50.0 ($p = 0.05$) T− = 5.0
210	13.20 ± 1.64	19.40 ± 2.66	47.0	2.577 ($p = 0.05$)	T+ = 51.5 ($p = 0.05$) T− = 3.5

[a] Soft compared with hard. [b] NS = not significant.

Table III—Flufenamic Acid Plasma Levels (Micrograms per Milliliter) in Nine Men at Various Times after the Administration of 200 mg in Hard or Soft Gelatin Capsules

Minutes	Mean ± SE		Percent[a]	Student's t Test[b]	Wilcoxon's Signed Rank Test[b]
	Hard	Soft			
90	6.33 ± 1.08	15.07 ± 0.70	138.1	6.608 ($p = 0.001$)	T+ = 45.0 ($p = 0.01$) T− = 0
180	6.79 ± 0.48	6.60 ± 0.52	−2.8	−0.406 (NS)	T+ = 16.6 (NS) T− = 28.5
360	2.21 ± 0.15	1.42 ± 0.19	−35.8	−3.310 ($p = 0.05$)	T+ = 3.0 ($p = 0.05$) T− = 42.0

[a] Soft compared with hard. [b] NS = not significant.

Mean plasma concentrations at the various time intervals were statistically analyzed for differences depending on the pharmaceutical forms as well as for differences in the mean areas under plasma concentration–time curves, calculated by means of the trapezoidal rule.

Statistical significance was evaluated by the Student parametric *t* test for paired data (3). Wilcoxon's (4) signed rank nonparametric test was also used and is particularly suitable small samples.

RESULTS AND DISCUSSION

In all of the dogs, the soft capsule produced, as compared to the hard type, higher plasma levels of flufenamic acid at each time interval, except for one animal at 30 min and another at 210 min. The average difference was statistically significant for the entire observation period, except at 30 min (Table I), and attained its maximum (47%) at 210 min. The average area described by the plasma concentration–time curve of flufenamic acid was significantly greater following the soft capsule as compared to the hard one (Table II). The average increase was 34% with a range of 12–116%.

In the human subjects, plasma levels of flufenamic acid following soft capsule administration were higher only at 90 min as compared to the hard type (in all subjects), and the average value at this time was more than double (Table III). The crossover comparison between plasma levels following hard and soft capsule administration was also carried out by adjusting concentrations in absolute values (micrograms per milliliter) into relative values (micrograms per milliliter divided by milligrams per kilogram). Statistical analysis of these recalculated data confirmed that the average peak concentration at 90 min was higher with soft capsules, both in dogs and in humans.

In dogs, the average area under the plasma concentration–time curve was greater with soft capsules. Since a crossover design was used and data were analyzed by paired comparisons, no drawback ensued that might have been caused by a difference in the per kilogram dosage of flufenamic acid in dogs. This involved a variation in the absorption rate from animal to animal. However, the conclusion of this study is limited because the time intervals for plasma sample collections in humans were not the best in order to obtain a satisfactory profile of the actual concentration–time curves of flufenamic acid in plasma. The results for humans must be considered preliminary.

Bearing these points in mind, it may be concluded that the soft gelatin capsule enables higher plasma concentrations of the drug to be attained as compared with the hard capsule. The biological availability of the drug was quantitatively increased. When dogs received the soft gelatin capsule, plasma concentrations of flufenamic acid were higher than those following administration of the hard capsule, even during the decreasing phase. An appropriate study in humans might achieve similar results.

The different bioavailability of flufenamic acid due to the pharmaceutical dosage form may be dependent on physicochemical factors, brought into play by adjuvants in the soft gelatin capsule, which effect more rapid and complete drug absorption. With the hard capsule, absorption of the drug probably takes place more slowly and incompletely. The role of these factors is substantiated by the fact that the difference in bioavailability of the two dosage forms could not be correlated with the difference in their dissolution rates *in vitro*. Inasmuch as latency, intensity, and duration of action depend on the magnitude of the plasma levels and on the rate of their reaching critical values and remaining above them, it is to be assumed that the type of dosage form greatly determines the course of effect of single doses of flufenamic acid.

REFERENCES

(1) J. G. Wagner, E. S. Gerard, and D. G. Kaiser, *Clin. Pharmacol. Ther.*, **7**, 610(1966).

(2) R. A. Buchanan, C. J. Eaton, S. T. Koeff, and A. W. Kinkel, *Curr. Ther. Res.*, **11**, 533(1969).

(3) W. C. Guenther, "Analysis of Variance," Prentice Hall, Englewood Cliffs, N.J., 1964.

(4) F. Wilcoxon, *Biometrics*, **1**, 80(1945).

ACKNOWLEDGMENTS AND ADDRESSES

Received July 29, 1974, from the *[*]Istituto di Farmacologia e Farmacognosia, University of Rome, Piazzale delle Scienze, 2 Rome, Italy,* the *[‡]Quality Control Department, Sigma-Tau, Pomezia, Italy,* and the *[§]Health Statistics, University of Rome, Rome, Italy.*

Accepted for publication May 30, 1975.

[x] To whom inquiries should be directed.

GLC Determination of Degradation of Two Related Amine Uptake Inhibitors

REX W. SOUTER ˣ **and ALAN DINNER**

Abstract □ A convenient GLC method was developed to assay the chemically related CNS agents *dl*-3-(*p*-trifluoromethylphenoxy)-*N*-methyl-3-phenylpropylamine (I*a*) and *dl*-3-(*o*-methoxyphenoxy)-*N*-methyl-3-phenylpropylamine (I*b*). Subsequently, this GLC method was used to monitor the stability of I*a* and I*b* in acidic and basic media. These CNS agents were stable in basic solution but labile under acid conditions, and the degradations of both compounds approximated pseudo-first-order kinetics. Products formed during the acid hydrolysis of I*a* and I*b* were identified and were shown not to interfere in the GLC assays of the parent ethers.

Keyphrases □ GLC—stability determination, 3-phenylpropylamines, CNS agents □ CNS agents—3-phenylpropylamines, GLC stability determination

After the synthesis of a potential new drug, a suitable analytical assay procedure is needed for stability studies. Ideally, this method should be facile, able to detect the drug at low levels, and valid in the presence of chemical degradation products of the drug.

This paper reports a method for the assays of the selective serotonin uptake inhibitor (1-3) *dl*-3-(*p*-trifluoromethylphenoxy)-*N*-methyl-3-phenylpropylamine (I*a*) and the norepinephrine uptake inhibitor (2) *dl*-3-(*o*-methoxyphenoxy)-*N*-methyl-3-phenylpropylamine (I*b*). Both compounds are currently under study as inhibitors of uptake into monoaminergic neurons in brain.

EXPERIMENTAL

Reagents—The solvents used were all of analytical reagent quality. The 99% *n*-pentacosane[1] used as internal standard, the OV-225 liquid phase[2], and the acid-washed, dimethyldichlorosilane-treated Chromosorb G[3] were all purchased materials.

Apparatus—A high-precision gas chromatograph was used[4]. Screw-capped vials[5] with septums[6] were used for all sample extractions.

Chromatographic Conditions—The column was a 0.9-m × 0.83-cm (3-ft × 0.25-in.) o.d. acid-washed, dimethyldichlorosilane-treated glass U-tube packed with 4% OV-225 on 80–100-mesh Chromosorb G. The oven was operated at 200° for studies of I*a* and at 215° for studies of I*b*. Helium was used as the carrier gas (after passing through a drying trap packed with 5A molecular sieves) at an approximate flow rate of 60 ml/min.

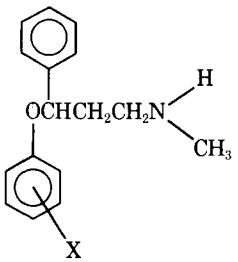

I*a*: X = *p*-CF_3
I*b*: X = *o*-OCH_3

Procedure—Peak areas were calculated using an on-line calculation program from the expanded RTE 2100 computer system[4]. Area ratios of sample–internal standard usually agreed within 1% for replicate injections.

For the degradation studies, a known amount (150–300 mg) of I*a* or I*b* as the hydrochloride salt was added to 100 ml of refluxing 0.1 *N* HCl. At various time intervals, aliquots of solution were removed and cooled in ice water. A 2-ml sample of each cooled aliquot was pipetted into the screw-capped septum vial. To this vial was added 7.4 *N* NH_4OH (to bring the pH to 7.5–8), and the solutions were mixed. Finally, 2.0 ml of a chloroform solution of the internal standard *n*-pentacosane (0.5–0.6 mg/ml) was added, the vial was capped, and the mixture was shaken for 2 min.

The two layers were allowed to separate, and then samples of the chloroform portion were injected into the GLC column. Plots of log [ether] *versus* time were constructed using a least-squares program available through a computer[7], and the slopes of the resulting straight lines were used to calculate the pseudo-first-order rate constants. Reactions were followed for at least two half-lives (C and D in Fig. 1). NMR spectra were obtained[8] using tetramethylsilane as the internal reference. Mass spectra were obtained on a gas chromatograph–mass spectrometer[9] unit at 70 ev.

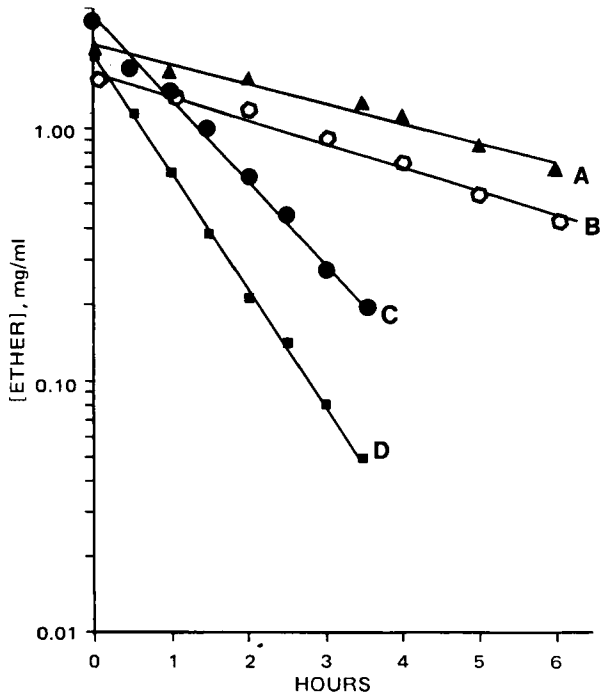

Figure 1—*Kinetic plots for acid degradation of* I*a and* I*b. Key: A,* I*a, initial measured concentration = 2.03 mg/ml, slope = −0.078; B,* I*a, initial measured concentration = 1.50 mg/ml, slope = −0.097; C,* I*b, initial measured concentration = 2.63 mg/ml, slope = −0.33; and D,* I*b, initial measured concentration = 1.97 mg/ml, slope = −0.46.*

[1] Lachat Chemicals, Mequon, Wis.
[2] Ohio Valley Specialty Chemicals, Marietta, Ohio.
[3] Johns-Manville, Denver, Colo.
[4] Model F&M 402, Hewlett-Packard, Avondale, Pa.
[5] No. 13028, Pierce Chemical Co., Rockford, Ill.
[6] Lined with Teflon, Canton Biomedical Products, Boulder, Colo.
[7] DEC-10, Digital Equipment Corp., Marlborough, Me.
[8] Varian T-60A, Varian Instrument Division, Palo Alto, Calif.
[9] LKB 9000S, LKB Instruments, Rockville, Md.

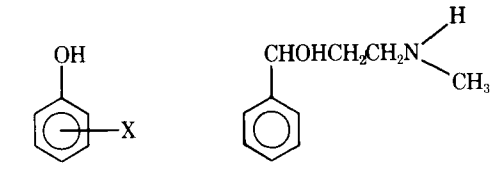

IIa: X = p-CF_3
IIb: X = o-OCH_3

III

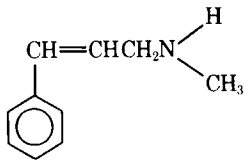

IV

Decomposition of *dl*-3-(*p*-Trifluoromethylphenoxy)-*N*-methyl-3-phenylpropylamine (Ia)—A solution of 300 mg (1 mmole) of Ia in 100 ml of 0.1 *N* aqueous hydrochloric acid was allowed to reflux for 24 hr. The solution was cooled, adjusted to pH 8 with 7.4 *N* NH_4OH, and then extracted with three 50-ml portions of chloroform. The chloroform layers were combined, dried over anhydrous magnesium sulfate, and finally concentrated on a rotary evaporator at 25°.

A portion of the concentrated chloroform solution was streaked onto a 500-μm TLC plate[10], and the plate was developed using methanol–acetic acid (90:10) as the eluant. Three zones were observed under 254-nm UV light (R_f 0.83, 0.65, and 0.55). The zones were scraped from the plate and eluted with chloroform, and the resulting solutions were evaporated. The fastest-moving zone was identified as *p*-trifluoromethylphenol (IIa); NMR (carbon tetrachloride): δ 7.65 (d, 2H, J = 8 Hz, aromatics), 6.9 (d, 2H, J = 8 Hz, aromatics), and 6.3 (s, 1H, OH); mass spectrum molecular ion at *m/e* 162, calculated for $C_7H_5F_3O$, 162; prominent fragmentation peak at *m/e* 143 ($p^+ - F$). TLC comparison with an authentic sample gave the same R_f values in two different solvent systems.

The middle zone was identified *via* IR comparison as unreacted starting material. The slowest-moving zone was identified as *N*-methyl-3-phenyl-3-hydroxypropylamine (III); NMR (deuterated methanol): δ 7.4 (s, 5H, aromatics), 4.9 (t, 1H, J = 6 Hz, benzylic H), 3.1 (t, 2H, J = 6 Hz, NCH_2—), 2.6 (s, 3H, NCH_3), and 2.1 (q, 2H, J = 6 Hz, $CHCH_2$—); mass spectrum molecular ion at *m/e* 165, calculated for $C_{10}H_{15}NO$, 165; major fragment at *m/e* 147 ($M^+ - H_2O$).

Decomposition of *dl*-3-(*o*-Methoxyphenoxy)-*N*-methyl-3-phenylpropylamine (Ib)—This material was degraded and worked up in a manner similar to that of Ia. Development of the thin-layer chromatogram revealed the presence of three zones (R_f 0.69, 0.65, and 0.55). The fastest-moving zone was shown to be guaiacol (*o*-methoxyphenol, IIb) *via* IR comparison with authentic material. The middle zone was unreacted starting material (IR comparison), and the slowest-moving zone was identified (as for Ia) as III.

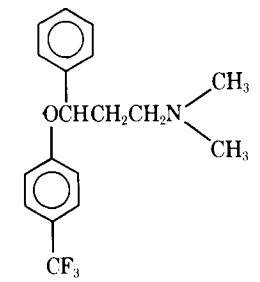

V

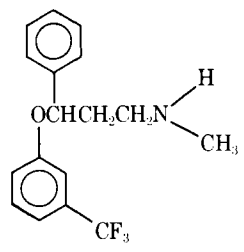

VI

[10] Silica gel F-254, EM Labs., Elmsford, N.Y.

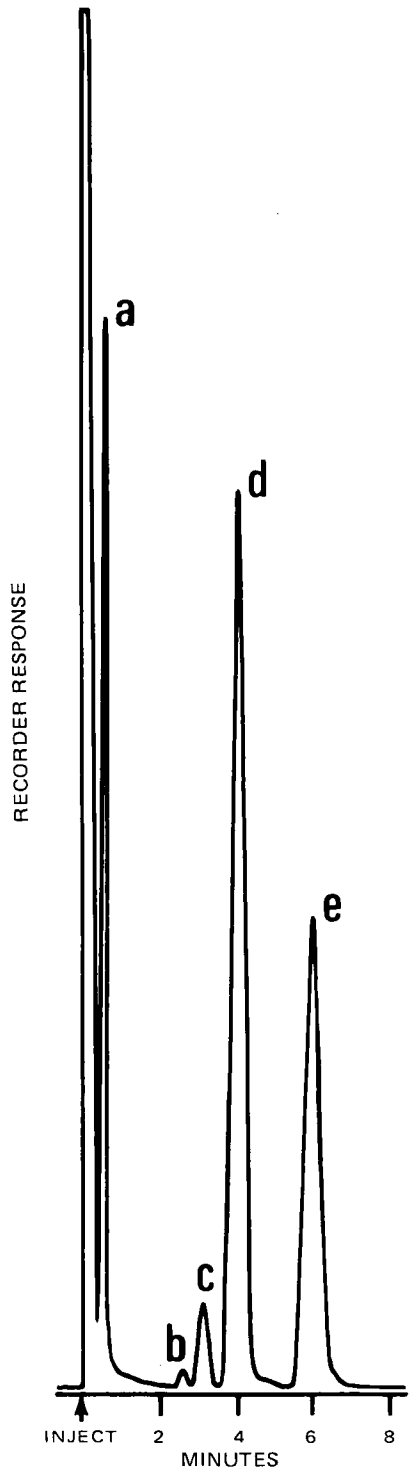

Figure 2—*Typical gas chromatogram of partially degraded Ia. Key: a,* p-*trifluoromethylphenol; b, V; c, VI; d,* Ia; *and e,* n-*pentacosane.*

RESULTS AND DISCUSSION

Calibration curves for Ia and Ib were obtained, and they re-

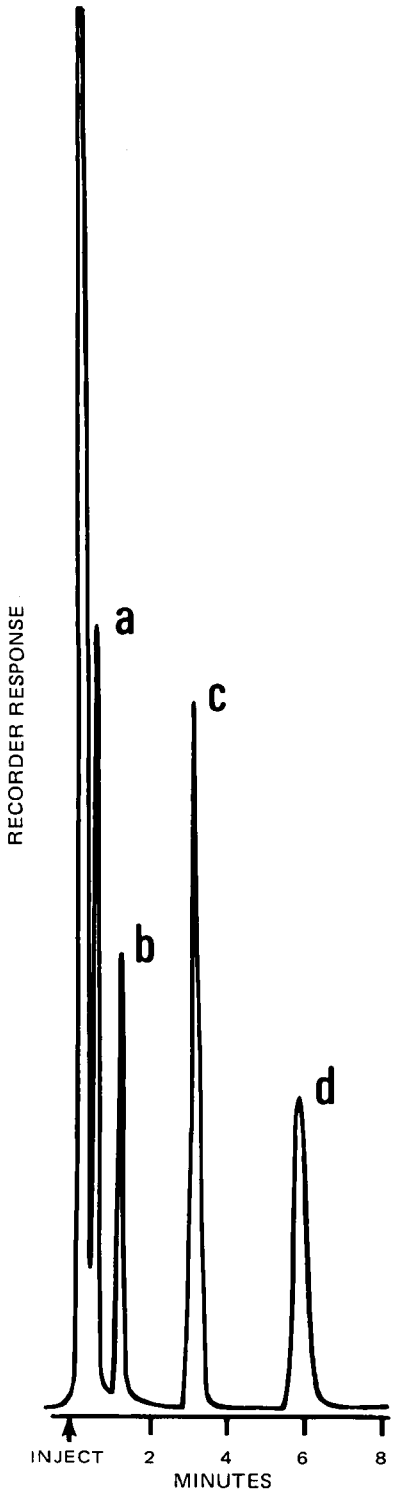

Figure 3—*Typical gas chromatogram of partially degraded Ib. Key: a, IIb; b, IV; c, n-pentacosane; and d, Ib.*

vealed a linear relationship between the peak area of compound–peak area of internal standard and the concentration of sample injected between 1.0×10^{-2} and 2.4 μg/μl. Quantities as low as 10 ng were detectable for either compound.

The kinetics of the acidic degradation of solutions of ethers Ia and Ib at two different starting concentrations are shown in Fig. 1. The degradations of both compounds approximate pseudo-first-order kinetics, with a k value of 0.20 hr^{-1} for Ia and of 0.90 hr^{-1} for Ib. Although these conditions are generally too mild for the cleavage of either aryl alkyl (4, 5) or dialkyl ethers (6, 7), the hydrolysis of aryl benzyl ethers is quite facile (8, 9). Benzyl phenyl ether itself has been cleaved in various solvents with hydrobromic acid at room temperature (10).

Literature reports of the solvolyses of other benzyl phenyl ethers (9, 10) suggest that the cleavage rates of the two compounds examined were not unusual.

The products of the acid-catalyzed cleavage of Ia were *p*-trifluoromethylphenol[11] (IIa) and *N*-methyl-3-phenyl-3-hydroxypropylamine (III), while Ib yielded *o*-methoxyphenol (IIb) and III. As expected, no benzyl halide was found since it would be hydrolyzed immediately under the reaction conditions (11) to the observed benzyl alcohol; no *O*-demethylation of Ib was noted.

The NMR, IR, and mass spectral data were consistent with the proposed structures. A combined GLC–mass spectral analysis of the product mixture from either Ia or Ib also revealed a small amount of material (1%) at m/e 147. The major fragments at m/e 146 and 117 $(C_6H_5CH{=}CHCH_2)^+$ strongly suggest IV as the likely structure. Injection of purified III into the gas chromatograph revealed no decomposition of IV. Hence, IV is generated from the acid-catalyzed dehydration of III in the reaction mixture.

Figures 2 and 3 represent typical chromatograms of partially degraded samples of Ia and Ib. Clearly, the degradation products do not interfere with the starting material or with the internal standard. In Fig. 2, peaks b and c represent impurities present in the Ia used. The identities of b and c were determined by use of GLC–mass spectrometry and by comparisons of chromatographic retention times with authentic samples. Peak b is 3-(*p*-trifluoromethylphenoxy)-*N*,*N*-dimethyl-3-phenylpropylamine (V), and peak c is 3-(*m*-trifluoromethylphenoxy)-*N*-methyl-3-phenylpropylamine (VI).

Attempted basic degradation of either Ia or Ib with 0.1 *N* aqueous sodium hydroxide at 100° resulted in complete recovery of starting material after 3 days. In general, alkali metals are required for the basic cleavage of benzyl aryl ethers (12).

REFERENCES

(1) D. Wong, J. Horn, F. Bymaster, K. Hauser, and B. Molloy, *Life Sci.*, **15**, 471(1974).

(2) D. Wong *et al.*, *Fed. Proc.*, **33**, 255(1974).

(3) R. Fuller, K. Perry, and B. Molloy, *Life Sci.*, **15**, 1161(1974).

(4) J. Bunnett, E. Bunzel, and K. Nahakedian, *J. Amer. Chem. Soc.*, **84**, 4136(1962).

(5) J. Bunnett and E. Bunzel, *ibid.*, **83**, 117(1961).

(6) R. Burwell, Jr., and M. Fuller, *ibid.*, **79**, 2332(1957).

(7) D. Jaques and J. Leiston, *J. Chem. Soc.*, **1961**, 4963.

(8) K. Kratzl and G. Mischke, *Monatsch. Chem.*, **94**, 753(1963).

(9) H. Hart and R. Elias, *J. Amer. Chem. Soc.*, **83**, 895(1961).

(10) A. Drummond and A. Eastham, *ibid.*, **79**, 3689(1957).

(11) R. Burwell, Jr., *Chem. Rev.*, **54**, 615(1954).

(12) P. Schorigin, *Chem. Ber.*, **57**, 1627(1924).

ACKNOWLEDGMENTS AND ADDRESSES

Received February 11, 1975, from *Lilly Research Laboratories, Indianapolis, IN 46206*

Accepted for publication June 4, 1975.

The authors thank Mr. Joseph Gregory and Mr. John Brunson for technical assistance and Mr. Kenneth Hauser for providing authentic samples of V and VI.

ˣ To whom inquiries should be directed.

[11] This material was shown to be a metabolite of Ia in the rat; C. J. Parli, unpublished results.

pKa Determination of Methaqualone

Keyphrases □ Methaqualone—spectrophotometric pKa determination □ pKa—spectrophotometric determination, methaqualone

To the Editor:

In a recent publication, Chatten *et al.* (1) reported the pKa value of methaqualone to be 3.56. The method used in their work was a potentiometric titration of the drug in a varying composition of acetone–water solvent systems. Methaqualone at three different molar concentrations was titrated to the half-neutralization point with standardized hydrochloric acid, and the pH was measured. The extrapolated pH values at infinite dilution of acetone were plotted against the molar concentration of the drug, and the extrapolated pH value of 3.56 from such a plot was reported as a pKa of methaqualone.

The pKa value thus obtained is questionable since the use of mixed solvents can produce anomalies in the pKa determination (2). There are two major complicating factors in the use of mixed solvents. First, the different solvating power of the two components creates new complexities; and second, the organic component contributes extra acidic and basic species to the solution. Although reproducible pH readings may be obtained in many mixed solvent systems, the pH meters are calibrated in aqueous buffers and pH values obtained under such conditions can be devoid of quantitative significance (3).

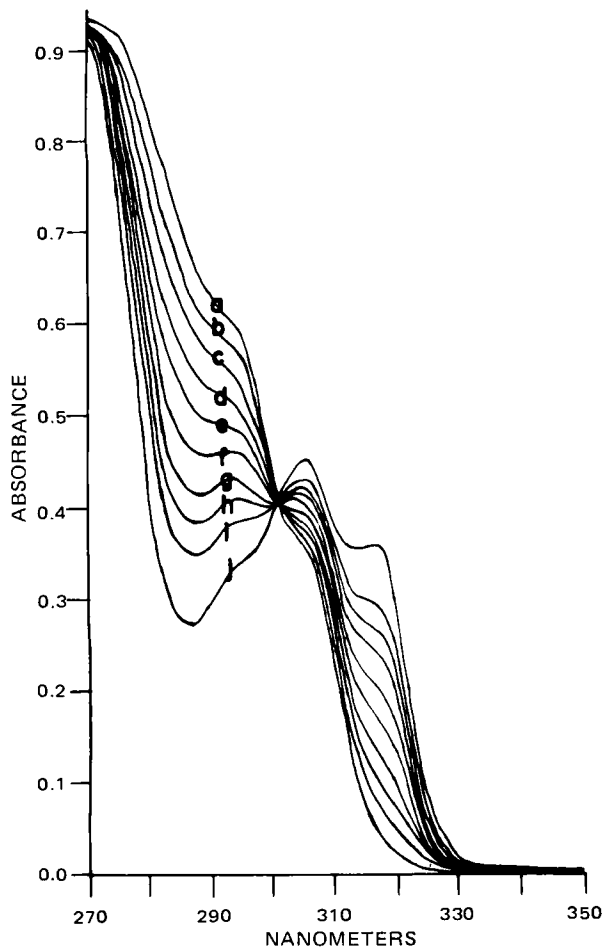

Figure 1—*Spectral changes of methaqualone in acidic media. Key: a, pH 1.05; b, pH 1.74; c, pH 1.96; d, pH 2.19; e, pH 2.37; f, pH 2.59; g, pH 2.79; h, pH 2.96; i, pH 3.17; and j, pH 4.56.*

Table I—Determination of pKa of Methaqualone by Spectrophotometric Method

pH	Absorbance (λ 286 nm)	pKa	Absorbance (λ 316 nm)	pKa
1.05	0.707	—	0.048	—
1.74	0.650	2.57	0.090	2.55
1.96	0.610	2.51	0.110	2.56
2.19	0.563	2.50	0.142	2.56
2.37	0.523	2.52	0.175	2.51
2.59	0.472	2.53	0.214	2.53
2.79	0.423	2.53	0.249	2.53
2.96	0.388	2.54	0.272	2.55
3.17	0.349	2.54	0.298	2.56
4.56	0.266	—	0.360	—
	Arithmetic mean	2.53	Arithmetic mean	2.54

For a sparingly soluble substance such as methaqualone, a UV spectrophotometric method can be used to determine the pKa value with no difficulty. In this laboratory, a spectrophotometric method was applied to measure pKa at two independent analytical wavelengths, λ 286 and 316 nm. The solution of methaqualone (1.24×10^{-4} *M*) was prepared in 0.1 *N* HCl to which 10 ml of 2 *M* KCl and 10 ml of 0.2 *M* Na_2HPO_4 were added to give a total volume of 500 ml with an ionic strength of 0.14.

Ten solutions with pH values ranging from 1.05 to 4.56 were prepared by adding a few drops of 5 *M* NaOH. The pH of each solution was measured using a pH meter[1] fitted with a glass–calomel electrode prior to absorbance reading[2]. The blank was the solvent without the sample. The spectra of 10 solutions thus obtained are shown in Fig. 1, with a well-defined isosbestic point at 301 nm. The pKa was calculated at λ 316 nm using:

$$\text{pKa} = \text{pH} + \log \frac{d_m - d}{d - d_i} \qquad \text{(Eq. 1)}$$

where d_m = absorbance of the unionized species, d = absorbance of the solution tested, and d_i = absorbance of the ionized species.

Table I shows the data obtained from the spectral analysis of methaqualone in different pH media and the pKa value calculated from two analytical wavelengths. The protolytic constant thus determined is in disagreement with the reported value of 3.56. In our opinion, the potentiometric method for the pKa determination of methaqualone using a mixed solvent system is unreliable for reasons already discussed. Our reported pKa value is in agreement with that published previously using a spectrophotometric

[1] Brinkmann pH meter 102.
[2] Cary 14 recording spectrophotometer.

method (pKa = 2.54) at the analytical wavelength, λ 316 nm (4). At the time of preparation of this manuscript, it was found[3] that the reported pKa value of methaqualone in the Schulman *et al.* (5) study was 2.59 ± 0.006 by absorptiometric and fluorometric pH titration. This result is additional evidence of the erratic pKa value reported by Chatten *et al.* (1).

(1) L. G. Chatten, R. E. Moskalyk, R. A. Locock, and F. J. Schaefer, *J. Pharm. Sci.*, **63**, 1294(1974).

(2) A. Albert and E. P. Serjeant, "Ionization Constants of Acids and Bases," Wiley, New York, N.Y., 1962, pp. 66, 67.

(3) R. F. Cookson, *Chem. Rev.*, **74**, 11(1974).

(4) D. M. Patel, A. J. Visalli, J. J. Zalipsky, and N. H. Reavey-Cantwell, in "Analytical Profiles of Drug Substances," vol. 4, Academic, New York, N.Y., 1975, p. 256.

(5) S. G. Schulman, J. M. Rutledge, and G. Torosian, *Anal. Chim. Acta*, **68**, 455(1974).

J. J. Zalipsky ˣ
D. M. Patel
R. J. Darnowski
N. H. Reavey-Cantwell
Analytical and Physical Chemistry Department
Research Division
William H. Rorer, Inc.
Fort Washington, PA 19034

Received September 11, 1975.
Accepted for publication December 16, 1975.
ˣ To whom inquiries should be directed.

[3] J. M. Rutledge, personal communication.

Application of Girard Reagent T to Radioimmunological Assay of Prednisolone in Plasma

Keyphrases □ Prednisolone—separation from hydrocortisone with Girard reagent T, applicability to radioimmunological determination □ Hydrocortisone—reaction with Girard reagent T, separation from prednisolone, plasma □ Girard reagent T—reaction with hydrocortisone, separation from prednisolone, plasma

To the Editor:

Due to the cross-reactivity between endogenous hydrocortisone and prednisolone, Sullivan *et al.* (1) suppressed the production of interfering endogenous hormone by pretreating the volunteers with dexamethasone in their recent bioavailability trial of this drug. In our study, we separated prednisolone from hydrocortisone by selectively forming the water-soluble derivative of the latter and extracting the prednisolone into the organic phase.

Lederer (2) reported that the rates of reaction of a number of steroid ketones with water-soluble Girard reagent T in an acetic acid–methanol mixture established the order of keto group reactivity to be Δ^4-3 ≫ 20 ≫ 11. It seems reasonable to expect that the reactivity of the $\Delta^{1,4}$-3 ketone function of prednisolone is much less than that of the Δ^4-3 ketone group of hydrocortisone on the basis of resonance and steric considerations. Thus, a water-soluble hydrazone derivative of hydrocortisone can be selectively formed in the presence of prednisolone.

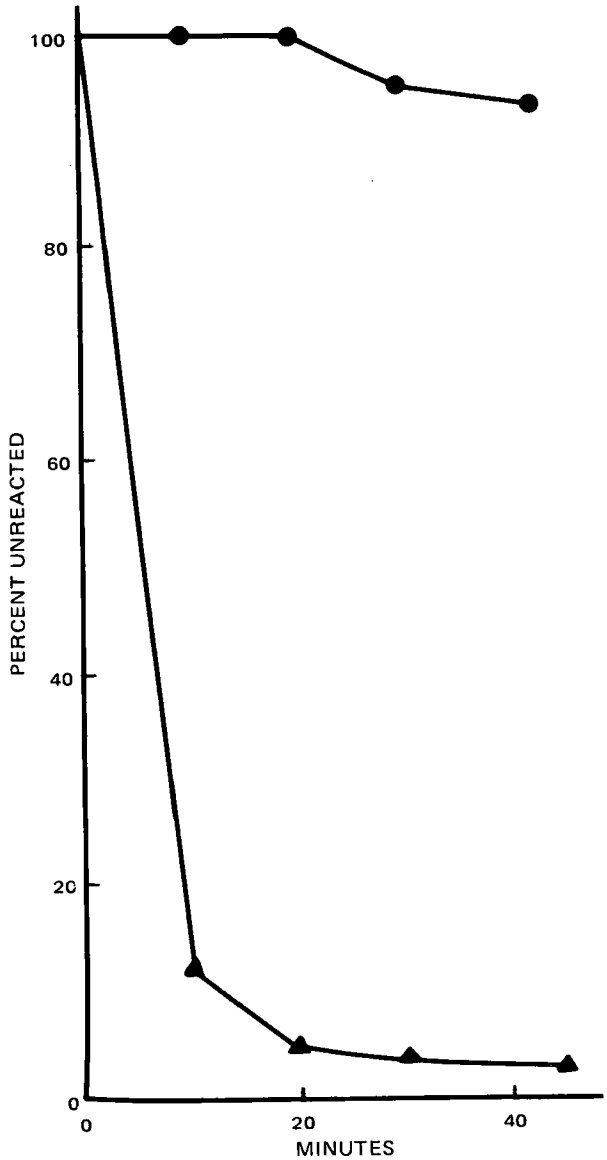

Figure 1—*Separation of prednisolone and hydrocortisone in plasma using Girard reagent T. Key:* ●, *prednisolone; and* ▲, *hydrocortisone.*

In our experiment, 1.0 ml of plasma was spiked with either 100,000 dpm of prednisolone (6,7-^{3}H)[1] plus 5 ng of cold carrier or 50,000 dpm of hydrocortisone (1,2-^{3}H)[2] plus 10 ng of cold carrier. Following the extraction of the drug into 5 ml of methylene chloride–ether (40:60), the dried residue was reacted with 50 μl of 10% Girard reagent T [dissolved in acetic acid–methanol (1:10)]. The reaction was stopped at 10, 20, 30, and 45 min by the addition of 0.5 ml of pH 8 phosphate buffer. The aqueous phase was extracted with 5 ml of methylene chloride–ether (40:60), the organic phase was transferred to a scintillation vial, and the solvent was evaporated under vacu-

[1] Specific activity = 40 Ci/mmole.
[2] Specific activity = 35 Ci/mmole.

method (pKa = 2.54) at the analytical wavelength, λ 316 nm (4). At the time of preparation of this manuscript, it was found[3] that the reported pKa value of methaqualone in the Schulman *et al.* (5) study was 2.59 ± 0.006 by absorptiometric and fluorometric pH titration. This result is additional evidence of the erratic pKa value reported by Chatten *et al.* (1).

(1) L. G. Chatten, R. E. Moskalyk, R. A. Locock, and F. J. Schaefer, *J. Pharm. Sci.*, **63**, 1294(1974).

(2) A. Albert and E. P. Serjeant, "Ionization Constants of Acids and Bases," Wiley, New York, N.Y., 1962, pp. 66, 67.

(3) R. F. Cookson, *Chem. Rev.*, **74**, 11(1974).

(4) D. M. Patel, A. J. Visalli, J. J. Zalipsky, and N. H. Reavey-Cantwell, in "Analytical Profiles of Drug Substances," vol. 4, Academic, New York, N.Y., 1975, p. 256.

(5) S. G. Schulman, J. M. Rutledge, and G. Torosian, *Anal. Chim. Acta*, **68**, 455(1974).

J. J. Zalipsky ˣ
D. M. Patel
R. J. Darnowski
N. H. Reavey-Cantwell
Analytical and Physical Chemistry Department
Research Division
William H. Rorer, Inc.
Fort Washington, PA 19034

Received September 11, 1975.
Accepted for publication December 16, 1975.
ˣ To whom inquiries should be directed.

[3] J. M. Rutledge, personal communication.

Application of Girard Reagent T to Radioimmunological Assay of Prednisolone in Plasma

Keyphrases □ Prednisolone—separation from hydrocortisone with Girard reagent T, applicability to radioimmunological determination □ Hydrocortisone—reaction with Girard reagent T, separation from prednisolone, plasma □ Girard reagent T—reaction with hydrocortisone, separation from prednisolone, plasma

To the Editor:

Due to the cross-reactivity between endogenous hydrocortisone and prednisolone, Sullivan *et al.* (1) suppressed the production of interfering endogenous hormone by pretreating the volunteers with dexamethasone in their recent bioavailability trial of this drug. In our study, we separated prednisolone from hydrocortisone by selectively forming the water-soluble derivative of the latter and extracting the prednisolone into the organic phase.

Lederer (2) reported that the rates of reaction of a number of steroid ketones with water-soluble Girard reagent T in an acetic acid–methanol mixture established the order of keto group reactivity to be Δ^4-3 ≫ 20 ≫ 11. It seems reasonable to expect that the reactivity of the $\Delta^{1,4}$-3 ketone function of prednisolone is much less than that of the Δ^4-3 ketone group of hydrocortisone on the basis of resonance and steric considerations. Thus, a water-soluble hydrazone derivative of hydrocortisone can be selectively formed in the presence of prednisolone.

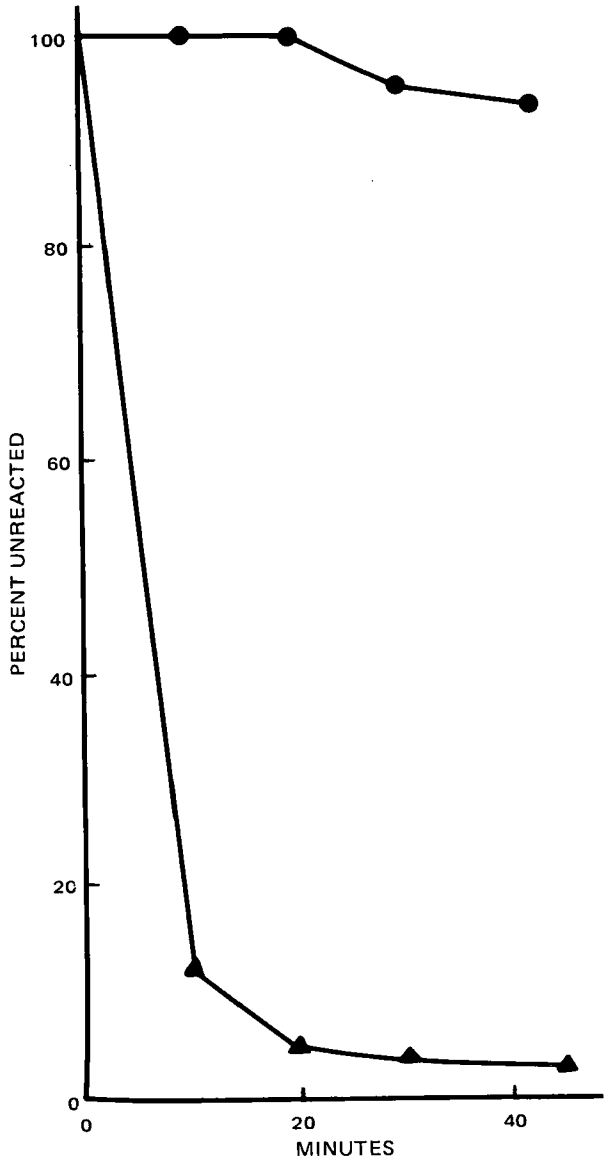

Figure 1—*Separation of prednisolone and hydrocortisone in plasma using Girard reagent T. Key:* ●, *prednisolone; and* ▲, *hydrocortisone.*

In our experiment, 1.0 ml of plasma was spiked with either 100,000 dpm of prednisolone (6,7-^{3}H)[1] plus 5 ng of cold carrier or 50,000 dpm of hydrocortisone (1,2-^{3}H)[2] plus 10 ng of cold carrier. Following the extraction of the drug into 5 ml of methylene chloride–ether (40:60), the dried residue was reacted with 50 μl of 10% Girard reagent T [dissolved in acetic acid–methanol (1:10)]. The reaction was stopped at 10, 20, 30, and 45 min by the addition of 0.5 ml of pH 8 phosphate buffer. The aqueous phase was extracted with 5 ml of methylene chloride–ether (40:60), the organic phase was transferred to a scintillation vial, and the solvent was evaporated under vacu-

[1] Specific activity = 40 Ci/mmole.
[2] Specific activity = 35 Ci/mmole.

um. The radioactivity was determined by a liquid scintillation technique.

The results (Fig. 1) indicated that 97% of the hydrocortisone had reacted within 45 min, whereas no appreciable reaction with prednisolone occurred.

We are currently attempting to adapt this separation procedure to a radioimmunoassay of prednisolone in plasma. The initial results are encouraging, and the Girard reagent T did not interfere with the radioimmunoassay of prednisolone. Details of this new radioimmunoassay procedure will be reported separately.

(1) T. J. Sullivan, R. G. Stoll, E. Sakmas, D. C. Blair, and J. G. Wagner, *J. Pharmacokinet. Biopharm.*, **2**, 29(1974).

(2) E. Lederer, *Trav. Members Soc. Chim. Biol.*, **24**, 1149(1942).

Jack C. K. Loo ˣ
Arnost B. Vilim
Nicole Jordan
James Moffatt
Drug Research Laboratories
Health Protection Branch
Tunney's Pasture, Ottawa
Canada K1A OL2

Received June 16, 1975.
Accepted for publication October 10, 1975.
ˣ To whom inquiries should be directed.

Pharmacokinetic Model to Describe Self-Induced Decreases in Steady-State Concentrations of Carbamazepine

Keyphrases □ Carbamazepine—self-induced decreases in steady-state serum concentrations, pharmacokinetic model proposed □ Pharmacokinetics—model proposed, description of self-induced decreases in steady-state serum concentrations of carbamazepine

To the Editor:

It has been reported that carbamazepine reduces the serum concentrations and elimination half-lives of several drugs, including itself, in several species (1–9). A study was performed to examine the behavior of serum carbamazepine levels during chronic administration of 6 mg/kg/day for 22 days to six normal drug-free human volunteers.

During the 3 weeks of treatment, there were significant decreases in average, maximum, and minimum (C_{min}) steady-state serum concentrations compared to values predicted from single-dose studies in the same subjects (Table I). By the end of the 3rd week, the average steady-state concentration was 50% of the level predicted from single-dose studies. In addition, the elimination half-life at the end of the 3rd week had decreased from 33.9 ± 3.5 hr[1] (single-dose determination) to 19.8 ± 4.0 hr[1]. Similar results recently were reported by Eichelbaum *et al.* (9); they found biological half-lives of 35.6 ± 15.3 hr following single doses and 20.9 ± 5 hr after 15–21 days of chronic treatment (200 mg/day) in four patients.

[1] The single-dose value was obtained from a nonlinear least-squares fit of the data to $C = A(e^{-KEt} - e^{-kat})$ using a MBDX85 computer program. The terminal half-life was obtained by nonlinear least-squares fit of the 8–72-hr data points.

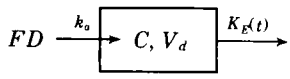

Scheme I

A literature review failed to produce a pharmacokinetic model that can be used to quantify and predict these self-induced decreases in steady-state concentrations. Several models were examined. The model proposed (Scheme I) is based on the observation that C_{min} appears to decrease at an exponential rate during multiple dosing with carbamazepine. The decrease in C_{min} is compatible with an exponential increase in the elimination rate constant (K_E) if one assumes that the drug is completely absorbed during the dosing interval. (This assumption is reasonable since the mean absorption half-life was 2.3 ± 1.1 hr and the dosing interval was 24 hr.)

In Scheme I, F is the fraction of dose D absorbed, k_a is a first-order absorption rate constant, and C is the concentration of drug in a single compartment of volume V_d. The term $K_E(t)$ represents an exponentially increasing elimination rate "constant," which is given by:

$$K_E(t) = K_E^{\infty} - (K_E^{\infty} - K_E^{0})e^{-K_I t} \qquad \text{(Eq. 1)}$$

where K_E^0 and K_E^∞ are the elimination rate constants at times zero and infinity, respectively, and K_I is a first-order rate constant. This model predicts that C_{min} decreases exponentially to an asymptotic minimum value.

Theoretical concentrations at any time t following multiple doses were approximated by:

$$C = \frac{FD}{V_d}\frac{k_a}{k_a - K_E(t)}\left[\left(\frac{1-e^{-nK_E(t)\tau}}{1-e^{-K_E(t)\tau}}\right)\times e^{-K_E(t)t} - \left(\frac{1-e^{-nk_a\tau}}{1-e^{-k_a\tau}}\right)e^{-k_a t}\right] \qquad \text{(Eq. 2)}$$

where n is the number of doses, and τ is the dosing interval.

Table I compares the experimentally observed mean serum concentrations with concentrations predicted using the proposed self-induction model as well as concentrations predicted using a one-compartment model with a *constant* elimination rate constant. Close agreement is observed between experimental values and predictions of the self-induction model, indicating that the proposed model is adequate to describe the pharmacokinetics of carbamazepine during chronic administration.

The phenomenon of self-induced decreases of steady-state levels during chronic dosing has significant clinical implications. The proposed pharmacokinetic model provides an adequate mathematical description of the rate of the process of self-induction. Also, this self-induction model allows the calculation of a dosage regimen that will maintain constant average concentrations at steady state even in the face of

um. The radioactivity was determined by a liquid scintillation technique.

The results (Fig. 1) indicated that 97% of the hydrocortisone had reacted within 45 min, whereas no appreciable reaction with prednisolone occurred.

We are currently attempting to adapt this separation procedure to a radioimmunoassay of prednisolone in plasma. The initial results are encouraging, and the Girard reagent T did not interfere with the radioimmunoassay of prednisolone. Details of this new radioimmunoassay procedure will be reported separately.

(1) T. J. Sullivan, R. G. Stoll, E. Sakmas, D. C. Blair, and J. G. Wagner, *J. Pharmacokinet. Biopharm.*, **2**, 29(1974).

(2) E. Lederer, *Trav. Members Soc. Chim. Biol.*, **24**, 1149(1942).

Jack C. K. Loo ˣ
Arnost B. Vilim
Nicole Jordan
James Moffatt
Drug Research Laboratories
Health Protection Branch
Tunney's Pasture, Ottawa
Canada K1A OL2

Received June 16, 1975.
Accepted for publication October 10, 1975.
ˣ To whom inquiries should be directed.

Pharmacokinetic Model to Describe Self-Induced Decreases in Steady-State Concentrations of Carbamazepine

Keyphrases □ Carbamazepine—self-induced decreases in steady-state serum concentrations, pharmacokinetic model proposed □ Pharmacokinetics—model proposed, description of self-induced decreases in steady-state serum concentrations of carbamazepine

To the Editor:

It has been reported that carbamazepine reduces the serum concentrations and elimination half-lives of several drugs, including itself, in several species (1–9). A study was performed to examine the behavior of serum carbamazepine levels during chronic administration of 6 mg/kg/day for 22 days to six normal drug-free human volunteers.

During the 3 weeks of treatment, there were significant decreases in average, maximum, and minimum (C_{min}) steady-state serum concentrations compared to values predicted from single-dose studies in the same subjects (Table I). By the end of the 3rd week, the average steady-state concentration was 50% of the level predicted from single-dose studies. In addition, the elimination half-life at the end of the 3rd week had decreased from 33.9 ± 3.5 hr[1] (single-dose determination) to 19.8 ± 4.0 hr[1]. Similar results recently were reported by Eichelbaum *et al.* (9); they found biological half-lives of 35.6 ± 15.3 hr following single doses and 20.9 ± 5 hr after 15–21 days of chronic treatment (200 mg/day) in four patients.

[1] The single-dose value was obtained from a nonlinear least-squares fit of the data to $C = A(e^{-KEt} - e^{-kat})$ using a MBDX85 computer program. The terminal half-life was obtained by nonlinear least-squares fit of the 8–72-hr data points.

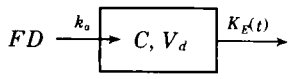

Scheme I

A literature review failed to produce a pharmacokinetic model that can be used to quantify and predict these self-induced decreases in steady-state concentrations. Several models were examined. The model proposed (Scheme I) is based on the observation that C_{min} appears to decrease at an exponential rate during multiple dosing with carbamazepine. The decrease in C_{min} is compatible with an exponential increase in the elimination rate constant (K_E) if one assumes that the drug is completely absorbed during the dosing interval. (This assumption is reasonable since the mean absorption half-life was 2.3 ± 1.1 hr and the dosing interval was 24 hr.)

In Scheme I, F is the fraction of dose D absorbed, k_a is a first-order absorption rate constant, and C is the concentration of drug in a single compartment of volume V_d. The term $K_E(t)$ represents an exponentially increasing elimination rate "constant," which is given by:

$$K_E(t) = K_E^{\infty} - (K_E^{\infty} - K_E^{0})e^{-K_I t} \qquad \text{(Eq. 1)}$$

where K_E^0 and K_E^∞ are the elimination rate constants at times zero and infinity, respectively, and K_I is a first-order rate constant. This model predicts that C_{min} decreases exponentially to an asymptotic minimum value.

Theoretical concentrations at any time t following multiple doses were approximated by:

$$C = \frac{FD}{V_d}\frac{k_a}{k_a - K_E(t)}\left[\left(\frac{1-e^{-nK_E(t)\tau}}{1-e^{-K_E(t)\tau}}\right)\times e^{-K_E(t)t} - \left(\frac{1-e^{-nk_a\tau}}{1-e^{-k_a\tau}}\right)e^{-k_a t}\right] \qquad \text{(Eq. 2)}$$

where n is the number of doses, and τ is the dosing interval.

Table I compares the experimentally observed mean serum concentrations with concentrations predicted using the proposed self-induction model as well as concentrations predicted using a one-compartment model with a *constant* elimination rate constant. Close agreement is observed between experimental values and predictions of the self-induction model, indicating that the proposed model is adequate to describe the pharmacokinetics of carbamazepine during chronic administration.

The phenomenon of self-induced decreases of steady-state levels during chronic dosing has significant clinical implications. The proposed pharmacokinetic model provides an adequate mathematical description of the rate of the process of self-induction. Also, this self-induction model allows the calculation of a dosage regimen that will maintain constant average concentrations at steady state even in the face of

Table I—Values of Observed Concentrations Compared to Values Predicted Using Single-Dose Data and Values Predicted Using the Self-Induction Model

Day	Hour	Concentration Predicted from Single-Dose Data, μg/ml	Observed Serum Concentration, μg/ml	Concentration Predicted Using Self-Induction Model, μg/ml
8	0	10.2	5.3	5.4
	2	13.4	8.9	9.3
	4	13.9	9.6	9.8
	6	13.5	9.0	9.6
	8	13.2	8.9	8.9
	12	12.5	7.8	8.3
	24	10.4	5.2	5.4
15	0	10.6	4.3	4.5
	2	13.6	7.8	8.2
	4	14.2	8.2	9.1
	6	13.6	7.6	8.2
	8	13.4	7.7	7.5
	12	13.0	6.5	6.5
	24	10.6	4.4	4.5
22	0	10.6	3.8	4.4
	2	13.6	7.1	8.0
	4	14.2	8.3	9.1
	6	13.6	8.0	8.6
	8	13.4	7.1	7.6
	12	13.0	6.3	6.5
	24	10.6	3.8	4.4
	48	6.4	1.8	1.9
	72	4.0	1.0	0.9

an increasing elimination rate constant, thus yielding more efficacious epilepsy therapy.

(1) H. Meinardi, in "Antiepileptic Drugs," D. M. Woodbury, J. K. Penry, and R. P. Schmidt, Eds., Raven, New York, N.Y., pp. 407–496.

(2) P. L. Morselli, M. Gerna, D. DeMaio, G. Zandra, F. Viani, and S. Garattini, presented at the Workshop on the Determination of Antiepileptic Drugs in Body Fluids II, Bethel, Federal Republic of Germany, May 1974.

(3) A. S. Troupin, J. R. Green, and R. H. Levy, *Neurology*, **24**, 863(1974).

(4) P. L. Morselli, P. Biandrate, A. Frigerio, and S. Garattini, *Eur. J. Clin. Invest.*, **2**, 297(1972).

(5) O. Penttila, P. J. Neuvonen, K. Aho, and R. Lehtovaara, *Brit. Med. J.*, **2**, 470(1974).

(6) J. Hansen, K. Siersbaek-Nielsen, and L. Skovsted, *Clin. Pharmacol. Ther.*, **12**, 539(1973).

(7) R. Ronfeld and L. Z. Benet, presented at the APhA Academy of Pharmaceutical Sciences, Chicago meeting, 1974.

(8) R. H. Levy, W. H. Pitlick, A. S. Troupin, J. R. Green, and J. M. Neal, *Clin. Pharmacol. Ther.*, **17**, 657(1975).

(9) M. Eichelbaum, K. Ekbom, L. Bertilsson, V. A. Ringberger, and A. Rane, *Eur. J. Clin. Pharmacol.*, **8**, 337(1975).

William H. Pitlick *
René H. Levy ˣ
Departments of Pharmaceutical Sciences and Neurological Surgery
School of Pharmacy and School of Medicine
University of Washington
Seattle, WA 98195

Allan S. Troupin
John R. Green †
Department of Neurological Surgery
School of Medicine
University of Washington
Seattle, WA 98195

Received May 27, 1975.
Accepted for publication November 21, 1975.
Supported in part by National Institutes of Health Grant RR-37 and by a research grant from Ciba-Geigy Corp.
Part of this research was performed at the Clinical Research Center of the University of Washington.

* Present address: School of Pharmacy, University of Pittsburgh, Pittsburgh, PA 15261
† Deceased.
ˣ To whom inquiries should be directed.

Pharmacokinetic Analysis of Renal Handling of Sulfamethizole

Keyphrases □ Sulfamethizole—renal excretion mechanisms, pharmacokinetic analysis □ Excretion, renal—sulfamethizole, pharmacokinetic analysis □ Pharmacokinetic analysis—renal excretion mechanisms, sulfamethizole

To the Editor:

It is important to clarify the renal excretion mechanisms of drugs when considering their effectiveness and safety. Weiner and Mudge (1) carried out extensive physiological studies of renal tubular excretion mechanisms, but studies have not been made on the quantitative relationship between secretion and reabsorption of drugs in the nephron. Previously, we elucidated the renal handling of sulfonamides by means of inhibitory experiments (2, 3); but since the conditions are harsh, there is a limitation in the application of this method to humans.

The present study was undertaken to establish an analytical method for renal excretion mechanisms of drugs under more suitable conditions to enable clinical applications to humans. For this purpose, renal handling of sulfamethizole was analyzed using an analog computer to determine the alteration of plasma concentration and clearance ratio after intravenous administration of a single dose of sulfamethizole.

Generally, the excretion of a drug from the kidney into urine is expressed by:

$$UV = (GFR)P_f + S - A \qquad \text{(Eq. 1)}$$

Table I—Values of Observed Concentrations Compared to Values Predicted Using Single-Dose Data and Values Predicted Using the Self-Induction Model

Day	Hour	Concentration Predicted from Single-Dose Data, μg/ml	Observed Serum Concentration, μg/ml	Concentration Predicted Using Self-Induction Model, μg/ml
8	0	10.2	5.3	5.4
	2	13.4	8.9	9.3
	4	13.9	9.6	9.8
	6	13.5	9.0	9.6
	8	13.2	8.9	8.9
	12	12.5	7.8	8.3
	24	10.4	5.2	5.4
15	0	10.6	4.3	4.5
	2	13.6	7.8	8.2
	4	14.2	8.2	9.1
	6	13.6	7.6	8.2
	8	13.4	7.7	7.5
	12	13.0	6.5	6.5
	24	10.6	4.4	4.5
22	0	10.6	3.8	4.4
	2	13.6	7.1	8.0
	4	14.2	8.3	9.1
	6	13.6	8.0	8.6
	8	13.4	7.1	7.6
	12	13.0	6.3	6.5
	24	10.6	3.8	4.4
	48	6.4	1.8	1.9
	72	4.0	1.0	0.9

an increasing elimination rate constant, thus yielding more efficacious epilepsy therapy.

(1) H. Meinardi, in "Antiepileptic Drugs," D. M. Woodbury, J. K. Penry, and R. P. Schmidt, Eds., Raven, New York, N.Y., pp. 407–496.

(2) P. L. Morselli, M. Gerna, D. DeMaio, G. Zandra, F. Viani, and S. Garattini, presented at the Workshop on the Determination of Antiepileptic Drugs in Body Fluids II, Bethel, Federal Republic of Germany, May 1974.

(3) A. S. Troupin, J. R. Green, and R. H. Levy, *Neurology*, **24**, 863(1974).

(4) P. L. Morselli, P. Biandrate, A. Frigerio, and S. Garattini, *Eur. J. Clin. Invest.*, **2**, 297(1972).

(5) O. Penttila, P. J. Neuvonen, K. Aho, and R. Lehtovaara, *Brit. Med. J.*, **2**, 470(1974).

(6) J. Hansen, K. Siersbaek-Nielsen, and L. Skovsted, *Clin. Pharmacol. Ther.*, **12**, 539(1973).

(7) R. Ronfeld and L. Z. Benet, presented at the APhA Academy of Pharmaceutical Sciences, Chicago meeting, 1974.

(8) R. H. Levy, W. H. Pitlick, A. S. Troupin, J. R. Green, and J. M. Neal, *Clin. Pharmacol. Ther.*, **17**, 657(1975).

(9) M. Eichelbaum, K. Ekbom, L. Bertilsson, V. A. Ringberger, and A. Rane, *Eur. J. Clin. Pharmacol.*, **8**, 337(1975).

William H. Pitlick *
René H. Levy ˣ
Departments of Pharmaceutical Sciences and Neurological Surgery
School of Pharmacy and School of Medicine
University of Washington
Seattle, WA 98195

Allan S. Troupin
John R. Green †
Department of Neurological Surgery
School of Medicine
University of Washington
Seattle, WA 98195

Received May 27, 1975.
Accepted for publication November 21, 1975.
Supported in part by National Institutes of Health Grant RR-37 and by a research grant from Ciba-Geigy Corp.
Part of this research was performed at the Clinical Research Center of the University of Washington.

* Present address: School of Pharmacy, University of Pittsburgh, Pittsburgh, PA 15261
† Deceased.
ˣ To whom inquiries should be directed.

Pharmacokinetic Analysis of Renal Handling of Sulfamethizole

Keyphrases □ Sulfamethizole—renal excretion mechanisms, pharmacokinetic analysis □ Excretion, renal—sulfamethizole, pharmacokinetic analysis □ Pharmacokinetic analysis—renal excretion mechanisms, sulfamethizole

To the Editor:

It is important to clarify the renal excretion mechanisms of drugs when considering their effectiveness and safety. Weiner and Mudge (1) carried out extensive physiological studies of renal tubular excretion mechanisms, but studies have not been made on the quantitative relationship between secretion and reabsorption of drugs in the nephron. Previously, we elucidated the renal handling of sulfonamides by means of inhibitory experiments (2, 3); but since the conditions are harsh, there is a limitation in the application of this method to humans.

The present study was undertaken to establish an analytical method for renal excretion mechanisms of drugs under more suitable conditions to enable clinical applications to humans. For this purpose, renal handling of sulfamethizole was analyzed using an analog computer to determine the alteration of plasma concentration and clearance ratio after intravenous administration of a single dose of sulfamethizole.

Generally, the excretion of a drug from the kidney into urine is expressed by:

$$UV = (GFR)P_f + S - A \qquad \text{(Eq. 1)}$$

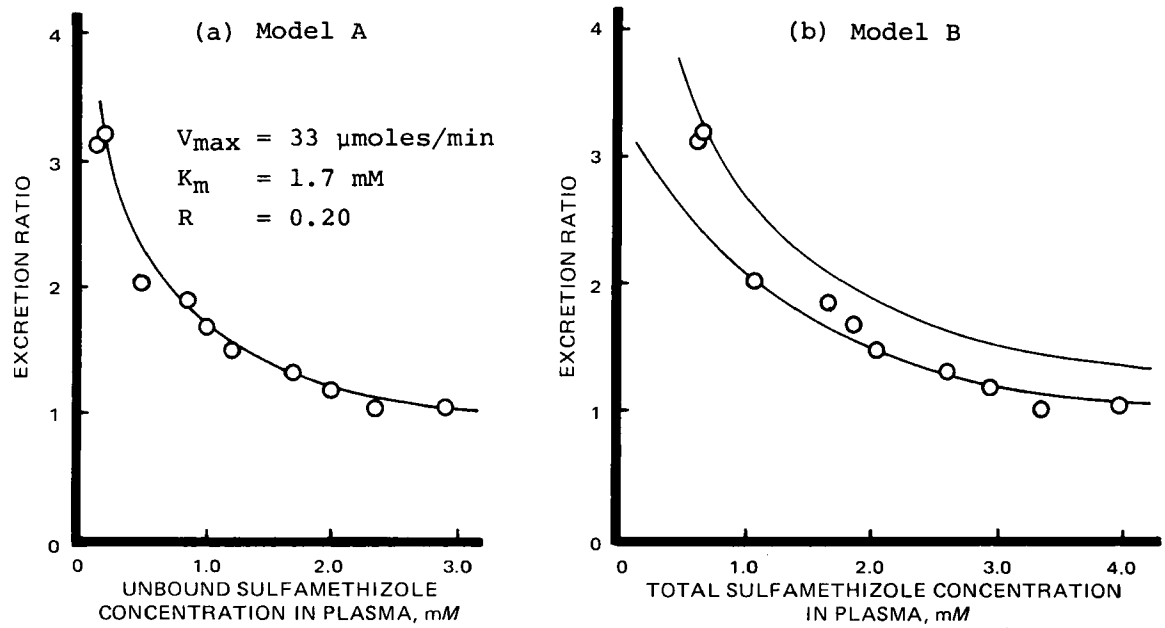

Figure 1—*Experimental data points and simulated computer curves. Each point represents renal clearance data. The solid line represents the computer-simulated curve. The upper solid line in Fig. 1b is the simulation curve for the data of a low plasma level and the lower curve is for the data of a high plasma level of sulfamethizole.*

where U is the drug concentration in urine, V is the urine flow rate, GFR is the glomerular filtration rate, P_f is the unbound drug concentration in plasma, S is the rate of secretion, and A is the rate of reabsorption. By assuming that a drug is reabsorbed by nonionic diffusion and that the rate of active secretion of a drug conforms to the Michaelis–Menten equation and is dependent upon the protein-free drug concentration in plasma, A and S can be expressed as:

$$A = (R)[(GFR)P_f + S] \quad \text{(Eq. 2)}$$

$$S = \frac{V_{max}P_f}{K_m + P_f} \quad \text{(Eq. 3)}$$

where R, V_{max}, and K_m indicate the reabsorption fraction, the maximum velocity of secretion, and the Michaelis constant, respectively. On the other hand, the clearance ratio corrected for plasma protein binding of the drug, ER (excretion ratio), is:

$$ER = \frac{UV}{(P_f)(GFR)} \quad \text{(Eq. 4)}$$

From Eqs. 1–4, ER can be expressed as:

$$ER = \left[1 + \frac{V_{max}}{(K_m + P_f)(GFR)}\right](1 - R) \quad \text{(Eq. 5)}$$

If the rate of active secretion is dependent upon the total concentration of the drug in plasma (P), Eq. 5 should be:

$$ER = \left[1 + \frac{V_{max}}{(K_m + P)(GFR)}\frac{P}{P_f}\right](1 - R) \quad \text{(Eq. 6)}$$

Equations 5 and 6 are programmed on the analog computer as model equations, Eq. 5 for Model A and Eq. 6 for Model B. In these equations, UV, P, P_f, and GFR are determined by the clearance method after administration of a single dose and V_{max}, K_m, and R are parameters.

Renal clearance experiments were performed by the single-injection technique using male New Zealand albino rabbits. Urine samples were collected at 5- and 10-min intervals, and blood samples were taken at 1 min before the midpoint of the urine collection periods. This 1 min indicates the delay time required for phenolsulfonphthalein to appear in the urine after intravenous injection in rabbits based on the experiment in humans (4). Experiments with the combination of the standard renal clearance and the secretory inhibition using iodopyracet (2) were also performed.

Inulin was used to determine the glomerular filtration rate. The plasma and urine samples were treated with Somogyi deproteinizing reagents (5) and then analyzed as follows: (*a*) sulfamethizole by the procedure of Bratton and Marshall (6), using 2-diethylaminoethyl-1-naphthylamine as the coupling agent (7); and (*b*) inulin by a modification of the Dische and Borenfreund method (8). Binding of sulfamethi-

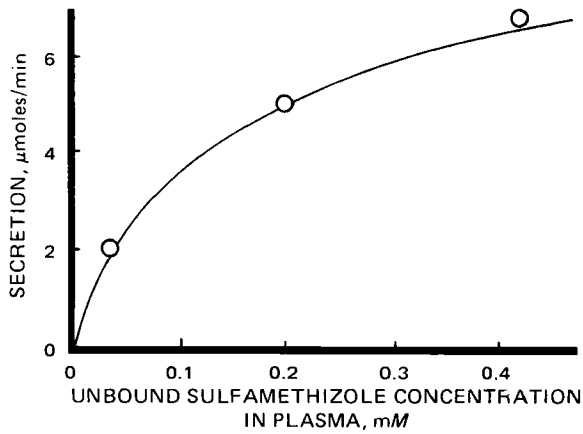

Figure 2—*Relationship between plasma concentration and renal tubular secretion of sulfamethizole. Each point represents the experimental data obtained by inhibitory experiments. The solid line represents the calculated curve of Model A.*

zole to rabbit plasma protein was determined by the membrane ultrafiltration technique (9). Analysis of the clearance data was performed using the analog computer.

The results are shown in Fig. 1. The simulation curve of Model A fitted well with the experimental data. However, in Model B, a fitting curve could not be obtained with any of the various parameters available. When the parameters were selected at the values given in Fig. 1*a*, the calculated curve of Model A agreed well with the experimental data obtained by inhibitory experiments (2, 3) (Fig. 2). From these results, it is considered that the tubular reabsorption of sulfamethizole can be explained by nonionic diffusion, while the tubular secretion can be explained by active transport that conforms to the Michaelis–Menten equation.

In addition, since Model A fits the experimental data, it can be presumed that the tubular secretion of sulfamethizole is dependent upon the unbound sulfamethizole concentration in plasma. Details of pharmacokinetic analyses of some sulfonamides and phenolsulfonphthalein using Model A will be described in a subsequent paper.

In conclusion, this analytical method permits analysis of a limited amount of experimental data on the renal excretion of sulfamethizole in a dynamic condition where the concentration in plasma varies with time after administration of a single dose. It also can be used to clarify the renal handling of sulfamethizole within a short period. This method is presently being applied to humans.

(1) I. M. Weiner and H. Mudge, *Amer. J. Med.*, **36**, 743(1964).
(2) T. Arita, R. Hori, E. Owada, and K. Takahashi, *Chem. Pharm. Bull.*, **17**, 2526(1969).
(3) E. Owada, K. Takahashi, R. Hori, and T. Arita, *ibid.*, **22**, 594(1974).
(4) H. W. Smith, W. Goldring, and H. Chasis, *J. Clin. Invest.*, **17**, 263(1937).
(5) M. Somogyi, *J. Biol. Chem.*, **86**, 655(1930).
(6) A. C. Bratton and E. K. Marshall, Jr., *ibid.*, **128**, 537(1939).
(7) T. Koizumi, T. Arita, and K. Kakemi, *Chem. Pharm. Bull.*, **12**, 413(1964).
(8) Z. Dische and E. Borenfreund, *J. Biol. Chem.*, **192**, 583(1951).
(9) E. Owada, R. Hori, and T. Arita, *Yakuzaigaku*, **33**, 125(1973).

Ryohei Hori [x]
Kosaku Sunayashiki
Akira Kamiya
Institute of Pharmaceutical Sciences
Hiroshima University School of Medicine
Kasumi 1-2-3, Hiroshima, Japan

Received August 27, 1975.
Accepted for publication December 1, 1975.
Supported in part by Grant 847093 from the Ministry of Education of Japan.
[x] To whom inquiries should be directed.

BOOKS

REVIEWS

A Textbook of Pharmaceutical Analysis, Second Edition. By KENNETH A. CONNORS. Wiley, 605 Third Avenue, New York, NY 10016, 1975. 15.5 × 23.5 cm. Price $18.95.

Many changes have been incorporated into the second edition of this classic textbook. A new chapter on analytical toxicology has been included which adds immeasurably to the topics covered. The analysis of drugs in blood and/or urine samples is fast becoming an important area of interest and responsibility for the clinical pharmacist. In a community pharmacy, knowledge of preferred qualitative screening methods for drugs allows the pharmacist to function better as a drug expert in his or her locality. Another addition to the book is a chapter that provides basic information on volumetric techniques. This is of tremendous value to those pharmacy schools where a separate course in quantitative analysis is no longer required due to changing curricula. New sections dealing with such topics as ion-selective electrodes, ORD and CD, NMR and ESR, mass spectrometry, and high-pressure liquid chromatography have also been added.

The material is presented in six sections, which are entitled Titrimetric Analysis, Physical and Instrumental Methods, Separation Techniques, Elemental Analysis, Functional Group Analysis, and General Topics. These sections are further divided into chapters where the various techniques and/or subjects are discussed. A theoretical treatment is presented initially followed by practical application of the methodology in drug identification and/or quantification.

At the end of each chapter, the author has included laboratory exercises and questions dealing with the application of the subject matter in that segment. Several experiments have been added to those chapters where none existed in the first edition and other existing experiments have been updated and/or changed. The book therefore functions suitably as a source of sound laboratory exercises which can be performed either totally or in part during the customary 3-hr lab period.

The book is effective in its scope, variety of experiments and problems, and presentation style. It is a must for any student interested in pharmaceutical analysis. The researcher may find the book to be a helpful source of information on almost any analytical technique. The second edition of this textbook is truly an exciting adventure.

Reviewed by J. T. Stewart
School of Pharmacy
University of Georgia
Athens, GA 30602

zole to rabbit plasma protein was determined by the membrane ultrafiltration technique (9). Analysis of the clearance data was performed using the analog computer.

The results are shown in Fig. 1. The simulation curve of Model A fitted well with the experimental data. However, in Model B, a fitting curve could not be obtained with any of the various parameters available. When the parameters were selected at the values given in Fig. 1*a*, the calculated curve of Model A agreed well with the experimental data obtained by inhibitory experiments (2, 3) (Fig. 2). From these results, it is considered that the tubular reabsorption of sulfamethizole can be explained by nonionic diffusion, while the tubular secretion can be explained by active transport that conforms to the Michaelis–Menten equation.

In addition, since Model A fits the experimental data, it can be presumed that the tubular secretion of sulfamethizole is dependent upon the unbound sulfamethizole concentration in plasma. Details of pharmacokinetic analyses of some sulfonamides and phenolsulfonphthalein using Model A will be described in a subsequent paper.

In conclusion, this analytical method permits analysis of a limited amount of experimental data on the renal excretion of sulfamethizole in a dynamic condition where the concentration in plasma varies with time after administration of a single dose. It also can be used to clarify the renal handling of sulfamethizole within a short period. This method is presently being applied to humans.

(1) I. M. Weiner and H. Mudge, *Amer. J. Med.*, **36**, 743(1964).
(2) T. Arita, R. Hori, E. Owada, and K. Takahashi, *Chem. Pharm. Bull.*, **17**, 2526(1969).
(3) E. Owada, K. Takahashi, R. Hori, and T. Arita, *ibid.*, **22**, 594(1974).
(4) H. W. Smith, W. Goldring, and H. Chasis, *J. Clin. Invest.*, **17**, 263(1937).
(5) M. Somogyi, *J. Biol. Chem.*, **86**, 655(1930).
(6) A. C. Bratton and E. K. Marshall, Jr., *ibid.*, **128**, 537(1939).
(7) T. Koizumi, T. Arita, and K. Kakemi, *Chem. Pharm. Bull.*, **12**, 413(1964).
(8) Z. Dische and E. Borenfreund, *J. Biol. Chem.*, **192**, 583(1951).
(9) E. Owada, R. Hori, and T. Arita, *Yakuzaigaku*, **33**, 125(1973).

Ryohei Hori [x]
Kosaku Sunayashiki
Akira Kamiya
Institute of Pharmaceutical Sciences
Hiroshima University School of Medicine
Kasumi 1-2-3, Hiroshima, Japan

Received August 27, 1975.
Accepted for publication December 1, 1975.
Supported in part by Grant 847093 from the Ministry of Education of Japan.
[x] To whom inquiries should be directed.

BOOKS

REVIEWS

A Textbook of Pharmaceutical Analysis, Second Edition. By KENNETH A. CONNORS. Wiley, 605 Third Avenue, New York, NY 10016, 1975. 15.5 × 23.5 cm. Price $18.95.

Many changes have been incorporated into the second edition of this classic textbook. A new chapter on analytical toxicology has been included which adds immeasurably to the topics covered. The analysis of drugs in blood and/or urine samples is fast becoming an important area of interest and responsibility for the clinical pharmacist. In a community pharmacy, knowledge of preferred qualitative screening methods for drugs allows the pharmacist to function better as a drug expert in his or her locality. Another addition to the book is a chapter that provides basic information on volumetric techniques. This is of tremendous value to those pharmacy schools where a separate course in quantitative analysis is no longer required due to changing curricula. New sections dealing with such topics as ion-selective electrodes, ORD and CD, NMR and ESR, mass spectrometry, and high-pressure liquid chromatography have also been added.

The material is presented in six sections, which are entitled Titrimetric Analysis, Physical and Instrumental Methods, Separation Techniques, Elemental Analysis, Functional Group Analysis, and General Topics. These sections are further divided into chapters where the various techniques and/or subjects are discussed. A theoretical treatment is presented initially followed by practical application of the methodology in drug identification and/or quantification.

At the end of each chapter, the author has included laboratory exercises and questions dealing with the application of the subject matter in that segment. Several experiments have been added to those chapters where none existed in the first edition and other existing experiments have been updated and/or changed. The book therefore functions suitably as a source of sound laboratory exercises which can be performed either totally or in part during the customary 3-hr lab period.

The book is effective in its scope, variety of experiments and problems, and presentation style. It is a must for any student interested in pharmaceutical analysis. The researcher may find the book to be a helpful source of information on almost any analytical technique. The second edition of this textbook is truly an exciting adventure.

Reviewed by J. T. Stewart
School of Pharmacy
University of Georgia
Athens, GA 30602

Physical Pharmaceutics. By E. SHOTTON and K. RIDGWAY. Oxford University Press, Ely House, London W.1, England, 1974. xiii+409 pp. 209 figs., 30 tables, 15.5 × 23.5 cm. Price £ 15.—$48.00. (Distributed in the United States by Oxford University Press, 200 Madison Ave., New York, NY 10016.)

The first eight chapters of this book (about 60% of the volume) are devoted to consideration of the physical–chemical principles involved or associated with some pharmaceutical phenomena, systems, and operations. Included are phase rule as applied to different systems, viscosity and flow of fluids, fluid mechanics, heat transfer, evaporation and drying, surface properties, disperse systems, and powders. Three of the remaining seven chapters deal with solid dosage forms, liquid dosage forms and aerosols, and radioactive pharmaceuticals. One chapter briefly describes the formulation of pharmaceutical preparations and one chapter briefly presents biopharmaceutics. There is a chapter on humidification and air-conditioning as well as one chapter on construction materials for manufacturing equipment and for packaging.

Although the first 60% of the book deals with physical–chemical principles, the authors have introduced many pharmaceutical examples to illustrate these principles. The last part of the volume considers various classes of pharmaceutical dosage forms and their manufacture.

This book is intended as a text for an introductory course in physical pharmaceutics in the undergraduate pharmacy curriculum. The basic principles are presented first and are then followed by a limited number of descriptions of unit operations with little emphasis on the latter. This procedure of treating unit operations briefly was followed to limit the size of the book and to direct its use to pharmacy students rather than to chemical engineers.

In the preface the authors have stated that some unevenness of coverage may have arisen from limiting the size of the volume so that the cost would not become prohibitive. The brevity of some chapters, especially those in the last part of the book, is noticeable and in spite of the cost it may be advisable to expand them (the chapters on pharmaceutical preparations, liquids, formulation of pharmaceutical preparations, and biopharmaceutics) in the second edition.

"Physical Pharmaceutics" is a well-written text and is illustrated nicely with clear line-drawing figures. It is not an "all-inclusive" type of text but rather is intended to be used in an introductory course for pharmacy students. A major consideration in the acceptance of the book will be the listed price.

Reviewed by Elmer M. Plein
School of Pharmacy
University of Washington
Seattle, WA 98195

Amino-acids, Peptides, and Proteins, Vol. 6. R. C. SHEPPARD, Senior Reporter. The Chemical Society, Burlington House, London, W1V OBN, England, 1975. 16 × 24 cm. 514 pp. Price £16.50.

This volume covers the pertinent papers relative to the chemistry of amino acids, peptides, and proteins published in 1973. The report is subdivided into the now familiar areas as covered by previous volumes in this series. However, in this sixth volume the chapter on metal derivatives is omitted. The areas reviewed are: amino acids; structural investigations of peptides and proteins; peptide synthesis, which also includes an appendix of syntheses reported during 1973; peptides with structural features not typical of proteins; and the most interesting area to this reviewer, chemical structure and biological activity. A comparison can be made of the amount of coverage given to each of these areas in Vol. 6 with those reported on in the previous five volumes. The areas of structural investigation (45%) and peptide synthesis (20%) comprise nearly two-thirds of this volume. The identical sections covered in the previous volumes of this series have similar percentages. Thus, it would appear that there has been little change in the emphasis of research in peptide chemistry over these past 6 years.

The reappearance in Vol. 5, and again in Vol. 6, of the chapter on chemical structure and biological activity is very welcome. Usually the biological activity, which provides practically all of the justification and motivation for synthetic peptide chemistry, receives little or no attention in many publications. This omission is hard to understand. Possibly the pressure to publish the synthesis of yet another peptide may be reason enough for some authors.

The sixth volume of the series of specialist reports on amino acids, peptides and proteins is an essential addition for any specialized library in the peptide field. The chapter on the structure and biological activities is alone worth the purchase of this volume.

Reviewed by Brian J. Johnson
Department of Microbiology
University of Alabama Medical School
Birmingham, AL 35294

Principles of Pharmaceutical Marketing, 2nd Ed. By MICKEY C. SMITH. Lea & Febiger, Philadelphia, Pa., 1975. 440 pp. 16 × 24 cm. Price $16.50.

The book is a major contribution for pharmaceutical scientists, pharmacists, and pharmacy students. It would be nothing less than naive and erroneous if we thought that the profession of pharmacy and the pharmaceutical industry feed on the physical sciences and technology alone. Professor Smith has, in one concise package, given us the means to learn about pharmaceutical marketing. Divided into six parts (containing 20 chapters), the book leads the reader through the nuances of the pharmaceutical market to an in-depth examination of products and the decisions and processes involved in administrative decisions regarding marketing. Next, the reader is introduced to the three main components of the marketing channels—manufacturers, wholesalers, and retailers—and from these through a splendid review of the elements involved in pricing and competition, advertising, and retailing and finally, before the summary, through an explanation of internal and external controls.

Paul Olsen's book of 30 years ago stood as one of the few references in this area until the 1968 publication of this book's first edition, which was the first product in the field with quantitative data. The major flaw of the 1968 work, namely the rapid obsolescence of data, has now been fully rectified with the publication of the 1975 second edition containing updated data throughout. Naturally, the book only superficially touches many areas, but that is a fair price to pay for a work that has delivered, in a coherent form, a review of such an immense area.

Complete comprehension should be possible by anyone engaged in any area of pharmaceutical endeavor. This reviewer recommends the book to those engaged in physical and biological science activities as an excellent vehicle to gain an understanding of what is involved in bringing a product to market and sustaining it there once a marketable substance is produced. Of course, the book should serve as a text in pharmaceutical marketing courses in colleges of pharmacy. Lastly, as a reference, the book is a virtual gold mine of industry statistics. Professor Smith has produced a most useful work.

Reviewed by
Albert I. Wertheimer
College of Pharmacy
University of Minnesota
Minneapolis, MN 55414

Physical Pharmaceutics. By E. SHOTTON and K. RIDGWAY. Oxford University Press, Ely House, London W.1, England, 1974. xiii+409 pp. 209 figs., 30 tables, 15.5 × 23.5 cm. Price £ 15.—$48.00. (Distributed in the United States by Oxford University Press, 200 Madison Ave., New York, NY 10016.)

The first eight chapters of this book (about 60% of the volume) are devoted to consideration of the physical–chemical principles involved or associated with some pharmaceutical phenomena, systems, and operations. Included are phase rule as applied to different systems, viscosity and flow of fluids, fluid mechanics, heat transfer, evaporation and drying, surface properties, disperse systems, and powders. Three of the remaining seven chapters deal with solid dosage forms, liquid dosage forms and aerosols, and radioactive pharmaceuticals. One chapter briefly describes the formulation of pharmaceutical preparations and one chapter briefly presents biopharmaceutics. There is a chapter on humidification and air-conditioning as well as one chapter on construction materials for manufacturing equipment and for packaging.

Although the first 60% of the book deals with physical–chemical principles, the authors have introduced many pharmaceutical examples to illustrate these principles. The last part of the volume considers various classes of pharmaceutical dosage forms and their manufacture.

This book is intended as a text for an introductory course in physical pharmaceutics in the undergraduate pharmacy curriculum. The basic principles are presented first and are then followed by a limited number of descriptions of unit operations with little emphasis on the latter. This procedure of treating unit operations briefly was followed to limit the size of the book and to direct its use to pharmacy students rather than to chemical engineers.

In the preface the authors have stated that some unevenness of coverage may have arisen from limiting the size of the volume so that the cost would not become prohibitive. The brevity of some chapters, especially those in the last part of the book, is noticeable and in spite of the cost it may be advisable to expand them (the chapters on pharmaceutical preparations, liquids, formulation of pharmaceutical preparations, and biopharmaceutics) in the second edition.

"Physical Pharmaceutics" is a well-written text and is illustrated nicely with clear line-drawing figures. It is not an "all-inclusive" type of text but rather is intended to be used in an introductory course for pharmacy students. A major consideration in the acceptance of the book will be the listed price.

Reviewed by Elmer M. Plein
School of Pharmacy
University of Washington
Seattle, WA 98195

Amino-acids, Peptides, and Proteins, Vol. 6. R. C. SHEPPARD, Senior Reporter. The Chemical Society, Burlington House, London, W1V OBN, England, 1975. 16 × 24 cm. 514 pp. Price £16.50.

This volume covers the pertinent papers relative to the chemistry of amino acids, peptides, and proteins published in 1973. The report is subdivided into the now familiar areas as covered by previous volumes in this series. However, in this sixth volume the chapter on metal derivatives is omitted. The areas reviewed are: amino acids; structural investigations of peptides and proteins; peptide synthesis, which also includes an appendix of syntheses reported during 1973; peptides with structural features not typical of proteins; and the most interesting area to this reviewer, chemical structure and biological activity. A comparison can be made of the amount of coverage given to each of these areas in Vol. 6 with those reported on in the previous five volumes. The areas of structural investigation (45%) and peptide synthesis (20%) comprise nearly two-thirds of this volume. The identical sections covered in the previous volumes of this series have similar percentages. Thus, it would appear that there has been little change in the emphasis of research in peptide chemistry over these past 6 years.

The reappearance in Vol. 5, and again in Vol. 6, of the chapter on chemical structure and biological activity is very welcome. Usually the biological activity, which provides practically all of the justification and motivation for synthetic peptide chemistry, receives little or no attention in many publications. This omission is hard to understand. Possibly the pressure to publish the synthesis of yet another peptide may be reason enough for some authors.

The sixth volume of the series of specialist reports on amino acids, peptides and proteins is an essential addition for any specialized library in the peptide field. The chapter on the structure and biological activities is alone worth the purchase of this volume.

Reviewed by Brian J. Johnson
Department of Microbiology
University of Alabama Medical School
Birmingham, AL 35294

Principles of Pharmaceutical Marketing, 2nd Ed. By MICKEY C. SMITH. Lea & Febiger, Philadelphia, Pa., 1975. 440 pp. 16 × 24 cm. Price $16.50.

The book is a major contribution for pharmaceutical scientists, pharmacists, and pharmacy students. It would be nothing less than naive and erroneous if we thought that the profession of pharmacy and the pharmaceutical industry feed on the physical sciences and technology alone. Professor Smith has, in one concise package, given us the means to learn about pharmaceutical marketing. Divided into six parts (containing 20 chapters), the book leads the reader through the nuances of the pharmaceutical market to an in-depth examination of products and the decisions and processes involved in administrative decisions regarding marketing. Next, the reader is introduced to the three main components of the marketing channels—manufacturers, wholesalers, and retailers—and from these through a splendid review of the elements involved in pricing and competition, advertising, and retailing and finally, before the summary, through an explanation of internal and external controls.

Paul Olsen's book of 30 years ago stood as one of the few references in this area until the 1968 publication of this book's first edition, which was the first product in the field with quantitative data. The major flaw of the 1968 work, namely the rapid obsolescence of data, has now been fully rectified with the publication of the 1975 second edition containing updated data throughout. Naturally, the book only superficially touches many areas, but that is a fair price to pay for a work that has delivered, in a coherent form, a review of such an immense area.

Complete comprehension should be possible by anyone engaged in any area of pharmaceutical endeavor. This reviewer recommends the book to those engaged in physical and biological science activities as an excellent vehicle to gain an understanding of what is involved in bringing a product to market and sustaining it there once a marketable substance is produced. Of course, the book should serve as a text in pharmaceutical marketing courses in colleges of pharmacy. Lastly, as a reference, the book is a virtual gold mine of industry statistics. Professor Smith has produced a most useful work.

Reviewed by
Albert I. Wertheimer
College of Pharmacy
University of Minnesota
Minneapolis, MN 55414

Physical Pharmaceutics. By E. SHOTTON and K. RIDGWAY. Oxford University Press, Ely House, London W.1, England, 1974. xiii+409 pp. 209 figs., 30 tables, 15.5 × 23.5 cm. Price £ 15.—$48.00. (Distributed in the United States by Oxford University Press, 200 Madison Ave., New York, NY 10016.)

The first eight chapters of this book (about 60% of the volume) are devoted to consideration of the physical–chemical principles involved or associated with some pharmaceutical phenomena, systems, and operations. Included are phase rule as applied to different systems, viscosity and flow of fluids, fluid mechanics, heat transfer, evaporation and drying, surface properties, disperse systems, and powders. Three of the remaining seven chapters deal with solid dosage forms, liquid dosage forms and aerosols, and radioactive pharmaceuticals. One chapter briefly describes the formulation of pharmaceutical preparations and one chapter briefly presents biopharmaceutics. There is a chapter on humidification and air-conditioning as well as one chapter on construction materials for manufacturing equipment and for packaging.

Although the first 60% of the book deals with physical–chemical principles, the authors have introduced many pharmaceutical examples to illustrate these principles. The last part of the volume considers various classes of pharmaceutical dosage forms and their manufacture.

This book is intended as a text for an introductory course in physical pharmaceutics in the undergraduate pharmacy curriculum. The basic principles are presented first and are then followed by a limited number of descriptions of unit operations with little emphasis on the latter. This procedure of treating unit operations briefly was followed to limit the size of the book and to direct its use to pharmacy students rather than to chemical engineers.

In the preface the authors have stated that some unevenness of coverage may have arisen from limiting the size of the volume so that the cost would not become prohibitive. The brevity of some chapters, especially those in the last part of the book, is noticeable and in spite of the cost it may be advisable to expand them (the chapters on pharmaceutical preparations, liquids, formulation of pharmaceutical preparations, and biopharmaceutics) in the second edition.

"Physical Pharmaceutics" is a well-written text and is illustrated nicely with clear line-drawing figures. It is not an "all-inclusive" type of text but rather is intended to be used in an introductory course for pharmacy students. A major consideration in the acceptance of the book will be the listed price.

Reviewed by Elmer M. Plein
School of Pharmacy
University of Washington
Seattle, WA 98195

Amino-acids, Peptides, and Proteins, Vol. 6. R. C. SHEPPARD, Senior Reporter. The Chemical Society, Burlington House, London, W1V OBN, England, 1975. 16 × 24 cm. 514 pp. Price £16.50.

This volume covers the pertinent papers relative to the chemistry of amino acids, peptides, and proteins published in 1973. The report is subdivided into the now familiar areas as covered by previous volumes in this series. However, in this sixth volume the chapter on metal derivatives is omitted. The areas reviewed are: amino acids; structural investigations of peptides and proteins; peptide synthesis, which also includes an appendix of syntheses reported during 1973; peptides with structural features not typical of proteins; and the most interesting area to this reviewer, chemical structure and biological activity. A comparison can be made of the amount of coverage given to each of these areas in Vol. 6 with those reported on in the previous five volumes. The areas of structural investigation (45%) and peptide synthesis (20%) comprise nearly two-thirds of this volume. The identical sections covered in the previous volumes of this series have similar percentages. Thus, it would appear that there has been little change in the emphasis of research in peptide chemistry over these past 6 years.

The reappearance in Vol. 5, and again in Vol. 6, of the chapter on chemical structure and biological activity is very welcome. Usually the biological activity, which provides practically all of the justification and motivation for synthetic peptide chemistry, receives little or no attention in many publications. This omission is hard to understand. Possibly the pressure to publish the synthesis of yet another peptide may be reason enough for some authors.

The sixth volume of the series of specialist reports on amino acids, peptides and proteins is an essential addition for any specialized library in the peptide field. The chapter on the structure and biological activities is alone worth the purchase of this volume.

Reviewed by Brian J. Johnson
Department of Microbiology
University of Alabama Medical School
Birmingham, AL 35294

Principles of Pharmaceutical Marketing, 2nd Ed. By MICKEY C. SMITH. Lea & Febiger, Philadelphia, Pa., 1975. 440 pp. 16 × 24 cm. Price $16.50.

The book is a major contribution for pharmaceutical scientists, pharmacists, and pharmacy students. It would be nothing less than naive and erroneous if we thought that the profession of pharmacy and the pharmaceutical industry feed on the physical sciences and technology alone. Professor Smith has, in one concise package, given us the means to learn about pharmaceutical marketing. Divided into six parts (containing 20 chapters), the book leads the reader through the nuances of the pharmaceutical market to an in-depth examination of products and the decisions and processes involved in administrative decisions regarding marketing. Next, the reader is introduced to the three main components of the marketing channels—manufacturers, wholesalers, and retailers—and from these through a splendid review of the elements involved in pricing and competition, advertising, and retailing and finally, before the summary, through an explanation of internal and external controls.

Paul Olsen's book of 30 years ago stood as one of the few references in this area until the 1968 publication of this book's first edition, which was the first product in the field with quantitative data. The major flaw of the 1968 work, namely the rapid obsolescence of data, has now been fully rectified with the publication of the 1975 second edition containing updated data throughout. Naturally, the book only superficially touches many areas, but that is a fair price to pay for a work that has delivered, in a coherent form, a review of such an immense area.

Complete comprehension should be possible by anyone engaged in any area of pharmaceutical endeavor. This reviewer recommends the book to those engaged in physical and biological science activities as an excellent vehicle to gain an understanding of what is involved in bringing a product to market and sustaining it there once a marketable substance is produced. Of course, the book should serve as a text in pharmaceutical marketing courses in colleges of pharmacy. Lastly, as a reference, the book is a virtual gold mine of industry statistics. Professor Smith has produced a most useful work.

Reviewed by
Albert I. Wertheimer
College of Pharmacy
University of Minnesota
Minneapolis, MN 55414

Predicted Compounds—Alleged Biological Activity

The IUPAC Commission on Medicinal Chemistry conducted a study of some of the consequences arising in the past decade from applying computer-assisted techniques to the quantitative analysis of relationships between structure and biological activity.

The IUPAC Commission recently published a report entitled " 'Predicted' Compounds with 'Alleged' Biological Activities from Analyses of Structure–Activity Relationships. Implications for Medicinal Chemists"[1]. The report examines the effects on patentability resulting from the publication of such "predicted" compounds that have not been synthesized and concludes with the following two recommendations:

1. Medicinal chemists who publish predictions of allegedly active compounds should be urged to consider it their responsibility to synthesize and test such compounds or to arrange to have this work done. "Predictions" *per se* are of little practical value unless the underlying hypotheses are tested experimentally.
2. Journal editors and editorial boards should consider the adoption of policies which discourage the publication of manuscripts containing "predictions" if they are not accompanied by the synthesis and testing of the predicted compounds.

Copies of the complete report are available from the IUPAC Secretariat, Bank Court Chambers, 2/3 Pound Way, Cowley Center, Oxford, OX4 3YF, United Kingdom, or from the undersigned.

A. I. Rachlin
IUPAC Commission on Medicinal Chemistry
c/o Hoffmann–La Roche Inc.
Nutley, NJ 07110

Received December 22, 1975.

[1] "IUPAC Information Bulletin," No. 49, Mar. 1975, pp. 12–20.

Bioavailability Information

For the past year, I have served as the Academy of Pharmaceutical Sciences' representative to the APhA Bioavailability Project Steering Committee. As I am sure you are aware, this Committee has been overseeing the writing of bioavailability monographs on selected drug products. The nine drugs to be studied in the third phase of the Project include: acetaminophen, chlordiazepoxide, conjugated estrogens, ferrous sulfate, meprobamate, papaverine (sustained release), penicillin V potassium, sulfisoxazole, and thyroid.

The discussion and analysis of information supplied by manufacturers and/or distributors of drug products are major factors of each monograph. However, one problem the Committee has encountered is correctly identifying the appropriate individual within a company to contact for information.

Since industrial pharmaceutical scientists reading this Journal are the primary individuals within their companies concerned with the bioavailability issue, I am asking each to determine if any their products is being evaluated. In addition, I would appreciate it if they would communicate with Dr. Richard P. Penna, Staff Project Director at APhA headquarters, the name of the appropriate individual within the firm who should be directly contacted to provide bioavailability information.

Leslie Z. Benet
Bioavailability Project Steering Committee
Professional Affairs Division
American Pharmaceutical Association
Washington, DC 20037

Received December 22, 1975.

Authors please note:

Page charges for contributed articles published in the *Journal of Pharmaceutical Sciences* will be $70 per printed page, effective July 1976. Recognizing that publication of research reports is an integral part of research, page charge costs should be considered as a part of research funding. Acceptance of manuscripts for publication is not contingent upon payment of page charges, since the editors have no knowledge regarding payment. However, the continued viability of scientific journals is contingent upon the sponsors of research assuming some of the responsibility for publication of the results of research.

Predicted Compounds—Alleged Biological Activity

The IUPAC Commission on Medicinal Chemistry conducted a study of some of the consequences arising in the past decade from applying computer-assisted techniques to the quantitative analysis of relationships between structure and biological activity.

The IUPAC Commission recently published a report entitled " 'Predicted' Compounds with 'Alleged' Biological Activities from Analyses of Structure–Activity Relationships. Implications for Medicinal Chemists"[1]. The report examines the effects on patentability resulting from the publication of such "predicted" compounds that have not been synthesized and concludes with the following two recommendations:

1. Medicinal chemists who publish predictions of allegedly active compounds should be urged to consider it their responsibility to synthesize and test such compounds or to arrange to have this work done. "Predictions" *per se* are of little practical value unless the underlying hypotheses are tested experimentally.
2. Journal editors and editorial boards should consider the adoption of policies which discourage the publication of manuscripts containing "predictions" if they are not accompanied by the synthesis and testing of the predicted compounds.

Copies of the complete report are available from the IUPAC Secretariat, Bank Court Chambers, 2/3 Pound Way, Cowley Center, Oxford, OX4 3YF, United Kingdom, or from the undersigned.

A. I. Rachlin
IUPAC Commission on Medicinal Chemistry
c/o Hoffmann–La Roche Inc.
Nutley, NJ 07110

Received December 22, 1975.

[1] "IUPAC Information Bulletin," No. 49, Mar. 1975, pp. 12–20.

Bioavailability Information

For the past year, I have served as the Academy of Pharmaceutical Sciences' representative to the APhA Bioavailability Project Steering Committee. As I am sure you are aware, this Committee has been overseeing the writing of bioavailability monographs on selected drug products. The nine drugs to be studied in the third phase of the Project include: acetaminophen, chlordiazepoxide, conjugated estrogens, ferrous sulfate, meprobamate, papaverine (sustained release), penicillin V potassium, sulfisoxazole, and thyroid.

The discussion and analysis of information supplied by manufacturers and/or distributors of drug products are major factors of each monograph. However, one problem the Committee has encountered is correctly identifying the appropriate individual within a company to contact for information.

Since industrial pharmaceutical scientists reading this Journal are the primary individuals within their companies concerned with the bioavailability issue, I am asking each to determine if any their products is being evaluated. In addition, I would appreciate it if they would communicate with Dr. Richard P. Penna, Staff Project Director at APhA headquarters, the name of the appropriate individual within the firm who should be directly contacted to provide bioavailability information.

Leslie Z. Benet
Bioavailability Project Steering Committee
Professional Affairs Division
American Pharmaceutical Association
Washington, DC 20037

Received December 22, 1975.

Authors please note:

Page charges for contributed articles published in the *Journal of Pharmaceutical Sciences* will be $70 per printed page, effective July 1976. Recognizing that publication of research reports is an integral part of research, page charge costs should be considered as a part of research funding. Acceptance of manuscripts for publication is not contingent upon payment of page charges, since the editors have no knowledge regarding payment. However, the continued viability of scientific journals is contingent upon the sponsors of research assuming some of the responsibility for publication of the results of research.

1976

March 25
Safety and Toxicity of Pharmaceuticals and Consumer Products, Annual Symposium, Chemical Institute of Canada, Holiday Inn, Don Valley-Eglinton, Toronto, Canada (Contact T. J. Carrothers, Bristol-Myers Products Canada Ltd., 99 Vanderhoof Ave., Toronto, Canada M4G 2H6)

March 25–29
National Drug Abuse Conference, Americana Hotel, New York, N.Y.

March 28–April 11
Basic Principles of Therapeutic Drug Monitoring, Pine Mountain Conference on Clinical Chemistry, Pine Mountain, Ga. (Contact W. G. Trawick, Georgia State University, Atlanta, GA 30303, 404-658-3120)

April 3–8
APhA Annual Meeting, New Orleans, La.

April 4–7
Proprietary Association, Annual Meeting, The Breakers, Palm Beach, Fla.

April 4–9
Centennial American Chemical Society Meeting, New York, N.Y. (Contact A. T. Winstead, American Chemical Society, 1155 16th St., N.W., Washington, DC 20036)

April 10–13
Society for Biomaterials, Annual Meeting, and International Biomaterials Symposium, Philadelphia, Pa. (Contact S. R. Pollack, Department of Metallurgy and Materials Science, University of Pennsylvania, Philadelphia, PA 19174)

April 18–24
Basic Pharmacokinetics and Biopharmaceutics Workshop, American Society of Clinical Pharmacology and Therapeutics, St. Augustine, Fla. (Contact Irene Garrett, Administrative Associate, 1826 N.W. 26th Way, Gainesville, FL 32605)

April 25–29
Food and Drug Law Institute, Annual Meeting, Del Coronado, Coronado, Calif.

April 26–May 1
Third International Symposium on Detection and Prevention of Cancer, Americana Hotel, New York, N.Y. (Contact Dr. Herbert E. Nieburgs, Mount Sinai School of Medicine, City University of New York, Fifth Ave. and 100th St., New York, NY 10029)

May 10–12
Pharmaceutical Manufacturers Association, Annual Meeting, The Greenbrier, White Sulphur Springs, W.Va.

May 17
APhA Academy of Pharmaceutical Sciences, Annual Midwestern Regional Meeting, Industrial Pharmaceutical Technology and Pharmaceutical Analysis and Control Sections, O'Hare Inn, Chicago, Ill. (Contact Dr. A. Amann, Abbott Laboratories, North Chicago, IL 60064)

May 18–21
International Symposium on Drug–Receptor and Drug–Enzyme Interactions: A Basic Approach, La Societe Chimique De Belgique and Les Facultes Universitaires Notre-Dame De La Paix, Namur, Belgium (Contact Prof. F. Durant, Departemente de Chimie, Facultes Notre-Dame De La Paix, 61, Rue de Bruxelles, B-5000 Namur, Belgium)

June 3–5
Annual Summer Symposium, American Chemical Society Division of Analytical Chemistry, Tempe, Ariz. (Contact R. S. Juvet, Arizona State University, Tempe, AZ 85281)

June 14–25
Design and Analysis of Scientific Experiments, Massachusetts Institute of Technology (Contact Director of the Summer Session, Room E19-356, Massachusetts Institute of Technology, Cambridge, MA 02139)

June 20–24
National Medicinal Chemistry Symposium, American Chemical Society Division of Medicinal Chemistry, University of Utah, Salt Lake City, Utah (Contact L. B. Townsend, Department of Biopharmaceutical Sciences, University of Utah, Salt Lake City, UT 84112)

June 21–23
International Symposium on Mass Spectrometry in Drug Metabolism, Milan, Italy (Contact Dr. A. Frigerio, Instituto di Richerche Farmacologiche Mario Negri, Via Eritrea 62, 20157, Milan, Italy)

June 27–July 1
American Medical Association, Annual Meeting, Dallas, Tex.

August 27–29
The European Symposium of the International Association of Forensic Toxicologists, State University of Ghent, Belgium (Contact Department of Toxicology, State University of Ghent, Hospitaalstraat 13, 9000 Ghent, Belgium)

August 29–September 2
American Chemical Society, National Meeting, San Francisco, Calif. (Contact A. T. Winstead, American Chemical Society, 1155 16th St., N.W., Washington, DC 20036)

October 7–10
American College of Apothecaries, Annual Meeting, Bellevue Stratford, Philadelphia, Pa.

October 17–21
American Public Health Association, Annual Meeting, Miami Beach, Fla.

October 18–21
Association of Official Analytical Chemists, Marriott Twin Bridges, Washington, D.C. (Contact L. G. Ensminger, AOAC, Box 540, Ben Franklin Station, Washington, DC 20044)

October 22
APhA Academy of Pharmaceutical Sciences, Annual Eastern Regional Meeting, Industrial Pharmaceutical Technology Section, Governor Morris Inn, Morristown, N.J. (Contact Dr. Arthur Goldberg, Applied Sciences, TDD, Hoffmann–La Roche Inc., Nutley, NJ 07110)

November 14–18
APhA Academy of Pharmaceutical Sciences, National Meeting, Carleton House Hotel, Orlando, Fla.

November 14–18
American Dental Association, Annual Meeting, Las Vegas, Nev.

November 14–20
Federation of Analytical Chemistry and Spectroscopy Societies, Annual Meeting, American Chemical Society Division of Analytical Chemistry and others, Civic Center, Philadelphia, Pa. (Contact C. White, Analytical Chemistry Division, Oak Ridge National Laboratories, Oak Ridge, TN 37830)

December 4–8
American Medical Association, Clinical Meeting, Philadelphia, Pa.

December 5–10
American Society of Hospital Pharmacists, Midyear Meeting, Anaheim, Calif.

December 14–15
Food and Drug Law Institute, Annual Meeting, Washington Hilton, Washington, D.C.

Items to be considered for inclusion or corrections should be addressed to:

J. Pharm. Sci. Calendar
2215 Constitution Avenue, N.W.
Washington, DC 20037

Journal of Pharmaceutical Sciences

APRIL 1976

VOLUME 65 NUMBER 4

MARY H. FERGUSON
Editor

L. LUAN CORRIGAN
Assistant Editor

SHELLY ELLIOTT
Production Editor

JANET D. SHOFF
Copy Editor

EDWARD G. FELDMANN
Contributing Editor

SAMUEL W. GOLDSTEIN
Contributing Editor

LELAND J. ARNEY
Publications Director

EDITORIAL ADVISORY BOARD

JOHN AUTIAN	HARRY B. KOSTENBAUDER
LYNN R. BRADY	CARL J. LINTNER, JR.
WILLIAM O. FOYE	DAVID E. MANN, JR.
WILLIAM J. JUSKO	GERALD J. PAPARIELLO

The *Journal of Pharmaceutical Sciences* is published monthly by the American Pharmaceutical Association at 2215 Constitution Ave., N.W., Washington, DC 20037. Second-class postage paid at Washington, D.C., and at additional mailing office.

All expressions of opinion and statements of supposed fact appearing in articles or editorials carried in this journal are published on the authority of the writer over whose name they appear and are not to be regarded as necessarily expressing the policies or views of the American Pharmaceutical Association.

Offices—Editorial, Advertising, and Subscription Offices: 2215 Constitution Ave., N.W., Washington, DC 20037. Printing Offices: 20th & Northampton Streets, Easton, PA 18042

Annual Subscriptions—United States and foreign, industrial and government institutions $50, educational institutions $50, individuals *for personal use only* $30; single copies $5. All foreign subscriptions add $5 for postage. Subscription rates are subject to change without notice. Members of the American Pharmaceutical Association may elect to receive the *Journal of Pharmaceutical Sciences* as a part of their annual $60 (foreign $65) APhA membership dues.

Claims—Missing numbers will not be supplied if dues or subscriptions are in arrears for more than 60 days or if claims are received more than 60 days after the date of the issue, or if loss was due to failure to give notice of change of address. The Association cannot accept responsibility for foreign delivery when its records indicate shipment has been made.

Change of Address—Members and subscribers should notify at once both the Post Office and the American Pharmaceutical Association, 2215 Constitution Ave., N.W., Washington, DC 20037, of any change of address.

© Copyright 1976, American Pharmaceutical Association, 2215 Constitution Ave., N.W., Washington, DC 20037; all rights reserved.

DISSOLUTION TEST BLOSSOMS

The USP Executive Committee is to be highly commended for its decisive action announced early this year, in adopting a policy to establish a dissolution test requirement for all USP and NF tablets and capsules. This action was a long time in coming and had to clear a multitude of major hurdles prior to its approval.

The history of the dissolution test could probably be traced back to 1961 when the first rumblings were heard that the tablet disintegration test, which at that time was a general requirement in USP and NF monographs, was not serving as effectively as had been generally assumed. Probably the earliest reports on this subject appeared in this Journal and came from pharmacy school research laboratories in San Francisco and Buffalo.

Initial efforts were directed at modifications of the disintegration test equipment, the test conditions, and the time limits. Although some significant improvement resulted, it became evident that—at least in the case of some drugs or some formulations—a more sophisticated type of test procedure was needed. By the mid-1960's, a number of studies were reported which indicated that measurement of the dissolution characteristics of a solid dosage form constituted a much more reliable index of the suitability of the product formulation than did even the modified and improved disintegration test. On this basis, it was suggested that the compendia consider adoption of the dissolution test with a view toward its replacing the disintegration test.

Recognizing the complexity and serious ramifications involved, the compendia officials appointed a joint panel reflecting wide experience, as well as a wide diversity of affiliations and viewpoints. Concurrently, developmental work was initiated and given a high priority in the laboratory jointly sponsored by the compendia.

But then a rather curious turn of events occurred. Resistance began to surface from various sources: opposition for ill-defined reasons came from many of the drug manufacturers; academic scientists each appeared to have personal preferences with respect to the design of the apparatus and the test methodology to be employed; and various elements within the regulatory agencies appeared to have different views, depending upon their respective roles in the scheme of drug regulation and surveillance. The net result was that a test specification, which appeared to have a general consensus of blessing and support, almost overnight deteriorated into a controversial "hot potato" beset by political, economic, and administrative overtones.

In late 1968, a decision was made by the National Formulary, with the support of the NF Board, to "bite the bullet" and to proceed with initial implementation of the dissolution test. Shortly thereafter, a similar decision to move forward was made by the USP. So it was that the first compendia dissolution test requirements to be adopted anywhere in the world appeared in six monographs each of the 1970 editions of the *NF* and *USP*.

Regrettably, this action did not still the criticism—some of which, undoubtedly, was justifiable but much of which appeared otherwise. Some constructive criticism was offered with a view toward making the procedure more reproducible, reliable, and indicative of drug product quality. Any refinements that would contribute to these characteristics were welcomed since the compendia officials recognized that the procedure, the apparatus, and the methodology were certainly less than perfect. Nevertheless, all evidence indicated that the general approach being followed represented the best available and that it constituted a significant contribution toward drug product standardization.

The continued criticism and controversy were largely responsible for the relatively little progress made in applying this requirement to additional monographs in the 1975 editions of the compendia. Ideally, the early 1970's should have been devoted to extending the dissolution requirement to a significant number of additional tablet and capsule monographs. Instead, most of the effort had to be directed at "reinventing the wheel," so to speak, by retracing much the same ground and reconfirming the same decisions that led up to the specification as it had already appeared in the 1970 editions.

Consequently, the recent announcement of the USP Executive Committee action constitutes a "great leap forward." We consider it welcome news and hope that the next few years will be marked by broad collaboration and general cooperation, with the result that the stated goal for the 1980 compendia will, in fact, be attained.

Edward G. Feldmann

Journal of Pharmaceutical Sciences

APRIL 1976
VOLUME 65 NUMBER 4

REVIEW ARTICLE

Arrhythmias and Antiarrhythmic Drugs: Mechanism of Action and Structure–Activity Relationships I ▲

P. H. MORGAN * and I. W. MATHISON ˣ

Keyphrases □ Antiarrhythmic drugs—classifications, mechanism of action, structure–activity relationships, review □ Structure–activity relationships—antiarrhythmic drugs, review □ Arrhythmias—related to changes in normal transmembrane action potential and electrophysiological parameters, antiarrhythmic drugs, review

CONTENTS

Development of Currently Used and Experimental Antiarrhythmic Drugs 467
Genesis of Arrhythmias 470
Electrophysiology of Heart 470
Theory of Arrhythmia Genesis 472
Disturbances in Impulse Formation and Conduction 472
Disturbances in Fast–Slow Response Relationship 473
Considerations of Rhythms and Arrhythms on Ionic and Molecular Level 474
Mechanism of Action of Antiarrhythmic Drugs 477
Nonspecific Action at Myocardial Membrane 477
Electrophysiological Effects on Transmembrane Action Potential 478
References 480

The drug therapy of disturbances in cardiac rhythm had its beginning in 1914 when Wenckebach (1) reported that the cardiac arrhythmia of a patient with malaria, being treated with cinchona alkaloids (which contain mainly quinine), was converted to normal sinus rhythm. In 1918, Frey (2) studied cinchonine, quinine, and quinidine (I) and found that all three had similar properties in converting atrial fibrillation to normal rhythm but that quinidine was the most potent. Since this initial use, quinidine has remained one of the most important and efficacious drugs for maintaining normal heart rhythm (3).

DEVELOPMENT OF CURRENTLY USED AND EXPERIMENTAL ANTIARRHYTHMIC DRUGS

In 1951, Mark *et al.* (4) found that procainamide (II) was effective as an antiarrhythmic agent; it has been widely used since then in treating arrhythmias. Southworth *et al.* (5) reported in 1950 that the local anesthetic lidocaine[1] (III) was successful in terminating ventricular tachycardia, and this drug has become important in the early treatment of ventricular arrhythmias associated with acute myocardial infarction due to its relatively safe intravenous route of administration.

Phenytoin[2] (IV), an anticonvulsant drug in use since 1938, was reported in 1958 to be effective in ventricular arrhythmias in humans (6). Since then, phenytoin has been used quite widely, particularly against ventricular arrhythmias caused by digitalis toxicity (3). Another drug discovered to have antiar-

▲ *Editor's note:* Part II of this article will appear in the May 1976 issue of the *Journal of Pharmaceutical Sciences.*

[1] Xylocaine or lignocaine.
[2] Dilantin.

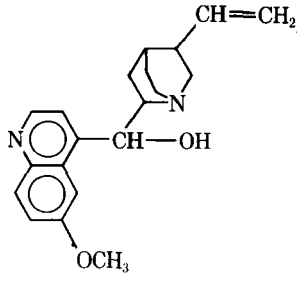

I

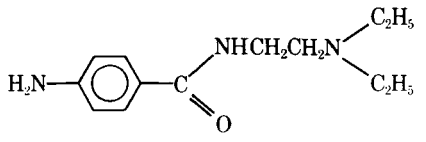

II

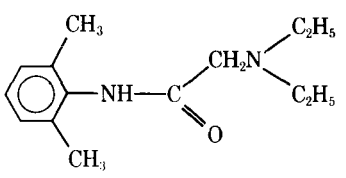

III

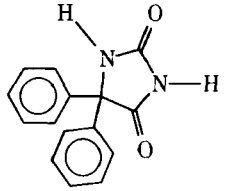

IV

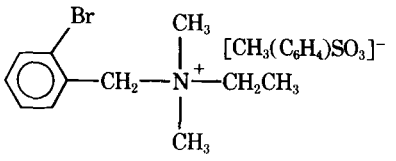

V

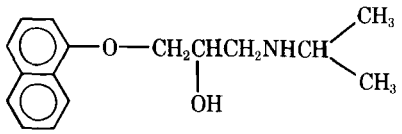

VI

rhythmic properties (7) is bretylium tosylate (V). Subsequent studies on bretylium showed that it is effective in the treatment of disturbances of ventricular rhythm that were not successfully abolished by conventional drugs; on this basis, it has achieved limited clinical use (3).

Propranolol (VI) also has gained widespread clinical use as an antiarrhythmic agent. This drug, developed in 1964, is a potent β-adrenergic blocking agent (8). However, subsequent studies indicated that propranolol had, in addition to β-blocking properties, a quinidine-like action on the heart (9, 10). Which of these factors represents the more important antiarrhythmic property is still a matter of controversy (11, 12), although it is generally accepted that β-blockade is the primary therapeutic effect at normal blood levels (13).

Several other drugs not normally classified as antiarrhythmic agents have been used in the therapy of certain cardiac rhythm disturbances, *e.g.*, digitalis (14). Many compounds in the early stages of pharmacological and clinical evaluation have proved to be effective in the treatment of experimentally induced arrhythmias in animals (15–25).

Disopyramide[3] (VII) is currently being used successfully in Europe and appears to manifest its antiarrhythmic properties in much the same way as quinidine while having a wider margin of safety (26, 27).

Verapamil (VIII), a derivative of papaverine, has been in clinical use in Europe since 1966. It is reported to be most successful against atrial fibrillation and flutters and paroxysmal supraventricular and preexcitatory tachycardia but less successful against ventricular arrhythmias. This drug has evoked considerable interest recently due to its novel mechanism of action (28–30).

Mexiletine[4] (IX) has successfully passed several clinical trials and has demonstrated efficacy against ventricular arrhythmias equal to, or greater than, currently available drugs (31, 32). In addition, mexiletine is reported to be effective when taken orally and to possess a long half-life in the body at effective levels without the toxic side effects seen with the most commonly used long-term oral antiarrhythmic drugs. A preliminary report of a pharmacokinetic study claimed that plasma mexiletine levels are linearly related to salivary concentrations (33). Use of this relationship is proposed as a rapid and convenient analytical method for determining blood drug levels during antiarrhythmic therapy.

A new drug, 2-amino-2′,6′-propionoxyxylidide hydrochloride (X), possessing a structure similar to lidocaine and mexiletine, has proved successful in treating experimental ventricular arrhythmias in animals (34). It is orally absorbed, has a rapid onset of action and long duration, and is currently being studied in humans.

Amiodarone[5] (XI), initially used in the treatment of angina pectoris (35), has been reported to be an effective antiarrhythmic agent after prolonged oral administration in both animals and humans (36). This drug possesses an unusual mechanism of action, mimicking the lengthening of the duration of the cardiac action potential seen in hypothyroidism, although no evidence of this condition has been reported in patients receiving the drug (37).

Aprindine (XII) is reported to be an orally effective, long-acting drug, efficacious in preventing ventricular arrhythmias associated with acute myocardial infarction (38, 39). One clinical study suggested that one dose per day is sufficient for maintenance therapy (40).

Another drug that has shown promising antiarrhythmic properties in animal tests is a decahydroquinoline derivative, 4-carbamoyloxy-1-[4-(4-fluorophenyl)-4-oxybutyl]decahydroquinoline[6] (XIII). It is reported to be orally effective and long acting, possessing similar actions on the heart as quinidine (41).

Propafenone[7] (XIV) underwent clinical trials in Germany and is effective in humans. Its effectiveness may result from both its β-adrenergic blocking properties and its local anesthetic, quinidine-like actions (42).

Diphenidol (XV) is reported to be efficacious in

[3] Norpace.

[4] Kö 1173.
[5] Cardarone.
[6] L 7810.
[7] 5A-79.

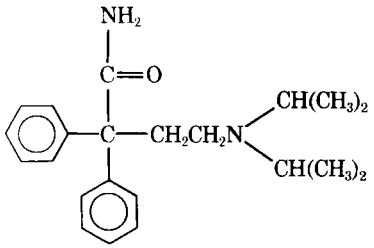

VII

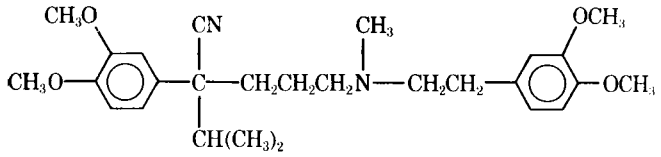

VIII

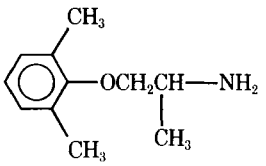

IX

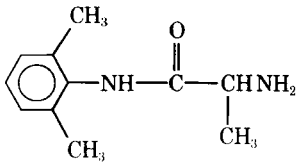

X

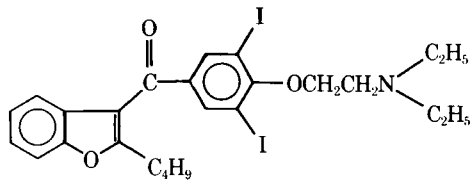

XI

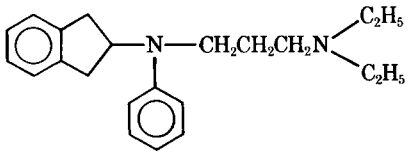

XII

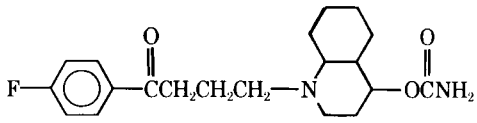

XIII

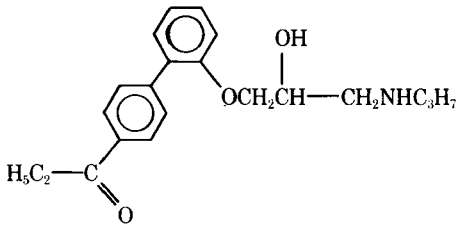

XIV

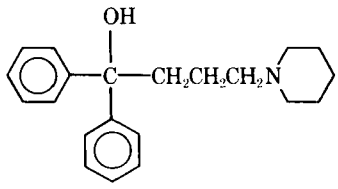

XV

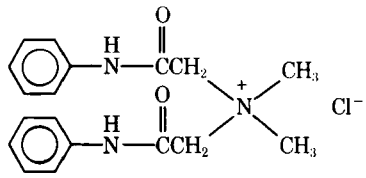

XVI

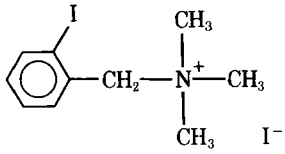

XVII

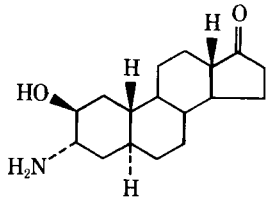

XVIII

both digitalis-induced arrhythmias in dogs and in digitalis intoxication in humans. Its usefulness as a clinical drug has been proposed (43).

N,N-Bis(phenylcarbamoylmethyl)dimethylammonium chloride[8] (XVI), a quaternary ammonium derivative of lidocaine synthesized several years ago (44), has recently received renewed interest as a supplement to lidocaine in intravenous treatment of arrhythmias in the coronary care unit (45). The compound is reported to be successful in the treatment of most types of ventricular arrhythmias and is suggested especially for arrhythmias that have proved refractory to other antiarrhythmic drugs (46). Compound XVI has a rapid onset of action and long duration. Moreover, due to the presence in the molecule of a permanently charged cation, it fails to pass through the blood–brain barrier and thus elicits much fewer central nervous system (CNS) side effects than does lidocaine (47).

o-Iodobenzyltrimethylammonium chloride[9] (XVII), an analog of bretylium, has demonstrated effectiveness in raising the ventricular fibrillation threshold to electroshock, preventing ventricular fibrillation in dogs suffering from experimentally induced myocardial infarction, and, in contrast to bretylium, reversing ouabain-induced arrhythmias. Compound XVII lacks the initial and potentially dangerous sympathomimetic effects of bretylium (48). The ^{131}I-labeled analog of XVII is highly localized in cardiac tissue and has been proposed as a heart scanning agent for use in radiology (49, 50).

A steroid, 3α-amino-5α-androstan-2β-ol-17-one[10] (XVIII), possesses potent antiarrhythmic activity (51, 52). Compound XVIII proved effective in antagonizing aconitine-induced arrhythmias in rats, being seven times more potent and five times less toxic than lidocaine by the intravenous route. The

[8] QX-572.

[9] UM-360.

[10] ORG-6001.

Table I—Etiological Factors that May Give Rise to Cardiac Arrhythmias[a]

Local cardiac factors
1. Hypertensive heart disease
2. Rheumatic, diphtheric, and viral types of heart disease
3. Degenerative states, especially coronary artery disease
4. Congenital abnormalities
5. Congestive heart failure

Cardiac factors resulting from disturbances in other organs
1. CNS (mediated by sympathetic and vagal stimulation)
2. Pulmonary disease (emphysema)
3. Endocrine (hypo- and hyperthyroidism, hypo- and hyperaldosteronism, diabetic acidosis, and hypoglycemia)
4. GI (fluid and electrolyte loss by vomiting and diarrhea)
5. Renal disturbances (renal insufficiency and alterations in fluid balance)

General factors
1. Infections and toxic states
2. Anemia and avitaminosis
3. Electrolyte disturbances
4. Drugs (digitalis, quinidine, and procainamide toxicity and toxicity from some general anesthetics used in surgery)

[a] Adapted, with permission, from Samuel Bellet, "Clinical Disorders of the Heart Beat," 3rd ed., Lea & Febiger, Philadelphia, Pa., 1971, p. 119.

compound was effective orally at a lower dose than lidocaine given intravenously and was similar to lidocaine in its potency in restoring ouabain-induced ventricular tachycardia and in correcting postmyocardial infarction arrhythmias in dogs. Protective doses of XVIII were effective 18 and 24 hr after intravenous and oral administrations, respectively. The compound lacks both local anesthetic activity *in vivo* and β-adrenergic blocking properties.

The appearance of several orally effective, long-acting, and less toxic antiarrhythmic agents should be encouraging to the clinician. Many new experimental drugs have been shown in clinical trials to be equally or more efficacious than the currently available choices while exhibiting an encouraging lack of toxic side effects. There has been a great and well-documented need for drugs possessing these properties for prophylactic treatment or prolonged maintenance of high-risk heart patients receiving antiarrhythmic therapy (13, 53, 54).

When considering the treatment of cardiac arrhythmias, choice of the most suitable agent must be based on a thorough knowledge of the basic pathological mechanism causing the disturbance (55, 56). Indeed, an arrhythmia is usually secondary to some primary pathological condition. Bellet (3) divided the factors into three groups: (*a*) local cardiac factors, (*b*) cardiac factors resulting from disturbances in other organs, and (*c*) general factors such as drug toxicity (Table I).

GENESIS OF ARRHYTHMIAS

Electrophysiology of Heart—The complexity of the genesis of arrhythmias becomes simplified somewhat when one considers the problem on a cellular level. This approach became possible in 1950 when the first transmembrane action potential of a single cardiac cell was recorded (57, 58), using a microelectrode developed previously (59). Subsequent studies during the last 20 years have led to a greater understanding of the cellular mechanisms by which arrhythmias are generated. The advances made since these beginnings were compiled and discussed in several excellent books and reviews (60–71), so only a brief introduction will be presented here. With this introduction, the reader will be able to understand better the following discussion on the effect of antiarrhythmic drugs on the transmembrane action potential.

Four inherent properties of cardiac muscle permit its performance as a pump. These properties are automaticity, conductivity, excitability, and contractility. Automaticity enables the heart to generate its own electrical stimulus spontaneously. This stimulus is normally generated in the specialized pacemaker or automatic cells in the sino-atrial node (S-A node). From this focal point, the stimulus is conducted to surrounding cells and other parts of the atria and ventricle by specialized conducting fibers.

Excitation of a cardiac cell may occur spontaneously (self-excitation) as in the automatic cells already described, or it may be the result of an external stimulus, *i.e.*, an artificial pacemaker. The pacemaker provides the spontaneous stimulus which is propagated throughout the heart in the form of an action potential. When the excitatory impulse encounters contractile cardiac cells, the myofibrils of these cells contract and provide the force by which the heart pumps the blood.

The transmembrane potential (difference) observed in all cardiac cells is about −90 mv in quiescent ventricular muscle fibers and Purkinje fibers and from −70 to −80 mv in atrial fibers; the cell interior is negative with respect to the exterior. This potential difference in muscle cells remains constant until excitation occurs; then the stimulus, in the form of a depolarizing current, reduces the potential difference across the membrane. If this potential is reduced from the resting potential (R.P.) of about −90 mv to a critical value (from −65 to −70 mv), called the threshold potential (T.P.), an action potential is produced.

The recorded action potential from canine ventricular muscle is illustrated in Fig. 1D. The curve representing the action potential is divided into five phases (0 through 4). Phase 0 is the rapid depolarization that occurs upon excitation. The difference in membrane potential decreases; during what is termed the overshoot, the inside of the cell actually becomes positive with relation to the outside.

Following depolarization, the cell begins the process of repolarization back to the resting potential (−90 mv). Repolarization in cardiac cells is a slow process, about 500 times longer than nerve cell repolarization. The first phase of repolarization (phase 1) is quite rapid and is then followed by a period of slow repolarization (phase 2 or the plateau). Repolarization speeds up again in phase 3 and completes the process by returning the transmembrane potential back to resting potential. Phase 4 is characterized by an interval of electrical quiescence in nonautomatic

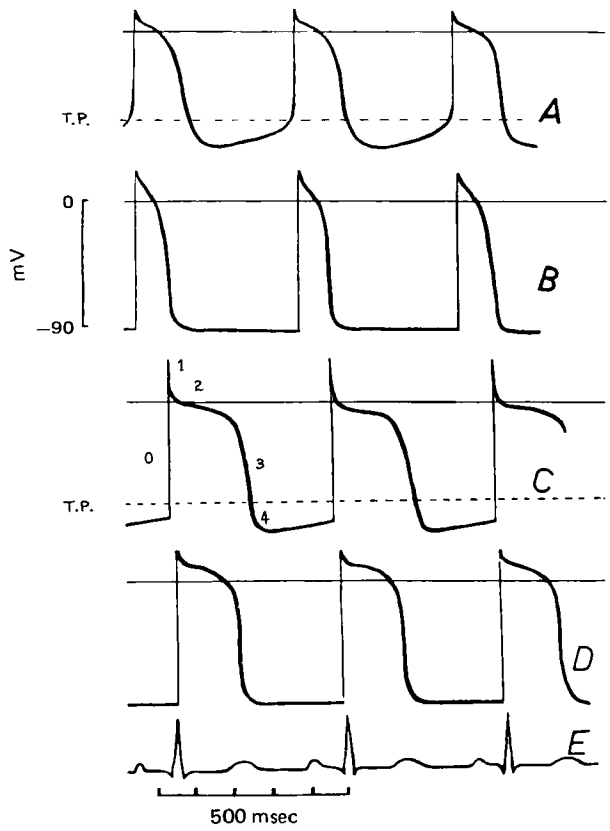

Figure 1—*Transmembrane action potentials recorded from cells of: (A) S-A node, (B) atrial muscle, (C) Purkinje system, and (D) ventricular muscle; on the same time axis is the ECG (E). The five recognized phases of the transmembrane action potential are numbered in the first complex of row C. Note diastolic depolarization and level of threshold potential (T.P.) in rows A and C. The difference in duration and configuration of action potentials from different cell types and the delay in A-V conduction are indicated by the delay in upstroke between B and C. [Reprinted, with permission, from W. Trautwein,* Pharmacol. Rev., *15, 279(1963) (Williams & Wilkins, Baltimore, Md.).]*

cardiac cells, such as ventricular or atrial muscle cells (Fig. 1B).

The action potentials for automatic heart cells are illustrated in Fig. 1. Figure 1A is a typical transmembrane action potential recorded from cells of the S-A node. The maximum diastolic potential reached in S-A nodal cells (−70 mv) is less than in the other types of heart cells. Also, the automatic cells exhibit spontaneous diastolic depolarization observed in the transmembrane action potential as the gradual rise in slope of phase 4. When the gradual decrease in potential difference reaches the threshold potential (about −50 mv in S-A nodal cells), rapid depolarization (phase 0) occurs. By this mechanism, the heart generates its own impulse, giving rise to the property of automaticity.

The automatic cells of the S-A node usually are the true pacemaker of the heart, since they fire at a faster rate than the other automatic cells. Automatic cells also are found in specialized atrial conduction fibers among certain cells in the atrio-ventricular node (A-V node) and in the His–Purkinje fibers. If, for any reason, the firing rate of the S-A nodal cells decreases, then other automatic cells, sometimes called latent pacemaker cells, can take over. However,

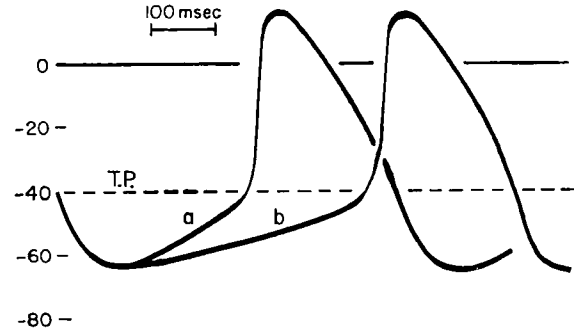

Figure 2—*Illustration of how changes in the slope of phase 4 or the rate of slow diastolic depolarization could be responsible for changes in the firing frequency of cardiac pacemaker cells. (Reprinted, with permission, from B. F. Hoffman and P. F. Cranefield, "Electrophysiology of the Heart," McGraw-Hill, New York, N.Y., 1960, p. 109.)*

under normal conditions, most automatic cardiac cells are excited by a propagated or conducted action potential (wave of depolarizing current) from the pacemaker before the slope of phase 4 reaches threshold potential.

The rate of firing of automatic cells may be altered as a result of a change in the slope of phase 4, a change in the magnitude of the threshold potential, and a change in the magnitude of the maximum diastolic potential (the potential at the conclusion of repolarization) (62). The effect of a change in the slope of phase 4 is illustrated in Fig. 2. The steeper slope (*a*) reaches threshold potential more rapidly than (*b*), resulting in a faster heart rate. On the other hand, a slower heart rate is observed when the slope of phase 4 is decreased.

The body exerts nervous control over the heart by way of the adrenergic (sympathetic) system, which on stimulation results in heart rate increases, and by the cholinergic (parasympathetic) system *via* the vagus nerve, which on stimulation results in a decrease in heart rate. The adrenergic mediators (endogenous and/or exogenous catecholamines) increase the slope of phase 4; the vagal mediator, acetylcholine, decreases the slope of phase 4. Both cause hyperpolarization (increased maximum diastolic potential). Therefore, the knowledge gained from the ability to record transmembrane action potentials has produced greater understanding of the mechanism of adrenergic and vagal control of the heart rate on the cellular level.

The effect of changes in the magnitude of the threshold potential on the rate of pacemaker firing is shown in Fig. 3. In the action potential (*a*), the threshold potential is about −50 mv (T.P.-1); in the action potential (*b*), the threshold potential has been raised to −40 mv (T.P.-2). It can be seen that (*b*) would fire at a slower rate than (*a*). Also, the maximum diastolic potential in the action potential (*c*) has been increased from about −60 mv (*d*) to −70 mv (*e*), resulting in a slowing of the heart rate.

The parameters of the transmembrane action potential that are important in a discussion of the mechanism of action of antiarrhythmic drugs are:

1. Action potential amplitude—the total potential change occurring during phase 0.

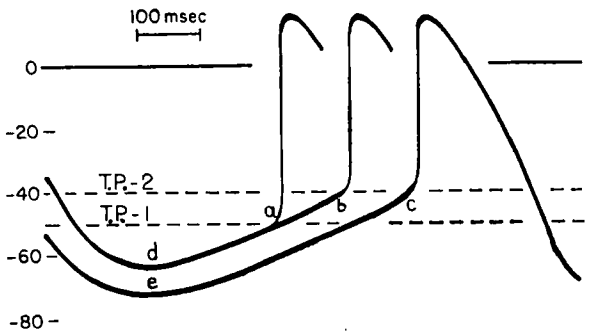

Figure 3—*Illustration of the effect of changes in threshold potential and maximum diastolic potential upon the heart rate. (Reprinted, with permission, from B. F. Hoffman and P. F. Cranefield, "Electrophysiology of the Heart," McGraw-Hill, New York, N.Y., 1960, p. 109.)*

2. Action potential duration—the time period from the start of phase 0 to the end of phase 3. Also, the time required for 50%, 90%, *etc.*, repolarization is sometimes reported as well as the time required to repolarize to some designated voltage.

3. Conduction velocity—the speed at which a stimulus or action potential is propagated.

4. Automaticity—determined by the slope of phase 4 (discussed previously).

5. Maximum upstroke velocity (v/sec)—the steepest slope of the rise of phase 0. This parameter is sometimes reported as average rising velocity.

6. Excitability—dependent upon the level of the threshold potential. For example, if the threshold potential is displaced toward zero potential and the difference between threshold potential and maximum diastolic potential is increased, a greater stimulus is required to effect depolarization.

7. Effective refractory period—period of repolarization during which no normal action potential can be elicited, although a weak, nonpropagated action potential can arise.

8. Absolute refractory period—period of action potential immediately following the start of repolarization during which no response to stimulus is possible. The cell is inexcitable during this period, which usually ends at approximately 50% repolarization.

9. Total refractory period—the resultant of the absolute and effective refractory periods.

10. Membrane responsiveness—the relationship of the maximum upstroke velocity to the level of membrane potential at which the action potential is initiated.

Theory of Arrhythmia Genesis—*Disturbances in Impulse Formation and Conduction*—Several excellent books and reviews are available on the genesis of arrhythmias with relation to changes in electrophysiological and transmembrane properties of the heart (3, 15, 64–69, 71–77).

The currently accepted theory on the mechanisms involved in the genesis of cardiac arrhythmias is that they may result from abnormal impulse formation, abnormal impulse conduction, or a combination of these factors (78). Bigger (79) outlined several factors that may be associated with genesis of arrhythmias (Table II). The disturbances in impulse formation and conduction, and theories as to the origin of the disturbances that cause arrhythmias, have been discussed in detail (64, 66, 68, 73, 74, 76, 77, 79–81).

Table II—Factors Associated with Cardiac Arrhythmias[a]

Disturbances of impulse formation (automaticity)
A. Alterations in normal automaticity
  1. Mechanism
    a. Changes in slope of phase 4 depolarization (ions, autonomic mediators, perfusion, and drugs)
    b. Changes in transmembrane voltage threshold (ions and drugs)
    c. Changes in maximal diastolic transmembrane voltage
    d. Currents flowing from adjacent cells
  2. Site-specialized tissues
    a. S-A node
    b. Atrial specialized fiber tracts
    c. Distal A-V node, bundle of His, bundle branches, and terminal Purkinje fibers
B. Abnormal automatic activity
  1. Mechanism
    a. Changes in repolarization (delayed or abbreviated)
    b. Persistent depolarization
    c. Currents flowing between adjacent cells
    d. After potentials
    e. Oscillatory behavior
  2. Site
    a. Specialized tissues (automatic cells)
    b. "Ordinary" atrial or ventricular myocardium

Disturbances of impulse propagation (conduction)
A. Mechanism
  1. Low transmembrane voltage
    a. Reduced maximal diastolic transmembrane voltage
    b. Transmembrane voltage reduced by spontaneous depolarization during phase 4 (only in specialized tissues)
    c. Incomplete repolarization
  2. Decreased membrane responsiveness
  3. Raised transmembrane voltage threshold
B. Type of conduction alteration
  1. Conduction delay (unidirectional or bidirectional)
    a. With reentrant activity
    b. Without reentrant activity
  2. Conduction failure (unidirectional or bidirectional)
    a. With reentrant activity
    b. Without reentrant activity
C. Site
  1. S-A node and atrium
  2. A-V node
  3. Ventricular muscle and Purkinje fiber junction
  4. Any cardiac tissue

[a] Adapted, with permission, from J. T. Bigger, Jr., in "Cardiac Arrhythmias: the Twenty-fifth Hahnemann Symposium," L. S. Dreifus and W. A. Likoff, Eds., Grune & Stratton, New York, N.Y., 1973, p. 31.

Arrhythmias due to disturbances in impulse formation are thought to be caused by changes in the rate of rise of diastolic depolarization (slope of phase 4). Changes in the slope result in alteration of the heart rate and/or development of new spontaneous ectopic focal discharges in latent pacemaker cells. The normal rate of rise of diastolic depolarization (phase 4) may be altered by an imbalance of the autonomic mediators, acetylcholine and the catecholamines, changes in extracellular ionic concentrations (potassium and calcium ions), hypoxia, changes in the concentration of carbon dioxide, excessive stretch of cardiac tissue, mechanical trauma, and weak electronic currents arising from myocardial ischemia or infarction (66).

Arrhythmias due to disturbances in conduction often are attributed to a phenomenon termed reentry or circus movement (82–86). A model of reentry was

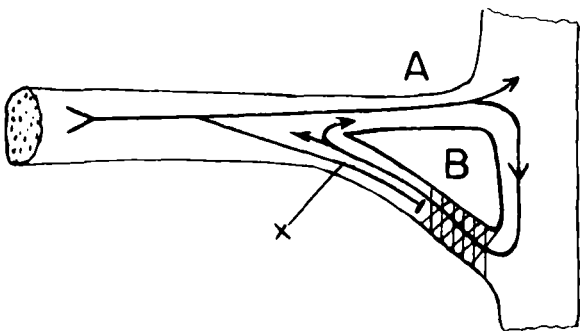

Figure 4—*Diagrammatic representation of arrhythmia due to unidirectional block, giving rise to reentry. This figure represents a peripheral part of the Purkinje system and attached ventricular muscle. The hatched area in branch B represents a unidirectional block to forward conduction. [Reprinted, with permission, from B. F. Hoffman,* Progr. Cardiovasc. Dis., *8, 319(1966) (Grune & Stratton, New York, N.Y.).]*

described by Hoffman (68) and is shown in Fig. 4. As illustrated, branch A possesses normal conduction whereas branch B has a unidirectional block to forward conduction. As shown by the arrows, the normally conducted impulse can enter the muscle fiber and then travel in a retrograde path back through branch B. If the cells that were previously excited by the normally conducted impulse (*i.e.*, at point X) have had time to reach an excitable stage in their action potential, they may be reexcited by the retrograde impulse after the impulse passes through the block area. This wave of reexcitation may then proceed around branch B, branch A, and the ventricular fiber in a circular movement. In this manner, a self-sustaining arrhythmia may arise.

On the other hand, as shown in Fig. 5, the block prevents retrograde conduction, and the conduction of the impulse through branch B is delayed by some mechanism. The impulse traversing branch B may excite the ventricular muscle at a time lapse sufficient for the action potential (i), elicited by the normally propagated impulse through branch A, to have repolarized to enable the delayed impulse to elicit a second action potential (ii).

Disturbances in Fast–Slow Response Relationship—Recently, the two types of electrical activity that have been detected in cardiac fibers and are manifested either in anatomically different tissue or in disease states have been recognized for their important role in the genesis of arrhythmias (72, 80, 81). One type of activity, termed the fast response, is characterized by cardiac fibers with a rapid rate of phase 0 depolarization as a result of a rapid influx of sodium ions. The fast response is found in atrial and ventricular muscle fibers and in fibers of the specialized conducting systems of the atria and ventricles. The rapid influx of sodium ions occurs through specific membrane channels and can be specifically blocked with tetradotoxin (87).

The fast fibers are characterized by a large resting potential (−90 mv), a threshold potential of about −70 mv, a rapid rate of rise of phase 0 of up to 1000 v/sec in Purkinje fibers, and a large amplitude (100–130 mv), all of which result in rapid conduction (0.5–5 m/sec). Such properties confer upon the fast

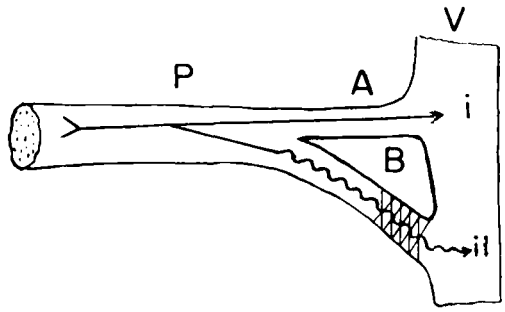

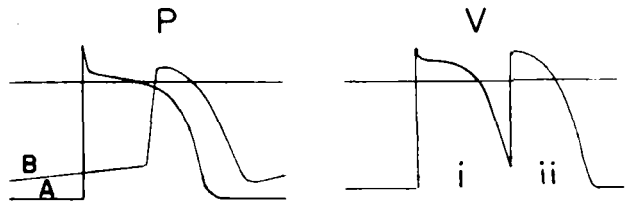

Figure 5—*Diagrammatic representation of arrhythmia due to delayed conduction. The drawing at the top represents a peripheral part of the Purkinje system (P) and attached ventricular muscle (V). In branch A, conduction proceeds at normal velocity and the action potential is shown below by trace A. In branch B, conduction velocity is reduced and unidirectional block is present in the hatched area. The locally recorded action potential is shown by trace B. The action potential in branch A elicits the ventricular action potential number i; the slowly propagating action potential in B initiates the second ventricular action potential, number ii. [Reprinted, with permission, from B. F. Hoffman,* Progr. Cardiovasc. Dis., *8, 319(1966) (Grune & Stratton, New York, N.Y.).]*

response a large safety factor for conduction, so that the minor electrical or anatomical aberrances do not interfere significantly with the spread of the impulse.

The fast fibers also possess a second, slow inward current, probably carried by calcium ions through separate, specific membrane channels not blocked by tetradotoxin. The slow current only becomes activated when the fast sodium-ion depolarizing current has lowered the transmembrane potential to about −55 mv. Since the slow channel consists of a low current and is slowly activated, it does not contribute significantly to phase 0. The slow inward current is also deactivated slowly and persists after rapid depolarization is complete, maintaining the membrane in a depolarized state. For this reason, the slow current is thought to be responsible for the prolonged plateau phase so characteristic of the cardiac action potential.

Fibers that exhibit only the slow response (slow fibers) are anatomically located in the S-A and A-V nodes, the A-V ring fibers, and the mitral and tricuspid valve leaflets. The slow rate of depolarization (1–10 v/sec), low resting potential (from −70 to −60 mv), and low amplitude (35–75 mv) of the transmembrane action potential result in relatively slow conduction (0.01–0.1 m/sec) of the impulse at a low safety factor. Although unaffected by tetradotoxin, the slow membrane channels can be selectively blocked by verapamil and its analog, 5-[(3,4-dimethoxyphenylethyl)methylamino]-2-propyl-2-(3,4,5-trimethoxy-

Table III—Comparison of Properties of Fast and Slow Inward Currents[a]

Electrophysiological Property	Fast Current	Slow Current
Activation plus inactivation kinetics dependent on extra cellular ion concentration of	Fast sodium ions	Slow calcium ions
Abolished by	Tetradotoxin	Verapamil, XIX, Mn, Co, Ni, La
Threshold of activation	−60– −70 mv	−30– −40 mv
Resting membrane potential	−80– −95 mv	−40– −70 mv
Conduction velocity	0.5–3.0 m/sec	0.01–0.1 m/sec
Overshoot	20–35 mv	0–15 mv
dv/dt of phase 0	200–1000 v/sec	1–10 v/sec
Transmembrane action potential amplitude	100–130 mv	35–75 mv
Response to stimulus	All-or-none	Dependent on characteristics of stimulus
Safety factor for conduction	High	Low
Recovery of excitability	Prompt; ends with repolarization	Delayed; outlasts full repolarization

[a] Reprinted, with permission, from D. P. Zipes, H. R. Besch, Jr., and A. M. Watanabe, *Circulation*, **51**, 761 (1975) (American Heart Association).

phenyl)valeronitrile[11] (XIX), and certain metal ions such as manganese (88). A comparison of the electrophysiological properties of fast and slow fibers is shown in Table III.

In addition to the slow and fast fibers, transitional fibers presumably convert the slow response generated by S-A nodal pacemaking cells into a fast response, which can then be safely conducted to the various regions of the heart.

The importance of the slow response in the genesis of arrhythmias was realized when it was discovered that disease states in fast fibers can disrupt the ionic mechanisms giving rise to normal action potentials and can lower the resting membrane potential. Under these conditions, the fast sodium-ion influx becomes partially or wholly inactivated and the slow current becomes predominant. The electrical properties associated with the slow response favor the genesis of arrhythmias since the large safety factor of the fast response is greatly diminished. Indeed, Cranefield (80) stated that "most and maybe all arrhythmias result either from slow conduction or rhythmic activity in a discrete and localized area of cells that show only slow response." Therefore, in the case of the slow response, the genesis of an arrhythmia may be said to arise from both disturbances in impulse formation and conduction.

Although the genesis of arrhythmias has been discussed in terms of changes in automaticity and disturbances of conduction, the actual mechanism probably is more complex, involving a combination of these and other factors which act in concert to disrupt the orderliness of heart rhythm. Mason and Braunwald (89) stated that "central to the perpetuation of arrhythmias is the non-homogeneous nature of myocardial tissue, in which a crucial relationship may exist between the number of impulse wavelets, pathlengths and muscle mass, the duration of the refractory period and the conduction velocity."

Considerations of Rhythms and Arrhythms on Ionic and Molecular Level—The most basic study of the mechanism of arrhythmias is at the biomolecular and ionic level. Every disturbance in heart rhythm, normal or abnormal, can ultimately be traced to changes in the ratios of intracellular to extracellular ionic concentrations, which are mediated by changes in the permeability of the cell membrane. This level of study is of greatest interest to the medicinal chemist, and this relatively new approach will be dealt with in some detail. Several recent reviews and books are available on the subject (60, 61, 63, 74, 79, 90–96).

The electrical activity observed in excitable tissue must have its origin in the movements of ions present in the tissue. Of primary importance in the genesis and maintenance of the electrical activity is the cell membrane separating aqueous solutions of different ionic composition. The most important ions in cardiac tissue are sodium, potassium, and calcium cations and chloride and intracellular organic anions. The membrane of excitable cells is selective in its permeability to ions, *the selectivity being dependent upon the potential across the membrane.*

In addition to the usual physicochemical forces which move ions across semipermeable membranes according to concentration gradients, the cell membrane is equipped with an "active transport" system. This system requires metabolic energy sources and moves or transports ions across the membrane against a concentration gradient (97–99). One active transport system has been termed the sodium–potassium exchange pump or, more simply, the sodium pump.

During the resting phase (phase 4) of excitable cells, the inside of the cell is electronegative relative to the outside. This potential difference is established by the active transport system, which maintains a high potassium-ion concentration inside the cell (37.5 times the extracellular concentration) and a high concentration of sodium ions outside the cell (7.5 times the intracellular concentration). The membrane is relatively impermeable to sodium ions and quite permeable to potassium ions during the resting phase. Therefore, a dynamic equilibrium is attained,

[11] D-600.

Table IV—Alleged Contribution of Various Ionic Channels to Phases of the Cardiac Action Potential[a]

Ion	Direction	Channel	Phase 0, Upstroke	Phase 1, Rapid Repolarization	Phase Notch	Phase 2, Plateau	Phase 3, Final Repolarization	Phase 4, Diastolic Depolarization
Sodium	Inward	i_{Na} (fast)	On	Off	—	—	—	—
		i_{Na} (slow)	—	—	On	Off	—	—
Chloride	Inward	i_{Cl}	—	On	Off	—	—	—
Calcium	Inward	i_{Ca}	On	—	—	—	Off	—
Potassium	Outward	i_{K1}	Off	—	—	—	On	—
		i_{X1}[c]	—	—	—	—	On	Off
		i_{X2}[c]	—	—	—[b]	—[b]	—[b]	—
		i_{Ks}	—	—	—	On	—	Off

[a] Adapted, with permission, from H. A. Fozzard and W. R. Gibbons, *Amer. J. Cardiol.*, 31, 182(1973). [b] Too slow to participate. [c] X_1 and X_2 are additional potassium channels.

which maintains the transmembrane potential at about −90 mv (in atrial and ventricular muscle fibers and Purkinje fibers), and is dependent on the active transport system to bring potassium ions in and carry sodium ions out of the cell.

When a resting cell is stimulated with an impulse large enough to decrease the membrane potential to the threshold potential, rapid depolarization occurs (phase 0). At this point, the permeability to sodium ions increases dramatically (permeability to sodium ions may become 10 times greater than that of potassium ions). The rapid influx of sodium ions normally results in a reversal of the membrane potential. The inside of the cell becomes positive with respect to the outside, as evidenced by an overshoot in the transmembrane action potential of about +30 mv. As a consequence of the influx of sodium ions, a sodium current is produced. This current acts as a depolarizing stimulus to adjacent cells and results in conduction of the impulse from cell to cell.

The slow diastolic depolarization characterized by the gradual rise in phase 4 of automatic cells apparently is due to a steady decrease in the permeability to potassium ions while a small permeability to sodium ions remains constant. The decreased permeability to potassium reduces the efflux of potassium ions out of the cell which, alone, would maintain the negativity of the transmembrane potential; however, the presence of the small steady influx of sodium ions slowly depolarizes the cell. When the slow "sodium leak" reduces the transmembrane potential to the threshold potential, the very rapid influx of sodium ions occurs almost as if a "gate" had been opened (13).

After depolarization, the cell begins the repolarization process to restore the transmembrane potential to its maximal resting value. While rapid depolarization is complete after about 1 msec, repolarization requires up to 500 msec. The mechanisms by which repolarization is accomplished are quite complex, and little was known until a voltage clamp technique was developed (100, 101) for studying cardiac fibers. With this technique, it became possible to differentiate the ion fluxes occurring throughout the action potential (102).

The application of this technique and interpretation of the results must be approached with due caution, as pointed out in an extensive and critical review (103). In spite of the difficulties involved, the procedure has enjoyed rapid growth and has led to an increased understanding of the ionic currents in excitable cardiac cell membranes (104–106).

In 1973, Fozzard and Gibbons (60) indicated that there appeared to be eight separate fluxes that apparently traverse different pores or channels in passing through the cardiac cell membrane. Table IV lists the separate channels and the contribution of each to the various phases of the cardiac action potentials. Figure 6 shows a characteristic cardiac action potential, with the arrows indicating the ionic fluxes asso-

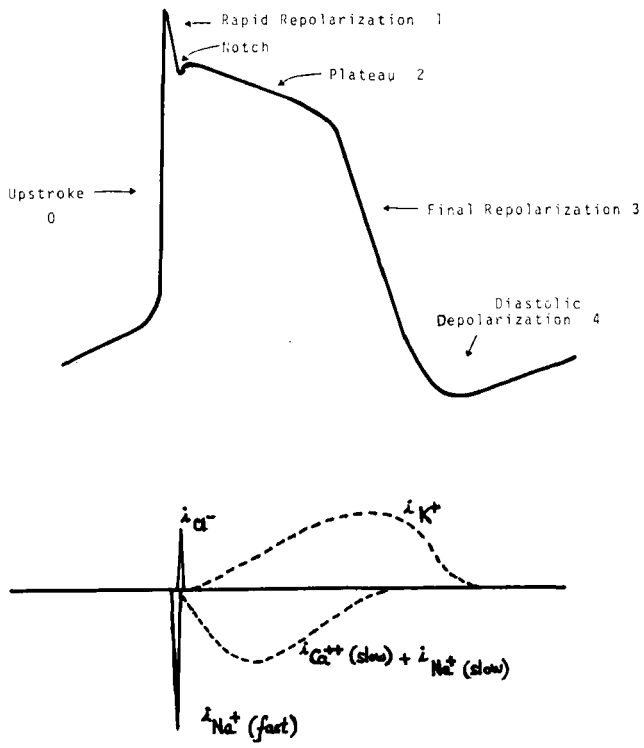

Figure 6—*(Top) Diagrammatic representation of a Purkinje fiber action potential. Each distinctive phase is labeled with the term used in the text where the ionic events related to it are discussed. (Bottom) Corresponding with each phase of the action potential is a diagrammatic representation of the contribution of the time-dependent membrane currents to each phase. The currents shown above the line make the inside of the cell more negative (repolarizing), whereas the currents below the line make the cell interior more positive (depolarizing).*

ciated with the phases of the action potential.

The rapid repolarization (phase 1) appears to result from a decrease in permeability to the influx of sodium ions. At the same time, an increase in permeability to the influx of chloride ions makes the interior of the cell more negative. The notch seen sometimes in Purkinje fibers results from a slow inward sodium flux, a shutting off of the chloride-ion channel, and the influx of calcium ions, the last being necessary for myofibril contraction. Therefore, the repolarization to more negative values is slowed or stopped momentarily.

However, repolarization proceeds slowly during the plateau (phase 2) as a result of the closing of the slow sodium-ion influx and the appearance of a small efflux of potassium. The final and more rapid repolarization (phase 3) seems to involve the shutting down of the inward calcium-ion flux and the efflux of potassium ions through two separate channels. Research on the identification and differentiation of ion channels in membranes is in an early stage, and further study doubtless will require modification of the current concept of ionic channels (60).

An understanding of the macromolecular mechanism for the opening and closing of ionic channels would be most interesting. However, few reports dealing with the problem are available. DeMello (107) presented some hypotheses and drew attention to the importance of membrane phospholipids in maintaining transmembrane potentials. This contention appears to be supported by the fact that electrical excitability can be conferred on a phospholipid bilayer separating two aqueous solutions containing different potassium-ion concentrations (108).

Szekeres and Papp (15, p. 20) reported a theory that postulates the existence of a carrier system of great transport capacity with the ability to accommodate the extremely strong ionic flux seen in phase 0. This carrier system is especially efficient in transporting sodium ions along their concentration gradient into the cell. The proposed system contains carrier molecules, each of which is assumed to contain three or four negatively charged ionic centers. As each carrier molecule binds one sodium ion, two or three negative centers remain free. These free negative ionic centers become electrically associated with the outer surface of the membrane, which is positive at resting potential. However, when the membrane becomes depolarized, the association is broken and each carrier molecule migrates rapidly to the inside of the membrane, carrying one sodium ion into the cell.

The amplitude of phase 0 is greatly dependent upon the value of the transmembrane potential. An increase in the amplitude of phase 0, according to the theory, is a result of more carrier molecules being able to become electrically associated with the outer surface of the membrane when there is a greater positive charge on the outer membrane surface. Conversely, if the resting potential of the membrane is low, fewer carrier molecules associate at the outer membrane surface and the amplitude of the depolarization phase is weaker.

Changeux *et al.* (109) attempted to put the ionic selectivity of the permeability change in excitable membranes on a sounder theoretical basis. They postulated the existence of "ionophores," macromolecular elements of the membrane that recognize the permeative ion at a selective site and transport it along the electrochemical gradient across the membrane. The capacity for selective transport of the particular ionophores involved in the excitation process changes upon excitation or depolarization by means of a structural or conformational change.

Several investigators reported that depolarization causes conformational changes in membrane-bound proteins of excitable cells. Clark and Strickholm (110) offered evidence that a conformational transition involving histidine groups of surface membrane proteins is involved in the action potential and ion permeability regulation in excitable membranes. Tasaki *et al.* (111) collected experimental data which suggest that an ion-dependent conformational change occurs upon excitation. Papakostidis *et al.* (112) reported that in proteins from excitable nerve cell membranes, a relatively large part of the protein occurs as an antiparallel β-structure in the presence of potassium ions. In the presence of sodium and calcium ions, the proteins are no longer in the β-structure but are largely in the helical form.

Although most reported studies were performed on excitable nerve cells rather than excitable cardiac cells, the molecular events probably are quite similar; it is unfortunate that cardiac fibers are more difficult to study than are nerve fibers.

In summary, sufficient evidence has been accumulated to justify theories proposing that the excitatory process in cardiac cells is basically governed by the interaction of membrane components with particular ions. This interaction results in ionic fluxes across the membrane. The maintenance of the resting potential seems to involve a mechanism requiring energy in the form of adenosine triphosphate, since inhibition of the formation or availability of adenosine triphosphate results in a reduction of the transmembrane potential over time (15, p. 315).

The depolarization and repolarization phases appear to depend on conformational changes of the components of the membrane, which open and close gates by allowing simple diffusion or, alternatively, inhibiting the influx or efflux of ions through the membrane. This conformational mobility is dependent upon the changing potential across the cell membrane. This is not surprising when one realizes that changes in potential can disrupt or cause formation of intra- and intermolecular dipole interactions, electrostatic charge interactions, hydrogen bonds, and other intra- and intermolecular associations. Therefore, any extraneous force that acts to: (*a*) disrupt the energy source of the ion pump or (*b*) change the normal ionic concentration of the exo- and/or endoplasm, as well as any agent that interacts with the membrane to cause a change in the proper conformational mobility required for normal action potential formation, may cause a disturbance of the heart rhythm.

MECHANISM OF ACTION OF ANTIARRHYTHMIC DRUGS

Recent attempts to explain the mode of action of antiarrhythmic drugs have been numerous. Complications are quickly evident when one considers the variety of the chemical structures of the drugs used to correct arrhythmias. In addition, most drugs with antiarrhythmic activity have other prominent pharmacological actions. Indeed, nearly all drugs in clinical use as antiarrhythmics were developed and used for some other pharmacological action. Only because of astute clinical observations of their effectiveness in correcting arrhythmias during treatment of the intended disease condition did it become apparent that the drugs were useful as antiarrhythmics. This situation apparently is due to the poor correlation between the activity found in experimental arrhythmias in animals and the therapeutic potencies in human patients (16, 113).

Szekeres and Papp (15, 16) divided antiarrhythmic drugs into two broad classes: specific and nonspecific. Specific antiarrhythmic drugs evoke their action primarily through an indirect mechanism such as altering a specific autonomic nervous response. β-Adrenergic blocking agents belong in this class. The specific antiarrhythmic drugs generally are similar in chemical structure and interact with a stereoselective receptor site.

Nonspecific Action at Myocardial Membrane—The nonspecific antiarrhythmic agents appear to act directly on the myocardial cell membrane, producing a cardiodepressant effect *via* changes in basic electrophysiological properties such as automaticity, excitability, conductivity, and refractoriness[12]. Quinidine (I) is the prototype of this class of agents; consequently, agents exhibiting this type of antiarrhythmic action are said to possess "quinidine-like" properties (16).

Propranolol[13] (VI), a β-adrenergic blocking (specific) agent used clinically as an antiarrhythmic, and other β-blocking compounds have been shown to elicit their beneficial effect primarily from inhibition of adrenergic stimulation; but at higher concentrations, their effect also is from a quinidine-like depression of the myocardium (13). The β-blocking properties are valuable assets to antiarrhythmic therapy, especially when the arrhythmia results from, or is sensitive to, adrenergic stimulation. On the other hand, quinidine and many other nonspecific antiarrhythmic agents have been shown to possess weak β-adrenergic blocking properties (13; 15, p. 301), which, in certain arrhythmias, can be beneficial to their action.

The mechanism by which the drug molecule interacts with the biological system is of primary importance in assaying the mode of action of drugs. Barlow (114) listed three possible mechanisms of interaction: (*a*) a process involving enzymes, (*b*) a process involving receptors, and (*c*) some physicochemical process. In the case of nonspecific antiarrhythmic drugs, most studies have shown that the depression of the myocardial membrane is not directly related to a concomitant suppression of the membrane enzyme, sodium–potassium adenosine triphosphatase, which provides high energy phosphates for operation of the ion transport system (15, p. 296; 65, p. 279; 89, p. 130).

The variety of chemical structures associated with nonspecific antiarrhythmic compounds and the differences observed in the actions of the drugs on electrophysiological parameters indicate that this class of agents probably does not act on specific receptor sites. Additional supportive evidence is that while the antiarrhythmic effect is altered in some ways by differences in stereochemistry, the antiarrhythmic "receptor" is not very stereoselective. For example, the resolution of racemic alprenolol, propranolol, and butidrine into their respecitve enantiomers indicated that only the *levo*-isomers are potent β-adrenergic blocking agents whereas both the *dextro*- and *levo*-isomers possess local anesthetic and antiarrhythmic activity (115–119). The differences in potency seen in closely related chemical structures, or in isomers of the same compounds, may be the result of greater bioavailability and specificity for cardiac tissue of one structure or isomer and not the result of stereoselective receptors (120, 121).

The consensus is that nonspecific or quinidine-like antiarrhythmic drugs act by a physicochemical process. Evidence has been obtained with studies on the interaction of local anesthetics (most antiarrhythmic drugs possess local anesthetic activity) with monomolecular films of membrane lipids extracted from nerve cells (94). These experiments indicated that the local anesthetic drugs penetrate the monolayer and increase the surface pressure, as if the drug molecules had penetrated the monolayer and caused it to expand. Also, the magnitude of the increase in surface pressure exactly paralleled the potency of the drugs in causing nerve block.

The results of this and other similar studies prompted Shanes (94) to suggest that local anesthetic drugs block conduction by penetrating the cell membrane between the pores of channels through which sodium ions pass across the membrane. Following penetration and occupation of the membrane, the drugs would tend to compress the channels and hinder their enlargement at times when an increased permeability is required. Shanes termed this type of drug action membrane stabilization. Subsequently, the phenothiazine tranquilizers, antihistamines, steroids, antiarrhythmic agents, and other drugs were found to decrease membrane permeability to sodium ions (122, 123).

Shanes strengthened his theory by finding that destabilizing or labilizing drugs (the veratrum alkaloids), which increase the membrane permeability to sodium, cause a gradual decrease in surface pressure of the monolayer. The change in pressure can be blocked by the same procedures used to block the veratrum alkaloid effect on nerve membranes: (*a*) addition of calcium, (*b*) lowering the pH, and (*c*) treatment with a local anesthetic drug (a membrane stabilizer) (94).

[12] The terms nonspecific, quinidine-like and Class I action, and cardiac membrane stabilization and myocardial depression are used interchangeably throughout this review.

[13] Inderal.

The nonspecific membrane-stabilizing effects of a series of β-adrenergic blocking agents were investigated using isolated nerve and myocardial tissue and erythrocyte ghosts and blood platelets (124–127). The local anesthetic properties, changes in myocardial conduction velocity, protection of human erythrocytes against hypotonic hemolysis, and inhibition of the active transport of serotonin across the blood platelet membrane were studied. In all cases, the results indicated that apart from the β-adrenergic blocking properties, these agents possess striking membrane-stabilizing properties at the concentrations studied. Also, evidence was obtained from morphological studies and from experiments using a fluorescent probe that the underlying mechanism of the membrane stabilization is a change in membrane protein conformation induced by adsorption to or absorption in the membrane by the drug molecules resulting in alterations in permeability.

A membrane expansion theory of anesthesia was proposed recently in which the anesthetic and other nonspecific nerve blocking drugs are said to adsorb to hydrophobic regions of membrane proteins, evoking conformational changes in the proteins and thus partially or wholly blocking the ionic conductance channels necessary for action potential production (128).

Other studies showed that membrane-stabilizing drugs inhibit the permeation of sodium ions through the membrane by complexing with a membrane phospholipid, which seems to be involved in the movement of ions across the membrane (94, 107).

Regardless of the specific macromolecular element of the membrane with which the stabilizing drug interacts, these drugs probably invade the cell membrane and alter ionic permeability by a physicochemical process. The physical properties of the drug that seem to be necessary include a pKa around 8.0–9.0, adequate lipid solubility, and appropriate chemical moieties. The molecular structure of most nonspecific antiarrhythmic drugs consists of three moieties, which presumably are necessary for activity: (*a*) a benzene ring or condensed aromatic portion connected to (*b*) a basic amino group, usually tertiary or secondary but in some cases primary, by way of (*c*) an ester, ether, amide, or hydroxyalkyl group capable of becoming involved in hydrogen bonding. These structural features are almost identical to those generally considered necessary for local anesthetic drugs (129).

Indeed, with very few exceptions, all nonspecific antiarrhythmic drugs and most β-adrenergic blocking drugs used to control rhythm disturbances are membrane-stabilizing agents and many possess local anesthetic activity (115–119, 130, 131). The strong connection between local anesthetic activity and antiarrhythmic activity undoubtedly stems from the membrane-stabilization properties of both classes.

Figure 7 depicts an oversimplified representation of the interaction of nonspecific, membrane-stabilizing antiarrhythmic drugs with a model membrane (132). It can be seen that incorporation of sufficient numbers of membrane-stabilizing molecules into the membrane obviously alters its function.

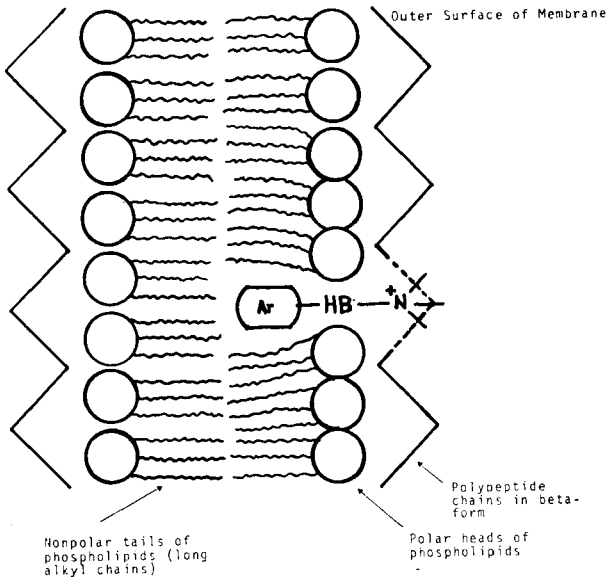

Figure 7—*Schematic illustration indicating possible molecular interaction of antiarrhythmic agents (or other membrane-stabilizing drugs) with a cell membrane. The portion of the drug molecule labeled Ar represents the aromatic ring usually contained in antiarrhythmics, while HB indicates the group that may become involved in hydrogen bonding. In this model interaction, it can be seen that the drug may alter the structure of both the outer protein layer and the phospholipid layer.*

It has been suggested that in addition to disturbances of the cardiac membrane conformation caused by the binding of antiarrhythmic drugs, the essential amino group may also play an important role (133, 134). This basic center has a sufficiently high pKa in all antiarrhythmic drugs (except phenytoin, which is weakly acidic) to cause it to be ionized significantly at physiological pH. The positioning of such a cation at the outer surface of the membrane may impede ionic transport as a result of its possible hydration and/or repellency of sodium ions and other cations (135).

In summary, there appears to be sufficient evidence to explain the action of nonspecific antiarrhythmic drugs on the basis of a *physical membrane occupancy theory*. This theory depends upon the ability of the drug to: (*a*) bind at cardiac membranes, (*b*) induce a change in the conformation of the membrane that will ultimately give the desired effects, and (*c*) present a charged amino group at or near the surface of the membrane.

Electrophysiological Effects on Transmembrane Action Potential—The effect of membrane-active agents on the permeability of ions can be observed by changes in parameters of the transmembrane action potential. Since the development of the technique for recording the transmembrane action potential of cardiac cells, many studies have elucidated the effects of antiarrhythmic drugs on these parameters. Numerous reviews of the subject have appeared (15–17, 23, 61, 65, 69–74, 76, 89, 94, 136–142).

In assessing the effect of antiarrhythmic drugs on the transmembrane action potential of isolated cardiac tissues, one must exercise due caution. The parameters of the transmembrane action potential are de-

Table V—Effects of Antiarrhythmic Agents on the Transmembrane Action Potential of Isolated Cardiac Tissue[a]

Agent	Type of Tissue[b]	Resting Potential	Amplitude	*dv/dt*	Membrane Responsiveness	Conduction Velocity	Duration	Refractory Period	Automaticity	Reference
Quinidine	Canine P.F.	0	↓	↓	↓	↓	↑	↑	↓	137, 148 149
Procainamide	Canine P.F.	0	↓	↓	↓	↓	↑	↑	↓	137, 148 149
Lidocaine	Canine P.F.	0	↓	↓	↓	↓	↓	↓	↓	150
Propranolol	Canine P.F.	0	↓	↓	↓	↓	↓	↓	↓	137, 148 149
Phenytoin	Canine P.F.	0	0	0, ↓[c]	↓[c], 0, ↑[d]	0, ↓[c]	↓	↓	↓	137, 148 149
Phenytoin	Rabbit A.M. and V.M.	0	0	↓	↓	↓	0	?	↓	151
Disopyramide	Canine P.F.	0	0	↓	↓	↓	↑	↑	↓	152, 153
Ajmaline	Canine P.F., A.M., and V.M.	0	↓	↓	↓	↓	↑[e], ↓[f]	?	↓	154
Mexiletine	Rabbit A.M. and V.M.	0	↓	↓	↓	↓	0	↑	0	155
Aprindine	Canine P.F.	↓	↓	↓	↓	↓	↓	↑	↓	40, 156
Verapamil	Canine P.F.	0	0	0	0, ↓	?	0, ↑[c]	0, ↑[c]	↓	28
Amiodarone[g]	Rabbit A.M. and V.M.	0	0	0	0	0	↑	↑	↓	157
Dimethyl quaternary propranolol[h]	Canine P.F.	0	↓	↓	↓	↓	↓	↓	↓	158
Bretylium	Rat A.M. and V.M.	0	↓	↓	↓	?	↑	↑	?	159

[a] 0 = no effect, ? = not reported, ↓ = decrease, ↑ = increase; and ↓ = questionable or slight effect. [b] P.F. = Purkinje fiber, A.M. = atrial muscle, and V.M. = ventricular muscle. [c] At high concentration only. [d] In acutely depressed fibers. [e] Atrial muscle and ventricular muscle. [f] Purkinje fiber. [g] After 6 weeks of treatment of whole animal. [h] UM-272.

pendent upon the ionic concentration of the medium or perfusate, especially the potassium concentration (23, 140, 143). Considerable confusion has resulted from studies on the effects of drugs when lower than normal physiological potassium concentrations have been used. Agreement over the interpretation of observed electrophysiological actions of drugs studied in isolated tissue and correlation to the clinical situation is complicated by several factors (144):

1. Disagreement exists over which dose of drug *in vitro* is comparable to the effective plasma concentration in humans.
2. Information is lacking on the effective drug content in myocardial tissue.
3. Fibers from different parts of the heart respond differently to comparable drug concentrations.
4. Abnormal or diseased tissues respond differently than normal tissue.
5. Small changes in ionic concentrations and pH can markedly influence the transmembrane action potential.
6. Important actions of the drug may be absent or overlooked in the experimental models.

In an attempt to remedy some of these problems, a technique was developed whereby isolated cardiac tissue is perfused with arterial blood from a donor animal and the effects of the drug on the whole animal and the isolated tissue are determined simultaneously (145, 146). Isolated diseased human cardiac tissues have been used in studies of the effects of drugs on the transmembrane action potential (147).

The effects of several antiarrhythmic drugs on various parameters of the transmembrane action potential of isolated cardiac tissue are given in Table V. There is still disagreement between some investigators over the effects listed for certain compounds, but the reviewers have attempted to extract the data from the most recent reviews and experimental studies. Vaughan Williams (23) reported that quinidine, procainamide, lidocaine, and phenytoin apparently elicit their action on the myocardium by depressing the maximum rate of depolarization, also called maximum upstroke velocity, represented by phase 0 in the transmembrane action potential. Lidocaine and phenytoin were previously thought to have no effect on the maximum rate of depolarization at therapeutic concentrations (160, 161). However, reinvestigation of these two drugs in a medium containing potassium concentrations more closely approaching physiological levels indicated that these drugs did indeed depress the maximum rate of depolarization at concentrations thought to correspond to therapeutic blood levels (23, 151, 162).

In addition to decreasing the rate of rise of the action potential, most of the quinidine-like group of drugs reduce heart rate and excitability of the myocardium without changing the resting potential (16). Also, conduction velocity is decreased and the effective refractory period is increased (61).

Apparently, the effects of these drugs result from their effect on sodium permeability. Upon excitation by an impulse, a less than normal increase in sodium permeability is observed, as though the gate that opens to allow the inrush of sodium is inhibited from opening fully (23). Therefore, the action potential rises less rapidly and there is less overshoot. This situation leads to a decrease in conduction velocity, since this parameter is dependent on the rate of rise, the overshoot, and the amplitude of phase 0.

After an action potential is initiated by the rapid

influx of sodium ions (phase 0), repolarization must proceed to a certain negative potential before the gate can reopen and allow the influx of sodium ions for production of a second action potential. The effective refractory period may be thought of as that point at which the repolarization has proceeded sufficiently for the rate of rise of a second excitation to be rapid enough to permit propagation of the impulse. Since quinidine and quinidine-like drugs inhibit the entry of sodium ions, repolarization must proceed further before the influx of sodium can become great enough to allow the minimum rate of rise for a propagated action potential (23). This is observed as an increase in the effective refractory period, an important property of antiarrhythmic drugs.

All quinidine-like drugs decrease the slope of phase 4 or the slow diastolic depolarization of automatic cells. This decrease is manifested by a decrease in automaticity. Additionally, the automaticity of cells responsible for the formation of ectopic impulses is depressed more than the automaticity of the S-A pacemaker, so the dominance of the normal cardiac pacemaker usually results (16).

From the preceding discussion, it appears that the effects of quinidine and quinidine-like drugs, at least on the electrical activity of fibers of isolated tissue, are due to induced changes in membrane permeability, particularly depression of sodium flux into the cell.

REFERENCES

(1) K. F. Wenckebach, "Die Unregelmässige Herztätigkeit und ihre Klinische Bedeutung," W. Engelmann, Leipzig, Germany, 1914, p. 173.

(2) W. Frey, *Klin. Wochenschr.*, **55,** 450(1918).

(3) S. Bellet, "Clinical Disorders of the Heart Beat," 3rd ed., Lea & Febiger, Philadelphia, Pa., 1971, chaps. 43–47.

(4) L. C. Mark, H. J. Kayden, J. M. Steele, J. R. Cooper, E. A. Rowenstine, and B. B. Brodie, *J. Pharmacol. Exp. Ther.*, **102,** 5(1951).

(5) J. L. Southworth, V. A. McKusick, E. C. Pierce, and F. L. Ranson, Jr., *J. Amer. Med. Ass.*, **143,** 717(1950).

(6) W. A. Leonard, *Arch. Intern. Med.*, **101,** 714(1958).

(7) P. E. Leveque, *Nature*, **207,** 203(1965).

(8) J. W. Black, A. F. Crowther, R. G. Shanks, L. H. Smith, and A. C. Dornhorst, *Lancet*, **1,** 1080(1964).

(9) W. G. Davis, *J. Pharm. Pharmacol.*, **22,** 284(1970).

(10) A. M. Barrett and V. A. Cullum, *Brit. J. Pharmacol.*, **34,** 43(1968).

(11) F. O. Apantaku, C. M. Baumgarten, and R. E. Ten Eick, *J. Pharmacol. Exp. Ther.*, **193,** 327(1975).

(12) W. P. Batsford, G. M. Weisfogel, S. H. Lau, and A. N. Damato, *Amer. Heart J.*, **88,** 733(1974).

(13) E. M. Vaughan Williams, *Advan. Drug Res.*, **9,** 69(1974).

(14) M. R. Rosen, A. L. Wit, and B. F. Hoffman, *Amer. Heart J.*, **89,** 391(1975).

(15) L. Szekeres and G. J. Papp, "Experimental Cardiac Arrhythmias and Antiarrhythmic Drugs," Akadémiai Kiadó, Budapest, Hungary, 1971.

(16) L. Szekeres and G. J. Papp, *Progr. Drug Res.*, **12,** 292(1968).

(17) A. L. Bassett and B. F. Hoffman, *Ann. Rev. Pharmacol.*, **11,** 143(1971).

(18) R. D. Tanz, *Ann. Rep. Med. Chem.*, **1,** 85(1965).

(19) C. F. Schwender, *ibid.*, **6,** 80(1970).

(20) G. W. Adelstein and R. R. Dean, *ibid.*, **9,** 67(1974).

(21) B. Clarkson, H. Tucker, and J. Wale, *ibid.*, **10,** 51(1975).

(22) J. E. Francis, *ibid.*, **10,** 65(1975).

(23) E. M. Vaughan Williams, *Schweiz. Med. Wochenschr.*, **103,** 262(1973).

(24) G. Faust and W. Fiedler, *Pharmazie*, **28,** 345(1973).

(25) "Drugs in Cardiology: Current Cardiovascular Topics," vol. I, parts 1 and 2, E. Donoso, Ed., Stratton Intercontinental Medical Book Corp., New York, N.Y., 1975.

(26) "A Seminar on Norpace, A New Antiarrhythmic Drug," *Angiology*, **26**(1), part 2 (1975).

(27) L. H. Vismara, D. T. Mason, and E. A. Amsterdam, *Clin. Pharmacol. Ther.*, **16,** 330(1974).

(28) M. R. Rosen, A. L. Wit, and B. F. Hoffman, *Amer. Heart J.*, **89,** 665(1975).

(29) W. W. Tse and J. Han, *Amer. J. Cardiol.*, **36,** 50(1975).

(30) H. J. Smith, B. N. Singh, H. D. Nisbet, and R. M. Norris, *Cardiovasc. Res.*, **9,** 569(1975).

(31) R. G. Talbot, *Amer. Heart J.*, **89,** 537(1975).

(32) R. W. F. Campbell, M. A. Dolder, L. F. Prescott, R. G. Talbot, A. Murray, and D. G. Julian, *Lancet*, **1**(7919), 1257(1975).

(33) A. H. Beckett and E. C. Chidomere, presented at Federation Internationale Pharmaceutique meeting, Sept. 1975, Dublin, Ireland.

(34) D. J. Coltart, T. B. Berndt, R. Kernoff, and D. C. Harrison, *Amer. J. Cardiol.*, **34,** 35(1974).

(35) R. Charlier, G. Deltour, A. Baudine, and F. Chaillet, *Arzneim.-Forsch.*, **18,** 1408(1968).

(36) C. Ferrero and M. B. Abderhamane, *G. Ital. Cardiol.*, **2,** 186(1972).

(37) E. M. Vaughan Williams, *Advan. Cardiol.*, **12,** 256(1974).

(38) F. Hagenmeijer and P. G. Hugenholtz, *Amer. J. Cardiol.*, **33,** 142(1974).

(39) G. Cheymol, J. C. Gilbert, and P. Mouille, *Thérapie*, **29,** 719(1974).

(40) H. Kesteloot, W. Van Mieghem, and H. DeGeest, *Acta Cardiol.*, **28,** 145(1973).

(41) E. E. Bagwell, P. Polster, and E. M. Vaughan Williams, *Brit. J. Pharmacol.*, **48,** 183(1973).

(42) O. A. Beck, E. Witt, and H. Hochrein, *Z. Kardiol.*, **64,** 179(1975).

(43) A. Felipe and S. Cecëna, *Amer. J. Cardiol.*, **33,** 130(1974).

(44) H. E. D'Amato and A. P. Truant, *Fed. Proc.*, **21,** 127(1962).

(45) L. Rydén, Å. Hjalmarson, H. Wasir, and L. Werkö, *Brit. Heart J.*, **36,** 811(1974).

(46) L. Rydén, Å. Hjalmarson, and A. Waldenström, *ibid.*, **37,** 426(1975).

(47) L. Rydén, B. Olsson, and J. Kvasnička, *Cardiovasc. Res.*, **9,** 81(1975).

(48) F. J. Kniffen, T. E. Lomas, R. E. Counsell, and B. R. Lucchesi, *J. Pharmacol. Exp. Ther.*, **192,** 120(1975).

(49) R. E. Counsell, T. Yu, V. V. Ranade, and A. Buswink, *J. Med. Chem.*, **16,** 1038(1973).

(50) E. A. Carr, Jr., R. E. Counsell, and M. Carroll, *Clin. Pharmacol. Ther.*, **14,** 132(1973).

(51) B. B. Vargaftig, M. F. Sugre, W. R. Buckett, and H. Van Riezen, *J. Pharm. Pharmacol.*, **27,** 697(1975).

(52) W. R. Buckett, F. A. Marwick, and B. B. Vargaftig, *Brit. J. Pharmacol.*, **54,** 3(1975).

(53) G. Breithardt, *Z. Kardiol.*, **63,** 401(1974).

(54) J. T. Bigger, Jr., *Amer. J. Med.*, **58,** 479(1975).

(55) B. F. Hoffman, M. R. Rosen, and A. L. Wit, *Amer. Heart J.*, **89,** 115(1975).

(56) *Ibid.*, **89,** 253(1975).

(57) L. A. Woodbury, J. W. Woodbury, and H. H. Hecht, *Circulation*, **1,** 264(1950).

(58) M. H. Draper and S. Weidmann, *J. Physiol. (London)*, **115,** 74(1951).

(59) G. Ling and R. W. Gerard, *J. Cell. Comp. Physiol.*, **34,** 383(1949).

(60) H. A. Fozzard and W. R. Gibbons, *Amer. J. Cardiol.*, **31,** 182(1973).

(61) C. B. Olsen and D. R. Waud, *Anesthesiology*, **33,** 520(1970).

(62) B. F. Hoffman and P. F. Cranefield, "Electrophysiology of the Heart," McGraw-Hill, New York, N.Y., 1960.

(63) "Electrical Phenomena in the Heart," W. C. DeMello, Ed., Academic, New York, N.Y., 1972.

(64) G. K. Moe and C. Mendez, *N. Engl. J. Med.*, **288,** 250(1973).

(65) "The Myocardial Cell; Structure, Function and Modifica-

tion by Cardiac Drugs," S. A. Briller and H. L. Conn, Jr., Eds., University of Pennsylvania Press, Philadelphia, Pa., 1966.
(66) B. F. Hoffman and P. F. Cranefield, *Amer. J. Med.*, **37**, 670(1964).
(67) "Cardiac Arrhythmias; The Twenty-Fifth Hahnemann Symposium," L. S. Dreifus and W. A. Likoff, Eds., Grune & Stratton, New York, N.Y., 1973.
(68) B. F. Hoffman, *Progr. Cardiovasc. Dis.*, **8**, 319(1966).
(69) W. Trautwein, *Pharmacol. Rev.*, **15**, 279(1963).
(70) J. Bureš, M. Petráň, and J. Zachar, "Electrophysiological Methods in Biological Research," 3rd ed., Academic, New York, N.Y., 1967.
(71) M. R. Rosen, A. L. Wit, and B. F. Hoffman, *Amer. Heart J.*, **88**, 380(1974).
(72) A. L. Wit, M. R. Rosen, and B. F. Hoffman, *ibid.*, **88**, 515(1974).
(73) C. R. Vander Ark and E. W. Reynolds, *Med. Clin. N. Amer.*, **53**, 1297(1969).
(74) J. T. Bigger, Jr., *Advan. Intern. Med.*, **18**, 251(1972).
(75) A. S. Leon and W. B. Abrams, *Amer. J. Med. Sci.*, **262**, 9(1971).
(76) D. H. Singer and R. E. Ten Eick, *Progr. Cardiovasc. Dis.*, **11**, 488(1969).
(77) H. Antoni, *Arch. Pharmacol.*, **269**, 177(1971).
(78) L. S. Dreifus, I. M. de Azevedo, and Y. Watanabe, *Amer. Heart J.*, **88**, 95(1974).
(79) J. T. Bigger, Jr., in "Cardiac Arrhythmias; The Twenty-Fifth Hahnemann Symposium," L. S. Dreifus and W. A. Likoff, Eds., Grune & Stratton, New York, N.Y., 1973, pp. 13–34.
(80) P. F. Cranefield, "The Conduction of the Cardiac Impulse—The Slow Response and Cardiac Arrhythmias," Futura, Mt. Kisco, N.Y., 1975.
(81) D. P. Zipes, H. R. Besch, Jr., and A. M. Watanabe, *Circulation*, **51**, 761(1975).
(82) G. K. Moe, *Rev. Physiol. Biochem. Exp. Pharmacol.*, **72**, 55(1975).
(83) G. K. Moe, *Coeur Méd. Interne.*, **13**, 581(1974).
(84) J. Geddes, M. J. Burgess, K. Millar, and J. A. Abildskov, *Amer. Heart J.*, **88**, 61(1974).
(85) A. L. Wit, M. R. Rosen, and B. F. Hoffman, *ibid.*, **88**, 664(1974).
(86) *Ibid.*, **88**, 798(1974).
(87) C. Y. Kao, *Pharmacol. Rev.*, **18**, 998(1966).
(88) D. P. Zipes and C. Mendez, *Circ. Res.*, **32**, 447(1973).
(89) D. T. Mason and E. Braunwald, *Mod. Trends Pharmacol. Ther.*, **1**, 112(1967).
(90) C. Fisch, *Circulation*, **47**, 408(1973).
(91) T. C. West, *Fed. Proc.*, **27**, 120(1968).
(92) D. H. Singer, R. Lazzara, and B. F. Hoffman, in "The Myocardial Cell," S. A. Briller and H. L. Conn, Jr., Eds., University of Pennsylvania Press, Philadelphia, Pa., 1966, pp. 73–110.
(93) D. P. Zipes, in "Cardiac Arrhythmias; The Twenty-Fifth Hahnemann Symposium," L. S. Dreifus and W. Likoff, Eds., Grune & Stratton, New York, N.Y., 1973, pp. 55–69.
(94) D. H. R. Gourley, "Interactions of Drugs with Cells," Charles C Thomas, Springfield, Ill., 1971, chap. 5. p. 79.
(95) S. Weidmann, *Ann. Rev. Physiol.*, **36**, 155(1974).
(96) D. Nobel, *Rec. Advan. Physiol.*, **9**, 1(1974).
(97) W. G. Nayler, in "Membranes and Ion Transport," vol. 2, E. E. Bittar, Ed., Wiley–Interscience, London, England, 1970, pp. 75–94.
(98) K. Koketsu, *Advan. Biophys.*, **2**, 77(1971).
(99) J. C. Skou, *Quart. Rev. Biophys.*, **7**, 401(1975).
(100) K. A. Deck, R. Kern, and W. Trautwein, *Pfluegers Arch. Ges. Physiol.*, **280**, 50(1964).
(101) H. H. Hecht, O. F. Hutter, and D. W. Lywood, *J. Physiol. (London)*, **1964**, 170P.
(102) M. Kohlhardt, B. Bauer, H. Krause, and A. Fleckenstein, *Pfluegers Arch. Ges. Physiol.*, **335**, 309(1972).
(103) E. A. Johnson and M. Lieberman, *Ann. Rev. Physiol.*, **33**, 479(1971).
(104) W. Trautwein, *Physiol. Rev.*, **53**, 793 (1973).
(105) T. Narahashi, *ibid.*, **54**, 813(1974).
(106) J. L. Walker and R. O. Ladle, in "Ion Selective Microelectrodes: Advances in Experimental Medicine and Biology," vol. 50, H. J. Berman and N. C. Hebert, Eds., Plenum, New York, N.Y., 1974, pp. 159–171.
(107) W. C. DeMello, in "Electrical Phenomena in the Heart," W. C. DeMello, Ed., Academic, New York, N.Y., 1972, chap. 3.
(108) P. Myeller and D. O. Rudin, *Nature*, **217**, 713(1968).
(109) J. P. Changeux, R. Blumenthal, M. Kasai, and T. Podleški, in "Molecular Properties of Drug Receptors," A Ciba Foundation Symposium, R. Porter and M. O'Connor, Eds., J. and A. Churchill, London, England, 1971, pp. 197–228.
(110) H. R. Clark and A. Strickholm, *Nature*, **234**, 470(1971).
(111) I. Tasaki, "Nerve Excitation," Charles C Thomas, Springfield, Ill., 1968.
(112) G. Papakostidis, G. Zundel, and E. Mehl, *Biochim. Biophys. Acta*, **288**, 277(1972).
(113) T. Baum, D. K. Eckfeld, A. T. Shropshire, G. Rowles, and L. L. Varner, *Arch. Int. Pharmacodyn. Ther.*, **193**, 149(1971).
(114) R. B. Barlow, *Soc. Chem. Ind. London, Rep. Progr. Appl. Chem.*, **51**, 169(1966).
(115) A. M. Barrett and V. A. Cullum, *Brit. J. Pharmacol.*, **34**, 43(1968).
(116) B. R. Madan, S. N. Mishra, and V. K. Khanna, *Arch. Int. Pharmacodyn. Ther.*, **182**, 121(1969).
(117) R. Howe and R. G. Shanks, *Nature*, **210**, 1336(1966).
(118) R. Ferrini, G. Miragoli, and G. Croce, *Arzneim.-Forsch.*, **18**, 829(1968).
(119) E. Musso and B. Taccardi, *Arch. Int. Pharmacodyn. Ther.*, **183**, 173(1970).
(120) E. M. Vaughan Williams, E. E. Bagwell, and B. N. Singh, *Cardiovasc. Res.*, **7**, 226(1973).
(121) Y. W. Cho, *Amer. Heart J.*, **85**, 648(1973).
(122) P. M. Seeman, *Int. Rev. Neurobiol.*, **9**, 145(1966).
(123) S. Roth and P. Seeman, *Nature (London)*, **231**, 284(1971).
(124) D. Hellenbrecht, *Arch. Pharmacol.*, **271**, 125(1971).
(125) B. Lemmer, G. Wiethold, D. Hellenbrecht, I. J. Bak, and H. Grobecker, *Arch. Pharmacol.*, **275**, 299(1972).
(126) G. Wiethold, B. Lemmer, D. Hellenbrecht, H. Grobecker, and D. Palm, *Arch. Pharmacol. (Suppl.)*, **274**, R125(1972).
(127) G. Wiethold, D. Hellenbrecht, B. Lemmer, and D. Palm, *Biochem. Pharmacol.*, **22**, 1437(1973).
(128) P. Seeman, *Experientia*, **30**, 759(1974).
(129) R. F. Doerge, in "Textbook of Organic Medicinal and Pharmaceutical Chemistry," 5th ed., C. O. Wilson, O. Gisvold, and R. F. Doerge, Eds., Lippincott, Philadelphia, Pa., 1966, chap. 22.
(130) K. Hermansen, *Brit. J. Pharmacol.*, **35**, 476(1969).
(131) W. G. Davis, *J. Pharm. Pharmacol.*, **22**, 284(1970).
(132) A. L. Lehninger, "Biochemistry, The Molecular Basis of Cell Structure and Function," Worth Publishers, New York, N.Y., 1970, p. 212.
(133) R. J. Luchi, H. L. Conn, and J. Helwig, *Amer. J. Cardiol.*, **10**, 252(1962).
(134) H. L. Conn, in "Advances in Cardiopulmonary Diseases," vol. 2, A. L. Banya and B. L. Gordon, Eds., Year Book Medical Publishers, Chicago, Ill., 1964, p. 286.
(135) I. W. Mathison, P. H. Morgan, R. R. Tidwell, and C. R. Handorf, *J. Pharm. Sci.*, **61**, 637(1972).
(136) "Cardiac Arrhythmias; The Twenty-Fifth Hahnemann Symposium," L. S. Dreifus and W. Likoff, Eds., Grune & Stratton, New York, N.Y., 1973, chap. 5.
(137) M. R. Rosen and B. F. Hoffman, *Circ. Res.*, **32**, 1(1973).
(138) E. M. Vaughan Williams, *Proc. Roy. Soc. Med.*, **62**, 75(1969).
(139) W. Lameijer and P. A. van Zwieten, *J. Pharm. Pharmacol.*, **25**, 168(1973).
(140) L. S. Gettes, *Amer. J. Cardiol.*, **28**, 526(1971).
(141) M. R. Rosen and H. Gelband, *Amer. Heart J.*, **81**, 428(1971).
(142) A. L. Bassett and A. L. Wit, *Progr. Drug Res.*, **17**, 33(1973).
(143) J. C. Pamintuan, L. S. Dreifus, and Y. Watanabe, *Amer. J. Cardiol.*, **26**, 512(1970); also, comments on this paper: B. N. Singh, *Amer. J. Cardiol.*, **28**, 240(1971), and reply: p. 241.
(144) B. I. Sasyniuk and R. I. Ogilvie, *Ann. Rev. Pharmacol.*, **15**, 131(1975).
(145) M. R. Rosen, H. Gelband, and B. F. Hoffman, *Circ. Res.*, **30**, 575(1972).
(146) M. R. Rosen, H. Gelband, and B. F. Hoffman, *Circulation*, **46**, 528(1972).
(147) K. Prasad, *Clin. Pharmacol. Ther.*, **18**, 22(1975).
(148) A. J. Atkinson, Jr., and R. Davison, *Ann. Rev. Med.*, **25**,

99(1974).
(149) B. F. Hoffman, M. R. Rosen, and A. L. Wit, *Amer. Heart J.*, **89**, 804(1975).
(150) *Ibid.*, **89**, 526(1975).
(151) B. N. Singh and E. M. Vaughan Williams, *Circ. Res.*, **29**, 286(1971).
(152) L. S. Dreifus, *Angiology*, **26**, 111(1975).
(153) B. K. Yeh, P.-K. Sung, and B. J. Scherlag, *J. Pharm. Sci.*, **62**, 1924(1973).
(154) R. Bojorges, G. Pastelin, S. Sanchez-Perez, R. Mendez, and E. Kabela, *J. Pharmacol. Exp. Ther.*, **193**, 182(1975).
(155) B. N. Singh and E. M. Vaughan Williams, *Brit. J. Pharmacol.*, **44**, 1(1972).
(156) K. Greenspan, M. Steinberg, D. Holland, and A. R. Freeman, *Amer. J. Cardiol.*, **33**, 140(1974).
(157) B. N. Singh and E. M. Vaughan Williams, *Brit. J. Pharmacol.*, **39**, 657(1970).
(158) M. R. Rosen, D. S. Miura, and P. Danilo, Jr., *J. Pharmacol. Exp. Ther.*, **193**, 209(1975).
(159) D. H. Namm, C. M. Wang, S. El-Sayad, and F. C. Copp, *ibid.*, **193**, 194(1975).
(160) L. D. Davis and J. V. Tempte, *Circ. Res.*, **24**, 639(1969).
(161) J. T. Bigger, Jr., and W. J. Mandel, *J. Clin. Invest.*, **49**, 63(1970).
(162) J. Wittig, "Influence of Hypoxia on the Action of Lignocaine," presented at the Workshop on Ions, Potentials and Rhythms of the Cardiac Muscle Research Group, Oxford, England, July 4, 1975.

ACKNOWLEDGMENTS AND ADDRESSES

Received from the *Division of Organic Chemistry, Department of Medicinal Chemistry, College of Pharmacy, University of Tennessee Center for the Health Sciences, Memphis, TN 38163*

The authors express their appreciation to Dr. Charles E. Kossmann, Dr. James R. Wennemark, and Dr. E. M. Vaughan Williams for useful discussions during the preparation of this review.

* Presently a Medical Research Council of Great Britain Research Fellow at Chelsea College, University of London, England.

ˣ To whom inquiries should be directed.

RESEARCH ARTICLES

Evaluation of Mannich Bases and Related Compounds as Inhibitors of Mitochondrial Function in Yeast and Inhibition of Blood Platelet Aggregation, Blood Clotting, and *In Vitro* Metabolism of 5-Dimethylamino-1-phenyl-1-penten-3-one Hydrochloride

J. R. DIMMOCK *ˣ, N. W. HAMON *, K. W. HINDMARSH *, D. G. MILLS *, L. E. NEGRAVE *, G. H. RANK ‡, and A. J. ROBERTSON ‡

Abstract □ 5-Dimethylamino-1-phenyl-1-penten-3-one hydrochloride (Ia) and 32 analogs were tested for inhibition of respiratory-dependent growth in *Saccharomyces cerevisiae*. Thirteen of the 33 compounds tested appeared to affect mitochondrial function, since the inhibition of respiratory-dependent growth was statistically greater than the inhibition of growth on fermentable energy sources. Inhibition of mitochondrial function in yeast and growth inhibition of an *in vitro* culture of human epidermoid carcinoma (KB) were positively correlated since 83% of the compounds tested either had mitochondrial-inhibiting properties and significant activity in the KB test or were inactive in both tests. Similarly, 78% of compounds tested showed murine toxicity and mitochondrial inhibition or had no effect on murine toxicity and yeast mitochondrial function. Injection of Ia into rats resulted in the appearance of blood in the urine and feces. Compound Ia inhibited adenosine diphosphate and collagen-induced aggregation of rat platelets but had no effect on blood clotting. TLC, following incubation of Ia with a rat liver extract, showed that the structure of Ia was not enzymatically modified and indicated activity *per se* on platelet aggregation and mitochondrial function.

Keyphrases □ Mannich bases—effect on mitochondrial function in yeast, human epidermoid carcinoma cultures, blood platelet aggregation, blood clotting, rats □ Mitochondrial activity—effect of Mannich bases and related compounds, yeast □ Blood platelet aggregation—effect of Mannich bases and related compounds, rats □ Coagulation, blood—effect of Mannich bases and related compounds, rats □ Structure-activity relationships—effect of Mannich bases and related compounds on mitochondrial function in yeast, human epidermoid carcinoma cultures, blood platelet aggregation and blood clotting, rats

Mannich bases have a wide range of biological activity including antineoplastic properties (1, 2), antimicrobial effects (3–5), analgesic activity (6), local anesthetic properties (7, 8), and psychotropic effects (9). To pursue a continuing interest in Mannich reactions (10–12) and α,β-unsaturated ketones (13, 14), several properties of a simple Mannich base, 5-dimethylamino-1-phenyl-1-penten-3-one (Ia), derived

99(1974).
(149) B. F. Hoffman, M. R. Rosen, and A. L. Wit, *Amer. Heart J.*, **89**, 804(1975).
(150) *Ibid.*, **89**, 526(1975).
(151) B. N. Singh and E. M. Vaughan Williams, *Circ. Res.*, **29**, 286(1971).
(152) L. S. Dreifus, *Angiology*, **26**, 111(1975).
(153) B. K. Yeh, P.-K. Sung, and B. J. Scherlag, *J. Pharm. Sci.*, **62**, 1924(1973).
(154) R. Bojorges, G. Pastelin, S. Sanchez-Perez, R. Mendez, and E. Kabela, *J. Pharmacol. Exp. Ther.*, **193**, 182(1975).
(155) B. N. Singh and E. M. Vaughan Williams, *Brit. J. Pharmacol.*, **44**, 1(1972).
(156) K. Greenspan, M. Steinberg, D. Holland, and A. R. Freeman, *Amer. J. Cardiol.*, **33**, 140(1974).
(157) B. N. Singh and E. M. Vaughan Williams, *Brit. J. Pharmacol.*, **39**, 657(1970).
(158) M. R. Rosen, D. S. Miura, and P. Danilo, Jr., *J. Pharmacol. Exp. Ther.*, **193**, 209(1975).
(159) D. H. Namm, C. M. Wang, S. El-Sayad, and F. C. Copp, *ibid.*, **193**, 194(1975).
(160) L. D. Davis and J. V. Tempte, *Circ. Res.*, **24**, 639(1969).
(161) J. T. Bigger, Jr., and W. J. Mandel, *J. Clin. Invest.*, **49**, 63(1970).
(162) J. Wittig, "Influence of Hypoxia on the Action of Lignocaine," presented at the Workshop on Ions, Potentials and Rhythms of the Cardiac Muscle Research Group, Oxford, England, July 4, 1975.

ACKNOWLEDGMENTS AND ADDRESSES

Received from the *Division of Organic Chemistry, Department of Medicinal Chemistry, College of Pharmacy, University of Tennessee Center for the Health Sciences, Memphis, TN 38163*

The authors express their appreciation to Dr. Charles E. Kossmann, Dr. James R. Wennemark, and Dr. E. M. Vaughan Williams for useful discussions during the preparation of this review.

* Presently a Medical Research Council of Great Britain Research Fellow at Chelsea College, University of London, England.

ˣ To whom inquiries should be directed.

RESEARCH ARTICLES

Evaluation of Mannich Bases and Related Compounds as Inhibitors of Mitochondrial Function in Yeast and Inhibition of Blood Platelet Aggregation, Blood Clotting, and *In Vitro* Metabolism of 5-Dimethylamino-1-phenyl-1-penten-3-one Hydrochloride

J. R. DIMMOCK *ˣ, N. W. HAMON *, K. W. HINDMARSH *, D. G. MILLS *, L. E. NEGRAVE *, G. H. RANK ‡, and A. J. ROBERTSON ‡

Abstract □ 5-Dimethylamino-1-phenyl-1-penten-3-one hydrochloride (Ia) and 32 analogs were tested for inhibition of respiratory-dependent growth in *Saccharomyces cerevisiae*. Thirteen of the 33 compounds tested appeared to affect mitochondrial function, since the inhibition of respiratory-dependent growth was statistically greater than the inhibition of growth on fermentable energy sources. Inhibition of mitochondrial function in yeast and growth inhibition of an *in vitro* culture of human epidermoid carcinoma (KB) were positively correlated since 83% of the compounds tested either had mitochondrial-inhibiting properties and significant activity in the KB test or were inactive in both tests. Similarly, 78% of compounds tested showed murine toxicity and mitochondrial inhibition or had no effect on murine toxicity and yeast mitochondrial function. Injection of Ia into rats resulted in the appearance of blood in the urine and feces. Compound Ia inhibited adenosine diphosphate and collagen-induced aggregation of rat platelets but had no effect on blood clotting. TLC, following incubation of Ia with a rat liver extract, showed that the structure of Ia was not enzymatically modified and indicated activity *per se* on platelet aggregation and mitochondrial function.

Keyphrases □ Mannich bases—effect on mitochondrial function in yeast, human epidermoid carcinoma cultures, blood platelet aggregation, blood clotting, rats □ Mitochondrial activity—effect of Mannich bases and related compounds, yeast □ Blood platelet aggregation—effect of Mannich bases and related compounds, rats □ Coagulation, blood—effect of Mannich bases and related compounds, rats □ Structure-activity relationships—effect of Mannich bases and related compounds on mitochondrial function in yeast, human epidermoid carcinoma cultures, blood platelet aggregation and blood clotting, rats

Mannich bases have a wide range of biological activity including antineoplastic properties (1, 2), antimicrobial effects (3–5), analgesic activity (6), local anesthetic properties (7, 8), and psychotropic effects (9). To pursue a continuing interest in Mannich reactions (10–12) and α,β-unsaturated ketones (13, 14), several properties of a simple Mannich base, 5-dimethylamino-1-phenyl-1-penten-3-one (Ia), derived

Table I—Effect on Yeast Mitochondria, Activity against the KB Tumor, and Mammalian Toxicity of Some Mannich Bases and Related Compounds

Compound	Concentration, mg/ml	Growth on Complex Ethanol Medium: Mean Area of Inhibition, mm²	Growth on Complex Ethanol Medium: SE	Growth on Complex Glucose Medium: Mean Area of Inhibition, mm²	Growth on Complex Glucose Medium: SE	KB[a]	Maximum[b] Tolerated Dose, Daily Injections, mg/kg	Maximum[b] Tolerated Dose, Injections Every 4 Days, mg/kg
Ia	5	32.4	4.5	0.0[c]	—	N.A.	100[d]	100[d]
Ib	5	70.4	9.4	0.0[c]	—	1.2	75	100
IIa	5	307.7	35.0	15.2	5.2	1.5	100	200
IIb	1	55.8	8.9	0.0[c]	—	2.4	<100	N.A.
IIc	1	102.2	16.5	0.0[c]	—	1.7	75	100
IId	1	123.2	10.5	41.5	15.4	1.0	12.5	50
IIe	1	41.5	5.6	0.0[c]	—	2.8	50	N.A.
IIf	1	128.7	8.9	27.9[c]	—	1.2	25	25
IIg	5	0	—	0	—	2.1	<100	100
IIh	5	11.16	6.83	27.9[c]	—	N.A.	N.A.	100[e]
IIIa	5	0	—	0	—	>100	N.A.	<100
IIIb	5	0	—	0	—	23	>400	N.A.
IIIc	5	0	—	0	—	>10	>400	>400[d]
IIId	5	0	—	0	—	30	>400	>400
IIIe	5	0	—	0	—	28	>400	>400
IIIf	5	0	—	0	—	N.A.	N.A.	>350[f]
IIIg	5	0	—	0	—	27	100	>400
IIIh	5	0	—	0	—	>100	N.A.	>400
IIIi	1	90.5	6.3	0.0[c]	—	24	50	100
IIIj	5	0	—	0	—	N.A.	N.A.	>400
IIIk	5	0	—	0	—	25	>400	>400
IIIl	5	0	—	0	—	N.A.	N.A.	>400
IIIm	5	100.9[c]	—	0.0[c]	—	N.A.	>175[g]	N.A.
IV	5	0	—	0	—	100	200	>400
Va	5	0	—	0	—	2.3	>200	>400
Vb	5	0	—	0	—	N.A.	N.A.	50[h]
VIa	5	369.5	15.7	46.4	8.8	6.4	>50	200
VIb	5	0	—	0	—	42	>10	10
VIc	1	194.9	11.8	0.0[c]	—	3.2	50	50
VId	5	0	—	0	—	>100	N.A.	>400
VIe	5	0	—	0	—	>10	200	200
VIIa	1	164.5	16.9	0.0[c]	—	N.A.	N.A.	>400[h]
VIIb	5	0	—	0	—	N.A.	>400	N.A.

[a] The figures, in micrograms per milliliter, in the KB cell culture screen indicate the dose inhibiting 50% growth of human epidermoid carcinoma of the nasopharynx in Eagle's medium. N.A. = result not available. With the exception of IV, the data are taken from Ref. 1 and are reproduced with permission. [b] In virtually all cases the compounds were injected intraperitoneally into the BDF_1 strain of mouse at doses of 400, 200, and 100 mg/kg. If toxicity appeared, the doses were reduced. The figures in the columns indicate 6/6 survivors. With the exception of Ia, IIh, IV, Vb, and VIIa, the data are taken from Ref. 1 and are reproduced with permission. N.A. = result not available. Daily injections were made for 9 days, and a total of three injections was given when injections were made every 4 days. [c] All five replicates gave the same value. [d] The CDF_1 strain of mouse was used. [e] Three BDF_1 strains of mice only were used. [f] One injection only at 350 mg/kg. [g] The DBA/2 strain of mouse was used. [h] Three BDF_1 strains of mice only were used, and two injections of compound were made.

from an α,β-unsaturated ketone, were studied, and the bioactivity of closely related analogs was examined.

RESULTS AND DISCUSSION

Compounds containing a benzylidene group attached to electron-withdrawing functions such as cyano and nitro moieties interfere with mitochondrial function (15), and certain anticancer agents interfere with mitochondria (16). To examine the possibility of Ia being a mitochondrial poison, a solution of this component was added to disks on complex ethanol medium and complex glucose medium which were inoculated with *Saccharomyces cerevisiae*. In the absence of mitochondrial function, the yeast will grow on complex glucose medium, which provides energy for growth by fermentation of glucose. However, the complex ethanol medium containing a nonfermentable energy source does not provide energy for the growth of the yeast if interference with mitochondrial function occurs. The antimitochondrial activity of Ia, an activity that is significantly more potent than established inhibitors such as chloramphenicol and tetracycline (17), is shown in Table I.

Further confirmation of Ia being a mitochondrial inhibitor was obtained by examining the effect on growth inhibition of *S. cerevisiae* when grown in liquid media containing nonfermentable energy sources (ethanol, glycerol, and acetate) and fermentable energy sources (glucose and galactose). Growth in complex galactose medium and minimal salts glucose medium containing fermentable energy sources required a concentration of Ia greatly exceeding that required for a 50% inhibition of growth in minimal salts ethanol medium, complex glycerol medium, and complex acetate medium, which contain nonfermentable energy sources (Table II).

Two structural analogs of Ia then were examined, in which one hydrogen atom of the methylene group vicinal to the ketone func-

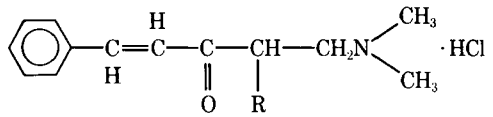

Ia: R = H
Ib: R = CH_3

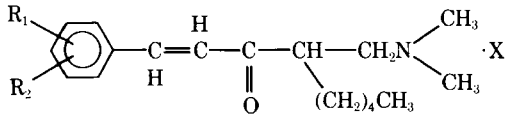

IIa: $R_1 = R_2 = H$, X = HCl
IIb: R_1 = 2-Cl, R_2 = H, X = HCl
IIc: R_1 = 4-Cl, R_2 = H, X = HCl
IId: R_1 = 2-Cl, R_2 = 4-Cl, X = HCl
IIe: R_1 = 2-Cl, R_2 = 6-Cl, X = HCl
IIf: R_1 = 3-Cl, R_2 = 4-Cl, X = HCl
IIg: R_1 = 4-Cl, R_2 = H, X = CH_3I
IIh: R_1 = 3-Cl, R_2 = 4-Cl, X = CH_3I

Table II—Growth Inhibition in Different Media[a] of *S. cerevisiae*

Compound	Medium	Concentration for 50% Inhibition of Growth, μg/ml
Ia	Minimal salts ethanol medium	51
	Complex glycerol medium	40
	Complex acetate medium	37
	Complex galactose medium	>1000
	Minimal salts glucose medium	780
Ib	Minimal salts ethanol medium	164[b]
	Minimal salts glucose medium	>1000
IIa	Minimal salts ethanol medium	90[c]
	Minimal salts glucose medium	385
IIIi	Minimal salts ethanol medium	73[d]
	Minimal salts glucose medium	287

[a] Cells were grown for 24 hr in a given liquid medium in the presence of the inhibitor. Growth is expressed as the percent of growth in the absence of inhibitor. [b] Mean of six determinations, SE = 5.36. [c] Mean of six determinations, SE = 4.28. [d] Mean of six determinations, SE = 2.72.

tion of Ia was replaced by a methyl group (Ib) or an *n*-pentyl function (IIa). Table I shows that both compounds inhibited mitochondrial function, a fact confirmed by growth inhibition studies using minimal salts ethanol medium and minimal salts glucose medium (Table II). Examination of Mannich bases related to IIa (namely, IIb–IIf) demonstrated that mitochondrial function was impaired. Quaternization of IIc gave IIg, which demonstrated no antimitochondrial properties. The related quaternary ammonium compound (IIh), which showed greater inhibition on complex glucose medium than on complex ethanol medium, presumably exerted its effect on yeast growth by interference with vital processes other than inhibition with mitochondrial function.

The ketones (III), which would be expected to be less water soluble than the related Mannich bases, did not inhibit mitochondrial function in yeast. The only exceptions were the quaternary ammonium compound (IIIi), which would be expected to be more water soluble than the related derivatives because it is fully ionized, and IIIm, which contains a shorter lipophilic aliphatic side chain than the corresponding unsubstituted compounds (IIIa and IIIj), indicating that solubility of these derivatives may play a part in the inhibition of mitochondrial function. Confirmation of the antimitochondrial activity of IIIi was found using liquid minimal salts glucose medium and minimal salts ethanol medium (Table II).

Mannich bases are capable of undergoing deamination to α,β-unsaturated ketones (10, 18), which may have possible significance *in vivo*. The potential breakdown products of IIc and IIf (namely, Va and Vb) were inactive as mitochondrial inhibitors under the test conditions. These results may indicate that the Mannich bases were active *per se* and did not break down to give the eliminated product. Alternatively, a hydrophilic dialkylamino group may be required to assist transportation to a site of action and liberate the corresponding unsaturated ketone (19).

The higher chemical and biological activity of allyl alcohol compared to the saturated analog (20, 21) may be due to the ability of allyl derivatives to function as biological alkylating agents because of the formation of carbonium ions. In the case of the substituted allyl alcohols (VIa–VIc), the carbonium ion is further stabilized by resonance due to the adjacent aromatic ring. The reduction of IIa led to VIa with a retention of antimitochondrial activity, but quaternization of VIa gave VIb, which was inactive. Reduction of IIb led to VIc, with nearly a fourfold increase in activity.

When masking of the polar group of Va and Vb occurred, utilizing the concept of latentiation (22) leading to the formation of the esters VId and VIe, mitochondrial function was abolished. This finding indicated that breakdown to the allyl alcohols does not occur in yeast cells or, alternatively, that the ester does not enter the cell. Possible changes in activity against yeast mitochondria were sought by reducing the α,β-unsaturated keto group of some of these derivatives. Reduction of IIf gave VIIa with a slight increase in inhibitory activity against yeast mitochondria; reduction of IIIa gave VIIb, and both compounds had no activity.

The KB test system gives an *in vitro* measure of the cytotoxicity of a compound and may indicate tumor-inhibiting properties (23).

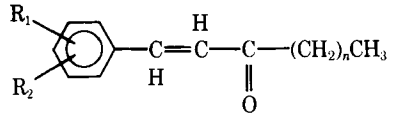

IIIa: $R_1 = R_2 = H$, $n = 5$
IIIb: R_1 = 2-Cl, $R_2 = H$, $n = 5$
IIIc: R_1 = 3-Cl, $R_2 = H$, $n = 5$
IIId: R_1 = 4-Cl, $R_2 = H$, $n = 5$
IIIe: R_1 = 2-Cl, R_2 = 4-Cl, $n = 5$
IIIf: R_1 = 2-Cl, R_2 = 6-Cl, $n = 5$
IIIg: R_1 = 3-Cl, R_2 = 4-Cl, $n = 5$
IIIh: R_1 = 4-$N(CH_3)_2$, $R_2 = H$, $n = 5$
IIIi: R_1 = 4-$\overset{+}{N}(CH_3)_3\overset{-}{I}$, $R_2 = H$, $n = 5$
IIIj: $R_1 = R_2 = H$, $n = 1$
IIIk: R_1 = 4-Cl, $R_2 = H$, $n = 1$
IIIl: R_1 = 4-NO_2, $R_2 = H$, $n = 1$
IIIm: $R_1 = R_2 = H$, $n = 0$

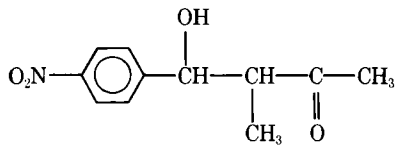

IV

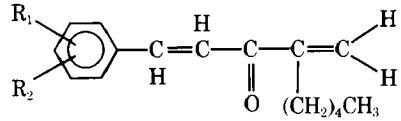

Va: R_1 = 4-Cl, $R_2 = H$
Vb: R_1 = 3-Cl, R_2 = 4-Cl

Significant activity in the KB test has been defined as the ability of a compound to inhibit 50% of the growth of human epidermoid carcinoma of the nasopharynx at a concentration of less than 4 μg/ml (24). The data in Table I were examined to see if a correlation existed between the effect on yeast mitochondria and KB toxicity. Of the 24 compounds for which data are available, 20 compounds (83%) either had mitochondrial-inhibiting properties and a minimal inhibitory concentration of less than 4 μg/ml in the KB test or failed to meet the criteria for activity in both tests.

The compounds in Table I were evaluated also for antineoplastic activity and murine toxicity (1) with the exception of Ia, IIh, IV, Vb, and VIIa, and the screening data for these compounds are given in Table III. Where data are available for mammalian toxicity, of the 19 compounds given daily at the maximum dose examined (*i.e.*, 400 mg/kg), 15 derivatives (79%) showed mitochondrial-inhibiting properties and mammalian toxicity or, alternatively, were inactive in inhibiting yeast mitochondria and caused no mortalities. Of the 26 compounds given every 4 days at the maximum dose administered (400 mg/kg), 21 (78%) showed toxicity and mitochondrial-inhibitory properties or showed no murine toxicity and did not inhibit yeast mitochondrial function. One may tentatively assume that interference with mitochondrial function is a factor in producing significant activity in the KB test system and also in producing mammalian toxicity.

Following injection of Ia into six rats at a dose of 100 mg/kg, the animals developed a paralysis of the hindlimbs within 2 hr. Although they recovered from this effect within 24 hr, death occurred in all animals within 36 hr. When Ia was administered at a dose of 50 mg/kg, blood was found in the feces and urine; this compound exerted a potent antidiuretic effect, a phenomenon that has been observed recently for IId and IIf (1). These results suggested that Ia might be interfering with normal hemostatic function of these animals, and studies were performed to determine if this compound was inhibiting blood clotting and/or platelet function.

The inhibitory effects of Ia on rat platelet aggregation induced by adenosine diphosphate and collagen are shown in Tables IV and V, respectively. Similar results were found when Ia was incubated for 5 min with human platelets. In this system, adenosine di-

Table III—Evaluation of Ia and Related Compounds against L-1210 Lymphoid Leukemia in Mice

Compound	Vehicle	Number of Animals Used	Dose Level[a], mg/kg	Frequency of Dose, days	Number of Injections	T/C, %[b]
Ia	Saline	6[c]	400 (0)	4	3	—
		6[c]	100	4	3	89
		6[c]	50	4	3	90
		6	100	1	9	88
		6	25	1	9	91
IIh	Hydroxypropylcellulose	3	400 (0)	4	2	—
		3	50	4	2	98
IV[d]	Hydroxypropylcellulose	6	400	4	3	98
		6	100	4	3	100
		6	400 (5)	1	9	92
		6	200	1	9	91
Vb	Dimethyl sulfoxide	3	400 (0)	4	2	—
		3	50	4	2	104
		3	25	4	2	114
VIIa	Hydroxypropylcellulose	3	400	4	2	117

[a] Drug was normally administered at 400, 200, and 100 mg/kg initially. The doses indicated are the maximum administered dose and the dose giving highest activity against L-1210 leukemia. If mortalities occurred, the number of survivors on Day 5 is indicated in brackets. [b] The value of T/C indicates the ratio of survival time of the treated mice over control mice, expressed as a percentage. A ratio of 125 or greater denotes significant activity. [c] The CDF_1 strain of mouse was used. [d] Compound inhibited 50% of the growth of human epidermoid carcinoma of the nasopharynx at 100 ppm (KB test).

Table IV—Reduction of Adenosine Diphosphate-Induced Aggregation Curve by Ia on Rat Blood Platelets

Concentration of Ia × 10^{-5} M	Curve Slope		Curve Height	
	Change, %	SE	Change, %	SE
13.2	8.6	±5.79	16.6	±2.35, $p < 0.005$
25.6	6.7	±9.55	31.4	±6.37, $p < 0.005$
48.8	37.9	±11.06, $p < 0.05$	68.6	±6.36, $p < 0.001$
88.9	62.1	±6.52, $p < 0.01$	91.9	±8.93, $p < 0.005$

phosphate-induced aggregation (curve height) was inhibited by 54.4% ± 4.37 *SEM* with 2.0 × 10^{-5} *M* Ia, by 76.3% ± 6.25 *SEM* with 6.0 × 10^{-5} *M* Ia, and by 100.0% ± 0.00 *SEM* with 15 × 10^{-5} *M* Ia. Collagen-induced aggregation of human platelets was completely inhibited by concentrations of Ia greater than 4 × 10^{-5} *M*.

The results of the prothrombin time, partial thromboplastin time, and activated partial thromboplastin time tests (Table VI) did not indicate the presence of a clotting defect in animals treated with Ia. There were no significant differences between the values found for these animals and for control rats. Compound Ia also did not have direct anticoagulant activity and did not hemolyze red cells *in vitro*. No metabolites of Ia were found following exposure of the compound to an active (determined by aniline hydroxylase activity) 9000×*g* supernatant fraction of rat liver for 20 min. The UV spectra obtained with the extract of the incubate and with a standard solution of Ia were identical, with one peak being present at 296 nm.

TLC did not reveal the presence of any metabolites from exposure of Ia to liver microsomes. The R_f value for Ia run on chloroform–methanol (95:5) was 0.19, and the R_f value for the extracted (alkaline) incubate was 0.18. In both cases, the spots were positive with Dragendorff's reagent and appeared as dark-brown spots following exposure to iodine vapor.

These observations suggest that Ia is active *per se* and that the presence of blood in the urine and feces of the treated rats is due in part to its inhibitory effect on platelet function.

Table V—Reduction of Collagen-Induced Aggregation Curve by Ia on Rat Blood Platelets

Concentration of Ia × 10^{-5} M	Curve Slope		Curve Height	
	Change, %	SE	Change, %	SE
10.9	21.1	±4.88, $p < 0.05$	26.3	±5.37, $p < 0.02$
21.3	52.4	±13.78, $p < 0.05$	64.8	±12.48, $p < 0.025$
40.8	94.6	±4.42, $p < 0.01$	97.5	±2.53, $p < 0.001$
75.5	100.0	±0.00, $p < 0.01$	100.0	±0.00, $p < 0.001$

Table VI—Effect of Ia on Prothrombin Time, Partial Thromboplastin Time, Activated Partial Thromboplastin Time, and Platelet Count in Rats

	Prothrombin Time, min	Partial Thromboplastin Time, min	Activated Partial Thromboplastin Time, min	Platelets				
				Count, mm^3	Lymphocytes, %	Polymorphs, %	Eosinophils, %	Monocytes, %
Untreated Rat 1	18.0	24.0	24.0	932,500	85	13	—	2
Untreated Rat 2	16.3	24.0	23.1	1,092,500	71	27	—	2
Rat 1	18.6	25.1	24.7	880,000	75	23	2	—
Rat 2	16.7	30.3	24.5	792,000	27	73	—	—
Rat 3	17.3	25.4	25.9	797,500	58	42	—	—
Rat 4	18.2	29.5	28.4	902,500	41	58	1	—

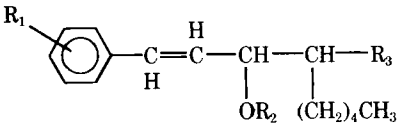

VI*a*: $R_1 = R_2 = H$, $R_3 = CH_2N(CH_3)_2 \cdot HCl$

VI*b*: $R_1 = R_2 = H$, $R_3 = CH_2\overset{+}{N}(CH_3)_3I$

VI*c*: $R_1 = 2\text{-}Cl$, $R_2 = H$, $R_3 = CH_2N(CH_3)_2 \cdot HCl$

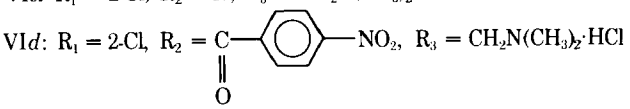

VI*d*: $R_1 = 2\text{-}Cl$, $R_2 = C(=O)$–C_6H_4–NO_2, $R_3 = CH_2N(CH_3)_2 \cdot HCl$

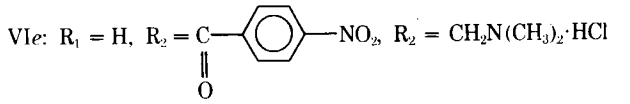

VI*e*: $R_1 = H$, $R_2 = C(=O)$–C_6H_4–NO_2, $R_3 = CH_2N(CH_3)_2 \cdot HCl$

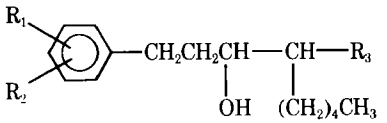

VII*a*: $R_1 = 3\text{-}Cl$, $R_2 = 4\text{-}Cl$, $R_3 = CH_2N(CH_3)_2 \cdot HCl$

VII*b*: $R_1 = R_2 = R_3 = H$

EXPERIMENTAL

Syntheses[1]—The Mannich bases listed in Table I were prepared as follows. 5-Dimethylamino-1-phenyl-1-penten-3-one hydrochloride (I*a*) was prepared by heating, under reflux, a mixture of benzylidene acetone (35.04 g, 0.240 mole), paraformaldehyde (7.64 g, 0.255 mole), dimethylamine hydrochloride (19.70 g, 0.242 mole), and hydrochloric acid (0.2 ml) in anhydrous alcohol (24 ml) for 12 hr. The crystals deposited (11.68 g) were removed and triturated with alcohol. Evaporation of the mother liquor to dryness followed by recrystallization of the residue gave a further crop of crystals (19.25 g). Recrystallization of the crystals from alcohol gave I*a* as colorless crystals (22.58 g, 40%), mp 157–158° [lit. (25) mp 157°].

The preparation of the derivatives I*b* and II*g* was described previously (1), and the syntheses of the Mannich bases (II*a*–II*f*) were reported elsewhere (10). (*E*)-1-(3,4-Dichlorophenyl)-4-dimethylamino-1-nonen-3-one methiodide (II*h*), prepared in a similar manner to II*g*, crystallized from alcohol as pale-yellow crystals (85%), mp 162.5°.

Anal.—Calc. for $C_{19}H_{28}Cl_2INO$: C, 47.10; H, 5.78; N, 2.89. Found: C, 47.03; H, 5.90; N, 2.91.

The syntheses of the α,β-unsaturated ketones (III*a*–III*l*) were reported previously (10, 26). Compound III*m* was obtained commercially[2], and its purity was checked by GLC. Compound IV, having the *threo*-configuration, was synthesized by the literature method (27). It crystallized from benzene–petroleum ether (3:1 v/v) as pale-yellow crystals (17%), mp 93–94.5° [lit. (28) mp 93–94°]; IR (potassium bromide): 3400 s (OH), 1705 s (C=O), and 1695 s (C=O) cm^{-1}; NMR (deuterochloroform): δ 8.12 (m, 2, aromatic H), 7.50 (m, 2, aromatic H), 4.87 (d, 1, $J_{4,3} = 8$ Hz, C_4H), 3.33 (s, 1, C_4OH, exchanged with D_2O), 2.93 (m, 1, C_3H), 2.22 (s, 3, C_1H_3), and 1.00 (d, 3, $J = 7.5$ Hz, C_3CH_3) ppm.

The preparation of the dienone (V*a*) was described previously (10). Analog V*b*, prepared in a similar manner from II*h*, crystallized as orange-yellow crystals from alcohol (78%), mp 37°. The mass spectrum showed *m/e* 296 as the parent peak.

Anal.—Calc. for $C_{16}H_{18}Cl_2O$: C, 64.64; H, 6.06; Cl, 23.90. Found: C, 64.49; H, 5.96; Cl, 24.18.

The samples of allylic alcohols and related esters (VI*a*–VI*e*) examined on complex glucose medium and complex ethanol medium were identical to those used in antineoplastic evaluations described previously (1); VI*a* and VI*b* were predominantly the *threo*-isomers, VI*c* and VI*e* were pure *threo*-isomers, and VI*d* was isomerically pure but of unknown relative stereochemistry (1, 14).

The preparation of the saturated alcohol (VII*a*) also was described previously (14). A suspension of Raney nickel (0.10 g approximately) in absolute alcohol (29) was added to a solution of 1-(3,4-dichlorophenyl)-4-dimethylaminomethyl-1-nonen-3-one hydrochloride (1.00 g, 0.00264 mole) in absolute alcohol (25 ml), and the mixture was hydrogenated in a Paar apparatus for 24 hr at 10–12 lb of pressure. The solution was filtered through diatomaceous earth[3], and evaporation of the solvent gave a pale-yellow liquid. This liquid crystallized on storage under vacuum. Repeated recrystallization from acetone afforded 1-(3,4-dichlorophenyl)-4-dimethylaminomethylnonan-3-ol hydrochloride (VII*b*) (0.4 g, 40%) as a pale-yellow solid, mp 103°. The mass spectrum showed *m/e* 345 as the parent peak.

Anal.—Calc. for $C_{18}H_{29}Cl_2NO \cdot HCl$: C, 56.45; H, 7.90; N, 3.66. Found: C, 55.48; H, 7.79; N, 3.60.

Inhibition of Mitochondrial Function—Complex glucose medium contained yeast extract (1%), bactopeptone (2%), glucose (2%), and agar (2%) in water and complex ethanol medium contained ethanol (1%) in place of glucose. The compounds (5.0 mg) were dissolved in 95% ethanol (1 ml), and 0.02 ml of the solution was applied to antibiotic disks (12.7 mm) placed on the surface of the plates containing complex glucose medium and complex ethanol medium previously spread with 0.2 ml of a culture of *S. cerevisiae*[4] grown for 48 hr in liquid complex ethanol medium.

The plates were incubated at 28° for 3 days, and the area of inhibition (square millimeters) surrounding the disk was determined. The area of growth inhibition on complex ethanol medium in excess of growth inhibition on complex glucose medium is a quantitative estimation of the inhibition of mitochondrial function. Each compound was initially tested at 5 mg/ml. Compounds that inhibited growth were then tested five times at 5 or 1 mg/ml.

For 50% growth inhibition studies (Table II) in liquid media, a diploid strain of *S. cerevisiae*[4] was initially grown to an early stationary phase in a liquid complex glucose medium. The medium, placed in 8 × 150-mm tubes, was inoculated to an optical density (640 nm) of 0.1 unit/ml. The inhibitors were added at concentrations of 1, 2.5, 5, 7.5, 10, 50, 100, 250, 500, 750, and 1000 μg/ml. After 24 hr of growth at 30°, the percentage growth was ascertained by the change in optical density and expressed as a percentage of the control. Minimal salts ethanol medium and minimal salts glucose medium contained ethanol (1%) and glucose (5%), respectively; complex acetate medium, complex glycerol medium, and complex galactose medium employed potassium acetate (2%), glycerol (4%), and galactose (2%), respectively.

The antineoplastic evaluation[5] of the compounds in Table III was conducted by intraperitoneal injection into the BDF_1 strain of mouse (24).

Administration of I*a* to Rats—The Mannich base (I*a*) was dissolved in sterile saline (0.9% w/v) and injected intraperitoneally into 40 male albino Wistar rats, 150–200 g, at a dose of 50 mg/kg in volumes of less than 1 ml. Ten control animals were injected with sterile saline. The rats were placed in metabolic cages, and the urine and feces were collected separately. Blood was detected visually in the urine and confirmed in both urine and feces by microscopic examination and the benzidine test (30).

After 24, 48, 72, and 120 hr, the urine output from 40 treated rats was 55, 100, 160, and 300 ml, respectively; the urine output from 10 control rats was 55, 70, 60, and 60 ml, respectively. No deaths occurred during the 5 days. Administration of I*a* at a dose of 100 mg/kg was undertaken using six animals.

Effect of I*a* on Blood Platelets—Whole blood was collected from the inferior vena cava of white, male, Wistar rats, 250–300 g, anesthetized with chloroform. Nine milliliters of whole blood was

[1] Melting points and boiling points are uncorrected. Elemental analyses were performed by Dr. F. B. Strauss, Microanalytical Laboratories, Oxford, England. GLC analysis utilized a Hewlett Packard 5750B research instrument, using a OV-101 on Chromosorb G column, HP80/100, 1.2 m × 0.3 cm (4 ft × 0.125 in.), at 140 and 170°. IR spectra were recorded on a Unicam SP-200 G spectrophotometer calibrated with polystyrene. A strong band intensity is designated s. NMR spectra were determined with a Varian T-60 machine, and the mass spectra were recorded on an AE1 MS-12 single-focusing mass spectrometer operated by Mr. D. Bain of the Department of Chemistry and Chemical Engineering, University of Saskatchewan, Saskatoon, Saskatchewan, Canada.

[2] Aldrich Chemical Co.

[3] Celite, Anachemia, Montreal, Quebec, Canada.

[4] Strain GR13 constructed in the Department of Biology, University of Saskatchewan, Saskatoon, Saskatchewan, Canada.

[5] Performed by the Drug Research and Development Division, National Cancer Institute, Bethesda, Md.

anticoagulated by mixing with 0.9 ml of aqueous trisodium citrate solution (3.8% w/v) in 13 × 100-mm Pyrex biological test tubes. The citrated whole blood was centrifuged at 750×*g* for 4 min to yield platelet-rich plasma.

Platelet aggregation was studied by a turbidimetric method (31) at 37°. Platelet-rich plasma, in 0.35-ml aliquots, was allowed to stand at room temperature for approximately 30 min before an experiment was begun. When adenosine diphosphate was the aggregating stimulus, a 1.35×10^{-5} *M* final concentration was employed. When collagen was the aggregation stimulus, a standard volume (0.1 ml) of collagen suspension was added. Experiments to determine the effects of I*a* on human blood platelets were performed as described previously (32).

Platelet aggregation was quantitated by measuring the slope of the aggregation curve and the maximum curve height attained within 5 min. The aggregation parameters of the curve employing I*a* were compared, by paired *t* test, to those of the control curve aggregated within 10 min (Tables IV and V).

Effects of I*a* on Blood Clotting—The hemolysis of red cells by I*a* was studied by a method outlined previously (33).

To determine if I*a* had any direct anticoagulant effect, saline solutions of I*a* and heparin were prepared (0.0, 0.1, 0.25, 0.5, 1.0, and 10.0 mg/ml). One-milliliter aliquots of these solutions were added to test tubes along with 0.9 ml of whole blood from male Wistar rats. The effects of I*a* were compared with those of heparin.

Prothrombin times were determined using a commercial rabbit brain thromboplastin[6], and partial thromboplastin[7] times and activated partial thromboplastin[7] times also were determined using commercial reagents.

In Vitro* Metabolism of I*a—*Tissue Preparation*—White, male Wistar rats, 200–350 g, which had been starved for 24 hr, were sacrificed by decapitation. Each liver was removed and placed in cold (4°) isotonic potassium chloride solution. To remove as much blood as possible, the liver was cut into small pieces into a second aliquot of cold isotonic potassium chloride solution.

Homogenization was carried out in 2 volumes of isotonic potassium chloride solution, using a homogenizer[8] operating at speed setting 40. Two grinding cycles of 5-sec duration, separated by 5 sec, were employed to produce a smooth liver homogenate. The homogenate was poured into two polycarbonate centrifuge tubes (28.7 × 103 mm) and centrifuged for 20 min (9000×*g*) in a refrigerated centrifuge[9]. The resulting supernatant layer was decanted and placed in a 50-ml beaker, which was kept in ice.

Substrates and Cofactors—The following solutions were prepared: 0.1 *M* phosphate buffer, 0.02 *M* magnesium chloride in distilled water, 0.02 *M* glucose 6-phosphate in 0.1 *M* phosphate buffer, 0.004 *M* nicotinamide adenosine dinucleotide phosphate in 0.1 *M* phosphate buffer, 0.005 *M* aniline hydrochloride in distilled water, and 0.01 *M* I*a* in 0.1 *M* phosphate buffer.

Enzyme Incubation—Three groups of incubation flasks were prepared.

1. To determine the enzyme activity of the 9000×*g* supernate, an aniline hydroxylase assay was performed by a modified method of LaDu *et al.* (34). The following items were added to five erlenmeyer flasks (25 ml): one glass bead (6 mm diameter), 1 ml of phosphate buffer, 1 ml of glucose 6-phosphate, 1 ml of nicotinamide adenosine dinucleotide phosphate, 1 ml of magnesium chloride, 1 ml of aniline hydrochloride solution, and 1 ml of the 9000×*g* supernatant homogenate.

2. To determine if enzymes present in the 9000×*g* supernate were altering the structure of I*a*, five incubation flasks were prepared as in Group 1, except that aniline hydrochloride was replaced with 1 ml of I*a* solution.

3. Five incubation flasks were also prepared to determine if I*a* had any effects on aniline hydroxylase activity. The contents of these flasks were similar to those in Group 1, except that 1 ml of I*a* solution replaced the 1 ml of phosphate buffer.

In all cases, control flasks were prepared in which the enzyme suspension was boiled prior to incubation. Incubation of aniline hydrochloride and aniline hydrochloride plus I*a* was of 20-min duration, while incubation of I*a* alone lasted 1 hr. All incubations were carried out in a shaking water bath at 37°. At the end of the incubation period, the reaction was stopped with 20% trichloroacetic acid, precipitated protein was removed by centrifugation, and the clear supernate was recovered. UV spectra were obtained on a control sample, a sample from the flask containing I*a*, and an aliquot of a standard solution of I*a*.

To isolate any metabolites of I*a* from the incubated samples, extractions were performed with chloroform at pH 2 and 9. The extracts were concentrated and spotted on TLC (silica gel G) and chromatographed using chloroform–methanol (95:5) as the developing solvent. Developed plates were treated with Dragendorff's reagent and exposed to iodine vapor. These experiments were repeated on five different occasions.

[6] Fibroplastin, BBL, Division of Bioquest, Cockeysville,.Md.
[7] Thrombofax and Activated Thrombofax, Ortho Diagnostics, Raritan, N.J.
[8] Virtis "45," Virtis Co., Gardiner, N.Y.
[9] International model B 20, International Equipment Co., Needham Heights, Mass.

REFERENCES

(1) J. R. Dimmock and W. G. Taylor, *J. Pharm. Sci.*, **64,** 241(1975).

(2) H. Schoenenberger, T. Bastig, L. Bindl, A. Adam, D. Adam, A. Petter, and W. Zwez, *Pharm. Acta Helv.*, **44,** 691(1969); through *Chem. Abstr.*, **72,** 65748f(1970).

(3) H. J. Florestano and M. E. Bahler, *J. Amer. Pharm. Ass., Sci. Ed.*, **45,** 320(1956).

(4) J. Sam and A. C. Thompson, *J. Pharm. Sci.*, **53,** 535(1964).

(5) W. L. Nobles and B. B. Thompson, *ibid.*, **53,** 1554(1964).

(6) R. Viterbo, M. Mastursi, and G. Perri, German pat. 2,241,578; through *Chem. Abstr.*, **80,** 108064q(1974).

(7) F. F. Blicke and E. S. Blake, *J. Amer. Chem. Soc.*, **52,** 235(1930).

(8) W. Wilson and Z. Y. Kyi, *J. Chem. Soc.*, **1952,** 1321.

(9) R. N. Shut, F. E. Ward, and R. Rodriguez, *J. Med. Chem.*, **15,** 301(1972).

(10) J. R. Dimmock and W. G. Taylor, *J. Pharm. Sci.*, **63,** 69(1974).

(11) J. R. Dimmock and W. A. Turner, *Can. J. Pharm. Sci.*, **9,** 33(1974).

(12) A. F. Casy, N. J. Harper, and J. R. Dimmock, *J. Chem. Soc.*, **1964,** 3635.

(13) J. R. Dimmock, P. D. Ralph, and P. L. Carter, *J. Chem. Soc. B*, **1968,** 698.

(14) W. G. Taylor and J. R. Dimmock, *Can. J. Chem.*, **52,** 2522(1974).

(15) C. R. Bovell, L. Packer, and G. R. Schontaum, *Arch. Biochem. Biophys.*, **95,** 379(1961).

(16) M. Gosalvez, M. Blanco, J. Hunter, M. Miko, and B. Chance, *Eur. J. Cancer*, **10,** 567(1974).

(17) G. H. Rank and N. T. Bech-Hansen, *Mol. Gen. Genet.*, **126,** 93(1973).

(18) J. A. Mollica, J. B. Smith, I. M. Nunes, and H. K. Govan, *J. Pharm. Sci.*, **59,** 1770(1970).

(19) P. N. Gordon, J. D. Johnston, and A. R. English, in "Antimicrobial Agents and Chemotherapy," G. L. Hobby, Ed., American Society for Microbiology, Bethesda, Md., 1965, p. 165.

(20) J. Packer and J. Vaughan, "A Modern Approach to Organic Chemistry," Oxford, London, England, 1958, p. 184.

(21) W. A. Uricchio, *Proc. Helmenthol. Soc. Wash.*, **18,** 136(1951); through *Chem. Abstr.*, **48,** 6650c(1954).

(22) N. J. Harper, in "Progress in Drug Research," vol. 4, E. Jucker, Ed., Birkhauser Verlag, Basel, Switzerland, 1962, p. 221.

(23) N. R. Farnsworth, *J. Pharm. Sci.*, **62** (5), iv(1973).

(24) R. I. Geran, N. H. Greenberg, M. M. MacDonald, A. M. Schumacher, and B. J. Abbott, *Cancer Chemother. Rep. (Part 3)*, **3** (2) (Sept. 1972).

(25) H. B. Nisbet, *J. Chem. Soc.*, **1938,** 1237.

(26) P. J. Smith, J. R. Dimmock, and W. G. Taylor, *Can. J. Chem.*, **50,** 871(1972).

(27) M. Stiles, R. R. Winkler, Y.-L. Chang, and L. Traynor, *J. Amer. Chem. Soc.*, **86,** 3337(1964).

(28) M. Stiles, D. Wolfe, and G. V. Hudson, *ibid.*, **81,** 628(1959).

(29) A. I. Vogel, "A Textbook of Practical Organic Chemistry," Longmans, Green, London, England, 1956, p. 871.

(30) W. R. Fearon, "An Introduction to Biochemistry," William Heinemann Medical Books, London, England, 1946, p. 459.

(31) G. U. R. Born, *Nature*, **194,** 927(1962).

(32) D. G. Mills, R. B. Philp, and M. Hirst, *Life Sci.*, **14,** 659(1974).

(33) M. J. Lynch, S. S. Raphael, L. D. Miller, P. D. Spare, and M. J. H. Inwood, "Medical Laboratory Technology and Clinical Pathology," Saunders, Philadelphia, Pa., 1969, p. 675.

(34) B. N. LaDu, H. G. Mandel, and E. L. Way, "Fundamentals of Drug Metabolism and Drug Disposition," Williams & Wilkins, Baltimore, Md., 1971, p. 571.

ACKNOWLEDGMENTS AND ADDRESSES

Received April 22, 1975, from the *College of Pharmacy and the ‡Department of Biology, University of Saskatchewan, Saskatoon, Saskatchewan, Canada, S7N 0W0.

Accepted for publication June 27, 1975.

The authors thank the Medical Research Council for the award of operating grants (MA-4761 and MA-5538) and a fellowship to D. G. Mills. Financial support to G. H. Rank by the National Cancer Institute of Canada is gratefully acknowledged. Funding by the Youth Employment Service Programme from the Government of Saskatchewan to L. E. Negrave is gratefully acknowledged. Dr. H. B. Wood, Jr., of the Drug Research and Development Division of the National Cancer Institute, Bethesda, Md., kindly supervised the screens employing L-1210 and KB test systems. The methods for carrying out the partial thromboplastin time and activated partial thromboplastin time were provided by Ortho Diagnostics, Raritan, N.J. The assistance of Mr. A. M. Qureshi in the synthesis of several compounds is acknowledged.

* To whom inquiries should be directed.

Controlled Drug Release from Polymeric Delivery Devices IV: *In Vitro–In Vivo* Correlation of Subcutaneous Release of Norgestomet from Hydrophilic Implants

YIE W. CHIEN ˣ and EDWARD P. K. LAU

Abstract □ The *in vitro* and *in vivo* releases of norgestomet from hydrophilic implants were found to follow a matrix-controlled ($Q - t^{1/2}$) process. The sorption of drug onto the implants was observed to obey the same mechanism but with a much smaller magnitude of the $Q/t^{1/2}$ value. The effect of the extent of cross-linking on the magnitude of drug release ($Q/t^{1/2}$) profiles was analyzed both theoretically and experimentally. The release of norgestomet from hydrophilic implants was found to be an energy-linked process. Two energy terms were calculated; the activation energy for matrix diffusion was 7.71 kcal/mole, and the heat of drug crystal solvation was 25–28.6 kcal/mole.

Keyphrases □ Drug release—controlled, norgestomet from hydrophilic polymeric delivery devices □ Norgestomet—subcutaneous release from hydrophilic implants, matrix-controlled kinetic mechanism □ Implants—hydrophilic, subcutaneous release of norgestomet □ Delivery devices—polymeric, hydrophilic implants, subcutaneous release of norgestomet

The controlled release profiles of ethynodiol diacetate[1], a progestin, from silicone matrixes were reported previously (1). *In vitro* release of the drug from such silicone-type vaginal devices followed either of two kinetic mechanisms, matrix controlled or partition controlled, depending on whether the diffusion across the polymer phase or the partitioning across the polymer–solution interface was the rate-limiting step (2). An 8-week investigation on the intravaginal release of ethynodiol diacetate in rabbits (3) demonstrated that the matrix-controlled process was the predominant mode of drug release *in vivo*. Subsequently, the authors also investigated the controlled release of progestins from popularly used (Long–Folkman-type) polysiloxane[2] capsules (4). In contrast to the matrix-controlled ($Q/t^{1/2}$) mechanism seen in the drug release from silicone matrixes, they observed a constant (Q/t) drug release rate (5).

It was established that the carriers prepared from silicone polymer are permeable only to lipophilic drugs, *e.g.*, steroids. The rate of drug release is linearly proportional to the polymer solubility (partition-controlled process) (5) or to the square root of the polymer solubility (matrix-controlled process) (1, 2) of a given drug species when all other factors are constant. Apparently, the solubility of drug molecules in polymer plays a rate-limiting role in the controlled release of drug from the silicone-type drug delivery devices.

In addition to studying the lipophilic silicone polymer, researchers in this laboratory have had an ongoing interest in the development of a biocompatible, hydrophilic polymer (hydrogel) as the drug delivery carrier. First introduced by Wichterle and Lim (6) for prosthetic implants and contact lenses, this purified hydrogel is nontoxic, transparent, autoclavable, chemically stable, pliable, and moldable. The unique characteristics of this polymer (different from the silicone polymer discussed earlier) are its hydrophilicity, conductivity, and extreme wettability. Hydrogel will absorb and elute, in addition to neutral species, ionizable compounds with a molecular weight of 8000 or less (7). Through controlled alteration of the amount of cross-linking agent, the monomer-to-water ratio, and the polymerization conditions, a range of masses is obtainable from compact gel to cellular sponge, with varying physical properties.

The purposes of this study were to analyze the mechanisms and rates of the controlled release of

[1] SC-11800.
[2] Silastic.

(33) M. J. Lynch, S. S. Raphael, L. D. Miller, P. D. Spare, and M. J. H. Inwood, "Medical Laboratory Technology and Clinical Pathology," Saunders, Philadelphia, Pa., 1969, p. 675.

(34) B. N. LaDu, H. G. Mandel, and E. L. Way, "Fundamentals of Drug Metabolism and Drug Disposition," Williams & Wilkins, Baltimore, Md., 1971, p. 571.

ACKNOWLEDGMENTS AND ADDRESSES

Received April 22, 1975, from the *College of Pharmacy and the ‡Department of Biology, University of Saskatchewan, Saskatoon, Saskatchewan, Canada, S7N 0W0.

Accepted for publication June 27, 1975.

The authors thank the Medical Research Council for the award of operating grants (MA-4761 and MA-5538) and a fellowship to D. G. Mills. Financial support to G. H. Rank by the National Cancer Institute of Canada is gratefully acknowledged. Funding by the Youth Employment Service Programme from the Government of Saskatchewan to L. E. Negrave is gratefully acknowledged. Dr. H. B. Wood, Jr., of the Drug Research and Development Division of the National Cancer Institute, Bethesda, Md., kindly supervised the screens employing L-1210 and KB test systems. The methods for carrying out the partial thromboplastin time and activated partial thromboplastin time were provided by Ortho Diagnostics, Raritan, N.J. The assistance of Mr. A. M. Qureshi in the synthesis of several compounds is acknowledged.

* To whom inquiries should be directed.

Controlled Drug Release from Polymeric Delivery Devices IV: *In Vitro–In Vivo* Correlation of Subcutaneous Release of Norgestomet from Hydrophilic Implants

YIE W. CHIEN ˣ and EDWARD P. K. LAU

Abstract □ The *in vitro* and *in vivo* releases of norgestomet from hydrophilic implants were found to follow a matrix-controlled ($Q - t^{1/2}$) process. The sorption of drug onto the implants was observed to obey the same mechanism but with a much smaller magnitude of the $Q/t^{1/2}$ value. The effect of the extent of cross-linking on the magnitude of drug release ($Q/t^{1/2}$) profiles was analyzed both theoretically and experimentally. The release of norgestomet from hydrophilic implants was found to be an energy-linked process. Two energy terms were calculated; the activation energy for matrix diffusion was 7.71 kcal/mole, and the heat of drug crystal solvation was 25–28.6 kcal/mole.

Keyphrases □ Drug release—controlled, norgestomet from hydrophilic polymeric delivery devices □ Norgestomet—subcutaneous release from hydrophilic implants, matrix-controlled kinetic mechanism □ Implants—hydrophilic, subcutaneous release of norgestomet □ Delivery devices—polymeric, hydrophilic implants, subcutaneous release of norgestomet

The controlled release profiles of ethynodiol diacetate[1], a progestin, from silicone matrixes were reported previously (1). *In vitro* release of the drug from such silicone-type vaginal devices followed either of two kinetic mechanisms, matrix controlled or partition controlled, depending on whether the diffusion across the polymer phase or the partitioning across the polymer–solution interface was the rate-limiting step (2). An 8-week investigation on the intravaginal release of ethynodiol diacetate in rabbits (3) demonstrated that the matrix-controlled process was the predominant mode of drug release *in vivo*. Subsequently, the authors also investigated the controlled release of progestins from popularly used (Long–Folkman-type) polysiloxane[2] capsules (4). In contrast to the matrix-controlled ($Q/t^{1/2}$) mechanism seen in the drug release from silicone matrixes, they observed a constant (Q/t) drug release rate (5).

It was established that the carriers prepared from silicone polymer are permeable only to lipophilic drugs, *e.g.*, steroids. The rate of drug release is linearly proportional to the polymer solubility (partition-controlled process) (5) or to the square root of the polymer solubility (matrix-controlled process) (1, 2) of a given drug species when all other factors are constant. Apparently, the solubility of drug molecules in polymer plays a rate-limiting role in the controlled release of drug from the silicone-type drug delivery devices.

In addition to studying the lipophilic silicone polymer, researchers in this laboratory have had an ongoing interest in the development of a biocompatible, hydrophilic polymer (hydrogel) as the drug delivery carrier. First introduced by Wichterle and Lim (6) for prosthetic implants and contact lenses, this purified hydrogel is nontoxic, transparent, autoclavable, chemically stable, pliable, and moldable. The unique characteristics of this polymer (different from the silicone polymer discussed earlier) are its hydrophilicity, conductivity, and extreme wettability. Hydrogel will absorb and elute, in addition to neutral species, ionizable compounds with a molecular weight of 8000 or less (7). Through controlled alteration of the amount of cross-linking agent, the monomer-to-water ratio, and the polymerization conditions, a range of masses is obtainable from compact gel to cellular sponge, with varying physical properties.

The purposes of this study were to analyze the mechanisms and rates of the controlled release of

[1] SC-11800.
[2] Silastic.

norgestomet (I) from hydrophilic implants and to investigate the correlations of *in vivo* and *in vitro* drug release profiles. Norgestomet is effective for the estrus synchronization in heifers.

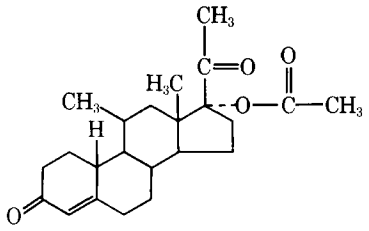

I

EXPERIMENTAL

Drug Delivery Devices—The delivery devices were prepared[3] first by polymerization from the water-soluble monomers of hydroxyethyl methacrylate to an alcohol-soluble, linear polymer[4]. Addition of the cross-linking agent ethylene dimethacrylate and an oxidizing catalyst yielded the three-dimensional ethylene glycomethacrylate gel[5] (II) (7).

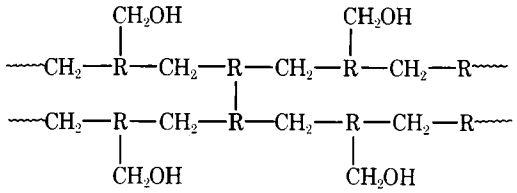

II

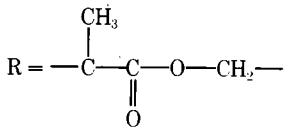

Various amounts of norgestomet may be impregnated in the hydrogel (II) by absorption by the dry polymer, incorporation into the gel plastic at the time of polymerization, or solution in the liquid linear polymer[4] (7).

Drug Release Systems—In Vitro *Studies*—In a dissolution flask, 300 ml of distilled water was maintained at 37°. At zero time, one rod of hydrogel (3 × 18 mm) was immersed with constant agitation (100 rpm) in this thermostated elution medium. The elution medium was sampled and renewed every 24 hr. The drug content in the samples was analyzed spectrophotometrically. The amount of norgestomet released from a unit surface area of hydrogel at a given day was calculated based on ϵ = 17,400 at λ_{max} = 242 nm.

In Vivo *Studies*—*In vivo* studies for three cross-links (*XL*) of hydrogel containing 5% norgestomet were conducted[6] in 39 cows. Cows were randomized into three lots of 13 each (A, B, and C). On Day 0, each cow in Lots A, B, and C was implanted in one of its ears with five implants of 1.2% *XL*, 4.8% *XL*, and 19.2% *XL*, respectively. The implants were placed in such a way as to minimize the possibility of their interfering with elution from each other. For analytical control purposes, two cows in each lot were implanted with a single nonmedicated hydrogel with corresponding cross-links. On Days 1, 2, 4, 8, and 16, one implant was removed from each cow and assayed for its residual drug content.

Hydrogel Sorption Studies—Ten rods of hydrogel (4.8% *XL*) containing no drug were immersed with shaking (80 oscillations/min) in 200 ml of aqueous solution of norgestomet (2×10^{-5} *M*) at 37°. Ten milliliters of sample was withdrawn every hour in the first 6 hr and then every day up to 5 days. After equilibration to 25°, the drug concentration in the sample was analyzed spectrophotometrically[7] and the amount of drug absorbed into the hydrogel (micrograms per square centimeter) was calculated as a function of time.

[3] HYDRO Med. Sciences, Inc., New Brunswick, N.J.
[4] Hydron S.
[5] Hydron.
[6] By Dr. Sam E. Curl, Texas Tech University, Lubbock, TX 79409
[7] Coleman 124 D double-beam spectrophotometer, Perkin-Elmer.

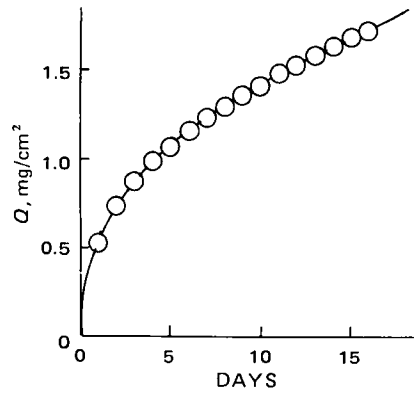

Figure 1—In vitro *cumulative amount of drug released (Q) per unit area of implant* versus *time for hydrogel implant (4.8% XL) containing 5% norgestomet.*

Determination of Solubility in Hydrogel—Five rods of hydrogel (4.8% *XL*) containing no drug were immersed with shaking (80 oscillations/min) in 200 ml of aqueous solution of norgestomet (2×10^{-5} *M*) at 37°. The drug concentration in the solution was monitored every day until a constant level was reached. Then the drug content absorbed into each rod of hydrogel was extracted with methanol for 3 days with constant shaking. The drug concentration in methanol was calculated and used to estimate the solubility of norgestomet in hydrogel. A solubility of 266.4 (±12.1) μg/cm³ was obtained.

RESULTS AND DISCUSSION

***In Vitro* Drug Release Studies**—The time course for the release of norgestomet from hydrogel implants at 37° is illustrated in Fig. 1. The cumulative amount of drug (Q) released from a unit surface area of implant is directly but not linearly proportional to the length of elution (in days). If the amount of drug (>36.3 mg/cm³) incorporated into a unit volume of hydrogel implant is greatly in excess of the polymer solubility (0.266 mg/ml) of drug, then most impregnated drug will be evenly dispersed in the polymeric matrix. In such a case, the release of drug from the hydrogel implant should follow the $Q - t^{1/2}$ relationship established by Higuchi (8), as demonstrated previously in the controlled release of ethynodiol diacetate from silicone vaginal devices (1–3):

$$Q = \sqrt{D_m(2A - C_p)C_p t} \qquad \text{(Eq. 1)}$$

where Q is the cumulative amount of drug released from a unit surface area of implant, D_m is the effective diffusivity of drug in polymeric matrix, A is the initial amount of drug incorporated in a unit volume of hydrogel, C_p is the solubility of drug in the hydrogel, and t is the time. In the present case, the drug content (A = 36.3 g/10³ cm³) incorporated into a unit volume of hydrogel is much higher than the solubility of drug in the hydrogel polymer (C_p = 0.266 g/10³ cm³); therefore, since $2A \gg C_p$, Eq. 1 may be simplified to:

$$Q = \sqrt{2D_m A C_p t} \qquad \text{(Eq. 2)}$$

According to Eq. 2, the cumulative amount of norgestomet released from the hydrogel, Q, should be linearly proportional to the square root of time ($t^{1/2}$). The nonlinear drug release profile ($Q - t$) shown in Fig. 1 is plotted in Fig. 2 according to Eq. 2. Apparently, the $Q - t^{1/2}$ relationship is also followed very well in the release of norgestomet from the hydrogel as ethynodiol diacetate was from silicone devices (1).

From the slope of the linear Q *versus* $t^{1/2}$ plot, the magnitude of drug release profile ($Q/t^{1/2}$) may be estimated. For the hydrogel implant with a degree of cross-linkage of 4.8%, the magnitude of the $Q/t^{1/2}$ value was found to be 0.396 mg/cm²/day$^{1/2}$. The influence of the extent of cross-linkage on the controlled-release profiles of norgestomet from hydrogel implants will be analyzed later.

***In Vivo* Drug Release Studies**—The release profile of norgestomet from a 4.8% cross-linked hydrogel device implanted subcu-

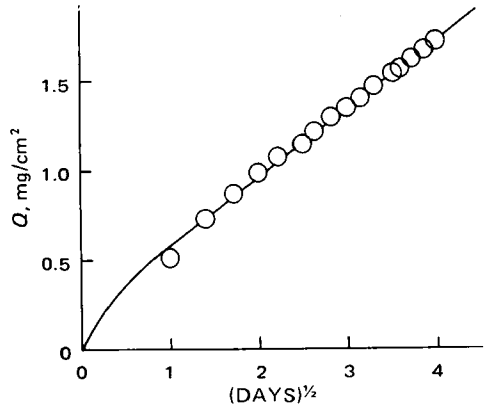

Figure 2—*Linear relationship between the* in vitro *cumulative amount of drug released (Q) per unit area of implant and the square root of time ($t^{1/2}$) following Eq. 2. The flux of drug release ($Q/t^{1/2}$) calculated from the slope is 0.396 mg/cm²/day$^{1/2}$.*

taneously in cows is shown in Fig. 3 according to Eq. 2. As demonstrated in the study of *in vitro* drug elution, the linear $Q - t^{1/2}$ relationship is also observed in the *in vivo* release of norgestomet. The agreement indicates that the same mechanism (matrix controlled) (1, 3) was followed in both *in vitro* and *in vivo* drug releases. The *in vivo* $Q/t^{1/2}$ value was also estimated from the slope of the $Q - t^{1/2}$ plot and found to be 0.504 mg/cm²/day$^{1/2}$. This magnitude of the $Q/t^{1/2}$ value is 27% higher than that estimated from the *in vitro* drug release profile (0.396 mg/cm²/day$^{1/2}$). This difference is obviously the result of the difference in the diffusional resistance between *in vivo* and *in vitro* cases (3).

Effect of Cross-Linking—In the process of hydrogel polymerization, varying amounts (1.2–19.2%) of ethylene dimethacrylate were added as a cross-linking agent for the cross-linking of a linear polymer[4] to a three-dimensional ethylene glycomethacrylate gel[5]. The addition of a cross-linking agent decreased the magnitude of $Q/t^{1/2}$ of norgestomet from the hydrogel (Table I). Both the *in vitro* and *in vivo* data for $Q/t^{1/2}$ were remarkably decreased as the extent of cross-linking increased.

In Eq. 2, only the matrix diffusivity (D_m), a rate-limiting parameter, appears to be sensitive to the degree of cross-linking (9), since it is directly proportional to the ratio of porosity (ϵ) over tortuosity (θ) (10) as follows:

$$D_m = D\frac{\epsilon}{\theta} \qquad \text{(Eq. 3)}$$

since the addition of a cross-linking agent results in a greater degree of polymer cross-linkage leading to the reduction in the mobility of the polymer chain and, consequently, a decrease in porosity (ϵ) as well as an increase in tortuosity (θ) for the diffusion of

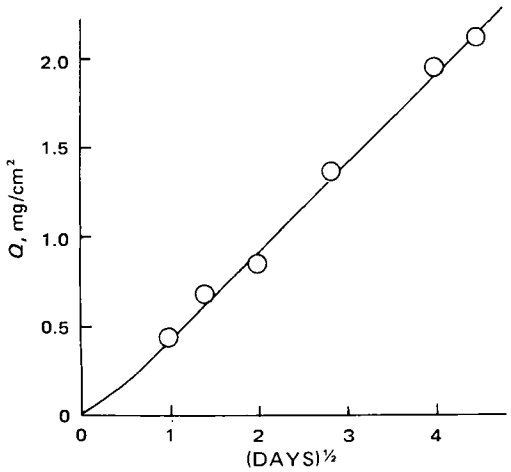

Figure 3—*Linear relationship between the* in vivo *cumulative amount of drug released (Q) per unit area of implant and the square root of time ($t^{1/2}$) following Eq. 2. The flux of drug release ($Q/t^{1/2}$) calculated from the slope is 0.504 mg/cm²/day$^{1/2}$.*

Table I—Effect of Extent of Cross-Linkage on the $Q/t^{1/2}$ Profiles of Norgestomet from Hydrogel Implants[a]

Cross-Linkage Extent, %	$Q/t^{1/2}$, mg/cm²/day$^{1/2}$	
	In Vitro	*In Vivo*
1.2	0.605	0.640
4.8	0.396	0.504
9.6	0.185	—
12.0	0.133	—
14.4	0.101	—
16.8	0.074	—
19.2	0.058	0.129

[a] Five percent drug per implant (total drug content = 6 mg).

drug in the polymer matrix. The term D is the intrinsic diffusivity of drug.

Equation 3 may be expressed alternatively to describe the influence of the extent of cross-linking (XL) on the effective matrix diffusivity (D_m):

$$D_m = kD/(XL) \qquad \text{(Eq. 4)}$$

since:

$$\epsilon/\theta = k/(XL) \qquad \text{(Eq. 5)}$$

where k is a proportionality constant. Substituting Eq. 4 for D_m in Eq. 2 gives:

$$Q/t^{1/2} = \sqrt{2kDAC_p}(XL)^{-1/2} \qquad \text{(Eq. 6)}$$

Equation 6 states that the magnitude of $Q/t^{1/2}$ values should be a direct function of the reciprocal of the square root of cross-linking agent added, $(XL)^{-1/2}$, with a slope defined by $(2kDAC_p)^{1/2}$. The relationship of $Q/t^{1/2}$ to $(XL)^{-1/2}$ is demonstrated in Fig. 4. Both *in vitro* and *in vivo* $Q/t^{1/2}$ values were linearly correlated with their corresponding $(XL)^{-1/2}$ data in the cross-linking range of 4.8–19.2% [$(XL)^{-1/2}$ = 4.56–2.28]. A higher effect on the magnitude of $Q/t^{1/2}$ value was observed when the cross-linking extent was below 4.8% [$(XL)^{-1/2}$ = 4.56]. The same kind of phenomenon was also observed in the diffusion of the gas molecules as small as nitrogen in natural rubber (9). The same type of trend was illustrated (insert in Fig. 4) when the effective diffusivity data were plotted against the reciprocal of the extent of cross-linking (Eq. 4).

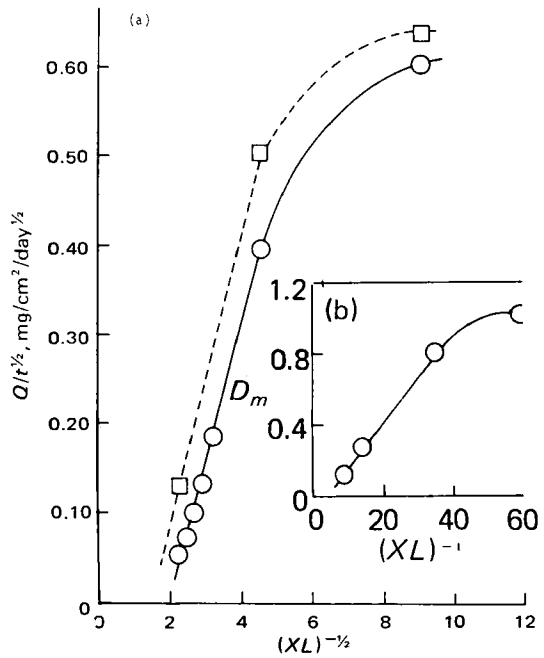

Figure 4—*(a) Relationship between the flux of drug release ($Q/t^{1/2}$) and the extent of cross-linking (XL) following Eq. 6. Key:* ○, *in vitro data; and* □, *in vivo data. (b) Relationship between* D_m *and* $(XL)^{-1}$ *(Eq. 4). (Data are from Ref. 9.)*

Table II—Effect of Extent of Cross-Linking (XL) on the Ratio of Porosity/Tortuosity (ϵ/θ) and the Effective Diffusivity of Drug in Polymer Matrix (D_m)

XL	ϵ/θ [a]	D_m [b], cm²/day
0.012	2.67	9.72×10^{-2}
0.048	0.67	2.42×10^{-2}
0.096	0.33	1.21×10^{-2}
0.120	0.27	9.72×10^{-3}
0.144	0.22	8.08×10^{-3}
0.168	0.19	6.93×10^{-3}
0.192	0.17	6.06×10^{-3}

[a] Calculated from Eq. 5, where $k = 3.20 \times 10^{-2}$. [b] Calculated from Eq. 4, where $k = 3.20 \times 10^{-2}$ and $D = 3.64 \times 10^{-2}$ cm²/day.

Figure 4 demonstrates that both *in vitro* and *in vivo* data followed the similar dependency of $Q/t^{1/2}$ on $(XL)^{-1/2}$.

The magnitude of the slope, $(2kDAC_p)^{1/2}$, of the linear region was estimated as 0.15 mg/cm²/day$^{1/2}$. By incorporating the values of D (3.64×10^{-2} cm²/day), A (36.3 g/10^3 cm³), and C_p (0.266 g/10^3 cm³), the magnitude of k, the proportionality constant relating ϵ/θ with $(XL)^{-1}$, may be computed. A value of 3.20×10^{-2} was obtained. Furthermore, the variation of ϵ/θ, the ratio of porosity to tortuosity, and of D_m, the effective diffusivity of drug in the hydrogel matrix, as a function of the extent of polymer cross-linking (XL) may be calculated from Eqs. 5 and 4, respectively (Table II). It is obvious that both the magnitudes of ϵ/θ and D_m values were decreased, except in the case with a cross-linkage of 0.012 (1.2% XL), as the extent of polymer cross-linking increased. Both the values of ϵ/θ and D_m for 1.2% XL were unrealistically high; *i.e.*, ϵ/θ should be less than unity (since $\epsilon \leq 1$ and $\theta \geq 1$) and D_m should also be smaller than D (3.64×10^{-2} cm²/day) (Eq. 3). These results are in agreement with observations discussed earlier (Fig. 4).

Effect of Temperature—The dependency of the drug release profiles on temperature is illustrated in Fig. 5. The higher the temperature, the greater the drug release $Q/t^{1/2}$ value (slope). This observation clearly indicates that the release of norgestomet from the hydrogel is an energy-linked process.

Inspection of Eq. 2 revealed that the magnitude of $Q/t^{1/2}$ values was directly proportional to the square root of the product of two energy-dependent parameters, C_P (polymer solubility) and D_m

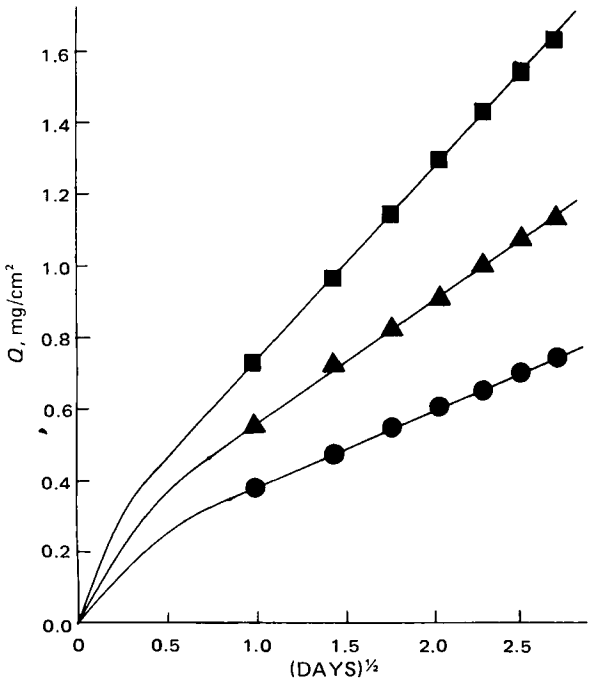

Figure 5—*Linear* $Q - t^{1/2}$ *relationship at various temperatures. Key:* ■, *45°;* ▲, *37°; and* ●, *25°. The* $Q/t^{1/2}$ *of drug release was calculated to be 0.522, 0.357, and 0.212 mg/cm²/day*$^{1/2}$, *respectively.*

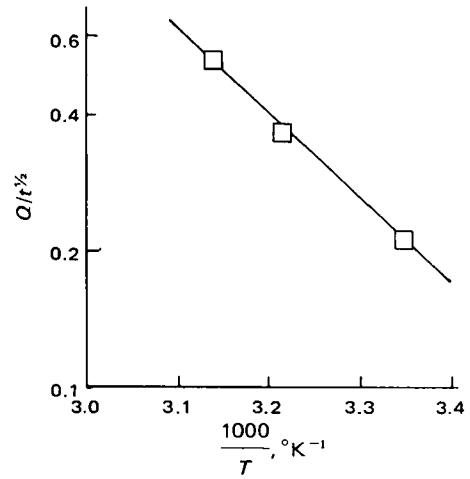

Figure 6—*Linear relationship between the flux of drug release* ($Q/t^{1/2}$) *and the reciprocal of temperature* (T^{-1}) *following Eq. 10. A value of 16.48 kcal/mole was obtained for the sum of* E_a *and* ΔH_f *[*$(T_m - T)/T_m$*].*

(matrix diffusivity), when the amount of drug ($2A$ term) incorporated was the same (a constant). Therefore, Eq. 2 may be expressed alternatively as:

$$\log (Q/t^{1/2}) = \tfrac{1}{2} \log (\text{constant}) + \tfrac{1}{2} \log D_m + \tfrac{1}{2} \log C_p \quad \text{(Eq. 7)}$$

It was known that (9):

$$\log D_m = \log D_0 - \frac{E_a}{2.303R} \frac{1}{T} \quad \text{(Eq. 8)}$$

where E_a is the energy of activation required for matrix diffusion, and (11):

$$\log C_p = -\frac{\Delta H_f}{2.303RT} \left(\frac{T_m - T}{T_m}\right) \quad \text{(Eq. 9)}$$

where ΔH_f is the energy required to increase the intermolecular distance in drug crystals, thus allowing drug molecules to dissociate from the crystal lattice and to dissolve into the polymer structure before molecular diffusion occurs, and T_m and T are the temperatures at which crystals melt and of the system examined, respectively.

Substituting Eqs. 8 and 9 for the D_m and C_p terms in Eq. 7, respectively, gives:

$$\log (Q/t^{1/2}) = \Sigma \log (\text{constant}) - \left[\frac{E_a}{4.606R} + \frac{\Delta H_f}{4.606R} \left(\frac{T_m - T}{T_m}\right)\right] \frac{1}{T} \quad \text{(Eq. 10)}$$

In the narrow temperature range (T = 298.15–318.15°K) investigated, it is assumed that the variation in $(T_m - T)/T_m$ term is quite small (T_m = 459.15°K) and may be approximated as a constant. If this first approximation is acceptable, then a linear relationship should be observed between log $(Q/t^{1/2})$ and T^{-1}. The result shown in Fig. 6 warrants this linearity. A value of 16.48 kcal/mole was calculated for $E_a + \Delta H_f [(T_m - T)/T_m]$. This energy term is a composite of E_a (activation energy for matrix diffusion) and ΔH_f (heat of crystal solvation) at a given temperature difference $[(T_m - T)/T_m]$.

The drug release profiles in Fig. 5 show a burst effect (12), with a higher initial release from the drug molecules accumulating on the matrix surface (1, 3). The values of lag time (t_{lag}) may be estimated from the negative time axis intercept on the initial stage of $Q - t$ (not $Q - t^{1/2}$) plots. The t_{lag} value is defined as:

$$t_{lag} = \frac{\delta^2}{3D_m} \quad \text{(Eq. 11)}$$

where δ is the effective thickness of a diffusion path.

Substituting Eq. 11 for the D_m term in Eq. 8 results in:

$$\log (t_{lag}) = -\log (\text{constant}) + \left(\frac{E_a}{2.303R}\right)\left(\frac{1}{T}\right) \quad \text{(Eq. 12)}$$

Equation 12 points out that a linear relationship exists between log (t_{lag}) and T^{-1} with a positive slope, which is defined by only the activation energy, E_a, for matrix diffusion. The linearity is

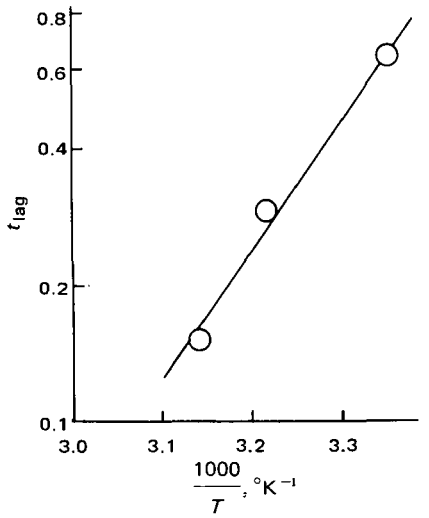

Figure 7—*Linear relationship between the lag time (t_{lag}) and the reciprocal of temperature (T^{-1}) following Eq. 12. From the slope, the activation energy (E_a) for diffusion was calculated to be 7.71 kcal/mole.*

demonstrated in Fig. 7. From the slope, the E_a value was estimated to be 7.71 kcal/mole. This value may then be applied to the estimation of the magnitude of ΔH_f at various values of the $(T_m - T)/T_m$ term. A range of 25–28.6 kcal/mole was obtained (Table III) for ΔH_f in the temperature range of 25–45°. The variation in both the magnitudes of ΔH_f and $(T_m - T)/T_m$ was quite small (only 12.5%) in this temperature range.

Sorption of Drug by Hydrogel Implants—In its dry state, the hydrogel is a compact and transparent polymer. In an aqueous solution, it tends to absorb water by virtue of its hydrophilicity and then to swell to a soft texture. A hydrogel implant with a cross-linking extent of 4.8% absorbed 54.6% of its weight of water, and its volume was increased 77.23% at the end of 7 days of immersion in water.

The sorption kinetics of norgestomet by hydrogel implants followed the same mechanism (Fig. 8) as in earlier analyses for the release of norgestomet from hydrogel implants. The profile of drug sorption ($Q'/t^{1/2}$) was calculated to be 4.92 mg/10^3 cm^2/day$^{1/2}$. Compared to the $Q/t^{1/2}$ of drug release (396 mg/10^3 cm^2/day$^{1/2}$),

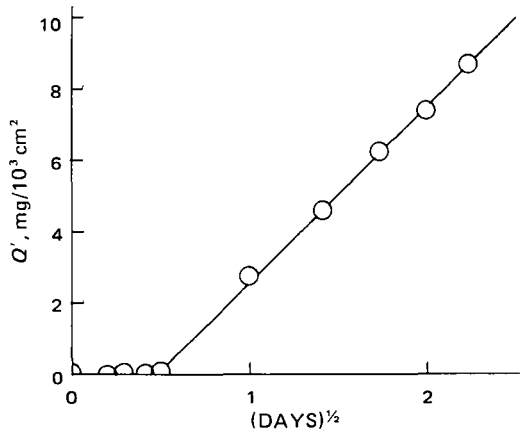

Figure 8—*Linear relationship between the cumulative amount (Q') of norgestomet adsorbed by a unit area of hydrogel implant* versus *time. The flux of drug release (Q'/t$^{1/2}$) was calculated from the slope and found to be 4.92 mg/10^3 cm^2/day$^{1/2}$.*

Table III—Calculation of the Heat of Crystal Solvation (ΔH_f) at Various Temperatures

Temperature	$(T_m - T)/T_m$[a]	ΔH_f[b], kcal/mole
25°	0.351	24.99
37°	0.325	26.98
45°	0.307	28.57

[a] T_m = 459.15°K. [b] ΔH_f was calculated from:

$$\Delta H_f = \frac{16.48 - E_a}{(T_m - T)/T_m} = \frac{8.77}{(T_m - T)/T_m}$$

since E_a = 7.71 kcal/mole.

this magnitude of drug sorption ($Q/t^{1/2}$) is insignificantly small (accounts for 1.24% only). This observation led to the conclusion that the release of norgestomet from hydrogel implants is an irreversible process under sink conditions.

It is concluded that, regardless of the difference in the physicochemical nature of polymer between hydrophilic hydrogel and lipophilic silicone delivery devices, the same theoretical model (Eq. 2) was followed for the release of drug molecules dispersing homogeneously throughout the polymeric matrixes. The same phenomenon was also observed in the delivery system prepared from polyethylene polymer (13).

REFERENCES

(1) Y. W. Chien, H. J. Lambert, and D. E. Grant, *J. Pharm. Sci.*, **63,** 365(1974).

(2) Y. W. Chien and H. J. Lambert, *ibid.*, **63,** 515(1974).

(3) Y. W. Chien, S. E. Mares, J. Berg, S. Huber, H. J. Lambert, and K. F. King, *ibid.*, **64,** 1776(1975).

(4) D. M. Long, Jr., and J. Folkman, U.S. pat. 3,279,996 (Oct. 18, 1966); through *Chem. Abstr.*, **66,** 5759g(1967).

(5) Y. W. Chien, "Abstracts," vol. 5, no. 1, APhA Academy of Pharmaceutical Sciences, San Francisco meeting, 1975, p. 125.

(6) O. Wichterle and D. Lim, *Nature*, **185,** 117(1961).

(7) S. Levowitz, J. N. LaGuerre, W. S. Calem, F. E. Gould, J. Scherrer, and H. Schoenfeld, *Trans. Amer. Soc. Artif. Intern. Organs*, **XIV,** 82(1968).

(8) T. Higuchi, *J. Pharm. Sci.*, **52,** 1145(1963).

(9) J. Crank and G. S. Park, "Diffusion in Polymers," Academic, New York, N.Y., 1968, chaps. 2, 3.

(10) P. Singh, S. J. Desai, A. P. Simonelli, and W. I. Higuchi, *J. Pharm. Sci.*, **57,** 217(1968).

(11) A. N. Martin, "Physical Pharmacy," Lea & Febiger, Philadelphia, Pa., 1969, chap. 14.

(12) R. W. Baker and H. K. Lonsdale, in "Controlled Release of Biologically Active Agents," A. C. Tanquary and R. E. Lacey, Eds., Plenum, New York, N.Y., 1974, p. 36.

(13) D. R. Kalwarf, M. R. Sikov, L. Smith, and R. Gordon, *Contraception*, **6,** 423(1972).

ACKNOWLEDGMENTS AND ADDRESSES

Received January 29, 1975, from the *Product Development Department, Searle Laboratories, Division of G. D. Searle & Co., Skokie, IL 60076*

Accepted for publication March 11, 1975.

Appreciation is extended to Mr. John Seul, Mr. William J. Shappee, and Miss Dianne M. Jefferson for conducting *in vitro* studies and also to Dr. George E. Short, Dr. Sam Curl, and Mrs. Grace Amir-Frazli for carrying out animal studies. The authors also thank Ms. Irene Wiggers and Ms. Suzanne Sering for help on manuscript preparation.

[x] To whom inquiries should be directed.

Modification of Diffusion Rates of Benzocaine from Topical Vehicles Using Sodium Salicylate as Complexing Agent

PETER YORK ˣ and ABDEL AZIS M. SALEH *

Abstract □ The release of benzocaine from various topical vehicles containing benzocaine, alone and in the presence of a complexing agent, sodium salicylate, was measured at 37° using dialysis through a cellulose membrane. Sodium salicylate had a marked effect on the release of benzocaine, depending upon the type of vehicle, with the largest increase observed for the water-miscible base, polyethylene glycol (macrogol ointment BPC). The amount of drug released from preparations containing 1% (w/w) and 2% (w/w) benzocaine in this vehicle depended upon the sodium salicylate concentration. Results are discussed in terms of the differing physical properties of the complexes formed.

Keyphrases □ Benzocaine—diffusion from topical vehicles, effect of sodium salicylate as complexing agent □ Sodium salicylate—effect on diffusion of benzocaine from topical vehicles □ Complex formation—effect on diffusion of benzocaine from topical vehicles, sodium salicylate as complexing agent □ Topical vehicles—effect of sodium salicylate on diffusion of benzocaine

Complexes result from donor–acceptor interactions between molecules and are used in pharmaceutical formulations in several ways. Certain complexes can solubilize otherwise insoluble material in a solvent [*e.g.*, the solubilization of xanthines by aromatic hydroxy acids (1)], and surfactants are widely used to solubilize pharmaceutical drugs (2). Improved stability of drugs can also result from complexation, as illustrated by the stabilization of solutions of certain local anesthetics by complexation with caffeine (3–5).

Drug–complex formation can also either improve or impair drug absorption and bioavailability, depending upon such factors as the oil–water partition coefficients of the drug and drug complex, the change in drug solubility, and the change in the diffusion rate of the drug through membranes when complexed (6–8). Absorption studies have generally related to GI absorption, and such effects in topical preparations have not been widely investigated.

There are two generally recognized methods for modifying drug release from topical preparations: (*a*) inclusion of a material in the base to modify the epidermal absorption barrier, and (*b*) alteration of the physical properties of the semisolid vehicle (9). Rates of drug release from such preparations can be followed by various *in vitro* and *in vivo* techniques (10), although prediction of release patterns is unreliable (10).

In a recent *in vivo* study, local anesthetic preparations were tested for their effectiveness in preventing itching and pain induced by an electric current. Only one of the 30 commercial formulations studied was efficient (11), and this preparation contained 20% (w/w) benzocaine. *In vitro* diffusion tests of ointment preparations of benzocaine also indicated significant variation of drug release from different types of vehicle (12).

In view of these reported variations and since many official and commercial benzocaine preparations contain less than 20% (w/w) of drug, the release of benzocaine from official and nonofficial semisolid topical vehicles was examined. The effect of adding sodium salicylate, which is known to form molecular complexes with benzocaine (13–15), also was studied to establish whether the *in vitro* release rate of benzocaine, measured using a dialysis cell, could be improved.

EXPERIMENTAL

Materials—Benzocaine[1] and sodium salicylate[2], official grades, were sieved through a 53-μm (300-mesh) sieve. Polyethylene glycol (macrogol) 300[3] and 4000[3], white soft paraffin[4], cetomacrogol emulsifying ointment[4], wool alcohols[4], hard paraffin[4], liquid paraffin[4], and wool fat[4], all official grades, were used as supplied.

The assay materials were 32% (w/w) hydrochloric acid[5], sodium nitrite[2] (analar), ammonium sulfamate[2] (laboratory reagent), and *N*-(1-naphthyl)ethylenediamine dihydrochloride[2] (laboratory reagent).

The cellulose dialysis cell membrane, prepared by splitting dialysis sacks[6] (inflated diameter 1.57 cm), was washed before use in distilled water.

Preparation of Bases—The vehicles studied are listed in Table I, and all constituents were incorporated on a weight per weight basis. No preservatives were included in the vehicles.

For Vehicles A and B, benzocaine and sodium salicylate, when present, were dissolved in polyethylene glycol 300, with the percentage of polyethylene glycol 300 being reduced appropriately. The ointment then was prepared by fusing the constituents at 60° and stirring until cold.

The solid materials were incorporated into Vehicle C at 50°, and the ointment then was stirred until cold.

For Vehicles D–G, benzocaine powder was suspended in the oily phase. Sodium salicylate, when present, was dissolved in the aqueous phase, with the proportions of the phase constituents being reduced appropriately. The two phases were heated separately to 50° and then mixed and stirred until cold.

Dialysis Equipment—The vehicle sample under test was tightly packed into a shallow steel dish, 3.12 cm in diameter and 0.62 cm in depth, fitted with a small flange. The surface of the vehicle was made smooth before applying the dialysis membrane to ensure intimate contact and removal of air. The membrane was secured by solidified hard paraffin wax above and below the small flange and then checked for leakage. The dish was located centrally, by means of a magnet, on the base of a 600-ml glass beaker containing 200 ml of distilled water (pH 5.2) at 37 ± 0.5°. This volume of water provided sink conditions for the diffusing benzocaine.

The distilled water was stirred at 75 rpm using a polytetrafluoroethylene plastic rectangular blade, 4.5 × 1.7 cm, connected by a glass rod, 6 mm in diameter, to a constant-speed motor[7]. The blade was positioned centrally in the beaker with the top of the 4.5-cm edge at the surface of the water.

[1] Hopkins and Williams Ltd., Chadwell Heath, Essex, England.
[2] B.D.H. Chemicls Ltd., Poole, England.
[3] Koch Light Laboratories Ltd., Colnebrook, England.
[4] Evans Medical Ltd., Speke, Liverpool, England.
[5] Merck Chemicals, Darmstadt, Germany.
[6] Sigma Chemicals, St. Louis, Mo.
[7] Citenco constant-speed motor K2.606, Citenco Ltd., Boreham Wood, Herts., England.

Table I—Composition and Type of Topical Vehicles Studied

Code	Name of Vehicle	Type of Vehicle	Benzocaine, % (w/w)	Sodium Salicylate, % (w/w)
A	Polyethylene glycol (macrogol ointment BPC)	Water miscible	1	0.0, 0.1, 0.25, 0.5, 1, 1.5, 2, 5, 10, 20
			2	0.0, 0.25, 0.5, 1, 2, 5, 10
B	Polyethylene glycol (macrogol ointment BPC), 90% (w/w), and distilled water, 10% (w/w)	Water miscible	1	0, 10
C	White soft paraffin BP	Oleaginous	1	0, 10
			5	0
D	Cetomacrogol cream BP	Oil-in-water emulsion cream	1	0, 10
E	Aqueous cream BP	Oil-in-water emulsion cream	1	0, 10
F	Wool alcohol cream[a]	Water-in-oil emulsion cream	1	0, 10
G	Hydrous wool fat BP	Water-in-oil emulsion cream	1	0, 10

[a] Composition: liquid paraffin, 30% (w/w); wool alcohols, 5% (w/w); white soft paraffin, 55% (w/w); and distilled water, 10% (w/w). For vehicle containing 1% (w/w) benzocaine and 10% (w/w) sodium salicylate, 44% (w/w) white soft paraffin was used.

Samples, 1 ml, were removed from time zero to 3 hr at 30-min intervals. A minimum of two diffusion experiments was performed for each vehicle composition.

Analytical Method—The assay for benzocaine was carried out using the diazo-coupling method of Bratton and Marshall (16) with minor modifications. A 1-ml sample was added to a 100-ml volumetric flask containing 50 ml of distilled water and 0.5 ml of 32% (w/w) hydrochloric acid; then 0.5 ml of 1% (w/v) sodium nitrite solution was added, and the contents were shaken for 3 min. Then 0.5 ml of 5% (w/v) ammonium sulfamate solution was added, and the solution was shaken for another 1 min. Then 1 ml of 0.5% (w/v) *N*-(1-naphthyl)ethylenediamine dihydrochloride solution was added, and the solution was diluted to volume with distilled water. After 10 min, the percentage transmission of the developed red color was determined at 545 nm[8] and the concentration of benzocaine was estimated from a calibration curve.

RESULTS AND DISCUSSION

Figure 1 shows the release of drug from plain vehicles containing 1% (w/w) benzocaine. Individual points are included for Vehicle A to illustrate the observed scatter of results. The points on the other curves represent averaged values. Similar scatter of results was observed for all subsequent experiments.

The curves in Fig. 1 indicate that the various vehicles exhibited differing rates of *in vitro* release of benzocaine. Their efficiency for releasing benzocaine was in the following order: water miscible > oil-in-water emulsion creams > white soft paraffin > water-in-oil emulsion creams.

All vehicles showed a curvilinear relationship between the total amount of benzocaine released and time. Vehicles A and B had an initial convex-upward section, while Vehicles C–G exhibited an initial concave-upward section.

With Vehicles A and B, slight swelling of the membrane occurred during the diffusion experiment due to water uptake into the dialysis cell. This result can be accounted for by the high osmotic pressure of the polyethylene glycol base, initially inducing water molecules to penetrate the membrane and enter into the cell. This effect would explain the "lag" period of approximately 60 min before the drug release rate became constant (Fig. 1). This effect was substantiated by the shorter period of slow release of 30 min for Vehicle B, the polyethylene glycol vehicle containing 10% (w/w) water.

In contrast, Vehicles C–G exhibited a faster initial release rate, which decreased to a constant rate after 60 min. This change in rate can be ascribed to the benzocaine in the layers adjacent to the membrane at the beginning of the experiment readily diffusing through the membrane. Subsequent availability of benzocaine for release depended upon diffusion of the drug through the vehicle to the membrane, and this diffusion was a slower process.

The benzocaine release data for Vehicles C–G all conformed to the mathematical relationship developed (17, 18), based on Fick's law, to describe the release of drugs from ointment bases in that straight-line relationships existed between the total amount of drug released and the square root of time.

It can be seen from Fig. 1 that the vehicles providing optimum release of benzocaine were the polyethylene glycol vehicles, A and B. The increase in solubility of benzocaine in the presence of polyethylene glycol 300 (15) and the water miscibility of the polyethylene glycol vehicle may be contributing factors in achieving improved release rates compared with the other vehicles. The drug release data for these two bases do not conform to the reported mathematical model (17, 18).

The effect of adding 10% (w/w) sodium salicylate, a material

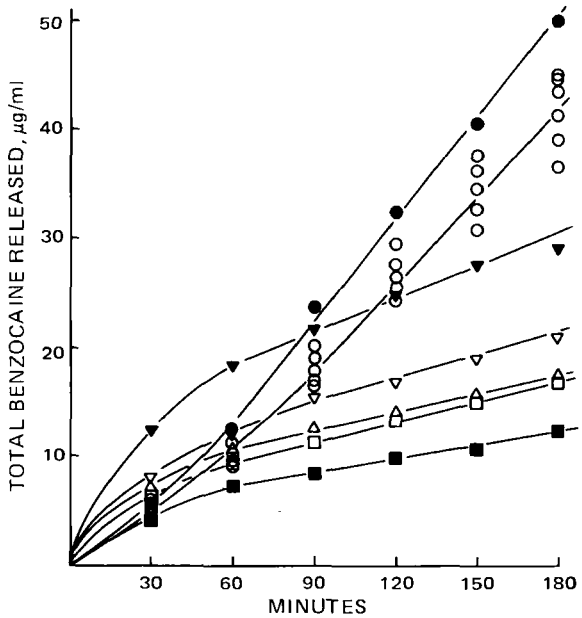

Figure 1—*Effect of type of topical vehicle on release of drug from preparations containing 1% (w/w) benzocaine. Key: ○, Vehicle A; ●, Vehicle B; △, Vehicle C; ▽, Vehicle D; ▼, Vehicle E; □, Vehicle F; and ■, Vehicle G. (To avoid confusion, individual experimental points are illustrated only for Vehicle A. Other points represent averaged values).*

[8] Eel 197 spectra colorimeter, Evans Electroselenium Ltd., Halstead, Essex, England.

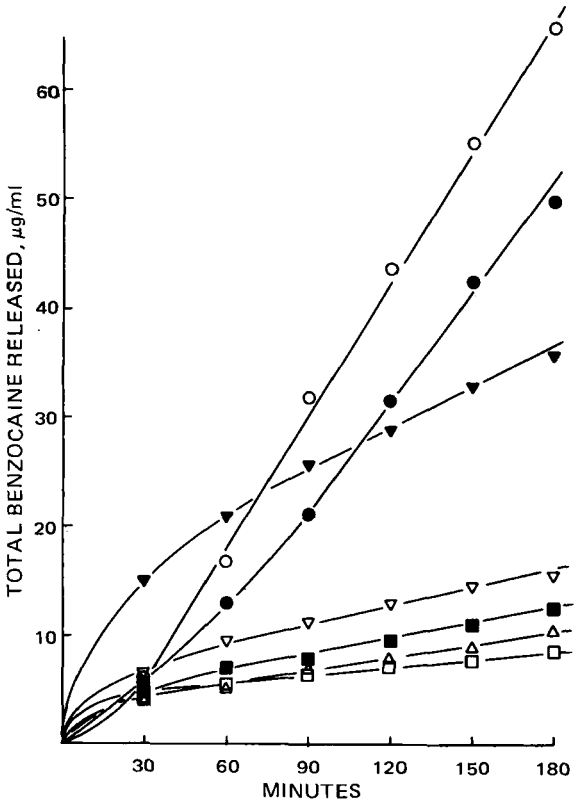

Figure 2—*Effect of type of topical vehicle on release of drug from preparations containing 1% (w/w) benzocaine and 10% (w/w) sodium salicylate. Key: see Fig. 1.*

known to complex with benzocaine (13–15), on the release rate of benzocaine from each vehicle is shown in Fig. 2. Three vehicles, A, B, and E, exhibited improved release profiles, while Vehicles C, D, and F showed decreased release profiles. For Vehicle G, the release rate remained unchanged. These differences can be attributed to possible changes in the partition coefficient of benzocaine in the vehicles containing sodium salicylate, the nonsolubility of sodium salicylate in the oily phases, and other factors such as solubility changes of the drug and drug complex (6–8).

The most significant increase occurred with Vehicle A, with an increase in amount of drug released of more than 60% after 2 hr compared with the plain vehicle. Since in this study the desired effect was to improve drug availability, this vehicle, polyethylene glycol (macrogol ointment BPC), was studied further, using two concentrations of benzocaine, 1 and 2% (w/w), with a series of concentrations of sodium salicylate (Table I).

Figure 3 shows graphs of the release of benzocaine from Vehicle A containing 1% (w/w) benzocaine and differing concentrations of sodium salicylate. To linearize these graphs and similar curves for 2% (w/w) benzocaine in Vehicle A, it was necessary to plot logarithm$_{10}$ of the total amount of benzocaine released *versus* logarithm$_{10}$ of the time in minutes (Fig. 4). Least-squares regression was carried out for all graphs, and the statistical data are given in Table II.

From these data, estimates of the total amount of benzocaine released after 2 hr from each studied preparation were made (Table II). Figure 5 shows the relationship between the total amount of drug released after 2 hr and the percent (w/w) sodium salicylate in Vehicle A for the 1 and 2% (w/w) benzocaine concentrations, together with the standard error of the individual points. Both curves exhibited a maximum at 0.25% (w/w) sodium salicylate followed by minima at 1.5 and 0.5% (w/w) sodium salicylate for Vehicle A containing 1 and 2% (w/w) benzocaine, respectively. A plateau section was then observed at higher sodium salicylate concentrations in both graphs.

A number of molecular complexing interactions took place within the polyethylene glycol vehicle containing both benzocaine and sodium salicylate since complexation reactions are known to occur

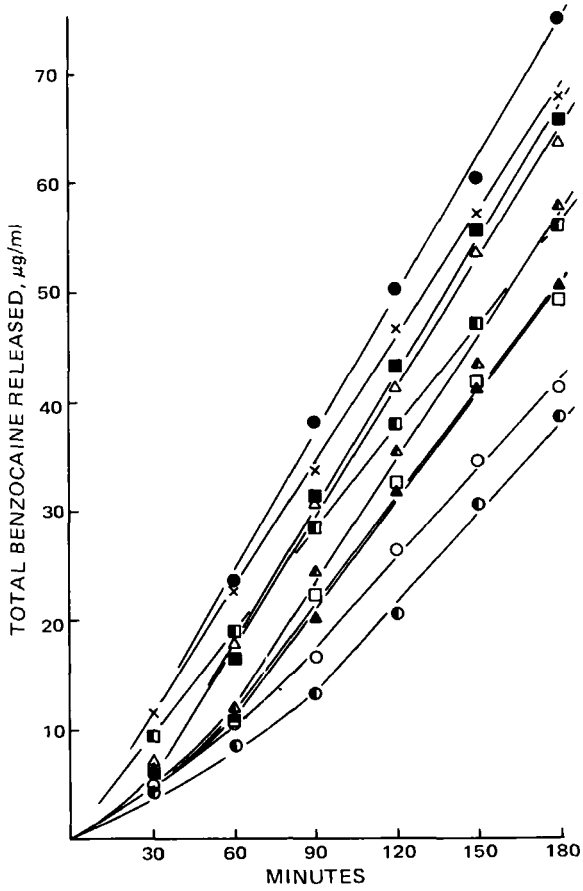

Figure 3—*Effect of increasing sodium salicylate concentration on release of drug from Vehicle A containing 1% (w/w) benzocaine. Key [sodium salicylate concentrations (1% w/w)]: ○, 0.0; ◐, 0.1; ●, 0.25; △, 0.5; ▲, 1.0; ▲, 1.5; □, 2.0; ◧, 5.0; ■, 10.0; and ×, 20.0.*

between both benzocaine and polyethylene glycol and benzocaine and sodium salicylate (15). Indeed, in concentrations of 5% of both complexing agents, benzocaine showed increased solubility compared with the presence of either polyethylene glycol or sodium salicylate alone, suggesting the possible formation of a multicomplex of the three different constituent molecules (15).

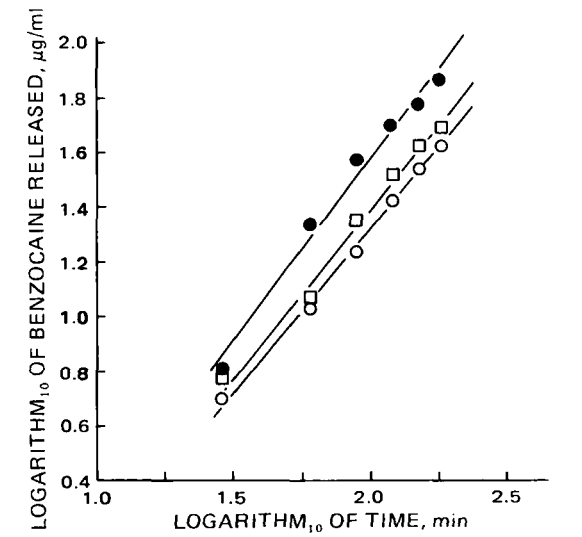

Figure 4—*Correlation between logarithm$_{10}$ of total benzocaine released and logarithm$_{10}$ of time for Vehicle A preparations containing 1% (w/w) benzocaine and different concentrations of sodium salicylate. Key: see Fig. 3.*

Table II—Summary of Calculated Statistical Parameters for Logarithm$_{10}$ Total Benzocaine Released *versus* Logarithm$_{10}$ Time in Minutes for Linear Regression

Vehicle	Sodium Salicylate, % (w/w)	Slope	Intercept	Correlation Coefficient	Calculated Total Amount of Benzocaine Released after 2 hr ± *SE*, μg/ml (p = 0.95, df = 4)[a]
Vehicle A + 1% (w/w) benzocaine	0.0	1.14	−0.960	0.970	25.76 ± 1.73
	0.1	1.09	−0.905	0.959	23.01 ± 2.02
	0.25	1.33	−1.084	0.991	48.08 ± 4.07
	0.5	1.28	−1.040	0.982	41.88 ± 3.47
	1.0	1.21	−0.987	0.997	33.88 ± 1.40
	1.5	1.12	−0.840	0.990	30.90 ± 1.40
	2.0	1.26	−1.130	0.998	30.97 ± 2.71
	5.0	0.98	−0.460	0.997	37.84 ± 2.29
	10.0	1.30	−1.082	0.965	42.07 ± 2.30
	20.0	0.95	−0.313	0.976	46.03 ± 1.61
Vehicle A + 2% (w/w) benzocaine	0.0	1.48	−1.276	0.998	63.39 ± 2.51
	0.25	1.19	−0.611	0.996	73.11 ± 1.06
	0.5	1.21	−0.907	0.992	40.74 ± 1.30
	1.0	1.28	−0.866	0.995	62.52 ± 1.83
	2.0	1.33	−0.984	0.939	60.39 ± 2.29
	5.0	1.42	−1.186	0.987	58.34 ± 1.76
	10.0	1.16	−0.612	0.989	63.24 ± 1.44

The relative solubility of benzocaine in its different complexed forms will differ, as will the rate of diffusion of the various complexes across the dialysis membrane, due to the different oil–water partition coefficients and size and charge changes of the complexes compared with the original form of the drug (7). Such changes in drug solubility in topical vehicles produce modification in drug availability, with slow release rates for drugs readily soluble in the base and faster release rates when the drug is less soluble (9). In addition, competition takes place between the complexing agents for the benzocaine molecules; the proportions of different complexes formed depend upon the relative affinities and binding strengths of the various complexes.

The summation of these interactions, solubility changes, competition, and other effects could account for the observed changes in the release rate of benzocaine with increasing concentrations of sodium salicylate.

The advantages of the polyethylene glycol vehicle and the presence of a complexing agent are shown by Fig. 6, which compares the release of benzocaine from two preparations. Vehicle C, containing 5% (w/w) benzocaine, is similar to an official benzocaine ointment preparation; Vehicle A, containing 1% (w/w) benzocaine and 0.25% (w/w) sodium salicylate, is the preparation that exhibited the optimum release of benzocaine for this concentration of drug. Although the latter system contained only one-fifth of the concentration of drug compared with the former, the total amount of benzocaine released after 2 hr was approximately 2.5 times greater than that observed for the preparation using white soft paraffin. The clinical significance of these findings using *in vivo* experiments is being established and will be presented in a future report.

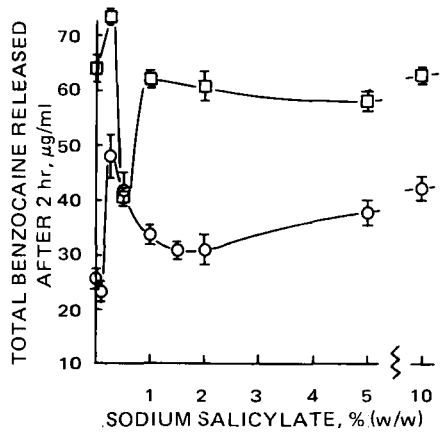

Figure 5—*Effect of increasing sodium salicylate concentration on the total amount of benzocaine released after 2 hr from Vehicle A. Key:* ○, *Vehicle A containing 1% (w/w) benzocaine; and* □, *Vehicle A containing 2% (w/w) benzocaine. (The bar lines represent ± 1* SE *from the calculated value.)*

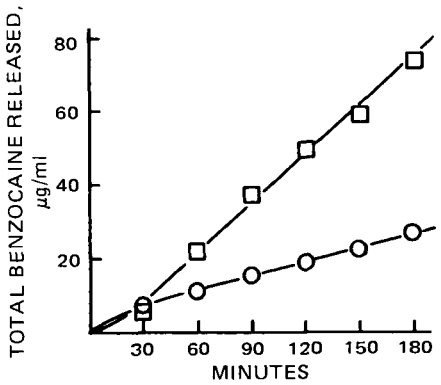

Figure 6—*Comparison of the release of benzocaine from two preparations. Key:* □, *Vehicle A containing 1% (w/w) benzocaine and 0.25% (w/w) sodium salicylate; and* ○, *Vehicle C containing 5% (w/w) benzocaine.*

CONCLUSIONS

1. The diffusion of benzocaine from various topical vehicles was studied using a dialysis cell fitted with a cellulose membrane. The rate of release for preparations containing 1% (w/w) benzocaine was in the following order: water-miscible vehicles > oil-in-water emulsion cream vehicles > white soft paraffin > water-in-oil emulsion cream vehicles.

2. The effect of sodium salicylate, an agent that complexes with benzocaine, on the rate of diffusion of drug was also investigated. The water-miscible base and aqueous cream vehicles exhibited increased release profiles.

3. The extent of the modifying effect on the release rate of drug by the complexing agent depended upon the concentration of sodium salicylate in the polyethylene glycol vehicle containing 1 and 2% (w/w) benzocaine. This result has been attributed to the formation of different types of complexes and to the differing solubilities and physical properties of these complexes.

REFERENCES

(1) T. Higuchi and A. Drubulis, *J. Pharm. Sci.*, **50**, 905(1961).

(2) B. A. Mulley, in "Advances in Pharmaceutical Sciences," vol. 1, H. S. Bean, A. H. Beckett, and J. E. Carless, Eds., Academic, London, England, 1964, p. 87.

(3) T. Higuchi and L. Lachman, *J. Amer. Pharm. Ass., Sci. Ed.*, **44**, 521(1955).
(4) J. C. Lach and W. A. Pauli, *Drug Stand.*, **27**, 104(1959).
(5) L. Lachman and T. Higuchi, *J. Amer. Pharm. Ass., Sci. Ed.*, **46**, 32(1957).
(6) G. Levy and T. Matsuzawa, *J. Pharm. Sci.*, **54**, 1003(1965).
(7) G. Levy and E. J. Mroszczak, *ibid.*, **57**, 235(1968).
(8) P. Singh, J. K. Guillory, T. D. Sokoloski, L. Z. Benet, and Y. N. Bhatia, *ibid.*, **55**, 63(1966).
(9) B. Idson, in "Topics in Medicinal Chemistry," vol. 4, J. L. Rabinowitz and R. M. Myerson, Eds., Wiley–Interscience, New York, N.Y., 1971, p. 207.
(10) P. Grasso and A. B. G. Lansdown, *J. Soc. Cosmet. Chem.*, **23**, 481(1972).
(11) J. Adriani and H. Dalili, *Anesth. Analg.*, **50**, 834(1971).
(12) J. W. Ayers and P. A. Laskar, *J. Pharm. Sci.*, **63**, 1402(1974).
(13) G. M. Ghali, A. M. Saleh, and M. M. Motawi, in "XII Conference of Pharmaceutical Sciences," Cairo, U.A.R., Nov. 1971, p. 117.
(14) G. M. Ghali, A. M. Saleh, and M. M. Motawi, in *ibid.*, p. 118.
(15) A. M. Saleh and P. York, *Pharm. Ind.*, in press.
(16) A. C. Bratton and E. K. Marshall, Jr., *J. Biol. Chem.*, **128**, 537(1939).
(17) T. Higuchi, *J. Soc. Cosmet. Chem.*, **11**, 85(1960).
(18) W. I. Higuchi, *J. Pharm. Sci.*, **51**, 802(1962).

ACKNOWLEDGMENTS AND ADDRESSES

Received April 4, 1975, from the *Department of Pharmaceutics, Faculty of Pharmacy, University of Khartoum, Khartoum, Sudan.*

Accepted for publication May 13, 1975.

* Present address: Department of Pharmaceutics, Faculty of Pharmacy, Alexandria University, Alexandria, U.A.R.

[x] To whom inquiries should be directed. Present address: Department of Pharmacy, Faculty of Medicine, University of Dar es Salaam, P.O. Box 20693, Dar es Salaam, Tanzania.

Gastric Acid Inactivation of Erythromycin Stearate in Solid Dosage Forms

B. G. BOGGIANO [x] and M. GLEESON

Abstract □ The effect of hydrochloric acid at pH 1.2–3.2 on erythromycin stearate and commercial dosage forms of erythromycin stearate was studied. Under all conditions examined, erythromycin was readily dissolved from the stearate as hydrochloride, and rapidly lost its biological activity in solution. The inclusion of pepsin in the test systems did not affect the results. Although formulation differences somewhat affected the rate of destruction, acid lability was exhibited by all products examined, except enteric-coated tablets. Amounts of acid considered to be normal in the fasting stomach contents of adults during the time likely for a dose to remain in the stomach caused 70–90% destruction within 15 min after the shells started to rupture. Amounts of hydrochloric acid appreciably less than 1 mEq, representing abnormally small quantities even in the fasting state, caused destruction ranging from 30 to 70% of the doses in 15 min. These results are not reconcilable with published statements that the sensitivity of erythromycin to gastric acid is overcome by providing the antibiotic in the form of stearate salt.

Keyphrases □ Erythromycin stearate—effect of hydrochloric acid at gastric pH, commercial dosage forms □ Gastric acid inactivation—erythromycin stearate, effect of hydrochloric acid at gastric pH, commercial dosage forms □ Antibiotics—erythromycin stearate, effect of hydrochloric acid at gastric pH, commercial dosage forms

Current knowledge appears to have rationalized most bioavailability issues with erythromycin. However, there remains the perplexing question of erratic blood levels from the stearate, particularly in the nonfasting stage. In a four-way crossover study on 12 subjects, the average peak serum level of erythromycin from the stearate was less than half that from the estolate following single 250-mg doses in fasting subjects (1). In the presence of food, the estolate showed no decrease in average peak serum levels but the levels from the stearate were greatly decreased, seven of the 12 subjects failing to show any absorption. Similar results were later found in a crossover study of 30 subjects in the nonfasting state (2).

BACKGROUND

The reduction in serum levels from the stearate in the presence of food could be due to increased gastric acidity or to the food *per se*. In one study (1), the presence of food did not reduce the absorption of the estolate; this finding suggests that the more likely reason for the reduced stearate levels could be increased gastric acidity.

The destructive effect of gastric acidity on unprotected erythromycin base has been known since Josselyn and Sylvester (3) reported an *in vivo* study in 1953. In the same year, they also reported a study on the stearate salt of erythromycin taken in suspension form, buffered with sodium citrate (4). They found that food did not reduce the absorption of erythromycin from the stearate and concluded that the less soluble stearate salt was resistant to gastric acid when taken in this form. Since then, unprotected solid dosage forms of erythromycin stearate have been marketed extensively.

The literature contains conflicting statements on the effect of gastric acidity on the stearate. In 1970 the *Medical Letter* (5) and in 1971 Wade (6) stated that erythromycin stearate is acid labile. However, more recently, Garrod and O'Grady (7) and Tolhurst *et al.* (8) claimed that the stearate is stable in the presence of gastric acid and that the base is liberated from it in the duodenum where it is absorbed. This divergence of published opinion and the low and erratic blood levels reported for solid dosage forms of the stearate suggested that an *in vitro* study of the effect of gastric acid on a range of solid pharmaceutical formulations of erythromycin stearate was warranted.

There has been no reported study on this topic. However, Stephens *et al.* (9) reported a measurement showing that unprocessed erythromycin stearate was rapidly inactivated by gastric acid. This finding contrasted markedly with their results on propionyl erythromycin lauryl sulfate (erythromycin estolate), which retained virtually full activity after prolonged exposure to gastric acid. The authors summarized the chemistry by explaining that propionyl

(3) T. Higuchi and L. Lachman, *J. Amer. Pharm. Ass., Sci. Ed.*, **44**, 521(1955).
(4) J. C. Lach and W. A. Pauli, *Drug Stand.*, **27**, 104(1959).
(5) L. Lachman and T. Higuchi, *J. Amer. Pharm. Ass., Sci. Ed.*, **46**, 32(1957).
(6) G. Levy and T. Matsuzawa, *J. Pharm. Sci.*, **54**, 1003(1965).
(7) G. Levy and E. J. Mroszczak, *ibid.*, **57**, 235(1968).
(8) P. Singh, J. K. Guillory, T. D. Sokoloski, L. Z. Benet, and Y. N. Bhatia, *ibid.*, **55**, 63(1966).
(9) B. Idson, in "Topics in Medicinal Chemistry," vol. 4, J. L. Rabinowitz and R. M. Myerson, Eds., Wiley–Interscience, New York, N.Y., 1971, p. 207.
(10) P. Grasso and A. B. G. Lansdown, *J. Soc. Cosmet. Chem.*, **23**, 481(1972).
(11) J. Adriani and H. Dalili, *Anesth. Analg.*, **50**, 834(1971).
(12) J. W. Ayers and P. A. Laskar, *J. Pharm. Sci.*, **63**, 1402(1974).
(13) G. M. Ghali, A. M. Saleh, and M. M. Motawi, in "XII Conference of Pharmaceutical Sciences," Cairo, U.A.R., Nov. 1971, p. 117.
(14) G. M. Ghali, A. M. Saleh, and M. M. Motawi, in *ibid.*, p. 118.
(15) A. M. Saleh and P. York, *Pharm. Ind.*, in press.
(16) A. C. Bratton and E. K. Marshall, Jr., *J. Biol. Chem.*, **128**, 537(1939).
(17) T. Higuchi, *J. Soc. Cosmet. Chem.*, **11**, 85(1960).
(18) W. I. Higuchi, *J. Pharm. Sci.*, **51**, 802(1962).

ACKNOWLEDGMENTS AND ADDRESSES

Received April 4, 1975, from the *Department of Pharmaceutics, Faculty of Pharmacy, University of Khartoum, Khartoum, Sudan.*

Accepted for publication May 13, 1975.

* Present address: Department of Pharmaceutics, Faculty of Pharmacy, Alexandria University, Alexandria, U.A.R.

[x] To whom inquiries should be directed. Present address: Department of Pharmacy, Faculty of Medicine, University of Dar es Salaam, P.O. Box 20693, Dar es Salaam, Tanzania.

Gastric Acid Inactivation of Erythromycin Stearate in Solid Dosage Forms

B. G. BOGGIANO [x] and M. GLEESON

Abstract □ The effect of hydrochloric acid at pH 1.2–3.2 on erythromycin stearate and commercial dosage forms of erythromycin stearate was studied. Under all conditions examined, erythromycin was readily dissolved from the stearate as hydrochloride, and rapidly lost its biological activity in solution. The inclusion of pepsin in the test systems did not affect the results. Although formulation differences somewhat affected the rate of destruction, acid lability was exhibited by all products examined, except enteric-coated tablets. Amounts of acid considered to be normal in the fasting stomach contents of adults during the time likely for a dose to remain in the stomach caused 70–90% destruction within 15 min after the shells started to rupture. Amounts of hydrochloric acid appreciably less than 1 mEq, representing abnormally small quantities even in the fasting state, caused destruction ranging from 30 to 70% of the doses in 15 min. These results are not reconcilable with published statements that the sensitivity of erythromycin to gastric acid is overcome by providing the antibiotic in the form of stearate salt.

Keyphrases □ Erythromycin stearate—effect of hydrochloric acid at gastric pH, commercial dosage forms □ Gastric acid inactivation—erythromycin stearate, effect of hydrochloric acid at gastric pH, commercial dosage forms □ Antibiotics—erythromycin stearate, effect of hydrochloric acid at gastric pH, commercial dosage forms

Current knowledge appears to have rationalized most bioavailability issues with erythromycin. However, there remains the perplexing question of erratic blood levels from the stearate, particularly in the nonfasting stage. In a four-way crossover study on 12 subjects, the average peak serum level of erythromycin from the stearate was less than half that from the estolate following single 250-mg doses in fasting subjects (1). In the presence of food, the estolate showed no decrease in average peak serum levels but the levels from the stearate were greatly decreased, seven of the 12 subjects failing to show any absorption. Similar results were later found in a crossover study of 30 subjects in the nonfasting state (2).

BACKGROUND

The reduction in serum levels from the stearate in the presence of food could be due to increased gastric acidity or to the food *per se*. In one study (1), the presence of food did not reduce the absorption of the estolate; this finding suggests that the more likely reason for the reduced stearate levels could be increased gastric acidity.

The destructive effect of gastric acidity on unprotected erythromycin base has been known since Josselyn and Sylvester (3) reported an *in vivo* study in 1953. In the same year, they also reported a study on the stearate salt of erythromycin taken in suspension form, buffered with sodium citrate (4). They found that food did not reduce the absorption of erythromycin from the stearate and concluded that the less soluble stearate salt was resistant to gastric acid when taken in this form. Since then, unprotected solid dosage forms of erythromycin stearate have been marketed extensively.

The literature contains conflicting statements on the effect of gastric acidity on the stearate. In 1970 the *Medical Letter* (5) and in 1971 Wade (6) stated that erythromycin stearate is acid labile. However, more recently, Garrod and O'Grady (7) and Tolhurst *et al.* (8) claimed that the stearate is stable in the presence of gastric acid and that the base is liberated from it in the duodenum where it is absorbed. This divergence of published opinion and the low and erratic blood levels reported for solid dosage forms of the stearate suggested that an *in vitro* study of the effect of gastric acid on a range of solid pharmaceutical formulations of erythromycin stearate was warranted.

There has been no reported study on this topic. However, Stephens *et al.* (9) reported a measurement showing that unprocessed erythromycin stearate was rapidly inactivated by gastric acid. This finding contrasted markedly with their results on propionyl erythromycin lauryl sulfate (erythromycin estolate), which retained virtually full activity after prolonged exposure to gastric acid. The authors summarized the chemistry by explaining that propionyl

Table I—Test Solutions

Solution	pH	Volume, ml	Hydrochloric Acid, mEq
1	1.2	50	4.2[a]
2	1.2	50	4.2
3	2.2	50	0.37
4	2.2	100	0.74
5	3.2	50	0.05
6	3.2	100	0.1

[a] With pepsin.

erythromycin (and erythromycin) dissolve in gastric juice and quickly lose their antibiotic activity. Carboxylic acid salts of these substances, even though water insoluble, behave similarly because the hydrochloric acid of gastric juice displaces the carboxylic acid and dissolves the antibiotic as the soluble hydrochloride salt. However, the estolate is a salt of the very strong acid, lauryl sulfuric acid, and gastric acid is not strong enough to displace the acid radical from the insoluble estolate; hence, it remains undissolved and potent for prolonged periods in gastric acid.

The following study was designed to expand on the observation by Stephens *et al.* (9) by examining *in vitro* the effect of acidity conditions on erythromycin stearate and solid pharmaceutical formulations of it. The purposes were to clarify conflicting published statements and to find a basis for understanding reported blood level results.

EXPERIMENTAL

Design—The study was divided into three parts: Study 1, the effect of hydrochloric acid on pure (unprocessed) erythromycin stearate, *i.e.*, the rate of dissolution of erythromycin from the stearate as hydrochloride; Study 2, the rate of inactivation of erythromycin when dissolved in hydrochloric acid; and Study 3, the rate of dissolution of erythromycin from commercial solid dosage forms when treated with a range of simulated gastric fluids.

Test Solutions—Approximately 4 mEq of hydrochloric acid was selected as a realistic simulation of the amount of gastric acid likely to be present over a 30-min period in a fasting adult, *i.e.*, the acid level expected to be present in the resting stomach contents (1–2 mEq) plus the average amount generated during 30 min without stimulation (~ 1 mEq every 15 min). In practice, larger amounts of hydrochloric acid could be present if the dose had been taken shortly before or after food. In selecting this amount of acid, several reference sources were used (10–12).

The effect of lower amounts of acid was also studied, including the very low level of 0.05 mEq to represent the situation in subjects markedly deficient in acid. The pH range of the test solutions was 1.2–3.2. A volume of 50 ml was selected for most tests, although in some cases 100 ml was used to obtain the desired balance of pH *versus* total acidity.

Six test solutions were selected (Table I). Several of these solutions were used for all three studies, depending on the pH and amount of hydrochloric acid required in each case. Solution 1 was simulated gastric fluid USP, containing pepsin and sodium chloride. Solution 2 was simply hydrochloric acid at the same pH and concentration for comparison with Solution 1 to assess whether pepsin contributed to breakdown. Solutions 3–6 were also dilutions of hydrochloric acid.

Exposure Times—There are ample references to stomach emptying times and to the $t_{1/2}$ (time for half the gastric contents to be emptied) following a meal. Buckler (13) quoted 2–6 hr for the former, and the latter was measured at slightly more than 1 hr (14, 15). However, times for which a single dose of medicament could be exposed to the gastric contents in the fasting state were more difficult to define. Based on previous work (16, 17), 30 min was selected as a conservatively realistic simulation of the time a solid dose would remain in an empty stomach. However, longer exposure times were also studied since doses could sometimes be taken in the presence of food and probably retained longer in the stomach.

Test Method—A test method was devised to give relatively quiescent conditions of exposure of the dose to the continuously moving solution, with no direct agitation applied to the dose itself.

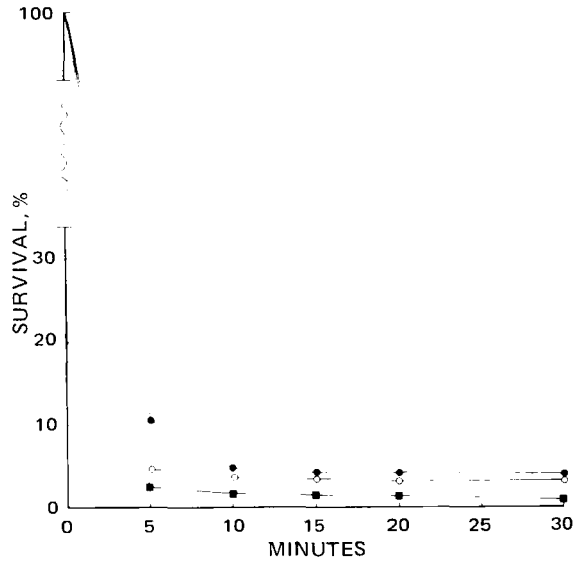

Figure 1—*Inactivation of erythromycin (250 mg, 0.34 mEq) in hydrochloric acid at different pH values. Key:* ■, *pH 1.2, 4.2 mEq;* ○, *pH 2.35, 0.74 mEq; and* ●, *pH 2.9, 0.45 mEq.*

For Studies 1 and 3 (see *Design*), the test solution was placed in a 100- or 200-ml round-bottom flask[1] and warmed to 37°. Erythromycin stearate (392 mg, equivalent to 250 mg of erythromycin), or a dose unit, was added and the stoppered flask was inclined at 45° and rotated at 30 rpm in a water bath controlled at 37 ± 0.5°. Capsules were prevented from floating by means of a glass loop made from a capillary tube.

For Study 3, the time of the first disruption of the shell and the appearance of the contents was recorded as the "disintegration time." Exposure periods were timed from the same point. After the appropriate exposure period, the solution was decanted quickly from the solid through Whatman 541 filter paper, the contents of the flask were washed with 15 ml of cold (18–20°) distilled water, and the washings were decanted through the filter. Four more washings were performed, *i.e.*, until free from acid, and the solid residue in the flask was transferred to the filter. The residue on the filter was dried to constant weight at 20° under vacuum. In Study 3, each residue was well mixed in an agate mortar to ensure homogeneity.

For Study 2, erythromycin base (250 mg, 0.34 mEq) was dissolved in the test solutions in a stoppered flask immersed in a 37° constant-temperature water bath. At intervals up to 30 min, 1-ml samples were removed and immediately diluted with 19 ml of pH 8.0, 0.8 *M* phosphate buffer. Solutions 2 and 4 were used (4.2 and 0.74 mEq of acid, respectively), and their final pH values were 1.2 and 2.35, respectively. A special solution also was used containing 0.45 mEq of hydrochloric acid in 100 ml. This was the lowest acidity–volume system capable of dissolving 250 mg of erythromycin, the final pH being 2.9.

Assays—Biological assays were performed on the dose residues and test solutions according to the cylinder-plate method of USP XVIII (p. 858), using *Sarcina lutea* as the test organism. The assay has the lower detectable limit of approximately 0.02 μg/ml.

Products Tested—A range of products was tested: nonenteric Capsule A from Source X, nonenteric Capsule B from Source Y, nonenteric Capsule C from Source Z, nonenteric film-coated Tablet A from Source X, and enteric-coated Tablet B from Source Y.

The same batch of each product was used throughout except for enteric-coated Tablet B; several batches of Tablet B were examined to check the reproducibility of its resistance to coat shedding in an acid medium. A separate dose unit was required for each individual experiment, *i.e.*, for each exposure period in each test solution. Thus, in addition to the normal limitations in experimental and assay reproducibility, each result contained a "deviation potential" because of the permitted variation in drug content between individual doses.

[1] Quickfit.

Table II—Erythromycin Surviving in Residues after Treatment of Erythromycin Stearate (392 mg, 0.34 mEq) with Solutions 2, 3, and 5

Exposure Time, min	Solution 2 (4.2 mEq)			Solution 3 (0.37 mEq)			Solution 5 (0.05 mEq)		
	Residue, mg	Surviving Erythromycin, mg	Survival, %	Residue, mg	Surviving Erythromycin, mg	Survival, %	Residue, mg	Surviving Erythromycin, mg	Survival, %
5	117	Nil	Nil	205	79	32	—	—	—
10	119	Nil	Nil	168	42	17	310	184	74
15	118	Nil	Nil	157	31	12	—	—	—
20	117	Nil	Nil	151	25	10	312	186	74
40	119	Nil	Nil	126	Nil	Nil	314	188	75
60	118	Nil	Nil	127	Nil	Nil	308	182	74

RESULTS

Study 1: Rate of Dissolution of Erythromycin from Unprocessed Erythromycin Stearate—The weights of the dried residues are given in Table II, together with weights and percentages of surviving erythromycin after treatment with Solutions 2, 3, and 5. All residues after testing against Solution 2 (pH 1.2, 4.2 mEq) and the 40- and 60-min residues after treatment with Solution 3 (pH 2.2, 0.37 mEq) were identified as pure stearic acid from their IR spectra (potassium bromide disk). The remaining residues were mixtures of erythromycin (stearate) and stearic acid.

The theoretical weight of stearic acid in each 392-mg sample of erythromycin stearate was 142 mg. The bulk of the stearic acid was deposited as an insoluble residue with part of it remaining in solution. Taking the undissolved portion as 126 mg (*vide* the final residue after treatment with Solution 3), the amount of erythromycin in the other residues was calculated by difference. Assays were not done for this series of tests, since this study was simply a pilot as a guide to the study on dosage forms.

In Solution 2, the acid represented a 12-fold stoichiometric excess. At this pH and excess acidity, full dissolution had occurred within 5 min. In Solution 3, which represented only about a 10% excess of acid, full dissolution of the erythromycin required 30–40 min. However, approximately 70% had been dissolved in 5 min. In Solution 5 (pH 3.2, 0.05 mEq), the amount of acid represented only about 15% of the stoichiometric equivalent of the test sample (0.34 mEq).

Although full dissolution of the erythromycin could not occur under these conditions, the actual proportion dissolved was in excess of the theoretical (26 *versus* 15%), with equilibrium being reached within 10 min. This finding can be explained on the basis of the intrinsic solubility of erythromycin base and some degree of catalytic behavior by the small level of hydrochloric acid. This particular experiment indicates the rapidity at which a trace of acid at relatively high pH could destroy at least its own equivalent of the stearate.

Study 2: Rate of Inactivation of Erythromycin at Three pH Values—The rates of inactivation of the erythromycin under the three test conditions are given graphically in Fig. 1. Under each condition, 90% or more of the antibiotic was inactivated in the first 5 min. The pH 1.2 condition (4.2 mEq) represented a relatively large excess of acid, but one that would not be abnormal *in vivo* even in the fasting state. The pH 2.35 (0.74 mEq) and pH 2.9 (0.45 mEq) conditions represented acidity levels appreciably lower than the average *in vivo* fasting situation with a relatively small excess of acid over antibiotic; but even under these conditions, the destruction of the antibiotic was almost as rapid as at pH 1.2.

If it is assumed that 0.34 mEq of hydrochloric acid displaces the stearic acid component and dissolves the erythromycin (Study 1), it is apparent that considerably less than 1 mEq of hydrochloric acid can concurrently dissolve and destroy at least two-thirds of a dose in 5 min.

Study 3: Rate of Dissolution of Erythromycin from Commercial Solid Dosage Forms—All products, except Tablet B, started to disintegrate at varying times in the test solutions. Tablet B had not shed its coat after 2 hr at 37° in the pH 1.2 medium. This product was checked for disintegration in simulated intestinal fluid BP, and disintegration was complete in times ranging from 10 to 22 min for 20 samples from different production batches. For the other products, the times of incipient disintegration are given in Table III.

Because it resisted disintegration in the acid medium, Tablet B was excluded from further study. All four of the remaining products were tested against pepsin-containing simulated gastric fluid USP (Solution 1, pH 1.2), but only Capsules A and B were tested against the nonpepsin-containing pH 1.2 medium (Solution 2) to obtain the comparative data on the effect of pepsin. All four products were tested against Solutions 3 and 4, but Solution 5 was excluded from this study. Only Capsule B was tested with Solution 6 (pH 3.2) since the very small amount of acid (0.1 mEq) made this information of minor interest.

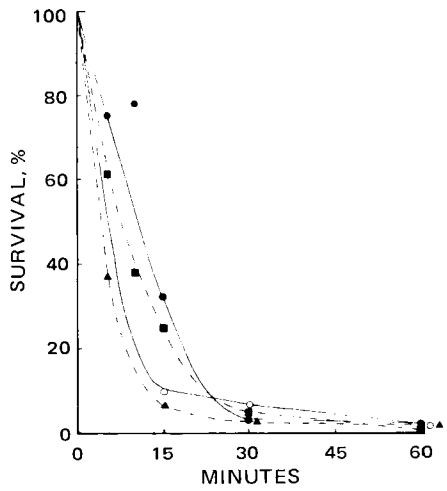

Figure 2—*Dissolution of erythromycin from nonenteric erythromycin stearate dosage forms treated with Solution 1 (pH 1.2, 4.2 mEq of hydrochloric acid, plus pepsin and sodium chloride). Key:* ●—●, *Capsule A;* ■- - - -■, *Capsule B;* O——O, *Capsule C; and* ▲- - - -▲, *Tablet A.*

Table III—Times of First Rupture of Shells or Coats of Nonenteric Dosage Forms

Product	Minutes					Mean Time, min
	Solution 1	Solution 2	Solution 3	Solution 4	Solution 6	
Capsule A	6, 4, 2, 2, 2	2, 3, 2, 2, 2	3, 3, 3, 6	4, 9, 3, 10, 10, 10	—	4.4
Capsule B	2, 2, 1, 2, 2	2, 2, 2, 2, 2	3, 2, 2, 2, 2, 2	2, 3, 2, 2, 2, 3	4, 2, 2, 2, 2, 2	2.1
Capsule C	2, 2, 2	—	3, 2, 3, 3	2, 3, 3, 3	—	2.5
Film-coated Tablet A	22, 20, 16, 11	—	13, 6, 7, 14, 10	7, 11, 3, 14	—	12.2

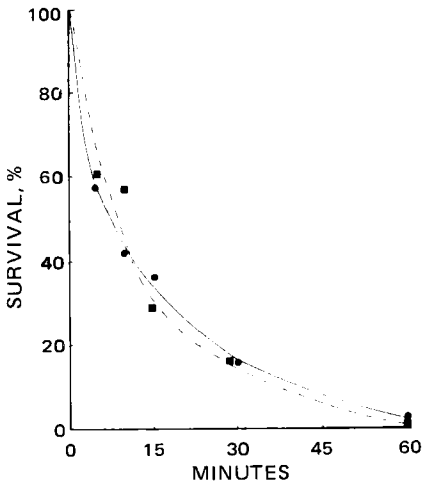

Figure 3—*Dissolution of erythromycin from nonenteric erythromycin stearate dosage forms treated with Solution 2 (pH 1.2, 4.2 mEq of hydrochloric acid, no pepsin). Key:* ●——●, *Capsule A; and* ■- - - -■, *Capsule B.*

The amounts of erythromycin surviving in the residues are given in Figs. 2–6. The percentage survival of erythromycin is quoted to the nearest 1% and relative to the nominal content of 250 mg/dose.

Solution 1 (pH 1.2, 4.2 mEq Acid with Pepsin)—Figure 2 shows that under these conditions all four nonenteric products were destroyed to degrees ranging from 70 to 90% in the first 15 min after the acid reached the contents. The most sensitive products were Capsule C and Tablet A, probably due to a lower proportion of buffering agent in these products. This amount of acid is approximately the amount likely to be available during a 30-min period in the resting stomach contents of adults.

Solution 2 (pH 1.2, 4.2 mEq Acid, No Pepsin)—Capsules A and B showed an almost identical destruction pattern (Fig. 3). Comparison with Fig. 2 does not suggest that pepsin significantly contributed to degradation, certainly not within the first 15 min by which time 70% of the erythromycin had been dissolved.

Solutions 3 and 4 (pH 2.2, 0.37 and 0.74 mEq Acid, Respectively)—The results in Figs. 4 and 5 show that degradation was again very rapid even at this higher pH and these low levels of acidity. On the average, it was of the order of 40 and 70%, respectively, in the first 15 min, apart from Capsule A which contained the highest amount of buffering agent. At these very low levels of acid, the presence of significant amounts of buffering agent could hinder degradation appreciably, since the amount of acid used was only slightly in excess of the chemical equivalent of erythromycin stearate. However, these levels of acid are well below those normally found even in the fasting stomach. The results using Solutions 1 and 2 show that with more normal amounts of acid, the quantity of buffers that can be incorporated in capsules or tablets fails to inhibit degradation significantly.

Solution 6 (pH 3.2, 0.1 mEq Acid)—The results on Capsule B (Fig. 6) were very erratic, but this is understandable with such a small amount of acid. Factors such as the rate of penetration of acid into the individual capsules used in each test would affect the results significantly, as would the permitted variation in content between individual capsules. Nevertheless, the figures indicate that approximately 30% of the erythromycin had been dissolved in about 15 min. Since the amount of acid represented 29% of the stoichiometric equivalent of erythromycin stearate, even a trace of acid at relatively high pH can rapidly dissolve approximately its own equivalent of erythromycin from the stearate, even in a dose containing a proportion of buffering agent.

DISCUSSION

The results show that erythromycin stearate is very sensitive to gastric acid *in vitro*, and any reduction in the rate and degree of inactivation is due to the nature of the pharmaceutical formulation. The 4.2 mEq of hydrochloric acid produced 70–90% destruction of all nonenteric products tested within 30 min, which included the time for disintegration of the shells. The period of most rapid degradation was the first 5 min after rupture of the shells. Furthermore, 0.74 mEq, which *in vivo* would represent a very low amount of gastric acid even in the fasting state, produced an average of 50–60% destruction within 15 min of shell disintegration.

It is difficult to relate these results directly to the *in vivo* situation. However, the study was designed to simulate as realistically

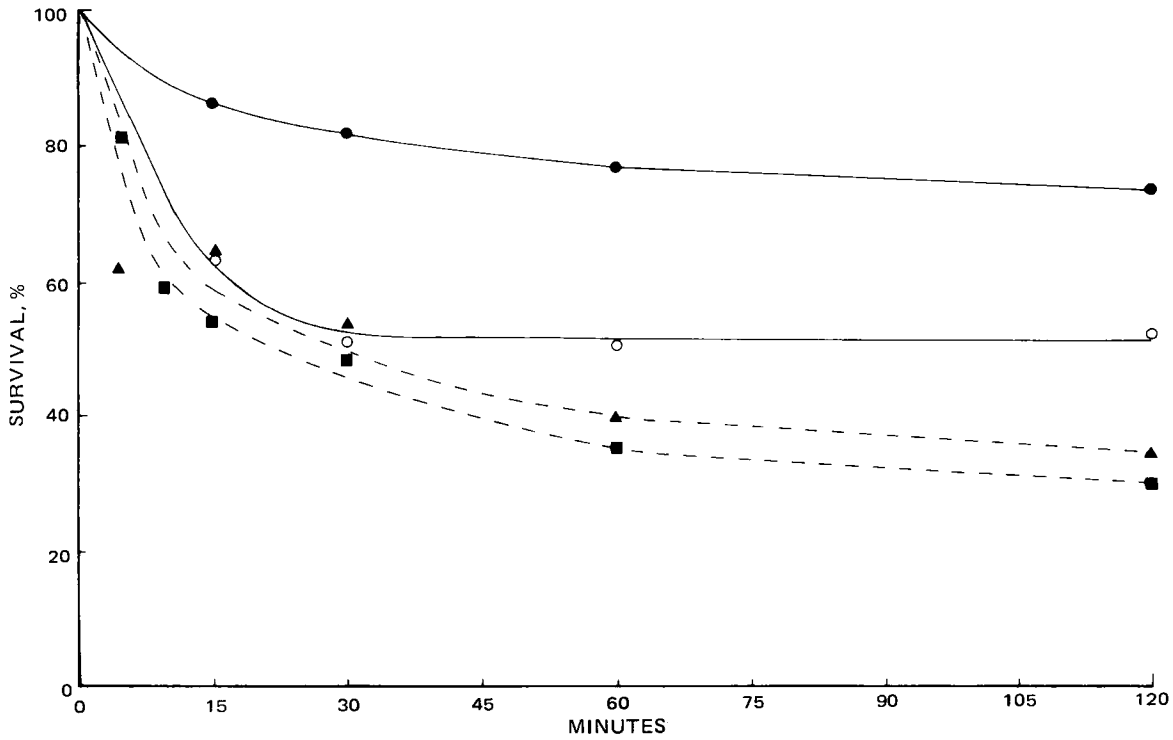

Figure 4—*Dissolution of erythromycin from nonenteric erythromycin stearate dosage forms treated with Solution 3 (pH 2.2, 0.37 mEq of hydrochloric acid). Key:* ●——●, *Capsule A;* ■- - - -■, *Capsule B;* O—O, *Capsule C; and* ▲- - - -▲, *Tablet A.*

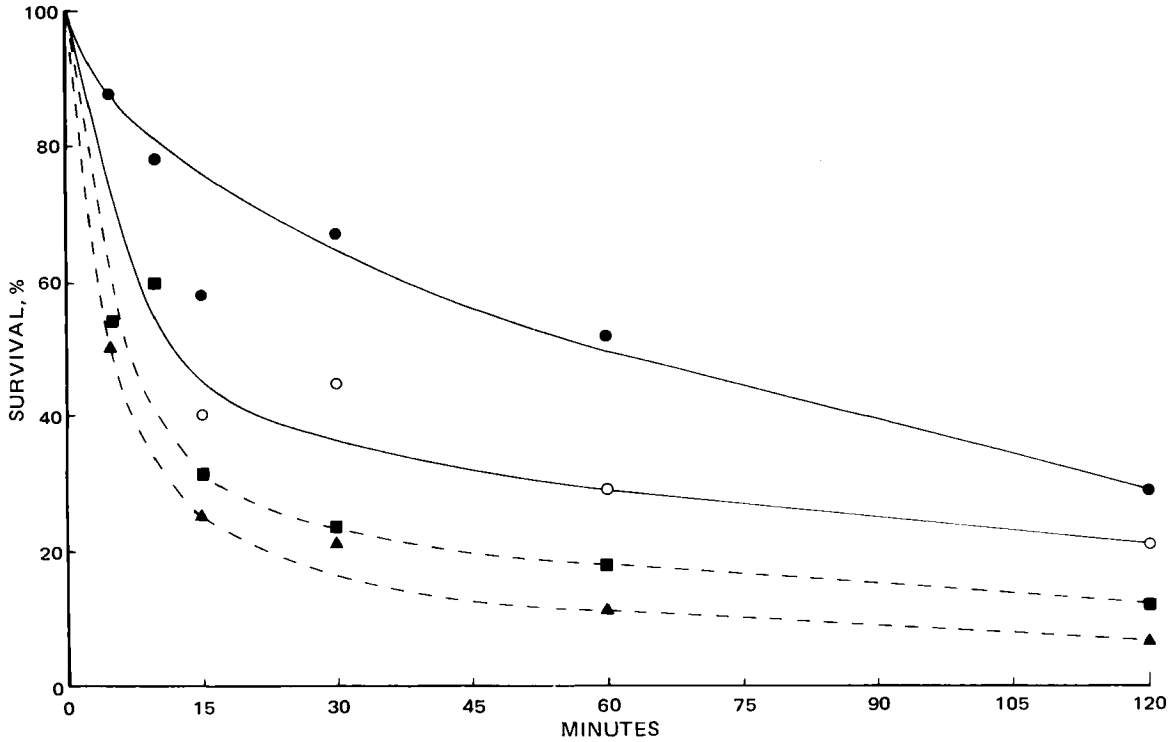

Figure 5—*Dissolution of erythromycin from nonenteric erythromycin stearate dosage forms treated with Solution 4 (pH 2.2, 0.74 mEq of hydrochloric acid). Key: ●——●, Capsule A; ■- - - -■, Capsule B; ○——○, Capsule C; and ▲- - - -▲, Tablet A.*

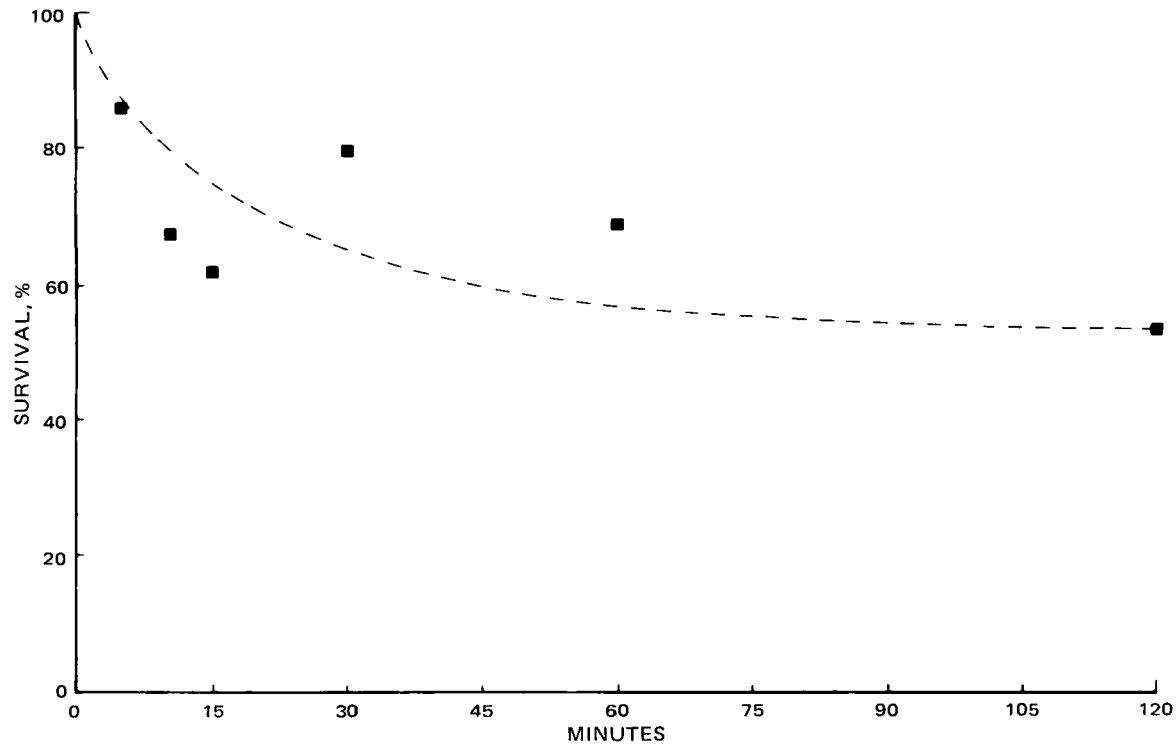

Figure 6—*Dissolution of erythromycin from Capsule B treated with Solution 6 (pH 3.2, 0.1 mEq of hydrochloric acid).*

as possible the range of acidity conditions found in the human stomach in the fasting state. The data show clearly that published statements on the acid stability of erythromycin stearate have been in error, and it is likely that a comparable degree of acid destruction occurs *in vivo*. This situation could account for the low serum levels found by Griffith and Black (1) compared to the estolate in fasting subjects and the much lower, or nonexistent, levels found by the same authors (1) and Bell (2) in nonfasting subjects.

REFERENCES

(1) R. S. Griffith and H. R. Black, *Amer. J. Med. Sci.*, **247**, 69(1964).

(2) S. M. Bell, *Med. J. Aust.*, **2**, 1280(1971).

(3) L. E. Josselyn and J. C. Sylvester, *Antibiot. Chemother.*, **1953**, 63.

(4) J. C. Sylvester and L. E. Josselyn, *ibid.*, **1953**, 930.

(5) *Med. Lett.*, **12**, 35(1970).
(6) D. N. Wade, *New Ethicals*, 12(10), 9(1971).
(7) L. P. Garrod and F. O'Grady, *Antibiot. Chemother.*, **1971**, 169.
(8) J. C. Tolhurst, G. Buckle, and S. W. Williams, "Chemotherapy with Antibiotics and Allied Drugs," 3rd ed., N.H.M.R.C., Australian Government Publishing Service, p. 78.
(9) V. C. Stephens, J. W. Conine, and H. W. Murphy, *J. Amer. Pharm. Ass., Sci. Ed.*, **48**, 620(1959).
(10) H. Varley, "Practical Clinical Biochemistry," William Heinemann Books Ltd., London, England, 1963, p. 258.
(11) G. F. Stening, *Mod. Med. Aust.*, **16**(5), 15(1973).
(12) F.D.A. Antacid Monograph, First Proposal, F.D.C. Reports, Special Supplement, Apr. 9, 1973.
(13) K. G. Buckler, *Gut*, **8**, 138(1967).
(14) G. H. Griffith, G. M. Owen, H. Campbell, and R. Shields, *Gastroenterology*, **54**, 1(1968).
(15) M. R. Colmer, G. M. Owen, and R. Shields, *Brit. Med. J.*, **2**, 448(1973).
(16) T. M. Feinblatt and E. A. Ferguson, *N. Engl. J. Med.*, **256**, 331(1957).
(17) J. Nimmo, R. C. Heading, P. Tothill, and L. F. Prescott, *Brit. Med. J.*, **1**, 587(1973).

ACKNOWLEDGMENTS AND ADDRESSES

Received November 7, 1973, from the *Research Division, F. H. Faulding & Co. Ltd., 48 Beans Road, Thebarton, South Australia, 5031.*

Accepted for publication June 11, 1975.

The authors thank D. R. Best of Hawthorn Park Research Laboratories Pty Ltd., Mittagong, New South Wales, Australia, for performing the biological assays.

[x] To whom inquiries should be directed.

Release and Elimination of ^{14}C-Fluphenazine Enanthate and Decanoate Esters Administered in Sesame Oil to Dogs

JACQUES DREYFUSS [x], JOHN J. ROSS, Jr., JAMES M. SHAW, IRVING MILLER, and ERIC C. SCHREIBER

Abstract □ The rates of release of ^{14}C-fluphenazine enanthate and ^{14}C-fluphenazine decanoate were compared in two groups of five male dogs. Each dog was given a single dose (2 mg/kg im) of either the enanthate or decanoate ester in sesame oil. The times required to attain maximum concentrations of radioactivity in plasma were 3.8 ± 0.5 days (±*SE*) for the enanthate ester and 10.6 ± 1.1 days for the decanoate ester ($p < 0.001$); maximum concentrations of radioactivity in the plasma at these times were 16.7 ± 1.1 and 11.1 ± 1.2 ng/ml, respectively ($p < 0.01$). However, 35 days after dosing, the concentrations of radioactivity in plasma were greater for the decanoate ester than for the enanthate ester. The times required for 50% of the dose to be excreted in the urine and feces were 7.8 ± 0.5 days for the enanthate ester and 22.6 ± 4.4 days for the decanoate ester ($p < 0.05$). The total amounts excreted in 35 days were 85.4 ± 1.8 and 68.8 ± 6.6% of the dose for the enanthate and decanoate esters, respectively; the average half-times for the rates of release of radioactivity from depot and body, as calculated from the data for total excretion, were 5.55 days for the enanthate ester and 15.4 days for the decanoate ester. Thirty-five days after dosing, the amount of the dose present in the injection site was 4.6 ± 1.6% for the enanthate ester and 18.6 ± 5.7% for the decanoate ester. Two groups of six dogs each were protected against the emetic effects of apomorphine more than twice as long by the decanoate ester than by the enanthate ester after the subcutaneous administration of single 8-mg/kg doses of either drug in sesame oil ($p < 0.05$). Based on measurements of total radioactivity, it was concluded that the decanoate ester was released from the depot at less than one-half the rate of the enanthate ester.

Keyphrases □ Fluphenazine—enanthate and decanoate esters, rates of release and elimination in urine and feces, dogs □ Elimination—renal and GI, fluphenazine enanthate and decanoate esters, dogs

Although many studies conducted in humans have demonstrated the clinical efficacy of long-acting esters of fluphenazine, there is little objective evidence to enable one to quantitate their slow-release characteristics. Such studies are difficult to conduct in humans for the following reasons:

1. Sufficient radioactivity cannot be administered to humans to allow for the detection of the low concentrations of the drug or its metabolites present in the circulation during a prolonged time.
2. It is generally not feasible, even under the best of circumstances, to collect excreta quantitatively over a month, especially when most radioactivity is excreted in the feces as it is with fluphenazine and its esters (1–3).
3. At the conclusion of the study, it is not possible to determine the amount of drug remaining in the depot at the injection site.

The relative rates of release of the enanthate (I*a*) and decanoate (I*b*) esters of ^{14}C-fluphenazine were compared in dogs because this species could be given

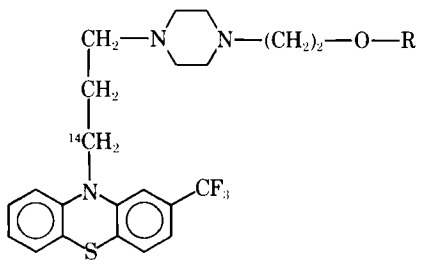

I*a*: R = $-C(=O)-(CH_2)_5CH_3$

I*b*: R = $-C(=O)-(CH_2)_8CH_3$

(5) *Med. Lett.*, **12**, 35(1970).
(6) D. N. Wade, *New Ethicals*, 12(10), 9(1971).
(7) L. P. Garrod and F. O'Grady, *Antibiot. Chemother.*, **1971**, 169.
(8) J. C. Tolhurst, G. Buckle, and S. W. Williams, "Chemotherapy with Antibiotics and Allied Drugs," 3rd ed., N.H.M.R.C., Australian Government Publishing Service, p. 78.
(9) V. C. Stephens, J. W. Conine, and H. W. Murphy, *J. Amer. Pharm. Ass., Sci. Ed.*, **48**, 620(1959).
(10) H. Varley, "Practical Clinical Biochemistry," William Heinemann Books Ltd., London, England, 1963, p. 258.
(11) G. F. Stening, *Mod. Med. Aust.*, **16**(5), 15(1973).
(12) F.D.A. Antacid Monograph, First Proposal, F.D.C. Reports, Special Supplement, Apr. 9, 1973.
(13) K. G. Buckler, *Gut*, **8**, 138(1967).
(14) G. H. Griffith, G. M. Owen, H. Campbell, and R. Shields, *Gastroenterology*, **54**, 1(1968).
(15) M. R. Colmer, G. M. Owen, and R. Shields, *Brit. Med. J.*, **2**, 448(1973).
(16) T. M. Feinblatt and E. A. Ferguson, *N. Engl. J. Med.*, **256**, 331(1957).
(17) J. Nimmo, R. C. Heading, P. Tothill, and L. F. Prescott, *Brit. Med. J.*, **1**, 587(1973).

ACKNOWLEDGMENTS AND ADDRESSES

Received November 7, 1973, from the *Research Division, F. H. Faulding & Co. Ltd., 48 Beans Road, Thebarton, South Australia, 5031.*

Accepted for publication June 11, 1975.

The authors thank D. R. Best of Hawthorn Park Research Laboratories Pty Ltd., Mittagong, New South Wales, Australia, for performing the biological assays.

[x] To whom inquiries should be directed.

Release and Elimination of ^{14}C-Fluphenazine Enanthate and Decanoate Esters Administered in Sesame Oil to Dogs

JACQUES DREYFUSS [x], JOHN J. ROSS, Jr., JAMES M. SHAW, IRVING MILLER, and ERIC C. SCHREIBER

Abstract □ The rates of release of ^{14}C-fluphenazine enanthate and ^{14}C-fluphenazine decanoate were compared in two groups of five male dogs. Each dog was given a single dose (2 mg/kg im) of either the enanthate or decanoate ester in sesame oil. The times required to attain maximum concentrations of radioactivity in plasma were 3.8 ± 0.5 days (±*SE*) for the enanthate ester and 10.6 ± 1.1 days for the decanoate ester ($p < 0.001$); maximum concentrations of radioactivity in the plasma at these times were 16.7 ± 1.1 and 11.1 ± 1.2 ng/ml, respectively ($p < 0.01$). However, 35 days after dosing, the concentrations of radioactivity in plasma were greater for the decanoate ester than for the enanthate ester. The times required for 50% of the dose to be excreted in the urine and feces were 7.8 ± 0.5 days for the enanthate ester and 22.6 ± 4.4 days for the decanoate ester ($p < 0.05$). The total amounts excreted in 35 days were 85.4 ± 1.8 and 68.8 ± 6.6% of the dose for the enanthate and decanoate esters, respectively; the average half-times for the rates of release of radioactivity from depot and body, as calculated from the data for total excretion, were 5.55 days for the enanthate ester and 15.4 days for the decanoate ester. Thirty-five days after dosing, the amount of the dose present in the injection site was 4.6 ± 1.6% for the enanthate ester and 18.6 ± 5.7% for the decanoate ester. Two groups of six dogs each were protected against the emetic effects of apomorphine more than twice as long by the decanoate ester than by the enanthate ester after the subcutaneous administration of single 8-mg/kg doses of either drug in sesame oil ($p < 0.05$). Based on measurements of total radioactivity, it was concluded that the decanoate ester was released from the depot at less than one-half the rate of the enanthate ester.

Keyphrases □ Fluphenazine—enanthate and decanoate esters, rates of release and elimination in urine and feces, dogs □ Elimination—renal and GI, fluphenazine enanthate and decanoate esters, dogs

Although many studies conducted in humans have demonstrated the clinical efficacy of long-acting esters of fluphenazine, there is little objective evidence to enable one to quantitate their slow-release characteristics. Such studies are difficult to conduct in humans for the following reasons:

1. Sufficient radioactivity cannot be administered to humans to allow for the detection of the low concentrations of the drug or its metabolites present in the circulation during a prolonged time.
2. It is generally not feasible, even under the best of circumstances, to collect excreta quantitatively over a month, especially when most radioactivity is excreted in the feces as it is with fluphenazine and its esters (1–3).
3. At the conclusion of the study, it is not possible to determine the amount of drug remaining in the depot at the injection site.

The relative rates of release of the enanthate (I*a*) and decanoate (I*b*) esters of ^{14}C-fluphenazine were compared in dogs because this species could be given

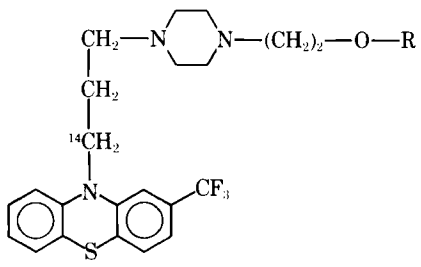

I*a*: R = $-C(=O)-(CH_2)_5CH_3$

I*b*: R = $-C(=O)-(CH_2)_8CH_3$

either ester (20 mg/0.5 ml of sesame oil) at approximately the same concentration as that most commonly given therapeutically to humans (25 mg/ml of sesame oil). Data published previously from studies of flupentixol decanoate indicate that the kinetics of drug release in dogs more closely resembles those found in humans than do the kinetics in rats (4).

EXPERIMENTAL

^{14}C-Fluphenazine enanthate or decanoate had a specific activity of 4.92 or 4.84 μCi/mg, respectively. These compounds were not less than 97% chemically and radiochemically pure.

Design—Each ester (41 mg) was dissolved in 1.0 ml of sesame oil containing 1.6% benzyl alcohol. Two groups of five purebred male beagles each were injected intramuscularly into the *biceps femoris* of the thigh muscle (0.5 ml of drug formulation/10 kg) with either the enanthate or decanoate ester. The enanthate ester was given at an average dose of 1.89 ± 0.11 mg/kg (±*SE*); the decanoate was given at an average dose of 2.03 ± 0.04 mg/kg.

The dogs were housed in metabolism cages that permitted the separate collection of urine and feces. Blood samples were drawn periodically for 35 days, and the total urinary and fecal excretions were collected daily for 35 days. Then the dogs were sacrificed by anesthesia with pentobarbital (30 mg/kg iv), followed by the rapid injection of 5 ml of a saturated solution of potassium chloride.

The dogs were necropsied, and selected tissues were analyzed for the presence of residual radioactivity. In addition, the entire musculature of both the left and right thighs was excised and analyzed, so that the amount of radioactivity remaining in the injection site could be determined.

Analysis of Plasma—A 0.8-ml plasma sample was dissolved in 4 ml of solubilizer[1], and the sample was counted with 15 ml of toluene scintillation fluid. This scintillation fluid contained, per liter of toluene, 5 g of 2,5-diphenyloxazole and 300 mg of 1,4-bis[2-(4-methyl-5-phenyloxazolyl)]benzene.

Analysis of Urine and Feces—Fecal samples were homogenized with 2–3 volumes of methanol; about 800 mg of homogenate was combusted[2]. Urine samples (1 ml) were counted directly in 15 ml of Bray's scintillation fluid (5).

Analysis of Tissues—Brain samples were homogenized in water in an all-glass homogenizer[3]; about 800 mg of homogenate was combusted. Certain portions of the eye (lens, cornea, aqueous and vitreous humors, and combined retina, choroid, and sclera) were combusted. Similarly, representative portions of omental fat (200 mg) and skin without hair (200 mg) were combusted. Samples of tissue from the heart, kidneys, liver, lungs, and thigh muscle were ground in a meat grinder; then about 800 mg of each well-mixed sample was combusted.

Counting of Samples—Radioactivity in each sample was measured by a liquid scintillation spectrometer[4]. Counting efficiency was determined with automatic external standardization and the use of previously prepared quench curves.

Duration of Protection against Apomorphine—Mongrel dogs were selected that consistently responded to the emetic effect of apomorphine (20 μg/kg iv) after the ingestion of a test meal. Two groups of six dogs each (three males and three females per group) were given, at the nape of the neck, equimolar doses of fluphenazine enanthate (8.0 mg/kg sc) or fluphenazine decanoate (8.6 mg/kg sc) in sesame oil containing 1.5% benzyl alcohol (1.6 ml/10 kg). Two control dogs (one male and one female) were given only sesame oil.

On the day after dosing, all dogs were given 20 μg/kg of apomorphine, followed in 1 day by 640 μg/kg of apomorphine. All dogs treated with either fluphenazine ester were protected from emesis on both days, whereas the two control dogs vomited consistently. The dogs dosed with either fluphenazine ester were then challenged at weekly intervals with apomorphine (640 μg/kg iv). If no emesis occurred, the same dose of apomorphine was used the next week. If emesis occurred, the dogs were challenged again on the same day, about 6 hr later, with one-half the dose of apomorphine.

The emetic dose given the next week depended upon the response of the previous week but was generally decreased by 50% if emesis occurred at any given dose. When a dog treated with either fluphenazine ester vomited after being challenged with 20 μg/kg of apomorphine, it was considered to be no longer protected and was withdrawn from the study. The control dogs were challenged each week throughout the study with 20 μg/kg of apomorphine and consistently showed emetic responses.

Analysis of Regression—Data obtained for the presence of radioactivity in the plasma, urine, feces, and urine plus feces for each dog were subjected to an analysis of linear exponential regression. The objective at this stage was to find the time interval over which the greatest correlation coefficient (r^2) could be obtained. The half-time ($T_{1/2}$ = 0.693/slope × ln 10) for each parameter was computed from the slope of the line for each dog. The average $T_{1/2}$ for each parameter for each drug was obtained by pooling the individual data points over the time interval having the greatest r^2 for *each* dog.

An analysis of variance (ANOVA) for each pooled regression was performed to determine whether the slope of the regression line was significantly different from zero. It was significant in all cases ($p < 0.0001$). In addition, a test for linearity of the regression was performed by partitioning the residual sum of squares into the sum of squares for pure error and for lack of fit (6). An F-test was performed by dividing the mean square due to lack of fit by the mean square due to pure error. These results were also significant in all cases ($p < 0.05$).

The adequacy of the regression coefficients was further tested by an examination of residuals for: (*a*) outliers, (*b*) randomness when plotted against time, and (*c*) randomness when plotted against the predicted dependent variable. The 95% tolerance intervals were computed according to standard procedures.

Tests for Correlation—The correlation between the average regression lines for urinary and fecal excretion of radioactivity after dosing with each drug was determined by calculating the coefficients for Pearson's Product and Spearman's Rank Order (7).

Analysis of Differences between Means—Initially, the means of all parameters were compared by a one-way analysis of variance (ANOVA). The values cited (probability > F) indicate the α-level of significance of the F-ratio for the hypothesis that the population means are equal. To determine whether the analysis of variance was valid, a test for the homogeneity of variances was performed (8). If the variances were equal ($p \leq 0.05$), the analysis of variance was considered valid. If the variances were unequal ($p \leq 0.05$), the analysis of variance was considered invalid and was replaced by a modified t-test (9).

RESULTS

Concentrations of Radioactivity in Plasma—The concentrations of radioactivity in the plasma of dogs after intramuscular doses of either ^{14}C-fluphenazine enanthate or decanoate are shown in Fig. 1. Concentrations of radioactivity were significantly different in the plasma of dogs given the enanthate or decanoate ester, except at 10, 13, and 16 days after dosing. One-half day after dogs had been dosed with the enanthate ester, greater concentrations of radioactivity were present in the plasma than in dogs dosed with the decanoate ester.

The maximum concentrations of radioactivity in plasma were greater and were attained earlier for the enanthate ester than for the decanoate ester. Thirty-five days after dosing with either ester, the concentrations of radioactivity in the plasma of the dogs dosed with the decanoate ester were significantly greater than they were in dogs given the enanthate ester.

Half-times of radioactivity in plasma were calculated as outlined under *Experimental*. The lines of best fit for the enanthate and decanoate esters, as obtained by analyses of regression, are shown in Fig. 2. The average half-lives obtained in this manner were 9.58 days for the enanthate ester and 33.6 days for the decanoate ester. Although the correlation coefficients obtained after dosing with the enanthate ester were slightly higher on the average when the time interval of 3–24 days was used, it was decided to extend the time interval to 35 days, thereby facilitating the comparison of the enanthate ester with the decanoate ester. In fact, this extension

[1] NCS solubilizer, Amersham/Searle Corp., Des Plaines, Ill.
[2] R. J. Harvey Instrument Corp., Hillsdale, N.J.
[3] Potter-Elvehjem, Fisher Scientific Co., Springfield, N.J.
[4] Packard Tri-Carb model 3380, Packard Instrument Co., Downers Grove, Ill.

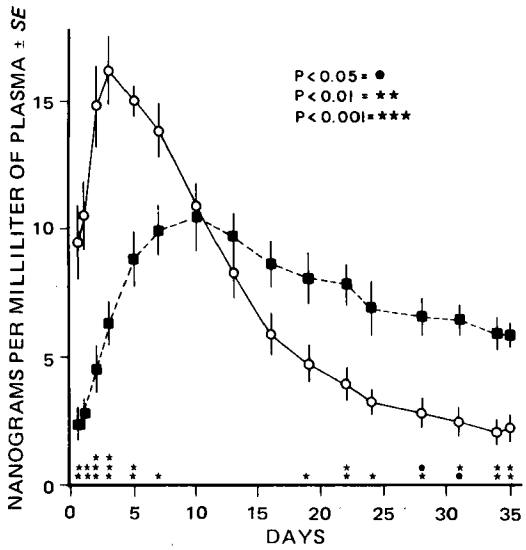

Figure 1—*Average concentrations of radioactivity in the plasma of dogs after the intramuscular administration of either fluphenazine enanthate or fluphenazine decanoate. Key:* ■, *^{14}C-fluphenazine decanoate; and* O, *^{14}C-fluphenazine enanthate.*

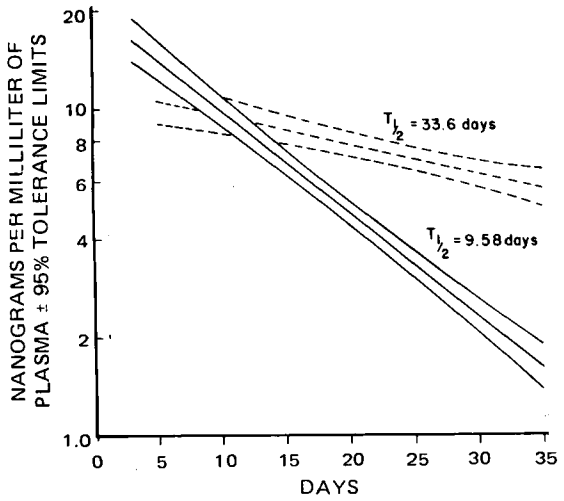

Figure 2—*Line of best fit and 95% tolerance limits for concentrations of radioactivity in the plasma of dogs dosed with either fluphenazine enanthate or fluphenazine decanoate. Key: - - -, ^{14}C-fluphenazine decanoate; and —, ^{14}C-fluphenazine enanthate.*

had only a minor effect on the half-lives obtained (8.38 *versus* 9.58 days).

Excretion of Radioactivity in the Urine and Feces—Urine and feces from each dog dosed with either ester were collected daily for 35 days. The average excretion of radioactivity by dogs dosed with either ester was mostly in the feces (66–81% of the dose); on the average, only 3–4% of the dose was excreted in the urine (Fig. 3). During the 35-day test, totals of 85 and 69% of the dose were excreted by dogs dosed with the enanthate and decanoate esters, respectively.

Lines of best fit were calculated for each ester for the total excretion of radioactivity. The total excretion of radioactivity (Fig. 4) indicated an average half-life of 5.55 days for the enanthate ester and 15.4 days for the decanoate ester. Figure 5 shows lines of best fit for the urinary and fecal excretion of radioactivity for each ester. The average slopes of the lines of best fit for the excretion of radioactivity in the urine and feces for each ester are parallel, as evidenced by the similar magnitude of the half-lives.

Correlation between the slopes for the urinary and fecal excretion of radioactivity by *each dog* dosed with either ester was statistically significant ($p < 0.0004$). We consider it very significant that

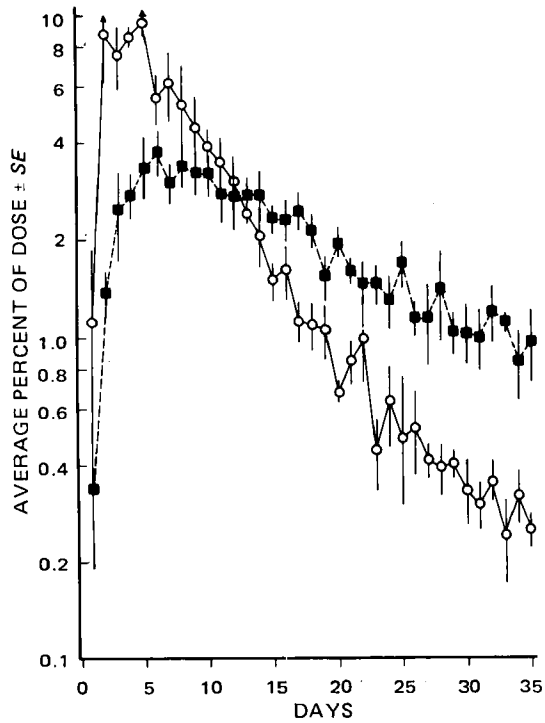

Figure 3—*Average daily excretion of radioactivity in the urine and feces of dogs after the intramuscular administration of either fluphenazine enanthate or fluphenazine decanoate. Key:* ■, *^{14}C-fluphenazine decanoate; and* O, *^{14}C-fluphenazine enanthate.*

the sets of lines, representing the enanthate and decanoate esters, have the same slope, even though one regression line represents urinary excretion and the other represents fecal excretion. In addition, the magnitudes of the slopes for each excretory route were different for the two esters.

Another way of comparing the rates of excretion of radioactivity for the two esters is by grouping the data on a weekly basis. Table I shows the amounts of radioactivity excreted on a weekly basis for each ester beginning with zero time and not just including the descending portion of each plot for excretion. The data clearly indicate, with high statistical significance, that the rate of release of radioactivity was greatest for the enanthate during the 1st week

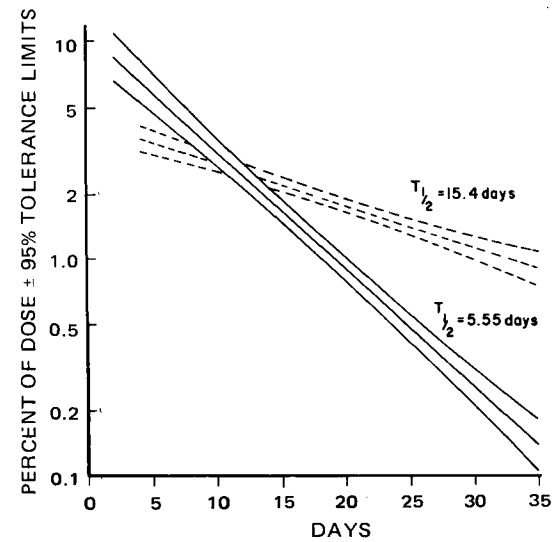

Figure 4—*Line of best fit and 95% tolerance limits for the total excretion of radioactivity by dogs after the intramuscular administration of either fluphenazine enanthate or fluphenazine decanoate. Key: - - -, ^{14}C-fluphenazine decanoate; and —, ^{14}C-fluphenazine enanthate.*

Table I—Weekly Excretion of Radioactivity after the Intramuscular Administration to Dogs of Either Fluphenazine Enanthate or Fluphenazine Decanoate

Weeks	Total Excretion, % of Dose ± *SE*		Statistical Significance
	Enanthate	Decanoate	
1	46.98 ± 2.62	17.07 ± 2.36	$p < 0.0001$
2	24.48 ± 1.76	20.80 ± 2.68	$p < 0.28$
3	7.87 ± 0.50	14.25 ± 1.06	$p < 0.0009$
4	3.95 ± 0.48	9.55 ± 0.86	$p < 0.0007$
5	2.12 ± 0.30	7.13 ± 0.32	$p < 0.0001$

after dosing but was greatest for the decanoate during the 2nd week after dosing. The data for both esters were not significantly different during the 2nd week, since the two curves cross each other at that time.

Residual Radioactivity in Selected Tissues and Drug Depot—The dogs were sacrificed 35 days after receiving either ester, and selected tissues were analyzed for residual radioactivity (Table II). In addition, the entire left thigh muscle of each dog, into which the drug had been injected, was excised and homogenized to determine how much radioactivity was still present in the depot. The right thigh muscle of each dog was processed similarly to provide a measure of the amounts of radioactivity that would ordinarily have localized in muscle from the presence of the drug in the circulation.

In dogs dosed with either ester, only traces of radioactivity were present in the blood, brain, nonpigmented portions of the eye, kidneys, omental fat, skin, and right thigh muscle. More appreciable amounts of radioactivity were found in the combined retina, choroid, and sclera of the eye, the liver, and the left thigh muscle. The binding of the phenothiazines to melanin is a well-established phenomenon (10, 11). The localization of radioactivity in the liver can be related to the biliary elimination of the fluphenazine esters.

Thirty-five days after dosing, radioactivity was still present in the injection sites of both groups of dogs: an average of about 5% of the dose for the enanthate ester and of about 19% for the decanoate ester. These amounts correlate with their relative rates of release from the depot, as evidenced by the relative half-times for excretion, and with their rates of release of radioactivity into the circulation.

Studies with Apomorphine—Pharmacological studies in dogs utilized the apomorphine test to determine the duration of action of long-acting neuroleptics. The decanoate ester protected dogs longer than did the enanthate ester ($p < 0.01$ for the response to 640 μg/kg of apomorphine by a Wilcoxon Rank Sum Test) (Table III). The ratio of protection against emesis (decanoate ester–enanthate ester) at any dose of apomorphine was slightly greater than 2. In addition, the decrease in the logarithm of the apomorphine dose with time was determined for each dog after dosing. The average slope, as determined from lines of best fit for *each dog*, was 2.88 times greater for the enanthate ester than for the decanoate ester ($p \leq 0.05$ by the Wilcoxon Rank Sum Test).

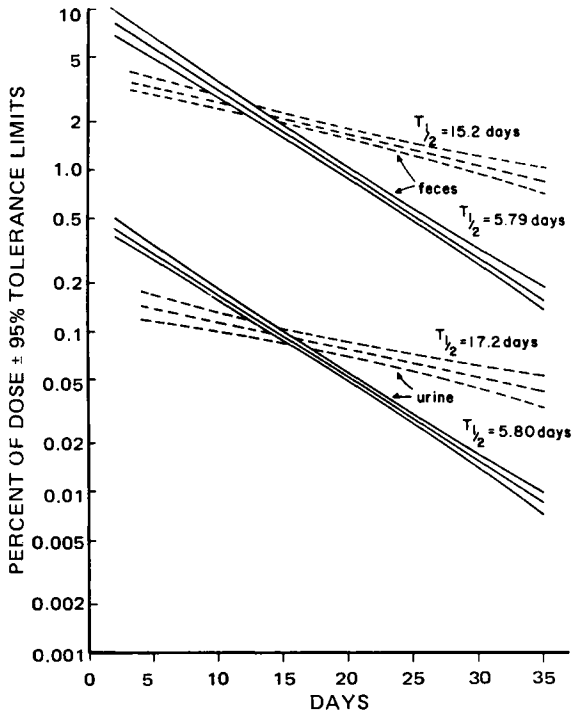

Figure 5—*Lines of best fit and 95% tolerance limits for the excretion of radioactivity in the urine or feces after the intramuscular administration of either fluphenazine enanthate or fluphenazine decanoate. Key: - - -, ^{14}C-fluphenazine decanoate; and —, ^{14}C-fluphenazine enanthate.*

DISCUSSION

A comparison of selected parameters for each dog given either ^{14}C-fluphenazine enanthate or ^{14}C-fluphenazine decanoate is shown in Table IV. This table shows arithmetic averages for each parameter and the statistical significance of the difference between each pair of values. During the entire study, 88–91% of the dose could be accounted for by the amounts of radioactivity excreted, the amounts present in the depot after 35 days, and the amounts remaining in certain tissues.

Table II—Average Residual Radioactivity Present in Selected Tissues of Dogs 35 Days after the Intramuscular Administration of Either Fluphenazine Enanthate or Fluphenazine Decanoate

Tissue	Fluphenazine Enanthate[a]		Fluphenazine Decanoate[a]	
	μg/g ± *SE*	% of Dose ± *SE*	μg/g ± *SE*	% of Dose ± *SE*
Brain	0.005 ± 0.001	0.002 ± 0.000	0.013 ± 0.002	0.004 ± 0.001
Combined retina, choroid, and sclera	0.53 ± 0.15	—	0.57 ± 0.17	—
Cornea	0.26 ± 0.23	—	0.022 ± 0.007	—
Aqueous humor	0.002 ± 0.001	—	0.004 ± 0.003	—
Vitreous humor	0.039 ± 0.020	—	0.030 ± 0.017	—
Lens	0.002 ± 0.001	—	0.003 ± 0.001	—
Kidneys	0.032 ± 0.004	0.010 ± 0.001	0.042 ± 0.009	0.010 ± 0.003
Liver	0.25 ± 0.05	0.46 ± 0.08	0.34 ± 0.05	0.49 ± 0.06
Omental fat	0.001 ± 0.001	—	0.011 ± 0.004	—
Skin	0.035 ± 0.008	—	0.032 ± 0.010	—
Left thigh muscle (contains injection site)	1.66 ± 0.52	4.65 ± 1.63	7.97 ± 2.34	18.66 ± 5.70
Right thigh muscle	0.009 ± 0.005	0.024 ± 0.011	0.021 ± 0.011	0.048 ± 0.023
Blood, μg/ml	0.001 ± 0.000	—	0.003 ± 0.001	—

[a] $n = 5$.

Table III—Protection against the Emetic Effect of Apomorphine Provided by Either Fluphenazine Enanthate or Fluphenazine Decanoate Administered Subcutaneously to Dogs

Dose of Apomorphine, μg/kg iv	Duration of Protection against Emesis (First Time for Emesis), Days ± *SE*		Ratio of Protective Effect, Decanoate/Enanthate
	Fluphenazine Enanthate[a]	Fluphenazine Decanoate[b]	
20	55 ± 6	124 ± 11[c]	2.25
40	46 ± 3	105 ± 7	2.31
80	45 ± 3	91 ± 8	2.02
160	40 ± 3	87 ± 9	2.18
320	38 ± 3	82 ± 9	2.16
640	34 ± 2	74 ± 6	2.18

[a] Using 8.0 mg/kg sc in 1.6 ml of sesame oil/10 kg of body weight. [b] Using 8.6 mg/kg sc in 1.6 ml of sesame oil/10 kg of body weight. [c] Two of the six dogs tested at this dose were still protected against the emetic effects of apomorphine 148 days after dosing.

The data of Table V show a complete comparison of the relevant half-times for release of radioactivity from the depot and the body for each ester, as calculated from the pooled regression data, rather than as the arithmetic averages. These data, based on measurements of total radioactivity, indicate that the decanoate ester was released at considerably less than one-half the rate of the enanthate ester. It is not clear why the half-times in plasma and excreta differed by a factor of almost 2. This finding might be explained by the inability to measure either unchanged parent ester. The possibility exists that the rate of excretion of radioactivity reflects the excretion of a metabolite, whereas the elimination of radioactivity from the plasma represents some combination of the elimination of the parent compound and a metabolite. However, in spite of this difference in absolute half-times between that found in plasma and excreta for both esters, the *ratio* of half-times for the decanoate–enanthate in plasma was still about 3:1.

The fact that the slopes of the regression lines for the urinary and fecal excretion of the enanthate and decanoate esters are similar for each drug, but different between the two drugs, suggests that the release of radioactivity from the oily depot may be the controlling factor that accounts for the different rates at which these esters are released from their sites of injection. However, other possibilities are not excluded by this finding of parallel slopes; *e.g.*, the hydrolysis of the ester bound could be the rate-limiting step.

Table V—Average Half-Times of Radioactivity in the Plasma and Excreta of Dogs after the Intramuscular Administration of Either Fluphenazine Enanthate or Fluphenazine Decanoate

Sample	$T_{1/2}$, Days		$T_{1/2}$ Decanoate
	Enanthate	Decanoate	$T_{1/2}$ Enanthate
Plasma	9.58	33.56	3.51
Urine	5.80	17.15	2.96
Feces	5.79	15.23	2.63
Urine + feces	5.55	15.39	2.77

Studies to answer this question were conducted recently and will be reported separately. Briefly, anesthetized dogs, whose bile ducts had been cannulated, were given intravenous doses of either the enanthate or decanoate ester of fluphenazine (1 mg/kg; unformulated). No unchanged ^{14}C-fluphenazine enanthate or ^{14}C-fluphenazine decanoate was present in the bile of these dogs in the earliest sample collected (0–1 hr). In addition, a large sample of blood was removed from the dogs 30 min after they had been dosed; extraction and chromatography of the plasma indicated that at least 79% of the radioactivity had been converted to free fluphenazine or its metabolites.

Moreover, when intravenous doses of either fluphenazine or its enanthate and decanoate esters were given to intact dogs (1 mg/kg), no sustained-release effect was obtained and similar concentrations of radioactivity were found in plasma. The kinetics of elimination of this radioactivity in plasma and its excretion in urine and feces were also comparable for all three compounds. These experiments demonstrate that the dog can rapidly hydrolyze either of these two esters and implicate the presence of the drugs in an oily depot as being responsible for sustained release. Earlier published findings on the disposition of ^{14}C-fluphenazine enanthate in dogs (1 mg/kg iv) also are consistent with this conclusion (2).

A difference between the duration of action of the decanoate ester relative to that of the enanthate ester in both the apomorphine test and the rates of release of radioactivity from the depot could be due to at least two factors. First, in the apomorphine study, the esters were administered subcutaneously rather than intramuscularly. Second, the volume of sesame oil given intramuscularly (0.5 ml/10 kg) was less than the volume given subcutaneously (1.6 ml/10 kg).

Studies of conditioned avoidance behavior in rats given single doses of either fluphenazine enanthate or decanoate revealed the

Table IV—Comparison of Selected Parameters after the Intramuscular Administration to Dogs of Either Fluphenazine Enanthate or Fluphenazine Decanoate in Sesame Oil

Parameter	Fluphenazine Enanthate	Fluphenazine Decanoate	Statistical Significance of the Difference between Means
Plasma concentration at 0.5 day, ng/ml	9.5 ± 1.5[a]	2.3 ± 0.7	$p < 0.005$
Time required to attain maximum plasma concentration, days	3.8 ± 0.5	10.6 ± 1.1	$p < 0.001$
Maximum plasma concentration, ng/ml	16.7 ± 1.1	11.1 ± 1.2	$p < 0.01$
Plasma concentration at 35 days, ng/ml	2.2 ± 0.5	6.1 ± 0.4	$p < 0.001$
Plasma half-time, days	9.58 ± 0.70	33.1 ± 3.9	$p < 0.01$
Urinary half-time, days	5.74 ± 0.50	11.7 ± 2.4	N.S.[b]
Fecal half-time, days	5.55 ± 0.39	13.8 ± 2.1	$p < 0.02$
Total excretion half-time, days	5.01 ± 0.54	13.7 ± 2.1	$p < 0.02$
Time required for 50% of dose to be excreted, days	7.8 ± 0.5	22.6 ± 4.4	$p < 0.05$
Amount of radioactivity excreted in urine in 35 days, % of dose	4.11 ± 0.13	2.96 ± 0.45	N.S.
Amount of radioactivity excreted in feces in 35 days, % of dose	81.29 ± 1.77	65.84 ± 6.33	N.S.
Amount of dose excreted in 35 days, %	85.40 ± 1.75	68.80 ± 6.63	N.S.
Amount of dose found in injection site after 35 days, %	4.62 ± 1.64	18.61 ± 5.71	$p < 0.1$
Total amount of dose recovered during entire study, %[c]	90.56 ± 1.10	88.04 ± 2.55	N.S.

[a] All values are the averages ± *SE*. [b] N.S. = not significant. [c] Includes the amounts present in certain tissues that contained residual radioactivity.

same spectrum of activity for both esters but a longer duration of action for the decanoate (12). Nymark *et al.* (13) reported on the prolonged neuroleptic effect of α-flupentixol decanoate in oil[5]. Subcutaneous doses of α-flupentixol decanoate provided protection against the emetic effects of apomorphine for 18–21 days, whereas comparable doses of α-flupentixol in oil provided protection for only 2–3 days. Nymark *et al.* (13) presumed that the decanoic acid ester of α-flupentixol, which is several thousand times more lipophilic than α-flupentixol, releases drug at a slower rate from the oily depot.

A comparison of concentrations of radioactivity in blood after the intramuscular injection of flupentixol decanoate into rats, dogs, or humans indicated that species differences exist in the rate of drug release from the depot (11). Rats and humans seemed to differ greatly in their relative rates of release, while dogs and humans apparently were more alike. These investigators (11) speculated that factors such as the different injection volumes leading to different degrees of spreading of the injected oil, as well as differences in blood flow through the injected muscle, may contribute to these observed species differences.

In studies of metabolism of flupentixol decanoate in rats and dogs, these two species behaved differently with respect to the rate at which the drug was released from an oily depot (14). Thus, rats showed maximum concentrations of radioactivity in blood within the first 24 hr after intramuscular dosing, whereas the maximum concentrations of radioactivity in blood of dogs were obtained 7 days after intramuscular dosing. These investigators (14) speculated that, since rats received a relatively greater volume of oil than did dogs, differences in the rates of release of drug from the depot were probably responsible for these varied effects.

Support for this concept is provided by an earlier study on the duration of action of subcutaneously administered testosterone and its propionate ester (15). That study showed that the amount of sesame oil used as a vehicle for the subcutaneous injection of testosterone or its propionate ester affected the duration of action of these two steroids. In the case of testosterone, sustained biological activity was prevented by the larger, and favored by the smaller, volume of oil. In the case of testosterone propionate, the larger volume of oil prolonged and intensified the compound's activity.

These investigators (15) pointed out that several factors can determine the rate of absorption of compounds from subcutaneous or intramuscular depots, including: (*a*) the absorbing area, which is proportional to the amount of solvent injected; (*b*) the ability, if any, of the solvent to bind the compound; (*c*) the rate at which the compound is released from the solvent; and (*d*) the rate at which the solvent itself is absorbed. In the case of the fluphenazine esters dissolved in sesame oil, it is not known which factors are involved in the difference in the rates of release of the enanthate and the decanoate from an oily depot.

Interesting studies have been published on some long-acting esters of pipotiazine (16). In rats that received intramuscular injections of pipotiazine palmitate and that were studied for 80 days, about 95% of the radioactivity present in the organism at any time was found in the region of the leg where the drug had been injected originally. Jørgensen *et al.* (14) reported similar observations for flupentixol decanoate. These observations provide further support for the idea that the prolonged duration of action of these compounds results primarily from their slow release from an oily depot.

Studies *in vitro* have shown that esterases in the plasma or tissues of the rat or dog are capable of hydrolyzing either the undecylenic or palmitic ester of pipotiazine (16), flupentixol decanoate (14), fluphenazine enanthate (2, 3), or fluphenazine decanoate[6]. From these studies, one can reasonably conclude that the parent neuroleptic molecule, rather than the intact ester, is responsible for the pharmacological action of these drugs.

[5] Viscoleo.

[6] J. Dreyfuss and J. M. Shaw, unpublished data.

REFERENCES

(1) J. Dreyfuss, J. J. Ross, Jr., and E. C. Schreiber, *J. Pharm. Sci.*, **60**, 821(1971).

(2) *Ibid.*, **60**, 829(1971).

(3) A. G. Ebert and S. M. Hess, *J. Pharmacol. Exp. Ther.*, **148**, 412(1965).

(4) A. Jørgensen and C. G. Gottfries, *Psychopharmacologia*, **27**, 1(1972).

(5) G. A. Bray, *Anal. Biochem.*, **1**, 279(1960).

(6) N. R. Draper and H. Smith, "Applied Regression Analysis," Wiley, New York, N.Y., 1966, p. 26.

(7) W. J. Conover, "Practical Nonparametric Statistics," Wiley, New York, N.Y., 1971, p. 243.

(8) W. J. Dixon and F. J. Massey, "Introduction to Statistical Analysis," McGraw-Hill, New York, N.Y., 1969, p. 111.

(9) *Ibid.*, p. 119.

(10) N. G. Lindquist and S. Ullberg, in "The Phenothiazines and Structurally Related Drugs," I. S. Forrest, C. J. Carr, and E. Usdin, Eds., Raven, New York, N.Y., 1974, p. 413.

(11) A. M. Potts, *Invest. Ophthalmol.*, **3**, 406(1964).

(12) A. J. Sanseigne, H. L. Yale, S. M. Hess, J. C. Burke, and Z. P. Horovitz, *Agressologie*, **9**, 3(1968).

(13) M. Nymark, K. F. Frank, V. Pedersen, V. Boeck, and I. M. Nielsen, *Acta Pharmacol. Toxicol.*, **33**, 363(1973).

(14) A. Jørgensen, K. F. Overø, and V. Hansen, *ibid.*, **29**, 339(1971).

(15) W. L. Honrath, A. Wolff, and A. Meli, *Steroids*, **2**, 425(1963).

(16) L. Julou, G. Bourat, R. Ducrot, J. Fournel, and C. Garret, *Acta Psychiat. Scand. Suppl.*, **241**, 9(1973).

ACKNOWLEDGMENTS AND ADDRESSES

Received March 7, 1975, from the *Departments of Drug Metabolism and Pharmacology, Squibb Institute for Medical Research, New Brunswick, NJ 08903*

Accepted for publication June 16, 1975.

The authors thank Mr. Peter Egli for synthesizing the radiolabeled fluphenazine esters, Mr. Carmen Mondi and Mrs. Louise Carter for excellent technical assistance, Dr. Morton Goldberg and Ms. Rita Fand for evaluating the duration of action studies with apomorphine, and Mr. Sal Meloni for preparing the illustrations.

[x] To whom inquiries should be directed.

Analysis of Butaclamol in Serum by Fluorescence Induction

J. HASEGAWA *, A. HURWITZ *x, G. KROL ‡, and R. DAVIES §

Abstract □ A sensitive TLC–fluorometric method was developed for the analysis of butaclamol, a benzo[6,7]cyclohepta[1,2,3-*de*]-pyrido[2,1-*a*]isoquinoline derivative, in serum. The method involves cyclohexane extraction of serum samples followed by TLC of the concentrated extracts. The developed TLC plates were sprayed with an oxidizing reagent and heated at 110°. Highly fluorescent spots were produced for butaclamol, which was well separated from metabolites and serum components. Fluorometric densitometry permitted quantitation with a sensitivity of 10 ng/spot application.

Keyphrases □ Butaclamol—TLC–fluorometric analysis, human serum □ TLC–fluorometry—analysis, butaclamol in human serum □ Fluorometry–TLC—analysis, butaclamol in human serum □ Tranquilizers—butaclamol, TLC–fluorometric analysis, human serum

Compounds of the benzo[6,7]cyclohepta[1,2,3-*de*]-pyrido[2,1-*a*]isoquinoline ring system have been prepared and shown to have potential use as neuroleptic agents (1). One important candidate was butaclamol hydrochloride (I).

Studies on orally and intravenously administered ^{14}C-butaclamol in dogs[1] receiving 1.5 mg/kg demonstrated peak serum levels of unchanged butaclamol corresponding to about 20 ng/ml. Therefore, a sensitive and specific quantitative analytical procedure for the drug in serum was required for studies in humans.

GC analysis using derivatization of the tertiary hydroxy function to the trimethylsilyl ether was useful but did not give adequate sensitivity for serum concentration determinations in the range required. Attempts to prepare derivatives suitable for electron-capture detection were unsuccessful.

UV spectrodensitometry after TLC also was unsuitable for blood level analyses because of insufficient sensitivity. Although butaclamol did not exhibit natural fluorescence, its oxidation products were highly fluorescent. Furthermore, studies indicated that oxidative induction of fluorescence could be accomplished directly on thin-layer plates.

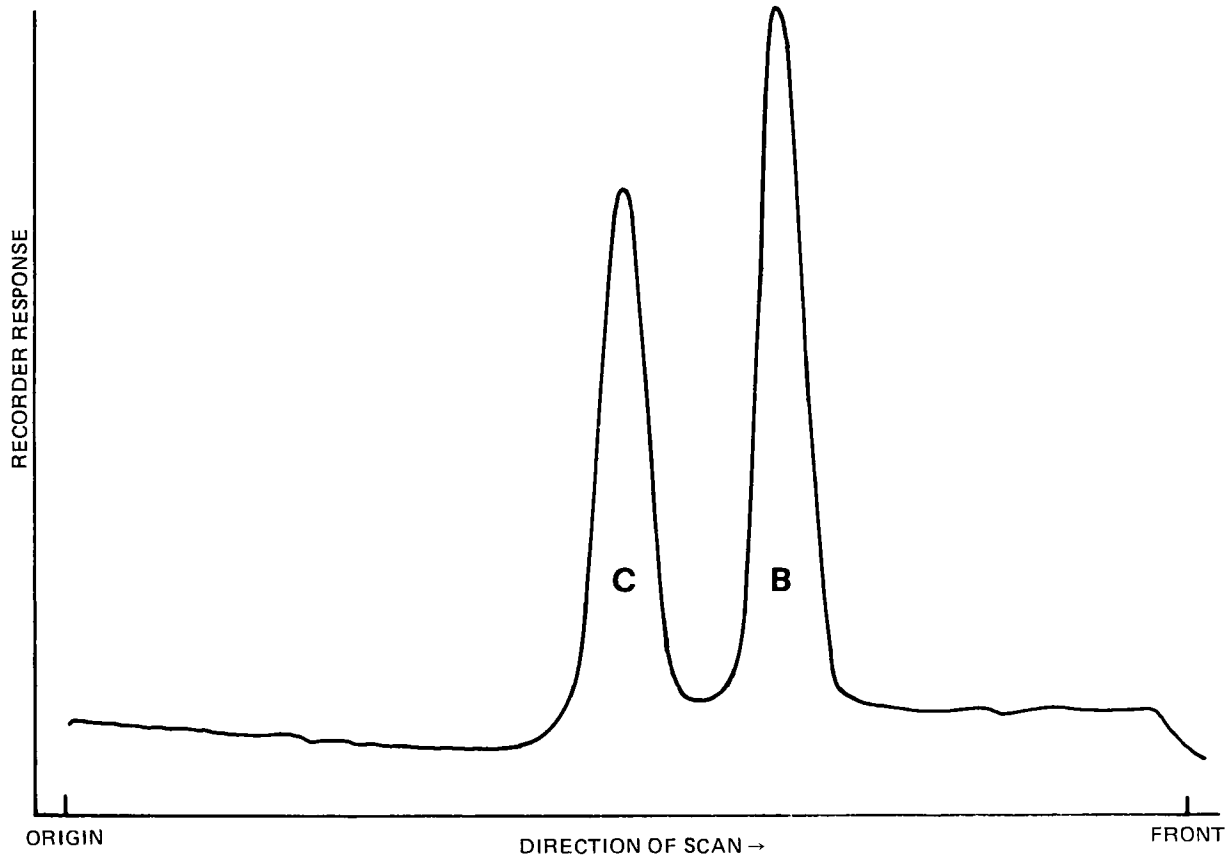

Figure 1—*Thin-layer chromatogram of butaclamol (B) and butaclamol* cis*-isomer (C).*

[1] M. Cayen, Department of Biochemistry, Ayerst Research Laboratories, Montreal, Quebec, Canada, unpublished data.

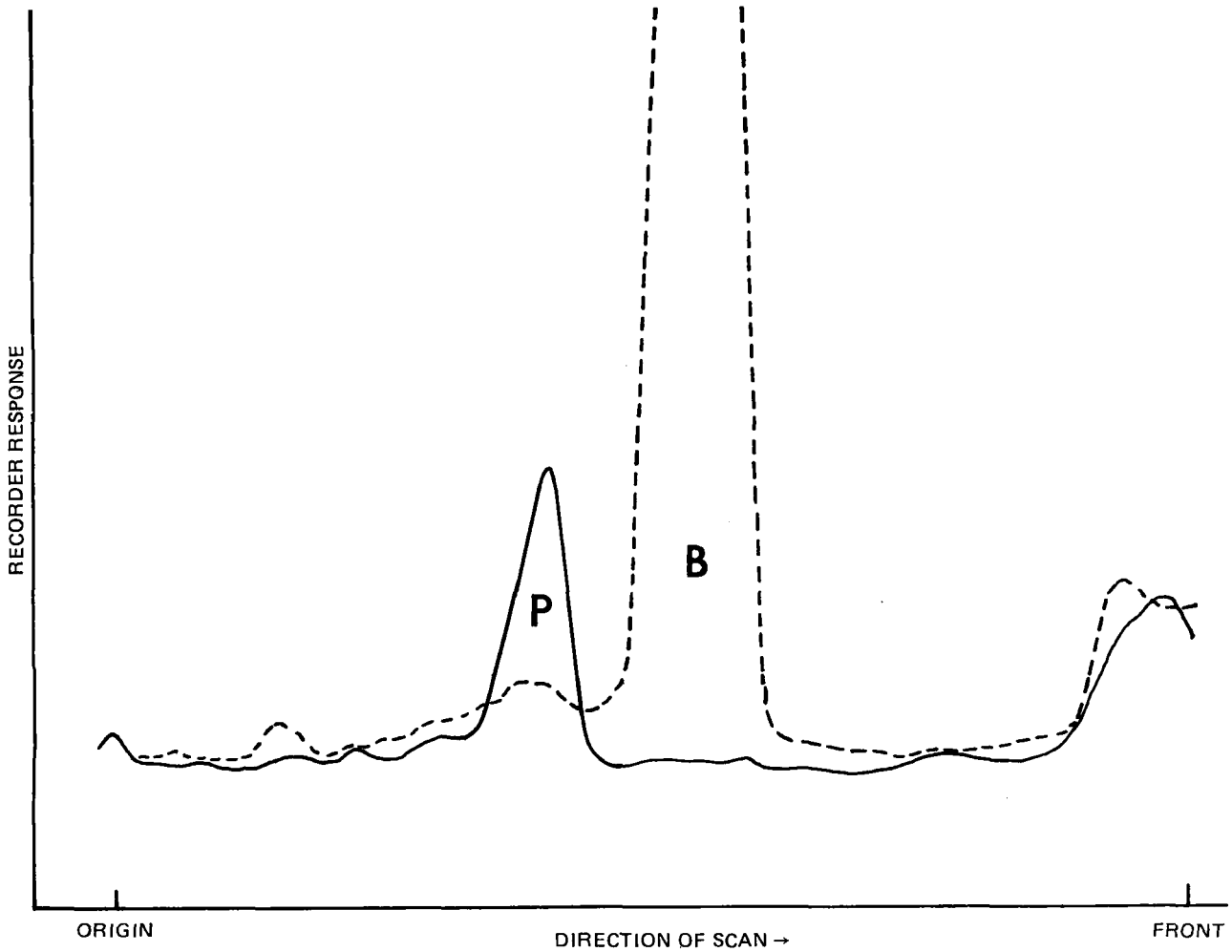

Figure 2—*Thin-layer chromatogram of butaclamol before and after reagent spraying. Key: —, before; - - -, after; P, oxidation products; and B, butaclamol.*

Although fluorescence behavior of *N*-heterocycles is not predictable, generally fluorescence can be observed where the influence of the lone electron pair of the nitrogen atom is negated in some way (2). For example, quinoline is nonfluorescent in neutral solution. However, in acid it has moderate fluorescence, presumably as a result of nitrogen atom lone pair protonation. To obtain the sensitivity needed for the anticipated serum concentration, a TLC procedure was developed to include oxidation on the plate.

Various oxidizing reagent sprays have been described (3). Several different sprays were evaluated with butaclamol, and the one giving the optimum response and stability was selected. The minimum quantifiable amount of butaclamol was 10 ng/spot; thus, this method could be used to quantitate 5 ng or less of drug/ml of serum.

EXPERIMENTAL

Reagents and Materials—TLC plates (20 × 20 cm) of silica gel[2] 60 F-254 with fluorescent indicator were used. All solvents and reagents were of analytical reagent grade, except for formic acid[3] (97%, practical) and zinc chloride[4] (dry, granular, ACS grade).

Developing Solvent System for TLC—A mixture of chloroform–ethyl acetate–ethanol–formic acid (36:36:25:3) was prepared and used in a saturated development chamber.

Fluorescence-Inducing Reagent Spray—Eighty milliliters of distilled water and 60 ml of hydrochloric acid were combined with stirring. When the solution cooled to room temperature, 20 ml of nitric acid, 1.5 g of manganese dioxide, and 1.5 g of zinc chloride were added and stirred for 30 min. The solution was then filtered with suction through a medium pore, sintered-glass funnel and transferred to a spray bottle. The solution was yellow initially but faded with time. This change had no apparent effect on the sensitivity of the spray, which was stable for at least 2 weeks.

Extraction—Five milliliters of serum and 10 ml of cyclohexane were shaken in a glass-stoppered centrifuge tube for 15 min and centrifuged; then 8 ml of the organic phase was removed to a clean tube. Ten milliliters of cyclohexane was again added to the serum, and the procedure was repeated with 10 ml of cyclohexane removed and combined with the initial extract. The combined extracts were evaporated to dryness under nitrogen at 50°[5].

To determine the extraction recovery obtained by this procedure, a known amount of the drug was spiked in human serum, extracted, and analyzed. Two extractions were required to minimize variability and to optimize recovery of butaclamol.

Chromatography and Detection—The extract residue was dissolved in 100 μl of cyclohexane by gently swirling the tube for about 30 sec. A 40-μl aliquot was taken and spotted in a prescored 1-cm TLC plate channel. Appropriate standards had been previously applied to separate channels.

The plate was developed in a saturated chamber until solvent

[2] E. Merck.
[3] Eastman Chemical.
[4] Fisher Scientific.

[5] N-Evap, Organomation Associates.

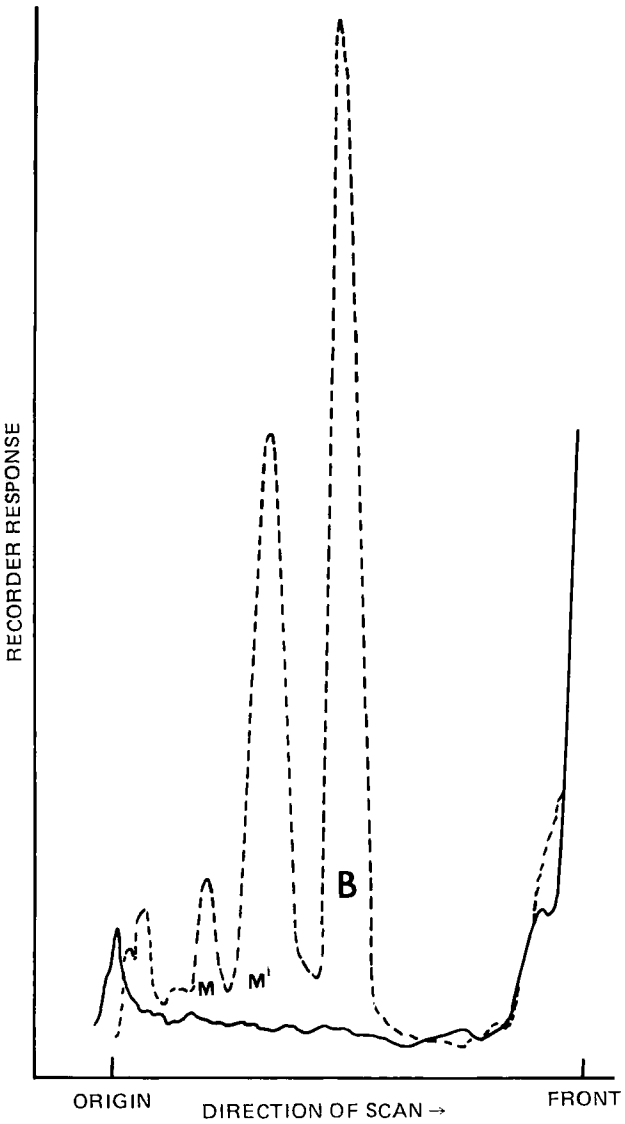

Figure 3—*Thin-layer chromatograms of serum samples from a dog where butaclamol corresponds to 54 ng/ml. Key: —, 0 hr; - - -, 2 hr; M and M', apparent metabolites; and B, butaclamol.*

front migration was about 16 cm, which took about 1 hr. The plate was then oven dried at 110° for 5 min, cooled briefly at room temperature, and finally sprayed. When saturated with spray, the plate was reheated at 110° for 30 min to induce oxidation.

Quantitation—The plates were scanned by spectrodensitometry[6] in the fluorescence mode. The excitation wavelength was 360 nm, and the emission wavelength was 710 nm. The quantitation of the unknown samples was based on a calibration curve obtained with a set of known reference samples. The observed chromatogram peak areas[7] were plotted against nanograms of reference sample applied to a given channel.

Animal Experiment—To assess the applicability of the assay method, a beagle dog, ~10 kg, was given 4 mg iv of butaclamol in 10 ml of 5% ethanol–water. At suitable time intervals before and after dosing, a 10-ml sample of blood was drawn, allowed to clot, and centrifuged. The serum was immediately frozen to await analysis.

Human Experiment—Five healthy male subjects between the ages of 18 and 55, with body weights between 45 and 90 kg and of a height proportional to size, were selected for study. A capsule dosage form containing 16 mg of butaclamol was administered, and a series of blood samples were drawn over the first 12 hr after dosing, with blank samples at zero time.

[6] Model SD3000, Schoeffel Instrument Corp.
[7] Honeywell recorder, Electronik 194, with disk integrator.

Table I—Recovery of Butaclamol from Spiked Human Serum

Concentration of Butaclamol in Spiked Sample, ng/ml	Concentration of Butaclamol Recovered, ng/ml	Recovery, % Butaclamol
10.0	9.2	92
10.0	9.2	92
10.0	9.0	90
10.0	9.5	95
10.0	10.2	102
20.0	19.4	97
20.0	19.4	97
20.0	18.8	94
20.0	17.2	86
30.0	28.1	94
30.0	27.6	92
30.0	29.1	97
30.0	27.3	91

RESULTS

Specificity—The specificity of the TLC separation was reflected by the observed baseline separation of butaclamol (I) from its *cis*-isomer (II) (Fig. 1) and from its oxidation products (Fig. 2). These oxidation products also could be distinguished from butaclamol by their natural fluorescence, observed prior to detection with the oxidizing spray reagent.

The natural fluorescence of the oxidation products and their higher polarity (low TLC R_f) may be due to a quaternary amine structure (III and IV) and unsaturation of the heterocyclic ring. Such structures were previously prepared and identified as oxidation products of related compounds of this series[8]. Oxidation on the TLC plate caused both increases and decreases in oxidation product fluorescence but a dramatic increase in the fluorescence for butaclamol (Fig. 2).

Several oxidizing sprays including potassium permanganate, hydrogen peroxide, and nitrohydrochloric acid were evaluated. All seemed to induce fluorescence of butaclamol. However, the selected reagent spray appeared to give the highest degree of induction with the best consistency and experimental ease.

A further demonstration of the specificity of the TLC separation is shown in Fig. 3. The chromatogram of blank dog serum is compared to that obtained for a 2-hr serum sample. Clearly, butaclamol was well separated from both serum components and two apparent metabolites, M and M'.

Calibration Line, Sensitivity, and Recovery—The lowest detectable amount of butaclamol was 2 ng/spot. Since an area under

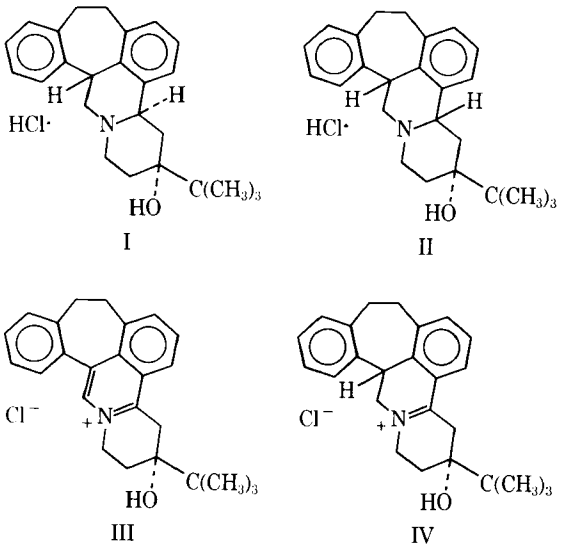

[8] L. Humber, Department of Chemistry, Ayerst Research Laboratories, Montreal, Quebec, Canada, unpublished data.

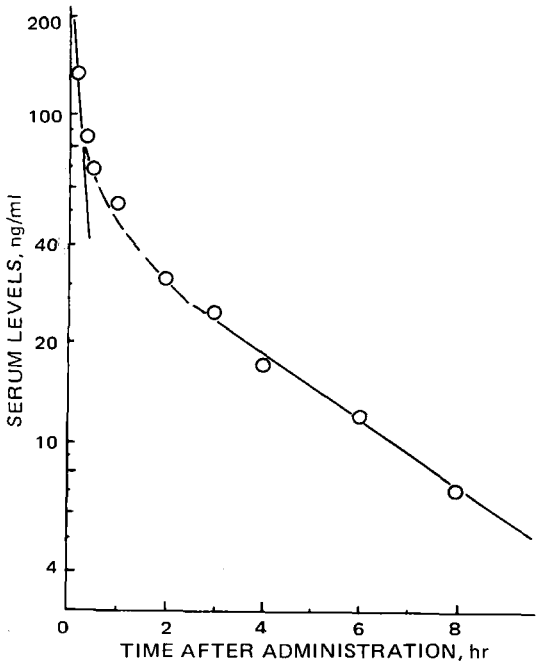

Figure 4—*Serum levels of butaclamol in a dog after intravenous administration of 4 mg. The half-life estimated for the β-phase was 3.0 hr.*

a peak of 10 relative area units can be integrated with good reproducibility, the lowest quantifiable amount was 10 ng/spot. The amount is equivalent to 5 ng/ml of serum concentration when a 40-μl sample is applied. Application of larger sample volumes would give a lower sensitivity limit. Five TLC plate spot applications ranging from 11 to 99 ng/spot gave the following calibration line: $\hat{X} = 12.50 + 3.227Y$, where $\hat{X}$ = estimated amount of butaclamol in nanograms per spot, and Y = observed relative peak area. The mean deviation from the regression line was 8.945, and the reproducibility expressed by $Syx/\bar{Y}$ was 4.71%.

A representative recovery experiment was carried out using 13 human serum samples spiked with three different known quantities of butaclamol (Table I). The mean recovery and standard deviation were 94 ± 4% with the range of 86–102%.

Serum Levels in Dog—The applicability of the assay method was tested with a dog. The serum concentration of butaclamol after administration of 4 mg iv is shown in Fig. 4. A biexponential decay with a half-life of 3.0 hr for the β-phase was observed.

Serum Levels in Humans—Mean serum butaclamol concentrations after a 16-mg oral administration in five healthy human volunteers are given in Fig. 5. A half-life for the β-phase was estimated to be 3 hr and was similar to the findings in dogs.

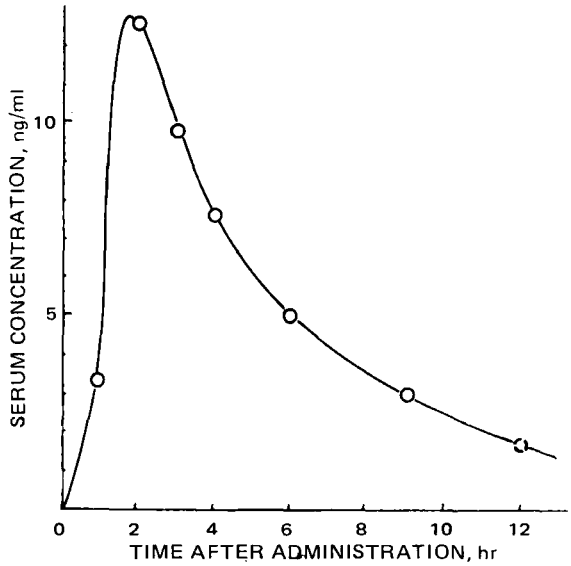

Figure 5—*Mean serum butaclamol concentration in five human volunteers after oral administration of 16 mg.*

REFERENCES

(1) F. T. Bruderlein, L. G. Humber, and K. Voith, *J. Med. Chem.*, **18**, 185(1975).

(2) E. Wehry and L. Rogers, "Fluorescence and Phosphorescence Analysis," Wiley, New York, N.Y., 1966, p. 92.

(3) "Thin Layer Chromatography," E. Stahl, Ed., Springer-Verlag, New York, N.Y., 1965.

ACKNOWLEDGMENTS AND ADDRESSES

Received May 7, 1975, from the *Pharmaceutical and ‡Analytical Research and Development Divisions, Ayerst Laboratories Inc., Rouses Point, NY 12979, and the §Department of Clinical Pharmacology, Ayerst, McKenna & Harrison, Ltd., Montreal, P.Q., Canada.

Accepted for publication June 16, 1975.

The authors gratefully acknowledge the assistance of Dr. B. Downey in the animal experiments and Dr. D. Chin and Dr. M. Kraml in the preparation and analysis of serum samples. They also thank R. Anstey, G. Boyden, J. Brisson, C. Carney, and R. DeAngelis for technical assistance and P. Schurman for the preparation of the figures.

ˣ To whom inquiries should be directed.

Bioavailability Assessment under Quasi- and Nonsteady-State Conditions II: Study Designs

K. C. YEH ˣ and K. C. KWAN

Abstract □ The flexibility of bioavailability assessment at quasi- and nonsteady state is demonstrated by systematically removing experimental constraints from the study design. Mathematical expressions are derived to describe each design variation. From the resultant solutions, it is evident that the proposed method can accommodate nonuniformities in dose, dosage interval, dosage regimen, dosing cycle, sampling interval, plasma half-life, washout period, and protocol adherence. Nominal requirements for the method are linear kinetics and mean plasma concentrations estimated over time intervals beginning and ending in the log–linear region.

Keyphrases □ Bioavailability—assessment under quasi- and nonsteady-state conditions, mathematical expressions, practical alternatives in study design □ Drug disposition—bioavailability assessment under quasi- and nonsteady-state conditions, mathematical expressions, practical alternatives in study design

In a previous report (1), the rationale for bioavailability estimations at quasi- and nonsteady state was presented. The advantage of the method over conventional approaches is that it needs neither steady-state plasma levels nor extended washout periods. Equations were derived to permit rigorous examination of the basic premise and underlying assumptions. In practice, however, some modification of these equations usually will be required to accommodate variations in experimental design.

The purpose of this article is to demonstrate the flexibility of the proposed method by considering some practical alternatives in study design. Accordingly, various experimental complexities will be introduced in a systematic manner. The corresponding mathematical expressions will be presented in closed form. The discussion will evolve from a relatively simple situation and will favor solutions in general form so that further extensions can be facilitated.

THEORETICAL: DESIGN VARIATIONS

The following equations were derived (1) on the assumptions that drug disposition obeys linear kinetics and that successive doses are administered during the log–linear region of the plasma concentration curve:

$$\bar{C}p^{(l)} = \bar{C}p^{(ss)}\,(1 - e^{-l\omega\tau}) \qquad \text{(Eq. 1)}$$

$$\bar{C}p^{(ss)} = \frac{F_x D}{\tau\omega V_0} \qquad \text{(Eq. 2)}$$

and:

$$\frac{F_y}{F_x} = \left[\frac{\bar{C}p^{(m+l)}}{\bar{C}p^{(l)}} - e^{-m\omega\tau}\right]\frac{(1 - e^{-l\omega\tau})}{(1 - e^{-m\omega\tau})} \qquad \text{(Eq. 3)}$$

where $\bar{C}p^{(l)}$ is the observed mean plasma concentration during the lth interval following the administration of l doses of formulation x; $\bar{C}p^{(ss)}$ is the mean plasma concentration at steady state, projected from $\bar{C}p^{(l)}$; $\bar{C}p^{(m+l)}$ is the observed mean plasma concentration during the $(m + l)$th dosage interval when l doses of formulation x are followed immediately by m doses of formulation y; τ is the dosage interval; ω is the terminal slope, which is assumed to be constant throughout; V_0 is an operational constant such that the product ωV_0 is equal to body drug clearance; and F_x and F_y are, respectively, the fraction, F, of the dose, D, absorbed from formulations x and y.

Equations 1–3 are descriptive of a simple and perhaps idealized situation, where the dosage interval, τ, is uniformly spaced around the clock, *e.g.*, when τ is equal to 8, 12, or 24 hr. However, when the drug is given more frequently than twice a day, a uniform dosing interval may not always be clinically relevant or compatible with the subject's normal sleeping habits. Thus, whenever feasible, dosing schedules should be modified so as to minimize unnecessary sources of inconvenience and noncompliance in bioavailability studies. Accordingly, alternative expressions to Eqs. 1–3 are needed to accommodate these and other variations in experimental design.

Dosing Intervals—Suppose a drug is given r doses daily with recurring dosage intervals $\tau_1, \tau_2, \ldots, \tau_r$ such that $\tau_1 + \tau_2 + \ldots + \tau_r = 24$ hr. The mean plasma concentrations during the first dosage interval on the Lth day and at steady state can be obtained by summing all administered doses, including the first dose on Day L; *i.e.*:

$$\bar{C}p^{(L,\tau_1)} = \bar{C}p^{(ss,\tau_1)}\left\{1 - \frac{\left[1 + \sum_{j=1}^{r-1}\left(\prod_{i=1}^{j} e^{\omega\tau_i}\right)\right]}{(e^{-24\omega})\left[\sum_{j=1}^{r}\left(\prod_{i=1}^{j} e^{\omega\tau_i}\right)\right]}(e^{-24L\omega})\right\} \qquad \text{(Eq. 4)}$$

and:

$$\bar{C}p^{(ss,\tau_1)} = \frac{FD}{\tau_1\omega V_0}\frac{(1 - e^{-\omega\tau_1})}{(1 - e^{-24\omega})}(e^{-24\omega})\left[\sum_{j=1}^{r}\left(\prod_{i=1}^{j} e^{\omega\tau_i}\right)\right] \qquad \text{(Eq. 5)}$$

where, in general, τ_i's need not be equal to one another[1]. It can be easily verified that Eq. 5 reduces to Eq. 2 when all τ_i's are equal. As an example of Eq. 5, consider a qid regimen in which doses are administered at 7 am, 11 am, 5 pm, and 10 pm. With $\tau_1 = 4$ hr, $\tau_2 = 6$ hr, $\tau_3 = 5$ hr, and $\tau_4 = 9$ hr:

$$\bar{C}p^{(ss,\tau_1)} = \frac{FD}{4\omega V_0}\frac{(1 - e^{-4\omega})}{(1 - e^{-24\omega})}[1 + e^{-20\omega} + e^{-14\omega} + e^{-9\omega}] \qquad \text{(Eq. 6)}$$

Obviously, the relative bioavailability between two formulations may be studied at nonsteady state in many ways. One of the simpler designs calls for estimations of both the mean plasma concentration and the terminal slope at the end of each treatment period. A typical dosing sequence in such a study is schematically depicted in Fig. 1*a*. During Period I, which lasts for L days, the standard formulation, s, is given r doses daily according to a prescribed regimen for $(L - 1)$ days, but only the first dose is given on Day L. Appropriate plasma samples are taken on Day L to permit estimations of $\bar{C}p^{(\mathrm{I},\tau_1)}$, the average plasma level during interval τ_1, and of ω_I, the terminal slope.

During Period II, which begins on Day $(L + 1)$ and lasts for M days, the same dosage regimen of r daily doses of formulation x is given for $(M - 1)$ days and then only the first dose on Day M. Appropriate estimates of $\bar{C}p^{(\mathrm{II},\tau_1)}$ and of ω_II are obtained from plasma samples taken on Day M. The purpose in giving only one dose on Day L of Period I and on Day M of Period II is to permit more extensive sampling of the terminal slopes. The elapsed time between the last dose of Treatment I and the first dose of Treatment II is defined as the washout period, which in this case is 1 day.

[1] In these and ensuing equations, the summation term is defined to be identically zero and the product term identically unity whenever the upper limit of the running index is smaller than the lower limit; *i.e.*: $\Sigma_a^b \equiv 0$ and $\Pi_a^b \equiv 1$, if $b < a$.

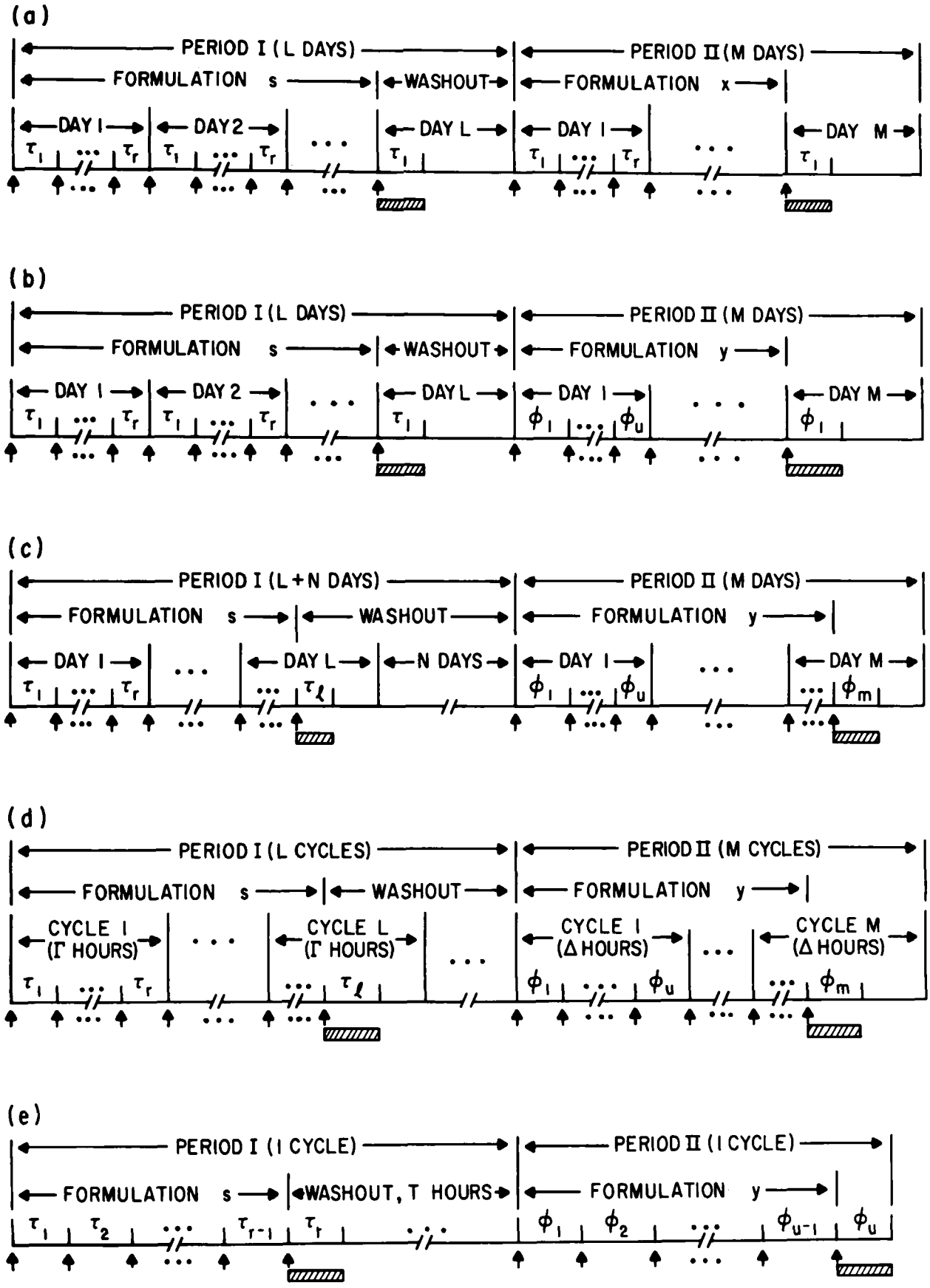

Figure 1—*Dosing schemes. Vertical arrows (↑) denote time of administration. Average plasma levels are determined in the last dosing interval of each treatment (shown in shaded area).*

By combining Eqs. 4 and 5, the mean plasma concentration during the first dosage interval, τ_1, on Day L becomes:

$$\bar{C}p^{(I,\tau_1)} = \frac{F_I D(1 - e^{-\omega_I \tau_1})}{\tau_1 \omega_I V_0 (1 - e^{-24\omega_I})} [R_1] \quad \text{(Eq. 7)}$$

where F_I is the fraction of the dose, D, absorbed from formulation s in Period I; ω_I is the observed terminal slope on Day L; and:

$$[R_1] = (e^{-24\omega_I}) \left[\sum_{j=1}^{r} \left(\prod_{i=1}^{j} e^{\omega_I \tau_i} \right) \right] - (e^{-24L\omega_I}) \left[1 + \sum_{j=1}^{r-1} \left(\prod_{i=1}^{j} e^{\omega_I \tau_i} \right) \right] \quad \text{(Eq. 8)}$$

The mean plasma level during τ_1 on Day M of Period II, $\bar{C}p^{(II,\tau_1)}$, is obtained by summing the residual contributions from formulation s during Period I, $\bar{C}p^s$, and the cumulative effects of formulation x during Period II, $\bar{C}p^x$:

$$\bar{C}p^s = \frac{F_I D[R_1]}{\tau_1 V_0 (1 - e^{-24\omega_I})} [e^{-24(\omega_I + M\omega_{II} - \omega_{II})}] \int_0^{\tau_1} e^{-\omega_{II} t'} dt' = \frac{F_I D[R_1] (1 - e^{-\omega_{II}\tau_1})}{\tau_1 \omega_{II} V_0 (1 - e^{-24\omega_I})} [e^{-24(\omega_I + M\omega_{II} - \omega_{II})}] \quad \text{(Eq. 9)}$$

and:

$$\bar{C}p^x = \frac{F_{II} D[R_2]}{\tau_1 V_0 (1 - e^{-24\omega_{II}})} \int_0^{\tau_1} e^{-\omega_{II} t'} dt' = \frac{F_{II} D[R_2] (1 - e^{-\omega_{II}\tau_1})}{\tau_1 \omega_{II} V_0 (1 - e^{-24\omega_{II}})} \quad \text{(Eq. 10)}$$

where t' is time from the last dose, *i.e.*, the morning dose on Day M of Period II; ω_{II} is the observed terminal slope; F_{II} denotes the fraction of dose D absorbed from formulation x during Period II; and:

$$[R_2] = (e^{-24\omega_{II}}) \left[\sum_{j=1}^{r} \left(\prod_{i=1}^{j} e^{\omega_{II} \tau_i} \right) \right] - (e^{-24M\omega_{II}}) \left[1 + \sum_{j=1}^{r-1} \left(\prod_{i=1}^{j} e^{\omega_{II} \tau_i} \right) \right] \quad \text{(Eq. 11)}$$

By combining Eqs. 9 and 10:

$$\bar{C}p^{(II,\tau_1)} = \frac{D(1 - e^{-\omega_{II}\tau_1})}{\tau_1 \omega_{II} V_0} \times \left\{ \frac{F_{II}[R_2]}{(1 - e^{-24\omega_{II}})} + \frac{F_I[R_1] [e^{-24(\omega_I + M\omega_{II} - \omega_{II})}]}{(1 - e^{-24\omega_I})} \right\} \quad \text{(Eq. 12)}$$

The bioavailability of formulation x relative to formulation s is given by Eq. 13, which is obtained by rearranging the ratio of Eq. 12 to Eq. 7:

$$\left(\frac{F_{II}}{F_I}\right)_{s/x} = \frac{[R_1](1 - e^{-24\omega_{II}})}{[R_2](1 - e^{-24\omega_I})} \times \left\{ \frac{\bar{C}p^{(II,\tau_1)} \omega_{II} (1 - e^{-\omega_I \tau_1})}{\bar{C}p^{(I,\tau_1)} \omega_I (1 - e^{-\omega_{II}\tau_1})} - e^{-24(\omega_I + M\omega_{II} - \omega_{II})} \right\} \quad \text{(Eq. 13)}$$

where the subscript s/x denotes the fact that formulation s is given in Period I and formulation x in Period II (Fig. 1*a*). The last term in Eq. 13 may be identified as the residue factor, because it reflects the effect of Treatment I on the observed mean plasma level, $\bar{C}p^{(II,\tau_1)}$. This term approaches zero as M approaches infinity, *i.e.*, at steady state. The ratio $\omega_{II}(1 - e^{-\omega_I\tau_1})/\omega_I(1 - e^{-\omega_{II}\tau_1})$ can be identified as a correction factor for the observed mean plasma levels in the event that the two terminal slopes are not identical.

Implicit in Eq. 13 is the assumption that V_0 remains constant but the terminal slope ω may change between treatments. For the special case of $L = M$ and $\omega_I = \omega_{II}$, Eq. 13 reduces to:

$$\left(\frac{f_{II}}{F_I}\right)_{s/x} = \frac{\bar{C}p^{(II,\tau_1)}}{\bar{C}p^{(I,\tau_1)}} - e^{-24M\omega} \quad \text{(Eq. 14)}$$

In Eqs. 7–13, ω_I and ω_{II} are used in the context that they represent the mean terminal slopes of their respective treatment periods. If $\omega_I \neq \omega_{II}$, possible causes of the observed difference are numerous and usually unknown. Among them are systematic changes arising from specific interactions between the drug and the host, random fluctuations in drug disposition, experimental error, and differences in absorption rate between formulations, for in theory at least the terminal slope may be the manifestation of a slow, first-order absorption rate.

In any event, it should be recognized that the use of ω_I and ω_{II} represents a simplified and possibly biased correction, which may result in an overestimation or an underestimation of the ratio (F_{II}/F_I). This problem of varying terminal slopes is, however, not unique with the proposed method but also pertains to steady-state comparisons. To compensate for these effects, a balanced crossover comparison of the treatments is desirable. Therefore, subsequent discussion assumes that each study design is a crossover comparison.

In a two-way crossover study, Eq. 13 is applicable to half of the subjects who received the depicted (Fig. 1*a*) sequence of formulation s for L days in Period I followed by formulation x for M days in Period II. For subjects in the complementary group who received formulation x for L days in Period I and formulation s for M days in Period II, the resultant bioavailability ratio becomes $(F_{II}/F_I)_{x/s}$. This result does not alter the general form of Eqs. 7–14 but merely means that the identification of formulations s and x with Periods I and II is reversed, *i.e.*:

$$\left(\frac{F_{II}}{F_I}\right)_{s/x} = \frac{F_x}{F_s} \quad \text{(Eq. 15)}$$

and:

$$\left(\frac{F_{II}}{F_I}\right)_{x/s} = \frac{F_s}{F_x} \quad \text{(Eq. 16)}$$

In addition, more estimates of ω_I and ω_{II} may be included in the design to observe better their time courses of change throughout the study. This may entail skipping dosages more than once per treatment. Alternatively, since successive doses are to be administered during the log-linear phase, it may be sufficiently reassuring to include a few strategically placed plasma sample points at the end of some selected dosage intervals.

Dosages and Dosage Regimens—Sometimes, bioavailability studies are performed to assess new formulations that differ from the standard formulation not only in potency but also in dosage regimen. Often, the new formulation may be one designed to deliver the same daily dosage at less frequent intervals.

Suppose formulation y is to be compared with formulation s in a crossover study. One dosing sequence in such a study is shown in Fig. 1*b*. During Period I, which lasts for L days, r doses of formulation s of potency D_I are given each day for $(L - 1)$ days, but only the first dose is administered on Day L. During Period II, which begins on Day $(L + 1)$, u doses of formulation y of potency D_{II} are given daily for $(M - 1)$ days, and again only one dose is given on Day M. In general, u may not be equal to r. Mean plasma concentrations and terminal slopes are determined on the last day of each treatment; the washout period is again 24 hr.

The expression for $\bar{C}p^{(I,\tau_1)}$ is analogous to Eq. 7, *i.e.*:

$$\bar{C}p^{(I,\tau_1)} = \frac{F_I D_I (1 - e^{-\omega_I \tau_1})[R_1]}{\omega_I \tau_1 V_0 (1 - e^{-24\omega_I})} \quad \text{(Eq. 17)}$$

where the subscript I is identified with formulation s. Also by analogy to Eq. 13 and defining the daily dosing intervals for formulation y as $\phi_1, \phi_2, \ldots, \phi_u$ such that $\phi_1 + \phi_2 + \ldots + \phi_u = 24$ hr, it can be shown that the mean plasma level, $\bar{C}p^{(II,\phi_1)}$, during the first dosage interval ϕ_1 on Day M of Period II is:

$$\bar{C}p^{(II,\phi_1)} = \frac{(1 - e^{-\omega_{II}\phi_1})}{\omega_{II}\phi_1 V_0} \times \left\{ \frac{F_{II} D_{II}[R_3]}{(1 - e^{-24\omega_{II}})} + \frac{F_I D_I[R_1]}{(1 - e^{-24\omega_I})} e^{-24(\omega_I + M\omega_{II} - \omega_{II})} \right\} \quad \text{(Eq. 18)}$$

where the subscript II is now identified with formulation y, and:

$$[R_3] = (e^{-24\omega_{II}}) \left[\sum_{j=1}^{u} \left(\prod_{i=1}^{j} e^{\omega_{II}\phi_i} \right) \right] - (e^{-24M\omega_{II}}) \left[1 + \sum_{j=1}^{u-1} \left(\prod_{i=1}^{j} e^{\omega_{II}\phi_i} \right) \right] \quad \text{(Eq. 19)}$$

Combining Eqs. 17 and 18 gives:

$$\left(\frac{F_{II}}{F_I}\right)_{s/y} = \frac{D_I[R_1](1 - e^{-24\omega_{II}})}{D_{II}[R_3](1 - e^{-24\omega_I})} \times \left\{ \frac{\bar{C}p^{(II,\phi_1)}(\phi_1\omega_{II})(1 - e^{-\omega_I\tau_1})}{\bar{C}p^{(I,\tau_1)}(\tau_1\omega_I)(1 - e^{-\omega_{II}\phi_1})} - e^{-24(\omega_I + M\omega_{II} - \omega_{II})} \right\} \quad \text{(Eq. 20)}$$

It is evident that Eq. 13 is a special case of Eq. 20 where $D_I = D_{II}$ and that a common daily dosage regimen is used for formulations s and y. The correction factor now includes the ratio ϕ_1/τ_1, which compensates for possible differences in the length of sampling intervals between treatments.

For subjects in the complementary group who received formula-

tion y (u daily doses) during Period I and formulation s (r daily doses) during Period II, the corresponding solution is:

$$\left(\frac{F_{II}}{F_I}\right)_{y/s} = \frac{D_I[R_4](1-e^{-24\omega_{II}})}{D_{II}[R_5](1-e^{-24\omega_I})} \times \left\{\frac{\bar{C}p^{(II,\tau_1)}(\tau_1\omega_{II})(1-e^{-\omega_I\phi_1})}{\bar{C}p^{(I,\phi_1)}(\phi_1\omega_I)(1-e^{-\omega_{II}\tau_1})} - e^{-24(\omega_I+M\omega_{II}-\omega_{II})}\right\} \quad \text{(Eq. 21)}$$

where:

$$[R_4] = (e^{-24\omega_I})\left[\sum_{j=1}^{u}\left(\prod_{i=1}^{j} e^{\omega_I\phi_i}\right)\right] - (e^{-24L\omega_I})\left[1+\sum_{j=1}^{u-1}\left(\prod_{i=1}^{j} e^{\omega_I\phi_i}\right)\right] \quad \text{(Eq. 22)}$$

and:

$$[R_5] = (e^{-24\omega_{II}})\left[\sum_{j=1}^{r}\left(\prod_{i=1}^{j} e^{\omega_{II}\tau_i}\right)\right] - (e^{-24M\omega_{II}})\left[1+\sum_{j=1}^{r-1}\left(\prod_{i=1}^{j} e^{\omega_{II}\tau_i}\right)\right] \quad \text{(Eq. 23)}$$

The quantity $[R_i]$ can be defined as the regimen factor, which serves to maintain proper accounting of the dosing sequence. More specifically, the regimen factor tracks the following: the total number of doses per treatment, the number of doses per day, the order among dosing intervals within the day, the number of days per treatment, and the order in which the treatments are administered. The systematic changes in $[R_i]$ among Eqs. 8, 11, 19, 22, and 23 should be noted in relation to the corresponding variations in dosing sequence. In subsequent discussion, these regimen factors will assume added significance as the complexity in experimental design increases.

Sampling Interval and Washout Period—Equations 4–23 were derived to accommodate experimental designs where estimates of mean plasma concentrations are confined to the first dosage interval on the last day of each treatment period and where the elapsed time between the last dose of the first treatment and the first dose of the second treatment is 24 hr. Expressions with greater general utility will be needed when neither condition prevails.

The general solution for the mean plasma concentration during interval τ_k on Day L following the repeated administration of r daily doses with recurring intervals $\tau_1, \tau_2, \ldots, \tau_k, \ldots, \tau_r$ may be represented by:

$$\bar{C}p^{(L,\tau_k)} = \bar{C}p^{(ss,\tau_k)}\left[1-\frac{[G]}{[H]}\right] \quad \text{(Eq. 24)}$$

where:

$$\bar{C}p^{(ss,\tau_k)} = \frac{FD[H](1-e^{-\omega\tau_k})}{\omega\tau_k V_0(1-e^{-24\omega})} \quad \text{(Eq. 25)}$$

$$[G] = (e^{-24L\omega})\left(\prod_{i=1}^{k-1} e^{-\omega\tau_i}\right)\left[1+\sum_{j=1}^{r-1}\left(\prod_{i=1}^{j} e^{\omega\tau_i}\right)\right] \quad \text{(Eq. 26)}$$

and:

$$[H] = (e^{\omega\tau_k})\left[\sum_{j=1}^{k}\left(\prod_{i=j}^{k} e^{-\omega\tau_i}\right)\right] + (e^{-24\omega})\left[\sum_{j=k}^{r-1}\left(\prod_{i=k}^{j} e^{\omega\tau_i}\right)\right] \quad \text{(Eq. 27)}$$

The working forms of Eqs. 26 and 27 are usually much simpler than their general forms. For example, the expressions for the case of $r = 3$ and $k = 2$ are:

$$[G] = (e^{-24L\omega})(1+e^{-\omega\tau_1}+e^{\omega\tau_2}) \quad \text{(Eq. 28)}$$

and:

$$[H] = 1+e^{-\omega\tau_1}+e^{-\omega(\tau_1+\tau_3)} \quad \text{(Eq. 29)}$$

It can be verified that Eqs. 24 and 25 reduce to Eqs. 4 and 5 when $k = 1$.

Suppose the experimental design includes a dosing scheme like that shown in Fig. 1c. As in Fig. 1b, formulation s is given in Period I and formulation y in Period II. However, instead of terminating Treatment I with the first dose on Day L, l doses of formulation s are administered on Day L. The mean plasma level $\bar{C}p^{(I,\tau_l)}$ is determined during the interval τ_l. Similarly, m doses of formulation y are given on Day M of Period II, and the mean plasma level $\bar{C}p^{(II,\phi_m)}$ is determined over ϕ_m. Terminal slopes ω_I and ω_{II} are estimated as before. Thus, if both treatment periods begin at the same clock hour and $l > 1$, the washout period is less than 24 hr when Treatment II begins on Day $(L+1)$.

On the other hand, the initiation of Treatment II may be postponed for N days (Fig. 1c) and the washout period is extended to $(24N + \Sigma_{i=l}^{r}\tau_i)$ hr. Under these circumstances, the bioavailability ratio is given by:

$$\left(\frac{F_{II}}{F_I}\right)_{s/y} = \frac{D_I[R_6](1-e^{-24\omega_{II}})}{D_{II}[R_7](1-e^{-24\omega_I})} \times \left\{\frac{\bar{C}p^{(II,\phi_m)}}{\bar{C}p^{(I,\tau_l)}}\frac{\omega_{II}\phi_m(1-e^{-\omega_I\tau_l})}{\omega_I\tau_l(1-e^{-\omega_{II}\phi_m})} - W\right\} \quad \text{(Eq. 30)}$$

where:

$$W = e^{-24(N\omega_I+M\omega_{II}-\omega_{II})}\left[\prod_{i=l}^{r} e^{-\omega_I\tau_i}\right]\left[\prod_{i=1}^{m-1} e^{-\omega_{II}\phi_i}\right] \quad \text{(Eq. 31)}$$

$$[R_6] = (e^{\omega_I\tau_l})\left[\sum_{j=1}^{l}\left(\prod_{i=j}^{l} e^{-\omega_I\tau_i}\right)\right] + (e^{-24\omega_I})\left[\sum_{j=l}^{r-1}\left(\prod_{i=l}^{j} e^{\omega_I\tau_i}\right)\right] - (e^{-24L\omega_I})\left(\prod_{i=1}^{l-1} e^{-\omega_I\tau_i}\right)\left[1+\sum_{j=1}^{r-1}\left(\prod_{i=1}^{j} e^{\omega_I\tau_i}\right)\right] \quad \text{(Eq. 32)}$$

and:

$$[R_7] = (e^{\omega_{II}\phi_m})\left[\sum_{j=1}^{m}\left(\prod_{i=j}^{m} e^{-\omega_{II}\phi_i}\right)\right] + (e^{-24\omega_{II}})\left[\sum_{j=m}^{u-1}\left(\prod_{i=m}^{j} e^{\omega_{II}\phi_i}\right)\right] - (e^{-24M\omega_{II}})\left(\prod_{i=1}^{m-1} e^{-\omega_{II}\phi_i}\right)\left[1+\sum_{j=1}^{u-1}\left(\prod_{i=1}^{j} e^{\omega_{II}\phi_i}\right)\right] \quad \text{(Eq. 33)}$$

In this case, the regimen factor $[R_i]$ has the added responsibility of tracking dosing intervals over which the mean plasma concentrations are determined. In general, $[R_i]$ represents the difference between $[G]$ and $[H]$ after appropriate substitutions therein.

The reason for skipping doses on Day L is to facilitate estimations of the terminal slope. Ideally, this elapsed time, or washout period, should only be long enough to provide a satisfactory estimate of ω. In the situations depicted in Figs. 1b and 1c, the difference in the length of the washout period is manifested in the terms $e^{-24\omega_I}$ and $(e^{-24N\omega_I})$ $[\Pi_{i=l}^{r} e^{-\omega_I\tau_i}]$ in Eqs. 20 and 31, respectively. This can be easily verified by noting that when $l = 1$ and $N = 0$, the two terms are identical:

$$\prod_{i=1}^{r} e^{-\omega_I\tau_i} = e^{-24\omega_I} \quad \text{(Eq. 34)}$$

Equation 30 is the most general form for the cases discussed so far. Experimental parameters and observed variables required for its application are summarized in Table I. The choice of design parameters is large, even in a simple two-way crossover study. For example, if $D_I = 2$ mg, $D_{II} = 5$ mg, $L = M = 2$ days, $N = 1$ day, $r = 2$, $u = l = m = 1$, $\tau_1 = 10$ hr, $\omega_I = 0.05$ hr^{-1}, $\omega_{II} = 0.06$ hr^{-1}, $\bar{C}p^{(I,\tau_1)} = 4$ ng/ml, and $\bar{C}p^{(II,\phi_1)} = 5$ ng/ml, it can be verified that the ratio F_{II}/F_I is equal to 1.067.

Dosing Cycles—Up to now, arguments have been developed on the basis that each dosing sequence repeats itself every 24 hr. This assumption is not unreasonable, since most current chronic therapy calls for medication at least once daily. Not coincidentally, in terms of study expedition, more frequent dosing also means that useful plasma concentrations can be attained sooner and study duration can be minimized. With increasing knowledge in chronopharmacology and controlled drug delivery systems, dosing cycles longer or shorter than 24 hr may become more meaningful for some drugs and dosage forms.

Suppose the dosing cycle for formulation s is Γ hr instead of 24 hr and that for formulation y is Δ hr. By reference to Fig. 1d, the mean plasma level of formulation s is estimated over the interval τ_l during the Lth cycle in Period I; the mean plasma level of formulation y is estimated over ϕ_m during the Mth cycle in Period II. The elapsed time between the last dose of treatment s and the first dose of treatment y is T hr. The solution for this design can be obtained by appropriate extensions of Eq. 30:

$$\left(\frac{F_{II}}{F_I}\right)_{s/y} = \frac{D_I[R_8](1-e^{-\Delta\omega_{II}})}{D_{II}[R_9](1-e^{-\Gamma\omega_I})} \times \left\{\frac{\bar{C}p^{(II,\phi_m)}\phi_m\omega_{II}(1-e^{-\omega_I\tau_l})}{\bar{C}p^{(I,\tau_l)}\tau_l\omega_I(1-e^{-\omega_{II}\phi_m})} - W\right\} \quad \text{(Eq. 35)}$$

Table I—Experimental Parameters and Observed Variables Applicable to Fig. 1c and Eq. 31

Parameters and Variables	Period I	Period II
Dosage potency	D_I	D_{II}
Length of period, days[a]	$L + N$	M
Length of cycle, hr	24	24
Number of doses per cycle	r	u
Dosage intervals, hr[b]	$\tau_1, \ldots, \tau_l, \ldots, \tau_r$	$\phi_1, \ldots, \phi_m, \ldots, \phi_u$
Last dose given[c]	lth dose on Day L	mth dose on Day M
Sampling interval, hr	τ_l	ϕ_m
Washout period, hr	$T = 24N + \sum_{i=l}^{r} \tau_i$	—
Terminal slope, hr^{-1}	ω_I	ω_{II}
Average plasma level	$\bar{C}p(I, \tau_l)$	$\bar{C}p(II, \phi_m)$

[a] N is optional; $N \geq 0$. [b] By definition, $\tau_1 + \tau_2 + \ldots + \tau_r = \phi_1 + \phi_2 + \ldots + \phi_u = 24$ hr, and all daily doses are assumed to begin at the same clock hour (*e.g.*, 8 am). [c] $r \geq l \geq 1$; $u \geq m \geq 1$.

where $\Gamma = \tau_1 + \tau_2 + \ldots + \tau_r$, $\Delta = \phi_1 + \phi_2 + \ldots + \phi_u$, and:

$$W = (e^{-\omega_I T}) \left(\prod_{i=1}^{m-1} e^{-\omega_{II}\phi_i} \right) [e^{-\omega_{II}\Delta(M-1)}] \quad \text{(Eq. 36)}$$

$$[R_8] = (e^{\omega_I \tau_l}) \left[\sum_{j=1}^{l} \left(\prod_{i=j}^{l} e^{-\omega_I \tau_i} \right) \right] + (e^{-\Gamma\omega_I}) \left[\sum_{j=l}^{r-1} \left(\prod_{i=l}^{j} e^{\omega_I \tau_i} \right) \right] - (e^{-\Gamma L \omega_I}) \left(\prod_{i=1}^{l-1} e^{-\omega_I \tau_i} \right) \left[1 + \sum_{j=1}^{r-1} \left(\prod_{i=1}^{j} e^{\omega_I \tau_i} \right) \right] \quad \text{(Eq. 37)}$$

$$[R_9] = (e^{\omega_{II}\phi_m}) \left[\sum_{j=1}^{m} \left(\prod_{i=j}^{m} e^{-\omega_{II}\phi_i} \right) \right] + (e^{-\Delta\omega_{II}}) \left[\prod_{j=m}^{u-1} \left(\prod_{i=m}^{j} e^{\omega_{II}\phi_i} \right) \right] - (e^{-\Delta M \omega_{II}}) \left(\prod_{i=1}^{m-1} e^{-\omega_{II}\phi_i} \right) \left[1 + \sum_{j=1}^{u-1} \left(\prod_{i=1}^{j} e^{\omega_{II}\phi_i} \right) \right] \quad \text{(Eq. 38)}$$

Thus, the lengths of dosing cycles also influence the regimen factors, $[R_i]$.

The very idea of a dosing cycle (of whatever length) demands unerring adherence to the prescribed regimen without which steady state can never be achieved and the equations so far developed cannot be applied. Therefore, the requirements for assessing bioavailability at quasi- and nonsteady state apparently are less demanding only with respect to study duration, not in exactitude. Accordingly, on purely pragmatic grounds, it is important that the proposed method accommodate those occasional deviations from perfect adherence to protocol.

Suppose a bioavailability study were to be performed such that Eq. 35 would apply. Suppose further that, in spite of best intentions, the prescribed dosage schedule could not be followed exactly but that the precise time for each dose was duly recorded. Under these circumstances, it is inconceivable that the integrity of the dosing cycles would have been preserved. Nevertheless, estimates of relative bioavailability are still possible by treating the entire Period I as a single dosing cycle for formulation s and treating the entire Period II as a single dosing cycle for formulation y. Mean plasma levels, $\bar{C}p^{(I,\tau_r)}$ and $\bar{C}p^{(II,\phi_u)}$, are determined during the last dosing interval of each treatment. This situation is schematically represented in Fig. 1e. The expression for this scheme represents a special case of Eq. 35, in which $M = L = 1$ with sampling intervals τ_r and ϕ_u. Substituting into Eq. 35 and simplifying give:

$$\left(\frac{F_{II}}{F_I}\right)_{s/y} = \frac{D_I}{D_{II}} [R] \times \left\{ \frac{\bar{C}p^{(II,\phi_u)}(1 - e^{-\omega_I \tau_r})\omega_{II}\phi_u}{\bar{C}p^{(I,\tau_r)}(1 - e^{-\omega_{II}\phi_u})\omega_I \tau_r} - (e^{-\omega_I T}) \left(\prod_{i=1}^{u-1} e^{-\omega_{II}\phi_i} \right) \right\} \quad \text{(Eq. 39)}$$

where:

$$[R] = \frac{\sum_{j=1}^{r} \left(\prod_{i=j}^{r-1} e^{-\omega_I \tau_i} \right)}{\sum_{j=1}^{u} \left(\prod_{i=j}^{u-1} e^{-\omega_{II}\phi_i} \right)} \quad \text{(Eq. 40)}$$

When recalling their intent, the relative simplicity of Eqs. 39 and 40 is ironic. They were derived to accommodate deviations from the prescribed regimen. Nevertheless, they suggest that mean plasma level determinations should always be confined to the last dosing interval of each treatment period and that each treatment period should be considered as a single dosing cycle even though protocol adherence may have been perfect. In practice, this approach should be preferred since the number of doses per treatment period need not be large under quasi- and nonsteady-state conditions.

In some instances, the doses ingested are not uniform throughout a given treatment period. Loading or booster doses may be intentionally given to raise the plasma levels initially or during the sampling interval, or the test subject may try to compensate for doses he or she accidentally missed. In either case, Eqs. 39 and 40 remain useful; their general formats need not be changed so long as all ingested doses are exact multiples of a common unit dose.

The number of terms in the denominator of the regimen factor, $[R]$, is always equal to the number of unit doses ingested within the corresponding treatment period. For example, if a unit dose D_I were to be given at 0, 8, 24, 32, 36, and 48 hr, the numerator of Eq. 40 would contain six terms: $e^{-48\omega_I} + e^{-40\omega_I} + e^{-24\omega_I} + e^{-16\omega_I} + e^{-12\omega_I} + 1$. However, if the doses were taken as one unit, each at 0 and 32 hr and as two units each at 24 and 48 hr, and nothing was taken at 8 and 36 hr, the six terms would become:

$$e^{-48\omega_I} + e^{-24\omega_I} + e^{-24\omega_I} + e^{-16\omega_I} + 1 + 1 = e^{-48\omega_I} + 2e^{-24\omega_I} + e^{-16\omega_I} + 2 \quad \text{(Eq. 41)}$$

Under these conditions, the booster, the loading, or the compensatory doses are merely multiples of unit doses given with zero dosage intervals.

It must be remembered that the proposed method is predicated on the assumption that successive doses are administered during the log-linear phase of plasma decay (1). On closer examination, however, this requirement can be relaxed to the extent that it applies only to the doses over which intervals the mean plasma levels are to be determined. It is not a constraint for all other doses. In other words, given an accurate record of the dosing sequence and its precise timing, it is sufficient that the mean plasma concentrations be determined over dosing intervals beginning and ending in the log-linear region. The justification for this conclusion is a consequence of the principles of superposition wherein the manifestation of log-linear plasma decay represents total accountability of the cumulative effects of all preceding dosages. The more restrictive requirement that successive doses must be administered during the log-linear region (1) is necessary only when dosage intervals are uniform.

Similarly, the constraint relative to continuing absorption during the log-linear phase (1) was necessary only because the relevant equations ignored the possibility that the terminal half-lives might differ between treatments. This constraint does not apply when estimates of ω are made in each treatment period.

SUMMARY AND CONCLUSIONS

An attempt has been made to examine the effect of potential constraints on the design of bioavailability studies under quasi- and nonsteady-state conditions. Given linear kinetics and mean plasma levels estimated over time intervals beginning and ending in the log-linear region, there appears to be no other constraints,

provided there is an accurate accounting of the doses ingested and their precise timing.

In general, the relative bioavailability between two formulations in a crossover study is a function of the ratio of their respective mean plasma concentrations at quasi- and nonsteady state. Appropriate correction factors may be introduced to compensate for the effects of dose, dosing sequence, half-life, sampling interval, and residuals. Each of these elements can be readily identified in the equations developed for each design variation.

Mathematical solutions in closed form have been derived for crossover studies in which: (*a*) the potency of the two treatments may be different, (*b*) time intervals between doses need not be uniform, (*c*) the daily dosage regimen for the two treatments may be different, (*d*) adjustments may be attempted for possible changes in half-life between treatments, (*e*) mean plasma concentrations may be sampled over any convenient dosing interval and need not be the same interval between treatment, (*f*) the elapsed time between the last dose of the first treatment and the first dose of the second treatment may be as long or as short as needed, (*g*) the dosage cycle of recurring sequences is not restricted to 24 hr and may differ between treatments, (*h*) treatment periods may vary in length, and (*i*) dosing sequences may be completely random, *i.e.*, acyclic.

Most of these design alternatives are equally applicable to comparisons at steady state. There is, however, one important difference. With the proposed method, steady-state plasma levels are inferred and, therefore, need not be experimentally attained. In this way, even though the dosing sequence may be acyclical, the corresponding steady state can be inferred by depicting the entire sequence as a single cycle repeated indefinitely. That is to say, steady state is more useful as a concept than an experimental reality.

The number of imaginable permutations in the design of bioavailability studies is limitless. Undoubtedly, many more will surface with time. No attempt has been made to consider any but the simplest of situations in the present discussion. Hopefully, sufficient details have been provided to permit useful extensions to more complex experimental designs.

REFERENCES

(1) K. C. Kwan, J. V. Bondi, and K. C. Yeh, *J. Pharm. Sci.*, **64**, 1639(1975).

ACKNOWLEDGMENTS AND ADDRESSES

Received January 31, 1975, from *Merck Sharp & Dohme Research Laboratories, West Point, PA 19486*

Accepted for publication June 17, 1975.

[x] To whom inquiries should be directed.

Correlation of Phase Inversion Temperature with Kinetics of Globule Coalescence for Emulsions Stabilized by a Polyoxyethylene Alkyl Ether

R. P. ENEVER

Abstract □ The phase inversion temperatures, globule coalescence rates, and long-term stability of oil-in-water emulsions stabilized by polyoxyethylene 4 cetyl ether were measured. Addition of sodium chloride to the aqueous phase depressed the phase inversion temperatures of the emulsions and the cloud point of the surfactant. Linear correlations were obtained between phase inversion temperature and cloud point and also between phase inversion temperature and the logarithm of the globule coalescence rate at constant temperature. This latter finding is consistent with a theory of emulsion type based upon the kinetics of coalescence. The programmed viscometric technique of determining inversion revealed the presence of a liquid crystalline phase below 35°, which contributes significantly to emulsion stability.

Keyphrases □ Emulsions—phase inversion temperature correlated with kinetics of globule coalescence, long-term stability measured, polyoxyethylene alkyl ether as stabilizer □ Polyoxyethylene alkyl ether—as stabilizer in emulsions □ Phase inversion temperature—emulsions, correlated with kinetics of globule coalescence □ Stability, long term—emulsions, polyoxyethylene alkyl ether as stabilizer

When oil-in-water emulsions stabilized by nonionic surfactants are heated, they may invert because of the decreased water solubility of the emulsifiers. This phenomenon has been examined extensively (1–3), particularly the relation between phase inversion temperature and formulation variables such as the hydrophilic–lipophilic balance (HLB) of the emulsifier, the nature and volume of the oil phase, and the presence of additives. The correlations obtained between emulsion stability and phase inversion temperature generally have been of a qualitative nature.

The work described here was concerned with the quantitative relationship between the phase inversion temperature and the rates of globule coalescence of a series of emulsions stabilized by a single nonionic surfactant. The relation of these parameters to long-term storage also was investigated. Emulsions with differing inversion temperatures and stabilities were produced by adding an electrolyte to their aqueous phases. The data were interpreted in terms of a quantitative kinetic theory for predicting emulsion type (4).

EXPERIMENTAL

Materials—The water was twice distilled from a quartz glass still. Liquid paraffin[1] was of BP quality. The surfactant[2], a commercial sample of polyoxyethylene cetyl ether containing an average of four ethylene oxide units (polyoxyethylene 4 cetyl ether), was used without purification (HLB 8.6). Sodium chloride[3] and glycerol[3] were analytical grade reagents.

Preparation of Emulsions—Oil-in-water emulsions were pre-

[1] Vestan grade A350, Fina S.A. Brussels, Belgium.
[2] Texofor A4, batch G964, Glovers Chemicals Ltd., Leeds, England.
[3] B.D.H. Chemicals Ltd., Poole, United Kingdom.

provided there is an accurate accounting of the doses ingested and their precise timing.

In general, the relative bioavailability between two formulations in a crossover study is a function of the ratio of their respective mean plasma concentrations at quasi- and nonsteady state. Appropriate correction factors may be introduced to compensate for the effects of dose, dosing sequence, half-life, sampling interval, and residuals. Each of these elements can be readily identified in the equations developed for each design variation.

Mathematical solutions in closed form have been derived for crossover studies in which: (*a*) the potency of the two treatments may be different, (*b*) time intervals between doses need not be uniform, (*c*) the daily dosage regimen for the two treatments may be different, (*d*) adjustments may be attempted for possible changes in half-life between treatments, (*e*) mean plasma concentrations may be sampled over any convenient dosing interval and need not be the same interval between treatment, (*f*) the elapsed time between the last dose of the first treatment and the first dose of the second treatment may be as long or as short as needed, (*g*) the dosage cycle of recurring sequences is not restricted to 24 hr and may differ between treatments, (*h*) treatment periods may vary in length, and (*i*) dosing sequences may be completely random, *i.e.*, acyclic.

Most of these design alternatives are equally applicable to comparisons at steady state. There is, however, one important difference. With the proposed method, steady-state plasma levels are inferred and, therefore, need not be experimentally attained. In this way, even though the dosing sequence may be acyclical, the corresponding steady state can be inferred by depicting the entire sequence as a single cycle repeated indefinitely. That is to say, steady state is more useful as a concept than an experimental reality.

The number of imaginable permutations in the design of bioavailability studies is limitless. Undoubtedly, many more will surface with time. No attempt has been made to consider any but the simplest of situations in the present discussion. Hopefully, sufficient details have been provided to permit useful extensions to more complex experimental designs.

REFERENCES

(1) K. C. Kwan, J. V. Bondi, and K. C. Yeh, *J. Pharm. Sci.*, **64**, 1639(1975).

ACKNOWLEDGMENTS AND ADDRESSES

Received January 31, 1975, from *Merck Sharp & Dohme Research Laboratories, West Point, PA 19486*

Accepted for publication June 17, 1975.

[x] To whom inquiries should be directed.

Correlation of Phase Inversion Temperature with Kinetics of Globule Coalescence for Emulsions Stabilized by a Polyoxyethylene Alkyl Ether

R. P. ENEVER

Abstract □ The phase inversion temperatures, globule coalescence rates, and long-term stability of oil-in-water emulsions stabilized by polyoxyethylene 4 cetyl ether were measured. Addition of sodium chloride to the aqueous phase depressed the phase inversion temperatures of the emulsions and the cloud point of the surfactant. Linear correlations were obtained between phase inversion temperature and cloud point and also between phase inversion temperature and the logarithm of the globule coalescence rate at constant temperature. This latter finding is consistent with a theory of emulsion type based upon the kinetics of coalescence. The programmed viscometric technique of determining inversion revealed the presence of a liquid crystalline phase below 35°, which contributes significantly to emulsion stability.

Keyphrases □ Emulsions—phase inversion temperature correlated with kinetics of globule coalescence, long-term stability measured, polyoxyethylene alkyl ether as stabilizer □ Polyoxyethylene alkyl ether—as stabilizer in emulsions □ Phase inversion temperature—emulsions, correlated with kinetics of globule coalescence □ Stability, long term—emulsions, polyoxyethylene alkyl ether as stabilizer

When oil-in-water emulsions stabilized by nonionic surfactants are heated, they may invert because of the decreased water solubility of the emulsifiers. This phenomenon has been examined extensively (1–3), particularly the relation between phase inversion temperature and formulation variables such as the hydrophilic–lipophilic balance (HLB) of the emulsifier, the nature and volume of the oil phase, and the presence of additives. The correlations obtained between emulsion stability and phase inversion temperature generally have been of a qualitative nature.

The work described here was concerned with the quantitative relationship between the phase inversion temperature and the rates of globule coalescence of a series of emulsions stabilized by a single nonionic surfactant. The relation of these parameters to long-term storage also was investigated. Emulsions with differing inversion temperatures and stabilities were produced by adding an electrolyte to their aqueous phases. The data were interpreted in terms of a quantitative kinetic theory for predicting emulsion type (4).

EXPERIMENTAL

Materials—The water was twice distilled from a quartz glass still. Liquid paraffin[1] was of BP quality. The surfactant[2], a commercial sample of polyoxyethylene cetyl ether containing an average of four ethylene oxide units (polyoxyethylene 4 cetyl ether), was used without purification (HLB 8.6). Sodium chloride[3] and glycerol[3] were analytical grade reagents.

Preparation of Emulsions—Oil-in-water emulsions were pre-

[1] Vestan grade A350, Fina S.A. Brussels, Belgium.
[2] Texofor A4, batch G964, Glovers Chemicals Ltd., Leeds, England.
[3] B.D.H. Chemicals Ltd., Poole, United Kingdom.

pared containing 27% (w/w) liquid paraffin, 3% (w/w) polyoxyethylene 4 cetyl ether, and 0.1–10.0% (w/w) sodium chloride.

The surfactant was dissolved in the oil by warming to 40°. The sodium chloride was dissolved in the water, and the appropriate quantity of the oil–surfactant mixture was added with continuous stirring. The coarse emulsion that formed was immediately homogenized[4]. Each emulsion was stored at room temperature for a minimum of 4 days to allow equilibration of the surfactant between the two phases and was rehomogenized before use.

Phase Inversion Temperatures—The phase inversion temperatures of emulsions were determined by the programmed temperature rise viscometric technique (5). An emulsion was continuously sheared in a cone and plate viscometer[5] at 266 sec^{-1} while the plate was heated at 0.5° min^{-1}. The torque output from the viscometer was displayed on an X–Y recorder against the amplified voltage signal from a thermocouple embedded in the plate.

The viscometer was fitted with a vapor hood to prevent evaporation of the aqueous phase of the emulsion. The gap width between the cone and the plate (average value 0.05 mm) was controlled with an automatic gap-setting unit. Inversion was detected as a pronounced increase in the apparent viscosity when the oil became the continuous phase of the emulsion. Four determinations were carried out on each emulsion, and the mean value was recorded (range ±0.5°).

Phase inversion temperatures were also determined by monitoring the specific conductivity[6] and temperature[7] of 60 ml of emulsion that was continuously agitated at 100 rpm with a small propeller stirrer. The emulsion was heated at a controlled rate of 0.5° min^{-1}. Inversion was detected as a rapid fall in specific conductivity below that of the aqueous phase used to prepare the emulsion. The results quoted are the means of four determinations.

Cloud Points—The cloud points of 0.05% (w/w) aqueous solutions of the surfactant containing 0.1–15.0% (w/w) sodium chloride were determined. Each solution was placed in a water-jacketed 2-cm path length spectrophotometer cell fitted with a thermocouple. A tungsten light source and phototransistor circuit were used to monitor the turbidity of the solution while it was heated at 0.5° min^{-1}.

The amplified phototransistor and thermocouple signals were displayed on an X–Y recorder, and the cloud point was detected as a sharp increase in the turbidity of the solution. Four determinations were carried out on each solution, and the mean value was recorded.

Globule Coalescence—Emulsion stability was assessed by measuring the change in the number of oil globules per milliliter with time (6). Samples of each emulsion were diluted 1 in 500 by volume with 40% (v/v) aqueous glycerol warmed to 35°. An aliquot was mounted in a 100-μm depth counting chamber[8] and allowed to stand for 1 hr at room temperature.

Subsequently, photomicrographs[9] were taken of five fields at ×800 magnification; negatives were enlarged[10] to give an overall magnification of ×1600. The globules in each field were counted, and the number of globules per milliliter of emulsion was calculated. At various time intervals, four samples were taken from each emulsion and the mean value for the 20 fields was calculated.

Creaming Rates—Emulsion samples were stored in 10-ml stoppered graduated measuring cylinders at 20° for up to 18 months. At 2-week intervals, the degrees of creaming and of separation of oil phase were assessed.

RESULTS AND DISCUSSION

Data for an emulsion containing 0.1% (w/w) sodium chloride obtained by the two methods of measuring phase inversion temperature are shown in Fig. 1. The apparent viscosity fell as the temperature was increased from 22°, and this fall was most marked at approximately 35°. Above 40°, the viscosity was essentially constant

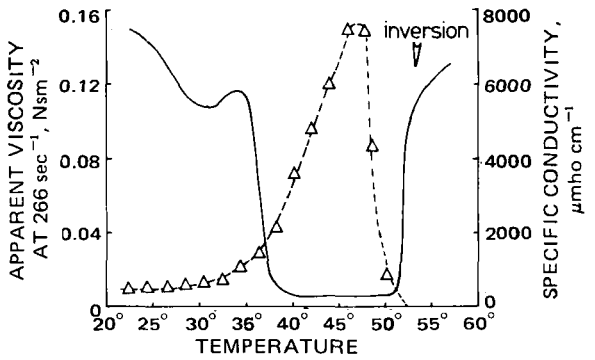

Figure 1—*Relationship between apparent viscosity and temperature (—) and between conductivity and temperature (- - -) for an emulsion containing 0.1% (w/w) sodium chloride.*

until inversion occurred with a rapid rise in viscosity. The discontinuity at 35° occurred in emulsions containing 0.1–6.0% (w/w) sodium chloride. Emulsions with higher sodium chloride contents inverted below this temperature.

Observation of emulsions using a hot-stage microscope[11] with polarized light showed that the discontinuity at 35° coincided with the disappearance of a liquid crystalline phase from the aqueous continuous medium. This finding was confirmed by separation of the emulsion phases by ultracentrifugation[12] at 250,000×g, followed by storage at temperatures above and below 35°. The reason for the small "shoulder" in the apparent viscosity curve just below 35° is not known but might be due to structural changes in the liquid crystalline phase prior to its disappearance.

The specific conductivity initially showed an increase with temperature, which also was most marked at the point of disappearance of the liquid crystalline phase. This result is to be expected since the decrease in viscosity will result in increased ionic mobility. Subsequently, conductivity fell sharply as the emulsion began to invert. There was good agreement between the values of phase inversion temperature obtained by the two methods.

This agreement is also evident in Fig. 2, where the phase inversion temperature was plotted against the sodium chloride concentration. The temperature of inversion fell with an increase in the sodium chloride concentration in a curvilinear manner. Similar relationships were reported for emulsions stabilized by various nonionic surfactants (3, 5). The variation in the cloud point of the emulsifier with the sodium chloride concentration was similar to that of the phase inversion temperature; in fact, a linear correlation was obtained between the inversion temperature and cloud point (r = 0.995).

Examples of globule coalescence data are plotted in Fig. 3. Results are for emulsions stored at 37° and show that there was a decrease in stability with an increasing sodium chloride concentration. It is evident that coalescence can be described by a first-order process; thus the slopes of the lines give the coalescence rate constants. The theory of coalescence developed by Van den Tempel (6) predicts this first-order relationship and has been found to hold for a number of emulsion systems (6, 7).

Figure 4 illustrates the effect of the liquid crystalline phase upon the rate of globule coalescence. The data, for an emulsion containing 2.0% (w/w) sodium chloride, show that the phase greatly enhanced emulsion stability. Above 35°, with disappearance of the phase, the rate of globule coalescence rapidly increased.

Linear correlations were obtained between the phase inversion temperature and the logarithm of globule coalescence rate constants at constant temperature for this emulsion series. Correlations were obtained both at 25 and 37° and thus exist in the presence and absence of the liquid crystalline phase, although the slope value at 37° is much greater (Fig. 5).

Davies (4) advanced a quantitative kinetic theory to account for the type of emulsion formed upon mixing oil and water. He considered that the relative rate constants for coalescence of oil globules in water (Rate 1) and water globules in oil (Rate 2) control emulsion type. For example, if Rate 2 is greater than Rate 1, the forma-

[4] Omerod URF-1 hand homogenizer, Omerod Engineers Ltd., Rochdale, England.
[5] Ferranti-Shirley, Ferranti Ltd., Moston, Manchester, England.
[6] Type PB/1 solid-state conductivity meter, L.T.H. Electronic Ltd., Luton, England.
[7] Type 1604 thermometer, Comark Electronic Ltd., Rustington, Sussex, England.
[8] Improved Neubauer cell, Hawksley and Sons Ltd., Lancing, England.
[9] Swift series 800 microscope fitted with Kodak Retina Reflex IV camera.
[10] Focomat 1c enlarger, E. Leitz GMBH, Wetzlar, Germany.
[11] Mettler FP5/FP52, Mettler Instrument A.G., Zurich, Switzerland.
[12] Omega II, Heraeus-Christ GMBH, West Germany.

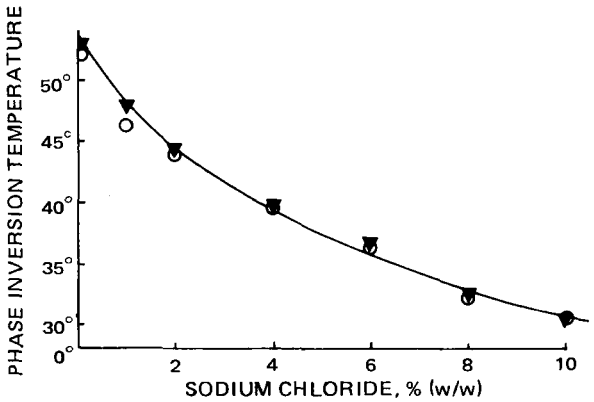

Figure 2—*Relationship between phase inversion temperature and sodium chloride concentration. Key: ▼, phase inversion temperature from viscosity data; and O, phase inversion temperature from conductivity data.*

tion of an oil-in-water emulsion is favored. For inversion of an oil-in-water emulsion to occur, Rate 1 must become large relative to Rate 2.

According to Davies (4):

$$\text{Rate 1} = A_1 \exp[(-0.24\psi_0^2 - \theta\textstyle\sum E_h)/RT] \qquad \text{(Eq. 1)}$$

where A_1 is a hydrodynamic collision factor (which takes into account the phase volume of oil and the viscosity of the continuous phase), ψ_0 is the electrical potential at the interface, θ is the fraction of interface covered by the surfactant, and ΣE_h is the total energy necessary to displace the water of hydration from the polar groupings of the surfactant prior to coalescence of the oil globules:

$$\text{Rate 2} = A_2 \exp(-600n\theta/RT) \qquad \text{(Eq. 2)}$$

where A_2 is a constant accounting for hydrodynamic factors, and n is the number of methylene groups in each surfactant hydrocarbon chain.

For emulsions stabilized by nonionic surfactants, the main stabilizing factors appear to be the viscosity and/or elasticity of the interfacial film and, most importantly, hindrance to close approach of the globules by the helical conformations of the hydrated polyoxyethylene chains. It is debatable, although unlikely, as to whether the surfactant contributes to the charge on the emulsion globules (8) and to the electrical forces of the repulsion. An increase in the temperature of the emulsion results in disruption of the hydrogen bonds linking water molecules to the ether oxygens of the polyoxyethylene chains. It follows that the value of ΣE_h falls with a rise in temperature, and this phenomenon is the major contribution to the increase in Rate 1. Provided the increase in Rate 2 is not significant relative to Rate 1, then, as has been shown in these experiments, inversion of an oil-in-water emulsion occurs.

Addition of sodium chloride to the emulsions also dehydrates

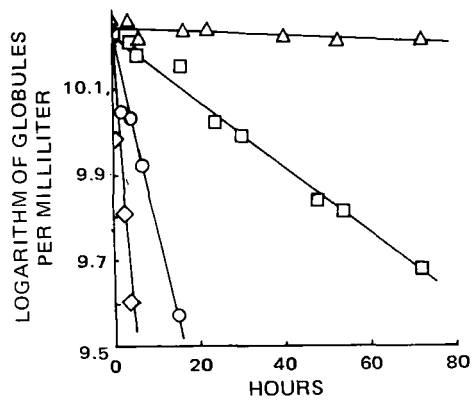

Figure 3—*Globule coalescence data for emulsions stored at 37°. Key [percent (w/w) sodium chloride]: △, 0.1; O, 2.0; □, 1.0; and ◇, 4.0%.*

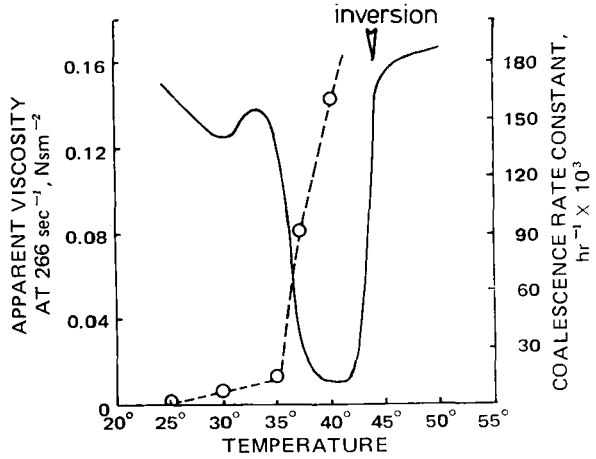

Figure 4—*Relationship between apparent viscosity and temperature (—) and between coalescence rate constant and temperature (- - -) for emulsions containing 2.0% (w/w) sodium chloride.*

the polyoxyethylene chains (3) and reduces ΣE_h. The electrolyte compresses the electrical double layer around the oil droplets and lowers ψ_0 as well, although, as already indicated, the electrical repulsion forces do not appear to play a significant role in stabilizing such emulsions (7). The net result should be a further increase in Rate 1 with an increasing sodium chloride content and a lowering of the temperature at which inversion occurs. The present experimental findings are in agreement with this hypothesis.

Equation 1 indicates that there is an inverse relationship between the logarithm of Rate 1 and ΣE_h. As Davies (4) pointed out, the cloud point temperature is related to the energy of dehydration of the surfactant; the present work with polyoxyethylene 4 cetyl ether found a linear correlation between the phase inversion temperature and the cloud point. Therefore, provided the electrical potential, ψ_0, makes little contribution to emulsion stability and the experimentally determined globule coalescence rate constants are a measure of Rate 1, the observed correlation between the phase inversion temperature and the logarithm of coalescence rate constant at constant temperature (Fig. 5) is consistent with the Davies hypothesis.

There was also a qualitative relationship between the phase inversion temperature and the degree of creaming and cracking of the emulsions on long-term storage at 20°. Figure 6 shows this relationship in the form of a plot of phase inversion temperature against the volume fraction of oil, water, and cream after 200 days of storage. It is evident that the lower the inversion temperature, the greater was the degree of separation of the phases. Nevertheless, these emulsions were not grossly unstable, since there was evi-

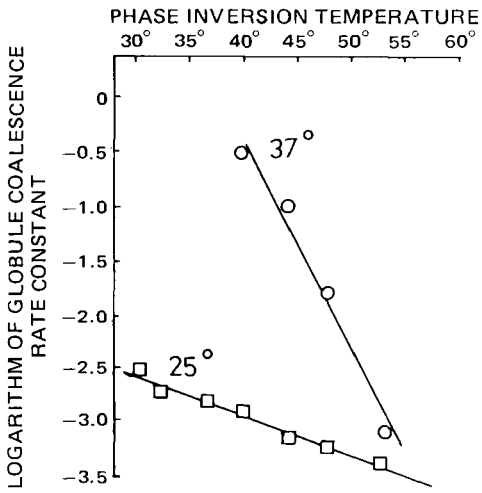

Figure 5—*Relationship between phase inversion temperature and logarithm of globule coalescence rate constant for emulsions stored at 25 and 37°.*

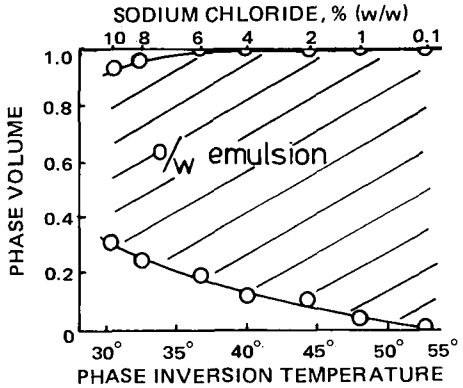

Figure 6—*Relationship between phase inversion temperature and volume fraction of oil, cream, and water after storage at 20° for 200 days.*

dence of cracking after 1 year of storage only with sodium chloride concentrations above 6.0% (w/w).

Shinoda and Saito (9) concluded that for satisfactory shelflife of emulsions stabilized by nonionic surfactants, the phase inversion temperature should be 25–70° above the storage temperature. Parkinson and Sherman (10) further developed this concept by examining the use of phase inversion temperature as an accelerated method for predicting emulsion stability. The relationships among the HLB of mixed emulsifier systems, the phase inversion temperatures, and the globule coalescence rates were investigated. The inversion temperatures were all greater than 85°, and a qualitative relationship was observed between the coalescence rate and the phase inversion temperature.

In comparison with the data of Shinoda and Saito (9) and Parkinson and Sherman (10), the inversion temperatures determined in the present work were considerably lower (ranging from 53.0 to 30.5°); one might be tempted to conclude that this result indicated unstable formulations. However, as with all accelerated test procedures, the primary requirement is that the stress applied should speed up, but not alter, the mechanism of deterioration operating at ambient temperatures. This work showed that the viscous liquid crystalline phase that disappears above approximately 35° has a considerable stabilizing influence on the emulsions. Although phase inversion temperature is a valuable method for ranking the emulsions in order of relative stability, its general applicability for predicting long-term stability is limited when phase changes occur on heating.

SUMMARY

1. The phase inversion temperatures of oil-in-water emulsions stabilized by polyoxyethylene 4 cetyl ether were determined by viscometric and conductimetric methods, and there was good agreement between the results. Addition of sodium chloride to the aqueous phases of the emulsions produced a lowering of the phase inversion temperature, and this result correlated with the fall in the cloud point of an aqueous solution of the surfactant.

2. The viscometric technique detected the presence of a liquid crystalline phase below approximately 35°.

3. Globule coalescence followed first-order kinetics. The liquid crystalline phase greatly influenced the rate of coalescence.

4. A linear correlation existed between the phase inversion temperature and the logarithm of the globule coalescence rate constant at a given temperature. This correlation was observed both in the presence and absence of the liquid crystalline phase. The finding was interpreted in terms of a quantitative kinetic theory of emulsion type.

5. A qualitative relationship was obtained between the degree of creaming and cracking of the emulsions on long-term storage and the phase inversion temperature.

REFERENCES

(1) K. Shinoda, *J. Colloid Interface Sci.*, **24**, 4(1967).

(2) H. Arai and K. Shinoda, *ibid.*, **25**, 396(1967).

(3) K. Shinoda and H. Takeda, *ibid.*, **32**, 642(1970).

(4) J. T. Davies, *Proc. Int. Congr. Surface Activity, 2nd, London*, **1**, 426(1957).

(5) V. B. Sunderland and R. P. Enever, *J. Pharm. Pharmacol.*, **24**, 804(1972).

(6) M. Van den Tempel, *Proc. Int. Congr. Surface Activity, 2nd, London*, **1**, 439(1957).

(7) P. H. Elworthy and A. T. Florence, *J. Pharm. Pharmacol.*, **21**, 70S(1969).

(8) P. Becher, *J. Colloid Sci.*, **17**, 325(1962).

(9) K. Shinoda and H. Saito, *J. Colloid Interface Sci.*, **30**, 258(1969).

(10) C. Parkinson and P. Sherman, *ibid.*, **41**, 328(1972).

ACKNOWLEDGMENTS AND ADDRESSES

Received April 28, 1975, from the *Department of Pharmaceutics, School of Pharmacy, University of London, Brunswick Square, London, WC1N 1AX, United Kingdom.*

Accepted for publication June 17, 1975.

Present address: Department of Pharmaceutical Chemistry, University of Kansas, Lawrence, KS 66044

Effect of Absorbents on Water Vapor Transmission of Free and Applied Polymer Films

ANTON H. AMANN

Abstract □ The influence of different types of absorbents on moisture transmission through free (cast films) and applied (coated tablets) polymer films was investigated. In free film studies, lubricated granulations were considered to be the absorbent. The compressed tablet was considered to be the absorbent in applied film studies. The results suggested that, using the same film formulation and film thickness in all cases, the polymer film reduced moisture absorption to the same degree, independent of the absorbent used, suggesting a constant moisture permeation. The results of the free film studies also simulated those of the applied films, allowing the correlation of the data.

Keyphrases □ Polymer films—free and applied, effect of different types of absorbents on moisture transmission □ Absorbents—effect on moisture transmission through free and applied polymer films

Numerous techniques have been developed and published for studying water vapor transmission properties of free films. The methods employed the utilization of permeability cups (1) or vapor transmission cells (2). The data obtained from free film studies allowed for quantification of factors influencing water vapor transmission such as film thickness, types of polymers used, cross-linking and crystallinity (3), plasticizers (4), and conditions surrounding the film as well as the method of film preparation (5).

In applied film studies, when tablets were coated with a polymer film, the rates of moisture uptake of tablet matrixes containing calcium chloride were determined as a function of film coat thickness and calcium chloride content of the matrix (6). These tablets were film coated with various lipophilic, hydrophilic, and mixed lipophilic–hydrophilic polymer systems. The results indicated that the water vapor transmission characteristics of applied films were different from those of free films. Recently (7), several model systems created a series of conditions intermediate between permeation through a free film and one applied to a tablet. It was shown that the physical characteristics of the absorbent influence the rate of water vapor transmission through the polymer film.

The objective of free film evaluation is to predict what may happen in the applied state. Therefore, one is confronted with certain limitations if free film studies are to exemplify the applied state. Two important considerations are: (*a*) solid dosage form or granulation on one side of the film, and (*b*) water vapor having a finite equilibrium level of absorption onto granules, powders, or tablets at any one temperature and vapor pressure.

In the past (2, 5–7), when data were evaluated using Fick's law in combination with Henry's law, the vapor pressure gradient was held constant and water vapor was to diffuse through a film and be absorbed into or by an infinite sink. Thus, a linear relationship was established when the transmitted water vapor was plotted *versus* time. If a finite equilibrium condition can be reached and the vapor pressure gradient changes with time, then a deviation from linearity might be expected.

The purposes of this paper are to present data showing what influences different types of absorbents have on water vapor transmission through free and applied polymer films and to establish a relationship between free and applied polymer films.

EXPERIMENTAL

Preparation of Cast Films—Twenty milliliters of hydroxypropyl methylcellulose[1] polymer solution was poured onto glass plates. Glass rings, with a diameter of 13.3 cm, were used to control the area of spreading. The composition of the polymer solution was: hydroxypropyl methylcellulose NF, 15 cps, 4.5 g; absolute alcohol USP, 45.0 ml; and methylene chloride, *q.s.*, 100.0 ml.

After the solvents were allowed to evaporate overnight, films were placed into a 40° chamber for 24 hr. Prior to using these films in water vapor transmission studies, they were equilibrated for at least 24 hr in a humidity chamber. Film thickness was determined by a micrometer and was found to be 8.0 ($\pm$0.5) $\times 10^{-3}$ cm.

Water Vapor Transmission Studies through Free Polymer Films—Permeability cups[2] were used to hold 25 g of various pharmaceutical granulations (hereafter referred to as absorbents). These absorbents represented six different dosage forms. The pretreated film was placed onto the cup and sealed with melted white ceresin wax[3]. The seal was allowed to cool before using the cell. The area of transmission was 41.7 cm^2.

Water vapor uptake was measured by placing these cups in a desiccant jar containing saturated sodium chloride solution. This procedure resulted in a vapor pressure condition of 17.8 mm Hg at 25° (8). The desiccant jar was placed in a controlled room at 25 $\pm$ 1°.

To ensure that moisture was not absorbed by, or transmitted through, the wax, a metal template was placed onto the cup and sealed with the wax. No weight changes occurred under the same conditions as were used for the free films.

At specified time intervals (*i.e.*, 8–12 hr), these cups were weighed on a top-loading balance having a precision of $\pm$1 mg.

Tablet Preparation—Six different types of absorbents (pharmaceutical granulations) were compressed into tablets. A 16-station rotary tablet machine, fitted with four deep cup punches, was employed. Hardness, tablet weight, and size of punches depended on the type of absorbent used. The tablets were coated by a continuous spray technique. Film thickness was determined by measuring, with a micrometer, 50 tablets before and after coating. Actual film thickness was 8.0 ($\pm$0.5) $\times 10^{-3}$ cm for all six coating runs.

The exposed surface area of the tablets was calculated from the punch specifications and height of the sidewall surface.

The coated tablets, along with uncoated tablets, were placed in a 40° oven for 1 week prior to moisture uptake studies.

Moisture Uptake Studies of Applied Polymer Films—Three sets of 20 coated tablets, as well as uncoated tablets, were placed in a petri dish and subjected to the same experimental design as free films.

Measurement of Water Vapor Transmission—As anticipated, in the presence of a polymer film a nonlinear relationship

[1] Shinetsu Chemical Co.
[2] Thwing Albert Instrument Co., Philadelphia, Pa.
[3] Strahl and Pitch, West Babylon, Long Island, N.Y.

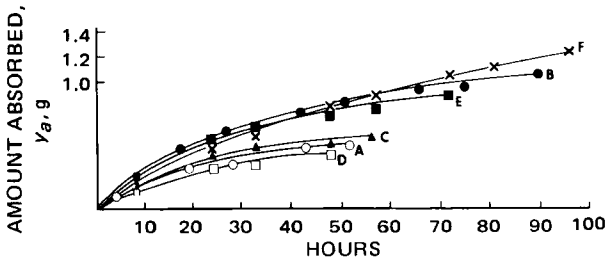

Figure 1—*Amount of moisture absorbed onto granules as a function of time in the presence of a polymer film. Key: ○, Formulation A; ●, Formulation B; ▲, Formulation C; □, Formulation D; ■, Formulation E; and ×, Formulation F.*

was found when the amount of moisture absorbed, y_a (considered to be a function of amount of moisture transmitted), was plotted *versus* time, t (Fig. 1). When the reciprocal functions were plotted ($1/y_a$ *versus* $1/t$), linearity was seen (Fig. 2). A possible explanation for this relationship is as follows.

If the vapor pressure gradient is held constant, then water vapor transmission follows the equation (9):

$$y_t = PA(p_0 - p)t \qquad \text{(Eq. 1)}$$

where y_t is the concentration of moisture transmitted at time t, A is the area of transmission, P is the average permeability coefficient as a function of the distance or length of the concentration gradient (usually film thickness), and $(p_0 - p)$ is the difference in vapor pressure between both sides of the film.

Should no moisture be present on one side of the film and should a limited space be available for moisture to occupy, then Henry's law would apply in that:

$$p = Sy_t \qquad \text{(Eq. 2)}$$

where S is a proportionality constant, relating pressure to the concentration of moisture. Equation 2 can be substituted into Eq. 1 when at $t = 0$, $y = 0$; then:

$$y_t = PA(p_0 - Sy_t)t \qquad \text{(Eq. 3)}$$

or:

$$y_t = PAp_0t - PASy_tt \qquad \text{(Eq. 4)}$$

Solving for y_t then gives:

$$y_t = (PAp_0t)/(1 + PASt) \qquad \text{(Eq. 5)}$$

Since the amount of moisture absorbed, y_a, is measured, a relationship can be established between the amount transmitted and the amount absorbed in the following manner. The rate of moisture transmission, $(dy/dt)_t$, can be expressed as:

$$(dy/dt)_t = -k_1Ap \qquad \text{(Eq. 6)}$$

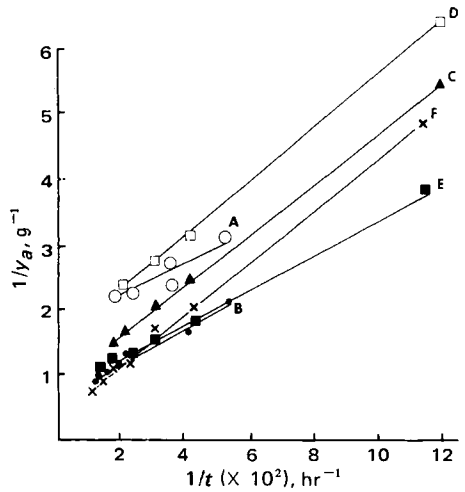

Figure 2—*Amount of moisture absorbed onto granules as a function of time in the presence of a polymer film. Data plotted according to Eq. 17. Key: see Fig. 1.*

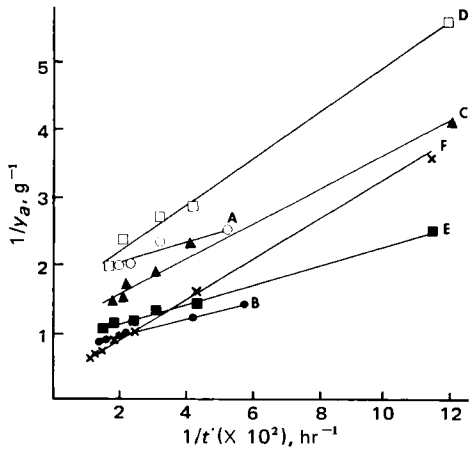

Figure 3—*Amount of moisture absorbed onto granules as a function of time in the absence of a polymer film. Data plotted according to Eq. 17. Key: see Fig. 1.*

where k_1 can be considered the moisture transmission constant. The absorption rate, $(dy/dt)_a$, can be expressed as:

$$(dy/dt)_a = k_2Ap - k_3x_a \qquad \text{(Eq. 7)}$$

where k_2 and k_3 are the absorption and desorption rate constants, respectively; and x_a is the amount of moisture absorbed, y_a, per unit weight of absorbent, m. If one assumes a steady-state condition, then the rate of moisture transmitted is equal to the rate of moisture absorbed. Thus, $(dy/dt)_t = (dy/dt)_a$ and:

$$-k_1Ap = k_2Ap - k_3x_a \qquad \text{(Eq. 8)}$$

Solving for the vapor pressure, p, then gives:

$$p = (k_3x_a)/(k_1 + k_2)A \qquad \text{(Eq. 9)}$$

By definition, the equilibrium constant, K_e, is equal to:

$$K_e = (k_1 + k_2)/k_3 \qquad \text{(Eq. 10)}$$

Then Eq. 9 can be expressed as:

$$p = x_a/K_eA \qquad \text{(Eq. 11)}$$

As mentioned before, when at $t = 0$, $p = 0$ and $y_a = 0$, then Henry's law (Eq. 2) can be applied and Eq. 11 can be written as:

$$y_t = x_a/K_eSA \qquad \text{(Eq. 12)}$$

Substitution of Eq. 12 into Eq. 5 then gives:

$$x_a/K_eSA = (PAp_0t)/(1 + PASt) \qquad \text{(Eq. 13)}$$

Since:

$$x_a = y_a/m \qquad \text{(Eq. 14)}$$

then:

$$y_a/mK_eSA = (PAp_0t)/(1 + PASt) \qquad \text{(Eq. 15)}$$

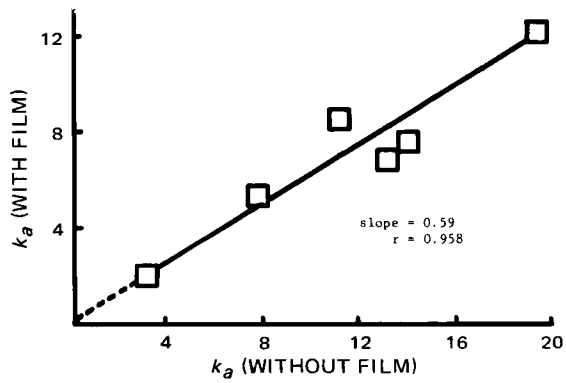

Figure 4—*Comparison of absorption rate constants from free film studies.*

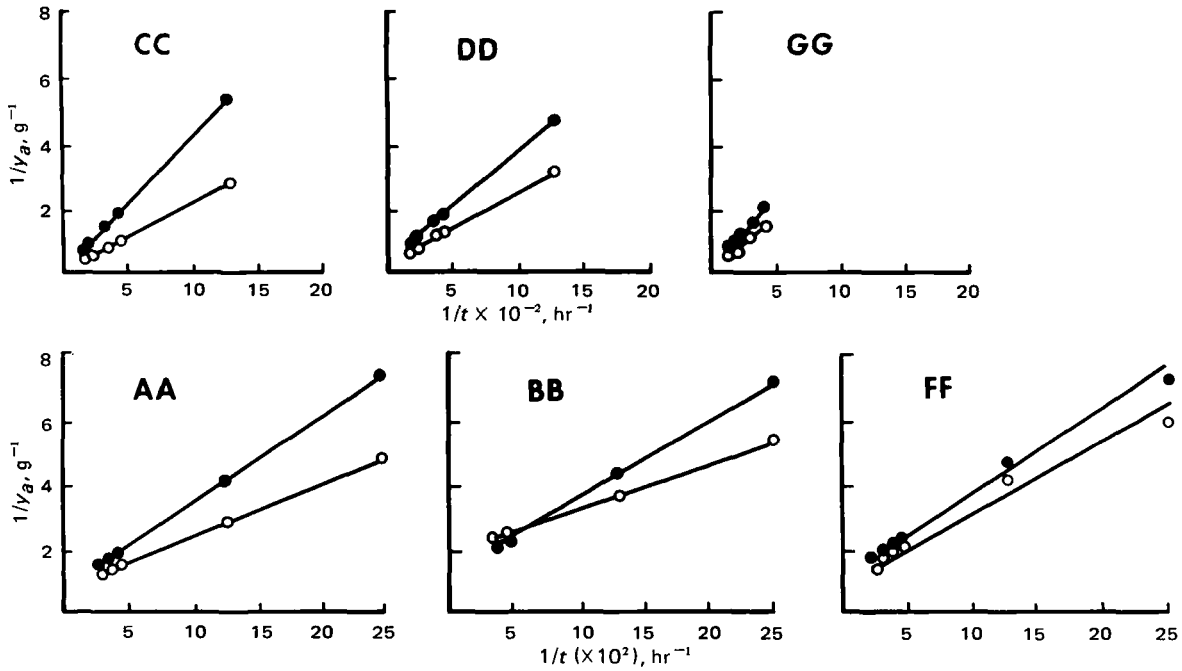

Figure 5—*Data for coated (○) and uncoated (●) tablets plotted according to Eq. 17.*

or:

$$mK_eSA/y_a = 1/(PAp_0t) + S/p_0 \quad \text{(Eq. 16)}$$

and, therefore:

$$1/y_a = 1/(SPK_eA^2mp_0)t + 1/K_eAmp_0 \quad \text{(Eq. 17)}$$

A plot of $1/y_a$ *versus* $1/t$ should yield a straight line. The following were calculated by plotting the data according to Eq. 17. The quantity SP was considered to be the apparent absorption rate constant, k_a:

$$k_a = 1/(\text{slope})K_eA^2mp_0 = (\text{intercept})/(\text{slope})(A) \quad \text{(Eq. 18)}$$

$$K_e = 1/(\text{intercept})Amp_0 \quad \text{(Eq. 19)}$$

The absorption in the absence of a polymer film was also plotted according to Eq. 17.

RESULTS AND DISCUSSION

The results of the absorption studies in the presence and absence of a polymer film are plotted in Figs. 2 and 3 according to Eq. 17. From the slopes and intercepts, the apparent absorption rates and equilibrium constants were calculated according to Eqs. 18 and 19 (Table I).

The presence of a polymer film (when the same formulation is compared) has no impact on the equilibrium constant (Table I).

Table I—Computation of the Rate Constants Derived from Eqs. 18 and 19, Using Pharmaceutical Granulations[a]

Formulation[b]	k_a, hr^{-1} cm^{-2} × 10^{-4}		K_e, cm^{-2} mm Hg^{-1} × 10^{-5}	
	Without Film	With Film	Without Film	With Film
D	10.97	9.01	3.50 (0.35)[c]	3.64 (0.12)[c]
F	2.92	2.16	15.40 (2.64)	13.47 (1.68)
C	7.79	5.61	5.99 (1.33)	6.49 (0.78)
A	19.40	12.20	3.39 (0.17)	3.59 (0.19)
E	13.92	7.57	6.26 (1.29)	7.59 (0.64)
B	13.52	6.98	7.48 (0.21)	7.81 (0.57)

[a] Area of transmission (A) = 41.70 cm^2, weight of powders (m) = 25.00 g, and vapor pressure (p_0) = 17.8 mm Hg. Film thickness was 8.0 × 10^{-3} cm. [b] See Figs. 2 and 3 for corresponding graph. [c] Represents ±95% confidence interval.

Because there is no difference in K_e, it appears that the limiting factor in the absorption process is the absorption of moisture onto granules and not diffusion through the polymer film. At equilibrium conditions, diffusion must occur at a much faster rate than absorption. Should the film be more of a controlling factor, a shift in K_e could be expected.

Comparison of the absorption rates shows that differences exist not only from one formulation to another but also when absorption is compared in the presence or absence of a polymer film. In all cases, absorption is much slower in the presence of a polymer film. The data appear to show that the polymer film has a variable diffusion rate. If the controlling factor is the polymer film and if the absorption rate is much greater than the permeation rate, no differences would be seen in the absorption rate when all of the different absorbents are compared in the presence of a polymer film. If this is the case, the vapor pressure differential would be constant on both sides of the film and linearity would be seen when y_a is plotted *versus* t, simulating a condition whereby moisture can be absorbed by, or diffuse into, an infinite sink.

The polymer film also can reduce absorption by acting as a barrier, which causes a change in vapor pressure with time. This method is ruled out since the slopes would be equal and independent of the absorbent, because (dy/dp) would be constant for any one film thickness at a given temperature and vapor pressure. The fact that the vapor pressure would probably change at a different rate, depending on the absorbent, would not cause a difference in k_a, because the slope would be a function of the average permeability coefficient.

Another alternative would be that the diffusion process has already occurred and that the polymer film actually presents an obstacle in absorption. This postulate is not unrealistic for several reasons. First, the polymer film is a relatively permeable species, and diffusion would be expected to occur much faster than the time required to reach equilibrium conditions. To reach equilibrium levels of absorption[4] took as long as 1 month. Second, the space between the granulation and the polymer film is very small, and a large concentration of water vapor would not be required to have a vapor pressure differential between both sides of the film of zero. The assumptions of this last alternative were used in developing Eq. 17. Therefore, at any given temperature and vapor pressure, the polymer film should be a constant barrier in reducing absorption.

[4] Equilibrium levels of moisture were determined for each granulation. However, the data are not included since no relationship existed between the total amount of moisture absorbed and K_e or k_a.

Table II—Computation of the Rate Constants Derived from Eqs. 18 and 19, Using Coated and Uncoated Tablets[a]

Formulation[b]	Area (A) of 20 Tablets, cm^2	Weight (m) of 20 Tablets, g	k_a, hr^{-1} cm^{-2} × 10^{-4}		K_e, cm^{-2} $mm\ Hg^{-1}$ × 10^{-5}	
			Uncoated	Coated	Uncoated	Coated
FF	76.30	22.14	9.97	7.93	4.72 (0.80)[c]	4.92 (0.76)[c]
GG	58.60	17.86	2.67	1.87	2.20 (0.21)	2.47 (0.27)
DD	73.20	17.03	3.60	2.23	2.39 (0.14)	2.21 (0.23)
BB	77.60	23.26	18.05	11.45	6.04 (1.31)	4.94 (0.31)
AA	65.20	13.38	11.91	7.08	7.60 (0.32)	6.38 (1.64)
CC	59.20	11.82	4.91	2.37	3.77 (1.60)	3.77 (1.60)

[a] Vapor pressure (p_0) = 17.8 mm Hg, and film thickness = 8.0 × 10^{-3} cm. [b] See Fig. 5 for corresponding graph. [c] Represents ±95% confidence interval.

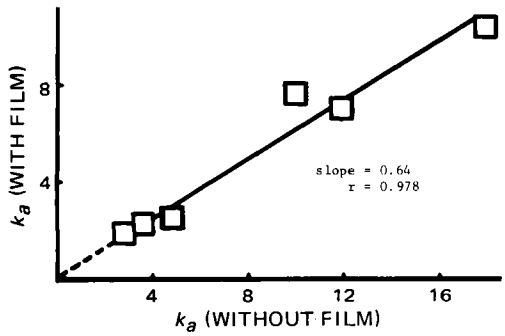

Figure 6—*Comparison of absorption rate constants from applied film studies (coated and uncoated tablets).*

To demonstrate this, the apparent absorption rates were plotted in Fig. 4. A good relationship appears to exist in that a reduction in the absorption rate of about 40%[5] can be attributed to the polymer film. This finding suggests that the total moisture and the amount absorbed at a given time interval are functions of the absorbent and that the degree to which a polymer film reduces absorption is constant and, apparently, independent of the absorbent.

As to film-coated tablets, the data obtained from these studies were treated as with free films (Fig. 5). As can be seen, linearity is obtained by plotting $1/y_a$ *versus* $1/t$ and common intercepts are obtained for each common tablet, with or without film coating.

The calculated equilibrium constants and absorption rates are given in Table II. The absorption rates are plotted in Fig. 6.

It appears that the same holds true for film-coated tablets as for free films in that the film retards moisture absorption by about 40% and is independent of the tablet formulation. Only the rate of absorption and the total amount absorbed are influenced by the tablet formulation.

When the results obtained with tablets and granules are considered, the mechanism by which a polymer film retards moisture apparently must be by altering or hindering the rate at which moisture diffuses to the absorption site. The presence of the film presents a constant barrier which slows the diffusion of moisture, resulting in a relationship such as that shown in Figs. 4 and 6. Therefore, the degree to which the polymer film retards absorption would be independent of the tablet or granule formulation and also independent of the physical nature of the solid matrix.

In conclusion, the absorbent does not influence moisture permeation through the film but, instead, the polymer film slows the absorption process. The results show that a very good correlation is obtained between free and applied films when subjected to this experimental design and treated according to Eq. 17.

Further investigation is needed to test the influence of film thickness, film formulation, vapor pressure, temperature, and tablet formulation factors, all of which can cause changes in moisture absorption.

[5] Calculated on the basis that:

$$[k_a(\text{without film}) - k_a(\text{with film})]/k_a(\text{without film}) \times 100\% = (1 - \text{slope}) \times 100\%$$

can be considered as the decrease in absorption attributed to the polymer film.

REFERENCES

(1) J. L. Kanig and H. Goodman, *J. Pharm. Sci.*, **51**, 77(1962).

(2) M. Patel, J. M. Patel, and A. P. Lemberger, *ibid.*, **53**, 286(1964).

(3) J. Crank and G. S. Park, "Diffusion in Polymers," Academic, New York, N.Y., 1968.

(4) R. R. Crawford and O. K. Esmerian, *J. Pharm. Sci.*, **60**, 312(1971).

(5) J. Swarbrick, A. H. Amann, and R. E. Lindstrom, *ibid.*, **61**, 1645(1972).

(6) G. S. Banker, A. Y. Gore, and J. Swarbrick, *J. Pharm. Pharmacol.*, **18**, 457(1966).

(7) A. H. Amann, R. E. Lindstrom, and J. Swarbrick, *J. Pharm. Sci.*, **63**, 931(1974).

(8) "International Critical Tables, III," McGraw-Hill, New York, N.Y., 1928, pp. 248–292.

(9) T. Kuriyama, M. Nobutoki, and M. Nakanishi, *J. Pharm. Sci.*, **59**, 1344(1970).

ACKNOWLEDGMENTS AND ADDRESSES

Received September 3, 1974, from the *Pharmaceutical Products Division, Abbott Laboratories, North Chicago, IL 60064*

Accepted for publication June 20, 1975.

The author acknowledges Mr. P. M. Palyok for technical assistance.

Present address: Adria Laboratories Inc., Wilmington, DE 19899

Conversion of Biguanides into Substituted *s*-Triazines Assayable by GC or Mass Fragmentography

DAVID ALKALAY ˣ, JOSEPH VOLK, and M. FRED BARTLETT

Abstract □ Substituted *s*-triazines were prepared by the treatment of biguanides with various organic acid anhydrides. This reaction permits the ready conversion of the hypoglycemic drugs phenformin, buformin, and metformin and of other analogous biguanides into compounds suitable for GC and mass fragmentographic determination with a high degree of sensitivity. Mass spectral data and Kováts retention indexes are presented for all *s*-triazines prepared for this study.

Keyphrases □ Biguanides—conversion into substituted *s*-triazines, GC and mass fragmentographic analysis □ *s*-Triazines, substituted—synthesized from biguanides, GC and mass fragmentographic analysis □ GC—analysis, *s*-triazines synthesized from biguanides □ Mass fragmentography—analysis, *s*-triazines synthesized from biguanides □ Hypoglycemic agents, oral—GC and mass fragmentographic analysis, *s*-triazines

Oral hypoglycemic agents are being used with 20–40% of diabetic patients (1). The two major groups of such drugs are the arylsulfonylureas and the biguanides. The latter include phenformin (I), buformin (II), and metformin (III), which are being widely used in the United States, Germany, and France, respectively (2).

Breidahl *et al.* (3) summarized current views on the yet uncertain mechanism of action of these compounds. Elucidation of this mechanism is hampered by the lack of suitable methodology for assaying biguanides in biological fluids. Published analytical procedures based on fluorescence, colorimetry, or UV absorption lack the necessary specificity and/or sensitivity (4–10). A GC method (11), involving pyrolytic conversion of biguanides into 2,4,6-triamino-1,3,5-triazines, apparently is suitable for assaying buformin in pharmaceutical preparations but not in biological specimens.

The acylation of biguanides has been known to yield *s*-triazines (12–16). The present article describes the use of this reaction for the reproducible conversion of biguanides into substituted *s*-triazines[1] suitable for GC and mass fragmentographic determination.

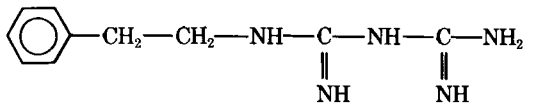

I

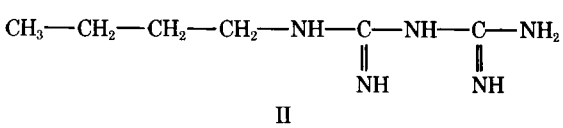

II

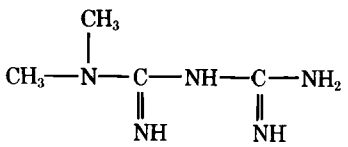

III

EXPERIMENTAL

Chemicals—The following reagents and solvents were used: amformin hydrochloride[2] (IV); buformin hydrochloride[2]; chlorodifluoroacetic anhydride[3]; dichlorofluoroacetic anhydride[4]; methylene chloride[5]; ether[6], anhydrous analytical reagent; 1-ethyl-1-phenethylbiguanide hydrochloride[7] (V), mp 165–166.5°; heptafluorobutyric anhydride[3]; *n*-hexane[5]; 38% hydrochloric acid[8], reagent; magnesium sulfate[8], anhydrous reagent; metformin hydrochloride[9]; 1-(*p*-methoxyphenethyl)biguanide hydrochloride[7] (VI), mp 171–172°; *d*-1-(α-methylphenethyl)biguanide nitrate[7] (VII), mp 141–142.5°, $[\alpha]_D^{25}$ +44.6° (2.16 g of VII in 100 ml of methanol); 1-(*p*-methylphenethyl)biguanide nitrate[7] (VIII), mp 159–160°; pentafluoropropionic anhydride[3]; phenformin hydrochloride[10]; phosphorus pentoxide[8], reagent; potassium hydroxide[8], reagent; sodium hydroxide[8], reagent; triethylamine[11]; and trifluoroacetic anhydride[12].

Preparation of *s*-Triazines—Two acylation methods were employed for the conversion of biguanides into substituted *s*-triazines.

Method A—Aqueous solutions of biguanide salts were made strongly alkaline with 10 *N* KOH and extracted with methylene chloride. Solvent evaporation gave the free bases. To 250-mg amounts of these bases, placed in 40-ml test tubes equipped with screw caps[13], was added 15 ml of a 3% solution of the appropriate organic acid anhydride in methylene chloride. The stoppered test tubes were heated at 50° for 10 min. After cooling, each sample was washed with 3 ml of 2 *N* NaOH. The organic phase was dried over anhydrous magnesium sulfate, filtered, and evaporated to dryness. The residues were recrystallized from solvent mixtures of ether and *n*-hexane.

Method B—One gram of biguanide salt and 1 ml of triethylamine were placed in a 5-ml acylation tube[14] and cooled to approximately −40°. Four milliliters of the appropriate organic acid anhydride was added to the mixture, and the tube was promptly sealed. Following the exothermic reaction, the tube was heated at 130° for 30 min. After cooling, the reaction mixture was partitioned between 25 ml of cold water and 100 ml of ether. The organic extract was washed consecutively with 1 *N* KOH, 1 *N* HCl, and water. It was dried over anhydrous magnesium sulfate, filtered, and evaporated to dryness. The residue was recrystallized from an ether and *n*-hexane solvent mixture.

Determination of Kováts Retention Indexes—Kováts index-

[1] While completing this investigation, the authors became aware of the independent development of a method for the determination in biological fluids of I–III after conversion into *s*-triazines [S. B. Matin, J. H. Karam, and P. H. Forsham, *Anal. Chem.*, **47**, 545(1975)].

[2] USV Pharmaceutical Corp., Tuckahoe, N.Y.

[3] Pierce Chemical Co., Rockford, Ill.

[4] Alfred Bader Chemicals, Division of Aldrich Chemical Co., Milwaukee, Wis.

[5] Nanograde solvent, Mallinckrodt Chemical Works, St. Louis, Mo.

[6] Mallinckrodt Chemical Works, St. Louis, Mo.

[7] Prepared by A. Wajngurt and M. A. Loo, Ciba-Geigy Corp., Ardsley, N.Y.

[8] J. T. Baker Chemical Co., Phillipsburg, N.J.

[9] Ciba-Geigy Ltd., Basle, Switzerland.

[10] Ciba-Geigy Corp., Summit, N.J.

[11] Eastman Kodak Co., Rochester, N.Y.

[12] Sequanal (grade) chemical, Pierce Chemical Co., Rockford, Ill.

[13] Lined with Teflon (du Pont).

[14] Regis Chemical Co., Morton Grove, Ill.

Table I—List of Substituted *s*-Triazines Derived from Biguanides

Compound	Name	Method	Yield[a], %
IX	2-Amino-4-phenethylamino-6-trifluoromethyl-*s*-triazine	B	64
X	2-Amino-4-pentafluoroethyl-6-phenethylamino-*s*-triazine	A	71
XI	2-Amino-4-heptafluoropropyl-6-phenethylamino-*s*-triazine	A	72
XII	2-Amino-4-chlorodifluoromethyl-6-phenethylamino-*s*-triazine	A	85
XIII	2-Amino-4-dichlorofluoromethyl-6-phenethylamino-*s*-triazine	A	64
XIV	2-Amino-4-(*p*-methylphenethyl)amino-6-trifluoromethyl-*s*-triazine	A	73
XV	2-Amino-4-(*p*-methylphenethyl)amino-6-pentafluoroethyl-*s*-triazine	A	67
XVI	2-Amino-4-heptafluoropropyl-6-(*p*-methylphenethyl)amino-*s*-triazine	A	60
XVII	2-Amino-4-chlorodifluoromethyl-6-(*p*-methylphenethyl)amino-*s*-triazine	A	73
XVIII	2-Amino-4-(*p*-methoxyphenethyl)amino-6-trifluoromethyl-*s*-triazine	B	68
XIX	2-Amino-4-(α-methylphenethyl)amino-6-trifluoromethyl-*s*-triazine	A	62
XX	2-Amino-4-(α-methylphenethyl)amino-6-pentafluoroethyl-*s*-triazine	A	83[b]
XXI	2-Amino-4-heptafluoropropyl-6-(α-methylphenethyl)amino-*s*-triazine	A	60
XXII	2-Amino-4-chlorodifluoromethyl-6-(α-methylphenethyl)amino-*s*-triazine	A	57
XXIII	2-Amino-4-(*N*-ethyl-*N*-phenethyl)amino-6-trifluoromethyl-*s*-triazine	B	23[b]
XXIV	2-Amino-4-(*N*-ethyl-*N*-phenethyl)amino-6-pentafluoroethyl-*s*-triazine	A	65[b]
XXV	2-Amino-4-(*N*-ethyl-*N*-phenethyl)amino-6-heptafluoropropyl-*s*-triazine	A	51
XXVI	2-Amino-4-chlorodifluoromethyl-6-(*N*-ethyl-*N*-phenethyl)amino-*s*-triazine	A	73
XXVII	2-Amino-4-butylamino-6-trifluoromethyl-*s*-triazine	B	61
XXVIII	2-Amino-4-butylamino-6-pentafluoroethyl-*s*-triazine	A	79
XXIX	2-Amino-4-butylamino-6-heptafluoropropyl-*s*-triazine	A	63
XXX	2-Amino-4-butylamino-6-chlorodifluoromethyl-*s*-triazine	A	90
XXXI	2-Amino-4-pentylamino-6-trifluoromethyl-*s*-triazine	B	77[b]
XXXII	2-Amino-4-pentafluoroethyl-6-pentylamino-*s*-triazine	A	80
XXXIII	2-Amino-4-heptafluoropropyl-6-pentylamino-*s*-triazine	A	54
XXXIV	2-Amino-4-chlorodifluoromethyl-6-pentylamino-*s*-triazine	A	89
XXXV	2-Amino-4-dimethylamino-6-trifluoromethyl-*s*-triazine	B	34

[a] Unless otherwise indicated, the yield is based on material melting within 3° of the analytical sample. [b] Yield based on material melting within 6° of the analytical sample.

es were calculated from the retention times of the investigated compounds and of selected normal saturated hydrocarbons (C_{15}, C_{16}, C_{17}, C_{18}, C_{20}, C_{22}, C_{24}, C_{26}, and C_{28}). The data were obtained on gas chromatographs equipped with flame-ionization detectors[15,16] and electron-capture (^{63}Ni or Sc^3H foils) detectors[16]. The glass columns [1.8 m (6 ft) × 2 mm i.d.] were filled with nonpolar or moderately polar packings[17]. Argon or nitrogen was used as the carrier gas with a flow rate of approximately 35 ml/min. The injector, detector, and column oven temperatures were maintained at 250, 280, and 210°, respectively.

RESULTS AND DISCUSSION

The substituted *s*-triazines prepared are listed in Table I. They were obtained in good yields by acylation of phenformin, buformin, metformin, and five analogous biguanides (IV–VIII). The latter were selected for use as possible internal standards when assaying the oral hypoglycemic compounds, I–III, in biological fluids. The choice of acylating agents was based on considerations of reactivity, anticipated volatility of the products, and the expectation that the halogenated substituted *s*-triazines will favor high sensitivity in GC detector response and will be suitable for mass fragmentography.

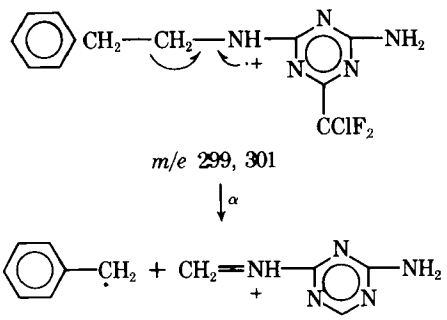

m/e 299, 301

m/e 208, 210

Scheme I

[15] Model 5000 gas chromatograph, Nuclear-Chicago, division of G. D. Searle and Co., Arlington Heights, Ill.
[16] Model 2100 gas chromatograph, Varian, Palo Alto, Calif.
[17] Three percent OV-1 or OV-17 on Chromosorb W HP, 80–100 mesh.

The *s*-triazines, IX–XXXV, are colorless crystalline compounds, whose physical properties are presented in Table II. The proposed structures are supported by elemental analysis results. Additional evidence was derived from the UV and NMR spectral data generated for IX, XVIII, XXVII, XXXI, and XXXV (Table III). The broad UV absorption maxima in the 273–284 and 213–215 nm regions are in agreement with the reported UV absorption of *s*-triazine (17). The NMR data are consistent with the assigned struc-

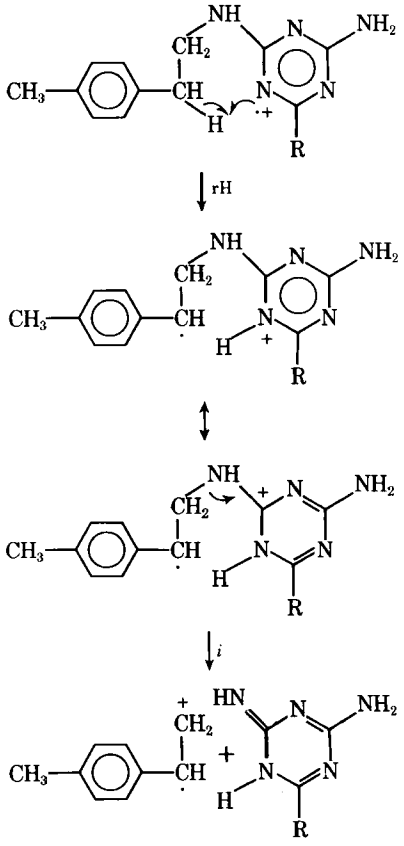

Scheme II

Table II—Analytical Data for Substituted *s*-Triazines Derived from Biguanides

Compound	Formula	Melting Point[a]	Analysis, %		Optical Rotation[b] $[\alpha]_D^{25}$
			Calc.	Found	
IX	$C_{12}H_{12}F_3N_5$	159.5–160°	C 50.88 H 4.27 N 24.73	50.86 4.56 24.93	—
X	$C_{13}H_{12}F_5N_5$	104–105°	C 46.85 H 3.63 N 21.02	46.87 3.93 21.34	—
XI	$C_{14}H_{12}F_7N_5$	109–110.5°	C 43.87 H 3.16 N 18.27	43.72 3.09 18.34	—
XII	$C_{12}H_{12}ClF_2N_5$	146–147°	C 48.09 H 4.04 N 23.37	47.80 3.99 23.20	—
XIII	$C_{12}H_{12}Cl_2FN_5$	105–106°	C 45.58 H 3.83 N 22.15	45.30 3.81 21.91	—
XIV	$C_{13}H_{14}F_3N_5$	185–186°	C 52.52 H 4.75 N 23.56	52.10 4.83 23.49	—
XV	$C_{14}H_{14}F_5N_5$	112–113°	C 48.41 H 4.06 N 20.17	48.18 3.96 20.21	—
XVI	$C_{15}H_{14}F_7N_5$	146.5–147.5°	C 45.32 H 3.55 N 17.63	45.23 3.82 17.69	—
XVII	$C_{13}H_{14}ClF_2N_5$	162–163°	C 49.76 H 4.50 N 22.32	49.69 4.90 22.35	—
XVIII	$C_{13}H_{14}F_3N_5O$	163.5–164.5°	C 49.84 H 4.50 N 22.36	50.23 4.58 22.21	—
XIX	$C_{13}H_{14}F_3N_5$	106–108°	C 52.52 H 4.75 N 23.56	52.28 4.79 23.37	+16.5° (c = 1.91)
XX	$C_{14}H_{14}F_5N_5$	78–79°	C 48.41 H 4.06 N 20.17	48.07 4.01 20.03	+25.0° (c = 1.23)
XXI	$C_{15}H_{14}F_7N_5$	56–57°	C 45.34 H 3.55 N 17.63	45.44 3.68 17.48	+20.1° (c = 1.98)
XXII	$C_{13}H_{14}ClF_2N_5$[c]	116–117°	C 48.37 H 4.68 N 21.70	48.26 4.45 21.59	+15.6° (c = 1.88)
XXIII	$C_{14}H_{16}F_3N_5$	107–108°	C 54.01 H 5.18 N 22.50	54.28 5.57 22.71	—
XXIV	$C_{15}H_{16}F_5N_5$	95–96°	C 49.86 H 4.46 N 19.38	50.15 4.60 19.36	—
XXV	$C_{16}H_{16}F_7N_5$	97.5–98.5°	C 46.72 H 3.92 N 17.03	46.80 3.89 17.07	—
XXVI	$C_{14}H_{16}ClF_2N_5$	97–98°	C 51.30 H 4.92 N 21.37	51.34 4.76 21.39	—
XXVII	$C_8H_{12}F_3N_5$	89–90°	C 40.85 H 5.14 N 29.78	40.78 5.38 29.74	—
XXVIII	$C_9H_{12}F_5N_5$	113–114°	C 37.90 H 4.24 N 24.56	37.92 4.30 24.51	—
XXIX	$C_{10}H_{12}F_7N_5$	88–89°	C 35.83 H 3.61 N 20.89	35.64 3.65 20.74	—
XXX	$C_8H_{12}ClF_2N_5$	103–104°	C 38.18 H 4.81 N 27.83	37.98 4.93 27.59	—
XXXI	$C_9H_{14}F_3N_5$	104–105°	C 43.37 H 5.66 N 28.10	43.04 5.85 27.99	—
XXXII	$C_{10}H_{14}F_5N_5$	116–117°	C 40.13 H 4.72 N 23.41	40.00 4.65 23.16	—
XXXIII	$C_{11}H_{14}F_7N_5$[d]	76–77.5°	C 35.97 H 4.39 N 19.07	36.03 4.22 18.86	—
XXXIV	$C_9H_{14}ClF_2N_5$	94–94.5°	C 40.68 H 5.31 N 26.36	40.70 5.44 26.19	—
XXXV	$C_6H_8F_3N_5$	153°	C 34.78 H 3.89 N 33.81	35.09 3.98 33.55	—

[a] Determined on a Thomas-Hoover capillary melting-point apparatus and reported uncorrected. [b] Optical rotation measurements were taken at 25° for the D (sodium) line, and "c" refers to milligrams of substance in 100 ml of methanolic solution. [c] Analyzed as the half-hydrate. [d] Analyzed as the monohydrate.

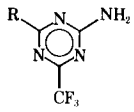

Table III—NMR and UV Spectra of Substituted *s*-Triazines Derived from Biguanides

Compound	R	NMR Spectra[a] δ, ppm	Assignment	Signal	Protons	UV Spectra[b] λ_{max}, nm (ε)
IX	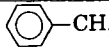	2.85	Ar—CH_2	t	2	273 (4041)
		3.67	N—CH_2	q	2	213 (35,609)
		5.50	C—NH, C—NH_2	br	3	—
		7.20	Ar—H	s	5	—
XVIII	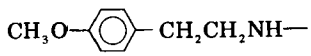	2.80	Ar—CH_2	t	2	284 (4698)
		3.65	N—CH_2	m	2	277 (5635)
		3.77	O—CH_3	s	3	215 (35,736)
		5.40	C—NH, C—NH_2	br	3	—
		6.80	Ar—H_m	d	2	—
		7.08	Ar—H_o	d	2	—
XXVII	$CH_3(CH_2)_3NH$—	0.90	C—CH_3	t	3	273 (3717)
		1.50	C—CH_2	m	4	213 (33,751)
		3.40	N—CH_2	q	2	—
		5.40	C—NH, C—NH_2	br	3	—
XXXI	$CH_3(CH_2)_4NH$—	0.90	C—CH_3	t	3	273 (3742)
		1.50	C—CH_2	m	6	213 (32,850)
		3.40	N—CH_2	q	2	—
		5.60	C—NH, C—NH_2	br	3	—
XXXV	$(CH_3)_2N$—	3.08	N—CH_3	s	6	278 (3430)
		7.40	C—NH_2	br	2	213 (27,433)

[a] Taken on a Varian XL-100 spectrometer with deuterated dimethyl sulfoxide solution of XXXV and deuterochloroform solutions of the remaining compounds, with tetramethylsilane as the internal reference. Singlet, broad singlet, doublet, triplet, quartet, and multiplet splittings are abbreviated s, br, d, t, q, and m, respectively. The H_m and H_o refer to protons in the *meta*- and *ortho*-positions of the *p*-methoxyphenethyl group of XVIII. [b] Determined in methanol with a Cary 14 instrument.

tures. Structural confirmation is provided also by the mass spectral data summarized in Table IV. They show the expected molecular ions and readily recognizable most abundant ion species (base peaks) for all synthetic *s*-triazines.

In the case of triazine XXXV, derived from metformin, the base peak is the molecular ion.

For IX–XIII and XIX–XXXIV, which constitute a majority of the investigated *s*-triazines, the base peak results from alpha cleavage of the molecular ion, as exemplified in Scheme I for the phenformin-derived triazine, XII. The monochloro-substituted triazines, XII, XXII, XXVI, XXX, and XXXIV, yield ^{35}Cl-substituted most abundant ions of the corresponding ^{37}Cl-substituted even electronic species in the expected 3:1 ratio of ^{35}Cl:^{37}Cl. The driving force for the cleavage is probably the electron-donating ability of the alkyl-substituted nitrogen atom.

The base peaks for XIV–XVIII appear to derive from a McLafferty rearrangement of the molecular ion followed by inductive cleavage with charge migration (Scheme II). Even among these *s*-

Table IV—GC and Mass Spectral Data for Substituted *s*-Triazines Derived from Biguanides

Compound	Kováts Indexes 3% OV-1	3% OV-17	Molecular Ion[a]	Most Abundant Ions[a] *m/e* > 60					
IX	2008	2430	283 (30)[b]	192 (100)	91 (43)	104 (38)	193 (20)		
X	1989	2360	333 (27)	242 (100)	91 (35)	104 (27)	243 (9)		
XI	2007	2339	383 (32)	292 (100)	91 (41)	104 (27)	293 (10)		
XII	2209	2667	299 (31)	208 (100)	91 (40)	210 (33)	104 (28)		
XIII	2359	2881	315 (32)	224 (100)	226 (65)	91 (34)	104 (34)	317 (21)	
XIV	2118	2518	297 (40)	118 (100)	192 (70)	105 (29)	180 (19)	117 (18)	119 (11)
XV	2097	2448	347 (33)	118 (100)	242 (71)	105 (31)	230 (18)	119 (16)	117 (9)
XVI	2112	2425	397 (27)	118 (100)	292 (47)	105 (30)	117 (18)	119 (15)	280 (14)
XVII	2295	2741	313 (20)	118 (100)	208 (49)	105 (34)	117 (22)	196 (17)	210 (16)
XVIII	2243	2715	313 (7)	134 (100)	121 (50)	192 (11)	135 (10)		
XIX	1988	2386	297 (3)	206 (100)	91 (24)	207 (10)	138 (8)		
XX	1972	2312	347 (5)	256 (100)	69 (13)	257 (11)	91 (10)		
XXI	1995	2318	397 (7)	306 (100)	69 (18)	91 (13)	307 (12)		
XXII	2171	2601	313 (2)	222 (100)	224 (31)	91 (17)	223 (9)		
XXIII	2014	2365	311 (25)	220 (100)	192 (50)	221 (16)	91 (11)		
XXIV	2025	2305	361 (16)	270 (100)	242 (40)	271 (13)	91 (8)		
XXV	2037	2276	411 (17)	320 (100)	292 (31)	91 (17)	321 (13)		
XXVI	2212	2583	327 (14)	236 (100)	238 (34)	208 (23)	91 (18)	237 (10)	
XXVII	1590	1871	235 (32)	192 (100)	193 (41)	206 (21)	179 (21)	138 (9)	
XXVIII	1575	1824	285 (30)	242 (100)	243 (52)	256 (40)	229 (22)	188 (11)	
XXIX	1590	1803	335 (33)	292 (100)	293 (46)	306 (32)	279 (18)	316 (11)	
XXX	1757	2047	251 (26)	208 (100)	209 (55)	210 (36)	222 (32)	195 (28)	216 (18)
XXXI	1672	1960	249 (31)	192 (100)	193 (43)	206 (22)	179 (18)	220 (14)	138 (9)
XXXII	1672	1915	299 (34)	242 (100)	243 (50)	256 (30)	270 (19)	229 (17)	280 (10)
XXXIII	1686	1894	349 (35)	292 (100)	293 (56)	306 (38)	320 (21)	279 (19)	330 (11)
XXXIV	1850	2150	265 (27)	208 (100)	209 (60)	210 (35)	222 (32)	195 (23)	236 (21)
XXXV	1378	1628	207 (100)	192 (73)	178 (20)	188 (13)			

[a] The mass spectral data were obtained on an AEI model MS 902 magnetic instrument at 70 ev. [b] The relative intensity of each ion is shown in parenthesis as percent of base peak value.

triazines, however, alpha cleavage in accordance with Scheme I is not insignificant. Thus, XIV–XVII, whose methyl substituent may be expected to have only a mild inductive effect, yield ions derived from alpha cleavage, with an abundance second only to that of the base peak.

The GC behavior of the *s*-triazines is good. They elute at moderate temperatures and give essentially symmetrical peaks. The Kováts retention indexes (Table IV) were obtained by computation of the appropriate logarithmic data (18). Independent determinations were also made by use of the Hupe (19) diagram. On the average, results by both methods differed by less than 0.05%.

The conversion of biguanides into substituted *s*-triazines was used for the development of GC and mass fragmentographic methods for assaying phenformin in biological fluids. This treatment permitted the determination of plasma and saliva drug concentration–time profiles and of urinary drug excretion rates following a 100-mg oral dose of phenformin to human volunteers (20). A similar assaying approach is applicable for buformin and metformin. A detailed description of the analytical methodology and its limitations will follow in a separate publication.

REFERENCES

(1) H. D. Breidahl, G. C. Ennis, F. I. R. Martin, J. R. Stawell, and P. Taft, *Drugs*, **3**, 204(1972).

(2) A. Loubatières, in "Oral Hypoglycaemic Agents," G. D. Campbell, Ed., Academic, New York, N.Y., 1969, chap. 1.

(3) H. D. Breidahl, G. C. Ennis, F. I. R. Martin, J. R. Stawell, and P. Taft, *Drugs*, **3**, 79(1972).

(4) R. E. Bailey, *Clin. Biochem.*, **3**, 23(1970).

(5) H. Hall, G. Ramachander, and J. M. Glassman, *Ann. N.Y. Acad. Sci.*, **148**, 601(1968).

(6) L. Freedman, M. Blitz, E. Gunsberg, and S. Zak, *J. Lab. Clin. Med.*, **58**, 662(1961).

(7) P. Pignard, *Ann. Biol. Clin.(Paris)*, **20**, 325(1962).

(8) R. Beckmann and G. Huebner, *Arzneim.-Forsch.*, **15**, 765(1965).

(9) E. R. Garrett and J. Tsau, *J. Pharm. Sci.*, **61**, 1404(1972).

(10) E. R. Garrett, J. Tsau, and P. H. Hinderling, *ibid.*, **61**, 1411(1972).

(11) J. A. F. Wickramasinghe and S. R. Shaw, *J. Chromatogr.*, **71**, 265(1972).

(12) R. Andreasch, *Monatsh. Chem.*, **48**, 145(1927).

(13) F. H. S. Curd and F. L. Rose, *J. Chem. Soc.*, **1946**, 362.

(14) J. T. Thurston (to American Cyanamid Co.), U.S. pat. 2,427,314 (1947); through *Chem. Abstr.*, **42**, 2286h(1948).

(15) A. Gruen (to J. R. Geigy A. G.), U.S. pat. 2,437,691 (1948); through *Chem. Abstr.*, **42**, 5475c(1948).

(16) G. P. Fraser and W. O. Kermack, *J. Chem. Soc.*, **1951**, 2682.

(17) C. Grundmann and A. Kreutzberger, *J. Amer. Chem. Soc.*, **76**, 5646(1954).

(18) E. Kováts, *Helv. Chim. Acta*, **41**, 1915(1958).

(19) K. P. Hupe, *J. Gas Chromatogr.*, **3**, 12(1965).

(20) D. Alkalay, L. Khemani, W. E. Wagner, Jr., and M. F. Bartlett, *J. Clin. Pharmacol.*, **15**, 446(1975).

ACKNOWLEDGMENTS AND ADDRESSES

Received March 31, 1975, from the *Research Department, Pharmaceuticals Division, Ciba-Geigy Corporation, Ardsley, NY 10502*

Accepted for publication June 20, 1975.

The authors are grateful to their colleagues from Research Services for providing the elemental analyses and all UV, NMR, and mass spectral data.

[x] To whom inquiries should be directed.

Correlation between Dissolution Characteristics and Absorption of Methaqualone from Solid Dosage Forms

P. B. CHEMBURKAR [*], R. D. SMYTH [x], J. D. BUEHLER, P. B. SHAH, R. S. JOSLIN, A. POLK, and N. H. REAVEY-CANTWELL

Abstract □ A methaqualone tablet in two strengths, 150 and 300 mg, was developed. The dissolution rate of an experimental formulation in pH 7.0 phosphate buffer, measured by the resin flask method, was shown to correlate with bioavailability in humans. The dissolution rate criterion was used to develop the final tablet formulation. Bioavailability of this formulation in two strengths was compared with a commercial capsule formulation and a slowly dissolving tablet formulation. Correlation between dissolution rate and bioavailability was shown in freshly prepared methaqualone tablet formulations. Bioavailability of tablets under accelerated stability testing conditions remained unaltered, whereas the dissolution rates in pH 7 phosphate buffer decreased, using the resin flask method. A rotating-flask method was developed, and dissolution in 0.1 *N* HCl at 2 rpm correlated with the bioavailability of both new and aged tablet formulations.

Keyphrases □ Methaqualone—solid dosage forms, dissolution rate correlated with bioavailability □ Dosage forms, solid—dissolution of methaqualone tablets correlated with bioavailability □ Dissolution—methaqualone tablets, correlated with bioavailability □ Bioavailability—methaqualone, correlated with dissolution of tablets

Methaqualone [2-methyl-3-(2-methylphenyl)-4-(3*H*)-quinazolinone] is a sedative–hypnotic and anticonvulsant compound of the 4-quinazolinone series (1). It is usually administered in tablet or capsule form, containing 150–300 mg of the base or hydrochloride salt. The pKa of the conjugate acid is 2.54, and its solubility is 0.3 mg/ml in water (2).

Peak serum levels have been observed within 2 hr after oral administration of methaqualone tablets (3). Other reports (4–6) also indicated the rapid absorption of methaqualone administered in various capsule and tablet formulations. Similar peak levels of methaqualone, within 2 hr, were reported for methaqualone–diphenhydramine hydrochloride tablets and capsules (7). Plasma and urinary excretion data were typical of a dissolution rate-limited process using 2-^{14}C-methaqualone capsules or tablets (4).

The effects of formulation variables on the dissolution of methaqualone were studied (8) in 0.1 *N* HCl, using Levy's beaker method (9); it was concluded

triazines, however, alpha cleavage in accordance with Scheme I is not insignificant. Thus, XIV–XVII, whose methyl substituent may be expected to have only a mild inductive effect, yield ions derived from alpha cleavage, with an abundance second only to that of the base peak.

The GC behavior of the *s*-triazines is good. They elute at moderate temperatures and give essentially symmetrical peaks. The Kováts retention indexes (Table IV) were obtained by computation of the appropriate logarithmic data (18). Independent determinations were also made by use of the Hupe (19) diagram. On the average, results by both methods differed by less than 0.05%.

The conversion of biguanides into substituted *s*-triazines was used for the development of GC and mass fragmentographic methods for assaying phenformin in biological fluids. This treatment permitted the determination of plasma and saliva drug concentration–time profiles and of urinary drug excretion rates following a 100-mg oral dose of phenformin to human volunteers (20). A similar assaying approach is applicable for buformin and metformin. A detailed description of the analytical methodology and its limitations will follow in a separate publication.

REFERENCES

(1) H. D. Breidahl, G. C. Ennis, F. I. R. Martin, J. R. Stawell, and P. Taft, *Drugs*, **3**, 204(1972).

(2) A. Loubatières, in "Oral Hypoglycaemic Agents," G. D. Campbell, Ed., Academic, New York, N.Y., 1969, chap. 1.

(3) H. D. Breidahl, G. C. Ennis, F. I. R. Martin, J. R. Stawell, and P. Taft, *Drugs*, **3**, 79(1972).

(4) R. E. Bailey, *Clin. Biochem.*, **3**, 23(1970).

(5) H. Hall, G. Ramachander, and J. M. Glassman, *Ann. N.Y. Acad. Sci.*, **148**, 601(1968).

(6) L. Freedman, M. Blitz, E. Gunsberg, and S. Zak, *J. Lab. Clin. Med.*, **58**, 662(1961).

(7) P. Pignard, *Ann. Biol. Clin.(Paris)*, **20**, 325(1962).

(8) R. Beckmann and G. Huebner, *Arzneim.-Forsch.*, **15**, 765(1965).

(9) E. R. Garrett and J. Tsau, *J. Pharm. Sci.*, **61**, 1404(1972).

(10) E. R. Garrett, J. Tsau, and P. H. Hinderling, *ibid.*, **61**, 1411(1972).

(11) J. A. F. Wickramasinghe and S. R. Shaw, *J. Chromatogr.*, **71**, 265(1972).

(12) R. Andreasch, *Monatsh. Chem.*, **48**, 145(1927).

(13) F. H. S. Curd and F. L. Rose, *J. Chem. Soc.*, **1946**, 362.

(14) J. T. Thurston (to American Cyanamid Co.), U.S. pat. 2,427,314 (1947); through *Chem. Abstr.*, **42**, 2286h(1948).

(15) A. Gruen (to J. R. Geigy A. G.), U.S. pat. 2,437,691 (1948); through *Chem. Abstr.*, **42**, 5475c(1948).

(16) G. P. Fraser and W. O. Kermack, *J. Chem. Soc.*, **1951**, 2682.

(17) C. Grundmann and A. Kreutzberger, *J. Amer. Chem. Soc.*, **76**, 5646(1954).

(18) E. Kováts, *Helv. Chim. Acta*, **41**, 1915(1958).

(19) K. P. Hupe, *J. Gas Chromatogr.*, **3**, 12(1965).

(20) D. Alkalay, L. Khemani, W. E. Wagner, Jr., and M. F. Bartlett, *J. Clin. Pharmacol.*, **15**, 446(1975).

ACKNOWLEDGMENTS AND ADDRESSES

Received March 31, 1975, from the *Research Department, Pharmaceuticals Division, Ciba-Geigy Corporation, Ardsley, NY 10502*

Accepted for publication June 20, 1975.

The authors are grateful to their colleagues from Research Services for providing the elemental analyses and all UV, NMR, and mass spectral data.

[x] To whom inquiries should be directed.

Correlation between Dissolution Characteristics and Absorption of Methaqualone from Solid Dosage Forms

P. B. CHEMBURKAR [*], R. D. SMYTH [x], J. D. BUEHLER, P. B. SHAH, R. S. JOSLIN, A. POLK, and N. H. REAVEY-CANTWELL

Abstract □ A methaqualone tablet in two strengths, 150 and 300 mg, was developed. The dissolution rate of an experimental formulation in pH 7.0 phosphate buffer, measured by the resin flask method, was shown to correlate with bioavailability in humans. The dissolution rate criterion was used to develop the final tablet formulation. Bioavailability of this formulation in two strengths was compared with a commercial capsule formulation and a slowly dissolving tablet formulation. Correlation between dissolution rate and bioavailability was shown in freshly prepared methaqualone tablet formulations. Bioavailability of tablets under accelerated stability testing conditions remained unaltered, whereas the dissolution rates in pH 7 phosphate buffer decreased, using the resin flask method. A rotating-flask method was developed, and dissolution in 0.1 *N* HCl at 2 rpm correlated with the bioavailability of both new and aged tablet formulations.

Keyphrases □ Methaqualone—solid dosage forms, dissolution rate correlated with bioavailability □ Dosage forms, solid—dissolution of methaqualone tablets correlated with bioavailability □ Dissolution—methaqualone tablets, correlated with bioavailability □ Bioavailability—methaqualone, correlated with dissolution of tablets

Methaqualone [2-methyl-3-(2-methylphenyl)-4-(3*H*)-quinazolinone] is a sedative–hypnotic and anticonvulsant compound of the 4-quinazolinone series (1). It is usually administered in tablet or capsule form, containing 150–300 mg of the base or hydrochloride salt. The pKa of the conjugate acid is 2.54, and its solubility is 0.3 mg/ml in water (2).

Peak serum levels have been observed within 2 hr after oral administration of methaqualone tablets (3). Other reports (4–6) also indicated the rapid absorption of methaqualone administered in various capsule and tablet formulations. Similar peak levels of methaqualone, within 2 hr, were reported for methaqualone–diphenhydramine hydrochloride tablets and capsules (7). Plasma and urinary excretion data were typical of a dissolution rate-limited process using 2-^{14}C-methaqualone capsules or tablets (4).

The effects of formulation variables on the dissolution of methaqualone were studied (8) in 0.1 *N* HCl, using Levy's beaker method (9); it was concluded

that no one technique or dissolution apparatus simulated *in vivo* conditions of methaqualone release from various tablet formulations. A relationship was shown between peak plasma levels of methaqualone in human subjects and the dissolution rates of tablets and capsules in pH 2 buffer (10).

The objective of this study was to develop a suitable *in vitro* dissolution technique that correlates with the bioavailability of newly prepared and aged methaqualone formulations.

EXPERIMENTAL

Dissolution Studies—*Resin Flask Method*—The procedure described by Poole (11) was modified to contain six separate stirring units chain driven by a common motor. Commercially available dissolution equipment[1] with a 5.1-cm (2-in.) stainless steel three-blade propeller[2] mounted on a stainless steel stirring shaft[3] was used. Stirrer speed was varied between 50 and 100 rpm. The volume of the dissolution medium was varied between 600 and 900 ml. Sampling of the medium and absorbance measurements were initially carried out manually but were later automated.

For the manual operation, samples (1.0 ml) of the dissolution fluid were removed at appropriate times by aspirating the fluid through a medium-grade, sintered-glass, gas dispersion tube into a pipet. The sample was diluted with 0.1 *N* NaOH, and the absorbance was determined at 236 nm.

For the automated operation, a medium-grade, sintered-glass, filter candle[4] was used as a filter. A peristaltic pump[5] was used to remove the dissolution medium simultaneously from three resin flasks, to filter and pump the filtrate into three flow-through cells[6], and then to return it to the resin flask; 600 and 900 ml of 0.1 *M* phosphate buffer (pH 7) were used for 150- and 300-mg methaqualone tablets, respectively.

All analyses were performed in triplicate. The absorbance of each sample was measured[7] and recorded[8] automatically with the aid of preset timers[9]. The absorbance was measured at 315 and 317 nm for the 150- and 300-mg methaqualone tablets, respectively. These wavelengths, rather than 236 nm (λ_{max}), were used since dilution of the sample for a reading at 236 nm would preclude recirculation of the sample in this closed system.

Rotating-Flask Method—The method described by Weintraub and Gibaldi (12) was used with a slight modification in the apparatus and with a dissolution medium volume of 600 ml of 0.1 *N* HCl. The rotation speed of the flask was varied between 0.5 and 6.0 rpm.

Accelerated Stability Testing—Tablets were stored at 40, 50, 60, 70, and 80° in closed containers. Unpackaged tablets were stored at room temperature and also at 40° in 80% relative humidity. Tablets packaged in blister packs were stored in 80% relative humidity. Tablets packaged in closed containers were stored in a light-temperature cycle cabinet (12 hr at 5° and 12 hr at 45°).

Formulations Studied—Table I lists the dosage form and the amount of methaqualone base or hydrochloride salt in the various formulations used.

Bioavailability Studies—All bioavailability studies were conducted in accordance with previously described procedures in normal fasted subjects (4). A 4 × 4 Latin-square design with three replications was used for Formulations A–D in 12 subjects. A 6 × 6 Latin-square design was used for Formulations P–U in six subjects. A completely randomized block design was used for Formulations C and K–N in three subjects.

Serum methaqualone levels were measured by a modification of the spectrofluorometric procedure of Brown and Smart (13). All data were subjected to an analysis of variance for the particular statistical design.

Table I—Formulations Used

Formulation	Dosage Form	Methaqualone: Chemical Form[a]	Methaqualone: Strength, mg
A	Tablet	Base	150
B	Tablet	Base	300
C	Tablet	Base	300
D	Capsule	Salt	200
P	Tablet	Base	300
Q	Capsule	Base	300
R	Tablet	Base	300
S	Tablet	Base	300
T	Tablet	Base	300
U	Capsule	Salt	200
K	Tablet	Base	150
L	Tablet	Base	150
M	Tablet	Base	150
N	Tablet	Base	150

[a] Methaqualone base is listed as base, and methaqualone hydrochloride salt is listed as salt.

RESULTS AND DISCUSSION

Preliminary dissolution studies using the resin flask technique with several methaqualone formulations in 0.1 and 0.01 *N* HCl showed no correlation between dissolution and bioavailability profiles. However, dissolution studies in phosphate buffer (pH 7) did show dissolution profiles that correlated with bioavailability data.

The dissolution in phosphate buffer, using the resin flask technique, was studied with Formulations A–D (Table II). The dissolution of 150-mg methaqualone tablets was studied in 600 ml of pH 7 phosphate buffer stirred at 60 rpm, and the dissolution of 300-mg tablets was studied in 900 ml of pH 7 phosphate buffer at 90 rpm. The rates of dissolution were equivalent at the different stirring speeds as shown by dissolving two 150-mg tablets in 900 ml of medium at 90 rpm.

The reproducibility of the dissolution procedure was confirmed with three sets of tablets from two lots of 300-mg tablets and one lot of 150-mg tablets. Three sets of capsules, from one lot of commercially marketed capsules containing 200 mg of methaqualone hydrochloride, were also studied for dissolution characteristics. The reproducibility of the dissolution analysis, as indicated by the standard deviation, was acceptable with all tablet formulations. However, the variation with the capsule formulation was much greater than with tablets.

This variation could be attributed to the difference in the mode of disintegration of tablets and capsules prior to dissolution. Tablets disintegrated immediately, and the methaqualone was instantly available for dissolution purposes. However, the dissolution characteristics of the capsule shell and physical interaction of the partially dissolved, solvated gelatin with the capsule contents introduced a variable time lag in the dissolution profile. Since the extent to which the gelatin hampered the dissolution differed from capsule to capsule, the variability in dissolution data for capsules was greater than that for tablets.

A 300-mg methaqualone formulation was developed in both capsule and tablet dosage forms. The dissolution profiles of these two formulations (P and Q) and four other formulations in pH 7 phosphate buffer are shown in Fig. 1. Tablet Formulations R and S were identical except that the methaqualone used was obtained from two different manufacturers. Formulations T and U were commercially available formulations in the forms of a tablet and a capsule containing 300 mg of methaqualone base and 200 mg of methaqualone hydrochloride, respectively.

The similarity in dissolution profiles of Formulations P, Q, T, and U is apparent. These profiles differ considerably from those of Formulations R and S. The bioavailability of these formulations was determined in six subjects. The average serum concentration profiles of methaqualone are shown in Fig. 1. The mean methaqualone serum concentrations at 0.5, 1, 2, and 3 hr of Formulations P, Q, T, and U are statistically equivalent and significantly different from Formulations R and S. Area under the curve (*AUC*) measure-

[1] Hanson Research Corp., Northridge, Calif.
[2] Catalog No. 8592-F25, Arthur H. Thomas, Philadelphia, Pa.
[3] Catalog No. 8592-F50, Arthur H. Thomas, Philadelphia, Pa.
[4] Catalog No. 4665-J588 J66, Arthur H. Thomas, Philadelphia, Pa.
[5] Model 7015, Cole Parmer, Chicago, Ill.
[6] Part 886655, Beckman Instrument Co., Fullerton, Calif.
[7] Model 210, Gilford Instrument Laboratories, Oberlin, Ohio.
[8] Leeds & Northrop, North Wales, Pa.
[9] Industrial Timer Corp., Parsippany, N.J.

Table II—Dissolution Profiles of Various Methaqualone Formulations[a]

Minutes	Methaqualone in Solution, $\bar{X}$ % ± SD				
	Formulation A[b]	Formulation A[c]	Formulation B[c]	Formulation C[c]	Formulation D[b]
10	63.2 ± 3.4	65.7 ± 2.0	57.9 ± 5.1	17.8 ± 2.7	18.0 ± 6.7
20	84.1 ± 2.2	80.5 ± 3.7	77.2 ± 4.0	29.6 ± 2.7	49.9 ± 8.8
30	92.5 ± 1.7	86.5 ± 4.5	85.3 ± 3.2	36.6 ± 2.8	71.4 ± 13.3
40	96.4 ± 1.5	89.7 ± 4.9	89.4 ± 2.8	41.6 ± 2.7	81.8 ± 13.2
50	98.2 ± 1.4	91.8 ± 5.2	92.1 ± 2.4	45.6 ± 2.6	87.2 ± 12.0
60	99.6 ± 1.4	92.8 ± 5.0	93.6 ± 2.1	48.8 ± 2.4	91.2 ± 11.3

[a] Dissolution was studied using the resin flask procedure with phosphate buffer (pH 7). Formulation A = 150-mg methaqualone tablet, Formulation B or C = 300-mg methaqualone tablet, and Formulation D = 200-mg methaqualone hydrochloride capsule. [b] Dissolution of one tablet (A) or one capsule (D) in 600 ml of buffer at 60 rpm. [c] Dissolution of two 150-mg tablets (A) or one 300-mg tablet (B or C) in 900 ml of buffer at 90 rpm.

Table III—Correlation of Dissolution and Area under the Serum Concentration Curve (*AUC*) with Various Formulations

AUC, μg hr/ml	Correlation Coefficient[a]					
	Dissolution Sampling Time, min					
	10	20	30	40	50	60
0–3	0.811[b]	0.979[c]	0.988[c]	0.987[c]	0.989[c]	0.990[c]
0–6	0.874[b]	0.986[c]	0.990[c]	0.985[c]	0.984[c]	0.987[c]

[a] Regression analysis of percent methaqualone in solution *versus* area under the curve with Formulations P-U. [b] Statistically significant, $p < 0.05$. [c] Statistically significant, $p < 0.001$.

ments at all testing intervals, *e.g.*, 0–0.5, 0–1, and 0–2 hr, confirmed these conclusions.

Formulations P, Q, T, and U dissolved very rapidly and reached a dissolution plateau of 95% in 30 min; they were rapidly absorbed and achieved equivalent peak serum concentrations within 1 hr. Formulations R and S, which dissolved slowly, did not reach 100% dissolution even after 60 min. These tablets were poorly absorbed and had lower serum levels throughout the experiment. The dissolution data obtained with Capsule U showed a lag period, consistent with the previous explanation for slower dissolution with capsule formulations.

Regression analysis of the serum *AUC* at 0 → 3 and 0 → 6 hr of Formulations P–U *versus* percent methaqualone in solution at 10, 20, 30, 40, 50, and 60 min indicated a highly significant correlation (Table III).

Subsequent studies resulted in the development of tablet Formulations A and B, containing 150 and 300 mg of methaqualone, respectively. The bioavailability of these formulations was compared to a slowly dissolving formulation (C) and a commercially available capsule formulation of methaqualone hydrochloride (D). There was no significant difference between the mean methaqualone serum concentrations at all sampling times for Formulations A, B, and D (Fig. 2). Peak serum concentrations of all four formulations were observed in 1–1.5 hr.

In this bioavailability experiment, the dose of methaqualone hydrochloride in Formulation D (349 mg of methaqualone base) was higher than in Formulations A and B; the peak serum concentrations were statistically equivalent. When the area under the curve for the 0–6-hr period for Formulation D was normalized to 300 mg of methaqualone base, the value obtained was 11.4 μg hr/ml as compared to 10.8 and 11.3 μg hr/ml for Formulations A and B, respectively.

The mean methaqualone serum concentrations and area under the curve of Formulation C were significantly lower than those of the other three formulations. The dissolution profiles in Fig. 2 predict that Formulation C should be lower in bioavailability than Formulations A, B, and D. When the lag time inherent in the dissolution profile of Capsule D is considered, the dissolution profiles

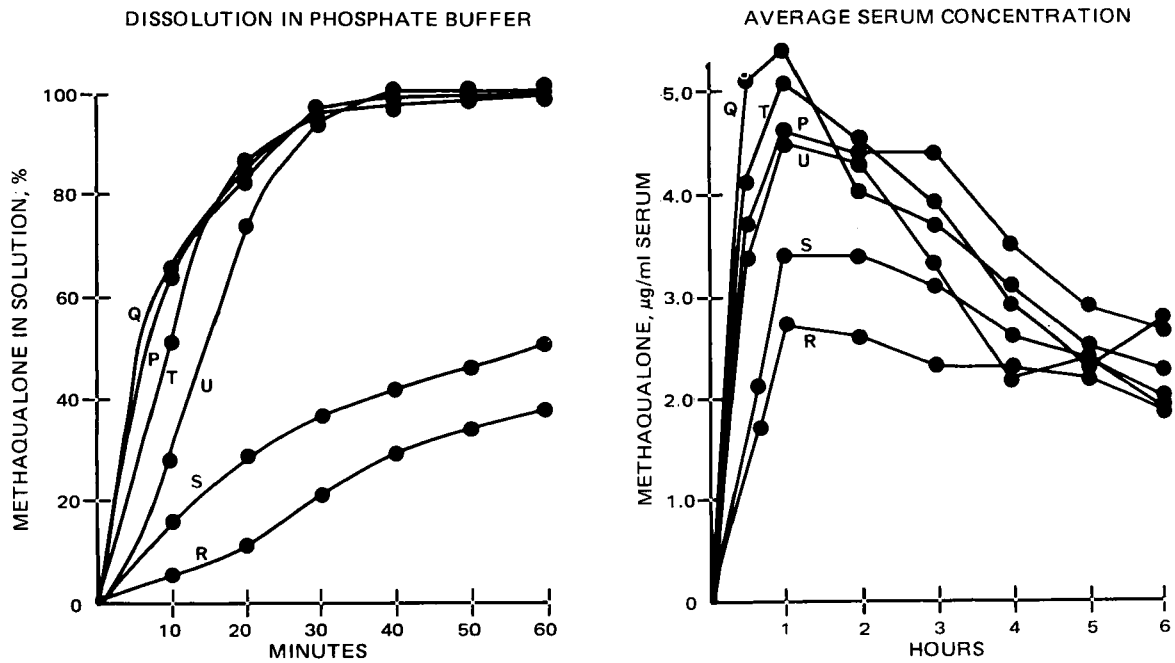

Figure 1—*Dissolution profiles measured by resin flask method for Formulations P–T in 900 ml of pH 7.0 phosphate buffer stirred at 90 rpm and for Formulation U in 600 ml of pH 7.0 phosphate buffer stirred at 60 rpm and average serum methaqualone levels for the formulations in six subjects with 600-mg dose.*

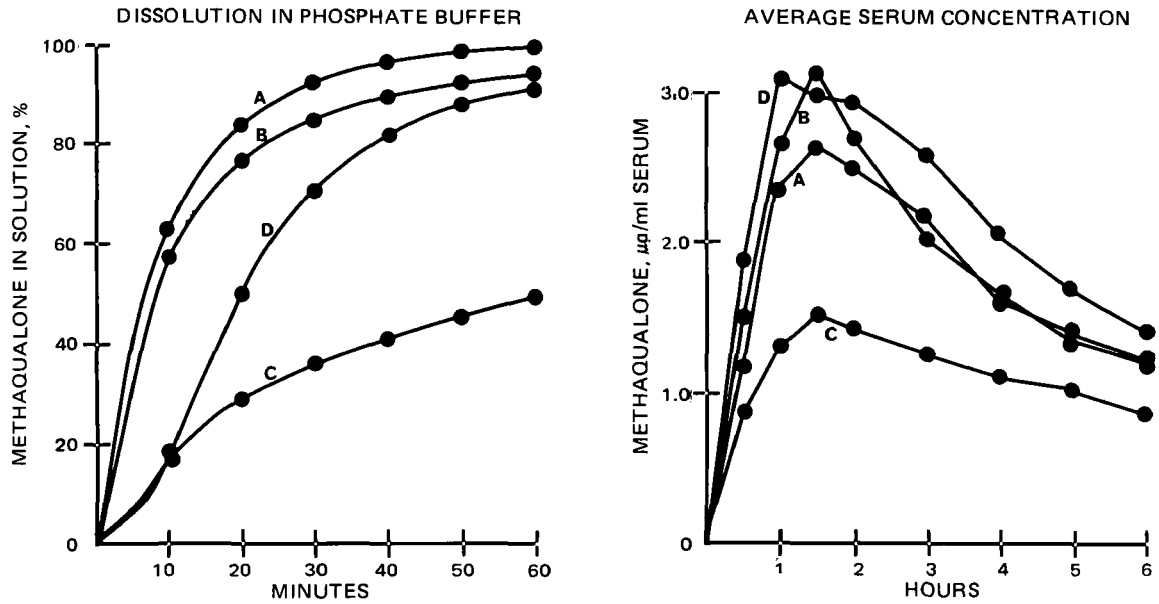

Figure 2—*Dissolution profiles measured by resin flask method for Formulations A, B, and D in 600 ml of pH 7.0 phosphate buffer stirred at 60 rpm and for Formulation C in 900 ml of pH 7.0 phosphate buffer stirred at 90 rpm and average serum methaqualone levels for the formulations in 12 subjects with 300-mg dose.*

for Formulations A, B, and D become similar. The dissolution profiles predicted that the bioavailability of 300 mg of methaqualone administered as one 300-mg tablet (Formulation B) or two 150-mg tablets (Formulation A) should be equivalent to each other and to capsule Formulation D.

Regression analyses of serum *AUC* 0 → 3 and *AUC* 0 → 6 *versus* percent dissolved in phosphate buffer are shown in Table IV. Statistically significant correlations were observed between percent dissolved in 40, 50, and 60 min and *AUC* 0 → 3 and 0 → 6 hr. Thus, the correlation previously established with the intermediate formulations (P–S) was observed with the final formulations (A and B). Equivalency in bioavailability of two strengths of a dosage form (150- and 300-mg tablets) was also demonstrated. This aspect is important and must be considered in the design and evaluation of drug products in various unit doses.

The final 150- and 300-mg methaqualone tablet formulations were tested for their chemical and physical stability by subjecting them to accelerated stability conditions, which included storing the tablets in open containers and subjecting them to high temperatures and high humidity. There was no change in the chemical stability of the methaqualone. The disintegration times of tablets stored at high temperatures increased slightly but never exceeded 10 min. The dissolution rates of tablets subjected to high humidity–high temperature conditions were considerably reduced (Table V).

Four different 150-mg methaqualone tablet formulations (K–N) with variable decreased dissolution rates were tested for their bioavailability in three subjects. The same three subjects were used throughout this phase of the study. The dissolution data and average serum methaqualone concentrations are shown in Table V.

Table IV—Correlation Coefficient of Percent Dissolved *versus* Area Under the Serum Level Curve (*AUC*) for Formulations A–D

AUC, μg hr/ml	Correlation Coefficient[a]					
	Dissolution Sampling Time, min					
	10	20	30	40	50	60
0–3	0.527	0.758	0.888	0.929[b]	0.943[b]	0.949[b]
0–6	0.500	0.747	0.890	0.937[b]	0.952[c]	0.960[c]

[a] Regression analysis of percent methaqualone in solution *versus* area under the curve with Formulations A–D. [b] Statistically significant, $p < 0.1$. [c] Statistically significant, $p < 0.05$.

The mean serum methaqualone concentrations of Formulations K–N were statistically equivalent. This finding is in contrast to their distinctly differing dissolution data. From the dissolution data, one would predict that Formulations M and N would be absorbed more slowly and to a lesser extent than Formulations K and L. Regression analysis showed no correlation between dissolution and bioavailability of aged samples.

The bioavailability of Formulation C, which had previously been demonstrated to have poor dissolution and poor bioavailability in a larger population, was also tested in these three subjects. Formulation C contained 300 mg of methaqualone. It was used as an intact tablet since cutting in half would tamper with the dosage form and change the surface characteristics. Table V lists the area under the curve for Formulation C, normalized to a 150-mg dose. Smyth *et al.* (4, 5) substantiated this normalization process. Normalization was carried out by halving the *AUC* for the 300-mg dose.

The serum levels in the three subjects for Formulation C were equivalent to those in a larger population. Thus, the data obtained with the other four formulations (K–N) were considered to be reflective of a larger population and clearly indicated that differing dissolution profiles of Formulations K–N in phosphate buffer did not correlate with their bioavailability in humans. When this discrepancy was observed between dissolution profiles using the resin flask method and the bioavailability data after administration of Formulation L, several other dissolution methods were investigated.

Dissolution rates were studied using the rotating-flask technique at speeds ranging from 0.5 to 6 rpm in 600 ml of 0.1 *N* HCl. Results obtained at 2 rpm and above were reproducible. Dissolution data obtained below 2 rpm showed differences between the formulations, which were not apparent in bioavailability. Dissolution studies by this method in pH 7.0 phosphate buffer also showed very poor correlation with bioavailability.

Dissolution data on Formulations L–N at 2 (Table VI) and 4 rpm were similar. Even though Formulation N was initially slow in dissolving, all three formulations released close to 100% of their contents into the dissolution medium after 40 min. Therefore, it appears that dissolution studies using the rotating-flask method may give the best correlation with bioavailability.

Bioavailability studies are usually conducted on freshly prepared formulations, because it is assumed that bioavailability will remain unaltered with age unless some physicochemical changes in the formulation are observed. However, little work has been reported on the correlation between dissolution rate and bioavailability of aged formulations. This report has shown that dissolution technology applied to freshly prepared formulations is not necessarily applicable to aged samples. Consequently, methods

Table V—Dissolution and Bioavailability Data on Stability Samples of Methaqualone Tablets

Time	Methaqualone in Solution, %[a]				
	Formulation K[b], 2 months at Room Temperature	Formulation L[b], 3 months in Light-Temperature Cycle	Formulation M[b], 7 months at 80% R.H. and Room Temperature	Formulation N[b], 8 months at 80% R.H. and 40°	Formulation C[b], 33 months at Room Temperature
0 min	0	0	0	0	0
10 min	53.7 ± 5.3	46.6 ± 2.7	18.2 ± 2.3	10.0 ± 1.6	3.3 ± 1.1
20 min	72.1 ± 6.3	67.8 ± 1.6	34.1 ± 4.4	18.2 ± 4.1	11.0 ± 0.6
30 min	81.0 ± 7.3	78.7 ± 0.6	45.9 ± 3.2	25.4 ± 6.2	16.6 ± 0.5
40 min	85.1 ± 7.0	84.4 ± 2.3	54.3 ± 4.2	31.4 ± 7.5	21.3 ± 1.0
50 min	87.7 ± 6.2	87.9 ± 1.4	60.1 ± 3.9	35.8 ± 8.4	25.9 ± 0.9
60 min	89.0 ± 5.2	90.5 ± 2.3	66.0 ± 4.2	39.8 ± 9.2	30.7 ± 0.6
	Serum Methaqualone, μg/ml[c]				
0 hr	0	0	0	0	0
0.5 hr	1.4 ± 0.3	1.5 ± 0.3	1.1 ± 0.5	1.3 ± 0.0	1.7 ± 0.2
1 hr	1.6 ± 0.3	1.9 ± 0.4	1.6 ± 0.2	1.7 ± 0.4	2.5 ± 0.5
1.5 hr	—	—	1.9 ± 0.6	2.3 ± 0.5	2.1 ± 0.6
2 hr	1.1 ± 0.1	1.4 ± 0.0	1.7 ± 0.6	1.4 ± 0.4	1.7 ± 0.3
3 hr	1.1 ± 0.2	1.1 ± 0.1	1.2 ± 0.3	0.8 ± 0.3	1.4 ± 0.3
4 hr	1.0 ± 0.2	0.8 ± 0.1	1.1 ± 0.4	0.6 ± 0.2	1.1 ± 0.2
5 hr	0.9 ± 0.3	0.7 ± 0.1	0.8 ± 0.2	0.5 ± 0.2	1.0 ± 0.3
6 hr	0.8 ± 0.1	0.7 ± 0.2	—	—	—
$AUC^{0-3\ hr}$, μg hr/ml	3.58	4.10	4.28	4.10	4.99 (2.49[d])
$AUC^{0-5\ hr}$, μg hr/ml	5.62	5.79	6.35	5.35	7.29 (3.65[d])

[a] Dissolution was measured using the resin flask method with phosphate buffer (pH 7). (See Table II for conditions.) Values are the average concentrations ± *SD*. [b] Formulations K-N = 150-mg methaqualone tablet identical to Formulation A but stored under various stability conditions, and Formulation C = 300-mg methaqualone tablet. (R.H. = relative humidity.) [c] Average data for bioavailability study in three subjects at a 150-mg methaqualone dose for Formulations K-N and at a 300-mg methaqualone dose for Formulation C ± *SD*. [d] Area under the curve normalized to 150-mg methaqualone dose.

Table VI—Dissolution of Methaqualone Tablets by the Rotating-Flask Method

Minutes	Methaqualone in Solution, %[a]			
	Formulation L[b]	Formulation M[b]	Formulation N[b]	Formulation C[b]
10	89.7 ± 7.3	88.9 ± 4.3	59.5 ± 6.0	27.9 ± 8.3
20	96.2 ± 5.4	96.2 ± 3.5	80.0 ± 6.1	45.5 ± 6.5
30	100 ± 3.2	100 ± 2.5	88.1 ± 4.9	58.1 ± 7.2
40[c]	—	—	92.2 ± 3.7	67.0 ± 3.2
50	—	—	94.9 ± 3.8	72.1 ± 4.9
60	—	—	96.3 ± 2.9	78.1 ± 6.8

[a] Using 600 ml of 0.1 *N* HCl at 37° in a 2-liter flask rotated at 2 rpm. Values are the average concentrations ± *SD*. [b] Formulations L-N = 150-mg methaqualone tablet identical to Formulation A but stored under various stability conditions, and Formulation C = 300-mg methaqualone tablet (see Table V). [c] Dissolution for Formulations L and M was stopped after 30 min.

that show correlation between dissolution characteristics and bioavailability of aged samples must be developed for each drug product.

REFERENCES

(1) A. H. Amin, D. R. Mehta, and S. S. Samartha, *Progr. Drug Res.*, **14**, 218(1970).

(2) D. M. Patel, A. J. Visalli, J. J. Zalipsky, and N. H. Reavey-Cantwell, in "Analytical Profiles of Drug Substances," vol. 4, K. Florey, Ed., Academic, New York, N.Y., 1975, p. 245.

(3) R. N. Morris, G. A. Gunderson, S. W. Babcock, and J. F. Zaroslinski, *Clin. Pharmacol. Ther.*, **13**, 719(1972).

(4) R. D. Smyth, J. K. Lee, A. Polk, P. B. Chemburkar, and A. M. Savacool, *J. Clin. Pharmacol.*, **13**, 391(1973).

(5) R. D. Smyth, P. B. Chemburkar, A. Polk, and J. K. Lee, "Abstracts," APhA Academy of Pharmaceutical Sciences, vol. 3, 1973, p. 48.

(6) R. D. Smyth, P. B. Chemburkar, P. P. Mathur, A. F. DeLong, A. Polk, P. B. Shah, R. S. Joslin, and N. H. Reavey-Cantwell, *J. Intern. Med. Res.*, **2**, 85(1974).

(7) M. E. Williams, M. J. Kendall, M. Mitchard, S. S. Davis, and R. Poxan, *Brit. J. Clin. Pharmacol.*, **1**, 99(1974).

(8) M. J. Alexis, M. P. Bandon, M. Delattre, A. DeMecheleer, M. J. Jehotte, M. P. Leduc, M. J. Leloup, M. J. Mathieu, I. Moran, M. M. Roland, and J. Stein, *J. Pharm. Belg.*, **26**, 252(1971).

(9) G. Levy and B. A. Hayes, *N. Engl. J. Med.*, **262**, 1953(1960).

(10) S. S. Davis, R. Poxan, M. Mitchard, and M. E. Williams, *Lancet*, **1**, 667(1973).

(11) J. W. Poole, *Drug Inform. Bull.*, **3**, 8(1969).

(12) H. Weintraub and M. Gibaldi, *J. Pharm. Sci.*, **59**, 1792(1970).

(13) S. S. Brown and G. A. Smart, *J. Pharm. Pharmacol.*, **21**, 466(1969).

ACKNOWLEDGMENTS AND ADDRESSES

Received March 27, 1974, from the *Research Laboratories, William H. Rorer, Inc., Fort Washington, PA 19034*

Accepted for publication June 25, 1975.

Presented in part at the Industrial Pharmaceutical Technology Section, Symposium on Drug Bioavailability, APhA Academy of Pharmaceutical Sciences, Boston, Mass., July 1973.

The authors gratefully acknowledge the assistance of T. Herczeg, J. K. Lee, P. W. Greco, and J. A. Jamison.

* Present address: Wyeth Laboratories, Radnor, PA 19087

ˣ To whom inquiries should be directed.

β-Hydroxynorleucine: Separation of Its Isomers and Biological Studies

THEODORE T. OTANI ˣ and MARY R. BRILEY

Abstract □ Separation of the four isomers of β-hydroxynorleucine was accomplished by partition column chromatography and asymmetric enzymatic hydrolysis of the *N*-chloroacetyl derivatives. From these, the corresponding *N*-chloroacetyl derivatives were made. The purity and configuration of each isomer of the free acid and *N*-chloroacetylated derivative were ascertained by: (*a*) paper chromatography in five solvent systems, (*b*) elemental analysis, (*c*) Van Slyke nitrous acid determination of primary amino nitrogen, (*d*) Van Slyke ninhydrin determination of α-carbonyl carbon, and (*e*) optical rotation. Comparison of the rate of enzymatic hydrolysis by hog renal acylase I of the *N*-chloroacetyl derivative of the L-isomers of each diastereomer showed that the acyl B isomer is a better substrate than the acyl A isomer, where A denotes the faster moving diastereomer and B denotes the slower moving diastereomer in a defined chromatographic solvent system. Microbiological assay using *Lactobacillus casei* in a system selected for screening for possible antitumor activity indicated that while none of the isomers as free amino acids had any growth inhibitory action, the *N*-acylated isomers showed modest but significant activity. The *N*-chloroacetyl derivative of the D-enantiomorph of diastereomer B exhibited the greatest growth inhibitory activity, showing about twice the activity of the other three isomers.

Keyphrases □ β-Hydroxynorleucine—isomers separated, *N*-chloroacetyl derivatives prepared, enzymatic hydrolysis and microbiological growth inhibitory activity of isomers compared □ Enantiomers—β-hydroxynorleucine, separation, comparison of biological activity □ Hydrolysis, enzymatic—isomers of β-hydroxynorleucine compared □ Microbiological assay—growth inhibitory activity of isomers of β-hydroxynorleucine compared

By using a general method for the chemical synthesis of β-hydroxy-α-amino acids, as described previously, 10 β-hydroxy-α-amino acids have been prepared thus far (1). When these amino acids were screened for probable antitumor activity by a microbiological method (2), it was noted that the *N*-chloroacetyl derivatives of β-hydroxyleucine and of β-hydroxynorleucine exhibited modest but significant degrees of inhibitory action (3).

The compounds as chemically prepared are racemic and probably diastereomeric mixtures; therefore, any biological activity exhibited by them would be the net effect of the action of each of the four isomers present, be it growth inhibitory, growth stimulatory, or inactive. The purposes of this article are to: (*a*) describe the isolation of the four isomers of each of these amino acids and the preparation of the corresponding *N*-acyl derivatives, and (*b*) report the findings of the study of the biological properties of these isomers using microbial systems.

EXPERIMENTAL

β-Hydroxynorleucine[1] was prepared as described previously (1).

The separation of the diastereomers was accomplished by means of partition column chromatography, with cellulose powder as the immobile phase. The solvent system consisted of methyl ethyl ketone–1-butanol–concentrated ammonia–water (3:5:1:1) (6) as described for the separation of the diastereomers of β-hydroxyhomomethionine and of β-hydroxymethoxinine (7). The resolution of the optical isomers was accomplished by use of hog renal acylase, as described by Greenstein (8).

RESULTS

Separation of Diastereomers of β-Hydroxynorleucine—A typical procedure for the separation of the diastereomers of β-hydroxynorleucine, similar to that described for the separation of the diastereomers of β-hydroxyhomomethionine and of β-hydroxymethoxinine (see Ref. 7 for details) is outlined here.

DL-β-Hydroxynorleucine AB[2] (250 mg, 1.69 mmoles) was dissolved in 4 ml of the methyl ethyl ketone solvent system, and the resulting solution was applied to a 25 × 150-cm column containing cellulose powder[3], which had been poured into the column as a slurry of the solvent system[4]. The column was eluted with the methyl ethyl ketone system at a flow rate of 0.2 ml/min at room temperature (22–25°)[5].

Three-milliliter fractions were collected. The fractions appearing between 309 and 343, 344 and 384, and 385 and 472 ml, containing isomer A, a mixture of isomers A and B, and isomer B, respectively, were collected and isolated from the solutions as described (7). The yields were 98.2 mg of isomer A (39.5%) and 94.0 mg of isomer B (37.5%), based on the initial weight of the mixture of the isomers. The unseparated portion, containing a mixture of isomers A and B, was similarly isolated by alcohol precipitation of the concentrated aqueous solution. The product was passed through a second column for further separation of the diastereomers.

The respective isomers yielded single spots when chromatographed in the methyl ethyl ketone system, each spot corresponding to one of the two spots of the original diastereomeric mixture (Table I). In addition, each diastereomer gave single ninhydrin-positive spots when chromatographed in four other solvent systems (Table I). The elemental analysis values were in agreement with those calculated for β-hydroxynorleucine (Table II). Manometric Van Slyke determinations of α-carbonyl carbon with ninhydrin (9) (Table III) and of primary amino nitrogen with nitrous acid (10) (Table IV) on the products yielded values in accordance with those expected for the α-amino carboxylic acid structure.

Resolution of Optical Isomers—Resolution of the optical antipodes was accomplished by asymmetric enzymatic hydrolysis of the racemic *N*-chloroacetyl derivatives followed by acid hydrolysis of the enzyme-resistant chloroacetyl D-isomer as described by Greenstein (8). Hog renal acylase[6] was used. The *N*-chloroacetyl derivatives for the resolution were prepared from the corresponding free amino acid by acylation under the conventional Schotten–Baumann conditions [*cf.*, Greenstein and Winitz (11)]. The yields of the acyl products ranged from 70 to 90%. The melting point of the *N*-chloroacetyl racemic A was 148.0–149.5° sharp; the melting point of the *N*-chloroacetyl racemic B was 137–138° sharp.

The yield of the unacylated L-isomer thus separated was about 80% and that of the D-isomer was about 55%. The extent of hydrol-

[1] β-Hydroxynorleucine = 2-amino-3-hydroxy-1-hexanoic acid. The preparation of this compound was reported previously (4, 5).

[2] The diastereomeric forms are here arbitrarily referred to as isomer A and isomer B, the former moving faster and the latter slower when chromatographed in the methyl ethyl ketone system.

[3] Whatman cellulose powder CF-11, H. Reeve Angel & Co., Clifton, N.J.

[4] In later experiments, dry cellulose powder was packed into the column with a tightly fitting Plexiglas plunger with about the same degree of separation of the isomers.

[5] Appropriate vents for the solvent reservoir and adequate ventilation for the removal of the solvent vapors during the fractionation were provided.

[6] Nutritional Biochemical Corp., Cleveland, Ohio. Activity was determined to be 4000 μmoles of acetylmethionine hydrolyzed per hour per milligram of protein nitrogen.

Table I—Chromatographic Data of the Diastereomers of β-Hydroxynorleucine[a]

Solvent System	R_f Diastereomer A	R_f Diastereomer B
Methyl ethyl ketone system[b]	0.38–0.49 (0.43)	0.30–0.40 (0.35)
77% Ethanol	0.50–0.60 (0.55)	0.53–0.61 (0.57)
80% Pyridine	0.54–0.65 (0.58)	0.58–0.68 (0.63)
Formic acid system[c]	0.61–0.73 (0.67)	0.66–0.76 (0.71)
Phenol system[d]	0.63–0.77 (0.69)	0.63–0.77 (0.70)

[a] Chromatographed on Whatman No. 1 chromatographic paper for 18–22 hr at 22–25°, ascending. Compounds were visualized by dipping the paper into a 0.25% acetone solution of ninhydrin and then warming the paper. Figures indicate the range of the R_f values; figures in the parentheses are the R_f values at the center of ninhydrin-positive spots. [b] Described in the text. [c] Formic acid–water–2-methyl-2-propanol (15:15:70). [d] Phenol saturated with 10% sodium citrate.

Table II—Elemental Analysis Data of the Diastereomers of β-Hydroxynorleucine[a]

Diastereomer	C, % Calc.[b]	C, % Obs.	H, % Calc.	H, % Obs.	N, % Calc.	N, % Obs.
A	48.96	48.87	8.90	9.01	9.52	9.41
B	48.96	48.70	8.90	9.01	9.52	9.25

[a] The analysis was performed by the staff of the Microanalytical Laboratory, National Institute of Arthritis, Metabolic, and Digestive Diseases, National Institutes of Health, Bethesda, Md. [b] Calculated for β-hydroxynorleucine, $C_6H_{13}NO_3$.

ysis of the digest in either case was followed by the Van Slyke nitrous acid method (10). Each free amino acid antipode yielded a single spot when chromatographed on paper in the methyl ethyl ketone system. Data on the identification and purity of these products are given in Table V.

Optically pure *N*-chloroacetyl L-derivatives were prepared by acylation of the optically pure L-amino acid, as described for the acylation of the racemic mixture. Optically pure *N*-chloroacetyl D-derivatives were isolated from this resolution mixture as described by Greenstein (8). The purity of the chloroacetyl derivatives separated from the digest was determined using the Van Slyke nitrous acid method; they yielded essentially no detectable amounts of nitrogen (Table VI).

Relative Rates of Enzymatic Hydrolysis of Diastereomers—Equimolar quantities of a racemic mixture of the *N*-chloroacetyl derivatives of diastereomers A and B were treated with the same solution of hog renal acylase I, and the rates of hydrolysis of these compounds were compared (Fig. 1).

The hydrolytic rates (averages of three determinations, calculated from the initial linear portion of the curve) were as follows: diastereomer A, 125 μmoles/hr/mg of protein nitrogen; and diastereomer B, 235 μmoles/hr/mg of protein nitrogen.

Microbiological Studies—The four isomers of β-hydroxynorleucine and their corresponding *N*-chloroacetyl derivatives were screened for possible antitumor activity using *Lactobacillus casei*[7] (ATCC 7469) in riboflavin-supplemented riboflavin assay medium[8], as described by Foley *et al.* (2). The level of riboflavin added was the minimal quantity required for maximal growth [*cf.*, (3)], which was determined here by assay to be 0.03 μg of riboflavin/ml, the final concentration of the assay system. The details of the assay procedure were described previously (3).

The range of concentration of the test compound studied was 100–1000 μg/ml (final concentration). The pH of the final assay system containing the highest concentration of the test compound determined in parallel nonsterile tubes differed no more than 0.07 pH unit from the control tubes containing no test compounds. The results are summarized in Tables VII and VIII.

Table III—Van Slyke Ninhydrin Determination of α-Carbonyl Carbon of the Diastereomers of β-Hydroxynorleucine[a]

	Diastereomer A	Diastereomer B
α-Carbon taken, mg	0.407	0.407
α-Carbon found, mg	0.396	0.400
Percent theory	97.1	98.5
Percent theory, alanine control	96.8	96.8

[a] Amino acid solution (1.0 ml) containing an equivalent of 0.407 mg of α-carbon treated with 1.0 ml of saturated picric acid solution pipetted into a reaction tube and 100 mg of ninhydrin added.

Table IV—Van Slyke Nitrous Acid Determination of Primary Amino Nitrogen of Diastereomers of β-Hydroxynorleucine[a]

	Diastereomer A	Diastereomer B
Primary amino nitrogen taken, mg	0.475	0.475
Primary amino nitrogen found, mg	0.496	0.495
Percent theory	104.2	104.2
Percent theory, leucine control	101.1	99.4

[a] Amino acid solution (1.0 ml) containing an equivalent of 0.475 mg of primary amino nitrogen diluted with 4.0 ml of water and treated with 1 ml of acetic acid and 2 ml of sodium nitrite solution (80 mg/100 ml).

Table V—Purity of the Isomers of β-Hydroxynorleucine[a]

Isomer	Optical Rotation[b], $[\alpha]_D^{22-24}$ Reported[d]	Optical Rotation[b], $[\alpha]_D^{22-24}$ Observed	Nitrogen[c], % Calc.	Nitrogen[c], % Found
L-A	+18.6	+19.1	9.52	9.39
D-A	−18.5	−20.6	9.52	9.68
L-B	+27.1	+26.2	9.52	9.22
D-B	−27.4	−27.1	9.52	9.58

[a] In all five solvent systems (Table I), a single spot appeared. [b] Optical rotation was determined on a Rudolph polarimeter model 80 with a sodium lamp using 100-mm tubes (bore size 3 mm) and a sample capacity of 0.7 ml; c 2, 5 *N* HCl. [c] Micro-Kjeldahl nitrogen analysis was performed by Mr. James F. Williams of this Laboratory. Calculated for $C_6H_{13}NO_3$. [d] Reference 4.

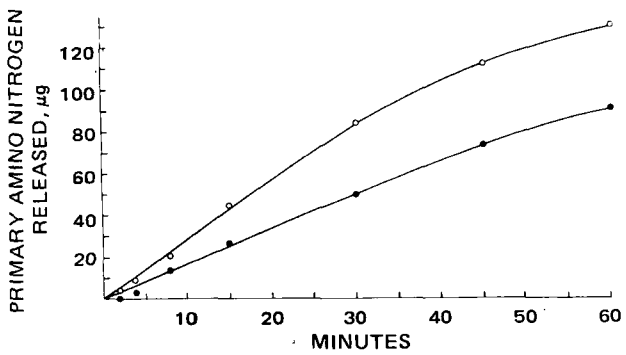

Figure 1—*Rates of hydrolysis of* N-*chloroacetyl-DL-β-hydroxynorleucine A and* N-*chloroacetyl-DL-β-hydroxynorleucine B by hog renal acylase I in 0.1* M *potassium phosphate buffer, pH 7.0,* T = *22–24°. Substrate concentration = 0.006* M *racemic mixture. Primary amino nitrogen was determined by the nitrous acid method of Van Slyke (10).*

[7] From the American Type Culture Collection, Rockville, Md.
[8] Difco Laboratories, Detroit, Mich.

Table VI—Purity of the Isomers of *N*-Chloroacetyl-β-hydroxynorleucine

Isomer[a]	Melting Point (Uncorrected)[b]	Optical Rotation[c], $[\alpha]^{21-24}$	Van Slyke Nitrous Acid Determination[d], % Primary Amino Nitrogen	C[e], %		H[e], %		N[e], %	
				Calc.	Obs.	Calc.	Obs.	Calc.	Obs.
L-A	101–104°	+27.2°	2	42.96	42.73	6.34	6.34	6.26	6.23
D-A	102–105°	−27.5°	2	42.96	43.25	6.34	6.58	6.26	6.18
L-B	144–146°	+12.0°	3	42.96	43.04	6.34	6.41	6.26	6.20
D-B	144–148°	−11.6°	0	42.96	43.20	6.34	6.50	6.26	6.32

[a] Ninhydrin reaction was negative for all isomers. Aqueous solution (concentration approximately 1 mg/ml) was spotted on paper, dried, treated with 0.25% acetone solution of ninhydrin, and warmed. [b] Melting points were determined on a Fisher–Johns melting-point block. [c] Optical rotation was determined on a Rudolph polarimeter model 80 with a sodium lamp. Conditions were as described in Table V; c 2, water. [d] Van Slyke nitrous acid determination of primary amino nitrogen, determined as described (*cf.*, Ref. 7). [e] Elemental analyses were performed by the staff of the Microanalytical Laboratory, National Institute of Arthritis, Metabolic, and Digestive Diseases, National Institutes of Health, Bethesda, Md. Calculated for $C_8H_{14}ClNO_4$.

None of the isomers of β-hydroxynorleucine as free amino acids affected the growth of *L. casei* in the system used (Table VII). However, when *N*-chloroacetylated, all four isomers showed some inhibition, with *N*-chloroacetyl-D-β-hydroxynorleucine B exhibiting about twice the growth inhibitory activity of the others (Table VIII).

DISCUSSION

The separation of the diastereomers by partition column chromatography yielded the pure isomers by a single passage of the diastereomeric mixture through the column. However, quantitative separation could not be accomplished by a single passage despite numerous attempts, varying such parameters as the geometry of the column, the particulate size of the cellulose powder, the mode of packing of the powder (solvent saturated or dry), and the flow rate.

Table VII—Effect of the Isomers of β-Hydroxynorleucine on the Growth of *L. casei* in Riboflavin Assay Medium[a]

Isomer	Turbidity[b], Klett Units (Red Filter)				Maximum Change, %
	0 μg/ml	100 μg/ml	500 μg/ml	1000 μg/ml	
L-A	188	184	187	188	0
D-A	188	184	182	180	−4
L-B	188	183	182	184	−2
D-B	188	186	184	183	−3
DL-AB	188	185	186	180	−4

[a] A typical experiment, representing five experiments. The turbidimetric figures are the averages of duplicates for that concentration. Maximum variation from mean = ±3 Klett units. [b] The instrument was set at zero against a sterile reagent blank which contained all components of the experimental tubes except the test compound and 0.05 ml of the normal saline solution that was used for washing the organism in place of the inoculum. The blank was kept in the refrigerator for the duration of the incubation of the experimental tubes. A sterility control, identical to the sterile reagent blank but incubated with the experimental tubes, was clear and read within the variation of the empty Klett tubes (±3 Klett units).

Table VIII—Effect of the Isomers of *N*-Chloroacetyl-β-hydroxynorleucine on the Growth of *L. casei* in Riboflavin Assay Medium

Isomer[a]	Turbidity[b], Klett Units				Maximum Change, %
	0 μg/ml	100 μg/ml	500 μg/ml	1000 μg/ml	
L-A	172	166	153	140	−19
D-A	172	162	153	134	−22
L-B	172	160	149	137	−20
D-B	172	166	129	84	−51
DL-AB	172	166	148	130	−24
Mercaptopurine	171	92	12	17	−93

[a] The pH of the test solutions was adjusted to 6 by the addition of 0.1 *N* NaOH. [b] See Table VII footnotes.

Although data are insufficient for assignment of the absolute configuration of the diastereomers, comparison of the chromatographic mobilities of these isomers in the Hardy–Holland solvent system (12) with the *threo-* and *erythro*-β-hydroxynorleucines of Buston and Bishop (5) indicates that diastereomer A, described here, corresponds to their *threo*-β-hydroxynorleucine and that diastereomer B corresponds to their *erythro*-β-hydroxynorleucine.

The four stereoisomeric forms of the free amino acid and of the *N*-chloroacetylated derivative were isolated by either Scheme I or II. The racemic diastereomers were separated by column chromatography followed by an enzymatic resolution of each racemic chloroacetyl diastereomer or by resolution of the racemic diastereomeric mixture followed by the separation of the optically homogeneous diastereomeric mixture by column chromatography.

It was noted that the optical purity of the products was retained in either route, *i.e.*, whether the separation of the diastereomers was followed by resolution or was performed on the optically ho-

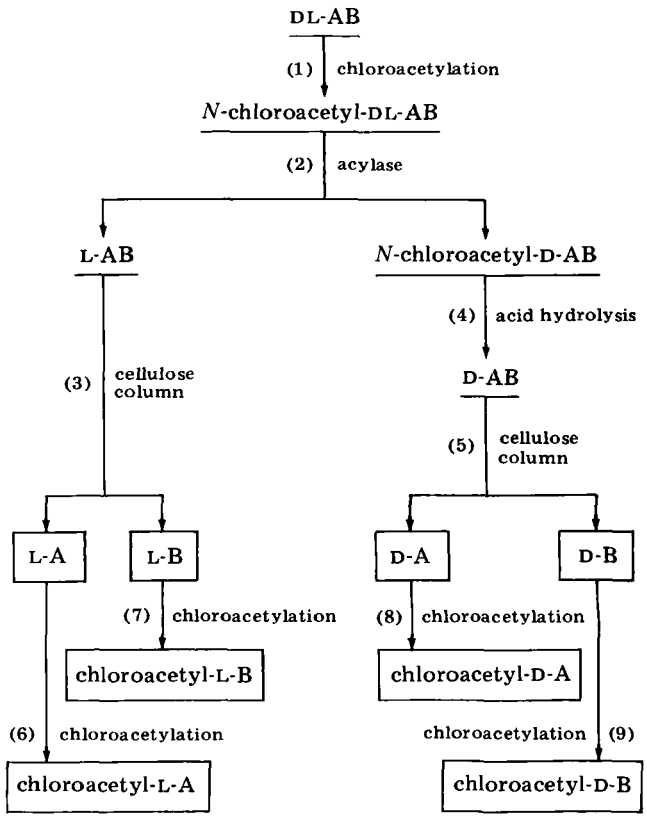

Scheme I—Separation of the isomers of β-hydroxynorleucine and their N-*chloroacetyl derivatives*

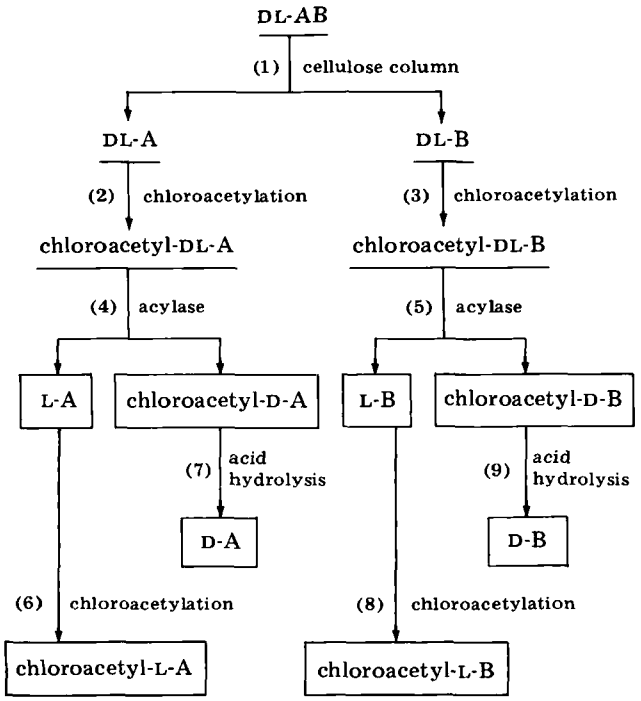

Scheme II—Separation of the isomers of β-hydroxynorleucine and their N*-chloroacetyl derivatives*

mogeneous diastereomeric mixture. The selection of the scheme to be used depends upon the compound desired. Hence, Scheme I (Table IX) was preferable for the isolation of the free amino acids because only five steps were required. Scheme II was more advantageous for the isolation of all four chloroacetylated isomers because only seven steps were required by this route as compared to the nine steps needed *via* Scheme I (Table IX).

Microbial studies confirmed earlier observation (3) that although the β-hydroxyamino acids as free acid were innocuous to the growth of *L. casei* in the system used here, their chloroacetylated derivatives were moderately growth inhibitory. However, the chloroacetyl D-B-isomer was twice as active as the other three isomers.

The apparent "activation" of these amino acids by acylation appears now to be unrelated to the hydrolytic rate of the *N*-acylated derivatives by acylase; apparently, the acyl D-derivatives of neither diastereomer were substrates of this enzyme in the resolution procedure. However, that the chloroacetyl group nevertheless contributes to the activity seems likely in view of the activity exhibited by the acylated derivatives of all four isomers and the inactivity of the unacylated mother compounds. It is interesting that despite the possible availability of a chloroacetyl group and an amino acid analog, L-β-hydroxynorleucine (either diastereomer), as a result of enzymatic hydrolysis, the acyl D-B-isomer exhibited the greatest activity.

If the activity shown by the chloroacetylated racemic diastereomeric mixture is due to a single isomer, isolation of this isomer should result in a compound four times as active as the mixture. In fact, however, there was noted only a twofold increase in activity. This observed twofold increase in activity by the chloroacetylated D-B-isomer could be explained on the basis that, contrary to the assumption of dilution of activity by the inert isomers, all four

Table IX—Comparison of Routes in the Isolation of Isomers of Free and Acylated β-Hydroxynorleucine

	Scheme I		Scheme II	
Treatment	For Preparation of Free Acid	For Preparation of *N*-Acylamino Acid	For Preparation of Free Acid	For Preparation of *N*-Acyl-Amino Acid
Chloroacetylation	1[a]	5	2	4
Enzymatic hydrolysis	1	1	2	2
Column chromatography	2	2	1	1
Acid hydrolysis	1	1	2	0
Total steps	5	9	7	7

[a] The number of operations required.

chloroacetylated isomers exhibited some growth inhibitory activity. Hence, the 24% inhibition shown by the chloroacetylated racemic diastereomeric mixture is probably the resultant action of all four chloroacetylated isomers, each contributing approximately a fourth of the total activity.

In view of the observation that certain of these compounds do exhibit some growth inhibitory activity in the microbial system selected for antitumor screening, further studies against mammalian tumors are indicated. The preparation of larger quantities of the optically pure diastereomers and their respective *N*-chloroacetyl derivatives is in progress.

REFERENCES

(1) T. T. Otani and M. Winitz, *Arch. Biochem. Biophys.*, **102,** 464(1963).

(2) G. E. Foley, R. E. McCarthy, V. M. Binns, E. E. Snell, B. M. Guirard, G. W. Kidder, V. C. Dewey, and P. S. Thayer, *Ann. N.Y. Acad. Sci.*, **76,** 413(1958).

(3) T. T. Otani, *Cancer Chemother. Rep.*, **38,** 25(1964).

(4) R. T. Adams and C. Niemann, *J. Amer. Chem. Soc.*, **73,** 4260(1951).

(5) H. W. Buston and J. Bishop, *J. Biol. Chem.*, **215,** 217(1955).

(6) Y. Ikutani, T. Okuda, and S. Akabori, *Bull. Chem. Soc. Jap.*, **33,** 582(1960).

(7) T. T. Otani and M. R. Briley, *J. Pharm. Sci.*, **63,** 1253(1974).

(8) J. P. Greenstein, in "Methods in Enzymology," vol. III, S. P. Colowick and N. O. Kaplan, Eds., Academic, New York, N.Y., 1957, p. 554.

(9) D. D. Van Slyke, R. T. Dillon, D. A. MacFadyen, and P. Hamilton, *J. Biol. Chem.*, **141,** 627(1941).

(10) D. D. Van Slyke, *ibid.*, **83,** 425(1929).

(11) J. P. Greenstein and M. Winitz, "Chemistry of the Amino Acids," vol. III, Wiley, New York, N.Y., 1961, p. 1834.

(12) T. L. Hardy and D. O. Holland, *Chem. Ind.*, **1952,** 855.

ACKNOWLEDGMENTS AND ADDRESSES

Received April 16, 1975, from the *Nucleic Acids Section, Laboratory of Physiology, National Cancer Institute, National Institutes of Health, Bethesda, MD 20014*

Accepted for publication June 20, 1975.

[x] To whom inquiries should be directed.

Evaluation of 2-Benzylidenecyclohexanones and 2,6-Bis(benzylidene)cyclohexanones for Antitumor and Cytotoxic Activity and as Inhibitors of Mitochondrial Function in Yeast: Metabolism Studies of (*E*)-2-Benzylidenecyclohexanone

J. R. DIMMOCK *x, N. W. HAMON *, K. W. HINDMARSH *, A. P. SELLAR *, W. A. TURNER *§, G. H. RANK ‡, and A. J. ROBERTSON ‡

Abstract □ Some 2-benzylidenecyclohexanones, 2,6-bis(benzylidene)cyclohexanones, and related compounds were evaluated for antitumor and cytotoxic activities; (*E*)-2-benzylidenecyclohexanone (I*a*) was shown to have significant cytotoxic properties and a potent inhibitory effect on yeast mitochondria. After intraperitoneal injection of I*a*, unchanged drug and a metabolite, tentatively identified as 2-(*p*-hydroxybenzyl)cyclohexanol, were found in the urine. No metabolites were found in the feces. Oral administration of I*a* afforded three unidentified metabolites in the urine and three unidentified metabolites in the feces.

Keyphrases □ Benzylidenecyclohexanones, substituted—evaluated for antitumor and cytotoxic activity, effect on mitochondrial function in yeast, metabolism studies □ Antitumor agents, potential—substituted benzylidenecyclohexanones evaluated □ Cytotoxic agents, potential—substituted benzylidenecyclohexanones evaluated □ Mitochondrial activity—substituted benzylidenecyclohexanones evaluated, yeast □ Structure–activity relationships—substituted benzylidenecyclohexanones evaluated for antitumor and cytotoxic activity, effect on mitochondrial function in yeast

Recently, some substituted 2-benzylidenecyclohexylamines were required as intermediates in the preparation of novel antineoplastic agents. The synthesis envisaged involved the preparation of the substituted 2-benzylidenecyclohexanones (I) followed by oximation to give the derivatives (V) to be reduced with lithium aluminum hydride to the desired substituted 2-benzylidenecyclohexylamines. The intermediate 2-benzylidenecyclohexanones are α,β-unsaturated ketones, a class of compounds known as alkylating agents (1–4) and possessing activity in various tumor systems (5, 6).

Recently, the preparation (7) and the antitumor and cytotoxic properties (5) of some substituted 1-phenyl-1-nonen-3-ones, which may be regarded as more flexible analogs of the substituted 2-benzylidenecyclohexanones, were described. In fact, the 1-nonen-3-ones are capable of adopting both (*S*)-*cis*- and (*S*)-*trans*-conformations whereas the compounds in Series I are locked in the (*S*)-*cis*-conformation. A comparison of the antitumor and cytotoxic properties of the two series of compounds may indicate some stereochemical requirements for activity in this group. It is well documented that in certain series the rigid analogs have higher pharmacological activity than the related acyclic derivatives (8, 9), although acyclic analogs of rigid cyclic compounds have enhanced biological activity (10–12) in other cases.

RESULTS AND DISCUSSION

The preparation of the compounds in Series I*a*–I*e*, II, III, and V was described previously (13, 14). Condensation between dichlorinated benzaldehydes and cyclohexanone led invariably to the bis compounds (III*b*–III*d*). In Series I and III, the compounds were shown by spectroscopic means to have the (*E*)- and (*E,E*)-configurations; II, prepared by UV irradiation from I*a*, was shown to have the (*Z*)-configuration. A representative 2-benzylidenecyclohexanone (I*a*) was reduced with lithium aluminum hydride to the corresponding alcohol (IV) with retention of the double bond, and it was considered that the oximes (V) derived from Series I would afford the required substituted 2-benzylidenecyclohexylamines on treatment with lithium aluminum hydride. However, reduction of V led to the formation of the epiminocyclohexanes (VI) (15).

With the exception of I*c* and III*a*, Compounds I–IV were given by intraperitoneal injection against the L-1210 lymphoid leukemia screen in mice, using the standard Q4D and QD1-9 protocols, at doses of 400–100 mg/kg and were found to be inactive. No toxicity was observed with the derivatives at 400 mg/kg with the exception of I*f*; with I*f* the dose had to be reduced to 50 mg/kg to prevent animal mortalities. The bis ketone (III*a*), assessed only using the Q4D protocol, was inactive. The cyclic derivatives thus resemble the related acyclic 1-phenyl-1-nonen-3-ones in showing no significant activity against L-1210 lymphoid leukemia and no murine toxicity except for the *para*-quaternary ammonium iodides.

The only difference in toxicity between the cyclic and acyclic series was the absence of toxicity in the unsubstituted compounds I*a* and II at a dose of 400 mg/kg whereas a dose of 100 mg/kg was fatal for the mice with the acyclic series. A marked difference in cytotoxicity existed between the stereoisomeric 2-benzylidenecyclohexanones in the KB screen, whereby the (*E*)-isomer was found to be approximately 17 times more active than the (*Z*)-isomer. The acyclic 1-phenyl-1-nonen-3-ones showed no activity in this screen at a concentration of 100 ppm, although I*b*–I*f* were similar in potency to the acyclic series of derivatives.

A number of biological alkylating agents, such as the nitrogen mustards, have five carbon atoms between the centers at which nucleophilic attack can occur (16); therefore, cross-linking between the N^7-atoms of near-opposite guanine residues of DNA may occur (17). With the 2,6-bis(benzylidene)cyclohexanones (III), the possibility of cross-linking occurring is conceivable if alkylation occurs at the benzylic carbon atom. However, the screening data indicated no significant activity in either the L-1210 or KB screen. Furthermore, high murine toxicity is absent, which may be associated with a failure for cross-linking due to steric impedence at the benzylic carbon atoms.

Possible explanations were sought for the wide variations in activity in the KB screen. Earlier work on α,β-unsaturated ketones had showed that polarity of the olefinic double bond (as measured by the τ values of the olefinic protons and IR carbonyl stretching frequencies) was dependent upon the Hammett and Taft values of the nuclear substituents (18). In Series I–III, no correlation between altered polarity of the charge on the benzylic carbon atom and KB activity could be seen. It is well known that in certain series of compounds, correlations exist between the planarity of the molecules and biological activity (19, 20). A clearcut evaluation indicating whether planarity of the molecules favors or retards cyto-

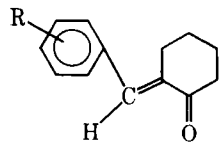

Ia: R = H
Ib: R = 2-Cl
Ic: R = 3-Cl
Id: R = 4-Cl
Ie: R = 4-$N(CH_3)_2$
If: R = 4-$N^+(CH_3)_3I^-$

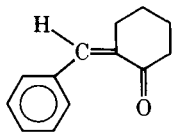

II

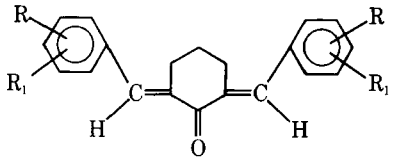

IIIa: R = R_1 = H
IIIb: R = 2-Cl, R_1 = 4-Cl
IIIc: R = 2-Cl, R_1 = 6-Cl
IIId: R = 3-Cl, R_1 = 4-Cl
IIIe: R = 4-$N(CH_3)_2$, R_1 = H

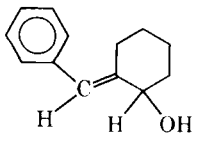

IV

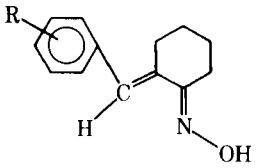

Va: R = H
Vb: R = 2-Cl
Vc: R = 4-Cl
Vd: R = 4-$N(CH_3)_2$

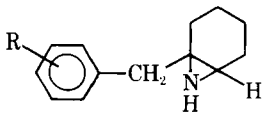

VIa: R = H
VIb: R = 2-Cl
VIc: R = 4-Cl

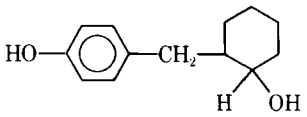

VII

toxic activity was not found, although the eight compounds that were more active than 100 ppm had, on average, a lower θ value than the four compounds that were inactive at 100 ppm.

Examination of the effect of the α,β-unsaturated ketones on yeast mitochondria suggested an explanation for the high activity of Ia. In the absence of mitochondrial function, the yeast will grow on complex glucose medium, which provides energy for growth by fermentation of glucose. However, the complex ethanol medium containing ethanol, a nonfermentable energy source, does not provide energy for the growth of the yeast if interference with mitochondrial function occurs. Table I shows that Ia is a potent mitochondrial poison, significantly more potent than certain established mitochondrial inhibitors such as chloramphenicol and tetracycline (21).

The selective effect on yeast mitochondria was confirmed by observing the threefold difference in concentration of Ia required to inhibit 50% of the growth of *Saccharomyces cerevisiae* on minimal salts ethanol medium and minimal salts glucose medium. Reduction of the carbonyl group of Ia with lithium aluminum hydride gave IV, shown by NMR evidence to have an equatorial hydroxyl group. The unsaturated alcohol IV had a similar absence of murine toxicity and activity against L-1210 leukemia as Ia but was approximately 150 times less potent in the KB screen. The drastic reduction in activity of IV may be due to facile hydrogen bonding preventing penetration *via* the cancer cell membrane to a site of action. Paradoxically, the compound showed significant activity against yeast mitochondria.

Table I—Assessment of the Cyclohexane Derivatives against the KB Tumor System and *S. cerevisiae*

Compound	KB Cell Culture Screen[a], μg/ml	Mean Area of Inhibition of Growth of *S. cerevisiae*, mm[b]		Interplanar Angle, θ[b]
		In Complex Ethanol Medium	In Complex Glucose Medium	
Ia	0.25	159.9[c]	0.0[d]	0
II	4.3	—	—	52
Ib	20	—	—	37
Ic	3.2	0	0	29
Id	21	—	—	0
Ie	>100	0	0	0
If	49	151.9[e]	85.4[f]	0
IIIa	29	0	0	0
IIIb	>100	0	0	52
IIIc	>100	0	0	63
IIId	16	0	0	33
IIIe	>100	0	0	0
IV	38	91.2[g]	0.0[d]	0

[a] Values indicate the dose inhibiting 50% of the growth of human epidermoid carcinoma of the nasopharynx in Eagle's medium. A compound should have an activity of 4 μg/ml or less to be considered as having significant cytotoxic activity. [b] Calculated using the absorption maxima described in Ref. 13, with the exception of If and IV which are described in this work. [c] *SE* 4.5. [d] All five replicates gave the same value. [e] *SE* 11.1. [f] *SE* 6.33. [g] *SE* 13.2.

Earlier work had shown the antitumor effect of oximes in the presence or absence of metals (22, 23), and aziridines have been used in the treatment of tumor systems (24). However, the cyclohexane derivatives (Va–Vd and VIa–VIc) were inactive in the intraperitoneal L-1210 system using the standard Q4D protocols. In the QD1-9 protocol, Va–Vd, VIa, and VIb were shown to be inactive at doses of 100–400 mg/kg. Toxicity was noted with all of the aziridines at 400 mg/kg.

The interesting level of cytotoxic activity of Ia and its efficacy as a mitochondrial inhibitor suggested its study for metabolism *in vivo*. Reduction of the olefinic double bond (25) and carbonyl group (26) of α,β-unsaturated ketones has taken place *in vivo*, as has the formation of the cysteine conjugates (27). The urine of rats, previously injected intraperitoneally with Ia, was extracted using a modification of the method of Curry (28) and shown by TLC to contain two components not present in the urine of control rats.

Mass spectrometry showed one component to be unreacted Ia and the other to be a metabolite possessing a molecular formula of $C_{13}H_{18}O_2$ (molecular ion: 206.1311; calculated for $C_{13}H_{18}O_2$: 206.1307). A loss of water from the parent peak gave an ion at *m/e* 188 with an accurate mass of 188.1194 (calculated for $C_{13}H_{16}O$: 188.1201), confirmed by the appropriate metastable peak at *m/e* 171.5; this finding suggested that a substituted cyclohexanol was present, loss of water being a major mass spectral pathway in the case of cyclohexanol (29). The mass spectrometry of a sample of 2-benzylcyclohexan-1-ol prepared by an unambiguous route showed loss of water as the major fragmentation pathway. A prominent peak at *m/e* 107 was attributed to a nuclear-hydroxylated benzyl group; since aromatic hydroxylation is favored in the *para*-position, evidence from mass spectrometry suggests the possibility of the metabolite being 2-(*p*-hydroxybenzyl)cyclohexan-1-ol (VII).

The acyclic α,β-unsaturated ketone, 1-phenyl-1-penten-3-one, was metabolized to the corresponding saturated alcohol, 1-phenylpentan-3-ol, and to 1-(*p*-hydroxyphenyl)pentan-3-one (26), indicating that complete reduction of the α,β-unsaturated keto group and aromatic hydroxylation occurred. TLC analysis indicated one component in each of the basic and amphoteric fractions, the sample in the amphoteric fraction having the same retention time as Ia. No metabolites were detected in the feces.

An examination of the efficiency of the extraction technique showed that Ia was extracted from control urine using the modified Curry technique with an efficiency of 11.4%. Use of liquid–liquid extraction techniques increased the efficiency to a little greater than 99.9%. Liquid–liquid extraction of urine at pH 9.0, 7.2, and 2.0 revealed only two components, one with an identical retention time to Ia. The quantity of unchanged drug found in urine after

Table II—Quantities of Unchanged Ia Obtained by Liquid–Liquid Continuous Extraction of Urine from Rats Previously Administered the Drug by Intraperitoneal Injection

Days after Injection	Unchanged Ia Found in Urine, %					
	400-mg/kg Dose Level			40-mg/kg Dose Level		
	pH 9.0	pH 7.2	pH 2.0	pH 9.0	pH 7.2	pH 2.0
1	0.50	0.10	—	0.54	0.06	—
2	0.13	—	—	0.07	—	—
3	0.02	—	—	—	—	—
4	—	—	—	—	—	—
	0.65	0.10	—	0.61	0.06	—
Total	0.75			0.67		

intraperitoneal injection was approximately 1%. Since the high dose used (400 mg/kg) could saturate enzyme systems, preventing metabolism of Ia, a lower dose of 40 mg/kg was used, but the quantity of unmetabolized Ia in the urine remained the same (Table II).

After oral administration of Ia, three metabolites were detected in the urine using either the modified Curry technique or liquid–liquid extraction. The GLC characteristics of one component had a retention time of unchanged Ia. The quantity of metabolites represented approximately 8.4% of the administered dose of which Ia was present to an extent of 0.66% (Table III). Examination of the feces after oral administration showed the presence of three metabolites by both Curry's modified method and the liquid–liquid extraction technique. The metabolites accounted for approximately 81% of the administered dose (Table IV). Repeated attempts to isolate the metabolites by preparative GLC proved unsuccessful. These metabolic studies indicated the presence of approximately 1% unconjugated metabolites and unchanged drug after intraperitoneal injection and approximately 89% of unchanged drug and unidentified metabolites after oral administration of Ia.

EXPERIMENTAL[1]

Preparation of Compounds

The preparation of Series Ia–Ie, II, III (13), V (14), and VI (15) was described previously.

(*E*)-2-(*p*-Dimethylaminobenzylidene)cyclohexanone Methiodide (If)—A solution of Ie (10.0 g, 0.04 mole) and methyl iodide (12.4 g, 0.08 mole) in anhydrous benzene (100 ml) was heated under reflux for 16 hr. The hot solution was filtered, and the residue was recrystallized from absolute ethanol to give If as bright-yellow crystals (6.6 g, 40%), mp 148–150°; IR (potassium bromide): 1615 (C=C) and 1682 (C=O) cm^{-1}; UV (alcohol): 280 (ϵ 13,590) and 219 (13,810) nm; NMR (deuterium oxide): δ 8.13–7.80 (m, 2, aromatic C^2H, C^6H), 7.80–7.47 (m, 2, aromatic C^3H, C^5H), 7.27 [t, 1, J = 2 Hz, $(CH_3)_3N^+C_6H_4CH$=], 3.77 [5.9, $(CH_3)_3N^+$], 3.07–2.53 (m, 2, C^3H_2), 2.80–2.33 (m, 2, C^6H_2), 2.17–1.50 (m, 4, C^4H_2, C^5H_2); mass spectrum: *m/e* 299 (parent peak).

Anal.—Calc. for $C_{16}H_{22}INO$: C, 51.76; H, 5.97. Found: C, 51.37; H, 6.01.

***cis*-2-Benzylcyclohexanol**—A solution of (*E*)-2-benzylidenecyclohexanone (Ia, 75.0 g, 0.403 mole) in dry ether (250 ml) was added to a suspension of lithium aluminum hydride (5.74 g, 0.151 mole) in dry ether (50 ml) and stirred at room temperature for 1 hr. After addition of water, the solvent was evaporated to give a pale-yellow syrup (73.0 g) which, on distillation, gave a colorless oil (63.4 g), bp 120°/0.3 mm. Recrystallization of the solidified distillate from petroleum ether[2] gave essentially IV as colorless crystals (52.3 g, 69%), mp 62.5° [lit. (31) mp 63–64°].

GLC analysis indicated the presence of two components (98:2) which could not be changed on repeated recrystallization; IR (potassium bromide): 3390 (OH) cm^{-1}; NMR (deuterochloroform): δ 7.53–7.00 (m, 5, C_6H_5), 6.55 (s, 1, C_6H_5CH=), 4.40–4.07 (m, 1, CH), 3.00–2.40 (m, 1, equatorial C^1H), 2.40–1.17 (m, 7, axial C^3H, C_4H_2, C^5H_2, C^6H_2), and 2.00 (s, 1, OH, exchanges with D_2O); mass spectrum: *m/e* (relative intensity) 188 (M^+, 100) and 170 (9).

Anal.—Calc. for $C_{13}H_{16}O$: C, 82.93; H, 8.57. Found: C, 82.81; H, 8.43.

A solution of IV (0.166 g) in ethanol (200 ml) was hydrogenated over 10% palladium-on-charcoal (0.251 g) at 51 psi for 24 hr. Removal of both catalyst and solvent gave *cis*-2-benzylcyclohexanol as a colorless oil (0.159 g, 95%), shown by GLC to be one component [lit. (32) *cis*-isomer as an oil, *trans*-isomer as a solid, mp 76–77°]; IR (smear): 3405 (OH) cm^{-1}; NMR (deuterochloroform): δ 7.37–7.00 (m, 5, C_6H_5), 3.87–3.63 (m, 1, CH), 3.40–2.97 (m, 1, C_2H), 2.77–2.23 (m, 2, $C_6H_5CH_2$), 2.07–0.63 (m, 8, C_3H_2, C_4H_2, C_5H_2, C_6H_2), and 1.68 (s, 1, OH, exchanges with D_2O); mass spectrum: *m/e* (relative intensity) 190 (M^+, 37) and 172 (100).

Inhibition of Mitochondrial Function

Complex glucose medium containing yeast extract (1%), bactopeptone (2%), glucose (2%), and agar (2%) in water and complex ethanol medium containing ethanol (4%) in place of glucose were employed. The compounds (5.0 mg) were dissolved in 95% ethanol (1 ml) and 0.02 ml of the solution was applied to antibiotic disks (12.7 mm). The disks were placed on the surface of the complex glucose medium and complex ethanol medium plates previously spread with 0.2 ml of a culture of *S. cerevisiae*[3] grown for 48 hr in liquid complex ethanol medium.

The plates were incubated at 28° for 3 days, and the area of inhibition (square millimeters) surrounding the disk was recorded. Five replicates for each compound were undertaken. The area of growth inhibition on complex ethanol medium in excess of growth inhibition on complex glucose medium is a quantitative estimation of the inhibition of mitochondrial function (Table I).

For growth inhibition studies of Ia, a diploid strain of *S. cerevisiae* homozygous for *ade* 2/*ade* 2[3] was grown to an early stationary phase in a liquid medium. The medium, placed in 8 × 150-mm tubes, was inoculated to an optical density (640 nm) of 0.1 unit/ml. The inhibitors were added at concentrations of 1, 2.5, 5, 7.5, 10, 50, 100, 250, 500, 750, and 1000 μg/ml of minimal salts glucose medium or minimal salts ethanol medium. After 24 hr of growth at 30°, the percentage growth was ascertained by the change in optical density and expressed as a percentage of the control.

Minimal salts ethanol medium contains 1% ethanol as a nonfermentable energy source, and minimal salts glucose medium employs 5% glucose as a fermentable energy source. Thus, growth in minimal salts ethanol medium is dependent upon mitochondrial function whereas growth on minimal salts glucose medium can occur by glycolysis. Six replicates were undertaken on minimal salts ethanol medium, and the concentration of Ia required to inhibit 50% of the growth of *S. cerevisiae* was 56.3 μg/ml, *SE* 10.77. The concentration required to inhibit 50% of the growth of the yeast on minimal salts glucose medium was 168 μg/ml.

[1] Boiling points and melting points are uncorrected. IR spectra were recorded on a Unicam SP-200G spectrophotometer calibrated with polystyrene. A Beckman DU spectrophotometer was employed for determining the UV spectra, using 1-cm quartz cells. NMR spectra were determined on a Varian T-60 instrument. Mass spectrometry was undertaken using an AEI MS12 single-focusing instrument operated by Mr. D. R. Bain, Department of Chemistry and Chemical Engineering, University of Saskatchewan, Saskatoon, and high-resolution mass spectrometry was carried out by Dr. D. Durden of the Department of Psychiatric Research, University Hospital, Saskatoon, Canada. Elemental analyses were carried out on a Coleman model 33 carbon–hydrogen analyzer by Mr. O. Douglas, College of Pharmacy, University of Saskatchewan, Saskatoon, Canada. GLC of the compounds synthesized was undertaken employing a Pye 104 gas chromatograph equipped with a flame-ionization detector and using 1.5-m × 0.6-cm (5-ft × 0.25-in.) o.d. glass columns packed with 4% SE-30 adsorbed onto acid-washed, silanized Chromosorb W (100–120 mesh). Nitrogen was used as the carrier gas at 55–60 ml/min, a detector temperature of 250°, and isothermal runs from 140 to 200°. GLC of the extracts obtained in the metabolism studies employed a Hewlett Packard 5750B instrument equipped with a flame-ionization detector and using 1.2-m × 0.3-cm (4-ft × 0.125-in.) o.d. stainless steel columns packed with 3% OV-101 on Chromosorb W (80–100 mesh H.P.). Nitrogen was the carrier gas at 40 ml/min; a detector and injection port temperature of 245° was maintained. Silica gel 7GF (J. T. Baker Chemical Co.) and silica gel 60HR (Merck) were used for TLC.

Adult male albino rats of the Wistar strain were housed individually in rat metabolism units with urine–feces separators (Econo-cage E110 metabolism unit, Maryland Plastics Inc.). They were allowed free access to food and water in a temperature- and humidity-controlled room having a 12-hr day/night cycle.

Evaluations of the compounds for antitumor and cytotoxic activity were carried out by the Drug Development Division, National Cancer Institute, Bethesda, Md., according to their protocols (30).

[2] Skelly F, Skelly Oil Co., Tulsa, Okla.

[3] Strain GR13 constructed in the Department of Biology, University of Saskatchewan, Saskatoon, Saskatchewan, Canada.

Table III—Percentage of Ia Excreted Unchanged and/or Converted into a Metabolite after Oral Administration

Days after Administration	Administered Dose Excreted, %								
	Component 1[a,b]			Component 2[c]			Component 3[d]		
	pH 9.0	pH 7.2	pH 2.0	pH 9.0	pH 7.2	pH 2.0	pH 9.0	pH 7.2	pH 2.0
1	0.54	0.12	—	0.29	0.24	4.75	1.72	—	—
2	—	—	—	0.05	0.04	—	0.59	—	—
3	—	—	—	—	—	—	0.02	—	—
Total	0.54	0.12	—	0.34	0.28	4.75	2.33	—	—
	0.66			5.37			2.33		

[a] Unchanged ketone. [b] Compound with a retention time of 2.60–2.63 min. [c] Compound with a retention time of 1.72–1.83 min. [d] Compound with a retention time of 5.21 min.

Examination of Rat Urine and Feces after Intraperitoneal Administration of Ia

Compound Ia (4.0000 g) was administered intraperitoneally in distilled water containing hydroxypropyl methylcellulose[4] to 40 male albino Wistar rats at a dose level of 400 mg/kg. The urine (test urine) and feces (test feces) were collected daily for 5 days and stored at −6°. Urine (control urine) and feces (control feces) were collected daily for 5 days from 10 male albino Wistar rats injected with distilled water containing hydroxypropyl methylcellulose.

Urine—The test urine (25 ml, pH 8.8) was extracted with ether (3 × 25 ml) to give an organic extract containing the basic (D) and neutral (C) fractions of urine. The aqueous phase was then acidified (pH 7.2) and extracted with ether (3 × 25 ml) to give an ethereal extract of the amphoteric (E) fraction. The aqueous phase was then acidified (pH 2.0) and extracted with ether (3 × 25 ml). The organic extract was washed immediately with aqueous sodium bicarbonate solution (5% w/v) (2 × 10 ml), and the two layers were separated into an aqueous phase (1) and an ethereal phase (1).

The aqueous phase (1) was acidified with hydrochloric acid (50% v/v) and extracted with ether (3 × 25 ml) to give an ethereal extract containing the strong acid (A) fraction. The ether layer (1) was washed with sodium hydroxide solution (0.45 *N*, 2 × 10 ml) to give an aqueous phase (2). The aqueous phase (2) was acidified immediately with hydrochloric acid (50% v/v) and extracted with ether (3 × 25 ml) to give an extract of the weakly acidic (B) fraction. Evaporation of the ethereal extracts gave Fractions A, B, E, and C-D. Control urine (25 ml) was extracted in a identical manner.

GLC—The fractions from both test and control urine were dissolved in ethanol, and 0.5–4-μl solutions were injected onto a GLC column at 190° (Fractions A and B) and 170° (Fractions C-D and E). The chromatograms of A and B showed similar constituents in both test and control urine. One extra peak was found in each of the C-D and E test fractions, with retention times of 0.60 and 1.95 min, respectively.

TLC—The test and control extracts of Fractions A and B were dissolved in ethanol and spotted onto silica gel 7GF. Upon development with chloroform–acetone (97:10), no compounds with R_f values differing from the control fractions appeared in the test fractions.

Fraction C-D from both test and normal urine was dissolved in ethanol and placed on silica gel 7GF plates. Development with chloroform–methanol (97:5) indicated a component with an R_f value of 0.70 found only in the test fraction. The test and control extracts of Fraction E were dissolved in ethanol, spotted onto silica gel 7GF plates, and developed with chloroform–methanol (97:5). A spot with an R_f value of 0.97 from the test urine appeared black under shortwave UV light, but the component with an R_f value of 0.97 from control urine appeared fluorescent blue.

A check that no degradation of the extracts from Fractions A, B, C-D, and E occurred on the silica gel was performed. The fractions were dissolved in ethanol and spotted onto silica gel plates. Two-dimensional chromatography in chloroform–acetone (97:10) for A and B and utilization of a developing mixture of chloroform and methanol (97:5) for C-D, E, and pure Ia showed no evidence of degradation.

Mass Spectrometry—The silica gel containing the black spot from the Fraction E test, R_f 0.97, was extracted with distilled acetone for 2–3 min. The solution was filtered through a sintered-glass filter and evaporated to dryness. The residue was then dissolved in ethanol, respotted on a silica gel 7GF plate, and developed in chloroform–methanol (97:5). The silica gel containing the one observable component, R_f 0.97, was removed from the plate, extracted with redistilled acetone for 2–3 min, filtered, evaporated to dryness, and rechromatographed on silica gel HR60.

The silica gel containing the black spot, R_f 0.97, was extracted with redistilled acetone, evaporated to dryness, and submitted for mass spectral analysis; mass spectrum: *m/e* (relative intensity) 186 (M^+, 75), 185 (100), 158 (13), 157 (15), 143 (15), 130 (25), 129 (46), 128 (31), 127 (13), 117 (33), 115 (54), 102 (17), 91 (79), 77 (33), and 67 (71). The mass spectrum for Ia showed *m/e* (relative intensity) 186 (M^+, 61), 185 (100), 158 (7), 157 (8), 143 (10), 130 (20), 129 (37), 128 (21), 127 (8), 117 (26), 115 (43), 102 (13), 91 (21), 77 (12), and 67 (43). A quantity of the extracted component was dissolved in ethanol and had a retention time of 1.96 min when 1.0 μl was injected onto a 3% OV-101 column at 170°.

The black spot, R_f 0.70, of Fraction D was extracted in a similar manner and submitted for mass spectrometry; mass spectrum: *m/e* (relative intensity) 206 (M^+, 11), 188 (30), 181 (9), 170 (10), 165 (7), 159 (10), 152 (7), 149 (16), 147 (9), 146 (7), 145 (14), 142 (7), 141 (9), 136 (7), 135 (34), 134 (25), 133 (11), 131 (14), 129 (14), 128 (11), 127 (7), 124 (10), 123 (98), 121 (21), 120 (100), 119 (25), 117 (11), 116 (7), 115 (18), 111 (7), 110 (7), 109 (13), 108 (24), 107 (99), 105 (14), 104 (7), 103 (9), 101 (7), 98 (7), 97 (21), 96 (9), 95 (14), 94 (16), 93 (9), 92 (18), 91 (62), 89 (9), 86 (9), 85 (9), 84 (9), 83 (16), 82 (11), 81 (25), 80 (9), 79 (28), 78 (15), 77 (43), 76 (7), 73 (10), 71 (14), 70 (10), 69 (24), 68 (7), 67)26), 66 (14), 65 (30), 63 (13), 60 (14), 59 (13), 58 (13), 57 (32), 56 (14), 55 (40), 54 (9), 53 (17), 52 (9), 51 (21), 50 (10), 45 (11), 44 (21), 43 (64), 42 (14), 41 (62), and 40 (9).

Feces—Feces (25.0 g) from the test rats were soaked in ether, ground in a mortar, and placed in a soxhlet extractor with ether (300 ml) for 66 hr. Evaporation of the ether gave a black residue, which was suspended in water (50 ml) and filtered. The aqueous extract (pH 4.2) was acidified (pH 2.0) with 1 *N* sulfuric acid, extracted with ether (3 × 75 ml) to give aqueous *a* and ether *a* layers. The aqueous *a* layer was basified (pH 7.2) with ammonium hydroxide solution and extracted with ether to give the ether extract containing the amphoteric (E) fraction. Basification of the aqueous *a* layer (pH 9.0) with ammonium hydroxide solution followed by extraction with ether gave an organic extract containing the basic (D) fraction.

The ether *a* layer was washed with freshly prepared sodium bi-

Table IV—Percentage of Metabolites of Ia Found in Feces after Oral Administration of Drug

Days after Administration	Administered Dose Excreted, %								
	Component 1			Component 2			Component 3		
	pH 9.0	pH 7.2	pH 2.0	pH 9.0	pH 7.2	pH 2.0	pH 9.0	pH 7.2	pH 2.0
1	—	10.90	—	—	15.68	—	—	24.78	—
2	—	10.14	—	—	11.65	—	—	27.88	—
3	—	—	—	—	—	—	—	—	—
Total	—	1.04	—	—	27.33	—	—	52.66	—
		81.03							

[4] Methocel HG, Dow Chemical of Canada, Ltd.

carbonate solution (5% w/v, 2 × 50 ml), and the two layers were separated, giving aqueous *b* and ether *b* layers. Acidification of the aqueous *b* layer with hydrochloric acid (50%) and extraction with ether gave an ethereal extract of the strong acid (A) fraction. The ether *b* layer was washed with aqueous sodium hydroxide solution (0.45 *N*, 2 × 100 ml) to give aqueous *c* and ether *c* layers. Acidification of the aqueous *c* layer with hydrochloric acid (50%) and extraction with ether gave an ethereal extract containing the weak acid (B) fraction. The ether *c* layer contained the neutral (C) fraction.

After water-soluble extraction, the black residue was dissolved in ether (50 ml). The ether layer was extracted with 1 *N* sulfuric acid, and the procedure was followed as described previously. Feces (26.0 g) from control rats were extracted in exactly the same manner. Evaporation of the ether gave Fractions A–E.

A second method of extraction for both test and control feces was undertaken in a similar manner to that described previously, except that the feces were soaked in methanol and then extracted with methanol for 66 hr. A third method of extraction of both test and control feces (90.0 g) used ether (600 ml) in a soxhlet extraction apparatus for 66 hr. The ether was evaporated to 200 ml and extracted as described previously, but there was no prior extraction of water-soluble materials.

TLC—The test and control fractions, A–E, obtained by the three extraction procedures were purified prior to investigation.

Ether was added to Fraction A and extracted with an equal volume of aqueous sodium hydroxide solution (0.45 *N*). After acidification of the aqueous layer with 1 *N* sulfuric acid, it was extracted exhaustively with ether. Fraction B was purified in a similar manner. Fraction C was added to a mixture of equal parts of hexane and ethanol. An equal amount of water was added, and the ethanol–water layer was removed by separation. The ethanol–water mixture was evaporated to dryness and dissolved in water, and the aqueous phase was extracted with ether. Ether was added to Fraction D, and the ethereal solution was shaken with an equal volume of 1 *N* sulfuric acid. The aqueous layer was then basified with 0.45 *N* sodium hydroxide solution and extracted with ether. Fraction E was purified in a similar manner. Finally, the ethereal extractions of test and control Fractions A–E were evaporated to dryness.

The purified residues obtained after the three extraction procedures were examined separately by TLC on silica gel. In each case, the developing solvent for Fractions A–C was a mixture of chloroform and acetone (97:10). For Fractions D and E, the solvent employed was a chloroform and methanol mixture (97:5). When the fractions of both test and control urine were examined, no additional spots appeared in the test fractions regardless of the method of extraction of the fecal material.

GLC—The purified extracts in ethanol (2.0–3.0 μl) from both test and control feces were injected onto a column at 190° (Fractions A–C) and 170° (Fractions D and E) under the conditions previously described. No additional peaks were evident in the test fractions.

Efficiency of Extraction Procedures for Isolating Ia from Urine—Compound Ia (1.0000 mg) was added to rat urine (25 ml) and extracted as described previously. Fraction E was diluted in ethanol to 0.8 ml. A sample of Ia was dissolved in ethanol and diluted to 0.8 ml. Samples of 0.6 μl of both ethanolic solutions were injected onto a GLC column at 170°, and the peak area of Fraction E was 11.40% that of the standard solution.

In a separate series of experiments, Ia (25.0000 mg) was mixed with control urine (100 ml, pH 8.6) and extracted with ether (200 ml) in a liquid–liquid continuous extraction apparatus for 24 hr. Samples of the extract (0.6 ml) were removed periodically, and 2.0-μl samples were injected onto a GLC column at 170°. The resultant peak area was compared with a peak area resulting from the injection (2.0 μl) of a solution of Ia (0.2500 mg in 1.0 ml of ethanol). The experiment was repeated, except that the urine was acidified to pH 7.2 prior to extraction. After 1, 2, 3, 4, 5, 6, and 24 hr, the percentage recovery of Ia from urine at pH 8.6 was 76.02, 77.11, 95.10, 99.13, 99.43, 99.93, and 99.49, respectively, and the percentage recovery of Ia from urine at pH 7.2 was 65.66, 74.73, 81.02, 88.40, 92.37, 96.68, and 96.38, respectively.

Quantitation of Unchanged Ia Excreted *via* Urine after Intraperitoneal Injection of Drug—Compound Ia (897.5000 mg) was administered to nine rats at a dose of 400 mg/kg. The urine was collected daily and extracted using the following procedure. The urine collected on Day 1 (231 ml, pH 7.3) was basified with ammonium hydroxide solution to pH 9.3 and extracted with ether (3 × 240 ml) to obtain an ethereal solution of the C-D fractions. The aqueous layer was acidified with 1 *N* sulfuric acid to pH 7.2 and extracted with ether (3 × 260 ml) to give an organic extract (742 ml) containing Fraction E.

The daily E fractions were diluted to 500 μl in ethanol. A standard curve of Ia in ethanol was prepared using the absolute calibration technique (33). Injections of 1.0 μl of the daily E fractions were also injected onto a GLC column. The resultant peak area was measured and compared with the standard curve to give the quantity of unchanged drug. The percentage of unchanged drug after 1, 2, 3, 4, 5, and 6 days was 0.50, 0.29, 0.26, 0.03, 0.00, and 0.00, respectively, *i.e.*, a total of 1.08%. The 11.40% extraction efficiency of this procedure and the volume of ether lost on extraction were considered in these calculations.

The quantitation of unchanged drug in urine using a liquid–liquid extraction procedure was undertaken. Compound Ia (404.0000 mg) was administered to five rats at a dose of 400 mg/kg, and the urine was collected daily. A urine sample (32 ml) collected after 1 day was basified to pH 9.0 with ammonium hydroxide and extracted with ether (360 ml) for 6 hr. The ethereal layer (270 ml) was separated, and the aqueous phase was acidified with sulfuric acid to pH 7.2 and extracted with ether (200 ml) for 6 hr. The ether was separated (165 ml), and the aqueous phase was further acidified to pH 2.0; ether (200 ml) was added, the solution was extracted for 6 hr, and the organic extract (165 ml) was separated.

Quantities of each of the ether extracts (2.0 μl) were injected onto a GLC column, and the peak areas were measured. A comparison with the standard curve indicated the quantity of unchanged Ia present. A correction factor for the volume of ether lost on extraction was made. Urine samples on Days 2, 3, and 4 were extracted in a similar manner and the results are in Table II.

In a further experiment, Ia (198.2000 mg) was administered to 25 rats at a dose of 40 mg/kg. The urine was collected daily and extracted using the liquid–liquid continuous extraction procedure at pH values of 9.0, 7.2, and 2.0, as outlined previously. The results are shown in Table II.

Examination of Rat Urine and Feces after Administration of Ia—Compound Ia (148.8000 mg), suspended in hydroxypropyl methylcellulose solution, was administered to 20 male albino Wistar rats at a dose level of 40 mg/kg. The urine and feces were collected for 3 days. Ten control rats were given only hydroxypropyl methylcellulose solution.

Test and control urines (40 ml) from each of the three daily urine samples were extracted in the same manner as for the intraperitoneal route to give Fractions A, B, C-D, and E. These fractions were dissolved in ethanol and injected onto a 3% OV-101 column in volumes of 4.0 μl. Fractions A, B, and E showed similar peaks in both test and control fractions. In Fraction C-D, three extra peaks appeared with retention times of 1.68, 2.61, and 6.11 min. The retention time of Ia under these conditions was 1.67 min.

Liquid–Liquid Continuous Extraction Procedure—Samples of test urine (40 ml) from each of the three daily urine collections were adjusted with alkali or acid to pH 9.0, 7.2, and 2.0 and extracted with ether for 6 hr using the liquid–liquid continuous extraction procedure. Control urine (40 ml) was extracted in a similar manner.

The fractions were dissolved in ethanol and injected onto a GLC 3% OV-101 column at 170°. The test urine of the pH 9.0 fraction contained three additional peaks with retention times of 1.83, 2.60, and 5.21 min. Under these conditions, Ia had retention times of 2.57–2.64 min. There were two extra peaks in the test sample of the pH 7.2 urine with retention times of 1.72 and 2.63 min; the retention time of Ia was 2.66 min under identical conditions. The pH 2.0 test urine had an extra peak with a retention time of 1.76 min.

Quantitation of Unchanged Drug and/or Metabolites—A sample of the evaporated urine fractions dissolved in ethanol (2.0–4.0 μl) was injected onto a GLC column, and the peak areas of the unchanged drug and/or metabolites were compared to a standard curve of Ia constructed by the method described earlier (33). The quantities of these compounds found in the urine are summarized in Table III and account for 8.36% of the administered dose.

A quantity of test urine from the liquid–liquid extraction (pH 9.0) was placed on an inactivated silica gel 7GF plate and developed in chloroform–methanol (97:5). A black spot, R_f 0.97, was seen in the extract from the test urine, and a fluorescent blue spot, R_f 0.96, was found in an extract from the control urine. The R_f

value of Ia was 0.97, appearing as a black spot under identical conditions. The plate was sprayed with an ethanolic solution of 2,4-dinitrophenylhydrazine (34); the spots in the test urine, R_f 0.96, and from Ia turned to an orange color but the spot with an R_f value of 0.96 in the control urine remained unchanged. The plate was sprayed with aqueous ferric chloride solution (5% w/v) (35), but no spots on the chromatogram changed their color.

Feces (30.0000 g) from both test and control rats were ground with a pestle and mortar and then extracted in a soxhlet apparatus for 48 hr with ether (185 ml). The ether was then extracted as described previously and separated into five fractions. GLC analysis of Fractions A, B, and E showed similar components. The test urine of Fractions C and D had one extra peak at 2.12 and 3.78 min, respectively.

Feces (30.0000 g) from each daily collection from the test rats were extracted by the liquid–liquid extraction procedure using ether for 24 hr. The ethereal extracts were evaporated to dryness, and distilled water (75 ml) was added. The pH was adjusted to 9.0, 7.2, and 2.0, and the solution was extracted with ether (200 ml) for 6 hr. The feces from the control rats were treated in a similar manner. GLC analysis (170°) showed similar components in the pH 9.0 and 2.0 fractions. There were three extra peaks in the pH 7.2 test fraction with retention times of 1.76, 10.30, and 23.95 min.

Quantitation of Metabolites in Feces—A sample of the extract (2.0–4.0 μl) was injected onto a GLC column at 170° under the conditions previously described, and the peak areas of the three components were compared to a standard curve of Ia similar to that described previously. The quantities of compounds found are summarized in Table IV.

A quantity of test (pH 7.2) and control feces extract was placed on an inactivated silica gel 7GF plate and developed in chloroform–methanol (97:5). A black spot appeared in the test extract, R_f 0.92, and a fluorescent blue spot, R_f 0.92, was found in the control extract. The plate was sprayed with 2,4-dinitrophenylhydrazine reagent, but no orange spots appeared. The plate was then sprayed with aqueous ferric chloride solution (5% w/v). A dark-green spot appeared in the test fraction at the R_f 0.92 spot but not in the control extract.

REFERENCES

(1) F. W. Menger and J. H. Smith, *J. Amer. Chem. Soc.*, **91,** 4211(1969).

(2) C. E. Lough, D. J. Currie, and H. L. Holmes, *Can. J. Chem.*, **46,** 771(1968).

(3) T. Posner, *Ber.*, **35,** 799(1902).

(4) *Ibid.*, **37,** 502(1904).

(5) J. R. Dimmock and W. G. Taylor, *J. Pharm. Sci.*, **64,** 181(1975).

(6) K.-H. Lee, H. Furukawa, and E.-S. Huang, *J. Med. Chem.*, **15,** 609(1972).

(7) J. R. Dimmock and W. G. Taylor, *J. Pharm. Sci.*, **63,** 69(1974).

(8) A. F. Casy, N. J. Harper, and J. R. Dimmock, *J. Chem. Soc.*, **1964,** 3635.

(9) S. F. Friess and H. D. Baldridge, *J. Amer. Chem. Soc.*, **78,** 2482(1956).

(10) M. S. Atwal, L. Bauer, S. N. Dixit, J. E. Gearien, M. Megaby, R. Morris, and C. Pokorny, *J. Med. Chem.*, **12,** 994(1969).

(11) M. May and D. J. Triggle, *J. Pharm. Sci.*, **57,** 511(1968).

(12) M. R. Boots, *J. Med. Chem.*, **12,** 426(1969).

(13) P. J. Smith, J. R. Dimmock, and W. A. Turner, *Can. J. Chem.*, **51,** 1458(1973).

(14) *Ibid.*, **51,** 1471(1973).

(15) J. R. Dimmock, W. A. Turner, P. J. Smith, and R. G. Sutherland, *Can. J. Chem.*, **51,** 427(1973).

(16) A. Albert, "Selective Toxicity," 5th ed., Chapman and Hall, London, England, 1973, p. 414.

(17) P. Brookes and P. D. Lawley, *Brit. Med. Bull.*, **20,** 91(1964).

(18) J. R. Dimmock, P. L. Carter, and P. D. Ralph, *J. Chem. Soc., B,* **1968,** 698.

(19) W. H. Laarhoven, R. J. F. Nivard, and E. Havinga, *Experientia,* **17,** 214(1961).

(20) A. J. H. Smit and F. Went, *Proc. Acad. Sci. Amsterdam,* **38,** 852(1935); through *Chem. Abstr.*, **30,** 2600[8](1936).

(21) G. H. Rank and N. T. Bech-Hansen, *Mol. Gen. Genet.*, **126,** 93(1973).

(22) K. Takamiya, *Gann,* **50,** 277(1959); through *Chem. Abstr.*, **54,** 6962i(1960).

(23) *Ibid.*, **50,** 265(1959); through *Chem. Abstr.*, **54,** 6962g(1960).

(24) J. A. Stock, in "Drug Design," vol. 2, E. J. Ariens, Ed., Academic, New York, N.Y., 1971, p. 535.

(25) I. M. Fraser, D. A. Fancher, and A. Strother, *Pharmacologist,* **10,** 203(1968).

(26) F. G. Fischer and H. J. Beilig, *Hoppe-Seylers Z. Physiol. Chem.*, **266,** 73(1940); R. T. Williams, "Detoxication Mechanisms," 2nd ed., Wiley, New York, N.Y., 1959, pp. 340, 341.

(27) J. E. Baer and K. H. Beyer, *Ann. Rev. Pharmacol.*, **6,** 1272(1966).

(28) A. C. Curry, "Poison Detection in Human Organs," 2nd ed., Charles C Thomas, Springfield, Ill., 1969, pp. 76, 77.

(29) H. Budzikiewicz, C. Djerassi, and D. H. Williams, "Mass Spectrometry of Organic Compounds," Holden-Day, San Francisco, Calif., 1967, p. 108.

(30) R. I. Geran, N. H. Greenberg, M. M. MacDonald, A. M. Schumacher, and B. J. Abbott, *Cancer Chemother. Rep. (Part 3),* **3** (2) (Sept. 1972).

(31) P. B. Russell, *J. Chem. Soc.*, **1954,** 1771.

(32) M. C. Dart and H. B. Henbest, *J. Chem. Soc.*, **1960,** 3563.

(33) M. Riedmann, *Xenobiotica,* **2,** 411(1973).

(34) E. Stahl, "Thin-Layer Chromatography," 2nd ed., Springer-Verlag, New York, N.Y., 1969, p. 871.

(35) *Ibid.*, p. 875.

ACKNOWLEDGMENTS AND ADDRESSES

Received April 22, 1975, from the *College of Pharmacy and the ‡Biology Department, College of Arts and Science, University of Saskatchewan, Saskatoon, Saskatchewan, Canada, S7N OWO.

Accepted for publication June 27, 1975.

The authors thank the Medical Research Council of Canada for financial support (Grant numbers MA-4761 and MA-5561) and for providing Studentships to A. P. Sellar and W. A. Turner. Financial support to G. H. Rank by the National Cancer Institute of Canada is gratefully acknowledged. Mr. M. S. Auyeung and Dr. G. B. Baker, College of Pharmacy, University of Saskatchewan, prepared four compounds described in this work and Mrs. L. Noble of the Department of Chemistry and Chemical Engineering, University of Saskatchewan, assisted with the preparative GLC. The authors thank Dr. H. B. Wood, Jr., Drug Research and Development Division, National Cancer Institute, Bethesda, Md., who arranged for the compounds to be screened against the L-1210 and KB tumor systems.

§ Present address: Pharmacy Department, College of Trades and Technology, St. John's, Newfoundland.

ˣ To whom inquiries should be directed.

Synthesis and α-Adrenolytic Activity of Chiral β-Haloethylamines

THOMAS N. RILEY ˣ and FRANK W. CRAWFORD

Abstract □ Several series of *N,N*-diaralkyl- and *N*-aryloxyalkyl-*N*-aralkyl-β-haloethylamines were synthesized containing centers of chirality in the aralkyl substituent and in the β-haloethyl moiety to study the stereoselectivity of α-adrenolytic activity of the β-haloethylamines. These compounds were synthesized from starting materials of known absolute configuration *via* synthetic schemes that did not alter the stereochemical integrity of the chiral centers. Evaluation of the α-adrenolytic activities of these β-haloethylamines on rat vas deferens indicated a variable degree of stereoselectivity of adrenergic blockade, which is interpreted in terms of drug–receptor interactions.

Keyphrases □ β-Haloethylamines, chiral—synthesis, stereoselectivity of α-adrenolytic activity studied, rats □ Enantiomers—β-haloethylamines, synthesis, stereoselectivity of α-adrenolytic activity studied, rats □ α-Adrenolytic activity—stereoselectivity of β-haloethylamines, rats □ Drug–receptor interactions—β-haloethylamines, stereoselectivity of α-adrenolytic activity studied, rats □ Structure–activity relationships—series of β-haloethylamines, stereoselectivity of adrenolytic activity studied, rats

The β-haloethylamines have found utility as therapeutic agents in the treatment of occlusive peripheral vascular disease and, primarily, as pharmacological tools in investigations of the α-adrenergic receptor (1, 2). The β-haloethylamines that produce a highly selective, irreversible antagonism of the α-adrenergic receptor can be structurally classified as either *N,N*-diaralkyl-β-haloethylamines (*e.g.*, dibenamine, I) or *N*-aralkyl-*N*-aryloxyalkyl-β-haloethylamines (*e.g.*, phenoxybenzamine, II, R = CH_3) (3).

While there is considerable information regarding the effect of structural modification on α-adrenolytic activity of the β-haloethylamines, only recently has evidence been obtained indicating that the α-receptor is stereoselective in its interaction with chiral β-haloethylamines. (*R*)-Phenoxybenzamine was reported to be approximately twice as active as the racemate and 14.5 times more potent than the (*S*)-antipode (4). The stereoselectivity of the α-adrenolytic activity of isomers of phenoxybenzamine was proposed to be due to an affinity difference for the receptor by the enantiomers as a result of conformational factors that influence the binding of the C-methyl group.

McLean *et al.* (5) reported on a series of α-adrenolytics containing the β-haloethylamine moiety incorporated into the structure of an agonist ligand, *N*-methyl-β-phenylethanolamine (III) (5). While these compounds were significantly less potent than phenoxybenzamine, their α-adrenolytic activity was characterized by a certain degree of stereoselectivity; (*S*)-III was approximately six times more potent than (*R*)-III. This stereoselectivity of action was opposite to that found in the interaction of β-phenylethanolamine agonists at the α-adrenergic receptor.

The objective of this study was to investigate more fully the stereochemical requirements for β-haloethylamine antagonism of the α-adrenergic receptor. The approach chosen was to design β-haloethylamines containing centers of chirality in the *N*-benzyl and the *N*-β-chloroethyl substituents of these compounds. Hence, β-haloethylamines IV and V were designed by introducing a center of chirality *via* α-methylation of the *N*-benzyl substituent of dibenamine and desmethylphenoxybenzamine (II, R=H). Similarly, β-haloethylamines VI and VII were designed by incorporation of an α-methyl group into the *N*-β-chloroethyl substituent of dibenamine and desmethylphenoxybenzamine. Hence, interpretation of the relative α-adrenolytic potencies of isomers IV–VII should provide useful information regarding both the structural and stereochemical requirements for β-haloethylamine antagonism of the α-adrenergic receptor.

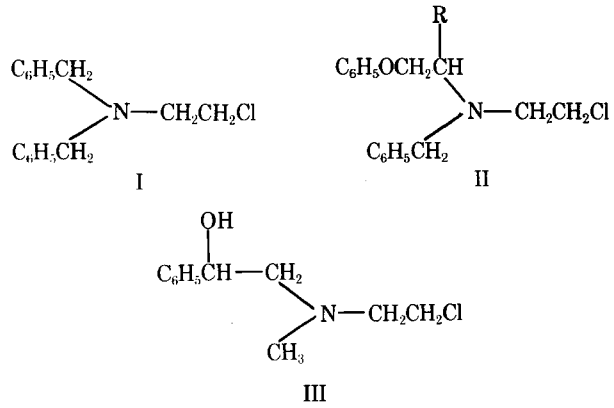

EXPERIMENTAL[1]

Chemistry—The syntheses of the desired chiral β-haloethylamines (IV–VII) were carried out in such a manner that the absolute configurations of the enantiomers were unequivocally determined. This objective was accomplished by utilizing starting materials of known absolute configuration and by utilizing synthetic reactions that maintained the stereochemical integrity of the chiral center.

The racemate and enantiomers of IV and V were synthesized utilizing the racemate and (*R*)-(+)- and (*S*)-(−)-antipodes of α-

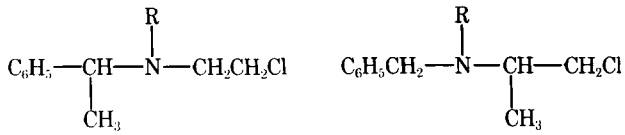

IV: R = $C_6H_5CH_2$
V: R = $C_6H_5OCH_2CH_2$

VI: R = $C_6H_5CH_2$
VII: R = $C_6H_5OCH_2CH_2$

[1] All melting points were determined with a Mel-Temp melting-point apparatus and are uncorrected. Elemental analyses were performed by Chemalytics, Inc., Tempe, Ariz. The IR spectra were obtained using a Perkin-Elmer 257 or a Beckman model 33 spectrophotometer. NMR spectra were obtained with a Jeolco C-60-HL spectrometer. Optical rotations were measured with a Perkin-Elmer 114 polarimeter, using a 5% sample concentration in 95% ethanol.

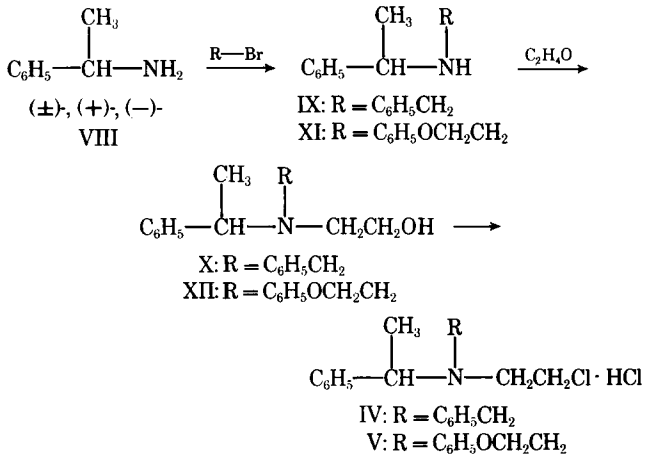

Scheme I

methylbenzylamine (VIII) (Scheme I). Benzylation of VIII was performed by condensation of VIII with benzaldehyde followed by borohydride reduction (Method A) or by treatment of VIII with benzyl bromide (Method B). It was recognized that synthesis by Method A could lead to racemization of the chiral center *via* tautomerization of the intermediate imine. However, a comparison of the optical rotations of the product, α-methyldibenzylamine (IX), obtained by treatment of the enantiomers of VIII according to either Method A or B, showed these values to be essentially identical, thereby indicating that racemization had not occurred in Method A.

The secondary amine (IX) was converted to the amino alcohol (X) by treatment with ethylene oxide, and X was converted to the β-chloroethylamine hydrochloride (IV) using thionyl chloride. Treatment of the racemate and enantiomers of VIII with 2-phenoxyethyl bromide gave the desired secondary amine (XI) in yields of approximately 75%. Hydroxyethylation of XI with ethylene oxide gave the amino alcohol (XII), which was converted to the β-chloroethylamine hydrochloride (V) using thionyl chloride in chloroform.

The racemate and enantiomers of VI and VII were synthesized from the racemate and (*R*)-(−)-alanine and (*S*)-(−)-alanine (XIII) (Scheme II). Alanine was benzoylated and reduced to *N*-benzylalaninol (XIV) by standard procedures (4). *N*-Benzylation of XIV using benzyl bromide in triethylamine gave good yields of the desired amino alcohol (XV), which was readily converted to the β-chloroethylamine analog (VI) upon treatment with thionyl chloride. *N*-2-Phenoxyethylation of XIV was carried out using 2-phenoxyethyl bromide in triethylamine; the resulting amino alcohol (XVI), upon treatment with thionyl chloride, gave the β-chloroethylamine analog (VII).

α-Methyldibenzylamine (IX)—*Method A*—A solution of 12.1 g (0.1 mole) of α-methylbenzylamine in 200 ml of dried benzene was treated with 10.6 g (0.1 mole) of benzaldehyde. After refluxing

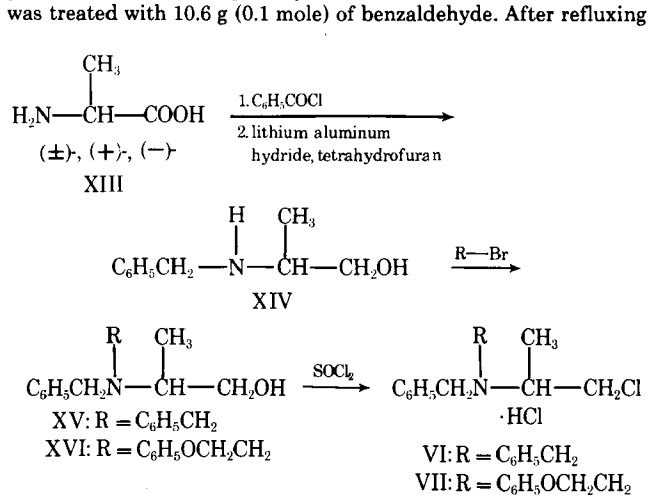

Scheme II

for 12 hr under a Dean–Stark apparatus, the solution was concentrated *in vacuo* to a yellow oil. This oil then was dissolved in 200 ml of an ethanolic suspension of 7.8 g (0.2 mole) of sodium borohydride. The reaction was refluxed overnight, treated with 25 ml of water, and filtered. The filtrate was concentrated *in vacuo;* the residue was dissolved in ether, dried (sodium sulfate), and concentrated *in vacuo;* and the light-yellow oil was distilled to yield 9.8 g (44%) of (±)-VIII, bp 118–121° (0.75 mm).

Treatment of (±)-VIII with ethereal hydrochloric acid followed by recrystallization from ethyl acetate provided (±)-VIII-HCl, mp 181–183° [lit. (6) mp 184°]; (*R*)-VIII, bp 110–115° (0.2 mm), $[\alpha]_D^{25}$ +52.0° [lit. (6) bp 171° (15 mm), $[\alpha]_D^{20}$ +29.7°]; and (*S*)-VIII, bp 112–115° (0.2 mm), $[\alpha]_D^{25}$ −53.2° [lit. (6) bp 171° (15 mm), $[\alpha]_D^{20}$ −39.9°]. The hydrochloride salts of (*R*)- and (*S*)-VIII were prepared in ethereal hydrochloric acid and recrystallized from ethyl acetate, mp 176–177° [lit. (6) mp 177°].

Method B—An ice-cooled solution of 12.1 g (0.1 mole) of α-methylbenzylamine in 200 ml of dry toluene was treated with 17.1 g (0.1 mole) of benzyl bromide added dropwise in a 20-ml solution of dry toluene. The reaction was refluxed for 3 hr and then concentrated *in vacuo*. The resulting oil was distilled to give 10.2 g (49%) of (±)-VIII. Similar treatment of (+)- and (−)-α-methylbenzylamines gave products whose physical data were identical to those obtained by Method A.

***N*-(2-Hydroxyethyl)-α-methyldibenzylamine (X)**—In an ice-cooled metal reaction bomb, 40.1 g (0.19 mole) of (±)-IX was treated with 9.7 g (0.22 mole) of ethylene oxide and 2 ml of water. The reaction mixture was heated at 110° for 12 hr and yielded an extremely viscous oil. Following distillation, 24 g (51%) of (±)-X was obtained, bp 150° (0.4 mm); (*R*)-X, bp 156–159° (0.15 mm), $[\alpha]_D^{25}$ + 27.4°; and (*S*)-X, bp 155–160° (0.15 mm), $[\alpha]_D^{25}$ −26.5°.

Anal.—Calc. for $C_{17}H_{21}NO$: C, 69.97; H, 7.60; N, 4.80. Found (±): C, 70.46; H, 7.82; N, 4.76; (*R*): C, 69.81; H, 7.60; N, 4.63; (*S*): C, 70.18, H, 7.77; N, 4.42.

***N*-(2-Chloroethyl)-α-methyldibenzylamine Hydrochloride (IV)**—An ice-cooled solution of 19 g (0.075 mole) of (±)-X in 100 ml of chloroform, previously saturated with dry hydrogen chloride gas, was treated with 11.0 g (0.1 mole) of thionyl chloride in 50 ml of chloroform. The reaction mixture was refluxed for 12 hr and then concentrated *in vacuo* to a viscous amber oil. A crystalline product was obtained by crystallization of the oil from ethyl acetate; 16.4 g (72%) of (±)-IV, mp 143–145°, was obtained after three recrystallizations from ethyl acetate. The enantiomers of X were obtained by an identical procedure: (*R*)-X, mp 176–177°, $[\alpha]_D^{25}$ + 18.2°; and (*S*)-X, mp 177–178°, $[\alpha]_D^{25}$ −18.1°.

Anal.—Calc. for $C_{17}H_{20}ClN{\cdot}HCl$: C, 65.81; H, 6.82; N, 4.51. Found (±): C, 65.79; H, 7.04; N. 4.24; (*R*): C, 65.79; H, 6.98; N, 4.65; (*S*): C, 65.77; H, 7.09; N, 4.13.

α-Methyl-*N*-(2-phenoxyethyl)benzylamine (XI)—A mixture of 12.1 g (0.1 mole) of (±)-VIII, 20 g (0.1 mole) of 2-phenoxyethyl bromide (prepared by treatment of 2-phenoxyethanol with phosphorus tribromide), and 10 g (0.1 mole) of triethylamine was prepared in a 45-ml metal reaction vessel. The sealed reaction vessel was heated at 100° for 12 hr, and a viscous oil was obtained. This oil was dissolved in chloroform and extracted with three 50-ml portions of water. The chloroform solution was dried (sodium sulfate) and concentrated *in vacuo*, and the resultant oil was distilled to give 18.4 g (75%) of (±)-XI, bp 120–127° (0.1 mm).

The enantiomers of VIII were treated in the same manner, providing (*R*)-XI, bp 126–129° (0.2 mm), $[\alpha]_D^{25}$ + 31.5°; and (*S*)-XI, bp 120–126° (0.1 mm), $[\alpha]_D^{24}$ −30.6°. The hydrochloride salts of the isomers of XI were prepared in ethereal hydrochloric acid providing (±)-XI-HCl, mp 151–153°; (*R*)-XI-HCl, mp 125–126°, $[\alpha]_D^{25}$ −10.5°; and (*S*)-XI-HCl, mp 124–126°, $[\alpha]_D^{25}$ + 10.0°.

Anal.—Calc. for $C_{16}H_{19}NO{\cdot}HCl$: C, 69.18; H, 7.26; N, 5.04. Found (±): C, 69.22; H, 7.06; N, 4.98; (*R*): C, 69.19; H, 7.18; N, 4.95; (*S*): C, 69.19; H, 7.30; N, 5.00.

***N*-(2-Hydroxyethyl)-*N*-(2-phenoxyethyl)-α-methylbenzylamine (XII)**—A mixture of 18.4 g (0.076 mole) of (±)-XI, 3.5 g (0.08 mole) of ethylene oxide, and 2 ml of water was prepared and sealed in a 45-ml metal reaction vessel. The vessel was heated at 120° for 17 hr, and the contents were distilled to afford 14.9 g (69%) of (±)-XII, bp 181–184° (0.2 mm). The enantiomers of XII were prepared in an identical manner, giving (*R*)-XII, bp 170–174° (0.12 mm), $[\alpha]_D^{25}$ +11.6°; and (*S*)-XII, bp 174–177° (0.16 mm), $[\alpha]_D^{25}$ −11.9°.

Anal.—Calc. for $C_{18}H_{23}NO_2$: C, 75.76; H, 8.12; N, 4.91. Found

(±): C, 75.04; H, 8.01; N, 5.15; (*R*): C, 75.39; H, 8.26; N, 5.14; (*S*): C, 75.32; H, 7.92; N, 4.88.

***N*-(2-Chloroethyl)-*N*-(2-phenoxyethyl)-α-methylbenzylamine Hydrochloride (V)**—Addition of 15 g (0.13 mole) of thionyl chloride to 10 g (0.035 mole) of (±)-XII in an ice-cooled chloroformic hydrochloric acid solution, followed by a 2-hr reflux period and workup as described in the preparation of (±)-IV, gave 4.8 g (40%) of (±)-V, mp 84–86°, after three recrystallizations from ethyl acetate. The enantiomers of V were similarly prepared, giving (*R*)-V, mp 106–107°, $[\alpha]_D^{25}$ +24.6°; and (*S*)-V, mp 106–108°, $[\alpha]_D^{25}$ −25.0°.

Anal.—Calc. for $C_{18}H_{22}ClNO{\cdot}HCl$: C, 63.53; H, 6.81; N, 4.12. Found (±): C, 63.57; H, 6.86; N, 3.83; (*R*): C, 63.87; H, 7.17; N, 3.93; (*S*): C, 63.50; H, 7.02; N, 4.35.

***N,N*-Dibenzyl-2-amino-1-propanol (XV)**—A solution of 13.7 g (0.08 mole) of benzyl bromide in 50 ml of dry toluene was added dropwise at room temperature to a stirred 250-ml solution of 10 g (0.06 mole) of (±)-XIV [prepared by lithium aluminum hydride in tetrahydrofuran reduction of (±)-*N*-benzoylalanine according to published procedures] (4) in dry toluene and 6 g of sodium carbonate in suspension. After addition of the benzyl bromide, the reaction was refluxed for 24 hr and filtered. Then the filtrate was concentrated *in vacuo* and the residue was distilled to afford 10.1 g (64%) of (±)-XV, bp 143–148° (0.1 mm).

The enantiomers of XV were prepared similarly from the enantiomers of XIV, providing (*R*)-XV, bp 144–149° (0.1 mm), $[\alpha]_D^{25}$ −34.8°; and (*S*)-XV, bp 142–148° (0.1 mm), $[\alpha]_D^{25}$ +35.1°. The hydrochloride salts of the isomers of XV were prepared in ethyl acetate saturated with hydrochloric acid. The salts were recrystallized to a stable melting point from ethyl acetate, providing (±)-XV-HCl, mp 181–183° [lit. (7) mp 180.5–182.5°]; (*R*)-XV-HCl, mp 140–142°; and (*S*)-XV-HCl, mp 142–144°.

Anal.—Calc. for $C_{17}H_{21}NO{\cdot}HCl$: C, 69.97; H, 7.60; N, 4.80. Found (±): C, 69.83; H, 7.85; N, 4.66; (*R*): C, 69.99; H, 7.38; N, 4.86; (*S*): C, 70.13; H, 7.61; N, 4.71.

***N*-(2-Chloro-1-methylethyl)dibenzylamine Hydrochloride (VI)**—A solution of 5.3 g (0.021 mole) of (±)-XV in 200 ml of dry, distilled benzene, previously saturated with hydrochloric acid, was cooled in an ice bath. Then 5.3 g (0.045 mole) of thionyl chloride in 50 ml of benzene was added. The reaction was allowed to warm to room temperature and then was refluxed for 12 hr. The solution was concentrated *in vacuo*, treated with three portions of 95% ethanol to destroy the unreacted thionyl chloride, and further concentrated *in vacuo*. A dark viscous oil, which crystallized on standing for 2 hr, was obtained. Recrystallization of the solid yielded 2.8 g (45%) of (±)-VI, mp 136–138° [lit. (8) mp 137–139°]. The enantiomers of XV were treated in an identical manner to provide (*R*)-VI, mp 167–168°, $[\alpha]_D^{25}$ −28.5°; and (*S*)-VI, mp 166–168°, $[\alpha]_D^{25}$ +26.2°.

Anal.—Calc. for $C_{17}H_{21}ClN{\cdot}HCl$: C, 65.81; H, 6.82; N, 4.51. Found (±): C, 66.35; H, 6.95; N, 4.53; (*R*): C, 65.74; H, 6.75; N, 4.54; (*S*): C, 65.98; H, 6.81; N, 4.42.

***N*-(2-Hydroxy-1-methylethyl)-*N*-(2-phenoxyethyl)benzylamine (XVI)**—A solution of 16.4 g (0.1 mole) of (±)-XIV in 200 ml of triethylamine was treated with 24 g (0.12 mole) of 2-phenoxyethyl bromide. The reaction was refluxed for 24 hr, after which the solvent was removed *in vacuo* and the resultant oil was distilled to provide 12.7 g (44%) of (±)-XVI, bp 190–198° (0.22 mm). The enantiomers of XIV were treated in an identical manner to yield (*R*)-XVI, bp 180–184° (0.08 mm), $[\alpha]_D^{25}$ −38.8°; and (*S*)-XVI, bp 186–190° (0.2 mm), $[\alpha]_D^{25}$ +39.5°.

Anal.—Calc. for $C_{18}H_{23}NO_2$: C, 75.75; H, 8.13; N, 4.91. Found (±): C, 75.52; H, 8.37; N, 4.97; (*R*): C, 76.61; H, 8.11; N, 5.10; (*S*): C, 75.92; H, 8.45; N, 4.91.

***N*-(2-Chloro-1-methylethyl)-*N*-(2-phenoxyethyl)benzylamine Hydrochloride (VII)**—A solution of 7 g (0.025 mole) of XVI and 3.6 g (0.03 mole) of thionyl chloride was prepared in chloroform, previously treated with hydrochloric acid. The solution was refluxed for 3 hr, concentrated *in vacuo*, and treated with three portions of ethanol with alternate *in vacuo* concentration. The resulting dark gummy material was crystallized from ethyl acetate to yield 3.7 g (44%) of (±)-VII which, after three recrystallizations from ethyl acetate, gave a white solid, mp 116–117°. The enantiomers of VII were likewise prepared from the enantiomers of XIV, giving (*R*)-VII, mp 122–124°, $[\alpha]_D^{25}$ +23.2°; and (*S*)-VII, mp 124–125°, $[\alpha]_D^{25}$ −22.5°.

Anal.—Calc. for $C_{18}H_{22}ClNO{\cdot}HCl$: C, 63.53; H, 6.81; N, 4.12. Found (±): C, 63.77; H, 6.88; N, 4.05; (*R*): C, 63.58; H, 6.72; N, 4.11; (*S*): C, 63.90; H, 7.12; N, 4.26.

Table I—α-Adrenolytic Activities of Chiral β-Chloroethylamines

Compound	Configuration	ED_{50}, mmole/ml
(±)-IV	—	12.0×10^{-8}
(+)-IV	*R*	7.0×10^{-8}
(−)-IV	*S*	22.0×10^{-8}
(±)-V	—	6.4×10^{-8}
(+)-V	*R*	6.1×10^{-8}
(−)-V	*S*	6.8×10^{-8}
(±)-VI	—	Inactive[a]
(−)-VI	*R*	Inactive[a]
(+)-VI	*S*	Inactive[a]
(±)-VII	—	75.0×10^{-8}
(+)-VII	*R*	34.0×10^{-8}
(−)-VII	*S*	24.0×10^{-8}
(±)-Phenoxybenzamine	—	1.5×10^{-8}

[a] The isomers of VI were deemed inactive in this study because they did not produce significant blockade of the contractile response of levarterenol of the rat vas deferens up to a concentration of 9.2×10^{-6} mmole/ml.

Pharmacology—Male, white rats, 200–375 g, were sacrificed with a sharp blow to the head. The vas deferens was removed in 2–3-cm strips and immediately placed in a bath of modified Krebs–Henseleit solution aerated by 95% oxygen and 5% carbon dioxide. In the test procedure, the vas deferens was mounted in a 25-ml bath of aerated Krebs–Henseleit solution and maintained at 37°. Tissues were allowed to equilibrate at least 30 min prior to the beginning of any experiment.

Contractile responses were recorded by means of a physiograph[2] with a chart speed of 0.01 cm/sec. The first step in the test procedure involved obtaining a contractile response to 5×10^{-5} *M* levarterenol [(−)-norepinephrine] (95% of maximum contraction). The next response to levarterenol was recorded after the tissue had stabilized, as indicated by a flat baseline. A given dose of β-haloethylamine was then added to the bath fluid; after 5 min, the tissue was washed, levarterenol was added, and the response was recorded. The percent decrease in the contractile response was calculated and represents the degree of adrenergic blockade.

A graphical correlation of percent blockade *versus* log concentration of the β-haloethylamine was then prepared, and the ED_{50} concentrations were taken from the graph. The ED_{50} values representing the concentration of β-haloethylamines (in millimoles per milliliter) required to reduce by 50% the response of the rat vas deferens to 5×10^{-5} *M* levarterenol after a 5-min exposure of the tissue to the antagonist are presented in Table I.

RESULTS AND DISCUSSION

The blockade of α-adrenergic receptors by β-haloethylamines has been characterized as being competitive irreversible in nature (9). To account for the biphasic nature of β-haloethylamine antagonism, Nickerson (10) proposed Scheme III for the mechanism of action of these agents. This proposal, later substantiated by Graham (11), suggests that the β-haloethylamine cyclizes in the biophase to form the pharmacologically active aziridinium ion, which then interacts in a reversible manner with the α-receptor to produce the initial competitive phase of antagonism. Following formation of the reversible aziridinium-ion–receptor complex, a nucleophile on the receptor becomes alkylated by the aziridinium ion to

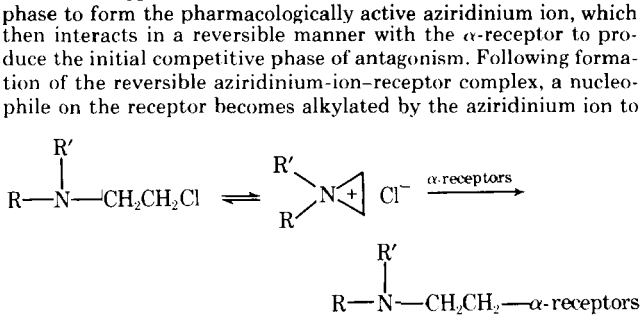

Scheme III

[2] DMP-4A.

establish irreversible blockade. Hence, the production of adrenergic antagonism by a β-haloethylamine is a function of the chemical reactivity of the molecule, which is of importance in the formation of the aziridinium ion, and the degree of structural and stereochemical complementarity of the aziridinium ion for the components of the α-receptor.

Hypothetical representations of the complex formed between the aziridinium ion and the α-receptor inferred a primary receptor binding role for the aryloxyalkyl substituent of the *N*-aryloxyalkyl-β-haloethylamines (12, 13). Similar descriptions of the interaction of an *N,N*-diaralkyl-β-haloethylamine with the α-receptor implicated a primary binding site on the receptor for the *N*-aralkyl substituent. However, it would appear that in the case of an *N*-aryloxyalkyl-*N*-aralkyl-β-haloethylamine (II), its primary interaction with the α-receptor involves preferential binding of the aryloxyalkyl substituent as opposed to binding of the aralkyl group. This conclusion is based upon the greater antagonistic potencies of the *N*-aryloxyalkyl-β-haloethylamines as compared to their *N*-aralkyl analogs (*e.g.*, phenoxybenzamine *versus* dibenamine) and confirmed by the results of this study that indicate greater potency for the *N*-phenoxyethyl-β-haloethylamines (V and VII) as compared to their *N*-benzyl analogs (IV and VI).

In addition, the lack of stereoselectivity of antagonistic action of the isomers of V suggests that the achiral phenoxyethyl substituent is primarily involved in receptor binding to the exclusion of an interaction of the chiral *N*-α-methylbenzyl substituent in these isomers. One would reasonably expect to observe a significant degree of stereoselectivity in the actions of the isomers of V if the *N*-α-methylbenzyl moiety was involved in binding the aziridinium ion of V to receptor components. Similarly, the relatively low level of stereoselectivity of α-antagonism exhibited by the isomers of IV [(*R*)/(*S*) ratio of 3.1] suggests that there is no great preference in binding of either the *N*-benzyl or the chiral *N*-α-methylethyl substituents of this β-haloethylamine at the receptor.

Previous studies of the effect of the α-methylation of the β-chloroethyl substituent of dibenamine indicated no change in potency as a result of this structural modification. However, a similar structural change in the phenoxybenzamine series is associated with a loss of antagonistic activity (14). The findings of this study are somewhat opposed to the literature reports in that the isomers of VI do not possess significant α-adrenolytic activity whereas the isomers of VII exhibit a fair degree of potency. The earlier studies of the effect of this structural modification on α-adrenolytic activity were carried out in whole animals (cat blood pressure changes), and the isomers of the dibenamine and phenoxybenzamine analogs were not studied.

Based upon the results obtained in this study, the general effect of α-methylation of the β-chloroethyl substituent in the β-haloethylamines is deleterious with regard to α-adrenolytic potency. The effect of this structural modification is so significantly deleterious to potency that VII is even less active than IV. The stereoselectivity of antagonistic potencies of the isomers of VII may be indicative of differences in receptor affinities for these compounds. However, numerous other factors may play a role in producing potency differences between enantiomeric β-haloethylamines (4, 5). These factors include differing modes of binding to the receptor, which could result in differing rates of receptor nucleophile alkylation; differences in rates of inhibition of levarterenol uptake sites; and the possibility of at least two different receptor subsites, which mediate the antagonism of β-haloethylamines at the adrenergic receptor.

Further, a comparison of the potencies of one series of isomers with a structurally related series of isomers is complicated by the possibility of differing rates of cyclization of the β-haloethylamines to the aziridinium ions. Additional study is required prior to explaining the nature of the stereoselectivity of α-adrenolytic potencies of the isomers of VII.

REFERENCES

(1) D. J. Triggle, "Neurotransmitter-Receptor Interactions," Academic, London, England, 1971, chap. IV.

(2) "The Pharmacological Basis of Therapeutics," 4th ed., L. S. Goodman and A. Gilman, Eds., Macmillan, New York, N.Y., 1970, p. 550.

(3) G. E. Ullyot and J. F. Kerwin, in "Medicinal Chemistry," vol. II, F. F. Blicke and C. M. Suter, Eds., Wiley, New York, N.Y., 1956, p. 234.

(4) P. S. Portoghese, T. N. Riley, and J. W. Miller, *J. Med. Chem.*, **14**, 561(1971).

(5) S. McLean, V. C. Swamy, D. Tomei, and D. J. Triggle, *ibid.*, **16**, 54(1973).

(6) K. Parck, *J. Pratk. Chem.*, **86**, 284(1913); through *Chem. Abstr.*, **7**, 3318(1914).

(7) J. F. Kerwin, G. E. Ullyot, R. C. Fuson, and C. L. Zirkle, *J. Amer. Chem. Soc.*, **69**, 2961(1947).

(8) J. F. Kerwin, G. C. Hall, F. J. Milnes, I. H. Witt, R. A. McLean, E. Macko, E. J. Fellows, and G. E. Ullyot, *ibid.*, **73**, 4162(1951).

(9) J. F. Moran, C. R. Triggle, and D. J. Triggle, *J. Pharm. Pharmacol.*, **21**, 38(1969).

(10) M. Nickerson, *Pharmacol. Rev.*, **1**, 27(1949).

(11) J. D. P. Graham, *Progr. Med. Chem.*, **2**, 132(1962).

(12) D. J. Triggle, *Advan. Drug Res.*, **2**, 173(1965).

(13) B. Belleau, *Proc. Int. Pharmacol. Meeting, 1st, Stockholm, 1961*, **7**, 75(1963).

(14) M. Nickerson and W. S. Gump, *J. Pharmacol. Exp. Ther.*, **97**, 25(1949).

ACKNOWLEDGMENTS AND ADDRESSES

Received May 19, 1975, from the *Department of Medicinal Chemistry, University of Mississippi, University, MS 38677*

Accepted for publication June 26, 1975.

Adapted in part from a thesis submitted by F. W. Crawford to the Graduate School, University of Mississippi, in partial fulfillment of the Master of Science degree requirements.

Supported by the Mississippi Heart Association and the Research Institute of Pharmaceutical Sciences, School of Pharmacy, University of Mississippi.

The authors acknowledge the assistance of Dr. James C. Murphy and Mr. Joseph M. Mauldin in carrying out the pharmacological evaluation of the compounds.

[x] To whom inquiries should be directed.

Hypocholesterolemic Agents III: Inhibition of β-Hydroxy-β-methylglutaryl Coenzyme A Reductase by Half Acid Esters of 1-(4-Biphenylyl)pentanol

KENNETH E. GUYER *, SHARON G. BOOTS, PAUL E. MARECKI, and MARVIN R. BOOTS ˣ

Abstract □ A series of half acid esters of 1-(4-biphenylyl)pentanol was synthesized and assayed for inhibition of rat liver β-hydroxy-β-methylglutaryl coenzyme A reductase. The number of methylenes separating the carboxyl and ester groups was varied from zero to six. A minimum of one methylene was required for reasonable activity. Further separation of the carboxyl and ester groups produced small changes in activity. Investigation of several isomeric (*cis* and *trans*) half acid esters indicated that activity was independent of configuration. Modification of the acid portion of the glutarate analog by incorporating a 3-hydroxyl group increased activity sixfold.

Keyphrases □ Hypocholesterolemic agents—series of half acid esters of 1-(4-biphenylyl)pentanol synthesized, effect on rat liver β-hydroxy-β-methylglutaryl coenzyme A reductase □ β-Hydroxy-β-methylglutaryl coenzyme A reductase—rat liver, effect of half acid esters of 1-(4-biphenylyl)pentanol □ 1-(4-Biphenylyl)pentanol—half acid ester series, synthesized, effect on rat liver β-hydroxy-β-methylglutaryl coenzyme A reductase

In an earlier report (1), an approach to the design of inhibitors of cholesterol biosynthesis as potential hypocholesterolemic agents was discussed. Specifically, the rationale for the inhibition of the target enzyme, β-hydroxy-β-methylglutaryl coenzyme A reductase, was presented. Previously, a series of arylalkyl hydrogen succinates and glutarates (I) was synthesized and found to be inhibitors of yeast β-hydroxy-β-methylglutaryl coenzyme A reductase. In this study, the alcohol portion of the acid esters was varied; maximum activity was obtained when R_1 = biphenyl and R_2 = *n*-butyl.

This paper describes the synthesis and assay of acid esters of 1-(4-biphenylyl)pentanol. Various diacids were utilized in an effort to determine the importance of the: (*a*) distance separating the free carboxyl and ester groups, (*b*) conformational relationship between the carboxyl and ester groups, and (*c*) hydroxyl group in the 3-position of substituted glutaric acid derivatives.

The recent availability of mammalian β-hydroxy-β-methylglutaryl coenzyme A reductase from rat liver (2) provided an enzyme source for the inhibition studies. Hopefully, these *in vitro* data would be more applicable to the selection of inhibitors for the *in vivo* studies in rats than the *in vitro* data obtained using the yeast reductase.

CHEMISTRY

Various half acid esters of 1-(4-biphenylyl)pentanol (1) were synthesized using five different procedures. Procedure A involved conversion of the diacid to the diacid chloride, followed by treatment of the diacid chloride with 1 equivalent of the alcohol. The reaction mixture was then treated with a sodium bicarbonate solution to hydrolyze the acid chloride present. Although statistical

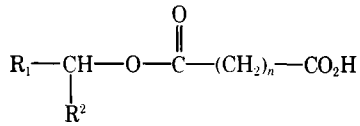

I: $n = 2$ or 3

yield would only be 50% using this procedure, the actual yields were much lower. This method was later replaced by Procedure D, which was much more versatile and used very mild and essentially neutral reaction conditions.

Procedure B involved the conversion of the diacid chloride to the diester using 2 equivalents of the substituted pentanol, followed by partial saponification. This method was also abandoned as a useful synthetic tool and replaced by Procedure D.

Procedure C, originally described by Palazzo *et al.* (3) and modified (1), involved treatment of the acid anhydride with the pentanol in pyridine (heated at reflux). This method gave low yields in many cases and was replaced by either Procedure D or E.

Procedure D, described originally by Büchi *et al.* (4), proved to be extremely useful. It often provided the desired monoester when other methods failed to give any of the desired product. It is the method of choice, especially when other functional groups are present in the starting diacid. This procedure involved the treatment of a diacid in chloroform at 25° with the substituted pentanol in the presence of *N,N*-dimethylformamide dineopentyl acetal.

Procedure E, originally described by Steglich and Höfle (5), also proved to be useful. The anhydride was treated with the substituted pentanol in dimethylformamide at 25° in the presence of 4-dimethylaminopyridine and triethylamine.

Synthesis of the monoester of 3-methoxy-3-methylglutaric acid was more involved because the starting diacid was not commercially available. A synthesis was devised starting with the known 4-hydroxy-4-methyl-1,6-heptadiene (XV, Scheme I) (6). Methylation of the hydroxyl group was effected by treatment with sodium hydride in dimethyl sulfoxide, followed by methyl iodide. Ozonolysis at −78°, followed by an oxidative workup using hydrogen peroxide in acetic acid, provided the methoxy diacid (XVII) in a 50% yield. Difficulty was encountered in the synthesis of the monoester (XIVc), and the only method that provided a respectable yield was Procedure D.

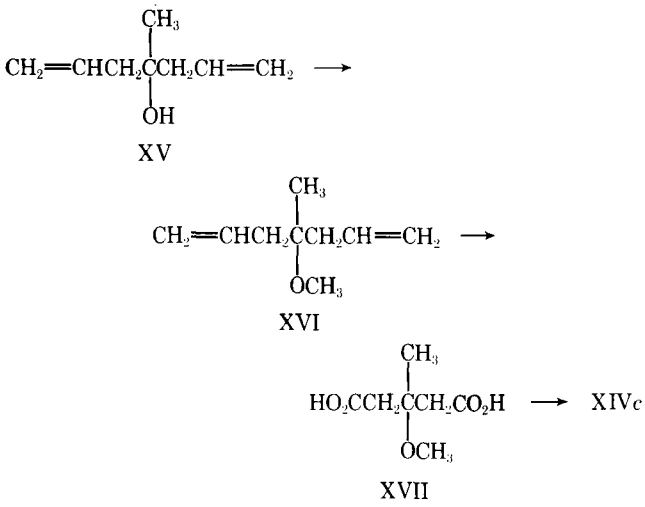

Scheme I

Table I—Properties of Monoesters of Dicarboxylic Acids

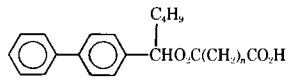

Compound	n	Procedure	Yield, %	Melting Point	Melting Point (Salt)	Formula	Analysis, %[a] Calc.	Found
IV*a*	0	A	19	Oil	169–170°	$C_{27}H_{30}N_2O_4S$	C 67.7	67.7
							H 6.3	6.4
							N 5.9	6.0
IV*b*	1	B	25	65–68°	—	$C_{20}H_{22}O_4$	C 73.6	73.8
							H 6.8	6.8
IV*c*	2	C	68	77–79°[b]	—	—	—	—
IV*d*	3	C	53	Oil[b]	122–123°	—	—	—
IV*e*	4	C	30	Oil	130–131°	$C_{31}H_{38}N_2O_4S$	C 69.6	69.5
							H 7.1	7.2
							N 5.2	5.2
IV*f*	5	B	21	Oil	126–127°	$C_{32}H_{40}N_2O_4S$	C 70.0	70.0
							H 7.3	7.4
							N 5.1	5.3
IV*g*	6	A	22	Oil	130–132°	$C_{33}H_{42}N_2O_4S$	C 70.5	70.3
							H 7.5	7.4
							N 5.0	5.2

[a] Analytical data were obtained on the solid monoesters, while the oils were characterized as their solid *S*-benzylthiuronium salts (1). [b] Described previously (1).

EXPERIMENTAL[1]

Reagents—The following were used: oxalyl chloride[2], malonyl chloride[3], fumaryl chloride[2], pimeloyl chloride[4], suberoyl chloride[5], *trans*-1,2-cyclobutanedicarboxylic acid chloride[3], maleic acid[3], β-hydroxy-β-methylglutaric acid[6], adipic anhydride (7), *cis*-1,2-cyclobutanedicarboxylic anhydride[3], *N,N*-dimethylformamide dineopentyl acetal[3], 4-dimethylaminopyridine[3], $NADP^+$[7], glucose 6-phosphate[7], torula yeast glucose 6-phosphate dehydrogenase[7], and β-hydroxy-β-methylglutaric-3-^{14}C acid[8].

Monoesters of Diacids—*Procedure A, Partial Esterification Using Diacid Chlorides: Monoesters IV*a, *IV*g, *X*b, *and XI*a—This example typifies the method (Schemes II and III) used to prepare these monoesters (Tables I and II). To a solution of 1.1 ml

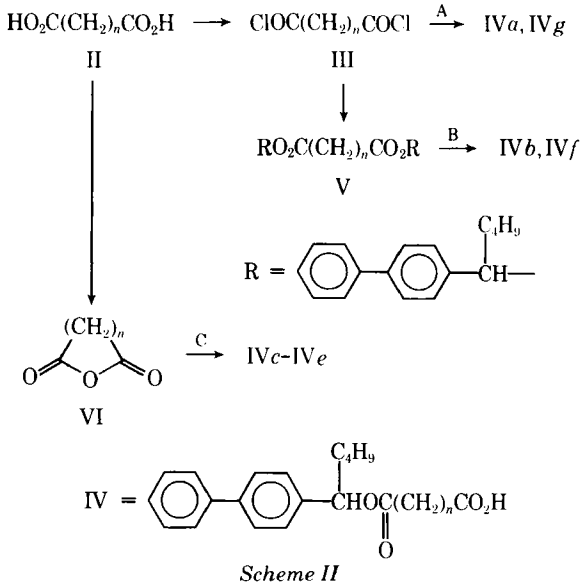

Scheme II

(0.01 mole) of fumaryl chloride in 10 ml of ether was added dropwise, with stirring, a solution of 2.4 g (0.01 mole) of 1-(4-biphenylyl)pentanol (1) in 20 ml of ether. The yellow solution was stirred at 25° for 21 hr, and then 10 ml of a 5% sodium bicarbonate solution was added. The mixture was stirred at 25° for 1.5 hr. Additional ether was added, and the aqueous phase was adjusted to pH 12 with a 5% sodium hydroxide solution.

The basic, aqueous extract was acidified to pH 2 with an ice-cold concentrated hydrochloric acid solution and then extracted with ether. The organic phase was washed with water and then with a saturated sodium chloride solution. The organic phase was dried over anhydrous sodium sulfate, and the solvent was removed under reduced pressure to afford 1.2 g of a beige solid.

Chromatography on 50 g of silicic acid (8) afforded 1.02 g (33%) of XI*a* as a white solid. An analytical specimen of XI*a*, mp 100–104°, was prepared by recrystallization from ethyl acetate–petroleum ether (bp 60–75°); IR ($CHCl_3$): 1710 (broad, acid and ester carbonyls) and 1642 (C=C) cm^{-1}; NMR ($CDCl_3$): δ 0.65–2.10 [broad, 9H, $CH_3(CH_2)_3$], 5.90 (t, J = 6 Hz, 1H, HCO_2C—), 6.90 (s, 2H, HC=CH), 7.24–7.70 (m, 9H, aromatic), and 8.85 (s, 1H, CO_2H) ppm.

*Procedure B, Partial Saponification of Diesters: Monoesters IV*b *and IV*f—This example typifies the method (Scheme II) used to prepare these monoesters. To a solution of 7.2 g (0.03 mole) of 1-(4-biphenylyl)pentanol (1) and 3.75 ml (0.03 mole) of *N,N*-dimethylaniline in 50 ml of ether was added, with stirring and cooling, a solution of 1.46 ml (0.015 mole) of malonyl chloride in 25 ml of ether. After the addition was complete, the reaction mixture was allowed to warm to 25°; it was heated at reflux for 2 hr and then

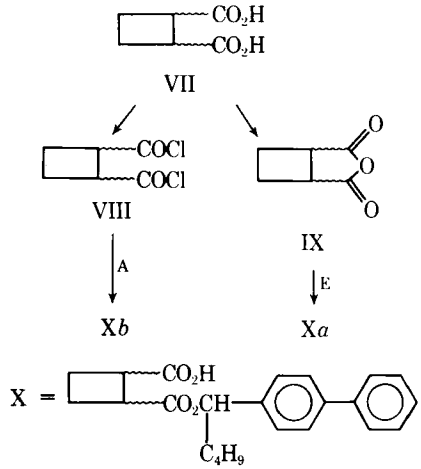

Scheme III

[1] Melting points were determined with a Thomas-Hoover capillary melting-point apparatus and are uncorrected. The elemental analyses were obtained from Galbraith Laboratories, Knoxville, Tenn. The IR spectra were determined using a Perkin-Elmer model 237 spectrophotometer. The NMR spectra were determined using a Perkin-Elmer model R-24 spectrometer in deuterochloroform, with tetramethylsilane as the internal reference.

[2] Eastman Organic Chemicals.

[3] Aldrich Chemical Co.

[4] Fisher Scientific Co.

[5] K and K Laboratories.

[6] Schwarz/Mann.

[7] Sigma Chemical Co.

[8] New England Nuclear.

Table II—Properties of Monoesters of Rigid Dicarboxylic Acids

Compound	Isomer	Procedure	Yield, %	Melting Point	Formula	Analysis, % Calc.	Found
X*a*	*cis*	E	78	126–128°	$C_{23}H_{26}O_4$	C 75.4 H 7.1	75.4 7.2
X*b*	*trans*	A	16	Oil	$C_{23}H_{26}O_4$	C 75.4 H 7.1	75.2 7.2
XI*a*	*trans*	A	33	100–104°	$C_{21}H_{22}O_4$	C 74.6 H 6.5	74.6 6.9
XI*b*	*cis*	D	72	109–112°	$C_{21}H_{22}O_4$	C 74.6 H 6.5	74.3 6.8

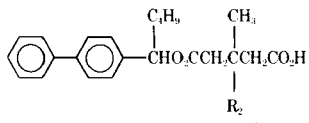

Table III—Properties of Monoesters of 3,3-Disubstituted Glutaric Acids

Compound	R_2	Procedure	Yield, %	Melting Point	Melting Point (Salt)	Formula	Analysis, %[a] Calc.	Found
XIV*a*	H	C	49	Oil	126–128°	$C_{31}H_{38}N_2O_4S$	C 69.6 H 7.1 N 5.2	69.7 7.0 5.3
XIV*b*	OH	D	29	Oil	108–109°	$C_{31}H_{38}N_2O_5S$	C 67.3 H 6.9 N 5.1	67.8 6.8 5.1
XIV*c*	OCH_3	D	59	Oil	94.5–96°	$C_{32}H_{40}N_2O_5S$	C 68.0 H 7.1 N 5.0	68.2 7.1 5.1

[a] The monoesters were characterized as their solid *S*-benzylthiuronium salts (1).

stirred at 25° for 17 hr. The resulting mixture was poured onto ice and filtered, and the organic phase was washed with a 5% hydrochloric acid solution, a 5% sodium hydroxide solution, water, and a saturated sodium chloride solution.

The organic phase was dried over anhydrous sodium sulfate, and the solvent was removed under reduced pressure to give 8.4 g of the diester as a yellow oil. A mixture of 3.2 g (0.006 mole) of the diester, 50 ml of 1,2-dimethoxyethane, 15 ml of water, and 1.7 ml of a 3.54 *N* potassium hydroxide solution was stirred at 25° for 17 hr. The resulting solution was extracted with ether, and the aqueous phase was acidified with a 5% hydrochloric acid solution. The resulting acidic aqueous extract was extracted with ether. The organic phase was washed with water and then with a saturated sodium chloride solution and was dried over anhydrous sodium sulfate. Then the solvent was removed under reduced pressure to afford 0.49 g (25%) of IV*b* as a yellow oil, which crystallized on standing.

Recrystallization from ether–petroleum ether (bp 60–75°) afforded an analytical specimen of IV*b* as a white solid, mp 65–68°; IR ($CHCl_3$): 1733 (broad, acid and ester carbonyls) cm^{-1}; NMR ($CDCl_3$): δ 0.70–2.20 [broad, 9H, $CH_3(CH_2)_3$], 3.48 (s, 2H, O=CCH_2C=O), 5.85 (t, J = 6 Hz, 1H, HCO_2C—), 7.25–7.75 (m, 9H, aromatic), and 10.10 (s, 1H, CO_2H) ppm.

Procedure C, Opening of Anhydrides in Pyridine: Monoesters IVc–IVe and XIVa—This procedure was described previously (1).

Procedure D, Partial Esterification Using Diacids: Monoesters XIb, XIVb, and XIVc—This example typifies the method (Scheme IV) used to prepare these monoesters (Table III). The method of Büchi *et al.* (4) was used. To a suspension of 0.870 g (0.0075 mole) of maleic acid in 40 ml of chloroform was added 2.25 g (0.0098 mole) of *N,N*-dimethylformamide dineopentyl acetal. A colorless solution resulted and was stirred at 25° for 10 min. To this solution was added 1.8 g (0.0075 mole) of 1-(4-biphenylyl)pentanol (1), and the resulting yellow solution was stirred at 25° for 84 hr. The solvent was removed under reduced pressure, and then the residue was added to ether.

The organic phase was washed with water and then twice with a 5% sodium hydroxide solution. The basic, aqueous extract was adjusted to pH 2 with a 5% hydrochloric acid solution and then was extracted with ethyl acetate. The organic phase was washed with water and then with a saturated sodium chloride solution. The organic phase was dried over anhydrous sodium sulfate, and then the solvent was removed under reduced pressure to afford 1.82 g (72%) of XI*b* as a white solid, mp 105–108°.

Recrystallization from ethyl acetate–petroleum ether (bp 60–75°) afforded an analytical specimen of XI*b* as white prisms, mp 109–112°; IR ($CHCl_3$): 1730 (broad, acid and ester carbonyls) and 1630 (C=C) cm^{-1}; NMR ($CDCl_3$): δ 0.70–2.20 [broad, 9H, $CH_3(CH_2)_3$], 5.85 (t, J = 6 Hz, 1H, HCO_2C—), 6.32 (s, 2H, HC=CH), 7.25–7.65 (m, 9H, aromatic), and 10.97 (s, 1H, CO_2H) ppm.

Procedure E, Opening of Anhydrides in the Presence of N,N-*Dimethylaminopyridine: Monoester Xa*—This example typifies the method (Scheme III) used to prepare this monoester. The procedure of Steglich and Höfle (5) was used. To a solution of 0.378 g (0.003 mole) of *cis*-1,2-cyclobutanedicarboxylic anhydride, 0.720 g (0.003 mole) of 1-(4-biphenylyl)pentanol (1), and 0.366 g (0.003 mole) of 4-dimethylaminopyridine in 10 ml of dimethylformamide (distilled from barium oxide) was added 0.6 ml (0.0045 mole) of

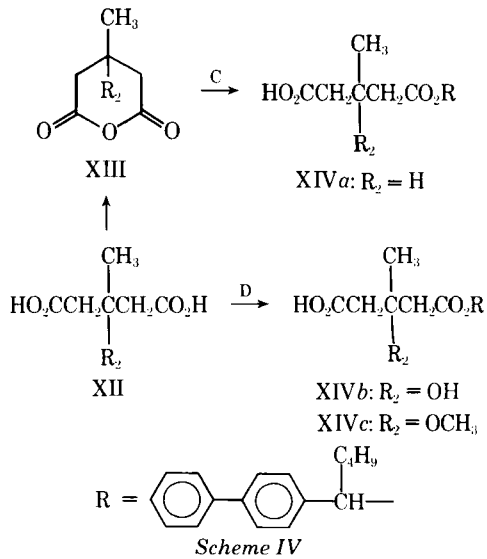

Scheme IV

triethylamine, and the solution was stirred at 25° for 24 hr. The mixture was poured on an ice–hydrochloric acid mixture and then extracted with ether.

The organic phase was washed with water and then twice with a 5% sodium hydroxide solution. The basic, aqueous extract was acidified with a 5% hydrochloric acid solution and then was extracted with ether. The organic phase was washed with water and a saturated sodium chloride solution and then was dried over anhydrous sodium sulfate. The solvent was removed under reduced pressure to afford 0.860 g (78%) of a yellow oil, which crystallized on standing.

Recrystallization from ethyl acetate–petroleum ether (bp 60–75°) afforded an analytical specimen of X*a* as a white solid, mp 126–128°; IR ($CHCl_3$): 1720 (broad, acid and ester carbonyls) cm^{-1}; NMR ($CDCl_3$): δ 0.54–2.40 [broad, 9H, $CH_3(CH_2)_3$], 3.30 (broad, s, 2H, $RO_2CCHCHCO_2$), 5.80 (t, J = 6 Hz, 1H, HCO_2C—), 7.20–7.70 (m, 9H, aromatic), and 11.20 (s, 1H, CO_2H) ppm.

Four-Step Synthesis of Monoester of 3-Methoxy-3-methylglutaric Acid (XIV*c*)—The method of Tschesche and Machleidt (6) was used for the synthesis of 4-hydroxy-4-methyl-1,6-heptadiene (XV), 89%, bp 51° (15 mm) [lit. (6) bp 50–51° (12 mm)].

The method of Anderson and Cree (9) was used for the preparation of 4-methoxy-4-methyl-1,6-heptadiene (XVI). To a suspension of 3.7 g (0.088 mole) of 57% sodium hydride in 50 ml of dry dimethyl sulfoxide was added dropwise at 25°, with stirring, 7.76 g (0.062 mole) of XV in 25 ml of dimethyl sulfoxide. The mixture was stirred until gas evolution ceased (2.5 hr). The suspension was cooled in an ice bath, and 26 g (0.18 mole) of methyl iodide was added in a dropwise manner. The mixture was allowed to warm to 25° and was stirred at 25° for 18 hr. Then it was poured into ether and water.

The organic phase was washed with water and a saturated sodium chloride solution and then was dried over anhydrous sodium sulfate. Removal of the solvent under reduced pressure afforded a brown liquid, which was distilled to give 5.64 g (65%) of XVI as a clear, colorless liquid, bp 149–151° (760 mm); IR (liquid film): 1645 (strong, C=C) cm^{-1}; NMR ($CDCl_3$): δ 1.10 (s, 3H, CH_3C), 2.25 [d, J = 7 Hz, 4H, $(C{=}CCH_2)_2$], 3.20 (s, 3H, CH_3O), 4.83–5.16 [m, 4H, $(C{=}CH_2)_2$], and 5.50–6.16 [m, 2H, $(CH{=}C)_2$] ppm.

Anal.—Calc. for $C_9H_{16}O$: C, 77.1; H, 11.5. Found: C, 77.2; H, 11.6.

The method of Tschesche and Machleidt (6) (Scheme I) was used for the preparation of 3-methoxy-3-methylglutaric acid (XVII). A solution containing 7.36 g (0.053 mole) of XVI, 7.0 ml of acetic acid, and 85 ml of methylene chloride was cooled in an acetone–dry ice bath. Ozone was passed through the solution for 3.5 hr, and the resulting blue solution was allowed to warm to 25°. To the clear, colorless solution was added 50 ml of acetic acid, and then the methylene chloride was removed under reduced pressure. To the residue were added 50 ml of acetic acid and 50 ml of 30% hydrogen peroxide; then the solution was heated at reflux for 8 hr.

Removal of the solvent under reduced pressure afforded 7.39 g of a colorless oil, which crystallized on standing. Recrystallization from ether–petroleum ether (bp 60–75°) gave 7.08 g (76%) of XVII as a white solid, mp 78–80°; IR ($CHCl_3$): 2500–2700 (broad, OH) and 1710 (CO_2H) cm^{-1}; NMR (acetone-d_6): δ 1.40 (s, 3H, CH_3C), 2.76 [s, 4H, $(CH_2)_2$], 3.26 (s, 3H, CH_3O), and 9.93 [s, 2H, $(CO_2H)_2$] ppm.

Anal.—Calc. for $C_7H_{12}O_5$: C, 47.7; H, 6.9. Found: C, 47.7; H, 7.0.

Procedure D (Scheme IV) was used to prepare the monoester XIV*c* from the synthesized diacid.

Preparation of Rat Liver Microsomes—Active rat liver microsomes containing β-hydroxy-β-methylglutaryl coenzyme A reductase activity were prepared according to Shapiro and Rodwell (10). Male Sprague–Dawley rats, ~100–130 g, were housed in an animal room in which light was provided from 7 am to 7 pm. Food[9] and water were available *ad libitum*. Between 12:05 and 12:30 am, the rats were stunned and decapitated.

The livers were excised into 0°, pH 6 homogenization buffer (30 m*M* ethylenediaminetetraacetic acid, 70 m*M* sodium chloride, and 10 m*M* β-mercaptoethanol). Then the livers were forced through a tissue press into 2.5 ml of 0° homogenization buffer per gram of liver prior to homogenization in a Potter–Elvehjem homogenizer with a pestle[10]. The homogenate was centrifuged twice for 15 min at 12,000×*g*, and the pellets were discarded. The supernate was centrifuged for 1 hr at 48,000×*g*; the resulting pellets were frozen in a dry ice–isopropyl alcohol bath. The tubes containing the frozen pellets were sealed[11] and stored at −60° for up to 3 weeks.

[9] Purina Laboratory Chow.

Table IV—Inhibition of β-Hydroxy-β-methylglutaryl Coenzyme A Reductase

Compound	*n*	Activity I/S[a]	Activity Inhibition, %
IV*a*	0	50[b]	36
IV*b*	1	6	50
IV*c*	2	11	50
IV*d*	3	11	50
IV*e*	4	7	50
IV*f*	5	20	50
IV*g*	6	20	50
X*a*		5[c]	50
X*b*		5[c]	50
XI*a*		3	50
XI*b*		5	50
XIV*a*		9	50
XIV*b*		1.5	50
XIV*c*		10	50

[a] The inhibition index, I/S, equals the ratio of the micromolar concentration of the inhibitor to the micromolar concentration of the substrate. At least two sets of duplicate determinations were used. [b] Insoluble at higher concentrations. [c] The assay mixture was saturated at these concentrations.

Assay of Enzyme Activity and Inhibition—Literature procedures (10–12) were modified. The rat liver microsomal pellet (obtained from about 3–4 g of minced liver) from one tube (described under *Preparation of Rat Liver Microsomes*) was suspended in 1.7 ml of homogenization buffer, pH 6.8. The assay system consisted of $NADP^+$ (9.7 μmoles), glucose 6-phosphate (59.7 μmoles), torula yeast glucose 6-phosphate dehydrogenase (5 units), 0.15 ml of the microsomal suspension containing about 2 mg of protein[12], and 0.1 ml of ethylene glycol monoethyl ether containing the inhibitor in a total volume of 2.9 ml.

Enzymatic activity was started by the addition of 0.1 ml of a solution containing 94 nmoles of *dl*-β-hydroxy-β-methylglutaryl-3-^{14}C coenzyme A (specific activity 890 dpm/nmole) (13). After 30 min of shaking incubation at 37°, the reaction was stopped by the addition of 0.2 ml of concentrated hydrochloric acid. Fifty microliters of an acetone solution containing 7×10^5 dpm (24 μmoles) of *dl*-mevalonolactone-5-^{3}H was added to the incubation mixture and allowed to stand overnight. The mixture was saturated with anhydrous sodium sulfate and then extracted three times with 10-ml portions of ether. The ether was evaporated at 30° under a nitrogen stream, and the residue was dissolved in 0.2 ml of acetone–water (9:1).

The solution was streaked on a silica gel thin-layer sheet[2] and developed with acetone–benzene (1:1). The area of the chromatogram containing the mevalonolactone, which corresponded to an R_f value between 0.6 and 1.0, was scraped into a liquid scintillation vial. Twenty milliliters of Bray's scintillation solution (15) was added, and ^{3}H and ^{14}C were determined simultaneously in a liquid scintillation counter[13]. Efficiency of counting was determined by the external standard method. Some variability in the inhibition data was noted between tubes of microsomes (even from the same liver preparation). For this reason, a standard inhibitor, 1-(4-biphenylyl)pentyl hydrogen succinate (IV*c*), was utilized routinely.

RESULTS AND DISCUSSION

The activity of IV*a*–IV*g*, X*a*, X*b*, XI*a*, XI*b*, and XIV*a*–XIV*c* as inhibitors of rat liver β-hydroxy-β-methylglutaryl coenzyme A reductase is shown in Table IV. To determine if the distance sepa-

[10] Teflon (du Pont).

[11] Parafilm.

[12] Protein was precipitated by 5% trichloroacetic acid to remove interference from β-mercaptoethanol, redissolved in 3% sodium hydroxide solution, and determined colorimetrically by the method of Lowry *et al.* (14).

[13] Nuclear Chicago Mark I.

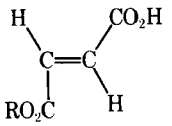

XI*a*

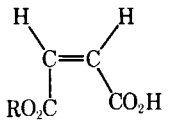

XI*b*

rating the carboxyl and ester groups was critical for activity, a series of monoesters related to I was prepared and assayed. The number (n) of methylene groups between the carboxyl and ester groups was varied from zero to six (IV*a*–IV*g*). While the data indicated that the distance between the groups was not highly critical, a minimum of one methylene group was required for reasonable activity, as shown by the decreased activity of IV*a* compared to IV*b*. Increasing the number of methylene groups from one to four did not alter the activity significantly. Further separation of the carboxyl and ester groups produced a decrease in activity (IV*f* and IV*g*).

The monoesters of several rigid dicarboxylic acids were investigated to determine if activity was dependent on the stereochemical relationship between the carboxyl and ester groups. The monoesters of *cis*- and *trans*-1,2-cyclobutanedicarboxylic acids (X*a* and X*b*) and the monoesters of fumaric and maleic acids (XI*a* and XI*b*) were studied. These rigid analogs were about two to three times more active than the corresponding flexible analog (IV*c*). However, the activity of the inhibitors does not appear to be strongly dependent on the stereochemical relationship between the carboxyl and ester groups.

Modifications of the glutarate analog (IV*d*) were made in an effort to provide inhibitors that resemble the glutaric acid portion of the substrate more closely. This was accomplished by incorporating a 3-methyl group (XIV*a*) and the 3-methyl-3-hydroxyl groups (XIV*b*). Compound XIV*a* was slightly more active than the unsubstituted glutarate analog (IV*d*), whereas XIV*b* was six times more active than XIV*a*. The methoxyl analog (XIV*c*) was investigated in an attempt to determine if the hydroxyl group in XIV*b* was acting as a hydrogen donor or hydrogen acceptor during binding to the enzyme. The decreased activity of XIV*c* compared to XIV*b* suggested that the hydroxyl group in XIV*b* was acting as a hydrogen donor in the binding interaction. However, an alternative explanation for the decreased activity of XIV*c* involves the steric bulk of the methoxyl group. If the steric bulk of the methoxyl group was responsible for the decreased activity, a greater decrease in activity would have been expected (see XIV*a* and XIV*c*).

REFERENCES

(1) M. R. Boots, S. G. Boots, C. M. Noble, and K. E. Guyer, *J. Pharm. Sci.*, **62**, 952(1973).

(2) T. C. Linn, *J. Biol. Chem.*, **242**, 984(1967).

(3) G. Palazzo, M. Tavella, and G. Strani, *J. Med. Pharm. Chem.*, **4**, 447(1961).

(4) H. Büchi, K. Steen, and A. Eschenmoser, *Angew. Chem. Int. Ed. Engl.*, **3**, 62(1964).

(5) W. Steglich and G. Höfle, *ibid.*, **8**, 981(1969).

(6) R. Tschesche and H. Machleidt, *Ann. Chem.*, **631**, 61(1960).

(7) J. W. Hill, *J. Amer. Chem. Soc.*, **52**, 4110(1930).

(8) H. Brockman and H. Muxfeldt, *Chem. Ber.*, **89**, 1379 (1956).

(9) D. M. Anderson and G. M. Cree, *Carbohyd. Res.*, **2**, 162(1966).

(10) D. J. Shapiro and V. W. Rodwell, *J. Biol. Chem.*, **246**, 3210(1971).

(11) D. J. Shapiro, R. L. Imblum, and V. W. Rodwell, *Anal. Biochem.*, **31**, 383(1969).

(12) S. Goldfarb and H. C. Pitot, *J. Lipid Res.*, **12**, 512 (1971).

(13) S. G. Boots, M. R. Boots, and K. E. Guyer, *J. Pharm. Sci.*, **60**, 614(1971).

(14) O. H. Lowry, N. J. Rosenbrough, A. L. Farr, and R. J. Randall, *J. Biol. Chem.*, **193**, 265(1951).

(15) G. A. Bray, *Anal. Biochem.*, **1**, 279(1960).

ACKNOWLEDGMENTS AND ADDRESSES

Received May 30, 1975, from the *Departments of Pharmaceutical Chemistry and Biochemistry, Medical College of Virginia Health Sciences Division, Virginia Commonwealth University, Richmond, VA 23298*

Accepted for publication June 27, 1975.

Presented in part at the Medical Sciences Section, Virginia Academy of Science, Norfolk meeting, May 1974.

Abstracted in part from a dissertation submitted by P. E. Marecki to Virginia Commonwealth University in partial fulfillment of the Doctor of Philosophy degree requirements.

Supported by a grant from the U.S. Public Health Service (HL-11768, National Heart and Lung Institute).

P. E. Marecki thanks the following for their generous support: National Institutes of Health, Traineeship GM484 (1970–1972); American Foundation for Pharmaceutical Education (1972–1974) (Sydnor Barksdale Penick Memorial Fellow, 1973–1974). Excellent technical assistance by Ms. Bonnie Frazier is gratefully acknowledged.

* Present address: Department of Biochemistry, Marshall University School of Medicine, Huntington, WV 25701

ˣ To whom inquiries should be directed.

N-Halo Derivatives III: Stabilization of Nitrogen–Chlorine Bond in *N*-Chloroamino Acid Derivatives

JAMES J. KAMINSKI, NICOLAE BODOR ˣ, and TAKERU HIGUCHI

Abstract □ The chlorination of α-amino acids and their related derivatives was investigated. A kinetic study of the stability of these *N*-chlorinated products led to an elucidation of the factors that significantly influence the stability and reactivity of the nitrogen–chlorine bond in these *N*-chloramines. From the kinetic investigations, a series of low chlorine potential, soft antimicrobial *N*-chloramines was developed based on derivatives of α-aminoisobutyric acid and related compounds.

Keyphrases □ *N*-Chloroamino acid derivatives—synthesis, kinetic stability study □ *N*-Halo derivatives—synthesis of *N*-chloroamino acid derivatives, kinetic stability study □ Antimicrobial agents—*N*-chloroamino acid derivatives, synthesis, kinetic stability study

Recently, the effect of chlorine directly bonded to nitrogen in *N*-chloramines was examined by photoelectron spectroscopy (1). The study was undertaken to define the interaction between the nitrogen and chlorine lone pairs in the *N*-chloro function. As a result of that investigation, the stability of the nitrogen–chlorine bond toward hydrolytic displacement and the antimicrobial activity of the *N*-chloramines could be correlated with the ionization potential of the nitrogen lone pair in the *N*-chloramines. For the *N*-chloramines investigated, the orbital energy (ionization potential) of the nitrogen lone pair was indicative of the degree of polarization in the nitrogen–chlorine bond. This observation suggested that the ionization potential of the nitrogen lone pair in *N*-chloramines would be a sensitive method for comparing the "chlorine potentials" (2, 3) of structurally different *N*-chloramines.

In continuing the investigation of the relationship between the antimicrobial activity of *N*-chloramines and the degree of polarization of the nitrogen–chlorine bond, a series of low chlorine potential *N*-chloramines was designed and investigated. It was hypothesized that the bactericidal action of *N*-chloramines was a manifestation of a chemical reaction involving the direct transfer of a positive chlorine from the *N*-chloramine to an appropriate receptor in the cell. This chemical reaction can effectively destroy or inhibit an enzymatic or a metabolic cell process, which results in the expiration of the organism.

By decreasing the polarity of the nitrogen–chlorine bond, the chemical reactivity of the *N*-chloramine would be minimized. These low chlorine potential *N*-chloramines would be less readily deactivated by extraneous reaction with denaturing agents and, therefore, would exhibit a high degree of antimicrobial activity against a broad spectrum of microorganisms. As a result, the low chlorine potential *N*-chloramines could more effectively exert their antimicrobial effect relative to higher chlorine potential *N*-chloramines.

In addition to decreasing the polarity of the nitrogen–chlorine bond, it was of interest to develop these low chlorine potential *N*-chloramines as "soft" antimicrobial agents. The soft nature of the *N*-chloramines rested primarily upon the mechanism of their antimicrobial action and the transient character of the *N*-chloramine precursor to generate nontoxic degradation products. If it is assumed that the transfer of positive chlorine from the *N*-chloramine to an appropriate receptor in the cell is primarily responsible for the antimicrobial effect of the *N*-chloramine, detoxification of the microorganism ultimately regenerates the parent molecule from which the *N*-chloramine is derived. By judiciously selecting the *N*-chloramine precursor from nontoxic entities and selectively incorporating specific functional groups susceptible toward hydrolysis, the inherent toxicity of the soft *N*-chloramine antimicrobial agents could be effectively controlled.

In the present study, a rational and systematic approach to the preparation of a class of low chlorine potential, soft antimicrobial *N*-chloramines was investigated. Based on the low polarity of the nitrogen–chlorine bond and the soft nature of the *N*-chloramines desired, the chlorination of α-amino acids and their related derivatives was examined. The results elucidated the factors that significantly influence the stability of these *N*-chloramines and other low chlorine potential *N*-chloramines in general. The stability and reactivity of a number of homologous *N*-chloroamino and *N,N*-dichloroamino derivatives were also investigated.

RESULTS AND DISCUSSION

The formation of *N*-chloro derivatives of amines has been accomplished principally by treatment of a solution of the amine (primary or secondary amine) with a source of "active" chlorine such as sodium hypochlorite or molecular chlorine. Although the degree of chlorination of the nitrogen atom can be controlled by the stoichiometric quantities of amine and/or chlorinating agent used in the synthesis, the reaction product can be influenced by factors such as the pH of the reaction medium and the concentration of the *N*-chloramine in solution. The *N*-chloroamino derivative tends to predominate in basic solution (pH > 9) whereas the *N,N*-dichloroamino derivative is favored in acidic solution (pH 4–6).

In addition, depending upon the concentration of the *N*-chloramine in solution, the *N,N*-dichloroamino derivative may be preferentially formed *via* the *N*-chloroamino derivative through a disproportionation process. Although iodometric analysis for positive chlorine is an insufficient criterion for product homogeneity, Metcalf (4) demonstrated that the *N*-chloroamino and *N,N*-dichlo-

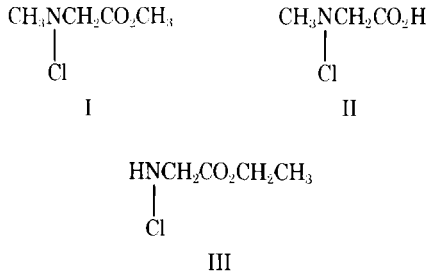

roamino derivatives have well-defined, characteristic UV absorption spectra, which can be used to determine product compositions.

To investigate a pure monochloroamino derivative from the chlorination of α-amino acids and their related derivatives, the initial studies concerned the preparation of methyl *N*-chlorosarcosinoate (I) and *N*-chlorosarcosine (II). The *N*-chloramines I and II were prepared by reaction of methyl sarcosinoate hydrochloride and sarcosine hydrochloride, respectively, with an aqueous solution of sodium hypochlorite. Compound I was isolated as a pale-yellow liquid whose UV absorption spectrum had a maximum absorbance at 264 nm, $\epsilon = 340\ M^{-1}\ cm^{-1}$. Compound I also gave satisfactory elemental analysis for positive chlorine, which was determined iodometrically. However, shortly after isolation, the *N*-chloramine underwent a spontaneous exothermic decomposition. Therefore, both I and II, as well as ethyl *N*-chloroglycinate (III), were prepared and their stability was investigated *in situ*.

The stability of the *N*-chloramines in solution was examined by following the rate of change in the concentration of positive chlorine iodometrically and/or monitoring the rate of change in absorbance at the wavelength of maximum absorption of the *N*-chloramine. The kinetic data obtained could be interpreted as first-order kinetic processes. The stability of the *N*-chloramines under the experimental conditions was characterized using the observed rate constant and the reaction half-life. Determination of the kinetic reaction constants for the *N*-chloramines was independent of the analytical method. That is, the observed rate constant and reaction half-life determined for the *N*-chloramine iodometrically were comparable to those determined spectrophotometrically.

Examination of the stability data for I–III (Table I) indicates several interesting observations. Comparison of the kinetic data for III relative to I indicates that the stability of the monochloroamino derivatives is not significantly influenced by the presence or absence of the N—H bond. Although the stability of I and III both appear to exhibit first-order behavior, the kinetic data for III are independent of the buffer concentration whereas the kinetic data for I are directly influenced by the buffer concentration.

The dichotomy of observing simple first-order kinetics for III and pseudo-first-order kinetics for I can be rationalized by considering that the monomolecular decomposition of III involves, as its rate-determining step, the loss of chloride ion from III to form the ion (IV). Subsequently, this reactive species can couple with another molecule of III to form the azo derivative (V) as suggested by Pinchuk *et al.* (5) (Scheme I).

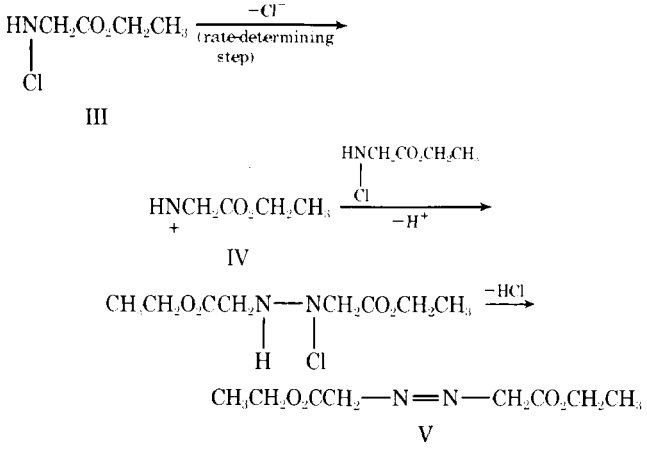

Scheme I

Table I—Stability of *N*-Chloroamino Acids and Related Derivatives

Compound	Buffer Concentration, M[a]	Rate Constant[b] $\times 10^{-2}$, min^{-1}	Half-Life, min	Correlation Coefficient[c]
I	0.1	1.12	61.9	0.999
	0.2	2.39	29.0	0.999
	0.25	3.02	22.9	0.999
	0.3	3.59	19.3	0.999
	0.4	4.77	14.5	0.999
	0.5	5.82	11.9	0.999
II	0.1	2.60[d]	26.7	0.998
	0.2	1.93[d]	35.9	0.999
	0.3	2.32[d]	29.9	0.992
	0.4	2.17[d]	31.9	0.999
	0.5	2.10[d]	33.0	0.999
III	0.25	13.2	5.3	0.999
	0.3	16.4	4.2	0.999
	0.4	18.0	3.9	0.999
	0.5	15.6	4.4	0.999

[a] Sodium dihydrogen phosphate, pH 7.0. [b] Rate constants were determined at 25° unless noted otherwise. [c] Correlation coefficients based on a linear regression analysis of the experimental data. [d] Rate constants were determined at 37°.

On the other hand, the direct relationship observed between the rate constants determined for I and the concentration of the buffer species suggests that the primary mechanism of decomposition proceeds through a bimolecular reaction between I and the phosphate buffer in a dehydrochlorination across the carbon–nitrogen bond in the *N*-chloramine. Graphical analysis of the kinetic data for I gives a rate constant equal to $0.15 \times 10^{-2}\ min^{-1}$ at zero buffer concentration (Fig. 1). Although two different hydrogen atoms adjacent to the nitrogen–chlorine bond are available for the elimination process, the dehydrochlorination is preferentially facilitated by the electron-withdrawing effect of the carbomethoxyl group in the *N*-chloramine (Scheme II).

In addition to the kinetic evidence supporting this mechanistic pathway for the decomposition of I, the decomposition product VII of I also was investigated indirectly. A solution of I that had undergone decomposition was examined spectrophotometrically and was found to be transparent in the 220–350-nm UV region. Addition of approximately a threefold excess of sodium hypochlorite, based on the initial concentration of I, to the decomposed so-

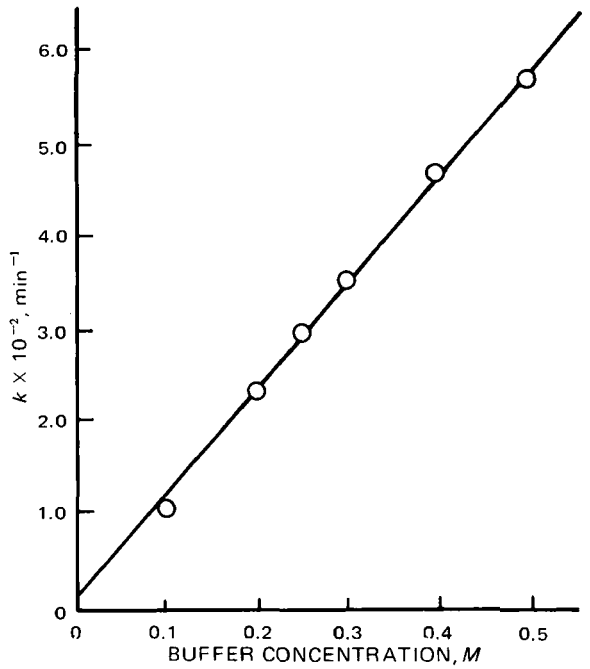

Figure 1—*Plot of the observed rate constant for the decomposition of I as a function of sodium dihydrogen phosphate concentration at pH 7.0 and 25°.*

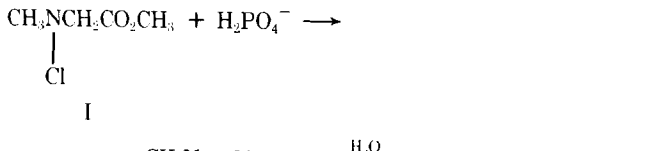

Scheme II

lution resulted in a product with an absorption maximum at 305 nm. This wavelength is characteristic for an *N,N*-dichloroamino species and is consistent with chlorination of methylamine (VII) to *N,N*-dichloromethylamine, λ_{max} 303 nm (4). Methylamine (VII) was formed *via* hydrolytic cleavage of the intermediate imine (VI), which had been initially formed in the dehydrochlorination (Scheme II).

The stability of *N*-chlorosarcosine (II) was investigated spectrophotometrically. Unlike the kinetic behavior observed in the decomposition of I, the reaction constants determined for the decomposition of II were independent of the buffer concentration. Therefore, the primary mechanistic pathway for the decomposition of II must proceed through a unimolecular degradation of II. This process also can be accounted for by a dehydrochlorination process. However, in this case, the dehydrochlorination of II is mediated by the decarboxylation of II itself. This mechanism is consistent with the buffer-independent rate constants observed for the decomposition of II.

Under the experimental conditions, II exists predominantly in the ionized carboxylate form. The ionization of the carboxyl group decreases the electrophilic character of the carbonyl group in II relative to I. Consequently, the importance of the α-hydrogen elimination pathway for the decomposition of the *N*-chloramine can be decreased. In summary, the kinetic behavior observed for the stability of I–III can be accounted for by changes in the mechanistic pathway through which the positive chlorine is lost in each *N*-chloramine.

With a better understanding of the proposed mechanisms that have been assumed responsible for the decomposition of I–III, the development of a unique class of *N*-chloroamino acid derivatives was initiated. This new class of low chlorine potential, soft antimicrobial *N*-chloramines was designed specifically to be incapable of dehydrochlorination by the decarboxylative route as well as by α-hydrogen elimination; synthetic amino acids geminally substituted at the α-carbon atom were primarily considered. In addition to this specific structural requirement, the synthetic amino acid chosen should ideally exhibit an inherently low toxicity. Based on these objectives, the *geminal*-dimethyl substitution at the α-carbon atom in α-aminoisobutyric acid and its inherent low toxicity suggested derivatization of this amino acid as the precursor of several *N*-chloramines. The initial investigations examined the chlorination of some homologous esters of α-aminoisobutyric acid (IX*a*–IX*f*).

In contrast to the *N*-chlorinated products of natural α-amino acids, the *N*-chloramines based on α-aminoisobutyric acid (X*a*–X*k*) were stable and could be purified, characterized, and stored in the neat state without exothermic or extensive decomposition. In addition, chlorination of the longer chain homologs (IX*b*–IX*f*) led to the preparation of both the *N*-chloroamino and *N,N*-dichloroamino derivatives. Although the initial investigations were directed toward examining the chlorination of relatively simple homologous esters of α-aminoisobutyric acid, the extension of these concepts toward the development of other related derivatives of α-aminoisobutyric acid with specifically desired physical–chemical

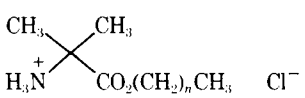

IX*a*: $n = 0$
IX*b*: $n = 5$
IX*c*: $n = 7$
IX*d*: $n = 11$
IX*e*: $n = 13$
IX*f*: $n = 17$

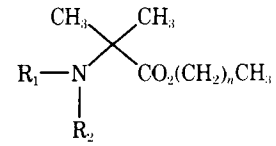

X*a*: R_1 = Cl, R_2 = Cl, $n = 0$
X*b*: R_1 = H, R_2 = Cl, $n = 5$
X*c*: R_1 = H, R_2 = Cl, $n = 7$
X*d*: R_1 = H, R_2 = Cl, $n = 11$
X*e*: R_1 = H, R_2 = Cl, $n = 13$
X*f*: R_1 = H, R_2 = Cl, $n = 17$
X*g*: R_1 = Cl, R_2 = Cl, $n = 5$
X*h*: R_1 = Cl, R_2 = Cl, $n = 7$
X*i*: R_1 = Cl, R_2 = Cl, $n = 11$
X*j*: R_1 = Cl, R_2 = Cl, $n = 13$
X*k*: R_1 = Cl, R_2 = Cl, $n = 17$

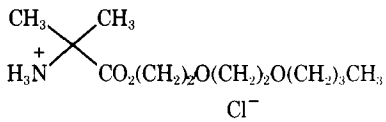

XI

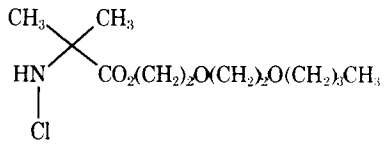

XII

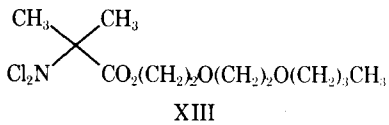

XIII

properties was equally feasible. For example, chlorination of 2-(2-*n*-butoxyethoxy)ethyl α-aminoisobutyrate hydrochloride (XI) gave the corresponding *N*-chloroamino (XII) and *N,N*-dichloroamino (XIII) derivatives.

Incorporation of the ether linkages in these *N*-chlorinated amino acid ester derivatives conferred advantageous water-solubilizing properties to XII and XIII while still retaining their surface-active characteristics. In addition to ester derivatization of α-aminoisobutyric acid, amide and peptide derivatives were considered. Representative of this approach, the 1,4-dichloro-2,2,5,5-tetramethyl-3,6-piperazinedione (XIV) was prepared. Due to the inherent low water solubility of this derivative, the *N*-chloramine could efficiently act as a sustained-release form of the active chlorine species.

The microbiological properties of these low chlorine potential, soft *N*-chloramine derivatives and other structurally related *N*-chloramine systems will be reported[1].

EXPERIMENTAL

Methyl *N*-Chlorosarcosinoate (I)—To a solution of 6.95 g (0.05 mole) of methyl sarcosinoate hydrochloride in 15 ml of water was added dropwise, with stirring, 65 ml (0.05 mole) of 0.78 *M* sodium hypochlorite solution. At the end of the addition, the reaction solution was adjusted to pH 7. The *N*-chloramine was extract-

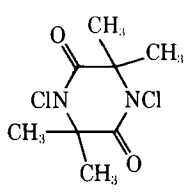

XIV

[1] J. J. Kaminski and N. Bodor, to be published.

ed into ethyl acetate. The aqueous layer was separated and extracted with ethyl acetate. The extracts were combined and dried over anhydrous sodium sulfate. Following filtration, the ethyl acetate was removed at room temperature under reduced pressure to afford 5.22 g (0.038 mole), 76%, of I as a pale-yellow liquid; UV (H_2O): λ_{max} 264 nm, $\epsilon = 340\ M^{-1}\ cm^{-1}$. The pale-yellow liquid underwent a spontaneous exothermic decomposition shortly after isolation.

Anal.—Calc. for $C_4H_8ClNO_2$: Cl, 25.8. Found: Cl, 24.8.

N-Chlorosarcosine (II)—Compound II was prepared *in situ* using a method described previously (4). Reaction of a solution of sarcosine hydrochloride buffered to pH 7 with an aqueous solution of sodium hypochlorite gave II; UV (H_2O): λ_{max} 268, $\epsilon = 310\ M^{-1}\ cm^{-1}$.

Ethyl N-Chloroglycinate (III)—Compound III was prepared *in situ* using a method described previously (4). Reaction of a solution of ethyl glycinate hydrochloride buffered to pH 7 with an aqueous solution of sodium hypochlorite gave III; UV (H_2O): λ_{max} 254 nm, $\epsilon = 339\ M^{-1}\ cm^{-1}$.

Methyl α-Aminoisobutyrate Hydrochloride (IX*a*)—To 30 ml (0.78 mole) of anhydrous methanol at −10° was added 7.9 ml (0.11 mole) of thionyl chloride at such a rate that the temperature was maintained below 0° during the addition. Then 10.3 g (0.10 mole) of α-aminoisobutyric acid was added in portions, with stirring, also at a rate such that the temperature was maintained below −5°. The reaction mixture was heated to and maintained at 58–60° for 2.5 hr. The methanol was removed under reduced pressure to afford a pale-yellow viscous liquid, which crystallized to an off-white solid on standing at room temperature. Trituration of this solid with anhydrous ether gave IX*a* as a white crystalline solid, 15.3 g (0.099 mole), 99%, mp 185–187°; IR (KBr): 1735 (C=O) cm^{-1}; PMR (D_2O): δ 1.63 (s, 6H) and 3.87 (s, 3H) ppm.

Anal.—Calc. for $C_6H_{12}ClNO_2$: C, 39.09; H, 7.88; N, 9.12. Found: C, 39.24; H, 8.01; N, 9.26.

***n*-Hexyl α-Aminoisobutyrate Hydrochloride (IX*b*)**—To 97.1 g (0.47 mole) of phosphorus pentachloride suspended in 940 ml of acetyl chloride was added 48.4 g (0.47 mole) of α-aminoisobutyric acid, and the resulting suspension was stirred at room temperature overnight. The amino acid chloride hydrochloride was removed from the reaction mixture by filtration and thoroughly washed with anhydrous ether under a nitrogen atmosphere. After drying *in vacuo* over calcium sulfate, the α-aminoisobutyryl chloride hydrochloride was obtained as a white powder, 72.96 g (0.46 mole), 98%, mp 139–141° dec.; IR (KBr): 1750 (C=O) cm^{-1}.

Anal.—Calc. for $C_4H_9Cl_2NO$: C, 30.40; H, 5.74; N, 8.89. Found: C, 31.24; H, 6.09; N, 9.15.

To 51.0 g (0.5 mole) of *n*-hexyl alcohol heated to 40° was added in portions over 10 min, with stirring, 15.7 g (0.1 mole) of α-aminoisobutyryl chloride hydrochloride, which was obtained as already described. The reaction mixture was purged with nitrogen and maintained at 75° for 3 hr. Cooling to room temperature gave a liquid mass from which the excess *n*-hexyl alcohol was removed by distillation *in vacuo*. The amino acid ester hydrochloride was crystallized by the addition of anhydrous ether and, after trituration overnight, was removed from the reaction mixture by filtration and thoroughly washed with anhydrous ether. After drying *in vacuo* over calcium sulfate, IX*b* was obtained as a white solid, 12.2 g (0.055 mole), 55%, mp 74–76°; IR (KBr): 1750 (C=O) cm^{-1}; PMR (D_2O): δ 10.7 (t, 3H), 1.3 (broad s, 8H), and 4.23 (broad t, 2H) ppm.

Anal.—Calc. for $C_{10}H_{22}ClNO_2$: C, 53.68; H, 9.91; N, 6.26. Found: C, 53.27; H, 10.06; N, 6.10.

By using the procedure described for the preparation of IX*b*, the following esters of α-aminoisobutyric acid were prepared.

n-*Octyl α-Aminoisobutyrate Hydrochloride* (*IX*c)—Melting point 79–82°; IR (KBr): 1750 (C=O) cm^{-1}; PMR (D_2O): δ 4.1 (t, 2H), 1.46 (s, 6H), 1.2 (broad s, 12H), and 0.7 (broad t, 3H) ppm.

Anal.—Calc. for $C_{12}H_{26}ClNO_2$: C, 57.24; H, 10.41; N, 5.56. Found: C, 57.14; H, 10.64; N, 5.36.

n-*Dodecyl α-Aminoisobutyrate Hydrochloride* (*IX*d)—Melting point 94–96°; IR (KBr): 1750 (C=O) cm^{-1}; PMR (dimethyl sulfoxide-d_6): δ 8.8 (broad s, 3H), 4.0 (t, 2H), 1.4 (s, 6H), 1.1 (broad s, 20H), and 0.7 (broad t, 3H) ppm.

Anal.—Calc. for $C_{16}H_{34}ClNO_2$: C, 62.41; H, 11.13; N, 4.55. Found: C, 61.62; H, 11.38; N, 4.21.

n-*Tetradecyl α-Aminoisobutyrate Hydrochloride* (*IX*e)—Melting point 96–97°; IR (KBr): 1750 (C=O) cm^{-1}; PMR (D_2O): δ 4.23 (broad t, 2H), 1.63 (s, 6H), 1.3 (broad s, 24H), and 1.1 (broad t, 3H) ppm.

Anal.—Calc. for $C_{18}H_{38}ClNO_2$: C, 64.69; H, 11.33; N, 4.18. Found: C, 64.17; H, 11.26; N, 3.95.

n-*Octadecyl α-Aminoisobutyrate Hydrochloride* (*IX*f)—Melting point 75–78°; IR (KBr): 2970 (CH), 2620 (N^+H), 1750 (C=O), and 1180 (CO) cm^{-1}.

Anal.—Calc. for $C_{22}H_{46}ClNO_2$: C, 67.39; H, 11.83; N, 3.57. Found: C, 66.84; H, 12.22; N, 3.17.

2-(2-n-Butoxyethoxy)ethyl α-Aminoisobutyrate Hydrochloride (*XI*)—Melting point 55–60°; IR (KBr): 2900 (CH), 1740 (C=O), and 1175 (CO) cm^{-1}; PMR (D_2O): δ 4.3–4.9 (m, 4H), 3.4–4.0 (m, 6H), 1.7 (s, 6H), 1.2–1.8 (m, 4H), and 0.9 (t, 3H) ppm.

Anal.—Calc. for $C_{12}H_{26}ClNO_4$: C, 50.78; H, 9.24; N, 4.94. Found: C, 50.39; H, 9.53; N, 5.00.

Methyl α-*N,N*-Dichloroaminoisobutyrate (X*a*) (5)—To 750 ml of 0.76 *M* sodium hypochlorite at 0° was added dropwise, with stirring, 39.1 g (0.26 mole) of III dissolved in 75 ml of water. The reaction mixture was adjusted to pH 4–6 by addition of 1 *M* HCl, and the suspension was stirred at 0° for 0.75 hr. The *N*-chloramine was extracted with methylene chloride, and the extracts were combined and dried over anhydrous sodium sulfate. Following filtration, the methylene chloride was removed under reduced pressure to afford a dark-yellow liquid. Distillation gave 33.48 g (0.18 mole), 69%, of X*a*, bp 34–38° (0.4 mm); IR (neat): 1750 (C=O) cm^{-1}; PMR ($CDCl_3$): δ 1.7 (s, 6H) and 3.37 (s, 3H) ppm; UV (H_2O): λ_{max} 305 nm, $\epsilon = 315\ M^{-1}\ cm^{-1}$.

Anal.—Calc. for $C_5H_9Cl_2NO_2$: C, 32.28; H, 4.88; N, 7.53. Found: C, 32.47; H, 5.03; N, 7.52.

***n*-Hexyl α-*N*-Chloroaminoisobutyrate (X*b*)**—To 65 ml of 0.75 *M* sodium hypochlorite at 0° was added 4.46 g (0.02 mole) of IV in portions over 5 min. The suspension was stirred vigorously at 0° for 1 hr. The *N*-chloramine was extracted into ether, and the extracts were combined and dried over anhydrous sodium sulfate. Following filtration, the ether was removed under reduced pressure to afford 4.12 g (0.019 mole), 95%, of X*b* as a pale-yellow liquid; IR (neat): 3280 (NH) and 1735 (C=O) cm^{-1}; PMR ($CDCl_3$): δ 5.0 (s, 1H), 4.2 (t, 2H), 1.43 (s, 6H), 1.32 (broad s, 8H), and 0.93 (broad t, 3H) ppm.

Anal.—Calc. for $C_{10}H_{20}ClNO_2$: C, 54.16; H, 9.09; N, 6.32. Found: C, 52.29; H, 9.21; N, 5.92.

By using the procedure described for the preparation of X*b*, the following α-*N*-chloroaminoisobutyrates were prepared.

n-*Octyl α-N-Chloroaminoisobutyrate* (*X*c)—R_f 0.21 (benzene, silica gel); IR (neat): 3300 (NH), 2960 (CH), 1750 (C=O), and 1150 (CO) cm^{-1}; PMR ($CDCl_3$): δ 5.0 (broad s, 1H), 4.2 (t, 2H), 1.4 (s, 6H), 1.37 (broad s, 12H), and 0.93 (broad t, 3H) ppm.

Anal.—Calc. for $C_{12}H_{24}ClNO_2$: C, 57.70; H, 9.68; N, 5.61. Found: C, 58.29; H, 10.09; N, 5.50.

n-*Dodecyl α-N-Chloroaminoisobutyrate* (*X*d)—R_f 0.24 (benzene, silica gel); IR (neat): 3300 (NH), 2970 (CH), 1740 (C=O), and 1140 (CO) cm^{-1}; PMR ($CDCl_3$): δ 5.0 (broad s, 1H), 4.2 (t, 2H), 1.4 (s, 6H), 1.3 (broad s, 20H), and 0.9 (broad t, 3H) ppm.

Anal.—Calc. for $C_{16}H_{32}ClNO_2$: C, 62.82; H, 10.55; N, 4.58. Found: C, 63.79; H, 11.24; N, 4.62.

n-*Tetradecyl α-N-Chloroaminoisobutyrate* (*X*e)—R_f 0.41 (benzene, silica gel); IR (neat): 3300 (NH), 2970 (CH), 1740 (C=O), and 1140 (CO) cm^{-1}; PMR ($CDCl_3$): δ 5.0 (broad s, 1H), 4.2 (t, 2H), 1.4 (s, 6H), 1.3 (broad s, 24H), and 0.9 (broad t, 3H) ppm.

Anal.—Calc. for $C_{18}H_{36}ClNO_2$: C, 64.74; H, 10.87; N, 4.20. Found: C, 65.02; H, 11.19; N, 3.68.

n-*Octadecyl α-N-Chloroaminoisobutyrate* (*X*f)—R_f 0.25 (benzene, silica gel); IR (neat): 3300 (NH), 2970 (CH), 1750 (C=O), and 1150 (CO) cm^{-1}; PMR ($CDCl_3$): δ 5.0 (broad s, 1H), 4.2 (t, 2H), 1.4 (s, 6H), 1.3 (broad s, 32H), and 0.9 (broad t, 3H) ppm.

Anal.—Calc. for $C_{22}H_{44}ClNO_2$: C, 65.39; H, 10.98; N, 3.47. Found: C, 66.77; H, 11.67; N, 2.99.

2-(2-n-Butoxyethoxy)ethyl α-N-Chloroaminoisobutyrate (*XII*)—IR (neat): 3295 (NH), 2960 (CH), 1740 (C=O), and 1130 (CO) cm^{-1}; PMR ($CDCl_3$): δ 5.0 (broad s, 1H), 4.3 (m, 2H), 3.2–4.0 (m, 8H), 1.4 (s, 6H), 1.8–1.2 (m, 4H), and 0.9 (t, 3H) ppm.

Anal.—Calc. for $C_{12}H_{24}ClNO_4$: C, 51.15; H, 8.58; N, 4.97. Found: C, 50.99; H, 8.56; N, 4.71.

***n*-Hexyl α-*N,N*-Dichloroaminoisobutyrate (X*g*)**—To 75 ml of 0.69 *M* sodium hypochlorite at 0° was added 4.46 g (0.02 mole) of IV in portions over 5 min. The reaction mixture was adjusted to pH 4–6 by the addition of 1 *M* HCl, and the suspension was vigor-

ously stirred at 0° for 1 hr. The *N*-chloramine was extracted into methylene chloride, and the extracts were combined and dried over anhydrous sodium sulfate. Following filtration, the methylene chloride was removed under reduced pressure to afford 3.71 g (0.015 mole), 75%, of a dark-yellow liquid. Chromatography on a magnesium silicate column with benzene–petroleum ether (75:25) (bp 30–60°) gave X*g* as a dark-yellow liquid, R_f 0.67 (benzene, silica gel); IR (neat): 2985 (CH), 1750 (C=O), and 1170 (CO) cm^{-1}; PMR ($CDCl_3$): δ 4.2 (t, 2H), 1.63 (s, 6H), 1.30 (broad s, 8H), and 0.90 (broad t, 3H) ppm.

Anal.—Calc. for $C_{10}H_{19}Cl_2NO_2$: C, 46.88; H, 7.48; N, 5.47. Found: C, 46.98; H, 7.69; N, 5.20.

Using the procedure described for the preparation of X*g*, the following α-*N,N*-dichloroaminoisobutyrates were prepared.

n-*Octyl* α-N,N-*Dichloroaminoisobutyrate* (*X*h)—R_f 0.69 (benzene, silica gel); IR (neat): 2980 (CH), 1750 (C=O), and 1160 (CO) cm^{-1}; PMR ($CDCl_3$): δ 4.2 (t, 2H), 1.7 (s, 6H), 1.3 (broad s, 12H), and 0.90 (broad t, 3H) ppm.

Anal.—Calc. for $C_{12}H_{23}Cl_2NO_2$: C, 50.71; H, 8.16; N, 4.93. Found: C, 50.77; H, 8.50; N, 4.46.

n-*Dodecyl* α-N,N-*Dichloroaminoisobutyrate* (*X*i)—R_f 0.70 (benzene, silica gel); IR (neat): 2970 (CH), 1750 (C=O), and 1170 (CO) cm^{-1}; PMR ($CDCl_3$): δ 4.2 (t, 2H), 1.7 (s, 6H), 1.3 (broad s, 20H), and 0.90 (broad t, 3H) ppm.

Anal.—Calc. for $C_{16}H_{31}Cl_2NO_2$: C, 56.46; H, 9.18; N, 4.12. Found: C, 56.74; H, 9.51; N, 3.81.

n-*Tetradecyl* α-N,N-*Dichloroaminoisobutyrate* (*X*j)—R_f 0.75 (benzene, silica gel); IR (neat): 2970 (CH), 1750 (C=O), and 1170 (CO) cm^{-1}; PMR ($CDCl_3$): δ 4.2 (t, 2H), 1.6 (s, 6H), 1.3 (broad s, 24H), and 0.9 (broad t, 3H) ppm.

Anal.—Calc. for $C_{18}H_{35}Cl_2NO_2$: C, 58.68; H, 9.58; N, 3.80. Found: C, 58.30; H, 9.94; N, 3.29.

n-*Octadecyl* α-N,N-*Dichloroaminoisobutyrate* (*X*k)—R_f 0.75 (benzene, silica gel); IR (neat): 2970 (CH), 1750 (C=O), and 1170 (CO) cm^{-1}; PMR ($CDCl_3$): δ 4.2 (t, 2H), 1.6 (2, 6H), 1.3 (broad s, 32H), and 0.90 (broad t, 3H) ppm.

Anal.—Calc. for $C_{22}H_{43}Cl_2NO_2$: C, 62.25; H, 10.21; N, 3.30. Found: C, 61.69; H, 10.53; N, 2.80.

2-(2-n-*Butoxyethoxy*)*ethyl* α-N,N-*Dichloroaminoisobutyrate* (*XIII*)—IR (neat): 2960 (CH), 1750 (C=O), and 1150 (CO) cm^{-1}; PMR ($CDCl_3$): δ 4.4 (m, 2H), 3.3–4.0 (m, 8H), 1.7 (s, 6H), 1.8–1.2 (m, 4H), and 0.9 (t, 3H) ppm.

Anal.—Calc. for $C_{12}H_{23}Cl_2NO_4$: C, 45.58; H, 7.33; N, 4.43. Found: C, 46.05; H, 7.60; N, 4.22.

1,4-Dichloro-2,2,5,5-tetramethyl-3,6-piperazinedione (XIV)—Through a mechanically stirred suspension of 29.95 g (0.17 mole) of 2,2,5,5-tetramethyl-3,6-piperazinedione (6) in 250 ml of water at 0° was bubbled chlorine gas for 1.5 hr. The white solid was isolated by filtration, washed thoroughly with cold water, and dried *in vacuo* over calcium sulfate to yield 38.20 g (0.16 mole), 94%, of XIV, mp 176.5–178°; IR (KBr): 1680 (C=O) cm^{-1}.

Anal.—Calc. for $C_8H_{12}Cl_2N_2O_2$: C, 40.18; H, 5.06; N, 11.72. Found: C, 40.49; H, 5.18; N, 11.64.

Kinetics for the Decomposition of I–III—*Iodometric Method*—For each determination of the reaction constants for I, a stock solution of 0.8×10^{-3} *M* I was prepared by reaction of methyl sarcosinoate hydrochloride (1 m*M*) with sodium hypochlorite (0.8 m*M*) in a final volume of 100 ml using the appropriate buffer solution. Periodically, samples were removed from the stock solution and the concentration of positive chlorine in the sample was determined iodometrically using 10^{-3} *M* sodium thiosulfate. Analysis as a first-order kinetic process gave the rate constants and half-lives listed in Table I.

Spectrophotometric Method—For each determination of the reaction constants for I–III, stock solutions of 0.8×10^{-3} *M* I–III were prepared by reaction of methyl sarcosinoate hydrochloride (1 m*M*), sarcosine hydrochloride (1 m*M*), and ethyl glycinate hydrochloride (1 m*M*), respectively, with sodium hypochlorite (0.8 m*M*) in a final volume of 100 ml using the appropriate buffer solution. In each case, the decrease in the wavelength of maximum absorbance for I (λ_{max} 264 nm), II (λ_{max} 268 nm), and III (λ_{max} 254 nm) was recorded as a function of time. Analysis as a first-order kinetic process gave the rate constants and half-lives reported in Table I.

REFERENCES

(1) N. Bodor, J. J. Kaminski, S. D. Worley, R. J. Colton, T. H. Lee, and J. W. Rabalais, *J. Pharm. Sci.*, **63**, 1387(1974).

(2) T. Higuchi, A. Hussain, and I. Pitman, *J. Chem. Soc., B*, **1969**, 626.

(3) I. Pitman, H. Dawn, T. Higuchi, and A. Hussain, *ibid.*, **1969**, 1230.

(4) W. S. Metcalf, *ibid.*, **1942**, 148.

(5) A. M. Pinchuk, L. N. Markovskii, and G. K. Bespalko, *Zh. Org. Khim.*, **7**, 2263 (1971),

(6) S. M. McElvain and E. H. Pryde, *J. Amer. Chem. Soc.*, **71**, 326(1949).

ACKNOWLEDGMENTS AND ADDRESSES

Received May 15, 1975, from *INTERx Research Corporation, Lawrence, KS 66044*

Accepted for publication June 27, 1975.

For Part II of this series, see: J. J. Kaminski and N. Bodor, *Tetrahedron*, in press.

[x] To whom inquiries should be directed.

Development of a Stable Sublingual Nitroglycerin Tablet II: Formulation and Evaluation of Tablets Containing Povidone

HO-LEUNG FUNG, S. K. YAP, and C. T. RHODES ˣ

Abstract □ Stable and pharmaceutically elegant sublingual nitroglycerin tablets were formulated using povidone to retard volatilization of the drug. Formulation and processing variables were investigated to produce an acceptable product. A blend of two grades of povidone, of different degrees of cross-linkage and water solubility, provided stable tablets which exhibited rapid disintegration. Directly compressed sublingual tablets made in this study retained over 80% of the initial nitroglycerin when exposed to the atmosphere at room temperature for 2 months. The direct compression tablets are of good appearance and low friability, and the formulation is readily compressed without problems. An interesting relationship among the hardness, disintegration time, and compaction pressure is described.

Keyphrases □ Nitroglycerin—sublingual tablets containing povidone, formulation and processing variables investigated, effect of compaction pressure on hardness and disintegration time □ Povidone—two grades used in sublingual nitroglycerin tablets, formulation and processing variables investigated □ Dosage forms—sublingual nitroglycerin tablets containing povidone, formulation and processing variables investigated

Recently, studies of the interaction between a number of pharmaceutically acceptable macromolecules and nitroglycerin were reported (1). Povidone substantially reduced the loss of nitroglycerin from test powder mixtures. Thus, it was felt that the design of nitroglycerin dosage forms containing povidone merited a full investigation.

When this study was initiated, molded nitroglycerin tablets were the most common sublingual dosage form used to provide rapid relief from the symptoms of angina. However, it seemed that there would be considerable advantages in producing directly compressed sublingual nitroglycerin tablets. In particular, the advantages of the direct compression process justified an attempt to exploit this technique. Some work indicated that there is potential for directly compressed nitroglycerin tablet formulations (2).

In this paper, formulation studies resulting in the development of stabilized nitroglycerin sublingual tablets are reported. These tablets are stable under most rigorous storage conditions, disintegrate rapidly, and compare favorably with existing commercial tablets.

EXPERIMENTAL

Materials—Two grades of povidone, designated types I[1] and II[2] (type I has a much lower degree of cross-linkage and an appreciably greater water solubility than type II), sucrose[3], corn starch[4], sodium starch glycolate[5], lactose USP[6], magnesium stearate[3], and a nitroglycerin–lactose mixture[7] containing 10% (w/w) of nitroglycerin were used without further purification.

Method—Molded tablets were prepared by dry mixing the component powders and then adding 1 ml of 50% (v/v) aqueous ethanol/12 g of powder as granulating fluid. The mass was then molded, and the formed tablets were allowed to dry at room temperature overnight.

The directly compressed tablets were prepared by a single-punch tablet press[8] with 5-cm beveled punches. The tablet components were mixed well by quartering. Tablets were prepared at seven different arbitrary compaction pressures from P_1, lowest, to P_7, highest. They were then evaluated for disintegration time using the USP apparatus. Friability was determined by a circular friabulator[9], 10 tablets being rotated for 15 min after a preliminary dedusting. Determination of weight loss after the operation allowed estimation of percentage friability. Tablet hardness values were measured using an electric hardness tester[10].

Physical stability of the tablets, in terms of nitroglycerin loss, was evaluated by storing samples of 40 tablets in open petri dishes at room temperature. The dishes were placed over 0.61 m (2 ft) apart to prevent migration of nitroglycerin between samples (1, 3, 4). The nitroglycerin content of the tablets was determined as a function of time using the assay technique described previously (5). For comparison purposes, two commercial brands of nitroglycerin tablets, Brands A[11] and B[12], were included in this study.

RESULTS AND DISCUSSION

Previously, it was shown that concentrations between 5 and 15% of povidone type I had a substantial stabilizing effect on nitroglycerin (1). Figure 1 shows the effect of varying the concentration of I on the hardness and disintegration time of molded sublingual nitroglycerin tablets containing 5% sucrose and lactose USP as the diluent. Increasing the proportion of I increased the hardness of the molded tablets until the concentration was about 10% (w/w),

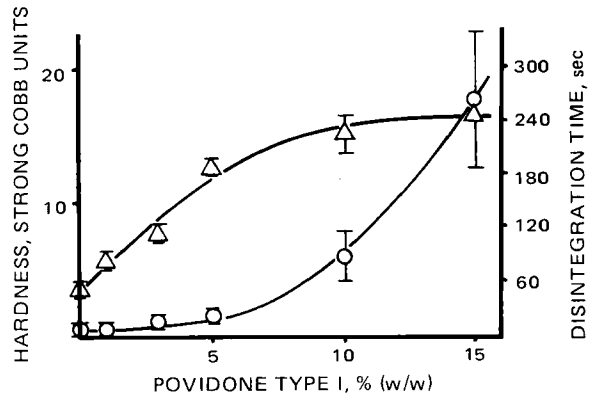

Figure 1—*Hardness (△) and disintegration time (○) of molded sublingual nitroglycerin tablets containing different proportions of povidone type I. Each data point represents the mean and standard deviation of six determinations.*

[1] Plasdone K-29-32, GAF Corp., New York, NY 10020
[2] Plasdone XL, GAF Corp., New York, NY 10020
[3] Fisher Scientific, Fair Lawn, NJ 07410
[4] Argo, Best Foods, Inc., Englewood Cliffs, NJ 07410
[5] Primojel K, Edward Mendell Co., Jefferson Valley, NY 10535
[6] Mallinckrodt Chemical Works, St. Louis, MO 63160
[7] ICI America, Tamaqua, PA 18252
[8] Erweka type TA3, Chemical and Pharmaceutical Co., New York, NY 10013
[9] Roche friabulator, Chemical and Pharmaceutical Co., New York, NY 10013
[10] Strong Cobb model PT102, J. H. Delmar and Sons, Chicago, IL 60625
[11] NitroPRN, 0.6 mg, Lot 4583044B, Warner-Chilcott, Morris Plains, NJ 07950
[12] Nitrostat, 0.6 mg, Lot MA153, Parke-Davis, Detroit, MI 48232

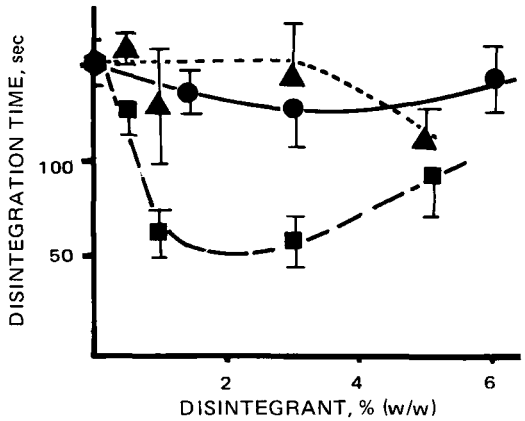

Figure 2—*Disintegration characteristics of molded sublingual nitroglycerin tablets containing 10% povidone type I and different concentrations of the disintegrant corn starch (●), sodium starch glycolate (▲), and povidone type II (■). Each data point represents the mean and standard deviation of six determinations.*

above which little change in hardness was observed. Conversely, an increase in the I concentration up to about 8% (w/w) had little effect on the disintegration time of the molded tablets. However, a quite abrupt increase in the disintegration time was detected above this value.

To retain the stabilizing effect of I without excessively long disintegration times, the percentage of this component was fixed at 10% (w/w). Although I did not have an excessive binding effect at the 10% level, it was still necessary to add a disintegrant. Following a preliminary screening, three materials—corn starch, sodium starch glycolate, and povidone type II (6)—were selected for detailed study. Figure 2 shows disintegration times for the molded tablets [containing 10% (w/w) I] as a function of disintegrant concentrations. Obviously, II offered the greater advantage in terms of diminution of disintegration time. Another advantage of including this material in the formulation was that it had a stabilizing action on nitroglycerin, albeit slightly less than that shown by I (Table I).

The formula (Formula I) selected for the molded tablet was:

nitroglycerin–lactose powder	*q.s.*
sucrose	5.0%
povidone type I	10.0%
povidone type II	2.0%
lactose monohydrate USP	to 100.0%

The poor weight uniformity, difficulty of preparation, and generally poor physical properties of these molded tablets stimulated study of direct compression tablets. The studies of the molded tablets had shown that the combination of povidone types I and II offers unique advantages in the formulation of nitroglycerin tablets. Therefore, this finding was exploited for the direct compression tablets. Of course, with a compressed tablet, the additional variable of compaction force can affect hardness–disintegration time relationships.

Figure 3 shows the effect of varying compaction pressure and percentage of II on the hardness and disintegration time of tablets containing 10% (w/w) I, 2% magnesium stearate, and lactose as the diluent. The effect of altering the concentration of II between 3 and 8% on disintegration time apparently was related to the effect of this substance on tablet hardness. With one exception, the data

Table I—Stability of Nitroglycerin in Lactose Powder Containing Povidone Type II upon Exposure to the Atmosphere at Room Temperature

	Percent Nitroglycerin Remaining in Powder in		
	7 Days	14 Days	28 Days
Control	37	6	5
With 10% (w/w) povidone type II	87	80	70

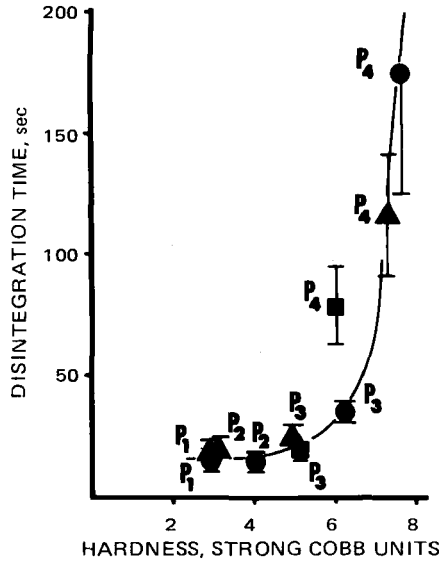

Figure 3—*Hardness and disintegration time of direct compression sublingual tablets containing 10% (w/w) povidone type I and 3% (●), 5% (▲), and 8% (■) of povidone type II produced under different compaction pressures. The* P *values indicate different compaction pressure from* P_1, *lowest, to* P_4, *highest.*

points derived from different concentrations of II and different compaction pressures fell on the same smooth curve. A concentration of 10% II was included in the selected formula. However, since the disintegration times of tablets containing 10% (w/w) I and 10% (w/w) II were still somewhat longer than desirable, another disintegrant was added to the formulation. Sodium starch glycolate, a water-soluble starch derivative having considerable potential in direct compression systems, was chosen for this purpose (7).

The selected direct compression formula (Formula II) was:

nitroglycerin–lactose powder	*q.s.*
sodium starch glycolate	1.0%
magnesium stearate	2.0%
povidone type I	10.0%
povidone type II	10.0%
lactose monohydrate USP	to 100.0%

which compresses to give tablets between 3.0 and 4.5 Strong Cobb hardness units.

The tablets prepared using Formula II have an elegant appearance, having a smooth, clean, white surface. The formula compresses readily; no evidence of "capping," "sticking," or other compression problems was detected. The excellent weight uniformity is indicative of good flow properties of the formulation (Table II). It is possible to reduce the concentration of magnesium stearate and still have good lubrication; reduction in the concentration of this component further decreases disintegration times. Of course, the final selection of optimum processing and formulation variables must depend on the type of tablet press used as well as the scale of production. In particular, the shorter dwell times on a rotary press might necessitate some minor changes. However, no major change is required.

Figure 4 shows the effect of variation in compaction pressure on the hardness and disintegration time of the compressed tablets. It is obvious that the disintegration time of the tablets remained essentially constant at less than 30 sec as long as the compaction pressure used produced tablet hardness of 5 Strong Cobb units or less. A further increase in compaction pressure caused only a slight increase in hardness but an exponential increase in the disintegration time of the tablets. In practice, tablet hardness of 3–4 Strong Cobb units is sufficient for sublingual tablets. Hence, this peculiar physical characteristic of povidone-stabilized direct compression nitroglycerin tablets is not a major quality control problem.

The interesting disintegration characteristics of direct compression nitroglycerin sublingual tablets containing povidone can, perhaps, be explained as follows. The disintegration of a tablet in a USP disintegration apparatus can be considered as consisting of two processes: bulk disintegration and surface erosion. In bulk dis-

Table II—Stability, Hardness, Disintegration Time, Friability, and Weight Uniformity of Brands A and B and Formula II

	Brand A (Compressed)	Brand B (Molded)	Formula II (Compressed)
Hardness, Strong Cobb units[a], mean (*SD*)	3.0 (0.3)	2.4 (0.2)	2.7 (0.4)
Disintegration time, sec[a], mean (*SD*)	7 (1)	23 (4)	14 (1)
Friability, %	1.2	6.7	1.3
Weight uniformity[b], mg, mean (*SD*)	33.1 (0.2)	35.6 (0.8)	77.2 (0.4)
Water-insoluble ingredients, % (means of three determinations)	60	0	12

[a] Determination of six tablets. [b] Determination of 10 tablets.

integration, capillary action or other mechanisms draw water into the tablet through pores, and subsequent swelling of the disintegrant ruptures the tablet structure. The fact that the disintegration time is essentially independent of compaction pressures between hardness values of 2–5 Strong Cobb units indicates that in such systems the rate of entry of water into the tablet is not rate determining and that bulk disintegration predominates in the overall disintegration of the tablet.

However, as compaction pressure is increased, tablet porosity decreases. Above a hardness of 5 units, the very different behavior may be due to reduction of tablet porosity beyond the critical value at which the reduction of the rate of water entry into the tablet diminishes the role of bulk disintegration in the total disintegration of the tablet. Therefore, as compaction pressure is increased, bulk disintegration decreases substantially and the slower surface erosion process predominates in the overall tablet disintegration. Detailed evaluation of compaction pressure and porosity would be required to elucidate fully the reasons for this interesting behavior.

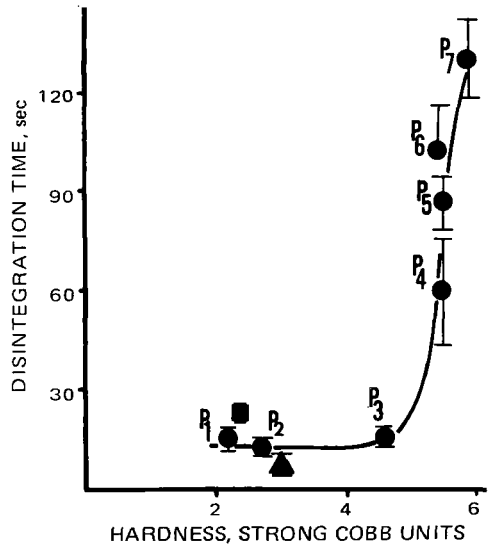

Figure 4—*Hardness and disintegration time of nitroglycerin sublingual tablets. Key: ●, Formula II; ▲, Brand A; and ■, Brand B. The* P *values indicate different compaction pressures. Each data point represents the mean and standard deviation of six determinations.*

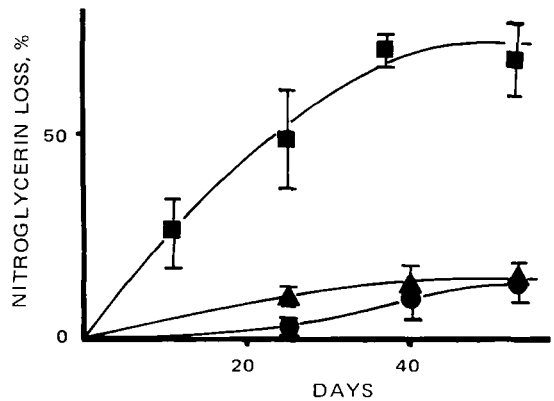

Figure 5—*Loss of nitroglycerin from Formula II (●), Brand A (▲), and Brand B (●) on exposure to the atmosphere on open petri dishes at room temperature. Each data point represents the mean and standard deviation of six single-tablet assays.*

The present authors previously reported (1) extraction experiments, which indicate that the formulation components used in this study are unlikely to affect biological availability adversely. Detailed clinical studies of nitroglycerin products, both tablets and ointments, would be useful.

Results of the comparative evaluations of the compressed tablets described in this study and commercially available tablets (Brand A, compressed, and Brand B, molded) are shown in Table II and Fig. 5. Even under the quite thorough test used in this investigation, the tablets prepared in this study and Brand A commercial tablets showed a high degree of stability. The test used was far more rigorous than one might expect in normal use.

It can be seen from Table II that the direct compression tablets described in this study compared favorably with Brands A and B in terms of weight uniformity and disintegration time. Table II also contains estimates of the percentage of water-insoluble ingredients in each of the three types of tablets. Estimates were obtained by shaking 100 tablets vigorously for 30 min with 30 ml of distilled water, filtering, and then weighing the residues. Brand B appears to be comprised entirely of water-soluble components; the product reported in this study had about 12% of water-insoluble material, while Brand A had approximately 60% (w/w) water-insoluble material. All three types of tablets had an acceptable "mouth feel," but some formulators might feel that 60% water-insoluble material in a sublingual tablet is high.

From the data presented, it is apparent that the direct compression tablet formulation reported herein compares very favorably with other recently introduced formulations which were developed to overcome the problem of nitroglycerin loss.

REFERENCES

(1) H.-L. Fung, S. K. Yap, and C. T. Rhodes, *J. Pharm. Sci.*, **63**, 1810(1974).

(2) M. D. Richman, C. D. Fox, and R. F. Shangraw, *ibid.*, **54**, 447(1965).

(3) S. A. Fusari, *ibid.*, **62**, 122(1973).

(4) *Ibid.*, **62**, 2012(1973).

(5) H.-L. Fung, P. Dalecki, E. Tse, and C. T. Rhodes, *J. Pharm. Sci.*, **62**, 696(1973).

(6) S. K. Kornblum and S. B. Stoopak, *ibid.*, **62**, 43(1973).

(7) K. A. Khan and C. T. Rhodes, *Pharm. Acta Helv.*, **47**, 153(1972).

ACKNOWLEDGMENTS AND ADDRESSES

Received April 3, 1975, from the *Department of Pharmaceutics, State University of New York at Buffalo, Buffalo, NY 14207*

Accepted for publication July 2, 1975.

Supported by the Pharmaceutical Division, Fisons Corp., Bedford, Mass.

[x] To whom inquiries should be directed. Present address: Department of Pharmacy, University of Rhode Island, Kingston, RI 02881

Isolation of Flindersiamine, Isoflindersiamine, and a New Alkaloid, Heliparvifoline, from *Helietta parvifolia* (Rutaceae)

P. T. O. CHANG, G. H. AYNILIAN *, G. A. CORDELL, M. TIN-WA, H. H. S. FONG, R. E. PERDUE, Jr. ‡, and N. R. FARNSWORTH ×

Abstract □ A phytochemical investigation of the leaves and twigs of *Helietta parvifolia* (Rutaceae) resulted in the isolation of heliparvifoline, a new furoquinoline alkaloid, in addition to the known bases flindersiamine and isoflindersiamine.

Keyphrases □ Alkaloids—flindersiamine, isoflindersiamine, and heliparvifoline isolated from *Helietta parvifolia* leaves and twigs, cytotoxicity evaluated □ *Helietta parvifolia*—leaves and twigs, alkaloids isolated, cytotoxicity evaluated □ Cytotoxicity—alkaloids from leaves and twigs of *Helietta parvifolia* isolated, evaluated

Helietta parvifolia (A. Gray) Benth (Rutaceae) is a tree native to Central and South America (1). Phytochemical studies on this plant have demonstrated the presence of the furoquinoline alkaloids flindersiamine (I) and kokusaginine (II) (2); the volatile oil components isosafrol, safrol, eugenol, and methyleugenol (2); an alkane, dotriacontane (3); and a straight-chain alcohol, tetracosanol (3).

The only other species of this genus investigated for its constituents is *H. longifoliata*, which yielded the pentacyclic triterpene isobauerenol (4), maculine (III) (5), limonin (6), dictamnine (IV) (7), 6-methoxydictamnine (V) (7), kokusaginine (II) (7), flindersiamine (I) (7), skimmianine (VI) (7), isodictamnine (VII) (7), and heliettin (8).

No pharmacological study or folkloric information has been reported concerning *Helietta* species. However, preliminary investigation showed that a 50% ethanol extract of *H. parvifolia* exhibits activity against the P-388 lymphocytic leukemia (T/C = 133%) in DBA/2 mice at a dose of 66 mg/kg[1]. The chloroform-soluble fraction obtained after partitioning the concentrated methanol extract of the plant between chloroform and water showed marginal activity against the P-388 leukemia (T/C = 129%) at a dose of 400 mg/kg. An extract representing the total alkaloids of this plant showed cytotoxicity against Eagle's 9KB carcinoma of the nasopharynx in cell culture (ED_{50} = 5.0 μg/ml)[1].

In view of the limited studies on the constituents of this plant and the preliminary results indicating activity in the 50% ethanol extract, the current study was initiated to isolate new potential antitumor agents from *H. parvifolia*.

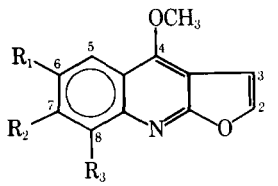

I: R_{1-2} = —OCH_2O—, R_3 = OCH_3
II: R_1 = OCH_3, R_2 = OCH_3, R_3 = H
III: R_{1-2} = —OCH_2O—, R_3 = H
IV: R_1 = H, R_2 = H, R_3 = H
V: R_1 = OCH_3, R_2 = H, R_3 = H
VI: R_1 = H, R_2 = OCH_3, R_3 = OCH_3
VIII: R_1 = OCH_3, R_2 = OH, R_3 = H
IX: R_1 = H, R_2 = OCH_3, R_3 = H

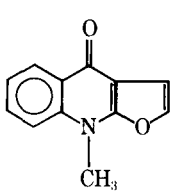

VII

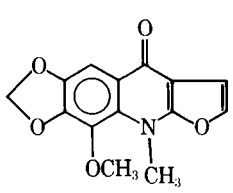

X

EXPERIMENTAL[2]

Plant Material—The plant material[3] was collected in Mexico during July 1972. The leaves and twigs were harvested, air dried, and milled to a coarse powder.

Preparation of Crude Alkaloid Fraction—Five kilograms of the plant material was extracted in a soxhlet apparatus for 36 hr with petroleum ether (bp 30–60°). After air drying, the defatted plant material was exhaustively extracted with methanol. The methanol extract yielded 502 g of residue after evaporation *in vacuo*.

A portion of the residue (450 g) was taken up in methanol (1 liter), and 2 *N* HCl (2 liters) was added. After thorough mixing, the methanol was removed *in vacuo*. The resulting acidic solution was made alkaline with 28% NH_4OH and extracted several times with chloroform until the final chloroform extract gave a negative alkaloid test with Mayer's reagent. The chloroform fractions were combined, dried over anhydrous sodium sulfate, filtered, and evaporated *in vacuo* to yield a residue (38 g).

Separation of Alkaloid Fraction—The major portion of the crude alkaloid fraction (33 g) was chromatographed on silica gel PE_{254}[4] (1.5 kg), employing benzene–chloroform–methanol (3:2:1) as the eluent. Fifty fractions (100 ml each) were collected (Column I). Fractions 14–26 were pooled and taken to dryness; then the residue was taken up in methanol, resulting in the formation of a crystalline compound (847 mg).

Based on the similarity of their TLC patterns on silica gel G

[1] The extracts were tested under the auspices of the Drug Research and Development branch of the National Cancer Institute. An extract is considered active if it causes a prolongation of life (T/C) in excess of 125% in the P-388 leukemia system and cytotoxic if it exhibits an $ED_{50} \leq 20$ μg/ml in the 9KB cell culture test system (9).

[2] All melting points were determined using a Köfler hot-stage instrument and are uncorrected. UV spectra were recorded on a Beckman model DB-G spectrophotometer using methanol as the solvent. IR spectra were recorded using a Beckman model 18-A spectrophotometer with polystyrene calibration at 1601 cm^{-1}. Intensities are reported as s (strong), m (medium), and w (weak). NMR spectra were recorded on a Varian Associates model T-60A instrument using tetramethylsilane as the internal standard. The chemical shifts are reported in parts per million (δ). Mass spectra were recorded using a Hitachi Perkin-Elmer model RMU-60 instrument.

[3] Voucher specimens were identified as *Helietta parvifolia* (Rutaceae) (CA-2022) by R. E. Perdue, Jr., and deposited at the Herbarium of the National Arboretum, Agricultural Research Service, U.S. Department of Agriculture, and at the Herbarium of the Department of Pharmacognosy and Pharmacology, College of Pharmacy, University of Illinois at the Medical Center.

[4] E. Merck, Darmstadt, Germany.

Table I—Chemical Shifts of Aromatic Protons in Selected Furoquinoline Alkaloids

	δ, Chemical Shift, ppm				δ, Chemical Shift, ppm			
	C-5	*ortho* Shift	*meta* Shift		C-8	*ortho* Shift	*meta* Shift	
6-Methoxydictamnine	7.50	0.61	0.06		7.90	0.60	0.02	0.05
7-Methoxydictamnine	8.10	0.66	0.01		7.25			
6,7-Dimethoxydictamnine	7.44				7.30	0.63		
Dictamnine	8.11				7.88			

plates[4], using Dragendorff's spray reagent and UV light as visualizing agents, the crystallization mother liquor (pooled fraction 14–26) was combined with fractions 27–41 and taken to dryness *in vacuo* to yield a residue (18 g). This residue was rechromatographed over a silica gel PF_{254} column (1.0 kg) (Column II), using chloroform as the eluent. A total of 303 fractions (100 ml each) was collected.

RESULTS AND DISCUSSION

Isolation and Identification of Flindersiamine (I)—The residue from pooled fractions 53–70, obtained from Column II, yielded a crystalline material (993 mg) from methanol. This material was shown to be identical to the compound isolated from fractions 14–26 (Column I) by mixed melting point and co-TLC. Recrystallization of one sample from methanol afforded an analytical sample, mp 205–206°; λ_{max} (methanol): 251 (log ε 4.91), 312 (4.17), and 325 (4.16) nm, indicating a 4-methoxyfuroquinoline moiety (10).

Mass spectral examination indicated a molecular ion at *m/e* 273 (100%). The fragmentation pattern, showing significant peaks at *m/e* 272 (55), 258 (9), 244 (44), 243 (27), 230 (40), 228 (47), 200 (15), and 172 (16), was identical with that reported for I (11). The NMR spectrum (dimethyl sulfoxide-d_6) showed two methoxy singlets at δ4.06 and 4.37; a singlet integrating for two protons at δ6.15, indicating the presence of a methylenedioxy group; two doublets (1H each) at δ7.38 (J = 2 Hz) and 7.97 (J = 2 Hz), indicating the presence of two furano protons; and a singlet (1H) at δ7.22, indicating the presence of an aromatic proton. The IR spectra of the isolate and reference flindersiamine[5] were superimposable, and the mixed melting point showed no depression, thus confirming the identity of the alkaloid.

Isolation and Characterization of Heliparvifoline (VIII)—The residue of pooled fractions 124–184, from Column II, yielded a crystalline material (239 mg) from methanol. This material, upon recrystallization from methanol, afforded an analytical sample, mp 245–247°. The UV spectrum exhibited absorption at λ_{max} (methanol): 247 (log ε 4.59), 313 (3.93), 324 (3.96), and 337 (3.89) nm, indicating a 4-methoxyfuroquinoline moiety (10). Upon addition of 0.1 *N* NaOH, the UV spectrum exhibited a bathochromic shift to 360 nm (log ε 3.99), suggesting the presence of a phenolic group. The original spectrum did not change upon the addition of 0.1 *N* HCl.

An IR spectrum (KBr) showed absorption bands at λ_{max} 3250–2500 (broad) (OH), 1625 (m), 1610 (s), 1550 (m), 1490 (s) (C=C), 1370 (s), 1270 (s), and 1050 (s) (=COC) cm^{-1}. Mass spectral examination indicated a molecular ion at *m/e* 245 (100%). Other significant peaks were observed at *m/e* 230 (55), 202 (19), 187 (10), 172 (15), and 159 (7). This fragmentation pattern is indicative of a dictamnine derivative (11).

The NMR spectrum (dimethyl sulfoxide-d_6) showed a broad singlet (1H) at δ3.37, which disappeared upon the addition of deuterium oxide. This signal was attributed to the presence of a phenolic proton. Two singlets (3H each), at δ3.90 and 4.40, suggested the presence of two methoxy groups, the downfield signal being due to the C-4 methoxy (12). Two singlets at δ7.20 and 7.43, each integrating for one proton, were assigned to two *para*-aromatic protons (at C-5 and C-8). Two doublets integrating for one proton each at δ7.92 and 7.38, with coupling constant J = 2 Hz, were assigned to C-2 and C-3 of the furan moiety, respectively. To determine the respective positions of the hydroxyl and methoxy groups on the aromatic ring, it was essential to assign the signals at δ7.20 and 7.43. Methylation with diazomethane at room temperature for 3 hr afforded kokusaginine (II) in high yield.

The NMR spectrum of II in dimethyl sulfoxide-d_6 showed three methoxy singlets at δ3.88, 3.92, and 4.40; two doublets integrating for one proton each at δ7.40 and 7.90 ppm (J = 2 Hz) for C-2 and C-3; and two singlets (1H each) at δ7.30 and 7.44, representing the two aromatic protons. To assign these resonances to the C-5 and C-8 protons of II, the aromatic regions of three additional compounds [6-methoxydictamnine (V), 7-methoxydictamnine (IX), and dictamnine (IV) itself] were examined.

The interpretation of the aromatic region in the NMR spectra of V and IX left little room for alternative explanations. In V, the two *ortho*-protons resonated at δ7.90 and 7.34; the latter was further coupled (J = 2 Hz) to a signal at δ7.50. In IX, the *ortho*-protons resonated at δ8.1 and 7.1; the latter was coupled (J = 2 Hz) to a signal at δ7.25.

There were two possible assignments for the δ7.30 and 7.44 resonances in II. It was felt that a decision could be made based on an examination of the effect of introducing an *ortho*-methoxy group on the chemical shift of an adjacent aromatic proton. In the absence of further structure modification, this shift would be expected to be reasonably consistent as a methoxy group is introduced at the 6- and 7-positions on the aromatic ring.

Table I shows the data for the four compounds under discussion, with a particular proton assignment selected for the aromatic protons of II. The shifts on introduction of a methoxy group *ortho* and *meta* to the C-5 and C-8 protons are also summarized in Table I. Introduction of a methoxy group consistently had the effect of shielding the adjacent *ortho*-proton by approximately δ0.62 and the *meta*-proton by approximately δ0.03. Therefore, the resonance at δ7.44 was assigned to the C-5 proton of II and that at δ7.30 was assigned to the C-8 proton, in agreement with a previous assignment (12).

The aromatic proton resonances remained to be assigned and thereby the position of the hydroxyl and methoxy groups in heliparvifoline.

In the methylation of heliparvifoline to II, the proton adjacent to the phenolic group was expected to experience the greatest shift. This proton, originally resonating at δ7.20, is deshielded by 0.1 ppm in II. This proton is at C-8 in II. Therefore, the phenolic group is located at C-7 in heliparvifoline.

An electron-releasing phenoxide ion is expected to cause increased shielding of the *ortho*-proton while affecting very little the *meta*-proton (13). Therefore, the resonance of the proton experiencing the greatest shift should be that due to the proton adjacent to the phenolic group. When the NMR spectrum of heliparvifoline was recorded in dimethyl sulfoxide-d_6 in the presence of a drop each of deuterium oxide and sodium deuteroxide, the resonance of the upfield aromatic proton was shifted from δ7.20 to 7.03 while the downfield proton was shifted from δ7.43 to 7.37. Thus, the hydroxyl group is located at the position adjacent to the proton resonating at δ7.20. This proton was previously assigned to the proton at C-8, thereby confirming the location of the hydroxyl group at C-7. Therefore, heliparvifoline has Structure VIII.

Isolation and Characterization of Isoflindersiamine (X)—Fractions 216–222, from Column II, were combined, taken to dryness, and dissolved in a minimum of hot methanol. From the cooled solution, 43 mg of a crystalline material was obtained. Recrystallization from methanol afforded an analytical sample, mp 212–213°; λ_{max} (methanol): 262 (log ε 4.32), 307 (3.60), 333 (3.73), and 348 (3.72) nm, indicating an *N*-methyl-4-furoquinoline moiety

[5] Supplied by Dr. E. Ritchie, Department of Organic Chemistry, University of Sidney, Sidney, N.S.W., Australia.

(14, 15). No change in the UV spectrum was observed upon the addition of either 0.1 *N* NaOH or 0.1 *N* HCl.

The IR spectrum (KBr) showed absorption bands at υ_{max} 3105 (w), 2950 (w), 2910 (w), 1610 (s), 1580 (w), 1450 (s) (C=C), 1470 (s) (CH_2), 1275 (s), 1050 (s) (=COC), and 930 (s) (CO) cm^{-1}. The NMR spectrum (dimethyl sulfoxide-d_6) showed two singlets (3H each) at δ4.00 and 4.10 ppm, representing one methoxy group at C-8 and one *N*-methyl group. A singlet integrating for two protons at δ6.23 ppm indicated the presence of a methylenedioxy group; two doublets at δ7.00 (J = 2 Hz) and 7.77 (J = 2 Hz) ppm, integrating for one proton each, were assigned to C-3 and C-2, respectively. A singlet integrating for one proton at δ7.50 ppm was assigned to a single aromatic proton.

Mass spectral examination indicated a molecular ion at *m/e* 273 (100%). The fragmentation pattern showed significant peaks at *m/e* 258 (42), 230 (9), 228 (12), 202 (5), 200 (6), and 172 (12). This fragmentation pattern differed from that of flindersiamine (I). The compound exhibited properties similar to those reported for isoflindersiamine (X) (16).

Previous work (16) had established a thermal isomerization of I to X. Repetition of this reaction[6] using the isolated I afforded X in 36% yield. The synthetic X exhibited identical UV, IR, mass, and NMR spectral data to the natural material, and a mixed melting-point determination showed no depression. The identity was therefore confirmed as X. Although not a new compound, this is the first reported natural occurrence of X.

Biological Activity—All three alkaloids isolated in this study were inactive in the 9KB cell culture and P-388 leukemia test systems.

SUMMARY

Separation of the chloroform-soluble alkaloid fraction of *H. parvifolia* by column chromatography resulted in the isolation of flindersiamine (I), isoflindersiamine (X), and a new furoquinoline alkaloid, heliparvifoline (VIII), whose structure was deduced by spectral means. The structure of X was confirmed by partial synthesis from I.

The copious yield of flindersiamine established it to be the major tertiary base in the aboveground parts of this plant. The quaternary alkaloid fraction of this plant is currently being investigated for the compound(s) responsible for the antileukemic and cytotoxic activities observed in the crude extracts.

[6] Flindersiamine (I) was heated in the presence of methyl iodide at 100° for 4 hr in a sealed tube. Crystallization from methanol afforded isoflindersiamine (X), mp 211–212°.

REFERENCES

(1) J. C. Willis, "A Dictionary of the Flowering Plants and Ferns," 7th ed., Cambridge University Press, London, England, 1966, p. 528.

(2) X. A. Dominguez, A. Canales, J. A. Garza, E. Gomez, and L. Garza, *Phytochemistry*, **10**, 1966(1971).

(3) X. A. Dominguez and A. Merijanian, *Rev. Latinoamer. Quim.*, **3**, 31(1972).

(4) D. F. Theumann and J. H. Comin, *Phytochemistry*, **8**, 781(1969).

(5) D. F. Theumann and J. H. Comin, *An. Asoc. Quim. Argent.*, **55**, 253(1967).

(6) J. C. Vitagliano and J. H. Comin, *ibid.*, **58**, 273(1970).

(7) C. A. Mammarella and J. H. Comin, *ibid.*, **59**, 239(1971).

(8) H. Pozzi, E. Sanchez, and J. H. Camin, *Tetrahedron*, **23**, 1129(1967).

(9) R. I. Geran, N. H. Greenberg, M. M. Macdonald, A. M. Schumacher, and B. J. Abbott, *Cancer Chemother. Rep. 3*, **3**, 1(1972).

(10) A. I. Scott, "Interpretation of Ultraviolet Spectra of Natural Products," Pergamon, New York, N.Y., 1964, p. 184.

(11) D. M. Glugston and D. B. Maclean, *Can. J. Chem.*, **43**, 2516(1965).

(12) A. V. Robertson, *Aust. J. Chem.*, **16**, 451(1963).

(13) R. J. Highet and P. F. Highet, *J. Org. Chem.*, **30**, 902(1965).

(14) F. W. Eastwood, G. K. Hughes, and E. Ritchie, *Aust. J. Chem.*, **7**, 87(1954).

(15) S. W. Pelletier, "Chemistry of the Alkaloids," Van Nostrand Reinhold, New York, N.Y., 1971, p. 356.

(16) F. A. L. Anet, P. T. Gilham, P. Gow, G. K. Hughes, and E. Ritchie, *Aust. J. Sci. Res. Ser. A, Phys. Sci.*, **5**, 412(1952).

ACKNOWLEDGMENTS AND ADDRESSES

Received August 22, 1974, from the *Department of Pharmacognosy and Pharmacology, College of Pharmacy, University of Illinois at the Medical Center, Chicago, IL 60612*

Accepted for publication July 8, 1975.

Supported by Research Contract NIH-NCI-C-72-2708 from the National Cancer Institute, National Institutes of Health, Department of Health, Education, and Welfare, Bethesda, MD 20014

* Present address: Abbott Laboratories, North Chicago, IL 60064

‡ Present address: Medical Plant Resources Laboratory, Agricultural Research Service, U.S. Department of Agriculture, Beltsville, MD 20705

x To whom inquiries should be directed.

Improved Transport Apparatus for Examining Diffusion of Drugs across Isolated Tissues and Synthetic Membranes

MARSHALL Z. BIBER and C. T. RHODES ˣ

Abstract □ A three-compartment diffusion apparatus that can accommodate synthetic as well as small isolated biological membranes such as rat intestine was developed and tested. The diffusion of drug from two outer donor cells into a central recipient cell allows for more membrane surface exposure and greater sensitivity in assaying as compared with previously published techniques. Reproducibility values for the synthetic membrane were equivalent to those obtained in more elaborate designs, while the reproducibility for biological membranes compared favorably with everted gut preparations and a similar diffusion apparatus. The clearance, per square centimeter of membrane, of salicylamide at pH 7.4 and 37° was 0.288 ml/hr/cm^2, which agreed with previous literature reports of different techniques. Although the diffusion through a synthetic membrane was more rapid, introduction of a nonionic surfactant enhanced the biological perfusion rate while having no significant effect on the synthetic barrier. The enhancement of the diffusion rate effected by 0.1 and 0.01% (w/v) surfactant was about twofold, rapid in onset, and not progressive, giving clearance values per square centimeter of 0.606 and 0.537 ml/hr/cm^2, respectively.

Keyphrases □ Diffusion—three-compartment apparatus developed, evaluated, and compared to other methods, synthetic membranes and isolated biological tissues studied using salicylamide □ Salicylamide—diffusion across synthetic membranes and isolated biological tissues, three-compartment apparatus developed, evaluated, and compared to other methods

Numerous methods have been devised to study the *in vitro* diffusion kinetics of drugs across biological and synthetic membranes. The most common of the biological studies involved some variation of the everted gut technique (1–6), while other systems were designed to accommodate one particular membrane (7–9). Not limited by the viability and size of living tissue, diffusion studies incorporating synthetic membranes have had more freedom in apparatus design (10–13).

Recently, Mayersohn and Suryasaputra (7) initiated studies of living tissue diffusion in an apparatus that can also accommodate synthetic membranes. Thus, both living and nonliving drug barriers can be studied under more identical conditions, the geometry of membrane placement and the mechanics of stirring being duplicated in both systems. Stirring of the serosal fluid, which cannot be readily achieved in everted guts, lends to a more uniform sampling, and elimination of eversion precludes any unnecessary damage to the tissue.

Ho (14) recently demonstrated that results obtained by the use of an apparatus such as that described by Doluisio *et al.* are, in part, dependent upon the sampling interval employed. Since the serosal compartment is not normally adequately stirred throughout the experiment, the sampling procedure in itself introduces additional stirring and enhances the diffusion. Thus, more frequently sampled experiments yield larger apparent diffusion rates. However, as mentioned previously (7, 10), the low diffusion area to recipient volume ratio is a major drawback to the diffusion cell method, the assay sample concentration being directly dependent upon this ratio.

This study concerns a modified model of the diffusion apparatus of Mayersohn and Suryasaputra (7), which allows for greater assay sensitivity (Fig. 1). The sandwiching in of the recipient cell, containing two membrane sections, with two donor cells obviously yields at least a twofold increase in diffusion area. In addition, it was possible to increase both the length and width of the diffusion window, thus exposing an even greater area to diffusion. The modified model allows for an apparent diffusion area of 5.9 cm^2, as compared to the 1.8 cm^2 achieved previously (Table I).

Since 20 ml of recipient solution was also used in this study, there was more than a threefold increase in the diffusion area–recipient volume ratio. In addition, the donor volume–diffusion area ratio was greatly increased, thus assuring a steady-state concentration gradient across the membrane. Donor solution concentrations decreased only 5.9 and 3.4% after 2-hr runs (salicylamide, 2 mg/ml) with and without surfactant, respectively.

EXPERIMENTAL

Materials—Figure 1 shows the three-compartment diffusion apparatus. The two outer donor compartments contain the appropriate mucosal solution, while the inner recipient compartment contains the serosal solution. The entire apparatus, with the exception of the securing bolts, wingnuts, and pins, was fabricated out of clear 95-mm (0.38-in.) plastic[1]. The water seal was facilitated by milling out a gasket around all four diffusion windows to give a plateau of minimal surface area.

A propeller stirrer[2] was used to agitate the recipient compartment; immersible magnetic stirrers[3], with 1.27-cm (0.5-in.) stirring bars[4], were used to stir the outer donor compartments. The removable recipient compartment cover has a silicone[5] gasket, giving a water seal when secured with small screws. The 48-mm (0.18-in.) securing bolts were set within the length of the diffusion windows so that the pressure could be distributed effectively to the mounting plateau where it is needed. [The bolts thus passed through the donor chambers *via* 63-mm (0.25-in.) diameter plastic tubing.]

The following reagent grade chemicals were employed: sodium chloride, potassium chloride, sodium bicarbonate, monobasic potassium phosphate, mercuric chloride, and ferric nitrate[6]. Salicylamide[7] (mp 140–142°) and the nonionic surfactant[8] polyoxy-

[1] Plexiglas, Rohm and Haas.
[2] Model 102, Talboy Engineering Corp.
[3] VWR Catalog No. 58947-055 (1972), Bronwill Scientific.
[4] Coated with Teflon (duPont).
[5] General Electric.
[6] Baker.
[7] Lot 711-1, Eastman Kodak.
[8] Brij 35, Lot 518, ICI American, Inc. (formerly Atlas).

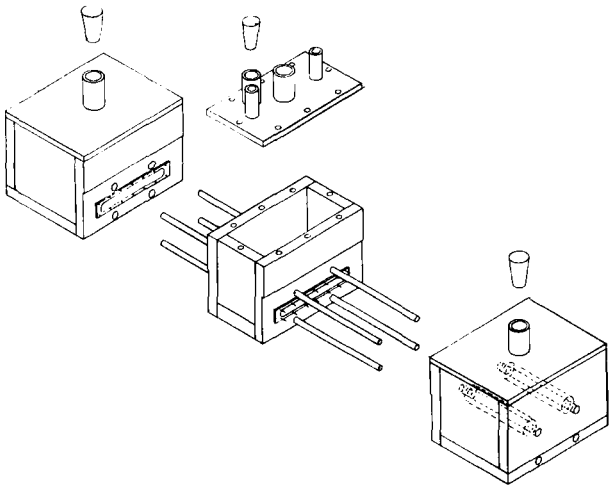

Figure 1—*Three-compartment diffusion apparatus. Inside dimensions are: outer (donor) cells, 50 × 72 × 50 mm; inner (recipient) cell, 32 × 72 × 50 mm; and diffusion windows, 5 × 70 mm.*

ethylene (23) lauryl ether (solid at room temperature) were the chemicals studied for diffusion characteristics. The gas mixtures were oxygen–carbon dioxide (95:5) and nitrogen–carbon dioxide (95:5). A regenerated cellulose[9] membrane, with a dry thickness of 2.5×10^{-3} cm (0.001 in.), was used as the synthetic membrane.

Procedure—*Living Membrane*—Male Sprague–Dawley rats (303–412 g), starved for 24 hr before use, were sacrificed in ether, and a midline abdominal incision was made to remove the small intestine at the pyloric sphincter. The intestine was immediately placed in Kreb's bicarbonate buffer, pH 7.4 (3, 5), at 10–15°; the buffer had been perfused previously with oxygen–carbon dioxide (95:5) for 20 min.

The initial 15 cm distal to the sphincter was discarded, and the first and second 10-cm sections thereafter were used for the diffusion runs. A 7-cm portion of each 10-cm section was sleeved on a rounded-end capillary tube, rinsed with buffer solution, cut lengthwise, and stretched over and secured by pins circumscribing the diffusion windows on the recipient compartment. A silicone[5] bung in the shape of the window was inserted to prevent the tissue from falling through during the mounting procedure.

After mounting the first segment with the mucosal surface facing the donor compartment, the appropriate donor cell was attached by guiding it on the bolts of the recipient compartment and securing it with wingnuts. The donor chamber was then filled with chilled buffer to bathe the tissue during the mounting of the second segment, which was treated similarly. The apparatus was then observed for 5 min to detect any mechanical or physiological leaks between compartments.

Once a good water seal was obtained, the donor compartments were rinsed and filled with buffered salicylamide solution, 2 mg/ml, previously perfused with oxygen–carbon dioxide. The compartments were then placed in a water bath maintained at 36.5 ± 1° throughout the experiment. *Via* thin polyethylene tubing[10], each compartment was constantly perfused with oxygen–carbon dioxide (washed through buffer solution) to maintain the pH at 7.4 ± 0.05. The run was commenced upon the addition of 20 ml of buffer solution to the recipient cell.

Synthetic Membrane—Regenerated cellulose, with a wet thickness of 34.7 ± 2.2 μm, was used as a comparison for the living tissue. Due to its thinness, it was necessary to use gaskets made out of plastic[11] to ensure a tight seal. Other than the use of a nitrogen–carbon dioxide (95:5) gas mixture instead of oxygen–carbon dioxide to maintain the buffer pH at 7.4, the synthetic runs were conducted in a similar fashion to the intestinal runs.

Studies on the effect of the stirring rate on the diffusion rate were conducted to optimize this important parameter in both donor and recipient compartments. An increase in the stirring rate of the recipient compartment to over 200 rpm caused an insignificant effect on the rate of drug diffusion. However, the rate was kept at about 250 rpm to ensure a homogeneous solution. Although the diffusion rate did not reach a maximum plateau value at 500 rpm in the donor compartments, the increase in diffusion was not significant enough to warrant such a high rate of stirring. A rate of 250 rpm was sufficient to minimize any stirring variance due to a fluctuation in the water pressure driving the immersible stirrers.

Table I—Comparison of Synthetic Membrane Diffusion Studies

Reference	Number of Determinations	Membrane	*RSD*, %	Temperature	Time of Experiment
10	23	Dimethyl	±6.29	37 ± 0.01°	—
12	5	Dimethyl	±7.0	37.3 ± 0.1°	8 hr
This study	12	Cellulose	±6.3	36.5 ± 1.0°	30 min

Assay—Ten-milliliter samples were taken from the recipient (serosal) compartment at 5-min intervals during the 1st hr of the run and every 10 min during the 2nd hr; the sample was replaced with 10 ml of fresh bicarbonate buffer. In calculation of transport rates, allowance was made for drug removed by sampling.

The salicylamide was assayed spectrophotometrically[12] at 540 nm and pH 1.5 using a modification of the Trinder method (15). The 10-ml samples were diluted to 25 ml with hydrochloric acid–potassium chloride buffer (pH 1.1) after the addition of 5 ml of Trinder's reagent. The samples from the intestinal studies were run through a 0.45-μm filter[13] to remove any tissue precipitate before a final adjustment to pH 1.5 was made.

A simple shake-foam test was used to detect the presence of surfactant in the serosal compartment. At the end of each diffusion study, a 5-ml serosal sample was shaken vigorously in a test tube for 5 sec and then observed; the time required for the foam to subside was noted. The results were compared with a calibration curve prepared from a range of known surfactant concentrations [1×10^{-1}–1×10^{-6}% (w/w)] in Kreb's bicarbonate buffer containing 0.2 mg/ml of salicylamide.

The foam time increased significantly for each 10-fold increment in surfactant concentration and was sensitive to 1×10^{-4}% (w/w). The foam time for a blank sample (no surfactant) was 124.6 ± 18 sec, as compared to a foam time of 4498 ± 322 sec for 0.0001% (w/v) surfactant. This difference was significant at the 99% level of confidence ($p < 0.01$).

RESULTS AND DISCUSSION

As can be seen from the data in Table I, the reproducibility of the synthetic membrane runs, with no surfactant, was equivalent to other diffusion apparatus. The reproducibility of seven intestinal runs with no surfactant compared favorably with previously reported data (Table II). Although the relative standard deviation was higher than that of everted gut studies, it compared well with the monodonor cell. The larger relative standard deviation can be explained in part by the greater age and weight variance of the rats. Rats used for the surfactant studies were younger (weighed less) and had a narrow weight range with a subsequent lower relative standard deviation, comparable with the everted intestinal studies (Table III).

As before (4, 6), there was no significant difference between the clearance rates for the 1st and 2nd hr of the intestinal runs. Thus, they were combined and included in Table III. Kreb's bicarbonate buffer was partly responsible for this effect; it has been shown to maintain biological material in a more constant and viable state than other buffer systems (5).

The surfactant's effect on the biological membrane was of rapid onset and was not progressive for at least 2 hr since the diffusion rate remained constant throughout the experiment. Current work

[9] Catalog No. 25225-260 (1972), VWR Scientific.
[10] Intramedic, Clay Adams.
[11] Parafilm, American Can Co.
[12] Perkin-Elmer 139.
[13] Millipore Corp.

Table II—Comparison of *In Vitro* Diffusion Studies Using Rat Intestine

Technique	pH of Kreb's Bicarbonate Buffer	Mucosal Surface Area, cm^2	Volume, ml: Mucosal Solution (Donor)	Volume, ml: Serosal Solution (Recipient)	Ratio of Diffusion Area to Recipient Volume	Ratio of Donor Volume to Diffusion Area	Donor Salicylamide Concentration, mg/ml	Number of Experiments	Clearance, ml/hr	Clearance, $ml/hr/cm^2$ ± *RSD*
Everted gut (3)	7.4	13.0 (7)	100	2	6.50	7.7	1.0	5	3.42	0.263 ± 4%
Single-donor cell apparatus (7)	7.4	1.79[a]	20	20	0.0894	11.2	4.0	7	0.287	0.160 ± 12%
Three-compartment apparatus (this study)	7.4 ± 0.05	5.9[a]	340	20	0.295	57.6	2.0	7	1.63	0–60 min, 0.276 ± 14.9% 60–120 min, 0.296 ± 19.3%

[a] Based on diffusion window dimensions.

Table III—Summary of Diffusion Studies Using Three-Compartment Apparatus

Membrane	Number of Experiments	Range of Rat Weights, g	Surfactant, % (w/v)	Clearance per Unit Area, $ml/hr/cm^2$: 0–60 min	60–120 min	0–120 min	Range[a]
Cellulose	12	—	0.0	1.114 ± 6.3	—	—	—
Cellulose	3	—	0.1	1.167 ± 5.2	—	—	—
Intestine	7	320–412	0.0	0.276 ± 14.9	0.296 ± 19.3	0.288 ± 16.75	—
Intestine	3	305–332	0.1	0.582 ± 7.7	0.630	0.606	0.533–0.686
Intestine	2	303–326	0.01	0.532 ± 7.2	0.538	0.537	0.505–0.553

[a] The 1st and 2nd hr are taken separately.

is being focused on the reversibility of this effect.

Wolfe *et al.* (4) showed, by removing the intestinal serosa and muscularis externa, that these tissues were the rate-limiting barriers in transport studies conducted on unstripped rat intestine. The increased diffusivity effected by the surfactant could be rationalized by either one or both of the following:

1. The surfactant increased the permeability of the muscularis externa and serosa.

2. The surfactant increased the partitioning of the drug into the inner, mucosal-side, tissue layers of the intestine, thus creating a greater concentration gradient across the muscularis externa and serosa.

The fact that the shake-foam test of recipient cell solutions showed no evidence of the surfactant's ability to cross the intestinal barrier makes the second explanation more probable.

Table II summarizes the results and pertinent apparatus parameters for the everted gut, single-donor cell, and our modified model. This study's clearance per square centimeter is more in agreement with the eversion technique than the Mayersohn cell. As mentioned previously (7), the possible distention of the everted gut would expose more of the convoluted surface to the muscosal solution, thereby increasing the clearance. Since the diffusion window was wider than in the previous cells, it was necessary to stretch the segment of intestine more during the mounting procedure, thus duplicating this distention. It was felt that stretching the tissue provided a more reproducible means of mounting, whereas it would be difficult to judge how much tissue was actually exposed in the window of an unstretched segment.

Preliminary studies were conducted on the effect of differences between the height of solutions in the donor and recipient cell on transport rates. Data obtained indicate that major effects are unlikely to be produced by variation in hydrostatic pressure. However, unless there is specific interest in investigating possible hydrostatic involvement in transport, it may be advantageous to use this apparatus with equal heights of solutions in all three compartments.

In conclusion, the economical and reproducible diffusion apparatus discussed here shows great potential for correlating *in vitro* drug diffusion between living and nonliving membranes. The increased surface area available for perfusion would make studies involving less viable tissue and/or slower diffusing drugs more amenable to current assay sensitivities. Further work is planned for other surfactant systems and drugs.

REFERENCES

(1) R. K. Crane and T. H. Wilson, *J. Appl. Physiol.*, **12,** 145(1958).

(2) T. H. Wilson and G. Wiseman, *J. Physiol.*, **123,** 116(1954).

(3) M. Mayersohn, M. Gibaldi, and B. Grundhofer, *J. Pharm. Sci.*, **60,** 1813(1971).

(4) D. Wolfe, S. C. Forland, and L. Z. Benet, *ibid.*, **62,** 200(1973).

(5) L. Z. Benet, J. M. Orr, R. H. Turner, and H. S. Webb, *ibid.*, **60,** 234(1971).

(6) M. Mayersohn and M. Gibaldi, *ibid.*, **60,** 225(1971).

(7) M. Mayersohn and K. Suryasaputra, *ibid.*, **62,** 681(1973).

(8) L. S. Shenouda and A. M. Mattocks, *ibid.*, **56,** 464(1967).

(9) A. J. Aguiar and M. A. Weiner, *ibid.*, **58,** 210(1969).

(10) G. L. Flynn and E. W. Smith, *ibid.*, **60,** 1713(1971).

(11) C. L. Olson, T. D. Sokoloski, S. N. Pagay, and D. Michaels, *Anal. Chem.*, **41,** 865(1969).

(12) E. R. Garrett and P. B. Chemburkar, *J. Pharm. Sci.*, **57,** 944(1968).

(13) A. L. Misra, A. Hunger, and H. Keberle, *J. Pharm. Pharmacol.*, **18,** 531(1966).

(14) N. Ho, paper presented at the APhA Academy of Pharmaceutical Sciences, New Orleans meeting, Nov. 1974.

(15) M. Z. Biber and C. T. Rhodes, *Clin. Chem. Acta*, **54,** 135(1974).

ACKNOWLEDGMENTS AND ADDRESSES

Received October 21, 1974, from the *Department of Pharmaceutics, State University of New York at Buffalo, Buffalo, NY 14207*

Accepted for publication July 1, 1975.

The authors acknowledge financial assistance from Merck Sharp and Dohme and Mr. Tanski for help in construction of the apparatus.

[x] To whom inquiries should be directed. Present address: Department of Pharmacy, University of Rhode Island, Kingston, RI 02881

Development of an Aerosol Dosage Form Containing Insulin

SHIH-WEI LEE * and JOHN J. SCIARRA *

Abstract □ An aerosol dosage form containing insulin was developed by suspending insulin zinc crystals in fluorocarbon propellant and using oleyl alcohol to improve the insulin suspension and to prevent valve clogging. A metered valve was used to control the amount of insulin delivered per actuation. The dose dispensed, sedimentation rate, and particle-size distribution of the aerosol formulation were evaluated. The potency of the insulin delivered from the aerosol containers stored at various temperatures and time intervals was determined using a radioimmunoassay. Based upon preliminary stability data, which were treated kinetically, it was noted that insulin aerosols stored in a refrigerator at 7° would have a predicted shelflife of approximately 19 years, whereas samples stored at 25 and 37° would have shelflives of 11 and 2 months, respectively. Long-term stability studies are indicated to establish this conclusion. On the basis of this study, it was concluded that an insulin-containing aerosol dosage form can be formulated and that a suitable dose of insulin can be dispensed using commercially available metered dose valves. The actual dose of insulin dispensed would have to be related to the degree of absorption of insulin one would normally expect when insulin is administered by the inhalation route.

Keyphrases □ Dosage forms—aerosol, insulin zinc suspension in fluorocarbon propellant, evaluation of dose dispensed, sedimentation rate, particle-size distribution, and insulin potency □ Aerosols—insulin zinc suspension in fluorocarbon propellant, evaluation of dose dispensed, sedimentation rate, particle-size distribution, and insulin potency □ Insulin zinc—aerosol dosage form, evaluation of dose dispensed, sedimentation rate, particle-size distribution, and insulin potency

Insulin, the drug of choice for diabetes mellitus, has been administered parenterally since its discovery. Clinical evidence has indicated that insulin can be delivered by inhalation, bringing about a reduction in the blood sugar level. The use of a liquefied gas as a vehicle to deliver insulin in the proper particle size and accurate dosage would make inhalation therapy simple and convenient compared to the use of atomizers or nebulizers. Since an aerosol dosage form is a self-contained complete unit, it can be used by the diabetic patient with little difficulty and should be readily acceptable for insulin administration.

The mechanism and molecular basis of action and clinical aspects of insulin were discussed previously (1). Since proteolytic enzymes inactivate the insulin molecule (2), insulin is completely ineffective when taken orally; subcutaneous injection has been the preferred route of administration. The effectiveness of insulin administered by inhalation was reported; a midget inhaler with an adapter with a narrow nozzle smaller than the opening of the patient's nostril was used (3).

In an animal study, insulin was administered in the form of fine spray (by nebulizer) to normal and hyperglycemic dogs (4), and the aerosol-administered insulin was almost as effective as a subcutaneous injection. Clinical studies were reported on the aerosol administration of insulin to human volunteers using a nebulizer[1] (5). The results indicated a hypoglycemic response in nondiabetic patients while the patients with diabetes mellitus showed an increase in plasma immunoreactive insulin and a decrease in plasma glucose concentration. It was suggested that insulin was absorbed through the respiratory mucous membrane and produced the hypoglycemic activity. Low absorption efficiency of insulin was found by the inhalation route, and approximately 10% of the aerosolized insulin was recovered based on comparisons of plasma immunoradioinsulin (6).

Methods for the *in vivo* detection of insulin have been described in the USP and by various workers (7–9). Several chromatographic methods also were reported (10–16).

The immunochemical assay (17) provided for the first time a procedure that could be used for commercial insulin. Baum *et al.* (18) modified the immunoassay method of Grodsky and Forsham (17) and Probst *et al.* (19) and reported that the method was accurate, fast, inexpensive, and specific for natural insulin.

The effect of temperature on the stability of commercial insulin preparations was studied using both a radioimmunoassay and the USP bioassay; the potency, as determined by the radioimmunoassay, compared favorably with data obtained by the USP rabbit assay (20).

The development of a suitable formulation system for an aerosol dosage form containing insulin and the physicochemical evaluation of the dosage form were the major concerns of this study. The physical evaluation of the suggested formulations was undertaken to determine the suitability of the formulation for clinical studies. Sedimentation, dose delivery, and particle-size distribution were deemed to be important aspects. In addition, the stability of the preparation under various temperature conditions was determined using a radioimmunoassay method.

EXPERIMENTAL

Insulin zinc crystals[2] USP and amorphous insulin powder were used. Each aerosol insulin preparation was formulated by adding 0.3 g (1.5%) of the appropriate insulin to a 30-ml plastic-coated glass aerosol container. A nonmetered aerosol valve (used as a closure) was crimped onto the bottle, and 19.7 g of dichlorodifluoromethane–dichlorotetrafluoroethane (50:50)[3] was added through the valve by the pressure fill method. Each aerosol was gently shaken and stored in a refrigerator at 7° for 24 hr.

Each insulin preparation was evaluated for redispersibility. Although both the insulin zinc crystals and the amorphous insulin

[1] Devilbiss Co., Toledo, Ohio.
[2] Beef insulin, Eli Lilly and Co., Indianapolis, Ind.
[3] Propellant 12/114 (50:50).

Table I—Evaluation of Selected Propellant Systems

Ingredient	Formula, % (w/w)									
	A	B	C	D	E	F	G	H	I	J
Insulin zinc crystals	2.18	2.18	2.18	2.18	2.18	2.18	2.18	2.18	2.18	2.18
Oleyl alcohol	6.54	6.54	6.54	6.54	6.54	6.54	6.54	6.54	6.54	6.54
Dichlorodifluoromethane—dichlorotetrafluoroethane (15:85)	91.28	—	—	—	—	—	—	—	—	—
Dichlorodifluoromethane—dichlorotetrafluoroethane (40:60)	—	91.28	—	—	—	—	—	—	—	—
Dichlorodifluoromethane—dichlorotetrafluoroethane (50:50)	—	—	91.28	—	—	—	—	—	—	—
Dichlorodifluoromethane—dichlorotetrafluoroethane (70:30)	—	—	—	91.28	—	—	—	—	—	—
Dichlorodifluoromethane	—	—	—	—	91.28	—	—	—	—	—
Difluoroethane	—	—	—	—	—	91.28	—	—	—	—
Monochlorodifluoroethane	—	—	—	—	—	—	91.28	—	—	—
Dichlorodifluoromethane—difluoroethane (90:10)	—	—	—	—	—	—	—	91.28	—	—
Dichlorodifluoromethane—monochlorodifluoroethane (80:20)	—	—	—	—	—	—	—	—	91.28	—
Dichlorodifluoromethane—monochlorodifluoroethane (90:10)	—	—	—	—	—	—	—	—	—	91.28
Suspension time, sec[a]	35	45	50	60	75	ND[b]	25	ND[b]	65	85

[a] Time required before first sign of settling noted. [b] ND = not dispersable.

could be easily redispersed, the insulin zinc crystals were selected for further study because this form exhibited greater redispersibility than the amorphous insulin.

To improve the suspendability of the insulin formulation, oleyl alcohol was added as a dispersing agent. Oleyl alcohol was also necessary as a lubricant for the metered valve to prevent valve clogging and to obtain uniform metering of the insulin dose. Insulin zinc (0.65 g) was accurately weighed (the amount was based on the assumption that 40 USP units of insulin would be dispensed when 70 mg of formulation was delivered through the aerosol valve) and transferred to a plastic-coated aerosol bottle. Oleyl alcohol, at levels of 5, 6.5, and 20%, was then added.

A 50-mg pressure fillable valve was crimped onto the bottle, and the propellant was added by the pressure method. The aerosols were gently shaken and stored in a refrigerator at 7° for 24 hr. The formulations were evaluated as to redispersibility immediately and at 1-, 2-, and 4-week intervals. Based upon these observations, 6.5% of oleyl alcohol was found to be suitable since the redispersion time (time necessary for the supernatant liquid to reach a value of 50%) increased from an initial value of 2.5 min to 12 min after 4 weeks.

Based upon these results, 2.18% of insulin zinc crystals and 6.5% of oleyl alcohol were used to determine the best propellant combination and concentration. Additional aerosols were prepared as previously indicated, except that varying propellant systems were used (Table I). Each aerosol was evaluated on the basis of the time required for settling to occur (Table I).

Evaluation of Formulation—On the basis of the results shown in Table I, the following formulation was selected for further study: insulin zinc crystals[4], 2.18% (w/w); oleyl alcohol[5], 6.54% (w/w); and dichlorodifluoromethane–monochlorodifluoroethane (90:10)[6], 91.28% (w/w).

Twenty grams of this formulation was placed into a 30-ml plastic-coated glass aerosol container along with the insulin zinc previously dispersed in the oleyl alcohol. The containers were purged of air by adding a few drops of propellant[3] to each container. A metered valve[7] (without a dip tube), which was previously determined to deliver approximately 70 mg of formulation or 40 units of insulin per actuation, was crimped onto each container.

Forty-eight containers were prepared, divided into three groups, and stored upright at 7, 25, and 37°. The dosage dispensed, sedimentation rate, and particle-size distribution of each sample was determined.

Dose Dispensed—Three aerosol units were tested initially and the tests were repeated for each storage condition after 24 hr and at 1-month intervals as follows. Each aerosol unit was fitted with an actuator, primed several times, and placed into a water bath at 21 ± 0.5° for at least 30 min. It was then dried, accurately weighed, actuated, and reweighed to determine the dose dispensed per actuation.

Repetitive doses were dispensed every 3 min. Ten readings for each unit were obtained; the average of 30 readings obtained at 7, 25, and 37° are shown in Fig. 1.

Sedimentation Rate—The sedimentation rate for the aerosol formulation was determined in the following manner. The outside of the plastic-coated aerosol bottles was calibrated with 10 equidistant lines. The containers were gently inverted five times to redisperse the solid. The time for the suspensoid to settle from the filling line by one, two, or more gradations was recorded, that is, the time for 10, 20%, *etc.*, of the supernatant liquid to appear.

The initial sedimentation rate was determined on the aerosol insulin samples stored at 7° for 24 hr. Monthly observations were made on the samples stored at 7, 25, and 37°. Samples stored at 7° were tested immediately after being taken from the refrigerator; samples stored at 25 and 37° were tested after being in a water bath at 21° for 30 min. The results shown in Table II represent the average of three determinations on each of three containers.

Particle-Size Analysis of Insulin Aerosols—The particle-size distribution of the aerosol insulin was determined by an impaction technique[8]. The sampling chamber (21, 22) was made from a 1000-ml round-bottom flask with an opening extending 45° to the body of the flask. An opening of approximately 7.6 cm was made in the bottom of the flask. The neck of the flask was about 4.4 cm in

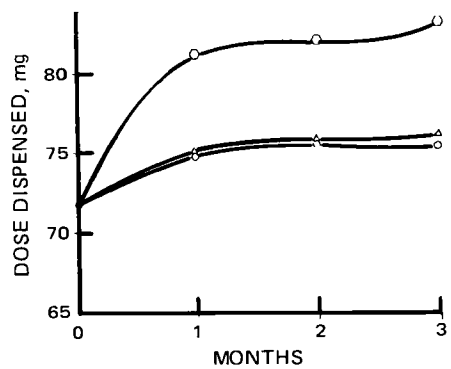

Figure 1—*Comparison of dose dispensed of insulin aerosols stored at different temperatures. Key:* ○, 7°; △, 25°; *and* ○, 37°.

[4] Lot 7AP06H, potency of 25.9 units/mg, Eli Lilly and Co.
[5] Adol 90, Lot 2237-M654-400, Ashland Chemical Co.
[6] Genetron 12/142b (90:10), Allied Chemical Co., Industrial Chemicals Division, New York, N.Y.
[7] B18F, 0.020 stainless steel stem, 50-mg housing, Neoprene gasket, VCA Inc., Bridgeport, Conn.
[8] Cascade impactor model DCI-6, Delron Research Products Co., Powell, Ohio.

Table II—Sedimentation of Aerosol Insulin Formulation at Varying Temperatures

Storage Time, Months	Supernatant Liquid, %	Time Required[a], min		
		7°	25°	37°
Initial	10	4.6	4.6	4.6
	20	5.7	5.7	5.7
	30	6.5	6.5	6.5
1	10	8.1	8.1	1.4
	20	13.6	2.3	1.7
	30	15.1	3.0	2.4
2	10	11.6	1.2	1.0
	20	15.3	1.5	1.5
	30	17.5	2.2	2.0
3	10	6.4	1.2	0.9
	20	9.5	1.6	1.3
	30	12.5	2.3	1.9

[a] Time required for 10%, 20%, *etc.*, of supernatant liquid to appear after gently shaking five times. Values are the averages of three determinations on each of three containers.

diameter, and its far end was slightly narrowed with an opening of 3.8 cm.

Samples were brought to ambient room temperature (23–25°). The impactor slides were accurately weighed and assembled in the impactor, and a vacuum of 44 cm Hg was applied. The weight of a sample was determined by weighing the aerosol container before and after removal of the sample.

Each container was fitted with an oral adapter, and the aerosol was actuated nine to 15 times into the sampling chamber. The time interval between each actuation was 20 sec so as to allow all of the sprayed sample to be drawn into the impactor. The vacuum was continued for 1 min after the last actuation and then slowly released. The glass slides were removed and accurately weighed to determine the difference in weight. This weight represented the amount of material deposited at each stage and is related to the particle size. The results shown in Table III represent the average of two determinations on each sample.

Preparation of Reagents for Radioassay—The dose of insulin delivered upon dispensing of the aerosol formulation stored at different temperatures and at intervals of 1, 2, and 3 months was determined by a radioimmunoassay[9]. Each kit contained the following reagents in 10-ml vials.

Buffer Solution—The buffer was dissolved in 200 ml of redistilled water and provided a pH 7.4 solution.

Dextran Gel[10]–Anti-Insulin Complex—The content of the vial was quantitatively transferred to a beaker containing a magnetic stirring rod. The vial was rinsed with 100 ml of the buffer solution in several portions, and the rinsings were added to the beaker with gentle and continuous stirring to form a homogeneous suspension.

Insulin Standard Solution—A lyophilized insulin standard, having an activity of 320 μunits/ml, was reconstituted in 4.0 ml of redistilled water.

Labeled Insulin Reagent—The lyophilized ^{125}I-insulin was reconstituted by adding 10 ml of the buffer solution.

Preparation of Standard Solution—The insulin standard solution was diluted with buffer to obtain suitable concentrations of insulin within the range of 3–320 μunits/ml.

Radioimmunoassay—*Dilution of Insulin Aerosol Formulation*—Serial dilutions of the aerosol formulation were required so that the strength of each dose would be within the range for the radioimmunoassay. A transfer device consisting of 13-gauge stainless steel tubing, 8.3 cm in length and affixed to an actuator, was used. A diluting solution of 0.005 *N* HCl at pH 2.5 and 0.1% bovine albumin was prepared.

The aerosol insulin preparations stored at 7, 25, and 37° were placed in a water bath at 21 ± 0.5° for 30 min. The samples were weighed and fitted with the transfer device. The aerosol was gently agitated and actuated once into approximately 200 ml of cold 0.0005 *N* HCl in a 300-ml beaker, which also contained a magnetic stirring rod. The actuator and transferring device were removed and rinsed with 0.0005 *N* HCl, and the rinsing was placed into the beaker.

[9] Phodebas insulin test kit, Pharmacia Laboratory Inc., Piscataway, N.J.
[10] Sephadex.

Table III—Particle-Size Distribution of Insulin Aerosol

Storage Time, Months	Particle Size, μ	Cumulative Weight Percent		
		7°	25°	37°
Initial	1.0	3.0	3.0	3.0
	2.0	14.7	14.7	14.7
	4.0	39.4	39.4	39.4
	8.0	74.3	74.3	74.3
	16.0	100	100	100
1	1.0	2.5	2.4	3.3
	2.0	10.0	12.1	15.7
	4.0	31.7	34.7	40.7
	8.0	66.2	66.9	72.9
	16.0	100	100	100
2	1.0	3.2	2.4	2.3
	2.0	13.5	12.1	13.2
	4.0	36.8	34.1	38.0
	8.0	69.5	68.6	72.1
	16.0	100	100	100
3	1.0	3.0	2.8	3.5
	2.0	13.1	13.3	15.8
	4.0	35.1	34.1	40.8
	8.0	67.6	68.4	73.9
	16.0	100	100	100

The aerosol container was reweighed so as to determine the weight of product expelled by one actuation. Then the solution was brought to room temprature and gently stirred for approximately 20 min using a magnetic stirrer. This procedure ensured the removal of any remaining propellant. The acid solution was transferred to a 500-ml volumetric flask. The beaker containing the solution was rinsed twice with about 100 ml of 0.005 *N* HCl, and the rinsings were added to the 500-ml volumetric flask and brought to volume with 0.005 *N* HCl.

A 0.5-ml aliquot of this solution was pipetted into a 25-ml volumetric flask and diluted to volume with 0.005 *N* HCl. This dilution then became the acid stock solution of insulin aerosol to be assayed. A 0.1-ml aliquot of the acid insulin stock solution was pipetted into 5 ml of the buffer contained in a test tube and gently stirred. This buffer dilution is referred to as the "unknown" in the radioimmunoassay. One aerosol unit from each of the three storage temperatures was treated in a similar manner. The procedure was then repeated on samples stored for 1, 2, and 3 months at these temperatures.

Dilution of Raw Insulin Zinc—About 1.2 mg of insulin zinc was accurately weighed and diluted in 0.005 *N* HCl. This diluted acid stock solution of the raw insulin zinc was also referred to as the "unknown" for further use in the radioimmunoassay. This solution was used as the standard when the potency of the insulin zinc used to prepare the aerosol formulation was determined.

Test Procedure for Radioimmunoassay—Sufficient plastic centrifuge tubes with round bottoms were labeled for duplicate assays of Standards A–H (Series 1) and the unknowns (Series 2). The radioimmunoassay procedure follows.

A 0.1-ml aliquot of Standards A–H, each one in duplicate, was pipetted into the tubes in Series 1. A 0.1-ml aliquot of each unknown, each one in duplicate, was pipetted into tubes in Series 2. A 0.1-ml aliquot of the ^{125}I-insulin solution was pipetted into each of the tubes in Series 1 and 2. A 1.0-ml aliquot of dextran gel–anti-insulin complex suspension was pipetted into each tube in Series 1 and 2. The suspension was stirred slowly and continuously to avoid foaming.

The tubes in Series 1 and 2 were stoppered and incubated overnight at room temperature by placing the tubes horizontally in a shaker[11]. The tubes in Series 1 and 2 were centrifuged at 2000×*g* for 2 min to remove droplets from the stoppers, and the stoppers were then removed.

The centrifugation was repeated, and the supernatant liquid was cautiously aspirated to approximately 5 mm from the bottom of each tube in Series 1 and 2. For this purpose, a collared suction nozzle coupled to a water aspirator was used. The collar was adjusted vertically to the correct height to avoid removal of particles.

The washing procedure was performed by adding 2 ml of 0.9% saline to each tube, centrifuging the tubes at 2000×*g* for 2 min,

[11] Radioimmunoassay shaker, Labindustries, Inc., Berkeley, Calif.

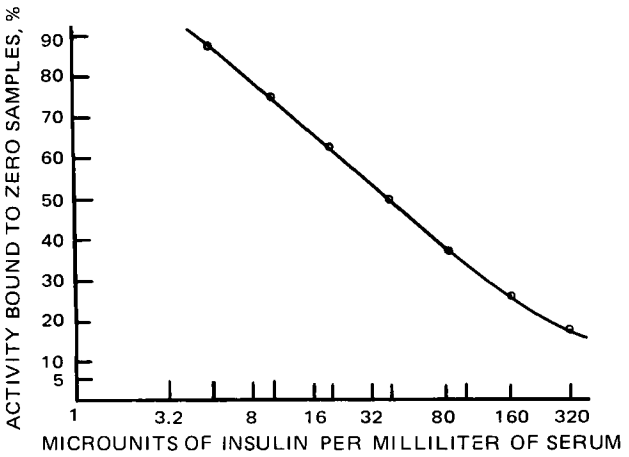

Figure 2—*Standard curve for radioimmunoassay of insulin aerosols: initial and 1-month samples.*

and withdrawing the supernatant liquid as just described. This washing procedure was performed three times, and the tubes were then stoppered.

The radioactivity in each tube in Series 1 and 2 was determined by using a gamma counter[12] set at a counting time of 4 min. The background radioactivity was checked by using an empty centrifuge tube.

Calculations—The mean count rate (*MCR*) for each standard was expressed as a percentage of the mean count rate of the "zeros." The background count was subtracted if significant. The percentage values of the mean count rate obtained for the insulin standards were plotted against the logarithm of insulin concentration on linear logarithmic paper, and a standard curve was constructed. The mean count rate for each "zero" and unknown was expressed in the same way as for the standards.

The concentration of insulin was read directly from the curve (microunits per milliliter) for each unknown sample. The value obtained was then multiplied by the dilution factor (1,250,000) to determine the amount of insulin delivered by one actuation of the aerosol. The results shown in Fig. 2 and Table IV represent the average of two determinations for each assay result.

RESULTS AND DISCUSSION

To improve the suspension of the insulin zinc crystals in the fluorocarbons, oleyl alcohol was added to the formulation. This dispersing agent served to wet the insulin zinc crystals, and its effectiveness was probably due to adsorption at the air–liquid and the solid–liquid interfaces, thereby reducing the contact angle and resulting in an improvement of wetting of the particles. Since each insulin particle was coated with a thin film of oleyl alcohol, which is miscible with fluorocarbons, this wetting process enhanced the dispersion of insulin zinc crystals in the fluorocarbons.

Furthermore, oleyl alcohol acts as a lubricant for the valve, thus preventing valve clogging. The quantity of oleyl alcohol used in this study was rather high. Lower percentages of the material resulted in a greater degree of caking of the insulin. By further reducing the particle size of the insulin, one possibly can reduce the amount of oleyl alcohol.

A preliminary study indicated that about 6.5% of oleyl alcohol would allow the insulin zinc to remain suspended for a long period when dichlorodifluoromethane was used as the propellant. However, further studies indicated that a blend of dichlorodifluoromethane–monochlorodifluoroethane (90:10) exhibited an even greater degree of suspension then dichlorodifluoromethane. This enhanced performance was attributed to the lower density of dichlorodifluoromethane–monochlorodifluoroethane than the density of dichlorodifluoromethane, so that the suspensoid was easier to suspend in the system and the duration of full suspension was longer. In addition, the combination of propellants is more polar than the pure propellant alone, thereby enhancing suspension. While other combinations of propellants could be used, this combination was best suited for the combination of insulin and oleyl alcohol.

[12] Gammacord-Ames Co., Division of Miles Labs., Elkhart, Ind.

Table IV—Summary of Radioimmunoassay Results of Insulin Aerosol

Samples	Amount Sampled, mg	Theoretical Insulin, Units	Recovery		Stability, %
			Units	%	
Insulin zinc (standard)	1.79	46.36	39.88	86.02	92.54
Initial	64.30	36.31	33.75	92.95	100.00
7°, 1 month	75.10	42.40	36.25	85.50	91.98
2 months	76.60	43.32	38.75	89.45	96.23
3 months	76.10	42.97	39.50	91.92	98.89
25°, 1 month	76.10	43.02	38.25	88.91	95.65
2 months	76.90	43.42	38.13	87.82	94.48
3 months	78.80	44.49	38.75	87.10	93.70
37°, 1 month	83.10	46.92	41.00	87.38	94.00
2 months	84.60	47.76	37.63	78.79	84.76
3 months	83.30	47.03	36.25	77.08	82.93

As can be seen from Fig. 1, the weight of formulation dispensed per actuation of the metered valve increased after 1 month. The metering tank of the valves used in this study was made of plastic, and the slight increase in weight dispensed may have been due to the swelling effect of the formulation on the plastic housing. However, the effect was pronounced with samples stored at 37° for 1–3 months; a combination of a swelling effect and heat upon the plastic housing probably caused it to expand, resulting in a greater weight dispensed. This could be avoided through use of a metered valve with a stainless steel housing or metering tank.

Statistical treatment of the data shown in Fig. 1 indicated that uniform dose dispensing was obtained in the aerosol preparations stored at 7 and 25°. Mean values of the results obtained over 3 months were in the range of 71.9–76.5 mg/dose with a standard deviation of 0.73–2.50 mg/dose. Over this 3-month stability study, the insulin units delivered per actuation ranged from an initial 40.6 to 43.2 USP units/dose at the end of the 3rd month; the highest standard deviation was ±1.41 USP units.

This satisfactory result can be seen easily from a plot obtained when the mean of each value was plotted against time (Fig. 1). The plot for 25° almost overlapped the plot for 7°. The paired t-test for significant difference indicated that there was no significant difference at the 95% confidence level between the doses dispensed of aerosols stored at 7° and those stored at 25° over 3 months (at n = 2, t = 2.410, which is less than the distribution of t = 4.303 at the 0.05 probability level).

The samples stored at 37° had a wider variation of dose dispensed over 3 months. The dose ranged from 71.9 mg initially to 83.2 mg at the end of the 3rd month. The highest standard deviation was ±6.78 mg/dose. The dose ranged from an initial 40.6 to 46.9 USP insulin units delivered per dose at the end of the 3rd month; the standard deviation was ±3.83 USP units/dose. The paired t-test for significant difference indicated the t value of 17.759 at two degrees of freedom was far greater than the t value of 4.303 at the 0.05 probability level. This finding indicates that there was a significant difference between the dose dispensed from aerosols stored at 37° and that of those stored at 7° over the 3-month period.

An increase in the sedimentation rate (decrease in suspension time) was observed with the aerosols stored at higher temperatures (25 and 37°). A large difference in suspension time was noticed when these samples were compared with times of samples stored at 7° (Table II). The longer suspension time, which occurred in the 7° samples, probably was due to the gradual decrease in the density of the propellant blend. At first, in samples stored in a refrigerator, the density of the propellant blend was heavier than that of the suspensoid (insulin zinc dispersion in oleyl alcohol). The suspensoid was lighter and floated to the top.

When a sample was taken out of the refrigerator, the sample temperature rose gradually to ambient temperature, and the density of the propellant blend decreased with an increase in temperature. At one point, the density of the propellant blend became equal to that of the suspensoid, which would aid in helping the suspended solids. As the temperature approached room temperature, the density of the propellant became less than that of the sus-

pensoid, resulting in an increase in sedimentation rate. This phenomenon provided a longer suspension time for the insulin aerosol when the aerosol was used immediately after being removed from the refrigerator.

The particle-size distribution of the insulin aerosols was determined. A cutoff point was made at the 16-μm level, since particles with a diameter of less than 10 μm are more significant for inhalation therapy; this figure also represents the upper limit of this technique. As indicated by Porush *et al.* (23), the optimum particle diameter for penetration into the pulmonary system is between 0.5 and 7 μm. Therefore, further analysis of the data of particle-size distribution (Table III) indicated that approximately 65–75% of the total sprayed insulin particles would have a particle size below 8 μm.

The "percent deposited" represents the percent of the total sprayed insulin that deposited on the lower four slides of the impactor, which, in turn, corresponded to a particle size of 1.0–8.0 μm. Particles in this size range can penetrate deep into the lungs and produce a biological effect. Therefore, if a higher percentage deposited would be more desirable, the particle size of insulin zinc crystals should be reduced further.

Table IV indicates a recovery of insulin by the radioimmunoassay method of 77–93%. The percentage of recovery was based on the assay result and its theoretical value. The low recovery also occurred in the initial assay of insulin zinc crystals and was due to normal assay variation. The variation is, however, within the limits established by the USP for insulin with a 95% fiducial limit of 87–115%. This assay variation for a single assay in this study was found to be ±6.54% at the 95% confidence level.

The precision of the radioimmunoassay was influenced by two major sources: (*a*) the variation encountered in preparing the standard curve, which was largely dependent upon volumetric errors and incomplete washing; and (*b*) the variation that occurred due to the diluting procedure and that attributed to the huge dilution factor in the successive dilution of insulin aerosols. Incomplete washing would be experienced if the washing procedure was performed twice instead of three times or if the collared suction nozzle was not placed deep enough to remove the unbound portion. If the nozzle was placed too deep, the dextran gel particles would then be removed. A lower count rate would result.

Another variation experienced during the dilution process of the insulin aerosol was the adsorption of insulin onto the glass walls. Since all volumetric flasks and beakers were made of Pyrex glass, the chance for insulin adsorption was relatively high. Therefore, 0.1% of bovine albumin was added to the diluent. The bovine albumin served as protein to precoat the glass walls and thus minimize insulin adsorption.

Within the scope of this study and in recognition of assay variations, the radioimmunoassay data demonstrated that insulin aerosols stored at 7° remained stable over 3 months while insulin aerosols stored at 25° showed some drop in potency. Samples stored at 37° showed a decline in potency. Based on percent stability, declines in potency of 6.0, 15.2, and 17.2% were observed in the 1st, 2nd, and 3rd months of storage, respectively, at 37°. However, for the purpose of predicting shelflife, the results of the radioimmunoassay for the insulin aerosols were analyzed using chemical kinetics.

Since the decomposition reaction was noted to follow first-order kinetics, the chemical stability of the insulin aerosol could be determined using the following equation:

$$\log \frac{C_0}{C} = \frac{kt}{2.303} \qquad \text{(Eq. 1)}$$

where C_0 is the initial potency, C is the potency at time t, and k is the rate constant.

According to the least-squares method and linear regression analysis, a new set of values for C_0 and C (in terms of percent stability) were calculated (Table V). By using the new values for C_0 and C in the analysis, estimates for $k_{7°}$, $k_{25°}$, and $k_{37°}$ were calculated according to Eq. 1.

The $k_{7°}$ result had a negative value, indicating an increase in potency with time. Apparently, this increase was due to the variation within the assay. Therefore, a better estimation for $k_{7°}$ can be obtained by the Arrhenius equation:

$$\log \frac{k_2}{k_1} = \frac{E_a(T_2 - T_1)}{2.303R(T_2T_1)} \qquad \text{(Eq. 2)}$$

Table V—Regression Analysis of Radioimmunoassay Results[a]

Storage Conditions of Samples	Stability, %	
	Original Values	New Values
7°, 1 month	91.98	92.245
2 months	96.23	95.700
3 months	98.89	99.155
25°, 1 month	95.65	95.585
2 months	94.48	94.610
3 months	93.70	93.635
37°, 1 month	94.00	92.765
2 months	84.76	87.230
3 months	82.93	81.695

[a] Data derived from results reported in Table IV.

where R is the gas constant, T is the absolute temperature, E_a is the energy of activation, and k_1 and k_2 are specific rate constants at T_1 and T_2, respectively.

In this case, E_a should first be calculated by using the known values for $k_{37°}$ and $k_{25°}$. Then the value for $k_{7°}$ should be calculated by using the known values for $k_{25°}$ and E_a. The results are as follows: $k_{25°} = 9.9 \times 10^{-3}$ (month^{-1}), $k_{37°} = 6.3 \times 10^{-2}$ (month^{-1}), $E_a = 28.3$ kcal/mole, and $k_{7°} = 4.58 \times 10^{-4}$ (month^{-1}).

Once the rate constant (k) is obtained, it can be used to estimate the time required for 10% of the insulin aerosol to degrade. This $t_{10\%}$ value is regarded as the shelflife of the product and can be calculated from:

$$t_{10\%} = \frac{0.104}{k} \qquad \text{(Eq. 3)}$$

Therefore, by using Eq. 3, the predicted shelflife of the insulin aerosol would be 19 years at 7°, 11 months at 25°, and only 2 months at 37°. The long predicted shelflife at 7° indicates that the insulin aerosol should be stored in a refrigerator. However, these predictions are based upon preliminary results obtained by assaying a limited number of samples. Additional samples should be studied under accelerated conditions and long-term storage.

SUMMARY AND CONCLUSIONS

Based upon the results obtained in this study, it was concluded that a stable aerosol dosage form containing insulin could be developed by suspending insulin zinc crystals in a propellant system with the aid of a dispersant and that this aerosol should be stored in a refrigerator. The dose dispensed per actuation was in the range of 40–43 USP insulin units for the samples stored at 7 and 25° while a higher dose was dispensed from the samples stored at 37°.

The particle-size distribution measured by the impactor was reliable and reproducible as long as the operating conditions were standardized. Approximately 65–75% deposition was obtained with the insulin aerosol stored at 7 and 25°. This percent deposited was defined as the percentage of total sprayed drug with particle diameters of 1–8 μm and able to penetrate deep into the pulmonary cavity to produce a biological effect.

As indicated by the radioimmunoassay, insulin zinc crystals can be formulated into an aerosol system and remain stable. The results indicated that the insulin potency of samples at 7 and 25° remained unchanged over 3 months. However, a decline in potency was noticed with the samples stored at 37° for 3 months. This decline would be simply due to the effect of heat on the insulin. No chemical incompatibilities between insulin zinc and oleyl alcohol or the propellant system were deduced from the results of the chemical stability study.

REFERENCES

(1) The American Diabetes Association, "Proceedings of 50th Anniversary Insulin Symposium," Indianapolis, Ind., 1971.

(2) "The Pharmacological Basis of Therapeutics," L. Goodman and A. Gilman, Eds., Macmillan, New York, N.Y., 1955, p. 1620.

(3) A. A. Ayer, *Antiseptic*, **51**, 1161(1954).

(4) A. R. Govinda-Rao, *Indian J. Physiol. Pharmacol.*, **3**, 161(1959).

(5) R. H. Waldman, T. C. Shipp, S. H. Wood, J. H. London, and F. M. Wigley, *Diabetes*, **20**, 552(1971).
(6) S. A. Berson and R. S. Yellow, *Methods Biochem. Anal.*, **12**, 69(1968).
(7) "The United States Pharmacopeia," 18th rev., Mack Publishing Co., Easton, Pa., 1970, p. 882.
(8) D. F. Waugh, R. E. Thompson, and R. J. Weimer, *J. Biol. Chem.*, **185**, 85(1950).
(9) G. M. Grodsky, *Biochem. J.*, **68**, 142(1958).
(10) R. R. Porter, *ibid.*, **53**, 320(1953).
(11) J. Porath and C. H. Li, *Biochim. Biophys. Acta*, **13**, 268(1954).
(12) W. Dickinson, *Nature*, **178**, 994(1956).
(13) F. A. Robinson and K. L. A. Fehr, *Biochem. J.*, **52**, 298(1952).
(14) G. Grodsky and H. Tarver, *Nature*, **177**, 223(1956).
(15) A. Light and M. V. Simpson, *ibid.*, **177**, 225(1956).
(16) E. L. Fenton, *Biochem. J.*, **71**, 507(1959).
(17) G. M. Grodsky and P. H. Forsham, *J. Clin. Invest.*, **39**, 1070(1960).
(18) W. E. Baum, W. F. Brown, and R. E. Crabtree, *J. Pharm. Sci.*, **53**, 738(1964).
(19) G. W. Probst, W. F. Brown, and H. J. Henry, *ibid.*, **55**, 1408(1966).
(20) W. O. Storvick and H. J. Henry, *Diabetes*, **17**, 499(1968).
(21) J. J. Sciarra, P. McGinly, and L. Izzo, *J. Soc. Cosmet. Chem.*, **22**, 385(1969).
(22) J. J. Sciarra and D. Adelman, *ibid.*, **22**, 867(1971).
(23) I. Porush, C. Thiel, and J. Young, *J. Amer. Pharm. Ass., Sci. Ed.*, **49**, 70(1960).

ACKNOWLEDGMENTS AND ADDRESSES

Received November 29, 1974, from the *Brooklyn College of Pharmacy, Long Island University, Brooklyn, NY 11216*, and the *College of Pharmacy and Allied Health Professions, St. John's University, Jamaica, NY 11439*

Accepted for publication June 26, 1975.

Presented at the Industrial Pharmaceutical Technology Section, APhA Academy of Pharmaceutical Sciences, New Orleans meeting, November 13, 1974.

Abstracted in part from a dissertation submitted by S.-W. Lee to St. John's University in partial fulfillment of the Doctor of Philosophy degree requirements.

The authors acknowledge the aid received from Dr. Edward Cheng in carrying out the radioimmunoassay of insulin.

* Present address: Pfizer, Inc., Brooklyn, N.Y.

ˣ To whom inquiries should be directed (at the Brooklyn College of Pharmacy).

Effect of Thermal Gelation on Dissolution from Coated Tablets

JOSEPH B. SCHWARTZ ˣ and THEODORE P. ALVINO *

Abstract □ Tablets with a methylcellulose coating were found to exhibit lower dissolution profiles than those coated with a hydroxypropyl methylcellulose coating at 37°, and the cause was investigated. The differences are attributed to thermal gelation of the methylcellulose at temperatures near 37°, which creates a barrier to the dissolution process and essentially changes the dissolution mechanism. This mechanism is substantiated by the fact that at temperatures below the gel point and at increased agitation, the effect disappears. The retarded dissolution effect is not peculiar to the drug involved.

Keyphrases □ Thermal gelation—effect on dissolution of methylcellulose-coated tablets □ Dissolution—methylcellulose-coated tablets, effect of thermal gelation □ Dosage forms—tablets, methylcellulose coated, effect of thermal gelation on dissolution □ Methylcellulose—tablet coating, effect of thermal gelation on dissolution

Polymers, particularly the cellulose polymers, are used in pharmacy as film formers for tablet coatings and as binding agents in a granulation step.

During the development of a coated tablet, several different polymers may be evaluated for various properties and their effects on the dosage form. Ideally, unless applied for a specific purpose, the coating used for a drug delivery system should not affect the efficiency with which the drug is delivered to the target site (1).

During a coating investigation, it was observed that identical core tablets coated with two different polymers exhibited widely different dissolution profiles. Differences in the polymers, methylcellulose[1] and hydroxypropyl methylcellulose[2], were investigated in an attempt to rationalize the observed dissolution differences.

EXPERIMENTAL

Core tablets containing the following components were prepared by standard direct compression techniques: dibasic calcium phosphate dihydrate, lactose USP, starch USP, purified wood cellulose[3], colloidal silicon dioxide[4], stearic acid, and magnesium stearate. Active ingredients included either aspirin or amitriptyline hydrochloride.

The coating consisting of only the polymer, and a yellow lake was applied by normal film-coating techniques. Approximately 2.9 mg of polymer was deposited per tablet. Dissolution measurements were carried out in the USP apparatus at 150 rpm, unless noted otherwise, in 0.1 *N* HCl. Solubility was measured according to the USP procedure.

RESULTS AND DISCUSSION

The dissolution profiles (Fig. 1) for the aspirin core tablet and the two corresponding coated tablets at 37° illustrate the difference in the methylcellulose coating. Aside from the lag time for the tablet coated with the hydroxypropyl polymer, the profile parallels that of the core tablet. The methylcellulose-coated tablet exhibits a slower release profile.

[1] Methocel MC 25 cps.
[2] Methocel 60 HG.
[3] Solka-Floc, B.W. 2030.
[4] Cab-O-Sil.

(5) R. H. Waldman, T. C. Shipp, S. H. Wood, J. H. London, and F. M. Wigley, *Diabetes*, **20**, 552(1971).
(6) S. A. Berson and R. S. Yellow, *Methods Biochem. Anal.*, **12**, 69(1968).
(7) "The United States Pharmacopeia," 18th rev., Mack Publishing Co., Easton, Pa., 1970, p. 882.
(8) D. F. Waugh, R. E. Thompson, and R. J. Weimer, *J. Biol. Chem.*, **185**, 85(1950).
(9) G. M. Grodsky, *Biochem. J.*, **68**, 142(1958).
(10) R. R. Porter, *ibid.*, **53**, 320(1953).
(11) J. Porath and C. H. Li, *Biochim. Biophys. Acta*, **13**, 268(1954).
(12) W. Dickinson, *Nature*, **178**, 994(1956).
(13) F. A. Robinson and K. L. A. Fehr, *Biochem. J.*, **52**, 298(1952).
(14) G. Grodsky and H. Tarver, *Nature*, **177**, 223(1956).
(15) A. Light and M. V. Simpson, *ibid.*, **177**, 225(1956).
(16) E. L. Fenton, *Biochem. J.*, **71**, 507(1959).
(17) G. M. Grodsky and P. H. Forsham, *J. Clin. Invest.*, **39**, 1070(1960).
(18) W. E. Baum, W. F. Brown, and R. E. Crabtree, *J. Pharm. Sci.*, **53**, 738(1964).
(19) G. W. Probst, W. F. Brown, and H. J. Henry, *ibid.*, **55**, 1408(1966).
(20) W. O. Storvick and H. J. Henry, *Diabetes*, **17**, 499(1968).
(21) J. J. Sciarra, P. McGinly, and L. Izzo, *J. Soc. Cosmet. Chem.*, **22**, 385(1969).
(22) J. J. Sciarra and D. Adelman, *ibid.*, **22**, 867(1971).
(23) I. Porush, C. Thiel, and J. Young, *J. Amer. Pharm. Ass., Sci. Ed.*, **49**, 70(1960).

ACKNOWLEDGMENTS AND ADDRESSES

Received November 29, 1974, from the *Brooklyn College of Pharmacy, Long Island University, Brooklyn, NY 11216*, and the *College of Pharmacy and Allied Health Professions, St. John's University, Jamaica, NY 11439*

Accepted for publication June 26, 1975.

Presented at the Industrial Pharmaceutical Technology Section, APhA Academy of Pharmaceutical Sciences, New Orleans meeting, November 13, 1974.

Abstracted in part from a dissertation submitted by S.-W. Lee to St. John's University in partial fulfillment of the Doctor of Philosophy degree requirements.

The authors acknowledge the aid received from Dr. Edward Cheng in carrying out the radioimmunoassay of insulin.

* Present address: Pfizer, Inc., Brooklyn, N.Y.

ˣ To whom inquiries should be directed (at the Brooklyn College of Pharmacy).

Effect of Thermal Gelation on Dissolution from Coated Tablets

JOSEPH B. SCHWARTZ ˣ and THEODORE P. ALVINO *

Abstract □ Tablets with a methylcellulose coating were found to exhibit lower dissolution profiles than those coated with a hydroxypropyl methylcellulose coating at 37°, and the cause was investigated. The differences are attributed to thermal gelation of the methylcellulose at temperatures near 37°, which creates a barrier to the dissolution process and essentially changes the dissolution mechanism. This mechanism is substantiated by the fact that at temperatures below the gel point and at increased agitation, the effect disappears. The retarded dissolution effect is not peculiar to the drug involved.

Keyphrases □ Thermal gelation—effect on dissolution of methylcellulose-coated tablets □ Dissolution—methylcellulose-coated tablets, effect of thermal gelation □ Dosage forms—tablets, methylcellulose coated, effect of thermal gelation on dissolution □ Methylcellulose—tablet coating, effect of thermal gelation on dissolution

Polymers, particularly the cellulose polymers, are used in pharmacy as film formers for tablet coatings and as binding agents in a granulation step.

During the development of a coated tablet, several different polymers may be evaluated for various properties and their effects on the dosage form. Ideally, unless applied for a specific purpose, the coating used for a drug delivery system should not affect the efficiency with which the drug is delivered to the target site (1).

During a coating investigation, it was observed that identical core tablets coated with two different polymers exhibited widely different dissolution profiles. Differences in the polymers, methylcellulose[1] and hydroxypropyl methylcellulose[2], were investigated in an attempt to rationalize the observed dissolution differences.

EXPERIMENTAL

Core tablets containing the following components were prepared by standard direct compression techniques: dibasic calcium phosphate dihydrate, lactose USP, starch USP, purified wood cellulose[3], colloidal silicon dioxide[4], stearic acid, and magnesium stearate. Active ingredients included either aspirin or amitriptyline hydrochloride.

The coating consisting of only the polymer, and a yellow lake was applied by normal film-coating techniques. Approximately 2.9 mg of polymer was deposited per tablet. Dissolution measurements were carried out in the USP apparatus at 150 rpm, unless noted otherwise, in 0.1 *N* HCl. Solubility was measured according to the USP procedure.

RESULTS AND DISCUSSION

The dissolution profiles (Fig. 1) for the aspirin core tablet and the two corresponding coated tablets at 37° illustrate the difference in the methylcellulose coating. Aside from the lag time for the tablet coated with the hydroxypropyl polymer, the profile parallels that of the core tablet. The methylcellulose-coated tablet exhibits a slower release profile.

[1] Methocel MC 25 cps.
[2] Methocel 60 HG.
[3] Solka-Floc, B.W. 2030.
[4] Cab-O-Sil.

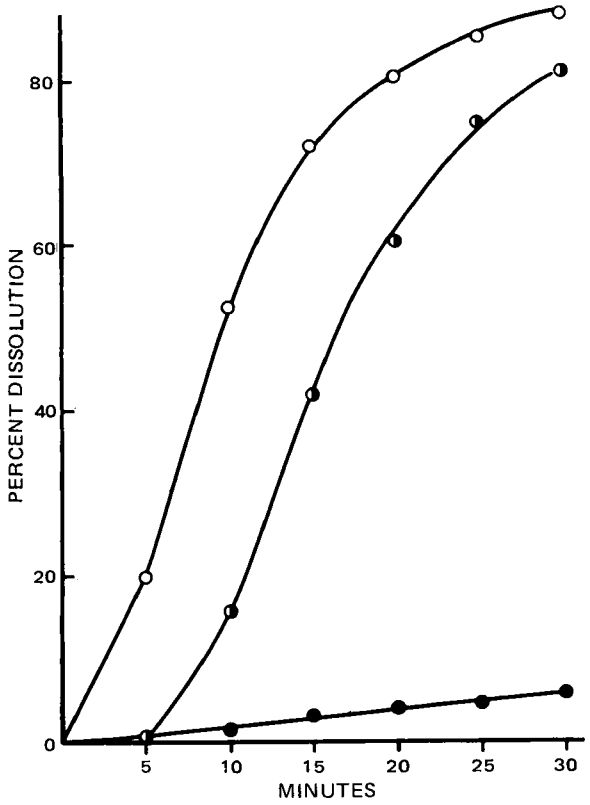

Figure 1—*Dissolution profiles for aspirin tablets at 37°. Key:* ○, *core tablet;* ◑, *hydroxypropyl methylcellulose coating; and* ●, *methylcellulose coating.*

Although both polymers are water soluble and the coating should not interfere with the dissolution process, these products do exhibit the property of thermal gelation, the phenomenon of gelation resulting from the application of heat. According to the product information (2), solutions of these cellulose derivatives gel on heating, whereas other gums, such as gelatin, gel only on cooling. Thermal gelation of these materials is a function of (among other factors) temperature and the type and concentration of polymer used.

If thermal gelation does occur, the gel formed by the tablet coating material may create a barrier to the dissolution process, *i.e.*, a change in the mechanism caused by a diffusion layer of polymer gel or by a very viscous polymer solution as it approaches the gel state. As the temperature of a methylcellulose solution is raised, hazing of the solution occurs just prior to gelation and viscosity may start to rise (2).

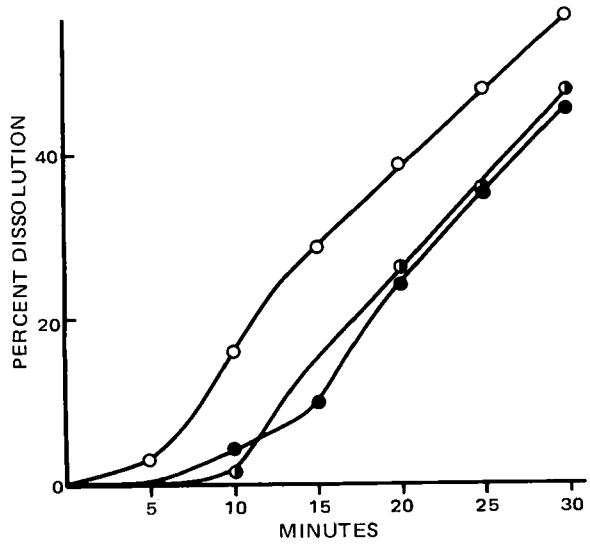

Figure 2—*Dissolution profiles for aspirin tablets at 21°. Key:* ○, *core tablet;* ◑, *hydroxypropyl methylcellulose coating; and* ●, *methylcellulose coating.*

If the phenomenon of thermal gelation is responsible for the slow dissolution rate of methylcellulose-coated tablets at 37°, then tablets coated with either polymer should give essentially the same profile at a temperature below the thermal gel point. Figure 2 shows the dissolution profiles for the aspirin tablets at 21°. Although the profiles for the core tablet and the hydroxypropyl polymer tablet are lower than those at 37°, as expected because of reduced solubility, the two coatings appear to yield equivalent results. However, the release from the methylcellulose-coated tablet is increased significantly over that at 37°.

Additional dissolution runs were also made at 26 and 31°. The 30-min dissolution figures are shown in Table I for all runs.

According to the Noyes–Whitney equation:

$$\frac{dw}{dt} = DS(C_s - C) \qquad \text{(Eq. 1)}$$

where w is the amount dissolved, t is the time, D is the diffusion coefficient, S is the surface area of the dissolving solid, C_s is solubility, and C is the concentration in the bulk.

At very low solute concentration in the dissolution medium, C may be ignored (3) and, by assuming D and S to be constant (*i.e.*, for initial dissolution rates), Eq. 1 may be integrated to yield:

$$w = kt \qquad \text{(Eq. 2)}$$

where $k = DSC_s$.

The slope of the initial points from a plot of percent released *versus* time for a given dissolution run yields the constant k', which equals $100k/w_0$, where w_0 is the initial amount of drug in the tablet. These values were calculated for the various dissolution runs (Table II).

The effect of temperature can be illustrated by the use of an Arrhenius plot (log k' *versus* the reciprocal of the absolute temperature). However, the term k' does contain the solubility term, C_s, which changes significantly with temperature (Table III).

Table I—Aspirin Dissolution at 30 min

Sample	Percent Released[a] at: 21°	26°	31°	37°
Core	56.41	66.22	73.84	88.01
Methylcellulose	45.19	10.35	7.62	5.82
Hydroxypropyl methylcellulose	47.56	63.95	77.28	81.08

[a] Mean of four runs.

Table II—Dissolution Rate Constants[a]

Temperature	Core Tablet (k')	Methylcellulose Coating (k')	Hydroxypropyl Methylcellulose Coating (k')
21°	2.539	0.985	1.526
26°	3.206	0.492	2.419
31°	3.067	0.290	3.034
37°	5.205	0.231	4.168

[a] See text.

Table III—Aspirin Solubility in 0.1 *N* HCl

Temperature[a]	Solubility × 10^2, moles/liter
21°	3.88
26°	4.82
31°	5.93
37°	7.55

[a] Measurements were made at 21 and 37°. Intermediate values were calculated by the Van't Hoff equation.

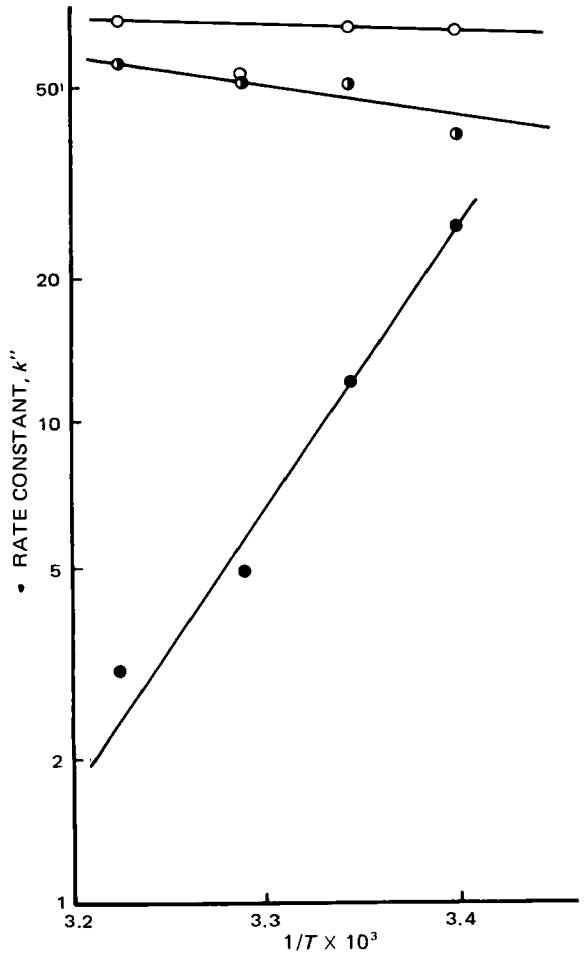

Figure 3—*Arrhenius plot showing effect of temperature on the rate constant k'' (see text). Key: ○, core tablet; ◑, hydroxypropyl methylcellulose coating; and ●, methylcellulose coating.*

The solubility effects can be separated by plotting the log k'' *versus* the reciprocal temperature (Fig. 3):

$$k'' = k'/C_s = 100\frac{DS}{w_0} \qquad \text{(Eq. 3)}$$

Changes noted in such a plot cannot then be attributed to a change in solubility when the solvent is assumed to be 0.1 *N* HCl.

The slopes in Fig. 3 for the core tablet and the hydroxypropyl polymer-coated tablet show slight decreases in the dissolution rate constant k'', which could be explained by a decrease in D as temperature is decreased. However, the data on the tablet with the methylcellulose coating show not only a positive slope but widely different values for k'', especially at higher temperatures. These values, of course, cannot be attributed to changes in D as a function of temperature, again if the solvent is assumed to be 0.1 *N* HCl.

The change in the sign of the slope indicates a difference in the mechanism for release with the methylcellulose polymer. The decrease in the k'' value with temperature can be explained simply by an increase in the viscosity of the dissolution medium. In such a case, the dissolution medium or barrier is no longer the 0.1 *N* HCl but a methylcellulose solution or methylcellulose gel with a concentration sufficient to lower D by increasing viscosity. The solubility, C_s, could also be lower in the methylcellulose solution than in the normal dissolution medium; but since the same concentration of polymer should exist for each methylcellulose-coated tablet and the C_s of the drug should increase with increasing temperature, the viscosity and, hence, the diffusion coefficient considerations appear to predominate.

Thus, the change in mechanism is attributed primarily to the presence of a barrier to dissolution in the form of a polymer solution or gel where the diffusion coefficient is much higher than that in the normal dissolution medium.

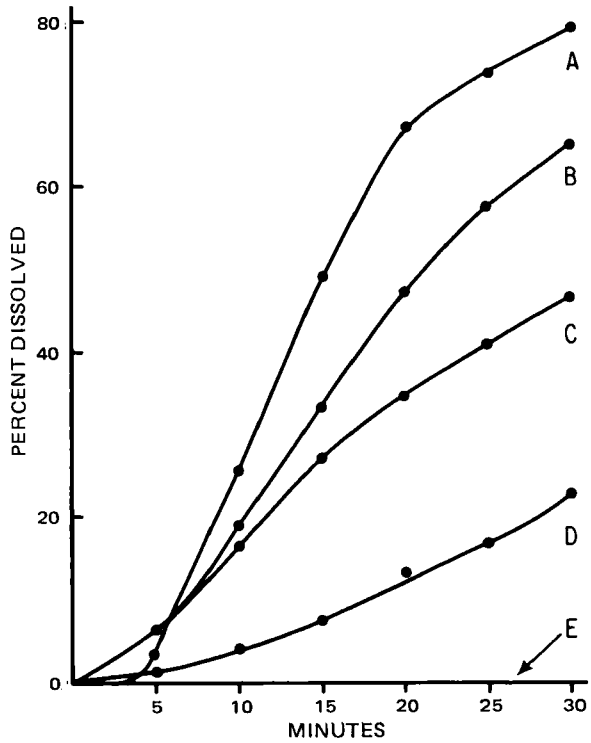

Figure 4—*Dissolution profiles for aspirin core tablets at 37° when methylcellulose has been added to the dissolution medium. Key (percent methylcellulose): A, 0.000387, B, 0.5; C, 1.0; D, 2.0; and E, 5.0.*

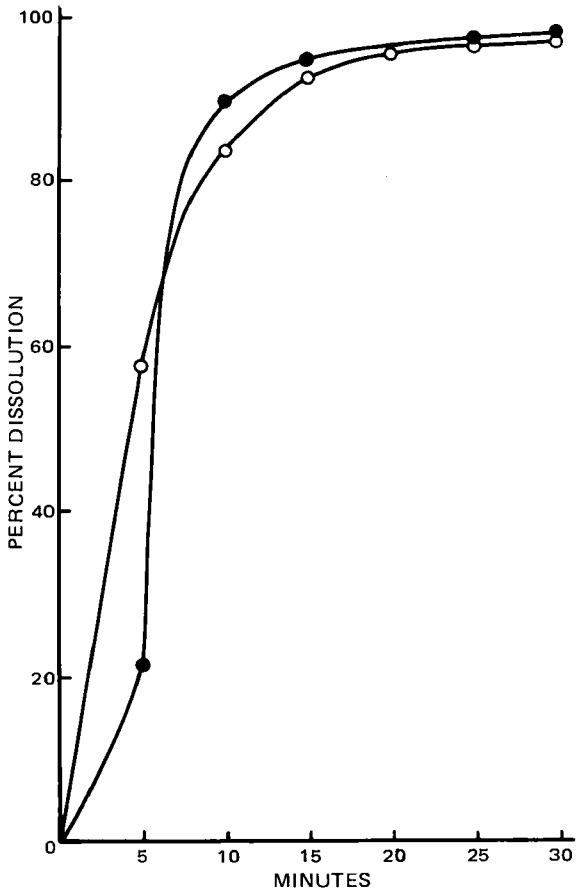

Figure 5—*Release profiles at 37° for aspirin tablets at 350 rpm. Key: ○, core tablet; and ●, methylcellulose coating.*

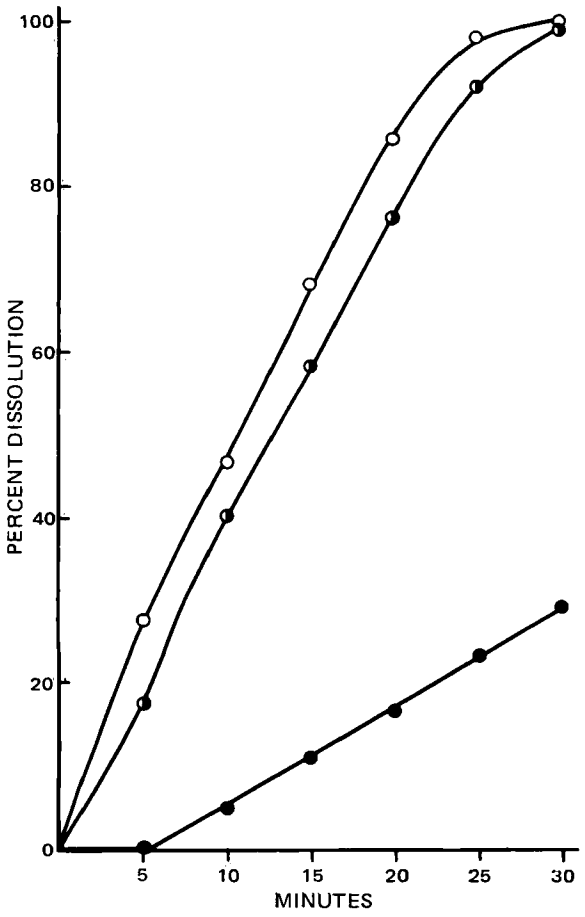

Figure 6—*Dissolution profiles at 37° for tablets containing amitriptyline hydrochloride. Key:* ○, *core tablet;* ◑, *hydroxypropyl methylcellulose coating; and* ●, *methylcellulose coating.*

To support this hypothesis, the effect on dissolution of the core tablet when the polymer concentration is increased in the dissolution medium is shown in Fig. 4. It is known that as the concentration of a given type of cellulose polymer increases, the thermal gel temperature decreases (2). The quantity of polymer in the coating of one tablet, when dispersed in the volume of solvent used for dissolution, is not sufficient to form a gel at the temperatures studied. The dissolution medium for curve A in Fig. 4 contains 2.9 mg of methylcellulose (0.000387%), and the profile is equivalent to that of the core tablet in the normal dissolution medium (Fig. 1).

As the concentration of methylcellulose is increased, the release rate decreases. At 5% polymer (Fig. 4, curve E), where gel structure was visually apparent, the gel-coated tablet was removed intact even after 15 min at a 500-rpm stirring rate.

These data indicate that it is not simply the presence of the polymer that retards dissolution but the concentration at the tablet surface. A very concentrated polymer solution probably exists at the surface of the methylcellulose-coated tablet—concentrated enough, in fact, to reduce the gel point to 37° or below. Even if gelation is incomplete, the polymer solution with its high viscosity provides a barrier to the dissolution process.

Agitation can affect the degree and apparent temperature of gelation, and continued agitation during gelation may break down the gel structure (2). The rotational speed of the dissolution basket was increased, and Fig. 5 shows that the release at 350 rpm for the methylcellulose-coated tablet is essentially equivalent to that of the core tablet.

To show that the decrease in release rate from the methylcellulose-coated product at 37° is not peculiar to the drug involved, the experiment was repeated using amitriptyline hydrochloride as the active ingredient. The release profiles for the core and coated tablets (Fig. 6) illustrate the differences.

The property of thermal gelation, although present in many polymers, is only of interest in this context when it occurs sufficiently near normal body temperatures to influence the rate of drug release. Where rapid release is required or where absorption might be controlled by the dissolution step, this phenomenon could be important and should be avoided.

REFERENCES

(1) L. C. Schroeter, in "Remington's Practice of Pharmacy," 14th ed., Mack Publishing Co., Easton, Pa., 1970, p. 1681.

(2) "Methocel Product Information," Dow Chemical Co., Midland, Mich., 1968.

(3) E. Nelson, *J. Amer. Pharm. Ass., Sci. Ed.*, **46**, 607(1957).

ACKNOWLEDGMENTS AND ADDRESSES

Received May 27, 1975, from the *Departments of Pharmaceutical Research and Development and Process Engineering and Development, Merck Sharp and Dohme Research Laboratories, West Point, PA 19486*

Accepted for publication July 8, 1975.

The authors acknowledge the helpful discussions of R. A. Castello and K. C. Kwan.

* Present address: Astra Pharmaceutical Products, Worcester, Mass.

ˣ To whom inquiries should be directed.

GLC Determination of Plasma Levels of Intact Chlorpropamide or Tolbutamide

K. K. MIDHA ˣ, I. J. McGILVERAY, and C. CHARETTE

Abstract □ A GLC procedure was developed for the quantitative estimation of intact chlorpropamide and tolbutamide concentrations in plasma; the drugs are used as mutual internal standards. After extraction of plasma containing the drug and internal standard with toluene, the dried residue is treated with ethereal diazomethane to form the methyl derivatives of tolbutamide and chlorpropamide. Aliquots of the ethereal solution are injected into a gas chromatograph equipped with a glass-lined injection port and glass column packed with a phenyl methyl silicone fluid (OV-25) on Chromosorb W, which facilitates the intact determination of the methyl derivatives of the drugs. The response to the flame-ionization detector was linear over a range of 0.20–25 μg/ml, with a 0.05-μg/ml limit of detectability for both drugs. The method compares favorably with a recently developed high-pressure liquid chromatographic procedure and is adequate for following blood level profiles of single doses of chlorpropamide (125 mg) and tolbutamide (250 mg). Mass spectral evidence showing that intact sulfonylureas are measured is presented.

Keyphrases □ Chlorpropamide—GLC analysis, plasma □ Tolbutamide—GLC analysis, plasma □ GLC—analysis, chlorpropamide and tolbutamide, plasma □ Antidiabetic agents—chlorpropamide and tolbutamide, GLC analysis, plasma

Chlorpropamide and tolbutamide, sulfonylurea derivatives, are widely used as oral hypoglycemic drugs in the treatment of diabetes. Most previously described procedures for the estimation of chlorpropamide and tolbutamide in biological fluids have been colorimetric or spectrophotometric methods (1–9). However, these methods suffer from a lack of specificity and/or sensitivity.

One GLC procedure for the estimation of plasma levels of chlorpropamide and tolbutamide involved methylation of the drugs with dimethyl sulfate prior to chromatography and detection with a flame-ionization detector (10). However, this procedure was found (11) to result in the degradation of the methylated derivatives of these drugs to methylated benzenesulfonamides in the injection port of the gas chromatograph. A similar GLC procedure involved methylation prior to chromatography (12).

The metabolism and pharmacokinetics of chlorpropamide were reviewed, and two assay methods were also described (13). One procedure utilized a GLC separation and quantitation with an electron-capture detector. The other was a high-speed liquid chromatographic (HSLC) procedure in which urinary metabolites of chlorpropamide were measured. Colorimetric and electron-capture methods were reported in which the nonspecific derivatives, *N*-propyl- and *N*-butyl-2,4-dinitroanilines, were formed by the reaction of 2,4-dinitrofluorobenzene with chlorpropamide and tolbutamide, respectively (14). These GLC procedures involved electron-capture detection or were nonspecific. Breakdown of the drugs to benzenesulfonamides in the injection port of the chromatograph appeared to be a problem in some cases (10–13).

The objective of the present study was to develop a simple and specific GLC procedure, employing flame-ionization detection for the determination of intact chlorpropamide and tolbutamide in plasma. This procedure was required for single-dose pharmacokinetic and bioavailability studies of these drugs.

EXPERIMENTAL

Reagents—Chlorpropamide[1], tolbutamide[2], toluene[3], and ether[4] were obtained commercially. Diazomethane was generated using a commercially available kit[5]. Plasma was obtained from the Red Cross Blood Bank. All other chemicals employed were analytical grade.

GLC—A gas chromatograph[6] equipped with a flame-ionization detector was employed. The column was coiled glass tubing, 1.83 m (6 ft) long by 3.0 mm i.d., packed with 5% phenyl methyl silicone fluid[7] (OV-25) on acid-washed, dimethyldichlorosilane-treated, high performance Chromosorb W[7] support (80–100 mesh).

The column was conditioned by maintaining the oven at 325° for 18 hr with low nitrogen flow. Operating conditions were: injection port temperature, 200°; column temperature, 220°; and detector temperature, 285°. The flow rate of nitrogen was 60 ml/min. Hydrogen and compressed air flow rates were adjusted to give maximum response.

Procedure—To 1-ml plasma samples in screw-capped[8] centrifuge tubes (20 ml) were added 1 ml of internal standard (7 μg of tolbutamide/ml for chlorpropamide or 4.25 μg of chlorpropamide/ml for tolbutamide) and 1.5 ml of 1 *N* HCl. The samples were extracted twice with 5-ml portions of toluene by shaking[9] for 10 min at 19 rpm, followed by centrifugation at 2500 rpm for 10 min. The 4- and 5-ml portions of the first and second toluene extracts, respectively, were transferred into a centrifuge tube (20 ml) containing 6 ml of 0.2 *M* phosphate buffer, pH 11.2

The tubes were mixed[9] for 10 min and then centrifuged for 10 min, after which the organic layer was discarded. The aqueous phosphate solution was acidified with 2.0 ml of 2 *N* HCl and extracted with 2 × 5-ml portions of toluene (mixed[9] 10 min, centrifuged 10 min). Four milliliters of the first extract and 5 ml from the second extract were transferred into an evaporating tube[10] (15). This combined toluene extract was evaporated to dryness at 85° under a stream of dry nitrogen.

An ethereal solution of diazomethane (0.5 ml) was added to the residue and left to react for 30 sec. The excess ethereal solution was evaporated at 45° under a stream of dry nitrogen to a volume of 25–50 μl, and aliquots (1–2 μl) were injected into a gas chromatograph equipped with a flame-ionization detector. The retention times of methylated chlorpropamide and tolbutamide were 4.50 and 5.90 min, respectively.

Standards and Calibration Curves—Chlorpropamide and tolbutamide standards were prepared by dissolving appropriate amounts of each in aqueous 0.01 *N* NaOH to obtain stock solutions of ≃50 μg/ml. Appropriate dilutions of these stock solutions were made to obtain concentrations over the 0.20–25.00-μg/ml range for chlorpropamide and tolbutamide.

[1] Chas. Pfizer & Co.
[2] Strong Cobb Arner of Canada, Fort Erie, Ontario, Canada.
[3] Caledon Laboratories, Georgetown, Ontario, Canada.
[4] Diethyl ether (anhydrous), Mallinckrodt Chemical Works Ltd., Montreal, Quebec, Canada.
[5] Catalog No. 710,025-0, Aldrich Chemical Co.
[6] Model 3920, Perkin-Elmer, Canada.
[7] Chromatographic Specialties, Brockville, Ontario, Canada.
[8] Lined with Teflon (duPont).
[9] Roto-Rack, Fisher Scientific Co., Montreal, Canada.
[10] Custom made by Canadian Laboratories Supplies Ltd., Montreal, Canada.

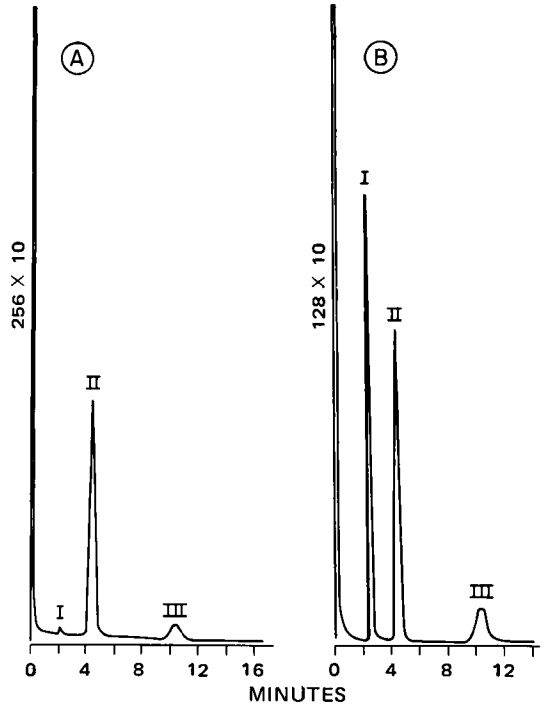

Figure 1—*Typical chromatograms of methylated chlorpropamide. Key: A, injection port temperature of 200°; and B, injection port temperature of 275°.*

Peak height ratios were calculated by dividing the height of the peak due to chlorpropamide or tolbutamide by the height of the other drug as the internal standard. Calibration curves were assembled from the results of spiked control plasma by plotting the peak height ratios against the concentrations of chlorpropamide or tolbutamide.

RESULTS AND DISCUSSION

Methylation of chlorpropamide with diazomethane gave three peaks (peaks I–III, Fig. 1A) with retention times of 2.2, 4.5, and 10.5 min, respectively, under the described GLC conditions. GLC–mass spectrometric[11] analysis of compounds giving rise to peaks I–III indicated that peak I was due to *N*-methyl-*p*-chlorobenzenesulfonamide (major ions at *m/e* 205–207, 175–177, and 111–113), peak II was due to *N*-methylchlorpropamide (diagnostic ions at *m/e* 261–263, 232–234, 226–228, 175–177, and 111–113), and peak III was due to a methyl enol ether of chlorpropamide, most likely the result of attack of diazomethane on carbonyl oxygen and loss of the more acidic sulfonamide proton (diagnostic ions at *m/e* 290–292, 258–260, 175–177, and 111–113).

Figure 1B shows a typical chromatogram of methylated chlorpropamide obtained with a complete glass system (*i.e.*, glass-lined injection port and glass column) with the injection port held at 275°. Figure 1A shows a typical chromatogram of methylated chlorpropamide obtained when the injection port temperature was dropped to 200°. From Fig. 1, it is apparent that the amount of *N*-methyl-*p*-chlorobenzenesulfonamide (peak I) increased at the expense of *N*-methylchlorpropamide (peak II) as the injection port temperature was raised. The amount of the methyl enol ether of chlorpropamide (peak III) did not seem to be influenced by the temperature changes in the injection port.

This thermal degradation of methylated chlorpropamide to *N*-methyl-*p*-chlorobenzenesulfonamide was tested by varying the injection port temperatures from 175 to 275°; 200° was best. At 175°, no decrease in the amount of *N*-methyl-*p*-chlorobenzenesulfonamide, as monitored by peak I, was observed. With injection port temperatures above 200°, the breakdown increased (Fig. 1B).

Similarly, methylation of tolbutamide with diazomethane and subsequent GLC analysis under similar conditions gave three peaks (peaks I–III, Fig. 2). GLC–mass spectral evidence indicated that peak I (retention time of 2.0 min) was due to *N*-methyl-*p*-toluenesulfonamide (major ions at *m/e* 185, 155, 141, 121, and 91), peak II (retention time of 5.9 min) was due to *N*-methyltolbutamide (diagnostic ions at *m/e* 241, 220, 212, 185, 155, 121, and 91), and peak III (retention time of 13.9 min) was due to a methyl enol ether of tolbutamide (diagnostic ions at *m/e* 284, 269, 255, 241, 184, 155, 121, and 91).

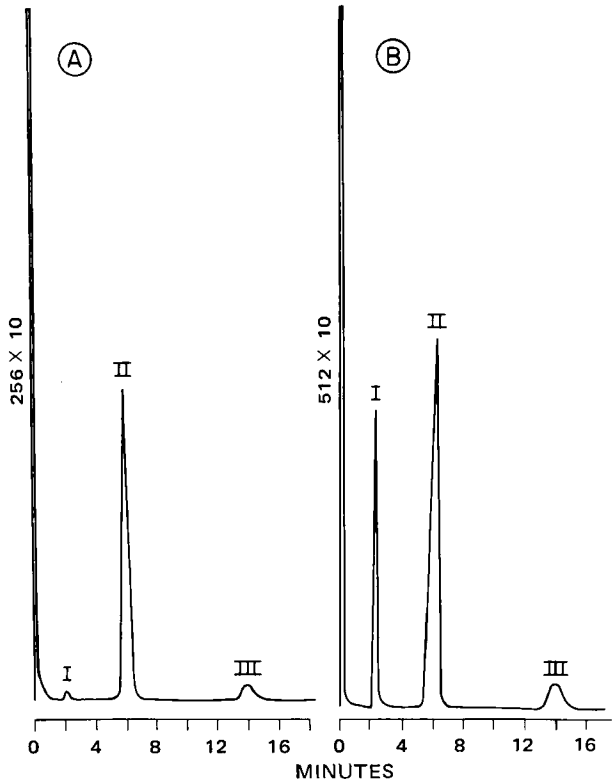

Figure 2—*Typical chromatograms of methylated tolbutamide. Key: A, injection port temperature of 200°; and B, injection port temperature of 275°.*

As the injection port temperature was dropped from 275 to 200° (Fig. 2), peak I due to *N*-methyl-*p*-toluenesulfonamide decreased and peak II due to *N*-methyltolbutamide increased. Thermal breakdown of methylated tolbutamide to *N*-methyl-*p*-toluenesulfonamide was reported previously (11), and it was observed (16) that methylation of tolbutamide also gave a methyl enol ether of tolbutamide as a minor product separate from the principal product *N*-methyltolbutamide.

The findings reported herein indicate that methylation of tolbutamide or chlorpropamide with diazomethane forms the desired *N*-methylated derivatives of these compounds together with minor amounts of methyl enol ethers. However, when the *N*-methylated derivatives were injected into the gas chromatograph, breakdown occurred to the respective *N*-methylbenzenesulfonamides. Careful choice of the injection port temperature minimized the breakdown of *N*-methyl derivatives of chlorpropamide and tolbutamide. Thus, the major peaks given by *N*-methylchlorpropamide (peak II, Fig. 1A) and *N*-methyltolbutamide (peak II, Fig. 2A) were used for the quantitative estimation of the respective drugs. Since these peaks were well resolved from each other (retention times of 4.5 and 5.9 min, respectively) under the study conditions and thermal breakdown was minimal when the injection port temperature was 200°, *N*-methyltolbutamide was used as an internal standard for *N*-methylchlorpropamide and vice versa.

Several other derivatization procedures, such as flash-heater methylation and methoxime formation with methoxyamine, were investigated in an attempt to form suitable derivatives of chlorpropamide and tolbutamide for GLC analysis. Flash-heater methylation of tolbutamide and chlorpropamide with trimethylanilinium hydroxide gave single peaks for each drug when a metal injection port was used. GLC–mass spectral analysis of these peaks indicated that *N,N*-dimethyl derivatives of benzenesulfonamides were

[11] Hitachi Perkin-Elmer model RMSU mass spectrometer coupled to a Perkin-Elmer model 990 gas chromatograph through a two-stage jet separator.

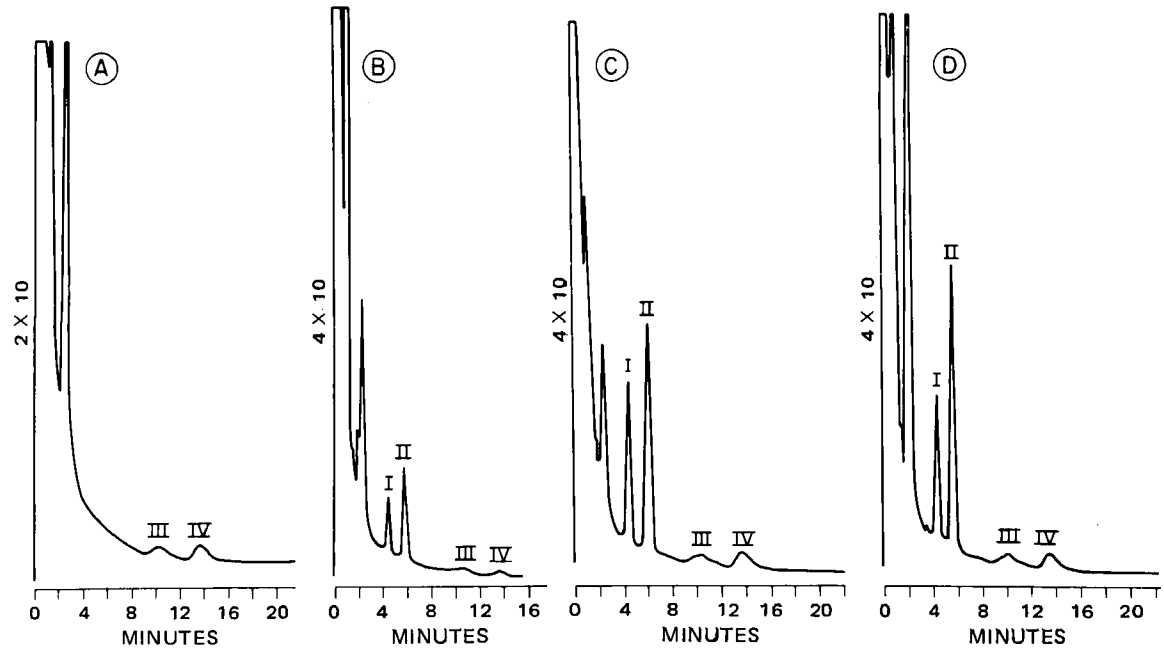

Figure 3—*Typical chromatograms of human plasma. Key: A, control plasma; B, plasma containing 4.25 μg/ml of chlorpropamide and 6.65 μg/ml of tolbutamide; C, plasma from a human volunteer who had been given 125 mg of chlorpropamide (amount is 4.75 μg); D, plasma from a human volunteer who had been given 500 mg of tolbutamide (amount is 15.10 μg); and peaks I and II, due to methylated chlorpropamide and tolbutamide, respectively.*

being formed. This observation is in agreement with previous results (17). This mode of derivatization was abandoned, since *p*-chlorobenzenesulfonamide, a metabolite of chlorpropamide[12], and *p*-toluenesulfonamide, a metabolite of tolbutamide[12], are extracted in the extraction procedure described and also undergo flash-heater methylation with trimethylanilinium hydroxide to *N,N*-dimethyl derivatives, which interfere in the analysis of these drugs.

Formation of methoxime derivatives of chlorpropamide and tolbutamide with methoxyamine hydrochloride in pyridine and subsequent GLC analysis gave a single peak for each drug on a column packed with a mixture of 1% dimethyl silicone fluid (OV-101) and 1% polyamide (Poly A-103). GLC–mass spectral analysis of these peaks indicated that the peaks were due to the respective benzenesulfonamides. Since these benzenesulfonamides are metabolites of these drugs[12], they would interfere.

Figure 3A shows a typical chromatogram obtained with control blank plasma processed as described under *Experimental* but with the internal standard, tolbutamide or chlorpropamide, omitted. Extraneous peaks III and IV at retention times 10.0 and 13.4 min, respectively, did not interfere with chlorpropamide and tolbutamide. Peaks appearing in the first 3 min after injection did not interfere with peak I (Fig. 3B) due to *N*-methylchlorpropamide or peak II (Fig. 3B) due to *N*-methyltolbutamide.

A chromatogram obtained when the method was applied to spiked plasma containing 4.25 μg of chlorpropamide and 6.65 μg of tolbutamide is shown in Fig. 3B. It is clear that the extraneous peaks do not interfere with the peaks due to chlorpropamide (peak I, 4.5 min) and tolbutamide (peak II, 5.9 min). Figure 3C shows a chromatogram obtained from a 72-hr plasma sample (1 ml) of a volunteer (73 kg) who received a commercial tablet of chlorpropamide (125 mg). Figure 3D shows a chromatogram obtained from a 24-hr plasma sample (1 ml) of a volunteer (73 kg) who received a commercial tablet of tolbutamide (500 mg).

The response of the flame-ionization detector to chlorpropamide and tolbutamide was linear with concentrations over the 0.20–25.00-μg/ml range. The ratio of the peak heights of chlorpropamide or tolbutamide and their respective internal standard (tolbutamide or chlorpropamide) plotted against concentration in the 0.20–25.00-μg/ml range gave straight lines passing through the origin (r = 1.0). Mean slope values of 0.146 ± 0.002 and 0.290 ± 0.003 were obtained for chlorpropamide and tolbutamide, respectively. The overall coefficients of variation were 3.4% (Table I) and 3.1% (Table II), respectively. The overall recoveries of chlorpropamide and tolbutamide from plasma were of the order of 72.1 ± 3.3 and 83.9 ± 1.5%, respectively (Table III). The described GLC procedure for tolbutamide and chlorpropamide appears specific since the known metabolites of both drugs do not interfere in the assay.

Table I—GLC Estimation of Chlorpropamide Added to 1 ml of Plasma

Chlorpropamide Added, μg	n	Mean Peak Height Ratio	Coefficient of Variation, CV, %[a]
0.212	4	0.049	6.05
0.425	4	0.085	0.91
0.920	3	0.143	4.03
1.840	3	0.303	3.81
3.680	3	0.553	2.09
7.360	4	1.137	2.72
13.800	3	2.093	4.12
23.000	3	3.350	3.44

[a] Mean CV = 3.40%, $y = mx$, where m = 0.146; and r = 1.0.

Table II—GLC Estimation of Tolbutamide Added to 1 ml of Plasma

Tolbutamide Added, μg	n	Mean Peak Height Ratio	Coefficient of Variation, CV, %[a]
0.332	4	0.095	4.19
0.665	4	0.191	1.62
1.330	4	0.466	3.52
3.325	8	0.993	3.21
6.650	6	1.964	3.73
13.300	5	3.860	3.05
26.200	4	7.744	2.47

[a] Mean CV = 3.11%, $y = mx$, where m = 0.290; and r = 1.0.

[12] There is some doubt about the status of these sulfonamides. While they occur in urine of patients treated with the drugs (13), the trace amounts suggest that they are degradation products rather than metabolites. They also occur as impurities in dosage forms and would interfere, as stated, in certain assays.

Table III—Recovery of Chlorpropamide and Tolbutamide from Plasma Determined by GLC Assay

Micrograms Added to 1 ml of Plasma	n	Mean Recovery, μg	Mean Recovery, %	*SD* of Percent Recovery
		Chlorpropamide		
3.68	4	2.71	73.63	4.77
7.36	4	5.19	70.59	1.76
Mean 72.11	3.27			
		Tolbutamide		
7.00	5	5.87	83.92	1.49

The major metabolites of tolbutamide are *p*-toluenesulfonamide[12], *p*-toluenesulfonylurea, hydroxytolbutamide, and carboxytolbutamide. When treated with diazomethane and chromatographed under the conditions described under *Experimental*, the metabolites gave retention times different from those of *N*-methyltolbutamide and *N*-methylchlorpropamide. *N*-Methyl-*p*-toluenesulfonamide had a retention time of 2.0 min. Methylated *p*-toluenesulfonylurea gave two peaks with retention times of 2.0 and 2.45 min. Methylated hydroxytolbutamide gave peaks with retention times of 9.7 and 23.6 min. Chromatography of carboxytolbutamide gave rise to two peaks with retention times of 10.8 and 12.9 min.

The major metabolites of chlorpropamide are *p*-chlorobenzenesulfonamide[12], *p*-chlorobenzenesulfonylurea, 2-hydroxychlorpropamide, and 3-hydroxychlorpropamide. None of these metabolites interfered with the assay; on methylation with diazomethane followed by chromatography under the described conditions, they gave retention times different from those of the methylated derivatives of the drug and the internal standard. Methylated *p*-chlorobenzenesulfonylurea gave two peaks with retention times of 2.2 and 2.7 min.

The peak of retention time 2.2 min was due to *N*-methyl-*p*-chlorobenzenesulfonamide, the breakdown product and perhaps a metabolite[12]. Methylated 2-hydroxychlorpropamide and methylated 3-hydroxychlorpropamide broke down mainly under the GLC conditions to give *N*-methyl-*p*-chlorobenzenesulfonamide. Minor peaks for intact methylated derivatives of alcohols, with retention times of 7.84 and 10.41 min, were well separated from those of methylated drug and the internal standard.

Application of the method to plasma level determination of chlorpropamide by GLC is shown in Fig. 4 where it is compared with a recently developed high-pressure liquid chromatographic (HPLC) procedure (18). A 125-mg dose of chlorpropamide (one-half of a tablet) was given to a healthy male volunteer (73 kg); blood was withdrawn at intervals over 168 hr, and aliquots of the plasma were assayed for chlorpropamide separately by the GLC and HPLC procedures. The methods compared favorably with an overall difference of 5.7%. When areas under the curves to 168 hr

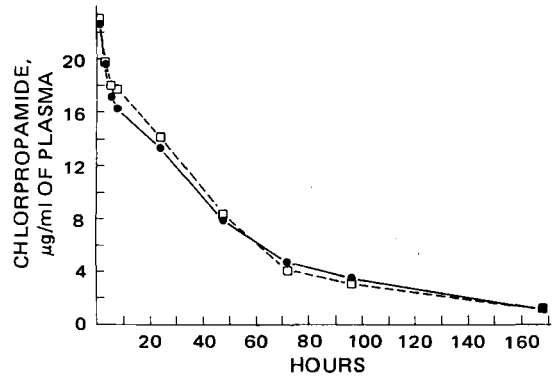

Figure 4—*Comparison of plasma chlorpropamide levels by GLC method with that of an HPLC method following a single oral dose of a 125-mg tablet of chlorpropamide to a human volunteer (73 kg). Key: ●, GLC method; and □, HPLC method.*

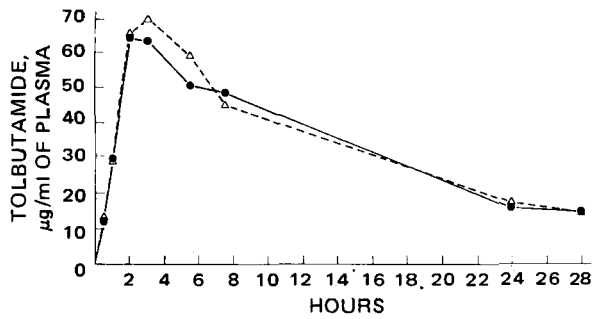

Figure 5—*Comparison of plasma tolbutamide levels by GLC method with that of an HPLC method following a single oral dose of a 500-mg tablet of tolbutamide to a human volunteer (73 kg). Key: ●, GLC method; and △, HPLC method.*

were compared, a difference of 1.1% was obtained. Application of the method to plasma level determinations of tolbutamide is demonstrated in Fig. 5, and comparison with a recently developed HPLC method (18) is also shown.

A 500-mg tablet of tolbutamide was given to a healthy male volunteer (73 kg); blood was withdrawn at intervals over 28 hr and analyzed separately by the GLC and HPLC procedures. The methods compared with an overall difference of 7.0%. When areas under the curves were compared to 28 hr, a difference of 1.9% was obtained.

The GLC method is simple, sensitive, and specific, because intact methylated chlorpropamide and tolbutamide are measured and the drugs are distinguished from their respective metabolites. The method can be employed for single- as well as multiple-dose pharmacokinetic studies. The procedure also gives promise of applicability to other sulfonylurea drugs.

REFERENCES

(1) H. Spingler and F. Kaiser, *Arzneim.-Forsch.*, **12**, 760(1956).

(2) A. A. Forist, W. L. Miller, J. Krake, and W. A. Struck, *Proc. Soc. Exp. Biol. Med.*, **96**, 180(1957).

(3) H. Spingler, *Klin. Wochenschr.*, **35**, 533(1957).

(4) E. Black and A. Norden, *Acta Pharmacol. Toxicol.*, **14**, 188(1968).

(5) T. J. Toolan and R. L. Wagner, *Ann. N.Y. Acad. Sci.*, **74**, 449(1958).

(6) I. Popa and A. Voicu, *Farmacia*, **10**, 399(1962).

(7) K. Kalinowski and R. Korzyliski, *Acta Pol. Pharm.*, **20**, 221(1963).

(8) R. H. Carmichael, *Clin. Chem.*, **5**, 597(1959).

(9) T. Chulski, *J. Lab. Clin. Med.*, **53**, 490(1959).

(10) K. Sabih and K. Sabih, *J. Pharm. Sci.*, **59**, 782(1970).

(11) D. L. Simmons, R. J. Ranz, and P. Picotte, *J. Chromatogr.*, **71**, 421(1972).

(12) L. F. Prescott and D. R. Redman, *J. Pharm. Pharmacol.*, **24**, 713(1972).

(13) J. A. Taylor, *Clin. Pharm. Ther.*, **13**, 710(1972).

(14) S. B. Matin and M. Rowland, *J. Pharm. Pharmacol.*, **25**, 186(1973).

(15) A. H. Beckett, *Dan. Tidsskr. Farm.*, **40**, 197(1966).

(16) W. F. Beyer, *Anal. Chem.*, **44**, 1312(1972).

(17) V. Aggarwal and I. Sunshine, *Clin. Chem.*, **20/2**, 200(1974).

(18) I. J. McGilveray, K. K. Midha, and S. Sved, presented at the Pharmaceutical Analysis and Control Section, APhA Academy of Pharmaceutical Sciences, New Orleans meeting, Nov. 1974.

ACKNOWLEDGMENTS AND ADDRESSES

Received May 19, 1975, from the *Drug Research Laboratories, Health Protection Branch, Health and Welfare Canada, Ottawa, Ontario K1A 0L2, Canada.*

Accepted for publication July 8, 1975.

Helpful discussions with Dr. S. Sved and Dr. D. V. C. Awang of the Drug Research Laboratories are gratefully acknowledged. The authors thank Mr. J. K. Cooper for technical assistance and Dr. A. W. By and Mr. J. C. Ethier for obtaining the mass spectra.

[x] To whom inquiries should be directed.

Mechanism of Action of Retinyl Compounds on Wound Healing IV: Effect of Desmethylretinoic Acid and Its Vinylogs on Granuloma Formation

K. H. LEE ˣ, CHERNG-CHYI FU, and MARVIN JUNG

Abstract □ The effect of side-chain length of desmethylretinoic acid on granuloma formation induced by implantation of cotton pellets was studied. As in the homologous series of retinoic acid studies, compounds with side chains shorter than retinoic acid were not active while compounds with side chains as long or longer than retinoic acid were active. The compound with a chain two carbons longer than retinoic acid was the most active. The hydroxyproline and hexosamine contents of the granuloma were analyzed. The mechanisms of action of these active compounds on wound healing are discussed.

Keyphrases □ Retinyl compounds—desmethylretinoic acid and vinylogs, wound-healing mechanism of action, effect on granuloma formation □ Desmethylretinoic acid and vinylogs—wound-healing mechanism of action, effect on granuloma formation □ Vitamin A-related compounds—desmethylretinoic acid and vinylogs, wound-healing mechanism of action, effect on granuloma formation □ Granuloma formation—effect of desmethylretinoic acid and vinylogs

It was reported previously that a few vitamin A (retinol) related compounds promote skin wound healing (1–3) and tissue regeneration (4) in rats. The structural relationship of a few naturally occurring compounds related to retinol was also studied (4). Recently, the effect of the length of the side chain of retinoic acid on granuloma formation induced by implanted cotton pellets was reported (5); compounds with side chains shorter than that of retinoic acid possessed no activity while compounds with longer side chains showed activity. The compound with a side chain carbons longer than retinoic acid showed higher activity than retinoic acid (5).

The present work concerned the effects of chain length of desmethylretinoic acid on granuloma formation induced by implanted cotton pellets. Compounds with side chains shorter than desmethylretinoic acid were not active. Compounds with side chains two or more carbons longer than desmethylretinoic acid were more active than desmethylretinoic acid and retinoic acid.

Both hydroxyproline and hexosamine contents of the granulomas induced by implanted cotton pellets in the presence of active compounds were greatly increased as compared with those present in the control granulomas. These active compounds are effective wound-healing agents. The mechanisms of action of these compounds on wound healing are discussed.

EXPERIMENTAL

Materials—The following were used: crystalline hydroxy-L-proline[1]; D-glucosamine hydrochloride[2], grade A; sodium hydride, 57% oil dispersion; lithium aluminum hydride powder[3], 97%; triethyl phosphite[4], 97%; β-ionone[4], n_D^{20} 1.584; trimethyl phosphonoacetate[4]; ethyl bromoacetate[4], 75%; tetrahydrofuran[4], 99.5%; *p*-dimethylaminobenzaldehyde[5], reagent grade; ether[6], anhydrous; phosphoric acid NF, 85%; manganese sulfate[6], monohydrate, analytical grade; potassium permanganate[6] USP, crystals; and dental cotton roll[7], size I.

Implantation of Cotton Pellet—The methods used in the preparation and implantation of cotton pellets were essentially the same as described previously (5).

On the 7th day after implantation, the animals were killed with ether. The granulomas were carefully removed and immediately weighed on a precision torsion balance[8]. After drying in an oven at 68° for 48 hr, the dry weight of the granuloma was taken.

Chemical Analysis—The granulomas were digested in the Pyrex digestion tube (5), and 1 ml of 6 *N* HCl was added to each granuloma. Each tube was sealed *in vacuo*, and the content was hydrolyzed at 140° in a constant-temperature heating block for 3 hr. After cooling to room temperature, the seal of the tube was broken and the content was carefully neutralized with 6 *N* NaOH.

The content was then filtered. The original digesting tube and the filter were rinsed several times with small portions of distilled water, and the filtrate with the washings was brought to volume. Aliquots were taken for hydroxyproline and hexosamine analysis according to the methods described by Woessner (6) and Cessi and Piliego (7), respectively.

Chemical Synthesis—The methods used for the synthesis of desmethylretinoic acid vinylogs basically followed published schemes (8). All reactions were carried out under nitrogen. Direct light was also avoided. The synthesis was carried out as shown in Scheme I.

2,6,6-Trimethyl-1-(2′-carboxy-1′-vinyl)cyclohex-1-ene (I) (Desmethyl C_{12} Acid)—The synthesis of this acid was described in detail previously (5).

2,6,6-Trimethyl-1-(4′-carboxybuta-1′,3′-dienyl)cyclohex-1-ene (V) (Desmethyl C_{14} Acid)—1. Synthesis of the C_{12} alcohol (II)—Fifteen grams of I (0.0773 mole) was dissolved in 80 ml of anhydrous ether. Lithium aluminum hydride (4.4 g, 0.116 mole) was placed in a round-bottom, three-necked flask with enough anhydrous ether to make a slurry. The mixture was brought to −15° with the aid of dry ice in acetone. The C_{12} acid solution was added dropwise into the mixture with stirring. The temperature was kept below −5°.

After all of the acid solution had been added, the reaction mixture was kept at room temperature with stirring for 1 hr. The mixture was then brought to 0°, and dilute sulfuric acid (1 *M*) was added dropwise to destroy any remaining lithium aluminum hydride. The mixture was then extracted with ether. The combined ether extract was washed once with water and then dehydrated with anhydrous magnesium sulfate overnight. The ether extract was filtered, and evaporation of ether gave 12.1 g (87% yield).

2. Synthesis of the C_{12} aldehyde (III)—A solution of 12.1 g (0.066 mole) of the C_{12} alcohol in anhydrous carbon tetrachloride was added dropwise into a flask containing 121.1 g of active manganese dioxide (9) and 500 ml of anhydrous carbon tetrachloride with vigorous stirring. The mixture was kept at room temperature with stirring for 4 hr. The manganese dioxide then was filtered by suction and washed several times with carbon tetrachloride. The carbon tetrachloride of the combined filtrates was evaporated, and the yield of the C_{12} aldehyde was 12 g (100%). The C_{12} aldehyde

[1] Sigma Chemical Co., St. Louis, Mo.
[2] Calbiochem, Los Angeles, Calif.
[3] Alpha Inorganics, Beverly, Mass.
[4] Aldrich Chemical Co., Milwaukee, Wis.
[5] Eastman Kodak Co., Rochester, N.Y.
[6] Mallinckrodt Chemical Works, St. Louis, Mo.
[7] Johnson and Johnson, New Brunswick, N.J.
[8] Roller-Smith.

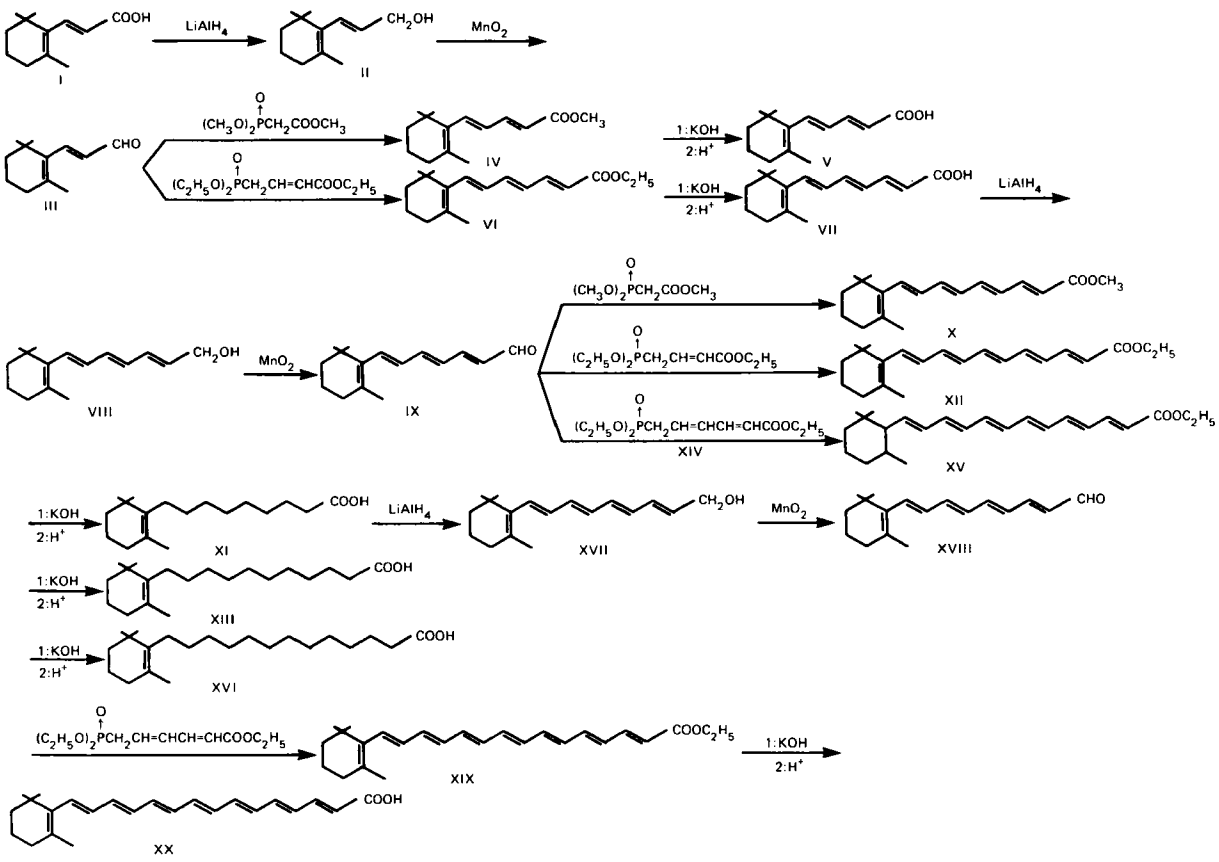

Scheme I

was used immediately in the next step.

3. Synthesis of the C_{14} ester (IV)—Sodium hydride [4.2 g (57%), 0.1 mole] was washed with anhydrous ether in a round-bottom, three-necked flask, and the ether was decanted. Dry tetrahydrofuran, 100 ml, was added to the washed sodium hydride. The suspension was brought to 0°.

Trimethyl phosphonoacetate (18.02 g, 0.1 mole) was added very slowly with stirring. The temperature was kept below 5°. The C_{12} aldehyde (12 g, 0.066 mole) dissolved in a small amount of tetrahydrofuran was added slowly. The mixture was allowed to warm to room temperature with stirring for 1 hr. Then the reaction mixture was brought to 0°, and saturated sodium chloride solution was added slowly and cautiously. The ester formed was extracted with petroleum ether. The petroleum ether was evaporated, and 11.2 g (73%, 0.048 mole) of the C_{14} ester was obtained.

4. Hydrolysis of the C_{14} ester—Ten grams of potassium hydroxide was dissolved in a mixture of 60 ml of water and 40 ml of ethanol. This alkaline solution, at 0°, was added to the ester with stirring, and this mixture was refluxed for 2–3 hr. At the end of hydrolysis, the ethanol was removed. After the addition of 100 ml of water, the aqueous solution was extracted with a small amount of ether to remove the unhydrolyzed ester.

The aqueous layer was acidified with dilute hydrochloric acid (6 *N*) at 0° to pH 4. The C_{14} acid was extracted with ether, and the combined ether extract was dried over magnesium sulfate. After evaporation of the ether, 7.45 g (63%) of crystalline C_{14} acid was obtained. The C_{14} acid was recrystallized from 60% ethanol.

2,6,6-Trimethyl-1-(6′-carboxyhexa-1′,3′,5′-trienyl)cyclohex-1-ene (VII) (Desmethyl C_{16} Acid)—Sodium hydride [4.66 g (57%), 0.11 mole] was washed with anhydrous ether and then suspended in anhydrous tetrahydrofuran at 0°. Triethyl phosphonocrotonate (27.75 g, 0.11 mole) was added slowly through a dropping funnel, and the mixture was stirred for 1 hr. Ten grams (0.055 mole) of III, dissolved in a small amount of tetrahydrofuran, was added slowly into the reaction mixture with stirring. The reaction mixture was left at room temperature with stirring for 1 hr and then brought back to 0°. A saturated sodium chloride solution was added very slowly. The C_{16} ester that formed was extracted with petroleum ether, and the petroleum ether was evaporated.

The ester was hydrolyzed in 100 ml of 10% KOH solution in 40% ethanol for 4 hr under reflux. At the end of hydrolysis, the ethanol was removed. After the addition of 100 ml of water, the aqueous solution was extracted with a small amount of ether to remove the unhydrolyzed ester and then acidified with dilute hydrochloric acid (6 *N*) at 0° to pH 5. The C_{16} acid was extracted with ether, and the combined ether extract was dried over anhydrous magnesium sulfate. After the ether was evaporated, 4.24 g (61%) of crystalline desmethyl C_{16} acid was obtained. The crude acid was recrystallized twice from 80% ethanol, mp 153–153.5°.

2,6,6-Trimethyl-1-(8′-carboxyocta-1′,3′,7′-tetraenyl)cyclohex-1-ene (XI) (Desmethylretinoic Acid)—Sodium hydride (2 g, 0.047 mole) was washed with anhydrous ether and then suspended in 100 ml of dry tetrahydrofuran. Trimethyl phosphonoacetate (8.8 g, 0.047 mole) was added slowly at 0°. After the addition was complete, the reaction mixture was kept at room temperature with stirring and brought back to 0°. The desmethyl C_{16} aldehyde (5 g, 0.0217 mole), dissolved in dry tetrahydrofuran, was added slowly to the reaction mixture with stirring. The reaction mixture was left at room temperature for 1 hr and then brought to 0°. Saturated sodium chloride solution was added to the mixture cautiously.

The desmethyl C_{18} ester was extracted with petroleum ether. The petroleum ether was removed, and 6.0 g of ester was obtained. The ester was then hydrolyzed in 100 ml of 10% KOH in 60% ethanol. After acidification and extraction, crude desmethylretinoic acid was obtained. The crude crystalline acid was recrystallized from ethanol.

2,6,6-Trimethyl-1-(10′-carboxydeca-1′,3′,5′,7′,9′-pentaenyl)cyclohex-1-ene (XIII) (Desmethyl C_{20} Acid)—The desmethyl C_{20} acid ethyl ester (XII) was synthesized from the desmethyl C_{16} aldehyde (IX) and triethyl phosphonocrotonate, using the same procedure as described for the synthesis of the desmethyl C_{20} acid ethyl ester, mp 98.5–99°; NMR ($CDCl_3$) (Fig. 1): δ 1.04 (s, *gem*-dimethyl), 1.3 (t, ester methyl), 1.72 (s, C-2 methyl), 4.22 (q, ester methyl), 5.85 (d, C-10 proton, J = 18 Hz), and 7.38 (q, C-9 proton).

Anal.—Calc. for $C_{22}H_{32}O_2$: C, 80.98; H, 9.20. Found: C, 80.73; H, 9.15.

The desmethyl C_{20} acid (XIII) was obtained from hydrolysis of XII in alcoholic potassium hydroxide solution, mp 187–188°; UV

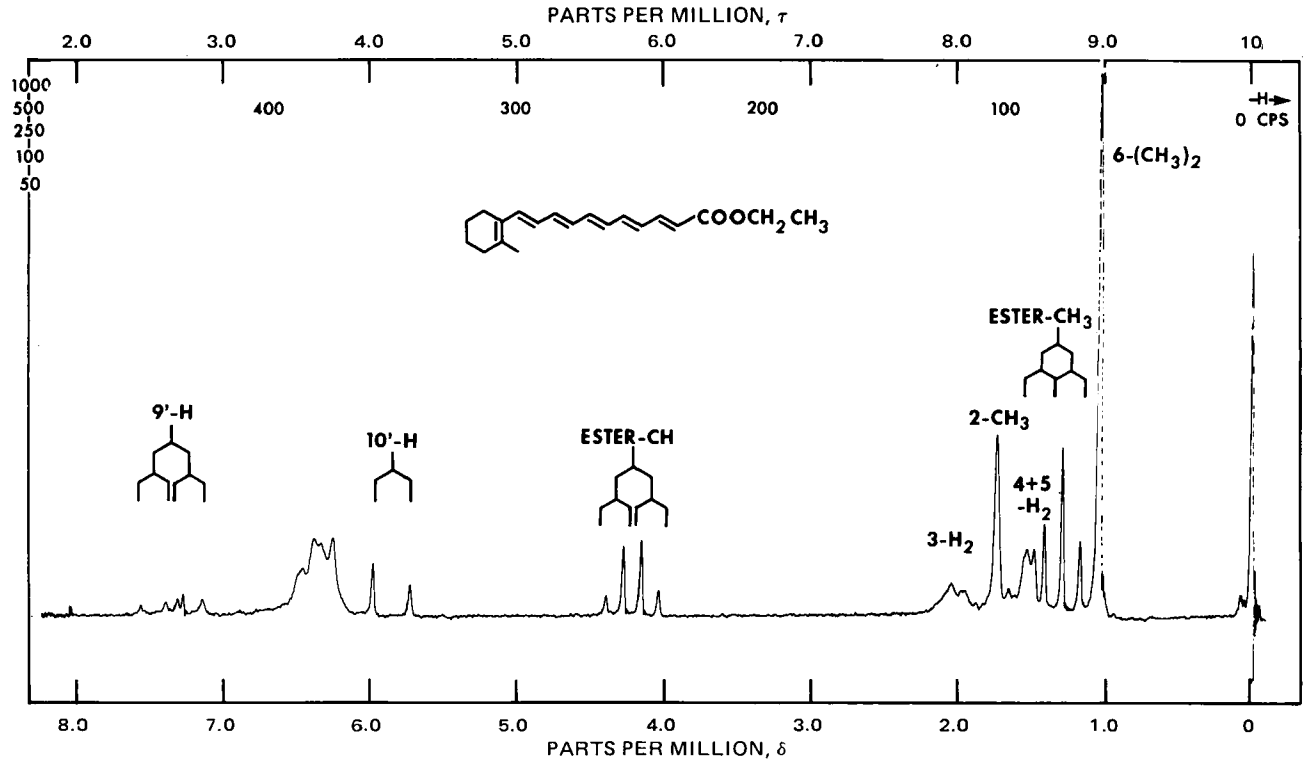

Figure 1—*NMR spectrum of XIII.*

(95% ethanol): λ_{max} 375 nm (ϵ 49,000).

Anal.—Calc. for $C_{20}H_{26}O_2$: C, 80.33; H, 8.72. Found: C, 80.55; H, 8.67.

2,6,6-Trimethyl-(12'-carboxyundeca-1',3',5',7',9',11'-hexaenyl)-cyclohex-1-ene (XVI) (Desmethyl C_{22} Acid)—The desmethyl C_{22} acid and ethyl ester (XV) were synthesized from IX and triethyl phosphonosorbate (XIV), and a 9.1% yield was obtained, mp 128–129°; NMR ($CDCl_3$) (Fig. 2): δ 1.04 (s, *gem*-dimethyl), 1.3 (t, ester methyl), 1.72 (s, C-2 methyl), 4.22 (q, ester methylene), 5.85 (d, C-12 proton, J = 15 Hz), and 7.38 (q, C-11 proton).

Anal.—Calc. for $C_{24}H_{32}O_2$: C, 81.81; H, 9.09. Found: C, 81.61; H, 8.98.

The desmethyl C_{22} acid (XVI) was obtained from hydrolysis of the desmethyl C_{22} ethyl ester in alcoholic potassium hydroxide solution, mp 193.5–195°; UV (95% ethanol): λ_{max} 396 nm (ϵ 74,200).

Anal.—Calc. for $C_{12}H_{28}O_2$: C, 81.48; H, 8.64. Found: C, 81.44; H, 8.67.

2,6,6-Trimethyl-1-(14'-carboxydodeca-1',3',5',7',9',11',13'-hept-

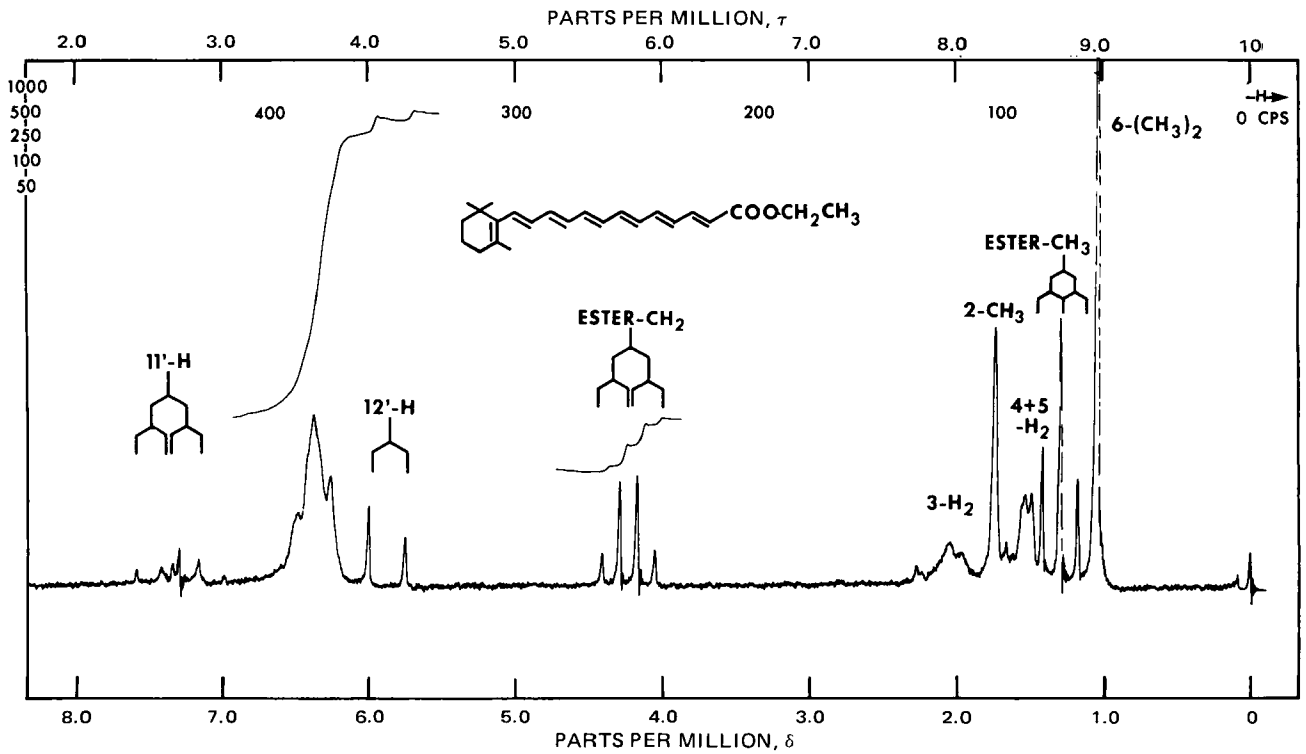

Figure 2—*NMR spectrum of XVI.*

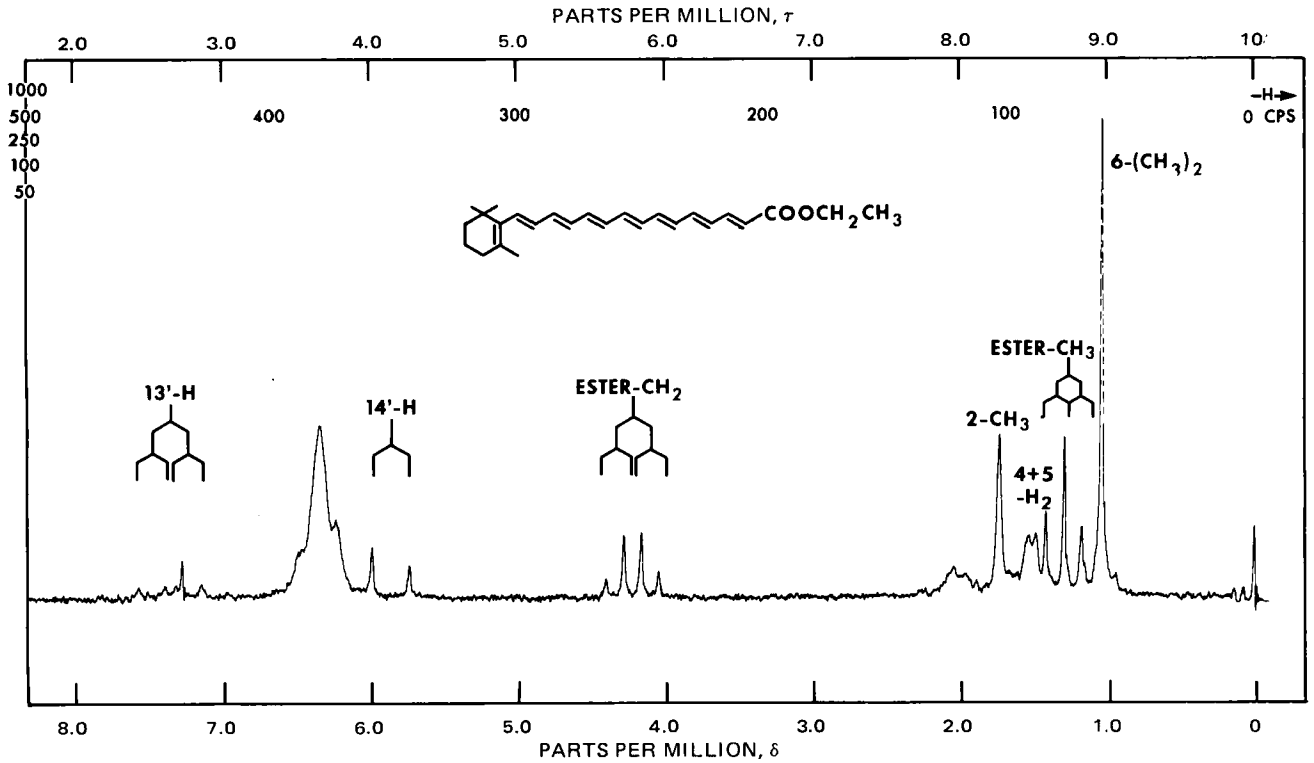

Figure 3—*NMR spectrum of XX.*

aenyl)cyclohex-1-ene (XX) (Desmethyl C_{24} Acid)—The desmethyl C_{24} acid and ethyl ester (XIX) were synthesized from the desmethyl C_{18} aldehyde (XVIII) and XIV, and a 2.2% yield was obtained, mp 158–159°; NMR ($CDCl_3$) (Fig. 3): δ 1.04 (s, *gem*-dimethyl), 1.3 (t, ester methyl), 1.72 (s, C-2 methyl), 4.22 (q, ester methylene), 5.85 (d, C-14 proton, J = 15 Hz), and 7.38 (q, C-13 proton).

Anal.—Calc. for $C_{26}H_{34}O_2$: C, 82.54; H, 8.99. Found: C, 82.36; H, 8.95.

Desmethyl C_{24} (XX) was obtained from hydrolysis of the desmethyl C_{24} acid ethyl ester in alcoholic potassium hydroxide solution, mp 202.5–203°; UV (95% ethanol): λ_{max} 415 nm (ε 85,200).

Anal.—Calc. for $C_{24}H_{30}O_2$: C, 82.38; H, 8.57. Found: C, 81.98; H, 8.30.

Triethyl Phosphonocrotonate (XIV)—Twenty-five grams of ethyl 4-bromocrotonate was placed in a three-necked flask and heated to 125° in an oil bath. Triethyl phosphite (21.5 g) was added dropwise, and the reaction was continued for 4 hr. Distillation *in vacuo* yielded 25 g of triethyl phosphonocrotonate (81.3%), bp 104–108°, 0.22 mm Hg.

RESULTS AND DISCUSSION

The structural formulas for the synthetic compounds are shown in Table I. The effects of these compounds on granuloma formation induced by implantation of cotton pellets are shown in Table II. Compounds with a side chain shorter than that of desmethylretinoic acid were not active while compounds with a side chain as long as or longer than that of desmethylretinoic acid were active. These findings are in agreement with the previous findings (4, 5) that, besides the 2,6,6-trimethylcyclohex-1-ene ring, the length of the side chain is also important for activity.

Desmethylretinoic acid was more active than retinoic acid. However, XIII, the compound with a chain two carbons longer than

Table I—Structural Formulas of Desmethylretinoic Acid Vinylogs

Compound Number	Structure	Trival Names
V	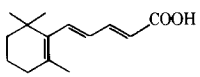	Desmethyl β-C_{14} acid
VII	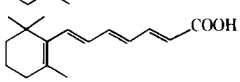	Desmethyl β-C_{16} acid
XI	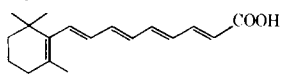	Desmethyl β-C_{18} acid or desmethylretinoic acid
XIII	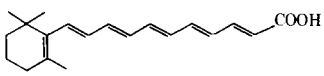	Desmethyl β-C_{20} acid
XVI	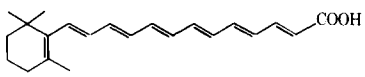	Desmethyl β-C_{22} acid
XX	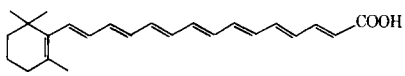	Desmethyl β-C_{24} acid

Table II—Effect of Desmethylretinoic Acid Vinylogs on Cotton Pellet-Induced Granuloma in Rats

Compound Number	Number of Animals	Granuloma Wet Weight, mg		Granuloma Weight, Experimental/Control	Granuloma Dry Weight, mg		Experimental/Control (p)
		Experimental	Control		Experimental	Control	
VII	6	238.6 ± 12.1	220.5 ± 12.2	1.1	29.0 ± 2.1	27.2 ± 2.1	1.1
XI	14	331.1 ± 14.8	208.8 ± 5.9	1.5	43.1 ± 2.6	25.5 ± 1.5	1.7
XIII	43	430.2 ± 8.1	205.0 ± 2.7	2.2	68.0 ± 1.5	23.9 ± 0.0	2.9
XVI	20	373.9 ± 8.6	202.9 ± 4.6	1.8	60.5 ± 1.6	24.9 ± 1.2	2.4
XX	6	340.3 ± 22.8	209.2 ± 4.4	1.6	51.6 ± 3.1	31.1 ± 2.0	1.7

desmethylretinoic acid, was considerably more active than its counterpart with two methyl groups on the side chain [β-C_{22} acid, 2,6,6-trimethyl-(10′-carboxy-3′,7′-dimethyldeca-1′,3′,5′,8′,9′-pentaenyl)cyclohex-1-ene] (5).

Compound XIII was the most active compound synthesized. Compound XIV was less active than XIII but was still more active than desmethylretinoic acid (XI or retinoic acid). It was also more active than its counterpart with two methyl groups on the side chain (β-C_{24} acid) (5). Even XX was a reasonably active compound.

Compounds XIII, XVI, and XX are new compounds. The NMR spectra of the esters of these acids are shown in Figs. 1–3.

Grindlay and Waugh (10) introduced a simple method for studying tissue regeneration. These workers used a polyvinyl sponge disk as a foreign body to induce granuloma formation or tissue regeneration. Jackson *et al.* (11) believed that the repair of connective tissue is the most basic feature in wound healing, and they used granulomas induced by the implanting polyvinyl sponge technique to study wound healing. It was shown previously that only retinyl derivatives that are active in increasing tensile strength of the healing wound also increase the size and weight of granuloma induced by either the cotton pellet or polyvinyl sponge (4, 5). Granuloma formation is a useful quantitative method for studying wound healing. All of the active synthetic compounds studied promote healing.

Sandberg and Zederfeldt (12) reported that the rate of gain in tensile strength and hydroxyproline in granuloma was directly related in rats or rabbits. For the present study, the effect of the active compounds on granuloma formation and the increase of hydroxyproline are shown in Tables III–VI. Meier *et al.* (13) used a cotton pellet as a foreign body to induce granuloma. Application of cortisone resulted in a diminution of granuloma size, which can be expressed quantitatively by determining its fresh or dry weight. Since then the method has been adapted as a standard assay for anti-inflammatory agents. Active retinyl compounds enhance granuloma formation, and it seems justified to call these compounds "inflammatory agents" (5, 14).

The effects of active retinyl derivatives on mucopolysaccharide synthesis were reported (4, 5). In this study, all compounds that stimulated granuloma formation also promoted mucopolysaccharide synthesis (Tables III–VI).

Inflammation and mucopolysaccharide synthesis are the two known important features in wound healing. Active retinyl derivatives reported previously (2, 14) and active compounds in the present experiment stimulated granuloma formation and promoted hydroxyproline and mucopolysaccharide synthesis. These results suggest that active retinyl compounds promote wound healing by inducing inflammation and increase the mucopolysaccharide synthesis mechanism of action.

Vitamin A or retinol has three distinct but unrelated major physiological functions. It is involved in the vision mechanism, it promotes growth, and it helps maintain a healthy epithelium. It is

Table III—Effect of XI on Hydroxyproline and Hexosamine Contents of Granuloma Induced by Cotton Pellets

	Control		Experimental
Number of animals	7		7
Granuloma dry weight, mg	25.1		48.8
Experimental/control		1.9	
Hydroxyproline weight, μg	291		425
Experimental/control		1.5	
Hydroxyproline, μg/granuloma, mg	11.5		8.7
Hexosamine weight, μg	24.3		5.3
Experimental/control		2.1	
Hexosamine, μg/granuloma, mg	9.7		10.5

Table IV—Effect of XIII on Hydroxyproline and Hexosamine Contents of Granuloma Induced by Cotton Pellets

	Control		Experimental
Number of animals	11		11
Granuloma dry weight, mg	21.3		67.3
Experimental/control		3.15	
Hydroxyproline weight, μg	277		736
Experimental/control		2.66	
Hydroxyproline, μg/granuloma, mg	12.9		10.9
Hexosamine weight, μg	201		480
Experimental/control		2.36	
Hexosamine, μg/granuloma, mg	9.4		7.0

Table V—Effect of XVI on Hydroxyproline and Hexosamine Contents of Granuloma Induced by Cotton Pellets

	Control		Experimental
Number of animals	8		8
Granuloma dry weight, mg	23.1		71.2
Experimental/control		3.06	
Hydroxyproline weight, μg	331		875
Experimental/control		2.64	
Hydroxyproline, μg/granuloma, mg	14.3		12.3
Hexosamine weight, μg	233		505
Experimental/control		2.13	
Hexosamine, μg/granuloma, mg	7.1		10.5

Table VI—Effect of XX on Hydroxyproline and Hexosamine Contents of Granuloma Induced by Cotton Pellets

	Control		Experimental
Number of animals	6		6
Granuloma dry weight, mg	30.0		47.9
Experimental/control		1.6	
Hydroxyproline weight, μg	350		600
Experimental/control		1.7	
Hydroxyproline, μg/granuloma, mg	11.7		12.6
Hexosamine weight, μg	284		460
Experimental/control		1.6	
Hexosamine, μg/granuloma, mg	9.5		9.6

well known that retinol can change reversibly to its aldehyde form (retinal) and irreversibly to its acid form (retinoic acid) in animal tissues. Retinal is responsible for the vision mechanism, but retinoic acid is not involved in this mechanism. Retinol, retinal, and retinoic acid promote growth, and any other change in structure of these molecules abolishes the growth-promoting activity.

Desmethylretinoic acid does not promote growth since it does not have methyl groups on the side chain. Being an acid, it cannot be involved in the vision mechanism. Desmethylretinoic acid promotes wound healing, and its action on epithelium is still not known. The relationships between healing and supporting a healthy epithelium are being studied.

REFERENCES

(1) K. H. Lee and T. G. Tong, *J. Pharm. Sci.*, **57**, 1238(1968).

(2) *Ibid.*, **58**, 773(1969).

(3) *Ibid.*, **59**, 851(1970).

(4) *Ibid.*, **59**, 1195(1970).

(5) K. H. Lee, C. C. Fu, M. R. Spencer, T. G. Tong, and R. Poon, *J. Pharm. Sci.*, **62**, 895(1973).

(6) J. F. Woessner, Jr., *Arch. Biochem. Biophys.*, **93**, 440(1961).

(7) C. Cessi and F. Piliego, *Biochem. J.*, **77**, 508(1960).

(8) P. J. van der Tempel and H. O. Herisman, *Tetrahedron*, **22**, 293(1966).

(9) S. Ball, T. W. Goodwin, and R. A. Morton, *Biochem. J.*, **42**, 516(1948).

(10) J. H. Grindlay and J. M. Waugh, *Arch. Surg.*, **63**, 633(1951).

(11) D. S. Jackson, D. B. Flinkinger, and J. E. Dunphy, *Ann. N.Y. Acad. Sci.*, **86**, 943(1960).

(12) N. Sandberg and B. Zederfeldt, *Acta Chim. Scand.*, **126**, 187(1963).

(13) R. Meier, W. Schuler, and P. Desaulles, *Experientia*, **6**, 469(1950).

(14) K. H. Lee and T. G. Tong, *J. Pharm. Sci.*, **59**, 1036(1970).

ACKNOWLEDGMENTS AND ADDRESSES

Received December 18, 1974, from the *School of Pharmacy, University of California, San Francisco, CA 94143*

Accepted for publication July 17, 1975.

Supported in part by Barnes-Hind Pharmaceuticals, Inc., Sunnyvale, Calif.

[x] To whom inquiries should be directed.

Solvent-Dependent Conformational System in Hydroxyureas Detected by NMR Spectroscopy

GEORGE R. PARKER [x], NANCY K. HILGENDORF, and JAMES G. LINDBERG *

Abstract □ The proton magnetic resonance spectra of the antileukemia agent hydroxyurea and substituted hydroxyureas in several solvents were recorded and correlated with structural features. Solvent-dependent differences in conformational preferences due to effects on internal hydrogen bonding, a temperature-dependent conformational feature, and the exchangeability of protons with deuterium oxide and acetone-d_6 were observed. The conformational features consistent with the spectral data are discussed.

Keyphrases □ Hydroxyurea and substituted hydroxyureas—NMR spectra correlated with structural features, solvent-dependent differences observed □ NMR spectroscopy—hydroxyurea and substituted hydroxyureas, spectra correlated with structural features, solvent-dependent differences observed □ Solvent-dependent conformational system—hydroxyurea and substituted hydroxyureas, detected by NMR spectroscopy □ Antileukemic agents—hydroxyurea, NMR spectra correlated with structural features

NMR spectroscopy has become a powerful tool for the determination of organic molecular structure, configurational stereochemistry, and conformational properties of molecules (1). Knowledge concerning the conformational properties of drugs at their site of action is essential to the understanding of the complex molecular mechanism of action (2).

An NMR analysis was conducted on a series of substituted analogs of the antileukemia agent hydroxyurea (I) to gain some insight into the conformational properties that might explain the relative biological inactivity of the 3-*N*-substituted analogs. Hydroxyurea has been observed to inhibit DNA synthesis in various biological systems (3–5) and exhibits

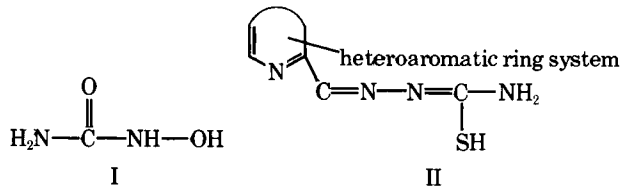

I II

activity against L-1210 lymphoid leukemia (6). The action of this compound has been attributed to the inhibition of the iron-dependent, allosterically controlled enzyme ribonucleoside diphosphate reductase (7–9) *via* a mechanism similar to that observed in a series of α-*N*-formylheteroaromatic thiosemicarbazones (II) (10).

In contrast to the rather large number of active analogs of II (72 of 97 compounds rated active *in vitro* and 51 of 97 active *in vivo*), only the ethyl and *n*-propyl analogs substituted at the 3-*N*-position and the methyl and ethyl 1-*N*-analogs of hydroxyurea were active *in vivo* against L-1210 lymphoid leukemia[1]. These biological data could be rationalized in terms of *in vivo* instability, poor transportability to the site of action, steric effects at the site of action, or conformational factors relevant to drug action, which this paper reports as a possibility in substituted hydroxyureas.

The molecular mechanism of action of I and II has

[1] Personal communication from the Cancer Chemotherapy National Screening Center of the National Cancer Institute.

well known that retinol can change reversibly to its aldehyde form (retinal) and irreversibly to its acid form (retinoic acid) in animal tissues. Retinal is responsible for the vision mechanism, but retinoic acid is not involved in this mechanism. Retinol, retinal, and retinoic acid promote growth, and any other change in structure of these molecules abolishes the growth-promoting activity.

Desmethylretinoic acid does not promote growth since it does not have methyl groups on the side chain. Being an acid, it cannot be involved in the vision mechanism. Desmethylretinoic acid promotes wound healing, and its action on epithelium is still not known. The relationships between healing and supporting a healthy epithelium are being studied.

REFERENCES

(1) K. H. Lee and T. G. Tong, *J. Pharm. Sci.*, **57**, 1238(1968).

(2) *Ibid.*, **58**, 773(1969).

(3) *Ibid.*, **59**, 851(1970).

(4) *Ibid.*, **59**, 1195(1970).

(5) K. H. Lee, C. C. Fu, M. R. Spencer, T. G. Tong, and R. Poon, *J. Pharm. Sci.*, **62**, 895(1973).

(6) J. F. Woessner, Jr., *Arch. Biochem. Biophys.*, **93**, 440(1961).

(7) C. Cessi and F. Piliego, *Biochem. J.*, **77**, 508(1960).

(8) P. J. van der Tempel and H. O. Herisman, *Tetrahedron*, **22**, 293(1966).

(9) S. Ball, T. W. Goodwin, and R. A. Morton, *Biochem. J.*, **42**, 516(1948).

(10) J. H. Grindlay and J. M. Waugh, *Arch. Surg.*, **63**, 633(1951).

(11) D. S. Jackson, D. B. Flinkinger, and J. E. Dunphy, *Ann. N.Y. Acad. Sci.*, **86**, 943(1960).

(12) N. Sandberg and B. Zederfeldt, *Acta Chim. Scand.*, **126**, 187(1963).

(13) R. Meier, W. Schuler, and P. Desaulles, *Experientia*, **6**, 469(1950).

(14) K. H. Lee and T. G. Tong, *J. Pharm. Sci.*, **59**, 1036(1970).

ACKNOWLEDGMENTS AND ADDRESSES

Received December 18, 1974, from the *School of Pharmacy, University of California, San Francisco, CA 94143*

Accepted for publication July 17, 1975.

Supported in part by Barnes-Hind Pharmaceuticals, Inc., Sunnyvale, Calif.

[x] To whom inquiries should be directed.

Solvent-Dependent Conformational System in Hydroxyureas Detected by NMR Spectroscopy

GEORGE R. PARKER [x], NANCY K. HILGENDORF, and JAMES G. LINDBERG *

Abstract □ The proton magnetic resonance spectra of the antileukemia agent hydroxyurea and substituted hydroxyureas in several solvents were recorded and correlated with structural features. Solvent-dependent differences in conformational preferences due to effects on internal hydrogen bonding, a temperature-dependent conformational feature, and the exchangeability of protons with deuterium oxide and acetone-d_6 were observed. The conformational features consistent with the spectral data are discussed.

Keyphrases □ Hydroxyurea and substituted hydroxyureas—NMR spectra correlated with structural features, solvent-dependent differences observed □ NMR spectroscopy—hydroxyurea and substituted hydroxyureas, spectra correlated with structural features, solvent-dependent differences observed □ Solvent-dependent conformational system—hydroxyurea and substituted hydroxyureas, detected by NMR spectroscopy □ Antileukemic agents—hydroxyurea, NMR spectra correlated with structural features

NMR spectroscopy has become a powerful tool for the determination of organic molecular structure, configurational stereochemistry, and conformational properties of molecules (1). Knowledge concerning the conformational properties of drugs at their site of action is essential to the understanding of the complex molecular mechanism of action (2).

An NMR analysis was conducted on a series of substituted analogs of the antileukemia agent hydroxyurea (I) to gain some insight into the conformational properties that might explain the relative biological inactivity of the 3-*N*-substituted analogs. Hydroxyurea has been observed to inhibit DNA synthesis in various biological systems (3–5) and exhibits

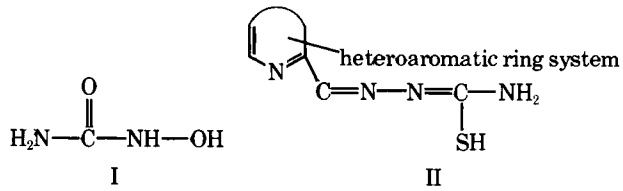

I II

activity against L-1210 lymphoid leukemia (6). The action of this compound has been attributed to the inhibition of the iron-dependent, allosterically controlled enzyme ribonucleoside diphosphate reductase (7–9) *via* a mechanism similar to that observed in a series of α-*N*-formylheteroaromatic thiosemicarbazones (II) (10).

In contrast to the rather large number of active analogs of II (72 of 97 compounds rated active *in vitro* and 51 of 97 active *in vivo*), only the ethyl and *n*-propyl analogs substituted at the 3-*N*-position and the methyl and ethyl 1-*N*-analogs of hydroxyurea were active *in vivo* against L-1210 lymphoid leukemia[1]. These biological data could be rationalized in terms of *in vivo* instability, poor transportability to the site of action, steric effects at the site of action, or conformational factors relevant to drug action, which this paper reports as a possibility in substituted hydroxyureas.

The molecular mechanism of action of I and II has

[1] Personal communication from the Cancer Chemotherapy National Screening Center of the National Cancer Institute.

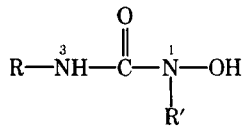

III

been proposed to involve ligand formation with enzymatic octahedral iron (11, 12), involving conformational planarity in the ligand molecule. NMR spectra of the substituted analogs of hydroxyurea (III) compared to hydroxyurea in various solvents indicated solvent-dependent conformational equilibria sensitive to the π-bond character between the 3-nitrogen and the carbonyl carbon and internal hydrogen bonding between the hydroxyl hydrogen and the carbonyl oxygen. This paper describes the NMR spectral data supporting this assertion.

The properties of internal hydrogen bonding and hindered rotation in hydroxyurea and its substituted derivatives due to this π-bond character may affect the acidity and complexing affinity toward ligand formation as well as *in vivo* stability and transportability. The resultant effect on pKa, lipid solubility, and conformational affinity toward ligand formation may influence the overall biological activity of these molecules. Other investigators may wish to consider these properties in the elucidation of the mechanism of action of hydroxyurea as an antileukemia agent and in the explanation of the reduced activity of substituted analogs as *in vivo* inhibitors of DNA synthesis.

EXPERIMENTAL

Materials—Hydroxyurea was purchased from a commercial source[2], and the 3-*N*-substituted analogs (Table I) were synthesized according to the original procedure (13) with reported modifications (14, 15). The 1-*N*-substituted analogs were made available for this study[3].

NMR Spectra—The NMR spectra were obtained using an NMR spectrometer[4] equipped with a variable temperature accessory. The chemical shift data were measured relative to tetramethylsilane[5] as an internal standard. Location of peaks (δ) is by parts per million downfield from the standard. Solvents for spectral data were acetone-d_6 (99%), pyridine-d_5 (99%), spectral grade pyridine, spectral grade tetrachloroethane, and deuterium oxide; all were obtained from commercial sources[6].

RESULTS

The NMR data for hydroxyurea and substituted analogs in various solvents and after deuterium oxide was added to the solvent appear in Table II. The spectrum of hydroxyurea in acetone-d_6 was somewhat difficult to obtain, since this derivative is the least soluble in this solvent. A low intensity spectrum showed a broad multiplet at 5.75 ppm and multiplets at 7.65 and 7.95 ppm in a ratio of 2:1:1.

Hydroxyurea in pyridine-d_5 appeared as signals in three general chemical shift regions: multiplets at 5.2 and 5.7 ppm, a singlet at 6.7 and a multiplet at 7.7 ppm, and multiplets at 8.4 and 9.1 ppm. The total integration for the signals in the three areas was 2:1:1. In a mixed solvent system of acetone-d_6–pyridine-d_5 (1:1), five distinct signals were observed: a broad multiplet at 6.8 ppm, sharp multiplets at 7.3 and 7.7 ppm, a sharp singlet at 8.7 ppm, and a broad multiplet at 9.1 ppm. A weaker and broad multiplet was also seen at 9.8 ppm, and the ratio of the signals between 6.8 and 7.7 ppm to those at 8.7–9.8 ppm was 3:1.

The addition of deuterium oxide to all of these systems produced an immediate loss of signals due to exchange, except for the deuterated water signal and weak signals at 5.2 and 6.4 ppm with hydroxyurea in pyridine-d_5. All of the spectra of hydroxyureas taken in acetone-d_6 showed a signal at around 3.0 ppm, which was found to be trace water in the acetone-d_6. This signal became larger when hydroxyureas were used that had traces of water in them.

In spectra of the 3-*N*-substituted hydroxyureas (IV–IX), the identification and assignment of three distinct signals downfield (for the two amino and the hydroxyl protons) was difficult for the *n*-propyl and the aromatic analogs of hydroxyurea in acetone-d_6. These signals were all observed for the isopropyl, *n*-butyl, and 1-*N*-substituted analogs of hydroxyurea in acetone-d_6, although the signal assigned to the hydroxyl proton (farthest downfield) rarely integrated as a single proton but rather as a fraction of a proton. The farthest downfield signal (integrated as one or nearly one proton) was observable in the 1-*N*-substituted analogs and in all spectra of compounds taken in pyridine-d_5.

Special attention was given to the isopropyl and *n*-butyl analogs (V and VI) in the 3-*N*-substituted series, since their spectra were different than what was expected. The methyl groups of the isopropyl analog in the solvents acetone-d_6, pyridine-d_5 (anhydrous and after water was added), pyridine (with trace water present), and tetrachloroethane at 36° appear in Fig. 1. The methyl peaks of V in the wet pyridine at 85° also appear in Fig. 1.

The methyl signal in acetone-d_6 appeared as unequal doublets and as three unequal doublets in pyridine rather than the expected doublet for the isopropyl group, and these doublets coalesced into a simple doublet after water was added. The coalescence was dependent on the amount of water or deuterium oxide added. The spectrum taken in spectral grade pyridine (not anhydrous) appeared as three doublets, all of substantial size, which changed relative peak heights at 85° but did not coalesce into two or one doublet.

The methyl groups appeared as a simple doublet in the solvent tetrachloroethane (selected as a suitable solvent for high temperature study) at the normal spectrometer temperature of 36°. The methine proton signal appeared to coalesce to a heptet from the complex signal, which appeared to be two overlapping heptets seen in acetone-d_6 and pyridine-d_5 prior to the addition of water or deuterium oxide.

Table I—Substituted Analogs of Hydroxyurea

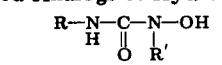

Compound	R	R′	Literature (14) Melting Point	Melting Point Found
IV	*n*-Propyl	H	128–129°	127–129°
V	Isopropyl	H	—	108–110°[a]
VI	*n*-Butyl	H	123–125°	122–125°
VII	Phenyl	H	142° dec.	141–142° dec.
VIII	*p*-Tolyl	H	151–153°	151–153°
IX	*p*-Chlorophenyl	H	171° dec.	170–171° dec.
X	H	Methyl	—	—
XI	H	Ethyl	—	—

[a] *Anal.*—Calc.: C, 40.66; H, 8.53; N, 23.72. Found: C, 40.47; H, 8.53; N, 24.04.

DISCUSSION

The use of NMR spectroscopy in the determination of structural and conformational properties of compounds related to urea and hydroxyurea was reviewed previously (16). The NMR data reported in this paper are similar to those in studies involving the effect of solvent (17) and of internal hydrogen bonding (18) on conformational properties of amides. In the hydroxyurea series in this study, a solvent-dependent conformational system was detected which may be partly due to internal hydrogen bonding.

In the hydroxyurea system (Scheme I), if hindrance to rotation

[2] Aldrich Chemical Co.
[3] Squibb Institute for Medical Research.
[4] Varian T60A, 60-MHz spectra.
[5] Stohler Isotope Chemical Co.
[6] Aldrich Chemical Co. and Stohler Isotope Chemical Co.

Table II—Data of Hydroxyureas in Various Solvents

Compound (Solvent)	Chemical Shift of Signals[a], δ
Hydroxyurea (I) (acetone-d_6)	5.75 (broad m, 1–2H, NH_2), 7.7 (m, 0.5H, NH), 8.0 (m, 1.5H, NH and OH)
I (acetone-d_6 plus deuterium oxide)	4.2 (DOH)
I (pyridine-d_5)	5.2 and 5.7 (m, 2H, NH_2), 6.7 (s) and 7.7 (m, 1H, NH), 8.4 (m) and 9.1 (broad s, 1H, OH)
I (pyridine-d_5 plus deuterium oxide)	3.2 (DOH), 5.2 and 6.4 (weak signals, ratio of 1:1)
I [pyridine-d_5–acetone-d_6 (1:1)]	6.8 (m), 7.3 (m) and 7.7 (m, 3H, NH_2 and NH), 8.7 (s), 9.1 (m), and 9.8 (broad m, 1H, OH)
3-*N*-(*n*-Propyl)hydroxyurea (IV) (acetone-d_6)	1.0 (t, 3H, CH_3), 1.55 (sextet, 2H, CH_2), 3.0 (m, 2H, CH_2), 6.2 and 7.0 (m, 1–2H, NH and/or OH)
IV (acetone-d_6 plus deuterium oxide)	1.0 (t, 3H, CH_3), 1.6 (sextet, 2H, CH_2), 3.15 (t, 2H, CH_2), 3.9 (DOH)
IV (pyridine-d_5)	0.9 (t, 3H, CH_3), 1.6 (sextet, 2H, CH_2), 3.5 (q, 2H, CH_2), 7.3 (m, 1H, NH), 9.6 (s, 1H, NH), 11.0 (m, 1H, OH)
IV (pyridine-d_5 plus deuterium oxide)	0.8 (t, 3H, CH_3), 1.5 (sextet, 2H, CH_2), 3.3 (complex t, 2H, CH_2), 5.4 (DOH), 7.3 (m, 0.3H, NH), 8.6 (s, 0.1H, NH), 9.4 (m, 0.2H, OH)
3-*N*-(Isopropyl)hydroxyurea (V) (acetone-d_6)	1.2 (2 pairs d, 6H, CH_3), 3.2 (H_2O), 3.9 (2 pairs heptet, 1H, CH), 6.3 (m, 1H, NH), 8.0 (m, 0.5H, NH), 8.4 (s, 0.5H, OH)
V (acetone-d_6 plus deuterium oxide)	1.1 (2 pairs d, 6H, CH_3), 3.8 (DOH), 3.9 (heptet, 1H, CH)
V (pyridine-d_5 anhydrous)	1.3 (2 pairs d, 6H, CH_3), 4.3 (octet, 1H, CH), 6.9 (d, 1H, NH), 8.8 (m, 1H, NH), 10.9 (m, 1H, OH)
V (pyridine-d_5 plus deuterium oxide)	1.2 (d, 6H, CH_3), 4.2 (m, 1H, CH), 5.3 (DOH), 6.9 (d, 0.3H, NH), 9.3 (m, 0.3H, NH or OH)
V (pyridine, trace water)	1.1 (3 pairs d, 6H, CH_3), 4.1 (complex nonet, 1H, CH)
V (tetrachloroethane)	1.1 (d, 6H, CH_3), 3.8 (heptet, 1H, CH)
3-*N*-(*n*-Butyl)hydroxyurea (VI) (acetone-d_6)	0.9 (m, 3H, CH_3) 1.5 (m, 4H, CH_2CH_2), 3.1 (m, 2H, CH_2 and H_2O), 6.5 (m, 1H, NH), 7.8 (m, 1H, NH), 8.3 (m, 1H, OH)
VI (acetone-d_6 plus deuterium oxide)	0.9 (t, 3H, CH_3), 1.4 (m, 4H, CH_2CH_2), 3.2 (m, 2H, CH_2N), 4.0 (DOH)
VI (pyridine-d_5)	0.9 (m, 3H, CH_3), 1.7 (m, 4H, CH_2CH_2), 3.5 (complex q, 2H, CH_2), 7.3 (m, 1H, NH), 9.3 (m, 1H, NH), 10.8 (broad m, 1H, OH)
VI (pyridine-d_5 plus deuterium oxide)	0.8 (m, 3H, CH_3), 1.4 (m, 4H, CH_2CH_2), 5.8 (DOH), 7.3 (m, 0.3H, NH)
3-*N*-(Phenyl)hydroxyurea (VII) (acetone-d_6)	3.2 (H_2O), 7.3 (m, 5H, C_6H_5), 8.3 (m, 1H, NH), 9.2 (m, 0.6H, NH), 10.0 (m, 0.3H, OH)
VII (acetone-d_6 plus deuterium oxide)	3.65 (DOH), 7.3 (m, 5H, C_6H_5)
3-*N*-(*p*-Tolyl)hydroxyurea (VIII) (acetone-d_6)	2.3 (s, 3H, CH_3), 3.0 (H_2O), 7.3 (m, 4H, C_6H_4), 8.7 (m, 0.5H, NH and/or OH)
VIII (acetone-d_6 plus deuterium oxide)	2.3 (s, 3H, CH_3), 3.8 (DOH), 7.3 (m, 4H, C_6H_4)
3-*N*-(*p*-Chlorophenyl)hydroxyurea (IX) (acetone-d_6)	3.0 (H_2O), 7.5 (m, 4H, C_6H_4), 8.4 (m, 0.5H, NH or OH)
IX (acetone-d_6 plus deuterium oxide)	3.9 (DOH), 8.5 (m, 4H, C_6H_4)
1-*N*-(Methyl)hydroxyurea (X) (acetone-d_6)	3.1 (s, 3H, CH_3), 6.2 (m, 2H, NH_2), 9.1 (m, 1H, OH)
X (acetone-d_6 plus deuterium oxide)	3.1 (s, 3H, CH_3), 3.8 (DOH), 6.2 (m, 0.25H, NH_2), 9.6 (m, 0.12H, OH)
X (pyridine-d_5)	2.7 (s, 3H, CH_3), 6.5 (m, 2H, NH_2), 8.7 (m, 1H, OH)
X (pyridine-d_5 plus deuterium oxide)	3.4 (s, 3H, CH_3), 5.8 (DOH), 6.2 (broad m, 1H, NH), 7.0 (m, 1H, NH)
1-*N*-(Ethyl)hydroxyurea (XI) (acetone-d_6)	1.1 (t, 3H, CH_3), 3.5 (q, 2H, CH_2), 6.2 (m, 2H, NH_2), 9.1 (m, 1H, OH)
XI (acetone-d_6 plus deuterium oxide)	1.1 (t, 3H, CH_3), 3.6 (complex q, 2H, CH_2), 3.9 (DOH)
XI (pyridine-d_5)	0.6 (t, 3H, CH_3), 3.2 (q, 2H, CH_2), 6.5 (m, 2H, NH_2), 10.7 (m, 1H, OH)
XI (pyridine-d_5 plus deuterium oxide)	1.2 (t, 3H, CH_3), 3.7 (q, 2H, CH_2), 5.8 (DOH), 6.8 (m, 0.3H, NH)

[a] Chemical shifts reported as δ in parts per million downfield from tetramethylsilane.

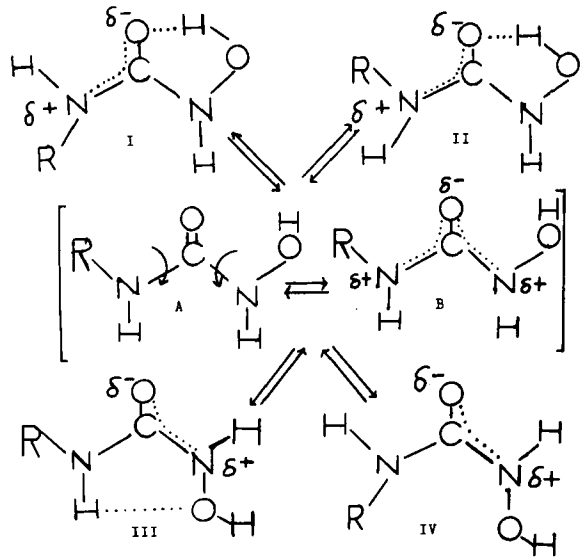

Scheme I—Conformers (I–IV) produced by rotation around 1-N-carbonyl and 3-N-carbonyl bonds by passing through some intermediate. Hypothetical intermediates A and B possess all sp^3 *bonds (A) or distribution of π-bond character all along the N—C—N system.*

around the nitrogen–carbonyl bonds is minimal, all four conformers are present in proportion to their thermodynamic stability in solution, but individual conformers are not discernible by NMR due to rapid interconversion between conformers. Hindered rotation about either the 1-*N*- or 3-*N*-carbonyl bond produces conformational isomers due to slow rotation with respect to the NMR time scale, and these isomers are observable in the NMR spectra.

The most conclusive proofs of conformational isomerization in this hydroxyurea series are the NMR spectra of the isopropyl analog (V) in various solvents. The addition of water and deuterium oxide to the systems produced changes in the spectra, which appear to indicate that internal hydrogen bonding is reduced by hydrogen bonding to solvent water (or deuterium oxide). This finding indicates that the conformational isomerization in the isopropyl analog, which is observed on the NMR time scale as complex doublets, is due to internal hydrogen bonding (I, II, and III in Scheme I); this bonding increases the amount of π-bond character between the 3-nitrogen and the carbonyl carbon.

The spectrum of the 3-*N*-(*n*-butyl) analog was also more complex than expected for a simple *n*-butyl group, and decoupling of the methylene group from the nitrogen (—CH_2CH_2NH) simplified the spectrum to some extent. Nevertheless, the uncoupled spectrum also can be interpreted as one derived from a hindered system where conformational isomers are present.

The isopropyl methyl groups of V appeared as a set of doublets in acetone-d_6, as three sets of doublets of about equal size in spectral grade pyridine (trace water present), and as three sets of doublets (one pair large and two pairs of much smaller but equal size)

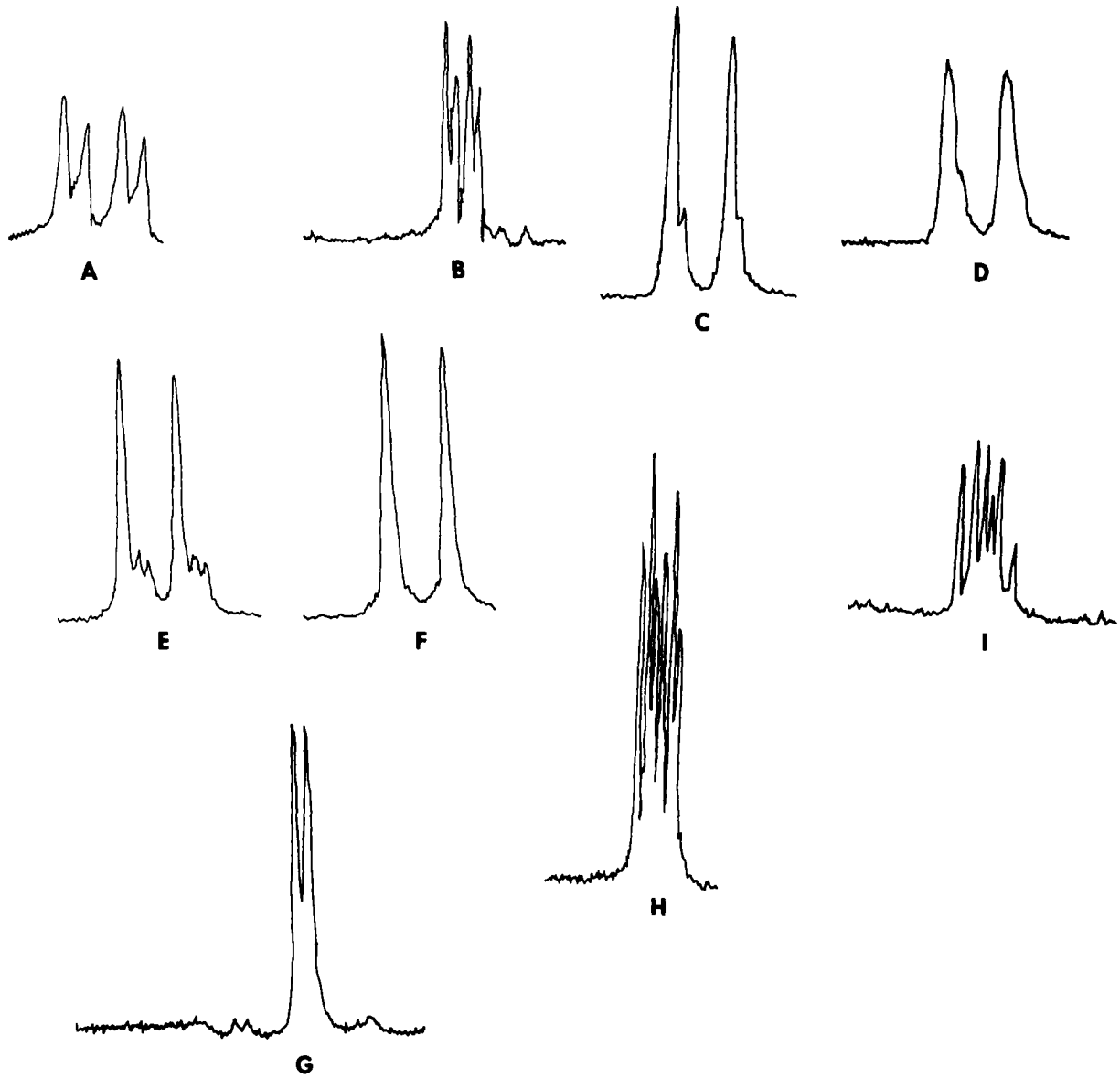

Figure 1—*Spectra of methyl peaks of 3-*N*-(isopropyl)hydroxyurea in various solvents. Key: A and B, in acetone-*d_6* with sweep width of 100 and 250 Hz, respectively; C and D, in the same solvent after water was added; E and F, in pyridine-*d_5* in solvent with trace water (E) and after water was added; H, in pyridine (trace water) at 85°; and I, in same solvent at 36°, as are all other spectra. G is spectrum in tetrachloroethane at 36°. Spectra C, D, E, and F had a sweep width of 100 Hz and G, H, and I had a sweep width of 500 Hz.*

in pyridine-d_5 at 36° (Fig. 1). All of these spectra coalesced into a simple doublet after sufficient water or deuterium oxide was added.

The NMR spectrum of the isopropyl analog in acetone-d_6 (Fig. 1; A and B were taken almost immediately after the acetone-d_6 was opened) can be rationalized as due to conformers where rotation was slowed on the NMR time scale and the isopropyl group was thus in the proximity of the carbonyl carbon or the carbonyl oxygen (Scheme II) for longer periods than would be expected if rotation around bonds was unhindered. In this system, hydrogen bonding internally between the hydroxyl and the carbonyl oxygen would promote an increase in π-bond character (3-nitrogen to carbonyl), separation of charge, and a change of hybridization state of the 3-nitrogen from sp^3 to sp^2 (Schemes I and II). When more water or deuterium oxide was added to this system, a simple doublet was observed, which might be rationalized as due to hydrogen bonding between the hydroxyl group and water and the carbonyl oxygen and water (or deuterium oxide).

If the π-character between the 1-nitrogen and carbonyl carbon is increased with a corresponding decrease in π-character between the 3-nitrogen and carbonyl *via* this hydrogen bonding with water, then faster rotation around the 3-*N*-carbonyl bond by the isopropyl group would be possible, and this result would be observed on the NMR time scale as a simple doublet. The observation of three sets of doublets in pyridine (I in Fig. 1) can be rationalized as due to a rotating conformational system (Scheme I), where four conformers are possible (I–IV). These conformers are due to rotations around the 1-*N*—carbonyl—3-*N* bonds and pass through some transition state existing somewhere between A and B.

The canonical form shown as A depicts the hydroxyurea system as entirely made up of sp^3 bonds between nitrogens and carbonyl carbon, and free and unhindered rotation would be possible. This system would be characterized as fast rotation on the NMR time scale, and the spectrum would be observed as a simple doublet in the case of the isopropyl group. The canonical form shown as B depicts a system where the π-bond character is equally distributed across the nitrogen–carbon–nitrogen system, with a resultant separation of charge. In this case, rotation is restricted due to the π-character of the bonds; if no rotation occurs, discrete conformers exist.

If π-bond character between 1-nitrogen and carbonyl carbon increases with a corresponding decrease in π-bond character at the 3-*N*-carbonyl bond in B, rotation around the 3-*N*-carbonyl bond would be allowed as long as internal hydrogen bonding (seen in Conformers I and II) did not prevent it. Changes in the hybridization state of the nitrogen–carbon–nitrogen system would allow

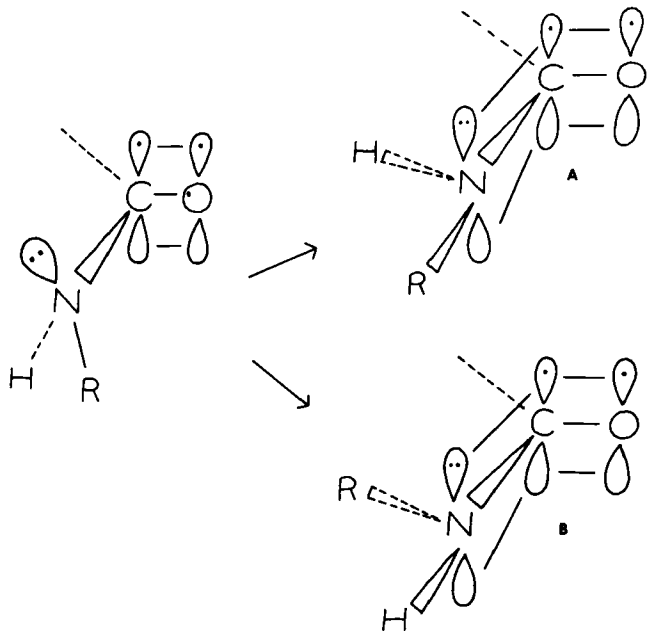

Scheme II—Change of hybridization state of 3-nitrogen from sp^3 *to* sp^2*, with resultant* π*-character of 3-N-carbonyl carbon bond producing conformational isomers A and B, which have the R group held rigid either in the environment of the carbonyl oxygen (A) or the carbonyl carbon (B).*

Conformers I–IV to form *via* rotation due to the sp^3 character of the bonds (similar to that in A). The speed of rotation between these conformers would be observable on the NMR time scale, and they would be seen as a single conformer if rotation and interconversion are fast or as individual conformers if rotation and interconversion are slow.

Conformer IV would probably be in the lowest population, since it is not stabilized by internal hydrogen bonding. Conformer III might not be observed if hydrogen bonding to solvent (such as acetone) is stronger than internal hydrogen bonding. The three sets of signals in pyridine then might be interpreted as due to Conformers I–III, and the two sets of peaks in acetone-d_6 might be interpreted as due to I and II. When a polar solvent (such as water or deuterium oxide) is added to the system, the amount of internal hydrogen bonding is decreased due to hydrogen bonding with solvent; thus, Conformers I–III are not as stable, and rotation and interconversion are more rapid. This result might explain why the addition of water or deuterium oxide to these systems produces NMR spectra where a simple doublet is observed rather than the complex sets of two or three doublets.

Conformer III, which depicts a restriction of rotation due to an increase in π-bond character between the 1-nitrogen and carbonyl and internal hydrogen bonding between the 3-*N*-proton and hydroxyl oxygen, might only be observable when the carbonyl carbon is stabilized by solvent such as the case of pyridine. The best representations of the system are not A and B but rather systems where there is some degree of sp^3 bond character, some π-bond character between 1-*N*-carbonyl and 3-*N*-carbonyl at all times, and the increase and/or decrease of the π-bond character allows the rotation in the systems through Conformers I–IV.

When a spectrum of the isopropyl analog was taken in tetrachloroethane (for a high temperature study), the isopropyl group appeared as a simple doublet at 36°. The coalescence of the peaks in a relatively nonpolar solvent (a dielectric constant of 8.2 compared to 78.5, 20.7, and 12.3 for water, acetone, and pyridine, respectively) was unexpected. The fact that the isopropyl group of V in tetrachloroethane produced a doublet could mean that: (*a*) the conformational mobility is fast on the NMR time scale, possibly due to fast interconversion (faster than that observed in acetone and pyridine); or (*b*) there is a greater preponderance of one conformation in this solvent.

Since the least polar solvent in this series produces a spectrum similar to that observed when the most polar agent (*i.e.*, water, *etc.*) is added to the solvents, both of these possibilities may be the explanation. Possibly, tetrachloroethane is the least able to stabilize the separation of charge that occurs in conformers where π-character is increased between the nitrogens and carbonyl carbon of the system (Conformers I–IV in Scheme I); thus, rotation about bonds and interconversion are very fast, and a simple doublet appears in the NMR spectrum. Tetrachloroethane could possibly be acting as a proton donator similar to chloroform, which would then stabilize Conformer IV (Scheme I), or possibly act by some mechanism to stabilize one particular conformer of the system in preference to all of the others. But these explanations seem less likely than the increase in speed of interconversion where charge is not separated and the conformers are not stabilized.

Although it is not possible to determine from the data presented whether conformational isomers due to restricted rotation are present in all of the substituted analogs, the NMR spectra of hydroxyurea (I) and other compounds of the series in various solvents indicate that the likelihood of conformational isomerization in the hydroxyurea series exists. The molecule hydroxyurea is structurally or conformationally different in the two solvents, acetone-d_6 and pyridine-d_5. Hydroxyurea may exchange with one solvent (acetone-d_6) and not with pyridine, but pyridine is the better base.

In acetone-d_6, it was difficult to determine whether the signal assigned to the hydroxyl proton represented one proton. However, it appeared that less than one proton was present, possibly due to immediate exchange with solvent. In pyridine, hydroxyurea appeared as three distinct signals in the ratio of 2:1:1, as would be expected for hydroxyurea. The spectrum of hydroxyurea in a mixed solvent system [acetone-d_6–pyridine-d_5 (1:1)] possessed three downfield signals equal to a single proton. This proton could be the hydroxyl proton in three different environments, as would be expected in Conformers I–III (Scheme I) where internal hydrogen bonding would stabilize these conformers.

The comparison of some compounds of this series in acetone-d_6 and pyridine-d_5 indicates that the hydroxyl proton is recognizable in the spectra of all compounds taken in pyridine, while only the 1-*N*-substituted analogs and the 3-*N*-isopropyl and *n*-butyl compounds show a recognizable hydroxyl signal. This observation might be attributed to a property of these analogs, such as a greater degree of internal hydrogen bonding or a stronger hydrogen bond, which protects these analogs from exchanging with the solvent acetone-d_6. While this process might be taking place, it is difficult to verify in this system since the exchange of the hydroxyl proton with deuterium of acetone-d_6 is dependent on the enolization of the acetone and the rate of this process can be increased if trace amounts of acid are added to these systems and observed as relatively fast exchange of the hydroxyl proton in the NMR spectra. Since the hydroxyureas in this series are not stable for long periods at room temperature and in solvents, trace amounts of acidic (or basic) residues might be catalyzing the enolization of the acetone-d_6, producing the exchange of the hydroxyl proton in certain analogs.

It is concluded from these data that conformational isomers are possible in hydroxyurea systems due to possible internal hydrogen bonding between the carbonyl oxygen and hydroxyl proton. This hydrogen bonding appears to be further stabilized in nonhydrogen bonding solvents, which are polar enough to stabilize the resultant separation of charge, and by substitution at the 3-nitrogen by bulky groups such as isopropyl.

The internal hydrogen bonding can be reduced by solvents such as acetone, which can hydrogen bond to hydroxyl, but this bonding continues to stabilize the conformers that are still hydrogen bonded. The internal hydrogen bonding is appreciably reduced by the addition of a polar hydrogen bonding solvent, such as water, which appears to promote separation of charge between the 1-nitrogen and the carbonyl carbon and thus allows free rotation around the 3-*N*-carbonyl axis. The use of a relatively nonpolar solvent such as tetrachloroethane appears to promote the conformational form that is most nonpolar (similar to canonical form A in Scheme I), which allows fast interconversion between Conformers I–IV due to free rotation around both the 1-*N*-carbonyl and the 3-*N*-carbonyl bonds.

Therefore, conformational isomers are likely in hydroxyurea systems. This property is more or less prevalent in various analogs under various conditions. Although the effect of this form of isomerization, if any, in biological systems cannot be ascertained at this time, the property is being considered as a possible factor in ex-

plaining the low *in vivo* antileukemic activity of substituted hydroxyureas. The potential interrelationship between internal hydrogen bonding and conformational isomerization as well as the resultant effect on the pKa of hydroxyurea molecules and biological transport to the site of action is currently being studied. Initial *in vitro* tests on ribonucleotide reductase (mammalian) by analogs IV–VI indicate enzyme inhibition activity[7] at about 10 times the concentration required with hydroxyurea (I). Therefore, some property involving transport of these molecules to their site of action might be involved in their pharmacodynamics.

REFERENCES

(1) N. S. Bhacca and D. H. Williams, "Applications of NMR Spectroscopy in Organic Chemistry," Holden-Day, San Francisco, Calif., 1964, pp. 135–158.

(2) A. F. Casy, in "Medicinal Chemistry," 3rd ed., A. Burger, Ed., Wiley–Interscience, New York, N.Y., 1970, pp. 81–107.

(3) F. S. Philips, S. S. Sternberg, A. P. Cronin, H. S. Schwartz, J. E. Sodergren, and P. M. Vidal, *Cancer Res.*, **25,** 1867(1967).

(4) W. C. Mohler, *Cancer Chemother.*, **34,** 1(1964).

(5) W. K. Sinclair, *Cancer Res.*, **27,** 297(1967).

(6) B. Stearns, L. Losee, and J. Bernstein, *J. Med. Pharm. Chem.*, **6,** 16(1963).

(7) I. H. Krakoff, *Int. Congr. Chemother. Proc., 5th,* **2,** 163(1967).

(8) P. Reichard, "The Biosynthesis of Deoxyribose," Wiley, New York, N.Y., 1968, p. 48, ref. 46.

(9) E. C. Moore and R. B. Hurlbert, *J. Biol. Chem.*, **241,** 4802(1966).

(10) F. A. French, E. J. Blanz, S. C. Shaddix, and R. W. Brockman, *J. Med. Chem.*, **17,** 172(1974).

(11) F. A. French, E. J. Blanz, J. R. DoAmaral, and D. A. French, *ibid.*, **13,** 1117(1970).

(12) E. C. Moore, N. S. Zedeck, K. C. Agrawal, and A. C. Sartorelli, *Biochemistry*, **9,** 4492(1970).

(13) W. Dresler and R. Stein, *Justus Liebigs Ann. Chem.*, **150,** 242(1869).

(14) R. E. Harmon, J. C. Dabrowiak, D. J. Brown, S. K. Gupta, M. Herbert, and D. Chitharanjan, *J. Med. Chem.*, **13,** 577(1970).

(15) G. Clifton, S. R. Bryant, and C. G. Skinner, *ibid.*, **13,** 377(1970).

(16) W. E. Stewart and T. H. Siddal, *Chem. Rev.*, **70,** 517(1970).

(17) F. Allmer, J. Kriz, and D. Doskocilova, *Collect. Czech. Chem. Commun.*, **38,** 3253(1973); E. W. Randall and J. D. Baldeschwieler, *J. Mol. Spectrosc.*, **8,** 365(1962); R. M. Moriarty, *J. Org. Chem.*, **28,** 1296(1963).

(18) B. F. Sagar, *J. Chem. Soc., B,* **1967,** 428.

[7] G. R. Parker and E. C. Moore, unpublished data.

ACKNOWLEDGMENTS AND ADDRESSES

Received October 30, 1974, from the *College of Pharmacy, Drake University, Des Moines, IA 50311*

Accepted for publication July 18, 1975.

Presented in part at the Medicinal Chemistry Section, APhA Academy of Pharmaceutical Sciences, Chicago meeting, August 1974.

Supported by the Drake University Research Council.

The authors thank Dr. David Abraham of the National Cancer Institute for supplying *in vivo* antileukemia data on hydroxyurea and 3-*N*-substituted analogs, Miss Barbara Stearns of the Squibb Institute for supplying the 1-*N*-substituted compounds and *in vivo* data on these compounds, and Dr. Lawrence Brown, Department of Chemistry, Drake University, for helpful suggestions.

* Department of Chemistry, Drake University, Des Moines, IA 50311

[x] To whom inquiries should be directed. Present address: Department of Medicinal Chemistry, College of Pharmacy, University of Houston, Houston, TX 77004

NOTES

Rapid Determination of Dimethyl Polysiloxane by Proton Magnetic Resonance Spectroscopy

M. L. ANHOURY, P. CROOY, R. DE NEYS [x], and A. LARIDANT

Abstract □ A new procedure is described for the quantitative extraction and determination of dimethyl polysiloxane by ^{1}H-NMR spectroscopy, using tetrachloroethylene as the solvent and dioxane as the internal reference.

Keyphrases □ Dimethyl polysiloxane—coatings, NMR analysis □ NMR spectroscopy—analysis, dimethyl polysiloxane coatings □ Silicones—NMR analysis of dimethyl polysiloxane coatings

The increasing use of silicones in drug, cosmetic, and food industries has given rise to various chemical and physical methods for the identification of this material. Several methods allow quantitative determinations of siloxane. Gravimetric (1) or volumetric (2) assays, visible or UV determination after mineralization (3–7), potentiometric titration (8), and IR (3, 6, 9–12) or atomic absorption spectroscopy (5, 12–14) determination after extraction have been reported.

A simple assay by NMR spectroscopy of the dimethyl polysiloxane (dimethicone) coating on needles of syringes is presented. This new technique compares favorably with the usual IR method.

EXPERIMENTAL

Method—Commercially available dimethyl polysiloxanes (I) [range of viscosity 0.65–10^6 centistokes (cS)] are silicone polymers in which each silicon atom of the polysiloxane chain is bonded to two methyl groups.

plaining the low *in vivo* antileukemic activity of substituted hydroxyureas. The potential interrelationship between internal hydrogen bonding and conformational isomerization as well as the resultant effect on the pKa of hydroxyurea molecules and biological transport to the site of action is currently being studied. Initial *in vitro* tests on ribonucleotide reductase (mammalian) by analogs IV–VI indicate enzyme inhibition activity[7] at about 10 times the concentration required with hydroxyurea (I). Therefore, some property involving transport of these molecules to their site of action might be involved in their pharmacodynamics.

REFERENCES

(1) N. S. Bhacca and D. H. Williams, "Applications of NMR Spectroscopy in Organic Chemistry," Holden-Day, San Francisco, Calif., 1964, pp. 135–158.

(2) A. F. Casy, in "Medicinal Chemistry," 3rd ed., A. Burger, Ed., Wiley–Interscience, New York, N.Y., 1970, pp. 81–107.

(3) F. S. Philips, S. S. Sternberg, A. P. Cronin, H. S. Schwartz, J. E. Sodergren, and P. M. Vidal, *Cancer Res.*, **25,** 1867(1967).

(4) W. C. Mohler, *Cancer Chemother.*, **34,** 1(1964).

(5) W. K. Sinclair, *Cancer Res.*, **27,** 297(1967).

(6) B. Stearns, L. Losee, and J. Bernstein, *J. Med. Pharm. Chem.*, **6,** 16(1963).

(7) I. H. Krakoff, *Int. Congr. Chemother. Proc., 5th,* **2,** 163(1967).

(8) P. Reichard, "The Biosynthesis of Deoxyribose," Wiley, New York, N.Y., 1968, p. 48, ref. 46.

(9) E. C. Moore and R. B. Hurlbert, *J. Biol. Chem.*, **241,** 4802(1966).

(10) F. A. French, E. J. Blanz, S. C. Shaddix, and R. W. Brockman, *J. Med. Chem.*, **17,** 172(1974).

(11) F. A. French, E. J. Blanz, J. R. DoAmaral, and D. A. French, *ibid.*, **13,** 1117(1970).

(12) E. C. Moore, N. S. Zedeck, K. C. Agrawal, and A. C. Sartorelli, *Biochemistry*, **9,** 4492(1970).

(13) W. Dresler and R. Stein, *Justus Liebigs Ann. Chem.*, **150,** 242(1869).

(14) R. E. Harmon, J. C. Dabrowiak, D. J. Brown, S. K. Gupta, M. Herbert, and D. Chitharanjan, *J. Med. Chem.*, **13,** 577(1970).

(15) G. Clifton, S. R. Bryant, and C. G. Skinner, *ibid.*, **13,** 377(1970).

(16) W. E. Stewart and T. H. Siddal, *Chem. Rev.*, **70,** 517(1970).

(17) F. Allmer, J. Kriz, and D. Doskocilova, *Collect. Czech. Chem. Commun.*, **38,** 3253(1973); E. W. Randall and J. D. Baldeschwieler, *J. Mol. Spectrosc.*, **8,** 365(1962); R. M. Moriarty, *J. Org. Chem.*, **28,** 1296(1963).

(18) B. F. Sagar, *J. Chem. Soc., B,* **1967,** 428.

[7] G. R. Parker and E. C. Moore, unpublished data.

ACKNOWLEDGMENTS AND ADDRESSES

Received October 30, 1974, from the *College of Pharmacy, Drake University, Des Moines, IA 50311*

Accepted for publication July 18, 1975.

Presented in part at the Medicinal Chemistry Section, APhA Academy of Pharmaceutical Sciences, Chicago meeting, August 1974.

Supported by the Drake University Research Council.

The authors thank Dr. David Abraham of the National Cancer Institute for supplying *in vivo* antileukemia data on hydroxyurea and 3-*N*-substituted analogs, Miss Barbara Stearns of the Squibb Institute for supplying the 1-*N*-substituted compounds and *in vivo* data on these compounds, and Dr. Lawrence Brown, Department of Chemistry, Drake University, for helpful suggestions.

* Department of Chemistry, Drake University, Des Moines, IA 50311

[x] To whom inquiries should be directed. Present address: Department of Medicinal Chemistry, College of Pharmacy, University of Houston, Houston, TX 77004

NOTES

Rapid Determination of Dimethyl Polysiloxane by Proton Magnetic Resonance Spectroscopy

M. L. ANHOURY, P. CROOY, R. DE NEYS [x], and A. LARIDANT

Abstract □ A new procedure is described for the quantitative extraction and determination of dimethyl polysiloxane by ^{1}H-NMR spectroscopy, using tetrachloroethylene as the solvent and dioxane as the internal reference.

Keyphrases □ Dimethyl polysiloxane—coatings, NMR analysis □ NMR spectroscopy—analysis, dimethyl polysiloxane coatings □ Silicones—NMR analysis of dimethyl polysiloxane coatings

The increasing use of silicones in drug, cosmetic, and food industries has given rise to various chemical and physical methods for the identification of this material. Several methods allow quantitative determinations of siloxane. Gravimetric (1) or volumetric (2) assays, visible or UV determination after mineralization (3–7), potentiometric titration (8), and IR (3, 6, 9–12) or atomic absorption spectroscopy (5, 12–14) determination after extraction have been reported.

A simple assay by NMR spectroscopy of the dimethyl polysiloxane (dimethicone) coating on needles of syringes is presented. This new technique compares favorably with the usual IR method.

EXPERIMENTAL

Method—Commercially available dimethyl polysiloxanes (I) [range of viscosity 0.65–10^6 centistokes (cS)] are silicone polymers in which each silicon atom of the polysiloxane chain is bonded to two methyl groups.

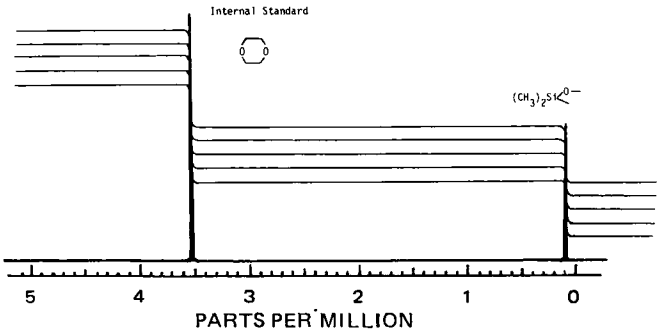

Figure 1—*Five traces of integral curve for analysis of dimethyl polysiloxane.*

Because of the presence of six equivalent hydrogen atoms per monomeric unit, I is a molecule of choice for quantitative estimations by NMR spectroscopy, showing a sharp singlet at δ 0.09 ppm (tetramethylsilane as reference). The area under a particular ^{1}H-NMR signal is directly proportional to the number of protons giving this signal and is easily obtained from the corresponding integral trace.

In a quantitative ^{1}H-NMR procedure (15), a particular integral value is related to a specific number of protons estimated by the inclusion of an internal standard in the solutions to be analyzed. Dioxane, at any suitable concentration (here at 0.4% v/v) in tetrachloroethylene, was chosen as a standard because it contains eight magnetically equivalent protons. Furthermore, tetrachloroethylene is a useful solvent both for the extraction of silicones and for ^{1}H-NMR spectroscopy.

Ratio values (R), defined as:

$$R = \frac{\text{mean value (mm) of integrals of } (CH_3)_2Si<^{O}- \text{ peak}}{\text{mean value (mm) of integrals of dioxane peak}} \quad \text{(Eq. 1)}$$

are obtained by five consecutive traces of the integral curve (Fig. 1) of the dioxane singlet at δ 3.53 ppm and the $(CH_3)_2Si<^{O}-$ singlet at δ 0.09 ppm.

Silicone is quantitatively estimated by comparing R values of solutions of unknown concentration in I with R values of standard solutions.

This new method and the usual IR assay are applied to I of different viscosities (20, 50, 200, 300, and 1000 cS). Silicones having a mean number of dimethyl siloxane units from 10 to about 350 are readily measured with these techniques.

Apparatus—NMR spectra were obtained on a 60-Hz spectrometer[1], and IR spectra were obtained on a double-beam spectrophotometer[2].

Reagents—Tetrachloroethylene, dioxane, and methylene chloride were spectroscopic grade solvents. Compounds I were commercially available silicones[3].

Procedures—*^{1}H-NMR Analysis*—Standard solutions were prepared with weighed samples of I of different viscosities. Linear regression of R, y, with concentration, x, was obtained with a range of 0–6.0 mg/ml from standard curves. The simple regression line of y on x calculated by the method of least squares was $y = 0.24x - 0.04$. A coefficient of correlation of 0.996 for more than 100 samples ascertained its significance. The regression passed through the origin, and the standard deviation of the intercept was 0.09.

IR Analysis—Control analyses were made by the IR method (9, 12), using the >Si—O— stretching band at 1090 cm^{-1} in methylene chloride solution. The calibration line related absorbance values with the concentration in the 0–2000-μg/ml range; the coefficient of correlation was 0.944.

Assay—*^{1}H-NMR Spectroscopy*—Metal needles, cut from 10 syringes pretreated with silicone, were collected in a flat-bottom flask of 3 ml and extracted by stirring for 5 min at room temperature with 1.0 ml of tetrachloroethylene–dioxane (99.6:0.4 v/v). NMR spectroscopy curves were made on 0.5-ml samples of the solution.

[1] Perkin-Elmer R 12.

[2] Beckman IR-4.

[3] The 360 medical fluids (20 and 200 cS) were supplied by Dow Corning Corp.; M 1028/50, 300, and 1000 cS were supplied by U.C.B., Belgium; and Baysilon M 300 (300 cS) was from Bayer, Germany.

Table I—Milligrams of the Silicone Recovered per Syringe

Assay	Silicone, mg	
	NMR Method	IR Method
1	0.148	0.154
2	0.151	0.154
3	0.152	0.148
4	0.150	0.152
5	0.150	0.147
6	0.149	0.153
7	0.150	0.150
8	0.151	0.152
Mean value	0.150	0.151
SD	1.25×10^{-3}	3.08×10^{-3}

Table II—Milligrams of the Silicone Recovered per Syringe as a Function of Concentration of the Lubrication Liquid Assay by NMR

Silicone in Lubrication Liquid, %	Silicone per Syringe, mg
20	0.15
10	0.05
7	0.04

Table III—Recovery of I

Lubrication Liquid[a], mg	Assay by NMR Method		Recovery, %
	R Values	Silicone, mg	
750.2	0.670	147.5	98.3
907.5	0.754	183.0	100.8
861.2	0.711	167.5	97.3
915.0	0.808	180.0	98.4
		Mean value	98.7

[a] Silicone (20%) in chloroform.

IR Spectroscopy—Needles, precoated with silicone, were stirred for 5 min at room temperature in methylene chloride (1.0 ml). The absorbance of the peak at 1090 cm^{-1} was compared with the standard curve.

RESULTS

Table I shows the data obtained by the two methods with eight groups of 10 syringes from the same batch. These needles were pretreated with a 20% (v/v) chloroform solution of I (360 medical fluid, 350 cS) as the lubrication liquid. The assays on batches treated with the lubrication liquid containing different concentrations of silicone are listed in Table II.

Recovery experiments (Table III) showed that 98.7% of I was recovered after a single extraction. Recovery experiments were done by coating sheets of glass with various weighed quantities of a 20% (w/v) chloroform solution of silicone. After evaporation of the chloroform, glass sheets were extracted with 50 ml of tetrachloroethylene–dioxane (99.6:0.4 v/v) and assayed by NMR.

REFERENCES

(1) D. Ridge and M. Todd, *J. Soc. Chem. Ind.*, **69**, 49(1950).

(2) J. Franc and K. Placek, *Collect. Czech. Chem. Commun.*, **38**, 513(1973).

(3) H. J. Horner, J. E. Weiler, and N. C. Angelotti, *Anal. Chem.*, **32**, 858(1960).

(4) R. Reverchon and Y. Legrand, *Chim. Anal.*, **47**, 194(1965).

(5) P. Neal, A. D. Campbell, D. Firestone, and M. H. Aldridge, *J. Amer. Oil Chem. Soc.*, **46**, 561(1969).

(6) L. de Lindemann and C. Bernardini, *Riv. Combust.*, **24**, 425(1970).

(7) A. Bradley and D. Altebrando, *Anal. Chem.*, **46**, 2061(1974).
(8) G. Schott and E. Popowski, *Z. Chem.*, **7**, 265(1968).
(9) P. Gantes, J. Barat, and H. Joly, *Ann. Fals. Exp. Chim.*, **63**, 174(1970).
(10) A. L. Smith and J. A. McHard, *Anal. Chem.*, **31**, 1174(1959).
(11) A. Pozefsky and M. E. Grenoble, *Drug Cosmet. Ind.*, **80**, 752(1957).
(12) T. Rihs, *Pharm. Acta Helv.*, **1971**, 550.
(13) J. R. Miller, J. J. Helprin, and J. S. Finlayson, *J. Pharm. Sci.*, **58**, 455(1969).
(14) E. Mario and R. E. Gerner, *ibid.*, **57**, 1243(1968).
(15) A. F. Casy, "P.M.R. Spectroscopy in Medicinal and Biological Chemistry," Academic, London, England, 1971.

ACKNOWLEDGMENTS AND ADDRESSES

Received November 29, 1973, from *Research & Development, Recherche et Industrie Thérapeutiques (R.I.T.), Rixensart 1330, Belgium.*

Accepted for publication June 12, 1975.

The authors express their gratitude to the Institut pour l'Encouragement de la Recherche Scientifique dans l'Industrie et l'Agriculture for the financial support given to this research.

[x] To whom inquiries should be directed.

NMR Determination of Enantiomers of 7-Chloro-3,3a-dihydro-2-methyl-2*H*,9*H*-isoxazolo[3,2-*b*][1,3]benzoxazin-9-one Using Chiral Shift Reagent, Tris[3-(heptafluorobutyryl)-*d*-camphorato]europium(III)

PHILIP REISBERG [x], IAN A. BRENNER, and JEROME I. BODIN

Abstract □ A simple NMR method was developed for the determination of the enantiomers of 7-chloro-3,3a-dihydro-2-methyl-2*H*,9*H*-isoxazolo[3,2-*b*][1,3]benzoxazin-9-one. Chiral shift reagent, tris[3-(heptafluorobutyryl)-*d*-camphorato]europium(III), causes the doublet assigned to the protons of the 2-methyl group, which normally appears at about 1.5 ppm, to split into two pairs of doublets and to shift downfield to about 2.0–3.5 ppm. The downfield pair of doublets represents the two enantiomers present in one racemate, designated as the β-form, while the upfield pair represents the enantiomers of the racemate designated as the α-form. From the integration of the area under the doublets, the relative concentration of all four enantiomers was determined.

Keyphrases □ NMR spectroscopy—determination, enantiomers of 7-chloro-3,3a-dihydro-2-methyl-2*H*,9*H*-isoxazolo[3,2-*b*][1,3]-benzoxazin-9-one using europium chiral shift reagent □ Europium—chiral shift reagent, use in NMR determination of enantiomers of substituted isoxazolo[3,2-*b*][1,3]benzoxazin-9-one □ Enantiomers—substituted isoxazolo[3,2-*b*][1,3]benzoxazin-9-one, NMR determination using europium chiral shift reagent □ Chiral shift reagent, europium—use in NMR determination of enantiomers of substituted isoxazolo[3,2-*b*][1,3]benzoxazin-9-one

The use of deuterated tris(1,1,1,2,2,3,3-heptafluoro-7,7-dimethyl-4,6-octanedionato)europium(III) shift reagent to determine the ratio of the diastereoisomers of 7-chloro-3,3a-dihydro-2-methyl-2*H*,9*H*-isoxazolo[3,2-*b*][1,3]benzoxazin-9-one[1] (I) was reported previously (1). An extension of this method to determine the enantiomers of each isomeric pair by use of the chiral shift reagent tris[3-(heptafluorobutyryl)-*d*-camphorato]europium(III) (II) has been successfully accomplished.

DISCUSSION

The use of lanthanide shift reagents in NMR spectroscopy in the last few years has been of great help in elucidating the structures of many organic compounds (2). With the introduction of the new optically active shift reagents (3), a new dimension was added to this approach. The chiral shift reagent can discriminate between enantiotropic groups and can separate peaks arising from the corresponding protons of a racemate. When the reagent is added to a chiral sample, pseudocontact shift differences are observed in the NMR spectrum.

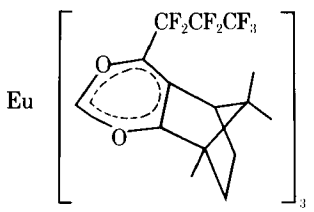

II

The successful determination of the optical purity of different types of compounds has been reported (4, 5). Chiral shift reagents also have been used to distinguish *meso-* from *dextro-* or *levo-*diastereoisomers of dimethyl 2,3-diaminosuccinate (6). As with the nonchiral lanthanide shift reagents, the europium chiral complexes produced a downfield shift while the praseodymium chiral complexes did the reverse.

Since I has two optically active centers, it can exist as four different stereoisomers. In this work the presence of the four stereoisomers was investigated by use of the chiral shift reagent.

EXPERIMENTAL

Apparatus—Spectra were obtained at 60 MHz using an analytical spectrophotometer[2]. A sweep time of 250 sec and a sweep width of 500 Hz were used, unless otherwise indicated; the δ-scale was used throughout. Tetramethylsilane (III), 1% (v/v) in deuterated chloroform[3], was used as the internal reference from which chemical shifts were measured.

Reagents and Chemicals—Compound I, α- and β-forms, was used (1). For the chiral shift reagent, a 0.3 *M* solution of II was

[1] Previously referred to in the literature as W-2395.

[2] Varian T-60.

[3] Norell Chemical Co., Landing, N.J.

(7) A. Bradley and D. Altebrando, *Anal. Chem.*, **46**, 2061(1974).
(8) G. Schott and E. Popowski, *Z. Chem.*, **7**, 265(1968).
(9) P. Gantes, J. Barat, and H. Joly, *Ann. Fals. Exp. Chim.*, **63**, 174(1970).
(10) A. L. Smith and J. A. McHard, *Anal. Chem.*, **31**, 1174(1959).
(11) A. Pozefsky and M. E. Grenoble, *Drug Cosmet. Ind.*, **80**, 752(1957).
(12) T. Rihs, *Pharm. Acta Helv.*, **1971**, 550.
(13) J. R. Miller, J. J. Helprin, and J. S. Finlayson, *J. Pharm. Sci.*, **58**, 455(1969).
(14) E. Mario and R. E. Gerner, *ibid.*, **57**, 1243(1968).
(15) A. F. Casy, "P.M.R. Spectroscopy in Medicinal and Biological Chemistry," Academic, London, England, 1971.

ACKNOWLEDGMENTS AND ADDRESSES

Received November 29, 1973, from *Research & Development, Recherche et Industrie Thérapeutiques (R.I.T.), Rixensart 1330, Belgium.*

Accepted for publication June 12, 1975.

The authors express their gratitude to the Institut pour l'Encouragement de la Recherche Scientifique dans l'Industrie et l'Agriculture for the financial support given to this research.

[x] To whom inquiries should be directed.

NMR Determination of Enantiomers of 7-Chloro-3,3a-dihydro-2-methyl-2*H*,9*H*-isoxazolo[3,2-*b*][1,3]benzoxazin-9-one Using Chiral Shift Reagent, Tris[3-(heptafluorobutyryl)-*d*-camphorato]europium(III)

PHILIP REISBERG [x], IAN A. BRENNER, and JEROME I. BODIN

Abstract □ A simple NMR method was developed for the determination of the enantiomers of 7-chloro-3,3a-dihydro-2-methyl-2*H*,9*H*-isoxazolo[3,2-*b*][1,3]benzoxazin-9-one. Chiral shift reagent, tris[3-(heptafluorobutyryl)-*d*-camphorato]europium(III), causes the doublet assigned to the protons of the 2-methyl group, which normally appears at about 1.5 ppm, to split into two pairs of doublets and to shift downfield to about 2.0–3.5 ppm. The downfield pair of doublets represents the two enantiomers present in one racemate, designated as the β-form, while the upfield pair represents the enantiomers of the racemate designated as the α-form. From the integration of the area under the doublets, the relative concentration of all four enantiomers was determined.

Keyphrases □ NMR spectroscopy—determination, enantiomers of 7-chloro-3,3a-dihydro-2-methyl-2*H*,9*H*-isoxazolo[3,2-*b*][1,3]-benzoxazin-9-one using europium chiral shift reagent □ Europium—chiral shift reagent, use in NMR determination of enantiomers of substituted isoxazolo[3,2-*b*][1,3]benzoxazin-9-one □ Enantiomers—substituted isoxazolo[3,2-*b*][1,3]benzoxazin-9-one, NMR determination using europium chiral shift reagent □ Chiral shift reagent, europium—use in NMR determination of enantiomers of substituted isoxazolo[3,2-*b*][1,3]benzoxazin-9-one

The use of deuterated tris(1,1,1,2,2,3,3-heptafluoro-7,7-dimethyl-4,6-octanedionato)europium(III) shift reagent to determine the ratio of the diastereoisomers of 7-chloro-3,3a-dihydro-2-methyl-2*H*,9*H*-isoxazolo[3,2-*b*][1,3]benzoxazin-9-one[1] (I) was reported previously (1). An extension of this method to determine the enantiomers of each isomeric pair by use of the chiral shift reagent tris[3-(heptafluorobutyryl)-*d*-camphorato]europium(III) (II) has been successfully accomplished.

DISCUSSION

The use of lanthanide shift reagents in NMR spectroscopy in the last few years has been of great help in elucidating the structures of many organic compounds (2). With the introduction of the new optically active shift reagents (3), a new dimension was added to this approach. The chiral shift reagent can discriminate between enantiotropic groups and can separate peaks arising from the corresponding protons of a racemate. When the reagent is added to a chiral sample, pseudocontact shift differences are observed in the NMR spectrum.

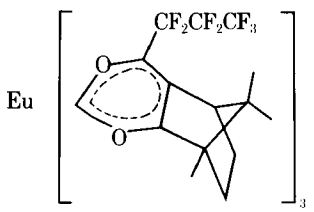

II

The successful determination of the optical purity of different types of compounds has been reported (4, 5). Chiral shift reagents also have been used to distinguish *meso-* from *dextro-* or *levo-*diastereoisomers of dimethyl 2,3-diaminosuccinate (6). As with the nonchiral lanthanide shift reagents, the europium chiral complexes produced a downfield shift while the praseodymium chiral complexes did the reverse.

Since I has two optically active centers, it can exist as four different stereoisomers. In this work the presence of the four stereoisomers was investigated by use of the chiral shift reagent.

EXPERIMENTAL

Apparatus—Spectra were obtained at 60 MHz using an analytical spectrophotometer[2]. A sweep time of 250 sec and a sweep width of 500 Hz were used, unless otherwise indicated; the δ-scale was used throughout. Tetramethylsilane (III), 1% (v/v) in deuterated chloroform[3], was used as the internal reference from which chemical shifts were measured.

Reagents and Chemicals—Compound I, α- and β-forms, was used (1). For the chiral shift reagent, a 0.3 *M* solution of II was

[1] Previously referred to in the literature as W-2395.

[2] Varian T-60.

[3] Norell Chemical Co., Landing, N.J.

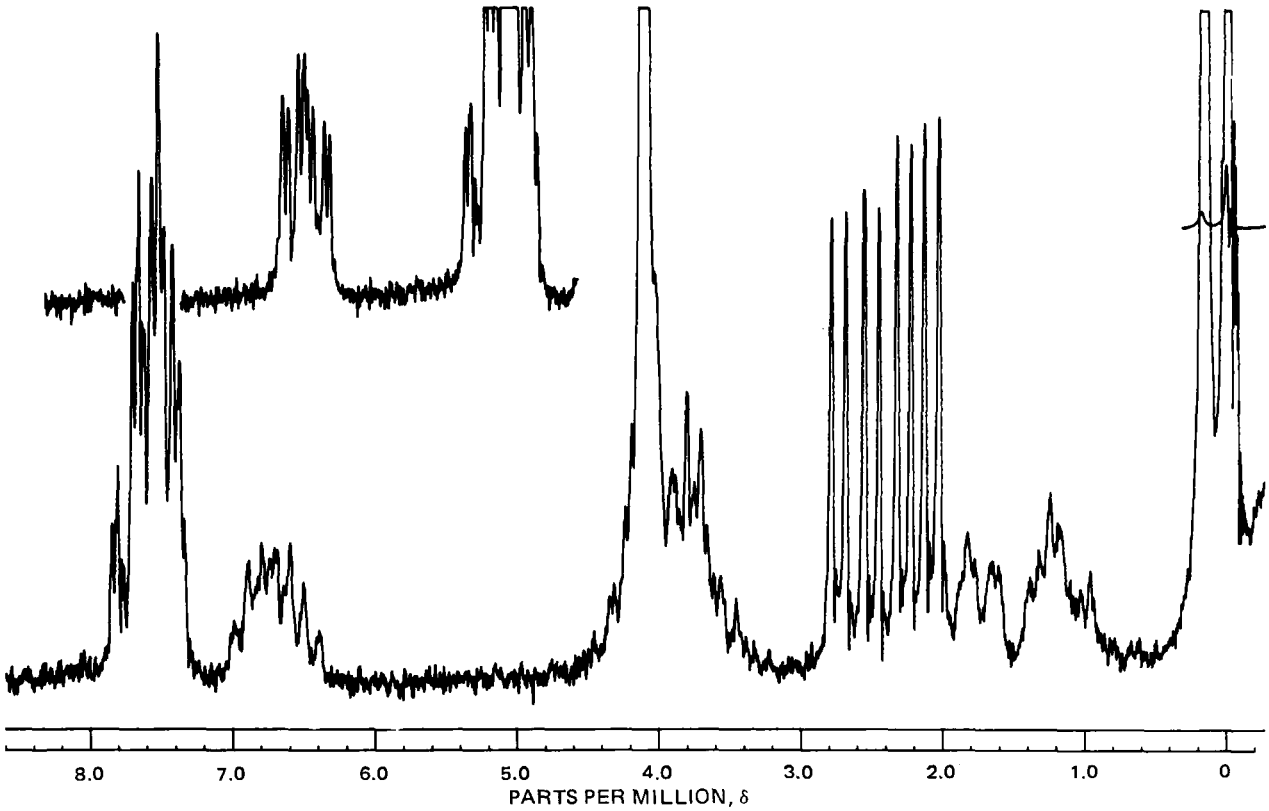

Figure 1—*NMR spectrum of prepared mixture of I [α-form–β-form (1:1)] using chiral shift reagent (II) dissolved in deuterochloroform as the solvent.*

prepared using deuterated chloroform containing 1% of III as the solvent.

Procedure—*Method A*—A solution of 25 mg of the α-form and 25 mg of the β-form was prepared by dissolving them in 0.4 ml of the chiral shift reagent. Then the NMR spectrum was obtained (Fig. 1).

Method B—A solution of 50 mg of I was obtained by dissolving it in 0.4 ml of the chiral shift reagent. The NMR spectrum was ob-

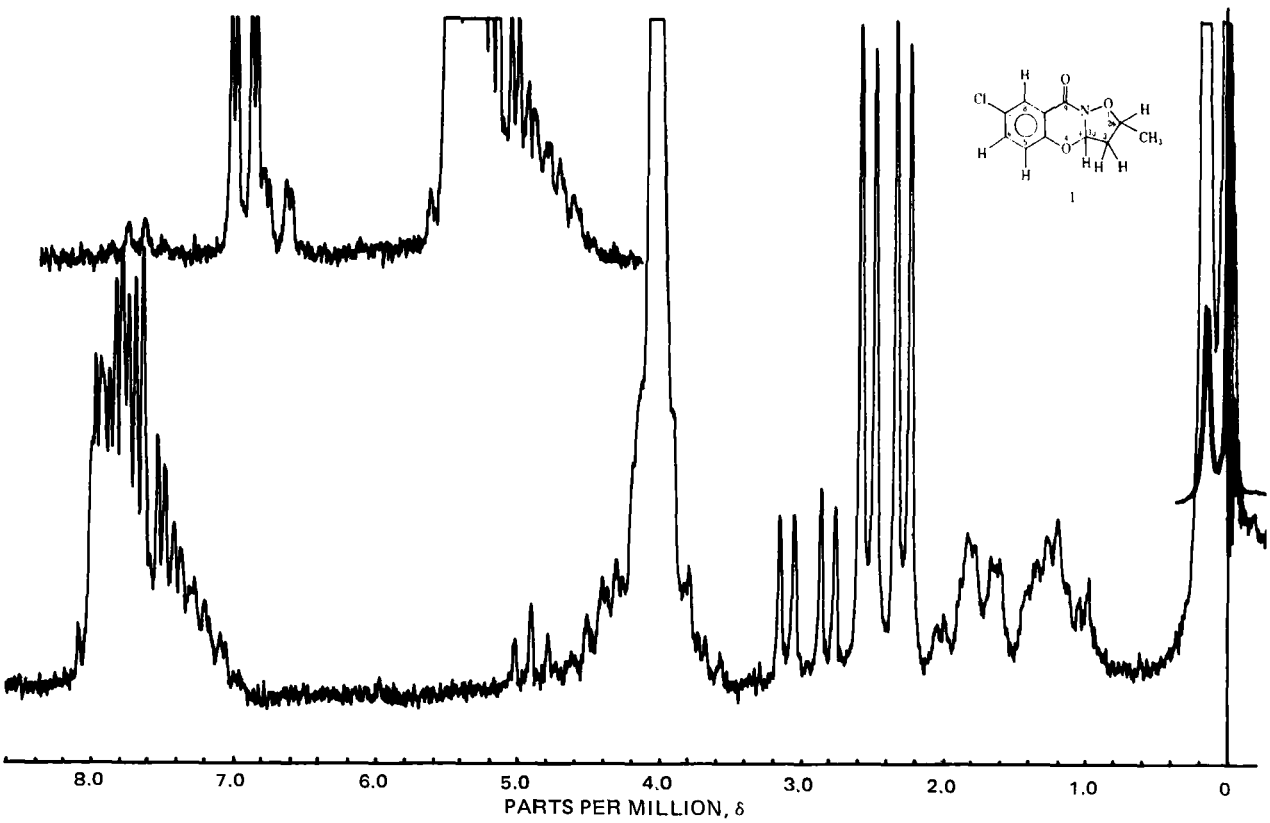

Figure 2—*NMR spectrum of I using chiral shift reagent (II) dissolved in deuterochloroform as the solvent.*

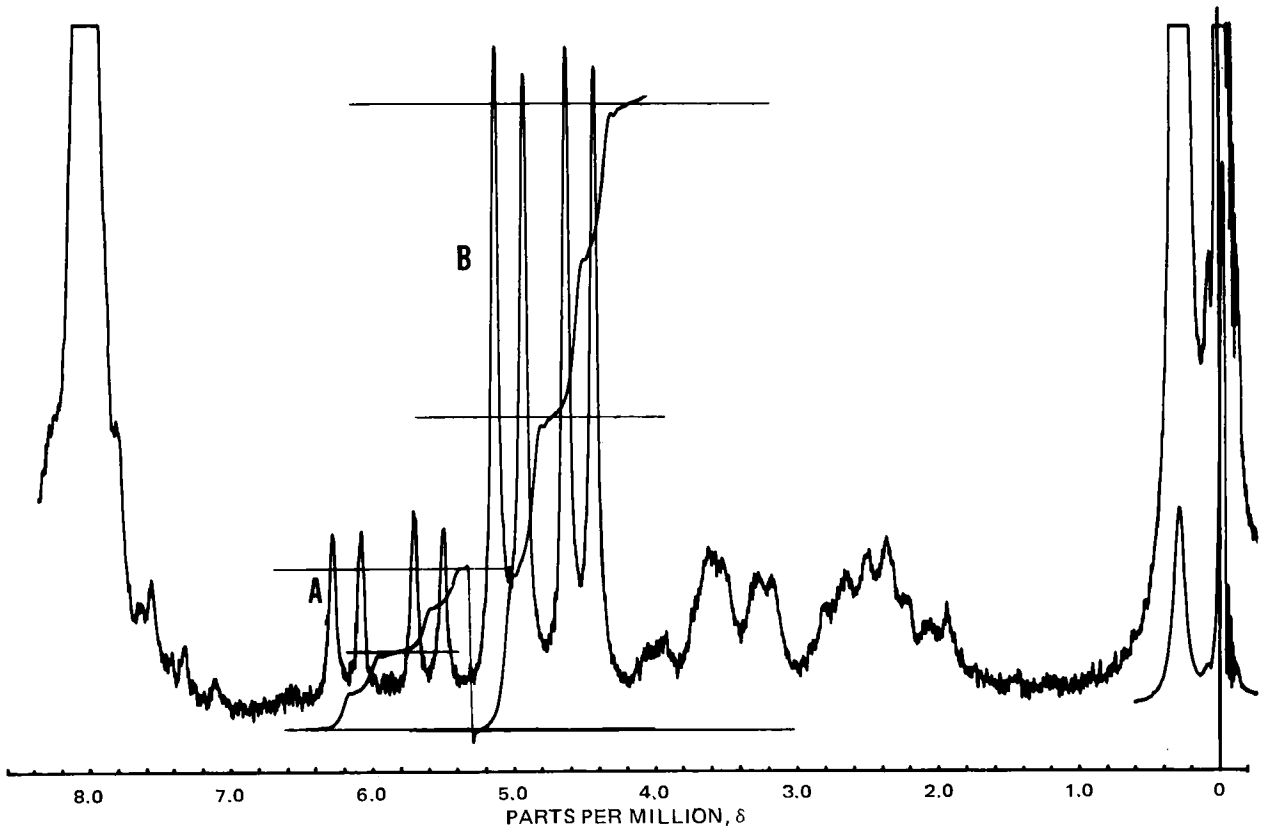

Figure 3—*Expansion of Fig. 2 to 250-Hz sweep width. Key: A, average = 34.00; B, average = 129.64; α-form = 129.64 (79.2%); β-form = 34.00 (20.8%); and Compound I = 163.64 (100%).*

tained at 500- and 250-Hz sweep widths (Figs. 2 and 3).

RESULTS

The NMR signal for the protons of the methyl group of the α- and β-forms of I appears as a pair of doublets in the 2.5–3.5-ppm region after addition of the lanthanide shift reagent (1). With the use of the chiral lanthanide shift reagent, the NMR signal for the protons of the methyl group of the α- and β-forms is further split into two pairs of doublets (Fig. 1). The two downfield doublets at about 2.5–3.0 ppm represent the two enantiomers present in the β-racemate, while two upfield doublets at about 2.0–2.5 ppm represent the two enantiomers present in the α-form.

The NMR signal for the protons of the methyl group in I in Figs. 2 and 3 also appears as two pairs of doublets; the two smaller downfield doublets correspond to the two enantiomers present in the β-form, while the two enantiomers of the α-form are found further upfield.

Integration of the area shows that I consists of a 79:21 mixture of the α- and β-racemates. The integrated values of the doublets of the α-form are equal to one another, and each represents 39.5% of the total area. The integrated values of the doublets of the β-form are also equal but only represent 10.5% of the total area. There is a slight difference in area for the enantiomers of the β-form, probably due to baseline elevation resulting in higher integral values.

By use of the chiral lanthanide shift reagent, the structure of I has been elucidated further.

REFERENCES

(1) P. Reisberg, I. A. Brenner, and J. I. Bodin, *J. Pharm. Sci.*, **63**, 1586(1974).

(2) C. C. Hinckley, *J. Amer. Chem. Soc.*, **91**, 5160(1969).

(3) H. L. Goering, J. N. Eikenberry, and G. S. Koermer, *ibid.*, **93**, 5913(1971).

(4) G. M. Whiteside and D. W. Lewis, *ibid.*, **93**, 5914(1971).

(5) R. R. Fraser, M. A. Petit, and J. K. Saunders, *Chem. Commun.*, **1971**, 1450.

(6) M. Kainosho, K. Ajisaki, W. H. Pirkle, and S. D. Beare, *J. Amer. Chem. Soc.*, **94**, 5924(1972).

ACKNOWLEDGMENTS AND ADDRESSES

Received May 8, 1975, from the *Analytical Research and Development Department, Carter-Wallace, Inc., Cranbury, NJ 08512*

Accepted for publication June 19, 1975.

The authors thank Dr. D. B. Reisner for providing samples of I and its α- and β-forms and for helpful discussions.

[x] To whom inquiries should be directed.

Comparison of Protective Effects of Ethylestrenol, Norbolethone, and Spironolactone against Lethality from Acute Doses of Parathion and Paraoxon in Female Rats

CASEY P. ROBINSON *x, PAUL W. SMITH ‡, JUDY K. McCONNELL *, and BOYD R. ENDECOTT ‡

Abstract □ Protection against the toxicity of parathion (increased LD_{50}) was provided by preadministered ethylestrenol and, to a lesser extent, by norbolethone and spironolactone. Ethylestrenol and norbolethone also offered protection against paraoxon toxicity. With ethylestrenol and spironolactone, the protection against parathion lethality was greater than that against paraoxon lethality.

Keyphrases □ Ethylestrenol—effect on toxicity of parathion and paraoxon, compared to norbolethone and spironolactone, rats □ Norbolethone—effect on toxicity of parathion and paraoxon, compared to ethylestrenol and spironolactone, rats □ Spironolactone—effect on toxicity of parathion and paraoxon, compared to ethylestrenol and norbolethone, rats □ Parathion—toxicity in rats, effect of ethylestrenol, norbolethone, and spironolactone □ Paraoxon—toxicity in rats, effect of ethylestrenol, norbolethone, and spironolactone

Several steroids, including ethylestrenol, norbolethone, and spironolactone, offer protection against a variety of toxins when the steroid is given for a period of time prior to challenge with the toxic agent (1). These "catatoxic" steroids induce drug-metabolizing enzymes, and this action has been proposed as the probable mechanism of their protective effect (2). Their effect on paraoxon toxicity has not been reported, and earlier experiments (1) with parathion did not allow an evaluation of the relative protective efficiency of the three agents mentioned here.

In this study, the effects of prior administration of these steroids on the LD_{50}'s of paraoxon and parathion in female rats were determined.

EXPERIMENTAL

Two hundred and twenty-two female, drug-naive, albino Holtzman rats, ~105 g, were used. They were given 10 mg of ethylestrenol, norbolethone, or spironolactone suspended in 1 ml of water or 1 ml of water only, by gastric tube, twice daily for 3 days and once on the 4th day. This dose and dosage schedule had been used previously and shown to be effective in protecting against a variety of toxins (1).

The organophosphorus compounds were dissolved in dimethyl sulfoxide and administered intraperitoneally 2–4 hr after the dose of steroid on the 4th day. Concentrations were adjusted so that the appropriate doses were contained in 0.1 ml of dimethyl sulfoxide/100 g of body weight. The rats were observed for 24 hr, and acute LD_{50}'s and their 95% confidence intervals were computed from the data obtained by the method of Finney (3).

RESULTS AND DISCUSSION

The results (Table I) show that the steroids afforded protection against parathion in the following order of effectiveness: ethylestrenol > norbolethone = spironolactone > control. The protection to paraoxon lethality afforded by ethylestrenol was greater than that afforded by norbolethone. Spironolactone did not protect against paraoxon toxicity. Ethylestrenol and norbolethone afforded more protection to parathion-poisoned rats than to those poisoned with paraoxon. Although ethylestrenol and norbolethone are anabolic agents and spironolactone is a diuretic, no differences in weight gain were observed ($p > 0.05$, the Student t test for unpaired data) during the 4 days of treatment.

Table I—Effect of Pretreatment with Spironolactone, Norbolethone, or Ethylestrenol on the Lethality of Parathion and Paraoxon in Female Rats

Pretreatment	Poison	LD_{50}[a], mg/kg	95% Confidence Interval
Water sham	Parathion	1.40	1.27–1.58
	Paraoxon	0.43	0.35–0.52
Spironolactone	Parathion	2.80	2.52–3.05
	Paraoxon	0.48	0.21–0.71
Norbolethone	Parathion	2.86	2.59–3.10
	Paraoxon	0.88	0.68–0.98
Ethylestrenol	Parathion	5.90	3.70–7.68
	Paraoxon	1.06	1.03–1.12

[a] Each LD_{50} was calculated from observations of the lethality of the poison at at least three dosage levels with seven to nine rats in each group.

Pretreatment with catatoxic steroids has been previously shown to increase the metabolism rate of various compounds (2). In this study, the protection afforded by two of the steroids was greater against parathion lethality than against paraoxon lethality. This finding indicates that enzymes that inactivate both parathion and its active metabolite paraoxon are being induced if only an increased rate of metabolism is involved in the protective effects. It has been demonstrated previously that the enzymes metabolizing parathion and paraoxon can both be induced (4).

However, an increase in the LD_{50} does not necessarily indicate an effect on the rate of inactivation of the toxin. The toxicity of paraoxon can also be altered by an alteration in its binding to relatively nonvital tissues (5, 6). Other factors such as an altered rate of absorption from the peritoneal cavity or an alteration in the permeability of the blood–brain barrier also may be involved in the observed changes in lethality.

REFERENCES

(1) H. Selye, *Arch. Environ. Health*, **21**, 706(1970).

(2) B. Solymoss, H. G. Classen, and S. Varga, *Proc. Soc. Exp. Biol. Med.*, **132**, 940(1969).

(3) D. J. Finney, "Probit Analysis," 3rd ed., Cambridge University Press, London, England, 1971.

(4) R. E. Poore and R. A. Neal, *Toxicol. Appl. Pharmacol.*, **23**, 759(1972).

(5) R. R. Lauwerys and S. D. Murphy, *ibid.*, **14**, 348(1969).

(6) A. J. Triolo, E. Mata, and J. M. Coon, *ibid.*, **17**, 174(1970).

ACKNOWLEDGMENTS AND ADDRESSES

Received December 13, 1974, from the *College of Pharmacy, University of Oklahoma, Norman, OK 73069, and the ‡Civil Aeromedical Institute, Federal Aviation Administration, Oklahoma City, OK 73125

Accepted for publication June 17, 1975.
Equipment and facilities were provided under FAA Task No. AM-B-73-TOX-2. Steroids were gifts of Organon, Inc. (ethylestrenol), Wyeth Labs., Inc. (norbolethone), and Searle and Co. (spironolactone).
[x] To whom inquiries should be directed.

Rapid GLC Determination of Fusaric Acid in Biological Fluids

KOCHY K. FUNG [x], ROBERT T. KODA, ROBERT F. MARONDE, and JORDAN L. COHEN

Abstract □ A simple, sensitive GLC assay was developed for fusaric acid, the active metabolite of bupicomide, to follow the disposition of this investigational antihypertensive agent in patients undergoing therapy. Fusaric acid is efficiently extracted from biological samples, derivatized by on-column methylation, and chromatographed using flame-ionization detection. An internal standard is utilized to quantitate results. The procedure is rapid and specific for fusaric acid, and has a lower limit of sensitivity of 0.1 μg/ml. The method is suitable for supporting pharmacokinetic studies of bupicomide following therapeutic doses in animals and humans.

Keyphrases □ Fusaric acid—active metabolite of bupicomide, GLC analysis, biological fluids □ GLC—analysis, fusaric acid (active metabolite of bupicomide), biological fluids □ Bupicomide—pharmacokinetic study by GLC analysis of fusaric acid metabolite, biological fluids

Fusaric acid (5-*n*-butylpicolinic acid) isolated from fungus culture filtrates was found to be a potent inhibitor of dopamine β-hydroxylase under both *in vitro* and *in vivo* (1) conditions and demonstrated significant hypotensive effects in animals (2–4) as well as in humans (5–6). Bupicomide[1], the amide derivative of fusaric acid, was reported to possess pharmacological activities similar to the parent compound (7).

Bupicomide is presently undergoing clinical trial as an antihypertensive agent. Studies using radiolabeled drug indicated that bupicomide underwent extensive metabolism rapidly when administered orally to animals (8). No unchanged drug was found by following the plasma time course of bupicomide. Only fusaric acid, a major metabolite, was identified.

Similar findings were reported in the same studies (8) after administration of a 15-mg/kg oral dose of bupicomide to humans. The biological half-life of fusaric acid was reported to be 8.7 hr in humans, utilizing a UV spectrophotometric procedure. However, for the analysis of fusaric acid in plasma, direct application of the UV assay to clinical studies involving therapeutic doses is limited by the lack of sensitivity and specificity.

The present work describes an analytical method in which fusaric acid is extracted from a biological sample along with an added internal standard into an organic solvent and subsequently is derivatized by on-column methylation for GLC determination. The procedure is applicable to blood and urine and is rapid enough to be performed routinely for clinical studies of patients on bupicomide therapy.

[1] Sch 10595.

EXPERIMENTAL

Reagents—All chemicals and solvents used were analytical reagent grade. The internal standard, *N*-*n*-butylphthalimide, was synthesized according to standard methods (9) by refluxing *n*-butylamine and phthalic anhydride in acetic acid. The crude product was recrystallized from alcohol–water before use, mp 32 ± 0.5° (10).

Procedure for Biological Samples—Blood samples were collected[2] and allowed to clot. The serum was separated by centrifugation and frozen until analysis. Spiked standards of fusaric acid in pooled serum were treated similarly. Urine samples also were collected, frozen, and stored until analysis.

A biological fluid, 0.5 ml, was transferred to a screw-capped[3] tube containing 2 μg of *N*-*n*-butylphthalimide, 0.5 ml of 0.1 *M* pH 4 citrate buffer that had been presaturated with sodium chloride, and 4.0 ml of methylene chloride. The mixture was mechanically shaken for 5 min and then centrifuged at 2200 rpm for 5 min to allow separation of the phases. The top layer was aspirated off, and the organic layer was decanted into a 5-ml vial[4] and evaporated to dryness under vacuum.

About 0.3 ml of acetone was used to wash the sides of the vial with intermittent vortex mixing. The acetone was removed under vacuum, and 10–15 μl of 0.1 *M* trimethylphenylammonium hydroxide[5] was added to the evaporated sample, followed by 1 min of vigorous vortex mixing. Then 1–2 μl of the mixture was injected into the gas chromatograph.

GLC—The assay was performed on a gas chromatograph[6] equipped with a flame-ionization detector. A 183-cm (6-ft) × 2-mm i.d. glass coiled column packed with 3% OV-1 on 100–120-mesh Gas Chrom Q[7] was used. GLC conditions were: column temperature, 150°; and detector and injector temperatures, 250°. The nitrogen carrier gas was maintained at 40 ml/min, while air and hydrogen flow rates were 250 and 30 ml/min, respectively. Methylation of the samples occurred in the injection port, with the derivatized product eluting as a sharp peak at ~6 min followed by the internal standard peak at ~7 min.

Injection could be resumed at ~12 min when the impurities had

[2] Vacutainers, no anticoagulant, Beckton, Dickinson and Co., Rutherford, N.J.
[3] Lined with Teflon (du Pont).
[4] Reacti-vial, Pierce Chemical Co., Rockford, Ill.
[5] Eastman Organic Chemicals, Rochester, N.Y.
[6] Varian model 2700 (Varian Aerograph, Walnut Creek, Calif.) equipped with a Hitachi Perkin-Elmer recorder, model 156.
[7] Applied Science Laboratories, State College, Pa.

Accepted for publication June 17, 1975.
Equipment and facilities were provided under FAA Task No. AM-B-73-TOX-2. Steroids were gifts of Organon, Inc. (ethylestrenol), Wyeth Labs., Inc. (norbolethone), and Searle and Co. (spironolactone).
[x] To whom inquiries should be directed.

Rapid GLC Determination of Fusaric Acid in Biological Fluids

KOCHY K. FUNG [x], ROBERT T. KODA, ROBERT F. MARONDE, and JORDAN L. COHEN

Abstract □ A simple, sensitive GLC assay was developed for fusaric acid, the active metabolite of bupicomide, to follow the disposition of this investigational antihypertensive agent in patients undergoing therapy. Fusaric acid is efficiently extracted from biological samples, derivatized by on-column methylation, and chromatographed using flame-ionization detection. An internal standard is utilized to quantitate results. The procedure is rapid and specific for fusaric acid, and has a lower limit of sensitivity of 0.1 μg/ml. The method is suitable for supporting pharmacokinetic studies of bupicomide following therapeutic doses in animals and humans.

Keyphrases □ Fusaric acid—active metabolite of bupicomide, GLC analysis, biological fluids □ GLC—analysis, fusaric acid (active metabolite of bupicomide), biological fluids □ Bupicomide—pharmacokinetic study by GLC analysis of fusaric acid metabolite, biological fluids

Fusaric acid (5-*n*-butylpicolinic acid) isolated from fungus culture filtrates was found to be a potent inhibitor of dopamine β-hydroxylase under both *in vitro* and *in vivo* (1) conditions and demonstrated significant hypotensive effects in animals (2–4) as well as in humans (5–6). Bupicomide[1], the amide derivative of fusaric acid, was reported to possess pharmacological activities similar to the parent compound (7).

Bupicomide is presently undergoing clinical trial as an antihypertensive agent. Studies using radiolabeled drug indicated that bupicomide underwent extensive metabolism rapidly when administered orally to animals (8). No unchanged drug was found by following the plasma time course of bupicomide. Only fusaric acid, a major metabolite, was identified.

Similar findings were reported in the same studies (8) after administration of a 15-mg/kg oral dose of bupicomide to humans. The biological half-life of fusaric acid was reported to be 8.7 hr in humans, utilizing a UV spectrophotometric procedure. However, for the analysis of fusaric acid in plasma, direct application of the UV assay to clinical studies involving therapeutic doses is limited by the lack of sensitivity and specificity.

The present work describes an analytical method in which fusaric acid is extracted from a biological sample along with an added internal standard into an organic solvent and subsequently is derivatized by on-column methylation for GLC determination. The procedure is applicable to blood and urine and is rapid enough to be performed routinely for clinical studies of patients on bupicomide therapy.

[1] Sch 10595.

EXPERIMENTAL

Reagents—All chemicals and solvents used were analytical reagent grade. The internal standard, *N*-*n*-butylphthalimide, was synthesized according to standard methods (9) by refluxing *n*-butylamine and phthalic anhydride in acetic acid. The crude product was recrystallized from alcohol–water before use, mp 32 ± 0.5° (10).

Procedure for Biological Samples—Blood samples were collected[2] and allowed to clot. The serum was separated by centrifugation and frozen until analysis. Spiked standards of fusaric acid in pooled serum were treated similarly. Urine samples also were collected, frozen, and stored until analysis.

A biological fluid, 0.5 ml, was transferred to a screw-capped[3] tube containing 2 μg of *N*-*n*-butylphthalimide, 0.5 ml of 0.1 *M* pH 4 citrate buffer that had been presaturated with sodium chloride, and 4.0 ml of methylene chloride. The mixture was mechanically shaken for 5 min and then centrifuged at 2200 rpm for 5 min to allow separation of the phases. The top layer was aspirated off, and the organic layer was decanted into a 5-ml vial[4] and evaporated to dryness under vacuum.

About 0.3 ml of acetone was used to wash the sides of the vial with intermittent vortex mixing. The acetone was removed under vacuum, and 10–15 μl of 0.1 *M* trimethylphenylammonium hydroxide[5] was added to the evaporated sample, followed by 1 min of vigorous vortex mixing. Then 1–2 μl of the mixture was injected into the gas chromatograph.

GLC—The assay was performed on a gas chromatograph[6] equipped with a flame-ionization detector. A 183-cm (6-ft) × 2-mm i.d. glass coiled column packed with 3% OV-1 on 100–120-mesh Gas Chrom Q[7] was used. GLC conditions were: column temperature, 150°; and detector and injector temperatures, 250°. The nitrogen carrier gas was maintained at 40 ml/min, while air and hydrogen flow rates were 250 and 30 ml/min, respectively. Methylation of the samples occurred in the injection port, with the derivatized product eluting as a sharp peak at ~6 min followed by the internal standard peak at ~7 min.

Injection could be resumed at ~12 min when the impurities had

[2] Vacutainers, no anticoagulant, Beckton, Dickinson and Co., Rutherford, N.J.
[3] Lined with Teflon (du Pont).
[4] Reacti-vial, Pierce Chemical Co., Rockford, Ill.
[5] Eastman Organic Chemicals, Rochester, N.Y.
[6] Varian model 2700 (Varian Aerograph, Walnut Creek, Calif.) equipped with a Hitachi Perkin-Elmer recorder, model 156.
[7] Applied Science Laboratories, State College, Pa.

Table I—Variation of Extraction of Fusaric Acid with pH

pH	Extraction of Fusaric Acid[a,b], %	
	0.1 *M* Citrate Buffer	0.1 *M* Citrate Buffer with 2 *M* NaCl
1.65	71.8	75.3
2.10	76.4	80.5
2.60	77.4	82.8
3.05	78.0	84.9
4.05	78.0	84.9
4.55	77.5	84.9
5.05	75.4	83.9
6.08	55.7	76.6

[a] Average of two determinations. [b] Based on equal volumes of methylene chloride and buffer solution.

been eluted from the column. At the end of the day, the column was reconditioned at 220° and periodically treated with a mixture of trimethylsilyl donors[8]. The detector was cleaned by sonication in acetone after several days of use. These steps ensured optimum efficiency and sensitivity of the system.

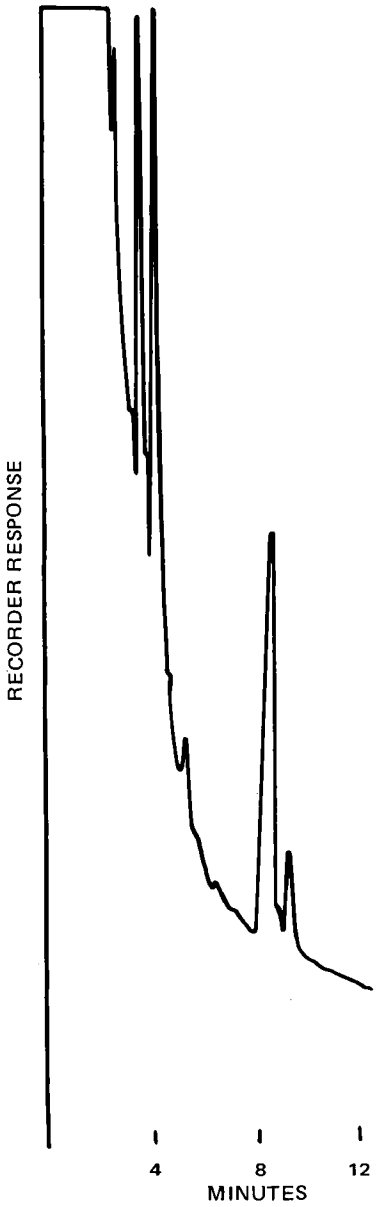

Figure 1—*Gas chromatogram of a serum control.*

[8] Silyl 8, Pierce Chemical Co., Rockford, Ill.

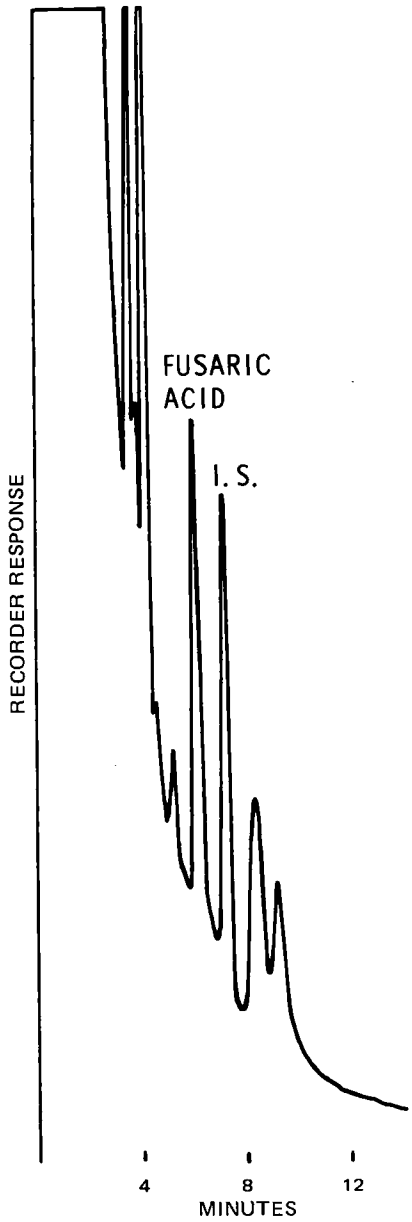

Figure 2—*Gas chromatogram of a serum sample of fusaric acid with the addition of* N-n-*butylphthalimide (I.S.) (fusaric acid concentration = 5.00 μg/ml;* N-n-*butylphthalimide concentration = 0.13 μg/μl injected).*

RESULTS AND DISCUSSION

The amphoteric nature of the fusaric acid molecule requires careful consideration of the extraction system to assure maximal extraction efficiency and minimum interference from biological samples. Methylene chloride was the solvent of choice. The variation in the percent recovery with pH was systematically examined (Table I). It was apparent that pH 4 was optimal and that the addition of salt not only enhanced the extraction but also made the percent recovery less dependent on the pH. Under the assay conditions, the recovery of fusaric acid from biological samples was better than 90%.

The addition of an internal standard to the samples prior to extraction eliminated the necessity of pipetting and allowed almost quantitative transfer of the extract. *N-n*-Butylphthalimide was selected because of its stability, purity, and extraction properties as well as its convenient retention time under the chromatographic conditions. Besides methylation, other alkylations of fusaric acid with triethyl-, propyl-, and butylammonium hydroxides were attempted to determine optimal sensitivity and specificity. However, after carrying through the procedure with plasma, serum, and

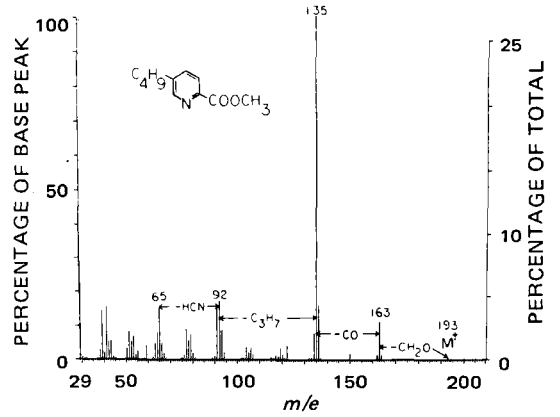

Figure 3—*GLC–mass spectrum of the methyl ester of fusaric acid.*

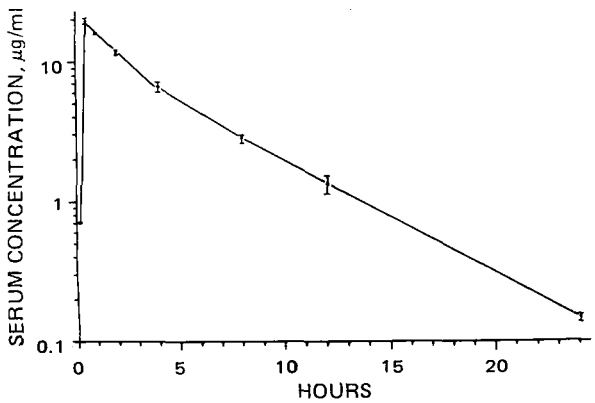

Figure 4—*Serum concentration of fusaric acid in a fasted normal volunteer following a single oral dose of 200 mg of bupicomide.*

urine blanks, only the methylated product eluted without interference.

Figures 1 and 2 represent typical chromatograms from extracted human serum control and sample, respectively. The sharpness of the peaks enabled the use of peak height ratios for quantitation. A linear standard curve, corresponding to original concentrations of fusaric acid of from 0.2 to 20 μg/ml, was obtained. The sensitivity limit was 10 ng of injected compound. Standard deviation at 1 μg/ml was 1.5% for five replicate samples.

Specimens containing higher concentrations were originally diluted with pooled serum and analyzed as already described. Subsequently, water was used to adjust all samples to 0.5 ml since no differences were observed in extraction efficiency. Serum samples with fusaric acid levels as high as 100 μg/ml were quantitated in this manner.

To ascertain the specificity of the method, the biological samples were analyzed by injection into a gas–liquid chromatograph interfaced with a mass spectrometer[9]. The resulting mass spectrum of the peak eluting at 6 min is shown in Fig. 3. It corresponded to the methyl ester of fusaric acid.

The applicability of the assay to clinical studies is demonstrated by following the serum time course of fusaric acid in a fasted normal volunteer after a single oral dose of 200 mg of bupicomide. Urine specimens from the same period were collected and analyzed (Figs. 4 and 5). The serum concentration of fusaric acid rose sharply, reaching peak levels within 1 hr, and then declined rapidly, with a half-life estimated to be 3.7 hr. Over a 24-hr period, only about 3.5% of the dose was excreted as fusaric acid.

While others (8, 11) obtained similar urinary data in animals, the half-life of fusaric acid in humans was reported to be 8.7 hr (8). Such discrepancy may be due to variations in the subjects, doses, or experimental conditions or, very likely, to the nonspecificity of the analytical method. Since fusaric acid has been demonstrated to undergo side-chain oxidations in the body (11), metabolites would

[9] Varian model CH-7, Varian Mat Divisions, Springfield, N.J.

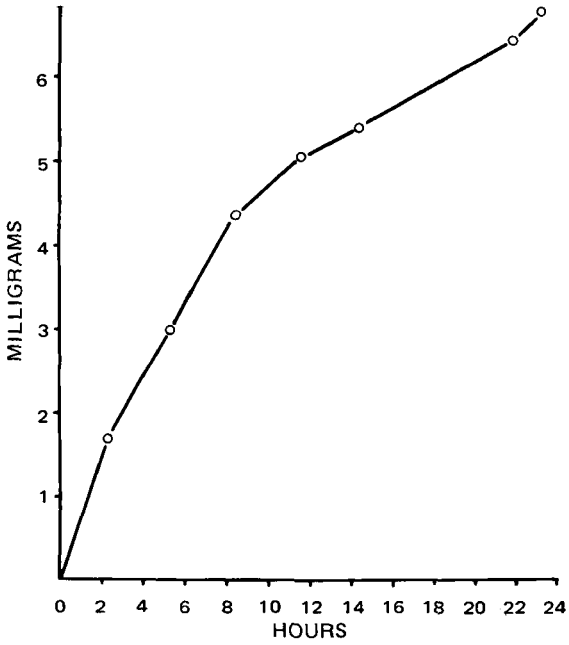

Figure 5—*Cumulative urinary excretion of fusaric acid in a fasted normal volunteer following a single oral dose of 200 mg of bupicomide.*

not be readily distinguishable from the parent compound when analyzed by the UV method. Apparent higher plasma concentration of fusaric acid would result, and the estimated half-life would appear longer.

The GLC procedure described here has been adapted for analyzing heart and brain tissue samples to delineate tissue distribution in rats. Additional studies are in progress to extend the method to other tissues and to determine the ultimate sensitivity requirements for establishing pharmacokinetic parameters in animals and humans.

REFERENCES

(1) T. Nagatsu, H. Hidaka, H. Kuzuya, and K. Takeya, *Biochem. Pharmacol.*, **19**, 35(1970).

(2) H. Suda, T. Takeuchi, T. Nagatsu, M. Matsuzaki, I. Matsumoto, and H. Umegawa, *Chem. Pharm. Bull.*, **17**, 2377(1969).

(3) H. Hidaka, T. Nagatsu, and K. Takeya, *J. Antibiot. (Tokyo), Ser. A*, **22**, 228(1969).

(4) I. Nagatsu, T. Nagatsu, K. Mitzutani, H. Umezawa, M. Matsuzaki, and T. Takeuchi, *Nature (London)*, **230**, 381(1971).

(5) F. Terasawa and M. Kameyama, *Jap. Circ. J.*, **35**, 339(1971).

(6) R. J. Matta and G. F. Wooten, *Clin. Pharmacol. Ther.*, **14**, 541(1973).

(7) C. A. Korduba, J. Veals, A. Wohl, S. Symchowicz, and I. I. A. Tabachnick, *J. Pharmacol. Exp. Ther.*, **184**, 671(1973).

(8) S. Symchowicz and M. Staub, *ibid.*, **191**, 324(1974).

(9) A. I. Vogel, "Elementary Practical Organic Chemistry," 3rd ed., Longmans, Green and Co. Ltd., London, England, 1961, p. 447.

(10) G. Vanags, *Acta Univ. Latv., Kim. Fak. Ser.*, **4**, 405(1939); through *Chem. Abstr.*, **34**, 1983b(1940).

(11) H. Umezawa, "Enzyme Inhibitors of Microbial Origin," 1st ed., University Park Press, Baltimore, Md., 1972, pp. 81, 83.

ACKNOWLEDGMENTS AND ADDRESSES

Received May 19, 1975, from the *Schools of Pharmacy and Medicine, University of Southern California, Los Angeles, CA 90033*

Accepted for publication June 18, 1975.

Supported in part by funds provided by Schering Corp., Bloomfield, N.J.

The authors thank Dr. Robert Spangenburg of the Schering Corp. for samples of bupicomide.

[x] To whom inquiries should be directed.

Determination of Nitrofurantoin in Urine by Reduction at Rotating Platinum Electrode

WILLIAM D. MASON ˣ and BEVERLY SANDMANN

Abstract □ The application of the reduction of nitrofurantoin at the rotating platinum electrode to the determination of the drug in the urine of clinical patients was evaluated and compared to a commonly used colorimetric method. The new electrochemical method was found to be faster and more efficient with precision and accuracy comparable to those of the colorimetric method.

Keyphrases □ Nitrofurantoin—electrochemical analysis, compared to colorimetric analysis, urine □ Electrochemical analysis—nitrofurantoin, urine, compared to colorimetric analysis □ Antibacterial agents—nitrofurantoin, electrochemical analysis, urine

The use of nitrofurantoin, 1-[(5-nitrofurfurylidene)amino]hydantoin, in the treatment of urinary tract infections is widely accepted (1). Due to the site of action, determination of the concentration of nitrofurantoin in urine is important for bioavailability studies and patient monitoring (2). The commonly used method for the determination of nitrofurantoin in urine is a colorimetric procedure (3–5), based on extraction of the drug into nitromethane followed by the formation of a nitrofurantoin–hyamine complex which absorbs at 400 nm.

A polarographic method was reported for the determination in urine, based on measuring the peak current of the differential polarogram resulting from reduction of the nitro group (6). A standard addition technique is employed to correct for possible differences in the diffusion constant of the drug in various urine samples.

Although the reported methods are sufficiently specific and sensitive, they involve cumbersome manipulative steps or the use of equipment frequently not available in laboratories doing clinical assays (*i.e.*, a differential or differential pulse polarograph). The rotating platinum electrode, because of the higher limiting currents possible with combined convection–diffusion-controlled mass transport, was considered a possible alternative to the common mercury electrodes.

The rotating platinum electrode may be used as the working electrode in a simple direct current procedure with high sensitivity. Thus, an investigation of the reduction of nitrofurantoin at the rotating platinum electrode, with the objective of developing a simple and rapid method for the determination of this drug in urine, was undertaken. The developed method is presented and compared to the commonly employed colorimetric method (3).

EXPERIMENTAL

Apparatus—The three-electrode cell with the rotating platinum electrode is shown in Fig. 1. The rotating platinum electrode is turned by a synchronous rotator[1] at the rate of 1800 rpm. The working and counter electrodes are made of platinum wire sealed in glass, and the reference electrode is a saturated calomel electrode[2]. The cell is designed to require 15 ml of solution for analysis and to permit rapid conversion from one sample to the next.

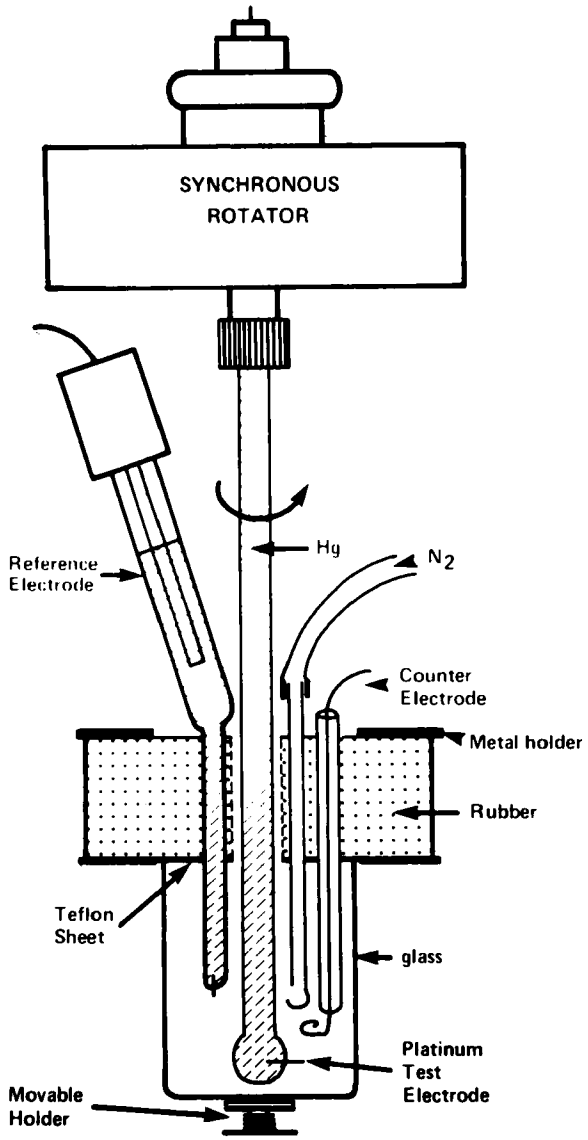

Figure 1—*Three-electrode cell for rotating platinum electrode.*

A dc polarography system[3] is used to record the current–voltage curves. All electrical leads are shielded, and the shields are connected to ground.

Chemicals—All chemicals were of the highest quality commercially available. Standard solutions of nitrofurantoin were prepared in dimethylformamide or acetone from a pure powder[4].

Procedures—Current–voltage curves were determined by placing about 15 ml of the test solution in the electrolysis cell, deaerating with nitrogen for 4 min with the voltage at 0 v *versus* the satu-

[1] S-76485, Sargent Welch Scientific Co.

[2] Coleman No. 3-152.

[3] Heath EU-401.

[4] Norwich Pharmacal Co., Norwich, N.Y.

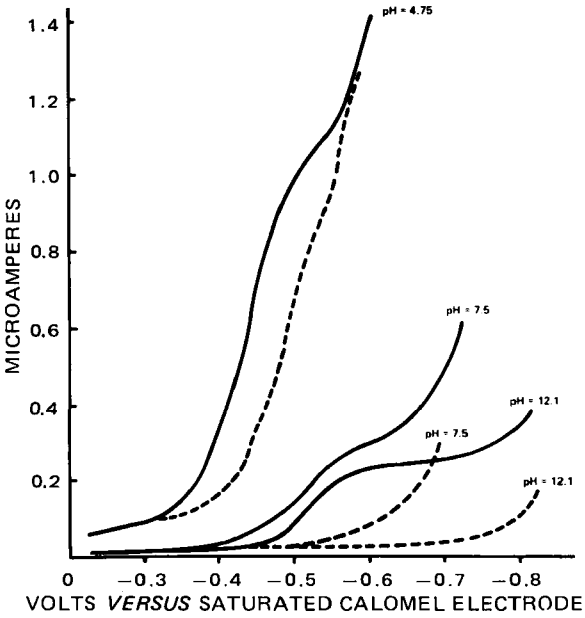

Figure 2—*Nitrofurantoin current voltage curve for 4-μg/ml solutions in various buffers. Key: —, nitrofurantoin; and - - -, buffer only.*

rated calomel electrode. Then the voltage was scanned cathodically at 5 mv/sec with the rotating platinum electrode turning at 1800 rpm. During the scan, the nitrogen atmosphere was maintained above the solution. Holding the electrode potential at 0 v *versus* the saturated calomel electrode during the deaeration period was necessary to condition the electrode.

Several buffer solutions were evaluated to determine their effects on the reduction wave of nitrofurantoin and the background current at the rotating platinum electrode. The buffers studied were 0.1 *M* H_2SO_4, 0.2 *M* HCl, 0.5 *M* sodium acetate (pH 4.75), 0.2 *M* sodium phosphate (pH 6.5 and 7.5), 0.5 *M* sodium phosphate (pH 6.5 and 7.5), 0.2 *M* sodium borate (pH 9.0 and 12.1), 0.5 *M* sodium borate (pH 9.0 and 12.1), and 0.25 *M* sodium hydroxide.

Urine samples were collected from 20 different hospitalized patients who were not taking nitrofurantoin or other drugs containing nitro groups. However, each patient was taking one or more of the following drugs: aspirin, acetaminophen, codeine, diazepam, chlordiazepoxide, phenytoin, phenobarbital, quinidine, or tolbutamide. Five milliliters of each urine sample was diluted to 50 ml in each buffer, and current–voltage scans were run. Then nitrofurantoin (to give 40 μg/ml) was added to each urine sample, and the current–voltage scans were repeated. These spiked urine samples also were assayed by the colorimetric method (3).

The accuracy and precision of the rotating platinum electrode method were compared to the colorimetric method (3) by analysis of urine samples from five patients taking nitrofurantoin for urinary infections. The rotating platinum electrode method consisted of pipetting 5.0 ml of the urine into a 50-ml volumetric flask and diluting to volume with 0.50 *M* borate buffer (pH 12.1). Then the current–voltage curve was determined, and the concentration was calculated from a calibration curve of limiting current *versus* nitrofurantoin concentration.

RESULTS AND DISCUSSION

The current–voltage curve for reduction of nitrofurantoin at the rotating platinum electrode is greatly dependent on the pH and molarity of the buffer system employed. In strong acid media, the nitrofurantoin wave and background current were not separated and thus were not useful for analysis. Figure 2 shows some typical current–voltage curves at three pH values; the more alkaline pH was required for a suitable current–voltage curve.

It also was noted that the higher molarity buffers (*i.e.*, 0.5 *versus* 0.2 *M*) gave sharper current–voltage curves. The current–voltage scans run in 0.25 *M* sodium hydroxide gave a limiting current, which demonstrated the lack of stability of nitrofurantoin in this medium. The limiting current decreased 17% in 10 min. In the 0.5

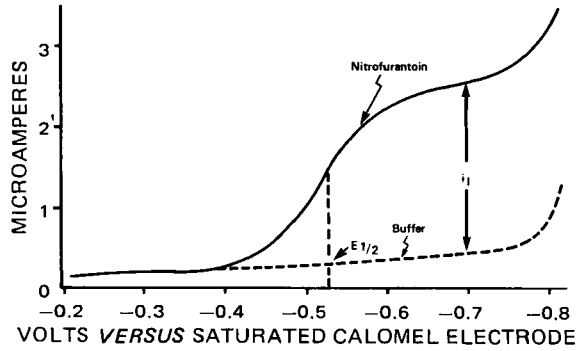

Figure 3—*Reduction of nitrofurantoin (4 μg/ml) in 0.50* M *borate buffer, pH 12.1.*

M sodium borate buffer (pH 12.1), the limiting current decreased 4.0% in 60 min. Thus, the borate buffer can be used in the analysis if test solutions are assayed within a few minutes of preparation.

Figure 3 shows a typical current–voltage curve for nitrofurantoin reduction at the rotating platinum electrode in 0.5 *M* sodium borate buffer. The half-wave potential was −0.53 v *versus* the saturated calomel electrode, and $E_{3/4}$–$E_{1/4}$ was 75 mv. The limiting current varied in a linear manner with the concentration of nitrofurantoin. A typical calibration curve between 0.50 and 15 μg/ml is expressed by:

$$i_l = \left(0.39 \frac{\mu\text{amp ml}}{\mu\text{g}}\right) C + 0.39\ \mu\text{amp} \qquad \text{(Eq. 1)}$$

with a regression coefficient of 0.98 when the limiting current was determined in triplicate at 0.5, 1, 2, 4, 8, 10, 14, and 15 μg/ml. Calibration plots determined at various times over a month did not differ more than 5.0% in either slope or intercept.

The current–voltage curves on the urine samples from patients not taking drugs with nitro groups showed no reduction waves and thus no potential interferences. The limiting current for nitrofurantoin (4.0 μg/ml) in 90% sodium borate buffer and 10% urine from the 20 patients not taking drugs with nitro groups ranged from 1.66 to 1.87 μamp. This study indicates the small potential error introduced by the urine from various sources and that interference due to commonly used drugs or their metabolites is unlikely.

The possible interferences of various antibiotics, particularly chloramphenicol, were not evaluated, because no patients were encountered who were taking such combinations. Indeed, clinicians indicate that such therapy seldom would be employed. The rotating platinum electrode method involves the reduction of the nitro group, so drugs (*i.e.*, nitroimidazoles and chloramphenicol) or drug metabolites containing nitro groups and appearing in high concentration in the urine would interfere.

Table I shows the comparative values and precision of the rotating platinum electrode method and the colorimetric method (3) for samples from five patients taking nitrofurantoin. The colorimetric method is more precise, but the mean values obtained are quite close.

SUMMARY

In summary, a relatively simple and fast method for the determination of nitrofurantoin in urine is presented. The method allows a triplicate analysis in 35 min, with only a slight loss in the

Table I—Comparative Analysis of Urine from Patients Taking Nitrofurantoin

Patient	Mean ± *SD*[a], μg/ml: Rotating Platinum Electrode Method	Mean ± *SD*[a], μg/ml: Colorimetric[b] Method
1	20.0 ± 0.5	21.2 ± 0.2
2	43.0 ± 1.0	44.0 ± 0.5
3	3.5 ± 0.5	3.8 ± 0.1
4	24.0 ± 0.8	23.0 ± 0.2
5	71.0 ± 1.5	69.0 ± 0.8

[a] Three assays on each sample. [b] Reference 3.

precision obtained with the longer colorimetric method. The new method does not require extraction steps or the addition of reagents, both of which take considerable time.

The method described is similiar to the method of Jones *et al.* (6) in that it is based on the electrochemical reduction of the nitro functional group in nitrofurantoin. The rotating platinum electrode method has the advantage over a previously used electrochemical method of not requiring a differential pulse polarograph or differential polarograph; it requires only a simple direct current polarograph, because of the relatively high sensitivity possible with a rotating electrode.

REFERENCES

(1) H. E. Paul and M. F. Paul, "Experimental Chemotherapy II," Academic, New York, N.Y., 1964, pp. 307–370.

(2) D. Cadwallader, "The Bioavailability of Drug Products (The APhA Bioavailability Pilot Project)," American Pharmaceutical Association, Washington, D.C., July 1973, p. 31.

(3) J. D. Conklin and R. D. Hollifield, *Clin. Chem.*, **11**, 926 (1965).

(4) *Ibid.*, **12**, 632(1966).

(5) *Ibid.*, **16**, 335(1970).

(6) B. M. Jones, R. J. M. Ratcliffe, and S. G. E. Stevens, *J. Pharm. Pharmacol., Suppl.*, **17**, 52-S(1965).

ACKNOWLEDGMENTS AND ADDRESSES

Received April 21, 1975, from the *School of Pharmacy, University of Missouri-Kansas City, Kansas City, MO 64108*

Accepted for publication June 25, 1975.

[x] To whom inquiries should be directed.

Simple Transformation Method for Predicting Plasma Drug Profiles from Dissolution Rates

D. P. VAUGHAN [x] and R. H. LEACH [‡]

Abstract □ A transformation factor is described which related *in vitro* drug dissolution from a preparation to the corresponding *in vivo* plasma drug concentrations. This factor, derived from the dissolution profile and the corresponding *in vivo* plasma concentration of a single formulation, was used to predict plasma concentration profiles of similar formulations simply from dissolution data.

Keyphrases □ Plasma drug profiles—predicted from dissolution rates, transformation factor described □ Dissolution rates—transformation factor described for prediction of plasma drug profiles

Frequently, the *in vivo* dissolution rate of an oral dosage form controls the rate at which a drug appears in plasma, and similar formulations of the same drug can have different therapeutic equivalences. Since drug absorption studies in humans are expensive and time consuming, *in vitro* dissolution data are frequently correlated with the biological availability of a drug from different preparations. The times to achieve 50% drug dissolution (t_{50}) usually are correlated with either maximal plasma drug concentrations or the areas under the plasma concentration–time curves (1).

Although these latter methods are useful, they are not designed to predict the plasma time course of a drug following administration of different preparations. One method of predicting plasma drug concentrations involves a detailed pharmacokinetic study of drug distribution and elimination after an oral aqueous dose and the derivation of an explicit function to describe *in vitro* drug dissolution from various preparations (2).

Alternatively, a curve follower or variable diode function generator can be used to input *in vitro* dissolution data directly into a pharmacokinetic model programmed on an analog computer (3).

To avoid detailed pharmacokinetic studies in humans, a simple transformation method was investigated for predicting plasma drug concentrations from *in vitro* dissolution data.

THEORY

Two independent functions of time, $f_1(t)$ and $f_2(t)$, can be related to each other at some specific value of time by an arbitrary transformation factor, $m(t)$, so that at time t:

$$f_1(t)m(t) = f_2(t) \qquad \text{(Eq. 1)}$$

Relating the two functions (Eq. 1) in this way does not necessarily imply a specific relationship between them. Similarly, *in vitro* dissolution characteristics of an oral drug preparation can be related to the corresponding *in vivo* plasma drug concentrations.

Without defining the distribution and elimination processes in the body, the plasma concentration of a drug obtained with some drug input process into the body can be related to the drug input by an operator, $m(t)$, such that:

$$\text{drug input}(t) = m(t)\ [\text{plasma drug concentration}(t)] \qquad \text{(Eq. 2)}$$

In Eq. 2, m is a collection of numbers which, together with the drug input, uniquely determines the plasma drug concentration for all $t \geq 0$. When considering plasma drug concentrations obtained after oral administration of a dosage formulation, Eq. 2 becomes:

$$\text{amount of drug released } \textit{in vivo} \text{ from formulation}(t) = m_i(t)\ [\text{plasma drug concentration}(t)] \qquad \text{(Eq. 3)}$$

where m_i is a collection of numbers which, together with the amount of drug released from the preparation at time t, uniquely determines the plasma drug concentration at time t for all $t \geq 0$.

Similarly, *in vitro* drug dissolution from an oral formulation can be related to the corresponding *in vivo* drug dissolution by an operator, $m_j(t)$:

$$\text{amount of drug dissolved in } \textit{in vitro} \text{ dissolution test from dosage formulation}(t), \textit{i.e.}, \text{dis}_j(t) = m_j(t) \times \text{amount of drug released } \textit{in vivo} \text{ from formulation}(t) \qquad \text{(Eq. 4)}$$

precision obtained with the longer colorimetric method. The new method does not require extraction steps or the addition of reagents, both of which take considerable time.

The method described is similiar to the method of Jones *et al.* (6) in that it is based on the electrochemical reduction of the nitro functional group in nitrofurantoin. The rotating platinum electrode method has the advantage over a previously used electrochemical method of not requiring a differential pulse polarograph or differential polarograph; it requires only a simple direct current polarograph, because of the relatively high sensitivity possible with a rotating electrode.

REFERENCES

(1) H. E. Paul and M. F. Paul, "Experimental Chemotherapy II," Academic, New York, N.Y., 1964, pp. 307–370.

(2) D. Cadwallader, "The Bioavailability of Drug Products (The APhA Bioavailability Pilot Project)," American Pharmaceutical Association, Washington, D.C., July 1973, p. 31.

(3) J. D. Conklin and R. D. Hollifield, *Clin. Chem.*, **11**, 926 (1965).

(4) *Ibid.*, **12**, 632(1966).

(5) *Ibid.*, **16**, 335(1970).

(6) B. M. Jones, R. J. M. Ratcliffe, and S. G. E. Stevens, *J. Pharm. Pharmacol., Suppl.*, **17**, 52-S(1965).

ACKNOWLEDGMENTS AND ADDRESSES

Received April 21, 1975, from the *School of Pharmacy, University of Missouri-Kansas City, Kansas City, MO 64108*

Accepted for publication June 25, 1975.

[x] To whom inquiries should be directed.

Simple Transformation Method for Predicting Plasma Drug Profiles from Dissolution Rates

D. P. VAUGHAN [x] and R. H. LEACH [‡]

Abstract □ A transformation factor is described which related *in vitro* drug dissolution from a preparation to the corresponding *in vivo* plasma drug concentrations. This factor, derived from the dissolution profile and the corresponding *in vivo* plasma concentration of a single formulation, was used to predict plasma concentration profiles of similar formulations simply from dissolution data.

Keyphrases □ Plasma drug profiles—predicted from dissolution rates, transformation factor described □ Dissolution rates—transformation factor described for prediction of plasma drug profiles

Frequently, the *in vivo* dissolution rate of an oral dosage form controls the rate at which a drug appears in plasma, and similar formulations of the same drug can have different therapeutic equivalences. Since drug absorption studies in humans are expensive and time consuming, *in vitro* dissolution data are frequently correlated with the biological availability of a drug from different preparations. The times to achieve 50% drug dissolution (t_{50}) usually are correlated with either maximal plasma drug concentrations or the areas under the plasma concentration–time curves (1).

Although these latter methods are useful, they are not designed to predict the plasma time course of a drug following administration of different preparations. One method of predicting plasma drug concentrations involves a detailed pharmacokinetic study of drug distribution and elimination after an oral aqueous dose and the derivation of an explicit function to describe *in vitro* drug dissolution from various preparations (2).

Alternatively, a curve follower or variable diode function generator can be used to input *in vitro* dissolution data directly into a pharmacokinetic model programmed on an analog computer (3).

To avoid detailed pharmacokinetic studies in humans, a simple transformation method was investigated for predicting plasma drug concentrations from *in vitro* dissolution data.

THEORY

Two independent functions of time, $f_1(t)$ and $f_2(t)$, can be related to each other at some specific value of time by an arbitrary transformation factor, $m(t)$, so that at time t:

$$f_1(t)m(t) = f_2(t) \qquad \text{(Eq. 1)}$$

Relating the two functions (Eq. 1) in this way does not necessarily imply a specific relationship between them. Similarly, *in vitro* dissolution characteristics of an oral drug preparation can be related to the corresponding *in vivo* plasma drug concentrations.

Without defining the distribution and elimination processes in the body, the plasma concentration of a drug obtained with some drug input process into the body can be related to the drug input by an operator, $m(t)$, such that:

$$\text{drug input}(t) = m(t)\ [\text{plasma drug concentration}(t)] \qquad \text{(Eq. 2)}$$

In Eq. 2, m is a collection of numbers which, together with the drug input, uniquely determines the plasma drug concentration for all $t \geq 0$. When considering plasma drug concentrations obtained after oral administration of a dosage formulation, Eq. 2 becomes:

$$\text{amount of drug released } \textit{in vivo} \text{ from formulation}(t) = m_i(t)\ [\text{plasma drug concentration}(t)] \qquad \text{(Eq. 3)}$$

where m_i is a collection of numbers which, together with the amount of drug released from the preparation at time t, uniquely determines the plasma drug concentration at time t for all $t \geq 0$.

Similarly, *in vitro* drug dissolution from an oral formulation can be related to the corresponding *in vivo* drug dissolution by an operator, $m_j(t)$:

$$\text{amount of drug dissolved in } \textit{in vitro} \text{ dissolution test from dosage formulation}(t), \textit{i.e.}, \text{dis}_j(t) = m_j(t) \times \text{amount of drug released } \textit{in vivo} \text{ from formulation}(t) \qquad \text{(Eq. 4)}$$

Combining Eqs. 3 and 4 gives:

$$\text{dis}_j(t) = m_i(t)m_j(t)[\text{plasma drug concentration}(t)] \quad \text{(Eq. 5)}$$

and from Eq. 5:

amount of drug dissolved at time t in *in vitro* dissolution test = $H(t) \times$ plasma drug concentration at time t obtained with oral drug preparation (Eq. 6)

Plasma drug concentrations are a function of both the pharmacokinetics of the drug within the body and the amount of drug absorbed. Since the latter is also a function of the amount of drug released from the preparation, H (Eq. 6) can be regarded as a transformation factor which simultaneously compensates for the kinetics of the drug and relates *in vitro* drug dissolution to *in vivo* drug dissolution.

If linear drug pharmacokinetics are assumed with respect to the dose, then H (Eq. 6) is a specific operator, and for two different formulations of the same drug:

$$\text{dis}_1(t) = H(t)C_{p1}(t) \quad \text{(Eq. 7)}$$

and:

$$\text{dis}_2(t) = H(t)C_{p2}(t) \quad \text{(Eq. 8)}$$

where C_{p1} and C_{p2} are plasma drug concentrations obtained with two different oral preparations of the same drug, and dis_1 and dis_2 are the corresponding amounts of drug released *in vitro* from these preparations.

The transformation factor H (Eq. 7) can be evaluated at different values of t from one *in vitro* dissolution curve and the corresponding *in vivo* plasma drug concentrations (Eq. 7). Calculated values of H can then be used to predict plasma drug concentrations for another preparation of the same drug from a knowledge of its dissolution profile obtained under identical conditions as those used for the first preparation.

EXPERIMENTAL

To demonstrate the application of Eqs. 7 and 8, the serum concentrations of total alprenolol were calculated from the data of Johansson *et al.* (4), and the results were compared with experimental observations (Table I). Johansson *et al.* (4) recorded the total serum concentration of alprenolol and its metabolites obtained with three sustained-release preparations (A, B, and C) at 0.25, 0.5, 1.0, 1.5, 2.0, and 3.0 hr after drug administration and measured the *in vitro* dissolution at time 1.0, 2.0, 4.0, and 6.0 hr.

Estimates of the *in vitro* drug dissolution at times corresponding with serum sample times were obtained by linear interpolation between the quoted values. The *in vitro* data (4) also were curve fitted to a polynomial using a least-squares fit by orthogonal polynomials, and the numerical value of the polynomial function itself was used in the calculation.

From the *in vivo* and interpolated *in vitro* data for Preparation A (dose ≡ 100 mg of alprenolol hydrochloride), the transformation factor of H was calculated at different times (Table I). This transformation factor was then used in conjunction with the interpolated *in vitro* data for Preparation C (dose ≡ 100 mg of alprenolol hydrochloride) to predict the *in vivo* serum concentrations.

Further examples of the application of Eqs. 7 and 8 are given in Fig. 1; predicted serum digoxin concentrations for two brands of digoxin tablets and predicted serum alprenolol concentrations for two sustained-release preparations [B and C (4)] are presented. Predicted serum drug concentrations are also compared with experimentally determined concentrations in Fig. 1. *In vitro* dissolution data and serum drug concentrations used in the calculations on digoxin were obtained from Fraser *et al.* (5), Preparation 3 was used to calculate H, and the serum levels of digoxin for Preparations 6 and 8 are predicted.

DISCUSSION

As indicated in Table I, the predicted serum drug concentrations (Fig. 1) obtained by the application of transformation factors (Eqs. 7 and 8) are in excellent agreement with the *in vivo* measurements. The discrepancies between predicted and measured digoxin

Table I—Calculation of the Transformation Factor H at Various Times (Eq. 7) from the *In Vitro* Dissolution of Alprenolol and *In Vivo* Serum Alprenolol Concentrations of Preparation A and the Application of H to the Prediction (Eq. 8) of the Serum Concentrations of Alprenolol Obtained with Preparation C[a]

Hours	Drug Released *In Vitro* from Preparation A (*i.e.*, dis_1), %		Serum Alprenolol Concentration Obtained with Preparation A (*i.e.*, C_{p1}), μg/g	$H(t) = \frac{\text{dis}_1}{C_{p1}}$		Drug Released *In Vitro* from Preparation C (*i.e.*, dis_2), %		Calculated Serum Concentration of Alprenolol for Preparation C (*i.e.*, dis_2/H), μg/g		*In Vivo* Serum Concentration of Alprenolol for Preparation C, μg/g	Difference in Calculated and Experimental Alprenolol Concentrations, %	
	a	*b*		*a*	*b*	*a*	*b*	*a*	*b*		*a*	*b*
0.25	15	17.9	0.08	187.5	223.72	7.5	8.54	0.04	0.04	0.03	+25.0	+25.0
0.5	30	32.34	0.68	44.12	47.56	15	15.65	0.34	0.33	0.32	+6.25	+3.13
1.0	60	55.56	1.56	38.46	35.62	29.5	27.58	0.77	0.77	0.77	0.0	0.0
1.5	70	72.15	1.85	37.84	39.0	36	36.85	0.95	0.94	0.9	+5.5	+4.44
2	79	83.16	1.99	39.69	41.79	42	43.80	1.05	1.05	1.00	+5.0	+5.0
3	87	92.80	1.82	47.8	50.99	50	53.03	1.05	1.04	1.1	—4.5	—5.45
4	94.5	93.11	1.48	63.85	62.91	58.5	57.9	0.92	0.92	0.98	—6.0	—6.0

[a] Columns *a* and *b* list data obtained using a linear and a polynominal interpolation of the *in vitro* dissolution data, respectively.

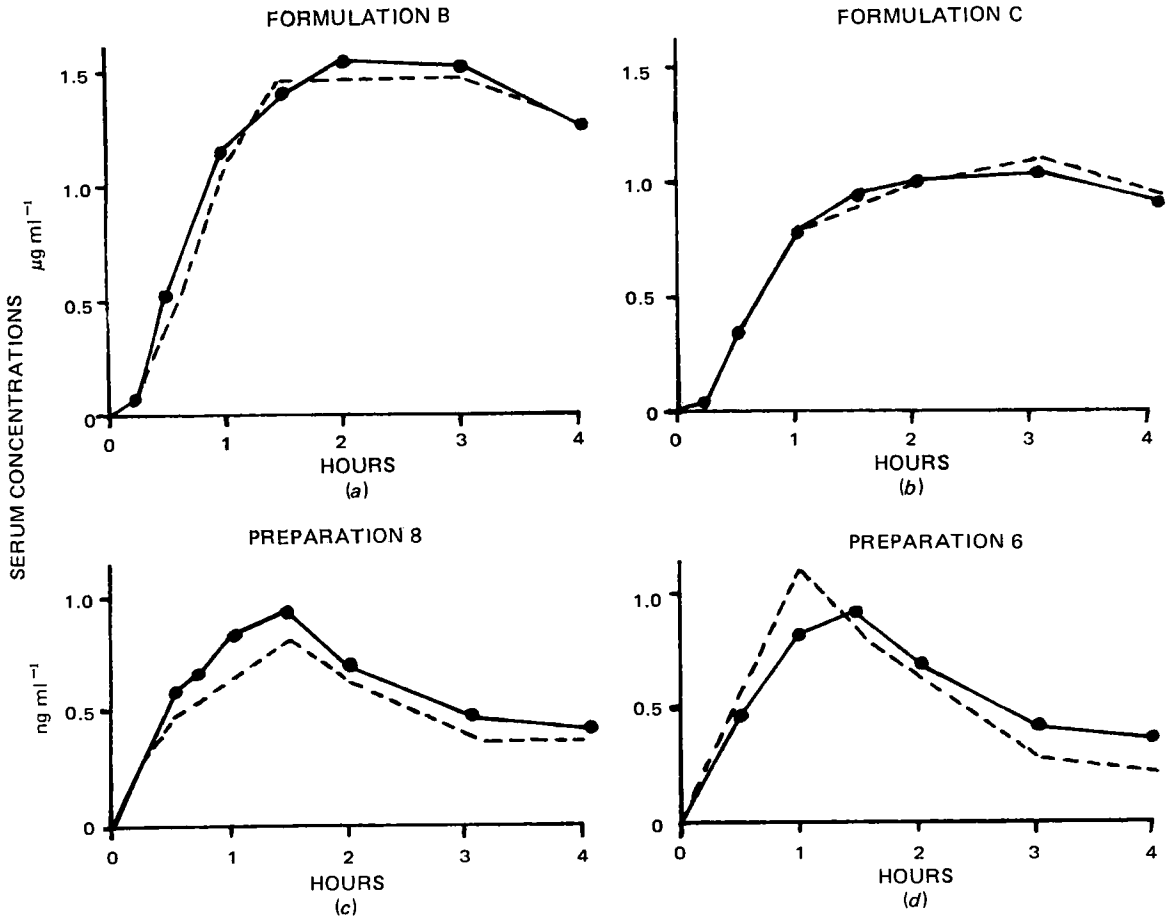

Figure 1—(a *and* b) *Predicted mean serum concentrations of total alprenolol after the administration of 100 mg of alprenolol hydrochloride in two different tablet formulations* (– ● –) *and the experimental* (- - -) *serum levels of alprenolol (experimental data from Ref. 4).* (c *and* d) *Predicted mean serum concentrations of digoxin after the administration of two brands of digoxin tablets* (– ● –) *and the experimental* (- - -) *serum levels of digoxin (experimental data from Ref. 5).*

concentrations can be largely ascribed to the errors[1] in the determination of digoxin by radioimmunoassay (5).

The transformation factors obtained by Eq. 7 and their subsequent applications (Eq. 8) are only valid during the time required to achieve complete or asymptotic *in vitro* dissolution. However, this period could be extended by decreasing the agitation rates in dissolution tests.

Since the transformation factor relates *in vivo* to *in vitro* dissolution, its application is valid only if the changes in *in vitro* dissolution mechanisms (*e.g.*, disintegration and disaggregation) between various formulations of the same drug are adequately mimicked *in vivo*. For example, transformation factors obtained from a tablet formulation are unlikely to apply to a capsule preparation since these two products could have different *in vivo* dissolution mechanisms. This restriction limits the general application of the method for predicting *in vivo* data from *in vitro* data.

However, provided the method is evaluated for a particular type of formulation, it could be applied as a control procedure for estimating the effects of *in vitro* dissolution changes on blood concentrations. This method of predicting blood concentrations (Eqs. 3 and 4) from *in vitro* dissolution data is independent of the processes governing drug release from a preparation, drug absorption, and the pharmacokinetics of drug distribution or elimination.

[1] The error is ±20–30% for serum digoxin <1 ng/ml; L. S. Culank, Clinical Chemistry Department, Queen Elizabeth Medical Centre, Birmingham B15 2TH, United Kingdom, personal communication, 1974.

In conclusion, the use of transformation factors can provide a rapid and simple method for predicting plasma drug concentrations from *in vitro* data.

REFERENCES

(1) J. G. Wagner, "Biopharmaceutics and Relevant Pharmacokinetics," Drug Intelligence Publications, Hamilton, Ill., 1971, chap. 18.

(2) R. G. Weigand and J. D. Taylor, *Biochem. Pharmacol.*, **3**, 256(1960).

(3) H. Stelmarck, J. R. Robinson, and S. P. Erikson, *J. Pharm. Sci.*, **54**, 1453(1965).

(4) R. Johansson, C. G. Regardh, and J. Sjögren, *Acta Pharm. Suecica*, **8**, 59(1971).

(5) E. J. Fraser, R. H. Leach, J. W. Poston, A. M. Bold, L. S. Culank, and A. B. Lipede, *J. Pharm. Pharmacol.*, **25**, 968(1973).

ACKNOWLEDGMENTS AND ADDRESSES

Received January 15, 1975, from the *School of Pharmacy and Biology, Sunderland Polytechnic, Sunderland SR1 3SD, United Kingdom, and the ‡Pharmaceutical Department, Queen Elizabeth Medical Centre, Birmingham B15 2TH, United Kingdom.

Accepted for publication June 20, 1975.

* To whom inquiries should be directed.

Protein-Binding Polyhedral Boranes II: DL-*S*-(10-Dimethylsulfidooctahydrodecaborane)methionine

P. M. JACOBS, R. L. SNEATH, Jr., A. H. SOLOWAY ˣ, and A. S. DEY

Abstract □ An analog of methionine, DL-*S*-(10-dimethylsulfidooctahydrodecaborane)methionine, was synthesized from fully protected homoserine. A protected dipeptide with glycine is described.

Keyphrases □ Boranes—synthesis of a decaboranemethionine derivative, a neutral polyhedral borane with protein-incorporating functions, potential tumor antibody-binding agent □ Protein binding—polyhedral borane synthesized, potential tumor antibody-binding agent □ Methionine analog—synthesis of a neutral polyhedral borane with protein-incorporating functions, potential tumor antibody-binding agent

The development of neutral polyhedral boranes with protein-incorporating functions offers the opportunity of binding such structures to tumor antibodies. Treatment of a tumor by neutron-capture therapy then could be quite specific (1–3). As part of continuing efforts in this area (4), DL-*S*-(10-dimethylsulfidooctahydrodecaborane)methionine (I), an analog of the amino acid methionine, substituted at the side-chain sulfur with a polyhedral borane, was synthesized.

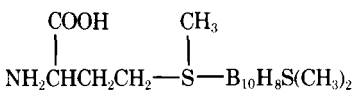

I

This work is providing the basis for several lines of research designed to synthesize a water-soluble, boron-containing polypeptide. This amino acid will be used to synthesize low and medium weight polymers to attach to tumor antibodies. In this way, large numbers of boron atoms can be localized in and at the level of the cell. Variable solubility characteristics of the products can be obtained by copolymerization with other amino acids

DISCUSSION

Compound I can by synthesized from DL-homoserine (II) or DL-homoserine lactone (5) (III) by the sequence outlined in Schemes I and II. Compound II or III is subjected to carbobenzyloxylation; then treatment of the sodium salt (IV) with *p*-nitrobenzyl toluenesulfonate (6) yields the *p*-nitrobenzyl ester (V). The toluenesulfonate (VI) is then formed by treatment of (V) with *p*-toluenesulfonyl chloride and pyridine. Reaction of VI with tetramethylammonium 1-methylsulfido-10-dimethylsulfidooctahydrodecaborane (7) results in the fully protected amino acid (VII).

This derivative can be partially or totally deprotected using routine methods of peptide chemistry, except that catalytic hydrogenation must be avoided since this procedure is known to degrade the borane cage (4). Some transformations are shown in Scheme II. Treatment of VII with sodium or potassium hydroxide in methanol or acetone at room temperature gives the free acid (VIII), which can be isolated through the dicyclohexylammonium salt. Reaction of VIII with hydrogen bromide in acetic acid yields the hydrobromide salt from which I can be isolated. This free amino acid is more soluble in methanol than in cold water, presumably due to the effect of the unusual side chain.

Compound VIII was also used to form a dipeptide (IX) by reaction with glycine ethyl ester and dicyclohexylcarbodiimide. Other coupling methods were not tested, but no difficulty is anticipated with the mixed anhydride or active ester methods, since this amino acid is stable to the reagents and conditions used.

EXPERIMENTAL[1]

***N*-Carbobenzoxy-DL-homoserine *p*-Nitrobenzyl Ester (V)**—*Method A*—The method was identical to that used previously for the preparation of the L-isomer (8). The yield was 22%, mp 108–110°; IR: 3400 (OH, NH), 1720 ($CH_2OC{=}ONH$), 1600, 1520, and 1350 (NO_2) cm^{-1}; NMR (deuterochloroform): δ 8.2 (2, d, aromatic), 7.4 (7, m, aromatic), 5.8 (1, d, NH), 5.25 (2, s, $NO_2C_6H_4CH_2$), 5.15 (2, s, $C_6H_5CH_2$), 4.5 (1, m, $NHCHCO$), 3.7 (2, q, CH_2OH), 2.8 (1, OH), and 2.0 (2, m, $CHCH_2CH_2OH$).

Anal.—Calc. for $C_{19}H_{20}N_2O_7$: C, 58.76; H, 5.19; N, 7.21. Found: C, 59.10; H, 4.94; N, 7.23.

Method B—Homoserine lactone *p*-toluenesulfonate (6) (40 g, 0.146 mole) was added to about 250 ml of water containing 25 g of sodium bicarbonate (0.31 mole). Benzyl chloroformate (23 ml, 0.16 mole) was added in four portions over 1 hr, and the mixture was allowed to stir for 3 hr more. Then the solution was extracted twice with 200 ml of ethyl acetate. The organic solution was washed with water, dried over sodium sulfate, and evaporated. Crystallization of the residue from ethyl acetate–hexane gave 20.5 g (60%), mp 108–110° [lit. (9) mp 110–112°].

The lactone (8 g, 34 mmoles) was dissolved in about 20 ml of methanol, and 4 *N* NaOH was added until the pH remained at 11 for 15 min (8 ml, 32 mmoles). Then the solution was evaporated to dryness several times with benzene. The residue was dissolved in 40 ml of dimethylformamide and 80 ml of acetone, *p*-nitrobenzyl toluenesulfonate (10.75 g, 35 mmoles) was added, and the mixture was refluxed for 1 hr. After evaporation, the residue was partitioned between ethyl acetate and water. The organic layer was dried over sodium sulfate and evaporated to give an oil. The oil crystallized from ether to give 11 g (89%) of white crystals, mp 88–93°. Recrystallization from ethyl acetate–hexane gave 7.94 g of an ester (64%), mp 108–110°, identical with that obtained by Method A.

***N*-Carbobenzoxy-*O*-*p*-toluenesulfonate-DL-homoserine *p*-Nitrobenzyl Ester (VI)**—Compound V (6.94 g, 17.9 mmoles) was dissolved in 40 ml of pyridine at 0°, and 4.78 g (25 mmoles) of *p*-toluenesulfonyl chloride was added. The reaction mixture was kept at 0° overnight. Ethyl acetate and iced 7 *N* H_2SO_4 were then added, and the layers separated. The organic layer was then washed with 2 *N* H_2SO_4, sodium bicarbonate solution, and saline, dried over sodium sulfate, and evaporated. The residue was crystallized from ethyl acetate–hexane to give 7.2 g (75%) of white crystals, mp 98–101°, and recrystallized to give 6.1 g, mp 102–104°; IR (potassium bromide): 3350 (NH), 1760 (ester), 1715 (CH_2O-C=O), 1600, 1520, 1370 (NO_2), 1350, and 1200 (OSO_2) cm^{-1}; NMR (deuterochloroform): δ 8.2 (2, d, $C_6H_4NO_2$), 7.7 (2, d, $C_6H_4NO_2$), 7.3 (9, m, aromatic), 5.4 (1, d, NH), 5.2 (2, s, $NO_2C_6H_4CH_2$), 5.1 (2, s, $C_6H_5CH_2$), 4.5 (1, m, —CH—), 4.1 (2, t, $—CH_2O—$), 2.5 (3, s, $CH_3C_6H_5$), and 2.2 (2, m, —CH—).

[1] Melting points were determined using a Mel-Temp melting-point apparatus and are corrected. Elemental analyses were performed by Midwest Microlab, Inc., Indianapolis, Ind. IR spectra were determined on a Perkin-Elmer 127 Infracord, and NMR spectra were determined on a Varian T-60. Silica gel hard-layer TLC plates were purchased from Analtech, Inc. Boron-containing compounds were visualized on TLC with an acidic 1% $PdCl_2$ spray.

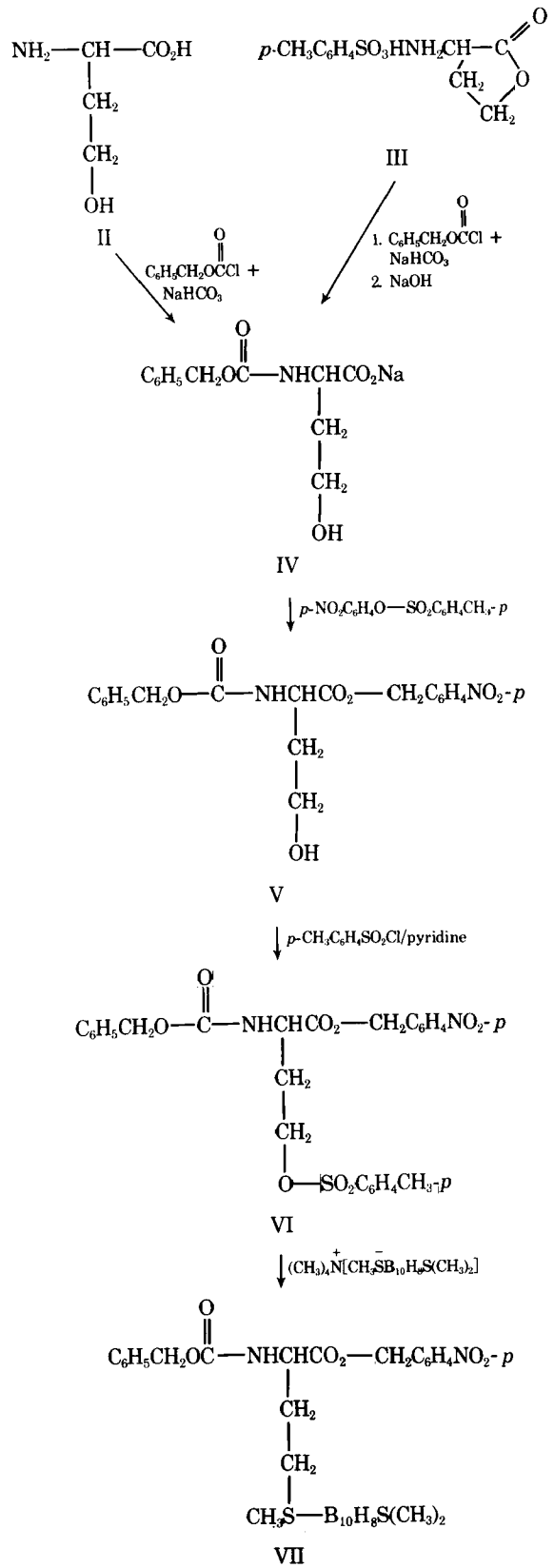

Scheme I

Anal.—Calc. for $C_{26}H_{26}N_2O_9S$: C, 57.56; H, 4.83; N, 5.16. Found: C, 57.46; H, 4.61; N, 5.23.

N-Carbobenzoxy-DL-S-(10-dimethylsulfidooctahydrodecaborane)methionine p-Nitrobenzyl Ester (VII)—Compound VI (1.2 g, 2.34 mmoles) was dissolved in acetone and added to a solution of tetramethylammonium 1-methylsulfido-10-dimethylsulfidooctahydrodecaborane (0.7 g, 2.34 mmoles) in 7 ml of dimethylformamide. Although a precipitate occurred within 1–2 min, TLC indicated only about 50% reaction after 12 hr at room temperature. After 45 min at 50°, all of the starting boron salt was reacted. Ethyl acetate was added and washed several times with water, dried over magnesium sulfate, and evaporated.

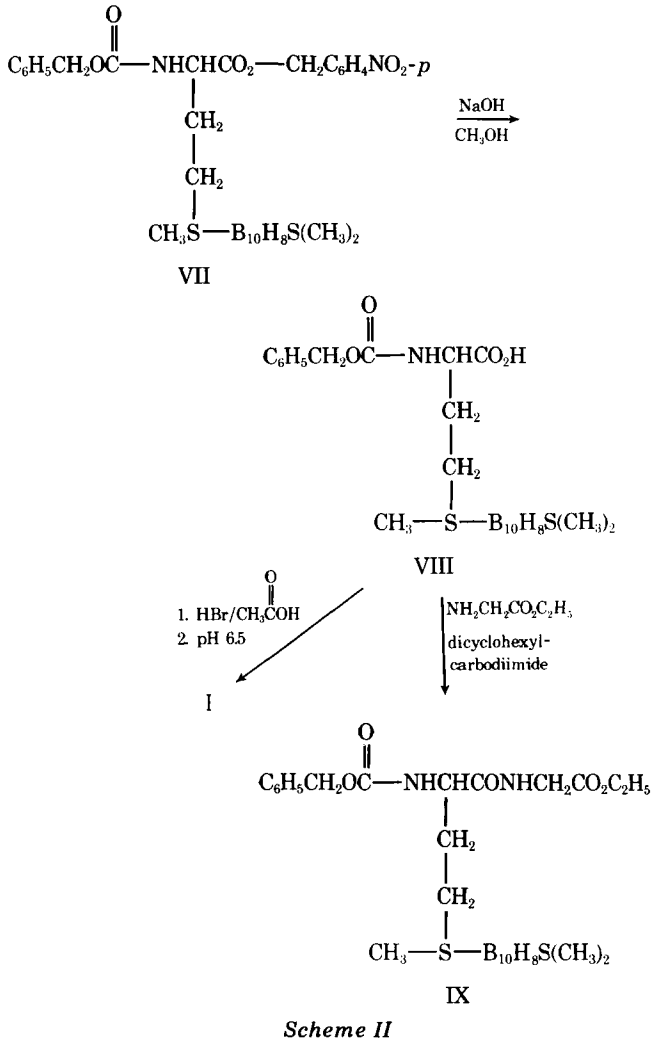

Scheme II

Chromatography of the resulting oil on silica gel–chloroform gave 1.2 g of an oil, which could be obtained as a noncrystalline foam by vacuum evaporation of a methanol or acetone solution, mp 59–65°; IR: 3150 (NH), 2500 (BH), 1750 (ester), 1720 (CH_2O-C=O), 1600, 1520, and 1360 (NO_2) cm^{-1}; NMR (deuterochloroform): δ 8.2 (2, d, $NO_2C_6H_4$), 7.6 (2, d, $NO_2C_6H_4$), 7.3 (5, s, C_6H_5), 7.0 (1, m, NH), 5.3 (2, s, $NO_2C_6H_4CH_2$), 5.1 (2, s, $C_6H_5CH_2$), 4.7 (1, m, —CH—), 3.6 (2, m, CH_2S), 3.1 (9, s, SCH_3), and 2.6 (2, m, —CH—).

Anal.—Calc. for $C_{22}H_{36}B_{10}N_2O_6S_2$: C, 44.26; H, 6.07; N, 4.69; S, 10.74. Found: C, 43.92; H, 6.08; N, 4.43; S, 10.52.

N-Carbobenzoxy-DL-S-(10-dimethylsulfidooctahydrodecaborane)methionine (VIII)—Compound VII (1.2 g, 2 mmoles) was stirred with 0.6 ml (2.4 mmoles) of 4 *N* NaOH in an acetone–water solution (15 ml) for 1 hr at room temperature. Water was added, and the mixture was extracted with ethyl acetate. The aqueous layer was acidified and extracted three times with ethyl acetate. The organic solution was dried over magnesium sulfate and evaporated to an oil. A solution of 0.6 ml of dicyclohexylamine in ethyl acetate was added, and 0.6 g (48%) of white crystals were obtained, mp 183–186°.

Recrystallization from methanol–acetone–ether–hexane gave 0.4 g, mp 187.5–190°; IR (potassium bromide): 3400 (NH), 2500 (BH), and 1720 (CH_2OC=O) cm^{-1}; NMR (dimethyl sulfoxide-d_6–deuterium oxide): δ 7.3 (5H, s, C_6H_5), 5.1 (2H, s, $C_6H_5CH_2$), 3.4 (1, m, —CH—), 3.0 (6H, s, SCH_3), 2.9 (3H, s, SCH_3), 2.5 (4H, m, $—CH_2CH_2—$), and 1.0–2.0 (22H, m, $2C_6H_{11}$).

Anal.—Calc. for $C_{27}H_{54}B_{10}N_2O_4S_2$: C, 50.45; H, 8.47. Found: C, 50.58; H, 8.33.

DL -S-(10 - Dimethylsulfidooctahydrodecaborane)methionine (I)—The oily free acid, VIII (1.4 g, 3 mmoles), was treated with 20 ml of 15% HBr–acetic acid for 1 hr. Ether was added, and the mixture was cooled. A white solid was obtained, which was recrystallized from methanol–ether, yielding 1 g, mp 152° dec. The hydrobromide salt (0.21 g) was suspended in water, and the pH was adjusted to 6 with dilute sodium hydroxide solution. The resulting white solid was insoluble in cold water but soluble in hot water and in methanol. It was ninhydrin positive and palladium chloride positive, and it had an R_f of 0.41 (methanol) and a melting point of 185°; IR (potassium bromide): 3550, 3350, broad (NH_2), 2980, 2900 (CH_2), 2500 (BH), 1600 (CO_2^-), 1500 (CH_2), 1400, 1320, 1040, and 1000 cm^{-1}.

A satisfactory microanalysis could not be obtained due to incomplete combustion and the formation of boron carbide.

***N*-Carbobenzoxy-DL-*S*-(10-dimethylsulfidooctahydrodecaborane)methionylglycine Ethyl Ester (IX)**—The dicyclohexylammonium salt of VIII (330 mg, 0.51 mmole) was converted to the acid by treatment with 2 *N* H_2SO_4 and extraction into ethyl acetate. After drying over magnesium sulfate and evaporation, the residue was dissolved in 10 ml of methylene chloride plus 1 ml of dimethylformamide and cooled to 0°. Glycine ethyl ester hydrochloride (140 mg, 1 mmole) was added along with 0.14 ml (1 mmole) of triethylamine. Dicyclohexylcarbodiimide (123 mg, 0.6 mmole) was then introduced. After the mixture was stirred overnight, it was filtered, evaporated, and partitioned between ethyl acetate and water.

The organic layer was washed sequentially with 2 *N* H_2SO_4, sodium bicarbonate solution, and saline. This layer was then dried over magnesium sulfate and evaporated. The residue was purified by preparatory TLC to give 50.2 mg of recovered acid VIII (R_f 0.57, methanol) and 89.9 mg of the dipeptide (R_f 0.25, 20% ethyl acetate–chloroform) as a noncrystalline foam, mp 81–83° (begins to change structure at 65°); IR (chloroform): 3400 (NH), 3030, 2930 (CH), 2500 (BH), 1720 (CH_2OC=ONH), 1705 (ester), 1670 (amide), and 1200 (ester) cm^{-1}; NMR (deuterochloroform): δ 7.3 (5H, s, C_6H_5), 5.5–6.0 (2H, m, 2NH), 3.9–4.3 (7H, m, $NHCH(CH_2CH_2$—$CONHCH_2COCH_2CH_3)$, and 3.0 (9H, d, 3SCH), and 1.0–1.5 (5H, m, CH_2CH_3 and $CHCH_2CH_2$).

Anal.—Calc. for $C_{19}H_{38}B_{10}N_2O_5S_2$: C, 41.75; H, 7.01; S, 11.71. Found: C, 42.03; H, 7.24; S, 11.91.

REFERENCES

(1) A. H. Soloway, G. L. Brownell, R. G. Ojemann, and W. H. Sweet, in "Preparation and Biomedical Applications of Labeled Molecules," Euratom, Brussels, Belgium, 1964, pp. 383–403.

(2) M. G. Hawthorne and R. J. Weiksema, *J. Med. Chem.*, **15** 449(1972).

(3) A. G. Mallinger, I. L. Jozwiak, Jr., and J. C. Carter, *Cancer Res.*, **32**, 1947(1972).

(4) R. L. Sneath, Jr., A. H. Soloway, and A. S. Dey, *J. Med. Chem.*, **17**, 796(1974).

(5) J. S. Morley and J. M. Smith, *J. Chem. Soc. (C)*, **1968**, 726.

(6) D. Theodoropoulos and J. Tsangaris, *J. Org. Chem.*, **29**, 2272(1964).

(7) W. H. Knoth, W. R. Herther, and E. L. Muetterties, *Inorg. Chem.*, **4**, 280(1965).

(8) C. S. Pande, J. Rudick, and R. Walter, *J. Org. Chem.*, **35**, 1440(1970).

(9) Y. Knobler and M. Frankel, *J. Chem. Soc.*, **1958**, 1629.

ACKNOWLEDGMENTS AND ADDRESSES

Received April 3, 1975, from the *Department of Medicinal Chemistry and Pharmacology, Northeastern University, Boston, MA 02115*

Accepted for publication June 20, 1975.

Supported in part by the National Institutes of Health through Grant P 101 CA 12246 and the Ruth M. Israel Fund for Cancer Research.

[x] To whom inquiries should be directed.

High-Speed Liquid Chromatographic Determination of Procaine in Pharmaceuticals

S. K. WAHBA KHALIL [x] and W. H. SHELVER

Abstract □ The operating conditions for a quantitative method of determining procaine in pharmaceutical preparations by high-speed liquid chromatography are described. The presence of decomposition products and the possible interference of other ingredients usually present in pharmaceutical preparations were found to have no effect. The method, because of its simplicity, is highly suited for routine analysis of pharmaceutical preparations containing procaine.

Keyphrases □ Procaine—high-speed liquid chromatographic analysis, pharmaceutical preparations □ High-speed liquid chromatography—analysis, procaine, pharmaceutical preparations

Several methods for the quantitative determination of procaine and its hydrochloride in pharmaceutical preparations are available. The USP XVIII (1) monographs for procaine hydrochloride and sterile procaine hydrochloride incorporate a method based on titration with standard sodium nitrite solution. This analytical scheme is satisfactory for the drug substance or its solution, but other substances containing a primary amine would interfere with the analysis. The assay for procaine hydrochloride in procaine hydrochloride injection requires an extraction procedure, followed by spectrophotometric determination (2). The USP does not recommend any method of assay for the procaine portion in penicillin G procaine, although a method is recommended for the penicillin moiety (3).

Several colorimetric (4–6), spectrophotometric (7), and acidimetric (8) methods have been developed for the determination of procaine. These methods show high sensitivity but do not have the specificity and simplicity that would be anticipated with a chromatographic procedure. In addition, since these procedures often require separation of the procaine from the interfering substances, they are quite time consuming.

Anal.—Calc. for $C_{27}H_{54}B_{10}N_2O_4S_2$: C, 50.45; H, 8.47. Found: C, 50.58; H, 8.33.

DL -S-(10 - Dimethylsulfidooctahydrodecaborane)methionine (I)—The oily free acid, VIII (1.4 g, 3 mmoles), was treated with 20 ml of 15% HBr–acetic acid for 1 hr. Ether was added, and the mixture was cooled. A white solid was obtained, which was recrystallized from methanol–ether, yielding 1 g, mp 152° dec. The hydrobromide salt (0.21 g) was suspended in water, and the pH was adjusted to 6 with dilute sodium hydroxide solution. The resulting white solid was insoluble in cold water but soluble in hot water and in methanol. It was ninhydrin positive and palladium chloride positive, and it had an R_f of 0.41 (methanol) and a melting point of 185°; IR (potassium bromide): 3550, 3350, broad (NH_2), 2980, 2900 (CH_2), 2500 (BH), 1600 (CO_2^-), 1500 (CH_2), 1400, 1320, 1040, and 1000 cm^{-1}.

A satisfactory microanalysis could not be obtained due to incomplete combustion and the formation of boron carbide.

***N*-Carbobenzoxy-DL-*S*-(10-dimethylsulfidooctahydrodecaborane)methionylglycine Ethyl Ester (IX)**—The dicyclohexylammonium salt of VIII (330 mg, 0.51 mmole) was converted to the acid by treatment with 2 *N* H_2SO_4 and extraction into ethyl acetate. After drying over magnesium sulfate and evaporation, the residue was dissolved in 10 ml of methylene chloride plus 1 ml of dimethylformamide and cooled to 0°. Glycine ethyl ester hydrochloride (140 mg, 1 mmole) was added along with 0.14 ml (1 mmole) of triethylamine. Dicyclohexylcarbodiimide (123 mg, 0.6 mmole) was then introduced. After the mixture was stirred overnight, it was filtered, evaporated, and partitioned between ethyl acetate and water.

The organic layer was washed sequentially with 2 *N* H_2SO_4, sodium bicarbonate solution, and saline. This layer was then dried over magnesium sulfate and evaporated. The residue was purified by preparatory TLC to give 50.2 mg of recovered acid VIII (R_f 0.57, methanol) and 89.9 mg of the dipeptide (R_f 0.25, 20% ethyl acetate–chloroform) as a noncrystalline foam, mp 81–83° (begins to change structure at 65°); IR (chloroform): 3400 (NH), 3030, 2930 (CH), 2500 (BH), 1720 (CH_2OC=ONH), 1705 (ester), 1670 (amide), and 1200 (ester) cm^{-1}; NMR (deuterochloroform): δ 7.3 (5H, s, C_6H_5), 5.5–6.0 (2H, m, 2NH), 3.9–4.3 (7H, m, $NHCH(CH_2CH_2$—$CONHCH_2COCH_2CH_3)$, and 3.0 (9H, d, 3SCH), and 1.0–1.5 (5H, m, CH_2CH_3 and $CHCH_2CH_2$).

Anal.—Calc. for $C_{19}H_{38}B_{10}N_2O_5S_2$: C, 41.75; H, 7.01; S, 11.71. Found: C, 42.03; H, 7.24; S, 11.91.

REFERENCES

(1) A. H. Soloway, G. L. Brownell, R. G. Ojemann, and W. H. Sweet, in "Preparation and Biomedical Applications of Labeled Molecules," Euratom, Brussels, Belgium, 1964, pp. 383–403.

(2) M. G. Hawthorne and R. J. Weiksema, *J. Med. Chem.*, **15** 449(1972).

(3) A. G. Mallinger, I. L. Jozwiak, Jr., and J. C. Carter, *Cancer Res.*, **32**, 1947(1972).

(4) R. L. Sneath, Jr., A. H. Soloway, and A. S. Dey, *J. Med. Chem.*, **17**, 796(1974).

(5) J. S. Morley and J. M. Smith, *J. Chem. Soc. (C)*, **1968**, 726.

(6) D. Theodoropoulos and J. Tsangaris, *J. Org. Chem.*, **29**, 2272(1964).

(7) W. H. Knoth, W. R. Herther, and E. L. Muetterties, *Inorg. Chem.*, **4**, 280(1965).

(8) C. S. Pande, J. Rudick, and R. Walter, *J. Org. Chem.*, **35**, 1440(1970).

(9) Y. Knobler and M. Frankel, *J. Chem. Soc.*, **1958**, 1629.

ACKNOWLEDGMENTS AND ADDRESSES

Received April 3, 1975, from the *Department of Medicinal Chemistry and Pharmacology, Northeastern University, Boston, MA 02115*

Accepted for publication June 20, 1975.

Supported in part by the National Institutes of Health through Grant P 101 CA 12246 and the Ruth M. Israel Fund for Cancer Research.

[x] To whom inquiries should be directed.

High-Speed Liquid Chromatographic Determination of Procaine in Pharmaceuticals

S. K. WAHBA KHALIL [x] and W. H. SHELVER

Abstract □ The operating conditions for a quantitative method of determining procaine in pharmaceutical preparations by high-speed liquid chromatography are described. The presence of decomposition products and the possible interference of other ingredients usually present in pharmaceutical preparations were found to have no effect. The method, because of its simplicity, is highly suited for routine analysis of pharmaceutical preparations containing procaine.

Keyphrases □ Procaine—high-speed liquid chromatographic analysis, pharmaceutical preparations □ High-speed liquid chromatography—analysis, procaine, pharmaceutical preparations

Several methods for the quantitative determination of procaine and its hydrochloride in pharmaceutical preparations are available. The USP XVIII (1) monographs for procaine hydrochloride and sterile procaine hydrochloride incorporate a method based on titration with standard sodium nitrite solution. This analytical scheme is satisfactory for the drug substance or its solution, but other substances containing a primary amine would interfere with the analysis. The assay for procaine hydrochloride in procaine hydrochloride injection requires an extraction procedure, followed by spectrophotometric determination (2). The USP does not recommend any method of assay for the procaine portion in penicillin G procaine, although a method is recommended for the penicillin moiety (3).

Several colorimetric (4–6), spectrophotometric (7), and acidimetric (8) methods have been developed for the determination of procaine. These methods show high sensitivity but do not have the specificity and simplicity that would be anticipated with a chromatographic procedure. In addition, since these procedures often require separation of the procaine from the interfering substances, they are quite time consuming.

Table I—Calibration Data for HSLC Procaine Analysis[a]

Concentration Added, μg/ml	Peak Area of Procaine / Peak Area of Standard	SD	CV
25[b]	0.318	0.0085	2.7
50[c]	0.672	0.0164	2.4
125[c]	1.608	0.0783	4.9

[a] Regression analysis gave the following equation: concentration = 0.927 + 78.05 (area of procaine/area of standard). [b] Average of nine replicate injections. [c] Average of five replicate injections.

This report describes a high-speed liquid chromatographic (HSLC) method. The method permits measurement of procaine in the presence of its degradation products and other chemicals commonly included with procaine in pharmaceutical products. This procedure was applied to several commercial preparations containing procaine[1].

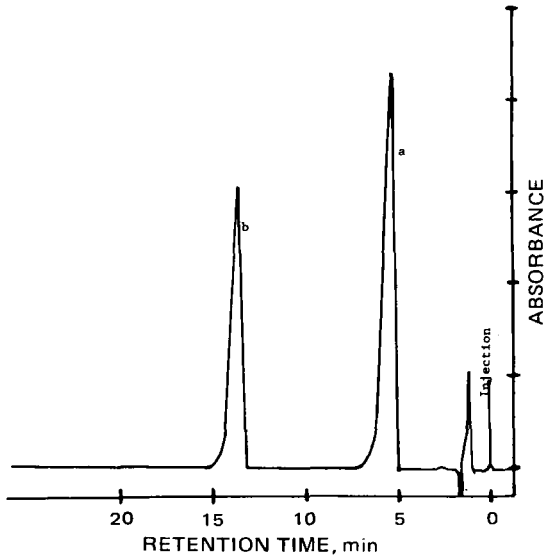

Figure 1—*Representative chromatogram. Key: a, pyrrocaine; and b, procaine.*

EXPERIMENTAL[2]

Reagents and Chemicals—Analytical grade procaine hydrochloride[3] and pyrrocaine hydrochloride[4] were used.

Mobile Phase—The mobile phase, consisting of 60% acetonitrile, 40% water, and 0.01% concentrated ammonium hydroxide solution (28%) was prepared daily. The mobile phase was degassed by applying a water aspirator vacuum to the solution for 10 min.

Internal Standard Solution—An aqueous solution of pyrrocaine hydrochloride, 1 mg/ml (calculated on the free base weight), was used.

Standard Procaine Hydrochloride Solution—A 5-mg/100 ml (calculated on the free base weight) procaine hydrochloride aqueous solution was used.

Conditions for Chromatographic Analysis—The degassed mobile phase was pumped through the column at a flow rate of 3 ml/min (1000–1500 psi) at room temperature until a stable baseline was obtained. Replicate 20-μl injections of a 1:1 mixture of the procaine hydrochloride and the pyrrocaine hydrochloride solutions were made using a 25-μl syringe[5]. The chromatogram was recorded[6] with a chart speed of 0.51 cm (0.2 in.)/min with the output from the UV monitor at 0.04 absorbance unit fed into the electronic integrator. The peak areas were measured using an electronic integrator.

Interferences—The possible interferences from *p*-aminobenzoic acid, diethylaminoethanol, and epinephrine were studied by adding different amounts to a standard procaine hydrochloride solution and performing the analysis.

Sample Preparation and Assay—For liquid preparations, measure an aliquot of the procaine preparation containing 10 mg of procaine, as the free base, into a 100-ml volumetric flask and dilute to volume with water. In case of penicillin procaine, weigh accurately about 10 mg of the powder, dissolve in water, and dilute to 100 ml with water. Mix an equal volume of the test solution with standard pyrrocaine solution, and inject 10 μl of the mixture. Calculate the amount of procaine by comparing with a standard.

Table II—Comparison between HSLC Method and Other Methods

Preparation	Labeled Amount, mg/ml	Recovery, % HSLC Mean	HSLC n[a]	HSLC CV	Other Methods Mean	Other Methods n	Other Methods CV
Procaine hydrochloride[b], 2-ml ampul	100	99.6	6	1.8	101.4[c]	3	0.8
Procaine hydrochloride[b], 2-ml ampul	1000	100.0	4	0.9	100.2[c]	2	0.2
Procaine hydrochloride[b] and adrenalin	100	100.0	4	0.4	100.6[d]	2	0.1
Penicillin G procaine	40	99.7	5	2.3	100.3[d]	2	0.1

[a] *n* = number of replicate determinations. [b] Novocain. [c] Volumetric determination using sodium nitrite. [d] Colorimetric determination using sodium nitrite and α-naphthylethylamine.

RESULTS AND DISCUSSION

The separation of amines by partitioning on-column requires suppression of the ionization of the amino group to obtain sharp peaks. The addition of a very small amount of ammonium hydroxide solution to the mobile phase gave excellent results and avoided the addition of any solid, such as ammonium carbonate, which could interfere with the operation of the chromatographic system by blocking the column, injection system, or detector. Utilization of a mobile phase consisting of 60% acetonitrile and 40% water modified with 0.01% ammonium hydroxide gave well-resolved sharp peaks for pyrrocaine and procaine with retention times of 5.6 and 14.3 min, respectively (Fig. 1).

Under these conditions, *p*-aminobenzoic acid, diethylaminoethanol, and epinephrine were eluted with the solvent front and thus did not interfere with the analysis. The output of the UV detector

[1] Obtained from the College of Pharmacy preparations laboratory.

[2] A Waters Associates liquid chromatograph (model 202) equipped with an M-6000 pump, a single-wavelength UV monitor (254 nm), a U6K Universal liquid chromatograph injector, an integrator (Hewlett Packard model 3370B) with digital printout, and a column containing octadecylsilane bonded to μCorasil (*μBondapak C 18*), 300 mm long × 4 mm i.d., obtained from Waters Associates, were used.

[3] Merck.

[4] Lot 64 C 025, Endo Laboratories.

[5] Precision Sampling Corp., Baton Rouge, La.

[6] Beckman 25.4-cm (10-in.) laboratory recorder model 1005.

was fed into the electronic integrator, and the ratio of the area of the procaine peak to the area of the internal standard (pyrrocaine) was calculated. Regression analysis of these data indicated excellent linearity and reproducibility (Table I). The amount of procaine that could be measured was as low as 0.25 μg of total free base injected.

Application of this method to four pharmaceutical dosage forms containing procaine was carried out to determine the suitability of the procedure for this type of analysis. The results of the HSLC method (Table II) were compared with the sodium nitrite titration or the colorimetric determination, which required an extraction. Although the coefficient of variation of the HSLC method is somewhat higher than the other method, it is sufficiently low to be acceptable. The agreement between the HSLC method and the other methods was excellent. The convenience of the HSLC method, together with its increased specificity and simplicity, makes this method a desirable alternative.

REFERENCES

(1) "The United States Pharmacopeia," 18th rev., Mack Publishing Co., Easton, Pa., 1970, pp. 543–545.

(2) *Ibid.*, p. 544.

(3) *Ibid.*, p. 545.

(4) F. J. Bandelin and C. R. Kemp, *Ind. Eng. Chem., Anal. Ed.*, **18**, 470(1946).

(5) W. J. Mader, H. S. Sterne, Jr., J. Rosin, and H. A. Frediani, *J. Amer. Pharm. Ass., Sci. Ed.*, **39**, 175(1950).

(6) D. C. Garratt, "The Quantitative Analysis of Drugs," 3rd ed., Charles C Thomas, Springfield, Ill., 1964, p. 190.

(7) M. Tátsuzawa, S. Hashiba, and A. Okawara, *Jap. Anal.*, **17**, 1116(1968).

(8) "The British Pharmacopoeia," The Pharmaceutical Press, London, England, 1968, p. 22.

ACKNOWLEDGMENTS AND ADDRESSES

Received April 4, 1975, from the *College of Pharmacy, North Dakota State University, Fargo, ND 58102*

Accepted for publication July 1, 1975.

[x] To whom inquiries should be directed.

GLC Analysis of Lidocaine in Blood Using an Alkaline Flame-Ionization Detector

T. R. IRGENS, W. M. HENDERSON, and W. H. SHELVER [x]

Abstract □ A method was developed for the quantitative GLC determination of lidocaine and its major metabolite monoethylglycinexylidide. By using the specificity of the alkaline flame-ionization detector, this simple analytical procedure is extremely sensitive, rapid, and easily performed.

Keyphrases □ Lidocaine—GLC analysis in blood □ Monoethylglycinexylidide—major metabolite of lidocaine, GLC analysis, blood □ GLC—analysis, lidocaine and monoethylglycinexylidide (major metabolite), blood □ Antiarrhythmics—lidocaine, GLC analysis in blood

The therapeutic and toxic effects of many drugs are directly related to the concentration of the drug and metabolites in the plasma of the patient. To regulate the dose properly, a rapid, precise, and specific procedure for measuring plasma concentrations of the drug and significant drug metabolites is required.

Lidocaine is used routinely in the acute management of ventricular arrhythmias, particularly those that occur during acute myocardial infarction. Lidocaine is metabolically dealkylated at the basic nitrogen (1, 2), and methods of measuring the monodealkylated product (3) monoethylglycinexylidide and the didealkylated product (4) glycinexylidide or both (5) have been developed. Lidocaine occasionally shows toxic side effects (6), and both monoethylglycinexylidide (7) and glycinexylidide (8) have been reported to have significant pharmacological actions that could contribute to the antiarrhythmic activity and to the side effects of lidocaine. Animal experiments suggest that monoethylglycinexylidide is the most potent (8).

Element-specific detectors such as the alkaline flame-ionization detector are useful for the analysis of compounds containing nitrogen (9). The alkaline flame-ionization detector has proven to be a suitable detector for monitoring drugs containing nitrogen (10–13).

Several investigators reported the quantitative determination of lidocaine by GLC, usually utilizing the flame-ionization detector (14–17); other workers utilized GLC–mass spectrometry (3, 4, 8). After this study was undertaken, a report appeared on the use of the alkaline flame-ionization detector (18) in the determination of lidocaine and its metabolites, but precision was reported only for a range of samples.

EXPERIMENTAL

Apparatus—The gas chromatograph[1] was equipped with an alkaline flame-ionization detector and a flame-ionization detector. An electronic integrator[2] was used for measuring peak areas. A glass U-shaped column, 1.8 m × 0.3 cm (6 ft × 0.125 in.), was packed with 3% KOH plus 2% polyethylene glycol[3] coated onto 80–100-mesh Chromosorb W DMSC/AW.

The column was conditioned at 240° for 24 hr, and the operating conditions were: oven temperature, 210°; detector temperature, 220°; and injection port temperature, 200°. Nitrogen was used as the carrier gas at a flow rate of 15 ml/min. Hydrogen and air were adjusted to give optimum recorder response. For this analysis, the hydrogen was set at 45 ml/min and air was at 290 ml/min.

Chemicals and Reagents—Lidocaine[4] and pyrrocaine[5] were

[1] Model 420, Packard Instrument Co., Downers Grove, Ill.
[2] Model 3370B, Hewlett-Packard Co., Palo Alto, Calif.
[3] Carbowax 20 M.
[4] Astra Pharmaceutical Products, Worcester, Mass.
[5] Endo Laboratories, Richmond Hill, N.Y.

was fed into the electronic integrator, and the ratio of the area of the procaine peak to the area of the internal standard (pyrrocaine) was calculated. Regression analysis of these data indicated excellent linearity and reproducibility (Table I). The amount of procaine that could be measured was as low as 0.25 μg of total free base injected.

Application of this method to four pharmaceutical dosage forms containing procaine was carried out to determine the suitability of the procedure for this type of analysis. The results of the HSLC method (Table II) were compared with the sodium nitrite titration or the colorimetric determination, which required an extraction. Although the coefficient of variation of the HSLC method is somewhat higher than the other method, it is sufficiently low to be acceptable. The agreement between the HSLC method and the other methods was excellent. The convenience of the HSLC method, together with its increased specificity and simplicity, makes this method a desirable alternative.

REFERENCES

(1) "The United States Pharmacopeia," 18th rev., Mack Publishing Co., Easton, Pa., 1970, pp. 543–545.

(2) *Ibid.*, p. 544.

(3) *Ibid.*, p. 545.

(4) F. J. Bandelin and C. R. Kemp, *Ind. Eng. Chem., Anal. Ed.*, **18**, 470(1946).

(5) W. J. Mader, H. S. Sterne, Jr., J. Rosin, and H. A. Frediani, *J. Amer. Pharm. Ass., Sci. Ed.*, **39**, 175(1950).

(6) D. C. Garratt, "The Quantitative Analysis of Drugs," 3rd ed., Charles C Thomas, Springfield, Ill., 1964, p. 190.

(7) M. Tátsuzawa, S. Hashiba, and A. Okawara, *Jap. Anal.*, **17**, 1116(1968).

(8) "The British Pharmacopoeia," The Pharmaceutical Press, London, England, 1968, p. 22.

ACKNOWLEDGMENTS AND ADDRESSES

Received April 4, 1975, from the *College of Pharmacy, North Dakota State University, Fargo, ND 58102*

Accepted for publication July 1, 1975.

[x] To whom inquiries should be directed.

GLC Analysis of Lidocaine in Blood Using an Alkaline Flame-Ionization Detector

T. R. IRGENS, W. M. HENDERSON, and W. H. SHELVER [x]

Abstract □ A method was developed for the quantitative GLC determination of lidocaine and its major metabolite monoethylglycinexylidide. By using the specificity of the alkaline flame-ionization detector, this simple analytical procedure is extremely sensitive, rapid, and easily performed.

Keyphrases □ Lidocaine—GLC analysis in blood □ Monoethylglycinexylidide—major metabolite of lidocaine, GLC analysis, blood □ GLC—analysis, lidocaine and monoethylglycinexylidide (major metabolite), blood □ Antiarrhythmics—lidocaine, GLC analysis in blood

The therapeutic and toxic effects of many drugs are directly related to the concentration of the drug and metabolites in the plasma of the patient. To regulate the dose properly, a rapid, precise, and specific procedure for measuring plasma concentrations of the drug and significant drug metabolites is required.

Lidocaine is used routinely in the acute management of ventricular arrhythmias, particularly those that occur during acute myocardial infarction. Lidocaine is metabolically dealkylated at the basic nitrogen (1, 2), and methods of measuring the monodealkylated product (3) monoethylglycinexylidide and the didealkylated product (4) glycinexylidide or both (5) have been developed. Lidocaine occasionally shows toxic side effects (6), and both monoethylglycinexylidide (7) and glycinexylidide (8) have been reported to have significant pharmacological actions that could contribute to the antiarrhythmic activity and to the side effects of lidocaine. Animal experiments suggest that monoethylglycinexylidide is the most potent (8).

Element-specific detectors such as the alkaline flame-ionization detector are useful for the analysis of compounds containing nitrogen (9). The alkaline flame-ionization detector has proven to be a suitable detector for monitoring drugs containing nitrogen (10–13).

Several investigators reported the quantitative determination of lidocaine by GLC, usually utilizing the flame-ionization detector (14–17); other workers utilized GLC–mass spectrometry (3, 4, 8). After this study was undertaken, a report appeared on the use of the alkaline flame-ionization detector (18) in the determination of lidocaine and its metabolites, but precision was reported only for a range of samples.

EXPERIMENTAL

Apparatus—The gas chromatograph[1] was equipped with an alkaline flame-ionization detector and a flame-ionization detector. An electronic integrator[2] was used for measuring peak areas. A glass U-shaped column, 1.8 m × 0.3 cm (6 ft × 0.125 in.), was packed with 3% KOH plus 2% polyethylene glycol[3] coated onto 80–100-mesh Chromosorb W DMSC/AW.

The column was conditioned at 240° for 24 hr, and the operating conditions were: oven temperature, 210°; detector temperature, 220°; and injection port temperature, 200°. Nitrogen was used as the carrier gas at a flow rate of 15 ml/min. Hydrogen and air were adjusted to give optimum recorder response. For this analysis, the hydrogen was set at 45 ml/min and air was at 290 ml/min.

Chemicals and Reagents—Lidocaine[4] and pyrrocaine[5] were

[1] Model 420, Packard Instrument Co., Downers Grove, Ill.
[2] Model 3370B, Hewlett-Packard Co., Palo Alto, Calif.
[3] Carbowax 20 M.
[4] Astra Pharmaceutical Products, Worcester, Mass.
[5] Endo Laboratories, Richmond Hill, N.Y.

Table I—Statistical Analysis of the Calibration Curve for Lidocaine and Monoethylglycinexylidide

Compound	Slope	*SE*	*r*	*n*
Monoethylglycinexylidide	0.511 (0.489–0.533)	0.010	0.998	12
Lidocaine	0.320 (0.311–0.330)	0.005	0.998	19

obtained from commercial sources. Monoethylglycinexylidide was synthesized using a modified procedure of Moore and Dalrymple (19). The melting point for monoethylglycinexylidide was 51° [lit. (4) mp 51°], and its NMR spectra were compatible with the proposed structure.

Procedure—Into a 20-ml screw-topped test tube was placed 2.5 ml of plasma containing lidocaine. To this tube was added 5 ml of a benzene solution containing pyrrocaine as the internal standard in a concentration of 5 μg/ml. Then 0.2 ml of 5 *N* sodium hydroxide was added to make the mixture alkaline.

The mixture was mixed for 15 min and then centrifuged for 5 min. The organic phase was transferred to a pear-shaped tube and evaporated to dryness on a water bath, equipped with a vacuum, at 50°. Fifty microliters of benzene was used to dissolve the residue. A 5-μl aliquot was injected directly on the column with a 10-μl microsyringe.

Calibration Curve—Samples for the lidocaine calibration ranged from 0.1 to 3 μg/ml. Five extractions were made at each concentration, and the calibration curve was plotted utilizing a linear regression line. Regression statistics are shown in Table I.

Samples for the monoethylglycinexylidide calibration curve ranged from 0.25 to 4 μg/ml, and the calibration curve was plotted utilizing a linear regression line. Regression statistics are shown in Table I.

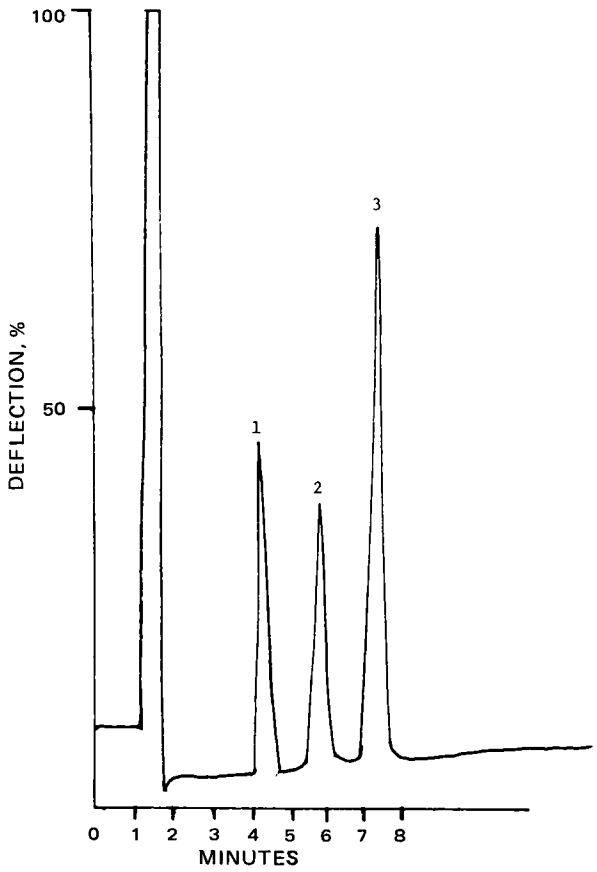

Figure 1—*Gas chromatographic separation of lidocaine (peak 1), monoethylglycinexylidide (peak 2), and pyrrocaine (peak 3). The sample contained 100 ng of lidocaine, 100 ng of monoethylglycinexylidide, and 500 ng of pyrrocaine.*

Table II—Precision of the Lidocaine Analysis at Different Plasma Levels

Plasma Concentration, μg/ml[a]	Coefficient of Variation, %
0.1	18.0
0.4	9.1
1.0	6.5
3.0	3.6

[a] Mean of five determinations.

Table III—Precision of the Monoethylglycinexylidide Analysis at Different Plasma Levels

Plasma Concentration, μg/ml[a]	Coefficient of Variation, %
0.25	5.53
0.50	3.16
2.0	2.27
4.0	1.91

[a] Mean of three determinations.

Relative Recovery—A standard solution in benzene of lidocaine-free base and pyrrocaine was prepared in a concentration that would be precisely the concentration attained after extraction of a 1-μg/ml lidocaine sample. The same procedure was followed for extraction of lidocaine, and a 2.5-ml aliquot was used and evaporated to dryness. The peak area ratios were recorded for the extraction and the standard solution. The mean relative recovery was 91.9% (SD = 5.0, n = 4). The mean relative recovery for monoethylglycinexylidide was 88.7% (SD = 3.65, n = 3)

RESULTS

Figure 1 shows a typical chromatogram of lidocaine, monoethylglycinexylidide, and pyrrocaine extracted from plasma. The retention times were 4 min for lidocaine, 6 min for monoethylglycinexylidide, and 7.5 min for pyrrocaine.

Peak area ratios were used to prepare calibration curves. The standard curve was linear over the range of 0.1–3 μg/ml of plasma for lidocaine and of 0.25–4 μg/ml of plasma for monoethylglycinexylidide. The precision of the extraction procedure for lidocaine was checked at the 0.1-, 0.4-, 1-, and 3-μg/ml levels. Five extractions were made at each concentration (Table II). For monoethylglycinexylidide, the precision was tested at 0.25, 0.5, 2.0, and 4 μg/ml of plasma (Table III).

As shown, subtherapeutic quantities of licocaine can be measured with a high degree of precision by this method. The column used gave excellent separation of lidocaine from the metabolite monoethylglycinexylidide, and no interference was noted from compounds normally present in blood.

REFERENCES

(1) J. Thomas and P. Meffin, *J. Med. Chem.*, **15**, 1046(1972).

(2) J. B. Keenaghan and R. N. Boyes, *J. Pharmacol. Exp. Ther.*, **180**, 454(1972).

(3) J. M. Strong and A. J. Atkinson, Jr., *Anal. Chem.*, **44**, 2287(1972).

(4) J. M. Strong, M. Parker, and A. J. Atkinson Jr., *Clin. Pharmacol. Ther.*, **14**, 67(1973).

(5) C. A. Difazio and R. E. Brown, *Anesthesiology*, **34**, 86(1971).

(6) R. Seldon and A. A. Sasahara, *J. Amer. Med. Ass.*, **202**, 908(1967).

(7) E. R. Smith and B. R. Duce, *J. Pharmacol. Exp. Ther.*, **179**, 580(1971).

(8) J. M. Strong, D. E. Mayfield, A. J. Atkinson, Jr., B. C. Burris, F. Raymond, and L. T. Webster, Jr., *Clin. Pharmacol. Ther.*, **17**, 184(1975).

(9) D. F. S. Natusch and T. M. Thorpe, *Anal. Chem.*, **45**, 1184A(1973).

(10) S. P. James and R. H. Waring, *J. Chromatogr.*, **78**, 417(1973).
(11) D. D. Breimer and J. M. Van Rossum, *ibid.*, **88**, 235(1974).
(12) L. T. Sennello and F. E. Kohn, *Anal. Chem.*, **46**, 752(1974).
(13) P. A. Toseland, M. Albani, and F. D. Gauchel, *Clin. Chem.*, **21**, 98(1975).
(14) H. M. Koehler and J. J. Hefferren, *J. Pharm. Sci.*, **53**, 745(1964).
(15) J. B. Keenaghan, *Anesthesiology*, **29**, 110(1968).
(16) G. A. Edhorn, *Can. Anaesth. Soc. J.*, **18**, 189(1971).
(17) N. Benowitz and M. Rowland, *Anesthesiology*, **39**, 639(1973).
(18) K. K. Adjepon-Yamoah and L. F. Prescott, *J. Pharm. Pharmacol.*, **26**, 889(1974).
(19) J. A. Moore and D. L. Dalrymple, "Experimental Methods in Organic Chemistry," Saunders, Philadelphia, Pa., 1971, pp. 181–184.

ACKNOWLEDGMENTS AND ADDRESSES

Received April 30, 1975, from the *College of Pharmacy, North Dakota State University, Fargo, ND 58102*
Accepted for publication June 18, 1975.
[x] To whom inquiries should be directed.

Onset of Enzyme Induction with Pregnenolone-16α-carbonitrile in Male and Female Rats

S. J. STOHS [x] and H. ROSENBERG

Abstract □ Male and female rats treated with a single 20-mg/kg ip dose of pregnenolone-16α-carbonitrile (PCN) produced parallel increases in hepatic cytochrome P-450 and aniline hydroxylase activity. However, the onset of increase in aniline hydroxylase activity and cytochrome P-450 content was slower in male than female animals. The maximal levels achieved in male rats were 89% of the values observed in the female animals. Furthermore, the hepatic aniline hydroxylase activity and P-450 content declined more rapidly in male than in female rats.

Keyphrases □ Pregnenolone-16α-carbonitrile—effect on hepatic cytochrome P-450 and aniline hydroxylase activity, male and female rats compared □ Cytochrome P-450 activity—effect of pregnenolone-16α-carbonitrile, male and female rats compared □ Aniline hydroxylase activity—effect of pregnenolone-16α-carbonitrile, male and female rats compared

3β-Hydroxypregn-5-ene-20-one-16α-carbonitrile, commonly known as pregnenolone-16α-carbonitrile or PCN (I), is a catatoxic steroid with no known hormonal activity. However, it is rapidly becoming well known as a potent inducer of hepatic enzymes (1–11). As is characteristic of enzyme inducers such as phenobarbital, I increases liver weight, cytochrome P-450 content, aniline hydroxylase, ethylmorphine *N*-demethylase, and cytochrome c reductase but does not increase the microsomal protein per gram of liver content (5).

Ultrastructural changes in rat hepatocytes following I treatment have been extensively examined (12–17). Compound I produced marked proliferation of smooth-surfaced endoplasmic reticulum, with disorganization of the rough endoplasmic reticulum occurring. Most cytoplasmic changes returned to normal within 10 days after the last I administration (15).

The potential for using I to promote detoxification of many xenobiotics exists; and when I is given to female rats several days before a toxicant, it can protect against a variety of substances (3). If I is to be useful in promoting xenobiotic detoxification, the rate of onset of enhanced hepatic drug-metabolizing activity must be determined since the applicability of I lies in its administration after a toxicant has been ingested by a patient.

All cited studies were conducted with female rats. Therefore, it was of interest to learn how quickly I can enhance the activity of the hepatic mixed function oxidase system in male rats and to compare these results with the onset, maximal effects, and duration of induction in female rats.

EXPERIMENTAL

Animal Pretreatment—Male and female rats[1], 120–140 g, were maintained on food[2] and tap water *ad libitum*. To determine the onset of action of I upon hepatic mixed function oxidase activity, both male and female rats were given a single dose of I (20 mg/kg ip) in 0.2% polysorbate 80 in isotonic saline or only the polysorbate 80–saline vehicle and sacrificed at various times after injection.

Hepatic aniline hydroxylase activity (nanomoles of *p*-aminophenol formed per minute per milligram of microsomal protein) and hepatic microsomal cytochrome P-450 content (nanomoles of P-450 per milligram of microsomal protein) were determined in control and experimental animals injected and sacrificed at corresponding times. Three control and three experimental rats were treated and sacrificed at each time point for each sex.

Enzyme, Protein, and Cytochrome P-450 Assays—The 10,000×*g* supernatant fraction was used to determine aniline hydroxylase activity, using an NADPH-generating system (18) and the assay technique of Kato and Gillette (19). Microsomal P-450 was determined by the method of Omura and Sato (20). Microsomal protein was measured by the Folin phenol method (21). These determinations were performed on three pairs of rats sacrificed at 10, 15, 20, 25, 30, 48, 60, and 72 hr after treatment. Averages in corresponding control and experimental groups were compared (Table I).

RESULTS AND DISCUSSION

The effect of a single injection of pregnenolone-16α-carbonitrile (I) at 20 mg/kg on the onset and time course of hepatic aniline hy-

[1] Sasco, Inc., Omaha, Neb.
[2] Purina Lab Chow.

(10) S. P. James and R. H. Waring, *J. Chromatogr.*, **78**, 417(1973).
(11) D. D. Breimer and J. M. Van Rossum, *ibid.*, **88**, 235(1974).
(12) L. T. Sennello and F. E. Kohn, *Anal. Chem.*, **46**, 752(1974).
(13) P. A. Toseland, M. Albani, and F. D. Gauchel, *Clin. Chem.*, **21**, 98(1975).
(14) H. M. Koehler and J. J. Hefferren, *J. Pharm. Sci.*, **53**, 745(1964).
(15) J. B. Keenaghan, *Anesthesiology*, **29**, 110(1968).
(16) G. A. Edhorn, *Can. Anaesth. Soc. J.*, **18**, 189(1971).
(17) N. Benowitz and M. Rowland, *Anesthesiology*, **39**, 639(1973).
(18) K. K. Adjepon-Yamoah and L. F. Prescott, *J. Pharm. Pharmacol.*, **26**, 889(1974).
(19) J. A. Moore and D. L. Dalrymple, "Experimental Methods in Organic Chemistry," Saunders, Philadelphia, Pa., 1971, pp. 181–184.

ACKNOWLEDGMENTS AND ADDRESSES

Received April 30, 1975, from the *College of Pharmacy, North Dakota State University, Fargo, ND 58102*
Accepted for publication June 18, 1975.
[x] To whom inquiries should be directed.

Onset of Enzyme Induction with Pregnenolone-16α-carbonitrile in Male and Female Rats

S. J. STOHS [x] and H. ROSENBERG

Abstract □ Male and female rats treated with a single 20-mg/kg ip dose of pregnenolone-16α-carbonitrile (PCN) produced parallel increases in hepatic cytochrome P-450 and aniline hydroxylase activity. However, the onset of increase in aniline hydroxylase activity and cytochrome P-450 content was slower in male than female animals. The maximal levels achieved in male rats were 89% of the values observed in the female animals. Furthermore, the hepatic aniline hydroxylase activity and P-450 content declined more rapidly in male than in female rats.

Keyphrases □ Pregnenolone-16α-carbonitrile—effect on hepatic cytochrome P-450 and aniline hydroxylase activity, male and female rats compared □ Cytochrome P-450 activity—effect of pregnenolone-16α-carbonitrile, male and female rats compared □ Aniline hydroxylase activity—effect of pregnenolone-16α-carbonitrile, male and female rats compared

3β-Hydroxypregn-5-ene-20-one-16α-carbonitrile, commonly known as pregnenolone-16α-carbonitrile or PCN (I), is a catatoxic steroid with no known hormonal activity. However, it is rapidly becoming well known as a potent inducer of hepatic enzymes (1–11). As is characteristic of enzyme inducers such as phenobarbital, I increases liver weight, cytochrome P-450 content, aniline hydroxylase, ethylmorphine *N*-demethylase, and cytochrome c reductase but does not increase the microsomal protein per gram of liver content (5).

Ultrastructural changes in rat hepatocytes following I treatment have been extensively examined (12–17). Compound I produced marked proliferation of smooth-surfaced endoplasmic reticulum, with disorganization of the rough endoplasmic reticulum occurring. Most cytoplasmic changes returned to normal within 10 days after the last I administration (15).

The potential for using I to promote detoxification of many xenobiotics exists; and when I is given to female rats several days before a toxicant, it can protect against a variety of substances (3). If I is to be useful in promoting xenobiotic detoxification, the rate of onset of enhanced hepatic drug-metabolizing activity must be determined since the applicability of I lies in its administration after a toxicant has been ingested by a patient.

All cited studies were conducted with female rats. Therefore, it was of interest to learn how quickly I can enhance the activity of the hepatic mixed function oxidase system in male rats and to compare these results with the onset, maximal effects, and duration of induction in female rats.

EXPERIMENTAL

Animal Pretreatment—Male and female rats[1], 120–140 g, were maintained on food[2] and tap water *ad libitum*. To determine the onset of action of I upon hepatic mixed function oxidase activity, both male and female rats were given a single dose of I (20 mg/kg ip) in 0.2% polysorbate 80 in isotonic saline or only the polysorbate 80–saline vehicle and sacrificed at various times after injection.

Hepatic aniline hydroxylase activity (nanomoles of *p*-aminophenol formed per minute per milligram of microsomal protein) and hepatic microsomal cytochrome P-450 content (nanomoles of P-450 per milligram of microsomal protein) were determined in control and experimental animals injected and sacrificed at corresponding times. Three control and three experimental rats were treated and sacrificed at each time point for each sex.

Enzyme, Protein, and Cytochrome P-450 Assays—The 10,000×*g* supernatant fraction was used to determine aniline hydroxylase activity, using an NADPH-generating system (18) and the assay technique of Kato and Gillette (19). Microsomal P-450 was determined by the method of Omura and Sato (20). Microsomal protein was measured by the Folin phenol method (21). These determinations were performed on three pairs of rats sacrificed at 10, 15, 20, 25, 30, 48, 60, and 72 hr after treatment. Averages in corresponding control and experimental groups were compared (Table I).

RESULTS AND DISCUSSION

The effect of a single injection of pregnenolone-16α-carbonitrile (I) at 20 mg/kg on the onset and time course of hepatic aniline hy-

[1] Sasco, Inc., Omaha, Neb.
[2] Purina Lab Chow.

Table I—Hepatic Aniline Hydroxylase Activity and Cytochrome P-450 Content in Male and Female Rats following a Single Dose of I[a]

Time after Treatment, hr	P-450 Content, % of Controls		Aniline Hydroxylase Activity, % of Controls	
	Male	Female	Male	Female
10	99	98	101	102
15	100	109	100	115
20	106	141	130	157
25	113	182	145	163
30	163	170	136	153
48	144	169	122	149
60	128	127	101	130
72	100	101	99	97

[a] Male and female rats were given a single dose of 20 mg/kg ip of I or the vehicle. Three animals from each group of both sexes were sacrificed at the times indicated. Aniline hydroxylase activity was determined as nanomoles of *p*-aminophenol formed per minute per milligram of microsomal protein. Hepatic microsomal cytochrome P-450 was determined as nanomoles of P-450 per milligram of microsomal protein. Each value is the mean of the treated animals over the mean of the control animals times 100.

droxylase activity and cytochrome P-450 content in male and female rats is given in Table I.

As can be seen, aniline hydroxylase activity in the female rats increased sharply at 20 hr after I administration and remained elevated at or above this level until 48 hr posttreatment. In both male and female rats, maximal aniline hydroxylase activity was observed 25 hr after I treatment; the maximum levels achieved in male rats were approximately 89% of those observed in female rats. The difference was not statistically significant due to the small number of animals used. In the male rats, the aniline hydroxylase activity did not remain elevated but began to fall rapidly and had returned to control levels by 60 hr after treatment.

In the female rats, hepatic cytochrome P-450 content was maximal at 25 hr after I treatment and remained elevated until 48 hr, after which it began to decline. In the male rats, peak levels of cytochrome P-450 were observed 30 hr after pretreatment and gradually declined thereafter, reaching control levels by 72 hr after I treatment. As with aniline hydroxylase activity, maximum P-450 levels in male rats were approximately 89% of the values observed in female rats. The difference between the maximum P-450 levels for male and female rats was not significant, although the differences at 20 and 25 hr after I treatment were significant at the $p < 0.05$ level.

Radzialowski (22) investigated the effect of I on bilirubin metabolism in male and female rats. After I pretreatment, the rate of bilirubin metabolism increased 56% in female rats but only 29% in male rats, supporting our general observations. Conney (23) discussed the sex differences involved in the metabolism of various compounds. It appears that in both the induced and uninduced states, female rats metabolize many xenobiotics more rapidly than male rats.

Following a single injection of I at 20 mg/kg, enzyme induction was not seen until at least 20 hr after administration. This time interval might be shortened by using larger doses and/or more frequent administration. Compound I might be useful in situations involving chronic toxicity. Whether I could be used for detoxification following acute toxicity by xenobiotics would depend on the agent and circumstances involved.

REFERENCES

(1) H. Selye, *Experientia*, **27**, 1445(1971).

(2) B. Solymoss, J. Werringloer, and S. Toth, *Steroids*, **17**, 427(1971).

(3) H. Selye and S. Szabo, *Psychopharmacology*, **24**, 430(1972).

(4) G. Zsigmond and B. Solymoss, *Proc. Soc. Exp. Biol. Med.*, **145**, 631(1974).

(5) A. Y. H. Lu, A. Somogyi, S. West, R. Kuntzman, and A. H. Conney, *Arch. Biochem. Biophys.*, **152**, 457(1972).

(6) Y. Taché, H. Selye, S. Szabo, and J. Taché, *J. Endocrinol.*, **58**, 233(1973).

(7) P. Kourounakis, S. Szabo, and H. Selye, *J. Pharm. Pharmacol.*, **25**, 670(1973).

(8) R. E. Talcott and S. J. Stohs, *Res. Commun. Chem. Pathol. Pharmacol.*, **5**, 663(1973).

(9) B. Tuchweber, J. Werringloer, and P. Kourounakis, *Biochem. Pharmacol.*, **23**, 513(1974).

(10) S. Szabo, P. Kourounakis, H. Selye, and O. da Silva, *J. Pharmacol. Exp. Ther.*, **188**, 45(1974).

(11) R. E. Talcott and S. J. Stohs, *Biochem. Pharmacol.*, **23**, 1221(1974).

(12) H. Selye, *Verh. Dtsch. Ges. Pathol.*, **56**, 191(1972).

(13) B. D. Garg, K. Kovacs, and B. Tuchweber, *Virchows Arch. B. Zellpathol.*, **12**, 61(1972).

(14) B. D. Garg, S. Szabo, B. Tuchweber, and K. Kovacs, *Hormone Res.*, **4**, 53(1973).

(15) B. D. Garg, B. Tuchweber, J. Werringloer, J. D. Khandekar, and K. Kovacs, *Acta Anat.*, **85**, 190(1973).

(16) J. D. Khandekar, B. D. Garg, B. Tuchweber, and K. Kovacs, *Rev. Can. Biol.*, **32**, 121(1973).

(17) T. Lindeborg and H. Glaumann, *Exp. Mol. Pathol.*, **21**, 313(1974).

(18) R. E. Talcott and S. J. Stohs, *J. Pharm. Sci.*, **61**, 296(1972).

(19) R. Kato and J. R. Gillette, *J. Pharmacol. Exp. Ther.*, **150**, 279(1965).

(20) T. Omura and R. Sato, *J. Biol. Chem.*, **239**, 2370(1964).

(21) O. H. Lowry, N. J. Rosenbrough, A. L. Farr, and R. J. Randall, *J. Biol. Chem.*, **193**, 265(1951).

(22) F. M. Radzialowski, *Biochem. Pharmacol.*, **22**, 1607(1973).

(23) A. H. Conney, *Pharmacol. Rev.*, **19**, 317(1967).

ACKNOWLEDGMENTS AND ADDRESSES

Received April 21, 1975, from the *Department of Medicinal Chemistry and Pharmacognosy, College of Pharmacy, University of Nebraska Medical Center, Lincoln, NE 68588*

Accepted for publication June 17, 1975.

Supported in part by a grant from the Nebraska Heart Association.

The pregnenolone-16α-carbonitrile was generously provided by The Upjohn Co. The authors also wish to thank Mr. Daniel Monaghan, Mr. Alan Schmaljohn, and Mrs. Laura Pape for technical assistance.

[x] To whom inquiries should be directed.

Conformational Populations for Antihistamines and Antihypertensives in Solution

NORMAN S. HAM

Abstract □ The conformations in aqueous solution were determined for the XCH_2CH_2N systems of some antihistamines (H_1-receptor antagonists) and some adrenergic neuron blocking agents, including the antihypertensive drugs guanethidine and guanoclor. The rotameric species thought to be the pharmacologically active one is often not the only rotamer present in solution.

Keyphrases ■ Antihistamines—containing the XCH_2CH_2N system, rotameric conformations in aqueous solution □ Antihypertensives—containing the XCH_2CH_2N system, rotameric conformations in aqueous solution □ Guanethidine—rotameric conformations in aqueous solution □ Guanoclor—rotameric conformations in aqueous solution

A considerable variety of pharmacological activity is observed among derivatives of 1,2-disubstituted ethanes, XCH_2CH_2Y, and this variety has led to many attempts to correlate the observed biological activity with the conformational preferences about the C—C single bond. In these compounds, three conformations are possible, depending on the relative dispositions of the substituents X and Y. In one, X and Y are in a *trans* relationship; and in two, X and Y are *gauche*. Generally, the energy differences between these rotamers are expected to be quite low (less than 42 kJ/mole), so all three rotamers may be present in solution at physiological pH.

Under these conditions, the proton magnetic resonance (PMR) spectrum is an average of the spectra of the individual rotamers (1). Although the spectral parameters can, in principle, provide rotameric populations, this is not always straightforward. The difficulties are partly experimental and numerical and partly interpretative (2). Recent work clarified the effects of the substituents X and Y on the parameters obtained from an analysis of the high-resolution PMR spectrum of the XCH_2CH_2Y system (3) (an *AA'BB'* spectrum), and quantitative rotameric populations can now be obtained.

Two clinically important examples of compounds containing the XCH_2CH_2N system are found among the antihistaminics and the antihypertensive agents. Conformational information for some representative molecules of these drug classes is presented here.

EXPERIMENTAL

The PMR spectra were recorded at 60, 90, and 100 MHz[1]. The spectral details for the antihistamines, aside from the chemical shift data, were reported earlier (4). The other compounds, except guanoclor, were run in the form of their salts as approximately 20% solutions in deuterium oxide. The solubility of guanoclor in deuterium oxide was only 0.25%.

The ethanic $-CH_2CH_2-$ portions of the PMR spectra were of the *AA'BB'* type. For many of the compounds, however, complete analysis of this part of the spectrum was made difficult by one or more complications due to overlapping absorptions, long-range couplings, unfavorable linewidths, or uncertainties in some parameters. However, the parameter N, the sum of the vicinal coupling constants J_{AB} and $J_{AB'}$, is estimated from the separation between the strongest pair of lines in one of the multiplets, either *A* or *B*, depending on which is clearer (2).

Pyrilamine Free Base—NMR ($CDCl_3$): δ 2.3 [s, 6H, $N(CH_3)_2$], 2.55 (m, 2H, CCH_2N, N = 14.6 Hz), 3.64 (m, 2H, NCH_2C, N = 14.6 Hz), 3.75 (s, 3H, OCH_3), 4.67 (s, 2H, benzyl CH_2), 7.0 (m, 7H, aromatic H), and 8.25 (m, 1H, pyridyl H_α).

Pyrilamine Maleate—NMR (D_2O): δ 3.06 [s, 6H, $^+N(CH_3)_2$], 3.8 (s, 3H, OCH_3), 3.48 (m, 2H, CCH_2N^+, N = 12.1 Hz), 4.02 (m, 2H, NCH_2C, N = 12.1 Hz), 4.67 (s, 2H, benzyl CH_2), 7.0 (m, 7H, aromatic H), and 8.25 (m, 1H, pyridyl H_α).

Tripelennamine Hydrochloride—NMR (D_2O): δ 3.17 [s, 6H, $^+N(CH_3)_2$], 3.53 (m, 2H, CCH_2N^+, N = 12.0 Hz), 4.08 (m, 2H, NCH_2C, N = 12.0 Hz), 4.83 (s, 2H, benzyl CH_2), 7.0 (m, 8H, aromatic H), and 8.3 (m, 1H, pyridyl H_α).

Methapyrilene Hydrochloride—NMR (D_2O): δ 3.07 [s, 6H, $^+N(CH_3)_2$], 3.45 (m, 2H, CCH_2N^+, N = 11.8 Hz), 3.98 (m, 2H, NCH_2C, N = 11.8 Hz), 7.1 (m, 6H, aromatic H and thienyl H), and 8.25 (m, 1H, pyridyl H_α).

Guanethidine Sulfate—NMR (D_2O): δ 1.7 (m, 10H, CCH_2C), 3.35 (m, 6H, NCH_2), and 3.60 (m, 2H, CCH_2NH, N = 13.4 Hz).

N-(*2-Morpholinoethyl*)*guanidine Sulfate*—NMR (D_2O): δ 2.60 (m, 6H, NCH_2, N = 13.0 and 9.5 Hz), 3.35 (m, 2H, CCH_2NH, N = 13.0 Hz), and 3.74 (m, 4H, $-OCH_2$, N = 9.5 Hz).

Diphenhydramine Hydrochloride—NMR (D_2O): δ 2.9 [s, 6H, $^+N(CH_3)_2$], 3.36 (m, 2H, CCH_2N, N = 10.1 Hz), 3.76 (m, 2H, OCH_2C, N = 10.1 Hz), 5.55 (s, 1H, >CH), and 7.4 (m, 10H, aromatic H).

Guanoclor Sulfate—NMR (D_2O): δ 3.54 (m, 2H, CCH_2N, N = 10.0 Hz), 4.48 (m, 2H, OCH_2C, N = 10.0 Hz), and 7.5 (m, 3H, aromatic H).

Quantitative interpretation of N values is based on the correlation between the vicinal coupling constants in the individual rotamers and the electronegativities of substituents X and Y derived by Abraham and Gatti (3). Relations for the parameter N as a function of n_t, the proportion of *trans*-rotamer, can be derived for the OCH_2CH_2N and NCH_2CH_2N fragments and are given in Eqs. 1 and 2, respectively (2):

$$N = 9.63 + 8.17n_t \quad \text{(Eq. 1)}$$

$$N = 10.51 + 7.39n_t \quad \text{(Eq. 2)}$$

In the absence of a complete analysis, the N value may be overestimated and the errors inherent in the correlations are such that the n_t values listed in Table I may be in error by ±5%.

RESULTS AND DISCUSSION

Antihistamines—Until recently, the known antagonists of histamine acted only on H_1-receptors such as those found in the gut and bronchi (5). Tertiary amine derivatives, *e.g.*, pyrilamine and tripelennamine, are typical agents of this type. These antihistamines might now be called H_1-receptor antagonists, since the discovery of the gastric secretory inhibitors based on imidazole-substituted butylthioureas has provided the pharmacological classification of H_2-receptor antagonists (6). Rotameric populations for the H_1-receptor antagonists of the XCH_2CH_2N type, for which qualitative conclusions were presented earlier (4), are given in Table I.

For the antagonists of the ethylenediamine type, there is a fall in the percentage of *trans*-rotamer when the aliphatic side-chain nitrogen atom is protonated. At physiological pH, this side-chain nitrogen atom will be protonated; Table I shows that only 20% of the

[1] Varian A60, HA100, and Bruker WH90 NMR spectrometers.

Table I—Spectral Parameter N, Proportions (n_t) of *trans*-Rotamer, and Biological Activity Data for Antihistamines and Antihypertensives

Compound	N, Hz	n_t	H_1-Receptor Antagonist pA_2 Value (9)	Adrenergic Neuron Blocking Activity (13,14)
	NCH_2CH_2N Types			
Pyrilamine base (deuterochloroform)	14.6[a]	0.56	—	—
Pyrilamine maleate (deuterium oxide)	12.1[a]	0.22	9.36	—
Tripelennamine hydrochloride (deuterium oxide)	12.0[a]	0.21	9.00	—
Methapyrilene hydrochloride (deuterium oxide)	11.8[a]	0.18	8.63	—
Guanethidine sulfate (deuterium oxide)	13.4	0.4	—	Active
N-(2-Morpholinoethyl)guanidine sulfate (deuterium oxide)	13.0	0.34	—	No activity
	OCH_2CH_2N Types			
Diphenhydramine hydrochloride (deuterium oxide)	10.1[a]	0.06	8.14	—
Xylocholine bromide (deuterium oxide)	10.1[b]	0.06	—	Active
Guanoclor sulfate (deuterium oxide)[c]	10.0	0.04	—	High activity
N-(2-Morpholinoethyl)guanidine sulfate (deuterium oxide)	9.5	0	—	No activity

[a] From Ref. 4. [b] From Ref. 16. [c] Guanoclor is [[2-(2,6-dichlorophenoxy)ethyl]amino]guanidine.

trans-rotamer is present in solution for the common antihistamine salts. In these compounds, which contain an α-pyridyl ring as well as a benzyl group, the *gauche*-form can be stabilized considerably by the hydrogen bond involving the heterocyclic nitrogen atom and the $^+NH(CH_3)_2$ group. This kind of intramolecular hydrogen bond, which was originally postulated to be a factor in determining the conformation of the histamine monocation (7), is more important with these antihistamines (80% *gauche*-rotamers) than with the corresponding methylated histamine derivative, 4(5)-(β-dimethylaminoethyl)imidazole (40% *gauche*-rotamers) (8).

Comparison of the ethylenediamine and ether type of antagonist shows that the order of decreasing pA_2 value (9) parallels the percentage of *trans*-rotamer. These observations lend support to the view that the *trans*-$XCCN^+$ conformation is the pharmacologically active one for H_1-receptor antagonism (10–12). However, the pharmacologically active species is then not the most abundant one in solution. This objection is not too serious because of the changes that may occur during drug–receptor binding and in view of the small energy differences between the rotamers (a population ratio of 4:1 implies an energy difference of about 4.2 kJ/mole).

Antihypertensives—Adrenergic neuronal blocking drugs form one group of clinically useful antihypertensive agents (13, 14). On nerve stimulation, these drugs act within the nerve terminal to prevent release of the adrenergic transmitter. Aside from xylocholine bromide (15, 16), the first compound with this action to be discovered, there is little information about either the solid-state or solution conformations of these compounds.

The common structural feature of these drugs seems to be a positively charged terminal group separated from a lipophilic ring structure (14); a number of these agents are 1,2-disubstituted ethanes. Table I summarizes the conformational populations for the ethanic chain of some molecules representative of these antihypertensives. The positively charged groups in these compounds are either trimethylammonium, the guanidinium ion, or the aminoguanidinium ion.

Augstein *et al.* (17), in discussing adrenergic neuron blocking activity of aryloxyethylguanidines and aryloxyethylaminoguanidines, suggested that activity results when the cationic head and the ring are separated by a distance similar to that found in sympathomimetic amines. Hydrogen bonds involving $O—HN^+$ were thought to be important in maintaining this distance, with a resulting O/N *gauche* disposition for the substituents of the ethanic side chain.

For compounds based on the OCCN system, Table I shows that the *gauche*-rotamers predominate either completely or very nearly so in aqueous solution. The observed *gauche* conformations of many choline derivatives have been ascribed to an electrostatic interaction between the oxygen and the cationic head and also to hydrogen bonds of the O—HC type (18). Although such a hydrogen bond has been inferred from the crystal structure of xylocholine (15), this type of hydrogen bond has been doubted (19). For other choline derivatives, recent opinion has favored an electrostatic interaction (2, 16, 20); but in the case of guanoclor, the NH group of the guanidinium head may provide extra stability through a six-membered ring involving the O—C—C—N—N—H atoms (17).

Comparison of the chemical shifts of phenocholine and xylocholine showed that for xylocholine in solution the aromatic ring was considerably restricted in rotation to a region orthogonal to the plane of the COC bond (2). The chemical shift of the OCH_2 protons for guanoclor indicates that the bulky *ortho*-dichloro substituents are also restricting rotation.

The NCCN system of guanethidine sulfate has about 40% of the *trans*-rotamer present in solution, whereas the morpholino compound has slightly less. These populations, when compared with those of the aryloxy compounds, can be understood in terms of weaker hydrogen bonds and/or weaker electrostatic effects, resulting from the replacement of an oxygen atom by a less electronegative nitrogen atom.

The percentages of *gauche*-rotamers deduced from the PMR spectra are in qualitative accord with the neuronal blocking activity; but the orientation and character of the ring structure are also important, as the inactivity of the morpholino compound shows. Whereas the lipophilic character of the morpholino ring is apparently unfavorable for adrenergic neuronal blocking activity, the ring inversions possible in the eight-membered ring in guanethidine can produce conformations similar to those found with the aryloxy compounds.

These results demonstrate the extent of the conformational flexibility of the antihistamines and antihypertensives in aqueous solution. Nevertheless, these results should not be applied directly to the *in vivo* situation of the drug–receptor complex, since there are probably a number of unknown conformational ramifications in the binding process.

REFERENCES

(1) L. M. Jackman and S. Sternhell, "Application of Nuclear Magnetic Resonance Spectroscopy in Organic Chemistry," 2nd ed., Pergamon Press, Oxford, England, 1969, p. 368.

(2) C. C. J. Culvenor and N. S. Ham, *Aust. J. Chem.*, **27**, 2191(1974).

(3) R. J. Abraham and G. Gatti, *J. Chem. Soc. B*, **1969**, 961.

(4) N. S. Ham, *J. Pharm. Sci.*, **60**, 1764(1971).

(5) A. S. F. Ash and H. O. Schild, *Brit. J. Pharmacol. Chemother.*, **27**, 427(1966).

(6) J. W. Black, W. A. M. Duncan, C. J. Durant, C. R. Ganellin, and E. M. Parsons, *Nature (London)*, **236**, 385(1972).

(7) C. Niemann and J. T. Hays, *J. Amer. Chem. Soc.*, **64**, 2288(1942).

(8) N. S. Ham, A. F. Casy, and R. R. Ison, *J. Med. Chem.*, **16**, 470(1973).

(9) R. B. Barlow, "Introduction to Chemical Pharmacology," Methuen, London, England, 1968, p. 357.

(10) L. B. Kier, *J. Med. Chem.*, **11**, 441(1968).

(11) A. F. Casy and R. R. Ison, *J. Pharm. Pharmacol.*, **22**, 270(1970).

(12) *Ibid.*, **22**, 368, 371(1970).

(13) R. P. Mull and R. A. Maxwell, in "Antihypertensive

Agents," E. Schlittler, Ed., Academic, New York, N.Y., 1967, p. 115.

(14) G. J. Durant, A. M. Roe, and A. L. Green, *Progr. Med. Chem.*, **7**, 124(1970).

(15) P. Coggon, A. T. McPhail, and A. M. Roe, *Nature (London)*, **224**, 1200(1969).

(16) P. Partington, J. Feeney, and A. S. V. Burgen, *Mol. Pharmacol.*, **8**, 269(1972).

(17) J. Augstein, S. M. Green, A. M. Monro, T. I. Wrigley, A. R. Katritzky, and G. J. Tiddy, *J. Med. Chem.*, **10**, 391(1967).

(18) M. Sundaralingam, *Nature (London)*, **217**, 35(1968).

(19) T. F. Brennan, F. K. Ross, W. C. Hamilton, and E. Shefter, *J. Pharm. Pharmacol.*, **22**, 724(1970).

(20) A. Makriyannis, K. F. Sullivan, and H. G. Mautner, *Proc. Nat. Acad. Sci. USA*, **69**, 3416(1972).

ACKNOWLEDGMENTS AND ADDRESSES

Received January 3, 1975, from *CSIRO, Division of Chemical Physics, P.O. Box 160, Clayton, Victoria 3168, Australia.*

Accepted for publication July 1, 1975.

The author is grateful to the following companies for providing samples: Ciba Laboratories (guanethidine and the morpholino compound) and Pfizer Ltd. (guanoclor). The help of M. E. Hughes, J. L. Little, and R. I. Willing in recording spectra is also gratefully acknowledged.

Determination of Hyoscyamine in BPC Mixtures

SALEH A. H. KHALIL ˣ **and SAWSAN EL-MASRY**

Abstract □ The hyoscyamine contents of four BPC mixtures (containing either belladonna or hyoscyamus tincture) were determined using the acid-dye technique. A sample size of 10 ml was required. The mean percentage recovery of hyoscyamine ranged from 99.73 to 101.03 from three mixtures; from the magnesium trisilicate and belladonna mixture, it was 94.8. The effects of pH and adsorption on the extraction of the alkaloid–dye complex from the mixtures examined are discussed.

Keyphrases □ Hyoscyamine—colorimetric determination using acid-dye technique, mixtures containing belladonna or hyoscyamus tincture □ Colorimetry—determination, hyoscyamine in mixtures, acid-dye technique

The current edition of the British Pharmaceutical Codex (BPC) lacks a quantitative method for the estimation of hyoscyamine content in mixtures containing either belladonna or hyoscyamus tincture. Instead, a TLC method is specified for testing the presence of tropane alkaloids in these mixtures (1). Recently, a colorimetric method based on the acid-dye technique was suggested for the microdetermination of hyoscyamine and scopolamine in synthetic mixtures (2).

The present work reports the suitability of the suggested method for the determination of hyoscyamine content in some BPC mixtures. The following mixtures were examined: aluminum hydroxide and belladonna; belladonna mixture, pediatric; magnesium trisilicate and belladonna; and potassium citrate and hyoscyamus.

EXPERIMENTAL

Materials—The materials used in preparation of the BPC mixtures were of either BP or BPC grade[1]. Belladonna and hyoscyamus tinctures BP[2], bromcresol purple[1], and reagent grade chloroform[1] were used.

Procedures—Hyoscyamine determination was carried out on the freshly prepared mixtures as follows:

Aluminum Hydroxide and Belladonna Mixture—Measure 10 ml of the mixture, add 10 ml of water (used to rinse the pipet), and centrifuge the diluted mixture for 3 min at 4000 rpm. To a 5-ml aliquot of the clear supernate, add 10 ml of McIlvaine buffer solution (pH 6.60 ± 0.05) and 10 ml of chloroform solution of bromcresol purple (4×10^{-4} *M*). Shake the mixture for 1 min and allow the layers to separate for 10 min.

Separate the chloroform layer containing the hyoscyamine–dye complex and reextract the aqueous layer with 3 × 10 ml of chloroform. To the combined chloroform extracts, add 15 ml of 0.1 *N* NaOH and shake to liberate the combined dye. Dilute the aqueous phase to 25 ml with 0.1 *N* NaOH and measure the absorbance at 580 nm[3].

Carry out a standard run under the same conditions using 0.25 ml of the standard hyoscyamine sulfate solution in 70% alcohol (containing the equivalent of 30 mg % of hyoscyamine base). Compare using a blank similarly prepared.

Belladonna Mixture, Pediatric—Measure 10 ml of the mixture and add about 0.5 ml of 0.1 *N* NaOH to adjust the pH to 6.6. Follow the procedure for the aluminum hydroxide and belladonna mixture, starting from "... add 10 ml of McIlvaine buffer solution...." Use 0.3 ml of the standard hyoscyamine sulfate solution containing the equivalent of 30 mg % of hyoscyamine base.

Potassium Citrate and Hyoscyamus Mixture—Measure 10 ml of the mixture, add 10 ml of water and 5 ml of ammonia T.S., and extract with 4 × 10 ml of chloroform. Evaporate the combined chloroform extracts and dissolve the residue in the 10 ml of McIlvaine buffer solution used in the assay. Follow the procedure for the aluminum hydroxide and belladonna mixture; use the 3 × 10-ml chloroform aliquots to rinse the container previously washed with the buffer.

For the standard run, use 2 ml of the standard hyoscyamine sulfate solution in 70% alcohol (containing the equivalent of 5 mg % of hyoscyamine base).

Magnesium Trisilicate and Belladonna Mixture—Measure 10 ml of the mixture, add 40 ml of 0.5 *N* HCl, and heat at 50° for 30 min with shaking. Cool and then centrifuge for 3 min at 4000 rpm. To a 10-ml aliquot of the supernate, add a few drops of 0.1 *N* NaOH to adjust the pH to 6.6. Follow the procedure for the aluminum hydroxide and belladonna mixture, starting from "... add 10 ml of McIlvaine buffer solution ...." Use 0.1 ml of the standard

[1] British Drug Houses Ltd., Poole, England.
[2] William Ransom and Son Ltd., Hitchin, Hertfordshire, England.
[3] Unicam SP 500 Series 2.

Agents," E. Schlittler, Ed., Academic, New York, N.Y., 1967, p. 115.

(14) G. J. Durant, A. M. Roe, and A. L. Green, *Progr. Med. Chem.*, **7**, 124(1970).

(15) P. Coggon, A. T. McPhail, and A. M. Roe, *Nature (London)*, **224**, 1200(1969).

(16) P. Partington, J. Feeney, and A. S. V. Burgen, *Mol. Pharmacol.*, **8**, 269(1972).

(17) J. Augstein, S. M. Green, A. M. Monro, T. I. Wrigley, A. R. Katritzky, and G. J. Tiddy, *J. Med. Chem.*, **10**, 391(1967).

(18) M. Sundaralingam, *Nature (London)*, **217**, 35(1968).

(19) T. F. Brennan, F. K. Ross, W. C. Hamilton, and E. Shefter, *J. Pharm. Pharmacol.*, **22**, 724(1970).

(20) A. Makriyannis, K. F. Sullivan, and H. G. Mautner, *Proc. Nat. Acad. Sci. USA*, **69**, 3416(1972).

ACKNOWLEDGMENTS AND ADDRESSES

Received January 3, 1975, from *CSIRO, Division of Chemical Physics, P.O. Box 160, Clayton, Victoria 3168, Australia.*

Accepted for publication July 1, 1975.

The author is grateful to the following companies for providing samples: Ciba Laboratories (guanethidine and the morpholino compound) and Pfizer Ltd. (guanoclor). The help of M. E. Hughes, J. L. Little, and R. I. Willing in recording spectra is also gratefully acknowledged.

Determination of Hyoscyamine in BPC Mixtures

SALEH A. H. KHALIL ˣ **and SAWSAN EL-MASRY**

Abstract □ The hyoscyamine contents of four BPC mixtures (containing either belladonna or hyoscyamus tincture) were determined using the acid-dye technique. A sample size of 10 ml was required. The mean percentage recovery of hyoscyamine ranged from 99.73 to 101.03 from three mixtures; from the magnesium trisilicate and belladonna mixture, it was 94.8. The effects of pH and adsorption on the extraction of the alkaloid–dye complex from the mixtures examined are discussed.

Keyphrases □ Hyoscyamine—colorimetric determination using acid-dye technique, mixtures containing belladonna or hyoscyamus tincture □ Colorimetry—determination, hyoscyamine in mixtures, acid-dye technique

The current edition of the British Pharmaceutical Codex (BPC) lacks a quantitative method for the estimation of hyoscyamine content in mixtures containing either belladonna or hyoscyamus tincture. Instead, a TLC method is specified for testing the presence of tropane alkaloids in these mixtures (1). Recently, a colorimetric method based on the acid-dye technique was suggested for the microdetermination of hyoscyamine and scopolamine in synthetic mixtures (2).

The present work reports the suitability of the suggested method for the determination of hyoscyamine content in some BPC mixtures. The following mixtures were examined: aluminum hydroxide and belladonna; belladonna mixture, pediatric; magnesium trisilicate and belladonna; and potassium citrate and hyoscyamus.

EXPERIMENTAL

Materials—The materials used in preparation of the BPC mixtures were of either BP or BPC grade[1]. Belladonna and hyoscyamus tinctures BP[2], bromcresol purple[1], and reagent grade chloroform[1] were used.

Procedures—Hyoscyamine determination was carried out on the freshly prepared mixtures as follows:

Aluminum Hydroxide and Belladonna Mixture—Measure 10 ml of the mixture, add 10 ml of water (used to rinse the pipet), and centrifuge the diluted mixture for 3 min at 4000 rpm. To a 5-ml aliquot of the clear supernate, add 10 ml of McIlvaine buffer solution (pH 6.60 ± 0.05) and 10 ml of chloroform solution of bromcresol purple (4×10^{-4} *M*). Shake the mixture for 1 min and allow the layers to separate for 10 min.

Separate the chloroform layer containing the hyoscyamine–dye complex and reextract the aqueous layer with 3 × 10 ml of chloroform. To the combined chloroform extracts, add 15 ml of 0.1 *N* NaOH and shake to liberate the combined dye. Dilute the aqueous phase to 25 ml with 0.1 *N* NaOH and measure the absorbance at 580 nm[3].

Carry out a standard run under the same conditions using 0.25 ml of the standard hyoscyamine sulfate solution in 70% alcohol (containing the equivalent of 30 mg % of hyoscyamine base). Compare using a blank similarly prepared.

Belladonna Mixture, Pediatric—Measure 10 ml of the mixture and add about 0.5 ml of 0.1 *N* NaOH to adjust the pH to 6.6. Follow the procedure for the aluminum hydroxide and belladonna mixture, starting from "... add 10 ml of McIlvaine buffer solution...." Use 0.3 ml of the standard hyoscyamine sulfate solution containing the equivalent of 30 mg % of hyoscyamine base.

Potassium Citrate and Hyoscyamus Mixture—Measure 10 ml of the mixture, add 10 ml of water and 5 ml of ammonia T.S., and extract with 4 × 10 ml of chloroform. Evaporate the combined chloroform extracts and dissolve the residue in the 10 ml of McIlvaine buffer solution used in the assay. Follow the procedure for the aluminum hydroxide and belladonna mixture; use the 3 × 10-ml chloroform aliquots to rinse the container previously washed with the buffer.

For the standard run, use 2 ml of the standard hyoscyamine sulfate solution in 70% alcohol (containing the equivalent of 5 mg % of hyoscyamine base).

Magnesium Trisilicate and Belladonna Mixture—Measure 10 ml of the mixture, add 40 ml of 0.5 *N* HCl, and heat at 50° for 30 min with shaking. Cool and then centrifuge for 3 min at 4000 rpm. To a 10-ml aliquot of the supernate, add a few drops of 0.1 *N* NaOH to adjust the pH to 6.6. Follow the procedure for the aluminum hydroxide and belladonna mixture, starting from "... add 10 ml of McIlvaine buffer solution ...." Use 0.1 ml of the standard

[1] British Drug Houses Ltd., Poole, England.
[2] William Ransom and Son Ltd., Hitchin, Hertfordshire, England.
[3] Unicam SP 500 Series 2.

Table I—Results of Replicate Determinations of Hyoscyamine in Four BPC Mixtures by the Acid-Dye Technique Using Bromcresol Purple at pH 6.6

Number of Runs	Hyoscyamine Recovery, % in Mixtures			
	Aluminum Hydroxide and Belladonna	Belladonna, Pediatric	Potassium Citrate and Hyoscyamus	Magnesium Trisilicate and Belladonna
1	98.2	98.9	100.5	95.4
2	98.8	101.9	98.7	94.8
3	101.1	100.8	102.8	95.7
4	99.0	99.7	99.3	94.3
5	98.5	102.4	101.8	95.6
6	100.7	101.8	101.2	93.5
7	98.4	101.7	99.0	94.1
8	101.9	99.6	98.9	95.4
9	99.1	99.7	101.9	93.7
10	101.6	102.8	101.2	95.5
Mean	99.73	101.03	100.53	94.8
SD, %	1.43	1.46	1.47	0.84
CV, %	1.43	1.45	1.46	0.88

hyoscyamine sulfate solution containing the equivalent of 30 mg % of hyoscyamine base.

RESULTS AND DISCUSSION

At pH 6.6, bromcresol purple was found to complex selectively with hyoscyamine. Neither scopolamine nor tropine (one of the hydrolytic products of hyoscyamine) interfered. Interference due to chlorophyll was less than 2%.

To test for the possible interference from the volatile bases that may be present in the tinctures, standard curves were made using heated[4] and unheated tinctures. Almost identical results were obtained for both. The calculated slopes of the linear plots were 0.195 and 0.191 for heated and unheated belladonna tinctures, respectively, and 0.350 and 0.345 for heated and unheated hyoscyamus tinctures, respectively. This finding may suggest that the volatile bases, if present in the tinctures, did not interfere with the assay procedure.

It is concluded, therefore, that the recommended method is specific for the determination of hyoscyamine in belladonna and hyoscyamus tinctures. Compared with the BP methods of assay, which yielded 30.1 mg % for belladonna tincture and 5.3 mg % for hyoscyamus tincture, the recommended method gave the hyoscyamine contents as 29.6 and 5.1 mg % for the two tinctures, respectively.

Application of the suggested method for the determination of hyoscyamine in some BPC mixtures without pH adjustment, preextraction, or desorption steps was unsuccessful, perhaps due to the effect of pH, interference of the components of the mixture during the extraction of the alkaloid–dye complex, or adsorption of hyoscyamine onto the solid ingredient(s) of the mixture. In the aluminum hydroxide and belladonna mixture, however, direct estimation yielded a mean recovery of 99.73% (Table I). Aluminum hydroxide gel[5] BP had no apparent adsorptive effect when belladonna tincture was added and the mixture was stored for 7 days at 25 ± 0.2°.

The pH of the belladonna mixture, pediatric, was 3.6 owing to the presence of benzoic acid. Direct determination of hyoscyamine, without preadjustment of pH, gave high percentages, from 110.2 to 113.0 (eight determinations). This result was due mainly to the effect of pH since low values favor the partitioning of the excess dye in chloroform. After adjustment to pH 6.6, the mean recovery was 101.03% (Table I).

Direct determination of hyoscyamine in the potassium citrate and hyoscyamus mixture, without preextraction, failed possibly due to the acidic pH (5.9) and the high electrolyte concentration of this mixture (30% potassium citrate and 5% citric acid). The average recovery obtained by direct determination was 138.2% (±2.9%, eight determinations). Preadjustment to pH 6.6 using 1 *N* NaOH decreased the average recovery to 126.4%. Therefore, the relatively high electrolyte concentration of the mixture "salted out" the excess dye, thereby increasing its partitioning in chloroform; consequently, high results were obtained. Preextraction with chloroform from an alkaline medium (as outlined under *Experimental*) overcame this problem, the average recovery obtained being 100.53% (Table I).

TLC[6] confirmed that the supernate of the magnesium trisilicate and belladonna mixture was almost completely devoid of hyoscyamine. This finding was attributable to the rapid adsorption of hyoscyamine on magnesium trisilicate (3), which amounted to about 93% (4). When the BPC procedure for testing the presence of belladonna alkaloids (1) was adopted, the mean recovery was 54.1% (±5.7%, six determinations). The low result was probably due to the incomplete elution of the adsorbed hyoscyamine by the acetone–ammonia mixture used. With the procedure described under *Experimental*, the average recovery was 94.8% (Table I).

Attempts were made to improve the recovery by elevating the temperature of digestion (50–70°), prolonging the digestion time (0.5–3 hr), or boiling with concentrated hydrochloric acid as suggested by Gupta and Euler (3). No significant improvement was obtained; the results varied from 93.9 to 96.2% (mean 94.11%). The hydrated silica gel, produced from magnesium trisilicate in acid medium, probably had some adsorptive effect, so complete recovery of hyoscyamine could not be obtained.

REFERENCES

(1) "British Pharmaceutical Codex," The Pharmaceutical Press, London, England, 1973, pp. 871, 872.

(2) S. El-Masry and S. A. H. Khalil, *J. Pharm. Sci.*, **62**, 1332(1973).

(3) V. D. Gupta and K. E. Euler, *ibid.*, **61**, 1458(1972).

(4) S. El-Masry and S. A. H. Khalil, *J. Pharm. Pharmacol.*, **26**, 243(1974).

ACKNOWLEDGMENTS AND ADDRESSES

Received September 25, 1974, from the *Department of Pharmacy and Pharmacology, College of Medicine, University of Benin, Benin City, Nigeria.*

Accepted for publication July 2, 1975.

Present address (of both authors): Faculty of Pharmacy, University of Alexandria, Alexandria, Arab Republic of Egypt.

[x] To whom inquiries should be directed.

[4] The tinctures were evaporated to dryness in the presence of a few drops of ammonia solution, and heating was continued for 15 min in the presence of a few drops of alcohol.

[5] Aludrox gel, Batch C.IG42, J. Wyeth & Brothers Ltd., Hants, England.

[6] Methanol–34.5% (w/w) ammonia (100:1) was the solvent system, and silica gel G (Merck) was the adsorbent.

Synthesis and Biological Evaluation of 1-(4-Hydroxy-2-oxo-2*H*-1-benzopyran-3-yl)pyridinium Hydroxide Inner Salt Derivatives

NATHANIEL GRIER [x] and ROBERT A. STRELITZ

Abstract □ Eight 1-(4-hydroxy-2-oxo-2*H*-1-benzopyran-3-yl)pyridinium hydroxide inner salts were synthesized, and the antibacterial, antifungal, anticoccidial, and anthelmintic activities were determined against different microorganisms, the protozoan *Eimeria tenella*, and trichostrongyle nematodes. All were noninhibitory to Gram-negative bacteria and the parasites. The pyridine, 4-benzylpyridine, and 2-isoquinoline inner salt derivatives controlled only *Rhizoctonia solani* of the four genera of fungi challenged.

Keyphrases □ Benzopyranylpyridinium salts, substituted—synthesized, antibacterial, antifungal, anticoccidial, anthelmintic activities evaluated □ Antibacterial agents, potential—series of substituted benzopyranylpyridinium salts synthesized, evaluated □ Antifungal agents, potential—series of substituted benzopyranylpyridinium salts synthesized, evaluated □ Anticoccidial agents, potential—series of substituted benzopyranylpyridinium salts synthesized, evaluated □ Anthelmintic agents, potential—series of substituted benzopyranylpyridinium salts synthesized, evaluated

4-Hydroxycoumarin and various 3-substituted derivatives have antimicrobial (1–3), anthelmintic (4), and insecticidal (4) properties of interest. An effort was directed to the synthesis of related compounds with possibly enhanced utility for the growth control of bacteria, fungi, protozoa, and helminths. Eight novel 1-(4-hydroxy-2-oxo-2*H*-1-benzopyran-3-yl)pyridinium hydroxide inner salt derivatives (I) were prepared by treatment of 3-bromo-4-hydroxycoumarin with pyridines (Scheme I).

2-Alkylpyridines and quinoline failed to yield I-type compounds, apparently because of steric hindrance; isoquinoline was converted to 2-(4-hydroxy-2-oxo-2*H*-1-benzopyran-3-yl)isoquinolinium hydroxide inner salt. A similar selectivity in betaine formation with dichloromaleimides was observed previously (5).

All of the compounds prepared are listed in Table I. When tested in preliminary screens for antimicrobial and antiparasitic properties, none exhibited sufficient inhibition and potency to encourage further study. The pyridine, 4-benzylpyridine, and 2-isoquinoline I inner salt derivatives suppressed growth of one fungus, but the eight compounds failed to suppress the growth of the Gram-negative bacteria, protozoan, and helminth at the maximum concentrations tested.

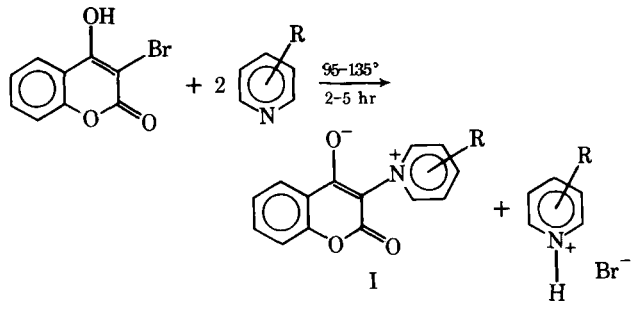

Scheme I

The pyridines were obtained from commercial sources, and 4-hydroxycoumarin was readily brominated using a known procedure (6).

DISCUSSION[1]

All of the compounds prepared were assayed for antimicrobial potency using the method of Conkey and Carlson (7). The microorganisms employed are associated with industrial and agricultural economic losses and include *Staphylococcus aureus* (ATCC 6538), *Aerobacter aerogenes*[2] (IPC 500), *Aureobasidium pullulans* (ATCC 9348), *Aspergillus niger* (ATCC 6275), *Rhizoctonia solani* (ATCC 16115), and *Verticillium albo-atrum*[3] (V3H). The compounds were dissolved or suspended in 25% methanol at concentrations of 1 mg/ml and diluted with hot sterile culture medium[4] to the desired strength. Concentrations of 1, 10, 50, and 100 μg/ml were used.

A culture medium containing the maximum concentration of 2.5% methanol failed to inhibit any of the microorganisms. All assays were run in duplicate. The control consisted of test medium medicated with 10 μg/ml of phenylmercuric acetate, which was totally effective.

The antimicrobial activities of the compounds at the 100-μg/ml concentration are reported in Table II. All but 1-(4-hydroxy-2-oxo-2*H*-1-benzopyran-3-yl)-4-*tert*-butylpyridinium hydroxide inner salt inhibited *S. aureus*. The 1-pyridinium, 1-(4-benzyl)pyridinium, and 2-isoquinolinium derivatives also prevented growth of *R. solani*. No activity was evident for any compound at the three lower concentrations.

An *in vitro* chemotherapy screen was run with Gram-negative bacteria such as *Escherichia coli*[5] (MSD 2017 and 3293), *Pseudomonas aeruginosa* (MSD 3210 and 3301), and *Proteus vulgaris* (MSD 1810). Stock solutions of the eight compounds containing 2 mg/ml of dimethyl sulfoxide were diluted with hot sterile culture medium[6] to provide concentrations of 200, 100, 80, 60, 40, 20, 10, 5, and 1 μg/ml.

A culture medium with the maximum concentration of 1% dimethyl sulfoxide as the solvent control was noninhibitory. All assays were run in duplicate. Tetracycline was used as a control and prevented growth completely at a concentration of 20 μg/ml. No test compounds were antibacterial at the indicated concentrations.

The betaines were evaluated in *in vitro* and *in vivo* parasitology assays (8, 9). Ova and larva of trichostrongyle nematodes, which cause helminthiasis, were subjected to a maximum concentration of 0.1 mg/ml of the test compounds and were unaffected. Thiabendazole, at a concentration of 1 μg/ml, suppressed both forms of the parasite.

The coccidiosis screen employed 2-week-old chicks fed a basal ration containing 0.05% (w/w) betaine. On the 2nd day of the experiment, an inoculum was administered orally containing 50,000 sporulated oocysts of the protozoan *Eimeria tenella*. After an additional 6 days, a comparative evaluation was made between the

[1] The broad spectrum antimicrobial test was run by the Product Development Laboratory, Chemical Division; all other screens were run in the Merck Sharp & Dohme Research Labs., Rahway, N.J.
[2] Institute of Paper Chemistry, Appleton, Wis.
[3] Collection n, University of California, Riverside, Calif.
[4] Difco tryptone glucose extract agar for bacteria and Difco Sabouraud maltose agar for the fungi.
[5] Field isolates.
[6] Difco brain heart infusion agar.

Table I—1-(4-Hydroxy-2-oxo-2*H*-1-benzopyran-3-yl)pyridinium Hydroxide Inner Salt Derivatives

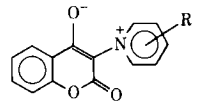

Compound	R	Melting Point	Yield, %	Recrystallization Solvent	Empirical Formula	Analysis, % Calc.	Found
I*a*	H	244–245°	38	Methanol	$C_{14}H_9NO_3$	C 70.29	70.00
						H 3.79	3.78
						N 5.86	5.81
I*b*	4-Methyl	>300°	34	Ethanol	$C_{15}H_{11}NO_3$	C 71.13	71.05
						H 4.38	4.41
						N 5.53	5.47
I*c*	4-Ethyl	253–256°	60	Tetrahydrofuran–petroleum ether (bp 30–60°)	$C_{16}H_{13}NO_3$	C 71.90	71.73
						H 4.90	4.91
						N 5.24	5.30
I*d*	4-*tert*-Butyl	288–290°	22	Isopropanol	$C_{18}H_{17}NO_3$	C 73.20	73.09
						H 5.80	5.75
						N 4.74	4.64
I*e*	4-Benzyl	195–198°	65	Isopropanol	$C_{21}H_{15}NO_3$	C 76.58	76.27
						H 4.59	4.79
						N 4.25	4.46
I*f*	3-Chloro	281–283°	20	Dimethylformamide	$C_{14}H_8ClNO_3$	C 61.44	60.92
						H 2.95	2.98
						N 5.12	4.96
						Cl 12.96	13.06
I*g*	3-Hydroxy	>350°	38	Ethanol	$C_{14}H_9NO_4$	C 65.88	65.40
						H 3.55	3.59
						N 5.49	5.76
I*h*	3,4-Benzo	299–300°	32	Isopropanol	$C_{18}H_{11}NO_3$	C 74.73	74.36
						H 3.83	3.57
						N 4.84	4.77

Table II—Antimicrobial Activity[a] of 1-(4-Hydroxy-2-oxo-2*H*-1-benzopyran-3-yl)pyridinium Hydroxide Inner Salts

Compound	*S. aureus*	*A. aerogenes*	*A. pullulans*	*A. niger*	*R. solani*	*V. albo-atrum*
I*a*	+	—	—	—	+	—
I*b*	+	—	—	—	—	—
I*c*	+	—	—	—	—	—
I*d*	—	—	—	—	—	—
I*e*	+	—	—	—	+	—
I*f*	+	—	—	—	—	—
I*g*	+	—	—	—	—	—
I*h*	+	—	—	—	+	—
Phenylmercuric acetate	+	+	+	+	+	+

[a] + = complete inhibition; — = no inhibition.

test group and control chicks fed the unmedicated diet. No activity was found for any compounds. Amprolium, at a concentration of 0.003% (w/w), controlled the infection.

EXPERIMENTAL[7]

The compounds (Table I), except I*g*, were prepared in the manner described for I*a*. No attempt was made to improve yields. Upon crystallization, all of the compounds were yellow crystalline solids; their IR spectra in mineral oil[8] mulls exhibited intensive absorption in the 1680–1600-cm^{-1} region. These bands probably involve strong mixing of two C⋯O and two C⋯C valence bond motions[9]:

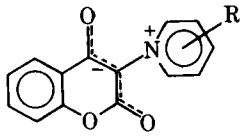

[7] Melting points were taken in open capillary tubes with a Thomas-Hoover apparatus and are uncorrected. IR spectra were obtained with a Perkin-Elmer model 621 grating spectrophotometer; TLC was performed with Analtech Inc. precoated plates.

[8] Nujol.

[9] The clarification of IR spectral band assignments in this region for coumarin and chromone structures was detailed by Büchi *et al.* (10).

1-(4-Hydroxy-2-oxo-2*H*-1-benzopyran-3-yl)pyridinium Hydroxide Inner Salt (I*a*)—Five grams (0.021 mole) of powdered 3-bromo-4-hydroxycoumarin was suspended in 25 ml of anhydrous pyridine, and the mixture was heated at 95° for 4 hr. The solution, which resulted shortly on warming, gradually deposited solids. After cooling to 20°, the mixture was suction filtered and the product was washed with cold methanol. The yield was 4.3 g (85.7%). Recrystallization from methanol (40 ml) provided 1.9 g (37.8%); single spot TLC on silica gel, R_f 0.45 [chloroform–methanol (9:1 v/v)].

3-Hydroxy-1-(4-hydroxy-2-oxo-2*H*-1-benzopyran-3-yl)pyridinium Hydroxide Inner Salt (I*g*)—A finely ground mixture of 1.2 g (0.005 mole) of 3-bromo-4-hydroxycoumarin and 0.95 g (0.01 mole) of 3-hydroxypyridine was heated in an oil bath at 135° for 2 hr. A clear melt was obtained at 95°. The liquid solidified on cooling and was then washed with cold ethanol; 0.8 g (63%) of betaine was isolated. Recrystallization of 0.5 g twice from 30–35 ml of dimethylformamide provided 0.3 g; single spot TLC on silica gel, R_f 0.44 [chloroform–methanol (9:1 v/v)].

REFERENCES

(1) L. Jurd, A. D. King, Jr., and K. Mihara, *Experientia*, **26**, 1281(1970).

(2) T. Toda, T. Tokunaga, T. Ouchida, K. Shiroya, and T. Nakamoto, *Chemotherapy (Tokyo)*, **6**, 91(1958).

(3) K. S. R. Krishna Mohan Rao and N. V. Subba Rao, *Indian J. Chem.*, **3**, 522(1965); *Proc. Indian Acad. Sci., Sect. A*, **67**, 42(1968).

(4) J. S. McIntyre, Jr., and A. R. Knight, U.S. pats. 3,509,177, 3,511,856, and 3,511,892 (1970).

(5) M. J. Karten, S. L. Shapiro, E. S. Isaacs, and L. Freedman, *J. Org. Chem.*, **30**, 2657(1965).

(6) C. F. Huebner and K. P. Link, *J. Amer. Chem. Soc.*, **67**, 99(1945).

(7) J. H. Conkey and J. A. Carlson, "Relative Toxicity of Biostatic Agents Suggested for Use in the Pulp and Paper Industry," Biological Control Committee of the American Paper and Pulp Association, New York, N.Y., 1963.

(8) J. D. Tiner, *Amer. J. Vet. Res.*, **26**, 1204(1965).

(9) E. C. McManus, W. C. Campbell, and A. C. Cuckler, *J. Parasitol.*, **59**, 1190(1968).

(10) G. Büchi, D. H. Klaubert, R. C. Shank, S. M. Weinreb, and G. N. Wogan, *J. Org. Chem.*, **36**, 1143(1971).

ACKNOWLEDGMENTS AND ADDRESSES

Received May 1, 1975, from the *Merck Sharp and Dohme Research Laboratories, Rahway, NJ 07065*

Accepted for publication July 2, 1975.

The authors thank Dr. A. W. Douglas for the IR data and interpretation and R. Boos for microanalyses.

[x] To whom inquiries should be directed.

Antimalarials V: Aminobenzothiazoles

EDWARD R. ATKINSON [x] and FELIX E. GRANCHELLI

Abstract □ Four mono- and dialkylated 4-aminobenzothiazoles (VII–X) were prepared as analogs of potent causal prophylactic drugs in the 8-aminoquinoline series. Compounds VII and VIII were toxic at 80 mg/kg in the chick; IX was inactive at 640 mg/kg. In a sporozoite-induced mouse test system, X was inactive at 30 mg/kg and toxic at 480 mg/kg. None of the compounds was active as a suppressive drug.

Keyphrases □ 4-Aminobenzothiazoles, mono- and dialkylated—synthesis, antimalarial activity screened □ Antimalarial agents, potential—mono- and dialkylated 4-aminobenzothiazoles screened □ Structure–activity relationships—mono- and dialkylated 4-aminobenzothiazoles, antimalarial activity

The history of the development of causal prophylactic antimalarials in the 6- and 8-aminoquinoline series, such as I and II, is well known; convenient summaries are available (1, 2). More recently developed additions to the series (III) are among its more potent members (3, 4).

The pharmacological analogy between quinolines and benzothiazoles was drawn first by Bogert and Abrahamson (5), who prepared 2-phenylbenzothiazole-6-carboxylic acid as an analog of cinchophen. Benzothiazole amino alcohols, having the side chain at the 6-position, were later found not to be curative

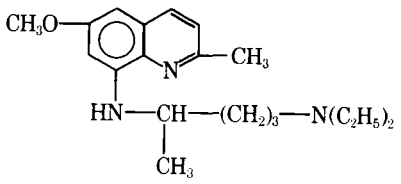

I

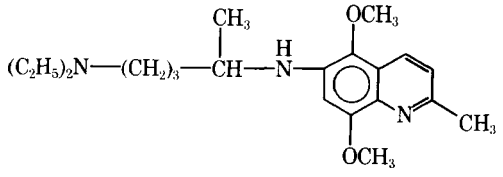

II

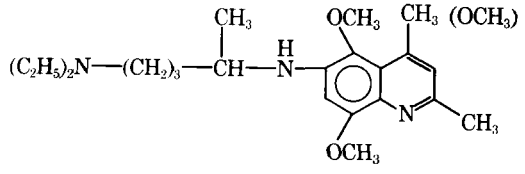

III

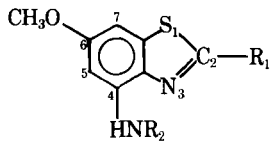

IV: $R_1 = CH_3$, $R_2 = (CH_2)_3N(C_2H_5)_2$

V: $R_1 = H$, $R_2 = NH(CH_2)_2N(C_2H_5)_2$

VI: $R_1 = CH_3$, $R_2 = NH(CH_2)_6N(C_2H_5)_2$

and to be highly toxic in mice at 160–640 mg/kg (6). A few other inactive benzothiazoles derived from 2-amino- or 2-mercaptobenzothiazole were reported (7). Compound IV was reported to be inactive (test system unreported) (8) and V was synthesized but not evaluated (9). Compound VI was found to be inactive (10) in the test system then in vogue (7).

Benzothiazoloquinones, as analogs of quinolinequinones, have been found to have effective prophylactic activity against *Plasmodium gallinaceum* in the chick (11).

The purposes of the present work were to prepare additional members of the 4-aminobenzothiazole series and to determine their prophylactic activity in a standard animal test system.

DISCUSSION

A general literature procedure (9) was used for the sequence 4-methoxy-2-nitroaniline → 1-chloro-6-methoxy-4-nitrobenzodithiazole (55%) → 1-hydroxy-6-methoxy-4-nitrobenzodithiazole (21%, but not isolated in most runs) → 6-methoxy-2-methyl-4-nitrobenzothiazole (43% overall from 1-chloro precursor) → 4-amino-6-methoxy-2-methylbenzothiazole (57%). The amine was alkylated by 3-dimethylaminopropyl chloride to give 4-(3-dimethylaminopropyl)amino-6-methoxy-2-methylbenzothiazole (VII·2HCl·H_2O, 24%).

The alkylation of 4-amino-6-methoxy-2-methylbenzothiazole by 2-bromo-5-diethylaminopentane (12) to VIII gave an unacceptable poor yield. An alternative procedure, recently used for the analogous alkylation of 1,4-dimethoxy-2-naphthylamine (13), involved the condensation of the amine with 5-diethylamino-2,2-dimethoxypentane followed by reduction of the intermediate anil by sodium borohydride. 4-(4-Diethylamino-2-methylbutyl)amino-6-methoxy-2-methylbenzothiazole (VIII·HCl·H_2O) was obtained in 21% yield.

The precursor for both IX and X was prepared from 1-hydroxy-6-methoxy-4-nitrobenzodithiazole (an intermediate in the 2-methyl series described previously) by the sequence 2-mercapto-4-methoxy-6-nitroaniline (9) (65%) → 2-(4-chlorophenyl)-6-methoxy-4-nitrobenzothiazole (85%) → 4-amino-2-(4-chlorophenyl)-6-methoxybenzothiazole (71%). Alkylation of the amine by 3-dimethylaminopropyl chloride gave 2-(4-chlorophenyl)-4-(3-dimethyl-

ACKNOWLEDGMENTS AND ADDRESSES

Received May 1, 1975, from the *Merck Sharp and Dohme Research Laboratories, Rahway, NJ 07065*

Accepted for publication July 2, 1975.

The authors thank Dr. A. W. Douglas for the IR data and interpretation and R. Boos for microanalyses.

[x] To whom inquiries should be directed.

Antimalarials V: Aminobenzothiazoles

EDWARD R. ATKINSON [x] and FELIX E. GRANCHELLI

Abstract □ Four mono- and dialkylated 4-aminobenzothiazoles (VII–X) were prepared as analogs of potent causal prophylactic drugs in the 8-aminoquinoline series. Compounds VII and VIII were toxic at 80 mg/kg in the chick; IX was inactive at 640 mg/kg. In a sporozoite-induced mouse test system, X was inactive at 30 mg/kg and toxic at 480 mg/kg. None of the compounds was active as a suppressive drug.

Keyphrases □ 4-Aminobenzothiazoles, mono- and dialkylated—synthesis, antimalarial activity screened □ Antimalarial agents, potential—mono- and dialkylated 4-aminobenzothiazoles screened □ Structure–activity relationships—mono- and dialkylated 4-aminobenzothiazoles, antimalarial activity

The history of the development of causal prophylactic antimalarials in the 6- and 8-aminoquinoline series, such as I and II, is well known; convenient summaries are available (1, 2). More recently developed additions to the series (III) are among its more potent members (3, 4).

The pharmacological analogy between quinolines and benzothiazoles was drawn first by Bogert and Abrahamson (5), who prepared 2-phenylbenzothiazole-6-carboxylic acid as an analog of cinchophen. Benzothiazole amino alcohols, having the side chain at the 6-position, were later found not to be curative

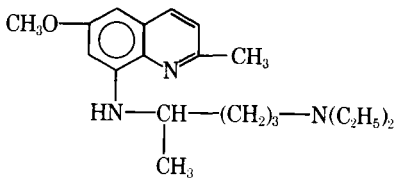

I

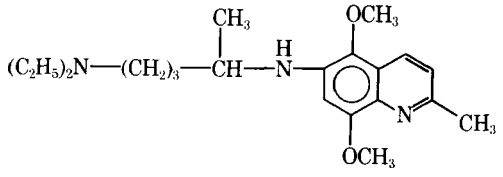

II

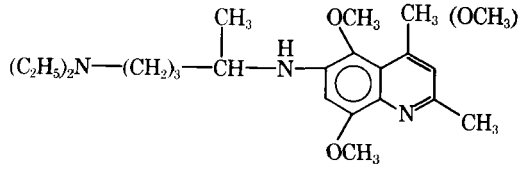

III

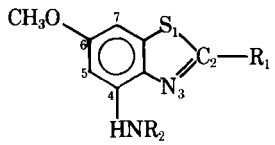

IV: $R_1 = CH_3$, $R_2 = (CH_2)_3N(C_2H_5)_2$

V: $R_1 = H$, $R_2 = NH(CH_2)_2N(C_2H_5)_2$

VI: $R_1 = CH_3$, $R_2 = NH(CH_2)_6N(C_2H_5)_2$

and to be highly toxic in mice at 160–640 mg/kg (6). A few other inactive benzothiazoles derived from 2-amino- or 2-mercaptobenzothiazole were reported (7). Compound IV was reported to be inactive (test system unreported) (8) and V was synthesized but not evaluated (9). Compound VI was found to be inactive (10) in the test system then in vogue (7).

Benzothiazoloquinones, as analogs of quinolinequinones, have been found to have effective prophylactic activity against *Plasmodium gallinaceum* in the chick (11).

The purposes of the present work were to prepare additional members of the 4-aminobenzothiazole series and to determine their prophylactic activity in a standard animal test system.

DISCUSSION

A general literature procedure (9) was used for the sequence 4-methoxy-2-nitroaniline → 1-chloro-6-methoxy-4-nitrobenzodithiazole (55%) → 1-hydroxy-6-methoxy-4-nitrobenzodithiazole (21%, but not isolated in most runs) → 6-methoxy-2-methyl-4-nitrobenzothiazole (43% overall from 1-chloro precursor) → 4-amino-6-methoxy-2-methylbenzothiazole (57%). The amine was alkylated by 3-dimethylaminopropyl chloride to give 4-(3-dimethylaminopropyl)amino-6-methoxy-2-methylbenzothiazole (VII·2HCl·H_2O, 24%).

The alkylation of 4-amino-6-methoxy-2-methylbenzothiazole by 2-bromo-5-diethylaminopentane (12) to VIII gave an unacceptable poor yield. An alternative procedure, recently used for the analogous alkylation of 1,4-dimethoxy-2-naphthylamine (13), involved the condensation of the amine with 5-diethylamino-2,2-dimethoxypentane followed by reduction of the intermediate anil by sodium borohydride. 4-(4-Diethylamino-2-methylbutyl)amino-6-methoxy-2-methylbenzothiazole (VIII·HCl·H_2O) was obtained in 21% yield.

The precursor for both IX and X was prepared from 1-hydroxy-6-methoxy-4-nitrobenzodithiazole (an intermediate in the 2-methyl series described previously) by the sequence 2-mercapto-4-methoxy-6-nitroaniline (9) (65%) → 2-(4-chlorophenyl)-6-methoxy-4-nitrobenzothiazole (85%) → 4-amino-2-(4-chlorophenyl)-6-methoxybenzothiazole (71%). Alkylation of the amine by 3-dimethylaminopropyl chloride gave 2-(4-chlorophenyl)-4-(3-dimethyl-

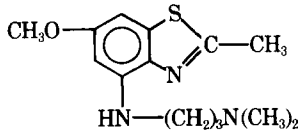

VII

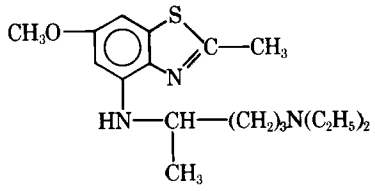

VIII

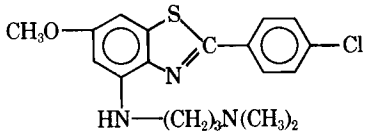

IX

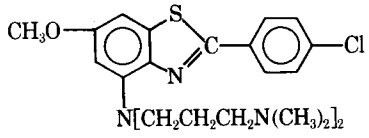

X

aminopropyl)amino-6-methoxybenzothiazole (IX, 50%). When an excess of alkylating agent was used, 4-[bis(3-dimethylaminopropyl)amino]-2-(4-chlorophenyl)-6-methoxybenzothiazole (X, 73%) was obtained.

Attempts to prepare an analog of VIII in the 2-(4-chlorophenyl) series failed when the reductive alkylation of the amine precursor could not be achieved as in the synthesis of VIII.

Compounds VII–X were examined in tests[1] designed to detect true causal prophylactic drugs (those that affect primary exoerythrocytic parasites). Against *P. gallinaceum* in a sporozoite-induced chick test (14), both VII and VIII caused toxic deaths at or above 80 mg/kg; IX caused no increase in mean survival time at 640 mg/kg, the highest dose tested. Compound X was examined in a sporozoite-induced mouse test system against *P. berghei yoelii* (15); it was inactive at 30 mg/kg and caused toxic deaths at 480 mg/kg. Primaquine prevents parasitemia at 30 mg/kg in this test.

Compounds VII, IX, and X were also tested for suppressive antimalarial activity in mice (16) and were found to be inactive at 640 mg/kg. The 4-amino precursors of VII and IX were also inactive in this test.

EXPERIMENTAL[2]

4-(3-Dimethylaminopropyl)amino-6-methoxy-2-methylbenzothiazole Dihydrochloride Monohydrate (VII·2HCl·H_2O)—A mixture of 5.6 g (0.0288 mole) of 3-dimethylaminopropyl chloride hydrochloride[3] and 30 ml of absolute ethyl alcohol was refluxed for 3 days, an alkylation procedure used successfully in the quinoline series (2). The mixture was allowed to stand at room temperature until separation of the hydrochloride salt of unreacted aminobenzothiazole stopped; 3.5 g was recovered. The filtrate then was diluted with 200 ml of water and extracted with ether to remove a small additional amount of unreacted amine.

The aqueous phase was made basic by addition of excess solid potassium carbonate and then extracted with ether. The ether extract was washed with saturated aqueous sodium chloride until neutral, dried over sodium sulfate, and evaporated to dryness to give 2.2 g of a green oil. Bulb-to-bulb distillation at 175–180°/0.01 mm gave 1.9 g (24%) of an almost colorless oil, which was converted in the usual way to a colorless dihydrochloride salt, mp 188–195° dec. (sealed capillary).

Anal.—Calc. for $C_{14}H_{21}N_3OS·2HCl·H_2O$: C, 45.41; H, 6.80; Cl, 19.15; N, 11.35. Found: C, 45.64; H, 6.29; Cl, 19.43; N, 11.33.

The hydrate character was assigned on the basis of the analysis and the NMR spectrum.

4-(4-Diethylamino-1-methylbutyl)amino-6-methoxy-2-methylbenzothiazole Dihydrochloride Monohydrate (VIII·2HCl·H_2O)—The general procedure was that described previously (13) for the alkylation of 1,4-dimethoxy-2-naphthylamine.

A mixture of 3 g (0.0155 mole) of 4-amino-6-methoxy-2-methylbenzothiazole, 3.55 g (0.0175 mole) of 5-diethylamino-2,2-dimethoxypentane, and 175 mg of *p*-toluenesulfonic acid was heated under nitrogen to 140° and held at that temperature for 24 hr. The methyl alcohol that formed during the reaction was collected and not allowed to return to the reaction mixture.

The dark-red viscous oil was dissolved in ether. The solution was washed with saturated aqueous sodium carbonate, dried over potassium carbonate, and evaporated to give 4.85 g (93%) of crude anil, whose spectrum showed strong absorption at 1665 cm^{-1}.

A solution of 1.45 g (0.037 mole) of sodium borohydride in 40 ml of absolute ethyl alcohol was added in one lot to a stirred solution of the crude anil in 100 ml of absolute ethyl alcohol at 0°. Stirring was continued under nitrogen for 24 hr at room temperature. The solution then was poured into 500 ml of water, and the mixture was extracted with ether. The extract was washed with saturated aqueous sodium chloride, dried over potassium carbonate, and evaporated to give 4.55 g of an oil. Distillation of the oil in a bulb-to-bulb apparatus gave a forecut of unalkylated aminobenzothiazole followed by 1.1 g of crude VII (base), bp 165–175°/0.01 mm, whose spectrum showed no absorption at 1665 cm^{-1}. However, NMR and elemental analyses clearly showed that a significant amount of unalkylated aminobenzothiazole still remained.

The crude oil was dissolved in chloroform–benzene (1:1), and the solution was passed through a 2 × 25-cm magnesium silicate[4] column, on which the unalkylated amine was not absorbed significantly. Elution of the column with the solvent mixture containing 5–10% methyl alcohol gave an oil; this oil was converted in the usual way to a hygroscopic dihydrochloride salt (VIII·2HCl·H_2O), mp 110° dec. (shrinks at 84°).

Anal.—Calc. for $C_{18}H_{29}N_3OS·2HCl·H_2O$: C, 50.69; H, 7.79; Cl, 16.63: N, 9.85; S, 7.52. Found: C, 50.64; H, 7.73; Cl, 16.53; N, 9.79; S, 7.67.

The hydrate character was assigned on the basis of the analysis and the NMR spectrum.

2-(4-Chlorophenyl)-6-methoxy-4-nitrobenzothiazole—The procedure was based on earlier preparations of 2-phenylbenzothiazoles (17, 18).

A mixture of 21 g (0.12 mole) of *p*-chlorobenzoyl chloride and 70 ml of *N,N*-dimethylaniline was purged with nitrogen, and then 14 g (0.07 mole) of freshly prepared 2-mercapto-4-methoxy-6-nitroaniline (9) was stirred in rapidly. The mixture warmed spontaneously to 50° and became very stiff. The temperature was then raised during 2 hr to 190° and held there for an additional hour; when the mixture was held at this temperature for longer times or when it was heated to reflux, yields were inferior.

The mixture was cooled and then stirred for 30 min with a mixture of 525 ml of 6 *N* HCl and 525 ml of chloroform. The aqueous phase was additionally extracted with chloroform. The combined chloroform phases were washed with 6 *N* HCl, water, aqueous sodium bicarbonate, saturated aqueous sodium chloride, and water. After drying over magnesium sulfate, they were evaporated under vacuum. The residual pasty solid was triturated with alcohol and filtered to give 19.1 g (85%), mp 167–171°. A sample for analysis, mp 170–171°, was obtained by recrystallization from ethyl alcohol–dimethoxyethane.

Anal.—Calc. for $C_{14}H_9ClN_2O_3S$: C, 52.43; H, 2.83; Cl, 11.05; N, 8.73. Found: C, 52.52; H, 2.88; Cl, 10.93; N, 8.68.

4-Amino-2-(4-chlorophenyl)-6-methoxybenzothiazole—A mixture of 20 g (0.061 mole) of the nitro compound, 70 g (0.31 mole) of stannous chloride dihydrate, 350 ml of 12 *N* HCl, and 5 g

[1] Test results were obtained by the Rane Laboratory, Miami, Fla., and by the Illinois Institute of Technology, Chicago, Ill., and were provided by the Walter Reed Army Institute of Research.

[2] Melting points were obtained in capillaries and are uncorrected. Elemental analyses were performed by Galbraith Laboratories, Inc., and by the late Dr. S. M. Nagy (Belmont, Mass.). Satisfactory IR and NMR spectra were recorded for all new compounds and for all important intermediates.

[3] Aldrich.

[4] Florisil.

of tin (30 mesh) was stirred at 70–90° and diluted with about 850 ml of acetic acid until the nitro compound dissolved. Heating at 90–95° was continued for 4 hr, and the mixture was allowed to cool overnight. A tin complex (18 g, mp 195°) separated. It was stirred with 20% NaOH for several hours, washed with water until neutral, and dried to give 12.5 g (71%), mp 160–164°. A sample for analysis, mp 169–174°, was obtained by recrystallization from acetic acid.

Anal.—Calc. for $C_{14}H_{11}ClN_2OS$: C, 57.83; H, 3.81; Cl, 12.19; N, 9.63; S, 11.03. Found: C, 57.69; H, 3.69; Cl, 12.26; N, 9.60; S, 11.10.

2-(4-Chlorophenyl)-4- (3-dimethylaminopropyl)amino -6-methoxybenzothiazole (IX)—A mixture of 2.32 g (0.008 mole) of 4-amino-2-(4-chlorophenyl)-6-methoxybenzothiazole, 0.34 g (0.008 mole) of sodium hydride (as a 57% suspension in mineral oil[5]), 1.0 g (0.008 mole) of 3-dimethylaminopropyl chloride, and 100 ml of dry toluene was stirred under nitrogen at 110–120° for 64 hr. The mixture was cooled to 0°, and 5 ml of water was added dropwise. The small aqueous layer was separated and extracted with toluene. The combined toluene solutions were dried over magnesium sulfate and taken to dryness under vacuum to give 2.9 g of a brown pasty solid. A thin-layer chromatogram [silica, benzene–hexane–methanol (5:3:2)] showed that a significant amount of unalkylated amine was present.

From a number of alternative purification procedures examined with the products or previous runs, the following was chosen. The solid was extracted with 60 ml of boiling hexane, and a small amount of insoluble gum was discarded. The hexane solution was cooled to 0° and deposited 1.5 g (50%) of yellow crystals, mp 93–96°. Recrystallization from boiling hexane gave a good recovery of material, mp 97–100°.

Anal.—Calc. for $C_{19}H_{22}ClN_3OS$: C, 60.71; H, 5.89; Cl, 9.43; N, 11.18; S, 8.53. Found: C, 60.68; H, 6.17; Cl, 9.16; N, 11.05; S, 8.28.

Unsuccessful alkylation reactions were attempted in refluxing ethyl alcohol, dimethylformamide at 70°, and diethylene glycol at 175°, in which reaction times of 3–4 days were used.

4-[Bis(3-dimethylaminopropyl)amino]-2-(4-chlorophenyl)-6-methoxybenzothiazole (X)—A solution of 4.35 g (0.036 mole) of 3-dimethylaminopropyl chloride in 20 ml of dry toluene was added dropwise to a stirred mixture of 2.63 g (0.009 mole) of 4-amino-2-(4-chlorophenyl)-6-methoxybenzothiazole, 1.65 g (0.039 mole) of sodium hydride (as a 57% dispersion in mineral oil[5], and 150 ml of dry toluene. Additional dry toluene was added to bring the mixture to a total volume of 250 ml, and the mixture was refluxed for 54 hr. When TLC showed that much unalkylated material remained, an additional 1.6 g of sodium hydride, 4.3 g of 3-dimethylaminopropyl chloride, and 20 ml of toluene were added.

After an additional 24-hr reaction time, unalkylated material was no longer present. The reaction mixture was treated with 40 ml of water, and the aqueous phase was extracted with toluene. The combined toluene phases were dried over magnesium sulfate and taken to dryness under vacuum. The pasty residue was triturated with cold petroleum ether, and the filterable solid (mp 85–89°; 3 g, 73%) was recrystallized from boiling hexane to give yellow needles, mp 89–90°.

Anal.—Calc. for $C_{24}H_{33}ClN_4OS$: C, 62.52; H, 7.21; Cl, 7.69; N, 12.15; S, 6.95. Found: C, 62.29; H, 7.27; Cl, 7.51; N, 11.88; S, 7.10.

[5] Alfa.

REFERENCES

(1) E. F. Elslager, M. P. Hutt, and L. M. Werbel, *J. Heterocycl. Chem.*, **6**, 99(1969).

(2) P. Nickel, L. Schrimpl, E. Fink, and O. Dann, *Justus Liebigs Ann. Chem.*, **744**, 119(1971).

(3) E. Fink, P. Nickel, and O. Dann, *Arzneim.-Forsch.*, **20**, 1775(1970).

(4) O. Dann, P. Nickel, and E. Fink, German Offen. 1,945,660 (1971).

(5) M. T. Bogert and E. M. Abrahamson, *J. Amer. Chem. Soc.*, **44**, 826(1922).

(6) A. Burger and S. N. Sawhney, *J. Med. Chem.*, **11**, 270(1968).

(7) G. R. Coatney, W. C. Cooper, N. B. Eddy, and J. Greenburg, Public Health Monograph No. 9, U.S. Government Printing Office, Washington, D.C., 1953, Table 106, p. 209.

(8) I. L. Knunyants and Z. V. Benevolenskaya, *J. Gen. Chem.*, **7**, 2471(1937); through *Chem. Abstr.*, **32**, 2119(1938).

(9) H. H. Fox and M. T. Bogert, *J. Amer. Chem. Soc.*, **61**, 2013(1939).

(10) M. L. Mercury, S. M. Vincent, and M. L. Sherrill, *ibid.*, **68**, 1594(1946).

(11) M. D. Friedman, P. L. Stotter, T. H. Porter, and K. Folkers, *J. Med. Chem.*, **16**, 1314(1973).

(12) R. C. Elderfield, W. J. Gensler, F. Brody, J. D. Head, S. C. Dickerman, L. Wiederhold, III, C. B. Kremer, H. A. Hageman, F. J. Kreysa, J. M. Griffing, S. M. Kupchan, B. Newman, and J. T. Maynard, *J. Amer. Chem. Soc.*, **68**, 1579(1946).

(13) D. J. McCaustland, P. L. Chien, C. C. Cheng, J. Novotny, W. L. Schreiner, and F. W. Starks, *J. Med. Chem.*, **16**, 1311(1973).

(14) L. Rane and D. S. Rane, *Proc. Helminthol. Soc. Washington*, **39**, 283(1972).

(15) M. E. King, A. M. Shefner, and M. D. Schneider, *ibid.*, **39**, 288(1972).

(16) T. S. Osdene, P. B. Russell, and L. Rane, *J. Med. Chem.*, **10**, 431(1967).

(17) H. D. Cossey, J. Judd, and F. F. Stephens, *J. Chem. Soc.*, **1965**, 954.

(18) M. P. Lankelma and A. E. Knauf, *J. Amer. Chem. Soc.*, **53**, 309(1931).

ACKNOWLEDGMENTS AND ADDRESSES

Received January 27, 1975, from *Arthur D. Little, Inc., Cambridge, MA 02140*

Accepted for publication July 8, 1975.

This article is Contribution No. 1327 of the Army Research Program on Malaria. The authors thank Dr. Richard E. Strube for helpful suggestions.

[x] To whom inquiries should be directed.

Effect of Polysorbate 80 on Apparent Partition Coefficient of Salicylic Acid and Its Absorption from the Rat Intestine

AHMED H. HIKAL ˣ, LARRY DYER, and SUI-WAI WONG

Abstract □ The effect of polysorbate 80 on the apparent partition coefficient of salicylic acid between chloroform and a 0.05 *M* phosphate buffer at pH 6.5 was investigated. Three different concentrations of the surfactant were studied: 0.001, 0.01, and 2.0% (w/v). Concentrations of polysorbate 80 equal to or above the CMC significantly increased the apparent partition coefficient of salicylic acid. A lower surfactant concentration did not produce a significant change in the apparent partition coefficient of the acid. Polysorbate 80 at the same three concentrations produced no significant change in the percent of salicylic acid absorbed from the rat intestine *in situ* when dissolved in a 0.05 *M* phosphate buffer at pH 6.5. When 2.0% (w/v) polysorbate 80 in the phosphate buffer was left inside the rat intestine for 1 hr, the permeability of the intestine to salicylic acid was not significantly changed.

Keyphrases □ Polysorbate 80—effect on apparent partition coefficient and absorption of salicylic acid, rat intestine □ Salicylic acid—apparent partition coefficient and absorption, rat intestine, effect of polysorbate 80 □ Surfactants—polysorbate 80, effect on apparent partition coefficient and absorption of salicylic acid, rat intestine □ Absorption, intestinal—salicylic acid, effect of polysorbate 80, rats □ Partition coefficient—salicylic acid, effect of polysorbate 80, rats

In recent years, several nonionic surfactants have been incorporated in pharmaceutical formulations to influence drug availability (1). Numerous studies also have dealt with various aspects of the effects of surfactants on drug absorption (2–18). Many observations reported in these studies seem contradictory. The source of this conflict might have been in the particular drug, surface-active agent, biological system, or experimental technique utilized.

To the best of these authors' knowledge, the effect of surfactants on the apparent partition coefficient of drugs has not been documented.

In the present study, an attempt was made to elucidate the effect of a nonionic surfactant (polysorbate 80) on the apparent partition coefficient of salicylic acid and to correlate this effect with the effect on the rate of absorption of salicylic acid from an *in situ* rat intestine. The influence of the surfactant on the permeability of the rat intestine to salicylic acid also was investigated.

EXPERIMENTAL

All chemicals and reagents were used as obtained without further purification.

Determination of Apparent Partition Coefficient—Phosphate buffer solution (0.05 *M*) and chloroform were first saturated, each with the other phase, by shaking[1] at room temperature for 24 hr. Salicylic acid[2], 30, 40, 50, 60, and 70 mg, was accurately weighed and placed in 125-ml glass-stoppered bottles. Forty milliliters of chloroform was added to each bottle, followed by 40 ml of the aqueous phase [0.05 *M* phosphate buffer containing 0.001, 0.01, or 2.0% (w/v) polysorbate 80[3]]. One bottle contained no salicylic acid and served as a blank; another bottle contained only a standard solution of salicylic acid (1 mg/ml) in the aqueous phase.

All bottles were placed on a horizontal shaker[4] and shaken at a speed of approximately 250 rpm for 24 hr. A portion of the aqueous layer (approximately 10 ml) was then transferred to a test tube and centrifuged[5] for 1 hr to break the emulsion formed in the polysorbate 80 solution. One milliliter of the clear aqueous layer was withdrawn for assay.

The concentration of salicylic acid in the chloroform layer was determined by difference, and the apparent partition coefficient was determined by dividing the concentration in chloroform by the concentration in the aqueous layer.

Absorption of Salicylic Acid from Rat Intestine—The technique used to study the absorption of salicylic acid from the rat intestine was similar to that developed by Doluisio *et al.* (19). Male albino rats, 200–450 g, were fasted for at least 24 hr, with water being allowed *ad libitum*. The rats were anesthetized with pentobarbital sodium[6], 50 mg/kg ip. The animals were kept warm during the experiment with an IR lamp.

Details of the cannulation and of the sample withdrawal procedures were reported previously (19). The cannulated intestine was flushed with 400–500 ml of normal saline before the salicylic acid solution was introduced. A 1.0-ml sample of the absorption solution was withdrawn at 10-min intervals for assay. Net water absorption was determined in separate experiments using phenolsulfonphthalein as a marker, and absorption values were corrected accordingly. Six animals were used for each phase of the experiment.

The following solutions were tested:

1. Salicylic acid, 1 mg/ml in a 0.05 *M* phosphate buffer at pH 6.5 (measured before addition of salicylic acid, changed to 6.2 after the acid was added).
2. Salicylic acid, 1 mg/ml in the phosphate buffer containing the following concentrations of polysorbate 80: 0.001, 0.01, and 2.0% (w/v).

Effect of Polysorbate 80 on Intestinal Membrane of Rats—To study the effect of polysorbate 80 on the intestinal membrane of the rat, a solution containing 2.0% (w/v) polysorbate 80 in the 0.05 *M* phosphate buffer was introduced into the cannulated intestine and left for 1 hr. The intestine was then flushed with normal saline, and the absorption of salicylic acid (1 mg/ml) in the phosphate buffer at pH 6.5 was studied as already described.

Treatment of Data—The Student *t* test was used to determine the significance of the differences observed in the apparent partition coefficients. A two-way analysis of variance was used to determine the significance of differences observed in the intestinal absorption data.

Assay of Salicylic Acid—The following procedure was used to determine salicylic acid, both in the partition coefficient experiments and the absorption experiments. One milliliter of the solution to be assayed was diluted with 20 ml of water, and 5.0 ml of Trinder's reagent (20) was added. The absorbance of the resulting solution was then measured at 526 nm[7]. In the intestinal absorption experiments, it was necessary to centrifuge the solutions after adding Trinder's reagent and to use the supernatant liquid for measuring the absorbance.

RESULTS

Table I lists the apparent partition coefficients of salicylic acid

[1] Eberbach shaker, Eberbach Corp., Ann Arbor, Mich.
[2] Fisher Scientific Co., Houston, Tex.
[3] Atlas Chemical Industries, Wilmington, Del.
[4] Shaker bath model 25, Precision Scientific Co., Chicago, Ill.
[5] Clinical centrifuge, International Equipment Co., Boston, Mass.
[6] Nembutal Sodium, Abbott Laboratories, North Chicago, Ill.
[7] Spectronic-20, Bausch and Lomb, Rochester, N.Y.

Table I—Apparent Partition Coefficient of Salicylic Acid in the Presence of Polysorbate 80

Polysorbate 80, % (w/v)	Apparent Partition Coefficient[a] (±SE)
None	0.021 (±0.002)
0.001	0.023 (±0.002)
0.01	0.031 (±0.003)
2.0	0.085 (±0.002)

[a] Chloroform–0.05 *M* phosphate buffer at pH 6.5.

in the 0.05 *M* phosphate buffer. The Student *t* test showed that the increases in the apparent partition coefficient produced by 0.01 and 2.0% (w/v) polysorbate 80 were significant ($p < 0.05$)(t values for $N_1 = N_2 = 5$ were 2.567 and 21.428, respectively); there was no significant change ($p > 0.05$) in the apparent partition coefficient in the presence of 0.001% (w/v) surfactant ($t = 0.670$).

The results of the intestinal absorption studies are given in Table II. A two-way analysis of variance showed that the differences observed in the percent absorbed with and without polysorbate 80 were not significant ($p > 0.05$) [F ratios for $\nu = 1/10$ were 0.920, 0.015, and 0.014 for 0.001, 0.01, and 2.0% (w/v) surfactant, respectively]. Therefore, polysorbate 80 at concentrations below, equal to, or above the critical micelle concentration (CMC) had no significant effect on the percent of salicylic acid absorbed from the rat intestine. Furthermore, a 2.0% (w/v) polysorbate 80 solution in phosphate buffer at pH 6.5, when left in the rat intestine for 1 hr, had no significant effect on the permeability of the intestine to salicylic acid (F ratio = 0.003).

DISCUSSION

The relationship between the apparent partition coefficients of drugs and their rates of diffusion across biological membranes has long been established (21). Drugs diffuse through membranes at rates directly proportional to their lipid–water partition coefficients. Chloroform often has been used to simulate the lipid phase (21).

Surfactants influence the absorption of drugs from solutions through various mechanisms (15). There are possible interactions between the surfactant and drug as well as between the surfactant and biological membrane. Drug–surfactant interactions seem to be related to the lipid solubility of the drug (2–4). Lipid-soluble drugs are more likely to interact with surfactant micelles than are lipid-insoluble drugs. In particular, surfactant concentration, whether it is below or above the CMC, is another determinant of drug–surfactant interactions (11).

Retardation of the absorption of lipid-soluble drugs in the presence of micellar concentrations of surfactants is postulated to be according to the following model (15):

1. A micellar solution consists of two phases, a micellar phase and the surrounding aqueous phase.
2. The partition ratio of drug between the micellar phase and the aqueous phase is constant, independent of drug concentration.
3. Absorption of the drug incorporated in the micelle is negligible.

Since the drug in the micellar phase is unavailable for absorption, the effective concentration of the drug is less than the apparent concentration, and a decreased absorption rate is observed.

Interactions between surfactants and biological membranes are related to the ionic nature of the surfactant (15) and, possibly, to the type of membrane studied. Anionic and cationic surfactants seem to have a greater influence on membrane permeability than do nonionic surfactants.

The current data (Table I) show that polysorbate 80 at concentrations equal to or higher than the CMC significantly increased the apparent partition coefficient of salicylic acid. This finding indicates that a complex is formed between the drug and the surfactant that is more soluble in chloroform than the drug alone. The fact that a surfactant concentration below the CMC did not significantly change the apparent partition coefficient of the drug indicates that the complex formed is most probably micellar in nature. Micellar complexation has been shown to occur between salicylic acid and another nonionic surfactant, polysorbate 60, in 0.1 *N* HCl (8).

Intestinal absorption data (Table II) indicate that concentrations of polysorbate 80 of up to 2.0% (w/v), considerably higher than the CMC of 0.01% (w/v), produced no significant change in the percent absorbed of salicylic acid. It is possible that the complex between polysorbate 80 and salicylic acid under the present experimental conditions is not very stable. A complex may dissociate at such a rate as not to be absorption rate limiting. The intestinal membrane itself also may have contributed to the rapid dissociation of the complex. In one study (22), complex formation between certain drugs (*e.g.*, codeine and aminopyrine) and dyes (*e.g.*, bromthymol blue and eosine B) markedly increased the apparent partition coefficients of the dyes but did not influence their absorption from an everted rat intestine. The intestinal membrane may have had a dissociating effect upon the complexes formed (22).

Another possibility is that micellar complexation did not occur under the present experimental conditions. Salicylic acid has a pKa of 3.0 (23) and would exist mostly in the unionized form in 0.1 *N* HCl. However, it exists mostly as salicylate anions in a buffer system at pH 6.5. It was demonstrated previously (13) that significant micellar complexation occurred between polysorbate 80 and the unionized form of secobarbital but not with the ionized form. However, despite the difference in complexation, the absorption of the ionized and unionized forms of secobarbital was influenced to the same extent by polysorbate 80 (13).

Surfactants also can alter the permeability of biological membranes. This effect seems to vary with the type of surfactant and the type of membrane studied. Polysorbate 80 enhanced the absorption of 4-aminoantipyrine in the goldfish by a direct effect on the biological membrane (14). However, polysorbate 80 had no effect on the permeability of the rat intestine to salicylamide (10). In the present study, when 2.0% (w/v) polysorbate 80 in the phosphate buffer at pH 6.5 was left in the rat intestine for 1 hr, the permeability of the membrane to salicylic acid was not significantly changed. The percent of salicylic acid absorbed in the pretreated intestine was almost the same as that without pretreatment (Table II).

Table II shows that there was a slight reduction in the percent absorbed in the presence of 0.001% (w/v) surfactant and that the animal-to-animal variation was large. The reduction is not statistically significant, and there is no explanation for the apparent large variation.

REFERENCES

(1) S. S. Ashan and S. M. Blaug, *Drug Stand.*, **28**, 95(1960).

(2) S. Riegelman and W. J. Crowell, *J. Amer. Pharm. Ass., Sci. Ed.*, **47**, 115(1958).

Table II—Percent of Salicylic Acid Absorbed over 60 min from the Rat Intestine[a]

Minutes	Polysorbate 80, % (w/v) None	0.001	0.01	2.0	None[b]
10	37.23 (1.20)	31.92 (4.33)	37.25 (1.38)	41.26 (1.44)	35.10 (2.10)
20	57.79 (1.55)	47.67 (7.81)	57.16 (2.31)	58.90 (2.21)	58.48 (3.87)
30	71.77 (1.03)	59.05 (8.62)	72.48 (2.09)	72.70 (1.21)	73.27 (3.20)
40	82.03 (1.03)	68.62 (7.17)	80.45 (2.05)	78.44 (0.79)	81.37 (3.31)
50	87.73 (1.07)	75.44 (5.80)	84.61 (1.87)	83.47 (0.87)	86.10 (1.79)
60	91.91 (0.70)	80.71 (4.28)	87.90 (1.36)	85.90 (0.97)	90.09 (1.34)

[a] Mean of six rats (±SE). [b] After a 2.0% polysorbate 80 solution was left in the intestine for 1 hr.

(3) *Ibid.*, **47**, 123(1958).
(4) *Ibid.*, **47**, 127(1958).
(5) P. M. Lish and J. H. Weikel, Jr., *Toxicol. Appl. Pharmacol.*, **1**, 501(1959).
(6) J. A. Nissim, *Nature*, **187**, 305(1960).
(7) H. Brise, *Acta Med. Scand.*, **376**, 47(1962).
(8) G. Levy and R. H. Reuning, *J. Pharm. Sci.*, **53**, 147(1964).
(9) K. Kakemi, T. Arita, and S. Muranishi, *Chem. Pharm. Bull.*, **13**, 976(1965).
(10) H. Yamada and R. Yamamoto, *ibid.*, **13**, 1279(1965).
(11) G. Levy, K. E. Miller, and R. H. Reuning, *J. Pharm. Sci.*, **55**, 394(1966).
(12) C. W. Whitworth and L. D. Yantis, *ibid.*, **56**, 1661(1967).
(13) G. Levy and J. A. Anello, *ibid.*, **57**, 101(1968).
(14) J. A. Anello and G. Levy, *ibid.*, **58**, 721(1969).
(15) M. Gibaldi and S. Feldman, *ibid.*, **59**, 579(1970).
(16) I. Utsumi, K. Kohno, and Y. Takeuchi, *Chem. Pharm. Bull.*, **21**, 1727(1973).
(17) I. Utsumi, K. Kohno, and Y. Takeuchi, *J. Pharm. Sci.*, **63**, 676(1974).
(18) T. S. Saginella, J. H. Perrin, J. J. Vallner, and P. Bass, *ibid.*, **63**, 790(1974).
(19) J. T. Doluisio, N. F. Billups, L. W. Dittert, E. T. Sugita, and J. V. Swintosky, *ibid.*, **58**, 1196(1969).
(20) P. Trinder, *Biochem. J.*, **57**, 301(1954).
(21) L. S. Schanker, *J. Med. Pharm. Chem.*, **2**, 343(1960).
(22) G. Levy and T. Matsuzawa, *J. Pharm. Sci.*, **54**, 1003(1965).
(23) A. N. Martin, J. Swarbrick, and A. Cammarata, in "Physical Pharmacy," 2nd ed., Lea & Febiger, Philadelphia, Pa., 1969, p. 194.

ACKNOWLEDGMENTS AND ADDRESSES

Received September 6, 1974, from the *College of Pharmacy, University of Houston, Houston, TX 77004*

Accepted for publication July 8, 1975.

Supported in part by a Limited Grant-in-Aid from the Faculty Research Support Program, University of Houston.

The authors thank Dr. James R. Brown, Quantitative Management Sciences, University of Houston, for assistance with the statistical analysis.

[x] To whom inquiries should be directed.

New Compounds: Synthesis of Aliphatic Seleno Amino Acids as Potential Pancreatic Imaging Agents

TSVI SADEH [*], MICHAEL A. DAVIS [‡x], and ROGER W. GIESE [§]

Abstract □ External imaging of the pancreas is made possible by taking advantage of that organ's large requirement for exogenous amino acids. The only successful approach thus far has been the substitution of selenium for the sulfur atom in amino acids naturally containing sulfur, specifically selenomethionine labeled with selenium-75. The synthesis of a class of selenium-containing amino acids has been undertaken where the selenium atom replaces a methylene group of common amino acids that do not contain a sulfur atom. Reported here are the synthesis and toxicological evaluation of one such analog, 3-[(2-aminoethyl)selenyl]alanine (L-4-selenalysine).

Keyphrases □ Seleno amino acids, aliphatic—synthesis of 3-[(2-aminoethyl)selenyl]alanine, potential pancreatic imaging agent, toxicological evaluation □ Amino acids, aliphatic—selenium substituted, synthesis of 3-[(2-aminoethyl)selenyl]alanine, potential pancreatic imaging agent, toxicological evaluation □ Pancreatic imaging agents, potential—3-[(2-aminoethyl)selenyl]alanine synthesized, toxicological evaluation

It is well known that the pancreas has a large requirement for exogenous amino acids. This specific characteristic was the basis for choosing radiolabeled amino acids to detect pancreatic tumors. Hansson (1) demonstrated this feature by using ^{14}C- and ^{35}S-labeled amino acids and proved that these compounds localized in the exocrine portion of the organ.

To obtain gamma-emitting amino acids for external detection and visualization of the pancreas, it was proposed to replace the sulfur atom in sulfur-containing amino acids such as methionine and cysteine. ^{75}Se-Selenomethionine was subsequently synthesized (2) but has achieved only limited clinical utility as a pancreatic imaging agent due to the unfavorable pancreas to liver concentration ratio. Several studies comparing ^{14}C-labeled amino acids showed that methionine has one of the poorest pancreas to liver ratios of all naturally occurring amino acids (3).

DISCUSSION

The sulfur analogs of numerous natural and synthetic amino acids have been synthesized but no attempts have been made to substitute selenium for the hetero sulfur atom. Compounds I–III are prime examples of reported sulfur analogs of common amino acids.

Compound I is a derivative of alanine, 3-[(2-aminoethyl)thio]alanine, but can also be considered as a hetero analog of lysine (4-thialysine). This compound has been shown to be a potent inhibitor of lysine utilization (4). Compound II, 3-methyl-3-(methylthio)alanine, is an isostere of isoleucine (4-thiaisoleucine and 4-thiaalloisoleucine) (5). α-Aminoadipic acid is a lysine precursor, and Compound III, 3-[(carboxymethyl)thio]alanine, can be viewed as a sulfur-containing α-aminoadipic acid (4-thia-α-aminoadipic acid) (6).

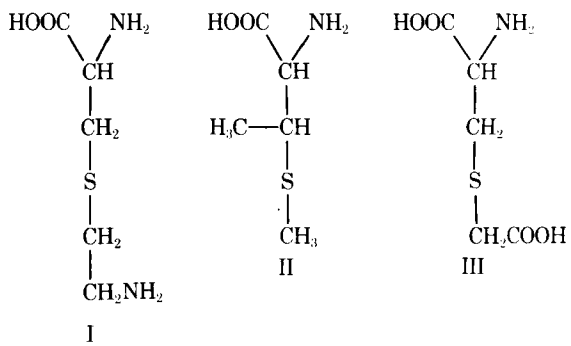

(3) *Ibid.*, **47**, 123(1958).
(4) *Ibid.*, **47**, 127(1958).
(5) P. M. Lish and J. H. Weikel, Jr., *Toxicol. Appl. Pharmacol.*, **1**, 501(1959).
(6) J. A. Nissim, *Nature*, **187**, 305(1960).
(7) H. Brise, *Acta Med. Scand.*, **376**, 47(1962).
(8) G. Levy and R. H. Reuning, *J. Pharm. Sci.*, **53**, 147(1964).
(9) K. Kakemi, T. Arita, and S. Muranishi, *Chem. Pharm. Bull.*, **13**, 976(1965).
(10) H. Yamada and R. Yamamoto, *ibid.*, **13**, 1279(1965).
(11) G. Levy, K. E. Miller, and R. H. Reuning, *J. Pharm. Sci.*, **55**, 394(1966).
(12) C. W. Whitworth and L. D. Yantis, *ibid.*, **56**, 1661(1967).
(13) G. Levy and J. A. Anello, *ibid.*, **57**, 101(1968).
(14) J. A. Anello and G. Levy, *ibid.*, **58**, 721(1969).
(15) M. Gibaldi and S. Feldman, *ibid.*, **59**, 579(1970).
(16) I. Utsumi, K. Kohno, and Y. Takeuchi, *Chem. Pharm. Bull.*, **21**, 1727(1973).
(17) I. Utsumi, K. Kohno, and Y. Takeuchi, *J. Pharm. Sci.*, **63**, 676(1974).
(18) T. S. Saginella, J. H. Perrin, J. J. Vallner, and P. Bass, *ibid.*, **63**, 790(1974).
(19) J. T. Doluisio, N. F. Billups, L. W. Dittert, E. T. Sugita, and J. V. Swintosky, *ibid.*, **58**, 1196(1969).
(20) P. Trinder, *Biochem. J.*, **57**, 301(1954).
(21) L. S. Schanker, *J. Med. Pharm. Chem.*, **2**, 343(1960).
(22) G. Levy and T. Matsuzawa, *J. Pharm. Sci.*, **54**, 1003(1965).
(23) A. N. Martin, J. Swarbrick, and A. Cammarata, in "Physical Pharmacy," 2nd ed., Lea & Febiger, Philadelphia, Pa., 1969, p. 194.

ACKNOWLEDGMENTS AND ADDRESSES

Received September 6, 1974, from the *College of Pharmacy, University of Houston, Houston, TX 77004*

Accepted for publication July 8, 1975.

Supported in part by a Limited Grant-in-Aid from the Faculty Research Support Program, University of Houston.

The authors thank Dr. James R. Brown, Quantitative Management Sciences, University of Houston, for assistance with the statistical analysis.

[x] To whom inquiries should be directed.

New Compounds: Synthesis of Aliphatic Seleno Amino Acids as Potential Pancreatic Imaging Agents

TSVI SADEH [*], MICHAEL A. DAVIS [‡x], and ROGER W. GIESE [§]

Abstract □ External imaging of the pancreas is made possible by taking advantage of that organ's large requirement for exogenous amino acids. The only successful approach thus far has been the substitution of selenium for the sulfur atom in amino acids naturally containing sulfur, specifically selenomethionine labeled with selenium-75. The synthesis of a class of selenium-containing amino acids has been undertaken where the selenium atom replaces a methylene group of common amino acids that do not contain a sulfur atom. Reported here are the synthesis and toxicological evaluation of one such analog, 3-[(2-aminoethyl)selenyl]alanine (L-4-selenalysine).

Keyphrases □ Seleno amino acids, aliphatic—synthesis of 3-[(2-aminoethyl)selenyl]alanine, potential pancreatic imaging agent, toxicological evaluation □ Amino acids, aliphatic—selenium substituted, synthesis of 3-[(2-aminoethyl)selenyl]alanine, potential pancreatic imaging agent, toxicological evaluation □ Pancreatic imaging agents, potential—3-[(2-aminoethyl)selenyl]alanine synthesized, toxicological evaluation

It is well known that the pancreas has a large requirement for exogenous amino acids. This specific characteristic was the basis for choosing radiolabeled amino acids to detect pancreatic tumors. Hansson (1) demonstrated this feature by using ^{14}C- and ^{35}S-labeled amino acids and proved that these compounds localized in the exocrine portion of the organ.

To obtain gamma-emitting amino acids for external detection and visualization of the pancreas, it was proposed to replace the sulfur atom in sulfur-containing amino acids such as methionine and cysteine. ^{75}Se-Selenomethionine was subsequently synthesized (2) but has achieved only limited clinical utility as a pancreatic imaging agent due to the unfavorable pancreas to liver concentration ratio. Several studies comparing ^{14}C-labeled amino acids showed that methionine has one of the poorest pancreas to liver ratios of all naturally occurring amino acids (3).

DISCUSSION

The sulfur analogs of numerous natural and synthetic amino acids have been synthesized but no attempts have been made to substitute selenium for the hetero sulfur atom. Compounds I–III are prime examples of reported sulfur analogs of common amino acids.

Compound I is a derivative of alanine, 3-[(2-aminoethyl)thio]alanine, but can also be considered as a hetero analog of lysine (4-thialysine). This compound has been shown to be a potent inhibitor of lysine utilization (4). Compound II, 3-methyl-3-(methylthio)alanine, is an isostere of isoleucine (4-thiaisoleucine and 4-thiaalloisoleucine) (5). α-Aminoadipic acid is a lysine precursor, and Compound III, 3-[(carboxymethyl)thio]alanine, can be viewed as a sulfur-containing α-aminoadipic acid (4-thia-α-aminoadipic acid) (6).

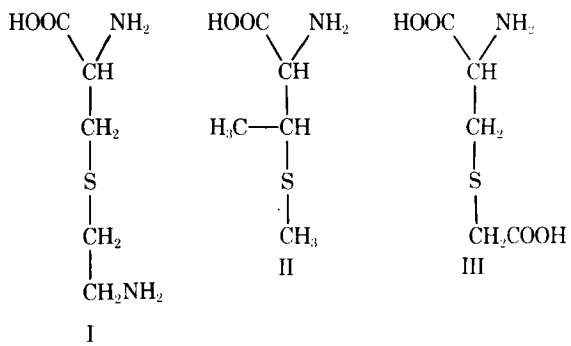

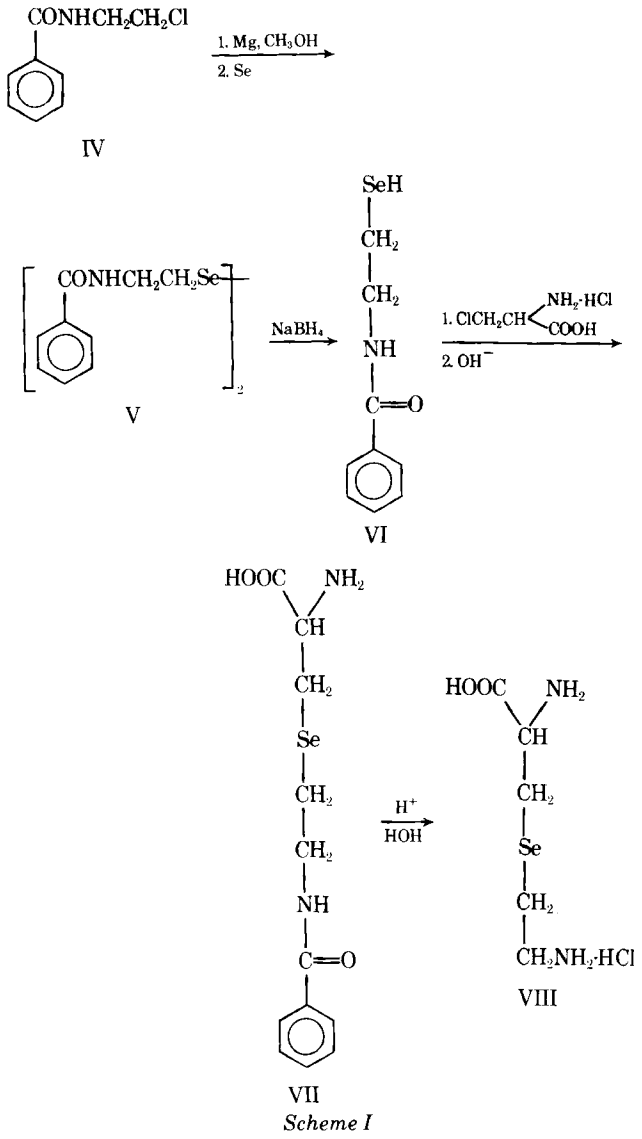

Scheme I

Interest in obtaining an improved agent for external visualization of the pancreas has led to an extensive synthetic program involving selenium-containing amino acids. This first report describes the successful synthesis and toxicological evaluation of 3-[(2-aminoethyl)selenyl]alanine (L-4-selenalysine), the selenium analog of I.

Chemistry—Reaction of benzoyl chloride with ethyleneimine gave *N*-(2-chloroethyl)benzamide (IV) in 75% yield (7). Refluxing IV with a solution of dimethoxydimagnesium diselenide (8) afforded bis[(2-aminoethyl)-*N*-benzoyl] diselenide (V) in 88% yield (9). Reduction of V with sodium borohydride or sodium amalgam gave (2-aminoethyl)-*N*-benzoylselenol (VI) which, upon subsequent treatment with L-3-chloroalanine (10), formed the sparingly soluble 3-[(2-aminoethyl)selenyl]-*N*-benzoylalanine (VII), also called ϵ-*N*-benzoyl-4-selenalysine.

Hydrolysis of VII with dilute hydrochloric acid led to the formation of the desired 3-[(2-aminoethyl)selenyl]alanine (L-4-selenalysine) (VIII), which was isolated as the monohydrochloride (overall yield 53%) (Scheme I). The analogous sulfur-containing compound (I) is well known (11).

Toxicology—Acute toxicity studies were carried out in Ness Ziona strain albino mice (20 ± 2 g). The LD_{50} for three different routes of administration, subcutaneous, intraperitoneal, and intravenous, was determined to be 130, 110, and 95 mg/kg, respectively. No physiological or behavioral changes were noted when sublethal doses were given.

Following the administration of lethal quantities, increased body activity accompanied by tremors, twitching, and labored breathing was readily apparent. Lethality was not immediate, however, but took place from 2 to 24 hr postadministration. When a dose four times the LD_{50} was given, death occurred within minutes. The relative lack of toxicity of selenalysine was an interesting finding since it had been shown that selenomethionine has an LD_{50} (intraperitoneal administration) of 4.25 mg/kg (12).

EXPERIMENTAL

Melting points[1] were determined for all of the solid compounds isolated, and elemental analyses[2] were performed for VII and VIII. Precoated silica gel plates[3] were used for TLC with the following solvent systems: A, 1-butanol–acetic acid–water (4:1:1); B, 96% ethanol–34% ammonium hydroxide (7:3); and C, methanol–isopropanol–34% ammonium hydroxide (5:3:2).

Plastic-backed TLC plates were found to have superior flow characteristics and higher resolving power compared to aluminum-backed plates, and all R_f values reported are for the plastic-backed plates. All synthetic reactions with selenium-containing compounds were performed in a hood because there is the possibility of hydrogen selenide release in several reactions.

Bis[(2-aminoethyl)-*N*-benzoyl]diselenide (V)—Compound IV (19.5 g), dissolved in methanol, was added to a methanolic solution of dimethoxydimagnesium diselenide (8 g of selenium) under gentle reflux. Refluxing was continued until the development of the typical golden-yellow color of organic diselenides was complete. The solution was then cooled, poured into cold water, and filtered. The precipitate was washed repeatedly with 10% HCl followed by a final rinse with cold water. This solid was crystallized from hot 96% ethanol, giving 20 g (88%), mp 144–145° [lit. (9) mp 144–145°].

(2-Aminoethyl)-*N*-benzoylselenol (VI, Not Isolated)—Compound V (22 g) was dissolved in 200 ml of ethanol and reduced with 5% sodium amalgam (100 g) or sodium borohydride (1.5 g) until the indicative diselenide color was discharged. Compound VI was not isolated but rather reacted immediately with chloroalanine to produce VII.

3-[(2-Aminoethyl)selenyl]-*N*-benzoylalanine (VII)—L-3-Chloroalanine hydrochloride (16 g) in aqueous solution was carefully neutralized with 10% NaOH and added to the solution of VI, which was kept at 35°. The stirred mixture was kept at pH 10 by the addition of 10% NaOH as required. A few crystals of sodium borohydride were added from time to time to prevent selenol oxidation.

After stirring at 35° for 3 hr, the solution was filtered, extracted with chloroform, brought to pH 6.5 with dilute acid, and left to crystallize. The material was purified by dissolution in the minimal volume of 10% HCl followed by filtration and reprecipitation by pH adjustment to 6.5 with ammonium hydroxide. The compound was recrystallized from boiling water, yielding 24.6 g (80%), mp 184°.

Anal.—Calc. for $C_{12}H_{16}N_2O_3Se$: C, 45.8; H, 5.1; N, 8.9; Se, 25.1. Found: C, 45.7; H, 5.2; N, 9.3; Se, 24.8.

3-[(2-Aminoethyl)selenyl]alanine (L-4-Selenalysine) (VIII)—Hydrolysis of VII was accomplished by refluxing in a 20-fold excess of 6 *N* HCl until a clear solution resulted (~3 hr). Upon cooling, benzoic acid crystallized out and was removed by filtration followed by an ether extraction of the filtrate. The aqueous phase was brought to pH 7 with ammonium hydroxide, whereupon any nonhydrolyzed starting material (VII) precipitated and was filtered off and recycled.

The filtrate was taken to dryness under vacuum, dissolved in a minimum volume of water, and refiltered. Absolute ethanol was added dropwise to the filtrate until the first sign of incipient turbidity appeared. The solution was then placed in the cold and allowed to crystallize upon standing (quantitative yield). Crystals of L-4-selenalysine monohydrochloride were obtained (small, colorless needles), mp 206°; TLC: one spot, R_f 0.78 (Solvent System B), R_f 0.76 (Solvent System C).

Anal.—Calc. for $C_5H_{13}ClN_2O_2Se$: C, 24.3; H, 5.3; Cl, 14.4; N, 11.3; Se, 31.9. Found: C, 24.4; H, 5.5; Cl, 14.4; N, 11.5; Se, 31.8.

[1] Gallenkamp capillary melting-point apparatus (uncorrected).

[2] Performed by Microanalytical Laboratory, Hebrew University, Jerusalem, Israel, and the Alfred Bernhardt Micro-Analytisches Laboratorium, Elback, German Federal Republic.

[3] C. Schleicher and Schull FR 1500 kieselgel.

Chromatography—L-3-Chloroalanine, because of its lability, must be applied to the TLC chromatogram as a fresh aqueous solution of the hydrochloride (1%) and dried immediately with a stream of warm air. The chromatogram was developed with Solvent System A, and the location of material was visualized by spraying with 1% ninhydrin in 1-butanol followed by heating at 80° until the pink spot of chloroalanine was clearly visible (about 7 min); R_f 0.31.

Comparative chromatography of L-lysine and the two isosteres, L-4-thialysine (I) and L-4-selenalysine (VIII) was carried out with their hydrochlorides. The highly polar nature of these amino acid hydrochlorides requires equally polar solvents for chromatographic separation, and Solvent Systems B and C were found to be satisfactory. The values for the hydrochloride of L-lysine, L-4-thialysine, and L-4-selenalysine were R_f 0.47, 0.75, and 0.78 in Solvent System B and R_f 0.37, 0.75, and 0.76 in Solvent System C, respectively. These results show the greater polarity of L-lysine compared to its sulfur and selenium analogs as well as the close similarity between the two hetero analogs.

REFERENCES

(1) E. Hansson, *Acta Physiol. Scand. Suppl.*, **1959**, 161.

(2) M. Blau and M. A. Bender, *Biochim. Biophys. Acta*, **49**, 389(1961).

(3) D. M. Taylor and M. F. Cottrall, "Radiopharmaceuticals and Labeled Compounds," vol. 1, IAEA, Vienna, Austria, 1973, p. 433.

(4) T. Shiota, J. E. Folk, and F. Tietze, *Arch. Biochem. Biophys.*, **77**, 373(1958).

(5) T. J. McCord, D. H. Cook, D. L. Tharp, and A. L. Davis, *J. Med. Chem.*, **8**, 290(1965).

(6) M. D. Armstrong and J. D. Lewis, *J. Org. Chem.*, **16**, 749(1951); M. D. Armstrong and J. D. Lewis, *J. Biol. Chem.*, **189**, 461(1951).

(7) H. Bestian, *Justus Liebigs Ann. Chem.*, **566**, 210(1950).

(8) W. H. H. Gunther, *J. Org. Chem.*, **32**, 3929(1967).

(9) W. H. H. Gunther and H. G. Mautner, *J. Amer. Chem. Soc.*, **82**, 2762(1960).

(10) E. Fischer and K. Raske, *Chem. Ber.*, **40**, 3717(1907).

(11) H. Lindley, *Nature*, **178**, 647(1956); H. Lindley, *Aust. J. Chem.*, **12**, 296(1959).

(12) H. L. Klug, D. F. Peterson, and A. L. Moxon, *Proc. S.D. Acad. Sci.*, **28**, 117(1949).

ACKNOWLEDGMENTS AND ADDRESSES

Received April 10, 1975, from the **Isotope Applications Department, Soreq Nuclear Research Centre, Yavne, Israel*, the *‡Department of Radiology, Harvard Medical School, Boston, MA 02115*, and the *§Department of Medicinal Chemistry and Pharmacology, Northeastern University College of Pharmacy and Allied Health Professions, Boston, MA 02115*

Accepted for publication July 1, 1975.

Supported in part by a grant from the New England Nuclear Corp. and by U.S. Public Health Service Grant GM 18674.

The authors are indebted to Dr. S. J. Adelstein, Dr. A. H. Soloway, and Dr. J. Gilat for encouraging this collaborative effort.

ˣ To whom inquiries should be directed.

New Compounds: Synthesis of *O*-(2,3,4,5,6-Pentafluorobenzyl)hydroxylamine Hydrochloride

GILBERT A. YOUNGDALE

Abstract □ Reaction of 2,3,4,5,6-pentafluorobenzyl bromide with *N*-hydroxyphthalimide produced *N*-(2,3,4,5,6-pentafluorobenzyloxy)phthalimide which, after hydrazinolysis and treatment with hydrogen chloride, yielded *O*-(2,3,4,5,6-pentafluorobenzyl)hydroxylamine hydrochloride. The latter compound was used to derivatize keto steroids for their analysis by electron-capture GLC.

Keyphrases □ *O*-(2,3,4,5,6-Pentafluorobenzyl)hydroxylamine hydrochloride—GLC derivatization reagent, synthesized from pentafluorobenzyl bromide □ GLC derivatization reagent—synthesis of *O*-(2,3,4,5,6-pentafluorobenzyl)hydroxylamine hydrochloride

A recent article (1) described the use of *O*-(2,3,4,5,6-pentafluorobenzyl)hydroxylamine hydrochloride (I) to derivatize keto steroids for their analysis by electron-capture GLC. The synthesis of I is reported in this article.

Synthesis of I was achieved following the general method of McKay *et al.* (2). Reaction of 2,3,4,5,6-pentafluorobenzyl bromide with *N*-hydroxyphthalimide produced *N*-(2,3,4,5,6-pentafluorobenzyloxy)-phthalimide which, after hydrazinolysis and treatment with anhydrous hydrogen chloride, yielded I (Scheme I).

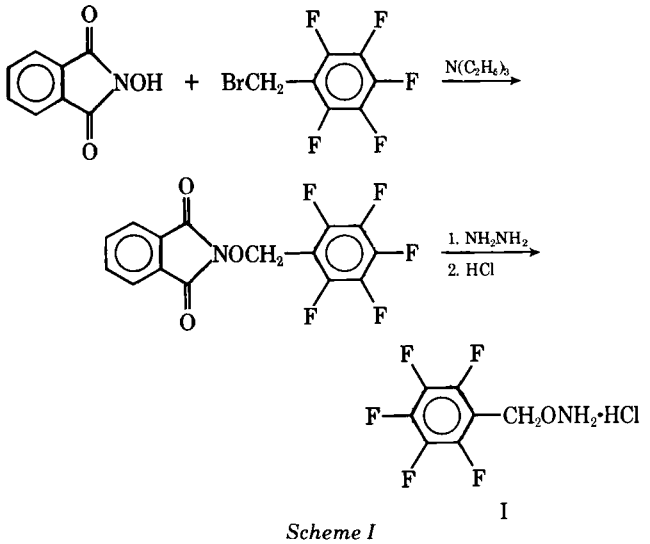

I

Scheme I

Chromatography—L-3-Chloroalanine, because of its lability, must be applied to the TLC chromatogram as a fresh aqueous solution of the hydrochloride (1%) and dried immediately with a stream of warm air. The chromatogram was developed with Solvent System A, and the location of material was visualized by spraying with 1% ninhydrin in 1-butanol followed by heating at 80° until the pink spot of chloroalanine was clearly visible (about 7 min); R_f 0.31.

Comparative chromatography of L-lysine and the two isosteres, L-4-thialysine (I) and L-4-selenalysine (VIII) was carried out with their hydrochlorides. The highly polar nature of these amino acid hydrochlorides requires equally polar solvents for chromatographic separation, and Solvent Systems B and C were found to be satisfactory. The values for the hydrochloride of L-lysine, L-4-thialysine, and L-4-selenalysine were R_f 0.47, 0.75, and 0.78 in Solvent System B and R_f 0.37, 0.75, and 0.76 in Solvent System C, respectively. These results show the greater polarity of L-lysine compared to its sulfur and selenium analogs as well as the close similarity between the two hetero analogs.

REFERENCES

(1) E. Hansson, *Acta Physiol. Scand. Suppl.*, **1959**, 161.

(2) M. Blau and M. A. Bender, *Biochim. Biophys. Acta*, **49**, 389(1961).

(3) D. M. Taylor and M. F. Cottrall, "Radiopharmaceuticals and Labeled Compounds," vol. 1, IAEA, Vienna, Austria, 1973, p. 433.

(4) T. Shiota, J. E. Folk, and F. Tietze, *Arch. Biochem. Biophys.*, **77**, 373(1958).

(5) T. J. McCord, D. H. Cook, D. L. Tharp, and A. L. Davis, *J. Med. Chem.*, **8**, 290(1965).

(6) M. D. Armstrong and J. D. Lewis, *J. Org. Chem.*, **16**, 749(1951); M. D. Armstrong and J. D. Lewis, *J. Biol. Chem.*, **189**, 461(1951).

(7) H. Bestian, *Justus Liebigs Ann. Chem.*, **566**, 210(1950).

(8) W. H. H. Gunther, *J. Org. Chem.*, **32**, 3929(1967).

(9) W. H. H. Gunther and H. G. Mautner, *J. Amer. Chem. Soc.*, **82**, 2762(1960).

(10) E. Fischer and K. Raske, *Chem. Ber.*, **40**, 3717(1907).

(11) H. Lindley, *Nature*, **178**, 647(1956); H. Lindley, *Aust. J. Chem.*, **12**, 296(1959).

(12) H. L. Klug, D. F. Peterson, and A. L. Moxon, *Proc. S.D. Acad. Sci.*, **28**, 117(1949).

ACKNOWLEDGMENTS AND ADDRESSES

Received April 10, 1975, from the **Isotope Applications Department, Soreq Nuclear Research Centre, Yavne, Israel*, the *‡Department of Radiology, Harvard Medical School, Boston, MA 02115*, and the *§Department of Medicinal Chemistry and Pharmacology, Northeastern University College of Pharmacy and Allied Health Professions, Boston, MA 02115*

Accepted for publication July 1, 1975.

Supported in part by a grant from the New England Nuclear Corp. and by U.S. Public Health Service Grant GM 18674.

The authors are indebted to Dr. S. J. Adelstein, Dr. A. H. Soloway, and Dr. J. Gilat for encouraging this collaborative effort.

ˣ To whom inquiries should be directed.

New Compounds: Synthesis of *O*-(2,3,4,5,6-Pentafluorobenzyl)hydroxylamine Hydrochloride

GILBERT A. YOUNGDALE

Abstract □ Reaction of 2,3,4,5,6-pentafluorobenzyl bromide with *N*-hydroxyphthalimide produced *N*-(2,3,4,5,6-pentafluorobenzyloxy)phthalimide which, after hydrazinolysis and treatment with hydrogen chloride, yielded *O*-(2,3,4,5,6-pentafluorobenzyl)hydroxylamine hydrochloride. The latter compound was used to derivatize keto steroids for their analysis by electron-capture GLC.

Keyphrases □ *O*-(2,3,4,5,6-Pentafluorobenzyl)hydroxylamine hydrochloride—GLC derivatization reagent, synthesized from pentafluorobenzyl bromide □ GLC derivatization reagent—synthesis of *O*-(2,3,4,5,6-pentafluorobenzyl)hydroxylamine hydrochloride

A recent article (1) described the use of *O*-(2,3,4,5,6-pentafluorobenzyl)hydroxylamine hydrochloride (I) to derivatize keto steroids for their analysis by electron-capture GLC. The synthesis of I is reported in this article.

Synthesis of I was achieved following the general method of McKay *et al.* (2). Reaction of 2,3,4,5,6-pentafluorobenzyl bromide with *N*-hydroxyphthalimide produced *N*-(2,3,4,5,6-pentafluorobenzyloxy)-phthalimide which, after hydrazinolysis and treatment with anhydrous hydrogen chloride, yielded I (Scheme I).

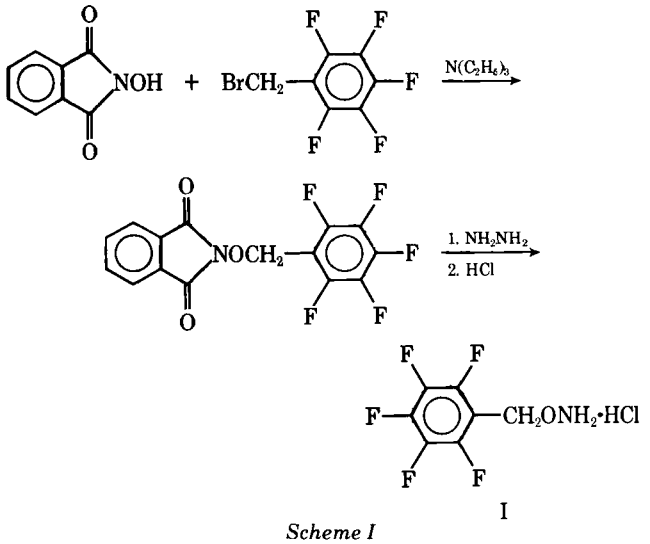

I

Scheme I

EXPERIMENTAL[1]

***N*-(2,3,4,5,6-Pentafluorobenzyloxy)phthalimide**—A mixture of 25 g (0.0957 mole) of 2,3,4,5,6-pentafluorobenzyl bromide, 15.6 g (0.0957 mole) of *N*-hydroxyphthalimide, 10.1 g (0.1 mole) of triethylamine, and 150 ml of dimethylformamide was stirred at room temperature for 19 hr and then on a steam bath for 2 hr. The majority of the solvent was removed under reduced pressure.

A solution of the residual material in methylene chloride was washed with 10% sodium carbonate solution and dried over anhydrous magnesium sulfate. The solvent was evaporated. Crystallization of the residue from acetone–hexane gave 27.4 g (83%) of buff crystals, mp 140–142°. An analytical sample was prepared by recrystallizing a portion from acetone–hexane, and buff crystals, mp 141–143°, were obtained.

Anal.—Calc. for $C_{15}H_6F_5NO_3$: C, 52.49; H, 1.76; F, 27.68. Found: C, 52.63; H, 1.76; F, 27.99.

***O*-(2,3,4,5,6-Pentafluorobenzyl)hydroxylamine Hydrochloride**—Fifteen grams (0.295 mole) of hydrazine hydrate was added to a suspension of 51.5 g (0.15 mole) of *N*-(2,3,4,5,6-pentafluorobenzyloxy)phthalimide in 87 ml of dimethylformamide and 870 ml of methanol at 60°. The mixture was stirred at ambient temperature for 3 hr and was then acidified to pH 2 by the addition of 2 *N* hydrochloric acid. The phthalylhydrazide was removed by filtration, and the filtrate was evaporated to dryness. The residue was treated with 200 ml of 2 *N* sodium hydroxide solution and extracted with ether (3 × 100 ml).

The combined ether extracts were dried over anhydrous magnesium sulfate, and anhydrous hydrogen chloride was bubbled through the ether solution. The solid which separated was collected by filtration, giving 31.1 g. Crystallization from ethanol gave 21.2 g, and an additional 5.1 g was obtained by concentrating the filtrate. The combined solids were recrystallized from ethanol, giving 20.4 g of white plates, mp 215° (sublimes[2]). An additional 4.2 g of white plates, mp 215° (sublimes[2]), was obtained by concentrating the filtrate. The total yield was 24.6 g (66%).

Anal.—Calc. for $C_7H_4F_5NO{\cdot}HCl$: C, 33.68; H, 2.02; Cl, 14.21; F, 38.06. Found: C, 33.77; H, 2.24; Cl, 14.29; F, 37.38.

[1] Melting points (Thomas Hoover apparatus) are corrected. The IR spectra were recorded on a Perkin-Elmer 241 spectrophotometer. NMR spectra were taken on a Varian A60 instrument. Mass spectra were recorded on a Consolidated Electrodynamics Corp. 21-110B mass spectrometer. The compounds were subjected to IR, NMR, and mass spectrometry, and the results were consistent with structures assigned.

[2] Drying the compound under high vacuum at elevated temperature will result in loss by sublimation.

REFERENCES

(1) K. T. Koshy, D. G. Kaiser, and A. L. VanDerSlik, *J. Chromatogr. Sci.*, **13**, 97(1975).

(2) A. F. McKay, D. L. Garmaise, G. Y. Paris, and S. Gelblum, *Can. J. Chem.*, **38**, 343(1960).

ACKNOWLEDGMENTS AND ADDRESSES

Received June 4, 1975, from the *Fertility Research Department, The Upjohn Company, Kalamazoo, MI 49001*

Accepted for publication June 25, 1975.

The author thanks D. J. Williams for technical assistance and the Physical and Analytical Chemistry Research Department of The Upjohn Co. for supplying analytical data.

New Compounds: Derivatives of Methyl 2-Aminoacetyl-4,5-dimethoxyphenylacetate

P. CATSOULACOS

Abstract □ Methyl 2-bromoacetyl-4,5-dimethoxyphenylacetate was prepared by reacting cupric bromide with methyl 2-acetyl-4,5-dimethoxyphenylacetate. Aminoacetyl derivatives formed on condensation of substituted *p*-aminobenzoic esters with the bromoacetyl derivative. Some prepared compounds were tested for local anesthetic and anti-inflammatory activities.

Keyphrases □ 2-Aminoacetyl-4,5-dimethoxyphenylacetate derivatives—synthesized, evaluated for local anesthetic and anti-inflammatory activity □ Anesthetics, local, potential—derivatives of 2-aminoacetyl-4,5-dimethoxyphenylacetate synthesized, evaluated □ Anti-inflammatory agents, potential—derivatives of 2-aminoacetyl-4,5-dimethoxyphenylacetate synthesized, evaluated

In view of the importance of the local anaesthetic activity of α-aminoketone derivatives (1–3), it was decided to condense methyl 2-bromoacetyl-4,5-dimethoxyphenylacetate with esters of *p*-aminobenzoic acid and *p*-aminosalicylic acid.

DISCUSSION

Methyl 2-acetyl-4,5-dimethoxyphenylacetate (I) (4) was halogenated with cupric bromide (5) to give the corresponding bromoacetyl derivative (II) in a 50% yield. Treatment of II with methyl and ethyl esters of *p*-aminobenzoic and *p*-aminosalicylic acid produced the aminoacetyl compounds (III) in good yields (Scheme I).

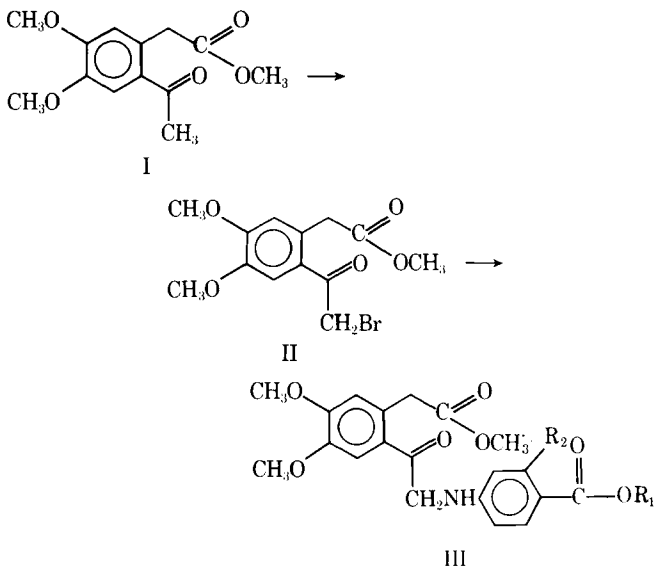

Scheme I

EXPERIMENTAL[1]

***N*-(2,3,4,5,6-Pentafluorobenzyloxy)phthalimide**—A mixture of 25 g (0.0957 mole) of 2,3,4,5,6-pentafluorobenzyl bromide, 15.6 g (0.0957 mole) of *N*-hydroxyphthalimide, 10.1 g (0.1 mole) of triethylamine, and 150 ml of dimethylformamide was stirred at room temperature for 19 hr and then on a steam bath for 2 hr. The majority of the solvent was removed under reduced pressure.

A solution of the residual material in methylene chloride was washed with 10% sodium carbonate solution and dried over anhydrous magnesium sulfate. The solvent was evaporated. Crystallization of the residue from acetone–hexane gave 27.4 g (83%) of buff crystals, mp 140–142°. An analytical sample was prepared by recrystallizing a portion from acetone–hexane, and buff crystals, mp 141–143°, were obtained.

Anal.—Calc. for $C_{15}H_6F_5NO_3$: C, 52.49; H, 1.76; F, 27.68. Found: C, 52.63; H, 1.76; F, 27.99.

***O*-(2,3,4,5,6-Pentafluorobenzyl)hydroxylamine Hydrochloride**—Fifteen grams (0.295 mole) of hydrazine hydrate was added to a suspension of 51.5 g (0.15 mole) of *N*-(2,3,4,5,6-pentafluorobenzyloxy)phthalimide in 87 ml of dimethylformamide and 870 ml of methanol at 60°. The mixture was stirred at ambient temperature for 3 hr and was then acidified to pH 2 by the addition of 2 *N* hydrochloric acid. The phthalylhydrazide was removed by filtration, and the filtrate was evaporated to dryness. The residue was treated with 200 ml of 2 *N* sodium hydroxide solution and extracted with ether (3 × 100 ml).

The combined ether extracts were dried over anhydrous magnesium sulfate, and anhydrous hydrogen chloride was bubbled through the ether solution. The solid which separated was collected by filtration, giving 31.1 g. Crystallization from ethanol gave 21.2 g, and an additional 5.1 g was obtained by concentrating the filtrate. The combined solids were recrystallized from ethanol, giving 20.4 g of white plates, mp 215° (sublimes[2]). An additional 4.2 g of white plates, mp 215° (sublimes[2]), was obtained by concentrating the filtrate. The total yield was 24.6 g (66%).

Anal.—Calc. for $C_7H_4F_5NO{\cdot}HCl$: C, 33.68; H, 2.02; Cl, 14.21; F, 38.06. Found: C, 33.77; H, 2.24; Cl, 14.29; F, 37.38.

[1] Melting points (Thomas Hoover apparatus) are corrected. The IR spectra were recorded on a Perkin-Elmer 241 spectrophotometer. NMR spectra were taken on a Varian A60 instrument. Mass spectra were recorded on a Consolidated Electrodynamics Corp. 21-110B mass spectrometer. The compounds were subjected to IR, NMR, and mass spectrometry, and the results were consistent with structures assigned.

[2] Drying the compound under high vacuum at elevated temperature will result in loss by sublimation.

REFERENCES

(1) K. T. Koshy, D. G. Kaiser, and A. L. VanDerSlik, *J. Chromatogr. Sci.*, **13**, 97(1975).

(2) A. F. McKay, D. L. Garmaise, G. Y. Paris, and S. Gelblum, *Can. J. Chem.*, **38**, 343(1960).

ACKNOWLEDGMENTS AND ADDRESSES

Received June 4, 1975, from the *Fertility Research Department, The Upjohn Company, Kalamazoo, MI 49001*

Accepted for publication June 25, 1975.

The author thanks D. J. Williams for technical assistance and the Physical and Analytical Chemistry Research Department of The Upjohn Co. for supplying analytical data.

New Compounds: Derivatives of Methyl 2-Aminoacetyl-4,5-dimethoxyphenylacetate

P. CATSOULACOS

Abstract □ Methyl 2-bromoacetyl-4,5-dimethoxyphenylacetate was prepared by reacting cupric bromide with methyl 2-acetyl-4,5-dimethoxyphenylacetate. Aminoacetyl derivatives formed on condensation of substituted *p*-aminobenzoic esters with the bromoacetyl derivative. Some prepared compounds were tested for local anesthetic and anti-inflammatory activities.

Keyphrases □ 2-Aminoacetyl-4,5-dimethoxyphenylacetate derivatives—synthesized, evaluated for local anesthetic and anti-inflammatory activity □ Anesthetics, local, potential—derivatives of 2-aminoacetyl-4,5-dimethoxyphenylacetate synthesized, evaluated □ Anti-inflammatory agents, potential—derivatives of 2-aminoacetyl-4,5-dimethoxyphenylacetate synthesized, evaluated

In view of the importance of the local anaesthetic activity of α-aminoketone derivatives (1–3), it was decided to condense methyl 2-bromoacetyl-4,5-dimethoxyphenylacetate with esters of *p*-aminobenzoic acid and *p*-aminosalicylic acid.

DISCUSSION

Methyl 2-acetyl-4,5-dimethoxyphenylacetate (I) (4) was halogenated with cupric bromide (5) to give the corresponding bromoacetyl derivative (II) in a 50% yield. Treatment of II with methyl and ethyl esters of *p*-aminobenzoic and *p*-aminosalicylic acid produced the aminoacetyl compounds (III) in good yields (Scheme I).

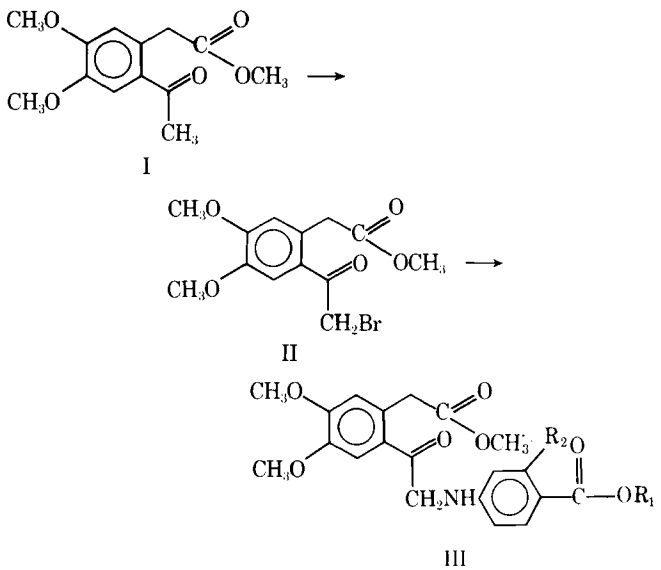

Scheme I

Table I—Anti-Inflammatory Evaluation of Two Derivatives of Methyl 2-Aminoacetyl-4,5-dimethoxyphenylacetate

Compound	Concentration, *M*	Inhibition, %
III*b*	5.4×10^{-6}	8
	5.1×10^{-7}	5
III*c*	1.6×10^{-5}	6
	1.6×10^{-6}	4

Table II—Physical Data of Methyl 2-Aminoacetyl-4,5-dimethoxyphenylacetate Derivatives

Compound	R_1	R_2	Yield, %	Melting Point	Recrystallization Solvent	Formula	Analysis, %	Calc.	Found
III*a*	CH_3	H	73	164–166°	Ethyl acetate	$C_{21}H_{23}NO_7$	C	62.84	62.95
							H	5.73	5.91
							N	3.49	3.48
III*b*	C_2H_5	H	79	154–155°	Ethyl acetate–hexane	$C_{22}H_{25}NO_7$	C	63.59	63.70
							H	6.07	6.10
							N	3.38	3.52
III*c*	CH_3	OH	63	184–186°	Chloroform–methanol	$C_{21}H_{23}NO_8$	C	60.42	60.54
							H	5.56	5.71
							N	3.36	3.43
III*d*	C_2H_5	OH	70	180–182°	Chloroform–methanol	$C_{22}H_{25}NO_8$	C	61.24	61.80
							H	5.84	6.20
							N	3.25	3.30

Compound IIIc, as its hydrochloride salt, was tested for local anesthetic activity in the guinea pig cornea and showed appreciable activity at a 0.5% (w/v) concentration, possessing an average activity of 40 min.

Compounds III*b* and III*c* were also tested *in vitro* for anti-inflammatory activity using the Tomlinson *et al.* (6) method (Table I).

EXPERIMENTAL[1]

Methyl 2-Bromoacetyl-4,5-dimethoxyphenylacetate (II)—Methyl 2-acetyl-4,5-dimethoxyphenylacetate (I), 50.4 g (0.2 mole), and cupric bromide, 89.4 g (0.4 mole), were dissolved in 1 liter of methanol, and the solution was heated under reflux for 3 hr. During this time, a white precipitate formed and the solution lightened in color. The reaction mixture, after filtration, was evaporated *in vacuo* to a paste. The paste was dissolved in chloroform.

The organic layer was washed with water, dried over sodium sulfate, and evaporated to yield a crystalline compound. Crystallization from ether gave 33.1 g (50%) of II, mp 112–114°; IR: ν_{max} 1735 ($COOCH_3$) and 1690 ($COCH_2Br$) cm^{-1}; NMR: τ 2.58 and 3.15 (two aromatic protons), 5.5 ($COCH_2Br$), 6 ($2CH_3O$), 6.05 (CH_2COOCH_3), and 6.25 ($COOCH_3$).

Anal.—Calc. for $C_{13}H_{15}BrO_5$: C, 47.13; H, 4.53. Found: C, 47.40; H, 4.62.

Methyl 2-Aminoacetyl-4,5-dimethoxyphenylacetate Derivatives—To a solution of II (3.31 g, 10 mmoles) in 150 ml of anhydrous benzene was added *p*-aminobenzoic or *p*-aminosalicylic ester (20 mmoles), and the mixture was heated under reflux for 5 hr. The solvent was evaporated under reduced pressure, and the residue was dissolved in chloroform. The organic layer was washed several times with water and dried over magnesium sulfate. After evaporation of the solvent, the residue was crystallized from the appropriate solvent.

IR and NMR spectra of the reported compounds were as expected. Physical data for the products obtained are given in Table II.

[1] Melting points were determined on a Gallenkamp melting-point apparatus and are uncorrected. IR spectra were recorded with a Perkin-Elmer 521 instrument in potassium bromide. NMR spectra were determined with a Varian Associates A-60 instrument, using deuterochloroform as the solvent and tetramethylsilane as the internal standard. Elemental analyses were performed by the Analytical Laboratory of the Chemistry Department, Nuclear Research Center "Demokritos."

REFERENCES

(1) J. Vacher, C. Lakatos, G. Rispat, and P. Duchene-Marulaz, *Arch. Int. Pharmacodyn. Ther.*, **1**, 165(1967).

(2) T. Teschigahara, *Folia Pharmacol. Jap.*, **58**, 67(1962); through *Chem. Abstr.*, **59**, 3240a(1963).

(3) N. Lofgren, U. Ragnarsson, and K. Sjoberg, *Acta Chem. Scand.*, **17**, 1252(1963).

(4) P. M. Chakrabarti, *Tetrahedron Lett., No. 22*, **1963**, 1771.

(5) J. K. Kochi, *J. Amer. Chem. Soc.*, **77**, 5274(1955).

(6) R. V. Tomlinson, H. J. Ringgold, M. C. Gureshi, and E. Forchielli, *Biochem. Biophys. Res. Commun.*, **46**, 552(1972).

ACKNOWLEDGMENTS AND ADDRESSES

Received February 25, 1975, from the *Greek Atomic Energy Commission, Nuclear Research Center "Demokritos," Chemistry Department, Athens, Greece.*

Accepted for publication July 3, 1975.

Testing of Heat Sealing by Thermal Analysis

Keyphrases ☐ Seals, heat—unit-dose packages, examined by calorimetry, IR spectroscopy, and thermomechanical analysis ☐ Containers, pharmaceutical—unit-dose packages, heat seals examined by calorimetry, IR spectroscopy, and thermomechanical analysis ☐ Packages, unit dose—heat seals examined by calorimetry, IR spectroscopy, and thermomechanical analysis

To the Editor:

The compendia seek to provide comprehensive standards for pharmaceutical containers. A moisture *permeation* standard for multiple-dose prescription containers has been presented (1, 2). Devising comparable standards for unit-dose packages is more difficult; not only must the moisture permeability characteristics of the component film and laminate be measured, but separate verification is required to determine the efficacy of the heat seal that must be formed for complete closure. This communication deals with the latter problem.

When laminates or films are suited for testing under reduced pressure, the efficacy of the heat seal is determined by vacuum testing. This procedure gives only "pass–fail" information. A physical or chemical determination, applicable to single packages, is needed for more meaningful data.

The characterization of high polymers, including films and laminates, by thermal methods is well established (3), and the high temperature glass transition, T_g, of film samples has been studied by thermomechanical analysis (4) with the sample stretched between two hooks. Linear expansion determinations (5) have correlated with the degree of molecular ordering in polyurethane elastomers.

The possibility exists that the heat-sealing event may modify the polymer's crystallinity, thus changing the melting characteristics or rheological behavior. Physical or chemical measurements can give evidence of the thermal history of the polymers. With this in mind, a few commercial unit-dose packages were examined by differential scanning calorimetry, multiple internal reflectance IR spectroscopy, and thermomechanical analysis. The manufacturers of the unit-dose packaged pharmaceutical products made available some samples that were visibly integral but deliberately designed to fail vacuum testing and some samples that passed vacuum testing. Initial results of this study are reported here.

High density polyethylene trays [0.55 mm (1 mil = 0.025 mm)], composed of a lid-stock of low density polyethylene-coated foil with paper overlay for labeling (0.15 mm), are used to package pilocarpine ophthalmic matrix[1]. Differential scanning calorimetry was performed on the following portions of the samples:

1. The low density polyethylene lid-stock, showing an endotherm from 105 to 110° and peaking at 107°.
2. The high density polyethylene tray, center section, showing an endotherm from 115 to 137° and peaking at 133°.
3. Samples cut from heat-sealed areas that: (*a*) passed vacuum testing or (*b*) failed vacuum testing.
4. Unsealed sandwiches prepared from untreated cuttings of the lid-stock and tray, incorporating both endotherms 1 and 2.

Comparisons of thermograms 3*a*, 3*b*, and 4 revealed no correlation in either the width or peak values of the endotherms or the individual heat of fusion values as represented by area *versus* sample weight. Therefore, no distinct correlation between the efficacy of the heat seal and differential scanning calorimetry was readily apparent. An initial X-ray diffraction crystallographic study[2] revealed no ready correlation between the efficacy of the seal and the fine structure of the diffractograms. Reflectance IR spectra obtained in our laboratory gave the expected functional group information but did not correlate with heat sealing.

In sharp contrast to this physical evidence, thermomechanical analysis gave substantial evidence of a correlation between the ability of the weighted probe to penetrate the sample and the efficacy of the heat seal of these high density polyethylene trays with the low density polyethylene-coated foil/paper lid-stock.

To make the thermomechanical measurement, a sample about 3–4 mm in diameter was cut from the tray, lid-stock, heat-sealed area or a sandwich of the tray and lid-stock was prepared. A 5-g weight was placed on top of the quartz probe shaft of the analyzer module[3]. The penetration of the quartz probe into the sample as the system was heated was detected by a moving-coil transducer located on the shaft between the sample and the weight pan, and this displacement *versus* temperature was displayed on the axis of the *x–y* recorder. Complete penetration of the high density polyethylene tray (0.55 mm) and the low density polyethylene foil/paper lid-stock (0.15 mm) made into an average 0.7-mm heat-sealed sandwich would be about 0.5 mm.

Full-scale vertical deflection of the primary pen was set to represent 1.0 mm. A secondary pen recorded the first derivative of the displacement. The results were as follows.

The penetration of the lid-stock alone corresponded exactly to the first endotherm of low density polyethylene of 100–115°, as determined in the differential scanning calorimetry mode.

Penetration of virgin high density polyethylene trays corresponded, at the onset of 135°, to the second endotherm determined in the differential scan-

[1] Ocusert Pilo-20 and 40, Alza Corp., Palo Alto, Calif.; W. J. Mader, Alza Corp., Palo Alto, Calif., personal communication.

[2] N. J. DeAngelis and G. J. Papariello, Wyeth Laboratories, Radnor, Pa., personal communication.

[3] Model 941 thermomechanical analysis accessory in conjunction with model 940 thermal analyzer, DuPont Instruments Division, Newark, Del.

ning calorimetry mode and was nearly complete on heating up to 180°. The softened polymer flowed up around the end of the penetration probe, engulfing the tip.

Thermograms of the tray and lid-stock sandwich were indicative of complete penetration of the high density polyethylene tray as well as the initial penetration of the lid-stock. The softened polymer, once again, flowed upward around the probe.

On well-sealed samples, only 1% of the material was penetrated in the region associated with the high density polyethylene endotherm. At 180°, penetration values were 0.005–0.016 mm (average of six measurements = 0.007 mm). No additional penetration was noted when the sample was heated to 300°. The polymer retained its shape with no evidence of flow.

On samples that failed the leak test, about 70% of the tray and lid-stock sandwich value was penetrated at 180°. Penetrations of 0.52–0.55 mm (average of six measurements = 0.53 mm) were noted at this temperature. Continued heating to 300° showed complete penetration.

Subsequent removal and physical examination of the high density polyethylene layer confirmed that the penetration was complete. Linear expansion caused the trays to be 5% thicker at 50° than at ambient temperatures at which caliper measurements were made.

During the sealing process, the polymer sandwich is subjected to a relatively high temperature under pressure for very short periods. To simulate the sealing process in our laboratories, centers were cut from the unsealed areas of the tray and lid-stock. The plastic top and backing were pressed together between two wooden slats with a screw clamp. Sections of plastic were heated below the melting point for 15 min at 65, 90, 95, 100, 110, 115, and 120°. Finally, at 120°, samples did not allow probe penetration, which was characteristic of a good seal and a more crystalline structure.

An unclamped center section of high density polyethylene alone was heated at only 110° for 15 min and became rigid and concave, giving a penetration curve characteristic of an essentially crystalline polymer. A sample heated beyond the melting point to 140° and then cooled contracted to a thick bar; this material was easily penetrated with a 5-g weight and was considered amorphous. Heating the sample of polyethylene below its melting point to 110 or 120° clearly allows a transition to a more crystalline form.

A sample of amorphous material was heated to 140° in the thermomechanical analysis system and held at that temperature under a 5-g weight. After 10 min, 75% of the sample's thickness had been penetrated; the entire sample was penetrated after 50 min. The crystalline sample was not penetrated in a similar experiment. A narrow probed, temperature-adjustable penetrometer probably could be designed for routine measurements after method development.

High density polyethylene is essentially crystalline when prepared: 95% crystalline by the Phillips process and 85% crystalline by the Zeigler process (6). When film is prepared and shaped, the polymer is heated under pressure to a white, essentially amorphous substance. The results of our testing indicate that the unheated centers and the improperly sealed sides of the unit-dose container are composed of this essentially amorphous material, which will flow (penetrate) at 140° at 5 g/3.14 mm^2. The well-sealed area of the container is composed of essentially crystalline polymer, which will not exhibit significant flow under a 5-g weight.

The flow index of polyethylene (7) is measured at 190° and 43.2 psi (30.5 g/3.14 mm^2). A crystalline portion of the tray was placed in the thermomechanical analysis test apparatus and heated to 190° under a 30-g weight, at which time the sample exhibited flow (penetration). After the sample was allowed to cool, a penetration test was performed using the 5-g weight. The sample then flowed at 140°, characteristic of the amorphous polymer. The degree of penetration is obviously a measure of the degree of crystallinity.

A correlation also was found between probe penetration and the efficacy of the heat seal of samples composed of 1.5-mil polyethylene/0.7-mil aluminum foil/0.67-mil polyethylene/1-mil transparent cellophane sealed to an identical strip[4]. The findings were complicated by inconsistent results caused by nonuniformity of the seal and the fact that there were three layers of plastic in the final product. Samples were taken from each of the four sides of the package. On the samples that failed the vacuum leak test, one end of the package tested as properly sealed, the sides tested the same, and the other end had such a poor seal that the sample separated during the test procedure. Therefore, at lower temperatures, one section of the sealing mechanism is less effective than the others. Even with these complications, differences were easily detected by thermomechanical analysis between acceptable and unacceptable containers.

The scope of applicability offered by thermomechanical analysis is uncertain with respect to pharmaceutical packaging, both in testing heat seals and characterizing batches of polymeric materials. The sealing process would have to cause changes in the polymers consistently. It is our experience that thermomechanical analysis is a more sensitive instrumental method for detecting transitions in polyethylene structure. Thermoplastic materials, which retain the ability to flow upon reheating, are used largely in unit-dose packaging and especially in the heat-sealing process; this area of promise for thermomechanical analyses needs to be surveyed. Experiments with polymers other than polyethylene and other strip packaging systems are in progress.

(1) "The United States Pharmacopeia," 19th rev., Mack Publishing Co., Easton, Pa., 1975, p. 647.

(2) "The National Formulary," 14th ed., Mack Publishing Co., Easton, Pa., 1975, p. 888.

(3) J. Mitchell, Jr., and J. Chiu, *Anal. Chem.*, **47**, 303R, 304R(1975).

(4) H. D. Burks, *J. Appl. Polym. Sci.*, **18**, 627(1974).

(5) G. W. Miller, *ibid.*, **15**, 39(1971).

[4] G. Irwin and J. J. Pierantozzi, Wyeth Laboratories, Radnor, Pa., personal communication.

(6) R. B. Seymour, "Modern Plastics Technology," Reston Publishing, Reston, Va., 1975, p. 167.
(7) *Ibid.*, p. 97.

Lee T. Grady
Jeanne T. Reamer ˣ
Drug Research and Testing Laboratory
United States Pharmacopeia
Rockville, MD 20852

Received August 25, 1975.
Accepted for publication January 7, 1976.
ˣ To whom inquiries should be directed.

Kinetics of Butaperazine Adsorption onto Quartz Cells

Keyphrases □ Butaperazine—adsorption onto quartz cells, kinetics □ Adsorption—butaperazine onto quartz cells, kinetics □ Tranquilizers—butaperazine, adsorption onto quartz cells, kinetics

To the Editor:

Kinetics of adsorption of drugs onto plastic and filtering materials are well documented (1–7). However, kinetics of adsorption of drugs onto quartz cells appear to be rarely reported. During our study on the interaction between butaperazine, an antipsychotic agent, and a saliva-stimulating device[1], we found that the fluorescent intensity of the butaperazine solution in cyclohexane stored in quartz cells decreased with time. Additional studies were carried out to explore this interaction, and the results of these preliminary studies are reported here.

The stock solution (2 mg/ml) of butaperazine maleate[2] was prepared in 95% ethanol. This solution was diluted with cyclohexane[3] in 100-ml volumetric flasks to concentrations of 2.0 and 0.14 μg/ml. Then 1 ml of 1 *N* NaOH solution was added, and the flasks were shaken to convert butaperazine maleate to its free base in cyclohexane. The cyclohexane was transferred immediately and directly into three quartz cells, which were then covered with lids.

Fluorescent intensities were measured immediately and every 5 min thereafter for 30 min with a fluorometer[4] at the excitation wavelength of 312 nm and the fluorescent wavelength of 498 nm. The average results, expressed in terms of percent of the initial fluorescent intensity as a function of time, are shown in Fig. 1. In the study with the higher initial concentration, the fluorescent intensity decreased to a constant 88% after 10 min. The decrease in intensity with the lower initial concentration followed an apparent first-order process with a half-life of 16 min.

These concentration-dependent decrease phenomena are consistent with the saturable adsorption theory. This contention is also supported by the following desorption study. Two cells were filled with 2 μg/ml of the butaperazine solution. After 10 min of adsorption equilibration, the solution in the cell was discarded and the cell was filled with pure cyclohexane. The fluorescent intensity of the solution was then measured as a function of time. The average results are also shown in Fig. 1. The average recovery into the fresh cyclohexane at 30 min was about 33%.

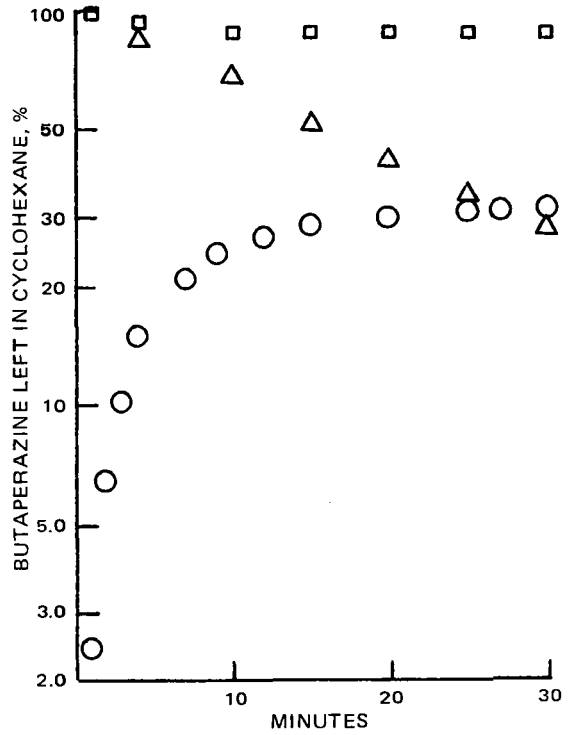

Figure 1—*Time course of the fluorescent intensity of cyclohexane solutions of butaperazine in the cell. Key:* □, *initial concentration of 2.0 μg/ml in the adsorption study;* △, *initial concentration of 0.14 μg/ml in the adsorption study; and* ○, *desorption study where the scale 100 is equivalent to 0.22 μg/ml when all adsorbed butaperazine was desorbed into cyclohexane.*

In all of these studies, the butaperazine solutions were protected from light irradiation whenever feasible. Adsorption of butaperazine onto the glassware was mentioned in one (8) of two recent papers (8, 9) describing similar fluorometric methods for the measurement of butaperazine concentrations in plasma. Moreover, in the present study, coating the cells with silicone[5] was ineffective in reducing the adsorption effect.

(1) A. H. Kapadia, W. L. Guess, and J. Autian, *J. Pharm. Sci.*, **53**, 720(1964).
(2) M. B. Rodell, R. Bodnar, W. L. Guess, and J. Autian, *ibid.*, **54**, 129(1965).
(3) S. Weisenfeld, S. Podolsky, L. Goldsmith, and L. Ziff, *Diabetes*, **17**, 766(1968).
(4) W. L. Chiou and L. D. Smith, *J. Pharm. Sci.*, **59**, 843(1970).
(5) K. Kakemi, H. Sezaki, E. Arakawa, L. Kirmura, and K. Ikeda, *Chem. Pharm. Bull.*, **19**, 2523(1971).
(6) P. Moorhatch and W. L. Chiou, *Amer. J. Hosp. Pharm.*, **31**, 72(1974).
(7) W. L. Chiou, *Can. J. Pharm. Sci.*, **10**, 112(1975).
(8) D. H. Manier, J. Sekerke, J. V. Dingelland, and M. K. El-Yousef, *Clin. Chim. Acta*, **57**, 225(1974).
(9) J. M. Davis, D. S. Janowsky, H. J. Sekerke, H. Manier, and M. K. El-Yousef, in "The Phenothiazines and Structurally Related Drugs," I. S. Forrest, C. J. Carr, and E. Usdin, Eds., Raven, New York, N.Y., 1974, p. 433.

[1] Parafilm, American Can Co., Neenah, Wis.
[2] A. H. Robins Co., Richmond, Va.
[3] Certified ACS grade, Fisher Scientific Co., Fair Lawn, N.J.
[4] Perkin-Elmer model 203 fluorescence spectrometer, Norwalk, Conn.
[5] Siliclad, Clay Adams, Division of Becton, Dickinson and Co., Parsippany, NJ 07054

(6) R. B. Seymour, "Modern Plastics Technology," Reston Publishing, Reston, Va., 1975, p. 167.
(7) *Ibid.*, p. 97.

Lee T. Grady
Jeanne T. Reamer ˣ
Drug Research and Testing Laboratory
United States Pharmacopeia
Rockville, MD 20852

Received August 25, 1975.
Accepted for publication January 7, 1976.
ˣ To whom inquiries should be directed.

Kinetics of Butaperazine Adsorption onto Quartz Cells

Keyphrases □ Butaperazine—adsorption onto quartz cells, kinetics □ Adsorption—butaperazine onto quartz cells, kinetics □ Tranquilizers—butaperazine, adsorption onto quartz cells, kinetics

To the Editor:

Kinetics of adsorption of drugs onto plastic and filtering materials are well documented (1–7). However, kinetics of adsorption of drugs onto quartz cells appear to be rarely reported. During our study on the interaction between butaperazine, an antipsychotic agent, and a saliva-stimulating device[1], we found that the fluorescent intensity of the butaperazine solution in cyclohexane stored in quartz cells decreased with time. Additional studies were carried out to explore this interaction, and the results of these preliminary studies are reported here.

The stock solution (2 mg/ml) of butaperazine maleate[2] was prepared in 95% ethanol. This solution was diluted with cyclohexane[3] in 100-ml volumetric flasks to concentrations of 2.0 and 0.14 μg/ml. Then 1 ml of 1 *N* NaOH solution was added, and the flasks were shaken to convert butaperazine maleate to its free base in cyclohexane. The cyclohexane was transferred immediately and directly into three quartz cells, which were then covered with lids.

Fluorescent intensities were measured immediately and every 5 min thereafter for 30 min with a fluorometer[4] at the excitation wavelength of 312 nm and the fluorescent wavelength of 498 nm. The average results, expressed in terms of percent of the initial fluorescent intensity as a function of time, are shown in Fig. 1. In the study with the higher initial concentration, the fluorescent intensity decreased to a constant 88% after 10 min. The decrease in intensity with the lower initial concentration followed an apparent first-order process with a half-life of 16 min.

These concentration-dependent decrease phenomena are consistent with the saturable adsorption theory. This contention is also supported by the following desorption study. Two cells were filled with 2 μg/ml of the butaperazine solution. After 10 min of adsorption equilibration, the solution in the cell was discarded and the cell was filled with pure cyclohexane. The fluorescent intensity of the solution was then measured as a function of time. The average results are also shown in Fig. 1. The average recovery into the fresh cyclohexane at 30 min was about 33%.

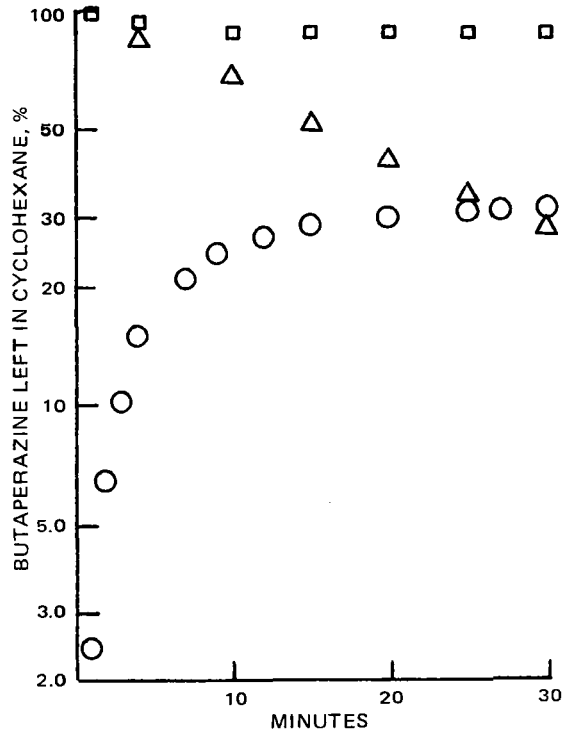

Figure 1—*Time course of the fluorescent intensity of cyclohexane solutions of butaperazine in the cell. Key:* □, *initial concentration of 2.0 μg/ml in the adsorption study;* △, *initial concentration of 0.14 μg/ml in the adsorption study; and* ○, *desorption study where the scale 100 is equivalent to 0.22 μg/ml when all adsorbed butaperazine was desorbed into cyclohexane.*

In all of these studies, the butaperazine solutions were protected from light irradiation whenever feasible. Adsorption of butaperazine onto the glassware was mentioned in one (8) of two recent papers (8, 9) describing similar fluorometric methods for the measurement of butaperazine concentrations in plasma. Moreover, in the present study, coating the cells with silicone[5] was ineffective in reducing the adsorption effect.

(1) A. H. Kapadia, W. L. Guess, and J. Autian, *J. Pharm. Sci.*, **53**, 720(1964).
(2) M. B. Rodell, R. Bodnar, W. L. Guess, and J. Autian, *ibid.*, **54**, 129(1965).
(3) S. Weisenfeld, S. Podolsky, L. Goldsmith, and L. Ziff, *Diabetes*, **17**, 766(1968).
(4) W. L. Chiou and L. D. Smith, *J. Pharm. Sci.*, **59**, 843(1970).
(5) K. Kakemi, H. Sezaki, E. Arakawa, L. Kirmura, and K. Ikeda, *Chem. Pharm. Bull.*, **19**, 2523(1971).
(6) P. Moorhatch and W. L. Chiou, *Amer. J. Hosp. Pharm.*, **31**, 72(1974).
(7) W. L. Chiou, *Can. J. Pharm. Sci.*, **10**, 112(1975).
(8) D. H. Manier, J. Sekerke, J. V. Dingelland, and M. K. El-Yousef, *Clin. Chim. Acta*, **57**, 225(1974).
(9) J. M. Davis, D. S. Janowsky, H. J. Sekerke, H. Manier, and M. K. El-Yousef, in "The Phenothiazines and Structurally Related Drugs," I. S. Forrest, C. J. Carr, and E. Usdin, Eds., Raven, New York, N.Y., 1974, p. 433.

[1] Parafilm, American Can Co., Neenah, Wis.
[2] A. H. Robins Co., Richmond, Va.
[3] Certified ACS grade, Fisher Scientific Co., Fair Lawn, N.J.
[4] Perkin-Elmer model 203 fluorescence spectrometer, Norwalk, Conn.
[5] Siliclad, Clay Adams, Division of Becton, Dickinson and Co., Parsippany, NJ 07054

Kun Chang
Win L. Chiou ˣ
Department of Pharmacy and
Clinical Pharmacokinetics Laboratory
College of Pharmacy
University of Illinois at
the Medical Center
Chicago, IL 60612

Received November 14, 1975.
Accepted for publication January 26, 1976.
ˣ To whom inquiries should be directed.

Differing Antitumor Activities of the Hydrochloride and Methiodide Salts of 1-Ethyl-3-(3′-dimethylaminopropyl)-carbodiimide

Keyphrases □ 1-Ethyl-3-(3′-dimethylaminopropyl)carbodiimide—hydrochloride and methiodide salts, antitumor activity compared, mice □ Antitumor agents, potential—1-ethyl-3-(3′-dimethylaminopropyl)carbodiimide, hydrochloride and methiodide salts compared, mice

To the Editor:

Cellular surface modifications effected by the reaction of mouse neuroblastoma C1300 and carcinoma TA3 cells with 1-ethyl-3-(3′-dimethylaminopropyl)-carbodiimide hydrochloride (II) have been demonstrated *in vitro* to result in an increased susceptibility of these cells to immune lysis by soluble antibodies (1). This carbodiimide derivative also has been shown to exert an *in vivo* antitumor activity. On the basis of the following lines of evidence, this activity appears to result from an enhanced host immune reactivity against drug-modified tumor cells:

1. Chemotherapeutic effectiveness against neuroblastoma C1300 solid tumors increases with increasing host levels of cytotoxic serum antibodies (1).

2. Drug inhibition of TA3 ascites carcinoma growth is not observed in hosts that have received an immunosuppressive 700-rad whole body dose of cobalt-60 radiation (2).

In addition to having chemotherapeutic potential, the *in vivo* action of this carbodiimide derivative may be useful for tumor diagnosis using the scintillation camera, since the enhancement of host immune reactions in neoplastic tissue could create a favorable condition for the selective uptake of radioisotopically labeled compounds (3).

On the basis of NMR and IR evidence, the water-soluble hydrochloride salt[1] (II) of the carbodiimide base 1-ethyl-3-(3′-dimethylaminopropyl)carbodiimide (I) has been found to exist in aqueous solution at physiological pH as an equilibrium mixture of two isomeric species: 7.4% open chain carbodiimide hydrochloride (II*a*) and 92.6% 2-ethylamino-3,3-dimethyl-3,4,5,6-tetrahydropyrimidine chloride (II*b*) (4, 5). Because of the structural complexity introduced by isomerism of II, we synthesized and tested the chemotherapeutic activity of the water-soluble carbodiimide salt 1-ethyl-3-(3′-dimethylaminopropyl)carbodiimide methiodide (III), which is formed by reaction of I with methyl iodide (4).

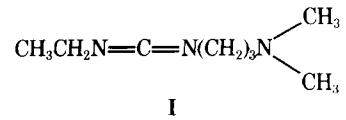

I

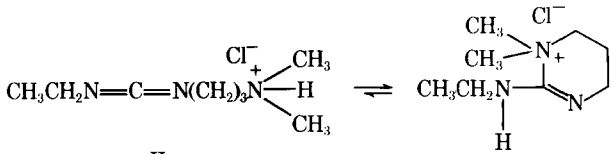

II*a* II*b*

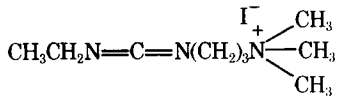

III

NMR and IR studies showed that III exists exclusively as the open chain carbodiimide at physiological pH (5). From a comparison of the biological effects of II and III, we sought to gain evidence as to whether the structural features of II—apart from its chemically reactive carbodiimino functionality—are important factors in the antitumor action exerted by this compound.

In vitro cytotoxicity assays were carried out to assess the relative abilities of II and III to increase the complement-dependent (6) antibody-mediated lysis of neuroblastoma C1300 target cells. The antiserum used was drawn from A/HeJ mice[2] bearing 21-day-old neuroblastoma C1300 tumors. The antiserum was added to test cultures so that the final dilution was 1:640 (v/v). Rabbit serum was absorbed with C1300 cells by the method of Boyse *et al.* (7) to remove naturally occurring toxic substances (8); the absorbed rabbit serum was then placed in test cultures at a final dilution of 1:40 (v/v) as a source of the complement.

Lysis of C1300 target cells was determined from the percentage release of the intracellular chromium-51 label during an 8-hr incubation at 37°. The method used to label C1300 target cells with chromium-51, the preparation of the antiserum and complement, and details of the cytotoxicity assay procedure were described previously (1). Compounds II and III were added to test cultures at an identical concentration of 0.16 m*M*. On the basis of drug tolerance studies, this concentration of carbodiimide was determined to be the maximum that was not toxic to C1300 cells over the 8-hr incubation used in all cytotoxicity assays.

Results of *in vitro* cytotoxicity assays are summarized in Table I. Neuroblastoma C1300 target cell lysis by A/HeJ immune serum increased significantly when II was added to test cultures (from 13.4 to 27.8%). Addition of the open chain carbodiimide III, however, did not lead to increased target cell immune lysis.

[1] Ott Chemical Co., Muskegon, Mich.

[2] Jackson Laboratory, Bar Harbor, Me.

Kun Chang
Win L. Chiou ˣ
Department of Pharmacy and
Clinical Pharmacokinetics Laboratory
College of Pharmacy
University of Illinois at
the Medical Center
Chicago, IL 60612

Received November 14, 1975.
Accepted for publication January 26, 1976.
ˣ To whom inquiries should be directed.

Differing Antitumor Activities of the Hydrochloride and Methiodide Salts of 1-Ethyl-3-(3′-dimethylaminopropyl)-carbodiimide

Keyphrases □ 1-Ethyl-3-(3′-dimethylaminopropyl)carbodiimide—hydrochloride and methiodide salts, antitumor activity compared, mice □ Antitumor agents, potential—1-ethyl-3-(3′-dimethylaminopropyl)carbodiimide, hydrochloride and methiodide salts compared, mice

To the Editor:

Cellular surface modifications effected by the reaction of mouse neuroblastoma C1300 and carcinoma TA3 cells with 1-ethyl-3-(3′-dimethylaminopropyl)-carbodiimide hydrochloride (II) have been demonstrated *in vitro* to result in an increased susceptibility of these cells to immune lysis by soluble antibodies (1). This carbodiimide derivative also has been shown to exert an *in vivo* antitumor activity. On the basis of the following lines of evidence, this activity appears to result from an enhanced host immune reactivity against drug-modified tumor cells:

1. Chemotherapeutic effectiveness against neuroblastoma C1300 solid tumors increases with increasing host levels of cytotoxic serum antibodies (1).

2. Drug inhibition of TA3 ascites carcinoma growth is not observed in hosts that have received an immunosuppressive 700-rad whole body dose of cobalt-60 radiation (2).

In addition to having chemotherapeutic potential, the *in vivo* action of this carbodiimide derivative may be useful for tumor diagnosis using the scintillation camera, since the enhancement of host immune reactions in neoplastic tissue could create a favorable condition for the selective uptake of radioisotopically labeled compounds (3).

On the basis of NMR and IR evidence, the water-soluble hydrochloride salt[1] (II) of the carbodiimide base 1-ethyl-3-(3′-dimethylaminopropyl)carbodiimide (I) has been found to exist in aqueous solution at physiological pH as an equilibrium mixture of two isomeric species: 7.4% open chain carbodiimide hydrochloride (II*a*) and 92.6% 2-ethylamino-3,3-dimethyl-3,4,5,6-tetrahydropyrimidine chloride (II*b*) (4, 5). Because of the structural complexity introduced by isomerism of II, we synthesized and tested the chemotherapeutic activity of the water-soluble carbodiimide salt 1-ethyl-3-(3′-dimethylaminopropyl)carbodiimide methiodide (III), which is formed by reaction of I with methyl iodide (4).

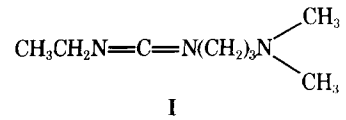

I

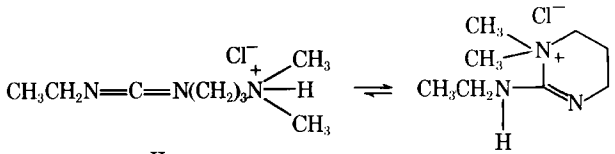

II*a* II*b*

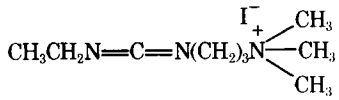

III

NMR and IR studies showed that III exists exclusively as the open chain carbodiimide at physiological pH (5). From a comparison of the biological effects of II and III, we sought to gain evidence as to whether the structural features of II—apart from its chemically reactive carbodiimino functionality—are important factors in the antitumor action exerted by this compound.

In vitro cytotoxicity assays were carried out to assess the relative abilities of II and III to increase the complement-dependent (6) antibody-mediated lysis of neuroblastoma C1300 target cells. The antiserum used was drawn from A/HeJ mice[2] bearing 21-day-old neuroblastoma C1300 tumors. The antiserum was added to test cultures so that the final dilution was 1:640 (v/v). Rabbit serum was absorbed with C1300 cells by the method of Boyse *et al.* (7) to remove naturally occurring toxic substances (8); the absorbed rabbit serum was then placed in test cultures at a final dilution of 1:40 (v/v) as a source of the complement.

Lysis of C1300 target cells was determined from the percentage release of the intracellular chromium-51 label during an 8-hr incubation at 37°. The method used to label C1300 target cells with chromium-51, the preparation of the antiserum and complement, and details of the cytotoxicity assay procedure were described previously (1). Compounds II and III were added to test cultures at an identical concentration of 0.16 m*M*. On the basis of drug tolerance studies, this concentration of carbodiimide was determined to be the maximum that was not toxic to C1300 cells over the 8-hr incubation used in all cytotoxicity assays.

Results of *in vitro* cytotoxicity assays are summarized in Table I. Neuroblastoma C1300 target cell lysis by A/HeJ immune serum increased significantly when II was added to test cultures (from 13.4 to 27.8%). Addition of the open chain carbodiimide III, however, did not lead to increased target cell immune lysis.

[1] Ott Chemical Co., Muskegon, Mich.

[2] Jackson Laboratory, Bar Harbor, Me.

Table I—Effect of Carbodiimide Derivatives on Neuroblastoma C1300 Immune Lysis

Serum and Dilution (v/v)	Complement-Dependent C1300 Target Cell Lysis[a], %		
	Serum	Serum + II (0.16 m*M*)	Serum + III (0.16 m*M*)
Immune A/HeJ[b] (1:640) + rabbit complement (1:40)	13.4 ± 2.1 (6)[c]	27.8 ± 2.5 (6)	13.2 ± 0.9 (2)

[a] The percentage of complement-dependent antibody-mediated C1300 target cell lysis was determined from the release of intracellular chromium-51 label during an 8-hr incubation at 37° (1). The percent lysis is expressed relative to a "background" release of chromium-51 label measured in control cultures. Contents of control cultures were the following: (*a*) C1300 target cells alone; (*b*) target cells and II (0.16 m*M*); (*c*) target cells and III (0.16 m*M*); (*d*) target cells and rabbit complement; (*e*) target cells, rabbit complement, and II (0.16 m*M*); (*f*) target cells, rabbit complement, and III (0.16 m*M*); (*g*) target cells and immune serum; (*h*) target cells, immune serum, and II (0.16 m*M*); and (*i*) target cells, immune serum, and III (0.16 m*M*). The average percent release of chromium-51 label did not differ significantly among these cultures and was 25.3 ± 0.7 (*SE*). Additional controls provided the following information: (*a*) a 1:640 dilution of serum from nonimmunized A/HeJ mice was not cytotoxic to C1300 target cells; and (b) antiserum from A/HeJ mice immunized against C1300 cells was not cytotoxic to unrelated target cells, specifically A/HeJ spleen cells. [b] Immune serum was drawn from syngeneic A/HeJ mice bearing 21-day-old C1300 solid tumors. [c] Mean ±*SE* (number of determinations).

Previous *in vivo* chemotherapy trials demonstrated that II exerts an antitumor activity against neuroblastoma C1300 tumors only during advanced stages of growth (3 weeks posttransplantation), when the host level of circulating cytotoxic antibody is high (1). This pattern of drug response is in distinct contrast to that observed with antimetabolites [*e.g.*, 6-thioguanine (1)], which are most effective against young, rapidly growing tumors. We, therefore, tested the relative chemotherapeutic effectiveness of II and III by administering these compounds to A/HeJ mice bearing 21-day-old neuroblastoma C1300 tumors. The procedures used for the preparation of tumors and injected drugs were described previously (1).

Compounds II and III were dissolved in 0.9% NaCl solution and injected intraperitoneally in a volume of 0.2 ml; control mice received 0.2 ml of 0.9% NaCl solution. The dosage of II and III used in chemotherapy trials, 50 mg/kg, was the maximum tolerated level for A/HeJ mice. The chemotherapeutic effect of II and III was measured as a *T/C* ratio, defined as the average tumor weight of drug-injected mice divided by the average tumor weight of 0.9% NaCl solution-injected mice at 7 days postinjection. Calculation of a T/C ratio was based on tumor weights from 10 pairs of mice; each drug-injected mouse was matched with a control 0.9% NaCl solution-injected mouse bearing a C1300 tumor of identical size and shape at the time of injection.

In vivo chemotherapy trials demonstrated that a 50-mg/kg ip dose of II exerted a significant inhibitory effect on the subsequent growth of 21-day-old C1300 tumors, with the T/C ratio at 7 days postinjection being 0.51. Based on the Student *t* test, the difference in the average weight of tumors from drug-injected and 0.9% NaCl-injected control mice was significant at $p < 0.001$. Compound III did not exert a statistically significant chemotherapeutic effect. Following administration of a 50-mg/kg ip dose of III to mice bearing 21-day-old C1300 tumors, the T/C ratio at 7 days postinjection was 0.94.

Results presented here thus indicate that the open chain carbodiimide III fails to enhance tumor immune lysis *in vitro* or to exert an antitumor effect *in vivo*, in distinct contrast to the activity demonstrated for the carbodiimide derivative (II). This observation indicates that the chemotherapeutic effect of II is not associated solely with its chemically reactive carbodiimino functional group but depends as well on other aspects of molecular structure.

In this regard, one principal difference between II and III is the permanent charge of the quaternary amine of III in contrast to the partially uncharged state of the tertiary amine of II*a* [pKa ~ 10.75 (5)]. As a consequence, II may partition into and chemically modify the tumor cell surface to a greater extent than III. The difference in charge character of II and III may also influence their metabolism, relative tissue distributions, and plasma clearance rates in a manner that favors a greater *in vivo* chemotherapeutic effect by II.

A second major structural difference between II and III is the existence of II predominantly as the reduced pyrimidine species (II*b*). The potential role of this structure in the antitumor activity of II remains obscure, but information could possibly be gained through the synthesis and biological testing *in vitro* and *in vivo* of new carbodiimide compounds that isomerize to form heterocyclic structures.

(1) R. A. Fawwaz, T. S. Tenforde, and W. H. Mehlberg, *Cancer Res.*, **35**, 679(1975).

(2) T. S. Tenforde, R. A. Fawwaz, and R. A. Grossman, *Experientia*, in press.

(3) R. A. Fawwaz and T. S. Tenforde, *Med. Hypotheses*, **1**, 29(1975).

(4) J. C. Sheehan, P. A. Cruickshank, and G. L. Boshart, *J. Org. Chem.*, **26**, 2525(1961).

(5) T. Tenforde, R. A. Fawwaz, N. K. Freeman, and N. Castagnoli, Jr., *ibid.*, **37**, 3372(1972).

(6) D. R. Schultz, "The Complement System," vol. 6 of "Monographs in Allergy," Karger, New York, N.Y., 1971.

(7) E. A. Boyse, L. Hubbard, E. Stockert, and M. E. Lamm, *Transplantation*, **10**, 446(1970).

(8) S. V. Boyden, *Advan. Immunol.*, **5**, 1(1966).

Tom S. Tenforde [x]
Rashid A. Fawwaz
Lawrence Berkeley Laboratory
Biology and Medicine Division
University of California
Berkeley, CA 94720

Neal Castagnoli, Jr.
Department of Pharmaceutical Sciences
School of Pharmacy
University of California
San Francisco, CA 94122

Received July 28, 1975.
Accepted for publication January 9, 1976.
Supported by U.S. Atomic Energy Commission Contract W-7405-eng-48 with the Lawrence Berkeley Laboratory.
The technical assistance of Alice Beckmann is gratefully acknowledged.

[x] To whom inquiries should be directed.

Antibiotics, Vol. III. Mechanism of Action of Antimicrobial and Antitumor Agents. Edited by JOHN W. CORCORAN and FRED E. HAHN. Springer-Verlag, 175 Fifth Ave., New York, NY 10010, 1975. 742 pp. 17 × 25 cm. Price $77.10.

The present volume is the third in the Antibiotics series published by Springer-Verlag. Volumes I and II which appeared in 1967 were edited by Gottlieb and Shaw. They were subtitled Mechanism of Action and Biosynthesis, respectively. Volume III is subtitled Mechanism of Action of Antimicrobial and Antitumor Agents and represents an updating and expansion of the material in Volume I, adding new topics and repeating those in which, in the opinion of the editors, there has been sufficient advance. The book consists of 46 chapters, each a short review of one or of a small group of closely related antibiotics. The chapters are divided into three sections according to the mechanism of action of the compounds.

The reviews, written by original contributors in the fields of the respective antibiotic, are for the most part excellent. For those for whom the volume is presumably intended (the research worker and advanced student), it will provide a welcome and valuable source of material that is otherwise scattered throughout the literature. For physicians and others primarily interested in the clinical use of antibiotics, however, the book will be of less value. Intentionally, no effort is made to distinguish by order or by emphasis those compounds clinically useful as antimicrobials, those clinically useful as antineoplastic agents, and those with no clinical application, and no effort is made to stress this aspect in the reviews themselves. Within the limits sets for it, however, the book can be strongly recommended, although the price, following the recent trend for volumes of this sort, will unfortunately put it out of the reach of many.

Reviewed by P. J. Creaven
Roswell Park Memorial Institute
Grace Cancer Drug Center
Buffalo, NY 14263

The Fate of Drugs in the Organism, A Bibliography Survey, Vols. 1 and 2. Edited by J. HIRTZ, Societe Francaise des Sciences et Techniques Pharmaceutiques Working Group. Marcel Dekker, Inc., 270 Madison Ave., New York, NY 10016, 1974 and 1975. 16 × 23 cm. 579 and 578 pp. Price $59.50 each.

These publications, the first of a new series, are divided into three parts: a sequentially numbered list of collected references, an analytical table of references arranged according to drug name, and an empirical formula table. In the analytical table, the content of each article is briefly analyzed using a series of 17 key words. In addition, the publication year and the total number of references quoted in the article are given.

While these publications do not intend to be exhaustive, they do attempt to locate information from various sources about the absorption, distribution, metabolism, and excretion of drugs and pull it together for easier use. Three thousand articles are included in each volume.

Staff Review

Neurological Complications of Oral Contraceptives. By EDWIN R. BICKERSTAFF. Oxford University Press, 200 Madison Avenue, New York, NY 10016, 1975. viii + 107 pp. 16.2 × 24 cm. Price $15.00.

This interesting little book was written by the Senior Consultant Neurologist at the Midland Centre for Neurosurgery and Neurology in Birmingham, England. The information contained in it is a blend of the author's own clinical experience and a somewhat modest review of the literature. Bickerstaff does acknowledge that he has not attempted to present an exhaustive review of the world's literature; unhappily, however, a few of the authors chosen to be cited may find their names misspelled. Such typographical errors, along with a few others, *in toto* are not numerous, except if one considers the small size of the book, 19 pages of which consist only of illustrative figures and their legends. These figures, incidentally, most of which are arteriograms, are excellent. However, since the author indicates that he is writing primarily for nonneurologists, much of his intended audience might better appreciate the figures if more of the latter contained arrowed labeling in addition to the legends.

The book is divided into five parts. The first and longest part, entitled Intracranial Vascular Disease, includes sections on the incidence and diagnosis of episodes of cerebral arterial insufficiency in healthy young women, patterns of cerebral arterial involvement, predisposing factors, possible etiology, symptomatology, investigation and clinical management, late prognosis, and intracranial venous occlusion. The remaining and much shorter four parts of the book are entitled Involuntary Movements, Neuro-opthalmological Disorders, Disorders of Cerebral or Cerebrovascular Function, *i.e.,* migraine and epilepsy, and, lastly, Miscellaneous Disorders.

A large section of Part I also is devoted to "the development of thought on the association between cerebrovascular disease and the use of oral contraceptives." The author has attempted to present an unbiased account by citing opinions from both sides of the controversy. Nevertheless, it is rather clear where the author's personal opinions lie. The reader, unfortunately, is not presented with the type of quantitative information needed to form an opinion. The reader is presented, instead, with statements such as "... occlusion of normal cerebral arteries in either stage of the reproductive cycle is, in practical terms, a great rarity, ...," and also with case histories of the author's patients who had been taking oral contraceptives and who had suffered neurological disorders. Cases in which it was indicated that the symptoms disappeared when the preparation was withdrawn, and reappeared when oral contraceptives were again administered, are certainly suggestive of an association. However, although the author stresses that the oral contraceptives should be withdrawn when certain neurological symptoms appear, a number of the case histories indicate recovery with no mention of whether or not the preparation was discontinued.

Furthermore, it would be hoped that in a book with the title "Neurological Complications of Oral Contraceptives," quantitative data might be found, estimating the actual incidence of most of the neurological disorders discussed, in the nonpregnant nonuser, nonpregnant user, pregnant, and puerperal populations. Incidentally, it should be pointed out that the author refers a number of times to low-estrogen preparations. The American reader should be aware, however, that most, if not all, of these comments refer to preparations containing 50 μg of estrogen. Combined preparations containing less than 50 μg of estrogen have appeared on the market much more recently in England than they have in the United States.

Perhaps the greatest value of this book lies in its detailed descriptions, with illustrative case histories, of the symptoms of various neurological disorders, particularly those due to cerebral arterial insufficiency and intracranial venous occlusion, and in its warning that a change in one's pattern of migrainous attack, again illustrated with case histories, could portend the development of a more serious vascular problem. Since an association between the use of oral contraceptives and cerebrovascular deficit certainly has not been disproven, the reader would probably do well to discontinue the use of oral contraceptives in patients exhibiting such symptoms.

Reviewed by Audrey S. Bingel
Department of Pharmacognosy and Pharmacology
University of Illinois College of Pharmacy
Chicago, IL 60612

Antibiotics, Vol. III. Mechanism of Action of Antimicrobial and Antitumor Agents. Edited by JOHN W. CORCORAN and FRED E. HAHN. Springer-Verlag, 175 Fifth Ave., New York, NY 10010, 1975. 742 pp. 17 × 25 cm. Price $77.10.

The present volume is the third in the Antibiotics series published by Springer-Verlag. Volumes I and II which appeared in 1967 were edited by Gottlieb and Shaw. They were subtitled Mechanism of Action and Biosynthesis, respectively. Volume III is subtitled Mechanism of Action of Antimicrobial and Antitumor Agents and represents an updating and expansion of the material in Volume I, adding new topics and repeating those in which, in the opinion of the editors, there has been sufficient advance. The book consists of 46 chapters, each a short review of one or of a small group of closely related antibiotics. The chapters are divided into three sections according to the mechanism of action of the compounds.

The reviews, written by original contributors in the fields of the respective antibiotic, are for the most part excellent. For those for whom the volume is presumably intended (the research worker and advanced student), it will provide a welcome and valuable source of material that is otherwise scattered throughout the literature. For physicians and others primarily interested in the clinical use of antibiotics, however, the book will be of less value. Intentionally, no effort is made to distinguish by order or by emphasis those compounds clinically useful as antimicrobials, those clinically useful as antineoplastic agents, and those with no clinical application, and no effort is made to stress this aspect in the reviews themselves. Within the limits sets for it, however, the book can be strongly recommended, although the price, following the recent trend for volumes of this sort, will unfortunately put it out of the reach of many.

Reviewed by P. J. Creaven
Roswell Park Memorial Institute
Grace Cancer Drug Center
Buffalo, NY 14263

The Fate of Drugs in the Organism, A Bibliography Survey, Vols. 1 and 2. Edited by J. HIRTZ, Societe Francaise des Sciences et Techniques Pharmaceutiques Working Group. Marcel Dekker, Inc., 270 Madison Ave., New York, NY 10016, 1974 and 1975. 16 × 23 cm. 579 and 578 pp. Price $59.50 each.

These publications, the first of a new series, are divided into three parts: a sequentially numbered list of collected references, an analytical table of references arranged according to drug name, and an empirical formula table. In the analytical table, the content of each article is briefly analyzed using a series of 17 key words. In addition, the publication year and the total number of references quoted in the article are given.

While these publications do not intend to be exhaustive, they do attempt to locate information from various sources about the absorption, distribution, metabolism, and excretion of drugs and pull it together for easier use. Three thousand articles are included in each volume.

Staff Review

Neurological Complications of Oral Contraceptives. By EDWIN R. BICKERSTAFF. Oxford University Press, 200 Madison Avenue, New York, NY 10016, 1975. viii + 107 pp. 16.2 × 24 cm. Price $15.00.

This interesting little book was written by the Senior Consultant Neurologist at the Midland Centre for Neurosurgery and Neurology in Birmingham, England. The information contained in it is a blend of the author's own clinical experience and a somewhat modest review of the literature. Bickerstaff does acknowledge that he has not attempted to present an exhaustive review of the world's literature; unhappily, however, a few of the authors chosen to be cited may find their names misspelled. Such typographical errors, along with a few others, *in toto* are not numerous, except if one considers the small size of the book, 19 pages of which consist only of illustrative figures and their legends. These figures, incidentally, most of which are arteriograms, are excellent. However, since the author indicates that he is writing primarily for nonneurologists, much of his intended audience might better appreciate the figures if more of the latter contained arrowed labeling in addition to the legends.

The book is divided into five parts. The first and longest part, entitled Intracranial Vascular Disease, includes sections on the incidence and diagnosis of episodes of cerebral arterial insufficiency in healthy young women, patterns of cerebral arterial involvement, predisposing factors, possible etiology, symptomatology, investigation and clinical management, late prognosis, and intracranial venous occlusion. The remaining and much shorter four parts of the book are entitled Involuntary Movements, Neuro-opthalmological Disorders, Disorders of Cerebral or Cerebrovascular Function, *i.e.,* migraine and epilepsy, and, lastly, Miscellaneous Disorders.

A large section of Part I also is devoted to "the development of thought on the association between cerebrovascular disease and the use of oral contraceptives." The author has attempted to present an unbiased account by citing opinions from both sides of the controversy. Nevertheless, it is rather clear where the author's personal opinions lie. The reader, unfortunately, is not presented with the type of quantitative information needed to form an opinion. The reader is presented, instead, with statements such as "... occlusion of normal cerebral arteries in either stage of the reproductive cycle is, in practical terms, a great rarity, ...," and also with case histories of the author's patients who had been taking oral contraceptives and who had suffered neurological disorders. Cases in which it was indicated that the symptoms disappeared when the preparation was withdrawn, and reappeared when oral contraceptives were again administered, are certainly suggestive of an association. However, although the author stresses that the oral contraceptives should be withdrawn when certain neurological symptoms appear, a number of the case histories indicate recovery with no mention of whether or not the preparation was discontinued.

Furthermore, it would be hoped that in a book with the title "Neurological Complications of Oral Contraceptives," quantitative data might be found, estimating the actual incidence of most of the neurological disorders discussed, in the nonpregnant nonuser, nonpregnant user, pregnant, and puerperal populations. Incidentally, it should be pointed out that the author refers a number of times to low-estrogen preparations. The American reader should be aware, however, that most, if not all, of these comments refer to preparations containing 50 μg of estrogen. Combined preparations containing less than 50 μg of estrogen have appeared on the market much more recently in England than they have in the United States.

Perhaps the greatest value of this book lies in its detailed descriptions, with illustrative case histories, of the symptoms of various neurological disorders, particularly those due to cerebral arterial insufficiency and intracranial venous occlusion, and in its warning that a change in one's pattern of migrainous attack, again illustrated with case histories, could portend the development of a more serious vascular problem. Since an association between the use of oral contraceptives and cerebrovascular deficit certainly has not been disproven, the reader would probably do well to discontinue the use of oral contraceptives in patients exhibiting such symptoms.

Reviewed by Audrey S. Bingel
Department of Pharmacognosy and Pharmacology
University of Illinois College of Pharmacy
Chicago, IL 60612

Antibiotics, Vol. III. Mechanism of Action of Antimicrobial and Antitumor Agents. Edited by JOHN W. CORCORAN and FRED E. HAHN. Springer-Verlag, 175 Fifth Ave., New York, NY 10010, 1975. 742 pp. 17 × 25 cm. Price $77.10.

The present volume is the third in the Antibiotics series published by Springer-Verlag. Volumes I and II which appeared in 1967 were edited by Gottlieb and Shaw. They were subtitled Mechanism of Action and Biosynthesis, respectively. Volume III is subtitled Mechanism of Action of Antimicrobial and Antitumor Agents and represents an updating and expansion of the material in Volume I, adding new topics and repeating those in which, in the opinion of the editors, there has been sufficient advance. The book consists of 46 chapters, each a short review of one or of a small group of closely related antibiotics. The chapters are divided into three sections according to the mechanism of action of the compounds.

The reviews, written by original contributors in the fields of the respective antibiotic, are for the most part excellent. For those for whom the volume is presumably intended (the research worker and advanced student), it will provide a welcome and valuable source of material that is otherwise scattered throughout the literature. For physicians and others primarily interested in the clinical use of antibiotics, however, the book will be of less value. Intentionally, no effort is made to distinguish by order or by emphasis those compounds clinically useful as antimicrobials, those clinically useful as antineoplastic agents, and those with no clinical application, and no effort is made to stress this aspect in the reviews themselves. Within the limits sets for it, however, the book can be strongly recommended, although the price, following the recent trend for volumes of this sort, will unfortunately put it out of the reach of many.

Reviewed by P. J. Creaven
Roswell Park Memorial Institute
Grace Cancer Drug Center
Buffalo, NY 14263

The Fate of Drugs in the Organism, A Bibliography Survey, Vols. 1 and 2. Edited by J. HIRTZ, Societe Francaise des Sciences et Techniques Pharmaceutiques Working Group. Marcel Dekker, Inc., 270 Madison Ave., New York, NY 10016, 1974 and 1975. 16 × 23 cm. 579 and 578 pp. Price $59.50 each.

These publications, the first of a new series, are divided into three parts: a sequentially numbered list of collected references, an analytical table of references arranged according to drug name, and an empirical formula table. In the analytical table, the content of each article is briefly analyzed using a series of 17 key words. In addition, the publication year and the total number of references quoted in the article are given.

While these publications do not intend to be exhaustive, they do attempt to locate information from various sources about the absorption, distribution, metabolism, and excretion of drugs and pull it together for easier use. Three thousand articles are included in each volume.

Staff Review

Neurological Complications of Oral Contraceptives. By EDWIN R. BICKERSTAFF. Oxford University Press, 200 Madison Avenue, New York, NY 10016, 1975. viii + 107 pp. 16.2 × 24 cm. Price $15.00.

This interesting little book was written by the Senior Consultant Neurologist at the Midland Centre for Neurosurgery and Neurology in Birmingham, England. The information contained in it is a blend of the author's own clinical experience and a somewhat modest review of the literature. Bickerstaff does acknowledge that he has not attempted to present an exhaustive review of the world's literature; unhappily, however, a few of the authors chosen to be cited may find their names misspelled. Such typographical errors, along with a few others, *in toto* are not numerous, except if one considers the small size of the book, 19 pages of which consist only of illustrative figures and their legends. These figures, incidentally, most of which are arteriograms, are excellent. However, since the author indicates that he is writing primarily for nonneurologists, much of his intended audience might better appreciate the figures if more of the latter contained arrowed labeling in addition to the legends.

The book is divided into five parts. The first and longest part, entitled Intracranial Vascular Disease, includes sections on the incidence and diagnosis of episodes of cerebral arterial insufficiency in healthy young women, patterns of cerebral arterial involvement, predisposing factors, possible etiology, symptomatology, investigation and clinical management, late prognosis, and intracranial venous occlusion. The remaining and much shorter four parts of the book are entitled Involuntary Movements, Neuro-opthalmological Disorders, Disorders of Cerebral or Cerebrovascular Function, *i.e.,* migraine and epilepsy, and, lastly, Miscellaneous Disorders.

A large section of Part I also is devoted to "the development of thought on the association between cerebrovascular disease and the use of oral contraceptives." The author has attempted to present an unbiased account by citing opinions from both sides of the controversy. Nevertheless, it is rather clear where the author's personal opinions lie. The reader, unfortunately, is not presented with the type of quantitative information needed to form an opinion. The reader is presented, instead, with statements such as "... occlusion of normal cerebral arteries in either stage of the reproductive cycle is, in practical terms, a great rarity, ...," and also with case histories of the author's patients who had been taking oral contraceptives and who had suffered neurological disorders. Cases in which it was indicated that the symptoms disappeared when the preparation was withdrawn, and reappeared when oral contraceptives were again administered, are certainly suggestive of an association. However, although the author stresses that the oral contraceptives should be withdrawn when certain neurological symptoms appear, a number of the case histories indicate recovery with no mention of whether or not the preparation was discontinued.

Furthermore, it would be hoped that in a book with the title "Neurological Complications of Oral Contraceptives," quantitative data might be found, estimating the actual incidence of most of the neurological disorders discussed, in the nonpregnant nonuser, nonpregnant user, pregnant, and puerperal populations. Incidentally, it should be pointed out that the author refers a number of times to low-estrogen preparations. The American reader should be aware, however, that most, if not all, of these comments refer to preparations containing 50 μg of estrogen. Combined preparations containing less than 50 μg of estrogen have appeared on the market much more recently in England than they have in the United States.

Perhaps the greatest value of this book lies in its detailed descriptions, with illustrative case histories, of the symptoms of various neurological disorders, particularly those due to cerebral arterial insufficiency and intracranial venous occlusion, and in its warning that a change in one's pattern of migrainous attack, again illustrated with case histories, could portend the development of a more serious vascular problem. Since an association between the use of oral contraceptives and cerebrovascular deficit certainly has not been disproven, the reader would probably do well to discontinue the use of oral contraceptives in patients exhibiting such symptoms.

Reviewed by Audrey S. Bingel
Department of Pharmacognosy and Pharmacology
University of Illinois College of Pharmacy
Chicago, IL 60612

Journal of Pharmaceutical Sciences

MAY 1976

VOLUME 65 NUMBER 5

MARY H. FERGUSON
Editor

L. LUAN CORRIGAN
Assistant Editor

SHELLY ELLIOTT
Production Editor

JANET D. SHOFF
Copy Editor

EDWARD G. FELDMANN
Contributing Editor

SAMUEL W. GOLDSTEIN
Contributing Editor

LELAND J. ARNEY
Publications Director

EDITORIAL ADVISORY BOARD

JOHN AUTIAN
LYNN R. BRADY
WILLIAM O. FOYE
WILLIAM J. JUSKO
HARRY B. KOSTENBAUDER
CARL J. LINTNER, JR.
DAVID E. MANN, JR.
GERALD J. PAPARIELLO

The *Journal of Pharmaceutical Sciences* is published monthly by the American Pharmaceutical Association at 2215 Constitution Ave., N.W., Washington, DC 20037. Second-class postage paid at Washington, D.C., and at additional mailing office.

All expressions of opinion and statements of supposed fact appearing in articles or editorials carried in this journal are published on the authority of the writer over whose name they appear and are not to be regarded as necessarily expressing the policies or views of the American Pharmaceutical Association.

Offices—Editorial, Advertising, and Subscription Offices: 2215 Constitution Ave., N.W., Washington, DC 20037. Printing Offices: 20th & Northampton Streets, Easton, PA 18042

Annual Subscriptions—United States and foreign, industrial and government institutions $50, educational institutions $50, individuals *for personal use only* $30; single copies $5. All foreign subscriptions add $5 for postage. Subscription rates are subject to change without notice. Members of the American Pharmaceutical Association may elect to receive the *Journal of Pharmaceutical Sciences* as a part of their annual $60 (foreign $65) APhA membership dues.

Claims—Missing numbers will not be supplied if dues or subscriptions are in arrears for more than 60 days or if claims are received more than 60 days after the date of the issue, or if loss was due to failure to give notice of change of address. The Association cannot accept responsibility for foreign delivery when its records indicate shipment has been made.

Change of Address—Members and subscribers should notify at once both the Post Office and the American Pharmaceutical Association, 2215 Constitution Ave., N.W., Washington, DC 20037, of any change of address.

© Copyright 1976, American Pharmaceutical Association, 2215 Constitution Ave., N.W., Washington, DC 20037; all rights reserved.

THE PRICE OF A "FREE PRESS"

Whenever election time rolls around, one hears a good many stories about Chicago politics, and how votes can be bought and sold if the price is right. This writer was born and raised in Chicago and can attest to the fact that many of these stories are all too true.

However, votes are not the only things in life that shouldn't be for sale but, nevertheless, are solicited, priced, and bought.

When our constitutional fathers wrote lofty guarantees about freedom of the press, they failed to foresee the impact and influence of those who would decide the placement of advertising—where, when, and how much. It is a sad but acknowledged fact that the editorial policies of many publications—in the lay press, as well as in the medical and pharmaceutical press—are strongly influenced, if not dictated, by the source of advertising dollars. This point has been made at various times relative to the cozy relationship which exists between one of our "sister professions" and the drug industry.

Woe be to the newspaper, journal, magazine, or other publication that dares to report that which does not please the advertisers! The old adage that "hell hath no fury like a woman scorned" is mild compared to the rage and retaliation that some advertisers will display when the medium they employ does something to displease them.

The prestigious *New York Times* apparently felt that it was immune to this phenomenon, because early this year it dared to run a five-part series on medical incompetence in which drug industry promotional and advertising practices came in for their share of criticism.

Well, it did not take long for the ax to fall. Just a few weeks later, the *Times* ran another story, this time headlined "Drug Ads Dropped Over *Times* Series." This story told how pharmaceutical concerns abruptly canceled advertising worth $500,000 from *Modern Medicine*, a magazine owned by The New York Times Company. This translated into a loss of 200 pages of drug company advertisements in the magazine. From the gist of the article, the cause and effect relationship between the series of articles and the canceled ads was made crystal clear.

Predictably, industry trade spokesmen, as well as others, have criticized the *Times* articles as bordering on the sensational. And perhaps there may be some justification for their viewpoint. On the other hand, other writers—including the editor of a prominent journal in the drug and cosmetic field—commented upon the *Times* series in quite favorable terms.

Be that as it may, all of this is "old hat" to APhA and its publications! It has been almost 10 years now since the Association dared to adopt certain policies and to carry reports of these policies in its publications. These actions similarly displeased a wide segment of the pharmaceutical industry.

Massive cancellations of advertising pages and meeting exhibit space were the immediate result. To their credit, a small but significant number of advertisers disdained this petty course. At any rate, to this day our ad sections are thin, and advertising revenue remains a very nominal source of APhA income. Consequently, APhA publications must be funded in other ways. In the case of the *Journal of Pharmaceutical Sciences*, subscription revenue, membership dues, and page charges now constitute the principal sources of revenue.

Rising costs, especially for paper and printing, have contributed greatly to major increases in the Journal expense budget over the past few years. Only so much can be done to absorb such costs, and one recent result has been the need to raise page charges, effective with the July 1976 issue. Concomitantly, steps are being taken to stimulate authors to pay page charges because there is some indication that the "payment is not mandatory" policy is being abused by certain authors.

Moreover, it has become necessary to establish a ceiling on the number of pages which may be published during the calendar year. This step has also been dictated by the need to control publication costs.

Hence, lack of adequate revenue prevents us from doing as much as we would like. In the case of this Journal, meager advertising income is one factor that has necessitated placing a lid on the number of pages available; and, in turn, this page limit is creating a backlog of accepted papers and longer delays in their publication. Regrettably, such is the price that has to be paid in order to maintain "a free press." —EGF

Journal of Pharmaceutical Sciences

MAY 1976

VOLUME 65 NUMBER 5

MARY H. FERGUSON
Editor

L. LUAN CORRIGAN
Assistant Editor

SHELLY ELLIOTT
Production Editor

JANET D. SHOFF
Copy Editor

EDWARD G. FELDMANN
Contributing Editor

SAMUEL W. GOLDSTEIN
Contributing Editor

LELAND J. ARNEY
Publications Director

EDITORIAL ADVISORY BOARD

JOHN AUTIAN
LYNN R. BRADY
WILLIAM O. FOYE
WILLIAM J. JUSKO
HARRY B. KOSTENBAUDER
CARL J. LINTNER, JR.
DAVID E. MANN, JR.
GERALD J. PAPARIELLO

The *Journal of Pharmaceutical Sciences* is published monthly by the American Pharmaceutical Association at 2215 Constitution Ave., N.W., Washington, DC 20037. Second-class postage paid at Washington, D.C., and at additional mailing office.

All expressions of opinion and statements of supposed fact appearing in articles or editorials carried in this journal are published on the authority of the writer over whose name they appear and are not to be regarded as necessarily expressing the policies or views of the American Pharmaceutical Association.

Offices—Editorial, Advertising, and Subscription Offices: 2215 Constitution Ave., N.W., Washington, DC 20037. Printing Offices: 20th & Northampton Streets, Easton, PA 18042

Annual Subscriptions—United States and foreign, industrial and government institutions $50, educational institutions $50, individuals *for personal use only* $30; single copies $5. All foreign subscriptions add $5 for postage. Subscription rates are subject to change without notice. Members of the American Pharmaceutical Association may elect to receive the *Journal of Pharmaceutical Sciences* as a part of their annual $60 (foreign $65) APhA membership dues.

Claims—Missing numbers will not be supplied if dues or subscriptions are in arrears for more than 60 days or if claims are received more than 60 days after the date of the issue, or if loss was due to failure to give notice of change of address. The Association cannot accept responsibility for foreign delivery when its records indicate shipment has been made.

Change of Address—Members and subscribers should notify at once both the Post Office and the American Pharmaceutical Association, 2215 Constitution Ave., N.W., Washington, DC 20037, of any change of address.

© Copyright 1976, American Pharmaceutical Association, 2215 Constitution Ave., N.W., Washington, DC 20037; all rights reserved.

THE PRICE OF A "FREE PRESS"

Whenever election time rolls around, one hears a good many stories about Chicago politics, and how votes can be bought and sold if the price is right. This writer was born and raised in Chicago and can attest to the fact that many of these stories are all too true.

However, votes are not the only things in life that shouldn't be for sale but, nevertheless, are solicited, priced, and bought.

When our constitutional fathers wrote lofty guarantees about freedom of the press, they failed to foresee the impact and influence of those who would decide the placement of advertising—where, when, and how much. It is a sad but acknowledged fact that the editorial policies of many publications—in the lay press, as well as in the medical and pharmaceutical press—are strongly influenced, if not dictated, by the source of advertising dollars. This point has been made at various times relative to the cozy relationship which exists between one of our "sister professions" and the drug industry.

Woe be to the newspaper, journal, magazine, or other publication that dares to report that which does not please the advertisers! The old adage that "hell hath no fury like a woman scorned" is mild compared to the rage and retaliation that some advertisers will display when the medium they employ does something to displease them.

The prestigious *New York Times* apparently felt that it was immune to this phenomenon, because early this year it dared to run a five-part series on medical incompetence in which drug industry promotional and advertising practices came in for their share of criticism.

Well, it did not take long for the ax to fall. Just a few weeks later, the *Times* ran another story, this time headlined "Drug Ads Dropped Over *Times* Series." This story told how pharmaceutical concerns abruptly canceled advertising worth $500,000 from *Modern Medicine*, a magazine owned by The New York Times Company. This translated into a loss of 200 pages of drug company advertisements in the magazine. From the gist of the article, the cause and effect relationship between the series of articles and the canceled ads was made crystal clear.

Predictably, industry trade spokesmen, as well as others, have criticized the *Times* articles as bordering on the sensational. And perhaps there may be some justification for their viewpoint. On the other hand, other writers—including the editor of a prominent journal in the drug and cosmetic field—commented upon the *Times* series in quite favorable terms.

Be that as it may, all of this is "old hat" to APhA and its publications! It has been almost 10 years now since the Association dared to adopt certain policies and to carry reports of these policies in its publications. These actions similarly displeased a wide segment of the pharmaceutical industry.

Massive cancellations of advertising pages and meeting exhibit space were the immediate result. To their credit, a small but significant number of advertisers disdained this petty course. At any rate, to this day our ad sections are thin, and advertising revenue remains a very nominal source of APhA income. Consequently, APhA publications must be funded in other ways. In the case of the *Journal of Pharmaceutical Sciences*, subscription revenue, membership dues, and page charges now constitute the principal sources of revenue.

Rising costs, especially for paper and printing, have contributed greatly to major increases in the Journal expense budget over the past few years. Only so much can be done to absorb such costs, and one recent result has been the need to raise page charges, effective with the July 1976 issue. Concomitantly, steps are being taken to stimulate authors to pay page charges because there is some indication that the "payment is not mandatory" policy is being abused by certain authors.

Moreover, it has become necessary to establish a ceiling on the number of pages which may be published during the calendar year. This step has also been dictated by the need to control publication costs.

Hence, lack of adequate revenue prevents us from doing as much as we would like. In the case of this Journal, meager advertising income is one factor that has necessitated placing a lid on the number of pages available; and, in turn, this page limit is creating a backlog of accepted papers and longer delays in their publication. Regrettably, such is the price that has to be paid in order to maintain "a free press." —EGF

Journal of Pharmaceutical Sciences

MAY 1976
VOLUME 65 NUMBER 5

REVIEW ARTICLE

Arrhythmias and Antiarrhythmic Drugs: Mechanism of Action and Structure–Activity Relationships II ▲

P. H. MORGAN * and I. W. MATHISON ˣ

Keyphrases □ Antiarrhythmic drugs—classifications, mechanism of action, structure–activity relationships, review □ Structure–activity relationships—antiarrhythmic drugs, review □ Arrhythmias—related to changes in normal transmembrane action potential and electrophysiological parameters, antiarrhythmic drugs, review

CONTENTS

Classifications of Antiarrhythmic Drugs 635
Structure–Activity Relationships 637
Nonspecific Antiarrhythmic Agents 637
Cardioselective β-Adrenergic Antagonists 644
References 647

CLASSIFICATIONS OF ANTIARRHYTHMIC DRUGS

Several attempts have been made to classify antiarrhythmic drugs according to their electrophysiological properties. Again, disagreement arises due to the complications mentioned earlier and due to the lack of agreement over which drug-induced changes in the transmembrane action potential are most responsible for the therapeutic action in humans. The measure of success of any classification depends upon its relevance to, and usefulness in, the clinical situation.

As discussed previously, Szekeres and Papp (15) divided antiarrhythmic drugs into two broad classes: (*a*) nonspecific, for the quinidine-like membrane-stabilizing drugs, and (*b*) specific, for the β-adrenergic blocking drugs.

Vaughan Williams (13, 163, 164) proposed four classes of drugs (Table VI). Class I includes the membrane-stabilizing drugs which interfere with sodium-ion influx during rapid depolarization, resulting in a decrease in the rate of rise (dv/dt) of phase 0.

Class II antiarrhythmic drugs include bretylium, propranolol, and other antisympathetic drugs in which little if any of their action is quinidine-like at therapeutic concentrations. This class includes drugs that are β-adrenergic blocking agents or that elicit their antisympathetic action by blocking the release of the sympathetic transmitters, epinephrine and norepinephrine. The blocking of sympathetic activity by these drugs is said to reduce the probability of arrhythmias, regardless of the nature of the precipitating factor (23).

Although Vaughan Williams classified bretylium as a Class II drug, eliciting its primary effect by β-adrenergic receptor blockade, Namm *et al.* (159) reported that bretylium exhibited Class I effects on rat atrium and ventricle muscle at concentrations previously thought to effect β-blockade only. The decrease in the rate of rise of phase 0 and the lengthening of the effective refractory period were essentially equal in normal and immunosympathectomized rats, indicating direct membrane depressant action rather than indirect effects from bretylium interacting with sympathetic neurons. *In vivo* and *in vitro*

▲ *Editor's note:* Part I of this article appeared in the April 1976 issue of the *Journal of Pharmaceutical Sciences*.

Table VI—Vaughan Williams' Classification of Antiarrhythmic Drugs

Class I	Class II	Class III	Class IV
Quinidine	Propranolol	Amiodarone	Verapamil
Procaine	Pronethalol	Oxyfedrine	XIX[b]
Procainamide	Bretylium	(Sotalol)[a]	
Lidocaine	Guanethidine	XX[a]	
Phenytoin	Alprenolol		
Disopyramide	Oxprenolol		
Ajmaline	Practolol		
Mexiletine	Sotalol		
(Propranolol)[c]	XX[d]		
(Alprenolol)[c]			
(Oxprenolol)[c]			

[a] These drugs have strong Class II action but also possess acute Class III action. [b] D-600. [c] These β-blocking agents possess Class I action only at high doses. [d] INPEA.

exposure of the myocardium to ^{14}C-bretylium showed that the drug was highly concentrated in the ventricle, and efflux studies indicated that the binding was tight, although slowly reversible. The subcellular distribution of the labeled drug bound to the ventricle suggested a binding to plasma membranes. The investigators concluded that their results indicate that underlying the antiarrhythmic action of bretylium is its accumulation in cardiac muscle cells and its direct effect on the electrophysiological properties of the membrane independent of any β-adrenergic receptor blockage.

The third class of antiarrhythmic drugs are those that affect the repolarization phase of the transmembrane action potential in contrast to the Class I drugs that affect the depolarization. Inhibition of repolarization causes an increase in the duration of the action potential. This has been found to occur in hypothyroid patients; in hyperthyroid patients, the action potential duration is decreased, which can result in atrial fibrillation.

After prolonged treatment (1–6 weeks) with amiodarone (157) or oxyfedrine (165, 166), a significant prolongation of repolarization and, hence, an increase in the absolute refractory period were observed and the effect did not appear to be linked with antithyroid action. The β-blocking agents, sotalol and *N*-isopropyl-1-(*p*-nitrophenyl)ethanolamine (XX) exhibit this action in addition to their Class II properties without the necessity of prolonged administration (167, 168).

Verapamil and its methoxy-substituted analog, XIX, belong to an apparent fourth class of antiarrhythmic agents. They are reported to have no significant effect on the rate of rise of phase 0, no β-blocking properties, and no effect on the repolarization phase except some shortening at 50% repolarization (28). Verapamil also is reported to be negatively inotropic (reduces the force of contraction). These effects are consistent with Vaughan Williams' postulate that verapamil probably elicits its antiarrhythmic activity by antagonizing the slow inward calcium-ion current associated with the slow response (13, 164). The slow response recently has been implicated in the genesis of arrhythmias arising in diseased tissue in which the fast response has been lost due to diminished resting potential (see earlier discussion of slow response).

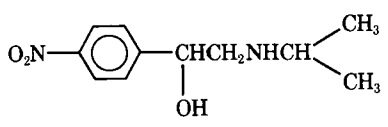

XX

Table VII—Hoffman's Classification of Antiarrhythmic Drugs

Group 1	Group 2	Group 3
Quinidine	Lidocaine	Bretylium
Procainamide	Phenytoin	
Propranolol		
Antazoline		
Ajmaline		
Disopyramide		

To summarize, the fundamental electrophysiological properties upon which Vaughan Williams' classification is based are: Class I, interference with fast sodium-ion influx of phase 0; Class II, antisympathetic action; Class III, prolongation of repolarization resulting in increased duration and refractory period; and Class IV, depression of the slow calcium-ion influx associated with the slow response. Vaughan Williams emphasized that a drug may elicit more than one class of action, but the class in which he placed them appears to describe their primary beneficial action (13).

A different classification was proposed by Hoffman and coworkers (17, 137, 170) which divides antiarrhythmic drugs into three groups (Table VII). The basis of Group 1 drug action is quinidine-like in that automaticity, membrane responsiveness, and dv/dt are decreased and conduction is slowed. Group 2 drugs also decrease automaticity but are claimed to increase membrane responsiveness, dv/dt, and conduction; lidocaine and phenytoin are included in this group. The actions of these drugs are in dispute because one group of investigators claimed that they are depressant and do not improve membrane responsiveness at normal potassium-ion levels (23, 148, 151, 162). Others maintain that phenytoin and possibly lidocaine do improve membrane responsiveness and conduction at lower drug concentrations, which more closely correspond to therapeutic blood levels in humans (144, 160, 161).

A third group is proposed for bretylium because it appears to act by a different mechanism of action than the first two groups. No attempt is made in this classification to distinguish between the indirect cardiac effects of β-adrenergic blockade and the direct effects of membrane-stabilizing drugs.

To recapitulate, Hoffman's classification divides antiarrhythmic drugs into: Group 1, those that express their beneficial action by depressing membrane responsiveness and conduction; Group 2, those whose beneficial action arises from increased membrane responsiveness and improved conduction; and Group 3, those whose mechanism of action appears to be different than the first two.

Cranefield (80) proposed that arrhythmias arise almost exclusively from slow response activity in a dis-

crete and localized focus of partially depressed fibers. Based upon this concept, he tentatively divided antiarrhythmic drugs into three classes: Class 1, those that affect the fast inward sodium-ion current (membrane stabilizers); Class 2, those that affect the slow inward calcium-ion current (verapamil and XIX); and Class 3, those that affect the transitional fibers. Cranefield's classification is similar in some ways to Vaughan Williams' in that Class 1 and Class 2 of the former correspond to Class I and Class IV of the latter, respectively. Apparently, further experimentation is necessary before any specific examples can be included in Class 3.

Sasyniuk and Ogilvie (144) stated recently that there is insufficient information on which to base a meaningful classification of antiarrhythmic drugs. However, they then observed that there appears to be two common actions for quinidine, procainamide, propranolol, lidocaine, and phenytoin. The first is that all five drugs are effective in suppressing automaticity in Purkinje fibers. The second is the ability to produce uniformity of the action potential duration and refractory period throughout the ventricular conducting system.

What becomes readily apparent in reviewing these different classifications is the lack of agreement over which observed electrophysiological change caused by a drug is most basic and eventually manifests itself therapeutically. Detailed knowledge of the biofunction of the macromolecular constituents of the excitable membrane could help clarify the confusion. Such knowledge may not be achieved for many years. However, as the sophistication of the voltage clamp technique advances, one may anticipate that investigations into the effects on each different ionic channel will lead to a more basic understanding and concise classification of the actions of antiarrhythmic drugs. Also, if the time comes when the contribution of each channel to the action potential can be measured accurately and a complete kinetic model can be constructed, it may become possible to describe and quantify mathematically the changes brought about by the actions of drugs.

STRUCTURE–ACTIVITY RELATIONSHIPS

Nonspecific Antiarrhythmic Agents—Szekeres and Papp (15) extensively reviewed the structure–activity relationships of antiarrhythmic drugs prior to 1970 and proposed a chemical classification of these agents. Conn (171) also reviewed the structure–activity relationships of antiarrhythmic drugs, primarily restricting his discussion to quinidine and its metabolites and procainamide. These investigations indicated that most antiarrhythmic drugs possess a tertiary amine group, which appears to be essential for activity. The presence of a benzene, pyridine, quinoline, or some other form of an aromatic ring system is also important, and this moiety is usually connected to the tertiary amine *via* a hydroxy-substituted alkyl chain, ester, or amide group (XXI–XXIV).

DiPalma and Lambert (172) indicated that methoxyl groups substituted on the aromatic ring portions of antiarrhythmic agents may enhance activity. For further classifications of other antiarrhythmic agents of different chemical structure, the reader is referred to Szekeres and Papp (15).

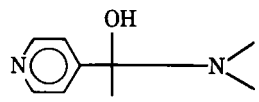

XXI

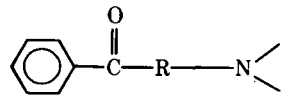

XXII: R = N or O

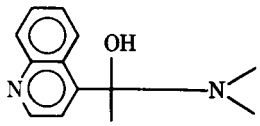

XXIII

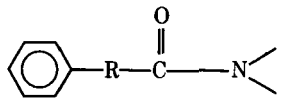

XXIV: R = N or O

The first attempt to determine the most potent compounds in a related series was by Frey in 1918 (2). He studied the antiarrhythmic potency of quinidine (I), quinine (XXV*a*), and cinchonine (XXVI); while all three possessed the ability to abolish atrial fibrillation, quinidine was the most potent. Gold *et al.* (173) compared the action of quinidine, quinine, cinchonine, and cinchonidine (XXV*b*) in slowing the rate of atrial circus movement and also found that quinidine was the most potent. Van Dongen and coworkers (174–177) reported on the action of several isomers and congeners of quinidine in increasing the myocardial resistance to arrhythmia-inducing levels of electrical shock. Some stereoselectivity was observed, but most compounds related to quinidine showed good activity.

Recently, a study determined the antiarrhythmic potency and acute toxicity in mice of quinidine and a series of 10 congeners, including various isomers (178). Eight of the 10 compounds possessed significant antiarrhythmic activity, although quinidine and dihydroquinidine (XXVII) were the most potent. In

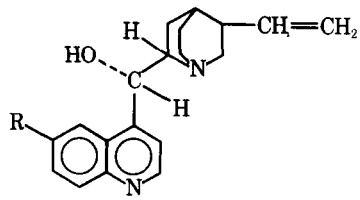

XXV*a*: R = CH_3O
XXV*b*: R = H

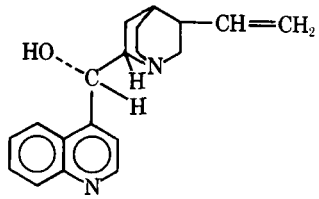

XXVI

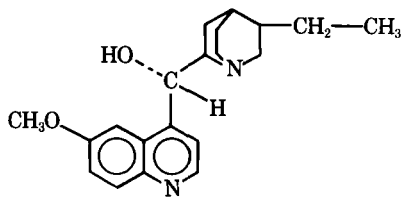

XXVII

this study, as in others (58, 179, 180), dihydroquinidine was shown to be slightly more potent than quinidine.

The antiarrhythmic potency was determined for a series of procainamide derivatives in which the *N*-ethyl substituents on the tertiary amine were modified or replaced (181). Replacement of both ethyl groups by related aliphatic groups (*i.e.*, isopropyl) greatly reduced activity, whereas replacement of only one ethyl group with an aromatic group greatly enhanced activity. A more recent structure–activity study on procainamide (II) involved amide reversal and *ortho*-methylation of the parent molecule (182). Results indicated that simple reversal of the amide group (XXVIII) in procainamide reduced activity about one-third whereas *ortho*-methylation (XXIX) of procainamide increased activity. The most active compounds were the *o*-methyl-substituted derivatives, in which the benzamido group of procainamide had been replaced by a benzoyl ester group (XXX).

Few structure–activity investigations that include physicochemical properties have been conducted on the nonspecific antiarrhythmic drugs, although those available have shown a correlation between physicochemical parameters (pKa and partition coefficient) and pharmacological potency. Studies on the effect of stereochemistry have been largely limited to differences in activity of diastereoisomers (*i.e.*, quinine and quinidine). However, optical isomerism (enantiomers) has been considered in the case of *d*- and *l*-propranolol and the other β-blocking agents in relation to their membrane-stabilizing properties. Activity is present in both the *d*- and *l*-forms with no significant difference in potency between the isomers (115–119).

This finding seems to imply that the differences in activity observed in studies involving diastereoisomers are probably due to differences in the physical properties of the isomers and not necessarily to differences in arrangement of the atoms in space. Since it seems likely that nonspecific antiarrhythmic activity may depend largely on the physical characteristics of the molecules, studies correlating these characteristics with the differences in activity, especially in a closely related series of active compounds, should be valuable in developing superior antiarrhythmic agents.

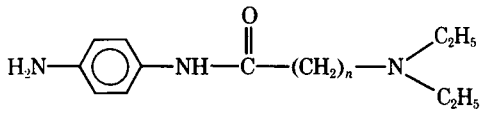

XXVIII: $n = 1$ or 2

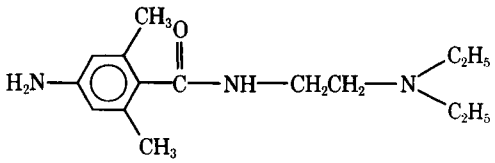

XXIX

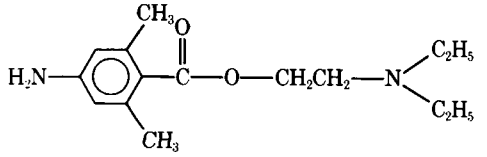

XXX

Investigations (183, 184) into the correlation between physicochemical properties and (*a*) β-blocking potency, (*b*) local anesthetic effect, and (*c*) myocardial membrane stabilization of a series of phenethanolamine and phenoxyisopropanolamine compounds led to the conclusion that there was a clear separation between β-blocking activity and the latter two actions. The physicochemical properties of these compounds were proposed to be determinants of their membrane affinity and, therefore, of their nonspecific pharmacological effects.

This proposal was further substantiated by quantitative correlations between surface activity, hydrophobicity (measured as octanol–water partition coefficient), local anesthesia, and changes in myocardial conduction velocity for β-adrenergic receptor blocking agents including VI, XX, pindolol (XXXI), alprenolol (XXXII), oxprenolol (XXXIII), practolol (XXXIV), sotalol (XXXV), 1-(3′-methylphenoxy)-2-hydroxy-3-isopropylaminopropane[14] (XXXVI), and 3-*tert*-butylamino-1-(6′-chloro-3′-methylphen-

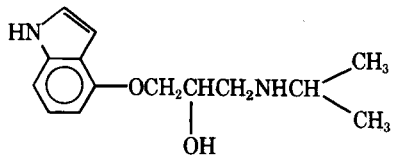

XXXI

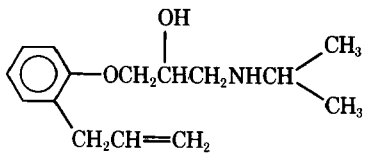

XXXII

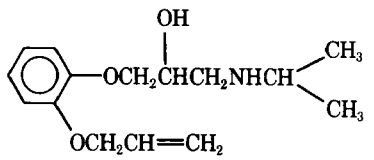

XXXIII

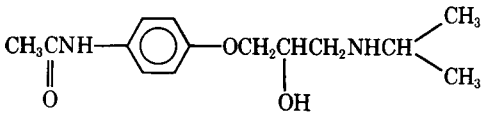

XXXIV

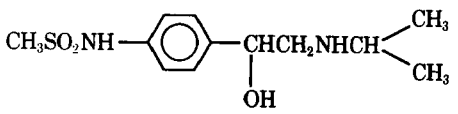

XXXV

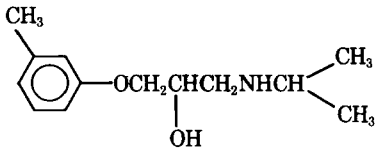

XXXVI

[14] Kö 592.

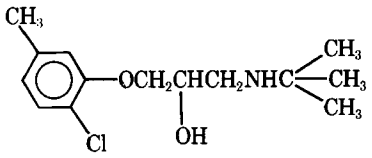

XXXVII

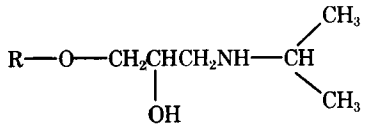

XXXVIII

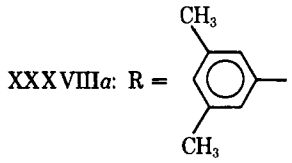

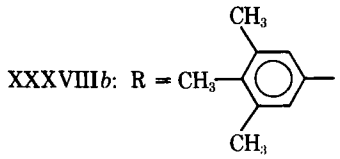

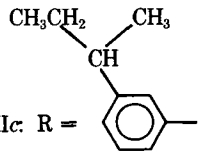

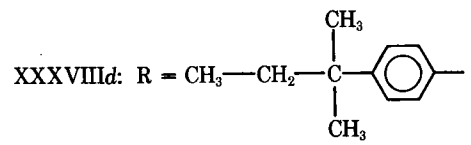

oxy)-2-propanol[15] (XXXVII) (185). A decrease in myocardial conduction velocity was considered a measure of membrane stabilization due to Class I action on cardiac fibers.

A close correlation was observed between the slowing of conduction, local anesthesia, the lowering of surface tension, and the partition coefficient, whether determined directly or calculated by the Hansch method (186, 187). Several conclusions were drawn as to the effect of various molecular modifications, all of which bear out that the nonspecific actions of the compounds studied increased in potency as the lipid solubility increased. This simple correlation allows the nonspecific actions of the series to be predicted with reasonable accuracy.

Two series of β-adrenergic receptor blocking drugs were subjected to a similar treatment in an effort to determine the effect of varying the degree of alkyl substitution on the phenyl ring in one series (XXXVI and XXXVIII*a–d*) and the effect of varying the size of alkyl substituents on the amino group in the other series (XXXIX*a–f*) (188). The difference in the degree of hydrophobicity ranged more than three orders of magnitude and was solely dependent on the sum of the hydrophobic contributions of the alkyl substituents. The degree of slowing of myocardial conduction was again used as a measure of the non-

[15] KL 255.

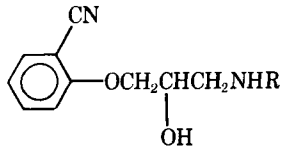

XXXIX

XXXIX*a*: R = −H
XXXIX*b*: R = −CH_3
XXXIX*c*: R = −CH_2−CH_3

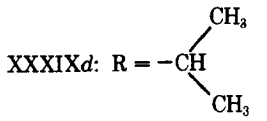

XXXIX*d*: R = −CH(CH$_3$)$_2$

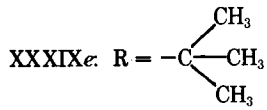

XXXIX*e*: R = −C(CH$_3$)$_3$

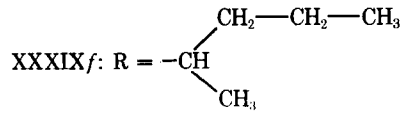

XXXIX*f*: R = −CH(CH$_2$CH$_3$)CH$_3$

specific action of the compounds, and their influence on the maximum rate of rise of intraventricular pressure (an index of the inotropic state of heart muscle) in anesthetized cats after β-blockade was measured *in vivo*. Both of these tests were purported by the authors to represent a measure of nonspecific cardiodepression.

The physicochemical and pharmacological data from both series of compounds were subjected to the Hansch analysis. This treatment revealed parabolic correlation equations between hydrophobicity and both pharmacological tests by plotting the log of the reciprocal IC_{50} or ED_{50} values *versus* log *P* (for interpretation of the parabolic case, see Ref. 189). The authors concluded that nonspecific cardiodepressant effects of β-blocking drugs can be predicted for given pharmacological systems by determination or calculation of the hydrophobicity of the drug molecules, irrespective of the site of the hydrophobic substituents.

A series of 11 bis(2-hydroxy-3-isopropylaminopropyl) ethers of dihydroxyarenes was synthesized, in which the points of substitution and the aromatic groups were varied (XL) (190). The compounds were evaluated for β-adrenergic receptor blocking action, local anesthesia, and myocardial depression in isolated guinea pig atrial muscle. The partition coefficients (octanol–pH 7.4 buffer) and dissociation constants were determined. Comparison of the β-blocking, local anesthetic, and antiarrhythmic (cardiodepressant) activities using multiple regression analysis indicated a good correlation between the latter two and insignificant correlation between β-blocking and the two nonspecific effects.

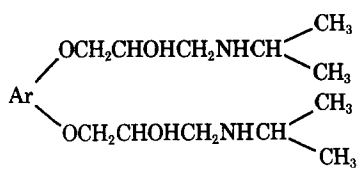

XL

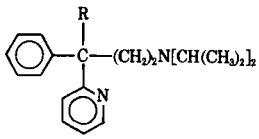

Table VIII—Data for Observed and Calculated Antiarrhythmic Potency[a]

Compound	R	π	IR, cm^{-1}, $\nu_{C=O}$	ln AP[b]		
				Obs.	Calc.[c]	Calc.[d]
1	—$CONCH_3N(CH_3)_2$	0.30	1640	2.254	2.276	2.276
2	—$CONHC_2H_5$	0.21	1656	1.891	1.936	1.965
3	—$CONHNHCH_3$	—0.35	1645	1.711	1.601	1.649
4	—$CO_2C_2H_5$	1.11	1733	1.677	1.518	1.603
5	—$CONHNHCOCH_3$	—0.57	1624	1.715	1.738	1.769
6	—$COCH_3$	0.75	1712	1.403	1.527	1.604
7	—$NHCOCH_3$	0.05	1679	1.313	1.419	1.492
8	—$CONHN{=}C(CH_3)_2$	0.21	1680	1.374	1.549	1.613
9[e]	—$CONH_2(H_3PO_4)$	0.00	1682	2.195		1.405
10	—$CONHNH_2$	—0.73	1622	1.407	1.624	1.663
11	—$CONHN(CH_3)_2$ (oxalate CH_3OH)	—0.59	1656	1.514	1.204	1.284
12	—CO_2CH_3	0.61[f]	1735	0.910	1.028	1.148
13	—$CONHC_6H_5$ ($H_2SO_4 \cdot 0.5H_2O$)	1.65	1683	2.935	2.818	2.795
14	—$CONHCH_3$	—0.31[g]	1661	1.404	1.379	1.449
15	—$CONHCH_2OH$	—0.82	1657	1.085	0.977	1.073

[a] Adapted, with permission, from T. K. Lin, Y. W. Chien, R. R. Dean, J. E. Dutt, H. W. Sause, C. H. Yon, and P. K. Yonan, *J. Med. Chem.*, **17**, 751(1974) (American Chemical Society, Washington, D.C.). [b] AP = 5 × MW × AR/1000, where MW is the molecular weight and AR is the activity ratio (described in Ref. 195). [c] The values were computed from an equation excluding disopyramide. [d] Including disopyramide. [e] Norpace. [f] This value was estimated by subtracting 0.5 from Compound 4. [g] This value was estimated by subtracting 0.5 from Compound 2.

Correlation of the physicochemical data and antiarrhythmic activity in a stepwise multiple regression analysis gave four optimal equations, two of which were parabolic. Inclusion of the log P and pKa terms provided the most relevant equation. Although the equations were unsuitable for predictive purposes, the authors claimed that they demonstrated the important role of lipophilicity since greater antiarrhythmic and local anesthetic potency resided in the compounds with higher partition coefficients.

Unfortunately, no mention was made of toxicity studies in any of these reports (185, 188, 190). However, there appears to be sufficient evidence that quantitative structure–activity relationship analyses can be of predictive value in assessing the cardiodepression of series of compounds designed to be β-adrenergic receptor blocking agents.

The only quantitative structure–activity relationship study of antiarrhythmic drugs considered to be Class I (Vaughan Williams classification) was performed on a series of disopyramide derivatives (Table VIII) (191–193) using a newly proposed quantum statistical method of analysis[16]. Briefly, the method is based on the rate and magnitude of the biological response being dependent upon two steps:

1. The drug molecule makes a Brownian-like motion from outside the cell to reach the receptor (determined by lipid solubility).

2. A binding mechanism between the receptor and drug molecule is established, which involves coupling of vibrational states between the receptor and the drug.

The probability of binding is related to the partition function of statistical mechanics associated with the quantum energy levels of the drug molecule. These quantum energy levels are observable by various spectral methods (IR and UV) and presumably describe the contribution to binding at the receptor site of involved functional groups of molecules having different electronic characteristics. The probability of eliciting a biological response is thus related to the probability of the drug being transported to the site of action (Step 1) and to the probability of the vibrational states of the receptor and active binding centers of the drug molecule being able to couple (Step 2).

This method was first used to analyze the antiarrhythmic activity of the series of disopyramide derivatives (Table VIII) synthesized previously (195). The compounds had structural modifications near the carbonyl group, which led to wide differences in the IR absorption peaks for the carbonyl group and to substantial differences in partition coefficients (octanol–pH 7.4 buffer). The antiarrhythmic potency (AP) was determined by dividing the mean maximal reduction in extrasystoles in the coronary artery-ligated dog by the mean effective dose. The equation used to evaluate the correlation between the two physical measurements and the antiarrhythmic potency was derived from the general equation:

$$\mathrm{AP} = \frac{d(\text{response})/dt}{1000C} = A p^{a1}(\text{Brownian}) \times p^{a2}(\text{binding}) \quad \text{(Eq. 1)}$$

where C = molar concentration, and A = proportionality constant. The final equation is:

$$\ln \mathrm{AP} = C_1 + C_2\pi - C_3\nu_{C=O} \quad \text{(Eq. 2)}$$

where π = partition coefficient, $\nu_{C=O}$ = IR absorption in wave numbers, and C_1, C_2, and C_3 are determined by multiple regression analysis. This equation was specifically derived for correlation of the antiarrhythmic potency of the compounds in Table VIII. By using Eq. 2, the antiarrhythmic potencies were calculated for the series and correlated remarkably

[16] For a critical review of methods using quantum mechanics in assessing biological data, see Ref. 194.

Table IX—Physical and Pharmacological Data (Mice) of 5-Substituted 2-Methyldecahydroisoquinolines

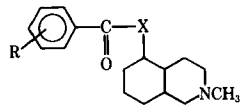

R	X	Isomer[a]	Pc[b]	P.R.[c]	T.R.[d]	T.I.[e]
3,4,5-$(OCH_3)_3$	O	*cis*	0.23	1.33	2.13	2.0
3,4,5-$(OCH_3)_3$	O	*trans*	0.50	2.22	2.46	2.8
3,4,5-$(OCH_3)_3$	NH	*cis*	2.98	0.75	0.66	3.6
3,4,5-$(OCH_3)_3$	NH	*trans*	3.83	1.00	0.65	4.8
Quinidine	—	—	—	1.00	1.00	3.1

[a]These are diastereoisomers; for a full description of the stereochemistry, see Ref. 197. [b]Octanol–water partition coefficient. [c]Potency ratio compared to quinidine. [d]Toxicity ratio compared to quinidine. [e]Therapeutic index = LD_{50}/ED_{50}.

well with the experimentally determined values. The results indicated that a combination of high lipid solubility and a low wave number should give a compound of optimal potency. Again, no mention was made of the correlation, if any, of the physicochemical parameters with toxicity.

The same group of investigators also mathematically correlated the plasma protein binding capacity and lipophilicity of a series of 20 disopyramide derivatives with structural variances in the amide moiety, the phenyl ring, and the pyridyl ring (196). By using multiple regression analyses, an equation was derived to describe a linear correlation of the extent of plasma binding with the differences in lipid solubility, irrespective of the site of the structural modification. A Scatchard analysis showed that the interaction involved only a primary binding site, postulated to be the planar phenyl ring that intercalates into the plasma protein helix. Similar binding and interaction were postulated previously as the mode of action of nonspecific antiarrhythmic drugs on myocardial cell membranes (Fig. 7).

Benzoyl ester and benzamido derivatives of *cis*- and *trans*-5-, 6-, and 8-amino- and hydroxy-2-methyldecahydroisoquinolines, respectively, were synthesized (197–202). The compounds demonstrated antiarrhythmic potency in inhibition of chloroform-induced ventricular fibrillation in mice (200–202) and in prolongation of the functional refractory period of isolated guinea pig atria (200, 203). Additionally, the effects of three of the more potent 8-substituted derivatives on the transmembrane action potential of isolated canine Purkinje fibers were investigated and shown to exhibit Class I behavior (203).

Although no quantitative structure–activity analyses were performed on the series of eight 5-substituted, 23 8-substituted, and 16 6-substituted derivatives, apparent dissociation constants and measures of lipophilicity were obtained. The latter values were obtained by determination of the partition coefficient (octanol–pH 7.4 buffer) or the percentage buccal absorption. The relevant structures, lipophilicity data, potency and toxicity ratios, and LD_{50}/ED_{50} ratios from the mouse screening tests are included in Tables IX–XI. Within the entire series of compounds, the pKa values did not differ significantly and were discounted as being responsible for the differences in potencies. However, lipophilicities varied widely and were related in each series to potency and

Table X—Physical and Pharmacological Data (Mice) of 6-Substituted 2-Methyldecahydroisoquinolines

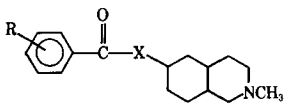

R	X	Isomer	Pc[a]	P.R.[a]	T.R.[a]	T.I.[a]
Quinidine	—	—	—	1.00	1.00	3.3
H	NH	*cis*	2.96	0.43	0.39	3.6
H	NH	*trans*	2.40	0.44	0.37	4.0
4-Cl	NH	*cis*	17.1	0.53	0.59	3.0
3,4-$(Cl)_2$	NH	*cis*	50.5	1.63	0.70	7.8
3,4-$(Cl)_2$	NH	*trans*	46.2	1.10	0.63	5.8
4-OCH_3	NH	*cis*	2.75	0.48	0.34	4.7
3,4-$(OCH_3)_2$	NH	*cis*	1.98	0.63	0.35	6.0
3,4-$(OCH_3)_2$	NH	*trans*	1.87	0.56	0.36	5.1
3,4,5-$(OCH_3)_3$	NH	*cis*[b]	1.15	0.82	0.41	6.7
3,4,5-$(OCH_3)_3$	NH	*trans*	1.28	0.69	0.50	4.6
3,4,5-$(OCH_3)_3$	NH	*cis*[b]	0.97	0.64	0.39	5.5
3,4,5-$(OCH_3)_3$	O	*cis*	7.68	1.70	0.98	5.8
3,4,5-$(OCH_3)_3$	O	*trans*	6.95	1.21	1.04	3.9
3,4-$(Cl)_2$	O	*cis*	145	0.86	0.40	7.1
3,4-$(Cl)_2$	O	*trans*	127	0.60	0.47	4.3

[a]See footnotes to Table IX. [b]These are two *cis*-diastereoisomers; see Ref. 199 for a full description of stereochemistry.

Table XI—Physical and Pharmacological Data (Mice) of 8-Substituted 2-Methyldecahydroisoquinolines

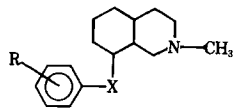

R	X	Isomer[a]	B.A.[b], %	P.R.[c]	T.R.[c]	T.I.[c]
Quinidine	—	—	—	1.00	1.00	3.3
H	CONH	*cis*	41	0.66	0.37	5.9
H	CONH	*trans*	43	0.65	0.37	5.9
2-(OCH_3)	CONH	*cis*	35	1.38	0.63	7.3
2-(OCH_3)	CONH	*trans*	41	0.91	0.70	4.3
4-(OCH_3)	CONH	*cis*	31	0.60	0.34	5.8
4-(OCH_3)	CONH	*trans*	34	0.82	0.36	7.6
3,4-$(OCH_3)_2$	CONH	*cis*	18	0.80	0.30	8.9
3,4-$(OCH_3)_2$	CONH	*trans*	27	0.98	0.33	9.8
3,4,5-$(OCH_3)_3$	CONH	*cis*	24	1.00	0.46	7.3
3,4,5-$(OCH_3)_3$	CONH	*trans*	31	1.29	0.64	6.7
4-Cl	CONH	*cis*	43	0.77	0.59	4.4
4-Cl	CONH	*trans*	54	0.80	0.56	4.8
3,4-$(Cl)_2$	CONH	*cis*	61	2.19	0.75	9.7
3,4-$(Cl)_2$	CONH	*trans*	59	1.48	0.41	12.0
H	SO_2NH	*cis*	30	0.57	0.37	5.2
H	SO_2NH	*trans*	37	0.46	0.48	3.3
H	COO	*cis*	82	0.65	0.59	3.7
4-Cl	COO	*cis*	87	0.62	0.44	4.7
4-Cl	COO	*trans*	85	1.10	0.70	5.2
3,4,5-$(OCH_3)_3$	COO	*cis*	71	0.99	1.23	2.6
3,4,5-$(OCH_3)_3$	COO	*trans*	70	2.16	1.58	4.5

[a]For a full description of the stereochemistry, see Ref. 198. [b]Percentage buccal absorption from pH 9.2 buffer. [c]See footnotes to Table IX.

toxicity, the more highly lipid-soluble compounds generally exhibiting the greater activity.

Comparison of the two *cis–trans*-diastereoisomeric pairs in the 5-substituted series revealed that the rigid, near-planar *trans*-isomers possessed higher partition coefficients and were more potent than the corresponding *cis*-isomers. A similar relationship was observed in several isomeric pairs of the 8-substituted series, which had significant differences in lipophilicity. For the isomeric pairs of near-equal lipophilicity, the *trans*-diastereomer was usually more potent. This finding prompted a proposal that the receptor area in or on the cardiac membrane possessed some degree of stereoselectivity favoring the *trans*-isomers (135). However, examination of the data in the 6-substituted series revealed that the *cis*-isomers

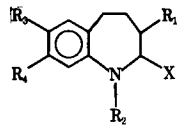

Table XII—Structures and Pharmacological Data (Mice) of 2,3,4,5-Tetrahydrobenzazepine Derivatives

R_1	R_2	R_3	R_4	X	ED_{50}[a], mg/kg	LD_{50}[a]	T.I.[b]
4-ClC_6H_5	$CH_2CH_2N[CH(CH_3)_2]_2$	H	H	=O	2.5	8	3.2
4-ClC_6H_5	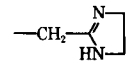	H	H	=O	14.5	70	4.8
H	$CH_2CH_2N[CH(CH_3)_2]_2$	OCH_3	H	=O	46	142	3.1
H	$CH_2CH_2N[CH(CH_3)_2]_2$	H	OCH_3	=O	68	171	2.5
4-ClC_6H_5	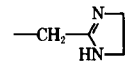	H	H	H_2	21	71	3.4
H	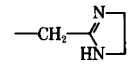	H	H	H_2	Inactive	104	—

[a] Administered intraperitoneally. [b] LD_{50}/ED_{50}.

were generally more potent, toxic, and lipophilic than the corresponding *trans*-isomers.

In the 6- and 8-benzamido derivatives, potency increased stepwise with the introduction of the 4-methoxy, 3,4-dimethoxy, and 3,4,5-trimethoxy moieties into the phenyl ring, although lipophilicity did not increase accordingly. This finding supports the claim of DiPalma and Lambert (172) mentioned earlier, and it is interesting to speculate that perhaps the methoxyl groups could be affecting the IR vibrational frequency of the carbonyl group and influencing potency as proposed by Lin *et al.* (193).

The stepwise introduction of chlorine atoms into the phenyl ring of the 6- and 8-benzamides according to the procedure reported by Topliss (204) resulted in compounds of increased lipid solubility and potency; from this scheme, the derivatives with the largest therapeutic index were obtained. There appeared to be no real advantage of one linkage between the decahydroisoquinoline ring and the aryl group over the others in the 8-substituted series, *i.e.*, ester, amide, or sulfonamide, although the esters were more lipophilic.

In assessing the importance of the point of attachment of the aryl ester or amide substituent, the 8-substituted compounds were generally more potent, with the 5- and 6-substituted compounds being nearly equipotent. The 5-substituted compounds were the most toxic, and the 6-substituted compounds were the least toxic. Again, lipophilicity appeared to be the most obvious determinant of potency.

A series of 14 derivatives of 2,3,4,5-tetrahydrobenzo[*b*]-1*H*-azepine was synthesized, and their toxicity in mice and potency in protecting mice against chloroform-induced ventricular fibrillation were determined (205). No measurements of pKa or lipid solubility were reported, although some comments as to optimal structural requirements were made. Lipophilic substituents (4-chlorophenyl) appeared to improve potency and increase toxicity. The presence of the 4-chlorophenyl or a methoxy substituent seemed necessary for antiarrhythmic activity, since the compound lacking both was inactive. The structures and pharmacological data are included in Table XII. The first compound in the table exhibited remarkable potency in this test as compared to quinidine and other standard antiarrhythmic drugs (206).

A series of 17-alkyl-substituted sparteines (XLI) was investigated for effects on the functional refractory period of isolated guinea pig atria (207). The alkyl substituents ranged from methyl to hexyl, and activity was demonstrated throughout the series. The 17-butyl derivative produced the greatest prolongation of the refractory period, suggesting an optimal chain length of four carbons. The increase in potency in passing from methyl to butyl was attributed to an increasingly stronger hydrophobic interaction between the alkyl substituents and the hydrophobic side chains in the excitable membrane protein. The investigators concluded that the hydrophobic interaction is as important as the attraction of the cationic group by Coulombic forces to fixed anionic sites in the membrane.

A series of 29 2-, 3-, and 4-substituted benzylamine derivatives related to α,α-dimethyl-4-($\alpha,\alpha,\beta,\beta$-tetrafluorophenethyl)benzylamine (XLII) was synthesized to examine the structural requirements for antiarrhythmic activity. The parent compound (XLII) is a new, orally effective, and long-acting antiarrhythmic agent presently undergoing clinical trials. The derivatives were evaluated for their efficacy in

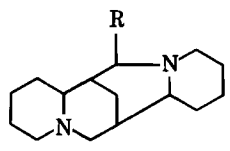

XLI

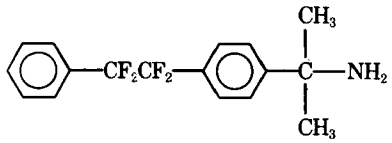

XLII

Table XIII—Structure and ED_{50} of Substituted Benzylamine Derivatives

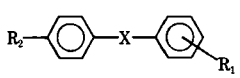

R_1	R_2	X	Isomer	ED_{50}[a], mg/kg
Quinidine	—	—	—	7.6
p-$C(CH_3)_2NH_2$	H	CF_2CF_2	—	0.60
p-$C(CH_3)_2NH_2$	H	CH_2CH_2	—	0.32
p-$C(CH_3)_2NH_2$	H	C≡C	—	0.80
p-$C(CH_3)_2NH_2$	OCH_3	C≡C	—	Inactive
p-$C(CH_3)_2NH_2$	CH_3	C≡C	—	5.0
p-$C(CH_3)_2NH_2$	F	C≡C	—	2.9
p-$C(CH_3)_2NH_2$	*n*-Butyl	C≡C	—	1.0
o-CH_2NH_2	H	C≡C	—	2.5
o-CH_2NH_2	F	C≡C	—	5.4
o-CH_2NH_2	CH_3	C≡C	—	1.7
o-CH_2NH_2	OCH_3	C≡C	—	0.65
o-CH_2NH_2	H	C=C	*cis*	Inactive
o-CH_2NH_2	H	C=C	*trans*	1.7
o-CH_2NH_2	OCH_3	C=C	*trans*	Inactive
o-CH_2NHCH_3	H	C=C	*trans*	2.4

[a] Administered intravenously.

Table XIV—Structure and Potency of Substituted 2-Phenylethyl-*N*-methylpiperidine Derivatives

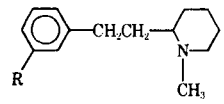

R	ED_{50}[a], mg/kg	P.R.[b]
Quinidine	83	1
NH_2	Inactive	—
$NHCOCH_3$	>50	—
OCH_3	>100	—
C_6H_5CONH	7.2	12
4-ClC_6H_4CONH	>25	<3.3
4-OHC_6H_4CONH	1.7	49
4-$NH_2C_6H_4CONH$	4.0	21
4-$CH_3COOC_6H_4CONH$	2.8	29
4-$OCH_3COOC_6H_4CONH$	7.1	12
3-$OCH_3COOC_6H_4CONH$	10	8.3
3,4-$(OCH_3)_2C_6H_3CONH$	10	8.3
3,5-$(OCH_3)_2C_6H_3CONH$	>50	<1.6
3,4,5-$(OCH_3)_3C_6H_2CONH$	39	2.1

[a] Administered intraperitoneally. [b] Potency ratio compared to quinidine.

preventing or controlling ventricular fibrillation after an experimentally induced infarction in anesthetized dogs.

Although no physicochemical properties were measured, the investigators deduced some molecular modifications which gave compounds as potent as XLII. Fourteen of the most active derivatives are shown in Table XIII. Replacement of the tetrafluoroethyl bridge with an ethylene unit gave increased potency, although the oral duration was reported to be shorter. Whereas substitution on the terminal phenylethynyl group in the *para*-substituted benzylamines decreased activity, similar substitution in the corresponding *ortho*-derivatives increased activity with the exception of the fluoro group. The effect of a 4-methoxy group in the *p*-phenylethynyl- and the *o*-phenylethenylbenzylamines was to abolish antiarrhythmic activity, whereas its presence in the *o*-phenylethynylbenzylamine produced the most potent compound of that series. The fact that activity resided exclusively in the *trans* geometrical isomer of the *cis*- and *trans*-phenylethenyl (X = CH=CH) derivatives may possibly indicate receptor stereoselectivity, although the effects of the differences in physicochemical properties of the pair (not reported) may play the major role in determining the presence or absence of activity.

A series of 28 compounds of the structural type shown in Table XIV was synthesized, and their potency in preventing chloroform-induced ventricular fibrillation was determined in mice (209). Of the more active compounds listed, it appears that polar, hydrophilic substituents (*i.e.*, *p*-OH, *p*-NH_2, and *p*-acetoxy) in the *para*-position of the benzamide ring impart greatest potency and that the presence of the lipophilic *p*-chloro group decreases potency. Increasing degrees of methoxy substitution gave no advantage insofar as potency was concerned. No toxicity or physicochemical data were reported for the compounds, although the *p*-benzamido, *p*-hydroxy, *p*-amino, *p*-acetoxy, and *p*-methoxybenzamido derivatives were selected for further testing.

A series of 49 5,5-disubstituted 3-aminoalkylhydantoins (XLIII) was synthesized and evaluated for their activity in preventing chloroform-induced ventricular fibrillation in mice and in delaying aconitine-induced arrhythmias in guinea pig atria (210). The β-pyridyl derivatives (XLIV and XLV) appeared to be the most promising, although no toxicity or physicochemical properties were reported. Advantageous molecular modifications were discussed.

An investigation into the metabolism of lidocaine prompted the examination of the antiarrhythmic potencies of the mono- and dideethylated metabolites (211). The *N*-monoethyl derivative and the primary amine derivatives were 0.8 and 0.1 times as potent as lidocaine, respectively, probably due in part to the anticipated fall in lipophilicity.

Quaternary ammonium derivatives of various antiarrhythmic drugs have been prepared as a means to limit their actions to effects on electrophysiological properties of the heart. Although the permanent cationic head does not diminish the antiarrhythmic potency of the drug in several cases, it does eliminate the toxic manifestations on the CNS, presumably because the charged species is unable to pass through the blood–brain barrier. Generally, quaternization appears to abolish β-blocking activity and either abolish or lessen local anesthetic properties. The latter effect apparently results from the greater difficulty of the permanently charged compounds in penetrating the nerve membrane as compared to the cardiac membrane. An additional attractive feature of the quaternized drugs is the longer duration of action when compared to the parent molecules.

This approach was employed in a study in which the dimethylammonium salts of propranolol, bunolol, XX, and dichloroisoproterenol were prepared and

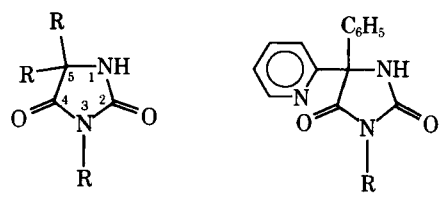

XLIII

XLIV: R = $CH_2CH_2N(CH_3)_2$

XLV: R = $CH_2CH(CH_3)CH_2N(CH_3)_2$

their pharmacological actions were compared with those of the parent compounds (212). In all four cases, quaternization abolished the β-blocking and local anesthetic activities and offered no protection against adrenergically induced arrhythmias, although some activity against ouabain-induced arrhythmias was observed.

Further studies on the dimethylammonium quaternary salt of propranolol[17] (XLVI) showed it to be effective against digitalis and myocardial infarction-induced arrhythmias in dogs (20). Rosen *et al.* (158) reported that XLVI demonstrated Class I behavior when applied to canine Purkinje fibers in concentrations similar to myocardial depressant concentrations of propranolol.

A series of 15 quaternary ammonium derivatives of lidocaine was synthesized, and their antiarrhythmic activity was determined (44). Although no details were included, all derivatives were reported to be effective; a consistent structure–activity relationship was observed throughout the series with regard to antiarrhythmic and other pharmacological and toxic activities. The optimal compound, XVI, recently received renewed interest and is undergoing clinical trials (22, 45–47).

The quaternary methylammonium derivative of lidocaine is as effective, or more so, than lidocaine in reversing ouabain-induced ventricular tachycardia by suppressing ectopic pacemakers, in reducing or abolishing arrhythmias resulting from experimentally produced myocardial infarction in dogs, and in raising the threshold for electrically induced fibrillation (150, 213, 214).

The activity of several antiarrhythmic compounds of widely differing molecular structures was correlated with their solubility and molecular volume (215). The physical properties of these molecules are of primary importance in determining their potency in inhibiting the automaticity of the ventricle induced by epinephrine. Therefore, the mechanism of membrane suppression by antiarrhythmic drugs may be similar to the general anesthetics (216), barbiturates (217), and local anesthetics (218), all of which appear to act in a nonspecific manner primarily resulting from their physical characteristics. This concept is consistent with the work of Frank (219), who postulated that general and local anesthetics and other drugs that depress excitable membranes by interfering with sodium influx during depolarization all act by a common mechanism which depends upon the physical properties of the molecules.

In summary, the more recent structure–activity relationship studies of nonspecific antiarrhythmic drugs offer no new information to necessitate alteration of the general structural requirements previously proposed (XXI–XXIV), with the exception that some primary and secondary amines also possess activity. The wide range of chemical structures found to possess antiarrhythmic acitivity, the dependence of potency on lipid solubility, and the lack of significant stereoselectivity at the site of action are all consistent with the proposed "physical membrane occupancy theory" of nonspecific antiarrhythmic action.

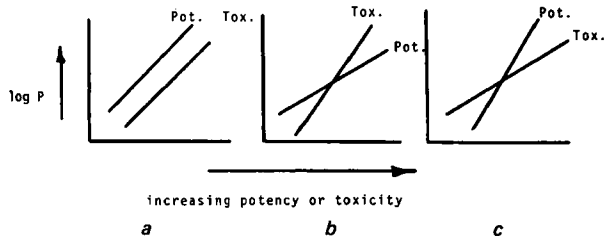

Figure 8—*Three possible ways potency (Pot.) and toxicity (Tox.) may relate to each other as lipophilicity (log P) increases.*

The most striking weakness of many studies reviewed was the lack of toxicity and physicochemical data for large series of structurally related compounds. These compounds would lend themselves readily to visual or quantitative structure–activity relationship analysis. The absence of toxicity data is surprising in view of the strong emphasis placed on early assessment of the ratio of acute toxicity to antiarrhythmic potency in a screening program (206, 220).

Attempts to correlate physicochemical properties with toxicity are also conspicuously absent in the quantitative structure–activity relationship investigations on antiarrhythmic drugs and other classes of drugs as well. Correlations predicting maximal potency alone are of limited use to the medicinal chemist in choosing the most promising compound for development unless information on toxicity trends is also available. If feasible, studies that detect correlations between physicochemical properties and the LD_{50}/ED_{50} ratio could be of great practical value.

More likely would be the determination of separate correlations of potency and toxicity with physicochemical properties. If, for example, both were linearly related to lipophilicity, the slopes of the plots of potency or toxicity *versus* the partition data in its appropriate form (Fig. 8) may relate to each other in one of three possible ways: (*a*) rates of increase in potency and toxicity parallel each other (Fig. 8*a*), (*b*) toxicity increases at a faster rate than potency (Fig. 8*b*), or (*c*) potency increases at a faster rate than toxicity (Fig. 8*c*). Obviously, knowledge of these relationships would prove useful in designing a drug with an optimum toxicity–potency ratio.

Of course, if no correlation between physicochemical properties and toxicity is observed, the toxicity of a whole range of active compounds would need to be determined to enable one to choose the optimal compound for development.

An irritating feature of many structure–activity relationship studies is the presentation of ED_{50} and LD_{50} data in milligrams per kilogram. It is totally invalid to relate potencies expressed in that way when the compounds of a series differ significantly in molecular weight. The data could be acceptably presented as millimoles per kilogram or micromoles per kilogram.

Cardioselective β-Adrenergic Antagonists—Structure–activity relationship studies on the β-blocking agents possessing antiarrhythmic activity

[17] UM-272.

Table XV—Structural Formulas of Some Myocardial Selective (+) and Nonselective (−) β-Adrenergic Receptor Antagonists

Ar—O—$CH_2CHOHCH_2NHR$

Compound	Ar	R	β_1 Selective	Reference
Propanolol	1-Naphthyl	$CH(CH_3)_2$	—	244
XLIX[a]	8-Thiochromanyl	$CH(CH_3)_2$	—	246
Pindolol	4-Indolyl	$CH(CH_3)_2$	—	244
Bifuralol	2-(7-Ethylfuranyl)	$C(CH_3)_3$	—	247
Bufetalol	2-Furfuryl	$C(CH_3)_3$	—	248
Timolol	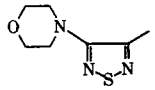	$C(CH_3)_3$	—	249
L[b]	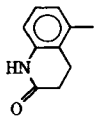	$C(CH_3)_3$	—	250, 251
LI	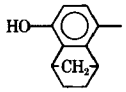	$C(CH_3)_3$	+	235
LII	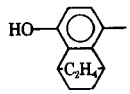	$C(CH_3)_3$	+	235
LIII	1-Naphthyl	3,4-$(OCH_3)_2C_6H_3CH_2CH_2$	+	236
LIV	p-$CH_3CONHC_6H_4$	3,4-$(OCH_3)_2C_6H_3CH_2CH_2$	++	236
LV	p-$C_6H_5CH_2CONHC_6H_4$	3,4-$(OCH_3)_2C_6H_3CH_2CH_2$	++	236
LVI	o-CH_2=$CHCH_2C_6H_4$	3,4-$(OCH_3)_2C_6H_3CH_2CH_2$	+	236
LVII	m-$CH_3C_6H_4$	3,4-$(OCH_3)_2C_6H_3CH_2CH_2$	+	236

[a] S-2395. [b] OPC-1085.

have been quite successful. The correlations seen between structure, physicochemical properties, and activity are highly indicative of a very stereoselective, defined receptor site. Structure–activity relationship investigations of β-blocking agents in general were discussed in several recent publications (17, 19–21, 115, 116, 118, 221–228).

Much recent attention has been directed to delineating structural requirements that impart cardioselectivity to β-adrenergic receptor antagonists. This work was given impetus in 1967 by the proposal that two types of β-adrenergic receptors existed (229). Lands *et al.* (229) found significant differences between the quantitative structure–activity correlation of β-adrenergic stimulants that mediate cardiac stimulation, lipolysis, and inhibition of small intestine motility and that of β-adrenergic stimulants responsible for bronchodilatation and vasodilation. The former were termed β_1- and the latter β_2-adrenergic effects. Although this classification remains a subject of controversy (21, 230, 231), it has become fairly well accepted.

Several successful attempts to synthesize β-receptor blocking agents eliciting β_1 actions (*e.g.*, block sympathetic drive of heart) to a much greater degree than β_2 actions (*e.g.*, block sympathetic-mediated bronchodilatation and vasodilation) have been reported. These findings prompted Levy and Wilkenfield (232) to categorize β-blocking drugs into three groups: (*a*) those that selectively block vascular and bronchial β-receptors, *e.g.*, butoxamine; (*b*) those that selectively block cardiac receptors, *e.g.*, practolol; and (*c*) those that block β-receptors in all tissues and are nonselective, *e.g.*, propranolol. The advantage of cardioselective β-blockade is that β_2-blockade in patients prone to bronchospasm could conceivably bring on breathing difficulty.

Some β-blocking agents investigated with respect to β_1/β_2 selectivity are listed in Tables XV and XVI. There is growing evidence from several structure–activity relationship studies that the presence of a *para*-substituent in the phenyl ring imparts greater β_1 activity while reducing overall β-blocking potency (233). Of course, the nature of the *para*-substituent is also important in determining the differential affinity of β-blockers. For example, sotalol, XX, 1-isopropylamino-3-(4-tolyloxy)-2-propanol[18] (XLVII), and 1-isopropylamino-3-(4-isopropylphenoxy)-2-propanol[19] (XLVIII) are *para*-substituted but exhibit no cardioselectivity. Also, some non-*para*-substituted β-blockers do possess cardioselectivity, *e.g.*, tolamolol, in which the *o*-methyl derivative is β_1 selective whereas the *p*-methyl derivative is not.

The effects on cardioselectivity of varying the size of the *N*-substituent in *o*-cyanophenoxypropanolamines were investigated (234). The affinity for the β_2-receptor was much more sensitive to this structural change than for the β_1-receptor. Whereas increasing the size of the *N*-substituent from hydrogen to *tert*-butyl increased β_1 affinity, it increased β_2 affinity at a much faster rate, resulting in the *N-tert*-butyl derivative (bunitrolol, Table XVI) being four times more potent on the β_2- than on the β_1-receptor. In contrast, the primary amine derivative (XXXVIII*a*), although less potent, had a sixfold greater affinity for the β_1-receptor.

A series of 34 derivatives of 3-amino-2-hydroxy-

[18] Kö 612.
[19] L 8429.

Table XVI—Structural Formulas of Some Myocardial Selective (+) and Nonselective (−) β-Adrenergic Receptor[a] Antagonists

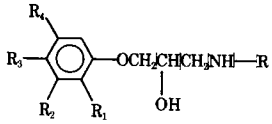

Compound	R_1	R_2	R_3	R_4	R	β_1 Selective	Reference
Practolol	H	H	$NHCOCH_3$	H	$CH(CH_3)_2$	+	120
o-Practolol	$NHCOCH_3$	H	H	H	$CH(CH_3)_2$	—	120
Alprenolol	CH_2—CH=CH_2	H	H	H	$CH(CH_3)_2$	—	237
p-Alprenolol	H	H	CH_2—CH=CH_2	H	$CH(CH_3)_2$	+	237
Oxprenolol	OCH_2—CH=CH_2	H	H	H	$CH(CH_3)_2$	—	120
p-Oxprenolol	H	H	OCH_2—CH=CH_2	H	$CH(CH_3)_2$	+	120
LVIII[b]	H	H	$OCH_2CH_2OCH_3$	H	$CH(CH_3)_2$	+	238
LIX[c]	H	H	$CH_2CH_2OCH_3$	H	$CH(CH_3)_2$	+	238
LX[d]	$COCH_3$	H	$NHCOC_3H_7$	H	$CH(CH_3)_2$	+	239
Trimepranol	CH_3	CH_3	$OCOCH_3$	CH_3	$CH(CH_3)_2$	—	240
LXI[e]	CH_3	CH_3	OH	CH_3	$CH(CH_3)_2$	—	240
LXII[f]	CH_3	CH_3	NH_2	CH_3	$CH(CH_3)_2$	—	240
LXIII[g]	CH_3	CH_3	$NHCOCH_3$	CH_3	$CH(CH_3)_2$	+	240
XLVII	H	H	CH_3	H	$CH(CH_3)_2$	—	221
LXIV	H	H	$CONH_2$	H	$CH(CH_3)_2$	—	241
LXV	H	H	H	$CONH_2$	$CH(CH_3)_2$	—	241
LXVI[h]	H	H	OCH_3	H	$C(CH_3)_3$	+	242
LXVII[i]	OCH_3	H	H	H	$C(CH_3)_3$	—	242
XLVIII	H	H	$C(CH_3)_2$	H	$CH(CH_3)_2$	—	242
Tolamolol	CH_3	H	H	H	$(CH_2)_2O$—C_6H_4—$CONH_2$	+	243
LXVIII	H	H	CH_3	H	$(CH_2)_2O$—C_6H_4—$CONH_2$	—	243
LXIX	H	H	$NHCOCH_3$	H	$(CH_2)_2OC_6H_4NHCOCH_3$	+	243
LXX	H	H	CH_2CONH_2	H	$(CH_2)_2O$—C_6H_4—$NHCOCH_3$	+	243
LXXI	H	H	$NHCOOC_2H_5$	H	$(CH_2)_2O$—C_6H_4—$NHCOCH_3$	+	243
LXXII	CH_3	H	$NHCOCH_3$	H	$(CH_2)_2O$—C_6H_4—$NHCOCH_3$	+	243
LXXIII	H	H	$NHCOC_2H_5$	H	$(CH_2)_2O$—C_6H_4—$NHCOCH_3$	+	243
LXXIV	H	H	$NHCOCH_3$	H	$(CH_2)_2O$—C_6H_4—NHCHO	+	243
Bunitrolol	CN	H	H	H	$C(CH_3)_3$	—	234
XXXVIII*a*	CN	H	H	H	H	+	234
Sotalol	H	H	$NHSO_2CH_3$	H	$CH(CH_3)_2$	—	244
Acebutolol	$COCH_3$	H	$NHCOCH_2CH_3$	H	$CH(CH_3)_2$	+	244
LXXV[j]	H	H	CH_2CONH_2	H	$CH(CH_3)_2$	+	245

[a] Adapted in part, with permission, from S. Zakhari, *Eur. J. Pharmacol.*, 29, 22(1974) (ASP Biological and Medical Press, Amsterdam, The Netherlands). [b] H 87/07. [c] H 93/26. [d] M + B 17803A. [e] VUBF 6502. [f] VUBF 8227. [g] VUBF 8101. [h] M 66368. [i] M 66527. [j] ICI 66082.

propoxy-1,2,3,4-tetrahydro-1,4-ethano- and 1,4-methanonaphthalenes (LXXVI, R_3 = CH_2 or C_2H_4) was synthesized, and the β_1- and β_2-blocking potency was determined (235). The results confirmed the importance of a *para*-substituent relative to the side chain. However, in contrast to the previous study, enhanced β_1 affinity resided in the *N-tert*-butyl (R_2) derivatives. The most cardioselective compounds possessed an 8-hydroxy group (R_1) and the *N-tert*-butyl group (LI and LII in Table XV).

The effect of varying the amino substituent on the β-blocking properties and cardioselectivity of a series of 1-amino-3-(*m*-tolyloxy)-2-propanols (LXXVII) was studied (236). The presence of an *N*-aralkyl (R) group was necessary to confer cardioselectivity, and the *N*-phenylethyl group was superior to the *N*-benzyl, *N*-phenylpropyl, or *N*-α-methylphenylethyl groups. The nature and position of substituents on the phenyl ring of the *N*-phenylethyl group had a profound effect on the degree of β_1 affinity, with the 3,4-dimethoxy (LVII in Table XV) group imparting the greatest cardioselectivity.

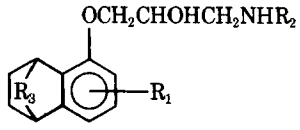

LXXVI

Subsequent investigation of the effects of varying the substituents on the phenoxy ring showed that the presence of more than one substituent caused a decrease in β_1 selectivity. The monosubstituents appeared to fall into two categories regarding their nature and position. For nonpolar substituents (alkyl or halogen), greater β_1 selectivity was observed when they were in the *ortho*- or *meta*-position; the presence of a polar substituent in the *meta*- or *para*-position conferred greater β_1 selectivity, the *para*-isomer generally giving the optimal β_1/β_2 ratio.

Since the 3,4-dimethoxyphenylethylamino group was shown to be unique in imparting β_1 selectivity, the effects of replacing the isopropyl moiety in propranolol, alprenolol, and practolol and its α-phenylacetanilide analog with the aforementioned group were investigated (LIII, LVI, LIV, and LV, respectively, in Table XV) (236). The β_1/β_2 ratio was improved in all four new compounds, particularly in the latter two compounds.

In assessing the importance of the reviewed investigations, there appears to be sufficient experimental evidence to justify some guidelines to chemists at-

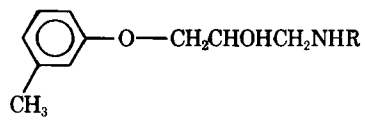

LXXVII

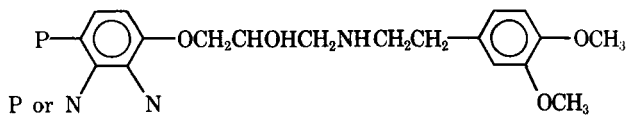

LXXVIII

tempting to synthesize cardioselective β-adrenergic blocking agents. Incorporation of an *N*-(3,4-dimethoxy)phenylethyl group into the basic structure (LXXVIII) and placement of a *para* or *meta* polar substituent (P) or an *ortho* or *meta* nonpolar substituent (N) onto the phenoxy ring appears to maximize the chances of success, although there are undoubtedly exceptions.

This review covers a wide range of topics. The intentions were to present the mechanism of action and structure–activity relationship studies of antiarrhythmic drugs with sufficient background material to enable the uninitiated reader to grasp more fully the complexities involved in the diagnosis and treatment of arrhythmias with drugs and to outline the basic research leading to antiarrhythmic drugs. The extensive literature citations will enable the reader to delve into this extremely fascinating area of chemotherapy.

REFERENCES

(163) E. M. Vaughan Williams, in "Symposium on Cardiac Arrhythmias," E. Sandoe, E. Flensted-Jensen, and K. M. Olson, Eds., A. B. Astra, Södertälje, Sweden, 1970, pp. 449–472.

(164) E. M. Vaughan Williams, "Antiarrhythmic Action in Relation to Ionic Currents," presented at the workshop on Ions, Potentials and Rhythms of the Cardiac Muscle Research Group, Oxford, England, July 4, 1975.

(165) P. Polster and E. M. Vaughan Williams, *Brit. J. Pharmacol.*, **47**, 187(1972).

(166) F. W. Eichbaum and W. J. Yasaka, *Eur. J. Pharmacol.*, **26**, 82(1974).

(167) B. N. Singh and E. M. Vaughan Williams, *Brit. J. Pharmacol.*, **39**, 679(1970).

(168) *Ibid.*, **43**, 10(1971).

(169) B. F. Hoffman and J. T. Bigger, Jr., in "Drill's Pharmacology in Medicine," 4th ed., J. R. DiPalma, Ed., McGraw-Hill, New York, N.Y., 1971, pp. 824–852.

(170) B. F. Hoffman, A. L. Wit, and M. R. Rosen, *Amer. Heart J.*, **88**, 95(1974).

(171) H. L. Conn, Jr., in "The Myocardial Cells; Structure, Function, and Modification by Cardiac Drugs," S. R. Briller and H. L. Conn, Jr., Eds., University of Pennsylvania Press, Philadelphia, Pa., 1966, pp. 269–296.

(172) J. R. DiPalma and J. J. Lambert, *Science*, **107**, 66(1948).

(173) H. Gold, W. Modell, and H. L. Otto, *Fed. Proc.*, **5**, 179(1946).

(174) K. Van Dongen and A. J. R. Sanches, *Arch. Int. Pharmacodyn. Ther.*, **55**, 52(1937).

(175) K. Van Dongen, *ibid.*, **58**, 193(1938).

(176) *Ibid.*, **58**, 279(1938).

(177) K. Van Dongen and A. Taal, *Arch. Int. Pharmacodyn. Ther.*, **81**, 129(1950).

(178) H. D. Christensen, K. H. Palmer, J. T. Gidley, and M. E. Wall, *Pharmacologist*, **12**, 305(1970).

(179) F. Alexander, H. Gold, L. N. Katz, and P. D. White, *J. Pharmacol. Exp. Ther.*, **90**, 191(1947).

(180) P. B. Hollander and H. R. Besch, *Arch. Int. Pharmacodyn. Ther.*, **178**, 407(1969).

(181) P. T. Thyrum, H. L. Conn, Jr., and R. J. Luchi, *ibid.*, **151**, 494(1964).

(182) D. K. Yung, M. M. Vohra, and I. Chu, *J. Pharm. Sci.*, **59**, 1405(1970).

(183) J. V. Levy, *Eur. J. Pharmacol.*, **2**, 250(1968).

(184) E. J. Ariëns, *Arch. Pharmacol. Exp. Pathol.*, **257**, 118(1967).

(185) D. Hellenbrecht, B. Lemmer, G. Wiethold, and H. Grobecker, *Arch. Pharmacol.*, **277**, 211(1973).

(186) C. Hansch and W. J. Dunn, III, *J. Pharm. Sci.*, **61**, 1(1972).

(187) M. S. Tute, *Advan. Drug Res.*, **6**, 1(1971).

(188) D. Hellenbrecht, K. F. Muller, and H. Grobecker, *Eur. J. Pharmacol.*, **29**, 223(1974).

(189) C. Hansch and J. M. Clayton, *J. Pharm. Sci.*, **62**, 1(1973).

(190) J. Zaagsma and W. T. Nauta, *J. Med. Chem.*, **17**, 507(1974).

(191) T. K. Lin, *ibid.*, **17**, 151(1974).

(192) *Ibid.*, **17**, 749(1974).

(193) T. K. Lin, Y. W. Chien, R. R. Dean, J. E. Dutt, H. W. Sause, C. H. Yen, and P. K. Yonan, *J. Med. Chem.*, **17**, 751 (1974).

(194) W. G. Richards and M. E. Black, *Progr. Med. Chem.*, **11**, 67(1975).

(195) C. H. Yen, H. S. Lowrie, and R. R. Dean, *J. Med. Chem.*, **17**, 1131(1972).

(196) Y. W. Chien, H. J. Lambert, and T. K. Lin, *J. Pharm. Sci.*, **64**, 961(1975).

(197) I. W. Mathison and R. C. Gueldner, *J. Org. Chem.*, **33**, 2510(1968).

(198) I. W. Mathison and P. H. Morgan, *ibid.*, **39**, 3210(1974).

(199) I. W. Mathison and R. R. Tidwell, *J. Chem. Soc.*, in press.

(200) I. W. Mathison, R. C. Gueldner, J. W. Lawson, S. J. Fowler, and E. R. Peters, *J. Med. Chem.*, **11**, 997(1968).

(201) I. W. Mathison and P. H. Morgan, *ibid.*, **17**, 1136(1974).

(202) I. W. Mathison and R. R. Tidwell, *ibid.*, **18**, 1227(1975).

(203) I. W. Mathison, P. H. Morgan, N. J. Wojciechowski, J. Bandura, and J. Wennemark, *J. Med. Chem.*, in press.

(204) J. G. Topliss, *ibid.*, **15**, 1006(1972).

(205) J. Huet, M. Martin, P. Linee, P. Lacroix, and P. Quiniou, *Eur. J. Med. Chem.*, **9**, 376(1974).

(206) J. W. Lawson, *J. Pharmacol. Exp. Ther.*, **160**, 22(1968).

(207) V. K. Engelmann, W. Raake, and A. Petter, *Arzneim.-Forsch.*, **24**, 759(1974).

(208) D. C. Remy, W. A. Van Saun, Jr., and E. L. Engelhardt, *J. Med. Chem.*, **18**, 142(1975).

(209) S. J. Dykstra, J. L. Minielli, J. E. Lawson, H. C. Ferguson, and K. W. Dungan, *ibid.*, **16**, 1015(1973).

(210) C. Casagrande, A. Galli, R. Ferrini, G. Miragoli, and G. Ferrari, *Farmaco*, **29**, 757(1974).

(211) R. G. Burney, C. A. Difazio, M. J. Peach, K. A. Petrie, and M. J. Sylvester, *Amer. Heart J.*, **88**, 765(1974).

(212) P. K. Lahiri and H. F. Hardman, *Arch. Int. Pharmacodyn. Ther.*, **210**, 197(1974).

(213) F. J. Kniffen, T. E. Lomas, N. L. Nobel-Allen, and B. R. Lucchesi, *Circulation*, **49**, 264(1974).

(214) R. A. Gillis, F. H. Thibodeaux, A. Raines, and F. G. Standaert, *ibid.*, **47**, 697(1973).

(215) L. Molinengo, *Eur. J. Pharmacol.*, **5**, 23(1968).

(216) J. Ferguson, "Mecanisme de la Narcose," CNRS, Paris, France, 1951, pp. 25–38.

(217) D. L. Tabern and E. F. Shelberg, *J. Amer. Chem. Soc.*, **55**, 328(1933).

(218) L. Molinengo, *Arch. Ital. Sci. Farmacol.*, **25**, 308(1960).

(219) G. B. Frank, *Fed. Proc.*, **27**, 132(1968).

(220) M. M. Winbury, *Ann. N.Y. Acad. Sci.*, **64**, 564(1956).

(221) H. Brunner, P. R. Hedwall, and M. Meier, *Arch. Pharmakol. Exp. Pathol.*, **269**, 219(1971).

(222) P. Somani and A. R. Laddu, *Eur. J. Pharmacol.*, **14**, 209(1971).

(223) J. V. Levy, *J. Pharm. Pharmacol.*, **20**, 813(1968).

(224) B. Belleau, *Ann. N.Y. Acad. Sci.*, **139**, 580(1967).

(225) G. J. Kelliher and J. Roberts, *Eur. J. Pharmacol.*, **20**, 243(1972).

(226) A. J. Ariëns, *Ann. N.Y. Acad. Sci.*, **139**, 606(1967).

(227) M. S. K. Shouri and T. J. Haley, *J. Pharm. Sci.*, **58**, 511(1969).

(228) J. D. Fitzgerald, *Int. J. Clin. Pharmacol. Biopharm.*, **11**, 235(1975).

(229) A. M. Lands, J. P. Arnold, J. P. McAuliff, F. P. Luduena, and T. G. Brown, Jr., *Nature (London)*, **214**, 597(1967).

(230) M. A. Wasserman and B. Levy, *J. Pharmacol. Exp. Ther.*, **188**, 357(1974).
(231) A. C. Dreyer and J. Offermeier, *Pharm. Res. Commun.*, **7**, 151(1975).
(232) B. Levy and B. E. Wilkenfield, *Fed. Proc.*, **29**, 1362(1970).
(233) S. Zakhari, *Eur. J. Pharmacol.*, **29**, 22(1974), and references cited therein.
(234) E. J. Mylecharane and C. Raper, *Arch. Int. Pharmacodyn. Ther.*, **202**, 163(1973).
(235) V. Vecchietti, F. Lauria, R. Tommasini, and M. Bergamaschi, *Eur. J. Med. Chem.*, **9**, 501(1974).
(236) M. L. Hoefle, S. G. Hastings, R. F. Meyer, R. M. Corey, A. Holmes, and C. D. Stratton, *J. Med. Chem.*, **18**, 148(1975).
(237) B. Åblad, M. Brograd, E. Carlsson, and L. Ek, *Eur. J. Pharmacol.*, **13**, 59(1970).
(238) B. Åblad, E. Carlsson, and L. Ek, *Life Sci.*, **12**, 107(1973).
(239) B. Levy, *Brit. J. Pharmacol.*, **47**, 398(1973).
(240) S. Zakhari and J. Drimal, "Is Acetamide Group Necessary for Selective β-Adrenoceptor Blockade?," presented at the Symposium on Pharmacodynamics of Circulation, Smolenice, Czechoslovakia, 1973.
(241) G. Shtacher, M. Erez, and S. Cohen, *J. Med. Chem.*, **16**, 516(1973).
(242) E. E. Bagwell and E. M. Vaughan Williams, *Brit. J. Pharmacol.*, **48**, 686(1973).
(243) J. Augstein, D. A. Cox, A. L. Ham, P. R. Leeming, and M. Snary, *J. Med. Chem.*, **16**, 1245(1973).
(244) A. M. Barrett, *Rec. Advan. Cardiol.*, **6**, 289(1973).
(245) A. M. Barrett, J. Carter, J. D. Fitzgerald, R. Hull, and D. LeCount, *Brit. J. Pharmacol.*, **48**, 340P(1973).
(246) M. Lauble, G. Cheymol, P. Mouille, J. C. Gilbert, and H. Schmitt, *Arch. Int. Pharmacodyn. Ther.*, **201**, 323(1973).
(247) J. R. Kilborn and P. Turner, *Brit. J. Clin. Pharmacol.*, **1**, 143(1974).
(248) *Drugs Today*, **10**, 332(1974).
(249) A. Seriabine, M. L. Torchina, J. M. Stavorski, C. T. Ludden, D. H. Minsker, and C. A. Stone, *Arch. Int. Pharmacodyn. Ther.*, **205**, 76(1973).
(250) K. Nakagawa, N. Murakami, S. Yoshizaki, M. Tominaga, H. Mori, Y. Yabuuchi, and S. Shintani, *J. Med. Chem.*, **17**, 529(1974).
(251) V. Yabuuchi and D. Kinoshita, *Jap. J. Pharmacol.*, **24**, 853(1974).

ACKNOWLEDGMENTS AND ADDRESSES

Received from the *Division of Organic Chemistry, Department of Medicinal Chemistry, College of Pharmacy, University of Tennessee Center for the Health Sciences, Memphis, TN 38163*

The authors express their appreciation to Dr. Charles E. Kossmann, Dr. James R. Wennemark, and Dr. E. M. Vaughan Williams for useful discussions during the preparation of this review.

* Presently a Medical Research Council of Great Britain Research Fellow at Chelsea College, University of London, England.

ˣ To whom inquiries should be directed.

RESEARCH ARTICLES

Programmed Diffusional Release Rate from Encapsulated Cosolvent System

FELIX THEEUWES ˣ, KAZUO ASHIDA*, and TAKERU HIGUCHI ‡

Abstract □ The programmed diffusional release rate of an active agent through a rate-controlling membrane from a cosolvent system is discussed. At initial conditions, the drug is present below saturation in solution in a solvent mixture, enclosed by the rate-controlling membrane; the solvent is composed of the main solvent and a cosolvent, which increases the drug solubility in the main solvent. During operation, the active agent and cosolvent diffuse from the capsule at a rate controlled by the membrane. Equations were derived describing the release rate of the active agent as a function of the permeability of the cosolvent and agent, the capsule dimensions, and the system's initial conditions. A great variety of release rate profiles can be programmed from declining to increasing delivery rate patterns as a function of time. Experimental data are presented for the drug progesterone in solution in cyclohexane with methyl, heptyl, or cetyl alcohol as the cosolvent in a polyethylene capsule. The theory qualitatively predicts the experimental results.

Keyphrases □ Diffusion—progesterone through rate-controlling membrane (polyethylene capsule), programmed release rate, cosolvent system □ Release rate, programmed—progesterone diffusion through rate-controlling membrane (polyethylene capsule) □ Drug delivery systems—progesterone diffusion through rate-controlling membrane (polyethylene capsule) □ Membranes, rate controlling—polyethylene capsule, progesterone diffusion □ Progesterone—diffusion through polyethylene capsule, programmed release rate □ Polyethylene capsule—rate-controlling membrane, progesterone diffusion, programmed release rate

During the past 5 years, considerable effort has been undertaken to achieve embodiments of a new class of dosage form, specified not by the quantity of drug but by the rate and duration of drug release (1). Both rate and duration are parameters that should be designed to be independent of the body environment in which the system is deployed.

The mechanism of diffusion provides one basis for accomplishing this objective. Such systems were discussed in detail in a recent review article (2). The release patterns are governed by Fick's law, and different time profiles are obtained, depending on the system design. Important well-known (2) release rate profiles are:

(230) M. A. Wasserman and B. Levy, *J. Pharmacol. Exp. Ther.*, **188**, 357(1974).
(231) A. C. Dreyer and J. Offermeier, *Pharm. Res. Commun.*, **7**, 151(1975).
(232) B. Levy and B. E. Wilkenfield, *Fed. Proc.*, **29**, 1362(1970).
(233) S. Zakhari, *Eur. J. Pharmacol.*, **29**, 22(1974), and references cited therein.
(234) E. J. Mylecharane and C. Raper, *Arch. Int. Pharmacodyn. Ther.*, **202**, 163(1973).
(235) V. Vecchietti, F. Lauria, R. Tommasini, and M. Bergamaschi, *Eur. J. Med. Chem.*, **9**, 501(1974).
(236) M. L. Hoefle, S. G. Hastings, R. F. Meyer, R. M. Corey, A. Holmes, and C. D. Stratton, *J. Med. Chem.*, **18**, 148(1975).
(237) B. Åblad, M. Brograd, E. Carlsson, and L. Ek, *Eur. J. Pharmacol.*, **13**, 59(1970).
(238) B. Åblad, E. Carlsson, and L. Ek, *Life Sci.*, **12**, 107(1973).
(239) B. Levy, *Brit. J. Pharmacol.*, **47**, 398(1973).
(240) S. Zakhari and J. Drimal, "Is Acetamide Group Necessary for Selective β-Adrenoceptor Blockade?," presented at the Symposium on Pharmacodynamics of Circulation, Smolenice, Czechoslovakia, 1973.
(241) G. Shtacher, M. Erez, and S. Cohen, *J. Med. Chem.*, **16**, 516(1973).
(242) E. E. Bagwell and E. M. Vaughan Williams, *Brit. J. Pharmacol.*, **48**, 686(1973).
(243) J. Augstein, D. A. Cox, A. L. Ham, P. R. Leeming, and M. Snary, *J. Med. Chem.*, **16**, 1245(1973).
(244) A. M. Barrett, *Rec. Advan. Cardiol.*, **6**, 289(1973).
(245) A. M. Barrett, J. Carter, J. D. Fitzgerald, R. Hull, and D. LeCount, *Brit. J. Pharmacol.*, **48**, 340P(1973).
(246) M. Lauble, G. Cheymol, P. Mouille, J. C. Gilbert, and H. Schmitt, *Arch. Int. Pharmacodyn. Ther.*, **201**, 323(1973).
(247) J. R. Kilborn and P. Turner, *Brit. J. Clin. Pharmacol.*, **1**, 143(1974).
(248) *Drugs Today*, **10**, 332(1974).
(249) A. Seriabine, M. L. Torchina, J. M. Stavorski, C. T. Ludden, D. H. Minsker, and C. A. Stone, *Arch. Int. Pharmacodyn. Ther.*, **205**, 76(1973).
(250) K. Nakagawa, N. Murakami, S. Yoshizaki, M. Tominaga, H. Mori, Y. Yabuuchi, and S. Shintani, *J. Med. Chem.*, **17**, 529(1974).
(251) V. Yabuuchi and D. Kinoshita, *Jap. J. Pharmacol.*, **24**, 853(1974).

ACKNOWLEDGMENTS AND ADDRESSES

Received from the *Division of Organic Chemistry, Department of Medicinal Chemistry, College of Pharmacy, University of Tennessee Center for the Health Sciences, Memphis, TN 38163*

The authors express their appreciation to Dr. Charles E. Kossmann, Dr. James R. Wennemark, and Dr. E. M. Vaughan Williams for useful discussions during the preparation of this review.

* Presently a Medical Research Council of Great Britain Research Fellow at Chelsea College, University of London, England.

ˣ To whom inquiries should be directed.

RESEARCH ARTICLES

Programmed Diffusional Release Rate from Encapsulated Cosolvent System

FELIX THEEUWES ˣ, KAZUO ASHIDA*, and TAKERU HIGUCHI ‡

Abstract □ The programmed diffusional release rate of an active agent through a rate-controlling membrane from a cosolvent system is discussed. At initial conditions, the drug is present below saturation in solution in a solvent mixture, enclosed by the rate-controlling membrane; the solvent is composed of the main solvent and a cosolvent, which increases the drug solubility in the main solvent. During operation, the active agent and cosolvent diffuse from the capsule at a rate controlled by the membrane. Equations were derived describing the release rate of the active agent as a function of the permeability of the cosolvent and agent, the capsule dimensions, and the system's initial conditions. A great variety of release rate profiles can be programmed from declining to increasing delivery rate patterns as a function of time. Experimental data are presented for the drug progesterone in solution in cyclohexane with methyl, heptyl, or cetyl alcohol as the cosolvent in a polyethylene capsule. The theory qualitatively predicts the experimental results.

Keyphrases □ Diffusion—progesterone through rate-controlling membrane (polyethylene capsule), programmed release rate, cosolvent system □ Release rate, programmed—progesterone diffusion through rate-controlling membrane (polyethylene capsule) □ Drug delivery systems—progesterone diffusion through rate-controlling membrane (polyethylene capsule) □ Membranes, rate controlling—polyethylene capsule, progesterone diffusion □ Progesterone—diffusion through polyethylene capsule, programmed release rate □ Polyethylene capsule—rate-controlling membrane, progesterone diffusion, programmed release rate

During the past 5 years, considerable effort has been undertaken to achieve embodiments of a new class of dosage form, specified not by the quantity of drug but by the rate and duration of drug release (1). Both rate and duration are parameters that should be designed to be independent of the body environment in which the system is deployed.

The mechanism of diffusion provides one basis for accomplishing this objective. Such systems were discussed in detail in a recent review article (2). The release patterns are governed by Fick's law, and different time profiles are obtained, depending on the system design. Important well-known (2) release rate profiles are:

1. Zero-order release, where the drug is released through a membrane of fixed dimensions from a source at constant thermodynamic activity.

2. Release from dispersed systems, where the release rate is inversely proportional to the square root of time (3, 4).

3. Release from a capsule containing the drug in solution where the release rate (dm/dt) decreases exponentially with time as:

$$\frac{dm}{dt} = A\left(\frac{P}{l}\right)C_0 \exp(-kt) \qquad \text{(Eq. 1)}$$

where A is the membrane area, l is the membrane thickness, P is the drug permeability through the membrane, and C_0 is the drug concentration at time $t = 0$ in the capsule. The rate constant, k, is defined as:

$$k = \frac{AP}{Vl} \qquad \text{(Eq. 2)}$$

where V is the capsule volume.

The three patterns discussed have a time profile constant or decreasing with time. In this paper, a system is discussed that can be programmed at a rate increasing, constant, or decreasing with time. The system consists of the drug in solution in a mixture of two solvents, contained in a capsule composed of a polymeric rate-controlling membrane. One of the two solvents, the main solvent, does not leave the capsule; the second solvent, the cosolvent, permeates through the membrane and, in turn, affects the thermodynamic activity of the drug in solution while the drug concentration continuously decreases.

In the system described here, the cosolvent was selected such that the drug solubility increases linearly in solution as a function of the cosolvent concentration. During the experiment, the capsule was suspended in the main solvent and the capsule wall served as the rate-controlling membrane for the drug and cosolvent.

The model systems studied consisted of a polyethylene capsule containing the drug progesterone in a solution of cyclohexane as the main solvent and methyl, heptyl, or cetyl alcohol as the cosolvent.

EXPERIMENTAL

Materials—Progesterone samples[1] were recrystallized from methyl alcohol to yield the crystalline form, mp 128°. All solvents were reagent grade and were used as received.

Solubility—The 37° solubility of progesterone in cyclohexane with alcohol as a cosolvent was determined using the solubility technique of Higuchi and Connors (5). Progesterone concentrations were determined spectrophotometrically at 232 nm in cyclohexane.

Diffusion—The permeability coefficients of progesterone, methyl alcohol, heptyl alcohol, and cetyl alcohol from cyclohexane through polyethylene into cyclohexane were determined for each compound separately. The experiments were carried out in a glass diffusion cell with a membrane area of 1.96 cm^2. Both sides of the cell were magnetically stirred. Polyethylene membranes, with a thickness of 5.8×10^{-3} cm, were used in the permeability experiments on the pure compound as well as in the cosolvent system diffusion experiments. The permeated amounts of progesterone were determined spectrophotometrically at 232 nm in cyclohexane. The permeated amounts of cosolvent were determined by GC.

In the cosolvent diffusion experiments, progesterone was dissolved at a known initial concentration, C_{Di}, smaller than the saturated value of C_{DS}, in a mixture of cyclohexane and cosolvent at concentration X_i. This solution was sealed into a polyethylene capsule and suspended in the first of a series of volumetric flasks containing cyclohexane. The flasks were shaken in a 37° bath. At regular time intervals, the capsule was transferred into a fresh flask in the same bath.

The content of each flask was analyzed, and the amount of progesterone released per unit time and area was calculated. The progesterone concentration on the downstream side was maintained at less than 5% of the concentration on the upstream side. The amounts of progesterone released were determined spectrophotometrically as in the solubility studies.

[1] Searle Chemicals.

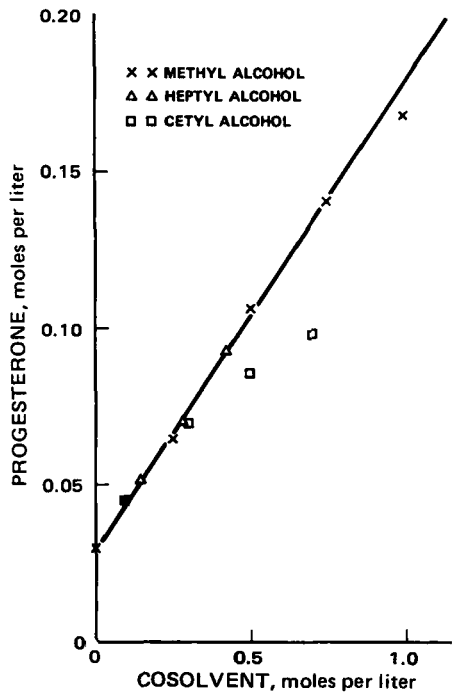

Figure 1—*Solubility of progesterone in cyclohexane as a function of cosolvent (methyl alcohol, heptyl alcohol, and cetyl alcohol) concentration.*

RESULTS

The solubility data of progesterone in the cyclohexane–alcohol cosolvent systems are plotted in Fig. 1. A linear solubility curve was obtained for the three cosolvents: methyl, heptyl, and cetyl alcohols. The intercept and initial slope were the same for the three cosolvents, and the curve can be represented by a single straight line:

$$C_{DS} = C_{DSO} + BX \qquad \text{(Eq. 3)}$$

where C_{DS} is the progesterone solubility in the system with X as the cosolvent concentration in moles per liter, C_{DSO} is the progesterone solubility in cyclohexane equal to 0.025 mole/liter, and $B = 0.15$ (moles per liter of progesterone/moles per liter of cosolvent) is the slope of the solubility curve.

The permeability coefficients for progesterone (P_D) and cosolvents (P_X) from cyclohexane through polyethylene are listed in Table I. The remaining parameters affecting the release phenome-

Table I—Experimental Permeability Coefficients through Polyethylene from Cyclohexane

Compound	Permeability Coefficient, cm^2/sec × 10^8
Progesterone	3.9
Methyl alcohol	5.1
Heptyl alcohol	1.9
Cetyl alcohol	0.45

Table II—Initial Progesterone and Cosolvent Concentrations and Capsule Dimensions

Cosolvent	Initial Concentration: Progesterone, C_{Di}, mole/liter	Initial Concentration: Cosolvent, X_i, mole/liter	Capsule Volume, cm^3	Membrane: Area, cm^2	Membrane: Thickness, cm
None	0.025	0	0.5	5.07	5.8×10^{-3}
Methyl alcohol	0.053	0.50	0.3	3.5	5.8×10^{-3}
Heptyl alcohol	0.053	0.50	0.35	4.0	5.8×10^{-3}
Cetyl alcohol	0.053	0.50	0.3	3.7	5.8×10^{-3}

non are listed in Table II, which gives the dimensions of the capsules and initial concentrations of cosolvent, X_i, and progesterone, C_{Di}, for each cosolvent experiment.

In the experiment listed in the first row of Table II, no cosolvent was used and the release rate declined exponentially according to Eq. 1. The experimental data are collectively presented in Fig. 2, in which the release rates are plotted for the cyclohexane and cosolvent systems. In these experiments, the same initial conditions and about the same capsule sizes were chosen. As seen earlier, the solubility curve represented by Eq. 3 is the same for each cosolvent system.

THEORETICAL

Derivation of Working Equations—In the following calculations, it is assumed that the cosolvent has no plasticizing effect on the membrane and that the cosolvent permeates from the capsule at a rate independent of the drug. It also is assumed that concentrations of the drugs and cosolvents in the membrane are in equilibrium with the inside and outside of the capsule at all times so that the bulk concentrations are directly related to the membrane surface concentrations[2] and the membrane can be treated as a thin membrane.

Under steady-state conditions in the membrane, it has been shown (6) that the drug permeation rate, dm/dt, is proportional to the fraction of saturation for a system obeying Henry's law:

$$\frac{dm}{dt} = \left(\frac{A}{l}\right) \bar{T} \left(\frac{C_D}{C_{DS}}\right) \quad \text{(Eq. 4)}$$

where A is the membrane area, l is the membrane thickness, and $\bar{T}$ is the transference coefficient (6):

$$\bar{T} = \frac{l}{A}\left(\frac{dm}{dt}\right)_{sat} = P_D C_{DS} \quad \text{(Eq. 5)}$$

In Eqs. 4 and 5, C_D and C_{DS} are the drug concentration and the drug concentration at saturation, respectively; $(dm/dt)_{sat}$ is the limiting mass permeation rate occurring from a saturated drug solution. The cosolvent system, progesterone–alcohol, has a saturated concentration, C_{DS}, represented by Eq. 3. Hence, Eqs. 4 and 3 result in:

$$\frac{dm}{dt} = \left(\frac{A}{l}\right) \bar{T} \left[\frac{C_D}{(C_{DSO} + BX)}\right] \quad \text{(Eq. 6)}$$

Since a steady state is assumed for the cosolvent as well as progesterone, Eq. 1 also applies to the cosolvent as long as the cosolvent leaves as an independent species. Thus, the concentration of cosolvent can be expressed by:

$$X = X_i \exp(-k_x t) \quad \text{(Eq. 7)}$$

where X_i is the initial cosolvent concentration, and k_x is:

$$k_x = \frac{AP_x}{Vl} \quad \text{(Eq. 8)}$$

For a capsule volume, V, the relation between the mass, m, of drug in solution and drug concentration, C_D, is given by:

$$m = C_D V \quad \text{(Eq. 9)}$$

Substituting Eqs. 9 and 7 into Eq. 6 results in:

$$\frac{dC_D}{C_D} = -\left(\frac{A}{l}\right)\left(\frac{\bar{T}}{V}\right) \frac{dt}{C_{DSO} + BX_i \exp(-k_x t)} \quad \text{(Eq. 10)}$$

The drug concentration, C_D, at each time, t, is obtained by integrating Eq. 10 from $t = 0$ from the initial drug concentration, C_{Di}, to C_D:

$$\int_{C_{Di}}^{C_D} \frac{dC_D}{C_D} = -\left(\frac{A}{l}\right)\left(\frac{\bar{T}}{V}\right) \int_0^t \frac{dt}{C_{DSO} + BX_i \exp(-k_x t)} \quad \text{(Eq. 11)}$$

The solution to Eq. 11 is given by:

$$\ln \frac{C_D}{C_{Di}} = -\left(\frac{A}{l}\right)\left(\frac{\bar{T}}{V}\right)\left[\frac{t}{C_{DSO}} + \frac{1}{C_{DSO}k_x} \ln \frac{C_{DSO} + BX_i \exp(-k_x t)}{C_{DSO} + BX_i}\right] \quad \text{(Eq. 12)}$$

To reduce the size of the expressions, substitute $\phi(t)$:

$$\phi(t) = t + \frac{1}{k_x} \ln \frac{C_{DSO} + BX_i \exp(-k_x t)}{C_{DSO} + BX_i} \quad \text{(Eq. 13)}$$

where $\bar{T}$ is the transference obtained from the system at unit activity and is given by:

$$\bar{T} = P_D C_{DSO} \quad \text{(Eq. 14)}$$

The final form of the delivery rate obtained from Eqs. 6 and 12–14 is given by:

$$\frac{dm}{dt} = \left(\frac{A}{l}\right)\bar{T} \frac{C_{Di} \exp[-k_D \phi(t)]}{C_{DSO} + BX_i \exp(-k_x t)} \quad \text{(Eq. 15)}$$

Equation 15 is the general expression for the delivery rate from a capsule containing drug in solution in a cosolvent system with a linear solubility curve. At $t = 0$, $\phi(t)$ reduces to zero and dm/dt reduces to Eq. 4 for $C_D = C_{Di}$. At $t \to \infty$, $\phi(t) \to \infty$ and dm/dt goes to zero. At $X_i = 0$, $\phi(t)$ is equal to t and Eq. 15 reduces to the simple case for a single solvent given by Eq. 1.

The maximum in the delivery rate is obtained when Eq. 16 holds:

$$\frac{d}{dt}\left(\frac{dm}{dt}\right) = 0 \quad \text{(Eq. 16)}$$

By differentiating Eq. 15 and equating to zero, the time, t_R, at which the maximum occurs is found to be:

$$t_R = \frac{lV}{AP_x} \ln \frac{P_x B X_i}{P_D C_{DSO}} \quad \text{(Eq. 17)}$$

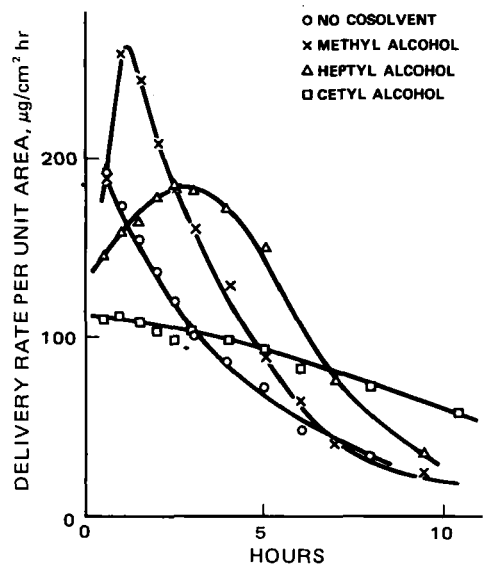

Figure 2—*Experimental release rates of progesterone from polyethylene capsules, containing cyclohexane as a primary solvent and an alcohol as the cosolvent, into cyclohexane.*

[2] This assumption will only be approximately true as hydrodynamic boundaries must be "crossed" at the interfaces (Ref. 7). Given the small permeability coefficients through the membrane and with the assumption that partition coefficients ≤1, these fluid boundaries would contribute negligibly to the diffusional resistance.

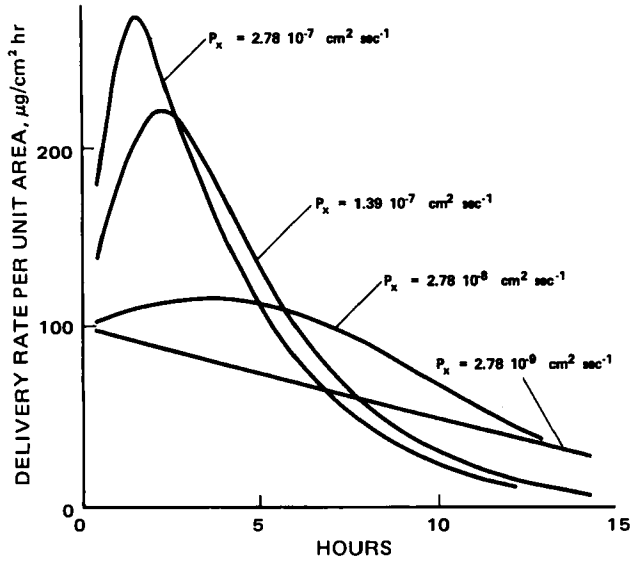

Figure 3—*Theoretical release rates of progesterone from polyethylene capsules calculated from Eq. 15 for different values of cosolvent permeability,* P_x.

From Eq. 17, it can be seen that t_R values exist only when $P_xBX_i > \bar{T}$. In other words, if $\bar{T} > P_xBX_i$, t_R is negative and no maximum exists. In this case, only decreasing rates are obtained.

It is notable that, if $P_xBX_i > \bar{T}$, the condition $t_R > 0$ is independent of the initial drug concentration, C_{Di}. Also, the time dependency of the rate in Eq. 15 is independent of C_{Di} and only the magnitude of the rate depends on C_{Di}.

As can be seen from Eq. 17, the maximum in the delivery rate can be programmed by selecting different cosolvents, in an homologous series, affecting mainly the permeability P_x. In Eq. 17, P_x appears both in the nominator and the denominator, resulting in a maximum value of t_R as a function of P_x; t_R is shortest for large values of P_x and increases with smaller P_x values to reach a maximum $t_{R,max}$ at P_{xm} before decreasing and becoming negative or ceasing to be real. The value P_{xm} at which the time t_R reaches a maximum can be obtained by differentiating Eq. 17 with respect to P_x and equating to zero. The value of P_{xm} is given by Eq. 18:

$$P_{xm} = e\left(\frac{\bar{T}}{BX_i}\right) \qquad \text{(Eq. 18)}$$

where e is the base of the natural logarithm.

The maximum time $t_{R,max}$ for a maximum rate is obtained by substituting Eq. 18 into Eq. 17, resulting in:

$$t_{R,max} = \frac{1}{e}\frac{lV}{A}\frac{BX_i}{\bar{T}} \qquad \text{(Eq. 19)}$$

$$t_{R,max} = \frac{lV}{AP_{xm}} \qquad \text{(Eq. 20)}$$

For cosolvent permeabilities P_x smaller than P_{xm}, $t_{R,max}$ decreases to reach the zero value at the cosolvent permeability P_{x0} given by:

$$P_{x0} = \frac{\bar{T}}{BX_i} \qquad \text{(Eq. 21)}$$

Numerical Calculations—The delivery rate per unit area, $(1/A)\ (dm/dt)$, was calculated from Eq. 15 using P_D given in Table I for an average sized capsule corresponding to Table II with V = 0.3 cm³, A = 3.7 cm², and $l = 5.8 \times 10^{-3}$ cm; initial conditions are C_{Di} = 0.053 mole/liter and X_i = 0.50 mole/liter. The cosolvent permeability was chosen at $P_x = 2.78 \times 10^{-9}$, 2.78×10^{-7}, 1.39×10^{-7}, and 2.78×10^{-9} cm²/sec. The theoretical curves are shown in Fig. 3.

Qualitatively, the experimental results of Fig. 2 agree with Fig. 3. At decreasing permeability of the cosolvent, the maximum in delivery rate decreases and shifts toward longer times as predicted by Eq. 17. At sufficiently low cosolvent permeability, the delivery rate decreases continuously and almost linearly with time, and a t_R does not exist.

The transference, $\bar{T}$, of progesterone through polyethylene submersed in cyclohexane is found to be 9.7×10^{-13} mole/cm sec, and

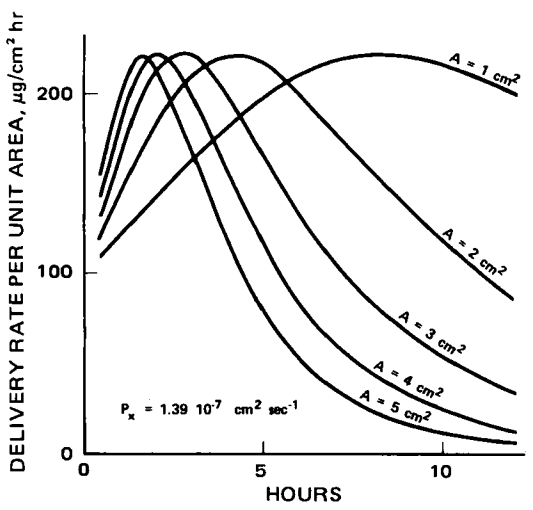

Figure 4—*Theoretical release rates of progesterone from polyethylene capsules calculated from Eq. 15 for different values of membrane area for the case satisfying* $P_xBX_i > \bar{T}$.

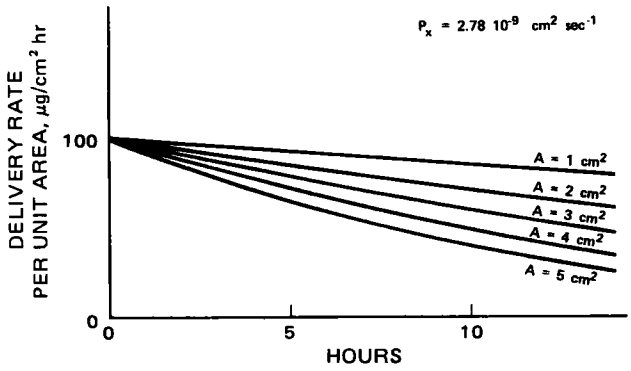

Figure 5—*Theoretical release rate of progesterone from polyethylene capsules calculated from Eq. 15 for different values of membrane area for the case satisfying* $\bar{T} > P_xBX_i$.

the progesterone flux at saturation, $(1/A)\ (dm/dt)_{sat}$, is 190 μg/cm² hr. This finding indicates, as shown in Figs. 2–4, that a supersaturated state is produced *in situ* and that supersaturation can be induced *via* facile equilibrium from the solvent into the membrane phase (6).

The cosolvent permeability, P_{xm}, for the alcohol series was calculated from Eq. 18 as $P_{xm} = 3.5 \times 10^{-8}$ cm²/sec, which would result in $t_{R,max}$ = 3.7 hr as calculated from Eq. 20. The cosolvent permeability at which $t_{R,max} = 0$ is calculated from Eq. 21: $P_{x0} = 1.3 \times 10^{-8}$ cm²/sec. The time at which the maximum in progesterone delivery rate occurs as a function of the alcohol cosolvent permeability is shown in Fig. 6. The calculations were carried out based on the initial experimental condition X_i = 0.5 mole/liter and an average sized capsule (Table II) using Eq. 17.

The membrane surface to capsule volume ratio of the system is very important for programming the device. In Figs. 4 and 5, typical fluxes are shown for systems characterized by $P_D = 3.9 \times 10^{-8}$ cm²/sec, V = 0.3 cm², and $l = 5.8 \times 10^{-3}$ cm. Initial concentrations are C_{Di} = 0.053 mole/liter and X_i = 0.50 mole/liter, and the membrane area was selected to be A = 1, 2, 3, 4, or 5 cm².

For Fig. 4, the cosolvent permeability was taken to be $P_x = 1.39 \times 10^{-7}$ cm²/sec. A P_x of 2.78×10^{-9} cm²/sec was assumed for Fig. 5. In Fig. 4, the maximum flux obtained is independent of membrane area. However, the onset of the maximum in flux occurs at longer times as the membrane area is reduced as predicted by Eq. 17. At low cosolvent permeability (Fig. 5), the flux becomes relatively invarient (zero-order rate) as the membrane area is reduced.

DISCUSSION

A cosolvent that enhances the drug solubility can be used to formulate the drug release rate in a controlled fashion. The drug re-

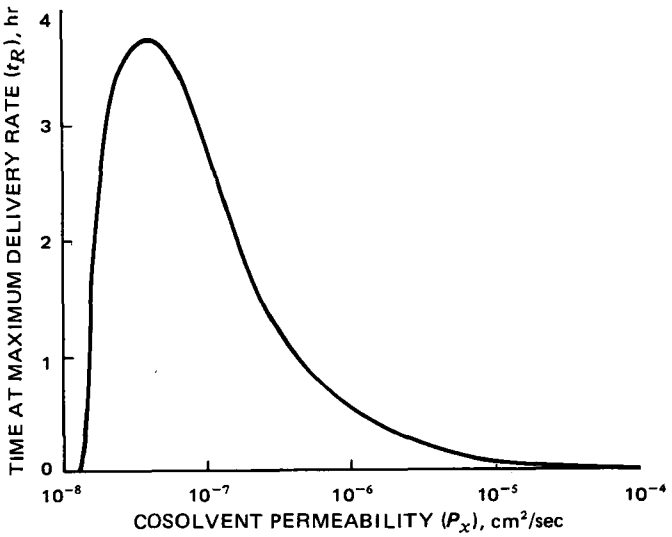

Figure 6—*Theoretical time at which a maximum in delivery rate occurs as calculated from Eq. 17 for progesterone diffusing from a polyethylene capsule (X_i = 0.5 mole/liter).*

lease rate from a cosolvent system with linear solubility characteristics is described by Eq. 15 as a first approximation. The release rate is equal to the product of the limiting rate, initial drug concentration, and a function of time. This time function is dependent on capsule dimensions, on drug and cosolvent permeabilities and solubility characteristics, and on the initial cosolvent concentration. The time function is independent of initial drug loading. The time function is flexible and can be programmed into shapes exhibiting a maximum at a predetermined time or into a declining time pattern. In the limit at zero cosolvent concentration, the time function reduces to a simple first-order (exponential decay) release.

Different release rate profiles were experimentally produced which are in qualitative agreement with the theory. It follows from the theory that no maximum is expected in the cetyl alcohol system, which has a P_x smaller than P_{x0}; for methyl and heptyl alcohols, a maximum is expected at 3.7 and 2.8 hr, respectively. The experimental permeability of heptyl alcohol is smaller than P_{xm} and, therefore, the maximum is expected to lie between 0 and 3.7 hr, the latter time being the maximum time, for maximum rate, expected for the system geometry. Experimental t_R times in excess of the theoretical maximum were not observed.

Since the theory as developed does not account for back-diffusion of cyclohexane, the influence of the cosolvent on membrane permeability characteristics, or for drug–cosolvent complexing (among other things), deviations can be expected where the membrane is affected by the presence of the cosolvent or where a strong cosolvent–drug interaction exists such that the complex diffuses as a separate species.

The release function predicts the attainment of a metastable, supersaturated state under certain tailored system conditions. A dosage form so designed could deliver a drug at rates exceeding those obtained from saturated solutions. During storage, the drug would remain in a stable solution state. When applied, a state of high thermodynamic activity can be produced *in situ* in a preprogrammed fashion.

REFERENCES

(1) F. E. Yates, H. Benson, R. Buckles, J. Urquhart, and A. Zaffaroni, in "Advances in Biomedical Engineering," vol. 5, J. F. Dickson, Ed., Academic, New York, N.Y., 1975.

(2) R. W. Baker and H. K. Lonsdale, in "Controlled Release of Biologically Active Agents," A. C. Tanquary and R. E. Lacey, Eds., Plenum, New York, N.Y., 1974, p. 15.

(3) T. Higuchi, *J. Soc. Cosmet. Chem.*, **11**, 85(1960).

(4) T. Higuchi, *J. Pharm. Sci.*, **50**, 874(1961).

(5) T. Higuchi and K. A. Connors, *Advan. Anal. Chem. Inst.*, **4**, 117(1965).

(6) F. Theeuwes, R. M. Gale, and R. W. Baker, *J. Membrane Sci.*, **1**, 3(1976).

(7) G. L. Flynn and S. H. Yalkowsky, *J. Pharm. Sci.*, **61**, 838(1972).

ACKNOWLEDGMENTS AND ADDRESSES

Received May 30, 1975, from *ALZA Research, Palo Alto, CA 94304*

Accepted for publication August 11, 1975.

F. Theeuwes thanks Dr. A. S. Michaels and Dr. R. W. Baker for their stimulating discussions on this subject and Scott Hamilton for the numerical computer evaluation of Eq. 15.

* Present address: Fujisawa Pharmaceutical Co. Ltd., 3 Doshomachi 4 Chome, Osaka, Japan.

‡ Present address: Pharmaceutical Chemistry Laboratory, University of Kansas, Lawrence, KS 66044

ˣ To whom inquiries should be directed.

Bioavailability of 17 Ampicillin Products

PHILIP L. WHYATT *, GERALD W. A. SLYWKA, ARMEN P. MELIKIAN, and MARVIN C. MEYER ˣ

Abstract □ The bioavailability of single lots of 250-mg ampicillin capsules, available from 17 distributors and/or manufacturers, was determined. Each product was evaluated in terms of the serum ampicillin levels achieved at 1, 2, 3, 4, 6, and 8 hr postadministration, the peak serum levels, the time of peak serum level, and the area under the serum level–time curve. There was no statistically significant difference ($p > 0.05$) between any of the 17 products tested.

Keyphrases □ Ampicillin—bioavailability of 17 products compared □ Bioavailability—ampicillin, 17 products compared □ Antibiotics—ampicillin, bioavailability of 17 products compared

It is well documented that while simple quantitative analysis of various drug dosage forms may indicate essentially identical drug content, the quantity of drug absorbed from the dosage form following oral administration may differ significantly from product to product (1–4). Ampicillin recently was categorized as a drug with "moderate risk potential" for bioavailability failures (5). Furthermore, the statement by

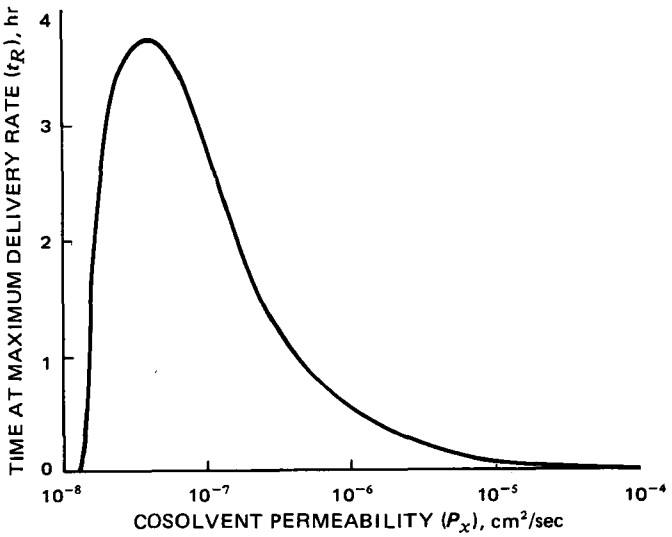

Figure 6—*Theoretical time at which a maximum in delivery rate occurs as calculated from Eq. 17 for progesterone diffusing from a polyethylene capsule (X_i = 0.5 mole/liter).*

lease rate from a cosolvent system with linear solubility characteristics is described by Eq. 15 as a first approximation. The release rate is equal to the product of the limiting rate, initial drug concentration, and a function of time. This time function is dependent on capsule dimensions, on drug and cosolvent permeabilities and solubility characteristics, and on the initial cosolvent concentration. The time function is independent of initial drug loading. The time function is flexible and can be programmed into shapes exhibiting a maximum at a predetermined time or into a declining time pattern. In the limit at zero cosolvent concentration, the time function reduces to a simple first-order (exponential decay) release.

Different release rate profiles were experimentally produced which are in qualitative agreement with the theory. It follows from the theory that no maximum is expected in the cetyl alcohol system, which has a P_x smaller than P_{x0}; for methyl and heptyl alcohols, a maximum is expected at 3.7 and 2.8 hr, respectively. The experimental permeability of heptyl alcohol is smaller than P_{xm} and, therefore, the maximum is expected to lie between 0 and 3.7 hr, the latter time being the maximum time, for maximum rate, expected for the system geometry. Experimental t_R times in excess of the theoretical maximum were not observed.

Since the theory as developed does not account for back-diffusion of cyclohexane, the influence of the cosolvent on membrane permeability characteristics, or for drug–cosolvent complexing (among other things), deviations can be expected where the membrane is affected by the presence of the cosolvent or where a strong cosolvent–drug interaction exists such that the complex diffuses as a separate species.

The release function predicts the attainment of a metastable, supersaturated state under certain tailored system conditions. A dosage form so designed could deliver a drug at rates exceeding those obtained from saturated solutions. During storage, the drug would remain in a stable solution state. When applied, a state of high thermodynamic activity can be produced *in situ* in a preprogrammed fashion.

REFERENCES

(1) F. E. Yates, H. Benson, R. Buckles, J. Urquhart, and A. Zaffaroni, in "Advances in Biomedical Engineering," vol. 5, J. F. Dickson, Ed., Academic, New York, N.Y., 1975.

(2) R. W. Baker and H. K. Lonsdale, in "Controlled Release of Biologically Active Agents," A. C. Tanquary and R. E. Lacey, Eds., Plenum, New York, N.Y., 1974, p. 15.

(3) T. Higuchi, *J. Soc. Cosmet. Chem.*, **11**, 85(1960).

(4) T. Higuchi, *J. Pharm. Sci.*, **50**, 874(1961).

(5) T. Higuchi and K. A. Connors, *Advan. Anal. Chem. Inst.*, **4**, 117(1965).

(6) F. Theeuwes, R. M. Gale, and R. W. Baker, *J. Membrane Sci.*, **1**, 3(1976).

(7) G. L. Flynn and S. H. Yalkowsky, *J. Pharm. Sci.*, **61**, 838(1972).

ACKNOWLEDGMENTS AND ADDRESSES

Received May 30, 1975, from *ALZA Research, Palo Alto, CA 94304*

Accepted for publication August 11, 1975.

F. Theeuwes thanks Dr. A. S. Michaels and Dr. R. W. Baker for their stimulating discussions on this subject and Scott Hamilton for the numerical computer evaluation of Eq. 15.

* Present address: Fujisawa Pharmaceutical Co. Ltd., 3 Doshomachi 4 Chome, Osaka, Japan.

‡ Present address: Pharmaceutical Chemistry Laboratory, University of Kansas, Lawrence, KS 66044

ˣ To whom inquiries should be directed.

Bioavailability of 17 Ampicillin Products

PHILIP L. WHYATT *, GERALD W. A. SLYWKA, ARMEN P. MELIKIAN, and MARVIN C. MEYER ˣ

Abstract □ The bioavailability of single lots of 250-mg ampicillin capsules, available from 17 distributors and/or manufacturers, was determined. Each product was evaluated in terms of the serum ampicillin levels achieved at 1, 2, 3, 4, 6, and 8 hr postadministration, the peak serum levels, the time of peak serum level, and the area under the serum level–time curve. There was no statistically significant difference ($p > 0.05$) between any of the 17 products tested.

Keyphrases □ Ampicillin—bioavailability of 17 products compared □ Bioavailability—ampicillin, 17 products compared □ Antibiotics—ampicillin, bioavailability of 17 products compared

It is well documented that while simple quantitative analysis of various drug dosage forms may indicate essentially identical drug content, the quantity of drug absorbed from the dosage form following oral administration may differ significantly from product to product (1–4). Ampicillin recently was categorized as a drug with "moderate risk potential" for bioavailability failures (5). Furthermore, the statement by

Table I—Ampicillin Capsules Employed in the Bioavailability Studies

Product[a]	Expiration Date	FDA Certified Potency[b]
1A,B,C	2/77	259
2A	12/74	248
3A	1/75	253
4A	1/75	260
5A	1/75	260
6A	11/74	256
2B	5/75	260
3B	5/76	249
4B	6/77	259[c]
5B	5/77	264
6B	7/74	246
2C	6/77	249
3C	2/76	255
4C	6/76	252
5C	10/75	254
6C	9/77	259
7C	7/76	274

[a] Products 1A, B, and C from Bristol Labs. (Polycillin), Lot A2116, manufactured by Bristol Labs.; Product 2A from Spencer-Mead, Lot 4746, manufactured by Biocraft Labs.; Product 3A from Paramount Surgical Supply Corp., Lot 2017-136, manufactured by Zenith Labs.; Product 4A from Vangard Labs., Lot 4774, manufactured by Biocraft Labs.; Product 5A from Wolins Pharmacal Corp., Lot 4774, manufactured by Biocraft Labs.; Product 6A from Columbia Medical Co., Lot 2017-126, manufactured by Zenith Labs.; Product 2B from Bocan Drug Co., Lot 201-3-B-102, manufactured by International Labs.; Product 3B from United Research Labs., Lot 2017-154, manufactured by Zenith Labs.; Product 4B from Wyeth Labs., Lot 1721636, manufactured by Wyeth Labs.; Product 5B from The Upjohn Co., Lot 199AW-D2, manufactured by Bristol Labs.; Product 6B from Squibb Pharmaceutical Co., Lot 2A622, manufactured by Squibb Pharmaceutical Co.; Product 2C from Smith Kline & French, Lot 32101, manufactured by Bristol Labs.; Product 3C from Beecham-Massengill, Lot Z7181RB, manufactured by Beecham-Massengill; Product 4C from Lederle Labs., Lot 334-101, manufactured by Beecham-Massengill; Product 5C from Ayerst Labs., Lot A6871PK, manufactured by Beecham-Massengill; Product 6C from Parke-Davis, Lot ML126, manufactured by Bristol Labs.; and Product 7C from Pfizer, Inc., Lot 24517, manufactured by Beecham-Massengill. [b] Expressed as milligrams of ampicillin per capsule. [c] Anhydrous ampicillin; all other products are ampicillin trihydrate.

the Drug Bioequivalence Panel of the Office of Technology Assessment (6) included ampicillin in the list of 24 drugs that exhibited differences in bioavailability between chemically equivalent products.

One study (7) compared three different 250-mg ampicillin products in a crossover experiment involving 12 human subjects. No statistically significant differences were noted in the bioavailability following oral administration. In contrast, a recent study (8) showed statistically significant differences in the bioavailability of the three 250-mg ampicillin products tested.

The present study was undertaken to provide bioavailability information on the currently marketed ampicillin products.

EXPERIMENTAL

Assay—The experimental design and the reported lack of stability of ampicillin in stored biological fluids (9, 10) required an assay method suitable for the rapid analysis of numerous samples. A microbiological, turbidimetric assay employing *Staphylococcus aureus*[1] was developed to quantitate serum ampicillin levels precisely and rapidly (10).

Venous blood samples were obtained following the oral administration of 250-mg capsules to human volunteers. The blood samples were allowed to clot, and the serum was separated within 30 min after collection and stored for no longer than 4 days at −10° until assayed.

[1] BMH 331-036, Baptist Memorial Hospital, Memphis, Tenn.

Table II—Experimental Design for Ampicillin Bioavailability Study, Series C[a]

	Week of Study						
Subject	1	2	3	4	5	6	7
1	1	2	7	3	6	4	5
2	1	2	7	3	6	4	5
3	2	3	1	4	7	5	6
4	2	3	1	4	7	5	6
5	3	4	2	5	1	6	7
6	3	4	2	5	1	6	7
7	4	5	3	6	2	7	1
8	4	5	3	6	2	7	1
9	5	6	4	7	3	1	2
10	5	6	4	7	3	1	2
11	6	7	5	1	4	2	3
12	6	7	5	1	4	2	3
13	7	1	6	2	5	3	4
14	7	1	6	2	5	3	4

[a] Each number within the matrix corresponds to a specific product code number. In Series A and B, Subjects 1–12 were used and six products were evaluated.

Clinical Study Protocol—The 14 male volunteers[2] had an average age of 24 years (range 20–38 years), an average height of 175.3 cm (range 167.6–190.5 cm), and an average weight of 75.5 kg (range 63.6–90.9 kg). Each volunteer was screened regarding general health and known drug allergies. All subjects underwent a hematologic and blood chemistry analysis[3] to ensure inclusion of only those subjects in good health. Each subject provided his informed written consent.

The bioavailability study of the 17 ampicillin products (Table I) was divided into three separate segments: Series A and B (12 subjects, 6 weeks, six products) and Series C (14 subjects, 7 weeks, seven products). Each subject received each drug in a sequence designed to minimize the influence of any cumulative or residual effects of preceding doses (11) (Table II). Product 1 was included in each series as a reference to permit comparisons.

All subjects were instructed to adhere to a standard protocol and to abstain from taking any medication for 1 week prior to and during each study. On the day of the study, following an overnight fast, each subject had an indwelling catheter[4] inserted into a forearm vein and a 10-ml blood sample was taken. A single ampicillin capsule was then swallowed with 240 ml (8 oz.) of water. No food or liquid other than water was permitted for 4 hr following ingestion of the dose. Ten-milliliter blood samples were withdrawn at 1, 2, 3, 4, 6, and 8 hr postadministration.

RESULTS AND DISCUSSION

Currently, antibiotic products must be certified for potency by the Food and Drug Administration (FDA), and each manufacturer was requested to provide the certification results (Table I).

There are almost 50 distributors of ampicillin products in the United States. However, FDA has approved the manufacture of ampicillin capsules by only the following eight companies: Beecham-Massengill Pharmaceutical, Biocraft Labs., Bristol Labs., International Labs., Linden Labs., E. R. Squibb & Sons, Wyeth Labs., and Zenith Labs. (9). This study encompassed all these manufacturers except Linden Labs.

To compare the relative bioavailability of 17 ampicillin products, four parameters describing the blood level curves were evaluated. These were: (*a*) serum concentrations achieved at 1, 2, 3, 4, 6, and 8 hr postadministration; (*b*) the peak serum concentration; (*c*) the time of peak concentration; and (*d*) the area under the serum concentration–time curve.

Serum Concentrations—The mean ampicillin serum levels observed are shown graphically in Figs. 1–3. Statistical analysis of these data revealed no significant differences ($p > 0.05$) between

[2] Recruited from the staff and student body of the University of Tennessee Center for the Health Sciences.
[3] SMA 12/60.
[4] Minicath PRN, Deseret Pharmaceutical Co., Sandy, Utah.

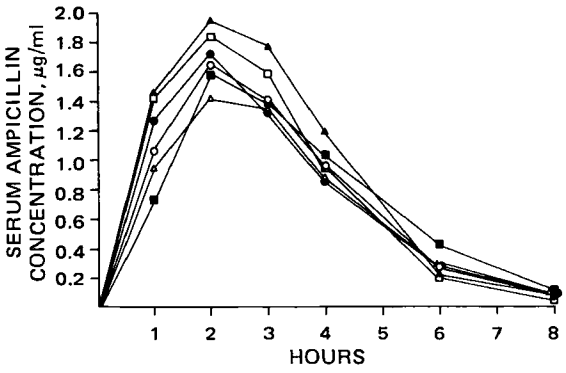

Figure 1—*Mean serum ampicillin levels for six products (Series A) administered to 12 subjects. Key: ●, Product 1A; ○, Product 2A; ■, Product 3A; □, Product 4A; ▲, Product 5A; and △, Product 6A. (See Table I for product code.)*

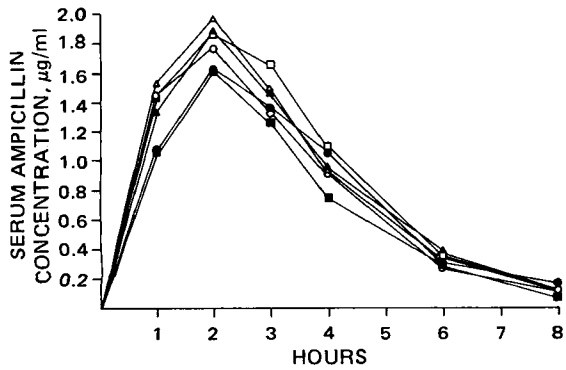

Figure 2—*Mean serum ampicillin levels for six products (Series B) administered to 12 subjects. Key: ●, Product 1B; ○, Product 2B; ■, Product 3B; □, Product 4B; ▲, Product 5B; and △, Product 6B. (See Table I for product code.)*

the products evaluated within each series in terms of the average serum levels at 1, 2, 3, 4, 6, and 8 hr postadministration.

Peak Serum Concentration—The magnitude of the peak serum level is a function of both the rate and extent of drug absorption. The average peak serum concentration for all tested products was 1.96 μg/ml (range 1.5–2.42 μg/ml). The analysis of variance for the peak serum level data showed no significant differences ($p > 0.05$) in peak serum level for any product tested.

Time of Peak Serum Concentration—This parameter is a function of the rate of drug absorption. The average time to achieve the peak serum concentration for all tested products was 2.14 hr (range 1.79–2.58 hr) after drug administration. A statistical analysis of the average time required to achieve the peak ampicillin serum levels for each product indicated no significant differences ($p > 0.05$).

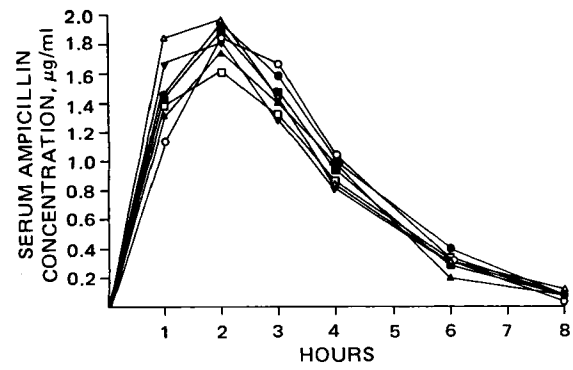

Figure 3—*Mean serum ampicillin levels for seven products (Series C) administered to 14 subjects. Key: ●, Product 1C; ○, Product 2C; ■, Product 3C; □, Product 4C; ▲, Product 5C; △, Product 6C; and ▼, Product 7C. (See Table I for product code.)*

Table III—Data for Series A

Product[a]	Summary of Average *AUC*: Average *AUC*[b], (μg/ml) × hr	*CV*, %	Percent Relative to Product 1A
5A	7.64 (0.74)	33.67	122.8
4A	6.96 (0.63)	31.52	111.9
3A	6.32 (0.47)	26.00	101.6
1A	6.22 (0.54)	30.01	100.0
2A	6.17 (0.58)	32.30	99.2
6A	5.74 (0.45)	27.44	92.3

Analysis of Variance for *AUC*

Source of Variance	Sum of Squares	Degrees of Freedom	Mean Squares	*F* Ratio
Between subjects				
Groups	2.684	5	0.537	0.039
Subjects within groups	81.547	6	13.591	
Within subjects				
Weeks	24.485	5	4.897	1.747
Products	27.899	5	5.580	1.991[c]
Product–week interaction	72.166	20	3.608	1.287
Error (within)	84.065	30	2.802	

[a] See Table I for products. [b] Average of 12 subjects; standard error in parentheses. [c] Not significant ($p > 0.05$).

Area under Serum Concentration-Time Curve (*AUC*)—The *AUC* values summarized (Tables III–V) are indicative of the relative amounts of ampicillin absorbed from each test product. Tables I–III also show the *AUC*'s for each product relative to reference Product 1. The *AUC* values were determined with the aid of a planimeter.

Approximately 25% of the serum level curves were sufficiently elevated at the terminal 8-hr sampling time to require the application of Eq. 1 for the estimation of the total *AUC*:

$$(AUC)_{0-\infty} = (AUC)_{0-8\,hr} + \frac{(C_s)_{8\,hr}}{K} \qquad \text{(Eq. 1)}$$

where $(C_s)_{8\,hr}$ is the serum ampicillin level at the 8-hr sampling time, and K is the elimination rate constant estimated from the terminal portion of a semilog plot of serum concentration *versus*

Table IV—Data for Series B

Product[a]	Summary of Average *AUC*: Average *AUC*[b], (μg/ml) × hr	*CV*, %	Percent Relative to Product 1B
4B	7.31 (0.40)	18.80	112.8
6B	7.22 (0.61)	29.23	111.4
5B	6.88 (0.30)	15.23	106.2
2B	6.53 (0.41)	21.99	100.8
1B	6.48 (0.39)	20.69	100.0
3B	5.88 (0.45)	26.40	90.7

Analysis of Variance for *AUC*

Source of Variance	Sum of Squares	Degrees of Freedom	Mean Squares	*F* Ratio
Between subjects				
Groups	16.302	5	3.260	0.610
Subjects within groups	32.088	6	5.348	
Within subjects				
Weeks	24.577	5	4.915	3.363
Products	17.090	5	3.418	2.339[c]
Product–week interaction	33.870	20	1.694	1.159
Error (within)	43.842	30	1.461	

[a] See Table I for products. [b] Average of 12 subjects; standard error in parentheses. [c] Not significant ($p > 0.05$).

Table V—Data for Series C

Summary of Average *AUC*

Product[a]	Average *AUC*[b], (μg/ml) × hr	*CV*, %	Percent Relative to Product 1C
1C	7.45 (0.56)	28.05	100.0
6C	7.38 (0.59)	29.96	99.1
7C	6.94 (0.51)	27.32	93.2
2C	6.83 (0.63)	34.56	91.7
3C	6.81 (0.69)	38.03	91.4
5C	6.45 (0.50)	28.89	86.6
4C	6.41 (0.54)	31.36	86.0

Analysis of Variance for *AUC*

Source of Variance	Sum of Squares	Degrees of Freedom	Mean Squares	*F* Ratio
Between subjects				
Groups	70.884	6	11.814	0.645
Subjects within groups	128.207	7	18.315	
Within subjects				
Weeks	34.115	6	5.685	2.152
Products	13.828	6	2.305	0.872[c]
Product–week interaction	80.304	30	2.677	1.013
Error (within)	110.972	42	2.642	

[a] See Table I for products. [b] Average of 14 subjects; standard error in parentheses. [c] Not significant ($p > 0.05$).

time. The mean half-life calculated from 64 individual serum level–time plots was 1.37 hr (*SE* 0.06). This value was in good agreement with previously reported values ranging from 1.0 to 1.3 hr (12, 13).

Tables III–V also summarize the statistical analysis of the *AUC* data. No statistically significant differences ($p > 0.05$) were observed for any tested product. Previous studies (14, 15) indicated that anhydrous ampicillin was approximately 8–17% better absorbed than the trihydrate form. Product 4B was the only anhydrous ampicillin evaluated. As indicated in Table IV, no statistically significant difference was observed between this product and the various trihydrate products tested.

The sensitivity of the experimental design was evaluated using the *F* ratio test described previously (7, 8). The differences in *AUC* between the product exhibiting the greatest mean *AUC* and the product exhibiting the lowest mean *AUC*, required for significance at the 0.05 level, were 18.3, 13.8, and 16.7% for Series A, B, and C, respectively. These differences indicated that the present study was more sensitive to differences in *AUC* than the work of Mayersohn and Endrenyi (7) but less sensitive than the study of MacLeod *et al.* (8). Application of the more stringent Newman–Keuls or Tukey test indicated that differences of 27.2, 20.5, and 25.6% for Series A, B, and C, respectively, would have been required for significance at the 0.05 level.

The absorption of ampicillin has been reported to exhibit considerable intrasubject and intersubject variability, with absorption following oral administration ranging from 20 to 70% of the dose (9). This study afforded an opportunity to investigate intrasubject variability upon repeated dosing, since each of 12 subjects took the reference Product 1 on three occasions, separated by at least 6 weeks. The *AUC*'s observed for these 12 subjects are shown in Table VI. Statistical analysis indicated no significant difference ($p > 0.05$) between the first, second, or third administration. However, several subjects, particularly Subjects 1 and 4, exhibited considerable variability in *AUC* between the three dose administrations. Subjects 8 and 9, who were identical twins, exhibited essentially the same average *AUC*'s.

Since several ampicillin products were manufactured by the same company but distributed by different companies, it was of interest to compare the bioavailability of presumably identical products administered to identical groups of subjects. Thus, Products 1C, 2C, and 6C were manufactured by the same company and were administered to the same subjects. Similarly, Products 1B and 5B, Products 3A and 6A, Products 3C, 4C, 5C, and 7C, and Products 2A, 4A, and 5A represent groups of products with identical manufacturers. A comparison of average *AUC* values among the individual products within each group indicates a maximum difference of only approximately 11%. This analysis further substantiates the methodology employed to assess the bioavailability of the ampicillin products, since those products for which little difference in absorption was anticipated exhibited very similar bioavailability.

Table VI—*AUC* for 12 Subjects Receiving Reference Product 1 on Three Separate Occasions[a]

Subject	Series A	Series B	Series C	Mean (*SE*)	*CV*, %
1	2.37	6.57	7.47	5.47 (1.57)	49.76
2	6.63	9.98	9.99	8.87 (1.11)	21.85
3	6.47	6.25	6.07	6.26 (0.11)	3.20
4	4.17	6.52	9.79	6.82 (1.63)	41.34
5	7.77	7.62	6.10	7.16 (0.53)	12.90
6	7.80	6.82	11.20	8.61 (1.32)	26.71
7	5.14	6.17	3.43	4.91 (0.80)	28.17
8	6.26	5.75	8.05	6.68 (0.70)	18.06
9	5.19	6.13	8.66	6.66 (1.04)	26.95
10	7.62	6.17	5.19	6.32 (0.71)	19.32
11	9.35	5.15	6.55	7.02 (1.23)	30.48
12	5.83	4.63	5.86	5.44 (0.40)	12.85
Mean	6.22	6.48	7.36		
SE	0.54	0.39	0.65		
CV, %	30.01	20.69	30.66		

[a] *AUC*'s expressed as (micrograms per milliliter) (hour).

REFERENCES

(1) "The Bioavailability of Drugs," B. B. Brodie and W. M. Heller, Eds., Proceedings of the Conference on Bioavailability at the National Academy of Sciences, Washington, D.C., Nov. 22–23, 1971.

(2) "Symposium on Formulation Factors Affecting Therapeutic Performance of Drug Products," *Drug Inform. Bull.*, Jan./June, 1969.

(3) G. H. Schneller, *J. Amer. Pharm. Ass.*, **NS9**, 455(1969).

(4) J. G. Wagner, "Biopharmaceutics and Relevant Pharmacokinetics," Drug Intelligence Publications, Hamilton, Ill., 1971, chap. 24.

(5) "Report of the Ad Hoc Committee on Drug Product Selection of the Academy of General Practice of Pharmacy and the Academy of Pharmaceutical Sciences," *J. Amer. Pharm. Ass.*, **NS13**, 278(1973).

(6) F-D-C Reports, **36** (28), A-3 (July 15, 1974).

(7) M. Mayersohn and L. Endrenyi, *Can. Med. Ass. J.*, **109**, 989(1973).

(8) C. MacLeod, H. Rabin, J. Ruedy, M. Caron, D. Zarowny, and R. O. Davies, *ibid.*, **107**, 203(1972).

(9) W. J. Jusko, in "The Bioavailability of Drug Products," The APhA Bioavailability Pilot Project, American Pharmaceutical Association, Washington, D.C., 1973, pp. 19–23.

(10) P. L. Whyatt, R. E. Dann, G. W. A. Slywka, and M. C. Meyer, *Antimicrob. Ag. Chemother.*, **6**, 811(1974).

(11) E. J. Williams, *Aust. J. Sci. Res. A*, **2**, 149(1949).

(12) W. J. Jusko and G. P. Lewis, *J. Pharm. Sci.*, **62**, 69(1973).

(13) W. M. M. Kirby, R. C. Gordon, and C. Regamey, *J. Infect. Dis.*, **129**, S154(1974).

(14) J. C. K. Loo, E. L. Foltz, H. Wallick, and K. C. Kwan, *Clin. Pharmacol. Ther.*, **16**, 35(1974).

(15) J. W. Poole, G. Owen, J. Silverio, J. N. Freyhof, and S. B. Roseman, *Curr. Ther. Res.*, **10**, 292(1968).

ACKNOWLEDGMENTS AND ADDRESSES

Received April 21, 1975, from the *Division of Drug Metabolism and Biopharmaceutics, Department of Medicinal Chemistry, College of Pharmacy, University of Tennessee Center for the Health Sciences, Memphis, TN 38163*

Accepted for publication June 11, 1975.

Supported in part by a contract from the Tennessee Department of Public Health and by U.S. Public Health Service Grant HL-09495.

The authors thank Mrs. Donna Phillips, Mrs. Diane Largent,

Mr. Keith Crawford, Miss Becky Watlington, Mrs. Ann Robinson, and Mrs. Irma Miller for technical assistance; Mrs. Ann McEachran for assistance in the statistical analysis of the data; Dr. Phillip Lieberman for providing the medical supervision for the study; and the 14 subjects who volunteered to participate in the study. Special thanks are extended to Mr. Herbert Bates, Pharmacist Consultant, Tennessee Department of Public Health, for encouragement and support.

* Department of Molecular Biology, College of Pharmacy, University of Tennessee Center for the Health Sciences, Memphis, TN 38163

[x] To whom inquiries should be directed.

Solubilities of Testosterone Propionate and Related Esters in Organic Solvents

KENNETH C. JAMES [x], CHU TEK NG, and PETER R. NOYCE *

Abstract □ The solubility parameters of a range of saturated hydrocarbons were calculated from vapor pressures and heats of vaporization. Solubilities of testosterone propionate were determined in these solvents at 25° and yielded solute solubility parameters which varied from solvent to solvent. The solubility parameter of testosterone propionate was determined by several other methods, and support was found for the previously published figure of 9.5 $cal^{1/2}\ cm^{-3/2}$. The geometric mean coefficient (l_{12}) in saturated hydrocarbons was found to be a rectilinear function of the branching ratio (r). The mean l_{12} of androstanolone and testosterone propionates was used to calculate the solubilities of other esters, giving good agreement with experimental results. IR data, presented as the sum of the shifts of the 3-keto and 17-ester carbonyl stretching frequencies in polar solvents, correlated rectilinearly with the geometric mean coefficients and the plot extrapolated to the l_{12} value of n-hexane, calculated from the branching ratio plot. Attempts to predict solubilities of other esters in polar solvents using l_{12} values achieved only limited success.

Keyphrases □ Testosterone propionate—related esters, solubility in various organic solvents □ Solubility—testosterone propionate and related esters in various organic solvents □ Hydrocarbons, saturated—solvents for testosterone propionate and related esters

The simplest model for a liquid solution is one where the solute and solvent have the same affinity for each other as they do for their own kind. Molecular distribution is then as random as can be permitted by molecular contact, and the solution is said to be ideal. Liquids that mix to form ideal solutions are mutually soluble in all proportions; but when the solute is a solid, solubility is limited because energy is necessary for liquefaction.

In real solutions, forces of intermolecular attraction are not uniform and like molecules tend to congregate together. When the solute and solvent have low polarities, thermal motion is sufficient to keep them randomly distributed, and solubility can be predicted (1) by:

$$-\ln X_2 = \frac{\Delta H^f}{R}\left[\frac{T_m - T}{T_m T}\right] + \frac{V_2\phi_1^2(\delta_1 - \delta_2)^2}{RT} \qquad \text{(Eq. 1)}$$

The first term on the right-hand side represents the natural logarithm of ideal solubility at temperature T; ΔH^f is the heat of fusion of the solute, and T_m is the melting point. The second term represents the contribution of the heat of mixing, which is assessed in terms of the solubility parameters δ_1 and δ_2, the square roots of the cohesive energy densities of solvent and solute, respectively. The term V_2 is the molar volume of the solute, and ϕ_1 is the volume fraction of the solvent.

Expansion of the $(\delta_1 - \delta_2)^2$ term gives the sum of the cohesive energy densities of solute and solvent minus twice their geometric mean, with the last term representing the energy gained in bringing the unlike molecules into contact. Cohesive energy has been equated with the energy of vaporization (1) and used to determine solubility parameters by:

$$\delta = \left[\frac{\Delta H^v - RT}{V}\right]^{1/2} \qquad \text{(Eq. 2)}$$

where ΔH^v represents heat of vaporization.

A solubility parameter of 9.5 $cal^{1/2}\ cm^{-3/2}$ was obtained for testosterone propionate (2) by a modification of the Chertkoff and Martin technique (3); this figure was confirmed later (4). Efforts at predicting solubilities in nonpolar solvents have been unsuccessful, however, and a reaffirmation of the value was sought.

EXPERIMENTAL

Materials—Steroid alcohols[1] and testosterone propionate[1] were obtained from a commercial source. Methods of characterization and preparation of the remaining esters were described previously (5). Saturated hydrocarbons were purchased from various sources; purities were never less than 97%. Research grade cyclohexane[2] (minimum purity 99.99%) was used for vapor pressure determinations. Anisole and carbon tetrachloride were of reagent grade and were fractionally distilled before use. Solubilities in these solvents were determined using previously described techniques (2, 6), and the remaining solubilities were taken from the literature (2, 7) (Table I).

Solubility Parameters—Nonpolar solvent solubility parameters, calculated from Eq. 2, are given in Table I. Some were obtained from published heats of vaporization (8); the remaining values were calculated from vapor pressures (9), corrected using (10):

$$\Delta H^v = \Delta H^v_{app}\, e^{-mT} \qquad \text{(Eq. 3)}$$

where ΔH^v represents the true heat of vaporization, ΔH^v_{app} is the experimental value at temperature T, and m is a constant. Polar solvent solubility parameters, taken from the literature (1), are

[1] Gifts from Organon Laboratories Ltd.
[2] British Drug Houses Ltd.

Mr. Keith Crawford, Miss Becky Watlington, Mrs. Ann Robinson, and Mrs. Irma Miller for technical assistance; Mrs. Ann McEachran for assistance in the statistical analysis of the data; Dr. Phillip Lieberman for providing the medical supervision for the study; and the 14 subjects who volunteered to participate in the study. Special thanks are extended to Mr. Herbert Bates, Pharmacist Consultant, Tennessee Department of Public Health, for encouragement and support.

* Department of Molecular Biology, College of Pharmacy, University of Tennessee Center for the Health Sciences, Memphis, TN 38163

[x] To whom inquiries should be directed.

Solubilities of Testosterone Propionate and Related Esters in Organic Solvents

KENNETH C. JAMES [x], CHU TEK NG, and PETER R. NOYCE *

Abstract □ The solubility parameters of a range of saturated hydrocarbons were calculated from vapor pressures and heats of vaporization. Solubilities of testosterone propionate were determined in these solvents at 25° and yielded solute solubility parameters which varied from solvent to solvent. The solubility parameter of testosterone propionate was determined by several other methods, and support was found for the previously published figure of 9.5 $cal^{1/2}\ cm^{-3/2}$. The geometric mean coefficient (l_{12}) in saturated hydrocarbons was found to be a rectilinear function of the branching ratio (r). The mean l_{12} of androstanolone and testosterone propionates was used to calculate the solubilities of other esters, giving good agreement with experimental results. IR data, presented as the sum of the shifts of the 3-keto and 17-ester carbonyl stretching frequencies in polar solvents, correlated rectilinearly with the geometric mean coefficients and the plot extrapolated to the l_{12} value of n-hexane, calculated from the branching ratio plot. Attempts to predict solubilities of other esters in polar solvents using l_{12} values achieved only limited success.

Keyphrases □ Testosterone propionate—related esters, solubility in various organic solvents □ Solubility—testosterone propionate and related esters in various organic solvents □ Hydrocarbons, saturated—solvents for testosterone propionate and related esters

The simplest model for a liquid solution is one where the solute and solvent have the same affinity for each other as they do for their own kind. Molecular distribution is then as random as can be permitted by molecular contact, and the solution is said to be ideal. Liquids that mix to form ideal solutions are mutually soluble in all proportions; but when the solute is a solid, solubility is limited because energy is necessary for liquefaction.

In real solutions, forces of intermolecular attraction are not uniform and like molecules tend to congregate together. When the solute and solvent have low polarities, thermal motion is sufficient to keep them randomly distributed, and solubility can be predicted (1) by:

$$-\ln X_2 = \frac{\Delta H^f}{R}\left[\frac{T_m - T}{T_m T}\right] + \frac{V_2\phi_1^2(\delta_1 - \delta_2)^2}{RT} \qquad \text{(Eq. 1)}$$

The first term on the right-hand side represents the natural logarithm of ideal solubility at temperature T; ΔH^f is the heat of fusion of the solute, and T_m is the melting point. The second term represents the contribution of the heat of mixing, which is assessed in terms of the solubility parameters δ_1 and δ_2, the square roots of the cohesive energy densities of solvent and solute, respectively. The term V_2 is the molar volume of the solute, and ϕ_1 is the volume fraction of the solvent.

Expansion of the $(\delta_1 - \delta_2)^2$ term gives the sum of the cohesive energy densities of solute and solvent minus twice their geometric mean, with the last term representing the energy gained in bringing the unlike molecules into contact. Cohesive energy has been equated with the energy of vaporization (1) and used to determine solubility parameters by:

$$\delta = \left[\frac{\Delta H^v - RT}{V}\right]^{1/2} \qquad \text{(Eq. 2)}$$

where ΔH^v represents heat of vaporization.

A solubility parameter of 9.5 $cal^{1/2}\ cm^{-3/2}$ was obtained for testosterone propionate (2) by a modification of the Chertkoff and Martin technique (3); this figure was confirmed later (4). Efforts at predicting solubilities in nonpolar solvents have been unsuccessful, however, and a reaffirmation of the value was sought.

EXPERIMENTAL

Materials—Steroid alcohols[1] and testosterone propionate[1] were obtained from a commercial source. Methods of characterization and preparation of the remaining esters were described previously (5). Saturated hydrocarbons were purchased from various sources; purities were never less than 97%. Research grade cyclohexane[2] (minimum purity 99.99%) was used for vapor pressure determinations. Anisole and carbon tetrachloride were of reagent grade and were fractionally distilled before use. Solubilities in these solvents were determined using previously described techniques (2, 6), and the remaining solubilities were taken from the literature (2, 7) (Table I).

Solubility Parameters—Nonpolar solvent solubility parameters, calculated from Eq. 2, are given in Table I. Some were obtained from published heats of vaporization (8); the remaining values were calculated from vapor pressures (9), corrected using (10):

$$\Delta H^v = \Delta H^v_{app}\, e^{-mT} \qquad \text{(Eq. 3)}$$

where ΔH^v represents the true heat of vaporization, ΔH^v_{app} is the experimental value at temperature T, and m is a constant. Polar solvent solubility parameters, taken from the literature (1), are

[1] Gifts from Organon Laboratories Ltd.
[2] British Drug Houses Ltd.

Table I—Solubilities and Related Data for Testosterone Propionate

Solvent	Mole Fraction Solubility, X_2	Solubility Parameter	Total Carbonyl Frequency Shift[a], cm^{-1}
1. *n*-Pentane	0.003[b]	7.05	—
2. *n*-Hexane	0.005[b]	7.26	0
3. *n*-Heptane	0.0058	7.42	—
4. *n*-Octane	0.0081	7.54	—
5. *n*-Nonane	0.0074	7.65	—
6. *n*-Decane	0.0095	7.72	—
7. *n*-Undecane	0.0085	7.81	—
8. *n*-Dodecane	0.0112	7.86	—
9. *n*-Hexadecane	0.0100	7.99	—
10. Cyclopentane	0.007[b]	8.11	—
11. Cyclohexane	0.012[b]	8.19	0
12. *cis*-Decahydronaphthalene	0.0170	8.58	—
13. *cis*-Hexahydroindan	0.0239	8.54	—
14. Methylcyclopentane	0.0107	7.95	—
15. Ethylcyclopentane	0.0131	7.95	—
16. Methylcyclohexane	0.0145	7.84	—
17. *n*-Propylcyclohexane	0.0100	7.94	—
18. Isopropylcyclohexane	0.0155	7.91	—
19. *n*-Butylcyclohexane	0.0141	7.94	—
20. *tert*-Butylcyclohexane	0.0153	7.77	—
21. Anisole	0.25[b] 0.251	—	24.6
22. Benzene	0.24[b] 0.260[c]	9.2[d]	17.1
23. Carbon disulfide	0.18[b]	10.0[d]	15.7
24. Carbon tetrachloride	0.16[b] 0.194	8.6[d]	14.7
25. Chlorobenzene	0.27[b]	9.5[d]	22.8
26. Chloroform	0.35[b]	9.2[d]	43.4
27. 1,2-Dichloroethane	0.27[b] 0.294[c]	9.8[d]	34.6
28. *trans*-1,2-Dichloroethylene	0.32[b]	9.0[d]	34.1
29. *cis*-1,2-Dichloroethylene	0.30[b]	9.1[d]	35.5
30. Nitrobenzene	0.22[b] 0.220[c]	10.0[d]	33.1
31. Tetrahydronaphthalene	0.20[b]	—	16.8
32. Toluene	0.20[b] 0.199[c]	8.9[d]	15.2
Bicyclohexyl	0.0165	—	—
Cyclooctane	0.0181	—	—
Ethylcyclohexane	0.0110	—	—

[a] Taken from Ref. 16. [b] Taken from Ref. 7. [c] Taken from Ref. 2. [d] Taken from Ref. 1.

given in Table I. Those of the solvent blends were calculated from the individual solvent values (11).

Determination of Vapor Pressures—The isotenisoscope technique of Smith and Menzies (12) was adopted. Experimental details are given elsewhere (13). Readings were corrected for capillary depression (14) and temperature and reduced to sea level (15). Mean results, each of five readings, were: cyclohexane, 13.05 ± 0.08 kNm^{-2}; saturated solution of testosterone propionate in cyclohexane, 11.60 ± 0.07 kNm^{-2}; and saturated solution of androstanolone propionate in cyclohexane, 11.53 ± 0.03 kNm^{-2} ($p = 0.01$).

Activity coefficients were calculated from the relative lowering of vapor pressure of cyclohexane, and solubility parameters were calculated by equating the natural logarithm of the result with the heat of mixing term in Eq. 1. The process yielded solubility parameters of 10.33 and 10.41 $cal^{1/2}\ cm^{-3/2}$ for androstanolone and testosterone propionates, respectively.

Ideal Solubilities—The values for testosterone esters were taken from James and Roberts (2). The remainder were calculated from heats of fusion, measured[3] and corrected for the heat capacity of the supercooled liquid (2) when necessary.

[3] Perkin-Elmer differential scanning calorimeter.

Miscellaneous Data—Solvent molar volumes were taken from Hildebrand *et al.* (1) when available, and the other values were calculated from published densities (15). Refractive indexes also were obtained from the literature (15). Molar volumes, 294 liters for testosterone propionate and 296 liters for androstanolone propionate, were those determined by Bowen (7). Volume fraction concentrations were calculated using a published procedure (2).

Geometric mean coefficients (l_{12}) were calculated by substituting observed solubilities in Eq. 6. A solubility parameter of 9.5 $cal^{1/2}\ cm^{-3/2}$ was assumed for testosterone propionate for these calculations, and those of the other esters were calculated from it using Hoy's constants (10). Spectral results were obtained using procedures described elsewhere (16, 17) (Table I).

DISCUSSION

Determination of Solubility Parameters—Hansen (18) considered that the calculation of solubility parameters from Eq. 2 was oversimplified when applied to polar solvents and split up the "overall" solubility parameter (δ) into dispersion (δ_d), polar (δ_p), and hydrogen-bonding (δ_h) components, as defined by:

$$\delta^2 = \delta_d^2 + \delta_p^2 + \delta_h^2 \qquad \text{(Eq. 4)}$$

Several lists of these parameters have been compiled (*e.g.*, 18, 19), but all are based on "volumes of solubility" and suitable only for semiquantitative predictions.

More precise figures can be employed by considering saturated hydrocarbons only, in which polar and hydrogen-bonding contributions are zero. The overall solubility parameter is then defined by Eq. 2 and can be calculated precisely from vapor pressures or heats of vaporization. Solubility parameters were not available in the literature for all of the saturated hydrocarbons examined here. Moreover, the rule of Hildebrand and Scott (20) frequently gave results at variance with published figures, throwing doubt on its reliability for evaluating unknown solubility parameters. The solubility parameters calculated from heats of vaporization compared favorably with those from other sources, when available, indicating that the hitherto unpublished solubility parameters obtained in this way would be reliable.

There still remained several saturated hydrocarbon solvents for which solubility parameters were required. Keller *et al.* (21) correlated the solubility parameters of 96 hydrocarbons with the Lorentz–Lorentz function $(n^2 - 1)/(n^2 + 2)$ and obtained a good rectilinear relationship. Since refractive indexes (n) were available for the unknown solvents (15), an attempt was made to calculate solubility parameters by this means. The straight-chain hydrocarbons showed excellent correlation; but when cyclic and branched-chain hydrocarbons were included, considerable scatter resulted. The overall standard deviation about the best rectilinear relationship was 0.24 $cal^{1/2}\ cm^{-3/2}$.

The method, therefore, appears suitable for predicting solubility parameters of straight-chain hydrocarbons, but results for the compounds for which solubility parameters were required in this work could be regarded only as approximate. Therefore, it was decided to use our own solubility parameters for nonpolar solvents, calculated from heats of vaporization and vapor pressures, and to consider only the solvents for which data were available.

The solubility parameter of testosterone propionate was calculated for each nonpolar solvent by substituting observed solubilities for X_2 in Eq. 1. Considerable variation was observed. The normal paraffins, for example, indicated that testosterone propionate had a solubility parameter between 9.9 and 10.0, while the solubility in cyclohexane gave a value of 10.4 $cal^{1/2}\ cm^{-3/2}$, which was confirmed by vapor pressure measurements.

Solubility parameters of nonvolatile solutes have been determined by plotting solubilities in a range of solvent blends against a solvent blend solubility parameter (3). Each plot went through a maximum, and the corresponding solubility parameter was equated to that of the solute. Similar procedures yielded a solubility parameter of 9.5 $cal^{1/2}\ cm^{-3/2}$ for testosterone propionate (2, 4). Polar solvents are normally required for this method, because of the limited solubility parameter range of nonpolar solvents. The method was repeated with testosterone propionate, using a large range of polar solvents.

The plot of solubility against the solvent solubility parameter showed considerable scatter, which could not be resolved into any

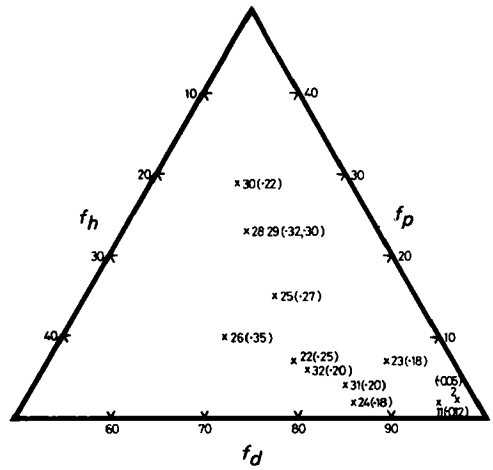

Figure 1—*Triangular solubility plot for testosterone propionate. Solvents are numbered in the manner indicated in Table I. Figures in parentheses represent mean solubilities.*

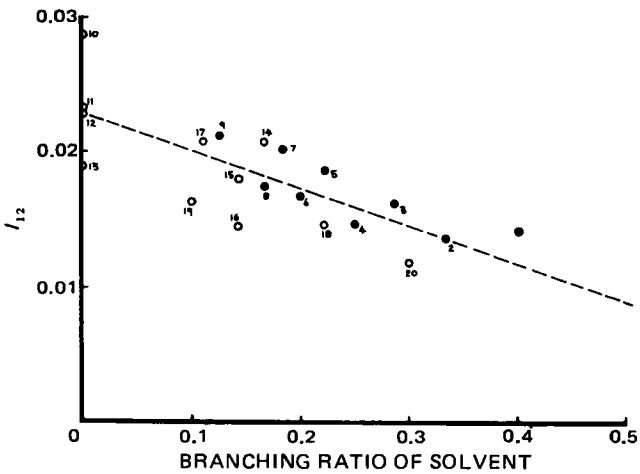

Figure 2—*Relationship between geometric mean coefficient and branching ratio. Solvents are numbered in the manner indicated in Table I.*

simple relationship and was attributed to variation in the shapes and sizes of the solvent molecules (22). To overcome this objection, studies were made on binary mixtures of nitrobenzene and toluene, which have similar shapes and molar volumes but different solubility parameters. The plot went smoothly through a maximum and indicated a solubility parameter for testosterone propionate in the region of 9.5 $cal^{1/2}$ $cm^{-3/2}$. A first derivative plot gave the precise value of 9.59 $cal^{1/2}$ $cm^{-3/2}$.

Plots without maxima were obtained when the procedure was repeated using blends of 1,2-dichloroethane with *cis-* and *trans-*1,2-dichloroethylenes, however. The reason for this result cannot be stated with certainty, but the fact that testosterone propionate forms some 1:2 complexes with 1,2-dichloroethane and chloroform through its 3-keto carbonyl group and only 1:1 complexes with the dichloroethylenes and aromatic solvents (16) may well be significant. It appears, therefore, that the answer obtained from this procedure is dependent on what solvents are used in the blends. Even with a range of different solvents, the results can be biased if a large proportion of the solvents react with the solute in a particular way, different from the rest. The result obtained with the nitrobenzene–toluene blends probably is reliable, because these two solvents are known to complex with testosterone propionate in a similar manner (16, 17).

Supporting evidence for the figure of 9.5 is available from sources not dependent on solubility data. The boiling point of testosterone propionate was determined by differential scanning calorimetry (7). Application of the Hildebrand and Scott (20) rule yielded a heat of vaporization of 23.03 kcal $mole^{-1}$, which gave a solubility parameter of 8.74 $cal^{1/2}$ $cm^{-3/2}$ when substituted into Eq. 2. More realistic solubility parameters were obtained by adding 0.6 unit to those calculated from the heats of vaporization (23). A value of 9.34 $cal^{1/2}$ $cm^{-3/2}$ was obtained by applying this correction to testosterone propionate, in fair agreement with that calculated from solubilities, considering the empirical nature of the derivation.

Another method for determining solubility parameters is expressed by (24):

$$\delta = \sqrt{\frac{\Sigma G}{V}} \qquad \text{(Eq. 5)}$$

where G is the partial molar attraction constant, and V is the molar volume. Insertion of G values from a recent compilation (10) in Eq. 5 gave a solubility parameter of 9.50 $cal^{1/2}$ $cm^{-3/2}$. Thus, although neither method was expected to give accurate results, they both provide independent supporting evidence that the solubility parameter is in the region of 9.5 $cal^{1/2}$ $cm^{-3/2}$.

Hansen (18) evaluated component solubility parameters (Eq. 4), using three-dimensional solubility diagrams, which were difficult to interpret. Teas (25) simplified the approach by using triangular diagrams, giving "areas" rather than "volumes" of solubility, defined in terms of functions of each component, such as the dispersive force function (f_d), equal to 100 (δ_d^2/δ^2). The technique is applied to testosterone propionate in Fig. 1. The area of maximum solubility indicates that a good solvent for testosterone propionate requires hydrogen-bonding and polar contributions of at least 10 on the Teas scale. If these contributions are too high, solvating ability will be reduced, as demonstrated by the solubilities in ethanol and water (2) and in nitrobenzene.

Chloroform appears to possess the optimum qualities; but in view of its complexing behavior, the significance of the result was regarded with suspicion and its position was ignored. The remainder of the points followed a logical pattern, with an area of maximum solubility in the region of $f_d = 65$, $f_p = 20$, and $f_h = 15$. The ideal characteristics could not be located precisely, because of the dearth of suitable solvents in this area. However, approximate component solubility parameter contributions suitable for solvent selection, assuming an overall value of 9.5 $cal^{1/2}$ $cm^{-3/2}$ (615 $J^{1/2}$ $m^{-3/2}$), are δ_d = 7.3 $cal^{1/2}$ $cm^{-3/2}$ (500 $J^{1/2}$ $m^{-3/2}$), δ_p = 4.2 $cal^{1/2}$ $cm^{-3/2}$ (270 $J^{1/2}$ $m^{-3/2}$), and δ_h = 3.7 $cal^{1/2}$ $cm^{-3/2}$ (240 $J^{1/2}$ $m^{-3/2}$).

Solubilities in Nonpolar Solvents—Hildebrand and Dymond (26) observed that solubilities in hydrocarbons depend on the degree of branching in the solvent molecule, which they assessed as a branching ratio (r), the number of methyl groups divided by the total number of carbon atoms. Hildebrand *et al.* (1) introduced an empirical coefficient (l_{12}) to improve the practicability of the geometric mean, extending Eq. 1 to Eq. 6:

$$-\ln X_2 = \frac{\Delta H^f}{R}\left[\frac{T_m - T}{T_m T}\right] + \frac{V_2 \phi_1^2}{RT}\left[(\delta_1 - \delta_2)^2 + 2 l_{12}\delta_1\delta_2\right] \qquad \text{(Eq. 6)}$$

A plot of l_{12} for testosterone propionate against the branching ratio is shown in Fig. 2. Least-squares analysis indicated a good rectilinear correlation (correlation coefficient = 0.822, $F_{1,18}$ = 37.4, and α 0.001 = 15.38) with a slope of 0.604. A similar plot and slope (0.664) were obtained with androstanolone propionate.

Table II—Observed and Calculated Solubilities in Cyclohexane

	Mole Fraction Solubility		
		Calculated	
	Observed	Eq. 1	Eq. 6
Androstanolone:			
Formate	0.003	0.010	0.002
Acetate	0.007	0.012	0.003
Butyrate	0.022	0.037	0.024
Nandrolone:			
Formate	0.009	0.027	0.007
Acetate	0.037	0.113	0.041
Propionate	0.084	0.424	0.156
Testosterone:			
Formate	0.004	0.039	0.009
Acetate	0.004	0.028	0.006
Butyrate	0.014	0.097	0.018
Valerate	0.018	0.088	0.017

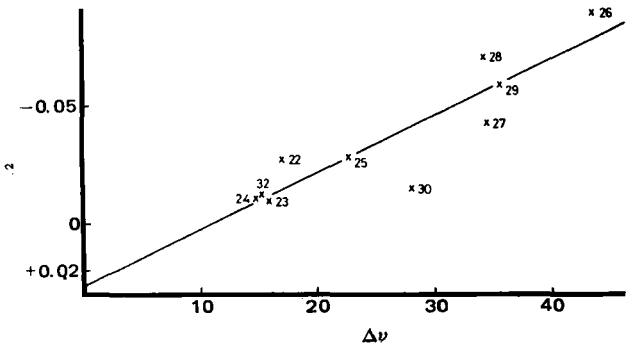

Figure 3—*Relationship between carbonyl stretching frequency shift and geometric mean coefficient. Solvents are numbered in the manner indicated in Table I.*

Ascent of the androstanolone and testosterone ester homologous series involves only small changes in molecular structure. Since l_{12} depends on the stereochemistry of the solute and solvent, it would be anticipated that the l_{12} for the propionate would be similar to those of adjacent esters. Table II shows solubilities of the lower androstanolone, nandrolone, and testosterone esters in cyclohexane, together with solubilities calculated using Eqs. 1 and 6. The mean l_{12} (0.022) for androstanolone and testosterone propionates was used in Eq. 6. An improvement was obtained by consideration of l_{12}; most predictions were good and, in all cases except that of androstanolone acetate, were significantly better than those in which the geometric mean was not corrected.

The terms δ_2 and l_{12} are interdependent; one can be set at any value, provided the other is adjusted to fit it. It appears that l_{12} would be a comparatively easy term to estimate in nonpolar solvents. It is suggested that, in view of the difficulties in obtaining solubility parameters for nonvolatile solutes, an arbitrary standard solubility parameter be used as the basis of a solubility parameter scale for steroids.

Testosterone propionate is a suitable standard substance, since it is readily available and comparatively inert. The figure of 9.5 $cal^{1/2}\ cm^{-3/2}$ is probably a good estimate of the solubility parameter of testosterone propionate. Solubility parameters of other steroids can be calculated from this value by using the procedures described by Small (24) and Hoy (10). The l_{12} values of key compounds, calculated from solubilities in a range of nonpolar solvents, could then be used as the basis of a scheme for estimating l_{12} values of other solutes, in the same way as was demonstrated with testosterone propionate.

Solubilities in Polar Solvents—While the three-component solubility parameter concept used here provides a means of selecting suitable solvents for testosterone propionate and similar compounds, the approach breaks down when applied to the prediction of solubilities in polar solvents because the observed values are in excess of ideal values while those predicted by Eq. 1 cannot exceed the ideal. It has been suggested that the high observed solubilities arise because complexation between solvent and solute gives a cohesive energy density between them greater than that predicted by the geometric mean assumption (22). Since the factor l_{12} corrects the differences between the solute to solvent cohesive energy densities and those predicted by the geometric mean (1), it should be influenced by complexing effects.

A plot of total carbonyl frequency shift, as an indicator of complexation, against l_{12} is illustrated in Fig. 3. The correlation is good, considering that l_{12} values represent small differences between large numbers. Solubility parameters were not available for anisole and tetrahydronaphthalene, which were, therefore, not included in the plot. A significant feature of this plot is that the linear regression line extrapolates to 0.025 at a frequency shift of zero, in good agreement with the l_{12} for *n*-hexane obtained from solubility data (Fig. 2). Scatter about the line could be due to steric effects for which a correcting factor, analogous to the *r* value of the saturated hydrocarbons, is difficult to assign.

Attempts to predict solubilities of other esters by substituting l_{12} values of testosterone propionate in Eq. 6 were disappointing. The limited success is probably due to the assumption that the esters interact identically with the solvent, which is an oversimplification. IR measurements, in fact, suggest significant ester to ester variation in complex stability. A three-variable treatment, in which the shifts induced by changing both ester and solvent are correlated with l_{12}, might achieve more success.

REFERENCES

(1) J. H. Hildebrand, J. M. Prausnitz, and R. L. Scott, "Regular and Related Solutions," Van Nostrand Reinhold, New York, N.Y., 1970.

(2) K. C. James and M. Roberts, *J. Pharm. Pharmacol.*, **20,** 709(1968).

(3) M. J. Chertkoff and A. N. Martin, *J. Amer. Pharm. Ass., Sci. Ed.*, **49,** 444(1960).

(4) D. B. Bowen and K. C. James, *J. Pharm. Pharmacol.*, **20,** 104S(1968).

(5) D. B. Bowen, K. C. James, and M. Roberts, *ibid.*, **22,** 518(1970).

(6) M. A. Q. Chaudry and K. C. James, *J. Med. Chem.*, **17,** 157(1974).

(7) D. B. Bowen, Ph.D. thesis, University of Wales, Cathays Park, Cardiff, Great Britain, 1969.

(8) F. D. Rossini, D. D. Wagman, W. H. Evans, S. Levine, and I. Jaffe, "Selected Values of Physical and Thermodynamic Properties of Hydrocarbons and Related Compounds," American Petroleum Institute Research Project 44, Carnegie Press, Pittsburgh, Pa., 1952.

(9) J. Timmermans, "Physical Constants of Pure Organic Compounds," Elsevier, Amsterdam, The Netherlands, 1950.

(10) K. L. Hoy, *J. Paint Technol.*, **42,** 76(1970).

(11) C. Sunwoo and H. Eisen, *J. Pharm. Sci.*, **60,** 238(1971).

(12) A. Smith and A. W. C. Menzies, *J. Amer. Chem. Soc.*, **32,** 1412(1910).

(13) C. T. Ng, Ph.D. thesis, University of Wales, Cathays Park, Cardiff, Great Britain, 1974.

(14) G. W. Thomson and D. R. Douslin, in "Technique of Chemistry," vol. 1, part 5, A. Weissberger and B. W. Rossiter, Eds., Interscience, New York, N.Y., 1971, p. 23.

(15) "Handbook of Chemistry and Physics," R. C. Weast, Ed., Chemical Rubber Co., Cleveland, Ohio, 1970.

(16) K. C. James and P. R. Noyce, *J. Pharm. Pharmacol.*, **22,** 109S(1970).

(17) K. C. James and P. R. Noyce, *J. Chem. Soc.*, **1971,** B2045.

(18) C. M. Hansen, *J. Paint Technol.*, **39,** 104(1967).

(19) C. M. Hansen and A. Beerbower, in "Kirk-Othmer Encyclopedia of Chemical Technology," 2nd ed., suppl. vol., A. Standen, Ed., Interscience, New York, N.Y., 1971, p. 889.

(20) J. H. Hildebrand and R. L. Scott, "Solubility of Nonelectrolytes," 3rd ed., Dover, New York, N.Y., 1964, p. 427.

(21) R. A. Keller, B. L. Karger, and L. R. Snyder, in "Gas Chromatography," R. Stock, Ed., Institute of Petroleum (London), Elsevier, London, England, 1971, p. 125.

(22) D. B. Bowen and K. C. James, *J. Pharm. Pharmacol.*, **22,** 104S(1970).

(23) R. L. Scott, *J. Chem. Educ.*, **30,** 542(1953).

(24) P. A. Small, *J. Appl. Chem.*, **3,** 71(1953).

(25) J. P. Teas, *J. Paint Technol.*, **40,** 19(1968).

(26) J. H. Hildebrand and J. Dymond, *Proc. Nat. Acad. Sci. USA*, **54,** 1001(1965).

ACKNOWLEDGMENTS AND ADDRESSES

Received March 10, 1975, from the *Welsh School of Pharmacy, University of Wales Institute of Science and Technology, Cathays Park, Cardiff, Great Britain.*

Accepted for publication July 14, 1975.

The authors acknowledge the award of research scholarships (to C. T. Ng and P. R. Noyce) of the University of Wales and are grateful to Organon Laboratories Ltd. for the gifts of steroids. They also thank Dr. D. B. Bowen for the use of some of his results.

* Present address: Department of Pharmacy, Chelsea College, University of London, London S.W.3, Great Britain.

ˣ To whom inquiries should be directed.

Synthesis of 3-Substituted Thieno[2,3-*d*]pyrimidin-4(3*H*)-one-2-mercaptoacetic Acids and Their Ethyl Esters for Pharmacological Screening

M. B. DEVANI *x, C. J. SHISHOO *, U. S. PATHAK *, S. H. PARIKH ‡, G. F. SHAH ‡, and A. C. PADHYA ‡

Abstract □ 3-Substituted thieno[2,3-*d*]pyrimidin-4(3*H*)-one-2-mercaptoacetic acids and their ethyl esters were synthesized from 2-mercaptothieno[2,3-*d*]pyrimidin-4(3*H*)-ones, which were obtained by cyclization of thienylthioureas in acidic medium. Analgesic, anti-inflammatory, and anticonvulsant activities were found in some of these compounds. Significant antimicrobial activity was exhibited by thienylthioureas.

Keyphrases □ Thienopyrimidinonemercaptoacetic acids and ethyl esters—synthesized, screened for analgesic, anti-inflammatory, anticonvulsant, and antimicrobial activity □ Structure–activity relationships—thienopyrimidinonemercaptoacetic acids and ethyl esters, screened for analgesic, anti-inflammatory, anticonvulsant, and antimicrobial activity □ Analgesic agents, potential—thienopyrimidinonemercaptoacetic acids and ethyl esters screened □ Anti-inflammatory agents, potential—thienopyrimidinonemercaptoacetic acids and ethyl esters screened □ Anticonvulsant agents, potential—thienopyrimidinonemercaptoacetic acids and ethyl esters screened □ Antimicrobial agents, potential—thienopyrimidinonemercaptoacetic acids and ethyl esters, screened

Pharmacological activities of 4-quinazolones have been extensively reviewed (1). The isosteric properties of benzene and thiophene are of interest to medicinal chemists. The concept of bioisosterism has been fully exploited and justified in the synthesis of thiophene analogs of established drug molecules (2, 3). Recently, 4-quinazolon-2-mercaptoacetic acids (I) were reported to possess significant anticonvulsant activity (4). Hypocholesterolemic, sedative, and antitussive properties were found in 2-mercapto-3,4-dihydrothieno[2,3-*d*]pyrimidin-4-one (5). Therefore, it was of interest to prepare the analog (V) of I for pharmacological screening.

DISCUSSION

Chemistry—3-Substituted thieno[2,3-*d*]pyrimidin-4(3*H*)-one-2-mercaptoacetic acid derivatives were synthesized starting with 2-amino-3-carbethoxythiophenes (II) (Scheme I). Compound II was readily available through the reaction of Gewald *et al.* (6). On reacting II with an alkyl or aryl isothiocyanate, a thiourea analog (III) was obtained. Compound III cyclized smoothly in ethanol saturated with dry hydrochloric acid to form 2-mercapto-3-substituted thieno[2,3-*d*]pyrimidin-4(3*H*)-one (IV). Refluxing IV with chloroacetic acid or its ethyl ester in the presence of potassium hydroxide yielded the corresponding 2-mercaptoacetic acid derivative (V).

When allylthioureas (XII and XXIII, Table I) were refluxed in ethanol saturated with dry hydrochloric acid, VI was obtained instead of the expected product (IV) (Scheme II).

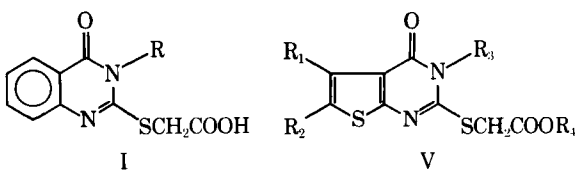

I V

Biological Activity—*Antimicrobial Study*—Thienylthioureas (Table I) were tested for antibacterial and antifungal activities. None of the compounds, at a concentration of 50 μg/ml, showed any appreciable inhibition of the growth of *Escherichia coli* (B-3-4), *Shigella shigae* (NCTC 8217), *Salmonella typhi* H901 (NCTC 3111), *Proteus ox* 19 (B-26-3), *Pseudomonas aeruginosa* (B-27-2), *Mycobacterium tuberculosis* (H37 Rv), *Candida albicans*[1], *Phialophora jeanselmei*[1], *Nocardia asteroides*[1], and *Aspergillus fumigatus*[1]. Compound IX was the most effective antibacterial agent against the Gram-positive organisms (Table II). In addition to antibacterial properties, VII, XII, XX, and XXVIII showed antifungal activity.

In general, thioureas having the terminal nitrogen substituted by a single short chain alkyl (C_1–C_4) or aralkyl group showed maximum activity. Replacement of a terminal alkyl group by an aryl group resulted in the loss of activity. Similar structure–activity relationships were observed with phenyl analogs (7).

Pharmacological Screening—Compounds VII, XIII, XVIII, XIX, XXVII, XXIX, XXXI, XXXIV, XXXVI, XXXVIII–LVII, and LIX were subjected to preliminary pharmacological screening for analgesic, anticonvulsant, and anti-inflammatory activities (Table III). Only two compounds (XLIX and LIV) showed protection (37.5%) against electric shock. None of the compounds had any appreciable protection against pentylenetetrazol-induced convulsions. Both *N*-benzylthiourea (XXIX) and its corresponding thienopyrimidine (XLIV) exhibited significant analgesic and anti-inflammatory activities. Maximum anti-inflammatory activity was found with thiazolothienopyrimidine (LIX).

EXPERIMENTAL

Synthesis—Crystallization solvents, yields, melting points, and analyses of the compounds synthesized are reported in Tables I, IV, and V. Melting points are uncorrected.

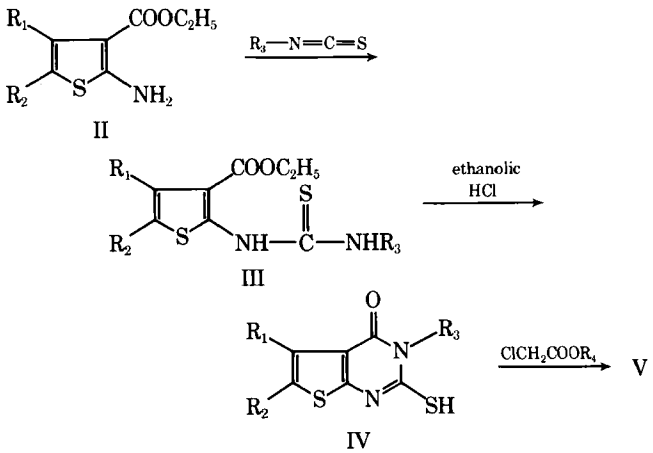

II III IV

Scheme I

[1] All India Institute of Medical Sciences Culture Collection.

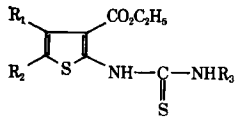

Table I—Physical Properties of Thienylthioureas

Compound	R_1	R_2	R_3	Melting Point	Yield, %	Crystallization Solvent	Molecular Formula	Analysis, % Calc.	Found
VII	CH_3	CH_3	CH_3	182–184°	80	Ethanol–chloroform	$C_{11}H_{16}N_2O_2S_2$	C 48.53	48.90
								H 5.88	6.10
VIII	CH_3	CH_3	C_2H_5	164–166°	82	Ethanol–chloroform	$C_{12}H_{18}N_2O_2S_2$	C 53.35	53.51
								H 6.29	6.12
IX	CH_3	CH_3	n-C_4H_9	128–130°	67	Ethanol	$C_{14}H_{22}N_2O_2S_2$	C 53.50	53.20
								H 7.00	6.90
X	CH_3	CH_3	n-C_6H_{13}	92–94°	78	Ethanol	$C_{16}H_{26}N_2O_2S_2$	C 56.14	56.00
								H 7.60	7.41
XI	CH_3	CH_3	cyclo-C_6H_{11}	179–181°	75	Ethanol	$C_{16}H_{24}N_2O_2S_2$	C 56.47	56.35
								H 7.06	7.27
XII	CH_3	CH_3	CH_2=$CHCH_2$	133–135°	70	Ethanol–chloroform	$C_{13}H_{18}N_2O_2S_2$	C 52.35	52.56
								H 6.04	6.31
XIII	CH_3	CH_3	$C_6H_5CH_2$	146–148°	65	Ethanol–chloroform	$C_{17}H_{20}N_2O_2S_2$	C 58.62	58.90
								H 5.75	6.00
XIV	CH_3	CH_3	C_6H_5	169–172°	74	Ethanol	$C_{16}H_{18}N_2O_2S_2$	C 57.48	57.22
								H 5.39	5.73
XV	CH_3	CH_3	2-$CH_3C_6H_4$	164–165°	70	Ethanol	$C_{17}H_{20}N_2O_2S_2$	C 58.62	58.85
								H 5.75	5.90
XVI	CH_3	CH_3	4-$CH_3C_6H_4$	169–171°	80	Ethanol	$C_{17}H_{20}N_2O_2S_2$	C 58.62	58.95
								H 5.75	6.05
								N 8.05	7.88
XVII	—$(CH_2)_3$—		C_2H_5	200–202°	72	Ethanol	$C_{13}H_{18}N_2O_2S_2$	C 52.35	52.52
								H 6.04	6.32
XVIII	—$(CH_2)_3$—		C_6H_5	183–185°	65	Ethanol–chloroform	$C_{17}H_{18}N_2O_2S_2$	C 58.96	59.20
								H 5.20	5.50
XIX	—$(CH_2)_3$—		4-$CH_3C_6H_4$	198–200°	60	Ethanol–chloroform	$C_{18}H_{20}N_2O_2S_2$	C 60.00	60.20
								H 5.55	5.87
XX	—$(CH_2)_4$—		CH_3	193–195°	80	Ethanol–chloroform	$C_{13}H_{18}N_2O_2S_2$	C 52.35	52.52
								H 6.04	6.25
XXI	—$(CH_2)_4$—		C_2H_5	161–164°	82	Ethanol–chloroform	$C_{14}H_{20}N_2O_2S_2$	C 53.85	53.91
								H 6.41	6.49
XXII	—$(CH_2)_4$—		n-C_6H_{13}	87–89°	73	Ethanol	$C_{18}H_{28}N_2O_2S_2$	C 58.70	58.79
								H 7.61	7.88
XXIII	—$(CH_2)_4$—		CH_2=$CHCH_2$	154–156°	85	Ethanol–chloroform	$C_{15}H_{20}N_2O_2S_2$	C 55.56	55.15
								H 6.17	6.26
								N 8.64	8.56
XXIV	—$(CH_2)_4$—		$C_6H_5CH_2$	136–138°	87	Ethanol–chloroform	$C_{19}H_{22}N_2O_2S_2$	C 60.96	61.15
								H 5.88	6.18
XXV	—$(CH_2)_4$—		C_6H_5	184–187°	82	Ethanol–chloroform	$C_{18}H_{20}N_2O_2S_2$	C 60.00	60.02
								H 5.55	5.87
XXVI	—$(CH_2)_4$—		3-$CH_3C_6H_4$	176–178°	84	Ethanol–chloroform	$C_{19}H_{22}N_2O_2S_2$	C 60.96	60.95
								H 5.88	5.92
XXVII	—$(CH_2)_4$—		4-$CH_3C_6H_4$	165–167°	80	Ethanol–chloroform	$C_{19}H_{22}N_2O_2S_2$	C 60.96	60.91
								H 5.88	5.71
XXVIII	—$(CH_2)_5$—		CH_2=$CHCH_2$	114–116°	76	Ethanol–chloroform	$C_{16}H_{22}N_2O_2S_2$	C 56.80	56.65
								H 6.51	6.64
XXIX	—$(CH_2)_5$—		$C_6H_5CH_2$	129–131°	70	Ethanol	$C_{20}H_{24}N_2O_2S_2$	C 61.86	61.59
								H 6.19	6.47
XXX	—$(CH_2)_5$—		4-$CH_3C_6H_4$	149–151°	70	Ethanol–chloroform	$C_{20}H_{24}N_2O_2S_2$	C 61.86	61.60
								H 6.19	6.49
								N 7.22	7.25

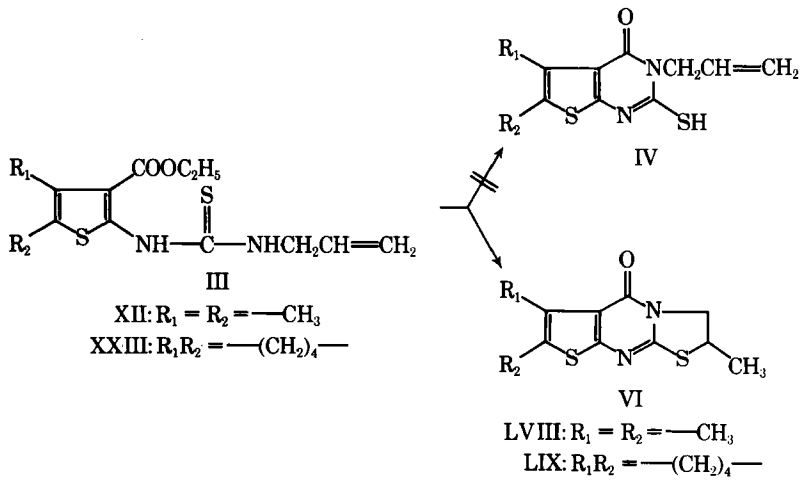

Scheme II

Table II—Antimicrobial Activity of Thienylthioureas (Minimum Inhibitory Concentration Values in Micrograms per Milliliter)

Compound	*Staphylococcus aureus* (NCTC 6571)	*Staphylococcus aureus*[a] (A/R)	*Sarcina lutea* (ATCC 9341)	*Bacillus subtilis* (NCTC 8236)	*Trychophyton mentagrophytes*[b]	*Microsporum gypseum*[b]
VII	50	25	25–50	50	50	50
IX	3.125	6.25	3.125	3.125	—	—
XII	50	50	50	50	50	50
XIII	25	50	25	50	—	—
XX	3.125	6.25	12.5	12.5	50	50
XXI	12.5	12.5	12.5	12.5	—	—
XXIII	12.5	12.5	12.5	25	—	—
XXIV	50	50	12.5	12.5	—	—
XXVIII	12.5	12.5	12.5	12.5	50	50

[a] Local isolate, Gram positive, coagulase positive, yellow pigment on potato medium, resistant to penicillin at 50 units. [b] All India Institute of Medical Sciences Culture Collection.

Preparation of N[1]*-4,5-Substituted Thienyl-*N[2]*-alkyl-(or aryl)-thiourea* (VII–XXX)—2-Amino-3-carbethoxy-4,5-substituted thiophene (6) (0.1 mole) was dissolved in hot ethanol (100 ml), and the appropriate isothiocyanate (0.11 mole) was added dropwise with stirring. The reaction mixture was refluxed on a steam bath for 5–6 hr. The mixture was cooled overnight, and the crude solid which separated was filtered and washed with ethanol. The product was dried and recrystallized from a suitable solvent (Table I).

*Preparation of 2-Mercapto-3,5,6-substituted Thieno[2,3-*d*]pyrimidin-4(*3H*)-one* (XXXI–XLVI)—A suspension of the appropriate N^1,N^2-substituted thiourea (0.05 mole) in ethanol saturated with dry hydrochloric acid (250 ml) was refluxed on a steam bath for 12 hr. The reaction mixture was cooled overnight in an ice box. The precipitated solid mass was filtered and washed with ethanol, and the dried product was recrystallized from an appropriate solvent (Table IV).

*Preparation of 3,5,6-Substituted Thieno[2,3-*d*]pyrimidin-4(*3H*)-one-2-mercaptoacetic Acid* (XLVII–LI)—A mixture of 2-mercapto-3,5,6-substituted thieno[2,3-*d*]pyrimidin-4(3*H*)-one (0.02 mole) and potassium hydroxide (0.04 mole) in ethanol (180 ml) was heated gently to obtain a clear solution. Chloroacetic acid (0.02 mole) dissolved in ethanol (10 ml) was added to the hot solution. The reaction mixture was refluxed for 6 hr on a steam bath and concentrated under vacuum. Dilute hydrochloric acid (10%) was added to obtain pH 5–6. The solid which precipitated was filtered, washed with water, and dried. Then the product was recrystallized from a suitable solvent (Table V).

*Preparation of Ethyl 3,5,6-Substituted Thieno[2,3-*d*]pyrimidin-4(*3H*)-one-2-mercaptoacetate* (LII–LVII)—To a mixture of 2-mercapto-3,5,6-substituted thieno[2,3-*d*]pyrimidin-4(3*H*)-one (0.02 mole) and potassium hydroxide (0.02 mole) in ethanol (180 ml) was added ethyl chloroacetate (0.02 mole) dissolved in ethanol (10 ml). The mixture was then refluxed for 8 hr. After cooling the reaction mixture overnight, the solid obtained was filtered, washed with water, and dried. Then the product was recrystallized from a suitable solvent (Table V).

*Preparation of 2,3-Dihydro-2,6,7-trimethylthieno[2,3-*d*]thiazolo[3,2-*a*]pyrimidin-5-one* (*LVIII*)—N^2-Allyl-N^1-[2-(3-carbethoxy-4,5-dimethylthienyl)]thiourea (14.9 g, 0.05 mole) in ethanol saturated with dry hydrochloric acid (250 ml) was prepared as described for XXXI–XLVI. When the product was recrystallized from ethanol, 7.8 g (70%) of crystalline material was obtained, mp 150–151°; IR ($CHCl_3$): 1660 cm^{-1} [C(=O)N]; UV: λ_{max} (ethanol) 210 (log ϵ 4.32), 274 (3.90), and 319 (4.10) nm; NMR ($CDCl_3$): δ 1.6 (d, 3H, C-2 methyl), 2.4 (s, 2H, C-6 methyl), 2.3 (s, 3H, C-7 methyl), and 3.9–4.6 (m, 3H, C-2 CH and C-3 CH_2).

Anal.—Calc. for $C_{11}H_{12}N_2OS_2$: C, 52.38; H, 4.76. Found: C, 52.60; H, 5.09.

*Preparation of 2-Methyl-2,3,6,7,8,9-hexahydrobenzo[*b*]thieno[2,3-*d*]thiazolo[3,2-*a*]pyrimidin-5-one* (*LIX*)—N^2-Allyl-N^1-[2-(3-carbethoxy-4,5,6,7-tetrahydrobenzo[*b*]thienyl)]thiourea (16.2 g, 0.05 mole) in ethanol saturated with dry hydrochloric acid (250 ml) was prepared as described for XXXI–XLVI. The product was recrystallized from ethanol to yield 11.15 g (77%) of crystalline material, mp 149–150°; IR ($CHCl_3$): 1675 cm^{-1} [C(=O)N]; UV: λ_{max} (ethanol): 211 (log ϵ 4.32), 275 (3.88), and 320 (4.14) nm; NMR ($CDCl_3$): δ 1.5 (d, 3H, C-2 methyl), 1.9 (t, 4H, C-7 CH_2 and C-8 CH_2), 2.7 (m, 4H, C-6 CH_2 and C-9 CH_2), and 4–4.7 (m, 3H, C-2 CH and C-3 CH_2).

Anal.—Calc. for $C_{13}H_{14}N_2OS_2$: C, 56.11; H, 5.03. Found: C, 56.22; H, 5.36.

Biological Screening—*Antimicrobial Testing*—The *in vitro* antibacterial and antifungal activities of VII–XVII, XX–XXVIII, and XXX were studied by a serial dilution technique (8), using dimethylformamide as the solvent. Dilutions were made so that in no instance was there more than 1% dimethylformamide in the test medium. At such concentrations, dimethylformamide has no inhibitory effect on the organisms.

Anticonvulsant Activity (9)—The following tests were performed on a group of eight mice of both sexes:

1. Maximum electric shock (induced using corneal electrode and a rectangular pulse of 50 mamp for 0.2 sec).

2. Pentylenetetrazol convulsions (compounds were administered orally at the dose level of 200 mg/kg followed by 100 mg/kg pentylenetetrazol[2] subcutaneously 1 hr later).

Analgesic Effect (10) (*Writhing Test, Acetic Acid*)—Oral doses (200 mg/kg) of the test compounds were administered to groups of female mice. After 15 min, the mice were injected with 0.1 ml/10 g of a 3% solution of acetic acid intraperitoneally; the number of writhing movements was recorded for 20 min.

Anti-Inflammatory Activity (11) (*Rat Paw Edema*)—Male rats (120–140 g) were divided into groups of four and fasted overnight. They were fed orally with the test compounds (200 mg/kg) as suspensions in 1% gum tragacanth. One hour later, 0.05 ml of 1% carrageenan in sterile saline was injected into the planter surface of one hindpaw in each animal. The volume of the paw was determined immediately and then 3 hr after the injection. The volume

Table III—Results of Pharmacological Screening[a]

Compound	Analgesia, % Inhibition	Anti-Inflammatory Activity, % Inhibition
XIII	20.0	—
XIX	—	14.0
XVI	—	13.6
XXIX	45.4	23.9
XXXI	—	23.5
XXXIV	—	25.0
XXXVI	—	16.6
XLI	—	15.9
XLIII	—	16.0
XLIV	45.0	16.6
LI	23.2	19.4
LIII	23.6	—
LIV	—	21.7
LVI	22.8	16.1
LIX	12.1	30.5
Aspirin (200 mg/kg)	55.0	—
Phenylbutazone (100 mg/kg)	—	60.0

[a] All compounds showed an LD_{50} of more than 1000 mg/kg po.

[2] Metrazol.

Table IV—Physical Properties of 2-Mercaptothieno[2,3-*d*]pyrimidin-4-ones

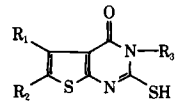

Compound	R_1	R_2	R_3	Melting Point	Yield, %	Crystallization Solvent	Molecular Formula	Analysis, % Calc.	Found
XXXI	CH_3	CH_3	CH_3	270–274°	80	Acetic acid	$C_9H_{10}N_2OS_2$	C 47.79 H 4.42 N 12.39	47.79 4.56 12.21
XXXII	CH_3	CH_3	CH_3CH_2	255–257°	81	Ethyl acetate	$C_{10}H_{12}N_2OS_2$	C 50.00 H 5.00	50.11 5.35
XXXIII	CH_3	CH_3	*n*-C_4H_9	201–202°	80	Ethanol	$C_{12}H_{16}N_2OS_2$	C 53.73 H 5.97	53.74 6.30
XXXIV	CH_3	CH_3	*n*-C_6H_{13}	172–175°	77	Ethanol–chloroform	$C_{14}H_{20}N_2OS_2$	C 56.76 H 6.76	57.04 6.95
XXXV	CH_3	CH_3	$C_6H_5CH_2$	235–240°	74	Acetic acid	$C_{15}H_{14}N_2OS_2$	C 59.60 H 4.64	59.58 4.95
XXXVI	CH_3	CH_3	C_6H_5	308–310°	72	Acetic acid	$C_{14}H_{12}N_2OS_2$	C 58.33 H 4.17	58.01 4.36
XXXVII	CH_3	CH_3	4-$CH_3C_6H_4$	220° dec.	71	Acetic acid	$C_{15}H_{14}N_2OS_2$	C 59.60 H 4.64 N 9.27	59.90 4.91 9.18
XXXVIII	—$(CH_2)_4$—		CH_3	298–301°	83	Acetic acid	$C_{11}H_{12}N_2OS_2$	C 52.38 H 4.76 N 11.11	52.32 5.04 10.86
XXXIX	—$(CH_2)_4$—		C_2H_5	259–261°	77	Acetic acid	$C_{12}H_{14}N_2OS_2$	C 54.14 H 5.26	53.95 5.43
XL	—$(CH_2)_4$—		*n*-C_6H_{13}	194–196°	69	Acetic acid	$C_{16}H_{22}N_2OS_2$	C 59.63 H 6.83 N 8.70	59.75 7.12 9.00
XLI	—$(CH_2)_4$—		$C_6H_5CH_2$	244–246°	67	2-Propanol–chloroform	$C_{17}H_{16}N_2OS_2$	C 62.20 H 4.88	62.49 5.13
XLII	—$(CH_2)_4$—		C_6H_5	315° dec.	72	Acetic acid	$C_{16}H_{14}N_2OS_2$	C 61.15 H 4.46 N 8.92	61.04 4.72 8.82
XLIII	—$(CH_2)_4$—		4-$CH_3C_6H_4$	280–283°	70	Acetic acid	$C_{17}H_{16}N_2OS_2$	C 62.20 H 4.88	61.98 5.10
XLIV	—$(CH_2)_5$—		$C_6H_5CH_2$	255–257°	71	Acetic acid	$C_{18}H_{18}N_2OS_2$	C 63.16 H 5.26	63.25 5.51
XLV	—$(CH_2)_5$—		C_6H_5	250–253°	72	Dioxane–ethanol	$C_{17}H_{16}N_2OS_2 \cdot 0.5H_2O$	C 60.53 H 5.04 N 8.31	60.44 4.99 8.32
XLVI	—$(CH_2)_5$—		3-$CH_3C_6H_4$	305° dec.	69	Acetic acid	$C_{18}H_{18}N_2OS_2$	C 63.16 H 5.26	63.20 5.49

Table V—Physical Properties of Thieno[2,3-*d*]pyrimidin-4-one-2-mercaptoacetic Acids and Ethyl Esters

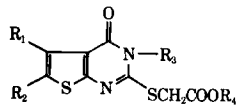

Compound	R_1	R_2	R_3	R_4	Melting Point	Yield, %	Crystallization Solvent	Molecular Formula	Analysis, % Calc.	Found
XLVII	CH_3	CH_3	CH_3	H	192–195°	87	Ethanol	$C_{11}H_{12}N_2O_3S_2$	C 46.48 H 4.23	46.81 4.52
XLVIII	—$(CH_2)_4$—		CH_3	H	187–190°	81	Ethanol	$C_{13}H_{14}N_2O_3S_2$	C 50.32 H 4.52	50.61 4.90
XLIX	—$(CH_2)_4$—		C_2H_5	H	188–190°	77	Ethanol	$C_{14}H_{16}N_2O_3S_2$	C 51.85 H 4.94 N 8.64	51.80 5.20 8.52
L	—$(CH_2)_4$—		C_6H_5	H	239–241°	50	Ethanol–chloroform	$C_{18}H_{16}N_2O_3S_2$	C 58.06 H 4.30	58.05 4.62
LI	—$(CH_2)_4$—		4-$CH_3C_6H_4$	H	245–247°	71	Ethanol–chloroform	$C_{19}H_{18}N_2O_3S_2$	C 59.07 H 4.66	58.98 4.93
LII	CH_3	CH_3	CH_3	C_2H_5	124–127°	65	Ethanol	$C_{13}H_{16}N_2O_3S_2$	C 50.00 H 5.13	50.00 5.30
LIII	—$(CH_2)_4$—		CH_3	C_2H_5	137–138°	68	Ethanol	$C_{15}H_{18}N_2O_3S_2$	C 53.25 H 5.33 N 8.28	53.61 5.69 8.45
LIV	—$(CH_2)_4$—		$C_6H_5CH_2$	C_2H_5	160–162°	90	Ethanol–chloroform	$C_{21}H_{22}N_2O_3S_2$	C 60.87 H 5.31 N 6.76	61.10 5.62 6.91
LV	—$(CH_2)_4$—		C_6H_5	C_2H_5	202–204°	55	Ethanol	$C_{20}H_{20}N_2O_3S_2$	C 60.00 H 5.00	60.01 5.19
LVI	—$(CH_2)_4$—		3-$CH_3C_6H_4$	C_2H_5	196–198°	85	Ethanol	$C_{21}H_{22}N_2O_3S_2$	C 60.87 H 5.31	60.93 5.63
LVII	—$(CH_2)_4$—		4-$CH_3C_6H_4$	C_2H_5	189–191°	78	Ethanol–chloroform	$C_{21}H_{22}N_2O_3S_2$	C 60.87 H 5.31	60.89 5.63

difference was calculated, and the anti-inflammatory effect was established from the results obtained.

Acute Toxicity—Mice of both sexes (15–20 g) were fasted for 2 hr. Suspensions (1% gum tragacanth) of the test compounds were administered orally, 0.1 ml/10 g of body weight. The LD_{50} was calculated after observation for 1 week (Table III).

REFERENCES

(1) A. H. Amin, D. R. Mehta, and S. S. Samarth, in "Progress in Drug Research," vol. 14, E. Jucker, Ed., Birkhaeuser Verlag, Basel, Switzerland, 1970, p. 218.

(2) W. L. Nobles and C. D. Blanton, *J. Pharm. Sci.*, **53**, 115(1964).

(3) M. Martin-Smith and S. T. Reid, *J. Med. Pharm. Chem.*, **1**, 507(1959).

(4) A. C. Glasser, L. Diamond, and G. Combs, *J. Pharm. Sci.*, **60**, 127(1971).

(5) F. Sauter, German offen. 2,210,503 (1972); through *Chem. Abstr.*, **77**, 164752n(1972).

(6) K. Gewald, E. Schinke, and H. Bottcher, *Chem. Ber.*, **99**, 94(1966).

(7) L. Doub, L. M. Richardson, D. R. Herbst, M. L. Black, O. L. Stevenson, L. L. Bambas, G. P. Youmans, and A. S. Youmans, *J. Amer. Chem. Soc.*, **80**, 2205(1958).

(8) "Mackie and McCartney's Handbook of Bacteriology," R. Cruickshank, Ed., E & S Livingstone Ltd., Edinburgh, Scotland, 1962, p. 407.

(9) G. F. Holland, D. A. Jaeger, R. L. Wagner, G. D. Laubach, W. M. McLamore, and S. Y. P'an, *J. Med. Pharm. Chem.*, **3**, 99(1961).

(10) L. B. Witkin, C. F. Heubner, F. Galdi, E. O'Keefe, P. Spitaletta, and A. J. Plummer, *J. Pharmacol. Exp. Ther.*, **133**, 400(1961).

(11) C. V. Winter, E. A. Risley, and G. W. Nuss, *Proc. Soc. Exp. Biol. Med.*, **111**, 544(1962).

ACKNOWLEDGMENTS AND ADDRESSES

Received February 4, 1975, from the **Department of Pharmaceutical Chemistry, L. M. College of Pharmacy, Ahmedabad-9, India, and the ‡Sarabhai Research Centre, Baroda-7, India.*

Accepted for publication July 8, 1975.

The authors thank Dr. C. S. Shah, L. M. College of Pharmacy, Ahmedabad-9, India, and Dr. V. Srinivasan, Sarabhai Research Centre, Baroda-7, India, for the facilities to carry out this work.

ˣ To whom inquiries should be directed.

Rapid and Sensitive Colorimetric Determination of Cobalt(II)

M. A. ELDAWY ˣ, A. S. TAWFIK *, and S. R. ELSHABOURI

Abstract □ A highly selective and sensitive spectrophotometric determination of cobalt(II) was developed. 7-Nitroso-8-hydroxyquinoline-5-sulfonic acid sodium salt was used as the chromogenic reagent for color development. Although other metals form colored chelates with the ligand, it was possible to develop a selective method using McIlvaine's pH 8 citric acid–phosphate buffer. Under these conditions, iron(II), iron(III), copper(II), zinc(II), and manganese(II), minerals likely to be compounded with cobalt(II) in geriatric formulations, do not interfere with the precision of the method or the color development. Calcium(II) and magnesium(II) do not form colored chelates with the used ligand. Hormones, vitamins, and additives likely to be present along with the cobalt ion in pharmaceutical formulations do not interfere. The sensitivity is 0.37 μg of cobalt(II)/ml of sample solution.

Keyphrases □ Cobalt(II)—colorimetric analysis, pharmaceutical formulations □ Colorimetry—analysis, cobalt(II) in pharmaceutical formulations □ Chelating agents—7-nitroso-8-hydroxyquinoline-5-sulfonic acid sodium salt used in colorimetric analysis of cobalt(II) in pharmaceutical formulations

Cobalt(II) salts are common ingredients in geriatric preparations along with other mineral salts, vitamins, and hormones. Various analytical procedures for the determination of cobalt(II) are available including volumetric (1), polarographic (2), colorimetric (3–7), fluorometric (8, 9), atomic absorption (10), ion-exchange chromatographic (11), and other miscellaneous (12) methods. Nevertheless, the analysis of cobalt(II) in multicomponent pharmaceutical preparations has not been frequently reported.

In a previous study (13), the chelating properties of 7-nitroso-8-hydroxyquinoline-5-sulfonic acid sodium salt were successfully used to develop a highly sensitive method for the determination of iron(II). Accordingly, it was decided to investigate the cobalt(II) complexing properties of this chelating agent to develop an analytical procedure for cobalt(II) that would not necessitate its prior separation from other mineral ions, vitamins, and hormones present in geriatric formulations.

EXPERIMENTAL

Apparatus—A recording spectrophotometer was used to determine the absorbance and obtain the spectra.

Materials—7-Nitroso-8-hydroxyquinoline-5-sulfonic acid sodium salt was prepared according to a reported method (14).

Cobalt sulfate, ferrous sulfate, copper sulfate, zinc sulfate, manganese sulfate, magnesium sulfate, calcium chloride, potassium chloride, hydrochloric acid, citric acid, disodium hydrogen phosphate, sodium acetate, acetic acid, and sodium carbonate were analytical grades.

Ethinyl estradiol, methyltestosterone, thiamine hydrochloride, riboflavin, pyridoxine hydrochloride, folic acid, cyanocobalamin, nicotinamide, ascorbic acid, starch, lactose, and glucose were pharmacopeial grades.

Reagents and Solutions—The following solution were used: ligand solution, 0.0025 *M* in double-distilled water; acetic acid–sodium acetate buffer, pH 3.42–5.89 (15); Clark and Lub's potassium chloride–hydrochloric acid buffer, pH 1.0–2.2 (16); McIlvaine's citric acid–phosphate buffer, pH 2.2–8.0 (16); and Sorensen's phosphate buffer, pH 5.0–8.0 (16). Double-distilled water was used throughout.

Standard Solution of Cobalt Sulfate ($CoSO_4 \cdot 7H_2O$, 0.005 M)—About 0.15 g of cobalt sulfate, accurately weighed, was placed in a 100-ml volumetric flask and dissolved and diluted to volume with water. Appropriate dilutions were made from this stock solution.

difference was calculated, and the anti-inflammatory effect was established from the results obtained.

Acute Toxicity—Mice of both sexes (15–20 g) were fasted for 2 hr. Suspensions (1% gum tragacanth) of the test compounds were administered orally, 0.1 ml/10 g of body weight. The LD_{50} was calculated after observation for 1 week (Table III).

REFERENCES

(1) A. H. Amin, D. R. Mehta, and S. S. Samarth, in "Progress in Drug Research," vol. 14, E. Jucker, Ed., Birkhaeuser Verlag, Basel, Switzerland, 1970, p. 218.

(2) W. L. Nobles and C. D. Blanton, *J. Pharm. Sci.*, **53**, 115(1964).

(3) M. Martin-Smith and S. T. Reid, *J. Med. Pharm. Chem.*, **1**, 507(1959).

(4) A. C. Glasser, L. Diamond, and G. Combs, *J. Pharm. Sci.*, **60**, 127(1971).

(5) F. Sauter, German offen. 2,210,503 (1972); through *Chem. Abstr.*, **77**, 164752n(1972).

(6) K. Gewald, E. Schinke, and H. Bottcher, *Chem. Ber.*, **99**, 94(1966).

(7) L. Doub, L. M. Richardson, D. R. Herbst, M. L. Black, O. L. Stevenson, L. L. Bambas, G. P. Youmans, and A. S. Youmans, *J. Amer. Chem. Soc.*, **80**, 2205(1958).

(8) "Mackie and McCartney's Handbook of Bacteriology," R. Cruickshank, Ed., E & S Livingstone Ltd., Edinburgh, Scotland, 1962, p. 407.

(9) G. F. Holland, D. A. Jaeger, R. L. Wagner, G. D. Laubach, W. M. McLamore, and S. Y. P'an, *J. Med. Pharm. Chem.*, **3**, 99(1961).

(10) L. B. Witkin, C. F. Heubner, F. Galdi, E. O'Keefe, P. Spitaletta, and A. J. Plummer, *J. Pharmacol. Exp. Ther.*, **133**, 400(1961).

(11) C. V. Winter, E. A. Risley, and G. W. Nuss, *Proc. Soc. Exp. Biol. Med.*, **111**, 544(1962).

ACKNOWLEDGMENTS AND ADDRESSES

Received February 4, 1975, from the **Department of Pharmaceutical Chemistry, L. M. College of Pharmacy, Ahmedabad-9, India, and the ‡Sarabhai Research Centre, Baroda-7, India.*

Accepted for publication July 8, 1975.

The authors thank Dr. C. S. Shah, L. M. College of Pharmacy, Ahmedabad-9, India, and Dr. V. Srinivasan, Sarabhai Research Centre, Baroda-7, India, for the facilities to carry out this work.

ˣ To whom inquiries should be directed.

Rapid and Sensitive Colorimetric Determination of Cobalt(II)

M. A. ELDAWY ˣ, A. S. TAWFIK *, and S. R. ELSHABOURI

Abstract □ A highly selective and sensitive spectrophotometric determination of cobalt(II) was developed. 7-Nitroso-8-hydroxyquinoline-5-sulfonic acid sodium salt was used as the chromogenic reagent for color development. Although other metals form colored chelates with the ligand, it was possible to develop a selective method using McIlvaine's pH 8 citric acid–phosphate buffer. Under these conditions, iron(II), iron(III), copper(II), zinc(II), and manganese(II), minerals likely to be compounded with cobalt(II) in geriatric formulations, do not interfere with the precision of the method or the color development. Calcium(II) and magnesium(II) do not form colored chelates with the used ligand. Hormones, vitamins, and additives likely to be present along with the cobalt ion in pharmaceutical formulations do not interfere. The sensitivity is 0.37 μg of cobalt(II)/ml of sample solution.

Keyphrases □ Cobalt(II)—colorimetric analysis, pharmaceutical formulations □ Colorimetry—analysis, cobalt(II) in pharmaceutical formulations □ Chelating agents—7-nitroso-8-hydroxyquinoline-5-sulfonic acid sodium salt used in colorimetric analysis of cobalt(II) in pharmaceutical formulations

Cobalt(II) salts are common ingredients in geriatric preparations along with other mineral salts, vitamins, and hormones. Various analytical procedures for the determination of cobalt(II) are available including volumetric (1), polarographic (2), colorimetric (3–7), fluorometric (8, 9), atomic absorption (10), ion-exchange chromatographic (11), and other miscellaneous (12) methods. Nevertheless, the analysis of cobalt(II) in multicomponent pharmaceutical preparations has not been frequently reported.

In a previous study (13), the chelating properties of 7-nitroso-8-hydroxyquinoline-5-sulfonic acid sodium salt were successfully used to develop a highly sensitive method for the determination of iron(II). Accordingly, it was decided to investigate the cobalt(II) complexing properties of this chelating agent to develop an analytical procedure for cobalt(II) that would not necessitate its prior separation from other mineral ions, vitamins, and hormones present in geriatric formulations.

EXPERIMENTAL

Apparatus—A recording spectrophotometer was used to determine the absorbance and obtain the spectra.

Materials—7-Nitroso-8-hydroxyquinoline-5-sulfonic acid sodium salt was prepared according to a reported method (14).

Cobalt sulfate, ferrous sulfate, copper sulfate, zinc sulfate, manganese sulfate, magnesium sulfate, calcium chloride, potassium chloride, hydrochloric acid, citric acid, disodium hydrogen phosphate, sodium acetate, acetic acid, and sodium carbonate were analytical grades.

Ethinyl estradiol, methyltestosterone, thiamine hydrochloride, riboflavin, pyridoxine hydrochloride, folic acid, cyanocobalamin, nicotinamide, ascorbic acid, starch, lactose, and glucose were pharmacopeial grades.

Reagents and Solutions—The following solution were used: ligand solution, 0.0025 *M* in double-distilled water; acetic acid–sodium acetate buffer, pH 3.42–5.89 (15); Clark and Lub's potassium chloride–hydrochloric acid buffer, pH 1.0–2.2 (16); McIlvaine's citric acid–phosphate buffer, pH 2.2–8.0 (16); and Sorensen's phosphate buffer, pH 5.0–8.0 (16). Double-distilled water was used throughout.

Standard Solution of Cobalt Sulfate ($CoSO_4 \cdot 7H_2O$, 0.005 M)—About 0.15 g of cobalt sulfate, accurately weighed, was placed in a 100-ml volumetric flask and dissolved and diluted to volume with water. Appropriate dilutions were made from this stock solution.

Table I—Continuous Variation Mixtures[a]

Component	Solution Number										
	1	2	3	4	5	6	7	8	9	10	11
Cobalt(II)[b]	0.0	0.2	0.4	0.6	0.8	1	1.2	1.4	1.6	1.8	2
Water	2.0	2.0	2.0	2.0	2.0	2	2.0	2.0	2.0	2.0	2
Reagent[b]	2.0	1.8	1.4	1.4	1.2	1	0.8	0.4	0.4	0.2	0

[a] Values are the volumes in milliliters. [b] Equimolar cobalt(II) and reagent stock solutions were used to prepare each mixture.

Preparation of Assay Solutions—*For Pure Cobalt Sulfate*—Appropriate volumes of the standard cobalt sulfate solution were used as the assay solutions.

For Synthetic Mixtures—An accurately measured volume of the synthetic mixture solution, equivalent to about 0.12 mg of cobalt sulfate, was transferred to a 10-ml volumetric flask and diluted to volume with water. This solution was the assay solution.

For Determination of Cobalt in Cyanocobalamin—About 5 mg of cyanocobalamin, accurately weighed, was placed in a small crucible, 1 drop of sulfuric acid was added, and the mixture was ignited for 30 min and then allowed to cool. One drop of sulfuric acid and 1 drop of nitric acid were added and the mixture was ignited again until no fumes appeared and the residue became violet in color. The residue was dissolved in 3 ml of distilled water and neutralized with solid sodium carbonate until effervescence ceased. It was then transferred quantitatively to a 10-ml volumetric flask, diluted to volume with distilled water, and filtered; the first portion of the filtrate was discarded. The clear filtrate was the assay solution.

Color Development—Into separate stoppered test tubes, each containing 4 ml of McIlvaine's citric acid–phosphate buffer, pH 8, was pipetted 2 ml of the ligand solution. After thorough mixing, 2 ml of the standard solution, 2 ml of the assay solution of appropriate dilution, and 2 ml of distilled water were added. The mixture was shaken thoroughly, and the absorbance of the standard and sample solutions was determined at 525 nm in 1-cm cells against the blank using a suitable spectrophotometer.

The concentration of cobalt(II) in the final sample solution (micrograms per milliliter) was obtained from a previously constructed standard calibration curve.

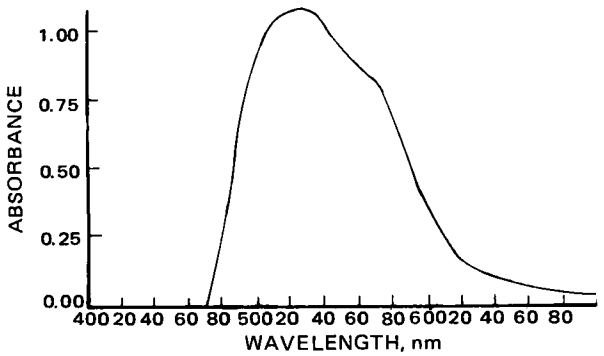

Figure 1—*Absorption spectrum for cobalt(II)–ligand complex in acetic acid–sodium acetate buffer, pH 5 [cobalt(II) = 5.4 μg/ml].*

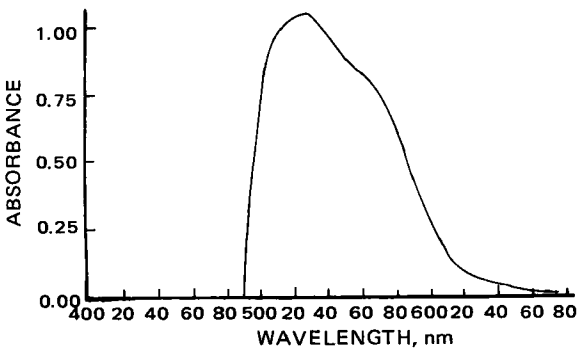

Figure 2—*Absorption spectrum for cobalt(II)–ligand complex in McIlvaine's citric acid–phosphate buffer, pH 8 [cobalt(II) = 3.67 μg/ml].*

Determination of Chelate Combining Ratio—Aqueous solutions of cobalt sulfate (0.001 *M*) and of the reagent (0.001 *M*) were prepared. Various amounts of each component were added to 11 test tubes. The concentrations of water and McIlvaine's citric acid–phosphate buffer, pH 8, remained constant in each mixture (Table I). The total number of moles was also kept constant. The absorbance of the solution in each tube was measured at 525 nm in a 1-cm cell against the blank using a suitable spectrophotometer.

RESULTS AND DISCUSSION

Acetic acid–sodium acetate buffer, pH 5, was used in the early stages of this work for the development of color of cobalt(II) with the ligand. The color developed immediately and exhibited λ_{max} at 525 nm (ϵ = 13,913) (Fig. 1). The relationship between absorbance at 525 nm and concentration was linear up to 5.86 μg/ml of cobalt(II)/ml of sample solution.

When trying to determine cobalt(II) in the presence of other metal ions, the method suffered from serious interferences. Other metal ions, namely zinc(II), manganese(II), iron(II), iron(III), and copper(II), absorbed at wavelengths close to that of the λ_{max} of the cobalt(II) complex. Accordingly, it was decided to investigate the chelation reaction to find out the proper system that would permit selective determination of cobalt(II) without interference from other metal ions. To achieve this objective, a series of buffer systems of various compositions and pH ranges was selected as vehicles for the development of the color reaction.

Variation of the pH of the acetic acid–sodium acetate buffer in the 3.42–5.89 range did not solve the problem due to the partial overlap of the other metal chelates near 525 nm, the λ_{max} of the cobalt chelate. Furthermore, low pH buffers such as that of Clark and Lub's (pH 1.0–2.2) failed to solve this problem.

When the pH of the medium was raised by the use of Sorensen's phosphate buffer, pH 5–8, the problem of interference was solved at pH 8. However, this procedure was hampered by the rather low absorptivity (ϵ = 9328) of the formed chelate, a fact that reflected itself upon the sensitivity of the method.

By using McIlvaine's citric acid–phosphate buffer solutions (pH 2.2–8.0), it was possible to attain proper conditions for the determination of cobalt(II) without interference from other metal ions and with high sensitivity (Table II). When a pH 8 solution of this buffer system was used as the milieu for color development, iron(II) and cobalt(II) formed colored chelates with absorption peaks at 710 and 525 nm, respectively. The other metal ions did not form any colored complexes under these conditions.

The absorption peak of iron(II) was sufficiently far from that of cobalt(II), thus permitting selective determination. The molecular absorptivity of the cobalt(II) complex as calculated from the absorption curve (Fig. 2) under these conditions was 18,478. The re-

Table II—Effect of McIlvaine's Citric Acid–Phosphate Buffer on Chelate Color Product of Cobalt(II)[a]

pH	λ_{max}, nm	*A*	λ_{max}, nm	*A*
2.2	400	0.7625	525	0.912
3	400	0.6750	525	1.112
4	440	0.6500	525	1.062
5	—	—	525	1.012
6	—	—	525	0.987
7	—	—	525	0.800
8	—	—	525	1.037

[a] Cobalt(II) = 3.67 μg/ml.

Table III—Determination of Cobalt(II) in the Presence of Hormones, Vitamins, Minerals, and Excipients Usually Found in Geriatric Preparations

Substances Added (per 0.12 mg Cobalt Sulfate), mg		Cobalt Sulfate Recovered[a]			
		mg	%	*SD*	*CV*
Ethinyl estradiol	0.01	0.1200	100.0 ± 0.2	0.30	0.30
Methyltestosterone	0.12	0.1200	100.0 ± 0.1	0.14	0.14
Thiamine hydrochloride	5.00	0.1199	99.9 ± 0.2	0.26	0.26
Riboflavin	2.50	0.1210	100.0 ± 0.1	0.14	0.13
Pyridoxine hydrochloride	0.50	0.1199	99.9 ± 0.6	0.90	0.90
Folic acid	0.50	0.1199	99.9 ± 0.2	0.26	0.26
Cyanocobalamin	0.001	0.1200	100.0 ± 0.0	0.00	0.00
Nicotinamide	5.00	0.1199	99.9 ± 0.3	0.41	0.41
Ascorbic acid	75.00	0.1210	100.8 ± 0.2	0.50	0.49
Ferrous sulfate	100.00	0.1210	100.8 ± 0.1	0.14	0.13
Zinc sulfate	1.50	0.1990	99.9 ± 0.3	0.26	0.26
Manganese chloride	1.50	0.1200	100.0 ± 0.2	0.30	0.30
Magnesium sulfate	100.00	0.1200	100.0 ± 0.1	0.00	0.00
Starch	100.00	0.1200	100.0 ± 0.0	0.00	0.00
Glucose	100.00	0.1200	100.0 ± 0.0	0.00	0.00
Lactose	100.00	0.1200	100.0 ± 0.0	0.00	0.00

[a] Average of three determinations.

lationship between absorbance and concentration was linear up to 4.44 μg of cobalt(II)/ml of sample solution; the lower limit for detection was 0.37 μg of cobalt(II)/ml of sample solution.

Under the conditions developed for the specific color formation, the combining ratio of the metal to ligand was determined by the method of continuous variation (17) and was found to be 1:3 (Fig. 3). This value is in agreement with the finding of Aly *et al.* (14), who, in a qualitative study, separated the cobalt(II)–ligand complex and determined its structure by elemental microanalysis.

The specificity of the method for the determination of cobalt(II) in the presence of other minerals, hormones, certain vitamins, and excipients likely to be present in geriatric formulations is shown in Table III. Several different amounts of standard solution, or several different weights of each ingredient shown in Table III, either singly or in admixture with all of the others, each approximating sample weights of commercial pharmaceutical dosage forms, were spiked with a known amount of cobalt sulfate and the analysis was performed. The average recovery of cobalt(II) from these synthetic mixtures ranged from 99.5 to 100.2%.

Application of this method for the determination of cobalt in cyanocobalamin gave a percentage recovery of 100.0 ± 0.3. Although the developed method might be suitable for certain formulations of relatively high cyanocobalamin content, it is not applicable to single-dose analysis of formulations with less than 12 μg of cyanocobalamin/dose.

The results demonstrate that the proposed method is applicable for the simultaneous determination of iron and cobalt. Only a single chromogen is used; the method is both simple and rapid. High sensitivity of the ligand chromogenic reagent facilitates the determination of submicrogram amounts of the elements. Moreover, the ligand is easily synthesized. Interferences under the developed condition are nil. The method is strongly recommended over other methods.

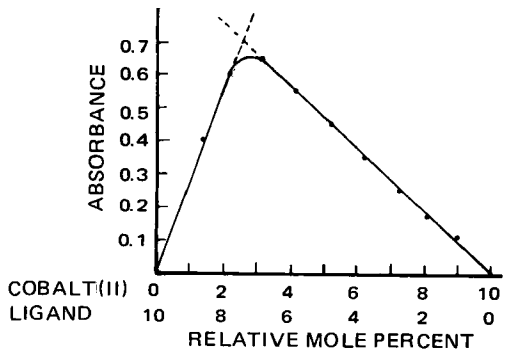

Figure 3—*Continuous variation plot for cobalt(II)–ligand complex in McIlvaine's citric acid–phosphate buffer.*

REFERENCES

(1) N. A. Bugrin and E. I. Zatula, *Farm. Zh.*, **25**, 54(1970); through *Chem. Abstr.*, **78**, 28989k(1973).

(2) K. H. Brainina and T. A. Krapivkina, *Zh. Anal. Khim.*, **22**, 1387(1967); through *Anal. Abstr.*, **16**, 3028(1969).

(3) D. W. Rogers, *Anal. Chem.*, **34**, 1657(1962).

(4) J. H. Billman and R. Chermin, *ibid.*, **36**, 552(1964).

(5) R. T. Pflaum and E. S. Tucher, *ibid.*, **43**, 459(1971).

(6) C. Zachariades and W. C. McGavock, *J. Pharm. Sci.*, **60**, 918(1971).

(7) S. Shibato, M. Furukawa, and K. Goto, *Talanta*, **20**, 426(1973).

(8) D. F. H. Wallach and T. L. Steck, *Anal. Chem.*, **35**, 1035(1963).

(9) K. E. Daughetry, R. J. Robinson, and J. I. Mueller, *ibid.*, **36**, 1098(1964).

(10) F. M. Farhan and M. Makhani, *J. Pharm. Sci.*, **59**, 1200(1970).

(11) J. P. Quinche and S. Quinche-Sax, *J. Chromatogr.*, **32**, 162(1968).

(12) A. I. Vogel, "A Text Book of Quantitative Inorganic Analysis Including Elementary Instrumental Analysis," 3rd ed., Longmans, New York, N.Y., pp. 529, 955.

(13) M. A. Eldawy, A. S. Tawfik, and S. R. Elshabouri, Abstracts of Papers, Third Pan-Arab Congress of Pharmaceutical Sciences, Baghdad, Iraq, Nov. 1972.

(14) M. M. Aly, M. Makhyoun, and S. Elezaby, *J. Inorg. Nucl. Chem.*, **35**, 2727(1973).

(15) A. I. Vogel, "A Text Book of Quantitative Inorganic Analysis Including Elementary Instrumental Analysis," 3rd ed., Longmans, New York, N.Y., p. 35.

(16) "Documenta Geigy, Scientific Tables," K. Dienn, Ed., J. R. Geigy, S. A., Basel, Switzerland, p. 314.

(17) H. Diehl and F. Lindstron, *Anal. Chem.*, **31**, 414(1969).

ACKNOWLEDGMENTS AND ADDRESSES

Received October 17, 1974, from the *Department of Pharmaceutical Chemistry, Faculty of Pharmacy, University of Assiut, Assiut, A.R. Egypt.*

Accepted for publication July 3, 1975.

Presented in part at the Third Pan-Arab Congress of Pharmaceutical Sciences, Baghdad, Iraq, November 1972.

Abstracted from a dissertation submitted by S. R. Elshabouri to the University of Assiut in partial fulfillment of the Doctor of Philosophy degree requirements.

* Present address: Elnasr Co. for Pharmaceutical Chemicals and Antibiotics, Abou Zaabal, Egypt.

‡ To whom inquiries should be directed. Present address: Department of Pharmaceutical Chemistry, Faculty of Pharmacy, University of Tanta, Tanta, Egypt.

GLC Analysis of Thioridazine, Mesoridazine, and Their Metabolites

EUGENE C. DINOVO ˣ, LOUIS A. GOTTSCHALK, BINA RANI NANDI, and PETER G. GEDDES

Abstract □ A GLC method for measuring thioridazine, mesoridazine, their metabolites, and possibly other phenothiazines was developed. By using this method, seven different phenothiazine derivatives, thioridazine, and six known thioridazine metabolites were extracted and separated. This method was tested by assaying plasma samples from 30 hospitalized psychiatric patients receiving thioridazine or mesoridazine.

Keyphrases □ Thioridazine and metabolites—GLC analysis, plasma □ Mesoridazine and metabolites—GLC analysis, plasma □ Phenothiazines—seven derivatives, GLC analysis, plasma □ GLC—analysis, thioridazine, mesoridazine, metabolites, and seven phenothiazine derivatives, plasma

Studies of thioridazine metabolism have been made difficult by the lack of specific methodologies for measuring thioridazine and its metabolites. The fluorometric method (1, 2), although sensitive, is not specific, because it measures the sum of the fluorescence of thioridazine and its metabolites (1, 3). Although phenothiazines and metabolites can be separated by TLC (3, 4), the components cannot be quantitated.

A GLC method specific for thioridazine was reported (5); but to study thioridazine metabolism and pharmacodynamics, a method capable of separating and quantitating thioridazine and its metabolites is needed. Therefore, the published method (5) was modified to measure thioridazine, mesoridazine [thioridazine (*S*)-sulfoxide], and five other known metabolites as well as other phenothiazines. Data are presented on the recovery, sensitivity, and precision of this method for thioridazine and mesoridazine and on the generality of the method. Plasma samples from 16 subjects receiving mesoridazine and 14 receiving thioridazine were analyzed with the described method (3).

EXPERIMENTAL

Reagents and Chemicals—Spectrophotometric grade heptane[1] was used; all other reagents were analytical reagent grade. Pure thioridazine, mesoridazine, and their metabolites[2] were used in the stock solutions, spiked plasma samples, and standards. Thioridazine, mesoridazine, thioridazine (*R*)-sulfoxide, and northioridazine (*S*)-sulfoxide were all used as the hydrochloride salts. Thioridazine disulfoxide, thioridazine (*S*)-sulfone, and northioridazine were used as the free bases. Chlorpromazine hydrochloride[3] was the internal standard.

The other phenothiazine drugs (perphenazine, trifluoperazine, prochlorperazine, and fluphenazine) were obtained[4] as tablets or ampuls, solubilized in distilled water, and used as such.

Plasma Samples—Spiked plasma samples were prepared by adding measured volumes of concentrated stock solution (0.5–1.0 mg/ml) to known measured quantities of pooled plasma[5]. Plasma dilutions due to addition of drugs were always less than 4%. Spiked plasma samples to be used as standards were prepared in a similar way but in bulk quantities (80–160 ml). Aliquots, 4 ml, were immediately pipetted into separate tubes, covered with parafilm, and kept frozen at −20° until use.

Plasma samples were also obtained from hospitalized psychiatric subjects receiving thioridazine (14 subjects) or mesoridazine (16 subjects). The plasma samples were frozen within 2 hr after blood was drawn and were kept frozen until use.

Extraction Procedure—To a 4-ml sample of plasma was added 2.5 ml of 1 *N* NaOH, and the solution was extracted twice with 5 ml of *n*-heptane–toluene (4:1 v/v) in a 15-ml screw-capped[6] culture tube for 30 min using a wrist-action shaker[7]. All samples for one or more patients and the standards were placed horizontally in a carrier box and shaken together.

The tubes were centrifuged and, if needed, the emulsion at the interface was broken up by stirring or freezing and the tubes were recentrifuged. The recovered heptane–toluene mixtures were pooled and transferred to a clean culture tube and similarly extracted with 2 ml of 0.1 *N* HCl for 30 min. The acid aqueous layer was then split into two aliquots: 0.5 ml for the spectrofluorometric assay and 1.4 ml for the GLC assay.

Fluorometric Assay—The fluorometric assay of Pacha (2) was used. To the 0.5-ml aliquot of the 0.1 *N* HCl layer were added 0.5 ml of 0.2 *N* H_2SO_4 and 100 μl of 0.1% $KMnO_4$. After 5 min, 100 μl of 0.2% H_2O_2 was added, and the fluorescence was read[8] at 355-nm excitation and 440-nm emission.

GLC Assay—To the 1.4-ml acid aliquot was added 0.8 ml of 2 *N* NaOH. The solution was extracted for 30 min with 100 μl of heptane–toluene containing chlorpromazine as the internal standard. The chlorpromazine–heptane–toluene mixture was prepared fresh each day of an experiment by mixing 100 μl of an ethanol mixture containing 8 mg of chlorpromazine hydrochloride/10 ml of absolute ethanol and 1.5 ml of heptane–toluene. For this extraction, glass-stoppered, conical, 3-ml tubes were shaken horizontally with a wrist-action shaker in a specially constructed carrier box.

GLC was performed using a chromatograph[9] with dual flame-ionization detectors. Two- to three-microliter aliquots of samples and standards were injected into 3% OV-17 on Chromosorb Q (100–120-mesh[10]) columns, 0.6 cm (0.25 in.) o.d., 1.8 m (6 ft) long, and 2 mm i.d. The conditions were as follows: column oven temperature, 275°; all other temperatures, 325°; column helium flow, 100 ml/min; hydrogen flow, 43 ml/min; and makeup helium flow, 108 ml/min. It is not essential to know the volume applied to the column since the same amount of chlorpromazine is present in all samples and can be used to normalize the calculations regardless of the actual concentration volumes.

The samples were run as are and, where needed, the heptane–toluene solution was concentrated by reduced pressure aspiration and rerun. The samples were concentrated to maximize the signal-to-noise ratio and, thus, increase the minimum detectable quantity. The concentration was performed in the same 3-ml conical centrifuge tubes after most of the aqueous layer was removed with a disposable pasteur pipet. This procedure adjusted the heptane layer in the narrow, conical section of the tube, facilitating removal of the organic layer with the microliter syringe for the GLC assay.

[1] Mallinckrodt Chemical Works, St. Louis, MO 63147
[2] Sandoz Pharmaceuticals, Hanover, NJ 07936
[3] Smith Kline and French Laboratories, Philadelphia, PA 19101
[4] Pharmacy of the Orange County Medical Center, Orange, Calif.
[5] Clinical Laboratory, Department of Pathology, Orange County Medical Center, Orange, Calif.
[6] Lined with Teflon (du Pont).
[7] Burrell Corp., Pittsburgh, Pa.
[8] Aminco-Bowman spectrophotofluorometer, American Instrument Co., Silver Spring, MD 20910
[9] GC-4 and Cliniscreen, Beckman Instruments, Fullerton, Calif.
[10] Applied Science Laboratories, Inc., State College, PA 16801

Table I—Effect of Concentrating the Heptane–Toluene Layer on the GLC Results

	Chlorpromazine				Mesoridazine			
Concentration	1×	3.8×	1×	3.6×	1×	3.8×	1×	3.6×
Peak height × attenuation × 10^{-3}, mm	60	246	64	212	3.1	9.8	3.5	13.2

Table II—Comparison of Fluorescence and GLC Mesoridazine Assays for Patient LB

	Time after Drug Administration, hr				
Assay Method	1	4	8	24	48
Fluorescent concentration, μg/ml plasma	4.25	5.10	2.98	1.49	0.43
GLC concentration, μg/ml plasma	3.03	4.11	0.98	0.35	—

Calculations—Three stock thioridazine, mesoridazine, and/or metabolite standards, 1, 5, and 10 μg/ml in 4 ml of plasma, kept frozen until use, were run together with the unknown samples. The response of the flame-ionization detector per microgram of drug was averaged over the three standards, and the average was used to calculate the concentration in the subjects' plasma samples. The equation used for the calculation incorporates corrections and normalizing factors for the volume of heptane–toluene recovered and for the concentrate volume differences as measured by the internal standard.

RESULTS AND DISCUSSION

To ascertain the effect of concentration on chlorpromazine and mesoridazine peak heights, several experiments were carried out as described under *Experimental*. Then, with a 100-μl syringe, most of the final heptane–toluene layer containing chlorpromazine and mesoridazine was removed, measured, and decanted into the conical part of a 3-ml conical centrifuge tube. An aliquot was assayed by GLC, the sample was concentrated by reduced pressure aspiration, the volume was measured with the syringe, and aliquots of the concentrate were assayed by GLC. The results in Table I show that the chlorpromazine peak heights reflected the concentration volumes and, therefore, could be used as a measure for the heptane–toluene volume.

Table II compares the results of fluorometric and GLC mesoridazine assays for Patient LB after a single intramuscular dose of 2 mg/kg. The fluorometric results were always greater than the GLC results, especially at the later times when little mesoridazine was measured by GLC while considerable amounts were seemingly still measurable by fluorescence. Fluorometrically, one is seeing a summation of the fluorescence of mesoridazine and its metabolites, while mesoridazine alone is measured by GLC. At the later times, metabolites are predominantly present, resulting in the greater disparity between the specific GLC and the nonspecific fluorometric results at these later times.

A GLC standard curve for mesoridazine was prepared using triplicate 4-ml spiked plasma samples and increasing concentrations of mesoridazine from 0.5 to 5 μg/ml. The results fell in a straight line. The line through the experimental points did not go through the origin, however, indicating a loss of drug during the assay procedure independent of drug concentration, perhaps due to nonspecific drug adhesion to the glassware. The drug lost in this way was less than 0.3 μg/assay. The mean and standard deviation of the mesoridazine peak height normalized to an attenuation of one for the 0.5-, 1.0-, 2.0-, 2.5-, and 5.0-μg/ml samples were 250 ± 115, 740 ± 105, 2100 ± 165, 2600 ± 225, and 5750 ± 135 mm, respectively.

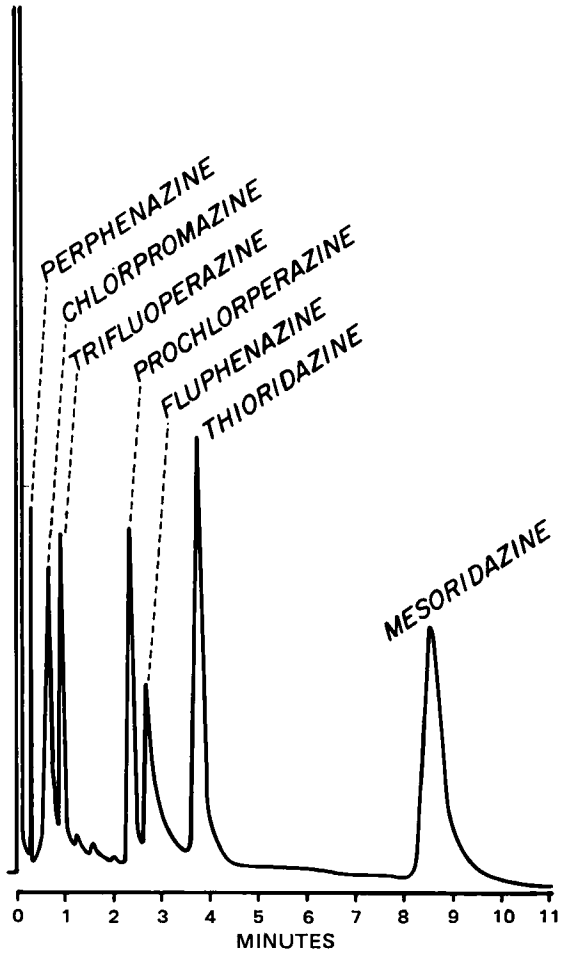

Figure 1—*Gas–liquid chromatogram of a mixture of seven phenothiazine derivatives. The seven phenothiazines were first run singly to find their elution time; then they were pooled and the mixture was injected into the gas chromatograph. The chromatographic conditions were set as indicated under* Experimental.

For a 4-ml plasma sample, the minimum detectable quantity was about 0.3 μg/ml of plasma without concentration. The minimum detectable quantity obtained with the inclusion of the concentration step was 0.05 μg/ml of plasma. The three standards should be included with every assay of unknown samples because of the slight fluctuations in sensitivity. The flame-ionization detector must be carefully optimized for good sensitivity. Relatively minor changes in helium or hydrogen flow can cause disproportionate changes in sensitivity.

The recoveries of parent drug and metabolites from water and plasma as measured by GLC are listed in Table III. The recoveries from water, especially for mesoridazine and thioridazine (*R*)-sulf-

Table III—Recoveries of Thioridazine, Mesoridazine, Thioridazine (*R*)-Sulfoxide, and Thioridazine (*S*)-Sulfone from Water and Plasma as Measured by GLC

	Thioridazine	Mesoridazine	Thioridazine (*S*)-Sulfone	Thioridazine (*R*)-Sulfoxide
Recovery from water, mean ± *SD* (*n* = 3), %	78 ± 0.5	83 ± 0.9	95 ± 0.5	87 ± 1.2
Recovery from plasma, mean ± *SD* (*n* = 8), %	77 ± 6	56 ± 4	82 ± 4	38 ± 3

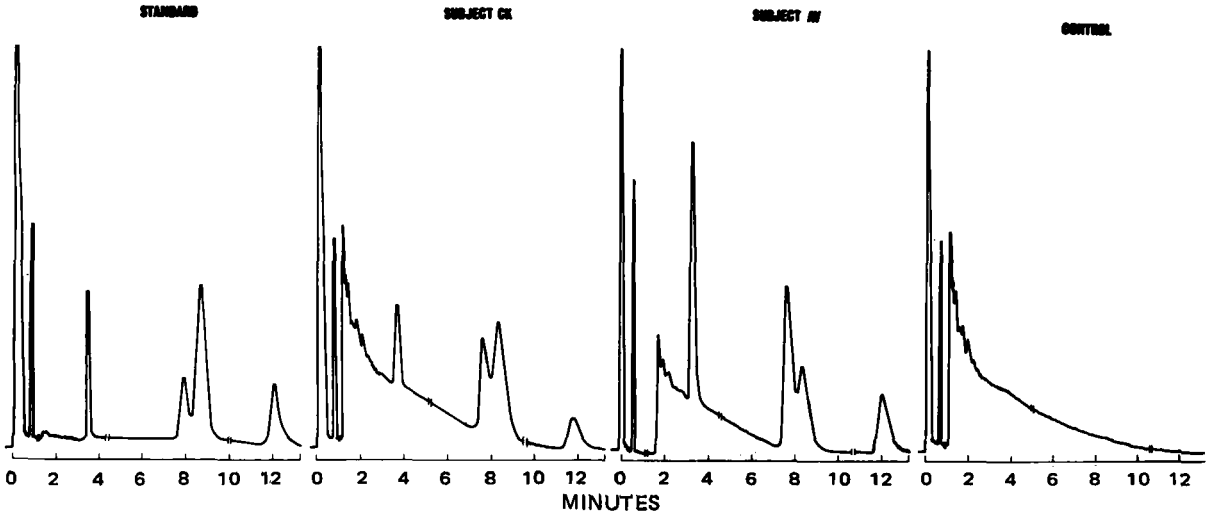

Figure 2—*Gas–liquid chromatograms of a standard, a control, and plasma from two hospitalized psychiatric subjects. The indentation marks (—‖—) signify changes in attenuation from 32,000 to 3200 to 1600 to 160 for the 5-μg/ml plasma standard and from 32,000 to 200 to 80 to 20 for the subject and control plasma samples at about 1.5, 4.5, and 10 min, respectively. Chlorpromazine at 0.6 min was used as the internal standard. Thioridazine, mesoridazine, thioridazine (S)-sulfone, and thioridazine (R)-sulfoxide eluted at about 3.4, 7.9, 8.3, and 12.1 min, respectively.*

oxide, were considerably greater than those from plasma. These data suggest a differential affinity of thioridazine and its metabolites for plasma binding sites. No corrections need to be made for affinity differences because the standards run concurrently with the unknown samples will have the same differential affinities and will thus correct for them.

The possibility that different plasma samples show different affinities for the drug and/or metabolites was investigated by using eight different plasma samples spiked with thioridazine and metabolites. The results (Table III) demonstrate that the differences in observed recoveries were within experimental error. The coefficients of variation for the plasma samples were 7.7, 7.1, 4.8, and 7.9% for thioridazine, mesoridazine, thioridazine (*S*)-sulfone, and thioridiazine (*R*)-sulfoxide, respectively.

The generality of the method is seen in Fig. 1 and Table IV. Figure 1 is a chromatogram of seven different phenothiazines pooled for this experiment. Table IV shows the retention time of several metabolites of thioridazine. The disulfoxide and disulfone metabolites are too polar to be optimally extracted into the heptane–toluene solvent at the pH indicated; however, they are readily extracted by methylene chloride.

A study of the pharmacodynamics of thioridazine and mesoridazine (3) showed a major unknown metabolite in the plasma of 21 human subjects receiving thioridazine or mesoridazine. This metabolite has now been identified (6) as thioridazine (*S*)-sulfone. The plasma concentration of thioridazine for nine subjects given a daily dose of thioridazine at 4 mg/kg po ranged from 1.35 to 6.87 μg/ml of plasma by the fluorometric method, with thioridazine hydrochloride as the standard, and from 0.16 to 2.1 μg/ml of plasma by the specific GLC method. Typical chromatograms of a standard and subject's plasma before and after drug treatment are shown in Fig. 2.

Table IV—Retention Time of Thioridazine and Its Metabolites.

	Minutes[a]
Thioridazine	3.6
Thioridazine (*S*)-sulfoxide	8.3
Thioridazine (*R*)-sulfoxide	12.8
Northioridazine	3.8
Northioridazine (*S*)-sulfoxide	8.7
Thioridazine disulfone	22.8[b]
Thioridazine disulfoxide	20.9[b]
Unknown component	9.1

[a] The elution time was measured from the rising leg of the solvent peak. [b] The extraction solvent was methylene chloride.

REFERENCES

(1) J. B. Ragland, V. G. Kinross-Wright, and R. S. Ragland, *Anal. Biochem.*, **12**, 60(1965).

(2) W. L. Pacha, *Experientia*, **25**, 103(1969).

(3) E. C. Dinovo, L. A. Gottschalk, E. P. Noble, and R. Biener, *Res. Commun. Chem. Pathol. Pharmacol.*, **1**, 489(1974).

(4) I. A. Zingales, *J. Chromatogr.*, **44**, 547(1969).

(5) S. H. Curry and G. P. Mould, *J. Pharm. Pharmacol.*, **21**, 174(1969).

(6) L. D. Gruenke, J. C. Craig, E. C. Dinovo, L. A. Gottschalk, and R. Biener, *Res. Commun. Chem. Pathol. Pharmacol.*, **10**, 221(1975).

ACKNOWLEDGMENTS AND ADDRESSES

Received May 1, 1975, from the *Neurochemistry Laboratory, Department of Psychiatry and Human Behavior, College of Medicine, University of California, Irvine, CA 92717*, the *Orange County Medical Center, Orange, CA 92668*, and the *Long Beach Veterans Administration Hospital, Long Beach, CA 90801*

Accepted for publication July 14, 1975.

Supported in part by a project grant (MH-20174) from the Psychopharmacology Branch, National Institute of Mental Health, and by a grant-in-aid from Sandoz Pharmaceuticals.

The metabolites were donated by Dr. J. J. Schwarz and Mr. Sidney Gimpel of Sandoz Pharmaceuticals.

[x] To whom inquiries should be directed (at the University of California, Irvine).

Effect of Phthalate Plasticizer on Blood Compatibility of Polyvinyl Chloride

S. W. KIM ˣ, R. V. PETERSEN, and E. S. LEE

Abstract □ The amount of a phthalate plasticizer on the surface of a sheet of polyvinyl chloride used in the fabrication of blood storage bags was quantified using attenuated total reflectance spectroscopy, water contact angle measurement, and weight loss due to methanol extraction. Water wettability increased as the amount of surface phthalate extracted by methanol increased, which indicates that the accumulation of phthalate on the surface increases hydrophobicity. The extraction of phthalate by methanol consists of two steps: (*a*) methanol first dissolves surface phthalate, and (*b*) phthalate in the bulk then diffuses through the surface. The adsorption of plasma proteins was investigated to determine the initial events as blood contacts the surface. The composition of adsorbed proteins on the methanol-cleansed surface differs from that on the uncleansed polyvinyl chloride surface. Albumin adsorption onto phthalate-contaminated surfaces is less than on cleansed surfaces while adsorption of γ-globulin and fibrinogen is greater on phthalate-contaminated surfaces. Protein adsorption can be related to surface thrombus formation. Increases in platelet numbers appeared on phthalate-contaminated surfaces as compared with methanol-treated surfaces. A phthalate may enhance platelet adhesion and aggregation when it exists on a polymer surface.

Keyphrases □ Phthalate plasticizer—effect of polyvinyl chloride on blood compatibility, quantified by attenuated total reflectance spectroscopy □ Polyvinyl chloride—blood compatibility, effect of phthalate plasticizer, quantified by attenuated total reflectance spectroscopy □ Attenuated total reflectance spectroscopy—measurement of effect of phthalate plasticizer on blood compatibility of polyvinyl chloride

Polyvinyl chloride plasticized with a phthalate ester, principally bis(2-ethylhexyl) phthalate (I), has been utilized in the fabrication of various medical devices such as blood storage bags, transfusion assemblies, and extracorporeal circulation devices used in cardiopulmonary bypass and renal hemodialysis units. It was recognized (1–3) that small quantities of additives, primarily I, are leached out of polyvinyl chloride by blood or various injectable solutions. Several investigators (4–12) quantitated the rate of extraction of I from blood storage bags (4–11), medical grade polyvinyl chloride tubing (4–6, 12), hemodialysis units (7), and cardiopulmonary bypass units (7) under various conditions and by various blood components. Of particular interest was the fact that hemodialysis units gave a zero-time concentration of 7.75 mg/100 ml and cardiopulmonary bypass tubing gave a zero-time concentration of 5.05 mg/100 ml in circulating blood (7).

In 1970, I was identified in tissues of human patients who had been transfused with blood stored in polyvinyl chloride blood storage bags (13). Similar observations subsequently were made in this laboratory and by other researchers (14–17) in studies on animals and humans directly exposed to polyvinyl chloride or to blood stored in polyvinyl chloride blood bags.

Although the effects of I on platelets and other formed elements of blood have been studied, little is known regarding the effects of I or other phthalates on the thrombogenicity of polymer surfaces. The studies reported here evaluate the alteration of polyvinyl chloride surface characteristics with the accumulation of I. It is postulated that exposed I on a polyvinyl chloride surface increases hydrophobicity, resulting in greater adsorption of γ-globulin and fibrinogen onto the surface, an important factor for platelet adhesion and aggregation (22).

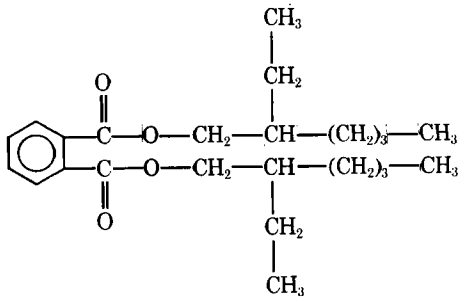

I

EXPERIMENTAL

Several experiments characterized the surface nature of polyvinyl chloride contaminated with I and the same material after extraction of I from the surface to determine the possible adverse effects of I upon contacting blood. The plastic used was a sheet of polyvinyl chloride supplied by a major manufacturer of blood bags used extensively in clinics and hospitals for the collection and storage of blood or blood fractions.

Since different batches vary considerably in composition and physical characteristics, polyvinyl chloride from a single batch was used in all studies. The age of the sheet ranged from about 6 to 8 months during the experiments. Similar formulations are employed in the manufacture of tubing used in blood administration assemblies and extracorporeal circulation devices.

Phthalate Extraction and Surface Characterization of Polyvinyl Chloride—Polyvinyl chloride samples (2 × 2.5 cm) were stored in 20 ml of methanol for varying periods. The quantity of I extracted was determined after drying at 50° for 15 min. Water contact angles were determined[1]. Attenuated total reflectance spectroscopy[2] was used to calculate the amount of surface phthalate.

The standard IR bands used were the carbonyl stretching vibration at 1720 cm^{-1} for phthalate ester and the methylene bending vibration at 1430 cm^{-1} for polyvinyl chloride. The plateau time was determined from the contact angle measurements and the weight of extracted phthalate. Surface phthalate was considered to be removed when the contact angle reached a plateau. The standard IR bands ratio, methanol extraction time, and decreasing weight of the sample provided data for the calibration curve for surface phthalate amounts.

Adsorption of Plasma Proteins on Polyvinyl Chloride Surfaces—The plasma protein solutions used consisted of albumin (human crystallized 4×), γ-globulin (bovine fraction II), and fi-

[1] Zisman goniometer, Rame-Hart, Inc.

[2] Perkin-Elmer model 521 grating IR spectrophotometer with Wilks Scientific Corp. attenuated total reflectance attachment.

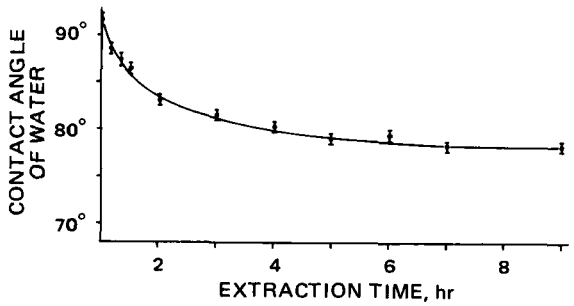

Figure 1—*Water contact angle as a function of methanol extraction time.*

brinogen (bovine fraction I) at physiological concentration ratios. In each experiment, one of the three proteins was radiolabeled with iodine-125. The polymer samples were clamped in cells designed for static adsorption. The samples were exposed for varying periods, following which they were rinsed with pH 7.4 isotonic phosphate buffer saline at a flow rate of 10 ml/sec for 1 min to remove excess solution (23).

The adsorbed amount of labeled protein was determined as a function of time by direct measurement of radioactivity on a section of polyvinyl chloride, using a scintillation counter[3]. The experiment was performed on phthalate-contaminated and methanol-extracted polyvinyl chloride surfaces. The latter was extracted with methanol overnight.

***Ex Vivo* Platelet Adhesion**—Phthalate-contaminated and methanol-extracted polyvinyl chloride surfaces were exposed to unheparinized animal blood. Sheep were cannulated, and the blood was allowed to flow through a specially designed polycarbonate cell wherein polyvinyl chloride was exposed to the flowing blood for 3 min by a technique described previously (22). The samples were rinsed with saline, and the platelets were fixed with glutaraldehyde and stained with Wright's staining solution. Twenty fields of each sample were used to determine the average number of platelets. A microscope[4] equipped with incident and transmitted light was used to visualize the platelets.

RESULTS AND DISCUSSION

Bulk phthalate constantly diffuses to the surface of polyvinyl chloride due to the concentration gradient. As shown in Fig. 1, the water contact angle decreases (wettability increases) as methanol extraction time increases until a plateau is reached, which requires about 6 hr at ambient temperature. The hydrophobic nature of the contaminated surface (water contact angle of 91.6°) decreases by dissolution of the surface phthalate until the plateau (water contact angle of 78.2°) is reached. The plateau contact angle can be considered the water contact angle on a pure polyvinyl chloride surface.

The amount of extracted phthalate starts with 0.00162 g/cm^2 at 10 min and increases asymptotically until the plateau quantity of

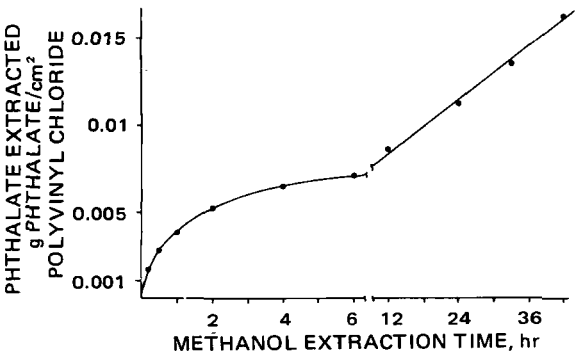

Figure 2—*Bis(2-ethylhexyl) phthalate (I) extraction as a function of methanol extraction time. The initial phase is a dissolution process followed by diffusion of bulk I through the surface.*

[3] Two-channel Nuclear Chicago model 725 liquid scintillation spectrometer.

[4] Nikon Apophot.

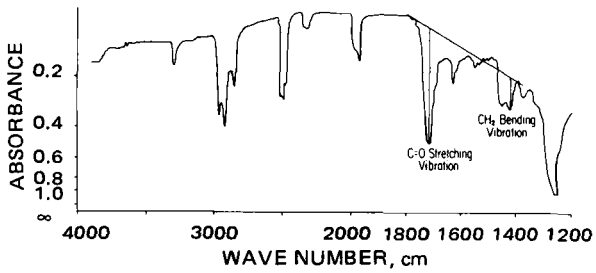

Figure 3—*Typical attenuated total reflectance tracing. The carbonyl stretching vibration for I is at 1720 cm^{-1}. The methylene bending vibration for polyvinyl chloride is at 1430 cm^{-1}.*

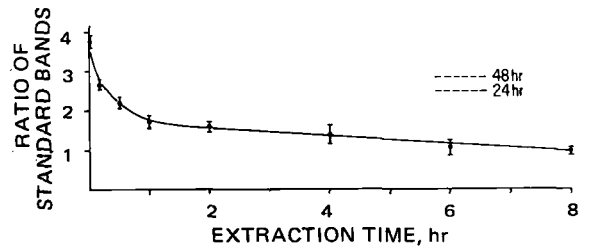

Figure 4—*I–polyvinyl chloride standard attenuated total reflectance bands ratio as a function of methanol extraction time. The dashes indicate surface I after 24 and 48 hr of air exposure following 6 hr of methanol extraction.*

0.00710 g/cm^2 is reached at 6 hr (Fig. 2). After 6 hr, the extracted amounts of phthalate increase linearly. The extraction and contact angle data indicate that surface phthalate is removed by a dissolution process. After dissolution of surface phthalate, bulk phthalate begins diffusion through the surface according to a linear curve fitting Fick's law of diffusion. These observations are valuable in obtaining the amount of surface phthalate and extraction time necessary for complete removal. There should be an overlapping step between dissolution and diffusion. The overlap would be expected to be indicated by a smooth curve at or near 6 hr rather than a sharp discontinuity.

A typical attenuated total reflectance tracing of polyvinyl chloride with surface phthalate is shown in Fig. 3. The characteristic band for I is at 1720 cm^{-1} for the carbonyl stretching vibration. A methylene bending vibration at 1430 cm^{-1} is characteristic of polyvinyl chloride. The peak for I includes the phthalate existing to a depth of approximately 1 μm. The ratio of the standard band of I to the polyvinyl chloride standard band *versus* methanol extraction time is plotted in Fig. 4. If a surface extraction time of 6 hr is assumed, a unique calibration curve is obtained to quantify the amount of phthalate existing on the surface. The calibration plot shown in Fig. 5 is a combination of Figs. 1, 2, and 4. Therefore, the quantity of surface phthalate can be determined using Fig. 5.

The kinetic curves for competitive protein adsorption are shown in Figs. 6–8. Albumin adsorption is greater on the methanol-cleansed surface. γ-Globulin and fibrinogen adsorptions are higher on the untreated polyvinyl chloride surfaces. It was noticed in ear-

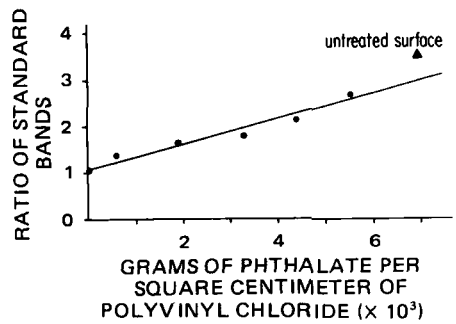

Figure 5—*Surface phthalate quantity measured as a function of the ratio of I–polyvinyl chloride standard attenuated total reflectance bands. Key: ▲, surface phthalate quantity on uncleansed polyvinyl chloride surface.*

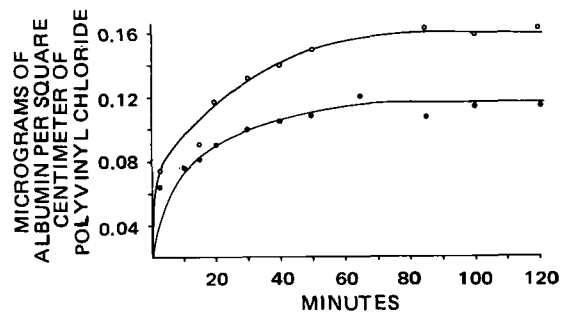

Figure 6—*Competitive adsorption of albumin from protein mixture. Key:* O, *methanol-extracted polyvinyl chloride surfaces; and* ●, *uncleansed polyvinyl chloride surfaces.*

lier studies (23, 24) that adsorbed protein amounts, plateau times, and adsorption rates depend upon the polymer surface. The governing factors might be the hydrophobic interaction between adsorbate and adsorbent, water structuring at the interface, hydrogen bonding, and the configurational entropy of proteins at the adsorbed sites.

In Fig. 6, it can be seen that the less hydrophobic extracted surface contains less phthalate, which increases albumin adsorption. However, the phthalate-containing surface shows an increase in adsorption of γ-globulin and fibrinogen when compared to the extracted surface (Figs. 7 and 8). When calculated on a weight percent basis after 2 min of adsorption, the phthalate-contaminated surface contained 6% albumin, 54% γ-globulin, and 40% fibrinogen; the extracted surface contained 19% albumin, 46% γ-globulin, and 35% fibrinogen. Following this initial determination, the weight percentages tended toward equalization over the 2 hr of observation. From these data, it can be seen that the initial events favor albumin adsorption onto the extracted surface; however, even pure polyvinyl chloride surfaces are not ideal for blood compatibility.

Another remarkable observation concerns the recontamination of the surface after methanol extraction. Polyvinyl chloride surfaces will recover the phthalate from the bulk polymer. After 1 day of exposure to air, 60% of the original quantity of surface I was restored *via* the diffusion process. After 2 days of exposure, 80% of the original quantity of I had diffused to the surface (Fig. 4).

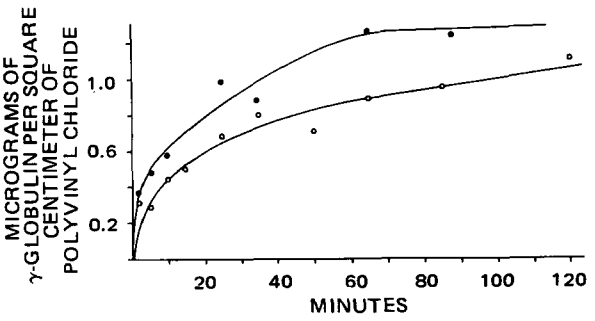

Figure 7—*Competitive adsorption of γ-globulin from protein mixture. Key:* O, *methanol-extracted polyvinyl chloride surfaces; and* ●, *uncleansed polyvinyl chloride surfaces.*

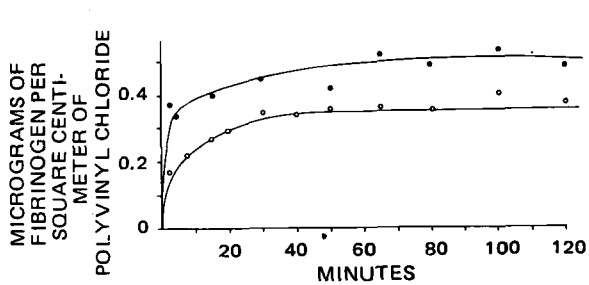

Figure 8—*Competitive adsorption of fibrinogen from protein mixture. Key:* O, *methanol-extracted polyvinyl chloride surfaces; and* ●, *uncleansed polyvinyl chloride surfaces.*

Two fibrinogen adsorption patterns were obtained, one for the original methanol-cleansed surface and the other following 2 days of air exposure after 6 hr of methanol extraction. In the latter, the fibrinogen adsorption pattern was similar to that on unextracted surfaces.

The number of adhered platelets differed for contaminated and extracted surfaces. According to the *ex vivo* study, the platelet counts were 3.1 ± 0.6/20,000 and 13.1 ± 2.8/20,000 μm^2 on methanol-extracted surfaces and untreated surfaces, respectively. Aggregated clumps of platelets also were observed on the untreated surfaces.

Although many extensive studies have been conducted on platelet adhesion and aggregation as related to hemostasis in the physiological environment (25, 26), few workers have focused on the foreign surface and certain chemical agents for aggregation. Since platelet adhesion to a surface and aggregation is the first observable event occurring in blood upon contact with a foreign surface, platelets play a major role in the *in vivo* initiation of thrombus formation on foreign surfaces.

Adenosine diphosphate, thrombin, collagen, and polylysine are platelet-aggregating agents (27). Adsorbed γ-globulin on a surface has been known to induce platelet aggregation on a surface (28). Fibrinogen has been shown to be an important factor for platelet adhesion to glass (29–31). However, it has not been fully explored whether or not plasticizers such as phthalate esters play a role as platelet-aggregating agents in the blood. When blood contacts a foreign surface, plasma proteins adsorb onto the surface until an equilibrium plateau is reached, and this proteinated surface determines the platelet adhesion. It was postulated (32) that glycosyl transferase on a platelet interacts, together with a nucleoside diphosphate monosaccharide and a divalent cation, with a glycoprotein acceptor adsorbed onto the foreign surface. The stability of the complex determines the strength and duration of the adhesion.

It has been shown that adsorbed γ-globulin and fibrinogen can be acceptors for enzyme complex formation while albumin is not. According to previous studies in this laboratory on competitive protein adsorption, the more hydrophobic polymers[5] adsorb fibrinogen and γ-globulin much faster than less hydrophobic polymers like polyurethane and dimethicone rubber (24). *Ex vivo* experiments have shown that about 10 times more platelets adhere to the more hydrophobic surfaces than to the polyurethane surfaces (22).

REFERENCES

(1) A. S. Trimble, B. S. Goldman, J. K. Yao, L. K. Kovats, and W. G. Bigelow, *Surgery*, **59**, 857(1966).

(2) W. L. Guess, J. Jacob, and J. Autian, *Drug Intel.*, **1**, 120(1967).

(3) W. L. Guess and S. Haberman, *J. Biomed. Mater. Res.*, **2**, 313(1968).

(4) R. J. Jaeger, Ph.D. dissertation, Johns Hopkins University, Baltimore, Md., 1971.

(5) R. J. Jaeger and R. J. Rubin, *Environ. Health Perspec.*, **3**, 53(1973).

(6) R. J. Jaeger and R. J. Rubin, *N. Engl. J. Med.*, **287**, 1114(1972).

(7) R. J. Jaeger and R. J. Rubin, *Environ. Health Perspec.*, **3**, 95(1973).

(8) M. S. Jacobson, R. Parkman, L. N. Button, R. J. Jaeger, and S. V. Kevy, *Res. Commun. Chem. Pathol. Pharmacol.*, **9**, 315(1974).

(9) J. Vessman and G. Rietz, *Int. Congr. IABS, 13th, Part A*, **27**, 205(1974).

(10) C. R. Valeri, T. J. Contreras, H. Feingold, R. H. Sheilby, and R. J. Jaeger, *Environ. Health Perspec.*, **3**, 102(1973).

(11) Y. L. Marcel and S. P. Noel, *Chem. Phys. Lipids*, **4**, 418(1970).

(12) R. E. Easterling, E. Johnson, and E. A. Napier, Jr., *Proc. Soc. Exp. Biol. Med.*, **147**, 572(1974).

(13) R. J. Jaeger and R. J. Rubin, *Science*, **170**, 460(1970).

(14) C. O. Schulz and R. J. Rubin, *Environ. Health Perspec.*, **3**, 123(1973).

[5] Teflon FEP.

(15) J. Autian, *ibid.*, **4**, 3(1973).
(16) L. S. Hillman, S. L. Goodwin, and W. R. Sherman, *N. Engl. J. Med.*, **292**, 381(1975).
(17) J. Mes, D. E. Coffin, and D. S. Campbell, *Bull. Environ. Contam. Toxicol.*, **12**, 721(1974).
(18) *Chem. Eng. News*, **Feb. 15, 1971**, 12.
(19) J. J. McNamara, M. D. Molot, and J. F. Stremple, *Ann. Surg.*, **172**, 334(1970).
(20) R. T. Solis and M. B. Gibbs, *Transfusion*, **12**, 245(1972).
(21) R. V. Moseley and D. B. Doty, *Ann. Surg.*, **171**, 329(1970).
(22) S. W. Kim, R. G. Lee, H. Oster, D. Coleman, J. D. Andrade, D. Lentz, and D. Olsen, *Trans. Amer. Soc. Artif. Int. Organs*, **20**, 449(1974).
(23) R. G. Lee and S. W. Kim, *J. Biomed. Mater. Res.*, **8**, 251(1974).
(24) R. G. Lee, C. Adamson, and S. W. Kim, *Thromb. Res.*, **4**, 485(1974).
(25) "Platelet Function and Thrombosis," P. M. Mannucci and S. Gorin, Eds., Plenum, New York, N.Y., 1972.
(26) "Platelet and Thrombosis," S. Sherry and A. Scriabine, Eds., University Park Press, Baltimore, Md., 1974.
(27) E. W. Salzman, *Fed. Proc.*, **30**, 1503(1971).
(28) M. A. Packham, G. Evans, M. F. Glynn, and J. F. Mustard, *J. Lab. Clin. Med.*, **73**, 686(1969).
(29) J. F. Mustard, M. F. Glynn, E. E. Nishizawa, and M. A. Packham, *Fed. Proc.*, **26**, 106(1967).
(30) R. G. Mason, M. S. Read, and K. M. Brinkhous, *Proc. Soc. Exp. Biol. Med.*, **137**, 680(1971).
(31) L. Vroman and A. L. Adams, *J. Biomed. Mater. Res.*, **3**, 43(1969).
(32) R. G. Lee and S. W. Kim, *ibid.*, **8**, 393(1974).

ACKNOWLEDGMENTS AND ADDRESSES

Received May 7, 1975, from the *Department of Applied Pharmaceutical Sciences, College of Pharmacy, University of Utah, Salt Lake City, UT 84112*

Accepted for publication July 16, 1975.

Supported in part by Contract NIH-NHLI-73-2908-B and in part by Grant PO1-HL-13738-04 (National Heart and Lung Institute).

The authors thank Dr. H. Oster and Dr. D. Olsen for their contributions to this work.

[x] To whom inquiries should be directed.

High-Pressure Liquid Chromatographic Determination of the 15-Epimer of Dinoprost in Bulk Drug

T. J. ROSEMAN [x], S. S. BUTLER, and S. L. DOUGLAS

Abstract □ The *p*-nitrophenacyl esters of dinoprost and its 15-epimer are well resolved using high-pressure liquid chromatography. Quantitation was achieved using the internal standard technique. The specially synthesized diphenylurea ester of cholic acid was found to be a model internal standard. Graphs of peak height ratios of the prostaglandin to the internal standard were linear with respect to the amount of prostaglandin injected, with the lower detection limit of the 15-epimer being about 0.5%. Data are presented that demonstrate the usefulness of this analytical technique in determining the concentration of the 15-epimer present during studies on the kinetics of decomposition of dinoprost.

Keyphrases □ Dinoprost—high-pressure liquid chromatographic analysis of 15-epimer in bulk drug □ High-pressure liquid chromatography—analysis, dinoprost and its 15-epimer □ Prostaglandins—dinoprost and its 15-epimer, analysis, high-pressure liquid chromatography

Development of stability-indicating assays is necessary for evaluating the feasibility of pharmaceutical dosage forms before clinical testing programs are initiated. Prostaglandins, for example, are being developed in many different drug delivery systems (1), *e.g.*, solutions, suppositories, and tablets, where the spectrum of decomposition products depends upon the particular prostaglandin and dosage form. To obtain accurate rate constants for the decomposition process, more than one analytical technique may be needed to distinguish between various degradation products.

A case in point is the separation and quantitation of the 15-epimer of dinoprost in the presence of dinoprost. It was reported previously that dilute solutions of dinoprost are unstable in acidic media (2), with a major route of degradation being epimerization of the C-15 hydroxyl group[1]. To date, the 15-epimer has not been resolved from dinoprost by GLC (3), but it can be separated by TLC in a reported solvent system (4).

Recently, however, radioisotopically labeled methyl esters were used to determine the 15-epimer content in a prostaglandin closely related to dinoprost (3), while the 15-epimer content in bulk dinoprost was determined using a refractive index detector on a high-pressure liquid chromatograph (5). High-pressure liquid chromatography (HPLC) was used to detect and quantitate various prostaglandins (6).

Utilizing the discovery that prostaglandins can be rapidly converted to *p*-nitrophenacyl esters for HPLC (7), a procedure is presented that quantitatively separates the 15-epimer from naturally occurring dinoprost. The procedure involves the reaction of the carboxylic acid group of the prostaglandin with *p*-nitrophenacyl bromide to yield the UV-absorbing *p*-nitrophenacyl ester. The derivatives are well separated and are quantitated using the internal standard technique. This analytical procedure is not only useful in calculating the amount of 15-epimer in bulk dinoprost but also can be utilized to determine the concentration of the 15-epimer in solution during studies on the kinetics of decomposition of dinoprost.

[1] T. J. Roseman, unpublished data.

(15) J. Autian, *ibid.*, **4**, 3(1973).
(16) L. S. Hillman, S. L. Goodwin, and W. R. Sherman, *N. Engl. J. Med.*, **292**, 381(1975).
(17) J. Mes, D. E. Coffin, and D. S. Campbell, *Bull. Environ. Contam. Toxicol.*, **12**, 721(1974).
(18) *Chem. Eng. News*, **Feb. 15, 1971**, 12.
(19) J. J. McNamara, M. D. Molot, and J. F. Stremple, *Ann. Surg.*, **172**, 334(1970).
(20) R. T. Solis and M. B. Gibbs, *Transfusion*, **12**, 245(1972).
(21) R. V. Moseley and D. B. Doty, *Ann. Surg.*, **171**, 329(1970).
(22) S. W. Kim, R. G. Lee, H. Oster, D. Coleman, J. D. Andrade, D. Lentz, and D. Olsen, *Trans. Amer. Soc. Artif. Int. Organs*, **20**, 449(1974).
(23) R. G. Lee and S. W. Kim, *J. Biomed. Mater. Res.*, **8**, 251(1974).
(24) R. G. Lee, C. Adamson, and S. W. Kim, *Thromb. Res.*, **4**, 485(1974).
(25) "Platelet Function and Thrombosis," P. M. Mannucci and S. Gorin, Eds., Plenum, New York, N.Y., 1972.
(26) "Platelet and Thrombosis," S. Sherry and A. Scriabine, Eds., University Park Press, Baltimore, Md., 1974.
(27) E. W. Salzman, *Fed. Proc.*, **30**, 1503(1971).
(28) M. A. Packham, G. Evans, M. F. Glynn, and J. F. Mustard, *J. Lab. Clin. Med.*, **73**, 686(1969).
(29) J. F. Mustard, M. F. Glynn, E. E. Nishizawa, and M. A. Packham, *Fed. Proc.*, **26**, 106(1967).
(30) R. G. Mason, M. S. Read, and K. M. Brinkhous, *Proc. Soc. Exp. Biol. Med.*, **137**, 680(1971).
(31) L. Vroman and A. L. Adams, *J. Biomed. Mater. Res.*, **3**, 43(1969).
(32) R. G. Lee and S. W. Kim, *ibid.*, **8**, 393(1974).

ACKNOWLEDGMENTS AND ADDRESSES

Received May 7, 1975, from the *Department of Applied Pharmaceutical Sciences, College of Pharmacy, University of Utah, Salt Lake City, UT 84112*

Accepted for publication July 16, 1975.

Supported in part by Contract NIH-NHLI-73-2908-B and in part by Grant PO1-HL-13738-04 (National Heart and Lung Institute).

The authors thank Dr. H. Oster and Dr. D. Olsen for their contributions to this work.

[x] To whom inquiries should be directed.

High-Pressure Liquid Chromatographic Determination of the 15-Epimer of Dinoprost in Bulk Drug

T. J. ROSEMAN [x], S. S. BUTLER, and S. L. DOUGLAS

Abstract □ The *p*-nitrophenacyl esters of dinoprost and its 15-epimer are well resolved using high-pressure liquid chromatography. Quantitation was achieved using the internal standard technique. The specially synthesized diphenylurea ester of cholic acid was found to be a model internal standard. Graphs of peak height ratios of the prostaglandin to the internal standard were linear with respect to the amount of prostaglandin injected, with the lower detection limit of the 15-epimer being about 0.5%. Data are presented that demonstrate the usefulness of this analytical technique in determining the concentration of the 15-epimer present during studies on the kinetics of decomposition of dinoprost.

Keyphrases □ Dinoprost—high-pressure liquid chromatographic analysis of 15-epimer in bulk drug □ High-pressure liquid chromatography—analysis, dinoprost and its 15-epimer □ Prostaglandins—dinoprost and its 15-epimer, analysis, high-pressure liquid chromatography

Development of stability-indicating assays is necessary for evaluating the feasibility of pharmaceutical dosage forms before clinical testing programs are initiated. Prostaglandins, for example, are being developed in many different drug delivery systems (1), *e.g.*, solutions, suppositories, and tablets, where the spectrum of decomposition products depends upon the particular prostaglandin and dosage form. To obtain accurate rate constants for the decomposition process, more than one analytical technique may be needed to distinguish between various degradation products.

A case in point is the separation and quantitation of the 15-epimer of dinoprost in the presence of dinoprost. It was reported previously that dilute solutions of dinoprost are unstable in acidic media (2), with a major route of degradation being epimerization of the C-15 hydroxyl group[1]. To date, the 15-epimer has not been resolved from dinoprost by GLC (3), but it can be separated by TLC in a reported solvent system (4).

Recently, however, radioisotopically labeled methyl esters were used to determine the 15-epimer content in a prostaglandin closely related to dinoprost (3), while the 15-epimer content in bulk dinoprost was determined using a refractive index detector on a high-pressure liquid chromatograph (5). High-pressure liquid chromatography (HPLC) was used to detect and quantitate various prostaglandins (6).

Utilizing the discovery that prostaglandins can be rapidly converted to *p*-nitrophenacyl esters for HPLC (7), a procedure is presented that quantitatively separates the 15-epimer from naturally occurring dinoprost. The procedure involves the reaction of the carboxylic acid group of the prostaglandin with *p*-nitrophenacyl bromide to yield the UV-absorbing *p*-nitrophenacyl ester. The derivatives are well separated and are quantitated using the internal standard technique. This analytical procedure is not only useful in calculating the amount of 15-epimer in bulk dinoprost but also can be utilized to determine the concentration of the 15-epimer in solution during studies on the kinetics of decomposition of dinoprost.

[1] T. J. Roseman, unpublished data.

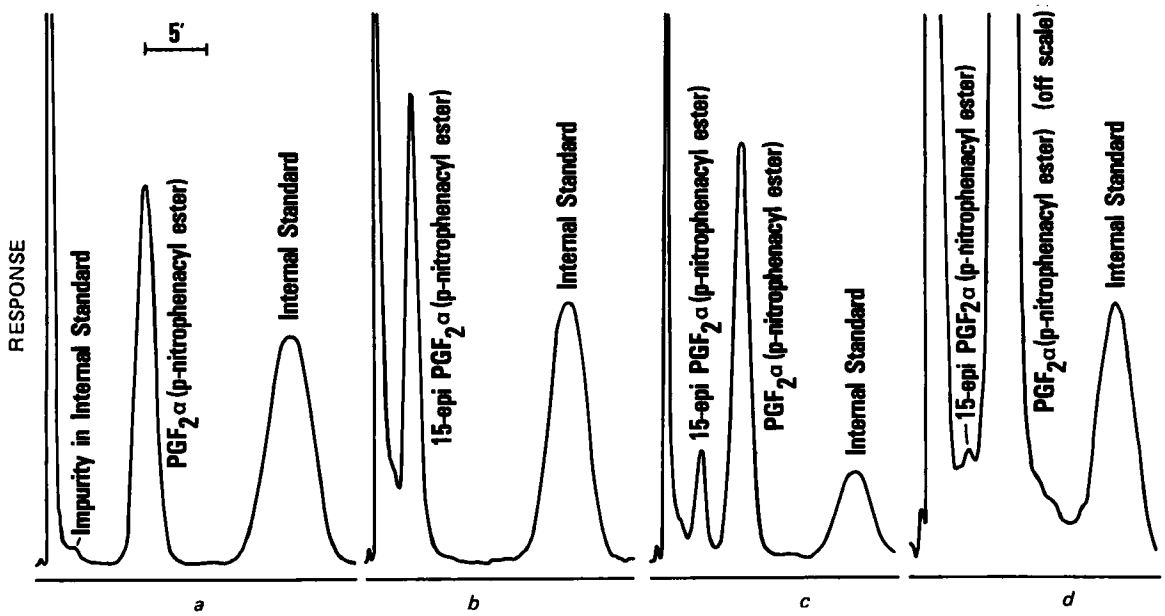

Figure 1—*High-pressure liquid chromatograms of* p-*nitrophenacyl esters of dinoprost ($PGF_{2\alpha}$) and its 15-epimer (15-epi $PGF_{2\alpha}$). (a and b) Concentration of internal standard = 3.75 mg/ml, attenuation = 16 × 10^{-2} aufs, and amount injected = 20 μg. (c) Concentration of internal standard = 1.25 mg/ml, attenuation = 16 × 10^{-2} aufs, and percent of 15-epimer = 16.7. (d) Concentration of internal standard = 0.42 mg/ml, attenuation = 2 × 10^{-2} aufs, and percent of 15-epimer = 1.0.*

EXPERIMENTAL

The prostaglandins[2], dinoprost, dinoprost tromethamine salt, and the 15-epimer were of high purity, being at least 99% pure by GLC and showing only one major zone by TLC. All of the solvents used were "distilled in glass" quality.

Preparation of Samples for Standard Curves—Samples for response curves were prepared from 5-mg/ml stock solutions of dinoprost (free acid) or its 15-epimer in chloroform. Aliquots of the stock solutions were pipetted into small vials and dried under nitrogen to yield the desired amount of prostaglandin.

The *p*-nitrophenacyl esters of dinoprost and its 15-epimer were prepared in the manner reported previously (7) as follows (Scheme I). Samples were dissolved in 0.5 ml of acetonitrile containing 12.2 mg/ml of *p*-nitrophenacyl bromide[3]. Then 5.6 μl of bis(isopropyl)ethylamine[4] (distilled one time) was added, and the mixture was allowed to react for 30 min at room temperature. Then 0.5 ml of the internal standard solution, 0.83–7.5 mg/ml of cholic acid diphenylurea ester in methanol, was added to the sample. Methanol was used to keep the internal standard in solution.

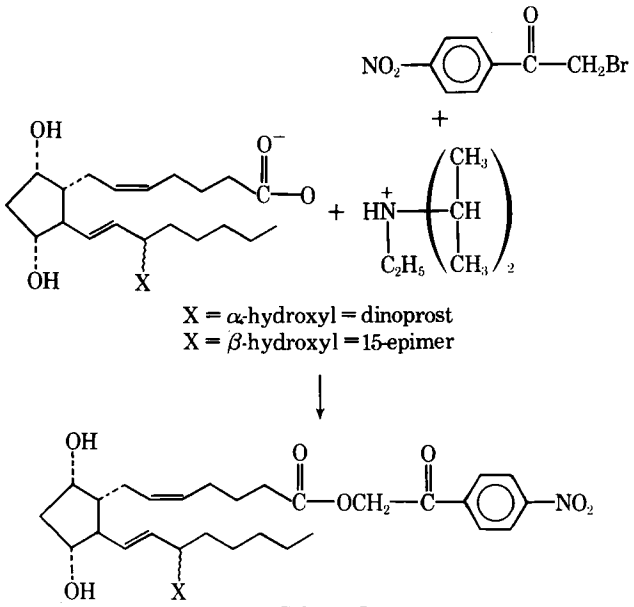

Scheme I

A 4-μl sample was injected into a high-pressure liquid chromatograph[5] within 3 hr under the following conditions: column, 1 m stainless steel (2.1 mm i.d.) packed with 20-μm silica gel[6]; detector, UV 254 nm; temperature, ambient; pressure, 2000 psi; flow rate, ~1 ml/min; and solvent mixture, acetonitrile–methylene chloride–water (50:50:1).

The internal standard concentration was reduced by a factor of three (to 1.25 mg/ml) when a concentration range of 5–20% (w/w) of the 15-epimer in dinoprost was quantitated. A further threefold reduction (to 0.42 mg/ml) was employed for levels below 5%. Samples were chromatographed within 3 hr after the reactants were added, since the ratio of derivatized prostaglandin to internal standard decreased gradually with time, *i.e.*, 15% over 3 days.

Extraction of Prostaglandins from Kinetic Experiments—To check for the presence of the 15-epimer under acidic and basic conditions using HPLC, aqueous solutions were first extracted and then derivatized as described. A 10-ml acidic sample of dinoprost (0.2 mg/ml as the tromethamine salt) from a kinetic run, stored for 30 days at 37° in pH 3.0 citric acid buffer, was pipetted into a 60-ml separator. The solution was then extracted with 3 × 15 ml of chloroform and evaporated to complete dryness with a stream of nitrogen. This extraction procedure yielded complete recovery of the prostaglandins. The dried extract was then derivatized as described.

For the study in the alkaline milieu, a solution containing 5 mg/ml equivalents of dinoprost as the tromethamine salt was stored for 10 months at 25° at pH 8.0. One milliliter was then placed in a separator, and the pH was lowered to 3 with citric acid buffer. The solution was extracted with 3 × 15 ml of chloroform and then reacted as described after the chloroform was dried under a stream of nitrogen. For this experiment, a reference sample was prepared by dissolving 5-mg equivalents of dinoprost as the tromethamine salt, in 1 ml of water and then extracted and analyzed as already described.

Synthesis of Internal Standard—The internal standard, cholic acid *p*-(3′-phenylureido)phenyl ester, commonly called the di-

[2] Obtained from the Pharmaceutical Research and Development Division, The Upjohn Co.

[3] 2-Bromo-4′-nitroacetophenone, practical grade, Eastman Organic Chemicals, Rochester, NY 14650

[4] Pfaltz-Bauer Co., Flushing, NY 11368

[5] Dupont 830 liquid chromatograph, DuPont Co., Wilmington, DE 19898

[6] LiChrosorb SI60, EM Laboratories, Inc., Elmsford, NY 10523. See Ref. 7 for the silica wash procedure.

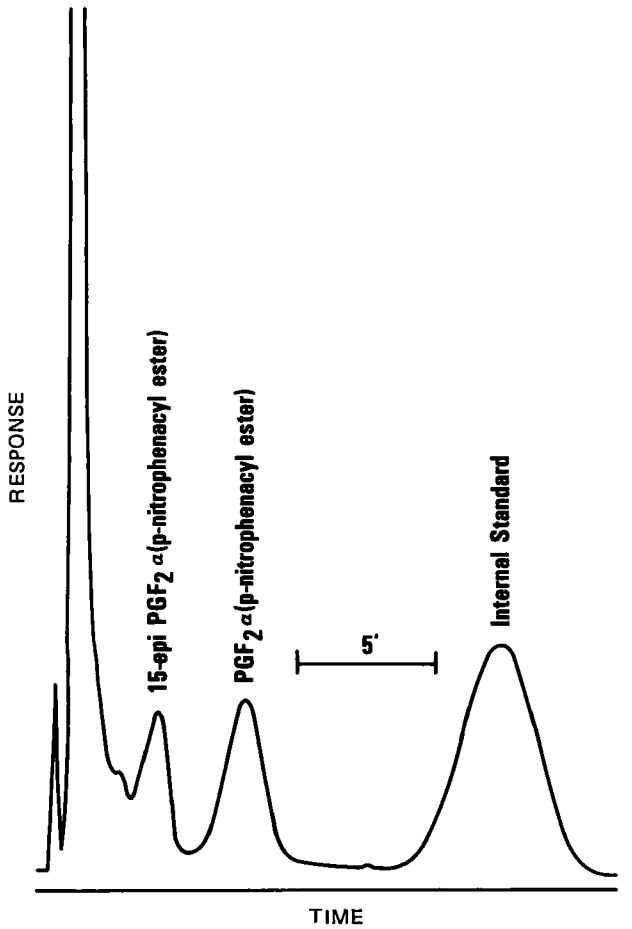

Figure 2—*Chromatogram of extracted sample from a kinetic experiment at pH 3.0. Internal standard concentration was 1.25 mg/ml, and the attenuation setting was 16 × 10^{-2} aufs.*

phenylurea ester of cholic acid, was prepared in the following manner.

A suspension of 4.0 g of cholic acid[7] in 50 ml of dry acetone was treated with 1.39 ml of triethylamine[8]. Immediate crystallization of the triethylamine salt occurred. While under a nitrogen atmosphere, the suspension was cooled to −10° and 1.35 ml of isobutyl chloroformate[9] was added. The mixture was maintained at −5–0° for 6 min before 2.2 g of *p*-hydroxydiphenylurea[10] in 15 ml of dry pyridine was added.

After 15 min at room temperature, the reaction mixture was diluted with 150 ml of ethyl acetate and washed with 2 × 150 ml of aqueous 5% citric acid followed by 2 × 100 ml of 0.1 *N* Na_2HPO_4[11] at pH 7.5. The organic phase was dried (sodium sulfate[11]) and evaporated to dryness. The compound was dissolved in 10 ml of chloroform–acetonitrile (3:7), filtered through 20 g of silica gel[12], and washed with 50 ml of the same solvent. The filtrate was concentrated and chromatographed over 300 g of silica gel 60.

The column was eluted with chloroform–acetonitrile (3:7) followed by chloroform–acetonitrile (1:4), acetonitrile, and, finally, acetonitrile–methanol (95:5). The first 1500 ml of eluent was discarded, and the product was found in the following 2000-ml fraction.

Evaporation of the solvent from the product fraction gave a white residue. This residue was crystallized from acetone by the addition of water, affording 0.85 g of product, mp 218–219°.

Anal.—Calc. for $C_{37}H_{50}N_2O_6$: C, 71.82; H, 8.14; N, 4.52. Found: C, 71.38; H, 7.61; N, 4.31.

[7] Nutritional Biochemicals Corp., Cleveland, OH 44128
[8] Matheson, Coleman and Bell, Norwood, OH 45212
[9] Eastman Organic Chemicals, Rochester, NY 14650
[10] Synthesized by reacting *p*-aminophenol with phenyl isocyanate, mp 218.8–220.3°.
[11] Analytical reagent, Mallinckrodt Chemical Works, St. Louis, MO 63160
[12] EM Laboratories, Elmsford, NY 10523

Table I—Peak Height Ratio (Prostaglandin–Internal Standard) of *p*-Nitrophenacyl Esters of Dinoprost and Its 15-Epimer as a Function of the Amount of Prostaglandin Injected

Micrograms Injected	Peak Height Ratio
Dinoprost	
1.22	0.098
4.12	0.342
12.4	0.982
20.8	1.77
15-Epimer	
0.40	0.039
2.00	0.210
4.00	0.350
12.0	1.08
20.0	1.84

Table II—Peak Height Ratio (Prostaglandin–Internal Standard) for the 15-Epimer (*p*-Nitrophenacyl Ester) in the Presence of Dinoprost (*p*-Nitrophenacyl Ester) for Low and High Concentrations of the 15-Epimer

Percent 15-Epimer Present	Peak Height Ratio
Low Concentration[a]	
0.50	0.056
1.0	0.125
2.0	0.273
High Concentration[b]	
2.0	0.150
5.7	0.413
9.1	0.652
16.7	1.21

[a] Internal standard concentration was 0.42 mg/ml, and attenuation was 2 × 10^{-2} aufs. [b] Internal standard concentration was 1.25 mg/ml, and attenuation was 16 × 10^{-2} aufs.

RESULTS AND DISCUSSION

Figure 1 shows typical chromatograms of dinoprost, its 15-epimer, and a mixture of the two. Baseline separation was achieved, with the epimer following directly after the solvent front. The internal standard, the diphenylurea ester of cholic acid, was nicely resolved after the dinoprost peak.

The use of an internal standard is quite helpful when quantitative studies are required. In this study, selection of an appropriate standard was a formidable task because (*a*) it should not decompose in the reaction medium, (*b*) it must be soluble in the reaction medium, and (*c*) it should have a retention time greater than dinoprost and yet elute in a reasonable time. This last requirement is necessary because the *p*-nitrophenacyl ester of the 15-epimer elutes before the ester of dinoprost and it would be difficult to resolve the internal standard peak in this region.

As a first attempt, many standard laboratory chemicals were chromatographed but did not meet these requirements. Since cholic acid has similar physicochemical properties as dinoprost (8), cholic acid derivatives were explored as possible internal standards. Commercially available compounds such as cholic acid, deoxycholic acid, and glycolic acid were unacceptable, so derivatives were synthesized. As shown in Fig. 1, the diphenylurea ester of cholic acid had sufficient polarity to yield an ideal retention time, and it did not degrade in the reaction medium. However, methanol was required to maintain it in solution.

Standard Curves—Table I lists the ratio of the peak heights of dinoprost and its 15-epimer to the internal standard height as a function of the amount of prostaglandin injected. Response curves were linear with respect to the amount injected in the regions under consideration. A plot of this ratio for the 15-epimer *versus* the percent of epimer present was also linear, as reflected by the data in Table II. The slope of this standard curve for the 15-epimer in the presence of dinoprost was comparable (within 13%) to that of the 15-epimer alone.

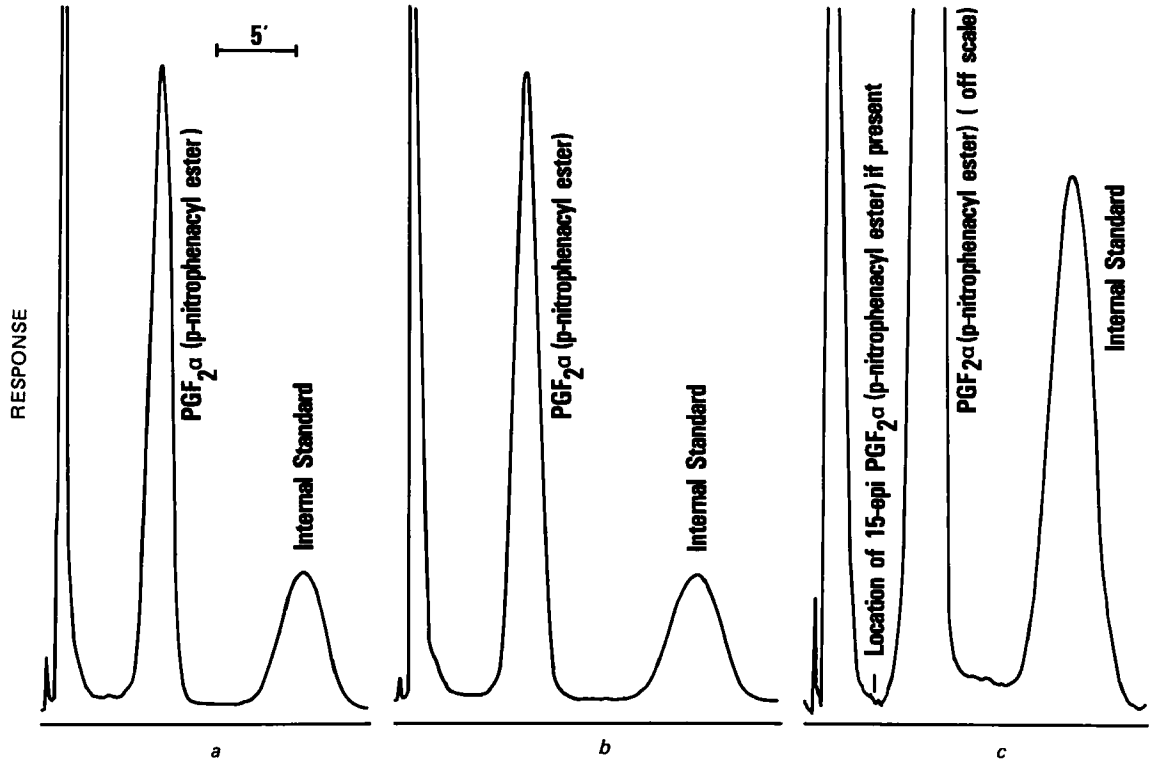

Figure 3—*High-pressure liquid chromatograms of the* p-*nitrophenacyl ester of dinoprost ($PGF_{2\alpha}$) from pH 8.0 solution stored for 10 months at 25°. Chromatograms do not show the presence of the 15-epimer (15-epi $PGF_{2\alpha}$). (a) Concentration of internal standard = 1.25 mg/ml, attenuation = 16 × 10^{-2} aufs, and sample was extracted standard of dinoprost tromethamine. (b) Concentration of internal standard = 1.25 mg/ml, attenuation = 16 × 10^{-2} aufs, and sample was extracted from solution stored at pH 8.0 for 10 months at 25°. (c) Concentration of internal standard = 1.25 mg/ml, attenuation = 4 × 10^{-2} aufs, and sample was extracted from solution stored at pH 8.0 for 10 months at 25°.*

To detect accurately 15-epimer concentrations of less than 2% (w/w) in dinoprost, it was necessary to lower the attenuation setting from 16 × 10^{-2} to 2 × 10^{-2} aufs and to lower the concentration of the internal standard. Linearity was achieved to a lower detectable limit of about 0.5% (Table II), which is an improvement over the level of detection reported previously (5). However, the slopes of the low and high concentration plots from the table were not equal (after accounting for differences in internal standard concentration). Presumably, this result was due to the significant baseline shifts that occur at high sensitivity settings (Fig. 1). Therefore, prostaglandin standards should be run under identical chromatographic conditions as the unknowns.

Determination of 15-Epimer Content in Acidic and Basic Dinoprost Solutions—Under acidic conditions, dinoprost forms the 15-epimer[1]. The epimer is not resolved by GLC but can be separated by TLC using the solvent system[13] of Hamberg and Samuelsson (4). One method to quantitate the epimer concentration requires the preliminary TLC separation followed by derivatization (silylation) for subsequent GLC analysis (9). This tedious process can be circumvented by using the one-step HPLC procedure described.

Figure 2 shows the chromatogram (HPLC) of an extracted dinoprost sample (after derivatization); the sample was stored at 37° for 30 days at pH 3.0. Two peaks were observed with retention times equal to dinoprost and its 15-epimer. Quantitation of the 15-epimer concentration showed that 40% conversion had taken place. In adsorption chromatography, it is expected that the less polar C-15 prostaglandin dehydration products, which also form under acidic conditions, elute in the solvent front.

In contrast to the solution stored under acidic conditions, the chromatograms in Fig. 3 show that at pH 8.0 no 15-epimer was detectable, even after 10 months of storage at 25°. In fact, when using this HPLC technique, dinoprost assayed at 103% of theory, indicating that dinoprost is quite stable under these circumstances.

The results of this investigation demonstrate that (*a*) the *p*-nitrophenacyl ester of 15-epimer of dinoprost can be used to determine its content in bulk dinoprost with HPLC and (*b*) this technique can be used to determine the concentration of the 15-epimer in dinoprost solutions stored for prolonged periods.

[13] Ethyl acetate–acetic acid–2,2,4-trimethylpentane–water (90:20:50:100); upper phase used.

REFERENCES

(1) T. O. Oesterling, W. Morozowich, and T. J. Roseman, *J. Pharm. Sci.*, **61**, 1861(1972).

(2) S. M. M. Karim, J. Devlin, and K. Hillier, *Eur. J. Pharmacol.*, **4**, 416(1968).

(3) M. F. Jones, *J. Pharm. Pharmacol.*, **25**, 900(1973).

(4) M. Hamberg and B. Samuelsson, *J. Biol. Chem.*, **241**, 257(1966).

(5) N. M. Weinshenker and A. Longwell, *Prostaglandins*, **2**, 207(1972).

(6) N. H. Andersen and E. M. K. Leovey, *ibid.*, **6**, 361(1974).

(7) W. Morozowich and S. L. Douglas, *ibid.*, **10**, 19(1975).

(8) T. J. Roseman and S. H. Yalkowsky, *J. Pharm. Sci.*, **62**, 1680(1973).

(9) T. J. Roseman, B. Sims, and R. G. Stehle, *Amer. J. Hosp. Pharm.*, **30**, 236(1973).

ACKNOWLEDGMENTS AND ADDRESSES

Received April 18, 1975, from the *Pharmacy Research Unit, The Upjohn Company, Kalamazoo, MI 49001*

Accepted for publication July 16, 1975.

Valuable discussions with Dr. Walter Morozowich were appreciated.

[x] To whom inquiries should be directed.

Effect of Edetate Disodium and Reduced Glutathione on Absorption of Acetazolamide from GI Tract of Rats

RONALD D. SCHOENWALD ˣ and RICHARD L. WARD

Abstract □ The absorption of acetazolamide suspensions from *in situ* rat gastric and intestinal loop segments was studied. In 1 hr, 66.2 and 64.3% remained unabsorbed from the rat stomach and intestine, respectively. Although 1% (w/v) reduced glutathione and 1% (w/v) (24 m*M*) edetate disodium had no effect on gastric absorption, drug absorption from the rat intestine (1 hr) was increased 1.5 and 2 times, respectively. It was hypothesized that the relatively poor intestinal absorption was due primarily to the formation of a pH-dependent (pH 4.5–10), nonabsorbable complex between acetazolamide and carbonic anhydrase present in the gut and that reduced glutathione acted as an inhibitor to promote intestinal absorption. Equilibrium dialysis studies showed that reduced glutathione could reduce the fraction of drug bound to human carbonic anhydrase B by one-half when present in a molar ratio 10 times that of acetazolamide; edetate disodium had no effect on the *in vitro* binding. It was, therefore, assumed that edetate disodium promoted an increase in intestinal absorption by altering the permeability of intestinal epithelium. Based upon present experimentation, however, the alteration of intestinal epithelium by reduced glutathione cannot be ruled out.

Keyphrases □ Acetazolamide—GI absorption, effect of edetate disodium and reduced glutathione, rats □ Edetate disodium—effect on GI absorption of acetazolamide, rats □ Glutathione, reduced—effect on GI absorption of acetazolamide, rats □ Absorption, GI—acetazolamide, effect of edetate disodium and reduced glutathione, rats

There is little information in the literature regarding the bioavailability of acetazolamide preparations. However, a plasma level comparison was presented recently (1) in which 500-mg acetazolamide compressed tablets and 500-mg sustained-release granules in capsule form were crossed over in human subjects. By comparing areas under the plasma level–time curves, it was found that the bioavailability of the sustained-release preparation was approximately one-half that of an equal dose of compressed tablets. Another study (2) reported nearly identical results.

One explanation for the reduced bioavailability of the sustained-release dosage form is that the intestinal transit time of the slow-release granules occurs at a rate faster than the drug can be released and subsequently absorbed, assuming the drug to be absorbed over a large portion of the small intestine. Conceivably, a preferential absorption site exists for acetazolamide. If acetazolamide is absorbed from a relatively small segment of the GI tract, then releasing drug after the slow release granules have passed that site would give a decreased extent of absorption compared to a rapidly dissolving tablet that releases drug before the site is reached.

The latter theory becomes more attractive by considering the results of a study by Coleman (3). In this study, the binding of acetazolamide to human carbonic anhydrase B was characterized at 4° at pH 2–11. Maximum binding occurred at pH 7, producing a 1:1 complex with an association constant of 1.25×10^7 L/M. At pH 4.5 and 10, only about 0.25 mole of acetazolamide was bound/mole of enzyme when free acetazolamide was equimolar to the enzyme at 2×10^{-5} M.

Since the GI pH is 1–3 in the stomach but occasionally as high as 5 following a meal and is 5–8 in the intestine (4), it is possible, based upon pH, that acetazolamide absorption in the intestine could be hindered by binding to carbonic anhydrase, if a sufficient concentration of enzyme existed. The concentration of carbonic anhydrase in the rat GI tract was reported (5) to be (μmoles/g wet tissue): stomach, 122; duodenum, 1.3; jejunum, 0.44; ileum, 0.32; and colon, 5.9. Although the enzyme is located intracellularly, normal extrusion of cells from human villi accounts for 250 g released into the intestine daily (6). Acetazolamide, bound to as large a molecule as carbonic anhydrase (mol. wt. = 30,000), would not be expected to transverse biological membranes passively.

Additional work by Coleman (3) showed that the binding was not only reversible and pH dependent but could be inhibited by cyanide and sulfide anions and required zinc ion. With this information, it was proposed that reduced glutathione, which contains a reactive sulfhydryl group, or edetate disodium, a chelating agent for zinc ion, could sufficiently inhibit the binding of acetazolamide and carbonic anhydrase and thus promote an increase in the rate and extent of absorption of acetazolamide in the intestine.

The present study was undertaken to examine the effects of reduced glutathione and edetate disodium on the GI absorption of acetazolamide from ligated loops of the rat GI tract.

EXPERIMENTAL

Test Animals—Male, Charles River strain rats, 240–340 g, were used for the absorption studies. The rats were fasted 14–20 hr prior to a given experiment, but water was allowed *ad libitum*.

Apparatus and Reagents—Acetazolamide USP[1], reduced glutathione[2], and human carbonic anhydrase B[3] were used as received. All other chemicals were reagent grade. A pH meter[4] and a ratio recording spectrophotometer[5] were used.

Solubility Determinations—Saturated solutions of acetazolamide in pH 4.0 McIlvaine's citrate buffer and pH 7.0 Sorensen's phosphate buffer were prepared at 25 and 37° and equilibrated for 24 hr in a shaker bath in the presence of excess acetazolamide. Aliquots were appropriately diluted with 0.1 N sodium hydroxide, and the absorbances were determined at 288 nm.

Drug Preparation—Drug suspensions were prepared by plac-

[1] Lederle Laboratories, Pearl River, N.Y.
[2] K and K Laboratories, Plainview, N.Y.
[3] Sigma Chemical Co., St. Louis, Mo.
[4] Beckman Zeromatic II.
[5] Beckman DK-2A.

ing 125 mg of acetazolamide in a 10-ml syringe and diluting to 5 ml with either McIlvaine's citrate buffer (pH 4.0) or Sorensen's phosphate buffer (pH 7.0) to give a final drug concentration of 25 mg/ml. Suspensions were also prepared containing 1% (w/v) reduced glutathione or 1% (w/v) edetate disodium, both of which dissolved in the buffer systems. Sodium chloride was added to maintain isotonicity. The suspensions were prepared 2–3 hr prior to use and shaken for maximum dissolution to take place.

***In Situ* Absorption Procedure**—The method of Levine *et al.* (7) was employed to study the absorption of acetazolamide from the GI tract of rats. In this procedure, the rats were anesthetized with urethan (1 g/kg ip). For the studies involving the stomach, ligatures were made proximal to the cardiac and pyloric sphincters. The pyloric ligature was tied; but prior to tying off the cardiac ligature, the drug suspension was injected into the stomach by means of a syringe and blunt needle.

The intestinal preparation was made by ligating the small intestine 1 cm proximal to the cecum and midway in the jejunum between the arterioles of the first intestinal and jejunal arteries. These positions were chosen because they could be easily reproduced, did not require removal of the intestine from the abdominal cavity, and, therefore, represented a minimal amount of handling.

Drug suspension was introduced *via* the jejunal ligature just prior to tying. After 60 min, either the tied stomach or intestinal segments were excised, cut open to expose the residual acetazolamide, and washed repeatedly with about 20 ml of a pH 9–10 sodium hydroxide solution. The solution was brought to a final volume of 25.0 ml and subsequently assayed for acetazolamide content.

Equilibrium Dialysis Studies—The binding of acetazolamide to carbonic anhydrase was determined using a dialyzing system consisting of a cylindrical plexiglass cell separated into two compartments (5-ml capacity on each side) by a dialyzing membrane[6]. The membranes were stored in isotonic buffer overnight and rinsed with fresh buffer before use. Acetazolamide was dissolved in isotonic pH 4.0 or 7.0 buffer and pipetted into one compartment of the cell, designated the external compartment.

The internal compartment contained human carbonic anhydrase and in some cases reduced glutathione or edetate disodium. Equilibrium dialysis was carried out at 37° for approximately 36 hr in a water bath equipped with a shaker[7]. The extent of binding was calculated from the concentration of free acetazolamide on the external side.

Analytical Methods—A 0.25-ml lumen sample was placed into a 5-ml volumetric flask and brought to volume with 0.1 *N* HCl. Then 2 ml was transferred to a 25-ml screw-capped glass culture tube, and 5 ml of isobutyl alcohol was added to extract the acetazolamide[8]. The two phases were shaken together for 5 min and centrifuged to facilitate separation of the layers. Then 4 ml of the isobutyl alcohol layer was removed and added to a small beaker containing about 0.5 g of anhydrous sodium sulfate to remove any water solubilized in the alcohol.

The isobutyl alcohol was decanted off, and a quantitative volume (about 3.5 ml) was added to another screw-capped glass culture tube containing 10.0 ml of 0.1 *N* sodium hydroxide. The two phases were shaken for 5 min and centrifuged, and the aqueous layer was measured for acetazolamide content against an appropriate blank at a fixed wavelength of 288 nm.

RESULTS AND DISCUSSION

Assay—To establish the reliability of the double-extraction assay procedure, isotonic buffer solutions were first added to ligated stomach and intestinal loops of the rat. After 60 min, the buffer solutions were collected from the respective loops, spiked with drug in concentrations of 0.2, 0.4, 0.6, and 0.75 mg/ml, and then extracted and assayed for acetazolamide content.

A constant percentage of drug was extracted from the lumen perfused buffers at each concentration, yielding averaged values of 72.5% ± 3.0 (n = 4) and 78.8% ± 4.2 (n = 4) for stomach and intestinal loop preparations, respectively. A nearly identical Beer's law relationship was followed with each set of data. Neither reduced glutathione nor edetate disodium interfered with the absorbance of acetazolamide at 288 nm.

Table I—Solubility of Acetazolamide at pH 4 and 7 and 25 and 37°

Buffer	pH	Solubility[a], mg/ml 25°	37°
McIlvaine's citric acid–phosphate	4.0	0.75 (0.0064)	1.38 (0.010)
Sorensen's phosphate	7.0	0.98 (0.0051)	2.09 (0.0058)

[a] Mean (±*SD*) where n = 3.

Acetazolamide Solubility—Table I gives the results of the solubility measurements at each pH and temperature. As the solvent pH approached the pKa of acetazolamide, 7.2 (8), its solubility improved as might be expected. Because of the limited solubility of acetazolamide at physiological pH values, suspension dosage forms were prepared.

Equilibrium Dialysis Results—Table II lists the concentrations studied as well as the results obtained for the binding of acetazolamide to human carbonic anhydrase at pH 4.0 and 7.0 with and without reduced glutathione and edetate disodium. At pH 7 and 37°, acetazolamide bound to human carbonic anhydrase to the extent of 19.0%[9] when present in a molar ratio (acetazolamide–carbonic anhydrase) of 3.0. By studying the same pH and concentration of acetazolamide and carbonic anhydrase but including reduced glutathione in a molar ratio of 10.0 to acetazolamide, the percent bound was reduced approximately one-half to 10.4%.

Edetate disodium, however, in molar ratios to acetazolamide of 29.0 and 290.0, showed no tendency toward inhibiting the binding at pH 7.0. At pH 4.0[10] and the same molar ratio of acetazolamide–carbonic anhydrase (3.0), no significant binding could be detected. The presence of either reduced glutathione or edetate disodium did not alter the pH 4.0 results.

***In Situ* Absorption Results**—Table III gives the results of the effect of edetate disodium and reduced glutathione on the absorption of acetazolamide from the stomach and intestine. Without the presence of adjuvants, 66.2 and 64.3% remained unabsorbed in the rat gastric and intestinal loop segments, respectively, in 1 hr. Although the duodenum and a section of the jejunum were not included in the intestinal loop segment, the intestinal segment as such would be expected to contain greater surface area and vascularity than the stomach preparation (8).

The relatively low absorption obtained for the intestine conflicts with the generally held belief that drug absorption occurs predominately from the intestine rather than the stomach (7). If it is assumed that the pH–partition hypothesis applies to acetazolamide and that greater vascularity and surface area exist in the intestinal loop than in the gastric loop, one would expect better intestinal absorption for the drug since its higher solubility at pH 7 (37°) permits an approximately equal concentration of unionized species (Table I: 1.38 mg/ml at pH 4 and 37° and 1.28 mg/ml at pH 7 and 37°) compared to pH 4.

In the presence of 1% (w/v) reduced glutathione and 1% (w/v) edetate disodium (24 m*M*), acetazolamide absorption in the stomach was not significantly improved (Table III). However, the intestinal results showed 2 and 1.5 times the extent of absorption at 1 hr when drug suspensions contained edetate disodium and reduced glutathione, respectively; both values were statistically significant. These results are qualitatively in agreement with the equilibrium dialysis results insofar as they support the hypothesis that the binding of carbonic anhydrase and acetazolamide could be inhibited in the presence of reduced glutathione at pH 7, potentially to promote acetazolamide absorption in the intestine but having no consequence on drug absorption from the stomach at pH 4.0.

Even though the stomach (parietal and epithelial cells) has the highest concentration of enzyme, its pH is unfavorable for binding.

[6] Dialyzing cellophane, Union Carbide Corp., New York, N.Y.
[7] American Optical model A002156, Dallas, Tex.
[8] Robert Goldman, Garden Laboratories, Springfield Gardens, N.Y., personal communication.

[9] Acetazolamide was found to bind to the dialysis cell and/or membrane on the order of 5.09 ± 2.1% (n = 5); the fraction bound was corrected accordingly.
[10] Because of the limited solubility of human carbonic anhydrase in pH 4.0 buffer, its concentration was reduced.

Table II—Binding of Acetazolamide to Human Carbonic Anhydrase B in the Presence and Absence of Edetate Disodium and Reduced Glutathione at 37° Using Equilibrium Dialysis

Determination	Concentration[a] Acetazolamide (×10⁵)	Human Carbonic Anhydrase B (×10⁵)	Reduced Glutathione (×10³)	Edetate Disodium (×10²)	pH	Percent Bound[b]
1	8.28	2.76	—	—	4.0[c]	0.930[d] (2.23)
2	8.28	2.76	0.828	—	4.0	0.160[d] (1.63)
3	8.28	2.76	—	1.2	4.0	−0.160[d] (3.30)
4	41.4	13.8	—	—	7.0[e]	19.0 (5.82)
5	41.4	13.8	4.14	—	7.0	10.4 (2.66)
6	41.4	13.8	—	1.2	7.0	20.4 (1.46)
7	41.4	13.8	—	12.0	7.0	19.1 (4.60)

[a] Expressed as molarity. [b] Mean (± *SD*) where $n = 3$ for Determinations 1–3, $n = 4$ for Determinations 4–6, and $n = 2$ for Determination 7. [c] McIlvaine's citric acid–phosphate buffer. [d] Taken as no perceptible binding. [e] Sorensen's phosphate buffer.

Table III—Effect of Edetate Disodium and Reduced Glutathione on Absorbance of Acetazolamide after 1 hr from the Rat Stomach (pH 4.0) and Intestinal (pH 7.0) Loop Segments

Experimental Conditions	Number of Gut Segments	Percent Unabsorbed[a]	*p*
Stomach			
Acetazolamide, pH 4.0[b]	5	66.2 (6.4)	—
Acetazolamide, 1% (w/v) reduced glutathione, pH 4.0	5	55.3 (12.2)	N.S.[c]
Acetazolamide, 1% (w/v) edetate disodium, pH 4.0	5	60.4 (9.52)	N.S.[c]
Intestine			
Acetazolamide, pH 7.0[d]	5	64.3 (3.52)	—
Acetazolamide, 1% (w/v) reduced glutathione, pH 7.0	5	45.4 (14.4)	0.02[e]
Acetazolamide, 1% (w/v) edetate disodium, pH 7.0	5	28.2 (10.4)	0.001[e]

[a] Mean (±*SD*). [b] McIlvaine's citric acid–phosphate buffer. [c] Paired *t*-test, N.S. = nonsignificant or $p > 0.05$ compared to drug alone in the stomach preparation. [d] Sorensen's phosphate buffer. [e] Paired *t*-test, compared to drug alone in intestinal loop segment.

Throughout the small intestine, however, the pH is favorable for maximum binding. The enhancement effect could not be attributed to an increase of acetazolamide solubility in the presence of reduced glutathione or edetate disodium. This was determined in an additional study in which excess acetazolamide was shaken in pH 7 buffer alone and with 1% (w/v) reduced glutathione and 1% (w/v) edetate disodium for 4 hr at 37°, the approximate total length of time the *in vivo* suspension dose was allowed to equilibrate. The solubility determinations, performed in triplicate, were all within a range of 2.0 mg/ml ± 5%.

It is conceivable that glutathione enhanced the *in situ* intestinal absorption of acetazolamide by altering the permeation of intestinal epithelium. Figure 1 depicts the physicochemical events proposed at the intestinal site of absorption. It is assumed that the rate of absorption is proportional to the concentration of free drug in solution, A_f. If it also can be assumed that a rapid, reversible

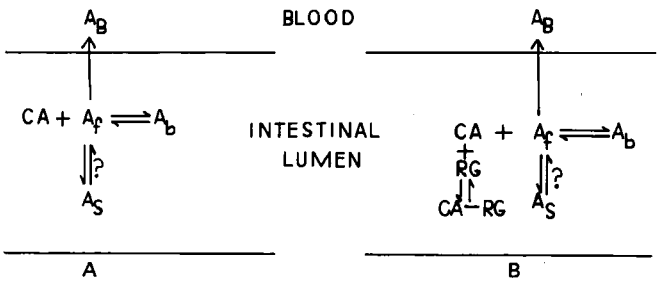

Figure 1—*Schematic representation of the hypothesized competitive mechanisms representing acetazolamide absorption in the rat intestinal tract at pH 7 in the presence (B) and absence (A) of the proposed inhibitor, reduced glutathione (RG). All symbols represent intestinal concentrations, where CA = carbonic anhydrase; A_f = free acetazolamide; A_b = hypothesized, bound, nonabsorbable complex; A_s = excess solid acetazolamide; and CA–RG = bound complex. The symbol ? questions the rapidity with which A_s can dissolve to maintain a constant A_f as free drug is absorbed from the intestinal lumen of the rat (A_B).*

equilibrium exists between the A_f and the postulated nonabsorbable complex of drug and carbonic anhydrase (Fig. 1A) and between A_f and excess solid drug, A_f would be expected to remain constant in spite of the fact that the fraction bound could be altered by the presence of reduced glutathione, RG (Fig. 1B). Excess solid could maintain the A_f regardless of the degree of binding that might occur; hence, the absorption rate and the amount of drug remaining in the intestinal lumen could only increase 1.5 times if the permeability of the absorbing membrane to acetazolamide increased due to the presence of reduced glutathione.

However, it was questioned whether the dissolution process near saturation levels would be rapid enough to maintain the A_f as drug was absorbed. An *in vitro* experiment was conducted to test the assumption that a rapid readjustment of the equilibrium exists between free drug in solution and excess solid under near saturation conditions (2 mg/ml) at 37°. Drug suspensions were prepared by placing 625 mg of acetazolamide into 25 ml of pH 7 buffer in a shaking water bath at 37°. After 3 hr, 1.0 ml of solution was filter pipetted and assayed for drug content; this value represented a zero-time value. Over the following hour, 3.0 ml was removed at 10-min intervals. An appropriate volume of pH 7 buffer was added at each 10-min interval to maintain the original volume of 25 ml.

The drug concentration was determined for each sample that was removed; the experiment was performed in triplicate. This sampling procedure represented an attempt to approximate the net rate that the absorbing membrane was removing drug from the intestinal lumen in the presence of reduced glutathione, *i.e.*, 45% remaining after 1 hr. After 3 hr of shaking at 37°, a concentration of 2.2 ± 0.075 mg/ml was measured. With each succeeding sample, the concentration of acetazolamide was lower. At the end of 1 hr, the concentration measured 1.91 ± 0.0095 mg/ml, which was statistically different from the zero-time value ($p < 0.03$) but greater than one would expect if no dissolution occurred under the experimental conditions or at 1.02 mg/ml.

Consequently, it is feasible that the absorption process occurs at a rate faster than the dissolution process, such that the increased amount of drug absorbed from the intestinal loop in the presence of reduced glutathione could be a consequence of competitive inhibition. However, the alteration of the intestinal epithelium by reduced glutathione cannot be ruled out without further experimen-

tation since the results are also compatible by this mechanism.

Edetate disodium has promoted an increase in intestinal (rat) absorption of salicylate anion (9), phenolsulfonphthalein (10), heparin (11), mannitol (11), inulin (11), decamethonium (11), and sulfanilic acid (11). It has been postulated that edetate disodium alters the aqueous permeability of the intestinal epithelium by depleting magnesium and calcium ions, resulting in separation of the epithelial cells of the rat intestine (12, 13). This mechanism is likewise suspected with acetazolamide, since the lack of effect of edetate disodium in inhibiting the binding of acetazolaminde to human carbonic anhydrase discounts the possibility of enzyme inactivation by removal of zinc ion. The possibility of edetate disodium acting as an *in vivo* inhibitor to the binding of acetazolamide to carbonic anhydrase is made more difficult by the fact that an endogenous source of free calcium exists to bind preferentially to the divalent edetate and to prevent calcium removal from the enzyme.

REFERENCES

(1) W. H. Havener, "Ocular Pharmacology," C. V. Mosby, St. Louis, Mo., 1970, p. 379.

(2) W. F. Bayne, G. Rodgers, and N. Crisologo, *J. Pharm. Sci.*, **64**, 402(1975).

(3) J. E. Coleman, *J. Biol. Chem.*, **242**, 5212(1967).

(4) M. Gibaldi, "Introduction to Biopharmaceutics," Lea & Febiger, Philadelphia, Pa., 1971, p. 13.

(5) T. H. Maren, *Physiol. Rev.*, **47**, 595(1967).

(6) H. W. Davenport, "Physiology of the Digestive Tract," 3rd ed., Year Book Medical Publishers, Chicago, Ill., 1971, p. 140.

(7) R. M. Levine, M. R. Blair, and B. J. Clark, *J. Pharmacol. Exp. Ther.*, **114**, 78(1955).

(8) "The Merck Index," 8th ed., Merck and Co., Rahway, N.J., 1968, p. 6.

(9) S. Feldman and M. Gibaldi, *J. Pharm. Sci.*, **58**, 967(1969).

(10) C. S. Tidball, *Amer. J. Physiol.*, **206**, 243(1964).

(11) L. S. Schanker and J. M. Johnson, *Biochem. Pharmacol.*, **8**, 421(1961).

(12) E. J. Masoro, in "Physiology and Biophysics III," T. C. Ruch and H. D. Patton, Eds., Saunders, Philadelphia, Pa., 1973, pp. 65, 66.

(13) T. Nadai, R. Kondo, A. Tatematsu, and H. Sezaki, *Chem. Pharm. Bull.*, **20**, 1139(1972).

ACKNOWLEDGMENTS AND ADDRESSES

Received May 12, 1975, from the *Department of Pharmaceutical Development, Alcon Laboratories, Inc., Fort Worth, TX 76101*

Accepted for publication July 14, 1975.

[x] To whom inquiries should be directed.

GLC Assay of Belladonna Extracts

DOROTHY K. WYATT [x], WILLIAM G. RICHARDSON [*], BRUCE McEWAN [*], JOHN M. WOODSIDE [*], and LEE T. GRADY

Abstract □ Samples of belladonna pilular and powdered extract and tincture from two suppliers were analyzed by GLC as a cooperative effort between two laboratories to develop methodology with substantial improvements in sensitivity, specificity, precision, and working time over the present official method. This goal was achieved, but marked differences in response of the individual extracts to different isolation schemes were noted.

Keyphrases □ Belladonna extract—GLC analysis in pharmaceutical formulations, suitability of anhydrous sodium sulfate in isolation, compared to official method □ Alkaloids, belladonna—GLC analysis in pharmaceutical formulations, suitability of anhydrous sodium sulfate in isolation, compared to official method □ Atropine—GLC analysis, pharmaceutical formulations of belladonna extract □ Scopolamine—GLC analysis, pharmaceutical formulations of belladonna extract □ Hyoscyamine—GLC analysis, pharmaceutical formulations of belladonna extract □ GLC—analysis, belladonna alkaloids, pharmaceutical formulations

Reliable GLC assays (1, 2) of atropine and scopolamine in dosage forms have come into general use in recent years and have been the basis of extensions (3) to other drug mixtures. Official titrimetric assays (4, 5) for the crude belladonna extracts (powdered and pilular) and the directly derived tincture are tedious, unspecific, and unreliable because of emulsion problems. Application of the GLC method to these mixtures of plant extracts would be desirable, and this paper reports the results of a cooperative effort between two laboratories to accomplish this goal. Some earlier assay work on plant extracts from belladonna by a GLC method was reported (6), and inaccuracies of the titrimetric approach also were noted then.

EXPERIMENTAL

All reagents were USP, NF, or ACS grade. Samples of pilular and powdered extracts were received from manufacturers, and the tincture was obtained locally. The optical isomers in atropine are not separated, so the combined atropine–hyoscyamine peak is expressed solely as atropine herein for convenience.

Chromatographic System[1]—A 1.2-m × 4-mm i.d. glass column packed with 3% methyl phenyl polysiloxane oil on 100–120-mesh acid-washed, flux-calcined, diatomaceous earth[2] was cured and conditioned as specified elsewhere (1, 2, 5). Minimal pledgets of silanized glass wool were used to minimize the catalytical conversion of atropine to apoatropine (6, 7). The column was maintained at 215°, and the injection port and flame-detector block temperatures were 240 and 245°, respectively; dry helium was used as a carrier gas at a flow rate of 65 ml/min. Electronic peak measurement was employed[3].

System Suitability—Chromatograph six to 10 injections of the assay preparation, and record peak areas as directed under *Procedure*. The analytical system is suitable for conducting this assay if the relative standard deviation for the ratio, R_A, calculated by the formula 100 × (standard deviation/mean ratio), does not exceed 2.0%; the resolution factor between A_H and A_A is not less than 5; and the tailing factor (the sum of the distances from peak center to the leading edge and to the tailing edge divided by twice the distance from the peak center to the leading edge), measured at 5% of the peak height of A_A, does not exceed 2.0.

[1] HP 5750B gas chromatograph with flame-ionization detector fitted for on-column injection.

[2] OV-17 on Gas Chrom Q, Applied Science Laboratories.

[3] Infotronics CRS 204 digital integrator.

tation since the results are also compatible by this mechanism.

Edetate disodium has promoted an increase in intestinal (rat) absorption of salicylate anion (9), phenolsulfonphthalein (10), heparin (11), mannitol (11), inulin (11), decamethonium (11), and sulfanilic acid (11). It has been postulated that edetate disodium alters the aqueous permeability of the intestinal epithelium by depleting magnesium and calcium ions, resulting in separation of the epithelial cells of the rat intestine (12, 13). This mechanism is likewise suspected with acetazolamide, since the lack of effect of edetate disodium in inhibiting the binding of acetazolaminde to human carbonic anhydrase discounts the possibility of enzyme inactivation by removal of zinc ion. The possibility of edetate disodium acting as an *in vivo* inhibitor to the binding of acetazolamide to carbonic anhydrase is made more difficult by the fact that an endogenous source of free calcium exists to bind preferentially to the divalent edetate and to prevent calcium removal from the enzyme.

REFERENCES

(1) W. H. Havener, "Ocular Pharmacology," C. V. Mosby, St. Louis, Mo., 1970, p. 379.

(2) W. F. Bayne, G. Rodgers, and N. Crisologo, *J. Pharm. Sci.*, **64**, 402(1975).

(3) J. E. Coleman, *J. Biol. Chem.*, **242**, 5212(1967).

(4) M. Gibaldi, "Introduction to Biopharmaceutics," Lea & Febiger, Philadelphia, Pa., 1971, p. 13.

(5) T. H. Maren, *Physiol. Rev.*, **47**, 595(1967).

(6) H. W. Davenport, "Physiology of the Digestive Tract," 3rd ed., Year Book Medical Publishers, Chicago, Ill., 1971, p. 140.

(7) R. M. Levine, M. R. Blair, and B. J. Clark, *J. Pharmacol. Exp. Ther.*, **114**, 78(1955).

(8) "The Merck Index," 8th ed., Merck and Co., Rahway, N.J., 1968, p. 6.

(9) S. Feldman and M. Gibaldi, *J. Pharm. Sci.*, **58**, 967(1969).

(10) C. S. Tidball, *Amer. J. Physiol.*, **206**, 243(1964).

(11) L. S. Schanker and J. M. Johnson, *Biochem. Pharmacol.*, **8**, 421(1961).

(12) E. J. Masoro, in "Physiology and Biophysics III," T. C. Ruch and H. D. Patton, Eds., Saunders, Philadelphia, Pa., 1973, pp. 65, 66.

(13) T. Nadai, R. Kondo, A. Tatematsu, and H. Sezaki, *Chem. Pharm. Bull.*, **20**, 1139(1972).

ACKNOWLEDGMENTS AND ADDRESSES

Received May 12, 1975, from the *Department of Pharmaceutical Development, Alcon Laboratories, Inc., Fort Worth, TX 76101*

Accepted for publication July 14, 1975.

[x] To whom inquiries should be directed.

GLC Assay of Belladonna Extracts

DOROTHY K. WYATT [x], WILLIAM G. RICHARDSON [*], BRUCE McEWAN [*], JOHN M. WOODSIDE [*], and LEE T. GRADY

Abstract □ Samples of belladonna pilular and powdered extract and tincture from two suppliers were analyzed by GLC as a cooperative effort between two laboratories to develop methodology with substantial improvements in sensitivity, specificity, precision, and working time over the present official method. This goal was achieved, but marked differences in response of the individual extracts to different isolation schemes were noted.

Keyphrases □ Belladonna extract—GLC analysis in pharmaceutical formulations, suitability of anhydrous sodium sulfate in isolation, compared to official method □ Alkaloids, belladonna—GLC analysis in pharmaceutical formulations, suitability of anhydrous sodium sulfate in isolation, compared to official method □ Atropine—GLC analysis, pharmaceutical formulations of belladonna extract □ Scopolamine—GLC analysis, pharmaceutical formulations of belladonna extract □ Hyoscyamine—GLC analysis, pharmaceutical formulations of belladonna extract □ GLC—analysis, belladonna alkaloids, pharmaceutical formulations

Reliable GLC assays (1, 2) of atropine and scopolamine in dosage forms have come into general use in recent years and have been the basis of extensions (3) to other drug mixtures. Official titrimetric assays (4, 5) for the crude belladonna extracts (powdered and pilular) and the directly derived tincture are tedious, unspecific, and unreliable because of emulsion problems. Application of the GLC method to these mixtures of plant extracts would be desirable, and this paper reports the results of a cooperative effort between two laboratories to accomplish this goal. Some earlier assay work on plant extracts from belladonna by a GLC method was reported (6), and inaccuracies of the titrimetric approach also were noted then.

EXPERIMENTAL

All reagents were USP, NF, or ACS grade. Samples of pilular and powdered extracts were received from manufacturers, and the tincture was obtained locally. The optical isomers in atropine are not separated, so the combined atropine–hyoscyamine peak is expressed solely as atropine herein for convenience.

Chromatographic System[1]—A 1.2-m × 4-mm i.d. glass column packed with 3% methyl phenyl polysiloxane oil on 100–120-mesh acid-washed, flux-calcined, diatomaceous earth[2] was cured and conditioned as specified elsewhere (1, 2, 5). Minimal pledgets of silanized glass wool were used to minimize the catalytical conversion of atropine to apoatropine (6, 7). The column was maintained at 215°, and the injection port and flame-detector block temperatures were 240 and 245°, respectively; dry helium was used as a carrier gas at a flow rate of 65 ml/min. Electronic peak measurement was employed[3].

System Suitability—Chromatograph six to 10 injections of the assay preparation, and record peak areas as directed under *Procedure*. The analytical system is suitable for conducting this assay if the relative standard deviation for the ratio, R_A, calculated by the formula 100 × (standard deviation/mean ratio), does not exceed 2.0%; the resolution factor between A_H and A_A is not less than 5; and the tailing factor (the sum of the distances from peak center to the leading edge and to the tailing edge divided by twice the distance from the peak center to the leading edge), measured at 5% of the peak height of A_A, does not exceed 2.0.

[1] HP 5750B gas chromatograph with flame-ionization detector fitted for on-column injection.

[2] OV-17 on Gas Chrom Q, Applied Science Laboratories.

[3] Infotronics CRS 204 digital integrator.

Anhydrous Sodium Sulfate—Transfer about 10 mg of atropine base, accurately weighed, to a 25-ml volumetric flask. Dilute to volume with 95% ethanol. Pipet 3.0 ml of this solution into each of two 60-ml separators and add about 10 ml of water, 1 ml of 1 *N* sodium hydroxide, and 10 ml of chloroform. Shake vigorously and allow the layers to separate. Then filter the organic phase from the first separator (Solution A) through phase-separating paper[4], suitably supported in a funnel, into a container and filter that from the second separator (Solution B) through about 30 g of anhydrous sodium sulfate (previously chloroform washed), supported with a small pledget of glass wool in a funnel, into a suitable container.

Extract a second time with 10 ml of chloroform and again collect the organic phase in a similar fashion. Evaporate the combined organic phases *in vacuo* to dryness and immediately add 1.0 ml of chloroform. Inject Solution A in duplicate and record the average peak area. Similarly inject and record Solution B. For the batch of reagent to be acceptable for use in this procedure, the two assay areas must be within 5% of each other.

Internal Standard Solution—Dissolve about 40 mg of USP homatropine hydrobromide reference standard, accurately weighed, in 0.1 *N* H_2SO_4 contained in a 50-ml volumetric flask. Then add 0.1 *N* H_2SO_4 to volume and mix. Prepare fresh daily.

Assay Preparation—Accurately weigh about 0.5 g of pilular or powdered extract and quantitatively transfer into a 125-ml conical flask. Add 40 ml of 0.1 *N* H_2SO_4. Heat to not more than 45° and stir the mixture to hasten solution. Decant the solution through medium-porosity filter paper into a 100-ml volumetric flask. Add two successive 20-ml portions of 0.1 *N* H_2SO_4, warming each, to wash the flask and filter each through the filter paper into the 100-ml volumetric flask. Dilute to volume with 0.1 *N* H_2SO_4 and mix.

Pipet 10 ml of this solution into a 60-ml separator. To the separator, add 1.0 ml of the internal standard solution and 15 ml of chloroform. Shake vigorously, allow the layers to separate, and discard the chloroform layer. [If there is an emulsion problem, a *mixed solvent* consisting of chloroform–2-propanol (10:3) can be substituted for chloroform throughout the extraction procedure.] Add another 15 ml of chloroform and extract again, discarding the chloroform phase. Add 15 ml of pH 9.5 phosphate buffer and sufficient 1 *N* sodium hydroxide solution, dropwise, so that the final pH is 9.0–9.5. Add 15 ml of chloroform, shake vigorously, and allow the layers to separate.

Filter the organic phase through 10 g of anhydrous sodium sulfate (previously chloroform washed), supported in a funnel with a small pledget of glass wool, into a suitable container. Extract again with two successive 15-ml portions of chloroform, collecting the clarified organic phase. Then wash the bed of sodium sulfate and the tip of the funnel with 5 ml of chloroform. Rapidly evaporate[5] the combined organic phase under reduced pressure, taking care not to heat the samples to greater than 45°. Add 1 ml of chloroform and mix to dissolve the alkaloids.

Proceed with belladonna tincture following the procedure outlined for the pilular and powdered extracts. However, in preparing the assay preparation, transfer 2.0 ml of the tincture instead of "10 ml of this solution" to a 60-ml separator containing 10 ml of 0.1 *N* H_2SO_4. Record from the standard curve the quantities, in milligrams, of atropine and scopolamine in the sample. Add the quantity of milligrams of atropine and scopolamine and multiply by 50 to obtain the milligrams of alkaloids per 100 ml.

Standard Preparation—Dissolve about 10 mg of USP scopolamine hydrobromide reference standard, accurately weighed, in 0.1 *N* H_2SO_4 contained in a 10-ml volumetric flask, add 0.1 *N* H_2SO_4 to volume, and mix. Label this Solution A. Dissolve about 20 mg of USP atropine sulfate reference standard, accurately weighed, in 0.1 *N* H_2SO_4 contained in a 50-ml volumetric flask, add 2.0 ml of Solution A and 0.1 *N* H_2SO_4 to volume, and mix. Prepare fresh daily.

Standard Curve—Pipet 1.0-, 2.0-, and 3.0-ml portions of the standard preparation into three 60-ml separators, respectively, and add 9.0, 8.0, and 7.0 ml of 0.1 *N* H_2SO_4, respectively. Proceed as directed under *Assay Preparation*, beginning with " . . . add 1.0 ml of the internal standard solution . . . ."

Extraction Blank—Transfer 10 ml of 0.1 *N* H_2SO_4 to a 60-ml separator. Proceed as directed under *Assay Preparation*, beginning with ". . . and 15 ml of chloroform. Shake vigorously." The blank chromatogram should contain no significant interferences at the locus of atropine, scopolamine, or homatropine.

Procedure—Inject a portion (about 5 μl) of each standard solution into a suitable gas chromatograph equipped with a flame-ionization detector. Measure the areas, A_A, A_H, and A_S, of the atropine, homatropine, and scopolamine peaks, respectively, in each chromatogram and calculate the ratios R_A and R_S by the formulas A_A/A_H and A_S/A_H. Plot the standard curves of the values of R_A and R_S against the amounts, in milligrams, of atropine and scopolamine in the solutions.

Calculate the amounts of atropine by the formula $W_a \times (0.8329/50) \times V$ and the amounts of scopolamine by the formula $W_s \times 0.2 \times (0.6921/50) \times V$, where W_a and W_s are the weights, in milligrams, of atropine sulfate and scopolamine hydrobromide, respectively; 0.8329 is the ratio of the molecular weights of atropine to atropine sulfate; 0.6921 is the ratio of the molecular weight of scopolamine to scopolamine hydrobromide; and V is the volume of the standard preparation.

Inject a portion of the assay preparation into the chromatograph and obtain a chromatogram as on the standard solutions. Measure the peak area of the atropine, homatropine, and scopolamine[6] peaks in the chromatogram and calculate the ratios r_A and r_S by the formulas a_A/a_H and a_S/a_H. From the standard curve, record the quantities, in milligrams, of atropine and scopolamine in the volume of sample taken. Add the quantity, in milligrams, of atropine and scopolamine and multiply by 10 to obtain the milligrams of alkaloids in the sample weight.

Alternative Assay Preparation—An earlier method developed in this laboratory consisted of an extraction scheme similar to the preceding procedure. However, in the earlier method, the internal standard, homatropine hydrobromide, was extracted as the base into chloroform; at the final evaporation stage of the analysis, 1 ml of this chloroform solution was added to the nearly dry sample. Initially, the sample (1 *versus* 0.5 g) was extracted into chloroform–ethanol (3:1).

Ten milliliters of this solution (2 ml of the tincture) was transferred to a separator, the solution was acidified with 10 ml of 0.1 *N* H_2SO_4, and most of the botanical components were extracted into chloroform and discarded. The remaining solution was made basic with 1 *N* sodium hydroxide, extracted twice with two 10-ml portions of chloroform, and evaporated to near dryness. The internal standard was added, and a 5-μl sample was injected for the assay of atropine. The solution was then concentrated further to ≤0.3 ml, and 10 μl of this solution was injected for the scopolamine analysis.

RESULTS AND DISCUSSION

Several years ago, GLC methods were developed for atropine and scopolamine dosage forms (1, 2). These methods have demonstrated consistent reliability and have been extended (3) to other drug mixtures. Some investigators (6) have applied earlier GLC technology to the analysis of belladonna. Chromatographic characteristics and problems of the alkaloids now are clearly appreciated (1, 2, 6, 7), so the application of a GLC assay to the extracts seems to be in order.

The belladonna extracts of commerce are complex and not fully defined with respect to composition, thermal history, age, and exact source. There are only two regular suppliers in this country, and rather surprising differences have come to light even with the limited sampling represented by the three extracts reported here. Indeed, the initial step chosen to begin the isolation sequence far outweighs all other analytical considerations combined. The initial isolation step in the recovery of drugs (or other analyses) from complex matrixes may well be the touchstone of the analytical method, but this fact is often obscured by excessive preoccupation with the often sophisticated and expensive instrumental systems subsequently used.

General Comments—Improved official methods for the determination of total alkaloidal concentration in the extracts and tinctures of belladonna have long been desired. The present offi-

[4] Whatman 1PS.

[5] Buchner Rotary Evap-O-Mix with VacTorr 20 portable pump and dry ice trap. Evaporation time should be not more than 1 hr.

[6] For increased scopolamine precision, concentrate the assay and standard preparations to 0.3 ml and inject 10 μl.

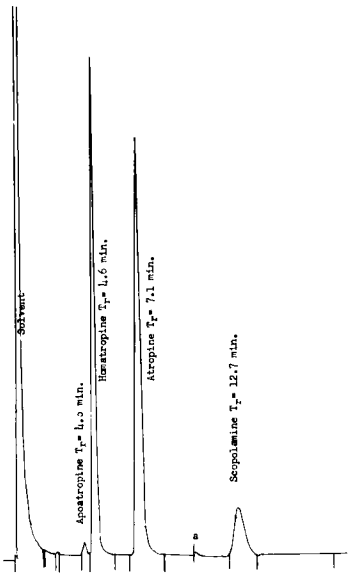

Figure 1—*Sample chromatogram of belladonna pilular extract. Key: a, a 10-fold decrease in attenuation.*

cial (4, 5) methods were in use before the 1930's and are imprecise, unspecific, and time consuming. They are based on isolation followed by acid–base titration and require multiple extractions for complete extraction of the drug. Fairly stable emulsions often are produced with each extraction step, so the extractions are unreliable and discouraging. The thermal instability of the alkaloids is well known, and breakdowns of the alkaloids by heat during this assay has been documented (6). Considering the nature of these alkaloids, the two 15-min dry-heating periods of the samples in air on a steam bath called for in the official procedure clearly can lead to substantial loss of alkaloidal content.

The isolation scheme presented here was chosen for its simplicity and similarity to the scheme used in the previously successful USP collaborative study (2) of atropine and scopolamine. The concentrations of plant materials are much lower than with the titrimetric assay procedure, so less emulsion potential exists. Two chloroform extractions from an acidified solution of the tincture and powdered and pilular extracts, as described in the *Procedure*, were sufficient to remove interfering plant materials, as shown by TLC monitoring of every individual extract along the isolation scheme.

The alkaloids were subsequently extracted into chloroform from the basified aqueous layer (pH 9.5 phosphate buffer was used instead of mineral alkali to minimize ester cleavage); 87.0% (pilular) and 87.6% (powder) of the alkaloids were recovered in the first extract, so that two additional extractions gave sufficient alkaloid recovery. The initial chloroform phases (acid extraction step) were also analyzed for atropine and scopolamine; none was found. An extraction blank is included in the procedure to monitor reagents for interfering impurities. Precision for the atropine standard carried through the procedure was 1.85% *RSD*, and chromatographic precision alone was 0.6% *RSD*. Standard curves, 0–4.5 μg of atropine, were rectilinear (correlation coefficient of 0.98, *SE* = 0.07, intercept of −0.02, based on 24 values over 14 days). A sample chromatogram is shown in Fig. 1.

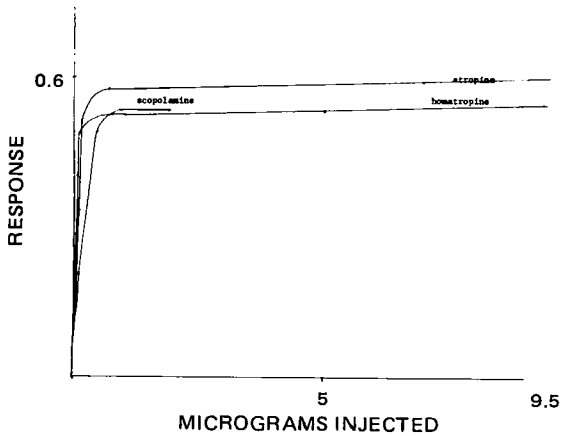

Figure 2—*Nonlinear adsorption data. Relative response times* C *of atropine, homatropine, and scopolamine* versus *anthracene: [(counts drug/counts anthracene)(weight anthracene/weight drug)] [C drug/C anthracene].*

Table I—Standard Addition Experiments

Sample	Type	Amount Added, %	Weighing	Prior Assay Value, % Atropine/ Atropine Added
I-A	Pilular	50	A	94.3, 95.6
			B	95.9, 95.9
			C	91.0, 90.1
			D	89.3, 89.3
				(average = 92.7)
I-B	Pilular	100	A	100.6, 99.8
			B	97.3, 99.2
			C	99.8, 99.8
				(average = 99.4)
I-C	Powdered	70	A	110.0, 108.0
			B	107.4, 108.8
			C	105.2, 108.4
			D	106.2, 114.1
			E	106.0
				(average = 108.2)

Nonlinear adsorption data or chromatographic recovery as a function of sample size for homatropine, atropine, and scopolamine *versus* anthracene are presented in Fig. 2. To eliminate the need for detector calibration (8), relative response values were multiplied by *C* drug/*C* anthracene, where *C* = [molecular weight/(12 × number of carbon atoms)]. Atropine and homatropine components exhibited minimal nonlinear adsorption in the region of the 3-μg sample sizes. Scopolamine recovery showed some nonlinearity and, therefore, decreased precision at its lower concentration, 0.3 μg, in the preparation used for the atropine analysis. The decreased precision in the scopolamine assay resulting from a single injection of about 0.3 μg of the drug, as opposed to ~2 μg following a concentration step and reinjection, did not substantially affect the total assay value of the belladonna extracts; therefore, the additional working time was not justifiable.

Standard addition experiments at 50, 100, and 70% of additional atropine, by pipet, with weighed amounts of previously assayed extracts resulted in recovery of added atropine of 92.7% (Lot A), 99.4% (Lot B), and 108.2% (Lot C), respectively (Table I). There still remained, however, a potential emulsion problem with the pilular extracts. This was most evident with Lot B of the pilular extract. An extraction medium of chloroform–2-propanol was substituted for chloroform throughout the procedure for this lot. As is evident, recovery using this modification was acceptable, but variable recovery due to extract lot differences is clearly indicated.

Extract Assays—When using the acid pretreatment scheme, total assay results (Laboratory I) for Supplier I were precise; the relative standard deviation values for Lots A–D were 1.1, 0.54, 0.63, and 1.02%, respectively. For Lots E and F from Supplier II, the relative standard deviations were 2.16 and 2.24%, respectively. Assay values are given in Table II. Assay values[7] for the tincture were higher than for the USP XVIII method. However, these are believed to reflect the true alkaloidal content. All samples had apoatropine contents not accounted for by injection port decomposition, probably due to the usual heat drying of the extracts during preparation. Indeed, it may develop that this content of apoatropine is an additional index of raw material quality.

Results for the Supplier II powdered extracts indicate a potential emulsion problem. A fourth extraction of the basic solution may be necessary in some cases to extract the alkaloids totally from other lots of a similar material. While complete solution in acid was evident for the pilular samples from Supplier I, such was

[7] These values were obtained before acquisition of a highly efficient vacuum pump that shortened evaporation time from several hours to less than 30 min.

Table II—Assay Results for Belladonna Alkaloids

Sample[a]	Weighing	Atropine, mg/g	Scopolamine, mg/g	Total Alkaloids[b], mg/g Average	
				Laboratory I	Laboratory II
Pilular Extract[c]					
I-A	A	12.59, 12.59	0.29, 0.31	12.81 ± 0.14	
	B	12.59, 12.65	0.29, 0.30	(*RSD* = 1.08%)	13.11
	C	12.57, 12.64	0.30, 0.30		13.63
	D	12.48, 12.44	0.29, 0.28		13.77
	E	12.25, 12.34	0.29, 0.29		
		(average = 12.51 ± 0.13, *RSD* = 1.07%)	(average = 0.29 ± 0.01, *RSD* = 2.87%).		(average = 13.50 ± 0.35, *RSD* = 2.58%)
I-B	A	11.21, 11.20	0.50, 0.50	11.71 ± 0.06	12.68
	B	11.18, 11.20	0.49, 0.50	(*RSD* = 0.54%)	12.54
	C	11.12, 11.18	0.48, 0.49		13.12
	D	11.30, 11.22	0.50, 0.49		
	E	11.30, 11.17	0.52, 0.53		
		(average = 11.21 ± 0.06, *RSD* = 0.49%)	(average = 0.50 ± 0.01, *RSD* = 2.59%)		(average = 12.78 ± 0.30, *RSD* = 2.37%)
II-E	A	11.23	0.51	11.55 ± 0.25	10.12
	B	11.07	0.58	(*RSD* = 2.16%)	11.49
	C	10.81	0.46		
		(average = 11.04 ± 0.21, *RSD* = 1.97%)	(average = 0.52 ± 0.06, *RSD* = 11.7%)		(average = 10.81 ± 0.97, *RSD* = 8.97%)
Powdered Extract[c]					
I-C	A	11.48, 11.34	0.20, 0.21	11.56 ± 0.07	11.12
	B	11.36, 11.34	0.18, 0.22	(*RSD* = 0.63%)	11.21
	C	11.36, 11.36	0.18, 0.22		11.30
	D	11.26, 11.47	0.20, 0.21		
	E	11.32, 11.28	0.22, 0.19		
		(average = 11.36 ± 0.07, *RSD* = 0.62%)	(average = 0.20 ± 0.02, *RSD* = 7.71%)		(average = 11.21 ± 0.09, *RSD* = 0.80%)
I-D	A	11.64, 11.58	0.11, 0.11	11.79 ± 0.12	11.82
	B	11.58, 11.58	0.09, 0.11	(*RSD* = 1.02%)	12.08
	C	11.74, 11.59	0.09, 0.09		12.21
	D	11.76, 11.68	0.10, 0.11		
	E	11.91, 11.80	0.12, 0.12		
		(average = 11.69 ± 0.11, *RSD* = 0.97%)	(average = 0.11 ± 0.01, *RSD* = 11.80%)		(average = 12.04 ± 0.20, *RSD* = 1.65%)
II-F	A	10.45	0.26	10.44 ± 0.23	11.16
	B	10.22	0.13	(*RSD* = 2.24%)	10.81
	C	10.15	0.12		(average = 10.99 ± 0.25, *RSD* = 2.25%)
		(average = 10.27 ± 0.16, *RSD* = 1.53%)	(average = 0.17 ± 0.08)		
		Atropine, mg/100 ml	Scopolamine, mg/100 ml		
Tincture[c]					
II-G		33.1	1.80	34.7 mg/100 ml	
		31.7	1.63		
		33.8			
		33.4			
		(average = 33.00 ± 0.93, *RSD* = 2.76%)			
USP XVIII assay		N.A.	N.A.	32.4, 31.2 } 31.8 mg/100 ml	

[a] Lots A, B, C, and D were from a single supplier; Lots E and F were from a second source. [b] All Laboratory I values are single-day, single-analyst, and single-analysis values. Second values reported are duplicate analyses of same weighing. Laboratory II conducted single determinations by two analysts on two different days. [c] Declared amounts: pilular extract, 12.5 mg/g; powdered extract, 12.5 mg/g; and tincture, 27–33 mg/100 ml.

Table III—Comparison of Assay Values for Original and Modified Methods

Extract	Code	Original Method: Weighings	Original Method: Total Alkaloids[a]	Modified Method: Weighings	Modified Method: Total Alkaloids[a]
Pilular	I-A	2	3.99	5	12.81
	II-E	5	11.78	5	11.55
Powdered	I-C	—	—	5	11.56
	II-F	3	7.08	3	10.44

[a] Average values expressed in milligrams per gram.

not the case for those from Supplier II. A single reextraction of the medium-porosity filter paper was used initially to remove the insoluble plant material, necessary to achieve total atropine–scopolamine extraction. Total assay results were still somewhat lower: 4.9% (Laboratory II) and 3% (Laboratory I), of which a 4.6% lower atropine value was noted.

An initial direct chloroform–alcohol (3:1) extraction of the alkaloids from the raw extracts was evaluated and was entirely successful for the Supplier II pilular extracts. However, when using this technique, Supplier I pilular extracts assayed at less than half the declared amount (Table III). The acid pretreatment scheme, on the other hand, yielded slightly lower Supplier II pilular extract results as compared to the organic extraction scheme. This substitution was weighed against the totally unsuccessful assay of the Supplier I pilular extracts and Supplier II powdered samples by the initial chloroform–alcohol extraction.

The identity of those solid additives necessary to produce a powdered extract needs further definition and standardization. Differences in manufacturing processes or sample constituents in the Supplier I samples clearly interfere with direct extraction with organic solvents; conversely, there appears to be similar problems with the acid extraction of Supplier II extracts, specifically lower assay values and the formation of emulsions.

Preliminary work in this laboratory included adding a portion of edetic acid during the initial part of the analysis, which increased the assay value of incompletely extracted samples by about 5%. As reported elsewhere (9), belladonna alkaloid plant material contains trace amounts of heavy metal ions[8], concentrated chiefly in the leaves. Presumably, these heavy metal contaminants plus iron from processing could be a significant source of variance between suppliers, sample extracts, but the problems encountered here are not sufficient cause to evaluate further heavy metal contamination as a possible error source.

An unsatisfactory lot of anhydrous sodium sulfate was also received in this laboratory. It lowered the assay values substantially by catalyzing on-column decomposition of the atropine samples as evidenced by the appearance of a classic decomposition in the peak envelope. Two OV-17 columns were prepared; on the first, preferential decomposition to apoatropine was observed. On the second, the atropine peak was merely severely distorted (both columns were suitable for atropine analysis). This batch of sodium sulfate did not differ from other batches in either composition or water content other than by a fourfold increase in calcium content as evidenced by X-ray methods. A reagent qualification test was developed.

[8] Heavy metal-ion contaminants include copper, molybdenum, manganese, chromium, nickel, vanadium, strontium, and barium.

REFERENCES

(1) R. O. Zimmerer, Jr., and L. T. Grady, *J. Pharm. Sci.*, **59,** 87(1970).

(2) L. T. Grady and R. O. Zimmerer, Jr., *ibid.*, **59,** 1324(1970).

(3) R. S. Santoro, P. P. Progner, E. A. Ambush, and D. E. Guttman, *ibid.*, **62,** 1346(1973).

(4) "The United States Pharmacopeia," 19th rev., Mack Publishing Co., Easton, Pa., 1975, pp. 46–48.

(5) "The National Formulary," 14th ed., Mack Publishing Co., Easton, Pa., 1975, pp. 58–61.

(6) M. J. Solomon, F. A. Crane, B. L. W. Chu, and E. S. Mika, *J. Pharm. Sci.*, **58,** 264(1969).

(7) E. Brochmann-Hanssen and A. B. Svendsen, *ibid.*, **51,** 1095(1962).

(8) B. J. Gudzinowicz, "Gas Chromatographic Analysis of Drugs and Pesticides," Dekker, New York, N.Y., 1967, p. 53.

(9) I. F. Gribovskaya and N. I. Grinkevich, *Agrokhimiya*, **10,** 124(1970).

ACKNOWLEDGMENTS AND ADDRESSES

Received March 10, 1975, from the *Drug Research and Testing Laboratory, United States Pharmacopeia, Rockville, MD 20852*

Accepted for publication July 17, 1975.

The authors acknowledge the technical assistance of Charles Chu.

* Control Analytical Department, Eli Lilly and Co., Indianapolis, IN 46206

[x] To whom inquiries should be directed.

Dissolution Rate Studies of Cholesterol Monohydrate in Bile Acid–Lecithin Solutions Using the Rotating-Disk Method

S. PRAKONGPAN, W. I. HIGUCHI, K. H. KWAN, and A. M. MOLOKHIA ˣ

Abstract □ A physical model approach was used to investigate cholesterol gallstone dissolution kinetics in simulated bile. Critical experimental and theoretical investigations simulating *in vivo* conditions showed that, in the bile acid–lecithin solutions, there is a significant interfacial barrier for both cholesterol gallstone and cholesterol monohydrate pellet dissolution. In the present study, the rotating-disk dissolution method and the accompanying Levich theory were applied to assess the contributions of the diffusion convection mass transfer resistance and of the interfacial barrier to the overall kinetics. Cholesterol dissolution rates in bile acid solutions were about 2–20 times slower than diffusion-controlled rates depending upon the degree of agitation. As found in previous studies, these rates in the presence of sufficient concentrations of dissolution accelerators approached the theoretical diffusion–convection-controlled rates. To account for the much slower dissolution rates in bile acid–lecithin solutions, two possible kinetic interpretations were investigated. The first is based upon slow crystal–micellar solution interfacial kinetics, and the second is based upon a slow rate of cholesterol solubilization in the aqueous diffusion layer. For the latter, an analytical mathematical solution was obtained.

Keyphrases □ Cholesterol monohydrate—dissolution rate studies in bile acid–lecithin solutions, rotating-disk method □ Bile acid–lecithin solutions—in cholesterol monohydrate dissolution rate studies, rotating-disk method □ Dissolution rate—cholesterol monohydrate in bile acid–lecithin solutions, rotating-disk method

Results of studies on the dissolution rate of human cholesterol gallstones and cholesterol monohydrate pellets in bile acid–lecithin solutions simulating bile were reported recently (1–4). An important finding was that there is a significant interfacial barrier for cholesterol gallstone and cholesterol monohydrate pellet dissolution in these bile–lecithin solutions. These studies also showed that when quaternary ammonium compounds were added to the solutions, the dissolution rates were enhanced dramatically and approached diffusion-controlled rates at sufficiently high concentrations.

These past studies involved experiments in which the gallstone and the cholesterol pellets were statically mounted in an assembly and solution agitation was accomplished by a paddle stirrer. The data were then analyzed by means of the conventional, semiempirical Nernst and Berthoud theories, involving the concept of an effective stagnant diffusion layer.

The purpose of the present report is to define more critically the baseline in bile acid–lecithin systems with and without the added dissolution rate accelerators. This approach is necessary for quantitative study of the structure–activity relationships for various medicinal agents capable of enhancing gallstone dissolution *in vivo*.

The rotating-disk method (5) and the accompanying Levich theory for analyzing the data are well suited for quantifying the contributions of the diffusion–convection mass transfer resistance and of the interfacial barrier and/or the solubilization kinetics in the diffusion layer to the overall kinetics. Thus, this experiment–theory combination was chosen for these baseline studies. Together with other independent experiments, this approach has been able to establish quantitatively the limiting kinetic behavior for cholesterol in bile acid–lecithin solutions.

THEORY

The dissolution process for a nonionic, nonreactive solid involves (*a*) the contact of the solvent with the solid interface, where (*b*) a physical reaction takes place. This reaction is followed by (*c*) the transport of the solute or products away from the interface into the bulk solution. In most cases of interest, since solvent contact occurs rapidly, steps (*b*) and/or (*c*) are generally considered to be rate determining.

The following discussion considers diffusion-controlled dissolution, interfacially controlled dissolution, and the situation when both may be important. An equation was derived (6) to account for both the interfacial resistance and the resistance for the transfer of the solute in solution from the vicinity of the solid surface into the bulk solvent under steady-state conditions:

$$\frac{dW}{dt} = J = \frac{A(C_s - C_b)}{h/D + 1/P} \qquad \text{(Eq. 1)}$$

where:

W = total amount of solid dissolved into solution at time t
J = dissolution rate
A = surface area of solid exposed to solution
D = diffusion coefficient of solute in the solvent
C_s = saturated concentration of solute
C_b = concentration of solute in the bulk
P = effective interfacial permeability coefficient
h = Nernst effective diffusion layer thickness

When surface equilibrium is rapid, $1/P$ is negligible and Eq. 1 becomes:

$$J = \frac{AD(C_s - C_b)}{h} \qquad \text{(Eq. 2)}$$

and the dissolution rate is determined by bulk transport only. When, on the other hand, equilibrium at the surface takes place slowly, $1/P$ is much greater than h/D and:

$$J = AP(C_s - C_b) \qquad \text{(Eq. 3)}$$

Then the dissolution rate is determined by the rate of solute transfer at or near the solid–solution interface, and it is interfacially controlled.

In the context of the Nernst diffusion layer theory, the total resistance for solute transfer from the solution immediately adjacent to the solid surface into the bulk is given by h/D, a purely diffusional term. In most dissolution situations, both convection and diffusion are expected to be important. Therefore, for the rotating-disk case, the effective diffusional resistance, h/D, may be equated to an appropriate function which includes the consideration of both processes. Thus, for the rotating-disk situation in which only diffusion and convection are important, the mass flux was given by Levich (5) as:

$$J = 0.62AD^{2/3}\nu^{-1/6}\omega^{1/2}(C_s - C_b) \qquad \text{(Eq. 4)}$$

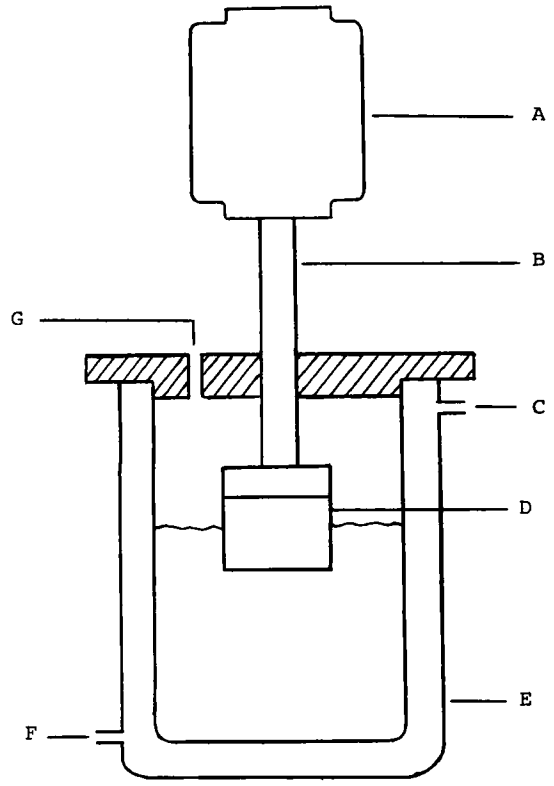

Figure 1—*Rotating-disk apparatus for dissolution rate studies. Key: A, constant-speed motor; B, rotating shaft; C, water outlet; D, removable disk containing pellet; E, water-jacketed beaker; F, water inlet; and G, sample port.*

where ν is the kinematic viscosity, and ω is the angular velocity of rotation.

The corresponding effective diffusion boundary layer thickness may be written as:

$$h = 1.612D^{1/3}\nu^{1/6}\omega^{-1/2} \quad \text{(Eq. 5)}$$

A closer approximation for the rotating-disk problem by Gregory and Riddiford (7) gives:

$$h = 1.805[0.8934 + 0.316(D/\nu)^{0.36}]D^{1/3}\nu^{1/6}\omega^{-1/2} \quad \text{(Eq. 6)}$$

Use of this value of h gives a 3% smaller theoretical dissolution rate than that predicted by Eq. 4 for $D/\nu \simeq 10^{-3}$.

In a purely bulk transport-controlled case, the observed dissolution rate should be essentially equal to the calculated flux (Eq. 4). If, however, the observed reaction rate is substantially lower than the calculated diffusion–convection flux, it may be concluded that the dissolution process is taking place in the interfacially controlled region.

EXPERIMENTAL

Materials—Sodium cholate[1] was used as received after the purity was checked with TLC. Recrystallized ^{14}C-labeled cholesterol monohydrate was prepared as previously described (3). A pure grade of egg lecithin was prepared using the method of Singleton *et al.* (8). The product was examined by TLC and shown to have very high purity.

Solubility and Diffusion Coefficient Determination—The methods described previously (3) were applied in this study.

Dissolution Rate Determination—Figure 1 is a schematic representation of the rotating-disk dissolution apparatus. It consists of three main parts: the outside water-jacketed beaker maintained at 37 ● 0.02°, the removable disk assembly, and the controlled-rotating device[2]. Figure 2 shows a schematic outline of the rotating disk with a pellet of the material under investigation mounted in place.

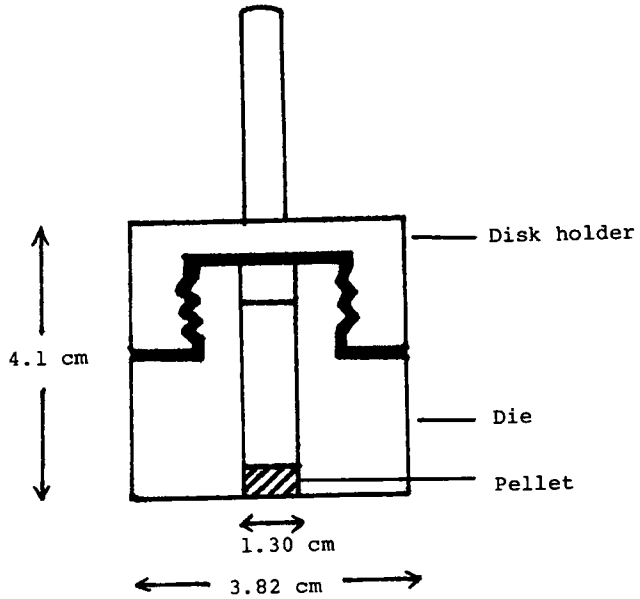

Figure 2—*Cross-section of removable disk assembly with pellet.*

Pellets of radioactive cholesterol monohydrate or benzoic acid were prepared by directly compressing 100 mg of the material in a die, 1.3 cm (0.5 in.) i.d., under a force of 1362 kg (3000 lb) using a laboratory press[3]. The die with the pellet was then firmly attached to the disk holder (Fig. 2).

For each dissolution run, 100 ml of solvent was pipetted into the beaker (Fig. 1). The rotating disk containing the pellet was then centered at about 1 cm below the solvent level so that the distances from the disk wall to the inner surface of the beaker exceeded 0.5 cm [these dimensions were shown (7) to provide adequate hydrodynamics within the system]. At the moment of contact between the pellet and the solvent, the motor and a timer were started simultaneously. Samples were withdrawn from the system by pipet at suitable time intervals for analysis in a liquid scintillation counter[4].

The rotational speeds tested varied from 20 to 600 rpm, corresponding to Reynolds numbers of 1100 and 32,600, respectively.

Benzoic acid was used as a model solute compound for assessing the geometry effects and the hydrodynamics within the system because benzoic acid has been known to dissolve by diffusion–convection control.

RESULTS AND DISCUSSION

Dissolution of Benzoic Acid—The results of the dissolution experiments of benzoic acid in 0.01 *N* hydrochloric acid are presented in Figs. 3 and 4. Figure 3 shows the relation between the amounts dissolved and time. The linear plots were obtained at all speeds of rotation, indicating constant rates during the time of each run.

When these dissolution rates were plotted *versus* the square root of the speed of rotation (Fig. 4), a linear relationship was obtained and was compared to the dissolution rates predicted by the Levich (5) theory (Eq. 4). However, the experimental rates were found to be about 14% lower than those predicted by the theory. This discrepancy is consistent with Riddiford's (9) views regarding the performance of rotating-disk geometries of the type used in the present study.

The benzoic acid data clearly show that diffusion–convection is the sole limiting step in the dissolution of benzoic acid in these experiments. The linear dependency of the dissolution rate J on $\omega^{1/2}$, even at high speeds of rotation, indicates that a fast equilibrium is taking place at the pellet surface.

Dissolution of ^{14}C-Cholesterol Monohydrate—Table I summarizes the experimental cholesterol monohydrate dissolution rate data together with the solubilities and diffusion coefficients in 2%

[1] Schwarz/Mann, Orangeburg, N.Y.
[2] Servodyne laboratory stirrer, Cole-Parmer Instrument Co., Chicago, Ill.
[3] Model B, Fred Carver, Inc., Summit, N.J.
[4] Beckman Instruments Inc., Fullerton, Calif.

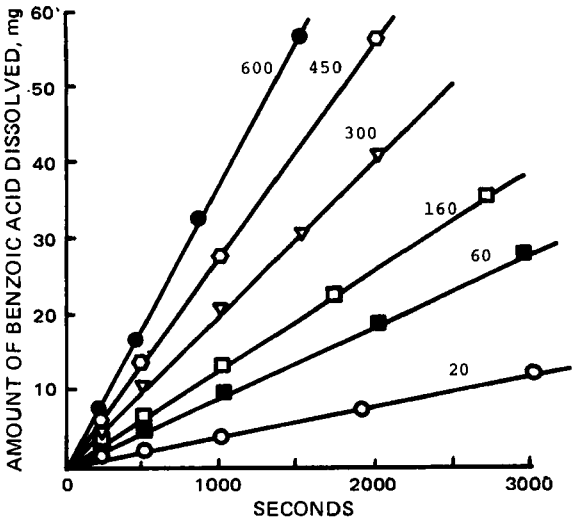

Figure 3—*Dissolution of benzoic acid pellets (A = 1.27 cm²) into 0.01 N HCl at various rotational speeds. Numbers on line refer to rotational speeds (revolutions per minute).*

bile acid and 2% bile acid–1% lecithin media with and without benzalkonium chloride.

To present the data in a more meaningful way, Eq. 4 was rearranged to:

$$J/0.62AD^{2/3}\nu^{-1/6}C_s = \omega^{1/2} \qquad \text{(Eq. 7)}$$

so that, for a diffusion-controlled dissolution, a plot of the left-hand side *versus* the right-hand side should give a straight line with a slope of unity. The presence of a significantly slow interfacial step should result in a significant negative deviation from linearity, and these deviations should increase with increasing $\omega^{1/2}$.

Figure 5 shows the cholesterol monohydrate dissolution rate data plotted according to Eq. 7. In the sodium cholate–lecithin solution (Table I and Fig. 5), the dissolution rates were essentially unaffected by changes in the rotation speeds; the results were close to those determined by the static pellet dissolution method (3). Thus, the interfacial resistance plays the dominant role as the rate-determining step in cholesterol monohydrate dissolution in synthetic bile, even at very low agitation.

Addition of benzalkonium chloride to the bile acid–lecithin system increased the rate of cholesterol monohydrate dissolution, as was found previously (4). As the concentration of benzalkonium chloride was varied from 0.25 to 2%, the dissolution behavior gradually changed from being largely interfacially controlled to being essentially diffusion controlled and quantitatively predicted by the Levich theory and the benzoic acid dissolution data (Table I and Fig. 5).

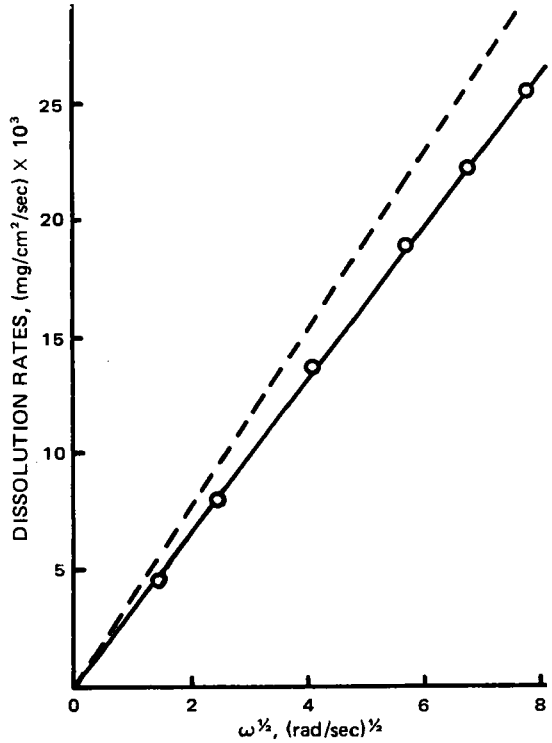

Figure 4—*Comparison between observed and predicted effects of stirring speed on the dissolution rate of a benzoic acid pellet in 0.01 N HCl at 37°. Key: —o—, observed; and - - - -, predicted by Eq. 4.*

Table II presents the effective permeability coefficients (P) for systems showing considerable interfacial resistance to cholesterol monohydrate dissolution. These values were calculated from the experimental rates using:

$$J' = \frac{A(C_s - C_b)}{1.612D^{-2/3}\nu^{1/6}\omega^{-1/2} + 1/P} \qquad \text{(Eq. 8)}$$

Table I—Dissolution Rates (J), Solubilities (C_s), and Diffusivities (D) of Cholesterol Monohydrate in Test Solutions

Solvent Media[a]			C_s,	$D \times 10^6$,	$J \times 10^4$, mg/cm²/sec			
C, %	L, %	BC, %	mg/ml	cm²/sec	20 rpm	60 rpm	300 rpm	600 rpm
2	—	—	0.53	2.17	0.23	0.26	0.33	0.39
2	1	—	1.05	1.491	0.11	0.13	0.15	0.16
2	1	0.25	1.20	1.30	1.05	1.62	2.20	2.37
2	1	0.50	1.55	1.30	2.74	4.60	8.12	9.01
2	1	1.0	2.20	1.29	3.61	6.14	11.2	15.7
2	1	2.0	3.30	1.40	4.82	9.87	22.4	29.6

[a] In 0.1 *M* phosphate buffer, pH 7.4. C = sodium cholate, L = lecithin, and BC = benzalkonium chloride.

Table II—Permeability Coefficient (P) of Cholesterol Monohydrate in Test Solutions

Solvent Media[a]			$P \times 10^4$, cm/sec				
C, %	L, %	BC, %	20 rpm	60 rpm	300 rpm	600 rpm	Mean ± SD[b]
2	—	—	0.54	0.54	0.66	0.77	0.656 ± 0.013
2	1	—	0.11	0.13	0.15	0.15	0.143 ± 0.001
2	1	0.25	1.50	2.14	2.35	2.38	2.29 ± 0.02
2	1	0.50	11.0	16.0	14.7	11.7	14.1 ± 2.2
2	1	1.0	8.19	13.0	14.2	19.6	15.6 ± 3.5

[a] In 0.1 *M* phosphate buffer, pH 7.4. C = sodium cholate, L = lecithin, and BC = benzalkonium chloride. [b] The value at 20 rpm is not included.

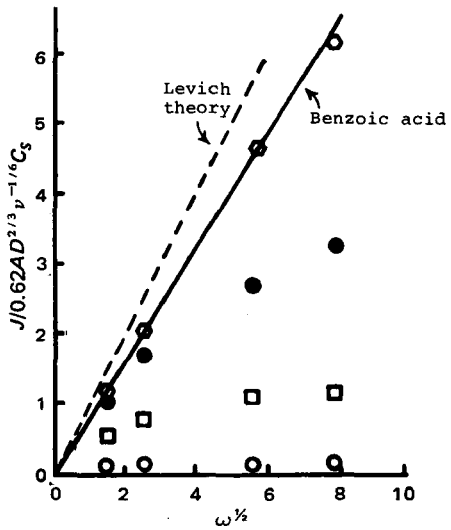

Figure 5—*Dissolution rates of cholesterol monohydrate in:* ○, *2% sodium cholate + 1% lecithin;* □, *2% sodium cholate + 1% lecithin + 0.25% benzalkonium chloride;* ●, *2% sodium cholate + 1% lecithin + 0.5% benzalkonium chloride; and* ○, *2% sodium cholate + 1% lecithin + 2% benzalkonium chloride in 0.1* M *phosphate buffer, pH 7.4.*

Equation 8 is obtained by substituting Eq. 5 into Eq. 1; J' refers to the corrected rate (based upon the benzoic acid data). Except at 20 rpm, the P values were essentially constant for each system. When the average P values were used to generate theoretical dissolution rates of cholesterol monohydrate, a good fit with the experimental rates was observed (Fig. 6).

Possible Physical Meaning of *P*—The permeability coefficient, P, may be shown to be associated with transfer kinetics at the crystal–solution interface or solubilization kinetics in the diffusion layer or both. When slow cholesterol transfer occurs at the cholesterol monohydrate crystal–solution interface, P may be considered to be a first-order reaction rate constant associated with this rate-determining process (1). If the process involves the slow solubilization of the aqueous free cholesterol by the micelles in the diffusion layer, P has an entirely different meaning.

The theoretical treatment for the latter case is presented in the *Appendix*, where it is shown that the two situations may have identical mathematical form from the hydrodynamic standpoint and may be considered to be mathematically equivalent if:

$$P = \frac{\sqrt{k_f D_f}}{K} \qquad \text{(Eq. 9)}$$

where k_f is the forward reaction rate constant, D_f is the diffusion coefficient of free cholesterol, and K is the equilibrium constant.

While more definitive experiments may be necessary before it can be determined which of the two mechanisms is more likely to be correct, the collective evidence strongly supports the crystal–solution interfacial reaction mechanism. One argument is that the mechanism based upon slow solubilization in the diffusion layer predicts that P would be proportional to the reciprocal of the square root of the micelle concentration. This can be seen from Eq. 9 since both k_f and K would be expected to be approximately proportional to the micelle concentration.

Other studies (2, 10) have shown, however, that at high ionic strength, P is either nearly constant or increases somewhat with increasing micelle concentrations over a 1–5% sodium cholate concentration range. Therefore, these data support the mechanism in which the slow step is kinetics at the crystal–solution interface and not the kinetics of cholesterol solubilization in the aqueous diffusion layer.

Other evidence supporting this viewpoint is that P has been found to be sensitive to electrolytes. Current studies in these laboratories indicate that P increases about fivefold when the phosphate buffer concentration is increased from 0.01 to 0.1 M. Also Surpuriya and Higuchi (10, 11) found similar electrolyte effects in their kinetic studies on the oil–water transport of cholesterol. These results are consistent with a micelle–interface interaction mechanism in which the close approach of a negatively charged micelle to a negatively charged surface is facilitated by counterions or by increasing ionic strength in general. Also, the strong influence of benzalkonium chloride upon P appears to be more consistent with a mechanism involving the interface than one involving micellar kinetics in the aqueous diffusion layer.

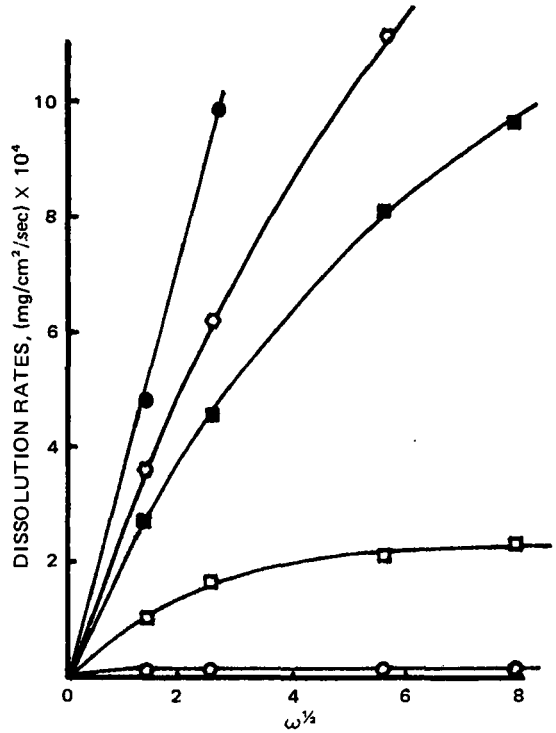

Figure 6—*Comparison of the theoretical (solid line) dissolution rates using average* P *values (Table II) with the experimental dissolution rates for cholesterol monohydrate pellets in:* ○, *2% sodium cholate + 1% lecithin;* □, *2% sodium cholate + 1% lecithin + 0.25% benzalkonium chloride;* ■, *2% sodium cholate + 1% lecithin + 0.5% benzalkonium chloride;* ○, *2% sodium cholate + 1% lecithin + 1% benzalkonium chloride; and* ●, *2% sodium cholate + 1% lecithin + 2% benzalkonium chloride.*

APPENDIX

The dissolution rate equation for nonequilibrium reaction kinetics in the diffusion layer is derived as follows. The reaction of cholesterol with the bile acid–lecithin micelles is given as:

$$C_f \underset{k_r}{\overset{k_1}{\rightleftharpoons}} C_m$$

Scheme I

and:

$$K = \frac{k_f}{k_r} \qquad \text{(Eq. A1)}$$

where:

C_f = concentration of free cholesterol
C_m = concentration of micellar cholesterol
k_f = forward reaction rate constant
k_r = reverse reaction rate constant
K = equilibrium constant

The steady-state diffusion equations for free and micellar cholesterol in the region $0 \leq x \leq h$ (the diffusion layer thickness) are:

$$D_f \frac{d^2C_f}{dx^2} - k_f\left(C_f - \frac{C_m}{K}\right) = 0 \qquad \text{(Eq. A2)}$$

$$D_m \frac{d^2C_m}{dx^2} + k_f\left(C_f - \frac{C_m}{K}\right) = 0 \qquad \text{(Eq. A3)}$$

where D_f is the diffusion coefficient of free cholesterol, and D_m is the diffusion coefficient of micellar cholesterol.

The boundary conditions at $x = 0$ are $C_f = C_f^0$, $C_m = C_m^0$, and $(dC_m/dx) = 0$. At $x = h$, $C_f = 0$ and $C_m = 0$.

Combining Eqs. A2 and A3 and integrating with these boundary conditions give:

$$C_f = \frac{D_m}{D_f} C_m + \left(C_f^0 + \frac{D_m C_m^0}{D_f}\right)\left(1 - \frac{x}{h}\right) \quad \text{(Eq. A4)}$$

for $(0 \leq x \leq h)$.

Substituting Eq. A4 into Eq. A3 and rearranging give:

$$\frac{d^2C_m}{dx^2} - \frac{k_f}{D_m}\left(\frac{D_m}{D_f} + \frac{1}{k}\right) C_m = -\frac{k_f}{D_m}\left(C_f^0 + \frac{D_m C_m^0}{D_f}\right)\left(1 - \frac{x}{h}\right) \quad \text{(Eq. A5)}$$

Equation A5 can be solved analytically for C_m to give:

$$C_m = \left[C_m^0 - \left(\frac{D_f C_f^0 + D_m C_m^0}{D_m + D_f/K}\right)\left(\frac{e^{x\sqrt{A}} - e^{-x\sqrt{A}}}{1 - e^{2h\sqrt{A}}}\right)\right] - \left(\frac{D_f C_f^0 + D_m C_m^0}{D_m + D_f/K}\right)\left(1 - \frac{x}{h}\right) \quad \text{(Eq. A6)}$$

where:

$$A = \left(\frac{k_f}{D_f} + \frac{k_f}{D_m K}\right) \quad \text{(Eq. A7)}$$

By differentiating Eq. A6 with $(dC_m/dx)_{x=0} = 0$, C_m^0 can be obtained algebraically:

$$C_m^0 = \frac{\frac{D_f C_f^0}{D_m + D_f/K}\left[1 + \frac{(1 - e^{2h\sqrt{A}})}{h\sqrt{A}(1 + e^{2h\sqrt{A}})}\right]}{1 - \left(\frac{D_m}{D_m + D_f/K}\right)\left(1 + \frac{(1 - e^{2h\sqrt{A}})}{h\sqrt{A}(1 + e^{2h\sqrt{A}})}\right)} \quad \text{(Eq. A8)}$$

The total diffusional flux of cholesterol is:

$$J = \frac{D_m C_m^0}{h} + \frac{D_f C_f^0}{h} \quad \text{(Eq. A9)}$$

and the flux from free cholesterol $(D_f C_f^0/h)$ can be neglected in this case. Substituting Eq. A8 into Eq. A9 and rearranging give:

$$J = \frac{D_m C_f^0}{h}\left[\frac{(1 - e^{2h\sqrt{A}}) + h\sqrt{A}(1 + e^{2h\sqrt{A}})}{\frac{h\sqrt{A}}{K}(1 + e^{2h\sqrt{A}}) - \frac{D_m}{D_f}(1 - e^{2h\sqrt{A}})}\right] \quad \text{(Eq. A10)}$$

For $h\sqrt{A} \gg 1$, Eq. A10 can be reduced to:

$$J = \frac{KC_f^0}{\frac{h}{D_m} + \frac{K}{\sqrt{k_f D_f}}} \quad \text{(Eq. A11)}$$

REFERENCES

(1) W. I. Higuchi, S. Prakongpan, V. Surpuriya, and F. Young, *Science*, **178**, 633(1972).

(2) W. I. Higuchi, V. Surpuriya, S. Prakongpan, and F. Young, *J. Pharm. Sci.*, **62**, 695(1973).

(3) W. I. Higuchi, S. Prakongpan, and F. Young, *ibid.*, **62**, 945(1973).

(4) *Ibid.*, **62**, 1207(1973).

(5) V. G. Levich, "Physicochemical Hydrodynamics," Prentice-Hall, Englewood Cliffs, N.J., 1962.

(6) A. Berthoud, *J. Chem. Phys.*, **10**, 624(1912).

(7) D. P. Gregory and A. C. Riddiford, *J. Chem. Soc.*, **1956**, 3756.

(8) W. S. Singleton, M. S. Gray, M. L. Brown, and J. L. White, *J. Amer. Oil Chem. Soc.*, **42**, 53(1965).

(9) A. C. Riddiford, in "Advances in Electrochemistry and Electrochemical Engineering," vol. 4, P. Delahay, Ed., Interscience, New York, N.Y., 1966, p. 47.

(10) V. Surpuriya and W. I. Higuchi, *J. Pharm. Sci.*, **61**, 375(1972).

(11) V. Surpuriya and W. I. Higuchi, *Biochim. Biophys. Acta*, **290**, 375(1972).

ACKNOWLEDGMENTS AND ADDRESSES

Received May 9, 1975, from the *College of Pharmacy, University of Michigan, Ann Arbor, MI 48104*

Accepted for publication July 16, 1975.

Supported by the National Institute of Arthritis, Metabolism and Digestive Diseases (Grant AM 16694).

The authors thank Dr. J. S. Schultz for help in developing the theory for the kinetics of solubilization in the diffusion layer.

[x] To whom inquiries should be directed.

Chlorpromazine Metabolism VII: New Quantitative Fluorometric Determination of Chlorpromazine and Its Sulfoxide

PUSHKAR N. KAUL [x], LLOYD R. WHITFIELD, and MERVIN L. CLARK

Abstract □ A new, sensitive assay is described for chlorpromazine and/or its sulfoxide. The method is based on reacting the tertiary amine base with 9-bromomethylacridine to form a quaternary compound which, on photolysis, yields highly fluorescent products that are determinable fluorometrically. The procedural steps were standardized, and an optimum assay procedure was developed. The method shows a less than 3% coefficient of variation when applied directly to chlorpromazine samples and is capable of determining 15–20 ng of the drug. The method is readily adaptable to clinical and bioavailability studies.

Keyphrases □ Chlorpromazine and its sulfoxide—fluorometric analysis after quaternization with 9-bromomethylacridine, pharmaceutical formulations and blood levels □ 9-Bromomethylacridine—quaternization reagent for fluorometric analysis of chlorpromazine and its sulfoxide, pharmaceutical formulations and blood levels □ Fluorometry—analysis, chlorpromazine and its sulfoxide, pharmaceutical formulations and blood levels □ Tranquilizers—chlorpromazine, fluorometric analysis, pharmaceutical formulations and blood levels

Of the many assay methods (1–12) developed for chlorpromazine, those possessing adequate sensitivity to determine its levels in blood include a GC method and its modifications (2, 3, 5), *in vitro* radioassay (6), radioimmunoassay (9, 10), and GC–mass spectrometry (4). The lack of precision in GC methods has been adequately reiterated (11–13). The *in vitro* radioquantitation method has not been applied successfully, perhaps because of its complicated nature and poor precision. A reported radioimmunoassay (9)

Combining Eqs. A2 and A3 and integrating with these boundary conditions give:

$$C_f = \frac{D_m}{D_f} C_m + \left(C_f^0 + \frac{D_m C_m^0}{D_f}\right)\left(1 - \frac{x}{h}\right) \quad \text{(Eq. A4)}$$

for $(0 \leq x \leq h)$.

Substituting Eq. A4 into Eq. A3 and rearranging give:

$$\frac{d^2C_m}{dx^2} - \frac{k_f}{D_m}\left(\frac{D_m}{D_f} + \frac{1}{k}\right) C_m = -\frac{k_f}{D_m}\left(C_f^0 + \frac{D_m C_m^0}{D_f}\right)\left(1 - \frac{x}{h}\right) \quad \text{(Eq. A5)}$$

Equation A5 can be solved analytically for C_m to give:

$$C_m = \left[C_m^0 - \left(\frac{D_f C_f^0 + D_m C_m^0}{D_m + D_f/K}\right)\left(\frac{e^{x\sqrt{A}} - e^{-x\sqrt{A}}}{1 - e^{2h\sqrt{A}}}\right)\right] - \left(\frac{D_f C_f^0 + D_m C_m^0}{D_m + D_f/K}\right)\left(1 - \frac{x}{h}\right) \quad \text{(Eq. A6)}$$

where:

$$A = \left(\frac{k_f}{D_f} + \frac{k_f}{D_m K}\right) \quad \text{(Eq. A7)}$$

By differentiating Eq. A6 with $(dC_m/dx)_{x=0} = 0$, C_m^0 can be obtained algebraically:

$$C_m^0 = \frac{\frac{D_f C_f^0}{D_m + D_f/K}\left[1 + \frac{(1 - e^{2h\sqrt{A}})}{h\sqrt{A}(1 + e^{2h\sqrt{A}})}\right]}{1 - \left(\frac{D_m}{D_m + D_f/K}\right)\left(1 + \frac{(1 - e^{2h\sqrt{A}})}{h\sqrt{A}(1 + e^{2h\sqrt{A}})}\right)} \quad \text{(Eq. A8)}$$

The total diffusional flux of cholesterol is:

$$J = \frac{D_m C_m^0}{h} + \frac{D_f C_f^0}{h} \quad \text{(Eq. A9)}$$

and the flux from free cholesterol $(D_f C_f^0/h)$ can be neglected in this case. Substituting Eq. A8 into Eq. A9 and rearranging give:

$$J = \frac{D_m C_f^0}{h}\left[\frac{(1 - e^{2h\sqrt{A}}) + h\sqrt{A}(1 + e^{2h\sqrt{A}})}{\frac{h\sqrt{A}}{K}(1 + e^{2h\sqrt{A}}) - \frac{D_m}{D_f}(1 - e^{2h\sqrt{A}})}\right] \quad \text{(Eq. A10)}$$

For $h\sqrt{A} \gg 1$, Eq. A10 can be reduced to:

$$J = \frac{KC_f^0}{\frac{h}{D_m} + \frac{K}{\sqrt{k_f D_f}}} \quad \text{(Eq. A11)}$$

REFERENCES

(1) W. I. Higuchi, S. Prakongpan, V. Surpuriya, and F. Young, *Science*, **178**, 633(1972).

(2) W. I. Higuchi, V. Surpuriya, S. Prakongpan, and F. Young, *J. Pharm. Sci.*, **62**, 695(1973).

(3) W. I. Higuchi, S. Prakongpan, and F. Young, *ibid.*, **62**, 945(1973).

(4) *Ibid.*, **62**, 1207(1973).

(5) V. G. Levich, "Physicochemical Hydrodynamics," Prentice-Hall, Englewood Cliffs, N.J., 1962.

(6) A. Berthoud, *J. Chem. Phys.*, **10**, 624(1912).

(7) D. P. Gregory and A. C. Riddiford, *J. Chem. Soc.*, **1956**, 3756.

(8) W. S. Singleton, M. S. Gray, M. L. Brown, and J. L. White, *J. Amer. Oil Chem. Soc.*, **42**, 53(1965).

(9) A. C. Riddiford, in "Advances in Electrochemistry and Electrochemical Engineering," vol. 4, P. Delahay, Ed., Interscience, New York, N.Y., 1966, p. 47.

(10) V. Surpuriya and W. I. Higuchi, *J. Pharm. Sci.*, **61**, 375(1972).

(11) V. Surpuriya and W. I. Higuchi, *Biochim. Biophys. Acta*, **290**, 375(1972).

ACKNOWLEDGMENTS AND ADDRESSES

Received May 9, 1975, from the *College of Pharmacy, University of Michigan, Ann Arbor, MI 48104*

Accepted for publication July 16, 1975.

Supported by the National Institute of Arthritis, Metabolism and Digestive Diseases (Grant AM 16694).

The authors thank Dr. J. S. Schultz for help in developing the theory for the kinetics of solubilization in the diffusion layer.

[x] To whom inquiries should be directed.

Chlorpromazine Metabolism VII: New Quantitative Fluorometric Determination of Chlorpromazine and Its Sulfoxide

PUSHKAR N. KAUL [x], LLOYD R. WHITFIELD, and MERVIN L. CLARK

Abstract □ A new, sensitive assay is described for chlorpromazine and/or its sulfoxide. The method is based on reacting the tertiary amine base with 9-bromomethylacridine to form a quaternary compound which, on photolysis, yields highly fluorescent products that are determinable fluorometrically. The procedural steps were standardized, and an optimum assay procedure was developed. The method shows a less than 3% coefficient of variation when applied directly to chlorpromazine samples and is capable of determining 15–20 ng of the drug. The method is readily adaptable to clinical and bioavailability studies.

Keyphrases □ Chlorpromazine and its sulfoxide—fluorometric analysis after quaternization with 9-bromomethylacridine, pharmaceutical formulations and blood levels □ 9-Bromomethylacridine—quaternization reagent for fluorometric analysis of chlorpromazine and its sulfoxide, pharmaceutical formulations and blood levels □ Fluorometry—analysis, chlorpromazine and its sulfoxide, pharmaceutical formulations and blood levels □ Tranquilizers—chlorpromazine, fluorometric analysis, pharmaceutical formulations and blood levels

Of the many assay methods (1–12) developed for chlorpromazine, those possessing adequate sensitivity to determine its levels in blood include a GC method and its modifications (2, 3, 5), *in vitro* radioassay (6), radioimmunoassay (9, 10), and GC–mass spectrometry (4). The lack of precision in GC methods has been adequately reiterated (11–13). The *in vitro* radioquantitation method has not been applied successfully, perhaps because of its complicated nature and poor precision. A reported radioimmunoassay (9)

is unable to differentiate between chlorpromazine and its 7-hydroxy metabolite, whereas a more recent method (10) remains to be assessed for its precision and clinical applicability. The GC–mass spectrometric method requires not only relatively expensive equipment but also specially trained personnel for day-to-day operation.

A new approach to assaying subnanomole quantities of chlorpromazine and its sulfoxide, adaptable to routine use in a clinical laboratory, was described previously (12, 14, 15). In essence, the method is based on reacting the appropriate tertiary amine with 9-bromomethylacridine to form a nonfluorescent quaternary compound. This product can be isolated by TLC and photolyzed to generate measurable fluorescence. The major component of the fluorescent photolytic products was shown to be 9-methylacridine (14, 15). Both the quaternization reaction and the photolysis are stoichiometric and reproducible.

This paper details the development and standardization of the evolved fluorometric method of assay for chlorpromazine and/or chlorpromazine 5-oxide (the sulfoxide), which invariably occurs as one metabolite of the drug.

EXPERIMENTAL

Materials and Equipment—The following were used: 9-bromomethylacridine, synthesized as described previously (14); chlorpromazine and chlorpromazine 5-oxide[1]; cadmium carbonate, cadmium bromide, lead oxide, mercuric cyanide, nickel carbonate, palladium carbonate, and zinc carbonate, all as catalysts; hydroquinone, cadmium sulfate, stannous chloride, and 2-chlorophenothiazine, all as antioxidants; acetone[2]; acetonitrile[2]; ammonium hydroxide[2]; benzene[2]; chloroform[2]; dichloromethane[2]; 1,2-dichloroethane[2]; *n*-hexane[2]; tetrahydrofuran[2]; 200-μm glass beads[3]; 100-μm thick silica gel TLC plates without fluorescent indicator and with terephthalate backing[4]; TLC saturation chambers[5]; a UV lamp emitting in the range of 200–300 nm (λ_{max} 254 nm)[6]; a microbalance; a pH meter; a sonicator; and vortex shakers.

General Assay Procedure—Chlorpromazine hydrochloride and/or its sulfoxide were converted to base by dissolving in 0.1 *N* NaOH. The base was extracted with *n*-hexane, and the solvent was evaporated. The appropriate base residue was dissolved in 100 μl of acetonitrile and reacted with excess 9-bromomethylacridine in the presence of glass beads as the catalyst. The reaction mixture was incubated at various temperatures for various times.

After the reaction period, the reaction mixture was used as such or evaporated to dryness and reconstituted to its original 100-μl volume. An aliquot was subjected to a TLC procedure to separate the quaternary salts. The isolated quaternary salts on the plates were photolyzed under UV light, and the fluorescent material was eluted with methanolic sulfuric acid for fluorometric determination[7].

Standardization of Reaction Conditions—The criteria for the evaluation of optimum reaction conditions were the magnitude and the precision of relative fluorescence produced in the final step of the general assay procedure. In the final application of the evolved assay procedure to blood, the drug in the biological fluid is generally extracted into the solvent. In this process, blood extractables are also extracted into the solvent. These extractables usually can interfere in the chemical reactions employed for assay purposes. Therefore, most experiments on standardization of the quaternization reaction were carried out in the presence of a blank blood extract.

Stoichiometry—To be useful as an analytical technique, the quaternization reaction as well as the photolyic reaction must be stoichiometric relative to the concentrations of the drugs to be assayed. Therefore, chlorpromazine and its sulfoxide, in amounts varying from 0.16 to 3.13 nmoles, were reacted with an excess of the acridine derivative and carried through the photolysis and fluorometric determination to establish the stoichiometry of the reaction.

9-Bromomethylacridine Concentration—Varying amounts of the acridine derivative, ranging from 50 to 313 nmoles, were added to a fixed quantity of chlorpromazine and reacted in the presence of 50 mg of glass beads for 18 hr at 50° to determine the amount of the reagent necessary to produce the most quaternary product.

Reaction Medium—The reaction of 3.13 nmoles of chlorpromazine with 94 nmoles of 9-bromomethylacridine in the presence of 50 mg of glass beads was carried out in organic solvents of varying polarity for 14 hr at 30° to determine the effect of solvent on the quaternization reaction.

Time–Temperature Dependence—Three sets of reaction tubes, with each tube containing 3.13 nmoles of the drug, 94 nmoles of the acridine reagent in 100 μl of acetonitrile, and 50 mg of glass beads, were allowed to react at 25, 50, and 70°. At definite times ranging from 1 to 18 hr, replicates of three tubes were removed from each temperature set and processed through the remainder of the general assay procedure to assess the progress of the reaction.

Catalysis—To accomplish the quaternization reaction in a relatively short time, various substances were evaluated as catalysts. Initial experiments revealed that inclusion of 200-μm glass beads increased the rate of formation of the reaction product significantly ($p < 0.05$) compared to the reaction not containing beads. Varying, but predetermined, weights of beads corresponding to known surface areas were added to the reaction mixtures, and their effect on the reaction was determined. The increase in surface area was accomplished either by increasing the quantity of beads or by crushing a fixed weight of beads to decrease the particle size.

The other agents tested as catalysts included cadmium carbonate (16), cadmium bromide, mercuric cyanide, nickel carbonate, palladium carbonate, zinc carbonate, and lead oxide.

Effect of Antioxidants—In the quaternization reaction of chlorpromazine, a minor product was invariably formed with an R_f value identical to that of the chlorpromazine sulfoxide quaternary product. This product might have been derived by quaternization of the sulfoxide present originally as a contaminant in the chlorpromazine stock, but TLC analysis of the chlorpromazine stock solution revealed that there was no detectable sulfoxide. Therefore, the secondary product might have resulted from oxidation of the drug to its sulfoxide during the quaternization reaction. If so, addition of a suitable antioxidant to the reaction mixture would inhibit this conversion.

On this basis, hydroquinone, cadmium sulfate, stannous chloride, and 2-chlorophenothiazine, all possessing a redox potential greater than that of the drug, were evaluated for their effectiveness in preventing the supposed oxidation. To the reaction mixture containing 3.13 nmoles of chlorpromazine in the presence of an eightfold molar quantity of the acridine derivative and 50 mg of glass beads were added twofold molar quantities of each antioxidant.

In other experiments, three different concentrations of chlorpromazine, with and without 12.6 nmoles of 2-chlorophenothiazine, were reacted with 94 nmoles of the acridine derivative in the presence of glass beads for 18 hr at 50°. The relative fluorescence values of the photolyzed quaternary product of the drug and its minor product each were separately analyzed by a two-factor analysis of variance, *i.e.*, 2-chlorophenothiazine (Factor A) and chlorpromazine concentration (Factor B).

Fractionation of Reaction Products—Various solvent systems and adsorbents for TLC were evaluated for their ability to separate the quaternary salts of chlorpromazine and its sulfoxide from the reactants, from the reaction by-products, and from each other. Fifty-two solvent systems were tested with alumina, different variants of cellulose, and polyamide plates. Another set of 81 solvent systems and some of their ratio variations were evaluated as the developing solvents with the silica gel plates. The presence

[1] Obtained from the Psychopharmacology Research Branch, National Institute of Mental Health.
[2] Nanograde or analytical reagent grade, Mallinckrodt Chemical Works, St. Louis, Mo.
[3] Arthur H. Thomas Co., Philadelphia, Pa.
[4] Eastman Kodak, Rochester, N.Y.
[5] Kensco, Oakland, Calif.
[6] Ultraviolet Products Ltd., San Gabriel, Calif.
[7] Aminco Bowman spectrophotofluorometer.

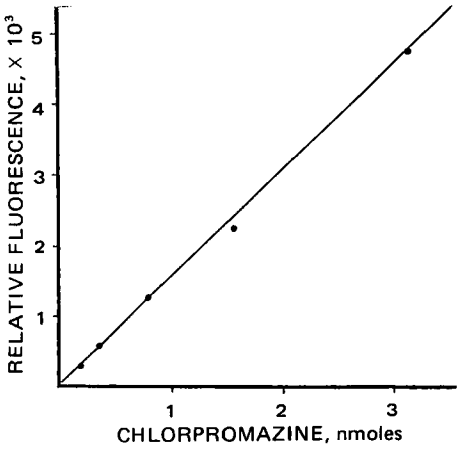

Figure 1—*Correlation between the quantity of chlorpromazine reacted with 9-bromomethylacridine and the relative fluorescence obtained following completion of the quaternization assay. Each point represents the mean of three values.*

of the phenothiazine nucleus at the spots that generated fluorescence following photolysis of the quaternary salts was confirmed by spraying the TLC plates with Forrest reagent (5% ferric chloride in 50% sulfuric acid) and noting the development of a pink color for chlorpromazine and a pinkish-purple color for the sulfoxide at their respective spots.

Photolysis—The quaternary ammonium product formed by the reaction of chlorpromazine with the acridine derivative had no fluorescence of its own. However, UV irradiation of the quaternary salt on a 100-μm silica gel TLC plate produced fluorescence. The stoichiometry of photolysis was determined by applying varying amounts of the isolated quaternary product to the silica gel plates, subjecting the plates to photolysis, eluting the fluorescent products thus generated, and measuring the fluorescence of the eluates. The relative rate of photolysis was determined with the UV lamp at different heights from the TLC plate. The products of photolysis were prepared on a large scale by preparative TLC for structure elucidation.

Determination of Fluorescence—For final quantitation in the assay procedure, the fluorescent products generated by photolysis on a spot were not fractionated to measure individual photolytic products. Instead, the spot was cut out and eluted by vortexing in 10 ml of 20% methanolic sulfuric acid (0.01 *N*), and the eluate was determined at excitation and emission wavelengths of 350 and 474 nm, respectively.

RESULTS AND DISCUSSION

The nature of the reaction between chlorpromazine and 9-bromomethylacridine to form a 1:1 quaternary adduct, the possible mechanism of photolysis of the quaternary product, and the characterization of the fluorescent products of photolysis were described previously (14). When various concentrations of the phenothiazine were reacted with an excess of the acridine reagent and the relative fluorescence of the corresponding photolyzed quaternary product was determined, a linear correlation was seen between the drug concentration and the fluorescence (Fig. 1).

Whenever chlorpromazine was reacted with the reagent in acetonitrile, a minor product with an R_f value equivalent to that of the quaternary product of the sulfoxide invariably developed.

Table I—Relative Yield of Quaternary Product Formed by Reacting Chlorpromazine with 9-Bromomethylacridine in Various Organic Solvents

Solvent	Maximum Yield ± *SD*, %
Acetonitrile	100 ± 1.2
Methanol	96 ± 1.5
Acetone	75 ± 1.6
Chloroform	62 ± 2.2
Tetrahydrofuran	16 ± 4.0

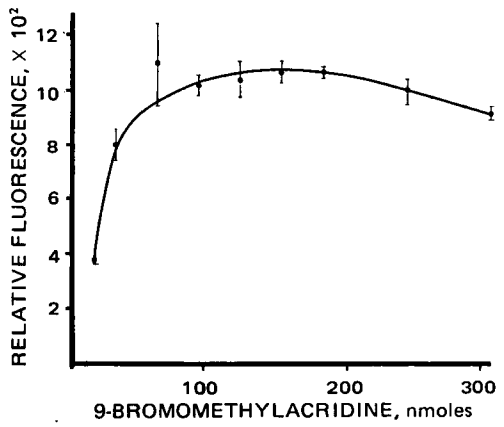

Figure 2—*Effect of varying concentrations of 9-bromomethylacridine on the formation of the quaternary product of chlorpromazine. Each point represents the mean of three values* ± SD.

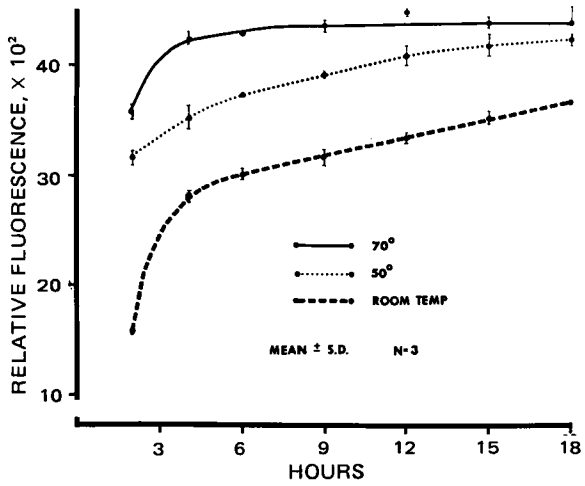

Figure 3—*Temperature dependence of the reaction of 3.13 nmoles of chlorpromazine in the presence of 94 nmoles of 9-bromomethylacridine reacted at 25, 50, and 70°. The points represent the mean of three values* ± SD.

However, in all cases during the standardization phase where 2-chlorophenothiazine was included as an antioxidant in the reaction mixture, the fluorescence value of this minor secondary spot was less than 5% of the value due to the major product of chlorpromazine. For this reason, the contribution of the minor spot was ignored in all analyses.

Reaction Conditions—The nucleophilic quaternization reaction was enhanced in relatively polar solvents (Table I). Although both acetonitrile (bp 81.6°) and methanol (bp 65.5°) appeared to facilitate the reaction, acetonitrile was selected for routine use due to its lower vapor pressure, resulting in relative ease and accuracy in the quantitative transfers involved in the assay procedure.

There was no significant difference ($p > 0.01$) in the fluorescence values resulting from the photolysis of the quaternary product of chlorpromazine formed when 94–250 nmoles of the acridine derivative were used relative to 3.13 nmoles of chlorpromazine (Fig. 2). Since higher concentrations of the acridine yielded significantly higher ($p < 0.05$) blank values, 94 nmoles was used for routine reactions.

The data in Fig. 3 indicate that the quaternization reaction was enhanced by increasing temperature. At 25°, the reaction proceeded to only 87% of the maximum. However, after an 18-hr reaction, there was no significant difference ($p > 0.05$) between the amounts of the quaternary salts formed at 50 and 70°. Occasionally, a few tubes of the higher temperature group showed additional spots, which were not observed in the tubes kept at 50°. For this reason, 50° was chosen as the optimum temperature for subsequent reactions. On completion of the reaction, the contents of all tubes were evaporated at room temperature, reconstituted in 100 μl of acetonitrile, and processed for the rest of the assay procedure.

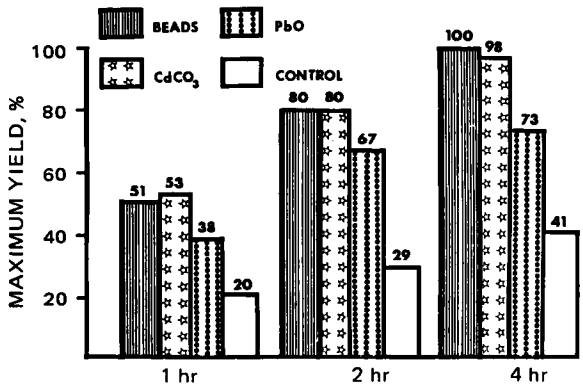

Figure 4—*Effect of 200-μm glass beads, cadmium carbonate ($CdCO_3$), and lead oxide (PbO) on the reaction of 3.13 nmoles of chlorpromazine with an excess of 9-bromomethylacridine at 50°*

The results of catalysis experiments indicated that glass beads and cadmium carbonate were equally effective as catalysts for the quaternization reaction (Fig. 4), whereas cadmium bromide, zinc carbonate, and other agents were of no value. A bead surface area of approximately 1 m^2, equivalent to 50 mg of glass beads/100-μl reaction volume, was optimum. Greater surface areas of glass beads had no further effect.

Of the various antioxidants used to prevent formation of the minor secondary product during the quaternization reaction, 2-chlorophenothiazine significantly ($p < 0.05$) reduced the formation. The other compounds had either no effect or actually caused a significant ($p < 0.05$) reduction in the formation of the primary reaction product, *i.e.*, the chlorpromazine quaternary compound. In the presence of the antioxidant, the relative values of the minor spot decreased as compared to those in its absence, with a corresponding increase in the primary product (Table II).

The statistical analysis on the data relative to the minor product is summarized in Table III. The data indicate that the presence of 2-chlorophenothiazine had a significant effect ($p < 0.05$) on the formation of the minor product. Also, the dependence of the minor spot on the concentration of chlorpromazine was significant ($p < 0.01$).

Separation of Reaction Products—On alumina, cellulose, and polyamide plates, the quaternary products moved best in relatively polar solvents. However, separation of the two quaternary salts of chlorpromazine and its sulfoxide from the excess reagent and other reaction by-products was difficult. *N,N*-Dimethylformamide–chloroform (7:30) was effective in separating the reaction by-products from the quaternary salts on the alumina plates but not on the cellulose and polyamide plates. Since the quaternary salts did not move from the origin in this system, benzene–dioxane–acetic acid (40:10:3) was required to move and separate the two salts. The fractionation, however, was far from satisfactory for accurate quantitative elution of the spots following photolysis. Therefore, the three adsorbents, *i.e.*, alumina, cellulose, and polyamide, were abandoned.

With the silica gel plates, only three of the 81 solvent systems tested were suitable. One of these utilized development of the plate in methanol–methylal–ammonium hydroxide (50:10:0.6) to move the reaction by-products, followed by development in butanol–acetic acid–water (50:10:40), which moved and separated the quaternary products of chlorpromazine (R_f 0.44) and its sulfoxide (R_f 0.39). However, 8–10 hr was required for development. Furthermore, the separations were not consistently reproducible.

Table III—Summary of the Two-Factor Analysis of Variance of Data Relative to Chlorpromazine Secondary Product

Variation	*SS*	*df*	*MS*	*F*
2-Chlorophenothiazine	1613.33	1	1613.33	7.69[a]
Chlorpromazine concentration	30621.66	2	15310.83	73.05[b]
2-Chlorophenothiazine × chlorpromazine concentration	771.60	2	385.83	1.84[c]
Error	5030.00	24	209.58	

[a] $p < 0.05$. [b] $p < 0.01$. [c] Not significant.

In the second system, the plates were predeveloped in methanol–methylal–benzene (2:2:1) to move the reaction by-products to the solvent front, followed by development in methanol–chloroform–benzene–ammonium hydroxide (35:16:10:5), which moved and separated the quaternary products of chlorpromazine (R_f 0.20) and its sulfoxide (R_f 0.26) from the blood blank. However, the development time was relatively long, the separations were inconsistent, and the fluorescence values following photolysis of the quaternary products lacked precision.

The third solvent system was acetonitrile–water (9:1). To date, this is the only system capable of simultaneously moving the reaction by-products to the solvent front and separating the two quaternary products from each other as well as from the blood blank. However, to increase the separation rather reproducibly, two sequential runs were found to be necessary. In this solvent system and with the TLC plates used in these studies, the quaternary salts of chlorpromazine and its sulfoxide have R_f values of 0.26 and 0.22, respectively.

Photolysis—Figure 5 shows that the correlation between the fluorescence yielded by photolysis and the amount of the quaternary compound in the spot was linear. Over 90% of the fluorescence was developed in 2–3 min with a lamp height of 9, 12, or 15 cm from the TLC plate (Fig. 6). As the time of photolysis increased, the fluorescence decreased, possibly due to the conversion of the fluorescent product(s) to less fluorescent congener(s). The loss of fluorescence was significant ($p < 0.05$) when photolysis times of 4 min or longer were used with either the 9- or 12-cm lamp height. With a 15-cm lamp height, however, no significant ($p > 0.05$) loss of fluorescence occurred until 7 min had elapsed. Therefore, a 15-cm lamp height was optimum for the assay procedure, although any height between 12 and 15 cm would be satisfactory for a 3-min photolysis period.

The fluorescent spot produced by photolysis of the quaternary salt on the silica gel TLC plate was developed in benzene–methanol (9:1) and found to resolve into three components. Of the total fluorescence, the primary component (R_f 0.70) represented about 85% while the other two minor spots represented about 7% (R_f 0.29) and 5% (R_f 0.79). A residual fluorescence remained at the point of origin and contributed about 1–3% of the total fluorescence; it may have been due to an unphotolyzed trace of the original quaternary salt. However, the overall photolytic yield of fluorescence, which is measured in the assay, was invariably constant for a particular concentration of the quaternary compound of chlorpromazine.

On comparing the physicochemical properties of the photolytic

Table II—Formation of the Major and Minor Quaternary Products of Chlorpromazine in the Presence and Absence of 2-Chlorophenothiazine

Chlorpromazine, ng/Sample	Without 2-Chlorophenothiazine		With 2-Chlorophenothiazine (12.6 nmoles)	
	Major Product	Minor Product	Major Product	Minor Product
100	508 ± 13.0[a]	14 ± 4.2	524 ± 29.7	7 ± 2.7
400	1720 ± 83.7	48 ± 4.5	1855 ± 97.5	40 ± 9.4
800	3520 ± 192	103 ± 30.9	3650 ± 150	74 ± 12.9

[a] Relative values. Mean ± *SD*; $n = 6$.

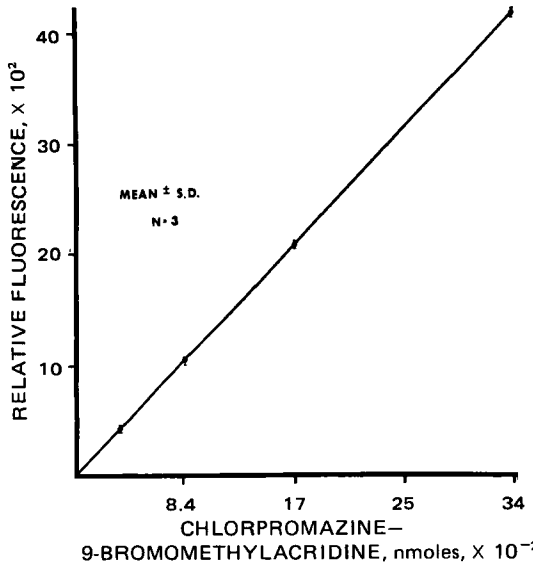

Figure 5—*Linear correlation between the quantity of chlorpromazine quaternary salt photolyzed on a silica gel TLC plate and the relative fluorescence generated. Each point represents the mean of three values* ± SD.

products with those of the synthesized authentic samples (23), the major component was found to be 9-methylacridine. The other two spots were 9-acridinemethanol and 9-acridinecarboxaldehyde, respectively, in the order of the magnitude of their fluorescence contribution.

Table IV shows that 90% of the maximum elutable fluorescence was eluted from the TLC spot by vortexing the cutout spot in 20% methanolic sulfuric acid (0.01 *N*) for 5 sec. There was no significant difference ($p > 0.05$) in the relative elutions at 10, 20, and 30 sec. A 20-sec vortexing time was chosen for the elution procedure.

Optimum Assay Procedure—To 0.063–3.13 nmoles (20 ng–1 μg) of chlorpromazine and/or its sulfoxide as base in a 1.5-ml stoppered polyethylene tube are added 94 nmoles of 9-bromomethylacridine and 0.22 μmole of 2-chlorophenothiazine in 100 μl of acetonitrile and 50 mg of 200-μm glass beads. The tube is stoppered and incubated at 50° for 18 hr. The reaction mixture is evaporated to dryness under nitrogen and reconstituted with 100 μl of acetonitrile. An aliquot of 10 μl is spotted on a 100-μm silica gel TLC plate with terephthalate backing and developed twice in acetonitrile–water (9:1).

The plate is dried at 80° for 15 min after each development and then placed at a distance of 12–15 cm under a UV lamp (λ_{max} 254 nm) for 3 min. The spot containing the generated fluorescent products is marked, cut out, transferred to a 50-ml centrifuge tube, and vortexed for 20 sec in 10 ml of 20% methanolic sulfuric acid (0.01 *N*). Then the tube is centrifuged for 3 min at 2250 rpm. The clear supernate is subjected to fluorometric determination at excitation and emission wavelengths of 350 and 474 nm, respectively.

Precision, Blanks, and Sensitivity—Replicate analyses on sets of different amounts of chlorpromazine and its sulfoxide bases, when carried out in the absence of blood blank, showed a very high precision, with a coefficient of variation within 0–3%. The reagent blanks invariably gave a reading of 100–120 units on the fluorometer, while the TLC plate blanks read 60–80. The fluorescence value relative to the quaternary product of 2 ng of chlorpromazine on a TLC spot read 250. Thus, as low as 60–100 pmoles of the drug and/or its sulfoxide can be determined by the assay.

Table IV—Time Required to Elute Fluorescent Products from Silica Gel Plates

Elution Time, sec	Maximum Eluted Fluorescence, %
5	91 ± 1.2
10	95 ± 2.3
20	97 ± 3.8
30	98 ± 2.2

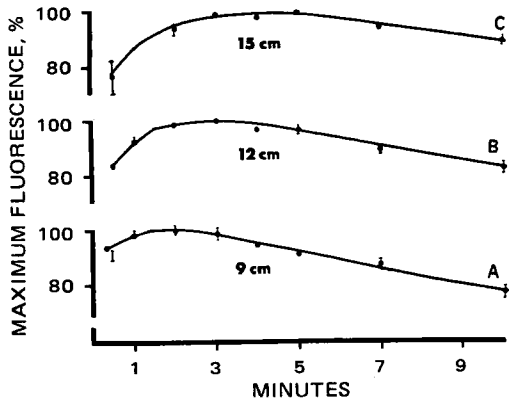

Figure 6—*Time-dependent photolysis of the quaternary product of chlorpromazine on a silica gel TLC plate with the UV lamp heights at 9 (A), 12 (B), and 15 (C) cm. Each point represents the mean of three values* ± *coefficient of variation.*

In the experiments carried out in the presence of blank blood extracts, the values of the total blank (including the contributions due to blood extractables, the reagent, and the TLC plate) ranged from 100 to 200, depending upon the source of blood. Although these blanks varied from blood to blood, the replicate values within a blood varied less than 5%.

Specificity—The method is specific for tertiary amine drugs. Primary and secondary amine metabolites of the drugs, as well as nonamine substances, do not interfere. Mixtures of tertiary amines, if present in the quaternization reaction, are difficult to fractionate for individual determinations. However, by adopting specific TLC procedures with particular adsorbents and solvents, the method can become selective and specific. For example, the described methodology has been specifically adapted for assaying chlorpromazine and its sulfoxide rather accurately, even when present together.

The quaternization fluorometric method should enable the study of dose–blood level–clinical response relationships for chlorpromazine and other drugs. Furthermore, with increasing emphasis being placed on the use of generic products, the potential of the method for conducting bioavailability and bioequivalence studies on tertiary amine drugs is obvious. If a further increase in the sensitivity of the method is accomplished by spotting a larger aliquot of the reaction mixture or similar other modifications, it would perhaps allow the study of localization and biotransformation of chlorpromazine in the relative brain areas reflective of the role or mechanism of action of the drug in the therapeutic regression of schizophrenic symptomatology. The method is currently being applied to clinical studies.

SUMMARY AND CONCLUSIONS

The need for a sensitive, accurate, and precise method for the quantitative determination of picomole quantities of chlorpromazine is fulfilled by the described quaternization assay. This method offers sensitivity in the 20–30-ng range with good accuracy. The coefficient of variation of most replicate analyses was 0–3%. The methodology requires instrumental and technical capabilities well within the scope of a routine clinical laboratory. Furthermore, the number of samples that can be analyzed by an individual per day is considerably larger than is possible with any GC method matching the sensitivity of the described fluorometric assay.

REFERENCES

(1) D. E. Johnson and H. P. Burchfield, "Lectures on Gas Chromatography, 1964; Agricultural and Biological Applications," Plenum, New York, N.Y., 1965, p. 109.

(2) S. H. Curry, *Agressologie*, **9**, 115(1968).

(3) C. G. Hammar and B. Holmstedt, *Experientia*, **24**, 98(1968).

(4) C. G. Hammar, D. Holmstedt, and R. Ryhage, *Anal. Biochem.*, **25**, 532(1968).

(5) S. H. Curry, *Anal. Chem.*, **40**, 1251(1968).

(6) D. H. Efron, S. R. Harris, A. A. Manian, and L. E. Gaudette, *Psychopharmacologia*, **19**, 207(1971).
(7) D. N. Teller, R. J. C. Levine, and H. C. B. Denber, *Agressologie*, **90**, 167(1968).
(8) T. J. Mellinger and C. E. Deller, *Anal. Chem.*, **36**, 1840(1964).
(9) K. Sawashima, R. Dixon, and S. Spector, *Fed. Proc.*, **33**, 571(1974).
(10) M. Shostak and J. Perel, *ibid.*, **34**, 780(1975).
(11) S. H. Curry, *Advan. Biochem. Psychopharmacol.*, **9**, 335(1974).
(12) P. N. Kaul and M. L. Clark, *Proc. ACNP*, in press.
(13) W. J. Turner, P. Turano, and S. Bodzinski, *ibid.*, in press.
(14) R. E. Lehr and P. N. Kaul, *J. Pharm. Sci.*, **64**, 950(1975).
(15) P. N. Kaul, R. E. Lehr, M. W. Conway, and L. R. Whitfield, *IRCS (Research on: Biomedical Technology; Pharmacology)*, **2**, 1343(1974).
(16) R. B. Conrow and S. Bernstein, *J. Org. Chem.*, **36**, 863(1971).

ACKNOWLEDGMENTS AND ADDRESSES

Received May 22, 1975, from the *University of Oklahoma and Central State Griffin Memorial Hospital, Norman, OK 73069*
Accepted for publication July 17, 1975.
Supported in part by U.S. Public Health Service Grant MH 21408-02.
The authors thank Dr. A. Manian, Psychopharmacology Research Branch of the National Institute of Mental Health, for supplying authentic samples of chlorpromazine and its metabolites and Dr. R. Lehr for synthesizing 9-bromomethylacridine.
[x] To whom inquiries should be directed (at 625 Elm Avenue, Norman, OK 73069).

Chlorpromazine Metabolism VIII: Blood Levels of Chlorpromazine and Its Sulfoxide in Schizophrenic Patients

PUSHKAR N. KAUL [x], LLOYD R. WHITFIELD, and MERVIN L. CLARK

Abstract □ A procedure was standardized for extracting chlorpromazine and its sulfoxide from the blood and for applying a recently developed fluorometric assay method to determine blood levels of these two compounds in schizophrenic patients receiving chlorpromazine therapy. The described methodology opens avenues for performing bioavailability and generic equivalence studies in humans.

Keyphrases □ Chlorpromazine and its sulfoxide—extraction from whole blood, fluorometric analysis □ Tranquilizers—chlorpromazine and its sulfoxide, extraction from whole blood, fluorometric analysis □ Fluorometry—analysis, chlorpromazine and its sulfoxide after extraction from whole blood

An approach to assaying chlorpromazine and its sulfoxide in relatively low concentrations was described recently (1–4). It utilizes quaternization of the tertiary amines with 9-bromomethylacridine and a photolytic process to generate fluorescent acridine derivatives in a stoichiometric fashion. The chief advantages of this methodology include a relatively high sensitivity, adequate for determining the clinically accrued blood levels; a high degree of precision, not present in any other method available for assaying chlorpromazine on a routine basis; and ease of analysis of a large number of samples simultaneously.

This paper describes the biological and clinical applications of the fluorometric methodology, preliminary to detailed clinical and pharmacokinetic studies on chlorpromazine currently in progress.

EXPERIMENTAL

Materials and Equipment—The materials and equipment were described previously (4). Isoamyl alcohol, 1-propanol, ether, toluene, *n*-heptane[1], and various chlorpromazine metabolites[2] were also used.

Assay Procedure—The optimum assay procedure, developed and standardized previously (4), was used except that chlorpromazine and its sulfoxide had to be isolated from the blood by an appropriate extraction procedure prior to application of the assay method. Therefore, the extraction procedure was standardized as to solvent, pH, and shake-time for optimum extraction.

Extraction Procedure—The use of sonicated whole blood was preferred over plasma, since chlorpromazine (5) as well as its metabolites (6, 7) is localized in the erythrocytes. The sample size was limited to 3 ml as in other assays (7), since volumes of 5 ml or less are clinically reasonable. However, larger volumes may be used if necessary when assaying chlorpromazine levels below 20 ng/ml.

Extraction Solvent—To seven sets of three tubes, each containing 3.16 nmoles of chlorpromazine in 3 ml of sonicated blood adjusted to pH 13, was added 10 ml each of various organic solvents in a 2:1 organic to aqueous volume ratio. The tubes were shaken for a constant time and centrifuged. A 9-ml aliquot of the organic solvent was removed and processed through the remainder of the procedure.

Extraction pH—A series of extraction tubes each contained a 3-ml sonicated blood sample with 3.16 nmoles of chlorpromazine and its sulfoxide. The samples were adjusted to various pH values between 9 and 14, with a set of three to five tubes per pH value. The samples were extracted for a constant time with *n*-hexane containing 1.5% isoamyl alcohol. The extracts were evaporated to dryness under nitrogen and at room temperature and processed through the assay procedure to determine the optimum pH for extraction.

Duration of Extraction—Sets of extraction tubes, with each tube containing fixed known quantities of chlorpromazine and its sulfoxide in 3-ml blood samples at pH 13 and 10 ml of an extraction solvent, were shaken horizontally in a mechanical shaker at 150 cpm for various lengths of time. The tubes were centrifuged,

[1] All nanograde or analytical reagent grade, Mallinckrodt Chemical Works, St. Louis, Mo.
[2] Obtained from the Psychopharmacology Research Branch, National Institute of Mental Health.

(6) D. H. Efron, S. R. Harris, A. A. Manian, and L. E. Gaudette, *Psychopharmacologia*, **19**, 207(1971).
(7) D. N. Teller, R. J. C. Levine, and H. C. B. Denber, *Agressologie*, **90**, 167(1968).
(8) T. J. Mellinger and C. E. Deller, *Anal. Chem.*, **36**, 1840(1964).
(9) K. Sawashima, R. Dixon, and S. Spector, *Fed. Proc.*, **33**, 571(1974).
(10) M. Shostak and J. Perel, *ibid.*, **34**, 780(1975).
(11) S. H. Curry, *Advan. Biochem. Psychopharmacol.*, **9**, 335(1974).
(12) P. N. Kaul and M. L. Clark, *Proc. ACNP*, in press.
(13) W. J. Turner, P. Turano, and S. Bodzinski, *ibid.*, in press.
(14) R. E. Lehr and P. N. Kaul, *J. Pharm. Sci.*, **64**, 950(1975).
(15) P. N. Kaul, R. E. Lehr, M. W. Conway, and L. R. Whitfield, *IRCS (Research on: Biomedical Technology; Pharmacology)*, **2**, 1343(1974).
(16) R. B. Conrow and S. Bernstein, *J. Org. Chem.*, **36**, 863(1971).

ACKNOWLEDGMENTS AND ADDRESSES

Received May 22, 1975, from the *University of Oklahoma and Central State Griffin Memorial Hospital, Norman, OK 73069*
Accepted for publication July 17, 1975.
Supported in part by U.S. Public Health Service Grant MH 21408-02.
The authors thank Dr. A. Manian, Psychopharmacology Research Branch of the National Institute of Mental Health, for supplying authentic samples of chlorpromazine and its metabolites and Dr. R. Lehr for synthesizing 9-bromomethylacridine.
[x] To whom inquiries should be directed (at 625 Elm Avenue, Norman, OK 73069).

Chlorpromazine Metabolism VIII: Blood Levels of Chlorpromazine and Its Sulfoxide in Schizophrenic Patients

PUSHKAR N. KAUL [x], LLOYD R. WHITFIELD, and MERVIN L. CLARK

Abstract □ A procedure was standardized for extracting chlorpromazine and its sulfoxide from the blood and for applying a recently developed fluorometric assay method to determine blood levels of these two compounds in schizophrenic patients receiving chlorpromazine therapy. The described methodology opens avenues for performing bioavailability and generic equivalence studies in humans.

Keyphrases □ Chlorpromazine and its sulfoxide—extraction from whole blood, fluorometric analysis □ Tranquilizers—chlorpromazine and its sulfoxide, extraction from whole blood, fluorometric analysis □ Fluorometry—analysis, chlorpromazine and its sulfoxide after extraction from whole blood

An approach to assaying chlorpromazine and its sulfoxide in relatively low concentrations was described recently (1–4). It utilizes quaternization of the tertiary amines with 9-bromomethylacridine and a photolytic process to generate fluorescent acridine derivatives in a stoichiometric fashion. The chief advantages of this methodology include a relatively high sensitivity, adequate for determining the clinically accrued blood levels; a high degree of precision, not present in any other method available for assaying chlorpromazine on a routine basis; and ease of analysis of a large number of samples simultaneously.

This paper describes the biological and clinical applications of the fluorometric methodology, preliminary to detailed clinical and pharmacokinetic studies on chlorpromazine currently in progress.

EXPERIMENTAL

Materials and Equipment—The materials and equipment were described previously (4). Isoamyl alcohol, 1-propanol, ether, toluene, *n*-heptane[1], and various chlorpromazine metabolites[2] were also used.

Assay Procedure—The optimum assay procedure, developed and standardized previously (4), was used except that chlorpromazine and its sulfoxide had to be isolated from the blood by an appropriate extraction procedure prior to application of the assay method. Therefore, the extraction procedure was standardized as to solvent, pH, and shake-time for optimum extraction.

Extraction Procedure—The use of sonicated whole blood was preferred over plasma, since chlorpromazine (5) as well as its metabolites (6, 7) is localized in the erythrocytes. The sample size was limited to 3 ml as in other assays (7), since volumes of 5 ml or less are clinically reasonable. However, larger volumes may be used if necessary when assaying chlorpromazine levels below 20 ng/ml.

Extraction Solvent—To seven sets of three tubes, each containing 3.16 nmoles of chlorpromazine in 3 ml of sonicated blood adjusted to pH 13, was added 10 ml each of various organic solvents in a 2:1 organic to aqueous volume ratio. The tubes were shaken for a constant time and centrifuged. A 9-ml aliquot of the organic solvent was removed and processed through the remainder of the procedure.

Extraction pH—A series of extraction tubes each contained a 3-ml sonicated blood sample with 3.16 nmoles of chlorpromazine and its sulfoxide. The samples were adjusted to various pH values between 9 and 14, with a set of three to five tubes per pH value. The samples were extracted for a constant time with *n*-hexane containing 1.5% isoamyl alcohol. The extracts were evaporated to dryness under nitrogen and at room temperature and processed through the assay procedure to determine the optimum pH for extraction.

Duration of Extraction—Sets of extraction tubes, with each tube containing fixed known quantities of chlorpromazine and its sulfoxide in 3-ml blood samples at pH 13 and 10 ml of an extraction solvent, were shaken horizontally in a mechanical shaker at 150 cpm for various lengths of time. The tubes were centrifuged,

[1] All nanograde or analytical reagent grade, Mallinckrodt Chemical Works, St. Louis, Mo.
[2] Obtained from the Psychopharmacology Research Branch, National Institute of Mental Health.

and appropriate aliquots of the organic phase were evaporated and processed by the assay procedure to determine the optimum shake-time for extraction.

Evaporation of Extract—After centrifugation for 10 min at 2250 rpm following the extraction phase, 9-ml aliquots of the organic layer from each tube were transferred to 30-ml Pyrex tubes and evaporated under nitrogen at different temperatures to approximately 0.5 ml. The concentrated extract was quantitatively transferred to a 1.5-ml stoppered polyethylene tube with the help of sequential rinses of 1.0, 0.5, and 0.5 ml of methanol. The solvent was evaporated to dryness and subjected to the assay procedure.

Addition and Recovery—Known quantities of chlorpromazine and its sulfoxide were added to 3-ml sonicated blood samples and processed through optimum extraction and assay procedures. The same quantities of the phenothiazines were also added directly to the quaternization reaction tubes and carried through the assay procedure.

Standard curves for the two compounds were obtained by adding varying amounts of each compound to naive human blood and then assaying the blood to determine the relative fluorescence corresponding to the various concentrations of the compounds.

Clinical Data—The standardized extraction and assay procedure is currently being used to analyze blood levels of chronic schizophrenic patients who received 200 or 600 mg/m^2/day po of chlorpromazine in four equally divided doses. A kinetic study was carried out on these patients at the beginning of therapy (Week 0) and at Weeks 4 and 12. For 3 days prior to and after each kinetic study, the patients were maintained on a standard liquid diet of uniform composition and calorie value.

On the day of the kinetic study, 120 mg/m^2 po of chlorpromazine hydrochloride in a syrup formulation was administered before breakfast. No food was given until 2 hr after the oral dose. Also, no medication was given following that single kinetic study dose until the 3rd day when the chlorpromazine four times a day schedule was resumed. No other drug was given to the patients. The blood samples were drawn by aseptic venipuncture before and at various time intervals after the kinetic study dose and kept frozen until assayed.

RESULTS AND DISCUSSION

The extraction efficiency of chlorpromazine was enhanced when the blood samples were extracted at pH 12–14 rather than at pH 9–11. A pH of 13 and above was chosen for routine extractions, because hydroxylated tertiary amine metabolites were not extracted into the organic solvent to any meaningful extent (less than 5%) at that pH. The optimum shake-time for extraction was 30 min.

Of the various organic solvents (Table I) evaluated for single-extraction efficiency, toluene, *n*-heptane, and *n*-hexane, all containing 1.5% isoamyl alcohol, were equally effective in extracting chlorpromazine from the blood at pH 13. Being a relatively lower boiling solvent, *n*-hexane was selected for routine extractions. Although ether was equally good, the quantitative transfers of this solvent were generally inaccurate due to its relatively high vapor pressure.

The evaporation of the organic extract was always carried out under nitrogen, since it is known that the phenothiazines are readily oxidizable. Of the various temperatures tested for suitability for evaporation of the extract, room temperature appeared to yield most consistent results.

Optimum Extraction Procedure—A 3-ml whole blood sample, containing chlorpromazine and its sulfoxide to be assayed, was sonicated in an extraction tube and adjusted to pH 13.0–13.5 with 2 *N* NaOH. Ten milliliters of *n*-hexane containing 1.5% isoamyl alcohol was added. The tube was stoppered, shaken horizontally on a mechanical shaker at 150 cpm for 30 min, and centrifuged. A 9-ml aliquot of the organic phase was transferred to another tube for evaporation to 0.5 ml at room temperature and under nitrogen.

The concentrate was quantitatively transferred to a 2.5-ml polyethylene reaction tube with the help of three sequential rinses of 1.0, 0.5, and 0.5 ml of methanol. The combined transfer rinses were evaporated to dryness at room temperature and under nitrogen. The residue was then treated with the quaternizing reagent and processed by the optimum assay procedure.

Addition and Recovery—Based on single extractions under optimum conditions of pH, shake-time, and solvent, the percent recoveries of various amounts of chlorpromazine added to blood ranged from 65 to 74% (Table II). The precision of replicate extractions was well within ±5%.

The data obtained by adding known amounts of chlorpromazine and its sulfoxide to 3-ml samples of blood and assaying by the combined extraction and assay procedure yielded linear standard curves for the two compounds over a concentration range of 20 ng–1 μg/ml.

Precision and Blanks—The precision of over 200 replicate (n = 2–5) sets of analyses, carried out over several months and expressed in terms of coefficient of variation, was ≤5% for nearly 80% of the total sets. Replicate analyses yielding a coefficient of variation larger than 10% are subject to a repeat assay in this laboratory. Considering the number and nature of various steps involved in the assay, the observed precision appeared fairly good.

The relative fluorescence values of blood blanks, inherently due to contributions of the blood extractables (drug unrelated) and the TLC plates, are shown in Table III. On the whole, the replicates of blank values within an experiment varied to a far less extent (<5%) than did the values between the experiments on different days. This variation was related to the variation in the source of blood. In routine analyses of chlorpromazine and its sulfoxide in blood, the corresponding fluorescence values of the blanks were subtracted from those of the unknown samples assayed, prior to computation of the unknown concentrations, with the help of standard curves.

Interference by Metabolites—The extraction procedure was designed to exclude all the hydroxylated metabolites of chlorpromazine. The primary and secondary amine metabolites, although extracted from the blood along with the drug and its sulfoxide, either do not react with the acridine reagent or their reaction products move to the solvent front along with the other relatively nonpolar reagent and reaction by-products when subjected to TLC with the acetonitrile–water system.

Theoretically, other nonhydroxylated metabolites of chlorpromazine, *e.g.*, 7-methoxychlorpromazine and its sulfoxide, should also be extractable if present in the blood of patients receiving chlorpromazine therapy. However, preliminary experiments indicated that this may not be a major problem. For example, when a 10-ml blood sample (at the peak absorption time) of a patient receiving a 1600-mg chronic daily dose of chlorpromazine was ex-

Table I—Relative Extractability of Chlorpromazine from Blood at pH 13 into Various Organic Solvents following Single Extraction for 30 min at 150 Shakes/min

Solvent	Maximum Extraction, %
n-Hexane	28
Benzene	38
15% 1-Propanol in hexane	43
3% Isoamyl alcohol in hexane	66
Ether	100
1.5% Isoamyl alcohol in *n*-heptane	100
1.5% Isoamyl alcohol in toluene	100
1.5% Isoamyl alcohol in *n*-hexane	100

Table II—Addition of Chlorpromazine to, and Its Recovery from, Whole Human Blood

Amount Added, ng/ml	Amount Recovered, ng/ml	Recovery, %
40	26 ± 1.6[a]	64.0 ± 2.9
60	39 ± 0.8	64.0 ± 1.4
100	71 ± 2.9	71.0 ± 2.6
400	279 ± 17.3	70.0 ± 3.7

[a] Mean ± *SD*; n = 2–4.

Table III—Relative Fluorescence Values of Various Blanks

Blank	Relative Fluorescence
Plate	70–90
Reaction (including plate blank)	100–120
Blood (including reaction blank)	120–220

Table IV—Blind Analyses of Spiked Blood Samples Containing Chlorpromazine and Its Sulfoxide

Chlorpromazine Concentration, ng/ml		Chlorpromazine Sulfoxide, ng/ml	
Added	Found	Added	Found
30.7[a]	29.0	30.3[a]	32.3
	27.5		30.6
	28.5		30.2
	25.0		33.1
	29.5		35.6
	$\bar{x}$[b] = 28.0 ± 1.88		$\bar{x}$ = 32.0 ± 2.20
139.0[c]	153.0	128.0[c]	115.0
	142.8		116.3
	140.0		112.0
	$\bar{x}$ = 145.0 ± 6.84		$\bar{x}$ = 114.0 ± 2.20
278.0[c]	278.0	256.0[c]	234.5
	251.5		224.3
	283.8		284.3
	$\bar{x}$ = 271.0 ± 17.20		$\bar{x}$ = 231.0 ± 6.90
256.0[a]	298.0	306.0[a]	313.0
	305.0		330.0
	311.0		333.0
	320.0		335.0
	295.0		325.0
	$\bar{x}$ = 306.0 ± 10.10		$\bar{x}$ = 327.0 ± 8.80

[a] Lyophilized plasma samples prepared by Dr. W. J. Turner, Central Islip State Hospital, Long Island, N.Y. [b] Mean ± *SD*. [c] Prepared at Central State Griffin Memorial Hospital.

tracted and the extract was subjected to TLC with methanol–ethyl acetate–acetic acid–water (17:56:17:10) as the developing solvent, 7-methoxychlorpromazine and its sulfoxide were nondetectable (authentic compounds used as reference). However, traces of promazine, its sulfoxide, and 7-methoxypromazine were detected. On elution, evaporation under nitrogen to dryness, and subjection to the described assay procedure, these promazine compounds at the peak absorption time together constituted nearly 30% of the steady-state blood level (800 ng/ml) of the patient measured in terms of chlorpromazine.

Considering that (*a*) the routine assay is based on only a 3-ml blood sample instead of 10 ml, (*b*) the usual therapeutically effective and clinically used dose of chlorpromazine is in the range of 150–600 mg/day (8), and (*c*) the steady-state blood levels[3] of the drug in a large number of patients receiving total daily oral doses of 200 and/or 600 mg/m^2 range from only 21 to 110 ng/ml, it appears reasonable that the interference due to these promazine metabolites, if present in other patients as well, may not be of major concern. However, this issue is being evaluated further.

Analysis of Unknowns—To determine the accuracy of the quaternization method when applied to blood or plasma, spiked samples were prepared and subsequently blind analyzed to determine the chlorpromazine and its sulfoxide concentrations. Table IV lists the results.

Patient Data—The developed and standardized assay methodology is currently being used in chronic clinical studies with schizophrenic patients aimed at correlating the orally given dose of chlorpromazine with its various pharmacokinetic parameters as well as the clinical responses observed. Figure 1 shows the absorption–elimination time profiles of chlorpromazine and its sulfoxide in a patient (C.D.) following ingestion of a single oral dose of 120 mg/m^2 of chlorpromazine (syrup formulation) on an empty stomach during Weeks 0, 4, and 12 of a chronic study.

The elimination of chlorpromazine in the blood of the same patient appeared to follow first-order kinetics, with a half-life of 3–4 hr and the elimination rate constant, k_e, of 17.3–22.3 × 10^{-2} hr^{-1} (Fig. 2). The elimination rate was significantly ($p < 0.05$) higher at Week 12 than at Week 0, suggesting a possible autoinduction caused by chlorpromazine and/or its metabolite(s) in the patient. However, this difference in half-lives may have been due to an intrasubject variation with time.

Application to Generic Bioequivalence—The full potential of

[3] Determined in this laboratory.

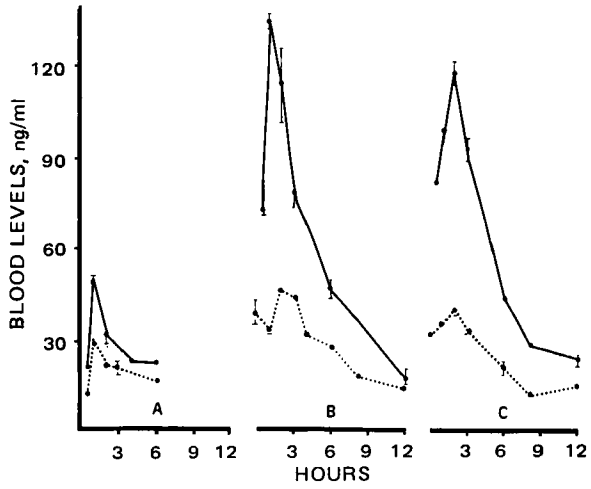

Figure 1—*Appearance and disappearance of chlorpromazine (——) and its sulfoxide (. . . .) in the blood of a chronic schizophrenic patient receiving 600 mg/m^2/day in four equally divided doses. The samples were drawn before and after giving the single oral kinetic dose (120 mg/m^2) of chlorpromazine on Weeks 0 (A), 4 (B), and 12 (C). Each point represents the mean of two values* ±SD.

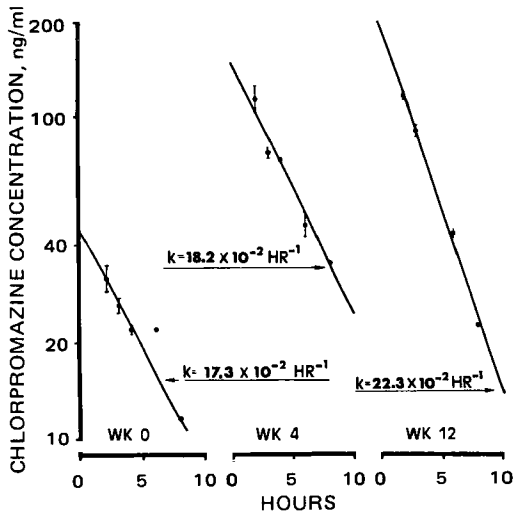

Figure 2—*Semilogarithmic plots of the data on elimination of chlorpromazine in a chronic schizophrenic patient receiving 600 mg/m^2/day in four equally divided doses. The blood samples were drawn before and after giving the single oral kinetic dose (120 mg/m^2) of chlorpromazine on Weeks 0, 4, and 12. Each point represents the mean of two values* ±SD.

the developed assay method may be gauged by realizing that it is applicable to many tertiary amine drugs other than chlorpromazine. Furthermore, assessment of the bioavailability of generic products that require an accurate and precise method of analysis makes this assay methodology valuable, particularly for drugs that show a large volume of distribution in the body. So far, atropine, amitriptyline, chlorprothixene, codeine, imipramine, morphine, pilocarpine, strychnine, and trifluoperazine have been found to react with 9-bromomethylacridine and produce fluorescent products upon photolysis. The stoichiometry of some of these reactions was found to hold over a wide range of concentrations. For example, Fig. 3 shows a concentration–fluorescence correlation with amitriptyline, chlorprothixene, and imipramine.

In a global cooperative assay study, 14 different laboratories were sent blind spiked plasma samples containing low and high concentrations of chlorpromazine and its sulfoxide. Of all the returns of data, the acridine fluorometric methodology appeared unmatched in terms of accuracy and precision (9).

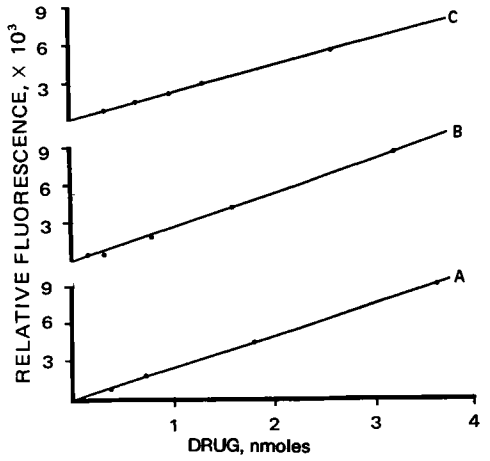

Figure 3—*Stoichiometric correlation of the direct reaction of imipramine (A), chlorprothixene (B), and amitriptyline (C) with 9-bromomethylacridine. Each point is the mean of three values.*

The described assay methodology has shown a specificity for tertiary amines, which precludes the possibility of interference due to the primary and secondary amine metabolites generally present in the blood of patients receiving drugs such as chlorpromazine (6, 7, 10) and amitriptyline (11, 12). However, the methodology does not presently discriminate between mixtures of tertiary amine drugs such as chlorpromazine and chlorprothixene. Nonetheless, it should be possible to differentiate the quaternary products of these drug mixtures by developing new TLC systems capable of such separations or by exploring electrophoresis prior to the photolytic step. These and other approaches are being attempted.

REFERENCES

(1) P. N. Kaul, R. E. Lehr, M. W. Conway, and L. R. Whitfield, *IRCS (Research on: Biomedical Technology; Pharmacology)*, **2**, 1343(1974).

(2) R. E. Lehr and P. N. Kaul, *J. Pharm. Sci.*, **64**, 950(1975).

(3) P. N. Kaul and M. L. Clark, *Proc. ACNP*, in press.

(4) P. N. Kaul, L. R. Whitfield, and M. L. Clark, *J. Pharm. Sci.*, **65**, 689(1976).

(5) P. Seeman and J. I. Weinstein, *Biochem. Pharmacol.*, **15**, 1743(1969).

(6) P. N. Kaul, M. J. Ticku, and M. L. Clark, *J. Pharm. Sci.*, **61**, 1753(1972).

(7) P. N. Kaul, M. W. Conway, M. J. Ticku, and M. L. Clark, *ibid.*, **61**, 581(1972).

(8) M. L. Clark, H. R. Ramsey, R. E. Ragland, D. K. Rahhal, E. A. Serafetinides, and J. P. Costiloe, *Psychopharmacologia*, **18**, 260(1970).

(9) W. J. Turner, P. Turano, and S. Bodzinski, *Proc. ACNP*, in press.

(10) P. Turano, J. E. March, W. J. Turner, and S. Merlis, *J. Med.*, **3**, 109(1972).

(11) H. B. Hucker and C. C. Porter, *Fed. Proc.*, **20**, 172(1961).

(12) U. Breyer and H. Remer, *Arch. Toxikol.*, **28**, 176(1971).

ACKNOWLEDGMENTS AND ADDRESSES

Received May 22, 1975, from the *University of Oklahoma and Central State Griffin Memorial Hospital, Norman, OK 73069*

Accepted for publication July 17, 1975.

The authors thank Dr. A. Manian, Psychopharmacology Research Branch of the National Institute of Mental Health, for supplying authentic samples of chlorpromazine and its metabolites.

ˣ To whom inquiries should be directed (at 625 Elm Avenue, Norman, OK 73069).

Effects of Various Hydrodynamic Conditions on Dissolution Rate Determinations

FRED L. UNDERWOOD * and DONALD E. CADWALLADER ˣ

Abstract □ An automated potentiometric procedure was used in dissolution rate studies to determine the effects of various hydrodynamic conditions on dissolution rate determinations. Changes in the hydrodynamics of the system resulted from using various sizes and shapes of dissolution vessels. Dissolution rate constants for benzoic acid prills in distilled water at pH-stat 6.2 were used as a measure of the agitation intensities present in the different shaped vessels. Great variations in the dissolution rates occurred in vessels with the same diameter and stirrer blade position when the shapes of the bottom of the vessel were varied. A similar order of dissolution rates was obtained at 100 and 150 rpm for the individual vessels at various propeller heights. The order differed from one vessel to another, depending on the shape of the bottom (concave, convex, or flat) of the vessel. In some cases, a change in the type of bottom resulted in the opposite order of rates for vessels with the same diameter.

Keyphrases □ Dissolution rate—benzoic acid, effect of varying hydrodynamic conditions by varying sizes and shapes of dissolution vessels □ Hydrodynamic conditions—effect on dissolution rate of benzoic acid by varying sizes and shapes of dissolution vessels □ Benzoic acid—dissolution rate, effect of varying hydrodynamic conditions by varying sizes and shapes of dissolution vessels

For several years, it has been recognized that the availability of a drug for GI absorption from solid dosage forms is often reflected by *in vitro* dissolution rates. This observation has stimulated research in dissolution rate studies. Many different variables, *e.g.*, particle size of dissolving substance, agitation intensity, temperature, and size and shape of the dissolution vessels can influence the dissolution rate of a substance.

Noyes and Whitney (1) made the first quantitative study of the dissolution process and derived an equation relating the dissolution rate to the surface area of the dissolving material. A relationship between dissolution rates and agitation intensity has been known to exist for some time, but relatively few studies have been carried out to show how various hydrodynamic conditions that can influence the agitation can affect the dissolution rate of a drug. The agita-

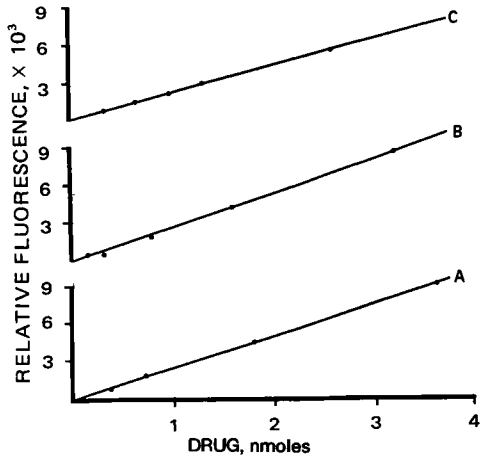

Figure 3—*Stoichiometric correlation of the direct reaction of imipramine (A), chlorprothixene (B), and amitriptyline (C) with 9-bromomethylacridine. Each point is the mean of three values.*

The described assay methodology has shown a specificity for tertiary amines, which precludes the possibility of interference due to the primary and secondary amine metabolites generally present in the blood of patients receiving drugs such as chlorpromazine (6, 7, 10) and amitriptyline (11, 12). However, the methodology does not presently discriminate between mixtures of tertiary amine drugs such as chlorpromazine and chlorprothixene. Nonetheless, it should be possible to differentiate the quaternary products of these drug mixtures by developing new TLC systems capable of such separations or by exploring electrophoresis prior to the photolytic step. These and other approaches are being attempted.

REFERENCES

(1) P. N. Kaul, R. E. Lehr, M. W. Conway, and L. R. Whitfield, *IRCS (Research on: Biomedical Technology; Pharmacology)*, **2**, 1343(1974).

(2) R. E. Lehr and P. N. Kaul, *J. Pharm. Sci.*, **64**, 950(1975).

(3) P. N. Kaul and M. L. Clark, *Proc. ACNP*, in press.

(4) P. N. Kaul, L. R. Whitfield, and M. L. Clark, *J. Pharm. Sci.*, **65**, 689(1976).

(5) P. Seeman and J. I. Weinstein, *Biochem. Pharmacol.*, **15**, 1743(1969).

(6) P. N. Kaul, M. J. Ticku, and M. L. Clark, *J. Pharm. Sci.*, **61**, 1753(1972).

(7) P. N. Kaul, M. W. Conway, M. J. Ticku, and M. L. Clark, *ibid.*, **61**, 581(1972).

(8) M. L. Clark, H. R. Ramsey, R. E. Ragland, D. K. Rahhal, E. A. Serafetinides, and J. P. Costiloe, *Psychopharmacologia*, **18**, 260(1970).

(9) W. J. Turner, P. Turano, and S. Bodzinski, *Proc. ACNP*, in press.

(10) P. Turano, J. E. March, W. J. Turner, and S. Merlis, *J. Med.*, **3**, 109(1972).

(11) H. B. Hucker and C. C. Porter, *Fed. Proc.*, **20**, 172(1961).

(12) U. Breyer and H. Remer, *Arch. Toxikol.*, **28**, 176(1971).

ACKNOWLEDGMENTS AND ADDRESSES

Received May 22, 1975, from the *University of Oklahoma and Central State Griffin Memorial Hospital, Norman, OK 73069*

Accepted for publication July 17, 1975.

The authors thank Dr. A. Manian, Psychopharmacology Research Branch of the National Institute of Mental Health, for supplying authentic samples of chlorpromazine and its metabolites.

ˣ To whom inquiries should be directed (at 625 Elm Avenue, Norman, OK 73069).

Effects of Various Hydrodynamic Conditions on Dissolution Rate Determinations

FRED L. UNDERWOOD * and DONALD E. CADWALLADER ˣ

Abstract □ An automated potentiometric procedure was used in dissolution rate studies to determine the effects of various hydrodynamic conditions on dissolution rate determinations. Changes in the hydrodynamics of the system resulted from using various sizes and shapes of dissolution vessels. Dissolution rate constants for benzoic acid prills in distilled water at pH-stat 6.2 were used as a measure of the agitation intensities present in the different shaped vessels. Great variations in the dissolution rates occurred in vessels with the same diameter and stirrer blade position when the shapes of the bottom of the vessel were varied. A similar order of dissolution rates was obtained at 100 and 150 rpm for the individual vessels at various propeller heights. The order differed from one vessel to another, depending on the shape of the bottom (concave, convex, or flat) of the vessel. In some cases, a change in the type of bottom resulted in the opposite order of rates for vessels with the same diameter.

Keyphrases □ Dissolution rate—benzoic acid, effect of varying hydrodynamic conditions by varying sizes and shapes of dissolution vessels □ Hydrodynamic conditions—effect on dissolution rate of benzoic acid by varying sizes and shapes of dissolution vessels □ Benzoic acid—dissolution rate, effect of varying hydrodynamic conditions by varying sizes and shapes of dissolution vessels

For several years, it has been recognized that the availability of a drug for GI absorption from solid dosage forms is often reflected by *in vitro* dissolution rates. This observation has stimulated research in dissolution rate studies. Many different variables, *e.g.*, particle size of dissolving substance, agitation intensity, temperature, and size and shape of the dissolution vessels can influence the dissolution rate of a substance.

Noyes and Whitney (1) made the first quantitative study of the dissolution process and derived an equation relating the dissolution rate to the surface area of the dissolving material. A relationship between dissolution rates and agitation intensity has been known to exist for some time, but relatively few studies have been carried out to show how various hydrodynamic conditions that can influence the agitation can affect the dissolution rate of a drug. The agita-

Table I—Sizes and Shapes of Dissolution Vessels

Outside Diameter, mm	Type of Bottom	500-ml Water Depth[a], mm
60	Flat	210
60	Concave	215
60	Convex	205
80	Flat	115
80	Concave	125
80	Convex	105
100	Flat	72
100	Concave	82
100	Convex	62

[a] This dimension is the height of the fluid surface from the bottom of the vessel when filled with 500 ml of distilled water at 37°.

tion effects on dissolution rates were studied using four vessels of different sizes and shapes (2). The effect of these different vessels on the dissolution rates was demonstrated; the vertical position of the agitator was varied in one vessel to study the effects of this variable on dissolution rates.

Hixson and Wilkens (3) conducted experiments in a series of geometrically similar cylindrical vessels, ranging in volume from 2.8 to 1338.7 liters (0.73 to 353 gallons), to study the performance of agitators in liquid–solid chemical systems. The same series of vessels was used to study the rate of dissolution of solids in liquids (4).

The flow patterns were compared in several geometrically dissimilar dissolution apparatus widely used in dissolution rate studies (5). Seven types of dissolution apparatus were tested to assess experimental reproducibility and apparatus variables and to examine the adherence of the kinetics of the dissolution process to theoretical rate laws (6). No attempt was made to examine the effect of changing variables such as agitation intensity, solvent volume, or geometry for a given apparatus. These studies appear to be the only reported experiments relating the effect of different geometrical shapes of dissolution vessels to dissolution rates.

Many types and shapes of containers are used in dissolution rate studies and testing procedures. Three commonly used ones are flat-bottom beakers (7), round-bottom vessels (8), and concave-bottom vessels (9). The purpose of this investigation was to show the effect of various hydrodynamic conditions, particularly the effect of different geometrically shaped dissolution vessels, on the dissolution rate of a model drug.

EXPERIMENTAL

Materials—Benzoic acid USP[1] was the model drug selected for these studies. Prills of benzoic acid were made by carefully melting benzoic acid powder (mp 122.4°) and spraying the melt into the air. The melt was aspirated into a preheated 1-ml tuberculin syringe fitted with a 1.27-cm (0.5-in.) 27-gauge stainless steel needle. The melt was sprayed into the air by pushing the plunger in rapidly. The droplets of benzoic acid formed spherical shapes while in the air, where they cooled and solidified. The prills were collected and separated into the desired size fraction (20–30 mesh) by sieving.

Equipment—A pH-stat instrumental setup[2] similar to that of

[1] Fisher Scientific Co.
[2] Radiometer–Copenhagen, 72 E. M. Drupvej, Copenhagen NV, Denmark.

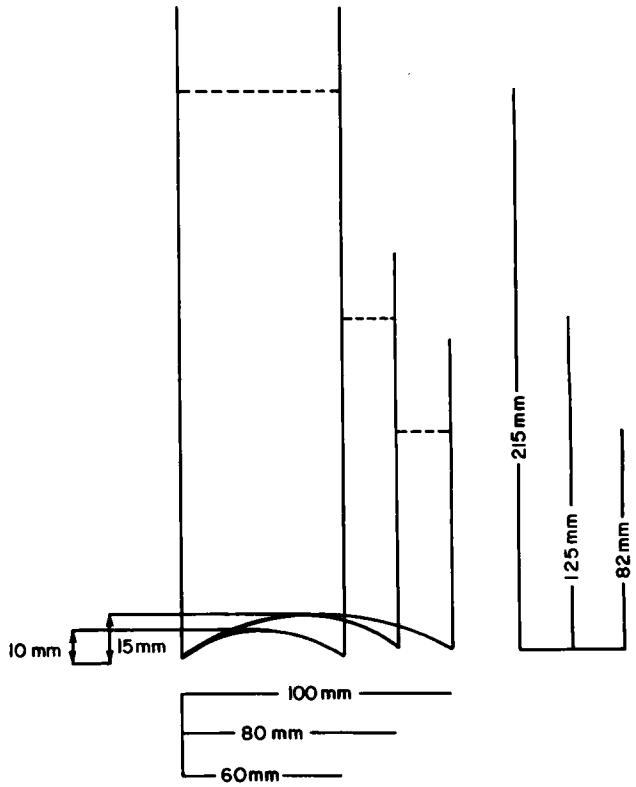

Figure 1—*Diagram of concave-bottom vessels. Broken lines (- - -) indicate water levels.*

Shah (10) was used. It consisted of an automated titrator with a pH meter, an autoburet unit, a titragraph recorder, and appropriate electrodes. The equipment recorded, as a function of time, the supply of correcting acid or base required to maintain a sample at a constant pH. A temperature compensator was used to compensate for slight pH variations at different temperatures.

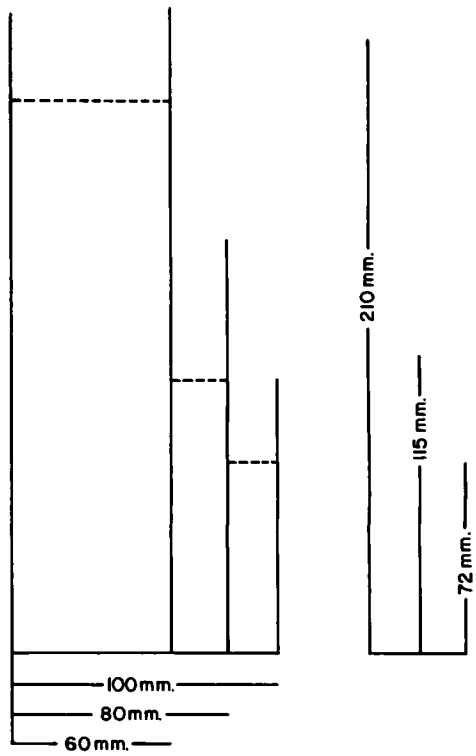

Figure 2—*Diagram of flat-bottom vessels. Broken lines (- - -) indicate water levels.*

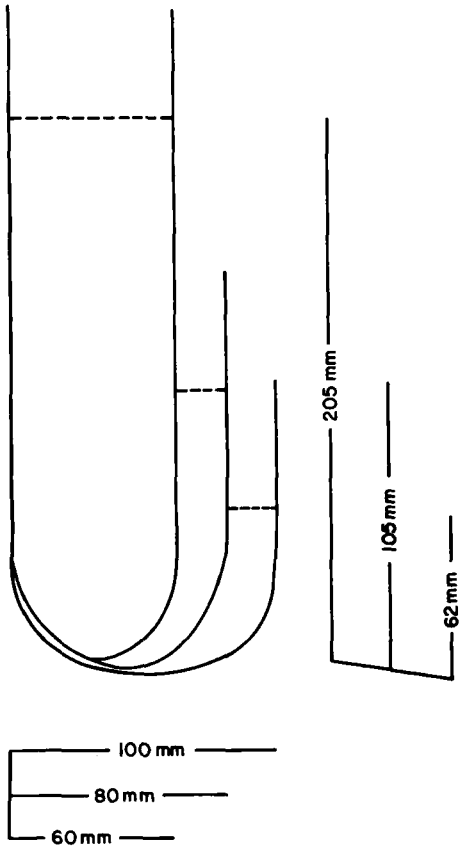

Figure 3—*Diagram of convex-bottom vessels. Broken lines (- - -) indicate water levels.*

The dissolution assembly used for the dissolution rate studies consisted of a double-walled glass-jacketed container and a constant-temperature circulating water bath[3]. This container could accommodate different types and sizes of dissolution vessels. Agitation was produced using a stainless steel marine-type propeller attached to a stainless steel shaft 8 mm in diameter. The propeller consisted of three round blades, 18 mm in diameter, set at 45° angles to the shaft. The propeller had a stirring diameter of 5 cm, and its speed was maintained at a constant rate by a constant-speed torque-controlled unit[4].

Nine glass dissolution vessels with different shaped bottoms were used. Their dimensions are presented in Table I, and diagrams are shown in Figs. 1–3.

Dissolution Studies—A volume of 500 ml of distilled water was placed in the dissolution vessel and brought to 37 ± 0.1° in the constant-temperature bath. A pH-stat of 6.2 was used in all experiments. The propeller was centered at a preselected distance from the bottom of the dissolution vessel, and an accurately weighed sample (0.50 g) of the drug was added to the dissolution medium while the stirrer was rotating at the desired speed. A dissolution rate profile of the drug was obtained directly from the chart recorder.

RESULTS AND DISCUSSION

Figures 4–6 and Table II summarize the data concerning the effect of various hydrodynamic conditions, associated with different shapes of vessels and propeller positions, on the dissolution rate of benzoic acid. Dissolution rate constants for the dissolution of benzoic acid prills under various conditions were calculated using the Hixson–Crowell cube root equation (11).

In the 60-mm convex-bottom vessel, the dissolution rates increased as the distance of the stirrer blade from the bottom of the vessel increased. The opposite results were obtained in the 60-mm concave-bottom vessel, where the dissolution rate decreased as the distance from the bottom of the vessel and the stirrer blade increased. In the 60-mm flat-bottom vessel, the dissolution rates decreased with increasing distances between the stirrer blade and vessel bottom up to 90 mm and then increased with increasing distances between the stirrer blade and vessel bottom. The same general pattern was observed at both 100 and 150 rpm (Figs. 4 and 5).

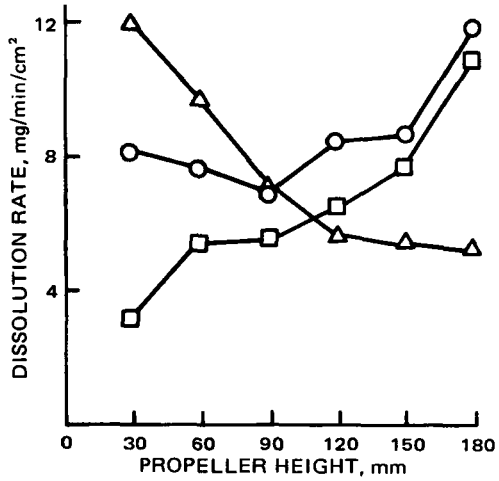

Figure 4—*Effect of propeller position and vessel shape on the dissolution rate of benzoic acid prills in 60-mm o.d. vessels at 100 rpm. Key: ○, flat bottom; □, convex bottom; and △, concave bottom.*

A comparison of the dissolution rates in the 80-mm vessels (Fig. 6) showed the same pattern for 100 and 150 rpm, but the pattern differed from the one shown in the 60-mm vessels. The dissolution rates decreased with increasing distances between the stirrer blade and vessel bottom in the 80-mm concave-bottom vessel and increased in the 80-mm flat-bottom vessel. In the 80-mm round-bottom vessel, the dissolution rate decreased when the distance be-

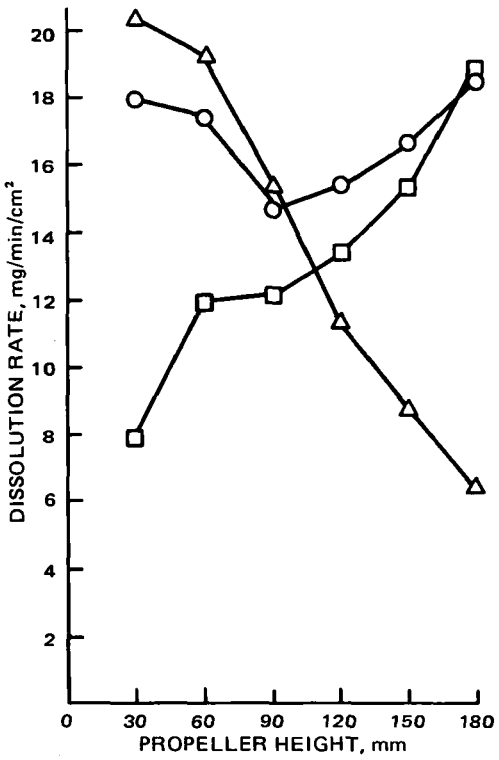

Figure 5—*Effect of propeller position and vessel shape on the dissolution rate of benzoic acid prills in 60-mm o.d. vessels at 150 rpm. Key: ○, flat bottom; □, convex bottom; and △, concave bottom.*

[3] Haake, Yellow Spring Instrument Co.,
[4] Master Servodyne System No. 4425, Cole-Palmer Instrument and Equipment Co., Chicago, Ill.

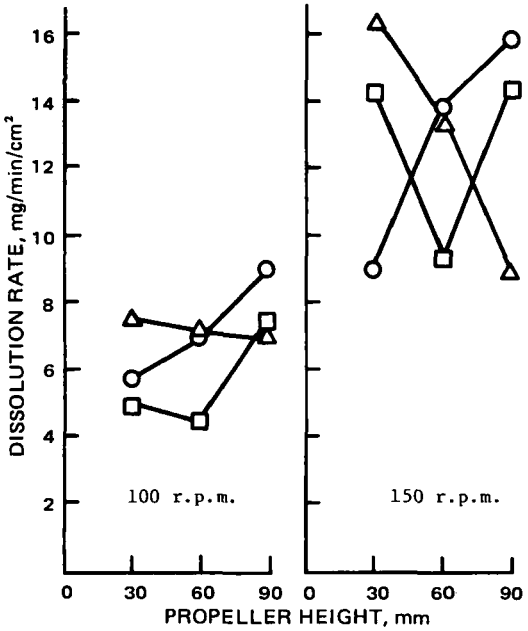

Figure 6—*Effect of propeller position and vessel shape on the dissolution rate of benzoic acid prills in 80-mm o.d. vessels. Key: ○, flat bottom; □, convex bottom; and △, concave bottom.*

tween the stirrer blade and vessel bottom was increased from 30 to 60 mm, and it increased when the distance was increased from 60 to 90 mm at 100 and 150 rpm.

The dissolution rates increased in all 100-mm vessels when the distances between the stirrer blade and the bottoms of the vessels were increased (Table II). However, variations in dissolution rates occurred between vessels having different shaped bottoms.

As seen in Figs. 4 and 5, the dissolution rates were relatively close together when the distance between the bottom of the vessels and stirrer blade was 90 mm. This finding indicated that approximately the same hydrodynamic conditions were present in the various shaped vessels when the propeller was positioned about midway in the dissolution vessels.

The results of this study emphasize the need for carefully scrutinizing *in vitro* dissolution rate data. This need is illustrated dramatically by the opposite order of dissolution rates obtained from experiments carried out in the 60-mm concave- and convex-bottom vessels. The results of this study indicate that the rate of solution of a drug formulation from a dosage form could pass the dissolution requirement using a vessel with one type of bottom and fail using another.

The wide range of dissolution rates obtained in the same vessels at various propeller heights and from different vessels at the same propeller height stresses the importance of propeller positions and vessel shapes in dissolution studies. The need for using the same size and shape vessels, identical stirrer blades, and the same stirrer blade positions for obtaining reproducible dissolution data in quality control or for reproducing results between laboratories is evident from the results obtained in this study.

There appears to be general agreement among those engaged in dissolution rate studies that a correlation between *in vitro* dissolution data and *in vivo* absorption data is of utmost importance. Levy *et al.* (12) pointed out the pronounced sensitivity of the dissolution rate of a drug in tablet form to small changes in agitation intensity. They also showed that small changes in agitation intensity as obtained by a change in stirring rate can yield results contrary to those obtained *in vivo* or with much greater differences from those observed in the clinical data. Results of this present study indicate that maintaining a constant shaped vessel and stirrer blade position in *in vitro* dissolution tests could be just as important as using a constant stirrer speed to maintain a constant agitation intensity.

Hixon and Crowell (2, 11, 13) thoroughly investigated the dependence of reaction velocity upon surface and agitation. In describing the nature of agitation on a liquid medium in a qualitative way, they concluded that it would be impossible to calculate the agitation of the total volume of the liquid as a continuous medium, since it varied from point to point. They also pointed out that the shape of the container was important, since it served in general to modify the motion generated in the fluid medium by the agitator. The results of this study tend to bear out their statements.

Table II—Dissolution Rate Constant (Milligrams per Minute per Square Centimeter) for Dissolution of Benzoic Acid Prills (20–30 Mesh) in Different Vessels at Various Propeller Heights at 100 and 150 rpm

Type[a] and Diameter of Vessel, mm	100 rpm		150 rpm	
	30 mm	60 mm	30 mm	60 mm
A-100	11.36	14.85	17.25	19.28
B-100	7.28	12.64	15.68	18.86
C-100	7.13	—	19.01	—

[a] A = flat-bottom vessel, B = convex-bottom vessel, and C = concave-bottom vessel.

REFERENCES

(1) A. A. Noyes and W. R. Whitney, *J. Amer. Chem. Soc.*, **19**, 930(1897).

(2) A. W. Hixson and J. H. Crowell, *Ind. Eng. Chem.*, **23**, 1160(1931).

(3) A. W. Hixson and G. S. Wilkens, *ibid.*, **25**, 1196(1933).

(4) A. W. Hixson and S. J. Baum, *ibid.*, **33**, 1433(1941).

(5) R. J. Withey and A. J. Bowker, *J. Pharm. Pharmacol.*, **24**, 345(1971).

(6) R. J. Withey, *ibid.*, **23**, 573(1971).

(7) G. Levy and B. A. Hayes, *N. Engl. J. Med.*, **262**, 1053(1960).

(8) P. J. Niebergall and J. E. Goyan, *J. Pharm. Sci.*, **52**, 29(1963).

(9) "The United States Pharmacopeia," 19th rev., Mack Publishing Co., Easton, Pa., 1974, p. 651.

(10) A. C. Shah, *J. Pharm. Sci.*, **60**, 1564(1971).

(11) A. W. Hixson and J. H. Crowell, *Ind. Eng. Chem.*, **23**, 923(1931).

(12) G. Levy, J. R. Leonards, and J. A. Procknall, *J. Pharm. Sci.*, **54**, 1719(1965).

(13) A. W. Hixson and J. H. Crowell, *Ind. Eng. Chem.*, **23**, 1002(1931).

ACKNOWLEDGMENTS AND ADDRESSES

Received March 20, 1975, from the *Department of Pharmacy, School of Pharmacy, University of Georgia, Athens, GA 30602*

Accepted for publication July 23, 1975.

Abstracted in part from a dissertation submitted by F. Underwood to the Graduate School, University of Georgia, in partial fulfillment of the Doctor of Philosophy degree requirements.

* Present address: School of Pharmacy, University of Arkansas, Little Rock, AR 72201

ˣ To whom inquiries should be directed.

Bumetanide: Radioimmunoassay and Pharmacokinetic Profile in Humans

W. R. DIXON ˣ, R. L. YOUNG, A. HOLAZO, M. L. JACK, R. E. WEINFELD, K. ALEXANDER, A. LIEBMAN, and S. A. KAPLAN

Abstract □ A simple, specific, and sensitive radioimmunoassay was developed for the determination of the diuretic bumetanide in plasma and urine. Antiserum to bumetanide was obtained from rabbits immunized with an immunogen prepared by covalently coupling the glycine conjugate of bumetanide to bovine serum albumin. Following extraction of the sample at pH 5.5 with ether, radioimmunoassay of the residue from the ether extract allows for the determination of bumetanide with a limit of sensitivity of about 1 ng/ml using 0.1 ml of plasma or urine. The specificity of the radioimmunoassay was established by comparison with specific radiometric and spectrofluorometric techniques. The pharmacokinetic profile of bumetanide in eight human subjects receiving single 2-mg oral doses of the drug was elucidated using the radioimmunoassay. The peak plasma levels ranged from 39 to 50 ng/ml at 1–4 hr after administration and declined with a mean apparent half-life of 1.17 hr. The mean plasma clearance rate was calculated to be 255 ml/min. During the first 24 hr, a mean of 43% of the bumetanide dose was excreted in the urine as intact drug.

Keyphrases □ Bumetanide—analysis, radioimmunoassay, plasma and urine, compared to radiometric and spectrofluorometric methods, pharmacokinetic profiles □ Radioimmunoassay—analysis, bumetanide, plasma and urine, compared to radiometric and spectrofluorometric methods □ Pharmacokinetics—bumetanide, plasma and urine, radioimmunoassay □ Diuretics—bumetanide, analysis, radioimmunoassay, plasma and urine, pharmacokinetic profiles

Bumetanide[1] (I) is a new sulfonamide diuretic and produces a rapid diuretic response with a short duration of action in humans (1, 2). Its pharmacological action is similar to that of furosemide, but it is 40–60 times more potent on a weight basis (1).

Two methods have been employed for the determination of bumetanide in biological samples. A spectrofluorometric technique (3), with modification (2), is capable of determining the drug in urine with a limit of sensitivity of about 100 ng/ml, and a GC method has similar sensitivity (4). In this laboratory, attempts to quantitate bumetanide in plasma and urine at levels below 100 ng/ml were unsuccessful using either spectrofluorometry or GC.

The development of a sensitive and specific radioimmunoassay is now reported for bumetanide. This method has permitted the elucidation of the blood level and urinary excretion profiles of this drug in humans.

EXPERIMENTAL

Preparation of Immunogen—*N*-(3-*n*-Butylamino-4-phenoxy-5-sulfamoylbenzoyl)glycine (II) was covalently coupled to bovine serum albumin by the mixed anhydride procedure of Erlanger *et al.* (5). Following exhaustive dialysis against 0.05 *M* tromethamine buffer (pH 9) and then distilled water, the immunogen was isolated by lyophilization. On the basis of its optical density at 326 nm in 0.1 *N* NaOH against a standard solution of bumetanide, it was estimated that this immunogen consisted of approximately 40 moles of the drug coupled to 1 mole of albumin.

Immunization and Antiserum Preparation—The lyophilized immunogen was dissolved in isotonic saline to give a 2-mg/ml solution. An equal volume of Freund's complete adjuvant[2] was added, and the mixture was emulsified. Two female New Zealand White rabbits were injected intradermally with 0.25 ml of the emulsion at four sites on the back. One month later, each rabbit received 1 mg of the immunogen subcutaneously as a solution in saline. Two weeks later, the rabbits were bled from the ear artery and the serum was harvested as previously described (6).

Radioimmunoassay Procedure—The following stock solutions were prepared:

1. Tritium-labeled bumetanide[3] (specific activity 16.63 mCi/mg); 150,000 cpm/ml in 0.01 *M* sodium phosphate buffer (pH 7.4).
2. Antiserum diluted 1:200 with buffer containing 0.1% bovine γ-globulin[4] and 0.1% sodium azide.
3. Sodium acetate buffer, 1 *M* (pH 5.5).
4. Standard solutions of 1, 5, 10, 20, 50, 100, and 200 ng/ml of unlabeled bumetanide in distilled water.

To generate a calibration curve relating displacement of bound ^{3}H-bumetanide by 0.1–20 ng of unlabeled drug, 0.1 ml of control plasma or urine was added to assay tubes (10 × 75 mm) containing 0.1 ml of each bumetanide standard. Two blanks also were included by adding 0.1 ml of the control plasma or urine to 0.1 ml of water. The unknown samples (0.1 ml) were then added to tubes containing 0.1 ml of water.

To each tube, 0.05 ml of sodium acetate buffer was added followed by 2 ml of ether. The bumetanide was extracted into the ether by vortexing for 5 sec. The tubes were then immersed in a shallow bath of 2-propanol–dry ice at −30°, and the aqueous phases froze solid within about 10 sec. The ether phases were de-

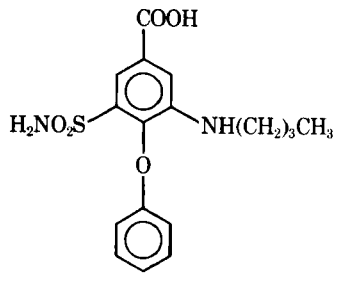

I

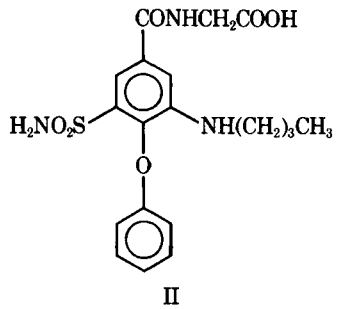

II

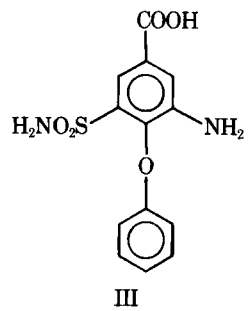

III

[1] 3-*n*-Butylamino-4-phenoxy-5-sulfamoxybenzoic acid.

[2] Grand Island Biological Co., Grand Island, N.Y.

[3] ^{3}H-Bumetanide was prepared by catalytic exchange in tritiated water and was purified by column chromatography.

[4] Miles Laboratories Inc., Kankakee, IL 60901

Table I—Levels of Bumetanide (Nanograms per Milliliter) in the Urine of Four Subjects[a] Who Received 2 mg of the Drug Orally as Measured by the Radioimmunoassay and Fluorometric Method

Collection Period, hr	Subject A		Subject B		Subject C		Subject D	
	Radioimmunoassay	Fluorometric Method	Radioimmunoassay	Fluorometric Method	Radioimmunoassay	Fluorometric Method	Radioimmunoassay	Fluorometric Method
0—2	151	143	160	172	173	219	200	218
2—4	182	193	184	214	202	242	—	—
4—6	120	120	148	147	273	278	240	236
6—8	68	n.m.[b]	23	n.m.	100	123	50	n.m.
8—10	26	n.m.	23	n.m.	18	n.m.	21	n.m.
10—12	15	n.m.	7	n.m.	5	n.m.	7	n.m.
12—24	9	n.m.	8	n.m.	n.m.	n.m.	7	n.m.

[a] These data were obtained during the developmental stages of the radioimmunoassay and are not included in the reported pharmacokinetic results. [b] n.m. = nonmeasurable.

canted into 12 × 75-mm tubes, and the solvent was evaporated by immersing the tubes in a water bath at 40° in a fume hood.

Each dry residue was dissolved in 0.6 ml of phosphate buffer, and 0.2 ml (30,000 cpm) of the ^{3}H-bumetanide solution was added. To each tube, except one blank, 0.2 ml of the diluted antiserum was added and the contents were mixed. After allowing the tubes to stand at 4° overnight, an equal volume (1 ml) of saturated ammonium sulfate was added to precipitate globulin-bound ^{3}H-bumetanide. The tubes were centrifuged at 3000 rpm at 2° for 30 min, and the supernates containing the unbound tracer were decanted into counting vials. After 1 drop of concentrated sulfuric acid was added, 10 ml of toluene scintillator[5] was added and the ^{3}H-bumetanide was extracted into the toluene by placing the covered vials in the vertical position on a reciprocating shaker and shaking for 10 min. Radioactivity in the samples was then determined.

All samples, including the standards and controls, were assayed in duplicate. The average of the tritium counts was used for calculation.

Spectrofluorometric and Radiometric Determinations of Bumetanide—A modification of the spectrofluorometric method of Østergaard *et al.* (3) was developed for the determination of bumetanide in urine. Briefly, the assay involved extraction of bumetanide from urine at pH 2 with ether, followed by TLC on silica gel using chloroform–methanol–acetic acid (85:10:5). The bumetanide (R_f 0.5) was eluted and dissolved in 1 *M* glycine buffer (pH 11.2). The fluorescence was then read in a fluorometer at an emission wavelength of 410 nm with excitation at 325 nm. The limit of sensitivity of this method was about 100 ng/ml of urine.

A radiometric method was used to determine the plasma levels of intact bumetanide in dogs given both oral and intravenous doses of ^{14}C-bumetanide. This procedure entailed an ethyl acetate extraction of acidified plasma and two-dimensional TLC of the concentrated extract with chloroform–methanol–acetic acid (85:10:5) followed by benzene–methanol–acetic acid (9:1:1). The radioactivity, migrating as cochromatographed authentic bumetanide, was determined and converted to nanograms per milliliter of bumetanide from the specific activity of the administered dose.

Clinical Protocol—Eight adult male volunteers, ages 21–60, were enrolled at the research ward[6] for 48 hr. Subjects with a history of renal disease or who were taking medication were excluded. Good health was established by a routine history and physical examination including vital signs, an ECG, and a laboratory battery consisting of complete blood count, urinalysis, fasting blood sugar, blood urea nitrogen, total protein and albumin, serum glutamic oxalic transaminase or serum glutamic pyruvic transaminase, serum bilirubin, alkaline phosphatase, sodium ions, potassium ions, chloride ions, and uric acid. Meals were standardized as to content and amount of fluid. Salt was withheld.

Subjects were admitted to the research ward 24 hr before the start of the study. Each subject was given 1000 ml of tap water to drink over 20–30 min, and then a control (predrug) 24-hr urine collection was initiated. The volume voided was measured. A 20-ml aliquot was taken, labeled with the subject's name, "predrug," and total volume voided, and frozen for shipment and subsequent assay.

On the second morning, the subjects were given 1000 ml of tap water to drink over 20–30 min before drug administration. Subjects were then given a single oral dose of 2 mg (two tablets) of bumetanide. Twelve-milliliter (oxalated) blood specimens were obtained at 0 (control), 0.5, 1.0, 1.5, 2, 4, 6, 10, 12, and 24 hr postadministration. The plasma was separated, labeled, and frozen for subsequent analysis.

Urine specimens (total volume voided) were collected at 0–2, 2–4, 4–6, 6–8, 8–10, 10–12, and 12–24 hr posttreatment. The volume of each specimen was measured, and the subjects were asked to drink an equivalent amount of water. A 20-ml aliquot from each time interval was labeled and frozen for shipment.

Determination of Pharmacokinetic Parameters—Areas under the plasma level–time curves ($0 \rightarrow \infty$) were estimated using the trapezoidal rule; the area from the last data point, $Cp(t)$, to infinity was calculated from the expression $Cp(t)/\beta$. The apparent half-life of elimination of bumetanide from plasma was determined by least-squares analysis of the terminal linear exponential segment of the plasma level–time curve. The apparent half-life of the drug was also calculated by least-squares analysis of the urinary excretion data using "sigma-minus" plots (7).

The total body clearance rate was determined by dividing the dose by the area under the plasma concentration–time curve ($0 \rightarrow \infty$). The latter calculation is made with the assumption that there is 100% bioavailability. The renal clearance rate was obtained by dividing the total amount of drug excreted intact in the urine by the area under the plasma level–time curve.

RESULTS

Antibody Production—Each rabbit produced antiserum capable of binding ^{3}H-bumetanide, as determined by comparison with control serum from nonimmunized rabbits. Almost identical and usable titers of antibodies were obtained from each rabbit at the first bleeding. All reported data were obtained using this first batch of pooled antiserum; 1 ml of a 1:1000 dilution was capable of binding about 70% of the 30,000 cpm of ^{3}H-bumetanide.

Radioimmunoassay Curve—Linearization of the calibration curve was achieved by plotting the percentage inhibition of binding of the ^{3}H-bumetanide, calculated as described previously (6), *versus* the concentration of unlabeled bumetanide on logit–log transformation graph paper[7]. An almost perfect straight line was obtained between 0.1 and 20 ng, resulting in a limit of sensitivity of about 1 ng/ml on analysis of 0.1 ml of plasma or urine. When employing the pooled variance estimate[8] from the replicate data from the whole calibration curve, the percentage inhibition of binding due to 0.1 ng of unlabeled bumetanide was significant at $p = 0.01$. The standard curves obtained in urine and plasma were virtually superimposable. Where necessary, urine samples were diluted with control urine to bring the bumetanide concentration within the limits of the calibration curve.

Recovery of ^{3}H-bumetanide added to plasma and extracted was 80 ± 2% (*SD*, $n = 6$), but no correction was made since standards and unknowns were processed in the same fashion.

Antiserum Specificity—The *N*-desbutyl derivative of bumeta-

[5] Omnifluor, New England Nuclear, Boston, MA 02118
[6] Deer Lodge Research Unit, Deer Lodge, Mont.
[7] TEAM, Box 25, Tamworth, NH 03886
[8] Statistical analyses were carried out by Mr. T. Lewinson, Hoffmann-La Roche Inc.

Table II—Plasma Levels and Urinary Excretion Data of Intact Bumetanide following 2-mg Single Oral Doses of Bumetanide

Hours	Plasma Levels in Eight Subjects, ng/ml							
	1	2	3	4	5	6	7	8
0.5	2.2	1.5	1.3	n.m.	27.5	5.3	n.m.	n.m.
1	13.0	29.5	11.9	4.0	41.0	24.5	12.0	2.2
1.5	44.0	43.0	25.0	6.6	25.5	53.0	38.5	3.8
2	38.0	42.0	38.5	26.2	17.0	63.0	30.5	11.8
4	19.0	16.8	12.6	41.5	7.8	12.8	29.0	49.5
6	1.4	3.7	1.3	11.8	1.3	8.6	9.4	7.3
8	n.m.[a]	3.3	n.m.	5.0	n.m.	4.6	2.3	2.6
10	n.m.	2.6	n.m.	3.0	1.2	2.4	3.3	n.m.
12	n.m.	n.m.	n.m.	n.m.	n.m.	n.m.	n.m.	n.m.
24	n.m.	n.m.	n.m.	n.m.	n.m.	n.m.	n.m.	n.m.
Interval Time, hr	Dose Excreted in Urine in Eight Subjects, %							
0—2	14.9	14.2	12.1	0.6	10.9	13.7	7.4	0.9
2—4	26.5	20.3	23.3	22.8	13.3	21.4	18.7	18.9
4—6	8.1	6.6	6.5	11.3	3.4	5.6	9.2	17.2
6—8	0.6	0.7	2.0	3.8	1.0	2.1	3.1	4.0
8—10	0.7	0.8	0.6	1.6	0.6	1.4	1.4	1.1
10—12	0.4	0.5	0.2	0.6	0.2	0.6	0.6	0.6
12—24	n.m.	0.8	0.4	0.6	0.2	0.4	0.3	0.1
Total 0—24	51.3	43.9	45.1	41.3	29.7	45.2	40.7	42.8

[a] n.m. = nonmeasurable.

nide (III), which has been reported as a metabolite in several animal species (8) but not specifically in the dog (3) or human, showed less than 0.5% cross-reactivity with the antiserum at a concentration necessary to cause 50% inhibition of the binding of the ^{3}H-bumetanide.

Comparison of Radioimmunoassay with Spectrofluorometric and Radiometric Determinations of Bumetanide—Samples of urine from four subjects who had received a 2-mg oral dose of bumetanide were assayed for intact drug by both the radioimmunoassay and the spectrofluorometric method, which had a limit of sensitivity of about 100 ng/ml. From Table I it can be seen that there was satisfactory agreement for the values (above 100 ng/ml) obtained using both methods. In the four samples for which the difference in values exceeded 10%, the fluorometric assay consistently gave the higher level. This result indicates that the radioimmunoassay is at least as specific as the spectrofluorometric assay, which did include a TLC separation step.

The specificity and accuracy of the radioimmunoassay for the determination of bumetanide in plasma were evaluated by analysis of plasma samples from three dogs who had received ^{14}C-bumetanide intravenously or orally. The levels of intact bumetanide were first determined by the radiometric technique. Samples (50 μl) were then assayed by the radioimmunoassay. The carbon-14 counts present in the aliquots taken for the radioimmunoassay were negligible relative to the amount of ^{3}H-bumetanide added.

The joint determinations were subjected to straight-line analysis by the method of Wald (9). The fitted intercept and slope (3.7; 1.04) were not significantly different ($p \leq 0.05$) from 0 and 1 with a correlation coefficient of 0.98 over a range of 32–540 ng/ml of bumetanide[8]. This finding showed that the radioimmunoassay was giving the same plasma levels in the dog as the radiometric assay that included a separation by TLC.

Pharmacokinetic Profile of Bumetanide in Humans—The plasma levels and urinary excretion data are presented in Table II. The plasma level data were evaluated for each subject in terms of the area under the plasma level curves, the maximum bumetanide level seen and the time of its occurrence, the apparent half-life of elimination of the drug from the plasma, and the plasma clearance rate. These pharmacokinetic parameters are presented in Table III.

Following oral administration of 2 mg of bumetanide, peak plasma levels were seen at 2.2 ± 0.4 (*SE*) hr and averaged 45 ± 3 ng/ml. The mean apparent half-life of bumetanide elimination was calculated from the plasma level data to be 1.2 ± 0.1 hr and was calculated from the urinary excretion of drug (sigma-minus plot) to be 1.6 ± 0.1 hr. The mean plasma clearance was 255 ± 26 ml/min, whereas the renal clearance was 107 ± 11 ml/min. By definition, the renal clearance is the fraction of plasma clearance that equals the fraction of the dose excreted unchanged in the urine (43 ± 2%).

DISCUSSION

The aim of the present investigation was to develop a specific radioimmunoassay for bumetanide, which, by virtue of its sensitivity, would allow the pharmacokinetic profile of this drug to be evaluated in humans following oral administration of a 2-mg dose. Previous attempts to determine the low levels of intact bumetanide that exist in plasma by either GC or spectrofluorometry were unsuccessful in this laboratory. This goal was achieved by producing an antiserum to bumetanide in the rabbit for the subsequent development of a radioimmunoassay. This radioimmunoassay proved to be about 100 times more sensitive than the GC and spectrofluorometric methods.

The specificity of the radioimmunoassay for measuring intact bumetanide was established in a number of ways. First, the antiserum was shown not to cross-react with the *N*-desbutyl derivative, the one reported metabolite of bumetanide (8). Second, when the plasma levels of bumetanide in dogs, who had received ^{14}C-bumetanide, were determined by the radioimmunoassay and a specific TLC–radiometric technique, no significant difference in the observed levels were found. Third, the concentrations of bumetanide in human urine, as determined by the radioimmunoassay, were in close agreement with those obtained using a specific spectrofluorometric method which involved the isolation of intact drug by TLC.

Further evidence for the specificity of the radioimmunoassay becomes apparent when one considers the observation of Davies *et al.* (2) that radioactivity in ether extracts of plasma and urine from subjects who had received ^{14}C-bumetanide accurately reflected the

Table III—Pharmacokinetic Profile of Bumetanide in Humans

Parameter	Subject								Mean	±*SE*
	1	2	3	4	5	6	7	8		
Area under plasma level curve (0→∞), ng/ml/hr	118.2	143.9	95.3	165.5	91.7	216.4	156.3	138.0	140.7	14.4
Time of peak plasma level, hr	1.5	1.5	2	4	1	2	1.5	4	2.2	0.4
Peak level, ng/ml	44.0	43.0	38.5	41.5	41.0	63.0	38.5	49.5	44.9	2.9
Apparent half-life of elimination, hr	0.8	1.1	0.8	1.6	1.1	1.8	1.1	0.9	1.2	0.1
Plasma clearance rate, ml/min	282.0	231.6	350.0	201.4	363.5	154.0	213.3	241.5	254.7	25.7
Dose of intact drug in 0—24-hr urine, %	51.3	43.9	45.1	41.3	29.7	45.2	40.7	42.8	42.5	2.2
Calculated apparent half-life of elimination, hr	1.1	2.0	1.6	1.8	1.6	1.8	1.5	1.1	1.6	0.1
Renal clearance rate, ml/min	144.7	101.7	157.9	83.2	108.0	69.6	86.8	103.4	106.9	10.7

amount of intact bumetanide present. This finding suggests that either no appreciable levels of metabolites were present or that bumetanide was selectively extracted by ether. In any event, the ether extraction step in the radioimmunoassay procedure should ensure that adequate specificity is obtained.

Although the major reason for the development of a radioimmunoassay for bumetanide was to obtain high sensitivity, the radioimmunoassay, due to its simplicity, allows a large number of samples to be assayed with relative ease compared to GC and spectrofluorometric methods.

In humans, the major portion of bumetanide excreted in the urine is excreted at the times when the plasma levels of bumetanide are at their peaks. These results suggest that the amount of excretion is proportional to the plasma level of bumetanide. This conclusion is further supported by the finding that the apparent half-lives calculated from either the urinary excretion data or the plasma level data are essentially the same.

Davies *et al.* (2) found that 47% of a 1-mg intravenous dose of ^{14}C-bumetanide was excreted in the urine within 3 days and that 16% was excreted in the feces within 8 days. Following the 2-mg oral dose of bumetanide to the eight subjects in this study, a mean of 43% of the dose was excreted in the urine during the 1st day, suggesting that these oral doses were completely absorbed. In addition, the mean renal clearance of bumetanide of 102 ml/min following intravenous administration to normal subjects (2) is in excellent agreement with the renal clearance of 107 ml/min found in the present study following oral administration. These results further suggest complete absorption of orally administered drug.

REFERENCES

(1) E. Bourke, M. J. A. Asbury, S. O'Sullivan, and P. B. B. Gatenby, *Eur. J. Pharmacol.*, **23**, 283(1973).

(2) D. L. Davies, A. F. Lant, N. R. Millard, A. J. Smith, J. W. Ward, and G. M. Wilson, *Clin. Pharmacol. Ther.*, **15**, 141(1973).

(3) E. H. Østergaard, M. P. Magnussen, C. K. Nielsen, E. Eilertsen, and H. H. Frey, *Arzneim.-Forsch.*, **22**, 66(1972).

(4) P. W. Feit, K. Roholt, and H. Sprensen, *J. Pharm. Sci.*, **62**, 375(1973).

(5) B. F. Erlanger, F. Borek, S. M. Beiser, and S. Lieberman, *J. Biol. Chem.*, **234**, 1090(1959).

(6) W. R. Dixon, J. Early, and E. Postma, *J. Pharm. Sci.*, **64**, 937(1975).

(7) B. K. Martin, *Brit. J. Pharmacol. Chemother.*, **29**, 181(1967).

(8) M. P. Magnussen and E. Eilertsen, *Arch. Pharmacol., Suppl.*, **282**, R61(1974).

(9) M. Kendall and S. Stuart, "The Advanced Theory of Statistics," vol. 2, Hafner, New York, N.Y., 1961, pp. 397–405.

ACKNOWLEDGMENTS AND ADDRESSES

Received April 30, 1975, from the *Department of Biochemistry and Drug Metabolism and the Chemical Research Division, Hoffmann-La Roche Inc., Nutley, NJ 07110*

Accepted for publication July 28, 1975.

[x] To whom inquiries should be directed.

Muscle Relaxant Properties of Chloramphenicol

SACHCHIDANANDA BANERJEE [x] and CHANDAN MITRA

Abstract □ Experiments with the guinea pig ileum, guinea pig trachea, rat fundal strip, rat colon, rat vas deferens, and toad heart indicated that chloramphenicol inhibited smooth muscles, decreasing both the height and frequency of spontaneous contraction. Chloramphenicol-induced relaxation was not mediated through adrenergic, cholinergic, or histaminergic mechanisms. The degree of muscle relaxation was related to the concentration of chloramphenicol, and the relaxant effect could be reversed by removing chloramphenicol from the site of action by washing. Its action appears to be direct on the muscle, possibly by interfering with the energy-generating mechanism.

Keyphrases □ Chloramphenicol—effect on smooth muscle relaxation, guinea pig □ Muscle relaxant activity—chloramphenicol, effect on smooth muscles, guinea pig □ Antibacterials—chloramphenicol, effect on smooth muscle relaxation, guinea pig

Chloramphenicol depresses the spontaneous movements of the rabbit ileum (1). It antagonizes the histamine- or acetylcholine-induced response of the rabbit ileum (1) and the dog bronchial chains (2). Chloramphenicol is 15–25 times more active than ephedrine in this respect (2).

This study was concerned with examining the muscle relaxant properties of chloramphenicol to understand its mode of action. Therefore, the effect of chloramphenicol was determined on different tissues containing smooth muscle such as the guinea pig ileum, rat fundal strip, rat colon, and rat uterus and in isolated organ systems representing the adrenergic, cholinergic, and histaminergic systems. The perfused toad heart, rabbit aortic strip, and rabbit ileum preparations were selected to examine the effect of chloramphenicol on the adrenergic system.

The perfused toad heart preparation exemplified a muscle system containing β-adrenergic receptors with strong autogenous contractile drive, whereas the aortic strip and rabbit ileum preparations represented muscle systems innervated with α-adrenergic receptors. The rabbit jejunum, having a muscle contractile system with a moderate autogenous drive, served as the model of the cholinergic system. The guinea pig trachea, having a muscle system with a weak autogenous contractile drive, served as the representative histaminergic system (3).

EXPERIMENTAL

Toad Heart Perfusion (Adrenergic System)—Toads (*Bufo melanostictus*) of either sex, 75–80 g, were pithed. The abdomen was opened by a midline incision, the pericardium was removed, and a venous cannula was inserted into one hepatic vein opening into the sinus venosus for perfusion with a Symes cannula. The perfusion fluid was frog–Ringer solution. A fine hook was fixed at the tip of the ventricle and was connected through a silk thread with an isotonic lever.

The drugs were injected into the rubber tube attached to the cannula to determine their effect on the spontaneously beating heart. The heart perfusion was continued for 30 min to attain equilibrium before any recordings were taken. For each experiment,

amount of intact bumetanide present. This finding suggests that either no appreciable levels of metabolites were present or that bumetanide was selectively extracted by ether. In any event, the ether extraction step in the radioimmunoassay procedure should ensure that adequate specificity is obtained.

Although the major reason for the development of a radioimmunoassay for bumetanide was to obtain high sensitivity, the radioimmunoassay, due to its simplicity, allows a large number of samples to be assayed with relative ease compared to GC and spectrofluorometric methods.

In humans, the major portion of bumetanide excreted in the urine is excreted at the times when the plasma levels of bumetanide are at their peaks. These results suggest that the amount of excretion is proportional to the plasma level of bumetanide. This conclusion is further supported by the finding that the apparent half-lives calculated from either the urinary excretion data or the plasma level data are essentially the same.

Davies *et al.* (2) found that 47% of a 1-mg intravenous dose of ^{14}C-bumetanide was excreted in the urine within 3 days and that 16% was excreted in the feces within 8 days. Following the 2-mg oral dose of bumetanide to the eight subjects in this study, a mean of 43% of the dose was excreted in the urine during the 1st day, suggesting that these oral doses were completely absorbed. In addition, the mean renal clearance of bumetanide of 102 ml/min following intravenous administration to normal subjects (2) is in excellent agreement with the renal clearance of 107 ml/min found in the present study following oral administration. These results further suggest complete absorption of orally administered drug.

REFERENCES

(1) E. Bourke, M. J. A. Asbury, S. O'Sullivan, and P. B. B. Gatenby, *Eur. J. Pharmacol.*, **23**, 283(1973).

(2) D. L. Davies, A. F. Lant, N. R. Millard, A. J. Smith, J. W. Ward, and G. M. Wilson, *Clin. Pharmacol. Ther.*, **15**, 141(1973).

(3) E. H. Østergaard, M. P. Magnussen, C. K. Nielsen, E. Eilertsen, and H. H. Frey, *Arzneim.-Forsch.*, **22**, 66(1972).

(4) P. W. Feit, K. Roholt, and H. Sprensen, *J. Pharm. Sci.*, **62**, 375(1973).

(5) B. F. Erlanger, F. Borek, S. M. Beiser, and S. Lieberman, *J. Biol. Chem.*, **234**, 1090(1959).

(6) W. R. Dixon, J. Early, and E. Postma, *J. Pharm. Sci.*, **64**, 937(1975).

(7) B. K. Martin, *Brit. J. Pharmacol. Chemother.*, **29**, 181(1967).

(8) M. P. Magnussen and E. Eilertsen, *Arch. Pharmacol., Suppl.*, **282**, R61(1974).

(9) M. Kendall and S. Stuart, "The Advanced Theory of Statistics," vol. 2, Hafner, New York, N.Y., 1961, pp. 397–405.

ACKNOWLEDGMENTS AND ADDRESSES

Received April 30, 1975, from the *Department of Biochemistry and Drug Metabolism and the Chemical Research Division, Hoffmann-La Roche Inc., Nutley, NJ 07110*

Accepted for publication July 28, 1975.

[x] To whom inquiries should be directed.

Muscle Relaxant Properties of Chloramphenicol

SACHCHIDANANDA BANERJEE [x] and CHANDAN MITRA

Abstract □ Experiments with the guinea pig ileum, guinea pig trachea, rat fundal strip, rat colon, rat vas deferens, and toad heart indicated that chloramphenicol inhibited smooth muscles, decreasing both the height and frequency of spontaneous contraction. Chloramphenicol-induced relaxation was not mediated through adrenergic, cholinergic, or histaminergic mechanisms. The degree of muscle relaxation was related to the concentration of chloramphenicol, and the relaxant effect could be reversed by removing chloramphenicol from the site of action by washing. Its action appears to be direct on the muscle, possibly by interfering with the energy-generating mechanism.

Keyphrases □ Chloramphenicol—effect on smooth muscle relaxation, guinea pig □ Muscle relaxant activity—chloramphenicol, effect on smooth muscles, guinea pig □ Antibacterials—chloramphenicol, effect on smooth muscle relaxation, guinea pig

Chloramphenicol depresses the spontaneous movements of the rabbit ileum (1). It antagonizes the histamine- or acetylcholine-induced response of the rabbit ileum (1) and the dog bronchial chains (2). Chloramphenicol is 15–25 times more active than ephedrine in this respect (2).

This study was concerned with examining the muscle relaxant properties of chloramphenicol to understand its mode of action. Therefore, the effect of chloramphenicol was determined on different tissues containing smooth muscle such as the guinea pig ileum, rat fundal strip, rat colon, and rat uterus and in isolated organ systems representing the adrenergic, cholinergic, and histaminergic systems. The perfused toad heart, rabbit aortic strip, and rabbit ileum preparations were selected to examine the effect of chloramphenicol on the adrenergic system.

The perfused toad heart preparation exemplified a muscle system containing β-adrenergic receptors with strong autogenous contractile drive, whereas the aortic strip and rabbit ileum preparations represented muscle systems innervated with α-adrenergic receptors. The rabbit jejunum, having a muscle contractile system with a moderate autogenous drive, served as the model of the cholinergic system. The guinea pig trachea, having a muscle system with a weak autogenous contractile drive, served as the representative histaminergic system (3).

EXPERIMENTAL

Toad Heart Perfusion (Adrenergic System)—Toads (*Bufo melanostictus*) of either sex, 75–80 g, were pithed. The abdomen was opened by a midline incision, the pericardium was removed, and a venous cannula was inserted into one hepatic vein opening into the sinus venosus for perfusion with a Symes cannula. The perfusion fluid was frog–Ringer solution. A fine hook was fixed at the tip of the ventricle and was connected through a silk thread with an isotonic lever.

The drugs were injected into the rubber tube attached to the cannula to determine their effect on the spontaneously beating heart. The heart perfusion was continued for 30 min to attain equilibrium before any recordings were taken. For each experiment,

the number of beats was counted for the first 2 min to obtain the frequency.

Rabbit Aortic Strips (Adrenergic System)—Albino rabbits, 1.5–3 kg, were decapitated after being stunned. The descending thoracic aorta was removed and placed in Krebs–Hensleit solution, and excess fat and connective tissue were removed. The aorta was cut along a closed spiral to form a continuous spiral strip from which small aortic strips, 0.4 mm thick, 2 mm wide, and 2.4 cm long, were prepared (4, 5). One end of the aortic strip was fixed at the base of the tissue chamber, having a volume of 30 ml and containing Krebs–Hensleit solution; the upper end was attached to an isotonic lever.

The lever was adjusted to provide an amplification of nine times and counterweighted to impart a tension of 4 g on the strip. The bath fluid was saturated with a mixture of 95% oxygen and 5% carbon dioxide and maintained at 37.5°. Under 4 g of tension, the strips immediately stretched about 40%, followed by a further stretch of 2–10% during the next 10–60 min. Because of this elongation, the strips were allowed to equilibrate for 2–3 hr before the effects of the drugs were studied.

Rabbit Ileum (Adrenergic System)—Albino rabbits were killed as already described. A section of 4 cm of ileum was excised through a midline incision on the abdomen. The contents of the intestine were removed by gentle washing of the lumen with Tyrode solution kept at 37.5°. A section of approximately 2–2.5 cm of ileum was suspended in a 30-ml organ bath containing Tyrode solution saturated with 95% oxygen and 5% carbon dioxide and maintained at 37.5°. The tissue was equilibrated for 30 min in the organ bath with frequent washings before any contraction was recorded.

Rabbit Jejunum (Cholinergic System)—The preparation was the same as that described for the rabbit ileum. A section of 4 cm of jejunum was excised, 20–30 cm posterior to the pylorus.

Guinea Pig Tracheal Chain (Histaminergic System)—Guinea pigs, 200–250 g, were killed by a blow on the head. The trachea was removed, washed with warm Krebs–Hensleit solution, and then sectioned into 12 rings of about the same width. The rings were connected in series by means of short loops of silk thread in such a way that the dorsal smooth muscle band was vertical in the chamber (6). The chain was suspended in the organ bath at 37.5°; the bath contained Krebs–Hensleit solution saturated with 95% oxygen and 5% carbon dioxide.

A light, sensitive isotonic writing lever with 12-fold magnification was used to record contraction or dilatation of the tracheal chain. The tracheal chain was equilibrated for 60–90 min in the organ bath with frequent washings prior to the recordings.

Other Preparations—Studies also were undertaken with the guinea pig ileum, rat fundal strip, rat colon, rat vas deferens, and rat estrous uterus preparation (7), with acetylcholine, histamine, 5-hydroxytryptamine, nicotine, and pituitrin being used as agonists. The organ bath and the recording device were the same as those described earlier.

Chloramphenicol and other drugs were dissolved or diluted in isotonic sodium chloride solution of pH 7 and added to the bath fluid in the least volume possible to produce minimal osmotic shock to the tissues.

RESULTS

Effect of Chloramphenicol on Isolated Guinea Pig Ileum—The agonists used were acetylcholine, histamine, 5-hydroxytryptamine, and nicotine. Significant alteration in the height of contraction of guinea pig ileum was observed only after relatively high doses of chloramphenicol. Changes in the height of contraction became evident at a concentration of 10 μg/ml of bath for acetylcholine, 20 μg/ml for 5-hydroxytryptamine and nicotine, and 40 μg/ml for histamine.

Incremental increases in concentrations of chloramphenicol from 10 to 320 μg/ml for agonist acetylcholine, from 40 to 640 μg/ml for agonist histamine, and from 20 to 320 μg/ml for agonist nicotine and 5-hydroxytryptamine produced progressive reductions in the height of contraction by the guinea pig ileum (Table I).

Effect of Chloramphenicol on Rat Fundal Strip—The agonist used was 5-hydroxytryptamine. Alterations in the height of contraction of the fundal strip were observed at a relatively high concentration of chloramphenicol (250 μg/ml of bath). Incremental increases in the concentration of chloramphenicol from 250 μg/ml to 2 mg/ml produced a linear reduction in the height of contraction (Table I).

Table I—Chloramphenicol-Induced Inhibition of Smooth Muscles Using Various Agonists

Tissue Preparation	Agonist, μg/ml Bath	Chloramphenicol, μg/ml Bath	Inhibition Compared to Agonist-Induced Contraction, %, Mean ± *SE*
Guinea pig ileum	Acetylcholine, 0.66	10	17 ± 2
		20	24 ± 3
		40	31 ± 4
		80	54 ± 8
		160	83 ± 2
		320	91 ± 2
	Histamine, 0.0031	40	11 ± 4
		80	25 ± 4
		160	48 ± 7
		320	78 ± 6
		640	90 ± 4
	5-Hydroxytryptamine, 0.43	20	25 ± 7
		40	28 ± 4
		80	44 ± 7
		160	64 ± 13
		320	87 ± 2
	Nicotine, 0.33	20	19 ± 6
		80	51 ± 6
		80	51 ± 12
		160	71 ± 8
		320	90 ± 4
Rat fundus strip	5-Hydroxytryptamine, 0.23	250	32 ± 5
		500	49 ± 4
		1000	72 ± 5
		2000	89 ± 4
Rat colon	5-Hydroxytryptamine, 0.1	10	10 ± 5
		20	20 ± 5
		20	29 ± 4
		80	40 ± 3
		160	62 ± 4
		320	80 ± 3
	Acetylcholine, 0.033	50	32 ± 2
		100	50 ± 1
		200	72 ± 4
		400	90 ± 4
Rat estrous uterus	Pituitrin, 0.033	20	6 ± 2
		40	14 ± 2
		80	24 ± 4
		160	50 ± 10
		320	92 ± 4
	5-Hydroxytryptamine, 0.008	2	15 ± 5
		4	18 ± 5
		8	14 ± 6
		16	24 ± 6
		32	46 ± 1
		64	93 ± 2
Rat vas deferns	Epinephrine, 2.0	160	17 ± 8
		320	26 ± 6
		640	37 ± 2
		1280	54 ± 5
		2560	81 ± 3

Effect of Chloramphenicol on Rat Colon—Alteration in the height of contraction of the rat colon was observed with 10 μg of chloramphenicol/ml of bath for the agonist 5-hydroxytryptamine and 50 μg of chloramphenicol/ml for the agonist acetylcholine. Incremental increases in chloramphenicol concentrations from 10 to 320 μg/ml for 5-hydroxytryptamine and from 50 to 400 μg/ml for acetylcholine produced a progressive reduction in the height of rat colon contraction (Table I).

Effect of Chloramphenicol on Rat Estrous Uterus—The agonists used were 5-hydroxytryptamine and pituitrin. Alterations in the height of contraction were observed with a concentration of chloramphenicol of 2 μg/ml of bath for the agonist 5-hydroxytryptamine and 20 μg/ml for pituitrin. Incremental increases in the concentration of chloramphenicol from 2 to 64 μg/ml for the agonist 5-hydroxytryptamine and from 20 to 320 μg/ml for pituitrin produced a progressive reduction in the height of contraction (Table I).

Effect of Chloramphenicol on Rat Vas Deferens—The agonist used was epinephrine. Alterations in the height of contraction

Table II—Chloramphenicol-Induced Inhibition of Rate (Frequency) and Height (Amplitude) of Contraction of Toad Heart

Dose of Chloramphenicol, mg	Inhibition, %[a]	
	Frequency per Minute	Amplitude, mm
0.25	6 ± 1	27 ± 5
0.5	3 ± 1	29 ± 5
1.0	4 ± 1	51 ± 2
2.0	4 ± 1	81 ± 4
4.0	15 ± 6	97 ± 2
8.0	68 ± 6	100 (total)

[a] Mean of seven observations ± *SE*.

were observed with a relatively high concentration of chloramphenicol, 160 μg/ml of bath. Incremental increases in the concentration of chloramphenicol from 160 to 2560 μg/ml produced a progressive reduction in the height of contraction (Table I).

Effect of Chloramphenicol on Perfused Toad Heart—Reductions in the rate and height of contraction of the spontaneously beating toad heart were observed only after a relatively high dose of chloramphenicol, 0.25 mg. Incremental increases in the dose of chloramphenicol from 0.25 to 8 mg produced a progressive reduction in the amplitude of contraction. The frequency of the beat, however, changed significantly only when the dose was increased to 4 mg. Higher concentrations produced a state of contracture of the heart (Table II).

To determine the efficacy of chloramphenicol on the reduction of force and rate of contraction of the heart, the agonists epinephrine and histamine were selected. Under controlled conditions, 3 mg of chloramphenicol produced an average reduction of the frequency by five beats/min and of amplitude by 57 mm. When the heart was stimulated with 0.2 μg of epinephrine, 3 mg of chloramphenicol produced an average reduction of the frequency by 13 beats/min and of amplitude by 42 mm. Similarly, after the heart was stimulated with 10 μg of histamine, the same dose of chloramphenicol led to an average reduction of frequency by 42 beats/min and of amplitude by 54 mm (Table III).

To ascertain that the action of chloramphenicol was direct and not mediated through inhibition or release of mediators, the effects of several blocking agents were studied. The efficacy of the block was tested by challenging the tissue with the appropriate agonist. After the addition of 0.2 μg of propranolol hydrochloride/ml in the perfusion fluid, no significant changes in frequency and amplitude from the control values were observed. The addition of 3 mg of chloramphenicol in the perfusion fluid in the presence of the challenger epinephrine and propranolol produced an average reduction of frequency of the heart beat by 21 beats/min and of amplitude by 47 mm below that of propranolol alone (Table III).

The addition of 0.25 μg of atropine sulfate/ml in the perfusion fluid did not significantly change either the frequency or the amplitude of the heart beat in comparison to the control values. After the adequacy of the atropine block was ascertained with 0.04 μg of acetylcholine, 3.3 mg of chloramphenicol produced an average reduction of 31 beats/min and a 48-mm reduction in the amplitude of contraction (Table III).

Physostigmine, 4.7 μg/ml in the perfusion fluid, did not significantly change either the frequency or the amplitude of the heart beat in comparison to the control values. The addition of the standard dose of 3.4 mg of chloramphenicol, in the presence of physostigmine in the perfusion fluid, reduced the frequency by 14 beats/min and the amplitude of contraction by 52 mm as compared to the control values (Table III).

Effect of Chloramphenicol on Isolated Rabbit Aortic Strip—The minimum amount of chloramphenicol required to produce relaxation in the isolated rabbit aortic strip was 0.5 mg/ml of bath. Increasing the concentration of chloramphenicol from 0.5 to 4 mg/ml produced a progressive reduction in the height of contraction by the aortic strip. The addition of an average dose of 16 μg of epinephrine/ml produced a sustained contraction of the aortic strip, which was found to be antagonized minimally by 0.5 mg and maximally by 4 mg of chloramphenicol/ml. The presence of chloramphenicol in the bath before the addition of epinephrine diminished the epinephrine response; the mean antagonism was 15, 31, 47, and 74% for 0.5, 1, 2, and 4 mg of chloramphenicol/ml, respectively. Chloramphenicol behaved as an adrenergic negator by inhibiting the epinephrine response (Table IV).

Epinephrine stimulation, 9 μg/ml, increased the force of contraction, which was inhibited by about 60% by the addition of phentolamine hydrochloride, 0.5 μg/ml of bath. Addition of 4 mg of chloramphenicol/ml to this preparation further reduced the height of contraction by about 89% (Table IV).

Effect of Chloramphenicol on Isolated Rabbit Ileum—Epinephrine, 0.267 μg/ml of bath, produced maximal relaxation. Increase in the concentration of epinephrine to 0.533 μg/ml diminished the relaxation response. Phentolamine hydrochloride was added to the bath, 2.5 μg/ml, and then epinephrine, 0.267 μg/ml,

Table III—Effect of Chloramphenicol on the Perfused Toad Heart in the Presence of Various Agonists and Blocking Agents[a]

Control	Effect of Chloramphenicol	Agonist or Blocker Used	Effect of Agonist or Blocker	Combined Effect of Agonist or Blocker plus Chloramphenicol
		Heart Beats per Minute		
63 ± 3	58 ± 5 (3 mg)	Epinephrine (0.2 μg)	71 ± 3	58 ± 6
63 ± 3	58 ± 5 (3 mg)	Histamine (10 μg)	68 ± 2	26 ± 5
58 ± 5	42 ± 9 (3 mg)	Propranolol (0.2 μg/ml)	54 ± 4	33 ± 8
65 ± 6	45 ± 7 (3.3 mg)	Atropine (0.25 μg/ml)	62 ± 5	31 ± 8
72 ± 6	58 ± 6 (3.4 mg)	Phyostigmine (4.7 μg/ml)	67 ± 5	53 ± 5
		Height of Contraction, mm		
67 ± 4	10 ± 2 (3 mg)	Epinephrine (0.2 μg)	80 ± 2	38 ± 8
67 ± 4	10 ± 2 (3 mg)	Histamine (10 μg)	54 ± 3	0 (complete inhibition)
51 ± 5	8 ± 3 (3 mg)	Propranolol (0.2 μg/ml)	49 ± 5	2 ± 1
50 ± 6	2 ± 0.5 (3.3 mg)	Atropine (0.25 μg/ml)	51 ± 6	3 ± 2
67 ± 4	10 ± 3 (3.4 mg)	Physostigmine (4.7 μg/ml)	60 ± 4	8 ± 3

[a] Values are means of seven observations ± *SE*. Figures in parentheses indicate the dose of the drug used. The dose is total dose in the case of chloramphenicol and agonists and per milliliter of perfusion fluid in the case of blocking agents. Differences in the values in columns 1 and 4 and in columns 2 and 5 are not statistically significant.

Table IV—Effect of Chloramphenicol on the Height of Contraction of the Isolated Rabbit Aortic Strip in the Presence of Agonists and Blocking Agents

Drug Used	Height of Contraction of Aortic Strip[a], mm
Epinephrine (16 μg/ml of bath)	43 ± 1
plus chloramphenicol (0.5 mg/ml)	34 ± 3
plus chloramphenicol (1 mg/ml)	29 ± 4
plus chloramphenicol (2 mg/ml)	23 ± 4
plus chloramphenicol (4 mg/ml)	9 ± 3
Epinephrine (9 μg/ml)	27 ± 6
Phentolamine (0.5 μg/ml) plus epinephrine (9 μg/ml)	11 ± 3
Phentolamine (0.5 μg/ml) plus chloramphenicol (4 mg/ml) plus epinephrine (9 μg/ml)	3 ± 1

[a] Values are means of six observations ± *SE*.

was added after 0.5 hr. This dose of phentolamine was sufficient to block the maximum epinephrine-induced relaxation, indicating the total block of α-adrenergic receptors. Chloramphenicol, 2 mg/ml, added with both blocker (2.5 μg/ml) and challenger (0.267 μg/ml) present, produced the same degree of relaxation as the control chloramphenicol response.

Effect of Chloramphenicol on Isolated Rabbit Jejunum—The minimum concentration of chloramphenicol to inhibit the frequency and amplitude of spontaneously occurring rhythmic pendular contraction was 250 μg/ml of bath. Incremental increases of chloramphenicol concentration from 250 μg/ml to 2 mg/ml induced a dose-dependent reduction in the frequency of spontaneous contractions. At concentrations above 2 mg/ml, the jejunum became paralyzed; the normal control rhythm could be restored after washing (Table V).

When the jejunum was stimulated with 0.01 μg of acetylcholine/ml, the frequency of pendular contractions, 10/min, did not increase. However, there was a marked increase in the tone, as evidenced by the uplift of the baseline in the record of jejunal contraction. The addition of 1 mg of chloramphenicol/ml in the presence of the same amount of acetylcholine led to a reduction of the frequency of contraction to 4.5/min. This rate was further reduced to 1.25/min when the concentration of chloramphenicol was increased to 2 mg/ml. When the dose of acetylcholine was increased to 0.02 μg/ml, the jejunal contraction could be reduced considerably by 1–2 mg of chloramphenicol/ml (Table V).

When barium chloride was added as a nonspecific stimulant in concentrations of 25 μg/ml, the frequency of jejunal contractions did not change significantly. Addition of chloramphenicol, 0.5–1.0 mg/ml, considerably reduced the frequency of jejunal contraction. The reduction was greater when the concentration of chloramphenicol was 1 mg/ml. The reduction could be reversed by the removal of chloramphenicol by washing (Table V).

Table V—Effect of Chloramphenicol on the Pendular Contractions of the Isolated Rabbit Jejunum

Drugs Used per Milliliter of Bath	Pendular Contractions per Minute[a]
Control	11 ± 1
Chloramphenicol (0.25 mg)	10 ± 1
Chloramphenicol (0.5 mg)	9 ± 1
Chloramphenicol (1.0 mg)	6 ± 1
Chloramphenicol (2.0 mg)	3 ± 1
Acetylcholine (0.01 μg)	10 ± 0.5
plus chloramphenicol (1 mg)	4.5 ± 1
plus chloramphenicol (2 mg)	1.25 ± 0.25
Acetylcholine (0.02 μg)	10 ± 0.3
plus chloramphenicol (1 mg)	3.5 ± 0.4
plus chloramphenicol (2 mg)	1.18 ± 0.2
Barium chloride (25 μg)	9.5 ± 1
plus chloramphenicol (0.5 mg)	5.5 ± 1
plus chloramphenicol (1 mg)	3.25 ± 0.4

[a] Values are means of six observations ± *SE*.

Table VI—Effect of Chloramphenicol on the Height of Contraction of Guinea Pig Trachea in the Presence of Agonist and Blocking Agents

Drugs Used per Milliliter of Bath	Height of Contraction[a], mm
Acetylcholine (4 μg)	15.5 ± 0.9
plus chloramphenicol (0.5 mg)	10.1 ± 0.7
plus chloramphenicol (1 mg)	8.0 ± 0.3
plus chloramphenicol (2 mg)	5.0 ± 0.8
plus chloramphenicol (4 mg)	2.0 ± 0.4
Histamine (7 μg)	22 ± 3.4
plus chloramphenicol (1 mg)	18 ± 2.3
plus chloramphenicol (2 mg)	11.5 ± 1.4
plus chloramphenicol (4 mg)	4.6 ± 1.0
Diphenhydramine (2.5 mg) plus histamine (7 μg)	5.3 ± 0.4
Diphenhydramine (2.5 mg) plus histamine (7 μg) plus chloramphenicol (1 mg)	4.0 ± 1.1
Propranolol (2.5 μg) plus histamine (7 μg)	20 ± 2.2
Propranolol (2.5 μg) plus histamine (7 μg) plus chloramphenicol (2 mg)	10 ± 1.1

[a] Values are means of six observations ± *SE*.

Effect of Chloramphenicol on Isolated Guinea Pig Trachea—The minimum amount of chloramphenicol required to produce relaxation in the guinea pig trachea was 0.5 mg/ml of bath. An increased concentration of chloramphenicol produced a dose-dependent reduction in the height of contraction. The addition of 4 μg of acetylcholine or of 7 μg of histamine/ml produced a sustained contraction of the trachea, which could be antagonized minimally by 0.5 mg of chloramphenicol in the case of acetylcholine and by 1.0 mg of chloramphenicol in the case of histamine and maximally in each instance by 4 mg/ml.

When chloramphenicol was added before the addition of histamine in the bath, the histamine response diminished. The inhibition was 19, 43, and 79% for 1, 2, and 4 mg of chloramphenicol/ml, respectively. The behavior of chloramphenicol was much like that of an antihistaminic drug. Similarly, chloramphenicol was added to the bath before the addition of acetylcholine and the acetylcholine response diminished. The inhibition was 38, 47, 68, and 87% for 0.5, 1, 2, and 4 mg of chloramphenicol/ml, respectively (Table VI).

Diphenhydramine hydrochloride, 2.5 μg/ml, inhibited the histamine response by approximately 76%. The addition of chloramphenicol in the bath, 1 mg/ml, further reduced the height of contraction; the total inhibition was 82%. Propranolol hydrochloride, 2.5 μg/ml, also reduced the histamine response (10%), but the addition of chloramphenicol to propranolol reduced the histamine response to a great extent (55%) (Table VI).

Effect of Chloramphenicol on Release of Calcium in Bath Fluid—In experiments with rabbit jejunum, calcium- and magnesium-free Tyrode solution was used to exclude the possibility of effects of chloramphenicol on these ions. The isoosmolarity of the fluid was maintained by the addition of extra sodium chloride. Control experiments with Tyrode solution containing the usual concentrations of calcium and magnesium were also undertaken.

After chloramphenicol was added to the bath to study its effect on the contraction of jejunum, no change in the concentration of calcium ion in the bath fluid could be observed. In experiments with rabbit aortic strips, calcium and magnesium concentrations in the bath fluid were maintained as usual. The presence of chloramphenicol did not influence the concentration of calcium in the bath, indicating no change in the availability of calcium to the tissues.

DISCUSSION

Chloramphenicol not only inhibited the autogenous contractile mechanism but was also active when the contractile drive was magnified by the use of agonists. The degree of muscle relaxation was related to the concentration of chloramphenicol in the bath. The action could be reversed by removing chloramphenicol by washing the organ preparation.

The force of contraction of the guinea pig trachea, enhanced by either histamine or acetylcholine, was reduced by the addition of chloramphenicol in the bath. Chloramphenicol, when added to the bath prior to the addition of histamine or acetylcholine, partially counteracted the action of the latter drugs. Chloramphenicol thus behaved as an antihistaminic or as an acetylcholine blocker. Furthermore, chloramphenicol reduced the force of contraction in the presence of propranolol (β-block) and diphenhydramine (histamine block).

In experiments with the toad heart, 0.2 μg of propranolol/ml blocked completely the maximal β-receptor-induced response. In experiments with tracheal chains, 2.5 μg of propranolol hydrochloride/ml was used, 12.5 times the dose used in toad heart experiments. Furthermore, Black and Stephenson (8) showed that the effect of epinephrine on the guinea pig tracheal chain could be antagonized by 0.1 μg/ml or less of pronethalol, a drug of one-tenth the potency compared to propranolol with regard to its β-adrenergic blocking property (9). It was, therefore, quite likely that the β-block was complete with 2.5 μg of propranolol hydrochloride/ml.

Diphenhydramine hydrochloride, 2.5 μg/ml, produced a relaxation of about 76% of the control histamine response. A further increase in the dose produced variable results. If a total block of histamine response by diphenhydramine hydrochloride was attained, no further relaxant effect by chloramphenicol could be demonstrated. Complete histaminergic block with diphenhydramine hydrochloride was not attempted. These findings indicated that chloramphenicol possibly did not act through either the adrenergic β-receptor or histaminergic receptor present in the tracheal tissue.

Similar action by chloramphenicol was observed in experiments with the toad heart. Chloramphenicol depressed the force and rate of contraction even in the presence of atropine sulfate and propranolol hydrochloride. Acetylcholine chloride, 0.04 μg, completely stopped the toad heart beat. Atropine sulfate, 0.25 μg/ml, completely blocked the effect of acetylcholine in all experiments. This dose of atropine sulfate exerted a maximum anticholinergic effect. Therefore, chloramphenicol-induced relaxation was not achieved through β-receptor blockade or cholinergic stimulation.

By gradually increasing the concentration of physostigmine in the perfusion fluid of control experiments with the toad heart, it was observed that physostigmine, 4.7 μg/ml of perfusion fluid, maximally potentiated the acetylcholine response, suggesting the achievement of maximal anticholinesterase activity. The maximal cholinesterase-inhibiting dose of physostigmine (4.7 μg/ml) alone in the perfusion fluid could not significantly inhibit either the rate or amplitude of contraction as compared to the control values (Table III). Chloramphenicol, 3.4 mg, produced a rate inhibition of 14 beats/min and an amplitude inhibition of 57 mm with respect to the control values. The response to chloramphenicol in the presence of physostigmine at the dose level of 4.7 μg/ml, which inhibited the cholinesterase enzyme completely, remained unaltered; *i.e.*, the difference between control chloramphenicol and chloramphenicol with physostigmine values was not statistically significant (Table III).

It, therefore, seems that the acetylcholinesterase inhibition by physostigmine could not provide further effective concentration of acetylcholine to achieve an enhanced cholinergic effect. If chloramphenicol promoted the release of acetylcholine, there would have been a significant difference between the chloramphenicol and chloramphenicol with physostigmine values. This result indicated the absence of involvement of acetylcholine in the characteristic chloramphenicol-induced muscle relaxation.

In the rabbit aortic strip preparation, chloramphenicol produced muscle relaxation even after a partial α-receptor block with phentolamine. But in the rabbit ileum preparation, chloramphenicol produced muscle relaxation even after a complete α-receptor block with phentolamine. This finding indicated that relaxation was not mediated through the α-receptor mechanism.

In experiments with the rabbit jejunum, which has a weak autogenous contractile drive, chloramphenicol reduced both the force and frequency of the spontaneously occurring pendular contraction. The minimum amount of chloramphenicol needed to demonstrate these effects was 250 μg/ml. The same amount of chloramphenicol was also needed to demonstrate its effects on the toad heart, which has a stronger spontaneous autogenous drive. To produce about 65% inhibition in the frequency of contraction, however, the amount of chloramphenicol needed per milliliter of bath was 1.5 mg for rabbit jejunum (Table V) and 8 mg for toad heart (Table II). This difference seemed to be logical. The toad heart has a greater autogenous contractile drive than the jejunum. To achieve the same percent inhibition, more chloramphenicol would seem necessary in the toad heart than in the jejunum.

The contractile force and frequency of contraction of the jejunum preparation, increased by pretreatment with acetylcholine, could be reduced by the addition of chloramphenicol in the bath (Table V), indicating that chloramphenicol could interfere with either drug-induced or spontaneously occurring contraction. The ability of chloramphenicol to antagonize the direct stimulation of the jejunum by barium chloride (Table V) indicated that chloramphenicol was interfering with the energy-generating mechanism (3).

Experiments with guinea pig ileum, rat fundal strip, rat colon, rat estrous uterus, and rat vas deferens, using various agonists, clearly demonstrated that chloramphenicol inhibited smooth muscles nonspecifically, acting as a nonspecific spasmolytic substance. From these observations, it may be concluded that chloramphenicol induces relaxation of smooth muscles by a direct action.

REFERENCES

(1) F. Leaders, C. B. Pittinger, and J. P. Long, *Antibiot. Chemother.*, **10**, 503(1960).

(2) G. Benzi, E. Bermudez, and E. Arrigoni, *J. Pharm. Sci.*, **59**, 556(1970).

(3) H. Kehl, *ibid.*, **62**, 723(1973).

(4) R. F. Furchgott and S. Bhadrakom, *J. Pharmacol. Exp. Ther.*, **108**, 129(1953).

(5) R. F. Furchgott, "Methods in Medical Research," vol. 8, Year Book Medical Publishers, Chicago, Ill., 1960, p. 177.

(6) J. C. Castillo and E. K. de Beer, *J. Pharmacol. Exp. Ther.*, **90**, 104(1947).

(7) R. A. Turner, "Screening Methods in Pharmacology," Academic Press, London, England, 1965.

(8) J. W. Black and T. S. Stephenson, *Lancet*, **2**, 311(1962).

(9) "The Pharmacological Basis of Therapeutics," L. S. Goodman and A. Gilman, Eds., Macmillan, London, England, 1970, p. 565.

ACKNOWLEDGMENTS AND ADDRESSES

Received December 9, 1974, from the *Research and Development Division, Dey's Medical Stores (Manufacturing) Private Limited, Calcutta-19, India.*

Accepted for publication July 22, 1975.

The authors thank Sri B. N. Dey, Dey's Medical Stores (Manufacturing) Limited, for the facilities provided.

[x] To whom inquiries should be directed.

Controlled Drug Permeation I: Controlled Release of Butamben through Silicone Membrane by Complexation

MASAHIRO NAKANO ˣ, KAZUHIKO JUNI, and TAKAICHI ARITA

Abstract □ The effects of caffeine, β-cyclodextrin, and povidone on the permeation behavior of butamben from saturated solutions in these complexing agents through a dimethyl polysiloxane membrane were investigated at 30°. In all systems, these agents increased the rate of release over the plain saturated drug solution. The effect was more pronounced with caffeine and β-cyclodextrin than with povidone. Interpretation of these results with the aid of solubility data for the corresponding systems led to the following generalization. For a fixed total (free and complexed) amount of drug available for release, sustained release is associated with systems containing more stable complexes. The practical value of this approach to the controlled release of drug is discussed.

Keyphrases □ Butamben—controlled release from saturated solutions through silicone membrane, effect of caffeine, β-cyclodextrin, and povidone as complexing agents □ Membrane permeation—controlled release of butamben from saturated solutions through silicone membrane, effect of caffeine, β-cyclodextrin, and povidone as complexing agents □ Drug delivery systems—controlled release of butamben from saturated solutions through silicone membrane, effect of caffeine, β-cyclodextrin, and povidone as complexing agents □ Complexation—effect of caffeine, β-cyclodextrin, and povidone on controlled release of butamben through silicone membrane □ Silicone membrane—controlled release of butamben, effect of caffeine, β-cyclodextrin, and povidone

Controlled release[1] of drugs has received much recent attention from the standpoint of increasing the effectiveness and decreasing the side effects in long-term administration of therapeutic agents (1). A controlled-release formulation or delivery system contains drug in polymeric material and can allow drug delivery to the target organ at controlled rates over a specified period. One form of these systems is a capsule of polymeric material filled with the drug in a solid or liquid state or with a suspension or solution of the drug in a fluid. The release of the drug is controlled by diffusion through the capsule walls.

To achieve constant release from a drug delivery system, the concentration gradient has to be maintained constant. A constant concentration gradient may be achieved by having either: (*a*) a large volume reservoir of drug in the solution (2) or (*b*) the drug in the solid phase (3) in the donor side of a membrane and a sink condition in the receptor side. Because of the difficulty in accommodating a large volume reservoir within the drug delivery system, suspensions are usually employed to maintain the drug concentration within the delivery system constant.

Suspensions, however, have their own problems such as sedimentation and particle-size growth of the dispersed solid during storage. Therefore, the possible use of complexation as the reservoir was examined as a way to sustain drug release over a specified period.

Complexation in pharmaceutical systems has been studied by many workers (4). Its possible role in accelerating or retarding drug permeation[1] through a silicone membrane has been reported (5, 6). In the present studies, the effects of three types of complexes on the permeation of a local anesthetic, butamben, were investigated. The complexes included were: (*a*) plane to plane, (*b*) inclusion, and (*c*) macromolecular.

Caffeine has been reported to form complexes with aromatic molecules, presumably of plane-to-plane stacking (7). β-Cyclodextrin, on the other hand, has been known to include drug molecules within its cavity (8). Povidone, a water-soluble polymer, has been studied as to its complexing tendencies with drugs (9).

THEORETICAL

When the transfer of drug from a donor solution to a receptor solution is considered (Fig. 1), Fick's law of diffusion may be written in the following form:

$$\frac{dM_t}{dt} = -DA\frac{dC_m}{dx} \qquad \text{(Eq. 1)}$$

where dM_t/dt = release rate, D = diffusivity in the membrane, A = surface area of the membrane, and dC_m/dx = concentration gradient in the membrane.

In the steady state, Eq. 1 may be written:

$$\frac{dM_t}{dt} = DA\frac{C_{m,d} - C_{m,r}}{l} = DA\frac{K_dC_d - K_rC_r}{l} \qquad \text{(Eq. 2)}$$

where $C_{m,d}$ and $C_{m,r}$ = drug concentrations in the membrane at the donor side and receptor side, respectively; K_d and K_r = distribution coefficients of the drug between the membrane and the donor solution and the membrane and the receptor solution, respectively; C_d and C_r = drug concentrations in the donor solution and the receptor solution, respectively; and l = thickness of the membrane.

If a sink condition is maintained in the receptor solution, C_r remains negligible compared to C_d. Then Eq. 2 can be simplified to:

$$\frac{dM_t}{dt} = \frac{DAK_d}{l}C_d = \frac{PA}{l}C_d \qquad \text{(Eq. 3)}$$

where $P = DK_d$ = permeability.

Case 1 (Zero-Order Release)—When a suspension is placed at the donor side, the drug concentration in the donor solution remains constant because loss of drug from the solution by permeation is constantly compensated for by the dissolution of solid drug (Fig. 1, Case 1). Equation 3 is then written:

$$\frac{dM_t}{dt} = \frac{DAK_d}{l}C_s \qquad \text{(Eq. 4)}$$

where C_s = solubility of the drug in the donor solution. Since all terms on the right-hand side of Eq. 4 are constant, the release rate of drug through the membrane is constant. A plot of the release rate against time gives a straight line parallel to the time axis (Fig. 2, Case 1).

Case 2 (First-Order Release)—When a plain saturated drug solution is placed in the donor compartment, the drug concentra-

[1] In this paper, "permeation" and "transport" refer to three successive processes of partition into, diffusion through, and partition out of the membrane, whereas "release" refers to the last process.

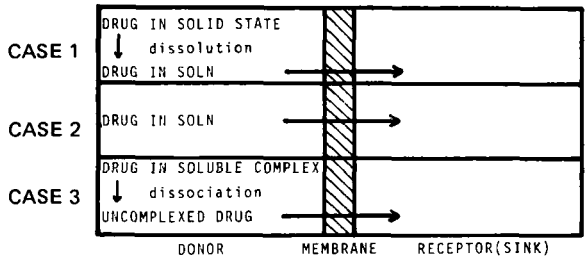

Figure 1—*Schematic representation of the permeation of drug from three different conditions (Cases 1–3) in the donor compartment.*

tion in the donor solution decreases with time as the drug permeates to the receptor solution (Fig. 1, Case 2). Under this condition, Eq. 3 becomes:

$$\frac{dM_t}{dt} = \frac{DAK_d}{l} C_s e^{-(DAK_d/lV)t} \qquad \text{(Eq. 5)}$$

where V = volume of the donor solution. Thus, the release rate plotted against time yields an exponential curve (Fig. 2, Case 2).

Case 3—When a saturated drug solution containing a complexing agent is placed in the donor compartment, the complexed drug may serve as a reservoir. Loss of uncomplexed (permeable) drug from the donor solution by permeation is partly compensated for by dissociation of the complex (Fig. 1, Case 3). Therefore, the concentration of permeable drug does not decrease as rapidly as in the plain solution (Case 2).

When the fraction of complexed drug is large, the concentration of permeable drug may be kept fairly constant and the release rate declines only slowly. A plot of the release rate against time gives a curve falling between a straight line (zero-order release) and an exponential curve (first-order release) (Fig. 2, Case 3).

EXPERIMENTAL

Materials—Medical grade dimethyl polysiloxane sheeting[2] in a labeled thickness of 5 mil (0.127 mm) was used. The following chemicals were obtained from commercial sources and used after characterization by differential scanning calorimetry and thermal gravimetric analysis but without further purification: butamben[3], reagent grade, mp 56.5°; benzocaine[4], Japanese Pharmacopeial grade, mp 89.0°; methylcellulose 4000 cps[5]; caffeine monohydrate[5], reagent grade; β-cyclodextrin[6]; and povidone[7].

Test Solutions—Solutions used in permeation studies were prepared in the following fashion. A suspension was prepared in a water-jacketed beaker maintained at 30° by stirring an excess amount of the local anesthetic in water or in 0.1% methylcellulose solution for 2 days with a magnetic stirrer. Saturated solutions were prepared similarly by stirring an excess of the local anesthetic in various vehicles and filtering through a sintered-glass disk just prior to diffusion studies.

Permeation Studies—The quasisteady-state diffusion cell previously described (5) was used. The cell was initially equilibrated overnight in a shaker bath maintained at 30° with 50 ml of distilled water in both arms. Water was removed by suction; 40 ml of 0.1 N HCl (to maintain a sink condition with respect to the permeable species in the receptor solution by protonating the permeated local anesthetic) was added to one arm, and an equal volume of a test solution was pipetted into another arm. All solutions were warmed to 30° before being placed into the cell.

The cell was mechanically shaken horizontally at a rate of 70 ± 2 strokes/min. With the suspension of drug in water only, instead of shaking the cell itself, the contents of both arms of the cell were stirred with propellers attached to electric motors to effect better dispersion of the solid drug. A 0.5-ml portion of the receptor solution was pipetted out at predetermined time intervals and diluted with pH 6 phosphate buffer. Subsequently, UV absorbance of the unprotonated local anesthetic was measured at 287 nm.

[2] Silastic nonreinforced, lot HH0842, Dow Corning, Midland, Mich.
[3] Tokyo Kasei, Tokyo, Japan.
[4] Torii Pharmaceuticals, Tokyo, Japan.
[5] Wako Pure Chemical Industries, Osaka, Japan.
[6] CPC International, Englewood Cliffs, N.J.
[7] K15, Daiichi Pure Chemicals, Tokyo, Japan.

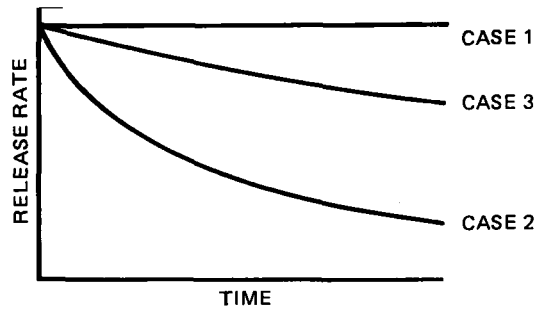

Figure 2—*Illustration of the time dependence of release rate for the three cases: 1, suspension; 2, saturated solution in water; and 3, saturated solution in solutions of complexing agents.*

Determination of Solubility—An excess of the local anesthetic was placed into each vial containing a complexing agent at various concentrations. The vials were then equilibrated at 30° by shaking for at least 24 hr. In the β-cyclodextrin system, where a complex with limited solubility was formed, a longer equilibration period (3 days) was required. Equilibrated mixtures were filtered quickly, and the filtrates were assayed for the local anesthetic as follows.

Analytical Methods—*Spectrophotometric Assay*—In the absence of any interfering material, the UV absorbance of butamben at 287 nm was used to determine the concentration of the local anesthetic that permeated into the receptor solution. The solubilities of the local anesthetic were similarly determined.

GLC Assay—In the presence of UV-absorbing interfering material (caffeine), the concentration of butamben was determined by GLC. A known amount of benzocaine (internal standard) was added to a sample solution, and water was vacuum evaporated. The residue was subsequently dissolved in 50 μl of chloroform, and a 2-μl portion of the chloroform solution was injected into the column.

GLC conditions were as follows: apparatus, gas chromatograph with a flame-ionization detector[8]; column, 2-m stainless steel with 1.5% OV-101 on Shimalite W (80–100 mesh)[5]; injection port temperature, 265°; column temperature, 173°; detector temperature, 275°; nitrogen (carrier gas) flow rate, 30 ml/min; hydrogen flow rate, 25 ml/min; and air flow rate, 940 ml/min. The retention times for benzocaine (as internal standard), butamben, and caffeine were 1.9, 3.6, and 4.3 min, respectively.

RESULTS AND DISCUSSION

Permeation behaviors of butamben from the suspensions in water and methylcellulose solution, from its saturated solutions in 2% solutions of various complexing agents, and from the plain saturated solution (no solid nor complexing agent) are shown in Fig. 3. When the suspensions were placed in the donor compartment, the concentration of drug in the receptor solution increased linearly with time, since a concentration gradient was maintained constant.

Although the solubility of the drug in 0.1% methylcellulose was the same as in water, the release rate of the drug was smaller from the methylcellulose suspension than from the propeller-stirred suspension in water, indicating that the better dispersion and reduced diffusion layer thickness around the solid in the latter favor the dissolution of the drug which, in turn, favors the transport of the drug. When the saturated solution was used as a donor solution, the rate of release decreased rapidly as concentration in the donor solution decreased. Only about 20% of the drug remained in the donor solution after 8 hr. When saturated solutions of the drug containing 2% complexing agents were used, the release curves fell between the line representing the permeation from the suspension and the curve for the plain solution, indicating that complexation has effects on the permeation pattern of the drug.

Before the effects of complexation on permeation are considered, it is appropriate to discuss the possibility of permeation of species other than the free (uncomplexed) drug, such as the complexing agents or the complexes, although this possibility was assumed not to be the case in the *Theoretical* section. Among the

[8] Shimadzu GC-4APF, Shimadzu Manufacturing Co., Kyoto, Japan.

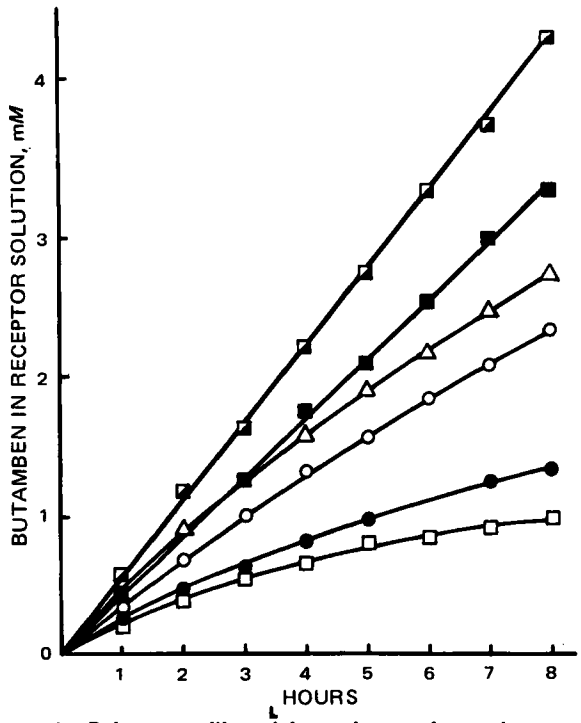

Figure 3—*Release profiles of butamben under various conditions. Key: ◪, suspension in water stirred by propeller; ■, suspension in 0.1% methylcellulose; △, saturated solution in 2% caffeine; ○, saturated solution in 1.1% β-cyclodextrin (see text); ●, saturated solution in 2% povidone; and □, saturated solution in water.*

complexing agents employed in this study, β-cyclodextrin and povidone are not expected to permeate through the membrane because they do not partition into the membrane. Caffeine, on the other hand, permeates very slowly. However, its much smaller permeability ($P = 8 \times 10^{-9}$ cm²/sec) (5) in comparison with that of butamben ($P = 6 \times 10^{-6}$ cm²/sec) warrants the assumption that the caffeine concentration in the donor solution remains essentially constant throughout the permeation study.

As for the permeation of the complexed species, the cyclodextrin and povidone complexes can be considered impermeable since these complexing agents do not partition into the silicone membrane. If the caffeine complex had permeated at a significant rate, the initial release rates of butamben from the caffeine system would have been much greater than those from the drug suspension, since six times as much drug is present in the caffeine system as in the saturated solution. This, however, was not the case. The permeability of the caffeine–butamben complex, if any, is expected to be much smaller than that of free butamben. Thus, the permeable species in the systems examined here is assumed to be essentially the free (uncomplexed) drug alone.

To gain insight into the influence of the degree of complexation on the permeation pattern of the drug, the solubilities of the drug in solutions of the complexing agents were also measured (Fig. 4). Solubility increased linearly with the concentration of caffeine and povidone, whereas β-cyclodextrin formed a complex with limited solubility (the solubility of the complex was about 7 m*M* at 30°). Stability constants calculated by the Higuchi and Connors equation (4) were 2.2×10^3, 61, and 2.9 M^{-1} for β-cyclodextrin, caffeine, and povidone (where the repeating unit was taken to be its molecular weight), respectively.

Figure 4 also provides information concerning the exact amounts of the free and complexed drug present in the donor solution of the three systems at zero time. At zero time, the amount of the free drug was the same in all systems. The drug solubilized by each 2% complexing agent is given by the corresponding *y*-axis values minus the solubility of the drug in plain water.

In the povidone system, the amount of the drug solubilized was small. The cumulative amount of the drug permeated in the 8-hr period, although larger than that from the saturated solution in water, was much smaller than in the other two systems.

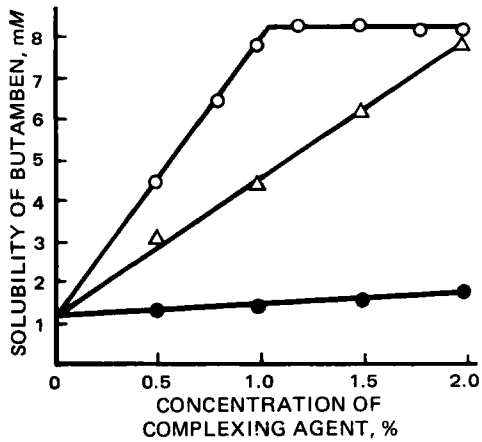

Figure 4—*Solubility profiles of butamben in solutions of three types of complexing agents. Key: ○, β-cyclodextrin; △, caffeine; and ●, povidone.*

With the β-cyclodextrin system, the donor solution at zero time contained only 1.1% total β-cyclodextrin instead of 2%; the difference, having precipitated as the solid complex, was removed from the system upon filtration. The total drug (free and complex) in the donor solution at zero time was estimated to be 0.33 mmole from the solubility diagram (Fig. 4). In the 2% caffeine system, the total drug was estimated similarly to be 0.31 mmole. Therefore, in these two systems, the total amount of drug available for permeation was comparable even with different stability constants. Consequently, if the permeation studies (Fig. 3) were continued to infinite time, the permeation profiles for these two systems would have converged to similar plateaus.

Under these circumstances, since β-cyclodextrin forms a complex with a greater stability constant, the concentration of the free drug (permeable species) in the β-cyclodextrin system during the initial stage of permeation tends to be smaller than that in the caffeine system and, consequently, the release rate is initially smaller. The permeation profiles presented in Fig. 3 for the first 8-hr period clearly indicate that the rate of release was initially smaller

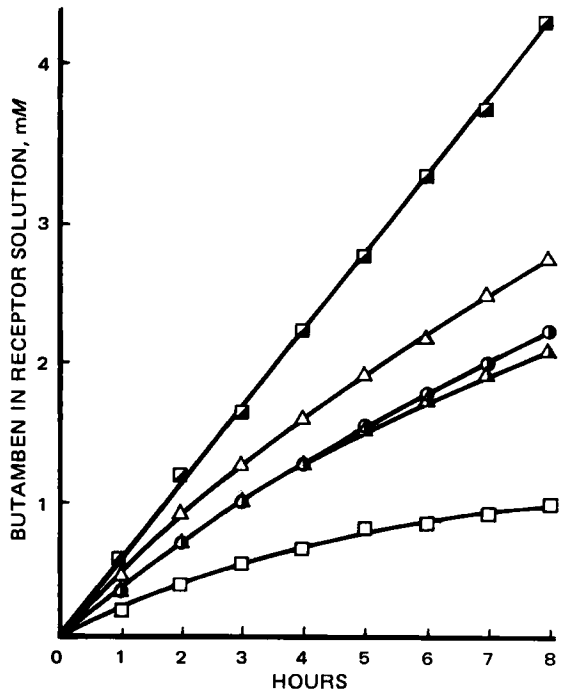

Figure 5—*Release profiles of butamben under various conditions. Key: ◪, suspension in water stirred by propeller; △, saturated solution in 2% caffeine; ◑, saturated solution in 1% β-cyclodextrin, ▲, saturated solution in 1% caffeine; and □, saturated solution in water.*

from the β-cyclodextrin system than from the caffeine system. Since the total drug available for release in these systems was comparable, the rate of release in the caffeine system must have declined faster than in the β-cyclodextrin system.

To confirm the present interpretation, the permeation study was repeated using the saturated solution of the drug in 1% β-cyclodextrin (Fig. 5). At this concentration, the solubility of the complex was not exceeded. As can be seen from Fig. 5, the total amount of the drug available for permeation was equal to that of the previously studied permeation from the saturated solution of drug in 2% caffeine (*i.e.*, 0.31 mmole). Therefore, the permeation profiles presented in Fig. 5 for the 2% caffeine system and the 1% β-cyclodextrin system should have a common plateau. If so, the faster initial rate of release in the 2% caffeine system must lead to a shorter release time than in the 1% β-cyclodextrin system. The following generalization may, therefore, be made. For a fixed amount of total (free and complexed) drug, the more stable the complex is, the greater is the tendency of the system to sustain the release of drug; *i.e.*, the release of drug extends over a longer period.

The permeation profile from 1% caffeine is also shown in Fig. 5. Since the amount of total drug in 1% β-cyclodextrin was greater than that in the 1% caffeine system (Fig. 4), more drug was expected to be released from the 1% β-cyclodextrin system than from the 1% caffeine system at infinite time, even though the release rates were identical during the first 5 hr.

The following conclusions may therefore be drawn for the release of drug from its saturated solution containing various amounts of complexing agents. If such systems are capable of forming soluble, membrane-impermeable complexes, the release rate of drug from such systems is greater than that from the plain saturated solution of the drug, although never exceeding that from the suspension in water. Control of the release profile of drug between these limits may be possible by means of a proper choice of complexing agents. It is evident that the more stable the complex is, the greater is the reservoir of the drug available for release.

It has also been shown that for a fixed amount of total drug (*i.e.*, fixed amount of complex since free drug is independent of the complexing agent), the more stable the complex is, the slower is the initial rate of release but the longer is the time required for complete release. Therefore, control of permeation of drug by means of complexation may find its practical value in obtaining slow sustained release from membrane-encapsulated dosage forms containing drug in solution.

REFERENCES

(1) D. R. Cowsar, in "Controlled Release of Biologically Active Agents," A. C. Tanquary and R. E. Lacey, Eds., Plenum, New York, N.Y., 1974, pp. 1–13.

(2) E. R. Garrett and P. B. Chemburkar, *J. Pharm. Sci.*, **57**, 944(1968).

(3) R. W. Baker and H. K. Lonsdale, in "Controlled Release of Biologically Active Agents," A. C. Tanquary and R. E. Lacey, Eds., Plenum, New York, N.Y., 1974, pp. 25–30.

(4) T. Higuchi and K. A. Connors, *Advan. Anal. Chem. Instr.*, **4**, 117(1965).

(5) M. Nakano and N. K. Patel, *J. Pharm. Sci.*, **59**, 77(1970).

(6) M. Nakano, *ibid.*, **60**, 571(1971).

(7) T. Higuchi and H. Kristiansen, *ibid.*, **59**, 1601(1970).

(8) J. L. Lach and J. Cohen, *ibid.*, **52**, 137(1963).

(9) T. Higuchi and R. Kuramoto, *J. Amer. Pharm. Ass., Sci. Ed.*, **43**, 393(1954).

ACKNOWLEDGMENTS AND ADDRESSES

Received March 31, 1975, from the *Faculty of Pharmaceutical Sciences, Hokkaido University, Sapporo 060, Japan.*

Accepted for publication July 21, 1975.

Supported by a grant from the Ministry of Education, Japan.

[x] To whom inquiries should be directed.

Tritiated Naltrexone Binding in Plasma from Several Species and Tissue Distribution in Mice

T. M. LUDDEN [*], L. MALSPEIS [*], J. D. BAGGOT [‡], T. D. SOKOLOSKI [*], S. G. FRANK [*], and R. H. REUNING [*x]

Abstract □ The binding of 15,16-^{3}H-naltrexone in human, monkey, dog, guinea pig, rat, and mouse plasma was investigated over a range of concentrations, including predicted therapeutic levels. Studies using equilibrium dialysis at 37° indicate that the extent of binding is independent of naltrexone concentration over the concentration range of 1–500 ng/ml for dog plasma and of 0.1–500 ng/ml for human, monkey, guinea pig, rat, and mouse plasma. The extent of naltrexone binding in plasma is similar in the six species studied, the range being from 20% bound in rat plasma to 26% in plasma from beagle and mongrel dogs. This relatively low extent of naltrexone binding in plasma is consistent with previous findings of a large apparent volume of distribution for this drug in the dog. To investigate further the distribution of tritiated naltrexone, the tissue levels of radioactivity in mice at 1, 5, and 15 min after intravenous administration of 8-^{3}H-naltrexone were determined. Naltrexone was rapidly distributed from plasma to tissues, with less than 4% of the dose being present in plasma at 1 min after injection.

Keyphrases □ Naltrexone—plasma protein binding in humans, monkeys, dogs, guinea pigs, rats, and mice, tissue distribution in mice □ Protein binding, plasma—naltrexone, humans, monkeys, dogs, guinea pigs, rats, and mice □ Distribution, tissue—naltrexone, mice □ Pharmacokinetics—naltrexone, humans, monkeys, dogs, guinea pigs, rats, and mice □ Antagonists, narcotic—naltrexone, pharmacokinetics, humans, monkeys, dogs, guinea pigs, rats, and mice

Naltrexone, a narcotic antagonist, has been suggested for use in the treatment of heroin dependence (1). Since narcotic antagonists provide no stimulus to the patient to return for frequent dosing (2), the availability of a sustained-release drug delivery system is desirable. Such potential delivery systems for naltrexone have been prepared and tested (3, 4).

It is well known that binding to plasma proteins can influence significantly the distribution of a drug, its pharmacokinetic profile, and its duration of phar-

from the β-cyclodextrin system than from the caffeine system. Since the total drug available for release in these systems was comparable, the rate of release in the caffeine system must have declined faster than in the β-cyclodextrin system.

To confirm the present interpretation, the permeation study was repeated using the saturated solution of the drug in 1% β-cyclodextrin (Fig. 5). At this concentration, the solubility of the complex was not exceeded. As can be seen from Fig. 5, the total amount of the drug available for permeation was equal to that of the previously studied permeation from the saturated solution of drug in 2% caffeine (*i.e.*, 0.31 mmole). Therefore, the permeation profiles presented in Fig. 5 for the 2% caffeine system and the 1% β-cyclodextrin system should have a common plateau. If so, the faster initial rate of release in the 2% caffeine system must lead to a shorter release time than in the 1% β-cyclodextrin system. The following generalization may, therefore, be made. For a fixed amount of total (free and complexed) drug, the more stable the complex is, the greater is the tendency of the system to sustain the release of drug; *i.e.*, the release of drug extends over a longer period.

The permeation profile from 1% caffeine is also shown in Fig. 5. Since the amount of total drug in 1% β-cyclodextrin was greater than that in the 1% caffeine system (Fig. 4), more drug was expected to be released from the 1% β-cyclodextrin system than from the 1% caffeine system at infinite time, even though the release rates were identical during the first 5 hr.

The following conclusions may therefore be drawn for the release of drug from its saturated solution containing various amounts of complexing agents. If such systems are capable of forming soluble, membrane-impermeable complexes, the release rate of drug from such systems is greater than that from the plain saturated solution of the drug, although never exceeding that from the suspension in water. Control of the release profile of drug between these limits may be possible by means of a proper choice of complexing agents. It is evident that the more stable the complex is, the greater is the reservoir of the drug available for release.

It has also been shown that for a fixed amount of total drug (*i.e.*, fixed amount of complex since free drug is independent of the complexing agent), the more stable the complex is, the slower is the initial rate of release but the longer is the time required for complete release. Therefore, control of permeation of drug by means of complexation may find its practical value in obtaining slow sustained release from membrane-encapsulated dosage forms containing drug in solution.

REFERENCES

(1) D. R. Cowsar, in "Controlled Release of Biologically Active Agents," A. C. Tanquary and R. E. Lacey, Eds., Plenum, New York, N.Y., 1974, pp. 1–13.

(2) E. R. Garrett and P. B. Chemburkar, *J. Pharm. Sci.*, **57**, 944(1968).

(3) R. W. Baker and H. K. Lonsdale, in "Controlled Release of Biologically Active Agents," A. C. Tanquary and R. E. Lacey, Eds., Plenum, New York, N.Y., 1974, pp. 25–30.

(4) T. Higuchi and K. A. Connors, *Advan. Anal. Chem. Instr.*, **4**, 117(1965).

(5) M. Nakano and N. K. Patel, *J. Pharm. Sci.*, **59**, 77(1970).

(6) M. Nakano, *ibid.*, **60**, 571(1971).

(7) T. Higuchi and H. Kristiansen, *ibid.*, **59**, 1601(1970).

(8) J. L. Lach and J. Cohen, *ibid.*, **52**, 137(1963).

(9) T. Higuchi and R. Kuramoto, *J. Amer. Pharm. Ass., Sci. Ed.*, **43**, 393(1954).

ACKNOWLEDGMENTS AND ADDRESSES

Received March 31, 1975, from the *Faculty of Pharmaceutical Sciences, Hokkaido University, Sapporo 060, Japan.*

Accepted for publication July 21, 1975.

Supported by a grant from the Ministry of Education, Japan.

[x] To whom inquiries should be directed.

Tritiated Naltrexone Binding in Plasma from Several Species and Tissue Distribution in Mice

T. M. LUDDEN [*], L. MALSPEIS [*], J. D. BAGGOT [‡], T. D. SOKOLOSKI [*], S. G. FRANK [*], and R. H. REUNING [*x]

Abstract □ The binding of 15,16-^{3}H-naltrexone in human, monkey, dog, guinea pig, rat, and mouse plasma was investigated over a range of concentrations, including predicted therapeutic levels. Studies using equilibrium dialysis at 37° indicate that the extent of binding is independent of naltrexone concentration over the concentration range of 1–500 ng/ml for dog plasma and of 0.1–500 ng/ml for human, monkey, guinea pig, rat, and mouse plasma. The extent of naltrexone binding in plasma is similar in the six species studied, the range being from 20% bound in rat plasma to 26% in plasma from beagle and mongrel dogs. This relatively low extent of naltrexone binding in plasma is consistent with previous findings of a large apparent volume of distribution for this drug in the dog. To investigate further the distribution of tritiated naltrexone, the tissue levels of radioactivity in mice at 1, 5, and 15 min after intravenous administration of 8-^{3}H-naltrexone were determined. Naltrexone was rapidly distributed from plasma to tissues, with less than 4% of the dose being present in plasma at 1 min after injection.

Keyphrases □ Naltrexone—plasma protein binding in humans, monkeys, dogs, guinea pigs, rats, and mice, tissue distribution in mice □ Protein binding, plasma—naltrexone, humans, monkeys, dogs, guinea pigs, rats, and mice □ Distribution, tissue—naltrexone, mice □ Pharmacokinetics—naltrexone, humans, monkeys, dogs, guinea pigs, rats, and mice □ Antagonists, narcotic—naltrexone, pharmacokinetics, humans, monkeys, dogs, guinea pigs, rats, and mice

Naltrexone, a narcotic antagonist, has been suggested for use in the treatment of heroin dependence (1). Since narcotic antagonists provide no stimulus to the patient to return for frequent dosing (2), the availability of a sustained-release drug delivery system is desirable. Such potential delivery systems for naltrexone have been prepared and tested (3, 4).

It is well known that binding to plasma proteins can influence significantly the distribution of a drug, its pharmacokinetic profile, and its duration of phar-

macological action (5, 6). Therefore, comparative data on naltrexone distribution and binding in several species and in humans must be available for rational development of model animal systems for: (*a*) pharmacokinetic analysis of naltrexone, (*b*) pharmacokinetic and pharmacological evaluation of sustained-release naltrexone delivery systems, and (*c*) toxicological analysis of naltrexone and its delivery systems.

The purposes of the present study were to determine the binding characteristics of naltrexone in plasma from humans, monkeys, dogs, guinea pigs, rats, and mice over a range of therapeutic plasma concentrations and to determine the extent of tissue distribution of radioactivity in the mouse at 1, 5, and 15 min after intravenous administration of tritiated naltrexone.

EXPERIMENTAL

Reagents—The analytical grade reagents used were chloroform, absolute methanol, 1-butanol, and benzene. Concentrated ammonium hydroxide, acetic acid, monobasic potassium phosphate, and dibasic sodium phosphate were reagent grade.

Purity and Exchangeability of 8-^{3}H- and 15,16-^{3}H-Naltrexone—To an ampul containing 4.64 mCi (2 mg) of 8-^{3}H-naltrexone[1] as a solid was added 4.0 ml of 10% absolute ethanol in benzene containing 2 mg of unlabeled naltrexone[2]. The final concentration was 1.16 mCi (1 mg)/ml. The sample of 15,16-^{3}H-naltrexone[3], 45.0 mCi (1 mg), was received dissolved in 10% ethanol in benzene. This solution was diluted to 100 ml with the same solvent, yielding a final concentration of 0.45 mCi (10 μg)/ml. These solutions were stored under nitrogen in a refrigerator. In the preparation of aqueous solutions from these stock solutions, the organic solvents were removed by evaporation in a stream of nitrogen prior to the addition of buffer.

The purity of the 8-^{3}H- and 15,16-^{3}H-naltrexone was checked periodically by TLC on 0.25-mm thick sheets of silica gel on aluminum[4]. Each radioactive naltrexone stock solution (1 μl) was spotted on the thin-layer sheets after applying 5 μg of unlabeled naltrexone in a volume of 5 μl of methanol. The solvent systems used were: A, chloroform–methanol–concentrated ammonium hydroxide (46 ml:4 ml:2 drops)[5]; B, methanol–1-butanol–benzene–water (60:15:10:15) (7); and C, 1-butanol–acetic acid–water (60:15:30) (7). The times required for development at room temperature in Solvent Systems A, B, and C were 50, 150, and 240 min, respectively.

To determine the distribution of radioactivity on the thin-layer sheets, the silica gel was removed in small, measured increments by scraping. These samples were then placed in liquid scintillation counting vials. Four milliliters of distilled water was added to each vial, and the mixture was suspended with 10 ml of an all-purpose scintillation fluid[6]. The samples were assayed in a liquid scintillation spectrometer[7] equipped with automatic external standardization. The degree of quenching did not vary significantly from vial to vial.

The exchangeability of 8-^{3}H-naltrexone was determined in the following manner. A solution containing 86 ng (0.1 μCi) in 10 ml of phosphate-buffered saline (0.01 *M* phosphate buffer made isotonic with saline, pH 7.4) was prepared. At various times after preparation of the solution, a 1.0-ml aliquot was removed and a 100-μl sample of this aliquot was placed in a counting vial along with 0.4 ml of phosphate-buffered saline and 10 ml of all-purpose scintillation fluid. This assay yielded the concentration of total radioactivity in the sample.

To the remaining 0.9 ml of the aliquot was added 0.9 ml of a suspension of dextran-coated charcoal (dextran, 62.5 mg; phosphate-buffered saline, 25 ml; and activated charcoal, 2.5 g). The mixture was shaken intermittently for 3–4 min and then gravity filtered through filter paper[8]. A 0.5-ml sample of the filtrate was assayed. This filtrate should have contained any tritiated water formed by exchange plus any nonadsorbed drug. Therefore, the radioactivity in the filtrate indicates the maximum extent to which exchange could have occurred.

Less than 0.5% of the total radioactivity occurred in the filtrate from 0 to 48 hr and less than 1% from 48 to 96 hr. Thus, there appears to be no appreciable exchange of label with water over the time studied. Similarly, the label of 15,16-^{3}H-naltrexone was shown to be stable (less than 0.5% radioactivity in filtrate) for at least 6 hr in phosphate-buffered saline.

The lack of appreciable exchange of the tritium label of 8-^{3}H-naltrexone with water *in vivo* is indicated by the essentially complete recovery of label, 97.9 ± 7.9% (mean ± *SD*), obtained in the distribution study described later. Any tritiated water formed would have been lost when the samples were dried prior to preparation for counting. Likewise, the label of 15,16-^{3}H-naltrexone has been shown not to exchange with water *in vivo* when, after administration to guinea pigs, essentially total recovery of tritium, 97.6 ± 2.7%, in the dried excreta was obtained under conditions similar to those described for the distribution study.

Blood Collection—Blood from two mongrel dogs, two foxhounds, 14 beagles, and three human subjects was collected in heparinized syringes by venipuncture. Guinea pigs, rats, and mice were lightly anesthetized with ether, decapitated, and bled into heparinized beakers. After the collection of blood from these species, plasma was separated by centrifugation and used within 24 hr (storage at 10°). Fresh monkey (*Macca mulatta*) plasma samples from two males and one female were received frozen and then thawed just prior to use.

Equilibrium Dialysis—Dialysis (8) was performed using equilibrium dialysis cells[9], the half-cells being separated by a strip of cellophane membrane[10]. One milliliter of plasma was placed in one half-cell; 1 ml of 0.16 *M* phosphate buffer, pH 7.4 (prepared by mixing 0.16 *M* KH_2PO_4 and 0.16 *M* Na_2HPO_4 in a volume ratio of approximately 1:4), containing the desired concentration of 15,16-^{3}H-naltrexone and unlabeled naltrexone was placed in the other half-cell. (The 15,16-^{3}H-naltrexone was used in the binding studies, because its high specific activity permitted the measurement of binding at concentrations down to 0.1 ng/ml.) Each half-cell contained a small glass bead to aid in mixing. The dialysis cells were wrapped in plastic and placed in a shaking water bath at 37°.

In some cases, buffer containing drug, 2 ng/ml, was dialyzed against buffer alone to demonstrate that equilibrium across the membrane had been achieved by 24 hr. At the end of 24 hr, the ratio of radioactivity on the side initially without drug to that initially with drug was 0.994 ± 0.039, $n = 4$.

After 24 hr, duplicate 0.1-ml samples were removed from each half-cell, placed in a liquid scintillation counting vial with 10 ml of scintillation cocktail[11], and assayed by liquid scintillation counting. Count rates were corrected for counting efficiency, as determined by an external standard and reference to a quench correction curve; results are expressed as concentration of naltrexone.

The percentage of total naltrexone in the plasma that was bound was calculated from:

$$\text{percentage bound} = \frac{C_p - (C_b \times F)}{C_p} \times 100\% \qquad \text{(Eq. 1)}$$

where C_p = naltrexone concentration in plasma, C_b = naltrexone concentration in buffer, and F = fraction of plasma that is water.

The fraction of plasma that is water, F in Eq. 1, is used to correct for the volume occupied by plasma solutes, mainly proteins. The values of F for humans, dogs, and rats are 0.94 (9), 0.93 (9), and 0.935 (10), respectively. Values of F for guinea pig and mouse plasma were determined to be 0.938 ± 0.009 and 0.935 ± 0.001, re-

[1] Lot 1620-124, provided under National Institute on Drug Abuse Contract HSM 42-73-184 with Research Triangle Institute, Research Triangle Park, N.C.
[2] Endo Laboratories, Inc., Garden City, N.Y.
[3] Lot 1681-17-6, provided under National Institute on Drug Abuse Contract HSM 42-73-184 with Research Triangle Institute, Research Triangle Park, N.C.
[4] E. M. Reagents, E. M. Laboratories, Elmsford, N.Y.
[5] This solvent system was suggested by Dr. J. A. Kepler, Research Triangle Institute, Research Triangle Park, N.C.
[6] Instagel, Packard Instrument Co., Downers Grove, Ill.
[7] Packard Tri-Carb model 3375, Parkard Instrument Co., Downers Grove, Ill.
[8] Whatman No. 1, W & R Balston, Ltd., Maidstone, England.
[9] Chemical Rubber Co., Cleveland, Ohio.
[10] Will Scientific, Rochester, N.Y.
[11] Aquasol, New England Nuclear, Boston, Mass.

Table I—TLC Analysis of Purity of 8-^{3}H-Naltrexone and 15,16-^{3}H-Naltrexone

Solvent System	8-^{3}H-Naltrexone R_f[a]	8-^{3}H-Naltrexone Percentage Recovered[b]	15,16-^{3}H-Naltrexone R_f[a]	15,16-^{3}H-Naltrexone Percentage Recovered[b]
A	0.43[c]	95.1	0.54[c]	97.4
B	0.36	97.2	0.33	97.7
C	0.31	98.8	0.32	98.2

[a] R_f value of authentic naltrexone. [b] Percentage of radioactivity recovered from the plate, corrected for plate background, at the R_f value corresponding to authentic naltrexone. [c] The R_f value of naltrexone in Solvent System A varied up to 20% from day to day, as indicated by iodine visualization.

spectively. There was insufficient monkey plasma available to determine its water content; therefore, the approximate value of 0.935 was used in the calculations.

Determination of Plasma Water—Six samples each of guinea pig and pooled mouse plasma were weighed in tared vials and dried at 100–110° to constant weight. The loss in weight upon drying was taken as the water content and expressed as the fraction of total plasma weight.

Dialysis of Plasma *versus* Ultrafiltrate of Plasma—During dialysis of plasma against a buffer such as the one used in this study, it is likely that the plasma concentrations of various small, diffusible molecules and ions are altered. In some cases, this alteration might change the binding of the compound being studied. To investigate this possibility, dog (foxhound) plasma was dialyzed against an ultrafiltrate of the same plasma using the following procedure.

Plasma (5 ml) was added to each of two membrane filter cones[12]; these cones had been soaked overnight in distilled water. The cones were drained and blotted before the addition of plasma. The filter cones were then placed in polycarbonate centrifuge tubes and centrifuged (2000×*g*) for 5 min to remove water trapped in the walls of the filters. After transferring the cones to dry centrifuge tubes, centrifugation was continued for 1 hr.

At the end of this time, about 4 ml of ultrafiltrate was collected from each tube. Since these filter cones retain substances with molecular weights greater than 50,000 daltons, the ultrafiltrate should be free of most plasma proteins but still contain the smaller plasma solutes. The dialysis of plasma *versus* plasma ultrafiltrate containing naltrexone was carried out as previously described. Controls, plasma *versus* buffer containing naltrexone, were dialyzed simultaneously. The initial concentration of 15,16-^{3}H-naltrexone in buffer or ultrafiltrate was 2 ng/ml.

Distribution of Radioactivity in Mouse Tissues after Intravenous Administration of 8-^{3}H-Naltrexone—Male, albino, CFl mice[13], 22–32 g, were injected *via* the tail vein with 8-^{3}H-naltrexone[14] and nonradiolabeled compound, 0.925 mg (40 μCi)/kg. A 50-μl syringe with 1-μl graduations[15] was used for drug administration. The injection solution was prepared by dissolving 17.4 μg (20 μCi) of 8-^{3}H-naltrexone and 445 μg of nonradiolabeled compound in 0.5 ml of phosphate-buffered saline to give a final concentration of 925 μg (40 μCi)/ml. This solution was freshly prepared on the day of an experiment.

The mice were sacrificed by decapitation at either 1, 5, or 15 min after the intravenous injection. Blood was collected in a heparinized beaker, and plasma and red cells were separated in a hematocrit tube by centrifugation. The brain, lungs, heart, spleen, liver, and kidneys were removed and placed in tared combustion cones[16] containing cellulose powder. Organs too large to be placed in one cone were divided and placed in as many cones as necessary. Samples of fat, muscle, skin, red cells, and plasma were also added to similarly prepared combustion cones, as was the portion of the tail containing the injection site.

The GI tract (stomach and small and large intestines) was homogenized[17] in 2 ml of water. Similarly, a homogenate of the carcass, predominantly muscle and bone, was prepared using 35 ml of water. Samples of GI and carcass homogenates were weighed into combustion cones. All organ, tissue, and homogenate samples were air dried a minimum of 16 hr before being oxidized[18]. During the combustion procedure, the tritiated water resulting from the oxidation was collected in liquid scintillation counting vials and 15 ml of scintillation liquid (naphthalene, 100 g; 2,5-diphenyloxazole, 5 g; 1,4-bis[2-(4-methyl-5-phenyloxazolyl)]benzene, 0.3 g; dioxane, 720 ml; toluene, 180 ml; and absolute methanol, 35 ml) was subsequently added. The samples were assayed by liquid scintillation counting as previously described.

The amount of radioactivity administered was determined by a similar assay of the tritiated water produced by oxidation of aliquots of a 1:1000 dilution of the injection solution. The percentage of administered radioactivity in each organ or tissue was then calculated. The total recovery of radioactivity in all tissue and organ samples plus the carcass was essentially complete, 97.9 ± 7.9% of the dose.

Table II—Binding of Naltrexone in Monkey, Guinea Pig, Rat, and Mouse Plasma over a Range of Relevant Concentrations[a]

Mean Assayed Total Concentration of Naltrexone in Plasma, ng/ml	Percentage Bound[b]	Mean Assayed Total Concentration of Naltrexone in Plasma, ng/ml	Percentage Bound[b]
Monkey		Guinea Pig	
0.108	18.9 ± 2.49	0.104	20.4 ± 2.78
7.73	21.3 ± 2.86	7.50	20.9 ± 2.43
527	20.7 ± 0.23	512	21.9 ± 4.46
Rat[c]		Mouse[d]	
0.0995	19.8 ± 2.3	0.104	23.1 ± 1.56
7.80	19.9 ± 1.35	7.80	21.9 ± 2.25
514	19.4 ± 1.82	517	23.3 ± 1.20

[a] Measurements made at 37° using equilibrium dialysis. [b] Mean ± *SD*; n = 6 for guinea pigs and rats, and n = 3 for monkeys and mice; n is the number of plasma samples, each from a different animal. [c] Each sample obtained by pooling plasma from two rats. [d] Each sample obtained by pooling plasma from 10 mice.

RESULTS

Purity of 8-^{3}H- and 15,16-^{3}H-Naltrexone—The R_f values of authentic naltrexone chromatographed in three solvent systems are presented in Table I together with the percentage of radioactivity corresponding to those R_f values. It is evident that the purities of 8-^{3}H-naltrexone and 15,16-^{3}H-naltrexone, as measured by this technique, are greater than 95 and 97%, respectively.

Dialysis of Plasma *versus* Plasma Ultrafiltrate—The percentages bound in dog plasma dialyzed against the ultrafiltrate and dog plasma dialyzed against 0.16 *M* phosphate buffer are 19.1 ± 2.4 and 21.3 ± 3.3, respectively, for seven determinations. There is no significant difference between these values (t test, $p > 0.05$), indicating that any diffusion of small molecules between plasma and phosphate buffer does not significantly alter the extent of naltrexone binding in plasma.

Concentration Studies—In Fig. 1, the relationship between percentage bound and plasma naltrexone concentration for three human subjects and two mongrel dogs is shown. The lines in Fig. 1 are the least-squares regression lines of best fit to the data points on a linear scale. (In Fig. 1, a log scale is used on the abscissa for ease of presentation.) For the human subjects, the slope of this line is 0.008 ± 0.003, which is significantly different from zero (t test, $p < 0.05$). However, when the data for each subject are fit individually, only the slope obtained with data from Subject TL is significantly different than zero.

The data obtained using plasma from two mongrel dogs give a line of best fit having a slope of 0.002 ± 0.005. This value, as well

[12] Type CF50A, Amicon Corp., Lexington, Mass.
[13] Carworth Farms.
[14] This form of tritiated naltrexone, having a lower specific activity, was the only radiolabeled material available at the time of the experiment.
[15] Hamilton Co., Reno, Nev.
[16] Packard Instrument Co., Downers Grove, Ill.
[17] Sorvall Omni-Mixer, Ivan Sorvall Inc., Norwalk, Conn.
[18] Tritium oxidizer model 300, Packard Instrument Co., Downers Grove, Ill.

Table III—Binding of Naltrexone in Plasma Obtained from Humans, Monkeys, Dogs, Guinea Pigs, Rats, and Mice

Species	n	Mean Assayed Total Concentration of Naltrexone in Plasma, ng/ml	Percentage Bound[a]
Human[b]	3	13.5	20.7 ± 0.47
Monkey[b]	3	7.73	21.3 ± 2.86
Dog[b]			
Mongrels	2	13.8	26.2
Beagles	14	13.3	26.8 ± 2.12
Foxhounds	2	12.7	20.2
Guinea pig[b]	6	7.50	20.9 ± 2.43
Rat[c]	6	7.80	19.9 ± 1.35
Mouse[d]	3	7.80	21.9 ± 2.25

[a] Mean ± SD. [b] n is the number of plasma samples, each from a different subject or animal. [c] n is the number of samples, each obtained by pooling plasma from two rats. [d] n is the number of samples, each obtained by pooling plasma from 10 mice.

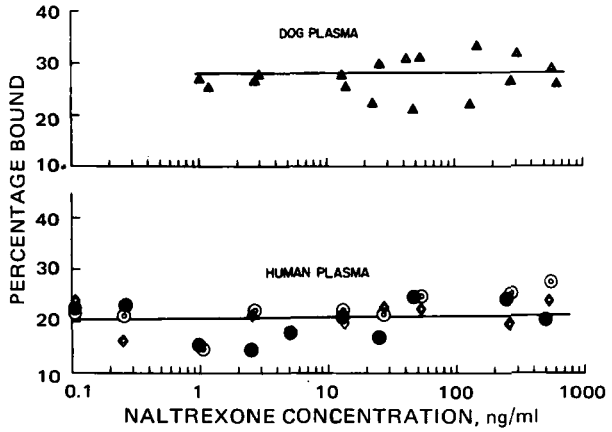

Figure 1—*Effect of concentration of naltrexone on the percentage of naltrexone bound in dog and human plasma at 37°. Key: ▲, Dog GS; △, Dog PS; ●, Human TM; ⊙, Human TL; and ◆, Human RR.*

as the values obtained when the data from each dog are fit individually, does not differ significantly from zero ($p > 0.05$). In any case, the very low values of these slopes indicate that the concentration of naltrexone has negligible influence on the percentage bound in human and dog plasma.

Similar results were obtained for the monkey, guinea pig, rat, and mouse. In Table II, the percentage bound in monkey, guinea pig, rat, and mouse plasma at low, intermediate, and high plasma concentrations is shown. These data clearly demonstrate that the plasma binding of naltrexone in these species is independent of naltrexone concentration over the large concentration range studied.

Species Comparisons—The percentage of naltrexone in plasma that is bound at comparable drug concentrations is given in Table III for the six species studied. None of the percentage bound values differs appreciably from one another.

Distribution of Radioactivity in the Mouse—The results of the distribution study in mice are presented in Table IV and Fig. 2. At 1 min after injection (injection time was 5–10 sec), less than 4% of the administered radioactivity remains in plasma. At 1–5 min postinjection, the radioactivity is distributed in rough proportion to tissue wet weight (except skin, kidneys, and lungs). However, at 15 min, 46% of the dose is localized in the organs of elimination, kidneys, liver, and GI tract, which represent only 20.3% of the body weight.

DISCUSSION

The percentage of naltrexone bound did not vary appreciably over the large concentration ranges of about 1–500 ng/ml (2.9×10^{-9} to 1.5×10^{-6} *M*) for dog plasma and of 0.1–500 ng/ml (2.9×10^{-10} to 1.5×10^{-6} *M*) for monkey, guinea pig, rat, mouse, and human plasma. Plasma binding that is independent of drug concentration also was reported for the basic drugs amphetamine (8), codeine (12), morphine (12, 13), pentazocine (14), and desipramine (15). The binding of methadone (16), quinidine (17), nicotine (18), propranolol (19), and the benzodiazepines (20) to plasma or albumin has been characterized as concentration dependent.

The binding of the adrenergic β-receptor antagonist alprenolol to human serum is concentration dependent while the binding to human serum albumin is not (21). This difference underlines the importance of using serum or plasma instead of purified protein fractions if the results of binding studies are to simulate conditions *in vivo*. There does not appear to be any relationship between the extent of binding of these basic drugs and whether or not the binding is concentration dependent. Thus, it is important to obtain binding data for basic drugs in several species so that this factor can be better understood. No significant species differences were noted in the binding of naltrexone in human, monkey, dog, guinea pig, rat, and mouse plasma. However, species differences have been found for other basic drugs such as amphetamine (9), codeine (12), morphine (12), propranolol (19), and desipramine (22).

Results of preliminary studies concerning the pharmacokinetics of naltrexone in dogs (foxhounds) indicate that this compound has a relatively large apparent volume of distribution (3.2–3.6 liters/kg) (23). This finding is consistent with the low extent of plasma binding observed in the present study; *i.e.*, most of the drug in plasma is free to cross capillary membranes readily and to accumulate in tissues.

The results of the present study concerning the pharmacokinetics of naltrexone in mouse tissues at 1, 5, and 15 min after intrave-

Table IV—Distribution of Radioactivity in the Mouse after Intravenous Administration of 8-^{3}H-Naltrexone, 1 mg/kg

Tissue	Percentage of Body Weight[a]	Concentration, μg Naltrexone Equivalent per g Wet Weight[b]			Percentage of Dose[b]		
		1 min	5 min	15 min	1 min	5 min	15 min
Brain	1.49 (0.25)	0.568 (0.069)	0.803 (0.063)	0.508 (0.233)	0.67 (0.12)	1.43 (0.18)	0.89 (0.47)
Lung	0.70 (0.14)	3.31 (0.87)	1.25 (0.19)	0.980 (0.175)	2.08 (0.85)	0.99 (0.12)	0.80 (0.13)
Heart	0.49 (0.09)	1.66 (0.37)	0.683 (0.060)	0.516 (0.051)	0.91 (0.20)	0.36 (0.04)	0.29 (0.07)
Spleen	0.35 (0.09)	1.19 (0.36)	1.25 (0.20)	0.883 (0.077)	0.34 (0.16)	0.44 (0.08)	0.38 (0.18)
Liver	5.50 (0.91)	1.40 (0.09)	3.26 (0.20)	3.81 (0.65)	6.27 (1.00)	20.6 (2.9)	23.1 (4.4)
Fat	—	0.222 (0.125)	0.349 (0.153)	0.359 (0.145)	—	—	—
Kidney	1.52 (0.11)	5.27 (0.98)	3.47 (0.46)	2.87 (0.34)	7.97 (1.62)	5.66 (1.11)	4.98 (0.66)
GI tract	13.3 (1.9)	0.98 (0.080)	1.06 (0.18)	1.27 (0.20)	11.8 (0.9)	16.9 (2.1)	17.8 (1.2)
Skin	16.6 (0.9)[c]	0.361 (0.074)	0.547 (0.192)	0.739 (0.238)	6.46 (1.30)	10.3 (3.4)	12.8 (4.3)
Muscle	39.9[d]	0.781 (0.280)	0.794 (0.098)	0.459 (0.054)	33.7 (12.4)	39.1 (1.2)	24.7 (2.4)
Plasma	5.1[d]	0.646 (0.179)	0.506 (0.095)	0.931 (0.060)	3.57 (1.02)	2.70 (0.41)	5.69 (0.69)
Red cells	4.98 (1.22)[e]	0.675 (0.062)	0.411 (0.024)	0.246 (0.029)	5.23 (1.97)	1.94 (0.29)	1.44 (0.19)
Injection site	—	—	—	—	7.30 (2.25)	3.79 (2.08)	2.93 (3.18)
Total					86.3	104.2	95.8

[a] Mean of 12 mice (except where noted), standard deviation in parenthesis. [b] n = 3. [c] n = 8. [d] From Ref. 11. [e] Calculated from the hematocrit (Hct) as follows: red cells, percent of body weight = 5.1% [Hct/(1 − Hct)].

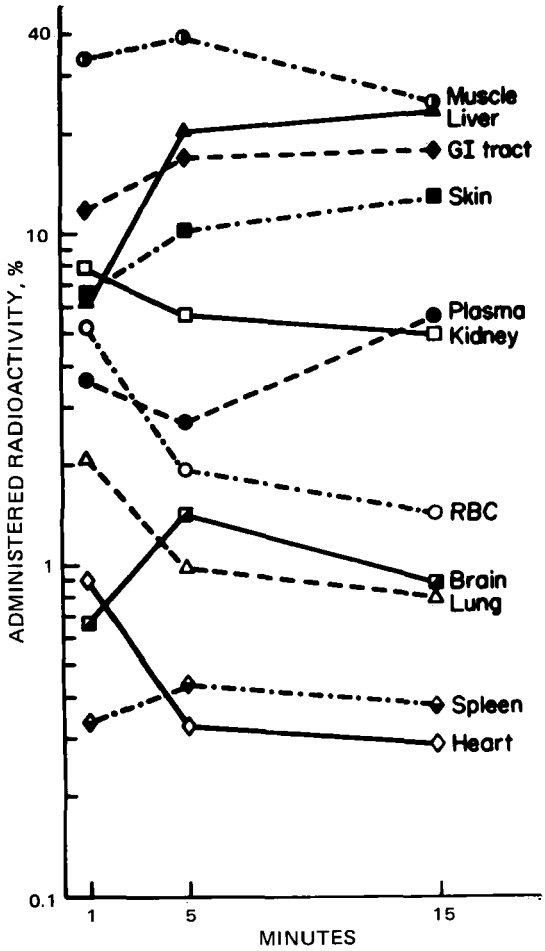

Figure 2—*Distribution of radioactivity in the mouse as a function of time after intravenous injection of 8-^{3}H-naltrexone. Each point represents the mean of three values.*

nous administration further illustrate the rapid and extensive distribution from plasma to body tissues; less than 4% of the administered radioactivity remains in plasma after 1 min. The amount of radioactivity in the brain reaches a maximum at 5 min (Fig. 2). A similar early peak in brain levels was reported for pentazocine (24).

The ratio of radioactivity concentration (expressed as micrograms of naltrexone equivalents per gram wet weight of tissue or fluid) in plasma to that in the red cell fraction increases with time (0.9 at 1 min, 1.2 at 5 min, and 3.8 at 15 min). This fact, plus the absolute increase in plasma radioactivity at 15 min, suggests that significant amounts of radiolabeled metabolites may be accumulating in plasma and that these are too polar to penetrate red cells readily. Thus, the distribution pattern, particularly at 15 min, may not be that of only unaltered naltrexone.

The low extent of binding suggests that potential interactions involving displacement from binding sites will not be a therapeutic problem with naltrexone (25). In addition, the concentration independence of binding over a wide concentration range indicates that this factor can be considered a constant in the interpretation of naltrexone pharmacokinetics.

REFERENCES

(1) W. R. Martin, D. R. Jasinski, and P. A. Mansky, *Arch. Gen. Psychiat.*, **28**, 784(1973).

(2) T. M. Maugh, II, *Science*, **177**, 249(1972).

(3) W. R. Martin and V. L. Sandquist, *Arch. Gen. Psychiat.*, **30**, 31(1974).

(4) A. P. Gray and D. S. Robinson, *J. Pharm. Sci.*, **63**, 159(1974).

(5) P. Keen, in "Handbook of Experimental Pharmacology," vol. 28, part 1, B. B. Brodie and J. R. Gillette, Eds., Springer-Verlag, New York, N.Y., 1971, pp. 213–233.

(6) P. G. Dayton, Z. H. Israili, and J. M. Perel, *Ann. N.Y. Acad. Sci.*, **226**, 172(1973).

(7) S. J. Mulé, *Anal. Chem.*, **36**, 1907(1964).

(8) J. D. Baggot, L. E. Davis, and C. A. Neff, *Biochem. Pharmacol.*, **21**, 1813(1972).

(9) "Handbook of Biological Data," W. S. Spector, Ed., W. B. Saunders, Philadelphia, Pa., 1956, p. 55.

(10) R. C. Lanman and L. S. Schanker, *Life Sci.*, **9**, part I, 1003(1970).

(11) J. J. Friedman, *Proc. Soc. Exp. Biol. Med.*, **88**, 323(1955).

(12) J. D. Baggot and L. E. Davis, *Amer. J. Vet. Res.*, **34**, 571(1973).

(13) G. D. Olsen, *Clin. Pharmacol. Ther.*, **17**, 31(1975).

(14) M. Ehrnebo, S. Agurell, L. O. Boreus, E. Gordon, and U. Lönroth, *Clin. Pharmacol. Ther.*, **16**, 424(1974).

(15) O. Borga, D. L. Azarnoff, G. Plym-Forshell, and F. Sjöqvist, *Biochem. Pharmacol.*, **18**, 2135(1969).

(16) G. D. Olsen, *Clin. Pharmacol. Ther.*, **14**, 338(1973).

(17) C. A. Neff, L. E. Davis, and J. D. Baggot, *Amer. J. Vet. Res.*, **33**, 1521(1972).

(18) C. R. Short and M. E. Tumbleson, *Toxicol. Appl. Pharmacol.*, **24**, 612(1973).

(19) G. H. Evans, A. S. Nies, and D. G. Shand, *J. Pharmacol. Exp. Ther.*, **186**, 114(1973).

(20) W. Müller and U. Wollert, *Naunyn-Schmiedebergs Arch. Pharmakol.*, **280**, 229(1973).

(21) K. A. Johansson, C. Appelgrn, K. O. Borg, and R. Elofsson, *Acta Pharm. Suecica*, **11**, 333(1974).

(22) O. Borga, D. L. Azarnoff, and F. Sjöqvist, *J. Pharm. Pharmacol.*, **20**, 571(1968).

(23) V. K. Batra, R. A. Sams, R. H. Reuning, and L. Malspeis, *Pharm. Abstr.*, **4**, 122(1974).

(24) N. J. Coroneos, N. P. Keaney, D. G. McDowall, V. W. A. Pickerodt, J. P. Glynn, and A. Robertson, *Brit. J. Pharmacol.*, **50**, 393(1974).

(25) P. T. Schoenemann, D. W. Yesair, J. J. Coffey, and F. T. Bullock, *Ann. N.Y. Acad. Sci.*, **226**, 162(1973).

ACKNOWLEDGMENTS AND ADDRESSES

Received March 28, 1975, from the *College of Pharmacy and the ‡College of Veterinary Medicine, Ohio State University, Columbus, OH 43210

Accepted for publication July 28, 1975.

Supported by Contract HSM 42-73-182 and Grant DA-00473 from the National Institute on Drug Abuse (NIDA), U.S. Department of Health, Education and Welfare, Rockville, Md.

The authors are indebted to Dr. J. A. Kepler for providing the tritiated naltrexone under NIDA Contract HSM 42-73-184 with Research Triangle Institute, Research Triangle Park, N.C., and to Dr. D. A. McCarthy, Parke-Davis & Co., Ann Arbor, Mich., for providing samples of monkey plasma.

‡ To whom inquiries should be directed.

Pharmacokinetic Model for Simultaneous Determination of Drug Levels in Organs and Tissues

C. N. CHEN and J. D. ANDRADE ˣ

Abstract □ An extension of the Bischoff–Dedrick pharmacokinetic model is presented. This model is derived from basic considerations of drug distribution with physiological and anatomical meaning. The Bischoff–Dedrick model can simultaneously predict drug distribution with time in blood, organs, and tissues of pharmacological interest. The parameters are applied to a 15-kg standard dog. The experimental kinetic data of thiopental in brain, plasma, liver, lean tissue, and adipose tissue in a dog are used to demonstrate the feasibility of the model. Allowable variations in the parameters are determined. In general, the kinetics of drug distribution in blood, organs, and tissues depend on the drug dosage, lipid solubility, partition coefficients, metabolism rate, excretion rate, protein binding, route of administration, sizes of organs and tissues, and blood flow rates through organs and tissues. These factors enter the kinetic model separately and explicitly so their effects on the kinetics of drug distribution can be studied to provide valuable information for optimal therapy.

Keyphrases □ Pharmacokinetic model—proposed for simultaneous determination of drug distribution with time in blood, organs, and tissues, demonstrated with thiopental in dogs □ Distribution, drug—simultaneous determination in blood, organs, and tissues, pharmacokinetic model, demonstrated with thiopental in dogs □ Thiopental—distribution in blood, organs, and tissues, pharmacokinetic model for simultaneous determination proposed, dogs

Drug concentration in blood is measured clinically because this procedure is easier and more convenient than the sampling of other tissues or fluids. Therefore, it has been used as an index of dose scheduling for therapeutics. Conventional pharmacokinetic models (1) correlate kinetic data of drug concentration in blood by using one or several exponential terms. Each exponential term in the conventional model represents a compartment; single or multiple compartments are used to curve fit the experimental kinetic data. The coefficients and rate constants in the pharmacokinetic equations are then determined from the curve-fit parameters.

Drug concentrations in blood with time depend on the drug dosage, lipid solubility, partition coefficients, metabolism rate, excretion rate, protein binding, and route of administration. Common pharmacokinetic models put all these factors into the rate constants and coefficients of the curve-fit equations. Unless the rate constants and coefficients can be expressed as explicit functions of related factors, they cannot be predicted without experimental kinetic data.

Some cardiac drugs, *e.g.*, digitalis, or ultrashort-acting barbiturates, *e.g.*, thiopental, have rather narrow margins of safety. Their kinetic distribution in blood may not provide sufficient information for adequate therapy. Digitalis kinetics in heart muscle and thiopental kinetics in brain can provide much better information for optimal therapy than the drug levels present in blood (2–4). Furthermore, knowledge of the drug distribution in blood, organs, and tissues may be necessary for providing optimal treatment. Conventional pharmacokinetic models cannot provide such information.

An entirely different approach to pharmacokinetic modeling was developed by Bischoff, Dedrick, and their coworkers (5–13), beginning in 1966. Their pharmacokinetic model simultaneously predicts the kinetics of drug distribution in blood, organs, and tissues of pharmacological interest. They successfully applied it to predict pharmacokinetics of thiopental (8), methotrexate (9, 12), and cytarabine (13). Bischoff and Dedrick (8) used the physiological parameters of a 70-kg standard male and a four-compartment model (blood, viscera, lean tissue, and adipose tissue) to simulate experimental kinetic data (2) of thiopental distribution in plasma, liver, lean tissue, and adipose tissue of the dog. They combined brain, heart, kidneys, liver, *etc.*, as a viscera compartment (8).

Since thiopental kinetics in the brain may provide valuable information for optimal therapy, an attempt was made to predict thiopental kinetics in the brain and, simultaneously, to predict thiopental kinetics in plasma, liver, lean tissue, and adipose tissue based on the physiological parameters of a 15-kg standard dog by using the Bischoff–Dedrick approach. The model can also be applied to study the pharmacokinetics of other drugs.

THEORETICAL

The data of Brodie *et al.* (2, 3) (Figs. 1 and 2), showing thiopental kinetics in plasma, liver, lean tissue, adipose tissue, and brain of the dog, were used to demonstrate the feasibility of the model. At least five body regions are defined: brain, liver, lean tissue, adipose tissue, and blood pool (blood volume in the capillary bed of any body region is included in that body region while the remaining blood is grouped together as another body region, called the blood pool). In mammals, blood from the GI area perfuses the liver. Thus, the GI tissues were added as another body region. Since there was little interest in the kinetics of thiopental in kidneys or heart, these and other organs were considered as another body region called viscera.

A diagram of blood circulation in the seven body regions is shown in Fig. 3. As blood flow carries the drug to the capillary bed where the drug diffuses into the tissue, each body region except the blood pool in Fig. 3 is further divided into two portions: the blood volume in the capillary bed and the tissue volume without blood. The physiological parameters of the model for a 15-kg standard dog are also shown in Fig. 3. A detailed discussion of the derivation of these parameters is presented in *Appendix I*.

Protein binding plays an important role in pharmacological effects and pharmacokinetics, since most drugs are bound to plasma proteins, especially to albumin and various tissue components (11). It is well recognized that not all macromolecules in blood or tissue are responsible for binding with the drug. Shen and Gibaldi (14) showed that the predicted thiopental concentrations in plasma and lean tissue, based on the total macromolecule content in organs and tissues, were substantially overestimated by the Bischoff–

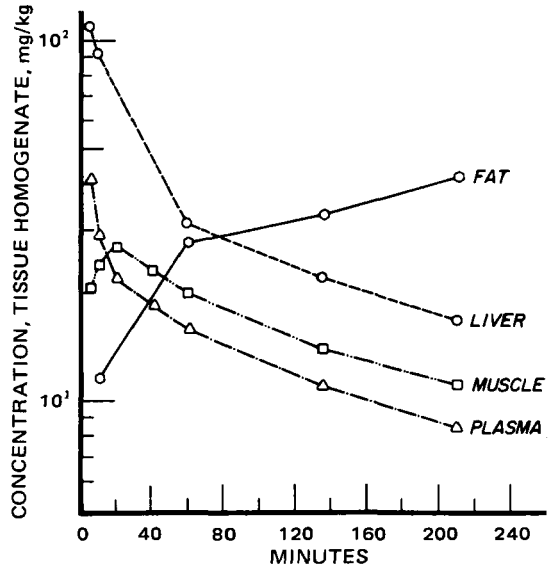

Figure 1—*Experimental thiopental concentrations in various tissues of a dog after 25 mg/kg iv (redrawn from Ref. 2).*

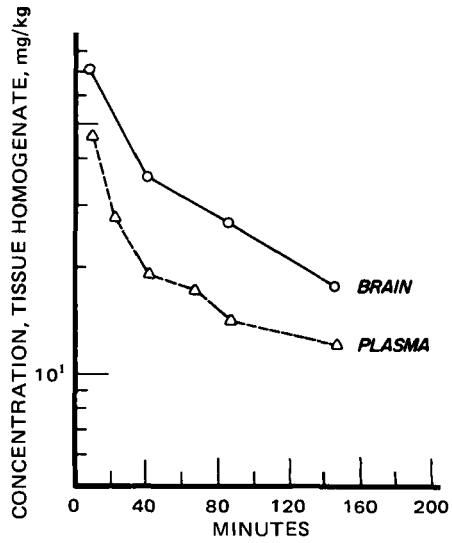

Figure 2—*Experimental thiopental concentrations in plasma and brain of a dog after 40 mg/kg iv (redrawn from Ref. 3).*

Dedrick model. Bischoff and Dedrick (7, 8) proposed the concept of effective protein fraction and applied it to their model for thiopental pharmacokinetics. In the addendum to Shen and Gibaldi's article (14), Bischoff and Dedrick favored the use of effective protein concentration rather than effective protein fraction utilizing:

$$C_T = F_W C + C_M X \qquad \text{(Eq. 1)}$$

where the total drug concentration (C_T) in blood or tissue is defined in terms of the volume fraction of water (F_W), free drug concentration (C), effective binding macromolecule concentration (C_M), and bound drug "concentration" (X, the amount of bound drug per unit of effective binding macromolecules). This approach obviates assuming unit densities, and there is no need for the two coefficients to be fractions that add up to unity.

Volume fractions of water in blood, organs, and tissues are available in the literature and in biological data handbooks. Table I lists calculated and reported values for volume fractions of water in organs and tissues of the dog. The volume fraction of water in the tissue portion of any body region can be calculated by:

$$V_{YzB}F_{W,B} + V_{YzT}F_{W,YzT} = (V_{YzB} + V_{YzT})F_{W,Yz} \qquad \text{(Eq. 2)}$$

where:

$F_{W,B}$ = volume fraction of water in blood
$F_{W,YzT}$ = volume fraction of water in tissue portion of Yz body region
$F_{W,Yz}$ = volume fraction of water in Yz body region
V_{YzB} = blood volume in Yz body region
V_{YzT} = tissue volume in Yz body region

The effective binding macromolecule concentration (C_M) in blood or tissue can be determined in terms of the fraction of bound drug (F) and the equilibrium relation between free and bound drug in blood or tissue. A detailed discussion of how effective binding macromolecule concentrations in blood and tissues were derived is presented in *Appendix II.*

The physical picture of dynamic drug distribution at any instant in any body region is as follows. The inflow drug (free and bound) mixes with the drug in the capillary bed and the mixed drug (free drug only) in the capillary bed then diffuses into the tissue. Both the changing free drug concentrations in blood water and tissue water disturb and then reestablish the equilibrium relations between free and bound drug in the capillary bed and the tissue. When a well-mixed state in the capillary bed is assumed, the outflow drug concentration (free and bound) from the body region is the same as that reestablished in the capillary bed.

For highly lipid-soluble drugs, the rate of mass transfer between blood in the capillary bed and tissue is so fast that, at any instant, the free drug concentration in tissue water effectively equals that in blood water. This condition was called the "flow-limiting condition" by Dedrick and Bischoff (7), who discussed mathematical details of the condition and found that highly lipid-soluble compounds, such as thiopental and aniline, approximate the condition.

The transient mass balance for any body region can be expressed as:

[accumulation rate of free drug and bound drug in both capillary bed and tissue portion] = [inflow rate of free drug and bound drug from blood pool and/or other body regions]

+ [drug injection rate, if any]

− [outflow rate of free drug and bound drug from body region]

− [metabolism rate and/or excretion rate of drug, if any]

(Eq. 3)

The mathematical equation of transient mass balance for body region Y (Fig. 4) is:

$$(F_{W,B}V_{YB} + F_{W,YT}V_{YT})\frac{dC_Y}{dt} + (C_{M,B}V_{YB})\frac{dX_{YB}}{dt} + (C_{M,YT}V_{YT})\frac{dX_{YT}}{dt} = Q_Y(F_{W,B}C_B + C_{M,B}X_B) - Q_Y(F_{W,B}C_Y + C_{M,B}X_{YB}) \qquad \text{(Eq. 4)}$$

where:

$$C_{M,B} = F_{Pl,B}C_{M,Pl} + (1 - F_{Pl,B})C_{M,RBC}$$

and:

C_B = free drug concentration in blood water from the blood pool (micromoles per liter)
C_Y = free drug concentration in blood water or tissue water of body region Y (micromoles per liter)
$C_{M,B}$ = effective binding macromolecule concentration in blood (kilograms per liter)
$C_{M,Pl}$ = effective binding macromolecule concentration in plasma (kilograms per liter)
$C_{M,RBC}$ = effective binding macromolecule concentration in red blood cells (kilograms per liter)
$C_{M,YT}$ = effective binding macromolecule concentration in tissue portion of body region Y (kilograms per liter)
$F_{W,B}$ = volume fraction of water in blood
$F_{W,YT}$ = volume fraction of water in tissue portion of body region Y

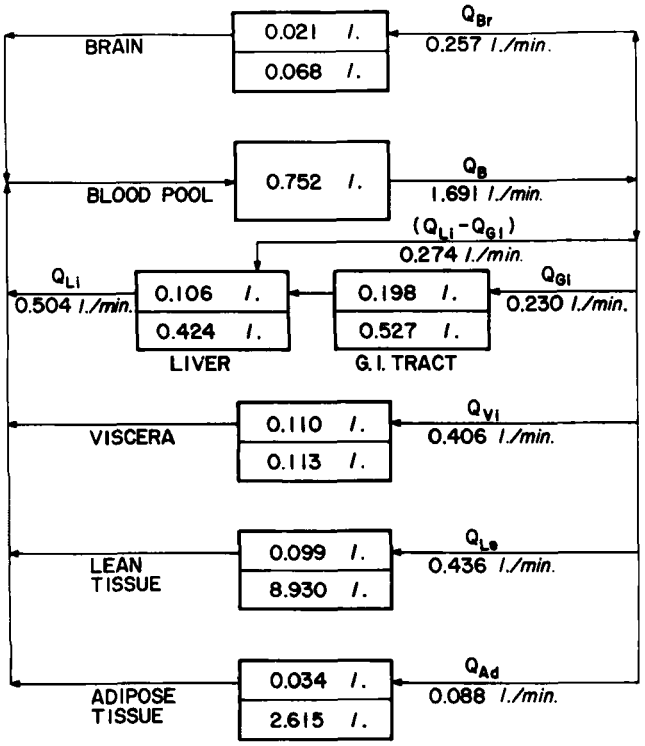

Figure 3—*Body regions and blood flow of a 15-kg dog.*

$F_{Pl,B}$ = volume fraction of plasma in blood
Q_Y = volumetric blood flow rate from body region Y (liters per minute)
t = time (minutes)
V_{YB} = blood volume in capillary bed of body region Y (liters)
V_{YT} = volume of tissue portion of body region Y (liters)
X_B = bound drug concentration (amount of bound drug per unit of effective binding macromolecules) from the blood pool (micromoles per kilogram)
X_{YB} = bound drug concentration in capillary bed of body region Y (micromoles per kilogram)
X_{YT} = bound drug concentration in tissue portion of body region Y (micromoles per kilogram)

The first term on the left-hand side of Eq. 4 represents the accumulation rate of free drug in both blood water and tissue water. The second and third terms indicate accumulation rates of bound drug in the capillary bed and in the tissue portion, respectively. The first term on the right-hand side of Eq. 4 represents the inflow rate of free drug and bound drug from the blood pool, and the second term indicates the outflow rate of free drug and bound drug from body region Y (Fig. 4).

Table I—Calculated and Reported Values for Volume Fractions of Water in Organs and Tissues of the Dog

Tissue (Yz)	$F_{W,Yz}$[a]	$F_{W,YzT}$[b]
Whole blood	0.800[c]	—
Plasma	0.930[c]	—
Red blood cells	0.640[c]	—
Whole brain	0.795[c]	0.794
Liver	0.746[c]	0.733
Intestines	0.757[c]	0.741
Heart	0.783[c]	0.775
Kidneys	0.802[c]	0.807
Viscera	0.791[d]	0.782
Lean tissue	0.776[c]	0.776
Adipose tissue	0.200[e]	0.192

[a] Reported values for volume fractions of water in various tissues. [b] Calculated values for volume fractions of water in tissue portions of various tissues. [c] P. L. Altman and D. S. Dittmer, "Biology Data Book," vol. 1, 2nd ed., Federation of American Societies for Experimental Biology, Bethesda, Md., 1972, pp. 19, 393, 394. [d] The value for volume fraction of water in viscera was calculated from heart and kidneys. [e] C. H. Best and N. B. Taylor, "The Living Body," 4th ed., Holt, Rinehart and Winston, New York, N.Y., 1966, p. 55.

Similarly, the transient mass balance was applied for each body region shown in Fig. 3. The goal was to predict thiopental kinetics in plasma. The blood was divided into plasma and red blood cells, using a hematocrit value of 45% (volume). The concept of effective binding macromolecule concentration in blood and various tissues (*Appendix II*) and the flow-limiting condition are applied to the following mathematical model.

For the blood pool:

$$F_{Pl,B} = 0.55 \qquad \text{(Eq. 5)}$$

$$C_{M,B} = F_{Pl,B}C_{M,Pl} + (1 - F_{Pl,B})C_{M,RBC} \qquad \text{(Eq. 6)}$$

The transient mass balance for the blood pool (Figs. 3 and 4) is:

$$\underbrace{(F_{W,B}V_B)\frac{dC_B}{dt}}_{\text{accumulation rate of free drug in blood pool}} + \underbrace{(C_{M,B}V_B)\frac{dX_B}{dt}}_{\text{accumulation rate of bound drug in blood pool}}$$

$$= \underbrace{Q_{Br}(F_{W,B}C_{Br} + C_{M,B}X_{BrB}) + Q_{Li}(F_{W,B}C_{Li} + C_{M,B}X_{LiB}) + Q_{Vi}(F_{W,B}C_{Vi} + C_{M,B}X_{ViB}) + Q_{Le}(F_{W,B}C_{Le} + C_{M,B}X_{LeB}) + Q_{Ad}(F_{W,B}C_{Ad} + C_{M,B}X_{AdB})}_{\text{summation of inflow rates of free and bound drug from five body regions}} + \underbrace{Mg(t)}_{\text{injection term}}$$

$$- \underbrace{Q_B(F_{W,B}C_B + C_{M,B}X_B)}_{\text{outflow rate of free and bound drug from blood pool}} \qquad \text{(Eq. 7)}$$

The particular symbols are defined under *Notation*.

The term $Mg(t)$ is the injection term, where M is the total amount of the drug injected and $g(t)$ is a normalized injection function (7, 8):

$$g(t) = 30\lambda(\lambda t)^2(1 - \lambda t)^2 \qquad \text{(Eq. 8)}$$

where λ is the reciprocal of the injection duration. The term $Mg(t)$ simulates a smooth injection and is convenient for computation (7, 8). Note that:

$$\int_0^{1/\lambda} g(t)\,dt = 1 \qquad \text{(Eq. 9)}$$

A similar mass balance for the liver (Li) gives:

$$\underbrace{(F_{W,B}V_{LiB} + F_{W,LiT}V_{LiT})\frac{dC_{Li}}{dt}}_{\text{accumulation rates of free drug in capillary bed and tissue portion of liver}} + \underbrace{(C_{M,B}V_{LiB})\frac{dX_{LiB}}{dt} + C_{M,LiT}V_{LiT})\frac{dX_{LiT}}{dt}}_{\text{accumulation rates of bound drug in capillary bed and tissue portion of liver}}$$

$$= \underbrace{(Q_{Li} - Q_{GI})(F_{W,B}C_B + C_{M,B}X_B)}_{\text{inflow rates of free and bound drug from blood pool}} + \underbrace{Q_{GI}(F_{W,B}C_{GI} + C_{M,B}X_{GIB})}_{\text{inflow rates of free and bound drug from GI area}}$$

$$- \underbrace{Q_{Li}(F_{W,B}C_{Li} + C_{M,B}X_{LiB})}_{\text{outflow rate of free and bound drug from liver}} - \underbrace{R_{Li}(C_{Li})}_{\text{metabolism rate of drug}} \qquad \text{(Eq. 10)}$$

The metabolism rate (7, 8) is written in the simple Michaelis–Menten form:

$$R_{Li}(C_{Li}) = \frac{k_{Li}C_{Li}}{k_{M,Li} + C_{Li}} \qquad \text{(Eq. 11)}$$

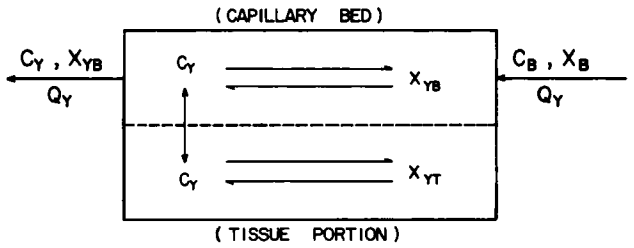

Figure 4—*Diagram of transient mass balance for the body region* Y *under the assumptions of a well-mixed state in the capillary bed and flow-limiting condition for highly lipid-soluble drugs.*

Since the metabolism mainly occurs in the liver, all metabolism of thiopental is assumed to occur in the liver. In general, similar terms could be added to other body regions if necessary. Mark (15) reported a value for the overall metabolism rate of thiopental as 15%/hr. The parameters (k_{Li} and $k_{M,Li}$) in Eq. 11 were empirically adjusted to provide values of k_{Li} = 5.68 μmoles/min and $k_{M,Li}$ = 4.0 μmoles/liter for a 15-kg standard dog. The remaining mass balances have similar forms.

For the brain (Br) region:

$$(F_{W,B}V_{BrB} + F_{W,BrT}V_{BrT})\frac{dC_{Br}}{dt} + (C_{M,B}V_{BrB})\frac{dX_{BrB}}{dt} + (C_{M,BrT}V_{BrT})\frac{dX_{BrT}}{dt} = Q_{Br}(F_{W,B}C_B + C_{M,B}X_B - F_{W,B}C_{Br} - C_{M,B}X_{BrB}) \quad \text{(Eq. 12)}$$

For the viscera (Vi) region:

$$(F_{W,B}V_{ViB} + F_{W,ViT}V_{ViT})\frac{dC_{Vi}}{dt} + (C_{M,B}V_{ViB})\frac{dX_{ViB}}{dt} + (C_{M,ViT}V_{ViT})\frac{dX_{ViT}}{dt} = Q_{Vi}(F_{W,B}C_B + C_{M,B}X_B - F_{W,B}C_{Vi} - C_{M,B}X_{ViB}) \quad \text{(Eq. 13)}$$

For the GI (GI) tissue region:

$$(F_{W,B}V_{GIB} + F_{W,GIT}V_{GIT})\frac{dC_{GI}}{dt} + (C_{M,B}V_{GIB})\frac{dX_{GIB}}{dt} + (C_{M,GIT}V_{GIT})\frac{dX_{GIT}}{dt} = Q_{GI}(F_{W,B}C_B + C_{M,B}X_B - F_{W,B}C_{GI} - C_{M,B}X_{GIB}) \quad \text{(Eq. 14)}$$

For the lean tissue (Le) region:

$$(F_{W,B}V_{LeB} + F_{W,LeT}V_{LeT})\frac{dC_{Le}}{dt} + (C_{M,B}V_{LeB})\frac{dX_{LeB}}{dt} + (C_{M,LeT}V_{LeT})\frac{dX_{LeT}}{dt} = Q_{Le}(F_{W,B}C_B + C_{M,B}X_B - F_{W,B}C_{Le} - C_{M,B}X_{LeB}) \quad \text{(Eq. 15)}$$

For the adipose tissue (Ad) region:

$$(F_{W,B}V_{AdB} + F_{W,AdT}V_{AdT})\frac{dC_{Ad}}{dt} + (C_{M,B}V_{AdB})\frac{dX_{AdB}}{dt} + (C_{M,AdT}V_{AdT})\frac{dX_{AdT}}{dt} = Q_{Ad}(F_{W,B}C_B + C_{M,B}X_B - F_{W,B}C_{Ad} - C_{M,B}X_{AdB}) \quad \text{(Eq. 16)}$$

Adipose tissue must be handled somewhat differently (*Appendix II*). It is worth noting that free drug concentrations and bound drug concentrations in all body regions (Fig. 3) are involved in Eq. 7, while the free drug concentration and bound drug concentration in the blood pool appear in all equations. Thus, each equation is not independent but interrelated to the others, constituting a set of simultaneous differential equations. There are 20 unknown variables (seven free drug concentrations in blood water or tissue water of the seven body regions and 13 bound drug concentrations in the capillary beds and tissue portions of the seven body regions) in Eqs. 7, 10, and 12–16. Seven equations can serve to solve only seven variables. Therefore, to solve the seven simultaneous equations, 13 remaining variables should be correlated to the seven selected variables by certain relationships.

Equilibrium relationships between free drug concentrations and bound drug concentrations in blood, organs, and tissues can be determined experimentally and provide the 13 relationships to solve the seven simultaneous differential equations. Actually, the equilibrium relationships between free and bound drug in the capillary beds of all body regions are the same. Hence, only seven equilibrium relations (one in the blood and six in the tissue portions of six body regions) are required.

Any equilibrium relation between free and bound drug in blood and various tissues can be determined by a general form of Langmuir adsorption (16, 17):

$$r = \sum_{i=1}^{n} \frac{N_i K_i C}{1 + K_i C} \quad \text{(Eq. 17)}$$

where:

r = moles of bound drug per mole of binding macromolecule (moles per mole)
C = free drug concentration (micromoles per liter)
N_i = average number of type i binding sites per molecule of binding macromolecule (moles per mole)
K_i = intrinsic association constant of type i binding site (liters per micromole)

Goldbaum and Smith (18) measured the binding of several barbiturates in 1% bovine serum albumin at drug levels of pharmacological interest. They correlated the observed data with the form of Langmuir adsorption for two types of binding sites:

$$r = \frac{N_1 K_1 C}{1 + K_1 C} + \frac{N_2 K_2 C}{1 + K_2 C} \quad \text{(Eq. 18)}$$

Bound drug concentration (X, micromoles of bound drug per kilogram of effective binding macromolecule) can be related to r, to be

Table II—Parameter Values for Kinetic Model of Thiopental in a 15-kg Dog

Parameter	Numerical Values
Effective binding macromolecule concentration[a], kg/liter	$C_{M,Pl}$ = 0.0146, $C_{M,RBC}$ = 0.0152, $C_{M,B}$ = 0.0149, $C_{M,BrT}$ = 0.0233, $C_{M,LiT}$ = 0.0408, $C_{M,GIT}$ = 0.0331, $C_{M,ViT}$ = 0.0409, $C_{M,LeT}$ = 0.0222, $C_{M,AdT}$ = 0.8700
Binding site constants (7, 8), μmoles/kg	B_1 = 18,400, B_2 = 305,000
Intrinsic association constant (7, 8), liters/μmole	K_1 = 0.060, K_2 = 0.000625
Lipid solubility constant (7, 8)	B_A = 100
Injection parameter[b]	M = 1420.45 μmoles, λ = 0.20 min^{-1}
Metabolism constant[b]	k_{Li} = 5.68 μmoles/min, $k_{M,Li}$ = 4.0 μmoles/liter

[a] For detailed calculation, see *Appendix II*. [b] The values were modified from Refs. 7 and 8 to suit the condition of 25 mg of thiopental/kg for a 15-kg dog.

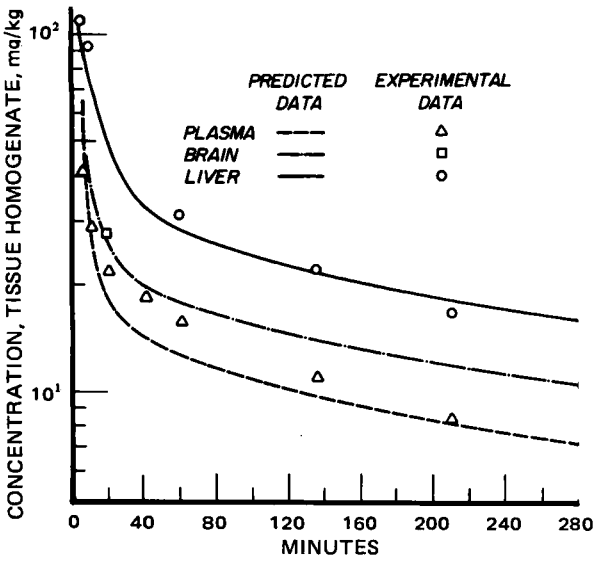

Figure 5—*Predicted and experimental thiopental concentrations in plasma, brain, and liver following 25 mg/kg iv.*

defined in terms of free drug concentration (C):

$$X = \frac{10^9}{M_P}(r) = \frac{B_1K_1C}{1+K_1C} + \frac{B_2K_2C}{1+K_2C} \qquad \text{(Eq. 19)}$$

where:

$$Bi = \frac{10^9}{M_P}(Ni)$$

where M_P = molecular weight of binding macromolecule; 68,000 was assumed for the albumin to calculate constant Bi shown in Table II.

Since no other equilibrium relationships are available, Eq. 19 with the constants in Table II was assumed to represent the equilibrium relation in blood, organs, and tissues as an approximation and was used to solve the simultaneous Eqs. 7, 10, and 12–16. This approximation is reasonable if the equilibrium relationships between free drug concentrations and bound drug concentrations in blood and various tissues of the dog have similar curve shapes to those measured in 1% bovine serum albumin by Goldbaum and Smith (18). It is assumed that the fractions of bound drug (thiopental) in blood, organs, and tissues of the dog are similar to those of the rabbit, which are available (18) and are used to calculate effective binding macromolecule concentrations (*Appendix II*). How close must they be for a reasonable approximation will be discussed later.

One may wonder whether the equilibria between free and bound drug in the body regions can be established so quickly that the equilibrium relationships can be applied to the equations of transient mass balances for the various body regions. Colowick and Womack (19), in their studies on binding of diffusible molecules by macromolecules, pointed out that the usual chemical equilibrium for the binding reaction can be reached quickly, suggesting that the equilibrium relationships between free and bound drug in blood and tissues can be applied to the equations of transient mass balances.

The term for the excretion rate is included in the general treatment (20). Since the excretion of unchanged thiopental is negligible (21), the term is omitted in this treatment.

RESULTS AND DISCUSSION

Analytical solutions of the simultaneous differential equations were not feasible because of nonlinearities caused by the binding terms. Therefore, Eqs. 7, 10, and 12–16 were solved by numerical methods (20). The numerical results for the dosage of 25 mg of thiopental/kg are presented in Figs. 5 and 6. The predicted kinetics in plasma and several organs and tissues of interest agree well with the experimental data (2).

The same mathematical model used to develop Eqs. 7, 10, and 12–16 was applied to predict the thiopental distribution in plasma and brain (3) shown in Fig. 2 by modifying some of the parameters in Table II to meet the new conditions. Because 40 mg of thiopental/kg was intravenously injected, the total amount of thiopental injected to a 15-kg dog was 2272.72 instead of 1420.45 μmoles and the injection duration was 8 min so that $\lambda = 0.125\ \text{min}^{-1}$. The predicted kinetics in plasma and brain also agree well with the experimental data (Fig. 7).

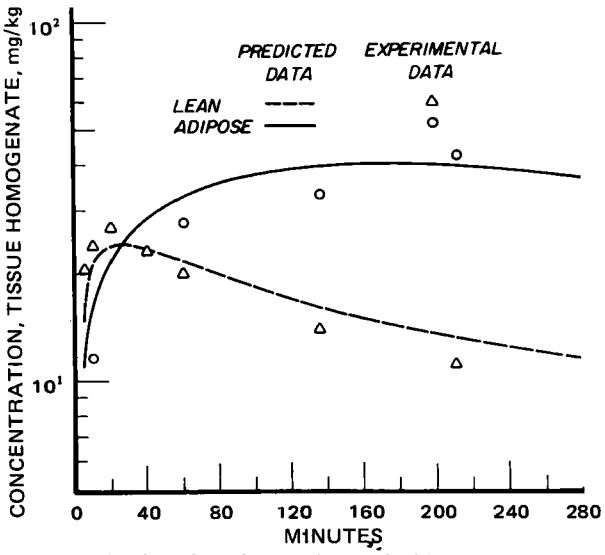

Figure 6—*Predicted and experimental thiopental concentrations in lean and adipose tissues following 25 mg/kg iv.*

Mathematical Model Testing—This mathematical model involves many parameters that must be known to certain degrees of accuracy. If the model is stable enough, some reasonable variations of the parameters should not appreciably change the results. Physiological parameters in Table I and Fig. 3 are statistical average values, which may be close to true values. Biochemical parameters in Table II are determined from experiment and are expected to deviate from true values. Because the true values for all parameters are unknown, the values for all parameters in Tables I and II and Fig. 3 were assumed to be standard values. The stability of the model was tested by comparing the numerical results from standard values for all parameters with those from a variation of ±10% of standard value for each of the following parameters:

1. ±10% variation of the volume of any body region
2. ±10% variation of the volume and the blood flow rate of any body region

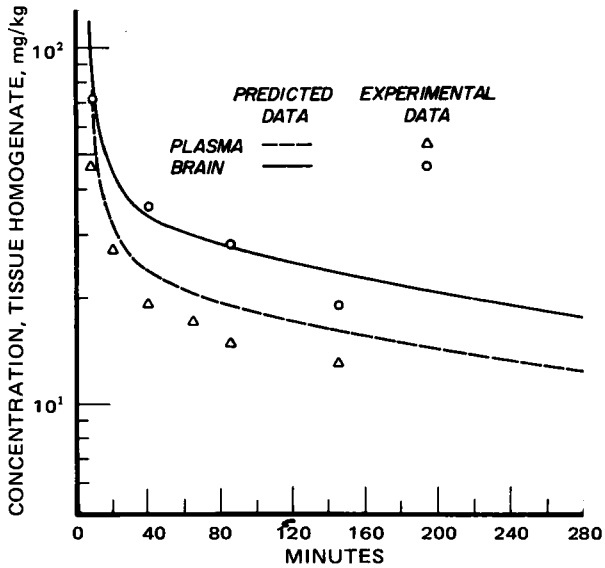

Figure 7—*Predicted and experimental thiopental concentrations in plasma and brain following 40 mg/kg iv.*

Table III—Volumes and Blood Supplies of Different Body Regions for a 15-kg Standard Dog

Tissue	Total Tissue Volume (Including Blood), liters	Tissue Volume (Excluding Blood[a]), liters	Blood Volume in Capillary Bed, liters	Blood Flow Rate, liters/min
Brain	0.089[b]	0.068	0.021[c]	0.257[d]
Liver	0.530[b]	0.424	0.106[e]	0.504[f]
Adrenals	0.002[b]	0.001	0.001[c]	0.034[d]
Kidneys	0.090[b]	0.025	0.065[c]	0.264[f]
Thyroid	0.003[b]	0.001	0.002[c]	0.027[d]
Heart	0.128[b]	0.086	0.042[c]	0.081[d]
GI	0.725[b]	0.527	0.198[e]	0.230[g]
Lean tissue	9.029[h]	8.930	0.099[f]	0.436[d]
Fatty marrow	0.480[i]	0.472	0.008[c]	0.020[d]
Fat	2.169[i]	2.143	0.026[c]	0.068[d]

[a] Calculated from total tissue volume minus blood volume in the capillary bed. [b] W. S. Spector, "Handbook of Biological Data," Saunders, Philadelphia, Pa., 1956, pp. 163, 283. [c] Calculated under the assumption that dogs and humans have the same ratio of blood volume in capillary bed to tissue volume without blood. [d] Calculated under the assumption that blood flow rate in certain tissues or organs have the same percentages of blood flow rate from the blood pool as that of standard man. [e] E. E. Selkurt, "Physiology," 2nd ed., Little, Brown, Boston, Mass., 1966, pp. 391–393. [f] D. S. Dittmer and R. M. Grebe, "Handbook of Circulation," Saunders, Philadelphia, Pa., 1959, pp. 71, 127, 129. [g] J. P. Delaney and J. Custer, *Circ. Res.*, 17, 394(1965). [h] Calculated under the assumption of 60.2% of body weight. [i] Calculated under the assumption that dogs and humans have the same percentage of body weight for the corresponding tissues.

3. ±10% variation of the value for each volume fraction of water in any body region
4. ±10% variation of the lipid solubility constant, B_A
5. ±10% variation of the metabolism constant, k_{Li}
6. ±10% variation of the binding site constants, Bi
7. ±10% and ±5% variation of the fractional data of bound drug in various tissues

The data (20) show that ±10% variation in each parameter, except fractional data of bound drug in various tissues, can be tolerated without significantly affecting the results. This finding verifies that the model is quite stable, allowing at least ±10% variations in all parameters but fractional data of bound drug where a ±5% variation is acceptable. This indicates that the values for fractions of bound drug in blood, organs, and tissues are more sensitive parameters than the others in the model and, therefore, must be determined more accurately.

Conclusions—Thiopental kinetics in brain are very important for anesthetic studies. The model not only predicts thiopental distribution in blood but also simultaneously provides thiopental kinetics in brain and other organs. Conventional pharmacokinetic models can never achieve this feature. One important feature of the model is that each equation is not independent but interrelated to the others.

One potential application is that if the model can be verified for a given drug in a species pharmacokinetically similar to humans, it can then be applied to predict human pharmacokinetics by making certain modifications in physiological and biochemical parameters. The experimentally observed drug distribution in plasma or blood can be used to compare with the corresponding kinetics predicted by the model. If they agree well, the predicted drug distribution in the other body regions that are difficult to sample may be expected to follow corresponding kinetic courses with confidence, even if they cannot be verified experimentally. Therefore, the model can provide valuable information for optimal therapeutic regimens.

Another potential application of the model is that the pharmacokinetics of some critical substances such as uric acid, creatinine, and urea in patients suffering from renal failure or of exogenous poisons in acutely intoxicated patients can be analyzed with respect to extracorporeal device treatments. In such cases, the extracorporeal device adds one more equation to the model system, and certain physiological parameters such as blood flow rates through organs and tissues must be modified. This type of analysis could lead to more optimal extracorporeal device treatment (20).

APPENDIX I: DETAILS OF PHYSIOLOGICAL PARAMETERS

The viscera body region shown in Fig. 3 includes kidneys, thyroid, heart, and adrenals; the adipose tissue body region contains fatty marrow and fat. The blood volume of the blood pool is from total blood volume (1.320 liters) minus the sum of the blood volumes of the other six body regions shown in Fig. 3. The blood flow rate from the blood pool is the sum of the blood flow rates from the other five body regions (excluding blood flow rate from the GI area) (Table III).

APPENDIX II

The effective binding macromolecule concentrations[1] (7, 14) in various tissues can be derived as follows. If there are D μmoles of drug contained in tissue homogenate of Yz body region with W liters of water (tissue water and blood water in the tissue homogenate) and P kg effective binding macromolecules out of total macromolecules in the tissue, the following relation can be established:

$$D = WC + PX \qquad \text{(Eq. A1)}$$

where C is free drug concentration in blood water or tissue water (micromoles per liter), and X is bound drug concentration (the amount of bound drug per unit of effective binding macromolecules) in the tissue (micromoles per kilogram). The fraction of bound drug in the tissue homogenate, F, is defined as $F = PX/D$. Substituting this into Eq. A1 gives:

$$D = (1-F)D + PX \qquad \text{(Eq. A2)}$$

When Eq. A2 is divided by the total volume of the tissue homogenate, it becomes:

$$C_T = (1-F)C_T + C_{M,Yz}X \qquad \text{(Eq. A3)}$$

where C_T is the total drug concentration, and $C_{M,Yz}$ is the effective binding macromolecule concentration of Yz tissue homogenate. This relationship can be further simplified:

$$C_{M,Yz} = \frac{FC_T}{X} \qquad \text{(Eq. A4)}$$

Substituting Eq. 19 into Eq. A4 gives:

$$C_{M,Yz} = FC_T \Big/ \left(\frac{B_1K_1C}{1+K_1C} + \frac{B_2K_2C}{1+K_2C}\right) \qquad \text{(Eq. A5)}$$

The effective binding macromolecule concentration in any tissue homogenate (Table IV) can be calculated by using Eq. A5 if the fraction of bound drug (F) in a certain total drug concentration (C_T) and the equilibrium relationship between the free drug concentration and bound drug concentration in the tissue homogenate are known.

The effective binding macromolecule concentration in the tissue portion (Table IV) can be calculated by the following equations,

[1] K. B. Bischoff, School of Chemical Engineering, Cornell University, Ithaca, NY 14850, and R. L. Dedrick, Biomedical Engineering and Instrumentation Branch, National Institutes of Health, Bethesda, MD 20014, personal communication

Table IV—Binding Parameters of Thiopental in Various Organs and Tissues of the Rabbit

Parameter	Liver	Heart	Kidneys	Brain	Lean Tissue	Red Blood Cells	Plasma, Undiluted	Viscera[a]	GI Tissue[a]
F^b	0.66	0.62	0.53	0.50	0.45	0.40	0.85	0.58	—
$C_{M,Yz}{}^c$	0.0356	0.0313	0.0235	0.0213	0.0221	0.0152	0.0146	0.0281	0.0281
$C_{M,YzT}{}^c$	0.0408	0.0393	0.0459	0.0233	0.0222	—	—	0.0409	0.0331

[a] Data shown were calculated by the method discussed in *Appendix II.* [b] Fractions of bound drug in organs and tissues except plasma were determined from tissue homogenate diluted to five volumes (18). [c] $C_{M,Yz}$ and $C_{M,YzT}$ are the effective binding macromolecule concentrations, which have been multiplied by five (dilution factor), in tissue homogenate and in the tissue portion, respectively. The values shown were calculated by the method discussed in *Appendix II.*

taking the liver as an example:

$$C_{M,B} = F_{Pl,B}C_{M,Pl} + (1 - F_{Pl,B})C_{M,RBC} \qquad \text{(Eq. A6)}$$

$$\frac{V_{LiB}}{V_{LiB}+V_{LiT}}C_{M,B} + \frac{V_{LiT}}{V_{LiB}+V_{LiT}}C_{M,LiT} = C_{M,Li} \qquad \text{(Eq. A7)}$$

The viscera body region consists of kidneys, heart, thyroid, and adrenals. Since the volume fraction of the thyroid and adrenals in the viscera is negligible and their fractional bound thiopental data are not available, effective binding macromolecule concentrations in kidneys (Ki) and heart (He) (Table IV) were used to calculate the effective binding macromolecule concentration in the viscera by the following equation:

$$C_{M,Vi} = \frac{V_{Ki}C_{M,Ki} + V_{He}C_{M,He}}{V_{Ki} + V_{He}} \qquad \text{(Eq. A8)}$$

Fractional bound drug data are not available for GI tissue, so its effective binding macromolecule concentration was not calculated. Therefore, the value of the effective binding macromolecule concentration in the viscera was assigned to the GI tissue. The effective binding macromolecule concentration in the GI tissue portion was then determined.

The tissue binding in adipose tissue[1] is somewhat different from that in other tissues and must be handled differently. The equilibrium relationship between free and bound drug in the capillary bed of adipose tissue is the same as Eq. 19:

$$X_{AdB} = C_{Ad}\left(\frac{B_1K_1}{1+K_1C_{Ad}} + \frac{B_2K_2}{1+K_2C_{Ad}}\right) \qquad \text{(Eq. A9)}$$

Total drug concentration in the capillary bed of adipose tissue, $C_{T,AdB}$, is defined as:

$$C_{T,AdB} = F_{W,B}C_{Ad} + C_{M,B}X_{AdB} \qquad \text{(Eq. A10)}$$

Substituting Eq. A9 into Eq. A10 gives:

$$C_{T,AdB} = C_{Ad}\left[F_{W,B} + C_{M,B}\left(\frac{B_1K_1}{1+K_1C_{Ad}} + \frac{B_2K_2}{1+K_2C_{Ad}}\right)\right] \qquad \text{(Eq. A11)}$$

The tissue "binding" by adipose tissue is primarily the lipid solubility for which a simple linear Henry's law solubility relationship can be used (7, 8). Thus, drug concentration in adipose tissue (X_{AdT}) is proportional to free drug concentration (C_{Ad}) in tissue water:

$$X_{AdT} = B_AC_{Ad} \qquad \text{(Eq. A12)}$$

Total drug concentration in adipose tissue portion ($C_{T,AdT}$) is defined as:

$$C_{T,AdT} = F_{W,AdT}C_{Ad} + C_{M,AdT}X_{AdT} \qquad \text{(Eq. A13)}$$

When Eq. A12 is substituted into Eq. A13, Eq. A13 becomes:

$$C_{T,AdT} = C_{Ad}(F_{W,AdT} + C_{M,AdT}B_A) \qquad \text{(Eq. A14)}$$

The partition coefficient of adipose tissue (K_{Ad}) is defined as the ratio of total drug concentration in adipose tissue to that in its blood:

$$K_{Ad} = \frac{C_{T,AdT}}{C_{T,AdB}} = \frac{F_{W,AdT} + C_{M,AdT}B_A}{F_{W,B} + C_{M,B}\left(\frac{B_1K_1}{1+K_1C_{Ad}} + \frac{B_2K_2}{1+K_2C_{Ad}}\right)} \qquad \text{(Eq. A15)}$$

Since[1] $K_{Ad} = 15$ and $B_A = 100$, at $C_{Ad} = 100$ (μmoles/liter), $C_{M,AdT}$, which can be solved by Eq. A15, is 0.870.

NOTATION

C_{Yz} = free drug concentration in tissue water or blood water of Yz body region (micromoles per liter)
$C_{M,Yz}$ = effective binding macromolecule concentration in Yz body region (kilograms per liter)
$C_{M,YzT}$ = effective binding macromolecule concentration in tissue portion of Yz body region (kilograms per liter)
$F_{W,B}$ = volume fraction of water in blood
$F_{W,YzT}$ = volume fraction of water in tissue portion of Yz body region
Q_B = blood flow rate from blood pool (liters per minute)
Q_{Yz} = blood flow rate from Yz body region (liters per minute)
V_{YzB} = blood volume within capillary bed of Yz body region (liters)
V_{YzT} = volume of tissue portion of Yz body region (liters)
X_{YzB} = bound drug concentration (amount of bound drug per unit of effective binding macromolecules) in capillary bed of Yz body region (micromoles per kilogram)
X_{YzT} = bound drug concentration (amount of bound drug per unit of effective binding macromolecules) in tissue portion of Yz body region (micromoles per kilogram)
Yz = various body regions and tissues

REFERENCES

(1) A. Rescigno and G. Segre, "Drug and Tracer Kinetics," 1st American ed., Blaisdell, Lexington, Mass., 1966.

(2) B. B. Brodie, E. Bernstein, and L. C. Mark, *J. Pharmacol. Exp. Ther.*, **105**, 421(1952).

(3) B. B. Brodie and C. A. M. Hogben, *J. Pharm. Pharmacol.*, **9**, 345(1957).

(4) "The Pharmacological Basis of Therapeutics," 4th ed., L. S. Goodman and A. Gilman, Eds., Macmillan, New York, N.Y., 1970.

(5) K. B. Bischoff and R. G. Brown, *Chem. Eng. Progr. Symp. Ser. No. 66*, **62**, 33(1966).

(6) K. B. Bischoff, in "Chemical Engineering in Medicine and Biology," D. Hershey, Ed., Plenum, New York, N.Y., 1967, p. 417.

(7) R. L. Dedrick and K. B. Bischoff, *Chem. Eng. Progr. Symp. Ser. No. 84*, **64**, 32(1968).

(8) K. B. Bischoff and R. L. Dedrick, *J. Pharm. Sci.*, **57**, 1346(1968).

(9) D. S. Zaharko, R. L. Dedrick, K. B. Bischoff, J. A. Longstreth, and V. T. Oliverio, *J. Nat. Cancer Inst.*, **46**, 775(1971).

(10) K. B. Bischoff, K. J. Himmelstein, R. L. Dedrick, and D. S. Zaharko, in "Chemical Engineering in Medicine," R. F. Gould, Ed., American Chemical Society, Washington, D.C., 1973, p. 47.

(11) R. L. Dedrick, D. D. Ferrester, and D. H. W. Ho, *Biochem. Pharmacol.*, **21**, 1(1972).

(12) R. L. Dedrick, D. S. Zaharko, and R. J. Lutz, *J. Pharm. Sci.*, **62**, 882(1973).

(13) R. L. Dedrick, D. D. Ferrester, T. N. Cannon, S. M. El Dareer, and L. B. Mellett, *Biochem. Pharmacol.*, **22**, 2405(1973).

(14) D. Shen and M. Gibaldi, *J. Pharm. Sci.*, **63**, 1698(1974).

(15) L. C. Mark, *Clin. Pharmacol. Ther.*, **4**, 504(1963).

(16) F. Karush, *J. Amer. Chem. Soc.*, **72**, 2705(1950).

(17) J. D. Teresi and J. M. Luck, *J. Biol. Chem.*, **194**, 823(1952).

(18) L. R. Goldbaum and P. K. Smith, *J. Pharmacol. Exp. Ther.*, **111**, 197(1954).

(19) S. P. Colowick and F. C. Womack, *J. Biol. Chem.*, **224**, 774(1969).

(20) C. N. Chen, Ph.D. dissertation, University of Utah, Salt Lake City, Utah, 1976.

(21) G. M. C. Masson and E. Beland, *Anesthesiology*, **6**, 483(1945).

ACKNOWLEDGMENTS AND ADDRESSES

Received May 1, 1975, from the *College of Engineering, College of Pharmacy, and the Institute for Biomedical Engineering, University of Utah, Salt Lake City, UT 84112*

Accepted for publication July 21, 1975.

The authors thank Dr. Sen-Maw Fang and Dr. David Gough for many helpful suggestions. They are particularly grateful to Dr. Kenneth B. Bischoff and Dr. Robert L. Dedrick for providing invaluable advice and information.

Supported in part by National Science Foundation Grant GH38996X and National Institutes of Health–Food and Drug Administration Grant FD 00480-01.

[x] To whom inquiries should be directed.

Hypocholesterolemic Agents IV: Inhibition of β-Hydroxy-β-methylglutaryl Coenzyme A Reductase by Arylalkenyl and Arylepoxy Hydrogen Succinates and Glutarates

MARVIN R. BOOTS*[x], PAUL E. MARECKI*, SHARON G. BOOTS*, and KENNETH E. GUYER[‡§]

Abstract □ Two series of half acid esters of succinic and glutaric acids were synthesized and assayed for inhibition of rat liver β-hydroxy-β-methylglutaryl coenzyme A reductase. Irreversible inhibition was studied by incorporation of a potential alkylating group (the epoxide function) into the side chain of the alcohol portion of the half acid esters. Incorporation of a terminal olefin function into the side chain of the alcohol portion of the half acid esters provided a group that could form a charge–transfer complex. Neither irreversible inhibition nor formation of a charge–transfer complex was indicated from these studies; however, the two series of half acid esters exhibited reversible inhibition.

Keyphrases □ Hypocholesterolemic agents, potential—series of arylalkenyl and arylepoxy hydrogen succinates and glutarates, synthesis, effect on β-hydroxy-β-methylglutaryl coenzyme A reductase □ Enzymes—β-hydroxy-β-methylglutaryl coenzyme A reductase, inhibition by series of arylalkenyl and arylepoxy hydrogen succinates and glutarates □ Succinates, arylalkenyl and arylepoxy—substituted series, synthesis, effect on β-hydroxy-β-methylglutaryl coenzyme A reductase □ Glutarates, arylalkenyl and arylepoxy—substituted series, synthesis, effect on β-hydroxy-β-methylglutaryl coenzyme A reductase

Previous reports (1, 2) presented an approach to the design of inhibitors of the enzyme β-hydroxy-β-methylglutaryl coenzyme A reductase as potential hypocholesterolemic agents. These studies led to the development of reversible inhibitors (I) of yeast and rat liver β-hydroxy-β-methylglutaryl coenzyme A reductase. Structure–activity relationships indicated that maximum activity was observed when R_1 = biphenylyl, R_2 = *n*-butyl, and n = 1–4.

This study describes the synthesis and assay of potential irreversible inhibitors (II) of β-hydroxy-β-methylglutaryl coenzyme A reductase based upon I.

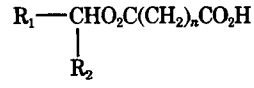

I: $n = 0$–6

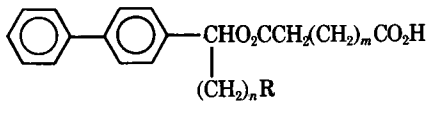

II: R = —CH(O)CH$_2$, n = 1–3, m = 1 or 2

III: R = —CH=CH$_2$, n = 1–3, m = 1 or 2

The epoxide group was selected as the potential alkylating group on the basis of its relatively small size and its reactivity with nucleophiles.

The arylalkenylcarbinols (V), which were precursors of the arylepoxycarbinols (VI) used in the synthesis of the epoxy acid esters (II), were also esterified to give the corresponding alkenyl acid esters (III). Not only were these alkenyl acid esters readily available from a synthetic point of view, but they also could provide useful information when assayed as potential reversible inhibitors. The possibility exists that the terminal olefinic bond found in these alkenyl acid esters might act as an electron donor in the formation of a charge–transfer complex. Alkenes are well known for acting as donors in the formation of a charge–transfer complex because of their electron-rich π-clouds (3).

EXPERIMENTAL[1]

Chemistry—The previously described method (1) of preparing the arylalkylcarbinols was used with only slight modifications. Alkenyl bromides were utilized and the resulting arylalkenylcarbi-

[1] Melting points were determined with a Thomas-Hoover capillary melting-point apparatus and are uncorrected. Elemental analyses were carried out by Mr. Paul E. Marecki, Department of Pharmaceutical Chemistry, and by Galbraith Laboratories, Knoxville, Tenn. IR spectra were determined using a Perkin-Elmer model 237 spectrophotometer. NMR spectra were determined using a Perkin-Elmer model R-24 spectrometer or a Varian Associates A-60 spectrometer in deuterochloroform, using tetramethylsilane as the internal reference.

(19) S. P. Colowick and F. C. Womack, *J. Biol. Chem.*, **224**, 774(1969).

(20) C. N. Chen, Ph.D. dissertation, University of Utah, Salt Lake City, Utah, 1976.

(21) G. M. C. Masson and E. Beland, *Anesthesiology*, **6**, 483(1945).

ACKNOWLEDGMENTS AND ADDRESSES

Received May 1, 1975, from the *College of Engineering, College of Pharmacy, and the Institute for Biomedical Engineering, University of Utah, Salt Lake City, UT 84112*

Accepted for publication July 21, 1975.

The authors thank Dr. Sen-Maw Fang and Dr. David Gough for many helpful suggestions. They are particularly grateful to Dr. Kenneth B. Bischoff and Dr. Robert L. Dedrick for providing invaluable advice and information.

Supported in part by National Science Foundation Grant GH38996X and National Institutes of Health–Food and Drug Administration Grant FD 00480-01.

[x] To whom inquiries should be directed.

Hypocholesterolemic Agents IV: Inhibition of β-Hydroxy-β-methylglutaryl Coenzyme A Reductase by Arylalkenyl and Arylepoxy Hydrogen Succinates and Glutarates

MARVIN R. BOOTS*[x], PAUL E. MARECKI*, SHARON G. BOOTS*, and KENNETH E. GUYER[‡§]

Abstract □ Two series of half acid esters of succinic and glutaric acids were synthesized and assayed for inhibition of rat liver β-hydroxy-β-methylglutaryl coenzyme A reductase. Irreversible inhibition was studied by incorporation of a potential alkylating group (the epoxide function) into the side chain of the alcohol portion of the half acid esters. Incorporation of a terminal olefin function into the side chain of the alcohol portion of the half acid esters provided a group that could form a charge–transfer complex. Neither irreversible inhibition nor formation of a charge–transfer complex was indicated from these studies; however, the two series of half acid esters exhibited reversible inhibition.

Keyphrases □ Hypocholesterolemic agents, potential—series of arylalkenyl and arylepoxy hydrogen succinates and glutarates, synthesis, effect on β-hydroxy-β-methylglutaryl coenzyme A reductase □ Enzymes—β-hydroxy-β-methylglutaryl coenzyme A reductase, inhibition by series of arylalkenyl and arylepoxy hydrogen succinates and glutarates □ Succinates, arylalkenyl and arylepoxy—substituted series, synthesis, effect on β-hydroxy-β-methylglutaryl coenzyme A reductase □ Glutarates, arylalkenyl and arylepoxy—substituted series, synthesis, effect on β-hydroxy-β-methylglutaryl coenzyme A reductase

Previous reports (1, 2) presented an approach to the design of inhibitors of the enzyme β-hydroxy-β-methylglutaryl coenzyme A reductase as potential hypocholesterolemic agents. These studies led to the development of reversible inhibitors (I) of yeast and rat liver β-hydroxy-β-methylglutaryl coenzyme A reductase. Structure–activity relationships indicated that maximum activity was observed when R_1 = biphenylyl, R_2 = *n*-butyl, and n = 1–4.

This study describes the synthesis and assay of potential irreversible inhibitors (II) of β-hydroxy-β-methylglutaryl coenzyme A reductase based upon I.

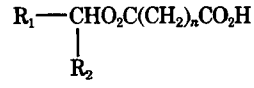

I: $n = 0$–6

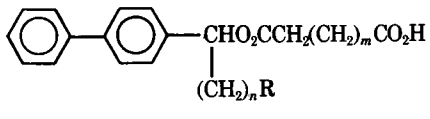

II: R = —CH(O)CH$_2$, n = 1–3, m = 1 or 2

III: R = —CH=CH$_2$, n = 1–3, m = 1 or 2

The epoxide group was selected as the potential alkylating group on the basis of its relatively small size and its reactivity with nucleophiles.

The arylalkenylcarbinols (V), which were precursors of the arylepoxycarbinols (VI) used in the synthesis of the epoxy acid esters (II), were also esterified to give the corresponding alkenyl acid esters (III). Not only were these alkenyl acid esters readily available from a synthetic point of view, but they also could provide useful information when assayed as potential reversible inhibitors. The possibility exists that the terminal olefinic bond found in these alkenyl acid esters might act as an electron donor in the formation of a charge–transfer complex. Alkenes are well known for acting as donors in the formation of a charge–transfer complex because of their electron-rich π-clouds (3).

EXPERIMENTAL[1]

Chemistry—The previously described method (1) of preparing the arylalkylcarbinols was used with only slight modifications. Alkenyl bromides were utilized and the resulting arylalkenylcarbi-

[1] Melting points were determined with a Thomas-Hoover capillary melting-point apparatus and are uncorrected. Elemental analyses were carried out by Mr. Paul E. Marecki, Department of Pharmaceutical Chemistry, and by Galbraith Laboratories, Knoxville, Tenn. IR spectra were determined using a Perkin-Elmer model 237 spectrophotometer. NMR spectra were determined using a Perkin-Elmer model R-24 spectrometer or a Varian Associates A-60 spectrometer in deuterochloroform, using tetramethylsilane as the internal reference.

Table I—Properties of Arylalkenylcarbinols and Arylepoxycarbinols

Compound	n	Yield, %	Physical Description	Formula	Analysis, % Calc.	Found
V	1	69	63.5–65°[a,b]	$C_{16}H_{16}O$	C 85.7 H 7.2	86.0 7.2
V	2	94	68–68.5°[a,b]	$C_{17}H_{18}O$	C 85.7 H 7.6	85.6 7.7
V	3	46	55–58°[a,b]	$C_{18}H_{20}O$	C 85.7 H 8.0	85.5 7.6
VI	1	97	Colorless liquid[b,c]	$C_{16}H_{16}O_2$	C 80.0 H 6.7	79.8 6.5
VI	2	96	Colorless liquid[b,c]	$C_{17}H_{18}O_2$	C 80.3 H 7.1	—[d] —
VI	3	92	Beige liquid[b,e]	$C_{18}H_{20}O_2$	C 80.6 H 7.5	80.6 7.2

[a] White solid. [b] IR spectra (chloroform) and NMR spectra (deuterochloroform) were consistent with the assigned structures. An example of each is given in the *Experimental* section. [c] Purified by molecular distillation. [d] No satisfactory analytical data could be obtained. [e] No purification was carried out.

nols (V) were epoxidized using *m*-chloroperbenzoic acid (Scheme I). The arylepoxycarbinols (VI) were then treated with either succinic or glutaric anhydride, using a modification of the method of Steglich and Höfle (4). This method afforded the desired epoxy acid esters (II). The arylalkenylcarbinols also were treated with succinic or glutaric anhydride to afford the alkenyl acid esters (III).

Preparation of Arylalkenylcarbinols—The arylalkenylcarbinols listed in Table I were prepared by the treatment of 4-biphenylcarboxaldehyde[2] with the appropriate Grignard reagent. 1-(4-Biphenylyl)-3-buten-1-ol (V, n = 1) was prepared using the method of Tschesche and Machleidt (5). 1-(4-Biphenylyl)-4-penten-1-ol (V, n = 2) and 1-(4-biphenylyl)-5-hexen-1-ol (V, n = 3) were prepared using a procedure described previously (1).

Table I lists the pertinent data for these compounds. An example of typical IR and NMR spectra is given here for 1-(4-biphenylyl)-3-buten-1-ol; IR ($CHCl_3$): 3590 (medium, OH) and 1640 (medium >C=CH_2) cm^{-1}; NMR ($CDCl_3$): δ 2.47 (t, 2H, CH_2), 2.68 (s, 1H, OH), 4.65 (t, 1H, R_3CH), 4.87–5.27 (m, 2H, >C=CH_2), 5.48–6.18 (m, 1H, CH=), and 7.20–7.70 (m, 9H, aromatic) ppm.

Preparation of Arylepoxycarbinols—The arylepoxycarbinols listed in Table I (VI, n = 1–3) were prepared by the treatment of the appropriate arylalkenylcarbinol with *m*-chloroperbenzoic acid. A typical example is given here. The method of Fieser and Fieser (6) was used. To a solution of 3.36 g (0.015 mole) of 1-(4-biphenylyl)-3-buten-1-ol (V, n = 1) in 25 ml of chloroform was added, in a dropwise manner with stirring and cooling in an ice bath, a solution of 5.06 g (0.025 mole) of 85% *m*-chloroperbenzoic acid in 100 ml of chloroform. The mixture was stirred at 25° for 18 hr, and a solution of freshly prepared 10% sodium sulfite (75 ml) was added (negative starch iodide test).

The organic phase was washed with 5% sodium bicarbonate, water, and then a saturated sodium chloride solution. The solution was dried over anhydrous sodium sulfate. Removal of the solvent under reduced pressure afforded 3.50 g (97%) of the arylepoxyalcohol (VI, n = 1) as a brown liquid. Molecular distillation using a Hickman still provided an analytical specimen as a colorless liquid; IR ($CHCl_3$): 3600 (medium, free OH), 3450 (medium, broad, hydrogen-bonded OH), and 835 (epoxide) cm^{-1}; NMR ($CDCl_3$): δ 1.90 (t, 2H, CH_2), 2.32–3.22 (m, 3H, $\overset{O}{\text{CH}}—CH_2$), 3.48 (s, 1H, OH), 4.84 (t, 1H, R_3CH), and 7.27–7.66 (m, 9H, aromatic) ppm.

Preparation of Alkenyl Acid Esters and Epoxy Acid Esters—The acid esters listed in Table II were prepared by a modification of the procedure of Steglich and Höfle (4) and Guyer *et al.* (2), except that the triethylamine was omitted and the reaction time was increased to 72 hr.

Assay of Enzyme Activity and Inhibition—Rat liver microsomes containing β-hydroxy-β-methylglutaryl coenzyme A reductase activity were prepared according to Shapiro and Rodwell (7). The assay procedure used was described previously (2). The enzyme incubation mixture consisted of $NADP^+$ (9.7 μmoles)[3], glucose 6-phosphate (59.7 μmoles)[3], torula yeast glucose 6-phosphate dehydrogenase (5 units)[3], microsomal protein (2 mg), 0.1 ml of ethylene glycol monoethyl ether containing the inhibitor, and sufficient assay buffer (30 m*M* edetic acid, 70 m*M* sodium chloride, and 10 m*M* β-mercaptoethanol, pH 6.8) to produce a total volume of 2.9 ml.

Enzymatic activity was initiated by the addition of 0.1 ml of a solution containing 94 nmoles (31 μ*M*) of 3-^{14}C-*dl*-β-hydroxy-β-methylglutaryl coenzyme A prepared (8) from 3-^{14}C-β-hydroxy-β-methylglutaric acid[4]. After 30 min of incubation, the reaction was stopped and 5-^{3}H-*dl*-mevalonolactone[4] was added. Mevalonolactone was extracted and isolated by TLC, and radioactivity was determined in a liquid scintillation counter[5].

Assay of Irreversible Enzyme Inhibition—The assay procedure used was that already described, except that the mixture was preincubated with the inhibitor at 37° for 20 min prior to the addition of the substrate. The inhibitor concentration used was that found to give the $(I/S)_{50\%}$ (Table III). Then 94 (31 μ*M*) or 517 (172 μ*M*) nmoles of the substrate was added.

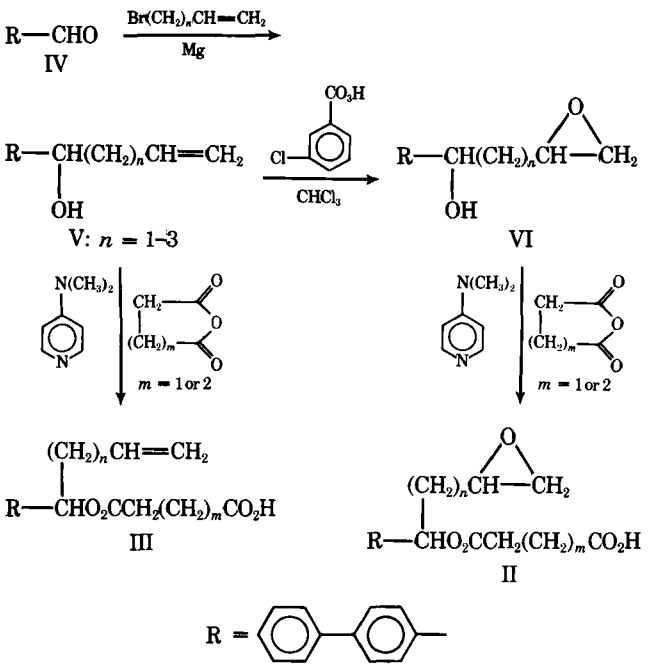

Scheme I

[2] Aldrich Chemical Co.

[3] Sigma Chemical Co.

[4] New England Nuclear.

[5] Nuclear-Chicago Mark I.

Table II—Properties of Arylalkenyl and Arylepoxy Acid Esters

Compound	*n*	*m*	Yield, %	Melting Point (Salt)	Formula	Analysis, %[a] Calc.	Found
III*a*	1	1	79	143–144°[b]	$C_{28}H_{30}N_2O_4S \cdot \frac{1}{2}H_2O$	C 67.3 H 6.2 N 5.6	67.4 6.2 5.6
III*b*	2	1	57	118–119°[b]	$C_{29}H_{32}N_2O_4S$	C 69.0 H 6.4 N 5.6	68.8 6.4 5.6
III*c*	3	1	58	125–127°[b]	$C_{30}H_{34}N_2O_4S \cdot 1H_2O$	C 67.2 H 6.3 N 5.2	67.3 6.5 5.3
III*d*	1	2	26	146.5–147°[b]	$C_{29}H_{32}N_2O_4S$	C 69.0 H 6.4 N 5.6	69.2 6.5 5.5
III*e*	2	2	38	122–123°[c]	$C_{30}H_{34}N_2O_4S \cdot \frac{1}{2}H_2O$	C 68.3 H 6.4 N 5.3	68.4 6.5 5.4
III*f*	3	2	42	100–101.5°[b]	$C_{31}H_{36}N_2O_4S$	C 68.7 H 6.6 N 5.2	68.3 6.5 4.8
II*a*	1	1	57	114–116°[c]	$C_{28}H_{30}N_2O_5S \cdot \frac{1}{2}H_2O$	C 65.2 H 6.0 N 5.4	65.3 6.0 5.4
II*b*	2	1	73	97–99°[c]	$C_{29}H_{32}N_2O_5S \cdot \frac{1}{2}H_2O$	C 65.8 H 6.0 N 5.3	65.7 6.1 5.4
II*c*	3	1	23	105–107°[b]	$C_{30}H_{34}N_2O_5S$	C 67.4 H 6.4 N 5.2	67.5 6.4 5.2
II*d*	1	2	47	132–133°[b]	$C_{29}H_{32}N_2O_5S \cdot \frac{1}{2}H_2O$	C 65.8 H 6.2 N 5.3	65.6 6.2 5.3
II*e*	2	2	42	115–117°[c]	$C_{30}H_{34}N_2O_5S \cdot \frac{1}{2}H_2O$	C 66.3 H 6.3 N 5.2	66.1 6.4 5.0
II*f*	3	2	27	79–82°[b]	$C_{31}H_{36}N_2O_5S \cdot \frac{1}{2}H_2O$	C 66.8 H 6.4 N 5.0	66.9 6.4 5.3

[a] The compounds were pale-yellow oils and were characterized as their solid *S*-benzylthiuronium salts (1). IR spectra (chloroform) and NMR spectra (deuterochloroform) were consistent with the assigned structures. [b] White solid. [c] Beige solid.

RESULTS AND DISCUSSION

The alkenyl acid esters (III*a*–III*f*) and the epoxy acid esters (II*a*–II*f*) were initially assayed using the procedure previously described (2) for determining potential reversible inhibitors of rat liver β-hydroxy-β-methylglutaryl coenzyme A reductase (Table III). Compounds VII*a* and VII*b* were included so that a comparison could be made between the alkenyl and epoxy acid esters and the corresponding inhibitors with only a hydrocarbon (*n*-butyl) side chain. The assay results shown in Table III indicate that these compounds (II*a*–II*f* and III*a*–III*f*) are indeed inhibitors with activity essentially comparable to VII*a* and VII*b*. No significant loss of activity was noted when either a terminal olefin or epoxide function was introduced into the side chain. The lack of increased activity of III*a*–III*f*, which contain the terminal olefin group, seems to indicate that no charge–transfer site has been located on the enzyme surface.

The epoxy acid esters (II*a*–II*f*) were then examined to determine whether the inhibition noted in Table III was reversible or irreversible. The epoxy acid ester II*d* was not evaluated for irreversible activity due to solubility problems. The epoxy acid esters were evaluated as irreversible inhibitors by preincubating the enzyme assay mixture with the inhibitor prior to the addition of substrate. The exposure of the inhibitors to the enzyme was limited to a rela-

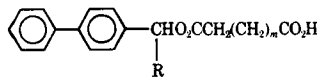

Table III—Inhibition of β-Hydroxy-β-methylglutaryl Coenzyme A Reductase

Compound	R	Activity[a], $(I/S)_{50\%}$, *m* = 1	Compound	Activity[a], $(I/S)_{50\%}$, *m* = 2
II*a*	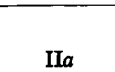	20	II*d*	13[b] (26%)
II*b*	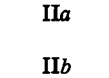	13	II*e*	13
II*c*		13	II*f*	10
III*a*	$CH_2CH{=}CH_2$	10	III*d*	9
III*b*	$(CH_2)_2CH{=}CH_2$	11	III*e*	11
III*c*	$(CH_2)_3CH{=}CH_2$	11	III*f*	8
VII*a*[c]	$(CH_2)_3CH_3$	11	VII*b*[d]	11

[a] The inhibition index, $(I/S)_{50\%}$, equals the ratio of the micromolar concentration of the inhibitor to the micromolar concentration of the substrate required to give 50% inhibition. At least two sets of duplicate determinations were used. [b] Insoluble at higher concentrations. [c] A standard inhibitor used routinely to provide comparability of each assay set (2). [d] Described previously (2).

tively short time (20 min) because of the instability of the enzyme to these conditions even in the absence of the inhibitors.

Two substrate concentrations (31 and 172 μM) were used in an attempt to detect any irreversible inhibition. In experiments utilizing 31 μM, the same degree of inhibition was observed as that previously found without prior exposure of the enzyme to the inhibitor (Table III). In experiments utilizing 172 μM, no inhibition was found. This substrate concentration was sufficient to eliminate all of the reversible inhibition exhibited by VIIa. Thus, it appears that the epoxy acid esters are inactive as irreversible inhibitors of the reductase.

REFERENCES

(1) M. R. Boots, S. G. Boots, C. M. Noble, and K. E. Guyer, *J. Pharm. Sci.*, **62**, 952(1973).

(2) K. E. Guyer, S. G. Boots, P. E. Marecki, and M. R. Boots, *ibid.*, **65**, 548(1976).

(3) B. R. Baker, "Design of Active-Site-Directed Irreversible Enzyme Inhibitors," Wiley, New York, N.Y., 1967, pp. 28–38.

(4) W. Steglich and G. Höfle, *Angew. Chem. Int. Ed.*, **8**, 981(1969).

(5) R. Tschesche and H. Machleidt, *Ann. Chem.*, **631**, 61(1960).

(6) L. F. Fieser and M. Fieser, "Reagents for Organic Synthesis," vol. 1, Wiley, New York, N.Y., 1967, p. 136.

(7) D. J. Shapiro and V. M. Rodwell, *J. Biol. Chem.*, **246**, 3210(1971).

(8) S. G. Boots, M. R. Boots, and K. E. Guyer, *J. Pharm. Sci.*, **60**, 614(1971).

ACKNOWLEDGMENTS AND ADDRESSES

Received July 3, 1975, from the *Department of Pharmaceutical Chemistry and the ‡Department of Biochemistry, Medical College of Virginia Health Sciences Division, Virginia Commonwealth University, Richmond, VA 23298

Accepted for publication August 8, 1975.

Presented at the Medical Sciences Section, Virginia Academy of Science, Norfolk meeting, May 1974.

Abstracted in part from a dissertation submitted by P. E. Marecki to Virginia Commonwealth University in partial fulfillment of the Doctor of Philosophy degree requirements.

Supported by a grant from the U.S. Public Health Service (HL-11768, National Heart and Lung Institute).

P. E. Marecki thanks the following for their generous support: National Institutes of Health, Traineeship GM484 (1970–1972); and the American Foundation for Pharmaceutical Education, 1972–1974 (Sydnor Barksdale Penick Memorial Fellow, 1973–1974).

Excellent technical assistance by Ms. Bonnie Frazier is gratefully acknowledged.

§ Present address: Department of Biochemistry, Marshall University School of Medicine, Huntington, WV 25701

ˣ To whom inquiries should be directed.

Continuous-Flow System for Determination of Diffusion Coefficients: Use of a Natural Membrane

GARNET G. SMITH * and GARNET E. PECK ˣ

Abstract □ A natural membrane was employed in an automated diffusion system. A mature male Mongolian gerbil sebaceous gland pad was excised and mounted into a suitable retainer so that the external surface was oriented toward the concentrated aqueous drug solution. Aqueous solutions of benzoic acid and the three commonly used parabens were studied. The gerbil sebaceous pad effectively prevented any diffusion of these drug solutions within 15 hr. Water by itself, however, was transported through the skin even against a pressure gradient. Although no apparent diffusion of these compounds occurred, a significant amount of drug was retained by the sebaceous pad. An expression for membrane–water partition coefficients could be calculated. Based upon thicknesses of natural and synthetic membranes, theoretical approximations of diffusion rates were found using lag time calculations.

Keyphrases □ Diffusion coefficients—determined in automated continuous-flow system, gerbil sebaceous pad □ Partition coefficients—determined in automated continuous-flow system, gerbil sebaceous pad □ Membranes, natural—gerbil sebaceous pad in automated continuous-flow system, diffusion coefficients

The outer surface of the skin is an unspecific, rugged, impermeable membrane, allowing few molecules to penetrate readily. This nonspecific barrier of the skin slows the transfer of all substances; severe chemical treatment may be required to increase the rate of penetration. When the epidermis is separated from the dermis, the epidermis retains all of the resistance to diffusion through skin.

Skin permeability has been studied for more than 50 years, and an enormous quantity of qualitative data has been generated. However, few reports have appeared on the methods or experiments for routine *in vitro* evaluation of the diffusion process in natural skin membranes.

An improvement in quantifying penetration rates came with the use of excised skin in diffusion cells (1). Diffusion cells employing excised skin are capable of producing rapid and reproducible results. Their use depends upon three assumptions.

1. Dead skin has the same permeability properties as living membranes, a relationship that has been shown to hold for several compounds (1).
2. In the diffusion cell, the penetrant must pass through the full thickness of the dermis; whereas in the natural state, the capillary network between the dermis and epidermis can remove the drug (2).
3. The excised skin surface properties remain constant for a reasonable length of time.

The chief advantage of the diffusion cell over the intact animal is the ease in measurement of the penetrant, which is not diluted or altered by the body (3).

EXPERIMENTAL

Chemicals—The drugs whose diffusion constants were to be

tively short time (20 min) because of the instability of the enzyme to these conditions even in the absence of the inhibitors.

Two substrate concentrations (31 and 172 μM) were used in an attempt to detect any irreversible inhibition. In experiments utilizing 31 μM, the same degree of inhibition was observed as that previously found without prior exposure of the enzyme to the inhibitor (Table III). In experiments utilizing 172 μM, no inhibition was found. This substrate concentration was sufficient to eliminate all of the reversible inhibition exhibited by VIIa. Thus, it appears that the epoxy acid esters are inactive as irreversible inhibitors of the reductase.

REFERENCES

(1) M. R. Boots, S. G. Boots, C. M. Noble, and K. E. Guyer, *J. Pharm. Sci.*, **62**, 952(1973).

(2) K. E. Guyer, S. G. Boots, P. E. Marecki, and M. R. Boots, *ibid.*, **65**, 548(1976).

(3) B. R. Baker, "Design of Active-Site-Directed Irreversible Enzyme Inhibitors," Wiley, New York, N.Y., 1967, pp. 28–38.

(4) W. Steglich and G. Höfle, *Angew. Chem. Int. Ed.*, **8**, 981(1969).

(5) R. Tschesche and H. Machleidt, *Ann. Chem.*, **631**, 61(1960).

(6) L. F. Fieser and M. Fieser, "Reagents for Organic Synthesis," vol. 1, Wiley, New York, N.Y., 1967, p. 136.

(7) D. J. Shapiro and V. M. Rodwell, *J. Biol. Chem.*, **246**, 3210(1971).

(8) S. G. Boots, M. R. Boots, and K. E. Guyer, *J. Pharm. Sci.*, **60**, 614(1971).

ACKNOWLEDGMENTS AND ADDRESSES

Received July 3, 1975, from the *Department of Pharmaceutical Chemistry and the ‡Department of Biochemistry, Medical College of Virginia Health Sciences Division, Virginia Commonwealth University, Richmond, VA 23298

Accepted for publication August 8, 1975.

Presented at the Medical Sciences Section, Virginia Academy of Science, Norfolk meeting, May 1974.

Abstracted in part from a dissertation submitted by P. E. Marecki to Virginia Commonwealth University in partial fulfillment of the Doctor of Philosophy degree requirements.

Supported by a grant from the U.S. Public Health Service (HL-11768, National Heart and Lung Institute).

P. E. Marecki thanks the following for their generous support: National Institutes of Health, Traineeship GM484 (1970–1972); and the American Foundation for Pharmaceutical Education, 1972–1974 (Sydnor Barksdale Penick Memorial Fellow, 1973–1974).

Excellent technical assistance by Ms. Bonnie Frazier is gratefully acknowledged.

§ Present address: Department of Biochemistry, Marshall University School of Medicine, Huntington, WV 25701

ˣ To whom inquiries should be directed.

Continuous-Flow System for Determination of Diffusion Coefficients: Use of a Natural Membrane

GARNET G. SMITH * and GARNET E. PECK ˣ

Abstract □ A natural membrane was employed in an automated diffusion system. A mature male Mongolian gerbil sebaceous gland pad was excised and mounted into a suitable retainer so that the external surface was oriented toward the concentrated aqueous drug solution. Aqueous solutions of benzoic acid and the three commonly used parabens were studied. The gerbil sebaceous pad effectively prevented any diffusion of these drug solutions within 15 hr. Water by itself, however, was transported through the skin even against a pressure gradient. Although no apparent diffusion of these compounds occurred, a significant amount of drug was retained by the sebaceous pad. An expression for membrane–water partition coefficients could be calculated. Based upon thicknesses of natural and synthetic membranes, theoretical approximations of diffusion rates were found using lag time calculations.

Keyphrases □ Diffusion coefficients—determined in automated continuous-flow system, gerbil sebaceous pad □ Partition coefficients—determined in automated continuous-flow system, gerbil sebaceous pad □ Membranes, natural—gerbil sebaceous pad in automated continuous-flow system, diffusion coefficients

The outer surface of the skin is an unspecific, rugged, impermeable membrane, allowing few molecules to penetrate readily. This nonspecific barrier of the skin slows the transfer of all substances; severe chemical treatment may be required to increase the rate of penetration. When the epidermis is separated from the dermis, the epidermis retains all of the resistance to diffusion through skin.

Skin permeability has been studied for more than 50 years, and an enormous quantity of qualitative data has been generated. However, few reports have appeared on the methods or experiments for routine *in vitro* evaluation of the diffusion process in natural skin membranes.

An improvement in quantifying penetration rates came with the use of excised skin in diffusion cells (1). Diffusion cells employing excised skin are capable of producing rapid and reproducible results. Their use depends upon three assumptions.

1. Dead skin has the same permeability properties as living membranes, a relationship that has been shown to hold for several compounds (1).
2. In the diffusion cell, the penetrant must pass through the full thickness of the dermis; whereas in the natural state, the capillary network between the dermis and epidermis can remove the drug (2).
3. The excised skin surface properties remain constant for a reasonable length of time.

The chief advantage of the diffusion cell over the intact animal is the ease in measurement of the penetrant, which is not diluted or altered by the body (3).

EXPERIMENTAL

Chemicals—The drugs whose diffusion constants were to be

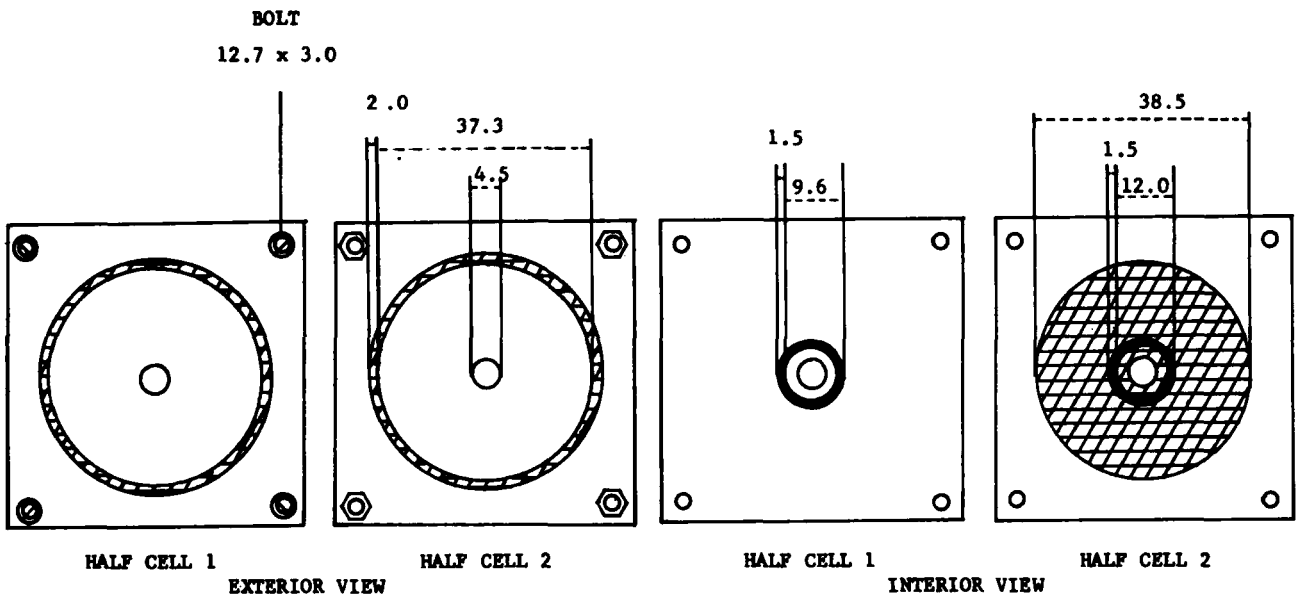

Figure 1—*Schematic diagram of the natural membrane retainer (dimensions in millimeters). Key: ▨, recessed region; and ■, elevated region.*

determined included reagent grade benzoic acid[1], methylparaben[2], propylparaben[3], and butylparaben[4].

Natural Membrane—The natural membrane used was the excised sebaceous gland pad from the mature male Mongolian gerbil. Glenn and Gray (4) described the biological and histological characteristics of the abdominal sebaceous gland pad of the gerbil (*Meriones unguiculatus*). The yellowish-brown, wax-coated secretory surface of the male pad extends up to 25 mm in length and 5 mm in width. The female pad is smaller and sometimes absent. The mature gerbil pad is easily detected in the midline of the abdomen. The sebaceous pad was selected because of its high concentration of sebum.

The animal was sacrificed, and the abdominal hair was depilated with standard animal shears. The sebaceous gland pad, with approximately 12 mm of surrounding skin, was removed using surgical scissors. Care was taken to remove only the skin and not connective tissue or peritoneal wall.

Diffusion Cell—The diffusion cell was a modification of one described previously (5–7). The sink side of the cell had two small side arms, 4 cm long and 0.635 cm i.d., placed near the bottom of the flask; one was directly opposite the large side arm, and the other was at right angles to it. In the center of the two washers[5] used to hold the membrane was located an opening to expose 4.42×10^{-1} cm^2 of the membrane. Stirring in both flasks was achieved by magnetic stirring bars rotating at 300 rpm.

Figure 1 shows a schematic diagram of the tissue holder. It was fabricated of 5-mm thick sheeting[5] and contained a hole in the center with a diameter of 4.5 mm to expose an area of 1.59×10^{-1} cm^2. This size opening corresponded to the width of the gerbil pad. The tissue holder design allowed the mounting of thick skin without leaking.

Automated Analysis System—Figure 2 is a schematic diagram of the experimental apparatus system. The diffusion cell was placed in a water bath maintained at 37.5°. To the two small side arms of the sink side was attached 1.0-cm o.d. Tygon tubing, which allowed the sink solution to pass through a flowcell[6] placed inside a spectrophotometer[7]. This arrangement was accomplished by circulating the fluid at a fixed flow rate using a peristaltic pump[8].

Initially, the action of the pump created sympathetic vibrations in the diffusion cell membrane, which exerted a force in addition to the concentration gradient on the diffusion process. To overcome this effect, two aspirator bottles were used as pressure release reservoirs. A 250-ml aspirator bottle was placed in line before the peristaltic pump, and a 500-ml aspirator bottle was placed after it. These reservoir tanks were partially filled with fluid and closed to the atmosphere so that the air over the fluid was compressed by the pumping action instead of the fluid, thus eliminating vibrations in the membrane.

A recent study described a slightly different diffusional system, used in the evaluation of a series of *p*-aminobenzoates (8). The cell used in that study had a diffusional area of 10 cm^2 and was made to utilize dimethyl polysiloxane membranes (9).

The spectrophotometer was connected to a recorder, which plotted the absorbance values as a function of time at a single wavelength.

Partition Coefficients—Equilibrium partition coefficients were determined at 37.5°. Equal aliquots of chloroform and aqueous drug solutions of known concentration were stirred together until equilibrium was attained. The aqueous phase was assayed spectrophotometrically.

RESULTS AND DISCUSSION

Water Transfer through Pad—The natural membrane, excised male gerbil sebaceous pad, was mounted into the automated diffusion system. The exterior surface of the skin was oriented toward the concentrated side of the diffusion cell. With the Y-tube stopcocks open, it was impossible to attain fluid equilibrium in the system. Even raising the pressure release reservoirs [Fig. 2, 45.7-cm (18-in.) pressure head] to excessive heights did not prevent water from being transferred out of the concentrated side of the cell. It appeared that water moved across the skin, even against a pressure gradient.

Fluid disappeared at the rate of approximately 0.14 ml/hr. By reversing the skin so that the interior surface of the membrane was exposed to the concentrated side of the diffusion cell, the fluid level on this side increased at the rate of approximately 0.07 ml/hr. These results indicated the possibility of facilitated transport of water through gerbil sebaceous pad since the water moved against a pressure gradient. Verification of this theory could be done by monitoring a substance, such as tritiated water, and following this movement through the sebaceous pad by another technique.

Bathing Solution of Pad—To preserve the integrity of the skin, lactated Ringer's solution replaced the water as solvent in the automated diffusion system and the stock solutions. A visible turbidity appeared in the sink side of the diffusion cell after a few hours (usually 6). The turbidity resulted in excessive "noise" on the recorder, making any spectral measurements impossible. By returning to the use of sterile water for injection, this turbidity did

[1] J. T. Baker Chemical Co., Phillipsburg, N.J.
[2] Heyden Newport Chemical Corp., New York, N.Y.
[3] Heyden Chemical Corp., New York, N.Y.
[4] Merck and Co., Inc., Rahway, N.J.
[5] Coated with Teflon (du Pont).
[6] One-milliliter volume cell, Scientific Glass Apparatus Co., Bloomfield, N.J.
[7] Beckman DB, Beckman Instruments, Fullerton, Calif.
[8] Zero-Max Co., Minneapolis, Minn.

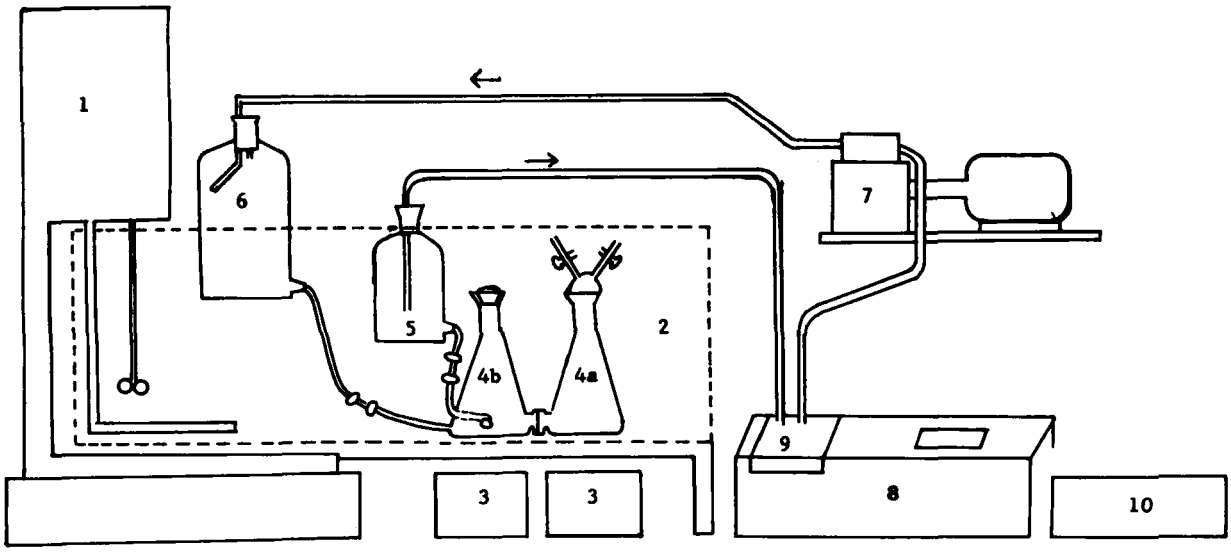

Figure 2—*Schematic diagram of the automated diffusion system. Key: 1, heater; 2, aquarium; 3, magnetic stirrer; 4a, diffusion cell, concentrated side; 4b, diffusion cell, sink side; 5, reservoir outflow; 6, reservoir inflow; 7, peristaltic pump; 8, spectrophotometer; 9, flowcell; and 10, recorder.*

not occur and constant monitoring of the UV absorbance was possible. Complex formation between the lactic acid of the Ringer's solution and some material leached from the sebaceous pad apparently produced this turbidity. This turbidity was seen only when Ringer's solution was used. Because of this reaction, distilled water only was used.

When one natural membrane was used for all experiments, severe decomposition of the membrane occurred after 3–5 days of determinations. Breakdown of the membrane was quickly noted by excessive noise on the recorder. These erratic absorbance values seemed to be due to a viscous decomposition product from the pad, which would coat the entire sink side of the diffusion system. Therefore, a new sebaceous pad was used for each experimental run and the absorbance values could be recorded over 15 hr.

Composition of Sebum—Sebum is a complex mixture of lipid substances whose detailed chemical composition is unknown (10). Sebum comprises the main portion of skin surface lipids (11); as much as 30% of this lipid material may consist of free fatty acids, more than half of which are saturated and unsaturated C_{16} and C_{18} acids with a wide range of branched and unbranched C_{14}, C_{15}, C_{17}, and some shorter carbon chain acids. The remaining materials are esterified acids, wax alcohols, squalene, sterols, and a small quantity of paraffin hydrocarbons (10, 11). There is no free cholesterol present in the gerbil sebum; it is apparently all esterified (12).

Sebum is essentially a hydrophobic oil; water will not spread over sebum but will immediately form droplets (13). Old sebum is chemically different from recently formed sebum and from the lipid droplets in the sebaceous cells (14). Kile *et al.* (15) studied the UV and IR spectra of sebum but found the interpretation of results difficult.

Drug Diffusion Studies—To separate the absorbance values for the particular diffusing drug from absorbances due to cellular components released from the skin, blank runs were made. Several blank experiments (at least five), in which no drug was placed in the concentrated side of the diffusion cell, were measured. Absorbance values for the blank were subtracted from the absorbance values obtained when a drug solution was present in the concentrated side of the diffusion cell.

Absorbance values, an average of five determinations using five different sebaceous pads, were found at two wavelengths of maximum absorbance, 227.5 and 256 nm, corresponding to those for benzoic acid and the parabens series, respectively. The absorbance units at 227.5 nm varied from 0.085 ± 0.015 at time zero to 0.096 ± 0.015 after 15 hr. At 256 nm, the same readings were 0.029 ± 0.015 at time zero to 0.032 ± 0.017 at 15 hr. The absorbance of the water in the concentrated side of the diffusion cell was found to be effectively zero at the end of each experiment.

Table I illustrates the average results of four determinations of the UV scan for the decomposition products of the sebaceous gland pad. The decomposition products from the inner surface of the gerbil sebaceous pad absorbed light throughout the entire UV spectrum, with maximum values in the 220–230-nm range. These absorbing materials apparently started leaching from the pad as soon as the pad was mounted.

The change in absorbance values with time was measured when 0.01 *M* benzoic acid solution was placed into the concentrated side of the diffusion cell. The absorbance units varied from 0.079 ± 0.016 at time zero to 0.093 ± 0.019 at 15 hr. By comparison with the blank values at 227.5 nm, there was little or no difference between these values at the same respective times. This finding indicates that apparently no net benzoic acid diffused across the entire thickness of the gerbil sebaceous gland pad.

The change in absorbance values with time was measured when the paraben solutions were placed into the concentrated side of the diffusion cell. The absorbance units varied from 0.029 ± 0.005 to 0.032 ± 0.007 for 0.01 *M* methylparaben solution, from 0.030 ± 0.002 to 0.031 ± 0.001 for 0.00248 *M* propylparaben solution, and from 0.027 ± 0.007 to 0.029 ± 0.009 for 0.00111 *M* butylparaben solution at times zero and 15 hr, respectively. Each absorbance value was an average of five individual values using five different sebaceous pads. A comparison of these absorbance values with those of the blank at 256 nm showed that no net transfer of the parabens through this natural membrane was observed.

Membrane–Water Partition Coefficients—At the termination of each individual experiment, the drug solution in the concentrated side of the diffusion cell was assayed spectrophotometrically. By subtracting this value from the known concentration placed there initially, a measure of the quantity of drug held by

Table I—UV Scan of a Sample of Gerbil Sebaceous Pad after 15 hr in Distilled Water

Wavelength, nm	Absorbance Units[a]	*SD*[b]
220	0.089	0.019
224	0.091	0.018
227.5	0.089	0.018
232	0.078	0.018
240	0.044	0.015
248	0.030	0.010
256	0.027	0.009
264	0.027	0.008
272	0.025	0.009
280	0.021	0.008
288	0.017	0.007
296	0.016	0.007
304	0.014	0.005
312	0.013	0.005
320	0.010	0.005

[a] Average of four individual values. [b] Determination from these four values.

Table II—Membrane–Water Partition Coefficients for the Gerbil Sebaceous Pad at 37.5°[a]

Drug	Trial Number	Amount of Drug Retained by Membrane, mg	Partition Coefficient, Membrane–Water, $\times 10^3$
Benzoic acid	1	1.45	3.93
	2	2.90	7.91
	3	2.22	6.40
	4	4.35	11.76
	5	2.18	5.92
	6	4.71	12.72
Mean		2.97	6.20
SD		1.19	3.16
Methylparaben	1	6.53	14.98
	2	2.18	4.98
	3	2.18	4.98
	4	5.16	11.53
	5	6.64	14.88
Mean		4.54	10.27
SD		2.00	4.49
Propylparaben	1	8.56	78.15
	2	3.19	27.78
	3	3.19	27.78
	4	3.77	33.08
	5	2.61	22.67
Mean		4.26	37.89
SD		2.18	20.40
Butylparaben	1	5.37	83.71
	2	3.05	45.85
	3	4.06	59.83
	4	2.47	35.49
	5	6.38	117.02
Mean		4.26	68.38
SD		1.45	29.20

[a] After a 15-hr exposure to water.

the skin was obtained. Table II shows the effective partition coefficient for the membrane to the water phase at 37.5°. As the polarity of the compound decreased (a higher membrane–water partition coefficient), more drug adhered to the sebaceous pad.

It is feasible that the natural membrane–water partition coefficient could be related to the chloroform–water or the octanol–water ratios. Table III summarizes these values. Figures 3–5 show semilogarithmic plots of the partition coefficient as a function of the number of carbons in the ester moiety of the solute. The slope in the case of the natural membrane–water partition coefficient (Fig. 3) is 0.26. This slope differs from that of chloroform–water (0.49) (Fig. 4) or octanol–water (0.54) (Fig. 5). This finding implies that previously reported assumptions (16, 17) that an organic phase can simulate the *in vivo* state in drug distribution are valid.

Considering the differences among Figs. 3–5, the retention of nonpolar compounds by the sebaceous gland pad must require the membrane to have some degree of polarity. Although the principal component of this skin is the hydrophobic material sebum, other materials must be present to impart some polarity to the membrane. The use of a purely nonpolar liquid as a model for the sebaceous pad would appear not to be valid. Levy and Mroszczak (18) verified this point by showing that a dye complexed with caffeine to make it more lipid soluble diffused at different rates through artificial barriers than across biological membranes. They concluded that an *in vitro* system of a lipid barrier separating two aqueous

Table III—Apparent Partition Coefficients of Aromatic Drugs

Drug	Partition Coefficient: Chloroform–Water	Partition Coefficient: Octanol–Water[a]
Benzoic acid	4.11	74.2
Methylparaben	4.77	91.2
Propylparaben	73.19	1096.0
Butylparaben	165.46	3715.0

[a] Values abstracted from L. Albert, C. Hansch, and D. Elkins, *Chem. Rev.*, 71, 525(1971).

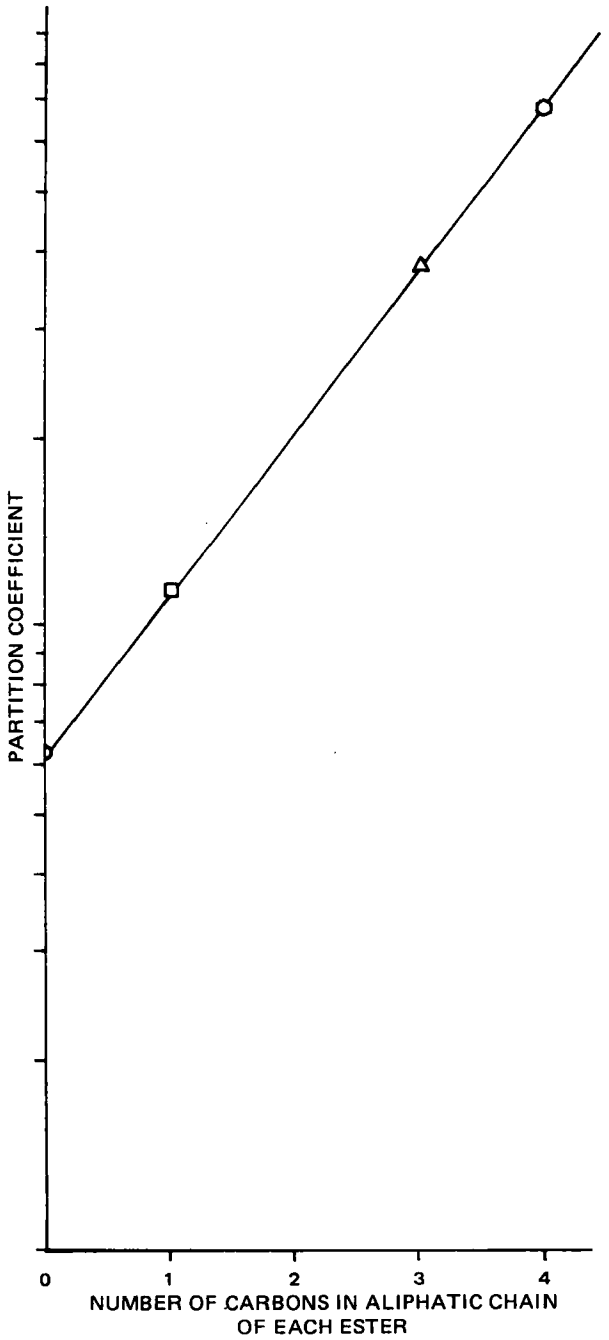

Figure 3—*Relationship between the natural membrane–water partition coefficient and the number of carbons in the aliphatic chain. Key:* ○, *benzoic acid;* □, *methylparaben;* △, *propylparaben; and* ○, *butylparaben.*

regions did not adequately reflect the *in vivo* situation for this complex. Treherne (2) showed that nonelectrolytes diffused across whole excised rabbit skin at rates proportional to their ether–water partition coefficients. The dielectric constant of ether is similar in value to that of chloroform.

All of the parabens are capable of sensitizing the skin; and since nonpolar compounds are retained to a greater extent by the gerbil sebaceous pad, this could explain some of their adverse effects (19). The best antifungal property is associated with butylparaben and could be directly related to its membrane–water partition coefficient being larger than that of the lower molecular weight parabens.

The significance of the thickness of a natural membrane in comparison to the synthetic membrane can be considered from a discussion of lag times. The lag time, t_L, by definition is the time interval before steady state is reached due to a finite diffusion veloc-

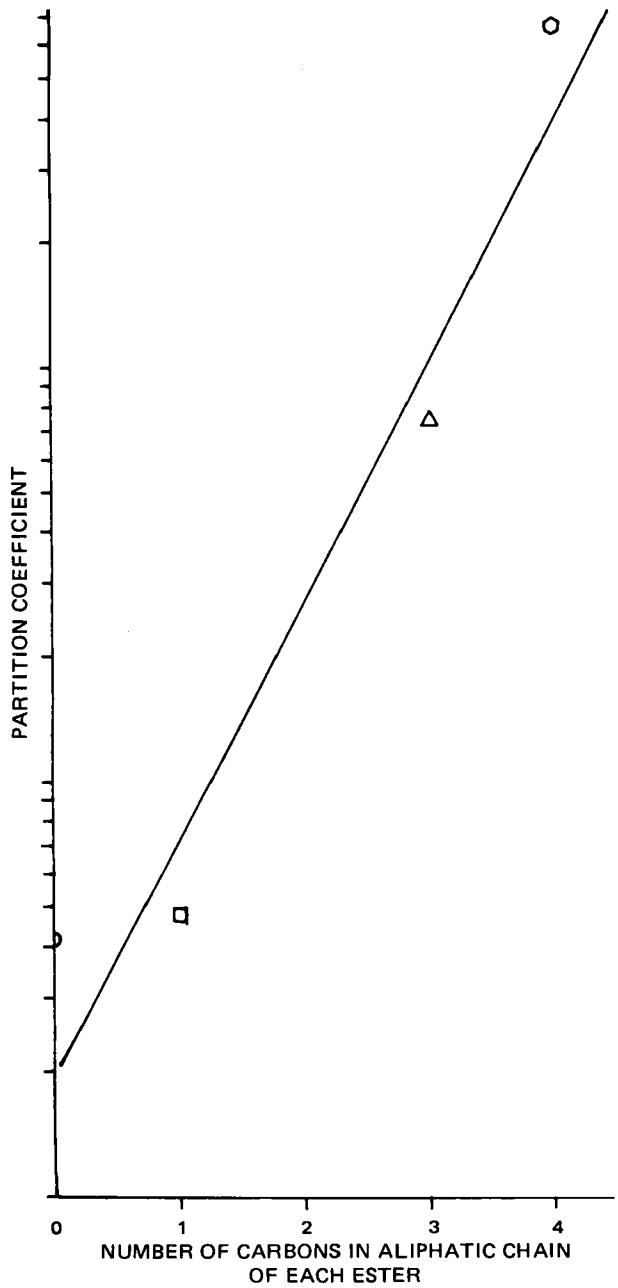

Figure 4—*Relationship between the chloroform–water partition coefficient and the number of carbons in the aliphatic chain. Key:* ○, *benzoic acid;* □, *methylparaben;* △, *propylparaben; and* ⬡, *butylparaben.*

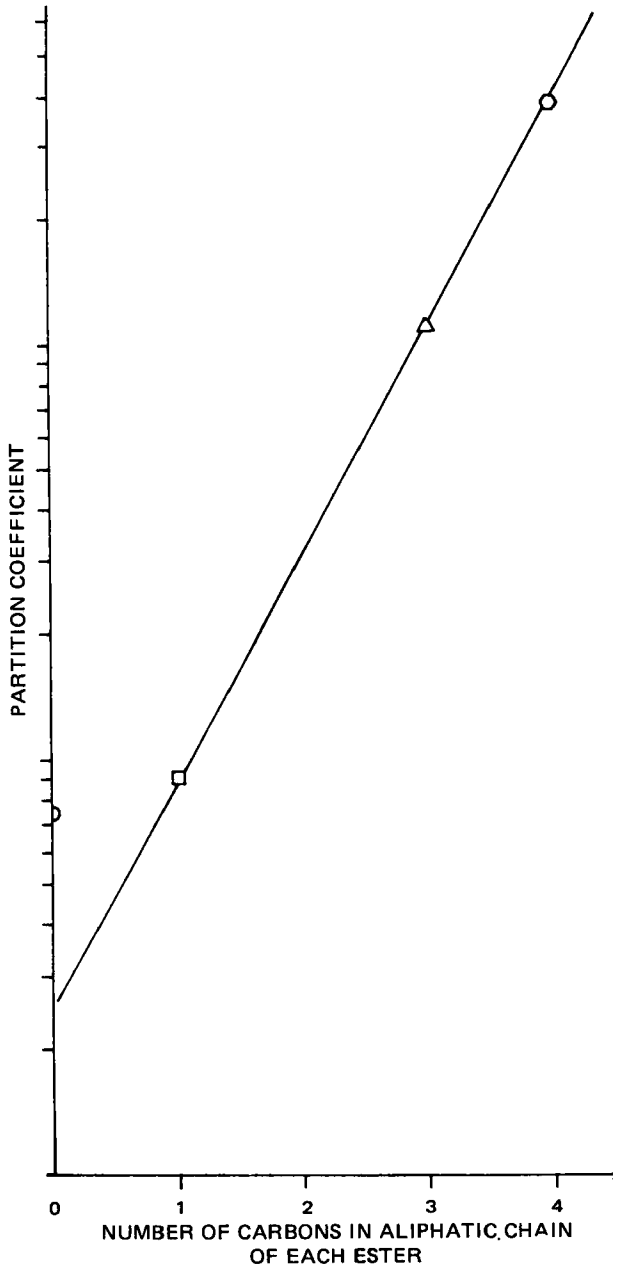

Figure 5—*Relationship between the octanol–water partition coefficient and the number of carbons in the aliphatic chain. Key:* ○, *benzoic acid;* □, *methylparaben;* △, *propylparaben; and* ⬡, *butylparaben.*

ity of the drug within the membrane. When the amount of drug diffusing is plotted against time, the resulting curve emerges from the origin with a very small slope and extends over a finite time period. The slope of the curve gradually increases with time to become a straight line (steady state). The intercept t_L on the time axis made by the asymptotic curve is:

$$t_L = \frac{h^2}{6D} \qquad \text{(Eq. 1)}$$

where h is the membrane thickness, and D is the diffusion coefficient. This equation is a simplified form of the more general expression (20). This relationship can be considered with respect to the diffusion coefficient for benzoic acid ($D = 1 \times 10^{-5}$ cm^2/sec approximately) through a microweb membrane (h = 0.013 cm) as compared to the gerbil skin (h = 0.08 cm before, or h = 0.18 cm after, swelling). The diffusion process through a microporous structure such as this synthetic cellulosic filter is assumed to be the same as through the skin. Although this assumption is false, such a situation would result in a diffusion coefficient of maximum value. By using Eq. 1, an equivalent thickness of 0.08 cm for a microweb membrane would yield a diffusion coefficient for benzoic acid approximately 38 times smaller than the same constant through the 0.013-cm synthetic membrane. Similarly, for the hydrated membrane, the diffusion rate would be 192 times slower than through the synthetic membrane.

By inserting these approximations back into Eq. 1, a comparison of lag times is possible for the three thicknesses of membrane (Table IV). From these approximations, it can be concluded that if the diffusion process in the gerbil sebaceous pad were the same as that through a cellulosic membrane, it would take about 29 hr before any measureable steady-state concentrations could be detected. This fact could possibly imply that the preparation of a synthetic membrane model to approximate the diffusion process through whole skin may be an exceedingly difficult task since the excised tissue could decompose before any drug passed into the sink. Zwolinski *et al.* (21) indicated that diffusion constants for

Table IV—Comparison of Theoretical Lag Times Based on Three Different Membrane Thicknesses

Membranes Thickness h, cm	Diffusion Coefficient D, cm^2/sec	Lag Time t_L, sec
Synthetic = 0.013	1×10^{-5}	2.8
Natural = 0.08	2.6×10^{-7}	4.1×10^{3}
Natural, hydrated = 0.18	5.2×10^{-8}	1.04×10^{5}

nonelectrolytes in natural membranes are 10^4–10^5 times smaller than their values in aqueous solutions, primarily due to higher activation energies.

SUMMARY

The following conclusions were found relative to this study:

1. The natural membrane used in an automated diffusion system was the excised sebaceous gland pad of the mature male Mongolian gerbil. To accommodate a membrane of such thickness, the fabrication of a new tissue holder was required.

2. Mounting of the sebaceous pad in an aqueous environment produced minimal decomposition of the skin over 15 hr. The use of lactated Ringer's solution to bathe the tissue resulted in a visible turbidity of the sink side of the diffusion cell. This turbidity apparently was caused by some complex formation within the gerbil pad and was not seen when high purity water was used.

3. Water was transferred across the skin against a fluid pressure gradient, indicating the possibility of facilitated transport.

4. No transfer of benzoic acid, methylparaben, propylparaben, and butylparaben was observed through the gerbil pad as indicated by a lack of change in drug concentration on the sink side of the cell after 15 hr of exposure in the cell.

5. Significant quantities of the drugs were retained by this natural membrane after 15 hr of exposure at 37.5° in the test cell. From these amounts retained, a membrane–water partition coefficient was calculated. It increased in value as the polarity of the diffusing substance decreased.

6. Plots were made relating the membrane–water partition coefficients for the drugs studied to those obtained for chloroform–water and octanol–water systems. Because of the differences in physicochemical properties between chloroform and octanol and the natural membrane, an *in vitro* organic phase can only approximate as a comparative model to the sebaceous pad.

7. The natural membrane incorporated sufficient water in the hydrated state in the automated diffusion system to increase its thickness by more than twice its original size. This observation was used to consider theoretical diffusion lag times based on thickness differences. This concept may require further consideration when designing membrane systems to approximate the natural membrane being proposed for a particular study.

REFERENCES

(1) R. T. Tregaer, "Physical Functions of Skin," Academic, New York, N.Y., 1966, pp. 1–52.

(2) J. E. Treherne, *J. Physiol.*, **133**, 171(1956).

(3) M. Ainsworth, *J. Soc. Cosmet. Chem.*, **11**, 69(1960).

(4) E. M. Glenn and J. Gray, *Endocrinology*, **76**, 1115(1965).

(5) L. S. Shenauda and A. M. Mattocks, *J. Pharm. Sci.*, **56**, 464(1967).

(6) S. J. Desai, P. Singh, A. P. Simonelli, and W. I. Higuchi, *ibid.*, **55**, 1224(1966).

(7) A. H. Goldberg and W. I. Higuchi, *ibid.*, **57**, 1583(1968).

(8) G. L. Flynn and S. H. Yalkowsky, *ibid.*, **61**, 838(1972).

(9) G. L. Flynn and E. W. Smith, *ibid.*, **60**, 1713(1971).

(10) F. J. Ebling, *J. Soc. Cosmet. Chem.*, **16**, 405(1965).

(11) "Advances in Biology of Skin," vol. 4, W. Montagna, R. A. Ellis, and A. F. Silver, Eds., Macmillan, New York, N.Y., 1963, pp. 19–30, 32–44, 110–123.

(12) W. F. Lever, "Histopathology of the Skin," 4th ed., Lippincott, Philadelphia, Pa., 1967, p. 22.

(13) K. K. Jones, M. C. Spencer, and S. A. Sanchez, *J. Invest. Dermatol.*, **17**, 213(1951).

(14) W. Montagna, *Anat. Rec.*, **104**, 243(1949).

(15) R. L. Kile, F. H. Snyder, and J. W. Haefele, *Arch. Dermatol. Syphilol.*, **61**, 792(1950).

(16) J. Perrin, *J. Pharm. Pharmacol.*, **19**, 25(1967).

(17) P. P. Lamy, *Pharm. Acta Helv.*, **44**, 79(1969).

(18) G. Levy and E. J. Mroszczak, *J. Pharm. Sci.*, **57**, 235(1968).

(19) "Remington's Pharmaceutical Sciences," 15th ed., Mack Publishing Co., Easton, Pa., 1975, pp. 1095, 1098.

(20) A. J. Aguiar and M. A. Weiner, *J. Pharm. Sci.*, **58**, 210(1969).

(21) B. J. Zwolinski, H. Eyring, and P. E. Reese, *J. Phys. Chem.*, **53**, 1426(1949).

ACKNOWLEDGMENTS AND ADDRESSES

Received February 22, 1972, from the *Department of Industrial and Physical Pharmacy, School of Pharmacy and Pharmacal Sciences, Purdue University, West Lafayette, IN 47907*

Accepted for publication July 31, 1975.

Supported by a David Ross Fellowship, Purdue Research Foundation.

The authors thank the reviewer for the time spent in preparing the review comments and suggestions.

* Present address: Pharmaceutical Manufacturing Development, The Upjohn Co., Kalamazoo, MI 49001

‡ To whom inquiries should be directed.

Nonspecific Effect of Bis(2-ethylhexyl) Phthalate on Hexobarbital Sleep Time

EWART A. SWINYARD[x], J. H. WOODHEAD, and R. V. PETERSEN

Abstract □ The data presented suggest that the intravenous or intraperitoneal administration of bis(2-ethylhexyl) phthalate prolongs hexobarbital sleep time in mice and rats by enlarging the lipophilic pool, a phenomenon that can be replicated by pretreatment of the animals with olive oil. These results call attention to the importance of considering the physical characteristics of a substance when evaluating its effect on a pharmacologically active agent.

Keyphrases □ Phthalate ester—bis(2-ethylhexyl) phthalate, effect on hexobarbital sleep time, mice, rats □ Hexobarbital—sleep time, effect of bis(2-ethylhexyl) phthalate, mice, rats □ Bis(2-ethylhexyl) phthalate—effect on hexobarbital sleep time, role of phthalate, physical properties, mice, rats

Previous studies (1, 2) showed that the increased hexobarbital sleep time induced in mice and rats by pretreatment with bis(2-ethylhexyl) phthalate (I) is unrelated to the increased sensitivity of the central nervous system to the barbiturate or to an effect of the plasticizer on the rate of hepatic metabolism of the hexobarbital. Confirmation of these findings in this laboratory prompted the investigation of the mechanism responsible for the potentiation of hexobarbital sleep time caused by I.

Although I is absorbed very slowly from the peritoneal cavity (25% of a given dose remains in the body of rats after 13 days) (3), it is rapidly cleared from the blood ($t_{1/2}$ = 4.5–9 min and is dose dependent) when administered intravenously (4). These observations and a report (5) indicating that a significant amount of I associates with the lipoprotein fraction of the blood suggested that I-induced prolongation of hexobarbital sleep time results from its physical properties and is a nonspecific function characteristic of lipophilic substances. The present report substantiates this hypothesis.

EXPERIMENTAL

Male albino mice (Carworth Farms, CF No. 1 strain) and male albino rats (Sprague–Dawley strain) were allowed free access to both food[1] and water except when they were removed from their cages for the experimental procedures. Compound I or olive oil was sonicated in either mouse or rat serum (81% of particulate < 2.7 μm) and administered intraperitoneally or intravenously in doses of 300 and 500 mg/kg in mice and rats, respectively. The volume administered was limited to 1 ml/100 g of body weight in mice and 1 ml/1000 g of body weight in rats.

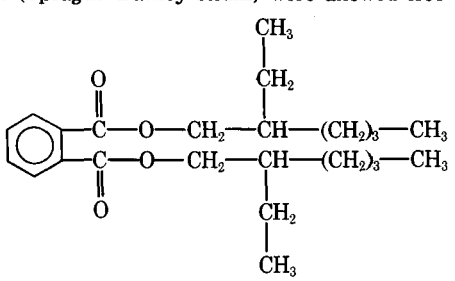

I

For the determination of hexobarbital sleep time, groups of randomly selected mice or rats were injected intravenously or intraperitoneally with I, olive oil, or the requisite volume of serum. At appropriate time intervals after the administration of I, olive oil, or serum, hexobarbital sodium was injected intravenously in a dose of 100 mg/kg in mice and 80 mg/kg in rats. The sleep time, in minutes, was measured from the end of the hexobarbital injection to the time each animal regained its righting reflex. The righting reflex was considered present when an animal placed on its back was able to right itself in three consecutive trials in 5 sec. The increases in sleep time in the drug-treated groups compared to the corresponding control group were calculated, and the significance of the differences was evaluated by an analysis of variance.

To determine the effect of the treatment on serum hexobarbital levels, groups of eight rats each were injected intravenously with I, olive oil, or the requisite volume of serum followed immediately by hexobarbital sodium, also given intravenously. Five minutes after the hexobarbital injection, blood was drawn from each animal and centrifuged. Hexobarbital was extracted from the serum with 1.5% isoamyl alcohol in heptane and measured in pH 11 buffer at 245 nm[2]. Samples containing I were also measured at pH 2, since I interfered with the hexobarbital reading at 245 nm in pH 11 buffer.

RESULTS AND DISCUSSION

The effect of I on hexobarbital sleep time in mice and rats is shown in Table I. In mice administered I intraperitoneally, hexobarbital sleep time increased significantly at all time intervals. The percent increase varied from 31 to 51% and was unrelated to the time interval between the administration of I and the hexobarbital. Indeed, 24 hr after I administration, hexobarbital sleep time was increased 46%. Similarly, hexobarbital sleep time was increased in rats by 23 and 44% 0.5 and 6 hr, respectively, after the intraperitoneal administration of I.

This prolonged effect after the intraperitoneal administration of I is undoubtedly related to its slow absorption from the peritoneal cavity and, hence, the maintenance of a rather constant level of I in the blood. In marked contrast to the results obtained by the intraperitoneal route, intravenously administered I in mice failed to increase the sleep time when hexobarbital was administered 1 or 4 hr later. In view of the short half-life of I (4), this result was attributed to its rapid clearance from the blood.

These observations, coupled with the confirmation of previous studies (1, 2) that I does not significantly affect the rate of hepatic metabolism of hexobarbital, emphasized the importance of the finding of Stern *et al.* (5) that when I is added to plasma a significant amount of the plasticizer becomes associated with the lipoprotein fraction. It was, therefore, hypothesized that the I increases the lipophilic reservoir for the hexobarbital and, consequently, prolongs hexobarbital sleep time by means of its physical

[1] Wayne Lab-Blox.
[2] Gilford 240 spectrophotometer.

Table I—Effect of I (300 mg/kg in Mouse Serum or 500 mg/kg in Rat Serum) on Hexobarbital (100 mg/kg iv in Mice or 80 mg/kg iv in Rats) Sleep Time in Mice and Rats

Time Interval between I and Hexobarbital, hr	Route of Administration of I	Mice				Rats			
		Sleep Time, min				Sleep Time, min			
		I Treated	Serum Control	% Increase	p Value	I Treated	Serum Control	% Increase	p Value
0.5	Intraperitoneal	39.0	25.9	51	<0.01	23.3	18.9	23	<0.03
1	Intraperitoneal	34.4	24.5	40	<0.03				
2	Intraperitoneal	35.3	24.5	44	<0.04				
6	Intraperitoneal	32.1	24.5	31	<0.01	25.7	17.9	44	<0.03
24	Intraperitoneal	28.9	19.9	46	<0.01				
1	Intravenous	24.0	23.5	—	—				
4	Intravenous	32.2	32.2	—	—				

characteristics. If this hypothesis is correct, I should also prolong sleep time when given intravenously, provided the hexobarbital is given before I is cleared from the blood. Furthermore, other lipophilic substances, such as olive oil, also should prolong hexobarbital sleep time.

To test this hypothesis, mice were injected intravenously with either I or olive oil in serum and immediately given hexobarbital by the same route. Olive oil in serum was also given by the intraperitoneal route of administration, and hexobarbital was administered intravenously 1 hr later. The results are shown in Table II;

Table II—Effect of I or Olive Oil (300 mg/kg in Mouse Serum) on Hexobarbital (100 mg/kg iv) Sleep Time in Mice

Drug	Route of Administration	Time Interval between Drug and Hexobarbital	Sleep Time, min		p Value
			Drug Treated	Serum Control	
I	Intravenous	Immediate	58.3	32.5	<0.01
Olive oil	Intravenous	Immediate	49.6	32.5	<0.01
Olive oil	Intraperitoneal	1 hr	44.9	30.9	<0.01

Table III—Effect of I or Olive Oil (500 mg/kg in Rat Serum) on Hexobarbital (80 mg/kg iv) Levels in Rat Serum

Drug	Micrograms of Hexobarbital per Milliliter of Serum	p Value
I	90	<0.01
Olive oil	80	<0.01
Control	70	<0.01

hexobarbital sleep time was increased by 79 and 53% after the intravenous administration of I and olive oil, respectively.

If the mechanism by which I and olive oil increase hexobarbital sleep time is by enlarging the lipophilic pool, a significantly greater amount of hexobarbital should be present in the serum of I- and olive oil-treated animals as compared to the controls. To evaluate this point, three groups of eight rats each were injected intravenously with I, olive oil, or the requisite volume of serum and then immediately injected with 80 mg/kg iv of hexobarbital sodium. Five minutes after the hexobarbital injection, blood was withdrawn from each animal and the concentration of hexobarbital was determined.

As shown in Table III, the concentration of hexobarbital was significantly increased in both I- and olive oil-treated animals. Thus, these data support the concept that the increase in hexobarbital sleep time induced by I is due to its physical characteristics, which enlarge the lipophilic reservoir for hexobarbital, and not to its pharmacological properties *per se*. These observations call attention to another factor that must be considered when evaluating the effect of substances on hexobarbital sleep time.

REFERENCES

(1) R. J. Rubin and R. J. Jaeger, *Environ. Health Perspect.*, **3**, 53(1973).

(2) J. W. Daniel and H. Bratt, *Toxicology*, **2**, 51(1974).

(3) R. J. Jaeger and R. J. Rubin, *Environ. Health Perspect.*, **3**, 95(1973).

(4) C. O. Schulz and R. J. Rubin, *ibid.*, **3**, 123(1973).

(5) I. Stern, J. Miripol, and R. Izzo, *Pharmacologist*, **16**, 283(1974).

ACKNOWLEDGMENTS AND ADDRESSES

Received May 27, 1975, from the *College of Pharmacy, University of Utah, Salt Lake City, UT 84112*

Accepted for publication July 8, 1975.

Supported in part by Contract NIH-NHLI-73-2908-B.

[x] To whom inquiries should be directed.

Interference by Butyl Rubber Stoppers in GLC Analysis for Theophylline

FRANCIS CHRZANOWSKI *, PAUL J. NIEBERGALL *x, ROBERT MAYOCK ‡, JOEL TAUBIN ‡, and EDWIN SUGITA *

Abstract □ During a study of the pharmacokinetics of theophylline using GLC analysis, unexpectedly high values occurred in a random manner. The cause of these abnormal values was investigated, and significant interference was observed when blood samples were drawn using evacuated glass tubes sealed with butyl rubber stoppers. *In vitro* tests using distilled water showed no apparent theophylline levels due to the additives in three commonly used tubes. However, when water was allowed to remain in contact with the butyl rubber stoppers for 1 min, an apparent theophylline content of as high as 5.5 μg/ml was observed. A contact time of 60 min resulted in apparent theophylline levels of as high as 52.3 μg/ml. It was concluded that a substance leached from the butyl rubber stoppers accounted for the spurious results.

Keyphrases □ Theophylline—GLC analysis, effect of butyl rubber stoppers, blood □ Butyl rubber—stoppers, effect on GLC analysis of theophylline, blood □ GLC—analysis, theophylline in blood, effect of butyl rubber stoppers

A convenient and widely used method for collecting blood samples employs an evacuated glass tube sealed with a butyl rubber stopper[1]. The sample is drawn by vacuum into the tube by means of a multiple sampling device formed from a needle with two points: one for venipuncture and the other for penetrating the butyl rubber cap. Up to 1 min is needed to obtain one 10-ml sample.

Because of the angle at which the tubes are usually held, blood is in contact with the cap almost immediately after it is punctured. Even after this brief period, materials that have a deleterious effect upon subsequent drug analysis for theophylline can be leached from the cap.

EXPERIMENTAL

A study of the pharmacokinetics of theophylline was performed using an assay (1) involving preliminary extraction of serum samples with 5% isopropyl alcohol in chloroform, evaporation of the extract to dryness, redissolution of the residue in 50 μl of solvent, and injection of a portion of the resulting solution into a gas chromatograph[2]. The solvent system and the column packing[3] (3% OV-17 on 100–120-mesh Chromosorb W-HP) were similar to those used for the chromatographic assay of a wide variety of drugs in biological fluids. In the collection of the blood specimens, a 19-gauge butterfly scalp needle with a three-way stopcock was used to obtain blood samples when the sampling intervals were relatively short; a normal saline infusion was used to keep the lines open.

Some subjects in the study chose to have the infusion set removed when the sampling interval reached 2 hr. Subsequent samples from these individuals were obtained using disposable syringes or evacuated glass tubes. The samples were allowed to clot and then were spun down. The caps were taken off fresh tubes, which were then filled with the serum harvested by means of disposable glass pipets. These tubes were sealed with cork or, if cork was not available, with butyl rubber stoppers. The serum samples were stored in a freezer until they could be assayed. Originally, no particular precautions were taken to keep either the fresh blood or the serum from contacting the rubber closures. From observations and inquiries, it was concluded that this procedure for the drawing and subsequent handling of the specimens is not uncommon.

At this point, abnormally high assay results began to occur in an apparently random manner. To discover the source of the problem, the effects of using tubes sealed with butyl rubber stoppers were investigated. The tubes investigated were: Type A (red cap), no additives in the glass tube; Type B (orange cap), potassium oxalate and sodium fluoride in the glass tube; Type C (lavender cap), tripotassium ethylenediaminetetraacetic acid and potassium sorbate in the tube; and Type D (green cap), heparin in the tube.

Each type of tube was opened, the butyl rubber cap was discarded, and a small amount of distilled water was added (Set A). After 30 min, a sample from each tube was carried through the entire extraction and analytical procedure. A second set (Set B) of tubes was studied. The capped tubes were held vertically with the caps down. The caps were then punctured with a stainless steel needle connected to a plastic disposable syringe containing distilled water.

It had been determined previously that neither the syringe nor the needle would interfere with the assay. The tubes were allowed to fill with distilled water, and samples were taken at 1 min (approximately the time needed to obtain a 10-ml sample) and at 5, 15, and 60 min. The samples were then carried through the extraction and assay procedure.

RESULTS

The chromatograms for the tubes in Set A showed no peaks other than the one due to the internal standard used in the procedure. Thus, the chemicals in the tubes and the glass or materials leaching from the glass were not causing the problem.

The chromatograms from the tubes in Set B showed, in addition to the peak due to the internal standard, a peak occurring at 12.8 min. This peak overlapped sufficiently with the normal theophylline peak at 13.1 min so that it could be, and indeed in the initial pharmacokinetic study apparently was, interpreted as being theophylline. Table I presents the apparent theophylline content obtained from each type of tube at the indicated time. Obviously, some material was being leached quite rapidly from the butyl rubber stoppers, and this substance was substantially interfering with the assay for theophylline.

DISCUSSION

The finding of apparent theophylline levels of up to 5.5 μg/ml within a contact time of approximately 1 min is impressive in view of the fact that the serum therapeutic level of this drug is 10–20 μg/ml. Although tubes are normally kept in a vertical position during transportation and storage, longer contact times between the samples and the butyl rubber stoppers are possible. Such contact

Table I—Apparent Theophylline Content Obtained from Distilled Water in Contact with Butyl Rubber Caps (Set B Tubes)

	Apparent Theophylline Content by Tube Type, μg/ml			
Minutes	A	B	C	D
1	1.1	4.9	5.5	2.6
5	23.2	13.2	35.9	25.2
15	28.1	22.1	46.5	40.3
60	44.3	39.4	52.3	47.5

[1] Vacutainer, Becton Dickinson, Rutherford, N.J.
[2] Varian Aerograph 2400, Walnut Creek, Calif.
[3] Supelco Inc., Bellefonte, Pa.

could result in apparent theophylline levels well above the therapeutic range.

A relatively large number of materials are used in the manufacture of butyl rubber stoppers, and the identification of the interfering material would be a major project. Telephone conversations with the manufacturer of the tubes led to no clues as to what the material might be. Therefore, the finding of this study indicates that any laboratories analyzing blood samples by GLC should determine whether the collection tubes will interfere with the analysis. Such an analysis can be performed quite easily by the methods used in this study.

REFERENCES

(1) F. A. Chrzanowski, P. J. Niebergall, J. G. Nikelly, E. T. Sugita, and R. L. Schnaare, *Biochem. Med.*, 11, 26(1974).

ACKNOWLEDGMENTS AND ADDRESSES

Received May 2, 1975, from the *Department of Pharmacy, Philadelphia College of Pharmacy and Science, Philadelphia, Pa., and the ‡Pulmonary Disease Section of the Department of Medicine, University of Pennsylvania School of Medicine, Philadelphia, Pa.

Accepted for publication July 3, 1975.

Supported in part by National Institutes of Health Clinical Research Center Grant RR 00040.

The authors acknowledge the comments and assistance of Dr. Karl Engelman, Director of the Clinical Research Center of the Hospital at the University of Pennsylvania.

‡ To whom inquiries should be directed. Present address: Marion Laboratories, Inc., Kansas City, MO 64137

Determination of Tinidazole in Tablets by dc Polarography

MARJAN SLAMNIK

Abstract □ A polarographic method was developed for determining tinidazole in tablets. The substance is extracted from the sample with water, pH 6.8 Britton–Robinson buffer is added to an aliquot, and the solution is polarographed at the dropping mercury electrode *versus* the saturated calomel electrode. The polarographic wave is well developed and enables a fairly precise quantitative determination. The method of standard addition is used.

Keyphrases □ Tinidazole—polarographic analysis, commercial tablets □ Polarography—analysis, tinidazole, commercial tablets □ Antitrichomonal agents—tinidazole, polarographic analysis, commercial tablets

Tinidazole[1], 1-[2-(ethylsulfonyl)ethyl]-2-methyl-5-nitro-1*H*-imidazole, is an antitrichomonal agent and has a chemical structure similar to that of metronidazole, 2-methyl-5-nitro-1*H*-imidazole-1-ethanol, *i.e.*, a 2-methyl-5-nitroimidazole ring. The mechanism of the polarographic reduction of metronidazole is known (1), and from the chemical similarity it can be concluded that tinidazole undergoes the same polarographic reduction mechanism. Tinidazole and metronidazole also have similar dc polarographic behavior including a four-electron reduction wave corresponding to the reduction of the nitro group, the same slope of the $E_{1/2} = f/\text{pH}$ plot, and close values of $E_{1/2}$.

For the quantitative determination of tinidazole, the more positive wave was used. This wave is evident in a Britton–Robinson buffer of pH 6.8 and has the $E_{1/2}$ at −0.47 v *versus* the saturated calomel electrode. The more negative wave, which is not well developed, does not interfere. Tinidazole is stable at pH 6.8.

[1] Pfizer Inc.

EXPERIMENTAL

Apparatus—A recording polarograph[2] was equipped for dc polarography and had a drop timer[3]. A dropping mercury electrode with an outflow velocity of 2 mg/sec at a height of 60 cm of the mercury head was used. It was placed in a standard beaker-type cell with a saturated calomel electrode.

Reagents and Chemicals—Britton–Robinson buffer, pH 6.8, was prepared by mixing 100 ml of Solution A and 50 ml of Solution B. Solution A consisted of 0.04 *M* acetic acid, 0.04 *M* orthophosphoric acid, and 0.04 *M* boric acid. Solution B was 0.2 *M* sodium hydroxide.

For the standard solution, 60 mg of tinidazole standard was dissolved in water in a 100-ml volumetric flask (amber glass).

Procedures—Weigh a portion of finely ground sample, 100–150 mg of tinidazole, into a 250-ml volumetric flask (amber glass). Add 200 ml of water, shake well for at least 30 min, and dilute to volume with water. Filter through filter paper with fine pores, discarding the first 20 ml of filtrate. Then pipet 5 ml of the clear filtrate into a 50-ml volumetric flask, add 0.3 ml of a 0.2% aqueous solution of polyethylene glycol ether of monoisooctylphenol[4] or the same amount of a 0.2% aqueous solution of gelatin, and dilute to volume with the Britton–Robinson buffer. Pipet 25 ml of the prepared solution into a polarographic cell and purge with oxygen-free nitrogen for 10–15 min. Record the polarogram *versus* the saturated calomel electrode from 0.0 to 0.9 v applied voltage on the dropping mercury electrode with the sensitivity of 7 μamp for the full scale of the recorder. Apply a suitable damping and use a drop timer, the drop time being 2–3 sec.

After obtaining the polarogram, add 1 ml of the standard solution to the solution in the cell, deaerate with oxygen-free nitrogen for 1 min, and again record the polarogram under the same conditions. Measure the wave heights H and h (Fig. 1) and calculate:

$$\text{mg of tinidazole per tablet} = \frac{ahb \times 1000}{(1.04H - h)(w)} \qquad \text{(Eq. 1)}$$

where a = milligrams of tinidazole reference standard in 100 ml of standard solution, w = weight of sample (milligrams) taken for the

[2] Polarimeter type PO 4, Radiometer, Copenhagen, Denmark.
[3] Type DLT 1, Radiometer, Copenhagen, Denmark.
[4] Triton X-100, Rohm & Haas Co.

could result in apparent theophylline levels well above the therapeutic range.

A relatively large number of materials are used in the manufacture of butyl rubber stoppers, and the identification of the interfering material would be a major project. Telephone conversations with the manufacturer of the tubes led to no clues as to what the material might be. Therefore, the finding of this study indicates that any laboratories analyzing blood samples by GLC should determine whether the collection tubes will interfere with the analysis. Such an analysis can be performed quite easily by the methods used in this study.

REFERENCES

(1) F. A. Chrzanowski, P. J. Niebergall, J. G. Nikelly, E. T. Sugita, and R. L. Schnaare, *Biochem. Med.*, 11, 26(1974).

ACKNOWLEDGMENTS AND ADDRESSES

Received May 2, 1975, from the *Department of Pharmacy, Philadelphia College of Pharmacy and Science, Philadelphia, Pa., and the ‡Pulmonary Disease Section of the Department of Medicine, University of Pennsylvania School of Medicine, Philadelphia, Pa.

Accepted for publication July 3, 1975.

Supported in part by National Institutes of Health Clinical Research Center Grant RR 00040.

The authors acknowledge the comments and assistance of Dr. Karl Engelman, Director of the Clinical Research Center of the Hospital at the University of Pennsylvania.

‡ To whom inquiries should be directed. Present address: Marion Laboratories, Inc., Kansas City, MO 64137

Determination of Tinidazole in Tablets by dc Polarography

MARJAN SLAMNIK

Abstract □ A polarographic method was developed for determining tinidazole in tablets. The substance is extracted from the sample with water, pH 6.8 Britton–Robinson buffer is added to an aliquot, and the solution is polarographed at the dropping mercury electrode *versus* the saturated calomel electrode. The polarographic wave is well developed and enables a fairly precise quantitative determination. The method of standard addition is used.

Keyphrases □ Tinidazole—polarographic analysis, commercial tablets □ Polarography—analysis, tinidazole, commercial tablets □ Antitrichomonal agents—tinidazole, polarographic analysis, commercial tablets

Tinidazole[1], 1-[2-(ethylsulfonyl)ethyl]-2-methyl-5-nitro-1*H*-imidazole, is an antitrichomonal agent and has a chemical structure similar to that of metronidazole, 2-methyl-5-nitro-1*H*-imidazole-1-ethanol, *i.e.*, a 2-methyl-5-nitroimidazole ring. The mechanism of the polarographic reduction of metronidazole is known (1), and from the chemical similarity it can be concluded that tinidazole undergoes the same polarographic reduction mechanism. Tinidazole and metronidazole also have similar dc polarographic behavior including a four-electron reduction wave corresponding to the reduction of the nitro group, the same slope of the $E_{1/2} = f/\text{pH}$ plot, and close values of $E_{1/2}$.

For the quantitative determination of tinidazole, the more positive wave was used. This wave is evident in a Britton–Robinson buffer of pH 6.8 and has the $E_{1/2}$ at −0.47 v *versus* the saturated calomel electrode. The more negative wave, which is not well developed, does not interfere. Tinidazole is stable at pH 6.8.

[1] Pfizer Inc.

EXPERIMENTAL

Apparatus—A recording polarograph[2] was equipped for dc polarography and had a drop timer[3]. A dropping mercury electrode with an outflow velocity of 2 mg/sec at a height of 60 cm of the mercury head was used. It was placed in a standard beaker-type cell with a saturated calomel electrode.

Reagents and Chemicals—Britton–Robinson buffer, pH 6.8, was prepared by mixing 100 ml of Solution A and 50 ml of Solution B. Solution A consisted of 0.04 *M* acetic acid, 0.04 *M* orthophosphoric acid, and 0.04 *M* boric acid. Solution B was 0.2 *M* sodium hydroxide.

For the standard solution, 60 mg of tinidazole standard was dissolved in water in a 100-ml volumetric flask (amber glass).

Procedures—Weigh a portion of finely ground sample, 100–150 mg of tinidazole, into a 250-ml volumetric flask (amber glass). Add 200 ml of water, shake well for at least 30 min, and dilute to volume with water. Filter through filter paper with fine pores, discarding the first 20 ml of filtrate. Then pipet 5 ml of the clear filtrate into a 50-ml volumetric flask, add 0.3 ml of a 0.2% aqueous solution of polyethylene glycol ether of monoisooctylphenol[4] or the same amount of a 0.2% aqueous solution of gelatin, and dilute to volume with the Britton–Robinson buffer. Pipet 25 ml of the prepared solution into a polarographic cell and purge with oxygen-free nitrogen for 10–15 min. Record the polarogram *versus* the saturated calomel electrode from 0.0 to 0.9 v applied voltage on the dropping mercury electrode with the sensitivity of 7 μamp for the full scale of the recorder. Apply a suitable damping and use a drop timer, the drop time being 2–3 sec.

After obtaining the polarogram, add 1 ml of the standard solution to the solution in the cell, deaerate with oxygen-free nitrogen for 1 min, and again record the polarogram under the same conditions. Measure the wave heights H and h (Fig. 1) and calculate:

$$\text{mg of tinidazole per tablet} = \frac{ahb \times 1000}{(1.04H - h)(w)} \qquad \text{(Eq. 1)}$$

where a = milligrams of tinidazole reference standard in 100 ml of standard solution, w = weight of sample (milligrams) taken for the

[2] Polarimeter type PO 4, Radiometer, Copenhagen, Denmark.
[3] Type DLT 1, Radiometer, Copenhagen, Denmark.
[4] Triton X-100, Rohm & Haas Co.

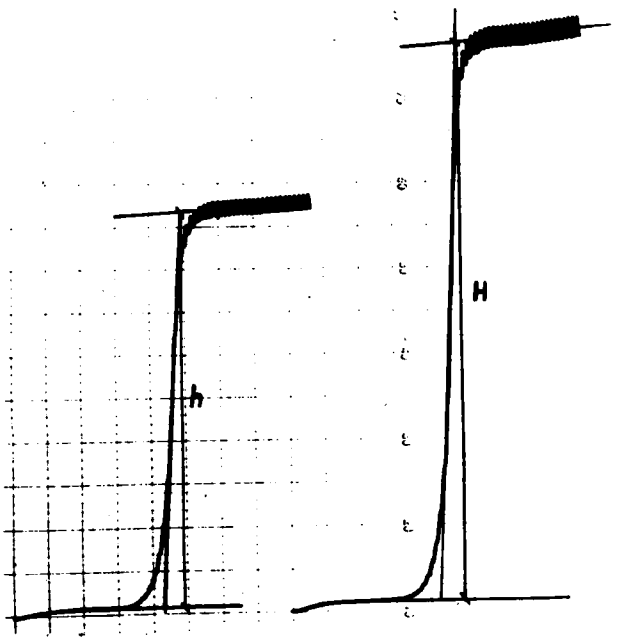

Figure 1—*Polarographic waves of tinidazole before and after standard addition.*

determination, h = wave height of tinidazole before standard addition, H = wave height of tinidazole after standard addition, and b = average weight of a tablet (grams).

RESULTS AND DISCUSSION

The polarographic wave of tinidazole obtained under the described conditions is well developed, and the precision of the proposed method is evident from Table I. The polarographic current was diffusion controlled and increased linearly with concentration in the range used for the determination.

The method of standard addition was preferred because it is more rapid than the concentration–diffusion current plot method.

Table I—Results of 10 Polarographic Analyses of Tinidazole in Tablets[a]

Analysis	Tinidazole per Tablet, mg
1	150
2	148
3	156
4	153
5	147
6	151
7	151
8	146
9	149
10	154
Average	150.5
SD	±2%

[a] Fasigyn tablets, Pfizer; analyzed by Pfizer Specification No. 3-FPS-255. This sample contains 152 mg of tinidazole/tablet.

Since the currents are diffusion controlled and possess the normal temperature coefficient of less than 2%/degree, no thermostating of the cell is necessary and the curves for the solution to be analyzed and for the solution after standard addition are recorded at room temperature.

REFERENCES

(1) D. Dumanović, J. Volke, and V. Vajgand, *J. Pharm. Pharmacol.*, 18, 507(1966).

ACKNOWLEDGMENTS AND ADDRESSES

Received April 4, 1975, from the *Research-Development Institute, KRKA Pharmaceutical and Chemical Works, Novo mesto, Yugoslavia.*

Accepted for publication July 2, 1975.

The author thanks Pfizer Inc. for samples and the Pfizer Inc. Publication Committee for help in the preparation of this paper. The author also gratefully acknowledges Dr. J. Volke, Polarographic Institute of J. Heyrovský, Prague, Czechoslovakia, for help in correcting this article.

Isolation of Pinastric Acid and Ergosterol from *Parmelia caperata* (L.) Arch.

T. SERRA and J. POLÓNIA ˣ

Abstract □ Among other common compounds, pinastric acid and ergosterol were isolated for the first time from *Parmelia caperata*. The isolation of these compounds is described; identification was made from the melting point and UV, IR, and mass spectral data.

Keyphrases □ Pinastric acid—isolated from *Parmelia caperata*, UV, IR, and mass spectral data □ Ergosterol—isolated from *Parmelia caperata*, UV, IR, and mass spectral data □ *Parmelia caperata*—isolation of pinastric acid and ergosterol, UV, IR, and mass spectral data □ Lichens—*Parmelia caperata*, isolation of pinastric acid and ergosterol, UV, IR, and mass spectral data

Parmelia caperata (L.) Arch. is a widely studied lichen (1), but there are no references to the identification of pulvinic acid derivatives and sterols among the several compounds isolated from this species. The present paper reports the extraction and identification of pinastric acid and ergosterol from a Portuguese specimen of *P. caperata*, in which several common compounds, such as (+)-usnic, caperatic, and protocetraric acids, also were found.

Pinastric acid is a methoxy derivative of vulpinic acid, the latter having shown antibiotic activity (2). Because of its chemical constitution, pinastric acid cannot be considered an artifact formed during extraction but may be a term in a probable biogenetic chain: pulvinic acid → vulpinic acid → pinastric acid → leparinic acid → leparinic acid methyl ether.

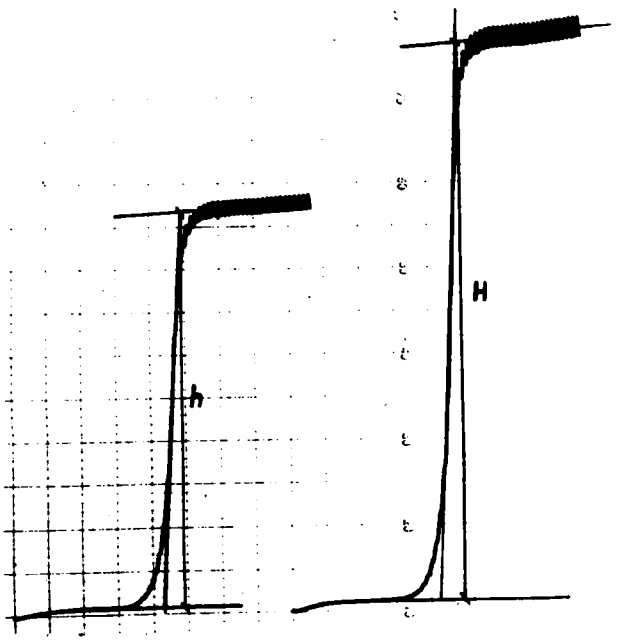

Figure 1—*Polarographic waves of tinidazole before and after standard addition.*

determination, h = wave height of tinidazole before standard addition, H = wave height of tinidazole after standard addition, and b = average weight of a tablet (grams).

RESULTS AND DISCUSSION

The polarographic wave of tinidazole obtained under the described conditions is well developed, and the precision of the proposed method is evident from Table I. The polarographic current was diffusion controlled and increased linearly with concentration in the range used for the determination.

The method of standard addition was preferred because it is more rapid than the concentration–diffusion current plot method.

Table I—Results of 10 Polarographic Analyses of Tinidazole in Tablets[a]

Analysis	Tinidazole per Tablet, mg
1	150
2	148
3	156
4	153
5	147
6	151
7	151
8	146
9	149
10	154
Average	150.5
SD	±2%

[a] Fasigyn tablets, Pfizer; analyzed by Pfizer Specification No. 3-FPS-255. This sample contains 152 mg of tinidazole/tablet.

Since the currents are diffusion controlled and possess the normal temperature coefficient of less than 2%/degree, no thermostating of the cell is necessary and the curves for the solution to be analyzed and for the solution after standard addition are recorded at room temperature.

REFERENCES

(1) D. Dumanović, J. Volke, and V. Vajgand, *J. Pharm. Pharmacol.*, 18, 507(1966).

ACKNOWLEDGMENTS AND ADDRESSES

Received April 4, 1975, from the *Research-Development Institute, KRKA Pharmaceutical and Chemical Works, Novo mesto, Yugoslavia.*

Accepted for publication July 2, 1975.

The author thanks Pfizer Inc. for samples and the Pfizer Inc. Publication Committee for help in the preparation of this paper. The author also gratefully acknowledges Dr. J. Volke, Polarographic Institute of J. Heyrovský, Prague, Czechoslovakia, for help in correcting this article.

Isolation of Pinastric Acid and Ergosterol from *Parmelia caperata* (L.) Arch.

T. SERRA and J. POLÓNIA ˣ

Abstract □ Among other common compounds, pinastric acid and ergosterol were isolated for the first time from *Parmelia caperata*. The isolation of these compounds is described; identification was made from the melting point and UV, IR, and mass spectral data.

Keyphrases □ Pinastric acid—isolated from *Parmelia caperata*, UV, IR, and mass spectral data □ Ergosterol—isolated from *Parmelia caperata*, UV, IR, and mass spectral data □ *Parmelia caperata*—isolation of pinastric acid and ergosterol, UV, IR, and mass spectral data □ Lichens—*Parmelia caperata*, isolation of pinastric acid and ergosterol, UV, IR, and mass spectral data

Parmelia caperata (L.) Arch. is a widely studied lichen (1), but there are no references to the identification of pulvinic acid derivatives and sterols among the several compounds isolated from this species. The present paper reports the extraction and identification of pinastric acid and ergosterol from a Portuguese specimen of *P. caperata*, in which several common compounds, such as (+)-usnic, caperatic, and protocetraric acids, also were found.

Pinastric acid is a methoxy derivative of vulpinic acid, the latter having shown antibiotic activity (2). Because of its chemical constitution, pinastric acid cannot be considered an artifact formed during extraction but may be a term in a probable biogenetic chain: pulvinic acid → vulpinic acid → pinastric acid → leparinic acid → leparinic acid methyl ether.

Ergosterol is widely distributed in plants. Although it has been found in several lichens (1), its isolation from *P. caperata* has not been reported. This compound also was identified by GC–mass spectrometry in the unsaponifiable matter of the same lichen species, along with several other sterols (3) presenting a common biogenetic relationship.

EXPERIMENTAL[1]

The air-dried lichen[2] (330 g) was extracted in a soxhlet apparatus with petroleum ether (bp 40–60°) until the solvent was colorless. By concentration of this extract under reduced pressure, an amorphous product was formed (2.5 g after washing with petroleum ether and drying). It showed, on TLC [Kieselgel G[3] plates activated at 110° for 30 min, thickness ~0.25 mm, developed with chloroform–acetone (80:20)], a spot corresponding to (+)-usnic acid, which was isolated and identified by melting point, $[\alpha]_D$, and UV, IR, and mass spectral data (1, 4, 5).

Further concentration of the petroleum ether extract to 50 ml gave another amorphous substance (675 mg), 105 mg of which was extracted by methanol. The resulting orange solution was submitted to TLC as described previously and showed spots corresponding to usnic acid, atranorin, and chloratranorin (?). It also showed a blue spot (R_f ~0.5), after spraying with anisic aldehyde (6), and a yellow spot (R_f ~0.4) in visible light, became red under UV (350 nm). On concentration and cooling of the methanolic solution, a small amount of orange rectangular plates was formed.

Recrystallization from methanol gave 5 mg of pinastric acid (corresponding to the yellow-red spot), mp 204–206°; UV: λ_{max} (methanol) 293 and 388 nm; λ_{min} 238 and 338 nm; IR: ν_{max} (potassium bromide) 3020, 2960, 2840, 2540, 1775, 1765, 1680, 1600, 1575, 1520, 1465, 1450, 1440, 1420, 1370, 1335, 1310, 1280, 1260, 1195, 1160, 1110, 1090, 1070, 1030, 965, 910, 850, 840, 820, 790, 775, 740, 710, and 700 cm^{-1}; mass spectrum: M^+ = 352 (24%), *m/e* (%) 353 (5), 321 (20), 320 (100), 308 (6), 294 (7), 293 (3), 292 (11), 278 (2), 265 (10), 264 (50), 237 (10), 234 (2), 209 (14), 208 (80), 175 (14), 165 (10), 164 (2), 149 (6), 148 (20), 147 (50), 146 (10), 145 (40), 135 (10), 120 (11), 119 (56), 118 (8), 117 (28), 105 (18), 91 (19), 90 (14), 89 (71), 77 (19), 76 (18), 65 (18), and 63 (18); m* 164 (264 → 208); m* 207.5 (264 → 234); m* 264 (293 → 278); m* 291 (352 → 320).

By concentration of mother liquors from which pinastric acid was separated, a small amount of colorless plates was obtained (7 mg). Recrystallization from methanol gave 5 mg of ergosterol[4], mp 159–161° (Liebermann positive). Only one spot (the blue one referred to previously) was obtained on TLC [chloroform–acetone (80:20) and benzene–dioxane–acetic acid (90:25:4)]; UV: λ_{max} (methanol) 271, 282, and 293 nm; IR: ν_{max} (potassium bromide) 3390, 2900, 2840, 1667, 1471, 1370, 1070, 1042, 990, 971, 835, and 800 cm^{-1}; mass spectrum: M^+ = 396 (100%), *m/e* (%) 397 (30), 337 (50), 271 (45), 253 (56), 251 (23), 211 (49), 199 (28), 197 (30), 185 (28), 183 (28), 158 (65), 157 (70), 145 (78), 143 (85), 119 (58), 109 (55), 107 (60), and 105 (75).

[1] Melting points were determined on a Kofler microscope and are uncorrected. UV spectra were determined on a Bausch & Lomb Spectronic 505 spectrophotometer. IR spectra were determined on a Perkin-Elmer 257 instrument, and only the major bands are quoted. Mass spectra were recorded on a Hitachi RMU-6M with an ionizing potential of 70 ev.

[2] The plant material was collected from *Pinus Pinaster* Sol. trees at Cortegaça, Portugal, in May 1972 and identified as *P. caperata* by Prof. C. Tavares. A voucher specimen is deposited in the Laboratório de Quimica Orgânica, Faculdade de Farmácia, Universidade do Porto, Portugal.

[3] Merck.

[4] All analytical determinations were compared with an authentic sample.

REFERENCES

(1) C. F. Culberson, "Chemical and Botanical Guide to Lichen Products," University of North Carolina Press, Chapel Hill, N.C., 1969, pp. 193, 409.

(2) T. Korzybski, Z. Kowszyk-Gindifer, and W. Kurylowicz, "Antibiotics—Origin, Nature and Properties," vol. II, Pergamon, Oxford, England, 1967, p. 1424.

(3) T. Serra and J. Polónia, "XXXI Congreso Luso-Español para el Progreso de las Ciencias, Coloquio M—Cromatografia Gaseosa en Asociacion con otras Tecnicas Auxiliares," Comunicacion No. 7, Cadiz, Spain, Apr. 1974.

(4) S. H. Harper and R. M. Letcher, *Proc. Trans. Rhodesian Sci. Ass.*, **51**, 156(1966).

(5) S. Huneck, C. Djerassi, D. Becher, M. von Ardenne, K. Steinfelder, and R. Tummler, *Tetrahedron*, **24**, 2707(1968).

(6) E. Stahl, "Thin-Layer Chromatography," Springer-Verlag, New York, N.Y., 1969, p. 695.

ACKNOWLEDGMENTS AND ADDRESSES

Received January 6, 1975, from the *Laboratório de Quimica Orgânica, Faculdade de Farmácia, Universidade do Porto, Portugal.*

Accepted for publication July 22, 1975.

Supported by the Instituto de Alta Cultura (Grants PFR/6 and PFR/3).

The authors thank C. J. Queirós de Oliveira and M. J. Guedes for technical assistance.

[x] To whom inquiries should be directed.

Quantitative NMR Analysis of a Four-Component Mixture of Phenylglycine Derivatives

R. J. WARREN [x], J. E. ZAREMBO, D. B. STAIGER, and A. POST

Abstract □ A rapid, accurate, and precise NMR analytical method for the analysis of phenylglycine, dihydrophenylglycine, tetrahydrophenylglycine, and cyclohexylglycine in combination with each other was developed. The method is based on the integration of the NMR signal characteristic of each component relative to the signal from tetramethylammonium bromide, which is added as an internal standard. No prior separation of the four components is required.

Keyphrases □ Phenylglycine and derivatives—NMR analysis in four-component mixture □ NMR spectroscopy—analysis, phenylglycine and derivatives in four-component mixture

NMR spectroscopy is being used increasingly for quantitative analysis of pharmaceuticals in dosage forms (1, 2) and chemical (3, 4) and isomeric (5) mixtures. The method offers advantages of speed, relatively good precision and accuracy, and ease of execution, and four components do not need to be sepa-

Ergosterol is widely distributed in plants. Although it has been found in several lichens (1), its isolation from *P. caperata* has not been reported. This compound also was identified by GC–mass spectrometry in the unsaponifiable matter of the same lichen species, along with several other sterols (3) presenting a common biogenetic relationship.

EXPERIMENTAL[1]

The air-dried lichen[2] (330 g) was extracted in a soxhlet apparatus with petroleum ether (bp 40–60°) until the solvent was colorless. By concentration of this extract under reduced pressure, an amorphous product was formed (2.5 g after washing with petroleum ether and drying). It showed, on TLC [Kieselgel G[3] plates activated at 110° for 30 min, thickness ~0.25 mm, developed with chloroform–acetone (80:20)], a spot corresponding to (+)-usnic acid, which was isolated and identified by melting point, $[\alpha]_D$, and UV, IR, and mass spectral data (1, 4, 5).

Further concentration of the petroleum ether extract to 50 ml gave another amorphous substance (675 mg), 105 mg of which was extracted by methanol. The resulting orange solution was submitted to TLC as described previously and showed spots corresponding to usnic acid, atranorin, and chloratranorin (?). It also showed a blue spot (R_f ~0.5), after spraying with anisic aldehyde (6), and a yellow spot (R_f ~0.4) in visible light, became red under UV (350 nm). On concentration and cooling of the methanolic solution, a small amount of orange rectangular plates was formed.

Recrystallization from methanol gave 5 mg of pinastric acid (corresponding to the yellow-red spot), mp 204–206°; UV: λ_{max} (methanol) 293 and 388 nm; λ_{min} 238 and 338 nm; IR: ν_{max} (potassium bromide) 3020, 2960, 2840, 2540, 1775, 1765, 1680, 1600, 1575, 1520, 1465, 1450, 1440, 1420, 1370, 1335, 1310, 1280, 1260, 1195, 1160, 1110, 1090, 1070, 1030, 965, 910, 850, 840, 820, 790, 775, 740, 710, and 700 cm^{-1}; mass spectrum: M^+ = 352 (24%), *m/e* (%) 353 (5), 321 (20), 320 (100), 308 (6), 294 (7), 293 (3), 292 (11), 278 (2), 265 (10), 264 (50), 237 (10), 234 (2), 209 (14), 208 (80), 175 (14), 165 (10), 164 (2), 149 (6), 148 (20), 147 (50), 146 (10), 145 (40), 135 (10), 120 (11), 119 (56), 118 (8), 117 (28), 105 (18), 91 (19), 90 (14), 89 (71), 77 (19), 76 (18), 65 (18), and 63 (18); m* 164 (264 → 208); m* 207.5 (264 → 234); m* 264 (293 → 278); m* 291 (352 → 320).

By concentration of mother liquors from which pinastric acid was separated, a small amount of colorless plates was obtained (7 mg). Recrystallization from methanol gave 5 mg of ergosterol[4], mp 159–161° (Liebermann positive). Only one spot (the blue one referred to previously) was obtained on TLC [chloroform–acetone (80:20) and benzene–dioxane–acetic acid (90:25:4)]; UV: λ_{max} (methanol) 271, 282, and 293 nm; IR: ν_{max} (potassium bromide) 3390, 2900, 2840, 1667, 1471, 1370, 1070, 1042, 990, 971, 835, and 800 cm^{-1}; mass spectrum: M^+ = 396 (100%), *m/e* (%) 397 (30), 337 (50), 271 (45), 253 (56), 251 (23), 211 (49), 199 (28), 197 (30), 185 (28), 183 (28), 158 (65), 157 (70), 145 (78), 143 (85), 119 (58), 109 (55), 107 (60), and 105 (75).

[1] Melting points were determined on a Kofler microscope and are uncorrected. UV spectra were determined on a Bausch & Lomb Spectronic 505 spectrophotometer. IR spectra were determined on a Perkin-Elmer 257 instrument, and only the major bands are quoted. Mass spectra were recorded on a Hitachi RMU-6M with an ionizing potential of 70 ev.

[2] The plant material was collected from *Pinus Pinaster* Sol. trees at Cortegaça, Portugal, in May 1972 and identified as *P. caperata* by Prof. C. Tavares. A voucher specimen is deposited in the Laboratório de Quimica Orgânica, Faculdade de Farmácia, Universidade do Porto, Portugal.

[3] Merck.

[4] All analytical determinations were compared with an authentic sample.

REFERENCES

(1) C. F. Culberson, "Chemical and Botanical Guide to Lichen Products," University of North Carolina Press, Chapel Hill, N.C., 1969, pp. 193, 409.

(2) T. Korzybski, Z. Kowszyk-Gindifer, and W. Kurylowicz, "Antibiotics—Origin, Nature and Properties," vol. II, Pergamon, Oxford, England, 1967, p. 1424.

(3) T. Serra and J. Polónia, "XXXI Congreso Luso-Español para el Progreso de las Ciencias, Coloquio M—Cromatografia Gaseosa en Asociacion con otras Tecnicas Auxiliares," Comunicacion No. 7, Cadiz, Spain, Apr. 1974.

(4) S. H. Harper and R. M. Letcher, *Proc. Trans. Rhodesian Sci. Ass.*, **51**, 156(1966).

(5) S. Huneck, C. Djerassi, D. Becher, M. von Ardenne, K. Steinfelder, and R. Tummler, *Tetrahedron*, **24**, 2707(1968).

(6) E. Stahl, "Thin-Layer Chromatography," Springer-Verlag, New York, N.Y., 1969, p. 695.

ACKNOWLEDGMENTS AND ADDRESSES

Received January 6, 1975, from the *Laboratório de Quimica Orgânica, Faculdade de Farmácia, Universidade do Porto, Portugal.*

Accepted for publication July 22, 1975.

Supported by the Instituto de Alta Cultura (Grants PFR/6 and PFR/3).

The authors thank C. J. Queirós de Oliveira and M. J. Guedes for technical assistance.

[x] To whom inquiries should be directed.

Quantitative NMR Analysis of a Four-Component Mixture of Phenylglycine Derivatives

R. J. WARREN [x], J. E. ZAREMBO, D. B. STAIGER, and A. POST

Abstract □ A rapid, accurate, and precise NMR analytical method for the analysis of phenylglycine, dihydrophenylglycine, tetrahydrophenylglycine, and cyclohexylglycine in combination with each other was developed. The method is based on the integration of the NMR signal characteristic of each component relative to the signal from tetramethylammonium bromide, which is added as an internal standard. No prior separation of the four components is required.

Keyphrases □ Phenylglycine and derivatives—NMR analysis in four-component mixture □ NMR spectroscopy—analysis, phenylglycine and derivatives in four-component mixture

NMR spectroscopy is being used increasingly for quantitative analysis of pharmaceuticals in dosage forms (1, 2) and chemical (3, 4) and isomeric (5) mixtures. The method offers advantages of speed, relatively good precision and accuracy, and ease of execution, and four components do not need to be sepa-

Table I—Chemical Shifts and Integration of Signal Characteristic of Individual Components

Component	Spectrum Integrated, Hz	Chemical Shift, ppm	Number of Protons
Phenylglycine	1000	7.60	5
Dihydrophenylglycine	300	2.84	4
Tetrahydrophenylglycine	1000	1.92	5
Cyclohexylglycine	300	1.25	5
Tetramethylammonium bromide	1000, 300	3.36	12

rated. The method described here is illustrative of the utility of NMR to determine complex mixtures of organic substances quantitatively without prior separation.

Catalytic reduction of dihydrophenylglycine usually results in a four-component mixture containing varying amounts of phenylglycine, tetrahydrophenylglycine, and cyclohexylglycine. In this laboratory, analysis of such mixtures have been carried out with an amino acid analyzer, a process that is much more time consuming than the NMR method presented here. The NMR method allows analysis of the bulk chemical with no prior separation and no treatment other than dissolving the sample in 2% DCl.

EXPERIMENTAL

Apparatus and Reagents—The following were used: a 90-MHz spectrometer[1], a five-place balance[2], a 2% DCl solution (prepared by diluting a stock solution[3] of 20% DCl 1 to 10 with deuterium oxide), tetramethylammonium bromide[4] (internal standard) (98% pure by titration), phenylglycine[4], tetrahydrophenylglycine[5], dihydrophenylglycine[5], and cyclohexylglycine[5].

Procedure—A sample (50–100 mg) containing dihydrophenylglycine as the major component and phenylglycine, tetrahydrophenylglycine, and cyclohexylglycine as minor components was accurately weighed into a small vial. A 10–20-mg quantity of tetramethylammonium bromide was accurately weighed and added to the vial. The resulting mixture was dissolved in 0.5 ml of 2% DCl solution. The NMR spectrum of the clear solution was obtained along with five integrations, using a 10-ppm sweep width and a 5-min sweep time. The portion of the spectrum from 4.0 to 0.5 ppm (δ scale) was rerun on a 300-Hz sweep width and a 5-min sweep time. This portion of the spectrum was integrated five times.

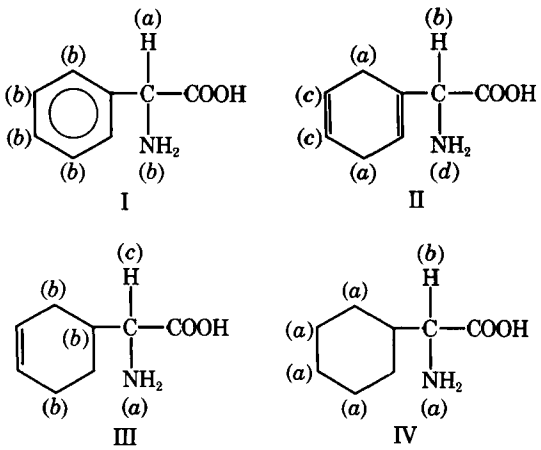

[1] Perkin-Elmer model R32.
[2] Model H16, Mettler.
[3] Thompson-Packard.
[4] Eastman Chemical Co.
[5] Prepared and assayed in these laboratories.

Table II—Analysis of Prepared Mixtures

Mixture	Components in Mixture	Weight Added, mg	Weight of Component Found by NMR	Percent Theory Recovered
1	Dihydrophenylglycine	66.93	66.34	99.1
	Phenylglycine	13.84	14.11	101.9
	Cyclohexylglycine	7.75	7.66	98.4
	Tetrahydrophenylglycine	6.91	7.32	105.9
	Tetramethylammonium bromide	11.59		
2	Dihydrophenylglycine	63.88	65.39	102.4
	Phenylglycine	15.71	15.05	95.8
	Cyclohexylglycine	10.13	10.17	100.4
	Tetrahydrophenylglycine	9.75	9.04	92.7
	Tetramethylammonium bromide	11.92		
3	Dihydrophenylglycine	48.74	49.42	101.4
	Phenylglycine	20.68	21.09	101.9
	Cyclohexylglycine	15.71	15.34	97.9
	Tetrahydrophenylglycine	12.02	11.30	94.0
	Tetramethylammonium bromide	14.08		
4	Dihydrophenylglycine	47.16	46.37	98.3
	Phenylglycine	9.76	9.46	96.9
	Cyclohexylglycine	13.06	13.75	105.3
	Tetrahydrophenylglycine	6.03	6.43	106.6
	Tetramethylammonium bromide	13.59		

The signal integrations used for calculating the individual components are summarized in Table I.

Each component in the sample was calculated using the average of five integrations according to:

$$\frac{\text{integral average}_{\text{sample}}}{\text{integral average}_{\text{TMAB}}} \times \frac{\text{equivalent weight}_{\text{sample}}}{\text{equivalent weight}_{\text{TMAB}}} \times \text{mg}_{\text{TMAB}} = \text{mg of component in mixture} \quad \text{(Eq. 1)}$$

where TMAB = tetramethylammonium bromide, and:

$$\text{equivalent weight} = \frac{\text{molecular weight}}{\text{number of protons integrated}} \quad \text{(Eq. 2)}$$

Equivalent weights are as follows: phenylglycine, 30.24; dihydrophenylglycine, 38.30; tetrahydrophenylglycine, 38.55; cyclohexylglycine, 31.24; and tetramethylammonium bromide, 12.84.

Tetrahydrophenylglycine is found by difference, *i.e.*, total weight of sample − (milligrams of phenylglycine + milligrams of dihydrophenylglycine + milligrams of cyclohexylglycine) = milligrams of tetrahydrophenylglycine.

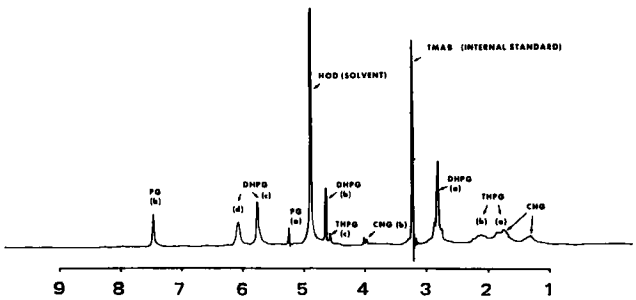

Figure 1—*NMR spectrum of four-component mixture of dihydrophenylglycine (DHPG), phenylglycine (PG), cyclohexylglycine (CHG), tetrahydrophenylglycine (THPG), and the internal standard tetramethylammonium bromide (TMAB).*

Table III—Statistical Analysis: Absolute Error and Percent Deviation from Average

Dihydrophenylglycine	Phenylglycine	Cyclohexylglycine	Tetrahydrophenylglycine
99.1	101.9	98.4	105.9
102.4	95.8	100.4	92.7
101.4	101.9	97.6	94.0
98.3	96.9	105.3	106.6
$\bar{x}$ = 100.3	99.1	100.4	99.8
σ = ±1.92	±3.24	±3.46	±7.47
RSD, % = 1.91	3.27	3.45	7.48

RESULTS AND DISCUSSION

The NMR spectrum of a four-component mixture with dihydrophenylglycine (II) as the major component and phenylglycine (I), tetrahydrophenylglycine (III), and cyclohexylglycine (IV) as minor components is shown in Fig. 1. Tetramethylammonium bromide was chosen as the internal standard because it is readily available and gives a single NMR signal at 3.36 ppm; this signal does not interfere with the NMR spectra of the four components.

The NMR signal characteristic of each component is indicated in Fig. 1 and listed in Table I. Once these characteristic NMR signals have been established and assigned, the method is straightforward. The remaining operation is to integrate the respective signals carefully relative to the signal of a known weight of the internal standard. These data are sufficient to calculate the amount of each component present in the mixture by Eqs. 1 and 2.

The results for a series of four-component mixtures prepared for analysis by the NMR method are shown in Table II. Since two components are present in amounts less than 10%, the accuracy and precision of this complex mixture are reasonably adequate (Table III). The tetrahydrophenylglycine content is found by difference due to the overlap of this signal with part of the NMR signal from cyclohexylglycine.

The developed method has the advantage over existing methods in that no prior separation of the components is required. An additional advantage is that qualitative identification of the individual components is obtained from their NMR spectra.

REFERENCES

(1) J. W. Turczan and B. A. Goldwitz, *J. Ass. Offic. Anal. Chem.*, **56**, 669(1973).

(2) E. B. Shenin, W. R. Benson, and M. M. Smith, Jr., *ibid.*, **56**, 124(1973).

(3) B. A. Goldwitz and J. W. Turczan, *J. Pharm. Sci.*, **62**, 115(1973).

(4) T. Huynh-Ngoc and G. Sirois, *ibid.*, **62**, 1335(1973).

(5) R. J. Warren and J. E. Zarembo, *ibid.*, **59**, 840(1970).

ACKNOWLEDGMENTS AND ADDRESSES

Received February 6, 1975, from *Research and Development, Smith Kline & French Laboratories, Philadelphia, PA 19101*

Accepted for publication July 8, 1975.

[x] To whom inquiries should be directed.

Electron-Capture GLC Determination of Phenylpropanolamine as a Pentafluorophenyloxazolidine Derivative

L. NEELAKANTAN and H. B. KOSTENBAUDER [x]

Abstract □ A simplified procedure is described for an electron-capture GLC determination of phenylpropanolamine in blood plasma. The method is based on derivatization of phenylpropanolamine with pentafluorobenzaldehyde at room temperature without prior extraction of the drug from plasma. The derivative, pentafluorophenyloxazolidine, is readily extracted from plasma into a small volume of hexane. Samples usually can be injected directly into the gas chromatograph without concentration of the hexane solution. Data are presented to illustrate the suitability of the method for dosage form bioavailability evaluation from plasma phenylpropanolamine levels achieved after acute oral administration of a typical dosage form.

Keyphrases □ Phenylpropanolamine—GLC analysis, plasma □ GLC—analysis, phenylpropanolamine, plasma □ Adrenergic agents—phenylpropanolamine, plasma

Previously reported methods for GLC determination of phenylalkanolamines and related compounds in plasma are based upon extraction of the amine from plasma followed by conversion to an electron-capturing perfluoroacyl- or pentafluorobenzaldehyde derivative (1–10). While this approach provides adequate sensitivity, the extraction procedure necessary to isolate the relatively water-soluble phenylalkanolamine from plasma sometimes gives rise to troublesome interfering peaks in the chromatogram.

A marked improvement in assay simplicity, together with excellent sensitivity and reliability, can be achieved by derivatization of phenylpropanolamine directly in plasma. The principle of the method involves reaction of the phenylpropanolamine in plasma with pentafluorobenzaldehyde to yield an electron-capturing derivative, which is then readily extracted into a small volume of hexane. The derivative forms within 1 hr at room temperature and is extremely stable under the assay conditions.

EXPERIMENTAL

Chromatographic Conditions—The gas chromatograph[1] was equipped with both an alkali flame-ionization detector and a 250-mCi tritium electron-capture detector. Glass columns, 2 m in length, 0.625 cm o.d., 0.20 cm i.d., were packed with 100–120-mesh

[1] Varian Aerograph model 2700, Varian Instrument Division, Palo Alto, Calif.

Table III—Statistical Analysis: Absolute Error and Percent Deviation from Average

Dihydrophenylglycine	Phenylglycine	Cyclohexylglycine	Tetrahydrophenylglycine
99.1	101.9	98.4	105.9
102.4	95.8	100.4	92.7
101.4	101.9	97.6	94.0
98.3	96.9	105.3	106.6
$\bar{x}$ = 100.3	99.1	100.4	99.8
σ = ±1.92	±3.24	±3.46	±7.47
RSD, % = 1.91	3.27	3.45	7.48

RESULTS AND DISCUSSION

The NMR spectrum of a four-component mixture with dihydrophenylglycine (II) as the major component and phenylglycine (I), tetrahydrophenylglycine (III), and cyclohexylglycine (IV) as minor components is shown in Fig. 1. Tetramethylammonium bromide was chosen as the internal standard because it is readily available and gives a single NMR signal at 3.36 ppm; this signal does not interfere with the NMR spectra of the four components.

The NMR signal characteristic of each component is indicated in Fig. 1 and listed in Table I. Once these characteristic NMR signals have been established and assigned, the method is straightforward. The remaining operation is to integrate the respective signals carefully relative to the signal of a known weight of the internal standard. These data are sufficient to calculate the amount of each component present in the mixture by Eqs. 1 and 2.

The results for a series of four-component mixtures prepared for analysis by the NMR method are shown in Table II. Since two components are present in amounts less than 10%, the accuracy and precision of this complex mixture are reasonably adequate (Table III). The tetrahydrophenylglycine content is found by difference due to the overlap of this signal with part of the NMR signal from cyclohexylglycine.

The developed method has the advantage over existing methods in that no prior separation of the components is required. An additional advantage is that qualitative identification of the individual components is obtained from their NMR spectra.

REFERENCES

(1) J. W. Turczan and B. A. Goldwitz, *J. Ass. Offic. Anal. Chem.*, **56**, 669(1973).

(2) E. B. Shenin, W. R. Benson, and M. M. Smith, Jr., *ibid.*, **56**, 124(1973).

(3) B. A. Goldwitz and J. W. Turczan, *J. Pharm. Sci.*, **62**, 115(1973).

(4) T. Huynh-Ngoc and G. Sirois, *ibid.*, **62**, 1335(1973).

(5) R. J. Warren and J. E. Zarembo, *ibid.*, **59**, 840(1970).

ACKNOWLEDGMENTS AND ADDRESSES

Received February 6, 1975, from *Research and Development, Smith Kline & French Laboratories, Philadelphia, PA 19101*

Accepted for publication July 8, 1975.

[x] To whom inquiries should be directed.

Electron-Capture GLC Determination of Phenylpropanolamine as a Pentafluorophenyloxazolidine Derivative

L. NEELAKANTAN and H. B. KOSTENBAUDER [x]

Abstract □ A simplified procedure is described for an electron-capture GLC determination of phenylpropanolamine in blood plasma. The method is based on derivatization of phenylpropanolamine with pentafluorobenzaldehyde at room temperature without prior extraction of the drug from plasma. The derivative, pentafluorophenyloxazolidine, is readily extracted from plasma into a small volume of hexane. Samples usually can be injected directly into the gas chromatograph without concentration of the hexane solution. Data are presented to illustrate the suitability of the method for dosage form bioavailability evaluation from plasma phenylpropanolamine levels achieved after acute oral administration of a typical dosage form.

Keyphrases □ Phenylpropanolamine—GLC analysis, plasma □ GLC—analysis, phenylpropanolamine, plasma □ Adrenergic agents—phenylpropanolamine, plasma

Previously reported methods for GLC determination of phenylalkanolamines and related compounds in plasma are based upon extraction of the amine from plasma followed by conversion to an electron-capturing perfluoroacyl- or pentafluorobenzaldehyde derivative (1–10). While this approach provides adequate sensitivity, the extraction procedure necessary to isolate the relatively water-soluble phenylalkanolamine from plasma sometimes gives rise to troublesome interfering peaks in the chromatogram.

A marked improvement in assay simplicity, together with excellent sensitivity and reliability, can be achieved by derivatization of phenylpropanolamine directly in plasma. The principle of the method involves reaction of the phenylpropanolamine in plasma with pentafluorobenzaldehyde to yield an electron-capturing derivative, which is then readily extracted into a small volume of hexane. The derivative forms within 1 hr at room temperature and is extremely stable under the assay conditions.

EXPERIMENTAL

Chromatographic Conditions—The gas chromatograph[1] was equipped with both an alkali flame-ionization detector and a 250-mCi tritium electron-capture detector. Glass columns, 2 m in length, 0.625 cm o.d., 0.20 cm i.d., were packed with 100–120-mesh

[1] Varian Aerograph model 2700, Varian Instrument Division, Palo Alto, Calif.

Gas Chrom Q coated with 1.25% OV-17[2]. Columns were conditioned for 36 hr at 275° and were treated *in situ* with a silylating agent[3]. Nitrogen carrier gas flow was 30 ml/min. For alkali flame-ionization detection, hydrogen flow was 27 ml/min and air flow was 300 ml/min. The column temperature was 190°, the injector temperature was 245°, and the detector temperature was 210°.

Reagents—The following were used: phenylpropanolamine hydrochloride NF; pentafluorobenzaldehyde[4], 98%; 2,4-dinitrofluorobenzene[4]; and hexane[5], pesticide grade. Other materials were reagent grade.

The marker, 2,4-dinitrophenyl-*N,N*-diethylamine, was prepared from 2,4-dinitrofluorobenzene and diethylamine and was twice recrystallized from ethanol.

The pentafluorobenzaldehyde, although adequately pure when fresh, gave numerous interfering peaks in the chromatogram within a few days after the original container was opened. Therefore, the aldehyde was shaken with an excess of saturated aqueous sodium bisulfite solution, and the precipitated aldehyde bisulfite compound was collected and recrystallized from aqueous ethanol. The aldehyde bisulfite compound is stable and can be stored for use in this form.

Estimation of Phenylpropanolamine in Plasma—Into 13-mm glass culture tubes (acid washed and siliconized[6]) were placed 3 ml of plasma, approximately 20 mg of aldehyde bisulfite reagent, two drops of 10% aqueous potassium hydroxide, and 2 ml of a hexane solution containing 640 ng of the marker, 2,4-dinitrophenyl-*N,N*-diethylamine. The tubes were capped[7] and rocked for 1 hr at room temperature while protected from direct light. The tubes were then centrifuged, and 2-μl samples of the hexane solution were injected into the gas chromatograph. The concentration of phenylpropanolamine in plasma was determined by comparison of peak height ratios and a standard curve.

Calibration Curve—Known amounts of phenylpropanolamine hydrochloride were added to 2.5 ml of human plasma, volume was made up to 3 ml with distilled water, and these solutions were carried through the same procedure as already described.

Similar standard curves were obtained by adding phenylpropanolamine hydrochloride to distilled water rather than to plasma.

RESULTS

Figure 1 shows a typical chromatogram for electron-capture

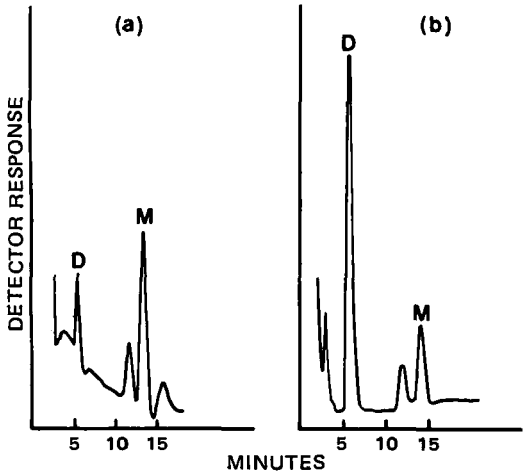

Figure 1—(a) *Chromatogram obtained after spiking 3 ml of pooled human plasma with phenylpropanolamine hydrochloride to provide a concentration of 13.3 ng/ml; attenuation 32.* (b) *Chromatogram obtained from assay of a 2-ml plasma sample from a human subject 4 hr after oral ingestion of 50 mg of phenylpropanolamine hydrochloride; attenuation 64. The symbols D and M refer to drug and marker peaks, respectively.*

[2] Applied Science Laboratories, State College, Pa.
[3] Silyl-8, Pierce Chemical Co., Rockford, Ill.
[4] Aldrich Chemical Co., Milwaukee, Wis.
[5] Matheson, Coleman and Bell, East Rutherford, N.J.
[6] Siliclad, Clay Adams, Division of Becton, Dickinson and Co., Parsippany, N.J.
[7] Stoppers lined with Teflon (du Pont).

Table I—Standard Curve Obtained for Derivatization, Extraction, and GLC Quantitation of Phenylpropanolamine Hydrochloride Added to Plasma and Water

Medium	Drug[a]/Marker[b]	Weight Ratio	Weight Ratio: Peak Height Ratio	Weight Ratio: Peak Height Ratio
Plasma	1.1 ng/32 ng	0.034	0.15	0.23
Plasma	2.2 ng/32 ng	0.069	0.33	0.21
Plasma	3.3 ng/32 ng	0.103	0.50	0.21
Plasma	5.5 ng/32 ng	0.172	0.86	0.20
Plasma	11.0 ng/32 ng	0.344	1.58	0.22
Plasma	200 ng/640 ng	0.312	1.55	0.20
Plasma	300 ng/640 ng	0.469	2.44	0.19
Plasma	400 ng/640 ng	0.625	3.09	0.20
Plasma	500 ng/640 ng	0.781	3.70	0.21
Water	300 ng/640 ng	0.469	2.28	0.21
Water	500 ng/640 ng	0.781	3.94	0.20
Water	0/640 ng	0	0.03	—
Plasma	0/640 ng	0	0.00	—

[a] Phenylpropanolamine hydrochloride in a 3-ml solution. [b] 2,4-Dinitrophenyl-*N,N*-diethylamine.

quantitation of phenylpropanolamine in spiked human plasma and in plasma obtained from a human subject after oral ingestion of a phenylpropanolamine dosage form.

Table I illustrates the linearity of a calibration curve obtained for phenylpropanolamine hydrochloride added to plasma in amounts ranging from 1.1 to 500 ng/3 ml of plasma. Data for four replicate determinations at 13 and 130 ng/ml indicate a relative standard deviation of less than 5% at both concentrations.

Figure 2 presents typical plasma levels of phenylpropanolamine in two human subjects who ingested 50 mg of phenylpropanolamine hydrochloride in tablet form after an overnight fast.

DISCUSSION

The principle of this analytical method rests on the reaction of pentafluorobenzaldehyde with phenylpropanolamine to form a derivative, which is proposed to be a pentafluorophenyloxazolidine (Scheme I). Reaction of β-aminoalcohols with aldehydes to produce oxazolidines was reported previously (11–14). In some cases, however, the product may exist as a mobile tautomeric system with the corresponding Schiff base.

Bergmann (15), in his comprehensive review, discussed the structure, reactions, and synthesis of oxazolidines. Neelakantan (16, 17) and Neelakantan and Molin-Case (18) did extensive studies on the stereospecific reaction of aromatic aldehydes with ephedrine and ψ-ephedrine. Indeed, this reaction is an induced asymmetric synthesis. The reaction of aldehyde bisulfites with ephedrine also pro-

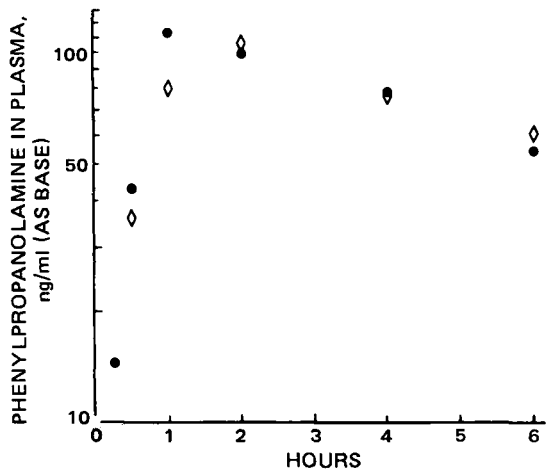

Figure 2—*Plasma phenylpropanolamine levels in two human subjects following ingestion of 50 mg of phenylpropanolamine hydrochloride in tablet form.*

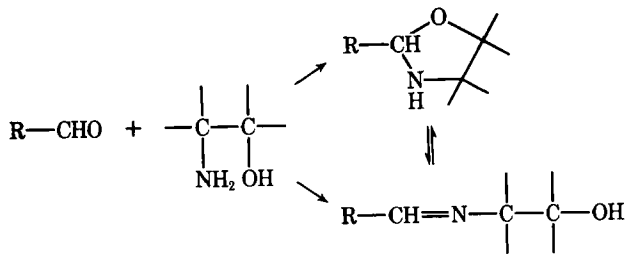

Scheme I

ceeds by a stereospecific mechanism. These α-aminoalkanesulfonates readily give the corresponding oxazolidines in the presence of base (17). The absolute configurations and structures were confirmed by X-ray diffraction for the benzaldehyde–ephedrine product (18).

In the present case, pentafluorobenzaldehyde or its bisulfite addition compound reacts with phenylpropanolamine in the presence of base. The product obtained is sparingly soluble in water and readily soluble in aprotic solvents such as hexane and benzene. The product is easily hydrolyzed by acids and very stable in aqueous base. The reaction involves facile splitting of water in an aqueous medium and goes to completion at room temperature in 1 hr. Both thermodynamic and steric factors probably contribute to the ease of formation of this oxazolidine.

Moffat and Horning (6) reported the formation of a Schiff base from pentafluorobenzaldehyde and β-hydroxy-β-phenylethylamine by heating in acetonitrile for 1 hr at 60° and, after addition of *N,O*-bis(trimethylsilyl)acetamide, further heating for 1 hr at 60°. Even in this case, however, formation of an oxazolidine, with subsequent ring opening with *N,O*-bis(trimethylsilyl)acetamide, cannot be ruled out. Indeed, the reactivity of oxazolidines cannot unambiguously be differentiated from that of Schiff bases in many chemical reactions. Physical properties such as boiling point, dipole moment, magnetic susceptibility, and UV spectra also cannot establish with certainty the structure of these products.

In mass fragmentography, benzyl cleavage would occur predominantly in both cases. Molecular refraction and IR spectra might be of assistance, but ^{13}C-NMR might be most useful. The ^{13}C-NMR spectra would be free of complications from the methylene protons. From the pronounced difference in the geometry of the two possible structures, it might be possible to assign the molecular structure of the reaction product. This study is in progress.

On the basis of currently available information, Scheme II is suggested for the derivatization.

Indirect evidence for the oxazolidine structure is provided from the reaction of both ephedrine and phenylpropanolamine with

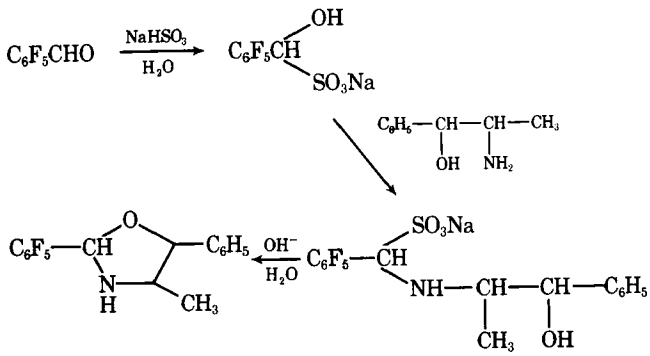

Scheme II

benzaldehyde. In both cases, the products are formed readily at room temperature. Both products are readily extracted with hexane, are stable to base, and are easily hydrolyzed by acid. Their respective retention time and sensitivity to an alkali flame-ionization detector are very similar.

Although the structure of the pentafluorobenzaldehyde–phenylpropanolamine derivative remains to be confirmed, the derivative provides a simple, reliable, and sensitive method for quantitation of phenylpropanolamine. No back-extractions or preliminary cleanups are involved. Since the reaction goes to completion at room temperature in 1 hr, there is no possibility of decomposition due to heating. The product is readily extracted into hexane, and usually no concentration of the hexane solution is required. If desired, however, the hexane extract can be concentrated by evaporation of solvent without loss of the derivative or marker.

The derivative has been shown to be stable in hexane for days. This derivative avoids problems such as partial hydrolysis of silyl ether groups in the presence of moisture, nitrogen to oxygen migrations, and similar complications which may arise with electron-capture derivatives of the perfluoroacyl type.

As shown in Fig. 1, spiked plasma samples yield several additional, unidentified, chromatographic peaks. These peaks also appear in drug-free plasma, but they do not interfere with phenylpropanolamine quantitation. Figure 2, illustrating typical plasma phenylpropanolamine levels following a single oral administration of 50 mg of phenylpropanolamine hydrochloride in tablet form, indicates that the assay procedure is quite adequate for assessment of bioavailability.

REFERENCES

(1) L. M. Cummins and M. J. Fourier, *Anal. Lett.*, **2**, 403(1969).

(2) R. B. Bruce and W. R. Maynard, Jr., *Anal. Chem.*, **41**, 977(1969).

(3) L. J. Dombrowski, P. M. Comi, and E. L. Pratt, *J. Pharm. Sci.*, **62**, 1761(1973).

(4) E. Anggard and G. Sedvall, *Anal. Chem.*, **41**, 1250(1969).

(5) G. R. Wilkinson, *Anal. Lett.*, **3**, 289(1970).

(6) A. C. Moffat and E. C. Horning, *Biochim. Biophys. Acta*, **222**, 248(1970).

(7) T. Walle and H. Ehrsson, *Acta Pharm. Suecica*, **8**, 27(1971).

(8) D. J. Edwards and K. Blau, *Anal. Biochem.*, **45**, 387(1972).

(9) Y. Maruyama and A. E. Takemori, *ibid.*, **49**, 240(1972).

(10) J. C. Lhuguenot and B. F. Maume, *J. Chromatogr. Sci.*, **12**, 411(1974).

(11) W. E. Noland and R. A. Johnson, *J. Org. Chem.*, **25**, 1155(1960).

(12) M. Senkus, *J. Amer. Chem. Soc.*, **62**, 1515(1945).

(13) E. D. Bergmann and H. Resnick, *J. Chem. Soc.*, **1956**, 1662.

(14) H. Pfanz and G. Kirshner, *Ann.*, **614**, 149(1958).

(15) E. D. Bergmann, *Chem. Rev.*, **53**, 309(1953).

(16) L. Neelakantan, *J. Org. Chem.*, **36**, 2253(1971).

(17) *Ibid.*, **36**, 2256(1971).

(18) L. Neelakantan and J. A. Molin-Case, *J. Org. Chem.*, **36**, 2261(1971).

ACKNOWLEDGMENTS AND ADDRESSES

Received November 20, 1974, from the *College of Pharmacy, University of Kentucky, Lexington, KY 40506*

Accepted for publication July 14, 1975.

Supported by a research grant from Warner-Lambert Research Institute, Morris Plains, N.J.

[x] To whom inquiries should be directed.

Interpretation of Distribution Coefficients of *p*-Alkylpyridines by a Modified Regular Solution Theory

KUANG C. YEH * and WILLIAM I. HIGUCHI ˣ

Abstract □ The hypothetical hexadecane–octane distribution coefficients for the alkylpyridines were deduced from the corresponding oil–water distribution data. The values were analyzed by a modified regular solution theory. A good correlation was noted by including the Flory–Huggins entropy factor in the calculation and by considering the deviation from the geometric mean assumption.

Keyphrases □ Alkylpyridines—distribution coefficients interpreted, modified regular solution theory □ Distribution coefficients—alkylpyridines, interpreted by modified regular solution theory

In a previous paper (1), a study of the distribution of *p*-alkylpyridines between various organic solvents and an aqueous sodium chloride solution was presented. The differences in the distribution coefficients were attributed to the differences in interactions between the solvents and the solute. The present report presents an analysis of the interactions of the solutes in the hydrocarbon solvents following the modified Scatchard–Hildebrand regular solution theory.

DISCUSSION

The infinite dilution activity coefficient of a nonpolar solute, n, in a polar solvent, i, γ_{ni}, has been described (2):

$$RT \ln(\gamma_{ni}) = V_n(\lambda_n - \lambda_i)^2 + V_n(\tau_i^2 - 2\Psi_{ni}) + RT[\ln(V_n/V_i) + 1 - (V_n/V_i)] \quad \text{(Eq. 1)}$$

where the V's are the molar volumes, and Ψ_{ni} is an induction energy density arising from dipole-induced dipole interactions. The λ's and τ are the nonpolar and polar solubility parameters, respectively, defined as $\lambda^2 = (E^{disp}/V)$ and $\tau^2 = (E^{polar}/V)$, where E^{disp} and E^{polar} are the nonpolar and polar molar cohesive energies, respectively. The three terms on the right-hand side of Eq. 1 represent the dispersion forces, the polar interaction forces, and the Flory–Huggins correction factor. The last term was added to account for the excess of mixing arising from the differences in the molecular size.

The geometric mean assumption involving the dispersion forces, as given by Eq. 1, is likely to be an oversimplification in polar mixtures where differences in molecular geometry and size are large. The inclusion of a deviation factor, l_{ni}, may be used to correct the defect.

Thus, the hypothetical distribution coefficient, $k_{h/o}$, for an alkylpyridine between hexadecane and octane may be expressed as:

$$k_{h/o} = (\gamma_{no}/\gamma_{nh}) \quad \text{(Eq. 2)}$$

or:

$$\log(k_{h/o}) = \frac{V_n}{2.303RT}[(\lambda_n - \lambda_o)^2 - (\lambda_n - \lambda_h)^2] + \frac{2V_n}{2.303RT}[\Psi_{no} - \Psi_{nh}] - \frac{2V_n\lambda_n}{2.303RT}(l_{nh}\lambda_h - l_{no}\lambda_o) + \frac{1}{2.303}[\ln(V_h/V_n) - (V_h - V_o)V_n/V_hV_o] \quad \text{(Eq. 3)}$$

Data Reduction—The $k_{h/o}$ for *p*-alkylpyridines may be computed from the following identity equation, using the experimentally determined oil–water distribution coefficients $k_{h/w}$ and $k_{o/w}$ (1):

$$\log(k_{h/o}) = \log(k_{h/w}) - \log(k_{o/w}) \quad \text{(Eq. 4)}$$

However, the possible effects of the mutual solubilities of the partitioning solvents on $k_{h/o}$ were evaluated first. The solubility of *n*-octane in water is 5.8×10^{-6} M at 25° (3). The presence of sodium chloride in the aqueous phase (1) would further reduce the solubility. The solubility of hexadecane in the aqueous phase would be even smaller due to the hydrophobic effect of the additional methylene groups (4). Thus, the effect of the hydrocarbon solubilities on $\log(k_{h/o})$ was assumed to be negligible.

The effect of water dissolved in the hydrocarbons, however, may not be insignificant. The solubility of water in hexadecane was determined (5) to be $[W]_h = 3 \times 10^{-3}$ M at 25°. The corresponding value in octane, $[W]_o = 4.7 \times 10^{-3}$ M, was estimated from the same source by interpolation. To estimate the hydration effect, the experimental data of Johnson *et al.* (6) on pyridine were used and an empirical relationship was noted:

$$[PW]_i/[P]_i = 1 \times 10^{-2} + 2.09 \times [W]_i \quad \text{(Eq. 5)}$$

where $[W]_i$ is the intrinsic water solubility in the nonpolar solvent i in units of moles per liter, and $[PW]_i/[P]_i$ is the ratio of concentrations of the pyridine–water complex and the unhydrated pyridine monomer in that solvent. The three species may be related by the equilibrium reaction shown in Scheme I:

$$P_i + W_i \rightleftharpoons PW_i$$

Scheme I

If it is assumed that the water solubilities are decreased by 3.3% in the presence of 1 M NaCl (7), then:

$$[W]_h = 0.967 \times 3 \times 10^{-3}\ M = 2.9 \times 10^{-3}\ M \quad \text{(Eq. 6a)}$$

$$[W]_o = 0.967 \times 4.7 \times 10^{-3}\ M = 4.54 \times 10^{-3}\ M \quad \text{(Eq. 6b)}$$

Substituting these values into Eq. 5, one obtains the corresponding ratios:

$$\frac{[PW]_h}{[P]_h} = 1 \times 10^{-2} + 2.09 \times 2.9 \times 10^{-3} = 1.61 \times 10^{-2} \quad \text{(Eq. 7a)}$$

$$\frac{[PW]_o}{[P]_o} = 1 \times 10^{-2} + 2.09 \times 4.54 \times 10^{-3} = 1.95 \times 10^{-2} \quad \text{(Eq. 7b)}$$

The ratio of the unhydrated pyridine to the total pyridine content in each solvent becomes:

$$\frac{[P]_h}{[P]_h + [PW]_h} = \frac{1}{1.0161} \quad \text{(Eq. 8a)}$$

$$\frac{[P]_o}{[P]_o + [PW]_o} = \frac{1}{1.0195} \quad \text{(Eq. 8b)}$$

Applying these ratios into Eq. 4 gives:

$$\log(k_{h/o}) = \log(k_{h/w}/1.0161) - \log(k_{o/w}/1.0195) \quad \text{(Eq. 9)}$$

where $k_{h/w}$ and $k_{o/w}$ are the experimental values.

It was further assumed that the two correction factors, 1.0161 and 1.0195, remain unchanged for the whole series, based on the reasoning that the stability of $[PW]_i$ may not be significantly affected by the chain length and that the net effect of the two factors is small. This treatment allows the comparison of experimentally deduced $k_{h/o}$ values for alkylpyridines with theoretical values based upon Eq. 3.

Table I—Distribution Coefficient between Hexadecane and Octane, Molar Volume, and the Estimated Nonpolar Solubility Parameter for *p*-Alkylpyridines at 25°

Solute	log ($k_{h/o}$)	V_n, ml	λ_n, (cal/ml)$^{1/2}$
Pyridine	0.162	80.88	9.88
4-Picoline	0.169	96.91	9.44
4-Ethylpyridine	0.149	113.15	9.24
4-Propylpyridine	0.127	129.74	9.03
4-Butylpyridine	0.104	146.49	8.86
4-Amylpyridine	0.082	163.09	8.73
4-Hexylpyridine	0.074	179.60	8.62
4-Heptylpyridine	0.062	195.90	8.53
4-Octylpyridine	0.031	212.11	8.46
4-Nonylpyridine	0.011	228.15	8.40

Table I lists the log($k_{h/o}$) values based on Eq. 9.

Evaluation of Parameters in Eq. 3 and Results—The induction energy density, Ψ_{ni}, has been suggested to be dependent upon the dielectric constant of the medium (8). Since both solvents were nonpolar, it was assumed that $\Psi_{nh} = \Psi_{no}$.

The nonpolar solubility parameters of pyridine (λ_p = 9.88) and the solvents (λ_h = 7.975 and λ_o = 7.554) were obtained from the literature (2, 8, 9).

The nonpolar cohesive energies of 4-picoline and 4-ethylpyridine, estimated from the aromatic homomorph plot (2), were found to be 8.64 and 9.67 kcal/mole, using critical temperatures of 643°K and 662°K, respectively. These critical temperatures were, in turn, calculated from the equation of Nokay (10). The homomorph of a molecule is defined as the equistructural hydrocarbon at the same reduced temperature and with the same molar volume as the polar molecule. The nonpolar cohesive energies of propylpyridine and the higher homologs were estimated by the method of Rheineck and Lin (11), who noted that the contribution of the methylene group in a homologous series to the cohesive energy is additive and that the value depends on the nature of the end group. For alkylpyridines, the value was estimated to be 0.92 kcal/mole. Since it has been shown that the polar induction energy of a long chain alkyl derivative remains essentially unchanged (12), the incremental nonpolar cohesive energy was equated to 0.92 kcal/mole. The corresponding λ_n values are shown in Table I.

Unfortunately, the deviation factors l_{nh} and l_{no} cannot be estimated reliably because neither the γ values nor any quantitative independent theories for the deviation factor are presently available. Therefore, any systematic *a priori* test of Eq. 3 is precluded for the present situation. However, an analysis of the data suggests that the resultant ($l_{nh}\lambda_h - l_{no}\lambda_o$) varies regularly with the chain length (Fig. 1). In the absence of further information, the smoothed linear least-squares values were used to construct the "best fit" curve B of Fig. 2.

Figure 2 is a graphic presentation of the three terms that contribute to the log($k_{h/o}$): the geometric mean term, the deviation

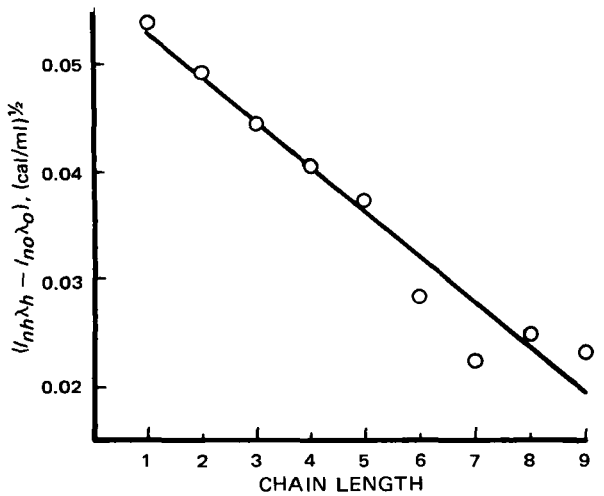

Figure 1—*Chain-length effect on the deviation terms in the hexadecane–octane solvent pair.*

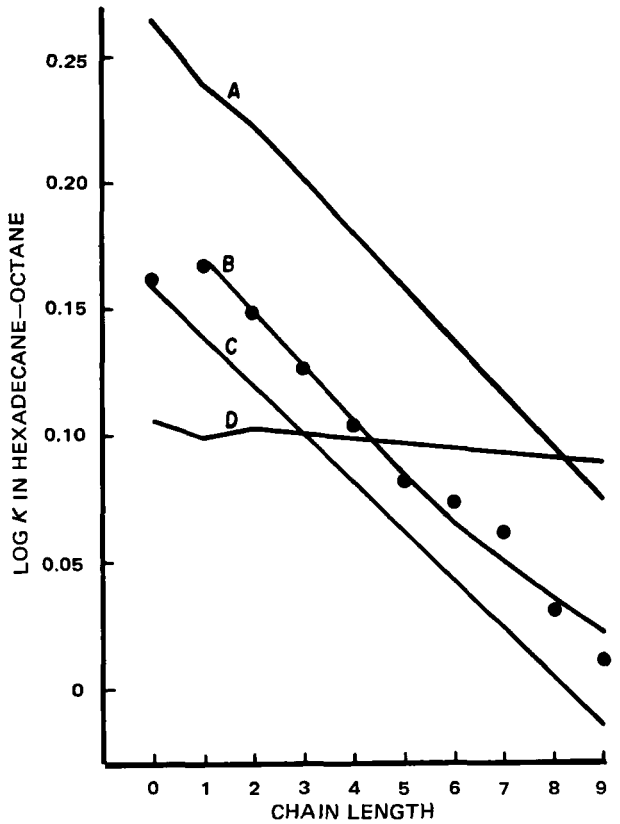

Figure 2—*Contribution of various terms to the distribution coefficients between hexadecane and octane. Key: A, geometric mean terms and Flory–Huggins terms; B, all three terms; C, Flory–Huggins terms alone; D, geometric mean terms alone; and ●, experimental data.*

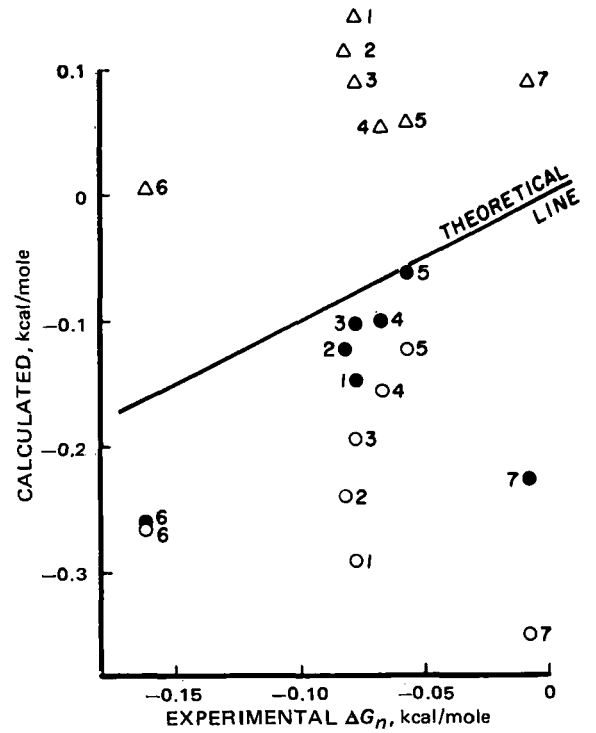

Figure 3—*Comparison of the calculated contributions to the experimental free energy (ΔG_n) of solution in nonpolar solvent n-octadecane at 35° (14). Key: 1, butane; 2, pentane; 3, hexane; 4, heptane; 5, octane; 6, cyclohexane; 7, benzene; △, geometric mean term; ●, geometric mean term plus Flory–Huggins factor; and ○, Flory–Huggins factor.*

term, and the Flory–Huggins factor. Curve D represents the contribution of the geometric mean term. Although it intersects the experimental data points and, therefore, is a good approximation by itself, it does not seem to account for the chain-length effect. The Flory–Huggins term is shown as line C, and this line is essentially parallel to the experimental values. The sums of the two terms are labeled line A. It is obvious that line A predicts a higher $\log(k_{h/o})$ than the observed values. Thus, to best describe the data, all three terms are apparently needed.

Application to Other Systems—Although the method of Prausnitz has been further extended to cover polar–polar mixtures (13), Eq. 3 cannot be applied to other solvent pairs reported previously because of the lack of means of estimating Ψ_{ni} and l_{ni} in polar mixtures. Furthermore, it was difficult to estimate reliable corrected $\log(k_{j/i})$ values from the oil–water partition data due to significant mutual solubilities of the solvents.

The introduction of the Flory–Huggins factor and the deviation term to Eq. 1 appears to be justified in at least nonpolar mixtures. In this case, the expression becomes:

$$RT \ln(\gamma_{ni}) = V_n(\lambda_n - \lambda_i)^2 + 2V_n l_{ni}\lambda_n\lambda_i + RT[\ln(V_n/V_i) + 1 - (V_n/V_i)] \quad \text{(Eq. 10)}$$

Figure 3 compares the calculated contributions from Eq. 10 and the experimental data of Cruickshank *et al.* (14). While the geometric mean term always gives nonnegative contribution to the free energy of solution, the combination of the geometric mean term and the Flory–Huggins factor seems to improve the correlation. The poor fit of cyclohexane and benzene suggests that the deviation term is an important factor for the two solutes whose molecular geometry differs greatly from that of the solvent *n*-octadecane.

REFERENCES

(1) K. C. Yeh and W. I. Higuchi, *J. Pharm. Sci.*, **65**, 80(1976).

(2) R. F. Weimer and J. M. Prausnitz, *Hydrocarbon Process.*, **44**, 237(1965).

(3) J. A. Riddick and W. B. Bunger, "Techniques of Chemistry, Organic Solvents. Physical Properties and Methods of Purification," vol. II, 3rd ed., Wiley–Interscience, New York, N.Y., 1970.

(4) G. Nemethy and H. A. Scheraga, *J. Chem. Phys.*, **36**, 3382, 3401(1962).

(5) P. Schartzberg, *J. Phys. Chem.*, **67**, 976(1963).

(6) J. R. Johnson, P. J. Kilpatrick, S. D. Christian, and H. E. Affsprung, *ibid.*, **72**, 3223(1968).

(7) R. A. Robins and R. H. Stokes, "Electrolyte Solutions," Academic, New York, N.Y., 1955.

(8) J. H. Hildebrand, J. M. Prausnitz, and R. L. Scott, "Regular and Related Solutions," Van Nostrand Reinhold, New York, N.Y., 1970.

(9) J. A. Larkin, D. V. Fenby, T. S. Gilman, and R. L. Scott, *J. Phys. Chem.*, **70**, 1959(1966).

(10) R. Nokay, *Chem. Eng.*, **Feb. 23, 1959**, 147.

(11) A. E. Rheineck and K. F. Lin, *J. Paint Technol.*, **40**, 611(1968).

(12) E. F. Meyer, T. A. Renner, and K. S. Stec, *J. Phys. Chem.*, **75**, 642(1971).

(13) J. G. Helpinstill and M. Van Winkle, *Ind. Eng. Chem. Process Des. Develop.*, **7**, 213(1968).

(14) A. J. B. Cruickshank, B. W. Gainey, and C. L. Young, *Trans. Faraday Soc.*, **64**, 337(1968).

ACKNOWLEDGMENTS AND ADDRESSES

Received June 27, 1974, from the *College of Pharmacy, University of Michigan, Ann Arbor, MI 48104*

Accepted for publication June 13, 1975.

Presented at the Basic Pharmaceutics Section, APhA Academy of Pharmaceutical Sciences, Houston meeting, April 1972.

Abstracted from a thesis submitted by K. C. Yeh to the University of Michigan in partial fulfillment of the Doctor of Philosophy degree requirements.

Supported in part by Training Grant 1T1-GM-1367 from the U.S. Public Health Service and in part by Grant GM-13368 from the National Institute of General Medical Sciences, U.S. Public Health Service, Bethesda, Md.

The authors thank Dr. J. M. Prausnitz, University of California, for helpful discussions on the polar interaction energies.

* Present address: Merck Sharp & Dohme Research Laboratories, West Point, PA 19486

ˣ To whom inquiries should be directed.

Reduction of Activity of Cyanocobalamin in the Presence of Methylparaben Sodium at Autoclave Temperature

S. YAZDANY ˣ and F. BADII

Abstract □ Reduction of activity of cyanocobalamin (vitamin B_{12}) due to degradation or interaction with methylparaben sodium was measured by UV spectrophotometry and microbial assay. TLC of the heated mixture showed two different spots, which indicate some alteration in the structure of the cyanocobalamin molecule in the presence of methylparaben sodium at 115° for 10 min. The losses were about 20% by UV measurements and 32% by microbial assay. The degree of loss was sufficient to suggest that methylparaben sodium might have considerable influence on the stability of pharmaceutical products containing cyanocobalamin. Methylparaben and sodium chloride had no effect on cyanocobalamin.

Keyphrases □ Cyanocobalamin—activity, effect of methylparaben sodium, autoclave temperature, pharmaceutical formulations □ Methylparaben sodium—effect on cyanocobalamin activity, autoclave temperature, pharmaceutical formulations □ Vitamins—cyanocobalamin, activity, effect of methylparaben sodium, autoclave temperature, pharmaceutical formulations

Methylparaben sodium is often used in the formulation of pharmaceutical products. A fairly extensive literature has developed on the incompatibilities of the parabens and macromolecule polymers. Patel and Kostenbauder (1) found that solubilization of parabens with nonionic surfactants involved binding effects. The interaction between methylcellulose and the parabens also was reported (2).

term, and the Flory–Huggins factor. Curve D represents the contribution of the geometric mean term. Although it intersects the experimental data points and, therefore, is a good approximation by itself, it does not seem to account for the chain-length effect. The Flory–Huggins term is shown as line C, and this line is essentially parallel to the experimental values. The sums of the two terms are labeled line A. It is obvious that line A predicts a higher $\log(k_{h/o})$ than the observed values. Thus, to best describe the data, all three terms are apparently needed.

Application to Other Systems—Although the method of Prausnitz has been further extended to cover polar–polar mixtures (13), Eq. 3 cannot be applied to other solvent pairs reported previously because of the lack of means of estimating Ψ_{ni} and l_{ni} in polar mixtures. Furthermore, it was difficult to estimate reliable corrected $\log(k_{j/i})$ values from the oil–water partition data due to significant mutual solubilities of the solvents.

The introduction of the Flory–Huggins factor and the deviation term to Eq. 1 appears to be justified in at least nonpolar mixtures. In this case, the expression becomes:

$$RT \ln(\gamma_{ni}) = V_n(\lambda_n - \lambda_i)^2 + 2V_n l_{ni}\lambda_n\lambda_i + RT[\ln(V_n/V_i) + 1 - (V_n/V_i)] \quad \text{(Eq. 10)}$$

Figure 3 compares the calculated contributions from Eq. 10 and the experimental data of Cruickshank *et al.* (14). While the geometric mean term always gives nonnegative contribution to the free energy of solution, the combination of the geometric mean term and the Flory–Huggins factor seems to improve the correlation. The poor fit of cyclohexane and benzene suggests that the deviation term is an important factor for the two solutes whose molecular geometry differs greatly from that of the solvent *n*-octadecane.

REFERENCES

(1) K. C. Yeh and W. I. Higuchi, *J. Pharm. Sci.*, **65**, 80(1976).

(2) R. F. Weimer and J. M. Prausnitz, *Hydrocarbon Process.*, **44**, 237(1965).

(3) J. A. Riddick and W. B. Bunger, "Techniques of Chemistry, Organic Solvents. Physical Properties and Methods of Purification," vol. II, 3rd ed., Wiley–Interscience, New York, N.Y., 1970.

(4) G. Nemethy and H. A. Scheraga, *J. Chem. Phys.*, **36**, 3382, 3401(1962).

(5) P. Schartzberg, *J. Phys. Chem.*, **67**, 976(1963).

(6) J. R. Johnson, P. J. Kilpatrick, S. D. Christian, and H. E. Affsprung, *ibid.*, **72**, 3223(1968).

(7) R. A. Robins and R. H. Stokes, "Electrolyte Solutions," Academic, New York, N.Y., 1955.

(8) J. H. Hildebrand, J. M. Prausnitz, and R. L. Scott, "Regular and Related Solutions," Van Nostrand Reinhold, New York, N.Y., 1970.

(9) J. A. Larkin, D. V. Fenby, T. S. Gilman, and R. L. Scott, *J. Phys. Chem.*, **70**, 1959(1966).

(10) R. Nokay, *Chem. Eng.*, **Feb. 23, 1959**, 147.

(11) A. E. Rheineck and K. F. Lin, *J. Paint Technol.*, **40**, 611(1968).

(12) E. F. Meyer, T. A. Renner, and K. S. Stec, *J. Phys. Chem.*, **75**, 642(1971).

(13) J. G. Helpinstill and M. Van Winkle, *Ind. Eng. Chem. Process Des. Develop.*, **7**, 213(1968).

(14) A. J. B. Cruickshank, B. W. Gainey, and C. L. Young, *Trans. Faraday Soc.*, **64**, 337(1968).

ACKNOWLEDGMENTS AND ADDRESSES

Received June 27, 1974, from the *College of Pharmacy, University of Michigan, Ann Arbor, MI 48104*

Accepted for publication June 13, 1975.

Presented at the Basic Pharmaceutics Section, APhA Academy of Pharmaceutical Sciences, Houston meeting, April 1972.

Abstracted from a thesis submitted by K. C. Yeh to the University of Michigan in partial fulfillment of the Doctor of Philosophy degree requirements.

Supported in part by Training Grant 1T1-GM-1367 from the U.S. Public Health Service and in part by Grant GM-13368 from the National Institute of General Medical Sciences, U.S. Public Health Service, Bethesda, Md.

The authors thank Dr. J. M. Prausnitz, University of California, for helpful discussions on the polar interaction energies.

* Present address: Merck Sharp & Dohme Research Laboratories, West Point, PA 19486

ˣ To whom inquiries should be directed.

Reduction of Activity of Cyanocobalamin in the Presence of Methylparaben Sodium at Autoclave Temperature

S. YAZDANY ˣ and F. BADII

Abstract □ Reduction of activity of cyanocobalamin (vitamin B_{12}) due to degradation or interaction with methylparaben sodium was measured by UV spectrophotometry and microbial assay. TLC of the heated mixture showed two different spots, which indicate some alteration in the structure of the cyanocobalamin molecule in the presence of methylparaben sodium at 115° for 10 min. The losses were about 20% by UV measurements and 32% by microbial assay. The degree of loss was sufficient to suggest that methylparaben sodium might have considerable influence on the stability of pharmaceutical products containing cyanocobalamin. Methylparaben and sodium chloride had no effect on cyanocobalamin.

Keyphrases □ Cyanocobalamin—activity, effect of methylparaben sodium, autoclave temperature, pharmaceutical formulations □ Methylparaben sodium—effect on cyanocobalamin activity, autoclave temperature, pharmaceutical formulations □ Vitamins—cyanocobalamin, activity, effect of methylparaben sodium, autoclave temperature, pharmaceutical formulations

Methylparaben sodium is often used in the formulation of pharmaceutical products. A fairly extensive literature has developed on the incompatibilities of the parabens and macromolecule polymers. Patel and Kostenbauder (1) found that solubilization of parabens with nonionic surfactants involved binding effects. The interaction between methylcellulose and the parabens also was reported (2).

Table I—Losses of Cyanocobalamin in the Presence of 0.1% Methylparaben Sodium Heated at 115° and Measured by UV Spectrophotometry

Cyanocobalamin Concentration, μg/ml	Reduction, %					
	Run 1	Run 2	Run 3	Run 4	Run 5	Mean ± *SD*
45	18.23	19.12	20.45	17.78	—	18.89 ± 1.17
30	22.64	18.39	22.64	20.00	21.00	20.92 ± 1.83
22.5	16.67	18.89	14.45	17.34	—	16.83 ± 1.84
15	17.07	18.20	16.00	—	—	17.09 ± 1.10

Table II—Losses in Activity of Cyanocobalamin in the Presence of 0.1% Methylparaben Sodium Heated at 115° in an Autoclave and Measured by Microbial Assay

Cyanocobalamin Concentration, μg/ml	Reduction, %				
	Run 1	Run 2	Run 3	Run 4	Mean ± *SD*
45	25.50	32.50	37.50	—	31.83 ± 5.99
30	31.50	34.50	—	—	33.00 ± 2.12
22.50	29.50	33.50	37.50	—	33.50 ± 4.00
15	26.50	31.00	37.00	36.20	32.67 ± 4.90

Although several reviews (3) devoted considerable discussion to the incompatibility that might arise from the interaction of a paraben with the containers, the incompatibility or inactivation that might arise from the interaction or binding of parabens with drugs of a large molecular nature has not been reported. However, the binding of parabens with some molecules such as polyethylene, povidone, and gelatin has been demonstrated (4). These observations suggest that generally unrecognized incompatibilities might exist in many pharmaceutical formulations and might markedly influence the release of the drug from a dosage form and alter the stability and assay of a drug. The present study was designed to investigate the possible interaction or binding effect of methylparaben sodium with cyanocobalamin (vitamin B_{12}) at the autoclave temperature (115° for 10 min).

EXPERIMENTAL

Materials—Methylparaben sodium[1], analytical grade, which was recrystallized three times from methanol, and cyanocobalamin USP were used after analysis by TLC and IR spectroscopy.

Methods—TLC, according to the method of Stahl (5), was performed on each preautoclaved (115° for 10 min) sample on fluorescent silica gel plates. The solvent system used was methanol–water (95:5) or butanol–acetic acid–0.66 *M* KH_2PO_4–methanol (36:18:36:10). Since cyanocobalamin and the interaction product were colored, no detecting reagent was used. Methylparaben sodium spots were detected by UV light.

The potency of cyanocobalamin was measured by the microbial method described in USP XVIII (6), using *Lactobacillus leichmannii* (ATCC 7830) as a test organism.

The UV analysis[2] at 360 nm (6) was the USP XVIII method.

RESULTS AND DISCUSSION

A decrease in the potency of several concentrations of cyanocobalamin in aqueous solution in the presence of methylparaben sodium at autoclave temperature (115° for 10 min) was investigated. The TLC method showed that the autoclave temperature had no effect on an aqueous solution of cyanocobalamin but confirmed the formation of a new compound in the presence of methylparaben sodium (Fig. 1).

Table I shows the percent reduction of cyanocobalamin measured by UV spectrophotometric method after autoclaving in the presence of methylparaben sodium. The increase in concentration of cyanocobalamin had no significant effect on the amount of reduction of cyanocobalamin measured by UV spectrophotometry. Pure cyanocobalamin was used at each stage under the same conditions as a control.

Table II shows the percent reduction of cyanocobalamin potency after autoclaving at 115° for 10 min in the presence of methylparaben sodium measured by microbial assay; the results show that the concentration of cyanocobalamin had little effect on the percent reduction. A comparison of the results obtained by the UV and microbial methods shows a higher reduction by the latter method, suggesting the reliability of the microbial assay.

The interaction or degradation of cyanocobalamin on methylparaben sodium appears to be similar to an interaction of a rubber stopper with methylparaben as described by Lachman *et al.* (7). It appears that substances having large molecular weights interact with methylparaben sodium and form new compounds.

Figure 1 illustrates the effect of methylparaben sodium with cy-

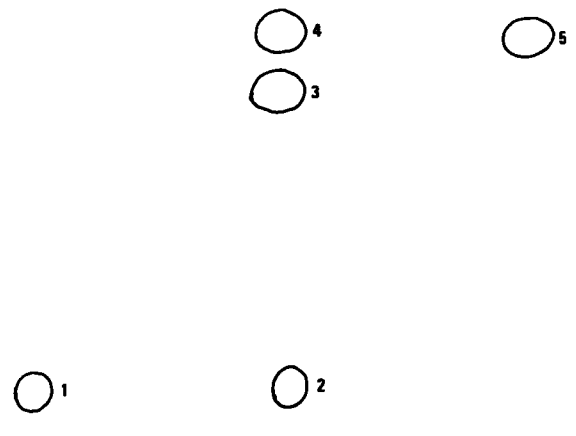

Figure 1—*Thin-layer chromatogram (silica gel) of cyanocobalamin. Key: 1, standard cyanocobalamin; 2, unbound part of cyanocobalamin; 3, bound part of cyanocobalamin with methylparaben sodium; 4, methylparaben sodium; and 5, standard sample of methylparaben sodium.*

[1] Merck.
[2] Varian-Tektron 635.

anocobalamin. The results are indicative of an interaction between these two substances and the formation of a new compound. The interaction is apparently enhanced by elevated temperatures. When the mixture was kept at room temperature for a long period, a small amount of a new compound was formed, suggesting a very low rate of deterioration of cyanocobalamin at room temperature.

Methylparaben and sodium chloride had no effect on cyanocobalamin in the same conditions, which rules out the effect of sodium ion in deterioration of cyanocobalamin.

REFERENCES

(1) N. K. Patel and H. B. Kostenbauder, *J. Amer. Pharm. Ass., Sci. Ed.*, **47**, 289(1958).

(2) W. T. Tillman and R. Kuramoto, *ibid.*, **46**, 214(1957).

(3) D. L. Wedderburn, "Advances in Pharmaceutical Science," vol. 1, Academic, New York, N.Y., 1964, p. 195.

(4) G. M. Miyawaki, N. K. Patel, and H. B. Kostenbauder, *J. Amer. Pharm. Ass., Sci. Ed.*, **48**, 315(1959).

(5) E. Stahl, *Pharmazie*, **11**, 633(1956).

(6) "The United States Pharmacopeia," 18th rev., Mack Publishing Co., Easton, Pa., 1970, p. 887.

(7) L. Lachman, S. Weinstein, G. Hopkins, S. Slack, P. Eisman, and J. Cooper, *J. Pharm. Sci.*, **51**, 224(1962).

ACKNOWLEDGMENTS AND ADDRESSES

Received February 27, 1975, from the *Department of Industrial Pharmacy and Drug Quality Control, School of Pharmacy, University of Tehran, Tehran, Iran.*

Accepted for publication July 11, 1975.

Supported by a research grant from the Ministry of Science and Higher Education of Iran.

The authors are grateful to Professor D. Kazemi and Professor I. Lalezari of Tehran University for their advice and encouragement.

[x] To whom inquiries should be directed.

Enhancement of Solubility of Drug Salts by Hydrophilic Counterions: Properties of Organic Salts of an Antimalarial Drug

S. AGHARKAR, S. LINDENBAUM [x], and T. HIGUCHI

Abstract □ Judicious choice of the salt form of a drug can greatly affect the aqueous solubility and formulation of the compound. The objective of this work was to demonstrate the effect of various counteranions on the aqueous solubility of the antimalarial agent α-(2-piperidyl)-3,6-bis(trifluoromethyl)-9-phenanthrenemethanol. Several organic salts of this drug were studied. The methods of synthesis, the apparent aqueous solubilities, and *in vitro* dissolution tests for these salts are reported. The lactate salt was 200 times as soluble as the hydrochloride salt. This enhanced solubility suggests that parenteral administration of this drug may now be feasible.

Keyphrases □ Solubility, aqueous—salts of substituted phenanthrenemethanol antimalarial agent, effect of hydrophilic counterions □ Salts—substituted phenanthrenemethanol antimalarial agent, effect of hydrophilic counterions on aqueous solubility □ Counterions, hydrophilic—effect on aqueous solubility of substituted phenanthrenemethanol antimalarial agent □ Antimalarial agents—α-(2-piperidyl) -3,6- bis(trifluoromethyl) -9- phenanthrenemethanol, salts, effect of hydrophilic counterions on aqueous solubility

It has been shown that organic acid salt forms of basic drugs, such as amines, have higher aqueous solubilities than their corresponding halide salts (1). This technique has found important application in the development of more soluble salt forms of drugs to improve their bioavailability and ease in formulation.

The objective of this work was to utilize previous findings (1) for α-(2-piperidyl)-3,6-bis(trifluoromethyl)-9-phenanthrenemethanol (I). The principles employed in choosing counterions to render a high molecular weight hydrophobic drug more water soluble are generally applicable.

Compound I has been shown to exhibit significant activity against infections with strains of *Plasmodium falciparum* resistant to chloroquine, quinine, and pyrimethamine (2). Because of two optically active centers, it can exist as any one of four possible stereoisomers or mixtures thereof. The absolute configuration of all of the isomers has been established (3). The work reported here was done with one racemic pair, referred to as "isomer a" by Carroll and Blackwell (3). They also showed that all four enantiomers are potent antimalarials and, therefore, no attempt was made to resolve the racemic mixture.

The apparent solubility of the hydrochloride salt of I and its free base was measured in water at 25°. Compound I, being large and hydrophobic, is only sligtly soluble as the hydrochloride salt (Table I). This poor solubility was suspected to be the main reason for its poor bioavailability. In all previous work, I was administered orally as the hydrochloride

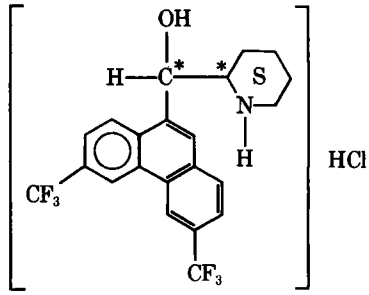

I

* = optically active centers

anocobalamin. The results are indicative of an interaction between these two substances and the formation of a new compound. The interaction is apparently enhanced by elevated temperatures. When the mixture was kept at room temperature for a long period, a small amount of a new compound was formed, suggesting a very low rate of deterioration of cyanocobalamin at room temperature.

Methylparaben and sodium chloride had no effect on cyanocobalamin in the same conditions, which rules out the effect of sodium ion in deterioration of cyanocobalamin.

REFERENCES

(1) N. K. Patel and H. B. Kostenbauder, *J. Amer. Pharm. Ass., Sci. Ed.*, **47**, 289(1958).

(2) W. T. Tillman and R. Kuramoto, *ibid.*, **46**, 214(1957).

(3) D. L. Wedderburn, "Advances in Pharmaceutical Science," vol. 1, Academic, New York, N.Y., 1964, p. 195.

(4) G. M. Miyawaki, N. K. Patel, and H. B. Kostenbauder, *J. Amer. Pharm. Ass., Sci. Ed.*, **48**, 315(1959).

(5) E. Stahl, *Pharmazie*, **11**, 633(1956).

(6) "The United States Pharmacopeia," 18th rev., Mack Publishing Co., Easton, Pa., 1970, p. 887.

(7) L. Lachman, S. Weinstein, G. Hopkins, S. Slack, P. Eisman, and J. Cooper, *J. Pharm. Sci.*, **51**, 224(1962).

ACKNOWLEDGMENTS AND ADDRESSES

Received February 27, 1975, from the *Department of Industrial Pharmacy and Drug Quality Control, School of Pharmacy, University of Tehran, Tehran, Iran.*

Accepted for publication July 11, 1975.

Supported by a research grant from the Ministry of Science and Higher Education of Iran.

The authors are grateful to Professor D. Kazemi and Professor I. Lalezari of Tehran University for their advice and encouragement.

[x] To whom inquiries should be directed.

Enhancement of Solubility of Drug Salts by Hydrophilic Counterions: Properties of Organic Salts of an Antimalarial Drug

S. AGHARKAR, S. LINDENBAUM [x], and T. HIGUCHI

Abstract □ Judicious choice of the salt form of a drug can greatly affect the aqueous solubility and formulation of the compound. The objective of this work was to demonstrate the effect of various counteranions on the aqueous solubility of the antimalarial agent α-(2-piperidyl)-3,6-bis(trifluoromethyl)-9-phenanthrenemethanol. Several organic salts of this drug were studied. The methods of synthesis, the apparent aqueous solubilities, and *in vitro* dissolution tests for these salts are reported. The lactate salt was 200 times as soluble as the hydrochloride salt. This enhanced solubility suggests that parenteral administration of this drug may now be feasible.

Keyphrases □ Solubility, aqueous—salts of substituted phenanthrenemethanol antimalarial agent, effect of hydrophilic counterions □ Salts—substituted phenanthrenemethanol antimalarial agent, effect of hydrophilic counterions on aqueous solubility □ Counterions, hydrophilic—effect on aqueous solubility of substituted phenanthrenemethanol antimalarial agent □ Antimalarial agents—α-(2-piperidyl) -3,6- bis(trifluoromethyl) -9- phenanthrenemethanol, salts, effect of hydrophilic counterions on aqueous solubility

It has been shown that organic acid salt forms of basic drugs, such as amines, have higher aqueous solubilities than their corresponding halide salts (1). This technique has found important application in the development of more soluble salt forms of drugs to improve their bioavailability and ease in formulation.

The objective of this work was to utilize previous findings (1) for α-(2-piperidyl)-3,6-bis(trifluoromethyl)-9-phenanthrenemethanol (I). The principles employed in choosing counterions to render a high molecular weight hydrophobic drug more water soluble are generally applicable.

Compound I has been shown to exhibit significant activity against infections with strains of *Plasmodium falciparum* resistant to chloroquine, quinine, and pyrimethamine (2). Because of two optically active centers, it can exist as any one of four possible stereoisomers or mixtures thereof. The absolute configuration of all of the isomers has been established (3). The work reported here was done with one racemic pair, referred to as "isomer a" by Carroll and Blackwell (3). They also showed that all four enantiomers are potent antimalarials and, therefore, no attempt was made to resolve the racemic mixture.

The apparent solubility of the hydrochloride salt of I and its free base was measured in water at 25°. Compound I, being large and hydrophobic, is only sligtly soluble as the hydrochloride salt (Table I). This poor solubility was suspected to be the main reason for its poor bioavailability. In all previous work, I was administered orally as the hydrochloride

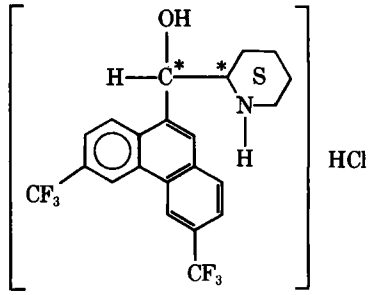

I

* = optically active centers

Table I—Apparent Solubilities and Melting Points of Salt Forms of I

Salt Form	Melting Point	Apparent Solubility[a]	pH of Saturated Solutions[a]
Hydrochloride	331°	12–15 mg/liter	5.79
Free base (I)	215°	7–8 mg/liter	
dl-Lactate	172° dec.	1.8–1.9 g/liter	3.8
l-Lactate	192–193° dec.	0.9–0.95 g/liter	
2-Hydroxyethane-1-sulfonate	250–252° dec.	0.62 g/liter	5.0
Methanesulfonate	290° dec.	0.3 g/liter	2.4
Sulfate	270° dec.	20 mg/liter	5.1
Sulfate		8 mg/liter[b]	

[a] At 25° in water. [b] At 25° in 0.1 *N* HCl.

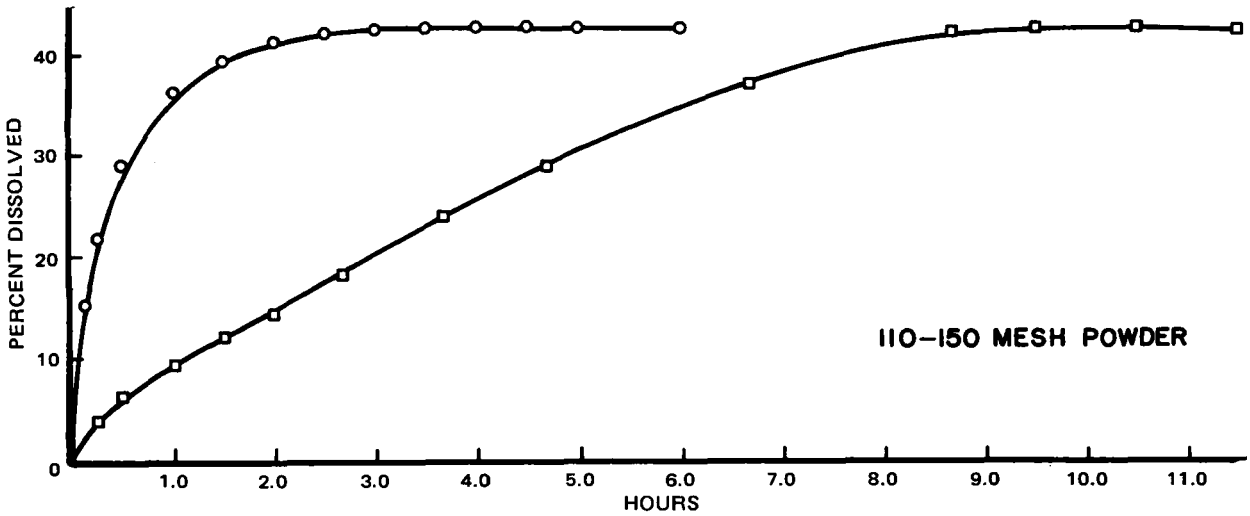

Figure 1—*Dissolution rate of hydrochloride salt of I in 0.1 N H_2SO_4 (○) and 0.1 N HCl (□) at 37°. Some of the solid was still floating on the surface after the rate of dissolution had leveled off, which may explain why the percent dissolved did not reach a value of 100.*

salt. Since stomach contents are rich in chloride ions, it is expected that the equilibrium represented by Scheme I will remain farther to the left, thus decreasing the solubility and the rate of solubilization of the hydrochloride salt of I, represented as BH^+Cl^-

$$BH^+Cl^-_{(solid)} \overset{K_{sp}}{\rightleftharpoons} (BH^+)_{aq} + (Cl^-)_{aq}$$

Scheme I

EXPERIMENTAL

The free base of I was prepared by the method of Carroll (4).

All salts were prepared by mixing a solution of I in 95% ethanol and a 50% excess of the stoichiometric amount of acid required for neutralization. The solution was stirred for about 2 hr. Excess solvent was evaporated, and the precipitated salt was filtered and recrystallized from methanol–water.

Salts were identified using IR[1], UV[2], and elemental analyses. Physicochemical properties of these salts are given in Table I. Apparent solubilities of these salts were measured by shaking excess salt at 25° in water for 3 days.

The equilibrium solutions were tested for the presence of decomposition products by TLC using silica plates. The solvent system was benzene–methanol–concentrated ammonium hydroxide (79:19:2). The freshly prepared solution and equilibrated solutions of salts of I showed a single spot (R_f 0.45) as detected by UV light and iodine vapor, thus indicating that the salt forms of I did not undergo any detectable degradation in the aqueous solutions over the equilibration period. A single spot was also observed using ethyl acetate–propyl alcohol–acetic acid–water (10:10:5:2) with an R_f of 0.68.

Aqueous concentrations were determined using a previously constructed Beer's law plot in the UV region at λ_{max} 252.5 nm. Dissolution tests were carried out on pure powder using an equivalent amount of each salt equal to 6.30 mg of I free base. A sample of 100–150-mesh powder in 500 ml of dissolution medium was used. The dissolution rate of the powder was monitored continuously at 252.5 nm using a flowcell. The USP dissolution test apparatus was employed without the basket, and the dissolution medium (Figs. 1 and 2) was maintained at 37° and stirred at 100 rpm.

RESULTS AND DISCUSSION

From Table I it can be seen that the lactate salt is approximately 200 times as soluble as the hydrochloride salt of I, the form used in the past.

Both the 2-hydroxyethane-1-sulfonate and lactate salts of I have

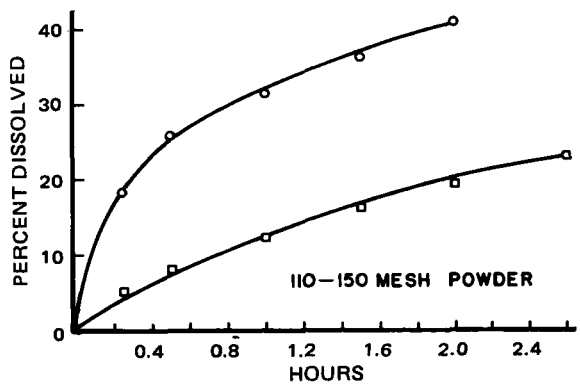

Figure 2—*Dissolution rate of the 2-hydroxyethane-1-sulfonate (○) and the hydrochloride (□) salts of I in 0.1 N HCl at 37°.*

[1] Beckman IR 33.
[2] Cary 14 or 15.

Table II—Apparent Solubility of 2-Hydroxyethane-1-sulfonate Salt of I at 25° in Commonly Used Parenteral Vehicles

Vehicle	Apparent Solubility, g/liter
20% Ethanol—20% glycerin in water	1.9
20% Propylene glycol—5% ethanol in water	0.6
10% Dextrose in water	0.75

lower melting points than the hydrochloride salt of I, suggesting that the enhanced solubility of these salts with organic anions is due in part to decreased crystal lattice energy. Also contributing to the increased solubility of these salts is the possibility of hydrogen bonding between the hydroxyl groups of the lactate and 2-hydroxyethane-1-sulfonate anions with the solvent.

The optical activity of lactic acid creates difficulties in defining the system studied due to the presence of several isomers with different physical properties. Therefore, it was decided to investigate the 2-hydroxyethane-1-sulfonate salt of I in more detail.

Since one objective of this work was to improve the aqueous solubility of I so that it could be administered parenterally, the apparent solubility of the 2-hydroxyethane-1-sulfonate salt of I in different commonly used vehicles was measured (Table II). As can be seen from Table II, the apparent solubility of I as the 2-hydroxyethane-1-sulfonate salt can be considerably increased by choice of the proper vehicle.

To provide evidence for the decrease in solubility of the hydrochloride salt of I due to the common-ion effect, it was decided to measure the apparent solubility of this salt as a function of chloride-ion concentration. When these data (Table III) were plotted as the molar concentration of the hydrochloride salt of I in solution as a function of the reciprocal of the chloride-ion concentration, a nonlinear curve was obtained. Therefore, it was not possible to calculate the solubility product constant (K_{sp}) of this salt (5).

The nonlinearity may be due to the presence of two diastereoisomers with different solubilities. Further work is required to ascertain the source of this nonlinear behavior. However, it is apparent that the solubility of the hydrochloride salt of I decreases considerably with an increase in the chloride-ion concentration.

The apparent solubility of the sulfate salt of I is slightly greater than that of the hydrochloride salt. However, in 0.1 *N* HCl, the solubility is approximately equal to that of the hydrochloride salt, probably due to the rapid conversion of the sulfate to the hydrochloride in 0.1 *N* HCl.

To substantiate the argument against the use of hydrochloride salts of amines due to the common-ion effect, dissolution rates of the hydrochloride salt of I were measured in 0.1 *N* HCl and in 0.1 *N* H_2SO_4 (Fig. 1). The study was conducted in acid solutions to avoid dissociation of the protonated base as shown in Scheme II.

The dissolution rate in 0.1 *N* H_2SO_4 is much faster than in 0.1 *N* HCl, thus supporting the hypothesis that the rate of dissolution and the solubility of the hydrochloride salt of I will be decreased by the common-ion effect in the medium rich in chloride ion.

$$(BH^+)_{aq} \rightleftharpoons B_{aq} + H^+_{aq}$$

Scheme II

Table III—Apparent Aqueous Solubility of the Hydrochloride Salt of I as a Function of Chloride-Ion Concentration at 25°

Apparent Solubility[a], moles/liter × 10^5	Total Chloride-Ion Concentration, moles/liter × 10^3
3	40.0
6.2	10.0
9.5	8.0
10.9	5.0
15.9	3.1
19.0	2.2
24.0	1.3

[a] Represents average of three measurements; range ±0.5–1%.

The dissolution rate of 2-hydroxyethane-1-sulfonate salt of I was also measured in 0.1 *N* HCl (Fig. 2). The dissolution rate of this salt is considerably greater than that of the hydrochloride salt.

The optimum oral therapeutic dose of the hydrochloride salt of I was determined to be 750 mg as a single dose (6). This high dose was probably necessary due to incomplete absorption from the GI tract. Since the organic salts of I reported in this work are considerably more soluble than the hydrochloride salt, the dose of these salts of I required to achieve the same therapeutic response as with the hydrochloride salt should be considerably reduced.

By using these newly prepared salts, it should now be possible to administer I in a parenteral dosage form for the treatment of malaria.

REFERENCES

(1) L. W. Dittert, T. Higuchi, and D. Reese, *J. Pharm. Sci.*, **53**, 1325(1964).

(2) F. Y. Wiselogle, "A Survey of Antimalarial Drugs 1941–1945," vol. II, Edwards, Ann Arbor, Mich., p. 1267.

(3) F. I. Carroll and J. T. Blackwell, *J. Med. Chem.*, **17**, 210(1974).

(4) F. I. Carroll, in IND Application Supplement No. 1 72, Walter Reed Army Institute of Research, Washington, D.C., Dec. 1970.

(5) J. N. Butler, "Ionic Equilibrium—A Mathematical Approach," Addison-Wesley, Reading, Mass., 1964, p. 37.

(6) C. J. Canfield, in IND Application Supplement No. 4, Section L, Walter Reed Army Institute of Research, Washington, D.C., Dec. 1972, p. 98.

ACKNOWLEDGMENTS AND ADDRESSES

Received January 8, 1975, from the *Department of Pharmaceutical Chemistry, McCollum Laboratories, University of Kansas, Lawrence, KS 66044*

Accepted for publication July 28, 1975.

Supported in part by a grant from the Department of the Army, U.S. Army Medical Research Development Command.

This paper is Contribution No. 1324 to the Army Research Program on Malaria, Contract DADA17-73-C-3125.

[x] To whom inquiries should be directed.

Errors Involved in Instantaneous Intravascular Input Assumptions

SARFARAZ NIAZI

Abstract □ A comparative evaluation of a zero-order input and the generally accepted instantaneous intravascular input assumption is made for two- and three-compartment open model systems. Equations are derived and a nomogram is prepared to calculate the magnitude of error involved in instantaneous input assumptions. It is suggested that all intravascular administrations be considered as zero-order inputs.

Keyphrases □ Pharmacokinetic models—errors in instantaneous intravascular input assumptions, two- and three-compartment open models □ Disposition, drug—pharmacokinetic models, errors in instantaneous intravascular input assumptions, two- and three-compartment open models

Pharmacokinetic modeling of drug disposition frequently has been used to characterize dosage regimens, toxicity profiles, and pharmacological responses (1–5). The pharmacokinetic parameters such as various compartment volume terms and the rate constants describing the intercompartmental transfer and elimination from the body often have been appropriately determined by quickly administering an intravascular dose and assuming that all of the drug is present in the central compartment when the kinetic processes of distribution and elimination begin (2).

Although the assumption of instantaneous intravascular administration simplifies the model, a detailed description of the model, including the kinetic processes during the period of administration, would eliminate possible errors due to this assumption. Also, this model can be used in instances where a prolonged administration is necessary to build up analyzable concentrations in the blood. The purposes of this paper are to evaluate comparatively the pharmacokinetic models with zero-order and instantaneous input and to offer a critique on the magnitude of error involved in the instantaneous intravascular input assumption.

THEORY

The disposition kinetics of many drugs can be more appropriately described in terms of multicompartment models than by assuming the body to be a single compartment (4) as depicted in Schemes I and II for the most commonly encountered two- and three-compartment open models. The kinetics of these models were analyzed assuming instantaneous input (6).

The time course of drug disposition following zero-order infusion in a two-compartment open model (Scheme I) was reported (2, 6):

$$\frac{x_1}{k_0} = \frac{(k_{21} - b_1)(1 - e^{-b_1\theta})}{b_1(b_2 - b_1)} e^{-b_1 t'} - \frac{(k_{21} - b_2)(1 - e^{-b_2\theta})}{b_2(b_2 - b_1)} e^{-b_2 t'} \quad \text{(Eq. 1)}$$

$$\frac{x_2}{k_0} = \frac{k_{12}(1 - e^{-b_1\theta})}{b_1(b_2 - b_1)} e^{-b_1 t'} - \frac{k_{12}(1 - e^{-b_2\theta})}{b_2(b_2 - b_1)} e^{-b_2 t'} \quad \text{(Eq. 2)}$$

where:

x_1, x_2 = amounts in the central and tissue compartments, respectively
b_1, b_2 = hybrid rate constants
k_0 = zero-order infusion rate
θ = duration of infusion
$t' = (t - \theta)$, time following infusion

A three-compartment open model with zero-order input is shown in Scheme II. A kinetic description of this model is:

$$\frac{dx_1}{dt} = k_0 + k_{21}x_2 + k_{31}x_3 - k_{12}x_1 - k_{13}x_1 - k_{el}e_1 \quad \text{(Eq. 3)}$$

$$\frac{dx_1}{dt} = k_0 + k_{21}x_2 + k_{31}x_3 - k_1x_1 \quad \text{(Eq. 4)}$$

$$\frac{dx_2}{dt} = k_{12}x_1 - k_{21}x_2 \quad \text{(Eq. 5)}$$

$$\frac{dx_3}{dt} = k_{13}x_1 - k_{31}x_3 \quad \text{(Eq. 6)}$$

with the conditions $x_1 = x_2 = x_3 = 0$ at $t = 0$. By using Laplace transforms, one can write:

$$(S + k_1)X_1 - k_{21}X_2 - k_{31}X_3 = k_0/S \quad \text{(Eq. 7)}$$

$$-k_{12}X_1 + (S + k_{21})X_2 = 0 \quad \text{(Eq. 8)}$$

$$-k_{13}X_1 + (S + k_{31})X_3 = 0 \quad \text{(Eq. 9)}$$

where X_1, X_2, and X_3 are Laplace transforms of x_1, x_2, and x_3, respectively.

When no complex roots are assumed:

$$\Delta = S(S + b_1)(S + b_2)(S + b_3) \quad \text{(Eq. 10)}$$

$$\Delta_{1,1} = k_0(S + k_{21})(S + k_{31}) \quad \text{(Eq. 11)}$$

$$\Delta_{1,2} = -k_0k_{12}(S + k_{31}) \quad \text{(Eq. 12)}$$

$$\Delta_{1,3} = k_0k_{13}(S + k_{21}) \quad \text{(Eq. 13)}$$

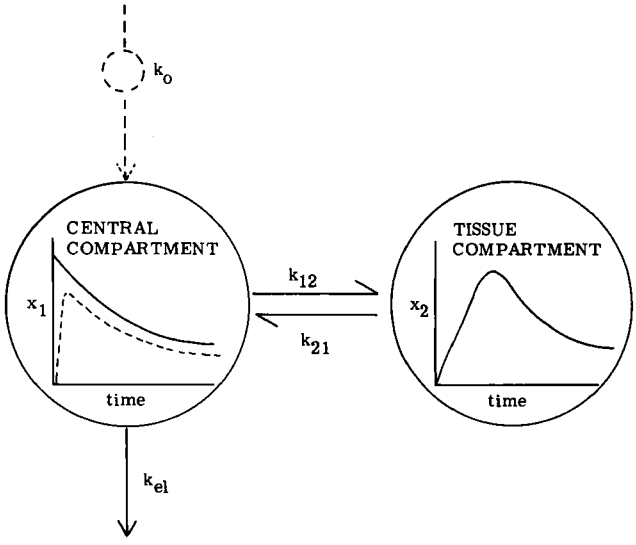

Scheme I—Two-compartment open model with instantaneous or zero-order input

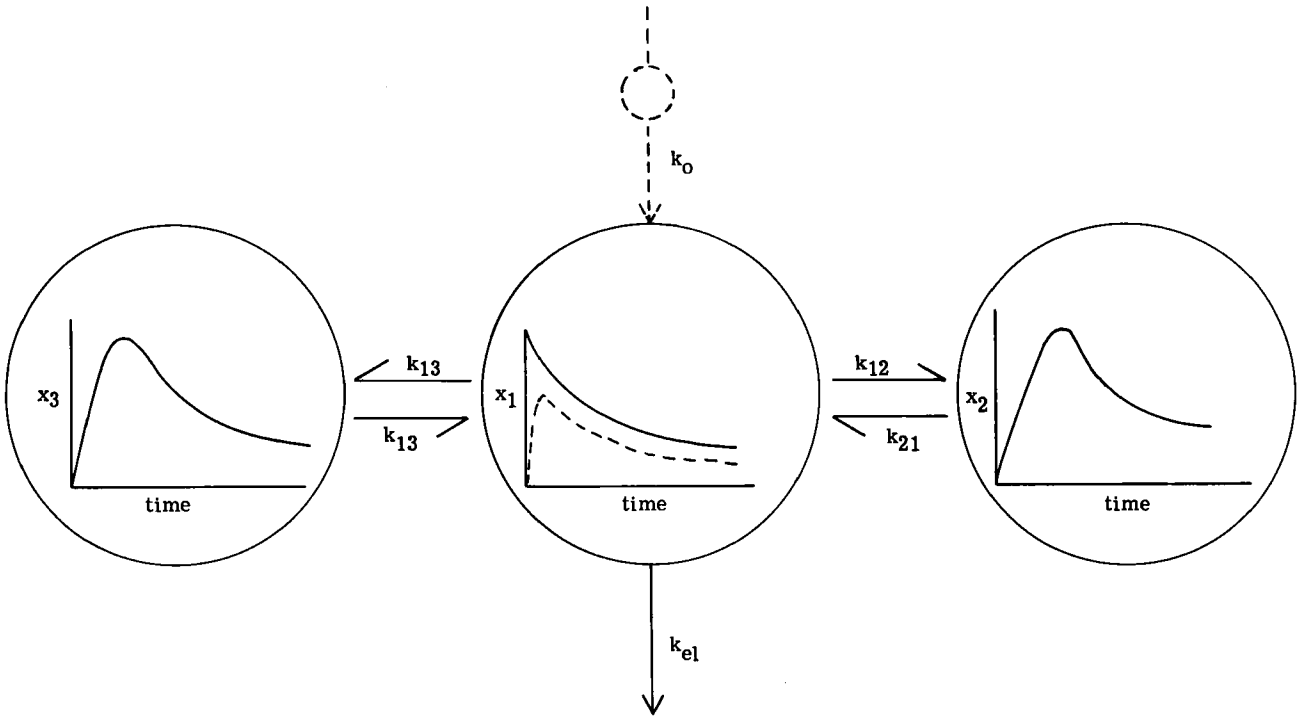

Scheme II—Three-compartment open model with instantaneous or zero-order input

and by Cramer's rule:

$$\frac{X_1}{k_0} = \frac{\Delta_{1,1}}{\Delta} = \frac{(-1)^2(S + k_{21})(S + k_{31})}{S(S + b_1)(S + b_2)(S + b_3)} \quad \text{(Eq. 14)}$$

$$\frac{X_2}{k_0} = \frac{\Delta_{1,2}}{\Delta} = -\frac{(-1)^3 k_{12}(S + k_{31})}{S(S + b_1)(S + b_2)(S + b_3)} \quad \text{(Eq. 15)}$$

$$\frac{X_3}{k_0} = \frac{\Delta_{1,3}}{\Delta} = \frac{(-1)^4 k_{13}(S + k_{21})}{S(S + b_1)(S + b_2)(S + b_3)} \quad \text{(Eq. 16)}$$

with the following solutions:

$$\frac{x_1}{k_0} = \frac{k_{21}k_{31}}{b_1b_2b_3} - \frac{(k_{21} - b_1)(k_{31} - b_1)}{b_1(b_2 - b_1)(b_3 - b_1)}e^{-b_1t} - \frac{(k_{21} - b_2)(k_{31} - b_2)}{b_2(b_1 - b_2)(b_3 - b_2)}e^{-b_2t} - \frac{(k_{21} - b_3)(k_{31} - b_3)}{b_3(b_1 - b_3)(b_2 - b_3)}e^{-b_3t} \quad \text{(Eq. 17)}$$

$$\frac{x_2}{k_0} = \frac{k_{31}k_{12}}{b_1b_2b_3} - \frac{k_{12}(k_{31} - b_1)}{b_1(b_2 - b_1)(b_3 - b_1)}e^{-b_1t} - \frac{k_{12}(k_{31} - b_2)}{b_2(b_1 - b_2)(b_3 - b_2)}e^{-b_2t} - \frac{k_{12}(k_{31} - b_3)}{b_3(b_1 - b_3)(b_2 - b_3)}e^{-b_3t} \quad \text{(Eq. 18)}$$

$$\frac{x_3}{k_0} = \frac{k_{21}k_{13}}{b_1b_2b_3} - \frac{k_{13}(k_{21} - b_1)}{b_1(b_2 - b_1)(b_3 - b_1)}e^{-b_1t} - \frac{k_{13}(k_{21} - b_2)}{b_2(b_1 - b_2)(b_3 - b_2)}e^{-b_2t} - \frac{k_{13}(k_{21} - b_3)}{b_3(b_1 - b_3)(b_2 - b_3)}e^{-b_3t} \quad \text{(Eq. 19)}$$

These equations describe the time course of drug disposition during the infusion period. If the infusion is abruptly ceased following time $t = \theta$, the input function corresponds to a rectangular pulse of length equal to θ. The Laplace transform for such an input is (7):

$$f(S) = \frac{k_0}{S}(1 - e^{-\theta S}) \quad \text{(Eq. 20)}$$

and since:

$$f(S)e^{-\theta S} = f(t - \theta) \quad \text{(Eq. 21)}$$

the functions described in Eqs. 17–19, minus their displaced counterparts by $t' = t - \theta$, describe the time course of drug disposition following the zero-order infusion period:

$$\frac{x_1}{k_0} = \frac{(k_{21} - b_1)(k_{31} - b_1)(1 - e^{-b_1\theta})}{b_1(b_2 - b_1)(b_3 - b_1)}e^{-b_1t'} + \frac{(k_{21} - b_2)(k_{31} - b_2)(1 - e^{-b_2\theta})}{b_2(b_1 - b_2)(b_3 - b_2)}e^{-b_2t'} + \frac{(k_{21} - b_3)(k_{31} - b_3)(1 - e^{-b_3\theta})}{b_3(b_2 - b_3)(b_1 - b_3)}e^{-b_3t'} \quad \text{(Eq. 22)}$$

$$\frac{x_2}{k_0} = \frac{k_{12}(k_{31} - b_1)(1 - e^{-b_1\theta})}{b_1(b_2 - b_1)(b_3 - b_1)}e^{-b_1t'} + \frac{k_{13}(k_{31} - b_2)(1 - e^{-b_2\theta})}{b_2(b_1 - b_2)(b_3 - b_2)}e^{-b_2t'} + \frac{k_{12}(k_{31} - b_3)(1 - e^{-b_3\theta})}{b_3(b_1 - b_3)(b_2 - b_3)}e^{-b_3t'} \quad \text{(Eq. 23)}$$

$$\frac{x_3}{k_0} = \frac{k_{13}(k_{21} - b_1)(1 - e^{-b_1\theta})}{b_1(b_2 - b_1)(b_3 - b_1)}e^{-b_1t'} + \frac{k_{13}(k_{21} - b_2)(1 - e^{-b_2\theta})}{b_2(b_1 - b_2)(b_3 - b_2)}e^{-b_2t'} + \frac{k_{13}(k_{21} - b_3)(1 - e^{-b_3\theta})}{b_3(b_1 - b_3)(b_2 - b_3)}e^{-b_3t'} \quad \text{(Eq. 24)}$$

DISCUSSION

The two-compartment open model was analyzed previously (8–10) incorporating zero-order input. In this paper, the main concerns are the error involved in instantaneous input assumptions in both two-and three-compartment open models and how these errors can be corrected following intravascular drug administration.

The equations presented describing the time course of drug disposition following the administration period can be modified to express the fraction of the administered dose remaining in the central compartment.

For the two-compartment model:

$$\frac{x_1}{k_0\theta} = \frac{(k_{21} - b_1)(1 - e^{-b_1\theta})}{b_1(b_2 - b_1)\theta}e^{-b_1t'} + \frac{(b_2 - k_{21})(1 - e^{-b_2\theta})}{b_2(b_2 - b_1)\theta}e^{-b_2t'} \quad \text{(Eq. 25)}$$

For the three-compartment model:

$$\frac{x_1}{k_0\theta} = \frac{(k_{21} - b_1)(k_{31} - b_1)(1 - e^{-b_1\theta})}{b_1(b_2 - b_1)(b_3 - b_1)\theta}e^{-b_1t'} + \frac{(k_{21} - b_2)(k_{31} - b_2)(1 - e^{-b_2\theta})}{b_2(b_1 - b_2)(b_3 - b_2)\theta}e^{-b_2t'} + \frac{(k_{21} - b_3)(k_{31} - b_3)(1 - e^{-b_3\theta})}{b_3(b_2 - b_3)(b_1 - b_3)\theta}e^{-b_3t'} \quad \text{(Eq. 26)}$$

since:

$$k_0\theta = \text{dose administered} \quad \text{(Eq. 27)}$$

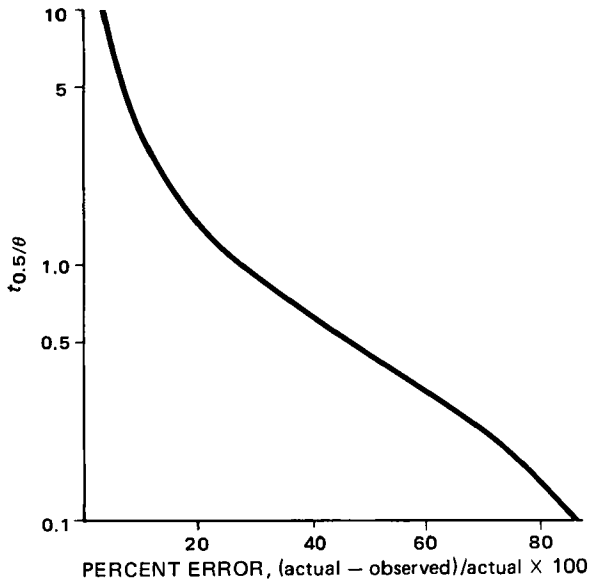

Figure 1—*Percent error involved in the intercept value, assuming instantaneous input at various* $t_{0.5/\theta}$ *ratios.*

A similar treatment of Eqs. 2, 18, and 19 gives the fraction of the administered dose remaining in the tissue compartments. Equations 25 and 26 also represent the ratio of concentration in the central compartment and the concentration at zero time if the total dose is instantaneously administered:

$$\frac{x_1}{k_0\theta} = \frac{c_1 v_1}{c_0 v_1} \qquad \text{(Eq. 28)}$$

where c_1 and c_0 are concentrations in the central compartment, and v_1 is its volume. These equations can be further simplified:

$$\frac{c_1}{c_0} = A_{21}\frac{(1-e^{-b_1\theta})}{b_1\theta}e^{-b_1t'} + A_{22}\frac{(1-e^{-b_2\theta})}{b_2\theta}e^{-b_2t'} \qquad \text{(Eq. 29)}$$

$$\frac{c_1}{c_0} = A_{31}\frac{(1-e^{-b_1\theta})}{b_1\theta}e^{-b_1t'} + A_{32}\frac{(1-e^{-b_2\theta})}{b_2\theta}e^{-b_2t'} + \frac{A_{33}(1-e^{-b_3\theta})}{b_3\theta}e^{-b_3t'} \qquad \text{(Eq. 30)}$$

such that (6) for the two-compartment model:

$$A_{21} + A_{22} = 1 \qquad \text{(Eq. 31)}$$

and for the three-compartment model:

$$A_{31} + A_{32} + A_{33} = 1 \qquad \text{(Eq. 32)}$$

In a model where an instantaneous input assumption is made, it is assumed that:

$$\frac{1 - e^{-b_i\theta}}{b_i\theta} = 1 \qquad \text{(Eq. 33)}$$

where i refers to the disposition phase. This factor is in each term of Eqs. 29 and 30. However, since this fraction (Eq. 33) is always less than 1, c_0 would invariably be underestimated if an instantaneous input is assumed without correcting the intercepts on the concentration–time plot. A reciprocal of Eq. 33 multiplied to the experimental intercept would correct this error. Figure 1 shows the percent error involved as a function of the disposition phase half-life and administration period ratio. A total error can be calculated easily by adding the errors involved in each disposition phase:

$$\text{total error, \%} = 100\sum_{i=1}^{n}\frac{\theta b_i - 1 + e^{-b_i\theta}}{\theta b_i} \qquad \text{(Eq. 34)}$$

For example, a detailed pharmacokinetic analysis of fluorocarbon aerosol propellants (11) showed that the blood concentration profile of dichlorodifluoromethane can be given by:

$$c_1 = 2379.6e^{-0.49499t} + 362.9e^{-0.08941t} + 18.2e^{-0.01026t} \qquad \text{(Eq. 35)}$$

following the administration of the fluorocarbon over 3 min. The cumulated error involved, from Fig. 1, is 62% if proper corrections are not made in the calculations. Therefore, the corrected equation should read:

$$c_1 = 4568.4e^{-0.49499t} + 413.7e^{-0.08941t} + 18.5e^{-0.01026t} \qquad \text{(Eq. 36)}$$

It is obvious that an instantaneous input assumption will always result in an error which can be easily corrected if the data are treated considering the intravascular administration as a zero-order input (Schemes I and II). Such modification is necessary to make the pharmacokinetic model more realistic, since there is no provision of a lag time in a continuous kinetic model.

These models also can be used for drugs that are too poorly soluble or too irritating to be administered by rapid intravenous injection and should be administered slowly over a long period. It is not necessary to achieve an equilibrium for the analysis of pharmacokinetic parameters as was suggested previously (8).

REFERENCES

(1) A. G. Goldstein, L. Aronow, and S. M. Kalman, "Principles of Drug Action," Wiley, New York, N.Y., 1974.

(2) J. G. Wagner, "Biopharmaceutics and Relevant Pharmacokinetics," 1st ed., Drug Intelligence Publications, Hamilton, Ill., 1971.

(3) G. Levy, *Clin. Pharmacol. Ther.*, **7**, 362(1966).

(4) S. Riegelman, J. Loo, and M. Rowland, *J. Pharm. Sci.*, **57**, 117(1968).

(5) L. W. Dittert, *Drug Intel. Clin. Pharm.*, **8**, 222(1974).

(6) A. Rescigno and G. Segre, "Drug and Tracer Kinetics," 1st ed., Blaisdell, New York, N.Y., 1966.

(7) P. A. McCollum and B. F. Brown, "Laplace Transform Tables and Theorems," Holt, Reinhart & Winston, Chicago, Ill., 1965.

(8) M. Gibaldi, *J. Pharm. Sci.*, **58**, 1133(1969).

(9) *Ibid.*, **58**, 327(1969).

(10) J. C. K. Loo and S. Riegelman, *J. Pharm. Sci.*, **59**, 53(1970).

(11) S. Niazi, Ph.D. dissertation, University of Illinois at the Medical Center, Chicago, Ill., 1974.

ACKNOWLEDGMENTS AND ADDRESSES

Received March 31, 1975, from the *Department of Pharmacy, College of Pharmacy, University of Illinois at the Medical Center, Chicago, IL 60612*

Accepted for publication July 9, 1975.

Correlations between Substituent Parameters of 4-Substituted Benzoic Acids and Their *In Vitro* Dissolution and Partitioning

J. H. COLLETT ˣ and L. KOO

Abstract □ The *in vitro* dissolution and partitioning of some 4-substituted benzoic acids from nondisintegrating disks was investigated using a water–octanol system. The rates of appearance of benzoic acids in the aqueous phase differed from the rates of appearance in octanol, probably due to back-transfer from the octanol phase. The suitability of the procedure for investigating the influence of molecular modification on *in vitro* dissolution and partitioning is considered. Correlations among the rates of appearance in octanol, the rates of appearance in an aqueous phase, and substituent parameters of benzoic acids were investigated. The best statistical fit was obtained using molecular orbital substituent indexes.

Keyphrases □ Benzoic acids, 4-substituted—*in vitro* dissolution and partitioning from nondisintegrating disks □ Dissolution—4-substituted benzoic acids, nondisintegrating disks, *in vitro* □ Partitioning—4-substituted benzoic acids, nondisintegrating disks, *in vitro* □ Structure–activity relationships—4-substituted benzoic acids, *in vitro* dissolution and partitioning from nondisintegrating disks

There has been considerable interest in the development of techniques capable of simulating drug absorption processes from solid dosage forms. Absorption processes involve dissolution of the drug followed by partitioning of the dissolved drug into a lipid membrane. However, these processes generally have been considered independently as dissolution (1, 2) and as partitioning systems (3). A single procedure combining the two systems was reported for simulation of the overall absorption process (4). The report was confined to the dissolution and partitioning of one drug.

In this work, the dissolution and partitioning of some substituted benzoic acids were measured. Relationships between the rates of appearance in aqueous and octanol phases and substituent parameters (5) of the compounds were investigated. Such relationships would be useful for the assessment of the effects of molecular modification on *in vitro* availability of drugs as measured by partitioning rates.

Previous correlations between structure and biological activity were limited to studies in which drugs were administered in solution. Results from these *in vitro* correlations may indicate the feasibility of assessing effects of molecular modification on biological activity following administration of solid dosage forms.

EXPERIMENTAL

Materials—Nondisintegrating disks of benzoic acid[1] and its 4-hydroxy, chloro, bromo, iodo, nitro, and methoxy[2] derivatives were prepared in a hydraulic press[3]. The compression pressure was 300 kg/m^2. Laboratory grade 1-octanol[2], which did not interfere with spectrophotometric assays, was used as the organic solvent; 200-ml volumes of 0.1 *N* HCl were used as the dissolution medium.

Apparatus—A modified rotating disk-type apparatus was used. The dissolution cell was described previously (6). The stirrer shaft was modified to take account of the two-phase system. A machined titanium disk holder was fitted into the base of the stirrer shaft so that a constant surface of disk was exposed to the dissolution medium.

Three propeller blades were attached to the shaft 1.5 cm above the upper edge of the disk holder. When octanol was in the cell, the lower edge of each blade was 2.3 cm above the octanol–aqueous phase boundary. The stirrer shaft was driven by an 80-rpm asynchronous motor[4].

Procedure—Octanol was presaturated with 0.1 *N* HCl; 0.1 *N* HCl was presaturated with octanol for 24 hr at 25 ± 0.1° prior to use.

A disk was fitted into the disk holder. Then 200 ml of 0.1 *N* HCl solution was placed in the dissolution cell, and the unit was assembled but not stirred. An equal volume of octanol was superimposed on the aqueous phase. After the stirrer motor was started, samples of octanol were removed at appropriate time intervals and assayed spectrophotometrically[5]. An equal volume of octanol was added to the cell after sampling.

A flow-through procedure was used to sample the aqueous medium. The solution was pumped by way of 1-mm diameter polyethylene tubing into a 0.1- or 1.0-cm path length flowcell in a spectrophotometer[6]. The flow rate of the solution was 7 ml/min. At any one time, less than 2 ml of the aqueous solution was out of the bulk solution.

RESULTS AND DISCUSSION

The rates of appearance of the benzoic acids in the aqueous phase were obtained from slopes of the concentration of drug dissolved in the aqueous phase as a function of time. Rates of appearance followed zero-order kinetics for at least the first 30 min prior to the attainment of a steady-state concentration in the aqueous phase. Rates of appearance in the octanol phase were obtained from slopes of the drug concentration in octanol against time. After an initial lag period, the rate of appearance in the octanol phase also could be described by zero-order kinetics.

A typical plot of the drug concentration in the aqueous and organic phases as a function of time is shown in Fig. 1. Rate constants for appearance of each compound in the aqueous and octanol layers are given in Table I. Included in the same table are rate constants for dissolution into an aqueous phase alone. The dissolution rate of drug into 0.1 *N* HCl and its appearance in the organic solvent phase were not equivalent as reported previously (2). However, according to Niebergall *et al.* (7), the results for benzoic acid into cyclohexane–octanol were a specific example of a general case.

The rate constant for the appearance in octanol of compounds other than benzoic acid and 4-hydroxybenzoic acid are similar to those for dissolution into an aqueous phase alone. This discrepancy can be accounted for. Khalil and Martin (3) reported that a lipid phase need not act as a perfect sink, and back-transfer of the drug from the lipid to aqueous phase can occur. Consequently, the appearance in octanol would be less than expected if back-transfer did not occur. Such a situation does not detract from using this system for assessment of the effects of structural changes in a molecule on its dissolution and partitioning. It does emphasize the

[1] Fisons A. R.
[2] Laboratory reagent, British Drug Houses Ltd.
[3] Apex type A14.
[4] Crouzet Ltd., France.
[5] Unicam SP 500.
[6] Cecil type CE202.

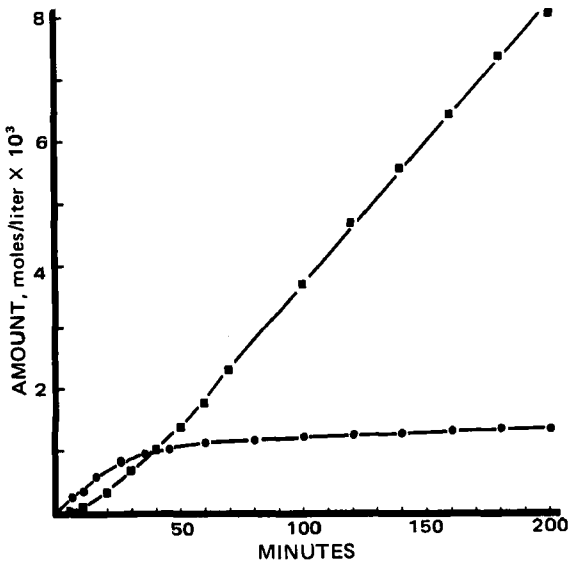

Figure 1—*Amounts of 4-hydroxybenzoic acid in 0.1* N *HCl* (●) *and octanol* (■) *as a function of time.*

need for care in the choice of an organic solvent as a model lipid layer.

Octanol has been used successfully as a reference solvent in studies correlating structure with biological activity (5). Substituent parameters used in quantitative structure–activity studies include π (where $\pi = \log P_x - \log P_H$; P_H is the partition coefficient of a parent compound, and P_x is that of a derivative); σ, the Hammett constant; and molecular orbital substituent indexes (8). Values of substituent indexes are given in Table II.

The relationship between the rate constant for appearance (k_p) in octanol and π is:

	n	r	s	F	
$\log k_p = -1.70(\pm 0.36)\pi - 5.17$	7	0.905	0.505	22.6	(Eq. 1)

when using a combination of σ and π, one obtains:

	n	r	s	F	
$\log k_p = -1.56(\pm 0.20)\pi - 0.63(\pm 0.05)\sigma - 5.15$	7	0.929	0.491	12.6	(Eq. 2)

Recently, Cammarata and Rogers (8) correlated π values for benzoic acids with appropriate electronic indexes. Excluding the values for nitro and iodobenzoic acids, the following equation relates the appearance in octanol to molecular orbital substituent indexes:

	n	r	s	F	
$\log k_p = 1.53(\pm 0.06)\ \Sigma_r' \lvert Q_r^T \rvert - 0.90(\pm 0.09)\ \Sigma_r' S_r^E - 3.99$	5	0.992	0.199	66.9	(Eq. 3)

There is only a slight improvement in correlation by inclusion of π and σ in the same relationship. The best fit is seen when molecular orbital substituent indexes are used. These indexes are specific for the substituent groups of benzoic acid, and this specificity may account for the improved fit over that seen with the more general π. The correlation of the partition rate with electronic indexes indicates that the change in the solvation shell around the substituent controls partitioning from a polar to nonpolar environment.

Correlations between rates of appearance (k_0) into the aqueous phase beneath octanol with the same substituent parameters lead to the following equations:

	n	r	s	F	
$\log k_0 = -1.74(\pm 0.36)\pi - 5.48$	7	0.910	0.503	24.1	(Eq. 4)
$\log k_0 = -1.60(\pm 0.20)\pi - 0.67(\pm 0.06)\sigma - 5.47$	7	0.935	0.479	14.0	(Eq. 5)
$\log k_0 = 1.69(\pm 0.07)\Sigma_r' \lvert Q_r^T \rvert - 0.92(\pm 0.09)\Sigma_r' S_r^E - 4.34$	5	0.992	0.199	66.9	(Eq. 6)

Table I—Rate Constants[a] for the Appearance of 4-Substituted Benzoic Acids in 0.1 *N* HCl and Octanol

Substituent	$k_0 \times 10^4$, moles/min/liter	$k_w \times 10^4$, moles/min/liter	$k_p \times 10^4$, moles/min/liter
H	13.67	38.10	30.66
OH	25.97	61.90	45.58
Cl	0.14	0.40	0.38
Br	0.06	0.15	0.16
I	0.03	0.06	0.06
NO_2	0.60	1.30	1.27
CH_3O	0.80	1.75	1.74

[a] k_0 is a zero-order rate constant for appearance in 0.1 *N* HCl layered with octanol; k_w is a zero-order dissolution rate constant into 0.1 *N* HCl; and k_p is a zero-order rate constant for appearance in octanol.

Table II—Substituent Parameters for 4-Substituted Benzoic Acids

Substituent	π[a]	σ[a]	$\Sigma' S^E$[b]	$\Sigma' \lvert Q^T \rvert$[b]
H	0	0	0.857	0.121
OH	−0.30	−0.37	1.870	0.945
Cl	0.87	0.23	2.863	0.081
Br	0.98	0.23	3.083	0.100
I	1.14	0.18	—	—
NO_2	0.02	0.78	—	—
CH_3O	0.08	−0.26	3.148	0.566

[a] From Ref. 5. [b] From Ref. 8.

The regression coefficients in each series are similar to those for (k_p), an indication of a rate-limiting process. Again, the best fit is obtained with electronic indexes. However, this is hardly surprising since these indexes are essentially a representation of solvation energy, which is a controlling factor in dissolution. The interrelationship between dissolution and π can be accounted for in the following manner. Hansch *et al.* (9) related the solubility of an organic liquid in water (S) to its partition coefficient between octanol and water (P) as:

$$\log \frac{1}{S} = a \log P + b \qquad \text{(Eq. 7)}$$

The dissolution rate of drug, k_{diss}, from a disk of fixed area under sink conditions may be expressed as:

$$k_{diss} = k' S_{sat} \qquad \text{(Eq. 8)}$$

where S_{sat} is the saturation solubility, and k' is a first-order rate constant. In saturated solutions with low solubility:

$$\log \frac{k'}{k_{diss}} = a \log P + b \qquad \text{(Eq. 9)}$$

i.e., the dissolution rate is related to the partition coefficient and π. While correlations between dissolution and partitioning and substituent parameters have been found, inferences regarding the effects of molecular modification on *in vivo* absorption cannot be made from these relationships. Nonetheless, the dissolution and partitioning system can be used as a screen for the effects of molecular modification on *in vitro* availability. Correlations with *in vivo* data may be possible when biological data are obtained following the administration of congeneric series of drugs as solid dosage forms.

REFERENCES

(1) D. E. Wurster and G. P. Polli, *J. Pharm. Sci.*, **53**, 311(1964).

(2) M. Gibaldi and S. Feldman, *ibid.*, **56**, 1238(1967).

(3) S. A. Khalil and A. N. Martin, *ibid.*, **56**, 1225(1967).

(4) P. J. Niebergall, M. Y. Patil, and E. T. Sugita, *ibid.*, **56**, 943(1967).

(5) C. Hansch and T. Fujita, *J. Amer. Chem. Soc.*, **86**, 1616(1964).

(6) J. H. Collett, J. A. Rees, and N. A. Dickinson, *J. Pharm. Pharmacol.*, **24**, 724(1972).

(7) P. J. Niebergall, E. T. Sugita, and R. L. Schnaare, *J. Pharm. Sci.*, **60**, 1575(1971).

(8) A. Cammarata and K. S. Rogers, *J. Med. Chem.*, **14**, 269(1971).

(9) C. Hansch, J. E. Quinlan, and G. L. Lawrence, *J. Org. Chem.*, **33**, 347(1968).

ACKNOWLEDGMENTS AND ADDRESSES

Received March 26, 1975, from the *Department of Pharmacy, University of Manchester, Manchester, United Kingdom.*

Accepted for publication July 10, 1975.

[x] To whom inquiries should be directed.

Sinoacutine from *Glaucium contortuplicatum* Boiss.

M. TIN-WA [*], N. R. FARNSWORTH [*x], and K. A. ZIRVI [‡]

Abstract □ A phytochemical investigation of *Glaucium contortuplicatum* Boiss. (Papaveraceae) resulted in the isolation of sinoacutine from this plant for the first time. Spectral evidence for the identity of the isolated compound as sinoacutine is presented.

Keyphrases □ *Glaucium contortuplicatum*—phytochemical investigation, whole plant extract, sinoacutine isolated □ Sinoacutine—isolated from whole plant extract of *Glaucium contortuplicatum* □ Alkaloids—sinoacutine isolated from whole plant extract of *Glaucium contortuplicatum*

A literature survey revealed that no chemical work had been reported on the title plant. A phytochemical investigation was initiated, and the isolation of dicentrine nitrate was reported (1).

The isolation and identification of sinoacutine from this plant are now reported. Sinoacutine was first isolated from the Chinese drug "Ching-fengteng," *Sinomenium acutum* Redh *et* Wils. (Menispermaceae) (2), and later from *Cassytha pubescens* R. Br. (Lauraceae) (3), *Croton flavens* L. (Euphorbiaceae) (4), *Corydalis pallida* var. *tenuis* (Fumariaceae) (5), and *Cocculus carolinus* D.C. (Menispermaceae) (6).

This is the first reported occurrence of sinoacutine in *Glaucium contortuplicatum*. Recently, it was reported to be present in *G. flavum* (7). Sinoacutine had been synthesized (8) and found to elicit mild antitussive properties (9).

EXPERIMENTAL[1]

A quantity (20 kg) of the air-dried and powdered whole plant was extracted with hot petroleum ether (bp 30–60°) for 36 hr and then with hot methanol for 72 hr. The alcoholic extract, after charcoal treatment and concentration, gave a large amount of inorganic nitrates and an alkaloid, dicentrine nitrate (1), which were removed by filtration. After trituration of the filtrate with acetone to remove sugars, the acetone-soluble portion was evaporated to dryness *in vacuo*, dissolved in water, made basic with ammonium hydroxide to pH 9, and extracted with chloroform. The chloroform extract was washed with water, dried over anhydrous sodium sulfate, and chromatographed over a column containing neutral aluminum oxide S.

Elution with benzene and treatment of the dried residue with acetone yielded colorless prisms of sinoacutine (150 mg), mp 194–197° dec. [lit. (4) mp 197–199°]; $[\alpha]_D^{26.5}$ −117.64° (c 0.81, ethanol) [lit. (4, 6) $[\alpha]_D^{23}$ −115.0° (c 1.03, ethanol), $[\alpha]_D^{28}$ −115.8° (c 1.0, ethanol)]; UV: λ_{max} (methanol) 214 (log ϵ 4.22), 240 (4.21), and 280 (3.72) nm [lit. (6) UV: λ_{max} (ethanol) 214 (log ϵ 4.40), 245 (4.30), and 280 (3.80) nm]. Major absorptions in the IR spectrum were at ν_{max} (KBr) 3450 (broad OH stretch), 1670, 1640, and 1610 cm^{-1} (cyclohexadienone system).

The NMR spectrum in deuterochloroform showed a three-proton singlet at δ 2.45 (NCH_3), two three-proton singlets at δ 3.73 and 3.84 (2-OCH_3), two one-proton singlets at δ 6.36 and 7.56 (two olefinic protons), and two barely resolved proton peaks at δ 6.70 and 6.75 (two aromatic protons), which were in close agreement with the literature values (6, 10). In addition, the four methylene bridge protons were located as two triplets centered at δ 1.16 and 3.66 as determined by irradiation.

Deuterium exchange experiments permitted the assignment of a broad peak centered at δ 6.2 to the phenolic proton. The remaining one methine and one methylene protons appeared between δ 2.0 and 3.4 but were complex and somewhat obscured by the NCH_3 signal; no further attempt was made to assign these protons. The mass spectrum gave a molecular ion at *m/e* 327, which was also the base peak, followed by other significant peaks at *m/e* 312 ($M^+ - CH_3$, 40%), 299 ($M^+ - CO$, 22%), and 284 ($M^+ - CO—CH_3$, 55%). The fragmentation pattern is similar to that of salutaridine (11), the enantiomer of sinoacutine.

The isolate was compared with a reference sample of sinoacutine[2] and was found identical in all respects (IR, UV, mass spectrometric, TLC, melting point, and R_f data), and a mixed melting point was not depressed.

[1] The plant material was collected near Shiraz, Iran, in April 1971 and was identified as *Glaucium contortuplicatum* Boiss. (Papaveraceae) by M. H. Bokhari, Department of Biology, Pahlavi University. A voucher specimen (DPH-G2740) representing the collection was deposited in the Department of Pharmacology Herbarium, Pahlavi University, Shiraz, Iran.

UV spectra were taken using a Beckman model D-G grating spectrophotometer. IR spectra were taken using a Beckman model IR 18 A spectrophotometer. Mass spectra were determined using a single-focusing Hitachi Perkin-Elmer model RMU-6D mass spectrometer, operating at 70 ev. NMR spectra were taken using a Varian T-60 instrument operating at 60 MHz. Optical rotations were recorded using a Carl Zeiss optical polarimeter. The melting-point and mixed melting-point determinations were made using a Kofler hot-stage melting-point apparatus.

REFERENCES

(1) K. A. Zirvi and P. H. Jones, *Pahlavi Med. J.*, **5**, 668(1974).

(2) J. S. Hsu, S. Y. Lo, and J. H. Chu, *Sci. Sinica*, **13**, 2016(1964).

(3) S. R. Johns, J. A. Lamberton, and A. A. Sioumis, *Aust. J. Chem.*, **19**, 2331(1966).

(4) K. L. Stuart, C. Chambers, and D. Byfield, *J. Chem. Soc. C*, **1969**, 1681.

(5) T. Kametani, M. Ihara, and T. Hondo, *ibid.*, **1970**, 1060.

(6) D. J. Slatkin, N. J. Doorenbos, J. E. Knapp, and P. L. Schiff, Jr., *J. Pharm. Sci.*, **61**, 1825(1972).

(7) L. D. Yakhontova, V. I. Sheichenko, and O. N. Tolkachev, *Khim. Prir. Soedin.*, **8**, 212(1974).

[2] A reference sample of sinoacutine was provided by D. J. Slatkin, Department of Pharmacognosy, School of Pharmacy, University of Pittsburgh.

(7) P. J. Niebergall, E. T. Sugita, and R. L. Schnaare, *J. Pharm. Sci.*, **60**, 1575(1971).

(8) A. Cammarata and K. S. Rogers, *J. Med. Chem.*, **14**, 269(1971).

(9) C. Hansch, J. E. Quinlan, and G. L. Lawrence, *J. Org. Chem.*, **33**, 347(1968).

ACKNOWLEDGMENTS AND ADDRESSES

Received March 26, 1975, from the *Department of Pharmacy, University of Manchester, Manchester, United Kingdom.*

Accepted for publication July 10, 1975.

[x] To whom inquiries should be directed.

Sinoacutine from *Glaucium contortuplicatum* Boiss.

M. TIN-WA [*], N. R. FARNSWORTH [*x], and K. A. ZIRVI [‡]

Abstract □ A phytochemical investigation of *Glaucium contortuplicatum* Boiss. (Papaveraceae) resulted in the isolation of sinoacutine from this plant for the first time. Spectral evidence for the identity of the isolated compound as sinoacutine is presented.

Keyphrases □ *Glaucium contortuplicatum*—phytochemical investigation, whole plant extract, sinoacutine isolated □ Sinoacutine—isolated from whole plant extract of *Glaucium contortuplicatum* □ Alkaloids—sinoacutine isolated from whole plant extract of *Glaucium contortuplicatum*

A literature survey revealed that no chemical work had been reported on the title plant. A phytochemical investigation was initiated, and the isolation of dicentrine nitrate was reported (1).

The isolation and identification of sinoacutine from this plant are now reported. Sinoacutine was first isolated from the Chinese drug "Ching-fengteng," *Sinomenium acutum* Redh *et* Wils. (Menispermaceae) (2), and later from *Cassytha pubescens* R. Br. (Lauraceae) (3), *Croton flavens* L. (Euphorbiaceae) (4), *Corydalis pallida* var. *tenuis* (Fumariaceae) (5), and *Cocculus carolinus* D.C. (Menispermaceae) (6).

This is the first reported occurrence of sinoacutine in *Glaucium contortuplicatum*. Recently, it was reported to be present in *G. flavum* (7). Sinoacutine had been synthesized (8) and found to elicit mild antitussive properties (9).

EXPERIMENTAL[1]

A quantity (20 kg) of the air-dried and powdered whole plant was extracted with hot petroleum ether (bp 30–60°) for 36 hr and then with hot methanol for 72 hr. The alcoholic extract, after charcoal treatment and concentration, gave a large amount of inorganic nitrates and an alkaloid, dicentrine nitrate (1), which were removed by filtration. After trituration of the filtrate with acetone to remove sugars, the acetone-soluble portion was evaporated to dryness *in vacuo*, dissolved in water, made basic with ammonium hydroxide to pH 9, and extracted with chloroform. The chloroform extract was washed with water, dried over anhydrous sodium sulfate, and chromatographed over a column containing neutral aluminum oxide S.

Elution with benzene and treatment of the dried residue with acetone yielded colorless prisms of sinoacutine (150 mg), mp 194–197° dec. [lit. (4) mp 197–199°]; $[\alpha]_D^{26.5}$ −117.64° (c 0.81, ethanol) [lit. (4, 6) $[\alpha]_D^{23}$ −115.0° (c 1.03, ethanol), $[\alpha]_D^{28}$ −115.8° (c 1.0, ethanol)]; UV: λ_{max} (methanol) 214 (log ϵ 4.22), 240 (4.21), and 280 (3.72) nm [lit. (6) UV: λ_{max} (ethanol) 214 (log ϵ 4.40), 245 (4.30), and 280 (3.80) nm]. Major absorptions in the IR spectrum were at ν_{max} (KBr) 3450 (broad OH stretch), 1670, 1640, and 1610 cm^{-1} (cyclohexadienone system).

The NMR spectrum in deuterochloroform showed a three-proton singlet at δ 2.45 (NCH_3), two three-proton singlets at δ 3.73 and 3.84 (2-OCH_3), two one-proton singlets at δ 6.36 and 7.56 (two olefinic protons), and two barely resolved proton peaks at δ 6.70 and 6.75 (two aromatic protons), which were in close agreement with the literature values (6, 10). In addition, the four methylene bridge protons were located as two triplets centered at δ 1.16 and 3.66 as determined by irradiation.

Deuterium exchange experiments permitted the assignment of a broad peak centered at δ 6.2 to the phenolic proton. The remaining one methine and one methylene protons appeared between δ 2.0 and 3.4 but were complex and somewhat obscured by the NCH_3 signal; no further attempt was made to assign these protons. The mass spectrum gave a molecular ion at *m/e* 327, which was also the base peak, followed by other significant peaks at *m/e* 312 ($M^+ - CH_3$, 40%), 299 ($M^+ - CO$, 22%), and 284 ($M^+ - CO—CH_3$, 55%). The fragmentation pattern is similar to that of salutaridine (11), the enantiomer of sinoacutine.

The isolate was compared with a reference sample of sinoacutine[2] and was found identical in all respects (IR, UV, mass spectrometric, TLC, melting point, and R_f data), and a mixed melting point was not depressed.

[1] The plant material was collected near Shiraz, Iran, in April 1971 and was identified as *Glaucium contortuplicatum* Boiss. (Papaveraceae) by M. H. Bokhari, Department of Biology, Pahlavi University. A voucher specimen (DPH-G2740) representing the collection was deposited in the Department of Pharmacology Herbarium, Pahlavi University, Shiraz, Iran.

UV spectra were taken using a Beckman model D-G grating spectrophotometer. IR spectra were taken using a Beckman model IR 18 A spectrophotometer. Mass spectra were determined using a single-focusing Hitachi Perkin-Elmer model RMU-6D mass spectrometer, operating at 70 ev. NMR spectra were taken using a Varian T-60 instrument operating at 60 MHz. Optical rotations were recorded using a Carl Zeiss optical polarimeter. The melting-point and mixed melting-point determinations were made using a Kofler hot-stage melting-point apparatus.

REFERENCES

(1) K. A. Zirvi and P. H. Jones, *Pahlavi Med. J.*, **5**, 668(1974).

(2) J. S. Hsu, S. Y. Lo, and J. H. Chu, *Sci. Sinica*, **13**, 2016(1964).

(3) S. R. Johns, J. A. Lamberton, and A. A. Sioumis, *Aust. J. Chem.*, **19**, 2331(1966).

(4) K. L. Stuart, C. Chambers, and D. Byfield, *J. Chem. Soc. C*, **1969**, 1681.

(5) T. Kametani, M. Ihara, and T. Hondo, *ibid.*, **1970**, 1060.

(6) D. J. Slatkin, N. J. Doorenbos, J. E. Knapp, and P. L. Schiff, Jr., *J. Pharm. Sci.*, **61**, 1825(1972).

(7) L. D. Yakhontova, V. I. Sheichenko, and O. N. Tolkachev, *Khim. Prir. Soedin.*, **8**, 212(1974).

[2] A reference sample of sinoacutine was provided by D. J. Slatkin, Department of Pharmacognosy, School of Pharmacy, University of Pittsburgh.

(8) T. Kametani, M. Ihara, K. Fukumolo, and H. Yagi, *J. Chem. Soc. C*, **1969**, 2030.
(9) V. V. Berezhinskaya, *Postep Dziedzinie Leku Rosl.*, **1972**, 164.
(10) D. H. R. Barton, G. W. Kirby, W. Steglich, G. M. Thomas, A. R. Battersby, T. A. Dobson, and H. Ramuz, *J. Chem. Soc.*, **1965**, 2423.
(11) D. M. S. Wheeler, T. H. Kinstler, and K. L. Rhinehart, *J. Amer. Chem. Soc.*, **89**, 4494(1967).

ACKNOWLEDGMENTS AND ADDRESSES

Received November 11, 1974, from the *Department of Pharmacognosy and Pharmacology, College of Pharmacy, University of Illinois at the Medical Center, Chicago, IL 60612, and the ‡Department of Pharmacology, School of Medicine, Pahlavi University, Shiraz, Iran.

Accepted for publication July 10, 1975.

ˣ To whom inquiries should be directed.

Effect of Sodium Salicylate on Hamster Cells *In Vitro*

M. RUBENSTEIN* §, D. GIACOMONI *, and L. M. PACHMAN ‡ˣ

Abstract □ Doses of sodium salicylate greater than 100 μg/ml increased the generation time of baby hamster kidney (BHK 21) cells in culture from 16 to 35 hr. Exposure to similar doses of salicylate for 18–44 hr resulted in a marked reduction of RNA synthesis. The species of RNA synthesized in the presence of sodium salicylate appeared to be similar to those synthesized by normal cells in the absence of sodium salicylate. Sodium salicylate did not alter the oxidative phosphorylation of BHK cells.

Keyphrases □ Sodium salicylate—effect on hamster kidney cells in culture, generation time, RNA synthesis □ Cell culture—hamster kidney cells, effect of sodium salicylate on generation and RNA synthesis □ RNA synthesis—hamster kidney cells in culture, effect of sodium salicylate □ Analgesics—sodium salicylate, effect on hamster kidney cells in culture, generation time, RNA synthesis

Aspirin is used to treat various rheumatic diseases. Sodium salicylate has been used as a probe for *in vitro* studies because its effect was similar to that of aspirin on DNA synthesis by stimulated lymphocytes *in vitro* (1). Sodium salicylate inhibited the *in vitro* protein, RNA, and DNA syntheses of human lymphocytes responding to phytohemagglutinin or antigen (1–3). Since great variability has been observed in the suppressive effect of sodium salicylate on human lymphocytes, a genetically defined cell line of baby hamster kidney (BHK 21) cells was selected as a model system to study the effect of salicylate on mammalian cells *in vitro*.

EXPERIMENTAL

Baby hamster kidney cells[1] (BHK 21) were grown as monolayers in a carbon dioxide incubator at 37° using Dulbecco modified Eagle's medium[2] supplemented with 10% fetal calf serum[3] and 10% tryptose phosphate broth[2]. The growth of cells was monitored by harvesting the monolayer after trypsinization and counting the cells using a hemocytometer[4]. Viability was determined by exclusion of 0.1% trypan blue dye.

Total "early labeled" RNA synthesis was determined by exposing the cells to ^{3}H-uridine[5] (2 μCi/ml) for 30 min. At the end of the exposure, sodium azide (0.2%) in saline was added and the cells were harvested and divided into two aliquots. One aliquot was used to measure the radioactivity incorporated in the 10% trichloroacetic acid-insoluble fraction; the other aliquot was used to determine the total DNA by the method of Seibert (4). RNA synthesis was measured as radioactivity incorporated per milligram of DNA.

To determine the effect of sodium salicylate[6] on the type of RNA molecules synthesized, exponentially growing cells were exposed to sodium salicylate (200 μg/ml) for 18 hr. After this incubation time, ^{3}H-uridine (2 μCi/ml) was added for 30 min. Then cells were harvested and mixed with cells that had been grown in the absence of sodium salicylate and similarly exposed to 0.5 μCi/ml of ^{14}C-uridine[5].

RNA was extracted from the cells as previously described (5). The sedimentation profile of the radioactive RNA was determined by layering an aliquot on top of a sucrose linear gradient [5–40% sucrose in 0.01 *M* sodium acetate (pH 5.1), 0.1 *M* NaCl, and 0.001 *M* edetate disodium] in a tube fitting the SW41 rotor of an ultracentrifuge[7].

After 17 hr of centrifugation at 4°, 0.5-ml fractions were collected from the top of the tube using a density gradient fractionator[8]. The fractionator recorded the optical density at 260 nm continuously. To each fraction, 1 ml of cold 20% trichloroacetic acid was added, followed by 5 ml of cold 10% trichloroacetic acid to precipitate RNA. The resulting sediment was collected over a 0.45-μm filter[9], and the acid-precipitable radioactivity was determined.

Determination of the oxidative phosphorylation and the hexose monophosphate shunt was adapted from the method previously described (6). In brief, 3 ml of medium containing 750,000 BHK cells was dispensed into 100-ml serum bottles[10], and sodium salicylate was added to triplicate flasks in a final concentration of 200 μg/ml. Control bottles were prepared containing fewer cells (500,000/3 ml) so that the numbers of cells in each category (sodium salicylate and control) would be equivalent at the end of the 24-hr incubation period.

After 24 hr of incubation, the medium was decanted from all bottles. The cell monolayer was washed with 0.85 *M* phosphate-buffered saline containing 1000 μg/ml of dextrose. To each culture, 3.0 ml of saline–dextrose containing 200 μg/ml of sodium salicylate or saline was added. ^{14}C-Glucose, labeled in the C-1 or C-6 position, was then added (0.5 μCi/ml). The bottles were immediately capped with rubber stoppers, from which were suspended ampuls containing 1.0 ml of a quaternary ammonium hydroxide[11].

[1] Obtained from Dr. C. Basilico.
[2] Grand Island Biological, Grand Island, N.Y.
[3] Flow Laboratories, Rockville, Md.
[4] Newbauer.
[5] New England Nuclear, Boston, Mass.
[6] Merck Chemical Division, Merck & Co., Rahway, N.J.
[7] Spinco L265, Beckman Instrument Co., Fullerton, Calif.
[8] Instrumentation Specialties Co., Lincoln, Neb.
[9] Millipore, Bedford, Mass.
[10] Bellco Glass, Inc., Vineland, N.J.
[11] Hyamine hydroxide, Packard, Downers Grove, Ill.

(8) T. Kametani, M. Ihara, K. Fukumolo, and H. Yagi, *J. Chem. Soc. C*, **1969**, 2030.
(9) V. V. Berezhinskaya, *Postep Dziedzinie Leku Rosl.*, **1972**, 164.
(10) D. H. R. Barton, G. W. Kirby, W. Steglich, G. M. Thomas, A. R. Battersby, T. A. Dobson, and H. Ramuz, *J. Chem. Soc.*, **1965**, 2423.
(11) D. M. S. Wheeler, T. H. Kinstler, and K. L. Rhinehart, *J. Amer. Chem. Soc.*, **89**, 4494(1967).

ACKNOWLEDGMENTS AND ADDRESSES

Received November 11, 1974, from the *Department of Pharmacognosy and Pharmacology, College of Pharmacy, University of Illinois at the Medical Center, Chicago, IL 60612, and the ‡Department of Pharmacology, School of Medicine, Pahlavi University, Shiraz, Iran.

Accepted for publication July 10, 1975.

ˣ To whom inquiries should be directed.

Effect of Sodium Salicylate on Hamster Cells *In Vitro*

M. RUBENSTEIN* §, D. GIACOMONI *, and L. M. PACHMAN ‡ˣ

Abstract □ Doses of sodium salicylate greater than 100 μg/ml increased the generation time of baby hamster kidney (BHK 21) cells in culture from 16 to 35 hr. Exposure to similar doses of salicylate for 18–44 hr resulted in a marked reduction of RNA synthesis. The species of RNA synthesized in the presence of sodium salicylate appeared to be similar to those synthesized by normal cells in the absence of sodium salicylate. Sodium salicylate did not alter the oxidative phosphorylation of BHK cells.

Keyphrases □ Sodium salicylate—effect on hamster kidney cells in culture, generation time, RNA synthesis □ Cell culture—hamster kidney cells, effect of sodium salicylate on generation and RNA synthesis □ RNA synthesis—hamster kidney cells in culture, effect of sodium salicylate □ Analgesics—sodium salicylate, effect on hamster kidney cells in culture, generation time, RNA synthesis

Aspirin is used to treat various rheumatic diseases. Sodium salicylate has been used as a probe for *in vitro* studies because its effect was similar to that of aspirin on DNA synthesis by stimulated lymphocytes *in vitro* (1). Sodium salicylate inhibited the *in vitro* protein, RNA, and DNA syntheses of human lymphocytes responding to phytohemagglutinin or antigen (1–3). Since great variability has been observed in the suppressive effect of sodium salicylate on human lymphocytes, a genetically defined cell line of baby hamster kidney (BHK 21) cells was selected as a model system to study the effect of salicylate on mammalian cells *in vitro*.

EXPERIMENTAL

Baby hamster kidney cells[1] (BHK 21) were grown as monolayers in a carbon dioxide incubator at 37° using Dulbecco modified Eagle's medium[2] supplemented with 10% fetal calf serum[3] and 10% tryptose phosphate broth[2]. The growth of cells was monitored by harvesting the monolayer after trypsinization and counting the cells using a hemocytometer[4]. Viability was determined by exclusion of 0.1% trypan blue dye.

Total "early labeled" RNA synthesis was determined by exposing the cells to ^{3}H-uridine[5] (2 μCi/ml) for 30 min. At the end of the exposure, sodium azide (0.2%) in saline was added and the cells were harvested and divided into two aliquots. One aliquot was used to measure the radioactivity incorporated in the 10% trichloroacetic acid-insoluble fraction; the other aliquot was used to determine the total DNA by the method of Seibert (4). RNA synthesis was measured as radioactivity incorporated per milligram of DNA.

To determine the effect of sodium salicylate[6] on the type of RNA molecules synthesized, exponentially growing cells were exposed to sodium salicylate (200 μg/ml) for 18 hr. After this incubation time, ^{3}H-uridine (2 μCi/ml) was added for 30 min. Then cells were harvested and mixed with cells that had been grown in the absence of sodium salicylate and similarly exposed to 0.5 μCi/ml of ^{14}C-uridine[5].

RNA was extracted from the cells as previously described (5). The sedimentation profile of the radioactive RNA was determined by layering an aliquot on top of a sucrose linear gradient [5–40% sucrose in 0.01 *M* sodium acetate (pH 5.1), 0.1 *M* NaCl, and 0.001 *M* edetate disodium] in a tube fitting the SW41 rotor of an ultracentrifuge[7].

After 17 hr of centrifugation at 4°, 0.5-ml fractions were collected from the top of the tube using a density gradient fractionator[8]. The fractionator recorded the optical density at 260 nm continuously. To each fraction, 1 ml of cold 20% trichloroacetic acid was added, followed by 5 ml of cold 10% trichloroacetic acid to precipitate RNA. The resulting sediment was collected over a 0.45-μm filter[9], and the acid-precipitable radioactivity was determined.

Determination of the oxidative phosphorylation and the hexose monophosphate shunt was adapted from the method previously described (6). In brief, 3 ml of medium containing 750,000 BHK cells was dispensed into 100-ml serum bottles[10], and sodium salicylate was added to triplicate flasks in a final concentration of 200 μg/ml. Control bottles were prepared containing fewer cells (500,000/3 ml) so that the numbers of cells in each category (sodium salicylate and control) would be equivalent at the end of the 24-hr incubation period.

After 24 hr of incubation, the medium was decanted from all bottles. The cell monolayer was washed with 0.85 *M* phosphate-buffered saline containing 1000 μg/ml of dextrose. To each culture, 3.0 ml of saline–dextrose containing 200 μg/ml of sodium salicylate or saline was added. ^{14}C-Glucose, labeled in the C-1 or C-6 position, was then added (0.5 μCi/ml). The bottles were immediately capped with rubber stoppers, from which were suspended ampuls containing 1.0 ml of a quaternary ammonium hydroxide[11].

[1] Obtained from Dr. C. Basilico.
[2] Grand Island Biological, Grand Island, N.Y.
[3] Flow Laboratories, Rockville, Md.
[4] Newbauer.
[5] New England Nuclear, Boston, Mass.
[6] Merck Chemical Division, Merck & Co., Rahway, N.J.
[7] Spinco L265, Beckman Instrument Co., Fullerton, Calif.
[8] Instrumentation Specialties Co., Lincoln, Neb.
[9] Millipore, Bedford, Mass.
[10] Bellco Glass, Inc., Vineland, N.J.
[11] Hyamine hydroxide, Packard, Downers Grove, Ill.

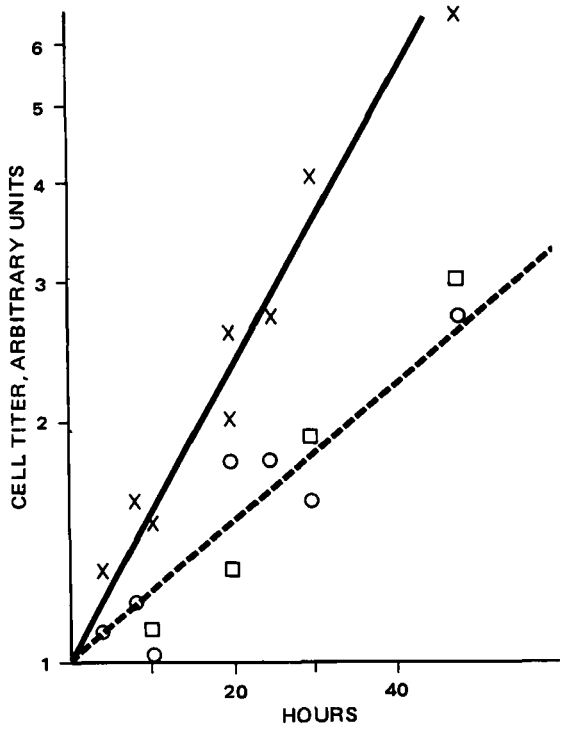

Figure 1—*Effect of sodium salicylate on growth of BHK 21 cells. BHK 21 cells were grown in the absence and in the presence of different amounts of sodium salicylate. The cell number at time 0 was given the value 1. Key: ×—, control (no salicylate added); □ - - - -, 100 μg/ml of sodium salicylate in the medium; and ○ - - - -, 200 μg/ml of sodium salicylate in the medium. Data from two experiments are presented.*

The bottles were incubated for 3 hr in a 37° water bath. Then the ampuls containing adsorbed ^{14}C-carbon dioxide were immediately removed, and their radioactivity was determined in a liquid scintillation counter[12].

Cell counts were done on the monolayer of the triplicate bottles, and the ^{14}C-carbon dioxide evolved was expressed as counts per minute per million cells.

RESULTS

The growth of BHK 21 cells in the presence of sodium salicylate was studied (Fig. 1). The addition of 100 μg/ml of sodium salicylate increased the generation time from 16 (control) to 35 hr. A higher concentration of sodium salicylate (200 μg/ml) did not increase the generation time further. The viability of the cells was more than 95% throughout the experiment.

The effect of sodium salicylate on the incorporation of ^{3}H-uridine by the cells during a 30-min exposure to the label (total early labeled RNA synthesis) was determined. When cells were incubated for 24 hr with 200 μg/ml of sodium salicylate, the incorporation of radiolabeled uridine was reduced by 37–60% with respect to controls. When the cells were incubated for 24 hr in the presence of 350 μg/ml of sodium salicylate, the reduction of incorporation was greater than 90%. After 44 hr of incubation with 200 μg/ml of sodium salicylate, incorporation was reduced by 80%.

When the effect of sodium salicylate on the type of RNA molecules synthesized in cells exposed for 18 hr to the drug was studied, the early labeled RNA was analyzed on a sucrose gradient. ^{3}H-RNA derived from sodium salicylate-treated cells and ^{14}C-RNA from controls were analyzed in the same gradient. This "double label" technique permits the comparison of the sedimentation pattern of the two RNA preparations in the same gradient, thus allowing the detection of even minor differences.

The profiles of the two RNA preparations (Fig. 2) were similar, indicating that there were no major qualitative differences in the early labeled RNA synthesized by cells grown in the presence or absence of salicylate. When early labeled RNA was extracted from BHK 21 cells exposed to sodium salicylate (200 μg/ml) for a longer period (48 hr) and similarly analyzed, a comparable sedimentation pattern was found.

[12] Mark I, Nuclear Chicago, Chicago, Ill.

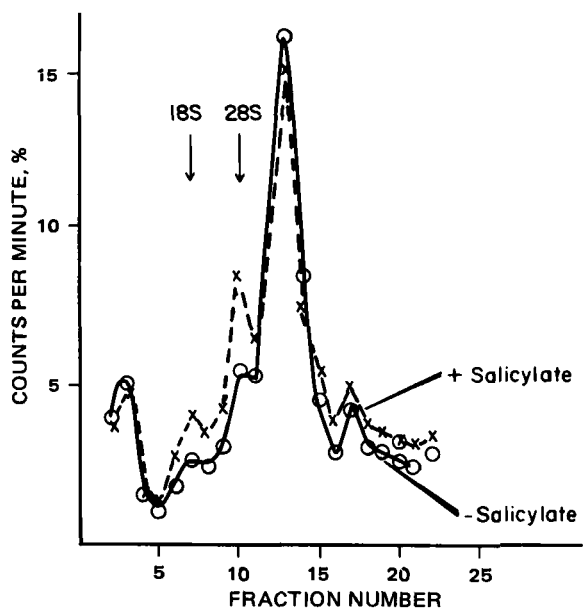

Figure 2—*Sucrose gradient analysis of RNA synthesized in the presence or absence of sodium salicylate. BHK 21 cells grown for 18 hr in the absence or presence of sodium salicylate (200 μg/ml) were exposed for 30 min to ^{14}C- and ^{3}H-labeled uridine, respectively, harvested, and pooled; RNA was extracted and analyzed on a sucrose gradient. The sedimentation positions of 18S and 28S RNA are indicated by arrows. The carbon-14 and tritium radioactivity are indicated as percent of total radioactivity of each isotope. Key: ○—, carbon-14 (RNA from control cultures); and × - - -, tritium (RNA from cells exposed to sodium salicylate).*

The effect of sodium salicylate (200 μg/ml) on the hexose monophosphate shunt and on the oxidative phosphorylation of BHK 21 cells was studied. The amount of ^{14}C-carbon dioxide evolved from 1-^{14}C-glucose (*via* both the mitochondria and the hexose monophosphate shunt) or 6-^{14}C-glucose (the mitochondria alone) was measured, and the C-1/C-6 ratio was compared with that of the controls (Table I). In sodium salicylate-treated cells, a decrease in carbon dioxide evolved from glucose labeled in C-1 and C-6 was observed, suggesting a lower metabolic activity. The ratio of C-1/C-6 remained the same (12.5), suggesting that there was no change in the way glucose was utilized.

DISCUSSION

BHK 21 cells (a genetically homogeneous mammalian cell line) were selected to avoid the differences in susceptibility to sodium salicylate of lymphocytes from different human donors. The data presented here show that the inhibition of synthesis of total early labeled RNA by sodium salicylate in these rapidly dividing cells is similar to the inhibition by salicylate of RNA synthesis in phytohemagglutinin-stimulated lymphocytes during a 4-hr period (1).

In the present studies, early labeled RNA synthesized by BHK 21 cells in the presence or absence of sodium salicylate had a simi-

Table I—Effect of Sodium Salicylate on Oxidation of Glucose by BHK 21 Cells

Sodium Salicylate, μg/ml	Carbon Diosicle from 1-^{14}C-Glucose[a] (C-1), cpm	Carbon Dioxide from 6-^{14}C-Glucose[a] (C-6), cpm	C-1/C-6[b]
0	6450 ± 400	517 ± 25	12.5
200	4200 ± 500	337 ± 80	12.5

[a] Average of triplicate determinations ± 95% confidence limits. [b] Ratio of the means.

lar sedimentation pattern. These two sets of experiments suggest that sodium salicylate, while reducing the RNA synthesizing ability of BHK 21 cells, affects the synthesis of all species of RNA to a similar degree. A marked decrease also was observed in the growth rate of these cells when exposed to sodium salicylate (100–200 μg/ml); this decrease could be the result of diminished RNA synthesis. Paine and Nagington (7) reported that similar doses of sodium salicylate decreased the growth rate of human embryonic kidney, lung, and heart cells but not of embryonic skin fibroblasts.

The observed decrease in RNA synthesis as well as the decrease in macromolecular synthesis by cells of different origins in the presence of salicylate (2) lends support to the hypothesis that salicylate generally interferes with cellular growth (1, 7, 8). However, the effect of sodium salicylate on the function of the specific cell type may be variable. Data presented in this paper suggest that sodium salicylate (200 μg/ml) does not affect mitochondrial activity of BHK 21 cells, since there is no increase in the ^{14}C-carbon dioxide evolved from 6-^{14}C-glucose.

Sodium salicylate (300 μg/ml) minimally increased both C-1- and C-6-derived carbon dioxide production by human polymorphonuclear cells but did not affect phagocytosis and bacterial killing, a phenomenon greatly dependent on hexose monophosphate shunt activity (9). The same concentration of sodium salicylate uncoupled oxidative phosphorylation of the lymphocytes and markedly impaired synthesis of DNA and RNA (1) as well as immunoglobulins (10). Therefore, it is speculated that the function of cell types more dependent on mitochondrial activity may be more susceptible to the inhibitory effects of sodium salicylate.

REFERENCES

(1) L. M. Pachman, N. B. Esterly, and R. D. A. Peterson, *J. Clin. Invest.*, **50**, 226(1971).

(2) M. T. H. Smith and P. D. Dawkins, *J. Pharm. Pharmacol.*, **23**, 729(1971).

(3) G. Opelz, P. I. Terasaki, and A. A. Hirata, *Lancet*, **2**, 478(1973).

(4) F. G. Seibert, *J. Biol. Chem.*, **133**, 593(1940).

(5) F. Amaldi, D. Giacomoni, and R. Zito-Bignami, *Eur. J. Biochem.*, **11**, 419(1969).

(6) L. M. Pachman, P. Jayanetra, and R. M. Rothberg, *J. Pediat.*, **52**, 823(1973).

(7) T. F. Paine, and J. Nagington, *Nature New Biol.*, **233**, 108(1971).

(8) T. M. Brody, *J. Pharmacol. Exp. Ther.*, **39**, 117(1956).

(9) L. M. Pachman, *Fed. Proc.*, **29**, 1392(1970).

(10) C. V. Alm and L. M. Pachman, *Experientia*, **27**, 924(1971).

ACKNOWLEDGMENTS AND ADDRESSES

Received September 3, 1974, from the *Department of Microbiology, University of Illinois at the Medical Center, Chicago, IL 60612 and the ‡Department of Pediatrics, Northwestern University, Children's Memorial Hospital, Chicago, IL 60614

Accepted for publication July 14, 1975.

Supported in part by a grant from the Illinois Chapter of the Arthritis Foundation, the Apfelbaum Foundation, and the Leukemia Research Foundation, Chicago, Ill.

The authors thank Sandra M. Baldwin for technical assistance.

§ Supported by U.S. Public Health Service Grant PHS A1 00335 in partial fulfillment of the Doctor of Philosophy degree requirements at the University of Illinois at the Medical Center.

ˣ To whom inquiries should be directed.

Antihemolytic and Antiproteolytic Properties of Substituted Thiosemicarbazidophenothiazines and Thiazolidonylphenothiazines

ANSHUMALI CHAUDHARI *, SUSHIL KUMAR *, SHIVA P. SINGH *‡, SURENDRA S. PARMAR *§ˣ, and VIRGIL I. STENBERG ‡

Abstract □ Antihemolytic and antiproteolytic properties of several 10-(1-acetyl-4-arylthiosemicarbazido)phenothiazines and their corresponding cyclized 10-(2-arylimino-3-acetylamino-4-thiazolidonyl)phenothiazines were investigated. *In vitro* protection of hypoosmotic hemolysis of human red blood cells by substituted thiosemicarbazidophenothiazines and substituted thiazolidonylphenothiazines was concentration dependent; the degree of protection ranged from 19 to 32 and 26 to 42%, respectively, at a final concentration of 0.1 m*M*. All phenothiazines exhibited antiproteolytic activity. The *in vitro* inhibition of trypsin-induced hydrolysis of bovine serum albumin by these phenothiazines was concentration dependent and competitive in nature; the degree of inhibition ranged from 30 to 50 and 32 to 79% for substituted thiosemicarbazidophenothiazines and substituted thiazolidonylphenothiazines, respectively, at a concentration of 1 m*M*. Cyclization of substituted thiosemicarbazidophenothiazines into the corresponding cyclized substituted thiazolidonylphenothiazines increased the antihemolytic and antiproteolytic effectiveness of these phenothiazines.

Keyphrases □ Phenothiazines, substituted—antihemolytic and antiproteolytic activities investigated □ Antihemolytic activity—substituted phenothiazines evaluated □ Antiproteolytic activity—substituted phenothiazines evaluated □ Structure–activity relationships—substituted phenothiazines evaluated for antihemolytic and antiproteolytic activities

It has been shown that the membrane-stabilizing effects of phenothiazine derivatives are reflected by delayed spontaneous hemolysis of red blood cells (1, 2). Phenothiazine derivatives also have been reported to exhibit anti-inflammatory effectiveness against formaldehyde-induced arthritis (3, 4). Recent studies indicated correlation between the antiproteolytic activity of amyrin acetates (5) and their anti-inflammatory activity (6). Furthermore, numerous psychotropic agents have been proposed to affect the physicochemical properties of cell membranes, accounting for the basis of their mechanism of action (7).

These observations prompted studies of the antihemolytic and antiproteolytic properties of some substituted thiosemicarbazidophenothiazines and their corresponding cyclized substituted thiazoli-

lar sedimentation pattern. These two sets of experiments suggest that sodium salicylate, while reducing the RNA synthesizing ability of BHK 21 cells, affects the synthesis of all species of RNA to a similar degree. A marked decrease also was observed in the growth rate of these cells when exposed to sodium salicylate (100–200 μg/ml); this decrease could be the result of diminished RNA synthesis. Paine and Nagington (7) reported that similar doses of sodium salicylate decreased the growth rate of human embryonic kidney, lung, and heart cells but not of embryonic skin fibroblasts.

The observed decrease in RNA synthesis as well as the decrease in macromolecular synthesis by cells of different origins in the presence of salicylate (2) lends support to the hypothesis that salicylate generally interferes with cellular growth (1, 7, 8). However, the effect of sodium salicylate on the function of the specific cell type may be variable. Data presented in this paper suggest that sodium salicylate (200 μg/ml) does not affect mitochondrial activity of BHK 21 cells, since there is no increase in the ^{14}C-carbon dioxide evolved from 6-^{14}C-glucose.

Sodium salicylate (300 μg/ml) minimally increased both C-1- and C-6-derived carbon dioxide production by human polymorphonuclear cells but did not affect phagocytosis and bacterial killing, a phenomenon greatly dependent on hexose monophosphate shunt activity (9). The same concentration of sodium salicylate uncoupled oxidative phosphorylation of the lymphocytes and markedly impaired synthesis of DNA and RNA (1) as well as immunoglobulins (10). Therefore, it is speculated that the function of cell types more dependent on mitochondrial activity may be more susceptible to the inhibitory effects of sodium salicylate.

REFERENCES

(1) L. M. Pachman, N. B. Esterly, and R. D. A. Peterson, *J. Clin. Invest.*, **50**, 226(1971).

(2) M. T. H. Smith and P. D. Dawkins, *J. Pharm. Pharmacol.*, **23**, 729(1971).

(3) G. Opelz, P. I. Terasaki, and A. A. Hirata, *Lancet*, **2**, 478(1973).

(4) F. G. Seibert, *J. Biol. Chem.*, **133**, 593(1940).

(5) F. Amaldi, D. Giacomoni, and R. Zito-Bignami, *Eur. J. Biochem.*, **11**, 419(1969).

(6) L. M. Pachman, P. Jayanetra, and R. M. Rothberg, *J. Pediat.*, **52**, 823(1973).

(7) T. F. Paine, and J. Nagington, *Nature New Biol.*, **233**, 108(1971).

(8) T. M. Brody, *J. Pharmacol. Exp. Ther.*, **39**, 117(1956).

(9) L. M. Pachman, *Fed. Proc.*, **29**, 1392(1970).

(10) C. V. Alm and L. M. Pachman, *Experientia*, **27**, 924(1971).

ACKNOWLEDGMENTS AND ADDRESSES

Received September 3, 1974, from the *Department of Microbiology, University of Illinois at the Medical Center, Chicago, IL 60612 and the ‡Department of Pediatrics, Northwestern University, Children's Memorial Hospital, Chicago, IL 60614

Accepted for publication July 14, 1975.

Supported in part by a grant from the Illinois Chapter of the Arthritis Foundation, the Apfelbaum Foundation, and the Leukemia Research Foundation, Chicago, Ill.

The authors thank Sandra M. Baldwin for technical assistance.

§ Supported by U.S. Public Health Service Grant PHS A1 00335 in partial fulfillment of the Doctor of Philosophy degree requirements at the University of Illinois at the Medical Center.

ˣ To whom inquiries should be directed.

Antihemolytic and Antiproteolytic Properties of Substituted Thiosemicarbazidophenothiazines and Thiazolidonylphenothiazines

ANSHUMALI CHAUDHARI *, SUSHIL KUMAR *, SHIVA P. SINGH *‡, SURENDRA S. PARMAR *§ˣ, and VIRGIL I. STENBERG ‡

Abstract □ Antihemolytic and antiproteolytic properties of several 10-(1-acetyl-4-arylthiosemicarbazido)phenothiazines and their corresponding cyclized 10-(2-arylimino-3-acetylamino-4-thiazolidonyl)phenothiazines were investigated. *In vitro* protection of hypoosmotic hemolysis of human red blood cells by substituted thiosemicarbazidophenothiazines and substituted thiazolidonylphenothiazines was concentration dependent; the degree of protection ranged from 19 to 32 and 26 to 42%, respectively, at a final concentration of 0.1 m*M*. All phenothiazines exhibited antiproteolytic activity. The *in vitro* inhibition of trypsin-induced hydrolysis of bovine serum albumin by these phenothiazines was concentration dependent and competitive in nature; the degree of inhibition ranged from 30 to 50 and 32 to 79% for substituted thiosemicarbazidophenothiazines and substituted thiazolidonylphenothiazines, respectively, at a concentration of 1 m*M*. Cyclization of substituted thiosemicarbazidophenothiazines into the corresponding cyclized substituted thiazolidonylphenothiazines increased the antihemolytic and antiproteolytic effectiveness of these phenothiazines.

Keyphrases □ Phenothiazines, substituted—antihemolytic and antiproteolytic activities investigated □ Antihemolytic activity—substituted phenothiazines evaluated □ Antiproteolytic activity—substituted phenothiazines evaluated □ Structure–activity relationships—substituted phenothiazines evaluated for antihemolytic and antiproteolytic activities

It has been shown that the membrane-stabilizing effects of phenothiazine derivatives are reflected by delayed spontaneous hemolysis of red blood cells (1, 2). Phenothiazine derivatives also have been reported to exhibit anti-inflammatory effectiveness against formaldehyde-induced arthritis (3, 4). Recent studies indicated correlation between the antiproteolytic activity of amyrin acetates (5) and their anti-inflammatory activity (6). Furthermore, numerous psychotropic agents have been proposed to affect the physicochemical properties of cell membranes, accounting for the basis of their mechanism of action (7).

These observations prompted studies of the antihemolytic and antiproteolytic properties of some substituted thiosemicarbazidophenothiazines and their corresponding cyclized substituted thiazoli-

Table I—Antihemolytic and Antiproteolytic Properties of 10-(1-Acetyl-4-arylthiosemicarbazido)phenothiazines[a]

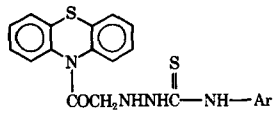

Compound	Ar	Protection of Hypoosmotic Hemolysis[b], %		Inhibition of Trypsin-Induced Hydrolysis of Bovine Serum Albumin[c], %		
		0.01 m*M*	0.1 m*M*	0.1 m*M*	0.5 m*M*	1.0 m*M*
I	C_6H_5	Nil[d]	24 ± 1.2	9 ± 0.7	22 ± 0.9	40 ± 1.0
II	2-$CH_3C_6H_4$	Nil	19 ± 1.0	Nil[d]	20 ± 0.6	36 ± 1.1
III	4-$CH_3C_6H_4$	Nil	20 ± 1.5	24 ± 1.0	27 ± 0.5	47 ± 0.6
IV	2-$OCH_3C_6H_4$	6 ± 1.4	26 ± 0.9	Nil	Nil	30 ± 0.9
V	4-$OCH_3C_6H_4$	Nil	20 ± 1.0	14 ± 0.8	20 ± 1.2	33 ± 0.5
VI	4-ClC_6H_4	11 ± 1.0	32 ± 1.2	17 ± 0.5	31 ± 1.3	42 ± 0.8
VII	4-BrC_6H_4	Nil	29 ± 1.0	18 ± 0.7	28 ± 0.5	45 ± 1.0
VIII	4-IC_6H_4	13 ± 1.1	32 ± 0.9	14 ± 0.6	15 ± 0.8	36 ± 1.2
IX	1-$C_{10}H_7$ (naphthyl)	Nil	20 ± 1.4	12 ± 1.0	40 ± 0.6	50 ± 0.6

[a] The assay procedure and the contents of the reaction mixture are as indicated in the text. Each experiment was done in duplicate, and the values indicate mean values of three separate experiments with ± standard error of the mean. [b] Antihemolytic activity was determined as protection against hypoosmotic hemolysis of human red blood cells by phenothiazine derivatives used at final concentrations of 0.01 and 0.1 m*M*. [c] The degree of inhibition of the activity of trypsin during hydrolysis of bovine serum albumin by phenothiazine derivatives was determined at the final concentrations of 0.1, 0.5, and 1.0 m*M*. [d] Represents experiments exhibiting no protection of hypoosmotic hemolysis and no inhibition of trypsin-induced hydrolysis of bovine serum albumin.

donylphenothiazines in an attempt to elucidate the biochemical basis for their anticonvulsant properties (8).

EXPERIMENTAL[1]

Determination of Hypoosmotic Hemolysis—Assay of hypoosmotic hemolysis was carried out by following the method reported earlier (9). Fresh heparinized human blood was oxygenated with a mixture of oxygen (90%) and carbon dioxide (10%) for 60 sec. To 0.1 ml of the whole blood was added 3 ml of a buffer solution (0.425% NaCl; sodium phosphate buffer, 5 m*M*, pH 7.4; total osmolality of 135 mosmoles/liter), with or without the test compounds. The tubes were shaken gently two or three times and then allowed to stand at room temperature (28–30°) for exactly 5 min. These tubes were then centrifuged for 5 min at 1000×*g* to separate the cells.

Under these conditions, hemolysis of the human blood cells occurred but in no case exceeded 50%. The absorbance of the supernate was read at 540 nm in a colorimeter. Percent protection was calculated by comparing the absorbance values observed in the presence of the substituted phenothiazines with those observed in the control tubes without the test compounds. The control values were represented as 100% hypoosmotic hemolysis. Absorbance values for the blank containing 0.1 ml of blood in 3 ml of 0.85% NaCl (normal saline) were substracted from the values obtained for both the control and the experimental tubes containing the test compounds.

All substituted phenothiazines were dissolved in the buffered saline solution of pH 7.4 (osmolality of 135 mosmoles/liter) and were used at a final concentration of 0.001–0.1 m*M*.

Assay of Proteolytic Activity of Trypsin—The antiproteolytic activity of substituted phenothiazines was determined by evaluating their ability to inhibit trypsin-induced hydrolysis of bovine serum albumin. The reaction mixture consisted of 0.05 *M* tromethamine buffer (pH 8.2), 0.075 mg of crystalline trypsin (1 g was sufficient to hydrolyze 250 g of casein), 0.03 m*M* bovine serum albumin, and water in a total volume of 1 ml. The substituted phenothiazines were dissolved in dimethylformamide and were used at final concentrations of 0.001–0.1 m*M*. An equivalent amount of dimethylformamide, added to the control tubes, had no effect on trypsin activity.

All substituted phenothiazines were preincubated with trypsin for 10 min prior to the addition of bovine serum albumin, and the reaction mixture was further incubated for 5 min after the addition of bovine serum albumin (5). The reaction was stopped by the addition of 5 ml of 15% (w/v) trichloroacetic acid solution. The acid-soluble products of protein breakdown, obtained after centrifugation, were determined (10) as an index of the enzyme activity. Suitable 0.5-ml aliquots of the acid-soluble supernatant solution were added to 5 ml of a freshly prepared mixture of 8% Na_2CO_3 solution and a solution containing 0.064% $CuSO_4$ and sodium potassium tartrate (0.12%) in equal volumes. The mixture was allowed to stand at room temperature for 10 min, and the absorbance was measured at 750 nm against a reagent blank in a spectrophotometer[2].

RESULTS AND DISCUSSION

The membrane-stabilizing property of phenothiazine derivatives was evaluated by determining the decrease in the degree of hypoosmotic hemolysis of human red blood cells. All 10-(1-acetyl-4-arylthiosemicarbazido)phenothiazines protected hypoosmotic hemolysis when used at a final concentration of 0.1 m*M*, and the degree of protection ranged from 19 to 32% (Table I). The use of 0.01 m*M* solutions of these compounds (except IV, VI, and VII) failed to provide protection from hypoosmotic hemolysis; IV, VI, and VII decreased hypoosmotic hemolysis by 6–13%.

In the present study, cyclization of substituted thiosemicarbazidophenothiazines into the corresponding 10-(2-arylimino-3-acetylamino-4-thiazolidonyl)phenothiazines resulted in the increased effectiveness of the cyclized compounds to provide protection against hypoosmotic hemolysis (Table II). The degree of protection observed with substituted thiazolidonylphenothiazines ranged from 26 to 42% at a final concentration of 0.1 m*M*. Compound VIII was an exception, since a slight decrease in its antihemolytic activity was observed on cyclization into XVII. The antihemolytic activity of these phenothiazines was concentration dependent, and greater protection from hypoosmotic hemolysis was observed with the use of higher concentrations.

The inhibitory effects of substituted thiosemicarbazidophenothiazines and their corresponding cyclized thiazolidonylphenothiazines on the hydrolysis of bovine serum albumin by trypsin are recorded in Tables I and II, respectively. All compounds were used at final concentrations of 0.1, 0.5, and 1.0 m*M*. The degree of inhibition of trypsin was concentration dependent and increased with a simultaneous increase in the concentration of these phenothiazine derivatives. Such an inhibition of trypsin-induced hydrolysis of bovine serum albumin ranged from 30 to 50% with substituted thiosemicarbazidophenothiazines (Table I) and from 32 to 79% with substituted thiazolidonylphenothiazines (Table II) at a final concentration of 1.0 m*M*. Thus, as was observed with antihemolytic activity, cyclization of 10-(1-acetyl-4-arylthiosemicarbazido)phenothiazines into the corresponding 10-(2-arylimino-3-acetylamino-4-thiazolidonyl)phenothiazines resulted in increased antiproteolytic activity.

[1] Commercial chemicals were obtained from Sigma Chemical Co., St. Louis, Mo. The syntheses and the physical constants of 10-(1-acetyl-4-arylthiosemicarbazido)phenothiazines and 10-(2-arylimino-3-acetylamino-4-thiazolidonyl)phenothiazines were reported earlier (8).

[2] Hitachi Perkin-Elmer spectrophotometer model 139.

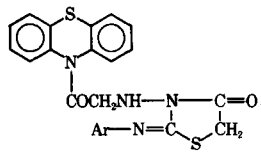

Table II—Antihemolytic and Antiproteolytic Properties of 10-(2-Arylimino-3-acetylamino-4-thiazolidonyl)phenothiazines[a]

Compound	Ar	Protection of Hypoosmotic Hemolysis, %		Inhibition of Trypsin-Induced Hydrolysis of Bovine Serum Albumin, %		
		0.01 m*M*	0.1 m*M*	0.1 m*M*	0.5 m*M*	1.0 m*M*
X	C_6H_5	24 ± 1.1	36 ± 1.0	5 ± 0.7	26 ± 0.5	65 ± 1.1
XI	2-$CH_3C_6H_4$	21 ± 1.2	36 ± 1.3	6 ± 0.8	27 ± 0.7	63 ± 0.6
XII	4-$CH_3C_6H_4$	18 ± 0.9	27 ± 1.1	4 ± 1.0	20 ± 1.0	59 ± 0.5
XIII	2-$OCH_3C_6H_4$	25 ± 1.5	37 ± 1.2	20 ± 0.7	33 ± 1.3	45 ± 0.8
XIV	4-$OCH_3C_6H_4$	19 ± 1.3	40 ± 0.9	4 ± 0.4	13 ± 0.7	32 ± 0.6
XV	4-ClC_6H_4	15 ± 1.0	30 ± 1.4	17 ± 0.8	26 ± 0.6	35 ± 0.9
XVI	4-BrC_6H_4	18 ± 0.9	42 ± 0.9	18 ± 0.7	50 ± 0.9	58 ± 0.7
XVII	4-IC_6H_4	12 ± 1.2	29 ± 1.1	24 ± 1.0	57 ± 0.8	79 ± 0.5
XVIII	1-$C_{10}H_7$ (naphthyl)	12 ± 1.1	26 ± 1.5	5 ± 0.8	24 ± 0.5	41 ± 1.0

[a] Assay procedures for the determination of antihemolytic and antiproteolytic properties of phenothiazine derivatives are as indicated in Table I.

In the present study, preincubation of these phenothiazine derivatives for 0, 10, 20, and 30 min (8) prior to the addition of bovine serum albumin in no way altered their antiproteolytic activity. These preincubation studies indicated a rapidly reversible nature of inhibition of trypsin by these phenothiazine derivatives during hydrolysis of bovine serum albumin. This finding was further supported by kinetic studies with 10-[2-(4-iodophenyl)imino-3-acetylamino-4-thiazolidonyl]phenothiazine (XVII); the method reported by Dixon (11) was followed for graphic evaluation of the nature of inhibition and determination of the K_i value for this inhibitor. As is evident from Fig. 1, XVII exhibited a competitive nature of inhibition of trypsin during hydrolysis of bovine serum albumin and possessed a K_i value of 0.12 m*M*.

These studies failed to provide any relationship between antihemolytic and antiproteolytic properties of phenothiazine derivatives and their chemical structure, so a definite structure–activity relationship was not exhibited (Tables I and II). The protection of hypoosmotic hemolysis indicated that these phenothiazines presumably prevent the various processes in the cell membranes, as reported earlier for other psychotropic drugs (12–14). However, the similarity between increased antihemolytic and antiproteolytic effectiveness observed in this study and a similar increase in anticonvulsant activity observed on cyclization of substituted thiosemicarbazidophenothiazines into the corresponding substituted thiazolidonylphenothiazines (8) provided evidence that antihemolytic and antiproteolytic activities may account for some biochemical effects for the anticonvulsant property of these phenothiazine derivatives.

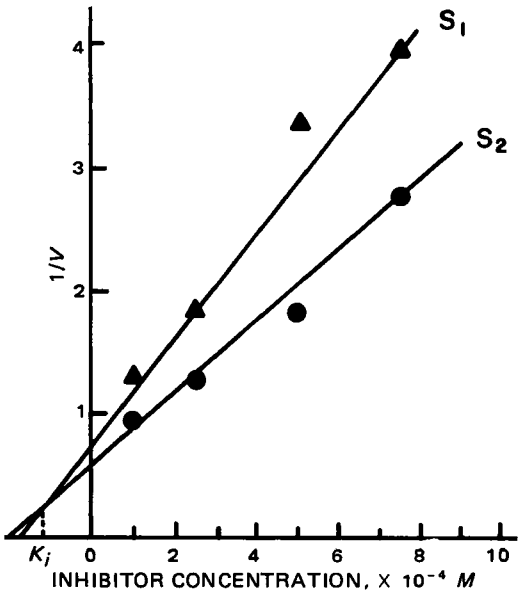

Figure 1—*Competitive inhibition of the activity of trypsin by XVII during hydrolysis of bovine serum albumin, where 1/V represents the reciprocal of the enzyme activity as determined by the amount of the products of protein breakdown using different concentrations of XVII. Assay procedures and the contents of the reaction mixture are as indicated in Table I. In all experiments, trypsin was incubated with XVII for 10 min prior to the addition of bovine serum albumin, which was used at two concentrations of 0.025 m*M (S_1, ▲) *and 0.033 m*M (S_2, ●). *The K_1 value (inhibitor constant) for XVII was 0.12 m*M *during trypsin-induced hydrolysis of bovine serum albumin.*

REFERENCES

(1) B. N. Halpern, B. Dreyfus, and G. Bourdon, *Presse Med.*, **58**, 1151(1950).

(2) H. Chaplin, Jr., H. Crawford, M. Cutbush, and P. L. Mollison, *J. Clin. Pathol.*, **5**, 91(1952).

(3) G. Wilhelmi, *Arch. Exp. Pathol. Pharmacol.*, **227**, 497(1956).

(4) J. R. Parratt and G. B. West, *Brit. J. Pharmacol.*, **13**, 65(1958).

(5) A. Chaudhari, A. K. Chaturvedi, S. S. Parmar, and S. J. Brumleve, *Res. Commun. Chem. Pathol. Pharmacol.*, **7**, 205(1974).

(6) M. B. Gupta, T. N. Bhalla, G. P. Gupta, C. P. Mitra, and K. P. Bhargava, *Eur. J. Pharmacol.*, **6**, 67(1969).

(7) M. Weatherall, in "Recent Advances in Pharmacology," 4th ed., J. M. Robson and R. S. Stacy, Eds., Churchill, London, England, 1968, p. 1.

(8) S. P. Singh, B. Ali, T. K. Auyong, S. S. Parmar, and B. De Boer, *J. Pharm. Sci.*, **65**, 391(1976).

(9) C. Dwivedi, R. D. Harbison, B. Ali, and S. S. Parmar, *ibid.*, **63**, 1124(1974).

(10) O. H. Lowry, N. J. Rosenbrough, A. L. Farr, and R. J. Randall, *J. Biol. Chem.*, **193**, 265(1951).

(11) M. Dixon, *Biochem. J.*, **55**, 170(1953).

(12) P. Seeman and J. Weinstein, *Biochem. Pharmacol.*, **15**, 1737(1966).

(13) A. Despopoulos, *ibid.*, **19**, 2907(1970).

(14) W. Mikikits, A. Mortara, and R. G. Spector, *Nature (London)*, **225**, 1150(1970).

ACKNOWLEDGMENTS AND ADDRESSES

Received May 27, 1975, from the *Department of Pharmacology and Therapeutics, King George's Medical College, Lucknow University, Lucknow 226003, India, and the Departments of ‡Chemistry and §Physiology and Pharmacology, University of North Dakota, Grand Forks, ND 58202

Accepted for publication July 14, 1975.

Supported in part by the U.S. Public Health Service, National Institutes of Health Grants 1 T01 HL-05939, 1 R01 DA00996-01, and GM-21590 and Career Development Award 1-K4-GM-09888 to V. I. Stenberg.

The authors thank Professor Stanley J. Brumleve and Professor Roland G. Severson for their advice and encouragement. Grateful acknowledgment is made to the Indian National Science Academy, New Delhi, India, and to the State Council of Scientific and Industrial Research, Uttar Pradesh, Lucknow, India, for providing Research Fellowships to A. Chaudhari and S. Kumar, respectively.

[x] To whom inquiries should be directed (at the University of North Dakota).

Spectrophotometric Determination of Diphenhydramine Hydrochloride Using Dipicrylamine

FADHIL A. SHAMSA [x] and ROSTAM H. MAGHSSOUDI

Abstract □ A spectrophotometric procedure for the determination of diphenhydramine hydrochloride based on the reaction with dipicrylamine was developed. A yellow complex forms and is easily extractable by chloroform at pH 5. The mole ratio of diphenhydramine hydrochloride to dipicrylamine in the complex is 1:3. The absorbance of the complex obeys Beer's law over the concentration range of 3–10 μg of diphenhydramine hydrochloride per ml of chloroform. This procedure can be carried out in the presence of other compounds without interference.

Keyphrases □ Diphenhydramine hydrochloride—spectrophotometric analysis, color complex with dipicrylamine, pharmaceutical formulations □ Dipicrylamine—color complex formation for spectrophotometric analysis of diphenhydramine hydrochloride, pharmaceutical formulations □ Spectrophotometry—analysis, diphenhydramine hydrochloride, pharmaceutical formulations □ Antihistaminic agents—diphenhydramine hydrochloride, spectrophotometric analysis, pharmaceutical formulations

5-(Hydroxymethyl)-2-furaldehyde is a well-known product of the Maillard reaction (1–3). It is frequently present in pharmaceutical preparations, particularly in syrups, and can interfere in the chemical analysis for active components.

USP XVIII (4) described a UV assay for diphenhydramine hydrochloride (I) elixir, in which 5-(hydroxymethyl)-2-furaldehyde interferes with the chemical analysis, the nonaqueous titrimetry for the powder, and also the UV assays for the capsule and injection preparations. The separation of the base on a cation exchanger, followed by quantitative spectrophotometric determination, was reported (5, 6).

A UV method was developed to measure the steam-distillable compound after hydrolysis and oxidation of diphenhydramine (7). An addition compound formation between diphenhydramine and tetrabromophenolphthalein ethyl ether in ethylene-dichloride was used (8), as was ion-pair formation between the amine and an indicator dye (9). Nonaqueous titrimetry and salt partition were used in analysis procedures for organic bases (10, 11).

Quantitative TLC also was described (12). A modification of the USP XVIII method was described in which the effect of 5- (hydroxymethyl)-2-furaldehyde was eliminated (13). A column chromatography procedure was reported for the separation of I from a capsule formulation with determination by UV (14). However, these methods lack the simplicity and sensitivity to determine microamounts of I.

The present study describes a direct, simple, and sensitive procedure for the determination of I spectrophotometrically. This method is applicable for powder, syrup, capsule, injection, and elixir dosage forms without interferences. The procedure depends on the formation of a complex between I and dipicrylamine (II) which is extractable by chloroform at pH 5. This method can be carried out successfully in the presence of 5-(hydroxymethyl)-2-furaldehyde and other compounds.

EXPERIMENTAL[1]

Reagents and Chemicals—A 0.001 *M* diphenhydramine hydrochloride (I) aqueous solution (USP reference standard) and a 0.001 *M* dipicrylamine (II) in 0.4% sodium carbonate solution were prepared. All buffers used were of the BP standard.

General Procedure—To a 50-ml separator were added 1-5 ml of 0.001 *M* I, 1 ml of 0.001 *M* II, and 10 ml of pH 5 buffer solution. The mixture was shaken, and the complex formed was extracted with 5, 3, and 2 ml of chloroform by vigorous shaking. The extracts were collected in a 10-ml volumetric flask and then diluted to volume with chloroform. The absorbance of the complex in chloroform was measured at 420 nm *versus* a similarly prepared blank. Any other pharmaceutical preparations should be diluted to contain less than 100 μg/ml of I and then analyzed as described.

RESULTS AND DISCUSSION

A yellow-colored complex with a maximum absorption at 420 nm developed (Fig. 1) when I reacted with II. It was completely extractable by chloroform at pH 5. A calibration curve was plotted for various concentrations of I. Beer's law was followed over the concentration range of 30–100 μg of I/10 ml of chloroform. The molar absorptivity was 1.45×10^4.

The effects of temperature, pH, and the presence of many compounds were studied. A pH of 5 gave optimum results and different temperatures had no effect on complex formation and extraction.

Effect of Other Compounds—To determine the effect of other compounds, a standard solution containing 90 μg of I and the compound in question were placed in a separator and analyzed by the described method. The following compounds did not interfere when added in the indicated amounts: ammonium chloride[2] (10 mg), menthol[2] (100 mg), sucrose[2] (100 mg), sodium citrate[2] (10 mg), saccharin sodium[2] (5 mg), acetaminophen[3] (10 mg), phenylephrine hydrochloride[3] (100 mg), ascorbic acid[3] (10 mg), 5-(hydroxymethyl)-2-furaldehyde[4] (20 mg), orange oil[5] (0.1 ml), cinna-

[1] A Coleman Junior II model 6/20 spectrophotometer with 1-cm glass cells and a Beckman 10 recorder were used. A Beckman H_3-type pH meter was used for pH measurements.
[2] Present with I in syrups.
[3] Components of a diphenhydramine capsule marketed as Flustop.
[4] Frequently present in syrups.
[5] Constituents of I elixir.

The authors thank Professor Stanley J. Brumleve and Professor Roland G. Severson for their advice and encouragement. Grateful acknowledgment is made to the Indian National Science Academy, New Delhi, India, and to the State Council of Scientific and Industrial Research, Uttar Pradesh, Lucknow, India, for providing Research Fellowships to A. Chaudhari and S. Kumar, respectively.

[x] To whom inquiries should be directed (at the University of North Dakota).

Spectrophotometric Determination of Diphenhydramine Hydrochloride Using Dipicrylamine

FADHIL A. SHAMSA [x] and ROSTAM H. MAGHSSOUDI

Abstract □ A spectrophotometric procedure for the determination of diphenhydramine hydrochloride based on the reaction with dipicrylamine was developed. A yellow complex forms and is easily extractable by chloroform at pH 5. The mole ratio of diphenhydramine hydrochloride to dipicrylamine in the complex is 1:3. The absorbance of the complex obeys Beer's law over the concentration range of 3–10 μg of diphenhydramine hydrochloride per ml of chloroform. This procedure can be carried out in the presence of other compounds without interference.

Keyphrases □ Diphenhydramine hydrochloride—spectrophotometric analysis, color complex with dipicrylamine, pharmaceutical formulations □ Dipicrylamine—color complex formation for spectrophotometric analysis of diphenhydramine hydrochloride, pharmaceutical formulations □ Spectrophotometry—analysis, diphenhydramine hydrochloride, pharmaceutical formulations □ Antihistaminic agents—diphenhydramine hydrochloride, spectrophotometric analysis, pharmaceutical formulations

5-(Hydroxymethyl)-2-furaldehyde is a well-known product of the Maillard reaction (1–3). It is frequently present in pharmaceutical preparations, particularly in syrups, and can interfere in the chemical analysis for active components.

USP XVIII (4) described a UV assay for diphenhydramine hydrochloride (I) elixir, in which 5-(hydroxymethyl)-2-furaldehyde interferes with the chemical analysis, the nonaqueous titrimetry for the powder, and also the UV assays for the capsule and injection preparations. The separation of the base on a cation exchanger, followed by quantitative spectrophotometric determination, was reported (5, 6).

A UV method was developed to measure the steam-distillable compound after hydrolysis and oxidation of diphenhydramine (7). An addition compound formation between diphenhydramine and tetrabromophenolphthalein ethyl ether in ethylene-dichloride was used (8), as was ion-pair formation between the amine and an indicator dye (9). Nonaqueous titrimetry and salt partition were used in analysis procedures for organic bases (10, 11).

Quantitative TLC also was described (12). A modification of the USP XVIII method was described in which the effect of 5- (hydroxymethyl)-2-furaldehyde was eliminated (13). A column chromatography procedure was reported for the separation of I from a capsule formulation with determination by UV (14). However, these methods lack the simplicity and sensitivity to determine microamounts of I.

The present study describes a direct, simple, and sensitive procedure for the determination of I spectrophotometrically. This method is applicable for powder, syrup, capsule, injection, and elixir dosage forms without interferences. The procedure depends on the formation of a complex between I and dipicrylamine (II) which is extractable by chloroform at pH 5. This method can be carried out successfully in the presence of 5-(hydroxymethyl)-2-furaldehyde and other compounds.

EXPERIMENTAL[1]

Reagents and Chemicals—A 0.001 *M* diphenhydramine hydrochloride (I) aqueous solution (USP reference standard) and a 0.001 *M* dipicrylamine (II) in 0.4% sodium carbonate solution were prepared. All buffers used were of the BP standard.

General Procedure—To a 50-ml separator were added 1-5 ml of 0.001 *M* I, 1 ml of 0.001 *M* II, and 10 ml of pH 5 buffer solution. The mixture was shaken, and the complex formed was extracted with 5, 3, and 2 ml of chloroform by vigorous shaking. The extracts were collected in a 10-ml volumetric flask and then diluted to volume with chloroform. The absorbance of the complex in chloroform was measured at 420 nm *versus* a similarly prepared blank. Any other pharmaceutical preparations should be diluted to contain less than 100 μg/ml of I and then analyzed as described.

RESULTS AND DISCUSSION

A yellow-colored complex with a maximum absorption at 420 nm developed (Fig. 1) when I reacted with II. It was completely extractable by chloroform at pH 5. A calibration curve was plotted for various concentrations of I. Beer's law was followed over the concentration range of 30–100 μg of I/10 ml of chloroform. The molar absorptivity was 1.45×10^4.

The effects of temperature, pH, and the presence of many compounds were studied. A pH of 5 gave optimum results and different temperatures had no effect on complex formation and extraction.

Effect of Other Compounds—To determine the effect of other compounds, a standard solution containing 90 μg of I and the compound in question were placed in a separator and analyzed by the described method. The following compounds did not interfere when added in the indicated amounts: ammonium chloride[2] (10 mg), menthol[2] (100 mg), sucrose[2] (100 mg), sodium citrate[2] (10 mg), saccharin sodium[2] (5 mg), acetaminophen[3] (10 mg), phenylephrine hydrochloride[3] (100 mg), ascorbic acid[3] (10 mg), 5-(hydroxymethyl)-2-furaldehyde[4] (20 mg), orange oil[5] (0.1 ml), cinna-

[1] A Coleman Junior II model 6/20 spectrophotometer with 1-cm glass cells and a Beckman 10 recorder were used. A Beckman H_3-type pH meter was used for pH measurements.
[2] Present with I in syrups.
[3] Components of a diphenhydramine capsule marketed as Flustop.
[4] Frequently present in syrups.
[5] Constituents of I elixir.

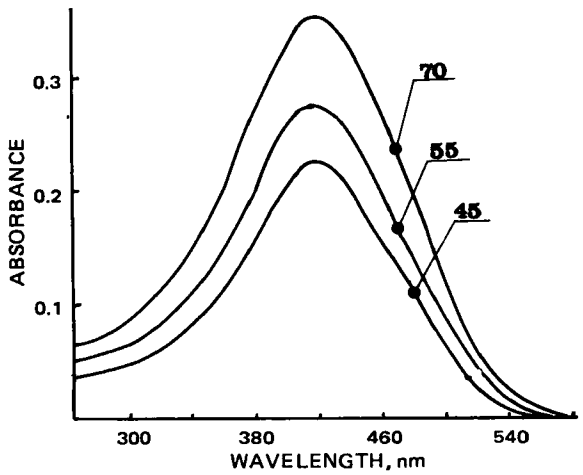

Figure 1—*Absorption spectra of the I–II complex at various I concentrations. (Numbers on curves indicate concentration of I in micrograms per 10 ml of chloroform.)*

mon oil[5] (0.003 ml), clove oil[5] (0.1 ml), coriander oil[5] (0.05 ml), anethol (0.2 ml), amaranth[5] (5 mg), and alcohol[5] (0.5 ml). The percent recovery of I from different synthetic pharmaceutical preparations is shown in Table I.

Stability of Complex—The I–II complex was very stable in chloroform and began to fade slowly only after 10 days. Before the extraction, the mixture was put in a boiling water bath for 30 min; the absorbance did not change after extraction with chloroform.

Nature of Complex—The mole ratio method (15) was employed to determine the composition of the I–II complex as follows.

The concentration of I was kept constant at 0.0002 *M* while the concentration of II was varied between 0.0001 and 0.002 *M*. Spectrophotometric measurements were made as already described.

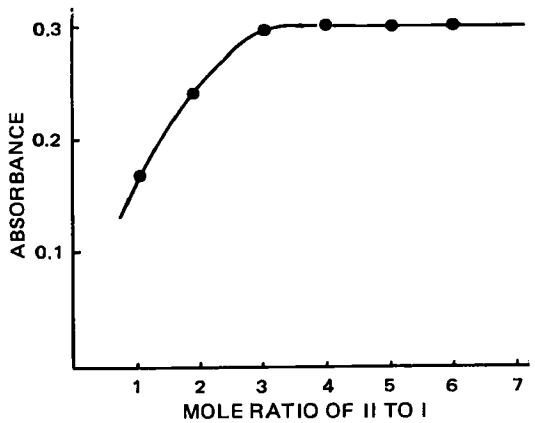

Figure 2—*Variation of the absorbance* versus *the mole ratio of II to I at 420 nm when the concentration of I was kept constant at 2* $\times 10^{-4}$ M.

Table I—Percent Recovery of Diphenhydramine Hydrochloride

Synthetic Preparation	I Added, μg	Absorbance Values: Before Addition	Absorbance Values: After Addition	Recovery, %	Deviation, %
Syrup	40	0.250	0.452	101.0	1
Capsule	40	0.250	0.450	100	0.0
Elixir	40	0.250	0.447	98.5	1.5
Injection	40	0.200	0.400	100	0.0
Capsules[a]	40	0.200	0.400	100	0.0

[a] The analysis was applied to Flustop capsules containing 400 mg of acetaminophen, 5 mg of phenylephrine hydrochloride, 10 mg of diphenhydramine hydrochloride, and 50 mg of ascorbic acid.

Figure 2 shows that the absorbance of the complex increased as the concentration of II was increased up to a I–II ratio of 1:3. The absorbance of the complex did not change with further increases, indicating a 1:3 ratio of I to II in the complex.

Precision and Accuracy—A set of 10 identical samples, each with a final I concentration of 90 μg, was treated according to the recommended procedure and the absorbances were measured. The percent accuracy and the confidence limits were calculated to be 1% and 89.1 ± 0.85 μg, respectively.

REFERENCES

(1) A. Gottschal and S. M. Partridge, *Nature*, **165**, 684(1950).
(2) J. E. Hodge, *J. Agr. Food Chem.*, **1**, 928(1953).
(3) S. Patton, *J. Dairy Sci.*, **38**, 457(1955).
(4) "The United States Pharmacopeia," 18th rev., Mack Publishing Co., Easton, Pa., 1970, pp. 207–210.
(5) F. De Fabrizio, *J. S. Afr. Chem. Inst.*, **20**, 194(1967).
(6) F. De Fabrizio, *J. Pharm. Sci.*, **59**, 1470(1970).
(7) J. E. Wallace, J. D. Biggs, and E. V. Dahl, *Anal. Chem.*, **38**, 831(1966).
(8) M. Tsubouchi, *Bull. Chem. Soc. Jap.*, **43**, 3164(1970).
(9) F. Matsui and W. N. French, *J. Pharm. Sci.*, **60**, 287(1971).
(10) C. A. Mainville and L. G. Chatten, *ibid.*, **53**, 154(1964).
(11) J. Levine, *ibid.*, **54**, 485(1965).
(12) S. Demir and J. Amal, *J. Fac. Pharm. Istanbul Univ.*, **5**, 80(1969).
(13) D. Woo, J. K. C. Yen, and K. R. Heimlich, *J. Pharm. Sci.*, **62**, 1993(1973).
(14) F. De Fabrizio, *ibid.*, **63**, 91(1974).
(15) J. H. Yoe and A. L. Jones, *Ind. Eng. Chem. Anal. Ed.*, **16**, 111(1944).

ACKNOWLEDGMENTS AND ADDRESSES

Received May 8, 1975, from the *Department of Pharmaceutical Chemistry, Faculty of Pharmacy, Tehran University, Tehran, Iran.*

Accepted for publication July 21, 1975.

[x] To whom inquiries should be directed.

Application of Trihydroxyindole Reaction to Methanesulfonanilides: Fluorometric Analysis for Soterenol and Mesuprine

TERRY T. KENSLER, DANA BROOKE ˣ, and DONNA M. WALKER*

Abstract □ Methanesulfonanilides, like soterenol and mesuprine, which are bioisosteric with adrenergic catecholamines, form fluorescent species when subjected to the trihydroxyindole reaction. Presumably, the fluorescence is due to adrenolutin-like species formed from aminochrome intermediates. Fluorescence was not induced in a relative of soterenol where a methyl group was added to the sulfonamido nitrogen, a fact that suggests the presence of a quinoid intermediate in the reaction scheme of soterenol. A ring isomer of soterenol, where the methanesulfonamido and hydroxyl groups were interchanged, produced only about 5% as much fluorescence response as soterenol. The soterenol counterparts to isoproterenol and isoproterenolsulfonic acid did not produce fluorescence when treated like soterenol. This finding and the fact that response was linear with concentration for soterenol and mesuprine suggest that a fluorometric analysis could be developed for these methanesulfonanilides.

Keyphrases □ Soterenol—fluorometric analysis after trihydroxyindole reaction, pharmaceutical formulations □ Mesuprine—fluorometric analysis after trihydroxyindole reaction, pharmaceutical formulations □ Trihydroxyindole reaction—with methanesulfonanilides, fluorometric analysis of soterenol and mesuprine □ Methanesulfonanilides—trihydroxyindole reaction applied, fluorometric analysis of soterenol and mesuprine □ Adrenergic agents—soterenol and mesuprine, fluorometric analysis, pharmaceutical formulations

Recently, Prasad *et al.* applied time-honored fluorometric methods to the analysis of epinephrine (1) and isoproterenol (2) in pharmaceuticals. These methods involved iodine oxidation of the catecholamine to the aminochrome, which was subsequently treated to form a fluorescent species. These reports suggested the possibility of fluorometric analyses of certain methanesulfonanilides, which are bioisosteric with catecholamines (3, 4). One such compound, soterenol (I), the methanesulfonamido counterpart of isoproterenol, is well known for its adrenergic activity.

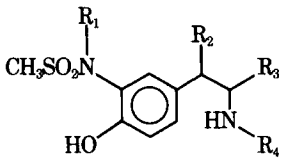

I: $R_1 = H$, $R_2 = OH$, $R_3 = H$, $R_4 = (CH_3)_2CH-$
II: $R_1 = H$, $R_2 = OH$, $R_3 = CH_3$, $R_4 = 4\text{-}(OCH_3)C_6H_4CH_2CH_2-$
III: $R_1 = CH_3$, $R_2 = OH$, $R_3 = H$, $R_4 = (CH_3)_2CH-$
IV: $R_1 = H$, $R_2 = SO_3H$, $R_3 = H$, $R_4 = (CH_3)_2CH-$

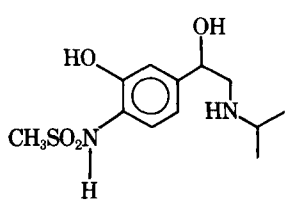

V

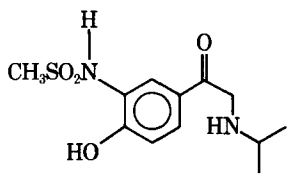

VI

The application of the trihydroxyindole reaction to the analysis of such compounds[1] as I and mesuprine (II) was attempted on the assumption that the sulfonamido group can act like a phenolic hydroxyl group during the formation of aminochromes and, subsequently, fluorescent adrenolutin-like derivatives. Experimental support of this supposition should be of general interest.

As will be seen, methanesulfonanilides like I and II do form fluorescent derivatives. Compounds III–VI were used to examine certain other aspects of the effect of substrate structure on the development of fluorescence.

EXPERIMENTAL

Reagents—Compounds I–VI as the appropriate salts were drawn from laboratory stock. The hydrochloride salts of I, II, V, and VI were prepared and described previously (4). The acetate salt of III is that described in a recent U.S. patent (5).

Compound IV, 1-(4-hydroxy-3-methanesulfonamidophenyl)-2-isopropylaminoethanesulfonic acid, was prepared[2] by heating a solution of equimolar amounts of I as the hydrochloride and sodium bisulfite at pH 6.8 under reflux for 5.5 hr. The solution was cooled and filtered, and the white solid was recrystallized once from 1 *N* HCl and once from water, giving IV, mp 288.5° dec. (corrected). The IR, NMR, UV, elemental, and TLC analyses were consistent with the one compound, IV.

Isoproterenol hydrochloride USP[3] was used as received. All other chemicals were either USP or reagent grade. The water was double distilled.

Buffer—Buffers, 0.1 *M* in citrate, were prepared by dissolving appropriate amounts of sodium citrate and citric acid in water and adjusting the pH with sodium hydroxide when necessary.

Iodine–Potassium Iodide Solution—A 0.001 *M* I_2 in 1.4% KI solution was prepared by diluting 1.0 ml of a 0.1 *M* I_2 (in 0.1 *M* KI) solution to 100 ml with 1.4% KI solution.

Sodium Ascorbate (0.2% in 5 *N* NaOH)—A 5.0-ml aliquot of a freshly prepared 2% solution of ascorbic acid was diluted to 50.0 ml in a volumetric flask with 5 *N* NaOH. This solution was used within 1 hr.

Apparatus—Fluorescence measurements were routinely taken using a ratio fluorometer[4] equipped with No. 405 narrow pass primary filters and a No. 2A-12 sharp cut secondary filter[5]. The fluorescence of each sample was recorded relative to an 1800-ppb quinine sulfate equivalent uranium glass reference bar. Emission spectra were recorded using a spectrophotofluorometer[6].

Procedure—Solutions for analysis, essentially 0.1 *M* in citrate, were prepared by diluting stock solutions of the substrates with citrate buffer. A 1.0-ml portion of the 0.001 *M* I_2 solution was added with agitation to a 10-ml volumetric flask containing 5.0 ml of the buffered sample. After a predetermined time, sodium ascorbate solution was added to volume and the solution was mixed. The rela-

[1] Soterenol and mesuprine have been cited as MJ 1992 and MJ 1987, respectively, in the scientific literature.
[2] D. G. Mikolasek, Mead Johnson and Co., personal communication.
[3] Gane's Chemical Works.
[4] Beckman model 772.
[5] Turner stock Nos. 110-812 and 110-818.
[6] Aminco-Bowman model 8202.

Table I—Fluorometric Measurements with Sulfonanilides and Isoproterenol

Compound	Sample, *M*	Iodine, *M*	pH	Fluoresce	Excitation[a], λ_{max}	Emission[a], λ_{max}
I	1.45×10^{-5}	0.001	5.5	Yes	425	505
II	1.20×10^{-5}	0.001	5.5	Yes	430	510
III	2.90×10^{-4}	0.005	4.0—7.1	No	—	—
IV	8.90×10^{-6}	0.001	5.5	No	—	—
V	6.88×10^{-5}	0.001	5.5	Yes	455	545
VI	1.23×10^{-5}	0.001	5.5	No	—	—
Isoproterenol	3.36×10^{-6}	0.001	4.0	Yes	420	510

[a] Excitation and emission wavelengths are from uncorrected spectra and are only approximate.

tive fluorescence developed was determined after 8–10 min with a reagent blank set at zero.

RESULTS AND DISCUSSION

Compounds I, II, and, to a lesser extent, V can be made to fluoresce by treatment with iodine followed by alkaline ascorbate. The readings are linear with substrate concentration, as illustrated for I and II in Fig. 1. The data of Fig. 1 were based on reaction with iodine at pH 5.5 (I for 15 min, II for 30 min) followed by addition of ascorbate solution with measurement of fluorescence 8–10 min later. The pH and time of the oxidation step were chosen to maximize reproducibility and convenience of sample handling. The time course of fluorescence development for II at three pH values is shown in Fig. 2.

The data of Fig. 1 are intended only to depict linearity of meter response *versus* concentration when a ratio fluorometer is used. When, however, fluorescence spectra are recorded by means of a spectrophotofluorometer for samples containing I or II, treated as described, the responses per mole of substrate, measured at λ_{max} (Table I), are virtually identical. Isoproterenol hydrochloride, oxidized at its optimal pH of 4.0 (2) for 10 min, developed approximately twice the fluorescence per mole. Oxidation of V (10 min at pH 5.5) produced only about one-twentieth of the response recorded for I as described previously[7].

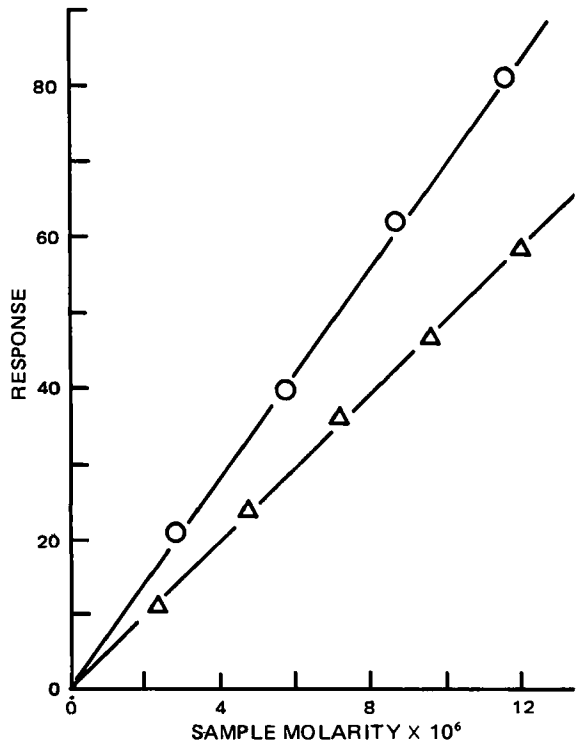

Figure 1—*Ratio of fluorometer response* versus *sample concentration for soterenol* (○) *and mesuprine* (△).

[7] Fluorescence readings were slightly higher if the oxidation was at pH 4.5. At both pH values, the readings were reasonably constant from 3 to 30 min.

These comparisons may aid in judging the reactivities of the substrates tested. However, because numerous factors affect the formation and stability of aminochrome intermediates and the adrenolutin-like fluorophores, the comparisons should be used cautiously. For example, the ultimate concentration of fluorophore can be adversely affected by side reactions such as the iodination of aminochromes. Mattok and Wilson (6, 7) showed that the rate of iodination depends upon iodine and iodide concentrations and is general base (buffer) catalyzed. Laverty and Taylor (8) showed that the oxidation of catecholamines to aminochromes was significantly influenced by buffer composition and pH.

No fluorescence was observed when III was treated under conditions that easily oxidized I. This was true even when the concentration of III (2.9×10^{-4} *M*) was 20 times the highest concentration used for I (1.45×10^{-5} *M*) and the iodine concentration was increased fivefold to 0.005 *M*. In these cases, the oxidation step was attempted for up to 1 hr at pH values ranging from 4.0 to 7.1.

This finding appears to be a parallel to the fact that guaiacolamines do not produce fluorescence under conditions that easily develop fluorescence in catecholamines. For example, normetanephrine produces fluorescence when treated with iodine only under alkaline conditions (8). Metanephrine and normetanephrine are oxidized by metaperiodate under acid conditions where the reaction probably involves loss of the O^3-methyl group (9). This finding indirectly supports the premise that fluorescence development from the methanesulfonanilides requires a quinoid-like intermediate (VII) similar to that proposed (9, 10) for the formation of aminochromes from catecholamines. An extension of this reasoning would support formation of an aminochrome intermediate (VIII) from the methanesulfonanilides. This structure is not unlike the stable *p*-nitrophenylhydrazone (IX) of adrenochrome (11).

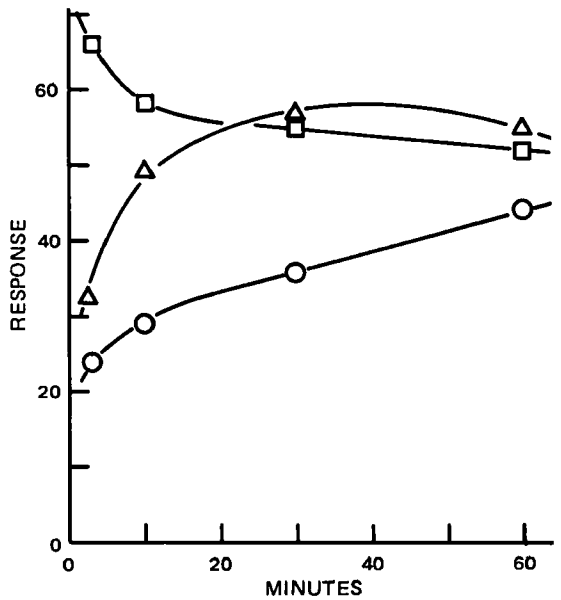

Figure 2—*Effect of time and pH of the oxidation step on the ultimate fluorescence of mesuprine. Buffers used were at pH 4.5* (○), *5.5* (△), *and 6.4* (□). *Mesuprine concentration was 1.2 × 10^{-5}* M.

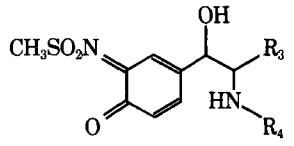

VII

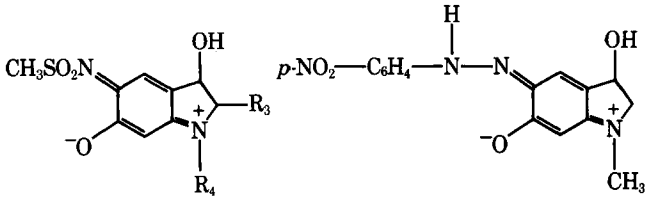

VIII IX

That V, an isomer of I differing only in the positions of the ring substituents, produced only about one-twentieth the fluorescence of I was somewhat surprising. No explanation is offered, but it is interesting to note that compounds in this series (*i.e.*, those with the methanesulfonamido group *para* to the ethanolamine side chain) also have considerably lower adrenergic potency (4).

Prasad *et al.* (2) showed that isoproterenol and isoproterenolsulfonic acid do not interfere with their fluorometric method. Similarly, the ketone VI and the sulfonic acid IV do not form fluorescent species under the conditions used to analyze I. These final tests were designed only to demonstrate the lack of interference from IV and VI and do not preclude the possibility that these compounds might form fluorescent derivatives under different conditions.

REFERENCES

(1) V. K. Prasad, R. A. Ricci, B. C. Nunning, and A. P. Granatek, *J. Pharm. Sci.*, **62**, 1130(1973).

(2) *Ibid.*, **62**, 1135(1973).

(3) A. A. Larsen and P. M. Lish, *Nature*, **203**, 1284(1964).

(4) A. A. Larsen, W. A. Gould, H. R. Roth, W. T. Comer, R. H. Uloth, K. W. Dungan, and P. M. Lish, *J. Med. Chem.*, **10**, 462(1967).

(5) A. A. Larsen and R. H. Uloth, U.S. pat. 3,660,487 (1972).

(6) G. L. Mattok and D. L. Wilson, *Can. J. Chem.*, **45**, 2473(1967).

(7) *Ibid.*, **45**, 1721(1967).

(8) R. Laverty and K. M. Taylor, *Anal. Biochem.*, **22**, 269(1968).

(9) R. A. Heacock and W. S. Powell, *Progr. Med. Chem.*, **9**, 275(1972).

(10) W. H. Harrison, *Arch. Biochem. Biophys.*, **101**, 116(1963).

(11) W. S. Powell and R. A. Heacock, *J. Chem. Soc. P1*, **1973**, 509.

ACKNOWLEDGMENTS AND ADDRESSES

Received March 21, 1975, from the *Division of Pharmaceutical Sciences, Mead Johnson Research Center, Mead Johnson and Company, Evansville, IN 47721*

Accepted for publication July 21, 1975.

The authors thank Dr. D. G. Mikolasek for providing analytical data on IV and other technical assistance. They also thank Dr. W. T. Comer for his interest and assistance and Dr. M. J. Bartek for help in recording fluorescence spectra.

* Present address: Armak Co., Chicago, Ill.

‡ To whom inquiries should be directed.

Thiocardenolides I: Synthesis and Biological Actions of 3β-Thiocyanato-14β-hydroxy-5β-card-20(22)-enolide

HANLEY N. ABRAMSON *‡, CHIAN L. HUANG *, THOMAS F. WU *, and THOMAS TOBIN ‡

Abstract □ The synthesis of a 3β-thiocyanatocardenolide is described. The compound exhibited about 0.1 times the cardiotonic effect of digitoxigenin in the isolated frog heart preparation. At a dosage of 20 mg/kg in the intact rat, it elicited ECG changes similar to those seen with a 10-mg/kg dose of digitoxigenin. Studies also revealed the new cardenolide to be a reversible inhibitor of sodium- and potassium-activated adenosine triphosphatase.

Keyphrases □ Thiocardenolides—3β-thiocyanato-14β-hydroxy-5β-card-20(22)-enolide synthesized, screened for cardiotonic activity and effect on sodium- and potassium-activated adenosine triphosphatase □ Cardiotonic agents, potential—3β-thiocyanato-14β-hydroxy-5β-card-20(22)-enolide synthesized and screened □ Adenosine triphosphatase, sodium and potassium activated—effect of 3β-thiocyanato-14β-hydroxy-5β-card-20(22)-enolide evaluated

Most naturally occurring cardioactive steroids are characterized by the presence of a free hydroxyl group at position 3β, as in digitoxigenin (I). While the changes in biological properties elicited by glycosidation, esterification, epimerization, and oxidation of the cardenolide 3β-hydroxyl group are well known and have been reviewed (1), nothing has been published concerning the effect of replacing the oxygen atom at position 3β by other heteroatoms such as nitrogen or sulfur.

The 3α- and 3β-aminodigitoxigenins were prepared (2), but their pharmacological actions were not described. Removal of the 3β-oxygen atom of I to give 3-deoxydigitoxigenin results in a compound that has cardiotonic activity on the isolated frog heart comparable to that of I (3, 4).

As part of a program to prepare and study the pharmacological actions of sulfur-containing cardenolides, the synthesis and biological properties of the 3β-thiocyanato analog (II) of I are now reported.

EXPERIMENTAL[1]

Chemistry—3β-Thiocyanato-14β-hydroxy-5β-card-20(22)-enolide (II) was prepared by a two-step sequence from 3-epidigitoxi-

[1] Melting points were taken on a Fisher-Johns melting-point stage and are uncorrected. UV absorption spectra were determined in 95% ethanol on a Beckman model DK2A recording spectrophotometer. IR absorption spectra were recorded on a Beckman model 8 recording spectrophotometer. NMR spectra were determined on a Varian EM 360 spectrometer. Microanalyses were conducted by Spang Microanalytical Laboratory, Ann Arbor, Mich. TLC was carried out with silica gel G. Column chromatography was carried out with silica gel 60 (Brinkmann 7734).

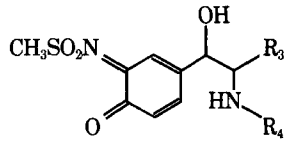

VII

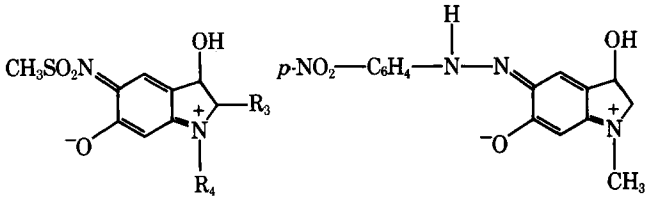

VIII IX

That V, an isomer of I differing only in the positions of the ring substituents, produced only about one-twentieth the fluorescence of I was somewhat surprising. No explanation is offered, but it is interesting to note that compounds in this series (*i.e.*, those with the methanesulfonamido group *para* to the ethanolamine side chain) also have considerably lower adrenergic potency (4).

Prasad *et al.* (2) showed that isoproterenol and isoproterenolsulfonic acid do not interfere with their fluorometric method. Similarly, the ketone VI and the sulfonic acid IV do not form fluorescent species under the conditions used to analyze I. These final tests were designed only to demonstrate the lack of interference from IV and VI and do not preclude the possibility that these compounds might form fluorescent derivatives under different conditions.

REFERENCES

(1) V. K. Prasad, R. A. Ricci, B. C. Nunning, and A. P. Granatek, *J. Pharm. Sci.*, **62**, 1130(1973).

(2) *Ibid.*, **62**, 1135(1973).

(3) A. A. Larsen and P. M. Lish, *Nature*, **203**, 1284(1964).

(4) A. A. Larsen, W. A. Gould, H. R. Roth, W. T. Comer, R. H. Uloth, K. W. Dungan, and P. M. Lish, *J. Med. Chem.*, **10**, 462(1967).

(5) A. A. Larsen and R. H. Uloth, U.S. pat. 3,660,487 (1972).

(6) G. L. Mattok and D. L. Wilson, *Can. J. Chem.*, **45**, 2473(1967).

(7) *Ibid.*, **45**, 1721(1967).

(8) R. Laverty and K. M. Taylor, *Anal. Biochem.*, **22**, 269(1968).

(9) R. A. Heacock and W. S. Powell, *Progr. Med. Chem.*, **9**, 275(1972).

(10) W. H. Harrison, *Arch. Biochem. Biophys.*, **101**, 116(1963).

(11) W. S. Powell and R. A. Heacock, *J. Chem. Soc. P1*, **1973**, 509.

ACKNOWLEDGMENTS AND ADDRESSES

Received March 21, 1975, from the *Division of Pharmaceutical Sciences, Mead Johnson Research Center, Mead Johnson and Company, Evansville, IN 47721*

Accepted for publication July 21, 1975.

The authors thank Dr. D. G. Mikolasek for providing analytical data on IV and other technical assistance. They also thank Dr. W. T. Comer for his interest and assistance and Dr. M. J. Bartek for help in recording fluorescence spectra.

* Present address: Armak Co., Chicago, Ill.

‡ To whom inquiries should be directed.

Thiocardenolides I: Synthesis and Biological Actions of 3β-Thiocyanato-14β-hydroxy-5β-card-20(22)-enolide

HANLEY N. ABRAMSON *‡, CHIAN L. HUANG *, THOMAS F. WU *, and THOMAS TOBIN ‡

Abstract □ The synthesis of a 3β-thiocyanatocardenolide is described. The compound exhibited about 0.1 times the cardiotonic effect of digitoxigenin in the isolated frog heart preparation. At a dosage of 20 mg/kg in the intact rat, it elicited ECG changes similar to those seen with a 10-mg/kg dose of digitoxigenin. Studies also revealed the new cardenolide to be a reversible inhibitor of sodium- and potassium-activated adenosine triphosphatase.

Keyphrases □ Thiocardenolides—3β-thiocyanato-14β-hydroxy-5β-card-20(22)-enolide synthesized, screened for cardiotonic activity and effect on sodium- and potassium-activated adenosine triphosphatase □ Cardiotonic agents, potential—3β-thiocyanato-14β-hydroxy-5β-card-20(22)-enolide synthesized and screened □ Adenosine triphosphatase, sodium and potassium activated—effect of 3β-thiocyanato-14β-hydroxy-5β-card-20(22)-enolide evaluated

Most naturally occurring cardioactive steroids are characterized by the presence of a free hydroxyl group at position 3β, as in digitoxigenin (I). While the changes in biological properties elicited by glycosidation, esterification, epimerization, and oxidation of the cardenolide 3β-hydroxyl group are well known and have been reviewed (1), nothing has been published concerning the effect of replacing the oxygen atom at position 3β by other heteroatoms such as nitrogen or sulfur.

The 3α- and 3β-aminodigitoxigenins were prepared (2), but their pharmacological actions were not described. Removal of the 3β-oxygen atom of I to give 3-deoxydigitoxigenin results in a compound that has cardiotonic activity on the isolated frog heart comparable to that of I (3, 4).

As part of a program to prepare and study the pharmacological actions of sulfur-containing cardenolides, the synthesis and biological properties of the 3β-thiocyanato analog (II) of I are now reported.

EXPERIMENTAL[1]

Chemistry—3β-Thiocyanato-14β-hydroxy-5β-card-20(22)-enolide (II) was prepared by a two-step sequence from 3-epidigitoxi-

[1] Melting points were taken on a Fisher-Johns melting-point stage and are uncorrected. UV absorption spectra were determined in 95% ethanol on a Beckman model DK2A recording spectrophotometer. IR absorption spectra were recorded on a Beckman model 8 recording spectrophotometer. NMR spectra were determined on a Varian EM 360 spectrometer. Microanalyses were conducted by Spang Microanalytical Laboratory, Ann Arbor, Mich. TLC was carried out with silica gel G. Column chromatography was carried out with silica gel 60 (Brinkmann 7734).

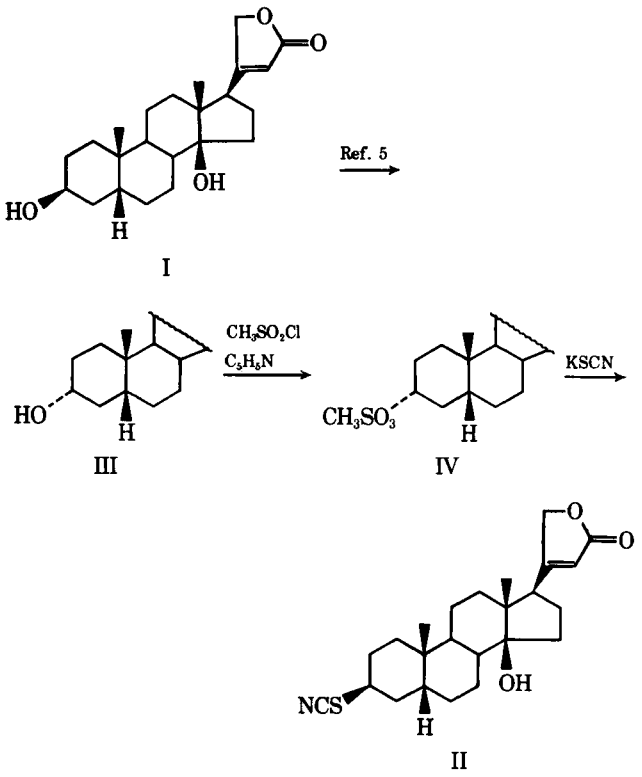

Scheme I

genin (III) (Scheme I). While the methanesulfonate ester (IV) of III was readily prepared, attempts to convert III to its *p*-toluenesulfonate ester, as described by Sawlewicz *et al.* (2), gave only starting material.

3α-Methanesulfonyloxy- 14β-hydroxy-5β-card-20(22) -enolide (IV)—A solution of 545 mg (1.46 mmoles) of III (5) in 10 ml of dry pyridine was cooled to 0° in an ice–salt bath and treated with 3.6 ml of freshly distilled methanesulfonyl chloride. The mixture was placed in the refrigerator for 3 hr. TLC [benzene–ethyl acetate (1:2)] showed the reaction to be complete. The reaction mixture then was poured onto ice, and the precipitate was collected by filtration, washed with water, and dried *in vacuo*.

The crude product weighed 617 mg (93% yield), mp 134–138°, and was suitable for use in the next reaction; IR: ν_{max} (chloroform) 3620 (OH), 1790 and 1745 (butenolide doublet), 1630 (C=C), and 1360 and 1170 (sulfonate doublet) cm^{-1}; UV: λ_{max} (ethanol) 217 nm (ϵ = 19,500); NMR ($CDCl_3$; tetramethylsilane as internal standard): δ 0.88 (3H, s, 18-CH_3), 0.93 (3H, s, 19-CH_3), 3.10 (3H, s, SO_2CH_3), 4.91 (2H, s, 21-CH_2), and 5.88 (1H, s, 22=CH—).

3β-Thiocyanato-14β-hydroxy-5β-card-20(22)-enolide (II)—A solution of IV (500 mg, 1.10 mmoles) and 250 mg (2.59 mmoles) of potassium thiocyanate in 6 ml of dimethylformamide was stirred at 100° for 2 hr. The reaction mixture was poured onto ice. The precipitate was filtered, washed with water, and dried *in vacuo*. The product was purified by column chromatography, using increasing concentrations of chloroform in benzene as the eluent. A total of 328 mg (72% yield) of pure II was eluted with chloroform–benzene (4:1). Recrystallization from acetone–water gave 229 mg, mp 234–234.5°; IR: ν_{max} (mineral oil) 3495 (OH), 2145 (sharp and medium, —SCN), 1790 and 1745 (butenolide doublet), and 1630 (C=C) cm^{-1}; UV: λ_{max} (ethanol) 216.5 nm (ϵ = 19,700); NMR (CD_3SOCD_3; tetramethylsilane as internal standard): δ 0.77 (3H, s, 18-CH_3), 0.93 (3H, s, 19-CH_3), 4.15 (1H, m, 3α-H), 4.90 (2H, s, 21-CH_2), and 5.94 (1H, s, 22=CH—).

Anal.—Calc. for $C_{24}H_{33}NO_3S$: C, 69.36; H, 8.00; N, 3.37; S, 7.72. Found: C, 69.37; H, 8.06; N, 3.42; S, 7.67.

While the thiocyanate anion may be considered to be an ambident nucleophile, the product II was identified as a thiocyanate rather than as an isothiocyanate on the basis of the IR spectrum. Thiocyanates show medium to strong, sharp absorption at 2170–2135 cm^{-1}, while isothiocyanates exhibit a very strong and broad band at 2150–2050 cm^{-1} (6). The multiplet centered at δ 4.15 in the NMR of II due to the deshielded equatorially oriented 3α-proton compares well with the value of δ 4.04 found for the equatorially oriented 3β-proton of 3α-thiocyanato-5α-steroids (7). Axial orientation of the proton at position 3 of II would be expected to result in absorption near δ 3.15 (7).

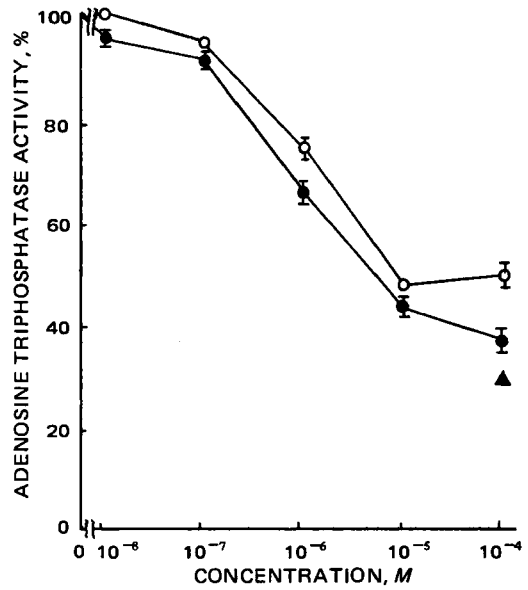

Figure 1—*Inhibition of a rat brain sodium- and potassium-activated adenosine triphosphatase preparation (10) (40 μg) in the presence of sodium (100 mmoles), potassium (15 mmoles), and adenosine triphosphate (5 mmoles) after incubation for 10 min at 37°. The average adenosine triphosphatase activity is 117 ± 4.0 μmoles P_i/mg protein/hr. Key: ○, inhibitory activity of II (means ± SE of determinations on six enzyme preparations); ●, inhibitory activity of I (means ± SE of determinations on four enzyme preparations); and ▲, inhibition by 10^{-4} M ouabain (mean of two determinations).*

Biological Evaluation—Isolated frog hearts (six preparations) were used to evaluate the cardiotonic effect of II according to Straub's method (8). Saline was used as the control, and digitoxigenin (I) was used as the reference standard. The frog hearts were perfused with Frog–Ringers solutions of both compounds, and the changes in chronotropic and inotropic responses were recorded on a smoked-drum chymograph. Analytically pure samples of II were used in the succeeding experiments.

The effect of II on the intact rat heart was studied using three animals. The animals were anesthetized with pentobarbital (45 mg/kg ip), and the cardiac actions were recorded on a polygraph recorder[2]. Saline was used as the control, and digitoxigenin was used as the standard.

All studies of sodium- and potassium-activated adenosine triphosphatase inhibition utilized the standard rat brain enzyme preparation (9) as modified by Tobin *et al.* (10). About 40 μg of the enzyme was incubated with 100 mmoles of sodium (Na^+), 15 mmoles of potassium (K^+), and 5 mmoles of adenosine triphosphate[3] for 10 min at 37°. The adenosine triphosphatase activity was measured and expressed as a percentage of the total enzyme activity [117 ± 4.0 μmoles of inorganic phosphate (P_i)/mg of protein/hr] at various concentrations of I and II. The results are presented in Fig. 1. The extent of inhibition by 10^{-4} *M* ouabain is indicated for comparison.

The effect of II on the equilibrium level of ^{3}H-ouabain binding to sodium- and potassium-activated adenosine triphosphatase was measured upon incubation of about 100 μg of the rat brain enzyme with 100 mmoles of sodium (Na^+), 0.2 mmole of magnesium (Mg^{+2}), and 5 mmoles of adenosine triphosphate at 37°. A tracer amount (3×10^{-10} mole) of ^{3}H-ouabain[4] (11.7 Ci/mmole) was added to the system at zero time. The counts per minute bound to

[2] Sanborn model 964.
[3] Sigma Chemical Co., St. Louis, Mo.
[4] New England Nuclear, Boston, Mass.

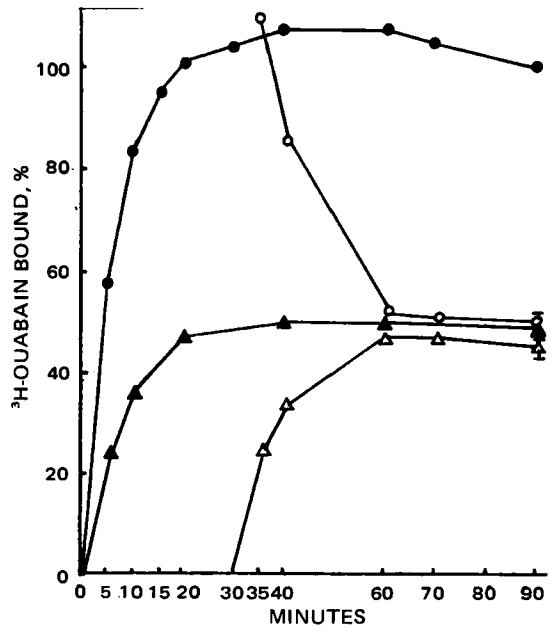

Figure 2—*Effect of II on the equilibrium level of ^{3}H-ouabain binding to a rat brain sodium- and potassium-activated adenosine triphosphatase preparation (10) (100 μg) in the presence of sodium (100 mmoles), magnesium (0.2 mmole), and adenosine triphosphate (5 mmoles) at 37°. Counts per minute of ^{3}H-ouabain at each time point is expressed as a percentage of the counts per minute of ^{3}H-ouabain bound at 90 min (equivalent to 11.4 ± 0.2 pmoles of ^{3}H-ouabain/mg of protein bound). All points are the means of experimental determinations on two different enzyme preparations, except for the 90-min data points which are the means ± SE of experimental determinations on four different enzyme preparations. Key: ●, control, 3 × 10^{-10} mole of ^{3}H-ouabain added at time zero; ▲, II (1 × 10^{-6} mole) and ^{3}H-ouabain added simultaneously; ○, II added 30 min after ^{3}H-ouabain; and △, ^{3}H-ouabain added 30 min after II.*

the enzyme was measured when: (*a*) ^{3}H-ouabain was added alone, (*b*) II was added to the binding system 30 min after the ^{3}H-ouabain, (*c*) II and ^{3}H-ouabain were added simultaneously, and (*d*) ^{3}H-ouabain was added 30 min after II. The results are summarized in Fig. 2. The number of counts per minute bound at each time point is expressed as a percentage of the number bound at 90 min in the presence of sodium ion and adenosine triphosphate, which was equivalent to 11.4 ± 0.2 pmoles of ^{3}H-ouabain/mg of protein bound.

In a study of the reversibility of the inhibition by II of sodium- and potassium-activated adenosine triphosphatase, about 400 μg of the enzyme was incubated with 100 mmoles of sodium chloride, 1 mmole of magnesium chloride, and 50 mmoles of tromethamine[3] (pH 7.4). The experiment was started by adding 0.1 mmole of adenosine triphosphate and 0.1 mmole of I or II or an equivalent volume of tromethamine buffer (control) to the system and incubating at 37° for 10 min.

At the end of this period, the enzyme was washed free of unreacted compound by twice centrifuging at 35,000×*g* and resuspending in 2 ml of tromethamine buffer. An aliquot was taken for protein estimation, and the enzyme was incubated at 37°. The adenosine triphosphatase activity of these preparations was expressed as a percentage of that of enzymes preincubated and washed in the absence of drugs, which averaged 152.6 ± 3.0 μmoles P_i/mg protein/hr. The results are shown in Fig. 3.

RESULTS AND DISCUSSION

In the isolated frog heart, no remarkable effect was seen in the dilution range of 1 × 10^{-5}–1 × 10^{-7} of II. At 1 × 10^{-4} dilution of II, the hearts responded with increased amplitude following a transient depressant response. A similar effect was observed with digitoxigenin at a dilution of 1 × 10^{-5}, except that no initial transient

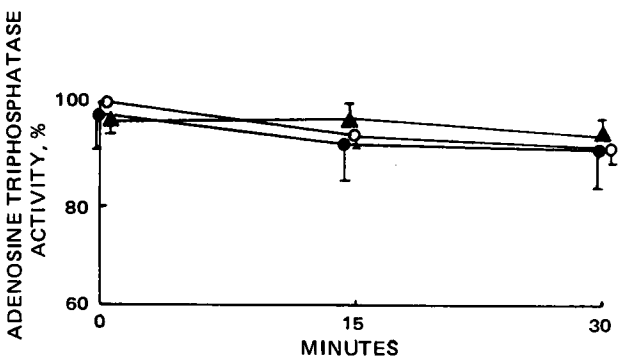

Figure 3—*Reversibility of inhibition of a rat brain sodium- and potassium-activated adenosine triphosphatase preparation (10) (400 μg) after incubation at 37° for 10 min in the presence of sodium (100 mmoles), magnesium (1 mmole), tromethamine buffer (50 mmoles, pH 7.4), adenosine triphosphate (0.1 mmole), and either I or II. Each time point represents the extent of adenosine triphosphatase activity (±SE of experimental determinations on four different enzyme preparations) after the enzyme has been washed free of either I or II and again incubated at 37°. Adenosine triphosphatase activity is expressed as a percentage of that of the enzymes preincubated and washed in the absence of drug, which averaged 152.6 ± 3.0 μmoles P_i/mg protein/hr. Key: ○, control (tromethamine buffer); ●, after incubating with 0.1 mmole of I and washing; and ▲, after incubating with 0.1 mmole of II and washing.*

depressant action was observed. At a dilution of 1 × 10^{-3}, II caused a decreased amplitude on the heart, which was not modified by atropine. Digitoxigenin exhibited the same response at a dilution of 1 × 10^{-4}. It is concluded that II has a stimulant action on the isolated frog heart at 1 × 10^{-4} dilution but a depressant effect at 1 × 10^{-3} dilution. The effect of II is thus about 0.1 that of digitoxigenin on the isolated frog heart.

Injection of 10 mg/kg iv of II had no noticeable effect on the lead II ECG of the intact rat heart. At a dosage level of 20 mg/kg, there was a decrease in the amplitude of the T wave and a reduction of the amplitude of the QRS complex. In general, the PR interval was prolonged with a shortened QT segment at 30 mg/kg. Similar responses were observed with digitoxigenin at lower doses (10 mg/kg).

The results of the interaction of II with sodium- and potassium-activated adenosine triphosphatase indicate that the inhibitory effect of II on the enzyme is slightly less than that of digitoxigenin (Fig. 1) and is reversible (Figs. 2 and 3). Figure 2 shows that the same equilibrium level of ^{3}H-ouabain was found regardless of the order of addition of the ligands, suggesting that II competes with the ouabain for the cardiotonic steroid binding site on the enzyme.

It thus appears that substitution of the 3β-hydroxyl group of digitoxigenin by a 3β-thiocyanato group does not seriously alter the ability of the cardenolide to interact at the steroid binding site of sodium- and potassium-activated adenosine triphosphatase, although there is a reduction in cardioactivity. This work is currently being expanded to a study of other thiocardenolides containing thiol and thioacetyl groupings at position 3β to ascertain whether it is possible to develop active-site-directed irreversible inhibitors of sodium- and potassium-activated adenosine triphosphatase that can act by the formation of disulfide bonds to the enzyme.

REFERENCES

(1) C. S. Davis and R. P. Halliday, in "Medicinal Chemistry," 3rd ed., part II, A. Burger, Ed., Wiley–Interscience, New York, N.Y., 1970, p. 1065.

(2) L. Sawlewicz, E. Weiss, H. H. A. Linde, and K. Meyer, *Helv. Chim. Acta*, **55**, 2452(1972).

(3) Y. Saito, Y. Kanemasa, and M. Okada, *Chem. Pharm. Bull.*, **18**, 629(1970).

(4) K. Takeda, T. Shigei, and S. Imai, *Experientia*, **26**, 867(1970).

(5) A. Yamada, *Chem. Pharm. Bull.*, **8**, 18(1960).
(6) M. B. Colthup, L. H. Daly, and S. B. Wiberley, "Introduction to Infrared and Raman Spectroscopy," Academic, New York, N.Y., 1964, p. 204.
(7) K. Tori and T. Komeno, *Tetrahedron*, **21**, 309(1965).
(8) W. Straub, *Biochem. Z.*, **75**, 132(1916).
(9) T. Akera and T. M. Brody, *Mol. Pharmacol.*, **5**, 605(1969).
(10) T. Tobin, T. Akera, C. S. Han, and T. M. Brody, *ibid.*, **10**, 501(1974).

ACKNOWLEDGMENTS AND ADDRESSES

Received November 25, 1974, from the *College of Pharmacy and Allied Health Professions, Wayne State University, Detroit, MI 48202, and the ‡Department of Pharmacology, Michigan State University, East Lansing, MI 48823

Accepted for publication July 16, 1975.

Supported by a grant from the Michigan Heart Association.

ˣ To whom inquiries should be directed.

Fluorometric Determination of Cephradine in Plasma

ANTHONY F. HEALDˣ, CALLIXTUS E. ITA, and ERIC C. SCHREIBER

Abstract □ A fluorometric method was developed for the determination of cephradine in plasma. A fluorescent product is formed when samples of deproteinized plasma containing cephradine are heated for 3 hr at 100° and pH 1. The fluorescence is determined in sodium hydroxide solution (pH 13.5) at excitation and emission wavelengths of 350 and 445 nm, respectively. Only 0.1 ml of plasma is required, and concentrations of cephradine as small as 0.1 μg/ml may be determined. In plasma samples from a dog taken over a 10-hr period after an intramuscular injection of 250 mg of cephradine, essentially similar concentrations of cephradine were obtained by the fluorometric method and a standard microbiological bioassay.

Keyphrases □ Cephradine—fluorometric analysis, compared to microbiological bioassay, plasma □ Fluorometry—analysis, cephradine in plasma □ Antibiotics—cephradine, fluorometric analysis, plasma

Cephradine (I), 7-[D-2-amino-2-(1,4-cyclohexadien-1-yl)acetamido]-3-methyl-8-oxo-5-thia-1-azabicyclo[4.2.0]oct-2-ene-2-carboxylic acid, is a semisynthetic cephalosporin (1). The concentration in biological fluids of cephradine, a poorly bound antibiotic, may be determined microbiologically (1). Colorimetric assays for cephalosporins (2) and cephradine (3) also have been reported.

During studies of the bioavailability of cephradine, it became desirable to develop a rapid, sensitive, chemical assay of the concentration of this antibiotic in plasma. Jusko (4) described a fluorometric assay for ampicillin that appeared to be specific for penicillins containing the structure enclosed by the dotted line in Structure I.

During initial attempts to adapt this assay to cephradine, plasma concentrations of cephradine less than 5–10 μg/ml could not be determined. Because the first step in the formation of a fluorescent product from ampicillin is the acid hydrolysis of the β-lactam ring, the greater stability of this ring in cephalosporins might be a major factor in the reduced sensitivity of the assay when applied to cephradine. The present sensitive analytical method for cephradine was developed by increasing the severity of the hydrolysis conditions.

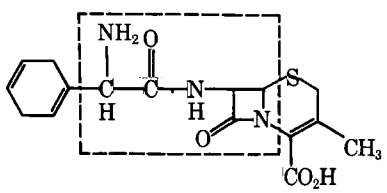

I

EXPERIMENTAL

Reagents—The following reagents were used: 10% aqueous trichloroacetic acid solution, 4 *N* sodium hydroxide solution, and 0.2 *M* potassium chloride–hydrochloric acid buffer, pH 1.0. Glass-distilled water was used throughout, and the use of polyethylene containers was avoided (5).

Cephradine Standard Curve—Cephradine standards were added to control plasma. Because of possible variations in the water content of separate batches of cephradine, each cephradine standard was calibrated microbiologically. All weights were expressed as micrograms or milligrams of microbiological activity. Aliquots of a stock solution of cephradine in water (100 μg/ml) were diluted with plasma to prepare a suitable range of working standards as well as a blank. Three 0.1-ml aliquots of each standard were carried through the procedure with each batch of plasma samples.

Microbiological Method—The concentration of cephradine in plasma samples was determined microbiologically by an agar-diffusion method, with *Sarcina lutea* (ATCC 9341) as the test organism.

Animal Experiment—Cephradine for injection (250 mg) was injected into the semitendinosus muscle of a male beagle dog (10.6 kg). Plasma was obtained at intervals for 10 hr, and the cephradine content of each sample was determined by both the spectrofluorometric and microbiological methods.

Fluorometric Assay Procedure—Fluorescence was measured[1] at excitation and emission wavelengths of 350 and 445 nm, respectively. The instrument was zeroed with a reagent blank and set to read 90% of full-scale deflection against a suitable cephradine standard, depending on the range of concentrations expected in the unknowns.

[1] Farrand Mark I spectrofluorometer.

(5) A. Yamada, *Chem. Pharm. Bull.*, **8**, 18(1960).
(6) M. B. Colthup, L. H. Daly, and S. B. Wiberley, "Introduction to Infrared and Raman Spectroscopy," Academic, New York, N.Y., 1964, p. 204.
(7) K. Tori and T. Komeno, *Tetrahedron*, **21**, 309(1965).
(8) W. Straub, *Biochem. Z.*, **75**, 132(1916).
(9) T. Akera and T. M. Brody, *Mol. Pharmacol.*, **5**, 605(1969).
(10) T. Tobin, T. Akera, C. S. Han, and T. M. Brody, *ibid.*, **10**, 501(1974).

ACKNOWLEDGMENTS AND ADDRESSES

Received November 25, 1974, from the *College of Pharmacy and Allied Health Professions, Wayne State University, Detroit, MI 48202, and the ‡Department of Pharmacology, Michigan State University, East Lansing, MI 48823

Accepted for publication July 16, 1975.

Supported by a grant from the Michigan Heart Association.

ˣ To whom inquiries should be directed.

Fluorometric Determination of Cephradine in Plasma

ANTHONY F. HEALDˣ, CALLIXTUS E. ITA, and ERIC C. SCHREIBER

Abstract □ A fluorometric method was developed for the determination of cephradine in plasma. A fluorescent product is formed when samples of deproteinized plasma containing cephradine are heated for 3 hr at 100° and pH 1. The fluorescence is determined in sodium hydroxide solution (pH 13.5) at excitation and emission wavelengths of 350 and 445 nm, respectively. Only 0.1 ml of plasma is required, and concentrations of cephradine as small as 0.1 μg/ml may be determined. In plasma samples from a dog taken over a 10-hr period after an intramuscular injection of 250 mg of cephradine, essentially similar concentrations of cephradine were obtained by the fluorometric method and a standard microbiological bioassay.

Keyphrases □ Cephradine—fluorometric analysis, compared to microbiological bioassay, plasma □ Fluorometry—analysis, cephradine in plasma □ Antibiotics—cephradine, fluorometric analysis, plasma

Cephradine (I), 7-[D-2-amino-2-(1,4-cyclohexadien-1-yl)acetamido]-3-methyl-8-oxo-5-thia-1-azabicyclo[4.2.0]oct-2-ene-2-carboxylic acid, is a semisynthetic cephalosporin (1). The concentration in biological fluids of cephradine, a poorly bound antibiotic, may be determined microbiologically (1). Colorimetric assays for cephalosporins (2) and cephradine (3) also have been reported.

During studies of the bioavailability of cephradine, it became desirable to develop a rapid, sensitive, chemical assay of the concentration of this antibiotic in plasma. Jusko (4) described a fluorometric assay for ampicillin that appeared to be specific for penicillins containing the structure enclosed by the dotted line in Structure I.

During initial attempts to adapt this assay to cephradine, plasma concentrations of cephradine less than 5–10 μg/ml could not be determined. Because the first step in the formation of a fluorescent product from ampicillin is the acid hydrolysis of the β-lactam ring, the greater stability of this ring in cephalosporins might be a major factor in the reduced sensitivity of the assay when applied to cephradine. The present sensitive analytical method for cephradine was developed by increasing the severity of the hydrolysis conditions.

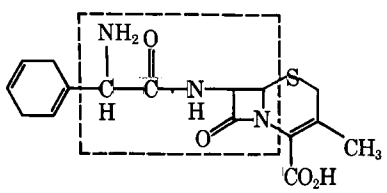

I

EXPERIMENTAL

Reagents—The following reagents were used: 10% aqueous trichloroacetic acid solution, 4 *N* sodium hydroxide solution, and 0.2 *M* potassium chloride–hydrochloric acid buffer, pH 1.0. Glass-distilled water was used throughout, and the use of polyethylene containers was avoided (5).

Cephradine Standard Curve—Cephradine standards were added to control plasma. Because of possible variations in the water content of separate batches of cephradine, each cephradine standard was calibrated microbiologically. All weights were expressed as micrograms or milligrams of microbiological activity. Aliquots of a stock solution of cephradine in water (100 μg/ml) were diluted with plasma to prepare a suitable range of working standards as well as a blank. Three 0.1-ml aliquots of each standard were carried through the procedure with each batch of plasma samples.

Microbiological Method—The concentration of cephradine in plasma samples was determined microbiologically by an agar-diffusion method, with *Sarcina lutea* (ATCC 9341) as the test organism.

Animal Experiment—Cephradine for injection (250 mg) was injected into the semitendinosus muscle of a male beagle dog (10.6 kg). Plasma was obtained at intervals for 10 hr, and the cephradine content of each sample was determined by both the spectrofluorometric and microbiological methods.

Fluorometric Assay Procedure—Fluorescence was measured[1] at excitation and emission wavelengths of 350 and 445 nm, respectively. The instrument was zeroed with a reagent blank and set to read 90% of full-scale deflection against a suitable cephradine standard, depending on the range of concentrations expected in the unknowns.

[1] Farrand Mark I spectrofluorometer.

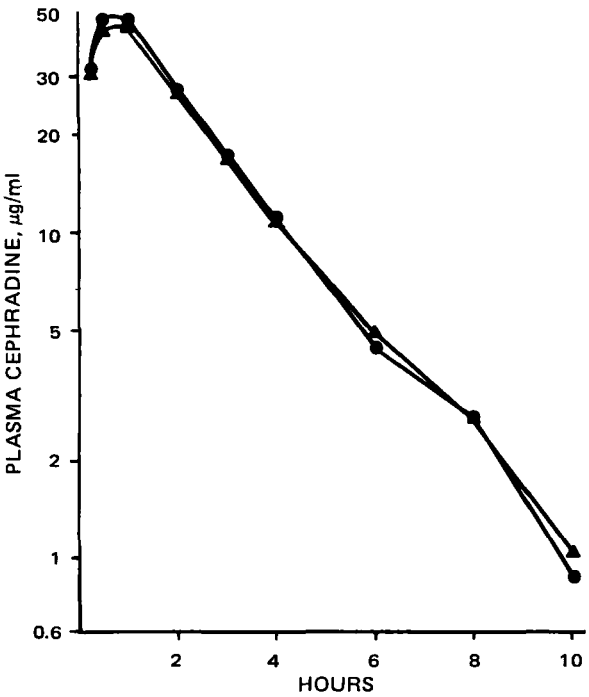

Figure 1—*Concentrations of cephradine in plasma from a male beagle dog after the intramuscular injection of 250 mg of cephradine. Key: ●, fluorometric assay; and ▲, microbiological assay.*

Duplicate samples were prepared by transferring 0.1-ml aliquots of each plasma sample to 2-ml centrifuge tubes. Trichloroacetic acid solution (1.0 ml) was added to each tube, the contents were mixed well, and the tubes were centrifuged for 5 min at 800×*g*. Portions (0.1 ml) of the supernate were transferred to graduated Pyrex centrifuge tubes, followed by 1.0 ml of pH 1.0 potassium chloride–hydrochloric acid buffer.

After mixing, each tube was capped with a glass marble and incubated at 100° for 3 hr. When the tubes had cooled to room temperature, the volumes were made up to 2 ml with distilled water. Sodium hydroxide solution (0.5 ml) was added to each tube, and the contents were mixed well. The fluorescence of each standard and unknown was determined, a standard curve was prepared, and the concentration of cephradine in each sample was read directly from the standard curve.

RESULTS AND DISCUSSION

The fluorescence of cephradine was linear over the range of 0.1–100 μg/ml of plasma. A sample of control plasma spiked with 0.1 μg of cephradine/ml gave a reading of 0.135 fluorescence unit, as compared to a reading of 0.01 unit for the control plasma. The coefficients of variation for triplicate samples of cephradine at different concentrations in plasma were 13% at 0.1 μg/ml, 5.8% at 0.5 μg/ml, 3.7% at 1.0 μg/ml, and 2.7% at 2.0 μg/ml. The coefficient of variation of the microbiological assay for five replicate samples was 3.5% at 0.5 μg/ml[2]. Although it appeared to be more precise, the microbiological assay required a much larger volume of plasma and was more time consuming than the fluorometric method.

Because they contain the structure enclosed by the dotted line in Structure I, cephalexin, ampicillin, and epicillin also react in this procedure, but other common cephalosporins and penicillins do not. Fluorescent material might possibly be derived from the hydrolysis products of cephradine. However, this is not a problem in *in vivo* studies, because cephradine is excreted unchanged (1). Both spectrofluorometric and microbiological methods gave similar results for the concentration of cephradine in plasma after its intramuscular injection (Fig. 1).

Conversion of cephradine to the fluorophore was not complete after the 3-hr incubation. Since most of the observed cephradine concentrations were in excess of 1 μg/ml of plasma, the operating convenience of the 3-hr hydrolysis time outweighed any gain in sensitivity that might have been obtained by prolonging the incubation. The hydrolysis time may be increased at the discretion of the investigator. Care should be taken that all standard and unknown samples are subjected to identical conditions of hydrolysis and cooling.

REFERENCES

(1) I. Weliky, H. H. Gadebusch, K. Kripalani, P. Arnow, and E. C. Schreiber, *Antimicrob. Ag. Chemother.*, **5**, 49(1974).

(2) L. P. Marelli, *J. Pharm. Sci.*, **61**, 1647(1972).

(3) J. Kirschbaum, *ibid.*, **63**, 923(1974).

(4) W. J. Jusko, *ibid.*, **60**, 728(1971).

(5) R. F. Chen, *Anal. Lett.*, **5**, 664(1972).

ACKNOWLEDGMENTS AND ADDRESSES

Received April 25, 1975, from the *Department of Drug Metabolism, E. R. Squibb & Sons, Inc., New Brunswick, NJ 08903*

Accepted for publication August 12, 1975.

[x] To whom inquiries should be directed.

[2] T. B. Platt, E. R. Squibb & Sons, Inc., personal communication.

Reduced Acid-Neutralizing Velocity of Spray-Dried Agglomerated Magnesium Carbonate

Keyphrases □ Magnesium carbonate, agglomerated—spray dried, acid-neutralizing velocity □ Spray drying—agglomerated magnesium carbonate, acid-neutralizing velocity □ Acid-neutralizing velocity—spray-dried agglomerated magnesium carbonate

To the Editor:

In a recent article by Kawashima and Takenaka (1), certain conclusions were made based on the Hixson–Crowell law (2). This law is based on the following assumptions: (*a*) the film theory of Nernst–Brunner (3, 4) holds; (*b*) sink conditions apply; (*c*) the particles are spherical; (*d*) the substance dissolves isotropically, *i.e.*, has a constant shape factor; (*e*) there is no (measurable) particle-size *versus* solubility dependence; and (*f*) the powder is monodispersed.

Kawashima and Takenaka (1) used a rearranged form of the Hixson–Crowell law to get the relationships between diffusion layer thickness and parameters such as the initial particle size of the sample, temperature, and rate of agitation. They observed that the diffusion layer thickness increases linearly with increasing particle size and decreases curvilinearly with increasing temperature or agitation rate. The rearranged equation used had the following form:

$$\frac{d}{dt}[C_L/C_e] = (DS_wC_e/X)\,[1 - (C_L/C_e)]^{5/3} \qquad \text{(Eq. 1)}$$

where:

C_L = concentration of solute (milligrams per milliliter)
C_e = equilibrium solubility (milligrams per milliliter)
S_w = specific surface area given by $6/(d_0\rho)$ (square centimeters per gram)
d_0 = mean particle diameter (centimeters)
D = diffusion coefficient (square centimeters per second)
ρ = true particle density (grams per milliliter)
X = diffusion layer thickness (centimeters)

The authors did not state the assumptions made in deriving Eq. 1 from the Hixson–Crowell law. These assumptions (except for sink condition) are the same as those that applied in deriving the Hixson–Crowell law itself, and the initial amount of the sample required (W_0) is given by the expression:

$$W_0 = VC_e = W_e \qquad \text{(Eq. 2)}$$

where V is the volume of the dissolution medium (milliliters), and W_e is the amount of solid required just to saturate the dissolution medium (grams).

For the dissolution studies, the authors (1) used salicylic acid and an initial weight of 0.5 g; they employed 450 ml of distilled water as the dissolution medium. They carried out their experiments at three different temperatures (27, 37, and 47°). The drawback in their experimental design is that the initial 0.5-g amount does not satisfy the condition of Eq. 2, *i.e.*, W_0 is different from W_e.

The United States Pharmacopeia lists the solubility of salicylic acid in distilled water at 25° as 0.0022 g/ml (5); therefore, the initial amount required for dissolution would be $W_0 = C_eV = 450 \times 0.0022 = 0.99$ g. Even at 25°, the amount used (0.5 g) falls short of this figure. Deviations would, of course, be much larger with increasing temperatures (*i.e.*, at 37 and 47°). It is obvious also that the amount used must change with temperature in the same ratio as the solubility changes.

Since the dissolution experiments carried out by Kawashima and Takenaka (1) were under conditions where $W_0 < W_e$, the proper nonsink equations for this condition would be the equations reported by Short *et al.* (6) and Patel and Carstensen (7). The Short–Sharkey–Rhodes equation in the form shown in Ref. 7 is:

$$\psi(W) = -\frac{DS_w{W_0}^{1/3}}{XV}t + \psi(W_0) \qquad \text{(Eq. 3)}$$

where:

$$\psi(W) = 0.5F^{-2}[\ln\{(U+F)^2/(F^2 - UF + U^2)\}] + \sqrt{3}F^{-2}\arctan[(2U - F)/(F\sqrt{3})] \qquad \text{(Eq. 4)}$$

where:

$$F^3 = W_e - W_0 \qquad \text{(Eq. 5)}$$

and:

$$W = U^3 = \text{amount (grams) of powder remaining} \qquad \text{(Eq. 6)}$$

According to the experimental conditions of Kawashima and Takenaka (1), Eq. 3 should have been used to describe the dissolution of salicylic acid and to calculate the diffusion layer thickness (X) from the slope of the dissolution profile. If Ref. 1 had contained tabulated values of C_L *versus* t, then Eq. 3 could have been used directly and, by knowing all values except X, X could have been calculated from the slope of ψ *versus* t plots.

Equation 3 has been used in this communication to reconstruct the dissolution profile for the conditions taken from Ref. 1. For one set of experiments carried out at 37° and 620 rpm, the values were as follows: t = 37°, $W_0 = 0.5$ g, $W_e = 1.44$ g (Table I), $D = 4.85 \times$

Table I—Calculated Initial Amount Required According to Eq. 1

Temperature	Solubility, g/ml	Initial Amount Required According to Eq. 1, $W_0 = C_e V$, g	Initial Amount Used, g
27°	0.00231	1.04	0.5
37°	0.00320[a]	1.44	0.5
47°	0.00465[b]	2.09	0.5

[a] Determined in this laboratory. [b] Reference 8.

10^{-6} cm²/sec, V = 450 ml, d_0 = 0.003 cm, ρ = 1.4 g/ml, and $X = 34 \times 10^{-4}$ cm. Then:

$$\psi(W) = \psi(W_0) - \frac{DS_w W_0^{1/3}}{XV} t = 1.326 - 0.0036t \quad \text{(Eq. 7)}$$

Equation 7 is obtained by substituting the given values in Eq. 3. It is important to note that the value of the diffusion layer (X) chosen here is taken from Ref. 1 but really it is an arbitrary value. The amount dissolved *versus* time is calculated under these conditions using Eq. 7 and is shown in Table II.

The data in Table II are treated according to Kawashima and Takenaka (1); the best-fit regression equation obtained was:

$$\log [d(C_L/C_e)/dt] = 2.16 \log \{1 - (C_L/C_e)\} - 2.613 \quad \text{(Eq. 8)}$$

with a correlation coefficient of 0.989. The theoretical slope of this plot is 1.66, which is in conflict with Eq. 8. The diffusion layer thickness value calculated from Eq. 8 is 90 μm, which also does not agree with the value used in Eq. 7 (X = 34 μm).

Therefore, it is demonstrated here that Eq. 1 is not an appropriate model to fit the experimental results of Ref. 1. The slope of 1.66 reported in Ref. 1 is also questionable.

The best method for calculating the diffusion layer thickness (X) for the experiments carried out in Ref. 1 would be to use data points where the total amount dissolved is less than 20% of W_e and to treat the data according to the Hixson–Crowell cube root law (2). This method was used for the first five data points in Table II and gave a diffusion layer thickness (X) of 39 μm, which is quite close to the chosen value of 34 μm.

Table II—Amount Dissolved *versus* Time Calculated Using Experimental Conditions from Ref. 1 and Eq. 7

W_L[a], g Dissolved	W, g Undissolved	$\psi(W)$, $g^{-2/3}$	Time, t, sec	$W_0^{1/3} - W^{1/3}$, $g^{1/3}$
0	0.5	1.326	0	0
0.05	0.45	1.268	16	0.027
0.1	0.40	1.203	34	0.057
0.15	0.35	1.130	54	0.089
0.20	0.30	1.046	78	0.124
0.25	0.25	0.945	101	0.164
0.30	0.20	0.833	137	
0.35	0.15	0.689	177	
0.40	0.10	0.499	230	
0.45	0.05	0.216	308	

[a] The W_L (grams) values were assumed, and $\psi(W)$ was calculated. By using this value of $\psi(W)$ and Eq. 7, the corresponding time value was calculated.

(1) Y. Kawashima and H. Takenaka, *J. Pharm. Sci.*, **63**, 1546(1974).
(2) A. Hixson and J. Crowell, *Ind. Eng. Chem.*, **23**, 923(1931).
(3) W. Nernst, *Z. Phys. Chem.*, **47**, 52(1904).
(4) E. Brunner, *ibid.*, **51**, 95(1905).
(5) "The United States Pharmacopeia," 15th rev., Mack Publishing Co., Easton, Pa., 1955, p. 623.
(6) M. P. Short, P. Sharkey, and C. T. Rhodes, *J. Pharm. Sci.*, **61**, 1732(1972).
(7) M. Patel and J. T. Carstensen, *ibid.*, **64**, 1651(1975).
(8) M. Kanke and K. Sekiguchi, *Chem. Pharm. Bull.*, **21**, 871(1973).

Mahendra Patel
School of Pharmacy
University of Wisconsin
Madison, WI 53706

Received August 29, 1975.
Accepted for publication February 13, 1976.

Reduced Acid-Neutralizing Velocity of Spray-Dried Agglomerated Magnesium Carbonate: A Response

Keyphrases □ Magnesium carbonate, agglomerated—spray dried, acid-neutralizing velocity □ Spray drying—agglomerated magnesium carbonate, acid-neutralizing velocity □ Acid-neutralizing velocity—spray-dried agglomerated magnesium carbonate

To the Editor:

It is appreciated that the estimates of the encapsulation ratio of spray-dried products depend on the method used for the calculation of diffusion layer thickness, and the validity of Patel's (1) general comments is accepted. However, his statement regarding the use of an initial weight of 0.5 g of salicylic acid in our studies requires modification.

In our investigations, samples of salicylic acid of 1.18, 1.55, and 2.24 g were placed in 450 ml of water at 27, 37, and 47°, respectively. This point is not immediately evident from our publication (2), since only the equilibrium concentration of solute was reported. Since flotation of part of the salicylic acid was observed at the initial stage of the dissolution study, a small excess of salicylic acid was added to the solvent. Therefore, our experimental conditions, where $W_0 \simeq W_e$, can meet the requirement for applying the rearranged equation (2) of the Hixon–Crowell cube root law (3). The slope of plots of data based on this equation was 1.66 over 80–90% of the total amount dissolved.

(1) M. Patel, *J. Pharm. Sci.*, **65**, 770(1976).
(2) Y. Kawashima and H. Takenaka, *ibid.*, **63**, 1546(1974).
(3) A. Hixon and J. Crowell, *Ind. Eng. Chem.*, **23**, 923(1931).

Y. Kawashima
Gifu College of Pharmacy
Mitahora, Gifu 502
Japan

Received October 8, 1975.
Accepted for publication January 13, 1976.

Table I—Calculated Initial Amount Required According to Eq. 1

Temperature	Solubility, g/ml	Initial Amount Required According to Eq. 1, $W_0 = C_e V$, g	Initial Amount Used, g
27°	0.00231	1.04	0.5
37°	0.00320[a]	1.44	0.5
47°	0.00465[b]	2.09	0.5

[a] Determined in this laboratory. [b] Reference 8.

10^{-6} cm²/sec, V = 450 ml, d_0 = 0.003 cm, ρ = 1.4 g/ml, and $X = 34 \times 10^{-4}$ cm. Then:

$$\psi(W) = \psi(W_0) - \frac{DS_w W_0^{1/3}}{XV} t = 1.326 - 0.0036t \quad \text{(Eq. 7)}$$

Equation 7 is obtained by substituting the given values in Eq. 3. It is important to note that the value of the diffusion layer (X) chosen here is taken from Ref. 1 but really it is an arbitrary value. The amount dissolved *versus* time is calculated under these conditions using Eq. 7 and is shown in Table II.

The data in Table II are treated according to Kawashima and Takenaka (1); the best-fit regression equation obtained was:

$$\log [d(C_L/C_e)/dt] = 2.16 \log \{1 - (C_L/C_e)\} - 2.613 \quad \text{(Eq. 8)}$$

with a correlation coefficient of 0.989. The theoretical slope of this plot is 1.66, which is in conflict with Eq. 8. The diffusion layer thickness value calculated from Eq. 8 is 90 μm, which also does not agree with the value used in Eq. 7 (X = 34 μm).

Therefore, it is demonstrated here that Eq. 1 is not an appropriate model to fit the experimental results of Ref. 1. The slope of 1.66 reported in Ref. 1 is also questionable.

The best method for calculating the diffusion layer thickness (X) for the experiments carried out in Ref. 1 would be to use data points where the total amount dissolved is less than 20% of W_e and to treat the data according to the Hixson–Crowell cube root law (2). This method was used for the first five data points in Table II and gave a diffusion layer thickness (X) of 39 μm, which is quite close to the chosen value of 34 μm.

Table II—Amount Dissolved *versus* Time Calculated Using Experimental Conditions from Ref. 1 and Eq. 7

W_L[a], g Dissolved	W, g Undissolved	$\psi(W)$, $g^{-2/3}$	Time, t, sec	$W_0^{1/3} - W^{1/3}$, $g^{1/3}$
0	0.5	1.326	0	0
0.05	0.45	1.268	16	0.027
0.1	0.40	1.203	34	0.057
0.15	0.35	1.130	54	0.089
0.20	0.30	1.046	78	0.124
0.25	0.25	0.945	101	0.164
0.30	0.20	0.833	137	
0.35	0.15	0.689	177	
0.40	0.10	0.499	230	
0.45	0.05	0.216	308	

[a] The W_L (grams) values were assumed, and $\psi(W)$ was calculated. By using this value of $\psi(W)$ and Eq. 7, the corresponding time value was calculated.

(1) Y. Kawashima and H. Takenaka, *J. Pharm. Sci.*, **63**, 1546(1974).
(2) A. Hixson and J. Crowell, *Ind. Eng. Chem.*, **23**, 923(1931).
(3) W. Nernst, *Z. Phys. Chem.*, **47**, 52(1904).
(4) E. Brunner, *ibid.*, **51**, 95(1905).
(5) "The United States Pharmacopeia," 15th rev., Mack Publishing Co., Easton, Pa., 1955, p. 623.
(6) M. P. Short, P. Sharkey, and C. T. Rhodes, *J. Pharm. Sci.*, **61**, 1732(1972).
(7) M. Patel and J. T. Carstensen, *ibid.*, **64**, 1651(1975).
(8) M. Kanke and K. Sekiguchi, *Chem. Pharm. Bull.*, **21**, 871(1973).

Mahendra Patel
School of Pharmacy
University of Wisconsin
Madison, WI 53706

Received August 29, 1975.
Accepted for publication February 13, 1976.

Reduced Acid-Neutralizing Velocity of Spray-Dried Agglomerated Magnesium Carbonate: A Response

Keyphrases □ Magnesium carbonate, agglomerated—spray dried, acid-neutralizing velocity □ Spray drying—agglomerated magnesium carbonate, acid-neutralizing velocity □ Acid-neutralizing velocity—spray-dried agglomerated magnesium carbonate

To the Editor:

It is appreciated that the estimates of the encapsulation ratio of spray-dried products depend on the method used for the calculation of diffusion layer thickness, and the validity of Patel's (1) general comments is accepted. However, his statement regarding the use of an initial weight of 0.5 g of salicylic acid in our studies requires modification.

In our investigations, samples of salicylic acid of 1.18, 1.55, and 2.24 g were placed in 450 ml of water at 27, 37, and 47°, respectively. This point is not immediately evident from our publication (2), since only the equilibrium concentration of solute was reported. Since flotation of part of the salicylic acid was observed at the initial stage of the dissolution study, a small excess of salicylic acid was added to the solvent. Therefore, our experimental conditions, where $W_0 \simeq W_e$, can meet the requirement for applying the rearranged equation (2) of the Hixon–Crowell cube root law (3). The slope of plots of data based on this equation was 1.66 over 80–90% of the total amount dissolved.

(1) M. Patel, *J. Pharm. Sci.*, **65**, 770(1976).
(2) Y. Kawashima and H. Takenaka, *ibid.*, **63**, 1546(1974).
(3) A. Hixon and J. Crowell, *Ind. Eng. Chem.*, **23**, 923(1931).

Y. Kawashima
Gifu College of Pharmacy
Mitahora, Gifu 502
Japan

Received October 8, 1975.
Accepted for publication January 13, 1976.

Shilajit I: Chemical Constituents

Keyphrases □ Shilajit—chemical constituents determined, compared to extracts of *Euphorbia royleana* plant □ *Euphorbia royleana* plant—chemical constituents determined, compared to extracts of shilajit (Indian rock exudate) □ Triterpenes—isolated from shilajit (Indian rock exudate) and *Euphorbia royleana* plant □ Benzcoumarins—isolated from shilajit (Indian rock exudate) and *Euphorbia royleana* plant □ Ellagic acid—isolated from shilajit (Indian rock exudate) and *Euphorbia royleana* plant

To the Editor:

Shilajit is a blackish-brown exudation from steep rocks of different formations found in the Himalayan regions of Uttar Pradesh, Himachal Pradesh, Jammu, and Kashmir. Aqueous solution of shilajit is used for treating hypertension, chronic bronchitis, asthma, genito-urinary infections, dropsy, and nervous disorders (1). However, the hazards of its collection and the scanty amount available prompt unscrupulous dealers to adulterate it with quercus gall, gums, and cow's urine. Therefore, it is essential to evaluate the chemical constituents of shilajit to assay its quality.

The current information relating to the chemical constituents of shilajit is only fragmentary. It was reported to contain resins, fatty acids, benzoic and hippuric acids, and albuminoids (1). A study of vegetation of the areas of shilajit-exuding rocks indicated (2) that *Euphorbia royleana* Boiss., a latex-bearing plant abundantly growing in the Western Himalayas, could be the source of organic constituents of shilajit. This postulate had not been tested before experimentally. Evidence is now presented to establish that the active principles of shilajit owe their origin primarily to *E. royleana* plants.

Extraction of shilajit with solvents of graded polarity yielded three different classes of organic compounds, (*a*) triterpenes and sterols; (*b*) aromatic carboxylic acids, ellagic acid, and 3,4-benzcoumarins; and (*c*) α-amino acids. The identity of the individual entities was established on the basis of physical and spectral properties of the compounds and their derivatives and, when possible, by direct comparison with authentic samples.

Desiccated and powdered shilajit[1] (200 g) was successively extracted with 500 ml of hot petroleum ether (bp 60–80°), chloroform, and methanol. The extracts were processed separately.

On column chromatography over neutral alumina (activity grade about IV), the petroleum ether extract (148 mg) afforded euphol (8 mg), taraxerol (22 mg), and sitosterol (18 mg) as well as two partially characterized triterpenes and a sterol as minor entities. The petroleum ether extract from the air-dried latex of *E. royleana*[1], collected from the top of shilajit-exuding rocks, yielded the same major constituents in 0.01, 0.08, and 0.03% yields, respectively. Previously, taraxerol, taraxeryl acetate, and glut-5-en-3β-yl acetate were reported (3, 4) in *E. royleana*.

From the chloroform extract (220 mg), benzoic acid (66 mg), *m*-hydroxybenzoic acid (11 mg), and three 3,4-benzcoumarins (I–III) were isolated by solvent extraction and column and preparative layer chromatography. Compound I (80 mg), colorless needles from acetone–hexane, mp 231–232°, $C_{13}H_8O_3$ (M^+, 212), showed UV absorption maxima at λ (ethanol) 232 (*A* 0.74), 248 (0.4), 278 (0.43), 303 (0.34), and 330 (0.23) nm. The IR absorption maxima were at ν (mineral oil) 3280 (OH) and 1698 (lactonic CO) cm^{-1}; the lactonic carbonyl absorption was shifted to ν 1742 cm^{-1} in the corresponding methyl ether. These properties are strikingly similar to those of hydroxycoumarins (5, 6).

The 60-MHz proton magnetic resonance (PMR) spectrum in trifluoroacetic acid showed a coupled set of three protons in the δ 7.0 region (involving an *ABC* system) and complex multiplets in the δ 8.3–7.5 region associated with four aromatic protons. In the mass spectrum, aside from the molecular ion peak, which is the base peak, significant fragment ion peaks appeared at *m/e* 184 (40%, 212 → 184 transition, m* 160), 156 (8), 155 (14), 128 (27), 127 (18), 126 (8), 115 (7), and 114 (6).

On the basis of these data, I was identified as 7-hydroxy-3,4-benzcoumarin. Hurtley (7) previously accomplished its synthesis while developing a convenient method of synthesis of 3,4-benzcoumarins by the condensation of reactive phenols with *o*-bromobenzoic acid with copper as a catalyst. Its spectral properties, however, were not recorded. Also, this study is the first demonstration of the natural occurrence of I.

Compound II (4 mg), mp 140–141°, $C_{14}H_{10}O_3$ (M^+, 226), was readily identified as the methyl ether of I. Compound III (7 mg), yellow needles from acetone, mp >360°, $C_{13}H_8O_4$ (M^+, 228, 100%), showed significant fragment ions at *m/e* 200 (35), 172 (5), 171 (12), and 144 (22). In the PMR spectrum, two coupled sets of three protons each appeared in the δ 7.5 and 7.0 regions and were assigned to two *ABC* systems. Compound III gave a diacetate, mp 208–209° (M^+, 312). The compound was assigned 2′,7-dihydroxy-3,4-benzcoumarin structure and was previously reported in castoreum (secretions from the scent glands of beaver) (8).

Benzoic and *m*-hydroxybenzoic acid and the three benzcoumarins (I–III) were also isolated from the latex of *E. royleana*. Additionally, the presence of a number of benzcoumarins, in the form of amino acid conjugates, was detected in the latex.

The methanol extract (2.8 g) was separated into two fractions by trituration with a moist solvent ether. In the ethereal extract, ellagic acid was detected readily by inspection of a paper chromatogram in Forestal solvent (9). Two minor, less polar, phenolic components also were detected in this fraction. The same compounds were detected as the major constituents in the

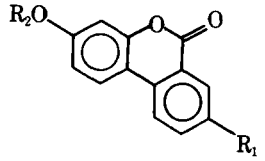

I: $R_1 = R_2 = H$
II: $R_1 = H, R_2 = CH_3$
III: $R_1 = OH, R_2 = H$

[1] Shilajit and the latex samples were collected, with the assistance of members of the Amalgamated Units, Central Council of Research in Indian Medicine and Homeopathy, Tarikhet, from Jorassi village, Almorah, India. A voucher specimen of each has been preserved at the Pharmaceutical Chemistry Research Laboratory, Department of Pharmaceutics, Banaras Hindu University.

corresponding extract of the latex of *E. royleana*. Ellagic acid and its 3,3′-dimethyl ether were previously reported in two other *Euphorbia* species (5).

The ether-insoluble fraction of the methanol extract showed a number of ninhydrin-positive spots, suggesting the presence of α-amino acids. It was dissolved in methanol and chromatographed[2]. Elution was carried out with increasing proportions of triethylamine in methanol. The identity of the amino acids was established by paper chromatography using authentic markers according to the method of Hardy *et al.* (10). Among the 18 free amino acids detected in the effluents, seven were identified. These were, in order of abundance, glycine, aspartic acid, methionine, asparagine, glutamic acid, tyrosine, and phenylalanine. The major amino acid composition in the latex of *E. royleana* was similar to that of shilajit.

(1) R. N. Chopra, K. L. Handa, and L. D. Kapoor, "Indigenous Drugs of India," 2nd ed., Dhar & Sons, Calcutta, India, 1958, p. 457.
(2) H. C. Pandey, *Nagarjun (India)*, **16**, 31(1973).
(3) R. C. Sharma, A. Zaman, and A. R. Kidwai, *Indian J. Chem.*, **2**, 254(1964).
(4) P. Sengupta and S. Ghosh, *J. Indian Chem. Soc.*, **42**, 543(1965).
(5) F. M. Dean, "Naturally Occurring Oxygen Ring Compounds," Butterworths, London, England, 1963, p. 220.
(6) F. Stitt, E. Gong, K. J. Palmer, and J. N. Shoolery, *J. Am. Chem. Soc.*, **81**, 4615(1959).
(7) W. R. H. Hurtley, *J. Chem. Soc.*, **1929**, 1870.
(8) E. Lederer, *ibid.*, **1949**, 2115.
(9) E. C. Bate-Smith, *Chem. Ind. (London)*, **1956**, R.32.
(10) T. L. Hardy, D. O. Holland, and J. H. C. Nayler, *Anal. Chem.*, **27**, 971(1955).

S. Ghosal ˣ
J. P. Reddy
Pharmaceutical Chemistry Research Laboratory
Department of Pharmaceutics
Banaras Hindu University
Varanasi-5, India
V. K. Lal
Amalgamated Units
Central Council for Research in
Indian Medicine and Homeopathy
Tarikhet, Almorah, India

Received November 28, 1975.
Accepted for publication February 23, 1976.
The authors are grateful to Dr. T. R. Govindachari, Ciba-Geigy Research Centre, Bombay, India, and Dr. R. K. Chaudhuri, Pharmazeutisches Institute, Bonn, Germany, for some spectral data, and to Mr. P. Joshi, Central Council for Research in Indian Medicine and Homeopathy, Tarikhet, India, for cooperation in this work.
ˣ To whom inquiries should be directed.

[2] Dowex-50-X8.

Failure of Prednisone to Alter Plasma Salicylate Concentrations in Dogs

Keyphrases □ Prednisone—effect on plasma salicylate concentrations, dogs □ Salicylate—plasma concentrations, effect of prednisone, dogs □ Interactions—prednisone and salicylate, dogs

To the Editor:

Drug interactions are important considerations in modern therapy. Among the important drug interactions are those affecting disposition of salicylates. Plasma salicylate concentrations are altered by agents such as ammonium chloride, ascorbic acid (1), aminobenzoic acid (2), and "nonsystemic" antacids (3).

An interaction of corticosteroids and salicylates was reported by Klinenberg and Miller (4). They observed a rise in plasma salicylate concentrations in four patients with rheumatoid arthritis as corticosteroid dosage was tapered and salicylate dosage remained constant. The magnitude of increased salicylate concentration was sufficient in one patient for the development of salicylate intoxication. These authors cited the tapering of corticosteroid as the mechanism responsible for the rise in plasma salicylate. This interaction has important implications, because corticosteroids and salicylates frequently are administered simultaneously in the treatment of diseases other than rheumatoid arthritis such as acute rheumatic fever. Because, to our knowledge, the interaction has not been confirmed, we studied the effect of prednisone treatment on plasma salicylate concentration in dogs.

Six mongrel dogs, 13–20 kg, were administered aspirin tablets orally (900 mg/dose, except Dog 6 which received 600 mg/dose) on an 8 am–2 pm–8 pm–2 am schedule. The dosage schedule resulted in average plasma salicylate concentrations between 10 and 20 mg %. Heparinized blood was drawn from each dog at 1 pm daily to monitor plasma salicylate concentrations. Once salicylate concentrations were stable, 10 mg of prednisone was administered orally once daily at 8 am to each dog for 6 days. The aspirin dosage schedule remained unchanged throughout prednisone administration. Plasma salicylate concentrations were determined by a reported method (5).

The salicylate concentrations on the 3 days prior to prednisone administration and on the last 3 days of prednisone administration were averaged for each dog and analyzed by the Student *t* test (paired comparison). Thus, each dog served as its own control for the comparison of aspirin treatment alone *versus* aspirin plus prednisone treatment.

Table I shows the average plasma salicylate concentrations of each dog before and during prednisone treatment. Prior to prednisone treatment, the mean salicylate concentration was 16.1 mg %. During prednisone therapy, the mean salicylate concentration was 17.3 mg %. Comparison of each dog's average plasma salicylate level before and during prednisone treatment by the paired *t* test showed no significant change ($p > 0.05$).

Table I—Average Plasma Salicylate Concentration (Milligrams Percent)

Dog	Before Prednisone	During Prednisone	Difference
1	19	18	−1
2	15	21	+6
3	17	13	−4
4	14	13	−1
5	18	23	+5
6	14	16	+2
Mean	16.1	17.3	1.2 ± 1.5

corresponding extract of the latex of *E. royleana*. Ellagic acid and its 3,3′-dimethyl ether were previously reported in two other *Euphorbia* species (5).

The ether-insoluble fraction of the methanol extract showed a number of ninhydrin-positive spots, suggesting the presence of α-amino acids. It was dissolved in methanol and chromatographed[2]. Elution was carried out with increasing proportions of triethylamine in methanol. The identity of the amino acids was established by paper chromatography using authentic markers according to the method of Hardy *et al.* (10). Among the 18 free amino acids detected in the effluents, seven were identified. These were, in order of abundance, glycine, aspartic acid, methionine, asparagine, glutamic acid, tyrosine, and phenylalanine. The major amino acid composition in the latex of *E. royleana* was similar to that of shilajit.

(1) R. N. Chopra, K. L. Handa, and L. D. Kapoor, "Indigenous Drugs of India," 2nd ed., Dhar & Sons, Calcutta, India, 1958, p. 457.
(2) H. C. Pandey, *Nagarjun (India)*, **16**, 31(1973).
(3) R. C. Sharma, A. Zaman, and A. R. Kidwai, *Indian J. Chem.*, **2**, 254(1964).
(4) P. Sengupta and S. Ghosh, *J. Indian Chem. Soc.*, **42**, 543(1965).
(5) F. M. Dean, "Naturally Occurring Oxygen Ring Compounds," Butterworths, London, England, 1963, p. 220.
(6) F. Stitt, E. Gong, K. J. Palmer, and J. N. Shoolery, *J. Am. Chem. Soc.*, **81**, 4615(1959).
(7) W. R. H. Hurtley, *J. Chem. Soc.*, **1929**, 1870.
(8) E. Lederer, *ibid.*, **1949**, 2115.
(9) E. C. Bate-Smith, *Chem. Ind. (London)*, **1956**, R.32.
(10) T. L. Hardy, D. O. Holland, and J. H. C. Nayler, *Anal. Chem.*, **27**, 971(1955).

S. Ghosal ˣ
J. P. Reddy
Pharmaceutical Chemistry Research Laboratory
Department of Pharmaceutics
Banaras Hindu University
Varanasi-5, India
V. K. Lal
Amalgamated Units
Central Council for Research in
Indian Medicine and Homeopathy
Tarikhet, Almorah, India

Received November 28, 1975.
Accepted for publication February 23, 1976.
The authors are grateful to Dr. T. R. Govindachari, Ciba-Geigy Research Centre, Bombay, India, and Dr. R. K. Chaudhuri, Pharmazeutisches Institute, Bonn, Germany, for some spectral data, and to Mr. P. Joshi, Central Council for Research in Indian Medicine and Homeopathy, Tarikhet, India, for cooperation in this work.
ˣ To whom inquiries should be directed.

[2] Dowex-50-X8.

Failure of Prednisone to Alter Plasma Salicylate Concentrations in Dogs

Keyphrases □ Prednisone—effect on plasma salicylate concentrations, dogs □ Salicylate—plasma concentrations, effect of prednisone, dogs □ Interactions—prednisone and salicylate, dogs

To the Editor:

Drug interactions are important considerations in modern therapy. Among the important drug interactions are those affecting disposition of salicylates. Plasma salicylate concentrations are altered by agents such as ammonium chloride, ascorbic acid (1), aminobenzoic acid (2), and "nonsystemic" antacids (3).

An interaction of corticosteroids and salicylates was reported by Klinenberg and Miller (4). They observed a rise in plasma salicylate concentrations in four patients with rheumatoid arthritis as corticosteroid dosage was tapered and salicylate dosage remained constant. The magnitude of increased salicylate concentration was sufficient in one patient for the development of salicylate intoxication. These authors cited the tapering of corticosteroid as the mechanism responsible for the rise in plasma salicylate. This interaction has important implications, because corticosteroids and salicylates frequently are administered simultaneously in the treatment of diseases other than rheumatoid arthritis such as acute rheumatic fever. Because, to our knowledge, the interaction has not been confirmed, we studied the effect of prednisone treatment on plasma salicylate concentration in dogs.

Six mongrel dogs, 13–20 kg, were administered aspirin tablets orally (900 mg/dose, except Dog 6 which received 600 mg/dose) on an 8 am–2 pm–8 pm–2 am schedule. The dosage schedule resulted in average plasma salicylate concentrations between 10 and 20 mg %. Heparinized blood was drawn from each dog at 1 pm daily to monitor plasma salicylate concentrations. Once salicylate concentrations were stable, 10 mg of prednisone was administered orally once daily at 8 am to each dog for 6 days. The aspirin dosage schedule remained unchanged throughout prednisone administration. Plasma salicylate concentrations were determined by a reported method (5).

The salicylate concentrations on the 3 days prior to prednisone administration and on the last 3 days of prednisone administration were averaged for each dog and analyzed by the Student *t* test (paired comparison). Thus, each dog served as its own control for the comparison of aspirin treatment alone *versus* aspirin plus prednisone treatment.

Table I shows the average plasma salicylate concentrations of each dog before and during prednisone treatment. Prior to prednisone treatment, the mean salicylate concentration was 16.1 mg %. During prednisone therapy, the mean salicylate concentration was 17.3 mg %. Comparison of each dog's average plasma salicylate level before and during prednisone treatment by the paired *t* test showed no significant change ($p > 0.05$).

Table I—Average Plasma Salicylate Concentration (Milligrams Percent)

Dog	Before Prednisone	During Prednisone	Difference
1	19	18	−1
2	15	21	+6
3	17	13	−4
4	14	13	−1
5	18	23	+5
6	14	16	+2
Mean	16.1	17.3	1.2 ± 1.5

The importance of recognizing an interaction between corticosteroids and salicylates is obvious. However, it is unclear from these data that the interaction exists, at least in the dog. Hansten (6) listed this interaction, citing the paper by Klinenberg and Miller (4). Their paper also was cited in a symposium on chronic salicylate therapy, but it was pointed out that their results were unconfirmed (7). Our results, showing that corticosteroids did not lower plasma salicylate concentrations in dogs, suggest the need to examine further the reported interaction between these drugs in humans.

(1) G. Levy and J. R. Leonards, *J. Am. Med. Ass.*, **217**, 81(1971).
(2) M. J. H. Smith and P. K. Smith, "The Salicylates," Interscience, New York, N.Y., 1966, pp. 34–43.
(3) G. Levy, T. Lampman, B. L. Kamath, and L. K. Garrettson, *N. Engl. J. Med.*, **293**, 323(1975).
(4) J. R. Klinenberg and F. Miller, *J. Am. Med. Ass.*, **194**, 601(1965).
(5) "Manual of Analytical Toxicology," I. Sunshine, Ed., Chemical Rubber Co., Cleveland, Ohio, 1971, pp. 307, 308.
(6) P. D. Hansten, "Drug Interactions," Lea & Febiger, Philadelphia, Pa., 1973, p. 172.
(7) K. Fremont-Smith, "Proceedings of the Conference on Effects of Chronic Salicylate Administration," U.S. Government Printing Office, Washington, D.C., 1966, p. 3.

Daniel K. Day ˣ
Harold E. Williamson
Robert J. Roberts

Division of Pediatric Clinical Pharmacology
Departments of Pharmacology and Pediatrics
College of Medicine
University of Iowa
Iowa City, IA 52242

Received January 30, 1976.
Accepted for publication March 1, 1976.
Supported by GM12675.
D. K. Day was supported by a Medical Student Research Fellowship in Pharmacology–Clinical Pharmacology from the Pharmaceutical Manufacturers Association Foundation.
ˣ To whom inquiries should be directed.

Spot Tests Used for Systematic Identification of Drugs of Abuse

Keyphrases □ Drugs of abuse—systematic identification using spot tests □ Abuse drugs—systematic identification using spot tests □ Spot tests—systematic identification of drugs of abuse

To the Editor:

A number of the observations reported by Masoud (1) are at variance with long accepted literature results (2–6) and our own observations. Our observations are based on tens of thousands of forensic samples which come into our laboratory each year and which are screened using the spot tests mentioned in Masoud's paper (1).

To ensure that these inconsistencies were not due to small differences in the composition of the spot test reagents commonly used in our laboratory and those of Masoud, we prepared reagents to the specifications of Masoud's paper. The observations reported here are based on these reagents. Samples in the range described by Masoud, *i.e.*, 1–2 mg, were used, and all tests were run in porcelain spot plates. The following serious inconsistencies were encountered.

1. In Table II of Masoud's paper under the caption "Alkaloids that Give Negative Tests with One or More Reagents":

(*a*) The table indicates that heroin and morphine give a positive Mayer, a positive Dragendorff, and a negative Wagner test. It is our observation that both give strong positive reactions with all three of these reagents.

(*b*) The table indicates that lysergide (LSD) gives negative results for all three of the alkaloidal tests. It is our observation that pure lysergide gives strong positives with these reagents. Some illicit samples, where the lysergide concentration is quite low, still give a positive Wagner test. The concentrations encountered in many illicit samples will be below the sensitivity limits of these spot tests.

(*c*) The table indicates negative tests with all three reagents for psilocybin. Our observation is that psilocybin gives a positive Wagner and a negative Mayer test.

2. In Table III, under the caption "Nonalkaloids that Give Positive Alkaloidal Tests with One or More Reagents": The table indicates that procaine and methylphenidate give a negative Mayer and a negative Wagner test. Our observation is that both these compounds give positive tests with both reagents.

3. In the discussion of the Marquis reagent on page 843:

(*a*) The discussion indicates that some nonopiates produce color reactions with the Marquis reagent very similar to those shown by the opiates. Ephedrine sulfate, amphetamine sulfate, methamphetamine hydrochloride, and meperidine are listed as examples. Our observation is that the colors produced by these compounds are not similar to the colors produced by the opiates. In fact, the orange to brown color reaction produced by ephedrine, amphetamine, and methamphetamine with the Marquis reagent is used in our laboratory and in most other crime laboratories as a screening test for these compounds (2–6).

(*b*) The discussion continues that these "false positives" are not documented in "other references known to the author." An extensive compilation of the colors produced with the Marquis reagent, which includes these compounds, is found in "Isolation and Identification of Drugs" (2), cited by Masoud as his Ref. 6. Furthermore, this information is in all modern references on forensic drug analysis (2–6).

4. In the discussion of cobalt thiocyanate on page 843: The author comments on the lack of specificity of this test in the identification of cocaine, due to other compounds giving the characteristic flaky pre-

The importance of recognizing an interaction between corticosteroids and salicylates is obvious. However, it is unclear from these data that the interaction exists, at least in the dog. Hansten (6) listed this interaction, citing the paper by Klinenberg and Miller (4). Their paper also was cited in a symposium on chronic salicylate therapy, but it was pointed out that their results were unconfirmed (7). Our results, showing that corticosteroids did not lower plasma salicylate concentrations in dogs, suggest the need to examine further the reported interaction between these drugs in humans.

(1) G. Levy and J. R. Leonards, *J. Am. Med. Ass.*, **217**, 81(1971).
(2) M. J. H. Smith and P. K. Smith, "The Salicylates," Interscience, New York, N.Y., 1966, pp. 34–43.
(3) G. Levy, T. Lampman, B. L. Kamath, and L. K. Garrettson, *N. Engl. J. Med.*, **293**, 323(1975).
(4) J. R. Klinenberg and F. Miller, *J. Am. Med. Ass.*, **194**, 601(1965).
(5) "Manual of Analytical Toxicology," I. Sunshine, Ed., Chemical Rubber Co., Cleveland, Ohio, 1971, pp. 307, 308.
(6) P. D. Hansten, "Drug Interactions," Lea & Febiger, Philadelphia, Pa., 1973, p. 172.
(7) K. Fremont-Smith, "Proceedings of the Conference on Effects of Chronic Salicylate Administration," U.S. Government Printing Office, Washington, D.C., 1966, p. 3.

Daniel K. Day ˣ
Harold E. Williamson
Robert J. Roberts

Division of Pediatric Clinical Pharmacology
Departments of Pharmacology and Pediatrics
College of Medicine
University of Iowa
Iowa City, IA 52242

Received January 30, 1976.
Accepted for publication March 1, 1976.
Supported by GM12675.
D. K. Day was supported by a Medical Student Research Fellowship in Pharmacology–Clinical Pharmacology from the Pharmaceutical Manufacturers Association Foundation.
ˣ To whom inquiries should be directed.

Spot Tests Used for Systematic Identification of Drugs of Abuse

Keyphrases □ Drugs of abuse—systematic identification using spot tests □ Abuse drugs—systematic identification using spot tests □ Spot tests—systematic identification of drugs of abuse

To the Editor:

A number of the observations reported by Masoud (1) are at variance with long accepted literature results (2–6) and our own observations. Our observations are based on tens of thousands of forensic samples which come into our laboratory each year and which are screened using the spot tests mentioned in Masoud's paper (1).

To ensure that these inconsistencies were not due to small differences in the composition of the spot test reagents commonly used in our laboratory and those of Masoud, we prepared reagents to the specifications of Masoud's paper. The observations reported here are based on these reagents. Samples in the range described by Masoud, *i.e.*, 1–2 mg, were used, and all tests were run in porcelain spot plates. The following serious inconsistencies were encountered.

1. In Table II of Masoud's paper under the caption "Alkaloids that Give Negative Tests with One or More Reagents":

(*a*) The table indicates that heroin and morphine give a positive Mayer, a positive Dragendorff, and a negative Wagner test. It is our observation that both give strong positive reactions with all three of these reagents.

(*b*) The table indicates that lysergide (LSD) gives negative results for all three of the alkaloidal tests. It is our observation that pure lysergide gives strong positives with these reagents. Some illicit samples, where the lysergide concentration is quite low, still give a positive Wagner test. The concentrations encountered in many illicit samples will be below the sensitivity limits of these spot tests.

(*c*) The table indicates negative tests with all three reagents for psilocybin. Our observation is that psilocybin gives a positive Wagner and a negative Mayer test.

2. In Table III, under the caption "Nonalkaloids that Give Positive Alkaloidal Tests with One or More Reagents": The table indicates that procaine and methylphenidate give a negative Mayer and a negative Wagner test. Our observation is that both these compounds give positive tests with both reagents.

3. In the discussion of the Marquis reagent on page 843:

(*a*) The discussion indicates that some nonopiates produce color reactions with the Marquis reagent very similar to those shown by the opiates. Ephedrine sulfate, amphetamine sulfate, methamphetamine hydrochloride, and meperidine are listed as examples. Our observation is that the colors produced by these compounds are not similar to the colors produced by the opiates. In fact, the orange to brown color reaction produced by ephedrine, amphetamine, and methamphetamine with the Marquis reagent is used in our laboratory and in most other crime laboratories as a screening test for these compounds (2–6).

(*b*) The discussion continues that these "false positives" are not documented in "other references known to the author." An extensive compilation of the colors produced with the Marquis reagent, which includes these compounds, is found in "Isolation and Identification of Drugs" (2), cited by Masoud as his Ref. 6. Furthermore, this information is in all modern references on forensic drug analysis (2–6).

4. In the discussion of cobalt thiocyanate on page 843: The author comments on the lack of specificity of this test in the identification of cocaine, due to other compounds giving the characteristic flaky pre-

cipitate. It is our observation that many other compounds do, in fact, produce this color reaction. However, a modification to the test, using stannous chloride solution (7), enhances the specificity.

For example, procaine, benzocaine, diphenhydramine, and cocaine do give a blue precipitate with cobalt thiocyanate reagent; but upon addition of stannous chloride solution, the blue precipitate disappears in the case of procaine, benzocaine, and diphenhydramine but remains unchanged with cocaine.

5. In the discussion of the Zwikker test on page 843: The discussion indicates that glutethimide gives a gray color with the Zwikker reagent, which is inconsistent with the blue-violet color reported by Clarke (2) for glutethimide and barbiturates. Our observations are in agreement with those of Clarke (2).

The reported results using reagents prepared according to the formulations in Masoud's paper (1) are in accord with our previous experience and the literature. Therefore, the inconsistencies between our experience and the results reported by Masoud cannot be due to small differences in the reagents used. We feel it is important that these observations be brought to the attention of the scientific community, since our chemists and those working in hundreds of other crime laboratories across the nation must defend their results in court under intense cross-examination. Frequently, under cross-examination, articles in the scientific literature at variance with the chemist's results are quoted to cast doubt on his or her credibility and to confuse the lay people of the jury.

(1) A. N. Masoud, *J. Pharm. Sci.*, **64**, 841(1975).

(2) E. G. C. Clarke, "Isolation and Identification of Drugs," The Pharmaceutical Press, London, England, 1971.

(3) F. Lundquist, "Methods of Forensic Science," vol. 1, Wiley, New York, N.Y., 1962, p. 1.

(4) A. A. Moenssens, R. E. Moses, and F. E. Inbau, "Scientific Evidence in Criminal Cases," Foundation Press, Mineola, N.Y., 1973.

(5) K. P. O'Brien and R. C. Sullivan, "Criminalistics Theory and Practice," Holbrook Press, Boston, Mass., 1972.

(6) R. F. Canaff, "Basic Training Program for Forensic Drug Chemists," Laboratory Division, Bureau of Narcotics and Dangerous Drugs, U.S. Department of Justice, Washington, D.C., 1972.

(7) A. P. Mathers, "Methods of Analysis," U.S. Internal Revenue Service, Publication 341, Washington, D.C., 1967, pp. 78, 137.

Charles V. Rorke [x]
H. A. Harris
Thomas Catalano
Crime Laboratory Section
New York City Police Department
New York, NY 10003

Sumer M. Dugar
Crime Laboratory
Baltimore Police Department
Baltimore, Md.

Received November 19, 1975.
Accepted for publication February 5, 1976.
We wish to thank Dr. Andrew Bartilucci, Dean of the College of Pharmacy and Allied Health Sciences and Director of the Drug Testing Laboratory, Pharmaceutical Services Institute, St. John's University, New York, N.Y., for bringing this article to our attention.

[x] To whom inquiries should be directed.

Spot Tests Used for Systematic Identification of Drugs of Abuse: A Response

Keyphrases □ Spot tests—systematic identification of drugs of abuse □ Drugs of abuse—systematic identification by spot tests □ Abuse drugs—systematic identification by spot tests

To the Editor:

The communication by Rorke *et al.* (1) in reference to an earlier paper (2) discussed a number of discrepancies between our results. We would like to deal with each point in the following discussion.

Wagner's Reaction with Heroin, Morphine, Psilocybin, Procaine, and Methylphenidate—The spot tests performed by Rorke *et al.* (1) were run in porcelain spot plates. This procedure is not in agreement with the use of small glass test tubes described in our work. This difference was found to be crucial since, in our laboratory, we shake the test tube upon the addition of the reagent as a general practice; this is not done when porcelain spot plates are used.

With the drugs of controversy, namely, heroin, morphine, psilocybin, procaine, and methylphenidate, when one or two drops of Wagner's reagent in the concentration used (1–2 mg) are added and the test tube is shaken, the initial precipitate disappears, which has caused the interpretation as a negative. However, we do agree with Rorke *et al.* that when spot plates are used and when three or more drops of Wagner's reagent are added, a positive reaction is observed.

Lysergide Detection and Reaction with Alkaloidal Spot Tests—In the original paper (2), under *Preparation of Samples*, it was mentioned that lysergide was detected in quantities as low as 5 μg. This concentration was used for the detection of lysergide by alkaloidal spot tests and the Ehrlich reagent. At these concentrations, lysergide is not detectable with all three alkaloidal reagents but is detectable with Ehrlich's reagent. Since many street samples contain concentrations below the sensitivity of the alkaloidal spot tests which are detectable by Ehrlich's reagent and for the sake of not missing such low concentrations, the worker should test the drug with Ehrlich's reagent even if it is negative to the alkaloidal spot tests. Rorke *et al.* (1) are correct, however, in pointing out that high concentrations of pure lysergide do give positive alkaloidal spot tests.

Reaction of Procaine and Methylphenidate with Mayer's Reagent—Procaine and methylphenidate formed a very slight precipitate with Mayer's reagent a few minutes after the reagent was added. This delayed, weak reaction differs from the instantaneous strong precipitate formed with most alkaloids. This difference was responsible for the controversy.

Marquis Reagent—In the earlier paper (2), it was mentioned that some nonopiates produced similar colors to those produced by opiates, and a few examples were given. Many of these colors are indeed very similar to those produced by opiates. For example, methapyrilene produces a black-purple color, as documented by

cipitate. It is our observation that many other compounds do, in fact, produce this color reaction. However, a modification to the test, using stannous chloride solution (7), enhances the specificity.

For example, procaine, benzocaine, diphenhydramine, and cocaine do give a blue precipitate with cobalt thiocyanate reagent; but upon addition of stannous chloride solution, the blue precipitate disappears in the case of procaine, benzocaine, and diphenhydramine but remains unchanged with cocaine.

5. In the discussion of the Zwikker test on page 843: The discussion indicates that glutethimide gives a gray color with the Zwikker reagent, which is inconsistent with the blue-violet color reported by Clarke (2) for glutethimide and barbiturates. Our observations are in agreement with those of Clarke (2).

The reported results using reagents prepared according to the formulations in Masoud's paper (1) are in accord with our previous experience and the literature. Therefore, the inconsistencies between our experience and the results reported by Masoud cannot be due to small differences in the reagents used. We feel it is important that these observations be brought to the attention of the scientific community, since our chemists and those working in hundreds of other crime laboratories across the nation must defend their results in court under intense cross-examination. Frequently, under cross-examination, articles in the scientific literature at variance with the chemist's results are quoted to cast doubt on his or her credibility and to confuse the lay people of the jury.

(1) A. N. Masoud, *J. Pharm. Sci.*, **64**, 841(1975).

(2) E. G. C. Clarke, "Isolation and Identification of Drugs," The Pharmaceutical Press, London, England, 1971.

(3) F. Lundquist, "Methods of Forensic Science," vol. 1, Wiley, New York, N.Y., 1962, p. 1.

(4) A. A. Moenssens, R. E. Moses, and F. E. Inbau, "Scientific Evidence in Criminal Cases," Foundation Press, Mineola, N.Y., 1973.

(5) K. P. O'Brien and R. C. Sullivan, "Criminalistics Theory and Practice," Holbrook Press, Boston, Mass., 1972.

(6) R. F. Canaff, "Basic Training Program for Forensic Drug Chemists," Laboratory Division, Bureau of Narcotics and Dangerous Drugs, U.S. Department of Justice, Washington, D.C., 1972.

(7) A. P. Mathers, "Methods of Analysis," U.S. Internal Revenue Service, Publication 341, Washington, D.C., 1967, pp. 78, 137.

Charles V. Rorke [x]
H. A. Harris
Thomas Catalano
Crime Laboratory Section
New York City Police Department
New York, NY 10003

Sumer M. Dugar
Crime Laboratory
Baltimore Police Department
Baltimore, Md.

Received November 19, 1975.
Accepted for publication February 5, 1976.
We wish to thank Dr. Andrew Bartilucci, Dean of the College of Pharmacy and Allied Health Sciences and Director of the Drug Testing Laboratory, Pharmaceutical Services Institute, St. John's University, New York, N.Y., for bringing this article to our attention.

[x] To whom inquiries should be directed.

Spot Tests Used for Systematic Identification of Drugs of Abuse: A Response

Keyphrases □ Spot tests—systematic identification of drugs of abuse □ Drugs of abuse—systematic identification by spot tests □ Abuse drugs—systematic identification by spot tests

To the Editor:

The communication by Rorke *et al.* (1) in reference to an earlier paper (2) discussed a number of discrepancies between our results. We would like to deal with each point in the following discussion.

Wagner's Reaction with Heroin, Morphine, Psilocybin, Procaine, and Methylphenidate—The spot tests performed by Rorke *et al.* (1) were run in porcelain spot plates. This procedure is not in agreement with the use of small glass test tubes described in our work. This difference was found to be crucial since, in our laboratory, we shake the test tube upon the addition of the reagent as a general practice; this is not done when porcelain spot plates are used.

With the drugs of controversy, namely, heroin, morphine, psilocybin, procaine, and methylphenidate, when one or two drops of Wagner's reagent in the concentration used (1–2 mg) are added and the test tube is shaken, the initial precipitate disappears, which has caused the interpretation as a negative. However, we do agree with Rorke *et al.* that when spot plates are used and when three or more drops of Wagner's reagent are added, a positive reaction is observed.

Lysergide Detection and Reaction with Alkaloidal Spot Tests—In the original paper (2), under *Preparation of Samples*, it was mentioned that lysergide was detected in quantities as low as 5 μg. This concentration was used for the detection of lysergide by alkaloidal spot tests and the Ehrlich reagent. At these concentrations, lysergide is not detectable with all three alkaloidal reagents but is detectable with Ehrlich's reagent. Since many street samples contain concentrations below the sensitivity of the alkaloidal spot tests which are detectable by Ehrlich's reagent and for the sake of not missing such low concentrations, the worker should test the drug with Ehrlich's reagent even if it is negative to the alkaloidal spot tests. Rorke *et al.* (1) are correct, however, in pointing out that high concentrations of pure lysergide do give positive alkaloidal spot tests.

Reaction of Procaine and Methylphenidate with Mayer's Reagent—Procaine and methylphenidate formed a very slight precipitate with Mayer's reagent a few minutes after the reagent was added. This delayed, weak reaction differs from the instantaneous strong precipitate formed with most alkaloids. This difference was responsible for the controversy.

Marquis Reagent—In the earlier paper (2), it was mentioned that some nonopiates produced similar colors to those produced by opiates, and a few examples were given. Many of these colors are indeed very similar to those produced by opiates. For example, methapyrilene produces a black-purple color, as documented by

Clarke (3). Indeed, some colors produced by other drugs (*e.g.*, ephedrine, amphetamine, and methamphetamine) may be identified by trained eyes, but untrained personnel should be warned of the possibility of misidentification, particularly when other extraneous material and colors are added to the drug as is the case with street drugs. As Clarke stated:

> *"The color given in any test depends on the quantity of material used and on its purity, and may be described differently by different individuals. To allow for this, the following lists must be used in as wide a sense as possible."*

Therefore, it is up to the worker to exercise his or her judgment in utilizing such color tests for the primary screening of these compounds.

Clarke's compilation of the colors produced with the Marquis reagent did not include ephedrine (3).

Cobalt Thiocyanate—Table IV in the earlier paper (2) included 14 compounds that gave a blue flaky precipitate with cobalt thiocyanate. Rorke *et al.* (1) suggested the use of stannous chloride to enhance the specificity of the test by differentiating between cocaine and procaine and between benzocaine and diphenhydramine; however, they did not mention the behavior of the other compounds listed in the table or of the many other compounds not included. They also failed to consider that many street samples contain mixtures of cocaine and procaine, which make this test worthless or, at best, very difficult to interpret.

The addition of stannous chloride to the blue flaky precipitate formed by such a mixture results in partial dissolution of the precipitate. This partial dissolution is very difficult to observe, and the mixture may be misidentified as cocaine. Rorke *et al.* (1) also failed to mention that the blue precipitate formed by methadone dissolves only partially in stannous chloride, which adds to the possibility of erroneous interpretation.

Therefore, it is our opinion that the use of stannous chloride does not add to the specificity of this test and may lead to erroneous results. For these reasons, it was not included in the scheme described in the original paper (1).

Zwikker's Test—The original paper (2) is in disagreement with Rorke *et al.* (1) and Clarke (3). We repeated the experiment using the reagents described and amobarbital, phenobarbital sodium, and secobarbital as reference standards. At the concentration of 2 mg of the barbiturates used, an instant blue-violet color developed, which was found to be very stable. At this concentration, no blue-violet color was developed with glutethimide. Instead, a yellow color developed, which changed upon standing to a gray color. However, very high concentrations of glutethimide, *i.e.*, more than 10 mg, produced a similar blue-violet color, which disappeared almost instantaneously and faded to a gray color within a few seconds. Therefore, we stand firmly by the results reported earlier (1).

In conclusion, we feel that this exchange with Rorke *et al.* (1) has clarified a number of points, which are examples of the many scientific variables between laboratories due to human differences and differences in methodology. This exchange has also demonstrated, as was pointed out previously (2), that these tests only provide preliminary information to help in the selection of the necessary confirmatory tests such as TLC and GLC. They also aid in the selection of the compound or compounds that are to be used as reference standards for the final identification by TLC or GLC.

Rorke *et al.* (1) pointed out the importance of such tests for chemists defending their results in the courts. We disagree with them in this statement. Results of spot tests should never be used as evidence in the courts.

(1) C. V. Rorke, H. A. Harris, T. Catalano, and S. M. Dugar, *J. Pharm. Sci.*, **65**, 774(1976).

(2) A. N. Masoud, *ibid.*, **64**, 841(1975).

(3) E. G. C. Clarke, "Isolation and Identification of Drugs," The Pharmaceutical Press, London, England, 1969, pp. 663–669.

Asaad N. Masoud ˣ
School of Pharmacy
Creighton University
Omaha, NE 68178

Donald J. Nittskoff
Analytical Laboratories of Ohio
Cleveland, OH 44110

Received December 19, 1975.
Accepted for publication February 26, 1976.
ˣ To whom inquiries should be directed.

Intramolecular and Intermolecular Transformations of Aspirin in Nonhydroxylic Solvents

Keyphrases □ Aspirin—intra- and intermolecular transformations in nonhydroxylic solvents, reaction mechanisms □ Transformations, intra- and intermolecular—acetylsalicylic acid in nonhydroxylic solvents, reaction mechanisms

To the Editor:

Much evidence has been presented (1–3) to suggest that the hydrolysis of ionized acetylsalicylic acid (aspirin) involves intramolecular general-base catalysis by the carboxylate anion and not, as previously supposed (4–8), an intramolecular nucleophilic catalysis with a kinetically significant intermediary formation of the mixed anhydride of salicylic and acetic acids. There seems, however, to be an equilibrium between acetylsalicylate and the anion of the mixed salicylic acetic anhydride (3, 9). But since the anhydride reverts to the starting ester much faster than it is hydrolyzed, the nucleophilic pathway is not a feasible hydrolytic route.

The hydrolysis of the ester group in acetylsalicylic acid is also catalyzed by the unionized carboxyl group (2, 10). In this case, nucleophilic catalysis may be involved because of a more favorable equilibrium constant for the formation of the protonated form rather than the ionized one of the mixed anhydride intermediate (10).

We have observed, and now wish to report, novel and unusual reactions of acetylsalicylic acid occurring in solutions of the acid in nonhydroxylic solvents.

Clarke (3). Indeed, some colors produced by other drugs (*e.g.*, ephedrine, amphetamine, and methamphetamine) may be identified by trained eyes, but untrained personnel should be warned of the possibility of misidentification, particularly when other extraneous material and colors are added to the drug as is the case with street drugs. As Clarke stated:

> *"The color given in any test depends on the quantity of material used and on its purity, and may be described differently by different individuals. To allow for this, the following lists must be used in as wide a sense as possible."*

Therefore, it is up to the worker to exercise his or her judgment in utilizing such color tests for the primary screening of these compounds.

Clarke's compilation of the colors produced with the Marquis reagent did not include ephedrine (3).

Cobalt Thiocyanate—Table IV in the earlier paper (2) included 14 compounds that gave a blue flaky precipitate with cobalt thiocyanate. Rorke *et al.* (1) suggested the use of stannous chloride to enhance the specificity of the test by differentiating between cocaine and procaine and between benzocaine and diphenhydramine; however, they did not mention the behavior of the other compounds listed in the table or of the many other compounds not included. They also failed to consider that many street samples contain mixtures of cocaine and procaine, which make this test worthless or, at best, very difficult to interpret.

The addition of stannous chloride to the blue flaky precipitate formed by such a mixture results in partial dissolution of the precipitate. This partial dissolution is very difficult to observe, and the mixture may be misidentified as cocaine. Rorke *et al.* (1) also failed to mention that the blue precipitate formed by methadone dissolves only partially in stannous chloride, which adds to the possibility of erroneous interpretation.

Therefore, it is our opinion that the use of stannous chloride does not add to the specificity of this test and may lead to erroneous results. For these reasons, it was not included in the scheme described in the original paper (1).

Zwikker's Test—The original paper (2) is in disagreement with Rorke *et al.* (1) and Clarke (3). We repeated the experiment using the reagents described and amobarbital, phenobarbital sodium, and secobarbital as reference standards. At the concentration of 2 mg of the barbiturates used, an instant blue-violet color developed, which was found to be very stable. At this concentration, no blue-violet color was developed with glutethimide. Instead, a yellow color developed, which changed upon standing to a gray color. However, very high concentrations of glutethimide, *i.e.*, more than 10 mg, produced a similar blue-violet color, which disappeared almost instantaneously and faded to a gray color within a few seconds. Therefore, we stand firmly by the results reported earlier (1).

In conclusion, we feel that this exchange with Rorke *et al.* (1) has clarified a number of points, which are examples of the many scientific variables between laboratories due to human differences and differences in methodology. This exchange has also demonstrated, as was pointed out previously (2), that these tests only provide preliminary information to help in the selection of the necessary confirmatory tests such as TLC and GLC. They also aid in the selection of the compound or compounds that are to be used as reference standards for the final identification by TLC or GLC.

Rorke *et al.* (1) pointed out the importance of such tests for chemists defending their results in the courts. We disagree with them in this statement. Results of spot tests should never be used as evidence in the courts.

(1) C. V. Rorke, H. A. Harris, T. Catalano, and S. M. Dugar, *J. Pharm. Sci.*, **65**, 774(1976).

(2) A. N. Masoud, *ibid.*, **64**, 841(1975).

(3) E. G. C. Clarke, "Isolation and Identification of Drugs," The Pharmaceutical Press, London, England, 1969, pp. 663–669.

Asaad N. Masoud ˣ
School of Pharmacy
Creighton University
Omaha, NE 68178

Donald J. Nittskoff
Analytical Laboratories of Ohio
Cleveland, OH 44110

Received December 19, 1975.
Accepted for publication February 26, 1976.
ˣ To whom inquiries should be directed.

Intramolecular and Intermolecular Transformations of Aspirin in Nonhydroxylic Solvents

Keyphrases □ Aspirin—intra- and intermolecular transformations in nonhydroxylic solvents, reaction mechanisms □ Transformations, intra- and intermolecular—acetylsalicylic acid in nonhydroxylic solvents, reaction mechanisms

To the Editor:

Much evidence has been presented (1–3) to suggest that the hydrolysis of ionized acetylsalicylic acid (aspirin) involves intramolecular general-base catalysis by the carboxylate anion and not, as previously supposed (4–8), an intramolecular nucleophilic catalysis with a kinetically significant intermediary formation of the mixed anhydride of salicylic and acetic acids. There seems, however, to be an equilibrium between acetylsalicylate and the anion of the mixed salicylic acetic anhydride (3, 9). But since the anhydride reverts to the starting ester much faster than it is hydrolyzed, the nucleophilic pathway is not a feasible hydrolytic route.

The hydrolysis of the ester group in acetylsalicylic acid is also catalyzed by the unionized carboxyl group (2, 10). In this case, nucleophilic catalysis may be involved because of a more favorable equilibrium constant for the formation of the protonated form rather than the ionized one of the mixed anhydride intermediate (10).

We have observed, and now wish to report, novel and unusual reactions of acetylsalicylic acid occurring in solutions of the acid in nonhydroxylic solvents.

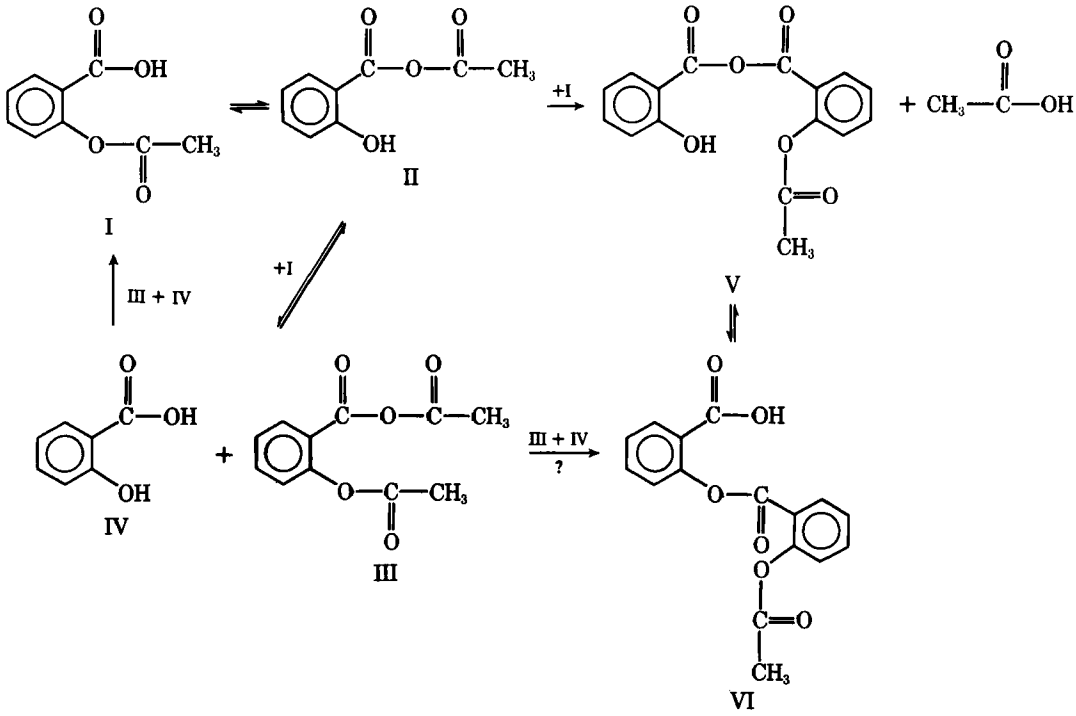

Scheme I

Acetylsalicylic acid (I, Scheme I) dissolved in various nonhydroxylic solvents (*e.g.*, benzene, ether, chloroform, ethyl acetate, acetone, and acetonitrile) was found to convert into several products. In alcohols such as methanol and propanol, I remained unchanged. This preliminary report presents only results obtained in benzene solutions.

On heating a solution of I in benzene (2–20 mg/ml) at 60°, an equilibrium between I and the mixed acetylsalicylic acetic anhydride (III) and salicylic acid (IV) was established after a few hours at concentrations corresponding to 74, 13, and 13 mole %, respectively, of the initial I concentration. At constant temperature, the rates of the reversible formation of both III and IV followed first-order kinetics for periods corresponding to two to three half-lives. Besides being formed in equimolar amounts, III and IV were produced at identical rates. The mixed anhydride III was determined quantitatively by an anhydride assay (11) after prior removal of the acid products (I and IV) by extraction with an aqueous phosphate buffer solution of pH 8 (11). Salicylic acid (IV) was determined either by direct spectrophotometric measurement at 320 nm (where I and IV do not interfere) after appropriate dilution of the reaction solution with benzene or by spectrophotometric analysis of an aqueous buffer (pH 7.4)-extracted reaction solution [this procedure, which is similar to that described by Gore *et al.* (12), was also used to determine undegraded I].

The identification of III was accomplished by IR (chloroform) and NMR (deuterochloroform) spectroscopy as well as by a quantitative UV determination of the amount of IV released by alkaline hydrolysis. In addition, by using a modification of the anhydride assay (11), which allows a selective determination of both an anhydride moiety and a reactive ester group like that in I (to be reported later), the compound was shown to contain equimolar amounts of anhydride and ester groups. On reaction with glycine in aqueous solution at pH 9.5, the anhydride produced *N*-salicyloylglycine in a yield of 25%.

We previously (13) thought, as have others (14), that the anhydride formed in benzene solutions of I was acetylsalicylic anhydride, but this is not correct. On prolonged standing of the solutions, however, a disproportionation of III to the symmetrical acetylsalicylic anhydride (and acetic anhydride) was observed to take place.

On further standing of the benzene solutions of I, a product shown to be acetylsalicylsalicylic acid (VI) was formed in considerable amounts. An approximate first-order half-life of 23 hr was observed at 60°. The product reached a maximal concentration corresponding to a net conversion of 58% of I. The identity of VI was established by comparison with authentic acetylsalicylsalicylic acid (15) by TLC using several developing systems, by GLC (16), and by alkaline hydrolysis to give first salicylsalicylic acid (a reaction used for spectrophotometric quantitation of VI) and then IV (15). Although more stable than I, VI, once formed, readily transformed as observed by means of TLC.

Although the reactions of I to give III and IV followed first-order kinetics, the observed rate constants associated with the production of either III or IV depended on the initial concentration of I (Fig. 1). However, this apparent paradoxical feature becomes understandable when it is borne in mind that the total change of the concentration of I is relatively small (26% of I is transformed). The pronounced saturation effect of the plot in Fig. 1 is indicative of the

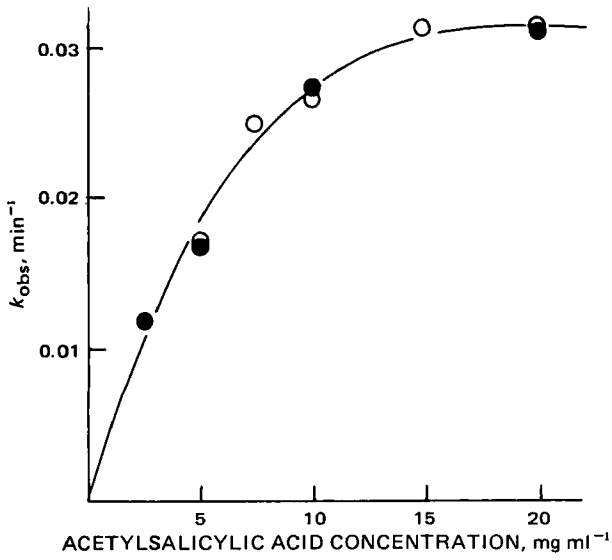

Figure 1—*Plot of observed first-order rate constants for formation of salicylic acid (●) and mixed acetylsalicylic acetic anhydride (○) at 60° in benzene solutions of acetylsalicylic acid as a function of the initial concentration of acetylsalicylic acid.*

presence of a metastable intermediate in the reactions and of a change in the rate-determining step with increasing concentrations of I; *i.e.*, the formation of the intermediate becomes rate limiting at the higher concentrations of I.

We interpret these results to mean that I, through an intramolecular addition of the carboxyl group to the ester carbonyl moiety, is converted into the mixed salicylic acetic anhydride (II), which then either returns to I or reacts at the anhydride moiety with the carboxyl group of a second molecule of I to produce III and IV (with attack on the acetyl carbonyl moiety of the anhydride) or to produce V (with attack on the salicyloyl carbonyl moiety) which, in turn, rearranges into VI (like II to I, Scheme I). Admittedly, other pathways can be imagined to lead to the formation of III, IV, and VI (*e.g.*, a reaction between two molecules of II), but it seems inevitable to postulate an intermediate formation of a mixed salicylic acetic anhydride (II). The *para*-substituted analog of I, *p*-acetoxybenzoic acid, completely fails to undergo any degradation in the present conditions.

A catalysis of all reactions shown in Scheme I was observed by triethylamine and also by benzene-insoluble materials such as magnesium hydroxide and magnesium carbonate. This finding apparently suggests that the ionized acetylsalicylate undergoes reactions *via* the anhydride II in nonhydroxylic solvents. A similar suggestion was advanced previously (17, 18).

The observations described may possibly contribute to an understanding of the mechanism of catalysis of reactions of I and related compounds in aqueous as well as in nonaqueous solutions [*cf.*, the recent paper by Kömives *et al.* (19) on aminolysis of I in acetonitrile]. Since preliminary experiments indicated that similar transformations of I can occur in the solid state at elevated temperatures, the results may become of relevance for the assessment of the stability of I formulations. This assessment has so far mostly been based on the conviction that IV and acetic acid are the only products of degradation (20).

As far as allergy to I is concerned, the formation of even small amounts of the immunogenic acetylsalicylsalicylic acid and acetylsalicylic anhydride should be avoided (21, 22). On the basis of the ready ability of the mixed acetylsalicylic acetic anhydride to salicyloylate amino groups as described here, this compound may most likely be as immunogenic as acetylsalicylsalicylic acid and acetylsalicylic anhydride.

(1) A. R. Fersht and A. J. Kirby, *J. Amer. Chem. Soc.*, **89**, 4853, 4857(1967).
(2) T. St. Pierre and W. P. Jencks, *ibid.*, **90**, 3817(1968).
(3) A. R. Fersht and A. J. Kirby, *ibid.*, **90**, 5818(1968).
(4) L. J. Edwards, *Trans. Faraday Soc.*, **46**, 723(1950).
(5) *Ibid.*, **48**, 696(1952).
(6) E. R. Garrett, *J. Amer. Chem. Soc.*, **79**, 3401(1957).
(7) M. L. Bender, F. Chloupek, and M. C. Neveu, *ibid.*, **80**, 5384(1958).
(8) M. L. Bender, *Chem. Rev.*, **60**, 53(1960).
(9) D. S. Kemp and T. D. Thibault, *J. Amer. Chem. Soc.*, **90**, 7154(1968).
(10) A. R. Fersht and A. J. Kirby, *ibid.*, **90**, 5826(1968).
(11) H. Bundgaard and C. Bundgaard, *J. Pharm. Pharmacol.*, **25**, 593(1973).
(12) A. Y. Gore, K. B. Naik, D. O. Kildsig, G. E. Peck, V. F. Smolen, and G. S. Banker, *J. Pharm. Sci.*, **57**, 1850(1968).
(13) H. Bundgaard, *J. Pharm. Pharmacol.*, **26**, 535(1974).
(14) J. Levine, *J. Pharm. Sci.*, **50**, 506(1961).
(15) H. Bundgaard, *J. Pharm. Pharmacol.*, **26**, 18(1974).
(16) S. Patel, J. H. Perrin, and J. J. Windheuser, *J. Pharm. Sci.*, **61**, 1794(1972).
(17) D. Davidson and L. Auerbach, *J. Amer. Chem. Soc.*, **75**, 5984(1953).
(18) D. E. Guttman, *J. Pharm. Sci.*, **57**, 1685(1968).
(19) T. Kömives, A. F. Márton, and F. Dutka, *Chem. Ind. (London)*, **1975**, 567.
(20) C. A. Kelly, *J. Pharm. Sci.*, **59**, 1053(1970).
(21) A. L. de Weck, *Int. Arch. Allergy Appl. Immunol.*, **41**, 393(1971).
(22) H. Bundgaard and A. L. de Weck, *ibid.*, **49**, 119(1975).

Hans Bundgaard ˣ
Claus Larsen
Department of Pharmaceutics
Royal Danish School of Pharmacy
2 Universitetsparken
DK-2100 Copenhagen
Denmark

Received December 22, 1975.
Accepted for publication February 9, 1976.
ˣ To whom inquiries should be directed.

Two New Diterpenes from *Stemodia maritima* L.

Keyphrases □ Diterpenes—isolated from aboveground portion of *Stemodia maritima*, PMR, IR, mass, and circular dichroism spectral identification □ *Stemodia maritima*—aboveground portion extracted, diterpenes isolated and identified □ Maritimol—isolated from *Stemodia maritima*, PMR, IR, mass, and circular dichroism spectral identification □ Stemodinol—isolated from *Stemodia maritima*, PMR, IR, mass, and circular dichroism spectral identification

To the Editor:

An investigation of the aboveground portion of

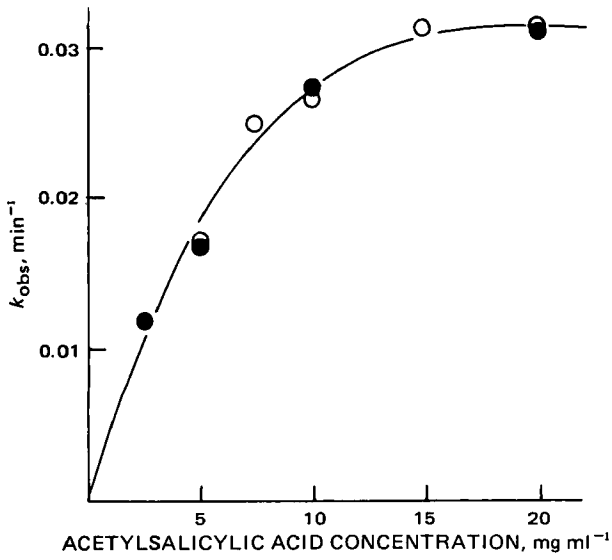

Figure 1—*Plot of observed first-order rate constants for formation of salicylic acid (●) and mixed acetylsalicylic acetic anhydride (○) at 60° in benzene solutions of acetylsalicylic acid as a function of the initial concentration of acetylsalicylic acid.*

presence of a metastable intermediate in the reactions and of a change in the rate-determining step with increasing concentrations of I; *i.e.*, the formation of the intermediate becomes rate limiting at the higher concentrations of I.

We interpret these results to mean that I, through an intramolecular addition of the carboxyl group to the ester carbonyl moiety, is converted into the mixed salicylic acetic anhydride (II), which then either returns to I or reacts at the anhydride moiety with the carboxyl group of a second molecule of I to produce III and IV (with attack on the acetyl carbonyl moiety of the anhydride) or to produce V (with attack on the salicyloyl carbonyl moiety) which, in turn, rearranges into VI (like II to I, Scheme I). Admittedly, other pathways can be imagined to lead to the formation of III, IV, and VI (*e.g.*, a reaction between two molecules of II), but it seems inevitable to postulate an intermediate formation of a mixed salicylic acetic anhydride (II). The *para*-substituted analog of I, *p*-acetoxybenzoic acid, completely fails to undergo any degradation in the present conditions.

A catalysis of all reactions shown in Scheme I was observed by triethylamine and also by benzene-insoluble materials such as magnesium hydroxide and magnesium carbonate. This finding apparently suggests that the ionized acetylsalicylate undergoes reactions *via* the anhydride II in nonhydroxylic solvents. A similar suggestion was advanced previously (17, 18).

The observations described may possibly contribute to an understanding of the mechanism of catalysis of reactions of I and related compounds in aqueous as well as in nonaqueous solutions [*cf.*, the recent paper by Kömives *et al.* (19) on aminolysis of I in acetonitrile]. Since preliminary experiments indicated that similar transformations of I can occur in the solid state at elevated temperatures, the results may become of relevance for the assessment of the stability of I formulations. This assessment has so far mostly been based on the conviction that IV and acetic acid are the only products of degradation (20).

As far as allergy to I is concerned, the formation of even small amounts of the immunogenic acetylsalicylsalicylic acid and acetylsalicylic anhydride should be avoided (21, 22). On the basis of the ready ability of the mixed acetylsalicylic acetic anhydride to salicyloylate amino groups as described here, this compound may most likely be as immunogenic as acetylsalicylsalicylic acid and acetylsalicylic anhydride.

(1) A. R. Fersht and A. J. Kirby, *J. Amer. Chem. Soc.*, **89**, 4853, 4857(1967).
(2) T. St. Pierre and W. P. Jencks, *ibid.*, **90**, 3817(1968).
(3) A. R. Fersht and A. J. Kirby, *ibid.*, **90**, 5818(1968).
(4) L. J. Edwards, *Trans. Faraday Soc.*, **46**, 723(1950).
(5) *Ibid.*, **48**, 696(1952).
(6) E. R. Garrett, *J. Amer. Chem. Soc.*, **79**, 3401(1957).
(7) M. L. Bender, F. Chloupek, and M. C. Neveu, *ibid.*, **80**, 5384(1958).
(8) M. L. Bender, *Chem. Rev.*, **60**, 53(1960).
(9) D. S. Kemp and T. D. Thibault, *J. Amer. Chem. Soc.*, **90**, 7154(1968).
(10) A. R. Fersht and A. J. Kirby, *ibid.*, **90**, 5826(1968).
(11) H. Bundgaard and C. Bundgaard, *J. Pharm. Pharmacol.*, **25**, 593(1973).
(12) A. Y. Gore, K. B. Naik, D. O. Kildsig, G. E. Peck, V. F. Smolen, and G. S. Banker, *J. Pharm. Sci.*, **57**, 1850(1968).
(13) H. Bundgaard, *J. Pharm. Pharmacol.*, **26**, 535(1974).
(14) J. Levine, *J. Pharm. Sci.*, **50**, 506(1961).
(15) H. Bundgaard, *J. Pharm. Pharmacol.*, **26**, 18(1974).
(16) S. Patel, J. H. Perrin, and J. J. Windheuser, *J. Pharm. Sci.*, **61**, 1794(1972).
(17) D. Davidson and L. Auerbach, *J. Amer. Chem. Soc.*, **75**, 5984(1953).
(18) D. E. Guttman, *J. Pharm. Sci.*, **57**, 1685(1968).
(19) T. Kömives, A. F. Márton, and F. Dutka, *Chem. Ind. (London)*, **1975**, 567.
(20) C. A. Kelly, *J. Pharm. Sci.*, **59**, 1053(1970).
(21) A. L. de Weck, *Int. Arch. Allergy Appl. Immunol.*, **41**, 393(1971).
(22) H. Bundgaard and A. L. de Weck, *ibid.*, **49**, 119(1975).

Hans Bundgaard ˣ
Claus Larsen
Department of Pharmaceutics
Royal Danish School of Pharmacy
2 Universitetsparken
DK-2100 Copenhagen
Denmark

Received December 22, 1975.
Accepted for publication February 9, 1976.
ˣ To whom inquiries should be directed.

Two New Diterpenes from *Stemodia maritima* L.

Keyphrases □ Diterpenes—isolated from aboveground portion of *Stemodia maritima*, PMR, IR, mass, and circular dichroism spectral identification □ *Stemodia maritima*—aboveground portion extracted, diterpenes isolated and identified □ Maritimol—isolated from *Stemodia maritima*, PMR, IR, mass, and circular dichroism spectral identification □ Stemodinol—isolated from *Stemodia maritima*, PMR, IR, mass, and circular dichroism spectral identification

To the Editor:

An investigation of the aboveground portion of

Stemodia maritima L. (Scrophulariaceae)[1] resulted in the isolation and identification of two new diterpenes containing an unusual tetracyclic skeleton. These new diterpenes have been named maritimol and stemodinol, and Structures I*a* and I*b* have been assigned to them, respectively.

Percolation of the dried, powdered, aboveground portion with petroleum ether (bp 40–60°) yielded a dark-green percolate. Concentration of the percolate yielded a yellowish-green precipitate, which was filtered and chromatographed over silica gel. Elution was initiated with *n*-hexane followed by increasing amounts of benzene in *n*-hexane, benzene, increasing amounts of chloroform in benzene, chloroform, and, finally, increasing amounts of methanol in chloroform. Elution with 3% methanol in chloroform yielded the two new diterpenes, which were obtained pure by crystallization.

While this study was in progress, a report appeared concerning the isolation and identification of stemodin (I*c*) and stemodinone (I*d*) from the leaves of *S. maritima* (1). The structures for these diterpenes containing the novel stemodane ring system were solved through a single-crystal X-ray analysis of stemodinone (1). These two diterpenes were also identified in this study[2].

Maritimol (I*a*) had a melting point of 169–170° (isopropyl ether) and $[\alpha]_D^{25}$ +3.7° (c 0.93, pyridine). It exhibited a parent ion peak at *m/e* 306.255, corresponding to the formula $C_{20}H_{34}O_2$ (calculated *m/e* 306.256), which was also supported by elemental analysis. The IR spectrum had an absorption at ν_{max} (KBr) 3340 cm^{-1}; the proton magnetic resonance (PMR) spectrum[3] indicated four methyl singlets at δ 0.86, 0.96, 1.03, and 1.11 and another signal at δ 3.20 (dd, 1H, J = 11, 5 Hz). This last signal shifted to δ 4.41 (dd, 1H, J = 11, 5 Hz) in the monoacetate (I*e*)[4], mp 152–153° (ethanol); $[\alpha]_D^{25}$ +12.0° (c 0.60, chloroform); IR: ν_{max} (KBr) 3570 and 1725 cm^{-1}; PMR: δ 0.90, 0.91, 0.98, 1.11, and 2.05 (s, 3H each).

Oxidation of maritimol with Jones reagent gave the ketone (I*f*)[4], mp 117–118° (ether); $[\alpha]_D^{25}$ −37.0° (c 0.80, chloroform); IR: ν_{max} ($CHCl_3$) 3620 and 1705 cm^{-1}; PMR: δ 1.10 and 1.13 (s, 6H each). The circular dichroism spectrum[5] of I*f* showed a negative Cotton effect, $[\theta]_{296}$ − 3225. These data suggest that maritimol (I*a*) is isomeric with stemodin (I*c*). Reduction of I*f* under Huang-Minlon (2) conditions produced the known desoxy derivative (I*g*)[6], which confirmed the stemodane ring system.

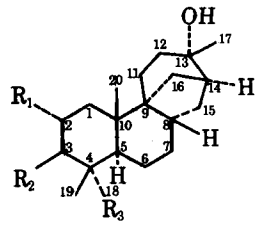

I*a*: R_1 = H, R_2 = OH, R_3 = CH_3
I*b*: R_1 = R_2 = H, R_3 = CH_2OH
I*c*: R_1 = OH, R_2 = H, R_3 = CH_3
I*d*: R_1 = =O, R_2 = H, R_3 = CH_3
I*e*: R_1 = H, R_2 = $OCOCH_3$, R_3 = CH_3
I*f*: R_1 = H, R_2 = =O, R_3 = CH_3
I*g*: R_1 = R_2 = H, R_3 = CH_3
I*h*: R_1 = Br, R_2 = =O, R_3 = CH_3
I*i*: R_1 = R_2 = H, R_3 = CH_2OCOCH_3
I*j*: R_1 = R_2 = H, R_3 = CHO

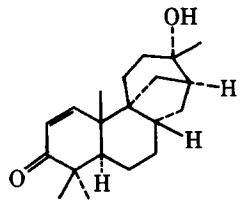

II

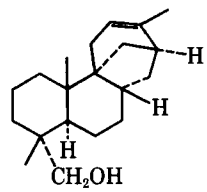

III

The secondary hydroxyl group could be located at C-1, C-3, C-11, or C-12 based on the PMR data. Treatment of I*f* with trimethylphenylammonium tribromide (3) yielded the monobromo derivative, I*h*, mp 99–100° dec. (ether); IR: ν_{max} ($CHCl_3$) 3620 and 1725 cm^{-1}. The presence of one bromine atom was confirmed by observing the peaks at *m/e* 384 (10%) and 382 (10%) in the mass spectrum. The PMR spectrum showed signals for four methyl groups and two double doublets (1H each) centered at δ 2.60 (J = 12, 5.5 Hz) and 4.90 (J = 13, 5.5 Hz), which form the *MX* portion of an *AMX* pattern, with the *A* portion being hidden under the methylene envelope (4).

Dehydrobromination of I*h*, using lithium carbonate and lithium bromide in dimethylformamide (3), yielded the α,β-unsaturated ketone II[7]; IR: ν_{max} ($CHCl_3$) 3620 and 1660 cm^{-1}; UV: λ_{max} (CH_3OH) 230 nm (ϵ 8200), signals for four methyl groups and two doublets (1H each) at δ 7.06 (J = 9.5 Hz) and 5.80 (J = 9.5 Hz). These data are consistent only with placement of the secondary hydroxyl at C-1 or C-3. Position C-1 was eliminated by applying the octant rule (5). The predicted sign of the Cotton effect for a ketone at C-1 would be positive; at C-3, it would be negative. The observed sign for I*f* is negative, and thus the ketone (and, hence, the hydroxyl) can be placed at C-3. Since one coupling constant for the C-3 proton is large (J = 11 Hz), this proton is placed axial

[1] The plant material was obtained from the Caribbean island of Curacao, where it is used for the treatment of venereal disease. The plant was identified, collected, and provided to us by Dr. Julia Morton; a voucher specimen was deposited in the Herbarium of the Department of Pharmacognosy, University of Mississippi.

[2] Stemodin [$C_{20}H_{34}O_2$ (*m/e* 306.254, calculated *m/e* 306.256; the formula was also supported by elemental analysis), mp 195–196°, $[\alpha]_D^{25}$ −2.8° (c 1.03, pyridine)] had physical and spectral properties in agreement with those reported previously (1). The acetate of stemodin was also prepared, and the data agreed with those previously reported (1). Stemodinone [$C_{20}H_{34}O_2$ (*m/e* 304.238, calculated *m/e* 304.240; the formula was also supported by elemental analysis), mp 212–213°, $[\alpha]_D^{25}$ +13.1° (c 0.90, chloroform)] had physical and spectral properties as reported previously (1). It was also prepared by Jones oxidation of stemodin (1).

[3] The PMR data for all compounds were obtained at 60 MHz using deuterochloroform and tetramethylsilane as the internal standard.

[4] The formula was supported by high-resolution mass spectral and/or elemental analyses.

[5] The circular dichroism measurements were performed on a Jasco model J-40 automatic recording spectropolarimeter using methanol as the solvent.

[6] Compound I*g* was prepared from stemodinone as described previously (1). The physical and spectral properties of I*g*[4] were in agreement with those reported previously. Compound I*g* was identical in all respects (melting point, mixed melting point, TLC, IR, and NMR) to the Huang-Minlon reduction product obtained from I*f* and I*j*.

[7] Compound II could not be obtained in crystalline form but was one spot on TLC; the formula $C_{20}H_{30}O_2$ was confirmed by high-resolution mass spectrometry.

and the hydroxyl can be equatorial. Thus, maritimol (I*a*) is stemodane-3β,13α-diol[8].

Stemodinol (I*b*) had a melting point of 182–183° (chloroform–*n*-hexane) and $[\alpha]_D^{25}$ +13.8° (c 1.01, pyridine). It exhibited a parent ion peak at *m/e* 306.256, corresponding to the formula $C_{20}H_{34}O_2$ (calculated *m/e* 306.256), which was also supported by elemental analysis. The IR spectrum had absorptions at ν_{max} ($CHCl_3$) 3620 and 3340 cm^{-1}. The PMR spectrum indicated the presence of three methyl singlets at δ 0.70, 0.90, and 1.11 and a pair of doublets forming an *AB* quartet at δ_A 3.37 (J = 10 Hz) and δ_B 2.85 (J = 10 Hz). The pair shifted to δ_A 3.77 (J = 11 Hz) and δ_B 3.62 (J = 11 Hz) in the monoacetate[4] (I*i*), mp 81–83° (ethanol–water); $[\alpha]_D^{25}$ +17.5° (c 0.40, chloroform); IR: ν_{max} (KBr) 3410 and 1735 cm^{-1}; PMR: δ 0.83, 0.95, 1.13, and 2.05 (s, 3H each).

Oxidation of I*b* with chromium trioxide–pyridine produced the aldehyde (I*j*)[4], mp 145–146°; IR: ν_{max} ($CHCl_3$) 3620 and 1730 cm^{-1}; PMR: δ 0.90, 1.03, 1.15 (s, 3H each), and 9.20 (s, 1H). These data suggest that stemodinol (I*b*) is also isomeric with stemodin (I*c*) and that I*b* contains a primary alcohol. Reduction of I*j* under Huang-Minlon conditions (2) gave the known desoxy derivative, I*g*[6]. Thus, stemodinol contains the same carbon skeleton as stemodin. The primary alcohol could be located at any one of four positions (C-17, C-18, C-19, or C-20).

The failure of I*b* to form an acetonide with cupric sulfate and acetone[9] and the formation of III by treatment of I*b* with 1% HCl in acetone eliminated C-17 as a possible location of the primary alcohol group. The dehydrated product, III[10], had ν_{max} ($CHCl_3$) 3640 and 3470 cm^{-1}; PMR: δ 0.78, 1.01 (s, 3H each), 1.65 (d, 3H, J = 1.5 Hz), 4.95 (1H, broad), and the *AB* quartet δ_A 3.34 (J = 10 Hz) and δ_B 3.10 (J = 10 Hz).

The location of the primary alcohol at C-18[11] is based on PMR data. The center of the *AB* quartet for hydroxymethyl groups and their corresponding acetates has been related to their positions at C-18 and C-19 (8). The *AB* quartet for I*b* and its acetate I*e* is centered at 197 and 222 Hz, respectively, consistent with placement of the primary alcohol at C-18. Additional evidence for this placement can be found by observing both the chemical shift and long-range coupling of the aldehydic proton in positions C-18 and C-19 (9). If the aldehyde were at C-19, the signal for the aldehydic proton would appear near δ 9.70 as a doublet (J = 1–2 Hz) (8) rather than as a singlet near δ 9.20 as in I*j*. Based on this evidence, the structure proposed for stemodinol (I*b*) is stemodane-13α,18-diol[8].

[8] The numbering used is that for the hypothetical hydrocarbon, stemodane, as proposed by the authors in Ref. 1. This differs from the numbering proposed for aphidicolane, a hydrocarbon differing in stereochemistry only at C-9, C-13, and C-14 (6).

[9] Compound I*b*, cupric sulfate, and acetone were stirred at room temperature for 3 days and only starting material was recovered.

[10] Compound III could not be obtained in crystalline form but was one spot on TLC; the formula $C_{20}H_{32}O$ was confirmed by high-resolution mass spectrometry.

[11] Although C-20 was also a possibility, it was ruled out on biogenetic grounds since there are no known examples of diterpenes with a primary alcohol at this position. Numerous examples occur with hydroxyl at C-18 or C-19 (7).

(1) P. S. Manchand, J. D. White, H. Wright, and J. Clardy, *J. Amer. Chem. Soc.*, **95**, 2705(1973).

(2) Huang-Minlon, *ibid.*, **71**, 3301(1949).

(3) A. G. González, B. M. Fraga, M. G. Hernández, and J. G. Luis, *Phytochemistry*, **12**, 1113(1973).

(4) N. S. Bhacca and D. H. Williams, "Applications of NMR Spectroscopy in Organic Chemistry: Illustrations from the Steroid Field," Holden-Day, San Francisco, Calif., 1966, chap. 3, p. 48.

(5) L. A. Mitscher and G. W. Clark, *Lloydia*, **35**, 311(1972).

(6) K. M. Brundret, W. Dalziel, B. Hesp, J. A. J. Harvis, and S. Neidle, *J. C. S. Chem. Commun.*, **1972**, 1027.

(7) T. K. Devon and A. I. Scott, "Handbook of Naturally Occurring Compounds," vol. II, Academic, New York, N.Y., 1972, pp. 281–384.

(8) A. Gaudemer, J. Polonsky, and E. Wenkert, *Bull. Soc. Chim. Fr.*, **1964**, 407.

(9) M. Fetizon, G. Moreau, and N. Moreau, *ibid.*, **1968**, 3295.

Charles D. Hufford
R. Oswaldo Guerrero
Norman J. Doorenbos [x]
Department of Pharmacognosy
School of Pharmacy
University of Mississippi
University, MS 38677

Received March 26, 1975.

Accepted for publication February 9, 1976.

Supported in part by the Research Institute of Pharmaceutical Sciences, School of Pharmacy, University of Mississippi.

We are grateful to Dr. Stephen Billets, Research Institute of Pharmaceutical Sciences, for the determination of the high-resolution mass spectral data and to Dr. Julia Morton for providing large amounts of plant material.

[x] To whom inquiries should be directed.

REVIEWS

Toxicology: The Basic Science of Poisons. Edited by L. J. CASARETT and J. DOULL. Macmillan, New York, N.Y., 1975. xiv + 768 pp., 49 figures, 112 tables. Price $23.95.

How often in an academic career do you receive a book for review about which you can honestly say you enjoyed getting it and reviewing it? Well, I have had the opportunity. For some 10 years, I have been teaching a graduate course in General Toxicology without a text, because none existed. Now arrives on the toxicology scene a most welcome text. I had the opportunity, during the summer Gordon Research Conference, to preview this book and the general opinion at that time was that we finally had a useful text for beginning courses in toxicology.

The book follows somewhat the same format as the classic text in pharmacology. I have pointed out to publishers over the past dozen years that what is needed in toxicology is an edited text along the same lines as the Goodman and Gilman text in pharmacology. Casarett and Doull have edited a 30-chapter text divided into four units. The initial unit deals with general principles of toxicology, covering quite well the scope of toxicology, absorption, distribution, excretion, metabolism of toxicants, and factors influencing toxicology. The only part of Unit I that is lacking is the chapter on toxicologic evaluation. It does not go into as much detail as is necessary to teach this aspect of toxicology. Hopefully, in future editions, this chapter will be written by a toxicologist whose expertise and daily job involve toxic evaluations (safety evaluations or assessment of hazards).

Unit II covers systemic toxicology in eight chapters. Essentially, a review of each system is included with discussion of the pathophysiology for specific chemicals. This section is lacking in a discussion of the largest organ of the body, the skin. It also lacks a chapter on the endocrine system.

Unit III deals with specific toxic agents under chapter headings as varied as Food Additives, Air Pollutants, Pesticides, Carcinogens, Social Poisons, Phytotoxicology, and Teratogens.

Unit IV is probably the most disappointing section of the text. This unit deals with the applications of toxicology, specifically Clinical Toxicology, Forensic Toxicology, Industrial Toxicology, Veterinary Toxicology, and Toxicology and the Law. Disappointing from the real point of view. The authors, in general, avoid putting into a chapter the real application of toxicology to their specific fields. It almost appears that they were writing to impress their colleagues rather than to inform a beginning student in toxicology. I am sure that these chapters will improve as Dr. Doull receives input from the users.

The text is very welcome and very useful for beginning courses in toxicology. It is not a perfect text, but neither was the first edition of Goodman and Gilman. Hopefully, future editions will contain chapters written by toxicologists with expertise in the area for which they were chosen to write.

This will be a classic text in toxicology. It will grow in size and wisdom as real toxicologists become involved in its preparation; many were involved in this first volume. I recommend its adoption for all beginning courses in General Toxicology, so that all future toxicologists would have a "standard of excellence" for a basic education in the basic science of Toxicology.

Reviewed by Charles L. Winek
Duquesne University
Pittsburgh, PA 15219

The Pharmacological Basis of Therapeutics, Fifth Edition. Edited by LOUIS S. GOODMAN and ALFRED GILMAN. Macmillan, 866 Third Ave., New York, NY 10022, 1975. 1704 pp. 19 × 27 cm. Price $30.00.

The fifth edition, published 34 years after the first, will undoubtedly continue to be one of the most useful pharmacology reference texts available.

The organization of the fifth edition is identical to the fourth edition, published in 1970. The 77 chapters reportedly underwent a thorough updating with respect to the mechanism of action and indication of use of older drugs and to the addition of important new drug entities. To prevent expansion of the fifth edition, less dynamic and outmoded sections were condensed or eliminated. As in the past, in areas where the number of therapeutic agents available is large, major discussion is focused on the well-established and effective prototypal drugs, while the numerous related compounds receive relatively brief descriptions. Therefore, the book is approximately 100 pages less than the fourth edition. There is also more discussion devoted to the pharmacokinetic principles of drugs. Other new entries include a discussion of the role of cyclic AMP as the "second messenger" and of the pharmacological effects of the prostaglandins.

"The Pharmacological Basis of Therapeutics" remains valuable as a complete and comprehensive text on pharmacology for all members of the health professions.

Staff Review

NOTICES

The Selectivity of Drugs. By ADRIEN ALBERT. John Wiley and Sons, Inc., 605 Third Ave., New York, NY 10016, 1975. 64 pp. 17 × 21 cm.

Current Developments in Psychopharmacology, Vol. 1. Edited by WALTER B. ESSMAN and L. VALZELLI. Spectrum Publication, Inc., 86-19 Sancho St., Holliswood, NY 11423, 1975. 345 pp. 16 × 24 cm.

Inhibitors of Nucleic Acid Synthesis. By HELGA KERSTEN and WALTER KERSTEN. Springer-Verlag, 175 Fifth Ave., New York, NY 10010, 1974. 184 pp. 17 × 24.5 cm. Price $27.90.

Cell Patterning. Ciba Foundation Symposium 29 (new series), Ciba-Geigy Corp., Summit, NJ 07901, 1975. 356 pp. 17 × 25 cm.

Effects of Drugs on Clinical Laboratory Tests. By D. S. YOUNG, L. C. PESTANER, and VAL GIBBERMAN. Clinical Pathology Dept., National Institutes of Health, Bethesda, MD 20014, 1975. 432 pp. 21 × 27.5 cm.

Les Applications Industrielles de la Microbiologie. By JACQUES RIVIERE. Masson et Cie, 120, Bd. Saint-Germain, Paris 6, France, 1975. 203 pp. 16 × 24 cm.

Young Inner City Families: Development of Ego Strength Under Stress. By MARGARET MORGAN LAWRENCE. Behavioral Publication, Inc., 72 Fifth Ave., New York, NY 10011, 1975. 139 pp. 14.5 × 21.5 cm. Price $10.95.

Size at Birth. Ciba Foundation Symposium 27 (new series). Ciba-Geigy Corp., Summit, NJ 07901. 408 pp. 17 × 24.5 cm.

Molds, Mushrooms, and Mycotoxins. By CLYDE M. CHRISTENSEN. University of Minnesota Press, Minneapolis, MN 55455, 1975. 264 pp. 15 × 23 cm. Price $11.50.

Psychopharmacology Communications, Vol. 1. Edited by EARL USDIN. Marcel Dekker, Inc., 270 Madison Ave., New York, NY 10016, 1975. 115 pp. 15 × 23 cm. Price $7.50.

Die Chemotherapeutischen und Pesticiden Wirkungen der Thiolreagenzien. By TIBOR ZSOLNAI. Akademiai Kiado of the Hungarian Academy of Science, Budapest V. Alkotmany U. 21, 1975. 415 pp. 17 × 24.5 cm. Price $26.00.

Weighing Designs (Statistics: Textbooks and Monographs Series, Vol. 12). By K. S. Banerjee. Marcel Dekker, Inc., 270 Madison Ave., New York, NY 10016, 1975. 141 pp. 16 × 24 cm. Price $12.75.

LSD—A Total Study. By D. V. SIVASANKAR. PJD Publications Ltd., Westbury, NY 1590, 1975. 960 pp. 16 × 24 cm. Price $29.75.

Pharmacotherapy and Psychotherapy: Paradoxes Problems and Progress, Vol. IX. Committee on Research. Group for the Advancement of Psychiatry, Inc., 419 Park Ave. S., New York, NY 10016, 1975. 176 pp. 16 × 20 cm. Price $6.00.

REVIEWS

Toxicology: The Basic Science of Poisons. Edited by L. J. CASARETT and J. DOULL. Macmillan, New York, N.Y., 1975. xiv + 768 pp., 49 figures, 112 tables. Price $23.95.

How often in an academic career do you receive a book for review about which you can honestly say you enjoyed getting it and reviewing it? Well, I have had the opportunity. For some 10 years, I have been teaching a graduate course in General Toxicology without a text, because none existed. Now arrives on the toxicology scene a most welcome text. I had the opportunity, during the summer Gordon Research Conference, to preview this book and the general opinion at that time was that we finally had a useful text for beginning courses in toxicology.

The book follows somewhat the same format as the classic text in pharmacology. I have pointed out to publishers over the past dozen years that what is needed in toxicology is an edited text along the same lines as the Goodman and Gilman text in pharmacology. Casarett and Doull have edited a 30-chapter text divided into four units. The initial unit deals with general principles of toxicology, covering quite well the scope of toxicology, absorption, distribution, excretion, metabolism of toxicants, and factors influencing toxicology. The only part of Unit I that is lacking is the chapter on toxicologic evaluation. It does not go into as much detail as is necessary to teach this aspect of toxicology. Hopefully, in future editions, this chapter will be written by a toxicologist whose expertise and daily job involve toxic evaluations (safety evaluations or assessment of hazards).

Unit II covers systemic toxicology in eight chapters. Essentially, a review of each system is included with discussion of the pathophysiology for specific chemicals. This section is lacking in a discussion of the largest organ of the body, the skin. It also lacks a chapter on the endocrine system.

Unit III deals with specific toxic agents under chapter headings as varied as Food Additives, Air Pollutants, Pesticides, Carcinogens, Social Poisons, Phytotoxicology, and Teratogens.

Unit IV is probably the most disappointing section of the text. This unit deals with the applications of toxicology, specifically Clinical Toxicology, Forensic Toxicology, Industrial Toxicology, Veterinary Toxicology, and Toxicology and the Law. Disappointing from the real point of view. The authors, in general, avoid putting into a chapter the real application of toxicology to their specific fields. It almost appears that they were writing to impress their colleagues rather than to inform a beginning student in toxicology. I am sure that these chapters will improve as Dr. Doull receives input from the users.

The text is very welcome and very useful for beginning courses in toxicology. It is not a perfect text, but neither was the first edition of Goodman and Gilman. Hopefully, future editions will contain chapters written by toxicologists with expertise in the area for which they were chosen to write.

This will be a classic text in toxicology. It will grow in size and wisdom as real toxicologists become involved in its preparation; many were involved in this first volume. I recommend its adoption for all beginning courses in General Toxicology, so that all future toxicologists would have a "standard of excellence" for a basic education in the basic science of Toxicology.

Reviewed by Charles L. Winek
Duquesne University
Pittsburgh, PA 15219

The Pharmacological Basis of Therapeutics, Fifth Edition. Edited by LOUIS S. GOODMAN and ALFRED GILMAN. Macmillan, 866 Third Ave., New York, NY 10022, 1975. 1704 pp. 19 × 27 cm. Price $30.00.

The fifth edition, published 34 years after the first, will undoubtedly continue to be one of the most useful pharmacology reference texts available.

The organization of the fifth edition is identical to the fourth edition, published in 1970. The 77 chapters reportedly underwent a thorough updating with respect to the mechanism of action and indication of use of older drugs and to the addition of important new drug entities. To prevent expansion of the fifth edition, less dynamic and outmoded sections were condensed or eliminated. As in the past, in areas where the number of therapeutic agents available is large, major discussion is focused on the well-established and effective prototypal drugs, while the numerous related compounds receive relatively brief descriptions. Therefore, the book is approximately 100 pages less than the fourth edition. There is also more discussion devoted to the pharmacokinetic principles of drugs. Other new entries include a discussion of the role of cyclic AMP as the "second messenger" and of the pharmacological effects of the prostaglandins.

"The Pharmacological Basis of Therapeutics" remains valuable as a complete and comprehensive text on pharmacology for all members of the health professions.

Staff Review

NOTICES

The Selectivity of Drugs. By ADRIEN ALBERT. John Wiley and Sons, Inc., 605 Third Ave., New York, NY 10016, 1975. 64 pp. 17 × 21 cm.

Current Developments in Psychopharmacology, Vol. 1. Edited by WALTER B. ESSMAN and L. VALZELLI. Spectrum Publication, Inc., 86-19 Sancho St., Holliswood, NY 11423, 1975. 345 pp. 16 × 24 cm.

Inhibitors of Nucleic Acid Synthesis. By HELGA KERSTEN and WALTER KERSTEN. Springer-Verlag, 175 Fifth Ave., New York, NY 10010, 1974. 184 pp. 17 × 24.5 cm. Price $27.90.

Cell Patterning. Ciba Foundation Symposium 29 (new series), Ciba-Geigy Corp., Summit, NJ 07901, 1975. 356 pp. 17 × 25 cm.

Effects of Drugs on Clinical Laboratory Tests. By D. S. YOUNG, L. C. PESTANER, and VAL GIBBERMAN. Clinical Pathology Dept., National Institutes of Health, Bethesda, MD 20014, 1975. 432 pp. 21 × 27.5 cm.

Les Applications Industrielles de la Microbiologie. By JACQUES RIVIERE. Masson et Cie, 120, Bd. Saint-Germain, Paris 6, France, 1975. 203 pp. 16 × 24 cm.

Young Inner City Families: Development of Ego Strength Under Stress. By MARGARET MORGAN LAWRENCE. Behavioral Publication, Inc., 72 Fifth Ave., New York, NY 10011, 1975. 139 pp. 14.5 × 21.5 cm. Price $10.95.

Size at Birth. Ciba Foundation Symposium 27 (new series). Ciba-Geigy Corp., Summit, NJ 07901. 408 pp. 17 × 24.5 cm.

Molds, Mushrooms, and Mycotoxins. By CLYDE M. CHRISTENSEN. University of Minnesota Press, Minneapolis, MN 55455, 1975. 264 pp. 15 × 23 cm. Price $11.50.

Psychopharmacology Communications, Vol. 1. Edited by EARL USDIN. Marcel Dekker, Inc., 270 Madison Ave., New York, NY 10016, 1975. 115 pp. 15 × 23 cm. Price $7.50.

Die Chemotherapeutischen und Pesticiden Wirkungen der Thiolreagenzien. By TIBOR ZSOLNAI. Akademiai Kiado of the Hungarian Academy of Science, Budapest V. Alkotmany U. 21, 1975. 415 pp. 17 × 24.5 cm. Price $26.00.

Weighing Designs (Statistics: Textbooks and Monographs Series, Vol. 12). By K. S. Banerjee. Marcel Dekker, Inc., 270 Madison Ave., New York, NY 10016, 1975. 141 pp. 16 × 24 cm. Price $12.75.

LSD—A Total Study. By D. V. SIVASANKAR. PJD Publications Ltd., Westbury, NY 1590, 1975. 960 pp. 16 × 24 cm. Price $29.75.

Pharmacotherapy and Psychotherapy: Paradoxes Problems and Progress, Vol. IX. Committee on Research. Group for the Advancement of Psychiatry, Inc., 419 Park Ave. S., New York, NY 10016, 1975. 176 pp. 16 × 20 cm. Price $6.00.

REVIEWS

Toxicology: The Basic Science of Poisons. Edited by L. J. CASARETT and J. DOULL. Macmillan, New York, N.Y., 1975. xiv + 768 pp., 49 figures, 112 tables. Price $23.95.

How often in an academic career do you receive a book for review about which you can honestly say you enjoyed getting it and reviewing it? Well, I have had the opportunity. For some 10 years, I have been teaching a graduate course in General Toxicology without a text, because none existed. Now arrives on the toxicology scene a most welcome text. I had the opportunity, during the summer Gordon Research Conference, to preview this book and the general opinion at that time was that we finally had a useful text for beginning courses in toxicology.

The book follows somewhat the same format as the classic text in pharmacology. I have pointed out to publishers over the past dozen years that what is needed in toxicology is an edited text along the same lines as the Goodman and Gilman text in pharmacology. Casarett and Doull have edited a 30-chapter text divided into four units. The initial unit deals with general principles of toxicology, covering quite well the scope of toxicology, absorption, distribution, excretion, metabolism of toxicants, and factors influencing toxicology. The only part of Unit I that is lacking is the chapter on toxicologic evaluation. It does not go into as much detail as is necessary to teach this aspect of toxicology. Hopefully, in future editions, this chapter will be written by a toxicologist whose expertise and daily job involve toxic evaluations (safety evaluations or assessment of hazards).

Unit II covers systemic toxicology in eight chapters. Essentially, a review of each system is included with discussion of the pathophysiology for specific chemicals. This section is lacking in a discussion of the largest organ of the body, the skin. It also lacks a chapter on the endocrine system.

Unit III deals with specific toxic agents under chapter headings as varied as Food Additives, Air Pollutants, Pesticides, Carcinogens, Social Poisons, Phytotoxicology, and Teratogens.

Unit IV is probably the most disappointing section of the text. This unit deals with the applications of toxicology, specifically Clinical Toxicology, Forensic Toxicology, Industrial Toxicology, Veterinary Toxicology, and Toxicology and the Law. Disappointing from the real point of view. The authors, in general, avoid putting into a chapter the real application of toxicology to their specific fields. It almost appears that they were writing to impress their colleagues rather than to inform a beginning student in toxicology. I am sure that these chapters will improve as Dr. Doull receives input from the users.

The text is very welcome and very useful for beginning courses in toxicology. It is not a perfect text, but neither was the first edition of Goodman and Gilman. Hopefully, future editions will contain chapters written by toxicologists with expertise in the area for which they were chosen to write.

This will be a classic text in toxicology. It will grow in size and wisdom as real toxicologists become involved in its preparation; many were involved in this first volume. I recommend its adoption for all beginning courses in General Toxicology, so that all future toxicologists would have a "standard of excellence" for a basic education in the basic science of Toxicology.

Reviewed by Charles L. Winek
Duquesne University
Pittsburgh, PA 15219

The Pharmacological Basis of Therapeutics, Fifth Edition. Edited by LOUIS S. GOODMAN and ALFRED GILMAN. Macmillan, 866 Third Ave., New York, NY 10022, 1975. 1704 pp. 19 × 27 cm. Price $30.00.

The fifth edition, published 34 years after the first, will undoubtedly continue to be one of the most useful pharmacology reference texts available.

The organization of the fifth edition is identical to the fourth edition, published in 1970. The 77 chapters reportedly underwent a thorough updating with respect to the mechanism of action and indication of use of older drugs and to the addition of important new drug entities. To prevent expansion of the fifth edition, less dynamic and outmoded sections were condensed or eliminated. As in the past, in areas where the number of therapeutic agents available is large, major discussion is focused on the well-established and effective prototypal drugs, while the numerous related compounds receive relatively brief descriptions. Therefore, the book is approximately 100 pages less than the fourth edition. There is also more discussion devoted to the pharmacokinetic principles of drugs. Other new entries include a discussion of the role of cyclic AMP as the "second messenger" and of the pharmacological effects of the prostaglandins.

"The Pharmacological Basis of Therapeutics" remains valuable as a complete and comprehensive text on pharmacology for all members of the health professions.

Staff Review

NOTICES

The Selectivity of Drugs. By ADRIEN ALBERT. John Wiley and Sons, Inc., 605 Third Ave., New York, NY 10016, 1975. 64 pp. 17 × 21 cm.

Current Developments in Psychopharmacology, Vol. 1. Edited by WALTER B. ESSMAN and L. VALZELLI. Spectrum Publication, Inc., 86-19 Sancho St., Holliswood, NY 11423, 1975. 345 pp. 16 × 24 cm.

Inhibitors of Nucleic Acid Synthesis. By HELGA KERSTEN and WALTER KERSTEN. Springer-Verlag, 175 Fifth Ave., New York, NY 10010, 1974. 184 pp. 17 × 24.5 cm. Price $27.90.

Cell Patterning. Ciba Foundation Symposium 29 (new series), Ciba-Geigy Corp., Summit, NJ 07901, 1975. 356 pp. 17 × 25 cm.

Effects of Drugs on Clinical Laboratory Tests. By D. S. YOUNG, L. C. PESTANER, and VAL GIBBERMAN. Clinical Pathology Dept., National Institutes of Health, Bethesda, MD 20014, 1975. 432 pp. 21 × 27.5 cm.

Les Applications Industrielles de la Microbiologie. By JACQUES RIVIERE. Masson et Cie, 120, Bd. Saint-Germain, Paris 6, France, 1975. 203 pp. 16 × 24 cm.

Young Inner City Families: Development of Ego Strength Under Stress. By MARGARET MORGAN LAWRENCE. Behavioral Publication, Inc., 72 Fifth Ave., New York, NY 10011, 1975. 139 pp. 14.5 × 21.5 cm. Price $10.95.

Size at Birth. Ciba Foundation Symposium 27 (new series). Ciba-Geigy Corp., Summit, NJ 07901. 408 pp. 17 × 24.5 cm.

Molds, Mushrooms, and Mycotoxins. By CLYDE M. CHRISTENSEN. University of Minnesota Press, Minneapolis, MN 55455, 1975. 264 pp. 15 × 23 cm. Price $11.50.

Psychopharmacology Communications, Vol. 1. Edited by EARL USDIN. Marcel Dekker, Inc., 270 Madison Ave., New York, NY 10016, 1975. 115 pp. 15 × 23 cm. Price $7.50.

Die Chemotherapeutischen und Pesticiden Wirkungen der Thiolreagenzien. By TIBOR ZSOLNAI. Akademiai Kiado of the Hungarian Academy of Science, Budapest V. Alkotmany U. 21, 1975. 415 pp. 17 × 24.5 cm. Price $26.00.

Weighing Designs (Statistics: Textbooks and Monographs Series, Vol. 12). By K. S. Banerjee. Marcel Dekker, Inc., 270 Madison Ave., New York, NY 10016, 1975. 141 pp. 16 × 24 cm. Price $12.75.

LSD—A Total Study. By D. V. SIVASANKAR. PJD Publications Ltd., Westbury, NY 1590, 1975. 960 pp. 16 × 24 cm. Price $29.75.

Pharmacotherapy and Psychotherapy: Paradoxes Problems and Progress, Vol. IX. Committee on Research. Group for the Advancement of Psychiatry, Inc., 419 Park Ave. S., New York, NY 10016, 1975. 176 pp. 16 × 20 cm. Price $6.00.

Manual of Psychiatric Therapeutics, Practical Psychiatry and Psychopharmacology. Edited by RICHARD I. SHADER. Little, Brown and Co., 34 Beacon St., Boston, MA 02106, 1975. 362 pp. 15 × 22 cm.

Central Cholinergic Systems and Behavior. By F. V. DeFEUDIS. Academic Press, 24–28 Oval Rd., London NW1 7DX, England, 1975. 223 pp. 15.5 × 24 cm. Price $15.75.

The Future of Philanthropic Foundations. Ciba Foundation Symposium 30 (new series). American Elsevier Publishing, 52 Vanderbilt Ave., New York, NY 10017, 1975. 240 pp. 17 × 25 cm.

Outcome of Severe Damage to the Central Nervous System. Ciba Foundation Symposium 34 (new series). Elsevier Scientific Publishing Co., Excerpta Medica, North Holland Publishing Co., P.O. Box 211, Amsterdam, The Netherlands, 1975. 354 pp. 17.5 × 24.5 cm.

The Structure and Function of Chromatin. Ciba Foundation Symposium 28 (new series). Associated Scientific Publishers, P.O. Box 211, Amsterdam, The Netherlands, 1975. 368 pp. 17 × 25 cm.

Behavioral Pharmacology. By SUSAN D. IVERSEN and LESLIE L. IVERSEN. Oxford University Press, 200 Madison Ave., New York, NY 10016, 1975. 310 pp. 14 × 21.5 cm. Price $10.95 cloth; $5.95 paper.

Radiological Health Training Resources, 1975. Division of Training and Medical Applications, USD/HEW, FDA, Bureau of Radiological Health, Rockville, MD 20852. 18 pp. 20 × 26.5 cm.

Psychopharmacology, A Biological Approach. By ROBERT A. LEVITT. John Wiley & Sons, Inc., 605 Third Ave., New York, NY 10016, 1975. 502 pp. 16 × 24 cm. Price $17.50.

Molecular Mechanisms of Gonadal Hormone Action: Advances in Sex Hormone Research, Vol. 1. By JOHN A. THOMAS and RADHEY L. SINGHAL. University Park Press, Chamber of Commerce Bldg., Baltimore, MD 21202, 1975. 399 pp. 16 × 24 cm. Price $32.50.

Handbook of Organosilicon Compounds, Vol. 1. By V. BAZANT MILAN HORAK, VACLAV CHVALOVSKY, and JAN SCHRAML. Marcel Dekker, Inc., 270 Madison Ave., New York, NY 10016, 1975. 761 pp. 16 × 25 cm. Price $75.00.

Nonproprietary Names for Pharmaceutical Substances. World Health Organization Technical Report Series No. 581. World Health Organization, Geneva, Switzerland, 1975. 32 pp. 14 × 20 cm. Price Sw. fr. 6.-.

Ophthalmica, Pharmazeutische Grundlagen ihrer Zubereitung, Band. 1. Wissenschaftliche Verlagsgesellschaft mbH, 7000 Stuttgart 1, Postfach 40, Germany, 1975. 558 pp. 15 × 20.5 cm. Price 80 DM.

Environmental Chemistry, Vol. 1. By G. EGLINTON. The Chemical Society, Burlington House, London W1V OBN, England, 1975. 199 pp. 14 × 21 cm. Price £7.00.

Psychiatry in Broad Perspective. By ROY R. GRINKER. Behavioral Publication, Inc., 72 Fifth Ave., New York, NY 10011, 1975. 262 pp. 14.5 × 22 cm. Price $14.95; $12.95 (students).

The Organic Constituents of Higher Plants. By TREVOR ROBINSON. Cordus Press, P.O. Box 587, North Amherst, MA 01059, 1975. 347 pp. 18 × 29 cm. Price $10.00.

Microcrystal Polymer Science. By O. A. BATTISTA. McGraw-Hill Book Co., 1221 Avenue of the Americas, New York, NY 10020, 1975. 208 pp. 16 × 22.5 cm. Price $18.50.

Research on Captive Populations

Our national debate about institutionalized research subjects is heating up. Recent revelations about army and CIA experimentation with LSD provide a chilling reminder of the arrogant disrespect for persons that can accompany the power that a cloak of secrecy brings. The National Commission for the Protection of Human Subjects of Biomedical and Behavioral Research is now turning its attention to research on soldiers, prisoners, inpatients, and other captive populations. The research community fears unwelcome new restrictions, and the air hangs heavy with concern, outrage, and polarization. A lot is at stake both for those whose focus is on the social benefits of research and for those—scientists and others—who recognize that how we treat our disadvantaged populations is a substantial indicator—and, indeed, a major determinant—of what sorts of persons we are.

Confined persons are desirable subjects largely because of what Franz J. Ingelfinger calls their "administrative eligibility." The structured circumstances that provide that eligibility also make such persons dependent on the decisions of others who, as commanding officers, wardens, or hospital staff, have substantial control over the potential subjects' lives. It is argued that their dependency makes coercion implicit unavoidably in their circumstances; hence the consent of such persons, even if fully informed, cannot be fully free. Thus, if informed consent freely given is a criterion of ethical acceptability, captive populations cannot ethically be used for research.

Yet this argument may prove too much. Coercion to some degree frequently seems implicit even in the provision of uncontroversial opportunities. Poor or unemployed persons, and even the professionally frustrated, if offered an opportunity for betterment, are pressured by their circumstances to seize the opportunities. No one argues that to provide such opportunities is generally unethical. Some prisoners claim a right to decide for themselves whether to participate in research programs, thereby to better their circumstances through compensation, relief of boredom, and opportunity to gain enhanced self-respect through altruistic service. A ban on such research would reflect a paternalistic decision to protect prisoners from such decisions.

Perhaps the dependency of captive populations does justify, or even require, paternalistic prevention of their participation in research. But that can be shown only by identifying those features of their dependency that make free choice impossible. Since all persons are dependent and constrained in various ways, the dependency of captive populations must be assessed against the broader backdrop of universal human dependency. The inquiry requires clarity about the relationships among the concepts of rewards, incentives, opportunities, dependency, coercion, freedom of choice, and the justifiability of paternalism. Such traditionally philosophical issues reveal immediate practical import in the context of debate about public regulation of scientific practice and should be given their due by the National Commission and by partisans in the debate.

Furthermore, it would be unfortunate to overweight the present facts of administrative eligibility. New forms of social organization can arise as needed, and one can easily imagine a league of research subjects, motivated by altruism, compensation, or social recognition, analogous to other socially beneficial, risk-accepting groups such as volunteer firefighters or the civil air patrol. Judgments about convenience provide shaky grounds indeed for conclusions about ethical acceptability. Conceptual clarity and sound arguments are what we need.

The cloak of secrecy that has shielded our programs of research on confined populations is rapidly lifting; much of what is revealed will not bear moral scrutiny. Notice has been served on universities, drug companies, national security organizations, and the scientific community at large that the search for truth will enjoy no procedural carte blanche. In the ensuing debate the scientific community's credit rating is at stake.

Samuel Gorovitz
Department of Philosophy
University of Maryland
College Park, MD 20742

Received February 13, 1976.

Authors please note:

Page charges for contributed articles published in the Journal of Pharmaceutical Sciences *will be $70 per printed page, effective July 1976. Recognizing that publication of research reports is an integral part of research, page charge costs should be considered as a part of research funding.*

Acceptance of manuscripts for publication is not contingent upon payment of page charges. However, the continued viability of scientific journals is contingent upon the sponsors of research assuming some of the responsibility for publication of the results of research.

1976

May 17
APhA Academy of Pharmaceutical Sciences, Annual Midwestern Regional Meeting, Industrial Pharmaceutical Technology and Pharmaceutical Analysis and Control Sections, O'Hare Inn, Chicago, Ill. (Contact Dr. A. Amann, Abbott Laboratories, North Chicago, IL 60064)

May 18–21
International Symposium on Drug–Receptor and Drug–Enzyme Interactions: A Basic Approach, La Societe Chimique De Belgique and Les Facultes Universitaires Notre-Dame De La Paix, Namur, Belgium (Contact Prof. F. Durant, Departemente de Chimie, Facultes Notre-Dame De La Paix, 61, Rue de Bruxelles, B-5000 Namur, Belgium)

June 3–5
Annual Summer Symposium, American Chemical Society Division of Analytical Chemistry, Tempe, Ariz. (Contact R. S. Juvet, Arizona State University, Tempe, AZ 85281)

June 8–10
Miles International Symposium, Kresge Auditorium, Massachusetts Institute of Technology, Cambridge, Mass. (Contact E. G. Bassett, Miles Laboratories, Inc., Elkart, IN 46514)

June 14–25
Design and Analysis of Scientific Experiments, Massachusetts Institute of Technology (Contact Director of the Summer Session, Room E19-356, Massachusetts Institute of Technology, Cambridge, MA 02139)

June 20–24
National Medicinal Chemistry Symposium, American Chemical Society Division of Medicinal Chemistry, University of Utah, Salt Lake City, Utah (Contact L. B. Townsend, Department of Biopharmaceutical Sciences, University of Utah, Salt Lake City, UT 84112)

June 21–23
International Symposium on Mass Spectrometry in Drug Metabolism, Milan, Italy (Contact Dr. A. Frigerio, Instituto di Richerche Farmacologiche Mario Negri, Via Eritrea 62, 20157, Milan, Italy)

June 23–25
Drug Information Association, Annual Meeting, St. Francis Hotel, San Francisco, Calif. (Contact W. S. Arrington, Wyeth Laboratories, P.O. Box 8299, Philadelphia, PA 19101)

June 25
Parenteral Drug Association, Mid-Summer Meeting, Hyatt Regency O'Hare, Chicago, Ill.

June 27–July 1
American Medical Association, Annual Meeting, Dallas, Tex.

July 11–16
American Society of Pharmacognosy, Annual Meeting, Mt. Telemark Lodge, Cable, Wis. (Contact Dr. J. M. Cassady, School of Pharmacy and Pharmacal Sciences, Purdue University, West Lafayette, IN 47907)

July 18–22
American Association of Colleges of Pharmacy, Leamington Hotel, Minneapolis, Minn.

August 4–6
American Academy of Clinical Toxicology, American Association of Poison Control Centers, and Canadian Academy of Clinical Toxicology, Annual Meeting, Olympia Hotel, Seattle, Wash.

August 9–13
Gordon Research Conferences, Medicinal Chemistry, Colby-Sawyer College, New London, N.H. (Contact Dr. A. M. Cruickshank, Director, Gordon Research Conferences, Pastore Chemical Laboratory, University of Rhode Island, Kingston, RI 02881)

August 15–19
American Society for Pharmacology and Experimental Therapeutics, Tulane University, New Orleans, La.

August 27–29
The European Symposium of the International Association of Forensic Toxicologists, State University of Ghent, Belgium (Contact Department of Toxicology, State University of Ghent, Hospitaalstraat 13, 9000 Ghent, Belgium)

August 29–September 2
American Chemical Society, National Meeting, San Francisco, Calif. (Contact A. T. Winstead, American Chemical Society, 1155 16th St., N.W., Washington, DC 20036)

September 6–11
International Congress of Pharmaceutical Sciences, Warsaw, Poland.

September 20–22
National Conference on Cancer Research and Clinical Investigation, American Cancer Society and National Cancer Institute, Regency Hyatt Atlanta Hotel, Atlanta, Ga. (Contact Dr. S. L. Arje, American Cancer Society, 777 3rd Ave., New York, NY 10017)

October 7–10
American College of Apothecaries, Annual Meeting, Bellevue Stratford, Philadelphia, Pa.

October 17–20
ASTM Committee E-19, Practice of Chromatography, North Shore Hilton Hotel, Chicago, Ill. (Contact Gerald Dupre, Biodynamics, Inc., Box 43, Mettlers Road, East Millstone, NJ 08874)

October 17–21
American Public Health Association, Annual Meeting, Miami Beach, Fla.

October 18–21
Association of Official Analytical Chemists, Marriott Twin Bridges, Washington, D.C. (Contact L. G. Ensminger, AOAC, Box 540, Ben Franklin Station, Washington, DC 20044)

October 22
APhA Academy of Pharmaceutical Sciences, Annual Eastern Regional Meeting, Industrial Pharmaceutical Technology Section, Cherry Hill Inn, Cherry Hill, N.J. (Contact Dr. Arthur Goldberg, Applied Sciences, TDD, Hoffmann–La Roche Inc., Nutley, NJ 07110)

November 14–18
APhA Academy of Pharmaceutical Sciences, National Meeting, Carleton House Hotel, Orlando, Fla.

November 14–18
American Dental Association, Annual Meeting, Las Vegas, Nev.

November 14–20
Federation of Analytical Chemistry and Spectroscopy Societies, Annual Meeting, American Chemical Society Division of Analytical Chemistry and others, Civic Center, Philadelphia, Pa. (Contact C. White, Analytical Chemistry Division, Oak Ridge National Laboratories, Oak Ridge, TN 37830)

December 4–8
American Medical Association, Clinical Meeting, Philadelphia, Pa.

December 5–10
American Society of Hospital Pharmacists, Midyear Meeting, Anaheim, Calif.

December 14–15
Food and Drug Law Institute, Annual Meeting, Washington Hilton, Washington, D.C.

1977

February 20–26
American Association for the Advancement of Science, Annual Meeting, Denver, Colo.

April 26–28
Pharmaceutical Manufacturers Association, Annual Convention, Boca Raton Hotel, Boca Raton, Fla.

May 14–19
APhA Annual Meeting, New York, N.Y.

May 15–18
Proprietary Association, Annual Meeting, The Greenbrier, White Sulphur Springs, W.Va.

June 18–23
American Medical Association, Annual Meeting, San Francisco, Calif.

Items to be considered for inclusion or corrections should be addressed to:

J. Pharm. Sci. Calendar
2215 Constitution Avenue, N.W.
Washington, DC 20037

Journal of Pharmaceutical Sciences

JUNE 1976

VOLUME 65 NUMBER 6

MARY H. FERGUSON
Editor

L. LUAN CORRIGAN
Assistant Editor

SHELLY ELLIOTT
Production Editor

JANET D. SHOFF
Copy Editor

EDWARD G. FELDMANN
Contributing Editor

SAMUEL W. GOLDSTEIN
Contributing Editor

LELAND J. ARNEY
Publications Director

EDITORIAL ADVISORY BOARD

JOHN AUTIAN	HARRY B. KOSTENBAUDER
LYNN R. BRADY	CARL J. LINTNER, JR.
WILLIAM O. FOYE	DAVID E. MANN, JR.
WILLIAM J. JUSKO	GERALD J. PAPARIELLO

The *Journal of Pharmaceutical Sciences* is published monthly by the American Pharmaceutical Association at 2215 Constitution Ave., N.W., Washington, DC 20037. Second-class postage paid at Washington, D.C., and at additional mailing office.

All expressions of opinion and statements of supposed fact appearing in articles or editorials carried in this journal are published on the authority of the writer over whose name they appear and are not to be regarded as necessarily expressing the policies or views of the American Pharmaceutical Association.

Offices—Editorial, Advertising, and Subscription Offices: 2215 Constitution Ave., N.W., Washington, DC 20037. Printing Offices: 20th & Northampton Streets, Easton, PA 18042

Annual Subscriptions—United States and foreign, industrial and government institutions $50, educational institutions $50, individuals *for personal use only* $30; single copies $5. All foreign subscriptions add $5 for postage. Subscription rates are subject to change without notice. Members of the American Pharmaceutical Association may elect to receive the *Journal of Pharmaceutical Sciences* as a part of their annual $60 (foreign $65) APhA membership dues.

Claims—Missing numbers will not be supplied if dues or subscriptions are in arrears for more than 60 days or if claims are received more than 60 days after the date of the issue, or if loss was due to failure to give notice of change of address. The Association cannot accept responsibility for foreign delivery when its records indicate shipment has been made.

Change of Address—Members and subscribers should notify at once both the Post Office and the American Pharmaceutical Association, 2215 Constitution Ave., N.W., Washington, DC 20037, of any change of address.

© Copyright 1976, American Pharmaceutical Association, 2215 Constitution Ave., N.W., Washington, DC 20037; all rights reserved.

A CHALLENGE TO THE DRUG INDUSTRY

For years we have been hearing about the so-called "drug lag," in which critics—predominately from the drug industry—have charged the federal government and, specifically, the Food and Drug Administration with being ultracautious and unduly conservative in granting approvals for the marketing of new drugs. It has been claimed that too much data are required, that the review process is too meticulous, and that the levels of demonstrated effectiveness and safety for new drug approval have been set too high. It is claimed that, as a consequence, drugs become available abroad many years before they are permitted to appear on the U.S. market.

Overnight, a situation has developed that has had the ironic effect of completely reversing these respective traditional stances. The government is now prodding, pushing, and exerting pressure on the drug industry to move quickly to mass produce and mass market a new pharmaceutical product. And the industry is in the position of being reluctant and hesitant because it has legitimate uncertainties about the safety and effectiveness of the drug preparation involved.

We refer, of course, to the swine flu vaccine and the goal of producing sufficient vaccine to immunize virtually the entire U.S. population by early winter of this year.

Testimony of knowledgeable witnesses at Congressional hearings in early April indicates that there are some legitimate questions as to the probable effectiveness of the vaccine—what percent of the immunized population will achieve positive protection—as well as concerns about the safety of the product. The latter presumably might be attributable either to individual allergic reactions, since egg cultures will be used in its production, or to faulty manufacturing procedures which could result in an entire batch being defective.

On the other hand, the predictions of the magnitude of the threat posed by a 1918-type epidemic make it clear that the nation must be prepared to accept certain risks in order to head off the possibility of a national health calamity.

Steps must be taken by the government agencies involved—the Food and Drug Administration for control and regulation, the Center for Disease Control for overseeing the program nationally, the National Institutes of Health for influenza research, and state and local governments as a pipeline for bringing the program to the community level—as well as the pharmaceutical industry to see that the hazards are minimized, while maximizing the hoped-for benefits.

Reportedly, the drug industry has been reluctant to undertake production of the vaccine in the absence of Congressional action granting immunity on grounds of either antitrust violations or product liability. Such concerns are understandable; the request for such immunity represents sound business practice.

However, as to product liability, whether due to anaphylactic reactions or the possibility of a faulty batch, such risks constitute the normal occupational hazards associated with the pharmaceutical manufacturing business. The only significant difference here is the brief timetable involved, which limits the amount of testing and study that can be conducted before the product goes into general distribution.

Such testing is important and its value must not be downplayed. However, it would seem to be a manageable problem—one that can be largely resolved by properly reallocating resources and personnel, even though this may mean disrupting the research timetables and production schedules for other drug products. Granting product liability immunity would establish a bad precedent and is fraught with other hazards.

As this column is being written, the vaccine program is still not completely resolved. However, all indications are that the pharmaceutical industry will respond positively and responsibly, with the result that adequate supplies of the vaccine will be available in time to undertake the nationwide immunization program, thereby heading off the epidemic threat. We commend those involved for accepting this challenge.

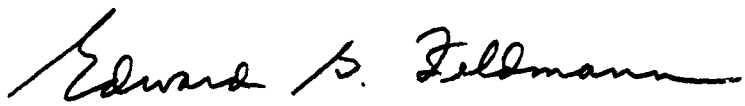

Journal of Pharmaceutical Sciences

JUNE 1976
VOLUME 65 NUMBER 6

REVIEW ARTICLE

Progesterone: An Overview and Recent Advances

MICHEL B. AUFRÈRE and HARRIET BENSON ˣ

Keyphrases □ Progesterone—production, metabolism, mechanism of action, effects, clinical use, toxicity, review □ Hormones—progesterone, production, metabolism, mechanism of action, effects, clinical use, toxicity, review □ Metabolism—progesterone, biosynthesis, concentration in body fluids and tissues, review □ Pharmacokinetics—progesterone, receptor characterization, nuclear interactions, receptor concentration, review □ Toxicity—progesterone, cell growth inhibition, prenatal and neonatal exposure, review □ Contraceptives—progesterone, metabolism, mechanism of action, effects, toxicity, review

CONTENTS

Production Rate and Metabolism 784
Production Rate in Humans 784
Biosynthesis 784
Concentration in Body Fluids and Tissues 784
Metabolism 785
Mechanism of Action 787
Receptor Characterization 787
Nuclear Interactions 788
Receptor Concentration 788
Effects on Reproductive Tissues and Functions 789
Hypothalamic–Pituitary–Ovarian Axis 789
Uterus 789
Sperm Migration and Capacitation 791
Implantation and Blastocyst Development 791
Direct Exposure of Uterine Lumen 791
Vagina 792
Mammary Gland 792
Other Effects 792
CNS 792
Cardiovascular System 793
Skeletal Growth and Weight Regulation 793
Microorganisms 793
Tumor Growth 794
Clinical Use 794
Carcinoma 794
Habitual Abortion 795
Gynecological Disorders 795
Contraception 795
Toxicity 795
Cell Growth Inhibition 795
Animal Toxicity Studies 795
Prenatal Exposure 796
Neonatal Exposure 797
References 797

Because of its major function in reproduction, the physiological role of progesterone has been widely studied in the human and various animal species for over 30 years. Endogenous as well as exogenous progesterone has specific and pronounced hormonal effects on the reproductive tract and, either directly or indirectly, exerts influence beyond the utero-vaginal locus. The primary emphasis in this review is on the role of progesterone in the regulation of human fertility.

Although several reviews have been written on compounds with progestational activity, only two recent texts address themselves specifically to progesterone rather than the synthetic analogs (1, 2); much has been reported, however, since the publication of these reviews 5 years ago. Rather than a broad comprehensive review of all progestational compounds and actions, this article gives an overview of the physiological effects of progesterone and selected recent studies that are significant and relevant to the

Table I—Progesterone Production Rate in Humans

Source	Production Rate (Range), mg/day	Reference
Males	0.75	6
Ovariectomized women	1.2	6
Follicular phase	0.75–2.5	7
	2.3–5.4	8
	4	6
Luteal phase	22–43	8
	30	6
	15–50	7
Pregnancy:		
15 weeks	92	9
27–40 weeks	334 (188–563)	8
27–31 weeks	263	9
35–36 weeks	250	10
Third trimester	322 (188–563)	9
Third trimester	210 (132–288)	7

role of progesterone in human reproduction. Recent developments relating to the mechanism of action of progesterone and the clinical application of its physiological and pharmacological properties have been included also.

PRODUCTION RATE AND METABOLISM

Production Rate in Humans—Progesterone is secreted by the ovaries (3), the placenta (4), and the adrenal glands of both male and female (5). The rate of production, estimated by isotopic dilution techniques with ^{14}C- or ^{3}H-labeled progesterone, ranges from mean values of 0.75 mg/day for young males and 1.2 mg/day for ovariectomized females to about 250 mg/day in late pregnancy when placental contribution is most substantial. The rate of production is 2.3–5.4 mg/day during the follicular phase of the menstrual cycle and 22–43 mg/day during the luteal phase. These progesterone production rates are summarized in Table I.

Biosynthesis—In several mammalian species, progesterone is synthesized from both tissue and circulating cholesterol, the tissue cholesterol being derived from acetate (11, 12). Cholesterol is transformed to pregnenolone, the immediate precursor of progesterone. Pregnenolone is then converted to progesterone by a combined dehydrogenase and isomerase reaction.

Ovarian Synthesis—The human ovarian biosynthesis of progesterone has been studied by *in vitro* incubations of slices or homogenates in the presence of various labeled precursors and, more recently, by *in vivo* perfusion methods (13–15). A conversion of acetate to progesterone has been shown in luteinized rat ovarian tissue (16, 17), in bovine luteal tissue (18, 19), and in human corpora lutea (19). This biogenesis in the ovary is not limited to the corpus luteum but occurs also in the human graafian follicle (20, 21).

A correctly timed action of the anterior pituitary gonadotropic hormones, follicle-stimulating hormone (FSH), and luteinizing hormone (LH) seems essential for the biogenesis of progesterone in the corpus luteum. Luteinizing hormone injection rapidly increases ovarian synthesis of progesterone and its release in the circulation (13) by stimulation of the enzymes responsible for the conversion of cholesterol to progesterone.

Table II—Progesterone Concentrations in Human Peripheral Plasma

Source	Concentration, μg/100 ml of Plasma	Reference
Males	0.028 ± 0.013	6
Ovariectomized women	0.039 ± 0.010	6
Follicular phase	0.023 ± 0.010	33
	0.032 ± 0.025	34
	0.040 ± 0.005	35
	0.12 ± 0.02	36
	0.113 ± 0.049	6
Luteal phase	1–2	34
	0.94 ± 0.093	35
	0.83 ± 0.58	36
	0.828 ± 0.634	33
	1.04 ± 0.32	6
Pregnancy:		
8th week	2.1 ± 0.8	37
19th week	4.0 ± 0.5	38
20th week	5.2 ± 0.5	37
34th week	19.7 ± 5.2	39
34th week	14.3 ± 0.6	38
34th week	12.7 ± 4.4	37
24 hr postpartum	1.9 ± 0.3	39

Placental Synthesis—The progesterone required for maintenance of human pregnancy originates in the placenta after the 2nd month of gestation (22, 23), reaching levels of 1–4 μg/g of tissue (4, 24, 25). Placental biosynthesis has been shown to occur in the absence of fetal organism (26) and maternal ovaries (27). The precursors for the synthesis of progesterone in the placenta are fetal pregnenolone (28, 29), fetal pregnenolone sulfate (30), and, possibly, maternal blood cholesterol (31).

Concentration in Body Fluids and Tissues—Newer methods of analysis have provided a clear measure of progesterone plasma levels during numerous physiological events. Uterine tissue concentrations have received less attention but do not seem to follow a distinct pattern.

Plasma Concentrations—The concentration of progesterone in human peripheral plasma is about 0.035 μg/100 ml for both males and ovariectomized females. In normal young women, the plasma hormone level is 0.03–0.12 μg/100 ml during the follicular phase of the cycle; after ovulation, it rises to a maximum of 1–2 μg/100 ml. This concentration is maintained until approximately 24 hr before the onset of menstruation, when it falls to the preovulatory value.

Luteal function can be estimated routinely by the determination of plasma progesterone. The plasma progesterone level increases gradually during pregnancy, reaching 12–20 μg/100 ml of plasma near term and dropping to 1.9 μg/100 ml of plasma 24 hr postpartum. No mean change in the plasma progesterone level is observed throughout labor (32). These data are summarized in Table II.

Because progesterone is produced by the corpus luteum, the progesterone concentration is substantially higher in human ovarian vein blood than in peripheral plasma. Progesterone in ovarian venous blood is less than 2 μg/100 ml of plasma during the follicular phase but rises to about 60 μg/100 ml of plasma during the luteal phase, a concentration comparable to

Table III—Progesterone Concentrations in Human Ovarian and Uterine Vein Blood

Phase of Menstrual Cycle	Concentration, μg/100 ml of Plasma	Reference
Follicular phase	<2 (ovarian)	40
	0.2–1.5 (ovarian)	41
Luteal phase	56.1 (ovarian)	40
	0.7–186 (ovarian)	41
Pregnancy:		
First half	8–97 (uterine)	42
8 weeks	14.8 (uterine)	43
8 weeks	34 (ovarian)	43
11.5 weeks	63 (ovarian)	43
23 weeks	30 (ovarian)	43
40 weeks	13 (ovarian)	43
40 weeks	100–310 (ovarian)	44
40 weeks	200–710 (uterine)	44

the highest level found during pregnancy at 11.5 weeks. During late gestation, levels of progesterone in the venous blood of the ovary are 30–300 μg/100 ml of plasma. The progesterone content of uterine venous blood reaches 14.8 μg/100 ml of plasma during the 8th week of pregnancy, exceeding the value in peripheral blood; later in gestation, it ranges from 8 to 710 μg/100 ml of plasma (Table III).

Uterine Tissue Concentrations—Efforts to measure the progesterone content of the myometrium during pregnancy have produced a range of concentrations of 4–63 μg/100 g of tissue (Table IV). The variations may reflect differences in assay methods or in local concentrations within the uterus or may result from time-varying concentrations during pregnancy (45). Progesterone levels have not been determined in nonpregnant myometrial tissues.

Progesterone concentrations in the human endometrium range from 0.5 to 16.8 μg/100 g of tissue during the menstrual cycle and from 8 to 58.9 μg/100 g of tissue during pregnancy (Table V). At any given time in the cycle, the measured level of progesterone in endometrial tissue depends upon several factors, such as the overall corpora lutea function and enzymatic activity controlling metabolic pathways and rates. Therefore, alterations from normal tissue concentrations of progesterone might be used to determine abnormal endometrial functions (52).

Metabolism—The absorption of exogenous progesterone in humans is rapid, irrespective of the route of administration. Because progesterone is almost completely metabolized in one passage through the GI mucosa and the liver, however, low doses administered orally are ineffective. Intramuscular injection of 25 mg of progesterone in oil or administration of 100 mg by the vaginal or rectal route achieves plasma levels equivalent to those seen during the luteal phase (53).

Table IV—Progesterone Concentrations in Human Myometrium during Pregnancy

Gestational Age	Concentration, μg/100 g of Tissue	Reference
10–19 weeks	11.1 ± 8.1	45
11 weeks	4.7, 20.7	46
12–41 weeks	5–16	47
Undated, pooled material	31–63	47
12–41 weeks	4–52	48
4th month	9	49
10th month	7–22	49
33–38 weeks	12.6 ± 9.7	45
35–40 weeks	19–57	50
40 weeks	1.7–7.9	46
39–42 weeks	12.4 ± 7.3	45

Table V—Progesterone Concentrations in Human Endometrium

Phase of Menstrual Cycle	Concentration, μg/100 g of Tissue	Reference
Follicular phase	2.5, 3.1	46
	0.5, 1.5	51
Luteal phase	4.8, 16.8	46
	1.2, 3.0	51
Pregnancy:		
11 weeks	58.9	46
40 weeks	8–18.5	46

In the bloodstream, endogenous and exogenous progesterone binds to plasma proteins. Early investigations on the binding of progesterone to serum components, using equilibrium dialysis, indicated a high affinity of the hormone for human serum albumin (88.9%) (54). Extremely low amounts of progesterone are found in erythrocytes (55) or platelets (54). It was shown more recently that pregnant guinea pig serum contains a progesterone-binding globulin (PBG), which is distinct from corticosteroid-binding globulin (CBG or transcortin) (56).

Progesterone-binding globulin has been purified to homogeneity and found to be a glycoprotein with high (48.7%) carbohydrate content, a molecular weight of 77,500 daltons, and an isoelectric point in the range of pH 2.8–3.6 (57, 58). The relative binding affinities of various steroids for the guinea pig progesterone-binding globulin have been determined (59); compounds displaying high affinity include 5α-pregnan-3,20-dione, 20α-hydroxypregn-4-en-3-one, and 21-hydroxypreg-4-en-3,20-dione as well as progesterone. An equilibrium association constant of $9 \times 10^8\ M^{-1}$ is calculated at 4.0° for the progesterone–progesterone-binding globulin 1:1 complex.

The reported half-life of intravenously injected progesterone in the human ranges widely, from 3 (10) to 90 (60) min. These and other half-life determinations were discussed by Thijssen and Zander (61) and by Fylling (62), who obtained plasma half-life values of 27 and 45 min, respectively. The metabolic clearance rate (MCR) of progesterone, determined from both single-injection and continuous infusion methods, ranges between 2510 and 2800 liters/day in normal women and remains constant through the menstrual cycle (63–65).

In spite of the large ovarian production of progesterone, its concentration in uterine tissues is low, primarily due to metabolism by the liver, since blood flow from the ovaries leads to systemic circulation. The low uterine concentration is also due to the high rate of metabolism of progesterone by the endometrium and myometrium. Based on the percent of progesterone metabolized in an *in vitro* incubation, the metabolic rate for proliferative human endometrial tissue is 0.99 μg of progesterone/(g of tissue-hr); human myometrial tissue metabolizes 0.11 μg/(g of tissue-hr) (66). Uterine weights vary greatly, depend-

ing on parity, race, and age. A mature female uterus, which may be considered to weigh approximately 110 g (67), metabolizes approximately 3 mg of progesterone/day.

Species- and sex-dependent variations occur in the metabolism of progesterone. Its human metabolism consists of various conversions, including reduction, hydroxylation, cleavage, and conjugation (60, 68). The reductive metabolism of progesterone is depicted in Scheme I. In humans, progesterone is mainly metabolized by the liver to 5β-pregnane-3α,20α-diol (pregnanediol). This and other metabolites are then conjugated in the liver with glucuronic acid and excreted by the kidney. Liver metabolism accounts for approximately two-thirds of all metabolic pathways.

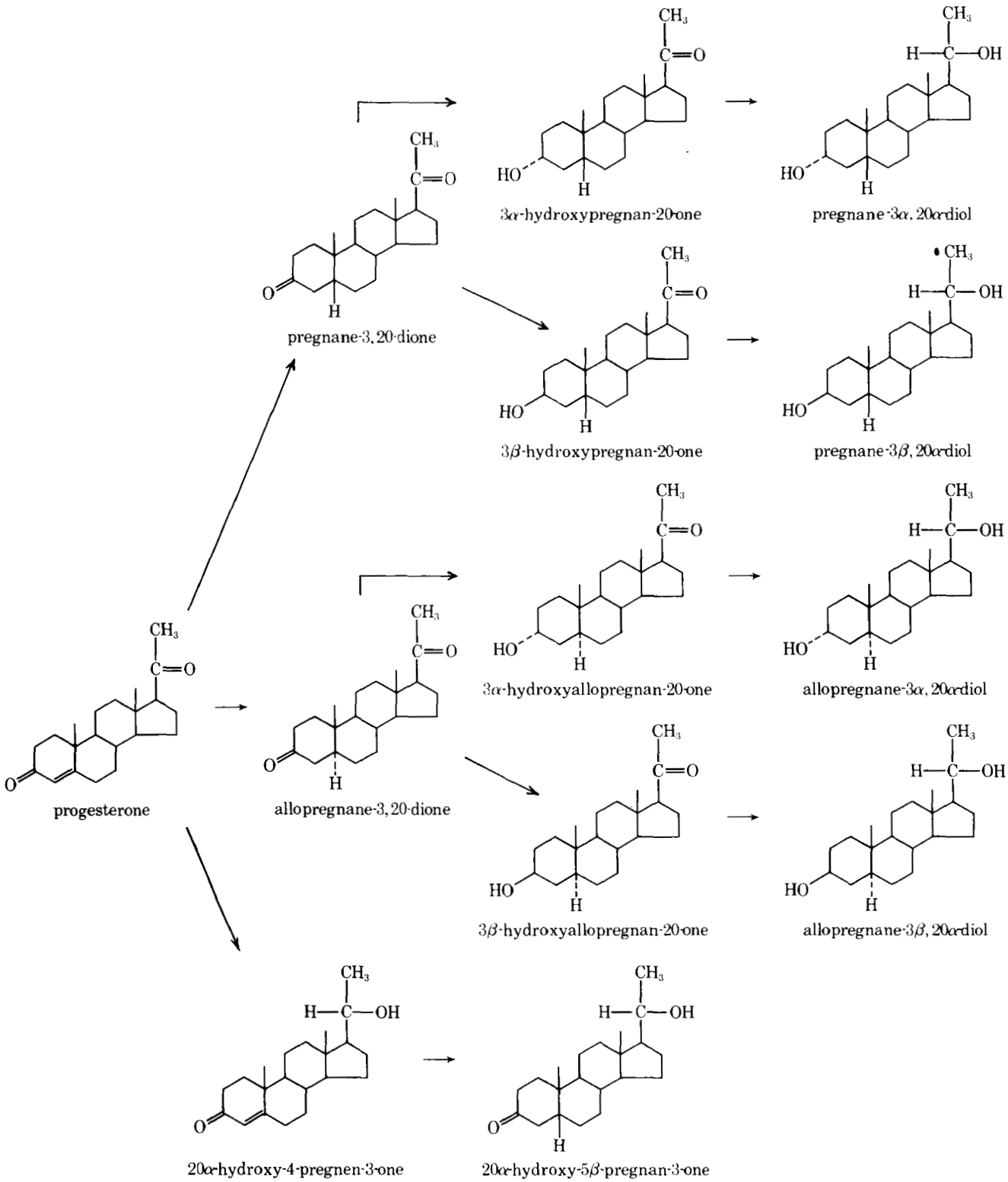

Scheme I—Major in vivo *human metabolic pathways of progesterone*

Following the injection of labeled progesterone, 50–60% of the excretion of progesterone metabolites is *via* the kidney; the second major excretory pathway, approximately 10%, is *via* the bile and feces (60). Overall recovery of labeled material accounts for up to 70% of an administered dose, the remainder being unaccounted for (69).

A highly significant correlation exists between serum progesterone concentration and urinary excretion of pregnanediol during the menstrual cycle (70). In some clinical investigations, only pregnanediol is measured as an index of progesterone secretion. For the detection of luteal activity, however, most clinical laboratories are abandoning the measurement of pregnanediol for the more definitive progesterone radioimmunoassay (70, 71). When labeled progesterone is injected in humans, a range of 6–27% is eliminated as urinary pregnanediol regardless of the dose of progesterone injected (72).

Hydroxylation of steroids by liver microsomes is affected by the same parameters that affect drug oxidation, suggesting that drugs and steroids are substrates for the same microsomal enzymes (73). Environmental chemicals [1,1,1-trichloro-2,2-bis(*p*-chlorophenyl)ethane (DDT) and chlordane] and drugs (phenobarbital) increase progesterone hydroxylase activity, resulting in a decrease in the concentration of progesterone and its metabolites in the brain and total body of the rat (74). This increase in metabolism is manifested *in vivo* by altered physiological responses, such as a decrease in the anesthetic action of large doses of progesterone.

In the human skin, metabolism of the hormone is accounted for by subcellular fractions shown to contain membrane-bound 5α-reductase and soluble 20α-hydroxysteroid dehydrogenase activity (75). Similar enzyme activities are observed in the rat pituitary gland (76). The metabolism of progesterone in the adrenal cortex leads to the production of corticosteroids (*e.g.*, cortisol and aldosterone). The formation of additional metabolites (hydroxylations and keto and alkene reductions) was reviewed by Kincl (77).

Among nonhuman primates, progesterone is also a major secretory product of the ovary. Its metabolism, however, differs from species to species. In the rhesus monkey, the diurnal change in progesterone secretion is a composite of fluctuations of ovarian and adrenal progesterone governed by different factors (78). In this species, the major urinary metabolite is androsterone, accounting for 6% of the progesterone administered (79); pregnanediol is isolated only in trace amounts (80). In the pigtail monkey, androsterone is the progesterone metabolite of quantitative importance (81).

Data for the chimpanzee and the baboon, on the other hand, show a progesterone metabolism pattern closer to that observed for humans. In immature chimpanzees, 7% of the injected dose of progesterone is recovered as pregnanediol (82). The chimpanzee placenta can also convert pregnenolone to progesterone (83). In the baboon, the major identified metabolites from intravenously administered progesterone are 11.7% androsterone and 31.4% for the 5α- and 5β-isomers of 3α,20α-pregnanediol (84, 85).

MECHANISM OF ACTION

A large body of accumulating evidence tends to support a unitary theory for the mechanism of action of steroid hormones. According to this theory, the steroids elicit a sequence of events, starting with the uptake of the steroid molecule into the target cell where the steroid binds to a specific cytoplasmic "receptor" protein. This receptor protein–steroid complex is then translocated to the nucleus where it binds to specific sites on the genome, thus inducing the transcription for a new, specific RNA. This RNA, in turn, results in the ribosomal synthesis of new proteins, which become the physiological expression of the specific steroid hormone. Recent reviews comprehensively cover the data on the various steps involved in the interaction of female steroid hormones with their target cells (86–88).

Receptor Characterization—The target cells responsive to progesterone contain high affinity, saturable cytoplasmic receptor proteins. Considerable evidence supports the hypothesis that the physiological manifestations of progesterone result from an initial interaction of the hormone with this specific receptor in the cytosol of the target cell. The identification of such a receptor must rely on the high specificity and high affinity of its interaction with progesterone.

The molecular interactions between progesterone and its receptor site are best studied with highly purified forms of the hormone–receptor complex. The isolation and partial purification of the progesterone receptor from various mammalian, including human, uterine tissues were recently reported (89–91). Subsequent to purification, the receptor–progesterone complex in human oviduct nuclei still retains its capacity for translocation and nuclear binding. Experiments are yet to be performed, however, where the hormone is removed from the receptor complex while the activity of the receptor is retained. Future work on the characterization and isolation of the progesterone receptor would be advanced by the use of identification ligands having optimal affinity for the receptor (92).

Partial characterization of the endometrial and myometrial progesterone–receptor complex indicates the binding macromolecules to be protein in nature. Much work recently has been performed to resolve whether the progesterone receptor is not, in fact, the corticosteroid-binding globulin (93, 94). Binding affinity studies (90, 95, 96) allow one to conclude that the endometrial and myometrial progesterone receptor is of tissue origin and has binding affinity distinct from that of corticosteroid-binding globulin.

Similarly, synthetic progestational agents show little affinity for corticosteroid-binding globulin but compete with progesterone for the cytosol binding site. This finding supports the suggestion that synthetic progestational agents act, at least in part, by interacting with receptors in target organs (95–97). Verma and Laumas (90), however, could not obtain

any competitive binding when using orally active progestational steroids. These results may be due to prolonged dialysis in the absence of glycerol, leading to rapid loss of high affinity progesterone binding activity (95, 98). In the hamster uterus, progesterone itself, not its metabolite 5α-pregnane-3,20-dione, mediates the progestational response by binding to the receptor site, indicating that initiation of the progestational response does not require conversion to this metabolite (99).

Ultracentrifugation in sucrose density gradients provides a practical means to differentiate among various forms of the receptor. The use of sedimentation rates to characterize receptor transformation for the estrogen–receptor complexes has been described (87). Even though the sedimentation behavior of steroid–receptor complexes varies according to concentration and ionic strength, it serves as a useful method to identify steroid–receptor complexes.

The sedimentation coefficient for the cytosol–progesterone receptor is about 4 S in sucrose density gradient centrifugation in the presence of 0.3 *M* KCl (90, 94). At low ionic strength (no potassium chloride), the aggregation occurs at 5 S and 8 S. Reported molecular weights for the receptor molecule monomer, calculated by various techniques, range between 60,000 and 110,000 daltons (89, 90). Binding is not covalent since the steroids are completely extractable with organic solvents. Published affinity constants vary between 1.0 and $3.4 \times 10^9\ M^{-1}$ (92, 96).

Nuclear Interactions—The nuclear steroid–receptor complex seems derived from the cytosol complex since cytosol receptor contents decrease as nuclear binding increases. The progesterone–receptor complex appears to bind the chick oviduct nuclei (a specific target tissue for progesterone) only after a time- and temperature-dependent transformation occurs. This transformation can be followed with ^{3}H-progesterone; the steroid–receptor complex becomes associated with the chromatin fractions (86).

The details of the molecular interactions between the receptor complex and chromatin fractions are not yet known, nor is the mechanism by which such interaction results in gene expression. Conceivably, the progesterone receptor consists of subunits that could play complementary roles in binding to the chromatin components responsible for acceptor activity (86, 88, 100).

In the estrogen-primed chick, progesterone increases the rate of synthesis of messenger RNA in the oviduct, an effect prevented by the administration of actinomycin D, an inhibitor of DNA-dependent RNA synthesis. If the biosynthesis of RNA is allowed to proceed, the oviduct synthesizes the hormone-dependent protein avidin.

After progesterone initiation of RNA biosynthesis, the hormone no longer seems necessary to evoke the resulting morphological changes. Consequently, total RNA extracted from progesterone-stimulated chick oviducts can induce the synthesis of avidin in estrogen-primed chicks. If no progesterone contamination is assumed, such a transfer method supports the concept that progesterone acts on the nucleus of target cells to promote synthesis of RNA (101). The morphological effects of progesterone (stimulation of cilia formation and secretory activity) can also be obtained by transfer of RNA extracted from progesterone-stimulated oviducts. The oviducts of the RNA-treated animals are almost indistinguishable from those that have undergone progesterone treatment (101).

Receptor Concentration—Theoretical and experimental approaches for the analysis of receptor concentration have been discussed (102). The concentration of progesterone receptor present in crude cytosol is approximately 3×10^{-9} mole/mg of protein (89, 103). The progesterone receptor concentration varies throughout the estrous cycle and is dependent on the action of both estrogen and progesterone (104, 105).

A single injection of estradiol (100 μg/kg) in castrated guinea pigs results in an eightfold increase in basal concentration of receptors after 20.5 hr (102). Similar results were obtained after diethylstilbestrol treatment in the chick oviduct (106). The established observation that, in most circumstances, progesterone can exert its biological effects only after estrogen priming is now understood in terms of the following scheme: estrogen → synthesis of progesterone receptor → progestational response. This increase in progesterone receptors after estradiol injection does not occur when actinomycin D or cycloheximide (an inhibitor of protein synthesis) is injected 15 min prior to the estradiol. Neither actinomycin D nor cycloheximide has any effect on receptor concentration when injected 20.5 hr after estradiol (time corresponding to maximum receptor concentration) (102). Following the estradiol treatment, the increase in concentration of progesterone receptor seems dependent on RNA and protein syntheses. The subsequent decrease in progesterone receptor is slow, with a receptor half-life of about 5 days.

The precise mechanism of receptor degradation is not understood. The injection of progesterone (1–10 mg) into estrogen-primed guinea pigs results in a rapid decrease in concentration of progesterone receptor. Very low concentrations of progesterone receptor are reached within 24 hr of progesterone injection and only slowly return to basal levels (102). This decrease in progesterone receptor concentration is not due to nuclear translocation (107) but may result either from an inactivation of the receptor protein or from changes in its binding behavior (since binding, not absolute receptor concentration, is measured).

The high levels of progesterone receptor during the follicular phase may, therefore, reflect the estrogen-dominated environment. On the other hand, a progesterone-dominated environment (*i.e.*, during the luteal phase) results in low levels of progesterone receptor. These observations are substantiated by the low concentrations of progesterone receptor present in subjects receiving oral contraceptives and during pregnancy.

In endometrial carcinoma, the concentration of progesterone receptor is low in undifferentiated tumors but relatively high in well-differentiated tu-

mors (108). Understanding the function of the receptor during the process of tumor differentiation may allow the prediction of the therapeutic response of tumor cells to treatment with progestational agents or other endocrine therapy. In human breast cancer, preliminary clinical results provide strong evidence for the hypothesis that only breast tumors containing progesterone receptors will show objective remission in response to endocrine therapy, *e.g.*, hypophysectomy or oophorectomy (109). During the malignant transformation of hormonal target tissue, the cells may not retain their ability to synthesize the hormone receptors. Patients with tumors containing both estrogen and progesterone receptors appear more likely to respond to endocrine therapy than if the tumors are without these receptors or only with estrogen receptors.

EFFECTS ON REPRODUCTIVE TISSUES AND FUNCTIONS

Hypothalamic–Pituitary–Ovarian Axis—Progesterone plays a relatively minor role during the early follicular stage of the menstrual cycle. Follicle-stimulating hormone secretion increases, promoting growth of the ovarian follicle. Follicular growth results in estrogen secretion and estrogen, in turn, seems to stimulate further follicular growth. Near the middle of the menstrual cycle, estrogen secretion peaks and stimulates or enhances the sudden release of luteinizing hormone. This transient increase in luteinizing hormone secretion results in high plasma luteinizing hormone levels causing ovulation. Accompanying the luteinizing hormone ovulatory surge, plasma follicle-stimulating hormone sharply rises. Luteinizing hormone seems to act directly on the follicle to cause release of the egg.

Following ovulation, the empty follicle rapidly becomes the corpus luteum, which secretes both progesterone and estrogen. In the human, increased progesterone synthesis may actually begin before ovulation (110, 111); it has been shown that by the time follicle-stimulating hormone and luteinizing hormone exhibit their peaks, the serum progesterone already has increased significantly (112). The ripe follicle is the probable source of this preovulatory progesterone (113), which at this point in the cycle may facilitate the release of luteinizing hormone. During the functional life of the corpus luteum (the luteal phase), the progesterone it produces reaches levels that inhibit hypothalamic cells controlling the formation or release of luteinizing hormone in the pituitary (114, 115).

We lack a cohesive understanding of which pituitary gonadotropin is most essential for the maintenance of the human corpus luteum. Luteinizing hormone can stimulate progesterone secretion and extend luteal life, yet other factors are involved since continuous treatment with luteinizing hormone or human chorionic gonadotropin (HCG) can extend luteal life for only a few days, the corpus luteum regressing during treatment. Regression of the corpus luteum abolishes the hormonal support provided to the secretory endometrium (116), leading to the endometrial sloughing of menstruation.

During pregnancy, the production of progesterone by the placenta (117–119) and the corpus luteum (3, 120) suppresses gonadotropin secretion and inhibits ovulation. The suppression of pituitary activity attained by progesterone administration includes adrenocorticotropin and growth hormone as well as gonadotropins. Such a broad range of pituitary inhibition suggests that the increased progesterone production during pregnancy is one major factor eliciting the shift from pituitary to placental dominance.

Progesterone exerts both stimulatory and inhibitory effects on ovulation (121). In some mammals (*e.g.*, rabbits and rats), progesterone, if given at a critical interval and dose, induces ovulation. This stimulatory effect of progesterone has been reviewed in detail (122). More emphasis, however, has been placed on progesterone's inhibition of ovulation, a concept that was a starting point for the development of oral contraception (123). Oral contraceptives containing both estrogenic and progestational analogs may interfere with fertility in several ways, but it is well established that, as presently used, their contraceptive action in humans results from suppression of follicle-stimulating hormone and luteinizing hormone and inhibition of ovulation.

Continuous administration of a progestational agent alone in sufficient doses also inhibits ovulation and abolishes the menstrual cycle for as long as therapy is continued. Smaller doses of progestational agents, as in the "mini-pill," also provide a contraceptive effect but do not disturb the menstrual cycle or ovulation. Progesterone injections, even in high doses, do not affect follicular maturation except in the late preovulation phase.

Autoradiograms of the hypothalamus of guinea pigs demonstrate a selective concentration of progesterone or its metabolites in the nuclei of certain neurons of the brain, providing supportive evidence for the presence of progesterone-sensitive sites in the hypothalamus (124). Nuclear binding of progesterone in hypothalamic neurons is further suggested as necessary for the production of the central hormonal action of progesterone.

Rat and baboon pituitary glands have the capacity to metabolize progesterone *via* 5α-reductase and 20α-hydroxysteroid dehydrogenase activity (125). This enzymatic activity within a target tissue has been interpreted as representing a mechanism by which progesterone may modulate certain pituitary and central nervous system (CNS) functions (76, 125).

Another approach in the elucidation of the interactions between hormonal and neural parameters responsible for estrus behavior has been to investigate the effects of ovarian steroids on the neuronal activity of brain monoamines (126). However, no clear picture has yet emerged from such studies due to experimental and interpretative problems.

Uterus—The primary target tissue for progesterone is the uterus. The sites of action are both the mucosal (endometrium) and muscular (myometrium)

portions. Progesterone enhances overall uterine growth (especially endometrial) resulting from estrogen priming. Subsequently, the endometrium differentiates and becomes ready for implantation of the blastocyst (secretory endometrium).

During the luteal phase of the menstrual cycle, the corpus luteum secretes estrogen and progesterone, causing the endometrium to become more tortuous and to produce a more mucous secretion with a high glycogen content. Endometrial growth is largely due to estrogen, while progesterone is responsible for the stromal changes and the increase in glycogen and glycoprotein in the glandular epithelium. These changes peak 7–8 days after ovulation, coincident with maximal progesterone secretion.

If implantation of a fertilized blastocyst does not occur, the secretory activity of the corpus luteum decreases, resulting in a measurable drop in progesterone production. This drop also may be partly due to an increase in ovarian 20α-hydroxysteroid dehydrogenase. With the fall in progesterone, the secretory endometrium can no longer be maintained, and it is sloughed (menstruation).

Endometrial Histology—Progesterone is considered responsible for the conversion of proliferative to secretory endometrium *in vivo* during the menstrual cycle. By adding progesterone (10 μg/ml) to a culture medium, glandular cells in the endometrial tissue are stimulated to secrete, and subnuclear vacuolation appears after 2–3 days. As the culture continues, the vacuoles disappear and secretion of mucopolysaccharides into the lumen of the glands occurs (127). Similar subnuclear vacuolation appears in the glandular cells of the endometrium in oophorectomized women after progesterone treatment.

Histochemically, this secretory effect is manifested by the increase in glycogen granules present in the cytoplasm and by changes in the apical villous borders of cells (128, 129). Glycogen granules first concentrate in the basal portion of the epithelial cells and then enter the secretory domes from which they detach as secretion globules. The substrates contained in the wall of the glandular epithelial cells are neutral or predominantly acid mucoids. These endometrial changes are well documented and have served historically as the basis of several bioassays for screening progestational agents.

After extended progestational therapy, the histochemical picture is one of focal pseudodecidual transformation of the stroma with glycogen accumulation and involution of the glands.

Protracted therapy provides a variety of changes encountered on a localized basis, including atypical secretion, exhaustion, and regression alternating with each other (129). Associated with the conversion of the endometrium to its secretory phase is an increase in the activity of most endometrial tissue enzymes (130–133).

Intrauterine Leukocytes—In most animal models (estrous, ovariectomized, and pseudopregnant), progesterone is generally found either to reduce or not to affect leukocyte levels in the uterus (134–137). Neutrophils and mononuclear cells are abundant in endometrial tissue during the menstrual flow, and mononuclear cells increase in association with the pseudodecidual stromal reaction occurring in the luteal phase.

Other observations have shown, however, that progesterone may also increase the number of the leukocytes present in oviductal tissues of cattle; such leukocytes release their products into the uterus at the start of the follicular phase, giving the uterus, under the influence of estrogen, its bactericidal properties. These leukocyte-like cells penetrate the lumen during early luteal stages of the estrous cycle and at early stages of pregnancy. The specific origin of these cells has not been determined; their morphology differs from the eosinophilic and neutrophilic polymorphonuclear cells present in genital tissues during inflammation (138).

Myometrial Activity—Human myometrial activity has been reviewed extensively (139, 140). As described by Moawad and Bengtsson (140), from Day 6 to Day 18 of a normal 28-day menstrual cycle the same type of activity is found, *i.e.*, frequent contractions (two to four per minute) of low amplitude (3–10 mm Hg) and short duration. After the 8th day preceding the next period, contractions of another type appear, with lower frequency (every 2–3 min), higher amplitude (around 25 mm Hg), and longer duration (1–2 min). These contractions gradually increase to a "prelabor-like" pattern 4 days before the next period. A further increase to "labor-like" activity is observed around the onset of bleeding.

The relative importance of the combined action of estrogen and progesterone is not known. The prelabor-like pattern corresponds with the presence of both estrogen and progesterone, whereas the labor-like pattern corresponds with the withdrawal of both hormones. In the nonpregnant woman, exogenous progesterone also induces the prelabor-like pattern of myometrial activity, resulting in contractions of lower frequency, longer duration, and higher amplitude (141).

In the pregnant uterus, most experiments indicate a depression of myometrial activity. Placental contribution of progesterone to the myometrium rather than the peripheral plasma progesterone may be responsible for this depression of myometrial activity (50, 142). In the rabbit, in which progesterone is known to have a blocking action on the myometrium, treatment with progesterone inhibits the myometrial stimulations caused by prostaglandin $F_{2\alpha}$ (dinoprost) (143). Agreement is still lacking on the physiological parameters that precipitate the onset of labor and, in particular, on the role (if any) of progesterone in the complex process of initiation and control of labor. In the human, the mean plasma progesterone remains unchanged prior to and throughout normal labor (32). In the case of premature labor, however, Csapo *et al.* (144) attributed the onset to a decrease in progesterone levels, caused perhaps by a failure in placental growth and function.

Electrophysiologically, progesterone has been suggested to act by inhibiting the movement of ions through the myometrial cell membrane (145). Like-

wise, inhibition of enzymes that are coupled to ionic movements and that are responsible for uterine muscle contraction would provide an alternative explanation. *In vitro,* progesterone does inhibit creatine phosphokinase activity (146) and, at high concentrations, adenosine triphosphatase activity (147).

Cervix—During the preovulatory phase of the cycle or following estrogen priming, the endocervical mucus is highly elastic and displays well-formed ferning (crystallized sodium chloride) upon drying. The rheological properties of this estrogenic mucus make it suitable for sperm penetration and survival. During the luteal phase, progesterone decreases the total volume of estrogenic mucus present in the endocervical canal (148), increases mucus viscosity, and decreases its "Spinnbarkeit" (length of the mucus thread) (149). Concomitant clouding of the mucus is due to the presence of polymorphonuclear leukocytes.

Progesterone (30 mg/week im), when administered without estrogen priming in ovariectomized women, causes no observable effect on the cervical mucosa. After an intramuscular injection of progesterone (5–10 mg), spermatozoa have difficulty in penetrating the mucus and in maintaining their motility. Progesterone, in oral doses of 10 mg/day to normal women, decreases both sperm population and sperm motility in the endocervical mucus following sexual intercourse (150). Intracervical silicone elastomer devices releasing progesterone display the expected progesterone effects; they inhibit secretion of preovulatory human cervical mucus, lower its Spinnbarkeit, and increase its viscosity (148).

Sperm Migration and Capacitation—Inhibition of sperm motility by progesterone is usually ascribed to secretory changes in the mucus production by the cervical crypts. In addition, progesterone released *in vitro* into cervical mucus inhibits sperm migration, suggesting that progesterone has a direct spermiostatic action (151). The relevance of this direct effect of progesterone on the regulation of fertility is not, however, established. Other factors that may play a role in the rate of sperm transfer have been studied: ciliary actions in the genital system, serotonin (152), oxytocin (153), and prostaglandins (154–156).

A specific hormonal balance seems necessary for sperm capacitation, a process involving changes in the spermatozoa necessary for penetration into eggs (157). An anticapacitating effect of progesterone was initially observed in rabbits (158). Further evidence was derived from experiments in which spermatozoa were incubated in the uterus of estrous rabbits pretreated with progesterone. In the progesterone-treated rabbits, only 2.1% of the ova were fertilized, as opposed to 63% after incubation in estrous rabbits without progesterone. Sperm capacitation was inhibited only in the uterus and not in the fallopian tubes.

Implantation and Blastocyst Development—The fertilized mammalian ovum generally reaches the uterus between 3 and 5 days after ovulation; in the uterus, the ovum requires a special environment, which is highly dependent on hormonal factors. Implantation of the fertilized ovum results in a rapid growth and differentiation at the implantation site, characterized by increased rates in the synthesis of nucleic acids and proteins. Results of reported studies are difficult to correlate due to species and experimental differences.

In the rabbit, for instance (159), survival of unimplanted fertilized eggs in the uterus depends on the presence of progesterone acting on the uterine epithelium and enabling the eggs to implant at the correct time. In most species, however, progesterone *per se* does not seem required for implantation but is essential for the initiation and maintenance of the decidualization and for the survival of the embryo. Ovariectomy in early pregnancy in the guinea pig does not prevent implantation, but subsequent degeneration of the decidua, ascribed to progesterone deficiency, results in embryonic death (160). If, however, progesterone administration is given following ovariectomy, pregnancy is maintained. Concurrent administration of small quantities of estrogen often reduces the amount of progesterone required (161).

In the rat, some inhibition of uterine receptivity occurs whenever the basic progesterone–estrogen sequence is disturbed. Receptivity in the uterus appears to be a local phenomenon, in that implantation can be inhibited in one part of the organ due to local administration of hormones while progressing normally in the rest of the uterus (160).

In spayed rats, the blastocyst can survive in the uterine lumen for several days in the absence of exogenous hormones (162). If progesterone (10 mg) is injected in such spayed rats, the blastocyst may survive for several weeks without implanting. This induction of dormancy in the blastocyst has been suggested to result from a hypothetical inhibitor produced by the uterus under the influence of progesterone as a protection to the embryo. A small dose of estrogen (1 μg) subsequent to progesterone injection removes the inhibition and leads to implantation. Normal development occurs provided progesterone treatment is continued.

Direct Exposure of Uterine Lumen—The direct exposure of the uterine lumen to exogenous progesterone has a contraceptive effect. Progesterone-filled silicone elastomer capsules inserted in the uterine horn of mature rabbits inhibit implantation of fertilized ovum (163). Similar capsules have also served as a contraceptive in human volunteers (164–166). Clinical efficacy studies with an intrauterine device that releases progesterone will be discussed later.

Morphological changes in the endometrium were observed in women having the progesterone-releasing system *in utero* but not in women wearing placebo devices (*i.e.,* containing no progesterone). The latter showed the usual endometrial picture of stromal edema and sometimes inflammatory cells. Delivery of progesterone to the endometrium causes a decidual transformation with a depression of the glandular development. The progesterone-releasing uterine system increases endometrial progesterone levels and decreases endometrial estradiol levels but causes no detectable change in the peripheral plasma levels of these steroids (51).

The specific mechanism of the contraceptive activity of intrauterine progesterone administration is unknown. Myometrial activity is unaffected in humans (167). Furthermore, no systemic effects from progesterone have been observed in rabbits (163), baboons (168), or humans (169). Contraceptive efficacy appears to depend on one or more changes within the uterine milieu: alteration of cervical mucus (170), disturbance of sperm capacitation (171–173), reduction of egg fertilization (171), endometrial suppression (170), and/or inhibition of nidation. Although the latter two effects seem the most likely mechanisms, the other factors may participate.

Vagina—Following estrogen priming, progesterone causes desquamation in the human vagina (174, 175). Desquamation occurs in clumps, the superficial cells being replaced by cells with basophilic cytoplasm and vesicular nuclei (149). In addition to shedding superficial layers, the thickness of the epithelium increases and progesterone may inhibit estrogen-induced vaginal cornification (176). The significance of an increase in the number of polymorphonuclear leukocytes, observable after 12 hr of an intravenous drip infusion of progesterone, is not known (177).

Mammary Gland—Mammary gland growth is a complex process involving other endocrine tissues besides the ovaries and the placenta (*e.g.*, pituitary and adrenals). Progesterone by itself, in sufficiently large doses, causes full development of the ductal and lobuloalveolar system of the mammary glands in intact and castrated rats, mice, and guinea pigs (178–180); priming by estrogen is not necessary to attain full development. Daily injections of 5–20 mg of progesterone in rhesus monkeys increase the size and number of lobules (181).

In the human, the alveolar proliferation caused by progesterone is most evident during pregnancy but is also operative during each luteal phase. The differences reported in the literature on this effect are partially due to marked species differences and to the inability to distinguish, in castrated but nonhypophysectomized animals, between a direct effect of progesterone on the mammary growth or an indirect action *via* the pituitary. In most experimental animals, the pituitary must remain intact if estrogen and progesterone are to affect mammary growth (180).

OTHER EFFECTS

As might be expected from its milligram per day production and wide body distribution, progesterone has sundry effects in addition to those on the reproductive organs. The effects of major interest in humans are summarized here. Reviews dealing with the effects of progesterone on other organ systems, including the effects on hepatic metabolism (182), the liver (183), respiration (184, 185), and the skin (186), have been published.

CNS—Progesterone exerts various effects on the CNS. The effect of progesterone on the hypothalamic–pituitary–ovarian axis has already been described. Sawyer *et al.* (187) reviewed the central effects of various hormones as they pertain to animal sexual behavior. Traditionally, the sharp falls in progesterone levels occurring at the end of each menstrual cycle and at the end of pregnancy have been implicated in premenstrual and postpartum disturbances in behavior (188–190).

The occurrence of depression or puerperal psychosis increases significantly during the 3 postpartum months (191). Serious psychological disturbances due solely to increased progesterone levels are, however, unlikely (192). Rather than investigating the role played by a unique agent (*i.e.*, progesterone) in pregnancy-related psychological phenomena, a more integrated approach encompassing a multiplicity of agents may better indicate possible correlations.

One clinical survey on the relationship between the incidence of migraine attacks and the stage of the menstrual cycle showed that the attacks occur regularly just before or during menstruation only in 13 out of 138 migraine patients (193). Most women with migraine, however, exhibited elevated plasma concentrations of both progesterone and estrogen throughout the menstrual cycle as compared to healthy migraine-free controls. This elevation in migraine patients was more marked in the late luteal phase. It must be kept in mind, however, that additional nonhormonal factors may be responsible for such results.

When progesterone (35 mg) is injected intraperitoneally into female rats, a deep anesthesia occurs within 15 min; if given subcutaneously, however, 100 mg is without effect (194, 195). A single intraperitoneal injection of progesterone (5 mg) into estrogen-primed rats shortens the periods of wakefulness and induces, in the hippocampal area, the appearance of EEG spikes similar to those of sleep (196).

Studying the uptake of labeled progesterone and two of its metabolites (pregnanolone and pregnanedione), Raisinghani *et al.* (197) concluded that pregnanolone mediates the anesthetic effect of progesterone. The median anesthetic dose in mice is 89 mg/kg iv (198). In the human, this effect has not had any practical application, although Merryman *et al.* (199) reported sleep induction in women within the first 15 min of an intravenous infusion of progesterone (500 mg). The hypnotic effect lasts for several hours and is dose dependent.

Progesterone increases, and estradiol decreases, the seizure threshold for rats given electroshock-induced convulsions (200). The administration of 5 mg/kg/day of progesterone significantly raises the seizure threshold in female rats but is without effect in males. This anticonvulsant effect in females is transient; after 20 days of treatment, a mild convulsant response is observed in both males and females. Progesterone is also effective in protecting dogs against induced convulsions.

Clinical studies with human epileptic patients appear consistent with animal results; the number of seizures definitely declines during the luteal phase of the menstrual cycle and increases immediately before, during, and just after menstruation. This exacerbation is thought to result from the drop in the progesterone secretion. Activations of abnormal EEG

patterns and precipitation of seizure occur with exogenous estrogen whereas a decrease in seizures is observed with premenstrual progesterone therapy (201, 202). This effect of progesterone on the CNS has not been clinically exploited, however, since other more advantageous therapeutic compounds are available.

Progesterone is associated with an increase in basal body temperature. In women, the basal body temperature is usually higher during the luteal phase of the cycle; the initial rise in temperature is widely assumed to coincide with ovulation. The pattern of basal body temperature, however, varies greatly from subject to subject. In addition, no increase in basal body temperature with ovulation is obtained in 12% of otherwise normal cycles (203). These factors indicate that this thermogenic effect cannot be used reliably for predicting ovulation. Body temperature also generally increases during the first 4 months of pregnancy (204).

The increase in basal body temperature is not mediated by the uterus, since this effect is also seen in males and hysterectomized females and there is no evidence of local uterine inflammation. After a single 10–15-mg injection of progesterone to males, temperature rises 0.3–0.9° (0.5–1.5°F) for 1–4 days (205). A minimum dose (~10 mg) is required to elicit this rise, beyond which, however, the response is not dose dependent. In the rat, the intact pituitary seems essential in eliciting this thermogenic action; it has been suggested that the hypothalamic thermoregulating centers are involved. On the other hand, neither ovariectomy nor thyroidectomy has any effect (206). It is assumed that the hypothalamic centers lose their responsiveness after extended exposure to progesterone because body temperature falls to pregestational follicular levels after the 4th month of pregnancy (204).

Cardiovascular System—High doses of exogenously administered progesterone can either elevate or lower blood pressure in various species. Daily subcutaneous doses of progesterone reduce blood pressure in rats (15 mg/kg) and dogs (20 mg/kg) with experimental nephrogenic hypertension (207). In studies with patients suffering from either primary or renal hypertension, progesterone (50–200 mg/day im for 10–16 days) significantly decreases blood pressure without loss of sodium (208, 209).

On the other hand, Horrobin (210) reported that prolonged treatment (60 days) of rabbits with large daily doses (25–50 mg) of progesterone results in a moderate (15–25 mm Hg) rise in systolic arterial pressure and causes renal lesions. This effect could be explained partially by considering the increase in aldosterone secretion that accompanies high doses of progesterone, whereas low doses of progesterone are ineffective in increasing aldosterone secretion (211). Moreover, progesterone is a precursor in the biosynthesis of aldosterone and other corticosteroids, a fact that may also explain the clinical finding that some Addisonian patients do well with little or no corticoid therapy during pregnancy.

A rise of systolic blood pressure in the range of 10 mm Hg is observed in certain women taking combined estrogen–progestogen oral contraceptives. A rise of similar magnitude observed with intravenous infusion of estrogens strongly suggests that the estrogen component is responsible for this effect observed with combined oral contraceptives (212).

Exogenous progesterone does not influence the plasma fibrinogen level in the rat, and no changes in platelet number can be observed (213).

Skeletal Growth and Weight Regulation—Injection of progesterone into intact mice (three weekly doses of 10 μg) retards growth, cartilage development, and ossification. In castrated mice of either sex, progesterone somewhat counteracts the effect of gonadectomy by restoring a more regular course of ossification (214). The treatment of rats with progesterone (1 mg/day im for 7 days) markedly decreases the rate of growth of their teeth (215). Plasma growth hormone concentrations after glucose and insulin administration are decreased significantly in normal subjects following progesterone administration (300–400 mg/day im for 3–5 days). Progesterone also impairs growth hormone response to arginine (216). Such observations suggest that placental production of progesterone contributes to the suppression of pituitary release of growth hormone observed in late human pregnancy.

Experiments with female rodents given progesterone at levels closely approximating those of pregnancy (217) indicate the following effects: water retention, protein anabolism (increased nitrogen retention), and appetite stimulation. It has been suggested that these actions are related to the direct influence of progesterone on the hypothalamic food-regulating centers (218). In rats, these effects of progesterone administration on the weight and composition of the body are not present in either males or castrated females (219) but are seen after ovary implantation (220). Hypophysectomy drastically reduces the weight response to progesterone; adrenalectomy, on the other hand, markedly increases it (221, 222).

In humans, nitrogen excretion (as urea) increases with a daily dose of 50 mg of progesterone. This catabolic effect, seen in both sexes and in hypophysectomized and ovariectomized subjects, has been attributed to an increased utilization of amino acids by the liver (223). Progesterone (100 mg/day im) has been used in conjunction with a low calorie diet, digitalis, and diuretics in the treatment of obese patients with alveolar hypoventilation. The therapeutic benefits from progesterone did not appear necessarily associated with weight loss from the treatment but were the result of stimulated ventilation and improvement in the pulmonary status of the obese patients (224).

Microorganisms—Antibacterial action against Gram-positive microorganisms is shown *in vitro* by progesterone (10–20 μg/ml). Progesterone exerts its bacteriostatic action on staphylococci primarily during the first 8 hr of incubation; the effect is reduced by the presence of oxygen (225). In the presence of 20 μg of progesterone/ml, there is a significant decrease in the oxidation by resting staphylococcal suspensions or utilization by staphylococci of pyruvate as an energy source during growth.

The effect of progesterone on Gram-negative organisms seems restricted to members of the genus *Neisseria;* strains of *N. gonorrhoeae* and *N. meningitidis* are sensitive to growth inhibition by progesterone (40 μg/ml) (226). The site of progesterone action appears to be in the cell membrane, where the hormone may bind to proteins (227). Although other factors could contribute, this growth inhibitory effect of progesterone correlates with the observation that, during the menstrual cycle, the lowest isolation rate for *N. gonorrhoeae* from cervical cultures occurs at the peak of progesterone activity (228).

Tumor Growth—A review by Kramer *et al.* (229) concluded that progesterone inhibits the growth of estrogen-induced tumors, except for enhancing the growth of pituitary adenoma. Lipschütz (230) was the first to demonstrate that the subcutaneous implantation of a progesterone pellet in guinea pigs (average absorption calculated to be 40 mg/day over 2 months) reduces the development of estradiol-induced tumors. Continuous administration of progesterone (20-mg pellets sc) also prevents the appearance of mammary tumors in rats exposed to the synergistic carcinogenic effect of radiation (800 Rads) and estrogen (231). In these experiments, progesterone had a protective effect against both the estrogen and combined estrogen–radiation treatments, because fewer tumors occurred on both the irradiated side and the nonirradiated side.

In experimental tumor induction with known carcinogens, tremendous variation in results has been observed, depending on the animal species and strain used and the methods of administering the carcinogens and hormones (232). Prolonged and high doses of progesterone (45 mg/mouse for 9 weeks) or synthetic progestational agents, if administered at a critical time, increased the effect of known carcinogens on the endocervical mucosa. Histological results indicated that parenteral administration of progesterone influences the maturation of 20-methylcholanthrene-induced endocervical carcinoma in mice. Progesterone had, however, no effect on the maturation of induced invasive carcinoma from the vagina and the exocervix (233, 234).

Progesterone (6 mg/week sc for 17 weeks) increased the frequency of metastasis when mammotropic pituitary tumors were transplanted in mice (235). Poel (236) found that progesterone (0.25 ml of 5% progesterone in peanut oil sc/week for 19 weeks) accelerated the development of 20-methylcholanthrene-induced mammary tumors in mice. When 7,12-dimethylbenz[*a*]anthracene (DMBA) was used as a carcinogen, mammary tumorigenesis was significantly enhanced by progesterone treatment if begun just before or after carcinogen administration in intact rats (237) or if given continuously after dimethylbenzanthracene treatment in hypothyroid rats (238). When, on the other hand, progesterone was administered before feeding dimethylbenzanthracene, it prevented the onset of mammary cancers (239) as shown by a reduction in tumor yield; continuation of progesterone after carcinogen administration, however, lessened this reduction in tumor yield (240).

The results of studies on the growth of malignant cells during progesterone administration in susceptible animal strains have questionable relevance in humans. Progesterone and progestational agents have been used successfully in humans in the treatment of endometrial carcinoma (241–246) and with more limited success in the treatment of mammary carcinoma (246). Animal testing, moreover, provides little evidence suggesting that progesterone is tumorigenic *per se.* Evidence that it enhances chemically induced tumorigenesis is at best debatable, considering the variation in response based on pharmacological factors, such as route of administration and local concentration of progesterone, and tumoral factors, such as homogeneity, degree of differentiation, and genetically determined hormonal responsiveness of the tumor cell population.

CLINICAL USE

Progesterone, with its short half-life and extensive degradation following ingestion, has been inconvenient to use effectively in the clinic. Because of these problems, orally effective, synthetic progestational agents frequently have been substituted (247, 248), perhaps unwisely in some cases, since synthetic progestogens recently have been linked with abnormal fetal development (249, 250). Recent successful clinical uses of progesterone have utilized its local administration to a given area, thereby reducing the loss of progesterone to systemic metabolism.

Carcinoma—The role of sex steroids in the development of carcinoma of the endometrium has been the subject of considerable investigation over the past 30 years. It has been suggested that, in some individuals, unopposed, protracted estrogen stimulation of the endometrium may eventually result in carcinoma (251, 252). Because progesterone has a profound modifying effect on the estrogen-prepared endometrium, progesterone has been investigated as a prophylactic and therapeutic drug in the overall management of patients with endometrial or breast cancer and adenomatous hyperplasia.

Patients with metastatic endometrial carcinoma were treated from 3.5 weeks to 4.5 years with progesterone (50 mg three times/week) or hydroxyprogesterone caproate (up to 1 g weekly) (253). In 32% of the cases, objective remissions were obtained, lasting from 1 month to 9 years. Remission rates were similar in studies using progestational agents for the treatment of recurrent endometrial adenocarcinoma (241–246). Regression of endometrial carcinoma following progesterone therapy is ascribed to a direct effect upon the cancer cell rather than to an indirect inhibition of pituitary tropic hormone release.

Progesterone treatment has proved of only limited value, with a success rate of 10%, in the regression of advanced mammary carcinomas (254). The hypothesis that estrogenic stimulation in the absence of sufficient progesterone secretion provides a favorable setting for mammary carcinoma (255) has not been tested epidemiologically.

In early studies on the use of progesterone therapy

for cervical carcinoma, Hertz (256, 257) administered intramuscular injections of 250 mg/day of progesterone to 17 women over periods ranging from 10 to 149 days (a total of 1.5–42.5 g of progesterone/patient). The regressive changes observed were not considered sufficient to justify the use of progesterone as a therapeutic agent in carcinoma of the cervix.

Preliminary studies with the use of progesterone suppositories for vaginal adenosis have been more promising. Using this local mode of hormone administration, five out of five patients achieved regression of their adenosis and a striking reduction in associated redness and inflammation while maintaining normal ovulatory function (258).

Habitual Abortion—The effectiveness of progesterone in protecting pregnancy is not established. Nevertheless, progesterone therapy is sometimes initiated in pregnant women with a history of habitual abortion and in pregnant women who experience blood staining, with or without abdominal cramps. Several medications and different routes of administration may be used, including vaginal, rectal, intramuscular, or intra-amniotic (259, 260). Progesterone (1000 mg/day) has also been administered orally to these patients from the beginning of pregnancy through at least the 36th week of gestation. Of the 52 women receiving oral progesterone and completing the study, 38 were able to maintain pregnancy and deliver full-term infants (261). Synthetic progestogens should not be substituted for progesterone because of their association with fetal masculinization (249) and teratogenicity (250).

Gynecological Disorders—Progesterone and synthetic progestogens have a wide clinical application in the treatment of gynecological disorders such as dysmenorrhea, amenorrhea, and dysfunctional uterine bleeding (247, 248, 262). Synthetic progestogens are used occasionally to attain less painful episodes in patients with primary dysmenorrhea. Progesterone is generally successful in the treatment of secondary amenorrhea. Such steroid therapy is essentially substitutive, replacing the missing endogenous ovarian hormones. For diagnosis of the cause of amenorrhea, a suitable test dose is 50 mg of progesterone injected twice (48 hr apart). Subsequent withdrawal bleeding indicates the production of endogenous estrogen, a responsive endometrium, and a nonpregnant state. Repeated induction of artificial menses usually requires an estrogen for 20 days, followed by a progestational agent for 5 days (248).

The underlying principle of progesterone therapy in the control of dysfunctional uterine bleeding is to raise the blood level of the steroid to a point capable of preventing further disintegration of the bleeding endometrium and then to withdraw the steroid abruptly, causing a rapid exfoliation of the superficial layers and nonsurgical curettage. An intramuscular injection of progesterone (25 mg/day for 5 days) is used to control uterine bleeding.

Contraception—Early studies on its use as an oral contraceptive showed that, at 300 mg/day (5th to 25th day of the menstrual cycle), progesterone was effective in preventing ovulation through four cycles (263). The related effect of larger doses of progesterone on gonadotropin excretion also has been investigated. Rothchild (264) found that continuous or intermittent intravenously administered progesterone (100–400 mg/day) for 10 days depressed the total amount of gonadotropin excreted into the urine. However, Paulsen *et al.* (265) found that oral progesterone at 1000 mg/day for 87 days did not have a significant effect on urinary gonadotropin excretion. The efficacy of progesterone as an oral contraceptive was never fully tested, because synthetic progestational agents, which were orally effective, were available.

Direct administration of progesterone to the uterine lumen, however, has been found a convenient and effective method of contraception (266, 267). In a preliminary clinical study, silicone elastomer devices releasing progesterone were placed in 109 women for two to 13 cycles (a total of 755 woman months). No pregnancies occurred with a functional device *in situ*. Two pregnancies did occur: one when the device was displaced into the cervix and the other when the device was not releasing progesterone. The devices caused suppression in the superficial portion of the endometrium, but a regular menstrual cycle was preserved (164–166).

This method of contraception has since been improved and extensively tested in over 4000 women. Progesterone is released at a rate of 65 μg/day from a T-shaped uterine system[1] for 1 year. At the end of the year, the system is replaced. The efficacy of the uterine system compares favorably with oral contraceptives (267) and it causes no extrauterine systemic steroid effects (169).

TOXICITY

Cell Growth Inhibition—Addition of high concentrations of progesterone (50–200 μg/ml) to tissue cultures of endometrial carcinoma cells is associated with inhibition of DNA synthesis, which results in a decrease in cell survival (246, 268). With adrenal cells, 50% inhibition of growth is accomplished with 7 μg/ml of progesterone (269). The cell growth inhibition value for chick heart ventricular cell cultures is 4 μg/ml of progesterone (270).

Animal Toxicity Studies—The intravenous LD_{50} of progesterone in propylene glycol (20 mg/ml) in rabbits is 26.5 mg/kg. The animals exhibit respiratory convulsions and opisthotonos; the primary cause of death is acute hypoxia (271). Such results, however, cannot reliably represent the acute toxicity of intravenously administered progesterone since propylene glycol itself has an intravenous LD_{50} of 3.2 ml/kg of rabbit body weight (271). The intraperitoneal LD_{100} of progesterone in peanut oil in rats is 327 mg/kg (272).

Oral administration (40 or 160 mg/kg/day) or subcutaneous injections (4 or 16 mg/kg/day) of progesterone suspended in 0.25% carboxymethylcellulose

[1] Progestasert System, Alza Corp., Palo Alto, CA 94304

were carried out for 26 weeks with both male and female rats (273). Mortality in tested animals did not differ from a control group. Gonads were atrophied in both males (prostate) and females (uterus) receiving the high subcutaneous dosage. Hematological values determined throughout the experiment were unremarkable, as were microscopic examinations of organ tissues at termination of the experiment. In males, body and organ weights did not differ from those of controls. The only significant changes at these dose levels occurred in female animals receiving subcutaneous treatment. These animals exhibited an increase in body and liver weights. This increase in liver weight was not significant, however, when expressed as a ratio to body weight.

Prenatal Exposure—Using an egg transfer technique, Dickmann (274) determined the effect of progesterone on the survival of rat morulae. Morulae degenerated in the uteri of recipients that had been ovariectomized and injected daily with 2 mg of progesterone. No deleterious effect to the blastocyst could be observed. Progesterone concentrations below 2 μg/ml produced no noticeable effects on the development of the mouse ova *in vitro*; concentrations above 4 μg/ml inhibited ova development by blocking cleavage, particularly at the blastula stage (275). This action was reversible, with ova resuming cleavage when placed in progesterone-free media.

Using subcontraceptive levels of progesterone in rabbits (2 mg sc near ovulation), Allen and Foote (276) concluded that progesterone suppressed the development of zygotes into blastocysts, but that once implanted successfully, all treated embryos developed normally and were equivalent to controls during their postnatal development. The mechanism of this action of progesterone on mammalian ova *in vitro* seems to result from an inhibition in transfer of amino acids or soluble proteins across the cell membrane, thereby inhibiting protein synthesis within the ovum (277).

Various progesterone effects on the fetus occur in the pregnant rat, depending upon dosage and time of administration. For instance, progesterone (5 mg/day im) injected on Days 16 through 19 had no effect, but the same dosage on Days 20 through 23 caused fetal death (278, 279). There is no agreement on the hypothesis that fetal death is related to the prolonged delay of parturition due to progesterone administration (279). In the pregnant swine, progesterone (2 mg/kg/day sc) between Day 0 and Day 25 of gestation did not increase the expected embryonic survival rate, indicating that early embryonal mortality is not due to a deficiency of progesterone in this species (280, 281).

In a study of the effects of some known teratogens (*e.g.*, ergocornine) on the course of gestation in rats, it was concluded that the mechanism for teratogenic action is mediated, at least in part, by a progesterone deficiency resulting from the use of the teratogen (282). The administration of 1 mg of ergocornine on the 8th day seriously disturbed pregnancy and increased the incidence of fetal malformations. Progesterone treatment (5 mg/day) given concomitantly with the teratogen allowed pregnancy to proceed according to a more normal pattern (282). The embryolethal effect of certain drugs, such as actinomycin D, is also decreased by progesterone treatment. For instance, subcutaneous injections of progesterone (4 mg/day between the 8th and 21st day of gestation) in actinomycin D-treated rats increased the number of live fetuses and reduced the number of nonviable implantations (283).

The possibility of fetal masculinization by progesterone treatment has been reviewed and experimentally investigated (284). Pregnant rats were treated from the 16th to the 19th day of gestation with 4–274 mg of progesterone (1–75 mg/day). All female fetuses exhibited normally developed genitalia, and it was concluded that there is little or no risk of masculinization of female infants.

Some cases of human female pseudohermaphroditism were reported following administration of synthetic progestogens during gestation to mothers treated for habitual or threatened abortion (285). These data describe synthetic progestogens that exhibit masculinizing properties and in no way argue against the use of progesterone (249). This virilizing effect of synthetic progestogens upon the female fetus seems to be attributable to the androgenic properties of the steroids, since it is well established that the administration of androgens during pregnancy leads to masculinization in both laboratory animals and humans (286).

Hagler *et al.* (287) summarized the effect of steroid administration to mothers during early pregnancy on the incidence of male pseudohermaphroditism. At that time (1963), there were only three cases where progesterone was given alone (37.5–200 mg iv weekly for up to 17 weeks), and in none did male pseudohermaphroditism occur. One infant was anencephalic, but there is no reason to believe that malformation was due to a progesterone effect.

Progesterone therapy, sometimes initiated in pregnant women, causes no adverse effect to the fetus. On the other hand, synthetic progestogens or estrogen–progestogen combinations—given in cases of threatened abortions, pregnancy tests, or as oral contraceptives—have been associated with a variety of congenital abnormalities. These include hypospadia (288), transposition of the great vessels (289), CNS malformation (290, 291), and other anomalies (292–294). These preliminary clinical findings clearly indicate the need to ascertain the absence of pregnancy before initiation of oral contraception (estrogen and/or synthetic progestogen) and strongly suggest that hormonal agents are contraindicated as pregnancy tests (250).

Studies of fetal development under the influence of progestational agents point out the need to differentiate clearly between the use of synthetic progestogens and progesterone (295). Progesterone, which is secreted in large quantities during gestation, is necessary to maintain the early stages of pregnancy. Progesterone has not been found harmful to the developing fetus and, in fact, may be beneficial to it (295, 296). Infants born to women using an intrauterine

device that releases progesterone to the uterine lumen have been normal[2].

Neonatal Exposure—Early postnatal damage in neonate rodents caused by estrogens or androgens can be blocked by progesterone. Progesterone (3 mg im) prevented the alteration of gonadal function produced by injecting androgen into female rats and estrogen into male rats (297). Such observations suggest that certain human hypogonadal syndromes or infertility may result in part from decreased or abnormal steroidogenesis during fetal life. The neonate mouse is highly sensitive to progesterone. The following pattern is observed: between 0 and 24 hr, LD_{50} = 70 mg/kg; between 49 and 72 hr, LD_{50} = 1200 mg/kg; and between 121 and 168 hr, LD_{50} = 2700 mg/kg (298).

These results suggest that the neonate mouse does not have the enzymatic ability necessary to metabolize the injected progesterone and that anatomical barriers preventing elevated concentrations in certain organ systems (*e.g.*, CNS) are not yet fully developed. The injection of a single dose of progesterone (1 mg) to 5-day-old female mice resulted in a delay in sexual maturity and a decrease in fertility of the animals, although estrous cycles were normal (299). Even though no dose–effect relationship has been established, proper progesterone level during the neonatal period appears essential for the adequate gonadal development and function.

REFERENCES

(1) "Pharmacology of the Endocrine System and Related Drugs: Progesterone, Progestational Drugs and Antifertility Agents," vol. I, International Encyclopedia of Pharmacology and Therapeutics, sect. 48, M. Tausk, Ed., Pergamon, New York, N.Y., 1971.

(2) "The Gestagens," Handbook of Experimental Pharmacology, vol. XXII/I, K. Junkmann, Ed., Springer-Verlag, New York, N.Y., 1968.

(3) J. Zander, F. Forbes, A. von Münstermann, and R. Neher, *J. Clin. Endocrinol. Metab.*, **18,** 337(1958).

(4) E. Diczfalusy, *Acta Endocrinol.*, **10,** 373(1952).

(5) A. M. Moses, J. Lobotsky, and C. W. Lloyd, *J. Clin. Endocrinol. Metab.*, **19,** 987(1959).

(6) A. Riondel, J. F. Tait, S. A. S. Tait, M. Gut, and B. Little, *ibid.*, **25,** 229(1965).

(7) T. J. Lin, S. C. Lin, F. Erlenmeyer, I. T. Kline, R. Underwood, R. Billiar, and B. Little, *ibid.*, **34,** 287(1972).

(8) O. V. Dominguez, G. D. Francois, M. Watanabe, and S. Solomon, *Proc. Meet. Endocrine Soc., 44th*, **35,** 17(1962).

(9) S. Solomon, M. Watanabe, O. V. Dominguez, M. J. Gray, C. I. Meekey, and E. A. H. Sims, *Excerpta Med. Found. Int. Congr. Ser.*, **51,** 267(1962).

(10) W. H. Pearlman, *Ciba Found. Colloq. Endocrinol.*, **11,** 233(1957).

(11) K. Block, *J. Biol. Chem.*, **157,** 661(1945).

(12) D. B. Bartosik and E. B. Romanoff, "The Gonads," K. W. Mc Kerns, Ed., North-Holland Publishing Co., Amsterdam, The Netherlands, 1969, p. 211.

(13) S. Dell'Acqua, S. Mancuso, M. Catelli, and A. Bompiani, *Acta Endocrinol.*, **75,** 368(1974).

(14) N. R. Mason and K. Savard, *Endocrinology*, **75,** 215(1964).

(15) B. I. Tamaoki and G. Pincus, *ibid.*, **69,** 527(1961).

(16) W. Y. Huang and W. H. Pearlman, *J. Biol. Chem.*, **237,** 1060(1962).

(17) B. F. Rice and A. Segaloff, *Acta Endocrinol.*, **51,** 131(1966).

(18) K. Savard and G. Telegdy, *Steroids, Suppl. II*, **1965,** 205.

(19) M. L. Sweat, D. Berliner, M. Bryson, C. Nabors, J. Haskell, and E. Holmstrom, *Biochim. Biophys. Acta*, **40,** 289(1960).

(20) K. J. Ryan and Z. Petro, *J. Clin. Endocrinol. Metab.*, **26,** 46(1966).

(21) K. J. Ryan and O. W. Smith, *J. Biol. Chem.*, **236,** 705(1961).

(22) M. E. Davis and E. J. Plotz, *Recent Progr. Horm. Res.*, **13,** 347(1957).

(23) H. W. Jones and P. G. Weil, *J. Amer. Med. Ass.*, **111,** 519(1938).

(24) H. A. Salhanick, M. W. Noall, M. X. Zarrow, and L. T. Samuels, *Science*, **115,** 708(1952).

(25) W. H. Pearlman and E. Cerceo, *Endocrinology*, **53,** 599(1953).

(26) O. Cassmer, *Acta Endocrinol., Suppl.*, **45,** 1(1959).

(27) E. Diczfalusy and U. Borell, *J. Clin. Endocrinol. Metab.*, **21,** 1119(1961).

(28) R. B. Jaffe, *Excerpta Med., Series No. 111*, **1966,** 547.

(29) R. Pion, R. B. Jaffe, G. Eriksson, N. Wiqvist, and E. Diczfalusy, *Acta Endocrinol.*, **48,** 234(1965).

(30) R. Palmer, G. Eriksson, N. Wiqvist, and E. Diczfalusy, *ibid.*, **52,** 598(1966).

(31) K. J. Ryan, R. A. Meigs, and Z. Petro, *Amer. J. Obstet. Gynecol.*, **96,** 676(1966).

(32) D. M. Okada, D. Tulchinsky, J. W. Ross, and C. J. Hobel, *ibid.*, **119,** 502(1974).

(33) S. Furuyama and C. A. Nugent, *Steroids*, **17,** 663(1971).

(34) E. D. B. Johansson, *Acta Endocrinol.*, **61,** 592(1969).

(35) C. M. Cargille, G. T. Ross, and T. Toshimi, *J. Clin. Endocrinol. Metab.*, **29,** 12(1969).

(36) C. Fassorra and M. Luisi, *Hormones*, **2,** 153(1971).

(37) E. D. B. Johansson, *Acta Endocrinol.*, **61,** 607(1969).

(38) A. Csapo, E. Knobil, H. Van der Molen, and W. Wiest, *Amer. J. Obstet. Gynecol.*, **110,** 630(1971).

(39) J. L. Llauró, B. Runnebaum, and J. Zander, *ibid.*, **101,** 867(1968).

(40) G. Mikhail, J. Zander, and W. M. Allen, *J. Clin. Endocrinol. Metab.*, **23,** 1267(1963).

(41) C. W. Lloyd, J. Lobotsky, D. T. Baird, J. H. McCracken, J. Weisz, M. Pupkin, J. Zanartu, and J. Puga, *ibid.*, **32,** 155(1971).

(42) F. Fuchs, A. R. Fuchs, and R. V. Short, *J. Endocrinol.*, **27,** 333(1963).

(43) G. Mikhail and W. M. Allen, *Amer. J. Obstet. Gynecol.*, **99,** 308(1967).

(44) W. J. LeMaire, P. W. Conly, A. Moffett, and W. W. Cleveland, *ibid.*, **108,** 132(1970).

(45) B. Runnebaum and J. Zander, *Acta Endocrinol., Suppl.*, **150,** 5(1971).

(46) I. Nilsson, *Acta Obstet. Gynecol. Scand.*, **51,** 117(1972).

(47) A. C. Barnes, D. Kumar, and J. A. Goodno, *Amer. J. Obstet. Gynecol.*, **84,** 1207(1962).

(48) D. Kumar and A. C. Barnes, *ibid.*, **92,** 717(1965).

(49) J. Zander and B. Runnebaum, *Acta Endocrinol.*, **54,** 19(1967).

(50) W. G. Wiest, *Steroids*, **10,** 279(1967).

(51) K. Hagenfeldt and B. M. Landgren, *J. Steroid Biochem.*, **6,** 895(1975).

(52) H. Grundsell, I. Nilsson, and S. Nordqvist, *Lancet*, **1,** 888(1973).

(53) E. D. B. Johansson, *Acta Obstet. Gynecol. Scand., Suppl.*, **19,** 17(1972).

(54) U. Westphal, B. D. Ashley, and G. L. Selden, *Arch. Biochem. Biophys.*, **92,** 441(1961).

(55) R. V. Short, *J. Endocrinol.*, **16,** 415(1958).

(56) R. M. Burton, G. B. Harding, N. Rust, and U. Westphal, *Steroids*, **17,** 1(1971).

(57) G. B. Harding, R. M. Burton, S. D. Stroupe, and U. Westphal, *Life Sci.*, **14,** 2405(1974).

(58) E. Milgrom, P. Allouch, M. Atger, and E. E. Baulieu, *J. Biol. Chem.*, **248,** 1106(1973).

(59) E. Milgrom, P. Allouch, and M. Atger, *Methods Enzymol.*, **36,** 120(1975).

(60) A. A. Sandberg and W. R. Slaunwhite, *J. Clin. Endocrinol. Metab.*, **18,** 253(1958).

[2] Alza Corp., Palo Alto, CA 94304, unpublished results.

(61) J. H. H. Thijssen and J. Zander, *Acta Endocrinol.*, **51,** 563(1966).
(62) P. Fylling, *ibid.*, **65,** 284(1970).
(63) T. J. Lin, R. B. Billiar, and B. Little, *J. Clin. Endocrinol. Metab.*, **35,** 879(1972).
(64) B. Little, R. B. Billiar, J. Bougas, and J. F. Tait, *ibid.*, **36,** 1222(1973).
(65) W. H. Pearlman, *Excerpta Med. Found. Int. Congr. Ser.*, **51,** Abst. 11, 15(1962).
(66) M. L. Sweat and M. J. Bryson, *Amer. J. Obstet. Gynecol.*, **106,** 193(1970).
(67) P. L. Langlois, *J. Reprod. Med.*, **4,** 31(1970).
(68) K. Fotherby, *Vitam. Horm. (N.Y.)*, **22,** 153(1964).
(69) M. E. Davis, E. J. Plotz, G. V. LeRoy, R. G. Gould, and H. Werbin, *Amer. J. Obstet. Gynecol.*, **72,** 740(1956).
(70) H. Askalani, M. Smuk, J. Sugar, P. Delvoye, C. Robyn, and J. Schwers, *ibid.*, **118,** 1054(1974).
(71) G. E. Abraham, G. B. Maroulis, and J. R. Marshall, *Obstet. Gynecol.*, **44,** 522(1974).
(72) R. A. Harkness, D. W. Davidson, and J. A. Strong, *Acta Endocrinol.*, **60,** 221(1969).
(73) A. H. Conney and J. J. Burns, *Science*, **178,** 576(1972).
(74) A. H. Conney, M. Jacobson, W. Levin, K. Scheidman, and R. Kuntzman, *J. Pharmacol. Exp. Ther.*, **154,** 310(1966).
(75) E. C. Gomez, P. Frost, and S. L. Hsia, *J. Invest. Dermatol.*, **64,** 240(1975).
(76) T. Tabei, H. Haga, W. L. Heinrichs, and W. L. Hermann, *Steroids*, **23,** 651(1974).
(77) F. A. Kincl, in "Pharmacology of the Endocrine System and Related Drugs: Progesterone, Progestational Drugs and Antifertility Agents," vol. I, International Encyclopedia of Pharmacology and Therapeutics, sect. 48, M. Tausk, Ed., Pergamon, New York, N.Y., 1971, pp. 13–64.
(78) H. G. Spies, C. J. Mahoney, R. L. Norman, D. K. Clifton, and J. A. Resko, *J. Clin. Endocrinol. Metab.*, **39,** 347(1974).
(79) T. M. Plant, V. H. T. James, and R. P. Michael, *J. Endocrinol.*, **51,** 751(1971).
(80) J. Chamberlain, B. A. Knights, and G. H. Thomas, *ibid.*, **28,** 235(1964).
(81) J. d'A. Jeffery, *ibid.*, **34,** 387(1966).
(82) L. P. Romanoff, M. Grace, E. M. Sugarman, and G. Pincus, *Gen. Comp. Endocrinol.*, **3,** 649(1963).
(83) T. Shinada and K. J. Ryan, *Steroids*, **21,** 233(1973).
(84) J. W. Goldzieher and L. R. Axelrod, *Gen. Comp. Endocrinol.*, **13,** 201(1969).
(85) B. D. Kulkarni, C. S. Kammer, and J. W. Goldzieher, *ibid.*, **14,** 68(1970).
(86) B. W. O'Malley and A. R. Means, *Science*, **183,** 610(1974).
(87) E. V. Jensen and E. R. DeSombre, *ibid.*, **182,** 126(1973).
(88) I. S. Edelman, *J. Steroid Biochem.*, **6,** 147(1975).
(89) R. G. Smith, C. A. Iramain, V. C. Buttram, and B. O'Malley, *Nature*, **253,** 271(1975).
(90) U. Verma and K. R. Laumas, *Biochim. Biophys. Acta*, **317,** 403(1973).
(91) W. T. Schrader, *Methods Enzymol.*, **36,** 187(1975).
(92) D. Philibert and J. P. Raynaud, *Contraception*, **10,** 457(1974).
(93) J. L. McGuire, C. D. Bariso, and B. S. Fuller, *Acta Endocrinol.*, **75,** 579(1974).
(94) P. C. Young and R. E. Cleary, *J. Clin. Endocrinol. Metab.*, **39,** 425(1974).
(95) D. V. Illingworth, G. P. Wood, G. L. Flickinger, and G. Mikhail, *ibid.*, **40,** 1001(1975).
(96) B. R. Rao, W. G. Wiest, and W. M. Allen, *Endocrinology*, **95,** 1275(1974).
(97) J. L. McGuire and C. DeDella, *ibid.*, **88,** 1099(1971).
(98) P. D. Feil, S. R. Glasser, D. O. Toft, and B. W. O'Malley, *ibid.*, **91,** 738(1972).
(99) W. W. Leavitt and C. J. Grossman, *Proc. Nat. Acad. Sci. USA*, **71,** 4341(1974).
(100) W. T. Schrader, S. H. Socher, and R. E. Buller, *Methods Enzymol.*, **36,** 292(1975).
(101) S. J. Segal, R. Ige, and M. Burgos, in "Physiology and Genetics of Reproduction," Part A, E. M. Coutinho and F. Fuchs, Eds., Plenum, New York, N.Y., 1973, pp. 99–112.
(102) E. Milgrom, M. Luu Thi, and E. E. Baulieu, *Acta Endocrinol., Suppl. 180,* **74,** 380(1973).
(103) M. Haukkamaa and T. Luukkainen, *J. Steroid Biochem.*, **5,** 447(1974).
(104) E. Milgrom, M. Atger, M. Perrot, and E. E. Baulieu, *Endocrinology*, **90,** 1071(1972).
(105) W. W. Leavitt, D. O. Toft, C. A. Strott, and B. W. O'Malley, *ibid.*, **94,** 1041(1974).
(106) D. O. Toft and B. W. O'Malley, *ibid.*, **90,** 1041(1972).
(107) E. Milgrom, M. Luu Thi, M. Atger, and E. E. Baulieu, *J. Biol. Chem.*, **248,** 6366(1973).
(108) K. Pollow, H. Luebbert, E. Boquoi, G. Kreuzer, and B. Pollow, *Endocrinology*, **96,** 319(1975).
(109) K. B. Horwitz, W. L. McGuire, O. H. Pearson, and A. Segaloff, *Science*, **189,** 726(1975).
(110) M. A. Yussman, M. L. Taymor, J. Miyara, and C. Phetteplace, *Fertil. Steril.*, **21,** 119(1970).
(111) U. Goebelsmann, A. R. Midgley, Jr., and R. B. Jaffe, *J. Clin. Endocrinol. Metab.*, **29,** 1222(1969).
(112) K. S. Moghissi, F. N. Syner, and T. N. Evans, *Amer. J. Obstet. Gynecol.*, **114,** 405(1972).
(113) E. Johansson and L. Wide, *Acta Endocrinol.*, **62,** 82(1969).
(114) S. M. McCann, *Amer. J. Physiol.*, **202,** 601(1962).
(115) V. C. Stevens and N. Vorys, *Obstet. Gynecol. Surv.*, **22,** 781(1967).
(116) R. V. Short, *Recent Progr. Horm. Res.*, **20,** 303(1964).
(117) F. C. Hagemenas and G. W. Kittinger, *Endocrinology*, **94,** 922(1974).
(118) L. P. Bengtsson and P. M. Ejarque, *Acta Obstet. Gynecol. Scand.*, **43,** 49(1964).
(119) P. M. Ejarque and L. P. Bengtsson, *Acta Endocrinol.*, **44,** 521(1962).
(120) W. M. Allen, *Gynecol. Invest.*, **5,** 142(1974).
(121) J. W. Everett, *Physiol. Rev.*, **44,** 373(1964).
(122) G. H. Zeilmaker, in "Pharmacology of the Endocrine System and Related Drugs: Progesterone, Progestational Drugs and Antifertility Agents," vol. I, International Encyclopedia of Pharmacology and Therapeutics, sect. 48, M. Tausk, Ed., Pergamon, New York, N.Y., 1971, pp. 331–352.
(123) G. Pincus, "The Control of Fertility," Academic, New York, N.Y., 1965.
(124) M. Sar and W. Stumpf, *Science*, **182,** 1266(1973).
(125) W. L. Herrmann, W. L. Heinrichs, and T. Tabei, *Amer. J. Obstet. Gynecol.*, **117,** 679(1973).
(126) A. Wirz-Justice, E. Hackmann, and M. Lichtsteiner, *J. Neurochem.*, **22,** 187(1974).
(127) E. I. Kohorn and R. Tchao, *J. Endocrinol.*, **45,** 401(1969).
(128) H. Schmidt-Matthiesen, "The Normal Human Endometrium," McGraw-Hill, New York, N.Y., 1963.
(129) H. Schmidt-Matthiesen, in "Pharmacology of the Endocrine System and Related Drugs: Progesterone, Progestational Drugs and Antifertility Agents," vol. I, International Encyclopedia of Pharmacology and Therapeutics, sect. 48, M. Tausk, Ed., Pergamon, New York, N.Y., 1971, pp. 457–486.
(130) A. Franceschelli, *Monit. Obstet. Ginecol. Endocrinol. Metab.*, **34,** 330(1963).
(131) W. Lindenschmidt and T. Zeile, *Zentralbl. Gynaekol.*, **84,** 577(1962).
(132) F. V. Lucas, *Amer. J. Obstet. Gynecol.*, **88,** 965(1964).
(133) W. Luh and H. Brandau, *Z. Geburtshilfe Gynaekol.*, **168,** 14(1967).
(134) A. P. Baker, F. Bergman, and K. G. Paul, *Acta Endocrinol.*, **54,** 696(1967).
(135) L. Bjersing and N. E. Borglin, *Acta Pathol. Microbiol. Scand.*, **60,** 27(1964).
(136) T. H. Brinsfield, H. W. Hawk, and H. F. Righter, *J. Reprod. Fert.*, **8,** 293(1964).
(137) H. W. Hawk, G. D. Turner, and T. H. Brinsfield, *Amer. J. Vet. Res.*, **24,** 595(1963).
(138) J. E. Nellor, *Anat. Rec.*, **151,** 171(1965).
(139) L. P. Bengtsson, in "Pharmacology of the Endocrine System and Related Drugs: Progesterone, Progestational Drugs and Antifertility Agents," vol. I, International Encyclopedia of Pharmacology and Therapeutics, sect. 48, M. Tausk, Ed., Pergamon, New York, N.Y., 1971, pp. 487–517.
(140) A. H. Moawad and L. P. Bengtsson, *Amer. J. Obstet. Gynecol.*, **98,** 1057(1967).
(141) L. P. Bengtsson, *Acta Obstet. Gynecol. Scand., Suppl. 6,*

49, 5(1970).
(142) A. I. Csapo, C. E. R. DeMattos, and M. B. DeSousa Filho, *Amer. J. Obstet. Gynecol.*, **87,** 793(1963).
(143) D. G. Porter and H. R. Behrman, *Nature*, **232,** 627(1971).
(144) A. I. Csapo, O. Pohanka, and H. L. Kaihola, *Brit. Med. J.*, **1,** 137(1974).
(145) J. M. Marshall and A. I. Csapo, *Endocrinology*, **68,** 1026(1961).
(146) A. Lanza, *J. Obstet. Gynaecol. Brit. Commonw.*, **81,** 568(1974).
(147) D. Kumar, P. R. Adams, and A. C. Barnes, *Nature*, **205,** 701(1965).
(148) M. Cohen, *Fertil. Steril.*, **21,** 715(1970).
(149) J. Ferin, in "Pharmacology of the Endocrine System and Related Drugs: Progesterone, Progestational Drugs and Antifertility Agents," vol. I, International Encyclopedia of Pharmacology and Therapeutics, sect. 48, M. Tausk, Ed., Pergamon, New York, N.Y., 1971, pp. 441–456.
(150) G. D. London and P. B. Lawrence, *Fertil. Steril.*, **18,** 1(1967).
(151) E. Kesserii, P. Camacho-Ortega, G. Laudahn, and G. Schöpflin, *ibid.*, **26,** 57(1975).
(152) T. Mann and L. C. Prosser, *Biol. Bull. (Woods Hole, Mass.)*, **125,** 384(1963).
(153) M. Freund, *Bibliogr. Reprod.*, **15,** 1(1970).
(154) M. Bygdeman, *Mem. Soc. Endocrinol.*, **14,** 49(1966).
(155) V. R. Pickles and R. J. Fitzpatrick, "Symposium on Endogenous Substances Affecting the Myometrium," vol. 14, Society for Endocrinology, Cambridge University Press, New York, N.Y., 1966.
(156) V. R. Pickles, W. J. Hall, P. C. Clegg, and T. J. Sullivan, in *ibid.*, p. 89.
(157) C. R. Austin, *Int. J. Fertil.*, **12,** 25(1967).
(158) M. C. Chang, *Endocrinology*, **63,** 619(1958).
(159) R. Deanesly, in "Marshall's Physiology of Reproduction," A. Parkes, Ed., Little, Brown, Boston, Mass., 1966.
(160) A. McLaren, *J. Reprod. Fertil., Suppl.*, **18,** 159(1973).
(161) R. Courrier, *Vitam. Horm. (N.Y.)*, **8,** 179(1950).
(162) G. Mayer, in "Delayed Implantation," A. C. Enders, Ed., University of Chicago Press, Chicago, Ill., 1963, pp. 213–228.
(163) B. Seshadri, Y. Gibor, and A. Scommegna, *Amer. J. Obstet. Gynecol.*, **109,** 536(1971).
(164) A. Scommegna, G. N. Pandya, M. Christ, A. W. Lee, and M. R. Cohen, *Fertil. Steril.*, **21,** 201(1970).
(165) A. Scommegna, *Atti Semin. Int. Sui Problemi Med. Sociale Controllo Fecondito*, **1972,** 161.
(166) G. N. Pandya and A. Scommegna, *Excerpta Med. Found. Int. Congr. Ser. No. 246*, **VII,** 103(1972).
(167) Y. Gibor, *Amer. J. Obstet. Gynecol.*, **109,** 542(1971).
(168) S. A. Tillson, B. B. Pharriss, and J. D. Neill, *J. Steroid Biochem.*, **5,** 376(1974).
(169) S. A. Tillson, M. Marian, R. Hudson, P. Wong, B. Pharriss, R. Aznar, and J. Martinez-Manautou, *Contraception*, **11,** 179(1975).
(170) J. Martinez-Manautou, M. Maqueo, R. Aznar, B. Pharriss, and A. Zaffaroni, *Amer. J. Obstet. Gynecol.*, **121,** 175(1975).
(171) M. C. Chang, *Endocrinology*, **81,** 1251(1967).
(172) M. Roland, *Bull. N. Y. Acad. Med.*, **45,** 681(1969).
(173) A. Rosado, J. J. Hicks, R. Aznar, and E. Mercado, *Contraception*, **9,** 39(1974).
(174) International Academy of Gynecological Cytology, *Acta Cytol.*, **3,** 197(1959).
(175) *Ibid.*, **4,** 221(1960).
(176) G. Jones and E. B. Astwood, *Endocrinology*, **30,** 295(1942).
(177) J. Ferin, J. Bonte, and J. Vassilopoulos, *Bull. Soc. R. Belge Gynecol. Obstet.*, **25,** 265(1955).
(178) G. K. Benson, A. T. Cowie, C. P. Cox, and S. A. Goldzveig, *J. Endocrinol.*, **15,** 126(1957).
(179) J. Hilgers, in "Pharmacology of the Endocrine System and Related Drugs: Progesterone, Progestational Drugs and Antifertility Agents," vol. I, International Encyclopedia of Pharmacology and Therapeutics, sect. 48, M. Tausk, Ed., Pergamon, New York, N.Y., 1971, pp. 83–101.
(180) H. Selye, *Proc. Soc. Exp. Biol. Med.*, **43,** 343(1940).
(181) C. G. Hartman and H. Speert, *Endocrinology*, **29,** 639(1941).
(182) D. G. Hall, M. S. Fahim, Z. Fahim, R. Der, and G. Dement, *J. Reprod. Med.*, **6,** 116(1971).
(183) C. S. Song and A. Kappas, *Vitam. Horm. (N.Y.)*, **26,** 147(1968).
(184) A. Kappas and R. H. Palmer, *Pharmacol. Rev.*, **15,** 123(1963).
(185) M. Kramer, L. Damrosch, and G. Klink, in "Die Gestagene, Handbook of Experimental Pharmacology," vol. XXII/I, K. Junkmann, Ed., Springer-Verlag, New York, N.Y., 1968, p. 512.
(186) C. A. De Groot, M. T. van der Lely, and R. Kooij, *Brit. J. Dermatol.*, **77,** 617(1965).
(187) C. H. Sawyer, M. Kawakami, and S. Kanematsu, *Res. Publ., Ass. Nerv. Ment. Dis.*, **43,** 59(1966).
(188) M. Tausk and J. De Visser, in "Pharmacology of the Endocrine System and Related Drugs: Progesterone, Progestational Drugs and Antifertility Agents," vol. I, International Encyclopedia of Pharmacology and Therapeutics, sect. 48, M. Tausk, Ed., Pergamon, New York, N.Y., 1971, pp. 375–387.
(189) D. A. Hamburg, *Res. Publ. Ass. Nerv. Ment. Dis.*, **43,** 251(1966).
(190) B. C. Little, R. J. Matta, and T. Zahn, *J. Nerv. Ment. Dis.*, **159,** 256(1974).
(191) F. T. Melges, *Psychosom. Med.*, **30,** 95(1968).
(192) K. Kyger and B. Webb, *Amer. J. Obstet. Gynecol.*, **113,**759(1972).
(193) M. T. Epstein, J. M. Hockaday, and T. D. R. Hockaday, *Lancet*, **1,** 543(1975).
(194) H. Selye, *J. Pharmacol.*, **73,** 127(1941).
(195) H. Selye, *Endocrinology*, **30,** 437(1942).
(196) F. Navratil-Brunel, thesis, Montpellier, France, 1967.
(197) K. H. Raisinghani, R. I. Dorfman, E. Forchielli, L. Gyermek, and G. Genther, *Acta Endocrinol.*, **57,** 395(1968).
(198) S. K. Figdor, M. J. Kodet, B. M. Bloom, E. J. Agnello, S. Y. Pan, and G. D. Laubach, *J. Pharmacol.*, **119,** 299(1957).
(199) W. Merryman, R. Boiman, L. Barnes, and J. Rothchild, *J. Clin. Endocrinol. Metab.*, **14,** 1567(1954).
(200) D. E. Wooley and P. S. Timiras, *Endocrinology*, **70,** 196(1962).
(201) J. Laidlaw, *Lancet*, **2,** 1235(1956).
(202) F. Morrell, *Neurology*, **9,** 352(1959).
(203) E. D. B. Johansson, U. Larsson-Cohn, and C. Gemzell, *Amer. J. Obstet. Gynecol.*, **113,** 933(1972).
(204) J. Klein, *Geburtshilfe Frauenheilkd.*, **11,** 418(1951).
(205) J. Rothchild and A. Barnes, *Endocrinology*, **50,** 485(1952).
(206) M. E. Freeman, J. K. Crissman, Jr., G. N. Louw, R. L. Butcher, and E. K. Inskeep, *ibid.*, **86,** 717(1970).
(207) J. G. Armstrong, *Proc. Soc. Exp. Biol. Med.*, **102,** 452(1959).
(208) J. Genest, W. Nowaczynski, E. Koiw, T. Sandor, and P. Biron, in "Essential Hypertension," K. D. Block and P. Cottier Eds., Springer-Verlag, Berlin, Germany, 1960 (English Edition, 1962), pp. 126–146.
(209) L. De Soldati, I. E. De Fortega, C. R. Pellegatta, and H. Cammarota, *Cardiologia*, **48,** 489(1966).
(210) D. F. Horrobin, *Lancet*, **1,** 1390(1972).
(211) G. Telegdy and K. Lissák, *Acta Physiol. Acad. Sci. Hung.*, **26,** 313(1965).
(212) R. J. Weir, *Lancet*, **1,** 467(1971).
(213) J. S. Noumoff, T. Schoendorf, W. Theiss, and F. K. Beller, *J. Reprod. Med.*, **9,** 55(1972).
(214) R. Silberberg and M. Silberberg, *Exp. Med. Surg.*, **23,** 157(1965).
(215) K. Masuda, *Nichidai Igaku Zasshi*, **19,** 3813(1960).
(216) S. K. Bhatia, D. Moore, and R. Kalkhoff, *J. Clin. Endocrinol. Metab.*, **35,** 364(1972).
(217) D. W. Bullock and B. Cook, *J. Endocrinol.*, **37,** 382(1967).
(218) A. D. Dewar, *J. Reprod. Fertil., Suppl.*, **9,** 17(1969).
(219) G. Bourdel and R. Jacquot, *Arch. Sci. Physiol.*, **19,** 99(1965).
(220) E. Hervey and G. R. Hervey, *J. Endocrinol.*, **37,** 361(1967).
(221) E. Hervey, G. R. Hervey, and P. M. Zamboanga, "Second International Congress on Hormonal Steroids," Excerpta Medica Foundation, Amsterdam, The Netherlands, 1966, p. 190.
(222) M. Tausk and J. De Visser, in "Pharmacology of the Endocrine System and Related Drugs: Progesterone, Progestational Drugs and Antifertility Agents," vol. I, International Encyclopedia

of Pharmacology and Therapeutics, sect. 48, M. Tausk, Ed., Pergamon, New York, N.Y., 1971, pp. 361–366.
(223) R. L. Landau and K. Lugibihl, in "Recent Progress in Hormone Research," vol. XVII, G. Pincus, Ed., Academic, New York, N.Y., 1961, pp. 249–281.
(224) R. S. Rivlin, *N. Engl. J. Med.*, **292,** 26(1975).
(225) W. Yotis and R. Stanke, *J. Bacteriol.*, **92,** 1285(1966).
(226) S. A. Morse and T. J. Fitzgerald, *Infect. Immunol.*, **10,** 1370(1974).
(227) M. Ciavatti, G. Michel, B. Chataing, and A. Jouvenceux, *Biochem. Med.*, **9,** 293(1974).
(228) M. L. Koch, *Amer. J. Obstet. Gynecol.*, **59,** 168(1950).
(229) M. Kramer, L. Damrosch, and G. Klink, in "Die Gestagene, Handbook of Experimental Pharmacology," vol. XXII/I, K. Junkmann, Ed., Springer-Verlag, New York, N.Y., 1968, pp. 597–679.
(230) A. Lipschütz, *J. Amer. Med. Ass.*, **120,** 171(1942).
(231) A. Segaloff, *Cancer Res.*, **33,** 1136(1973).
(232) K. A. Karande and K. J. Ranadive, *Brit. J. Cancer,* **28,** 299(1973).
(233) S. Reboud and G. Pageaut, *Nature,* **241,** 398(1973).
(234) S. Blanzat-Reboud and A. Russfield, *Amer. J. Obstet. Gynecol.*, **103,** 46(1969).
(235) W. E. Poel and H. Haran-Ghera, *Lancet,* **2,** 970(1963).
(236) W. E. Poel, *Brit. J. Cancer,* **19,** 824(1965).
(237) A. G. Jabara and A. G. Harcourt, *Pathology,* **2,** 115(1970).
(238) A. G. Jabara and J. S. Maritz, *Brit. J. Cancer,* **28,** 161(1973).
(239) G. S. Kledzik, C. J. Bradley, and J. Meites, *Cancer Res.*, **34,** 2953(1974).
(240) A. Jabara, P. H. Toyne, and A. G. Harcourt, *Brit. J. Cancer,* **27,** 63(1973).
(241) W. Wentz, *Obstet. Gynecol.*, **24,** 370(1964).
(242) J. B. Bonte, *Acta Obstet. Gynecol. Scand., Suppl. 19,* **51,** 21(1972).
(243) G. Malkasian, D. G. Decker, E. Mussey, and C. E. Johnson, *Amer. J. Obstet. Gynecol.*, **110,** 15(1971).
(244) J. G. Peck and D. A. Boyes, *ibid.*, **103,** 90(1969).
(245) J. A. Collins and D. M. Jewkes, *ibid.*, **120,** 779(1974).
(246) B. A. Stoll, *Clin. Obstet. Gynecol.*, **16** (4), 130(1973).
(247) M. Roland, "Progestogen Therapy," Charles C Thomas, Springfield, Ill., 1965.
(248) S. L. Israel, "Diagnosis and Treatment of Menstrual Disorders and Sterility," 5th ed., Harper and Row, New York, N.Y., 1967, pp. 214–216.
(249) L. Wilkins, *J. Amer. Med. Ass.*, **172,** 1028(1960).
(250) A. H. Nora and J. J. Nora, *Arch. Environ. Health,* **30,** 17(1975).
(251) L. G. Crowley and S. A. Duwe, *Calif. Med.*, **110,** 139(1969).
(252) S. B. Gusberg, *Obstet. Gynecol.*, **30,** 287(1967).
(253) R. M. Kelley and W. H. Baker, *Cancer Res.*, **25,** 1190(1965).
(254) D. Gordon, B. N. Horwitt, A. Segaloff, P. Murison, and J. V. Schlosser, *Cancer,* **5,** 275(1952).
(255) B. M. Sherman and S. G. Korenman, *ibid.*, **33,** 1306(1974).
(256) R. Hertz, *J. Amer. Med. Ass.*, **154,** 1114(1954).
(257) R. Hertz, J. K. Cramer, J. P. Young, and B. B. Westfall, *J. Nat. Cancer Inst.*, **11,** 867(1951).
(258) A. L. Herbst, S. J. Robboy, G. J. McDonald, and R. E. Scully, *Amer. J. Obstet. Gynecol.*, **118,** 607(1974).
(259) C. H. Hendricks, W. E. Brenner, R. A. Gabel, and T. Kerenyi, in "Brook Lodge Symposium on Progesterone," A. C. Barnes, Ed., Pergamon, New York, N.Y., 1961, pp. 53–64.
(260) S. J. Nillius and E. D. Johansson, *Amer. J. Obstet. Gynecol.*, **110,** 470(1971).
(261) J. E. Seidl, J. A. Epstein, and H. S. Kupperman, *Int. J. Fertil.*, **3,** 349(1958).
(262) P. H. Berczeller, I. S. Young, and H. S. Kupperman, *Clin. Pharmacol. Ther.*, **5,** 216(1964).
(263) G. Pincus, *Vitam. Horm. (N.Y.)*, **17,** 307(1959).
(264) I. Rothchild, *J. Clin. Endocrinol. Metab.*, **17,** 754(1957).
(265) C. A. Paulsen, D. J. Moore, R. T. Roscoe, and C. G. Heller, *Acta Endocrinol., Suppl.*, **51,** 203(1960).
(266) A. Zaffaroni, *Acta Endocrinol., Suppl. 185,* **75,** 423(1974).
(267) B. B. Pharriss, R. Erickson, J. Bashaw, S. Hoff, V. A. Place, and A. Zaffaroni, *Fertil. Steril.*, **25,** 915(1974).
(268) E. I. Kohorn and R. Tchao, *J. Obstet. Gynaecol. Brit. Commonw.*, **75,** 1262(1968).
(269) D. Perlman, N. H. Guiffre, S. A. Brindle, and S. C. Pan, *Proc. Soc. Exp. Biol. Med.*, **111,** 623(1962).
(270) S. Biswas, J. D. Macdougall, and R. P. Cook, *Brit. J. Exp. Pathol.*, **45,** 13(1964).
(271) W. J. Rappoport, B. Goldstein, and A. L. Haskings, *Obstet. Gynecol.*, **9,** 497(1957).
(272) W. S. Spector, "Handbook of Toxicology," vol. I, Saunders, Philadelphia, Pa., 1956, p. 246.
(273) H. W. Rudel and F. A. Kincl, in "Pharmacology of the Endocrine System and Related Drugs: Progesterone, Progestational Drugs and Antifertility Agents," vol. I, International Encyclopedia of Pharmacology and Therapeutics, sect. 48, M. Tausk, Ed., Pergamon, New York, N.Y., 1971, pp. 405–409.
(274) Z. Dickmann, *Fertil. Steril.*, **21,** 541(1970).
(275) W. K. Whitten, *J. Endocrinol.*, **16,** 80(1957).
(276) M. C. Allen and R. H. Foote, *Fertil. Steril.*, **24,** 220(1973).
(277) J. C. Daniel and J. D. Levy, *J. Reprod. Fertil.*, **7,** 323(1964).
(278) H. C. Moore, *Acta Endocrinol., Suppl.*, **51,** 911(1960).
(279) H. C. Moore, *J. Obstet. Gynaecol. Brit. Commonw.*, **68,** 570(1961).
(280) H. G. Spies, D. R. Zimmerman, H. L. Self, and L. E. Casida, *J. Anim. Sci.*, **18,** 163(1959).
(281) P. H. Sammelwitz, P. J. Dziuk, and A. V. Nabandov, *ibid.*, **15,** 1211(1956).
(282) G. Carpent and L. Desclin, *Endocrinology,* **84,** 315(1969).
(283) G. Carpent and L. Desclin, *C. R. Acad. Sci., Ser. D,* **264,** 2933(1967).
(284) R. Mey, *Geburtshilfe Frauenheilkd.*, **23,** 615(1963).
(285) G. K. Suchowsky and K. Junkmann, *Endocrinology,* **68,** 341(1961).
(286) L. Wilkins, H. W. Jones, G. H. Holman, and R. S. Stempfel, Jr., *J. Clin. Endocrinol. Metab.*, **18,** 559(1958).
(287) S. Hagler, A. Schultz, H. Hankin, and R. H. Kunstadter, *Amer. J. Dis. Child.*, **106,** 586(1963).
(288) D. Aarskog, *Birth Defects,* **7,** 122(1971).
(289) E. P. Levy, *Lancet,* **1,** 611(1973).
(290) I. Gal, *Nature,* **240,** 241(1972).
(291) L. E. Sever, *ibid.*, **242,** 410(1973).
(292) R. L. Kaufman, *Lancet,* **1,** 1396(1973).
(293) J. J. Nora and A. H. Nora, *ibid.*, **1,** 941(1973).
(294) D. T. Janerich, J. M. Piper, and D. M. Glebatis, *N. Engl. J. Med.*, **291,** 697(1974).
(295) A. Jost, *Clin. Pharmacol. Ther.*, **14,** 714(1973).
(296) J. L. Marx, *Science,* **180,** 174(1973).
(297) F. A. Kincl and M. Maqueo, *Endocrinology,* **77,** 859(1965).
(298) D. A. Karnofsky, P. J. Hamre, and G. Hysom, *Proc. Soc. Exp. Biol. Med.*, **79,** 641(1952).
(299) T. V. Purandare, S. R. Munshi, and S. S. Rao, *J. Reprod. Fertil.*, **38,** 247(1974).

ACKNOWLEDGMENTS AND ADDRESSES

Received from *Alza Corporation, Palo Alto, CA 94304*
The authors thank Dr. V. Place and Dr. B. Pharriss for their careful study of the manuscript, and B. Klompus and C. Record for their valuable assistance.
[x] To whom inquiries should be directed.

Comparison of Several Molecular Topological Indexes with Molecular Surface Area in Aqueous Solubility Estimation

G. L. AMIDON ˣ and S. T. ANIK

Abstract □ The molecular topological indexes proposed by Wiener (Wiener number), Hosoya (*Z*-value), and Randic (branching index) were correlated with computed molecular surface areas and aqueous solubilities for the monofunctional aliphatic alcohols, ethers, ketones, aldehydes, carboxylic acids, esters, and hydrocarbons. Comparison of the indexes with molecular surface area indicates that all three indexes (or simple modifications) correlate with molecular surface area and, although computed in different manners, reflect molecular topology. Comparison of the correlations of log solubility with the several indexes leads to the following conclusions: (*a*) the branching index works well for aliphatic, acyclic monofunctional compounds but not cyclic aliphatic compounds; (*b*) the square root of the Wiener number correlates less satisfactorily with log solubility than the other indexes but more correctly handles cyclic compounds (when generalized after Hosoya); (*c*) correlations of log solubility with the log *Z*-value are satisfactory, but the index is difficult to compute; and (*d*) the molecular surface area represents the single best parameter with which to correlate and estimate aqueous solubility due to its generality. However, for a restricted series of compounds, the branching index is perhaps the most useful index by virtue of its simplicity.

Keyphrases □ Topological indexes—Wiener number, *Z*-value, and branching (connectivity) index compared, correlated with molecular surface areas and aqueous solubilities, various monofunctional compounds □ Solubility, aqueous—correlated with topological indexes, various monofunctional compounds □ Wiener number—correlated with other topological indexes, molecular surface areas, and aqueous solubilities, various monofunctional compounds □ *Z*-value—correlated with other topological indexes, molecular surface areas, and aqueous solubilities, various monofunctional compounds □ Molecular connectivity—correlated with other topological indexes, molecular surface areas, and aqueous solubilities, various monofunctional compounds

The development of atomic and group "constants" that may be used in estimating the physical, chemical, and biological properties of organic compounds has been the subject of considerable research. The interest in such parameters results from the need or desire to estimate the properties of compounds that are unknown or for which the required experimental data are lacking. Examples of such parameters and approaches are numerous (1–11).

Approaches to the determination of the atomic or group parameters may be divided into two groups:

1. Those that directly reduce the molecular or bulk property to atomic contributions (*e.g.*, parachor, polarizability, refractive index, and partition coefficient).
2. Those that try to correlate the molecular or bulk property with an index computed from molecular structure (*e.g.*, correlations with computed surface areas and Wiener number).

An alternative approach, which does not necessarily imply an assumed additivity of the molecular and bulk properties from atomic contributions, is the correlation of one property with another (*e.g.*, partition coefficient with solubility and solubility with solubility parameter). There is probably no "best" parameter or approach due to the generally inevitable trade off between simplicity and accuracy. However, from an accuracy point of view, correlations between closely related physical properties are perhaps the best but require experimental data for at least one physical property.

Approaches 1 and 2 have the potential (and very de-

Table I—Summary of −Log Solubility (Molal), Total Surface Area (TSA), Wiener Number (*W*), Log *W*, *Z*-Value (*Z*), Log *Z*, and Branching Index (*B*) for Saturated Hydrocarbons

Compound	Structure	−Log Solubility	TSA, Å²	*W*	$\sqrt{W}$	*Z*[a]	Log *Z*	*B*
Methane		—	152.2	—	—	1	0	0
Ethane	—	—	191.7	1	1	2	0.301	1.000
Propane		—	223.5	4	2	3	0.477	1.414
n-Butane		2.63	255.2	10	3.16	5	0.699	1.914
Isobutane		2.55	249.1	6	2.45	4	0.602	1.732
n-Pentane		3.27	287.0	20	4.47	8	0.903	2.414
2-Methylbutane		3.18	274.6	18	4.24	7	0.845	2.270
Neopentane		3.13	270.1	12	3.46	5	0.699	2.000

(*continued*)

Table I—(*Continued*)

Compound	Structure	−Log Solubility	TSA, Å²	*W*	$\sqrt{W}$	*Z*[a]	Log *Z*	*B*
Cyclopentane		2.65	—	15	3.87	11	1.04	2.500
n-Hexane		3.95	319	35	5.92	13	1.11	2.914
3-Methylpentane		3.83	300.1	31	5.57	12	1.08	2.808
2,2-Dimethylbutane		3.67	290.8	26	5.10	9	0.954	2.561
Cyclohexane		3.18	279.1	27	5.20	18	1.26	3.000
n-Heptane		4.53	351	56	7.48	21	1.32	3.414
2,4-Dimethylpentane		4.39	324.7	48	6.93	15	1.18	3.126
(*e*)-Methylcyclohexane		3.85	304.9	42	6.48	26	1.41	3.394
Cycloheptane		3.52	301.9	42	6.48	29	1.46	3.500
n-Octane	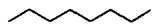	5.24	383	84	9.17	34	1.53	3.914
1-*cis*-2-Dimethylcyclohexane		4.26	315.5	60	7.75	39	1.59	3.805
Cyclooctane		4.15	322.6	64	8.00	47	1.67	4.000
2,2,4-Trimethylpentane		4.13	338.9	66	8.12	19	1.28	3.417

[a] Most tabulated values are from the compilation in Refs. 6 and 7; remaining values were computed from definitions (see text).

sirable) capability of estimating the physical properties of unknown compounds and, therefore, have a great attraction for "design" programs. Although they are generally limited by the additivity assumption, the nonadditivity can be at least partially accounted for by relaxing the atomic additivity to a group additivity; however, this approach causes an increase in the number of parameters required for estimation as well as a reduction in the generality and the ease of computation.

This report centers on the second approach since it was shown previously (10) that, at least in the case of molecular surface area correlations, it leads to a natural reduction in the number of parameters required for the estimation of aqueous solubilities. Molecular surface area, the Wiener number (*W*), Hosoya's *Z*-value (*Z*), and Randic's branching index (*B*) will be considered with the objective of assessing the value and limitations of the various approaches with respect to solubility estimation.

COMPUTATION OF TOPOLOGICAL INDEXES

Molecular Surface Area—Molecular surface areas were computed using the method developed by Hermann (9). An alternative method for estimating numbers related to molecular surface areas was employed by Harris *et al.* (12). This method has the advantage of not involving numerical computations but has the disadvantage of not allowing precise determination of the functional group surface areas[1].

Wiener Number—The Wiener number (*W*), called the path number by Wiener (3, 4), is defined as the sum of the distances between all pairs of carbon atoms in the molecule in terms of carbon–carbon bonds. It is computed by multiplying the number of carbon atoms on one side of any bond by the number on the other side of the bond and summing these values for all bonds. For example, for 3-ethylpentane, $W = 48$:

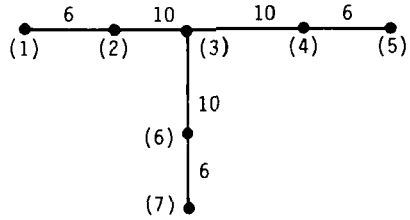

An alternative method of calculation of the Wiener number, suggested by Hosoya (6) and convenient for generalizing *W* to cyclic compounds, is to take *W* as one-half of the sum of the elements of the distance matrix, *D*, whose element d_{ij} is the number of bonds for the shortest path between atoms *i* and *j* with $d_{ii} = 0$. For this example, $W = 96/2 = 48$:

atom number	1	2	3	4	5	6	7	row sum
1	0	1	2	3	4	3	4	17
2	1	0	1	2	3	2	3	12
3	2	1	0	1	2	1	2	9
4	3	2	1	0	1	2	3	12
5	4	3	2	1	0	3	4	17
6	3	2	1	2	3	0	1	12
7	4	3	2	3	4	1	0	17
							total	96

Z-Values—The topological index, *Z*, was defined by Hosoya (6, 7) as follows. Let $p(k)$ be the number of ways in which *k* bonds can be chosen from a given molecule (or graph, *G*) such that no two of them are connected. Then:

$$Z = \sum_{i=0}^{N} p(i) \qquad \text{(Eq. 1)}$$

with $p(0) = 1$ and $p(1)$ = number of bonds, *N*. This example gives $p(0)$

[1] An additional problem associated with the use of the numbers reported by Harris *et al.* (12) is that the conformations considered were not specified. Some type of averaging over possible conformations for a given compound was indicated but not precisely stated.

Table II—Normalized Solubility and Indexes

Compound	Structure	Log Solubility	−Normalized Log Solubility	Normalized TSA	Normalized W	Normalized $\sqrt{W}$	Normalized Z	Normalized Log Z	Normalized B
Methane		—	1.00	1	—	—	1	1	—
Ethane		—	2.00	2	2	2	2	2	2
Propane		—	3.00	3	3	3	3	3	3
n-Butane		−2.63	4.00	4	4	4	4	4	4
Isobutane		−2.55	3.88	3.90	2.4	3.1	3.2	3.44	3.62
n-Pentane		−3.27	5.00	5	5	5	5	5	5
2-Methylbutane		−3.18	4.86	4.78	4.5	4.74	4.38	4.68	4.70
Neopentane		−3.13	4.79	4.71	3.0	3.87	3.13	3.87	4.14
Cyclopentane		−2.65	4.05	—	3.75	4.33	6.88	5.76	5.18
n-Hexane	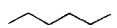	−3.95	−6.00	6	6	6	6	6	6
3-Methylpentane		−3.83	5.82	5.64	5.31	5.65	5.54	5.83	5.78
2,2-Dimethylbutane		−3.67	5.57	5.47	4.46	5.17	4.15	5.16	5.27
Cyclohexane	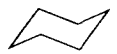	−3.18	4.83	5.25	4.63	5.27	8.31	6.8	6.18
n-Heptane	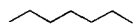	−4.53	7.00	7	7	7	7	7	7
2,4-Dimethylpentane		−4.39	6.78	6.48	6.0	6.49	5.0	6.26	6.41
Methylcyclohexane		−3.85	5.95	6.08	5.25	6.06	8.67	7.48	6.96
Cycloheptane		−3.52	5.44	6.02	5.25	6.06	9.67	7.74	7.18
n-Octane		−5.24	8.00	8	8	8	8	8	8
1-*cis*-2-Dimethylcyclohexane		−4.26	6.50	6.59	5.71	6.76	9.18	8.31	7.78
Cyclooctane		−4.15	6.34	6.74	6.10	6.97	11.06	8.73	8.18
2,2,4-Trimethylpentane		−4.13	6.31	7.08	6.29	7.08	4.47	6.69	6.98

[a]These values were computed using Eq. 4.

Table III—Results of Regression Analysis of Normalized Log Aqueous Solubility *versus* the Normalized Indexes for (*a*) Cyclic and Acyclic Hydrocarbons and (*b*) Acyclic Hydrocarbons Alone: Model N Log (Solubility) = $\theta_0 + \theta_1$ (N Index)

Index	θ_1	θ_0	r	s
		Acyclic and Cyclic		
NTSA	0.934	0.287	0.968	0.281
$N\overline{W}$	0.730	1.90	0.924	0.428
$N\sqrt{W}$	0.781	1.25	0.944	0.371
NZ	0.215	4.36	0.487	0.978
N log Z	0.504	2.60	0.755	0.734
NB	0.636	1.85	0.840	0.609
		Acyclic		
NTSA	0.946	0.304	0.980	0.262
$N\overline{W}$	0.714	1.98	0.932	0.471
$N\sqrt{W}$	0.811	1.20	0.965	0.343
NZ	0.720	2.08	0.848	0.688
N log Z	0.870	0.890	0.972	0.306
NB	0.887	0.722	0.975	0.288

= 1, $p(1) = 6$, $p(2) = 9$, $p(3) = 4$, and $p(i > 3) = 0$, which gives $Z = 20$. The Z-values for the various hydrocarbons considered in this study were taken directly from Ref. 6.

Branching Index[2]—The branching index, B, is defined (11) as follows. Assign to each (nonhydrogen) atom a value of $1/\sqrt{\nu}$, where ν is the number of nonhydrogen (*i.e.*, non-CH) bonds in which the atom is involved. The bond or edge index is given by the product of the values associated with the terminal atoms of that particular bond. Thus:

$$B = \sum_{\text{all bonds}} 1/\sqrt{\nu_i \nu_j} \qquad \text{(Eq. 2)}$$

and for example:

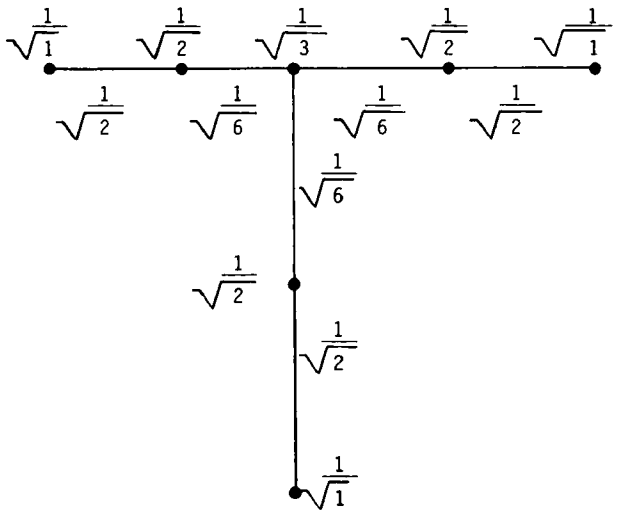

$$B = 3\left(\frac{1}{\sqrt{2}}\right) + 3\left(\frac{1}{\sqrt{6}}\right) = 3.3461 \qquad \text{(Eq. 3)}$$

RESULTS AND DISCUSSION

Comparison of Indexes—Table I presents log aqueous solubility, computed total surface areas (TSA) (with a solvent radius of 1.5 Å), W, $\sqrt{W}$, Z, log Z, and B for various hydrocarbons. Several observations can be made on inspection of Table I. First, while TSA and B increase linearly with chain length, W and Z do not. However, $\sqrt{W}$ and log Z increase in a nearly linear manner with chain length. Second, TSA and W decrease on cyclization, while Z and B increase. These trends suggest that $\sqrt{W}$ and log Z should be considered for correlation purposes and that Z (and log Z) and B will not satisfactorily treat both acyclic and cyclic compounds without a modification in their definitions.

Table IV—Atoms Contributing to Functional Group Terms

Compounds	Functional Group
Alcohols	R–(O-H)
Ethers	R–(O)–R′
Ketones, aldehydes	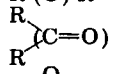
Acids, esters	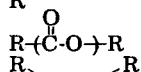
Olefins	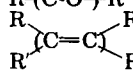

For more detailed comparison, it is convenient to normalize the data in Table I. Each entry in Table I has been normalized in the following manner:

$$\text{normalized property or index} = N\left\{\frac{\text{property or index for the compound}}{\text{property or index for the corresponding normal compound}}\right\} \qquad \text{(Eq. 4)}$$

where N is the number of nonhydrogen atoms (recorded in Table II). This normalization linearizes all indexes with chain length and allows direct comparisons to be made with respect to the effect of branching on the index. The general trends in the table can be illustrated by considering the six carbon isomers. By comparing the normalized indexes with the normalized solubilities, it is observed that the TSA and B indexes more closely reproduce the solubility trends while W and Z exhibit far too dramatic decreases with branching. Log Z and $\sqrt{W}$ are considerably better in this respect. Again, only TSA and W, or $\sqrt{W}$, correctly reproduce the trend for cyclic compounds.

Table III presents the results of a regression analysis using normalized solubilities and indexes. A theoretically perfect index, in addition to giving good r and s values, would have a slope of 1.0 (θ_1 in Table III), ignoring experimental error. From the table, it is clear that, for all compounds, the TSA parameter correlates best. When restricting attention to acyclic compounds, it is observed that TSA, $\sqrt{W}$, log Z, and B all work reasonably well. In making a decision as to the "best" index, the following considerations apply. The $\sqrt{W}$ is somewhat less satisfactory overall but is relatively easy to compute and handles cyclic compounds more correctly. Log Z is reasonably good but difficult to compute and incorrectly treats cyclic compounds; B and TSA are about equally good for acyclic compounds, while TSA is definitely superior overall but requires rather involved numerical computations[3].

Branching Index *versus* Surface Area—From the preceding analysis, it appears that the surface area and the branching index methods represent the most promising approaches, one from the point of view of generality and the other from the point of view of simplicity. These two approaches will now be compared for their ability to correlate with aqueous solubilities using monofunctional aliphatic compounds. Cyclic compounds are omitted from the data sets since, as noted previously, the branching index, as presently defined, does not adequately treat ring structures[4].

In the subsequent analysis, the computed indexes are used directly rather than the normalized values. The solubility data and the treatment of functional groups using the TSA index are the same as in previous studies (10, 15). For the branching index, the edge or bond values is divided by one-half and assigned to atoms. The index for a given atom is just one-half the sum of the incident edge or bond values. For example, on 3-methyl-1-butanol:

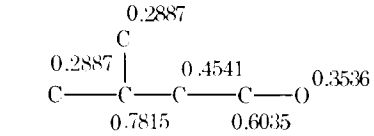

[2] Kier *et al.* (13) referred to B as the connectivity index and gave it the symbol χ.

[3] However, an easily executable computer program is available (14).

[4] See, however, Ref. 13.

Table V—Regression Analysis Model[a]: Log Solubility = θ_1HYB + θ_2 FGB + θ_3 FGI + θ_0 for Acyclic Monofunctional Compounds

Compounds[b]	θ_1[c]	θ_2[c]	θ_3[c]	θ_0[c]	r	s
Hydrocarbons (12)	−1.15 (0.08)	0	0	−0.59 (0.23)	0.976	0.182
Alcohols (83)	−1.16 (0.02)	−4.5 (0.34)	4.5 (0.11)	−0.57 (0.05)	0.996	0.118
Ethers (39)	−1.25 (0.04)	−2.7 (0.49)	3.9 (0.26)	−0.34 (0.12)	0.997	0.135
Ketones, aldehydes (47)	−1.15 (0.04)	0.5 (0.46)	1.9 (0.33)	−0.59 (0.11)	0.994	0.171
Esters (69)	−0.98 (0.02)	0.5 (0.32)	1.4 (0.37)	−1.05 (0.07)	0.994	0.151
Acids (23)	−1.16 (0.05)	−2.0 (2.2)	4.0 (2.2)	−0.56 (0.13)	0.996	0.185
Olefins (22)	−1.20 (0.05)	−0.7 (0.53)	−0.1 (0.35)	−0.47 (0.15)	0.989	0.157

[a] HYB = hydrocarbon branching index, FGB = functional group branching index, and FGI = functional group index. [b] Value in parenthesis is the number of data points. Data sets for the monofunctional compounds included the 12 hydrocarbons. [c] Value in parenthesis is the standard error.

Table VI—Regression Model[a]: Log Solubility = θ_1 HYSA + θ_2FGSA + θ_3FGI + θ_0 for Acyclic Monofunctional Compounds

Compounds[b]	θ_1[c]	θ_2[c]	θ_3[c]	θ_0[c]	r	s
Hydrocarbons (12)	−0.0193 (0.0013)	0	0	2.1 (0.38)	0.980	0.169
Alcohols (83)	−0.0187 (0.0003)	−0.023 (0.002)	3.4 (0.11)	2.0 (0.12)	0.991	0.177
Ethers (39)	−0.0201 (0.0006)	−0.060 (0.007)	3.44 (0.09)	2.4 (0.19)	0.997	0.124
Ketones, aldehydes (47)	−0.0185 (0.0005)	−0.034 (0.003)	3.6 (0.12)	1.9 (0.17)	0.995	0.157
Esters (69)	−0.0164 (0.0004)	−0.029 (0.003)	3.6 (0.14)	1.3 (0.15)	0.991	0.188
Acids (23)	−0.0195 (0.0008)	−0.036 (0.007)	4.3 (0.50)	2.2 (0.25)	0.997	0.167
Olefins (22)	−0.0199 (0.0009)	−0.021 (0.010)	0.5 (3.5)	2.3 (0.27)	0.988	0.163

[a] HYSA = hydrocarbon surface area, FGSA = functional group surface area, and FGI = functional group index. [b] Value in parenthesis is the number of data points. Data sets for the monofunctional compounds included the 12 hydrocarbons. [c] Value in parenthesis is the standard error.

and B = 2.7701. The value of 0.3536 can now be identified with the functional group, and a value of 2.4165 can be given to the hydrocarbon part of the molecule. Functional group indexes (FGI) and hydrocarbon indexes (HYI) were computed for all monofunctional compounds in this manner. Table IV shows the atoms considered as contributing to the functional group. The results of regression analysis are presented in Table V, and the corresponding results using molecular surface area are listed in Table VI (15). These data indicate that the branching index and surface area approaches are about equally successful, with perhaps some preference given to the branching index.

A discussion of the various terms in these regression equations is essentially the same as that for surface area (15). However, one point to be noted is the low value for the FGI coefficient for ketones, aldehydes, and esters. This is a result of treating the double bond (*e.g.*, $R_1R_2C{=}O$) as contributing two edges to each vertex. If the homomorph approach (15) is chosen and the index is computed using a hydrocarbon with the same number of nonhydrogen atoms, the FGI coefficients become very similar to those values using the surface area approach.

Another point is the high standard error associated with the FGI and FGB coefficients of the fatty acids in Table V. This is a result of the high correlation between these two parameters (due to the fact the FGB is almost a constant in this series). Removing, for example, the FGB term gives essentially the same r and s values as are given in Table V and low standard errors for the remaining parameters.

From a practical point of view, the branching index is very appealing. When studies are restricted, for example, to a homologous series of aliphatic substituents, the index provides effective carbon numbers that may be used in correlations (Table II). Its simplicity, however, is a disadvantage relative to surface area on at least three counts: (*a*) its inadequate treatment of cyclic compounds, (*b*) its insensitivity to conformational and stereochemical differences, and (*c*) its inability to treat hydrophobic (intra- and intermolecular) association. A molecule that might typify all of these problems is cholesterol. The branching index would give a single value for this molecule, while its physical properties would depend markedly on the conformational and stereochemical disposition of its atoms and perhaps on intramolecular hydrophobic association (15).

If an index is to account for these effects, it must consider distances between nonbonded atoms. There is no doubt that the branching index could be modified and extended by adding additional factors and extending its definition[5]. However, care must be taken not to lose its attractive simplicity.

SUMMARY AND CONCLUSIONS

The results of these studies indicate that all of the indexes considered can be used (or easily modified) to give reasonable results. However, the parameters of choice would probably be surface area for its generality and the branching index for its simplicity. When studying homologous series effects, the branching index may be particularly useful.

REFERENCES

(1) R. C. Reid and T. K. Sherwood, "The Properties of Gases and Liquids," 2nd ed., McGraw-Hill, New York, N.Y., 1966.

(2) A. Bondi, "Physical Properties of Molecular Crystals, Liquids and Glasses," Wiley, New York, N.Y., 1968.

(3) H. Wiener, *J. Am. Chem. Soc.*, **69,** 17(1947).

(4) H. Wiener, *J. Phys. Chem.*, **52,** 425(1948).

(5) J. R. Platt, *ibid.*, **56,** 328(1952).

(6) H. Hosoya, *Bull. Chem. Soc., Jpn.*, **44,** 2332(1971).

(7) *Ibid.*, **45,** 3415(1972).

(8) A. Leo, C. Hansch, and D. Elkins, *Chem. Rev.*, **71,** 525(1971).

(9) R. Hermann, *J. Phys. Chem.*, **76,** 2754(1972).

(10) G. L. Amidon, S. H. Yalkowsky, and S. Leung, *J. Pharm. Sci.*, **63,** 1858(1974).

(11) M. Randic, *J. Am. Chem. Soc.*, **97,** 6609(1975).

(12) M. H. Harris, T. Higuchi, and J. H. Rytting, *J. Phys. Chem.*, **77,** 2694(1973).

(13) L. B. Kier, L. H. Hall, W. J. Murray, and M. Randić, *J. Pharm. Sci.*, **64,** 1971(1975).

(14) "QCPE 225," Quantum Chemistry Program Exchange, Chemistry Department, Indiana University, Bloomington, IN 47401

(15) G. L. Amidon, S. H. Yalkowsky, S. T. Anik, and S. C. Valvani, *J. Phys. Chem.*, **79,** 2239(1975).

[5] See, for example, Platt's discussion of the Wiener number (5).

ACKNOWLEDGMENTS AND ADDRESSES

Received July 2, 1975, from the *Center for Health Sciences, School of Pharmacy, University of Wisconsin, Madison, WI 53706*
Accepted for publication August 25, 1975.

Presented in part at the APhA Academy of Pharmaceutical Sciences, Atlanta meeting, November 1975.

The authors thank Dr. Randic for a preprint of his manuscript on the branching index.

[x] To whom inquiries should be directed.

Continuous Dissolution Rate Determination as a Function of the pH of the Medium

P. TURI [x], M. DAUVOIS, and A. F. MICHAELIS

Abstract □ A method was developed for varying the pH of the medium during dissolution rate studies of timed-release tablets with the aid of compressed, totally soluble, alkaline powder mixtures. Commercial as well as experimental timed-release capsules or tablets were used as models, and dissolution rates were determined at pH 1.1, 2.4, and 7.4. The system can be applied to other pH values or other variations of the dissolution medium (*e.g.*, ionic strength) to: (*a*) correlate *in vitro* release rates with bioavailability data, (*b*) discriminate between alternative formulations during dosage form development, or (*c*) serve as a selective control procedure for a series of sustained-release dosage forms.

Keyphrases □ Dissolution rate—timed-release tablets, continuous determination as a function of pH □ Dosage forms—timed-release tablets, dissolution rate, continuous determination as a function of pH □ Tromethamine—buffer system for dissolution rate studies of timed-release tablets as a function of pH

Among the many parameters that influence the *in vitro* release rates of pharmaceuticals from timed-release dosage forms[1], the pH of the medium is particularly important, because these forms are designed to release their active ingredient(s) for a prolonged period (usually 8–12 hr). During this time interval, solid oral pharmaceutical formulations (such as tablets or capsules) pass from the stomach to the duodenum and on through the lower intestinal tract. Throughout this passage, they are exposed to a pH gradient ranging approximately from 1 to 8. [This range is narrower for healthy adults. The average pH of gastric fluid in men is about 1.9, while it is reported to be approximately 2.6 for women (2). The pH of the duodenal secretion for both men and women varies from 5.8 to 7.6 (3).]

This study was designed to evaluate a relatively simple method for determining the dissolution rates of timed-release solid dosage forms as a function of the pH of the medium. Model capsules and tablets were selected to meet the following requirements: (*a*) good solubility throughout the tested pH range, and (*b*) availability of a rapid assay procedure compatible with the system. The basic procedure was developed to allow for adjustment of the medium to other than the initial pH values or for the introduction of further changes (*e.g.*, ionic strength, viscosity, and composition of the medium).

[1] The term "timed release" is defined in NF XIV (1).

Alkaline phosphates and tromethamine [tris(hydroxymethyl)aminomethane] have been applied or recommended for modifying the pH of the medium (4–6), particularly for testing the dissolution rates of delayed-release formulations. In this study, completely soluble compressed tablets of these agents were formulated and used as the simplest way of achieving "in process" pH changes.

EXPERIMENTAL

Apparatus—The dissolution rate apparatus was fully described previously (6). The drug substance is extracted by a continuously flowing dissolution medium from the solid dosage forms, using a flow-through dissolution cell held at constant temperature (37°). The liquid moves through a flow-through cell, and the concentration is monitored spectrophotometrically (or by another suitable instrument). A typical set of dissolution curves is shown in Fig. 1.

Dissolution Media—Hydrochloric acid (0.1 *N*) was used as the initial dissolution fluid. The pH of this medium was changed by adding increasing amounts of tromethamine[2].

Within the scope of this study, the dissolution rates were determined at pH 1.1, 2.4, and 7.4. It was found practical to formulate 3.0-g tablets containing 1.4 g of tromethamine, 1.54 g of sucrose USP, and 0.06 g of polyethylene glycol 6000[3].

The thoroughly mixed powder was compressed directly with the aid of a manual hydraulic press[4] [compression force of 2270 kg (5000 lb)]. The excipients of the tablets were selected to form a tablet that dissolves completely in an aqueous medium and does not significantly absorb light between the wavelengths of 300 and 240 nm.

By adding four or five of these tablets, which contain 5.6 or 7.0 g of tromethamine, respectively, to the initial 500 ml of dissolution medium, the desired pH value of 2.4 or 7.4 was obtained without fluid interchange of the flowing system (Table I). (The tromethamine tablets dissolve in the medium in about 90 sec.)

Pharmaceutical Preparations—Commercially available theophylline capsules contained 259.2 mg of theophylline in coated pellets. The average total weight of the pellets in the size 0 capsules was 640.0 mg.

Phenylpropanolamine hydrochloride tablets were incorporated in an experimental timed-release matrix. [Phenylpropanolamine tablets or capsules were the subjects of several recent studies (6–8) due to their increasing therapeutic importance].

Dissolution Rate Testing Procedure—A predetermined volume of 0.1 *N* hydrochloric acid was added to each of six 1-liter beakers. For the theophylline capsules, 1000 ml was used; for the phenylpropanolamine hydrochloride tablets, 500 ml was used. The beakers were

[2] Ultrapure grade, 99.9%; Aldrich Chemical Co., Milwaukee, Wis.
[3] Sentry, Union Carbide Corp., New York, N.Y.
[4] Carver laboratory press model C, Fred S. Carver, Inc., Monomonee Falls, WI 53051

ACKNOWLEDGMENTS AND ADDRESSES

Received July 2, 1975, from the *Center for Health Sciences, School of Pharmacy, University of Wisconsin, Madison, WI 53706*
Accepted for publication August 25, 1975.

Presented in part at the APhA Academy of Pharmaceutical Sciences, Atlanta meeting, November 1975.

The authors thank Dr. Randic for a preprint of his manuscript on the branching index.

[x] To whom inquiries should be directed.

Continuous Dissolution Rate Determination as a Function of the pH of the Medium

P. TURI [x], M. DAUVOIS, and A. F. MICHAELIS

Abstract □ A method was developed for varying the pH of the medium during dissolution rate studies of timed-release tablets with the aid of compressed, totally soluble, alkaline powder mixtures. Commercial as well as experimental timed-release capsules or tablets were used as models, and dissolution rates were determined at pH 1.1, 2.4, and 7.4. The system can be applied to other pH values or other variations of the dissolution medium (*e.g.*, ionic strength) to: (*a*) correlate *in vitro* release rates with bioavailability data, (*b*) discriminate between alternative formulations during dosage form development, or (*c*) serve as a selective control procedure for a series of sustained-release dosage forms.

Keyphrases □ Dissolution rate—timed-release tablets, continuous determination as a function of pH □ Dosage forms—timed-release tablets, dissolution rate, continuous determination as a function of pH □ Tromethamine—buffer system for dissolution rate studies of timed-release tablets as a function of pH

Among the many parameters that influence the *in vitro* release rates of pharmaceuticals from timed-release dosage forms[1], the pH of the medium is particularly important, because these forms are designed to release their active ingredient(s) for a prolonged period (usually 8–12 hr). During this time interval, solid oral pharmaceutical formulations (such as tablets or capsules) pass from the stomach to the duodenum and on through the lower intestinal tract. Throughout this passage, they are exposed to a pH gradient ranging approximately from 1 to 8. [This range is narrower for healthy adults. The average pH of gastric fluid in men is about 1.9, while it is reported to be approximately 2.6 for women (2). The pH of the duodenal secretion for both men and women varies from 5.8 to 7.6 (3).]

This study was designed to evaluate a relatively simple method for determining the dissolution rates of timed-release solid dosage forms as a function of the pH of the medium. Model capsules and tablets were selected to meet the following requirements: (*a*) good solubility throughout the tested pH range, and (*b*) availability of a rapid assay procedure compatible with the system. The basic procedure was developed to allow for adjustment of the medium to other than the initial pH values or for the introduction of further changes (*e.g.*, ionic strength, viscosity, and composition of the medium).

[1] The term "timed release" is defined in NF XIV (1).

Alkaline phosphates and tromethamine [tris(hydroxymethyl)aminomethane] have been applied or recommended for modifying the pH of the medium (4–6), particularly for testing the dissolution rates of delayed-release formulations. In this study, completely soluble compressed tablets of these agents were formulated and used as the simplest way of achieving "in process" pH changes.

EXPERIMENTAL

Apparatus—The dissolution rate apparatus was fully described previously (6). The drug substance is extracted by a continuously flowing dissolution medium from the solid dosage forms, using a flow-through dissolution cell held at constant temperature (37°). The liquid moves through a flow-through cell, and the concentration is monitored spectrophotometrically (or by another suitable instrument). A typical set of dissolution curves is shown in Fig. 1.

Dissolution Media—Hydrochloric acid (0.1 *N*) was used as the initial dissolution fluid. The pH of this medium was changed by adding increasing amounts of tromethamine[2].

Within the scope of this study, the dissolution rates were determined at pH 1.1, 2.4, and 7.4. It was found practical to formulate 3.0-g tablets containing 1.4 g of tromethamine, 1.54 g of sucrose USP, and 0.06 g of polyethylene glycol 6000[3].

The thoroughly mixed powder was compressed directly with the aid of a manual hydraulic press[4] [compression force of 2270 kg (5000 lb)]. The excipients of the tablets were selected to form a tablet that dissolves completely in an aqueous medium and does not significantly absorb light between the wavelengths of 300 and 240 nm.

By adding four or five of these tablets, which contain 5.6 or 7.0 g of tromethamine, respectively, to the initial 500 ml of dissolution medium, the desired pH value of 2.4 or 7.4 was obtained without fluid interchange of the flowing system (Table I). (The tromethamine tablets dissolve in the medium in about 90 sec.)

Pharmaceutical Preparations—Commercially available theophylline capsules contained 259.2 mg of theophylline in coated pellets. The average total weight of the pellets in the size 0 capsules was 640.0 mg.

Phenylpropanolamine hydrochloride tablets were incorporated in an experimental timed-release matrix. [Phenylpropanolamine tablets or capsules were the subjects of several recent studies (6–8) due to their increasing therapeutic importance].

Dissolution Rate Testing Procedure—A predetermined volume of 0.1 *N* hydrochloric acid was added to each of six 1-liter beakers. For the theophylline capsules, 1000 ml was used; for the phenylpropanolamine hydrochloride tablets, 500 ml was used. The beakers were

[2] Ultrapure grade, 99.9%; Aldrich Chemical Co., Milwaukee, Wis.
[3] Sentry, Union Carbide Corp., New York, N.Y.
[4] Carver laboratory press model C, Fred S. Carver, Inc., Monomonee Falls, WI 53051

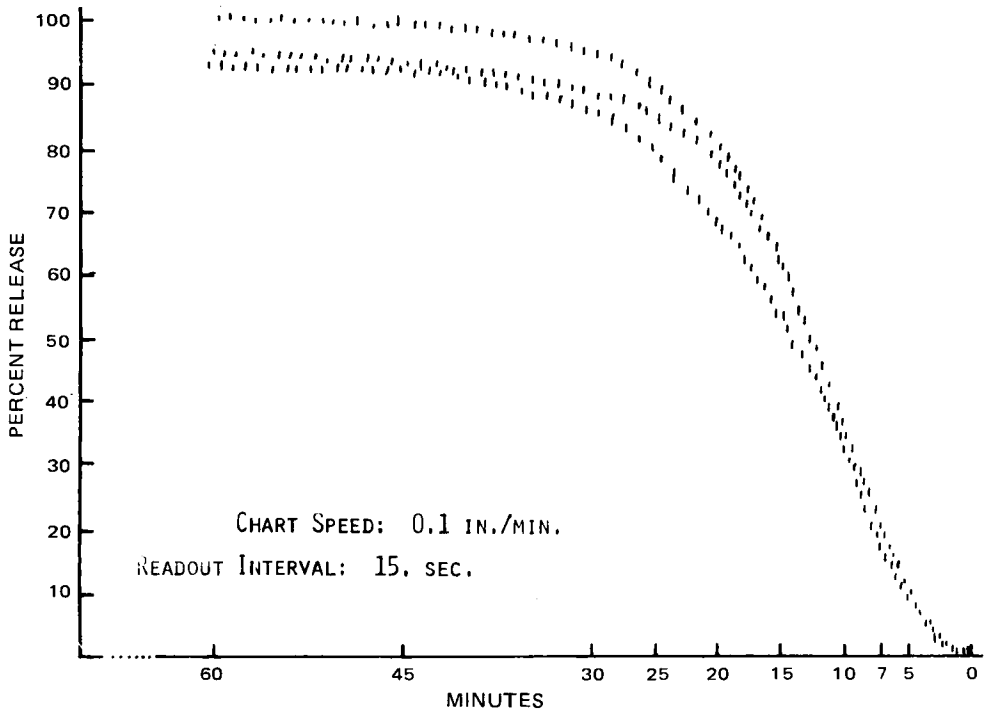

Figure 1—*Typical dissolution rate curves (three individual tablets).*

immersed in the larger constant-temperature water bath of the continuous release rate apparatus.

One dosage unit was inserted into each of five dissolution cells. The medium flowing out from the sixth beaker provided continuous baseline reference throughout the testing. The concentration of the solute in the dissolution medium was determined spectrophotometrically from the absorbance values at the approximate wavelength of the maximum absorbance (theophylline, 268 nm; phenylpropanolamine hydrochloride, 257 nm).

After 1 hr, the required number of tromethamine tablets was added to each beaker to shift the pH to 2.4. Similarly, after the 2nd hr, the pH was readjusted to 7.4 with additional tromethamine tablets.

RESULTS AND DISCUSSION

Dissolution curves obtained on the tested formulations are shown in Figs. 2 and 3.

The dissolution rate of solid particles in fluid media is described by the Noyes–Whitney equation (9):

$$\frac{da}{dt} = KS(C_s - C) \qquad \text{(Eq. 1)}$$

where da/dt, the rate of dissolution, is the amount of drug substance dissolved in a time unit; $(C_s - C)$ is the concentration gradient (the difference between the concentration of the saturated solution and the actual concentration in the medium at a given time); S is the surface area of the undissolved solute; and K is a constant, combining a large number of factors that may influence the dissolution rate.

Table I—pH Dependence of the Medium[a]

Amount of Tromethamine Added, g	pH[b]
0	1.1
5.6	2.4
6.0	2.7
6.4	7.1
7.0	7.4

[a] Initial dissolution medium was 500 ml of 0.1 *N* hydrochloric acid. [b] Variations equal ±0.1 pH unit. A Metrohm pH meter, model E300 (Metrohm Ltd., Herisau, Switzerland) was used.

These additional factors include the characteristics of the dissolution medium (*e.g.*, pH, ionic strength, and surface tension), the rates of stirring and/or the flow rates of the medium, physicochemical properties of the solute (*e.g.*, particle size), composition of the pharmaceutical formulation (*e.g.*, types and amounts of excipients), compression force, geometry of the tablets, types of capsules, and many other factors, which have been intensively studied (6–8, 10–17).

A series of papers dealt with the particular kinetics of the drug release from wax matrixes (5, 18–20) and from polymeric films (21).

For a given pharmaceutical formulation, if the other listed factors are reasonably constant, the pH of the medium may be the rate-determining factor. Therefore, Eq. 1 may be simplified as follows:

$$\frac{da}{dt} = K_1[f(\text{pH})](C_s - C) \qquad \text{(Eq. 2)}$$

where $f(\text{pH})$ represents a variable dependent upon the pH of the dissolution medium, and K_1 represents all other (constant) factors. Furthermore, under normal dissolution rate conditions, C_s is much larger than C and, for practical purposes, the concentration gradient can be substituted by C_s. As shown in Table II, the concentration gradient variation for the phenylpropanolamine hydrochloride tablets is negligible ($\Delta = 0.035\%$); it is very small (<2.5%) even for the theophylline capsules.

Manufacturers of timed-release dosage forms have recognized the possibility of utilizing the pH variations of the GI system, and pH dependence is often the basis of a timed-release delivery system.

The objective of this study was not to simulate physiological conditions but only to test *in vitro* dissolution rates in a simplified continuous system, as a means for establishing product uniformity and obtaining important information regarding the pH dependence of the dissolution rate from various pharmaceutical formulations. The initial pH 1.1 was selected as a value near the pH of simulated gastric fluid USP; pH 2.4 and 7.4 were also included since they are characteristic values in the actual range of gastric and duodenal secretions in humans (2, 3). The dosage units were exposed first for 1-hr periods at pH 1.1 and then at 2.4; thereafter, the operation of the dissolution apparatus was continued at pH 7.4 for 3–4 hr. If desired, the procedure may be varied by using different or additional pH values of the medium for shorter or longer times.

There are several methods of changing the pH of the medium. An efficient, but very tedious, way is described in NF XIV (1). It uses five individual rotating bottles and requires, after each scheduled period (ranging from 60 to 120 min): (*a*) the decanting of the medium (retaining "as much residue as is conveniently possible"), (*b*) the

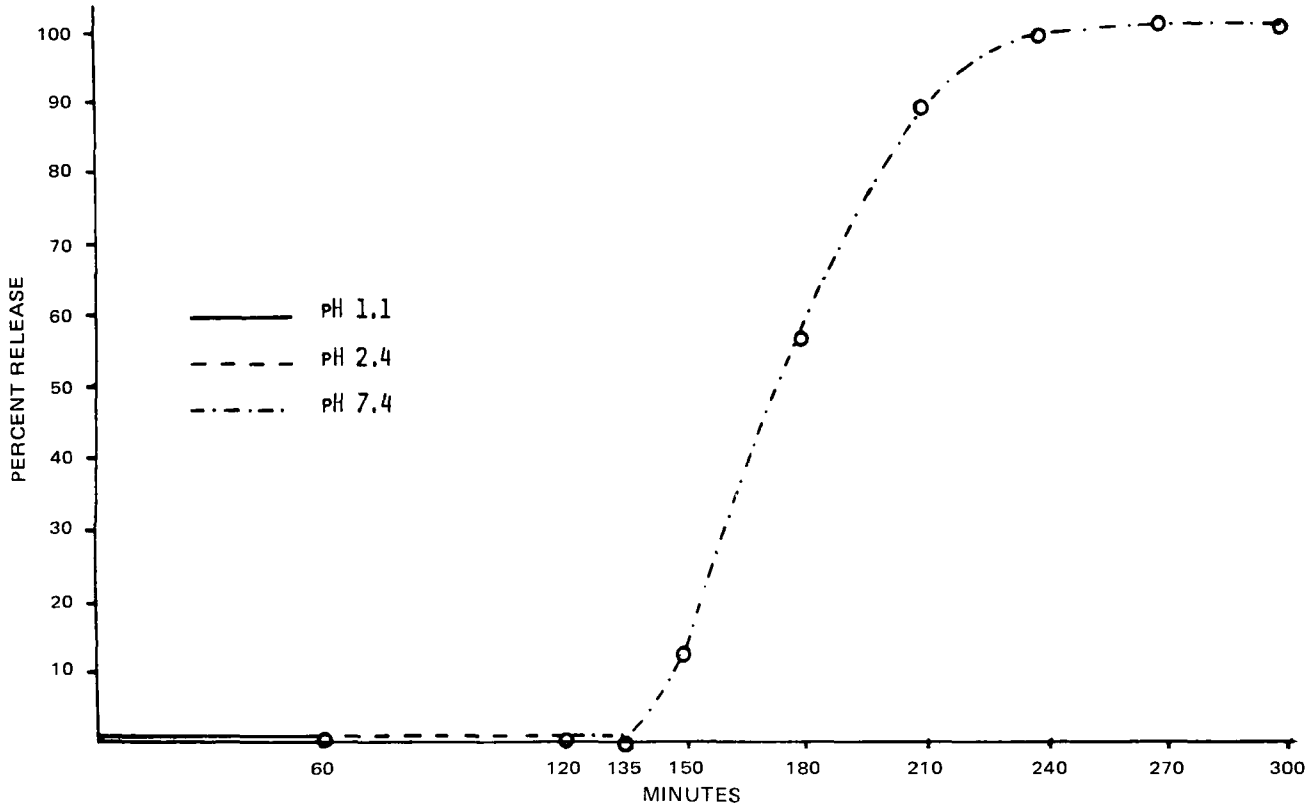

Figure 2—*Dissolution curve of theophylline capsules, 259.2 mg. Data points represent the average of four capsules. Linear regression analysis (from* t_{135} *to* t_{210}*) showed a rate of 0.98%/min* (r = 0.97).

quantitative returning of the inadvertently removed residual particles by washing them from the screens into the test bottles, (*c*) the gradual replacement of the dissolution medium of increasing pH values (from pH 1.2 to 7.5), and (*d*) the assaying of the residues. Besides the time-consuming and inconvenient operation, an additional disadvantage of this official method is that the number of residues (and, therefore, the number of parallel data) decreases at each subsequent step); at pH 7.5, only a single value can be obtained.

Other methods require the withdrawal of an assay sample at certain times and the replacement of the withdrawn volume with the same or with a different medium. These techniques involve not only a correction for the withdrawn amount (which can be simply calcu-

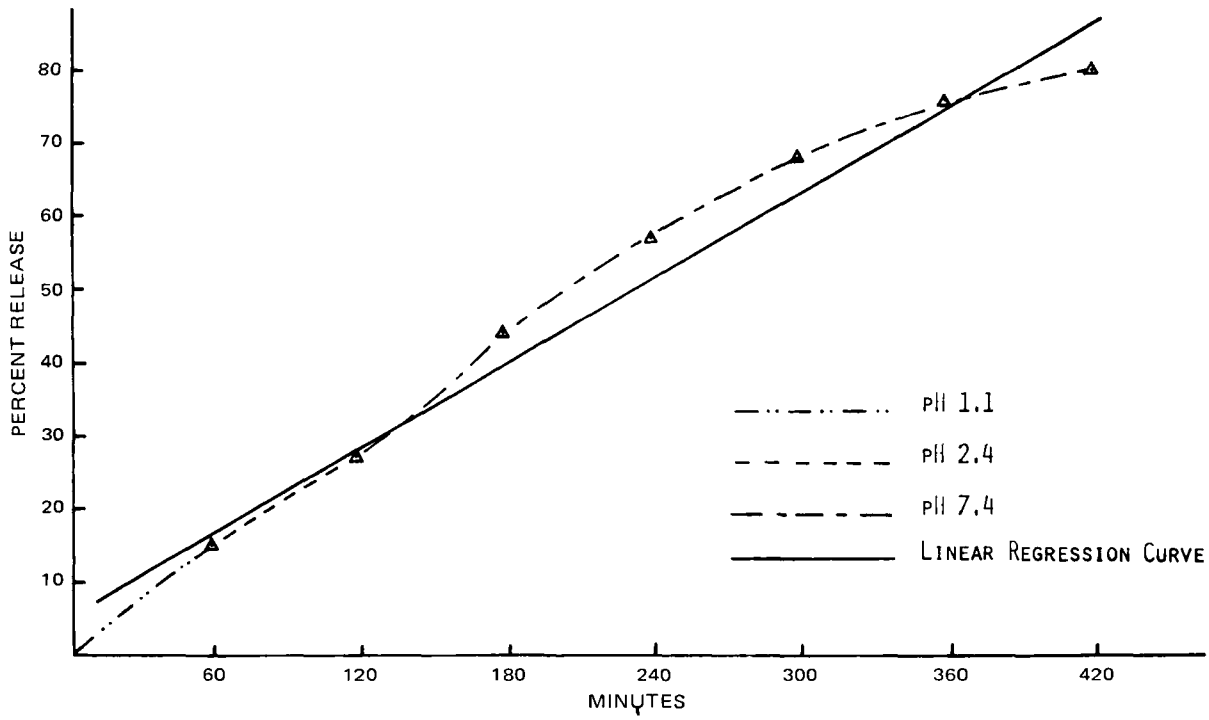

Figure 3—*Dissolution curve of experimental phenylpropanolamine hydrochloride tablets, 75 mg. Data points represent the average of five tablets. Linear regression analysis showed a rate of 0.19%/min* (r = 0.99).

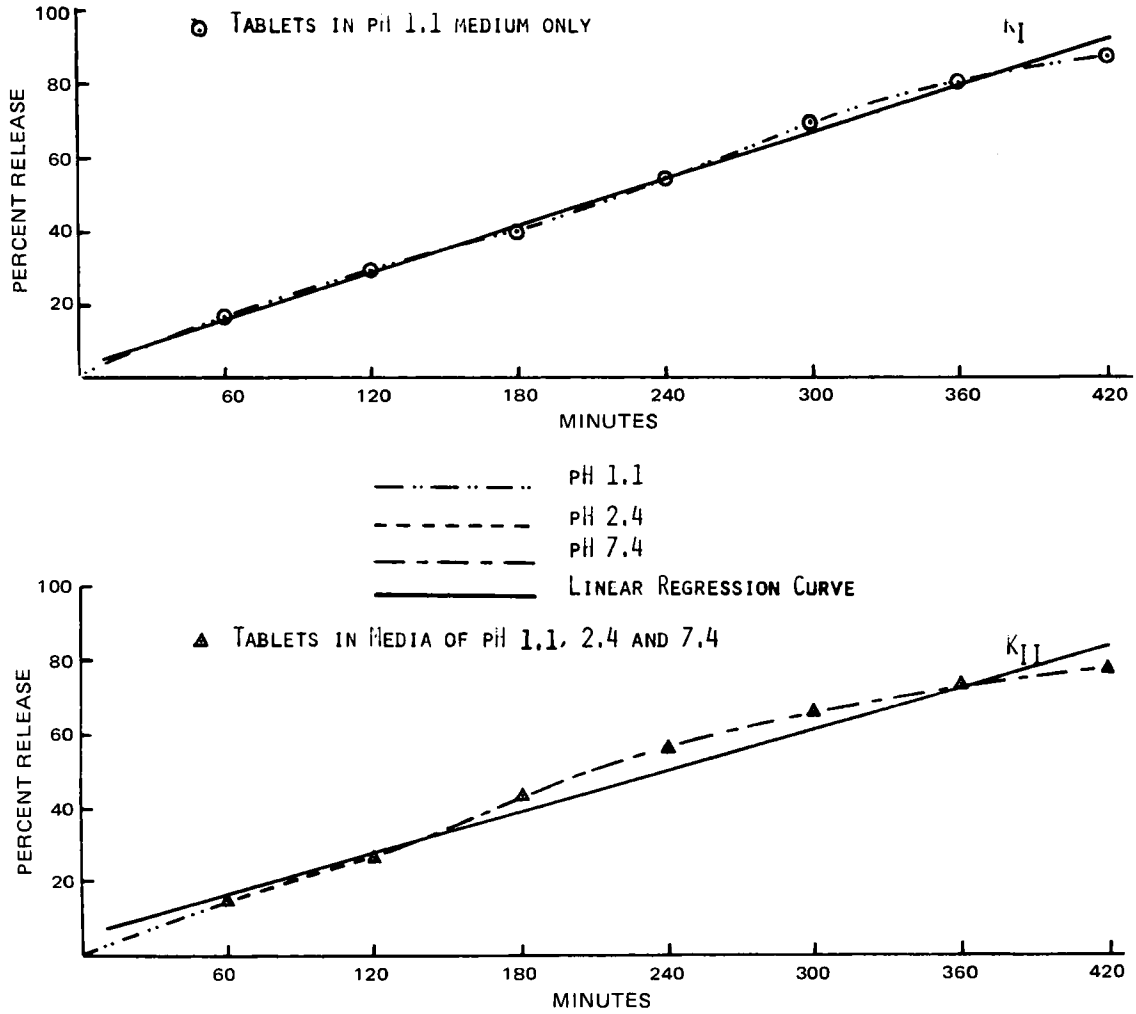

Figure 4—*Phenylpropanolamine hydrochloride tablets (comparative dissolution curves).*

lated), but also an actual change of the solute–solvent ratio. If the assay procedure or other factors necessitate comparatively larger volumes of withdrawals, the results are grossly distorted since, with the repeated replacements, less and less solute is extracted with more and more solvent. To overcome this problem, tromethamine tablets were selected. They not only change the pH of the medium without significantly changing its volume but also stabilize the pH since the hydrochloric acid–tromethamine combination is a standard buffering system (4).

Table II—Concentration Gradients in Dissolution Systems[a] at 37°

pH	Concentration Gradient ($G = C_s - C$)	Theophylline Capsules[b]	Phenylpropanolamine Hydrochloride Tablets[c]
1.1	G_{max}	1.207	42.780
	G_{min}	1.181	42.765
	$\Delta\%$	2.154	0.035
2.4	G_{max}	1.053	42.560
	G_{min}	1.027	42.545
	$\Delta\%$	2.469	0.035
7.4	G_{max}	1.120	43.110
	G_{min}	1.094	43.095
	$\Delta\%$	2.331	0.035

[a] G = concentration gradient ($C_s - C$); G_{max} = ($C_s - C$) at t_0; G_{min} = ($C_s - C$) at t_∞; C_s = saturation concentration (g/100 ml); C = concentration of the solute in the total dissolution medium (g/100 ml); and $\Delta\% = [(G_{max} - G_{min})/G_{max}] \times 100$. [b] Unit dosage = 259.2 mg; volume of the medium = 1000 ml. [c] Unit dosage = 75.0 mg; volume of the medium = 500 ml.

Another alkalizing agent, trisodium phosphate, was also considered in preliminary experiments. Due to its high water of crystallization content (56.9%), it was quite difficult to prepare the required large tablets. Additionally, there was a significant volume increase of the medium compared to the volume required for tromethamine tablets, which was only 0.7% at pH 2.4 and less than 0.75% at pH 7.4.

The dissolution curve of the commercial theophylline capsules indicated a 120-min lag time during acidic medium exposure, which corresponds to the claim that the pellets are enteric coated. After adjustment to pH 7.4, a typical S-shaped curve was obtained. After an induction period of 15 min (during which the enteric coating dissolved), the release began and continued at an almost constant rate of 0.98%/min. The release was practically complete in 2 hr after commencement of nonacidic exposure (Fig. 2).

The dissolution curve of the phenylpropanolamine hydrochloride tablets was quite different, because this formulation was designed to be pH independent in terms of release rate. Release began immediately and continued throughout the 7 hr of testing at about the same rate (0.19%/min) regardless of the pH of the medium. This result represents almost a zero-order release rate, independent of the pH of the medium within the applied limits (Fig. 3).

Figure 4 confirms this observation. In another test series, the medium was kept at pH 1.1 for 7 hr. The two curves (representing constant and variable pH conditions) show only a small rate difference (K_I = 0.21%/min; K_{II} = 0.19%/min).

CONCLUSIONS

With a simple procedural modification of a continuous dissolution rate system (namely, by adding to an initial dissolution medium of pH 1.1, at predetermined intervals, the appropriate amount of tromethamine in completely soluble tablets), the pH of the medium can

be increased and buffered as desired without any significant change in the volume of the medium. The method may serve as a highly automated alternative to the rotating-bottle method described in the official compendia. It offers the following advantages:

1. The operation of the system is very simple, and the system permits variation of conditions as required by the assay method.

2. While the system is basically designed to test the pH dependence of the dissolution rate of solid dosage forms, it may be easily adapted for determining the influence of other factors. Its flexibility may be particularly useful if *in vitro* simulation of *in vivo* bioavailability data is desired.

REFERENCES

(1) "The National Formulary," 14th ed., Mack Publishing Co., Easton, Pa., 1975, pp. 985, 986.

(2) G. Dotevall, *Acta Med. Scand.*, **170**, 59(1951).

(3) P. L. Altman, in "Blood and Other Body Fluids," D. S. Dittmer, Ed., Biological Handbooks, Federation of American Societies for Experimental Biology, Washington, D.C., 1961, pp. 416, 417.

(4) L. C. Schroeter and J. G. Wagner, *J. Pharm. Sci.*, **51**, 957(1962).

(5) F. Sjuib, A. P. Simonelli, and W. I. Higuchi, *ibid.*, **61**, 1381(1972).

(6) C. Cakiryildiz, P. J. Mehta, W. Rahmen, and D. Schoenleber, *ibid.*, **64**, 1692(1975).

(7) F. W. Goodhart, R. H. McCoy, and F. C. Ninger, *ibid.*, **62**, 304(1973).

(8) *Ibid.*, **63**, 1748(1974).

(9) H. Noyes and W. Whitney, *Z. Phys. Chem.*, **23**, 689(1897).

(10) J. G. Wagner, "Biopharmaceutics and Relevant Pharmacokinetics," 1st ed., Drug Intelligence Publications, Hamilton, Ill., 1971, pp. 115–120.

(11) J. E. Tingstad and S. Riegelman, *J. Pharm. Sci.*, **59**, 692(1970).

(12) R. E. Shepherd, J. C. Brice, and L. H. Luzzi, *ibid.*, **61**, 1152(1972).

(13) J. Cobby, M. Mayersohn, and G. C. Walker, *ibid.*, **63**, 725(1974).

(14) *Ibid.*, **63**, 732(1974).

(15) H. G. Kwee and G. A. Ulex, *Pharm. Ind.*, **36**, 576(1974).

(16) A. A. Ismail, M. W. Goudah, and M. M. Motawi, *ibid.*, **36**, 735(1974).

(17) J. B. Johnson, P. G. Kennedy, and S. H. Rubin, *J. Pharm. Sci.*, **63**, 1931(1974).

(18) J. B. Schwartz, A. P. Simonelli, and W. I. Higuchi, *ibid.*, **57**, 274(1968).

(19) *Ibid.*, **57**, 278(1968).

(20) F. Sjuib, A. P. Simonelli, and W. I. Higuchi, *J. Pharm. Sci.*, **61**, 1374(1972).

(21) M. Doubrow and M. Friedman, *ibid.*, **64**, 76(1975).

ACKNOWLEDGMENTS AND ADDRESSES

Received May 7, 1975, from the *Pharmacy and Analytical Research Department, Sandoz Inc., East Hanover, NJ 07936*

Accepted for publication August 27, 1975.

Presented at the Pharmaceutical Analysis and Control Section, APhA Academy of Pharmaceutical Sciences, San Francisco meeting, April 1975.

The authors thank Dr. Saul S. Kornblum for helpful discussions and Mr. Dennis Feltz for technical assistance.

[x] To whom inquiries should be directed.

Isolation of 10,11-Epoxide of Protriptyline in Rat Urine after Protriptyline Administration

V. ROVEI, G. BELVEDERE, C. PANTAROTTO, and A. FRIGERIO [x]

Abstract □ The 10,11-epoxide, 10-hydroxy, and 10,11-dihydrodiol metabolites of protriptyline were identified in rat urine collected after the administration of 40 mg/kg ip of protriptyline. Mass spectrometric characterization confirmed the structure of these metabolites.

Keyphrases □ Protriptyline—three metabolites isolated from rat urine, characterized by TLC, GLC, and GLC–mass spectrometry □ Metabolites—protriptyline, isolated from rat urine, characterized by TLC, GLC, and GLC–mass spectrometry □ Antidepressant agents—protriptyline, three metabolites isolated from rat urine, characterized by TLC, GLC, and GLC–mass spectrometry

Epoxides are intermediates in the biological conversion of the aromatic ring system into the corresponding dihydrodiols (1). However, the instability of these metabolites has made their isolation and direct identification in biological fluids difficult.

The isolation from rat urine of the 10,11-epoxide of carbamazepine (2) after administration of carbamazepine, a drug with tricyclic structure, prompted a systematic investigation on the metabolism of other drugs with the same tricyclic structure. During this study, 10,11-epoxides and *N*-desmethyl metabolites of cyproheptadine (3) and cyclobenzaprine (4) were identified.

This report summarizes findings on the metabolism of protriptyline (*N*-methyl-5*H*-dibenzo[*a*,*d*]cycloheptene-5-propylamine) (I), a drug possessing antidepressant activity (5). The 10,11-epoxide, 10,11-dihydrodiol, and 10-hydroxy metabolites of protriptyline were isolated and characterized by means of TLC, GLC, and GLC–mass spectrometry in rat urine after protriptyline administration.

EXPERIMENTAL

Biological Samples—Two male Sprague–Dawley rats, 200 g, were injected with 40 mg/kg ip of protriptyline hydrochloride[1] dissolved in saline. Following drug administration, urine samples were collected at various times over 48 hr and kept frozen until analyses were performed.

After addition of drug to untreated rat urine and incubation at 37° for 48 hr, no degradation of the product occurred.

Treatment of Biological Samples—Urine samples (20 ml)

[1] Donated by Merck Sharp and Dohme, Rahway, N.J.

be increased and buffered as desired without any significant change in the volume of the medium. The method may serve as a highly automated alternative to the rotating-bottle method described in the official compendia. It offers the following advantages:

1. The operation of the system is very simple, and the system permits variation of conditions as required by the assay method.

2. While the system is basically designed to test the pH dependence of the dissolution rate of solid dosage forms, it may be easily adapted for determining the influence of other factors. Its flexibility may be particularly useful if *in vitro* simulation of *in vivo* bioavailability data is desired.

REFERENCES

(1) "The National Formulary," 14th ed., Mack Publishing Co., Easton, Pa., 1975, pp. 985, 986.

(2) G. Dotevall, *Acta Med. Scand.*, **170**, 59(1951).

(3) P. L. Altman, in "Blood and Other Body Fluids," D. S. Dittmer, Ed., Biological Handbooks, Federation of American Societies for Experimental Biology, Washington, D.C., 1961, pp. 416, 417.

(4) L. C. Schroeter and J. G. Wagner, *J. Pharm. Sci.*, **51**, 957(1962).

(5) F. Sjuib, A. P. Simonelli, and W. I. Higuchi, *ibid.*, **61**, 1381(1972).

(6) C. Cakiryildiz, P. J. Mehta, W. Rahmen, and D. Schoenleber, *ibid.*, **64**, 1692(1975).

(7) F. W. Goodhart, R. H. McCoy, and F. C. Ninger, *ibid.*, **62**, 304(1973).

(8) *Ibid.*, **63**, 1748(1974).

(9) H. Noyes and W. Whitney, *Z. Phys. Chem.*, **23**, 689(1897).

(10) J. G. Wagner, "Biopharmaceutics and Relevant Pharmacokinetics," 1st ed., Drug Intelligence Publications, Hamilton, Ill., 1971, pp. 115–120.

(11) J. E. Tingstad and S. Riegelman, *J. Pharm. Sci.*, **59**, 692(1970).

(12) R. E. Shepherd, J. C. Brice, and L. H. Luzzi, *ibid.*, **61**, 1152(1972).

(13) J. Cobby, M. Mayersohn, and G. C. Walker, *ibid.*, **63**, 725(1974).

(14) *Ibid.*, **63**, 732(1974).

(15) H. G. Kwee and G. A. Ulex, *Pharm. Ind.*, **36**, 576(1974).

(16) A. A. Ismail, M. W. Goudah, and M. M. Motawi, *ibid.*, **36**, 735(1974).

(17) J. B. Johnson, P. G. Kennedy, and S. H. Rubin, *J. Pharm. Sci.*, **63**, 1931(1974).

(18) J. B. Schwartz, A. P. Simonelli, and W. I. Higuchi, *ibid.*, **57**, 274(1968).

(19) *Ibid.*, **57**, 278(1968).

(20) F. Sjuib, A. P. Simonelli, and W. I. Higuchi, *J. Pharm. Sci.*, **61**, 1374(1972).

(21) M. Doubrow and M. Friedman, *ibid.*, **64**, 76(1975).

ACKNOWLEDGMENTS AND ADDRESSES

Received May 7, 1975, from the *Pharmacy and Analytical Research Department, Sandoz Inc., East Hanover, NJ 07936*

Accepted for publication August 27, 1975.

Presented at the Pharmaceutical Analysis and Control Section, APhA Academy of Pharmaceutical Sciences, San Francisco meeting, April 1975.

The authors thank Dr. Saul S. Kornblum for helpful discussions and Mr. Dennis Feltz for technical assistance.

[x] To whom inquiries should be directed.

Isolation of 10,11-Epoxide of Protriptyline in Rat Urine after Protriptyline Administration

V. ROVEI, G. BELVEDERE, C. PANTAROTTO, and A. FRIGERIO [x]

Abstract □ The 10,11-epoxide, 10-hydroxy, and 10,11-dihydrodiol metabolites of protriptyline were identified in rat urine collected after the administration of 40 mg/kg ip of protriptyline. Mass spectrometric characterization confirmed the structure of these metabolites.

Keyphrases □ Protriptyline—three metabolites isolated from rat urine, characterized by TLC, GLC, and GLC–mass spectrometry □ Metabolites—protriptyline, isolated from rat urine, characterized by TLC, GLC, and GLC–mass spectrometry □ Antidepressant agents—protriptyline, three metabolites isolated from rat urine, characterized by TLC, GLC, and GLC–mass spectrometry

Epoxides are intermediates in the biological conversion of the aromatic ring system into the corresponding dihydrodiols (1). However, the instability of these metabolites has made their isolation and direct identification in biological fluids difficult.

The isolation from rat urine of the 10,11-epoxide of carbamazepine (2) after administration of carbamazepine, a drug with tricyclic structure, prompted a systematic investigation on the metabolism of other drugs with the same tricyclic structure. During this study, 10,11-epoxides and *N*-desmethyl metabolites of cyproheptadine (3) and cyclobenzaprine (4) were identified.

This report summarizes findings on the metabolism of protriptyline (*N*-methyl-5*H*-dibenzo[*a*,*d*]cycloheptene-5-propylamine) (I), a drug possessing antidepressant activity (5). The 10,11-epoxide, 10,11-dihydrodiol, and 10-hydroxy metabolites of protriptyline were isolated and characterized by means of TLC, GLC, and GLC–mass spectrometry in rat urine after protriptyline administration.

EXPERIMENTAL

Biological Samples—Two male Sprague–Dawley rats, 200 g, were injected with 40 mg/kg ip of protriptyline hydrochloride[1] dissolved in saline. Following drug administration, urine samples were collected at various times over 48 hr and kept frozen until analyses were performed.

After addition of drug to untreated rat urine and incubation at 37° for 48 hr, no degradation of the product occurred.

Treatment of Biological Samples—Urine samples (20 ml)

[1] Donated by Merck Sharp and Dohme, Rahway, N.J.

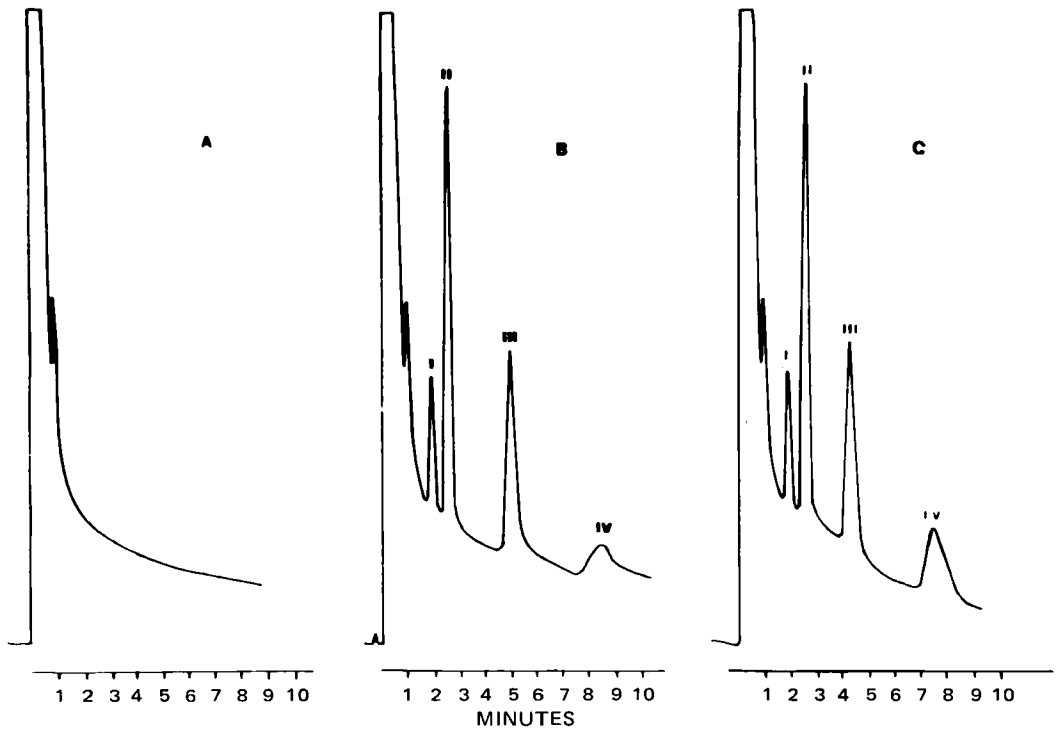

Figure 1—*Gas–liquid chromatograms. Key: A, urine blank; B, urine of rats treated with protriptyline (I), 40 mg/kg ip; and C, urine of rats treated with protriptyline after flash methylation with trimethylanilinium hydroxide.*

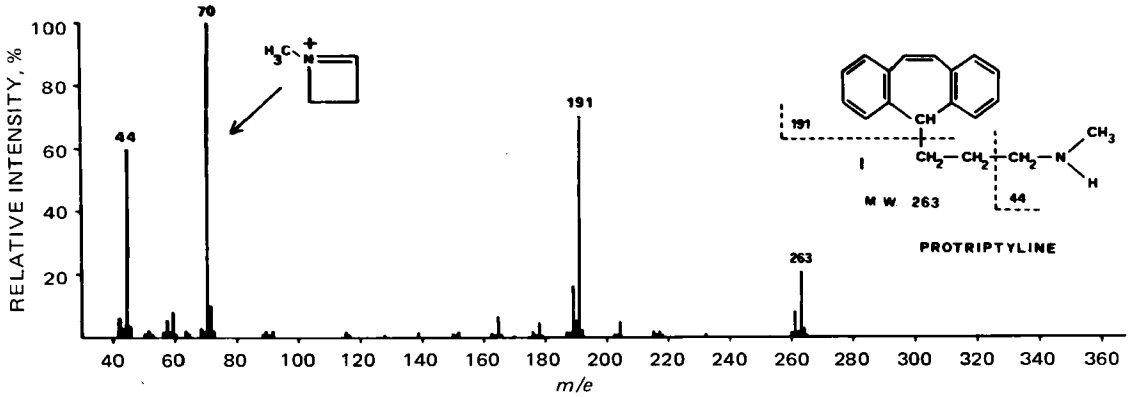

Figure 2—*Mass spectrum of authentic protriptyline (I). A similar mass spectrum was obtained by introducing the corresponding eluted TLC spot by a direct inlet system or GLC procedure.*

were adjusted to pH 9 with 1 *N* NaOH and extracted twice with ethyl acetate (20 ml).

The organic phase was concentrated to dryness under reduced pressure. After the addition of 0.2 ml of methanol, the material obtained was used for TLC, GLC, and mass spectral analysis.

Incubation with β-Glucuronidase—After extraction of free metabolites, the urine samples were incubated with β-glucuronidase[2]. Then 0.5 ml of the enzyme was added to 10 ml of urine, adjusted at pH 4.5 with acetate buffer (1 *M*), and the samples were incubated at 37° for 12 hr. The incubate was extracted twice with ethyl acetate (10 ml), evaporated to dryness, and analyzed by the described techniques.

General Procedures—Thin-layer chromatograms were prepared on 5 × 20-cm glass plates precoated with silica gel F-254[3] and developed at room temperature with *n*-hexane–diethylamine (50:50 v/v). Protriptyline and the possible metabolites were visualized with UV light at 254 and 361 nm (Table I).

GLC analyses were performed on a gas chromatograph[4] equipped with a flame-ionization detector. The chromatographic column consisted of glass tubing (2 m long and 4 mm i.d.) packed with 100–120-mesh Gas Chrom Q and coated with 3% OV-17[5]. The operating conditions were: injection port temperature, 300°; oven temperature, 290°; nitrogen (carrier gas) flow rate, 30 ml/min; hydrogen flow rate, 20 ml/min; and air flow rate, 300 ml/min.

Table I—R_f Values of Protriptyline and Its Metabolites on Thin-Layer Chromatogram[a]

Compound	R_f in Solvent System[b]
Protriptyline (I)	0.47
Metabolite II	0.36
Metabolite III	0.08
Metabolite IV	0.28

[a] Silica gel F-254 (0.25 mm). [b] *n*-Hexane–diethylamine (50:50 v/v).

[2] Boehringer.
[3] Merck.
[4] Carlo Erba Fractovap Gl.
[5] Applied Science Laboratories.

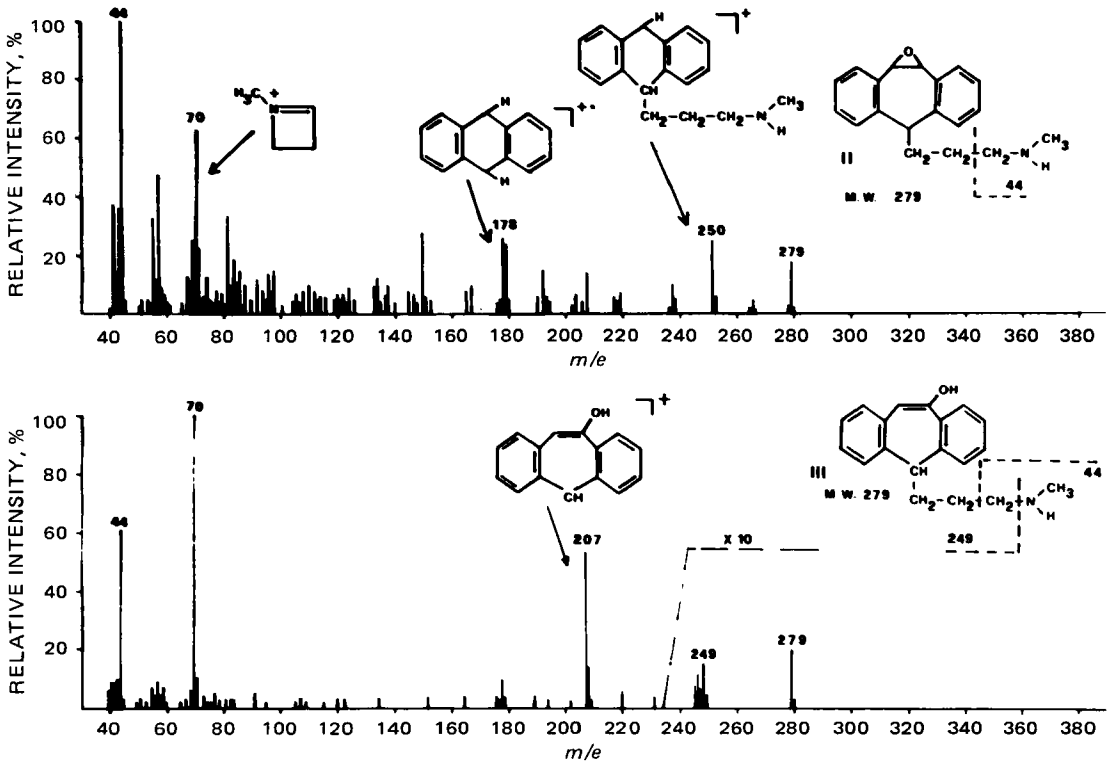

Figure 3—*Mass spectra of II (top panel) and III (bottom panel) obtained by introducing the corresponding eluted TLC spots by a direct inlet system or GLC procedure.*

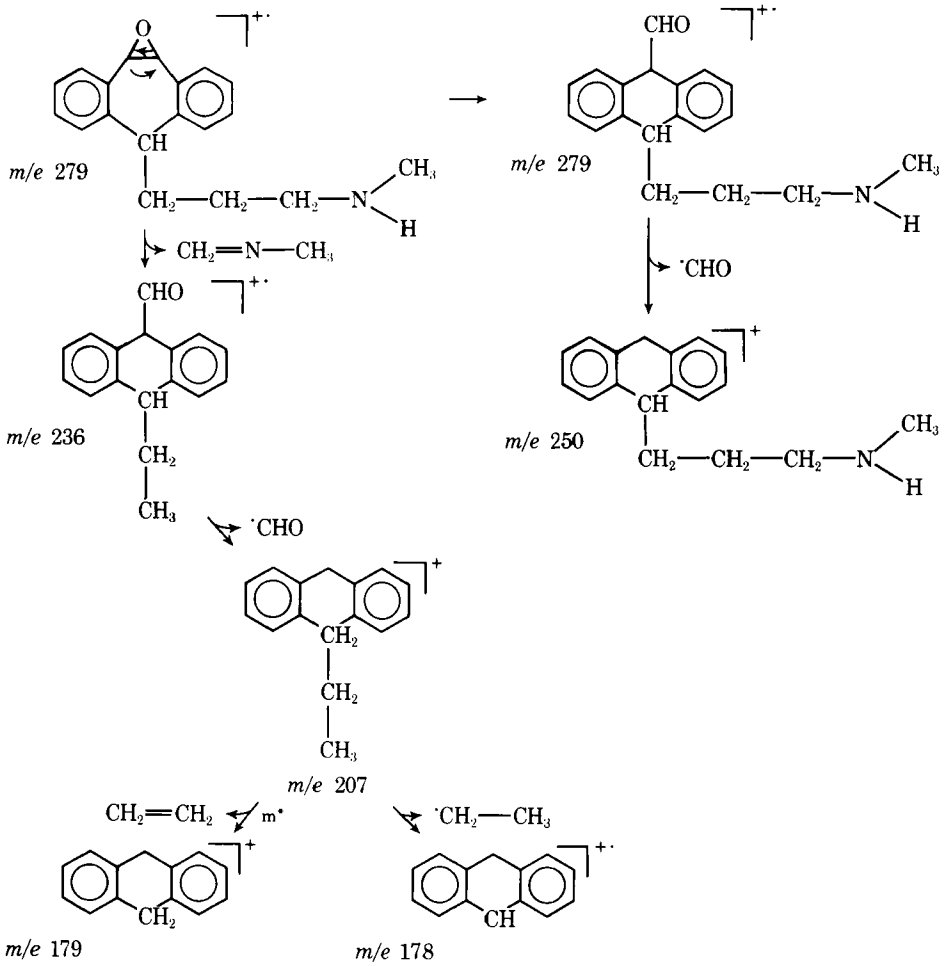

Scheme I—Suggested fragmentation pathway of the 10,11-epoxide of protriptyline. (No exact mass measurements were included in the parent ion or fragments, and only a few metastable ions were available to support the fragmentation scheme.)

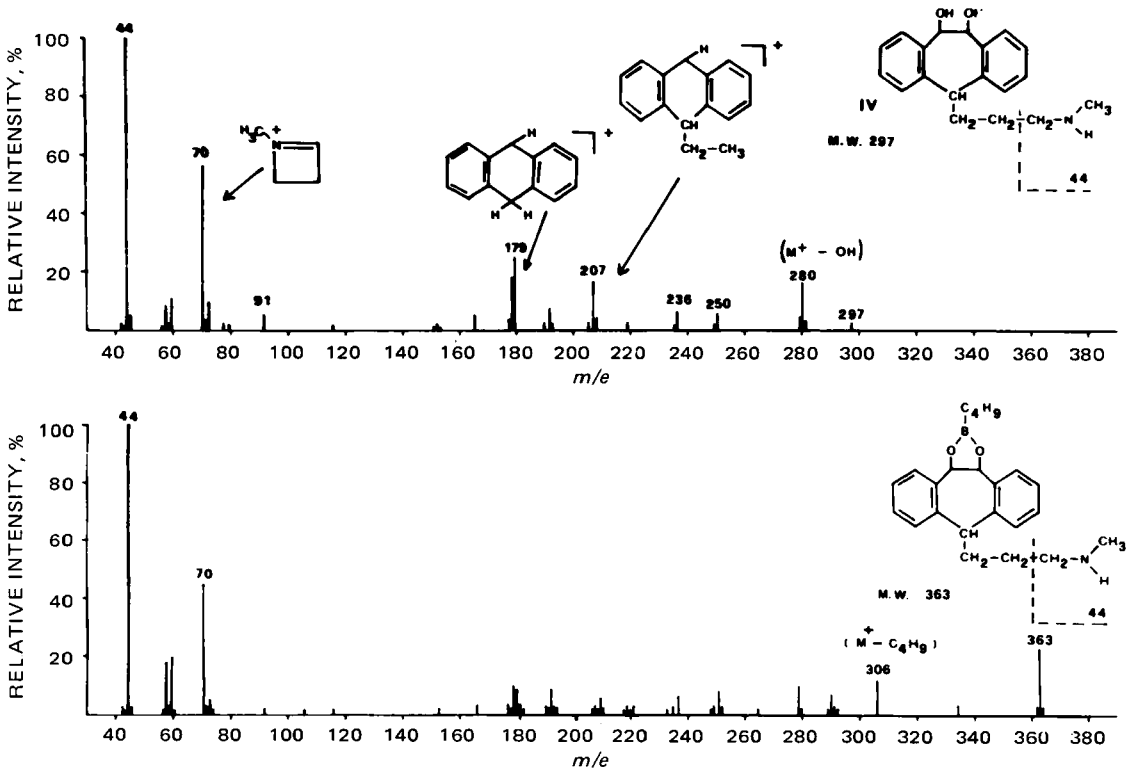

Figure 4—*Mass spectra of IV obtained by introducing the corresponding eluted TLC spot by a direct inlet system or GLC procedure (top panel) and after on-column reaction with* n*-butylboronic acid (bottom panel).*

A gas chromatograph–mass spectrometer[6] was used at the following conditions: energy of ionization beam, 70 ev; ion source temperature, 290°; and trap current, 60 μamp. Sample introduction was carried out by a direct inlet system at a probe temperature of 150° or by a GLC procedure utilizing a glass column (2 m long and 4 mm i.d.) packed with 3% OV-17 on 100–120-mesh Gas Chrom Q. The following conditions were used: injector temperature, 300°; oven temperature, 290°; and helium (carrier gas) flow rate, 30 ml/min.

RESULTS AND DISCUSSION

The ethyl acetate extract, obtained from 20 ml of rat urine, was concentrated to dryness, redissolved in 200 μl of methanol, spotted on a TLC plate, and developed with the described solvent system. The urine extracts of rats treated with the drug contained four spots, not present in the urine of control rats, with the R_f reported in Table I.

TLC of the extracts of the urine after incubation with β-glucuronidase showed two spots, with R_f 0.08 and 0.28, not present in the control urine extracts. The GLC analysis showed four peaks in the treated urine sample (Fig. 1).

Identification of the unchanged I (spot with R_f 0.47 and first GLC peak) was carried out by comparison with the mass spectrum of the standard drug (Fig. 2). The molecular ion is at *m/e* 263, and the peak at *m/e* 191 is characteristic of the tricyclic structure. The peak at *m/e* 44 and 70 (base peak) were due to the aliphatic chain cleavage.

The second GLC peak, corresponding to the spot with R_f 0.36, was identified as the 10,11-epoxide (II) of protriptyline (Fig. 3). The mass spectrum presented a molecular ion at *m/e* 279, which suggested the introduction of an oxygen atom into the drug molecule. The failure of this substance to react with trimethylanilinium hydroxide and the loss of 29 amu (ĊHO) from the molecular ion (Scheme I) to give an intense peak at *m/e* 250 suggested the presence of an epoxidic structure.

After isolation of II on TLC and treatment with 1 *N* HCl, it was possible to obtain a product with R_f 0.28. The spot was eluted with methanol. The material, analyzed by direct introduction into the ion source of the mass spectrometer, showed a spectrum corresponding to the 10,11-dihydrodiol (IV) of protriptyline (Fig. 4).

This spot was also analyzed by GLC–mass spectrometry after on-column reaction with *n*-butylboronic acid (Scheme II). A com-

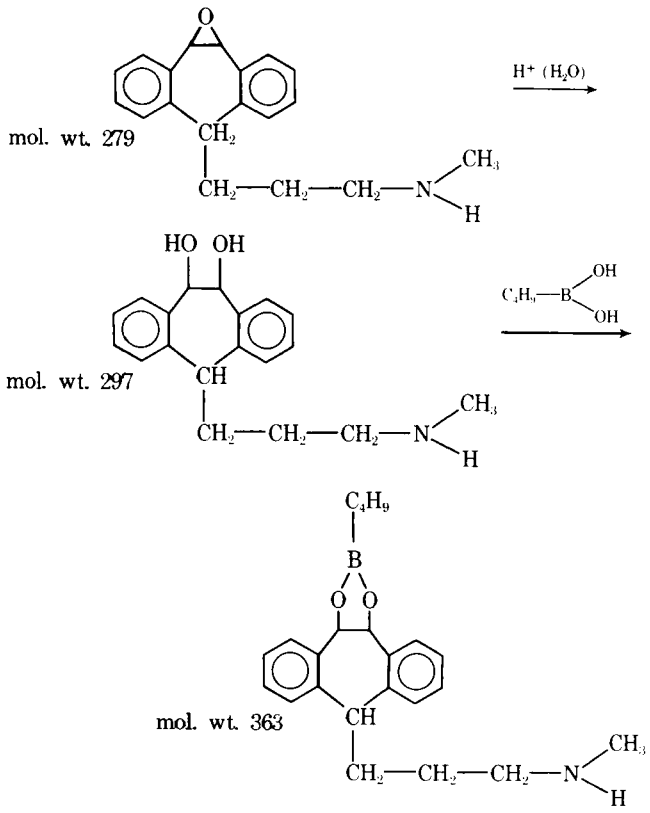

Scheme II—Reaction of the 10,11-dihydrodiol metabolite (obtained from the 10,11-epoxide of protriptyline) with n*-butylboronic acid.*

[6] LKB model 9000.

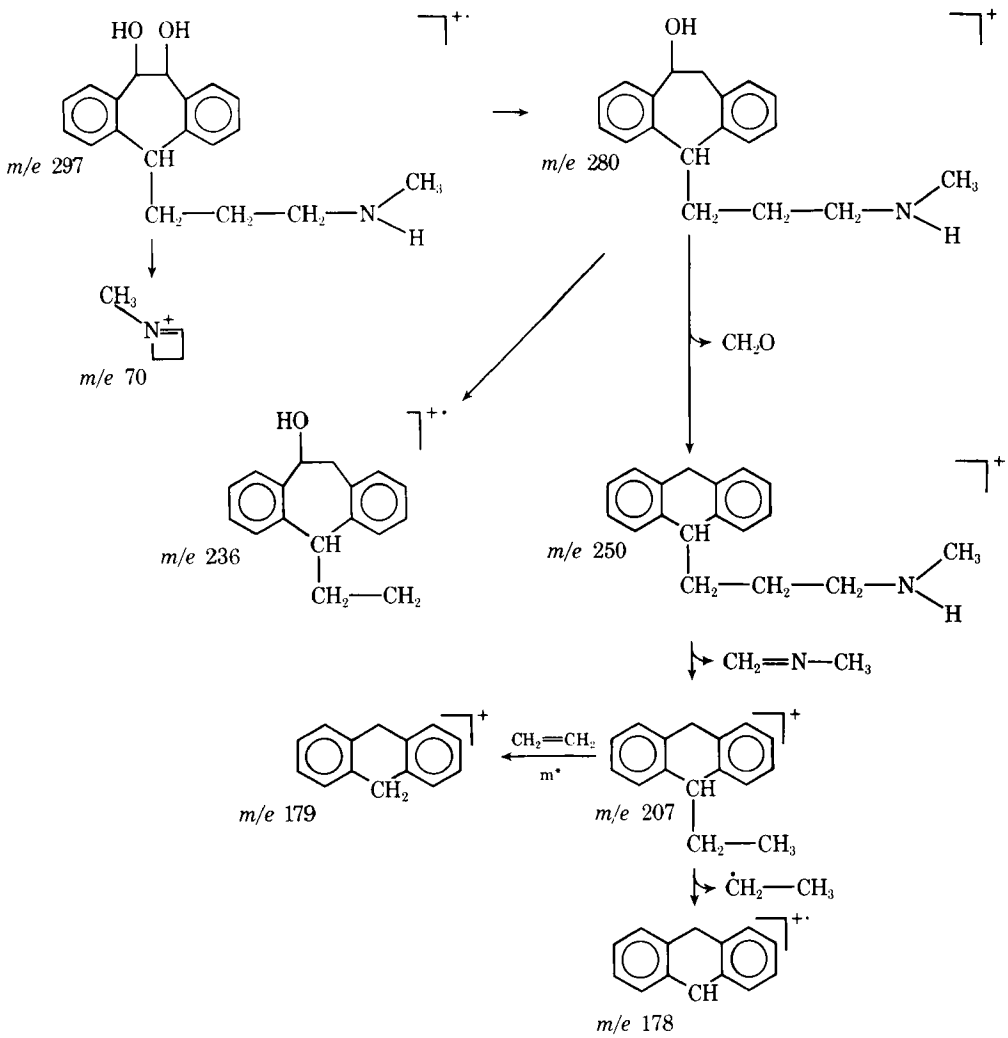

Scheme III—Suggested fragmentation pathway of the 10,11-dihydrodiol of protriptyline. (No exact mass measurements were included in the parent ion or fragments, and only a few metastable ions were available to support the fragmentation scheme.)

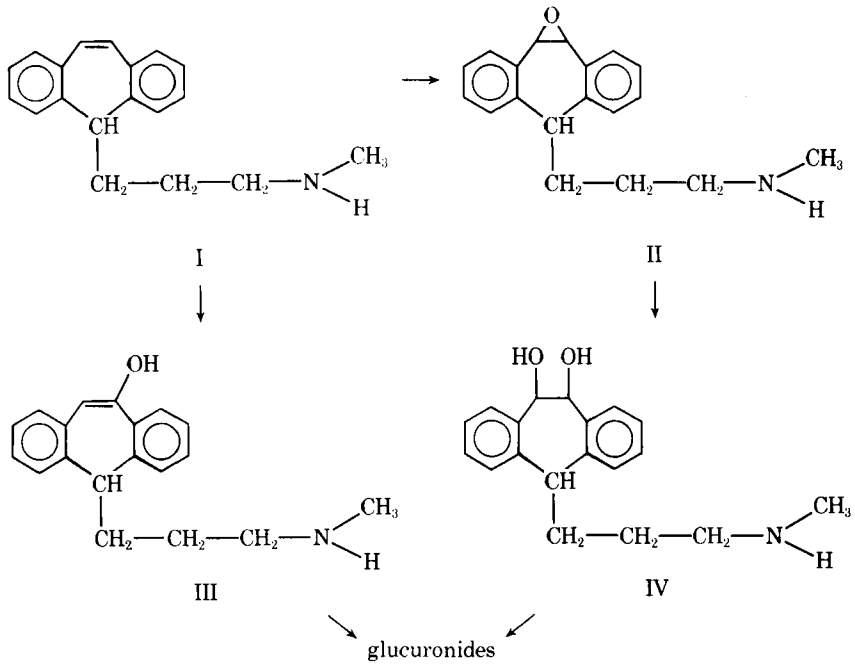

Scheme IV—Metabolic pathway of protriptyline (I).

pound was obtained with the molecular ion at *m/e* 363, corresponding to the *n*-butylboronate of the diol (Fig. 4). Furthermore, the TLC, GLC, and mass spectral properties of the diol were compared to those of a synthetic sample of the 10,11-dihydrodiol of protriptyline[7].

The second metabolite (third GLC peak) presented a spot at R_f 0.08 and was identified as the 10-hydroxy (III) metabolite previously detected (6).

The mass spectrum (Fig. 2) showed a molecular ion at *m/e* 279 and a very intense peak at *m/e* 207, suggesting the introduction of an oxygen atom into the tricyclic part of the molecule during the biotransformation. In this case, however, the GLC analysis, after methylation of the substance with trimethylanilinium hydroxide, revealed a shift of the GLC peak (Fig. 1C). The mass spectrum showed a corresponding shift of the molecular ion of 14 amu (methylation), proving the presence of a hydroxylated metabolite.

The last metabolite, the 10,11-dihydrodiol, previously identified by Sisenwine *et al.* (6), had an R_f 0.28 value and was the fourth GLC peak. The mass spectrum showed the molecular ion at *m/e* 297. The most important ions were at *m/e* 280 (−17 amu from the peak at *m/e* 297) and 179, arising from the ion at *m/e* 207 by loss of ethylene (the presence of a metastable ion confirmed this transition).

The study of fragmentation (Scheme III), the reaction of derivatization with *n*-butylboronic acid, as described here, and the comparison with the synthetic product established the structure of this metabolite.

A possible, but not proven, metabolic pathway of protriptyline is reported in Scheme IV. The drug may be transformed into the 10-hydroxy or 10,11-epoxide metabolite, which is metabolized to the 10,11-dihydrodiol. Both the mono- and dihydroxylated metabolites are also present in rat urines as glucuronides.

These findings are in agreement with the generally accepted hypothesis that epoxides represent the intermediates of aromatic and nonaromatic diols (7). In this investigation, the epoxide formed from protriptyline appears to be a stable metabolite, which could be isolated from and identified in urine.

[7] Donated by Italseber, Milan, Italy.

REFERENCES

(1) E. Boyland, *Biochem. Soc. Symp.*, **5**, 40(1950).

(2) A. Frigerio, R. Fanelli, P. Biandrate, G. Passerini, P. L. Morselli, and S. Garattini, *J. Pharm. Sci.*, **61**, 1144(1972).

(3) A. Frigerio, N. Sossi, G. Belvedere, C. Pantarotto, and S. Garattini, *ibid.*, **63**, 1536(1974).

(4) G. Belvedere, C. Pantarotto, V. Rovei, and A. Frigerio, *ibid.*, **65**, 815(1976).

(5) A. J. Ayd, Jr., *Lippincott's Med. Sci.*, **1968**, 54.

(6) S. F. Sisenwine, C. O. Tio, S. R. Shrader, and H. W. Ruelius, *J. Pharmacol. Exp. Ther.*, **175**, 51(1970).

(7) M. G. Horning, D. J. Harvey, E. C. Horning, and R. M. Hill, in "Proceedings of the International Symposium on Gas Chromatography–Mass Spectrometry," A. Frigerio, Ed., Isle of Elba, Italy, 1972, p. 403.

ACKNOWLEDGMENTS AND ADDRESSES

Received March 31, 1975, from the *Istituto di Ricerche Farmacologiche "Mario Negri," Via Eritrea 62, 20157 Milan, Italy.*

Accepted for publication July 23, 1975.

The authors thank Dr. M. Zanol for technical assistance.

[x] To whom inquiries should be directed.

Identification of 10,11-Epoxide and Other Cyclobenzaprine Metabolites Isolated from Rat Urine

G. BELVEDERE, C. PANTAROTTO, V. ROVEI, and A. FRIGERIO [x]

Abstract □ Cyclobenzaprine (40 mg/kg ip) was administered to rats, and six urinary metabolites of this drug were identified. They were the 10,11-epoxide, the *N*-oxide, the desmethyl derivative, the hydroxylated and desmethylhydroxylated compounds, and the *N*-oxide hydroxylated at the 10- or 11-position. Mass spectrometric analysis confirmed their structures.

Keyphrases □ Cyclobenzaprine metabolites—six isolated from rat urine, TLC, GLC, and mass spectral identification □ Metabolites, cyclobenzaprine—six isolated from rat urine, TLC, GLC, and mass spectral identification □ Sedatives—cyclobenzaprine, six metabolites isolated from rat urine, TLC, GLC, and mass spectral identification

Previous studies in this laboratory established that tricyclic compounds such as carbamazepine (1), cyproheptadine (2), and protriptyline (3) can be transformed into stable epoxides in the 10,11-position and isolated from human and rat urine. This investigation was concerned with another compound with antidepressant activity and possessing a tricyclic structure, cyclobenzaprine (*N,N*-dimethyl-5*H*-dibenzo[*a,d*]cycloheptene-$\Delta^{5,\gamma}$-propylamine) (I) (4).

Six metabolites were identified by using TLC, GLC, and mass spectrometric techniques. They were the 10,11-epoxide (V), the *N*-oxide (II), the desmethyl derivative (III), the hydroxylated (VI) and desmethylhydroxylated (VII) compounds, and the *N*-oxide hydroxylated (IV) at the 10- or 11-position.

EXPERIMENTAL

Biological Samples—Two male Sprague–Dawley rats, 200 g, were injected intraperitoneally with 40 mg/kg of cyclobenzaprine hydrochloride[1] dissolved in 0.9% NaCl. Urine was collected at various times over 48 hr following drug administration and frozen until analysis.

The drug, added to untreated rat urine and analyzed after 48 hr, did not show formation of any degradation products.

[1] Donated by Merck Sharp and Dohme, Rahway, N.J.

pound was obtained with the molecular ion at *m/e* 363, corresponding to the *n*-butylboronate of the diol (Fig. 4). Furthermore, the TLC, GLC, and mass spectral properties of the diol were compared to those of a synthetic sample of the 10,11-dihydrodiol of protriptyline[7].

The second metabolite (third GLC peak) presented a spot at R_f 0.08 and was identified as the 10-hydroxy (III) metabolite previously detected (6).

The mass spectrum (Fig. 2) showed a molecular ion at *m/e* 279 and a very intense peak at *m/e* 207, suggesting the introduction of an oxygen atom into the tricyclic part of the molecule during the biotransformation. In this case, however, the GLC analysis, after methylation of the substance with trimethylanilinium hydroxide, revealed a shift of the GLC peak (Fig. 1C). The mass spectrum showed a corresponding shift of the molecular ion of 14 amu (methylation), proving the presence of a hydroxylated metabolite.

The last metabolite, the 10,11-dihydrodiol, previously identified by Sisenwine *et al.* (6), had an R_f 0.28 value and was the fourth GLC peak. The mass spectrum showed the molecular ion at *m/e* 297. The most important ions were at *m/e* 280 (−17 amu from the peak at *m/e* 297) and 179, arising from the ion at *m/e* 207 by loss of ethylene (the presence of a metastable ion confirmed this transition).

The study of fragmentation (Scheme III), the reaction of derivatization with *n*-butylboronic acid, as described here, and the comparison with the synthetic product established the structure of this metabolite.

A possible, but not proven, metabolic pathway of protriptyline is reported in Scheme IV. The drug may be transformed into the 10-hydroxy or 10,11-epoxide metabolite, which is metabolized to the 10,11-dihydrodiol. Both the mono- and dihydroxylated metabolites are also present in rat urines as glucuronides.

These findings are in agreement with the generally accepted hypothesis that epoxides represent the intermediates of aromatic and nonaromatic diols (7). In this investigation, the epoxide formed from protriptyline appears to be a stable metabolite, which could be isolated from and identified in urine.

[7] Donated by Italseber, Milan, Italy.

REFERENCES

(1) E. Boyland, *Biochem. Soc. Symp.*, **5**, 40(1950).

(2) A. Frigerio, R. Fanelli, P. Biandrate, G. Passerini, P. L. Morselli, and S. Garattini, *J. Pharm. Sci.*, **61**, 1144(1972).

(3) A. Frigerio, N. Sossi, G. Belvedere, C. Pantarotto, and S. Garattini, *ibid.*, **63**, 1536(1974).

(4) G. Belvedere, C. Pantarotto, V. Rovei, and A. Frigerio, *ibid.*, **65**, 815(1976).

(5) A. J. Ayd, Jr., *Lippincott's Med. Sci.*, **1968**, 54.

(6) S. F. Sisenwine, C. O. Tio, S. R. Shrader, and H. W. Ruelius, *J. Pharmacol. Exp. Ther.*, **175**, 51(1970).

(7) M. G. Horning, D. J. Harvey, E. C. Horning, and R. M. Hill, in "Proceedings of the International Symposium on Gas Chromatography–Mass Spectrometry," A. Frigerio, Ed., Isle of Elba, Italy, 1972, p. 403.

ACKNOWLEDGMENTS AND ADDRESSES

Received March 31, 1975, from the *Istituto di Ricerche Farmacologiche "Mario Negri," Via Eritrea 62, 20157 Milan, Italy.*

Accepted for publication July 23, 1975.

The authors thank Dr. M. Zanol for technical assistance.

[x] To whom inquiries should be directed.

Identification of 10,11-Epoxide and Other Cyclobenzaprine Metabolites Isolated from Rat Urine

G. BELVEDERE, C. PANTAROTTO, V. ROVEI, and A. FRIGERIO [x]

Abstract □ Cyclobenzaprine (40 mg/kg ip) was administered to rats, and six urinary metabolites of this drug were identified. They were the 10,11-epoxide, the *N*-oxide, the desmethyl derivative, the hydroxylated and desmethylhydroxylated compounds, and the *N*-oxide hydroxylated at the 10- or 11-position. Mass spectrometric analysis confirmed their structures.

Keyphrases □ Cyclobenzaprine metabolites—six isolated from rat urine, TLC, GLC, and mass spectral identification □ Metabolites, cyclobenzaprine—six isolated from rat urine, TLC, GLC, and mass spectral identification □ Sedatives—cyclobenzaprine, six metabolites isolated from rat urine, TLC, GLC, and mass spectral identification

Previous studies in this laboratory established that tricyclic compounds such as carbamazepine (1), cyproheptadine (2), and protriptyline (3) can be transformed into stable epoxides in the 10,11-position and isolated from human and rat urine. This investigation was concerned with another compound with antidepressant activity and possessing a tricyclic structure, cyclobenzaprine (*N,N*-dimethyl-5*H*-dibenzo[*a,d*]cycloheptene-$\Delta^{5,\gamma}$-propylamine) (I) (4).

Six metabolites were identified by using TLC, GLC, and mass spectrometric techniques. They were the 10,11-epoxide (V), the *N*-oxide (II), the desmethyl derivative (III), the hydroxylated (VI) and desmethylhydroxylated (VII) compounds, and the *N*-oxide hydroxylated (IV) at the 10- or 11-position.

EXPERIMENTAL

Biological Samples—Two male Sprague–Dawley rats, 200 g, were injected intraperitoneally with 40 mg/kg of cyclobenzaprine hydrochloride[1] dissolved in 0.9% NaCl. Urine was collected at various times over 48 hr following drug administration and frozen until analysis.

The drug, added to untreated rat urine and analyzed after 48 hr, did not show formation of any degradation products.

[1] Donated by Merck Sharp and Dohme, Rahway, N.J.

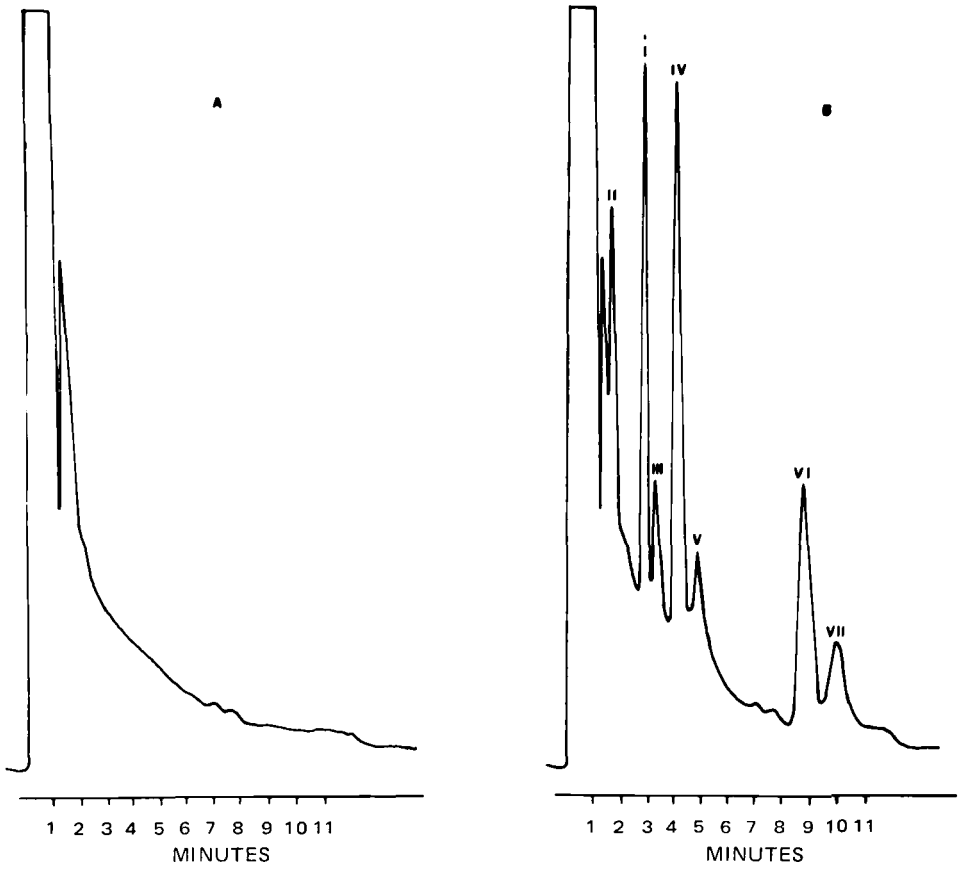

Figure 1—*Gas-liquid chromatograms of: A, urine blank; and B, urine of rats treated with I, 40 mg/kg ip.*

Table I—R_f Values of Cyclobenzaprine (I) and Its Metabolites on Thin-Layer Chromatograms[a]

Compound	R_f in Solvent System[b]	
	A	B
I	0.72	0.50
Metabolite II	0.16	0.00
Metabolite III	0.51	0.44
Metabolite IV	0.06	0.00
Metabolite V	0.68	0.40
Metabolite VI	0.46	0.35
Metabolite VII	0.19	0.23

[a] Silica gel F-254 (0.25 mm). [b] A = cyclohexane–2-propanol–methanol–diethylamine (60:25:10:5 v/v), and B = cyclohexane–diethylamine–toluene–methanol (75:10:10:5 v/v).

Treatment of Biological Samples—Urine samples (10–20 ml) were adjusted to pH 9 with 1 *N* NaOH and extracted with ethyl acetate (20–40 ml). The organic phase was concentrated to dryness in a water bath at 65° under a gentle stream of nitrogen. This material was then used for TLC, GLC, and mass spectral analyses.

Incubation with β-Glucuronidase—Incubation of urine samples was carried out after exhaustive extraction of the drug and the free metabolites with ethyl acetate. To 5 ml of urine adjusted at pH 4.5 with 1 *M* acetate buffer (5 ml) was added 0.5 ml of β-glucuronidase[2], and the samples were incubated at 37° for 12 hr. The incubate was extracted with ethyl acetate (5 ml), dried, and analyzed by the described techniques.

General Procedures—Thin-layer chromatograms were prepared on 5 × 20-cm glass plates precoated with silica gel F-254[3] and developed in the solvent systems shown in Table I. Cyclobenzaprine and the possible metabolites were visualized under UV light at 254 and 361 nm.

GLC determinations were performed on a gas chromatograph[4] equipped with a flame-ionization detector. The chromatographic column consisted of glass tubing, 2 m long and 4 mm i.d., packed with 100–120-mesh Gas Chrom Q and coated with 3% OV-17[5]. The operating conditions were: injection port temperature, 290°; oven temperature, 270°; nitrogen (carrier gas) flow rate, 50 ml/min; hydrogen flow rate, 20 ml/min; and air flow rate, 300 ml/min.

A GLC–mass spectrometer–computer system[6] was used at the following conditions: energy of the ionization beam, 70 ev; ion source temperature, 100°; and ionization current, 200 μamp. Sample introduction was carried out by a direct inlet system at a probe temperature of 120° or by a GLC procedure. This GLC procedure utilized a glass column, 2 m long and 4 mm i.d., packed with 3% OV-17 on 100–120-mesh Gas Chrom Q at the following conditions: injector temperature, 290°; oven temperature, 270°; and helium (carrier gas) flow rate, 30 ml/min.

Synthesis of 10,11-Epoxide (V)—Cyclobenzaprine hydrochloride (20 mmoles) was dissolved in water–methanol (1:1) (100 ml), and a mixture of 2 ml of acetonitrile and 5 ml of a 30% solution of hydrogen peroxide was added at various intervals. The pH was kept constant at 9–10 with 1 *N* NaOH until oxygen evolved.

After 48 hr at room temperature, the reaction mixture was extracted twice with an equal volume of methylene chloride, dried over sodium sulfate, and evaporated. To reduce the *N*-oxide obtained from V, a water solution of 1 *N* $Na_2S_2O_4 \cdot 7H_2O$ was added and the reaction was followed with the gas chromatograph.

The solution was then extracted twice with 15 ml of methylene chloride, and the organic layer was washed with 15 ml of 5% NH_4Cl. The organic phase was fractionated on a silica gel column, 60 × 2 cm, eluted with cyclohexane–chloroform–diethylamine (85:10:5 v/v). The fractions collected (2 ml) were examined by GLC, and those containing the epoxide were pooled and evaporated.

The epoxide yield, crystallized from methylene chloride, was 60%,

[2] Boehringer.
[3] Merck.
[4] Carlo Erba Fractovap G1.
[5] Applied Science Laboratories.
[6] Finnigan quadrupole model 3100 and computer model 6000.

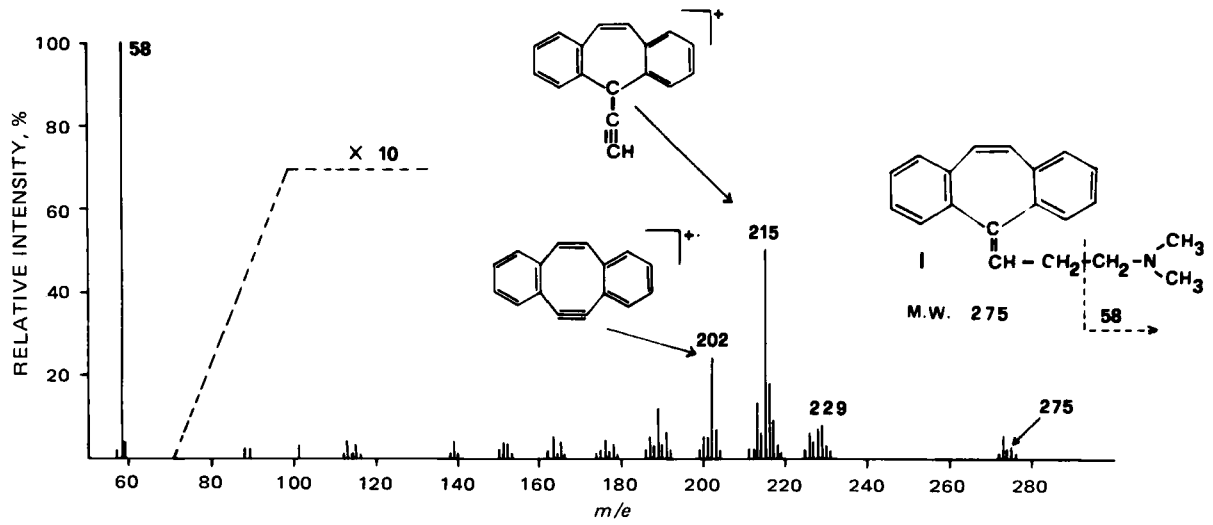

Figure 2—*Mass spectrum of authentic I. A similar spectrum was obtained by introducing the corresponding eluted TLC spots by the direct inlet system or GLC procedure.*

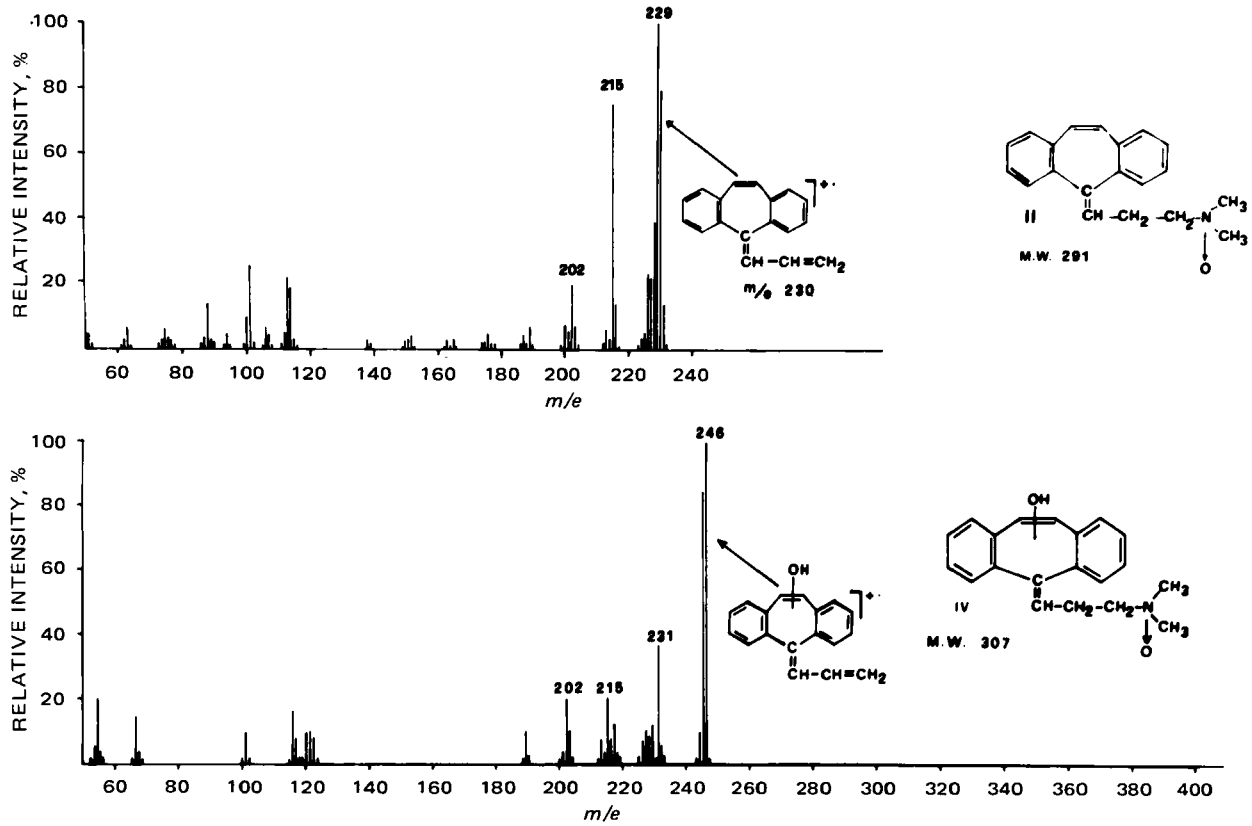

Figure 3—*Mass spectra of II and IV obtained by introducing the eluted TLC spots by the direct inlet system or GLC procedure.*

mp 97–100°. The compound showed R_f values at 0.72 and 0.50 R_f in Solvent Systems A and B (Table I), respectively; NMR[7] ($CDCl_3$): δ 4.2 (s, 2H, HCO epoxide), 2.8 [s, $N(CH_3)_2$], and 7.1–7.4 (m, 8H, aromatic proton).

RESULTS

The ethyl acetate extract of urine obtained from rats treated with I (40 mg/kg ip) was concentrated to dryness, redissolved in 100 μl of methanol, spotted on a TLC plate, and developed in Solvent Systems A and B. In contrast to the extract obtained from urine of untreated animals, seven spots were obtained; their R_f values are reported in Table I. Two metabolites (VI and VII) were also present in extracts obtained after β-glucuronidase treatment of the urine.

The extract of treated urine was also injected into the gas chromatograph, giving rise to seven peaks not present in the blank (Fig. 1).

The second GLC peak showed a retention time corresponding to that of authentic I. The R_f values of 0.72 and 0.50 (Table I) in Solvent Systems A and B, respectively, were identical to those of the starting drug. Furthermore, the mass spectrum (Fig. 2) of the compound was indistinguishable from the one obtained with authentic I.

Identification of Metabolites II and IV—The mass spectrum of the methanolic eluate from the spot at R_f 0.16 (Solvent System A) and the GLC–mass spectrum of the first peak exhibited a molecular ion at *m/e* 230 (Fig. 3). The structure elucidated by the mass spectrum

[7] Varian A60.

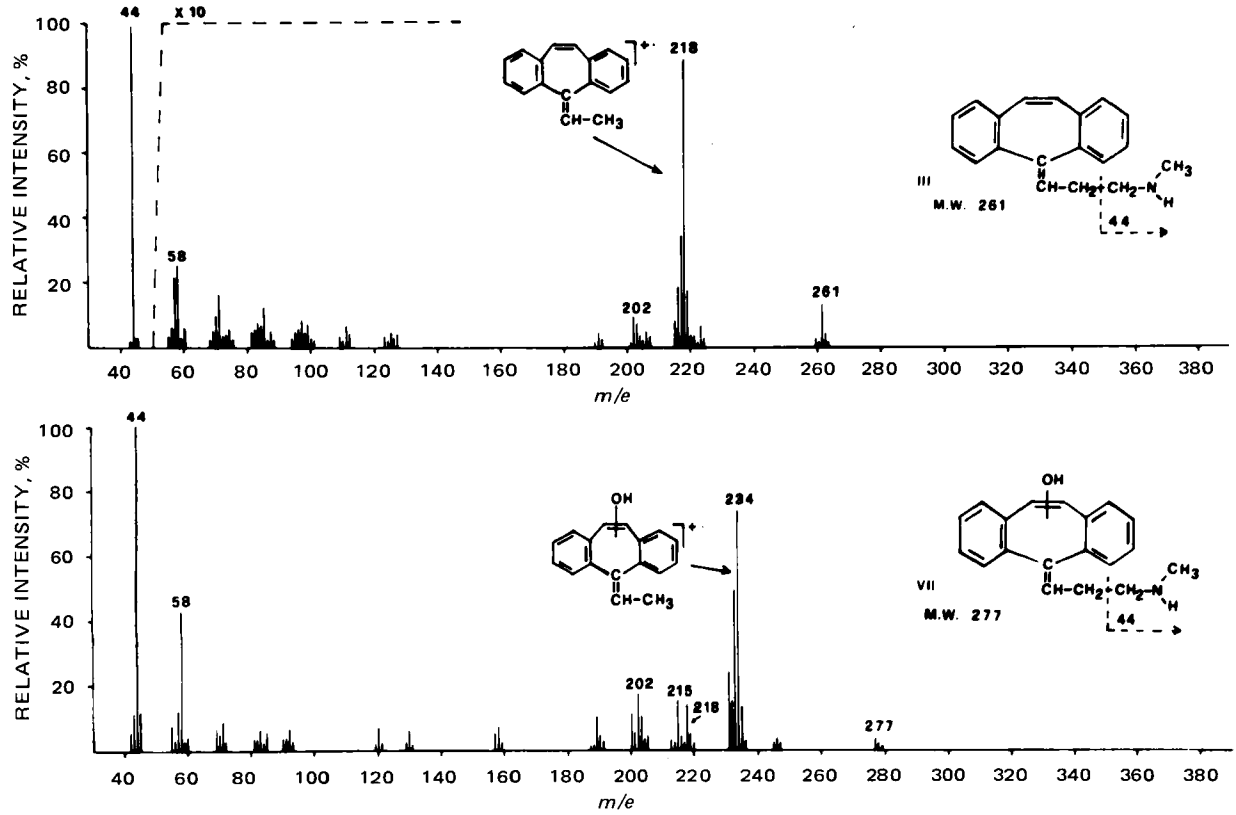

Figure 4—*Mass spectra of III and VII obtained by introducing the eluted TLC spots by the direct inlet system or GLC procedure.*

was the hydrocarbon VIII (Scheme I), which resulted from the Cope reaction of the *N*-oxide II in the injection port during GLC analysis (5). Therefore, the original identity of the TLC spot at R_f 0.16 in Solvent System A was II.

The fourth GLC peak, obtained from the injection of the eluate of the spot at R_f 0.06 (Solvent System A), gave rise to the mass spectrum in Fig. 3 when analyzed by GLC–mass spectrometry.

The higher polarity of this compound, demonstrated by a lower R_f

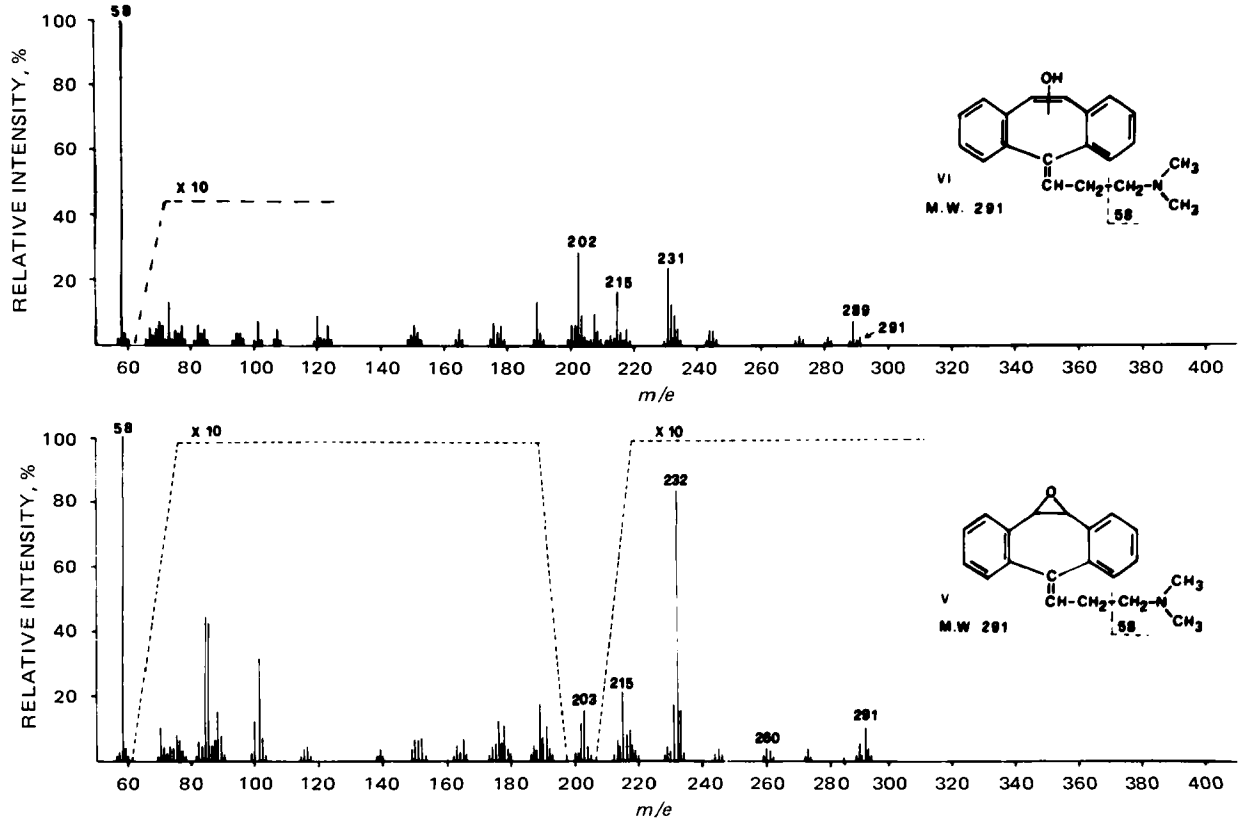

Figure 5—*Mass spectra of VI and the synthesized V obtained by introducing the eluted TLC spots by the direct inlet system or GLC procedure.*

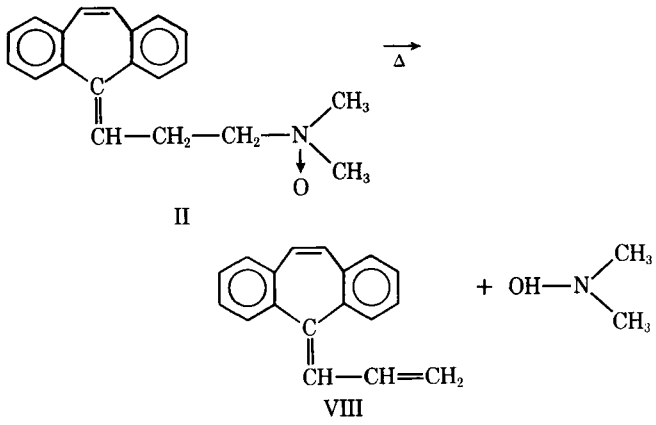

II

VIII

Scheme I—Cope thermal degradation of cyclobenzaprine N-*oxide*

value than that of the *N*-oxide and by a molecular ion at *m/e* 246 (16 amu more than the *N*-oxide), was consistent with the introduction of an oxygen atom into the 10- or 11-position of the *N*-oxide molecule, giving rise to IV. The presence of the hydroxyl group also was confirmed by on-column methylation with trimethylanilinium hydroxide.

This procedure gave rise to a GLC peak that, after mass spectral analysis, showed a mass spectrum in which the molecular ion was shifted to 14 amu, confirming the introduction of a methyl group.

As in the case of the *N*-oxide, the hydroxyl compound underwent the Cope reaction with the thermal loss of dimethylhydroxylamine.

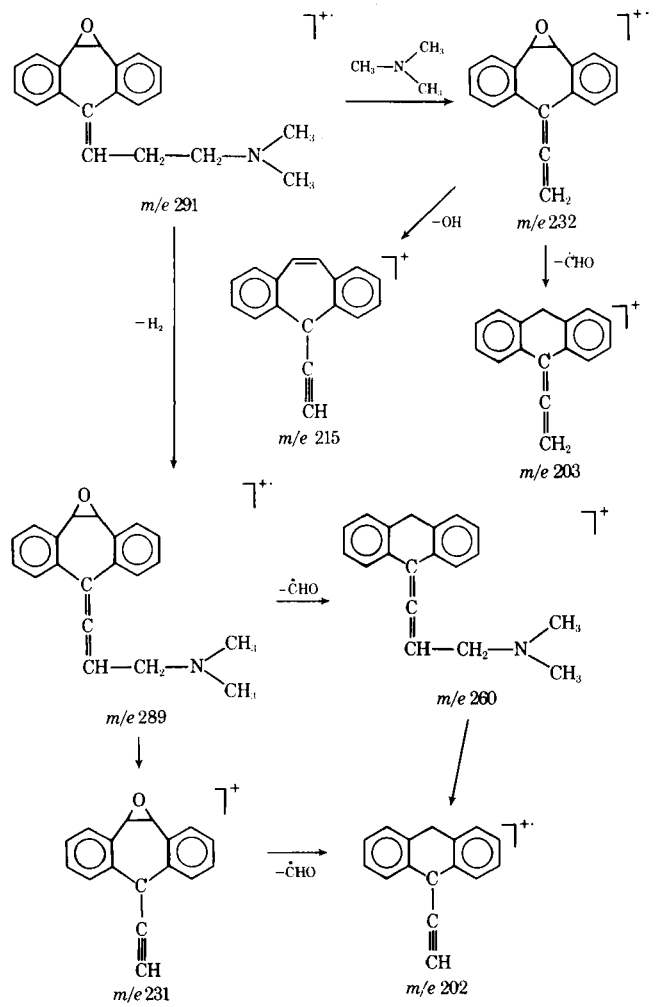

Scheme II—Suggested fragmentation pathway of the 10,11-epoxide of cyclobenzaprine. (No exact mass measurements were included in the parent ions or fragments, and only a few metastable ions were available to support the fragmentation scheme.)

Identification of Metabolites III and VII—The third GLC peak corresponded to a substance with R_f values of 0.51 and 0.44 in Solvent Systems A and B, respectively. The mass spectrum obtained by GLC or the direct inlet system showed the molecular ion at *m/e* 261 (Fig. 4), suggesting the loss of a methyl group in respect to I. The fragmentation pathway, showing the base peak at *m/e* 44 and a radical ion at *m/e* 218 (Fig. 4), confirmed a structure corresponding to the desmethylcyclobenzaprine.

The hydroxydesmethyl derivative was identified as the seventh GLC peak and corresponded to the TLC spots at R_f 0.19 and 0.23 in Solvent Systems A and B, respectively. The mass spectrum (Fig. 4) showed a molecular ion at *m/e* 277 due to the introduction of an oxygen atom into the 10- or 11-position of the drug molecule. After on-column treatment with trimethylanilinium hydroxide of the eluate of the TLC spots, a mass spectrum of the GLC peak was obtained with the molecular ion at *m/e* 305, confirming the structure of the metabolite. This compound also was present after incubation of the urine with β-glucuronidase.

Identification of Metabolites V and VI—The mass spectrum (Fig. 5) of the fifth GLC peak corresponded to a compound with the molecular ion at *m/e* 291 and R_f values of 0.68 and 0.41 in Solvent Systems A and B, respectively.

The hypothesis of the presence of an epoxide derivative of I was

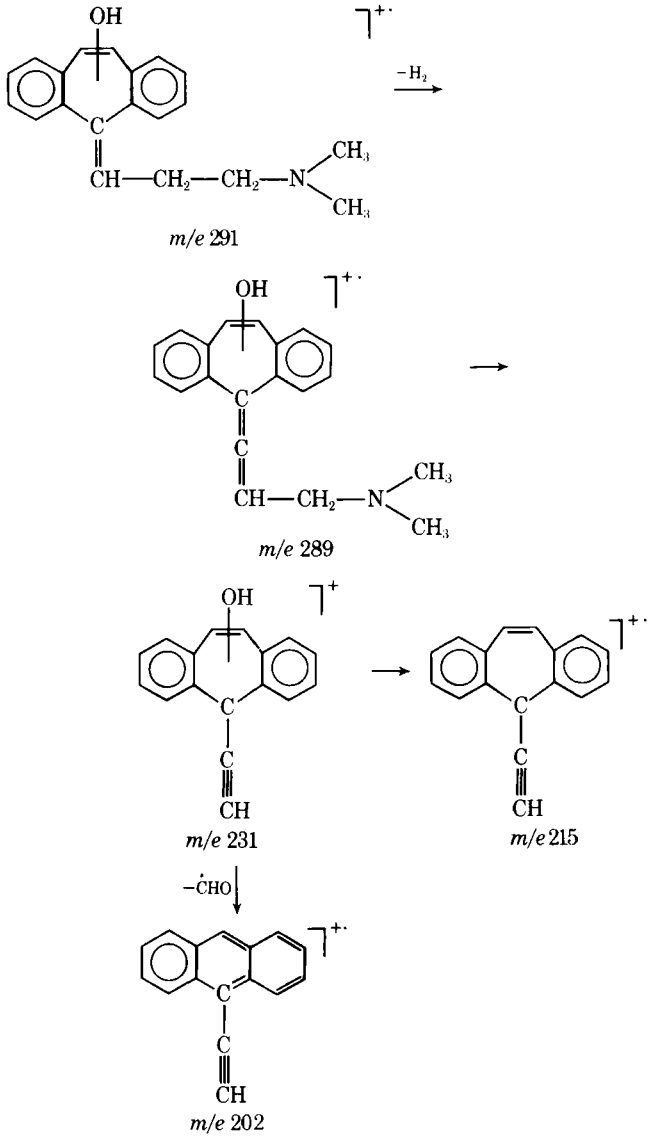

Scheme III—Suggested fragmentation pathway of hydroxycyclobenzaprine. (No exact mass measurements were included in the parent ions or fragments, and only a few metastable ions were available to support the fragmentation scheme.)

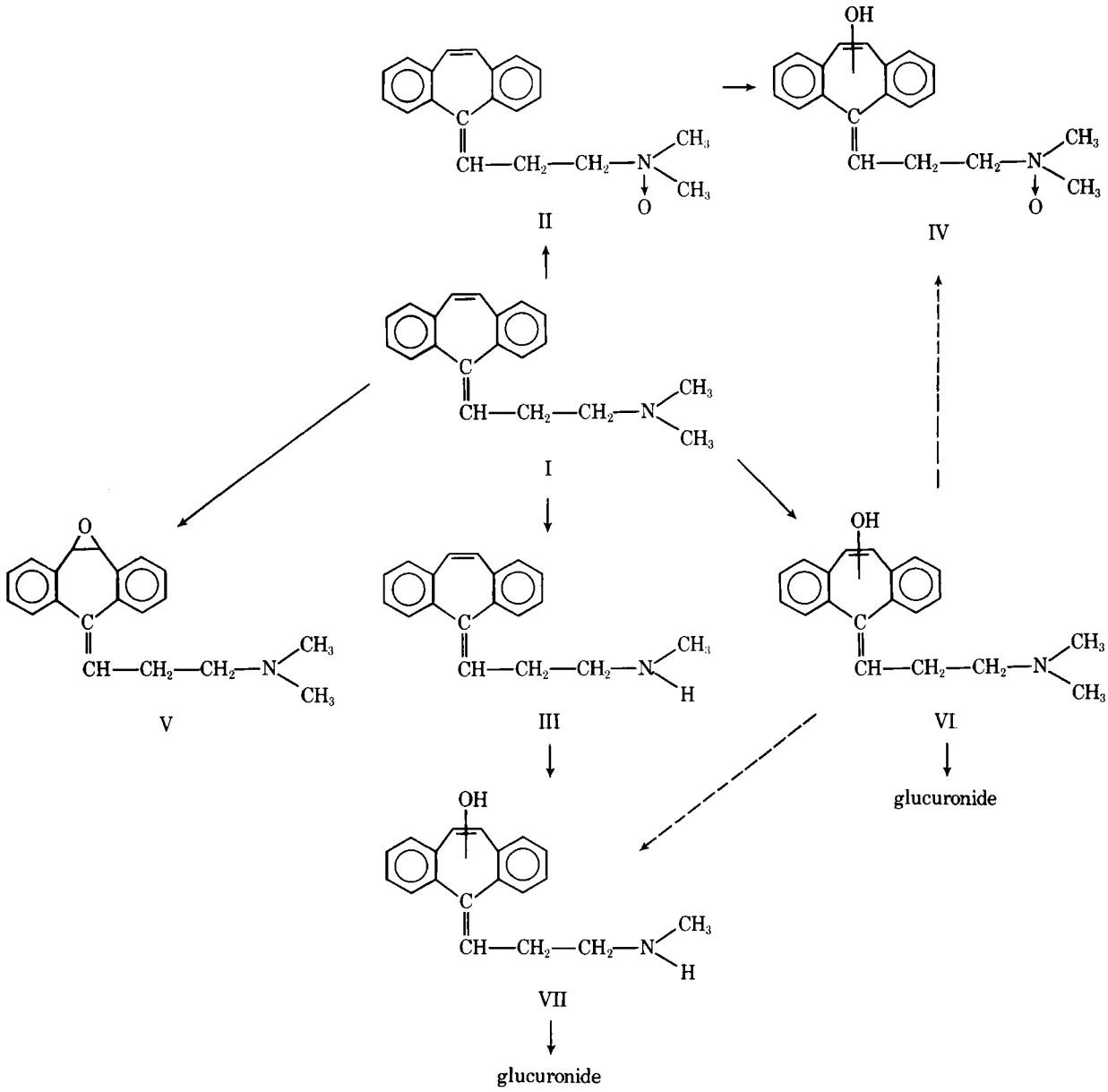

Scheme IV—Metabolic pathway of cyclobenzaprine in vivo.

supported by the fact that the molecular ion corresponded to the introduction of an oxygen atom into the drug molecule and by the failure in the methylation of the compound with trimethylanilinium hydroxide or diazomethane.

Moreover, the mass spectral, GLC, and TLC behavior of this metabolite was identical to that of a sample of the synthesized 10,11-epoxide of cyclobenzaprine. The fragmentation pathway of Metabolite V is reported in Scheme II.

The corresponding hydroxyl derivative of I gave rise to the sixth peak in the gas chromatogram. Its mass spectrum (Fig. 5) showed a molecular weight, 291, identical to that of the epoxide. However, there were different features in the fragmentation pathway (Scheme III) and, in addition, this compound reacted with trimethylanilinium hydroxide and formed a methylated product.

The hydroxycyclobenzaprine also was found in the β-glucuronidase-treated urine sample extracted with ethyl acetate.

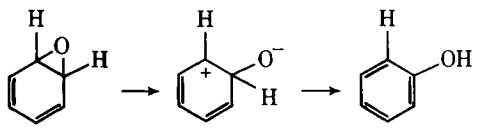

Scheme V

DISCUSSION

Scheme IV shows the metabolic pathway of cyclobenzaprine. The metabolic transformation of the drug probably occurs by oxidation of the nitrogen on the side chain to give II, by oxidation of the 10,11 double bond with formation of V and VI, and with loss of a methyl group giving rise to III. Metabolites II and III undergo a secondary transformation with oxygenation of the ethylenic double bond. Metabolites VI and VII also are present as glucuronide conjugates.

The loss of ĊHO to give the ions at *m/e* 260, 203, and 202 (Scheme II) seems to exclude the presence of the epoxide at the double bond of the aliphatic chain. Moreover, the TLC, GLC, and mass spectral properties of the metabolite are identical to those of the synthetic product which was unequivocally proven by NMR to be the cyclobenzaprine 10,11-epoxide.

The position of the hydroxyl group on the 10- or 11-carbon atom was assigned to Compounds IV, VI, and VII on the basis of methylation studies and mass spectral analysis. These compounds reacted immediately (5 min) with diazomethane, while prolonged (2 hr) reaction times were necessary for aromatic hydroxyl groups (6).

Moreover, the fragmentation pathway of V and VI (Schemes II and III) shows that both compounds give rise to the same radical ion at *m/e* 202 by loss of HĊO and contraction of the seven-membered ring.

Some reports (7, 8) have stated that the formation of monohydroxyl

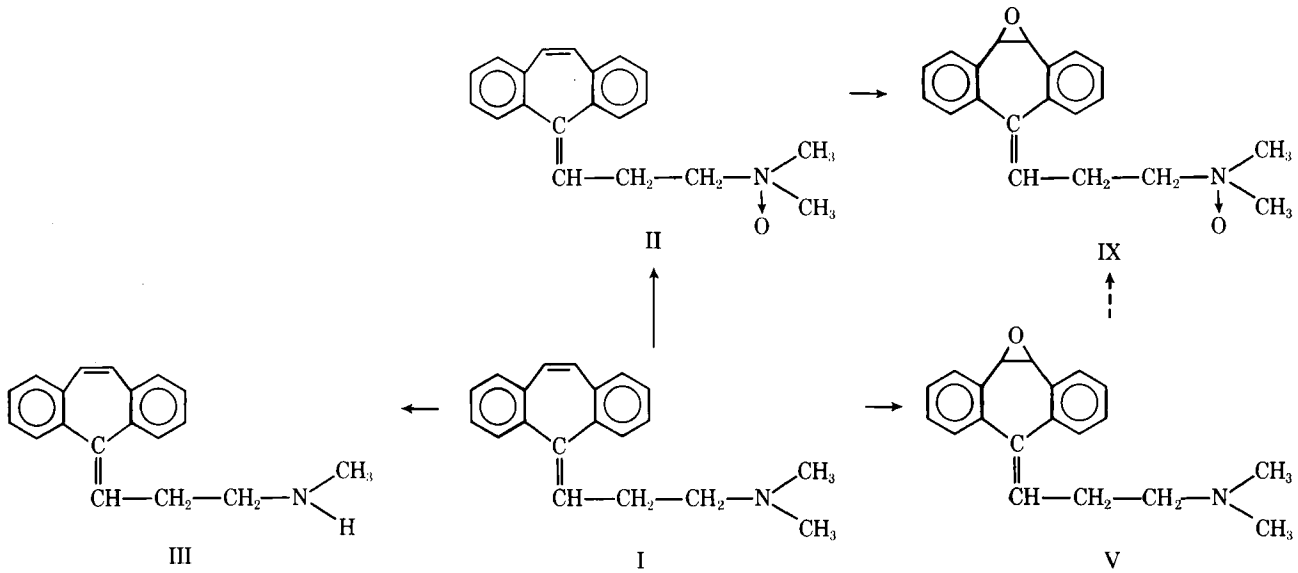

Scheme VI—Metabolic pathway of cyclobenzaprine incubated with microsomes.

derivatives, when an epoxide was present in the metabolic pathway, occurred by a nonenzymatic rearrangement of the epoxide (Scheme V). In our case, however, it was established that the formation of the hydroxylated metabolites was not due to a chemical modification of the epoxide molecule. In fact, after incubating the synthetic epoxide with control rat urine for 48 hr at 37°, no degradation of the compound was observed with TLC, GLC, and mass spectral techniques.

An unresolved problem at the present time is the positioning of the hydroxyl group at the 10- or 11-carbon of the ethylenic bridge.

The chemical evidence of an isomerism of the hydroxyl group, in respect to the double bond in the side chain, is evident because two different structures, IX and X, can be drawn. Moreover, the thin-layer chromatogram has a spot that, when eluted with methanol, shows the identical GLC retention time and mass spectrum of Metabolite VI but a different R_f value (0.27, Solvent System B).

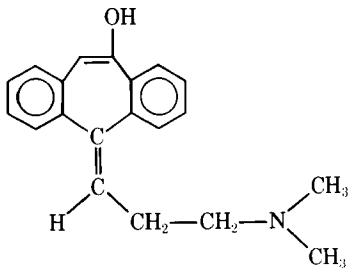

IX

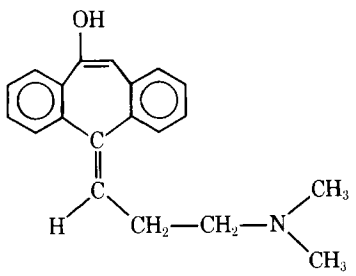

X

It can be argued from these data that the 10- and 11-positions are not the same from the chemical point of view but that the enzymatic introduction of oxygen is possible in both positions.

This investigation adds a new example of the formation of an epoxide when there is a double bond (10,11-position) of a tricyclic structure. This epoxide is obviously not highly reactive, since it can be isolated from urine and from liver microsomal enzymes (the metabolic pathway *in vitro* is reported in Scheme VI) (9). Studies in progress also indicate that this epoxide has pharmacological activity.

REFERENCES

(1) A. Frigerio, R. Fanelli, P. Biandrate, G. Passerini, P. L. Morselli, and S. Garattini, *J. Pharm. Sci.*, **61**, 1144(1972).

(2) A. Frigerio, N. Sossi, G. Belvedere, C. Pantarotto, and S. Garattini, *ibid.*, **63**, 1536(1974).

(3) V. Rovei, G. Belvedere, C. Pantarotto, and A. Frigerio, *ibid.*, **65**, 810(1976).

(4) J. Metyšová, J. Metyš, and Z. Votava, *Arch. Int. Pharmacodyn. Ther.*, **144**, 481(1963).

(5) G. Belvedere, V. Rovei, C. Pantarotto, and A. Frigerio, *Biomed. Mass Spectrom.*, **1**, 329(1974).

(6) M. G. Horning, C. Butler, D. J. Harvey, R. M. Hill, and T. E. Zion, *Res. Commun. Chem. Pathol.*, **6**, 565(1973).

(7) D. M. Jerina, J. W. Daly, B. Witkop, P. Zaltzman-Nirenberg, and S. Udenfriend, *Biochemistry*, **9**, 147(1970).

(8) D. Jerina, J. Daly, B. Witkop, P. Zaltzman-Nirenberg, and S. Udenfriend, *Arch. Biochem. Biophys.*, **128**, 176(1968).

(9) G. Belvedere, V. Rovei, C. Pantarotto, and A. Frigerio, *Xenobiotica*, in press.

ACKNOWLEDGMENTS AND ADDRESSES

Received March 31, 1975, from the *Istituto di Ricerche Farmacologiche "Mario Negri," Via Eritrea 62, 20157 Milan, Italy.*

Accepted for publication August 11, 1975.

[x] To whom inquiries should be directed.

Influence of Route of Administration on Physiological Availability of Levodopa in Dogs

STANLEY COTLER, ALICE HOLAZO, HAROLD G. BOXENBAUM, and STANLEY A. KAPLAN ˣ

Abstract □ The physiological basis for the reduced levodopa bioavailability following oral administration was investigated. Four dogs received single 25-mg/kg doses of ^{14}C-levodopa on three separate occasions in a crossover fashion *via* hepatoportal catheter, intravenous, and oral administrations. Plasma and urine specimens were analyzed for intact levodopa and total radioactivity. The ratios of areas under the plasma concentration–time curves following hepatoportal and intravenous administrations were close to unity, and the shapes of the curves were virtually identical. Following oral administration, however, significant reductions in the areas under the plasma concentration–time curves were observed. These data indicate that the physiologically impaired bioavailability of orally administered levodopa occurs almost exclusively as a result of metabolic degradation within the GI lumen and/or gut wall.

Keyphrases □ Levodopa—bioavailability, effect of route of administration, oral, intravenous, and hepatoportal catheter compared, dogs □ Bioavailability—levodopa, effect of route of administration, dogs □ Administration route—levodopa, oral, intravenous, and hepatoportal catheter compared, bioavailability, dogs

For many drugs, quantitative differences in pharmacological response and/or toxicity were observed when identical drug doses were administered by oral *versus* parenteral routes. An example is the antiarrhythmic agent lidocaine (1), which was therapeutically less active and produced more nausea when administered orally than when administered intravenously to dogs.

Such differences in therapeutic activity may frequently be understood by investigation of the physiological, biochemical, and pharmacokinetic characteristics of drug absorption. Information about these parameters may contribute to the pharmacological and toxicological profile of a drug by allowing the investigator to understand the basis of the observed differences in activity. In addition, the findings may suggest a means of defining or overcoming potential problem areas in drug development.

BACKGROUND

Bioavailability is determined most frequently by comparison of blood level–time curve shapes and areas following oral and intravenous administrations. In instances where bioavailability is incomplete, the ratio of oral to intravenous blood level curve areas is less than unity. This result may arise for a variety of reasons, which may be physicochemical and/or physiological in nature, including poor dissolution of the drug in the GI fluids, poor permeability of the drug across the GI mucosa, gut wall metabolism, metabolism by GI bacteria, enzymatic metabolism in the luminal contents, and first-pass liver metabolism.

Levodopa is an example of a drug exhibiting reduced oral bioavailability. Since the initial report of its isolation from *Vicia faba* beans by Guggenheim (2), levodopa has been the subject of numerous investigations. Interestingly, Guggenheim administered the compound to himself and was the first to note the emetic properties. Subsequent to the discovery of levodopa decarboxylase (2), levodopa and dopamine were proposed as intermediates in the biosynthesis of norepinephrine and epinephrine from L-tyrosine (Scheme I).

Dopamine was first identified as a normal brain constituent in 1957 (2). It was determined upon autopsy that patients suffering from the incapacitating effects of parkinsonism exhibited depleted dopamine levels in certain areas of the brain (3). Cotzias (4) became involved with levodopa as a result of his work with Chilean miners suffering from chronic manganese poisoning. He observed a similarity in the clinical manifestations of manganese poisoning and parkinsonism and began fruitful studies on parkinsonian brain abnormalities and their control.

Clinical treatment of parkinsonism involves the administration of levodopa, since dopamine itself cannot cross the blood–brain barrier (5). Once across the blood–brain barrier, levodopa can be biotransformed to dopamine and exert its effect. Satisfactory absorption of orally administered levodopa from the GI tract is an obvious prerequisite for therapeutic efficacy. Considerable interpatient variability in plasma levodopa concentrations has been observed (6) and may be indicative of variability in bioavailability.

Prior to systemic absorption of levodopa, the GI milieu may reduce significantly the amount of levodopa available (7). Biotransformation products subsequently may alter gastric secretion and motility; one such group of products, the phenylcarboxylic acids, may contribute to the drug's nauseating effect (7). In rats, the presence of an active transport absorption system (passive diffusion playing only a minor role) makes levodopa unique, since this process may be inhibited by a lack of molecular oxygen and the presence of other amino acids.

The existence of a similar levodopa absorption pattern in humans could explain some problems associated with the variability in absorption and bioavailability of the various dosage forms (8). Granerus *et al.* (9) calculated that only about 26% or less of the ingested dose reaches sytemic circulation and suggested that the remainder was decarboxylated in the intestines. However, these studies did not distinguish between possible first-pass liver and intestinal metabolism.

Coutinho *et al.* (10) administered radiolabeled levodopa to dogs and reported higher intact plasma levels and corresponding areas under the plasma concentration–time curves following intravenous administration as compared to oral administration of equivalent doses. Their data indicated that approximately 70–75% of the intravenous and 57–70% of the orally administered radioactivity were excreted in the urine over 72 hr, with levodopa and dopamine accounting for a small percentage of the excretion products. Approximately 3.0–7.0% of the intravenous or oral doses was excreted in the feces.

The efficiency of absorption of total radioactivity ranged between 83.0 and 92.0% of the administered dose. However, when calculated by area analysis, only 22.0–30.0% of the administered oral dose reached the systemic circulation as intact levodopa. These findings suggested that the remainder of the absorbed dose, approximately 60.0%, was biotransformed in the GI tract prior to absorption and/or in the liver during its first pass prior to reaching the general circulation.

The present investigation with levodopa was undertaken to elucidate the mechanism(s) responsible for the reduced oral levodopa bioavailability. Plasma level profiles of levodopa in each dog were compared subsequent to intravenous, hepatoportal, and oral administrations. Comparisons within the same animals permitted determination of the relative contributions of GI and first-pass liver metabolism to the observed reduced levodopa bioavailability.

EXPERIMENTAL

Hepatoportal Cannulation—Four beagle dogs, 10–14.2 kg, were anesthetized with 25–30-mg/kg iv doses of pentobarbital sodium. An incision was made on the left lateral portion of the body, and the spleen was exteriorized. An area of approximately 3 cm of a small tributary of the splenic vein adjacent to the spleen was cleared of

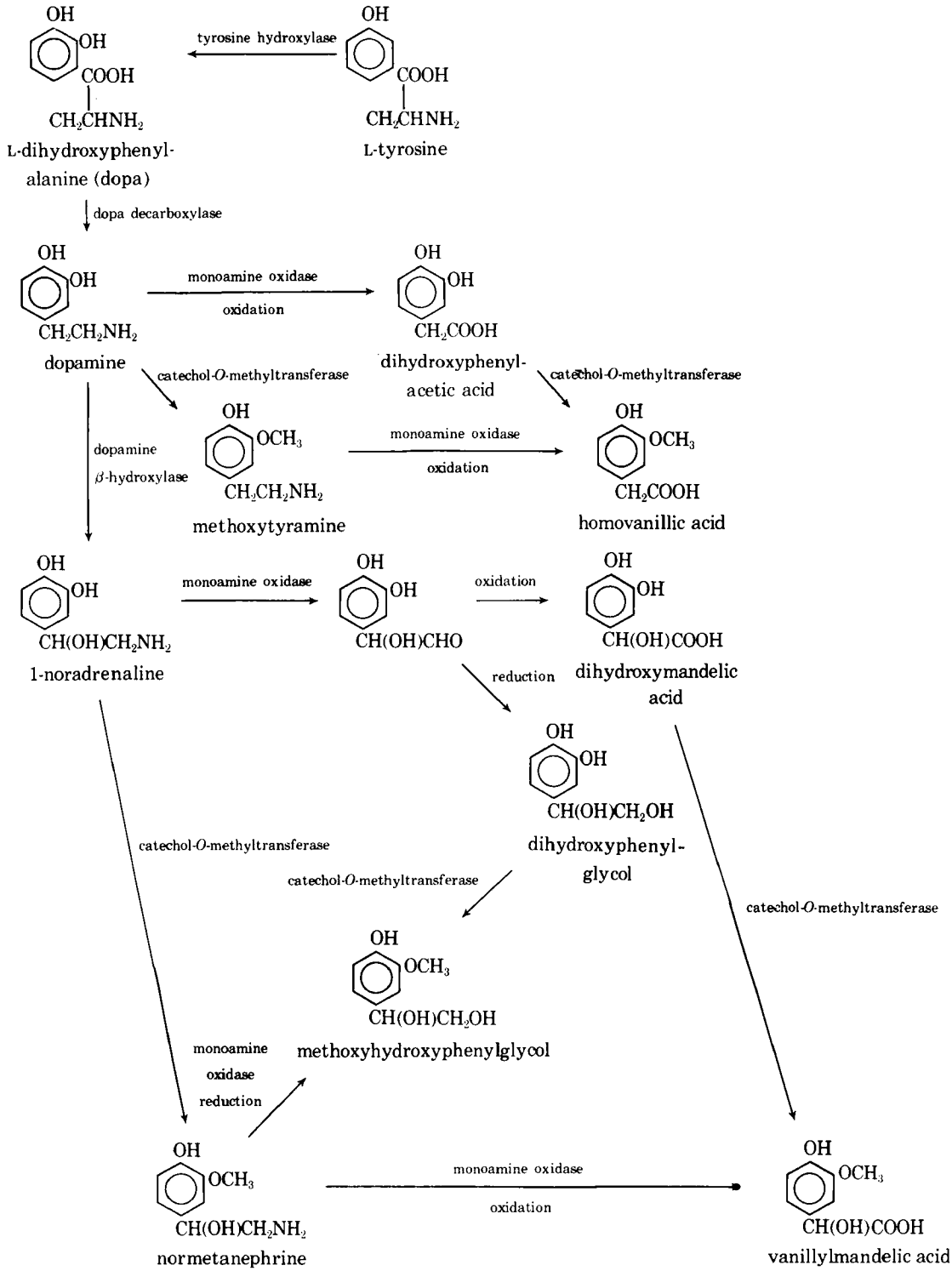

Scheme I—Metabolic pathway of levodopa

surrounding tissue. The vein was tied distally with "0" size silk, and a small incision was made in the vein through which a catheter[1] was introduced.

The catheter used for chronic intravascular implantation consisted of tubing, 0.147 cm o.d. and 0.086 cm i.d.[2], inserted over a 19-gauge, 2.54-cm disposable needle[3] to which a one-way stopcock[4] was attached. The catheter was extended into the hepatic portal vein so that its tip was brought just to the liver. The spleen was returned to its normal position, the free end of the catheter was exteriorized through a stab wound, and the incision closed.

The hepatoportal vein catheter was reintroduced into the stab wound just under the skin and brought through the loose subcutaneous tissue on the left lateral side and exteriorized in the area of the middle of the rib cage. The catheter was protected from damage, by the animal, by securing it in a pocket of a jacket[5]. The dogs were allowed to recover for approximately 1 week. A radiopaque solution,

[1] Coated with Teflon (du Pont).
[2] Teflon tubing, Alpha Wire Co., Elizabeth, N.J.
[3] B. D. 5686, Rutherford, N.J.
[4] B. D. 3154, Rutherford, N.J.
[5] Alice B. King Co., Los Angeles, Calif.

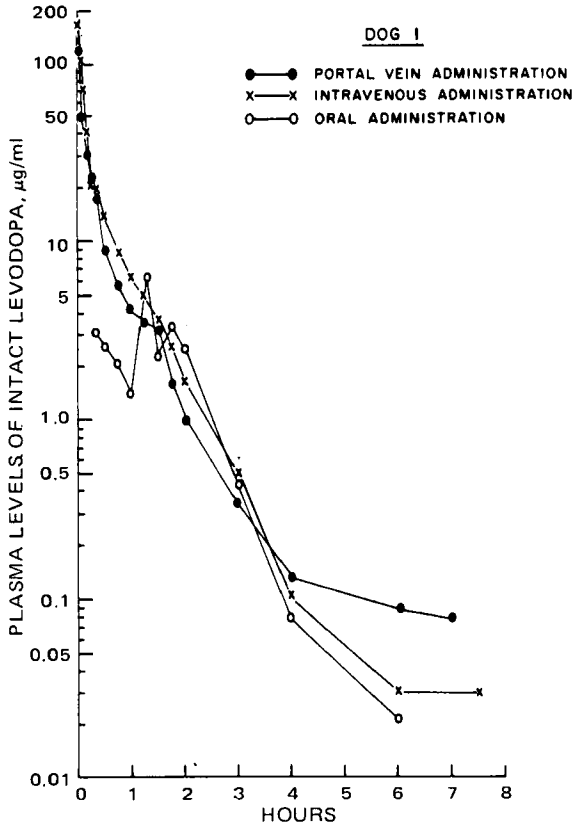

Figure 1—*Intact levodopa plasma levels following intravenous, hepatoportal, and oral administrations of 25-mg/kg doses of levodopa to Dog 1.*

diatrizoate sodium[6], was used for a subsequent X-ray to ensure that the catheter was in its proper position prior to initiating the studies.

The hepatoportal catheter allowed for the rapid administration of drug into the hepatic portal vein, assuring 100% passage of the dose through the liver prior to entering the systemic circulation and completely bypassing the GI tract.

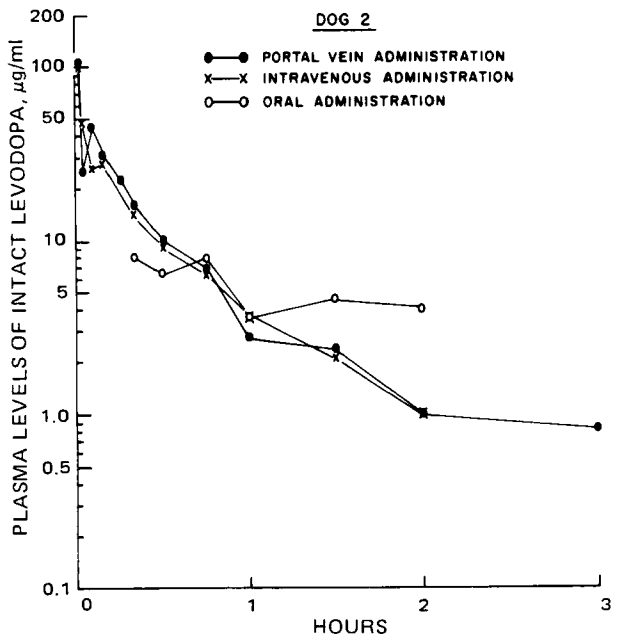

Figure 2—*Intact levodopa plasma levels following intravenous, hepatoportal, and oral administrations of 25-mg/kg doses of levodopa to Dog 2.*

[6] Hypaque, Winthrop Laboratories, New York, N.Y.

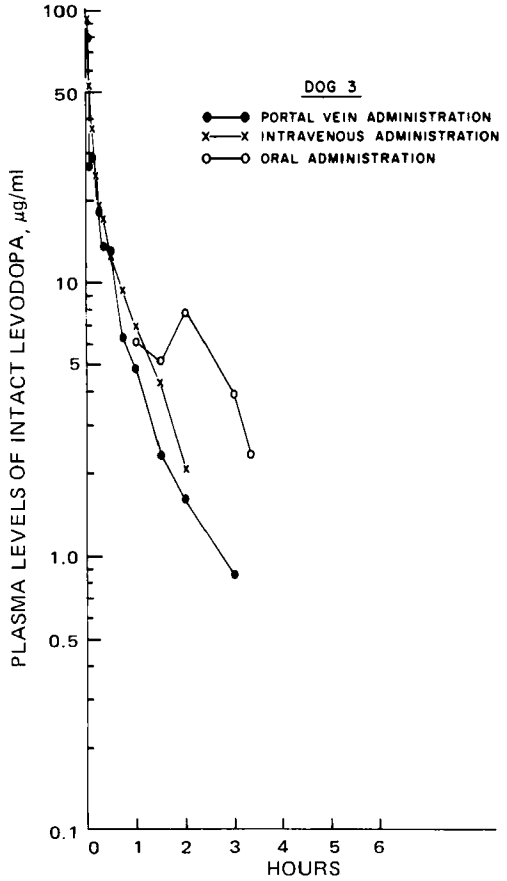

Figure 3—*Intact levodopa plasma levels following intravenous, hepatoportal, and oral administrations of 25-mg/kg doses of levodopa to Dog 3.*

Study Design—Four unanesthetized, fasted dogs (24 hr) with previously implanted hepatic portal vein catheters were used in a three-way crossover experiment. A minimum of 2 weeks elapsed between drug administrations. Levodopa was dissolved immediately prior to administration in 11 ml of 0.27 *N* hydrochloric acid.

In the first of the three administrations, 25-mg/kg doses of 2-^{14}C-levodopa (specific activity of 0.3 μCi/mg) were administered as a bolus into the hepatic portal vein. In the second administration, the 25-mg/kg doses of ^{14}C-levodopa were administered intravenously as a bolus to each dog *via* a catheter in the jugular vein. The third administration to each dog consisted of 25-mg/kg doses of solid ^{14}C-levodopa (in hand-packed gelatin capsules) administered orally.

Ten-milliliter blood specimens were obtained by venipuncture at the time intervals indicated in Figs. 1–4, with the first specimen obtained 1 min following intravenous and hepatoportal administrations and 10 min following oral administration. The blood was immediately transferred to tubes containing 0.2 ml of heparin (10,000 units/ml) and 10 mg of metabisulfite. The specimens were spun down in a refrigerated centrifuge, and the plasma was separated, frozen, and subsequently analyzed for intact levodopa and total radioactivity. The total volume of urine voided was collected at 24-hr intervals from 24 hr prior to dosing to 96 hr postdosing, and total carbon-14 radioactivity levels were determined.

Intravenous and hepatoportal administrations resulted in emesis 3–5 min postadministration. Oral administration resulted in emesis 20–32 min postadministration. In all cases, emesis fluid was collected and the radioactivity content was determined. Radioactivity was not detectable in the emesis fluid following either parenteral route of administration. Recoverable radioactivity of the emesis fluid following oral administration was determined, and the doses were corrected as indicated in Table I.

Analytical Procedure (11)—Heparinized blood specimens, with 10 mg of metabisulfite added to stabilize the levodopa at the time of collection, were chilled immediately in an ice bath. The plasma was

Table I—Pharmacokinetic Parameters of Levodopa in the Dog

	Dog 1			Dog 2			Dog 3			Dog 4		
	Intravenous	Hepatoportal	Oral	Intravenous	Hepatoportal	Oral	Intravenous	Hepatoportal	Oral	Intravenous	Hepatoportal	Oral
Levodopa dose, mg	300	300	300	256	265	269	335	335	368	212	250	250
Dose retained, mg	300	300	267	256	265	82	335	355	234	212	250	250
Dog weight, kg	12.0	12.0	12.0	10.2	10.6	10.8	13.4	14.2	14.7	10.0	10.0	10.0
Dose, mg/kg	25	25	22.3	25	25	7.5	25	25	15.9	21.2	25	25
A, μg/ml	161	87.3	—	156	65.6	—	78.4	72.7	—	132	110.2	—
B, μg/ml	26.3	11.2	—	24.2	4.5	—	23.9	21.7	—	19.4	26.1	—
α, hr^{-1}	14.58	7.44	—	42.30	4.64	—	17.46	17.50	—	19.50	16.60	—
β, hr^{-1}	1.37	1.09	1.21	1.66	0.63	—	1.21	1.42	0.60	1.24	1.63	1.09
$0.693/\beta$, hr	0.51	0.64	0.57	0.42	1.10	—	0.57	0.49	—	0.69	0.43	0.64
k_{12}, hr^{-1}	6.54	—	—	27.06	—	—	9.42	—	—	10.38	—	—
k_{21}, hr^{-1}	3.23	—	—	7.14	—	—	5.00	—	—	3.57	—	—
k_{10}, hr^{-1}	6.18	—	—	9.90	—	—	4.21	—	—	6.78	—	—
V_1, ml	1605	—	—	1412	—	—	3274	—	—	1397	—	—
Area under plasma level curve, μg/ml/hr	29.7	22.5	7.2[a]	18.4	19.6	10.0[a]	22.2	19.3	16.5[a]	22.3	23.3	5.2
Ratio areas compared to iv	—	0.76	0.24	—	1.06	0.54	—	0.84	0.74	—	1.04	0.22
Total carbon-14 excreted in urine, 0–96 hr, % of dose	75	121	62	65	76	88	89	100	116	73	89	94
Ratio carbon-14 excreted in urine compared to iv	—	1.6	0.83	—	1.2	1.4	—	1.1	1.3	—	1.2	1.3

[a] Area corrected for dose equivalent of 25 mg/kg.

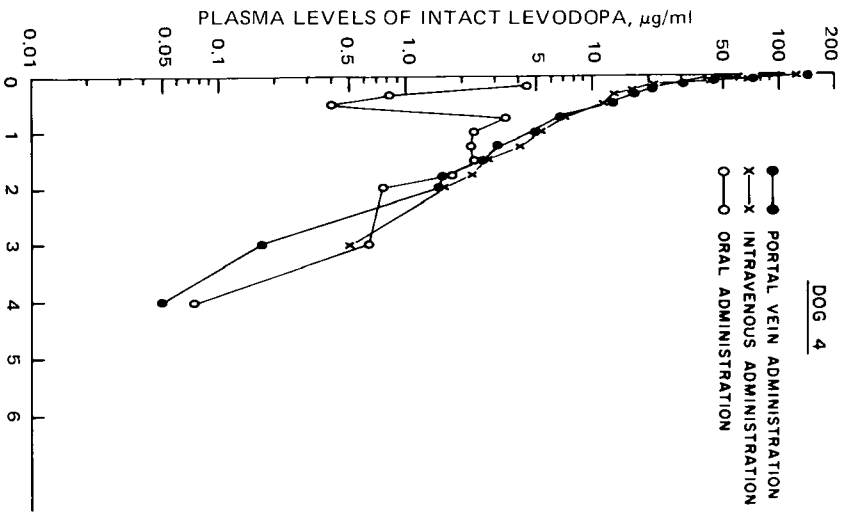

Figure 4—*Intact levodopa plasma levels following intravenous, hepatoportal, and oral administrations of 25-mg/kg doses of levodopa to Dog 4.*

separated in a refrigerated centrifuge. A 0.5-ml aliquot of plasma or a 0.2-ml aliquot of urine was added to 10 ml of scintillation solution[7] and counted for total radioactivity in a scintillation counter[8].

A second aliquot of 0.2 ml of plasma was added to 1.0 ml of a 20-mg/ml solution of edetic acid. One milliliter of water and 2 drops of a 2% solution of naphthoresorcinol in ethyl alcohol were added, and the specimen was mixed. Subsequently, 0.1 ml of 5 *N* sodium hydroxide was added, and the mixture was allowed to stand at room temperature for 5 min. The aqueous layer was washed once with 1 ml of 1-butanol. One milliliter of the aqueous layer was saturated with 0.5 g of sodium chloride and then acidified with 0.1 ml of 6 *N* hydrochloric acid. The levodopa derivative was extracted with 2 ml of ethylhexanol, with a mean (*SE*) recovery of 88.4 ± 1.9%, and determined spectrofluorometrically with excitation at 440 nm and emission at 470 nm.

RESULTS

Intact plasma levodopa levels in the four dogs are presented in Figs. 1–4 following all three routes of administration. Visual inspection of the intravenous and hepatoportal intact plasma level curves for each dog (Figs. 1–4) indicate that their overall disposition profiles were virtually identical. The areas under the plasma level–time curves were calculated using the trapezoidal rule. The (hepatoportal–intravenous) ratio of the areas under the plasma level curves ranged from 0.76 to 1.06, with a mean of 0.93. This ratio closely approximates unity and suggests that the liver did not substantially contribute to the reduced physiological availability of orally administered levodopa.

The corresponding (oral–intravenous) ratio of areas under the plasma level curves ranged from 0.23 to 0.74, with a mean of 0.44. This decreased area under the oral plasma level curves for unchanged levodopa when compared with the corresponding values obtained following the hepatoportal and intravenous administrations indicates

[7] Aquasol, New England Nuclear.
[8] Packard Tri-Carb model 3380.

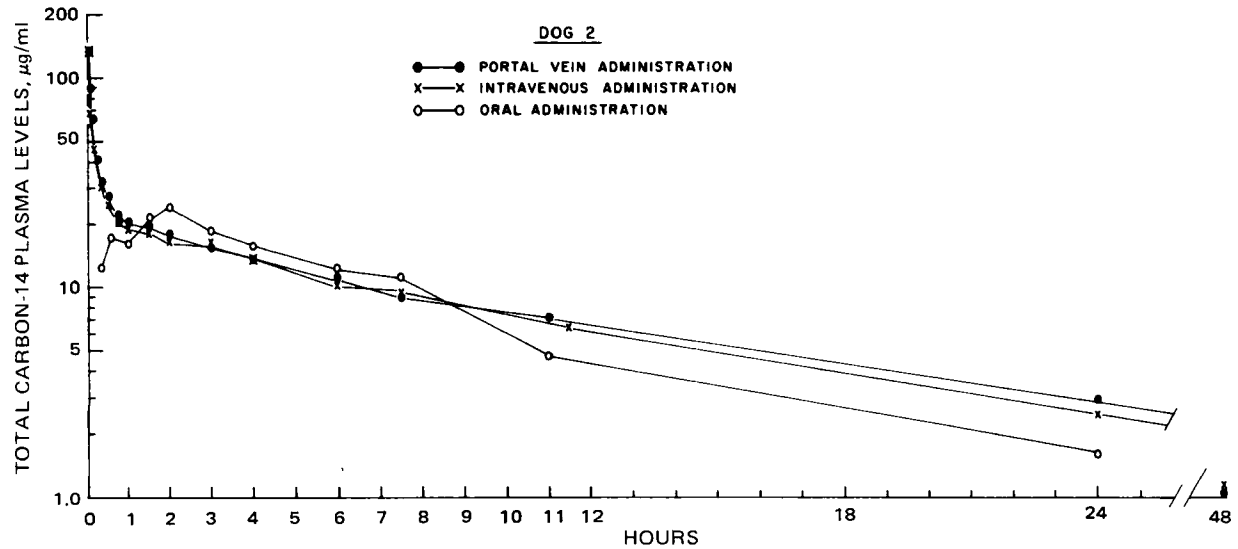

Figure 5—*Total carbon-14 plasma levels following intravenous, hepatoportal, and oral administrations of 25-mg/kg doses of levodopa to Dog 2.*

that the organ responsible for the reduced bioavailability of orally administered levodopa is the GI tract and not the liver.

The relatively complete recovery of administered total carbon-14 radioactivity in the urine following all three routes of administration (Table I) suggests complete absorption of the administered radioactive dose. Complete oral absorption of the administered dose is further confirmed by the comparable areas under the plasma level curves of total carbon-14 levels following all three routes of administration, as exemplified in Fig. 5 for one dog.

Following rapid intravenous injection of levodopa in the four dogs, plasma concentration–time curves could be described satisfactorily by a biexponential equation (12):

$$Cp = Ae^{-\alpha t} + Be^{-\beta t} \qquad \text{(Eq. 1)}$$

where t is time in minutes, Cp is plasma concentration (micrograms per milliliter) at time t; α and β are macroscopic rate constants having units of hours^{-1}, and A and B are coefficients having units of micrograms per milliliter. Initial estimates of the parameters A, B, α, and β were determined by appropriate graphical analysis (12). Initially, it was assumed that the plasma concentration–time data were consistent with the two-compartment open model (12) shown in Scheme II, where Compartments 1 and 2 are the central and peripheral compartments, respectively; k_{12}, k_{21}, and k_{10} are first-order microscopic rate constants (hours^{-1}) representing distribution and elimination processes; Cp is the concentration of drug (micrograms per milliliter) in Compartment 1 at time t (hours); and V_1 is the volume (milliliters) of Compartment 1.

The biexponential equation was fitted to the observed data using the NONLIN program (13), which uses an adaptation of Hartley's modification of the Gauss–Newton method for the fitting of nonlinear regression functions by least squares. Graphical estimates of A, B, α, and β were converted (12) to estimates of k_{12}, k_{21}, k_{10}, and V_1. These latter parameters were used as initial estimates for the program and were directly iterated. A weighting factor of $1/(Cp)^2$ was used in the analysis. Final estimates of the four parameters were converted to the parameters A, B, α, and β. Table I shows the results of these computer analyses. Visual inspection of the observed points about the fitted curves indicated a satisfactory randomness of scatter. Percent coefficients of variation (14) of the parameters k_{12}, k_{21}, k_{10}, and V_1 averaged 23.1, 12.3, 8.31, and 15.8%, respectively.

The question arises, however, as to the appropriateness of this model. Numerous *in vitro* studies indicated that extracts prepared from various animal tissues (15) are capable of decarboxylating levodopa. The wide variety of tissues capable of metabolizing levodopa alludes to the possibility that aromatic L-amino acid decarboxylase activity exists to varying degrees in virtually all regions of the body. Therefore, a more appropriate pharmacokinetic model might contain an irreversible elimination–metabolism step from both the central and peripheral compartments. However, an explicit solution to the parameters of such a model does not exist, except in the special situation where information on metabolite disposition is available (16).

Alternatively, if one assumes or calculates the ratio of elimination rate constants from the peripheral and central compartments, the model parameters may be solved (17, 18). Unfortunately, the present body of information with respect to the relative importance of the various dog tissues in the decarboxylation of levodopa is insufficient to permit even a rough approximation of this ratio. Consequently, the model-independent pharmacokinetic parameters A, B, α, and β may be considered to hold the greatest significance at this time.

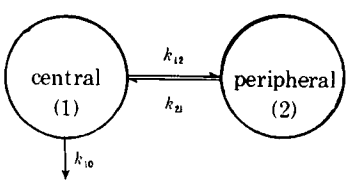

Scheme II—Two-compartment open model

DISCUSSION

The data in this study indicate that an orally administered dose of levodopa will be absorbed completely in terms of total radioactivity administered. However, the bioavailability of intact levodopa to the general circulation is reduced by a factor of at least one-half when administered orally. The ratios of areas under the intact levodopa plasma concentration–time curves following the hepatoportal vein administration and intravenous administration approximated unity, and the shapes of these curves were virtually identical within the same dog.

This observation indicates that the first pass of levodopa through the liver does not appreciably contribute to the reduced bioavailability observed following oral administration. The corresponding areas under the intact levodopa plasma concentration–time curves following oral administration were reduced significantly. These observations confirm that the physiologically impaired bioavailability of orally administered levodopa occurs virtually exclusively in the GI tract.

Rivera-Calimlim *et al.* (19) investigated the *in vitro* metabolism of ^{14}C-levodopa by incubating the drug with rat gastric and intestinal everted sacs and separating the drug and metabolites from tissue and serosal and mucosal fluids. These investigators demonstrated that extensive metabolism occurred and was associated with high levels of metabolites in both gastric and intestinal tissues and fluids. This metabolism occurred as a result of the decarboxylase activity in these tissues. The investigators also were able to show a significant inhibition of metabolism when ^{14}C-levodopa was incubated with tissues from rats pretreated with the decarboxylase inhibitor α-methylhydrazine, confirming that the decarboxylase enzymes were promoting metabolism.

Taubin and Landsberg (20) showed that, following intraperitoneal and intravenous administrations of levodopa to the rat, the duodenum

and ileum formed dopamine and *O*-methylated metabolites in greater amounts than in other tissues; they suggested that the rat gut has specific mechanisms for the uptake and metabolism of levodopa. Further studies (21) showed that, following intravenous administration to the rat, the total radioactivity levels in the duodenum exceeded by 10-fold the levels observed in the plasma, heart, or stomach and that the duodenal *O*-methylation reaction was predominantly localized in the mucosa.

All these findings are consistent with the conclusion reported herein: that the GI tract is virtually exclusively responsible for reduced physiological bioavailability of levodopa following oral administration. These findings are also consistent with other studies (22) indicating that coadministration of decarboxylase inhibitors can produce higher plasma levels following oral administration. However, the higher plasma levels probably also are due to inhibition of decarboxylase enzymes throughout other parts of the body. Since the therapeutic utility of levodopa depends upon adequate absorption of intact drug into the systemic circulation, the high doses needed for efficacy probably are required, in large part, because of the extensive biotransformation of levodopa in the GI tract.

Bianchine *et al.* (23) studied the absorption of levodopa in human subjects with uncomplicated parkinsonism following the oral administration of 500 mg of ^{14}C-levodopa. Negligible radioactivity was recovered in both the stools and expired air of these patients. Over 80% of the radioactivity was recovered in the urine, indicating virtually complete oral absorption of the administered radioactivity in humans. The investigators further showed that, by minimizing the duration of exposure of levodopa to the gastric mucosa, they could increase serum levodopa levels. Patients with slow gastric emptying exhibited the lowest serum drug levels, whereas patients receiving the levodopa *via* a direct duodenal infusion exhibited the highest levels. Rivera-Calimlim *et al.* (24) showed that higher serum levodopa levels occurred at earlier times in gastrectomized patients and that the lowest serum levels were observed in one patient who had retained the drug in the stomach for 7 hr. These clinical observations are indicative of GI metabolism as the basis for the reduced oral bioavailability of levodopa.

Clinical investigators administering the decarboxylase inhibitor benserazide [*N*-*dl*-seryl-*N*-(1,2,3-trihydrobenzyl)hydrazine] concomitantly with levodopa demonstrated increased serum levodopa levels (25–28). This procedure allowed for the reduction of the levodopa dose in a group of 20 parkinsonian patients (27) and resulted in fewer side effects. Benserazide does not pass the blood–brain barrier (28, 29) but inhibits extracerebral decarboxylase activity, allowing for greater systemic and brain levels of intact levodopa and a reduction in dose.

In conclusion, the data presented here indicate that substantially more intact levodopa reaches the systemic circulation following the intravenous and hepatoportal parenteral routes of administration than *via* oral administration. Such findings confirm that the physiologically impaired bioavailability of orally administered levodopa occurs virtually exclusively in the GI tract. The overall absorption characteristics of levodopa appear to be similar in dogs and humans, suggesting that in humans the physiologically impaired and variable absorption of orally administered levodopa results from its metabolism in the GI tract.

REFERENCES

(1) R. N. Boyes, H. J. Adams, and B. R. Duce, *J. Pharmacol. Exp. Ther.*, **174**, 1(1970).

(2) A. Carlsson, *Acta Neurol. Scand.*, **48**, Suppl. 51, 11(1972).

(3) R. M. Brogden, T. M. Speight, and G. S. Avery, *Drug*, **2**, 262(1971).

(4) G. C. Cotzias, *Hosp. Pract.*, **4**, 35(1969).

(5) W. Birkmayer, W. Danielcyk, E. Newmayer, and P. Rieder, *J. Neural Transm.*, **34**, 133(1973).

(6) S. Bergman, G. Curzon, J. Friedel, R. B. Godwin-Austen, C. D. Mardsen, and J. D. Parkes, *Br. J. Clin. Pharmacol.*, **1**, 417(1974)

(7) L. Rivera-Calimlim, C. A. Dujovne, J. P. Morgan, L. Lasagna, and J. R. Bianchine, *Eur. J. Clin. Invest.*, **1**, 313(1971).

(8) D. N. Wade, D. T. Mearrick, and J. L. Morris, *Nature*, **242**, 463(1973).

(9) A. Granerus, R. Jagenburg, and A. Svanborg, *Arch. Pharmacol.*, **280**, 429(1973).

(10) C. B. Coutinho, H. E. Spiegel, S. A. Kaplan, M. Yu, R. Christian, J. J. Carbone, J. Symington, J. A. Cheripko, M. Lewis, A. Touchin, and T. Crews, *J. Pharm. Sci.*, **60**, 1014(1971).

(11) R. Montalbo, W. A. Diel, and A. G. Glazko, *Clin. Res.*, **20**, 411(1972).

(12) S. Riegelman, J. C. K. Loo, and M. Rowland, *J. Pharm. Sci.*, **57**, 117(1968).

(13) C. M. Metzler, G. L. Elfring, and A. J. McEwen, "A Users Manual for NONLIN and Associated Programs," The Upjohn Co., Kalamazoo, MI 49001, Apr. 1974.

(14) H. G. Boxenbaum, S. Riegelman, and R. M. Elashoff, *J. Pharmacokinet. Biopharm.*, **2**, 123(1974).

(15) W. Lovenberg, H. Weissbach, and S. Udenfriend, *J. Biol. Chem.*, **237**, 89(1962).

(16) M. Rowland, L. Z. Benet, and S. Riegelman, *J. Pharm. Sci.*, **59**, 364(1970).

(17) T. Suzuki and Y. Saitoh, *Chem. Pharm. Bull.*, **21**, 1458(1973).

(18) D. Lalka, W. J. Jusko, and T. J. Bardos, *J. Pharm. Sci.*, **64**, 230(1975).

(19) L. Rivera-Calimlim, J. P. Morgan, C. A. Dujovne, J. R. Bianchine, and L. Lasagna, *Biochem. Pharmacol.*, **20**, 3051(1971).

(20) H. L. Taubin and L. Landsberg, *Clin. Res.*, **20**, 872(1972).

(21) L. Landsberg, M. Berardino, and P. Silva, *ibid.*, **22**, 321A(1974).

(22) D. S. Tandon and L. Rivera-Calimlim, *Fed. Proc.*, **33**, 498(1974).

(23) J. R. Bianchine, L. Rivera-Calimlim, J. P. Morgan, C. A. Dujovne, and L. Lasagna, *Ann. N.Y. Acad. Sci.*, **179**, 126(1971).

(24) L. Rivera-Calimlim, J. P. Morgan, C. A. Dujovne, J. R. Bianchine, and L. Lasagna, *J. Clin. Invest.*, **49**, 79a(1970).

(25) A. Pletscher and G. Bartholini, *Clin. Res. Ther.*, **12**, 344(1971).

(26) E. M. Miller and L. Wiener, *Neurology*, **5**, 482(1974).

(27) A. Barbeau, L. Gillo-Joffroy, and H. Mars, *Clin. Res. Ther.*, **12**, 353(1972).

(28) W. Birkmayer and E. Neumayer, *Z. Neurol.*, **202**, 257 (1972).

(29) G. Bartholini, W. P. Burkard, A. Pletscher, and H. M. Bates, *Nature*, **25**, 852(1967).

ACKNOWLEDGMENTS AND ADDRESSES

Received July 21, 1975, from the *Department of Biochemistry and Drug Metabolism, Hoffmann–La Roche Inc., Nutley NJ 07110*

Accepted for publication September 4, 1975.

[x] To whom inquiries should be directed.

Rheological Evaluation of Hog Gastric Mucin as a Model Mucus System

CHRISTOPHER MARRIOTT and IAN W. KELLAWAY ˣ

Abstract □ The rheological evaluation of preparations containing 10, 15, 20, and 25% powdered hog gastric mucin was carried out over the 13–48° temperature range using rotational and creep viscometry. The preparations were almost viscous, and no elastic behavior was demonstrated. The addition of borate ions frequently produced a slight decrease in viscosity. Tetracycline hydrochloride decreased the viscosity of the 10 and 25% materials, although the addition of this compound to fresh gastric and bronchial mucous gels markedly increased viscosity. The model is, therefore, only suitable in limited circumstances as a basis for the evaluation of the effect of drugs on gastric mucus.

Keyphrases □ Mucus system, gastric—rheological evaluation using rotational and creep viscometry, effect of borate ions and tetracycline on viscosity □ Rheological evaluation—gastric mucus system, rotational and creep viscometry □ Viscometry—rotational and creep, rheological evaluation of gastric mucus system □ Viscosity—gastric mucus system, effect of borate ions and tetracycline

Because of the heterogeneous nature of the natural mucous secretions of the body, many model systems have been suggested for use in the assessment of flow behavior and the effect of drugs *in vitro*. Some examples of studied systems are saliva (1, 2), egg white (3), alginates (4), and powdered hog stomach (5). A recently described technique uses the last material as a model system for the assessment of mucolytic drugs (6). It also has been used to evaluate the effect of mucus on the bioavailability of drugs both *in vivo* (7) and *in vitro* (8). The principal advantage of such a model is that it is freely available commercially, so it is not subject to the problems associated with the collection of mucous gels from animals.

However, previous studies with this material never established that the system produced after the addition of powdered hog stomach to water in any way resembled the mucous gel secreted in the stomach. The purposes of this study were to investigate the rheological properties of the systems produced with hog gastric mucin and to compare them with those of the gastric mucous gel obtained from fresh pig stomach.

EXPERIMENTAL

Preparation of Samples—Powdered porcine stomach mucin[1] was added to glass-distilled water and stirred to achieve dispersion. The resultant suspension was then allowed to equilibrate for 16 hr at 4°. Final concentrations of 10, 15, 20, and 25% (w/v) were used.

Sodium borate[2], when required, was dissolved in the water used for the preparation of the mucin suspension and was in contact with the mucin for the entire equilibration period.

Gastric mucous gel was obtained from the stomachs of freshly slaughtered domestic pigs (*Scrofa domestica*), which had been starved for approximately 48 hr. The stomachs were opened, and the gel was removed from the antral regions.

Human bronchial mucus was collected from hospitalized patients suffering from various chest conditions. Homogenized batches were prepared by the method reported by Marriott and Richards (9).

Tetracycline hydrochloride[3] was added to the samples 30 min prior to measurement. This short equilibration time was used because of the possibility of breakdown of the tetracycline solutions over longer periods and because it was shown previously to be adequate for any effects to be induced (10).

Rotational Viscometry—Flow curve (rheogram) determinations were carried out using an automatic rotational viscometer[4] in conjunction with an x–y recorder[5], which permitted flow curves to be plotted directly. The cup and bob measuring geometry was used, and the size of the unit was varied according to the viscosity of the sample.

The sample was loaded into the viscometer at 20°, and a sufficient time was allowed for the attainment of temperature equilibrium. The flow curve was determined using a sweep time of 120 sec and a maximum shear rate of 195 sec^{-1}. The temperature was then increased by increments of approximately 5°, and a flow curve was determined at

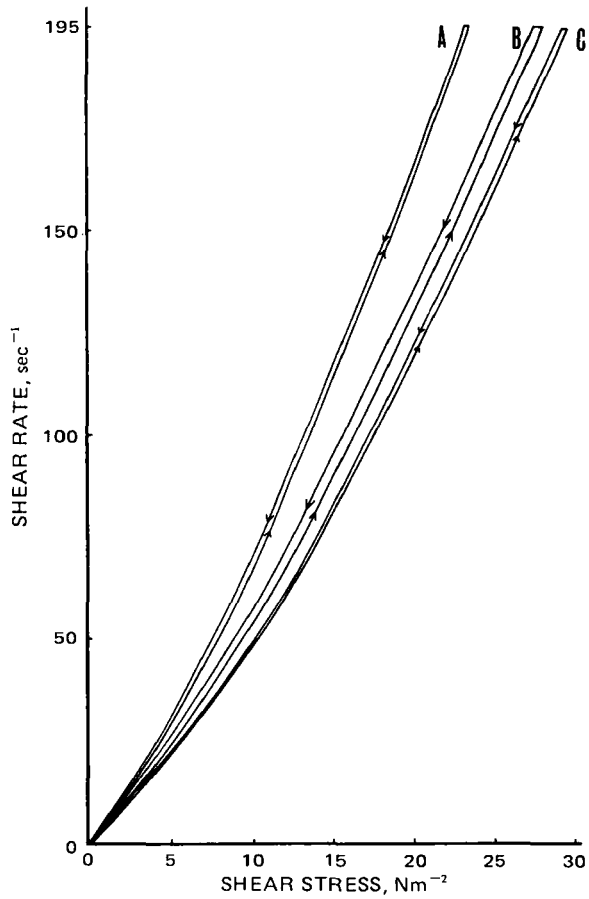

Figure 1—*Examples of flow curves obtained with the 10% mucin preparation using a sweep time of 120 sec. Key: A, 10% mucin plus 1% tetracycline hydrochloride at 33.8°; B, 10% mucin plus 1% sodium borate at 33.5°; and C, 10% mucin at 31.4°.*

[1] Crude, Type II, Sigma London Chemical Co. Ltd., London, United Kingdom.
[2] AnalaR, British Drug Houses, Poole, United Kingdom.
[3] The Boots Co. Ltd., Nottingham, United Kingdom.
[4] Rheomat 30 viscometer with Rheoscan programming unit, Contraves, A.G. Zurich, Switzerland.
[5] Farnell Instruments Ltd., Wetherby, United Kingdom.

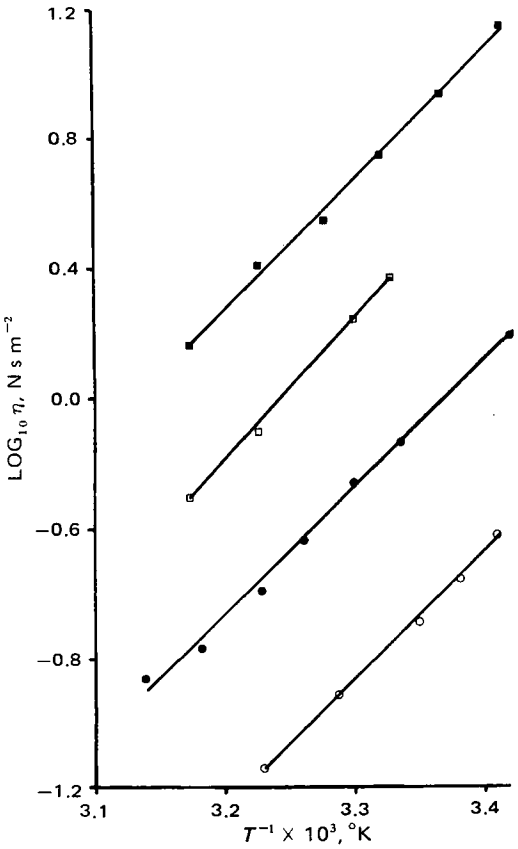

Figure 2—*Viscosity, measured by rotational viscometry, of 10, 15, 20, and 25% mucin preparations plotted logarithmically as a function of the reciprocal of the absolute temperature.*

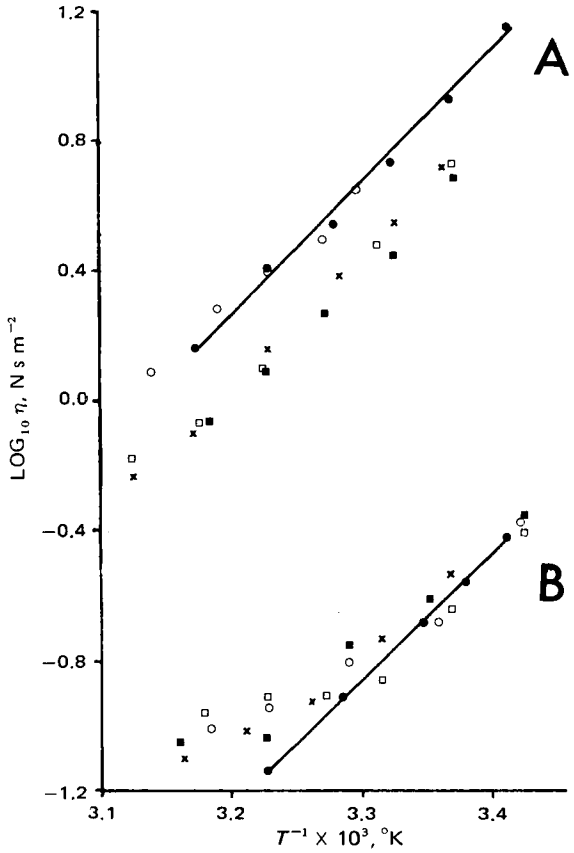

Figure 3—*Effect on viscosity, measured by rotational viscometry, of the addition of various amounts of sodium borate to (A) 25% and (B) 10% mucin preparations. In each case, the line drawn represents the mucin preparation without sodium borate. Key: ●, 0%; ○, 0.1%; ■, 0.25%; □, 0.5%; and ×, 1.0%.*

each temperature. The apparent viscosity, η, was calculated from the reciprocal of the slope of the linear portion of the curve recorded at an increasing shear rate.

Viscosity determinations were carried out with 10, 15, 20, and 25% (w/v) mucin preparations.

Creep Viscometry—This technique permits the evaluation of the viscoelastic properties of a material by measuring the compliance of the material at low shear stresses.

An air turbine viscometer with cone and plate geometry, capable of producing the low stresses, was used (11). Samples were loaded into the gap between the cone and plate, and a suitable period was allowed to attain temperature equilibrium. A small, constant stress was applied to the sample, and the resultant deformation was followed as a function of time. The temperature was then increased by approximately 5° increments, and determinations were made at several temperatures between 15 and 40°.

The residual shear viscosity, η_0, was calculated from the reciprocal of the slope of the linear strain–time plot for the mucin preparations. When creep curves typical of viscoelastic materials were produced, they were analyzed into discrete spectra using a computer program (2).

RESULTS

Some examples of the flow curves obtained with the 10% system are shown in Fig. 1. A small degree of hysteresis was apparent and was not altered by addition of either borate ions or tetracycline. In all cases, similar results were obtained when the experimental temperature was approached from a higher as well as from a lower temperature.

The derived viscosity values from the continuous shear viscometry are shown in Fig. 2, where log viscosity, η, has been plotted against the reciprocal of the absolute temperature to produce the typical Arrhenius plot. The viscosity increased with an increase in the concentration of the mucin, and the gradient of the slope was similar in each case.

When sodium borate was added to the 25% mucin system in concentrations between 0.1 and 1.0%, a slight decrease in viscosity was observed with all but the lowest concentration (Fig. 3). The gradients were again similar in all cases, in direct contrast to results obtained using the same concentrations of sodium borate with the 10% mucin preparations. Although little alteration was observed in the absolute value of the viscosity, a distinct deviation from linearity was apparent in the curves, particularly at higher temperatures.

A similar trend is demonstrated in Fig. 4, which shows the effect of tetracycline hydrochloride on the mucin preparations in the presence and absence of borate ions. Once more the additives decreased viscosity for both 10 and 25% mucin preparations, but deviation of the curves from linearity was observed in the latter case.

The evaluation of the samples by creep viscometry produced the type of creep compliance curve shown in Fig. 5. The mucin systems did not exhibit any marked degree of viscoelasticity since the curves are linear at times greater than 240 sec and not the exponential curves characteristic of viscoelastic materials. Such behavior approaches that of purely viscous systems, which would produce a straight line passing through the origin. The experimentally obtained curves (Fig. 5) may not be analyzed by means of the usual discrete spectral analysis (12), and the only information readily obtainable is the residual viscosity, η_0, calculated from the reciprocal of the slope.

The Arrhenius plot constructed from these results is shown in Fig. 6 for 15, 20, and 25% preparations. No results could be obtained with the 10% system because of the insensitivity of the technique when applied to such materials. However, linear curves with similar slopes were obtained for the three concentrations investigated, and once more it is apparent that the addition of 1% tetracycline hydrochloride produced a decrease in viscosity of the 25% mucin preparation.

A creep compliance curve obtained from gastric mucous gel obtained from the pig stomach is shown in Fig. 7. The curve is typical of those obtained with uncross-linked polymer systems that are viscoelastic (12), and obvious differences exist between this curve and those shown in Fig. 5. When 1% tetracycline hydrochloride was added,

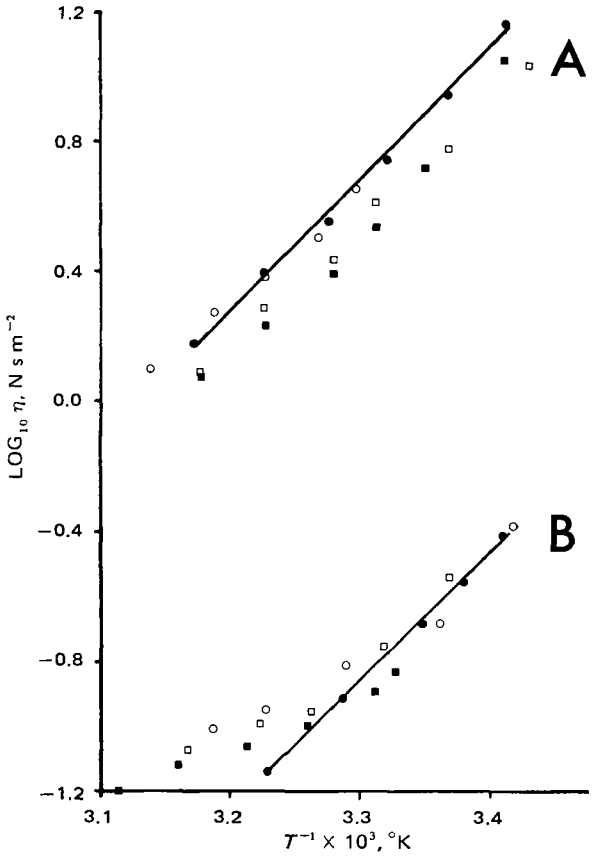

Figure 4—*Effect of tetracycline hydrochloride (1%) on the viscosity measured by rotational viscometry of (A) 25% and (B) 10% mucin preparations. In each case, the lines drawn represent the untreated samples. Key: ●, no additive; ○, 0.1% sodium borate; ■, 1% tetracycline hydrochloride; and □, 0.1% sodium borate and 1% tetracycline hydrochloride.*

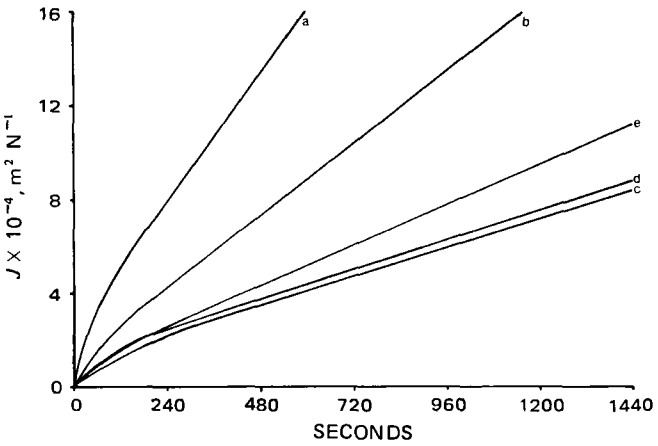

Figure 5—*Creep compliance curves for 15, 20, and 25% mucin preparations. The residual viscosity, η_0, was calculated from the reciprocal of the slope of the linear portions. Key: a, 15% mucin; b, 20% mucin; c, 25% mucin; d, 25% mucin plus 1% sodium borate; and e, 25% mucin plus 1% tetracycline hydrochloride.*

an increase in the structure of the gel was produced. This effect is similar to that described previously for homogenized bronchial mucous gels (Fig. 8) (10). Since in all cases the curves are of the shape expected for viscoelastic materials, they can be analyzed in terms of a mechanical model (Table I).

DISCUSSION

The nature of the material produced when dried hog gastric mucin is added to water is difficult to describe. It does possess some characteristic stickiness of mucous gels and does to some extent exhibit a "rubbery" consistency. However, it is obvious from the results that the material does not possess any innate elastic behavior and is almost purely viscous (Fig. 5). Also, although the viscosity of the preparation increases with increasing mucin concentration, the fact that the slopes of the Arrhenius plots remain parallel indicates that no increase in interaction between the molecules has occurred.

It has been suggested that the lack of a coherent gel structure may be overcome by the inclusion of borate ions in the mucin preparations (6). This suggestion could not be substantiated, since the addition of such ions usually produced a decrease in viscosity (Figs. 3 and 4). Since borate ions are universal cross-linking agents, it is tempting to assume that the mucin does not contain glycoprotein, which is generally considered to be responsible for the gel-like nature of mucus (13). However, Deman *et al.* (5) demonstrated a reduction in viscosity after incubation of a mucin preparation with neuramidase, indicating the presence of a sialic acid containing glycoprotein. Other workers (14) separated a glycoprotein from this material, and it appears that the reason why no gel is produced is due to the low percentage of glycoprotein present and/or to the high concentration of cellular contaminants in such a preparation.

However, the presence of some glycoprotein in the mucin, albeit at low concentration, may permit the use of the model system in the investigation of the effect of drugs on the physical properties of gastric mucus and the evaluation of the effect of mucus as a barrier to drug absorption. Davis *et al.* (6) claimed that the action of mucolytic drugs, which decrease viscosity, can be demonstrated using 10% hog gastric mucin. However, such a model also should be capable of demonstrating the effect of compounds that increase viscosity of mucous gels.

It was reported recently that the tetracycline antibiotics, particularly tetracycline and oxytetracycline, are capable of producing large increases in the viscosity of bronchial mucus (8). The addition of 1% tetracycline hydrochloride produced no increase in the viscosity of the mucin systems. Indeed, in all instances a small decrease in viscosity was apparent. This result is obviously not the true tetracycline effect, since a vast increase in structure was produced when a similar concentration was added to gastric mucus (Table I). This effect is substantiated by results obtained with bronchial mucus, indicating that it is not a function of the source of the mucous gel.

It is interesting to compare the viscosities of the natural gastric mucus and mucin preparations. Even the 25% material is 10 times less viscous than gastric mucous gel (Fig. 6 and Table I), necessitating the use of unreasonably high concentrations of mucin if the model is to

Table I—Values of Parameters Derived from the Creep Curves for Gastric and Bronchial Mucus before and after the Addition of 1% Tetracycline Hydrochloride[a]

Material	Additive	J_0, $m^2 N^{-1}$	η_0, $N s m^{-2}$	J_1, $m^2 N^{-1}$	J_2, $m^2 N^{-1}$	J_3, $m^2 N^{-1}$	τ_1, sec	τ_2, sec	τ_3, sec
Gastric mucus	—	0.0129	42,837	0.0115	0.0040	0.0071	831	201	31
Gastric mucus	1% Tetracycline hydrochloride	0.0038	543,819	0.0030	0.0028	0.0011	573	123	30
Bronchial mucus	—	0.0145	44,164	0.0323	0.0017		648	10	
Bronchial mucus	1% Tetracycline hydrochloride	0.0059	438,222	0.0103	0.0023		441	30	

[a] J_0 is the instantaneous compliance; η_0 is the residual shear viscosity; and J_1, τ_1, *etc.*, are the compliance and retardation times of the Voigt units necessary to fit the exponential portion of the curves.

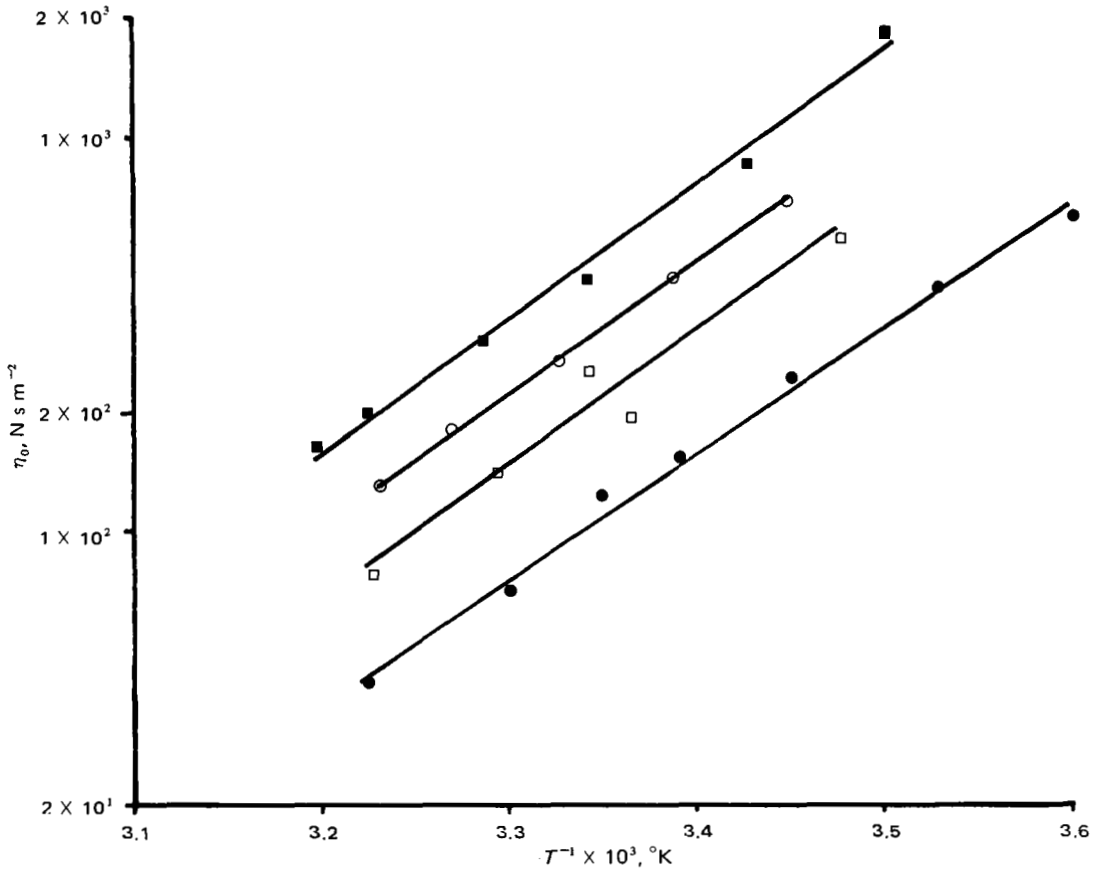

Figure 6—*Effect of temperature on the residual viscosity, η_0, calculated from the creep compliance curves for 15, 20, and 25% mucin preparations. Key: ■, 25% mucin; ○, 25% mucin plus 1% tetracycline hydrochloride; □, 20% mucin; and ●, 15% mucin.*

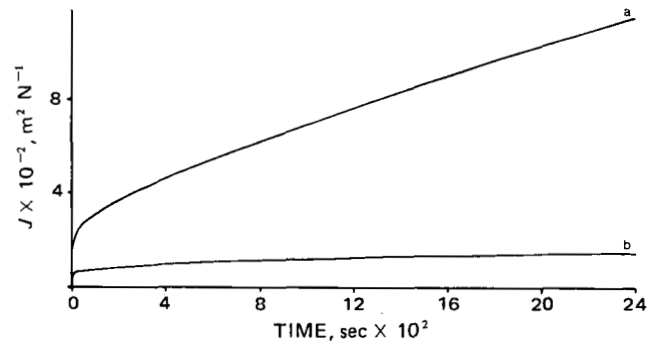

Figure 7—*Creep compliance curves for (a) fresh gastric mucous gel and (b) after the addition of 1% tetracycline hydrochloride.*

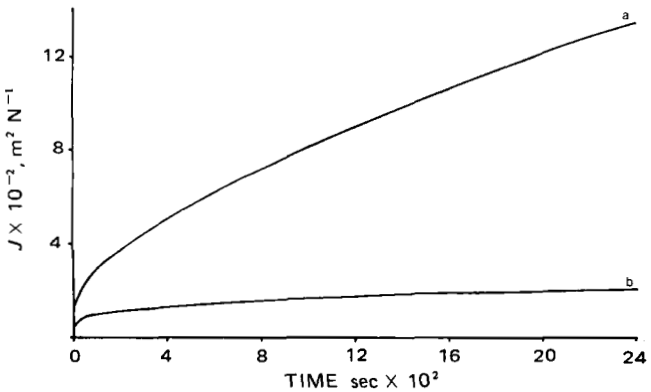

Figure 8—*Creep compliance curves for (a) homogenized bronchial mucous gel and (b) after the addition of 1% tetracycline hydrochloride.*

be realistic. However, the viscosity of human gastric aspirate was found to possess a similar viscosity to that of the 10% mucin when measured by rotational viscometry (15).

Therefore, the use of preparations containing dried hog gastric mucin as model systems for gastric mucous gels apparently is justified only when investigating compounds that decrease viscosity. The marked inability of the model to demonstrate any increase in viscosity with compounds such as tetracycline may limit its usefulness in screening tests. Indeed, with this model such compounds may even appear to possess mucolytic properties. However, if these limitations are considered, the mucin preparation may serve as a useful model for gastric mucus, although it is unlikely that its use in a screening test for agents that reduce the viscosity of bronchial mucus is justified.

REFERENCES

(1) S. S. Davis, *Rheol. Acta*, **10**, 28(1971).

(2) C. Marriott and L. I. Irons, *Biorheology*, **11**, 119(1974).

(3) S. S. Davis, *Bull. Physio-Pathol. Respir.*, **9**, 47(1973).

(4) M. King, A. Gilboa, F. A. Meyer, and A. Silberberg, *Amer. Rev. Resp. Dis.*, **110**, 740(1974).

(5) J. Deman, M. Mareel, and E. Bruyneel, *Biochim. Biophys. Acta*, **297**, 486(1973).

(6) S. S. Davis, A. Inglis, D. McNeil, and S. Scobie, *J. Pharm. Pharmacol.*, **26**, 64P(1974).

(7) B. W. Barry and M. P. Braybrooks, *ibid.*, **26**, 64P(1974).

(8) I. W. Kellaway and C. Marriott, *ibid.*, **25**, 167P(1973).

(9) C. Marriott and J. H. Richards, *Biorheology*, **11**, 129(1974).

(10) C. Marriott and I. W. Kellaway, *ibid.*, **12**, 391(1975).

(11) C. Marriott, L. I. Irons, and E. R. Harris, *J. Phys. E*, **6**, 200(1973).

(12) J. D. Ferry, "Viscoelastic Properties of Polymers," 2nd ed., Wiley, New York, N.Y., 1970.

(13) A. Allen and D. Snary, *Gut*, **13**, 666(1972).

(14) D. R. Strombeck and D. Harrold, *Infect. Immun.*, **10**, 1266(1974).

(15) J. N. R. Curt and R. Pringle, *Gut*, **10**, 931(1969).

ACKNOWLEDGMENTS AND ADDRESSES

Received May 19, 1975, from the *Pharmaceutics Research Unit, University of Nottingham, University Park, Nottingham, NG7 2RD, United Kingdom.*

Accepted for publication August 5, 1975.

For the gifts of compounds used in this study, grateful acknowledgment is made to the Boots Co. Ltd.

[x] To whom inquiries should be directed.

Absorption and Distribution of Radioactivity from Suppositories Containing ^{3}H-Benzocaine in Rats

JAMES W. AYRES [x], DUANGCHIT LORSKULSINT, ALBERT LOCK, LYNDA KUHL, and PAUL A. LASKAR

Abstract □ The effects of the suppository vehicle, drug concentration, and nonionic surfactants on *in vitro* benzocaine dialysis through a cellulose membrane and on rectal absorption in rats of total radioactivity following administration of ^{3}H-benzocaine were investigated. *In vitro* dialysis correlated quite well with *in vivo* absorption, and drug release was greater from water-soluble vehicles than from oleaginous vehicles. Inclusion of a nonionic hydrophilic or lipophilic surfactant in cocoa butter resulted in a statistically significant increase for *in vitro* drug release, while a lipophilic surfactant showed little effect *in vivo* and a hydrophilic surfactant depressed release *in vivo*. Both types of surfactant had small effects on release from polyethylene glycol. *In vitro* release of benzocaine from some commercially available suppositories was compared with experimental preparations. Variation in blood radioactivity following administration of the same concentration of ^{3}H-benzocaine in the same dosage form in male and female rats is reported.

Keyphrases □ Absorption—benzocaine from suppositories, effect of vehicle, drug concentration, and nonionic surfactants, rats □ Distribution—benzocaine from suppositories, effect of vehicle, drug concentration, and nonionic surfactants, rats □ Benzocaine—absorption and distribution from suppositories, rats □ Suppositories—absorption and distribution of benzocaine, rats □ Dosage forms—suppositories, absorption and distribution of benzocaine, rats

It is well recognized that formulation factors can influence the availability of a drug from a dosage form. Surface-active agents included in dosage forms may exert their effects on the active ingredient, the dosage form itself, or the membrane at the absorption site. Surfactants have been reported to increase and to decrease the absorption of drugs (1). Moreover, varying the concentrations of a surfactant can enhance or retard drug absorption, depending on the type of surfactant and whether or not micelle formation occurs (1).

The complex mechanisms of surfactant effects on drug absorption were reviewed previously (2). The *in vitro* release of benzocaine from ointment vehicles was reported (3) and compared (4) to the rate of absorption and resulting total blood level radioactivity following rectal administration of 20% ^{3}H-benzocaine (ethyl *p*-aminobenzoate) from ointment vehicles in rats. This paper reports the effects of suppository vehicles, variations in drug concentration, and the presence of a nonionic hydrophilic or lipophilic surfactant on the *in vitro* dialysis of benzocaine and the absorption of ^{3}H-benzocaine in rats.

EXPERIMENTAL

Dosage Form Preparation—All suppositories were prepared by the fusion method, and commercial products were used as received. The reagents and equipment used were similar to those reported previously (3, 4). Additional materials used in the present experiment were: dialysis membrane, available as a 2.54-cm (1-in.) × 30.5-m (100-ft) roll[1]; cocoa butter[2]; polysorbate 80[3]; and sorbitan monooleate[4].

For *in vivo* studies, ^{3}H-benzocaine was dissolved in the polyethylene glycol vehicle (75% polyethylene glycol 1000 and 25% polyethylene glycol 4000) or suspended in the cocoa butter vehicle. Suppository vehicles containing ^{3}H-benzocaine were poured into plastic, disposable, U-80 insulin syringes, which were refrigerated until completely congealed. The tips of the syringes were cut off, and the excess semisolid was removed.

A suppository volume of 0.5 ml was used for the experiment. The amount of surfactant used was too small to weigh directly, and the aliquot method was used for preparation.

***In Vitro* Dialysis**—Dialysis tubing was cut into 10-cm lengths and soaked for at least 24 hr in distilled water. At the time of the test, the tubing was closed and weighted at one end by tying with a thin strip of the dialysis tubing to a glass stopper. The suppository was introduced into the tubing followed by 2.5 ml of distilled water. The top was tied to form a container, which was as nearly full as possible without loss of water.

The sample was then placed in a 600-ml beaker containing 500 ml of distilled water maintained at 37.5°. It floated upward, being held near the center of the container by the glass stopper weight. At the appropriate time periods, 5-ml samples were pipetted from the beaker and 5 ml of distilled water (37.5°) was returned to the beaker. Care was taken to draw each sample from as close to the same place in the beaker as possible and to avoid stirring.

Analytical Method—The analysis of the benzocaine released during the *in vitro* test was carried out by the method of Matsumoto *et al.* (5). Aliquot portions of a sample solution were pipetted into a test tube followed by 2 *N* HCl (2 ml) and 0.2% $NaNO_2$ (0.4 ml), and the mixture was shaken for 5 min. Then 0.5% $NH_4SO_3NH_2$ (0.4 ml) was added, and the mixture was shaken for 3 min. *N*-(2-Diethylaminoethyl)-1-naphthylamine hydrochloride (1.0 ml of 0.5%) was then added with shaking.

After 30 min of intermittent shaking, the percent transmittance was measured at 550 nm and the concentration of benzocaine was determined from a standard curve.

***In Vivo* Studies**—Female Sprague–Dawley rats were used for all experiments except the male *versus* female study. Animal weights varied between 100 and 280 g. Surgical preparation, cannulation,

[1] Seamless regenerated cellulose dialysis tubing, Catalog No. 25225-226, VWR Scientific Supplies, Portland, Ore.
[2] Hershey Food Corp., Hershey, Pa.
[3] Tween 80, J. T. Baker, Phillipsburg, N.J.
[4] Span 80, J. T. Baker, Phillipsburg, N.J.

ACKNOWLEDGMENTS AND ADDRESSES

Received May 19, 1975, from the *Pharmaceutics Research Unit, University of Nottingham, University Park, Nottingham, NG7 2RD, United Kingdom.*

Accepted for publication August 5, 1975.

For the gifts of compounds used in this study, grateful acknowledgment is made to the Boots Co. Ltd.

[x] To whom inquiries should be directed.

Absorption and Distribution of Radioactivity from Suppositories Containing ^{3}H-Benzocaine in Rats

JAMES W. AYRES [x], DUANGCHIT LORSKULSINT, ALBERT LOCK, LYNDA KUHL, and PAUL A. LASKAR

Abstract □ The effects of the suppository vehicle, drug concentration, and nonionic surfactants on *in vitro* benzocaine dialysis through a cellulose membrane and on rectal absorption in rats of total radioactivity following administration of ^{3}H-benzocaine were investigated. *In vitro* dialysis correlated quite well with *in vivo* absorption, and drug release was greater from water-soluble vehicles than from oleaginous vehicles. Inclusion of a nonionic hydrophilic or lipophilic surfactant in cocoa butter resulted in a statistically significant increase for *in vitro* drug release, while a lipophilic surfactant showed little effect *in vivo* and a hydrophilic surfactant depressed release *in vivo*. Both types of surfactant had small effects on release from polyethylene glycol. *In vitro* release of benzocaine from some commercially available suppositories was compared with experimental preparations. Variation in blood radioactivity following administration of the same concentration of ^{3}H-benzocaine in the same dosage form in male and female rats is reported.

Keyphrases □ Absorption—benzocaine from suppositories, effect of vehicle, drug concentration, and nonionic surfactants, rats □ Distribution—benzocaine from suppositories, effect of vehicle, drug concentration, and nonionic surfactants, rats □ Benzocaine—absorption and distribution from suppositories, rats □ Suppositories—absorption and distribution of benzocaine, rats □ Dosage forms—suppositories, absorption and distribution of benzocaine, rats

It is well recognized that formulation factors can influence the availability of a drug from a dosage form. Surface-active agents included in dosage forms may exert their effects on the active ingredient, the dosage form itself, or the membrane at the absorption site. Surfactants have been reported to increase and to decrease the absorption of drugs (1). Moreover, varying the concentrations of a surfactant can enhance or retard drug absorption, depending on the type of surfactant and whether or not micelle formation occurs (1).

The complex mechanisms of surfactant effects on drug absorption were reviewed previously (2). The *in vitro* release of benzocaine from ointment vehicles was reported (3) and compared (4) to the rate of absorption and resulting total blood level radioactivity following rectal administration of 20% ^{3}H-benzocaine (ethyl *p*-aminobenzoate) from ointment vehicles in rats. This paper reports the effects of suppository vehicles, variations in drug concentration, and the presence of a nonionic hydrophilic or lipophilic surfactant on the *in vitro* dialysis of benzocaine and the absorption of ^{3}H-benzocaine in rats.

EXPERIMENTAL

Dosage Form Preparation—All suppositories were prepared by the fusion method, and commercial products were used as received. The reagents and equipment used were similar to those reported previously (3, 4). Additional materials used in the present experiment were: dialysis membrane, available as a 2.54-cm (1-in.) × 30.5-m (100-ft) roll[1]; cocoa butter[2]; polysorbate 80[3]; and sorbitan monooleate[4].

For *in vivo* studies, ^{3}H-benzocaine was dissolved in the polyethylene glycol vehicle (75% polyethylene glycol 1000 and 25% polyethylene glycol 4000) or suspended in the cocoa butter vehicle. Suppository vehicles containing ^{3}H-benzocaine were poured into plastic, disposable, U-80 insulin syringes, which were refrigerated until completely congealed. The tips of the syringes were cut off, and the excess semisolid was removed.

A suppository volume of 0.5 ml was used for the experiment. The amount of surfactant used was too small to weigh directly, and the aliquot method was used for preparation.

***In Vitro* Dialysis**—Dialysis tubing was cut into 10-cm lengths and soaked for at least 24 hr in distilled water. At the time of the test, the tubing was closed and weighted at one end by tying with a thin strip of the dialysis tubing to a glass stopper. The suppository was introduced into the tubing followed by 2.5 ml of distilled water. The top was tied to form a container, which was as nearly full as possible without loss of water.

The sample was then placed in a 600-ml beaker containing 500 ml of distilled water maintained at 37.5°. It floated upward, being held near the center of the container by the glass stopper weight. At the appropriate time periods, 5-ml samples were pipetted from the beaker and 5 ml of distilled water (37.5°) was returned to the beaker. Care was taken to draw each sample from as close to the same place in the beaker as possible and to avoid stirring.

Analytical Method—The analysis of the benzocaine released during the *in vitro* test was carried out by the method of Matsumoto *et al.* (5). Aliquot portions of a sample solution were pipetted into a test tube followed by 2 *N* HCl (2 ml) and 0.2% $NaNO_2$ (0.4 ml), and the mixture was shaken for 5 min. Then 0.5% $NH_4SO_3NH_2$ (0.4 ml) was added, and the mixture was shaken for 3 min. *N*-(2-Diethylaminoethyl)-1-naphthylamine hydrochloride (1.0 ml of 0.5%) was then added with shaking.

After 30 min of intermittent shaking, the percent transmittance was measured at 550 nm and the concentration of benzocaine was determined from a standard curve.

***In Vivo* Studies**—Female Sprague–Dawley rats were used for all experiments except the male *versus* female study. Animal weights varied between 100 and 280 g. Surgical preparation, cannulation,

[1] Seamless regenerated cellulose dialysis tubing, Catalog No. 25225-226, VWR Scientific Supplies, Portland, Ore.
[2] Hershey Food Corp., Hershey, Pa.
[3] Tween 80, J. T. Baker, Phillipsburg, N.J.
[4] Span 80, J. T. Baker, Phillipsburg, N.J.

Table I—Composition and Benzocaine Concentration of Various Types of Suppository Bases

Suppository	Vehicle	Surfactant	Average Weight for Dialysis Study[a], g	Benzocaine, %	Total Benzocaine for Dialysis, mg	Total Benzocaine Dialyzed in 5 hr, mg	Percent Dialyzed in 5 hr	Average Weight for *In Vivo* Release[b], g	Total ^{3}H-Benzocaine Available for *In Vivo* Release, mg
A	Polyethylene glycol[c]	None	—	20	—	—	—	0.579	115.8
B	Polyethylene glycol	None	2.35	10	235.0	80.5	34.3	0.573	57.3
C	Polyethylene glycol	None	—	5	—	—	—	0.567	28.4
D	Polyethylene glycol	None	2.41	3	72.3	57.0	78.8	0.569	17.1
E	Polyethylene glycol	Sorbitan monooleate, 1%	2.42	3	72.6	60.5	83.3	0.558	16.7
F	Polyethylene glycol	Sorbitan monooleate, 0.5%	2.42	3	72.6	45.8	63.0	0.554	16.6
G	Polyethylene glycol	Polysorbate 80, 1%	2.41	3	72.3	57.8	79.9	0.552	16.6
H	Polyethylene glycol	Polysorbate 80, 0.05%	2.33	3	69.9	55.5	79.4	0.556	16.7
I	Polyethylene glycol	None	—	1	—	—	—	0.581	5.8
J	Cocoa butter	None	—	20	—	—	—	0.510	102.0
K	Cocoa butter[d]	None	1.63	10	163.0	22.9	14.0	0.510	51.0
L	Cocoa butter	None	1.74	3	53.2	10.0	18.8	0.475	14.2
M	Cocoa butter	Sorbitan monooleate, 1%	1.77	3	53.1	11.9	22.4	0.438	13.1
N	Cocoa butter	Sorbitan monooleate, 0.05%	1.76	3	52.8	12.4	23.5	0.443	13.3
O	Cocoa butter	Polysorbate 80, 1%	1.67	3	50.1	13.9	27.6	0.468	14.0
P	Cocoa butter	Polysorbate 80, 0.05%	1.60	3	48.0	11.7	24.4	0.460	13.8
Q	Oleaginous[e,f]	Unknown	2.14	11	235.0	17.5	7.5	—	—
R	Cocoa butter[e,g]	Unknown	2.65	4.9	130.0	15.5	12.0	—	—
S	Cocoa butter[e,h]	Unknown	2.40	5.4	130.0	13.2	10.1	—	—

[a] Average weight of 10 suppositories. [b] Average weight of six or more suppositories. [c] Polyethylene glycol vehicle consisted of polyethylene glycol 1000 (75%) and polyethylene glycol 4000 (25%). [d] Hershey's. [e] Commercially available product. [f] Also contains hexachlorophene, ephedrine sulfate, and bismuth subgallate. [g] Also contains oxyquinoline sulfate, zinc oxide, menthol, and balsam peru. [h] Also contains ephedrine sulfate, oxyquinoline sulfate, zinc oxide, bismuth subgallate, and balsam peru.

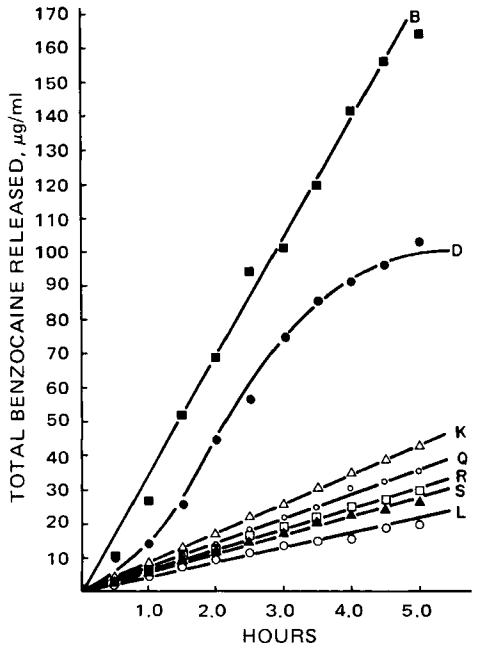

Figure 1—*Effect of suppository vehicle composition on release of drug from preparations containing benzocaine. Key: see Table I.*

blood sample collection, and blood analysis methodology were followed as previously reported (4).

RESULTS AND DISCUSSION

Table I shows the composition of suppositories selected for the investigation of variations in dialysis and rate of release for absorption of benzocaine. Figure 1 illustrates the variation in drug release of some experimental suppository formulations and the commercial products investigated. Since the active ingredient content of many commercial products is reported as a percentage, rather than an amount, Products A–P were prepared on a percentage weight per weight basis. The specific gravity of the polyethylene glycol vehicle used was about 1.4

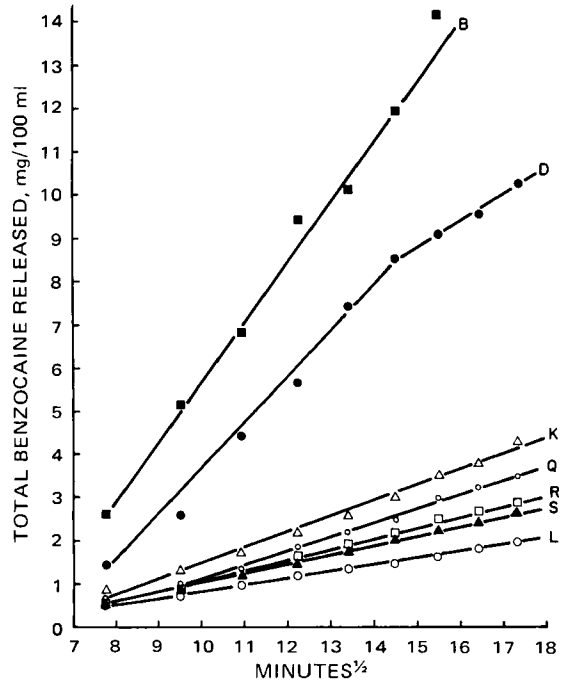

Figure 2—*Relationship between total mass of drug dialyzed and time$^{1/2}$. Key: see Table I.*

Table II—Summary of Calculated Statistical Parameters

Product	Intercept (b_0)	*SE* of Intercept	Regression Coefficient (b_1)	*SE* of Regression Coefficient
B	−88.9583	4.2313	113.5101	2.4429
D	−62.6965	7.3624	76.0611	4.2507
E	−90.9342	8.1531	96.8973	4.5225
F	−69.2085	5.8930	74.6488	3.2689
G	−76.7483	5.5375	87.5097	3.0717
H	−81.1662	4.4574	86.9697	2.4725
K	−21.1737	1.3366	27.8889	0.7717
L	−6.8433	0.5277	11.6569	0.3047
M	−8.5915	0.3772	14.3776	0.2178
N	−10.7434	0.5166	15.6600	0.2982
O	−10.6500	1.3357	17.8333	0.7712
P	−8.6347	0.6929	14.5876	0.4001
Q	−18.4070	1.0351	23.6619	0.5976
R	−11.9034	0.5641	16.9296	0.3257
S	−13.0224	0.8578	18.6843	0.4952

times that of the cocoa butter, and this difference was reflected in the variation in the total amount of benzocaine present in suppositories containing the same percent of benzocaine but different vehicles.

The total mass of drug transferred from semisolids under the conditions of the *in vitro* experiment was nearly linear with respect to the square root of time for the times investigated (Fig. 2). The linear portions of such benzocaine release curves were used in generating a linear least-squares regression line, and comparisons among the estimated parameters (Table II) were made (Table III) using the usual null hypothesis. The data points for Product D were approximated with two linear portions (Fig. 2), and the line for the early time period was arbitrarily chosen for statistical comparisons (Tables II and III).

In vitro testing of suppositories involves many considerations and some compromises in simulating conditions operating during rectal absorption. The conditions (6) that should be emulated are: (*a*) an average temperature of 36.9°; (*b*) water not present in the liquid state but present in the semisolid feces, which are 77–82% water; (*c*) rectal mucosa acting as a semipermeable membrane, allowing passage of water both away from and into the blood, depending on the osmotic gradient; (*d*) practically no peristaltic movement; (*e*) pressure on rectal contents varying from 0 to 50 cm of water, according to posture; and (*f*) possible presence of feces.

In normal people, fecal material is present in the rectum just prior to defecation only (7). Most of the time, this organ is free of solid matter which could physically interfere with absorption. Therefore, it is not necessary to introduce a material for *in vitro* testing that would simulate the presence of feces. It is necessary, however, to expose the dosage form to some fluid so that the drug has an opportunity to dissolve. While this exposure may seem to violate Condition *b*, a positive correlation between *in vitro* testing and *in vivo* results would indicate that such exposure to fluids is acceptable for testing purposes.

Testing at body temperature is critical, especially for products that melt in the rectum. Conditions *a* and *c* are readily satisfied by using a temperature-controlled water bath and placing the suppository inside a commercially available, semipermeable, dialysis membrane tubing. Condition *d* can be met by placing the dosage form in an unstirred medium. Although this procedure may allow a buildup of drug around the dosage form, which can slow drug release, such a static dialysis method may have a closer relationship to the absorption of drugs through a biological membrane than dialysis when the bulk phase is stirred.

The data reported here were obtained using a simple dialysis procedure, without stirring of the bulk receptor phase, which exposed the suppositories tested to a single, uniform pressure and approximated to some degree Conditions *a*, *c*, and *d*.

Examination of the results for the commercial products (Fig. 1) reveals less release from the 11% preparation than the 10% preparation and somewhat greater release from the 4.9% preparation than the 5.4% preparation, although the latter difference is not significant. Formulation factors other than concentration that could be playing a role include the presence of other ingredients that might interact with the benzocaine as well as different vehicle effects. The experimental cocoa butter formulations were completely melted within 10 min and the polyethylene glycol vehicles were dissolved within 1 hr. There was, however, no visible change in any commercial product during the 5-hr dialysis period. Each commercial suppository retained its shape, al-

Table III—Individual Comparisons Made[a]

Products	S	R	Q	P	O	N	M	L	K	H	G	F	E	D	B
B	—	—	*	—	—	—	—	—	*	*	*	*	*	*	—
D	—	—	—	—	—	—	—	*	*	ns	ns	ns	*	—	
E	—	—	—	—	—	—	*	—	—	—	ns	*	—		
F	—	—	—	—	—	*	*	—	—	~*	—	—			
G	—	—	—	—	*	—	—	—	—	ns	—				
H	—	—	—	*	—	—	—	—	—	—					
K	—	—	*	*	*	*	*	*	—						
L	*	*	—	*	*	*	*	—							
M	*	*	*	—	*	*	—								
N	*	ns	*	~*	—	—									
O	ns	ns	*	*	—										
P	*	*	*	—											
Q	*	*	—												
R	ns	—													
S	—														

[a] Comparisons among rates of benzocaine release from the semisolid as measured by the regression coefficient of the total benzocaine released with respect to the square root of time were made. All of these comparisons are not statistically independent. Therefore, when a comparison is noted as significant at the 95% confidence level, it is meant that the rates of release of benzocaine for the two products under comparison are likely to be different but at a confidence level slightly less than 95%. The result is that some of the differences in release rate noted as ~* might not prove to be significantly different under more rigorous testing; ns = not significant, ~* = barely significant, * = significant, and — = not tested for significance.

though they all became somewhat more pliable at the end of the experiment than at the beginning.

The dialysis of drug from saturated benzocaine solutions was studied, and the ratio of total benzocaine to free benzocaine increased proportionately as the concentration of a nonionic hydrophilic surfactant[3] was increased from 0 to 7%. Addition of the surfactant to a solution containing a fixed amount of benzocaine increased the dialysis rate compared to a solution without surfactant (5, 8). Therefore, 0.05 and 1.0% of sorbitan monooleate or polysorbate 80 were incorporated into both the polyethylene glycol and the cocoa butter vehicle containing 3% benzocaine.

Figure 3 shows the effect on the cocoa butter suppositories and the increase in the amount and rate of benzocaine released. The greatest increase in release was due to the presence of 1% polysorbate 80. Since the membrane was not controlling the rate of diffusion (as evidenced by increasing diffusion with an increased concentration), the surfactant must have been increasing the rate of dissolution of the drug. This finding is consistent with work showing that an increase in benzocaine dialysis from surfactant-containing solutions is due to the increased solubilization of the drug because of surfactant–drug interactions, followed by a rapid release of free drug as dialysis takes place (5, 8).

Figure 4 shows the results of dialysis from polyethylene glycol suppositories containing surfactants. Between 63 and 80% of the active ingredient was released (Table I).

It is not possible to use the actual amount of drug released from the different products (Table I) as a measure of the effect of the vehicle on dialysis of drug, since the amount present varies with the product considered. The percent of drug released, however, can be used for this purpose. The total released from the polyethylene glycol vehicle containing 10% benzocaine was almost 2.5 times the total released from the corresponding cocoa butter preparation when the percent benzocaine dialyzed was considered. The ratio was 2.9 to 4.2 when comparing the corresponding preparations containing 3% benzocaine. When considering the release from the 3 *versus* 10% preparations of a single vehicle type, it can be seen that the 10% formulation released a larger amount of drug but a smaller percent of drug during the dialysis period (Table I).

Various concentrations of ^{3}H-benzocaine in suppository dosage forms with and without surfactant (Table I) were selected for *in vivo* testing and were inserted into the rectum of female Sprague–Dawley rats. Blood samples (0.1 ml) were taken from the inferior vena cava at 5, 10, 20, 30, 40, 60, 90, 120, 180, 240, and 300 min, and the total

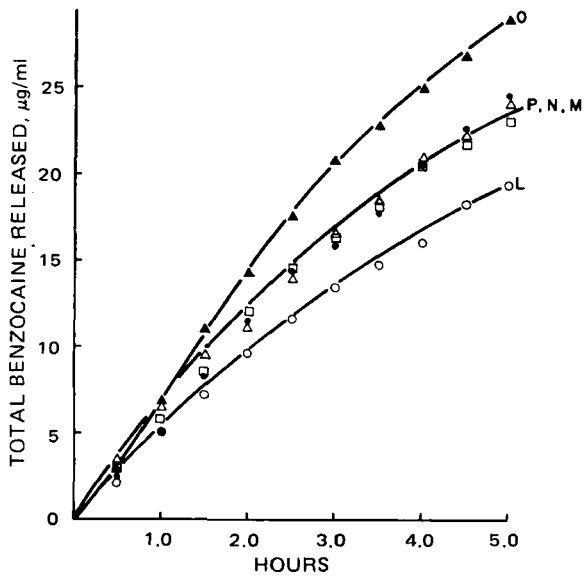

Figure 3—*Effect of surfactants on drug release from cocoa butter suppositories. Key: see Table I.*

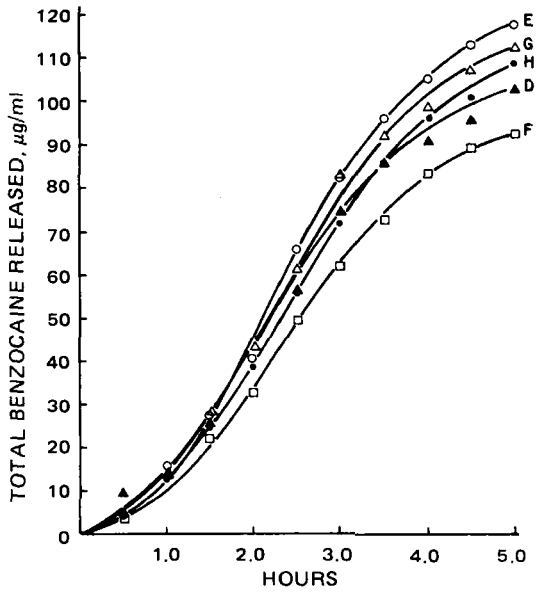

Figure 4—*Effect of surfactants on drug release from polyethylene glycol suppositories. Key: see Table I.*

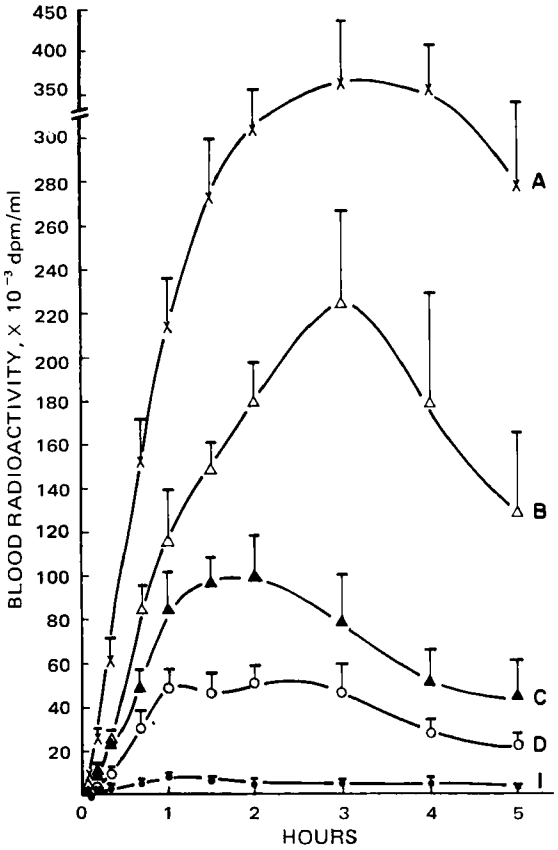

Figure 5—*Blood radioactivity after the application of ^{3}H-benzocaine in a polyethylene glycol suppository vehicle. Key: see Table I. A* t*-value larger than the critical* t*-value was obtained for all point comparisons except curve I* versus *B at 5 and 10 min; curve C* versus *B at 5, 10, 20, and 300 min; and curve B* versus *A at 180 min. (One side of the standard error of the mean is shown.)*

radioactivity present was determined. The means of the radioactivity detected are shown in Figs. 5–9.

Statistical analysis using unequal variance techniques indicated that weight variation among animals accounted for less than 5% of the variation following different dosage formulations. The standard error of the mean is included in some figures but not in others due to crowding. A point-by-point comparison of the means obtained at each sample time for the nonlinear curves was made using the Student *t* test (95% confidence level), and the results are summarized in the figure legends.

Due to the relatively large dispersion of experimental values, the ability to distinguish between mean values, which appear quite distinct, is compromised. An example of this situation can be seen when comparing the results from Formulation A *versus* Formulation B in Fig. 5 for the 180-min sample. The mean values for A and B were significantly different for each sample time (95% confidence level) except at 180 min due to the relatively large variances at that time. Increasing the number of animals in the study may have resulted in a significant difference in this case.

The blood level radioactivities from different concentrations of ^{3}H-benzocaine in polyethylene glycol suppositories (1, 3, 5, 10, and 20%) and cocoa butter suppositories (3, 10, and 20%) are shown in Figs. 5 and 6. Increasing the concentration of ^{3}H-benzocaine in both polyethylene glycol and cocoa butter suppository bases resulted in a higher total radioactivity in the blood. Since the volume of suppositories was equal with every concentration of drug administered, the total dose was increased by increasing the drug concentration. Both concentration and variation in total dose may be causes for the difference in the shape of the blood level curves using the same suppository vehicle.

It is clear from Fig. 5 that an increase in the ^{3}H-benzocaine in polyethylene glycol increased the area under the curve up to 5 hr. Although this finding indicates an increase in the amount of drug being absorbed from the rectum, since the drug had to be absorbed

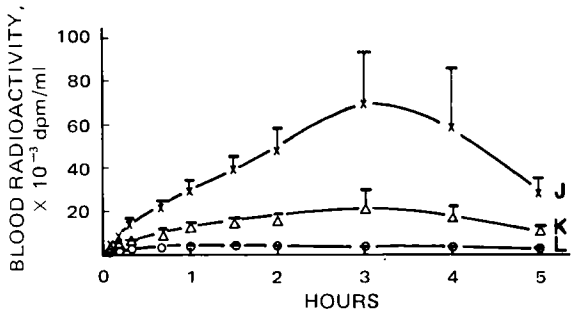

Figure 6—*Blood radioactivity after the application of ^{3}H-benzocaine in a cocoa butter suppository vehicle. Key: see Table I. A* t*-value larger than the critical* t*-value was obtained for all point comparisons except curve L* versus *K at 180 min, curve L* versus *J at 240 min, and curve K* versus *J at 180 and 240 min. (One side of the standard error of the mean is shown.)*

for the radioactivity to appear, under the conditions of this experiment the total radioactivity represents several metabolites rather than intact drug (4). Therefore, no pharmacokinetic analysis using the blood level radioactivity *versus* time curves was done in the present experiment.

A previous *in vitro* study (3) found that an increased concentration of benzocaine in polyethylene glycol ointment caused a decrease in release through a dialysis membrane. That decrease was explained on the basis of a decreased solubility and precipitation of the benzocaine in a polyethylene glycol–water solution, which formed under the *in vitro* conditions. This effect was not observed during the current dialysis experiments and is apparently not occurring *in vivo*, as evidenced by increasing absorption from an increased concentration of drug in this water-soluble vehicle.

The absorption from a cocoa butter suspension of drug is much less in rate and amount when compared to equal concentrations of drug in polyethylene glycol (Fig. 6). The latter vehicle is water soluble and can dissolve in the rectum. Benzocaine was dissolved in the polyethylene glycol vehicle and, therefore, was available to partition into the rectal fluids and the rectal mucosa during liquefaction (dissolution) of the polyethylene glycol. Cocoa butter does not dissolve but melts in the rectum.

Before liquefaction, dissolution of drug in rectal fluids is limited to the drug located at the surface of the suppository. Diffusion through the semisolid suppository is probably of little importance, since melting occurs readily at body temperature. After liquefaction, the

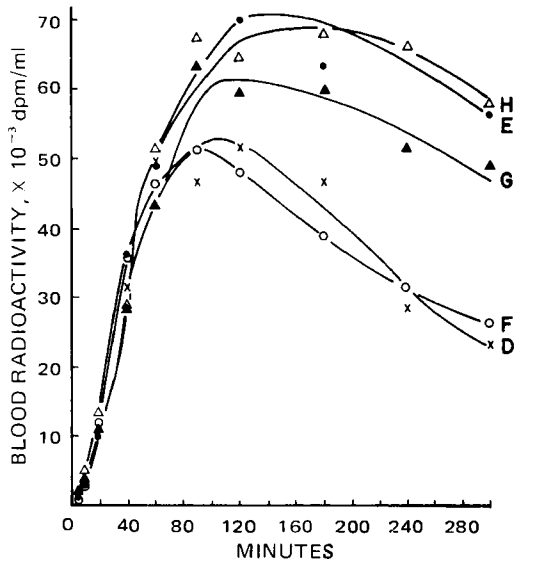

Figure 7—*Blood radioactivity after the application of 3% ^{3}H-benzocaine and surfactants in a polyethylene glycol vehicle. Key: see Table I. A* t*-value larger than the critical* t*-value was only obtained for point comparisons on curve D* versus *E after 240 min, curve D* versus *G after 240 min, curve E* versus *F after 240 min, and curve F* versus *H at 90 min.*

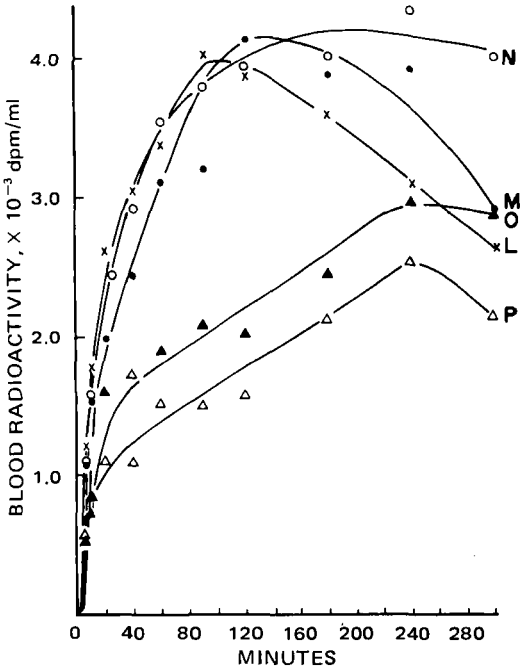

Figure 8—*Blood radioactivity after the application of 3% ^{3}H-benzocaine and surfactants in a cocoa butter suppository vehicle. Key: see Table I. A t-value larger than the critical t-value was found for at least half of the points when comparing the curves of L* versus *O, L* versus *P, M* versus *P, N* versus *O, and N* versus *P.*

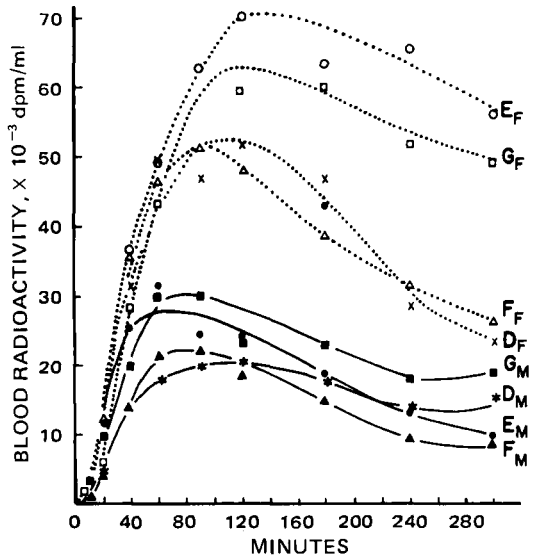

Figure 9—*Comparison of blood radioactivity following 3% ^{3}H-benzocaine in a polyethylene glycol vehicle in male and female rats. Key: see Table I. A t-value larger than the critical t-value was found for point comparisons of male* versus *female rats receiving the same formulation except for the first 60 min for E_F* versus *E_M and G_F* versus *G_M. (The F subscript is for female rats, and the M subscript is for male rats.)*

suspended drug would be coated with melted cocoa butter, which is much less viscous than the original semisolid.

Some drug may be exposed to the rectal fluids for rapid dissolution, but most drug would still have an oleaginous coating in which the drug has a very low solubility. The drug would have to diffuse through this coating before absorption could occur. Therefore, the slower drug absorption from the cocoa butter is not surprising, since the drug particles would be coated by a hydrophobic substance in which the drug has a low solubility.

Surfactants were included in the 3% ^{3}H-benzocaine in polyethylene glycol and cocoa butter suppositories to determine if the presence of a nonionic hydrophilic or lipophilic surfactant would affect the rate or amount of benzocaine absorption. Incorporation of a 1% lipophilic or 0.05 or 1% hydrophilic surfactant in the polyethylene glycol vehicle resulted in an apparent increase in total blood radioactivity (Fig. 7) for times beyond 180 min, although the range of values was wide enough for the differences of the means to be not statistically significant at most times.

With 3% ^{3}H-benzocaine in cocoa butter base, the lipophilic surfactant in both concentrations studied (1 and 0.05%) showed no significant influence on the amount absorbed (Fig. 8). However, the hydrophilic surfactant in both concentrations studied decreased the total counts in the blood significantly with most times under investigation.

Table III shows that for the products in Fig. 4 the release rates of only Formulations D and E were significantly different *in vitro*. All products were essentially the same *in vivo* with respect to the rate of drug release. All products with surfactant in cocoa butter, however, demonstrated a significant increase in the rate of drug release *in vitro*, but the only significant effect *in vivo* was a decrease in release with 1% polysorbate 80. In some cases the *in vitro* method did not accurately predict the *in vivo* effect. In these cases there were relatively small actual differences for the *in vitro* system, although the differences were statistically significant.

In the earlier part of the study, some experiments were run to measure the blood level concentration of radioactivity *versus* time using male rats. Female rats showed a total radioactivity in the blood about twice that of male rats (Fig. 9) when the same dosage form was administered. These differences could be due to differences in the rate of absorption, biotransformation, distribution, or excretion. Absorption across rectal membranes is usually considered to be a passive diffusion process. In passive diffusion, either the release of drug from the vehicle or drug dissolution in rectal fluids would be the rate-limiting step for absorption, especially with a drug like benzocaine which has a low water solubility.

The decreased rate of appearance of radioactivity in the blood from 20% ^{3}H-benzocaine in the cocoa butter vehicle compared to 20% ^{3}H-benzocaine in polyethylene glycol indicates that the rate of absorption is dependent on the amount of drug released from the vehicle and presented to the rectal mucosa, at least for the concentrations of drug studied here. Since the same vehicle and drug concentration were administered to males and females, it is unlikely that the observed differences were due to differences in absorption. Furthermore, the differences probably were not due to differences in excretion half-life of the parent drug or of identical amounts of the same metabolites in males or females because most drugs are excreted by a first-order process in either sex.

Excretion of total radioactivity and loss from the bloodstream may be different in males and females if metabolism is occurring at different rates and if different amounts of metabolites are available for excretion. One possible explanation for the results could be that males were metabolizing the drug to more polar products faster than the females and the more polar products were being cleared from the bloodstream more rapidly than the parent drug. Another possible explanation could be that distribution of the molecules containing radioactivity was different for male and female rats. Further work involving tissue distribution and metabolism is underway in these laboratories to determine which possibility is correct.

SUMMARY AND CONCLUSIONS

A simple dialysis method was used to measure the release of benzocaine from various experimental and commercially available suppositories. Wide variations were found in the amount of benzocaine dialyzed. Small differences, which were detectable *in vitro*, were not seen *in vivo* in rats, although substantial differences *in vitro* were correlated well with experimental results obtained *in vivo*.

Benzocaine was dialyzed and absorbed rectally in rats more rapidly from a polyethylene glycol vehicle than from cocoa butter, and the effects of the surfactants tested were variable. Rectal administration of the same concentration of ^{3}H-benzocaine in the same vehicle to male and female rats results in lower blood radioactivity *versus* time curves for the male rats.

Some formulation factor other than the concentration of benzocaine affected the relative amounts of benzocaine released *in vitro* from the commercially available products examined. Although the dialysis method is useful for evaluating the effects of formulation on drug

release from suppositories, the desirable release rate for the specific drug investigated has not been determined since its minimum effective concentration is not known. Considerably more research is needed in this area.

REFERENCES

(1) W. W. Davis and W. E. Wright, in "Pharmacology and the Skin," W. Montagna, E. J. Vanscott, and R. B. Stoughton, Eds., Appleton-Century Crofts, New York, N.Y., 1972, pp. 37–39.

(2) M. Gibaldi and S. Feldman, *J. Pharm. Sci.*, **59**, 579(1970).

(3) J. W. Ayres and P. A. Laskar, *ibid.*, **63**, 1402(1974).

(4) J. W. Ayres, D. Lorskulsint, and A. Lock, *ibid.*, **64**, 1958(1975).

(5) H. Matsumoto, H. Matsumura, and S. Iguchi, *Chem. Pharm. Bull.*, **14**, 385(1966).

(6) I. Setnikar and S. Fantelli, *J. Pharm. Sci.*, **51**, 566(1962).

(7) E. Nasset, in "Medical Physiology," 12th ed., P. Bard, Ed., C. V. Mosby, St. Louis, Mo., 1968, p. 559.

(8) H. Matsumoto, H. Matsumura, and S. Iguchi, *Chem. Pharm. Bull.*, **14**, 391(1966).

ACKNOWLEDGMENTS AND ADDRESSES

Received February 26, 1975, from the *Department of Pharmaceutical Science, School of Pharmacy, Oregon State University, Corvallis, OR 97331*

Accepted for publication August 11, 1975.

Abstracted in part from the thesis submitted by D. Lorskulsint to the Graduate School, Oregon State University, in partial fulfillment of the Master of Science degree requirements.

Supported in part by Biomedical Sciences Support Grant RR 07079.

[x] To whom inquiries should be directed.

Attainment of Highly Uniform Solid Drug Dispersions Employing Molecular Scale Drug Entrapment in Polymeric Latices

A. B. LARSON [*] and G. S. BANKER [x]

Abstract □ The uniformity of distribution attainable for an amine drug in solid dispersions prepared using a molecular scale entrapment procedure was investigated. Excellent reproducibility of drug content throughout the entire entrapment product was demonstrated in both flocculated (high drug levels) and deflocculated (low drug levels) systems. Drug content and content uniformity were found to be predictable for deflocculated systems, even at high drug dilution ratios. Milling or particle-size fractionation appeared to have no effect on the distribution of drug throughout the solid dispersion entrapment products. Dry blending was inferior to molecular scale drug entrapment in distributing small quantities of drug uniformly.

Keyphrases □ Dispersions, solid—amine drugs, uniformity of distribution, molecular scale entrapment procedure, flocculated and deflocculated systems □ Molecular scale drug entrapment—utilized to prepare solid dispersions of amine drugs, uniformity of distribution studied □ Distribution uniformity—amine drugs in solid dispersions studied, molecular scale entrapment procedure, effect of milling or particle-size fractionation □ Amine drugs—uniformity of distribution in solid dispersions, molecular scale drug entrapment procedure

Safety, efficacy, and reliability are the three basic criteria that define the quality of any well-designed pharmaceutical dosage form. High standards of drug product quality are necessary for the protection of the public, and one important facet of quality assurance is the maintenance of content uniformity. Content uniformity directly bears on each of the three criteria defining drug product quality. The importance of content uniformity in solid unit dosage forms to the consumer's health, safety, and welfare becomes obvious when one considers the potency of many drugs in use today.

BACKGROUND

Failure to meet content uniformity specifications in a solid dosage form may be attributed to weight variation between dosage units or improper mixing (nonhomogeneity of drug distribution). Another factor resulting in inaccuracies of drug content in tablets, capsules, or powders is drug segregation. Improper mixing leading to nonuniformity can result from the inherent difficulty in setting the "ideal mixing time" for high dilution solid dosage forms. Homogeneity of a potent active ingredient throughout a powder mix is highly dependent on particle size and shape, particle-size distribution, density, moisture, and charge. Furthermore, the size, efficiency, and type of mixer can make a difference when choosing a mixing time specification.

A "perfect mix" for a powder formulation would be exemplified by a three-dimensional location of drug plus excipient in space, in which every drug particle is the same size and is the same distance in all planes from every other drug particle. Two miscible liquids most closely approach (in practice) a perfect mix, since mixing occurs at a molecular level and is completely random. This result is never attained in powder blending due to the finite number of particles involved and the factors previously listed that may contribute to unmixing or segregation. However, a reasonable mix is possible if there are enough particles per drug dose and if the optimum mixing time is selected after carrying out adequate testing and sampling of the powder blend.

A high degree of mixedness achieved in a powder mix, however, does not necessarily mean the final product will meet content uniformity specifications. Segregation can occur when the mix is removed from the mixer, transferred to another point in the plant, or subsequently treated by other processing procedures. Furthermore, for capsules and tablets, nonuniform flow and subsequent weight variation could hinder unit-to-unit drug content even more.

In addition to these manufacturing problems, other problems concerning the control of content uniformity include analytical methods and statistical procedures. To allow content uniformity determinations on individual unit dosage forms, the assay methods must be accurate, reliable, and specific as well as sufficiently sensi-

release from suppositories, the desirable release rate for the specific drug investigated has not been determined since its minimum effective concentration is not known. Considerably more research is needed in this area.

REFERENCES

(1) W. W. Davis and W. E. Wright, in "Pharmacology and the Skin," W. Montagna, E. J. Vanscott, and R. B. Stoughton, Eds., Appleton-Century Crofts, New York, N.Y., 1972, pp. 37–39.

(2) M. Gibaldi and S. Feldman, *J. Pharm. Sci.*, **59**, 579(1970).

(3) J. W. Ayres and P. A. Laskar, *ibid.*, **63**, 1402(1974).

(4) J. W. Ayres, D. Lorskulsint, and A. Lock, *ibid.*, **64**, 1958(1975).

(5) H. Matsumoto, H. Matsumura, and S. Iguchi, *Chem. Pharm. Bull.*, **14**, 385(1966).

(6) I. Setnikar and S. Fantelli, *J. Pharm. Sci.*, **51**, 566(1962).

(7) E. Nasset, in "Medical Physiology," 12th ed., P. Bard, Ed., C. V. Mosby, St. Louis, Mo., 1968, p. 559.

(8) H. Matsumoto, H. Matsumura, and S. Iguchi, *Chem. Pharm. Bull.*, **14**, 391(1966).

ACKNOWLEDGMENTS AND ADDRESSES

Received February 26, 1975, from the *Department of Pharmaceutical Science, School of Pharmacy, Oregon State University, Corvallis, OR 97331*

Accepted for publication August 11, 1975.

Abstracted in part from the thesis submitted by D. Lorskulsint to the Graduate School, Oregon State University, in partial fulfillment of the Master of Science degree requirements.

Supported in part by Biomedical Sciences Support Grant RR 07079.

[x] To whom inquiries should be directed.

Attainment of Highly Uniform Solid Drug Dispersions Employing Molecular Scale Drug Entrapment in Polymeric Latices

A. B. LARSON [*] and G. S. BANKER [x]

Abstract □ The uniformity of distribution attainable for an amine drug in solid dispersions prepared using a molecular scale entrapment procedure was investigated. Excellent reproducibility of drug content throughout the entire entrapment product was demonstrated in both flocculated (high drug levels) and deflocculated (low drug levels) systems. Drug content and content uniformity were found to be predictable for deflocculated systems, even at high drug dilution ratios. Milling or particle-size fractionation appeared to have no effect on the distribution of drug throughout the solid dispersion entrapment products. Dry blending was inferior to molecular scale drug entrapment in distributing small quantities of drug uniformly.

Keyphrases □ Dispersions, solid—amine drugs, uniformity of distribution, molecular scale entrapment procedure, flocculated and deflocculated systems □ Molecular scale drug entrapment—utilized to prepare solid dispersions of amine drugs, uniformity of distribution studied □ Distribution uniformity—amine drugs in solid dispersions studied, molecular scale entrapment procedure, effect of milling or particle-size fractionation □ Amine drugs—uniformity of distribution in solid dispersions, molecular scale drug entrapment procedure

Safety, efficacy, and reliability are the three basic criteria that define the quality of any well-designed pharmaceutical dosage form. High standards of drug product quality are necessary for the protection of the public, and one important facet of quality assurance is the maintenance of content uniformity. Content uniformity directly bears on each of the three criteria defining drug product quality. The importance of content uniformity in solid unit dosage forms to the consumer's health, safety, and welfare becomes obvious when one considers the potency of many drugs in use today.

BACKGROUND

Failure to meet content uniformity specifications in a solid dosage form may be attributed to weight variation between dosage units or improper mixing (nonhomogeneity of drug distribution). Another factor resulting in inaccuracies of drug content in tablets, capsules, or powders is drug segregation. Improper mixing leading to nonuniformity can result from the inherent difficulty in setting the "ideal mixing time" for high dilution solid dosage forms. Homogeneity of a potent active ingredient throughout a powder mix is highly dependent on particle size and shape, particle-size distribution, density, moisture, and charge. Furthermore, the size, efficiency, and type of mixer can make a difference when choosing a mixing time specification.

A "perfect mix" for a powder formulation would be exemplified by a three-dimensional location of drug plus excipient in space, in which every drug particle is the same size and is the same distance in all planes from every other drug particle. Two miscible liquids most closely approach (in practice) a perfect mix, since mixing occurs at a molecular level and is completely random. This result is never attained in powder blending due to the finite number of particles involved and the factors previously listed that may contribute to unmixing or segregation. However, a reasonable mix is possible if there are enough particles per drug dose and if the optimum mixing time is selected after carrying out adequate testing and sampling of the powder blend.

A high degree of mixedness achieved in a powder mix, however, does not necessarily mean the final product will meet content uniformity specifications. Segregation can occur when the mix is removed from the mixer, transferred to another point in the plant, or subsequently treated by other processing procedures. Furthermore, for capsules and tablets, nonuniform flow and subsequent weight variation could hinder unit-to-unit drug content even more.

In addition to these manufacturing problems, other problems concerning the control of content uniformity include analytical methods and statistical procedures. To allow content uniformity determinations on individual unit dosage forms, the assay methods must be accurate, reliable, and specific as well as sufficiently sensi-

tive and precise. Statisticians are constantly seeking reliable and improved procedures by which a batch or lot may be judged acceptable or unacceptable by a minimum amount of sampling.

Recent investigations (1–7) of a novel physicochemical process, termed molecular scale drug entrapment, have been described. This process has broad application to the preparation of solid drug dispersions as sustained-release systems. Emphasis has been placed on reproducibility and reliability of such entrapment as a precise way of controlling the rate of drug delivery; however, little attention has been given to the process as a precise method of distributing drug uniformly throughout a powder mix. The basis for the molecular scale concept is the addition of a solution phase (Avogadro's number of particles per mole) to a colloidal polymer dispersion, commonly called a latex, which has been estimated to contain 10^{14} particles/ml of dispersion. Various physical or physicochemical means may then be employed to recover the solid dispersion.

X-ray diffraction studies demonstrated that distribution of an amine drug using this solid dispersion entrapment technique (3) occurred at the molecular level. However, no attempt was made to exploit the apparent distributing property of molecular scale drug entrapment as a potentially superior method of achieving a high order of content uniformity in solid unit dosage forms.

EXPERIMENTAL

Materials and Equipment—A linear, anionically charged, acrylic copolymer[1] composed of acrylic and methacrylic acids and esters, having a molecular weight exceeding 300,000, was supplied in latex form; it contained 40 ± 0.5% solids. The amine used in this study was methapyrilene hydrochloride NF[2], and all reagents used were analytical grade.

Liquid mixing was done by a mixer[3] equipped with a 5.1-cm (2-in.) diameter, marine-type propeller. An ultracentrifuge[4], using a No. 42 rotor and 96-ml polyallomar tubes, was employed to isolate mechanically the polymer phase of the colloidal latex drug formulations.

Micronization was accomplished using a fluid energy mill[5], while classification of granules and powders was carried out using a set of standard sieves. Densities of solid materials were determined utilizing an air compression pycnometer[6], and moisture contents were obtained using a moisture balance[7]. All solids blending was done in a metal blender[8], and analyses were performed with a spectrophotofluorometer[9].

Analytical Method—The basis for the assay technique used was given by Pearlman (8), who found that antihistamines with a nitrogen atom *ortho* to a pyridine nitrogen develop fluorescence when reacted with excess cyanogen bromide. Five milliliters of the methapyrilene solution to be assayed was pipetted into a 50-ml volumetric flask. To this solution, 2 ml of freshly prepared saturated cyanogen bromide solution was added. After stoppering and agitating, the mixture was allowed to stand at least 1 hr (fluorescence remained constant from 1 to 24 hr) before analysis. Because of the dangerous fumes caused by cyanogen bromide, any solution containing this substance was covered and kept under a hood.

Solutions for calibration curves were identical to unknowns except for drug content and ranged from 1.0×10^{-3} to 15×10^{-3} m*M*. Straight-line relationships resulted when the log relative intensity was plotted against the log of the drug concentration. All samples were read in a fluorometer (slit arrangement 3) with the excitation wavelength at 345 nm and emission at 407 nm. The precision of the fluorometric assay was determined by performing five replicate assays on aliquots of several methapyrilene standard solutions. Relative standard deviations of ±1.8 and 1.1% were found at 2×10^{-3} and 10×10^{-3} m*M* methapyrilene concentration levels, respectively.

[1] Rohm and Haas, Philadelphia, Pa.
[2] Abbott Laboratories, North Chicago, Ill.
[3] Model V7 Lightning, Type 70537, Mixing Equipment Co., Rochester, N.Y.
[4] Beckman L2-65B, Spinco Division, Beckman Instruments, Palo Alto, Calif.
[5] Gem T, George W. Helme Co., Rochester, N.Y.
[6] Beckman Instruments, Fullerton, Calif.
[7] Central Scientific Co., Chicago, Ill.
[8] Twin-Shell, Patterson-Kelly, East Stroudsburg, Pa.
[9] Aminco-Bowman, American Instrument Co., Silver Spring, Md.

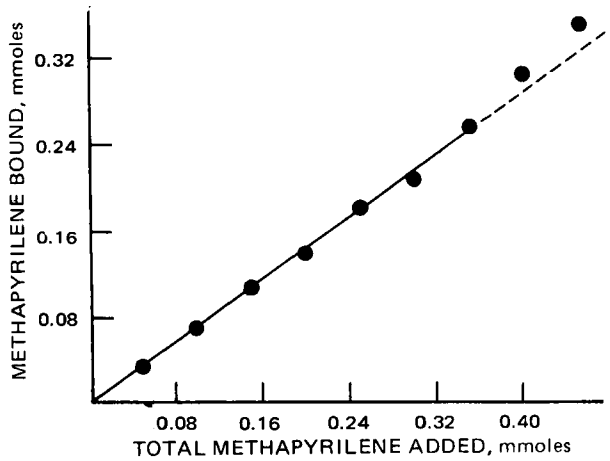

Figure 1—*Entrapment relationship between millimoles of methapyrilene bound and the millimoles of methapyrilene added to the latex.*

Preparation and Sampling of Polymeric Drug Dispersions—Formulations consisting of 50 ml of drug solution and 50 ml of polymer latex were mixed for 3 min at 300 rpm at room temperature. It was previously determined that temperature had no effect on the process and that equilibrium was established in 30 min (5). After a 30+ min equilibrium time, the systems, whether deflocculated or flocculated, were ultracentrifuged for 1 hr at 30,000 rpm. The supernates were retained for analysis as well as the precipitates.

The precipitates were pulverized and allowed to dry at 40°. It was determined that 12 hr was an adequate drying time. From each polymeric drug dispersion, 10 200-mg samples were chosen completely at random and with no regard to particle size or position in total population. These samples were dissolved in 0.2 *N* NaOH and analyzed with respect to drug content.

One formulation, consisting of 50 ml of 0.10 m*M* methapyrilene hydrochloride and 50 ml of latex, was prepared as already described for a micronization study. After drying, however, the isolated polymer product of this formulation was ground in a mortar and subsequently fed into a fluid energy mill using dry nitrogen at 54.5 kg (120 lb)/in.^{2} and a constant feed rate. The uniformity of distribution of drug throughout the micronized product was compared to the uniformity of distribution throughout a similar, but nonmicronized, product.

Uniformity of Distribution by Dry Blending as Compared to Molecular Scale Drug Entrapment—An entrapment formulation yielding a 1:10,000 dilution of methapyrilene to polymer was chosen for comparison to the following dry blended formulations: Formula I—methapyrilene hydrochloride, 100 mg, and lactose,

Table I—Typical Data for Distribution of Methapyrilene in the Isolated Dried Product of a Polymer Latex–Drug Formulation[a]

Sample[b]	Amount of Methapyrilene per 200 mg of Isolated Dried Product, μg
1	20.3
2	18.6
3	19.8
4	19.3
5	20.2
6	20.0
7	19.4
8	20.3
9	19.8
10	18.9
Average	19.7
SD	0.6

[a] This particular formulation consisted of 50 ml of a 0.5 m*M* methapyrilene hydrochloride solution and 50 ml of Acrysol ASE-75. [b] Samples were drawn at random from the isolated dried product.

Table II—Reproducibility of Methapyrilene Content in Samples of Solid Dispersions Obtained from a Flocculated Polymer Latex

Formulation[a]	Concentration of "Drug Solution"[a], m*M*	$\bar{X}$[b], mg	*RSD*
1	100	7.739 ± 0.132[c]	1.7
2	60	5.495 ± 0.181	3.3
3	15	1.778 ± 0.052	1.9
4	14	1.444 ± 0.045	3.1
5	10	0.959 ± 0.039	4.1
6	2	0.217 ± 0.009	3.9

[a] A formulation consisted of 50 ml of methapyrilene hydrochloride "drug solution" and 50 ml of Acrysol ASE-75. [b] Represents an average of 10 randomly selected samples drawn from the isolated dried product. [c] Standard deviation.

1000 g; and Formula II—methapyrilene hydrochloride, 100 mg, and flocculated polymer, 1000 g.

All ingredients were dried overnight at 40° and characterized as to particle size, density, and moisture content. The same basic procedure was used for mixing and sampling for Formulas I and II. First, a premix was made by adding about 300 g of diluent by geometric dilution to 100 mg of methapyrilene. To break up any lumps or agglomerates, the premix then was sized through a 60-mesh screen. The premix was then placed into a metal V-blender, and about 300 g more of diluent was added and allowed to mix for 5 min. Finally, the remaining diluent was added and blending was allowed to occur for 5 more min.

At this juncture, 4–5 g of mix was removed from the left top, bottom, and right top portions of the mixer and stored in tight containers for future analysis. Similarly, 4–5 g of mix was taken and stored after the following mixing times (in minutes): 10, 15, 20, 30, 45, and 60. From each of the three regional samples at each time interval, 20 200-mg samples were randomly selected and analyzed for drug content.

RESULTS AND DISCUSSION

The drug may be entrapped from solution by addition to a polymer latex, with the latex being isolated or separated by physicochemical means such as coagulation or by mechanical means such as ultracentrifugation.

At very low methapyrilene concentrations, a linear entrapment relationship appears to exist up to the point where flocculation begins (0.35–0.50 mmoles added) (Fig. 1). When the method of least squares is performed on the data in the range of 0.05–0.35 mmole added, the equation becomes:

$$\text{millimoles of bound methapyrilene} = (0.685) \times \text{millimoles of methapyrilene added} \quad \text{(Eq. 1)}$$

The fact that high levels of drug caused the latex to flocculate and low levels did not will be the subject of a future paper on mechanisms and factors affecting entrapment. Certainly, the direct relationship as seen in this region allows one to predict the amount of methapyrilene bound when other amounts of the same order of magnitude are added to the system. These findings also confirm that a drug–polymer dispersion may be formed independent of flocculation.

Table IV—Some Physical Characteristics of the Dry Mixing Components

Characteristic	Methapyrilene Hydrochloride	Lactose	Polymer[a]
Sieve fraction	80–100	80–100	80–100
Density	1.170	1.529[b]	1.342
Moisture content	0.2	0.0	0.0

[a] The isolated dried product was prepared from a flocculated latex system consisting of 4000 ml of 0.8 *M* KCl and 4000 ml of Acrysol ASE-75. [b] Literature value = 1.53 (17).

Table I illustrates the uniformity of distribution of a formulation consisting of 50 ml of 0.2 m*M* methapyrilene hydrochloride and 50 ml of latex. Since nearly 10% of the entire population was sampled, it is reasonable that inferences concerning the entire population are well justified.

Chiou and Riegelman (9) surveyed various types of solid dispersions but reported none of the techniques as improving solids mixing.

The data of Table I are typical of the uniformity of distribution data attained with entrapment formulations. This particular formulation did not appear to coagulate (flocculate) the latex; however, all formulations were treated similarly. The amount of drug present was normalized for what a 200-mg sample of polymeric drug dispersion should contain. With the normalized values, simple statistics (10–16) were used to treat the data. If it is assumed that the sampling data represent the entire population, a high degree of reproducibility of methapyrilene content throughout the isolated dried product is indicated. In fact, 19.7 ± 0.6 μg represents a mere 3.0% deviation from the mean amount found.

By employing this approach for all formulations, whether flocculated or deflocculated, data were accrued, treated, and summarized as shown in Tables II and III. The data indicate a high degree of uniformity of distribution in all of the solid dispersions, as shown by the low values of the relative deviation (percent deviation of a single determination from the mean amount found).

In the flocculated formulations (Table II), milligram amounts found distributed in 200 mg of dispersion are shown, with the percent deviations of drug content from the mean ranging from 1.7 to 4.1%. Table III shows the uniformity of distribution of drug in deflocculated systems. The relative deviations are lower for the deflocculated systems, ranging from only 1.6 to 3.0%. Among the several important differences that exist between Tables II and III are: (*a*) the presence or absence of flocculation, (*b*) higher percent deviations with flocculated systems, and (*c*) predictability of drug content in drug dispersions produced from deflocculated systems. When examining the data of Tables II and III, it should be remembered that a relative standard deviation of ±1.1–±1.8% was attributable to assay error (precision) over the concentration range employed.

The presence or absence of flocculation looms important in the isolation step. Due to the colloidal or near colloidal size of the particles in a polymer latex, isolation of the product in a deflocculated or peptized state cannot be accomplished by filtration or ordinary

Table III—Reproducibility of Methapyrilene Content in Samples of Solid Dispersions Obtained from a Deflocculated Polymer Latex

Formulation[a]	Concentration of "Drug Solution"[a], m*M*	$\bar{X}$[b], μg	*RSD*	Predicted $\bar{X}$[c], μg	Deviation from Predicted $\bar{X}$, %
1	1.00	88.1 ± 1.6[d]	1.8	94.2	6.5
2	0.50	44.9 ± 0.7	1.6	47.1	4.7
3	0.40	38.9 ± 0.7	1.8	37.7	3.2
4	0.20	19.7 ± 0.6	3.0	18.8	4.8
5	0.10	9.6 ± 0.2	2.1	9.4	2.1
6[e]	0.10	9.7 ± 0.2	2.1	9.4	3.1

[a] A formulation consisted of 50 ml of methapyrilene hydrochloride "drug solution" and 50 ml of Acrysol ASE-75. [b] Represents an average of 10 randomly selected samples drawn from the isolated dried product. [c] Predicted from Eq. 1. [d] Standard deviation. [e] Micronized granulation.

Table V—Drug Content Uniformity of 1:10,000 Blended Drug–Lactose and Drug–Polymer Physical Mixtures Obtained from Three Blender Sites at Various Mixing Times

Mixing Time, min	Lactose Formulation[a]				Polymer Formulation[a]			
	Top Left	Bottom	Top Right	$\bar{X}$[b]	Top Left	Bottom	Top Right	$\bar{X}$
	Micrograms per 200 mg of Mix							
5	23.3 ± 4.7[c]	22.1 ± 3.7	19.2 ± 1.8	21.5 ± 4.0	19.1 ± 4.1[d]	21.0 ± 5.1	21.7 ± 3.8	20.6 ± 4.4
10	22.0 ± 3.2	19.7 ± 2.8	21.1 ± 2.2	20.9 ± 2.9	17.3 ± 1.9[d]	19.0 ± 3.9	16.4 ± 2.0	17.6 ± 2.9
15	20.0 ± 3.1	22.8 ± 2.9	22.6 ± 3.2	21.8 ± 3.2	20.2 ± 5.1	19.4 ± 4.4	20.9 ± 4.8	20.2 ± 4.7
20	21.5 ± 2.9	21.8 ± 3.4	21.8 ± 2.9	21.7 ± 3.0	22.0 ± 4.2[d]	19.8 ± 5.0	20.6 ± 3.6	20.8 ± 4.3
30	19.0 ± 3.5	20.4 ± 2.5	20.0 ± 2.4	19.8 ± 2.9	20.8 ± 3.1	20.4 ± 3.1	23.1 ± 3.4	21.5 ± 3.4
45	18.4 ± 2.2	17.5 ± 2.3	18.1 ± 2.1	18.0 ± 2.2	19.6 ± 2.3	19.3 ± 2.3	17.4 ± 2.4	18.9 ± 2.5
60	16.5 ± 1.6	16.9 ± 1.9	16.5 ± 1.3	16.5 ± 1.4	18.6 ± 2.6	19.5 ± 3.1	19.7 ± 3.1	19.2 ± 2.9

[a] Formulations consisted of 100 mg of methapyrilene hydrochloride and 1000 g of diluent (lactose or polymer). [b] $\bar{X}$ represents average drug content based on all samples (top left, bottom, and top right) taken from the V-blender at a particular mixing time. [c] Standard deviation. [d] Drug content based on $n = 10$; all others are based on $n = 20$.

laboratory centrifugation but is possible by ultracentrifugation. Flocculated systems are readily isolated by filtration or centrifugation and their recovery, in general, is much simpler.

Probably the most important difference between the two types of systems is that uniformity of distribution can be reliably predicted for deflocculated systems (Scheme I and Table III). In only one case do percent deviations vary above the 5% level, illustrating that reliable predictability may be attained. Such prediction capability would allow a formulator to design, with mathematical certainty, a highly uniform product at any drug dilution ratio or dosage level desired.

No linear relationship existed for predicting the amount bound for flocculated systems, as can be seen from examination of Table II, although good batch-to-batch reproducibility for such systems was found previously (1, 2).

The ratios of mean amount found (column labeled $\bar{X}$) to sample weight (200 mg in each case) in Tables II and III vary on a weight-to-weight basis from 1:26 to 1:20,800 dilutions. Since even higher dilutions may be made, the dilution capability of polymer latex-produced solid dispersions has obvious implications when potent, low dose drugs are formulated. Formulations 5 and 6 of Table III correspond to dilutions of more than 1:20,000.

Another important property of entrapment products is apparent from a micronization experiment. The data in question are exemplified by Formulations 5 and 6 as listed in Table III. Formulations 5 and 6 are identical, except that 6 represents a micronized system. The results suggest that particle size does not make any difference when selecting samples from the isolated dried product for distribution studies. The fact that the strong forces of micronization do not reduce product uniformity by an effect of segregating drug and polymer is further evidence of a solid dispersion system. Since particle-size reduction and classification are important unit operations for solid dosage forms, the fact that milling the entrapment product does not affect drug distribution makes the molecular scale entrapment process that much more advantageous over conventional dry blending.

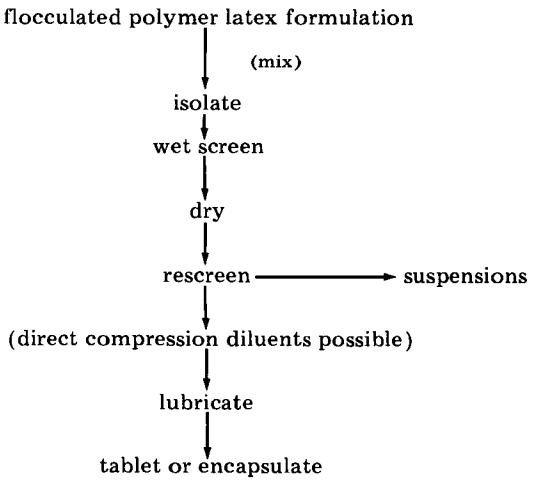

Scheme I—General scheme for scale-up of latex-generated solid dispersion systems

Uniformity of Distribution by Dry Blending as Compared to Molecular Scale Drug Entrapment—The dry mixing components were of the same sieve fraction and had little or no moisture content (Table IV). Good agreement was seen for the experimental density value (1.529) and the literature value (1.53) (Table IV). A greater density difference existed between the components of Formula I than between the components of Formula II (see *Experimental*).

Sampling results for the lactose and polymer physical mixtures are presented in Table V, which lists the average methapyrilene content in 200-mg samples taken from the three regions of the blender at various time intervals. To gain more information as to the homogeneity and deviation from the theoretical drug content of the dry blending process, the data of Table V are expressed as seen in Tables VI (lactose diluent) and VII (polymer diluent). Theoretically, each 200-mg sample should have contained 20 μg of methapyrilene if a perfect mix was attained.

The general picture that emerges from Tables V–VII is that the usual segregation and mixing problems of dry mixing are difficult to obviate, even when using only two components that are essentially the same size and have little or no moisture content. Definite similarities and differences existed between the lactose and polymer formulations. On the basis of homogeneity and predictability of drug content, both systems appeared to reach an optimum mixing time of 45 min, after which content uniformity in the analyzed samples dropped.

The drop in methapyrilene content after 45 min was quite rapid for the lactose formulation but gradual for the polymer formulation. Such an effect seems reasonable after considering the density differences (Table IV); however, other factors might include particle-size distribution, shape, and charge (18–24). Compared to the harder polymer particles, the softer lactose particles would be more likely to be susceptible to attrition or breakdown by bombarding against each other or the walls of the mixer. A wider particle-size distribution or a change to a more irregular shape may have contributed to the segregation and unmixing. Charge effects were not characterized, but a Plexiglas V-blender was purposely not used to minimize the creation of any charge.

Although the V-blender may be a very efficient mixer, a high degree of mixedness was not achieved for the two cases studied at many mixing times. The data in Tables VI and VII reveal that it was difficult to get within ±15% of the mean amount found, and below ±10% was only obtained when the theoretical content was too low or the methapyrilene content was not reproducible throughout all of the blend. Furthermore, as great as ±55% deviation occurred between sampling units, a situation mathematically predicted by Train (24).

These high dilution formulations thus suffer from the problems of segregation, unmixing, and the selection of a specific optimum mixing time. Treating these formulations as granulations could compound the difficulties in obtaining content uniformity due to poor or nonuniform flow and subsequent weight variation of tablets.

Under the conditions of this study, it appeared that the "best possible mix" for the dry blend formulations was attained after 45

Table VI—Homogeneity and Deviation from Theoretical Methapyrilene Content in 1:10,000 Drug–Lactose Physical Mixtures[a]

Mixing Time, min	RSD				Percent Deviation of Mean Amount Found from Theoretical Drug Content[b]			
	Top Left	Bottom	Top Right	$\bar{C}$[c]	Top Left	Bottom	Top Right	$\bar{T}$[d]
5	20.2	16.7	9.4	18.6	16.5	10.5	4.0	7.5
10	14.5	14.2	10.4	13.9	10.0	1.5	5.5	4.5
15	15.5	12.7	13.7	14.7	0.0	14.0	13.0	9.0
20	13.5	15.6	13.3	13.8	7.5	9.0	9.0	8.5
30	18.4	12.3	12.0	14.6	5.0	2.0	0.0	1.0
45	12.0	13.1	11.6	12.2	8.0	12.5	9.5	10.0
60	9.7	11.2	7.9	8.5	17.5	15.5	17.5	17.5

[a] The formulation consisted of 100 mg of methapyrilene and 1000 g of lactose. See Table V for corresponding mean values at the various time intervals. [b] Theoretical drug content equals 20 μg/200 mg of mix. [c] C represents the relative standard deviation based on the corresponding $\bar{X}$. [d] $\bar{T}$ represents the percent deviation of $\bar{X}$ from theoretical drug content.

min of mixing. Table VIII gives the results for a methapyrilene molecular scale drug entrapment formulation and also compares the results for the optimum mixes when methapyrilene was dry blended with lactose and polymer as diluents. All formulations were designed theoretically to yield 20 μg of methapyrilene/200 mg of sample, that is, a 1:10,000 ratio of drug to diluent. Even when particle size is controlled by mixing only 80–100-mesh material, the data clearly show that predictability and uniform distribution are much less for the dry-blended formulations than the solid dispersion entrapment product. The reproducibility of methapyrilene throughout the entrapment product was very satisfactory, deviating from the mean amount found by only 3.0% (compared to dry blending), and the deviation from the theoretical content was only 1.5%.

When considering the previous data and what has been established about molecular scale drug entrapment solid dispersions, several advantageous features of entrapment as a method of distributing drugs uniformly throughout a mix become evident. First, segregation due to density, particle size, and particle-size distribution are not serious problems as in dry blending. Entrapment occurs in solution to form a solid dispersion product following isolation and drying. The amount of drug entrapment is both predictable and uniformly distributed throughout the isolated dried product. Furthermore, milling or micronization does not adversely affect drug content or drug uniformity in an entrapment formulation.

In addition, temperature, rate of mixing, length of time between interaction, and separation do not substantially affect the results or the uniformity of results. The molecular scale entrapment method does not require the use of elevated temperatures to produce drug solution in a melt or drug fusion, as is required in other preparative methods for solid dispersions. The mixing time to at-

Table VII—Reproducibility and Predictability of Methapyrilene Content in Samples of a High Dilution Drug–Polymer Formulation[a]

Mixing Time, min	RSD				Percent Deviation of Mean Amount Found from Theoretical Drug Content[b]			
	Top Left	Bottom	Top Right	$\bar{C}$[c]	Top Left	Bottom	Top Right	$\bar{T}$[d]
5	21.5	24.3	17.5	21.4	4.5	5.0	8.5	7.0
10	11.0	20.5	12.2	16.5	13.5	5.0	13.0	12.5
15	25.2	22.7	23.0	23.3	1.0	3.0	4.5	1.0
20	19.1	25.3	17.5	20.7	10.0	1.0	3.0	4.0
30	14.9	15.2	14.7	15.8	4.0	2.0	15.5	2.5
45	11.7	11.9	13.8	13.2	2.0	3.5	13.0	5.5
60	14.0	15.9	15.7	15.1	7.0	2.5	1.5	4.0

[a] The formulation consisted of 100 mg of methapyrilene hydrochloride and 1000 g of polymer. See Table V for corresponding mean values at the various time intervals. [b] Theoretical drug content equals 20 μg/200 mg of mix. [c] C represents the relative standard deviation based on the corresponding $\bar{X}$. [d] $\bar{T}$ represents the percent deviation of $\bar{X}$ from theoretical drug content.

Table VIII—Comparison of Uniformity of Drug Distribution of 1:10,000 Physical Mixtures with a 1:10,000 Solid Dispersion

	Molecular Scale Drug Entrapment	Dry Blending I	Dry Blending II
Formulation constituents	0.20 m*M* I[a] 50 ml Latex[b] 50 ml	I 100 mg Lactose 1000 g	I 100 mg Polymer 1000 g
Mixing time, min	3	45	45
Sieve fractions	—	80–100	80–100
Mean amount per 200 mg sample, μg	19.7 ± 0.6	Top left 18.4 ± 2.2 Bottom 17.5 ± 2.3 Top right 18.1 ± 2.1 Overall[c] 18.0 ± 2.2	Top left 19.6 ± 2.3 Bottom 19.3 ± 2.3 Top right 17.4 ± 2.4 Overall 18.9 ± 2.5
RSD	3.0	Top left 12.0 Bottom 13.1 Top right 11.6 Overall 12.2	Top left 11.7 Bottom 11.9 Top right 13.8 Overall 13.2
Percent deviation of mean amount found from theoretical	1.5	Top left 8.0 Bottom 12.5 Top right 9.5 Overall 10.0	Top left 2.0 Bottom 3.5 Top right 13.0 Overall 5.5

[a] I = methapyrilene hydrochloride. [b] Latex = Acrysol ASE-75. [c] Overall values are based on all samples (top left, bottom, and top right) taken from the V-blender at the indicated mixing time.

tain, as well as the number of operations to produce, the uniform distribution of drug in granular solids is much less and more specific for latex-generated solid dispersions. Therefore, simpler, more specific manufacturing instructions are possible. Direct compression ingredients and lubricants can be added, or lubricants can be added to the entrapment product and tableted directly, with weight variation being the major factor impairing content uniformity. Entrapment may be compared to wet granulation as far as time to produce a finished tablet; availability and effectiveness do not appear to be problems for molecular scale drug entrapment (1–7).

For scale-up operations, a general scheme might include the steps indicated in Scheme I. The molecular scale drug entrapment method described herein appears to have great potential for distributing drugs uniformly, especially low dose, highly potent drugs where the usual blending techniques may be inadequate or unreliable.

REFERENCES

(1) H. Goodman, Ph.D. thesis, Purdue University, West Lafayette, Ind., 1962.

(2) H. Goodman and G. S. Banker, *J. Pharm. Sci.*, **59**, 1131(1970).

(3) G. T. Rhodes, K. Wai, and G. S. Banker, *ibid.*, **59**, 1578(1970).

(4) *Ibid.*, **59**, 1581(1970).

(5) L. K. Benedict, Ph.D. thesis, Purdue University, West Lafayette, Ind., 1966.

(6) G. S. Banker and H. Goodman, U.S. pat. 3,608,063 (Sept. 21, 1971).

(7) G. S. Banker, U.S. pat. 3,629,392 (Dec. 21, 1971).

(8) E. Pearlman, *J. Pharmacol. Exp. Ther.*, **95**, 465(1949).

(9) W. L. Chiou and S. Riegelman, *J. Pharm. Sci.*, **60**, 1281(1971).

(10) E. R. Garrett, *ibid.*, **51**, 672(1962).

(11) M. M. Tuckerman, *ibid.*, **51**, 700(1962).

(12) E. R. Garrett and E. C. Olson, *ibid.*, **51**, 764(1962).

(13) W. A. Wallis and H. V. Roberts, "Statistics—A New Approach," Free Press of Glencoe, Brooklyn, N.Y., 1963.

(14) A. J. Duncan, "Quality Control and Industrial Statistics," Richard D. Irwin, Homewood, Ill., 1957.

(15) N. M. Downie and R. W. Heath, "Basic Statistical Methods," Harper and Row, New York, N.Y., 1965.

(16) D. A. Skoog and D. M. West, "Fundamentals of Analytical Chemistry," Holt, Rinehart, and Winston, New York, N.Y., 1963.

(17) "The Merck Index," 7th ed., Merck & Co., Rahway, N.J., 1960, p. 594.

(18) P. J. Lloyd, P. C. M. Yeung, and D. C. Freshwater, *J. Soc. Cosmet. Chem.*, **21**, 205(1970).

(19) G. T. King, *Chem. Proc. Eng.*, **46**, 617(1964).

(20) J. L. Olsen and E. G. Rippie, *J. Pharm. Sci.*, **53**, 147(1964).

(21) E. G. Rippie, J. L. Olsen, and M. D. Faiman, *ibid.*, **53**, 1360(1964).

(22) M. D. Faiman and E. G. Rippie, *ibid.*, **54**, 719(1965).

(23) K. A. Lees, *J. Pharm. Pharmacol., Suppl.*, **15**, 43T(1963).

(24) D. Train, *J. Amer. Pharm. Ass., Sci. Ed.*, **49**, 265(1960).

ACKNOWLEDGMENTS AND ADDRESSES

Received November 28, 1973, from the *Industrial and Physical Pharmacy Department, School of Pharmacy and Pharmacal Sciences, Purdue University, Lafayette, IN 47907*

Accepted for publication July 31, 1975.

Presented at the Industrial Pharmaceutical Technology Section, APhA Academy of Pharmaceutical Sciences, San Diego meeting, November 1973.

Supported by the Purdue Research Foundation.

* Present address: Dorsey Laboratories, Division of Sandoz-Wander, Inc., Lincoln, NE 68506

[x] To whom inquiries should be directed.

Contact Angles and Wetting of Pharmaceutical Powders

C. F. LERK [x], A. J. M. SCHOONEN, and J. T. FELL *

Abstract □ Contact angles of pharmaceutical powders were determined by the h–ϵ method, which consists essentially of measuring the maximum height of a drop of liquid formed on a presaturated compact of the material. Determinations with aspirin as the test material indicate that the measured value is independent of the particle size of the powder and the porosity of the cake. The method was extended to include determinations on mixed powder systems. The results show that the hydrophobic material dominates with large particle-size powders; with small particle sizes, a linear relationship between the cosine of the contact angle of the mixed system and the proportion of the components is obtained. Results are presented for a wide variety of materials of pharmaceutical interest.

Keyphrases □ Powders, pharmaceutical—contact angles and wetting determined by h–ϵ method, effect of particle size and porosity of cake □ Contact angles—pharmaceutical powders, determined by h–ϵ method, effect of particle size and porosity of cake □ Wetting—pharmaceutical powders, effect of particle size and porosity of cake □ Aspirin powder—contact angles and wetting determined by h–ϵ method, effect of particle size and porosity of cake

The wetting of solid materials usually implies the replacement of air on the surface of a solid by a liquid. In addition to the components of the system, the type of wetting is also important. Osterhof and Bartell (1) distinguished between three types of wetting, namely those of adhesion, immersion, and spreading. The distinction between these three types may be made by considering the model, suggested by Parfitt (2), of a solid cube being immersed in a liquid (Fig. 1).

THEORY

The energy changes that take place when these processes occur may be written in terms of the measurable quantities of the liquid–vapor interfacial tension and the contact angle. If it is assumed that the solid surface before wetting is in equilibrium with the vapor of the liquid (1, 2), then:

$$W_a = -\gamma_{LV^\circ}(\cos\theta + 1) \qquad \text{(Eq. 1)}$$

$$W_i = -\gamma_{LV^\circ}\cos\theta \qquad \text{(Eq. 2)}$$

$$W_s = -\gamma_{LV^\circ}(\cos\theta - 1) \qquad \text{(Eq. 3)}$$

tain, as well as the number of operations to produce, the uniform distribution of drug in granular solids is much less and more specific for latex-generated solid dispersions. Therefore, simpler, more specific manufacturing instructions are possible. Direct compression ingredients and lubricants can be added, or lubricants can be added to the entrapment product and tableted directly, with weight variation being the major factor impairing content uniformity. Entrapment may be compared to wet granulation as far as time to produce a finished tablet; availability and effectiveness do not appear to be problems for molecular scale drug entrapment (1–7).

For scale-up operations, a general scheme might include the steps indicated in Scheme I. The molecular scale drug entrapment method described herein appears to have great potential for distributing drugs uniformly, especially low dose, highly potent drugs where the usual blending techniques may be inadequate or unreliable.

REFERENCES

(1) H. Goodman, Ph.D. thesis, Purdue University, West Lafayette, Ind., 1962.

(2) H. Goodman and G. S. Banker, *J. Pharm. Sci.*, **59**, 1131(1970).

(3) G. T. Rhodes, K. Wai, and G. S. Banker, *ibid.*, **59**, 1578(1970).

(4) *Ibid.*, **59**, 1581(1970).

(5) L. K. Benedict, Ph.D. thesis, Purdue University, West Lafayette, Ind., 1966.

(6) G. S. Banker and H. Goodman, U.S. pat. 3,608,063 (Sept. 21, 1971).

(7) G. S. Banker, U.S. pat. 3,629,392 (Dec. 21, 1971).

(8) E. Pearlman, *J. Pharmacol. Exp. Ther.*, **95**, 465(1949).

(9) W. L. Chiou and S. Riegelman, *J. Pharm. Sci.*, **60**, 1281(1971).

(10) E. R. Garrett, *ibid.*, **51**, 672(1962).

(11) M. M. Tuckerman, *ibid.*, **51**, 700(1962).

(12) E. R. Garrett and E. C. Olson, *ibid.*, **51**, 764(1962).

(13) W. A. Wallis and H. V. Roberts, "Statistics—A New Approach," Free Press of Glencoe, Brooklyn, N.Y., 1963.

(14) A. J. Duncan, "Quality Control and Industrial Statistics," Richard D. Irwin, Homewood, Ill., 1957.

(15) N. M. Downie and R. W. Heath, "Basic Statistical Methods," Harper and Row, New York, N.Y., 1965.

(16) D. A. Skoog and D. M. West, "Fundamentals of Analytical Chemistry," Holt, Rinehart, and Winston, New York, N.Y., 1963.

(17) "The Merck Index," 7th ed., Merck & Co., Rahway, N.J., 1960, p. 594.

(18) P. J. Lloyd, P. C. M. Yeung, and D. C. Freshwater, *J. Soc. Cosmet. Chem.*, **21**, 205(1970).

(19) G. T. King, *Chem. Proc. Eng.*, **46**, 617(1964).

(20) J. L. Olsen and E. G. Rippie, *J. Pharm. Sci.*, **53**, 147(1964).

(21) E. G. Rippie, J. L. Olsen, and M. D. Faiman, *ibid.*, **53**, 1360(1964).

(22) M. D. Faiman and E. G. Rippie, *ibid.*, **54**, 719(1965).

(23) K. A. Lees, *J. Pharm. Pharmacol., Suppl.*, **15**, 43T(1963).

(24) D. Train, *J. Amer. Pharm. Ass., Sci. Ed.*, **49**, 265(1960).

ACKNOWLEDGMENTS AND ADDRESSES

Received November 28, 1973, from the *Industrial and Physical Pharmacy Department, School of Pharmacy and Pharmacal Sciences, Purdue University, Lafayette, IN 47907*

Accepted for publication July 31, 1975.

Presented at the Industrial Pharmaceutical Technology Section, APhA Academy of Pharmaceutical Sciences, San Diego meeting, November 1973.

Supported by the Purdue Research Foundation.

* Present address: Dorsey Laboratories, Division of Sandoz-Wander, Inc., Lincoln, NE 68506

[x] To whom inquiries should be directed.

Contact Angles and Wetting of Pharmaceutical Powders

C. F. LERK [x], A. J. M. SCHOONEN, and J. T. FELL *

Abstract □ Contact angles of pharmaceutical powders were determined by the h–ϵ method, which consists essentially of measuring the maximum height of a drop of liquid formed on a presaturated compact of the material. Determinations with aspirin as the test material indicate that the measured value is independent of the particle size of the powder and the porosity of the cake. The method was extended to include determinations on mixed powder systems. The results show that the hydrophobic material dominates with large particle-size powders; with small particle sizes, a linear relationship between the cosine of the contact angle of the mixed system and the proportion of the components is obtained. Results are presented for a wide variety of materials of pharmaceutical interest.

Keyphrases □ Powders, pharmaceutical—contact angles and wetting determined by h–ϵ method, effect of particle size and porosity of cake □ Contact angles—pharmaceutical powders, determined by h–ϵ method, effect of particle size and porosity of cake □ Wetting—pharmaceutical powders, effect of particle size and porosity of cake □ Aspirin powder—contact angles and wetting determined by h–ϵ method, effect of particle size and porosity of cake

The wetting of solid materials usually implies the replacement of air on the surface of a solid by a liquid. In addition to the components of the system, the type of wetting is also important. Osterhof and Bartell (1) distinguished between three types of wetting, namely those of adhesion, immersion, and spreading. The distinction between these three types may be made by considering the model, suggested by Parfitt (2), of a solid cube being immersed in a liquid (Fig. 1).

THEORY

The energy changes that take place when these processes occur may be written in terms of the measurable quantities of the liquid–vapor interfacial tension and the contact angle. If it is assumed that the solid surface before wetting is in equilibrium with the vapor of the liquid (1, 2), then:

$$W_a = -\gamma_{LV^\circ}(\cos\theta + 1) \qquad \text{(Eq. 1)}$$

$$W_i = -\gamma_{LV^\circ}\cos\theta \qquad \text{(Eq. 2)}$$

$$W_s = -\gamma_{LV^\circ}(\cos\theta - 1) \qquad \text{(Eq. 3)}$$

Table I—Measured Values of Contact Angles of Materials of Pharmaceutical Interest

Material	Standard	Surface Tension, dynes/cm	Density Liquid, g/cm³	Density Solid, g/cm³	Porosity[a]	Drop Height[a], cm	cos θ	θ°
Acetaminophen[b]	BP	67.7	1.000	1.27	0.298	0.185	0.514	59
Aminosalicylic acid[b]	USP	68.3	0.998	1.52	0.363	0.170	0.534	57
Aspirin[c]	Ph. Ned.	59.4	1.001	1.40			See Table II	
Caffeine[c]	Ph. Ned.	60.3	1.001	1.23	0.185	0.102	0.736	43
Chloramphenicol[d]	Ph. Ned.	63.2	1.000	1.51	0.150	0.199	0.513	59
Chloramphenicol palmitate[e]	—	71.7	0.999	1.20	0.199	0.510	−0.569	125
Dicalcium phosphate dihydrate[f]	—	72.3	0.999	2.40	—	~0.000	~1.000	0
Hexobarbital[c]	Ph. Ned.	67.1	0.999	1.35	0.164	0.399	0.041	88
Lactose[c]	Ph. Ned.	71.6	1.071	1.54	0.135	0.057	0.868	30
Magnesium stearate[c]	Ph. Ned.	72.3	0.999	1.07	0.224	0.503	−0.520	121
Potassium chloride[g]	Analytical grade	74.5	1.160	1.98	0.048	0.028	0.935	21
Phenacetin[c]	Ph. Ned.	61.5	0.999	1.33	0.179	0.313	0.202	78
Phenobarbital[c]	Ph. Ned.	71.8	1.000	1.33	0.261	0.263	0.347	70
Polyethylene[h], high density	Laboratory reagent	72.3	0.999	0.94	0.233	0.425	−0.182	100
Salicylic acid[c]	Ph. Ned.	63.3	0.999	1.42	0.185	0.404	−0.224	103
Sodium chloride[c]	Ph. Ned.	76.3	1.190	2.17	0.093	0.046	0.885	28
Sulfadiazine[c]	Ph. Ned.	72.2	0.999	1.48	0.168	0.287	0.328	71
Polytef[h]	Laboratory reagent	72.3	0.999	2.39	0.036	0.462	−0.385	113

[a] See Table III. [b] A. C. F., Amsterdam, The Netherlands. [c] Lamers and Indemans, 's-Hertogenbosch, The Netherlands. [d] Pharmachemie, Haarlem, The Netherlands. [e] Nogepha, Amsterdam, The Netherlands. [f] Emcompress Special, Ed. Mendell Co., New York, N.Y. [g] Merck, Darmstadt, West Germany. [h] British Drug Houses, Poole, England.

where W_a, W_i, and W_s are the changes in free surface energy for the adhesion, immersion, and spreading processes, respectively; γ_{LV^0} is the liquid–vapor interfacial tension; and θ is the contact angle. For the process of wetting to occur, the appropriate value of W must be negative. Since γ_{LV^0} is always positive, the wetting process is determined by $\cos\theta$. Thus, measurements of the contact angle will give useful indications of wettability.

Pharmaceutically, wetting is not an end in itself but is the preliminary step in another process, *e.g.*, dispersion or dissolution, both *in vitro* and *in vivo*. In the preparation of dispersions, surfactants are often employed to aid in the wetting of insoluble powders (3). The role of wetting in the dissolution of drugs is not established.

Solvang and Finholt (4) stated that the change to a hydrophilic character probably was responsible for the increased dissolution rate of hydrophobic drugs after granulation with a binder. Kawashima *et al.* (5) concluded that improvement in wetting caused the increased dissolution rate of salicylic acid powder after spray drying with acacia. Allen and Davies (6) reported increases in the dissolution rate and amount of absorption of a highly lipid-soluble drug after admixture with lactose, seemingly due to increased wettability.

Newton and Razzo (7), however, after a detailed study on the release of drugs from hard gelatin capsules, concluded that wetting was not the controlling feature of drug release from capsules. The contact angle is one parameter controlling the penetration of liquids into capillaries in capsules and tablets; but evidence of the importance of the penetration rate in, for example, the subsequent dissolution of a drug from capsules is conflicting (8, 9).

Measurements of the contact angle of tablet surfaces have been undertaken to optimize film-coating techniques (10–12) and to

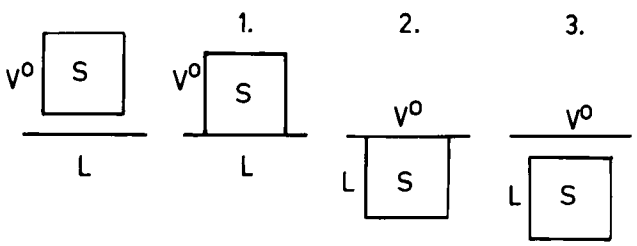

Figure 1—*Stages involved in the complete wetting of a solid cube (S) by a liquid (L). Key: 1, adhesional wetting; 2, immersional wetting; and 3, spreading wetting.*

study drug release from matrixes (13). In view of the importance of wetting and the scarcity of data available, it was decided to measure the contact angles of pharmaceutical powders.

Direct measurement of the contact angle of powders is not feasible; an indirect method must be used. Heertjes and Kossen (14) examined the methods available, and their results indicate the superiority of the h–ϵ method. This technique was adopted for this study.

The theory and technique of the h–ϵ method were described previously (15, 16) and extended (17). Essentially, a drop of liquid is formed on a cake of the test material, which has been previously saturated with the liquid. By using the equation of Padday (18), relating the height of a large liquid drop to the contact angle, and by correcting for "surface porosity," the contact angle may be determined. The relationships derived previously (16, 17) are:

$$\text{for } \theta > 90^\circ \qquad \cos\theta = -1 + \sqrt{(2 - Bh^2)\frac{2}{3(1-\epsilon_V)}} \qquad \text{(Eq. 4)}$$

$$\text{for } \theta < 90^\circ \qquad \cos\theta = 1 - \sqrt{\frac{2}{3(1-\epsilon_V)}Bh^2} \qquad \text{(Eq. 5)}$$

where h is the height of the liquid drop, ϵ_V is the volume porosity of the cake, and $B = \rho_L g/2\gamma_{LV^0}$, where ρ_L is the liquid density, and g is the acceleration due to gravity. In the derivation of these equations, assumptions are made that allow the determination of surface porosity in terms of the measurable volume porosity.

These equations apply to single materials. Pharmaceutical systems are, however, frequently mixtures and may be treated as follows. The mixture considered is a two-component system compressed into a porous cake and saturated with an appropriate liquid. Let f be the area fraction of Component 1 particles and $1 - f$ be the area fraction of Component 2 particles. If ϵ_S is the surface porosity, *i.e.*, the fraction of the solid surface wet by the drop, then:

$$(\gamma_{S_{1,2}V^0})_{por} = \epsilon_S\gamma_{LV^0} + (1-\epsilon_S)\gamma_{S_{1,2}V^0} \qquad \text{(Eq. 6)}$$

and:

$$\gamma_{S_{1,2}V^0} = f\gamma_{S_1V^0} + (1-f)\gamma_{S_2V^0} \qquad \text{(Eq. 7)}$$

where γ is the interfacial tension; and the subscripts S_1, S_2, $S_{1,2}$, por, V^0, and L refer to Solid 1, Solid 2, the solid mixture, the porous system, the vapor, and the liquid, respectively. Hence, com-

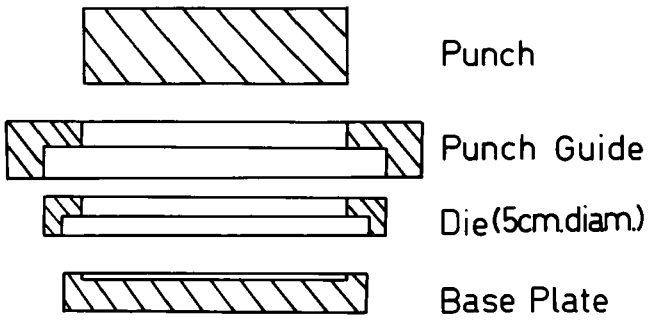

Figure 2—*Assembly for producing compacts for contact angle determination.*

bining Eqs. 6 and 7 gives:

$$(\gamma_{S_{1,2}V^\circ})_{por} = \epsilon_S\gamma_{LV^\circ} + (1-\epsilon_S)[f\gamma_{S_1V^\circ} + (1-f)\gamma_{S_2V^\circ}] \quad \text{(Eq. 8)}$$

Similarly:

$$(\gamma_{S_{1,2}L})_{por} = (1-\epsilon_S)\gamma_{S_{1,2}L} \quad \text{(Eq. 9)}$$

and:

$$\gamma_{S_{1,2}L} = f\gamma_{S_1L} + (1-f)\gamma_{S_2L} \quad \text{(Eq. 10)}$$

Thus, combining Eqs. 9 and 10 gives:

$$(\gamma_{S_{1,2}L})_{por} = (1-\epsilon_S)[f\gamma_{S_1L} + (1-f)\gamma_{S_2L}] \quad \text{(Eq. 11)}$$

Young's equation (18) for a porous mass consisting of two components may be written:

$$\cos\theta' = \frac{(\gamma_{S_{1,2}V^\circ})_{por} - (\gamma_{S_{1,2}L})_{por}}{\gamma_{LV^\circ}} \quad \text{(Eq. 12)}$$

where θ' is the apparent contact angle of the liquid on the porous mixed system. Substituting Eqs. 8 and 11 into Eq. 12 and rearranging give:

$$\cos\theta' = \epsilon_S + (1-\epsilon_S)(f)\frac{\gamma_{S_1V^\circ} - \gamma_{S_1L}}{\gamma_{LV^\circ}} + (1-\epsilon_S)(1-f)\frac{\gamma_{S_2V^\circ} - \gamma_{S_2L}}{\gamma_{LV^\circ}} \quad \text{(Eq. 13)}$$

which gives:

$$\cos\theta' = \epsilon_S + (1-\epsilon_S)[f\cos\theta_1 + (1-f)\cos\theta_2] \quad \text{(Eq. 14)}$$

where θ_1 and θ_2 are the contact angles of the liquid against Solids 1 and 2, respectively. From the work of Cassie (19):

$$f\cos\theta_1 + (1-f)\cos\theta_2 = \cos\theta_{1,2} \quad \text{(Eq. 15)}$$

where $\theta_{1,2}$ is the contact angle of the liquid against the mixed system. Hence, substituting Eq. 15 into Eq. 14 gives:

$$\cos\theta' = \epsilon_S + (1-\epsilon_S)\cos\theta_{1,2} \quad \text{(Eq. 16)}$$

The equation of Padday (18) written for a saturated porous mixed mass is:

$$\cos\theta = 1 - \frac{\rho_L g}{2\gamma_{LV^\circ}}h^2 = 1 - Bh^2 \quad \text{(Eq. 17)}$$

Combining Eqs. 16 and 17 gives:

$$\cos\theta_{1,2} = 1 - \frac{B}{1-\epsilon_S}h^2 \quad \text{(Eq. 18)}$$

This equation is analogous to those derived previously (16, 17) and can be treated in a similar manner to determine $\cos\theta_{1,2}$ by means of Eqs. 4 and 5.

EXPERIMENTAL

Materials—The materials used, together with the suppliers and relevant standards, are listed in Table I. They usually were used as supplied to give values that may be better guides to behavior under practical conditions. Where size fractions were required, initial sieving was carried out on a vibration sieve machine[1], followed by sieving of the required size fraction using an air jet sieve[2]. Milled samples were produced by an air jet mill[3]. Saturated solutions of the materials were prepared by allowing excess solid to equilibrate with distilled water in a constant-temperature room (23°).

Table II—Contact Angles of Aspirin of Varying Particle Sizes and Porosities

Size Fraction, μm	Porosity	Drop Height, cm	cos θ	θ°
125–180	0.093	0.286	0.297	73
150–210	0.105	0.297	0.262	75
150–210	0.141	0.287	0.272	74
150–210	0.246	0.262	0.291	73
600–850	0.075	0.299	0.269	73
Unfractionated[a]	0.145	0.292	0.265	75

[a] Mean particle size by air permeability = 13 μm.

Methods—*Contact Angle Measurements*—These measurements were carried out as detailed by Kossen and Heertjes (16). Compacts of the test powder were prepared using the arrangement shown in Fig. 2. After application of the required pressure, the punch, the punch guide, and the die were removed, leaving the cake of material in the base plate. The pressures used were as low as possible, consistent with the production of a stable cake, and were applied by means of a hydraulic press[4] and measured by a load cell[5]. In general, the pressure applied was between 100 and 200 kg/cm^2.

Porosities were calculated from a knowledge of the sample weight and dimensions. Presaturation of the compacted powder bed was accomplished either by spraying or, where possible, by simply dropping liquid onto the compact. Saturated solutions of the test materials were used to prevent dissolution.

After saturation, the cake plus base plate was placed on a horizontal table and surrounded by a cover equipped with viewing windows and a small hole to allow entry of a fine needle. The appropriate saturated solution was slowly dropped onto the cake surface from the needle, and readings of the drop height were taken with a cathetometer[6] until additional drops caused no increase in height. The contact angle was calculated from the appropriate equation, 4 or 5. All measurements were carried out at 23° and at least in duplicate.

Liquid and Solid Properties—The densities and surface tensions of the liquids and the densities of the solids were determined by a balance[7], a tensiometer[8], and an air comparison pycnometer[9], respectively. The liquid measurements were carried out at 23°.

RESULTS AND DISCUSSION

Initial experiments were conducted to assess the influence of particle size and porosity on the calculated contact angle. Aspirin was chosen as the test material because it is readily available in a range of particle sizes and forms stable compacts at low pressures. The results from the determinations are given in Table II. As can be seen, despite the assumptions implicit in the method, the results from a wide variety of particle sizes and porosities were remarkably consistent. This consistency was also observed (16) for organic liquids on ground sodium chloride compacts of different porosity. The extension of these determinations to changes both in porosity and particle size confirms the usefulness of the method.

The results from the samples produced by air jet milling are

[1] E. M. L. type 200-67, Haver and Boecker, Oelde, West Germany.
[2] Alpine Machinery Ltd., Augsburg, West Germany.
[3] Gem. T. Helme Chemicals Inc., Helmetta, N.J.
[4] M-30, Research and Industrial Instruments, London, England.
[5] WASA, Sonco, N. V. Rotterdam, The Netherlands.
[6] Precision Tool and Instrument Co., Surrey, England.
[7] Mohr, G. Kern, Ebingen, West Germany.
[8] Du Nuoy K 8600, Krüss, Hamburg, West Germany.
[9] Model 930, Beckman Instruments Ned. N. V., Amsterdam, The Netherlands.

Table III—Variation of Contact Angle of Aspirin with Time after Jet Milling

Time after Milling, hr	Porosity[a]	Drop Height[a], cm	cos θ	θ°
0	0.267	0.415	−0.275	106
24	0.339	0.359	−0.028	91
30	0.337	0.334	−0.036	87
48	0.312	0.292	+0.173	80
72	0.331	0.268	+0.230	77
120	0.343	0.268	+0.223	77

[a]These values are the means of more than one determination as a guide to the porosities used and the drop heights attained. To calculate cos θ, each set of values was treated as an individual, and the cos θ value in the table is the mean of the individual values.

shown in Table III. The initial high values of the contact angle immediately after milling fell with time to a value slightly higher than the mean of the values observed for the unmilled size fractions. This result indicates a change in the surface characteristics of the material, induced by the milling process, which is slowly reversible (UV assay confirmed no degradation had occurred on milling). Such effects may be brought about during milling, for example, by the creation of clean surfaces, formation of electrostatic charges, or changes in polymorphic form. The underlying cause of the observed changes in contact angle after milling was not investigated, but the results show that the technique provides a sensitive measure of the surface characteristics of a material.

Table I shows the results from a wide range of pharmaceutical materials together with other relevant information. The wide spectrum of values of these common materials should be noted. In all cases, it was possible to prepare and saturate the cake of material without disrupting its structure. For materials exhibiting contact angles above 90°, *e.g.*, magnesium stearate, saturation of the cake is impossible by spraying or dropping liquid onto the surface; the drop is merely formed on the dry compact. The theoretical derivation of the equation for angles above 90° takes this fact into account. The value for polyethylene (100°) and polytef (113°) are included to show the good agreement between these values and those

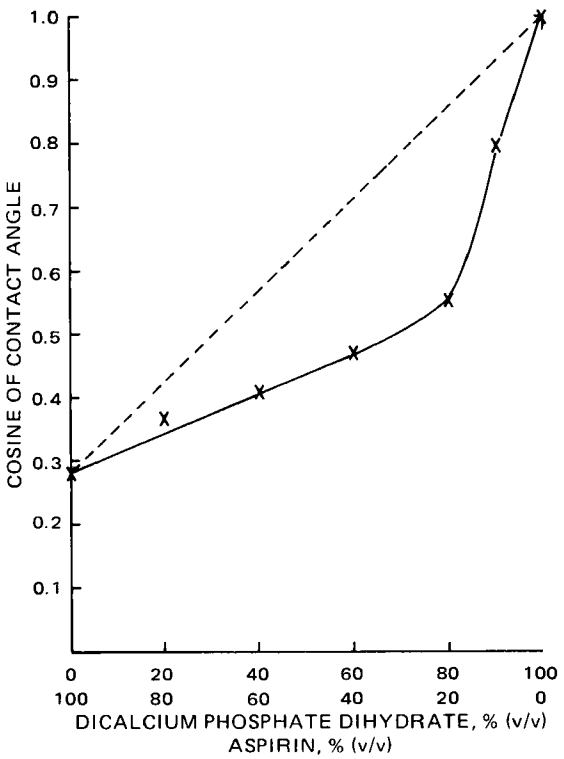

Figure 3—*Cosines of the contact angles of mixtures of dicalcium phosphate dihydrate and aspirin, 150–210-μm size fraction. Key: - - -, theoretical line; and ×, experimental points.*

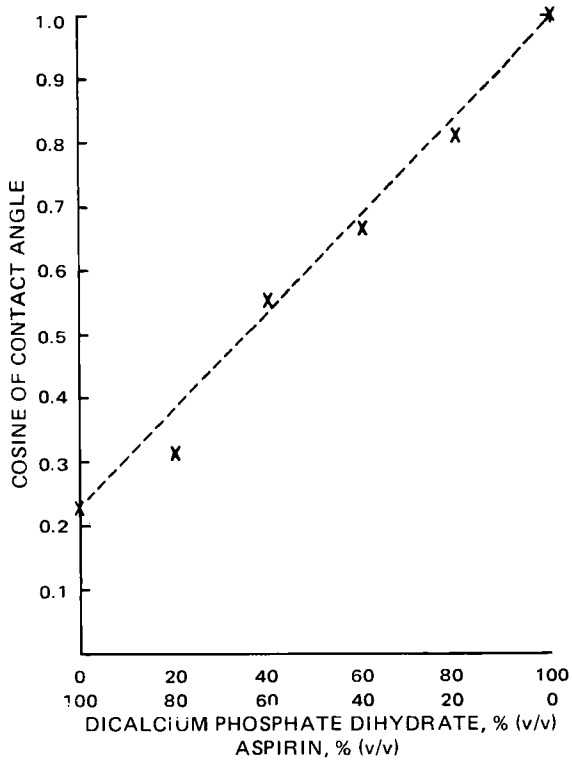

Figure 4—*Cosines of the contact angles of mixtures of dicalcium phosphate dihydrate and aspirin, jet-milled fraction. Key: - - -, theoretical line; and ×, experimental points.*

of 94° for polyethylene (20) and of 108° for polytef (21) determined by more conventional means.

To study the contact angle of mixtures, the system of aspirin–dicalcium phosphate dihydrate[10] was chosen. Spreading on a saturated dicalcium phosphate compact was rapid, and no drop height could be measured. Hence, its contact angle may be taken to be 0° or nearly so. The work of Cassie (19) indicates that there should be a linear relationship between the cosine of the contact angle of a heterogeneous surface and the area fraction of the components (Eq. 15).

The results for mixtures of 150–210-μm particles and jet-milled particles are presented in Figs. 3 and 4. For particles with a narrow size distribution that are not too irregular in shape, the volume fraction of each component may be considered to be equivalent to the area fraction on the surface of the compact. This is the case for the materials chosen. For the large particle-size powders, the results do not obey the relationship of Cassie (19), the hydrophobic fraction being more dominant. The jet-milled mixtures, however, show a close correlation.

The case of contact angles on heterogeneous surfaces was analyzed theoretically (22). One conclusion was that the hydrophobic fraction of the surface would be dominant for advancing angles. As the size of the heterogeneities in the surface became smaller, then the angles would more closely correspond to Cassie's curve (19). In the present experiments, advancing angles were determined, and the results fit in with these concepts. As the particle size was reduced, *i.e.*, the size of the heterogeneities in the surface became smaller, the hydrophobic portion of the surface became less dominant. The results agree more closely with the expected linear relation.

The work described demonstrates the usefulness of the h–ϵ method for the determination of contact angles of pharmaceutical powders and powder mixtures. The importance of these measurements in formulation is currently being studied.

REFERENCES

(1) H. J. Osterhof and F. E. J. Bartell, *Phys. Chem.*, **34**, 1399(1930).

[10] Emcompress Special, Ed. Mendell & Co. New York, N.Y.

(2) G. D. Parfitt, "Dispersion of Powders in Liquids," Elsevier, Amsterdam, The Netherlands, 1969.
(3) W. I. Higuchi, N. F. H. Ho, and A. H. Goldberg, in "Theory and Practice of Industrial Pharmacy," L. Lachman, H. A. Lieberman, and J. L. Kanig, Eds., Lea & Febiger, Philadelphia, Pa., 1970, pp. 120–136.
(4) S. Solvang and P. Finholt, *J. Pharm. Sci.*, **59**, 49(1970).
(5) Y. Kawashima, M. Saito, and H. Takenaka, *J. Pharm. Pharmacol.*, **27**, 1(1975).
(6) J. G. Allen and C. A. Davies, *ibid.*, **27**, 50(1975).
(7) J. M. Newton and F. N. Razzo, *J. Pharm. Pharmacol. Suppl.*, **26**, 30P(1974).
(8) G. Rowley and J. M. Newton, *J. Pharm. Pharmacol.*, **22**, 966(1970).
(9) J. C. Samyn and W. Y. Jung, *J. Pharm. Sci.*, **59**, 169(1970).
(10) J. A. Wood and S. W. Harder, *Can. J. Pharm. Sci.*, **5**, 18(1970).
(11) S. W. Harder, D. A. Zuck, and J. A. Wood, *ibid.*, **6**, 63(1971).
(12) L. Ehrhardt, L. Patt, and E. Schindler, *Pharm. Ind.*, **35**, 719(1973).
(13) P. Singh, D. J. Desai, A. P. Simonelli, and W. I. Higuchi, *J. Pharm. Sci.*, **57**, 217(1968).
(14) P. M. Heertjes and N. W. F. Kossen, *Powder Technol.*, **1**, 33(1967).
(15) N. W. F. Kossen, Thesis, Delft, The Netherlands, 1965.
(16) N. W. F. Kossen and P. M. Heertjes, *Chem. Eng. Sci.*, **20**, 593(1965).
(17) W. C. Witvoet, Ph.D. thesis, Delft, The Netherlands, 1971.
(18) J. F. Padday, in "Proceedings of the Second International Congress on Surface Activity," vol. 3, Butterworths, London, England, 1951, pp. 81–121.
(19) A. B. D. Cassie, *Discuss. Faraday Soc.*, **3**, 11(1948).
(20) H. W. Fox and W. A. Zisman, *J. Colloid Sci.*, **7**, 426(1952).
(21) *Ibid.*, **5**, 514(1950).
(22) R. E. Johnson, Jr., and R. H. Dettre, in "Surface and Colloid Science," vol. 2, E. Matijević, Ed., Wiley, New York, N.Y., 1969, pp. 85–153.

ACKNOWLEDGMENTS AND ADDRESSES

Received May 27, 1975, from the *Laboratory for Pharmaceutical Technology, The University, Ant. Deusinglaan 2, Groningen 8004, The Netherlands.*

Accepted for publication August 8, 1975.

The authors thank K. Zuurman for technical assistance and the Z.W.O. for the award of a grant to J. T. Fell.

* On leave of absence from the Department of Pharmacy, The University, Manchester M13 9PL, England.

ˣ To whom inquiries should be directed.

In Vivo and *In Vitro* Evaluation of a Microencapsulated Narcotic Antagonist

NORBERT MASON *, CURT THIES *ˣ, and THEODORE J. CICERO ‡§

Abstract □ Injectable microcapsules containing 75% (w/w) cyclazocine, a narcotic antagonist, were prepared with *dl*-poly(lactic acid) as the coating material. Capsule fractions falling between 105 and 295 μm released about 90% of their cyclazocine in 8 days of rotating-bottle extraction at 37° in pH 7.4 phosphate buffer. Although larger capsules released the drug somewhat more slowly, all capsules released cyclazocine far more rapidly than an ideal capsule should. This rapid release is attributed to macroscopic defects located in the capsule walls. The ability of the capsules to block the action of morphine *in vivo* was assessed by injection of a sesame seed oil suspension into Holtzman rats. A hot-plate test procedure was used to evaluate animal behavior. Capsule doses of 100–250 mg/kg to rats caused significant antagonism of morphine's analgesic effect for 14 days after injection. By Day 17, no antagonism occurred, indicating that the capsules completely released the drug *in vivo* between 14 and 17 days after injection.

Keyphrases □ Cyclazocine—injectable microcapsules, *in vivo* and *in vitro* release evaluated □ Microcapsules, injectable—*in vivo* and *in vitro* release of cyclazocine evaluated □ Dosage forms—injectable microcapsules, *in vivo* and *in vitro* release of cyclazocine evaluated □ Narcotic antagonists—cyclazocine, *in vivo* and *in vitro* release from injectable microcapsules evaluated

A significant problem in the long-term treatment and rehabilitation of heroin addicts is their pronounced tendency to undergo drug relapse. One possible means of circumventing this problem would be the injection or implantation of sustained-release preparations of narcotic antagonists, which would, in effect, inoculate the patient against heroin for a prescribed period, preferably 1 month or more. Theoretically, the repeated administration of such a preparation could provide a therapeutically effective level of antagonist for an indefinite treatment period.

An injectable sustained-release formulation must satisfy these requirements:

1. It must be biocompatible and provide uniform sustained release of the antagonist for a specified time.
2. Once the drug has been released, the delivery system must be biodegradable within a relatively brief time.
3. The microcapsules must be easily injected through hypodermic needles of sufficiently small size to be tolerated by patients.
4. The total amount of drug administered to the patient must not approach toxic levels to minimize any risk associated with accidental failure of the delivery system.

Narcotic antagonist formulations that meet several, but not necessarily all, of these requirements were reported recently. Insoluble salts and salt complexes of cyclazocine and naloxone were formulated (1), and several preparations significantly increased the duration of narcotic antagonist activity in mice. Prepared particulate cyclazocine–poly(lactic acid) composites provided sustained release *in vivo* and *in vitro* (2). However, the particles contained only 21% (w/w) of drug and required a 12-gauge needle for injection.

The technique of microencapsulation may provide

(2) G. D. Parfitt, "Dispersion of Powders in Liquids," Elsevier, Amsterdam, The Netherlands, 1969.
(3) W. I. Higuchi, N. F. H. Ho, and A. H. Goldberg, in "Theory and Practice of Industrial Pharmacy," L. Lachman, H. A. Lieberman, and J. L. Kanig, Eds., Lea & Febiger, Philadelphia, Pa., 1970, pp. 120–136.
(4) S. Solvang and P. Finholt, *J. Pharm. Sci.*, **59**, 49(1970).
(5) Y. Kawashima, M. Saito, and H. Takenaka, *J. Pharm. Pharmacol.*, **27**, 1(1975).
(6) J. G. Allen and C. A. Davies, *ibid.*, **27**, 50(1975).
(7) J. M. Newton and F. N. Razzo, *J. Pharm. Pharmacol. Suppl.*, **26**, 30P(1974).
(8) G. Rowley and J. M. Newton, *J. Pharm. Pharmacol.*, **22**, 966(1970).
(9) J. C. Samyn and W. Y. Jung, *J. Pharm. Sci.*, **59**, 169(1970).
(10) J. A. Wood and S. W. Harder, *Can. J. Pharm. Sci.*, **5**, 18(1970).
(11) S. W. Harder, D. A. Zuck, and J. A. Wood, *ibid.*, **6**, 63(1971).
(12) L. Ehrhardt, L. Patt, and E. Schindler, *Pharm. Ind.*, **35**, 719(1973).
(13) P. Singh, D. J. Desai, A. P. Simonelli, and W. I. Higuchi, *J. Pharm. Sci.*, **57**, 217(1968).
(14) P. M. Heertjes and N. W. F. Kossen, *Powder Technol.*, **1**, 33(1967).
(15) N. W. F. Kossen, Thesis, Delft, The Netherlands, 1965.
(16) N. W. F. Kossen and P. M. Heertjes, *Chem. Eng. Sci.*, **20**, 593(1965).
(17) W. C. Witvoet, Ph.D. thesis, Delft, The Netherlands, 1971.
(18) J. F. Padday, in "Proceedings of the Second International Congress on Surface Activity," vol. 3, Butterworths, London, England, 1951, pp. 81–121.
(19) A. B. D. Cassie, *Discuss. Faraday Soc.*, **3**, 11(1948).
(20) H. W. Fox and W. A. Zisman, *J. Colloid Sci.*, **7**, 426(1952).
(21) *Ibid.*, **5**, 514(1950).
(22) R. E. Johnson, Jr., and R. H. Dettre, in "Surface and Colloid Science," vol. 2, E. Matijević, Ed., Wiley, New York, N.Y., 1969, pp. 85–153.

ACKNOWLEDGMENTS AND ADDRESSES

Received May 27, 1975, from the *Laboratory for Pharmaceutical Technology, The University, Ant. Deusinglaan 2, Groningen 8004, The Netherlands.*

Accepted for publication August 8, 1975.

The authors thank K. Zuurman for technical assistance and the Z.W.O. for the award of a grant to J. T. Fell.

* On leave of absence from the Department of Pharmacy, The University, Manchester M13 9PL, England.

ˣ To whom inquiries should be directed.

In Vivo and *In Vitro* Evaluation of a Microencapsulated Narcotic Antagonist

NORBERT MASON *, CURT THIES *ˣ, and THEODORE J. CICERO ‡§

Abstract □ Injectable microcapsules containing 75% (w/w) cyclazocine, a narcotic antagonist, were prepared with *dl*-poly(lactic acid) as the coating material. Capsule fractions falling between 105 and 295 μm released about 90% of their cyclazocine in 8 days of rotating-bottle extraction at 37° in pH 7.4 phosphate buffer. Although larger capsules released the drug somewhat more slowly, all capsules released cyclazocine far more rapidly than an ideal capsule should. This rapid release is attributed to macroscopic defects located in the capsule walls. The ability of the capsules to block the action of morphine *in vivo* was assessed by injection of a sesame seed oil suspension into Holtzman rats. A hot-plate test procedure was used to evaluate animal behavior. Capsule doses of 100–250 mg/kg to rats caused significant antagonism of morphine's analgesic effect for 14 days after injection. By Day 17, no antagonism occurred, indicating that the capsules completely released the drug *in vivo* between 14 and 17 days after injection.

Keyphrases □ Cyclazocine—injectable microcapsules, *in vivo* and *in vitro* release evaluated □ Microcapsules, injectable—*in vivo* and *in vitro* release of cyclazocine evaluated □ Dosage forms—injectable microcapsules, *in vivo* and *in vitro* release of cyclazocine evaluated □ Narcotic antagonists—cyclazocine, *in vivo* and *in vitro* release from injectable microcapsules evaluated

A significant problem in the long-term treatment and rehabilitation of heroin addicts is their pronounced tendency to undergo drug relapse. One possible means of circumventing this problem would be the injection or implantation of sustained-release preparations of narcotic antagonists, which would, in effect, inoculate the patient against heroin for a prescribed period, preferably 1 month or more. Theoretically, the repeated administration of such a preparation could provide a therapeutically effective level of antagonist for an indefinite treatment period.

An injectable sustained-release formulation must satisfy these requirements:

1. It must be biocompatible and provide uniform sustained release of the antagonist for a specified time.
2. Once the drug has been released, the delivery system must be biodegradable within a relatively brief time.
3. The microcapsules must be easily injected through hypodermic needles of sufficiently small size to be tolerated by patients.
4. The total amount of drug administered to the patient must not approach toxic levels to minimize any risk associated with accidental failure of the delivery system.

Narcotic antagonist formulations that meet several, but not necessarily all, of these requirements were reported recently. Insoluble salts and salt complexes of cyclazocine and naloxone were formulated (1), and several preparations significantly increased the duration of narcotic antagonist activity in mice. Prepared particulate cyclazocine–poly(lactic acid) composites provided sustained release *in vivo* and *in vitro* (2). However, the particles contained only 21% (w/w) of drug and required a 12-gauge needle for injection.

The technique of microencapsulation may provide

a means of preparing narcotic antagonist formulations that are effective longer than those prepared to date, carry a higher drug content, and are capable of being injected through small needles. Microencapsulation is a process whereby individual drug particles are coated to retard the rate of drug dissolution (3). Although few polymers have characteristics that make them acceptable for injectable microcapsule-coating applications, a polymer that appears to be suitable is *dl*-poly(lactic acid). Accordingly, *dl*-poly(lactic acid) was used to prepare microcapsules containing cyclazocine, a narcotic antagonist. This paper describes the *in vivo* and *in vitro* performance of these capsules.

EXPERIMENTAL

Microencapsulation—Microcapsules containing cyclazocine were prepared with additive-free *dl*-poly(lactic acid)[1]. The capsules contained, on the average, 75% (w/w) cyclazocine and 25% (w/w) *dl*-poly(lactic acid). Several capsule sizes were isolated: 105–177, 177–295, and 295–595 μm. For each fraction, the smaller number given represents the size of the rectangular screen opening that retained the microcapsule, whereas the larger number represents the size of the rectangular screen opening through which the capsules passed. All capsule fractions used were isolated from the same capsule batch.

***In Vitro* Evaluation**—The *in vitro* release properties of the capsules were evaluated in a commercially available rotating-bottle apparatus[2] (40 rpm) at 37° in pH 7.4 phosphate buffer. The concentration of cyclazocine in the extracting solution was established spectrophotometrically by using the 278-nm band characteristic of cyclazocine. Release results are plotted as percent cyclazocine extracted from the capsule *versus* time.

Each data point reported was obtained with a separate test sample. The test samples consisted of 15 mg of capsules suspended in 75 ml of buffer. The 15-mg capsule weight was selected to minimize weighing errors, whereas the 75-ml volume of buffer filled the sample reservoirs. When a 15-mg capsule was used with 75 ml of buffer, complete cyclazocine extraction from the capsules yielded a concentration of 14.4 mg of drug/100 ml of buffer. This value is well below the saturation solubility of cyclazocine in pH 7.4 phosphate buffer at 37° (46 mg/100 ml). However, drug concentration in the extracting solution exceeded 15% of the saturation value once the capsules released 50% or more of their active contents.

The permeability of cyclazocine through *dl*-poly(lactic acid) films at 37° was measured by a procedure similar to one published previously (4). Membranes of 0.5–1-mil thickness were cast from solution onto a glass surface and placed in glass diffusion cells. The cells contained 12 ml of liquid on each side of the membrane and were rotated (~10 rpm) in a vertical plane at 37°. A saturated solution of cyclazocine was maintained on one side of the membrane (Side 1); only buffer was present initially on the other side (Side 2). The permeability of cyclazocine through the *dl*-poly(lactic acid) membrane was calculated from the rate of cyclazocine buildup on Side 2 of the dialysis cell, which was established spectroscopically (278 nm).

***In Vivo* Evaluation**—Pharmacological *in vivo* evaluations of the cyclazocine microcapsules were carried out in male Holtzman rats weighing between 125 and 150 g at the time of injection. Microcapsules were suspended in sesame seed oil at a constant drug to suspending medium ratio of 25 mg/ml. An 18-gauge needle was used to inject 177–295-μm capsules; 295–595-μm capsules were injected with a 16-gauge needle. The capsules were injected subcutaneously between the shoulder blades.

Different groups of rats ($n = 7$) were used for each test day following the injection. Rats were never tested more than once. In addition to the rats receiving microencapsulated cyclazocine, groups of rats ($n = 7$) were also injected with an equivalent amount of unencapsulated cyclazocine (dose calculated as 75% of the microcapsule dosage) suspended in sesame seed oil. Other rats ($n = 7$) were injected with the suspending medium free of drug.

At known intervals after injection of the microcapsules, unencapsulated cyclazocine, or sesame seed oil vehicle, the degree of antagonism of an ED_{80} dose of morphine (10 mg/kg) was evaluated using the hot-plate method described previously (5). The degree of analgesia produced by morphine in the three groups was established 45 min after the subcutaneous injection of the narcotic.

[1] Supplied by Dr. Donald Wise, Dynatech R/D Co., Cambridge, Mass.
[2] Manufactured by Ernest Menhold, Lester, Pa.

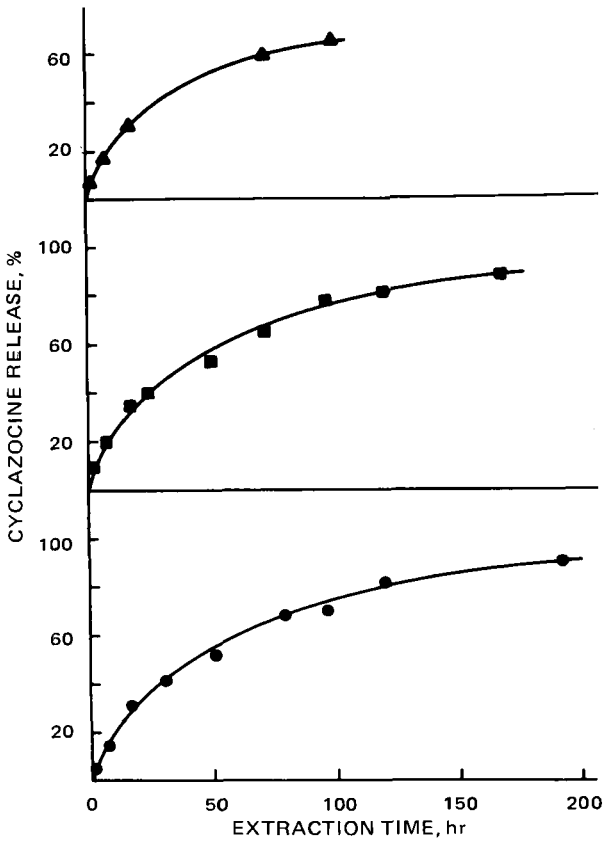

Figure 1—*Rate of cyclazocine extraction from* dl-*poly(lactic acid) microcapsules at 37° and pH 7.4. Key:* ●, *105–177-μm capsules;* ■, *177–295-μm capsules; and* ▲, *295–595-μm capsules.*

In the hot-plate method, analgesia is defined as an increase in reaction time over baseline levels. The response usually consists of licking the paws or, less frequently, jumping out of the restraining cylinder. A cutoff point of 30 sec on the hot plate after morphine injection was established to prevent injury to the paws. The maximum possible analgesic effect, as assayed by the hot-plate method, would thus be 30 sec minus the baseline reaction time. The degree of agonism of a given dose of morphine was determined by:

$$\frac{\text{reaction time after morphine} - \text{baseline reaction time}}{30\text{ sec} - \text{baseline reaction time}} \times 100 = \text{percent agonism} \quad \text{(Eq. 1)}$$

In the present studies, a dose of morphine was used that produced approximately 80% agonism (*i.e.*, ED_{80}) on the hot plate. The degree of antagonism of this dose of morphine was determined by:

$$\left(1 - \frac{\text{percent agonism of morphine plus drug}}{\text{percent agonism of morphine only}}\right) \times 100 = \text{percent antagonism} \quad \text{(Eq. 2)}$$

The percent antagonism of an ED_{80} dose of morphine was determined at 4, 7, 14, 17, and 21 days after the administration of microencapsulated cyclazocine, uncapsulated cyclazocine, or sesame seed oil.

RESULTS AND DISCUSSION

Figure 1 contains *in vitro* release curves for the various capsule fractions evaluated. Cyclazocine release was nonlinear under the extraction conditions used and declined steadily as extraction continued. About 8 days of extraction was needed to remove 90% of the cyclazocine from the 105–177- and 177–295-μm capsules. Capsules in the 295–595-μm fraction released 64% of the drug in 100 hr. They

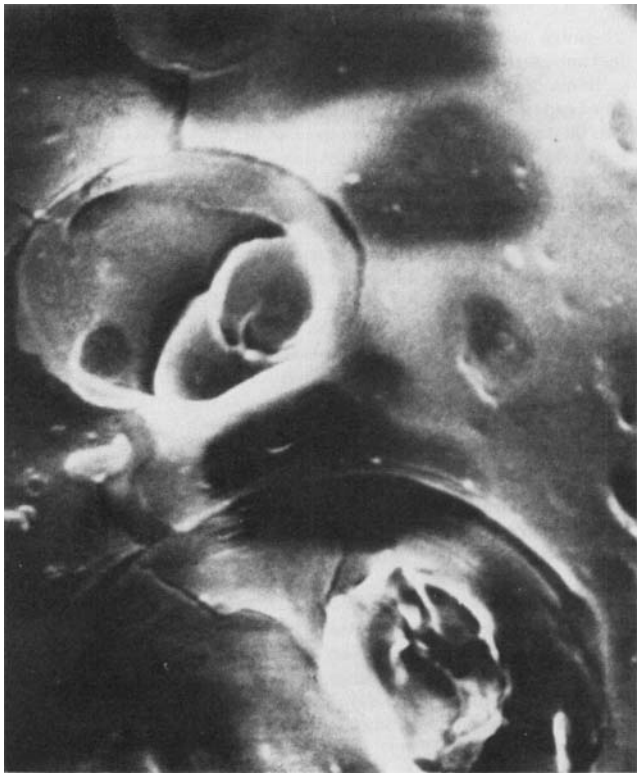

Figure 2—*Scanning electron micrograph of surface of* dl-*poly(lactic acid) microcapsule (105–177-μm fraction) containing cyclazocine (magnification = 2500×).*

appeared to release cyclazocine at a somewhat slower rate than the smaller capsules as extraction progressed, but the difference was not great. Unencapsulated cyclazocine dissolved completely in buffer within 2 hr, so the *dl*-poly(lactic acid) capsule walls clearly retarded cyclazocine release. However, the capsules released their cyclazocine considerably faster than they should have due to defects in the capsule coating.

Direct evidence that the capsule coatings contain defects is provided by the scanning electron micrograph shown in Fig. 2. This micrograph is representative of cyclazocine capsule surfaces and shows that such surfaces are irregular and cratered. The irregularities and craters represent weak points in the capsule wall and provide sites for accelerated transport of cyclazocine from the capsules. The craters could extend to the cyclazocine surface and thereby provide direct routes for passage of cyclazocine from the capsules. Although this possibility cannot be completely discounted, the ability of the capsules to provide cyclazocine release over at least a 9-day period suggests that few craters extend completely to the cyclazocine surface.

The permeability of a large drug molecule such as cyclazocine through a defect-free unswollen polymeric film in which it is insoluble would be expected to be very low. Thus, measurements of permeability through solvent-cast films should provide an estimate of permeability against which the performance of microcapsules may be compared. Accordingly, the permeability of cyclazocine through solvent-cast *dl*-poly(lactic acid) films was determined as discussed under *Experimental*. These measurements yielded permeability values of 2.9 and 3.0×10^{-11} cm^2/sec at 37°.

From the average of these values, the time required for a spherical 200-μm diameter capsule of uniform wall thickness (assumed to be 7.2 μm) to lose 50% of its drug [initially 80% (w/w) cyclazocine] was calculated. The interior of the capsules was assumed to be a saturated solution of cyclazocine; the extracting medium outside the capsule was assumed to contain no cyclazocine. Ideal capsules, obeying these boundary conditions, should give zero-order cyclazocine release and require 28.6 months of extraction to remove 50% of the drug. This calculated half-life for ideal capsules is about 300 times greater than that achieved by the cyclazocine capsules used in this study.

Presumably, most of the difference between observed and calculated rates of cyclazocine release was due to macroscopic defects in the polymer membrane like those shown in Fig. 2. One cannot ignore the possibility that nonuniform capsule wall thicknesses will always result when irregularly shaped solids are encapsulated and thereby make it impossible to prepare capsules with the maximum possible lifetime. Shear forces imposed upon the embryo capsules during the encapsulation process also may always contribute to wall nonuniformity and have the same effect. Nevertheless, the measured permeability coefficient for cyclazocine diffusing through a *dl*-poly(lactic acid) membrane was low and indicates that the concept of preparing truly long-acting cyclazocine capsules with *dl*-poly(lactic acid) is a valid one. Minimizing the capsule wall defects (Fig. 2) should lead to capsules with substantially longer lifetimes than the ones prepared to date.

Even though the cyclazocine microcapsules prepared for this study did not have defect-free coatings, they provided *in vitro* release for 8 or more days. Thus, their *in vivo* performance was evaluated. In preliminary studies, 105–177-μm cyclazocine capsules, suspended in 0.1% aqueous methylcellulose, were injected into rats at a dose level of 50 mg/kg. After 2 days, rats were tested on the hot plate after the injection of an ED_{100} dose of morphine (15 mg/kg). Such a high morphine dose was selected to provide a stringent test of the *in vivo* microcapsule performance in these preliminary studies. The analgesic effects of this morphine dose were antagonized by over 88% after the 2-day postinjection interval. Control animals that received only aqueous methylcellulose showed no antagonism of morphine's effect.

These preliminary data established that the cyclazocine capsules provided antagonism of a rather high dose of morphine for at least 2 days. However, these studies also revealed that the aqueous methylcellulose solution was inadequate as a suspending medium. Because this solution was so dilute, the capsules settled rapidly, thereby making it difficult to achieve an even suspension. Instead of using more concentrated aqueous methylcellulose solutions, sesame seed oil was used exclusively as the suspending medium for subsequent *in vivo* microcapsule evaluations. It gave relatively stable capsule dispersions, which were readily injected in a reproducible manner.

Table I summarizes the *in vivo* performance of several cyclazocine capsule fractions injected into rats with sesame seed oil as the suspending agent. These data show that the cyclazocine capsules pro-

Table I—Percent Antagonism of an ED_{80} Dose of Morphine (10 mg/kg) by Sesame Seed Oil, Unencapsulated Cyclazocine, and Microencapsulated Cyclazocine[a]

	Cyclazocine Dose, mg/kg	Days after Injection				
		4	7	14	17	21
Sesame seed oil	0	0	0	0	0	0
Unencapsulated cyclazocine	75	100.0 (0)	2.0 (0—7.8)	0	0	0
	175	100.0 (0)	4.4 (0—11.3)	0	0	0
Microencapsulated cyclazocine	100[b]	100.0 (0)	100 (0)	61.4 (27.8—93.9)	—	—
	250[c]	100.0 (0)	81.9 (65.3—90.9)	95.5 (84.6—100)	0	0

[a]Microencapsulated cyclazocine doses are reported as milligrams of capsules per kilogram body weight. Since the capsules contain 75% (w/w) drug, approximately this percentage was given as unencapsulated cyclazocine. An equal volume of sesame seed oil was given to controls. Groups of seven rats were used for each dose and time interval. Numbers in parentheses are the range of antagonism values measured at that point; other numbers are mean percent antagonism. [b]Capsule size of 177–295 μm. [c]Capsule sizes of 177–295 and 295–595 μm. Since there was no difference between capsule sizes in terms of their *in vivo* effectiveness, the data were pooled.

vided a high degree of antagonism toward an ED_{80} dose of morphine (10 mg/kg) for at least 14 days after injection. For comparative purposes, it should be noted that all encapsulated cyclazocine doses administered showed negligible blockade toward morphine 7 days after injection. How long the capsules effectively block the morphine challenge dose does not appear to vary with the capsule dose administered, at least over the dose range examined.

A dose of at least 100-mg capsules (72 mg of encapsulated drug/kg rat) was sufficient to produce a high degree of antagonism for up to 14 days after injection. Increasing the amount of capsules injected to 250 mg/kg also provided a high degree of antagonism for at least 14 days. As was the case with the 100-mg/kg capsule dose, no antagonism occurred 17 or 21 days after injection. The capsules, regardless of the amount injected, apparently completed release of drug sometime between 14 and 17 days after injection. This *in vivo* lifetime is not substantially greater than the *in vitro* lifetime of the capsules as determined by the rotating-bottle technique. Thus, longer acting injectable cyclazocine capsule formations will require capsules with polymer walls with fewer defects.

The *in vivo* performance of the cyclazocine capsules evaluated appeared to be independent of their size. Consistent with the *in vitro* release data shown in Fig. 1, there was little difference *in vivo* between 177–295- and 295–575-μm capsules. Since all capsule fractions had approximately the same cyclazocine content initially (75% w/w), the larger capsules, by virtue of having a thicker polymer coating, should release their payload at a significantly slower rate. The fact that they did not, either *in vitro* or *in vivo*, provides further evidence that the *dl*-poly(lactic acid) capsule coatings are at present defective.

For an injectable drug delivery device, the active ingredient should ideally be released at some uniform rate that provides a therapeutic drug level *in vivo* throughout the entire lifetime of the device. Once empty, the activity of the device should decline rapidly in a predictable manner until it has no ability to block the action of morphine. With such a device, successive injections could be given and overlap of drug release from two injections would be minimal.

The microcapsules utilized here approached this ideal behavior. A 250-mg/kg dose of 177–295- or 295–595-μm capsules provided 88–100% antagonism to morphine 14 days after injection and 0% antagonism 17–21 days after injection. It was not possible to ascertain precisely how fast the capsules declined, but clearly they went from a high degree of activity to zero activity within 3–7 days.

A significant factor in the successful administration of injectable microcapsules is the size of the needle required for injection. Complete delivery of capsules requires a needle with an internal diameter at least three times greater than that of the largest capsule. Otherwise, capsules lodge in the needle itself or at the constriction in the syringe where it joins the needle, and the amount actually injected is less than expected. Thus, an 18-gauge needle is required to administer 177–295-μm capsules, and a 16-gauge needle is needed for 295–595-μm capsules. Therefore, injectable capsules to be administered with a 21-gauge needle, the size used clinically for many intramuscular injections, must be less than 170 μm in diameter.

In conclusion, this study demonstrates that injectable microcapsules capable of providing prolonged effective *in vivo* release of a drug can be prepared. The capsules used so far have defect-filled coatings and release their drug content far more rapidly than predicted. Nevertheless, they can provide at least 2 weeks of activity *in vivo* when administered at a relatively high dose. They fall short of the 1-month or more lifetime desired, but formulation of such capsules should prove useful immediately in animal studies of narcotics and narcotic antagonists. These capsules also should serve as a promising first step in the development of a clinically useful sustained-release preparation. Since the capsules described in this paper release drug at a rate estimated to be 300 times greater than that of ideal *dl*-poly(lactic acid) capsules, there is considerable room for improving capsule quality. Efforts are being made to this end.

REFERENCES

(1) A. P. Gray and D. S. Robinson, in "Advances in Biochemical Psychopharmacology," vol. 8, M. C. Brande, L. S. Harris, E. L. May, J. P. Smith, and J. E. Villarreal, Eds., Raven, New York, N.Y., 1974, p. 555.

(2) J. H. R. Woodland, S. Yolles, D. A. Blake, R. Helrich, and F. J. Meyer, *J. Med. Chem.*, **16**, 897(1973).

(3) J. Bakan and J. Anderson, in "The Theory and Practice of Industrial Pharmacy," J. L. Kanig, L. Lachman, and H. A. Lieberman, Eds., Lea & Febiger, Philadelphia, Pa., 1970, chap. 13.

(4) N. S. Mason, O. Lindan, and R. E. Sparks, *Chem. Eng. Symp. Series*, **67**, 114, 139(1971).

(5) T. J. Cicero and E. R. Meyer, *J. Pharmacol. Exp. Ther.*, **184**, 404(1973).

ACKNOWLEDGMENTS AND ADDRESSES

Received March 6, 1975, from the **Department of Chemical Engineering, Washington University, St. Louis, MO 63130*, and the *‡Department of Psychiatry, Washington University School of Medicine, St. Louis, MO 63110*

Accepted for publication August 11, 1975.

Supported in part by U.S. Public Health Service Grants DA-00109 and DA-00259 and by National Institute on Drug Abuse Contract HSM-42-73-265.

The authors acknowledge the technical assistance of G. Lapka and E. R. Meyer.

§ Recipient of Research Scientist Development Award AA-70180.

ˣ To whom inquiries should be directed.

Molecular Orbital Calculations for Parabens: A Possible Mechanism of Action

KENNETH S. ALEXANDER, HAROLD PETERSEN, Jr., JOSEPH G. TURCOTTE, and ANTHONY N. PARUTA ˣ

Abstract □ Molecular orbital calculations were carried out on the series benzoic acid, *p*-hydroxybenzoic acid, methylparaben, and ethylparaben. The characteristic trends of this entire series of preservatives are demonstrated by these members. The computer program used was Iterated Extended Hückel Theory. These systems were characterized in terms of atomic charge distributions, effect of hydroxyl and ester groups (both sterically and electronically), preferred molecular conformations, and distinguishing features of molecular orbitals. Through this approach, it was hoped that a common mode of action for all members of this series could be detected and that the trend(s) in this feature would correlate with known trends in activity of members of this series.

Keyphrases □ Orbitals, molecular—calculations for substituted benzoic acid series, atomic charge distributions, effect of hydroxyl and ester groups, preferred conformations, pharmacokinetics, structure–activity relationships □ Benzoic acids, substituted—molecular orbital calculations, pharmacokinetics, structure–activity relationships □ Pharmacokinetics—substituted benzoic acids, related to molecular orbital calculations □ Structure–activity relationships—substituted benzoic acids, molecular orbital calculations related to mechanism of action □ Preservatives—substituted benzoic acids, molecular orbital calculations, pharmacokinetics, structure–activity relationships

During the past 10 years, the mechanics of interaction between drugs and receptor sites have been intensively scrutinized in the hope of describing these interactions and their nature, rate, and steric dependence in terms of chemical and physical parameters. Several investigators (1–10) attempted to relate molecular parameters such as bond lengths, acid–base character, energy levels, and orbital types to drug action (activity).

Because drug systems are extremely complex, a simplistic correlation between activity and some scaling factor of molecular parameters has not often been found. The mechanism of action of phenol-type disinfectants has been discussed from the point of view that phenol interrupts cellular transport and permits "leakage" of essential cell constituents into the extracellular fluids (11–13).

Various organic acids have been shown to elicit different antibacterial mechanisms of action depending on their molecular structure. It is the molecular structure of these acids that influences the ease with which they penetrate the cell, the part of the cell they attack, or the chemical nature of their attack (14).

The possible mode of action of benzoic acid has been postulated to be membrane action and competition with coenzymes (15). To date, the esters of *p*-hydroxybenzoic acid and vanillic acid are thought to act in the same manner as benzoic acid; however, further study is required to clarify or substantiate this hypothesis.

EXPERIMENTAL

The Iterated Extended Hückel Theory molecular orbital calculations were carried out by computer[1]. The program, a modification of Hoffmann's Extended Hückel Theory (EHT) program (16), was designed to iterate until charge consistency was attained. Input parameters were chosen that have been widely used in the application of semiempirical LCAO methods. This choice gave the calculations a relevance not obtainable with other, less well-recognized parameters. These input parameters included the molecular cartesian coordinates, Slater-type orbital exponents, a rough guess at atomic charges, valence state ionization potentials, a test limit of 0.002 (in units of charge distribution) to define a converged distribution, a weighing factor of 9/10 to control the charge correction with each iteration, and the maximum number of iterations to be carried out.

Cartesian coordinates were calculated by use of the CORCAL computer program (17), for which the input data included the molecular geometry in terms of bond angles, bond lengths, bond attachments, and dihedral angles. The molecules were situated with the phenyl ring in the x–y-plane, with the x-axis in the direction of the ester fragment. Upon rotation of the carbonyl fragment out of this plane, the carbonyl oxygen was directed in the positive z-direction.

The crystal-morphological X-ray data used to generate these coordinates were obtained for benzoic acid from the work of Sim *et al.* (18). Estimates of corresponding data for esters of *p*-hydroxybenzoic acid were based upon previously established crystallographic work for esters of various types, such that bond angles and bond lengths represent typical values (19–24).

Values for the orbital exponents, derived from Slater's rules, were as follows: carbon 2*s* and 2*p*, 1.625; nitrogen 2*s* and 2*p*, 1.95; oxygen 2*s* and 2*p*, 2.275; and hydrogen 1*s*, 1.2. The value of 1.2 for the hydrogen 1*s* orbital has been found to produce better results in several applications than the traditional value of 1.0.

Valence state ionization potentials given previously, (25, 26) were used as coulomb integrals, which, in turn, were used to obtain resonance integrals by use of the Cusachs formula (27).

All calculations were carried out with iteration to charge consistency. In this procedure, coulomb integrals were adjusted for atomic charge after each iteration, and the calculation was repeated until input and output charges matched within the present limit of 0.002 unit of charge.

RESULTS AND DISCUSSION

If one accepts the premise that a pattern of essential atoms and groups in a drug molecule must bear some distinct relationship to complimentary features on a receptor molecule, then it follows that the spatial relationships of these essential moieties must be identified in order to relate structure to biological activity. Therefore, an understanding of the electron density distributions within the various fragments of the drug moiety and an understanding of the drug molecule stereochemistry are critical to a deduction of the nature and/or topology of the receptor.

Important also is the relationship among the molecular orbital-calculated conformation, the X-ray crystallographic-determined conformation, and the conformation of a substance in solution. To this end, it must be remembered that molecular orbital calculations are carried out on a single isolated molecule, without considering the perturbations introduced by a neighboring molecule(s) or solvent, and crystal studies are done on a molecule frozen into an array of its kind. The solution-derived conformations are those of a molecule surrounded by solvent.

A recent question regarding molecular orbital-calculated conformations has been raised as to whether drug molecules treated in

[1] IBM 360/50.

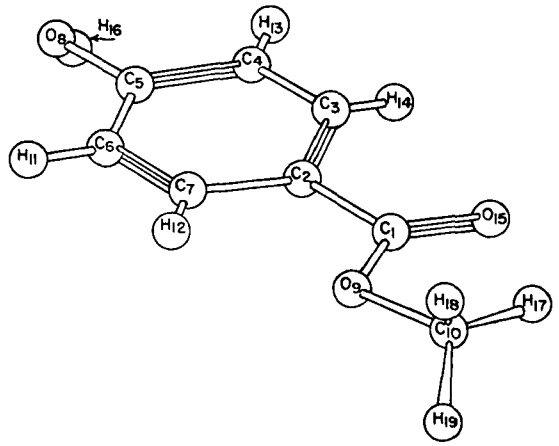

Figure 1—*Illustration of methylparaben in the planar,* cis-*conformation. See* Discussion *and Table I.*

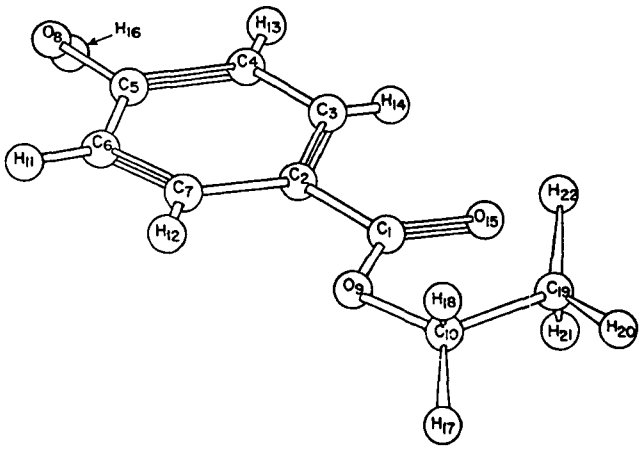

Figure 3—*Illustration of ethylparaben in the planar,* cis-*conformation. See* Discussion *and Table I.*

such a manner can be used to map complementary features of a receptor (28). Two working hypotheses have evolved in an effort to answer this question. One hypothesis, used in molecular orbital studies, is that these molecules engage the receptor in their preferred conformations. An alternative hypothesis is that the receptor is capable of a significant perturbation influence on a drug molecule within its vicinity and that a nonpreferred conformation engages the receptor. This hypothesis is not in violation of the concept that optimum stereochemistry maximizes efficacy, since the perturbed conformation could arise from the initial presentation of the drug molecule in its preferred conformation (29–32).

The graphic representation of several configurations considered in this study are given in Figs. 1–4. In Fig. 1, the methyl ester fragment of methylparaben is shown coplanar with the ring and the methyl group is directed toward the carbonyl oxygen. This arrangement can be called the "planar, *cis*"-conformation ("*cis*" implying that the carbonyl oxygen and methyl carbon are *cis* with respect to the C-1—O-9 axis). A rotation of 90° about the C-1—C-2 bond axis produces a "perpendicular, *cis*"-conformation. Subsequent rotation by 180° about the C-1—O-9 bond axis yields the "perpendicular, *trans*"-conformation (Fig. 2).

A planar, *cis*-conformation of ethylparaben is given in Fig. 3. A 180° rotation about the O-9—C-10 bond axis yields the planar, *trans*-conformation. Three perpendicular conformations were studied. A perpendicular, *cis*-conformation is obtained by a 90° rotation of the ethyl ester fragment about the C-1—C-2 axis of the planar, *cis*-conformation. A perpendicular, *trans*-conformation (perpendicular, *trans* A in Tables I and II) is obtained by an analogous rotation about the C-1—C-2 axis in the planar, *trans*-conformation. Subsequent 180° rotation about the C-1—O-9 bond axis in the planar, *trans*-conformation yields the conformation shown in Fig. 4 (perpendicular, *trans* B in Table II).

Other conformations not shown in this series are the "planar" configurations of benzoic acid and *p*-hydroxybenzoic acid in which the carboxyl group is coplanar with the ring (carboxyl hydrogen *cis* to carbonyl group), and the "perpendicular" configurations of these two systems in which the carboxyl group lies in a plane perpendicular ring. Table I illustrates the charge distributions within the various compounds and conformations studied. Table II shows the total molecular energy as well as that of the Highest Filled Molecular Orbital (HFMO) and Lowest Empty Molecular Orbital (LEMO).

From resonance arguments, it can be said that *p*-hydroxybenzoic acid as well as its esters forms stable resonance structures when the carboxyl group is coplanar with the ring. Therefore, it is expected that molecular conformers that tend to retain these configurations would be more stable than conformers that restrict this resonance. However, the relationship of molecular orbital theory, X-ray crystallography, and solution and biological conformers must be kept in mind as the analysis of the data progresses.

The following analysis of the data uses a charge/HFMO/LEMO/configurational energy approach to study effects of various substituents and conformers, both by trends and by discontinuities within these trends.

The analysis can best be carried out by considering the compounds as they relate to each other by a common parameter.

Energies—From the total energies given in Table II, it can be

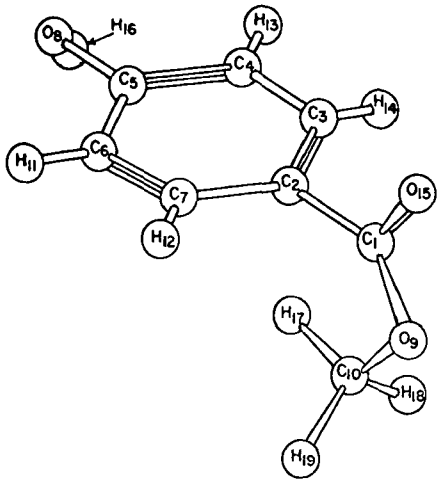

Figure 2—*Illustration of methylparaben in the perpendicular,* trans-*conformation. See* Discussion *and Table I.*

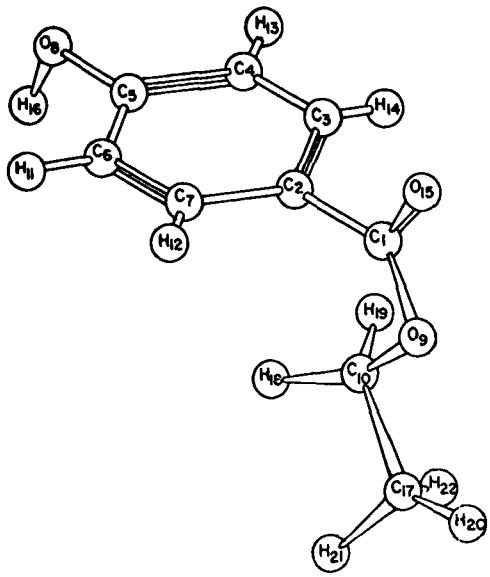

Figure 4—*Illustration of ethylparaben in the perpendicular,* trans-*conformation. See* Discussion *and Table I.*

Table I—Net Molecular Fragment[a] or Atomic Charge Distributions

Compound	Figure or Conformation	H—O	C-5	[b]	C-2—C-1	O-15	—C(=O)—O—R	O-9	R
Benzoic acid	Planar	—	0.004	0.050	0.183	−0.285	−0.183	−0.172	0.125
Benzoic acid	Perpendicular	—	0.0006	0.048	0.184	−0.286	−0.180	−0.171	0.128
p-Hydroxybenzoic acid	Planar	−0.132	0.088	0.189	0.178	−0.286	−0.195	−0.178	0.125
p-Hydroxybenzoic acid	Perpendicular	−0.176	0.084	0.205	0.194	−0.281	−0.168	−0.170	0.129
Methylparaben	1	−0.172	0.086	0.192	0.170	−0.293	−0.156	−0.208	0.210
Methylparaben	Perpendicular, *cis*	−0.186	0.081	0.184	0.166	−0.296	−0.157	−0.213	0.220
Methylparaben	2	−0.186	0.077	0.201	0.192	−0.299	−0.146	−0.207	0.220
Ethylparaben	3	−0.157	0.087	0.184	0.167	−0.278	−0.142	−0.217	0.218
Ethylparaben	Perpendicular, *cis*	−0.180	0.080	0.180	0.178	−0.274	−0.131	−0.210	0.207
Ethylparaben	Planar, *trans*	−0.158	0.086	0.180	0.159	−0.299	−0.153	−0.218	0.236
Ethylparaben	Perpendicular, *trans* A	−0.180	0.083	0.198	0.184	−0.291	−0.154	−0.206	0.196
Ethylparaben	4	−0.184	0.077	0.182	0.176	−0.300	−0.128	−0.210	0.247

[a] Entries in each column are the sum of the net atomic charges for each atom indicated in the column headings. [b] The hydrogens attached to the ring have been ignored.

seen that the most stable conformations are exhibited in compounds that have a planar and linear configuration, as expected; the next most stable conformation in the ester series is the perpendicular dangling chain (under the ring and down). Conformational changes are also reflected in changes in the LEMO energies but not to a great extent in the HFMO energies.

All planar conformations exhibit a LEMO energy of 8.6 ± 0.2 ev, and all perpendicular conformations exhibit a LEMO energy of 7.7 ± 0.2 ev. With only the exception of the planar and perpendicular, *cis*-conformation of ethylparaben, all esters as well as the parent acid and hydroxy derivative exhibit HFMO energy of 10.3 ± 0.2 ev.

Several additional comparisons can be made in terms of the total energies within the ethyl ester series:

1. The destabilization exhibited in the total energy and in the LEMO energy caused by rotating the ester group out of the plane of the phenyl ring (planar *versus* perpendicular, *cis* or planar *versus* perpendicular, *trans*) parallels the change in the methyl ester series and in *p*-hydroxybenzoic acid itself.

2. Of the two cases where there is a linear extension of the ethyl group away from the ring (planar and perpendicular, *trans*), the planar case is again more stable.

3. In the two planar cases, hooked and linear (planar, *cis versus* planar, *trans*), there is an increase in stabilization when going from the hooked to the linear configuration.

4. In the perpendicular-and-under-the-ring-and-down configuration (Fig. 4), the molecule is quite comparable to the most stable conformation (planar, *trans*); in this orientation, the whole ester substituent cannot participate in resonance stabilization or hydrogen-bonding stabilization, as is possible in the planar, *cis* molecule.

These comparisons lead to the conclusions that the molecule will tend to resonance stabilize if given a chance [this is also evident throughout the whole series (Table II) and is primarily reflected in the more stable energy of the LEMO as well as in the total energy] and that there is no significant evidence that intramolecular hydrogen bonding exists or plays an important role in molecular stabilization.

Charge Distribution—It is expected that absence of a *para*-substituent would markedly decrease the tendency for resonance stabilization and minimize charge redistribution with conformational changes. This result is shown in Table I in the case of benzoic acid. In *p*-hydroxybenzoic acid, however, where such stabilization can take place, there is a significant redistribution of charge with conformational change.

As the carboxyl group is moved from a position perpendicular to the plane of the phenyl ring to a coplanar position, there is a generalized redistribution of charge, notably involving a more negative charge on the hydroxyl fragment in the perpendicular case, when resonance is prevented. A maximum or near maximum negative charge is also observed in the ester cases when resonance is prevented, *i.e.*, when the ester fragment is perpendicular to the phenyl ring.

LEMO and HFMO Character—When considering possible charge-transfer or Lewis acid–base mechanisms of action, consideration is generally given to the HFMO and LEMO of a molecule as a result of energy matching criteria. In this instance, HFMO energies are significantly higher than the energy of the next highest filled molecular orbital, as expected, but the first *two* empty molecular orbitals are nearly degenerate in cases where the ester fragment is perpendicular to the phenyl ring. In the planar conformations, the second empty molecular orbital is significantly higher in energy than the first and need not be considered.

Comparisons show that when the members of this series are held in a planar conformation in which the alkyl portion of the ester fragment is directed away from the carbonyl oxygen (*trans*), the

Table II—Total Molecular, HFMO, and LEMO Energies[a]

Compound	Conformation	Figure	Total	HFMO	LEMO
Benzoic acid	Planar	—	−748	−10.453	−8.796
Benzoic acid	Perpendicular	—	−748	−10.416	−7.925
p-Hydroxybenzoic acid	Planar	—	−862	−10.394	−8.610
p-Hydroxybenzoic acid	Perpendicular	—	−861	−10.449	−7.801
Methylparaben	Planar, *cis*	1	−953	−10.203	−8.598
Methylparaben	Perpendicular, *cis*	—	−946	−10.117	−7.658
Methylparaben	Perpendicular, *trans*	2	−951	−10.158	−7.597
Ethylparaben	Planar, *cis*	3	−1045	−8.642	−8.590
Ethylparaben	Perpendicular, *cis*	—	−1042	−8.680	−7.722
Ethylparaben	Planar, *trans*	—	−1049	−10.157	−8.521
Ethylparaben	Perpendicular, *trans* A	—	−1044	−10.146	−7.694
Ethylparaben	Perpendicular, *trans* B	4	−1045	−10.124	−7.636

[a] All energies are given in electron volts (ev).

HFMO's are all very similar. When the alkyl group of the ethyl ester is oriented in close proximity to the carbonyl groups (*cis*) in either the planar or perpendicular orientation, the HFMO contains antibonding contributions from the methyl fragment and the energy of this orbital is destabilized with respect to the HFMO's of other members of the series.

The LEMO character falls into two categories, either a delocalized π-type or an antibonding carbonyl π-interaction. When planar, the LEMO's of all members of this series are delocalized orbitals over the ring and carbonyl group. When the ester fragment is perpendicular to the ring, the LEMO and second empty molecular orbital form a near degenerate set of molecular orbitals in which one is an antibonding carbonyl π-orbital and the other is a delocalized π-orbital different from those in the planar cases.

While these characteristics cannot substantiate a specific mechanism of action for members of this series, the use of these results for formulations of possible modes of action is possible. In this hypothesis, it is assumed that all members of the series function in a similar fashion; that is, the known increase in biological activity with alkyl group length is assumed to result from an increasingly facilitated mode of action as the chain is lengthened.

In two conformations, there is a series-wide similarity in several properties. First, when the molecules are held in a planar configuration in which the ester fragment is extended at the maximum distance from the carbonyl group and also in the planar configuration of benzoic acid, the energies are all at the configurational minimum for each member. The charge distribution (Table I) also shows a minimum charge on the hydroxyl group (corresponding to resonance stabilization, which is maximized in this orientation), and the HFMO and LEMO characters and energies are all very similar.

Second, when the next most stable conformer is examined, the perpendicular, *trans*-conformer of methylparaben and the ethylparaben conformation shown in Fig. 4, as well as the perpendicular conformation of *p*-hydroxybenzoic acid, are included. In this series, the negative charge is maximized on the hydroxyl group (resonance is prevented), the HFMO energy and character is very similar for all members, and the first two empty molecular orbitals form a near degenerate set, which is virtually identical in both cases.

The remaining conformers have fewer similar characteristics and/or are higher in energy.

While it is entirely possible for the biological activity of the parabens to be associated with the most stable configuration of each member of the series, it is also possible that it is related to the ability of these molecules and/or receptor sites to be mutually perturbed. Hence, hypotheses of action could be based on either ground-state geometry or the next most preferred geometry. This latter possibility and the similar characteristics of all members of the series and proposed receptor site (discussed later) when in this geometry suggest a mechanism in which the alkyl group of the ester fragment is directed downward from the ring. In this conformation, all of these compounds may react with a similar sized receptor site on a bacterial cell wall or membrane, for example.

Since these conformations of the perpendicular methyl and ethyl esters differ only by the length of the ester chain, lengthening of this chain could serve to increase still further the lipid solubility or site stability of the compound (discussed later). Previous solubility studies (23) substantiated this idea. In comparing the spatial requirements of this conformation with that of the most stable conformer, it also should be noted that the receptor site geometry would be required to change with the increasing alkyl group size of the ester in its most stable geometry (planar, with the alkyl group extending away from the carbonyl group). With this working hypothesis, a reasonable receptor site would be one consisting of a lipid area or areas in which alkyl groups of varying lengths for the ester chain are solubilized, sites of positive or negative charge resulting from ionic or ion–dipole interactions with protein functional groups, and relatively uncharged areas composed of hydrocarbon fragments. Such a general model utilizing these features is given in Scheme I. This scheme suggests an interaction of these intact esters with the site such that their alkyl ester group would be buried in the lipid pool, the phenyl group would be in the vicinity of a relatively nonreactive hydrocarbon fragment, and the hydroxyl fragment would be attached to a center of positive charge.

As indicated previously, the negative charge on the hydroxyl

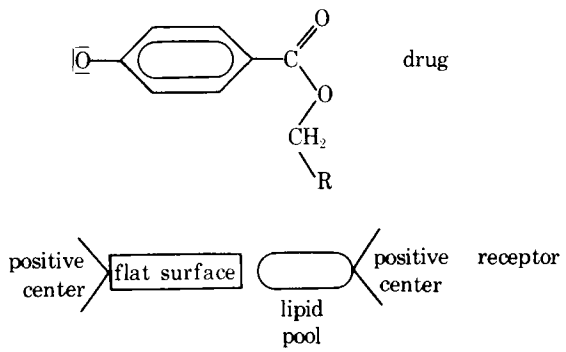

Scheme I—Theoretical receptor for the postulated active form of the paraben preservatives

group is maximized in the perpendicular conformation. With such a model, it is not unreasonable that all paraben esters would present a −10.4-ev lone-pair molecular orbital primarily localized on the carbonyl oxygen and a pair of nearly degenerate empty molecular orbitals of carbonyl antibonding π^* and delocalized ring π symmetries at −7.6 ev, which could interact by a charge-transfer or an acid–base interaction with molecules and thereby prevent normal cell membrane transport. Notably, all parabens could operate in a similar fashion at the molecular level, and the increase in effectiveness as a series is ascended would be directly proportional to the solubility of the compound. Therefore, solubility (at a receptor site and in transport) could become a primary factor in determining the amount of drug reaching the receptor site and interacting with the site, superseding the factor of chemical reaction whose characteristics change with alkyl chain lengthening.

Such a mechanism easily rationalizes the observed trend in activity from phenol < benzoic acid < *p*-hydroxybenzoic acid < ester and in the ester series from methyl < ethyl < propyl < butyl. *p*-Hydroxybenzoic acid would not be as lipid soluble as the methyl ester and may not readily be at such a site. Phenol and benzoic acid, while they may engage in the same mechanism of action, do not have the same functional groups to act in precisely the same manner as the later members of the series.

According to this hypothesis, the activity of these compounds should increase as the lipid portion of the molecule, the ester chain, becomes larger, since it may act as an anchor to retain the molecule at the site for a longer period. If sufficient sites are filled, cell function may be interrupted, causing the observed biological effect. As noted, biological activity does indeed increase as the ester chain increases.

In conclusion, Iterated Extended Hückel Theory molecular orbital calculations were carried out on a series of parabens. By use of characteristics common to all members of the series when each is held in a configurationally similar geometry, a working hypothesis was constructed for a mode of action for members of this series. In this proposed model, each member interacts with a receptor site through dipole–dipole interactions at the hydroxyl group and lipid solubilization of the ester alkyl fragment when the ester fragment is perpendicular to the ring plane. Each member also presents a -10.4 ± 0.2 ev HFMO of lone-pair symmetry on the carbonyl oxygen and a pair of nearly degenerate empty molecular orbitals of delocalized ring π and carbonyl antibonding π^* symmetries at −7.6 ev, which can interact with other portions of a receptor site or possibly restrict the activity of another molecular system through an acid–base or charge-transfer mechanism.

REFERENCES

(1) L. B. Kier, *J. Med. Chem.*, **11**, 441(1968).

(2) L. B. Kier, *Mol. Pharmacol.*, **4**, 20(1968).

(3) L. B. Kier, *J. Pharm. Sci.*, **59**, 112(1970).

(4) A. Pullman and B. Pullman, *Nature*, **196**, 228(1963).

(5) *Ibid.*, **199**, 4892(1965).

(6) J. S. Dewar, "The Molecular Orbital Theory of Organic Chemistry," McGraw-Hill, New York, N.Y., 1969.

(7) A. Streitweiser, Jr., "Molecular Orbital Theory for Organic Chemists," Wiley, New York, N.Y., 1961.

(8) J. D. Roberts, "Notes on Molecular Orbital Calculations," W. A. Benjamin, New York, N.Y., 1962.

(9) W. P. Purcell and K. Sundstrem, *J. Med. Chem.*, **12**, 18(1969).
(10) A. N. Martin and R. S. Schnaare, *J. Pharm. Sci.*, **54**, 1707(1965).
(11) E. F. Gale and E. S. Taylor, *J. Gen. Microbiol.*, **1**, 77 (1947).
(12) P. Maurice, *Proc. Soc. Appl. Bacteriol.*, **15**, 144(1952).
(13) J. Judis, *J. Pharm. Sci.*, **51**, 261(1962).
(14) M. Von Schelhorn, *Food Technol.*, **7**, 97(1953).
(15) O. Wyss, "Advances in Food Research," vol. I, Academic, New York, N.Y., 1948.
(16) R. Hoffmann and W. N. Lipscomb, *J. Chem. Phys.*, **36**, 2179, 3489(1962).
(17) Quantum Chemistry Program Exchange, Chemistry Department, Indiana University, No. 20.
(18) G. A. Sim, J. M. Robertson, and T. H. Goodwin, *Acta Crystallogr.*, **8**, 157(1955).
(19) R. Hulme and J. C. Scruton, *J. Chem. Soc., A*, **1967**, 2448.
(20) H. Giller-Panraud, *Bull. Soc. Chim. Fr.*, **1967**, 1988.
(21) C. Scheringer, *Z. Kristallogr.*, **119**, 273(1963).
(22) L. Manojlovic, *Acta Crystallogr. (B)*, **24**, 326(1968).
(23) M. Alleaume, G. Salas-Cimingo, and J. Decap, *C. R. Acad. Sci. Fr., C*, **262**, 416(1966).
(24) T. F. Lai and R. E. Marsh, *Acta Crystallogr.*, **22**, 885(1967).
(25) L. Basch, A. Viste, and H. Gray, *J. Chem. Phys.*, **44**, 10(1966).
(26) L. Basch, A. Viste, and H. Gray, *Theor. Chim. Acta*, **3**, 458(1965).
(27) L. C. Cusachs and J. R. Linn, Jr., *J. Chem. Phys.*, **46**, 2912(1967).
(28) L. B. Kier, "Molecular Orbital Theory in Drug Research," Academic, New York, N.Y., 1971.
(29) R. S. Mulliken, *J. Amer. Chem. Soc.*, **74**, 811(1952).
(30) R. Hoffmann, *J. Chem. Phys.*, **39**, 1397(1963).
(31) J. A. Pope, D. P. Santry, and G. A. Segal, *ibid.*, **43**, 5129(1965).
(32) R. Hoffmann and W. N. Lipscomb, *ibid.*, **36**, 3489(1962); **37**, 2872(1962); **36**, 2179(1962).

ACKNOWLEDGMENTS AND ADDRESSES

Received March 15, 1974, from the *College of Pharmacy, University of Rhode Island, Kingston, RI 02881*

Accepted for publication August 8, 1975.

Abstracted in part from a dissertation submitted by K. S. Alexander to the Graduate School, University of Rhode Island, in partial fulfillment of the Doctor of Philosophy degree requirements.

[x] To whom inquiries should be directed.

Controlled Flocculation of Coarse Suspensions by Colloidally Dispersed Solids I: Interaction of Bismuth Subnitrate with Bentonite

HANS SCHOTT

Abstract □ Deflocculated suspensions of coarse powders tend to cake as the individual particles settle out and form compact, cohesive sediments. Limited flocculation results in looser sediments because the settled-out flocs incorporate large amounts of the liquid suspending medium. Controlled flocculation of bismuth subnitrate suspensions was achieved by the addition of small amounts of bentonite. The interaction of the coarse, positively charged bismuth subnitrate particles in aqueous suspension with negatively charged, colloidally dispersed bentonite was investigated by measuring electrophoretic mobility, sedimentation volume, and viscosity. Gradual addition of bentonite dispersion to bismuth subnitrate suspensions first reduced the ζ-potential of the bismuth subnitrate particles from +28 mv to zero, then inverted it, and finally caused it to level off at −20 mv for bismuth subnitrate–bentonite weight ratios below 200. Owing to the much greater specific surface area of bentonite, the surface of the bismuth subnitrate lath-shaped crystals was completely covered by 0.5% of its weight in clay platelets. Adhesion was promoted by electrovalences between surface bismuthyl ions and cation-exchange sites of the clay and by secondary valences. The charge neutralization of bismuth subnitrate by bentonite was a heterocoagulation process: the addition of small amounts of the clay flocculated the bismuth subnitrate suspensions and eliminated caking. While the ζ-potential of the bismuth subnitrate particles leveled off when their surface was saturated with bentonite platelets, sedimentation volume and viscosity continued to increase when the clay concentration was increased further while maintaining the bismuth subnitrate concentration constant. The excess, nonadsorbed bentonite formed the characteristic house-of-cards structure, incorporating the bentonite-coated bismuth subnitrate particles as cornerstones.

Keyphrases □ Flocculation, controlled—coarse suspensions by colloidally dispersed solids, interaction of bismuth subnitrate with bentonite □ Suspensions, coarse—controlled flocculation by colloidally dispersed solids, interaction of bismuth subnitrate with bentonite □ Colloidal dispersions—controlled flocculation of coarse suspensions, interaction of bismuth subnitrate with bentonite □ Bismuth subnitrate—coarse suspension, controlled flocculation by colloidally dispersed bentonite □ Bentonite—colloidal dispersion, controlled flocculation of coarse suspension of bismuth subnitrate

The kinetic units in extensively deflocculated suspensions are primary particles or small aggregates. When approaching the bottom of the container during sedimentation, these particles can slip past one another, each seeking the lowest possible point, and settle down next to each other. They pack efficiently to produce compact, dense solid layers. The interparticle attraction in such compact sediments is high because the interparticle distances are small and the London–van der Waals forces, which decrease approximately with the seventh power of the distance, are consequently appreciable. Such conditions frequently lead to caking or claying, an undesirable phenomenon because it produces sediments that require extensive agitation for redispersion (1).

The kinetic units in flocculated suspensions are larger aggregates or flocs. They bridge easily when settling out and produce loose, voluminous sediments containing large amounts of trapped liquid suspending medium. Such sediments are easily redispersed into the original

(9) W. P. Purcell and K. Sundstrem, *J. Med. Chem.*, **12**, 18(1969).
(10) A. N. Martin and R. S. Schnaare, *J. Pharm. Sci.*, **54**, 1707(1965).
(11) E. F. Gale and E. S. Taylor, *J. Gen. Microbiol.*, **1**, 77 (1947).
(12) P. Maurice, *Proc. Soc. Appl. Bacteriol.*, **15**, 144(1952).
(13) J. Judis, *J. Pharm. Sci.*, **51**, 261(1962).
(14) M. Von Schelhorn, *Food Technol.*, **7**, 97(1953).
(15) O. Wyss, "Advances in Food Research," vol. I, Academic, New York, N.Y., 1948.
(16) R. Hoffmann and W. N. Lipscomb, *J. Chem. Phys.*, **36**, 2179, 3489(1962).
(17) Quantum Chemistry Program Exchange, Chemistry Department, Indiana University, No. 20.
(18) G. A. Sim, J. M. Robertson, and T. H. Goodwin, *Acta Crystallogr.*, **8**, 157(1955).
(19) R. Hulme and J. C. Scruton, *J. Chem. Soc., A*, **1967**, 2448.
(20) H. Giller-Panraud, *Bull. Soc. Chim. Fr.*, **1967**, 1988.
(21) C. Scheringer, *Z. Kristallogr.*, **119**, 273(1963).
(22) L. Manojlovic, *Acta Crystallogr. (B)*, **24**, 326(1968).
(23) M. Alleaume, G. Salas-Cimingo, and J. Decap, *C. R. Acad. Sci. Fr., C*, **262**, 416(1966).
(24) T. F. Lai and R. E. Marsh, *Acta Crystallogr.*, **22**, 885(1967).
(25) L. Basch, A. Viste, and H. Gray, *J. Chem. Phys.*, **44**, 10(1966).
(26) L. Basch, A. Viste, and H. Gray, *Theor. Chim. Acta*, **3**, 458(1965).
(27) L. C. Cusachs and J. R. Linn, Jr., *J. Chem. Phys.*, **46**, 2912(1967).
(28) L. B. Kier, "Molecular Orbital Theory in Drug Research," Academic, New York, N.Y., 1971.
(29) R. S. Mulliken, *J. Amer. Chem. Soc.*, **74**, 811(1952).
(30) R. Hoffmann, *J. Chem. Phys.*, **39**, 1397(1963).
(31) J. A. Pope, D. P. Santry, and G. A. Segal, *ibid.*, **43**, 5129(1965).
(32) R. Hoffmann and W. N. Lipscomb, *ibid.*, **36**, 3489(1962); **37**, 2872(1962); **36**, 2179(1962).

ACKNOWLEDGMENTS AND ADDRESSES

Received March 15, 1974, from the *College of Pharmacy, University of Rhode Island, Kingston, RI 02881*

Accepted for publication August 8, 1975.

Abstracted in part from a dissertation submitted by K. S. Alexander to the Graduate School, University of Rhode Island, in partial fulfillment of the Doctor of Philosophy degree requirements.

[x] To whom inquiries should be directed.

Controlled Flocculation of Coarse Suspensions by Colloidally Dispersed Solids I: Interaction of Bismuth Subnitrate with Bentonite

HANS SCHOTT

Abstract □ Deflocculated suspensions of coarse powders tend to cake as the individual particles settle out and form compact, cohesive sediments. Limited flocculation results in looser sediments because the settled-out flocs incorporate large amounts of the liquid suspending medium. Controlled flocculation of bismuth subnitrate suspensions was achieved by the addition of small amounts of bentonite. The interaction of the coarse, positively charged bismuth subnitrate particles in aqueous suspension with negatively charged, colloidally dispersed bentonite was investigated by measuring electrophoretic mobility, sedimentation volume, and viscosity. Gradual addition of bentonite dispersion to bismuth subnitrate suspensions first reduced the ζ-potential of the bismuth subnitrate particles from +28 mv to zero, then inverted it, and finally caused it to level off at −20 mv for bismuth subnitrate–bentonite weight ratios below 200. Owing to the much greater specific surface area of bentonite, the surface of the bismuth subnitrate lath-shaped crystals was completely covered by 0.5% of its weight in clay platelets. Adhesion was promoted by electrovalences between surface bismuthyl ions and cation-exchange sites of the clay and by secondary valences. The charge neutralization of bismuth subnitrate by bentonite was a heterocoagulation process: the addition of small amounts of the clay flocculated the bismuth subnitrate suspensions and eliminated caking. While the ζ-potential of the bismuth subnitrate particles leveled off when their surface was saturated with bentonite platelets, sedimentation volume and viscosity continued to increase when the clay concentration was increased further while maintaining the bismuth subnitrate concentration constant. The excess, nonadsorbed bentonite formed the characteristic house-of-cards structure, incorporating the bentonite-coated bismuth subnitrate particles as cornerstones.

Keyphrases □ Flocculation, controlled—coarse suspensions by colloidally dispersed solids, interaction of bismuth subnitrate with bentonite □ Suspensions, coarse—controlled flocculation by colloidally dispersed solids, interaction of bismuth subnitrate with bentonite □ Colloidal dispersions—controlled flocculation of coarse suspensions, interaction of bismuth subnitrate with bentonite □ Bismuth subnitrate—coarse suspension, controlled flocculation by colloidally dispersed bentonite □ Bentonite—colloidal dispersion, controlled flocculation of coarse suspension of bismuth subnitrate

The kinetic units in extensively deflocculated suspensions are primary particles or small aggregates. When approaching the bottom of the container during sedimentation, these particles can slip past one another, each seeking the lowest possible point, and settle down next to each other. They pack efficiently to produce compact, dense solid layers. The interparticle attraction in such compact sediments is high because the interparticle distances are small and the London–van der Waals forces, which decrease approximately with the seventh power of the distance, are consequently appreciable. Such conditions frequently lead to caking or claying, an undesirable phenomenon because it produces sediments that require extensive agitation for redispersion (1).

The kinetic units in flocculated suspensions are larger aggregates or flocs. They bridge easily when settling out and produce loose, voluminous sediments containing large amounts of trapped liquid suspending medium. Such sediments are easily redispersed into the original

flocs by shaking (1). These facts led to the development of the concept of controlled flocculation (2–7). By reducing the absolute value of the ζ-potential of the suspended particles, the van der Waals attractive forces between the particles overcome the coulombic repulsive forces. As a result, the primary particles adhere to one another in suspension and subsequently settle out as flocs, producing voluminous and readily redispersed sediments.

There are several techniques for causing suspensions to flocculate. According to the Schulze–Hardy rule and the underlying Derjaguin–Landau–Verwey–Overbeek theory, suspensions are flocculated most efficiently, *i.e.*, at the lowest additive concentrations, by the addition of electrolytes where the counterion (the ion whose charge has the opposite sign of the charge of the particles) has a high valence (1, 7, 8). Additives that constitute exceptions to the Schulze–Hardy rule, promoting flocculation at much lower than predicted concentrations, include ionic surfactants and potential-determining ions of charge opposite in sign to that of the particles (1, 8). Flocculation by the addition of sensitizing levels of polyelectrolytes or other water-soluble polymers (1, 3, 7) is, according to the author's practical experience, difficult to control; small overdoses of polymeric flocculating agents may bring about peptization. These various techniques for producing controlled flocculation have been applied to suspensions of organic and inorganic pharmaceuticals (9–14).

The purpose of the present work was to investigate the use of colloidal dispersions of fine particle size to reduce the absolute value of the ζ-potential of coarse medicinal suspensions of opposite charge, thereby causing these suspensions to flocculate and to produce voluminous, easily redispersible sediments. It represents an extension of the concept of heterocoagulation (15, 16) to combinations of fine colloidal dispersions and coarse suspensions of opposite charges. Positively charged bismuth subnitrate was selected as the coarse particulate drug (4–6) while sodium bentonite represented the finely dispersed colloid. Much smaller amounts of the colloidal material than of the coarse solid are required for flocculation because the former has a far greater specific surface area.

The interaction of bentonite in aqueous dispersion with the coarse, negatively charged solid, microcrystalline cellulose, was reported previously (17).

EXPERIMENTAL

Materials—The two batches of bismuth subnitrate NF employed were designated Batch A[1] and Batch B[2]. Sodium bentonite[3] and the cation-exchange resin[4] were also commercial products. Water was double distilled. All other chemicals were ACS reagent grade.

Methods—Bentonite dispersions were prepared by slurrying 1 or 2% clay in a blender[5] with water. The dispersions were decanted from settled-out grit after 48 hr of standing. This step reduced their solids contents to 0.88 or 1.98% (w/w), as determined by drying aliquots to constant weight at 125°. These dispersions were quite alkaline (pH 9.2–9.6) and might, therefore, have promoted additional hydrolysis of the bismuth subnitrate. Neutralization of the sodium bentonite by means of an acid would have added foreign electrolytes and might have leached some aluminum from the clay platelets. To avoid these undesirable effects, a small aliquot of the sodium bentonite dispersion was run through the cation-exchange resin in the hydrogen form. Enough of the acid bentonite dispersion (pH 2.0–2.2) was immediately added to the original, alkaline dispersion to lower the pH of the latter to between 5.2 and 5.5. The clay in these dispersions is referred to as sodium/hydrogen bentonite.

On standing, the pH of the sodium/hydrogen bentonite dispersions gradually increased by as much as 1 unit during the first 3–4 weeks and then became constant. The dispersions used in the present experiments were aged for over 4 weeks. Their pH values stabilized between 6.0 and 6.6.

The bismuth subnitrate suspension was prepared by the following successive steps: slurrying 120 g of powder with 600 ml of water, dispersing in a blender at top speed for 10 min, letting stand for 48 hr, filtering through a Büchner funnel (pH of filtrate = 1.44), washing three times with water, twice more resuspending in 500 ml of water by means of a blender, letting stand overnight, filtering (pH of filtrates = 1.6–1.9), washing once with water, and resuspending in the required volume of water by means of a blender. The final suspension was used for subsequent measurements within 8 hr. This procedure was designed to stabilize the composition of the surface layers of the bismuth subnitrate particles by causing surface hydrolysis to take place during the preparation of the suspension rather than during the measurements.

The solids contents of the three bismuth subnitrate suspensions employed, measured by withdrawing aliquots while the suspensions were being stirred and drying to constant weight at 105°, were 14.95, 17.72, and 23.46% (w/w).

To measure sedimentation volumes, 50-ml portions of the bismuth subnitrate suspension and measured volumes of water and sodium/hydrogen bentonite dispersion were pipetted, in that order, into 100-ml graduated cylinders equipped with standard taper stoppers. The water was added to bring the total volume to 70 ml for the first series and to 100 ml for the second. In the few instances where lower bismuth subnitrate–bentonite ratios were desired, some of the clear supernate of the 50-ml bismuth subnitrate suspension placed in the graduated cylinder was withdrawn and the 100-ml volumes were completed with clay dispersion. The contents were mixed by shaking, and sedimentation volumes were read after standing at rest for various lengths of time. The values were rounded to the nearest 0.5 ml. Measurements of pH were made with a combination glass and silver–silver chloride electrode and a digital pH meter[6]. When measuring the pH of the suspensions with two electrodes, equilibration times were far longer.

Microelectrophoresis measurements were made with a commercial instrument[7] using the molybdenum anode and an acrylic cell. The cell constant and equations for calculating specific conductance from current intensity, electrophoretic mobility from velocity of migration, and ζ-potential from electrophoretic mobility are given in Ref. 18.

Microelectrophoresis measurements are always made in very dilute suspensions to permit the determination of the velocity of migration of individual particles. The bentonite dispersions were diluted 1:100. The suspensions of bismuth subnitrate and the mixtures of clay dispersions and bismuth subnitrate suspensions were filtered and washed three times with water immediately prior to measuring electrophoretic mobilities to prevent hydrolysis of bismuth subnitrate from turning the suspensions acid. The washed solids were redispersed in water or in 0.001 or 0.01 *M* potassium chloride by manual shaking. Redispersing them briefly by means of a vortex genie shaker instead of manually did not change the mobility values significantly. In mixtures containing particles of bentonite and bismuth subnitrate, only the latter were used for mobility measurement. Their much larger size made them easily distinguishable from the much smaller clay particles. The pH values of the diluted mixtures were determined at the end of the electrophoresis measurements.

Viscosity measurements were made with a rotational instrument[8], using the largest (No. 1) spindle with the guard in place. The instrument was recalibrated with a 60% (w/w) sucrose solution. During

[1] Lot E 63465, Ruger Chemical Co., Irvington, N.J.
[2] Amend Drug and Chemical Co., New York, N.Y.
[3] Volclay bentonite BC dust, American Colloid Co., Skokie, Ill.
[4] Amberlite IR-120, Mallinckrodt Chemical Works, St. Louis, Mo.
[5] Waring.
[6] Sargent-Welch digital pH meter model NX.
[7] Zeta-Meter, Zeta-Meter, Inc., New York, N.Y.
[8] Brookfield Synchro-Lectric viscometer, model LVT, Brookfield Engineering Laboratories, Stoughton, Mass.

Table I—Composition of Sodium/Hydrogen Bentonite–Bismuth Subnitrate Mixtures

Mixture	Bentonite, % (w/w)	Bismuth Subnitrate, % (w/w)	Weight Ratio (Bismuth Subnitrate / Bentonite)
1	0	13.18	∞
2	0.00114	13.18	11,560
3	0.00568	13.18	2,320
4	0.0114	13.18	1,160
5	0.0568	13.18	230
6	0.1136	13.17	115
7	0.2270	13.16	60
8	0	7.95	∞
9	0.0188	7.95	420
10	0.0375	7.95	210
11	0.187	7.94	40
12	0.374	7.93	20
13	0.561	7.92	14
14	0.747	7.91	10
15	0.932	7.90	8.5
16	1.320	7.88	6
17	1.651	7.86	5

viscosity measurements of the suspensions, sedimentation of solid particles caused the shear stress (torque divisions) to drift downward. To prevent the settling out of solids from giving spuriously low viscosity values, the beaker containing the suspension was placed on a magnetic stirrer. Enough clearance was left between the bottom of the beaker and the viscometer guard to accommodate the stirring bar.

The suspension was stirred to distribute the sediment uniformly. Immediately after the stirring was stopped, the clutch of the viscometer was released and the reading was taken. While this technique did not permit the observation of thixotropic phenomena, the measurements could be made before appreciable sedimentation occurred and were, therefore, reproducible. Results are expressed as apparent viscosity in centipoises at 60 rpm. Temperature was constant at 24–25°.

The following technique was used to determine the effect of increasing concentrations of bentonite on the viscosity of bismuth subnitrate suspensions. The viscosity of a 750-ml portion of a suspension containing 26.7% (w/w) bismuth subnitrate was measured in a 800-ml beaker. The suspension was then permitted to undergo sedimentation. A 5-ml portion of clear supernate was removed, and 5 ml of a 2.19% dispersion of sodium/hydrogen bentonite was gradually added with stirring. After measuring the viscosity again and letting the suspension stand at rest, subsequent small portions of clear supernate were replaced by equal volumes of bentonite dispersion. Viscosity measurements were performed after each addition of clay. While the concentration of sodium/hydrogen bentonite was thus gradually increased, the concentration of bismuth subnitrate and the volume of the suspension remained essentially constant.

The last mixture had a high enough viscosity to make measurements at lower speeds. The revolutions per minute values were changed from 6 to 12 to 30 to 60 and back to 30 to 12 to 6. After each change of speed, the suspension had to be stirred to resuspend the sediment.

RESULTS

Two series of mixtures were made for the electrophoresis and sedimentation measurements. Each contained a constant level of bismuth subnitrate but a different amount of sodium/hydrogen bentonite. Sedimentation volumes and electrophoretic mobility were measured for each mixture. The compositions of the mixtures are listed in Table I.

Sedimentation Volumes—Sedimentation volumes for the 17 mixtures, measured after 1 or 1.5 and 18 hr, are listed in Table II. Sedimentation volumes after 18, 42, and 66 hr were the same. Therefore, the 18-hr values correspond to infinite time. The pH values are those of the filtrate, taken 18 hr after the bentonite dispersion and bismuth subnitrate suspension were mixed. The acidity is due to nitric acid produced by hydrolysis of the latter.

Electrophoretic Mobility—Electrophoretic mobilities for the mixtures of solids and their standard deviations are given in Table III. Each listed mobility value represents the average of 10 individual measurements, and the standard deviation is that of the average. Negative values indicate negative charges, which caused the particles to migrate to the positive pole. The factor to convert mobility values, in (micrometers per second)/(volts per centimeter), to ζ-potentials

Table II—Sedimentation Volumes of Sodium/Hydrogen Bentonite–Bismuth Subnitrate[a] Mixtures[b]

Mixture	Sedimentation Volume, ml, after 1 or 1.5 hr[c]	Sedimentation Volume, ml, after 18 hr	pH of Filtrate after 18 hr
1	5[d]	5[d]	1.40
2	5[d]	5	1.40
3	6[d]	6	1.38
4	6.5[e]	6.5	1.37
5	8	7	1.36
6	12.5	9.5	1.35
7	14	12	1.37
8	7[d]	7[d]	—
9	7.5	7	1.51
10	9	7.5	1.49
11	22	21	1.72
12	35.5	32	1.73
13	52	43	1.75
14	60.5	51	1.75
15	82[d]	59	1.77
16	97.5	85	1.86
17	100[f]	88	1.93

[a] Bismuth subnitrate Batch A. [b] Total volume of Mixtures 1–7 was 70 ml and that of Mixtures 8–17 was 100 ml. [c] At 1.5 hr after mixing for Mixtures 1–7 and at 1.0 hr after mixing for Mixtures 8–17. [d] Supernate quite cloudy. [e] Supernate slightly cloudy. [f] No noticeable sedimentation and no separation of supernate of lower solids contents.

Table III—Electrophoretic Mobility Values of Sodium/Hydrogen Bentonite, Bismuth Subnitrate[a], and Their Mixtures[b]

Mixture	Mobility ± s[c], (μm/sec / v/cm)	Specific Conductance, μmhos/cm	pH
	In Water		
—[d]	−3.39 ± 0.07	40	7.7
—[e]	−3.04 ± 0.08	20	6.6
1	+2.20 ± 0.09	5	5.1
2	+2.08 ± 0.14	10	5.2
3	+2.34 ± 0.21	10	5.2
4	+0.53 ± 0.05	5	5.3
5	−0.81 ± 0.23	30	4.5
6	−1.67 ± 0.03	20	4.4
7	−1.61 ± 0.09	30	4.5
7[f]	+1.57 ± 0.14	160	3.5
8	+2.30 ± 0.11	100	4.0
9	−1.31 ± 0.12	30	5.9
12	−1.36 ± 0.09	30	6.3
13	−1.66 ± 0.08, −1.60 ± 0.09	30, 30	6.3, 6.0
16	−1.80 ± 0.13, −1.97 ± 0.18	10, 50	6.0, 6.0
	In 0.001 *M* KCl		
9	−2.37 ± 0.32	200	4.7
10	−2.05 ± 0.13	210	4.6
11	−2.37 ± 0.11	200	4.6
12	−2.36 ± 0.11	200	4.5
13	−2.08 ± 0.13, −2.11 ± 0.09	230, 200	4.3, 4.4
14	−2.16 ± 0.15	200	4.6
15	−2.37 ± 0.13	200	4.5
16	−2.16 ± 0.07	200	5.9
	In 0.01 *M* KCl		
13	−2.70 ± 0.09	1350	4.2
16	−2.75 ± 0.04	1350	—

[a] Bismuth subnitrate Batch A. [b] For mixtures of bentonite and bismuth subnitrate particles, mobility values refer to the latter only. [c] Average of 10 measurements ± SD of the average. [d] Pure sodium bentonite. [e] Sodium/hydrogen bentonite. [f] After triturating with mortar and pestle in water.

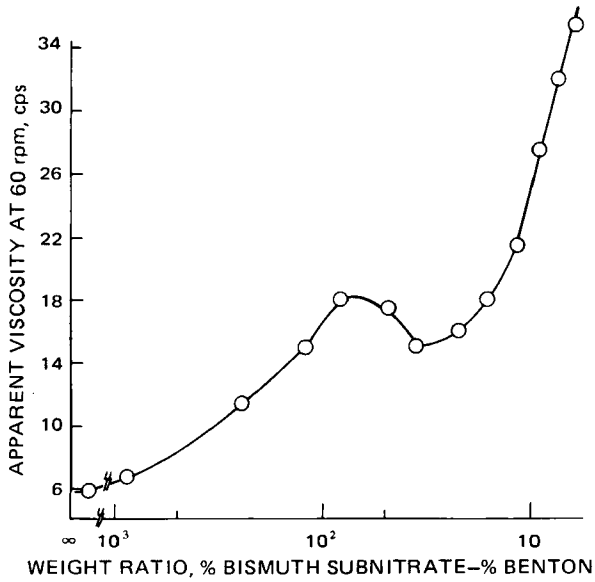

Figure 1—*Apparent viscosity as a function of composition, expressed as the weight ratio (percent bismuth subnitrate–percent bentonite), for a series of mixtures containing 26.73% (w/w) bismuth subnitrate.*

in millivolts is 12.9 according to the Smoluchowski equation at 25° (1, 18). At comparable pH and ionic strength, Batch B of bismuth subnitrate had twice the electrophoretic mobility of Batch A. For mixtures containing both bentonite and bismuth subnitrate, mobility values refer to particles of the latter only.

Viscosity—The apparent viscosity at 60 rpm as a function of the concentration ratio of bismuth subnitrate to sodium/hydrogen bentonite at a constant bismuth subnitrate concentration is shown in Fig. 1. The small maximum in viscosity followed by the shallow minimum in the range of concentration or weight ratios between 100 and 20 was replicated in a duplicate run. Figure 2 contains the consistency curve of the mixture with the lowest bismuth subnitrate–bentonite weight ratio and its apparent viscosity as a function of revolutions per minute. The two plots represent typical pseudoplastic behavior common to suspensions and dispersions with relatively low volume fractions of the disperse solid phase (19).

Caking—Caking or claying of bismuth subnitrate suspensions was negligible for mixtures with bismuth subnitrate–bentonite weight ratios of 1200 or less. The sediments of these mixtures, formed after standing at rest for an hour or a week, were completely resuspended by inverting the container or by brief, gentle stirring. Thus, the addition of 0.1% bentonite, based on the weight of bismuth subnitrate, eliminated claying, which was severe in the absence of bentonite.

DISCUSSION

Bismuth subnitrate Batch A consisted largely of lath-shaped crystals (20). The average edge size, determined by microscopic examination, was approximately 3 μm. For cubes of density 4.92 g/cm^3, this dimension corresponds to a specific surface area in the neighborhood of 4300 cm^2/g.

Bentonite consists of elemental lamellas or individual lattice layers having a thickness of 9.4 Å (21). According to previous studies based on electron micrographs of diluted, dried, and shadow-cast dispersions, the primary particles of the type of bentonite employed here, when fully dispersed in water, are packets averaging 3–4 lamellas. This corresponds to an average thickness of 3.5 × 9.4 = 33 Å, not counting the water sheets intercalated between the lattice layers (22–24). The intracrystalline water is lost upon drying. At a density of 2.83 g/cm^3, platelets with a thickness of 33 Å have a specific surface area in the neighborhood of 2 × 10^6 cm^2/g, a value about 460 times greater than the specific surface area of Batch A. The average diameter of the primary clay platelets is 0.2 μm (22).

Thus, the primary bentonite particles in water are extremely thin and, hence, very flexible platelets. They were found to deposit on the surface of cotton fabric (22) and pulp fibers (24) from aqueous dispersions lying flat and molding themselves intimately to those surfaces, forming an uninterrupted film. This film averaged a mere 28–38 Å in thickness. Therefore, it replicated the topography of the cellulose substrates so completely that its presence could not be detected by electron micrographs of surface replicas. Cotton fabrics and paper covered by this very thin clay film had appearances identical to the original materials without the clay. On burning the cellulose substrates, the infusible clay film remained behind as a shrunken surface replica, preserving microscopic details of the topography of those substrates (22, 24). The adhesion of bentonite to cotton and paper occurs presumably by hydrogen bonds between the oxygen ions covering the clay platelets and the hydroxyl groups of cellulose.

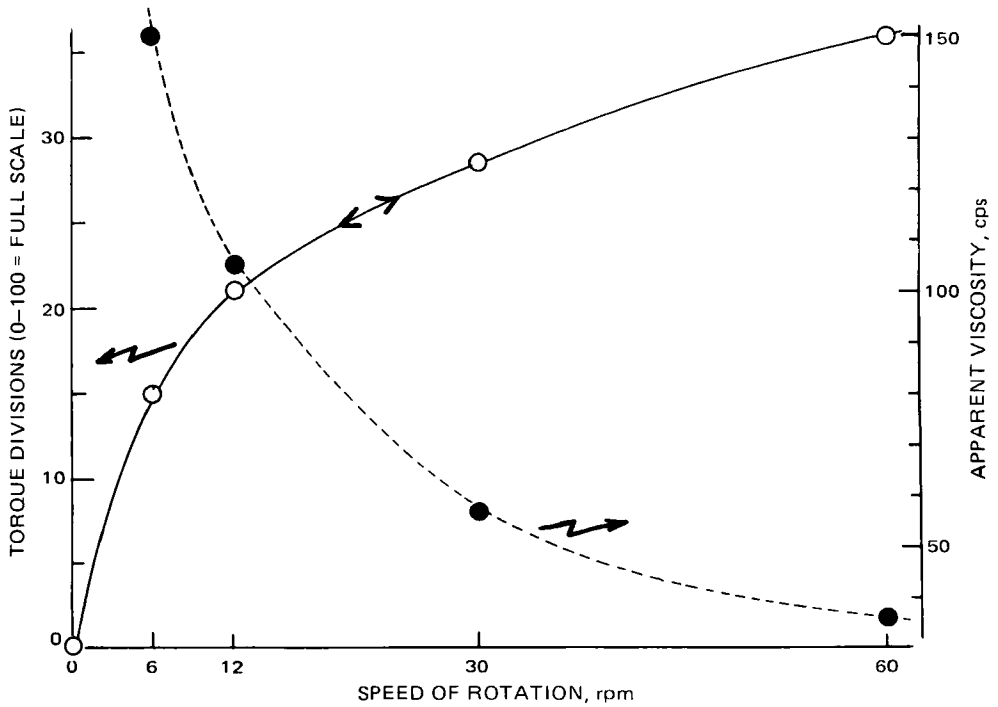

Figure 2—*Consistency curve and apparent viscosity as a function of rotational speed for a mixture of 26.73% bismuth subnitrate and 4.31% bentonite.*

The situation in the bentonite–bismuth subnitrate system appears to be analogous. In an aqueous dispersion, the sodium/hydrogen bentonite exists as very thin platelets. Partial substitution of sodium by hydrogen counterions did not alter the degree of dispersion of the bentonite in water (24). The clay platelets coat the large, lath-shaped bismuth subnitrate particles. The adhesion of the bentonite platelets to a bismuth subnitrate substrate is even stronger than to the cellulose substrates, because coulombic forces between the negatively charged clay and the positively charged bismuth subnitrate particles are superimposed on the van der Waals forces of attraction.

Bentonite particles owe their negative charge chiefly to cation-exchange sites, which are, in effect, silicic acid groups built into the clay lattice through isomorphous replacement of aluminum ions (Al^{+3}) by magnesium ions (Mg^{+2}) and silicon ions (Si^{+4}) by aluminum ions (Al^{+3}) (21). The counterions here are sodium and hydrogen cations. The electric charge of bismuth subnitrate particles in weakly alkaline, neutral, and acid media is positive because of an excess of bismuthyl cations over nitrate anions in the surface layer. The counterions are nitrate anions. When a bentonite dispersion is added to a bismuth subnitrate suspension, the extremely thin and smaller clay platelets lie flat against the surface of the coarse bismuth subnitrate crystals and adhere them. As the bismuth subnitrate surfaces become coated with bentonite platelets, their nitrate counterions are replaced by silicate ions embedded in the bentonite platelets. The sodium and hydrogen countercations of the latter pair off with the nitrate counteranions of the former, as illustrated in Fig. 3.

This arrangement is corroborated by the electrophoresis data of Table III. The addition of increasing amounts of bentonite dispersion to bismuth subnitrate suspensions gradually reduced the positive electrophoretic mobility or ζ-potential of the bismuth subnitrate particles to zero. This trend is shown by Mixtures 1–4 in Table III. Zero mobility corresponds to zero net charge, which indicates that the positive charges in the still bare portions of the surface of a bismuth subnitrate particle are equal in magnitude to the negative charges of the portions of that surface covered by sorbed bentonite platelets.

Further addition of bentonite beyond the amount that reduced the mobility of the bismuth subnitrate particles to zero inverted the sign of the mobility and conferred increasingly greater negative mobility values to these particles. This result is shown by Mixtures 5 and 6. The reason for the charge inversion is that the positively charged surfaces of the bismuth subnitrate crystals became more extensively covered with negatively charged bentonite platelets beyond the equivalence point. The net negative charge arises from the negative silicate ions in the outer face of sorbed clay platelets whose other face is attached to the surface of a bismuth subnitrate particle (Fig. 3).

However, the negative mobility values reached a limit. Despite continued increases in bentonite concentration, the electrophoretic mobility and the ζ-potential in water leveled off at -1.57 ± 0.25 (μm/sec)/(v/cm) and -20 ± 3 mv, respectively, for Mixtures 6, 7, 9, 12, 13, and 16. The level-off value for the negative mobility of bismuth subnitrate particles covered with bentonite platelets was one-half of the mobility of the bentonite platelets by themselves, which was -3.0 (μm/sec)/(v/cm). This finding is to be expected, because the cation-exchange sites in one of the two faces of a sorbed clay platelet are in contact with, and neutralized by, the bismuth subnitrate substrate. Only the negative charges in the outer face of a sorbed platelet, which are in contact with water and give rise to an electric double layer, contribute to the ζ-potential. In 0.001 *M* KCl, the plateau values for Mixtures 9–16 were -2.2 and -29 for mobility and ζ-potential, respectively.

The addition of bentonite to bismuth subnitrate to produce mixtures having bismuth subnitrate–bentonite weight ratios below 230 (in Mixtures 1–7, which contained 13% bismuth subnitrate) or below 420 (in Mixtures 9–16, which contained 8% bismuth subnitrate) caused no further increase in the negative values of electrophoretic mobility or ζ-potential. Evidently, the positively charged bismuth subnitrate particles became completely covered with negatively charged bentonite platelets at weight ratios below 230 (Mixture 5), producing saturation sorption. That ratio must be greater than the ratio of Mixture 6, namely, 115, because the bismuth subnitrate particles in that mixture already reached the plateau mobility.

It is of interest to compare the specific surface areas of bentonite and bismuth subnitrate with the weight ratio at which saturation sorption was reached. If the specific surface area of bentonite is 460 times greater than that of bismuth subnitrate, the bentonite platelets should completely cover the surface of the bismuth subnitrate particles at a bismuth subnitrate–bentonite weight ratio of 230. This

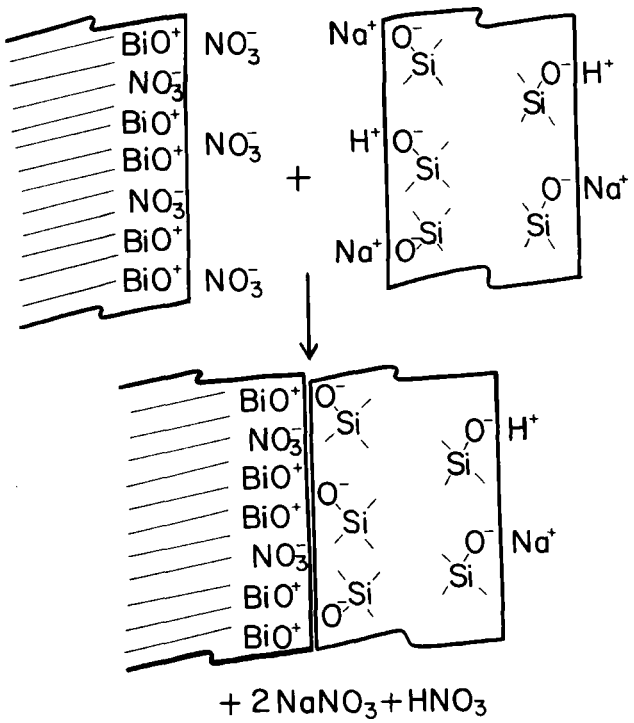

Figure 3—*Schematic representation in cross-section of the sorption of a segment of a bentonite platelet onto the surface of a bismuth subnitrate particle.*

value is one-half of the bentonite–bismuth subnitrate surface area ratio, because only one face of a bentonite platelet can contact a bismuth subnitrate surface and cover it. The effective surface area of bentonite for covering a solid substrate is, therefore, only one-half of the total value.

The weight ratio for complete coverage of bismuth subnitrate by a monolayer of nonoverlapping lamellas of bentonite 33 Å thick is 230. In practice, the sorbed clay platelets are likely to overlap. This overlapping reduces the effective specific surface area of bentonite dispersed in water and places the weight ratio for complete coverage or saturation sorption at below 230. The fact that this result is identical with the one obtained by electrophoresis is coincidental, because there is a gap between the weight ratios of Mixtures 5 and 6 and because the specific surface areas are only approximate values. The fact that the values obtained by electrophoresis and geometrical considerations are at least of the same order of magnitude corroborates the physical picture sketched in Fig. 3.

When Mixture 7 was triturated prior to electrophoresis measurements, fresh bismuth subnitrate surface was exposed, which was not previously in contact with, and therefore had not become coated by, bentonite. This fresh surface was positively charged and conferred positive values to the ζ-potential of the bismuth subnitrate particles.

A noteworthy feature of Table III is that the negative values of electrophoretic mobility and ζ-potential became more negative for a given mixture as the medium was changed from water to 0.001 and 0.01 *M* KCl. The usual effect of increasing ionic strength is to reduce the absolute values of electrophoretic mobility and ζ-potential. The present unusual behavior was reported for pure bentonite dispersed in aqueous solutions of the chlorides and sulfates of sodium and potassium (25).

Comparison of Table I with II and inspection of Fig. 4 show that the sedimentation volumes increased monotonically with decreasing bismuth subnitrate–bentonite weight ratios. For the mixtures containing 13% bismuth subnitrate (Mixtures 1–7), the rate of increase in sedimentation volume with a decreasing weight ratio was greatest in the vicinity of Mixture 5. Likewise, at approximately this same composition, the electrophoretic mobility of the bismuth subnitrate particles underwent the greatest variation, including a change in sign, and had the smallest absolute values. Small absolute values for mobility and ζ-potential cause the electrostatic repulsion between particles to be weak, promoting flocculation and large sedimentation volumes. The two curves in Fig. 4, representing electrophoretic mo-

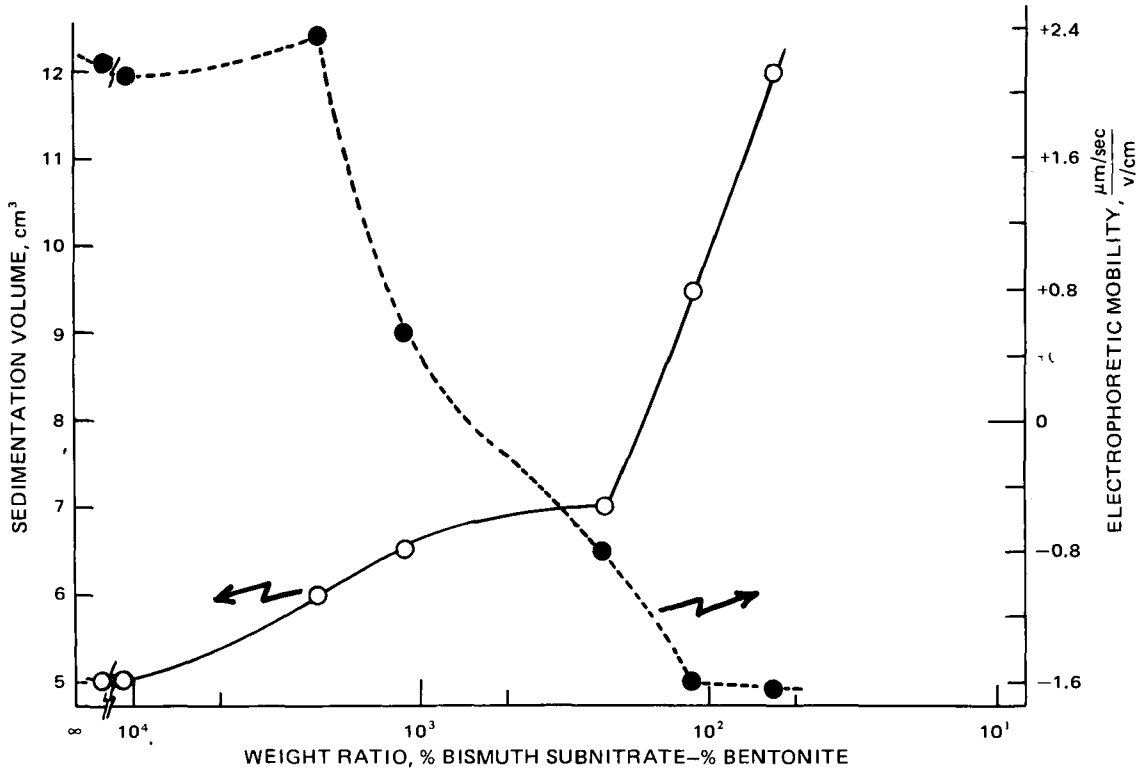

Figure 4—*Electrophoretic mobility and sedimentation volume at infinite time for Mixtures 1–7 as a function of the weight ratio (percent bismuth subnitrate–percent bentonite).*

bility and sedimentation volume as a function of the bismuth subnitrate–bentonite weight ratio, have approximately a mirror-image relationship, except that the latter curve does not level off even at the highest clay concentrations employed.

The sedimentation volumes continued to increase with decreasing bismuth subnitrate–bentonite weight ratios or increasing bentonite concentrations in the range of compositions where the electrophoretic mobility had reached a rather high and constant negative value, *i.e.*, for Mixtures 6 and 7 and 9–17. This finding is ascribed to the formation of the characteristic thixotropic house-of-cards structure (21) by the excess, free, or nonadsorbed bentonite. This scaffolding is due to the attraction between the positively charged edges and the negatively charged faces of the bentonite platelets (21). It probably incorporates as cornerstones the coarse bismuth subnitrate particles covered with a film of sorbed bentonite.

The viscosity measurements of Fig. 1 are in qualitative agreement with the results of the electrophoresis and sedimentation volume measurements. At infinite and very high bismuth subnitrate–bentonite ratios, the bismuth subnitrate particles have high positive charges and repel one another. Consequently, their suspension is deflocculated and has a low viscosity (19) as well as a small sedimentation volume. As the bismuth subnitrate–bentonite weight ratio decreases and the absolute value of the positive ζ-potential approaches zero, increasing flocculation produces higher viscosities. With further decreases in the weight ratio, as the ζ-potential turns increasingly negative, the bismuth subnitrate particles are peptized and the viscosity drops again. At still lower weight ratios, while the negative ζ-potential levels off because the surface of the bismuth subnitrate particles is saturated with bentonite, the viscosity begins to increase for the same reason that caused continued increases in the sedimentation volume, namely, the excess, nonadsorbed bentonite forms a house-of-cards structure.

The maximum and minimum in the plot of viscosity *versus* the bismuth subnitrate–bentonite weight ratio of Fig. 1 occur at a lower ratio than the one at which the electrophoretic mobility and sedimentation volume *versus* weight ratio plots of Fig. 4 undergo their sharpest changes. The difference may be ascribed to a difference in bismuth subnitrate concentration. The suspensions used to measure viscosities contained twice as much bismuth subnitrate than those used to measure sedimentation volumes.

Caking was relieved by two different mechanisms. At low bentonite concentrations, between bismuth subnitrate–bentonite weight ratios of approximately 1200 and 230, the sorbed clay reduced the high positive ζ-potential of the bismuth subnitrate particles to zero or to small positive or negative values. In the absence of strong electrostatic repulsion between the bismuth subnitrate particles, they flocculated in suspension and produced large sedimentation volumes. This mechanism is applicable to all finely dispersed colloidal solids of opposite charge; their specific surface area must be much higher than that of the coarse particulate drug.

At higher bentonite concentrations, for bismuth subnitrate–bentonite weight ratios below 230, enough bentonite was present to coat the bismuth subnitrate particles completely with clay platelets. At those levels, the house-of-cards structure of bentonite, which incorporated and thereby agglomerated the bentonite-covered bismuth subnitrate particles, was responsible for preventing those particles from forming compact sediments. This flocculation occurred despite the fact that the clay-coated particles had a negative ζ-potential large enough to prevent flocculation in the absence of nonadsorbed or free bentonite. This mechanism for relieving caking is only operative with finely dispersed colloidal solids of opposite charge that are also capable of producing structural viscosity at low concentrations.

REFERENCES

(1) K. J. Mysels, "Introduction to Colloid Chemistry," Wiley–Interscience, New York, N.Y., 1959, chap. 4.

(2) E. N. Hiestand, *Proc. Am. Assoc. Coll. Pharm., Teach. Semin.*, **13**, 125(1961).

(3) E. N. Hiestand, *J. Pharm. Sci.*, **53**, 1(1964).

(4) B. A. Haines and A. N. Martin, *ibid.*, **50**, 228(1961).

(5) *Ibid.*, **50**, 753(1961).

(6) *Ibid.*, **50**, 756(1961).

(7) A. N. Martin, J. Swarbrick, and A. Cammarata, "Physical Pharmacy," 2nd ed., Lea & Febiger, Philadelphia, Pa., 1969, pp. 461–526.

(8) H. Schott and A. N. Martin, in "American Pharmacy," 7th ed., L. W. Dittert, Ed., Lippincott, Philadelphia, Pa., 1974, chap. 6.

(9) R. G. Wilson and B. Ecanow, *J. Pharm. Sci.*, **52**, 757(1963).

(10) B. A. Matthews and C. T. Rhodes, *ibid.*, **57**, 569(1968).

(11) R. D. C. Jones, B. A. Matthews, and C. T. Rhodes, *ibid.*, **59**, 518(1970).

(12) J. V. Bondi, R. L. Schnaare, P. J. Niebergall, and E. T. Sugita, *ibid.*, **62**, 1731(1973).
(13) M. P. Short and C. T. Rhodes, *Can. J. Pharm. Sci.*, **8**, 46(1973).
(14) A. Felmeister, G. M. Kuchtyak, S. Koziol, and C. J. Felmeister, *J. Pharm. Sci.*, **62**, 2026(1973).
(15) B. V. Derjaguin, *Discuss. Faraday Soc.*, **18**, 85(1954).
(16) R. Hogg, T. W. Healey, and D. W. Fuerstenau, *Trans. Faraday Soc.*, **62**, 1638(1966).
(17) H. Schott, *J. Pharm. Sci.*, **59**, 1492(1970).
(18) H. Schott and C. Y. Young, *ibid.*, **61**, 182(1972).
(19) E. K. Fischer, "Colloidal Dispersions," Wiley, New York, N.Y., 1950, chaps. 4 and 5.
(20) "Hagers Handbuch der Pharmazeutischen Praxis," vol. I, G. Frerichs, G. Arends, and H. Zoernig, Eds., Springer-Verlag, Berlin, Germany, 1949, p. 681.
(21) H. van Olphen, "An Introduction to Clay Colloid Chemistry," Wiley–Interscience, New York, N.Y., 1963, chap. 6.
(22) H. Schott, *Text. Res. J.*, **35**, 612(1965).
(23) *Ibid.*, **40**, 924(1970).
(24) H. Schott, *Tappi*, **54**, 748(1971).
(25) H. Bergseth, *Kolloid-Z.*, **179**, 67(1961).

ACKNOWLEDGMENTS AND ADDRESSES

Received July 1, 1975, from the *School of Pharmacy, Temple University, Philadelphia, PA 19140*

Accepted for publication August 13, 1975.

Presented at the Basic Pharmaceutics Section, APhA Academy of Pharmaceutical Sciences, Atlanta meeting, November 1975.

Urinary Excretion of Probenecid and Its Metabolites in Humans as a Function of Dose

SRIKUMARAN MELETHIL * and WALTER D. CONWAY ˣ

Abstract □ A GLC assay was used to study the excretion of probenecid and its metabolites in the urine of human subjects following oral doses of 0.5, 1, and 2 g. From 75 to 88% of the dose was found in the urine. The major metabolite, probenecid acyl glucuronide, accounted for 34–47% of the dose. Approximately equal amounts (10–15%) of the mono-*N*-propyl, secondary alcohol, and carboxylic acid metabolites were excreted in the unconjugated form with only traces in the conjugated form. The primary alcohol metabolite was not found in measurable amounts. The terminal half-lives for excretion of all metabolites were in the range of 4–6 hr, were independent of dose, and were limited by their rates of formation. A prolonged time course of excretion of the metabolites, particularly at higher doses, suggests that probenecid, being poorly soluble in water, precipitates from solution in the GI tract, forming a depot of drug from which absorption is dissolution rate limited. The urinary excretion of unchanged probenecid, which accounts for 4–13% of the dose, is dependent on both the pH and flow rate of urine.

Keyphrases □ Probenecid and metabolites—urinary excretion as a function of dose □ Excretion, urinary—probenecid and metabolites, effect of dose □ Uricosuric agents—probenecid and metabolites, effect of dose □ Metabolism—probenecid, urinary excretion as a function of dose

Probenecid, 4-[(dipropylamino)sulfonyl]benzoic acid, was introduced as an uricosuric agent in 1951. However, only recently has its metabolic fate in humans and animals been fully elucidated (1–4). Studies of the disposition of the drug generally have used ^{14}C-labeled probenecid, and studies in humans have been limited by the need for a convenient nonradioactive assay. A GLC assay of the methyl esters of probenecid and its metabolites was employed for studies in rats (1, 4). The GLC assay of the propyl esters was utilized in the present study of the urinary excretion of probenecid and its metabolites in humans.

The plasma half-life of probenecid has been reported to increase with increasing dose and has been attributed to a decreased rate of metabolism at higher doses (5, 6). Unfortunately, in the human study (5), the determinations of plasma half-lives were not conducted over a sufficiently long period to be certain that distributive equilibrium had been achieved. In the dog study (6), the period over which plasma levels were measured was not indicated. Therefore, it is not clear whether this reported dose-dependent plasma decline of probenecid is real or simply the artifactual result of an inadequate sampling protocol. Therefore, the effect of increasing doses of probenecid on the urinary excretion of the drug and its metabolites in humans was investigated.

EXPERIMENTAL

Method—Unconjugated probenecid and its unconjugated metabolites were extracted with methylene chloride from urine acidified with 5 *N* HCl, converted to the propyl esters with diazopropane, and quantitated by GLC. A stainless steel column (2.8 mm × 2 m) packed with 10% OV-1 on 80–100-mesh Chromosorb W-HP was used. The gas chromatograph[1] was fitted with a flame-ionization detector. Operating parameters were: column temperature, 250°; injection port temperature, 280°; nitrogen carrier gas flow, 23 ml/min; and sensitivity, 2.5×10^{-11} amp full scale. *N,N*-Dibenzyl-(2,5-dimethylbenzene)sulfonamide was used as the internal standard. Optimum column performance was maintained by occasional injection of a silylating mixture[2] followed by overnight conditioning of the column.

Total drug and metabolites were determined by heating the acidified urine for 2 hr at 100° before extraction, derivatization, and chromatography[3]. Metabolites were synthesized as reported earlier (1, 4).

Protocol—Two healthy male subjects (Subject 1, 27 years, 58 kg; Subject 2, 42 years, 61.4 kg) did not ingest other drugs or alcoholic beverages for 2 days prior and 3 days after ingestion of probenecid. After fasting overnight, the initial morning urine sample was taken for use as an analytical control. Since the absorption of many drugs having poor water solubility is known to be dissolution rate limited, the dose of probenecid (0.5, 1, and 2 g) was administered orally in solution. The drug[4] was dissolved in 200 ml of 2–3% sodium bicarbonate, the minimum quantity required for complete solution. In one case (2-g dose, Subject 2), the dose was dissolved in 200 ml of dilute

[1] Perkin-Elmer Mark II.
[2] Silyl-8, Pierce Chemical Co., Rockford, Ill.
[3] The analytical procedures were reported in detail (7).
[4] Pure drug powder, Merck Sharp and Dohme, West Point, Pa.

(12) J. V. Bondi, R. L. Schnaare, P. J. Niebergall, and E. T. Sugita, *ibid.*, **62**, 1731(1973).
(13) M. P. Short and C. T. Rhodes, *Can. J. Pharm. Sci.*, **8**, 46(1973).
(14) A. Felmeister, G. M. Kuchtyak, S. Koziol, and C. J. Felmeister, *J. Pharm. Sci.*, **62**, 2026(1973).
(15) B. V. Derjaguin, *Discuss. Faraday Soc.*, **18**, 85(1954).
(16) R. Hogg, T. W. Healey, and D. W. Fuerstenau, *Trans. Faraday Soc.*, **62**, 1638(1966).
(17) H. Schott, *J. Pharm. Sci.*, **59**, 1492(1970).
(18) H. Schott and C. Y. Young, *ibid.*, **61**, 182(1972).
(19) E. K. Fischer, "Colloidal Dispersions," Wiley, New York, N.Y., 1950, chaps. 4 and 5.
(20) "Hagers Handbuch der Pharmazeutischen Praxis," vol. I, G. Frerichs, G. Arends, and H. Zoernig, Eds., Springer-Verlag, Berlin, Germany, 1949, p. 681.
(21) H. van Olphen, "An Introduction to Clay Colloid Chemistry," Wiley–Interscience, New York, N.Y., 1963, chap. 6.
(22) H. Schott, *Text. Res. J.*, **35**, 612(1965).
(23) *Ibid.*, **40**, 924(1970).
(24) H. Schott, *Tappi*, **54**, 748(1971).
(25) H. Bergseth, *Kolloid-Z.*, **179**, 67(1961).

ACKNOWLEDGMENTS AND ADDRESSES

Received July 1, 1975, from the *School of Pharmacy, Temple University, Philadelphia, PA 19140*

Accepted for publication August 13, 1975.

Presented at the Basic Pharmaceutics Section, APhA Academy of Pharmaceutical Sciences, Atlanta meeting, November 1975.

Urinary Excretion of Probenecid and Its Metabolites in Humans as a Function of Dose

SRIKUMARAN MELETHIL * and WALTER D. CONWAY ˣ

Abstract □ A GLC assay was used to study the excretion of probenecid and its metabolites in the urine of human subjects following oral doses of 0.5, 1, and 2 g. From 75 to 88% of the dose was found in the urine. The major metabolite, probenecid acyl glucuronide, accounted for 34–47% of the dose. Approximately equal amounts (10–15%) of the mono-*N*-propyl, secondary alcohol, and carboxylic acid metabolites were excreted in the unconjugated form with only traces in the conjugated form. The primary alcohol metabolite was not found in measurable amounts. The terminal half-lives for excretion of all metabolites were in the range of 4–6 hr, were independent of dose, and were limited by their rates of formation. A prolonged time course of excretion of the metabolites, particularly at higher doses, suggests that probenecid, being poorly soluble in water, precipitates from solution in the GI tract, forming a depot of drug from which absorption is dissolution rate limited. The urinary excretion of unchanged probenecid, which accounts for 4–13% of the dose, is dependent on both the pH and flow rate of urine.

Keyphrases □ Probenecid and metabolites—urinary excretion as a function of dose □ Excretion, urinary—probenecid and metabolites, effect of dose □ Uricosuric agents—probenecid and metabolites, effect of dose □ Metabolism—probenecid, urinary excretion as a function of dose

Probenecid, 4-[(dipropylamino)sulfonyl]benzoic acid, was introduced as an uricosuric agent in 1951. However, only recently has its metabolic fate in humans and animals been fully elucidated (1–4). Studies of the disposition of the drug generally have used ^{14}C-labeled probenecid, and studies in humans have been limited by the need for a convenient nonradioactive assay. A GLC assay of the methyl esters of probenecid and its metabolites was employed for studies in rats (1, 4). The GLC assay of the propyl esters was utilized in the present study of the urinary excretion of probenecid and its metabolites in humans.

The plasma half-life of probenecid has been reported to increase with increasing dose and has been attributed to a decreased rate of metabolism at higher doses (5, 6). Unfortunately, in the human study (5), the determinations of plasma half-lives were not conducted over a sufficiently long period to be certain that distributive equilibrium had been achieved. In the dog study (6), the period over which plasma levels were measured was not indicated. Therefore, it is not clear whether this reported dose-dependent plasma decline of probenecid is real or simply the artifactual result of an inadequate sampling protocol. Therefore, the effect of increasing doses of probenecid on the urinary excretion of the drug and its metabolites in humans was investigated.

EXPERIMENTAL

Method—Unconjugated probenecid and its unconjugated metabolites were extracted with methylene chloride from urine acidified with 5 *N* HCl, converted to the propyl esters with diazopropane, and quantitated by GLC. A stainless steel column (2.8 mm × 2 m) packed with 10% OV-1 on 80–100-mesh Chromosorb W-HP was used. The gas chromatograph[1] was fitted with a flame-ionization detector. Operating parameters were: column temperature, 250°; injection port temperature, 280°; nitrogen carrier gas flow, 23 ml/min; and sensitivity, 2.5×10^{-11} amp full scale. *N,N*-Dibenzyl-(2,5-dimethylbenzene)sulfonamide was used as the internal standard. Optimum column performance was maintained by occasional injection of a silylating mixture[2] followed by overnight conditioning of the column.

Total drug and metabolites were determined by heating the acidified urine for 2 hr at 100° before extraction, derivatization, and chromatography[3]. Metabolites were synthesized as reported earlier (1, 4).

Protocol—Two healthy male subjects (Subject 1, 27 years, 58 kg; Subject 2, 42 years, 61.4 kg) did not ingest other drugs or alcoholic beverages for 2 days prior and 3 days after ingestion of probenecid. After fasting overnight, the initial morning urine sample was taken for use as an analytical control. Since the absorption of many drugs having poor water solubility is known to be dissolution rate limited, the dose of probenecid (0.5, 1, and 2 g) was administered orally in solution. The drug[4] was dissolved in 200 ml of 2–3% sodium bicarbonate, the minimum quantity required for complete solution. In one case (2-g dose, Subject 2), the dose was dissolved in 200 ml of dilute

[1] Perkin-Elmer Mark II.
[2] Silyl-8, Pierce Chemical Co., Rockford, Ill.
[3] The analytical procedures were reported in detail (7).
[4] Pure drug powder, Merck Sharp and Dohme, West Point, Pa.

Table I—Excretion of Probenecid and Its Metabolites in the Urine of Human Subjects[a]

Subject	Dose, mg	Total Excreted, % of Dose	Relative Amounts of Probenecid and Metabolites Excreted, % of Total Urinary Excretion				
			Probenecid	Probenecid Acyl Glucuronide	Mono-*N*-propyl Metabolite[b]	Carboxylic Acid Metabolite[b]	Secondary Alcohol Metabolite[b]
1	500	80.7	16.5	41.8	10.5	15.0	16.3
	1000	76.7	10.7	47.2	11.0	15.4	15.9
	2000	87.8	10.3	38.6	15.8	17.1	18.7
2	500	86.4	4.8	55.6	13.8	11.0	15.8
	500	87.3	8.9	54.3	10.1	11.6	15.1
	1000	87.2	4.5	50.8	14.4	13.2	17.0
	2000	84.2	5.4	51.1	15.3	14.0	14.2

[a] Amounts represent the total of each metabolite excreted over periods of approximately 48, 72, and 85 hr following the 0.5-, 1.0-, and 2.0-g doses, respectively. [b] Free form only; conjugated form amounted to less than 3% of dose.

sodium hydroxide, which gave a solution of pH 7. This change allowed an examination of the effect of the medium on the disposition of the drug.

No solid food or beverages were ingested for 2 hr after medication. To stimulate urine flow, 100 ml of water was taken each hour for 7 hr after medication. Urine was collected every 2 hr for the first 8 hr and then *ad libitum* until no drug or metabolites were detectable in urine (48–85 hr). The urine volume was measured and the pH was determined[5] immediately, and the samples were then stored in a freezer until analyzed. Periodic analysis of selected urine samples showed that the composition of urine remained unchanged during storage. At least a 2-week interval was allowed before administering a second dose to either subject.

RESULTS AND DISCUSSION

Excretion of Probenecid and Its Metabolites in Urine—It is apparent from Table I that 80–88% of orally administered probenecid was recovered from urine, mainly in the form of the conjugated drug and its oxidized metabolites. Perel *et al.* (2) also recovered a mean of about 75% of a 2.0-g oral dose of ^{14}C-labeled probenecid in the 0–48-hr urine of two subjects. The lack of complete recovery may suggest incomplete absorption and/or enterohepatic cycling of the drug. However, the consistent recovery over the range of doses from 0.5 to 2.0 g suggests that absorption is at least constant, if not complete, and, therefore, supports the idea that some drug is excreted in bile and eliminated in the feces because of incomplete reabsorption. Verification of biliary excretion would require intravenous administration of the drug, for which it is difficult to obtain the necessary permission using human subjects[6].

The results in Table I also show that the relative amounts excreted in the form of the various metabolites remains essentially unchanged at the three doses. These results, therefore, do not support the earlier speculation (5) that the rate of metabolism is slower at the higher (2.0

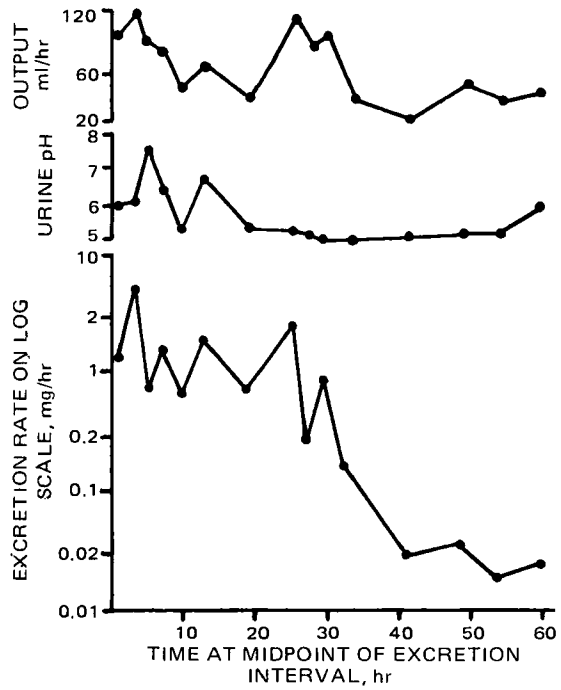

Figure 1—*Semilogarithmic plot of urinary excretion rate of probenecid and plots of urinary pH and urinary output against the time of midpoints of the excretion intervals for Subject 2 following a 1-g dose of probenecid.*

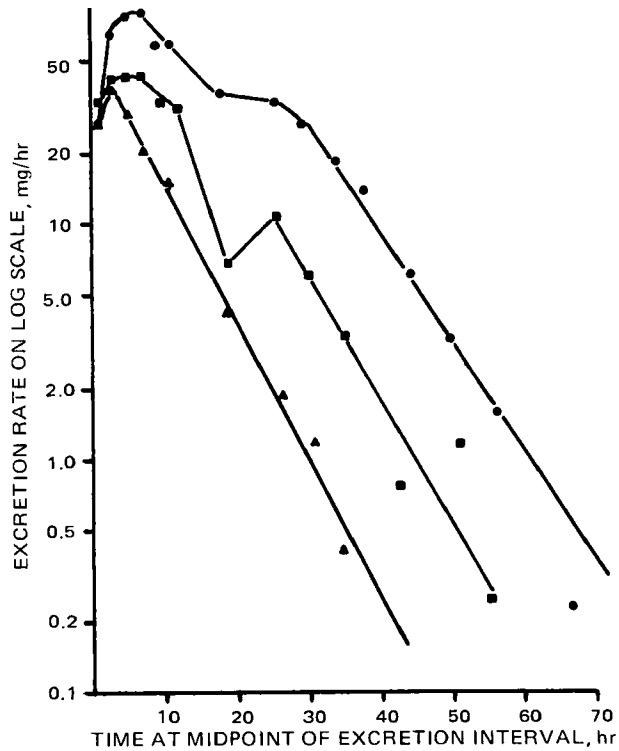

Figure 2—*Semilogarithmic plot of urinary excretion rate of probenecid metabolites against the time of midpoints of the excretion intervals for Subject 1 following 0.5- (▲), 1.0- (■), and 2.0- (●) g doses of probenecid. Excretion rate is expressed in terms of the amount (milligrams) of probenecid molecularly equivalent to the metabolites excreted.*

[5] Beckman Expandomatic pH meter, Beckman Instruments Inc., Fullerton, Calif.

[6] M. Gibaldi, State University of New York, Buffalo, N.Y., personal communication.

Table II—Terminal Half-Lives (in Hours) of Probenecid as Determined from Urinary Excretion Data for Different Metabolites at Various Doses[a]

Subject	Dose, mg	Mono-*N*-propyl Metabolite	Carboxylic Acid Metabolite	Secondary Alcohol Metabolite	Probenecid Acyl Glucuronide	Sum of Metabolites	
						Sigma-Minus	Excretion Rate
1	500	4.95	4.61	5.23	4.77	4.37	5.16
	1000	6.43	7.11	6.87	5.78	5.39	5.79
	2000	5.88	5.91	5.68	5.37	5.80	5.89
2	500	4.73	4.33	5.52	4.72	4.20	4.90
	500	4.27	5.32	4.61	4.94	4.91	5.43
	1000	4.71	5.12	5.52	4.55	5.95	5.44
	2000	4.04	4.37	4.58	4.08	5.51	5.36

[a] Obtained from slopes of the regression lines calculated for the apparently linear terminal portion of the plots. The *r* (coefficient of regression) values in all cases ranged from 0.92 to 0.99.

g) dose as compared to that at the lower dose (0.5 g). One would expect a decrease in the rate of metabolism at higher doses to result from the saturation of one or more metabolic pathways, thereby converting the apparent first-order kinetics observed for the particular pathway at lower doses to a zero-order process. This result would be reflected in an altered pattern of urinary metabolites at saturation doses as compared with lower doses, which was not observed.

These results, therefore, suggest that no individual metabolic pathway is saturated, since it would be unreasonable to expect all pathways to exhibit an equal degree of saturation as a function of dose. A single rate-limiting step common to all metabolic pathways, which is saturable at high doses, might be postulated. For example, transport of the drug to the site(s) of metabolism might be capacity limited, but such a thesis is difficult to reconcile with present-day knowledge of drug metabolism.

The relative amounts of metabolites recovered in urine in this study are in excellent agreement with those reported by Perel *et al.* (2). They found that about 2% of the dose was excreted as the primary alcohol metabolite, which was not found in measurable quantities in the present study. This finding is consistent with *in vitro* studies where the primary alcohol metabolite was observed to be readily oxidized to the carboxylic acid (8).

Effect of Urine pH and Urine Flow Rate on Excretion of Unchanged Probenecid—While the fractions of the administered dose excreted in the forms of conjugated probenecid and its oxidation products were about the same for both subjects (Table I), there was a two- to three-fold difference in the fraction excreted as unchanged probenecid by the two subjects. It is well known that probenecid is almost totally reabsorbed from renal tubules, thus reducing its excretion in urine in unchanged form to trace amounts (2–5), particularly where the urine is acidic. In dogs and humans, where metabolic alkalosis was induced by intravenous infusion of sodium bicarbonate, the renal clearance of probenecid increased greatly (9, 10).

This pH-dependent elimination of probenecid explains the differences in the urinary excretion of the drug observed in the present study. The pH of blank urine samples collected from Subject 1 was close to neutral (pH 6–7); for Subject 2, the pH was generally about 1 unit lower. A corresponding difference in pH was noticeable following administration of probenecid, particularly in the first few hours. As a result of the administration of a considerable amount of sodium bicarbonate solution, the urine pH typically rose to about 8–8.5 in Subject 1; it rose to only 7–7.5 in Subject 2. Therefore, it is

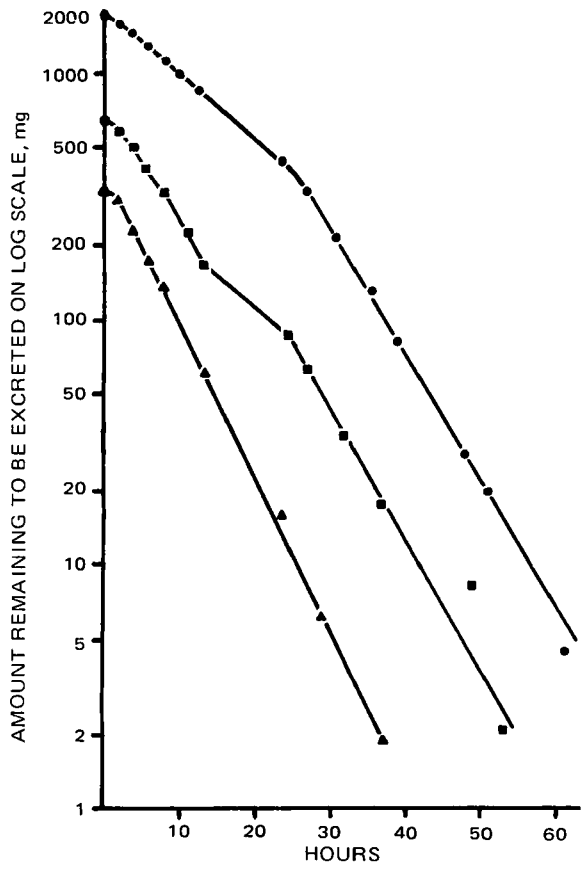

Figure 3—*Semilogarithmic plot of amount of probenecid metabolites remaining to be excreted (sigma-minus) against time for Subject 1 following 0.5- (▲), 1.0- (■), and 2.0- (●) g doses of probenecid. Amounts (milligrams) are expressed as probenecid molecularly equivalent to the metabolites.*

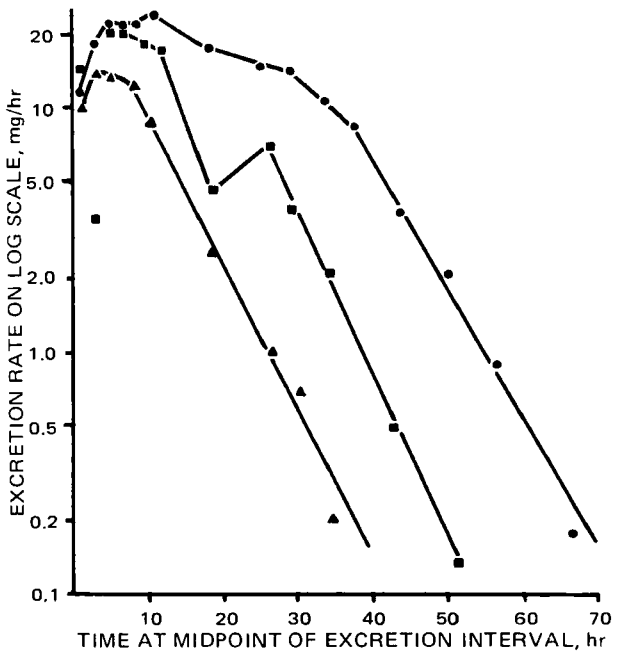

Figure 4—*Semilogarithmic plot of urinary excretion rate of probenecid acyl glucuronide against the time of midpoints of the excretion intervals for Subject 1 following 0.5- (▲), 1.0- (■), and 2.0- (●) g doses of probenecid.*

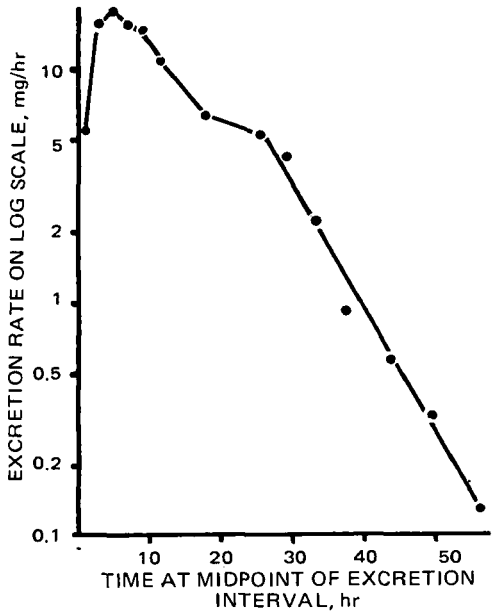

Figure 5—*Semilogarithmic plot of urinary excretion rate of the secondary alcohol metabolite against the time of midpoints of the excretion intervals for Subject 1 following a 2.0-g dose of probenecid. Excretion rate is expressed in terms of the amount (milligrams) of probenecid molecularly equivalent to the metabolites excreted.*

not surprising that a larger fraction of the dose was excreted unchanged in Subject 1 as compared to Subject 2.

There was no direct correlation between urinary pH and renal excretion of probenecid in this study. Probenecid is a weak acid with a pKa of 3.4 and is, therefore, completely ionized (>99.9%) at pH values of 6.4 and greater. Even at pH 5.0, the lowest urine pH observed in this study, 97.6% of the drug would exist in the ionized form. The present results indicate that the tubular reabsorption of probenecid is essentially complete even when the urine pH is well above the pKa of the drug. A completely quantitative explanation for this observation

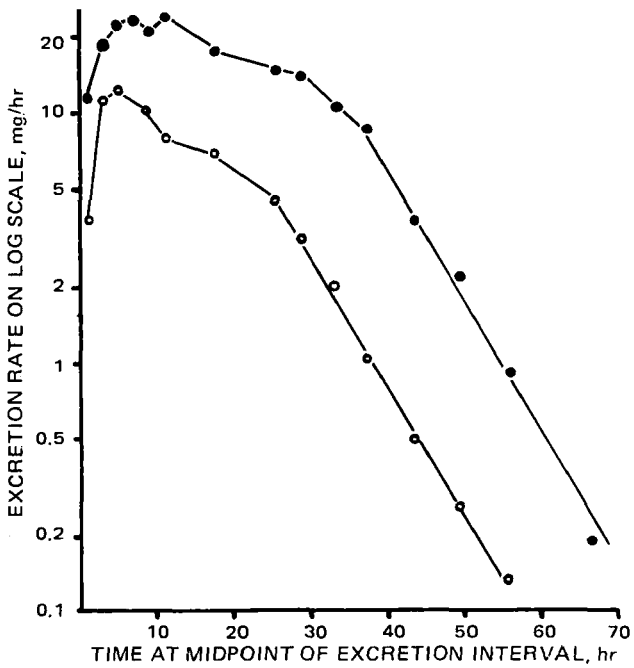

Figure 6—*Semilogarithmic plot of urinary excretion rate of probenecid acyl glucuronide (●) and the mono-N-propyl metabolite (○) in Subject 1 following a 2.0-g dose of probenecid. Excretion rate is expressed in terms of the amount (milligrams) of probenecid molecularly equivalent to the metabolites excreted.*

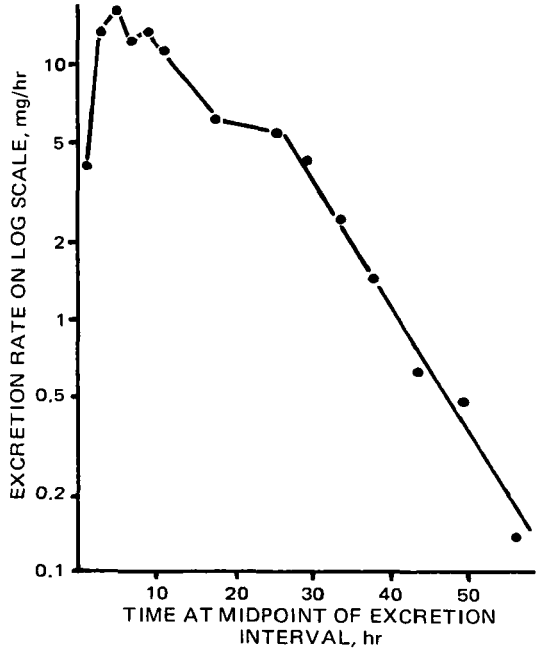

Figure 7—*Semilogarithmic plot of urinary excretion rate of the carboxylic acid metabolite against the time of midpoints of the excretion intervals for Subject 1 following a 2.0-g dose of probenecid. Excretion rate is expressed in terms of the amount (milligrams) of probenecid molecularly equivalent to the metabolites excreted.*

is difficult to formulate, since renal tubular reabsorption of a drug is dependent on both its physicochemical properties (pKa and lipid solubility) and the urine flow rate. The task is further complicated by the lack of information relating the pH of the tubular fluids at various segments of the nephron to the final urine pH.

It was reported that the urinary excretion of probenecid by dogs is flow rate dependent (9). A dependence on flow rate was also apparent in both subjects in the present study. A typical illustration is shown in Fig. 1. Over the interval from 20 to 55 hr, where the pH remained constant, the excretion pattern of probenecid mimicked the pattern for urine flow rate.

In view of the dependence of probenecid elimination on both urine pH and urine flow rate and because of the prolonged period required for absorption of the orally administered drug, a meaningful elimination half-life for probenecid cannot be obtained from plots, such as Fig. 1, of the unchanged drug excreted in urine.

Time Course of Urinary Excretion of Probenecid and Its Metabolites—The urinary excretion data were analyzed by the techniques suggested by Martin (11). Excretion rate plots and sigma-minus plots for the total drug excreted by Subject 1, as expressed by the sum of probenecid metabolites, are presented in Figs. 2 and 3. An excretion rate plot for probenecid acyl glucuronide is presented in Fig. 4. Figures 5–7 show the excretion rate plots for individual metabolites in Subject 1 following the 2.0-g dose. Corresponding plots of the data for Subject 2 were very similar. Half-lives for the excretion of individual metabolites for both subjects were estimated from regression lines calculated for the terminal portions of the plots and are summarized in Table II.

The results in Table II and Figs. 5–7 show that the half-lives for excretion of each metabolite do not differ significantly. Figures 5–7 show that the shapes of the excretion curves are similar for all metabolites, suggesting that each metabolite does not affect excretion of the others. The last two columns in Table II show that the half-lives calculated from the total dose excreted, as measured by the sum of all metabolites, are also in good agreement with those based on excretion of individual metabolites. The apparent half-lives calculated from the terminal portions of these curves for all doses lie in the range of about 4–7 hr. However, at any one dose, the variation in half-lives for individual metabolites is much less.

These results strongly suggest that the overall rate of metabolism is much slower than the rate of excretion in the dose range studied. In addition, negligible amounts of probenecid are excreted during the terminal phase where linear elimination kinetics are observed.

Therefore, the half-life of elimination by metabolism, obtained from the urinary excretion plots, represents the half-life for elimination of probenecid during the terminal excretion phase and is represented as such in Table II.

It can be seen from Figs. 2 and 3 that the time required for elimination of the dose is extended appreciably as the dose is increased. This appears to be due to a prolonged absorption of the drug. The apparent absorptive phase was about 10 hr for the 0.5-g dose and increased to 30–40 hr for the 2.0-g dose. The curvature in the sigma-minus plots at the 2.0-g dose suggests some type of saturation. In this connection, it is interesting to examine the excretion of the major metabolite, probenecid acyl glucuronide.

The maximum excretion rate was roughly constant at about 20 mg/hr over 5–30 hr for the 2.0-g dose for both subjects. Data from Subject 1 are presented in Fig. 4. For the 1-g dose, the maximum excretion rate was also about 20 mg/hr over 5–20 hr. For the 0.5-g dose, the excretion rate reached a maximum of approximately 15 mg/hr about 5 hr after medication and immediately began to decline.

The other metabolites exhibited similar plateaus in their excretion rate plots as shown in Figs. 5–7, where the excretion rates of the mono-*N*-propyl, carboxylic acid, and secondary alcohol metabolites are also seen to plateau at about 10–15 mg/hr. This parallel can be seen in Table I, which demonstrates that the fractions of the drug recovered in urine in the form of these metabolites are about equal. This apparent saturation could result from a single rate-limiting step in a sequential process of metabolism as mentioned earlier. Saturation of urinary excretion offers another possible explanation, but the results of Perel *et al.* (2) indicate that urinary excretion is not saturated.

The poor solubility of probenecid in water suggests a more likely explanation. The solubility of probenecid in water at 37° was determined to be about 50 μg/ml. Therefore, higher doses of the drug administered in solution possibly could have precipitated in the GI tract. The presence of insoluble probenecid in the GI tract would cause the absorption process to be dissolution rate limited (zero order), making the drug available for metabolism at a constant rate until all precipitated drug redissolved. Blood level data, as well as excretion data following intravenous administration of probenecid, would be useful in further resolving the mechanism of absorption, distribution, and elimination of the drug.

REFERENCES

(1) A. M. Guarino, W. D. Conway, and H. M. Fales, *Eur. J. Pharmacol.*, **8**, 244(1969).

(2) J. M. Perel, R. F. Cunningham, H. M. Fales, and P. G. Dayton, *Life Sci.*, **9** (Part I), 1337(1970).

(3) K. Sabih, C. D. Klaassen, and K. Sabih, *J. Pharm. Sci.*, **60**, 745(1971).

(4) W. D. Conway and S. K. Melethil, *ibid.*, **63**, 1551(1974).

(5) P. G. Dayton, T. F. Yu, W. Chen, L. Berger, L. A. West, and A. B. Gutman, *J. Pharmacol. Exp. Ther.*, **140**, 278(1963).

(6) P. G. Dayton, S. A. Cucinell, M. Weiss, and J. M. Perel, *ibid.*, **158**, 305(1967).

(7) W. D. Conway and S. Melethil, *J. Chromatogr.*, **115**, 222(1975).

(8) Z. H. Israeli, R. F. Cunningham, and P. G. Dayton, *Fed. Proc.*, **30**, 226(1971).

(9) I. M. Weiner, J. A. Washington, and G. H. Mudge, *Bull. Johns Hopkins Hosp.*, **106**, 333(1960).

(10) J. M. Perel, P. G. Dayton, T. F. Yu, and A. B. Gutman, *Eur. J. Clin. Pharmacol.*, **3**, 106(1971).

(11) B. K. Martin, *Br. J. Pharmacol. Chemother.*, **29**, 181(1967).

ACKNOWLEDGMENTS AND ADDRESSES

Received August 26, 1974, from the *Department of Pharmaceutics, School of Pharmacy, State University of New York at Buffalo, Buffalo, NY 14207*

Accepted for publication August 15, 1975.

Presented at the APhA Academy of Pharmaceutical Sciences, Chicago meeting, August 1974.

Supported in part by General Research Support Grant 5-S01 RR 05454-10 from the National Institutes of Health, Bethesda, MD 20014

* Present address: College of Pharmacy, North Dakota State University, Fargo, ND 58102

ˣ To whom inquiries should be directed.

Rapid Determination of Theophylline in Human Plasma by High-Pressure Liquid Chromatography

ORVILLE H. WEDDLE ˣ and WILLIAM D. MASON

Abstract □ A rapid, specific, high-pressure liquid chromatographic method for the determination of theophylline in plasma was developed. The procedure is fast enough (21 min from receipt of blood to reporting value) to be used for emergency determinations. The sensitivity, precision, and accuracy are sufficient for routine monitoring of therapeutic levels in patients. The assay is specific enough to be valid in the presence of caffeine and theobromine. Metabolites of theophylline as well as a number of drugs do not interfere with the assay.

Keyphrases □ Theophylline—high-pressure liquid chromatographic analysis, plasma □ High-pressure liquid chromatography—analysis, theophylline, plasma □ Relaxants, smooth muscle—theophylline, high-pressure liquid chromatographic analysis, plasma

Many patients receive theophylline for the prevention and treatment of asthmatic attacks. Several investigations showed good correlation between the plasma concentrations of theophylline and the improvement of pulmonary function in asthmatic patients (1–3). Recent reviews of pharmacokinetic control of drug therapy (4, 5) suggested that monitoring of blood theophylline levels can contribute significantly to the control of therapy of asthmatics. Unfortunately, these benefits are of limited application to the emergency care situation. Present methods of analysis either lack specificity or are too time consuming to contribute to the rapid adjustment of theophylline levels in the patient admitted for acute asthmatic attack where a subtherapeutic theophylline level may or may not be a contributing cause.

The method of theophylline analysis most widely used at present is that of Schack and Waxler (6). This procedure is not suited to monitoring theophylline therapy in many emergency situations since caffeine, theobromine, and other dietary xanthines that may be present in the patient are not distinguished from theophylline. It is used where patients can be placed on

Therefore, the half-life of elimination by metabolism, obtained from the urinary excretion plots, represents the half-life for elimination of probenecid during the terminal excretion phase and is represented as such in Table II.

It can be seen from Figs. 2 and 3 that the time required for elimination of the dose is extended appreciably as the dose is increased. This appears to be due to a prolonged absorption of the drug. The apparent absorptive phase was about 10 hr for the 0.5-g dose and increased to 30–40 hr for the 2.0-g dose. The curvature in the sigma-minus plots at the 2.0-g dose suggests some type of saturation. In this connection, it is interesting to examine the excretion of the major metabolite, probenecid acyl glucuronide.

The maximum excretion rate was roughly constant at about 20 mg/hr over 5–30 hr for the 2.0-g dose for both subjects. Data from Subject 1 are presented in Fig. 4. For the 1-g dose, the maximum excretion rate was also about 20 mg/hr over 5–20 hr. For the 0.5-g dose, the excretion rate reached a maximum of approximately 15 mg/hr about 5 hr after medication and immediately began to decline.

The other metabolites exhibited similar plateaus in their excretion rate plots as shown in Figs. 5–7, where the excretion rates of the mono-*N*-propyl, carboxylic acid, and secondary alcohol metabolites are also seen to plateau at about 10–15 mg/hr. This parallel can be seen in Table I, which demonstrates that the fractions of the drug recovered in urine in the form of these metabolites are about equal. This apparent saturation could result from a single rate-limiting step in a sequential process of metabolism as mentioned earlier. Saturation of urinary excretion offers another possible explanation, but the results of Perel *et al.* (2) indicate that urinary excretion is not saturated.

The poor solubility of probenecid in water suggests a more likely explanation. The solubility of probenecid in water at 37° was determined to be about 50 μg/ml. Therefore, higher doses of the drug administered in solution possibly could have precipitated in the GI tract. The presence of insoluble probenecid in the GI tract would cause the absorption process to be dissolution rate limited (zero order), making the drug available for metabolism at a constant rate until all precipitated drug redissolved. Blood level data, as well as excretion data following intravenous administration of probenecid, would be useful in further resolving the mechanism of absorption, distribution, and elimination of the drug.

REFERENCES

(1) A. M. Guarino, W. D. Conway, and H. M. Fales, *Eur. J. Pharmacol.*, **8**, 244(1969).

(2) J. M. Perel, R. F. Cunningham, H. M. Fales, and P. G. Dayton, *Life Sci.*, **9** (Part I), 1337(1970).

(3) K. Sabih, C. D. Klaassen, and K. Sabih, *J. Pharm. Sci.*, **60**, 745(1971).

(4) W. D. Conway and S. K. Melethil, *ibid.*, **63**, 1551(1974).

(5) P. G. Dayton, T. F. Yu, W. Chen, L. Berger, L. A. West, and A. B. Gutman, *J. Pharmacol. Exp. Ther.*, **140**, 278(1963).

(6) P. G. Dayton, S. A. Cucinell, M. Weiss, and J. M. Perel, *ibid.*, **158**, 305(1967).

(7) W. D. Conway and S. Melethil, *J. Chromatogr.*, **115**, 222(1975).

(8) Z. H. Israeli, R. F. Cunningham, and P. G. Dayton, *Fed. Proc.*, **30**, 226(1971).

(9) I. M. Weiner, J. A. Washington, and G. H. Mudge, *Bull. Johns Hopkins Hosp.*, **106**, 333(1960).

(10) J. M. Perel, P. G. Dayton, T. F. Yu, and A. B. Gutman, *Eur. J. Clin. Pharmacol.*, **3**, 106(1971).

(11) B. K. Martin, *Br. J. Pharmacol. Chemother.*, **29**, 181(1967).

ACKNOWLEDGMENTS AND ADDRESSES

Received August 26, 1974, from the *Department of Pharmaceutics, School of Pharmacy, State University of New York at Buffalo, Buffalo, NY 14207*

Accepted for publication August 15, 1975.

Presented at the APhA Academy of Pharmaceutical Sciences, Chicago meeting, August 1974.

Supported in part by General Research Support Grant 5-S01 RR 05454-10 from the National Institutes of Health, Bethesda, MD 20014

* Present address: College of Pharmacy, North Dakota State University, Fargo, ND 58102

ˣ To whom inquiries should be directed.

Rapid Determination of Theophylline in Human Plasma by High-Pressure Liquid Chromatography

ORVILLE H. WEDDLE ˣ and WILLIAM D. MASON

Abstract □ A rapid, specific, high-pressure liquid chromatographic method for the determination of theophylline in plasma was developed. The procedure is fast enough (21 min from receipt of blood to reporting value) to be used for emergency determinations. The sensitivity, precision, and accuracy are sufficient for routine monitoring of therapeutic levels in patients. The assay is specific enough to be valid in the presence of caffeine and theobromine. Metabolites of theophylline as well as a number of drugs do not interfere with the assay.

Keyphrases □ Theophylline—high-pressure liquid chromatographic analysis, plasma □ High-pressure liquid chromatography—analysis, theophylline, plasma □ Relaxants, smooth muscle—theophylline, high-pressure liquid chromatographic analysis, plasma

Many patients receive theophylline for the prevention and treatment of asthmatic attacks. Several investigations showed good correlation between the plasma concentrations of theophylline and the improvement of pulmonary function in asthmatic patients (1–3). Recent reviews of pharmacokinetic control of drug therapy (4, 5) suggested that monitoring of blood theophylline levels can contribute significantly to the control of therapy of asthmatics. Unfortunately, these benefits are of limited application to the emergency care situation. Present methods of analysis either lack specificity or are too time consuming to contribute to the rapid adjustment of theophylline levels in the patient admitted for acute asthmatic attack where a subtherapeutic theophylline level may or may not be a contributing cause.

The method of theophylline analysis most widely used at present is that of Schack and Waxler (6). This procedure is not suited to monitoring theophylline therapy in many emergency situations since caffeine, theobromine, and other dietary xanthines that may be present in the patient are not distinguished from theophylline. It is used where patients can be placed on

dietary restrictions for at least 24 hr prior to analysis. Gupta and Lundberg (7) used differential spectrophotometry to measure blood theophylline levels. No data were given on the effects of caffeine and theobromine on their assay.

Several assays have been reported that are specific enough to measure theophylline in the presence of caffeine, theobromine, and other interfering substances. These assays can be evaluated further by estimating the time required for a duplicate assay (T_d). This time should be the total time from receipt of a whole blood sample to reporting of results.

Shah and Riegelman (8) reported a GC method that distinguished theophylline from its metabolites and from caffeine. They used a separation procedure involving four extraction steps so that a T_d of 1 hr or more can be estimated from their data. Thompson *et al.* (9) described a high-pressure liquid chromatographic (HPLC) method for the determination of theophylline and its metabolites in blood and urine. Theophylline was well separated from caffeine, theobromine, and the metabolites of theophylline, caffeine, and theobromine. Analysis time was decreased by the finding that diluted plasma could be injected directly on column. On the other hand, the retention time of theophylline on the column was 20 min so the T_d might have been about 1 hr. Finally, Manion *et al.* (10) used a reversed-phase, gradient elution, HPLC method for theophylline. Since the chromatographic run lasted about 30 min, the T_d might have been more than 1 hr.

Thus, assays have been developed that are specific enough to determine blood theophylline levels in the presence of dietary xanthines and their metabolites. A need remains, however, for a method that is not only specific but fast enough to be used in emergency treatment. This paper describes a method with a T_d of 21 min. The method has been shown to measure accurately theophylline levels in the presence of caffeine, theobromine, theophylline metabolites, and a number of drugs often present in patients taking theophylline.

EXPERIMENTAL

Materials—UV grade hexane[1], 2-butanol[1], methanol[1], USP theophylline reference standard[2], theobromine[3], caffeine[4], and 3-methylxanthine[5] were used as obtained.

Apparatus—A high-pressure liquid chromatograph[6] equipped with a "septumless" injection port and a fixed wavelength (280 nm) UV absorption detector was used. The detector was operated at 0.01 absorbance unit full scale for most samples.

Chromatographic Parameters—The mobile phase contained 1% distilled water, 5% methanol, and 25% 2-butanol in *n*-hexane. The mobile phase was pumped at 3.33 ml/min at 25° through a stainless steel column (30.48 cm × 4 mm i.d.) packed with a high efficiency absorption packing[7]. It was found that connecting 25 cm of 0.25-mm i.d. tubing to the output of the UV detector flowcell made it unnecessary to "degas" the mobile phase. Aliquots (150 μl) of the extraction solution were injected directly on-column with a 250-μl syringe[8] using a stop-flow technique.

[1] Burdick and Jackson Laboratories, Muskegon, Mich.
[2] U.S.P.C. Inc., Rockville, Md.
[3] Mallinckrodt Chemical Works, St. Louis, Mo.
[4] Eastman Organic Chemicals, Rochester, N.Y.
[5] CYCLO Chemical Corp., Los Angeles, Calif.
[6] Model 4100, Varian Aerograph, Walnut Creek, Calif.
[7] μ-Porasil, Waters Associates, Milford, Mass.
[8] Model 725, Hamilton Co., Reno, Nev.

Table I—Separation of Theophylline from Other Compounds by HPLC[a]

Compound	Quantity of Solution[b] Injected: Volume, μl	Quantity of Solution[b] Injected: Concentration, μg/ml	Retention Time, min
Theophylline	10	25	2.9
Caffeine	10	50	5.9
Theobromine	100	10	7.4
3-Methylxanthine	100	0.5	3.5
1-Methyluric acid	100	5.0	6.6
1,3-Dimethyluric acid	100	Saturated	9.1

[a] μ-Porasil, conditions as described in the text. [b] Extraction solvent described in text.

Analytical Procedure—Two 0.5-ml aliquots of each plasma sample to be analyzed were placed in 15-ml screw-topped centrifuge tubes. Each tube received 0.3 ml of saturated ammonium sulfate solution and 5.0 ml of 40% 2-butanol in *n*-hexane. The two tubes were vortexed together for 30 sec and then centrifuged for 2 min at 3400 rpm. After centrifugation, 150 μl of the supernate from the first tube was drawn up into a 250-μl syringe[8] and injected into the chromatograph.

Six minutes after the first injection, 150 μl from the second tube was injected. Four minutes after the second injection, the chromatogram was removed and the peak heights were measured in millimeters. The peak heights were converted to plasma theophylline concentrations by comparison to a standard curve.

Preparation of Standard Curve—A theophylline stock solution of 0.500 μg/μl was prepared by dissolving a weighed sample of drug standard in methanol. Aliquots of 5, 10, 15, 20, 25, and 30 μl were added to 15-ml screw-topped centrifuge tubes. After the methanol was evaporated with a nitrogen stream at ambient temperature, 0.5 ml of pooled human plasma was added to each tube. The tubes were vortexed to dissolve the theophylline and then extracted and analyzed by the described procedure.

Fifteen analyses were done at each concentration: 5, 10, 15, 20, 25, and 30 μg/ml. The heights of the chromatogram peaks were measured in millimeters, and the average and standard deviation of the peak heights were taken at each concentration. A straight-line fit of the data was made by linear regression analysis, and the correlation coefficient was determined.

Evaluation of Accuracy and Precision—The accuracy and precision of the method were evaluated by performing 60 duplicate analyses on spiked samples of human plasma. Fifteen duplicate analyses were performed at each concentration: 5, 10, 15, and 20 μg/ml. The spiked samples were prepared by adding appropriate aliquots of the 0.50-μg/ml stock solution to 15-ml centrifuge tubes, evaporating the methanol in a nitrogen stream, and then dissolving the theophylline in 0.5-ml aliquots of plasma from selected plasma samples.

The 60 plasma samples used were left over from blood samples originally drawn for analyses of phenobarbital, phenytoin, quinidine, procainamide, or salicylate from patients known not to be receiving theophylline preparations. After preparation, the spiked samples were analyzed as described, and the mean and standard deviation of the measured values were determined.

Evaluation of Interferences—The retention times of caffeine, theobromine, 3-methylxanthine, 1-methyluric acid, and 1,3-dimethyluric acid were determined by injection of solutions of these drugs in the extraction solvent into the liquid chromatograph. The volumes and concentrations injected, as well as the retention times determined, are given in Table I. Possible interferences from quinidine, primidone, phenobarbital, phenytoin, salicylic acid, aspirin, diazepam, chlordiazepoxide, and ephedrine were evaluated by performing the theophylline analysis on samples of plasma from patients receiving these drugs but not theophylline. In each case, the patient sample had therapeutic levels of the drug being evaluated for possible interference.

RESULTS AND DISCUSSION

Figure 1*b* shows the chromatogram for a single 150-μl injection of the extract of a plasma sample to which 15 μg/ml of theophylline had

Table II—Accuracy and Precision of Theophylline HPLC Assay

Theophylline Added, μg/ml	Theophylline Found[a], μg/ml	SD, %
5	5.09	4.54
10	9.89	2.43
15	14.98	2.42
20	19.78	2.07

[a] Mean of 15 assays, each done in duplicate.

been added. The method described under *Analytical Procedure* was used. Figure 1*a* shows the chromatogram of a 150-μl injection of a plasma sample that was extracted in exactly the same way but with no added theophylline. The peaks and baseline variations due to the addition of 150 μl of extraction solvent plus components extracted from plasma are seen to be complete prior to the theophylline peak.

The theophylline peak heights measured on the chromatograms were plotted against the concentration of theophylline in the plasma standard solutions in preparing a standard curve. When 15 plasma samples at each concentration (5, 10, 15, 20, 25, and 30 μg/ml, *i.e.*, a total of 90 determinations) were assayed, the line obtained by linear regression was described by $y = 8.21x - 2.52$ with a correlation coefficient of 1.00. Additional plasma standards were run from time to time over 4 months, during which 43 theophylline determinations were made on patient samples. The slope and intercept of the standard curve did not vary more than 5% during this period.

The accuracy and precision of the method are shown in Table II. The low percent standard deviations over the clinical range (10–20 μg/ml) show that the method is precise enough for normal clinical analysis problems. The higher percent standard deviation at 5 μg/ml suggests that the method might not be suitable for more exacting research studies in the subtherapeutic concentration range.

The retention times of a number of different substances that might interfere with theophylline determinations are given in Table I. All of these compounds were well separated from theophylline. In clinical samples, a small peak was often seen at the 3-methylxanthine position. Another small, broad peak was frequently seen at the caffeine position. Peaks corresponding to 1-methyluric acid and 1,3-dimethyluric acid were not seen, and they probably were not extracted.

A number of drugs that might be taken by patients also taking theophylline were tested for interference with the theophylline assay.

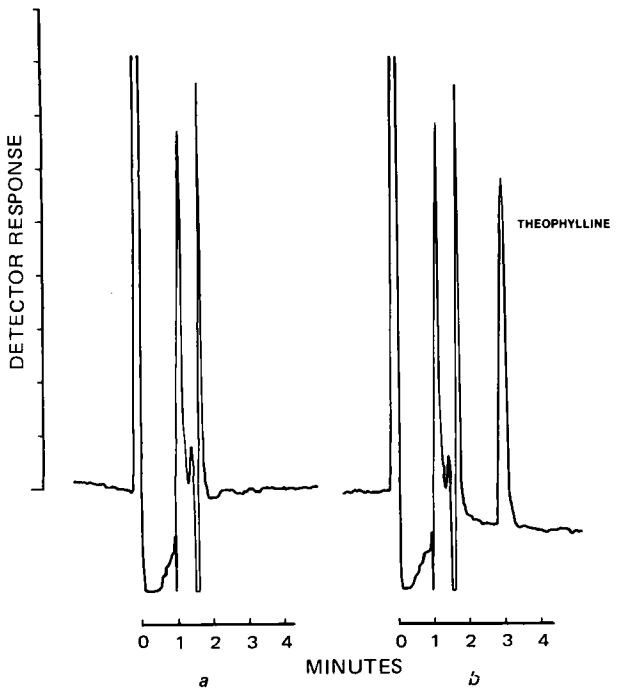

Figure 1—*High-pressure liquid chromatograms of human plasma extracts. Key:* a, *control plasma; and* b, *plasma containing 15.0 μg of theophylline/ml.*

Table III—Total Time Required for Duplicate Analysis of Whole Blood Samples for Theophylline[a]

Analytical Step	Time Required, min
Blood centrifugation	5.0
Pipetting of plasma and reagents	1.0
Vortexing	1.0
Centrifugation to separate phases	2.0
Handling of extract until first injection	1.0
Chromatographic time from first injection until second injection	6.0
Chromatographic time from second injection until removal of chart	4.0
Measuring peaks and calculation	1.0
Total time	21.0

[a] Conditions as described in the text.

Plasma samples from patients having therapeutic levels of phenobarbital, phenytoin, primidone, acetylsalicylate, ephedrine, diazepam, or chlordiazepoxide but no theophylline were analyzed. The samples were extracted and chromatographed in exactly the same way as for a theophylline analysis. In none of these cases was there a peak that would have given a false theophylline value. In some cases, this result was due to the fact that the potentially interfering drug or its metabolites did not extract under the assay conditions.

Table III illustrates that this quantitative assay can be done in 21 min from receipt of blood sample to reporting of data. Several measures were taken to attain this speed. Pipetting time was decreased by use of a transfer pipet[9] for plasma and for saturated ammonium sulfate. A dispenser[10] was used for the extraction solvent. The mobile phase velocity was the maximum the pump[6] would deliver. A mobile phase composition was chosen that gave the shortest retention time for theophylline which still allowed resolution of the theophylline peak from the 3-methylxanthine peak.

Quantization by peak height without an internal standard minimized the calculation time. The combination of normal-phase chromatography with an organic solvent extraction step minimized turnaround time since substances more polar than theophylline that would have been retained longer on the column were mostly eliminated by the extraction step. Finally, it is seen in Table I that the retention times of any caffeine or theobromine in the first extract would cause them to come off the column after injection of the second extract. In practice, if the second extract was injected 6 min after the first, the caffeine and theobromine peaks from the first extract came off the column before any theophylline in the second extract and did not interfere.

All of these timesaving steps were used in the analyses in which the accuracy and precision data were obtained. Thus, an analysis fast enough for emergency determinations has accuracy and precision sufficient for the routine monitoring of theophylline therapy.

REFERENCES

(1) P. A. Mitenko and R. I. Ogilvie, *N. Eng. J. Med.*, **289**, 600(1973).

(2) R. H. Jackson, J. I. McHenry, F. B. Moreland, W. J. Raymer, and R. L. Etter, *Dis. Chest*, **45**, 75(1964).

(3) R. Maselli, G. L. Casal, and E. F. Ellis, *J. Pediat.*, **76**, 777(1970).

(4) "Clinical Pharmacokinetics," G. Levy, Ed., APhA Academy of Pharmaceutical Sciences, Washington, D.C., 1974.

(5) V. Marks, W. E. Lindup, and E. M. Baylis, *Adv. Clin. Chem.*, **16**, 47(1973).

(6) J. A. Schack and S. H. Waxler, *J. Pharmacol. Exp. Ther.*, **97**, 283(1949).

(7) R. C. Gupta and G. D. Lundberg, *Anal. Chem.*, **45**, 2403(1973).

(8) V. P. Shah and S. Riegelman, *J. Pharm. Sci.*, **63**, 1283(1974).

(9) R. D. Thompson, H. T. Nagasawa, and J. W. Jenne, *J. Lab. Clin. Med.*, **84**, 584(1974).

[9] Model 0010-29 Biopette, Schwarz/Mann, Orangeburg, N.Y.

[10] A 10-ml Repipet, Labindustries, Berkeley, Calif.

(10) C. V. Manion, D. W. Shoeman, and D. L. Azaroff, *J. Chromatogr.*, **101**, 169(1974).

ACKNOWLEDGMENTS AND ADDRESSES

Received May 16, 1975, from the *School of Pharmacy, University of Missouri–Kansas City, Kansas City, MO 64108*

Accepted for publication August 13, 1975.

Supported in part by Grant D08PE05146-01 from the Department of Health, Education, and Welfare.

The authors thank the Clinical Pharmacy Faculty of the University of Missouri–Kansas City for assistance in this project.

[x] To whom inquiries should be directed.

Nitrofurantoin Solubility in Aqueous Urea and Creatinine Solutions

LIAN-KAUN CHEN, DONALD E. CADWALLADER [x], and HUNG WON JUN

Abstract □ Experiments were carried out to determine the effect of urea and creatinine on the solubility of nitrofurantoin in water at different temperature and pH conditions. The addition of urea to aqueous media increased nitrofurantoin solubility up to a maximum concentration level and then decreased solubility at higher urea concentrations. The amount of urea needed to bring about maximum nitrofurantoin solubility was dependent on temperature and ranged between 1.75 and 2.50%. Spectral studies suggest a possible interaction between urea and nitrofurantoin molecules. Nitrofurantoin solubility increased with an increasing creatinine concentration ranging from 0.05 to 1.6%. Spectral studies indicate a strong interaction between creatinine and nitrofurantoin molecules in solution. The combined effect of urea and creatinine on the solubility of nitrofurantoin could account for the absence of crystalluria with this drug, even though unusually high concentrations in urine have been reported.

Keyphrases □ Nitrofurantoin—solubility in aqueous solutions, effect of urea and creatinine, varying temperature and pH □ Urea—effect on aqueous solubility of nitrofurantoin, varying temperature and pH □ Creatinine—effect on aqueous solubility of nitrofurantoin, varying temperature and pH □ Solubility—nitrofurantoin in aqueous solutions, effect of urea and creatinine, varying temperature and pH

Nitrofurantoin, 1-[(5-nitrofurfurylidene)amino]-hydantoin, is an antibacterial agent widely used to treat urinary tract infections. It is a weak acid (pKa 7.2) possessing relatively low aqueous solubility characteristics. Solubility at 37° was reported to be 190 mg/liter in distilled water (1) and 125 mg/liter in pH 4.8 water (2). Bates *et al.*[1] (3) reported the solubility of this drug in water at pH 1.12 and 7.20 to be 154 and 374 mg/liter, respectively.

Nitrofurantoin concentrations in urine ranged from 250 to 500 mg/liter after 200 mg was administered every 6 hr to an 80-kg patient (4). Urine concentrations of 200–400 mg/liter were reported (5), and maximum urine nitrofurantoin concentrations ranged from 158 to 372 mg/liter in nine normal individuals, each of whom received a 100-mg tablet of drug every 4 hr for four doses (6). Although unusually high concentrations of nitrofurantoin are found in the urine, no case of crystalluria associated with nitrofurantoin therapy has been reported. These observations suggest that substances normally present in urine might affect the aqueous solubility of nitrofurantoin.

Preliminary findings indicated that urea initially increased nitrofurantoin solubility at low urea concentrations and then decreased solubility at higher urea concentrations (7). In the present study, an attempt was made to ascertain the effect of urea and another urine component, creatinine, on nitrofurantoin solubility at various temperatures and pH conditions.

EXPERIMENTAL

Materials—Nitrofurantoin[2] was used as received without further purification. Nitromethane[3] was spectrophotometric grade; urea, methyl alcohol, citric acid, creatinine[4], hydrochloric acid, disodium phosphate, and potassium chloride were reagent grade. A high molecular weight quaternary ammonium hydroxide solution[5] was diluted with absolute methanol to 0.04 *M*.

Equipment—A rotating apparatus[6], capable of holding multiple samples, was immersed in a water bath kept at constant temperature by a controlled-temperature circulating pump[7]. The pH values of aqueous systems were measured using a pH meter[8].

Preparation of Solution—McIlvaine's buffer solutions (pH 3–7) (8) were prepared by mixing appropriate volumes of 0.1 *M* citric acid and 0.2 *M* disodium phosphate solutions in deionized water.

Stock solutions of 0.2 *M* potassium chloride and 0.2 *M* hydrochloric acid were prepared with deionized water. Appropriate portions of the two were mixed and diluted to make the hydrochloric acid buffer solutions (pH 1.2–2.0). A 0.1 *M* hydrochloric acid solution was used for the pH 1.12 medium.

Appropriate amounts of urea and creatinine were dissolved in deionized distilled water or in various pH buffer solutions to make urea solutions ranging from 0.25 to 10% and creatinine solutions ranging from 0.05 to 2.0%.

Solubility Studies—Excess nitrofurantoin (~50 mg) was added to 40 ml of the appropriate test solution in a screw-capped bottle of 45-ml capacity. The tightly closed container was placed in a water bath at various temperatures (24, 30, 37, and 45 ± 0.1°) and rotated

[1] T. R. Bates, School of Pharmacy, State University of New York at Buffalo, personal communication. A lower value was erroneously reported in Ref. 3.

[2] A pure sample (Lot. E3769) was supplied by Eaton Laboratories, Norwich, N.Y.

[3] Aldrich Chemical Co., Milwaukee, Wis.

[4] Nutritional Biochemicals Corp., Cleveland, Ohio.

[5] Hyamine, Sigma Chemical Co., St. Louis, Mo.

[6] Menold, Lester, Pa.

[7] Haake E52, Berlin-Lichterfeid, West Germany.

[8] Photovolt-digicord, W. H. Curtin & Co.

(10) C. V. Manion, D. W. Shoeman, and D. L. Azaroff, *J. Chromatogr.*, **101**, 169(1974).

ACKNOWLEDGMENTS AND ADDRESSES

Received May 16, 1975, from the *School of Pharmacy, University of Missouri–Kansas City, Kansas City, MO 64108*

Accepted for publication August 13, 1975.

Supported in part by Grant D08PE05146-01 from the Department of Health, Education, and Welfare.

The authors thank the Clinical Pharmacy Faculty of the University of Missouri–Kansas City for assistance in this project.

[x] To whom inquiries should be directed.

Nitrofurantoin Solubility in Aqueous Urea and Creatinine Solutions

LIAN-KAUN CHEN, DONALD E. CADWALLADER [x], and HUNG WON JUN

Abstract □ Experiments were carried out to determine the effect of urea and creatinine on the solubility of nitrofurantoin in water at different temperature and pH conditions. The addition of urea to aqueous media increased nitrofurantoin solubility up to a maximum concentration level and then decreased solubility at higher urea concentrations. The amount of urea needed to bring about maximum nitrofurantoin solubility was dependent on temperature and ranged between 1.75 and 2.50%. Spectral studies suggest a possible interaction between urea and nitrofurantoin molecules. Nitrofurantoin solubility increased with an increasing creatinine concentration ranging from 0.05 to 1.6%. Spectral studies indicate a strong interaction between creatinine and nitrofurantoin molecules in solution. The combined effect of urea and creatinine on the solubility of nitrofurantoin could account for the absence of crystalluria with this drug, even though unusually high concentrations in urine have been reported.

Keyphrases □ Nitrofurantoin—solubility in aqueous solutions, effect of urea and creatinine, varying temperature and pH □ Urea—effect on aqueous solubility of nitrofurantoin, varying temperature and pH □ Creatinine—effect on aqueous solubility of nitrofurantoin, varying temperature and pH □ Solubility—nitrofurantoin in aqueous solutions, effect of urea and creatinine, varying temperature and pH

Nitrofurantoin, 1-[(5-nitrofurfurylidene)amino]-hydantoin, is an antibacterial agent widely used to treat urinary tract infections. It is a weak acid (pKa 7.2) possessing relatively low aqueous solubility characteristics. Solubility at 37° was reported to be 190 mg/liter in distilled water (1) and 125 mg/liter in pH 4.8 water (2). Bates *et al.*[1] (3) reported the solubility of this drug in water at pH 1.12 and 7.20 to be 154 and 374 mg/liter, respectively.

Nitrofurantoin concentrations in urine ranged from 250 to 500 mg/liter after 200 mg was administered every 6 hr to an 80-kg patient (4). Urine concentrations of 200–400 mg/liter were reported (5), and maximum urine nitrofurantoin concentrations ranged from 158 to 372 mg/liter in nine normal individuals, each of whom received a 100-mg tablet of drug every 4 hr for four doses (6). Although unusually high concentrations of nitrofurantoin are found in the urine, no case of crystalluria associated with nitrofurantoin therapy has been reported. These observations suggest that substances normally present in urine might affect the aqueous solubility of nitrofurantoin.

Preliminary findings indicated that urea initially increased nitrofurantoin solubility at low urea concentrations and then decreased solubility at higher urea concentrations (7). In the present study, an attempt was made to ascertain the effect of urea and another urine component, creatinine, on nitrofurantoin solubility at various temperatures and pH conditions.

EXPERIMENTAL

Materials—Nitrofurantoin[2] was used as received without further purification. Nitromethane[3] was spectrophotometric grade; urea, methyl alcohol, citric acid, creatinine[4], hydrochloric acid, disodium phosphate, and potassium chloride were reagent grade. A high molecular weight quaternary ammonium hydroxide solution[5] was diluted with absolute methanol to 0.04 *M*.

Equipment—A rotating apparatus[6], capable of holding multiple samples, was immersed in a water bath kept at constant temperature by a controlled-temperature circulating pump[7]. The pH values of aqueous systems were measured using a pH meter[8].

Preparation of Solution—McIlvaine's buffer solutions (pH 3–7) (8) were prepared by mixing appropriate volumes of 0.1 *M* citric acid and 0.2 *M* disodium phosphate solutions in deionized water.

Stock solutions of 0.2 *M* potassium chloride and 0.2 *M* hydrochloric acid were prepared with deionized water. Appropriate portions of the two were mixed and diluted to make the hydrochloric acid buffer solutions (pH 1.2–2.0). A 0.1 *M* hydrochloric acid solution was used for the pH 1.12 medium.

Appropriate amounts of urea and creatinine were dissolved in deionized distilled water or in various pH buffer solutions to make urea solutions ranging from 0.25 to 10% and creatinine solutions ranging from 0.05 to 2.0%.

Solubility Studies—Excess nitrofurantoin (~50 mg) was added to 40 ml of the appropriate test solution in a screw-capped bottle of 45-ml capacity. The tightly closed container was placed in a water bath at various temperatures (24, 30, 37, and 45 ± 0.1°) and rotated

[1] T. R. Bates, School of Pharmacy, State University of New York at Buffalo, personal communication. A lower value was erroneously reported in Ref. 3.

[2] A pure sample (Lot. E3769) was supplied by Eaton Laboratories, Norwich, N.Y.

[3] Aldrich Chemical Co., Milwaukee, Wis.

[4] Nutritional Biochemicals Corp., Cleveland, Ohio.

[5] Hyamine, Sigma Chemical Co., St. Louis, Mo.

[6] Menold, Lester, Pa.

[7] Haake E52, Berlin-Lichterfeid, West Germany.

[8] Photovolt-digicord, W. H. Curtin & Co.

Table I—Solubilities and Enthalpy Values of Nitrofurantoin in Distilled Water

Temperature	Solubility, mg/liter	Mole Fraction × 10^6	Enthalpy (ΔH)[a], kcal/mole
24°	79.5	6.01	18.70
30°	113.4	8.57	4.60
37°	174.1	13.16	4.37
45°	251.2	18.99	2.95

[a]Enthalpy values were calculated using the tangent of the van't Hoff plot at different temperatures.

for at least 24 hr. Preliminary experiments indicated that equilibrium was established within 12–18 hr.

After equilibrium, the test solutions were subjected to filtration[9] (0.45-μm pore size). The filtrate was diluted with deionized distilled water to make a solution of proper concentration (40–100 mg/liter) for spectrophotometric assay. At least five experimental runs were carried out for each test medium.

Assay Procedure—The assay procedure was adapted from Conklin and Hollifield (9). A mixture of 4.0 ml of 0.1 *N* hydrochloric acid, 1.0 ml of sample solution, and 10.0 ml of nitromethane was placed in a separator and shaken for 2 min. The mixture was allowed to separate into two clear layers, and an 8.0-ml portion of the nitromethane layer (bottom layer) was removed and centrifuged for 5 min. Then a 4.0-ml portion of this nitromethane solution and 0.5 ml of 0.04 *M* quaternary ammonium hydroxide methanolic solution were thoroughly mixed in a test tube, and the absorbance of the resulting solution was measured at 400 nm[10].

Nitromethane, which was treated with 1.0 ml of distilled water, 4.0 ml of 0.1 *N* hydrochloric acid, and 0.5 ml of quaternary ammonium hydroxide methanolic solution, was used as the blank. The absorbance readings were converted to concentration values (milligrams per liter) using a standard Beer–Lambert plot.

Spectral Studies—Difference spectroscopy (tandem technique) (10) was used to study the possible interactions between nitrofurantoin and urea and between nitrofurantoin and creatinine. Identical amounts of nitrofurantoin solution (20 mg/liter) and blanks were placed in both the reference and sample compartments, and the baseline was determined using a recording spectrophotometer[10]. Appropriate buffer solutions were used as blanks in both compartments.

A 10–50-μl amount of 30% urea stock solution containing 20 mg/liter of nitrofurantoin was added[11] to the nitrofurantoin solution in the sample compartment. An equal amount of plain 30% urea solution was added to the blank in the reference compartment. The spectrum was scanned and recorded between 500 and 230 nm. Additional amounts of stock solution were added, and the spectra were recorded. The same procedure was used for a creatinine–nitrofurantoin system in which a 5% creatinine stock solution was added to the nitrofurantoin solution (20 mg/liter).

RESULTS AND DISCUSSION

Solubility in Water and Buffer Media—The present study reports the solubility of nitrofurantoin in distilled water over a range of temperatures. These data served as a means of explaining the thermodynamic properties of nitrofurantoin in aqueous solutions. As shown in Table I, the solubilities of this drug increased at higher temperatures (endothermic), and the heat of solution (ΔH) varied at different temperatures. The variation in the enthalpy of the systems may be due to the formation of intermolecular interaction between the drug molecules.

A plot of the logarithm of the solute mole fraction against the reciprocal of the absolute temperature (van't Hoff plot) was found to be curvilinear. This graphic representation is frequently employed to determine the presence of molecular association in solution, and curvature of this plot suggests the possible occurrence of molecular interactions. Hildebrand and Scott (11) suggested the use of the van't Hoff plot for this purpose. In addition, when the logarithm of the solute mole fraction was plotted against the logarithm of the absolute temperature, the line was linear. This type of plot also has been used to predict the effects of temperature on the solubility of various compounds (12).

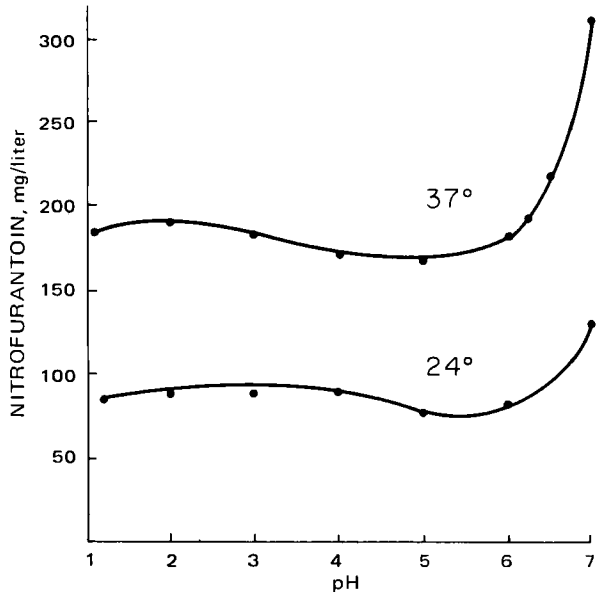

Figure 1—*Effect of pH on nitrofurantoin solubility in water.*

The solubility of nitrofurantoin in water was determined in this study at various hydronium-ion concentrations. Figure 1 depicts the effect of pH on the solubility of this drug. A large increase in solubility, starting at pH 6, was due to ionization of the drug (pKa 7.2) in the solution. This figure also shows that the solubility of nitrofurantoin was slightly higher at pH 2–3 than at about pH 5. This phenomenon might be explained by electron dislocalization of the molecule at the lower pH values, resulting in higher solubilities. Electron dislocalization in the nitrofurantoin molecule is possible due to the existence of three nitrogen atoms, each containing unshared electron pairs and conjugated double bonds.

The determined solubilities of nitrofurantoin are generally in good agreement with previously reported values. Paul *et al.* (6) found the nitrofurantoin solubility in distilled water to be 190 mg/liter at 37°; the value in the current study was 174 mg/liter. They also determined the solubility in pH 5 buffer to be 155 mg/liter. This value is in fair agreement with the value of 168 mg/liter reported in this study. The solubility value obtained in this study in 0.1 *N* hydrochloric acid (pH 1.12) at 37° (177 mg/liter) was slightly higher than the value of 154 mg/liter recently reported[1] (3).

Effect of Urea on Nitrofurantoin Solubility—Figures 2–5 summarize the data concerning the effect of urea on nitrofurantoin solubility in water and buffer. The addition of urea to aqueous media first increased nitrofurantoin solubility up to a maximum level and then decreased solubility at higher urea concentrations. After the maximum solubility was reached at an optimal urea concentration, nitrofurantoin solubility abruptly decreased to a level considerably lower than its solubility in distilled water.

Figure 2 illustrates this unusual solubility behavior of nitrofurantoin in water as a function of urea concentrations. At all temperatures studied, similar solubility curves were obtained. However, the amounts of urea needed for the maximum solubility of nitrofurantoin varied at different temperatures, ranging from 1.75 to 2.5% between 24 and 45°.

Figure 3 shows a linear correlation between the concentration of urea that produced maximum nitrofurantoin solubility in water and temperatures of the system. The slope of the line could be used for the prediction of urea concentrations exhibiting the maximum solubilizing effect at different temperatures. Although the pH of 5% urea in water was around 7.8, the solubility of nitrofurantoin did not increase in these solutions; in fact, the solubility of nitrofurantoin in 5% urea was much lower than in distilled water at 24, 30, and 37°.

When the temperature of the system was kept constant, the pH of the solution did not seem to affect the optimal urea concentrations at which the maximum solubility of nitrofurantoin was obtained.

[9] Millipore.
[10] Cary 118 spectrophotometer.
[11] Hamilton microliter syringe.

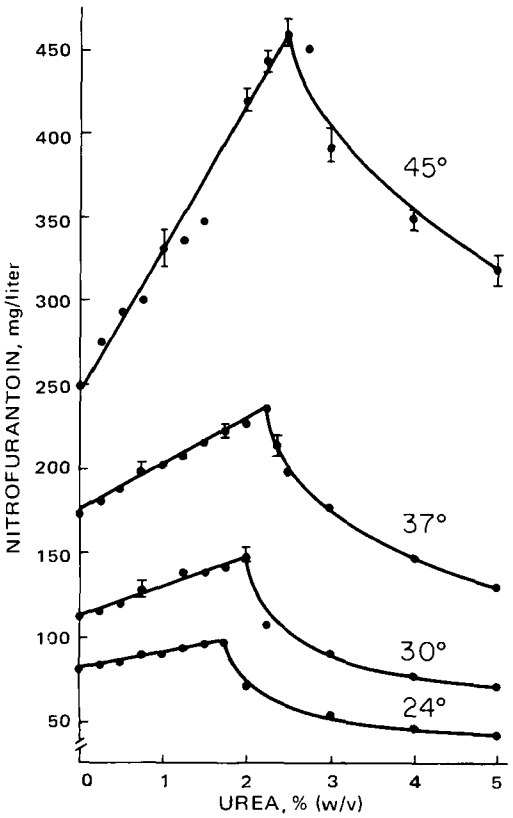

Figure 2—*Nitrofurantoin solubility in aqueous urea solutions at different temperatures.*

Figures 4 and 5 show the effects of hydronium-ion concentration on the amount of urea exhibiting the maximum solubilizing effect. The concentrations of urea needed for the maximum nitrofurantoin solubility were equal in different pH solutions used. The addition of urea to the buffer solutions did not significantly change the pH of the systems.

The findings that urea did increase the aqueous solubility of nitrofurantoin up to an optimum level might explain the elevated solubilities of this drug in urine frequently reported (5, 6). Concentrations of urea in the urine are normally in the neighborhood of 2% (13, 14).

The effect of urea on the aqueous solubility of organic compounds has been widely studied. Urea has been shown to increase the water solubility of chloramphenicol (15, 16) and acetaminophen (17) and to decrease the solubility of sulfathiazole (18). Mukerjee and Ghosh (19) reported the solubility of methylene blue to be 30 times higher in 10 *M* urea solution than in water. In a recent investigation, 1–5 *M* urea increased the water solubility of methyl *p*-hydroxybenzoate (20).

The effects of urea and thiourea on the solubility of benzoic and salicylic acids also were studied (21, 22), and it was inferred that the interaction of urea with salicylic acid was relatively complex but that

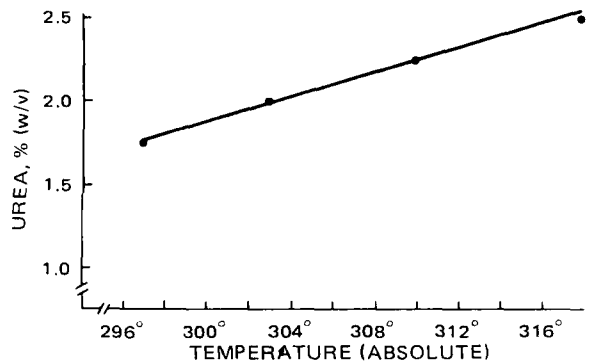

Figure 3—*Effect of temperature on the concentration of urea that provides maximum nitrofurantoin solubility in water.*

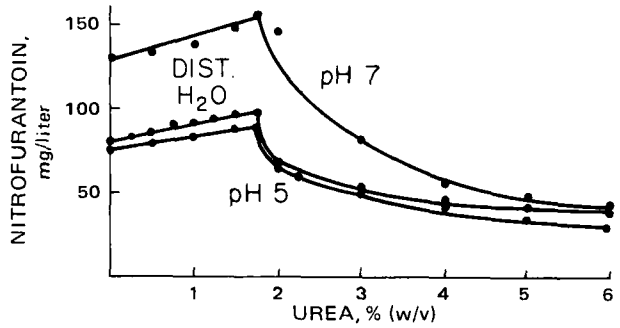

Figure 4—*Effect of pH on nitrofurantoin solubility in urea solutions at 24°.*

increases in the solubility of these compounds were due to formation of soluble complexes. Feldman and Gibaldi (23), however, concluded that the enhanced solubility of benzoic and salicylic acids in urea and alkylurea solutions did not involve complexation. They proposed that urea and alkylurea solubilized benzoic and salicylic acids by "breaking up" water clusters surrounding the nonpolar molecule, increasing the entropy of the system, and producing a "driving" force for the solubilization.

Thus, the literature reports indicate that urea exhibits two distinctly opposite effects as to its ability to change the solubility of various organic compounds in aqueous solutions, and there are also contradictory reports as to the mechanism of the urea effect on the solubility of various compounds. In studying the effect of urea on hydrocarbon solubility, Wetlaufer *et al.* (24) suggested several mechanisms to explain the increased solubility of hydrocarbons in aqueous urea solutions: (*a*) the solute is solely dissolved by the urea, (*b*) urea alters the structure of water so as to enhance solvation of the solute by water molecules, and (*c*) solute molecules are solvated both by urea and water molecules. These proposed mechanisms, however, usually have been associated with increased solubility of compounds at relatively high urea concentrations (1–5 *M*). There is no conclusive evidence to support any one mechanism whereby urea changes solubilities.

In the present study, because of the unusual behavior of the system (first an increase followed by a considerable decrease in nitrofurantoin solubility), a single explanation of the phenomenon is most difficult. A similar phenomenon was reported for the effect of urea on the solubility of tetracycline in water (25). The increased solubility of tetracycline was attributed in part to the formation of a nonclathrate complex; the complex continued to form up to a point (maximum

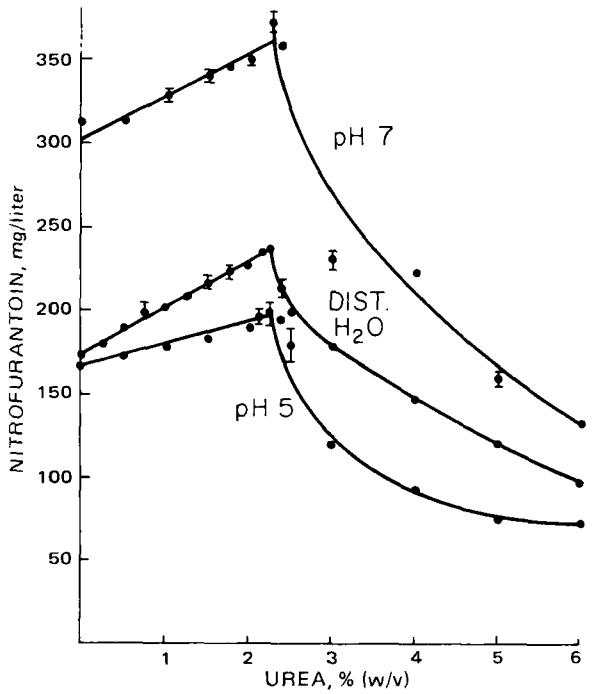

Figure 5—*Effect of pH on nitrofurantoin in urea solutions at 37°.*

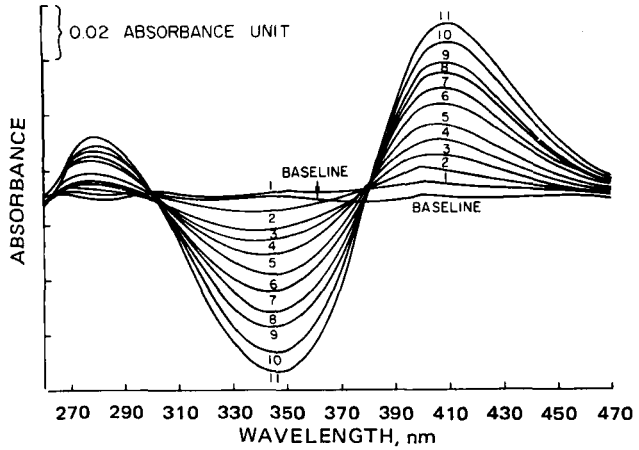

Figure 6—*Difference spectra of nitrofurantoin–urea in pH 7 buffer solution. Key [percent (w/v) urea in solution]: 1, 0.15; 2, 1.08; 3, 2.09; 4, 3.03; 5, 3.91; 6, 5.0; 7, 6.0; 8, 6.91; 9, 7.78; 10, 9.31; and 11, 10.65. All solutions contained the identical concentration of nitrofurantoin (20 mg/liter).*

solubility attained in 2.25 *M* urea at 35°), which can be considered the solubility limit of the complex. Higuchi and Ikeda (26) also found a similar solubility behavior with digoxin in aqueous hydroquinone solutions.

To examine the mechanism(s) of the urea effect on the solubility of nitrofurantoin, spectral properties of the system were studied. Analysis of the spectra (Fig. 6) suggests some type of interaction between nitrofurantoin and urea molecules. In practice, it has been generally recognized that many experimental problems associated with detecting and measuring spectral changes are greatly simplified by using difference spectral techniques (10). Instead of comparing the spectrum of nitrofurantoin with the spectrum of the mixture of nitrofurantoin and urea, the difference spectra of these substances were obtained and compared (Fig. 6). A distinctive new maximum band appeared at 410 nm when urea was added to the nitrofurantoin solution. The normal maximum band for nitrofurantoin in the visible range at pH 7 was at 375 nm. This large spectral shift (35 nm) is a strong indication of molecular interaction between urea and nitrofurantoin molecules. There was also an appreciable band at 345 nm (normally 310 for nitrofurantoin at pH 7). These spectral changes usually indicate conformational changes occurring in and/or near the main chromophore of the drug.

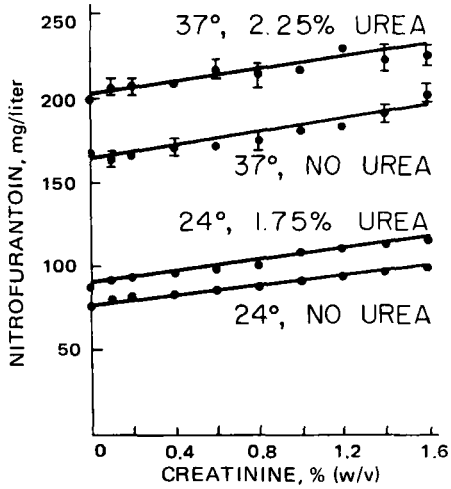

Figure 8—*Effect of creatinine on nitrofurantoin solubility in pH 5 aqueous medium (with and without urea) at 24 and 37°.*

Although no attempts were made in this study to quantitate the stoichiometry of the urea–nitrofurantoin interaction, preliminary spectral studies do indicate that the intensities of the spectral changes are directly proportional to the urea concentrations in the system. In addition, the presence of isosbestic points at 380 and 300 nm in the difference spectra (Fig. 6) suggests that the nature of the interaction between nitrofurantoin and urea molecules is of a specific type rather than a nonspecific interaction. The proposed intermolecular complexation may explain the increased solubility of nitrofurantoin at low urea concentrations.

On the other hand, the abrupt decrease in nitrofurantoin solubility when urea concentrations reach 1.75–2.5% at different temperatures might be explained by a salting-out effect. It is possible that when urea is added in an excessive amount, nitrofurantoin or its complex would

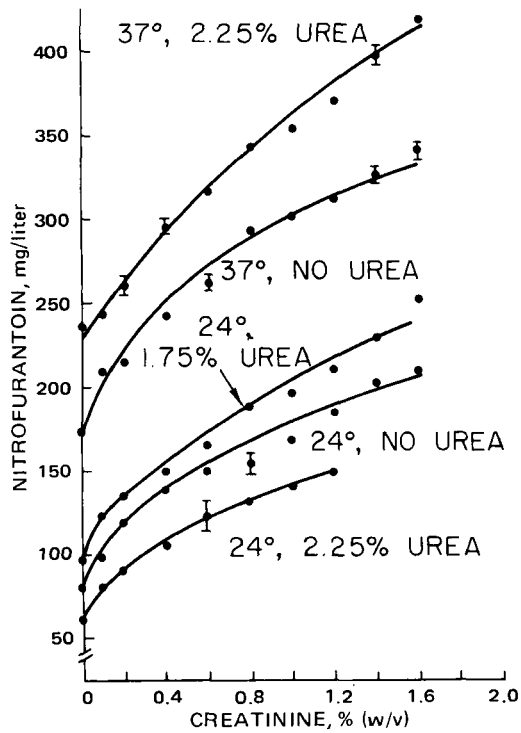

Figure 7—*Effect of creatinine on nitrofurantoin solubility in distilled water (with and without urea) at 24 and 37°.*

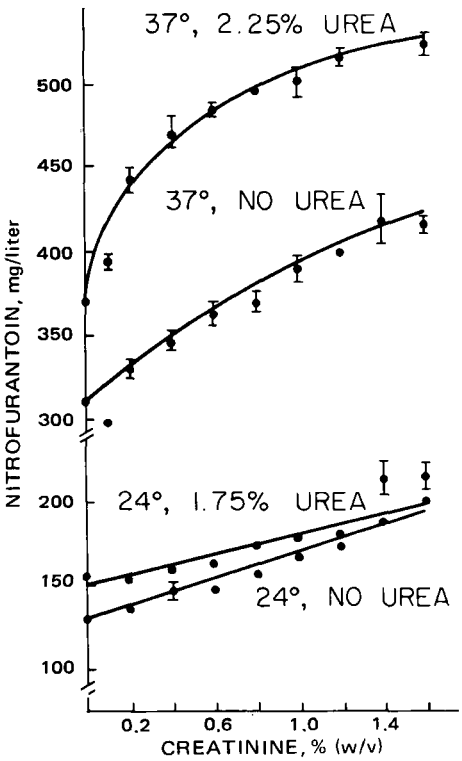

Figure 9—*Effect of creatinine on nitrofurantoin solubility in pH 7 aqueous medium (with and without urea) at 24 and 37°.*

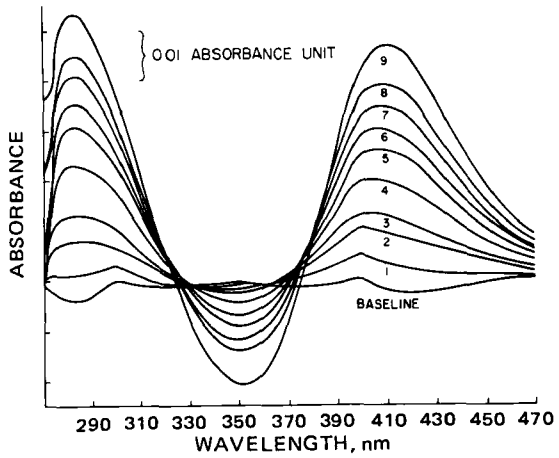

Figure 10—*Difference spectra of nitrofurantoin–creatinine in pH 7 buffer solution. Key [for percent (w/v) creatinine in solution]: 1, 0.122; 2, 0.238; 3, 0.349; 4, 0.555; 5, 0.746; 6, 0.918; 7, 1.078; 8, 1.226; and 9, 1.49. All solutions contained the identical concentration of nitrofurantoin (20 mg/liter).*

be precipitated. The breakdown of water structure might account for the increase in solubility at lower urea concentrations; however, disruption of the water structure probably would not occur at the low urea concentrations used in this study. The paradoxical behavior of nitrofurantoin in urea solutions makes it difficult to propose an unequivocal mechanism for the unusual solubility phenomenon.

Effect of Creatinine on Nitrofurantoin Solubility—The effect of creatinine on the aqueous solubility of nitrofurantoin at 24 and 37° is summarized in Figs. 7–9. As shown in these figures, the nitrofurantoin solubility was increased significantly in the presence of creatinine, even in relatively low creatinine concentrations (0.05–1.6%). The increases in the solubility of nitrofurantoin in 1.6% creatinine solution compared to distilled water at 24 and 37° were from 80 to 190 mg/liter and from 170 to 330 mg/liter, respectively. However, the general solubilizing effect of creatinine did not seem to be affected by temperature, pH, or addition of urea to the system.

On the other hand, creatinine enhanced the maximum solubility of nitrofurantoin in urea solutions. When creatinine was added to the solutions containing the optimal urea concentrations that exhibited the maximum solubility effect (2.25% at 37° and 1.75% at 24°), the maximum nitrofurantoin solubility was further increased. The solubility of nitrofurantoin was also increased by creatinine at a urea concentration (2.25% at 24°) that reduced nitrofurantoin solubility (Fig. 7). These findings lend support to the idea that the lack of crystalluria with nitrofurantoin, a compound of limited water solubility, is due to the combined solubilizing effect of urea and creatinine. The additional solubilizing effect of creatinine would offset the solubility-decreasing effect of urea which might occur at an unusually high urea concentration (higher than 2.0%) in the urine.

The spectra for nitrofurantoin–creatinine solutions (Fig. 10) indicate a possible interaction between the two compounds. There were two strong positive bands at 283 and 410 nm and a negative band at 352 nm. These spectral shifts were similar to those for nitrofurantoin–urea interactions and suggest a steric effect in the chromophore group. The presence of isosbestic points at 375 and 325 nm indicates that the interaction is of a specific type.

REFERENCES

(1) H. E. Paul and M. F. Paul, in "Experimental Chemotherapy," vol. II, R. J. Schnitzer and F. Hawking, Eds., Academic, New York, N.Y., 1964, p. 334.

(2) M. F. Paul, R. C. Bender, and E. G. Nohle, *Am. J. Physiol.*, **197**, 580(1959).

(3) T. R. Bates, J. M. Young, C. M. Wu, and H. A. Rosenberg, *J. Pharm. Sci.*, **63**, 643(1974).

(4) W. A. Richards, E. Riss, E. H. Kass, and M. Finland, *Arch. Intern. Med.*, **96**, 437(1955).

(5) E. H. Beutner, J. J. Petronio, H. E. Lind, H. M. Trafton, and M. Correia-Branco, "Antibiotics Annual 1954–1955," H. Welch and F. Marti-Ibanez, Eds., Medical Encyclopedia Inc., New York, N.Y., 1955, p. 988.

(6) M. F. Paul, C. Harrington, R. C. Bender, E. Nohle, and M. J. Bryson, *Proc. Soc. Exp. Biol. Med.*, **125**, 941(1967).

(7) D. E. Cadwallader, H. W. Jun, and L.-K. Chen, *J. Pharm. Sci.*, **64**, 886(1975).

(8) T. C. McIlvaine, *J. Biol. Chem.*, **49**, 183(1921).

(9) J. D. Conklin and R. D. Hollifield, *Clin. Chem.*, **11**, 925 (1965).

(10) T. T. Herskovits, in "Methods in Enzymology," vol. XI, C. H. W. Hirs, Ed., Academic, New York, N.Y., 1967, pp. 748–775.

(11) J. H. Hildebrand and R. L. Scott, "The Solubility of Nonelectrolytes," 3rd ed., Reinhold, New York, N.Y., 1964, pp. 273–285.

(12) J. H. Hildebrand, *J. Chem. Phys.*, **20**, 190(1952).

(13) H. A. Harper, "Review of Physiological Chemistry," 14th ed., Lange Medical, Los Altos, Calif., 1973, p. 398.

(14) A. White, P. H. Handler, and E. L. Smith, "Principles of Biochemistry," 3rd ed., McGraw-Hill, New York, N.Y., 1964, p. 737.

(15) K. Sekiguchi, N. Obi, and Y. Ueda, *Chem. Pharm. Bull.*, **12**, 134(1964).

(16) A. H. Goldberg, M. Gibaldi, J. L. Kanig, and M. Mayersohn, *J. Pharm. Sci.*, **55**, 581(1966).

(17) A. H. Goldberg, M. Gibaldi, and J. L. Kanig, *ibid.*, **55**, 482(1966).

(18) K. Sekiguchi and N. Obi, *Chem. Pharm. Bull.*, **9**, 866(1961).

(19) P. Mukerjee and A. K. Ghosh, *J. Phys. Chem.*, **67**, 193(1963).

(20) C. McDonald and E. Lindstrom, *J. Pharm. Pharmacol.*, **26**, 39(1974).

(21) S. Bolton, *J. Pharm. Sci.*, **52**, 1071(1963).

(22) D. M. Altwein, J. N. Delgado, and F. P. Cosgrove, *ibid.*, **54**, 603(1965).

(23) S. Feldman and M. Gibaldi, *ibid.*, **56**, 370(1967).

(24) D. B. Wetlaufer, S. K. Malik, L. Stoller, and R. L. Coffin, *J. Am. Chem. Soc.*, **86**, 509(1964).

(25) V. Naggar, N. A. Daabis, and M. M. Motawi, *Pharmazie*, **29**, 122(1974).

(26) T. Higuchi and M. Ikeda, *J. Pharm. Sci.*, **63**, 809(1974).

ACKNOWLEDGMENTS AND ADDRESSES

Received March 20, 1975, from the *Department of Pharmacy, School of Pharmacy, University of Georgia, Athens, GA 30602*

Accepted for publication August 15, 1975.

Abstracted in part from a thesis submitted by L.-K. Chen to the Graduate School, University of Georgia, in partial fulfillment of the Master of Science degree requirements.

[x] To whom inquiries should be directed.

Interaction of Dantrolene Sodium with Human Serum Albumin

J. J. VALLNER [x], L. A. STERNSON, and D. L. PARSONS

Abstract □ The binding of dantrolene sodium to human serum albumin was studied by fluorescence quenching and difference spectrophotometry. The association constant was calculated from each method of measurement and was large. This binding affinity may be of importance in the clinical setting, since competitive displacement of anionic drug by concurrently administered agents can occur. Consequently, the displacement of dantrolene from albumin was examined with a wide range of drugs. To gain insight into the characteristics of drug–albumin binding, the interaction of drug with cationic, anionic, and nonionic surfactants was also studied. Additions of drug to solutions of either the anionic or nonionic surfactant failed to result in a perturbation with the difference spectral technique. However, dantrolene added to the cationic resin produced a difference spectrum analogous to that observed with the drug–protein interaction.

Keyphrases □ Dantrolene sodium—binding to human serum albumin, fluorescence quenching and difference spectrophotometry, interaction with cationic, anionic, and nonionic surfactants □ Albumin, human serum—binding to dantrolene sodium, fluorescence quenching and difference spectrophotometry □ Fluorescence quenching—study of binding of dantrolene sodium to human serum albumin □ Difference spectrophotometry—study of binding of dantrolene sodium to human serum albumin □ Surfactants—cationic, anionic, and nonionic, interaction with dantrolene sodium □ Drug–protein binding—dantrolene sodium to human serum albumin

Most drugs are bound to serum albumin. Protein binding is an important factor in the distribution, metabolism, excretion, and activity of any administered chemical substance; only the fraction of drug unbound exerts pharmacological activity (1). The binding interaction is generally thought to occur through noncovalent forces, *i.e.*, hydrogen bonds and electrostatic, van der Waal, or hydrophobic interactions.

The binding equilibrium is often described by an association constant or constants together with the number of sites exhibiting each association constant. Such information is useful in establishing a proper dosage regimen (1). It is also of importance when two or more drugs that strongly bind to protein and compete for the same binding sites are administered concurrently. Higher free (unbound) drug concentrations are thereby produced and may precipitate a toxic response. Such increases in pharmacological activity of the displaced drug often necessitate an adjustment in dosage.

The binding to human serum albumin of a new drug should be examined, especially if the drug is an acidic molecule, because competitive binding with serum protein among acidic drugs has been shown to be particularly significant (2, 3). Recently, dantrolene sodium[1], 1-[[5-(4-nitrophenyl)furfurylidene]amino]-hydantoin sodium hydrate, a new muscle relaxant which apparently acts directly and selectively on skeletal muscle (4–6), was released for use in the United States.

Despite possessing a pKa of about 7.5 (7), dantrolene sodium has limited solubility at pH 7.4. The acidic and hydrophobic nature of the dantrolene molecule suggests that it may have a high affinity (binding constant) for serum albumin. However, the measurement of this affinity is made more difficult by the associated low solubility of dantrolene, as was demonstrated previously with various lipophilic drugs (8). The interaction of dantrolene with albumin was determined by difference spectrophotometry and fluorescence quenching measurements. Such techniques can detect small changes with suitable accuracy, and they appeared to be the most advantageous techniques for studying the interaction with protein of a drug with limited water solubility.

The propensity for other drugs to displace dantrolene from albumin binding sites also was determined from difference spectrophotometric measurements and may be of clinical importance in consideration of multiple drug therapy.

EXPERIMENTAL

Materials—The human serum albumin used had been investigated previously for purity[2] (9). Warfarin sodium[3], clofibrate[4], decamethonium bromide[5], propranolol hydrochloride[6], tolazoline hydrochloride[7], tolbutamide[8], isopropamide iodide[9], prochlorperazine[9], and ethacrynic acid[10] were used as received. Phenobarbital, secobarbital, and aspirin were USP grade; other materials were reagent grade. All solutions were prepared in deionized water.

Binding Studies—In all binding studies, the protein (1.45×10^{-6}–1.45×10^{-4} *M*) was dissolved in Sorensen's phosphate buffer (0.066 *M* NaH_2PO_4, 0.066 *M* K_2HPO_4) adjusted to pH 7.4. However, due to the solubility problems, stock solutions of dantrolene sodium were prepared (3.57×10^{-4} *M*) in deionized water adjusted to pH 9.0–10.0 with sodium hydroxide. Microliter[11] aliquots of drug were added to the protein solution, and such additions produced no more than 0.15 pH unit changes in the protein solutions as determined with a glass hydrogen-ion sensitive electrode.

For the competition studies, the displacing drug was dissolved in the same buffer solution as the protein, and again no significant changes in pH were observed during the binding studies.

Fluorescence—Solutions of albumin were prepared over the concentration range from 1.45×10^{-6} to 4.35×10^{-5} *M* at 22°, and each solution was carried through the following procedure. The fluorescent intensity of the native protein solution was recorded[12] at excitation and emission wavelengths of 289 and 357 nm, respectively. Microliter aliquots of dantrolene stock solution were subsequently added (to give a final concentration of drug from 3.6×10^{-6} to 9.22×10^{-5} *M* in the cell), and their effect on fluorescent intensity was

[1] Dantrium, Eaton Laboratories, Norwich, N.Y.

[2] Lot MX2519, 5-2526, Armour Pharmaceutical Co.
[3] Endo Laboratories, Garden City, N.Y.
[4] Ayerst, New York, N.Y.
[5] Burroughs Wellcome, Greenville, N.C.
[6] Inderal, Ayerst, New York, N.Y.
[7] Ciba Pharmaceuticals, Summit, N.J.
[8] Upjohn, Kalamazoo, Mich.
[9] SKF Laboratories, Philadelphia, Pa.
[10] Merck Sharp and Dohme Research Laboratories, Rahway, N.J.
[11] Hamilton Co., Reno, Nev.
[12] Aminco-Bowman spectrofluorometer.

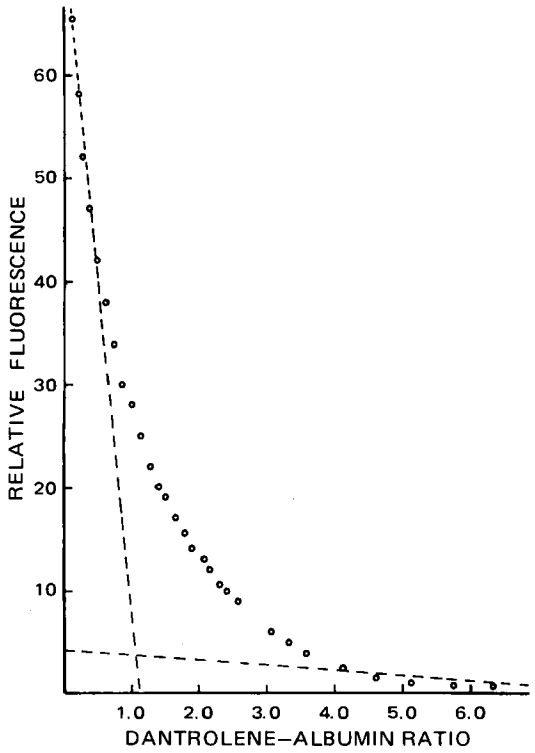

Figure 1—*Example of fluorescence quenching of human serum albumin by dantrolene. Intensity of albumin tryptophan fluorescence was monitored at 357 nm while exciting at 289 nm. Albumin concentration was 1.45 × 10⁻⁶ M.*

determined. At the selected wavelengths, the drug did not contribute to the fluorescence.

The protein concentration was kept constant throughout each quenching (binding) study so as not to contribute to the observed decreased fluorescence by having made the drug stock solution in the appropriate protein solution. Drug to protein ratios in the experiments ranged from 0.073 to 82. All dantrolene solutions were subjected to TLC on 0.25-mm silica gel 60 F-254 plates [developing solvent of chloroform–acetone (3:7)] to determine if chemical breakdown of the drug was occurring.

Experiments were repeated with all solutions and with the sample compartment maintained at 40°.

Difference Spectrophotometry—UV–visible spectra of dantrolene sodium (2.97×10^{-5} *M*) solutions were recorded[13] and showed maxima[14] at 392 nm ($a_m = 2.15 \times 10^4$) and 311 nm ($a_m = 1.40 \times 10^4$). For difference spectroscopy studies, the tandem cell technique was employed (10) in the split beam mode[13]. This technique is capable of measuring small differences from the baseline, due often to binding of the small molecule to the protein, provided that attention is paid to the particular requirement of keeping both protein and drug concentrations the same in the reference and sample compartments.

The baseline was obtained by placing the protein solution in one cell of the reference beam and buffer alone in the other cell of the reference beam; the sample compartment contained exactly the same solutions. Dantrolene was added to the buffer cell in the reference beam and the protein cell in the sample beam (at equal concentrations) to give final concentrations of drug ranging from 2.9×10^{-6} to 3.8×10^{-5} *M*.

To maintain a constant protein concentration throughout the titration, each addition of drug to the protein solution in the sample compartment was accompanied by the concomitant addition of an equal volume of albumin solution at a concentration twice that in the cell (*i.e.*, for titration of 1% albumin solutions, a 2% albumin solution was used to adjust protein concentrations). Similarly, drug concentration was maintained equally in both beams during titration by the addition of an equal volume of buffer to the cell containing drug and buffer in the reference compartment. Resulting difference spectra were subsequently recorded.

Drug–Surfactant Interactions—Difference spectroscopy studies were repeated in an identical manner to that already described, except that a 0.025% cetrimonium bromide, 0.025% sodium lauryl sulfate, or 0.1% octoxynol[15] solution was used in place of the protein.

Displacement Experiments—The competition between a number of acidic drugs for protein-bound dantrolene also was examined by difference spectroscopy. At a selected protein concentration of 3.62×10^{-5} *M* and a dantrolene concentration of 1.11×10^{-5} *M* (where it was determined that the drug was present mainly on a single class of sites), the effects on the difference spectrum after addition of various displacing drugs were examined. For this segment of the experiment, only the dantrolene–albumin difference spectrum resulting from perturbation in the visible wavelength region was investigated. The specific requirement for the variety of displacing drugs added was that they had no absorbance of their own above 340 nm.

Table I—Results of the Quenching of Native Human Serum Albumin Fluorescence by Dantrolene[a]

Albumin Concentration, *M*	Mole Ratio (*n*)	Association Constant × 10^{-5} M^{-1}
4.35×10^{-5}	0.95	3.9
2.90×10^{-5}	1.32	3.3
1.45×10^{-5}	1.68	2.3
7.25×10^{-6}	1.60	4.3
1.45×10^{-6}	1.15	5.4

[a] Excitation was at 289 nm and emission was at 357 nm in 1-cm cells at 22 ± 1°.

RESULTS

Dantrolene sodium was shown to bind to protein by the techniques of fluorescence quenching and difference spectroscopy. Fluorescence quenching measurements were based on the fact that albumin contains a single tryptophan residue that emits radiation at 357 nm when irradiated at 289 nm. Interaction of small molecules with human serum albumin, which results in a perturbation of the environment surrounding the tryptophan, is often sensed by reduction in fluorescent intensity attributed to the amino acid. Addition of dantrolene sodium (in concentrations ranging from 2.92×10^{-6} to 9.22×10^{-5} *M*) to protein solutions resulted in a quenching of the native fluorescence of the protein.

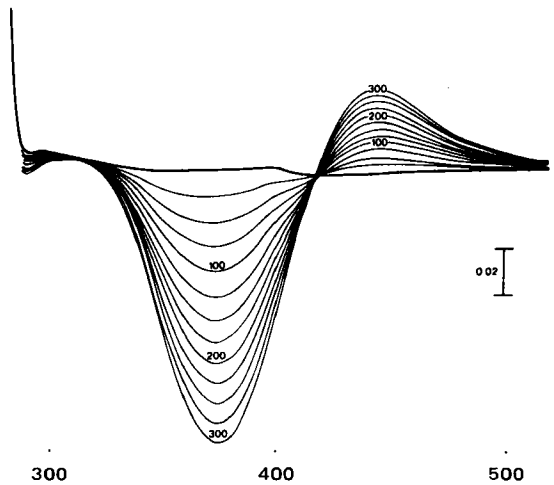

Figure 2—*Difference spectrophotometric titration of 1.45×10^{-4} M human serum albumin with dantrolene sodium. Each curve represents the addition of 25 μl of dantrolene solution (3.57×10^{-4} M) to 3 ml (initially) of buffer in the reference compartment and to 3 ml of protein in the sample compartment. The numbers 100, 200, and 300 denote microliters of dantrolene added for the difference spectrum to be obtained.*

[13] Cary 118 spectrophotometer, Cary Instruments, Monrovia, Calif.
[14] J. J. Vallner, unpublished observations.
[15] Triton X-100, Rohm and Haas.

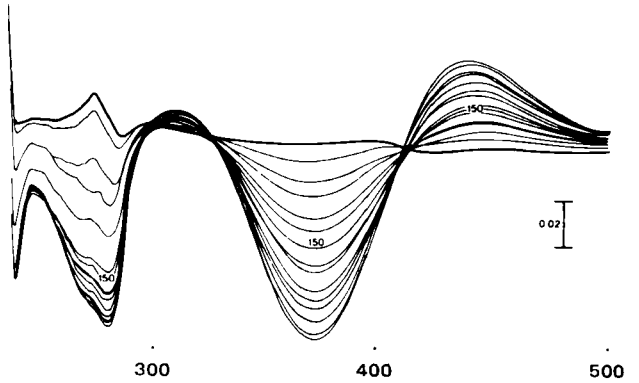

Figure 3—*Difference spectrophotometric titration of 7.25 × 10^{-5} M human serum albumin with dantrolene sodium. Interaction in the UV region is clearly indicated. (See caption of Fig. 2.)*

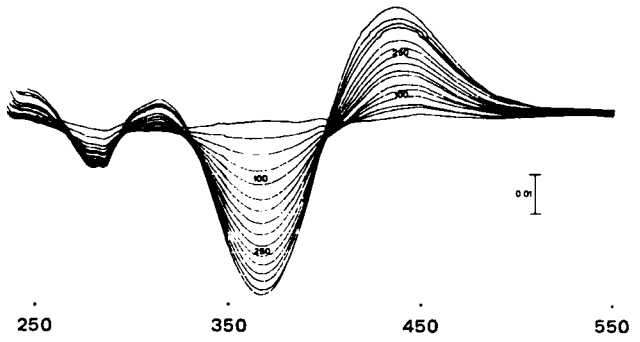

Figure 5—*Difference spectrophotometric titration of 1.45 × 10^{-5} M human serum albumin with dantrolene sodium. (See caption of Fig. 2.)*

A typical titration curve for the drug–albumin interaction is shown in Fig. 1. Extrapolation of the linear portions of these experimental titration curves gave the stoichiometric point from which the mole ratio (n) of dantrolene bound to protein was obtained (11). Association constants for the interaction of drug with protein were also calculated from the titration curves (Table I).

Quenching titrations also were performed at 40° at albumin concentrations of 1.45 × 10^{-5} and 4.35 × 10^{-5} M. At this higher temperature, the magnitude of the binding constants was reduced 30 ± 1%.

It was previously observed that chemical breakdown of dantrolene occurs in solution over 48 hr. To determine if degradation of dantrolene takes place during binding studies, all dantrolene solutions were subjected to TLC analysis upon conclusion of the experiment. Development of chromatograms with acetone–chloroform (7:3) plus 1% acetic acid revealed a single spot (R_f 0.51) attributable to the parent drug molecule. In two instances, a second, less intense spot (R_f 0.08) was also observed, representing the solution breakdown product. In these two instances, the data were discarded.

Interactions between serum albumin and dantrolene were also examined by difference spectrophotometry. Difference absorption spectra for the association of drug with protein in phosphate buffer (Figs. 2–6) are characterized by positive peaks at 443 ± 3 and 315 ± 1 nm and negative peaks at 371 ± 4 and 285 ± 3 nm. The absorption spectrum of dantrolene in buffer solution (pH 7.4) is characterized by peaks at 392, 311, and 223 nm. Families of curves were generated by the incremental addition of dantrolene to protein solutions of fixed concentration: 0.05, 0.1, 0.25, 0.5, and 1% in albumin. At the 1% protein level, difference peaks in the UV region were obscured by excessive absorption by protein.

Adequate precautions (as described under *Experimental*) were taken to maintain equivalent concentrations of drug and protein in both the sample and reference beam so that the curves must be the result of an interaction between dantrolene and albumin.

Absorbance titration curves (Fig. 7) were generated by plotting the change in absorbance (measured as difference in intensity of the 445-nm peak and 370-nm trough) *versus* the drug concentration at a constant protein level. Increasing concentrations of drug produced linearly increasing absorbance changes (r = 0.998 ± 0.001). The curve remained linear and did not level off (saturate) at higher drug concentration. The absence of a typical saturation curve (concave downward) may be due to solubility limitations rather than to the drug–albumin interaction itself. The solubility of dantrolene in aqueous solution at pH 7.4 is very low, so the drug concentration range over which binding was studied could not exceed the solubility limit (about 1 × 10^{-4} M). This concentration may not be high enough to saturate available binding sites, so a leveling off of the curve may not be observed.

Double reciprocal plots of the slope of titration curves described in Fig. 7 *versus* the protein concentration were constructed as shown in Fig. 8 and gave a straight line (r = 0.996 ± 0.001) with an intercept corresponding to the change in absorbance of dantrolene in the presence of an infinite amount of albumin. The association constant for the interaction was estimated from this plot to be 4.34 × 10^4 M^{-1}. (The amount of bound and free drug could not be determined due to linear increases in the change in absorbance *versus* added dantrolene concentration plots. Thus, the method of analysis was exactly analogous to that used in Michaelis–Menten kinetics.)

To elucidate the characteristics of the binding occurring between dantrolene and albumin, the interaction of drug with surface-active agents was studied. Difference spectra were generated as already described, except that surfactant was substituted for protein. Studies were conducted using anionic (sodium lauryl sulfate), cationic (cetrimonium bromide), and nonionic (octoxynol) surfactants at levels above the critical micelle concentration (CMC). The addition of drug to solutions of either the anionic or nonionic surfactant failed to result in a perturbation of the baseline, even at drug concentrations of 3 × 10^{-5} M. Addition of drug to the solution of cationic resin produced a difference spectrum (Fig. 9) characterized by a peak at 430 nm and a trough at 365 nm. The intensity of the spectrum was proportional to the concentration of drug added. This bathochromic shift of the dantrolene difference spectrum was analogous to the shift observed with the drug–protein interaction.

The propensity for other drugs to affect the interaction of dantrolene with albumin was also investigated by difference spectrophotometry. Studies were carried out at a constant concentration of dantrolene and protein, known to generate a significantly intense

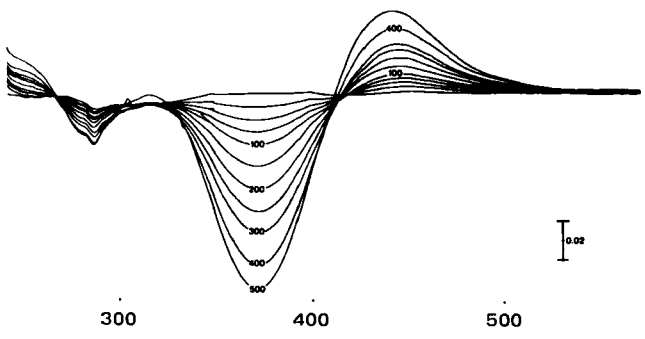

Figure 4—*Difference spectrophotometric titration of 3.63 × 10^{-5} M human serum albumin with dantrolene sodium. (See caption of Fig. 2.)*

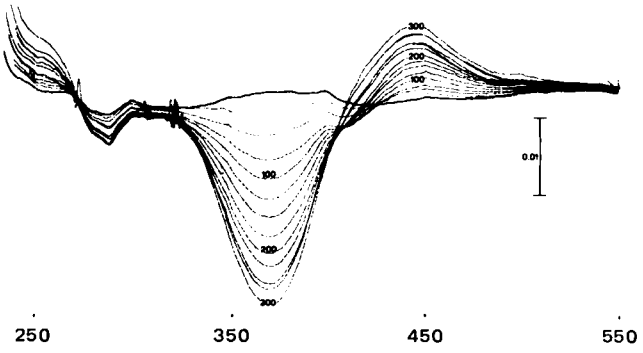

Figure 6—*Difference spectrophotometric titration of 7.25 × 10^{-6} M human serum albumin with dantrolene sodium. (See caption of Fig. 2.)*

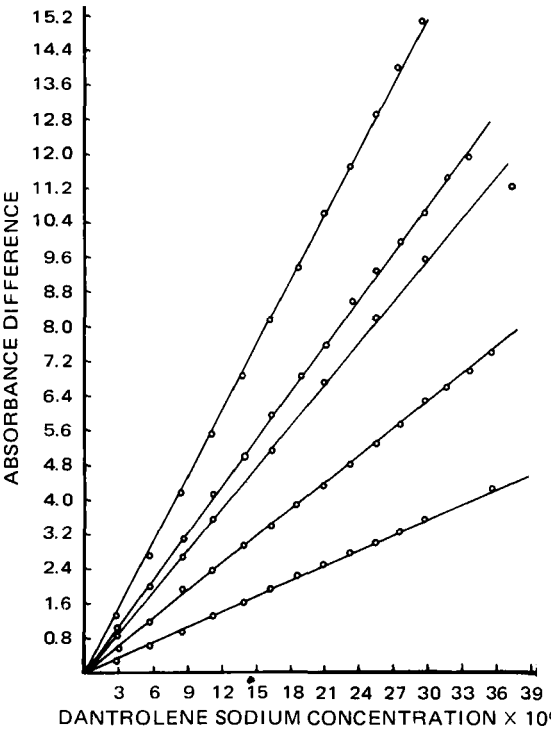

Figure 7—*Plots of absorbance difference × 10^2 (from 445-nm peak to 370-nm trough)* versus *dantrolene sodium concentration at constant protein concentrations. From the largest to smallest slope, the curves are in the order 1.45 × 10^{-4}, 7.25 × 10^{-5}, 3.63 × 10^{-5}, 1.45 × 10^{-5}, and 7.25 × 10^{-6} M human serum albumin.*

absorbance difference spectrum yet with a small enough drug to protein ratio to ensure considerable binding of dantrolene at the primary site. A drug to protein ratio of 0.32 was selected for initial studies. Displacing drug was added to both the reference beam (in buffer) and sample beam (in the dantrolene–protein solution), and the concentration of all species present was kept constant in both compartments.

The data in Table II indicate that some small, but measurable, differences (±6% changes) resulted for a number of added antagonists. These random effects are thought to be indicative of no significant displacement of the bound dantrolene. Three of the antagonists, however, did give large effects on the bound drug.

DISCUSSION

Both quenching fluorescence and difference spectrophotometric measurements support the fact that dantrolene interacts with albumin. The intensity of this interaction was calculated as an association constant from both the emission and absorption spectra. The magnitude of this constant was approximately one order of magnitude greater when calculated from quenching fluorescence data than from values obtained from difference spectrophotometric measurements. Other investigators (12) previously reported that the calculation of association constants from fluorescence measurements yielded values indicative of higher binding affinities than did values obtained by other methods.

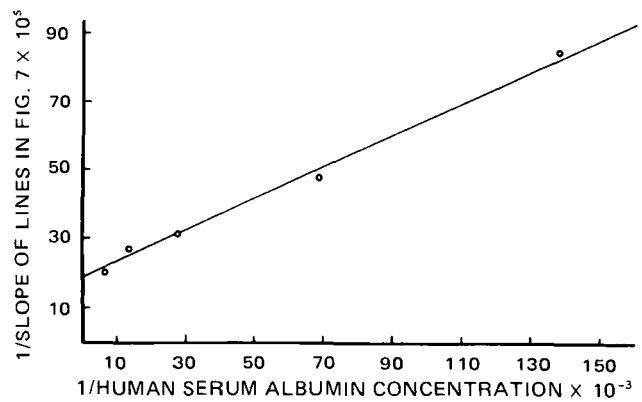

Figure 8—*Plot of reciprocal of slopes of Fig. 7* versus *reciprocal of human serum albumin concentration. (See text for explanation.)*

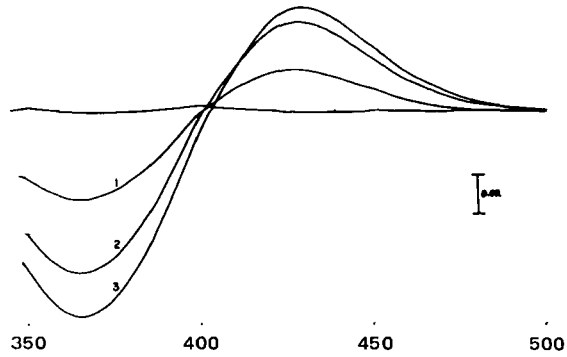

Figure 9—*Difference spectra of the interaction between cetrimonium bromide and dantrolene sodium. Cetrimonium bromide concentration was constant at 0.025%. Dantrolene concentrations were 1.11 × 10^{-5} (curve 1), 2.09 × 10^{-5} (curve 2), and 2.54 × 10^{-5} (curve 3)* M.

The native fluorescence of human serum albumin resides in a single tryptophan residue incorporated into an apparently hydrophobic region of the protein (13, 14). This region is postulated to be a high affinity site, involved in the binding of anionic drugs with the protein. Interaction of drug with this site perturbs the tryptophan environment, decreasing the fluorescent intensity of the protein. Fluorescence quenching measurements of drug–protein interactions are only sensitive to perturbations in the tryptophan residue. Secondary binding at sites remote from the fluorescent moiety are not detected.

Association constants calculated from absorption difference spectral data are more responsive to general alterations in the drug molecule environment due to interaction with protein and are, therefore, also sensitive to interactions not involving the tryptophan-containing region. Association constants calculated from difference spectral data may represent a weighted average of several binding sites. Since the tryptophan-containing region is reported to be the "high affinity site" for anionic drugs, if one assumes that additional sites have lower affinity for interaction with the drug, association constants calculated from difference spectra will be of lower value than constants obtained by monitoring fluorescence quenching.

Close examination of Figs. 2–6 suggests that dantrolene interacts with at least two sites on the protein. At a high protein concentration

Table II—Competition for Dantrolene Binding on Human Serum Albumin by a Variety of Drugs[a]

Drug Concentration, *M*	Change in Bound Dantrolene in Presence of Competition[b], %
Decamethonium bromide, 2.75 × 10^{-4}	0
Isopropamide iodide, 3.67 × 10^{-4}	0
Tolazoline hydrochloride, 3.44 × 10^{-4}	—6[c]
Prochlorperazine, 7.51 × 10^{-5}	+4
Propranolol hydrochloride, 1.10 × 10^{-4}	0
Ethacrynic acid, 1.24 × 10^{-4}	—1
Aspirin, 6.94 × 10^{-4}	—5
Secobarbital, 1.86 × 10^{-4}	+6
Phenobarbital, 2.81 × 10^{-4}	+6
Warfarin, 1.45 × 10^{-4}	—19
Clofibrate, 1.63 × 10^{-4}, 3.28 × 10^{-4}	—16, —33
Tolbutamide, 2.88 × 10^{-5}, 5.77 × 10^{-5}	+33, +44

[a] The dantrolene concentration was 1.15 × 10^{-5} *M* (where it is assumed that most of the drug is bound to the primary class of site; see *Discussion*) and the albumin concentration was 3.025 × 10^{-5} *M* (drug/protein = 0.317). [b] Each number given is an average of three separate experiments. [c] Numbers reflecting ±6% change in bound dantrolene are assumed to be indicative of no real displacement effect.

(Fig. 2), a distinct isosbestic point is maintained throughout the titration of protein with drug, suggestive of a single binding site. At lower concentrations of protein (0.25 and 0.50%), however, a more complicated family of difference spectra was recorded. Curves obtained at lower concentrations of drug pass through the isosbestic point; when the drug to protein ratio exceeded 1:3, the crossover point shifted to shorter wavelengths and the distinct isosbestic point was lost. The general shape of the difference spectra underwent no significant changes with titration by drug.

These results suggest that dantrolene interacts with a high affinity site on human serum albumin which becomes occupied at some drug to protein ratio, so additional drug must bind to secondary sites. Association constants calculated from difference spectra *(i.e.,* from plots of absorbance in the visible region *versus* concentration) then represent a weighted average of these multiple sites.

Secondary binding sites were detected also at lower protein concentrations from difference spectra generated in the UV region. Titration of albumin with drug yielded a family of spectra with troughs at 285 nm, which were saturable and contained an isosbestic point at 268 nm.

Plots of absorbance changes (445 minus 370 nm) *versus* dantrolene concentration (Fig. 7) at constant protein levels failed to show saturation of binding; *i.e.,* the curves remained linear and did not level off. This failure to observe saturation may result in part from the very limited solubility of dantrolene. Lack of saturation also may be due to multiple binding sites of equal affinity, but this possibility seems remote. Alternatively, self-association between dantrolene molecules through stacking or charge transfer complexation could account for the observed lack of saturation. Initial solvent studies carried out in these laboratories support the contention that dantrolene molecules can stack in a hydrophobic environment.

When dantrolene was dissolved in a solution containing the cationic detergent cetrimonium bromide (Fig. 9), the spectral shift was qualitatively very similar to that when drug became bound to protein. Very little effect on the difference absorption spectrum was seen at cetrimonium bromide concentrations below the CMC (0.02% w/v) (15) or in the presence of sodium lauryl sulfate or octoxynol. The shift toward longer wavelengths when dantrolene becomes bound to albumin and the effect seen when drug interacts with cetrimonium bromide suggest that the protein binding site for dantrolene consists of a cationic charge near a large hydrophobic site to accommodate the unsaturated rings.

Competition studies showed that a significant reduction of dantrolene binding occurred in the presence of the tightly bound warfarin (16, 17) and clofibrate (8), while basic drugs and the relatively weakly bound acidic drugs did not displace any dantrolene. The probability that warfarin, clofibrate, and dantrolene share some common binding site is thus enhanced. The situation with tolbutamide as the competing drug is somewhat peculiar. Tolbutamide has a binding constant of about $4–7 \times 10^4$ liters/mole (18, 19) and, as compared to clofibrate, would be expected to displace dantrolene. However, the presence of tolbutamide increased dantrolene binding. It can be speculated that tolbutamide may cause either a change in albumin conformation or a change in conformation during competition with the dantrolene molecule. Further work is underway to examine this increased binding phenomenon and the seemingly rapid breakdown of dantrolene in solution.

REFERENCES

(1) B. K. Martin, *Nature*, **207**, 274(1965).

(2) H. M. Solomon, *Proc. Int. Congr. Pharmacol. 4th*, **4**, 169(1970).

(3) C. M. Kunin, *J. Lab. Clin. Med.*, **65**, 416(1965).

(4) H. R. Snyder, C. S. Davis, R. K. Bickerton, and R. P. Halliday, *J. Med. Chem.*, **10**, 807(1967).

(5) L. J. Honkomp, R. P. Halliday, and F. L. Wessels, *Pharmacologist*, **12**, 201(1970).

(6) K. O. Ellis and J. F. Carpenter, *Fed. Proc.*, **30**, 670(1971).

(7) Literature on dantrolene sodium (Dantrium), Eaton Laboratories, Norwich, N.Y.

(8) J. H. Perrin, J. J. Vallner, and D. A. Nelson, *Biochem. Pharmacol.*, **24**, 769(1975).

(9) J. H. Perrin and J. J. Vallner, *J. Pharm. Sci.*, **64**, 1508(1975).

(10) A. S. Brill and H. E. Sandberg, *Biophys. J.*, **8**, 664(1968).

(11) N. A. Attalah and G. F. Lata, *Biochim. Biophys. Acta*, **168**, 321(1968).

(12) C. F. Chignell, *Mol. Pharmacol.*, **6**, 3(1970).

(13) J. B. Swaney and I. M. Klotz, *Biochemistry*, **9**, 2570(1970).

(14) J. J. Vallner, Ph.D. thesis, University of Wisconsin, Madison, Wis., 1974.

(15) C. F. Chignell, *Mol. Pharmacol.*, **5**, 455(1969).

(16) R. A. O'Reilly, *ibid.*, **7**, 209(1971).

(17) J. H. Perrin and D. A. Nelson, *Life Sci.*, **11**, 277(1972).

(18) J. Judis, *J. Pharm. Sci.*, **61**, 89(1972).

(19) J. H. Perrin and D. A. Nelson, *J. Pharm. Pharmacol.*, **25**, 129(1973).

ACKNOWLEDGMENTS AND ADDRESSES

Received May 30, 1975, from the *School of Pharmacy, University of Georgia, Athens, GA 30602*

Accepted for publication September 3, 1975.

The authors thank Dr. T. Higuchi and Dr. J. H. Perrin for helpful advice and discussion.

[x] To whom inquiries should be directed.

Identification and Quantitative GLC Determination of Iproniazid in Human Urine

R. M. de SAGHER, A. P. De LEENHEER ˣ, and A. E. CLAEYS

Abstract □ A GLC method for the specific identification and quantitation of iproniazid, a potent monoamine oxidase inhibitor drug, is described. The free drug is isolated from urine samples by two-phase extraction reinforced with salting out. Identification and quantitative determination at the microgram level are done on aliquots of the chloroform extract by GLC, using the 2-butyl analog as an internal standard. Iproniazid and potentially interfering compounds present in the extracts are also identified by GLC–mass spectrometry and TLC for supporting evidence of the GLC method's specificity.

Keyphrases □ Iproniazid—GLC analysis, urine □ GLC—analysis, iproniazid in urine □ Monoamine oxidase inhibitors—iproniazid, GLC analysis, urine □ CNS stimulants—iproniazid, GLC analysis, urine

Iproniazid (I) is a monoamine oxidase inhibitor drug used in Europe as a central stimulant in the treatment of mental depression. This drug is extensively metabolized, principally by hydrolysis into isonicotinic acid and isopropylhydrazine and to a lesser extent by dealkylation into isoniazid and acetone. Iproniazid, ^{14}C-labeled on the carbonyl group, was injected into rats; 98% of the label was recovered in the first 24-hr urine collection (1). Iproniazid, ^{14}C-labeled on the 2-carbon of the isopropyl group, was administered to rats, mice, and humans (2, 3). In rats and mice (2), about 15% of the label was excreted in urine (one-third as unchanged drug), but the greatest portion was expired as $^{14}CO_2$. Oral administration to two human patients (3) resulted in urinary excretion of the label of 10–13% totally and traces to 3% of free drug.

A quantitative method was described that used the sodium nitropentacyanoferroate reagent to determine the urinary concentration of iproniazid in patients receiving therapeutic doses (75–100 mg) (4). Of the iproniazid administered orally, about 10% was found as unchanged drug and a much larger quantity was detected as isonicotinic acid. The cyanogen bromide–ammonia reaction was used to examine the urinary excretion in nine normal persons dosed with iproniazid (5). Within 48 hr following administration of a 250-mg dose, about 16% was excreted as unchanged drug and 50% was excreted as isonicotinic acid. Many questions arise, however, as to the specificity of both spectrophotometric methods based on the sodium nitropentacyanoferroate or the cyanogen bromide–ammonia reaction.

The present report concerns the development of a specific and sensitive GLC determination of iproniazid in urine samples of patients receiving therapeutic doses.

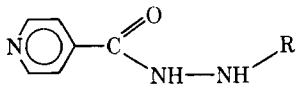

I: R = $CH(CH_3)_2$
II: R = $CH(CH_3)(CH_2CH_3)$

Table I—Case Histories of Major Iproniazid Therapy

Patient	Sex and Age (years)	Body Weight, kg	Daily Dose of Orally Administered Drugs
1	Male, 28	77	Iproniazid, 50 mg
2	Female, 42	73	Iproniazid, 75 mg Methotrimeprazine[a], 75 mg
3	Male, 54	86	Iproniazid, 50 mg Amobarbital[b], 150 mg Diazepam[c], 7.5 mg Thioridazine[d], 37.5 mg
4	Male, 29	79	Iproniazid, 50 mg Diazepam[c], 5 mg Fluphenazine hydrochloride[e], 1 mg
5	Female, 58	86	Iproniazid, 25 mg Fluphenazine hydrochloride[e], 1 mg

[a] Nozinan. [b] Amytal. [c] Valium. [d] Mellaril. [e] Sevinol.

EXPERIMENTAL

Reagents—Iproniazid[1] was obtained from iproniazid phosphate as reported previously (6). The internal standard, 1-isonicotinoyl-2-(2-butyl)hydrazine (II), was synthesized according to Yale *et al.* (7) and by the method described earlier (6). All inorganic and organic chemicals used were reagent grade. High purity nitrogen was employed for evaporation of extracts.

Collection of Urine Samples—Urine samples were collected without preservative on successive days from a volunteer (Subject 1) and four psychiatric patients (Subjects 2–5) to whom known amounts of iproniazid were administered orally. The urine outputs of Subject 1 were assembled and analyzed separately after administration of a single 50-mg dose of iproniazid. The four psychiatric patients were under a daily combined drug therapy for at least 3 months (Table I) including iproniazid (75, 50, 50, and 25 mg, respectively). Their successive 24-hr urine outputs were collected, homogenized, and stored at −7° until analyzed.

Extraction Procedure—To each 200-ml sample, or the total volume if less was available, of urine in a 1-liter separator were added 84 g of ammonium sulfate and 2 ml of 12 *N* HCl. The solution was extracted three times with 100 ml of peroxide-free ether (freshly distilled over hydroquinone, reagent grade), and the ether layers were discarded. The aqueous phase was made basic with 5 ml of 13 *N* NaOH and again extracted three times with 100 ml of ether. Then the ether layers were back-extracted three times with fresh 25-ml portions of 0.1 *N* HCl.

The combined acidic solutions were washed three times with 50 ml of chloroform. Then 31 g of ammonium sulfate and 1.5 ml of 13 *N* NaOH were added, and the aqueous solution was extracted three times with 50 ml of chloroform. After addition of the internal standard (II, 115 μg for Subject 1 and 216 μg for Subjects 2–5 and recovery experiments), the chloroform phase was dried over anhydrous sodium sulfate, filtered, and concentrated to a smaller volume in a rotary evaporator[2].

The solution was finally evaporated to dryness in a waterbath at 40° under a nitrogen stream in 15-ml silanized conical centrifuge tubes. The residue was dissolved with the aid of a mixer[3] in 100 μl of chloroform.

GLC—A gas chromatograph[4] equipped with dual flame-ionization

[1] Marsilid.
[2] Rotavapor Büchi, Flawil, Switzerland.
[3] Grindomat Retsch, Haan, West Germany.
[4] Varian Aerograph 2800, Walnut Creek, Calif.

Table II—Partition Coefficients of Iproniazid

Extracted Phase	Extractant: Chloroform	Extractant: Ether
0.26 *N* NH_4OH	0.35	0.02
0.26 *N* NaOH	<0.01	<0.01
0.1 *N* HCl	<0.01	<0.01
Aqueous ammonium sulfate–ammonium hydroxide[a]	13	2.0
Aqueous ammonium sulfate–hydrochloric acid[b]	<0.01	<0.01

[a] Forty grams of ammonium sulfate + 2 ml of 13 *N* NH_4OH/100 ml of aqueous phase. [b] Forty grams of ammonium sulfate + 2 ml of 12 *N* HCl/100 ml of aqueous phase.

detectors was used for single-column operation. The column consisted of 5% 50:50 cyanoethylmethyl dimethyl silicone gum[5] coated on 80–100-mesh diatomaceous earth[6] and packed in a 2.5-m × 2-mm i.d. spiral silanized glass column. Conditioning was performed for at least 12 hr at 220° with a carrier gas (nitrogen) flow of about 5 ml/min and then for a few hours at operating conditions.

Analyses were carried out isothermally at an oven temperature of 180° with the injector and detector blocks maintained a few degrees higher. Nitrogen was used as the carrier gas at a linear velocity, $\bar{u}_o$, of 14.3 cm/sec (measured with methane). The hydrogen and air flow rates were adjusted to give optimum sensitivity and good stability: hydrogen, 24–38 ml/min; and air, 250–550 ml/min.

The detectors were connected to the electrometer and, *via* an electronic integrator[7], to a 0–1-mv range recorder[8]. The attenuation settings employed were 2×10^{-11} amp/mv for the electrometer,

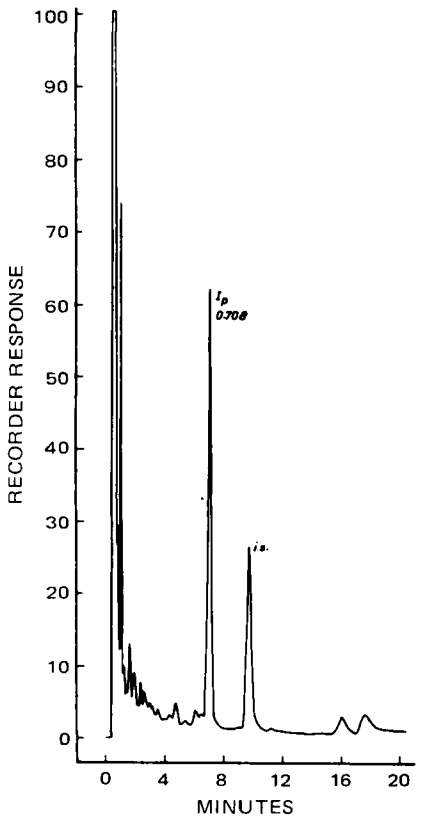

Figure 1—*Gas chromatogram of a urine extract from Subject 1. The column was 5% 50:50 cyanoethylmethyl dimethyl silicone gum* (T = *180°*, $\bar{u}_o$ = *14.3 cm/sec*); Ip = *iproniazid, and* is = *internal standard.*

[5] XE-60.
[6] Gas Chrom Q.
[7] Infotronics CRS 104, Houston, Tex.
[8] Varian Aerograph A25, Walnut Creek, Calif.

Table III—Recoveries of Iproniazid Added to Human Urine Samples

Iproniazid Added to 200 ml of Urine, μg	Iproniazid Recovered, μg	Recoveries, %
50	37.5	75.1
100	81.1	81.1
150	116.0	77.3
200	154.1	77.1
300	242.2	80.7
400	312.0	78.0
	Mean value ± *SD*, %	78.2 ± 2.3

whereas the electronic integrator input/output attenuator was used at ×5, ×10, or ×20.

All injections were made on-column with a 10-μl syringe[9], using an injection volume of approximately 1 μl.

Calculations—Calibration factors, k_i, were determined by measuring corresponding peak areas on chromatograms from the calibration series consisting of five different solutions of equal weight increments:

$$k_i = A_{Ip}w_{is}/A_{is}w_{Ip} \qquad \text{(Eq. 1)}$$

where A_{Ip} and A_{is} and w_{Ip} and w_{is} are peak areas and weights of iproniazid (*Ip*) and internal standard (*is*), respectively. For each calibration series, the mean calibration factor, $\bar{k}$, was calculated.

Results for urine samples, C_u (micrograms per 100 ml), were found by:

$$C_u = \frac{100}{0.78v}\,\frac{1}{\bar{k}}\,\frac{A_{Ip}'}{A_{is}'}\,w_{is} \qquad \text{(Eq. 2)}$$

where 100/0.78*v* is the conversion factor for an overall recovery of 78% and an extracted volume, *v* (milliliters), of urine; $\bar{k}$ is the mean calibration factor; A_{Ip}' and A_{is}' are peak areas of iproniazid as present in the chromatogram of the urine extract and the internal standard added to the chloroform phase, respectively; and w_{is} is the weight (micrograms) of the internal standard added to the chloroform extract prior to evaporation.

The urinary excretion, E_u, or percent of administered dose of iproniazid per 24 hr, recovered as unchanged drug, was calculated as follows:

$$E_u = C_uV/D \qquad \text{(Eq. 3)}$$

where C_u (micrograms per 100 ml) is the urinary concentration of iproniazid, *V* (milliliters) is the total 24-hr urinary output, and *D* (micrograms) is the amount of iproniazid administered orally in a 24-hr period.

GLC–Mass Spectrometry—All mass spectra were obtained on a gas chromatograph–mass spectrometer[10] using two column systems: (*a*) 1% polyamide resin[11] on diatomaceous earth[12] (80–100 mesh) in a spiral silanized glass column (2 m × 3.0 mm i.d.) at 200°, and (*b*) 5% cyanopropyl phenyl silicone gum[13] on diatomaceous earth[6] (80–100 mesh) in a spiral silanized glass column (1.9 m × 2.5 mm i.d.) at 197°. Helium, at a flow rate of 30 ml/min, was used as a carrier gas on both columns.

The chromatographic pattern was followed by recording the total ion current at an electron energy of 20 ev with the aid of a 0–5-mv recorder. Mass spectra were always scanned on the leading edge near the top of each peak at an electron energy of 70 ev. Injections were made on-column with the aid of a 10-μl syringe[9], using an injection volume of 1–4 μl.

TLC—Aliquots of 2 and 5 or 10 μl of extracts, obtained without addition of the internal standard, together with 1, 2, and 5 or 10 μg of iproniazid were spotted in a point or as a 2-cm line at 3 cm from the lower edge of 250-μm plates, prepared with equal parts of silica gel HF_{254}[14] and cellulose MN 300[15].

Two solvent systems were employed: (A) chloroform–methanol–13

[9] Hamilton 701N, Whittier, Calif.
[10] LKB 9000S, Bromma, Sweden.
[11] Versamid-930.
[12] Varaport 30.
[13] OV-225.
[14] Merck, Darmstadt, West Germany.
[15] Macherey, Nagel & Co, Düren, West Germany.

Table IV—Results for the Urinary Excretion of Iproniazid after Single-Dose Administration of 50 mg

Hours[a]	Urinary Concentration, C_u, μg/100 ml	Urinary Excretion, E_u, %	Rate of Excretion, $\Delta Ae/\Delta t$, μg/hr	Midpoint of Excretion Interval, t, hr
1.7	192	0.33	95.9	0.85
4.5	424	0.73	130.4	3.10
6.5	298	1.00	250.5	5.50
8.5	292	0.69	173.5	7.50
12.0	284	0.95	135.7	10.25
14.0	275	0.49	122.5	13.0
23.0	331	1.26	69.9	18.5
26.0	130	0.24	40.0	24.5
32.5	69	0.41	31.8	29.25
34.7	47	0.10	23.6	33.6

[a] Time in hours after oral intake of iproniazid.

N NH_4OH (90:10:1), and (B) benzene–methanol–diethylamine (90:10:1). After development, the plates were sprayed with phosphomolybdic acid reagent (8, 9) for visualization. For this reagent (8, 9), 5 g of phosphomolybdic acid[14] was dissolved in 100 ml of ethanol; after spraying, the TLC plates were exposed in a tank to ammonia vapors for 1 min.

RESULTS AND DISCUSSION

GLC of iproniazid, with its 2-butyl analog as an internal standard, was originally developed on three column systems, *i.e.*, 1% polyamide resin[11], 5% 50:50 cyanoethylmethyl dimethyl silicone gum[5], and 5% cyanopropyl phenyl silicone gum[13] (10). Separation of both compounds affords no problem, whereas quantitative measurement of iproniazid, determined on the calibration series, is feasible with a standard deviation, $\sigma_{\bar{k}}$, of about 1% or less. This excellent figure is undoubtedly due to the close structural similarity between the compound to be determined (iproniazid) and the internal standard (2-butyl analog) used.

To develop a logical extraction procedure for urine samples, partition coefficients of iproniazid between chloroform or ether and an aqueous basic or acidic phase were measured on the 5% 50:50 cyanoethylmethyl dimethyl silicone gum[5] column operated at 160° (Table II). These data indicate that iproniazid is better extracted from an aqueous ammonium sulfate–ammonium hydroxide solution with chloroform. However, the first isolation step is done with ether, because it is a more selective solvent with regard to the more apolar biological compounds and yields cleaner extracts.

Back-extraction from ether is then performed with an appropriate volume (3 × 25 ml) of 0.1 *N* HCl. Final transfer to the organic phase is achieved after alkalinization and addition of ammonium sulfate with the aid of chloroform. Six 200-ml urine samples spiked with amounts (50–400 μg) in the range anticipated for therapeutic levels of iproniazid were examined under the described conditions. Results obtained on the 5% 50:50 cyanoethylmethyl dimethyl silicone gum[5] column at 180° are presented in Table III and show a recovery relative to the internal standard of 78.2 ± 2.3%.

This performance seems acceptable, especially in view of the poor extractibility of iproniazid from an aqueous solution by double-phase extraction with organic solvents. In our experience, there is no other solution to overcome this effect than by a salting-out procedure. Although this salting-out technique increases the extraction capacity for iproniazid, it also coextracts many unwanted products as noticed in multiple analyses of blank urine samples. Small, but potentially interfering, peaks occur in all chromatographic patterns. For this reason, a careful comparison of the three GLC column systems, by injecting extracts of blank urine samples, was done at the beginning of these studies.

Quantitative determination on the 1% polyamide resin[11] column was given up because of interference from cotinine present in the extracts of urine of patients (smokers). Cotinine might be separated successfully from iproniazid by lowering the oven temperature to 150°, but this change results in lengthy analysis times. On the 5% cyanopropyl silicone gum[13] column, dibutyl phthalate was an artifact that overlapped with the internal standard under the experimental conditions. Therefore, all further analyses were carried out using the 5% 50:50 cyanoethylmethyl dimethyl silicone gum[5] column at 180°. It separated entirely unwanted products from the compound to be determined (iproniazid) and the internal standard.

Identification of the unwanted products by GLC–mass spectrometry revealed the presence of cotinine and hydroxycotinine (both normal metabolites of nicotine ingested by smokers), dibutyl phthalate (an artifact of organic solvents), and the xanthine derivatives (normal metabolites for coffee drinkers from caffeine) theobromine (3,7-dimethylxanthine) and paraxanthine (1,7-dimethyl-

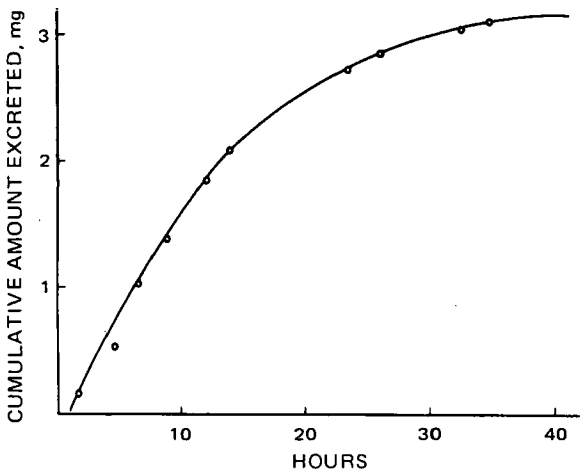

Figure 2—*Cumulative amount of iproniazid excreted in urine as a function of time for single-dose administration of 50 mg.*

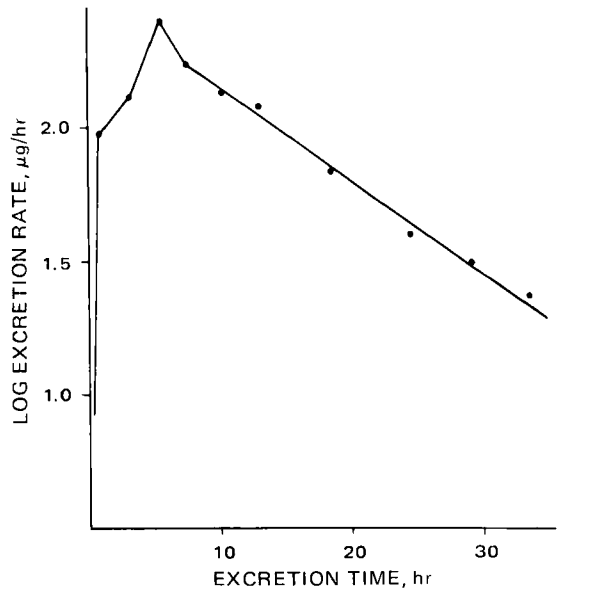

Figure 3—*Plot of the logarithm of the urinary excretion rate,* ΔAe/Δt, versus *the excretion time,* t.

Table V—Quantitative Results of GLC Determination of Iproniazid in Urine Samples of Psychiatric Patients Receiving Drug Therapy

Subject	Sample	Urinary Concentration, C_u, μg/100 ml	Urinary Excretion, E_u, %
2	1	178	3.89
	2	7	0.28
	3	120	3.29
	4	113	3.72
	5	165	4.02
3	1	125	2.42
	2	90	3.26
	3	107	2.80
	4	132	2.48
	5	193	3.85
4	1	156	7.37
	2	345	8.61
	3	140	3.41
	4	193	5.76
	5	264	6.07
5	1	46	2.72
	2	19	0.67
	3	22	0.34
	4	77	3.72
	5	60	3.14
	6	14	0.59

xanthine). With the exception of paraxanthine, which was detected only by comparison of its mass spectral data with those reported in the literature (11, 12), these compounds had identical retention characteristics on GLC analysis with authentic samples. No interference of the other drugs used or their metabolites was noticed in the chromatographic region where iproniazid and the internal standard eluted.

For verification of the specificity of results, aliquots of some urine extracts of psychiatric patients were examined by GLC–mass spectrometry. In all cases, iproniazid and the internal standard were positively identified by their mass spectral characteristics. Furthermore, other 200-ml aliquots of all urine samples of psychiatric patients were taken through the extraction procedure without the addition of the internal standard at the chloroform phase and chromatographed in Solvent Systems A and B by TLC. Except for one case, iproniazid was easily detected in all urine extracts (solvent system and R_f value: A, 0.6; and B, 0.3). Blank urine extracts developed in the same mobile phases did not yield interfering bands (spots).

Iproniazid was administered in a single dose of 50 mg to one subject, and successive urine outputs were collected and analyzed separately. A representative chromatogram is shown in Fig. 1. Results for the urinary excretion of free drug as a function of time is presented in Table IV. It appears that 6.21% of the orally administered dose of iproniazid was excreted cumulatively in urine within 34.7 hr (Fig. 2). These data can be treated to provide some pharmacokinetic information. Therefore, if it is assumed that the rate of excretion is proportional to the plasma concentration, then the proportionality constant is renal clearance, and a rate of excretion plot will parallel the plasma concentration curve. The latter allows one to determine the half-life.

From least-squares curve fit calculations performed on the last seven data ($\Delta Ae/\Delta t$ *versus* time), the exponential function $\Delta Ae/\Delta t = 310.1\, e^{-0.0785t}$ was found with a coefficient of correlation $r = 0.996$. The plot of log rate of excretion *versus* time (Fig. 3) indicates a half-life of 8.8 hr, which agrees well with results obtained by Koechlin *et al.* (3). Indeed, these authors indicated that the fall-off of the curves of the rates of urinary excretion of radioactivity reveals the presence of at least two components, with half-lives of approximately 10 and 17–20 hr, respectively. Comparison with our results identifies the first compound as free iproniazid.

Similar percent urinary excretion results were obtained for four psychiatric patients to whom doses of 25–75 mg of iproniazid were orally administered each day. A typical gas chromatogram of a urine extract from a psychiatric patient dosed with 75 mg of iproniazid is given in Fig. 4. Results for the percent urinary excretions of iproniazid in 24 hr are given in Table V. Under these conditions, 2–8% of the daily dose ingested was excreted in the 24-hr urine outputs.

The urinary excretion rate of iproniazid occurs rather slowly, as seen from results for Subject 1. Compared to iproclozide, another monoamine oxidase inhibitor drug described previously (13), the urinary excretion rate of iproniazid is about 15–20 times higher and the excretion persists for a much longer time after drug administration.

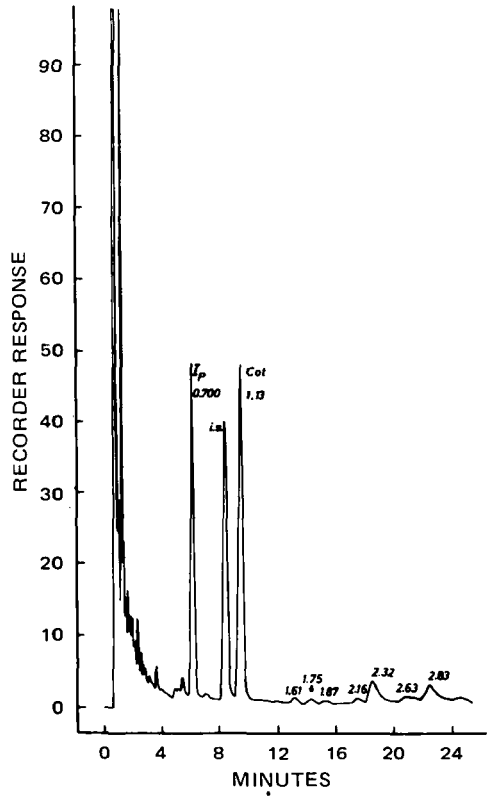

Figure 4—*Gas chromatogram of a urine extract from Subject 2. The column was 5% 50:50 cyanoethylmethyl dimethyl silicone gum (T = 180°, $\bar{u}_o$ = 14.3 cm/sec); Ip = iproniazid, is = internal standard, and Cot = cotinine).*

REFERENCES

(1) V. Nair, *Biochem. Pharmacol.*, **3**, 78(1959).

(2) B. Koechlin and V. Iliev, *Ann. N.Y. Acad. Sci.*, **80**, 864(1959).

(3) B. A. Koechlin, M. A. Schwartz, and W. E. Oberhaensli, *J. Pharmacol. Exp. Ther.*, **138**, 11(1962).

(4) K. B. Björnesjö and B. Jarnulf, *Scand. J. Clin. Lab. Invest.*, **14**, 408(1962).

(5) E. De Ritter, L. Drekter, J. Scheiner, and S. H. Rubin, *Proc. Soc. Exp. Biol. Med.*, **79**, 654(1952).

(6) R. M. de Sagher, A. P. De Leenheer, and A. E. Claeys, *J. Chromatogr. Sci.*, in press.

(7) H. L. Yale, K. Losee, J. Martins, M. Holsing, F. M. Perry, and J. Bernstein, *J. Am. Chem. Soc.*, **75**, 1933(1953).

(8) E. Schmid, E. Hoppe, C. Meythaler, Jr., and L. Zicha, *Arzneim.-Forsch.*, **13**, 969(1963).

(9) J. Drabner and W. Schwerd, *Z. Anal. Chem.*, **243**, 92(1968).

(10) R. M. de Sagher, A. P. De Leenheer, and A. E. Claeys, *J. Chromatogr. Sci.*, in press.

(11) C. D. Scott, "Advances in Clinical Chemistry," vol. 15, Academic, New York, N.Y., 1972, p. 28.

(12) H. Budzikiewicz, C. Djerassi, and D. H. Williams, "Structure Elucidation of Natural Products by Mass Spectrometry," vol. 1, Holden-Day, San Francisco, Calif., 1964, p. 214.

(13) R. M. de Sagher, A. P. De Leenheer, and A. E. Claeys, *Anal. Chem.*, **47**, 1144(1975).

ACKNOWLEDGMENTS AND ADDRESSES

Received May 20, 1975, from the *Laboratorium voor Analytische Chemie en Laboratoria voor Medische Biochemie en voor Klinische Analyse, Faculteit van de Farmaceutische Wetenschappen, Rijksuniversiteit, Academisch Ziekenhuis, 135 De Pintelaan,*

9000-Gent, Belgium.
Accepted for publication September 5, 1975.
The authors thank Mrs. A. Cruyl, recipient of a fellowship from the National Research Foundation (N.F.W.O.), for obtaining the mass spectra. They also are indebted to the National Foundation for Medical Research (F.G.W.O.) for supporting this work through Grants 20007 and 20210.
[x] To whom inquiries should be directed.

Solubilization as a Method for Studying Self-Association: Solubility of Naphthalene in the Bile Salt Sodium Cholate and the Complex Pattern of Its Aggregation

PASUPATI MUKERJEE [x] and JOHN R. CARDINAL [*]

Abstract □ Solubilization of uncharged, slightly soluble solutes is shown to be a useful approach for investigating patterns of self-association. The solubility of naphthalene in aqueous solutions of sodium cholate was determined over the concentration range of 0–0.20 mole/liter at 25°. Bile salts such as sodium cholate have many detergent-like properties and exhibit hydrophobic self-association in aqueous solutions. It has become customary to describe this aggregation using the model of micelle formation. The naphthalene solubility data show that the CMC for sodium cholate is not well defined. Comparison with solubilization in a typical micelle-forming system, sodium decanesulfonate, shows clearly that sodium cholate does not resemble a micelle-forming system. Further examination of the solubility data in terms of mutual association of naphthalene with aggregate species shows that the self-association of sodium cholate is not consistent with the formation of (*a*) only large micelles containing 10 or more monomers, (*b*) only dimers, (*c*) dimers and large micelles, and (*d*) any unique oligomer or multimer. A complex pattern of association, including the formation of dimers and one or more higher oligomers, is indicated.

Keyphrases □ Solubilization—method for study of self-association, naphthalene in aqueous solutions of sodium cholate compared to sodium decanesulfonate □ Micelle formation—solubilization of naphthalene in aqueous sodium cholate solutions compared to sodium decanesulfonate, method for study of self-association □ Naphthalene—solubility in aqueous sodium cholate solutions, method for study of self-association □ Sodium cholate—solvent for naphthalene, method for study of self-association

Bile salts are considered to be physiological surfactants (1–3). In common with ordinary surfactants or detergents, they contain a large hydrophobic moiety, which is responsible for their ability to emulsify and solubilize fats and lipids. Like detergents, they exhibit a tendency toward hydrophobic self-association (aggregation) in aqueous solution (1–8).

It has become customary to describe this aggregation using the model of detergent micelles (1–3). As discussed recently (9), hydrophobic self-association in aqueous solution can have very different patterns, depending upon the structure of the hydrophobic solutes. Fundamental requirements of an extensive cooperativity of self-association in the early stages of growth for a micelle-forming pattern of self-association and the existence of a critical micellization concentration (CMC) are not satisfied by all molecular structures.

The purposes of the present work were to examine how well the micellar model applies to the self-association of sodium cholate and to investigate the more general problem of how the solubilization by aggregates of a slightly soluble, uncharged solute can be used to provide information about self-association of aggregating solutes.

EXPERIMENTAL

Materials—Cholic acid[1] was recrystallized according to the method of Hofmann (10). Naphthalene[2] was purified by sublimation before use.

Apparatus—Absorbance measurements were made using silica cells of 1-cm path length in a spectrophotometer[3]. The constant-temperature bath for the solubilization studies was equipped with a thermoregulator[4], and the temperature was maintained at 25 ± 0.1°.

Solubility Experiments—Stock solutions of sodium cholate were obtained by titration of weighed quantities of cholic acid to pH 8–9 with sodium hydroxide solutions. These solutions were then brought to volume with double-distilled water. The desired concentrations of sodium cholate were prepared by volumetric dilution of this stock solution.

For the solubilization studies, 5 ml of a solution of sodium cholate was placed in a 2-dram vial to which naphthalene crystals were added in amounts more than sufficient to produce saturation. The vials were covered[5], sealed with parafilm, capped, placed in a water bath, and rotated at 25 ± 0.1° for 3 days. After this time, an appropriate volume, usually 2 ml, was withdrawn with a pipet whose tip had been covered with glass wool to filter excess crystals of naphthalene remaining in the solution.

The sample of cholate solution was quickly diluted to an appropriate volume with double-distilled water. The samples were always added to a volume of water close to that needed for the final volume to prevent precipitation of solid naphthalene crystals and to reduce loss of naphthalene by evaporation. Because of the volatility of naphthalene and its low solubility in water, losses due to evaporation on extensive handling of aqueous solutions can be serious.

[1] Aldrich Chemical Co., Milwaukee, WI 53233
[2] Baker and Adamson quality, Allied Chemicals, Morristown, N.J.
[3] Cary 16.
[4] Model 20, Bronwill Scientific, Rochester, N.Y.
[5] With a liner of Teflon (du Pont).

9000-Gent, Belgium.
Accepted for publication September 5, 1975.
The authors thank Mrs. A. Cruyl, recipient of a fellowship from the National Research Foundation (N.F.W.O.), for obtaining the mass spectra. They also are indebted to the National Foundation for Medical Research (F.G.W.O.) for supporting this work through Grants 20007 and 20210.
[x] To whom inquiries should be directed.

Solubilization as a Method for Studying Self-Association: Solubility of Naphthalene in the Bile Salt Sodium Cholate and the Complex Pattern of Its Aggregation

PASUPATI MUKERJEE [x] and JOHN R. CARDINAL [*]

Abstract □ Solubilization of uncharged, slightly soluble solutes is shown to be a useful approach for investigating patterns of self-association. The solubility of naphthalene in aqueous solutions of sodium cholate was determined over the concentration range of 0–0.20 mole/liter at 25°. Bile salts such as sodium cholate have many detergent-like properties and exhibit hydrophobic self-association in aqueous solutions. It has become customary to describe this aggregation using the model of micelle formation. The naphthalene solubility data show that the CMC for sodium cholate is not well defined. Comparison with solubilization in a typical micelle-forming system, sodium decanesulfonate, shows clearly that sodium cholate does not resemble a micelle-forming system. Further examination of the solubility data in terms of mutual association of naphthalene with aggregate species shows that the self-association of sodium cholate is not consistent with the formation of (*a*) only large micelles containing 10 or more monomers, (*b*) only dimers, (*c*) dimers and large micelles, and (*d*) any unique oligomer or multimer. A complex pattern of association, including the formation of dimers and one or more higher oligomers, is indicated.

Keyphrases □ Solubilization—method for study of self-association, naphthalene in aqueous solutions of sodium cholate compared to sodium decanesulfonate □ Micelle formation—solubilization of naphthalene in aqueous sodium cholate solutions compared to sodium decanesulfonate, method for study of self-association □ Naphthalene—solubility in aqueous sodium cholate solutions, method for study of self-association □ Sodium cholate—solvent for naphthalene, method for study of self-association

Bile salts are considered to be physiological surfactants (1–3). In common with ordinary surfactants or detergents, they contain a large hydrophobic moiety, which is responsible for their ability to emulsify and solubilize fats and lipids. Like detergents, they exhibit a tendency toward hydrophobic self-association (aggregation) in aqueous solution (1–8).

It has become customary to describe this aggregation using the model of detergent micelles (1–3). As discussed recently (9), hydrophobic self-association in aqueous solution can have very different patterns, depending upon the structure of the hydrophobic solutes. Fundamental requirements of an extensive cooperativity of self-association in the early stages of growth for a micelle-forming pattern of self-association and the existence of a critical micellization concentration (CMC) are not satisfied by all molecular structures.

The purposes of the present work were to examine how well the micellar model applies to the self-association of sodium cholate and to investigate the more general problem of how the solubilization by aggregates of a slightly soluble, uncharged solute can be used to provide information about self-association of aggregating solutes.

EXPERIMENTAL

Materials—Cholic acid[1] was recrystallized according to the method of Hofmann (10). Naphthalene[2] was purified by sublimation before use.

Apparatus—Absorbance measurements were made using silica cells of 1-cm path length in a spectrophotometer[3]. The constant-temperature bath for the solubilization studies was equipped with a thermoregulator[4], and the temperature was maintained at 25 ± 0.1°.

Solubility Experiments—Stock solutions of sodium cholate were obtained by titration of weighed quantities of cholic acid to pH 8–9 with sodium hydroxide solutions. These solutions were then brought to volume with double-distilled water. The desired concentrations of sodium cholate were prepared by volumetric dilution of this stock solution.

For the solubilization studies, 5 ml of a solution of sodium cholate was placed in a 2-dram vial to which naphthalene crystals were added in amounts more than sufficient to produce saturation. The vials were covered[5], sealed with parafilm, capped, placed in a water bath, and rotated at 25 ± 0.1° for 3 days. After this time, an appropriate volume, usually 2 ml, was withdrawn with a pipet whose tip had been covered with glass wool to filter excess crystals of naphthalene remaining in the solution.

The sample of cholate solution was quickly diluted to an appropriate volume with double-distilled water. The samples were always added to a volume of water close to that needed for the final volume to prevent precipitation of solid naphthalene crystals and to reduce loss of naphthalene by evaporation. Because of the volatility of naphthalene and its low solubility in water, losses due to evaporation on extensive handling of aqueous solutions can be serious.

[1] Aldrich Chemical Co., Milwaukee, WI 53233
[2] Baker and Adamson quality, Allied Chemicals, Morristown, N.J.
[3] Cary 16.
[4] Model 20, Bronwill Scientific, Rochester, N.Y.
[5] With a liner of Teflon (du Pont).

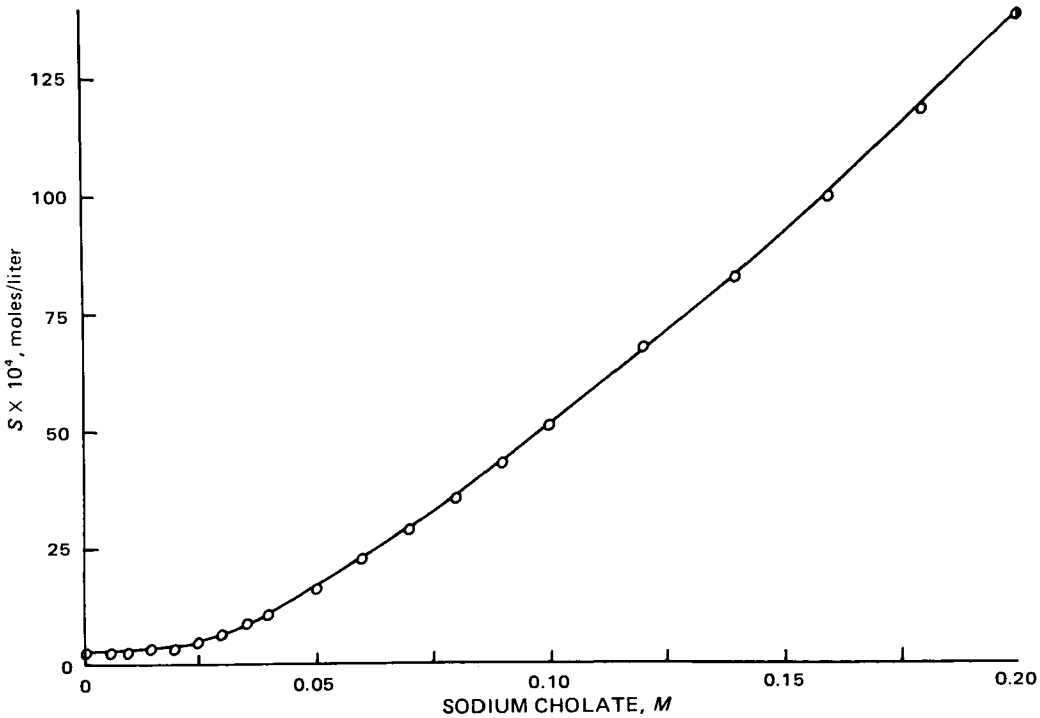

Figure 1—*Solubility of naphthalene, S, in aqueous solutions of sodium cholate at 25°.*

The concentration of naphthalene was determined by absorbance measurements at 276.0 nm. The wavelength of maximum absorbance of naphthalene changes with the increasing concentration of sodium cholate. This effect is negligible, however, when the concentration is low. Solutions at high concentrations of sodium cholate were always diluted to concentrations less than 0.007 *M* before absorbance measurements were performed.

The molar absorptivity of naphthalene was determined at 276.0 nm by dilution of a concentrated solution of naphthalene in a 50% water–methanol (v/v) mixture with sufficient water to reduce the methanol concentration to less than 0.5%. The value of the absorptivity was 5.070×10^3 liters/mole cm. This value compares favorably with the values of 4.946×10^3 and 4.927×10^3 reported (11) for two different samples of naphthalene determined by essentially the same technique.

RESULTS

The solubility, *S*, in moles per liter of naphthalene in water and sodium cholate solutions up to 0.2 *M* is shown in Fig. 1. Each value is the average of three to six determinations. The solubility in water was 2.55×10^{-4} *M*, as compared to the 2.62×10^{-4} *M* value found by Gordon and Thorne (11). This small difference appears to be due mainly to different estimates of molar absorptivities. The average absorbance measurements of saturated solutions of naphthalene in water agree within 0.2%.

DISCUSSION

The variation in the solubility of naphthalene with sodium cholate concentration (Fig. 1) is qualitatively similar to the results of numerous investigations reporting the solubilization of slightly soluble, uncharged, hydrophobic solutes by aggregating micelle-forming surfactants (12–14). The solubility changes relatively little below a certain concentration range and increases comparatively rapidly above this range. This rapid increase is generally attributed to the formation of micelles.

Such solubilization data are frequently used to determine CMC values (3, 12). This discussion will be concerned primarily with the meaning and significance of any such CMC value for sodium cholate and how solubilization data of the kind presented can be used to derive limited information on the pattern of self-association exhibited by aggregating hydrophobic solutes.

Limiting Association Concentrations—Some investigators (5, 7) suggested that bile salts, including sodium cholate, have three limiting association concentrations. According to this picture, the association begins above limit 1, but all of the added bile salt does not associate to form higher aggregates until above limit 2. Limits 2 and 3 are associated with changes in the aggregation numbers. Below limit 2, the aggregation numbers for sodium cholate fall in the 2–5 range; between limits 2 and 3, the aggregation number is about 5; above limit 3, the aggregation number is in the 15–20 range. For sodium cholate, these limiting concentrations are: limit 1, 0.013–0.015 *M*; limit 2, 0.045–0.050 *M*; and limit 3, 0.09–0.11 *M*.

The solubility data in Fig. 1 appear to be best represented by a smooth curve, with little evidence of any distinct "kink" or "break" at the limiting concentrations mentioned previously. To illustrate this point further, the ratio of the increment in solubility, $\Delta S = S_2 - S_1$, between adjacent concentrations and the increment in concentration, $\Delta C = C_2 - C_1$, were calculated, and $\Delta S/\Delta C$ was plotted against the mean concentration, $\bar{C} = (C_2 + C_1)/2$ (Fig. 2).

The value of $\Delta S/\Delta C$ thus calculated is *approximately* equivalent to the rate of change of *S* with *C*; $\Delta S/\Delta C$ measures the average value of the rate of change of *S* with *C* over the concentration range $C_2 - C_1$. It is subject to the error inherent in small increments such as ΔS or ΔC. It avoids, however, the uncertainties of differentiation by graphical or other means, which sometime involve subjective interpolations of data. The procedure is similar to that used previously (15, 16) for specific conductance (κ) data of ionic surfactants, in which 10^3

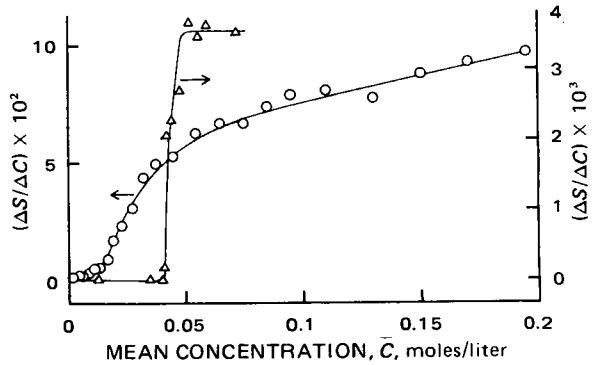

Figure 2—*The* ΔS/ΔC versus C̄ *plots (see text for definition). Key:* ○, *naphthalene in sodium cholate; and* △, *Orange OT in sodium decanesulfonate [based on data from Schott (14)].*

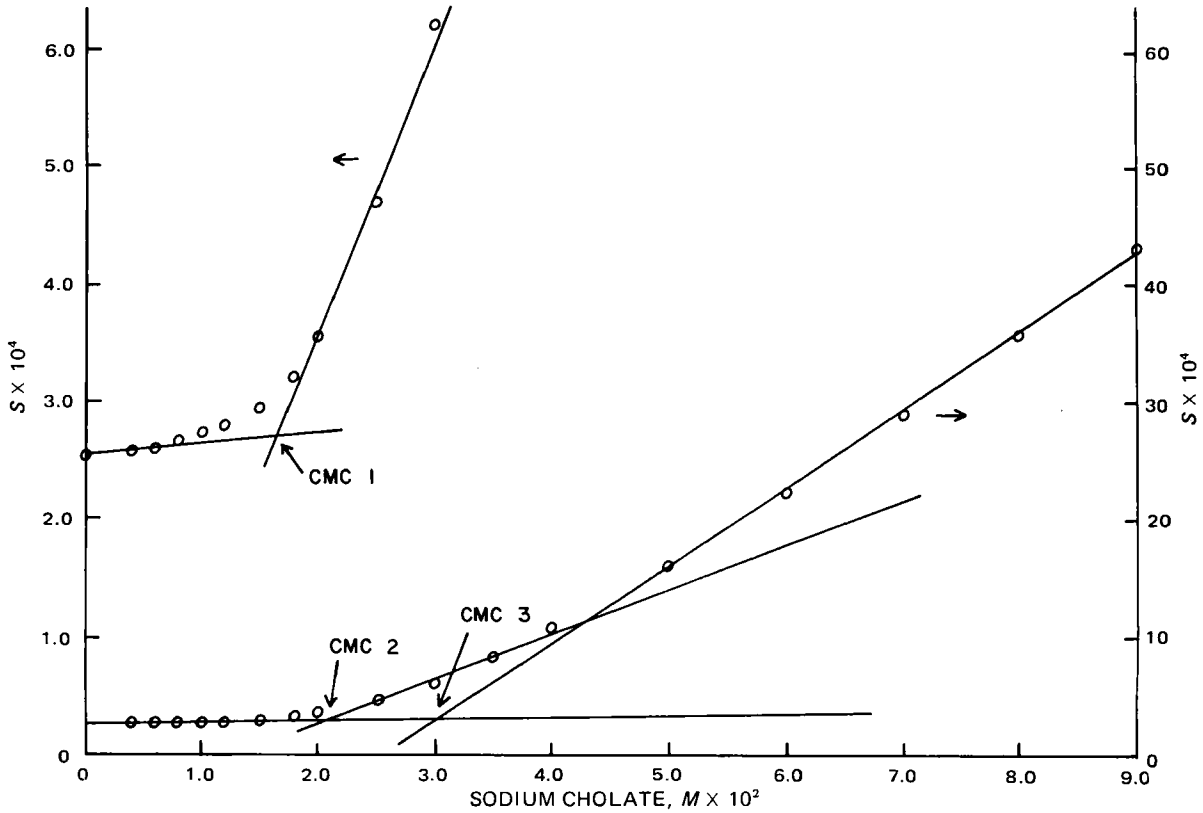

Figure 3—*Three different apparent CMC values from naphthalene solubilization data in sodium cholate* (S *in moles per liter*).

$\Delta\kappa/\Delta C$, the differential equivalent conductivity, is plotted against the mean concentration to demonstrate the abrupt transition brought about by micelle formation at the CMC in solutions of ionic surfactants containing flexible chains.

For comparison with a typical ionic detergent, Fig. 2 includes a $\Delta S/\Delta C$ *versus* $\bar{C}$ plot from the careful measurements of the solubility of Orange OT, a slightly soluble uncharged dye, in sodium decanesulfonate reported by Schott (14). The nearly vertical rise in $\Delta S/\Delta C$ for Orange OT in a typical detergent, sodium decanesulfonate, in the CMC region shows the effect of highly cooperative self-association, which leads to the beginning of the formation of large micelles at about the CMC (9, 15). The $\Delta S/\Delta C$ of naphthalene in sodium cholate shows no such abrupt transition. The mild upturn at about 0.017 *M* is followed by a continuous rise in $\Delta S/\Delta C$ over nearly a factor of 10 in concentration. In particular, there is no evidence of any other limiting association concentration across which $\Delta S/\Delta C$ shows any sharp rise. Therefore, it was concluded that the postulate of several limiting association concentrations is not tenable for sodium cholate.

CMC—Solubilization data of the kind presented in Fig. 1 are used to determine the CMC's of bile salts (3). In Fig. 3, the data below 0.09 *M* sodium cholate are plotted to examine the significance of this CMC. If the CMC is estimated by the usual procedure of linear extrapolations of data below and above the CMC (12), very different CMC values are obtained, depending upon what sections of the data are used. Three such apparent CMC values are indicated in Fig. 3. Depending upon which portion of the solubility curve is used, apparent CMC values can be obtained at 1.6, 2.0, or 3.0×10^{-2} *M*.

For surfactants with flexible chains forming micelles, such solubilization data do not allow a variation of more than 1–2% in the CMC value when using data over roughly a factor of 1.5–2 in concentrations below and above the CMC to locate the CMC (13, 14). Although many CMC data for sodium cholate and other bile salts are reported in the literature from similar studies (3), their significance is clearly rather limited. In particular, if some data in the transition region are absent, the CMC determination may *appear to be* quite reliable.

The problems associated with the determination of precise CMC values of bile salts and similar rigid molecules were pointed out previously (9, 12). In their compilation and evaluation of CMC data (12), Mukerjee and Mysels chose not to include any value for the bile salts. They pointed out "that the existence of a c.m.c. requires that higher multimers be relatively more stable than the small oligomers and that this requirement is met most commonly when the monomeric unit is a flexible chain."

Hydrophobic solutes with rigid monomers, such as bile salts and fused ring aromatic or heteroaromatic compounds, are expected to have rather diffuse and extended concentration ranges over which the degree of aggregation increases from low to high values (9, 12). The patterns of self-association they exhibit are different from micellar self-association involving extensive cooperativity in the early stages of growth (9). Nevertheless, such systems often lend themselves to the application of the micellar hypothesis if an apparent CMC value is obtained from limited data used in an uncritical fashion (9). If the CMC values are used to estimate monomer and micelle concentrations and thermodynamic quantities associated with micelle formation, rather serious errors of interpretation become likely (9).

ASSOCIATION MODELS

The preceding discussion of the nature of the solubilization of naphthalene by sodium cholate indicates strongly that the pattern of its self-association does not resemble that of micelle-forming surfactants containing flexible chains. Further examination of the solubility data provide some additional insight into the nature of the self-association. In this analysis, the solubilization of naphthalene as a typical uncharged, slightly soluble solute is used as a marker for the extent of association. If the monomer concentration is denoted by $[b_1]$ and an aggregate, b_n, forms according to Scheme I:

$$nb_1 \rightleftharpoons b_n$$

Scheme I

the formation of b_n is governed by the equilibrium constant β_n:

$$\beta_n = \frac{[b_n]}{[b_1]^n} \qquad \text{(Eq. 1)}$$

Then the amount solubilized, defined as $\Delta N = S - S_0$, where S is the solubility in the presence of sodium cholate and S_0 is the solubility in pure water, can be written as:

$$\Delta N = Kn[b_n] \qquad \text{(Eq. 2)}$$

where $n[b_n]$ is the monomer-equivalent concentration of the aggregate, and K is a proportionality constant. Equation 2 is valid because the activity of the solubilizate, naphthalene, is constant in these experiments under saturation conditions. Thus, if a series of mutual association equilibria between b_n and naphthalene, N, are postulated (Scheme II):

$$b_n + N \overset{K_1}{\rightleftharpoons} b_nN,\ b_n + 2N \overset{K_2}{\rightleftharpoons} b_nN_2, \ldots$$

Scheme II

the total amount of naphthalene solubilized is given by:

$$\Delta N = \sum_{i=1}^{\infty} i[b_nN_i] = \sum_{i=1}^{\infty} iK_i[b_n][N]^i \qquad \text{(Eq. 3)}$$

At saturation:

$$\Delta N = [b_n] \sum_{i=1}^{\infty} iK_i[S_0]^i \qquad \text{(Eq. 4)}$$

i.e., ΔN is proportional to $[b_n]$ (Eq. 2). The postulated equilibria assume ideality and neglect charge effects and counterion binding (17–20). These effects will be discussed later. For approximate treatment, the contribution of the $[b_nN_i]$ species to the total concentration, C, also is neglected so that:

$$C = [b_1] + n[b_n] \qquad \text{(Eq. 5)}$$

The ratio $\Delta N/C$ has values of 0.005 at 0.02 M, 0.021 at 0.04 M, 0.033 at 0.06 M, 0.049 at 0.1 M, and 0.068 at the highest concentration 0.2 M. The neglect of the aggregates containing naphthalene is not a serious approximation, particularly in dilute solutions (see later discussion).

To examine some specific models of association, log ΔN was plotted against log C and compared with predictions of the models (Fig. 4). The data at the lowest concentrations are rather uncertain because small differences in solubilities are involved. Some estimated error bars are indicated. The uncertainty of ΔN decreases rapidly with an increasing concentration of sodium cholate. At the higher concentrations, if C is corrected for the $[b_nN_i]$ species, the experimental curve would become steeper or, conversely, the calculated curves would be less steep.

Dimer Model—Several investigations (7, 21) indicate that the degree of aggregation for sodium cholate in the absence of electrolyte is about two. This dimer model can be shown to be inconsistent with our data. If a low value of 1.0 liter/mole is used for the dimerization constant, β_2 ($n = 2$ in Eq. 1), and the ΔN value at 0.015 M is fitted with the appropriate K value (Eq. 2) of 0.092 liter/mole, curve 2 is obtained. This curve is consistent with the data at the lowest concentrations but falls considerably below the experimental curve at higher concentrations. When using a higher value of 20.0 liters/mole for β_2 and fitting again at 0.015 M with the appropriate K value, curve 3 is obtained, which deviates more than curve 2 at the higher concentrations from curve 1.

The calculations have so far neglected charge effects, which are certainly important for self-association of ions. Upon applying corrections for activity coefficient variations using the Debye–Hückel limiting law for dimerization of monovalent ions according to Ghosh and Mukerjee (20), it is found that β_2 increases by a factor of 2.5 as the ionic strength increases from 0.01 to 0.25. If a further correction is applied for the shielding of the charges in the dimer, *i.e.*, reduction of the charge–charge repulsion of the dimer on increasing the ionic strength (22), β_2 can increase even more at higher ionic strengths. However, if it is assumed that these factors increase β_2 by a factor as large as 10, from 20 to 200 liters/mole as the concentration changes from 0.015 to 0.2 M, point 4 is obtained (Fig. 4). The improvement is only very slight.

Unique Oligomer Model—The possibility of the formation of any other unique oligomer, such as a tetramer, can be tested in a similar manner. Curve 5 in Fig. 4 shows, for example, that a 10-mer model ($n = 10$ in Eqs. 1 and 2 and Scheme I) fitted at the 0.015 M concentration is unsatisfactory, particularly in dilute solutions. A more general approach is outlined here and should apply to a variety of systems.

By neglecting charge effects and assuming ideality, *i.e.*, the applicability of Schemes I and II and Eqs. 1–5, one has:

$$C = [b_1] + n\beta_n[b_1]^n \qquad \text{(Eq. 6)}$$

and:

$$\Delta N = Kn\beta_n[b_1]^n \qquad \text{(Eq. 7)}$$

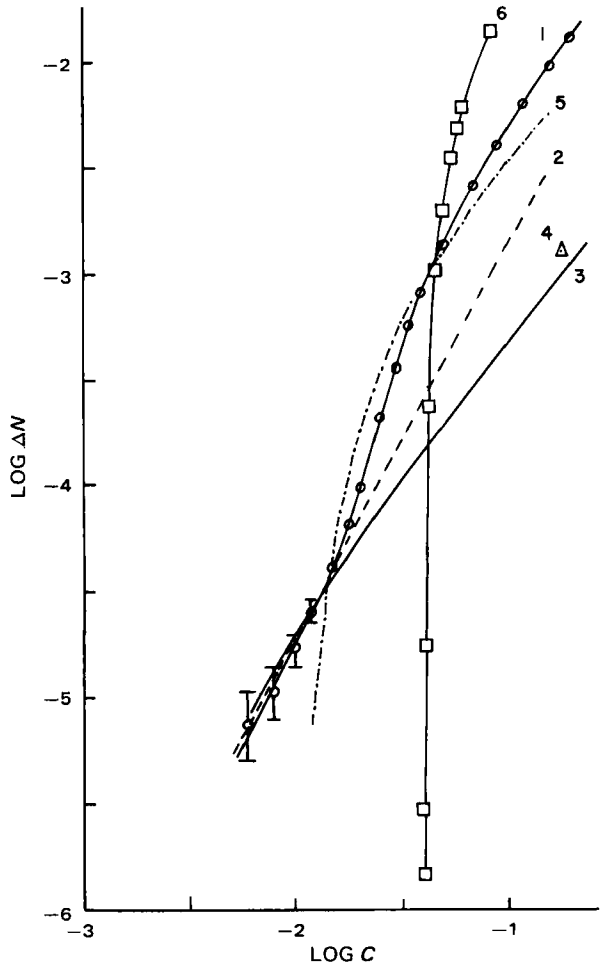

Figure 4—*Logarithm of the increase in concentration of the solubilizate, $\Delta N = S - S_0$, where S_0 is the solubility in the absence of surfactant, plotted against logarithm of the surfactant concentration. Key: ○, curve 1, naphthalene in sodium cholate; □, curve 6, Orange OT in sodium decanesulfonate [based on data from Schott (14)]; curve 2, dimer model with a low dimerization constant (1.0 liter/mole); curve 3, dimer model with a high dimerization constant (20 liters/mole); Δ, point 4, effect of applying several corrections (see text) on the dimer model of curve 3; and curve 5, the 10-mer model. All theoretical models (curves 2, 3, and 5) are fitted to the experimental curve (curve 1) at about 0.015* M.

such that:

$$R = \frac{d \ln \Delta N}{d \ln C} = \frac{(Kn^2\beta_n[b_1]^{n-1})([b_1] + n\beta_n[b_1]^n)}{(1 + n^2\beta_n[b_1]^{n-1})(Kn\beta_n[b_1]^n)} \qquad \text{(Eq. 8)}$$

where R measures the slope of the log ΔN *versus* log C curve in Fig. 4. The value of R according to Eq. 8 is maximum in dilute solutions: $R \to n$ as $C \to 0$. The value of R decreases continuously from n as C increases and approaches unity at high concentrations. The experimental curve in Fig. 4 shows a slope of about 2 in dilute solutions, indicating formation of dimers. The slope, however, *increases* with concentration to a maximum of about 3.4 and then decreases at higher concentrations. The data are thus inconsistent with the formation of any unique oligomer or multimer with a constant aggregation number.

In Eq. 6, the contribution of the aggregates containing naphthalene, *i.e.*, the b_nN_i species, are neglected. If these are included, then, by using Eq. 1 and Scheme II, C is given by:

$$C = [b_1] + n\beta_n[b_1]^n + n\sum_{i=1}^{\infty}[b_nN_i] =$$

$$[b_1] + n\beta_n[b_1]^n(1 + \sum_{i=1}^{\infty} K_iS_0{}^i) \qquad \text{(Eq. 9)}$$

Under saturation conditions, $\Sigma_{i=1}^{\infty} K_i S_0^i$ is a constant. If the full equation (Eq. 9) is used to derive R, the limiting values of R at low concentrations ($r \rightarrow n$ as $C \rightarrow 0$) or high concentrations ($R \rightarrow 1$ as $C \rightarrow \infty$) are not affected. However, the values of R at intermediate concentrations are changed.

When ionic surfactants form large micelles, counterion binding becomes very important (17–19). The mass action approach here (18) is represented by Scheme III:

$$nb_1^- + m\mathrm{Na}^+ \rightleftharpoons b_n^{-(n-m)}$$

Scheme III

where b_1^- is the monomer, Na^+ is a representative counterion, and n is the aggregation number, the charge of the micelle, b_n, being $-(n - m)$. If this equilibrium is governed by the equilibrium constant β^*, as given by:

$$\beta^* = \frac{[b_n]^{-(n-m)}}{[b_1^-]^n[\mathrm{Na}^+]^m} \qquad \text{(Eq. 10)}$$

and if Eq. 2 continues to apply, *i.e.*, the solubilization under saturation conditions is proportional to the micelle concentration, then it can be shown by proper substitution in Eqs. 6 and 7 that $(d \ln \Delta N)/(d \ln C) \rightarrow n + m$ as $C \rightarrow 0$. Thus, the solubilization increases more rapidly with concentration because of counterion participation. This limiting slope again remains unaffected if $[b_n N_i]$ species are included in C. When n is large, close to the CMC, under these idealized conditions, $R \rightarrow n + m$ when the solubilization just becomes appreciable.

The data of Schott (14) on the solubilization of Orange OT by sodium decanesulfonate, when plotted on a log–log scale (curve 6, Fig. 4), give a limiting mean value of 80 ± 20 for R at the four lowest concentrations reported. These concentrations are all actually below the reported CMC but are within about 10% of it. Since the value of m is frequently found to be about $2n/3$ (17–19), this would correspond to an aggregation number of about 48 for the micelles of sodium decanesulfonate. Because of the low absorbance measurements involved, this value is unlikely to be accurate. It is, however, consistent with the formation of large micelles by sodium decanesulfonate close to the CMC or below it.

Aggregation Model for Sodium Cholate—This analysis indicates that the self-association of sodium cholate involves dimerization as well as the formation of higher aggregates. More detailed analysis of the data rapidly loses significance because of the uncertainties of the assumed models. Thus, if the model of a dimer and one higher multimer is used, the uncertainty due to the unknown counterion binding of the higher multimer becomes serious. If ideality is assumed and counterion participation is neglected, a value of n of about 5 is derived for the inflection point of the log–log plot of Fig. 4, where the maximum slope is 3.4. Because of counterion participation, the true value of n is likely to be lower.

Further evidence that the average value of n remains low even at higher concentrations is indicated by Fig. 2. Thus, whereas $\Delta S/\Delta C$ is nearly independent of concentration for ordinary detergents from a concentration only about 10% above the CMC, as indicated by the results of sodium decanesulfonate in Fig. 2 and many results in the literature (12–14), it increases continuously for naphthalene in sodium cholate solutions by 25% as the concentration increases from 0.1 to 0.2 *M*, *i.e.*, in a range some five to 10 times the apparent CMC values. Thus, even at these high concentrations, the composition of the aggregates, as reflected in their solubilization capacity, changes markedly with concentration.

It was concluded, therefore, that the self-association of sodium cholate, as revealed by the solubilization of naphthalene, is inconsistent with (*a*) a micellar pattern of association involving only large aggregates; (*b*) the formation of any single oligomer, including a dimer; and (*c*) the formation of dimers and large aggregates. A complex pattern of association including the formation of dimers and one or more higher oligomers is indicated. Whether the aggregation involves open-ended continued association of the kind exhibited by the stacking interactions of planar molecules (9) or whether it is more complex remains to be investigated.

REFERENCES

(1) A. F. Hofmann and D. M. Small, *Annu. Rev. Med.*, **18**, 333(1967).

(2) M. C. Carey and D. M. Small, *Am. J. Med.*, **49**, 590(1970).

(3) D. M. Small, in "The Bile Acids," P. P. Nair and D. Kritchevsky, Eds., Plenum, New York, N.Y., 1971, chap. 8.

(4) S. A. Johnston and J. W. McBain, *Proc. R. Soc. London, Ser. A*, **181**, 119(1943).

(5) P. Ekwall, K. Fontell, and A. Sten, *Proc. Int. Congr. Surf. Act., 2nd*, **1957**, 397.

(6) K. Fontell, *Kolloid Z. Z. Polym.*, **244**, 246(1971).

(7) *Ibid.*, **244**, 253(1971).

(8) *Ibid.*, **250**, 333(1972).

(9) P. Mukerjee, *J. Pharm. Sci.*, **63**, 972(1974).

(10) A. F. Hofmann, *Acta Chem. Scand.*, **17**, 173(1963).

(11) J. E. Gordon and R. L. Thorne, *J. Phys. Chem.*, **71**, 4390(1967).

(12) P. Mukerjee and K. J. Mysels, "Critical Micelle Concentrations of Aqueous Surfactant Systems," NSRDS-NBS 36, U. S. Government Printing Office, Washington, D.C., 1971.

(13) R. J. Williams, J. N. Phillips, and K. J. Mysels, *Trans. Faraday Soc.*, **51**, 728(1955).

(14) H. Schott, *J. Phys. Chem.*, **70**, 2966(1966).

(15) G. S. Hartley, "Aqueous Solutions of Paraffin-Chain Salts," Hermann, Paris, France, 1936.

(16) K. J. Mysels and R. J. Otter, *J. Colloid Sci.*, **16**, 462(1961).

(17) K. Shinoda, T. Nakagawa, B. Tamamushi, and T. Isemura, "Colloidal Surfactants," Academic, New York, N.Y., 1963.

(18) P. Mukerjee, *Adv. Colloid Interface Sci.*, **1**, 241(1967).

(19) P. Mukerjee, K. J. Mysels, and P. Kapauan, *J. Phys. Chem.*, **71**, 4166(1967).

(20) A. K. Ghosh and P. Mukerjee, *J. Am. Chem. Soc.*, **92**, 6408(1970).

(21) D. M. Small, *Adv. Chem. Ser.*, **84**, 31(1968).

(22) P. Mukerjee, *J. Phys. Chem.*, **62**, 1397(1958).

ACKNOWLEDGMENTS AND ADDRESSES

Received July 21, 1975, from the *School of Pharmacy, University of Wisconsin, Madison, WI 53706*

Accepted for publication August 13, 1975.

Presented in part at the Basic Pharmaceutics Section, APhA Academy of Pharmaceutical Sciences, San Francisco meeting, April 1975.

Abstracted in part from a dissertation submitted by J. R. Cardinal to the University of Wisconsin in partial fulfillment of the Doctor of Philosophy degree requirements.

Supported by the Wisconsin Alumni Research Foundation and Public Health Service Research Grant AM 17281-01.

* Present address: College of Pharmacy, University of Utah, Salt Lake City, UT 84112

[x] To whom inquiries should be directed.

Iodometric and Spectrophotometric Assays for Cephradine after Its Hydrolysis with a β-Lactamase

B. MAY FRANTZ

Abstract □ Iodometric and spectrophotometric methods were developed for the analysis of the new antibiotic cephradine. The procedures are modifications of known methods but are novel in employing a specific β-lactamase for hydrolysis of the β-lactam ring of the cephalosporin molecule. The iodometric method is rapid, precise, and accurate, but it requires fairly large amounts of cephradine. The spectrophotometric method, using differential UV absorption at 260 nm, is more rapid and more sensitive than the iodometric method but somewhat less accurate. Both methods proved useful for the routine assay of cephradine in certain formulations.

Keyphrases □ Cephradine—iodometric and spectrophotometric analyses, pharmaceutical formulations □ Iodometry—analysis, cephradine, pharmaceutical formulations □ Spectrophotometry—analysis, cephradine, pharmaceutical formulations □ Antibiotics—cephradine, iodometric and spectrophotometric analyses, pharmaceutical formulations

Many assay methods for the cephalosporins have been developed from procedures originally utilized for the assay of penicillins and have been based primarily on the presence of the β-lactam ring in both classes of antibiotics. Although microbiological assays using agar diffusion (1) or photometric (2) procedures are preferred for the determination of cephalosporins in pharmaceutical preparations, body fluids, and formulations being studied for long-term stability, they are imprecise and tedious.

Chemical methods commonly used for the assay of β-lactam antibiotics are based on determining the products formed after hydrolysis of the β-lactam ring. The methods include an iodometric procedure (3), the hydroxylamine procedure (4), a manometric assay (5), and an alkalimetric method (6). All of these chemical methods can be performed rapidly but sometimes lack the specificity of the microbiological assays. This lack of specificity is particularly true of the hydroxylamine method, since many amides, anhydrides, esters, aldehydes, and ketones react with hydroxylamine and give rise to erroneous results.

The iodometric method, which is based on the measurement of the penicilloic acid formed upon alkaline hydrolysis of penicillin, is more specific. Direct spectrophotometric methods for cephalosporins (7) and, more recently, for penicillin (8) have been reported but have not been used extensively in the routine analysis of these antibiotics.

Although Alicino (9) successfully applied the iodometric assay to the determination of cephalosporin C, attempts in this laboratory to apply this method to the determination of cephradine {7-[D-(−)-2-amino-2-(1,4-cyclohexadien-1-yl)acetamido]-3-methyl-8-oxo-5-thia-1-azabicyclo[4.2.0]oct-2-ene-2-carboxylic acid} in formulations being studied for long-term stability gave erratic results. The recent development[1] in this laboratory of a β-lactamase (EC 3.5.2.6) with a high specificity toward cephradine and such related cephalosporins as cephalexin (7-[D-2-amino-2-phenylacetamido] - 3 - methyl-8-oxo-5-thia-1-azabicyclo-[4.2.0]oct-2-ene-2-carboxylic acid) prompted the development of an analytical method based on the iodometric procedure but using the enzyme for the specific hydrolysis of the β-lactam ring.

At the same time, a spectrophotometric assay for cephradine was developed, using the β-lactamase for hydrolysis. It is based on the assay described (7) for screening compounds for β-lactamase sensitivity and is similar to a published assay (10) in which the decrease in the characteristic UV absorption of the cephalosporin was determined after enzymatic hydrolysis.

[1] Unpublished data.

EXPERIMENTAL

Chemicals—All chemicals were reagent grade. 7-Aminodeacetoxycephalosporanic acid[2], cephradine[3] used for standard solutions, and penicillin G potassium[4] were house products.

Enzymes—The β-lactamase, called cephradinase, was prepared essentially as described by Hennessey and Richmond (11), with the following exceptions: sodium β-glycerophosphate was omitted from the culture medium; the organism used was a species of *Enterobacter* originally isolated as a secondary infection from a cancer patient and now part of the Squibb Microbiology Culture Collection (SC 8415); the medium was inoculated with 1.0 ml of a 5.0-ml suspension of the organism washed from a slant of yeast beef agar with 0.1% peptone water; the inducer used was cephradine; and growth of the culture was continued for 67 hr.

The enzyme used in the assays was a crude preparation of the β-lactamase obtained by sonication of the cells in 0.1 *M* phosphate buffer, pH 8.0, and removal of the cell debris by centrifugation. The enzyme was diluted in 0.1 *M* phosphate buffer, pH 8.0. The unit of activity of this enzyme has been defined as the number of micromoles of cephradine hydrolyzed per hour by 1 ml of enzyme solution at room temperature (23–25°). Penicillinase concentrate[5], with an activity of 1×10^6 kinetic units/ml, was diluted 100 times in 0.1 *M* phosphate buffer, pH 7.0, before use.

Preparation of Solutions—Phosphate buffers and phthalate buffer were prepared as described previously (12). A 0.01 *N* sodium thiosulfate solution was prepared from a 0.1 *N* sodium thiosulfate solution that had been standardized against potassium iodate. A 0.0094 *N* iodine solution was prepared from a 0.1 *N* iodine solution and standardized by direct titration against the 0.01 *N* sodium thiosulfate solution.

Methods—All incubations were carried out at room temperature (23–25°). Unless otherwise stated, cephradinase (β-lactamase) solutions with activities of approximately 50 units/ml were used.

Iodometric Assay Using Enzymatic Hydrolysis—Cephradine samples or standards were prepared in 0.1 *M* phosphate buffer, pH 7.0, to give final concentrations of approximately 500 μg/ml (450-μg/ml potency). Duplicate 5.0-ml aliquots of a cephradine sample solution were incubated with 2.0 ml of cephradinase solution for 30 min. A third 5.0-ml aliquot was used as a control and was incubated with 2.0 ml of 0.1 *M* phosphate buffer, pH 8.0, for the same time.

[2] Lot 2005/C-1005, Squibb Chemical Development Laboratories, New Brunswick, N.J.

[3] Cephradine dihydrate, Lot NN005NB, biological potency 900 μg/mg, Squibb, New Brunswick, N.J.

[4] Potassium penicillin G-4 (1590 units/mg), Squibb, New Brunswick, N.J.

[5] Baltimore Biological Laboratories, Cockeysville, Md.

This procedure was repeated for a standard solution containing an accurately weighed, known amount of cephradine at a concentration of approximately 500 μg/ml (450-μg/ml potency). Then 10 ml of 0.3 *M* phthalate buffer, pH 4.5, and 10.00 ml of 0.0094 *N* iodine solution were pipetted into each flask. After each flask had been swirled to mix the contents completely, it was stoppered and left to stand in the dark for 30 ± 1 min. The solutions were then titrated with 0.01 *N* sodium thiosulfate, using 2 ml of starch solution as the end-point indicator.

The amount of cephradine in an unknown sample was calculated as follows:

$$\text{cephradine (mg)} = \frac{[\text{amount thiosulfate(control)} - \text{amount thiosulfate(sample)} \times \text{sample volume}]}{\text{iodine titer} \times 5 \times \text{sample weight (mg)}} \quad \text{(Eq. 1)}$$

where 5 = volume of sample or control in each flask, sample volume = volume of original sample solution, thiosulfate = 0.01 *N* sodium thiosulfate solution, and iodine titer = volume of 0.0094 *N* iodine solution consumed by 1 mg of cephradine after treatment with cephradinase. The iodine titer is determined from the titration values obtained with the *standard* cephradine solution and is calculated as follows:

$$\text{iodine titer (ml/mg)} = \frac{[\text{amount thiosulfate(control)} - \text{amount thiosulfate(sample)}]}{\frac{\text{standard weight (mg)} \times 5}{50}} \quad \text{(Eq. 2)}$$

Once the amount of cephradine in an unknown sample was calculated, the potency of the sample was obtained by multiplying the cephradine concentration obtained by the potency of the cephradine standard.

Spectrophotometric Assay—Cephradine samples or standard, prepared in water, were assayed in digests containing 1.5 ml of 0.01 *M* phosphate buffer, pH 8.0, which contained 0.001 *M* dithiothreitol, 0.5 ml of cephradinase solution (~10 units of activity), and cephradine solution (containing 10–100 μg, equivalent to a potency of 9–90 μg) in a total volume of 3.0 ml. Controls were set up for each sample or standard solution and contained 0.5 ml of cephradinase, which had been boiled for 30 min, in place of active enzyme.

The duration of incubation was determined by the activity of the enzyme preparation used and was always calculated to be greater than the time required for the enzyme to hydrolyze completely the maximum amount of cephradine estimated to be present in the samples to be assayed. As a rule, the activities of the enzyme preparations used in the assay were such that incubation times no longer than 45 min were required for the complete hydrolysis of the cephradine. The sample or standard cephradine solutions were always added last to the assay or control digests. The digests were then immediately mixed, covered, and left to incubate.

The absorbances of the sample and control digests were measured at 260 nm[6]. The instrument was initially adjusted to zero absorption with a blank assay digest, containing water instead of cephradine solution, in the reference cell and a blank control digest in the sample cell. Matched 1-cm silica cells with a spectral range of 220–2500 nm were used for the measurements. The absorbances of the standard and sample digests were then read in the same manner, with the assay mixture in the reference cell and the assay control mixture in the sample cell.

A standard curve of absorption *versus* amount of cephradine was prepared each day that the assay was performed, using standards ranging in concentration from 10 to 100 μg of cephradine/ml of water (9–90-μg/ml potency) prepared in water from pure cephradine dihydrate with a known potency of 900 μg/mg. Standards and sample solutions were always assayed in duplicate on the day of their preparation. The concentration of cephradine in an unknown sample was determined directly from the standard curve, and the potency of the sample was obtained by multiplying the concentration by the potency of the cephradine standard.

Iodometric Assay Using Alkaline Hydrolysis—This method, a direct modification of the method originally described by Alicino (9), was developed in these laboratories[7]. Cephradine samples and controls were prepared as described in the iodometric method using enzymatic hydrolysis; but instead of enzyme, the samples were incubated with 2 ml of 3 *N* sodium hydroxide solution for 30 min. Then 2 ml of 3 *N* hydrochloric acid was added to the sample mixtures. No additions were made to the controls.

Then 10 ml of 0.3 *M* phthalate buffer, pH 4.5, and 10.00 ml of 0.0094 *N* iodine solution were added to each flask; the flasks were left to stand in the dark for 30 ± 1 min and were then titrated with 0.01 *N* sodium thiosulfate solution, as described previously. Cephradine potencies were calculated as they had been after enzymatic hydrolysis.

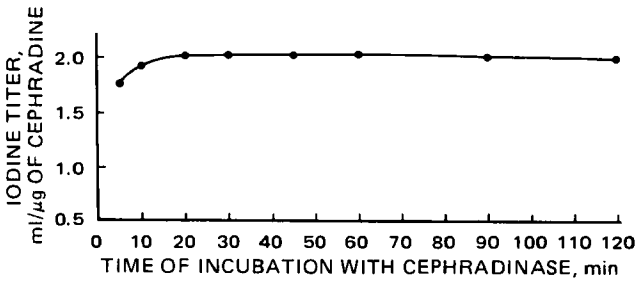

Figure 1—*Iodine titer* versus *time of incubation with cephradinase. Standard solutions of cephradine, with concentrations of approximately 500 μg/ml, were incubated with 2.0-ml aliquots of cephradinase for the periods shown and were then treated with iodine for 30 ± 1 min and titrated with sodium thiosulfate solution as described under* Methods.

RESULTS

Iodometric Assay—Certain experiments were carried out to determine the optimum conditions for running the assay.

Since the iodine titer, required for the calculation of cephradine concentration in unknown samples, was determined directly from the cephradine standard assayed at the same time as the unknown samples, the construction of a standard curve was unnecessary. The iodine titer was found to have almost the same value from day to day and varied only slightly as a result of slight changes in the concentration of the iodine and sodium thiosulfate solutions used in the iodometric procedure.

The iodine titer was affected, however, by the duration of incubation of cephradine with the cephradinase. This effect was investigated in an experiment in which a standard solution of cephradine, with a concentration of 569 μg/ml in 0.1 *M* phosphate buffer, pH 7.0, was incubated for various times with the enzyme at room temperature. Controls were incubated with 0.1 *M* phosphate buffer, pH 8.0, in parallel with the samples. At the end of each incubation period, samples were assayed as already described.

Figure 1 shows that for the particular enzyme preparation used in this experiment (activity of 47.7 units/ml), the iodine titer increased with the duration of incubation with cephradinase up to 20 min, remained constant until 60 min, and then declined slightly until 120 min. Therefore, for routine determinations of cephradine in solutions containing the drug in concentrations of approximately 500 μg/ml, a cephradinase preparation with an activity of approximately 50 units/ml was sufficiently active to bring about complete hydrolysis of the β-lactam substrate within 30 min without any change in iodine titer.

Optimal Time of Iodination—Although the original iodometric method for the assay of penicillin preparations described by Alicino (3) required the incubation of the hydrolyzed β-lactam compound with excess iodine for 30 min, the more recently described procedure (13) requires only 15 min of incubation with excess iodine. This difference led to attempts to determine the optimal time of iodination for cephradine hydrolyzed by cephradinase.

Standard solutions of cephradine in 0.1 *M* phosphate buffer, pH 7.0, with a concentration of approximately 500 μg/ml, were incubated with the enzyme for 30 min. Controls, incubated with 0.1 *M* phosphate buffer, pH 8.0, were run in parallel. After the 30-min incubation period, all digests were treated with 10 ml of 0.3 *M* phthalate buffer, pH 4.5, and 10.00 ml of 0.0094 *N* iodine solution. After rapid and thorough mixing, the iodinated solutions were left in the dark at room tem-

[6] Beckman DB recording spectrophotometer, Beckman Instruments, Inc., Fullerton, Calif.

[7] F. M. Russo-Alesi, personal communication.

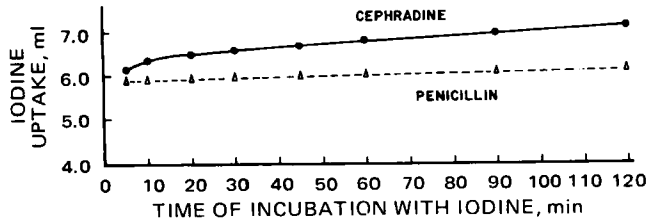

Figure 2—*Effect of time of iodination on iodine uptake. Standard solutions of cephradine, with concentrations of approximately 500 μg/ml, were incubated with cephradinase for 30 min. They were then treated with 10 ml of phthalate buffer and incubated with 10.00 ml of 0.0094* N *iodine solution for the periods shown. They then were titrated with sodium thiosulfate solution as described under* Methods. *Exactly the same procedure was followed for penicillin, except that the hydrolyzing enzyme was penicillinase.*

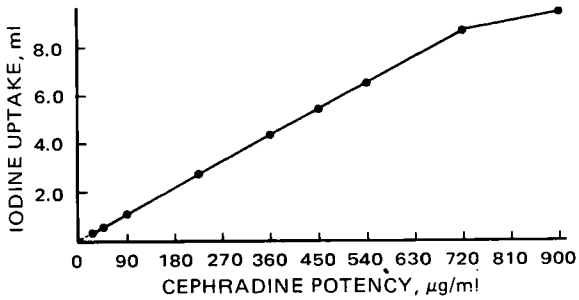

Figure 3—*Limits of the iodometric assay for cephradine using cephradinase for hydrolysis. Standard solutions of cephradine, with the potencies shown, were hydrolyzed with cephradinase and assayed by the iodometric procedure as described under* Methods.

perature for various intervals, which were precisely timed with a stopwatch. Thereafter, the iodine uptake was determined by titration with sodium thiosulfate, as described.

Figure 2 shows that when cephradinase was used to hydrolyze the β-lactam ring, the increase in iodine uptake with time was very slow after the first 20 min of iodination. Iodine uptake continued to increase as the iodination time progressed and did not reach a constant value. The same figure shows iodine uptake *versus* time of iodination for penicillin G potassium hydrolyzed by penicillinase. Here, too, iodine uptake increased slowly as the iodination time progressed, but the increase was slower and iodine uptake appeared to remain constant after 90 min of iodination. Since iodine uptake for cephradine hydrolyzed by cephradinase increased slowly with an increase in iodination time, the standard period of iodination, established as 30 ± 1 min, was timed precisely with a stopwatch.

Precision—The precision of the procedure was determined from analyses of solutions of cephradine made on 3 consecutive days by two operators. Standard solutions of cephradine in 0.1 *M* phosphate buffer, pH 7.0, approximately 500 μg/ml (450-μg/ml potency), were prepared on each day of assay and were used by both operators. A single sample solution of cephradine prepared in the same buffer, approximately 500 μg/ml (450-μg/ml potency), was prepared on each day of assay and was used by both operators.

Each operator assayed the sample solution 10 times each day, with controls being run in parallel for each two sample assay digests. The results (Table I) showed good reproducibility. For the 60 determinations, the recovery was 99.3%, the standard deviation of the mean was 10.2 (n = 60), and the relative standard deviation was 1.14%.

Sensitivity—The sensitivity of the procedure was determined by assaying a series of cephradine standard solutions [10–1000 μg/ml (potency of 9–900 μg/ml)] prepared in 0.1 *M* phosphate buffer, pH 7.0. Figure 3 shows that the relationship between iodine uptake and potency was linear between 25 and 720 μg/ml. Because of low iodine uptake and concomitantly greater thiosulfate titration values, the method was unworkable at cephradine potencies less than 25 μg/ml.

In addition to the daily determination of iodine titer, the linearity of the relationship between iodine uptake and potency of cephradine also obviated the need to construct a complete standard curve each day that the assay was performed. It was concluded that use of a single standard solution of cephradine, with a potency between 25 and 720 μg/ml, would be sufficient to determine the iodine titer in routine analyses.

Effect of 7-Aminodeacetoxycephalosporanic Acid—Since 7-aminodeacetoxycephalosporanic acid is an intermediate in the production of cephradine and has a typical β-lactam ring structure, its possible interference in the iodometric assay was investigated. A standard solution of cephradine in 0.1 *M* phosphate buffer, pH 7.0, with a concentration of 503 μg/ml was assayed in the presence of 7-aminodeacetoxycephalosporanic acid representing 1–20% of the weight of cephradine in the reaction mixture. Reaction mixtures and controls were assayed as described under *Methods;* the results (Table II) showed that 7-aminodeacetoxycephalosporanic acid did not interfere in the assay; *i.e.*, there was no significant change in the concentration obtained when cephradine was assayed in the presence of its precursor.

In another experiment, iodine uptake by 7-aminodeacetoxycephalosporanic acid after treatment with cephradinase was compared with that after treatment of the compound with alkali, as described for cephradine under *Methods.* The results (Table III) showed that almost no iodine was taken up by 7-aminodeacetoxycephalosporanic acid after treatment with the enzyme, whereas substantial amounts were consumed after treatment with alkali. From these results, it was concluded that 7-aminodeacetoxycephalosporanic acid was not readily hydrolyzed by cephradinase and that contaminating amounts of the precursor would not affect the results of an iodometric assay of cephradine that used the enzyme for hydrolysis of the β-lactam ring. In contrast, for the method using alkaline hydrolysis, contaminating amounts of 7-aminodeacetoxycephalosporanic acid would be expected to give erroneously high concentrations of cephradine.

Comparison with Bioassay and Alkali Iodometric Method—The iodometric method using enzymatic hydrolysis was compared with a turbidimetric bioassay, in which *Streptococcus faecalis* (ATCC 10541) was the test organism (2), and with the iodometric method involving alkaline hydrolysis. Solutions (~500 μg/ml) of six cephradine powders in 0.1 *M* phosphate buffer, pH 7.0, were prepared for the two iodometric assays; solutions (~250 μg/ml) of cephradine in 0.1 *M* phosphate buffer, pH 3.5, were prepared for the bioassay. The solutions were assayed by each method, on 2 consecutive days, fresh solutions and standards being prepared for each day of assay.

The potencies obtained for the cephradine powders (some of which had been stored at high temperatures for several years) used in this

Table I—Precision of the Enzyme Iodometric Method for Cephradine[a]

Operator	Potency Range, μg/ml	Mean Potency, μg/ml	*SD* of Mean (n = 60)
1	912–867	893	10.2
2	902–887	895	

[a] Assays were carried out by the procedure described under *Methods.* Relative standard deviation = 1.14%. Three samples were analyzed 30 times.

Table II—Effect of 7-Aminodeacetoxycephalosporanic Acid on the Potency of Cephradine as Determined by Enzyme Iodometric Assay[a]

Amount of 7-Aminodeacetoxycephalosporanic Acid Added to Cephradine, % (w/w)	Observed Potency, μg/mg	Change in Observed Potency, %
0.0	891.2	—
1.0	891.2	0
2.0	891.1	0
5.0	891.2	0
10.0	895.6	+0.5
20.0	895.8	+0.5

[a] Results are the means of duplicate determinations. Assays were carried out as described under *Methods.* Reaction mixtures were prepared to contain 4.0 ml of a standard solution of cephradine (concentration of 503 μg/ml) and 1.0 ml of a solution of 7-aminodeacetoxycephalosporanic acid containing 1–20% 7-aminodeacetoxycephalosporanic acid by weight of the amount of cephradine in the reaction mixture.

Table III—Iodine Uptake by 7-Aminodeacetoxycephalosporanic Acid and Cephradine after Treatment with Alkali or Cephradinase for 30 min[a]

Compound in Solution	Iodine Uptake[b] After Alkali[c] Treatment	Iodine Uptake[b] After Cephradinase[d] Treatment
Cephradine (530 μg/ml)	1.64	2.19
7-Aminodeacetoxy-cephalosporanic acid (510 μg/ml)	1.76	0.01
7-Aminodeacetoxy-cephalosporanic acid (102 μg/ml)	1.34	0.01
7-Aminodeacetoxy-cephalosporanic acid (5.1 μg/ml)	0	0

[a] Results are the means of duplicate determinations. [b] Iodine uptake = milliliters per milligram of 7-aminodeacetoxycephalosporanic acid or cephradine. [c] Iodometric assays involving alkaline hydrolysis were carried out as described under *Methods*. [d] Iodometric assays involving enzymatic hydrolysis were carried out as described under *Methods*.

experiment are given in Table IV. These results showed that the potencies determined by the iodometric method involving cephradinase hydrolysis agreed well with those obtained by bioassay, except when loss of bioactivity exceeded 50%. In contrast, the potencies determined by the alkali iodometric assay always showed poor agreement with the results of the bioassay.

Spectrophotometric Assay—Standard curves for the determination of cephradine potencies by spectrophotometric analysis after enzymatic hydrolysis of the β-lactam ring were prepared from the difference between absorbances obtained after reaction at room temperature of the cephradine standards with cephradinase and with cephradinase boiled for 30 min. The standard curves obtained were always linear, passing through the origin, and obeyed Beer's law for potencies of cephradine between 1 and 300 μg/ml.

Precision and Accuracy—The precision and accuracy were determined by assaying standard solutions of pure cephradine dihydrate of the same concentration (40 μg/ml, potency of 36 μg/ml) on 3 consecutive days. For a total of 60 determinations carried out by one operator over the 3-day period (n = 20/day), the recovery was 99.2%, the standard deviation of the mean was 1.52 (n = 60), and the relative standard deviation was 4.28%.

Sensitivity—With 1-cm light path length cells, the assay could be used to measure cephradine potencies as low as 1 μg/ml and as high as 300 μg/ml. This range possibly could be extended by using cells of different path lengths.

Table IV—Comparative Potencies of Cephradine in Bulk Powders[a]

Sample	Cephradine Potency, μg/mg: Cephradinase Iodometric Assay[b]	Alkali Iodometric Assay[c]	Bioassay[d]
NN054ND	813	979	812
NN059ND	843	991	854
NN061ND	846	980	778
NN054ND (large bottle)	578	744	578
NN059ND (large bottle)	466	643	424
NN061ND (large bottle)	464	639	405

[a] Results are the means of duplicate determinations on 2 consecutive days. Unless otherwise noted, the powders were stored at 50° in standard bottles for more than 2 years. [b] Iodometric assays involving enzymatic hydrolysis were carried out as described under *Methods*. [c] Iodometric assays involving alkaline hydrolysis were carried out as described under *Methods*. [d] Bioassays were carried out by the turbidimetric method (2).

Table V—Potency of Cephradine Formulations Determined by Spectrophotometric Assay and Bioassay[a]

Formulation	Spectrophotometric Assay[b]	Bioassay[c]
Capsules	480.3	482.0
Oral suspensions	39.8	38.7
Powders for reconstitution for injection	300.3	288.7

[a] Results are the means of duplicate determinations on 10 samples of each formulation. Cephradine potency is given as milligrams per capsule, milligrams per gram (oral suspension), or milligrams per vial (powder). [b] Spectrophotometric assays were carried out as described under *Methods*. [c] Bioassays were carried out by the turbidimetric method (2).

Comparison with Bioassay—Since the spectrophotometric method was intended for use in routine assays of cephradine in powders and other formulations, it was compared with the more commonly used bioassay in a series of experiments. The bioassay routinely used in these laboratories was a turbidimetric method (2), employing *S. faecalis* as the test organism. Accordingly, a series of capsules containing cephradine was analyzed in duplicate by both methods.

The results (Table V) showed that there was good agreement between the results obtained for this formulation. With other cephradine formulations, however, the spectrophotometric method gave consistently greater potency values compared with the bioassay (Table V). A similar discrepancy was also observed when the method was used to determine the potencies of cephradine powders stored for long periods at high temperatures. Table VI shows that, although the spectrophotometric method did indicate a loss of potency in certain samples, the potency loss was not as great as that indicated by the bioassay.

DISCUSSION

An iodometric assay of cephradine that uses the β-lactamase, cephradinase, in place of alkali for hydrolysis of the β-lactam ring was developed as a modification of the original iodometric method described by Alicino (3, 9). The procedure is relatively straightforward, accurate, and precise and gives reproducible results. It also is more specific than the original iodometric method that used alkaline hydrolysis[7], probably due to the more specific hydrolysis of the β-lactam ring by the enzyme.

However, the method cannot differentiate cephradine from other cephalosporins, such as cephalexin, which are substrates of the enzyme. These compounds can be readily assayed by exactly the same procedure as that described for use with cephradine. For each new cephalosporin, however, new reaction conditions (*e.g.*, time of incubation with the enzyme and time of iodination) have to be established. Interference in the method by the penicillins is unlikely, because these compounds are hydrolyzed by the enzyme only very slowly.

The method proved to be as accurate as the bioassay in determining the potencies of cephradine bulk formulations used in long-term stability studies, but it has the advantage of being more precise and

Table VI—Potencies of Cephradine Powders Subjected to Long-Term Storage as Determined by Spectrophotometric Assay and Bioassay[a]

Sample Number and Storage Conditions	Cephradine Potency, μg/mg: Spectrophotometric Assay[b]	Bioassay[c]
59, 5°	978	867
59, 50°	915	774
59 Bulk, 50°	537	484
61, 5°	946	903
61, 50°	910	791
61 Bulk, 50°	581	500

[a] Results are the means of duplicate determinations. [b] Spectrophotometric assays were carried out as described under *Methods*. [c] Bioassays were carried out by the turbidimetric method (2).

more rapid to perform than the bioassay. Although the procedure can be used to assay cephradine with a potency as low as 25 μg/ml, it lacks the sensitivity of the bioassay.

Since iodine was added to the reaction mixtures only after hydrolysis of the cephradine by cephradinase had been completed, a possible decrease in activity of the enzyme resulting from contact with the iodine was unimportant. The enzyme itself did not take up any iodine during the iodination procedure. The reaction was carried out at room temperature for the sake of simplicity but, from the results reported by others (14, 15), hydrolysis of the β-lactam ring at higher temperatures would be expected to give a more rapid assay and could lead to the development of an automated procedure similar to that reported by Lindstrom and Nordstrom (16).

The spectrophotometric method described was developed as a modification of certain methods used to assay β-lactamase activity (14, 17). It is similar to the procedures described for penicillin (18), for cephalosporin C (10), and for ampicillin (19). The procedure appears to be unique, however, in quantitating the amount of cephradine by measuring the difference between the absorption at 260 nm of enzymically hydrolyzed and nonhydrolyzed samples of the antibiotic. Use of a double-beam instrument and comparison of a hydrolzed sample with its nonhydrolyzed control yielded a direct reading of the amount of cephradine present. Also, at the wavelength used, this method of reading the absorbances eliminated the effects of absorbance of nonantibiotic material and enzyme.

The method proved to be quick, simple, and precise and gave reliable quantitative results. It has the advantage of requiring only small amounts of cephradine, and the range of the assay is limited only by the capabilities of the spectrophotometer. The assay is specific for cephalosporins, since the other major group of β-lactam-containing antibiotics, the penicillins, are poor substrates of the enzyme[1] and do not exhibit absorption maxima at 260 nm (8). Like the enzyme iodometric assay, this procedure cannot be expected to distinguish between cephradine and other cephalosporins that also serve as substrates for the enzyme[1].

Although the results obtained by this procedure in the assay of cephradine in dry-filled capsules compared favorably with those of the bioassay, high results obtained in the assay of other formulations made the method less accurate than the bioassay. The procedure also proved unsatisfactory for determining potencies of cephradine powders stored for long periods. Although the spectrophotometric assay showed decreases in potency of these powders that had been stored at high temperatures for 2 years, the decreases were not as great as those shown by the bioassay. The procedure also gave higher results than the bioassay for powders stored at 5°.

This discrepancy was probably attributable to the formation of nonbioactive or less bioactive products containing a β-lactam ring from cephradine during its storage. As noted for other antibiotics (10), the difference between the results of the chemical (spectrophotometric) assay and the bioassay of cephradine increased significantly and progressively as degradation of the drug proceeded.

Of the two chemical methods described, the iodometric appears to be the more suitable for determining the potency and stability of cephradine. The spectrophotometric method, which is more rapid but less accurate than the iodometric assay, should be the method of choice when a rapid determination of relative change in potency is desired.

REFERENCES

(1) R. J. Simmons, in "Analytical Microbiology," vol. 2, F. Kavanagh, Ed., Academic, New York, N.Y., 1972, pp. 193–205.

(2) D. Pitkin, P. Actor, W. Holl, A. Post, and J. A. Weisbach, *Antimicrob. Ag. Chemother.*, **5**, 223(1974).

(3) J. F. Alicino, *Ind. Chem. Eng., Anal. Ed.*, **18**, 619(1946).

(4) J. H. Ford, *Anal. Chem.*, **19**, 1004(1947).

(5) R. J. Henry and R. D. Housewright, *J. Biol. Chem.*, **167**, 559(1947).

(6) W. S. Wise and G. H. Twigg, *Analyst*, **75**, 106(1950).

(7) C. H. O'Callaghan, P. W. Muggleton, and G. W. Ross, *Antimicrob. Ag. Chemother.*, **1968**, 57.

(8) A. Samuni, *Anal. Biochem.*, **63**, 17(1975).

(9) J. F. Alicino, *Anal. Chem.*, **33**, 648(1961).

(10) L. P. Marelli, in "Cephalosporins and Penicillins, Chemistry and Biology," E. H. Flynn, Ed., Academic, New York, N.Y., 1972, pp. 609–635.

(11) T. D. Hennessey and M. H. Richmond, *Biochem. J.*, **109**, 469(1968).

(12) G. Gomori, in "Methods in Enzymology," vol. 1, S. P. Colowick and N. O. Kaplan, Eds., Academic, New York, N.Y., 1955, pp. 138–146.

(13) "Code of Federal Regulations," Title 21, Section 141 a.35(b), June 1, 1974.

(14) G. W. Ross, K. V. Chanter, A. M. Harris, S. M. Kirby, M. J. Marshall, and C. H. O'Callaghan, *Anal. Biochem.*, **54**, 9(1973).

(15) C. J. Perret, *Nature (London)*, **174**, 1012(1954).

(16) E. B. Lindstrom and K. Nordstrom, *Antimicrob. Ag. Chemother.*, **1**, 100(1972).

(17) L. D. Sabath, M. Jago, and E. P. Abraham, *Biochem. J.*, **96**, 739(1965).

(18) S. G. Waley, *ibid.*, **139**, 789(1974).

(19) J. A. T. Jansson, *Biochim. Biophys. Acta*, **99**, 171(1965).

ACKNOWLEDGMENTS AND ADDRESSES

Received July 7, 1975, from *Analytical Research and Development, Squibb Institute for Medical Research, New Brunswick, NJ 08903*

Accepted for publication September 4, 1975.

The author thanks Dr. G. A. Brewer, Jr., Dr. K. Florey, Dr. T. B. Platt, and Mr. F. M. Russo-Alesi for helpful discussions concerning this work, Mr. J. Gentile for performing the bioassays, and Ms. Maria Ioffreda for technical assistance.

Interactions of Nucleic Acid Bases with Catechol: UV Studies

FAHAD A. AL-OBEIDI and HANNA N. BORAZAN ˣ

Abstract □ UV absorption studies on weak interactions of adenine, cytosine, thymine, and uracil with catechol in aqueous solutions containing 0.1 *N* HCl gave evidence for the formation of charge transfer complexes. The absorptions of these complexes were found in the UV region at longer wavelengths than those of the pure components. It was possible to calculate various thermodynamic parameters and molar extinction coefficients at different wavelengths. The biological significance of the results is discussed.

Keyphrases □ Nucleic acid bases—adenine, cytosine, thymine, and uracil, interaction with catechol, UV absorption studies □ Catechol—interaction with adenine, cytosine, thymine, and uracil, UV absorption studies □ Complex formation—adenine, cytosine, thymine, and uracil, with catechol, UV absorption studies □ UV spectrophotometry—absorption studies, interactions of adenine, cytosine, thymine, and uracil, with catechol

Catechols are widely distributed in nature and have many biological and biochemical actions (1–3). Catechol forms the aromatic nucleus of the sympathomimetics, the catecholamines.

Nucleic acids carry the genetic information required for the synthesis of different types of proteins and enzymes (4, 5). Therefore, nucleic acids seemed to be possible targets for the action of many drugs, either directly or indirectly. The interactions between nucleic acids and some drugs were studied previously (6). Indirect actions were attributed to the interference of drugs with protein synthesis; some induce and others inhibit protein synthesis (7, 8).

To shed some light upon the nature of the adrenergic receptors, the nature of the complexes between biopolymers and those compounds needs to be investigated. To be systematic in these studies, the interactions between nucleic acid bases and catechol in aqueous solutions containing 0.1 *N* HCl were investigated spectroscopically at different temperatures.

EXPERIMENTAL

Catechol[1], thymine[1], cytosine[1], a standard solution of hydrochloric acid[1], adenine[2], and uracil[2] were obtained commercially. All chemicals, except catechol, were used without further purification. Catechol was purified by sublimation under reduced pressure (9) and kept in dark-brown bottles in a refrigerator. The sublimed catechol had the correct melting point (104°).

The solutions studied, prepared by dilution, contained a fixed concentration of nucleic acid bases (0.02 *M*) with different concentrations of catechol (0.3–0.8 *M*) in 0.1 *N* HCl. All solutions were freshly prepared and their spectra were recorded in rectangular 1-cm pathlength cells within 12 hr. Most operations were performed in a room with subdued lighting, to minimize photooxidation of catechol, at 18–20°.

The spectrophotometer[3] was checked and calibrated by using oxide film[4] at the beginning of each experiment. A thermostated cell holder[4] was used to maintain constant temperatures throughout the measurements.

When working at temperatures below room temperature, the cell holder was connected to a constant-temperature circulator and refrigerator[5]. To avoid water condensations at the surfaces of the cells at low temperatures, the cell compartment was flushed with nitrogen gas.

The baseline was recorded before running the spectra of a given set of solutions, using 0.1 *N* HCl in the cells of sample and reference compartments. The absorbance was measured by fixing wavelengths to minimize errors arising from steepness of the absorption spectra.

RESULTS

At the wavelengths investigated, the UV absorbances of catechol and all nucleic acid bases, when measured separately at different concentrations, were temperature independent. The absorbances depended only on concentration, as one would expect if no form of interaction is taking place.

The representative spectra presented in Fig. 1 show that the UV absorptions of the mixed substances were shifted from the absorptions of the individual pure substances toward longer wavelengths. Similar spectra were obtained for the other combinations studied. In most cases, the absorption spectra of the mixed substances were outside the region of absorptions of the pure compounds.

To calculate the absorbances of a complex, the absorptivities of the reacting compounds were calculated at different wavelengths. The absorbance of a complex at a given wavelength was estimated from the difference between the absorbance of a mixture and the sum of the absorbances of the pure components at concentrations identical to those used in the mixture. The experimental data used to calculate equilibrium constants (Table I) were actually measured in regions where the absorption of the free components was as small as possible and that of the complex was appreciable. The accuracy of the measurements was ±0.005 absorbance unit.

The following simple mathematical model:

$$A + D = AD \qquad \text{(Eq. 1)}$$

is proposed for calculating the equilibrium constants from the Benesi–Hildebrand equation:

$$\frac{(A_0)}{A_\lambda^{AD}} = \frac{1}{\epsilon_\lambda^{AD}} + \frac{1}{K_c^{AD}\epsilon_\lambda^{AD}(D_0)} \qquad \text{(Eq. 2)}$$

where (A_0) and (D_0) are the initial concentrations of the reactant species, A_λ^{AD} is the absorbance of the complex at the wavelength λ, ϵ_λ^{AD} is the molar absorptivity, and K_c^{AD} is the equilibrium constant.

The values of K_c^{AD} and ϵ_λ^{AD} may be obtained graphically from the slope and intercept of a plot of $(A_0)/A_\lambda^{AD}$ *versus* $1/(D_0)$, with (A_0) being kept constant. To minimize experimental errors, the slopes and intercepts were determined by the method of least squares. Plots of Eq. 2 for cytosine–catechol and uracil–catechol combinations are presented in Figs. 2 and 3, respectively. The intercepts calculated varied slightly with temperature for all combinations studied. By assuming the molar absorptivities to be constant over the temperature range studied, an average value was calculated from the values obtained when working at different temperatures. Thus, intercepts drawn in Figs. 2 and 3 actually represent the average.

Various thermodynamic parameters for different interactions between nucleic acid bases and catechol were calculated from the following equation:

$$\log K = -\frac{\Delta H^0}{2.303RT} + \text{constant} \qquad \text{(Eq. 3)}$$

[1] BDH Chemical Co., Poole, England.
[2] Hopkin and Williams Chemical Co., Chadwell Heath, Essex, England.
[3] Perkin-Elmer UV-visible model 402.
[4] Holmium.
[5] Model FK2, Haake Instrument Co.

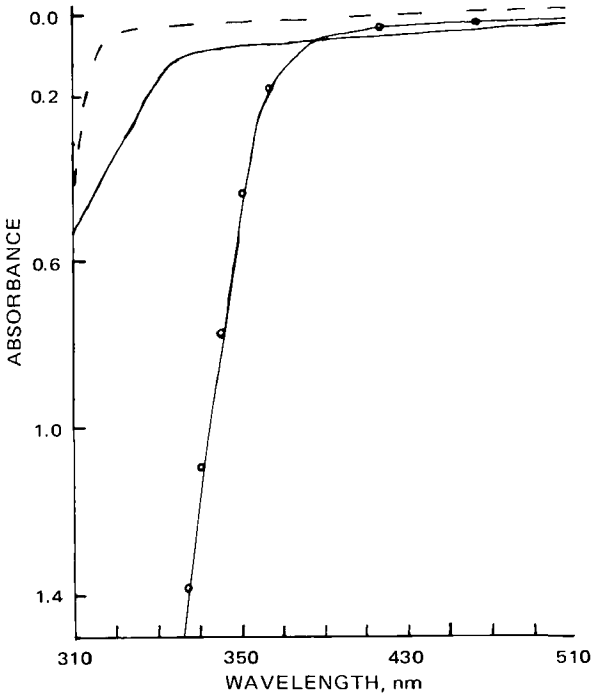

Figure 1—*Absorption spectra of 0.8* M *catechol* (——) *and* 2×10^{-2} M *cytosine* (- - -). *The* O–O–O *line represents a difference spectrum of 0.8* M *catechol plus* 2×10^{-2} M *cytosine* versus 2×10^{-2} M *cytosine. All solutions were in 0.1* N *HCl, and the measurements were at 18°.*

Therefore, a plot of log K *versus* the reciprocal of the absolute temperature, $1/T$, should give a linear slope of $-\Delta H^0/2.303R$ if the standard enthalpy change of the reaction, ΔH^0, does not depend on temperature; R is the gas constant. The Gibbs free energy change of a reaction, ΔG^0, can be related to changes in the standard enthalpy, entropy, ΔS^0, and equilibrium constant according to the following relationships:

$$\Delta G^0 = \Delta H^0 - T\,\Delta S^0 \qquad \text{(Eq. 4)}$$

$$\Delta G^0 = -RT \ln K \qquad \text{(Eq. 5)}$$

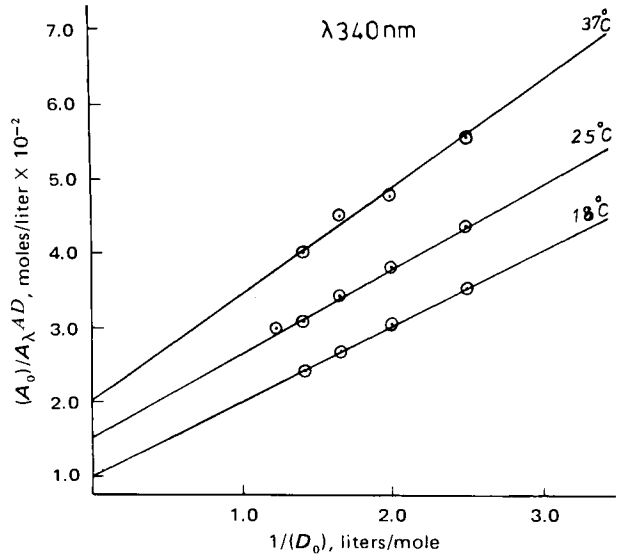

Figure 2—*Plots of* $(A_0)/A_\lambda^{AD}$ versus $1/(D_0)$ *of catechol solutions containing cytosine in 0.1* N *HCl at different temperatures. Cytosine total concentration,* (A_0), $= 2 \times 10^{-2}$ M, *and catechol total concentrations,* (D_0), $=$ *0.3–0.8* M; A_λ^{AD} *represents the absorbance of the complex at the wavelength. Curves have same intercepts as that of 18°. They were separated to avoid crowding.*

Table I—Equilibrium Constants (K), Standard Free Energy (ΔG°), Standard Enthalpy (ΔH°), and Standard Entropy (ΔS°) Changes Associated with the Interactions of Nucleic Acid Bases with Catechol in Aqueous Solutions Containing 0.1 N HCl Together with Molar Absorptivities (ϵ) at Different Wavelengths (λ)

Temperature ±0.5°	K, M^{-1} ±0.01	ΔG°, kcal/mole	ΔH°, kcal/mole	ΔS°, cal/deg/mole ±0.1
		Adenine—Catechol		
9°	1.69	−0.294		
18°	1.59	−0.264	−1.015	−2.6
37°	1.44	−0.226		
λ = 340 nm; ϵ = 21				
		Cytosine—Catechol		
18°	1.00	0.000		
25°	0.93	0.027	−3.295	−11.3
37°	0.71	0.203		
λ = 340 nm; ϵ = 100			λ = 350 nm; ϵ = 43.5	
		Thymine—Catechol		
8°	1.64	−0.276		
18°	1.40	−0.194	−2.541	−8.1
25°	1.27	−0.139		
λ = 310 nm; ϵ = 71.4				
8°	1.30	−0.146		
18°	1.10	−0.055	−2.615	−8.8
25°	1.01	−0.003		
λ = 314 nm; ϵ = 47.2				
		Uracil—Catechol		
6°	0.64	0.246		
18°	0.51	0.374	−2.842	−11.0
25°	0.48	0.410		
37°	0.39	0.518		
λ = 306 nm; ϵ = 119.8				
6°	0.49	0.394		
18°	0.38	0.533	−3.564	−14.0
25°	0.32	0.625		
37°	0.26	0.745		
λ = 310 nm; ϵ = 96.1				

Representative plots of Eq. 3 are shown in Figs. 4 and 5. The slopes and intercepts were also calculated statistically. The thermodynamic parameters calculated from these equations are summarized in Table I.

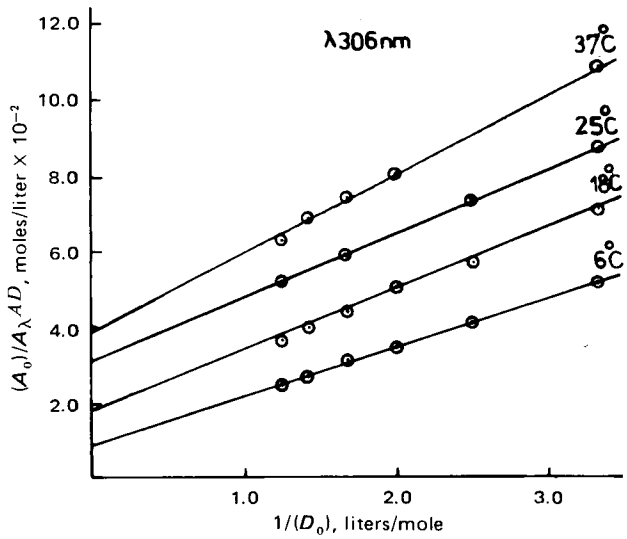

Figure 3—*Plots of* $(A_0)/A_\lambda^{AD}$ versus $1/(D_0)$ *of catechol solutions containing uracil in 0.1* N *HCl at different temperatures. Uracil total concentration,* (A_0), $= 2 \times 10^{-2}$ M, *and catechol total concentrations,* (D_0), $=$ *0.3–0.8* M; A_λ^{AD} *represents the absorbance of the complex at the wavelength. Curves have same intercepts as that of 6°. They were separated to avoid crowding.*

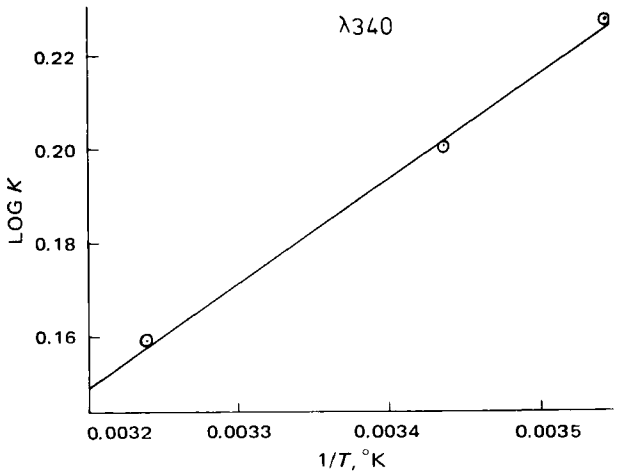

Figure 4—*Log* K *of the adenine–catechol interaction* versus *1*/T.

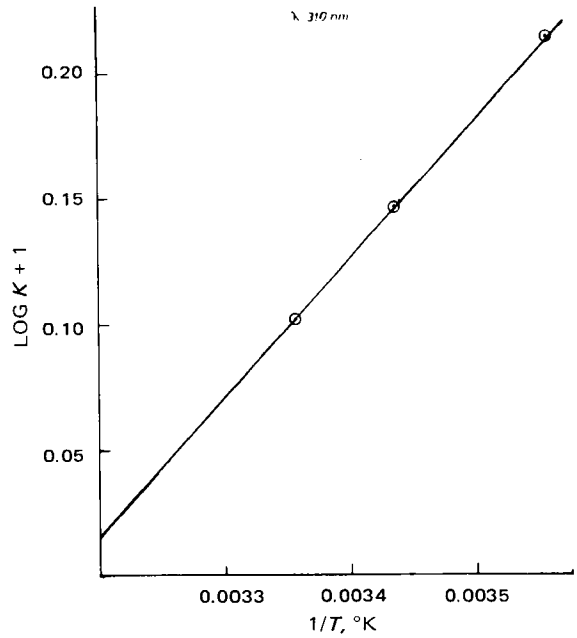

Figure 5—*Log* K *of the thymine–catechol interaction* versus *1*/T.

DISCUSSION

The differences in electronegativity and charge density existing between the molecules concerned account for the differences in their electronic properties. A charge transfer interaction can occur between different molecules or different regions within the same molecule as a result of inequalities in the sharing of electrons. The absorption of light by such weakly bonded donor–acceptor complexes is attributed to the so-called charge transfer transition.

Catechols are known to have strong electron donor properties when forming complexes with many substances (10). When catechol is mixed in solution with hydroquinone, the spectrum changes rapidly to that of a semiquinone. This effect is enhanced when oxygen is bubbled into the solution and can be attributed to charge transfer complex formation between catechol and oxygen; oxygen acts as the electron acceptor and catechol acts as the electron donor. As a result of the formation of such a complex, the oxidative power of oxygen is increased. Indeed, it was also observed that dehydrogenation of the coenzyme model 1-benzyl-1,4-dihydronicotinamide pyridinium salt is catalyzed by catechol in the presence of oxygen (11).

Nucleic acid bases also have been shown to form charge transfer complexes with many compounds (12). In those studies, nucleic acid bases were considered as the electron donors.

The electron donor–acceptor property of a molecule varies according to the environment. Thus, positively charged molecules are more likely to act as electron acceptors relative to neutral or negatively charged ones when forming complexes. The experimental results obtained here can be explained on a similar basis, *i.e.*, charge transfer complexes are formed between nucleic acid bases and catechol.

The electron donor ability of a molecule or an atom is usually measured by the ionization potential. The magnitude of the ionization potential is essentially equal to that of the binding energy of the highest occupied molecular orbital. In an analogous manner, the electron acceptor ability of a molecule or an atom can be measured by its electron affinity. However, the electron affinity is not equal to the binding energy of the lowest empty molecular orbital, because adding an electron to the lowest empty molecular orbital will alter the positions of all energy levels in the molecular or atomic orbitals.

The greater the electron affinity, the greater is the tendency of the molecule to act as an electron acceptor; the smaller the value of the ionization potential, the greater is the ability of a molecule or an atom to act as an electron donor. At present, no data are available on the ionization potential and electron affinity of catechol. Therefore, the electron donor or acceptor ability of catechol relative to various nucleic acid bases cannot be assigned.

Helene *et al.* (13), when studying the fluorescence of tyrosine or tyramine in mixed aggregates with nucleic acid bases, demonstrated fluorescence quenching of the phenol nucleus. They ascribed this phenomenon to electron transfer from the excited phenol ring to the purine or pyrimidine rings. One would expect that the electron-donating ability of catechol is greater than that of phenol, since it contains an extra electron-donating group. When these observations are applied to the present studies, catechol is considered as an electron donor and the nucleic acid bases are considered as electron acceptors.

It is observed from Table I that the order of the equilibrium constants of the interactions between nucleic acid bases and catechol is as follows: adenine–catechol > thymine–catechol > cytosine–catechol > uracil–catechol. Table I also makes clear that the ΔH^0 values of these complexes cannot be correlated with their equilibrium constants or their ΔG^0 values. The order of their enthalpy of formation is the reverse of that of the standard entropy change associated with such reactions. Higher values are observed for those of the uracil–catechol combination at a wavelength of 310 nm.

To explain the differences in the various thermodynamic parameters in terms of the specificity of these interactions, the degree and sites of protonation of the interacting molecules must be considered. Pullman and Pullman (14) classified the types of nitrogen present in nucleic acid bases and concluded that they all carry formal negative charges. Therefore, these atoms were considered to be the sites of protonation and alkylation. Spectrophotometric studies also indicated the ring nitrogens to be the principal site of attack by protons. However, the electronic charge on ring nitrogens cannot be taken solely as the measure of basicity of the nitrogen-containing heterocyclic compounds such as purine and pyrimidine derivatives (15).

Nakajima and Pullman (16) pointed out the significance of a coulombic integral between the lone pair of electrons on nitrogens and other π-electrons. The pKa's of the various nucleic acid bases and the positions of the most basic nitrogens were calculated (16). The net electronic charges on the carbonyl oxygens of uracil and thymine were found to be more negative compared to other atoms in the two molecules, ranging from −0.45 to −0.46. It may be concluded that the sites of initial protonation are nitrogen numbers 1 and 3 of adenine and cytosine, respectively, and the carbonyl oxygens of uracil and thymine.

The pKa of catechol at 25° and at an ionic strength of 0.18 was found to be 9.173 ± 0.002 (17). Therefore, all of the nucleic acid bases and catechol are protonated at the working pH.

The complex formation between all nucleic acid bases and catechol presumably occurs through parallel stacking. This mechanism of interaction in aqueous solutions has been suggested by many investigators for both self-association and complexation of nucleic acid bases, nucleosides, and similar systems (18–21).

Structural changes in nucleic acid bases seem to play a role in determining ΔH^0 and ΔS^0 values for the various interactions; for example, introducing a methyl group into uracil to give a thymine molecule leads to an appreciable change in these two parameters. This change can be explained on the basis of the net effect of two opposing factors, the steric and electronic effects imparted by the methyl group. A great change in entropy also reflects great changes in the structure of the solvent. As shown in Table I, a high degree of entropy change seems to be the determining factor for the magnitude of ΔG^0 and the formation of these complexes at the expense of ΔH^0.

No relationship was found between the magnitude of the equilibrium constants and the dipole moments of the nucleic acid bases. A fairly good correlation can be observed between equilibrium constants and the polarizability of the bases, consistent with the observations made by Broom *et al.* (19).

Table I shows the wavelength independence of the equilibrium constant of the reaction between cytosine and catechol that could indicate the formation of one type of complex (22). In the case of thymine–catechol and uracil–catechol interactions, the equilibrium constants were, however, wavelength dependent due to the formation of more than one type of complex in solution (22). The equilibrium constants decreased with an increase in wavelength.

Furthermore, Borazan (23), in explaining experimental results on complexation of the naturally occurring nucleosides and related compounds in dilute aqueous solutions (24–27), pointed out that multiple consecutive equilibria possibly can exist. Thus, for similar systems, such as the present case, plots of Eq. 2 that lead to linear slopes do not necessarily mean simple equilibrium situations as presented in Eq. 1. It may very well be that extinction coefficients of various associated forms and combinations of equilibrium constants for the multiple consecutive processes follow certain patterns such that linear slopes can be generated from the equation.

Finally, it is hoped that the discovery of the charge transfer phenomenon between nucleic acid bases and catechol will help in understanding the mechanism of action of catechol-containing substances in living systems at a more fundamental level.

CONCLUSION

Evidence was obtained from UV absorption studies for the existence of charge transfer complexes between nucleic acid bases and catechol in aqueous solutions containing 0.1 *N* HCl. It was possible to measure the absorbances of these complexes at different wavelengths in the UV region and to calculate thermodynamic parameters together with molar extinction coefficients from a simple mathematical model.

The results obtained indicate that these reactions are relatively specific and that they have, in most cases, a high heat of formation. In general, the equilibrium constants were found to be less than 2. Various thermodynamic parameters calculated from working at different wavelengths gave different values in many cases, indicating the formation of complexes having different stoichiometries.

REFERENCES

(1) B. Pullman and A. Pullman, "Quantum Biochemistry," Wiley, New York, N.Y., 1963, p. 471.

(2) H. R. Mahler and E. H. Cordes, "Biological Chemistry," Harper International Ed., Harper & Row, New York, N.Y., and John Weatherhill, Inc., Tokyo, Japan, 1971, p. 641.

(3) *Ibid.*, p. 646.

(4) J. D. Watson, "Molecular Biology of the Gene," 2nd ed., Benjamin, Menlo Park, Calif., 1970, p. 327.

(5) *Ibid.*, p. 355.

(6) M. J. Waring, *Nature*, **219**, 1320(1968).

(7) J. D. Watson, "Molecular Biology of the Gene," 2nd ed., Benjamin, Menlo Park, Calif., 1970, p. 553.

(8) V. M. Ingram, "Biosynthesis of Macromolecules," 2nd ed., Benjamin, Menlo Park, Calif., 1972, p. 212.

(9) A. I. Vogel, "Practical Organic Chemistry," 3rd ed., Longmans, Green and Co., London, England, 1964, p. 156.

(10) M. A. Slifkin, "Charge Transfer Interactions of Biomolecules," Academic, London, England, 1971, p. 214.

(11) G. Cilento and K. Zinner, *Biochim. Biophys. Acta*, **120**, 84(1966).

(12) M. A. Slifkin, "Charge Transfer Interactions of Biomolecules," Academic, London, England, 1971, pp. 76–95.

(13) C. Helene, T. Montenay-Garestier, and J. L. Dimicoli, *Biochim. Biophys. Acta*, **254**, 349(1971).

(14) B. Pullman and A. Pullman, "Quantum Biochemistry," Wiley, New York, N.Y., 1963, pp. 230–238.

(15) *Ibid.*, p. 231.

(16) T. Nakajima and A. Pullman, *J. Chim. Phys.*, **1958**, 793.

(17) R. F. Jameson and M. F. Wilson, *J. Chem. Soc., Dalton Trans.*, **23**, 2610(1972).

(18) P. O. P. Ts'o, I. S. Melvin, and A. C. Olson, *J. Am. Chem. Soc.*, **85**, 1289(1963).

(19) A. D. Broom, M. P. Schweizer, and P. O. P. Ts'o, *ibid*, **89**, 3612 (1967).

(20) J. L. Dimicoli and C. Helene, *ibid.*, **95**, 1036(1973).

(21) M. P. Schweizer, A. D. Broom, P. O. P. Ts'o, and D. P. Hollis, *ibid.*, **90**, 1042(1968).

(22) G. D. Johnson and R. E. Bowen, *ibid.*, **87**, 1655(1965).

(23) H. N. Borazan, *J. Pharm. Sci.*, **64**, 770(1975).

(24) F. M. Goyan and H. N. Borazan, *ibid*, **57**, 861(1968).

(25) H. N. Borazan, Ph.D. thesis, University of California, San Francisco, Calif., 1969.

(26) H. N. Borazan and F. M. Goyan, *J. Pharm. Sci.*, **62**, 923(1973).

(27) H. N. Borazan, *ibid.*, **62**, 1982(1973).

ACKNOWLEDGMENTS AND ADDRESSES

Received March 18, 1975, from the *Department of Pharmaceutical Chemistry, College of Pharmacy, University of Baghdad, Baghdad, Republic of Iraq.*

Accepted for publication September 4, 1975.

Abstracted in part from a dissertation submitted by F. A. Al-Obeidi to the University of Baghdad in partial fulfillment of the Master of Science degree requirements.

The authors thank Professor Hatif H. Al-Jalil for his encouragement during the investigation. They also thank the University of Baghdad for the financial support of this work.

[x] To whom inquiries should be directed.

In Vitro Adsorption of Various Pharmaceuticals to Montmorillonite

JAMES W. McGINITY ˣ and JOHN L. LACH

Abstract □ Dissolution and dialysis studies showed that cationic drugs and certain nonionic drugs bind strongly to montmorillonite clay. The quantity of drug bound by one unit of clay varied considerably. Anionic drugs were weakly bound, and less bioavailability problems would be anticipated with these medicinals. The mechanism of binding of cationic drugs to montmorillonite was proposed as a two-step process: a cation-exchange reaction followed by strong surface chemisorption.

Keyphrases □ Montmorillonite—*in vitro* adsorption by various pharmaceuticals, dissolution and dialysis studies, mechanism of binding □ Adsorption—various pharmaceuticals to montmorillonite *in vitro*, dissolution and dialysis studies, mechanism of binding □ Clay adsorbents—montmorillonite, *in vitro* adsorption by various pharmaceuticals, dissolution and dialysis studies, mechanism of binding

Montmorillonite, a complex colloidal magnesium aluminum silicate clay, is widely used in cosmetics and pharmaceuticals. It is available in several grades for special applications, a factor that has increased its potential in formulation. The general properties of montmorillonite were reviewed previously (1).

Various grades of montmorillonite were studied for use as disintegrants, binders, and lubricants (2). Another study (3) found that the procedure used to incorporate montmorillonite as the disintegrating agent affects the disintegration time of compressed tablets. Other reports concern the use of montmorillonite as a disintegrating (4–6) and granulating (7) agent. Recently, the influence of electrolytes on the desorption of neomycin from attapulgite and montmorillonite clays was investigated (8).

For many organic compounds, the mechanism of interaction with unneutralized montmorillonite was ion exchange (9). This mechanism also was suggested (10) for the inactivation of cationic antiseptics by a suspension of another montmorillonite clay, bentonite.

Surface adsorption was suggested as the mechanism in the interaction between montmorillonite and benzoic acid (11). This report discussed whether solutes are adsorbed on the surface or in the interlaminar space of neutralized montmorillonite as proposed earlier (12).

Although the literature contains numerous examples of montmorillonite performing different functions in pharmaceutical dosage forms, few reports concern the availability or dissolution of the drug from such dosage forms. The purposes of these studies were to determine the types of drugs that bind to montmorillonite, to investigate the extent of binding *via* dissolution–dialysis studies, and to shed light on the complex nature of binding between drugs and montmorillonite clay.

EXPERIMENTAL

Materials—The following were used: amphetamine sulfate[1], chlorpheniramine maleate[2], propoxyphene hydrochloride[3], caffeine[4], anhydrous theophylline NF, sodium salicylate NF, sulfanilamide NF, and montmorillonite[5]. The cellulose membrane[6] had an average pore diameter of 50 Å, an average dry thickness of 0.001 cm (0.00055 in.), and an average rewet thickness of 0.003 cm (0.00128 in.).

Preparation of Drug–Montmorillonite Sample—Montmorillonite flakes were ground and passed through a No. 60 sieve. The desired quantity of clay was weighed and added to sufficient deionized water, warmed to 80°, to make a 1% (w/v) suspension. Then the mixture was stirred with a magnetic stirrer and allowed to hydrate for 12 hr at room temperature.

A dilute solution of the drug was added slowly while the mixture was stirred vigorously. After drying under vacuum at temperatures below 35°, the sample was weighed, ground, passed through a No. 60 sieve, and then rotated end-over-end in a capped bottle for 2 hr to ensure uniformity. Such complexes with the different drugs were prepared by varying the amount of montmorillonite.

Unless otherwise stated, montmorillonite regular was the grade of clay used. Some studies utilized montmorillonite neutral, while others employed nonaqueous solvents for the equilibrating medium.

To assess the influence of electrolytes on the binding of drugs to regular montmorillonite, clay suspensions were prepared in 500-ml volumetric flasks. The magma was prepared as previously described, using 2 g of montmorillonite and 200 ml of warm deionized water. The 500 mg of drug was added either before or after the addition of the electrolyte. Each step in this process was allowed to stand and equilibrate for 12 hr at room temperature before the next component was added.

The pharmaceutical complexes discussed in this report are written as x:y, where x represents the quantity of drug and y represents the quantity of montmorillonite. For example, 1:10 represents 1 g of drug/10 g of clay.

The diffuse reflectance spectroscopy investigation employed 1:10 drug–montmorillonite adsorbates, prepared as the equilibrated sample and the physical mix. Chlorpheniramine maleate was the drug studied. Water was used as the solvent for equilibration, and the physically mixed sample was prepared by light trituration of the drug and clay. The montmorillonite used for the reference and the physical mix was hydrated and dried so it would be in the same physical state as the equilibrated sample. All powders were passed through a No. 100-mesh screen.

Apparatus for Dissolution–Dialysis Studies—The Lach dissolution–dialysis cell utilized for these studies consisted of two plexiglass compartments. The dissolution compartment (A) was separated from the dialysate (B) by a cellophane membrane. This apparatus was described previously and utilized in an earlier study (13). In all studies, 600 ml of medium was used in Compartment A and 350 ml was in the flask attached to Compartment B. The sample size varied for each drug as the ratio of drug to montmorillonite was changed.

The equilibrated sample was accurately weighed and added to the dissolution medium *via* the orifice in Compartment A. No problems were encountered in the wetting of the samples. However, some pure drugs did not wet readily; when aggregates formed at the surface, they were lightly broken up with a microspatula within seconds of adding the drug to the medium. Aliquots of 3 ml were withdrawn from Compartment A at periodic intervals by a pipet adapted with a sintered-glass filter of medium porosity.

Similarly, samples were extracted from the dialysate flask. These aliquots were appropriately diluted, and absorbance measurements were determined at the required wavelengths[7]. To maintain a constant

[1] J. H. Walker & Co., Mount Vernon, N.Y.

[2] Schering Corp., Union, N.J.
[3] Eli Lilly & Co., Indianapolis, Ind.
[4] Eastman-Kodak, Rochester, N.Y.
[5] Veegum, regular and neutral grades, R. T. Vanderbilt Co., New York, N.Y.
[6] Neflex dialysis membrane, Union Carbide Corp., New York, N.Y.
[7] Gilford model 240 spectrophotometer.

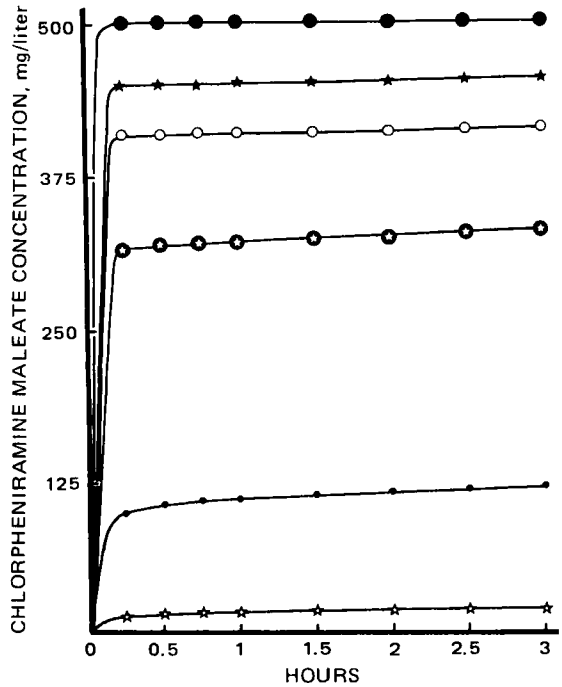

Figure 1—*Dissolution profiles of chlorpheniramine maleate–montmorillonite samples in different drug–excipient ratios in 0.1 N HCl at 25°. Key: ●, drug alone; ★, 1:0.5; ○, 1:1; ◎, 1:2; •, 1:5; and ☆, 1:10 and 1:20.*

volume in both compartments after the removal of samples from A and B, the same volume of fresh dissolution and dialysate medium was replaced. Accumulation corrections were made for removed samples.

RESULTS AND DISCUSSION

Dissolution data obtained with the dissolution–dialysis cell for various drug–montmorillonite complexes indicated the quantity of drug released from the complex. In some instances, however, a better index of true availability of a drug may be determined *via* dialysis studies. Not only the drug but also the drug–excipient complex is often estimated when working with macromolecules, giving erroneous results for dissolution determinations. This problem exists if the excipient is a high molecular weight, water-soluble material. Such a complex could pass through the filtering device used for sampling and thereby indicate an increase in dissolution rate over that of the pure drug.

The three cationic drugs chosen for investigation were chlorpheniramine maleate, amphetamine sulfate, and propoxyphene hydrochloride.

Chlorpheniramine Maleate–Montmorillonite—The dissolution data for the drug–montmorillonite samples, containing 300 mg of chlorpheniramine maleate with varying amounts of clay, in 0.1 *N* HCl are presented in Fig. 1. The initial increase in the amount of drug in solution represented the quantity of drug uncomplexed with the clay. The plateau effect suggested that the drug was strongly bound to the montmorillonite and that desorption was very slow in an acid medium. Particles of the complex appeared not to rehydrate in acid solution, as evidenced by the slight cloudiness of the dissolution medium, by the minimal increase in the viscosity of the medium, and by the gritty texture of the undissolved particles at the conclusion of each experiment.

The dialysis plots in Fig. 2 showed that drug release from the complex followed the same order as in the family of curves for the dissolution profiles. After 3 hr, 20% of the pure drug had dialyzed into Compartment B when no clay was present in the sample.

It can be assumed that the total quantity of antihistamine released after 15 min was due to uncomplexed or free drug. A plot of the concentration of chlorpheniramine maleate in solution after 15 min *versus* the percent of montmorillonite in the various solid complexes appears in Fig. 3. By extrapolating the curve to the *x*-axis, it was possible to determine the quantity of montmorillonite required to complex a

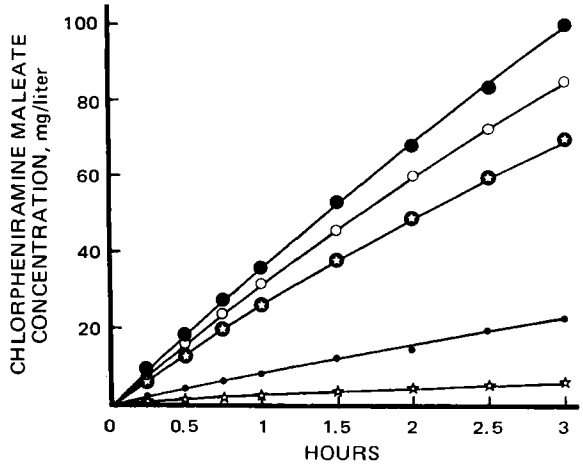

Figure 2—*Dialysis profiles of chlorpheniramine maleate–montmorillonite samples in different drug–excipient ratios in 0.1 N HCl at 25°. Key: ●, drug alone; ○, 1:1; ◎, 1:2; •, 1:5; and ☆, 1:10 and 1:20.*

certain amount of drug. According to this plot, a chlorpheniramine maleate–montmorillonite sample must contain 87% montmorillonite to complex all of the drug, *i.e.*, a ratio of 13:87 or 1:6.7. Therefore, 6.7 g of montmorillonite removes 1 g of drug from solution. If higher ratios are present, *i.e.*, greater than 6.7 g of clay/g of drug, no free drug would be available and only drug released from the complex would be detected. A more extensive treatment of the data derived from such a plot will be discussed with the propoxyphene hydrochloride–montmorillonite system.

Amphetamine Sulfate–Montmorillonite—All samples investigated contained 800 mg of amphetamine sulfate. The dissolution profiles (Fig. 4) showed that this drug was less tightly bound to montmorillonite than chlorpheniramine maleate. When the dissolution curves were compared for both drugs (Figs. 1 and 4) present as the 1:5 complex, the slight increase in the slope of the profile for the amphetamine complex represented an increase of 5% of drug concentration in the acid medium after 3 hr. As for chlorpheniramine maleate, the dialysis data for each complex were clearly separated and occurred in the same rank order as the family of curves for the dissolution plots.

Figure 4 also shows a marked difference in the amount of drug released from the 1:10 and 1:20 complexes, indicating that a higher ratio

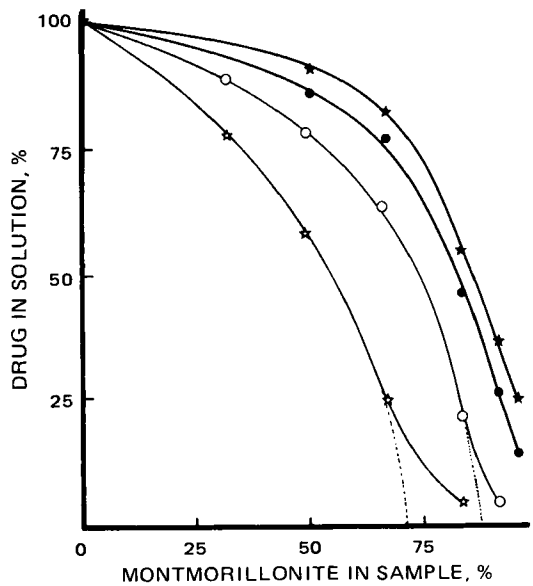

Figure 3—*Influence of the percent montmorillonite in the drug–clay adsorbate on the amount of drug in solution after a certain time period. Key: ☆, propoxyphene hydrochloride after 15 min; ○, chlorpheniramine maleate after 15 min; ●, amphetamine sulfate after 15 min; and ★, amphetamine sulfate after 30 min.*

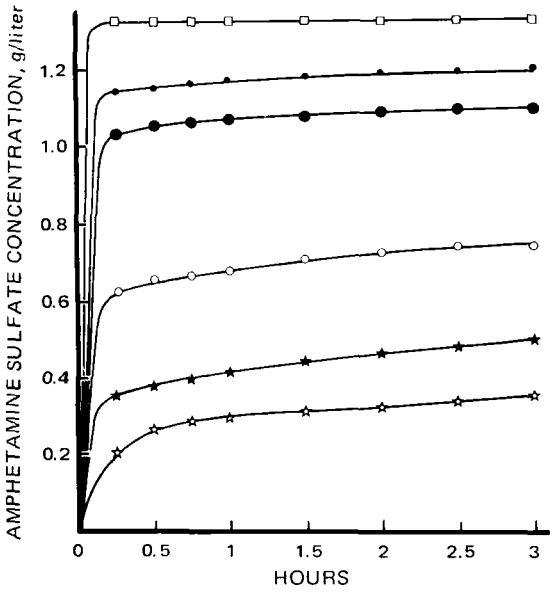

Figure 4—*Dissolution profiles of amphetamine sulfate–montmorillonite samples in different drug–excipient ratios in 0.1 N HCl at 25°. Key:* □, *drug alone;* •, *1:1;* ●, *1:2;* ○, *1:5;* ★, *1:10; and* ☆, *1:20.*

than 1:20 might be required to complex all of the drug. A plot of the amount of amphetamine sulfate in solution as a function of the percent of montmorillonite in the solid sample is shown in Fig. 3. The separation between the curves represents the quantity of drug released from the sample from 15 min to 3 hr for a particular ratio of drug and excipient.

However, extrapolation of these plots indicates that more than 100% montmorillonite would be required in a drug–montmorillonite complex to remove all drug from solution. One possible explanation is that a desorption process is taking place in the first 15 min. Thus, when the drug is desorbed from the complex in an acid medium, only a limited amount of data can be obtained using this method; the maximum adsorptive capacity of the clay cannot be derived from these profiles.

Propoxyphene Hydrochloride–Montmorillonite—The dissolution profiles for the montmorillonite complexes of this drug are illustrated in Fig. 5. All samples contained 800 mg of propoxyphene

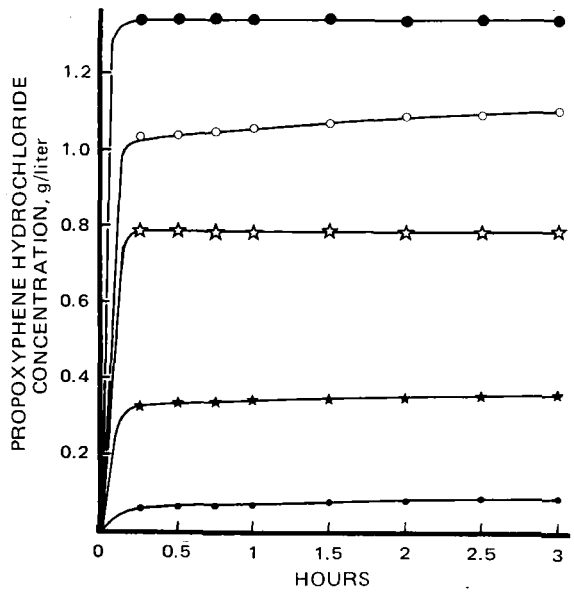

Figure 5—*Dissolution profiles of propoxyphene hydrochloride–montmorillonite samples in different drug–excipient ratios in 0.1 N HCl at 25°. Key:* ●, *drug alone;* ○, *1:0.5;* ☆, *1:1;* ★, *1:2; and* •, *1:5.*

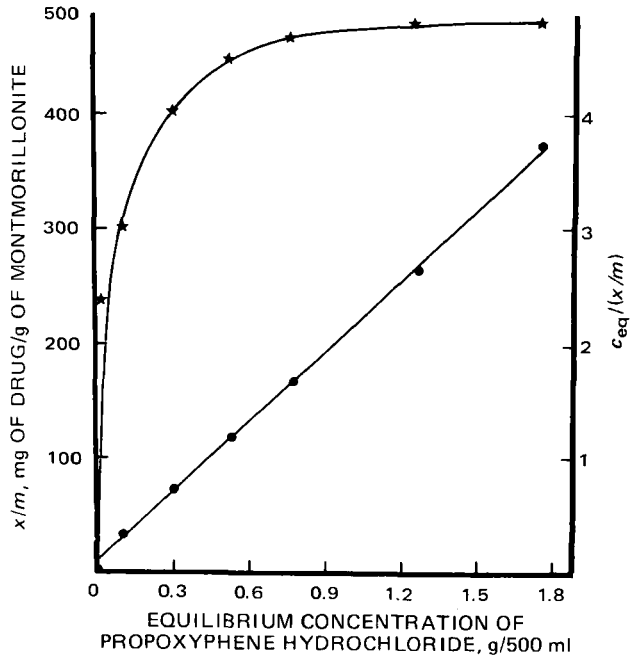

Figure 6—*Adsorption isotherm for propoxyphene hydrochloride by montmorillonite. Key:* ★, x/m versus *equilibrium concentration; and* ●, c_{eq}/(x/m) versus *equilibrium concentration.*

hydrochloride with varying amounts of montmorillonite clay. The dissolution data indicated that propoxyphene was very strongly bound, and the presence of the plateau in the dissolution profiles demonstrated that little drug was released in the acid solution. The dialysis data for the various drug–clay complexes appeared in the same rank order as the dissolution profiles.

Figure 6 shows the data plotted according to the Langmuir equation (14), which may be written as:

$$\frac{c}{x/m} = \frac{1}{ab} + \frac{c}{b} \qquad \text{(Eq. 1)}$$

where c is the equilibrium concentration of solute, x/m is the mass of solute (x) per gram (m) of the adsorbate, b is the constant called the "adsorptive capacity," and a is the constant called the "adsorption coefficient." The linear adsorption isotherm denoted monomolecular adsorption of drug to the clay. If deviations from linearity in the plot of $c/(x/m)$ *versus* c had occurred, the presence of a weak, electrostatically bound second layer of drug molecules would have been indicated. This effect was not observed; propoxyphene appeared to be monomolecularly adsorbed.

In addition, the b value or maximum adsorptive capacity of montmorillonite for this drug may be calculated. By extrapolating the plateau region of the curve in Fig. 6 back to the y-axis, the intercept gives the value for b equal to 480. The value of b can also be calculated from the linear plot and is equal to the reciprocal of the slope (b = 490). Therefore, the maximum amount of propoxyphene hydrochloride that 1 g of montmorillonite can adsorb is approximately 485 mg (approximately a 1:2.1 ratio).

The amount of propoxyphene hydrochloride in solution after 15 min, as a function of montmorillonite concentration, appears in Fig. 3. By extrapolating the curve to the x-axis, it can be shown that the sample must contain 71% clay to remove all drug from solution. Therefore, 1 g of drug was removed from solution by 2.3 g of clay. Thus, by utilizing dissolution data collected after 15 min for the various drug–excipient ratios in the acid medium, the maximum adsorptive capacity of the clay for propoxyphene was calculated to be 410 mg/g of montmorillonite.

The discrepancy between these two experimentally determined b values (410 *versus* 485) could partly be due to the slight amount of desorption of drug from the clay during the first 15 min. However, the higher value of b was determined from equilibrated liquid mixtures of hydrated clay and drug. The lower b value was determined from solid dehydrated particles of drug–montmorillonite complex in the acid medium. It is possible that during the slow dehydrating process, as water is removed, there is a slight but continuous change in the

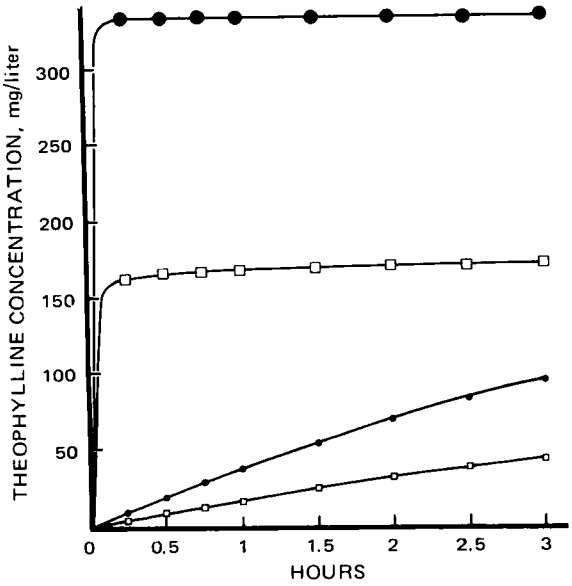

Figure 7—*Dissolution and dialysis profiles of theophylline–montmorillonite samples in different drug–excipient ratios in 0.1 N HCl at 25°. Key: ●, dissolution, drug alone; □, dissolution, 1:5; •, dialysis, drug alone; and ▫, dialysis, 1:5.*

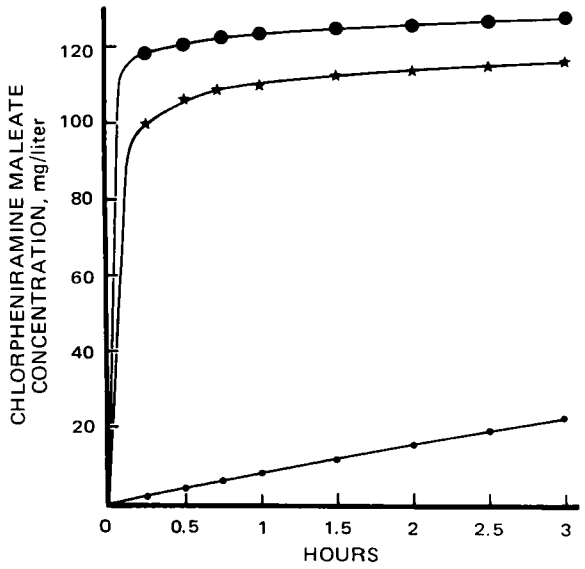

Figure 8—*Dissolution and dialysis profiles of a 1:5 chlorpheniramine maleate–montmorillonite sample, prepared from different grades of montmorillonite and run in 0.1 N HCl at 25°. Key: ●, dissolution, neutral montmorillonite; ★, dissolution, regular montmorillonite; and •, dialysis, neutral montmorillonite and regular montmorillonite.*

position of the equilibrium between drug adsorbed and free drug in solution (Scheme I). The pH of the medium may also affect this equilibrium.

$$\underset{\text{(free drug)}}{\text{drug} + \text{clay}} \rightleftharpoons \underset{\text{(complex drug)}}{\text{drug–clay}}$$

Scheme I

Anionic Drugs–Montmorillonite—In contrast to cationic-type drugs, which produced a thick curdy precipitate when added to the montmorillonite suspension, the addition of anionic drugs (*e.g.*, sodium salts of organic medicinals) simply caused a slight increase in viscosity. This effect was similar to that seen when an electrolyte such as sodium chloride was added to a suspension of montmorillonite.

This increase in viscosity was also evidenced when the nonionized drug sulfanilamide was added to the montmorillonite magma. This drug forms the anionic salt due to the many metal cations free in solution and the slightly alkaline pH of the suspension.

Since dissolution studies with these drug–montmorillonite adsorbates in an acid medium indicated that over 90% of drug was released after 30 min, fewer bioavailability problems would be anticipated with these systems.

Amphoteric Drugs–Montmorillonite—Both the nonionic xanthines theophylline and caffeine were found to bind moderately to montmorillonite. All samples contained 200 mg of the active ingredient with varying amounts of the clay. The dissolution and dialysis profiles for theophylline (Fig. 7) show approximately 50% of release from the 1:5 complex as compared to pure drug. The 1:5 complex of caffeine and montmorillonite released 42% of the drug into the dissolution medium. The appearance of the montmorillonite suspension after the addition of either xanthine indicated an increase in viscosity, as displayed by anionic drugs, plus a small degree of clumping, as exhibited by cationic drugs. This finding suggests that mechanisms other than physical adsorption were taking place.

The release profiles appear to confirm this deduction. Binding of theophylline appeared to be approximately of the same magnitude as amphetamine sulfate, although the amphetamine was more available from the complex in the acid medium. Caffeine (1,3,7-trimethylxanthine) and theophylline (1,3-dimethylxanthine) differ by the additional methyl group present on the caffeine molecule, so this functional group could account for 8% more caffeine than theophylline being bound by the same quantity of montmorillonite.

Introductory Mechanistic Studies—Bornstein (15) thoroughly reviewed the various types of bonding involved in drug–excipient interactions. The two limiting types of adsorption, physical and chemisorption, were discussed extensively by Monkhouse and Lach (16). Generally, the type of adsorption in most systems is not clear, although the extremes are easily distinguishable. It would be advantageous to characterize the nature of the surface of excipients if one were to examine the type of drug–excipient interaction closely. Unfortunately, the exact nature of very few surfaces is well understood.

Studies with anionic drugs and nonionics that form anionic moieties in the montmorillonite suspension showed that these drugs were bound weakly and were readily released from the drug–montmorillonite adsorbate. This reversibility of binding, leading to high concentrations of drug in the acid medium, was indicative of physical adsorption where weak van der Waals bonds were probably involved.

Additional experiments with respect to other effects were conducted utilizing drugs that were strongly bound to montmorillonite. Chlorpheniramine maleate and propoxyphene hydrochloride were the cationic drugs of choice.

The addition of a surfactant, polysorbate 80[8], to the acid medium prior to the 1:5 chlorpheniramine maleate–montmorillonite sample had little effect. The 4% increase in drug concentration in the medium after 3 hr indicated that forces stronger than physical adsorption were involved.

To investigate whether the pH of the clay was a key factor in the binding of cationic drugs, samples were prepared with chlorpheniramine maleate using both neutral (pH 7–7.5) and regular grade montmorillonite (pH 8.5–9). Release profiles of samples prepared from different grades of montmorillonite appear in Fig. 8. Dissolution studies showed that an additional 4% of the total drug was released from the neutral montmorillonite compared to the regular clay. This small difference may be explained by comparing the hydration of the two clays. The specially treated neutral montmorillonite does not hydrate nearly as well as the regular grade. This condition could result in less sites being exposed and available for drug adsorption, accounting for the difference seen in the dissolution profiles.

The lower content of sodium and potassium ions in the neutral clay may also be a factor. The dialysis profiles are the same for both grades of clay. The possibility exists for the formation of a quaternary nitrogen group in the drug molecule during the equilibration process. Quaternaries pass lipid or cellophane membranes at a much slower rate than does an uncharged drug moiety. This fact could account for a reduction in the dialysis rate of the drug from the neutral montmorillonite sample sufficient to render the dialysis profile identical with that found from the regular clay.

The effect of the equilibrating solvent on the binding of drugs to montmorillonite also was investigated using solvents of varying

[8] Tween 80.

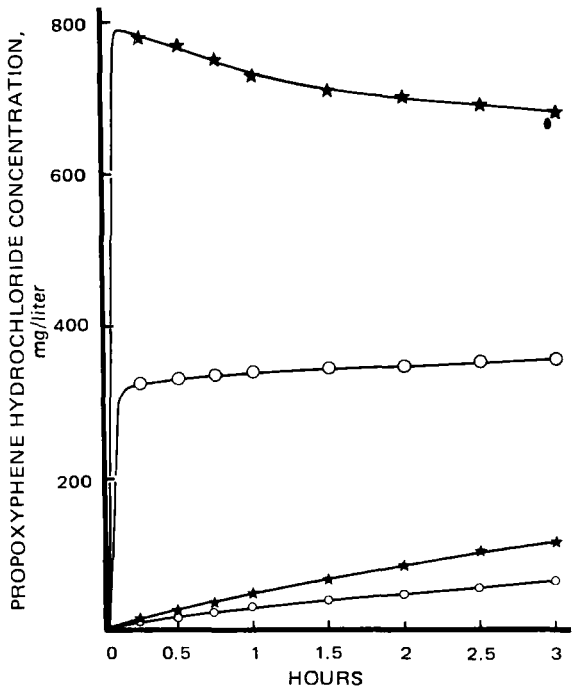

Figure 9—*Dissolution and dialysis profiles of a 1:2 propoxyphene hydrochloride–montmorillonite sample in 0.1 N HCl at 25°. Key: ★, dissolution, propoxyphene base equilibrated in methanol; ○, dissolution, propoxyphene hydrochloride equilibrated in water; ✶, dialysis, propoxyphene base equilibrated in methanol; and ○, dialysis, propoxyphene hydrochloride equilibrated in water.*

polarities. Carstensen and Su (11) showed that organic solutes free of cation-exchangeable groups adsorbed on the surface of neutralized montmorillonite and did not penetrate to the interior of the crystal. They showed that the nonionic drugs benzoic acid and diazepam (17), when equilibrated in nonaqueous solvents, were bound to neutral montmorillonite *via* an ion–dipole interaction. Since a surface physical adsorption was the proposed mechanism of binding, these authors stated that the montmorillonite adsorbates were bioavailable. Since their adsorption studies were carried out under nonaqueous conditions, it would be difficult to predict the bioavailability of drugs from the montmorillonite adsorbates without additional data.

When propoxyphene, which contains no cation-exchangeable groups, was added to a methanolic suspension of regular montmorillonite, no interaction was visible. Figure 9 shows the dissolution and dialysis profiles for propoxyphene base equilibrated in methanol and the drug hydrochloride salt equilibrated in water. Both samples were prepared as the 1:2 drug–montmorillonite complex and contained the same quantity of propoxyphene.

The dissolution curves in this figure are interesting; *e.g.*, over twice the quantity of drug was immediately released in solution from the methanol-equilibrated sample compared to the sample equilibrated in water. In this system, some of the base probably was bound *via* an ion–dipole type of surface adsorption, as suggested by Carstensen and Su (18). However, since only 60% of the drug was in solution after 15 min, this does suggest that forces stronger than those present in ion–dipole binding were responsible for the remaining 40% of the drug being strongly bound to the clay.

The "salting-out" phenomenon, evidenced by a decrease in the concentration of free drug in solution, could be due to the readsorption of drug back onto the clay. Propoxyphene in an acid medium is readily soluble since it forms the hydrochloride salt. In this ionized form, it can occupy sites on the montmorillonite where the base would not bind. Thus, in an acid medium the binding of the base to the montmorillonite would occur *via* the same mechanism as the hydrochloride salt under aqueous conditions.

However, when a cationic salt was equilibrated with regular montmorillonite using solvents of varying polarities (Table I), the binding and release profiles of the drug in the acid medium were very similar (Fig. 10). Consequently, it appears that if a drug is present as its cationic moiety, it would bind strongly to montmorillonite irrespective of the equilibrating solvent.

Table I—Influence of the Dielectric Constants of Equilibrating Solvent on Release of Chlorpheniramine from a 1:5 Drug–Montmorillonite Complex in 0.1 *N* HCl at 25°

Solvent	Dielectric Constant[a]	Chlorpheniramine in Solution, % After 15 min	Chlorpheniramine in Solution, % After 60 min
Water	78.5	19.8	23.3
Methyl alcohol	31.5	19.2	22.8
Acetone	19.1	19.9	22.3
Isopropyl alcohol	18.0	23.3	23.6

[a] Dielectric constants at 25°; from Ref. 23.

Wai and Banker (9), using radioactive sodium, confirmed the original claim by Grim (19) concerning the presence of exchangeable cations in montmorillonite clays. From their studies conducted in aqueous medium, Wai and Banker found that sodium in montmorillonite existed as the exchangeable cation as well as the free electrolyte. They concluded from their sorption profiles that, in an alcohol medium, the hydrochloride salts of the alkaloidal drugs studied were bound to the montmorillonite *via* cation exchange, surface adsorption, or a combination of both mechanisms or that they did not bind at all.

Studies in these laboratories suggested that cation exchange was one possible mechanism responsible for these interactions, although others also should be considered. The linear Langmuir adsorption isotherms found by Carstensen and Su (11, 18) in nonaqueous media and also obtained in this investigation (Fig. 6) in aqueous media seemed to indicate that surface adsorption was occurring rather than intercalation. It was also found that cationic drugs bind much stronger than anionic drugs. Since the surface of the montmorillonite carries a strong negative charge, it is possible that the drug was bound *via* a chemisorption interaction between the negative charge of the clay and the positive charge of the cationic moiety.

Figure 11 displays the influence of magnesium and sodium ions added to the montmorillonite suspension before and after the solution of chlorpheniramine maleate. Sodium chloride had a greater influence when added to the preformed complex than when it was added to the suspension before the drug. The opposite was true for magnesium chloride. When electrolytes were added to the clay suspension, an increase in viscosity was visible. This effect was not evident when the salts were added to the drug–clay suspension; the suspension had already lost the elegant stable appearance of the montmorillonite magma.

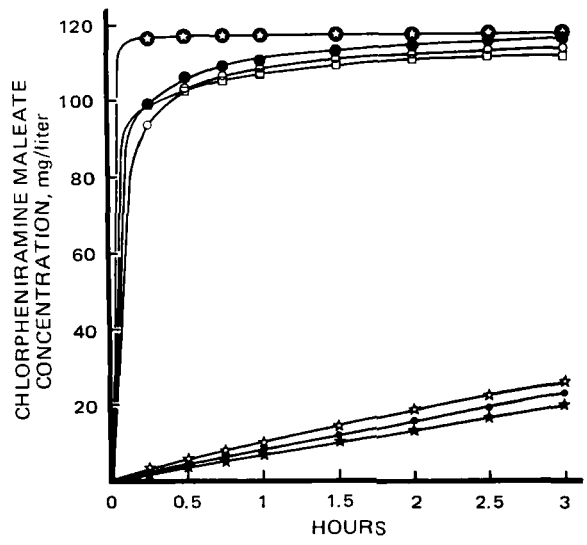

Figure 10—*Effect of preparing the sample in different solvents on the dissolution and dialysis profiles of a 1:5 chlorpheniramine maleate–montmorillonite sample in 0.1 N HCl at 25°. Key: ◎, dissolution, isopropyl alcohol; ●, dissolution, water; □, dissolution, acetone; ○, dissolution, methyl alcohol; ☆, dialysis, isopropyl alcohol; •, dialysis, water and methyl alcohol; and ★, dialysis, acetone.*

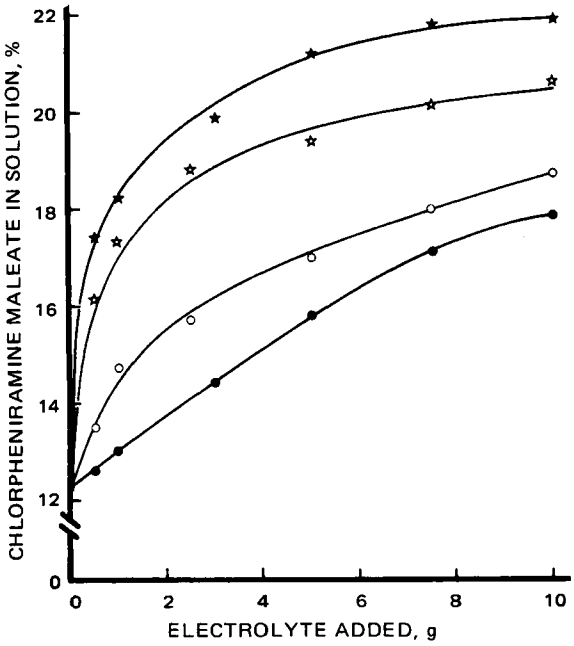

Figure 11—*Effect of electrolytes added to the montmorillonite suspension before (closed symbols) and after (open symbols) chlorpheniramine maleate. Key: ☆, ★, magnesium chloride (anhydrous); and ○, ●, sodium chloride.*

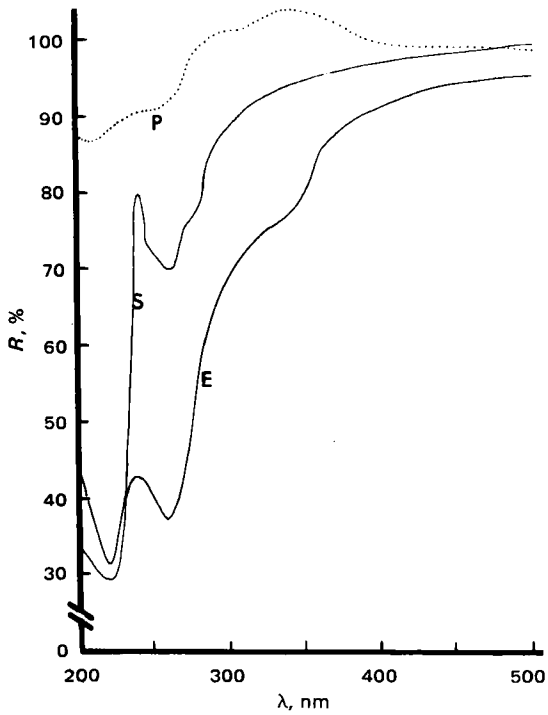

Figure 12—*Diffuse reflectance spectroscopy and UV spectra for chlorpheniramine maleate. Key: P, physical mix (diffuse reflectance spectroscopy); E, equilibrated (diffuse reflectance spectroscopy); and S, solution (UV, % T versus λ). Scale: % R = % T.*

When magnesium chloride solution was added to the montmorillonite suspension, it seemed logical that magnesium ions, being divalent, would be adsorbed to the clay surface more strongly than the singly charged sodium ions. This result would help explain why the divalent ions produced a higher concentration of free drug in solution than the monovalent ions. As the concentration of electrolyte was increased, the equilibrium would be in favor of exchange, making readsorption of drug onto the clay unlikely.

Although 10 g of sodium chloride added to the complex produced only a 7% increase in free drug in solution, this increase represented close to a 50% increase in the free drug concentration prior to the addition of the electrolyte. The degree of binding and amount of drug released were concentration dependent; *e.g.*, less free drug was found in solution if the volume was adjusted to 250 ml instead of 500 ml, all other parameters being constant.

The technique of diffuse reflectance spectroscopy was proposed by Lach and Bornstein (20–22) as a useful tool for the investigation of solid–solid interactions in pharmaceutical dosage forms. Diffuse reflectance spectroscopy was employed in the montmorillonite systems to study the surface interaction of drugs with the clay.

The diffuse reflectance spectrographs of percent reflectance *versus* wavelength for the physical and equilibrated sample appear in Fig. 12. Both samples contained the same quantity of drug. The lower reflectance (or higher absorbance) of the equilibrated sample signifies that the drug is surface coated onto the clay particles. The separation of peaks is not seen with the physical mix. The Kubelka–Munk theory predicts that the amount of radiant energy adsorbed will be directly proportional to the concentration of the adsorbing species present on the surface. Since little surface coating would be expected for the physical mix, most of the light beams are reflected.

At 340 nm, a shoulder appears in the equilibrated sample. The physical mix displays a peak at this wavelength, with reflectance being slightly greater than 100%. This finding cannot be fully explained at this time.

The S profile represents an aqueous solution spectrum of the drug (percent transmittance *versus* λ). The valleys for S occur at 223 and 262 nm. The valleys for reflective curve E for the equilibrated sample represent peaks of absorption and occur at 222 and 263 nm. This result indicates that the chromophores responsible for absorption at these wavelengths are not chemisorbed to the montmorillonite. The presence of a shoulder at 250 nm in profile S, not visible in profile E, and the shoulder at 271 nm in profile S, which is bathochromically shifted to 348 nm in profile E, are all indications of chemisorption.

SUMMARY AND CONCLUSIONS

The dissolution and dialysis results of this investigation indicated that cationic drugs and certain nonionic drugs bind tenaciously to montmorillonite clay. Anionic drugs and nonionics which exist as anionics, following their addition to the montmorillonite suspension, bind very weakly to the clay and pass rapidly into solution. The quantity of drug bound to the clay varied considerably from drug to drug.

For cationic drugs, it was proposed that the initial step in the binding mechanism was cation exchange. The cationic drug moiety exchanged with the bound metallic cation of the montmorillonite and then was bound to the clay *via* a strong chemisorption interaction between the positive charge of the drug and the negative charge on the clay surface. Reasons to support this two-step mechanism are as follows:

1. The quantity of chemisorbed drug was dependent on ionic concentration. As the salt content was increased, the binding of the drug decreased and less exchange took place. If electrolytes were added to the preformed drug–montmorillonite adsorbate in suspension, then the concentration of free drug in solution again increased. Readsorption of drug did not occur since the vacant sites on the clay were immediately reoccupied by the cations of the electrolyte.
2. Cationic drugs are readily soluble in hydrochloric acid, but very little drug was released from the adsorbate in this medium. This irreversible binding of the drug to montmorillonite was indicative of chemisorption.

The binding of the cationic salts to regular montmorillonite was very similar to that for the neutral grade of the clay. Consequently, the effect of the pH of the montmorillonite suspension appeared to be minimal on this drug–excipient interaction.

Diffuse reflectance spectroscopy studies suggested that specific functional groups in the drug molecule interact with the montmorillonite.

Finally, if one was not cognizant of interactions of montmorillonite with cationic drugs, then aqueous or nonaqueous solvents used in a wet granulation procedure would precipitate an interaction between the drug and clay excipient to decrease initial blood levels of the active substance. This problem would be particularly serious for drugs with low dosage, such as the antihistamines where immediate therapeutic levels of drug are required.

REFERENCES

(1) M. Barr, *Am. Perfum. Cosmet.*, **78**, 37(1963).
(2) K. Wai, G. DeKay, and G. S. Banker, *J. Pharm. Sci.*, **55**, 1244(1966).
(3) A. D. Nair and V. N. Bhatia, *J. Am. Pharm. Ass., Sci. Ed.*, **46**, 131(1957).
(4) H. M. Gross and C. H. Becker, *ibid.*, **41**, 157(1952).
(5) A. Firouzabadian and L. Huyck, *ibid.*, **43**, 248(1954).
(6) J. B. Ward and A. Trachtenberg, *Drug Cosmet. Ind.*, **91**, 35(1962).
(7) R. P. Patel and A. S. Rana, *Indian J. Pharm.*, **19** (Jan. 1957).
(8) J. W. McGinity and J. A. Hill, *J. Pharm. Sci.*, **64**, 1566(1975).
(9) K. Wai and G. S. Banker, *ibid.*, **55**, 1215(1966).
(10) W. A. Harris, *Aust. J. Pharm.*, **42**, 583(1961).
(11) J. T. Carstensen and K. S. E. Su, *J. Pharm. Sci.*, **60**, 733(1971).
(12) D. M. C. MacEwan and O. Talib-Uddin, *Colloq. Int. C. N. R. S.*, **10**, 24(1948).
(13) R. E. Northern, J. L. Lach, and J. H. Fincher, *J. Am. Hosp. Pharm.*, **30**, 622(1975).
(14) I. Langmuir, *J. Am. Chem. Soc.*, **39**, 1848(1917).
(15) M. Bornstein, Ph.D. thesis, University of Iowa, Iowa City, Iowa, 1966.
(16) D. C. Monkhouse and J. L. Lach, *Can. J. Pharm. Sci.*, **7**, 29(1972).
(17) J. Carstensen and K. S. E. Su, *J. Pharm. Sci.*, **61**, 139(1972).
(18) *Ibid.*, **61**, 420(1972).
(19) R. E. Grim, *J. Geol.*, **50**, 225(1942).
(20) J. L. Lach and M. Bornstein, *J. Pharm. Sci.*, **54**, 1730(1965).
(21) M. Bornstein and J. L. Lach, *ibid.*, **55**, 1033(1966).
(22) J. L. Lach and M. Bornstein, *ibid.*, **55**, 1040(1966).
(23) J. T. Carstensen, "Theory of Pharmaceutical Systems," vol. I, Academic, New York, N.Y., 1972, p. 132.

ACKNOWLEDGMENTS AND ADDRESSES

Received June 19, 1975, from the *College of Pharmacy, University of Iowa, Iowa City, IA 52240*

Accepted for publication September 10, 1975.

[x] To whom inquiries should be directed. Present address: School of Pharmacy, Texas Southern University, Houston, TX 77004

NOTES

α- and β-Halomorphides: Stereochemistry, Analgesic Potency, Toxicity, and Interaction with Narcotic Receptors *In Vitro*

HERMAN J. C. YEH [*], RAYMOND S. WILSON [*], WERNER A. KLEE [‡], and ARTHUR E. JACOBSON [*x]

Abstract □ The configuration of the halogen on the C-ring of several α- and β-halomorphides was determined by NMR. The analgesic potencies of these halomorphides and their interactions with narcotic receptors in rat brain homogenate were measured, as was the toxicity of the α- and β-chloromorphides. The halomorphides were examined as possible irreversible binders to the narcotic receptor.

Keyphrases □ Halomorphides, α and β—NMR determination of configuration of halogen on C-ring, analgesic potencies, toxicity, interaction with narcotic receptors studied □ Stereochemistry—α- and β-halomorphides, NMR determination of configuration of halogen on C-ring □ NMR—determination of configuration of halogen on C-ring of α- and β-halomorphides □ Analgesic agents—potency of α- and β-halomorphides compared □ Toxicity—α- and β-halomorphides compared

Recently, β-chloromorphide was found as a constituent of a clandestine opiate sample and was identified by comparison with a known sample (physical properties and mass and IR spectra) (1). Apparently the toxicity of this compound is unknown and the configuration of the halogen is uncertain, although its preparation, physical properties, and some biological data were described (2, 3).

α-Chloromorphide was isolated in this laboratory from a reaction between morphine and dimethylchloroformiminium chloride. Samples[1] of the known α- and β-chloromorphides, as well as the β-bromo- and β-iodomorphides, were obtained, and their biological activities and NMR spectra were determined. (From the NMR spectra, the configuration of the halide about the C-6 and C-8 positions in the C-ring could be deduced.)

IR spectral data were used to differentiate α-substituted codides (substituted on the C-6 position of the C-ring of the codide) from the β-substituted compounds (C-8-substituted compounds) (4). A relatively strong band at 940 cm^{-1} characterized the α-compounds, in agreement with a previous report (4). The β-compounds possessed a 900-cm^{-1} band and a 935–940-cm^{-1} band (medium to weak). NMR was used to differentiate clearly the α- and β-halomorphides and to obtain the orientation of halogen on the C-ring.

[1] Samples were obtained from Dr. E. L. May, National Institutes of Health.

REFERENCES

(1) M. Barr, *Am. Perfum. Cosmet.*, **78**, 37(1963).
(2) K. Wai, G. DeKay, and G. S. Banker, *J. Pharm. Sci.*, **55**, 1244(1966).
(3) A. D. Nair and V. N. Bhatia, *J. Am. Pharm. Ass., Sci. Ed.*, **46**, 131(1957).
(4) H. M. Gross and C. H. Becker, *ibid.*, **41**, 157(1952).
(5) A. Firouzabadian and L. Huyck, *ibid.*, **43**, 248(1954).
(6) J. B. Ward and A. Trachtenberg, *Drug Cosmet. Ind.*, **91**, 35(1962).
(7) R. P. Patel and A. S. Rana, *Indian J. Pharm.*, **19** (Jan. 1957).
(8) J. W. McGinity and J. A. Hill, *J. Pharm. Sci.*, **64**, 1566(1975).
(9) K. Wai and G. S. Banker, *ibid.*, **55**, 1215(1966).
(10) W. A. Harris, *Aust. J. Pharm.*, **42**, 583(1961).
(11) J. T. Carstensen and K. S. E. Su, *J. Pharm. Sci.*, **60**, 733(1971).
(12) D. M. C. MacEwan and O. Talib-Uddin, *Colloq. Int. C. N. R. S.*, **10**, 24(1948).
(13) R. E. Northern, J. L. Lach, and J. H. Fincher, *J. Am. Hosp. Pharm.*, **30**, 622(1975).
(14) I. Langmuir, *J. Am. Chem. Soc.*, **39**, 1848(1917).
(15) M. Bornstein, Ph.D. thesis, University of Iowa, Iowa City, Iowa, 1966.
(16) D. C. Monkhouse and J. L. Lach, *Can. J. Pharm. Sci.*, **7**, 29(1972).
(17) J. Carstensen and K. S. E. Su, *J. Pharm. Sci.*, **61**, 139(1972).
(18) *Ibid.*, **61**, 420(1972).
(19) R. E. Grim, *J. Geol.*, **50**, 225(1942).
(20) J. L. Lach and M. Bornstein, *J. Pharm. Sci.*, **54**, 1730(1965).
(21) M. Bornstein and J. L. Lach, *ibid.*, **55**, 1033(1966).
(22) J. L. Lach and M. Bornstein, *ibid.*, **55**, 1040(1966).
(23) J. T. Carstensen, "Theory of Pharmaceutical Systems," vol. I, Academic, New York, N.Y., 1972, p. 132.

ACKNOWLEDGMENTS AND ADDRESSES

Received June 19, 1975, from the *College of Pharmacy, University of Iowa, Iowa City, IA 52240*

Accepted for publication September 10, 1975.

[x] To whom inquiries should be directed. Present address: School of Pharmacy, Texas Southern University, Houston, TX 77004

NOTES

α- and β-Halomorphides: Stereochemistry, Analgesic Potency, Toxicity, and Interaction with Narcotic Receptors *In Vitro*

HERMAN J. C. YEH [*], RAYMOND S. WILSON [*], WERNER A. KLEE [‡], and ARTHUR E. JACOBSON [*x]

Abstract □ The configuration of the halogen on the C-ring of several α- and β-halomorphides was determined by NMR. The analgesic potencies of these halomorphides and their interactions with narcotic receptors in rat brain homogenate were measured, as was the toxicity of the α- and β-chloromorphides. The halomorphides were examined as possible irreversible binders to the narcotic receptor.

Keyphrases □ Halomorphides, α and β—NMR determination of configuration of halogen on C-ring, analgesic potencies, toxicity, interaction with narcotic receptors studied □ Stereochemistry—α- and β-halomorphides, NMR determination of configuration of halogen on C-ring □ NMR—determination of configuration of halogen on C-ring of α- and β-halomorphides □ Analgesic agents—potency of α- and β-halomorphides compared □ Toxicity—α- and β-halomorphides compared

Recently, β-chloromorphide was found as a constituent of a clandestine opiate sample and was identified by comparison with a known sample (physical properties and mass and IR spectra) (1). Apparently the toxicity of this compound is unknown and the configuration of the halogen is uncertain, although its preparation, physical properties, and some biological data were described (2, 3).

α-Chloromorphide was isolated in this laboratory from a reaction between morphine and dimethylchloroformiminium chloride. Samples[1] of the known α- and β-chloromorphides, as well as the β-bromo- and β-iodomorphides, were obtained, and their biological activities and NMR spectra were determined. (From the NMR spectra, the configuration of the halide about the C-6 and C-8 positions in the C-ring could be deduced.)

IR spectral data were used to differentiate α-substituted codides (substituted on the C-6 position of the C-ring of the codide) from the β-substituted compounds (C-8-substituted compounds) (4). A relatively strong band at 940 cm^{-1} characterized the α-compounds, in agreement with a previous report (4). The β-compounds possessed a 900-cm^{-1} band and a 935–940-cm^{-1} band (medium to weak). NMR was used to differentiate clearly the α- and β-halomorphides and to obtain the orientation of halogen on the C-ring.

[1] Samples were obtained from Dr. E. L. May, National Institutes of Health.

Table I—NMR Spectra of the α- and β-Halomorphides

Compound	δ[a], ppm: Proton Number 5	6	7	8	14	J, Hz: 5,6	5,7	5,8	6,7	6,8	7,8	8,14
α-Chloromorphide[b]	4.95	4.51	5.96	5.69	3.08	1.0	1.0	—	5.7	<1.0	9.6	1.8
β-Chloromorphide	4.96	5.71	5.86	4.0	2.54	3.3	—	1.4	10.4	2.2	1.4	9.9
β-Bromomorphide	5.16	5.72	6.05	4.19	3.16	3.3	—	1.6	10.4	2.3	1.8	9.6
β-Iodomorphide	5.14	5.82	5.93	4.07	2.96	3.0	—	1.8	10.2	1.9	1.2	9.8
Isocodeine	4.77	4.21	5.94	5.58	3.08	1.2	1.0	—	5.7	—	9.6	1.8
Codeine	4.85	4.14	5.67	5.26	2.66	6.4	1.3	—	1.8	3.1	10.0	2.3

[a] In deuterated methanol. [b] Probe at 50° to improve the solubility.

The α- and β-halomorphides were of interest also because it was found (5, 6) that thiol groups may exist at, or near, narcotic receptor sites (alkylating agents and heavy metals destroy receptor activity). Since the thiol, acting as a nucleophile, conceivably could interact with halomorphides, it was of interest to see whether these substrates would bind irreversibly with the narcotic receptor. Stork and Clarke (4) showed that the halomorphides, which are allylic halides, can react with various nucleophiles such as piperidine and thioethanol by an S_N2' mechanism. Thus, α-chloromorphide (I), β-chloromorphide (II), β-bromomorphide (III), and β-iodomorphide (IV) were examined for their ability to bind to the presumed narcotic receptors in rat brain homogenates and for analgesic potency *in vivo*. The α- and β-chloromorphides also were examined for acute toxicity in mice.

EXPERIMENTAL[2]

α-Chloromorphide (I)—Dimethylchloroformiminium chloride (7) (known to formylate phenols and alcohols) reacted exothermically with morphine hydrate (1.42 g, 0.05 mole) in dimethylformamide (10 ml). The yellow solution was stirred (20 min) and poured on ice, and a 10% solution of sodium carbonate was used to neutralize the solution. It was extracted with methylene chloride and dried over magnesium sulfate.

Removal of the solvent gave 1.7 g of a mixture of two compounds (by TLC). α-Chloromorphide (0.8 g) was isolated by utilizing its relative insolubility in hot acetone. The other compound in the mixture was formylmorphine, since prepared by other methods[1]. The I base was recrystallized from a mixture of acetone, methanol, and water, mp 192–194° [lit. (2) mp 193°]; mass spectrum: 303 (M^+), 305, and 268 (base).

Anal.—Calc. for $C_{17}H_{18}ClNO_2$: C, 67.21; H, 5.97; N, 4.61. Found: C, 67.24; H, 6.07; N, 4.35.

The other halomorphides were obtained from the original collection of Small and Lutz (2), who described their preparation and the preparation of the comparably substituted codides.

β-Chloromorphide (II)—The sample had a melting point of 184–188° [lit. (2) mp 188°]; mass spectrum: 303 (M^+), 305, and 268 (base).

Anal.—Calc. for $C_{17}H_{18}ClNO_2$: C, 67.21; H, 5.97; N, 4.61. Found: C, 66.93; H, 5.72; N, 4.38.

β-Bromomorphide Hydrochloride Monohydrate (III)—The sample was recrystallized from methanol–acetone, mp 191.5–193°; mass spectrum: 347 (M^+), 349, and 268 (base). It was dried for 20 hr at 100° before analysis.

Anal.—Calc. for $C_{17}H_{21}BrClNO_3$: C, 50.70; H, 5.26; N, 3.48. Found: C, 50.31; H, 5.22; N, 3.31.

β-Iodomorphide Acid Tartrate Monohydrate (IV)—The sample was recrystallized from acetone–methanol, mp 148.5–152.5°; mass spectrum: 395 (M^+) and 268 (base).

Anal.—Calc. for $C_{21}H_{26}INO_9$: C, 44.77; H, 4.65; N, 2.49. Found: C, 44.88; H, 4.62; N, 2.41.

RESULTS AND DISCUSSION

Stereochemistry—The structure of the α-chloromorphide (I) isolated from the dimethylchloroformiminium chloride reaction was established by the comparison of its NMR, IR, and mass spectra and melting point with those of the known sample[2]. The configuration about C-6 was deduced from NMR data. The coupling constants associated with the C-5, C-6, C-7, C-8, and C-14 protons in I were nearly identical with those in isocodeine (V) (8, 9) (Table I) and quite different from those in codeine (VI). The pertinent protons of codeine (9) also are listed in Table I. The protons in I at C-5, C-6, and C-8 were deshielded, as anticipated, compared with isocodeine. Thus, I can confidently be placed in the 6-iso series, in which the chlorine atom is axially oriented on the C-ring of morphine (above the plane of the ring).

The NMR spectrum of β-chloromorphide (II) showed a considerable shift of several protons from their positions in codeine or isocodeine. The spectrum of II was consistent with the presence of the halogen at the C-8 position and the double-bond between C-6 and C-7. The coupling constant observed between the C-8 and

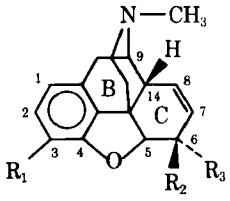

	R_1	R_2	R_3
I, α-chloromorphide	OH	Cl	H
V, isocodeine	OCH_3	OH	H
VI, codeine	OCH_3	H	OH
VII, morphine	OH	H	OH

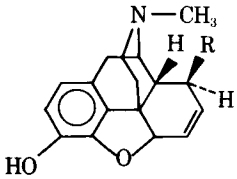

	R
II, β-chloromorphide	Cl
III, β-bromomorphide hydrocloride	Br
IV, β-iodomorphide acid tartrate	I

[2] Melting points (Fisher-Johns apparatus) are corrected. IR data were obtained as Nujol mulls on a Perkin-Elmer 257 instrument. Mass spectra were from a Finnigan 1015D with a model 6000 data collection system, using electron impact (100 ev). NMR spectra were obtained in deuterated methanol on a Varian HA-100. The probe was maintained at 30°, except where indicated. Spin decoupling was obtained in the usual manner. Microanalyses were performed by the Laboratory of Chemistry's Section on Microanalytical Services and Instrumentation. Pharmacological assays were performed by Mrs. Louise Atwell, Medicinal Chemistry Section, Laboratory of Chemistry.

Table II—Analgesic Potency, Toxicity, and Receptor Binding Affinity of the α- and β-Halomorphides

Compound	ED_{50}[a,b]	O[c]	P[d]	D[e]	LD_{50}[a,b]	EC_{50}[f]
α-Chloromorphide[g]	0.07 (0.05—0.1)	3.8	15.9	121	49.7 (42.3—58.4)	7
β-Chloromorphide[g]	0.8 (0.5—1.1)	2.9	19.8	105	280.9 (247—320)	3
β-Bromomorphide hydrochloride	0.60 (0.44—0.83)	2.6	19.4	136	—	10
β-Iodomorphide acid tartrate	0.39 (0.27—0.56)	3.4	44.6	144	—	20
Morphine hydrochloride	1.2 (0.9—1.3)	3.8	28.2	145	576 (558—594)	3

[a] Numbers in parentheses represent 95% confidence limits as obtained by probit analysis. LD is the acute 24-hr toxicity (10 animals for each of four or five dose levels). [b] Subcutaneous injection in mice, milligrams per kilogram, using the hot-plate assay (see Refs. 11 and 12). [c] Onset of analgesia in minutes. [d] Peak time at which maximal analgesic response is observed in minutes. [e] Duration of analgesia in minutes. [f] Effective concentration of drug required to inhibit stereospecific ^{3}H-dihydromorphine binding to rat brain homogenate by 50% in nanomoles. [g] Base, dissolved in dilute hydrochloric acid.

C-14 protons (9.9 Hz) is indicative of an equatorially oriented chlorine atom (10) (in the plane of the ring, as opposed to the C-8 hydrogen atom which is axially oriented below the plane). The C-14 proton is known to be axially oriented on morphine's C-ring [J_{ax-ax} = 8–10 Hz (10)]. Double-irradiation experiments confirmed the observed couplings.

The NMR spectra of the β-bromo- and iodomorphides were very similar to the spectrum of the β-chloromorphide. The coupling constants observed between C-6 and C-7, C-7 and C-8, and C-5 and C-6 were nearly identical to those in β-chloromorphide. Therefore, they must also have their halides equatorially oriented on the C-ring at C-8.

The monograph of Small and Lutz (2) contains errors in the assignments of the position and the configuration of the halogen in the halomorphides. The alpha and beta nomenclature was originally conceived to denote configuration about the C-6 position in the codides. α-Chloromorphide, for example, was presumed to have the same configuration about the C-6 position as the hydroxyl has in morphine and codeine (equatorially oriented on the C-ring). β-Chloromorphide was presumed to have the reverse (axial) position at C-6 (2).

The alpha and beta nomenclature was retained in this paper to avoid confusion. However, the α-halogen designation in this paper relates to the C-6 iso configuration (axial orientation at C-6), and the β-designation relates to the C-8 equatorially substituted position. It is not possible to use "pseudo" or "allopseudo" nomenclature for C-8-substituted compounds in the morphine series, since the name "pseudomorphine" has been used to denote the C-2-coupled dimer of morphine (2). In the codeine series, the C-8-substituted compounds are denoted pseudohalocodides (allopseudo related to a C-8 iso compound).

Perhaps a more precise way of describing the position and configuration of the halogen would be to name α-chloromorphide as 6β-chloromorphide and β-chloromorphide as 8β-chloromorphide[3].

Pharmacology—*Analgesic Potency and Toxicity*—The β-chloro-, bromo-, and iodomorphides were generally more potent than morphine (Table II) in mice in the hot-plate test for analgesia (11, 12). The α-chloromorphide had 10–15 times the potency of morphine and was considerably more toxic in mice than was morphine or the β-chloromorphide (Table II).

Receptor Binding—When using the usual *in vitro* techniques (13) for measuring substrate binding to narcotic receptors from rat brain homogenates, only β-chloromorphide exhibited a binding affinity exactly comparable to morphine, although all of the compounds bound well to the receptors. Transport to the receptor *in vivo* may play an important part in the observed activity of these compounds. Whether for this or other reasons, these compounds generally do not exhibit binding affinity to the narcotic receptors in accord with their analgesic potencies *in vivo*.

None of these halomorphides was observed to bind irreversibly to the narcotic receptors *in vitro* in experiments where rat brain preparations were incubated with 10^{-6}–10^{-8} *M* halomorphide at 37° for up to 2 hr, washed, and then assayed for unreacted receptors.

SUMMARY AND CONCLUSIONS

The α- and β-halomorphides were found to have a C-6 axial and C-8 equatorial halide, respectively. These are potent analgesics *in vivo* with, presumably, all of the liabilities associated with morphine. Also, the toxicities of the examined chloromorphides were greater than morphine. Therefore, the presence of chloromorphide in illicit opiate samples would appear to present an additional hazard to opiate addicts.

The inability of these compounds to act as irreversible inhibitors of the narcotic receptors *in vitro* might be ascribable to the chemical stability of the various compounds or to a rapid equilibrium with the receptors (no one molecule of the analgesic may interact with the receptor long enough to undergo the irreversible reaction). Or, perhaps, the thiol groups, if present on the receptor, may be too far from the area of the primary interaction or may be inaccessable when the receptor is occupied by opiate.

REFERENCES

(1) G. J. Herman and M.-N. N. Kan, *Biomed. Mass Spec.*, **1**, 350(1974).

(2) L. F. Small and R. E. Lutz, "Chemistry of the Opium Alkaloids," Supplement No. 103 to the Public Health Reports, U.S. Government Printing Office, Washington, D.C., 1932.

(3) N. B. Eddy, H. Halbach, and O. J. Braenden, *Bull. WHO*, **13**, 937(1955).

(4) G. Stork and F. H. Clarke, *J. Amer. Chem. Soc.*, **78**, 4619(1956).

(5) E. J. Simon, J. M. Hiller, and I. Adelman, *Proc. Nat. Acad. Sci. USA*, **70**, 1947(1973).

(6) H. A. Wilson, G. W. Pasternak, and S. H. Snyder, *Nature*, **253**, 448(1975).

(7) L. F. Fieser and M. Fieser, "Reagents for Organic Synthesis," vol. 1, Wiley, New York, N.Y., 1967, p. 287.

(8) L. J. Sargent and A. E. Jacobson, *J. Med. Chem.*, **15**, 843(1972).

(9) A. E. Jacobson, H. J. C. Yeh, and L. J. Sargent, *Org. Magn. Reson.*, **4**, 875(1972).

(10) R. M. Silverstein, G. C. Bassler, and T. C. Morrill, "Spectrometric Identification of Organic Compounds," 3rd ed., Wiley, New York, N.Y., 1974.

(11) N. B. Eddy and D. Leimbach, *J. Pharmacol. Exp. Ther.*, **107**, 385(1953).

(12) A. E. Jacobson and E. L. May, *J. Med. Chem.*, **8**, 563(1965); see Ref. 9 therein.

(13) W. A. Klee and R. A. Streaty, *Nature*, **248**, 61(1974).

ACKNOWLEDGMENTS AND ADDRESSES

Received May 19, 1975, from the *Laboratory of Chemistry, National Institute of Arthritis, Metabolism and Digestive Diseases, National Institutes of Health, Bethesda, MD 20014, and the ‡Laboratory of General and Comparative Biochemistry, National Institute of Mental Health, Bethesda, MD 20014

Accepted for publication July 29, 1975.

The authors thank Dr. Everette L. May for the samples of the halomorphides and Mrs. Louise Atwell for the analgesic and toxicological data.

‡ To whom inquiries should be directed.

[3] The authors thank the reviewer for this suggestion.

Relationship between Acute Toxicity in Mice and Polymorphic Forms of Polyene Antibiotics

G. GHIELMETTI, T. BRUZZESE ˣ, C. BIANCHI, and F. RECUSANI

Abstract □ Marked differences in LD_{50} values were found between various batches of polyene antibiotics (mepartricin and nystatin) after intraperitoneal administration in suspension to mice. Such differences do not seem attributable to the particle size but to different molecular spatial arrangements of the products, which modify their solubility and biological availability. In the samples obtained by chemical treatments of some batches of the polyene substances, it has been possible to change the toxicity drastically and then to bring it back to its original value.

Keyphrases □ Toxicity—relationship to polymorphic forms of polyene antibiotics mepartricin and nystatin, mice □ Polymorphic forms—polyene antibiotics mepartricin and nystatin, relationship to toxicity in mice □ Antibiotics, polyene—mepartricin and nystatin, polymorphic forms related to toxicity, mice □ Mepartricin—polymorphic forms related to toxicity, mice □ Nystatin—polymorphic forms related to toxicity, mice

In continuing chemical and biological studies of mepartricin[1], a semisynthetic polyene antibiotic with high antifungal and antiprotozoal activities (1, 2), it was observed that various batches differed considerably in acute toxicity after intraperitoneal administration (LD_{50} ip) in suspension to mice. These differences did not seem to be justified on the basis of the physicochemical and microbiological analyses, since all samples showed properties within well-defined limits of potency, and on the basis of TLC, NMR, IR, and UV evidence.

The toxicity values of many natural polyenes reported in the literature also show marked discrepancies. For example, the LD_{50} of intraperitoneal nystatin was found to be 8–14 (3), 20–26 (4), or about 200 (5) mg/kg according to different investigations. And the LD_{50} of intraperitoneal amphotericin B under the same experimental conditions seemed to be <99 (6), 280 (7), or even >1200 (8) mg/kg.

Bennet *et al.* (9) attempted to explain the difference in toxicity of various samples of amphotericin B by attributing the variability to the different particle sizes. But preliminary tests with mepartricin showed that this explanation does not apply here because no correlation between the LD_{50} values (intraperitoneal) and the size of the particles was seen. Therefore, it was postulated that occasional modifications of the isolation or purification methods of mepartricin, nystatin, or other polyenes might have given rise to products of different solubility, bioavailability, and toxicity as a result of polymorphic modifications, as reported for other classes of drugs (10).

To support this hypothesis, a few batches of mepartricin and nystatin were selected. A sample from each batch (Sample 1, Table I) was treated twice with organic solvents, the first treatment modifying the crystallographic forms (Sample 2) and the second returning it to the original form (Sample 3). All samples were sieved to keep the particle size uniform, and they were analyzed to control eventual differences in purity. Their solubility and LD_{50} values after intraperitoneal administration in suspension to mice were determined. In some samples, the acute toxicity was determined also after suitable solubilization to obtain values independent of the crystalline structure.

[1] Previously referred to in the literature as partricin methyl ester or SPA-S-160.

EXPERIMENTAL

Materials and Methods—Mepartricin was prepared according to a reported method (11). On the basis of preliminary acute toxicity tests in mice by intraperitoneal administration in suspension, four batches of product with very different LD_{50} values were chosen (Table I). Nystatin was a commercial product, and a batch of high[2] toxicity and one of low[3] toxicity were selected. The original Samples 1 of the two polyenes were treated with organic solvents by one of four methods, A–D, to give Samples 2 and then Samples 3. After treatment, they were passed through a stainless steel sieve of 4450 mesh/cm^2 (sieve opening 0.090 mm)[4]. Particle sizes ranging between 4 and 12 μm were obtained for all samples. Analytical controls by elemental analysis, determination of NMR, IR, and UV spectra, TLC, and testing for antifungal activity were also performed. The modifications of solubility and toxicity were then measured.

TLC—TLC was performed on silica gel[5] with a solvent system of butanol–ethanol–acetone–25% ammonium hydroxide (2:5:1:3). The spots were detected by exposure to UV light and had R_f values of about 0.8 for mepartricin and 0.43 for nystatin.

Antifungal Activity—Antifungal activity was determined by a turbidimetric method (12), suitably modified, that compared the growth inhibition of *Saccharomyces cerevisiae*[6] (ATCC 9763) under the influence of the test samples and known quantities of standard mepartricin and nystatin.

The test strain was cultivated for 18 hr at 37° in a broth containing 1% peptone[7], 0.5% yeast extract[8], and 2% glucose[9]. Then 1.7 ml of suspension was inoculated in 100 ml of a broth of the same composition.

The mepartricin standard was dissolved in dimethyl sulfoxide (1000 μg/ml) and diluted with sterile distilled water. Then 1 ml was added to the inoculated culture medium (9 ml) to obtain the final concentrations of 0.15, 0.20, 0.25, 0.30, and 0.35 μg of polyene compound in 10 ml of broth. After 5 hr of incubation at 37°, the absorbance was determined[10] at 580 nm. Values were plotted on the arithmetic scale of semilogarithmic paper with concentrations on the logarithmic scale, giving a five-point standard response line.

The test samples of mepartricin were worked up in the same way to give the midconcentration of 0.25 μg/10 ml. Then the absorbance was determined, and the potency was calculated from the standard response line.

[2] Batch 7208/P 0866, C.F.M., Milan, Italy.
[3] Batch 134, Gianni, Milan, Italy.
[4] No. 35, UNI Italian series, corresponding to 170 mesh, ASTM series.
[5] Kieselgel F_{254}, Merck, Darmstadt, Germany.
[6] Istituto Sieroterapico Milanese, Milan, Italy.
[7] Baltimore Biological Laboratory, Baltimore, Md.
[8] Difco, Detroit, Mich.
[9] Merck, Darmstadt, Germany.
[10] Spectronic 20, Bausch & Lomb, Rochester, N.Y.

Table I—Solubility of Samples of Mepartricin and Nystatin and Acute Toxicity in Mice following Administration of Aqueous Suspensions and Solutions

Compound (Batch Number)	Sample (Preparation Method)[a]	Microbiol Activity, units/mg[b]	Solubility, units/ml[c]	Acute Toxicity in Mice, LD_{50}, mg/kg (Confidence Limits, $p = 0.05$)		
				Intraperitoneal Suspension	Intraperitoneal Solution	Intravenous Solution
Mepartricin (P.149)	1 (B)	2590	12.196	19.5 (18.1–21.0)	—	—
	2 (A)	2525	3.507	126.3 (91.7–174.0)	—	—
	3 (B)	2632	10.085	22.7 (20.2–25.6)	—	—
Mepartricin (LS/11)	1 (A)	2375	3.539	77.7 (70.3–85.8)	—	—
	2 (B)	2352	12.617	15.4 (14.3–16.8)	—	—
	3 (A)	2357	3.905	100.4 (77.1–133.4)	—	—
Mepartricin (P.166)	1 (A)	2802	4.405	216.1 (144.9–322.3)	13.6 (12.2–14.5)	5.3 (4.4–6.4)
	2 (B)	2803	14.476	19.2 (16.7–22.1)	11.1 (10.5–12.3)	4.9 (4.2–5.7)
	3 (A)	2761	3.809	194.3 (163.8–230.4)	12.2 (11.1–13.3)	5.4 (4.9–6.0)
Mepartricin (P.167)	1 (B)	2455	12.326	14.1 (10.5–18.7)	12.5 (11.4–13.6)	5.3 (4.4–6.3)
	2 (A)	3020	4.798	114.2 (103.0–126.5)	11.6 (10.3–12.9)	4.3 (3.8–4.8)
	3 (B)	3010	14.700	8.8 (8.3–9.3)	11.3 (10.4–12.2)	4.7 (3.9–5.7)
Nystatin (7208/P 0866)	1[d]	4575	8.835	88.5 (77.1–101.5)	5.7 (4.8–6.8)	5.7 (4.7–6.9)
	2 (C)	5245	4.605	519.4 (458.4–577.2)	6.1 (5.5–6.9)	5.3 (4.4–6.4)
	3 (D)	4856	8.210	89.5 (81.4–97.1)	6.9 (5.8–8.2)	5.1 (4.0–6.6)
Nystatin (134)	1[d]	5120	3.925	200.9 (144.7–278.9)	5.5 (4.9–6.3)	6.6 (6.0–7.3)
	2 (D)	4142	8.120	23.2 (20.3–26.8)	5.1 (4.1–6.2)	5.8 (4.3–7.9)
	3 (C)	4905	4.127	635.4 (415.4–971.9)	4.4 (3.8–5.1)	8.3 (7.2–9.5)

[a] Sample 1 represents the original batch. Samples 2 and 3 were obtained in order by subsequent treatments. [b] Against the respective standard samples of mepartricin and nystatin. Note that the first polyene has a minimum inhibitory concentration against *Saccharomyces cerevisiae* and against *Candida albicans* below 0.1 unit/ml, while nystatin has minimum inhibitory concentration values of about 5 units/ml; thus 1 unit of mepartricin is much more potent than 1 unit of nystatin. [c] In aqueous solution of sodium lauryl sulfate at the concentration of 1% for mepartricin and at the concentration of 0.1% for nystatin. [d] Commercial sample.

The same procedure was followed with the standard and test samples of nystatin, using concentrations 50-fold higher.

Solubility Tests—Since the two polyenes were too sparingly soluble in distilled water and formed cloudy solutions, which could not be clarified by filtering or centrifuging, the tests were performed in a 1% solution of sodium lauryl sulfate for mepartricin and in a 0.1% solution of sodium lauryl sulfate for nystatin. Accurate and reproducible results for the various samples were obtained.

Suspensions containing 1% of the polyene in these solvents were prepared and stored in darkness at 4° with slow agitation; samples were taken after 1, 8, 24, and 48 hr. Every sample was carefully filtered on a porous membrane, and the solution was immediately subjected to microbiological assay. The results were constant in time and were expressed as the mean of the values for different samples.

Chemistry—*Method A*—Mepartricin (5 g) was treated with 150 ml of methylene chloride–methanol (9:1) at room temperature. The solution was evaporated to dryness at 35–40° under reduced pressure. The oily residue solidified on standing, forming a compact yellow solid, which was pulverized through a screen and dried *in vacuo* at room temperature until complete elimination of the solvent. The product was obtained in the form of layered plates with polygonal surfaces and regular contours.

Method B—Mepartricin (5 g) was treated with 100 ml of acetone–water (8:2) and heated to incipient boiling. The solution was rapidly cooled to room temperature, and 800 ml of ether was added with agitation. The precipitate was collected by filtration and dried *in vacuo* at room temperature, giving almost quantitative yields of yellow rounded granules with porous surfaces and irregular contours.

Method C—Nystatin (5 g) was treated with 50 ml of water saturated with methyl ethyl ketone and heated carefully to 60° with agitation. A partial solution was obtained from which the product rapidly began to separate by crystallization.

After a few minutes, heating was stopped. The mixture was slowly cooled to 10° in 1 hr with agitation. The precipitate was isolated by filtration, washed with acetone, and dried *in vacuo* at room temperature. Yellow needle crystals were obtained.

Method D—Nystatin (5 g) was dissolved in 200 ml of chloroform–methanol–ammonium hydroxide (7:2.5:0.5). The solution was evaporated to dryness *in vacuo* at a temperature below 25° to minimize the degradation of the product; this procedure was followed by trituration through a screen and drying *in vacuo* at room temperature. The product was obtained as yellow rounded granules with porous surfaces.

Pharmacology—The acute toxicity was determined in male and female Swiss mice, 18–22 g, by intraperitoneal administration of mepartricin or nystatin suspensions and, for a few samples, by intraperitoneal and intravenous administrations of solutions. Not less than eight groups of 10 mice each were used in each test. The mortality recorded in 7 days of observation served for calculating the LD_{50} by the Thompson (13) method of moving averages as described by Weil (14).

The compounds, sieved as already described, were suspended in carboxymethylcellulose (0.5% w/v), polysorbate 80 (0.05% w/v), and benzyl alcohol (0.5% v/v) and injected in the constant volume of 0.2 ml/10 g. When solutions were used, the compounds were dissolved in dimethyl sulfoxide with a sodium lauryl sulfate addition (62.5 mg of active agent in 0.45 ml of dimethyl sulfoxide and 125 mg of sodium lauryl sulfate in 25 ml of water). Stock solutions were prepared immediately before use, diluted with water as need-

ed, and injected intraperitoneally and intravenously in the constant volume of 0.2 ml/10 g.

In each test, the interval between doses was calculated with the geometric factor of 1.26 so that the logarithms of successive dosage levels differed by a constant (0.1).

The method of Thompson (13) and Weil (14) for calculating LD_{50} values was preferred to the usual method of Litchfield and Wilcoxon (15) for its simplicity, provided that the logarithm of successive dosage levels differed by a constant and that the number of animals used was the same in each group. The results obtained with the two methods are quite similar.

RESULTS AND DISCUSSION

The batches of mepartricin and nystatin, the samples obtained by the sequence of treatments, and the data of microbiological activity, solubility, and toxicity are described in Table I. These data indicate that, by varying the treatment method, it is possible to obtain samples of higher or lower solubility and, consequently, of very different acute toxicity after intraperitoneal administration in suspension.

For example, Sample 1 of mepartricin, Batch P.166, obtained by Method A, showed relatively low solubility and reduced toxicity, with an LD_{50} in mice of 216.1 mg/kg. When treated according to Method B, it became the more soluble and more toxic Sample 2 (LD_{50} ip 19.2 mg/kg). Treating Sample 2 by Method A then provided Sample 3, of relatively low solubility and toxicity (LD_{50} ip 194.3 mg/kg) like Sample 1. This return to the initial characteristics is obviously important in demonstrating that the changes of toxicity are not the result of a variation in the amount of eventual impurities during the treatment, as confirmed by the usual chemical and microbiological controls.

Furthermore, when the toxicity was determined by the same method but in solution, the differences between the treated Samples 2 and 3 and the original Sample 1 proved to be insignificant, with LD_{50} values for mepartricin Batch P.166 between 11.1 and 13.6 mg/kg, thus demonstrating their essential equivalence under identical bioavailability conditions and confirming the hypothesis concerning the influence of the crystal structure.

Analogous results were obtained when the solutions were administered intravenously, the LD_{50}'s being between 4.9 and 5.4 mg/kg. When the data for the more soluble mepartricin samples are compared, the toxicity in suspension proves to be comparable to that of the solutions, demonstrating a very high bioavailability of these materials. In contrast, more sparingly soluble samples exhibit a much lower *in vivo* utilization and toxicity than in solution.

In conclusion, the principal reason for the variability of the acute toxicity test results obtained with different batches of mepartricin and nystatin suspensions, seems to be attributable to differences in crystal structure, *i.e.*, the existence of polymorphic forms. The same might be true for many other polyenes cited in the literature, and this finding would explain the differences in toxicity data found by different laboratories. Consequently, it is imperative to standardize the methods of the final isolation of the products to have constant toxicity.

These results also suggest that, when a drug of inherently low bioavailability is to be used undissolved in various dosage forms, it may be advantageous to conduct pharmacological tests with several batches of different LD_{50} values (intraperitoneal) to choose the one with the best activity–toxicity ratio. Knowledge of the corresponding acute toxicity of the suitable solubilized product may give further indications as to the possibility of increasing the bioavailability of the undissolved product.

REFERENCES

(1) T. Bruzzese and R. Ferrari, Brit. pat. appl. 52,271 (Nov. 3, 1970).

(2) T. Bruzzese, I. Binda, A. Di Nardo, G. Ghielmetti, and M. Riva, *Experientia*, **28**, 1515(1972).

(3) H. Umezawa, "Index of Antibiotics from Actinomycetes," University of Tokyo, Tokyo, Japan, 1967, p. 474.

(4) E. L. Hazen and R. Brown, *Proc. Soc. Exp. Biol. Med.*, **76**, 93(1951).

(5) "The Merck Index," 8th ed., Merck & Co., Rahway, N.J., 1968, p. 753.

(6) D. P. Bonner, W. Mechlinski, and C. P. Schaffner, *J. Antibiot.*, **25**, 261(1972).

(7) B. A. Steinberg, W. P. Jambor, L. O. Suydam, and A. Soriano, *Antibiot. Ann.*, **1955–56**, 574.

(8) T. H. Sternberg, E. T. Wright, and M. Oura, *ibid.*, **1955–56**, 566.

(9) J. E. Bennet, G. J. Hill, II, W. T. Butler, and C. W. Emmons, "Antimicrobial Agents and Chemotherapy 1963," American Society for Microbiology, Ann Arbor, Mich., 1964, p. 745.

(10) J. Haleblian and W. McCrone, *J. Pharm. Sci.*, **58**, 911(1969).

(11) T. Bruzzese, M. Cambieri, and F. Recusani, *ibid.*, **64**, 462(1975).

(12) F. Kavanagh, "Analytical Microbiology," vol. II, Academic, New York, N.Y., 1972, p. 148.

(13) W. Thompson, *Bacteriol. Rev.*, **11**, 115(1947).

(14) C. Weil, *Biometrics*, **8**, 249(1952).

(15) J. T. Litchfield and F. Wilcoxon, *J. Pharmacol. Exp. Ther.*, **96**, 99(1949).

ACKNOWLEDGMENTS AND ADDRESSES

Received July 31, 1974, from the *Research Laboratories, SPA–Società Prodotti Antibiotici S.p.A., Via Biella 8, 20143 Milano, Italy.*

Accepted for publication July 25, 1975.

[x] To whom inquiries should be directed.

New Synthesis of Substituted Pyrrolo[1,2-*a*][1,3]diazepine and Its Pharmacological Activity

J. WALTER SOWELL, Sr. *, and C. DeWITT BLANTON, Jr. ˣ

Abstract □ A facile route for the synthesis of the substituted pyrrolo[1,2-*a*][1,3]diazepine nucleus from readily available starting material is reported. The compound was tested for antimalarial activity in mice, antineoplastic activity in mice, acute hypotensive activity in rats and dogs, effect on cholesterol–lipoprotein levels in rats, anti-inflammatory activity in rats, antiviral activity in mice, CNS depressant or stimulant activity in mice, diuretic activity in fasted rats, and antidiabetic activity in rats. Hypotensive activity of relatively short duration was observed in rats. The compound lacked positive pharmacological activity in the remaining tests.

Keyphrases □ Pyrrolo[1,2-*a*][1,3]diazepine, substituted—synthesis, antimalarial, antineoplastic, antiviral, and CNS activity in mice, hypotensive, anti-inflammatory, diuretic, and antidiabetic activity in rats □ Hypotensive agents, potential—substituted pyrrolo[1,2-*a*][1,3]diazepine screened, rats

Since the first synthesis of chlordiazepoxide was reported (1, 2) and it was shown to possess antianxiety activity (3, 4), there has been a tremendous interest in the 1,4-benzodiazepines as potential medicinal agents. In addition to chlordiazepoxide, diazepam (I), oxazepam, and flurazepam have been marketed in the United States for their psychopharmacological properties. Research directed toward nuclear substitution of the 1,4-benzodiazepine nucleus has been prolific, but less attention (5–7) has been given to isosteric modifications of the benzene ring in this nucleus. A few reports (8–10) have described the amidine (II) and saturated derivative (III).

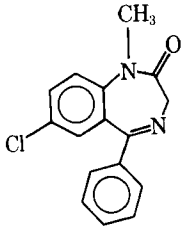

I

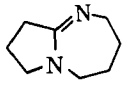

II

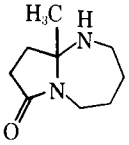

III

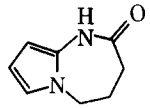

IV

This report describes a new synthesis for the 1*H*-pyrrolo[1,2-*a*][1,3]diazepine (IV) analog and preliminary pharmacology.

DISCUSSION

Chemistry—Acylation of 2-amino-3-cyano-4,5-dimethylpyrrole (V, Scheme I) (11) with 4-chlorobutyryl chloride in the presence of triethylamine gave the corresponding amide (VI). Upon treating a suspension of VI in absolute ethanol with potassium *tert*-butoxide, 9-cyano-7,8-dimethyl-2-oxo-1*H*-2,3,4,5-tetrahydropyrrolo[1,2-*a*]-[1,3]diazepine (VII) was obtained in good yields. One can visualize the diazepine (VII) formation proceeding through pyrrolyl anion formation followed by nucleophilic displacement of the halogen.

An alternative route to VII was investigated. Acylation of 1-acetyl-2-amino-3-cyano-4,5-dimethylpyrrole[1] (VIII) (12) with 4-chlorobutyryl chloride gave 1-acetyl-2-(4-chlorobutyramido)-3-cyano-4,5-dimethylpyrrole (IX, Scheme I). Ring closure to yield VII was achieved by refluxing IX in a hydroalcoholic solution containing sodium hydroxide. Reports (12, 13) indicated that 1-acetylpyrrole and derivatives thereof are susceptible to cleavage in alkaline media. Following the deacetylation, ring formation probably proceeds through pyrrolyl-anion formation and subsequent nucleophilic displacement of the halogen to yield VII.

Structural assignment was confirmed by elemental analysis and IR, NMR, and mass spectral data. The NMR spectrum of VII showed singlets at 2.03 and 2.10 ppm, which integrated for three protons each. These peaks were assigned to the protons on the methyl groups at the 7- and 8-positions. The complex multiplet between 2.2 and 2.7 ppm, integrating for four protons, was assigned to the protons of the methylenes at the 3- and 4-positions. A triplet centered at 4.15 ppm, integrating for two protons, was assigned to the protons of the methylene at the 5-position. A broad singlet centered at 10.55 ppm, integrating for one proton, was assigned to the proton of the nitrogen at the 1-position.

The mass spectrum of VII gave the parent ion at 203 mass units, corresponding to the molecular formula of $C_{11}H_{13}N_3O$. A strong peak at 160 amu (203 − 43 amu) showed the presence of X. A peak at 43 amu indicated the cleavage of —NHCO— from the parent structure.

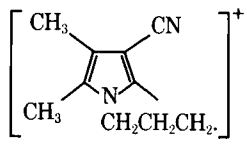

X

Biological Activity—The new pyrrolodiazepine (VII) was submitted to a variety of biological screens. Antimalarial test results[2] showed that the compound was inactive against *Plasmodium berghei* in mice by the method of Osdene *et al.* (14). The diazepine (VII) was inactive when tested against L-1210 and P-388 leukemia according to standard protocol[3] (15, 16).

Pharmacological test data were obtained[4] for: (*a*) acute hypotensive action in rats, (*b*) effect on cholesterol–lipoprotein levels in rats by a modified procedure of Tensho *et al.* (17), (*c*) anti-inflammatory activity (hindpaw edema) in rats (18), (*d*) *in vivo* antiviral (encephalomycarditis) activity in mice[5], (*e*) preliminary central nervous system depressant or stimulant activity in mice[6], (*f*) diuretic activity

[1] Compound VIII was prepared by direct ring closure from 3-acetamido-2-butanone and malononitrile in the standard Gewald (11) condensation. The expected elemental analyses and NMR and IR spectra were obtained.

[2] Provided by the Walter Reed Army Institute of Research.

[3] The Division of Cancer Treatment, National Cancer Institute, National Institutes of Health.

[4] From The Upjohn Co.'s biological evaluation program.

[5] The compound is administered to mice, 100 mg/kg ip, before and after intranasal infection with encephalomycarditis virus. A three-stage sequential system is used to classify the compound as active or inactive on the basis of mortality in groups of 10 mice/stage.

[6] The compound is administered to a group of mice, 100 mg/kg ip. Observations, 30 min after dosing, are made on spontaneous effects (loss of righting reflex, depression, stimulation, or convulsions) and autonomic symptoms. Then nicotine sulfate is injected intravenously, and observations on tonic or running convulsions and lethality are recorded.

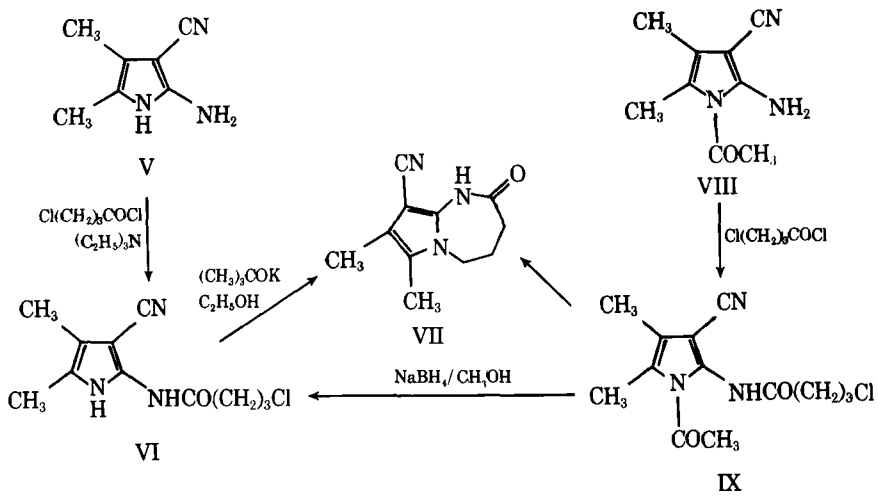

Scheme I

in fasted rats (19), and (*g*) antidiabetic activity in rats (20). Except for the acute hypotensive screen, VII did not exhibit significant activity in any of these tests. A single 50-mg/kg oral dose administered to two rats produced an average change in the mean arterial pressure from initial values of −17 and −6 mm Hg at 4 and 24 hr, respectively. The depressor activity was of relatively short duration. No hypotensive activity was observed when VII was evaluated in dogs, but further ring modification may yield compounds of more medicinal interest.

EXPERIMENTAL[7]

1-Acetyl-2-(4-chlorobutyramido)-3-cyano-4,5-dimethylpyrrole (IX)—A solution of VIII (12) (7.5 g, 0.0425 mole) in 75 ml of tetrahydrofuran and 45 ml of acetonitrile was continuously stirred in an ice bath while 4-chlorobutyryl chloride (3.3 g, 0.0234 mole) was added. After the addition was complete, the solution was stirred for an additional 30 min at this temperature. During this time, a heavy precipitate was formed. The reaction was allowed to continue for an additional hour at 50°.

The precipitate was removed by filtration and washed with 100 ml of tetrahydrofuran, and the combined filtrates were evaporated *in vacuo* to yield an oily, light-tan residue. This residue was shaken with 50 ml of cyclohexane, and solidification of the oil was obtained. The crude product (4.5 g, 75%) was recrystallized from benzene–cyclohexane to yield a white product homogeneous on TLC (ethyl acetate, R_f 0.53; tetrahydrofuran, R_f 0.59; chloroform, R_f 0.34), mp 120–121°; IR (potassium bromide): 3200, 2215, 1720, 1665, 1600, 1570, 1485, 1310, and 985 cm^{-1}; NMR (deuterochloroform): δ 2.03 (s, 3H, CH_3 at C-4 or C-5), 2.29 (s, 3H, CH_3 at C-5 or C-4), 2.00–2.40 (m, 2H, H's on the methylene that are beta to the carbonyl of the amide at C-2), 2.57 (s, 3H, CH_3 of acetyl), 2.60 (t, 2H, —$COCH_2$—), 3.62 (t, 2H, J = 6.0 Hz, —CH_2Cl), and 8.88 (s, 1H, NH of amide); UV λ_{max} (methanol): 209 (ϵ 13,300) and 284 (9800) nm.

Anal.—Calc. for $C_{13}H_{16}ClN_3O_2$: C, 55.42; H, 5.72; N, 14.91. Found: C, 55.28; H, 5.81; N, 14.86.

2-(4-Chlorobutyramide)-3-cyano-4,5-dimethylpyrrole (VI)—*Method I*—A solution of V (11) (6.75 g, 0.05 mole) and triethylamine (5.05 g, 0.05 mole) in 150 ml of tetrahydrofuran was cooled to −50° in a dry ice–acetone bath, and 4-chlorobutyryl chloride (7.05 g, 0.05 mole) was added. Immediately upon addition of the acid chloride, a heavy precipitate formed. The dry ice–acetone bath was removed, and the contents of the vessel were stirred vigorously as the mixture warmed to room temperature. After 30 min at room temperature, the reaction mixture was heated at 40° for 30 min.

The triethylamine hydrochloride was removed by filtration and washed with tetrahydrofuran. The combined filtrates were diluted with 300 ml of water to yield a light-tan solid, which was collected by filtration, washed with water, and air dried. The crude amide (9.8 g, 81.7%) was recrystallized three times from benzene–cyclohexane to yield white, fluffy crystals [homogeneous on TLC (ethyl acetate, R_f 0.57)], mp 170–171°; IR (potassium bromide): 3250, 3160, 2220, 1670, 1620, 1600, 1510, 1470, 1450, 1330, 1250, 1225, and 1125 cm^{-1}; NMR (deuterochloroform): δ 2.05 (s, 3H, CH_3 at C-4 or C-5), 2.10 (s, 3H, CH_3 at C-5 or C-4), 2.20–2.80 (m, 4H, —$COCH_2CH_2$—), 3.65 (t, 2H, J = 6.0 Hz, —CH_2Cl), 9.75 (s, 1H, —HNCO—), and 10.30 (s, 1H, N_1H); UV λ_{max} (methanol): 210 (ϵ 9990) and 284 (8190) nm.

Anal.—Calc. for $C_{11}H_{14}ClN_3O$: C, 55.12; H, 5.89; N, 17.53. Found: C, 54.97; H, 6.00; N, 17.58.

Method II—A solution of IX (2 g, 0.007 mole) in 25 ml of absolute methanol was treated with sodium borohydride (1.0 g, 0.027 mole) with stirring. After the addition was complete, the solution was stirred for 3 min and then poured into an ice–water mixture. The pH was adjusted to 7 with acetic acid, and the precipitate was collected, washed with water, and air dried.

The crude product (1.55 g, 91%) was recrystallized from benzene–cyclohexane and characterized as VI by the IR spectrum and melting point (168–169°). [The lability of the N^1-acetyl group under alkaline or alcoholic conditions (13) apparently accounts for the product obtained in this reaction.]

9-Cyano-7,8-dimethyl-2-oxo-1*H*-2,3,4,5-tetrahydropyrrolo-[1,2-*a*][1,3]diazepine (VII)—*Method I*—A suspension of IX (1.0 g, 0.00355 mole) in 75 ml of water and 25 ml of 95% ethanol was treated with sodium hydroxide (4.7 ml of 0.75 *N*, 0.00355 mole). The mixture was refluxed with continuous stirring for 20 hr, during which time a clear solution was obtained. The ethanol was removed, and a solid precipitated from the aqueous solution. This solid was collected by filtration, washed with water, and air dried.

The crude product (0.075 g, 10.4%)[8] was recrystallized three times from benzene–cyclohexane to yield a pale-pink powder [homogeneous on TLC (ethyl acetate, R_f 0.42; tetrahydrofuran, R_f 0.55)], mp 181–182°; IR (potassium bromide): 3300, 2200, 1670, 1600, 1550, 1450, 1400, 1280, 1225, 1120, and 750 cm^{-1}; NMR (deuterochloroform): δ 2.03 (s, 3H, CH_3 at C-8 or C-7), 2.10 (s, 3H, CH_3 at C-7 or C-8), 2.20–2.70 (m, 4H, —$COCH_2CH_2$—), 4.15 (t, 2H, J = 6.7 Hz, —NCH_2—), and 10.55 (broad s, 1H, amide NH); mol. wt. (mass spectra): calc., 203, and found, 203.

Anal.—Calc. for $C_{11}H_{13}N_3O$: C, 65.01; H, 6.45; N, 20.67. Found: C, 65.08; H, 6.49; N, 20.84.

Method II—A suspension of VI (4.8 g, 0.02 mole) in 75 ml of absolute ethanol was treated with potassium *tert*-butoxide (2.45 g, 0.022 mole). The suspension was heated to reflux and then stirred at room temperature for 10 days. (Subsequent experiments revealed that heating was not necessary to obtain similar results. Furthermore, stirring the reaction mixture overnight at room temperature gave

[7] Melting points were determined on a Thomas-Hoover apparatus (capillary method) and are uncorrected. The NMR spectra were determined on a Hitachi Perkin-Elmer R 20A high-resolution NMR spectrometer, using tetramethylsilane as the internal reference. IR spectra were determined on a Perkin-Elmer 237B grating spectrophotometer, using the potassium bromide technique. UV spectra were determined in methanol solution with a Perkin-Elmer 202 UV–visible spectrophotometer. Elemental analyses were determined by Atlantic Microlab, Inc., Atlanta, Ga. TLC was performed on Eastman chromatogram sheets, type 6060 (silica gel).

[8] The low yield may be rationalized as a result of the release of acetate not being sufficiently basic to form the pyrrolyl anion for subsequent ring closure.

identical results.) The alcoholic suspension was diluted with 25 ml of water (starting material and other by-products are soluble in the aqueous alkaline medium), and the precipitate was collected by filtration, washed with water, and air dried. The compound (3.1 g, 76.2%) melted at 181–182° and exhibited identical spectral and physical data as the material from Method I.

REFERENCES

(1) L. H. Sternbach and E. Reeder, *J. Org. Chem.*, **26**, 1111(1961).

(2) S. Garattini, E. Mussini, and L. O. Randall, "The Benzodiazepines," Raven, New York, N.Y., 1973.

(3) L. O. Randall, W. Schallek, G. A. Heise, E. F. Keith, and R. E. Bagdon, *J. Pharmacol. Exp. Ther.*, **129**, 163(1960).

(4) G. A. Archer and L. H. Sternbach, *Chem. Rev.*, **68**, 747(1968).

(5) R. Littell and D. Allen, *J. Med. Chem.*, **8**, 722(1965).

(6) H. A. DeWald, I. C. Nordin, Y. J. L'Italien, and R. F. Parcell, *ibid.*, **16**, 1346(1973).

(7) M. Nakanishi, T. Tahara, K. Araki, M. Shiroki, T. Tsumagari, and Y. Takigawa, *ibid.*, **16**, 214(1973).

(8) Farbenfabriken Bayer A.-G., French pat. 1,491,791 (1967); through *Chem. Abstr.*, **69**, P67412d(1968).

(9) H. Horst and U. Bahr, British pat. 1,134,613 (1968); through *Chem. Abstr.*, **70**, P29589e(1969).

(10) H. Wollweber, J. Kurz, and W. Nägele, *Arch. Pharm.*, **304**, 774(1971).

(11) K. Gewald, *Z. Chem.*, **1**, 349(1961).

(12) S. Sunder, M.S. thesis, Auburn University, Auburn, Ala., 1968, p. 52.

(13) W. A. Remers, R. H. Roth, G. J. Gibbs, and M. J. Weiss, *J. Org. Chem.*, **36**, 1232(1971).

(14) T. S. Osdene, P. B. Russell, and L. Rane, *J. Med. Chem.*, **10**, 431(1967).

(15) R. I. Geran, H. N. Greenberg, M. M. MacDonald, A. M. Schumacker, and B. J. Abbott, *Cancer Chemother. Rep.*, **3**, 1(1972).

(16) Instruction Booklet 14, "Screening Data Summary Interpretation," Drug Research and Development, Chemotherapy, National Cancer Institute, Bethesda, Md., 1972.

(17) A. Tensho, I. Shimizu, T. Takenawa, H. Kikuchi, and T. Rukujo, *J. Pharm. Soc. Jpn.*, **92**, 879(1972).

(18) E. M. Glenn, B. J. Bowman, W. Kooyers, T. Koslowske, and M. L. Meyers, *J. Pharmacol. Exp. Ther.*, **155**, 157(1967).

(19) L. L. Shaletzky, B. F. Graham, and J. Szmuszkovicz, *J. Med. Chem.*, **12**, 977(1969).

(20) G. C. Gerritsen and W. E. Dulin, *J. Pharmacol. Exp. Ther.*, **150**, 491(1965).

ACKNOWLEDGMENTS AND ADDRESSES

Received July 10, 1975, from the *Department of Medicinal Chemistry, School of Pharmacy, University of Georgia, Athens, GA 30602*

Accepted for publication August 13, 1975.

Adapted in part from a thesis submitted by J. W. Sowell to the University of Georgia in partial fulfillment of the Doctor of Philosophy degree requirements.

Supported in part by Public Health Service Research Grant MH16422 from the National Institutes of Health.

Antimalarial test results were provided through the courtesy of Dr. T. R. Sweeney, Walter Reed Army Institute of Research. Antineoplastic data were made available through the courtesy of Dr. H. B. Wood, Jr., Drug Development Branch, Drug Research and Development, Division of Cancer Treatment, National Cancer Institute. Pharmacological test results from personnel of The Upjohn Co. were provided through the courtesy of Dr. Paul O'Connell, Biological Screening Office, The Upjohn Co., Kalamazoo, Mich. Mass spectral data were provided through the courtesy of the Southeast Environmental Research Laboratory, Athens, Ga.

* Present address: School of Pharmacy, University of South Carolina, Columbia, S.C.

ˣ To whom inquiries should be directed.

Partition Coefficients of Selected Pyridine Carbamates and Comparisons with Their Acetylcholinesterase and Butyrylcholinesterase Inhibitory Potencies

O. ELMO MILLNER, Jr. *, and WILLIAM P. PURCELL ˣ

Abstract □ Partition coefficients of a series of 2-substituted 3-(*N,N*-dimethyl)carbamyloxypyridines were determined in an octanol–buffer (pH 7.4) system. The values obtained were compared with the inhibitory potencies of acetylcholinesterase and butyrylcholinesterase. No significant difference was found for the role of hydrophobicity in the two enzyme systems.

Keyphrases □ Partition coefficients—substituted pyridine carbamates, compared with acetylcholinesterase and butyrylcholinesterase inhibitory potencies □ Pyridine carbamates, substituted—partition coefficients compared with acetylcholinesterase and butyrylcholinesterase inhibitory potencies □ Acetylcholinesterase—inhibition by substituted pyridine carbamates compared to their partition coefficients □ Butyrylcholinesterase—inhibition by substituted pyridine carbamates compared to their partition coefficients □ Enzymes—acetylcholinesterase and butyrylcholinesterase, inhibition by substituted pyridine carbamates compared to their partition coefficients

Previously (1), the synthesis and enzymatic evaluation of some pyridine carbamates were reported, and the compounds were used as enzyme inhibitors in a comparative study of the active centers of acetylcholinesterase and butyrylcholinesterase. Fundamental differences in acetylcholinesterase and butyrylcholinesterase regarding their interaction with the selected carbamate inhibitors were presented (1). No results were included, however, on the effect of any chemical or physical properties of the inhibitor molecules on inhibitory activity. The purpose of this paper is to report results of a study on the contribution of relative hydrophobicities to the inhibition of acetylcholinesterase and butyrylcholinesterase by the selected carbamates (1).

Limited literature results comparing the active

identical results.) The alcoholic suspension was diluted with 25 ml of water (starting material and other by-products are soluble in the aqueous alkaline medium), and the precipitate was collected by filtration, washed with water, and air dried. The compound (3.1 g, 76.2%) melted at 181–182° and exhibited identical spectral and physical data as the material from Method I.

REFERENCES

(1) L. H. Sternbach and E. Reeder, *J. Org. Chem.*, **26**, 1111(1961).

(2) S. Garattini, E. Mussini, and L. O. Randall, "The Benzodiazepines," Raven, New York, N.Y., 1973.

(3) L. O. Randall, W. Schallek, G. A. Heise, E. F. Keith, and R. E. Bagdon, *J. Pharmacol. Exp. Ther.*, **129**, 163(1960).

(4) G. A. Archer and L. H. Sternbach, *Chem. Rev.*, **68**, 747(1968).

(5) R. Littell and D. Allen, *J. Med. Chem.*, **8**, 722(1965).

(6) H. A. DeWald, I. C. Nordin, Y. J. L'Italien, and R. F. Parcell, *ibid.*, **16**, 1346(1973).

(7) M. Nakanishi, T. Tahara, K. Araki, M. Shiroki, T. Tsumagari, and Y. Takigawa, *ibid.*, **16**, 214(1973).

(8) Farbenfabriken Bayer A.-G., French pat. 1,491,791 (1967); through *Chem. Abstr.*, **69**, P67412d(1968).

(9) H. Horst and U. Bahr, British pat. 1,134,613 (1968); through *Chem. Abstr.*, **70**, P29589e(1969).

(10) H. Wollweber, J. Kurz, and W. Nägele, *Arch. Pharm.*, **304**, 774(1971).

(11) K. Gewald, *Z. Chem.*, **1**, 349(1961).

(12) S. Sunder, M.S. thesis, Auburn University, Auburn, Ala., 1968, p. 52.

(13) W. A. Remers, R. H. Roth, G. J. Gibbs, and M. J. Weiss, *J. Org. Chem.*, **36**, 1232(1971).

(14) T. S. Osdene, P. B. Russell, and L. Rane, *J. Med. Chem.*, **10**, 431(1967).

(15) R. I. Geran, H. N. Greenberg, M. M. MacDonald, A. M. Schumacker, and B. J. Abbott, *Cancer Chemother. Rep.*, **3**, 1(1972).

(16) Instruction Booklet 14, "Screening Data Summary Interpretation," Drug Research and Development, Chemotherapy, National Cancer Institute, Bethesda, Md., 1972.

(17) A. Tensho, I. Shimizu, T. Takenawa, H. Kikuchi, and T. Rukujo, *J. Pharm. Soc. Jpn.*, **92**, 879(1972).

(18) E. M. Glenn, B. J. Bowman, W. Kooyers, T. Koslowske, and M. L. Meyers, *J. Pharmacol. Exp. Ther.*, **155**, 157(1967).

(19) L. L. Shaletzky, B. F. Graham, and J. Szmuszkovicz, *J. Med. Chem.*, **12**, 977(1969).

(20) G. C. Gerritsen and W. E. Dulin, *J. Pharmacol. Exp. Ther.*, **150**, 491(1965).

ACKNOWLEDGMENTS AND ADDRESSES

Received July 10, 1975, from the *Department of Medicinal Chemistry, School of Pharmacy, University of Georgia, Athens, GA 30602*

Accepted for publication August 13, 1975.

Adapted in part from a thesis submitted by J. W. Sowell to the University of Georgia in partial fulfillment of the Doctor of Philosophy degree requirements.

Supported in part by Public Health Service Research Grant MH16422 from the National Institutes of Health.

Antimalarial test results were provided through the courtesy of Dr. T. R. Sweeney, Walter Reed Army Institute of Research. Antineoplastic data were made available through the courtesy of Dr. H. B. Wood, Jr., Drug Development Branch, Drug Research and Development, Division of Cancer Treatment, National Cancer Institute. Pharmacological test results from personnel of The Upjohn Co. were provided through the courtesy of Dr. Paul O'Connell, Biological Screening Office, The Upjohn Co., Kalamazoo, Mich. Mass spectral data were provided through the courtesy of the Southeast Environmental Research Laboratory, Athens, Ga.

* Present address: School of Pharmacy, University of South Carolina, Columbia, S.C.

ˣ To whom inquiries should be directed.

Partition Coefficients of Selected Pyridine Carbamates and Comparisons with Their Acetylcholinesterase and Butyrylcholinesterase Inhibitory Potencies

O. ELMO MILLNER, Jr. *, and WILLIAM P. PURCELL ˣ

Abstract □ Partition coefficients of a series of 2-substituted 3-(*N,N*-dimethyl)carbamyloxypyridines were determined in an octanol–buffer (pH 7.4) system. The values obtained were compared with the inhibitory potencies of acetylcholinesterase and butyrylcholinesterase. No significant difference was found for the role of hydrophobicity in the two enzyme systems.

Keyphrases □ Partition coefficients—substituted pyridine carbamates, compared with acetylcholinesterase and butyrylcholinesterase inhibitory potencies □ Pyridine carbamates, substituted—partition coefficients compared with acetylcholinesterase and butyrylcholinesterase inhibitory potencies □ Acetylcholinesterase—inhibition by substituted pyridine carbamates compared to their partition coefficients □ Butyrylcholinesterase—inhibition by substituted pyridine carbamates compared to their partition coefficients □ Enzymes—acetylcholinesterase and butyrylcholinesterase, inhibition by substituted pyridine carbamates compared to their partition coefficients

Previously (1), the synthesis and enzymatic evaluation of some pyridine carbamates were reported, and the compounds were used as enzyme inhibitors in a comparative study of the active centers of acetylcholinesterase and butyrylcholinesterase. Fundamental differences in acetylcholinesterase and butyrylcholinesterase regarding their interaction with the selected carbamate inhibitors were presented (1). No results were included, however, on the effect of any chemical or physical properties of the inhibitor molecules on inhibitory activity. The purpose of this paper is to report results of a study on the contribution of relative hydrophobicities to the inhibition of acetylcholinesterase and butyrylcholinesterase by the selected carbamates (1).

Limited literature results comparing the active

Table I—Partition Coefficients (P) and I_{50} Values of Selected Carbamates

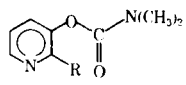

Compound	R	$P \pm SD$[a]	Acetylcholinesterase $I_{50} \times 10^5 M$	Butyrylcholinesterase $I_{50} \times 10^5 M$
I	H	—[b]	—[b]	—[b]
II	Cl	11.08 ± 0.61[a]	6.1 (±0.3)[c]	8.75 (±0.44)[c]
III	Br	13.74 ± 0.40[a]	2.15 (±0.11)[c]	6.0 (±0.3)[c]
IV	I	18.26 ± 0.91[a]	0.900 (±0.045)[c]	1.950 (±0.012)[c]
V	NO_2	3.46 ± 0.25[a]	7.9 (±0.4)[c]	19.0 (±1.0)[c]
VI	$CH_2N(CH_3)_2$	0.422 ± 0.068[a]	0.490 (±0.024)[c]	0.144 (±0.007)[c]
VII	$CH_2\overset{+}{N}(CH_3)_3$	—	0.360 (±0.018)[c]	0.135 (±0.007)[c]

[a] Standard deviation ($\sqrt{\Sigma y^2/n}$) of six determinations. [b] Compound underwent immediate autohydrolysis in water. [c] Experimental error determined by repeated measurements for one compound. See Ref. 1.

centers of acetylcholinesterase and butyrylcholinesterase that indicated a difference in the hydrophobic nature of the "nonesteratic" site of acetylcholinesterase and butyrylcholinesterase (2, 3) were based upon qualitative observations; hydrophobicity was assumed to increase with, and increase in, the alkyl nature of organophosphorus inhibitors (3) and pyridine acetate substrates (2). A quantitative assessment of the role of hydrophobic interactions in the inhibition of acetylcholinesterase and butyrylcholinesterase should aid in comparing the hydrophobic nature of the active centers of acetylcholinesterase and butyrylcholinesterase. For this reason, partition coefficients in the octanol–water system (4) were measured as quantitative indexes of hydrophobicity.

EXPERIMENTAL

The synthesis and enzymatic evaluation of the selected compounds were reported previously (1).

Partition Coefficients—Partition coefficients were determined in the octanol–water system (5, 6). Measurements were made using an aqueous phase consisting of 0.1 M phosphate buffer adjusted to pH 7.4. The aqueous phase was shaken vigorously with purified octanol to saturate it with octanol and vice versa so that the phase composition would remain constant during the partition process.

Partitioning was done in 50-ml glass-stoppered centrifuge tubes. A specially designed shaking apparatus was used to ensure vigorous shaking and thorough mixing. The amounts of compound and relative volumes of the two phases were varied. In this manner, any dependence of partitioning on solubility effect (*e.g.*, saturation of one phase with a compound) could be detected. The filled tubes were shaken for 10 min and centifuged until both phases were completely separated. Six determinations were made in this manner for each compound.

Concentrations in the two phases were determined by UV absorption. Absorbance *versus* concentration was determined in both the octanol and the aqueous phases to ensure linearity of absorbance with concentration in both phases in the concentration range used.

Regression Analyses—Linear regressions were performed using a computer program modified from the original program (7).

RESULTS AND DISCUSSION

The results of the partitioning measurements along with the I_{50} values of the respective compounds are given in Table I[1]. Since I undergoes rapid autohydrolysis in aqueous solution, there is no partition coefficient or I_{50} value for this compound.

If one compares the acetylcholinesterase and butyrylcholinesterase inhibitory activities with log P, VI clearly does not fall in line with the other compounds. The tertiary amine substituent of VI is largely protonated at pH 7.4, resulting in its low apparent partition coefficient (8).

The observation that inhibitory activity increases as the van der Waals radii of the halogen in the 2-position increase leads to the speculation that the inhibitory activity of carbamates that are quasisubstrates of cholinesterase, *i.e.*, progressive inhibitors, may be related to the ability of the carbamate to create an anhydrous environment at the catalytic center of the cholinesterase. Since these inhibitors have been shown to carbamylate (1), any condition that facilitates the rate of carbamylation should also increase inhibitory activity. The hydrolysis of carbamates is thought to proceed *via* a mechanism including a nucleophilic attack on the carbonyl carbon similar to the hydrolysis of acetylcholine (9). Weaver and Hutchison (10) showed that, in a nonenzymatic system, nucleophilicity is increased by anhydrous conditions.

The relative hydrophobicities of the halogen should increase with an increase in surface area of the nonpolar group (11, 12). The amount of structured water that is broken down when a hydrophobic moiety leaves the aqueous environment is directly proportional to the gain in the positive entropy for the transfer (11, 13) and, thus, to the strength of the hydrophobic interaction. The hypothesis of Belleau and Lacasse (14) is that the function of the third methyl group of acetylcholine, which has been shown not to contribute to the affinity of acetylcholine for the enzyme, acetylcholinesterase (15), is to expel water from the active site of acetylcholinesterase. The creation of a more anhydrous environment could serve to increase the rate of carbamylation (and thus the inhibitory potencies) by the halogen-substituted pyridine carbamates.

[1] *Note added in proof:* Even though the partition coefficients in Table I are apparent partition coefficients, the true partition coefficients should be the same, since ionization is not present. An exception to this is Compound XI, of course.

REFERENCES

(1) O. E. Millner, Jr., J. W. Stanley, and W. P. Purcell, *J. Med. Chem.*, **17**, 13(1974).

(2) K.-B. Augustinsson, *Biochim. Biophys. Acta*, **128**, 351(1966).

(3) M. I. Kabachnik, A. P. Brestkin, N. N. Godoviko, M. J. Michelson, E. V. Rozengart, and V. I. Rozengart, *Pharmacol. Rev.*, **22**, 355(1970).

(4) A. Leo, C. Hansch, and C. Church, *J. Med. Chem.*, **12**, 766(1969).

(5) A. Leo, C. Hansch, and D. Elkins, *Chem. Rev.*, **71**, 525(1971).

(6) A. Leo and C. Hansch, *J. Org. Chem.*, **36**, 1539(1971).

(7) A. J. Capato, "Single and Multiple Linear Regression Analysis Program," IBM Data Processing Systems, New York, N.Y., 1967.

(8) D. D. Perrin, "Dissociation Constants of Organic Bases in Aqueous Solution," Butterworths Scientific Publications, London, England, 1965.

(9) R. D. O'Brien, *Mol. Pharmacol.*, **4**, 121(1968).

(10) W. M. Weaver and J. D. Hutchison, *J. Amer. Chem. Soc.*, **86**, 261(1964).

(11) G. Nemethy, *Angew. Chem. Int. Ed.*, **6**, 195(1967).

(12) H. S. Frank and M. W. Evans, *J. Chem. Phys.*, **13**, 507(1945).

(13) G. Nemethy and H. A. Scheraga, *ibid.*, **36**, 3401(1962).

(14) B. Belleau and C. Lacasse, *J. Chem.*, **7**, 768(1964).

(15) I. B. Wilson and E. Cabib, *J. Amer. Chem. Soc.*, 78, 202(1956).

ACKNOWLEDGMENTS AND ADDRESSES

Received June 23, 1975, from the *Drug Design Division, University of Tennessee, Center for the Health Sciences, Memphis, TN 38163*

Accepted for publication August 4, 1975.

Abstracted in part from a dissertation submitted by O. E. Millner, Jr., to the University of Tennessee in partial fulfillment of the Doctor of Philosophy degree requirements.

Supported by the U.S. Public Health Service through a National Institutes of Health Traineeship (GM-02052) and by the University of Tennessee Cardiovascular Computer Project (HL-09495).

* NIH Trainee (GM-02052). Present address: Research and Development, Norwich Pharmacal Co., Norwich, NY 13815

ˣ To whom inquiries should be directed.

Potential Antitumor Agents: A Cytotoxic Cardenolide from *Coronilla varia* L.

MARTIN WILLIAMS * and JOHN M. CASSADY ˣ

Abstract □ An alcoholic extract of the seeds of *Coronilla varia* L. showed inhibitory activity against KB cells in culture and was fractionated through a series of partitions, column chromatography, and preparative layer chromatography to yield hyrcanoside, daphnoretin, scopoletin, and umbelliferone. Hyrcanoside was also tested in the PS mouse leukemia assay and showed borderline activity.

Keyphrases □ *Coronilla varia*—seeds, alcoholic extract, cardenolide and three coumarins isolated and identified, cytotoxic and antileukemic activity screened □ Cardenolides—hyrcanoside isolated from *Coronilla varia* seeds, cytotoxic and antileukemic activity screened □ Coumarins—isolated from alcoholic extract of *Coronilla varia* seeds, cytotoxic and antileukemic activity screened □ Cytotoxic compounds—alcoholic extract of *Coronilla varia* seeds, cytotoxic and antileukemic activity screened □ Antitumor agents, potential—alcoholic extract of *Coronilla varia* seeds, cardenolide and three coumarins isolated and screened □ Antileukemic agents, potential—alcoholic extract of *Coronilla varia* seeds, cardenolide and three coumarins isolated and screened

An alcoholic extract of the seeds of *Coronilla varia* L. (var. Penngift) (family Leguminosae) was found to have inhibitory activity against cells derived from human carcinoma of the nasopharynx (KB)[1]. Systematic fractionation of the extract led to the isolation of two cardenolides, one of which was identified as hyrcanoside (I); three coumarins, daphnoretin (II), scopoletin (III), and umbelliferone (IV); and two unidentified compounds. Compounds I–IV have been reported to occur in Russian varieties of *C. varia* (1, 2), and III and IV have also been shown to occur in *C. varia* (var. Penngift) (3). There is considerable interest in varieties of *C. varia* as potential forage crops (4, 5) and in soil erosion control, and recent publications dealing with toxic constituents have appeared (6, 7).

DISCUSSION

An outline of the general fractionation and chromatographic procedures are given in the *Experimental* section, and the biological data

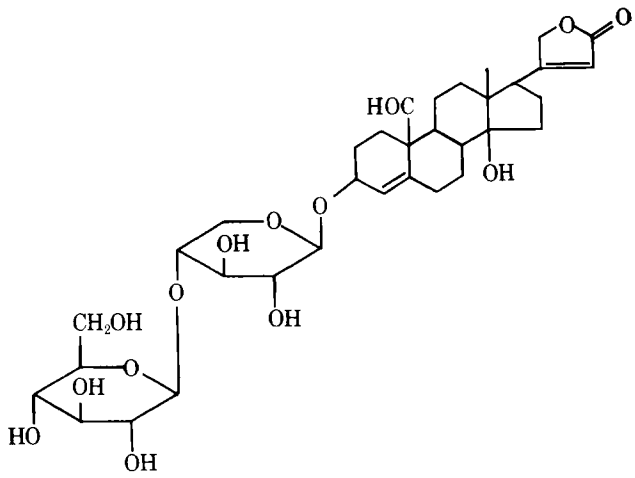

I

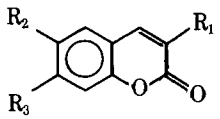

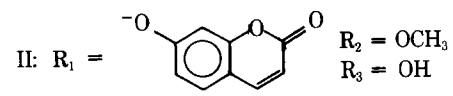

III: R_1 = H, R_2 = OCH_3, R_3 = OH
IV: R_1 = H, R_2 = H, R_3 = OH

are presented in Table I. The concentrated alcoholic fraction (C) from percolation of the powdered seed material with ethanol was partitioned between chloroform and water, resulting in concentration of the cytotoxic activity in the aqueous phase (C). Further partitioning of the aqueous phase with mixtures of chloroform and ethanol in various proportions and with 1-butanol brought the activity into the organic phase. Chromatography of Fraction E on silicic acid yielded the coumarins and an unidentified cardenolide with an R_f of 0.56. Chromatography of Fractions G and H on silicic acid, followed by preparative layer chromatography on silica gel, gave hyrcanoside (I) from Fraction G and two unidentified compounds, R_f 0.49 and 0.39, from Fraction H.

Solid 1 (L) obtained from the chloroform fraction (E) was identified as daphnoretin (II) on the basis of a comparison of physical and spectral properties with literature values. Solid 2 (M) and Solid 3 (N) were identified as scopoletin (III) and umbelliferone (IV) by direct comparison of physical and spectral properties with those of authentic

[1] The cell culture and mouse leukemia assays were performed under the auspices of the Division of Cancer Treatment, Drug Research and Development, National Cancer Institute, according to the procedure given in *Cancer Chemother. Rep.*, 25, 22(1962). In KB, a purified substance is considered active if it shows an $ED_{50} \leq 4$ μg/ml. In PS, a compound is considered active if it shows an increase in lifespan (ILS) of ≥25% relative to controls.

(15) I. B. Wilson and E. Cabib, *J. Amer. Chem. Soc.*, 78, 202(1956).

ACKNOWLEDGMENTS AND ADDRESSES

Received June 23, 1975, from the *Drug Design Division, University of Tennessee, Center for the Health Sciences, Memphis, TN 38163*

Accepted for publication August 4, 1975.

Abstracted in part from a dissertation submitted by O. E. Millner, Jr., to the University of Tennessee in partial fulfillment of the Doctor of Philosophy degree requirements.

Supported by the U.S. Public Health Service through a National Institutes of Health Traineeship (GM-02052) and by the University of Tennessee Cardiovascular Computer Project (HL-09495).

* NIH Trainee (GM-02052). Present address: Research and Development, Norwich Pharmacal Co., Norwich, NY 13815

ˣ To whom inquiries should be directed.

Potential Antitumor Agents: A Cytotoxic Cardenolide from *Coronilla varia* L.

MARTIN WILLIAMS * and JOHN M. CASSADY ˣ

Abstract □ An alcoholic extract of the seeds of *Coronilla varia* L. showed inhibitory activity against KB cells in culture and was fractionated through a series of partitions, column chromatography, and preparative layer chromatography to yield hyrcanoside, daphnoretin, scopoletin, and umbelliferone. Hyrcanoside was also tested in the PS mouse leukemia assay and showed borderline activity.

Keyphrases □ *Coronilla varia*—seeds, alcoholic extract, cardenolide and three coumarins isolated and identified, cytotoxic and antileukemic activity screened □ Cardenolides—hyrcanoside isolated from *Coronilla varia* seeds, cytotoxic and antileukemic activity screened □ Coumarins—isolated from alcoholic extract of *Coronilla varia* seeds, cytotoxic and antileukemic activity screened □ Cytotoxic compounds—alcoholic extract of *Coronilla varia* seeds, cytotoxic and antileukemic activity screened □ Antitumor agents, potential—alcoholic extract of *Coronilla varia* seeds, cardenolide and three coumarins isolated and screened □ Antileukemic agents, potential—alcoholic extract of *Coronilla varia* seeds, cardenolide and three coumarins isolated and screened

An alcoholic extract of the seeds of *Coronilla varia* L. (var. Penngift) (family Leguminosae) was found to have inhibitory activity against cells derived from human carcinoma of the nasopharynx (KB)[1]. Systematic fractionation of the extract led to the isolation of two cardenolides, one of which was identified as hyrcanoside (I); three coumarins, daphnoretin (II), scopoletin (III), and umbelliferone (IV); and two unidentified compounds. Compounds I–IV have been reported to occur in Russian varieties of *C. varia* (1, 2), and III and IV have also been shown to occur in *C. varia* (var. Penngift) (3). There is considerable interest in varieties of *C. varia* as potential forage crops (4, 5) and in soil erosion control, and recent publications dealing with toxic constituents have appeared (6, 7).

DISCUSSION

An outline of the general fractionation and chromatographic procedures are given in the *Experimental* section, and the biological data

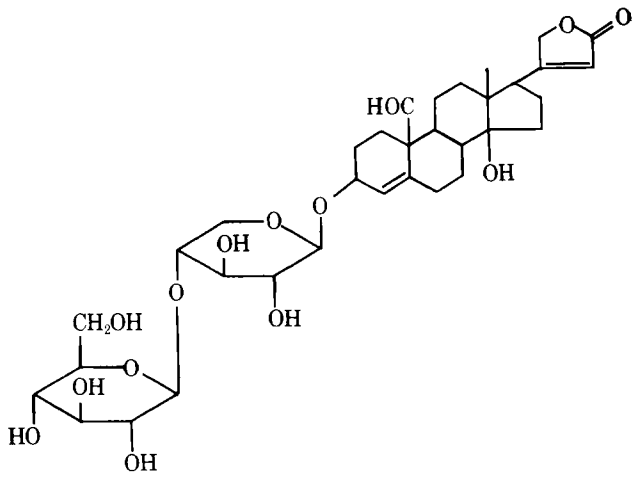

I

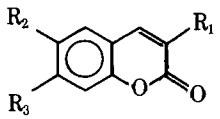

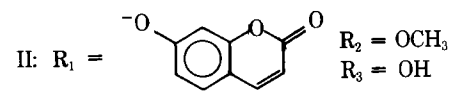

III: R_1 = H, R_2 = OCH_3, R_3 = OH
IV: R_1 = H, R_2 = H, R_3 = OH

are presented in Table I. The concentrated alcoholic fraction (C) from percolation of the powdered seed material with ethanol was partitioned between chloroform and water, resulting in concentration of the cytotoxic activity in the aqueous phase (C). Further partitioning of the aqueous phase with mixtures of chloroform and ethanol in various proportions and with 1-butanol brought the activity into the organic phase. Chromatography of Fraction E on silicic acid yielded the coumarins and an unidentified cardenolide with an R_f of 0.56. Chromatography of Fractions G and H on silicic acid, followed by preparative layer chromatography on silica gel, gave hyrcanoside (I) from Fraction G and two unidentified compounds, R_f 0.49 and 0.39, from Fraction H.

Solid 1 (L) obtained from the chloroform fraction (E) was identified as daphnoretin (II) on the basis of a comparison of physical and spectral properties with literature values. Solid 2 (M) and Solid 3 (N) were identified as scopoletin (III) and umbelliferone (IV) by direct comparison of physical and spectral properties with those of authentic

[1] The cell culture and mouse leukemia assays were performed under the auspices of the Division of Cancer Treatment, Drug Research and Development, National Cancer Institute, according to the procedure given in *Cancer Chemother. Rep.*, 25, 22(1962). In KB, a purified substance is considered active if it shows an $ED_{50} \leq 4$ μg/ml. In PS, a compound is considered active if it shows an increase in lifespan (ILS) of ≥25% relative to controls.

Table I—Cytotoxicity of Fractions from *C. varia* (11.0 kg, Seeds)

	Fraction	Weight, g	ED_{50} in 9KB, μg/ml
A	Hexane	500	100.00
B	Precipitate 1	36	45.0
C	Aqueous I		8.3
D	Precipitate 2	15	41.0
E	Chloroform	16	28.0
F	Organic I	17	3.1
G	Organic II	58	2.5
H	Organic III	131	2.6
I	Precipitate 3	36	2.6
J	Butanol	125	5.5
K	Aqueous II	950	100.0
L	Daphnoretin	0.263	43.0
M	Scopoletin	0.055	100.0
N	Umbelliferone	0.050	33.0
O	Unidentified cardenolide (R_f 0.56)	0.10	2.5
P	Hyrcanoside[a]	0.96	0.1, 0.7

[a] In the PS system, the percent T/C at 1.25 mg/kg was 133.

samples of these compounds. Solid 4 (O) was only tentatively identified as a cardenolide-type compound on the basis of its positive Kedde's reaction, characteristic NMR pattern, and IR spectrum.

Solid 5 (P), obtained from the organic Fraction II (G), was identified as hyrcanoside (I) on the basis of comparison of its physical and spectral properties with that of an authentic reference sample of hyrcanoside[2]. There was no depression in the melting point when a mixed melting point was determined with P and reference hyrcanoside, and the IR spectra of both P and the reference hyrcanoside were identical.

Organic Fraction III was not investigated further, even though active since a major component of the fraction was hyrcanoside. Precipitate 1 (B), obtained during the concentration of the ethanol extract, and Precipitate 2 (D), obtained during the concentration of the chloroform extract, were both found to be crude samples of daphnoretin (II). Precipitate 3 (I), obtained during the concentration of the 1-butanol extract, also was found to be a crude sample of hyrcanoside (I).

Biological activity in the KB system was determined for all fractions obtained through the general fractionation scheme and for all solids obtained during the chromatographic procedures. Since fractions containing the cardenolide glycosides were more active than the others, the cytotoxicity of the plant appears to be due to the presence of these glycosides in the seed. Hyrcanoside, the major glycoside present in the seeds, showed the maximum activity and probably accounted for most of the activity of the total seed extract.

EXPERIMENTAL[3]

Plant Material[4]—The seeds of *C. varia* L. (var. Penngift) (F.C. 40619) were powdered through an 80-mesh screen.

Extraction and Initial Separation—The powdered seed material (11.0 kg) was first extracted with *n*-hexane, and removal of the solvent left 500 g of hexane fraction. The defatted seed powder was then percolated at room temperature with 70% ethanol until the extract was almost colorless. Upon concentration of the ethanol extract under reduced pressure at about 80°, 36 g of Precipitate 1 (B) was obtained. The aqueous extract obtained after removal of the ethanol was then partitioned between chloroform and water. The aqueous phase was extracted three additional times with chloroform.

The combined chloroform extract, upon concentration, yielded 15 g of Precipitate 2 (D) and 16 g of chloroform Fraction E. The aqueous Fraction I (C) was then extracted four times with chloroform–ethanol (8.5:1.5). Upon concentration of the combined extract, it yielded 17 g of organic Fraction I (F). The aqueous phase was further extracted four times with chloroform–ethanol (2:1), which yielded 58 g of organic Fraction II (G). The aqueous phase was then extracted with chloroform–ethanol (1:1), which yielded 131 g of organic Fraction III (H). Finally, the aqueous phase was extracted four times with 1-butanol. The combined butanol extract, upon concentration, yielded 36 g of Precipitate 3 (I) and 125 g of the 1-butanol fraction (J). The aqueous phase was then freeze dried to yield 950 g of aqueous Fraction II (K).

Isolation of Daphnoretin (II), Scopoletin (III), and Umbelliferone (IV) from Fraction E—A sample of about 3 g of chloroform Fraction E was placed in a glass column previously packed with silicic acid (100 mesh). The elution was carried out with 1000 ml each of the following solvent mixtures: 5, 10, 15, 20, 25, 30, and 50% methanol in chloroform. A total of 425 tubes was collected and then combined into 10 fractions on the basis of TLC[5] results. Four of these fractions (1, 3, 5, and 8) were homogeneous and, upon concentration, yielded 52 mg of Solid 1 (L), 11 mg of Solid 2 (M), 10 mg of Solid 3 (N), and 26 mg of Solid 4 (O), respectively.

Solid 1 (L) and Daphnoretin (II)—Recrystallization from tetrahydrofuran–methanol yielded daphnoretin, mp 246–247°; IR ν_{max} (KBr): 3400 (OH), 3050 (aromatic CH), 2900 (aliphatic CH), 1715 (unsaturated lactone), ≈1600 (olefin), and 1275 (C—O, C=O stretch) cm^{-1}; NMR ($CDCl_3$): δ 3.90 (3H, singlet, CH_3O attached to aromatic system), 6.50 and 8.25 (each 1H, doublets, coupled vinyl protons), 7.25 and 7.35 (each 1H, doublets, coupled aromatic protons), and 7.05, 7.85, 7.95, and 8.10 (each 1H, singlets, aromatic protons); UV λ_{max} (CH_3OH) (log ε): 227 (4.17), 266 (3.85), 323 (4.28), and 345 (4.29) nm. The mass spectrum showed the molecular ion at *m/e* 352. Comparison (IR, UV, NMR, and mass spectra) of the isolated Solid 1 (L) with the literature values for daphnoretin showed that they were identical.

Solid 2 (M) and Scopoletin (III)—Recrystallization from acetone yielded scopoletin, mp 203–204°; IR ν_{max} (KBr): 3425 (OH), 3025 (aromatic CH), 2900 (aliphatic CH), 1710 (unsaturated lactone), ≈1600 (olefin), and 1275 (C—O, C=O stretch) cm^{-1}; NMR ($CDCl_3$) (dimethyl sulfoxide): δ 3.26 (1H, broad singlet, OH), 4.30 (3H, singlet, CH_3O attached to aromatic system), 6.30 and 8.10 (each 1H, doublets, coupled vinyl protons), and 7.00 and 7.70 (each 1H, singlets, aromatic protons); UV λ_{max} (CH_3OH) (log ε): 230 (4.23), 255 (2.76), 295 (2.81), and 345 (3.97) nm. The mass spectrum showed the molecular ion at *m/e* 192. Comparison (IR, UV, NMR, and mass spectra and mixed melting point) of the isolated Solid 2 (M) with authentic scopoletin showed that the two were indistinguishable.

Solid 3 (N) and Umbelliferone (IV)—Recrystallization from water yielded umbelliferone, mp 223–224°; IR ν_{max} (KBr): 3300 (OH), 1705 (unsaturated lactone), ≈ 1600 (olefin), and 1275 (C—O, C=O stretch) cm^{-1}; NMR ($CDCl_3$) (dimethyl sulfoxide): δ 3.22 (1H, broad singlet, OH), 6.21 and 8.15 (each 1H, doublets, coupled vinyl protons), 6.95 and 7.70 (each 1H, doublets, coupled aromatic protons), and 7.00 (1H, singlet, aromatic proton); UV λ_{max} (CH_3OH) (log ε): 244 (3.56), 257 (3.43), 322 (4.25), and 328 (4.27) nm. The mass spectrum showed the molecular ion at *m/e* 162. Comparison (IR, UV, NMR, and mass spectra and melting point) of the isolated Solid 3 (N) with authentic umbelliferone showed that the two were indistinguishable.

Isolation of Hyrcanoside (I) from Fraction G—A sample of about 10 g of the organic Fraction II (G) was placed in a glass column packed with silicic acid (100 mesh). Elution was first carried out with 1000 ml of chloroform followed by 1000 ml each of the following solvent mixtures: 10, 25, 50, and 75% ethanol in chloroform and then with 1000 ml each of 5 and 25% aqueous ethanol. A total of 540 tubes was collected and combined into 14 fractions on the basis of the TLC results. These fractions were then pooled into active (fractions 2–6) and inactive fractions on the basis of the biological testing data.

The combined active fraction was subjected to preparative layer chromatography. A sample of about 0.48 g was streaked on a precoated 2-mm thick preparative layer silica gel G plate with fluorescent indicator. The plate was developed in a chromatographic tank containing 100 ml of chloroform–ethanol (2:1). After development, the plate was examined under UV and four bands were marked. Each

[2] The authors are grateful to Dr. N. F. Komissarenko, Karkov Chemical and Pharmaceutical Research Institute, Lenningrad, USSR, for an authentic sample of hyrcanoside. Comparison samples of the other compounds were available in collection at Purdue University.

[3] Melting points were determined on a Mel-Temp capillary melting-point apparatus and are uncorrected. The IR spectra were obtained as potassium bromide pellets on a Beckman IR-33 spectrophotometer. UV spectra were taken in methanol on a Perkin-Elmer model Coleman 125 spectrophotometer. NMR spectra were recorded on a Jeol 100-MHz spectrometer. Low-resolution mass spectra were obtained on a Hitachi RMU-6A spectrometer.

[4] Obtained from Dr. Paul R. Henson, Crops Research Division, Agricultural Research Service, U.S. Department of Agriculture, Beltsville, Md.

[5] Analytical TLC was done on Brinkmann precoated silica gel G plates (0.25 mm thick) without fluorescent indicator. The solvent system of chloroform–ethanol (2:1) was used as the mobile phase. After development, the plate was sprayed with 3,5-dinitrobenzoic acid reagent.

band was scraped separately, extracted with methanol, and concentrated. The extract from the second band yielded 160 mg of Solid 5 (P).

Solid 5 (P) and Hyrcanoside (I)—Recrystallization from methanol yielded hyrcanoside, mp 205–208°; IR ν_{max} (KBr): 3430 (OH), 2940 (aliphatic CH), 2870 (aldehyde CH), 1740 (aldehyde carbonyl), 1720 (unsaturated lactone), and 1620 (olefin) cm^{-1}. The NMR (dimethyl sulfoxide) spectrum was complicated due to the presence of numerous methylene and hydroxy protons. However, it clearly showed the presence of the methyl and vinyl protons and also the aldehyde proton; UV λ_{max} (CH_3OH) (log ϵ): 230 (4.10), 290 (1.65), and 322 (1.54) nm. Comparison (IR, UV, NMR, mixed melting point, and cochromatography in three different solvent systems[6]) of the isolated Solid 5 (P) with an authentic sample of hyrcanoside showed the two to be indistinguishable.

REFERENCES

(1) N. F. Komissarenko and I. G. Zoz, *Rastit. Resur.*, **5**, 178(1969).

(2) R. B. Bagirov and N. F. Komissarenko, *Khim. Prir. Soedin.*, **2**, 251(1966).

(3) K. J. Pilju, *Diss. Abstr. Int. B*, **31**, 7048(1971).

(4) J. S. Shenk, M. L. Risins, and R. F. Barnes, *Agron. J.*, **66**, 13(1974).

(5) R. F. Barnes, G. W. Fissel, and J. S. Shenk, *ibid.*, **66**, 72(1974).

(6) R. T. Sherwood, M. Shamma, J. L. Moniot, and J. R. Kroschewsky, *Phytochemistry*, **12**, 2275(1973).

(7) D. L. Gustine, J. S. Shenk, B. G. Moyer, and R. F. Barnes, *Agron. J.*, **66**, 636(1974).

[6] The solvent systems used were: 1, chloroform–ethanol (2:1); 2, chloroform–tetrahydrofuran–*N*-methylformamide–methanol (50:50:7:18); and 3, chloroform–acetone–methanol (6:2:2).

ACKNOWLEDGMENTS AND ADDRESSES

Received April 30, 1975, from the *Department of Medicinal Chemistry and Pharmacognosy, School of Pharmacy and Pharmacal Sciences, Purdue University, West Lafayette, IN 47907*

Accepted for publication August 13, 1975.

Supported by Public Health Service Research Grant CA-11715 from the National Cancer Institute.

The authors thank Dr. Jonathan Hartwell, Division of Cancer Treatment, National Cancer Institute, for cooperation in arranging to obtain the testing reported, and Dr. Robert F. Barnes, Crops Research, U.S. Department of Agriculture, Pennsylvania State University, for valuable discussions concerning this research.

Previous paper in this series: G. A. Howie, P. E. Manni, and J. M. Cassady, *J. Med. Chem.*, **17**, 840(1974).

* Present address: College of Pharmacy, University of Kentucky, Lexington, KY 40506

x To whom inquiries should be directed.

Pharmacology of Malnutrition III: Binding of Digoxin to Normal and Kwashiorkor Serum

N. BUCHANAN *x, L. A. VAN DER WALT ‡, and B. STRICKWOLD *

Abstract □ Digoxin binding to normal and kwashiorkor serum was studied and found to be inferior in the latter. Digoxin should be used with care in hypoalbuminemic patients.

Keyphrases □ Digoxin—serum protein binding, normal and kwashiorkor serum □ Protein binding—digoxin, normal and kwashiorkor serum □ Malnutritic serum—digoxin binding, compared to normal serum □ Cardiotonic agents—digoxin, serum protein binding, normal and kwashiorkor serum

Circulating digoxin is known to be approximately 25% bound and 75% free in serum, the sole binding protein being albumin (1). Cardiac disease, associated with rheumatic fever, hypertension, and cardiomyopathy, is commonly seen in developing countries with concomitant poor nutrition. An *in vitro* study was thus performed to assess the effect of hypoalbuminemia on digoxin binding.

EXPERIMENTAL

Normal serum (albumin concentration of 3.75 g/100 ml) was obtained, with consent, from a patient hospitalized for an orthopedic disorder. Pooled kwashiorkor serum (albumin concentration of 2.4 g/100 ml) was obtained from several children admitted to a metabolic unit for various studies. Such serum was collected prior to the child's receiving therapy to avoid the presence of any competitive binders.

Tritiated digoxin[1] had a specific activity of 10,000 mCi/mmole and a mass concentration of 88,000 μg/ml. This solution was diluted with deionized water so that ultimately aliquots of the diluted solution could be added to 5-ml batches of normal and kwashiorkor serum, producing final digoxin concentrations of 0.1, 0.2, 0.3, 0.4, 0.5, 1.0, and 5 ng/ml.

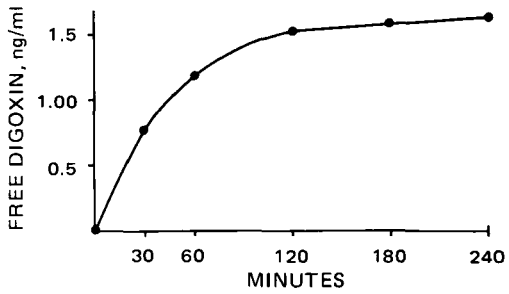

Figure 1—*Curve showing the equilibration time for ^3H-digoxin to be 180 min, there being no statistically significant increase in the free digoxin concentration between the 3- and 4-hr samples* ($p > 0.2$).

The serum was then dialyzed by equilibrium dialysis (2) at 37°, using 0.4 ml of serum for each dialysis. The equilibration time for ^3H-digoxin was 180 min (Fig. 1), but in practice each run was extended to 240 min. Ten dialyses were performed at each concentration; the digoxin concentrations in the original serum, dialyzed serum, and dialyzate were assessed by liquid scintillation counting[2]. The efficiency for tritium was 38.6%, and each specimen was assayed to give a counting error of 0.7% or less. The amount of digoxin in each sample was calculated directly from these data.

[1] Radiochemical Centre, Amersham, United Kingdom.

[2] Packard Tri-Carb liquid scintillation counter.

band was scraped separately, extracted with methanol, and concentrated. The extract from the second band yielded 160 mg of Solid 5 (P).

Solid 5 (P) and Hyrcanoside (I)—Recrystallization from methanol yielded hyrcanoside, mp 205–208°; IR ν_{max} (KBr): 3430 (OH), 2940 (aliphatic CH), 2870 (aldehyde CH), 1740 (aldehyde carbonyl), 1720 (unsaturated lactone), and 1620 (olefin) cm^{-1}. The NMR (dimethyl sulfoxide) spectrum was complicated due to the presence of numerous methylene and hydroxy protons. However, it clearly showed the presence of the methyl and vinyl protons and also the aldehyde proton; UV λ_{max} (CH_3OH) (log ϵ): 230 (4.10), 290 (1.65), and 322 (1.54) nm. Comparison (IR, UV, NMR, mixed melting point, and cochromatography in three different solvent systems[6]) of the isolated Solid 5 (P) with an authentic sample of hyrcanoside showed the two to be indistinguishable.

REFERENCES

(1) N. F. Komissarenko and I. G. Zoz, *Rastit. Resur.*, **5**, 178(1969).

(2) R. B. Bagirov and N. F. Komissarenko, *Khim. Prir. Soedin.*, **2**, 251(1966).

(3) K. J. Pilju, *Diss. Abstr. Int. B*, **31**, 7048(1971).

(4) J. S. Shenk, M. L. Risins, and R. F. Barnes, *Agron. J.*, **66**, 13(1974).

(5) R. F. Barnes, G. W. Fissel, and J. S. Shenk, *ibid.*, **66**, 72(1974).

(6) R. T. Sherwood, M. Shamma, J. L. Moniot, and J. R. Kroschewsky, *Phytochemistry*, **12**, 2275(1973).

(7) D. L. Gustine, J. S. Shenk, B. G. Moyer, and R. F. Barnes, *Agron. J.*, **66**, 636(1974).

[6] The solvent systems used were: 1, chloroform–ethanol (2:1); 2, chloroform–tetrahydrofuran–*N*-methylformamide–methanol (50:50:7:18); and 3, chloroform–acetone–methanol (6:2:2).

ACKNOWLEDGMENTS AND ADDRESSES

Received April 30, 1975, from the *Department of Medicinal Chemistry and Pharmacognosy, School of Pharmacy and Pharmacal Sciences, Purdue University, West Lafayette, IN 47907*

Accepted for publication August 13, 1975.

Supported by Public Health Service Research Grant CA-11715 from the National Cancer Institute.

The authors thank Dr. Jonathan Hartwell, Division of Cancer Treatment, National Cancer Institute, for cooperation in arranging to obtain the testing reported, and Dr. Robert F. Barnes, Crops Research, U.S. Department of Agriculture, Pennsylvania State University, for valuable discussions concerning this research.

Previous paper in this series: G. A. Howie, P. E. Manni, and J. M. Cassady, *J. Med. Chem.*, **17**, 840(1974).

* Present address: College of Pharmacy, University of Kentucky, Lexington, KY 40506

x To whom inquiries should be directed.

Pharmacology of Malnutrition III: Binding of Digoxin to Normal and Kwashiorkor Serum

N. BUCHANAN *x, L. A. VAN DER WALT ‡, and B. STRICKWOLD *

Abstract □ Digoxin binding to normal and kwashiorkor serum was studied and found to be inferior in the latter. Digoxin should be used with care in hypoalbuminemic patients.

Keyphrases □ Digoxin—serum protein binding, normal and kwashiorkor serum □ Protein binding—digoxin, normal and kwashiorkor serum □ Malnutritic serum—digoxin binding, compared to normal serum □ Cardiotonic agents—digoxin, serum protein binding, normal and kwashiorkor serum

Circulating digoxin is known to be approximately 25% bound and 75% free in serum, the sole binding protein being albumin (1). Cardiac disease, associated with rheumatic fever, hypertension, and cardiomyopathy, is commonly seen in developing countries with concomitant poor nutrition. An *in vitro* study was thus performed to assess the effect of hypoalbuminemia on digoxin binding.

EXPERIMENTAL

Normal serum (albumin concentration of 3.75 g/100 ml) was obtained, with consent, from a patient hospitalized for an orthopedic disorder. Pooled kwashiorkor serum (albumin concentration of 2.4 g/100 ml) was obtained from several children admitted to a metabolic unit for various studies. Such serum was collected prior to the child's receiving therapy to avoid the presence of any competitive binders.

Tritiated digoxin[1] had a specific activity of 10,000 mCi/mmole and a mass concentration of 88,000 μg/ml. This solution was diluted with deionized water so that ultimately aliquots of the diluted solution could be added to 5-ml batches of normal and kwashiorkor serum, producing final digoxin concentrations of 0.1, 0.2, 0.3, 0.4, 0.5, 1.0, and 5 ng/ml.

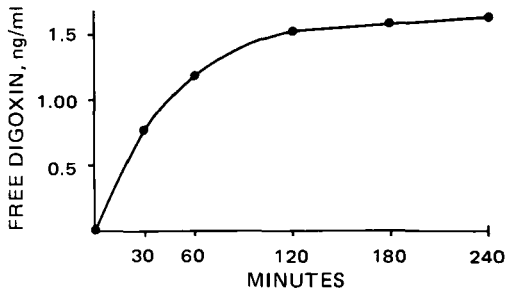

Figure 1—*Curve showing the equilibration time for ^3H-digoxin to be 180 min, there being no statistically significant increase in the free digoxin concentration between the 3- and 4-hr samples* ($p > 0.2$).

The serum was then dialyzed by equilibrium dialysis (2) at 37°, using 0.4 ml of serum for each dialysis. The equilibration time for ^3H-digoxin was 180 min (Fig. 1), but in practice each run was extended to 240 min. Ten dialyses were performed at each concentration; the digoxin concentrations in the original serum, dialyzed serum, and dialyzate were assessed by liquid scintillation counting[2]. The efficiency for tritium was 38.6%, and each specimen was assayed to give a counting error of 0.7% or less. The amount of digoxin in each sample was calculated directly from these data.

[1] Radiochemical Centre, Amersham, United Kingdom.

[2] Packard Tri-Carb liquid scintillation counter.

Table I—Results of Equilibrium Dialysis Studies on the Binding of ^{3}H-Digoxin to Normal and Kwashiorkor Serum

Total Serum Digoxin Concentration, ng/ml	Normal Serum			Kwashiorkor Serum		
	Free Digoxin, ng/ml	Bound Digoxin, ng/ml	Digoxin Bound, %	Free Digoxin, ng/ml	Bound Digoxin, ng/ml	Digoxin Bound, %
0.1	0.084 (0.00)[a]	0.015 (0.00)	15	0.098 (0.00)	0.006 (0.00)	5.8
0.2	0.162 (0.001)	0.038 (0.00)	19	0.18 (0.00)	0.013 (0.001)	8.8
0.3	0.236 (0.008)	0.064 (0.00)	21.3	0.28 (0.015)	0.017 (0.001)	5.8
0.4	0.292 (0.009)	0.108 (0.005)	27	0.035 (0.002)	0.029 (0.005)	7.7
0.5	0.374 (0.006)	0.126 (0.007)	25.2	0.48 (0.025)	0.042 (0.002)	8.0
1.0	0.876 (0.08)	0.108 (0.006)	11	0.94 (0.02)	0.059 (0.002)	5.9
5.0	4.48 (0.29)	0.24 (0.2)	5.0	4.64 (0.21)	0.06 (0.001)	1.3

[a] Values in parentheses represent standard deviation.

RESULTS

The bound and free digoxin concentrations at various total serum digoxin concentrations are shown in Table I. The free concentrations differed significantly between the two groups ($p < 0.01$), as did the bound concentrations ($p = 0.005$).

The differences in binding up to 1 ng/ml are depicted in Figs. 2 and 3, where lines of best fit are employed. In normal serum, only a small amount of digoxin was bound.

From Table I, it can be seen that there was a progressive rise in the amount bound up to 0.5 mg/ml, where there was about 25% binding, after which there was a relative fall off. In kwashiorkor serum, the degree of binding was appreciably less.

DISCUSSION

A considerable difference of opinion exists concerning the digoxin concentrations associated with toxicity. Doherty and Kane (3) found toxicity to be associated almost invariably with a serum concentration of greater than 3 ng/ml. Cree *et al.* (4) felt that concentrations of approximately 1.5 ng/ml were therapeutically adequate. Zeegers *et al.* (5) observed a mean concentration of 1.6 ± 0.7 ng/ml in nonintoxicated patients as opposed to 4.4 ± 0.9 ng/ml in intoxicated patients. Butler (6) observed an overlap in serum concentrations between nonintoxicated and intoxicated groups; 85% of the latter had serum concentrations above 2 ng/ml.

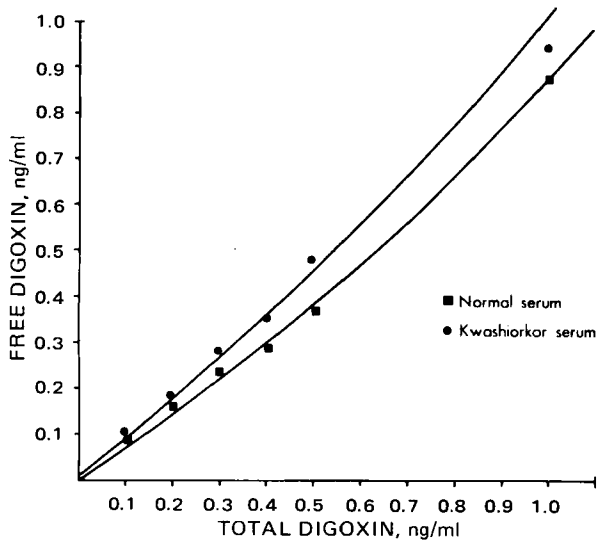

Figure 2—*Relationship of free digoxin in normal serum compared to that in kwashiorkor serum. The difference is significant* (t = *3.39*, n = *5*, p < *0.01*).

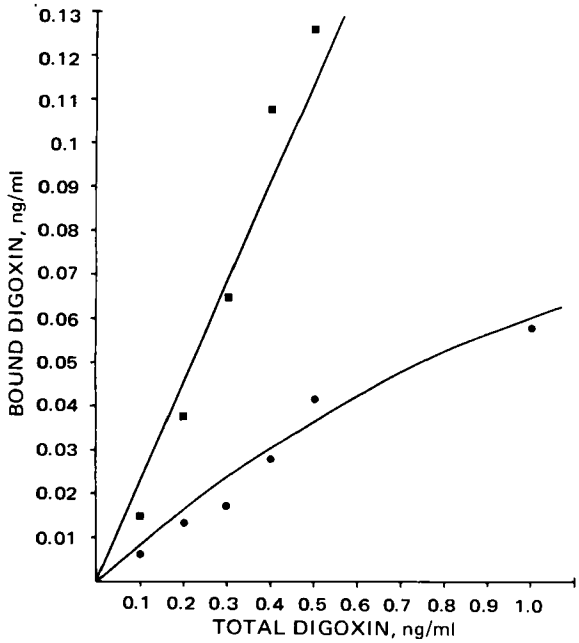

Figure 3—*Difference between the amounts of bound digoxin in normal and kwashiorkor serum. The difference is significant* (t = *4.08*, n = *5*, p = *0.005*).

The problem of digitalis toxicity is rendered even more complex because the tissue (cardiac muscle) digoxin concentrations probably are of most importance. The heart to serum concentration is known to vary from 17:1 to 35:1 (mean of 29:1) (6). The variability is as yet unexplained, although such factors as renal function play a part (7).

It is of interest to speculate that this variability may be related to the amount of free digoxin present in the serum and, hence, to the serum albumin concentration. The present study demonstrates that about 25% of serum digoxin is protein bound in normal serum and that binding is saturated at about 0.5 ng/ml total concentration. Thereafter, a progressive increase in the free concentration is observed. This situation is even more marked in the presence of hypoalbuminemia.

In the context of malnutrition, it is known that the serum albumin, serum potassium, and the total body potassium concentrations are depressed (8). These factors, especially when present concomitantly, are liable to produce digitalis intoxication and should probably be considered when treating malnourished persons with cardiac disease.

REFERENCES

(1) D. C. Evered, *Eur. J. Pharmacol.*, 18, 236(1972).

(2) N. Buchanan and C. Eyberg, *S. Afr. Med. J.*, **48**, 1867 (1974).

(3) J. E. Doherty and J. J. Kane, *Drugs*, **6**, 182(1973).

(4) J. E. Cree, D. J. Coltart, and M. R. Howard, *Brit. Med. J.*, **1**, 443(1973).

(5) J. J. W. Zeegers, A. H. J. Maas, A. F. Willebrands, H. H. Kruyswijk, and G. Jambroes, *Clin. Chim. Acta*, **44**, 109(1973).

(6) V. P. Butler, *N. Engl. J. Med.*, **283**, 1150(1970).

(7) W. J. Jusko and M. Weintraub, *Clin. Pharmacol. Ther.*, **16**, 449(1974).

(8) J. C. Waterlow and G. A. O. Alleyne, *Advan. Prot. Chem.*, **25**, 117(1971).

ACKNOWLEDGMENTS AND ADDRESSES

Received May 27, 1975, from the *Metabolic and Nutrition Unit, Department of Paediatrics, Baragwanath Hospital, P.O. Bertsham, Tvl., South Africa 2013, and the ‡School of Pathology, South African Institute for Medical Research, Johannesburg, South Africa.

Accepted for publication August 8, 1975.

The authors are indebted to the S. A. Medical Research Council for financial support, to Dr. D. C. Evered (Newcastle, United Kingdom) for advice, and to Professor J. D. L. Hansen for assistance with the manuscript.

ˣ To whom inquiries should be directed.

Influence of pH and Route of Injection on Acute Toxicity of Tetracycline in Mice

ROBERT T. WIVAGG, JAMES M. JAFFE, and JOHN L. COLAIZZI ˣ

Abstract □ Some LD_{50} determinations for tetracycline hydrochloride in mice were carried out over a range of pH values, using both the intraperitoneal and the subcutaneous routes of injection. Depending on the pH of the formulation, either water or a solvent system of water and 60% (v/v) propylene glycol was employed thus ensuring complete solution of the drug at all pH values tested. Higher LD_{50} values were obtained with the subcutaneous route than with the intraperitoneal route. With either route of administration, there was a trend toward lowest LD_{50} value occurrence at the isoelectric pH of tetracycline. Actual statistical significance was achieved for the intraperitoneal route only when LD_{50} values obtained at the isoelectric pH were compared with either of the more acidic pH values.

Keyphrases □ Tetracycline—effect of pH and route of injection on acute toxicity, mice □ pH—effect on acute toxicity of tetracycline, mice □ Injection route—subcutaneous *versus* intraperitoneal, effect on acute toxicity of tetracycline, mice □ Toxicity—tetracycline, effect of pH and route of injection, mice □ Antibiotics—tetracycline, effect of pH and route of injection on acute toxicity, mice

The acute toxicity of a drug is usually defined in terms of an LD_{50} value, which is the milligrams per kilogram dose of a drug that, on the average, will kill one-half of the group of test animals of a certain species under specified and controlled conditions following administration of a single dose (1). In the required acute toxicity testing performed on new drug entities, two factors that can influence the experimental results with a parenterally administered drug are its formulation and route of injection (2). For example, it has been demonstrated that intraperitoneal injections of a nitrogen mustard in mice at two different pH values resulted in different LD_{50} values, which could be accounted for on the basis of absorption rate differences resulting from pH–partition effects (3, 4). Other studies revealed that the route of injection may have either substantial effects on acute toxicity, as with procaine, or relatively small effects, as with isoniazid (5).

For the tetracycline class of antibiotics, maximum lipid solubility occurs at the isoelectric pH (pH_{iso}); for tetracycline itself, it occurs around pH 5.6 (6). The relative lipid solubility of tetracycline then decreases as the pH is raised or lowered on either side of the pH_{iso}. Thus, the objective of this study was to determine if there is a significant difference in acute toxicity values, as determined in mice receiving tetracycline injections, when the formulation pH is altered or when the route of parenteral administration is changed.

EXPERIMENTAL

Preparation of Tetracycline Solutions—Aqueous solutions of tetracycline hydrochloride[1] or solutions containing 60% (v/v) propylene glycol[2] were prepared immediately before injection. Both solutions contained 20 mg of tetracycline hydrochloride/ml. The propylene glycol–aqueous vehicle was necessary due to the minimal water solubility of tetracycline hydrochloride around the pH_{iso}, which resulted in marked precipitation when water alone was employed as the solvent. The pH values of the solution were adjusted using 1 *N* NaOH to 2.45, 8.20, and 11.00 in water and to 3.00, 5.50, and 9.00 in the propylene glycol–water solvent mixture.

LD_{50} Determinations—The LD_{50} was determined by the method of Litchfield and Wilcoxon (7) as suggested by the Food and Drug Administration (8). This method employs logarithmic probability graph paper and nomographs as the basis of the calculation.

For each test (*i.e.*, for each different pH of a given solvent system by a particular route of administration), 25 male albino mice[3], ~20 g, were randomly divided into five groups of five animals. The mice were injected with the appropriate dose of tetracycline hydrochloride on a milligrams per kilogram basis, employing the appropriate pH–solvent system. Doses for every one of the six pH–solvent systems tested were administered to each of the five groups in the following manner: one dose at the approximate LD_{50} value, previously estimated experimentally, and two doses above and two doses below this median point.

The exact doses were determined by converting the experimentally estimated doses to log scale and separating each dose by ap-

[1] Tetracycline hydrochloride, lot 174-010, donated by Lederle Laboratories, Division of American Cyanamid Co., Pearl River, N.Y.

[2] Propylene glycol, Ruger Chemical Co., Irvington, N.Y.

[3] Swiss-Webster male albino mice, Hilltop Farms, Scottdale, Pa.

(2) N. Buchanan and C. Eyberg, *S. Afr. Med. J.*, **48**, 1867 (1974).

(3) J. E. Doherty and J. J. Kane, *Drugs*, **6**, 182(1973).

(4) J. E. Cree, D. J. Coltart, and M. R. Howard, *Brit. Med. J.*, **1**, 443(1973).

(5) J. J. W. Zeegers, A. H. J. Maas, A. F. Willebrands, H. H. Kruyswijk, and G. Jambroes, *Clin. Chim. Acta*, **44**, 109(1973).

(6) V. P. Butler, *N. Engl. J. Med.*, **283**, 1150(1970).

(7) W. J. Jusko and M. Weintraub, *Clin. Pharmacol. Ther.*, **16**, 449(1974).

(8) J. C. Waterlow and G. A. O. Alleyne, *Advan. Prot. Chem.*, **25**, 117(1971).

ACKNOWLEDGMENTS AND ADDRESSES

Received May 27, 1975, from the *Metabolic and Nutrition Unit, Department of Paediatrics, Baragwanath Hospital, P.O. Bertsham, Tvl., South Africa 2013, and the ‡School of Pathology, South African Institute for Medical Research, Johannesburg, South Africa.

Accepted for publication August 8, 1975.

The authors are indebted to the S. A. Medical Research Council for financial support, to Dr. D. C. Evered (Newcastle, United Kingdom) for advice, and to Professor J. D. L. Hansen for assistance with the manuscript.

ˣ To whom inquiries should be directed.

Influence of pH and Route of Injection on Acute Toxicity of Tetracycline in Mice

ROBERT T. WIVAGG, JAMES M. JAFFE, and JOHN L. COLAIZZI ˣ

Abstract □ Some LD_{50} determinations for tetracycline hydrochloride in mice were carried out over a range of pH values, using both the intraperitoneal and the subcutaneous routes of injection. Depending on the pH of the formulation, either water or a solvent system of water and 60% (v/v) propylene glycol was employed thus ensuring complete solution of the drug at all pH values tested. Higher LD_{50} values were obtained with the subcutaneous route than with the intraperitoneal route. With either route of administration, there was a trend toward lowest LD_{50} value occurrence at the isoelectric pH of tetracycline. Actual statistical significance was achieved for the intraperitoneal route only when LD_{50} values obtained at the isoelectric pH were compared with either of the more acidic pH values.

Keyphrases □ Tetracycline—effect of pH and route of injection on acute toxicity, mice □ pH—effect on acute toxicity of tetracycline, mice □ Injection route—subcutaneous *versus* intraperitoneal, effect on acute toxicity of tetracycline, mice □ Toxicity—tetracycline, effect of pH and route of injection, mice □ Antibiotics—tetracycline, effect of pH and route of injection on acute toxicity, mice

The acute toxicity of a drug is usually defined in terms of an LD_{50} value, which is the milligrams per kilogram dose of a drug that, on the average, will kill one-half of the group of test animals of a certain species under specified and controlled conditions following administration of a single dose (1). In the required acute toxicity testing performed on new drug entities, two factors that can influence the experimental results with a parenterally administered drug are its formulation and route of injection (2). For example, it has been demonstrated that intraperitoneal injections of a nitrogen mustard in mice at two different pH values resulted in different LD_{50} values, which could be accounted for on the basis of absorption rate differences resulting from pH–partition effects (3, 4). Other studies revealed that the route of injection may have either substantial effects on acute toxicity, as with procaine, or relatively small effects, as with isoniazid (5).

For the tetracycline class of antibiotics, maximum lipid solubility occurs at the isoelectric pH (pH_{iso}); for tetracycline itself, it occurs around pH 5.6 (6). The relative lipid solubility of tetracycline then decreases as the pH is raised or lowered on either side of the pH_{iso}. Thus, the objective of this study was to determine if there is a significant difference in acute toxicity values, as determined in mice receiving tetracycline injections, when the formulation pH is altered or when the route of parenteral administration is changed.

EXPERIMENTAL

Preparation of Tetracycline Solutions—Aqueous solutions of tetracycline hydrochloride[1] or solutions containing 60% (v/v) propylene glycol[2] were prepared immediately before injection. Both solutions contained 20 mg of tetracycline hydrochloride/ml. The propylene glycol–aqueous vehicle was necessary due to the minimal water solubility of tetracycline hydrochloride around the pH_{iso}, which resulted in marked precipitation when water alone was employed as the solvent. The pH values of the solution were adjusted using 1 *N* NaOH to 2.45, 8.20, and 11.00 in water and to 3.00, 5.50, and 9.00 in the propylene glycol–water solvent mixture.

LD_{50} Determinations—The LD_{50} was determined by the method of Litchfield and Wilcoxon (7) as suggested by the Food and Drug Administration (8). This method employs logarithmic probability graph paper and nomographs as the basis of the calculation.

For each test (*i.e.*, for each different pH of a given solvent system by a particular route of administration), 25 male albino mice[3], ~20 g, were randomly divided into five groups of five animals. The mice were injected with the appropriate dose of tetracycline hydrochloride on a milligrams per kilogram basis, employing the appropriate pH–solvent system. Doses for every one of the six pH–solvent systems tested were administered to each of the five groups in the following manner: one dose at the approximate LD_{50} value, previously estimated experimentally, and two doses above and two doses below this median point.

The exact doses were determined by converting the experimentally estimated doses to log scale and separating each dose by ap-

[1] Tetracycline hydrochloride, lot 174-010, donated by Lederle Laboratories, Division of American Cyanamid Co., Pearl River, N.Y.

[2] Propylene glycol, Ruger Chemical Co., Irvington, N.Y.

[3] Swiss-Webster male albino mice, Hilltop Farms, Scottdale, Pa.

Table I—Mean LD_{50} Values with 95% Confidence Limits[a] and Potency Ratios for Tetracycline Hydrochloride at Various pH Values and with Various Solvent Systems and Routes of Parenteral Administration in Mice

Vehicle and Route of Administration	LD_{50} and Confidence Limits, mg/kg			Potency Ratio and Confidence Limits		
	pH 2.45	pH 8.20	pH 11.00	pH 2.45 *versus* 8.20	pH 2.45 *versus* 11.00	pH 8.20 *versus* 11.00
Aqueous vehicle						
Intraperitoneal	485 (452–519)	366 (302–442)	415 (343–502)	1.33[b] (1.10–1.60)	1.17[c] (0.97–1.41)	1.13[c] (0.86–1.48)
Subcutaneous	673 (510–888)	651 (449–944)	657 (355–1215)	1.03[c] (0.65–1.63)	1.02[c] (0.52–1.99)	1.01[c] (0.49–2.07)
	pH 3.00	pH 5.50	pH 9.00	pH 3.00 *versus* 5.50	pH 3.00 *versus* 9.00	pH 5.50 *versus* 9.00
Propylene glycol–aqueous vehicle						
Intraperitoneal	475 (420–537)	327 (262–409)	377 (320–455)	1.45[b] (1.13–1.86)	1.26[b] (1.02–1.56)	1.15[c] (0.88–1.51)
Subcutaneous	681 (497–932)	623 (498–779)	652 (438–971)	1.09[c] (0.75–1.59)	1.04[c] (0.63–1.73)	1.05[c] (0.67–1.65)

[a] Shown within parentheses. [b] Statistically significant ($p < 0.05$). [c] Not statistically significant ($p > 0.05$).

proximately 0.1 log unit (8). Each test solution was administered, in a volume sufficient to provide the desired dose, by the intraperitoneal and subcutaneous routes to two separate sets of mice. The mice were then observed for 48 hr following injection, and the number of deaths for each of the five separate dosage groups was recorded for each set.

A control group of mice also was employed by administering the same vehicle including any additives, but devoid of tetracycline, on the appropriate volume per kilogram basis by the route of administration being employed.

RESULTS

The results of this study (Table I and Fig. 1) indicate that tetracycline hydrochloride, when administered to mice by the intraperitoneal route, produced greater toxicity in the pH_{iso} region (approximately pH 5.5) of tetracycline. The data suggest a trend toward decreasing toxicity as the pH is decreased or increased from the pH_{iso} value. The results of a potency ratio test[4] performed on the data (Table I) indicated that the LD_{50} values for pH 2.45 and 3.00 were significantly higher than the LD_{50} values at the pH_{iso}. However, as Table I shows, for those pH values above the pH_{iso}, statistically significant differences for LD_{50} values were not shown by the potency ratio test. This observation is probably due to the greater variability in the amounts of tetracycline required to produce death in the test animals at these higher pH regions.

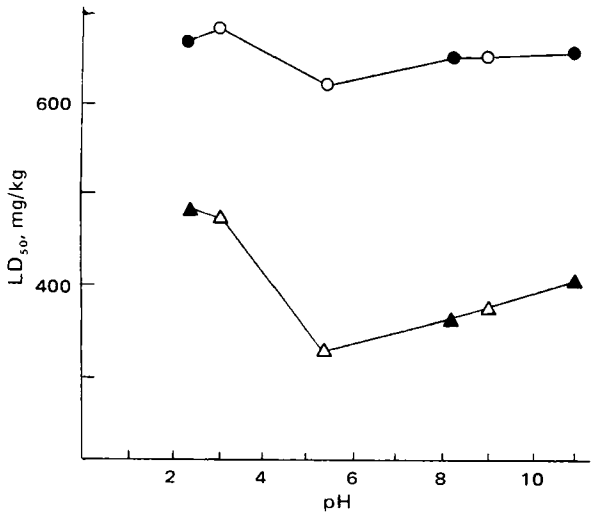

Figure 1—*Comparison of LD_{50} values for tetracycline hydrochloride at different pH values. Key: ●, subcutaneous route, water solvent; ○, subcutaneous route, water–propylene glycol solvent; ▲, intraperitoneal route, water solvent; and △, intraperitoneal route, water–propylene glycol solvent.*

[4] A test that compares the LD_{50} values obtained at separate pH levels and indicates if there is a statistically significant difference (5% level) between their toxicity values (7).

Figure 1 and Table I also show the results obtained when tetracycline hydrochloride was administered by the subcutaneous route. The general pattern was similar to the trend observed for the intraperitoneal route, with the greatest apparent toxicity occurring near the pH_{iso}. However, the magnitude of change was not as great, and the potency ratio test failed to demonstrate statistical significance at the 5% level.

The control group of mice, which received only drug-free solutions, showed no toxicity at any pH value by either route of administration.

DISCUSSION

The results of this study demonstrate that significant alterations in the acute toxicity characteristics of parenterally administered tetracycline hydrochloride may occur when either formulation pH or route of administration varies. Changing the pH of a tetracycline solution produced significant changes in the LD_{50} values when the drug was administered by the intraperitoneal route of administration in mice. When tetracycline was administered by the subcutaneous route, a similar trend of increased toxicity near the pH_{iso} region was also observed, but the differences were not statistically significant ($p > 0.05$). This finding could be attributed to the much slower absorption rates generally associated with the subcutaneous route, particularly in comparison with the intraperitoneal route (9).

Since the tetracycline moiety forms a zwitterionic species (6), the pH values selected were such that one experimental value would result in a tetracycline solution with a pH close to the maximum concentration of the zwitterionic form of the drug. The other pH values selected were far enough on either side of the pH_{iso} to represent a relatively high cationic species (pH 2.45–3.00) or a relatively high anionic species (pH 8.20–11.00) of the drug.

The results obtained, using the intraperitoneal route of administration, indicate that maximum zwitterionic species concentration results in the greatest toxicity for this compound. This finding appears to be due to the fact that when tetracycline hydrochloride exists as a zwitterion, it is at its pH of greatest lipid solubility (4). Since increased lipid solubility can generally increase the rate of drug absorption (10), it would follow that the zwitterionic pH produces greater toxicity since the drug is more rapidly absorbed when administered in this manner. For pH values above and below the pH_{iso}, tetracycline is in a less lipid-soluble form than for the zwitterionic pH region; therefore, it would tend to be less rapidly absorbed.

When attempts were made to maintain the pH of the tetracycline solutions employed in this study in the vicinity of the pH_{iso}

(5.5), a precipitate occurred immediately in a solvent system composed of water alone. Precipitate formation was finally avoided by the use of a solvent mixture of 60% propylene glycol in water. To check for the effect of solvent system throughout the test pH range, the propylene glycol–water mixture was used again in the cationic and anionic pH ranges. This evaluation as to possible solvent effects that might alter LD_{50} determinations revealed that the solvent mixture, as employed in this study, had little or no apparent influence on the absorption, as reflected by the toxicity data. Therefore, the data obtained using the propylene glycol–water solution could be pooled with the aqueous data to yield results indicative of alterations in the toxicological characteristics of tetracycline.

REFERENCES

(1) T. Loomis, "Essentials of Toxicology," 1st ed., Lea & Febiger, Philadelphia, Pa., 1968, pp. 13–24.

(2) G. Levy and W. Barr, *Ration. Drug Ther.*, **6**, 1(1972).

(3) J. H. Cutts and I. G. Walker, *Cancer Res.*, **26** (Part 1), 1386(1966).

(4) B. E. Ballard, *J. Pharm. Sci.*, **57**, 356(1968).

(5) T. Loomis, "Essentials of Toxicology," 1st ed., Lea & Febiger, Philadelphia, Pa., 1968, pp. 57–69.

(6) J. L. Colaizzi and P. R. Klink, *J. Pharm. Sci.*, **58**, 1184(1969).

(7) J. Litchfield and F. Wilcoxon, *J. Pharmacol. Exp. Ther.*, **96**, 99(1949).

(8) Staff of Division of Pharmacology, "Appraisal of the Safety of Chemicals in Foods, Drugs, and Cosmetics," 2nd ed., Association of Food and Drug Offices of the United States, Topeka, Kan., 1965, pp. 16–25.

(9) "The Pharmacological Basis of Therapeutics," 4th ed., L. S. Goodman and A. Gilman, Eds., Macmillan, New York, N.Y., 1970, p. 7.

(10) A. Albert, *Pharmacol. Rev.*, **4**, 136(1952).

ACKNOWLEDGMENTS AND ADDRESSES

Received May 19, 1975, from the *Department of Pharmaceutics, School of Pharmacy, University of Pittsburgh, Pittsburgh, PA 15261*

Accepted for publication August 8, 1975.

[x] To whom inquiries should be directed.

Antileukemic and Other Constituents of *Tithonia tagitiflora* Desf.

RAGHWENDRA PAL, D. K. KULSHRESHTHA, and R. P. RASTOGI [x]

Abstract □ Phytochemical investigation of *Tithonia tagitiflora* has led to isolation of six new germacranolides, tagitinins A, B, C, D, E, and F, β-sitosterol, and its β-D-glucoside. Among these, tagitinin F possesses antileukemic activity.

Keyphrases □ *Tithonia tagitiflora*—whole plant alcoholic extract, isolation of six new germacranolides, β-sitosterol, and its β-D-glucoside, screened for antileukemic activity □ Germacranolides—six new tagitinins isolated from whole plant extract of *Tithonia tagitiflora*, screened for antileukemic activity □ β-Sitosterol and its β-D-glucoside—isolated from whole plant extract of *Tithonia tagitiflora* □ Antileukemic agents, potential—constituents isolated from whole plant extract of *Tithonia tagitiflora* screened

Tithonia tagitiflora Desf. (Compositae) is an American plant which has become naturalized in the Khandala region. Only one species of this genus, namely *T. tubaeformis*, has undergone chemical investigation, resulting in the characterization of a new flavone, tithonine (1), and a novel germacranolide, orizabin (2).

In the screening program for tumor inhibitors from plant sources (3), the alcoholic extract of *T. tagitiflora* showed significant activity against P-388 lymphocytic leukemia (PS). The results of the subsequent studies leading to the isolation of the various constituents together with their biological data are described here[1].

[1] The plant material was identified as *Tithonia tagitiflora* Desf. (Compositae) by Mr. B. N. Mehrotra, Section of Botany, Central Drug Research Institute, Lucknow, India. A voucher (preserved) specimen (No. 2499), representing material collected for this investigation, is available for inspection at the Herbarium of the Institute.

EXPERIMENTAL

The reported melting points are uncorrected. Spots on TLC were visualized with 1% ceric sulfate in 2 *N* H_2SO_4 using silica gel plates and with alkaline potassium permanganate using neutral alumina plates.

Isolation of Constituents—The alcoholic extract of the dried plant material (11.0 kg) was extracted with benzene. The residual portion was partitioned with 1-butanol–water. The benzene-soluble material was defatted with *n*-hexane, and the insoluble fraction was decolorized with charcoal in ethanol, which yielded a light-green viscous mass (165 g). This residue showed eight spots on TLC which were designated as α (R_f 0.55 in ethyl acetate saturated with water + 10% methanol), A [R_f 0.44 in chloroform–ethyl acetate (1:1)], B, C, D, E, F, and G [R_f 0.22, 0.27, 0.33, 0.40, 0.47, and 0.58, respectively, in benzene–ethyl acetate (2:1)] on neutral alumina plates. A portion of the residue (68 g) was subjected to a gross fractionation over silica gel (1 kg) as shown in Table I.

The residue from fractions 3–5, on repeated crystallization from methanol, gave substance G, mp 136° (4.0 g).

The residue from fraction 7 (7.7 g) was rechromatographed over neutral alumina (activity of 2.5, 350 g). The residue (1.5 g) from the benzene–ethyl acetate (9:1) eluate crystallized from hexane–benzene, mp 128–130° (tagitinin F, 0.75 g), and the benzene–ethyl acetate (7:3) eluate (1.44 g) crystallized in a similar manner to yield tagitinin E, mp 208–210°, 0.50 g.

Fraction 9 (Table I, 4.2 g) was rechromatographed over neutral alumina. The benzene–ethyl acetate (7:3) eluate (1.11 g), on repeated crystallization from benzene–hexane, gave tagitinin D, mp 138–140° (0.45 g). The residue from the benzene–ethyl acetate (3:2) eluate (0.80 g) was rechromatographed over silica gel impregnated with silver nitrate (12%), and the benzene–ethyl acetate (3:2) eluate yielded pure tagitinin C (0.33 g) as colorless powder.

Rechromatography of fraction 10 (Table I, 5.0 g) over neutral alumina yielded a benzene–ethyl acetate (1:1) eluate (1.15 g), which crystallized from acetone–isopropyl ether, mp 125–126° (tagitinin

(5.5), a precipitate occurred immediately in a solvent system composed of water alone. Precipitate formation was finally avoided by the use of a solvent mixture of 60% propylene glycol in water. To check for the effect of solvent system throughout the test pH range, the propylene glycol–water mixture was used again in the cationic and anionic pH ranges. This evaluation as to possible solvent effects that might alter LD_{50} determinations revealed that the solvent mixture, as employed in this study, had little or no apparent influence on the absorption, as reflected by the toxicity data. Therefore, the data obtained using the propylene glycol–water solution could be pooled with the aqueous data to yield results indicative of alterations in the toxicological characteristics of tetracycline.

REFERENCES

(1) T. Loomis, "Essentials of Toxicology," 1st ed., Lea & Febiger, Philadelphia, Pa., 1968, pp. 13–24.

(2) G. Levy and W. Barr, *Ration. Drug Ther.*, **6**, 1(1972).

(3) J. H. Cutts and I. G. Walker, *Cancer Res.*, **26** (Part 1), 1386(1966).

(4) B. E. Ballard, *J. Pharm. Sci.*, **57**, 356(1968).

(5) T. Loomis, "Essentials of Toxicology," 1st ed., Lea & Febiger, Philadelphia, Pa., 1968, pp. 57–69.

(6) J. L. Colaizzi and P. R. Klink, *J. Pharm. Sci.*, **58**, 1184(1969).

(7) J. Litchfield and F. Wilcoxon, *J. Pharmacol. Exp. Ther.*, **96**, 99(1949).

(8) Staff of Division of Pharmacology, "Appraisal of the Safety of Chemicals in Foods, Drugs, and Cosmetics," 2nd ed., Association of Food and Drug Offices of the United States, Topeka, Kan., 1965, pp. 16–25.

(9) "The Pharmacological Basis of Therapeutics," 4th ed., L. S. Goodman and A. Gilman, Eds., Macmillan, New York, N.Y., 1970, p. 7.

(10) A. Albert, *Pharmacol. Rev.*, **4**, 136(1952).

ACKNOWLEDGMENTS AND ADDRESSES

Received May 19, 1975, from the *Department of Pharmaceutics, School of Pharmacy, University of Pittsburgh, Pittsburgh, PA 15261*

Accepted for publication August 8, 1975.

[x] To whom inquiries should be directed.

Antileukemic and Other Constituents of *Tithonia tagitiflora* Desf.

RAGHWENDRA PAL, D. K. KULSHRESHTHA, and R. P. RASTOGI [x]

Abstract □ Phytochemical investigation of *Tithonia tagitiflora* has led to isolation of six new germacranolides, tagitinins A, B, C, D, E, and F, β-sitosterol, and its β-D-glucoside. Among these, tagitinin F possesses antileukemic activity.

Keyphrases □ *Tithonia tagitiflora*—whole plant alcoholic extract, isolation of six new germacranolides, β-sitosterol, and its β-D-glucoside, screened for antileukemic activity □ Germacranolides—six new tagitinins isolated from whole plant extract of *Tithonia tagitiflora*, screened for antileukemic activity □ β-Sitosterol and its β-D-glucoside—isolated from whole plant extract of *Tithonia tagitiflora* □ Antileukemic agents, potential—constituents isolated from whole plant extract of *Tithonia tagitiflora* screened

Tithonia tagitiflora Desf. (Compositae) is an American plant which has become naturalized in the Khandala region. Only one species of this genus, namely *T. tubaeformis*, has undergone chemical investigation, resulting in the characterization of a new flavone, tithonine (1), and a novel germacranolide, orizabin (2).

In the screening program for tumor inhibitors from plant sources (3), the alcoholic extract of *T. tagitiflora* showed significant activity against P-388 lymphocytic leukemia (PS). The results of the subsequent studies leading to the isolation of the various constituents together with their biological data are described here[1].

[1] The plant material was identified as *Tithonia tagitiflora* Desf. (Compositae) by Mr. B. N. Mehrotra, Section of Botany, Central Drug Research Institute, Lucknow, India. A voucher (preserved) specimen (No. 2499), representing material collected for this investigation, is available for inspection at the Herbarium of the Institute.

EXPERIMENTAL

The reported melting points are uncorrected. Spots on TLC were visualized with 1% ceric sulfate in 2 *N* H_2SO_4 using silica gel plates and with alkaline potassium permanganate using neutral alumina plates.

Isolation of Constituents—The alcoholic extract of the dried plant material (11.0 kg) was extracted with benzene. The residual portion was partitioned with 1-butanol–water. The benzene-soluble material was defatted with *n*-hexane, and the insoluble fraction was decolorized with charcoal in ethanol, which yielded a light-green viscous mass (165 g). This residue showed eight spots on TLC which were designated as α (R_f 0.55 in ethyl acetate saturated with water + 10% methanol), A [R_f 0.44 in chloroform–ethyl acetate (1:1)], B, C, D, E, F, and G [R_f 0.22, 0.27, 0.33, 0.40, 0.47, and 0.58, respectively, in benzene–ethyl acetate (2:1)] on neutral alumina plates. A portion of the residue (68 g) was subjected to a gross fractionation over silica gel (1 kg) as shown in Table I.

The residue from fractions 3–5, on repeated crystallization from methanol, gave substance G, mp 136° (4.0 g).

The residue from fraction 7 (7.7 g) was rechromatographed over neutral alumina (activity of 2.5, 350 g). The residue (1.5 g) from the benzene–ethyl acetate (9:1) eluate crystallized from hexane–benzene, mp 128–130° (tagitinin F, 0.75 g), and the benzene–ethyl acetate (7:3) eluate (1.44 g) crystallized in a similar manner to yield tagitinin E, mp 208–210°, 0.50 g.

Fraction 9 (Table I, 4.2 g) was rechromatographed over neutral alumina. The benzene–ethyl acetate (7:3) eluate (1.11 g), on repeated crystallization from benzene–hexane, gave tagitinin D, mp 138–140° (0.45 g). The residue from the benzene–ethyl acetate (3:2) eluate (0.80 g) was rechromatographed over silica gel impregnated with silver nitrate (12%), and the benzene–ethyl acetate (3:2) eluate yielded pure tagitinin C (0.33 g) as colorless powder.

Rechromatography of fraction 10 (Table I, 5.0 g) over neutral alumina yielded a benzene–ethyl acetate (1:1) eluate (1.15 g), which crystallized from acetone–isopropyl ether, mp 125–126° (tagitinin

Table I—Chromatography of the Defatted Benzene-Soluble Fraction (68 g)

Fraction Number	Eluant	Weight, g	TLC[a]
1—2	Benzene	1.4	St
3—5	Benzene—ethyl acetate (4:1)	10.0	St, G
6	Benzene—ethyl acetate (3:1)	8.7	G, F (E)
7	Benzene—ethyl acetate (3:1)	7.7	F, E (D), (G)
8	Benzene—ethyl acetate (2:1)	4.9	D, (E), (C)
9	Benzene—ethyl acetate (2:1)	4.2	D, C, (B), St
10	Benzene—ethyl acetate (1:1)	5.0	B, (C), (A)
11	Benzene—ethyl acetate (1:1)	2.6	A, (B)
12	Benzene—ethyl acetate (1:2)	4.8	A, St
13	Benzene—ethyl acetate (1:2)	2.8	A, (α), St
14—15	Benzene—ethyl acetate (1:3)	6.8	A, α, St
16—17	Ethyl acetate	3.2	α, St
18—19	Ethyl acetate—ethanol (9:1)	3.5	St

[a] St = streaking; spots in parentheses indicate minor constituents.

B, 0.55 g). Similarly, the residue from fractions 14–15 (Table I, 6.8 g) was rechromatographed over silica gel. The benzene–ethyl acetate (1:3) eluate (5.34 g) crystallized from chloroform–hexane, mp 168–170° (tagitinin A, 4.7 g), and ethyl acetate eluate (0.66 g) gave substance α, mp 277–278° (0.28 g).

Tagitinins A, B, and D–F were obtained as colorless needles, and C was an amorphous powder. When heated with hydroxylamine hydrochloride, they gave a magenta color. The yields of the chemical constituents and their physical data are given in Table II.

Biological Activity—Anticancer screening against P-388 lymphocytic leukemia (PS) in mice was carried out according to the National Institutes of Health protocol (4). The activity data of the total alcoholic extract (A), the defatted benzene-soluble fraction (B), and tagitinin F are given in Table III. Other fractions of the extract and the remaining tagitinins (A–E) did not show any activity. The butanol-soluble fraction showed marginal activity only at a dose of 35 mg/kg (T/C 130).

DISCUSSION

The alcoholic extract of the plant (A) was fractionated into benzene- and butanol-soluble fractions. The benzene-soluble fraction was defatted with petroleum ether, whereby the total activity was found to be localized in the insoluble residue (B, Table III). Fraction B was subjected to repeated chromatography over silica gel and neutral alumina, resulting in the isolation of eight substances designated as α, A, B, C, D, E, F, and G in order of increasing R_f values. Substances A–F, being new, are named as tagitinins.

Table III—Activity of Plant Extract and Its Fractions in PS System

Materials Tested	Dose, mg/kg	Survivors[a], Number Taken on Day 5	Median Survival Time, days, Treated/Control	T/C[b], %	Status
Alcoholic extract A	800	6/6	13.3/10.0	133	Active
	400	6/6	14/10.0	140	Active
NSC No. B67 1964	200	6/6	15/10.0	150	Active
	100	6/6	14.4/10.0	144	Active
	50	6/6	11.8/10.0	118	Inactive
	25	6/6	10.6/10.0	106	Inactive
Fraction B	40	3/6	—	—	Toxic
	20	6/6	12.7/10.0	127	Active
	10	5/6	12.1/10.0	121	Inactive
	5	6/6	13.3/10.0	133	Active
	2	6/6	10.0/10.0	109	Inactive
Tagitinin F	50	4/4	16.1/10.0	161	Active
	25	4/4	15.5/10.0	155	Active
	12.5	4/4	16.1/10.0	161	Active

[a] Number is a measure of toxicity; 4/6 or 66.6% survival is considered to be nontoxic. [b] Treated/control (T/C) is also survival time of the test mice with respect to the survival of control mice. It is expressed as percent obtained by: (median survival time of treated mice/median survival time of control mice) × 100. A T/C value greater than 125 is considered as active.

All of these tagitinins were bitter in taste and gave a positive hydroxamic acid test for an ester or lactone group. All of them exhibited characteristic IR bands in the regions of 1760 cm^{-1} for α,β-unsaturated-γ-lactone and 1730 cm^{-1} for an ester grouping. In addition, they showed strong UV absorption characteristics of an α,β-unsaturated-γ-lactone chromophore (Table II).

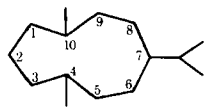

I

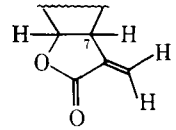

II

On the basis of physicochemical studies, they were found to be sesquiterpenoids, having the germacrane skeleton (I), an α,β-unsaturated-γ-lactone with an *exo*-methylene (II), and isobutyric ester groupings at C-6–C-8 and C-8–C-6. The differences were only in the oxygenation pattern and unsaturation at C-1, C-2, C-3, C-4, C-5, and C-10. Only tagitinin F showed antitumor activity in the P-388 system.

Table II—Substances Isolated from *T. tagitiflora*

Substance	Molecular Formula[a]	Melting Point ($[\alpha]_D$)	IR, cm^{-1}	UV, nm	Yield[b], %
Tagitinin A[c]	$C_{19}H_{28}O_7$	168—170° (−154°)	1757, 1732 1665, 890	215 (11,420)	0.1068
Tagitinin B[c]	$C_{19}H_{26}O_7$	125° (−142°)	1755, 1727 1642, 1157 890	214 (12,993)	0.0124
Tagitinin C[c]	$C_{19}H_{24}O_6$	Amorphous (−204°)	1757, 1727 1665, 886	212, 248 (16,280, 10,842)	0.0091
Tagitinin D[c]	$C_{19}H_{28}O_6$	138—140° (−137°)	1770, 1720 1665, 890	218 (18,900)	0.0101
Tagitinin E[c]	$C_{19}H_{26}O_6$	207—210° (−101°)	1760, 1730 1655, 890	213 (9,460)	0.1230
Tagitinin F[c]	$C_{19}H_{24}O_6$	128—130° (−144°)	1760, 1730 1655, 877	215 (12,240)	0.0173
α (β-sitosterol-β-D-glucoside)	$C_{35}H_{60}O_6$	277—278° (−45°)	—	—	0.0063
G (β-sitosterol)	$C_{29}H_{50}O$	136° (−39°)	—	—	0.0045

[a] Molecular formulas were deduced by carbon–hydrogen analyses and mass spectra (M^+). [b] Based on the weight of dry plant. [c] Indicates new substance.

REFERENCES

(1) J. Correa and M. L. Cervera, *Bull. Soc. Chim. Fr.*, **1971**, 475.

(2) A. Romo de Vivar, J. Romo, A. A. Ortega, E. Diaz, and M. A. Carino, *Rev. Latinoam. Quim.*, **2**, 38(1971).

(3) D. S. Bhakuni, M. L. Dhar, M. M. Dhar, B. N. Dhawan, B. Gupta, and R. C. Srimal, *Indian J. Exp. Biol.*, **9**, 91(1971).

(4) *Cancer Chemother. Rep.*, **3**, 1(1972).

ACKNOWLEDGMENTS AND ADDRESSES

Received March 27, 1975, from the *Division of Medicinal Chemistry, Central Drug Research Institute, Lucknow, India.*

Accepted for publication September 4, 1975.

The authors thank Mr. J. Saran and his associates for the microanalyses, Mr. R. K. Mukherji for the IR spectra, and Mr. Edward Samson for technical assistance. The plant material was collected under a program sponsored by the National Institutes of Health, Bethesda, Md., for the development of anticancer agents of plant origin (PL-480, Grant 134304), and the anticancer screening data were obtained from the Cancer Chemotherapy National Service Center, National Cancer Institute, Bethesda, Md.

This paper is Communication No. 2006 from the Central Drug Research Institute, Lucknow, India, and Part I of "Chemical Studies on *Tithonia tagitiflora* Desf."

[x] To whom inquiries should be directed.

Conformationally Defined Adrenergic Agents I: Potentiation of Levarterenol in Rat Vas Deferens by *endo*- and *exo*-2-Aminobenzobicyclo[2.2.2]octenes, Conformationally Defined Analogs of Amphetamine

GARY L. GRUNEWALD [*x], JAMES A. RUTH [*], TIMOTHY R. KROBOTH [*], BHARAT V. KAMDAR [*], POPAT N. PATIL [‡], and KADIM N. SALMAN [‡]

Abstract □ Four conformationally defined analogs of amphetamine were synthesized and studied for their ability to potentiate the action of levarterenol on the isolated vas deferens from reserpine-treated rats. The compounds also were studied for indirect adrenergic agonist activity in the same test system. A definite stereochemical correlation was demonstrated in each case, the *exo*-isomers being considerably more active than their *endo*-counterparts both in potentiation and in indirect activity. The more active isomers of each pair correspond to an *anti*-periplanar conformation of amphetamine. The compounds are probably acting by inhibition of the neuronal amine uptake mechanism, since none of the compounds was a direct-acting agonist itself. These results are discussed in relationship to other previously reported, conformationally defined, amphetamine analogs.

Keyphrases □ Adrenergic agents—conformationally defined analogs of amphetamine, potentiation of levarterenol in rat vas deferens □ Levarterenol—potentiation by conformationally defined analogs of amphetamine, rat vas deferens □ Amphetamines—conformationally defined analogs synthesized, potentiation of levarterenol in rat vas deferens □ Structure–activity relationships—conformationally defined analogs of amphetamine, potentiation of levarterenol in rat vas deferens

One recent technique for probing the nature of agonist–receptor interactions is the study of conformationally defined analogs of the agonists in question to quantitate the stereochemical requirements for biological activity. While such an approach has found considerable application in the areas of cholinergic agonists (1–5), on phenethanolamine systems (6–11), and dopaminergic agonists (12), relatively few examples of conformationally defined analogs of amphetamine have been reported and definite structure–activity relationships are noticeably scant.

Tranylcypromine (*trans*-2-phenylcyclopropylamine) (I) was considerably more potent than the *cis*-isomer (II) in its ability to inhibit catecholamine uptake into synaptosomes from the rat hypothalamus and corpus striatum (13). Similarly, 2-aminoindan (III) was more efficacious than 1-aminoindan (IV) in the same experiments. These results suggested that the fully extended, or *anti*-periplanar, conformation of amphetamine was the important spatial disposition necessary for inhibition of the neuronal uptake mechanism.

The synthesis of a series of 2-amino-3-phenyl-*trans*-decalins (V–VIII) was reported (14). Surprisingly, all of these compounds decreased the motor activity in mice at similar dosage levels so that no correlation of activity with stereochemistry could be discerned. The compounds were also surveyed (15, 16) as inhibitors of 5-hydroxytryptamine and histamine uptake in rabbit

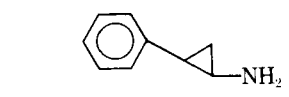

I

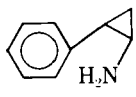

II

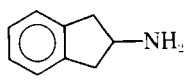

III

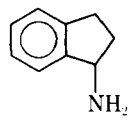

IV

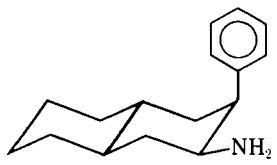

V

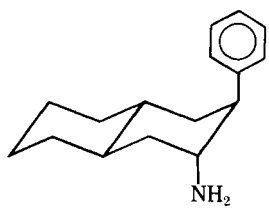

VI

REFERENCES

(1) J. Correa and M. L. Cervera, *Bull. Soc. Chim. Fr.*, **1971**, 475.

(2) A. Romo de Vivar, J. Romo, A. A. Ortega, E. Diaz, and M. A. Carino, *Rev. Latinoam. Quim.*, **2**, 38(1971).

(3) D. S. Bhakuni, M. L. Dhar, M. M. Dhar, B. N. Dhawan, B. Gupta, and R. C. Srimal, *Indian J. Exp. Biol.*, **9**, 91(1971).

(4) *Cancer Chemother. Rep.*, **3**, 1(1972).

ACKNOWLEDGMENTS AND ADDRESSES

Received March 27, 1975, from the *Division of Medicinal Chemistry, Central Drug Research Institute, Lucknow, India.*

Accepted for publication September 4, 1975.

The authors thank Mr. J. Saran and his associates for the microanalyses, Mr. R. K. Mukherji for the IR spectra, and Mr. Edward Samson for technical assistance. The plant material was collected under a program sponsored by the National Institutes of Health, Bethesda, Md., for the development of anticancer agents of plant origin (PL-480, Grant 134304), and the anticancer screening data were obtained from the Cancer Chemotherapy National Service Center, National Cancer Institute, Bethesda, Md.

This paper is Communication No. 2006 from the Central Drug Research Institute, Lucknow, India, and Part I of "Chemical Studies on *Tithonia tagitiflora* Desf."

[x] To whom inquiries should be directed.

Conformationally Defined Adrenergic Agents I: Potentiation of Levarterenol in Rat Vas Deferens by *endo*- and *exo*-2-Aminobenzobicyclo[2.2.2]octenes, Conformationally Defined Analogs of Amphetamine

GARY L. GRUNEWALD [*x], JAMES A. RUTH [*], TIMOTHY R. KROBOTH [*], BHARAT V. KAMDAR [*], POPAT N. PATIL [‡], and KADIM N. SALMAN [‡]

Abstract □ Four conformationally defined analogs of amphetamine were synthesized and studied for their ability to potentiate the action of levarterenol on the isolated vas deferens from reserpine-treated rats. The compounds also were studied for indirect adrenergic agonist activity in the same test system. A definite stereochemical correlation was demonstrated in each case, the *exo*-isomers being considerably more active than their *endo*-counterparts both in potentiation and in indirect activity. The more active isomers of each pair correspond to an *anti*-periplanar conformation of amphetamine. The compounds are probably acting by inhibition of the neuronal amine uptake mechanism, since none of the compounds was a direct-acting agonist itself. These results are discussed in relationship to other previously reported, conformationally defined, amphetamine analogs.

Keyphrases □ Adrenergic agents—conformationally defined analogs of amphetamine, potentiation of levarterenol in rat vas deferens □ Levarterenol—potentiation by conformationally defined analogs of amphetamine, rat vas deferens □ Amphetamines—conformationally defined analogs synthesized, potentiation of levarterenol in rat vas deferens □ Structure–activity relationships—conformationally defined analogs of amphetamine, potentiation of levarterenol in rat vas deferens

One recent technique for probing the nature of agonist–receptor interactions is the study of conformationally defined analogs of the agonists in question to quantitate the stereochemical requirements for biological activity. While such an approach has found considerable application in the areas of cholinergic agonists (1–5), on phenethanolamine systems (6–11), and dopaminergic agonists (12), relatively few examples of conformationally defined analogs of amphetamine have been reported and definite structure–activity relationships are noticeably scant.

Tranylcypromine (*trans*-2-phenylcyclopropylamine) (I) was considerably more potent than the *cis*-isomer (II) in its ability to inhibit catecholamine uptake into synaptosomes from the rat hypothalamus and corpus striatum (13). Similarly, 2-aminoindan (III) was more efficacious than 1-aminoindan (IV) in the same experiments. These results suggested that the fully extended, or *anti*-periplanar, conformation of amphetamine was the important spatial disposition necessary for inhibition of the neuronal uptake mechanism.

The synthesis of a series of 2-amino-3-phenyl-*trans*-decalins (V–VIII) was reported (14). Surprisingly, all of these compounds decreased the motor activity in mice at similar dosage levels so that no correlation of activity with stereochemistry could be discerned. The compounds were also surveyed (15, 16) as inhibitors of 5-hydroxytryptamine and histamine uptake in rabbit

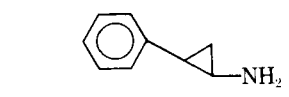

I

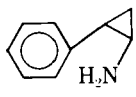

II

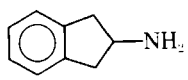

III

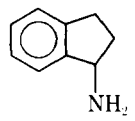

IV

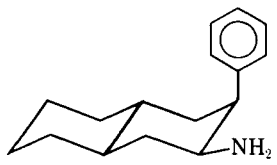

V

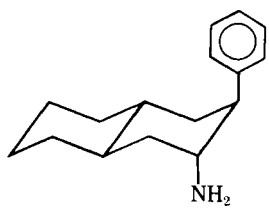

VI

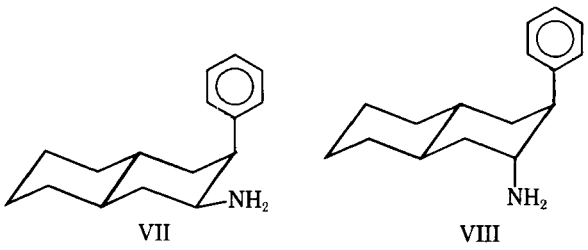

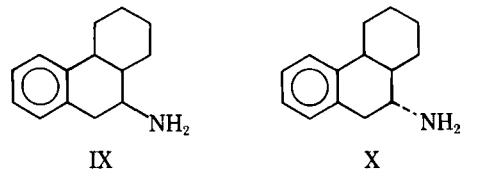

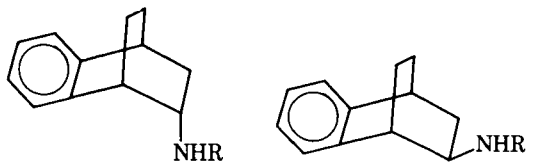

XI: R = H
XIII: R = CH_3

XII: R = H
XIV: R = CH_3

platelets, but no clearcut structure–activity relationship was observed.

The amphetamine analogs 10*a*- and 10*e*-aminooctahydrophenanthrenes (IX and X) were synthesized, and neither compound produced amphetamine-like effects in mice (17).

In an effort to delineate further stereochemical requirements for adrenergic activity, *endo*- and *exo*-2-aminobenzobicyclo- [2.2.2]octenes[1] (XI and XII) and *endo*- and *exo*-*N*-methyl-2-aminobenzobicyclo[2.2.2]-octenes (XIII and XIV) were synthesized and studied for agonist activity. The spatial arrangements in the *endo*- and *exo*-amino compounds offer an excellent approximation of the *gauche*- and *anti*-periplanar conformations, respectively, of amphetamine.

The tricyclic model system has the additional advantages of: (*a*) introducing fewer extraneous carbon

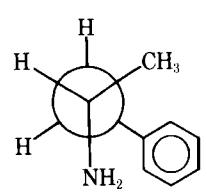

gauche-amphetamine

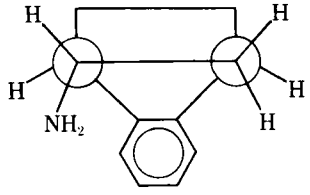

endo-amine (XI)

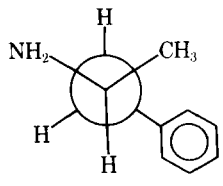

anti-periplanar amphetamine

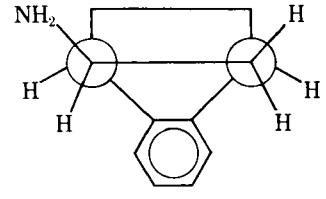

exo-amine (XII)

[1] In Chemical Abstracts nomenclature: *endo*- and *exo*-9-amino-1,2,3,4-tetrahydro-1,4-ethanonaphthalenes.

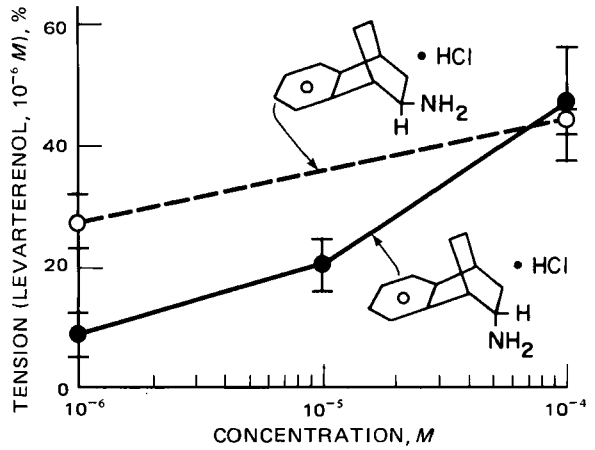

Figure 1—*Potentiation of levarterenol (10^{-6} M) on the reserpine-pretreated rat vas deferens* (n = 3–5) *in the presence of various concentrations of XI and XII. On each tissue, maximal effect of 3 × 10^{-4} M levarterenol was considered as 100; the change in tension is expressed as the percent of this maximum. The average response to 10^{-6} M levarterenol without a drug was 22 ± 2%* (n = 7). *Values in excess of this represent potentiation by the amphetamine analog. In those few cases where the control value was less than 20% (levarterenol alone), the value in the presence of the amphetamine analog was still greater than the control* (i.e., *potentiation*).

atoms, which could increase steric bulk or lipophilicity of the test compounds, as compared with the Smissman and Nelson models; and (*b*) holding the phenyl ring in a fixed orientation, similar to that observed in the amphetamine crystal structure (18) and to the low energy conformations predicted by molecular orbital calculations (19).

EXPERIMENTAL

The test compounds were prepared by the method of Kitahonoki *et al.* (20, 21).

Male, albino, Sprague–Dawley-derived rats[2], 200–710 g, were used. The rats received reserpine (5 mg/kg ip) 18–22 hr prior to the experiment.

The animals were decapitated, and the vas deferens was quickly removed, cleaned of blood vessels and fatty tissue, and mounted in a 10-ml jacketed tissue bath containing modified Krebs solution of the following composition (millimoles per liter of double-distilled water): NaCl, 118; KCl, 4.7; $MgCl_2 \cdot 6H_2O$, 0.54; $CaCl_2 \cdot 2H_2O$, 2.5; Na_2HPO_4, 1.0; $NaHCO_3$, 2.5; and glucose, 11. Edetic acid, 10 mg/liter, was added to retard the spontaneous oxidation of levarterenol [(−)-norepinephrine]. A mixture of 95% oxygen and 5% carbon dioxide was bubbled through the solution, and the temperature was kept at 37 ± 0.5°.

Responses of vas deferens to drugs were recorded isometrically under 0.25 g of tension *via* a force-displacement transducer on a polygraph. The tissues were left to equilibrate for 1 hr with frequent washing with new aliquots of Krebs solution. The response of the untreated vas deferens from one side was recorded to a standard dose of 1 × 10^{-6} *M* levarterenol which usually produced contraction between 20 and 30% of the maximum. The tissue was washed thoroughly until it returned to baseline, and a dose of 3 × 10^{-4} *M* levarterenol was given to produce 100% contraction.

The vas deferens from the contralateral side was incubated with a given concentration of the test compound for 15 min, and then the standard dose of 1 × 10^{-6} *M* levarterenol was given to test the response of the tissue. Subsequently, the tissue was washed several times and the response to levarterenol (3 × 10^{-4} *M*) was obtained. The change in response to a 1 × 10^{-6} *M* dose of levarterenol was calculated as a percent in terms of the maximum response obtained with a 3 × 10^{-4} *M* dose of levarterenol. At least three different concentrations of each compound were used.

[2] Obtained from Harlan or Lab Supply, Cumberland, Ind.

Table I—Effects of XI and XII on the Normal Rat Vas Deferens

Compound	Tension (with Minimum and Maximum Range), %					
	3×10^{-5} *M*		1×10^{-4} *M*		3×10^{-4} *M*	
	a[a]	b[b]	a	b	a	b
XI	0, $n = 2$	0	0, $n = 2$	2 (0–3)	9 (3–12), $n = 3$	12 (7–18)
XII	1 (0–2), $n = 2$	8 (3–13)	2, $n = 3$	11 (3–17)	5 (4–5), $n = 3$	13 (10–18)

[a] a = response within 1 min. [b] b = response within 5 min.

In another series of experiments, the indirect activity of XI and XII was tested. Normal (nonreserpinized) rat vas deferens was set up as already described and left to equilibrate before the start of the experiment. The activity of the compounds was tested at three different concentrations for 5 min. The tissue was then washed, and phenylpropanolamine in the same concentration as the test compound was added to serve as internal control. Subsequently, it was washed away, and a dose of 3×10^{-4} *M* levarterenol was given to attain a response that served as the 100% effect. The effects of the compounds under test as well as those of the internal control were calculated as percent changes in tension of the maximum response in the same tissue.

On the day of the experiment, drug solutions were prepared fresh in saline containing 0.05% of sodium metabisulfite to prevent autoxidation of catecholamines.

Levarterenol was used as the free base and dissolved with the aid of a few drops of 0.1 *N* HCl.

RESULTS AND DISCUSSION

Table I shows the activity of the amphetamine analogs XI and XII as indirect agonists in the normal rat vas deferens preparation. Both compounds possessed an immediate indirect action effect characterized by a sudden change in tension and a delayed action characterized by individual spikes. The *exo*-amino compound (XII) was more potent than the *endo*-amino compound (XI) in this effect at lower concentrations and equipotent at 3×10^{-4} *M*. Both XI and XII were less potent than phenylpropanolamine.

Figures 1 and 2 show the activity of XI–XIV as agents potentiating the effect of applied levarterenol in a reserpinized rat vas deferens preparation. For both R = H and R = CH_3, the results are quite striking. There was a pronounced increase in the ability to potentiate the action of levarterenol with the two *exo*-amines (XII and XIV),

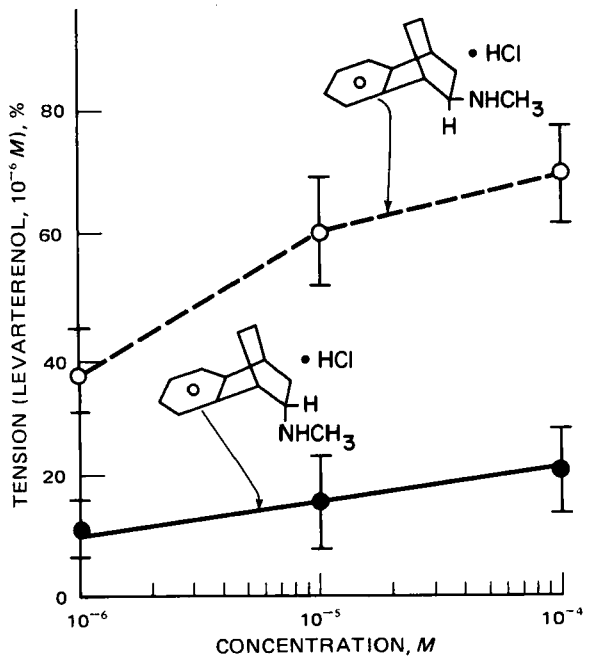

Figure 2—*Potentiation of levarterenol (10^{-6} M) on the reserpine-pretreated rat vas deferens* (n = 4) *in the presence of various concentrations of XIII and XIV. Experimental conditions were identical to those described in Fig. 1.*

which correspond to the fully extended or *anti*-periplanar conformation of amphetamine.

Most activity in the test compounds probably can be ascribed to a blockade of the neuronal uptake mechanism, since the compounds themselves are only indirect acting agonists and since the preparation studied was reserpine treated. These results suggest that, at least in this particular system, a definite stereochemical preference is seen at the neuronal amine uptake pump. Further experiments are required to demonstrate whether a component of the activity could be due to inhibition of monoamine oxidase. However, with amphetamine itself, such monoamine oxidase inhibition effects are usually negligible until concentrations of 10^{-4}–10^{-3} *M* are reached (22).

The results are quite significant in view of the lack of structure–activity relationship observed in most systems mentioned earlier (23). Whereas the results parallel quite well the structural preferences observed for tranylcypromine (I), similar correlations were not observed in the Smissman and Nelson systems. Because of the increased bulk of each of those systems, the lack of activity observed might be due to steric effects or to changes in lipophilicity of the compounds that render them incapable of binding at the neuronal uptake sites.

Other studies to be reported[3], dealing with the release of tritiated amines from rat hypothalamus and corpus striatum, further demonstrate a striking preference for the *exo*-amines, corresponding to a fully extended amphetamine conformation. These findings are consistent with a lack of appreciable monoamine oxidase inhibition.

Similarly, unpublished results[4] with a specific methamphetamine antibody demonstrate a pronounced binding of the fully extended *exo*-amines (XII and XIV) and no affinity for the *endo*-isomers (XI and XIII).

Whereas the crystal structure (18) of dextroamphetamine sulfate shows the molecule to exist in an extended conformation, molecular orbital calculations (19) demonstrate three energetically equivalent low energy conformations: the *anti*-periplanar as well as two *gauche*-conformations. Since the energy surfaces for the *gauche*-conformations are considerably larger than those for the *trans*-conformations, a prediction would be that the folded or *gauche*-conformations would predominate in solution at room temperature. Since these experiments suggest that the *anti*-periplanar conformation is more important in blockade of the uptake mechanism, caution is in order before extrapolation of the more populated conformation obtained from theoretical calculations to the conformation most likely to be physiologically active.

Additional work is underway in these laboratories to elaborate the nature of action of these compounds on the amine uptake mechanism.

REFERENCES

(1) E. E. Smissman, W. L. Nelson, J. B. LaPidus, and J. L. Day, *J. Med. Chem.*, **9**, 458(1966).

(2) E. E. Smissman and G. A. Chappell, *ibid.*, **12**, 432(1969).

(3) E. E. Smissman, R. T. Borchardt, and K. B. Schowen, *ibid.*, **15**, 545(1972).

(4) E. E. Smissman and G. R. Parker, *ibid.*, **16**, 23(1973).

(5) C. Y. Chiou, J. P. Long, J. G. Cannon, and P. D. Armstrong, *J. Pharmacol. Exp. Ther.*, **166**, 243(1969).

[3] In conjunction with C.O. Rutledge, Department of Pharmacology and Toxicology, University of Kansas, Lawrence, KS 66045

[4] In conjunction with B. Faraj, Department of Radiology, School of Medicine, Emory University, Atlanta, GA 30322. *Note added in proof:* This article has now been published. B. A. Faraj, Z. H. Israili, N. E. Kight, E. E. Smissman, and T. L. Pazdernik, *J. Med. Chem.*, **19**, 20(1976).

(6) E. E. Smissman and W. H. Gastrock, *J. Med. Chem.*, **11**, 860(1968).
(7) E. E. Smissman and G. H. Chappell, *ibid.*, **12**, 429(1969).
(8) E. E. Smissman and S. El-Antably, *ibid.*, **14**, 30(1971).
(9) E. E. Smissman and R. T. Borchardt, *ibid.*, **14**, 377(1971).
(10) *Ibid.*, **14**, 383(1971).
(11) W. L. Nelson and D. D. Miller, *J. Med. Chem.*, **13**, 807(1970).
(12) J. G. Cannon, J. C. Kim, and M. A. Aleem, *ibid.*, **15**, 348(1972).
(13) A. S. Horn and S. H. Snyder, *J. Pharmacol. Exp. Ther.*, **180**, 523(1972).
(14) E. E. Smissman and T. L. Pazdernik, *J. Med. Chem.*, **16**, 18(1973).
(15) J. Tuomisto, E. E. Smissman, T. L. Pazdernik, and E. J. Walaszek, *J. Pharm. Sci.*, **63**, 1708(1974).
(16) J. Tuomisto, E. J. Walaszek, E. E. Smissman, and T. L. Pazdernik, *ibid.*, **63**, 1714(1974).
(17) W. L. Nelson and B. E. Sherwood, *ibid.*, **63**, 1468(1974).
(18) R. Bergin and D. Carlstrom, *Acta Crystallogr.*, **B27**, 2146(1971).
(19) B. Pullman, J.-L. Coubiels, P. Courriere, and J.-P. Gervois, *J. Med. Chem.*, **15**, 17(1972).
(20) K. Kitahonoki, Y. Takano, and H. Takahashi, *Tetrahedron*, **24**, 4605(1968).
(21) K. Kitahonoki and Y. Takano, *Tetrahedron Lett.*, **1963**, 1597.
(22) G. R. Wenger and C. O. Rutledge, *J. Pharmacol. Exp. Ther.*, **189**, 725(1974).
(23) P. N. Patil, D. D. Miller, and U. Trendelenburg, *Pharmacol. Rev.*, **26**, 323(1974).

ACKNOWLEDGMENTS AND ADDRESSES

Received June 16, 1975, from the **Department of Medicinal Chemistry, School of Pharmacy, University of Kansas, Lawrence, KS 66045,* and the *‡Division of Pharmacology, College of Pharmacy, Ohio State University, Columbus, OH 43210*

Accepted for publication August 15, 1975.

Supported by the Kansas Heart Association, the University of Kansas General Research Fund, and the National Institutes of Health (Training Grant GM-1341 and Research Grants GM-17859 and NS-09350). The receipt of National Institutes of Health Postdoctoral Fellowship GM-55798-01 by J. A. Ruth is gratefully acknowledged.

[x] To whom inquiries should be directed.

Major Alkaloids of *Glaucium flavum* Grantz, Population Ghom

I. LALEZARI [x], A. SHAFIEE, and M. MAHJOUR

Abstract □ *Glaucium flavum* Grantz, population Ghom, contains 1.24% dicentrine, 0.89% bulbocapnine, and 0.05% salutaridine in dry aerial parts and root of the flowering plant. These alkaloids were detected for the first time in the *Glaucium* genus.

Keyphrases □ *Glaucium flavum*—dried whole plant extract, dicentrine, bulbocapnine, and salutaridine isolated and identified □ Alkaloids—dicentrine, bulbocapnine, and salutaridine isolated from *Glaucium flavum* whole plant extract □ Dicentrine—isolated from *Glaucium flavum* whole plant extract □ Bulbocapnine—isolated from *Glaucium flavum* whole plant extract □ Salutaridine—isolated from *Glaucium flavum* whole plant extract

In a continuation of chemotaxonomic studies of Iranian wild Papaveraceae (1–4), the major alkaloids of *Glaucium flavum* Grantz[1], a perennial wild plant scattered near the salt lake of Ghom, in the southern part of Tehran at about 900 m above sea level, were isolated and identified. The height of the plant is about 60 cm. The plant blooms from April until September. The four petals are yellow with orange spots on the base. The fruit consists of a long silique.

The total alkaloid content of this plant (dried aerial parts and root) was found to be 3.12%. TLC of the total alkaloids revealed that two major alkaloids existed. The dominant alkaloid was dicentrine (I) (1.24%). The second major alkaloid was bulbocapnine (II) (0.89%). A third alkaloid was separated from the total alkaloid and

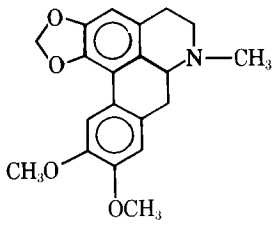

I

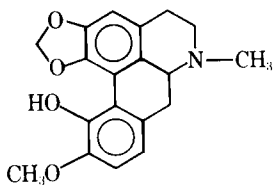

II

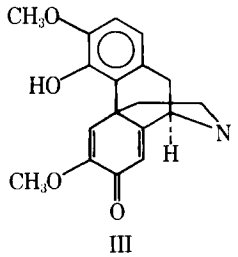

III

was identified as salutaridine (III) (0.05%).

The structures were assigned on the basis of physical properties, elemental analysis, and spectral data. The isolated salutaridine was identical with an authentic sample.

A literature survey (5–7) revealed that none of these alkaloids was reported previously in the *Glaucium* genus.

Several minor alkaloids were detected in this plant. The structure elucidation of the minor alkaloids is under investigation.

[1] The plant was identified by Professor H. Golgolab, Tehran University, and Professor K. Hummel, Tubingen University. A herbarium sample was deposited in the Herbarium of the College of Pharmacy, Tehran University.

(6) E. E. Smissman and W. H. Gastrock, *J. Med. Chem.*, **11**, 860(1968).
(7) E. E. Smissman and G. H. Chappell, *ibid.*, **12**, 429(1969).
(8) E. E. Smissman and S. El-Antably, *ibid.*, **14**, 30(1971).
(9) E. E. Smissman and R. T. Borchardt, *ibid.*, **14**, 377(1971).
(10) *Ibid.*, **14**, 383(1971).
(11) W. L. Nelson and D. D. Miller, *J. Med. Chem.*, **13**, 807(1970).
(12) J. G. Cannon, J. C. Kim, and M. A. Aleem, *ibid.*, **15**, 348(1972).
(13) A. S. Horn and S. H. Snyder, *J. Pharmacol. Exp. Ther.*, **180**, 523(1972).
(14) E. E. Smissman and T. L. Pazdernik, *J. Med. Chem.*, **16**, 18(1973).
(15) J. Tuomisto, E. E. Smissman, T. L. Pazdernik, and E. J. Walaszek, *J. Pharm. Sci.*, **63**, 1708(1974).
(16) J. Tuomisto, E. J. Walaszek, E. E. Smissman, and T. L. Pazdernik, *ibid.*, **63**, 1714(1974).
(17) W. L. Nelson and B. E. Sherwood, *ibid.*, **63**, 1468(1974).
(18) R. Bergin and D. Carlstrom, *Acta Crystallogr.*, **B27**, 2146(1971).
(19) B. Pullman, J.-L. Coubiels, P. Courriere, and J.-P. Gervois, *J. Med. Chem.*, **15**, 17(1972).
(20) K. Kitahonoki, Y. Takano, and H. Takahashi, *Tetrahedron*, **24**, 4605(1968).
(21) K. Kitahonoki and Y. Takano, *Tetrahedron Lett.*, **1963**, 1597.
(22) G. R. Wenger and C. O. Rutledge, *J. Pharmacol. Exp. Ther.*, **189**, 725(1974).
(23) P. N. Patil, D. D. Miller, and U. Trendelenburg, *Pharmacol. Rev.*, **26**, 323(1974).

ACKNOWLEDGMENTS AND ADDRESSES

Received June 16, 1975, from the **Department of Medicinal Chemistry, School of Pharmacy, University of Kansas, Lawrence, KS 66045,* and the *‡Division of Pharmacology, College of Pharmacy, Ohio State University, Columbus, OH 43210*

Accepted for publication August 15, 1975.

Supported by the Kansas Heart Association, the University of Kansas General Research Fund, and the National Institutes of Health (Training Grant GM-1341 and Research Grants GM-17859 and NS-09350). The receipt of National Institutes of Health Postdoctoral Fellowship GM-55798-01 by J. A. Ruth is gratefully acknowledged.

[x] To whom inquiries should be directed.

Major Alkaloids of *Glaucium flavum* Grantz, Population Ghom

I. LALEZARI [x], A. SHAFIEE, and M. MAHJOUR

Abstract □ *Glaucium flavum* Grantz, population Ghom, contains 1.24% dicentrine, 0.89% bulbocapnine, and 0.05% salutaridine in dry aerial parts and root of the flowering plant. These alkaloids were detected for the first time in the *Glaucium* genus.

Keyphrases □ *Glaucium flavum*—dried whole plant extract, dicentrine, bulbocapnine, and salutaridine isolated and identified □ Alkaloids—dicentrine, bulbocapnine, and salutaridine isolated from *Glaucium flavum* whole plant extract □ Dicentrine—isolated from *Glaucium flavum* whole plant extract □ Bulbocapnine—isolated from *Glaucium flavum* whole plant extract □ Salutaridine—isolated from *Glaucium flavum* whole plant extract

In a continuation of chemotaxonomic studies of Iranian wild Papaveraceae (1–4), the major alkaloids of *Glaucium flavum* Grantz[1], a perennial wild plant scattered near the salt lake of Ghom, in the southern part of Tehran at about 900 m above sea level, were isolated and identified. The height of the plant is about 60 cm. The plant blooms from April until September. The four petals are yellow with orange spots on the base. The fruit consists of a long silique.

The total alkaloid content of this plant (dried aerial parts and root) was found to be 3.12%. TLC of the total alkaloids revealed that two major alkaloids existed. The dominant alkaloid was dicentrine (I) (1.24%). The second major alkaloid was bulbocapnine (II) (0.89%). A third alkaloid was separated from the total alkaloid and

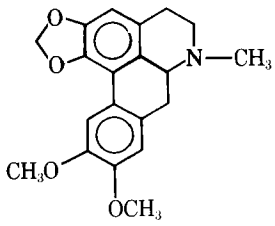

I

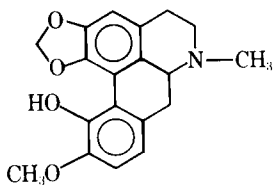

II

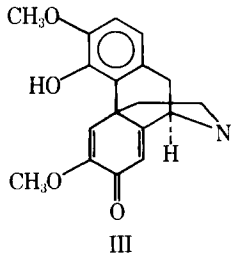

III

was identified as salutaridine (III) (0.05%).

The structures were assigned on the basis of physical properties, elemental analysis, and spectral data. The isolated salutaridine was identical with an authentic sample.

A literature survey (5–7) revealed that none of these alkaloids was reported previously in the *Glaucium* genus.

Several minor alkaloids were detected in this plant. The structure elucidation of the minor alkaloids is under investigation.

[1] The plant was identified by Professor H. Golgolab, Tehran University, and Professor K. Hummel, Tubingen University. A herbarium sample was deposited in the Herbarium of the College of Pharmacy, Tehran University.

EXPERIMENTAL[2]

Plant Material—The whole aerial parts and roots were collected during May, air dried in the shade, finally dried at 60° to a constant weight, and powdered so that all material passed a mesh not greater than 0.5 mm.

Extraction—Powdered plant material, 100 g, was moistened with 100 ml of 15% ammonia and stirred with 600 ml of chloroform at room temperature for 1 hr. The extraction was repeated four times. After evaporation of the solvent, the dark oily residue was extracted with 50 ml of 5% sulfuric acid. The solution was filtered and extracted with petroleum ether (3 × 20 ml) to remove the colored material.

The aqueous layer was made alkaline with 15% ammonia and extracted with chloroform (4 × 25 ml). After evaporation of the solvent, the dry residue (3.12 g) was subjected to preparative TLC on silica gel plates, using petroleum ether–chloroform–diethylamine (70:20:10) as the eluting solvent.

Dicentrine—The first major fraction was extracted with chloroform–methanol (85:15) and recrystallized from ethanol to give 1.24 g of I, mp 166–169° [lit. (8) mp 168–169°]; molecular weight by mass spectroscopy *m/e* 339; UV: λ_{max} (CH_3OH) 303 ($E^{1\%}_{1cm}$ 494) and 280 ($E^{1\%}_{1cm}$ 400) nm; IR (KBr): 1600, 1575, 1508, 1466, 1389, 1312, 1266, 1242, 1212, 1098, 1040, 955, 865, 838, and 769 cm^{-1}; NMR ($CDCl_3$): τ 7.46 (s, 3H, NCH_3), 6.1 (s, 6H, OCH_3), 4.0 (d, 2H, CH_2), 3.47 (s, 1H, aromatic), and 2.28 (s, 1H, aromatic)[3].

Anal.—Calc. for $C_{20}H_{21}NO_4$: C, 70.78; H, 6.24; N, 4.13. Found: C, 70.69; H, 6.30; N, 4.11.

Bulbocapnine—The second major fraction was extracted in a way similar to that used for dicentrine to give 0.89 g of II, mp 199–200° [lit. (11) mp 199°]; molecular weight by mass spectroscopy *m/e* 325; UV: λ_{max} (CH_3OH) 303 ($E^{1\%}_{1cm}$ 214), 275 ($E^{1\%}_{1cm}$ 370), and 268 ($E^{1\%}_{1cm}$ 432) nm; IR (KBr): 3175, 1645, 1618, 1515, 1488, 1466, 1404, 1299, 1235, 1136, 1082, 1062, 1033, 998, 959, 934, 853, 827, 806, and 735 cm^{-1}; NMR ($CDCl_3$): τ 7.44 (s, 3H, NCH_3), 6.1 (s, 3H, OCH_3), 3.97 (d, 2H, CH_2), 3.36 (s, 1H, aromatic), and 3.16 (s, 2H, aromatic)[4].

[2] Melting points were taken on a Kofler hot-stage microscope and are uncorrected. UV spectra were obtained on a Varian Techtron 635 instrument. IR spectra were recorded on a Leitz model III spectrograph. NMR spectra were obtained on a Varian T60A instrument, using tetramethylsilane as the internal standard. Mass spectra were recorded on a Varian Mat III spectrograph.

[3] NMR data were identical with those reported in the literature (9) for dicentrine.

[4] UV and NMR data were identical with those reported in the literature (10, 11) for bulbocapnine.

Anal.—Calc. for $C_{19}H_{19}NO_4$: C, 70.78; H, 6.24; N, 4.13. Found: C, 70.69; H, 6.20; N, 4.23.

Salutaridine—The third fraction was extracted as already described and recrystallized from ether to give 0.05 g of III, mp 197–199° [lit. (4) mp 196–198°]. The isolated material was identical to an authentic sample of salutaridine according to melting-point, mixed-melting point, IR, UV, NMR, and mass spectroscopic analyses (4).

Anal.—Calc. for $C_{19}H_{21}NO_4$: C, 69.72; H, 6.42; N, 4.28. Found: C, 70.01; H, 6.43; N, 4.31.

REFERENCES

(1) N. Sharghi and I. Lalezari, *Nature*, **213**, 1244(1967).

(2) I. Lalezari, A. Shafiee, and P. Nasseri, *J. Pharm. Sci.*, **62**, 1718(1973).

(3) I. Lalezari, P. Nasseri, and R. Asgharian, *ibid.*, **63**, 1331(1974).

(4) A. Shafiee, I. Lalezari, P. Nasseri-Nouri, and R. Asgharian, *ibid.*, **64**, 1570(1975).

(5) F. Santavy, in "The Alkaloids," vol. 12, R. H. Manske and H. L. Holmes, Eds., Academic, New York, N.Y., 1970, p. 337.

(6) I. Ribas, J. Sueiras, and L. Castedo, *Tetrahedron Lett.*, **1971**, 3093.

(7) *Ibid.*, **1972**, 2033.

(8) Y. Asahina, *Arch. Pharm.*, **247**, 201(1909).

(9) W. H. Baarschers, R. R. Arndt, K. Pachler, J. A. Weisbach, and B. Douglas, *J. Chem. Soc.*, **1964**, 4778.

(10) M. Freund and W. Josephi, *Ann. Chem.*, **277**, 10(1893).

(11) V. Brustier, P. Bourbon, R. Aloy, and G. Broussy, *Trav. Soc. Pharm., Montpellier*, **14**, 137(1954).

ACKNOWLEDGMENTS AND ADDRESSES

Received March 3, 1975, from the *Department of Chemistry, College of Pharmacy, University of Tehran, Tehran, Iran.*

Accepted for publication August 18, 1975.

Supported by Grant 13 of the International Foundation for Science and by a grant from the research division of Tehran University.

The authors are grateful to Dr. E. Levy, Weizmann Institute of Science, Rehovot, Israel, for advice.

This paper is the fifth in a series on plant alkaloids.

[x] To whom inquiries should be directed.

Simultaneous Quantitative GLC Determination of Chlorpheniramine Maleate and Phenylpropanolamine Hydrochloride in a Cold Tablet Preparation

R. E. MADSEN [*] and D. F. MAGIN [x]

Abstract □ A GLC method was developed for the simultaneous determinations of chlorpheniramine maleate and phenylpropanolamine hydrochloride in a cold tablet preparation containing a large amount of aspirin. The method utilizes a solid sampling device to eliminate interference from solvent, and it is rapid and precise. The total analysis time is less than 1.5 hr, thereby permitting its use for quality control purposes.

Keyphrases □ Chlorpheniramine maleate—GLC analysis, commercial cold tablets □ Phenylpropanolamine hydrochloride—GLC analysis, commercial cold tablets □ GLC—analysis, simultaneous, chlorpheniramine maleate and phenylpropanolamine hydrochloride, commercial cold tablets □ Dosage forms—commercial cold tablets, simultaneous GLC analysis of chlorpheniramine maleate and phenylpropanolamine hydrochloride

Analyses of chlorpheniramine maleate and phenylpropanolamine hydrochloride have been performed in various formulations by several means. Partition (1, 2), ion-exchange (3), liquid (4), and gas (5) chromatography are among the forms applied to these analyses. The purpose of this study was to develop a rapid, precise, and simple method for the simultaneous determination of chlorpheniramine maleate and phenylpropanolamine

EXPERIMENTAL[2]

Plant Material—The whole aerial parts and roots were collected during May, air dried in the shade, finally dried at 60° to a constant weight, and powdered so that all material passed a mesh not greater than 0.5 mm.

Extraction—Powdered plant material, 100 g, was moistened with 100 ml of 15% ammonia and stirred with 600 ml of chloroform at room temperature for 1 hr. The extraction was repeated four times. After evaporation of the solvent, the dark oily residue was extracted with 50 ml of 5% sulfuric acid. The solution was filtered and extracted with petroleum ether (3 × 20 ml) to remove the colored material.

The aqueous layer was made alkaline with 15% ammonia and extracted with chloroform (4 × 25 ml). After evaporation of the solvent, the dry residue (3.12 g) was subjected to preparative TLC on silica gel plates, using petroleum ether–chloroform–diethylamine (70:20:10) as the eluting solvent.

Dicentrine—The first major fraction was extracted with chloroform–methanol (85:15) and recrystallized from ethanol to give 1.24 g of I, mp 166–169° [lit. (8) mp 168–169°]; molecular weight by mass spectroscopy *m/e* 339; UV: λ_{max} (CH_3OH) 303 ($E^{1\%}_{1cm}$ 494) and 280 ($E^{1\%}_{1cm}$ 400) nm; IR (KBr): 1600, 1575, 1508, 1466, 1389, 1312, 1266, 1242, 1212, 1098, 1040, 955, 865, 838, and 769 cm^{-1}; NMR ($CDCl_3$): τ 7.46 (s, 3H, NCH_3), 6.1 (s, 6H, OCH_3), 4.0 (d, 2H, CH_2), 3.47 (s, 1H, aromatic), and 2.28 (s, 1H, aromatic)[3].

Anal.—Calc. for $C_{20}H_{21}NO_4$: C, 70.78; H, 6.24; N, 4.13. Found: C, 70.69; H, 6.30; N, 4.11.

Bulbocapnine—The second major fraction was extracted in a way similar to that used for dicentrine to give 0.89 g of II, mp 199–200° [lit. (11) mp 199°]; molecular weight by mass spectroscopy *m/e* 325; UV: λ_{max} (CH_3OH) 303 ($E^{1\%}_{1cm}$ 214), 275 ($E^{1\%}_{1cm}$ 370), and 268 ($E^{1\%}_{1cm}$ 432) nm; IR (KBr): 3175, 1645, 1618, 1515, 1488, 1466, 1404, 1299, 1235, 1136, 1082, 1062, 1033, 998, 959, 934, 853, 827, 806, and 735 cm^{-1}; NMR ($CDCl_3$): τ 7.44 (s, 3H, NCH_3), 6.1 (s, 3H, OCH_3), 3.97 (d, 2H, CH_2), 3.36 (s, 1H, aromatic), and 3.16 (s, 2H, aromatic)[4].

[2] Melting points were taken on a Kofler hot-stage microscope and are uncorrected. UV spectra were obtained on a Varian Techtron 635 instrument. IR spectra were recorded on a Leitz model III spectrograph. NMR spectra were obtained on a Varian T60A instrument, using tetramethylsilane as the internal standard. Mass spectra were recorded on a Varian Mat III spectrograph.

[3] NMR data were identical with those reported in the literature (9) for dicentrine.

[4] UV and NMR data were identical with those reported in the literature (10, 11) for bulbocapnine.

Anal.—Calc. for $C_{19}H_{19}NO_4$: C, 70.78; H, 6.24; N, 4.13. Found: C, 70.69; H, 6.20; N, 4.23.

Salutaridine—The third fraction was extracted as already described and recrystallized from ether to give 0.05 g of III, mp 197–199° [lit. (4) mp 196–198°]. The isolated material was identical to an authentic sample of salutaridine according to melting-point, mixed-melting point, IR, UV, NMR, and mass spectroscopic analyses (4).

Anal.—Calc. for $C_{19}H_{21}NO_4$: C, 69.72; H, 6.42; N, 4.28. Found: C, 70.01; H, 6.43; N, 4.31.

REFERENCES

(1) N. Sharghi and I. Lalezari, *Nature*, **213**, 1244(1967).

(2) I. Lalezari, A. Shafiee, and P. Nasseri, *J. Pharm. Sci.*, **62**, 1718(1973).

(3) I. Lalezari, P. Nasseri, and R. Asgharian, *ibid.*, **63**, 1331(1974).

(4) A. Shafiee, I. Lalezari, P. Nasseri-Nouri, and R. Asgharian, *ibid.*, **64**, 1570(1975).

(5) F. Santavy, in "The Alkaloids," vol. 12, R. H. Manske and H. L. Holmes, Eds., Academic, New York, N.Y., 1970, p. 337.

(6) I. Ribas, J. Sueiras, and L. Castedo, *Tetrahedron Lett.*, **1971**, 3093.

(7) *Ibid.*, **1972**, 2033.

(8) Y. Asahina, *Arch. Pharm.*, **247**, 201(1909).

(9) W. H. Baarschers, R. R. Arndt, K. Pachler, J. A. Weisbach, and B. Douglas, *J. Chem. Soc.*, **1964**, 4778.

(10) M. Freund and W. Josephi, *Ann. Chem.*, **277**, 10(1893).

(11) V. Brustier, P. Bourbon, R. Aloy, and G. Broussy, *Trav. Soc. Pharm., Montpellier*, **14**, 137(1954).

ACKNOWLEDGMENTS AND ADDRESSES

Received March 3, 1975, from the *Department of Chemistry, College of Pharmacy, University of Tehran, Tehran, Iran.*

Accepted for publication August 18, 1975.

Supported by Grant 13 of the International Foundation for Science and by a grant from the research division of Tehran University.

The authors are grateful to Dr. E. Levy, Weizmann Institute of Science, Rehovot, Israel, for advice.

This paper is the fifth in a series on plant alkaloids.

[x] To whom inquiries should be directed.

Simultaneous Quantitative GLC Determination of Chlorpheniramine Maleate and Phenylpropanolamine Hydrochloride in a Cold Tablet Preparation

R. E. MADSEN [*] and D. F. MAGIN [x]

Abstract □ A GLC method was developed for the simultaneous determinations of chlorpheniramine maleate and phenylpropanolamine hydrochloride in a cold tablet preparation containing a large amount of aspirin. The method utilizes a solid sampling device to eliminate interference from solvent, and it is rapid and precise. The total analysis time is less than 1.5 hr, thereby permitting its use for quality control purposes.

Keyphrases □ Chlorpheniramine maleate—GLC analysis, commercial cold tablets □ Phenylpropanolamine hydrochloride—GLC analysis, commercial cold tablets □ GLC—analysis, simultaneous, chlorpheniramine maleate and phenylpropanolamine hydrochloride, commercial cold tablets □ Dosage forms—commercial cold tablets, simultaneous GLC analysis of chlorpheniramine maleate and phenylpropanolamine hydrochloride

Analyses of chlorpheniramine maleate and phenylpropanolamine hydrochloride have been performed in various formulations by several means. Partition (1, 2), ion-exchange (3), liquid (4), and gas (5) chromatography are among the forms applied to these analyses. The purpose of this study was to develop a rapid, precise, and simple method for the simultaneous determination of chlorpheniramine maleate and phenylpropanolamine

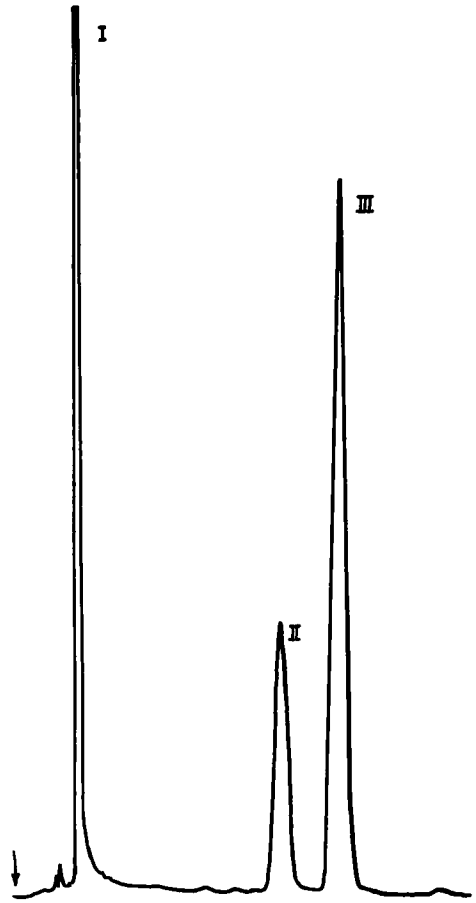

Figure 1—*Separation of phenylpropanolamine (I) and chlorpheniramine (II), using n-tetracosane (III) as an internal standard. Conditions are described in the text.*

hydrochloride in a cold tablet preparation containing a large amount of aspirin. The method is applicable to quality control procedures.

EXPERIMENTAL

Instrumentation—A gas chromatograph[1] fitted with a solid sampling device[2], was equipped with dual flame-ionization detectors. The column used was 1.8 m (6 ft) × 4 mm glass, packed with 3% OV-17 on 100–120-mesh Gas Chrom Q[3]. Helium was used as the carrier gas at a flow rate of 20 ml/min, and the air and hydrogen flows were set to maximize detector response. Temperatures were as follows: injector, 250°; column oven, 230°; and manifold, 250°. The signal was fed to a data processor[4], which calculated the results using the internal standard method.

Standard Solution[5]—Transfer 125.0 mg of reference phenylpropanolamine hydrochloride and 20.0 mg of reference chlorpheniramine maleate to the same 10-ml volumetric flask. Dissolve and dilute to volume with water.

Internal Standard Solution—Transfer 75.0 mg of reference *n*-tetracosane to a 25-ml volumetric flask. Dissolve and dilute to volume with chloroform.

Sample Preparation—Finely grind not less than 20 tablets and transfer a portion equivalent to two tablet weights to a 50-ml glass-stoppered centrifuge tube. Add 10.0 ml of chloroform and mix gently. Add 10 ml of 1 *N* sodium hydroxide, stopper, and shake vigorously for 1 min. Centrifuge to clarify the chloroform layer. Transfer 5.0 ml of the chloroform to a glass-stoppered test tube and evaporate just to dryness on a steam bath with the aid of a stream of air. Redissolve the residue in 1.0 ml of the internal standard solution.

Standard Preparation—Proceed as described for the sample preparation, substituting 2.0 ml of the standard solution for the ground tablet mixture.

Procedure—Transfer 2-μl portions[6] of the sample and standard preparations to separate aluminum capsules of the solid sampling device. Evaporate the chloroform and seal the capsules. Introduce the preparations into the gas chromatograph equilibrated at the given conditions.

The phenylpropanolamine elutes first at a retention time of 0.85 min, the chlorpheniramine next at 4.63 min, and the *n*-tetracosane last at 5.76 min (Fig. 1).

RESULTS AND DISCUSSION

Preliminary experimentation indicated that the solvent (chloroform) must be removed before the phenylpropanolamine content can be determined reproducibly. This step was accomplished through the use of the solid sampling device. No interference was noticed from aspirin in concentrations of 325 mg/tablet.

Verification tests, in triplicate, were run by two analysts on two separate samples of ground tablets. The results indicated amounts of 2.05 mg/tablet of chlorpheniramine maleate (label claim 2.0 mg/tablet) with a range of 2.02–2.08 mg/tablet and a *RSD* of ±1.2%. For the phenylpropanolamine hydrochloride, the value found was 12.22 mg/tablet (label claim 12.5 mg/tablet) with a range of 12.12–12.32 mg/tablet and a *RSD* of ±0.7%.

REFERENCES

(1) "Official Methods of Analysis," 10th ed., Association of Official Analytical Chemists, Washington, D.C., Sections 32.002, 32.013–32.016, 32.072–32.078, 1965.

(2) T. D. Boyle and J. Levine, *J. Ass. Offic. Anal. Chem.*, **51**, 191(1968).

(3) D. J. Smith, *ibid.*, **53**, 116(1970).

(4) A. Menyharth, F. P. Mahn, and J. E. Heveran, *J. Pharm. Sci.*, **63**, 431(1974).

(5) A. C. Celeste and M. V. Polito, *J. Ass. Offic. Anal. Chem.*, **49**, 541(1966).

ACKNOWLEDGMENTS AND ADDRESSES

Received July 18, 1975, from the *Quality Control Department, Winthrop Laboratories, Division of Sterling Drug, Rensselaer, NY 12144*

Accepted for publication September 4, 1975.

* Present address: Sterling Drug, Inc., McPherson, KS 67460

x To whom inquiries should be directed. Present address: Philip Morris Research Center, Richmond, VA 23261

[1] Perkin-Elmer model 900.
[2] Perkin-Elmer model MS-41.
[3] Supelco, Inc., Bellefonte, Pa.
[4] Perkin-Elmer PEP-1.
[5] All reference standards were obtained from Sterling Winthrop Research Institute, Rensselaer, N.Y.

[6] A Hamilton 25-μl syringe equipped with a repeating dispenser was used.

GLC Analysis of Lidocaine in Plasma Using a Novel Nitrogen-Sensitive Detector

H. B. HUCKER ˣ and S. C. STAUFFER

Abstract □ A simple, rapid GLC method for the determination of therapeutic levels of lidocaine in plasma or blood is described. After extraction with benzene from alkalinized plasma, the compound is analyzed by GLC using a nitrogen-sensitive detector. Quantitation is accomplished using an internal standard and a standard curve, which was linear over the 0.1–10-μg range. The limit of detection was approximately 10 ng/ml. Recovery of the parent compound was essentially quantitative. Plasma data are presented to demonstrate the utility of the method.

Keyphrases □ Lidocaine—GLC analysis, plasma or blood □ GLC—analysis, lidocaine, plasma or blood □ Anesthetics, local—lidocaine, GLC analysis, plasma or blood

Lidocaine has long been used as a local anesthetic agent and, in recent years, has been widely employed intravenously in the treatment of ventricular arrhythmias (1). Since desirable pharmacological effects require blood levels of approximately 1.5 μg/ml, whereas toxic side effects are observed at concentrations of 3 μg/ml (1), it is important to monitor lidocaine concentrations in patients undergoing therapy.

Several GLC methods using flame-ionization detection for the quantitative determination of lidocaine have been described (2–5). Assay of the drug by mass fragmentography also has been demonstrated (6). However, the use of a nitrogen detector to measure lidocaine in the GLC effluent appeared to offer advantages of sensitivity, rapidity, and specificity; a procedure for lidocaine using this technology is presented here.

EXPERIMENTAL

Reagents—Benzene[1], lidocaine hydrochloride, and ethylmethylglycinexylidide hydrochloride[2] were used. Drug concentrations were calculated as the free base.

Apparatus—A gas chromatograph fitted with a 1.8-m (6-ft) × 2-mm (i.d.) glass column, packed with 3% OV-17 on Gas Chrom Q (100–120 mesh), and a nitrogen–phosphorus detector were used[3]. Operating temperatures were 200, 260, and 265° for the column oven, injector, and interface (detector), respectively. Flow rates were 50, 4, and 100 ml/min for the carrier gas (helium), hydrogen, and air, respectively. A 1-mv recorder was used[4].

Procedure—Dog or human plasma (1 ml), the internal standard (ethylmethylglycinexylidide, 1 or 5 μg in 0.1 ml of water), 0.5 *N* NaOH (1 ml), and benzene (1 ml) were shaken in a 13-ml glass-stoppered centrifuge tube for 5 min. After centrifugation, 5 μl of the organic phase was injected directly into the chromatographic column[5].

Six male dogs (7.6–10 kg) were anesthetized with pentobarbital and given a continuous intravenous infusion of either 0.06 or 0.25 mg/kg/min of lidocaine in 5% dextrose in water. Blood samples were drawn at specified times into heparinized syringes and immediately centrifuged, and the plasma was separated. The concentration of lidocaine in the plasma was measured by using a calibration curve constructed by analyses of normal plasma spiked with known amounts of lidocaine and plotting the peak height ratio (lidocaine–internal standard) *versus* the lidocaine concentration. The peak height ratio was linearly related to the concentration of lidocaine over a range of 0.1–10 μg of lidocaine/ml of plasma.

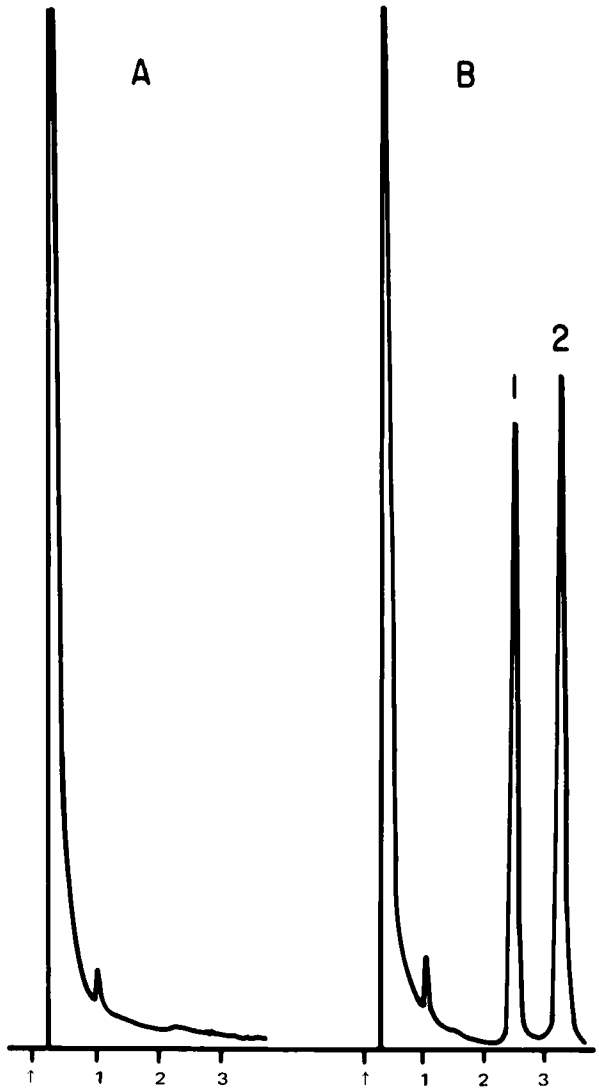

Figure 1—*Chromatograms of: A, a blank plasma extract; and B, an extract of plasma from a dog infused with lidocaine (0.06 mg/kg/min). Sample represents a concentration of 1.20 μg/ml with the equivalent of 6 ng injected. Key: 1, methylethylglycinexylidide (internal standard); and 2, lidocaine. Recorder attenuation was 10 × 5.*

RESULTS AND DISCUSSION

The reproducibility of the method was examined by analysis of plasma samples (1 ml) containing known concentrations of lidocaine (0.1–10 μg/ml) (Table I). The recovery of lidocaine was estimated by

[1] Burdick and Jackson Laboratories, Muskegon, Mich.
[2] Astra Pharmaceutical Products, Worcester, Mass.
[3] Model 3920, Perkin-Elmer Corp., Norwalk, Conn.
[4] Model 56, Leeds & Northrup Co., North Wales, Pa.
[5] Mass spectra were obtained on an LKB-9000S combined gas chromatograph–mass spectrometer. The spectra of the 3.3-min peak attributed to lidocaine in dosed dog plasma were essentially identical to those of authentic drug. A molecular ion was observed at *m/e* 234, and characteristic fragment ions were at *m/e* 219, 163, 148, 120, and 86 (base peak), in accordance with previously reported results (6).

Table I—Precision of Lidocaine Assay by GLC with a Nitrogen Detector

Lidocaine, μg/ml	Peak Height Ratio ± *SD*
0.1	0.08 ± 0.00 (n = 4)
0.5	0.44 ± 0.01 (n = 4)
1.0	0.85 ± 0.04 (n = 6)
2.5	2.10 ± 0.21 (n = 4)
5.0	4.00 ± 0.21 (n = 2)
10.0	8.28 ± 0.10 (n = 2)

comparison of peak heights of lidocaine standards with those obtained after extraction of the drug added to plasma over a concentration range of 0.1–5 μg/ml and was found to be quantitative (100.7 ± 6.6% *SD* for dog plasma and 103.2 ± 6.4% for human plasma). No interfering peaks were present in blank plasma extracts (Fig. 1); the retention times of lidocaine and internal standard were 3.3 and 2.5 min, respectively. The limit of lidocaine detection was approximately 10 ng/ml. Whole blood was as satisfactory for analysis as plasma.

Plasma levels of lidocaine in dogs given the drug by continuous intravenous infusion of different doses are shown in Table II. The levels in each group approached a constant value at 70 min, indicating that steady-state levels had nearly been achieved. Dose and plasma level appeared to be correlated, since increasing the dose by a factor of four caused a nearly proportional rise in plasma concentration.

The results indicate that the present method is satisfactory for routine clinical use, since the blood levels required in humans to achieve antiarrhythmic activity, 1.5 μg/ml (1), are the same as those measured in dogs by the new procedure. The present method would permit rapid monitoring of clinical samples; by avoiding an evaporation step, the entire analysis (using whole blood) may be completed in 10 min or less.

Although the use of a thermionic detector for analysis of other nitrogen-containing drugs was reported previously (7, 8), the nitrogen detector used in the present study is of a substantially different design than previous apparatus; it was described in detail elsewhere (9, 10). The thermionic source, a rubidium silicate glass bead in the new detector, is electrically heated and thus freed from dependence upon the flame as a source of thermal energy. Consequently, detector performance is independent of the heretofore critical factors of shape and temperature of the flame and the area of its contact with the alkali surface (11, 12), with an attendant increase in stability (10). Additional sensitivity is also gained since the hydrogen flow requirement is greatly reduced.

These advantages indicate that GLC analysis of many drugs using the new nitrogen detector is worth investigation. A preliminary report on the analysis of stimulants in this manner appeared previously (13).

During the preparation of this manuscript, two procedures for the determination of lidocaine using a nitrogen detector of conventional design appeared (14, 15). Both procedures entailed more steps than are required using the method described in the present paper.

Table II—Plasma Levels of Lidocaine in Dogs after Continuous Intravenous Infusion of Lidocaine

Minutes	Lidocaine Plasma Concentration[a]	
	Group 1	Group 2
10	3.22 ± 0.14	0.95 ± 0.11
20	3.86 ± 0.11	1.24 ± 0.14
30	4.48 ± 0.25	1.35 ± 0.19
40	4.74 ± 0.29	1.41 ± 0.23
50	4.86 ± 0.11	1.53 ± 0.25
70	5.56 ± 0.84	1.61 ± 0.29

[a] Expressed as micrograms of lidocaine per milliliter of plasma ± *SD*. Group 1 (two dogs) received 0.25 mg of lidocaine/kg/min; Group 2 (three dogs) received 0.06 mg/kg/min.

REFERENCES

(1) D. C. Harrison and E. L. Alderman, *Mod. Treat.*, **9**, 139(1972).

(2) J. B. Keenaghan, *Anesthesiology*, **29**, 110(1968).

(3) J. B. Keenaghan and R. N. Boyes, *J. Pharmacol. Exp. Ther.*, **180**, 454(1972).

(4) G. T. Tucker, *Anesthesiology*, **32**, 255(1970)

(5) G. Svinhufvud, B. Örtengren, and S.-E. Jacobsson, *Scand. J. Clin. Lab. Invest.*, **17**, 162(1965).

(6) J. M. Strong and A. J. Atkinson, *Anal. Chem.*, **44**, 2287(1972).

(7) M. Riedmann, *J. Chromatogr.*, **92**, 55(1974).

(8) D. D. Breimer and J. M. Van Rossum, *ibid.*, **88**, 235(1974).

(9) B. Kolb and J. Bischoff, *J. Chromatogr. Sci.*, **12**, 625(1974).

(10) M. J. Hartigan, J. E. Purcell, M. Novotný, M. L. McConnell, and M. L. Lee, *J. Chromatogr.*, **99**, 339(1974).

(11) S. Lakota and W. A. Aue, *ibid.*, **44**, 472(1969).

(12) K. O. Gerhardt and W. A. Aue, *ibid.*, **52**, 47(1970).

(13) F. L. Vandemark and R. F. Adams, *Clin. Chem.*, **20**, 861(1974).

(14) K. K. Adjepon-Yamoah and L. F. Prescott, *J. Pharm. Pharmacol.*, **26**, 889(1974).

(15) J. D. Cameron, *Clin. Chim. Acta*, **56**, 307(1974).

ACKNOWLEDGMENTS AND ADDRESSES

Received May 22, 1975, from the *Merck Institute for Therapeutic Research, West Point, PA 19486*

Accepted for publication September 4, 1975.

The authors are grateful to Dr. M. L. Torchiana for providing the samples of dog plasma, to J. B. Keenaghan for the gift of ethylmethylglycinexylidide, and Dr. A. G. Zacchei for the mass spectra.

[x] To whom inquiries should be directed.

Synthesis and Antimalarial Activity of Dibenz[c,e]azepine Derivatives

ANN M. WARNER and JOHN L. NEUMEYER ˣ

Abstract □ A series of 6-alkyl-2,10-bis(trifluoromethyl)-5*H*-dibenz[*c,e*]azepines were synthesized *via* a condensation reaction between 5,5′-bis(trifluoromethyl)-2,2′-diformylbiphenyl and the appropriate amine. These compounds were screened for antimalarial activity and were found to be inactive.

Keyphrases □ Dibenz[*c,e*]azepine derivatives—synthesis, antimalarial activity □ Antimalarial agents, potential—dibenz[*c,e*]azepines synthesized and screened □ Structure–activity relationships—dibenz[*c,e*]azepines synthesized and screened for antimalarial activity

A number of aminoalkyl derivatives of 10,11-dihydrodibenz[*b,f*]azepine (1) related to imipramine (I) were prepared and evaluated for their psychotropic activity (2). Other dibenz[*b,e*]azepine derivatives (II) were prepared due to the relationship of such compounds to the antihistamines of the benzylaniline type (3). The dibenz[*c,e*]azepines (III) were investigated primarily for their α-adrenergic blocking activity; one example, azepetine (III*a*), is a potent α-adrenergic blocking agent and has been used to treat peripheral vascular diseases (4).

After completing a study of the antimalarial activity of a series of 9,10-dihydrophenanthrene amino alcohols (5) with 3- and/or 6-trifluoromethyl substituents (IV), it was decided that an investigation of the antimalarial activity of the analogous 6-alkyl-2,10-bis(trifluoromethyl)-5*H*-dibenz[*c,e*]azepine derivatives (III*b*–III*e*) would be of interest.

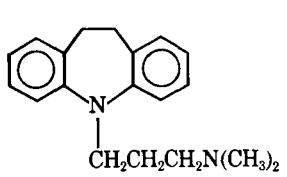

I

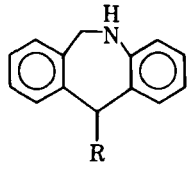

II

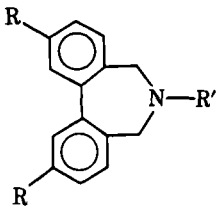

III*a*: R = H, R′ = $CH_2CH{=}CH_2$
III*b*: R = CF_3, R′ = $(CH_2)_3N(CH_2CH_3)_2$
III*c*: R = CF_3, R′ = $CH_2CH{=}CH_2$
III*d*: R = CF_3, R′ = $CH(COOH)CH_2C_6H_5$
III*e*: R = CF_3, R′ = $(CH_2)_4CH(NH_2)COOH$

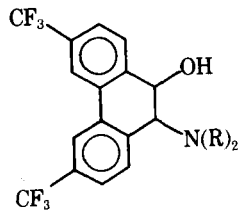

IV

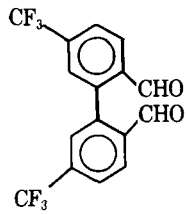

V

EXPERIMENTAL[1]

Biological Activity—The dibenz[*c,e*]azepine derivatives (III*b*–III*e*) were tested for antimalarial activity using mice infected with *Plasmodium berghei*[2] or chicks infected with *P. gallinaceum*. None of the compounds tested caused any increase in mean survival time of more than 2 days in the mouse screen, and they were considered inactive in the chick screen. The compounds tested were not lethal to mice at the dosages tested (640 mg/kg).

Chemistry—Compounds III*b*–III*e* were prepared by allowing 5,5′-bis(trifluoromethyl)-2,2′-diformylbiphenyl (V) to react with an appropriate amine in the presence of sodium hydrosulfite by the procedure of Hawthorne *et al.* (6). The dialdehyde V was prepared by the ozonolysis of 3,6-bis(trifluoromethyl)phenanthrene by the procedure described (5).

*6-(3-Diethylaminopropyl)-6,7-dihydro-2,10-bis(trifluoromethyl)-5*H*-dibenz*[c,e]*azepine Dihydrochloride* (*III*b)—According to the procedure of Hawthorne *et al.* (6), V (1.7 g, 0.005 mole) was allowed to react with *N,N*-diethylaminopropylamine (1.3 g, 0.01 mole) and sodium hydrosulfite (6.0 g, 0.038 mole). The reaction mixture was extracted with chloroform (3 × 25 ml), and the chloroform solution was dried (sodium sulfate) and treated with 50 ml of saturated chloroform–hydrochloric acid. The resulting solution was taken to dryness *in vacuo*, yielding 2.3 g (88%) of hygroscopic crystalline material, mp 108°; NMR: δ 7.2–7.8 (m), 3.4 (s), 2.5 (q), and 0.9–2.0 (m) ppm.

Anal.—Calc. for $C_{23}H_{26}F_6N_2{\cdot}2HCl{\cdot}\frac{1}{2}H_2O$: C, 52.26; H, 5.52; N, 5.30. Found: C, 52.26; H, 5.46; N, 5.20.

*6-(2-Propenyl)-6,7-dihydro-2,10-bis(trifluoromethyl)-5*H*-dibenz*[c,e]*azepine Hydrochloride* (*III*c)—Compound III*c* was similarly prepared from V (2.0 g, 0.006 mole) and allylamine (0.76 g, 0.017 mole). The mixture was extracted with ether, dried (sodium sulfate), and evaporated *in vacuo* to give a pale-yellow solid. This solid was recrystallized from carbon tetrachloride, mp 202–206°, redissolved in ether, and treated with ether–hydrochloric acid. The ether was removed *in vacuo* to give a yellow solid which was washed with carbon tetrachloride and then sublimed (110°/0.5 mm) to give 1.6 g (74%) of white crystals, mp 120° (sintering), 185–187° (clear melt); NMR: δ 7.4–7.8 (m), 5.0–6.2 (m), and 3.2–3.5 (m) ppm.

Anal.—Calc. for $C_{19}H_{16}ClF_6N{\cdot}\frac{1}{2}H_2O$: C, 54.75; H, 4.11; N, 3.36. Found: C, 55.12; H, 4.24; N, 3.13.

L-*6-(1-Benzyl-1-carboxyethyl)-6,7-dihydro-2,10-bis(trifluoromethyl)-5*H*-dibenz*[c,e]*azepine* (*III*d)—This compound was similarly prepared from V (1.0 g, 0.003 mole), L-phenylalanine (0.71 g, 0.004 mole), and sodium hydrosulfite (3.3 g, 0.018 mole). This mixture was allowed to react in methanol (20 ml) and phosphate buffer (25 ml, pH 7.6) at reflux for 12 hr. The reaction mixture was then cooled and acidified to pH 5 with 5% aqueous hydrochloric acid. The precipitate was collected and washed with 5% aqueous hydrochloric acid, water, and ether to give white crystals. The product, III*d*, was recrystallized from acetone to give 1.1 g (79%), mp 207–207.5°; NMR: δ 7.2–8.3 (m) and 3.4–4.8 (m) ppm.

[1] Melting points were determined on a Thomas-Hoover melting-point apparatus and are uncorrected. The microanalyses were determined by Galbraith Laboratories, Inc., Knoxville, Tenn. NMR spectra were recorded on a Varian T-60 spectrometer, with tetramethylsilane as the internal standard. Spectral data were recorded on a Beckman IR-10 spectrometer, and UV spectra were recorded with a Beckman DB-G grating spectrophotometer.

[2] Tests were carried out in five mice infected with *P. berghei* at 40, 160, and 640 mg/kg in the screening facility of Dr. L. Rane of the University of Miami. Chicks were infected with *P. gallinaceum* fatal to 100% of untreated controls within 3–4 days. An increase of at least 100% survival time of treated animals was considered as active (7).

Anal.—Calc. for $C_{25}H_{19}F_6NO_2$: C, 62.63; H, 3.99; N, 2.92. Found: C, 62.66; H, 4.20; N, 3.24.

L-*6-(5-Amino-5-carboxypentyl)-6,7-dihydro-2,10-bis(trifluoromethyl)-5H-dibenz*[c,e]*azepine Dihydrobromide* (*IIIe*)—α-Carbobenzoxy-L-lysine (1.29 g, 0.004 mole), 1.52 g (0.004 mole) of V, and sodium hydrosulfite (5.3 g, 0.03 mole) were allowed to react by the procedure of Hawthorne *et al.* (6). The reaction mixture was filtered to give a white solid, which was recrystallized from acetone to give 0.5 g (19%), mp 199–201°. This solid was treated with 5 ml of hydrobromic acid–acetic acid (30–32%) at room temperature for 1 hr. Upon addition of ether, the product precipitated and was collected. Recrystallization from ethanol–ether gave 0.43 g (93%) of white powder, mp 230–232°; NMR: δ 7.4–8.0 (m), 5.0–5.5 (m), 3.4–4.2 (m), 2.8–3.2 (m), and 1.0–2.1 (m) ppm.

Anal.—Calc. for $C_{22}H_{22}F_6N_2O_2 \cdot 2HBr$: C, 42.47; H, 3.89; N, 4.50. Found: C, 43.07; H, 4.28; N, 4.53.

REFERENCES

(1) L. J. Kricka and A. Ledwith, *Chem. Rev.*, **74**, 101(1974), and references cited therein.

(2) F. Hafliger and V. Burckhardt, in "Psychopharmacological Agents," vol. 1, M. Gordon, Ed., Academic, New York, N.Y., 1964, chap. 3.

(3) M. Protiva, *Farmaco, Ed. Sci.*, **21**, 76(1966).

(4) W. Wenner, *J. Org. Chem.*, **16**, 1475(1951); *ibid.*, **17**, 523, 1451(1952).

(5) A. S. Dey and J. L. Neumeyer, *J. Med. Chem.*, **17**, 1095(1974).

(6) J. Hawthorne, E. Mehelic, M. Morgan, and M. Witt, *J. Org. Chem.*, **28**, 2831(1963).

(7) T. S. Osdene, P. B. Russell, and L. Rane, *J. Med. Chem.*, **10**, 431(1967).

ACKNOWLEDGMENTS AND ADDRESSES

Received July 14, 1975, from the *Department of Medicinal Chemistry and Pharmacology, College of Pharmacy and Allied Health Professions, Northeastern University, Boston, MA 02115*

Accepted for publication September 10, 1975.

Supported in part by National Institutes of Health Grant 5F026M 21065.

The authors thank Dr. E. A. Steck of the Walter Reed Army Institute of Research for making available the results of the antimalarial screening data.

ˣ To whom inquiries should be directed.

Synthesis and Activity of (*R*)-(−)-*m*-Trimethylacetoxy-α-[(methylamino)methyl]benzyl Alcohol Hydrochloride: A Prodrug Form of (*R*)-(−)-Phenylephrine

SUN-SHINE YUAN and NICOLAE BODOR ˣ

Abstract □ Optically pure (*R*)-(−)-*m*-trimethylacetoxy-α-[(methylamino)methyl]benzyl alcohol hydrochloride was synthesized by the following sequence: (*R*)-(−)-phenylephrine was condensed with acetone in the presence of calcium carbide to give an oxazolidine derivative and then treated with thallous ethoxide in ether followed by trimethylacetyl chloride to yield the phenolic ester. Finally, the oxazolidine ring was cleaved by one equivalent of hydrogen chloride in ethanol. Condensation of phenylephrine with benzaldehyde, with or without solvents, gave either 1,1,2-trimethyl-4,6-dihydroxy-1,2,3,4-tetrahydroisoquinoline or a mixture of side-chain oxazolidine and the tetrahydroisoquinoline. Condensation of epinephrine with opianic acid in pyridine also gave a tetrahydroisoquinoline only. When applied on rabbit eyes, the prodrug (*R*)-(−)-*m*-trimethylacetoxy-α-[(methylamino)methyl]benzyl alcohol hydrochloride exhibited an unexpected, three times higher mydriatic activity than the corresponding racemic prodrug and was 15 times more active than the parent, (*R*)-(−)-phenylephrine.

Keyphrases □ Phenylephrine prodrug—(*R*)-(−)-*m*-trimethylacetoxy-α-[(methylamino)methyl]benzyl alcohol hydrochloride synthesized, mydriatic activity screened □ Prodrugs—(*R*)-(−)-*m*-trimethylacetoxy-α-[(methylamino)methyl]benzyl alcohol hydrochloride synthesized, mydriatic activity screened □ Mydriatic agents, potential — (*R*)-(−)-*m*-trimethylacetoxy-α-[(methylamino)methyl]benzyl alcohol hydrochloride synthesized and screened

Phenylephrine, *m*-hydroxy-α-[(methylamino)-methyl]benzyl alcohol, is a well-known sympathomimetic amine and is used topically as a nasal decongestant and as a mydriatic. Its levorotatory isomer is generally used because, as in the case of other adrenergic agents, the (*R*)-(−)-form is significantly (about 10 times) more potent (1) than the dextro-form. Therefore, the racemic mixture is about one-half as active as the (*R*)-(−)-form. High therapeutic concentrations (up to 10%) even of the (*R*)-(−)-form must, however, be used topically because of the low permeability of the molecule due to its polar, hydrophilic functions. Consequently, only small portions of the relatively high concentration solutions used are absorbed topically (for example, transcorneally).

To overcome this disadvantage, the use of more lipophilic prodrugs[1] (2) was suggested (3). Indeed, one corresponding racemic ester, *m*-trimethylacetoxy-α-[(methylamino)methyl]benzyl alcohol, was shown to possess higher biological activity and greater stability than the parent drug, (*R*)-(−)-phenylephrine, as a result of the greater lipid solubility and the masking of the labile phenolic hydroxyl group. As shown later, the increase in biological activity is significant; the racemic prodrug is about five times more effective as a mydriatic than the (*R*)-(−)-phenylephrine [the same mydriatic effect could be achieved with a 0.5% solution of (±)-prophenylephrine as with a 2.5% solution of (−)-phenylephrine solution]. As in the case of the parent drug,

[1] The expression "prodrug" denotes a derivative of a known and proven drug, which, due to its improved physicochemical properties, increases the bioavailability of the proven drug. The derivative is transformed by an enzymatic or chemical process into the proven drug before reaching it and/or at the site(s) of action. As applied in the present context, an improved form of phenylephrine is a prodrug form which, due to its improved topical (*i.e.*, corneal) absorptivity, increases the topical bioavailability of the drug. After absorption, the drug is released by an enzymatic and/or chemical process. See, for example, Ref. 2.

Anal.—Calc. for $C_{25}H_{19}F_6NO_2$: C, 62.63; H, 3.99; N, 2.92. Found: C, 62.66; H, 4.20; N, 3.24.

L-*6-(5-Amino-5-carboxypentyl)-6,7-dihydro-2,10-bis(trifluoromethyl)-5H-dibenz*[c,e]*azepine Dihydrobromide* (*IIIe*)—α-Carbobenzoxy-L-lysine (1.29 g, 0.004 mole), 1.52 g (0.004 mole) of V, and sodium hydrosulfite (5.3 g, 0.03 mole) were allowed to react by the procedure of Hawthorne *et al.* (6). The reaction mixture was filtered to give a white solid, which was recrystallized from acetone to give 0.5 g (19%), mp 199–201°. This solid was treated with 5 ml of hydrobromic acid–acetic acid (30–32%) at room temperature for 1 hr. Upon addition of ether, the product precipitated and was collected. Recrystallization from ethanol–ether gave 0.43 g (93%) of white powder, mp 230–232°; NMR: δ 7.4–8.0 (m), 5.0–5.5 (m), 3.4–4.2 (m), 2.8–3.2 (m), and 1.0–2.1 (m) ppm.

Anal.—Calc. for $C_{22}H_{22}F_6N_2O_2 \cdot 2HBr$: C, 42.47; H, 3.89; N, 4.50. Found: C, 43.07; H, 4.28; N, 4.53.

REFERENCES

(1) L. J. Kricka and A. Ledwith, *Chem. Rev.*, **74**, 101(1974), and references cited therein.

(2) F. Hafliger and V. Burckhardt, in "Psychopharmacological Agents," vol. 1, M. Gordon, Ed., Academic, New York, N.Y., 1964, chap. 3.

(3) M. Protiva, *Farmaco, Ed. Sci.*, **21**, 76(1966).

(4) W. Wenner, *J. Org. Chem.*, **16**, 1475(1951); *ibid.*, **17**, 523, 1451(1952).

(5) A. S. Dey and J. L. Neumeyer, *J. Med. Chem.*, **17**, 1095(1974).

(6) J. Hawthorne, E. Mehelic, M. Morgan, and M. Witt, *J. Org. Chem.*, **28**, 2831(1963).

(7) T. S. Osdene, P. B. Russell, and L. Rane, *J. Med. Chem.*, **10**, 431(1967).

ACKNOWLEDGMENTS AND ADDRESSES

Received July 14, 1975, from the *Department of Medicinal Chemistry and Pharmacology, College of Pharmacy and Allied Health Professions, Northeastern University, Boston, MA 02115*

Accepted for publication September 10, 1975.

Supported in part by National Institutes of Health Grant 5F026M 21065.

The authors thank Dr. E. A. Steck of the Walter Reed Army Institute of Research for making available the results of the antimalarial screening data.

ˣ To whom inquiries should be directed.

Synthesis and Activity of (*R*)-(−)-*m*-Trimethylacetoxy-α-[(methylamino)methyl]benzyl Alcohol Hydrochloride: A Prodrug Form of (*R*)-(−)-Phenylephrine

SUN-SHINE YUAN and NICOLAE BODOR ˣ

Abstract □ Optically pure (*R*)-(−)-*m*-trimethylacetoxy-α-[(methylamino)methyl]benzyl alcohol hydrochloride was synthesized by the following sequence: (*R*)-(−)-phenylephrine was condensed with acetone in the presence of calcium carbide to give an oxazolidine derivative and then treated with thallous ethoxide in ether followed by trimethylacetyl chloride to yield the phenolic ester. Finally, the oxazolidine ring was cleaved by one equivalent of hydrogen chloride in ethanol. Condensation of phenylephrine with benzaldehyde, with or without solvents, gave either 1,1,2-trimethyl-4,6-dihydroxy-1,2,3,4-tetrahydroisoquinoline or a mixture of side-chain oxazolidine and the tetrahydroisoquinoline. Condensation of epinephrine with opianic acid in pyridine also gave a tetrahydroisoquinoline only. When applied on rabbit eyes, the prodrug (*R*)-(−)-*m*-trimethylacetoxy-α-[(methylamino)methyl]benzyl alcohol hydrochloride exhibited an unexpected, three times higher mydriatic activity than the corresponding racemic prodrug and was 15 times more active than the parent, (*R*)-(−)-phenylephrine.

Keyphrases □ Phenylephrine prodrug—(*R*)-(−)-*m*-trimethylacetoxy-α-[(methylamino)methyl]benzyl alcohol hydrochloride synthesized, mydriatic activity screened □ Prodrugs—(*R*)-(−)-*m*-trimethylacetoxy-α-[(methylamino)methyl]benzyl alcohol hydrochloride synthesized, mydriatic activity screened □ Mydriatic agents, potential — (*R*)-(−)-*m*-trimethylacetoxy-α-[(methylamino)methyl]benzyl alcohol hydrochloride synthesized and screened

Phenylephrine, *m*-hydroxy-α-[(methylamino)-methyl]benzyl alcohol, is a well-known sympathomimetic amine and is used topically as a nasal decongestant and as a mydriatic. Its levorotatory isomer is generally used because, as in the case of other adrenergic agents, the (*R*)-(−)-form is significantly (about 10 times) more potent (1) than the dextro-form. Therefore, the racemic mixture is about one-half as active as the (*R*)-(−)-form. High therapeutic concentrations (up to 10%) even of the (*R*)-(−)-form must, however, be used topically because of the low permeability of the molecule due to its polar, hydrophilic functions. Consequently, only small portions of the relatively high concentration solutions used are absorbed topically (for example, transcorneally).

To overcome this disadvantage, the use of more lipophilic prodrugs[1] (2) was suggested (3). Indeed, one corresponding racemic ester, *m*-trimethylacetoxy-α-[(methylamino)methyl]benzyl alcohol, was shown to possess higher biological activity and greater stability than the parent drug, (*R*)-(−)-phenylephrine, as a result of the greater lipid solubility and the masking of the labile phenolic hydroxyl group. As shown later, the increase in biological activity is significant; the racemic prodrug is about five times more effective as a mydriatic than the (*R*)-(−)-phenylephrine [the same mydriatic effect could be achieved with a 0.5% solution of (±)-prophenylephrine as with a 2.5% solution of (−)-phenylephrine solution]. As in the case of the parent drug,

[1] The expression "prodrug" denotes a derivative of a known and proven drug, which, due to its improved physicochemical properties, increases the bioavailability of the proven drug. The derivative is transformed by an enzymatic or chemical process into the proven drug before reaching it and/or at the site(s) of action. As applied in the present context, an improved form of phenylephrine is a prodrug form which, due to its improved topical (*i.e.*, corneal) absorptivity, increases the topical bioavailability of the drug. After absorption, the drug is released by an enzymatic and/or chemical process. See, for example, Ref. 2.

a further increase in the relative potency can be expected by using the corresponding pivalate derivative of the levorotatory isomer, which should be about 10 times more potent than the parent (−)-phenylephrine.

Since there is no direct way for selective acylation of the phenolic hydroxyl group in phenylephrine, the (±)-pivalylphenylephrine was prepared (3) by reduction of the acylated *N*-benzylketone precursor. Resolving the racemic pivalate would be an unreliable way for obtaining the (*R*)-(−)-form, since it would be difficult to prevent the cleavage of the ester function during the resolution, particularly during the epimerization step in recycling.

This paper reports an easy synthetic procedure for preparing the optically pure (*R*)-(−)-enantiomer of *m*-pivalylphenylephrine as well as its comparative mydriatic effectiveness.

DISCUSSION

Chemistry—The synthetic scheme started from the optically active (*R*)-(−)-phenylephrine (I, Scheme I), in which the ethanolamine side chain was protected by the formation of an oxazolidine ring (4) as the result of the reaction with a ketone such as acetone. Compound II was easily formed using calcium carbide (5) as a dehydrating agent. The oxazolidine (II) was treated with thallous ethoxide in ether (6), and the formed thallous salt was reacted without isolation with trimethylacetyl chloride to afford the ester (III). The oxazolidine ring was then cleaved using one equivalent of hydrogen chloride in ethanol to give the optically active prodrug (IV). The optical purity of IV was confirmed by hydrolyzing it back to the parent, (*R*)-(−)-phenylephrine hydrochloride, and no change in the original optical rotation was observed.

Scheme I obviously can be used for the synthesis of the racemic derivative and for the preparation of other esters by replacing the pivalyl chloride with the corresponding acyl halide.

Contrary to these results, Kametani *et al.* (7) showed that the condensation of phenylephrine and acetone in alcoholic solvents did not result in the oxazolidine (II) but the tetrahydroisoquinoline isomer (V). On the other hand, Bretschneider (8) observed that the condensation of phenylephrine with cyclohexane, used also as the solvent, at higher temperature resulted in the oxazolidine (VI) in good yield.

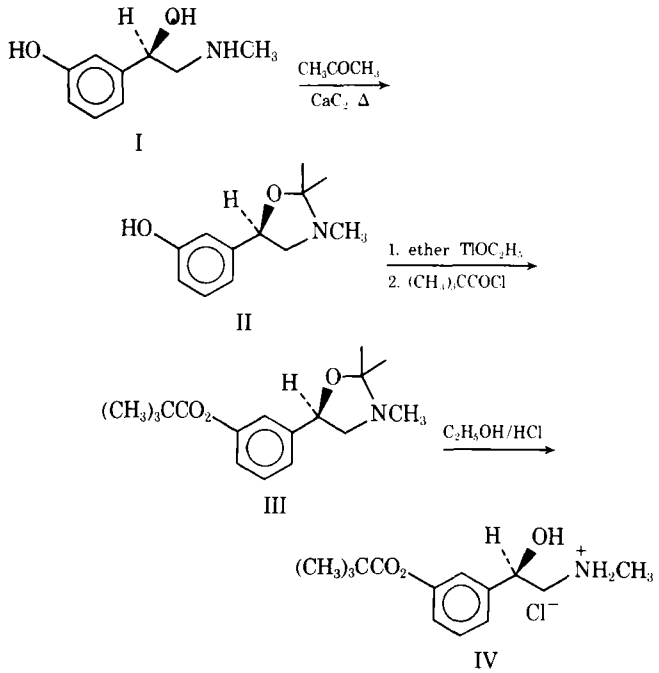

Scheme I

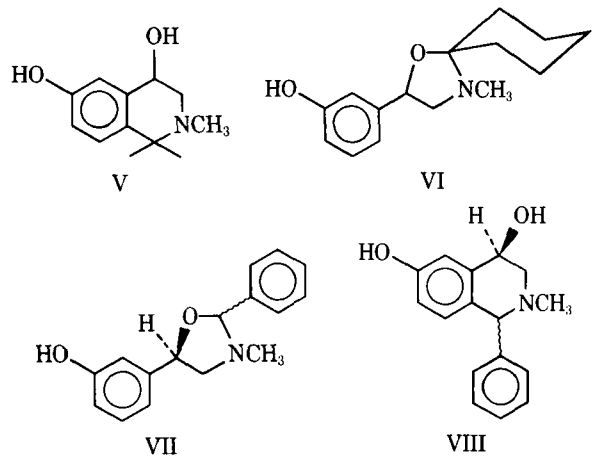

The preparation of the oxazolidine (VII) was recently reported (9) from benzaldehyde and phenylephrine. However, when using the experimental conditions given, the present authors found that a 1:1 mixture of VII and the tetrahydroisoquinoline (VIII) was formed. The condensation products were always formed exclusively in neat benzaldehyde or in pyridine as a solvent.

The analogous condensation of epinephrine with opianic acid in pyridine, as reported by Bretschneider (8), was reexamined. It was found that the product was not the oxazolidine (IX), as suggested by Bretschneider (8), but the tetrahydroisoquinoline (X), as clearly supported by the NMR spectrum (1 *M* Na_2CO_3 in D_2O): δ 7.1 (s, 2, C-5′ and C-6′), 6.8 (s, 1, C-5), 6.1 (s, 1, C-6), 5.2 (m, 1, C*H*OH), 4.4 (s, 1, CHN), 3.9 (s, 6, OCH_3), 3.2–2.6 (*ABX*, 2, CH_2N), and 2.2 (s, 3, NCH_3) ppm.

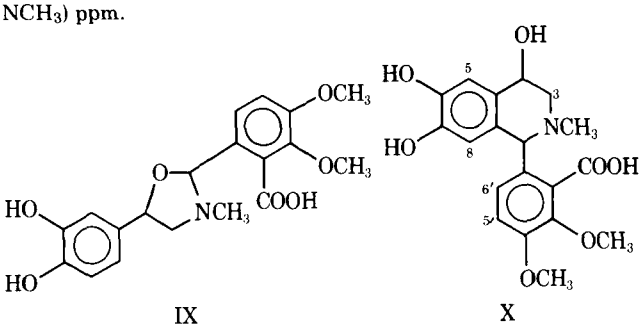

Mydriatic Activity—The mydriatic effectiveness of the pivalate (IV) thus prepared was then studied to confirm the expected increased activity as compared to (*R*)-(−)-phenylephrine and to the (*R,S*)-(±)-pivalate. The mydriatic activity was studied by measuring the change in pupillary diameters of male and female white rabbit eyes as a function of time and dose, following instillation of 50 μl of isotonic solutions of the compounds studied. Figure 1 shows the comparison

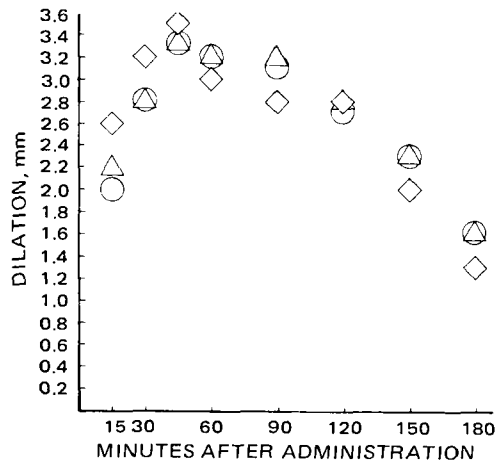

Figure 1—*Equivalent mydriatic responses of rabbit eyes elicited by (−)- and (±)-m-pivalylphenylephrine hydrochloride (prodrug) and (−)-phenylephrine hydrochloride solutions. Key: ○, 0.15% (−)-prodrug; △, 0.5% (±)-prodrug; and ◇, 2.5% (−)-phenylephrine.*

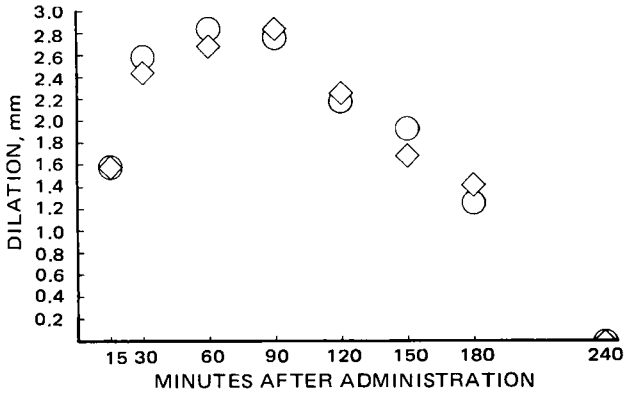

Figure 2—*Equivalent mydriatic responses of rabbit eyes elicited by (−)- and (±)-m-pivalylphenylephrine hydrochloride (prodrug) solutions. Key: ◇, 0.1% (−)-prodrug; and ○, 0.3% (±)-prodrug.*

of 2.5% of (*R*)-(−)-phenylephrine hydrochloride[2], 0.5% of (*R,S*)-*m*-trimethylacetoxy-α-[(methylamino)methyl]benzyl alcohol hydrochloride, and 0.15% of (*R*)-(−)-*m*-trimethylacetoxy-α-[(methylamino)methyl]benzyl alcohol hydrochloride.

All compounds tested elicited practically the same mydriatic effect at the concentrations studied, which proves the significant increase in activity by pivalation of the *m*-hydroxyl group of phenylephrine. However, it is surprising that the (*R*)-form was approximately three times more active than the racemic (*R,S*)-pivalate. To verify this unexpected result, numerous studies were performed using other concentrations (Fig. 2). The data verify that the (*R*)-(−)-form is indeed three times more active than the racemic form and, thus, about 15 times more potent a mydriatic as the free (*R*)-(−)-phenylephrine. The free (*R*)-(−)-phenylephrine is faster acting, although the effect decreases faster.

EXPERIMENTAL[3]

(*R*)-(−)-2,2,3-Trimethyl-5-(*m*-hydroxyphenyl)-1,3-oxazolidine (II)—(*R*)-(−)-Phenylephrine (I) (9.0 g, 0.05 mole), acetone (1 liter), and calcium carbide (4.0 g, 0.06 mole) were heated together at reflux with stirring for 24 hr. The solid material formed was filtered off, and the filtrate was concentrated *in vacuo*. The residue was crystallized in an acetone–hexane mixture to give 7.0 g of II (70%), mp 118–120°, $[\alpha]_D^{25}$ −17.9° (c 5, CH_3OH); IR (KBr): 2980, 2860, 2700, 1600, 1450, 1260, and 1120 cm^{-1}; NMR (CD_3COCD_3): δ 7.4–6.6 (m, 4), 5.2 (broad, 1), 5.0 (t, 1, J = 7 Hz), 3.3 (dd, 1, J = 7 and 9 Hz), 2.7 (dd, 1, J = 7 and 9 Hz), 2.4 (s, 3), and 1.3 (s, 6) ppm.

Anal.—Calc. for $C_{12}H_{17}NO_2$: C, 69.6; H, 8.2; N, 6.8. Found: C, 70.0; H, 8.4; N, 6.7.

A solution of II in methanol was stored at room temperature for 12 hr. After evaporating the solvent, pure (*R*)-(−)-phenylephrine was isolated.

(*R*) - (−) - 2,2,3-Trimethyl-5-(*m*-trimethylacetoxyphenyl)-1,3-oxazolidine (III)—To a solution of II (1.32 g, 6.38 mmoles) in 60 ml of ether was added thallous ethoxide (1.59 g, 6.38 mmoles), and the mixture was stirred at room temperature for 1 hr. Pivalyl chloride (0.79 ml, 6.38 mmoles) was then added, and stirring was maintained for 2 additional hr. The solid material formed in the reaction was filtered, and the filtrate was evaporated to dryness to give 1.8 g of an oily product, III (95%); $[\alpha]_D^{25}$ −10.6° (c 5, C_2H_5OH); IR (neat): 2960, 1760, 1610, 1590, 1480, 1450, 1370, 1360, 1260, 1230, 1140, and 1105 cm^{-1}; NMR (CCl_4): δ 7.4–6.8 (m, 4), 5.0 (t, 1, J = 7 Hz), 3.3 (dd, 1, J = 7 and 9 Hz), 2.8 (dd, 1, J = 7 and 9 Hz), 2.3 (s, 3), 1.4 (s, 9), and 1.3 (s, 6) ppm.

Anal.—Calc. for $C_{17}H_{25}NO_3$: C, 70.2; H, 8.6; N, 4.8. Found: C, 70.1; H, 8.8; N, 4.9.

(*R*)-(−)-*m*-(Trimethylacetoxy)-α-[(methylamino)methyl]benzyl Alcohol Hydrochloride (IV)—Compound III (1.8 g, 6.2 mmoles) in 60 ml of ether was treated with hydrogen chloride gas until the solution was no longer turbid. This mixture was then evaporated to dryness, and the residue was dissolved in a small amount of ethanol and then diluted with hexane. The hydrolysis and crystallization took place in the solution to give 1.2 g of the final product, IV (70%), mp 128–130°; $[\alpha]_D^{25}$ −36.7° (c 5, C_2H_5OH); IR (KBr): 3370, 2960, 2795, 2420, 1750, 1610, 1590, 1460, 1240, and 1110 cm^{-1}; NMR (CD_3COCD_3–D_2O): δ 7.5–6.8 (m, 4), 5.3 (dd, 1, J = 5 and 10 Hz), 3.8 (broad, 3), 3.4 (m, 2), 2.9 (s, 3), and 1.4 (s, 9) ppm.

Anal.—Calc. for $C_{14}H_{22}ClNO_3$: C, 58.4; H, 7.7; N, 4.9. Found: C, 58.4; H, 7.7; N, 4.6.

A solution of IV (1 g) in 10 ml of methanol containing 1 ml of concentrated hydrochloric acid was heated to reflux for 24 hr. The solvent was then removed *in vacuo* to give 0.7 g (90% yield) of (*R*)-(−)-phenylephrine hydrochloride, $[\alpha]_D^{25}$ −47.0° (c 5, C_2H_5OH) [lit. (10) $[\alpha]_D^{25}$ −46.2° (c 1)].

Condensation of Phenylephrine and Benzaldehyde—Racemic phenylephrine (0.83 g, 5 mmoles), benzaldehyde (0.55 ml, 5 mmoles), and benzene (100 ml) were placed in a flask attached with a Dean–Stark trap. The mixture was heated to reflux for 8 hr until 0.1 ml of water was collected. The solvent was partially removed, and the oxazolidine (VII) crystallized first (0.5 g, 38%), mp 215° dec.; IR (KBr): 3200, 1600, 1480, 1290, 1050, and 1000 cm^{-1}; NMR (CD_3COCD_3): δ 10.9 (m, 1), 7.4–6.5 (m, 9), 4.8 (m, 1, C-5), 4.6 (s, 1, C-2), 3.2–2.5 (m, 2, CH_2N), and 2.3 (s, 3, NCH_3) ppm.

The mother liquor was then evaporated to give 0.5 g (38%) of VIII, mp 110–112° [lit. (7) mp 90°]; IR (KBr): 3600, 3240, 2400, 1620, 1510, 1460, 1330, 1310, and 1240 cm^{-1}; NMR (CD_3COCD_3): δ 7.4–7.0 (m, 7), 6.4 (s, 1), 5 (m, 1), 4.2 (s, 1), 3.2 (m, 1, OH), 3.2 (m, 1), 2.5 (m, 1) and 2.2 (s, 3, NCH_3) ppm.

Condensation of Epinephrine with Opianic Acid—Racemic epinephrine (183 mg, 1 mmole) and opianic acid (210 mg, 1 mmole) were heated along with pyridine (10 ml) at 80–90° for 2 hr. After cooling, the product crystallized to give 150 mg of IX (40%), mp 245° dec. [lit. (8) mp 230° dec.); IR (KBr): 3500, 2460, 1610, 1580, 1530, 1480, 1450, 1420, 1380, 1280, 1260, and 1060 cm^{-1}. As in Bretschneider's study (8), purification attempts did not yield analytically pure material.

Mydriatic Experiments—Solutions of IV, the (*R,S*)-isomer of IV (3), and (*R*)-(−)-phenylephrine hydrochloride were prepared by dissolving the material in 0.9% saline solution. Standard doses of 50 μl were applied to male and female rabbit eyes, and pupillary changes were measured in a light- and temperature-controlled room. Amounts of dilation, in millimeters, were measured at 15-min intervals in the 1st hr and at 30-min intervals thereafter. The differences in the same animal between the pupil diameter of the eye with drug applied against the other eye with saline were observed. Each point is the average of five and/or six independent experiments.

REFERENCES

(1) A. M. Lands, V. L. Nash, H. R. Granger, and B. L. Dertinger, *J. Pharmacol. Exp. Ther.*, **89**, 382(1947).

(2) A. A. Sinkula and S. H. Yalkowsky, *J. Pharm. Sci.*, **64**, 181(1975).

(3) A. A. Hussain and J. E. Truelove, U.S. pat. 3,825,583 (July 23, 1974).

(4) R. Kelly and V. VanRheenen, *Tetrahedron Lett.*, **1973**, 1709.

(5) M. M. Maglio and C. A. Burger, *J. Am. Chem. Soc.*, **68**, 529(1946).

(6) E. C. Taylor, G. W. McLay, and A. McKillop, *ibid.*, **90**, 2422(1968).

(7) T. Kametani, F. Saton, H. Agui, K. Ueki, K. Kagasawa, M. Hiiragi, H. Ishimaru, and S. Horie, *Chem. Pharm. Bull.*, **18**, 1161(1970).

(8) H. Bretschneider, *Monatsch.*, **77**, 117(1947).

(9) L. Neelakantan, *J. Org. Chem.*, **36**, 2256(1971).

(10) "Dictionary of Organic Compounds," 4th ed., Oxford University Press, New York, N.Y., 1965.

ACKNOWLEDGMENTS AND ADDRESSES

Received August 4, 1975, from *INTERx Research Corporation, Lawrence, KS 66044*

Accepted for publication September 5, 1975.

The authors thank Mr. Richard Roller for help in determining the mydriatic activity of the various compounds.

[x] To whom inquiries should be directed.

[2] Neo-Synephrine.

[3] Melting points were taken in a Thomas Hoover capillary melting-point apparatus and are uncorrected. NMR spectra were measured in a Varian T-60 NMR spectrometer. IR spectra were taken in a Beckman 33 instrument. Optical rotations were measured using a Carl Zeiss polarimeter. Elemental analyses were performed by the medicinal chemistry laboratory of the University of Kansas, Lawrence, Kans.

Loss of Fluoride during Tablet Production

Keyphrases □ Fluoride—content in tablets prepared by wet granulation method, effect of processing, dyes, flavors, citric acid, and lubricants □ Tablets—wet granulation preparation, fluoride content, effect of processing, dyes, flavors, citric acid, and lubricants □ Dosage forms—tablets, wet granulation preparation, fluoride content, effect of processing, dyes, flavors, citric acid, and lubricants

To the Editor:

In response to a request from the College of Dentistry of the University of Iowa, colored and flavored chewable tablets containing 0.25, 0.50, and 1.00 mg of fluoride ion were designed and manufactured in lots of 10,000. Since most commercial fluoride tablets are small (approximately 100 mg), the concept was to design large, hard tablets that would require a strong bite followed by chewing to crush them and concomitantly to impact particles into the crevices of the teeth. Therefore, the fluoride would be available in the oral cavity for a longer time than is provided by a conventional tablet that is swallowed intact. To enhance chewing and appeal, flavors and colors were added.

After preliminary formulation, a 600-mg cherry-flavored tablet containing 1.0 mg of fluoride was selected for evaluation. The tablets were prepared by the wet granulation method. Mannitol, sodium fluoride, and saccharin sodium were blended in a twin-shell blender[1], granulated with a gelatin solution, and passed through a mill[2]. The wet granulation was dried in an oven[3] at 50° for 6 hr, and the dried granulation then was passed through a mill[2].

Magnesium stearate, colloidal silica[4], spray-dried stearic acid, and commercial flavor were blended with the dry granulation. Tablets were prepared with a single-punch tablet machine[5] and compressed to a hardness of 20 ± 1 kg using a 1.27-cm punch and die set. The fluoride content was within compendial specifications as assayed by the USP method (1) and the method of Daines and Morse (2).

By using this basic formulation, tablets with other flavors and dyes were prepared and then evaluated by a panel of children[6]. Because orange and lemon-lime were the most popular flavors, orange tablets containing 0.25 mg of fluoride and lemon-lime tablets containing 0.50 mg of fluoride were prepared in developmental lots of 10,000. Although operational and physical characteristics were satisfactory, analysis showed that these tablets contained less than 50% of the intended amount of fluoride.

Since the three formulations were similar except for the dyes, flavors, and flavor enhancer (citric acid), solutions were prepared of all three formulations and of each formulation omitting singularly the dye, flavor, citric acid, magnesium stearate, stearic acid, or colloidal silica. Analysis by specific ion electrode and chemical assays showed that the desired amount of fluoride was present in all solutions.

To determine the effect of processing on the loss of fluoride, lots of 10,000 tablets were prepared similar to the solutions but omitting singularly the dye, flavor, citric acid, magnesium stearate, stearic acid, or colloidal silica. Samples of the dry blend, the wet granulation, the dried granulation, and the tablets were analyzed. It was found that the dyes, flavors, and lubricants did not affect the fluoride content. All formulations containing citric acid were substandard after drying.

Since the wet granulation containing citric acid had the proper amount of fluoride before drying, it appears that fluoride loss is caused by the loss of hydrogen fluoride formed by the interaction of sodium fluoride and citric acid during the drying cycle. Deletion of citric acid from the formulations eliminated the problem of fluoride loss.

When drying moistened mixtures containing sodium fluoride and citric acid, a mild drying temperature of 50° promotes the loss of fluoride, presumably by loss of hydrogen fluoride vapor.

(1) "The United States Pharmacopeia," 19th rev., Mack Publishing Co., Easton, Pa., 1975, p. 460.

(2) T. L. Daines and K. W. Morse, *J. Chem. Educ.*, **51**, 680(1974).

Moshe Sabo
James F. Caputo
Eugene L. Parrott[x]
College of Pharmacy
University of Iowa
Iowa City, IA 52242

Received January 19, 1976.
Accepted for publication March 25, 1976.
[x] To whom inquiries should be directed.

[1] Patterson-Kelly Co.
[2] Fitzpatrick comminuting machine model D.
[3] Colton drying cabinet model E.
[4] Cab-O-Sil, G. L. Cabot Corp.
[5] Manesty model F3.
[6] Selected by the Department of Pedodontics.

Fundamentals of Clinical Pharmacokinetics. By JOHN G. WAGNER. Drug Intelligence Publications, Hamilton, IL 62341, 1975. xvi + 461 pp. 18 × 26 cm. Price $37.50

This text is the second in the series on pharmacokinetics by the author. The previous text, "Biopharmaceutics and Relevent Pharmacokinetics" (Drug Intelligence Publications, Hamilton, Ill., 1971) describes in detail the methodology and equations used in pharmacokinetics, with particular emphasis on the derivation of these equations. The present text, on the other hand, deals more closely with the clinical applications of these equations. The intent of the present text is ". . . to organize much of the knowledge of pharmacokinetics, with particular emphasis on human data, so that it may ultimately be useful in the clinical use of drugs." This objective is well carried out by the author.

The book begins with an introductory chapter, which generally describes the applications and importance of pharmacokinetics. The second chapter presents the basic pharmacokinetic equations for linear models, which are then used in the third chapter in the discussion of dosage regimen calculations. Chapters 4 and 5 describe absorption models and methods for estimating absorption rate constants, followed by a chapter discussing the use of LaPlace transforms for linear models. Chapters 7 and 8 contain an up-to-date discussion of nonlinear pharmacokinetics and a relatively short discussion of statistical methods useful in evaluating blood level data.

Chapter 9 discusses the relationship between drug concentration and response and the kinetics of pharmacological response, followed by a discussion of bioavailability in Chapter 10. Chapter 11 is a particularly worthwhile one, in which a thorough and current review of the effects of normal and pathologic physiology on pharmacokinetics is contained. The final chapter contains a discussion and computer program listing of automated methods of pharmacokinetic analysis. In addition to an extensive and thorough subject index, the text also contains an author citation index which should prove useful.

Most of the chapters are well written and presented in such a way that persons not thoroughly acquainted with pharmacokinetics can still understand the basic principles of the topic under discussion. Each chapter is followed by several review questions and/or problems, illustrating the principles discussed in the chapter.

This book presents one of the best and most comprehensive discussions of clinical pharmacokinetics available today. The book should be an excellent addition to the reference shelf of scientists involved in basic or clinical research. Although some sections of the book may be too advanced for many fifth-year students, it certainly should be useful in teaching Pharm.D. and graduate level courses. Of particular interest are the many examples using actual data and the generous use of references for the topics being discussed.

Although the pharmacokinetic terminology used throughout the text is not internally consistant from chapter to chapter, it may be useful in introducing the reader to differences in nomenclature routinely found in the literature. The text uses set type rather than photo offset, which is a distinct improvement over the previous text in this series. The only negative feature of the book is its price, which probably places it out of reach of most undergraduate and many graduate students.

Reviewed by William G. Crouthamel
School of Pharmacy
University of Maryland at Baltimore
Baltimore, MD 21201

Pharmacology and Pharmacokinetics. Edited by TORSTEN TEORELL, ROBERT L. DEDRICK, and PETER G. CANDLIFFE. Plenum Press, 227 West 17th Street, New York, NY 10011, 1974. 16 × 23.5 cm. 388 pp. Price $24.50.

In the fall of 1972, approximately 60 leading pharmacologists and pharmacokineticists convened to pay tribute to Professor Torsten Teorell on his retirement from the Chair of Physiology at Upsala University. The stated purpose of the program was "to review the present status, describe or formulate the pertinent problems, and finally delineate, if possible, the best ways of solving these problems" in pharmacokinetics. This volume, which includes 21 contributed papers and discussion summaries of each, represents the proceedings of that conference held at the John E. Fogarty International Center for Advanced Study in the Health Sciences, National Institutes of Health.

The presentations were mostly review in nature, sometimes didactic but only rarely provocative. Topics ranged from theoretical and practical considerations in modeling, interspecies scaling, and drug design to general discussions on the effects of disease, of physical, physiological, and genetic factors, and of concomitant therapy and the route of administration on drug biotransformation, distribution, and excretion; to specific applications in anticoagulant and cancer chemotherapy and in the treatment of depression and other neuropsychiatric disorders. In most cases, some prior knowledge of the author's work, or at least familiarity with the field, is presumed.

In many ways, this volume is an album of self-portraits by many of the pioneers in pharmacokinetics. It is also an accurate status report on the progress and frustrations of an emerging discipline during the first 50 years of development. While its sentimental value may have been flawed by the separate publication of approximately one-half of its titles in the *Journal of Pharmacokinetics and Biopharmaceutics*, its historical significance has not been thereby diminished.

Reviewed by K. C. Kwan
Merck Sharp and Dohme Research Laboratories
West Point, PA 19486

Remington's Pharmaceutical Sciences. 15th Edition. Edited under the direction of ARTHUR OSOL and JOHN E. HOOVER. Mack Publishing Co., Easton, PA 18042, 1975. 21 × 29 cm.

Acquaintance with every aspect of current information about drugs, including chemical, pharmaceutical, and toxicological, as well as areas of medicine relevant to drug therapy, is increasingly necessary for pharmacists to serve as members of the health professions team. The presentation of such diverse knowledge is the principal objective of this, the 15th edition of "Remington's Pharmaceutical Sciences."

Although every chapter has been revised, many rewritten, and several added, the most extensive revisions and additions are in those areas useful in preparing the pharmacist for the role of drug information specialist.

The section on Pharmaceutical and Medicinal Agents has been expanded to 33 chapters and includes new chapters on the pharmacological aspects of drug abuse, adverse effects, and interactions of drugs. The group on Biological Products now contains a chapter on principles of immunology. Chapters on bioavailability, bioequivalency testing, and stability of pharmaceutical products have been added to the Pharmaceutical Preparations section. Four new and two entirely rewritten chapters have been added to the section on Pharmaceutical Practice, which reflects the patient-oriented approach to pharmacy practice.

This volume is highly recommended as a comprehensive and up-to-date source of information on all facets of the pharmaceutical sciences and their application to pharmacy practice.

Staff Review

NOTICES

European Pharmacopoeia. Vol. III. Published under the direction of the Council of Europe. Maisonneuve, S.A., 57-Sainte-Ruffine, France, 1975. 464 pp. 16 x 25 cm.

Pesticide Selectivity. Edited by JOSEPH C. STREET. Dekker, 270 Madison Ave., New York, NY 10016, 1975. 197 pp. 15.5 x 23.5 cm. Price $18.50.

Fundamentals of Clinical Pharmacokinetics. By JOHN G. WAGNER. Drug Intelligence Publications, Hamilton, IL 62341, 1975. xvi + 461 pp. 18 × 26 cm. Price $37.50

This text is the second in the series on pharmacokinetics by the author. The previous text, "Biopharmaceutics and Relevent Pharmacokinetics" (Drug Intelligence Publications, Hamilton, Ill., 1971) describes in detail the methodology and equations used in pharmacokinetics, with particular emphasis on the derivation of these equations. The present text, on the other hand, deals more closely with the clinical applications of these equations. The intent of the present text is ". . . to organize much of the knowledge of pharmacokinetics, with particular emphasis on human data, so that it may ultimately be useful in the clinical use of drugs." This objective is well carried out by the author.

The book begins with an introductory chapter, which generally describes the applications and importance of pharmacokinetics. The second chapter presents the basic pharmacokinetic equations for linear models, which are then used in the third chapter in the discussion of dosage regimen calculations. Chapters 4 and 5 describe absorption models and methods for estimating absorption rate constants, followed by a chapter discussing the use of LaPlace transforms for linear models. Chapters 7 and 8 contain an up-to-date discussion of nonlinear pharmacokinetics and a relatively short discussion of statistical methods useful in evaluating blood level data.

Chapter 9 discusses the relationship between drug concentration and response and the kinetics of pharmacological response, followed by a discussion of bioavailability in Chapter 10. Chapter 11 is a particularly worthwhile one, in which a thorough and current review of the effects of normal and pathologic physiology on pharmacokinetics is contained. The final chapter contains a discussion and computer program listing of automated methods of pharmacokinetic analysis. In addition to an extensive and thorough subject index, the text also contains an author citation index which should prove useful.

Most of the chapters are well written and presented in such a way that persons not thoroughly acquainted with pharmacokinetics can still understand the basic principles of the topic under discussion. Each chapter is followed by several review questions and/or problems, illustrating the principles discussed in the chapter.

This book presents one of the best and most comprehensive discussions of clinical pharmacokinetics available today. The book should be an excellent addition to the reference shelf of scientists involved in basic or clinical research. Although some sections of the book may be too advanced for many fifth-year students, it certainly should be useful in teaching Pharm.D. and graduate level courses. Of particular interest are the many examples using actual data and the generous use of references for the topics being discussed.

Although the pharmacokinetic terminology used throughout the text is not internally consistant from chapter to chapter, it may be useful in introducing the reader to differences in nomenclature routinely found in the literature. The text uses set type rather than photo offset, which is a distinct improvement over the previous text in this series. The only negative feature of the book is its price, which probably places it out of reach of most undergraduate and many graduate students.

Reviewed by William G. Crouthamel
School of Pharmacy
University of Maryland at Baltimore
Baltimore, MD 21201

Pharmacology and Pharmacokinetics. Edited by TORSTEN TEORELL, ROBERT L. DEDRICK, and PETER G. CANDLIFFE. Plenum Press, 227 West 17th Street, New York, NY 10011, 1974. 16 × 23.5 cm. 388 pp. Price $24.50.

In the fall of 1972, approximately 60 leading pharmacologists and pharmacokineticists convened to pay tribute to Professor Torsten Teorell on his retirement from the Chair of Physiology at Upsala University. The stated purpose of the program was "to review the present status, describe or formulate the pertinent problems, and finally delineate, if possible, the best ways of solving these problems" in pharmacokinetics. This volume, which includes 21 contributed papers and discussion summaries of each, represents the proceedings of that conference held at the John E. Fogarty International Center for Advanced Study in the Health Sciences, National Institutes of Health.

The presentations were mostly review in nature, sometimes didactic but only rarely provocative. Topics ranged from theoretical and practical considerations in modeling, interspecies scaling, and drug design to general discussions on the effects of disease, of physical, physiological, and genetic factors, and of concomitant therapy and the route of administration on drug biotransformation, distribution, and excretion; to specific applications in anticoagulant and cancer chemotherapy and in the treatment of depression and other neuropsychiatric disorders. In most cases, some prior knowledge of the author's work, or at least familiarity with the field, is presumed.

In many ways, this volume is an album of self-portraits by many of the pioneers in pharmacokinetics. It is also an accurate status report on the progress and frustrations of an emerging discipline during the first 50 years of development. While its sentimental value may have been flawed by the separate publication of approximately one-half of its titles in the *Journal of Pharmacokinetics and Biopharmaceutics*, its historical significance has not been thereby diminished.

Reviewed by K. C. Kwan
Merck Sharp and Dohme Research Laboratories
West Point, PA 19486

Remington's Pharmaceutical Sciences. 15th Edition. Edited under the direction of ARTHUR OSOL and JOHN E. HOOVER. Mack Publishing Co., Easton, PA 18042, 1975. 21 × 29 cm.

Acquaintance with every aspect of current information about drugs, including chemical, pharmaceutical, and toxicological, as well as areas of medicine relevant to drug therapy, is increasingly necessary for pharmacists to serve as members of the health professions team. The presentation of such diverse knowledge is the principal objective of this, the 15th edition of "Remington's Pharmaceutical Sciences."

Although every chapter has been revised, many rewritten, and several added, the most extensive revisions and additions are in those areas useful in preparing the pharmacist for the role of drug information specialist.

The section on Pharmaceutical and Medicinal Agents has been expanded to 33 chapters and includes new chapters on the pharmacological aspects of drug abuse, adverse effects, and interactions of drugs. The group on Biological Products now contains a chapter on principles of immunology. Chapters on bioavailability, bioequivalency testing, and stability of pharmaceutical products have been added to the Pharmaceutical Preparations section. Four new and two entirely rewritten chapters have been added to the section on Pharmaceutical Practice, which reflects the patient-oriented approach to pharmacy practice.

This volume is highly recommended as a comprehensive and up-to-date source of information on all facets of the pharmaceutical sciences and their application to pharmacy practice.

Staff Review

NOTICES

European Pharmacopoeia. Vol. III. Published under the direction of the Council of Europe. Maisonneuve, S.A., 57-Sainte-Ruffine, France, 1975. 464 pp. 16 x 25 cm.

Pesticide Selectivity. Edited by JOSEPH C. STREET. Dekker, 270 Madison Ave., New York, NY 10016, 1975. 197 pp. 15.5 x 23.5 cm. Price $18.50.

Fundamentals of Clinical Pharmacokinetics. By JOHN G. WAGNER. Drug Intelligence Publications, Hamilton, IL 62341, 1975. xvi + 461 pp. 18 × 26 cm. Price $37.50

This text is the second in the series on pharmacokinetics by the author. The previous text, "Biopharmaceutics and Relevent Pharmacokinetics" (Drug Intelligence Publications, Hamilton, Ill., 1971) describes in detail the methodology and equations used in pharmacokinetics, with particular emphasis on the derivation of these equations. The present text, on the other hand, deals more closely with the clinical applications of these equations. The intent of the present text is ". . . to organize much of the knowledge of pharmacokinetics, with particular emphasis on human data, so that it may ultimately be useful in the clinical use of drugs." This objective is well carried out by the author.

The book begins with an introductory chapter, which generally describes the applications and importance of pharmacokinetics. The second chapter presents the basic pharmacokinetic equations for linear models, which are then used in the third chapter in the discussion of dosage regimen calculations. Chapters 4 and 5 describe absorption models and methods for estimating absorption rate constants, followed by a chapter discussing the use of LaPlace transforms for linear models. Chapters 7 and 8 contain an up-to-date discussion of nonlinear pharmacokinetics and a relatively short discussion of statistical methods useful in evaluating blood level data.

Chapter 9 discusses the relationship between drug concentration and response and the kinetics of pharmacological response, followed by a discussion of bioavailability in Chapter 10. Chapter 11 is a particularly worthwhile one, in which a thorough and current review of the effects of normal and pathologic physiology on pharmacokinetics is contained. The final chapter contains a discussion and computer program listing of automated methods of pharmacokinetic analysis. In addition to an extensive and thorough subject index, the text also contains an author citation index which should prove useful.

Most of the chapters are well written and presented in such a way that persons not thoroughly acquainted with pharmacokinetics can still understand the basic principles of the topic under discussion. Each chapter is followed by several review questions and/or problems, illustrating the principles discussed in the chapter.

This book presents one of the best and most comprehensive discussions of clinical pharmacokinetics available today. The book should be an excellent addition to the reference shelf of scientists involved in basic or clinical research. Although some sections of the book may be too advanced for many fifth-year students, it certainly should be useful in teaching Pharm.D. and graduate level courses. Of particular interest are the many examples using actual data and the generous use of references for the topics being discussed.

Although the pharmacokinetic terminology used throughout the text is not internally consistant from chapter to chapter, it may be useful in introducing the reader to differences in nomenclature routinely found in the literature. The text uses set type rather than photo offset, which is a distinct improvement over the previous text in this series. The only negative feature of the book is its price, which probably places it out of reach of most undergraduate and many graduate students.

Reviewed by William G. Crouthamel
School of Pharmacy
University of Maryland at Baltimore
Baltimore, MD 21201

Pharmacology and Pharmacokinetics. Edited by TORSTEN TEORELL, ROBERT L. DEDRICK, and PETER G. CANDLIFFE. Plenum Press, 227 West 17th Street, New York, NY 10011, 1974. 16 × 23.5 cm. 388 pp. Price $24.50.

In the fall of 1972, approximately 60 leading pharmacologists and pharmacokineticists convened to pay tribute to Professor Torsten Teorell on his retirement from the Chair of Physiology at Upsala University. The stated purpose of the program was "to review the present status, describe or formulate the pertinent problems, and finally delineate, if possible, the best ways of solving these problems" in pharmacokinetics. This volume, which includes 21 contributed papers and discussion summaries of each, represents the proceedings of that conference held at the John E. Fogarty International Center for Advanced Study in the Health Sciences, National Institutes of Health.

The presentations were mostly review in nature, sometimes didactic but only rarely provocative. Topics ranged from theoretical and practical considerations in modeling, interspecies scaling, and drug design to general discussions on the effects of disease, of physical, physiological, and genetic factors, and of concomitant therapy and the route of administration on drug biotransformation, distribution, and excretion; to specific applications in anticoagulant and cancer chemotherapy and in the treatment of depression and other neuropsychiatric disorders. In most cases, some prior knowledge of the author's work, or at least familiarity with the field, is presumed.

In many ways, this volume is an album of self-portraits by many of the pioneers in pharmacokinetics. It is also an accurate status report on the progress and frustrations of an emerging discipline during the first 50 years of development. While its sentimental value may have been flawed by the separate publication of approximately one-half of its titles in the *Journal of Pharmacokinetics and Biopharmaceutics*, its historical significance has not been thereby diminished.

Reviewed by K. C. Kwan
Merck Sharp and Dohme Research Laboratories
West Point, PA 19486

Remington's Pharmaceutical Sciences. 15th Edition. Edited under the direction of ARTHUR OSOL and JOHN E. HOOVER. Mack Publishing Co., Easton, PA 18042, 1975. 21 × 29 cm.

Acquaintance with every aspect of current information about drugs, including chemical, pharmaceutical, and toxicological, as well as areas of medicine relevant to drug therapy, is increasingly necessary for pharmacists to serve as members of the health professions team. The presentation of such diverse knowledge is the principal objective of this, the 15th edition of "Remington's Pharmaceutical Sciences."

Although every chapter has been revised, many rewritten, and several added, the most extensive revisions and additions are in those areas useful in preparing the pharmacist for the role of drug information specialist.

The section on Pharmaceutical and Medicinal Agents has been expanded to 33 chapters and includes new chapters on the pharmacological aspects of drug abuse, adverse effects, and interactions of drugs. The group on Biological Products now contains a chapter on principles of immunology. Chapters on bioavailability, bioequivalency testing, and stability of pharmaceutical products have been added to the Pharmaceutical Preparations section. Four new and two entirely rewritten chapters have been added to the section on Pharmaceutical Practice, which reflects the patient-oriented approach to pharmacy practice.

This volume is highly recommended as a comprehensive and up-to-date source of information on all facets of the pharmaceutical sciences and their application to pharmacy practice.

Staff Review

NOTICES

European Pharmacopoeia. Vol. III. Published under the direction of the Council of Europe. Maisonneuve, S.A., 57-Sainte-Ruffine, France, 1975. 464 pp. 16 x 25 cm.

Pesticide Selectivity. Edited by JOSEPH C. STREET. Dekker, 270 Madison Ave., New York, NY 10016, 1975. 197 pp. 15.5 x 23.5 cm. Price $18.50.

Journal of Pharmaceutical Sciences

JULY 1976

VOLUME 65 NUMBER 7

MARY H. FERGUSON
Editor

L. LUAN CORRIGAN
Assistant Editor

SHELLY ELLIOTT
Production Editor

JANET D. SHOFF
Copy Editor

EDWARD G. FELDMANN
Contributing Editor

SAMUEL W. GOLDSTEIN
Contributing Editor

LELAND J. ARNEY
Publications Director

EDITORIAL ADVISORY BOARD

JOHN AUTIAN	HARRY B. KOSTENBAUDER
LYNN R. BRADY	CARL J. LINTNER, JR.
WILLIAM O. FOYE	DAVID E. MANN, JR.
WILLIAM J. JUSKO	GERALD J. PAPARIELLO

The *Journal of Pharmaceutical Sciences* is published monthly by the American Pharmaceutical Association at 2215 Constitution Ave., N.W., Washington, DC 20037. Second-class postage paid at Washington, D.C., and at additional mailing office.

All expressions of opinion and statements of supposed fact appearing in articles or editorials carried in this journal are published on the authority of the writer over whose name they appear and are not to be regarded as necessarily expressing the policies or views of the American Pharmaceutical Association.

Offices—Editorial, Advertising, and Subscription Offices: 2215 Constitution Ave., N.W., Washington, DC 20037. Printing Offices: 20th & Northampton Streets, Easton, PA 18042

Annual Subscriptions—United States and foreign, industrial and government institutions $50, educational institutions $50, individuals *for personal use only* $30; single copies $5. All foreign subscriptions add $5 for postage. Subscription rates are subject to change without notice. Members of the American Pharmaceutical Association may elect to receive the *Journal of Pharmaceutical Sciences* as a part of their annual $60 (foreign $65) APhA membership dues.

Claims—Missing numbers will not be supplied if dues or subscriptions are in arrears for more than 60 days or if claims are received more than 60 days after the date of the issue, or if loss was due to failure to give notice of change of address. The Association cannot accept responsibility for foreign delivery when its records indicate shipment has been made.

Change of Address—Members and subscribers should notify at once both the Post Office and the American Pharmaceutical Association, 2215 Constitution Ave., N.W., Washington, DC 20037, of any change of address.

© Copyright 1976, American Pharmaceutical Association, 2215 Constitution Ave., N.W., Washington, DC 20037; all rights reserved.

SELF-SERVING TRADE SECRETS

If one of the "pollsters" who conduct opinion surveys were to ask a representative sample of Americans as to whether industry "trade secrets" should be adequately protected by law from forced disclosure—as, for example, under the Freedom of Information Act—one could safely predict that the response would be overwhelmingly in favor of such protection. The concept of trade secrets is a fundamental tenet of the capitalistic system, and one to which we ourselves subscribe.

Divergence of views arises when individuals are asked whether particular kinds of information are properly classified as trade secrets. Specifically, it is in this respect that we find that we must disagree—and disagree strongly—with a position articulated by spokesmen for the Pharmaceutical Manufacturers Association.

This spring, three of their top staff officials testified before the HEW Review Panel on New Drug Regulation; and they addressed the subjects of retaining control of drug testing under industry, rather than government auspices, and of adopting an additional phase in the clinical testing of new drugs in terms that made a rather credible and persuasive case for the industry position.

On the other hand, on the subject of trade secrets, we feel that the PMA presented a position that is self-serving to the detriment of the common good and the public welfare. Their prepared statement read in part:

> *"Much of the company information in question is data relating to safety and efficacy of new drugs. This information represents the results of many years of animal and clinical testing at enormous cost to the sponsoring company. The data would be of particular value to companies wishing to market competing products, in that expenditure of large amounts of research and testing time and money could be avoided . . . .*
>
> *"We urge your committee to evaluate critically the current FDA thinking that data supporting new drugs should not be protected from public disclosure. FDA has recently testified that the incentive to conduct new drug research is best protected by the U.S. patent laws and that limited FDA protection of safety and efficacy data is contrary to the public interest.*
>
> *"We strongly disagree with this premise. Although patent protection is essential for drug research, animal and clinical data generated by the new drug originator should not be handed out by the FDA to competitors so as to obviate the need to conduct any clinical research with follow-on versions of the new drugs."*

For our part, we strongly disagree with this approach for two reasons. First, we believe that patient welfare demands that health care practitioners using a drug should have ready and convenient access to all clinical data relating to that drug's safety and efficacy. And second, we believe that purely economic profit considerations are not sufficient to justify requiring duplicative clinical testing with the inherent risks to the subjects or patients involved.

We do agree that competitors ought not get "a free ride" by unjustly and unfairly benefiting from the work of others. However, there are other means to achieve this objective without resorting to secrecy of data that are critical to the informed use of a new drug.

Specifically, we object to PMA's cavalier dismissal of the patent system as the most appropriate vehicle for this purpose. We would remind the PMA that the patent system was, in fact, established to provide just this kind of industry protection. If the PMA feels that the system is not working satisfactorily for some reason, then the proper remedy is to modify the patent system, and not to hide and lock up information which may either save lives or prevent needless deaths.

Edward G. Feldmann

Journal of Pharmaceutical Sciences

JULY 1976

VOLUME 65 NUMBER 7

MARY H. FERGUSON
Editor

L. LUAN CORRIGAN
Assistant Editor

SHELLY ELLIOTT
Production Editor

JANET D. SHOFF
Copy Editor

EDWARD G. FELDMANN
Contributing Editor

SAMUEL W. GOLDSTEIN
Contributing Editor

LELAND J. ARNEY
Publications Director

EDITORIAL ADVISORY BOARD

JOHN AUTIAN	HARRY B. KOSTENBAUDER
LYNN R. BRADY	CARL J. LINTNER, JR.
WILLIAM O. FOYE	DAVID E. MANN, JR.
WILLIAM J. JUSKO	GERALD J. PAPARIELLO

The *Journal of Pharmaceutical Sciences* is published monthly by the American Pharmaceutical Association at 2215 Constitution Ave., N.W., Washington, DC 20037. Second-class postage paid at Washington, D.C., and at additional mailing office.

All expressions of opinion and statements of supposed fact appearing in articles or editorials carried in this journal are published on the authority of the writer over whose name they appear and are not to be regarded as necessarily expressing the policies or views of the American Pharmaceutical Association.

Offices—Editorial, Advertising, and Subscription Offices: 2215 Constitution Ave., N.W., Washington, DC 20037. Printing Offices: 20th & Northampton Streets, Easton, PA 18042

Annual Subscriptions—United States and foreign, industrial and government institutions $50, educational institutions $50, individuals *for personal use only* $30; single copies $5. All foreign subscriptions add $5 for postage. Subscription rates are subject to change without notice. Members of the American Pharmaceutical Association may elect to receive the *Journal of Pharmaceutical Sciences* as a part of their annual $60 (foreign $65) APhA membership dues.

Claims—Missing numbers will not be supplied if dues or subscriptions are in arrears for more than 60 days or if claims are received more than 60 days after the date of the issue, or if loss was due to failure to give notice of change of address. The Association cannot accept responsibility for foreign delivery when its records indicate shipment has been made.

Change of Address—Members and subscribers should notify at once both the Post Office and the American Pharmaceutical Association, 2215 Constitution Ave., N.W., Washington, DC 20037, of any change of address.

© Copyright 1976, American Pharmaceutical Association, 2215 Constitution Ave., N.W., Washington, DC 20037; all rights reserved.

SELF-SERVING TRADE SECRETS

If one of the "pollsters" who conduct opinion surveys were to ask a representative sample of Americans as to whether industry "trade secrets" should be adequately protected by law from forced disclosure—as, for example, under the Freedom of Information Act—one could safely predict that the response would be overwhelmingly in favor of such protection. The concept of trade secrets is a fundamental tenet of the capitalistic system, and one to which we ourselves subscribe.

Divergence of views arises when individuals are asked whether particular kinds of information are properly classified as trade secrets. Specifically, it is in this respect that we find that we must disagree—and disagree strongly—with a position articulated by spokesmen for the Pharmaceutical Manufacturers Association.

This spring, three of their top staff officials testified before the HEW Review Panel on New Drug Regulation; and they addressed the subjects of retaining control of drug testing under industry, rather than government auspices, and of adopting an additional phase in the clinical testing of new drugs in terms that made a rather credible and persuasive case for the industry position.

On the other hand, on the subject of trade secrets, we feel that the PMA presented a position that is self-serving to the detriment of the common good and the public welfare. Their prepared statement read in part:

> *"Much of the company information in question is data relating to safety and efficacy of new drugs. This information represents the results of many years of animal and clinical testing at enormous cost to the sponsoring company. The data would be of particular value to companies wishing to market competing products, in that expenditure of large amounts of research and testing time and money could be avoided . . . .*
>
> *"We urge your committee to evaluate critically the current FDA thinking that data supporting new drugs should not be protected from public disclosure. FDA has recently testified that the incentive to conduct new drug research is best protected by the U.S. patent laws and that limited FDA protection of safety and efficacy data is contrary to the public interest.*
>
> *"We strongly disagree with this premise. Although patent protection is essential for drug research, animal and clinical data generated by the new drug originator should not be handed out by the FDA to competitors so as to obviate the need to conduct any clinical research with follow-on versions of the new drugs."*

For our part, we strongly disagree with this approach for two reasons. First, we believe that patient welfare demands that health care practitioners using a drug should have ready and convenient access to all clinical data relating to that drug's safety and efficacy. And second, we believe that purely economic profit considerations are not sufficient to justify requiring duplicative clinical testing with the inherent risks to the subjects or patients involved.

We do agree that competitors ought not get "a free ride" by unjustly and unfairly benefiting from the work of others. However, there are other means to achieve this objective without resorting to secrecy of data that are critical to the informed use of a new drug.

Specifically, we object to PMA's cavalier dismissal of the patent system as the most appropriate vehicle for this purpose. We would remind the PMA that the patent system was, in fact, established to provide just this kind of industry protection. If the PMA feels that the system is not working satisfactorily for some reason, then the proper remedy is to modify the patent system, and not to hide and lock up information which may either save lives or prevent needless deaths.

Edward G. Feldmann

Journal of Pharmaceutical Sciences

JULY 1976
VOLUME 65 NUMBER 7

REVIEW ARTICLE

Pharmaceutical Sciences—1975: Literature Review of Pharmaceutics I ▲

FRANK W. GOODHART *x **and MARTIN L. EICHMAN** ‡

Keyphrases □ Pharmaceutical sciences—1975 literature review of pharmaceutics □ Technology, pharmaceutical—sterility, dosage forms, cosmetics, packaging equipment, dental products, biomedical devices, 1975 literature review □ Stability—solids, solutions, injectable products, antibiotics, and vitamins, kinetics, 1975 literature review □ Dosage forms—tablets, suspensions, emulsions, suppositories, aerosols, controlled-release devices, 1975 literature review □ Cosmetics—formulation and technology, microbiological contamination, 1975 literature review □ Instrumentation—in pharmaceutical technology, 1975 literature review □ Literature review—pharmaceutical sciences, 1975

CONTENTS

General Pharmacy 935
Preservatives 936
Flavor, Aroma, and Color 937
Stability 937
Solids 938
Solutions 938
Injectable Products 939
Kinetics 940
Antibiotics 940
Vitamins 941
Pharmaceutical Technology 941
Sterile Products 941
Ophthalmics 943
Sterility and Sterilization 943
Tablets and Capsules 943
Comminution, Mixing, Granulating, and Drying 944
Powder and Granule Characteristics 944
Compression 945
Effects of Excipients 945
Tablet Coating 946
Suspensions 946
Emulsions 947
Semisolids 947
Suppositories 947
Aerosols 948
Controlled-Release Preparations 948
Cosmetics 949
Microbiological Contamination 949
Formulation and Technology 949
Packaging 951
Instruments and Equipment 951
Dental Products and Materials 952
Biomedical Devices and Materials 952
References 952

This review article is a continuation of the annual review of pharmaceutics begun in 1963. As in past reviews in this series (1–14), the scope has been limited to the overall area of pharmaceutics since other specific subjects in pharmaceutical sciences are published elsewhere. The authors have used selected sections of *Chemical Abstracts* as well as 40 journals as the sources for this article.

It is hoped that this review will be of continued usefulness to the pharmaceutical scientist whenever pharmaceutical information is needed. The overall format remains essentially the same as that of the last several years; however, some changes have been made to reflect minor organizational improvements.

GENERAL PHARMACY

Two articles reported on the pharmaceutical industry; the first (15) reviewed the development of the industry, drug nomenclature, drug regulation, product classification, research, manufacturing, and quality control. The second (16) summarized the development

▲ *Editor's note:* Part II of this article will appear in the August 1976 issue of the *Journal of Pharmaceutical Sciences.*

of the pharmaceutical industry in Poland over the last 30 years. Process capability analysis, a quality control tool utilizing computer and statistical analysis, was described using data from laboratories and manufacturers (17).

A review of the drugs of veterinary medicine included topics such as drug products, commercial usage, manufacturing, distributing firms, compounding, ranges of application, and commercial forms (18). The types of infant formulas together with their composition as well as the compositions of human and cow milks were reported (19). Digestive and electrolyte problems sometimes occur because of measurement errors. A review of current aspects of pharmaceutics covered chemical stability, physical pharmacy, drug dissolution and absorption, microbiological studies, particulate contamination, and packaging (20).

Preservatives—The use of preservatives in biological products as currently regulated in the pharmacopoeias of various European countries, the United States, and the European Pharmacopoeia and by the World Health Organization was discussed (21). With six microorganisms as test organisms, a method was developed for testing liquid pharmaceutical preparations which centered on whether preservatives were needed. A 0.1% methylparaben–propylparaben mixture (8:2) preserved adequately, being more effective than a 0.05% mixture or 0.1% methylparaben (22).

The effectiveness of three preservatives currently used in various multiple-dose biological products was measured by monitoring the number of viable cells present at 7-day intervals following inoculation of 10^5 cells/ml of product (23). Certain toxoids, vaccines, and antiserums of blood group A were selected containing thimerosal, phenol, and sodium azide as preservatives. A significant difference in the ability of each type of preservative to reduce the number of viable organisms was found.

The availability of preservatives in emulsified systems was reported. The equations used to characterize the interaction of preservatives with other components of the formulation, particularly nonionic surfactants, were questioned; some equations were said to overestimate grossly the total concentration of preservative necessary to provide the required free concentration (24). Another paper reported on the interrelationship between preservative activity and the amounts of both oil and emulsifier (25). A standard cream formulation was used to evaluate thimerosal[1] sodium, *p*-chlorocresol, and a methylparaben–propylparaben mixture with a number of microorganisms; thimerosal sodium was the most effective (26).

Frequently isolated microorganisms from aqueous based products are *Pseudomonas cepacia* and *Ps. putida*; *Ps. aeruginosa* had increased resistance to various antimicrobials when grown in water (27). The partitioning of methyl-, ethyl-, propyl-, and butylparabens into flavoring oils from aqueous systems was studied and found to be dependent on the concentration of flavoring oil, the pH of the aqueous medium, and the nature and concentration of additives (28). Five preservatives were evaluated for their effectiveness in simple syrup after challenge by a number of test microorganisms (29). Benzoic acid was most effective at pH 3, and thimerosal sodium and benzyl alcohol were the most effective at pH 5.5.

The interaction between saccharin sodium and various parabens was demonstrated by solubility studies (30). The interaction of sorbic acid and parabens with nonionic agents was stronger than with polyethylene glycol 400, 1500, or 4000 when tested by serial dilution or dialysis methods (31). The combination of propylparaben with octyl gallate was about 10% more effective than octyl gallate alone in retarding the autoxidation of ethyl oleate (32). Differences were less pronounced when the same paraben was used in conjunction with nordihydroguaiaretic acid or butylated hydroxyanisole. Binding studies of methylparaben and chloroxylenol with sodium lauryl sulfate suggested that the palisade layer of the sodium lauryl sulfate represents the secondary binding sites of cetomacrogol (33).

The role of some nonionic additives to saturated dialdehyde solutions can display powerful bactericidal synergism when added in the proper proportion (34). Three formaldehyde-releasing cosmetic preservatives were studied to determine their quantitative release (35). The importance of neutralization of free formalin in biological products before freeze drying was stressed (36). The presence of free formalin, which is concentrated during the freeze-drying process, can have a deleterious effect on the antigens and adversely affect the immunogenicity of the product. It was demonstrated that pH and concentration were insignificant in determining the free aldehyde content in aqueous glutaraldehyde solutions (37). Therefore, the rates at which equilibria are established are important in determining antibacterial activity. The effects of aminosidine (paromomycin) with and without organism pretreatment with bacteriostatic agents were studied (38). The minimum concentration for cidal action increased with increasing concentrations of nutrients and with decreasing pH.

The activity of a number of other preservatives and antioxidants was studied. Commercial glycerin, analyzed for microbial contamination, showed no growth; therefore, its antimicrobial activity was determined using four organisms (39). After 7 days, significant bacterial concentrations were present. Catgut contamination with up to 94×10^6 nonsporulating microorganisms/ml (23 strains) was completely sterilized after a 24-hr exposure to ethanol (40). Alkylparabens are capable of being degraded to phenol by bacteria (41). It was suggested that ester hydrolysis occurs in the presence of *Ps. aeruginosa* with subsequent decarboxylation in the presence of *Klebsiella aerogines*. Butyl-, propyl-, ethyl-, and methylparabens showed a broad spectrum of activity against microorganisms most commonly contaminating pharmaceutical products (42). In general, they were more active against fungi than against bacteria and more active against Gram-positive than against Gram-negative bacteria. The activity of paraben mixtures was additive and complementary.

Thimerosal was compatible with more eye drop for-

[1] Merthiolate, Lilly.

Table I—Additional References on Preservatives

Reference	Topic
46	Microwave sanitization of color additives used in cosmetics
47	Preservatives used in biological reagents and their stability
48	Effectiveness of bronopol and five other compounds as cosmetic preservatives
49	Review of classification of preservatives according to their chemical structure and bactericidal activity
50	Review of preservation of cosmetics
51	Review of antimicrobial preservatives for pharmaceuticals and cosmetics
52	Investigation and determination of alkyl esters of *p*-hydroxybenzoic acid, sorbic acid, and benzoic acid
53	Spoilage of surfactants in cosmetic products and evaluation of bis(trichloromethyl)sulfone (chlorosulfons)
54	Usnic acid as a natural preservative deodorant and antimicrobial agent in cosmetic systems
55	Comparative antioxidant activity of 6-hydroxy-5,7,8-trimethyl-2-chromancarboxylic acid and other antioxidant compounds
56	Antioxidants used in pharmaceutical formulations and their determination by TLC
57	Antimicrobial preservatives in biologics
58	Essential oils as possible preservatives in cosmetic products

mulations than was chlorhexidine acetate, but the latter inhibited *Ps. aeruginosa* and *Candida albicans* faster than did thimerosal (43). Thimerosal had no adverse effect on purified meningococcal polysaccharide vaccines of serol A or C when used at a 0.01% concentration (44). The addition of disodium ethylenediaminetetraacetate (edetate disodium) prolonged antibiotic activity during storage in liquid or complex dry media at temperatures of 26° or less and exerted antimicrobial activity against common bacteria, especially *Bacillus subtilis* (45).

Additional references on preservatives are listed in Table I.

Flavor, Aroma, and Color—The formulation of liquid pharmaceutical products was reviewed with particular emphasis on the choice of sweeteners, flavor enhancers, flavors, and colors as well as various stability aspects (59). Amino acid esters of acetaminophen were less bitter than the parent drug but were susceptible to hydrolysis, thus making them unacceptable for liquid formulations (60). The palatability of carbon slurries was improved by the addition of thickening agents, sodium alginate, carboxymethylcellulose sodium, carrageenan, bentonite, and gelatin (61). The adsorption properties of the charcoals investigated were not affected by the thickeners.

The physical, chemical, organoleptic, and metabolic properties of fructose were compared to sucrose, dextrose, and high fructose corn syrup (62). The replacement of sucrose by lower costing high fructose corn syrup was discussed (63). Another article discussed the properties of high levulose (fructose) corn syrups and reported taste comparisons to sucrose and invert sugars (64).

A review of the formulation, life, fixation, and solubilization of perfume material and the use of instrumentation to control perfume formulations was presented (65). The decrease of odorant concentration in the gas phase after application of an odor eliminator and specific solvents was quantitatively determined by GC. It was shown that the so-called odor eliminators have no selectivity for malodorous materials (66). Numerous essential oils and aromatic chemicals commonly used in soap perfumes were tested for safety, and results were presented to assist perfume compounders in selecting odorant materials (67).

The Food and Drug Administration (FDA) status of food colorants was reviewed, and a list of approved food color additives exempt from certification was presented (68). A computerized color-matching and batch correction method was described for use by cosmetic manufacturers (69). The surface color of a series of color dispersions containing certified dyes in sucrose syrup was examined using an integrating sphere colorimeter (70). Color differences were calculated to develop color specifications for tablets, liquids, and creams. The stability of betalaine, a mixture of natural red beet pigments, was determined (71).

Additional references on flavor, aroma, and color are given in Table II.

Stability—A review of the factors that limit drug stability, with emphasis on traces of multivalent elements and the role of chelating agents, was published (91). The poor stability of certain pharmaceuticals containing polyethylene glycols was attributed to the presence of peroxide; however, peroxide levels can be reduced by pretreatment with water and butylated hydroxytoluene or propyl gallate in concentrations of 0.005–0.05% (92). Under normal storage conditions and on sterilization, the peroxide number of polyethylene glycol and its alkyl ethers increased to a significant level with oxidation, showing the characteristics of a chain reaction (93). The peroxide formation rate was increased by increasing temperature, the presence of copper ions, decreasing pH, surfactant concentration, and prior treatments such as bleaching or heat sterilization.

A method for the rapid determination of oxidation

Table II—Additional References on Flavor, Aroma, and Color

Reference	Topic
72	Instrumental methods for measurement of texture, color, and flavor
73	Codex Alimentarius: the way to a worldwide food and flavor regulation
74	Flavors: the future and the FDA
75	International standardization of essential oils
76	Components of Japanese spearmint oil
77	Methodological approach to flavoring
78	Physiological aspects of food flavoring
79	Food and cosmetic toxicology; monographs on fragrance of raw materials
80	Monographs on fragrance of raw materials, 1,1-dimethyl-2-phenylethanol
81	Monographs on fragrance of raw materials, α,α-dimethylphenethyl acetate
82	Sensory properties of acetals and ketals of 1-phenyl-1,2-ethanediol
83	Progress in perfumery and flavoring materials (31st annual article)
84	Flavoring of pharmaceutical products
85	Pharmaceutical aromatization and its relation to olfactory and gustatory phenomena in drug ingestion
86	Perfumery and chemistry, a symbiosis of art and science
87	Ceylon cinnamon bark oil: its use as a fragrance and flavor and its toxicity
88	Use of FD&C lakes to replace soluble dyes
89	Use and stability of carotenoid esters as colorants
90	Use of carotenoids as food colorants

stability of cosmetics was described in which the test material was heated to 120° and oxygen was blown into it (94). The disadvantages of accelerated tests for determining the stability of perfume components or perfumed products, such as talcs, and the possible lack of correlation between results of accelerated tests and actual market product performance were discussed (95). The correlation between long-term stability tests and accelerated tests conducted at higher temperatures was investigated.

Other general references on drug stability are listed in Table III.

Solids—The stability of aspirin in tablets was reviewed (106). The decomposition of acetylsalicylic acid (aspirin), acetyl-5-nitrosalicylic acid, and acetyl-5-chlorosalicylic acid in the solid state by water vapor was studied to elucidate the decomposition mechanisms of organic crystals by water vapor (107). A kinetic analysis was given as well as the results of a microscopic examination and comparative rates for the three compounds. The effects of formulation methodology and excipients on the stability of aspirin tablets were reported; comparisons included both wet and dry granulation methods and the effect of buffers (108).

In digitalis leaf capsules, purpurea glycosides A and B were most stable when digitalis powder was prepared by lyophilization (109). In tablets, the direct compression method was better than two granulation methods with respect to lanatoside content, both after preparation and after storage. Increased dissolution rates of phenylbutazone tablets BP on aging were reported, and the tendency toward longer dissolution could be simulated in short periods by using elevated temperatures (110).

Several brands of stabilized nitroglycerin tablets were studied, and one brand was superior to all others when placed under stress conditions (111). The same tablets were stable in medication cups for 7 days or in foil–foil or foil–cello strips. In another study, the stability of solid pharmaceutical compositions containing nitroglycerin was highly dependent on temperature and the type of container (112). Products were generally stable at 20°; but at 40°, tablets in hard gelatin capsules and timed-release tablets with compressed diffusion pellets showed especially low stability.

The influence of light, time of storage, and relative humidity of the surrounding atmosphere on the surface color and total color content of effervescent colored mouthwash tablets was studied (113). There appeared to be no correlation between fading at the surface of the tablets and the actual concentration of the coloring agent when measured in solution. The recovery of two aromatic ingredients from gum arabic, lactose, and potato starch supports and starch[2] capsules by extraction before and after 1 year of storage at 4° showed that the capsules provided the most stable form (114).

The effect of various additives on the rate of transformation of the metastable anhydrous succinylsulfathiazole Form I to the water-stable dihydrate Form II in aqueous suspensions was studied (115). Some additives, such as methylcellulose, showed significant transformation-retarding effects; others, such as glycerin, increased the rate of transformation. In another study by the same researchers, the transformation was studied by using a projecting microscope; particle-size distribution of Form I succinylsulfathiazole was determined (116).

Other references on the stability of solids are listed in Table IV.

Solutions—Methyldopa syrup preparations were made by dispersing tablets into unpreserved simple syrup and acidified simple syrup (128). Both preparations were stable after 14 days of storage in the dark. The hydrolysis of pilocarpine in carbomer hydrogels was studied and related to viscosity (129). The hydrolysis of procaine was also studied in the same gel system at pH 6, and the influence of ionic strength was determined (130). The activation energy was not influenced by the viscosity of the medium, but the second-order rate constant was significantly reduced. The rate constant–pH profile of the rate of sulfite-induced disappearance of epinephrine from aqueous solution under anaerobic conditions was determined at 81° in the 3.63–5.00 pH range at an ionic strength of 0.2 (131). The aerobic rate showed buffer catalysis above pH 4.4, and metabisulfite was more catalytic than either bisulfite or acetone bisulfite.

The hydronium-ion-catalyzed racemization of 0.2% levarterenol bitartrate in water was found to be dependent on the ionic strength and polarity of the solvent

Table III—Additional References on Drug Stability

Reference	Topic
96	Hydrolytic degradation of drugs
97	Drug stability trials
98	Purification and stability of ^{125}I-insulin
99	Factorial design for testing drug stability
100	Stability of prostaglandins
101	Incompatibility phenomena of galenic pharmaceutical preparations
102	Review of stability testing of pharmaceuticals
103	Influence of physical factors (heat, humidity, atmospheric pressure, and solar irradiation) on stability of pharmaceuticals
104	Room temperature stability of drug products labeled for refrigerated storage
105	Aging inhibition of aluminum hydroxide by mannitol and fructose

Table IV—Additional References on Stability of Solids

Reference	Topic
117	Microencapsulation and stability of ferrous sulfate microcapsules
118	Microencapsulation of three easily oxidized drugs [ascorbic acid, methylene blue, and phenazone (antipyrine)]
119	Photolytic decomposition of ethionamide salts
120	Effect of preservatives on stability of short ragweed pollen extract
121	Stability of antigen E in commercially prepared ragweed pollen extracts
122	Stabilization of dihydroepiandrosterone enanthate in powder mixtures
123	Solid-state decomposition of *para*-substituted salicylic acids
124	Decomposition of *p*-aminosalicylic acid in solid state
125	Prediction of shelflife of menthyl valerate tablets
126	Use of diffuse reflectance spectroscopy in preformulation screening and final product control
127	Stability of a tablet containing L-ascorbic acid and ferrous nicotinate

[2] Dry Flo.

(132). The stability of scopolamine hydrobromide drops, 0.25%, was significantly increased by addition of 2.5% polyvinyl alcohol or 1% polyacrylamide, and the preparations were not harmed by heat sterilization (133). Oral insulin preparations, particularly water-in-oil and micelle insulin emulsions as a means of protecting insulin from digestive enzymes, were reviewed (134).

Photodecomposition of a number of compounds was reported. The critical micelle concentration (CMC) of three phenothiazine derivatives, chlorpromazine, triflupromazine, and homophenazine, was studied by several means to determine the degree of aggregation (135). In a second study, the photoinstability of these compounds was shown to be dependent on their colloidal characteristics (136). Both sodium dodecylbenzenesulfonate and sodium dodecyl (lauryl) sulfate were decomposed by UV light at 254 nm (137).

A study of the effects of various storage conditions on the rate and products of degradation of the quinolinemethanol antimalarial agent, α-[(dibutylamino)-methyl]- 6,8-dichloro-2- (3′,4′-dichlorophenyl)-4-quinolinemethanol, was reported (138). Thioridazine hydrochloride in aqueous solution was subjected to high temperature (80°) as well as UV radiation of 254 nm (139). One decomposition product was isolated after heat treatment, but eight products were isolated and identified by TLC and other techniques. Solutions of thiacetazone (amithiozone) were decomposed by exposure to a 250-w mercury lamp, and the resulting irradiated solutions were characterized by several methods (140).

The stability of aspirin in decaglycerol tetraoleate, octaoleate, and decaoleate was studied at various temperatures (141). Fatty acid esters of acetaminophen were prepared with the acetate and all even-numbered fatty acids through the octadecanoate (142). Hydrolysis at pH 7.8 in the presence of lipase demonstrated that the short chain esters were hydrolyzed at the most rapid rate whereas the longer chain esters were the most stable of the group. The decomposition of amitriptyline hydrochloride was investigated in aqueous solution, and three major decomposition products were identified (143).

The hydrolytic degradation of 5-azacytidine was studied as a function of pH, temperature, and buffer concentration (144). The apparent first-order rate constants associated with formation of 5-azacytosine and 5-azauracil were reported. The hydrolysis of mazindol in aqueous solutions at various temperatures, pH values up to 7.6, and an ionic strength of 0.2 was studied (145). Kinetic relationships were reported as well as the effect of various buffers. Ergotoxine solutions at pH 3–4 decomposed due to hydrolysis of salt forms, but an accelerated decomposition occurred due to oxidation at pH less than 3 (146).

Changes in the color of amidopyrine (aminopyrine) solutions were due to the presence of noramidopyrine impurities formed at the alkylation stage during production (147). The oxidation rate of *N*-hydroxyamphetamine and *N*-hydroxyphentermine in aqueous solution was shown to be pH dependent, with oxidation taking place around the pKa (148). Kinetic equations for the hydrolysis of narcotine (noscapine) and lactonization of narcotic acid were published (149). Oxidative degradation products of phenothiazine in a hydroalcoholic solution saturated with oxygen were isolated after storage in the dark at 80° for 96 hr (150).

Table V—Additional References on Stability of Drugs in Solution

Reference	Topic
158	Stability of 1,4-benzodiazepines
159	Quantitation of barbiturate stability by TLC
160	Molecular orbital study on solvolysis of aspirin derivatives and acyl-α-chymotrypsin
161	Quantitation of procaine stability by TLC
162	Stability of *p*-aminosalicylic acid in malt extract
163	Stability of amphetaminil
164	Stability of aza analogs of methaqualone
165	Accelerated degradation of nonsteroid anti-inflammatory drugs at carbon black–water interface
166	Stability of tetrahydrocannabinols
167	Stability of oxyfedrine
168	Solvolytic decomposition of certain ethionamide salts
169	Stability of cocarboxylase hydrochloride
170	Effect of temperature on hydrolysis of carboxylase hydrochloride
171	Penicillamine as stabilizer of apomorphinium chloride solutions
172	Stability of nafiverine in aqueous solution
173	Bisulfite-ion-catalyzed degradation of fluorouracil
174	Stability of 1,3-bis(2-chloroethyl)-1-nitrosourea in aqueous solutions
175	Kinetics of hydrolysis of cytosine, cytidine, and arabinosylcytosine
176	Effect of briefly heating cyclophosphamide solutions

Streptokinase stability measured at various temperatures and times up to 48 hr was excellent in gelatin and 3% albumin solutions, intermediate in 10% dextran and 5% levulose (fructose), and poor in isotonic sodium chloride solution, 5% glucose, and Michaelis buffer solutions (151). The kinetics of indomethacin hydrolysis in ethanol–water and polyethylene glycol–water mixtures at pH 7–10 were reported (152). The decomposition of codeine and codeine phosphate was first order in aqueous solution, and the rate was accelerated by increasing the pH (153). The stability of a codeine phosphate syrup was attributed to the presence of sucrose and citric acid, which inhibited the autoxidation process (154).

Factors that participate in the decomposition reactions of itobarbital (butalbital) in tromethamine buffer were studied by differences observed in equilibrium constants, and second-order rate constants were subsequently calculated (155). The degradation of hexobarbital in alkaline aqueous solutions was investigated at pH 10.5 and 13 in a 5–40° temperature range, and a degradation scheme was proposed (156). The hydrolysis of chlordiazepoxide was determined over a broad pH range; both general acid catalysis and general base catalysis were observed, with a number of specific buffer ions having an accelerating conversion to lactam (157).

Other papers dealing with the stability of drugs in solution are listed in Table V.

Injectable Products—Three dexamethasone injections were found to be unstable when exposed to light; a light-resistant container was suggested for this product (177). The hydrolytic degradation of atropine sulfate was studied in an aqueous solution at pH 8 by a nonisothermal method (178, 179). The stability of a commercial product[3] containing amidopyrine (amino-

[3] Rheopyrin.

pyrine) and phenylbutazone was determined (180). Phenylbutazone was stable but amidopyrine was not. The autoxidation decomposition of glaucine hydrochloride injection was second order; the effects of pH, temperature, ionic strength, and traces of metallic ions on the reaction rate were studied (181).

The half-life, optimal pH, and general stability were determined for an injectable form of gentamicin (182). Eight decomposition products of morphine hydrochloride injection were identified by two-dimensional TLC (183). One decomposition product, dehydromorphine, was identified; solutions sealed under an inert gas were much more stable. In nonsulfite-containing solutions of morphine sulfate stored for 1 year, morphine *N*-oxide and 2,2′-dihydromorphine were found (184). In sulfite-stabilized solutions, dehydromorphine-8-sulfonic acid was identified.

Additional references on the stability of injectable products are listed in Table VI.

Kinetics—A continuous nonisothermal–isothermal method for stability prediction was developed (195). The experimental procedure involved changing the temperature of the samples being studied until degradation was rapid enough to proceed at a convenient isothermal rate for a sufficient number of half-lives. A multilevel nonisothermal method that estimates stability from the degradation ratio after a specific period of a straight temperature increase was proposed (196). It was suggested that Weibull probability paper be used, rather than the usual methods, because of its convenience and accuracy for prediction of reaction kinetics (197). Examples of its usefulness include acetylsalicylic acid (aspirin) and ascorbic acid solutions. Two computation procedures for the study of drug stability were described, one for comparison of high temperature degradation of drugs contained in different formulations and the other for estimation of stability prediction based on the Arrhenius law (198).

Other topics on kinetics include a kinetic study of melting (199), a computerized program to model the hydrolysis of local anesthetic drugs (200), the kinetics of the most frequent complex drug degradation reactions (201), a calculation flow chart for application of reaction kinetics in stability testing (202), and the kinetics and mechanism of aqueous degradation of Baker's Antifol (NSC 113,423) (203).

Table VI—Additional References on Stability of Injectable Products

Reference	Topic
185	Stability of hydroxyzine hydrochloride and atropine sulfate mixture
186	Stability of dopamine hydrochloride in large-volume parenteral solutions
187	Compatibility of papaverine hydrochloride with other injectable solutions
188	Stability and compatibility of nafcillin sodium injection
189	Connections between plasma quality and impurities of γ-globulin and albumin preparations
190	Predicting drug stability in parenteral mixtures
191	Stabilization of aminazine (chlorpromazine) solution for injection
192	Stability of amino acid infusion solutions
193	Stabilization of aminazine solution for injection
194	Properties of mannitol injection after repeated autoclaving

Antibiotics—The stabilities of three antibiotics (chloramphenicol, tetracycline, and phenoxybenzyl penicillin), all solid dosage forms in conventional packages, were determined at high temperature and humidity conditions which simulated storage on ships in tropical zones (204). Kinetic analyses were carried out, and a recommendation was made for special protective packaging. A comparative study of cephalosporins in an aqueous solution over a broad pH range was reported (205). The log k_{pH}–pH profiles for the hydrolyses of cephalothin, cephaloridine, cephaloglycin, and some related compounds were given.

The chemical stability of penicillin G potassium intravenous infusion solutions was related to the initial pH of the solutions and the ability of the buffer to maintain a constant pH during aging (206). Carefully prepared and purified penicillin G sodium was quite stable for long periods even at 30° and was more stable at pH 6–7 than at pH 5.0–5.5 (207). Ampicillin was degraded 10% in a 0.9% sodium chloride solution during 24 hr, whereas 5–12% decomposition took place in dextrose solutions within 2 hr (208). Another study reported that ampicillin partially degraded in an aqueous solution to yield ordered molecules with molecular weights varying between 1000 and 5000 (209).

Addition of 1% polysorbate 80[4], polysorbate 60[4], or ethanol decreased the degradation of ampicillin sodium; however, antioxidants such as rongalite, sodium dithionite, sodium metabisulfite, sodium bisulfite, sodium sulfite, and sodium ascorbate accelerated the degradation of the antibiotic (210). The influence of concentration, vehicle, dextrose, and temperature on the stability of oxacillin sodium solutions was determined using a chemical kinetic approach (211). The degradation of carbenicillin sodium in aqueous solution at constant ionic strength, a pH range of 1–10.7, and a temperature of 35° was reported to be first order (212). Maximum stability was at pH 6.5, and anions were found to catalyze the reaction.

The stability of oxytetracycline hydrochloride in solution was studied in 0.1 *N* hydrochloric acid and at pH 3–7 (213). The stability and physical compatibility of tobramycin sulfate in commonly used intravenous fluids were evaluated; most solutions were stable for 48 hr at room temperature (214). Storage of gentamicin solutions at pH 4 and 60° for 35–180 days did not significantly affect the concentration of the preparation, but its concentration decreased 8–30% at a pH greater than 4 (215). In another comprehensive report, the hydrolysis of gentamicin injections was studied as a function of time, temperature, and pH (216). The most favorable pH was reported to be in the 6–8 range, which gave gentamicin sulfate injections a stability up to 3 years.

No loss in the activity of neocarzinostatin injection occurred during 2 years of storage at 8°, but it was inactivated by reducing agents such as bisulfite and ascorbic acid as well as by urea and thiourea (217). Kinetic studies on the inactivation of the drug in aqueous solution showed that thermal inactivation was an apparent first-order reaction (218). In solid form, am-

[4] Tween.

photericin B and amphotericin B methyl ester free base exhibited similar stability, but acid salts of the methyl ester derivative stored under identical conditions were less stable (219). In solution, amphotericin B was generally more stable than its methyl ester salts.

Polyethylene glycol gels containing 1% concentrations of four antibiotics [chloramphenicol, tetracycline, erythromycin, and stamycin (mystatin)] were examined by TLC after 3 or 9 months of storage (220). Decomposition products and the activity of these preparations were reported. Cephapirin sodium was shown to be stable as a dry powder at high temperature and at 25° for 33 months (221). Aqueous solubility exceeded 500 mg/ml, and reconstituted solutions were stable. The stability of hamycin–tetracycline hydrochloride mixtures in capsules with various diluents was studied (222). Mannitol was the best diluent, with lactose the next best.

Several other antibiotic stability studies were reported including the X-ray diffraction characteristics of Bulgarian tetracycline (223), the effect of cupric ion and sodium lauryl sulfate on the degradation rate of penicillin G (224), and the stability of cephradine in infusion solutions (225).

Vitamins—Syrups containing ascorbic acid and B complex vitamins could be stabilized by replacing sucrose, vanillin, and various aldehyde-rich essential oils with sorbitol, saccharin sodium, citric acid, edetate disodium, and essence of banana or apple (226). The improved formula had a better taste and was less discolored after 18 months of storage at room temperature in the dark. Ascorbic acid tablets were reported to have the greatest stability when prepared by direct compression with a mixture of microcrystalline cellulose and milk sugar and then coated with a colored nonaqueous suspension of Eudragit (227).

Cupric and ferric ions had the most deleterious effect on ascorbic acid stability (228). Other salts such as sodium glycerophosphate, cobalt chloride, and calcium gluconate had little effect while manganese sulfate was practically without effect. Because of its antioxidant and chelating properties, 2,3-dimercaptopropane sodium sulfonate was reported to be a better stabilizer for ascorbic acid injection solutions than metabisulfite, cysteine, and ethylenediaminetetraacetic (edetic) acid (229). A kinetic study of the degradation of ascorbyl monolaurate in aqueous solution under aerobic conditions was reported (230). The rate of degradation was determined at 45, 60, and 80° at pH 3.1–10.1 and an ionic strength of 0.1. A microencapsulation technique for ascorbic acid using polyethylene glycol was developed (231).

Vitamin B_{12} (cyanocobalamin) was formulated by various methods into tablets containing thiamine and pyridoxine (232). In an ordinary formulation, a 43.6% loss of B_{12} occurred in 2 years. Alternative formulations such as use of B_{12} granules, multilayer tablets, or application of the vitamin in the sugar coating syrup greatly enhanced the stability. The transamination reaction of the thiazole moiety of thiamine by aromatic amine in the presence of bisulfite was studied kinetically and found to be second order with respect to thiamine and the aromatic amine, whereas the reaction rate was independent of the concentration of bisulfite (233).

Table VII—Additional References on Vitamin Stability

Reference	Topic
237	Vitamin D_3 stability in solubilized aqueous solutions
238	Stability of vitamin D_2 (ergocalciferol) tetraacetylglucoside
239	Vitamin A palmitate stability in solubilized systems
240	Influence of antioxidant compounds on stability of cod liver oil
241	Stability of riboflavin in tablets and injectable solutions
242	Review of vitamin B_{12} formulation
243	Stability of ascorbic acid tablets with special talcs

A kinetic study was made of the effect of 9-aminomethylacridan on the electronic excited states of riboflavin 5-phosphate to postulate a mechanism for the flavor-sensitized oxidation, and several mechanisms were suggested (234). Riboflavin was fused with urea, various ureides, and hydrotropic salts, which improved the solubility of the vitamin (235). The effect of these substances on hydrolytic and photolytic decomposition was reported, and thiourea and sodium salicylate gave maximum stabilizing effectiveness against both types of decomposition. The effect of selected antioxidants on the stability of vitamin D_3 (cholecalciferol) in solubilized aqueous solutions was reported (236). With ascorbic acid and nordihydroguaiaretic acid or butylated hydroxyanisole, 82% of the original amount of vitamin D_3 remained; without antioxidant, only 57% of the vitamin remained.

Additional references on vitamin stability are listed in Table VII.

PHARMACEUTICAL TECHNOLOGY

Sterile Products—A symposium was presented to review regulatory guidelines prohibiting the use of asbestos and glass fiber filters in the preparation of parenteral products (244). The principles of parenteral product formulation were reviewed and included methods of blood level modification, solubility, stability, and isotonicity considerations (245). Training for personnel to be employed in sterile product manufacturing was reported (246, 247). Incompatibilities occurring upon the addition of drugs to intravenous fluids and drug interactions in syringes were discussed with regard to the practice of adding multiple drugs to injections in hospitals (248). The chemical and physical compatibility of metampicillin sodium and sodium phosphocreatinine with other compounds was determined in solution (249), and the compatibility of four kinds of vitamin B_1 (thiamine hydrochloride) derivatives with 126 other parenteral solutions was reported (250).

The design and development of an elastomeric closure formulation were reviewed, including factors that affect polymer selection and functional performance as well as procedures for determining the general chemical, toxicological, and functional characteristics of a new closure formulation (251). Comparative chemical testing of plugs from three countries used for sealing infusion bottles was examined according to the criteria in Hungarian Pharmacopoeia VI. All three plugs met all standards for heavy metal contamination, acidity–alkalinity, and reducing substances; one plug did not meet the requirements for ammonia content (252).

The migration of zinc stabilizer from plasticized polyvinyl chloride was studied using blood serum, water, and other blood serum products (253). The profiles and rates of extraction of zinc and zinc mercaptobenzothiazole from rubber stoppers were evaluated, and the mechanism of extraction was found to be diffusion controlled (254). Blood plasma stored in plastic bags was found to contain 40–120 μg/ml of bis(2-ethylhexyl) phthalate (255). The perfusates from polyvinyl chloride hemodialysis tubings were investigated, and diethyl phthalate as well as other unidentifiable substances were found (256). Another study reported the presence of bis(2-ethylhexyl) phthalate in plastic bags used for the storage of transfusion blood (257).

According to a *Federal Register* notice, filters must not be of asbestos or glass unless the product cannot be manufactured without it, in which case an additional filter of 0.22 or 0.45 μm subsequently must be used (258). Cellulose particles of 15-μm size were injected into the tail veins of mice, and granulomas were later detected in the lungs and kidneys (259). The literature covering phlebitis as associated with intravenous administration of drugs was reviewed (260). The incidence of infusion phlebitis was found to be significantly reduced when an in-line 0.45-μm membrane filter was used (261). The greatest reduction of infusion phlebitis was in the filter groups receiving unbuffered solutions and no set change over 72 hr of therapy. In two other reports, no significant differences were found in the incidence of infusion phlebitis between groups utilizing in-line final filtration devices and those not using such devices (262, 263).

Particulates from natural rubber stoppers were formed after autoclaving, and it was suggested that stoppers should be sterilized by ethylene oxide (264). A study was conducted to determine the effectiveness of 0.22- and 0.45-μm pore size membrane filters in retaining microorganisms over 72 hr (265). With lactated Ringer's injection, the 0.45-μm filter was effective in retaining all microorganisms for 6 hr; however, *Escherichia coli* and *Ps. aeruginosa* began passing between 6 and 8 hr after seeding. No microorganisms passed through the 0.22-μm filter during the 72-hr study period.

A number of articles reported on methods of detecting particles in intravenous fluids; the methods were scanning electron microscopy (266), the Emhart Autoskan inspection system using the EVOP method (267), the Coulter counter (268, 269), the Nucleopore Prototron counter (270), and detection of scattered light from particulates using a laser beam (271). The feasibility of using membrane filters to remove particles from intravenous infusions of amphotericin B in dextrose 5% (a colloidal solution) was studied using six commercial membrane filters of pore sizes from 0.45 to 1.0 μm (272). The effects on particulate matter and stability of three parenteral containers of 0.9% sodium chloride injection were studied (273). A correlation appeared to exist between the quantity of particulate matter and the amount of unfiltered drug solution added.

A system for providing pyrogen-free water for pharmaceutical manufacturing was described; the aspects discussed included source, distillation, storage, distribution, and quality maintenance (274). Two papers described the principles, applications, and limitations of the Limulus test for pyrogen in parenteral drugs (275, 276). The effect of antibiotics and osmotic change on the release of endotoxin by bacteria retained on intravenous in-line filters was studied (277). An aseptic system for prefilling radiopharmaceutical kit vials and syringes was described (278). The system combines ultrafiltration with a method for monitoring for bacterial contamination and can be used for any vial- or syringe-filling operation.

Glass infusion bottles treated with ammonium chloride and made in Hungary were compared to borosilicate glass bottles (279). Buffered solutions retained a similar pH in each type of bottle, but solutions of higher pH decomposed the surface of treated bottles. Seven brands of intravenous fluid administration sets were studied to determine their functionality as measured by the most consistent flow rates, effect of the type of fluid container, and ability to determine the theoretical amounts of fluid (280). A method was described to measure changes in pressure inside a bottle during autoclaving without determining the integrity of the seal; if the rubber liner was unable to maintain the seal, air leaked slowly from the bottle during both the heating up and early sterilization period (281).

A new method for intermittent administration of intravenous fluids, which maintains the advantages of the piggyback system but at a lower cost, was described (282). A prototype in-line intravenous final filter with a large filtration area and an air elimination feature was evaluated (283). Freezing-point and differential thermal analysis data were presented for 19 pharmaceutical preparations (284). By means of thermal treatments or modification of different pharmaceutical formulas, it may be possible to modify the thermal behavior of these solutions to improve the quality of lyophilized products.

Numerous reports on specific parenteral product formulations appeared in the literature. The apparent solubility of hexamethylmelamine in aqueous solutions suitable for intravenous use was increased by complexation with gentisic acid (285). Six parenteral mannitol solutions analyzed for 5-hydroxymethylfurfural showed various levels of this impurity (286). Peroxide levels of ethyl oleate were lowered by treatment with an aqueous solution of sodium metabisulfite and hydrochloric acid followed by aqueous sodium carbonate (287). Sodium sulfate was added, and the oil was filtered and stored in well-filled containers protected from light.

Silicone coating of bottles prolonged the lifetime of parenteral sodium bicarbonate solutions, and those prepared with edetate disodium and hydrochloric acid were stable for 5 months (288). Sodium bicarbonate injection solution saturated to pH 7.3 with carbon dioxide and stabilized with edetate disodium remained clear during 3 years of storage at room temperature (289). The preparation of a glycerol solution for intravenous administration of sodium ascorbate was described (290). A method for the preparation and standardization of nitroglycerin injection was reported (291).

Other papers on various aspects of sterile products are listed in Table VIII.

Table VIII—Additional References on Sterile Products

Reference	Topic
292	Fat emulsion vehicle for intravenous administration of an aqueous insoluble drug
293	Preparation of sorbitol-containing solutions for intravenous infusion
294	Hyperosmolar cold-storage kidney preservative solution
295	Development of long-term stable blood-substituting solution
296	Evaluation of preparations of patent blue (alphazurine 2G) dye for parenteral use
297	Yttrium-90 citrate colloid for radioisotope synovectomy
298	Relationship among colloid association, physical stability, and acute toxicity on azo dyes in injection solutions
299	Recommended methods for compounding intravenous admixtures in hospitals
300	Soaking time in bottle-washing machines
301	Review of injectable solution formulation
302	Selection of optimum manufacturing systems for injectable solutions
303	Carrier solutions for low level intravenous insulin infusion
304	Preparation and control of sterile solutions of arginine monohydrochloride for clinical practice
305	Characterization and purification of insulin
306	Toxicity of intravenous benzyl alcohol
307	Combination of prodigiozan with glycine
308	Use of inactivators in evaluation of disinfectants
309	Variability of heparin preparations in clinical use
310	Incompatibilities of drugs for intravenous administration

Ophthalmics—The retention of technetium Tc 99m by human and rabbit eyes was decreased by blinking and, in decreasing order of activity, by saline solution, 1% methylcellulose, 1.4% polyvinyl alcohol, and white petrolatum–mineral oil (6:4) ointment (311). By using a stationary dialysis technique, it was found that the release of procaine hydrochloride in eye drops was retarded in solutions of methylcellulose and polyvinylpyrrolidone (povidone) but was not affected by carboxymethylcellulose; atropine sulfate was significantly retarded by carboxymethylcellulose (312). Drocinonide phosphate potassium formed an insoluble complex with neomycin sulfate in aqueous solution (313). Dibasic sodium phosphate was employed in an ophthalmic formulation to prevent the formation of this precipitate without affecting the stability of the steroid or the bioactivity of the antibiotic.

An aqueous neutral epinephrine[5] eye drop formulation containing 0.5 *M* borax, 0.3 *M* boric acid, phenylmercuric nitrate, 0.0002 *M* sodium metabisulfite, 0.3 *M* 8-hydroxyquinoline, and 0.02 *M* buffer, adjusted to pH 7 with sodium hydroxide, was recommended (314). The formulation packaged under nitrogen showed almost no decomposition after 5 months. The effects of wetting and suspending agents on the formulation of hydrocortisone acetate eye drops were determined (315). Octoxynol[6] and cetylpyridinium bromide were better wetting agents than benzalkonium chloride and polysorbate 80. Similarly, 1% polyvinyl alcohol with 0.1% octoxynol[6] was the most satisfactory suspending agent. It was shown in rabbits that when polyvinyl alcohol and methylcellulose were compared on a viscosity basis, there was essentially no difference in the two vehicles with regard to their influence on ocular drug bioavailability (316). The relationship between viscosity and contact time or drainage loss was discussed.

[5] Adrenalin, Parke-Davis.
[6] Triton X-100, Rohm and Haas.

Table IX—Additional References on Ophthalmics

Reference	Topic
320	Purification of cod liver oil for ophthalmological use with aid of adsorbents
321	Use of dimethyldodecylbenzylammonium chloride for eye drops containing pilocarpine hydrochloride
322	Review of formulation aspects of eye lotions
323	Review of preparation of eye drops
324	Formulation and technology of ophthalmological preparations
325	Preparation of ophthalmological preparations in pharmacy
326	Structure stability of ointment gels
327	New process for manufacture of sterile ophthalmic ointments
328	Antipseudomonal activity of contact lens solutions

The history, uses, and composition of conventional hard lenses, scleral lenses, and soft lenses were discussed (317). The composition and use of cleaning and disinfecting products were reviewed, as well as the indications for use of soft lenses. The requirements relating to antimicrobial activity of solutions employed for storing, cleaning, and wetting contact lenses were reviewed; the activities of preservatives and sterilizing agents employed in these products were discussed (318). Soluble ophthalmic inserts were made from various plastics and contained drugs such as neomycin, kanamycin, atropine, pilocarpine, and dexamethasone; activity was obtained for 34–72 hr (319).

Additional reports on ophthalmics are listed in Table IX.

Sterility and Sterilization—The techniques and equipment needed for obtaining clean and sterile air were surveyed (329). The design and use of a sterile holding tank and its integration with high-speed vial-filling lines were reported (330). Six commercially available biological indicator systems containing spores of *Bacillus stearothermophilus* were evaluated for resistance to 121 and 131° (250 and 270° F) saturated steam, and some manufacturers' labeled claims were not substantiated in the study (331).

The effect of holding heated and unheated *B. stearothermophilus* spores for 0, 40, 80, and 120 min in parenteral and buffer solutions at 0 and 22° was determined (332). The holding time, holding temperature, and the solution affected the number of organisms that were able to form colonies. Immersion of rubber and plastic medical equipment in a 0.5% aqueous solution of chlorhexidine gluconate at 70° produced complete sterility in 3 hr insofar as live bacteria and their vegetative forms and mold spores were concerned (333).

Additional references on sterility and sterilization are listed in Table X.

Tablets and Capsules—Recent progress in tablet technology and its application in the development of new tablet formulas were reviewed (362). A report discussed instruments used to determine tablet properties and forces in tableting (363). A book on tablet manufacture was published (364). Evolutionary operation as it applies to optimizing tablet manufacture was discussed, with particular reference to translating research formulations to production more efficiently (365). In a publication on the factors that influence the physical

Table X—Additional References on Sterility and Sterilization

Reference	Topic
334	Review of pertinent aspects of dosimetry in radiation sterilization equipment and choice of optimum parameters for sterilization of medical products
335	Effect of gamma irradiation on properties of polymeric materials
336	Surface area stability of micronized steroids sterilized by irradiation
337	Influence of steam and temperature on sterilizing action of ethylene oxide–etoxiate gas mixtures
338	Selection of sterilization process for parenteral solutions
339	Review of ethylene oxide sterilization and other types of chemical sterilization
340	Selection of packaging materials for medical products satisfactory for sterilization process
341	Challenge tests for antimicrobial agents
342	Chemical sterilants for aseptic packaging
343	Quality control of absolute bacteria removal filters
344	Manufacture of sterile topical products
345	Review of ethylene oxide sterilization
346	Sterilization of 33% ethanol with steam
347	Gas sterilization for medical purposes
348	New ways to sterilize ointment bases and oils
349	Sterilization by filtration in pharmaceutical industry
350	Effectiveness of ethylene oxide gas sterilization
351	Propylene oxide as sterilizing agent
352	Sterility testing of radiopharmaceuticals
353	Effect of gamma radiation on pilocarpine hydrochloride
354	Radiation sterilization of 0.9% sodium chloride ampuls and procaine powder
355	Effect of gamma irradiation on properties of polymeric materials
356	Optimum conditions for ethylene oxide sterilization of syringe barrels
357	Efficiency of ethylene oxide sterilization of plastic products for medical purposes
358	Sterilization of medical supplies using ethylene oxide
359	General principles of sterilization with ethylene oxide
360	Bulk sterilization of powders
361	Radiation sterilization of dextran irradiated in the dry state

properties of tablets, it was reported that an increase of the capillary network as a function of time involved structural changes reflecting the physical properties of tablets (366).

Gelatin capsules appearing in various pharmacopeias were reviewed (367). Soft gelatin capsules did not dissolve in simulated gastric fluid in the presence or absence of pepsin after 60 min (368). After exposure to this treatment, they generally disintegrated in simulated intestinal fluid of pH 7.5 in the presence of pancreatin within 4 min. Methods for preparing enteric hard gelatin capsules were reviewed with a description of the original technique used for enterocaps (369). The dosator system of a Zanasi LZ/64 capsule-filling machine was modified and fitted with strain gauges; these were used to measure the forces on the powder being filled during compaction and ejection (370). Special preparation techniques were reported, including decreasing the crystallinity of aspirin by spray drying with surfactants (371), microencapsulation of charcoal (372), and a review of microencapsulation (373).

Comminution, Mixing, Granulating, and Drying—Certain aspects of particulate contamination in tablet manufacture were discussed (374). The methods and equipment employed for granulation were reviewed (375). Methods were developed to test the consistency of granulates by a penetrometer measurement and the hardness (plasticity) by the Brinell number (376). The evaluation of flow properties of powders and granulated materials with respect to the preparation of solid dosage forms was reviewed (377). Intragranular migration of sodium chloride in granules made by the wet massing of heavy kaolin BP with salt solution was studied in batches dried by fluidization and by a vacuum tumbling method (378). The larger granules from the fluidized batch exhibited considerable intragranular variation while vacuum-dried granules had less migration.

A factorial design was found useful in the preparation of spherical particles by an extrusion–spheronization process (379). Another study, using the same apparatus, reported on formulations containing microcrystalline cellulose as well as spheronization speeds (380). Different stages in massing a granulation were measured by strain gauges and power input (381). Properties of the final granulation were independent of the addition rate of the binder solution and massing time but dependent on the amount of water in the binder solution. An air suspension technique was found to be satisfactory for the coating of moisture-sensitive materials with aqueous systems (382). The data demonstrated that solvent-sensitive materials can be encapsulated with little effect on the material when proper drying conditions are maintained.

Tablet crushing strength was greatly reduced when mixing times were prolonged in blends of amylose and magnesium stearate, and this finding was attributed to a lubricant film on the substrate (383). The mixing of antipyrine with lactose was followed by using colored lactose as the third component (384). The degree of mixing in a twin-shell blender was determined by making color measurements. The homogeneity of milled and unmilled cyclopenthiazide (1%) was determined in both coarse and fine lactose (385). The milled material demonstrated a segregating effect. The Nauta mixer was used to evaluate the mixing of a multicomponent tablet preblend of phenobarbitone (phenobarbital), butobarbitone (butethal), quinalbarbitone (secobarbital), and lactose; each component behaved in a unique manner (386, 387). The application of nonparametric statistics to the sampling in solids mixing was reported (388). The mixing of solid particles during fluidization in a conical apparatus was described (389).

The use and advantages of microwave radiation to dry tablet granulations were described, and available equipment was mentioned (390). The effects of the granule size and density on the drying rate kinetics of tablet granulations were studied, using lactose and sulfathiazole granules prepared with acacia mucilage and povidone solution (391). In a study comparing granulations prepared by the fluidized-bed method and by the traditional process, flow properties of fluidized-bed-dried granulations were generally better than those that were oven dried (392). In another study by the same group, tablets of lactose and phenacetin made by both processes were characterized (393). The kinetics of drying granulated sulfadimezine and its stability at various temperatures were reported (394).

Powder and Granule Characteristics—A continuum theory for the flow of granular materials with incompressible granules was described (395). Powder failure testing equipment was used successfully to study the effect of glidants on the flowability of two cohesive pharmaceutical powders, lactose and calcium hydrogen

phosphate, using the flow factor as the flowability parameter (396). Fine silica, magnesium stearate, and talc were investigated as glidants, and an optimum concentration was observed beyond which no further increase in flowability occurred. Static and dynamic wall pressures, measured by a small pressure-sensitive radiopill in axial–symmetrical and plain–strain experimental Perspex mass flow hoppers, were reported (397). The experimental results suggested the existence of radial stress fields in the convergent section of the hoppers and agreed with theoretical results.

A method of size grading powders using an automated sedimentation balance was described (398). The effectiveness of siliconized talc on the flow rates of L-ascorbic acid, aspirin, sulfaguanidine, sulfathiazole, oxytetracycline[7], and chloramphenicol palmitate was investigated (399). All materials except chloramphenicol palmitate showed a remarkable increase in their flow rate under the influence of siliconized talc as compared to nonsiliconized talc. The relationship between water absorption by δ-D-gluconolactone and subsequent drying was determined by a crushing strength measurement, and it was suggested that caking was caused by solid bridges formed by crystallization (400).

Compression—The surface acidity of compressed calcium and cadmium sulfates was measured after compression at various forces and temperatures, and acidities of both solids varied on compression (401). Powder X-ray diffraction, differential thermal analysis, and IR absorption were used to study the relationship between acidity and structural changes. The physical properties of tablets of identical composition but prepared by three different processes (wet granulation, dry granulation, and direct compression) were studied as a function of compressive force (402). Methods for determining the energetic work involved in tablet compression were presented and were applicable in predicting properties and quality of tablets (403).

The compaction behavior of various materials such as potassium chloride and lactose was studied and compared (404). Different particle sizes of lactose and potassium citrate were compacted, and the strain was measured at relatively low compaction forces (405). The yield strength and consolidation behavior were compared to those obtained for potassium and sodium chlorides. In another report on the same materials, various aspects of the physics of tablet compression were described further (406). A direct compression mixture of dicalcium phosphate and a cation-exchange resin was evaluated for disintegration and dissolution characteristics after compression at different compaction forces (407).

Compressed tablets of aspirin, dicalcium phosphate dihydrate, calcium phosphatocarbonate, alumina, and microcrystalline cellulose were made at several compaction pressures by a standardized technique, and their disintegration properties were evaluated by measuring particle sizes (408). The transmission of force to the die wall was measured by a piezoelectric sensor, and compression cycles of lactose granules of different shapes were compared (409). Two other studies on die wall pressures resulting from tablet compression were published (410, 411).

The pore structure of tablets made from wet massed granules and from crystalline granules was compared (412). The pore structure of a polymer compact was dependent upon the morphology of the initial particle and the mechanism of compaction (413). Mercury intrusion porosimetry was used to study both effects, and scanning electron photographs were used to confirm the interpretation obtained from mercury penetration. The rate of dissolution of sulfamethoxydiazine (sulfameter) tablets in three formulations of various moisture levels and compressed at various force levels was determined (414). Factors of interest in the physics of tablet compression including important features of granulated materials were reviewed (415).

Effects of Excipients—A factorial design was used to evaluate the compatibility between drugs and excipients in multicomponent mixtures (416). Chemical interactions could be detected and quantified in multicomponent mixtures, and the excipients responsible for them could be pinpointed. Nine direct compression fillers were evaluated for physical stability, compressibility, and lubricity with an instrumented tablet press (417). Four grades of commercially available microcrystalline cellulose were examined for appearance, particle-size distribution, specific surface area, pore size distribution, and surface energy (418).

The disintegration behavior of three direct compression formulations containing microcrystalline cellulose was reported (419). Aspirin tablets made by the dry method had good properties when microcrystalline cellulose, carboxymethylcellulose, ethylcellulose, carboxymethyl starch, anhydrous lactose, polyvinylpyrrolidone (povidone), dextrose[8], Silartex, and crystalline lactose binders were used (420). Sulfanilamide tablets made with various starches were evaluated for *in vitro* dissolution rates; barley starch was superior to plain starch and rice, wheat, potato, and arrowroot starches in giving the lowest disintegration time and highest release (421). Various excipients (potato starch, tricalcium phosphate, wheat starch, talc, and magnesium stearate) were evaluated in sulfanilamide tablet formulations (422). Properties of the granulations and compressed tablets were reported.

Starch sodium glycolate was evaluated as a disintegrant in tablets of sodium benzoate and calcium lactate and compared with starch and cellulose (423). Disintegration and dissolution were best with starch sodium glycolate. The same compound was evaluated by another investigator in direct compression formulations and was found to be a better disintegrant than alginic acid, corn starch, and microcrystalline cellulose (424). In another study, carboxymethyl starch was found superior to corn, wheat, potato, and rice starches but less effective than guar gum and magnesium aluminum stearate (425).

Additional references on excipients, *i.e.*, disintegrants, binders, and other substances that impart spe-

[7] Terramycin, Pfizer.

[8] Celutab, Penick and Ford.

Table XI—Additional References on Excipients

Reference	Topic
426	Water sorption properties of starch, carboxymethylcellulose sodium, sodium starch glycolate, and a cation-exchange resin
427	Evaluation of different viscosity grades of carboxymethylcellulose sodium as tablet disintegrants
428	Influence of surfactants on dissolution rate
429	Effect of tragacanth on disintegration time of tablets
430	Preparation of effervescent tablets
431	Use of sugarcane wax in preparation of tablets having prolonged action
432	Techniques for preparing slow-release drug forms for oral administration
433	Influence of moisture on rate of dissolution of sulfamethoxydiazine (sulfameter) tablets
434	Factors affecting dissolution rate of tablets
435	Effect of binders on physical standards and dissolution characteristics of ephedrine hydrochloride tablets
436	Influence of cellulose derivatives on physical properties of tablets
437	Interaction between hydroxyzine and dicalcium phosphate dihydrate
438	Use of native bentonite for direct tableting
439	Nu-Tab as a chewable direct compression carrier
440–443	Materials as dry binders for direct compression of tablets
444	Comparative evaluation of excipients for direct compression
445	Starch-containing cachets
446	Effect of various starches on physical properties of sulfaguanidine tablets
447	Review of components and formulation of effervescent tablets
448	Use of mannitol in tablets and other formulations
449	Formulation of mercaptopurine tablets
450	Optimum conditions for tableting 2-mercaptobenzothiazole with papaverine hydrochloride
451	Evaluation of binding substances used for the granulation of medical carbon
452	Optimum conditions for tableting 2-mercaptobenzothiazole with levomycetin (chloramphenicol)
453	Effect of techniques and components on formulation of nitrofurantoin tablets
454	Development of optimum technology for 2-mercaptobenzothiazole tablets
455	Use of colloidal silicon dioxide in pharmaceutical preparations including tablets
456	Intragranular starch: comparison of starch USP and modified corn starch
457	Direct compression of sulfamethoxydiazine (sulfameter) polymorphic forms
458	Methyl vinyl ether–maleic anhydride copolymer as a dry binder for direct compression
459	Dry binders for direct compression in tablet manufacture
460	Comparative study of lubricants in direct compression
461	Disintegration behavior of three direct compression formulations containing microcrystalline cellulose

cial properties to tablets, are listed in Table XI.

Tablet Coating—The composition of enteric coatings, the methods of application, the theory of enteric coatings and their properties, and factors affecting disintegration time and stomach emptying were discussed (462). Tablet film coatings, film-coating materials, plasticizers, and solvents used to ensure drug protection and good *in vivo* diffusion were reviewed (463). Film coating by the immersion tube process, where both coating solution and liquid are applied within the tablet bed, was reported (464). Zein and hydroxypropyl methylcellulose and various plasticizers were evaluated for film coating tablets (465). Application of hydroxypropyl methylcellulose from an ethanol–chloroform solution was carried out at various temperatures and flow rates, and the strength of the coatings was evaluated (466).

Three different subcoating powders were evaluated by application in simple syrup or gelatin–acacia syrup (467). A suspension coating containing polyvinylpyrrolidone (povidone), magnesium carbonate, talc, titanium dioxide, colloidal silicon dioxide[9], and water was used for coating tablets (468). The disintegration, dissolution, and stability of cyclothiazide and reserpine tablets were examined initially and periodically up to 1 year at various temperatures (469). Polyvinyl alcohol coating and sugar coating were compared and evaluated (470). A microscope photometer was used to measure the color uniformity and gloss of tablets (471). The influence of processing variables and type of dye on color uniformity was reported, and the use of the instrument to optimize the polishing of coated tablets was discussed.

Suspensions—The history of water-soluble gums (*e.g.*, seaweed extracts) was discussed including the effect of climatic conditions, collections, and harvestings, and some predictions about their future were reported (472). Factors affecting the stability of aggregates in dispersed systems were reported; the ζ-potential, the pH of the system, the electrolyte forms, and the surfactant type and concentration that affect stability of aggregates of dispersed drugs were discussed (473).

The stability of suspensions was discussed by viewing agglomeration as a process of microscopic segregation (474). The influence of size and porosity of agglomerates on the rate of settling was demonstrated with the aid of theoretical and experimental results. The viscosity compatibility of acacia, methylcellulose, and tragacanth with ethanol was reported, and it was found that the addition of colloidal silica counteracted the viscosity decrease caused by alcohol addition (475). The mechanism of coagulation of particles in suspensions during freeze–thaw cycles was reviewed (476).

Acacia and sodium alginate powders were sterilized by cobalt-60 irradiation to a total dose of 2.5 Mrad with no increase in residual radioactivity as a result of the treatment (477). The viscosities of acacia solutions were somewhat reduced by the treatment, while the viscosities of sodium alginate solutions were greatly reduced. It was concluded that this dose of irradiation was not an appropriate method of sterilization for these gums. Erythromycin and sulfadimezine were formulated into suspensions for treatment of bovine mastitis using polyethyl siloxane and esilon-5; physical and chemical stability studies were carried out (478).

The suspension-stabilizing ability of five suspending agents used for sulfisomidine suspensions was studied, and the addition of sodium citrate increased the sedimentation volume and degree of flocculation in suspensions containing carboxymethylcellulose sodium (479). Aluminum hydroxide gel was found to lose reactivity on aging or dilution with double-distilled water (480). The loss of reactivity was directly related to the degree of dilution, but dilution with dioxane or mother liquor had no effect on reactivity. The stability of sulfadimezine suspensions was studied using bentonite, methylcellulose, and carboxymethylcellulose sodium (481).

[9] Aerosil.

Emulsions—Various aspects of the formation and breaking of emulsions were reviewed (482). A modified phase inversion method was compared to the original method for the determination of the emulsifying potential of polysorbates 60 and 80 (483). The mechanism of phase inversion and surfactant location on the formulation of oil-in-water emulsions was reported (484). The effects of heat, agitation, and rheological properties on the production of emulsions on an industrial scale were studied, and a laboratory procedure was adopted for simulating large-scale production (485). The effects of tank size and impeller on the degree of liquid–liquid dispersion by mechanical agitation were studied (486). The influence of pH, emulsifier, and accelerated aging on preservative requirements of oil-in-water emulsions was reported (487).

Emulsions of mineral oil and cottonseed oil stabilized by nonionic surfactants have a substantial ζ-potential (488). The hydrophilic–lipophilic balance of surfactants was determined by using the emulsifier solvent power which, in turn, was related to ethanol value (489). A method for determining ethanol value was given. The formation and stability of emulsions made from 1:1 mixtures of water and octane were studied using various types and concentrations of surfactants (490). The phase inversion method was used to determine hydrophilic–lipophilic balance values of paraffin oil, rape oil, methyl silicone oil, olive oil, soybean oil, and oleic acid, using nonphenol adducts of ethylene oxide and other surfactants (491). The hydrophilic–lipophilic balance values obtained were comparable to values obtained by the Griffin procedure. The dielectric behavior of reverse emulsions during flocculation was studied (492).

The release of benzoic acid from oil-in-water emulsions was studied, and a dependence on the hydrophilic–lipophilic balance of the emulsifier, the viscosity, and the degree of dispersion was found (493). Oil-in-water emulsions of perfluorooctyl bromide for use as radiopaque media were stable and nonirritating (494). The particle-size distribution of a fluorocarbon emulsion was determined by centrifugal sedimentation (495).

Additional reports on emulsions are listed in Table XII.

Semisolids—The mechanical and storage effects on various ointment bases were studied (501). The influence of purity, components affecting pH, homogenization, and storage time on the color changes of zinc oxide paste with 20% resorcinol was followed by reflectance measurements (502). All factors, especially alkaline ingredients, affected the decomposition of resorcinol. The application properties of creams and ointment bases were reviewed (503). By means of fluid mechanics, subjective spreadability, viscosity, and stickiness perceived with the fingers were predicted (504). The effectiveness of different comminution techniques for salicylic acid and prednisolone was reported (505).

The water absorbancy of ointments containing polyethylene glycols, carbomer 934, emulsifiers, cetyl alcohol, and zinc stearate was determined (506). The quality and stability of ointments containing zinc oxide and one containing zinc oxide, fish oil, petrolatum, and lanolin were studied (507). The release of sulfathiazole and salicylic acid from white petrolatum containing ethoxylated surfactants of varying ethylene oxide chain lengths was evaluated by a dialysis method (508). The release rates of benzocaine[10] from two ointment bases were compared using an *in vitro* dialysis method as well as an *in vivo* method by determining blood levels in rabbits (509). Various methods were evaluated for determining the dispersion of benzocaine in ointments (510).

A study was undertaken to determine the water absorption capacities of pastes used in the treatment of conditions encountered particularly in veterinary medicine (511). The purposes of the study were to develop an *in vitro* method for the measurement of the absorptive rate and capacity of the pastes and to measure formulation effects and effects due to the physical state of the formulation.

Additional references on semisolids are listed in Table XIII.

Suppositories—A review on suppository formulation, especially the choice criteria for excipients, was published (531). Five bases were evaluated for suitability in preparing suppositories containing antibiotics (532). One base was suitable for oxacillin sodium, chloramphenicol was stable in two bases, while tetracycline hydrochloride was stable in all bases except polyethylene glycol. The release of these three antibiotics was studied by an *in vitro* method (533). The influence of preparation techniques and the composition

Table XII—Additional References on Emulsions

Reference	Topic
496	Preparation and stability of cosmetic water-in-oil emulsions
497	Use of hydrophilic–lipophilic balance system for studying paraffin emulsion
498	Emulsion for insulating and protecting the skin
499	Transparent emulsions
500	Cosmetic emulsions

Table XIII—Additional References on Semisolids

Reference	Topic
512	Tocopherol acetate ointments
513	Effect of limonin–limonene mixture on tissue permeability
514	Semisolid bases containing hydroxypropylcellulose
515	Effect of emulsifier on hydration number of petrolatum
516, 517	Use of hydrogenated cod liver oil in ointment preparation
518	Testing quality of pharmaceutical petrolatum
519	Review of emulsions and emulsion ointment bases
520	Study of air inclusion in ointments
521	Rheological interaction of emulsifiers with ointment bases
522	Stability of vitamins A and D_3 (cholecalciferol) in oil and water emulsions
523	Use of diethylene glycol stearate as emulsifier in ointment bases
524	Technological review of ophthalmic ointments
525	Coagulation structure formation in protective ointments
526	Properties of cold cream with triethanolamine and beeswax as emulsifying agents
527	Preparation of commercial petrolatum products from Soviet petrolatum
528	Rheological study of ointments containing ethonium and dodeconium additives
529	Topical vehicle design
530	Gelled vegetable oils as ointment bases using aluminum stearates

[10] Anesthesin, Abbott.

of aminophylline suppositories were examined 8 months after preparation (534). With some formulations and techniques, the unwanted late effects of the interaction between the active ingredients and vehicles could be prevented. A method of preparing hemorrhoidal suppositories of good quality was suggested (535).

A model system was developed for evaluating drug absorption in the rabbit doe (536). Drug disappearance from the drug reservoir followed first-order kinetics and was reproducible. The mechanical strengths and elastic moduli of blocks of polyethylene glycol with a range of molecular weights were determined (537). The release characteristics of prednisolone from similar blocks were determined and were correlated with the physical properties of the polyethylene glycols.

The bioavailability of aspirin from five brands of aspirin rectal suppositories was determined in an adult panel (538). At best, only 40% of the dose was available, but four out of five brands gave substantially lower absorption. The absorption of chloramphenicol from three types of suppository bases was studied in the rabbit (539). The absorption was higher with emulsified bases than with oleaginous bases. Surfactants in concentrations above the CMC had no effect on the release of soluble phenazone (antipyrine) or propylphenazone (540). Indomethacin release from suppositories containing polyoxyethylene decreased with the increasing molecular weight of the polymer (541). Also, indomethacin was absorbed into the bloodstream of rabbits faster when administered in polyethylene glycol suppositories than from those made with a glyceride base (542).

Chloramphenicol bioavailability was tested in rabbits and compared using various routes of administration: intravenous, intramuscular, rectal from an oil-in-water base, and oral (543). Physiological availability was highest for the suppository due to the first-pass effect of the liver.

Suppositories containing aspirin, dimethylaminophenazone (aminopyrine), phenacetin, and sulfanilamide of three different particle-size distributions were prepared (544). The effect of particle size on finished suppository physical properties was reported.

Coloring of suppositories was achieved by incorporation of colored powdered cellulose, which was made by treating with an alcoholic solution of a food coloring and drying (545). Color measurements were made, and the light fastness was determined. The use of insoluble organic coloring agents, mainly lake dyes, in suppositories was described (546).

Additional references on suppositories are listed in Table XIV.

Aerosols—A number of review articles appeared in the literature, including reviews of aerosol techniques (552), physicochemical systems for formulating pharmaceutical aerosols (553), aerosol hair products (554), the technology of aerosol cosmetics (555), aerosol foams (556), and alternatives to aerosols (557).

Table XIV—Additional References on Suppositories

Reference	Topic
547	Preparation of suppositories containing digitalis powder
548	Effect of melting point of suppositories on membrane diffusion
549	Use of Suppocire BML in suppositories
550	Thermal expansion of glycerol esters of some higher fatty acids used in suppository bases
551	Review of rectal administration of drugs

The causes of respiratory irritation by deodorant sprays that provoked cough were investigated, and several deodorant spray formulations were quantitatively evaluated for cough stimulation in a large number of subjects (558). A dexamethasone timed-release aerosol, employing the drug in microcapsules, was developed and evaluated (559). An aerosol dosage form of insulin was developed by dispersing insulin zinc crystals in a fluorocarbon propellant along with a dispersant (560).

A method of stabilization of nonionic aerosol emulsions was reported (561). Fatty alcohols in the propellant were added to the aqueous surfactant phase, which formed a surfactant–fatty alcohol complex. The binding of three fluorocarbon surfactants in an aqueous 5% human albumin solution was studied using the partition method, and the fraction of fluorocarbon bound was highly dependent on fluorocarbon concentrations (562). A new particle-size analysis technique of aerosols and fine powders was developed using an ultramicroscope and a sedimentation method (563).

The physicomechanical factors affecting spray from aerosol cans with centrifugal nozzles were studied using aqueous glycerin solutions (564). A practical method of employing carbon dioxide in cosmetic aerosols was presented; although it is not the ideal propellant, it does offer some advantages (565). Other articles discussed aerosol propellants (566, 567).

Controlled-Release Preparations—Cyclic iminocarbonates of dextran with coenzyme B_{12}, insulin, levarterenol, amphetamine, and procaine[11] were prepared and exhibited prolonged activity and increased stability (568). Sustained-release formulations of diphenhydramine hydrochloride were made using carnauba wax and stearyl alcohol, and some diluents also were evaluated for their effect on drug release (569). A new sustained-release tablet formulation of procainamide, in which the active component particles were coated with a thermoplastic substance, was tested *in vitro* and *in vivo* (570). It was reported that a sustained-release ascorbic acid tablet was not as bioavailable as an ordinary tablet, and this finding was attributed to ascorbic acid absorption, predominantly in the proximal small intestine (571).

The release of potassium from six different commercial formulations was compared, and the rate of release was markedly dependent on composition (572). In another study, three brands of slow-release potassium chloride tablets were tested for *in vitro* dissolution, using the Tingstad–Riegelman apparatus and a specific potassium-ion electrode as the monitoring device (573). A slow-release preparation of lithium sulfate was made by dispersion of the drug in a fat (574). Plasma levels of this new preparation and lithium carbonate tablets were obtained, and a higher frequency of diarrhea with the

[11] Novocain, Winthrop.

slow-release preparation was noted. The *in vitro* releases of six brands of quinidine bisulfate tablets were determined; four tablets were long acting, one was enteric coated, and one plain (575). Great differences were found in the quinidine release, depending on pH and time. The addition of starch to phenobarbital capsules increased the drug release rate (576).

Variables affecting the release of a drug from an inert plastic matrix were reviewed (577). The rate of release of water-soluble inorganic salts from tablets employing a polyethylene matrix was studied (578). Eight different slow-release tablet formulations on the Spanish market were examined for various physical properties as well as dissolution (579). The application of microencapsulation to alter the release properties of drugs was reported (580, 581).

The release of steroids and steroid esters from various drug delivery systems including water, vegetable oils, and polymer implants *in vivo* and *in vitro* was discussed (582). The controlled release of anticancer agents from composites with poly(lactic acid) was studied in rats (583). Silicone rubber implants were impregnated with drug by treatment with solutions of chloramphenicol or lincomycin hydrochloride (584). The release of these antibiotics from the implants was tested with *Sarcina lutea* as the test organism. The intravaginal release of ethynodiol diacetate from silicone devices in rabbits was studied, and *in vitro–in vivo* correlations were made (585). The release of progesterone from solid silicone rubber implants in sheep was superior to implants made from silicone rubber tubing containing solid progesterone (586). The release of caffeine and salicylic acid from cast ethylcellulose films was described, and release rate data were analyzed (587).

Various types of matrixes (plastics, waxes, and ion-exchange resins) used to control the release of drugs and the factors that affect their release were reviewed (588). The delivery of drugs from soft contact lenses composed of hydroxyethyl methacrylate–vinylpyrrolidinone polymer or polyhydroxyethyl methacrylate was discussed (589). Factors affecting the permeability of drugs through polymeric matrixes were described in quantitative terms, with particular reference to the use of pilocarpine.

A new delivery system for drugs, the osmotic pump, which delivers the agent by an osmotic process at a controlled rate, was reported (590). With immobilized enzymes, drug release in microcapsules was found to be zero order (591). The release of nicotinamide, isoniazid, acetylsalicylic acid (aspirin), and nalidixic acid from ion-exchange resins was studied (592). The kinetics of release of carbutamide from polymethacrylic acid derivatives were reported (593).

Additional references on controlled-release preparations are listed in Table XV.

Table XV—Additional References on Controlled-Release Preparations

Reference	Topic
594	Review of oral sustained-release and prolonged-action medication
595	Dry sustained-release oral drugs
596	Prolonged-action tablets prepared using vegetable mucilage
597	Significance of matrixes in prolonged-release oral administration
598	Preparation of coated micropellets and their use in pharmacy
599	Long acting steroid preparations
600	Evaluation of release rate of active substances from oral forms of drugs with prolonged action
601	Principles of retardation
602	Use of selected permeable membranes for biocompatible drug delivery systems
603	Oral retard preparation of verapamil hydrochloride

Cosmetics—*Microbiological Contamination*—A membrane filtration method for estimation of *Ps. aeruginosa* contamination of an oily cream was described (604). Various bactericides used in cosmetics and their activity were reviewed (605). The procedure for the preservation of talc according to the French and Italian pharmacopoeias was examined, antibacterial compounds were evaluated, and the manufacture of sterile talc for cosmetics was reported (606). Ethylene oxide sterilization of cosmetics was discussed, with particular reference to the proportion of residual amounts and reaction products that can cause toxicity problems (607).

Formulation and Technology—Similarities and differences in the development of a cosmetic product and that of a pharmaceutical preparation were reviewed (608). The responsibility of the cosmetic chemist to the public, as reinforced by legal codes requiring a product to match its promise to the consumer, was discussed (609).

Factors that determine the skin irritation potential of soaps and detergents were studied (610). Strongly anionic surfactants such as sodium lauryl sulfate had considerable activity, whereas nonionic ethoxylates had a minimal effect on the stratum corneum. Another study reported a new analytical approach for estimating the chemical interaction between surfactants resembling human skin and hair (611). The percutaneous absorption of some ^{14}C-labeled anionic surfactants was measured *in vivo* in rats after both consumer-type applications and applications of longer duration (612). Results obtained using isolated rat skin and human epidermis were compared. The absorption of ^{3}H-labeled triclosan[12] through rat skin treated with shampoo and with aerosol deodorant was measured (613). The concept of exaggerated exposure in topical irritancy and sensitization testing was discussed (614).

The structure and composition of the outer layers of the skin, the usefulness of various emulsions, and active ingredients useful in cosmetics were reviewed (615). Advantages and disadvantages of different methods for the determination of skin lipids were presented (616). The three disorders of the skin lipid systems that are of concern with seborrhea and related diseases were the amount, the composition, and the physical behavior of the lipid film on the skin's surface. The last factor was the most important.

A skin cream containing lactic acid or sodium lactate and adjusted to pH 4 was more beneficial for skin dryness and flaking than were control lotions (617). Measurements on extensibility and water-holding capacity

[12] Irgasan DP 300.

in isolated animal corneum showed that conventional humectants such as glycerol, sorbitol, and sodium lactate could be effective but the effect was lost when rinsed with water. Lactic acid was also effective and did not lose its effect when rinsed with water. The skin-moisturizing effect of baby oil was studied using 106 adult females who exhibited roughened, cracked, and inflamed skin of the elbows, knees, shins, and heels (618).

The experimental design and data analysis procedures associated with axillar antiperspirant tests were discussed; a new procedure, which does not require preliminary testing or establishment of "control ratios," was suggested (619). Silica gel moisture-absorbing tins strapped to the body side of the axilla were used to evaluate the effectiveness of antiperspirant agents under normal and near normal conditions (620). New trends in the formulation and testing technology of antiperspirant preparations were reviewed (621). One study involved the inhalational, histological, and dermatological aspects of aluminum chlorhydroxide, an active constituent in antiperspirant preparations (622).

^{35}S-Labeled zinc pyrithione in a shampoo formulation was adsorbed onto hair and skin; the degree of adsorption was dependent on time, pH, temperature, and concentration (623). The velocity of an aerosol hair spray was determined by measuring the gas velocity within the spray with a pilot-static tube (624). Measurements of the capture and penetration of hair spray droplets into a model array of hair fibers indicated that coarse sprays gave better penetration than fine sprays. The fastness of human hair colorings to crocking, washing, water, and light was determined (625). The causes of split ends of hair were reviewed (626). The usefulness and effect of hair conditioners, lacquers, setting lotions, and rinses on hair were reviewed (627).

A hairless mouse was used as an experimental model for evaluating the effectiveness of sunscreen preparations; the best protection was obtained with two sunscreens, 5.4% *p*-dimethylaminobenzoic acid and 2.7% alkyl *p*-aminobenzoate (628). Solar protective preparations were evaluated by *in vivo* and *in vitro* techniques (629). In another study, the photoprotective capabilities of propyl gallate, acetylcysteine, ascorbic acid, and 30 other compounds were tested, and no correlation between *in vivo* and *in vitro* effectiveness was identified (630). The effectiveness of titanium dioxide incorporated into 11 formulations was evaluated *in vitro* and *in vivo* (631).

A number of physical methods using a tensiometer[13] were used to characterize dentifrices and other semisolids (632). The cleaning power of toothpaste was evaluated by allowing stain to build up on teeth for 5 weeks using a nonabrasive toothpaste and then testing the cleaning activity of new pastes to remove stain (633). A mathematical relationship was developed to express the ability to remove stain. The physical characteristics of solid particles and heterogeneities in the liquid phase(s) of a toothpaste as it is extruded from the tube were studied by electron microscopic techniques (634).

[13] Instron.

Table XVI—Additional References on Formulation and Technology of Cosmetics

Reference	Topic
635	Aerobic microflora of outer eye
636	Formulation of high foaming cosmetic products
637	Aspects of skin penetration by collagen and proline
638	Microemulsions: formation and stabilization
639	Surfactants in personal care products
640	History of perfume industry
641	Raw materials for perfume industry
642	Adhesion and fixing of perfumes
643	Cosmetic emulsions, creams, and milks
644	Chemical constituents of skin and effects of cosmetics on skin
645	Methods of evaluating hair lacquers
646	Manufacturing methods and emulsion stability of cosmetic water–oil emulsions
647	Formulation of cosmetic emulsions
648	Review of hair straighteners
649	Review of face powders
650	Review of foundation makeup
651	Review of hand creams and lotions
652	Lipstick formula variations and lipstick properties
653	Classification and utilization of lanolin derivatives
654	Sarcosinates as base products for cosmetics
655	Review of polyethylene glycols
656	Review of emulsified and solid fragrances
657	Fingernail elongators and accessory nail preparations
658	Review of bath preparations
659	Review of shampoos
660	Review of depilatories
661	Preshave and aftershave preparations
662	Review of shaving preparations: soaps, creams, oils, and lotions
663	Sulfosuccinic acid half esters and their use in cosmetics
664	Gelatin hydrolysate use in cosmetic creams
665	Review of mouthwashes
666	Properties of cold cream with triethanolamine and beeswax as emulsifying agents
667	Review of cleansing creams and lotions
668	Role of essential fatty acids in regulatory processes of malpighian cell membranes
669	Body care aids
670	Synthetic bar soaps from sodium primary alkylsulfonates
671	Toilet soaps with disinfecting and therapeutic prophylactic additives
672	Hair conditioner formulation
673	Use of polyoxyethylene 20 sorbitan isostearate as emulsifier and solubilizer for cosmetics, drugs, and toiletries
674	Pigment dispersion technology for cosmetic application
675	Use of acyl lactylates in cosmetics and toiletries
676	Peroxides in polyethylene glycols and polyethylene glycol derivatives
677	Vegetable lecithin in cosmetic lotions
678	Cosmetic application of high oleic safflower oil
679	Role of research in development of cosmetic products
680	Evaluation of synthetic oily materials as bases for lipsticks, cleansing milks, and foundation emulsions
681	Determination of required hydrophilic–lipophilic balance of oil-in-water emulsions by phase inversion titration
682	Biphasic gels
683	Use of silicones in formulation of eye shadow sticks
684	Physical properties of basic aluminum complexes as related to their efficacy
685	Shampoo formulations
686	Cellulose polymers in cosmetics and toiletries
687	Cationic surfactants in low pH shampoos
688	Shampoo surfactants
689	Collaborative study of rabbit eye irritation tests
690	Dandruff and its treatment
691	Aerosol foam shampoos
692	Microbiology of shampoos
693	Trends and aspects of contemporary shampoos
694	Theory and practice of shampooing
695	Perspiratio insensibilis control by specific associations of lipids
696	Cosmetic regulation in Germany; main facts of 1974 law
697	Stability of basic aluminum chlorides in antiperspirant formulations
698	Lipstick formula variations and lipstick properties
699	Use of microencapsulation in cosmetics

Table XVI—(*Continued*)

Reference	Topic
700	Conditioning shampoos; digest of patents issued in 1970–1974
701	Critical review of antiperspirant efficacy testing
702	Role of prostaglandins in UV erythema
703	Analysis of shampoos containing anionic and nonionic surfactants
704	Assessment of auxiliary detergents in shampoo mixtures
705	Use of hydroxypropylcellulose acetates as gelling agents for organic solvents
706	Protective skin care
707	Direction of international perfumery
708	Importance of acetylenic compounds in perfumery
709	Utility of amine oxides in oil/water cosmetic systems
710	Occurrence of *Ps. aeruginosa* and *Staphylococcus aureus* in orbital area
711	Action and fate of sodium pyridinethione applied topically to rabbits
712	Implications of enlarged European Economic Community on quality and safety of cosmetics
713	Detection of chrysotile asbestos in talcs by differential thermal analysis
714	Properties of ethoxylated lanolin derivatives and their effect on cosmetic application
715	Cholesterol in cosmetic formulation
716	Cosmetic activity of emulsions
717	Phytogels and their possible cosmetic uses
718	Conditioning shampoo containing a mixture of wax and rosin
719	Cosmetic uses, structure, and asbestos contamination of talc
720	Cosmetic emulsion compounding
721	Use of cosmetic water-in-oil emulsions
722	Waxes in cosmetic preparations
723	Use of surfactants in cosmetics
724	Perfuming cosmetic products
725	Use of chelation as stabilizer in cosmetics
726	Practice of compounding cosmetic emulsions
727	Potential applications of urea for skin disease
728	Quaternary ammonium compounds in cosmetics
729	Shorter methods for evaluating antidandruff agents
730	Animal model for estimating relative sting potential of shampoos
731	Influence of protein vehicles on penetrability of sunscreens

Additional references on cosmetic formulation and technology are listed in Table XVI.

Packaging—The requirements of plastic materials for pharmaceutical packaging were reviewed (732). An identification method for pharmaceutical containers and packaging materials by IR spectroscopy was described, and a compilation of spectra was included (733). Extraction rates of marker compounds from rubber closures for parenteral use were reported (734). A model for predicting the maximum vinyl chloride concentration in bottle contents was developed from knowledge of the vinyl chloride monomer in polyvinyl chloride bottles (735). Octyltin-stabilized polyvinyl chloride was analyzed using food-simulating solvent to replace actual products (736).

The stability of promethazine hydrochloride solutions was compared in polyethylene and glass containers (737). Red-colored plastic and brown glass gave the best protection. Methods for the determination of synthetic organic colors in plastic packages for pharmaceutical use were reported (738), and trace amounts of colorant released to pharmaceutical preparations were detected. Various single-unit packages for syrups dispensed in hospitals were evaluated, and stabilities were determined (739). A study was made on the blister packaging of pharmaceutical products which included a description of the process, materials used for packaging, suitable machinery, and limitations (740). Various silicates were found to have a protective effect on aluminum tubes filled with toothpastes and shaving creams. This finding was attributed to the formation of a colloidal aluminum silicate on the aluminum surface, which was dependent on pH and the concentration of the corrosive agent (741).

Table XVII—Additional References on Packaging

Reference	Topic
742	Development of mechanical methods of testing child-proof containers
743	Packaging primer for drugs and cosmetics; polyethylene and polypropylene
744	Problems of using thermoplastic containers for dermal pharmaceutical products
745	Review of packaging in pharmaceutical industry
746	Environmental influence on seal performance
747	Use of adhesive-cohesive polyethylene to form cold-seal pouches
748	Properties of polyethylene in flexible packaging
749	New child-resistant closure systems for use in United Kingdom
750	Low adhesion properties of package laminates for peel property
751	Closures and seals for pharmaceutical containers
752	Sachet filling and forming machines
753	Testing and control of plastic containers for pharmaceuticals
754	Problems of labeling small and awkwardly shaped items

Additional references on packaging are listed in Table XVII.

Instruments and Equipment—The advantages of an electropolished stainless steel surface over mechanical surface treatment were discussed (755). The preliminary planning, design, and construction of a new sterile manufacturing plant were reported (756). The application of reverse osmosis for purification of water for sterile products was reviewed (757). The effect of the size of the tank and impeller on liquid–liquid dispersions by mechanical agitation was studied (758). The control of airborne dust was discussed, including such factors as filter types, ducts, and hooding devices (759).

Automatic checkweighers currently available were listed, and their pharmaceutical applicability was described (760). The use of a programmed checkweighing system in the packaging of drugs and cosmetics was discussed (761). Processes and equipment for agglomerating, instantizing, and spray drying food products were surveyed (762). Newer techniques mentioned were the steam-swept wheel process, the two-stage drying process, and a combination spray dryer–fluidized bed. The applicability of the Poisson distribution to suspension spray drying was studied (763). *In vivo* studies

Table XVIII—Additional References on Instruments and Equipment

Reference	Topic
765	Automatic placement of valves and tips on aerosol cans
766	Equipment for cosmetic and pharmaceutical industries
767	Aspects of electronic weighing
768	New, inexpensive device for making individually prepared capsules
769	Establishment of a nuclear pharmacy
770	Effect of method of freezing and pulverization of pancreas gland on yield of insulin

Table XIX—Additional References on Dental Products and Materials

Reference	Topic
774	Bond strength of dental amalgam joined to cast silver–tin alloys
775	Effects of sand blasting on surface of silver–tin alloy casts
776	Rugosimetric evaluation of two brands of amalgams using two techniques
777	Effect of particle sizes on compressive strength of dental silicate cements
778	Etching techniques for pit and fissure sealants
779	Factors influencing creep behavior of poly(methyl methacrylate) cements
780	Comparison of effects of linear and cyclic phosphates on adsorption of proteins by human enamel
781	Enhancement of antiplaque value of antibacterial agents by enamel-conditioning methods
782	Kinetics and mechanisms of reactions of human tooth enamel in buffered solutions of high fluoride concentrations
783	Laboratory properties of polyacrylate cement
784	Effect of salts commonly found in tap water on expansion of inlays

Table XX—References on Biomedical Devices and Materials

Reference	Topic
785	Evaluation of a metal–ceramic composite hip prosthesis
786	Composite implants for orthopedic applications; *in vivo* evaluation of candidate resins
787	Chronic heparin anticoagulant in dogs by continuous infusion with a totally implantable pump
788	Third-generation artificial kidney; pH and concentration control
789	Porous calcium sulfate dihydrate as a biodegradable implant in bone
790	Thermodifferential analysis of ceramic implants
791	Comparison between mercury and lithium chemical systems for pacemaker energy source applications
792	Soft tissue response to series of dense ceramic materials and two clinically used biomaterials
793	Hydrophilic polymers for biomedical materials
794	Required properties for biofunctional materials
795	Interfacial behavior of ceramic implants
796	Engineering and biological studies of metallic implant materials
797	Materials characterization of implantable porous electrodes
798	Polymeric materials for medicinal products of frequent use
799	Review of thrombogenic behavior of polymers and polymers potentially useful as implants
800	Method for methacrylate polymer (Hydron) impregnation of silicone rubber
801	Compatibility and versatility of natural and synthetic polymers as biomedical materials
802	Characterization and evaluation of springy polypropylene as prosthetic device
803	*In vitro* investigation of the anodic dissolution and capacitative behavior of 316L stainless steel as surgical orthopedic implant material
804	*In vitro* studies of lipid uptake by medical grade silicone rubbers used for heart valve balls
805	Physical characteristics and performance of synthetic wound dressings
806	Biological testing of surface-modified acrylic polymers
807	Absorbable artificial vas deferens for vasovasotomy
808	Medical use of organic porous polymer membrane
809	Review on polymer prosthesis and sutures
810	Development of biomedical polymers emphasizing collagen
811	Slow crack growth in acrylic bone cement
812	Survey of metallic implant materials
813	Review of materials for biomedical applications
814	Fractography of poly(methyl methacrylates)
815	Microstructure of two-phase poly(methyl methacrylates)
816	Review of chemical and physical properties of methacrylate polymer (Hydron)

with human volunteers compared the neutralizing effect of various antacid dosage forms using the Heidelberg capsule (764). A suspension and chewable tablet gave similar results, whereas a tablet for swallowing gave less prompt effects and a shorter duration of action.

Additional references on instruments and equipment are listed in Table XVIII.

Dental Products and Materials—A literature review of dental materials was published (771). Properties of dentifrices, including the function of a dentifrice, therapeutic dentifrices, dentifrice ingredients, abrasives, surfactants, humectants, binders, flavors, and fluorine compounds were reviewed (772). The absorption, distribution in body fluids, and bioavailability of fluoride were studied after various doses (773). The concentration of fluoride in saliva and plasma was found to be nearly equal.

Additional references on dental products and materials are listed in Table XIX.

Biomedical Devices and Materials—This year a separate section on implants, prosthetic devices, and the materials used in them is included because of increased research and development in these areas. References on these topics are listed in Table XX.

REFERENCES

(1) W. J. McKeehan, *J. Pharm. Sci.*, **52**, 613(1963).
(2) W. J. McKeehan and L. C. Lappas, *ibid.*, **53**, 695(1964).
(3) L. C. Lappas and R. E. Dempski, *ibid.*, **54**, 931(1965).
(4) R. E. Dempski and G. P. Polli, *ibid.*, **55**, 645(1966).
(5) G. P. Polli and L. J. Ravin, *ibid.*, **56**, 781(1967).
(6) L. J. Ravin and P. D. Bernardo, *ibid.*, **57**, 1075(1968).
(7) P. D. Bernardo and E. J. Russo, *ibid.*, **58**, 777(1969).
(8) E. J. Russo and T. L. Benney, *ibid.*, **59**, 883(1970).
(9) T. L. Benney and W. E. Hamlin, *ibid.*, **60**, 959(1971).
(10) W. E. Hamlin and A. C. Shah, *ibid.*, **61**, 989(1972).
(11) A. C. Shah and A. K. Herd, *ibid.*, **62**, 1033(1973).
(12) *Ibid.*, **62**, 1217(1973).
(13) A. K. Herd and J. K. Haleblian, *J. Pharm. Sci.*, **63**, 995(1974).
(14) J. K. Haleblian and F. W. Goodhart, *ibid.*, **64**, 1085(1975).
(15) L. H. Werner, *Handb. Ind. Chem., 7th Ed.*, **1974**, 597; through *Chem. Abstr.*, **82**, 21742b(1975).
(16) H. Tarchalska, *Przem. Chem.*, **53**, 436(1974); through *Chem. Abstr.*, **82**, 21746f(1975).
(17) B. G. Laroque and F. R. Grover, *Can. Pharm. J.*, **108**, 26(1975); through *Chem. Abstr.*, **82**, 160152x(1975).
(18) C. Walter, "The Drugs of Veterinary Medicine," 1973; through *Chem. Abstr.*, **82**, 90055s(1975).
(19) G. W. John and P. P. Lamy, *Am. J. Pharm.*, **147**, 101 (1975).
(20) W. Lund, R. J. McBride, J. B. Murray, and G. Smith, *Pharm. J.*, **214**, 322(1975); through *Chem. Abstr.*, **83**, 15526p(1975).
(21) H. Mengel, *Dev. Biol. Stand.*, **24**, 233(1974); through *Chem. Abstr.*, **82**, 103048u(1975).
(22) L. Smith, K. Jensen, and T. Mikkelsen, *Arch. Pharm. Chem.*, **81**, 1175(1974); through *Chem. Abstr.*, **82**, 175203p(1975).
(23) J. F. Farber and M. Rench, *Dev. Biol. Stand.*, **24**, 213(1974); through *Chem. Abstr.*, **82**, 103066y(1975).
(24) A. G. Mitchell and S. J. A. Kazmi, *Can. J. Pharm. Sci.*, **10**, 67(1975).
(25) G. H. Konning, *ibid.*, **9**, 103(1974); through *Chem. Abstr.*, **82**, 90028k(1975).
(26) R. Genova, L. Monti, and S. Casadio, *Bull. Tech., Gatefosse SFPA*, **68**, 48(1974); through *Chem. Abstr.*, **83**, 152281u(1975).
(27) C. L. Goldman, *Drug Cosmet. Ind.*, **117**(1), 40(1975).
(28) P. B. Chemburkar and R. S. Joslin, *J. Pharm. Sci.*, **64**, 414(1975).
(29) L. Adam, E. Szantho, I. Gered, and O. Horvath, *Rev. Med.*, **20**, 209(1974); through *Chem. Abstr.*, **83**, 48147u(1975).
(30) A. A. Kassem, H. A. F. Mahrous, A. E. Swealem, and N.

Rofael, *J. Drug Res.*, **6**, 185(1974); through *Chem. Abstr.*, **82**, 64406n(1975).

(31) I. M. Pertsev, D. I. Dmitrievskii, G. S. Bashura, and M. K. Pilipenko, *Farm. Zh. (Kiev)*, **30**, 43(1975); through *Chem. Abstr.*, **83**, 152263q(1975).

(32) M. T. Riera, *Cienc. Ind. Farm.*, **4**, 3(1972); through *Chem. Abstr.*, **83**, 15559b(1975).

(33) M. J. Crooks and K. F. Brown, *Aust. J. Pharm. Sci.*, **3**, 93(1974); through *Chem. Abstr.*, **83**, 329266z(1975).

(34) R. M. G. Boucher, *Can. J. Pharm. Sci.*, **10**, 1(1975).

(35) E. P. Sheppard and C. H. Wilson, *J. Soc. Cosmet. Chem.*, **25**, 655(1974).

(36) P. L. Altieri, S. Berman, and J. P. Lowenthal, *Dev. Biol. Stand.*, **24**, 71(1974); through *Chem. Abstr.*, **82**, 103060s(1975).

(37) C. E. Holloway and F. H. Dean, *J. Pharm. Sci.*, **64**, 1078(1975).

(38) E. R. Garrett and J. K. Lewis, *ibid.*, **64**, 1936(1975).

(39) E. J. Mariani, Jr., C. J. Libbey, and W. Litsky, *Dev. Ind. Microbiol.*, **14**, 356(1973); through *Chem. Abstr.*, **82**, 64368b(1975).

(40) W. Kedzia, B. Kedzia, and A. Szumala, *Ann. Pharm. (Poznan)*, **11**, 37(1975); through *Chem. Abstr.*, **83**, 33009b(1975).

(41) R. Nakamori, F. Tanaka, T. Nojiri, H. Yoshino, and M. Okumura, *J. Pharm. Sci.*, **64**, 1071(1975).

(42) J. E. McDavid, *Dev. Biol. Stand.*, **24**, 49(1974); through *Chem. Abstr.*, **82**, 116024h(1975).

(43) M. Kostolowska, L. Krowczynski, and E. Jania, *Farm. Pol.*, **30**, 993(1974); through *Chem. Abstr.*, **83**, 15570y(1975).

(44) J. V. Sorrentino and W. A. Hankins, *Dev. Biol. Stand.*, **24**, 107(1974); through *Chem. Abstr.*, **82**, 116025j(1975).

(45) N. Plishko, *Svinovodstvo (Moscow)*, **1**, 26(1975); through *Chem. Abstr.*, **82**, 160210n(1975).

(46) S. B. Jasnow and J. L. Smith, *Appl. Microbiol.*, **30**, 205(1975); through *Chem. Abstr.*, **83**, 168323v(1975).

(47) I. Batty, E. Harris, and A. Gasson, *Dev. Biol. Stand.*, **24**, 131(1974); through *Chem. Abstr.*, **82**, 103062u(1975).

(48) E. Seroczynska, *Tluszcze, Srodki Piorace, Kosmet.*, **18**, 362(1974); through *Chem. Abstr.*, **82**, 144810e(1975).

(49) H. Leszczynska-Bakal and T. Smazynski, *ibid.*, **19**, 53(1975); through *Chem. Abstr.*, **83**, 103187j(1975).

(50) J. Schimmel and M. N. Slotsky, *Cosmet., Sci. Technol., 2nd Ed.*, **3**, 391(1974); through *Chem. Abstr.*, **83**, 103110d(1975).

(51) K. H. Wallhaeusser, *Drugs Made Ger.*, **17**, 103(1974); through *Chem. Abstr.*, **83**, 15514h(1975).

(52) O. N. Yalcindag, *Kim. Sanayi*, **22**, 47(1974); through *Chem. Abstr.*, **82**, 77014h(1975).

(53) J. B. Urgell, *Cosmet. Perfum.*, **90**(3), 55(1975).

(54) M. Fontana and G. Prosperio, *Riv. Ital. Essenze, Profumi, Piante Off., Aromi, Saponi, Cosmet., Aerosol*, **56**, 315(1974); through *Chem. Abstr.*, **82**, 47615n(1975).

(55) W. M. Cort, J. W. Scott, and J. H. Harley, *Food Technol.*, **29**(11), 46(1975).

(56) O. N. Yalcindag, *Kim. Sanayi*, **22**, 161(1974); through *Chem. Abstr.*, **83**, 103170y(1975).

(57) K. H. Wallhaeusser, *Pharm. Ind.*, **36**, 716(1974); through *Chem. Abstr.*, **82**, 103040k(1975).

(58) H. P. Munzig and H. Schels, *Tluszcze, Srodki Piorace, Kosmet.*, **18**, 355(1974); through *Chem. Abstr.*, **82**, 129170c(1975).

(59) G. E. Schumacher, *Perspect. Clin. Pharm.*, **1972**, 368; through *Chem. Abstr.*, **82**, 64352s(1975).

(60) I. M. Kovach, *Diss. Abstr. Int.*, **36**, 734-B(1975).

(61) M. Manes and J. P. Mann, Jr., *Clin. Toxicol.*, **7**, 355(1974); through *Chem. Abstr.*, **82**, 47699t(1975).

(62) T. E. Doty and E. Vanninen, *Food Technol.*, **29**(11), 34(1975).

(63) J. W. Robinson, *Food Eng.*, **47**(5), 57(1975).

(64) K. C. Fruin and B. L. Scallet, *Food Technol.*, **29**(11), 40(1975).

(65) M. S. Balsam, *Cosmet., Sci. Technol., 2nd Ed.*, **2**, 599(1972); through *Chem. Abstr.*, **82**, 7551g(1975).

(66) E. Paukner and V. Hudewenz, *J. Soc. Cosmet. Chem.*, **26**, 235(1975).

(67) T. Fujii, S. Furukawa, and S. Suzuki, *Cosmet. Perfum.*, **90**(9), 37(1975).

(68) A. Weissler, *Food Technol.*, **29**(5), 38(1975).

(69) G. S. Roye, *Cosmet. Perfum.*, **90**(4), 25(1975).

(70) F. M. Bogdansky, *J. Pharm. Sci.*, **64**, 323(1975).

(71) J. H. von Elbe, *Food Technol.*, **29**(5), 42(1975).

(72) A. C. Noble, *ibid.*, **29**(12), 56(1975).

(73) J. Stofberg, *Cosmet. Perfum.*, **90**(10), 71(1975).

(74) R. Angelotti, *ibid.*, **90**(8), 43(1975).

(75) Anon., *ibid.*, **90**(2), 86(1975).

(76) T. Nagasawa, K. Umemoto, T. Tsuneya, and M. Shiga, *Koryo*, **108**, 45(1974); through *Chem. Abstr.*, **82**, 129171d(1975).

(77) H. M. Gattefosse, *Bull. Tech., Gattefosse SFPA*, **67**, 33(1972); through *Chem. Abstr.*, **82**, 7563n(1975).

(78) K. L. Franzen and J. E. Kinsella, *Chem. Ind.*, **Dec. 1975**, 505.

(79) D. L. J. Opdyke, *Food Cosmet. Toxicol.*, **12** Suppl. (Monographs on Fragrance of Raw Materials) (1974); through *Chem. Abstr.*, **83**, 15488c(1975).

(80) *Ibid.*, **12**, 531(1974); through *Chem. Abstr.*, **82**, 144803e(1975).

(81) *Ibid.*, **12**, 533(1974); through *Chem. Abstr.*, **82**, 144804f(1975).

(82) K. Kulka and J. W. Dittrick, *Cosmet. Perfum.*, **90**(2), 90(1975).

(83) P. Z. Bedoukian, *ibid.*, **90**(4), 49(1975).

(84) A. Verain, M. Traisnel, and M. Rouset, *Afinidad*, **31**, 351(1974); through *Chem. Abstr.*, **82**, 89989t(1975).

(85) M. Traisnel, A. Verain, and M. Rouzet, *Labo-Pharma—Probl. Tech.*, **23**, 481(1975); through *Chem. Abstr.*, **83**, 120690k(1975).

(86) H. R. Wagner, *Proc. Soc. Anal. Chem.*, **11**, 273(1974); through *Chem. Abstr.*, **83**, 15466u(1975).

(87) D. L. J. Opdyke, *Food Cosmet. Toxicol.*, **13**, 111(1975); through *Chem. Abstr.*, **83**, 15465t(1975).

(88) C. A. Signorino and E. Furmanski, *Food Eng.*, **47**(5), 76(1975).

(89) T. Philip, *Food Technol.*, **29**(5), 50(1975).

(90) J. C. Bauernfeind, *ibid.*, **29**(5), 48(1975).

(91) A. Staglavska, *Farmatsiva (Moscow)*, **23**, 75(1974); through *Chem. Abstr.*, **82**, 47657c(1975).

(92) J. W. McGinity, J. A. Hill, and A. L. LaVia, *J. Pharm. Sci.*, **64**, 356(1975).

(93) R. Hamburger, E. Azaz, and M. Donbrow, *Pharm. Acta Helv.*, **50**, 10(1975); through *Chem. Abstr.*, **82**, 144903n(1975).

(94) N. Yanishlieva and A. Popov, *Seifen, Oele, Fette, Wachse*, **101**, 185(1975); through *Chem. Abstr.*, **83**, 120653a(1975).

(95) G. W. Holzner, *Riechst., Aromen., Koerperpflegem*, **25**, 66(1975); through *Chem. Abstr.*, **83**, 168325x(1975).

(96) A. Dominguez-Gil and R. Cardoniga, *Medicamenta, Ed. Farm.*, **45**, 9(1975); through *Chem. Abstr.*, **83**, 103172a(1975).

(97) M. Kingsford, *Aust. J. Pharm. Sci.*, **4**, 23(1975); through *Chem. Abstr.*, **83**, 103180b(1975).

(98) L. E. Quihillalt, J. A. Arciprete, and A. E. A. Mitta, *Argent., Com. Nac. Engery At.*, [*Inf.*], **1974**, 378; through *Chem. Abstr.*, **83**, 15532n(1975).

(99) H. Stricker, *Pharm. Ind.*, **37**, 446(1975); through *Chem. Abstr.*, **83**, 168340y(1975).

(100) B. R. Hajratwala, *Aust. J. Pharm. Sci.*, **5**, 39(1975); through *Chem. Abstr.*, **83**, 152224c(1975).

(101) E. Nuernberg, *Dtsch. Apoth.-Ztg.*, **114**, 1411, 1715(1974); through *Chem. Abstr.*, **82**, 34973c(1975).

(102) M. De la Fernandez and R. Carmona, *Cienc. Ind. Farm.*, **4**, 257(1972); through *Chem. Abstr.*, **82**, 160129v(1975).

(103) J. L. Kiger, *Rev. Int. Serv. Sante Armees Terre, Mer Air*, **47**, 707(1974); through *Chem. Abstr.*, **82**, 160144w(1975).

(104) R. Wolfert and R. Cox, *Am. J. Hosp. Pharm.*, **32**, 585(1975).

(105) G. J. Rhee and B. S. Yu, *Yakhak Hoe Chi*, **18**, 20(1974); through *Chem. Abstr.*, **83**, 120723y(1975).

(106) L. Tomasini, D. Naplatanova, and M. Zakharieva, *Farmatsiya (Sofia)*, **24**, 57(1974); through *Chem. Abstr.*, **82**, 7566r(1975).

(107) J. Hasegawa, M. Hanano, and S. Awazu, *Chem. Pharm. Bull.*, **23**, 86(1975).

(108) H. Delonca, J. Joachim, G. Joachim, and A. Cantos, *Farmaco. Ed. Prat.*, **30**, 89(1975); through *Chem. Abstr.*, **83**, 136795j(1975).

(109) S. M. Khafagy, A. N. Girgis, and N. Rofael, *J. Drug Res.*, **6**, 55(1974); through *Chem. Abstr.*, **82**, 129242c(1975).

(110) D. Barrett and J. T. Fell, *J. Pharm. Sci.*, **64**, 335(1975).

(111) B. Dorsch and R. Shangraw, *Hosp. Pharm.*, **32**, 795(1975).

(112) K. Thoma and R. Groening, *Pharm. Ind.*, **36**, 876(1974); through *Chem. Abstr.*, **82**, 129236d(1975).

(113) N. Harb and D. J. Voaden, *J. Hosp. Pharm.*, **32**, 144(1974); through *Chem. Abstr.*, **82**, 34987k(1975).

(114) S. Basquin and M. Traisnel, *Sci. Tech. Pharm.*, **3**, 413(1974); through *Chem. Abstr.*, **82**, 160155a(1975).

(115) A. R. Ebian, M. A. Moustafa, S. A. Khalil, and M. M. Motawi, *J. Pharm. Sci.*, **64**, 1481(1975).

(116) M. A. Moustafa, A. R. Ebian, S. A. Khalil, and M. M. Motawi, *ibid.*, **64,** 1485(1975).

(117) M. A. El-Egakey, F. El-Khawas, A. G. Iskander, and M. M. Abd El-Khalek, *J. Drug Res.*, **6,** 169(1974); through *Chem. Abstr.*, **82,** 77071z(1975).

(118) M. A. El-Egakey, F. El-Khawas, A. G. Iskander, and M. M. Abd El-Khalek, *Pharmazie,* **29,** 466(1974); through *Chem. Abstr.*, **82,** 21788w(1975).

(119) E. Pawelczyk and S. Domeracki, *Acta Pol. Pharm.*, **31,** 315(1974); through *Chem. Abstr.*, **82,** 116044q(1975).

(120) H. Baer and M. L. Hooton, *Dev. Biol. Stand.*, **24,** 115(1974); through *Chem. Abstr.*, **82,** 116026k(1975).

(121) J. G. Center, N. Shuller, and L. D. Zeleznick, *J. Allergy Clin. Immunol.*, **54,** 305(1974); through *Chem. Abstr.*, **82,** 77026p(1975).

(122) M. Amin, A. Seeger, K. Prezewowsky, and P. Fuchs, *Pharm. Acta Helv.*, **49,** 117(1974); through *Chem. Abstr.*, **82,** 47693m(1975).

(123) P. Pothisiri and J. T. Carstensen, *J. Pharm. Sci.*, **64,** 1931(1975).

(124) J. T. Carstensen and P. Pothisiri, *ibid.*, **64,** 37(1975).

(125) A. I. Artem'ev, *Farmatsiya (Moscow)*, **24,** 60(1975); through *Chem. Abstr.*, **83,** 152286z(1975).

(126) D. G. Pope and J. L. Lach, *Pharm. Acta Helv.*, **50,** 165(1975); through *Chem. Abstr.*, **83,** 103184f(1975).

(127) A. A. Kassem and W. Darwish, *Bull. Fac. Pharm., Cairo Univ.*, **11,** 123(1972); through *Chem. Abstr.*, **82,** 64438z(1975).

(128) D. W. Newton, A. G. Rogers, C. H. Becker, and G. Torosian, *Am. J. Hosp. Pharm.*, **32,** 817(1975).

(129) B. Testa and J. C. Etter, *Can. J. Pharm. Sci.*, **10,** 16(1975).

(130) *Ibid.*, **10,** 20(1975).

(131) B. R. Hajratwala, *J. Pharm. Sci.*, **64,** 45(1975).

(132) A. E. M. El-Nimr, A. A. Kassem, and M. A. Kassem, *Pharmazie,* **30,** 216(1975); through *Chem. Abstr.*, **83,** 15606q(1975).

(133) T. S. Kondrat'eva and L. N. Pirozhnikova, *Farmatsiya (Moscow)*, **24,** 29(1975); through *Chem. Abstr.*, **83,** 103215s(1975).

(134) H. Abe and Y. Shigeta, *Farumashia,* **11,** 519(1975); through *Chem. Abstr.*, **83,** 152225d(1975).

(135) K. Thoma and E. Vasters, *Pharm. Ztg.*, **119,** 1430(1974); through *Chem. Abstr.*, **82,** 77035r(1975).

(136) *Ibid.*, **119,** 1591(1974); through *Chem. Abstr.*, **82,** 77038u(1975).

(137) S. Hagiwara, *Kyoto Furitsu Daigaku Gakujutsu Hokoku: Rigaku, Seikatsu Kagaku,* **25,** 19(1974); through *Chem. Abstr.*, **82,** 172953x(1975).

(138) H. Okada, V. Stella, J. Haslam, and N. Yata, *J. Pharm. Sci.*, **64,** 1650(1975).

(139) E. Pawelczyk and B. Marciniec, *Pharmazie,* **29,** 585(1974); through *Chem. Abstr.*, **82,** 77047w(1975).

(140) L. Molnar and M. Sivak, *ibid.*, **29,** 417(1974); through *Chem. Abstr.*, **82,** 21771k(1975).

(141) C. W. Whitworth and A. F. Asker, *J. Pharm. Sci.*, **64,** 2018(1975).

(142) C. T. Bauguess, F. Sadik, J. H. Fincher, and C. W. Hartman, *ibid.*, **64,** 117(1975).

(143) R. P. Enever, A. L. W. Po, B. J. Millard, and E. Shotton, *ibid.*, **64,** 1497(1975).

(144) R. E. Notari and J. L. DeYoung, *ibid.*, **64,** 1148(1975).

(145) H. V. Maulding, P. Turi, D. Grossman, and J. P. Nazareno, *ibid.*, **64,** 1833(1975).

(146) J. Kosir-Bizili and B. Meden, *Farm. Vestn. (Ljubljana)*, **25,** 101(1974); through *Chem. Abstr.*, **82,** 21766n(1975).

(147) A. David and G. Horvath, *Farmatsiya (Moscow)*, **24,** 36(1975); through *Chem. Abstr.*, **83,** 103216t(1975).

(148) B. Lindeke, E. Anderson, G. Lundkvist, U. Jonsson, and S. O. Eriksson, *Acta Pharm. Suec.*, **12,** 183(1975); through *Chem. Abstr.*, **83,** 103211n(1975).

(149) E. Pawelczyk and M. Zajac, *Pol. J. Pharmacol. Pharm.*, **27,** 69(1975); through *Chem. Abstr.*, **83,** 103200h(1975).

(150) H. Roseboom and J. A. Fresen, *Pharm. Acta Helv.*, **50,** 55(1975); through *Chem. Abstr.*, **83,** 15580b(1975).

(151) M. Martin and H. Auel, *Thromb. Diath. Haemorrh.*, **33,** 586(1975); through *Chem. Abstr.*, **83,** 168380m(1975).

(152) H. Krasowska, *Acta Pharm. Jugosl.*, **24,** 193(1974); through *Chem. Abstr.*, **82,** 116047t(1975).

(153) E. Pawelczyk and R. Wachowiak, *Herba Pol.*, **20,** 253(1974); through *Chem. Abstr.*, **83,** 32971x(1975).

(154) R. Wachowiak, *ibid.*, **20,** 356(1974); through *Chem. Abstr.*, **83,** 48140m(1975).

(155) D. O. Escudero, *An. Fac. Vet. Leon, Univ. Oviedo,* **19,** 13(1973); through *Chem. Abstr.*, **83,** 103204n(1975).

(156) A. B. Hansen and S. S. Larsen, *Arch. Pharm. Chemi, Sci. Ed.*, **3,** 7(1975); through *Chem. Abstr.*, **83,** 120729e(1975).

(157) H. V. Maulding, J. P. Nazareno, J. E. Pearson, and A. F. Michaelis, *J. Pharm. Sci.*, **64,** 278(1975).

(158) W. Mayer, S. Erbe, G. Wolf, and R. Voigt, *Pharmazie,* **29,** 700(1974); through *Chem. Abstr.*, **82,** 160163b(1975).

(159) H. V. Maulding, J. Polesuk, and D. Rosenbaum, *J. Pharm. Sci.*, **64,** 272(1975).

(160) H. Umeyama, *Chem. Pharm. Bull.*, **22,** 2518(1974); through *Chem. Abstr.*, **82,** 90019h(1975).

(161) H. V. Maulding and A. F. Michaelis, *J. Pharm. Sci.*, **64,** 275(1975).

(162) A. K. Madan and S. R. Jain, *Indian J. Pharm.*, **36,** 76(1974); through *Chem. Abstr.*, **82,** 21780n(1975).

(163) H. Honecker and H. Coper, *Arzneim-Forsch.*, **25,** 442(1975); through *Chem. Abstr.*, **83,** 152261n(1975).

(164) H. Poehlmann and S. Pfeifer, *Pharmazie,* **30,** 162(1975); through *Chem. Abstr.*, **83,** 120733b(1975).

(165) J. Noda, H. Sakamoto, and T. Nagai, *Chem. Pharm. Bull.*, **23,** 445(1975).

(166) E. R. Garrett and J. Tsau, *J. Pharm. Sci.*, **63,** 1563(1974).

(167) W. Brandt, *Arzneim.-Forsch.*, **25,** 856(1975); through *Chem. Abstr.*, **83,** 168389w(1975).

(168) E. Pawelczyk and S. Domeracki, *Acta Pol. Pharm.*, **31,** 305(1974); through *Chem. Abstr.*, **82,** 116045r(1975).

(169) T. V. Koval'chuk, T. I. Shakh, R. A. Galii, and V. G. Krasnova, *Farm. Zh. (Kiev)*, **30,** 38(1975); through *Chem. Abstr.*, **83,** 152279z(1975).

(170) T. V. Koval'chuk, T. I. Shakh, V. G. Krasnova, N. N. Kovaleva, P. I. Yakovenko, A. V. Chudnova, E. N. Yankovskaya, V. S. Sotnikov, and V. V. Smirnov, *Farmatsiya (Moscow)*, **24,** 63(1975); through *Chem. Abstr.*, **83,** 152287a(1975).

(171) V. Springer, M. Struhar, M. Heliova, J. Majer, and M. Chalabala, *Cesk. Farm.*, **23,** 356(1974); through *Chem. Abstr.*, **82,** 175202n(1975).

(172) S. Naito and T. Yamamoto, *J. Pharm. Sci.*, **64,** 253(1975).

(173) G. S. Rork and I. H. Pitman, *ibid.*, **64,** 216(1975).

(174) P. A. Laskar, *Diss. Abstr. Int.*, **35,** 3424-B(1975).

(175) J. L. DeYoung, *ibid.*, **35,** 4011-B(1975).

(176) D. Brooke, J. A. Scott, and R. J. Bequette, *Am. J. Hosp. Pharm.*, **32,** 44(1975).

(177) S. Shimizu, K. Yana, K. Furukawa, T. Takeda, Y. Mizuuchi, K. Narita, and T. Sato, *Iryo,* **27,** 742(1973); through *Chem. Abstr.*, **82,** 175190g(1975).

(178) A. Dominquez-Gil, R. Cadorniga, and A. Valls, *Cienc. Ind. Farm.*, **7,** 163(1975); through *Chem. Abstr.*, **83,** 168387u(1975).

(179) A. Dominguez-Gil, R. Cadorniga, and M. Bao, *ibid.*, **7,** 168(1975); through *Chem. Abstr.*, **83,** 168388v(1975).

(180) L. Vida and G. Vastagh, *Acta Pharm. Hung.*, **44,** 173(1974); through *Chem. Abstr.*, **82,** 21779u(1975).

(181) J. Lutomski and J. Wisniewski, *Herba Pol.*, **20,** 40(1974); through *Chem. Abstr.*, **82,** 34983f(1975).

(182) S. Bardarov and D. Mitev, *Arch. Union Med. Balk.*, **12,** 17(1974); through *Chem. Abstr.*, **82,** 21768q(1975).

(183) S. Kanafarska-Mlotkowska, *Acta Pol. Pharm.*, **30,** 297(1973); through *Chem. Abstr.*, **82,** 129237e(1975).

(184) H. Hammerstingl and H. Trapmann, *Fresenius' Z. Anal. Chem.*, **274,** 30(1975); through *Chem. Abstr.*, **83,** 103227x(1975).

(185) M. G. Beatrice, W. F. Stanaszek, L. V. Allen, G. K. Stanton, and T. R. Covington, *Am. J. Hosp. Pharm.*, **32,** 1133(1975).

(186) L. Gardella, J. Zaroslinski, and L. Possley, *ibid.*, **32,** 575 (1975).

(187) F. Kaczmarczyk and F. Modrzejewski, *Farm. Pol.*, **30,** 1001(1974); through *Chem. Abstr.*, **83,** 15571z(1975).

(188) E. Parker and H. Levin, *Am. J. Hosp. Pharm.*, **32,** 943(1975).

(189) I. Toth, F. Peterfy, and B. Boros, *Ann. Immunol. Hung.*, **17,** 67(1973); through *Chem. Abstr.*, **83,** 168364j(1975).

(190) N. F. H. Ho, *Perspect. Clin. Pharm.*, **1972,** 421; through *Chem. Abstr.*, **82,** 47650v(1975).

(191) D. M. Ruzhitskii and O. D. Ruzhitskaya, *Farm. Zh. (Kiev)*, **29,** 78(1974); through *Chem. Abstr.*, **82,** 90026h(1975).

(192) H. Seydel and R. Voigt, *Pharmazie,* **29,** 468(1974); through *Chem. Abstr.*, **82,** 7604b(1975).

(193) D. M. Ruzhitskii and O. D. Ruzhitskaya, *Farm. Zh. (Kiev)*, **29,** 78(1974); through *Chem. Abstr.*, **82,** 90026h(1975).

(194) B. S. R. Murty and J. N. Kapoor, *Am. J. Hosp. Pharm.*, **32,** 826(1975).
(195) M. A. Zoglio, H. V. Maulding, W. H. Streng, and W. C. Vincek, *J. Pharm. Sci.*, **64,** 1381(1975).
(196) N. Okusa, *Chem. Pharm. Bull.*, **23,** 803(1975).
(197) *Ibid.*, **23,** 794(1975).
(198) G. Neri, G. Guadagnini, and R. Mannucci, *Farmaco, Ed. Prat.*, **29,** 289(1974); through *Chem. Abstr.*, **82,** 77046v(1975).
(199) P. Vergnon and B. Drevon, *Lyon Pharm.*, **25,** 541(1974); through *Chem. Abstr.*, **82,** 89992p(1975).
(200) W. J. Irwin, *Pharm. J.*, **215,** 400(1975).
(201) T. Hermann, *Farm. Pol.*, **31,** 369(1975); through *Chem. Abstr.*, **83,** 152238k(1975).
(202) W. Grimm and J. P. Hugger, *Pharm. Ind.*, **36,** 437(1974); through *Chem. Abstr.*, **82,** 7599b(1975).
(203) Y.-c. J. Wang, *Diss. Abstr. Int.*, **35,** 5351-B(1975).
(204) H. Wasiak, *Rozpr. Wydz. 3: Nauk Mat.-Przyr., Gdansk. Tow. Nauk.*, **7,** 291(1973); through *Chem. Abstr.*, **82,** 7631h(1975).
(205) T. Yamana, A. Tsuji, K. Kanayama, and O. Nakano, *J. Antibiot.*, **27,** 1000(1974); through *Chem. Abstr.*, **82,** 90024f(1975).
(206) R. E. Lindsay and S. L. Hem, *Drug Dev. Commun.*, **1,** 211 (1974); through *Chem. Abstr.*, **83,** 15605p(1975).
(207) E. Brandl, F. Gapp, F. Knauseder, H. Kuntscher, and K. Riedl, *Sci. Pharm.*, **42,** 209(1974); through *Chem. Abstr.*, **83,** 32956w(1975).
(208) J. Ashwin, *Pharm. J.*, **214,** 487(1975).
(209) B. T. Butcher, M. K. Stanfield, G. T. Stewart, and R. Zemelman, *Liq. Cryst., Int. Liq. Cryst. Conf., [Pap], 3rd, Pt. 2,* **1970,** 687; through *Chem. Abstr.*, **82,** 90025g(1975).
(210) J. W. Kim, M. H. Lee, and S. K. Kim, *Yakhak Hoeji,* **17,** 27(1973); through *Chem. Abstr.*, **82,** 21765m(1975).
(211) D. Chatterji, P. K. Hiranaka, and J. F. Gallelli, *Am. J. Hosp. Pharm.*, **32,** 1130(1975).
(212) H. Zia, M. Tehrani, and R. Zargarbashi, *Can. J. Pharm. Sci.*, **9,** 112(1974); through *Chem. Abstr.*, **82,** 90029m(1975).
(213) I. Racz, *Acta Pharm. Hung.*, **44,** 227(1974); through *Chem. Abstr.*, **82,** 103081z(1975).
(214) R. Bergstrom, A. Fites, and J. Lamb, *Am. J. Hosp. Pharm.*, **32,** 887(1975).
(215) V. D. Kartseva, Y. A. Portnoi, N. A. Vakulenko, N. G. Kruzhkova, and E. M. Savitskaya, *Antibiotiki (Moscow),* **20,** 514(1975); through *Chem. Abstr.*, **83,** 120746h(1975).
(216) D. Mitev, *Farmatsiva (Sofia),* **24,** 45(1974); through *Chem. Abstr.*, **82,** 64401g(1975).
(217) M. Kohno, F. Ishii, I. Haneda, Y. Koyama, and M. Kikuchi, *Jpn. J. Antibiot.*, **27,** 715(1974); through *Chem. Abstr.*, **83,** 15573b(1975).
(218) M. Kohno, I. Haneda, Y. Koyama, and M. Kikuchi, *ibid.*, **27,** 707(1974); through *Chem. Abstr.*, **83,** 15574c(1975).
(219) D. P. Bonner, W. Mechlinski, and C. P. Schaffner, *J. Antibiot.*, **28,** 132(1975).
(220) E. Szantho, L. Adam, E. Peteanu, and L. Domokos, *Rev. Med. (Tirgu-Mures, Rom.),* **20,** 89(1974); through *Chem. Abstr.*, **80,** 21783r(1975).
(221) V. K. Prasad, W. H. Johns, M. W. Wingate, M. M. Mihotic, B. J. Southard, M. A. Kaplan, and A. P. Granatek, *Curr. Ther. Res., Clin. Exp.*, **16,** 1214(1974); through *Chem. Abstr.*, **82,** 129209x(1975).
(222) B. M. Trivedi and M. T. Rupareliya, *Hind. Antibiot. Bull.*, **16,** 175(1974); through *Chem. Abstr.*, **83,** 32957x(1975).
(223) S. Burdarov, D. Mitev, and I. Kolev, *Suvrem. Med.*, **25,** 29(1974); through *Chem. Abstr.*, **82,** 47677j(1975).
(224) J. T. H. Ong, *Diss. Abstr. Int.*, **35,** 4849-B(1975).
(225) D. Adam, *Muench. Med. Wochenschr.*, **116,** 1945(1974); through *Chem. Abstr.*, **82,** 77040p(1975).
(226) S. A. Ismaiel and E. A. Ismaiel, *Pharmazie,* **30,** 59(1975); through *Chem. Abstr.*, **82,** 144917v(1975).
(227) R. Ionova, E. Velikova, I. Filipov, and M. Luna, *Tr. Nauchnoiszled. Kim.-Farm. Inst.*, **9,** 417(1974); through *Chem. Abstr.*, **83,** 103206q(1975).
(228) B. K. Gupta, *Pharmastudent,* **17,** 28(1973); through *Chem. Abstr.*, **82,** 21756j(1975).
(229) S. P. Gladkikh, O. P. Belozerova, S. G. Mikhailova, and V. A. Karmanova, *Farmatsiya (Moscow),* **23,** 65(1974); through *Chem. Abstr.*, **82,** 64428w(1975).
(230) T. Tukamoto, S. Ozeki, M. Hasegawa, and F. Hattori, *Yakugaku Zasshi,* **94,** 917(1974); through *Chem. Abstr.*, **82,** 21778t(1975).
(231) M. A. El-Egakey, F. El-Khawas, A. G. Iskandar, and M. M. Abdel-Khalek, *Pharmazie,* **29,** 466(1974); through *Chem. Abstr.*, **82,** 21788w(1975).
(232) A. A. Kassem and W. Darwish, *Bull. Fac. Pharm. Cairo Univ.*, **11,** 129(1972); through *Chem. Abstr.*, **82,** 7596a(1975).
(233) Y. Otagiri, K. Uekama, and K. Ikeda, *Chem. Pharm. Bull.*, **23,** 13(1975).
(234) V. H. Mihranian, *Diss. Abstr. Int.*, **36,** 2822-B(1975).
(235) A. M. Saleh, *Pharmazie,* **29,** 474(1974); through *Chem. Abstr.*, **82,** 64413n(1975).
(236) R. Adamski, J. Sawicka, and B. Kosmider, *Farm. Pol.*, **30,** 1017(1974); through *Chem. Abstr.*, **83,** 32959z(1975).
(237) R. Adamski and J. Sawicka, *Herba Pol.*, **20,** 57(1974); through *Chem. Abstr.*, **82,** 64392e(1975).
(238) K. Shirai and S. Saito, *Vitamins,* **49,** 339(1975); through *Chem. Abstr.*, **83,** 152290w(1975).
(239) R. Adamski and J. Sawicka, *Herba Pol.*, **20,** 50(1974); through *Chem. Abstr.*, **82,** 34984g(1975).
(240) A. Fiebig and J. Kozlowska, *Ann. Acad. Med. Gedanensis,* **4,** 91(1974); through *Chem. Abstr.*, **83,** 15558a(1975).
(241) I. Selmiciu, E. Gafitanu, I. Popovici, and A. Pastia, *Rev. Med.-Chir.*, **78,** 433(1974); through *Chem. Abstr.*, **82,** 64439a(1975).
(242) S. Goldstein and A. Duca, *Rev. Chim. (Bucharest),* **25,** 279(1974); through *Chem. Abstr.*, **82,** 64362v(1975).
(243) D. B. A. Narayana and R. L. Khare, *Indian J. Pharm.*, **37,** 46(1975); through *Chem. Abstr.*, **83,** 136805n(1975).
(244) A. R. Casola, H. Newmark, and J. C. Cole, *Bull. Parenter. Drug Assoc.*, **29,** 216(1975).
(245) A. P. Simonelli and D. S. Dresback, *Perspect. Clin. Pharm.*, **1972,** 390; through *Chem. Abstr.*, **82,** 47649b(1975).
(246) R. A. Padovano, *Bull. Parenter. Drug Assoc.*, **29,** 210(1975).
(247) K. E. Avis, *ibid.*, **29,** 205(1975).
(248) P. F. D'Arcy, *Ir. J. Med. Sci.*, **143**(4, Suppl.), 93(1974); through *Chem. Abstr.*, **82,** 116032j(1975).
(249) M. V. Rinati and L. Fleischmann, *Farmaco, Ed. Prat.*, **30,** 211(1975); through *Chem. Abstr.*, **83,** 120742d(1975).
(250) A. Koshiro, H. Yamamoto, K. Matsuoka, K. Takahama, A. Hoshida, T. Ogawa, C. Yonekawa, T. Nakano, and T. Kobayashi, *Kyushu Yakugakkai Kaiho,* **28,** 33(1974); through *Chem. Abstr.*, **83,** 120725a(1975).
(251) F. M. Keim, *Bull. Parenter. Drug Assoc.*, **29,** 46(1975).
(252) J. Varga and I. Molnar, *Ann. Immunol. Hung.*, **17,** 273(1973); through *Chem. Abstr.*, **83,** 33007z(1975).
(253) M. Brzezicka-Bak, W. Zabojszcz, and W. Zalewski, *Polim. Med.*, **5,** 73(1975); through *Chem. Abstr.*, **83,** 168414a(1975).
(254) J. B. Boyette, *Diss. Abstr. Int.*, **36,** 733-B(1975).
(255) J. Vessman and G. Rietz, *Dev. Biol. Stand.*, **27,** 205(1974); through *Chem. Abstr.*, **82,** 21800u(1975).
(256) J. Neergaard, B. Nielsen, V. Faurby, D. H. Christensen, and O. F. Nielsen, *Nephron,* **14,** 263(1975); through *Chem. Abstr.*, **82,** 47714u(1975).
(257) S. Hasuike, E. Ueda, M. Sasaki, H. Iwaki, K. Yamada, and M. Marugami, *Igaku No Ayumi,* **90,** 796(1974); through *Chem. Abstr.*, **82,** 47715v(1975).
(258) *Fed. Regist.*, **40,** 11865(1975); through *Chem. Abstr.*, **83,** 15529s(1975).
(259) R. Purkiss, *J. Pharm. Pharmacol.*, **27,** 291(1975).
(260) S. J. Turco, *Bull. Parenter. Drug Assoc.*, **29,** 89(1975).
(261) P. DeLuca, R. Rapp, B. Bivins, H. McKean, and W. Griffen, *Am. J. Hosp. Pharm.*, **32,** 1001(1975).
(262) R. G. Swift, Jr., D. M. Searcy, and A. S. Pickard, *Drug. Intell. Clin. Pharm.*, **9,** 76(1975).
(263) *Ibid.*, **9,** 76(1975).
(264) W. J. Parsons, *Pharm. J.*, **214,** 553(1975).
(265) S. Rusmin, M. B. Althauser, and P. P. DeLuca, *Am. J. Hosp. Pharm.*, **32,** 373(1975).
(266) R. S. Levinson, L. V. Allen, W. F. Stanaszek, and S. Mills, *ibid.*, **32,** 1137(1975).
(267) T. N. Di Gaetano, *Bull. Parenter. Drug Assoc.*, **29,** 183(1975).
(268) S. M. Blaug and R. E. Sarabia, *ibid.*, **29,** 74(1975).
(269) R. Davis, R. Karuhn, J. Graf, and J. Stockham, *ibid.*, **29,** 98(1975).
(270) M. J. Groves, *Pharm. J.*, **213,** 581(1974).
(271) M. C. Porter, *Bull. Parenter. Drug Assoc.*, **29,** 169(1975).
(272) R. C. Huber and C. Riffkin, *Am. J. Hosp. Pharm.*, **32,** 173(1975).
(273) T. F. Stokes, E. D. Sumner, and T. E. Needham, *ibid.*, **32,**

821(1975).
(274) J. C. Holcombe, *Bull. Parenter. Drug Assoc.*, **29,** 153(1975).
(275) J. F. Cooper, *ibid.*, **29,** 122(1975).
(276) D. Krueger, G. Zimmermann, and G. Hebold, *Arzneim.-Forsch.*, **25,** 160(1975); through *Chem. Abstr.*, **82,** 175157b(1975).
(277) S. Rusmin and P. P. DeLuca, *Am. J. Hosp. Pharm.*, **32,** 378(1975).
(278) J. Dirksen and R. Larsen, *ibid.*, **32,** 1031(1975).
(279) E. Regos and K. Horvath, *Ann. Immunol. Hung.*, **17,** 269(1973); through *Chem. Abstr.*, **83,** 33006y(1975).
(280) J. L. Demoruelle, W. L. Harrison, and R. E. Flora, *Am. J. Hosp. Pharm.*, **32,** 177(1975).
(281) M. C. Allwood, R. Hambleton, and S. Beverley, *J. Pharm. Sci.*, **64,** 333(1975).
(282) J. Paxinos and T. Samuels, *Am. J. Hosp. Pharm.*, **32,** 892(1975).
(283) R. Rapp, B. Bivins, H. Schroeder, and P. DeLuca, *ibid.*, **32,** 1253(1975).
(284) E. Soler Peix, *Cienc. Ind. Farm.*, **6,** 341(1974); through *Chem. Abstr.*, **82,** 160189q(1975).
(285) B. Kreilgard, T. Higuchi, and A. J. Repta, *J. Pharm. Sci.*, **64,** 1850(1975).
(286) Z. Kubiak and A. Latka, *Farm. Pol.*, **31,** 25(1975); through *Chem. Abstr.*, **83,** 32967a(1975).
(287) D. A. Yassa and L. N. Gadel-Rub, *Pharmazie*, **30,** 339(1975); through *Chem. Abstr.*, **83,** 103235y(1975).
(288) A. Biernacki, Z. Galecki, and W. Chawlowski, *Farm. Pol.*, **31,** 385(1975); through *Chem. Abstr.*, **83,** 152322h(1975).
(289) H. Nerlo, M. Lojko-Krasowska, and A. Kosior, *ibid.*, **31,** 381(1975); through *Chem. Abstr.*, **83,** 152321g(1975).
(290) P. F. Kryshen, V. S. Sotnikov, V. V. Smirnov, and D. V. Utkin, *Farm. Zh. (Kiev)*, **30,** 49(1975); through *Chem. Abstr.*, **83,** 152293z(1975).
(291) T. W. Dean and D. C. Baun, *Am. J. Hosp. Pharm.*, **32,** 1036(1975).
(292) C. Fortner, W. Grove, D. Bowie, and M. Walker, *ibid.*, **32,** 582(1975).
(293) I. Ferenczi-Szirovicza and L. Mod, *Gyogyszereszet*, **19,** 128(1975); through *Chem. Abstr.*, **83,** 120775s(1975).
(294) J. Y. Masuda, R. N. Bleich, and J. H. Beckerman, *Am. J. Hosp. Pharm.*, **32,** 397(1975).
(295) R. S. Shpak, *Farm. Zh. (Kiev)*, **30,** 57(1975); through *Chem. Abstr.*, **83,** 152295b(1975).
(296) D. Newton, A. Rogers, C. Becker, and G. Torosian, *Am. J. Hosp. Pharm.*, **32,** 912(1975).
(297) B. Bowen, J. Darracott, E. Garnett, and R. Tomlinson, *ibid.*, **32,** 1027(1975).
(298) K. Thoma and D. Steinbach, *Pharm. Ind.*, **37,** 347(1975); through *Chem. Abstr.*, **83,** 168374n(1975).
(299) National Coordinating Committee on Large Volume Parenterals, *Am. J. Hosp. Pharm.*, **32,** 261(1975).
(300) W. Leipner, *Brauwelt*, **115,** 173(1975); through *Chem. Abstr.*, **82,** 126899m(1975).
(301) A. Carlier and L. T. Thuy, *Sci. Tech. Pharm.*, **3,** 345(1974); through *Chem. Abstr.*, **82,** 129188q(1975).
(302) M. R. Prin-Lombardo, *ibid.*, **3,** 355(1974); through *Chem. Abstr.*, **82,** 129256k(1975).
(303) E. W. Kraegen, L. Lazarus, H. Meler, L. Campbell, and Y. O. Chia, *Br. Med. J.*, **3,** 64(1975); through *Chem. Abstr.*, **83,** 168411x(1975).
(304) L. Lomolino, *Boll. Soc. Ital. Farm. Osp.*, **20,** 27(1974); through *Chem. Abstr.*, **82,** 7621e(1975).
(305) I. A. Mirsky, *Methods Invest. Diagn. Endocrinol.*, **2B,** 823(1973); through *Chem. Abstr.*, **83,** 152223b(1975).
(306) R. P. Evens, *Drug Intell. Clin. Pharm.*, **9,** 154(1975).
(307) L. A. Taranenko, G. E. Vaisberg, E. K. Berezina, and Z. V. Ermol'eva, *Antibiotiki (Moscow)*, **19,** 593(1974); through *Chem. Abstr.*, **82,** 47704r(1975).
(308) I. H. MacKinnon, *J. Hyg.*, **73,** 189(1974); through *Chem. Abstr.*, **82,** 47653y(1975).
(309) L. B. Jaques and L. W. Kavanagh, *Thromb. Diath. Haemorrh., Suppl.*, **56,** 171(1973); through *Chem. Abstr.*, **83,** 168354f(1975).
(310) W. R. Kramer, A. S. Inglott, and R. J. Cluxton, Jr., *Perspect. Clin. Pharm.*, **1972,** 438; through *Chem. Abstr.*, **82,** 38317q(1975).
(311) R. Hardberger, C. Hanna, and C. M. Boyd, *Arch. Ophthalmol.*, **93,** 42(1975); through *Chem. Abstr.*, **82,** 116057w(1975).
(312) B. S. Nath and D. M. Shingbal, *Indian J. Pharm.*, **36,** 107(1974); through *Chem. Abstr.*, **82,** 116035n(1975).
(313) J. W. McGinity and R. L. Brown, *J. Pharm. Sci.*, **64,** 1258(1975).
(314) M. Hamnett, *Hosp. Pharm.*, **33,** 70(1975); through *Chem. Abstr.*, **83,** 136852a(1975).
(315) A. S. Lee, *ibid.*, **32,** 125(1974); through *Chem. Abstr.*, **82,** 64435w(1975).
(316) T. F. Patton and J. R. Robinson, *J. Pharm. Sci.*, **64,** 1312(1975).
(317) R. A. Koetting, *J. Am. Pharm. Assoc.*, **NS 15,** 575(1975).
(318) R. M. E. Richards, *Pharm. J.*, **214,** 452(1975).
(319) Y. F. Maichuk, *Lancet*, **7899,** 173(1975).
(320) S. Mlotkowska, J. Kozlowska, J. Felczak, and B. Pankowska, *Farm. Pol.*, **31,** 31(1975); through *Chem. Abstr.*, **83,** 15533p(1975).
(321) T. S. Kondrat'eva and N. Van Ki, *Farmatsiya (Moscow)*, **24,** 70(1975); through *Chem. Abstr.*, **83,** 152288b(1975).
(322) J. D. Mullins, *Cosmet., Sci. Technol., 2nd Ed.*, **2,** 581(1972); through *Chem. Abstr.*, **82,** 21745e(1975).
(323) N. Takagi, *Nippon Shika Ishikai Zasshi*, **27,** 1081(1975); through *Chem. Abstr.*, **83,** 120681h(1975).
(324) M. Danilovic, *Arh. Farm.*, **24,** 345(1974); through *Chem. Abstr.*, **83,** 136751s(1975).
(325) N. Tufegdzic, *ibid.*, **24,** 357(1974); through *Chem. Abstr.*, **83,** 136752t(1975).
(326) G. Kedvessy and I. Eros, *Dtsch. Apoth.-Ztg.*, **114,** 1349(1974); through *Chem. Abstr.*, **82,** 34972b(1975).
(327) G. G. Smith, D. E. Fonner, and J. C. Griffin, *Bull. Parenter. Drug Assoc.*, **29,** 18(1975).
(328) R. M. E. Richards, *J. Pharm. Pharmacol.*, **27,** 381(1975).
(329) *Manuf. Chem Aerosol News*, **46**(3), 39(1975).
(330) W. A. Pauli, T. L. Grimes, D. E. Fonner, and J. C. Griffin, *Bull. Parenter. Drug Assoc.*, **29,** 163(1975).
(331) J. R. Gillis, *ibid.*, **29,** 111(1975).
(332) I. J. Pflug, M. Scheyer, G. M. Smith, and R. G. Holcomb, *ibid.*, **29,** 131(1975).
(333) W. Jurczyk, B. Kedzia, W. Kedzia, J. Masiakowski, and I. Salus, *Anest., Reanim., Internsywna Ter.*, **6,** 329(1974); through *Chem. Abstr.*, **82,** 144931v(1975).
(334) K. Krishnamurthy, *India, A.E.C., Bhabha At. Res. Cent., BARC-743* (1974); through *Chem. Abstr.*, **82,** 89994r(1975).
(335) M. V. Postrigan, L. A. Nikitina, L. B. Raikhlin, and A. I. Krivonosov, *Med. Tekh.*, **Apr. 1974,** 7; through *Chem. Abstr.*, **82,** 90047r(1975).
(336) L. Illum and N. Moeller, *Arch. Pharm. Chemi, Sci. Ed.*, **12,** 167(1974); through *Chem. Abstr.*, **83,** 32955v(1975).
(337) A. Jordy, *Pharm. Ind.*, **37,** 23(1975); through *Chem. Abstr.*, **83,** 48180z(1975).
(338) M. S. Korczynski, C. L. Peterson, and K. Schawel, *Bull. Parenter. Drug Assoc.*, **29,** 146(1975).
(339) A. M. Kayser, *Misc. Pap.–Landbouwhogesch. Wageningen*, **Sept. 1971,** 89; through *Chem. Abstr.*, **82,** 89990m(1975).
(340) D. Kalinska, *Probl. Tech. Med.*, **5,** 401(1974); through *Chem. Abstr.*, **82,** 175149a(1975).
(341) D. J. C. Davies and D. A. Norton, *J. Pharm. Pharmacol.*, **27,** 383(1975).
(342) R. T. Toledo, *Food Technol.*, **29**(5), 102(1975).
(343) D. B. Pall, *Bull. Parenter. Drug Assoc.*, **29,** 192(1975).
(344) A. R. Longworth, *ibid.*, **29,** 238(1975).
(345) J. J. Roxan, *Aust. J. Pharm. Sci.*, **2,** 65(1973); through *Chem. Abstr.*, **82,** 103034m(1975).
(346) M. B. Revzin, *Farmatsiya (Moscow)*, **24,** 66(1975); through *Chem. Abstr.*, **82,** 175220s(1975).
(347) T. Wegrzecki, *Probl. Tech. Med.*, **5,** 411(1974); through *Chem. Abstr.*, **82,** 175150u(1975).
(348) S. Gallinger, *Parfuem. Kosmet.*, **56,** 90(1975); through *Chem. Abstr.*, **83,** 120627v(1975).
(349) K. H. Wallhaeusser, *Pharm. Ind.*, **37,** 10(1975); through *Chem. Abstr.*, **83,** 48098d(1975).
(350) K. Zych, *Probl. Tech. Med.*, **5,** 395(1974); through *Chem. Abstr.*, **82,** 15517m(1975).
(351) A. Hart and M. W. Brown, *Appl. Microbiol.*, **28,** 1069(1974); through *Chem. Abstr.*, **82,** 77086h(1975).
(352) M. Chen, B. A. Rhodes, S. M. Larson, and H. N. Wagner, Jr., *J. Nucl. Med.*, **15,** 1142(1974); through *Chem. Abstr.*, **82,** 77085g(1975).
(353) H. Altorfer and X. Perlia, *Pharm. Acta Helv.*, **49,** 205(1974);

through *Chem. Abstr.*, **82,** 77062x(1975).

(354) V. S. Bondar, K. F. Kulesh, and F. A. Konev, *Farm. Zh. (Kiev),* **29,** 66(1974); through *Chem. Abstr.,* **82,** 77051t(1975).

(355) M. V. Postrigan, L. A. Nikitina, L. B. Raikhlin, and A. I. Krivonosov, *Med. Tekh.*, **4,** 7(1974); through *Chem. Abstr.,* **82,** 90047r(1975).

(356) M. Malinowska, *Probl. Tech. Med.*, **5,** 391(1974); through *Chem. Abstr.*, **83,** 15628y(1975).

(357) I. Sniezynska, M. Kucharzewski, M. Fidecki, and J. Sniezynski, *ibid.*, **5,** 375(1974); through *Chem. Abstr.*, **83,** 15626w(1975).

(358) S. Matuszczak, *ibid.*, **5,** 385(1974); through *Chem. Abstr.*, **83,** 15627x(1975).

(359) J. Borucka and E. Swedrowska, *ibid.*, **5,** 367(1974); through *Chem. Abstr.*, **83,** 15516k(1975).

(360) J. H. Scott-Foster, G. Magee, and M. J. Griffin, *Powder Technol. Publ. Ser.*, **2,** 37(1973); through *Chem. Abstr.*, **82,** 64471e(1975).

(361) S. Bachman, A. Zegota, and H. Zegota, *Probl. Tech. Med.*, **4,** 331(1973); through *Chem. Abstr.*, **82,** 7597b(1975).

(362) C. J. De Blaey, *Informationsdienst, Arbeitsgem. Pharm. Verfahrenstech.*, **20,** 224(1974); through *Chem. Abstr.*, **82,** 129196r(1975).

(363) C. Fauli, E. Parera, and P. Gabarro, *Cienc. Ind. Farm.*, **5,** 230(1973); through *Chem. Abstr.*, **82,** 129194p(1975).

(364) J. C. Johnson, "Tablet Manufacture," 1974; through *Chem. Abstr.*, **82,** 64475j(1975).

(365) M. H. Rubenstein, *Drug Cosmet. Ind.*, **116**(4), 44(1975).

(366) M. G. Horvath and G. Kedvessy, *Acta Pharm. Hung.*, **44,** 221(1974); through *Chem. Abstr.*, **82,** 103080y(1975).

(367) B. E. Jones and J. V. Tornblom, *Pharm. Acta Helv.*, **50,** 33(1975); through *Chem. Abstr.*, **83,** 15523k(1975).

(368) H. L. M. Cox, D. D. Breimer, and G. Freeke, *Pharm. Weekbl.*, **109,** 1018(1974); through *Chem. Abstr.*, **82,** 64397k(1975).

(369) J. M. Aiache, J. L. Vidal, S. Aiache, A. Jeanneret, and F. Cornat, *Labo-Pharma—Probl. Tech.*, **22,** 457(1974); through *Chem. Abstr.*, **82,** 21759n(1975).

(370) G. C. Cole and G. May, *J. Pharm. Pharmacol.*, **27,** 353(1975).

(371) H. Junginger, *Pharm. Ind.*, **36,** 333(1974); through *Chem. Abstr.*, **82,** 34996n(1975).

(372) M. Morishita, M. Fukushima, and Y. Inaba, *Am. Chem. Soc., Div. Org. Coat. Plast. Chem., Pap.*, **33,** 603(1973); through *Chem. Abstr.*, **82,** 175207t(1975).

(373) A. Djordjevic, *Arh. Farm.*, **25,** 99(1975); through *Chem. Abstr.*, **83,** 136775c(1975).

(374) W. Altenschmidt and T. Liske, *Drugs Made Ger.*, **15,** 11(1972); through *Chem. Abstr.*, **82,** 21747g(1975).

(375) R. Wood, *Manuf. Chem. Aerosol News*, **46**(6), 23(1975).

(376) E. U. Hunyadvari, *Acta Pharm. Hung.*, **45,** 110(1975); through *Chem. Abstr.*, **83,** 168373m(1975).

(377) H. Egermann, *Informationsdienst, Arbeitsgem. Pharm. Verfahrenstech.*, **20,** 8(1974); through *Chem. Abstr.*, **82,** 64358y(1975).

(378) D. N. Travers, *J. Pharm. Pharmacol.*, **27,** 516(1975).

(379) H. Malinowski and W. Smith, *J. Pharm. Sci.*, **64,** 1688(1975).

(380) K. C. Lee, S. H. Min, S. Rhee, Y. B. Kim, and C. W. Lee, *Yakhak Hoe Chi,* **18,** 236(1974); through *Chem. Abstr.,* **83,** 120786w(1975).

(381) N. O. Lindberg, L. Leander, L. Wenngren, H. Helgesen, and B. Reenstierna, *Acta Pharm. Suec.*, **11,** 603(1974); through *Chem. Abstr.*, **82,** 129245f(1975).

(382) H. Hall and T. M. Hinkes, *Am. Chem. Soc., Div. Org. Coat. Plast. Chem., Pap.*, **33,** 545(1973); through *Chem. Abstr.*, **82,** 175221t(1975).

(383) G. K. Bolhuis, C. F. Lerk, H. T. Zijlstra, and A. H. De Boer, *Pharm. Weekbl.*, **110,** 317(1975); through *Chem. Abstr.*, **83,** 32985e(1975).

(384) Y. Matsuda, S. Hayashi, and J. Okada, *Funsai,* **19,** 35(1974); through *Chem. Abstr.*, **82,** 175182f(1975).

(385) M. C. R. Johnson, *Pharm. Acta Helv.*, **50,** 60(1975); through *Chem. Abstr.*, **83,** 15582d(1975).

(386) P. Cook and J. A. Hersey, *Powder Technol.*, **9,** 257(1974).

(387) P. Cook and J. A. Hersey, *Aust. J. Pharm. Sci.*, **3,** 49(1974); through *Chem. Abstr.*, **82,** 77036s(1975).

(388) F. S. Lai, R. H. Wang, and L. T. Fan, *Powder Technol.*, **10,** 13(1974).

(389) L. M. Klyueva and N. I. Gel'perin, *Khim-Farm Zh.*, **8,** 37(1974); through *Chem. Abstr.*, **82,** 64416r(1975).

(390) D. N. Travers and R. J. Meredith, *Manuf. Chem. Aerosol News,* **46**(8), 37(1975).

(391) W. O. Opankunle, B. R. Bhutani, and V. N. Bhatia, *J. Pharm. Sci.*, **64,** 1023(1975).

(392) B. Kovacs, M. Gtarmathy, and L. Gyarmati, *Gyogyszereszet,* **18,** 284(1974); through *Chem. Abstr.*, **82,** 7619k(1975).

(393) *Ibid.*, **18,** 288(1974); through *Chem. Abstr.*, **82,** 7620d(1975).

(394) V. N. Pashchenko, V. N. Denisov, R. I. Moskalenko, and N. N. Myl'nikova, *Khim. Khim. Tekhnol., Obl. Nauchno-Tekh. Konf., [Mater], 4th,* **2,** 136(1973); through *Chem. Abstr.*, **82,** 116049v(1975).

(395) S. C. Cowin, *Powder Technol.*, **9,** 61(1974).

(396) P. York, *J. Pharm. Sci.*, **64,** 1216(1975).

(397) V. L. Rao and D. Venkateswarlu, *Powder Technol.*, **10,** 143(1974).

(398) J. D. Topham, *J. Pharm. Pharmacol.*, **27,** 6(1975).

(399) A. Kassem and S. Said, *Can. J. Pharm. Sci.*, **10,** 92(1975).

(400) A. Otsuka, K. Shamoto, K. Danjo, H. Sunada, and Y. Shioji, *Chem. Pharm. Bull.*, **23,** 673(1975).

(401) T. Kawakami, *Nippon Kagaku Kaishi,* 11, 2035(1974); through *Chem. Abstr.*, **82,** 35272k(1975).

(402) B. Selmeczi, *Arch. Pharm.*, **307,** 755(1974); through *Chem. Abstr.*, **82,** 35003y(1975).

(403) C. J. DeBlaey, *Diss. Abstr. Int.*, **35,** 4011-B(1975).

(404) J. Okada and Y. Fukumori, *Chem. Pharm. Bull.*, **23,** 326(1975).

(405) J. A. Hersey, E. T. Cole, and J. E. Rees, *Powder Technol. Publ. Ser.*, **4,** 165(1974); through *Chem. Abstr.*, **82,** 21767p(1975).

(406) J. A. Hersey, E. T. Cole, and J. E. Rees, *Pharm. Acta Helv.*, **50,** 28(1975); through *Chem. Abstr.*, **82,** 129231y(1975).

(407) K. A. Khan and C. T. Rhodes, *ibid.*, **49,** 258(1974); through *Chem. Abstr.*, **82,** 129228c(1975).

(408) K. A. Khan and C. T. Rhodes, *J. Pharm. Sci.*, **64,** 444(1975).

(409) E. Shotton and B. A. Obiorah, *ibid.*, **64,** 1216(1975).

(410) V. A. Belousov, E. E. Kol'man-Ivanov, I. E. Semenov-Ezhov, N. A. Stepanov, and I. P. Sukharev, *Khim.-Farm. Zh.*, **8,** 41(1974); through *Chem. Abstr.*, **82,** 64446a(1975).

(411) M. J. Jarvinen and M. J. Juslin, *Farm. Aikak.*, **83,** 1(1974); through *Chem. Abstr.*, **82,** 7600x(1975).

(412) A. B. Selkirk, *Powder Technol.*, **10,** 37(1974).

(413) H. K. Palmer and R. C. Rowe, *ibid.*, **10,** 225(1974).

(414) G. P. Betinetti and F. Giordano, *Farmaco, Ed. Prat.*, **29,** 395(1974); through *Chem. Abstr.*, **82,** 21773n(1975).

(415) E. Parera and C. Fauli, *Cienc. Ind. Farm.*, **4,** 263(1972); through *Chem. Abstr.*, **82,** 160130p(1975).

(416) H. Leuenberger and W. Becher, *Pharm. Acta Helv.*, **50,** 88(1975); through *Chem. Abstr.*, **83,** 32983c(1975).

(417) D. R. Savello, *Diss. Abstr. Int.*, **36,** 1159-B(1975).

(418) K. Marshall and D. Sixsmith, *Drug Dev. Commun.*, **1,** 51(1974); through *Chem. Abstr.*, **82,** 77041q(1975).

(419) K. Khan and C. T. Rhodes, *Can. J. Pharm. Sci.*, **10,** 62(1975); through *Chem. Abstr.*, **83,** 103210m(1975).

(420) H. Delonca, J. Joachim, P. Suvikrom, and G. Joachim, *Farmaco, Ed. Prat.*, **30,** 165(1975); through *Chem. Abstr.*, **83,** 136843y(1975).

(421) V. J. Keshri, T. Chakrabarti, and G. P. Srivastava, *Indian J. Pharm.*, **36,** 100(1974); through *Chem. Abstr.*, **82,** 175196p(1975).

(422) M. Y. Ambandh, J. Paris, O. Mangenot, F. Puisieux, and D. Duchene, *J. Pharm. Belg.*, **29,** 523(1974); through *Chem. Abstr.*, **83,** 136800g(1975).

(423) K. Kolarski, L. Krowczynski, and M. Nowak-Goss, *Farm. Pol.*, **30,** 989(1974); through *Chem. Abstr.*, **83,** 32958y(1975).

(424) E. Mendell, *Pharm. Acta Helv.*, **49,** 248(1974); through *Chem. Abstr.*, **82,** 129227b(1975).

(425) A. M. Sakr, A. A. Kassem, and N. A. Farrag, *Pharm. Ind.*, **37,** 283(1975); through *Chem. Abstr.*, **83,** 103233w(1975).

(426) K. A. Khan and C. T. Rhodes, *J. Pharm. Sci.*, **64,** 447(1975).

(427) K. A. Khan and C. T. Rhodes, *Pharm. Acta Helv.*, **50,** 99(1975); through *Chem. Abstr.*, **83,** 48157x(1975).

(428) R. Huettenrauch, U. Zahn, and J. Jacob, *Pharmazie,* **30,** 57(1975); through *Chem. Abstr.*, **82,** 160171c(1975).

(429) S. Gecgil and G. Bayraktar-Alpmen, *J. Pharm. Belg.*, **29,** 352(1974); through *Chem. Abstr.*, **82,** 47706t(1975).

(430) M. Chalabala, *Acta Fac. Pharm. Univ. Comenianae,* **27**(5), 7(1975); through *Chem. Abstr.*, **83,** 168406z(1975).

(431) I. Lopez and E. Orban, *Rev. Mex. Cienc. Farm.*, **5,** 1(1974); through *Chem. Abstr.*, **83,** 15600h(1975).

(432) M. del C. Gomez Carrasco, E. Quesada Nieto, and M. S. Socias Manzano, *An. R. Acad. Farm.*, **40,** 305(1974); through *Chem.*

Abstr., **82**, 64353t(1975).

(433) G. P. Betinetti and F. Giordano, *Farmaco, Id. Prat.*, **29**, 395(1974); through *Chem. Abstr.*, **82**, 21773n(1975).

(434) J. S. Morcillo, A. Cerezo, and J. M. Sune, *Cienc. Ind. Farm.*, **6**, 206(1974); through *Chem. Abstr.*, **82**, 64348v(1975).

(435) A. M. Sakr, H. M. Elsabbagh, A. A. Kassem, and A. H. Shalaby, *Arch. Pharm. Chemi, Sci. Ed.*, **2**, 153(1974); through *Chem. Abstr.*, **82**, 160178k(1975).

(436) B. Selmeczi, A. Keresztes, and J. Rapo, *Acta Pharm. Hung.*, **45**, 28(1975); through *Chem. Abstr.*, **83**, 48146t(1975).

(437) R. Denayer and J. Galer, *J. Pharm. Belg.*, **30**, 147(1975); through *Chem. Abstr.*, **83**, 152266t(1975).

(438) Y. S. Shumakov, *Farm. Zh. (Kiev)*, **29**, 49(1974); through *Chem. Abstr.*, **82**, 116051q(1975).

(439) R. W. Mendes, M. R. Gupta, I. A. Katz, and J. A. O'Neil, *Drug Cosmet. Ind.*, **115**(6), 42(1974).

(440) A. F. Asker, K. M. Saied, and M. M. Abdel-Khalek, *Pharmazie*, **30**, 373(1975); through *Chem. Abstr.*, **83**, 136787h(1975).

(441) *Ibid.*, **30**, 463(1975); through *Chem. Abstr.*, **83**, 136824t(1975).

(442) *Ibid.*, **30**, 377(1975); through *Chem. Abstr.*, **83**, 136830s(1975).

(443) *Ibid.*, **30**, 466(1975); through *Chem. Abstr.*, **83**, 136849e(1975).

(444) C. F. Lerk, G. K. Bolhuis, and A. H. De Boer, *Pharm. Weekbl.*, **109**, 945(1974); through *Chem. Abstr.*, **82**, 34998q(1975).

(445) R. F. Weir, J. Franz, J. E. Rees, and H. Sucker, *Pharm. Ind.*, **36**, 651(1974); through *Chem. Abstr.*, **82**, 129240a(1975).

(446) A. M. Sakr, A. A. Kassem, and N. A. Farrag, *ibid.*, **36**, 799(1974); through *Chem. Abstr.*, **82**, 129232z(1975).

(447) J. M. Aiache, *Pharm. Acta Helv.*, **49**, 169(1974); through *Chem. Abstr.*, **82**, 77024m(1975).

(448) H. H. Kavarna, *Indian Chem. Manuf.*, **12**, 17(1974); through *Chem. Abstr.*, **82**, 77020g(1975).

(449) H. Nerlo, W. Czarnecki, and T. Wolski, *Acta Pol. Pharm.*, **31**, 351(1974); through *Chem. Abstr.*, **82**, 77074c(1975).

(450) V. O. Likhoded, *Farm. Zh. (Kiev)*, **29**, 89(1974); through *Chem. Abstr.*, **82**, 77072a(1975).

(451) K. Kolarski, L. Krowczynski, and F. Koza, *Farm. Pol.*, **30**, 757(1974); through *Chem. Abstr.*, **82**, 77067c(1975).

(452) V. O. Likhoded, *Farm. Zh. (Kiev)*, **29**, 73(1974); through *Chem. Abstr.*, **82**, 116052r(1975).

(453) E. Parera, C. Fauli, J. Cemeli, and A. Del Pozo, *Cienc. Ind. Farm.*, **6**, 406(1974); through *Chem. Abstr.*, **83**, 15599q(1975).

(454) V. A. Likhoded, D. V. Proshunina, V. T. Pozdnyakova, and E. O. Gubiv, *Farm. Zh. (Kiev)*, **30**, 63(1975); through *Chem. Abstr.*, **83**, 152296c(1975).

(455) I. Eros, *Gyogyszereszet*, **19**, 215(1975); through *Chem. Abstr.*, **83**, 120685n(1975).

(456) J. B. Schwartz, E. T. Martin, and E. J. Dehner, *J. Pharm. Sci.*, **64**, 328(1975).

(457) U. Conte, P. Colombo, C. Caramella, G. P. Bettinetti, F. Giordano, and A. La Manna, *Farmaco, Ed. Prat.*, **30**, 194(1975); through *Chem. Abstr.*, **83**, 48154u(1975).

(458) F. El-Khawas, M. A. El-Egakev, M. M. Abd-El-Khalek, and R. M. El-Rasnedy, *Pharm. Ind.*, **36**, 657(1974); through *Chem. Abstr.*, **82**, 129241b(1975).

(459) A. F. Asker, K. M. Saied, and M. M. Abdel-Khalek, *Pharmazie*, **30**, 236(1975); through *Chem. Abstr.*, **83**, 15607r(1975).

(460) L. Delattre and J. Gillard, *Bull. Tech., Gattefosse SFPA*, **67**, 67(1972); through *Chem. Abstr.*, **82**, 7618j(1975).

(461) K. Khan and C. T. Rhodes, *Can. J. Pharm. Sci.*, **10**, 62(1975).

(462) J. G. Wagner, *Biopharm. Relevant Pharmacokinet.*, **1971** 158; through *Chem. Abstr.*, **82**, 34965b(1975).

(463) O. Laguna, L. T. Thuy, D. Duchene, and M. Seiller, *Sci. Tech. Pharm.*, **4**, 91(1975); through *Chem. Abstr.*, **83**, 168355g(1975).

(464) W. Rothe and G. Groppenbaecher, *Drugs Made Ger.*, **17**, 42(1974); through *Chem. Abstr.*, **82**, 35015d(1975).

(465) O. Laguna, L. T. Thuy, and D. Lefort des Ylouses, *Ann. Pharm. Fr.*, **32**, 641(1974); through *Chem. Abstr.*, **83**, 48152s(1975).

(466) T. A. Groshovyi, V. T. Pozdniakova, and Y. B. Borisenko, *Farm. Zh. (Kiev)*, **30**, 80(1975); through *Chem. Abstr.*, **83**, 48160t(1975).

(467) M. L. A. P. De Castro, J. H. F. Bueno, and J. A. Legendre, *Rev. Fac. Farm. Odontol. Araraquara*, **6**, 157(1972); through *Chem. Abstr.*, **83**, 32974a(1975).

(468) P. D. Pashnev, R. M. Safiulin, and N. A. Bugrim, *Khim-Farm. Zh.*, **9**, 38(1975); through *Chem. Abstr.*, **83**, 15593h(1975).

(469) J. W. Warren and E. J. Rowe, *Can. J. Pharm. Sci.*, **10**, 40(1975).

(470) R. Huettenrauch and S. Fricke, *Pharmazie*, **30**, 305(1975); through *Chem. Abstr.*, **83**, 103234x(1975).

(471) B. A. Matthews, S. Matsumoto, and M. Shibata, *Drug Dev. Commun.*, **1**, 303(1975); through *Chem. Abstr.*, **83**, 152297d(1975).

(472) G. Meer, W. A. Meer, and J. Tinker, *Food Technol.*, **29**(11), 22(1975).

(473) G. S. Bashura and V. A. Zamirailo, *Farm. Zh. (Kiev)*, **30**, 74(1975); through *Chem. Abstr.*, **83**, 32934n(1975).

(474) B. Koglin, *J. Soc. Cosmet. Chem.*, **26**, 439(1975).

(475) Z. D. Konye, *Gyogyszereszet*, **19**, 16(1975); through *Chem. Abstr.*, **82**, 160187n(1975).

(476) A. Nakamura, *Hyomen*, **13**, 1(1975); through *Chem. Abstr.*, **82**, 160143v(1975).

(477) A. W. Hartman, R. U. Nesbitt, Jr., F. M. Smith, and N. O. Nuessle, *J. Pharm. Sci.*, **64**, 802(1975).

(478) M. T. Alyushin, J. Vetra, L. Vaiders, and N. I. Skopets, *Vet.-Zhivotnovod.*, **1973**, 42; through *Chem. Abstr.*, **82**, 47702p(1975).

(479) A. A. Kassem, M. A. Moustafa, and F. S. Ghazy, *J. Drug Res.*, **6**, 77(1974); through *Chem. Abstr.*, **83**, 136853b(1975).

(480) N. J. Kerkhof, J. L. White, and S. L. Hem, *J. Pharm. Sci.*, **64**, 940(1975).

(481) V. A. Davydova, *Vopr. Farm. Dal'nem Vostoke*, **1**, 30(1973); through *Chem. Abstr.*, **83**, 103228y(1975).

(482) K. Ridgway, *Pharm. J.*, **213**, 583(1974).

(483) J. A. Castera and J. M. Sune, *Ars Pharm.*, **14**, 11(1973); through *Chem. Abstr.*, **83**, 15565a(1975).

(484) T. J. Lin, H. Kurihara, and H. Ohta, *J. Soc. Cosmet. Chem.*, **26**, 121(1975).

(485) W. Heers, *Fette, Seifen. Anstrichm.*, **76**, 420(1974); through *Chem. Abstr.*, **82**, 47982e(1975).

(486) S. Tsukiyama and A. Takamura, *Chem. Pharm. Bull.*, **23**, 616(1975).

(487) G. Jacobs, S. M. Henry, and V. F. Cotty, *J. Soc. Cosmet. Chem.*, **26**, 105(1975).

(488) P. Becher and S. Tahara, *Chem. Phys. Chem. Anwendungstech. Grenzflaechenaktiven Stoffe, Ber. Int. Kongr., 6th*, **2**, 519(1972); through *Chem. Abstr.*, **82**, 22124p(1975).

(489) G. Rimlinger, *Relata Tech. Chim. Biol. Appl.*, **5**, 513(1973); through *Chem. Abstr.*, **82**, 7841b(1975).

(490) A. A. Abramzon, G. B. Kryzhanovskaya, and E. S. Roskin, *Izv. Vyssh. Uchebn. Zaved., Khim. Khim. Tekhnol.*, **17**, 1150(1974); through *Chem. Abstr.*, **82**, 22119r(1975).

(491) A. Walter, J. Bertram, and G. Ahlers, *Dtsch. Apoth.-Ztg.*, **115**, 1135(1975); through *Chem. Abstr.*, **83**, 168381n(1975).

(492) A. I. Derevyanko, I. P. Sapon, T. Z. Sotskova, and O. D. Kurilenko, *Ukr. Khim. Zh. (Russ. Ed.)*, **40**, 937(1974); through *Chem. Abstr.*, **82**, 22118q(1975).

(493) E. Minkov, R. Ovcharov, D. Mikhailova, S. Bogdanova, M. Kasarova, and K. Koburova, *Pharm. Ind.*, **36**, 446(1974); through *Chem. Abstr.*, **82**, 21762h(1975).

(494) A. S. Arambulo, M.-S. Lie, A. L. Rosen, G. Dobben, and D. M. Long, *Drug Dev. Commun.*, **1**, 73(1974); through *Chem. Abstr.*, **82**, 77070y(1975).

(495) K. Yokoyama, A. Suzuki, I. Utsumi, and R. Naito, *Chem. Pharm. Bull.*, **22**, 2966(1974); through *Chem. Abstr.*, **82**, 77391d(1975).

(496) K. G. Ludwig, *Riv. Ital. Essenze, Profumi, Piante Off., Aromi, Saponi, Cosmet., Aerosol*, **56**, 478(1974); through *Chem. Abstr.*, **82**, 47625r(1975).

(497) L. Marszall, *Farm. Pol.*, **31**, 49(1975); through *Chem. Abstr.*, **83**, 15584f(1975).

(498) A. B. Balzan, *Fachh. Chemigr., Lithogr., Tiefdruck*, **3**, 173(1974); through *Chem. Abstr.*, **82**, 21720t(1975).

(499) G. Nahmias, *Inf. Chim.*, **124**, 221(1973); through *Chem. Abstr.*, **82**, 22108m(1975).

(500) C. Fox, *Surfactant Sci. Ser.*, **6**, 701(1974); through *Chem. Abstr.*, **82**, 47614m(1975).

(501) K. Pintye-Hodi, *Pharmazie*, **29**, 594(1974); through *Chem. Abstr.*, **82**, 21789x(1975).

(502) M. Melichar and M. Pokorna, *Cesk. Farm.*, **23**, 264(1974); through *Chem. Abstr.*, **82**, 144878h(1975).

(503) F. Neuwald, *Fette, Seifen, Anstrichm.*, **76**, 447(1974); through *Chem. Abstr.*, **82**, 64364x(1975).

(504) M. L. DeMartine and E. L. Cussler, *J. Pharm. Sci.*, **64**, 976(1975).

(505) J. Koegel, W. Horsch, and A. Jaeckel, *Pharmazie*, **30**, 311(1975); through *Chem. Abstr.*, **83**, 103208s(1975).

(506) J. A. Freitas and M. F. Guedes, *Rev. Port. Farm.*, **23**, 575(1973); through *Chem. Abstr.*, **82**, 64403j(1975).
(507) M. Sarsunova, B. Gremenova, K. Chladekova, and E. Neuschlova, *Cesk. Farm.*, **23**, 179(1974); through *Chem. Abstr.*, **82**, 64444y(1975).
(508) A. Meriaux-Brochu and J. Paiement, *J. Pharm. Sci.*, **64**, 1055(1975).
(509) V. V. Vasilenko, V. M. Gretskii, A. Z. Knizhnik, and O. V. Krasnova, *Farmatsiya (Moscow)*, **23**, 7(1974); through *Chem. Abstr.*, **82**, 129213u(1975).
(510) G. Haese and V. Jahn, *Pharm. Prax.*, **7**, 155(1974); through *Chem. Abstr.*, **82**, 34997p(1975).
(511) G. C. Dhaliwal, D. A. Zuck, and J. A. Wood, *Can. J. Pharm. Sci.*, **10**, 48(1975).
(512) H. Nerlo and W. Czarnecki, *Farm. Pol.*, **30**, 1095(1974); through *Chem. Abstr.*, **83**, 32982b(1975).
(513) *Manuf. Chem. Aerosol News*, **46**(3), 53(1975).
(514) Y. Machida and T. Nagai, *Chem. Pharm. Bull.*, **23**, 1003(1975).
(515) M. Danilovic and M. Stupar, *Arh. Farm.*, **24**, 49(1974); through *Chem. Abstr.*, **82**, 160186m(1975).
(516) W. Stozkowska, *Acta Pol. Pharm.*, **31**, 357(1974); through *Chem. Abstr.*, **82**, 90045p(1975).
(517) *Ibid.*, **31**, 663(1974); through *Chem. Abstr.*, **82**, 160200m(1975).
(518) J. Korbar-Smid, F. Kozjek, and M. Bozic, *Acta Pharm. Jugosl.*, **24**, 231(1974); through *Chem. Abstr.*, **82**, 103055u(1975).
(519) P. Braeckman, *Farm. Tijdschr. Belg.*, **52**, 47(1975); through *Chem. Abstr.*, **83**, 48107f(1975).
(520) S. Wahlgren and C. Fuehrer, *Pharmazie*, **30**, 97(1975); through *Chem. Abstr.*, **83**, 48121f(1975).
(521) E. Ugri Hunyadvari and I. Eros, *Acta Pharm. Hung.*, **45**, 19(1975); through *Chem. Abstr.*, **83**, 48145s(1975).
(522) K. Bolewski, B. Olejniczak, T. M. Stawinski, and G. Uchman, *Farm. Pol.*, **30**, 829(1974); through *Chem. Abstr.*, **82**, 144879j(1975).
(523) S. A. Iktisamov, *Mater. Nauchn. Konf. Alma-At. Gos. Med. Inst., 43rd*, **1971**, 436; through *Chem. Abstr.*, **82**, 90044n(1975).
(524) A. Velazquez, *Ars Pharm.*, **14**, 89(1973); through *Chem. Abstr.*, **83**, 15518n(1975).
(525) Z. I. Glon, *Poverkhn. Yavleniya Dispersn. Sistemakh*, **3**, 58(1974); through *Chem. Abstr.*, **83**, 103217u(1975).
(526) N. Tufegdzic and S. Mazic, *Acta Pharm. Jugosl.*, **4**, 107(1974); through *Chem. Abstr.*, **82**, 21719z(1975).
(527) U. Bogs and W. Helbig, *Pharmazie*, **29**, 712(1974); through *Chem. Abstr.*, **82**, 64448c(1975).
(528) P. I. Zaerko, Y. V. Tretinnik, and N. N. Kruglitskii, *Farm. Zh. (Kiev)*, **30**, 53(1975); through *Chem. Abstr.*, **83**, 152294a(1975).
(529) B. Idson, *Cosmet. Perfum.*, **90**(1), 25(1975).
(530) H. Schott and C. M. Ofner, *Drug Cosmet. Ind.*, **117**(2), 42(1975).
(531) M. Pruvost, *Sci. Tech. Pharm.*, **4**, 101(1975); through *Chem. Abstr.*, **83**, 168356h(1975).
(532) A. Zaremba and L. Krowczynski, *Acta Pol. Pharm.*, **31**, 769(1974); through *Chem. Abstr.*, **83**, 103231u(1975).
(533) *Ibid.*, **31**, 775(1974); through *Chem. Abstr.*, **83**, 103230t(1975).
(534) L. Gyarmati, K. Koritsanszky, and V. Vajda, *Gyogyszereszet*, **18**, 324(1974); through *Chem. Abstr.*, **82**, 77066b(1975).
(535) J. Spitael, *Farm. Tijdschr. Belg.*, **52**, 142(1975); through *Chem. Abstr.*, **83**, 103237a(1975).
(536) T. Yotsuyanagi, A. Molokhia, S. Hwang, N. F. H. Ho, G. L. Flynn, and W. I. Higuchi, *J. Pharm. Sci.*, **64**, 71(1975).
(537) I. W. Kellaway and C. Marriott, *ibid.*, **64**, 1162(1975).
(538) M. Gibaldi and B. Grundhofer, *ibid.*, **64**, 1064(1975).
(539) H. Matsumaru, T. Takubo, S. Tsuchiya, M. Hiura, and Y. Sugiura, *Tokyo Yakka Daigaku Kenkyu Nempo*, **24**, 418(1974); through *Chem. Abstr.*, **83**, 168408b(1975).
(540) L. Turakka and V. E. Krogerus, *Farm. Aikak.*, **83**, 59(1974); through *Chem. Abstr.*, **82**, 64409r(1975).
(541) H. Krasowska, L. Krowczynski, and E. Kocelak, *Farm. Pol.*, **31**, 291(1975); through *Chem. Abstr.*, **83**, 168378s(1975).
(542) S. Bartkowicz, J. Swierczek, and A. Siudek, *ibid.*, **31**, 297(1975); through *Chem. Abstr.*, **83**, 168379t(1975).
(543) H. Matsumaru, T. Takubo, S. Tsuchiya, and Y. Sugiura, *Tokyo Yakka Daigaku Kenkyu Nempo*, **24**, 413(1974); through *Chem. Abstr.*, **83**, 168392s(1975).
(544) B. W. Mueller, *Pharm. Ind.*, **36**, 943(1974); through *Chem. Abstr.*, **82**, 129247h(1975).
(545) E. Graf and V. Meyer, *ibid.*, **36**, 429(1974); through *Chem. Abstr.*, **82**, 21785t(1975).
(546) E. Spiess and C. Mathis, *Sci. Tech. Pharm.*, **3**, 231(1974); through *Chem. Abstr.*, **82**, 64437y(1975).
(547) O. Bugnariu, *Farmacia (Bucharest)*, **22**, 419(1974); through *Chem. Abstr.*, **83**, 32977b(1975).
(548) L. Waginaire, *Bull. Tech., Gattefosse SFPA*, **67**, 20(1972); through *Chem. Abstr.*, **82**, 47674f(1975).
(549) C. Merinero, C. Fauli, J. Cemeli, and A. Del Pozo, *Cienc. Ind. Farm.*, **4**, 250(1972); through *Chem. Abstr.*, **82**, 160197r(1975).
(550) I. Lichnerova and M. Chalabala, *Cesk. Farm.*, **23**, 219(1974); through *Chem. Abstr.*, **82**, 64426u(1975).
(551) N. Senior, *Adv. Pharm. Sci.*, **4**, 363(1974); through *Chem. Abstr.*, **82**, 129200n(1975).
(552) B. Schroeder, *Parfums, Cosmet., Aromes*, **2**, 59(1975); through *Chem. Abstr.*, **83**, 136690w(1975).
(553) D. Rodringuez Devesa, *Cienc. Ind. Farm.*, **4**, 225(1972); through *Chem. Abstr.*, **82**, 116013d(1975).
(554) S. Shernov, *Cosmet., Sci. Technol., 2nd Ed.*, **2**, 487(1972); through *Chem. Abstr.*, **82**, 7547k(1975).
(555) M. J. Root, *ibid.*, **2**, 417(1972); through *Chem. Abstr.*, **82**, 7546j(1975).
(556) *Drug Cosmet. Ind.*, **116**(6), 65(1975).
(557) M. Sorkin, *ibid.*, **117**(5), 34(1975).
(558) E. M. Staal, W. Bree, and P. L. C. A. Rijnbeek, *J. Soc. Cosmet. Chem.*, **26**, 509(1975).
(559) W. Feinstein and J. J. Sciarra, *J. Pharm. Sci.*, **64**, 408(1975).
(560) S. W. Lee, *Diss. Abstr. Int.*, **35**, 4012-B(1975).
(561) P. A. Sanders, *J. Soc. Cosmet. Chem.*, **25**, 581(1974).
(562) W. L. Chiou and J. H. Hsiao, *J. Pharm. Sci.*, **64**, 1052(1975).
(563) T. Yoshida, Y. Kousaka, and K. Okuyama, *Ind. Eng. Chem., Fundam.*, **14**, 47(1975); through *Chem. Abstr.*, **82**, 77383c(1975).
(564) M. N. Martyntseva, V. M. Tsetlin, B. Ya Mar'yasin, and K. P. Nazhestkin, *Khim.-Farm. Zh.*, **8**, 35(1974); through *Chem. Abstr.*, **82**, 64445z(1975).
(565) L. W. Haase, *Cosmet. Perfum.*, **90**(8), 31(1975).
(566) A. Stamm and R. Hug, *Labo-Pharm—Probl. Tech.*, **22**, 687(1974); through *Chem. Abstr.*, **82**, 103036p(1975).
(567) *Ibid.*, **22**, 839(1974); through *Chem. Abstr.*, **83**, 120697t(1975).
(568) L. Molteni and F. Scrollini, *Eur. J. Med. Chem.-Chim. Ther.*, **9**, 618(1974); through *Chem. Abstr.*, **83**, 48130h(1975).
(569) S. C. Dave, T. Chakrabarti, and G. P. Srivastava, *Indian J. Pharm.*, **36**, 94(1974); through *Chem. Abstr.*, **82**, 175195n(1975).
(570) D. Fremstad, S. Dahl, S. Jacobsen, P. K. M. Lunde, K. J. Nadland, A. A. Marthinsen, T. Waaler, and K. H. Landmark, *Eur. J. Clin. Pharmacol.*, **6**, 251(1973); through *Chem. Abstr.*, **82**, 90043m(1975).
(571) G. Leopold, J. Breuer, and F. Loebich, *IRCS Med. Sci.: Libr. Compend.*, **3**, 74(1975); through *Chem. Abstr.*, **83**, 15598p(1975).
(572) E. Kristoffersson, A. Kaukinene, and R. Krististoffersson, *Farm. Aikak.*, **83**, 51(1974); through *Chem. Abstr.*, **82**, 64408q(1975).
(573) W. H. Thomas and G. F. Cooney, *Aust. J. Pharm. Sci.*, **3**, 37(1974); through *Chem. Abstr.*, **82**, 90006b(1975).
(574) G. Persson, *Acta Psychiatr. Scand.*, **50**, 174(1974); through *Chem. Abstr.*, **82**, 21770j(1975).
(575) E. Kristoffersson and L. Niemi, *Farm. Aikak.*, **83**, 19(1974); through *Chem. Abstr.*, **82**, 21763j(1975).
(576) S. P. Bell and J. T. Fell, *Can. J. Pharm. Sci.*, **9**, 119(1974); through *Chem. Abstr.*, **82**, 90030e(1975).
(577) *Manuf. Chem. Aerosol News*, **46**(3), 23(1975).
(578) R. Huettenrauch and U. Schmeiss, *Pharmazie*, **30**, 536(1975); through *Chem. Abstr.*, **83**, 183356b(1975).
(579) M. C. Gomez, J. M. Sune, and A. Cerezo, *Cienc. Ind. Farm.*, **7**, 100(1975); through *Chem. Abstr.*, **83**, 103236z(1975).
(580) P. Speiser, *Labo-Pharma—Probl. Tech.*, **22**, 976(1974); through *Chem. Abstr.*, **83**, 136782c(1975).
(581) P. L. Madan, J. C. Price, and L. A. Luzzi, *Am. Chem. Soc., Div. Org. Coat. Plast. Chem., Pap.*, **33**, 589(1973); through *Chem. Abstr.*, **82**, 175206s(1975).
(582) J. Van der Vies, *J. Steroid Biochem.*, **6**, 215(1975); through *Chem. Abstr.*, **83**, 136754v(1975).
(583) S. Yolles, T. D. Leafe, and F. J. Meyer, *J. Pharm. Sci.*, **64**, 115(1975).
(584) M. F. Refojo and D. A. Thomas, *Ophthalmic Res.*, **7**, 33(1974); through *Chem. Abstr.*, **82**, 64443x(1975).
(585) Y. W. Chien, S. E. Mares, J. Berg, S. Huber, H. J. Lambert, and K. F. King, *J. Pharm. Sci.*, **64**, 1776(1975).

(586) N. F. Cunningham, N. Saba, and P. G. Millar, *J. Reprod. Fertil.*, **43**, 555(1975); through *Chem. Abstr.*, **83**, 120785v(1975).
(587) M. Donbrow and M. Friedman, *J. Pharm. Sci.*, **64**, 76(1975).
(588) M. Soledad Socias and A. Cerezo, *Cienc. Ind. Farm.*, **4**, 302(1972); through *Chem. Abstr.*, **82**, 103045r(1975).
(589) J. W. Shell and R. W. Baker, *Ann. Ophthalmol.*, **6**, 1037(1974); through *Chem. Abstr.*, **82**, 103104j(1975).
(590) F. Theeuwes, *J. Pharm. Sci.*, **64**, 1987(1975).
(591) L. B. Wingard, Jr., "Insolubilized Enzymes," 1974, p. 179; through *Chem. Abstr.*, **82**, 90018g(1975).
(592) I. Stivic and R. Senjkovic, *Acta Pharm. Jugosl.*, **24**, 249(1974); through *Chem. Abstr.*, **82**, 116048u(1975).
(593) B. H. Lippold and B. C. Lippolds, *Pharm. Ind.*, **36**, 432(1974); through *Chem. Abstr.*, **82**, 21761g(1975).
(594) J. G. Wagner, *Biopharm. Relevant Pharmacokinet.*, **1971**, 148; through *Chem. Abstr.*, **82**, 34964a(1975).
(595) R. De Neve, *Farm. Tijdschr. Belg.*, **51**, 282(1974); through *Chem. Abstr.*, **82**, 47641t(1975).
(596) J. Porebski, *Acta Pol. Pharm.*, **32**, 121(1975); through *Chem. Abstr.*, **83**, 136845a(1975).
(597) M. S. Socias and A. Cerezo, *Cienc. Ind. Farm.*, **5**, 114(1973); through *Chem. Abstr.*, **82**, 129193n(1975).
(598) G. Rothgang, *Informationsdienst, Arbeitsgem. Pharm. Verfahrenstech.*, **20**, 39(1974); through *Chem. Abstr.*, **82**, 7575t(1975).
(599) A. Vermeulen, *Acta Clin. Belg.*, **30**, 48(1975); through *Chem. Abstr.*, **83**, 103171z(1975).
(600) A. Grzesiczak, *Farm. Pol.*, **30**, 539(1974); through *Chem. Abstr.*, **82**, 21760f(1975).
(601) R. Huettenrauch, *Pharmazie*, **30**, 3(1975); through *Chem. Abstr.*, **82**, 116010a(1975).
(602) A. S. Michaels, *Am. Chem. Soc., Div. Org. Coat. Plast. Chem., Pap.*, **34**, 559(1974); through *Chem. Abstr.*, **83**, 197721d(1975).
(603) D. Mayer, M. Raschack, and K. Kesselring, *Arzneim.-Forsch.*, **25**, 1272(1975); through *Chem. Abstr.*, **83**, 197758w(1975).
(604) A. Hart and M. B. Ratansi, *J. Pharm. Pharmacol.*, **27**, 142(1975).
(605) G. Schmidt, *Seifen, Oele, Fette, Wachse*, **101**, 281(1975); through *Chem. Abstr.*, **83**, 120628w(1975).
(606) R. Selleri, O. Caldini, G. Orralesi, S. Facchini, and C. Rossi, *Boll. Chim. Farm.*, **113**, 617(1974); through *Chem. Abstr.*, **83**, 48091w(1975).
(607) D. E. Alguire, *Cosmet. Perfum.*, **90**(11), 21(1975).
(608) J. C. Etter, *Mitt. Geb. Lebensmittelunters. Hyg.*, **65**, 23(1974); through *Chem. Abstr.*, **82**, 160090a(1975).
(609) J. B. Wilkinson, *J. Soc. Cosmet. Chem.*, **26**, 497(1975).
(610) C. Prottey and T. Ferguson, *ibid.*, **26**, 29(1975).
(611) C. M. Pelejer, F. Balaguer, J. G. Dominquez, and J. L. Parra, *Cosmet. Perfum.*, **90**(3), 77(1975).
(612) D. Howes, *J. Soc. Cosmet. Chem.*, **26**, 47(1975).
(613) J. G. Black and D. Howes, *ibid.*, **26**, 205(1975).
(614) N. J. VanAbbe, P. Nicholas, and E. Boon, *ibid.*, **26**, 173(1975).
(615) F. Greiter, *Parfuem. Kosmet.*, **56**, 60(1975); through *Chem. Abstr.*, **83**, 120621p(1975).
(616) H. Tronnier, *J. Soc. Cosmet. Chem.*, **26**, 141(1975).
(617) J. D. Middleton, *ibid.*, **25**, 519(1974).
(618) E. R. Jolly and C. A. Sloughly, *ibid.*, **26**, 227(1975).
(619) W. M. Wooding and P. Finkelstein, *ibid.*, **26**, 225(1975).
(620) M. W. Steed, *ibid.*, **26**, 17(1975).
(621) E. Jungermann, *ibid.*, **25**, 621(1974).
(622) K. Rieger, J. Gross, H. Hollander, and W. Weigand, *ibid.*, **26**, 531(1975).
(623) T. Okumura, S. Hayashi, and S. Horin, *Cosmet. Perfum.*, **90**(3), 101(1975).
(624) R. W. Rance, *J. Soc. Cosmet. Chem.*, **25**, 545(1974).
(625) H. Beyer and G. A. Erlemann, *Parfuem. Kosmet.*, **55**, 221(1974); through *Chem. Abstr.*, **82**, 47623p(1975).
(626) V. Robinson, *Cosmet. Perfum.*, **90**(11), 25(1975).
(627) F. J. Berger and G. H. Megerle, *Cosmet., Sci. Technol., 2nd Ed.*, **2**, 345(1972); through *Chem. Abstr.*, **82**, 7545h(1975).
(628) H. Wolska, A. Langner, and F. N. Marzulli, *J. Soc. Cosmet. Chem.*, **25**, 639(1974).
(629) G. A. Groves, *Cosmet. Perfum.*, **90**(11), 36(1975).
(630) G. Kahn and M. C. Curry, *Arch. Dermatol.*, **109**, 510(1974); through *Chem. Abstr.*, **82**, 51359z(1975).
(631) T. M. MacLeod and W. Frain-Bell, *Br. J. Dermatol.*, **92**, 149(1975); through *Chem. Abstr.*, **83**, 32978e(1975).
(632) M. Block, *J. Soc. Cosmet. Chem.*, **26**, 189(1975).
(633) W. B. Davis and D. A. Rees, *ibid.*, **26**, 217(1975).
(634) W. B. Davis and A. C. MacDonald, *ibid.*, **26**, 477(1975).
(635) J. F. McConville and D. W. Anderson, Jr., *ibid.*, **26**, 83(1975).
(636) I. R. Schmolka, *ibid.*, **25**, 593(1974).
(637) M. Nagelschmidt and H. Struck, *Arch. Dermatol. Forsch.*, **250**, 237(1974); through *Chem. Abstr.*, **82**, 144825p(1975).
(638) H. L. Rosano, *J. Soc. Cosmet. Chem.*, **25**, 609(1974).
(639) J. T. Foley, *Drug Cosmet. Ind.*, **117**(5), 44(1975).
(640) M. Vogelmann, *Chem-Ztg.*, **99**, 49(1975); through *Chem. Abstr.*, **83**, 32898d(1975).
(641) U. Harder, *ibid.*, **99**, 54(1975); through *Chem. Abstr.*, **83**, 32899e(1975).
(642) W. Sturm and G. Mansfeld, *ibid.*, **99**, 69(1975); through *Chem. Abstr.*, **83**, 32913e(1975).
(643) E. R. Simo, *Cienc. Ind. Farm.*, **5**, 147(1973); through *Chem. Abstr.*, **82**, 129167g(1975).
(644) K. Kabzinska, *Tluszcze, Srodki Piorace, Kosmet.*, **18**, 342(1974); through *Chem. Abstr.*, **82**, 129162b(1975).
(645) A. Baldyga and L. Salamon, *ibid.*, **18**, 263(1974); through *Chem. Abstr.*, **82**, 129175h(1975).
(646) K. G. Ludwig and P. Hameyer, *Parfuem. Kosmet.*, **55**, 253(1974); through *Chem. Abstr.*, **82**, 76980h(1975).
(647) K. Kuczera, *Riechst., Aromen, Koerperpflegem.*, **24**, 335(1974); through *Chem. Abstr.*, **82**, 76969m(1975).
(648) G. G. Kolar and A. Miller, *Cosmet., Sci. Technol., 2nd Ed.*, **2**, 251(1972); through *Chem. Abstr.*, **82**, 76967j(1975).
(649) L. Farber, *ibid.*, **1**, 335(1972); through *Chem. Abstr.*, **82**, 76966h(1975).
(650) J. G. Fiedler, *ibid.*, 1, 317(1972); through *Chem. Abstr.*, **82**, 76965g(1975).
(651) S. J. Strianse, *ibid.*, **1**, 179(1972); through *Chem. Abstr.*, **82**, 76964f(1975).
(652) G. Van Ham and H. Boos, *Cosmet. Perfum.*, **90**(6), 27(1975).
(653) C. Chemtob, *Sci. Tech. Pharm.*, **3**, 479(1974); through *Chem. Abstr.*, **83**, 15513g(1975).
(654) L. Moldovanyi and W. Hungerbuehler, *IQ*, **74**, 11(1975); through *Chem. Abstr.*, **83**, 103114h(1975).
(655) G. Cholakova, *Farmatsiya (Sofia)*, **24**, 63(1974); through *Chem. Abstr.*, **82**, 7567s(1975).
(656) R. F. Schuler, *Cosmet. Sci. Technol., 2nd Ed.*, **2**, 635(1972); through *Chem. Abstr.*, **82**, 7552h(1975).
(657) L. J. Viola, *ibid.*, **2**, 543(1972); through *Chem. Abstr.*, **82**, 7550f(1975).
(658) R. E. Saute, *ibid.*, **2**, 503(1972); through *Chem. Abstr.*, **82**, 7548m(1975).
(659) D. H. Powers, N. D. Stiegelmeyer, and E. W. Lang, *ibid.*, **2**, 73(1972); through *Chem. Abstr.*, **82**, 7544g(1975).
(660) R. H. Barry, *ibid.*, **2**, 39(1972); through *Chem. Abstr.*, **82**, 7543f(1975).
(661) S. A. Bell, *ibid.*, **2**, 13(1972); through *Chem. Abstr.*, **82**, 7542e(1975).
(662) W. R. Schubert, *ibid.*, **2**, 1(1972); through *Chem. Abstr.*, **82**, 7541d(1975).
(663) H. Casotti, *Tenside Deterg.*, **11**, 202(1974); through *Chem. Abstr.*, **82**, 5553k(1975).
(664) A. G. Strenkovskaya, N. B. Vysotskaya, A. S. Gusarova, N. A. Krasnikova, E. P. Krysin, E. D. Glinka, K. M. Mel'nikov, O. B. Zobova, E. V. Kabanova, and R. N. Kalinina, *Maslo-Zhir. Prom-st.*, **Oct. 1974**, p. 26; through *Chem. Abstr.*, **82**, 64320e(1975).
(665) M. W. Rosenthal, *Cosmet. Sci. Technol., 2nd Ed.*, **1**, 533(1972); through *Chem. Abstr.*, **82**, 21744d(1975).
(666) N. Tufegdzic and S. Mazic, *Acta Pharm. Jugosl.*, **4**, 107(1974); through *Chem. Abstr.*, **82**, 21719z(1975).
(667) E. J. Masters, *Cosmet., Sci. Technol., 2nd Ed.*, **1**, 1(1972); through *Chem. Abstr.*, **82**, 21700m(1975).
(668) M. Cambrai, *J. Soc. Cosmet. Chem.*, **26**, 485(1975).
(669) H. Janistyn, "Handbook of Cosmetics and Perfumes, Volume 3: Body Care Aids," 2nd ed., 1973; through *Chem. Abstr.*, **83**, 152185r(1975).
(670) B. N. Tyutyunnikov, V. M. Kovalev, Z. I. Bukhshtab, V. S. Karetnikova, V. A. Kopysev, and M. V. Zotova, *Maslo-Zhir. Prom-st.*, **1975**(6), 25; through *Chem. Abstr.*, **83**, 149504p(1975).
(671) I. M. Tovbin and N. M. Zaliopo, *ibid.*, **1975** (7), 18; through *Chem. Abstr.*, **83**, 149494k(1975).
(672) H. Kroke, *Cosmet. Perfum.*, **90**(11), 31(1975).
(673) M. L. Schlossman and S. J. LaBruto, *ibid.*, **90**(11), 14(1975).
(674) J. L. Slack, *ibid.*, **90**(9), 55(1975).

(675) F. Baiocchi, D. Jennings, and A. J. Del Vecchio, *ibid.*, **90**(9), 31(1975).
(676) M. M. Reiger, *ibid.*, **90**(9), 12(1975).
(677) N. A. Harb, *ibid.*, **90**(1), 39(1975).
(678) W. F. Bernholz and R. Hoen, *ibid.*, **90**(1), 43(1975).
(679) K. Laden, *ibid.*, **90**(1), 37(1975).
(680) A. A. Kassem and S. A. Said, *ibid.*, **90**(1), 31(1975).
(681) L. Marszall, *ibid.*, **90**(2), 37(1975).
(682) G. Proserpio and V. Mariotti, *ibid.*, **90**(2), 41(1975).
(683) A. A. Kassem, S. A. Said, and A. A. Kassem, Jr., *ibid.*, **90**(2), 33(1975).
(684) E. S. Bretschneider, A. M. Rubino, and J. L. Jones, Jr., *ibid.*, **90**(2), 27(1975).
(685) G. S. Kass, *ibid.*, **90**(3), 105(1975).
(686) R. G. Rufe, *ibid.*, **90**(3), 93(1975).
(687) T. G. Schoenberg, *ibid.*, **90**(3), 89(1975).
(688) G. Barker, *ibid.*, **90**(3), 69(1975).
(689) F. N. Marzulli and D. I. Ruggles, *ibid.*, **90**(3), 65(1975).
(690) A. M. Kligman, *ibid.*, **90**(3), 63(1975).
(691) H. Ace, *ibid.*, **90**(3), 61(1975).
(692) J. I. Yablonski and C. L. Goldman, *ibid.*, **90**(3), 45(1975).
(693) T. Gerstein, *ibid.*, **90**(3), 35(1975).
(694) C. A. Rader and W. S. Tolgyesi, *ibid.*, **90**(3), 29(1975).
(695) R. M. Handjani-Vila, B. Rondot, and F. Lachampt, *ibid.*, **90**(4), 39(1975).
(696) G. Van Ham, *ibid.*, **90**(4), 34(1975).
(697) J. J. Margres, A. M. Rubino, and E. S. Bretschneider, *ibid.*, **90**(6), 36(1975).
(698) G. Van Ham and H. Boos, *ibid.*, **90**(6), 27(1975).
(699) M. D. DeGennaro and L. A. Luzzi, *ibid.*, **90**(7), 25(1975).
(700) P. Alexander, *ibid.*, **90**(7), 21(1975).
(701) R. Marcy, *ibid.*, **90**(7), 33(1975).
(702) W. H. Eaglstein, *ibid.*, **90**(8), 25(1975).
(703) D. H. Kirby, F. D. Barbuscio, W. Metzger, and J. Hourihan, *ibid.*, **90**(8), 19(1975).
(704) A. J. Harris, K. C. James, and M. Powell, *ibid.*, **90**(10), 23(1975).
(705) J. Teng, J. M. Lucas, and B. L. Scallet, *ibid.*, **90**(10), 32(1975).
(706) D. Osteroth, *ibid.*, **90**(10), 45(1975).
(707) F. Camail, *ibid.*, **90**(10), 74(1975).
(708) P. Z. Dedoukian, *ibid.*, **90**(10), 77(1975).
(709) B. Like, R. Sorrentino, and A. Petrocci, *J. Soc. Cosmet. Chem.*, **26**, 155(1975).
(710) J. F. McConville and D. W. Anderson, Jr., *ibid.*, **26**, 169(1975).
(711) H. C. S. Howlett and N. J. Van Abbe, *ibid.*, **26**, 3(1975).
(712) D. M. Gabriel, *ibid.*, **26**, 65(1975).
(713) W. Luckewicz, *ibid.*, **26**, 431(1975).
(714) J. P. McCarthy and M. L. Schlossman, *ibid.*, **26**, 523(1975).
(715) E. S. Lower, *Drug Cosmet. Ind.*, **116**(4), 57(1975).
(716) G. Rimlinger, *Labo-Pharma—Probl. Tech.*, **23**, 163(1975); through *Chem. Abstr.*, **83**, 183282z(1975).
(717) G. Proserpio and C. Pirro, *Riv. Ital. Essenze, Profumi, Piante Off., Aromi, Saponi, Cosmet., Aerosol*, **56**, 473(1974); through *Chem. Abstr.*, **82**, 34946w(1975).
(718) *Res. Discl.*, **127**, 5(1974); through *Chem. Abstr.*, **83**, 48090v(1975).
(719) R. J. Chudzikowski, *Soap Perfum. Cosmet.*, **48**, 56(1975); through *Chem. Abstr.*, **83**, 48081t(1975).
(720) K. Kuczera, *Riechst., Aromen, Koerperpflegem.*, **25**, 6(1975); through *Chem. Abstr.*, **83**, 120619u(1975).
(721) W. Heers, *Seifen, Oele, Fette, Wachse*, **101**, 71(1975); through *Chem. Abstr.*, **83**, 120620n(1975).
(722) R. Demeter, *ibid.*, **101**, 249(1975); through *Chem. Abstr.*, **83**, 120623r(1975).
(723) S. Rajagopalan, *Chem. Eng. World*, **10**, 52(1975); through *Chem. Abstr.*, **83**, 120626u(1975).
(724) J. Clotet, *Cienc. Ind. Farm.*, **4**, 269(1972); through *Chem. Abstr.*, **82**, 175126r(1975).
(725) A. Stahlavska, *Prum. Potravin*, **25**, 256(1974); through *Chem. Abstr.*, **82**, 34932p(1975).
(726) K. Kuczera, *Riechst., Aromen, Koerperpflegem.*, **25**, 6(1975); through *Chem. Abstr.*, **83**, 120619u(1975).
(727) F. Gonzalo-Bilbao, *Farm. Nueva*, **39**, 779(1974); through *Chem. Abstr.*, **82**, 144805g(1975).
(728) J. M. Quack and A. K. Reng, *Parfuem. Kosmet.*, **56**, 157(1975); through *Chem. Abstr.*, **83**, 197687x(1975).
(729) J. J. Leyden, K. J. McGinley, and A. M. Kligman, *J. Soc. Cosmet. Chem.*, **26**, 573(1975).
(730) R. W. Shanahan and C. O. Ward, *ibid.*, **26**, 581(1975).
(731) O. J. Lorenzetti, J. Boltralik, E. Busby, and B. Fortenberry, *ibid.*, **26**, 593(1975).
(732) V. Leoni, *Farmaco, Ed. Prat.*, **30**, 3(1975); through *Chem. Abstr.*, **82**, 116009g(1975).
(733) J. Bersier, W. Walter, and H. G. Wenzel, *Pharm. Ind.*, **36**, 588(1974); through *Chem. Abstr.*, **82**, 47639y(1975).
(734) J. B. Boyett and K. E. Avis, *Bull. Parenter. Drug Assoc.*, **29**, 1(1975).
(735) G. A. Daniels and D. E. Proctor, *Mod. Packag.*, **48**(4), 45(1975).
(736) A. A. Keller, A. W. Sheldon, and I. Simmons, *ibid.*, **48**(8), 42(1975).
(737) T. Beyrich, W. Zywica, D. Kottke, B. Kemna, and W. Thiele, *Pharmazie*, **29**, 517(1974); through *Chem. Abstr.*, **82**, 7608f(1975).
(738) F. Pellerin, J. L. Kiger, and J. Caporal-Gautier, *Ann. Pharm. Fr.*, **32**, 427(1974); through *Chem. Abstr.*, **82**, 90052p(1975).
(739) A. Hiort, K. Karlsson, U. Meresaar, and S. O. Nilsson, *Sven. Farm. Tidskr.*, **78**, 896(1974); through *Chem. Abstr.*, **82**, 160210q(1975).
(740) *Societe Francaise des Sciences et Techniques Pharmaceutiques, Sci. Tech. Pharm.*, **4**, 291(1975); through *Chem. Abstr.*, **83**, 197777b(1975).
(741) K. Kozhukharov and M. Nedev, *Farmatsiya (Sofia)*, **24**, 50(1974); through *Chem. Abstr.*, **82**, 64323h(1975).
(742) R. Gartside and J. W. L. Carter, *Pharm. J.*, **215**, 168(1975).
(743) S. Sacharow, *Drug Cosmet. Ind.*, **117**(5), 48(1975).
(744) F. Neuwald, *Pharm. Ind.*, **36**, 881(1974); through *Chem. Abstr.*, **82**, 116017h(1975).
(745) K. Mojsiejuk, *Przem. Chem.*, **54**, 224(1975); through *Chem. Abstr.*, **83**, 15524m(1975).
(746) A. Hirsch, F. X. Spiegel, and N. Floresca, *Mod. Packag.*, **48**(2), 34(1975).
(747) Anon., *ibid.*, **48**(2), 23(1975).
(748) S. Sacharow, *Food Eng.*, **47**(9), 64(1975).
(749) R. Wood, *Manuf. Chem. Aerosol News*, **46**(8), 41(1975).
(750) A. Hirsch, *Mod. Packag.*, **48**(10), 38(1975).
(751) R. Povey, *Manuf. Chem. Aerosol News*, **46**(6), 33(1975).
(752) P. Bathe, *ibid.*, **46**(10), 29(1975).
(753) J. Cooper, "Plastic Containers for Pharmaceuticals—Testing and Control," WHO Offset Publication No. 4, 1974; through *Chem. Abstr.*, **82**, 64476k(1975).
(754) P. Bathe, *Manuf. Chem. Aerosol News*, **46**(11), 39(1975).
(755) T. L. Grimes, D. E. Fonner, J. C. Griffen, and L. R. Rathbun, *Bull. Parenter. Drug Assoc.*, **29**, 64(1975).
(756) A. D. Woods, *ibid.*, **29**, 26(1975).
(757) G. H. Klumb, *ibid.*, **29**, 261(1975).
(758) S. Tsukiyama and A. Takamura, *Chem. Pharm. Bull.*, **23**, 616(1975).
(759) A. E. Llewelyn, *Manuf. Chem. Aerosol News*, **46**(9), 53(1975).
(760) R. Wood, *ibid.*, **46**(7), 25(1975).
(761) W. P. Hall, *ibid.*, **46**(7), 29(1975).
(762) J. D. Jensen, *Food Technol.*, **29**(6), 60(1975).
(763) Z. Shindle and I. Gallily, *J. Colloid. Interface Sci.*, **52**, 538(1975).
(764) G. Ekenved and A. Walan, *Scand. J. Gastroenterol.*, **10**, 267(1975); through *Chem. Abstr.*, **83**, 152292y(1975).
(765) *Manuf. Chem. Aerosol News*, **46**(3), 48(1975).
(766) *Ibid.*, **46**(4), 43(1975).
(767) K. Ridgway, *Pharm. J.*, **215**, 332(1975).
(768) G. R. Thompson and A. Cunningham, *J. Pharm. Sci.*, **64**, 320(1975).
(769) W. Porter, R. Ice, and K. Hetzel, *Am. J. Hosp. Pharm.*, **32**, 1023(1975).
(770) N. Aleksandrova, V. Makarov, E. Kaukhcheshvili, V. L. Konstantinov, and N. D. Sidorova, *Myasn. Ind. SSSR*, **Sept. 1974**, 23; through *Chem. Abstr.*, **82**, 64376c(1975).
(771) C. F. Valcke, *J. Dent. Assoc. S. Afr.*, **30**, 409(1975); through *Chem. Abstr.*, **83**, 103178g(1975).
(772) S. D. Gershon and M. Pader, *Cosmet., Sci. Technol., 2nd Ed.*, **18**, 423(1972); through *Chem. Abstr.*, **82**, 21743c(1975).
(773) D. Henschler, W. Beuttner, and J. Patz, *Calcium Metab. Bone Metab. Bone Dis.*, [*Proc. Eur. Symp. Calcif. Tissues*], **10**, 111(1973); through *Chem. Abstr.*, **83**, 157683m(1975).
(774) J. Dos Santos, Jr., D. M. Fichman, D. Guidi, and R. C. Real de Carvalho, *Rev. Fac. Odontol. Univ. Sao Paulo*, **12**, 85(1974);

through *Chem. Abstr.*, **83,** 152301a(1975).

(775) J. Dos Santos, Jr., D. M. Fichman, and D. Guidi, *ibid.*, **12,** 187(1974); through *Chem. Abstr.*, **83,** 152302b(1975).

(776) D. M Fichman, *ibid.*, **12,** 49(1974); through *Chem. Abstr.*, **83,** 152300z(1975).

(777) A. A. Correa and L. Steagall, *ibid.*, **12,** 43(1974); through *Chem. Abstr.*, **83,** 152299f(1975).

(778) Y. Takahashi, T. Matsukubo, and M. Takeuchi, *Shika Gakuho*, **75,** 804(1975); through *Chem. Abstr.*, **83,** 152236h(1975).

(779) R. W. Treharne and N. Brown, *J. Biomed. Mater. Res.*, **9,** 81(1975); through *Chem. Abstr.*, **83,** 168432e(1975).

(780) J. M. Briscoe, Jr., and K. M. Pruitt, *J. Dent. Res.*, **54,** 504(1975); through *Chem. Abstr.*, **83,** 108229j(1975).

(781) S. Katz and K. Park, *ibid.*, **54,** 540(1975); through *Chem. Abstr.*, **83,** 108230c(1975).

(782) W. I. Higuchi, S. C. Valvani, and J. J. Hefferren, *Arch. Oral Biol.*, **19,** 737(1974); through *Chem. Abstr.*, **82,** 132804t(1975).

(783) J. Dnebosky and J. Komrska, *Stomatol. Zpr.*, **1973**(2), 78; through *Chem. Abstr.*, **83,** 183354z(1975).

(784) W. Sledziewski and K. Baetz, *J. Dent. Assoc. S. Afr.*, **30,** 603(1975); through *Chem. Abstr.*, **83,** 183378k(1975).

(785) S. F. Hulbert, H. L. Richbourg, J. J. Klawitter, and B. W. Sauer, *J. Biomed. Mater, Res.*, **9,** 189(1975); through *Chem. Abstr.*, **83,** 168433f(1975).

(786) M. L. Jacobs and J. Black, *ibid.*, **9,** 221(1975); through *Chem. Abstr.*, **83,** 168434g(1975).

(787) T. D. Rohde, P. J. Blackshear, R. L. Varco, and H. Buchwald, *Trans., Am. Soc. Artif. Intern. Organs*, **21,** 510(1975); through *Chem. Abstr.*, **83,** 168426f(1975).

(788) F. Lai, M. Scott, R. Tankersley, H. Wayt, L. Green, R. Rhodes, and A. Zelman, *ibid.*, **21,** 346(1975); through *Chem. Abstr.*, **83,** 168425e(1975).

(789) J. W. Frame, *J. Dent.*, **3,** 177(1975); through *Chem. Abstr.*, **83,** 183379m(1975).

(790) L. Cini, A. Pizzo-Ferrato, C. Trentani, S. Sandrolini, and M. Paltrinieri, *J. Biomed. Mater. Res.*, **9,** 441(1975); through *Chem. Abstr.*, **83,** 183377j(1975).

(791) M. Mosharrafa, *Biomed. Sci. Instrum.*, **11,** 157(1975); through *Chem. Abstr.*, **83,** 168446n(1975).

(792) W. C. Richardson, Jr., S. F. Hulbert, J. J. Klawitter, and B. W. Sauer, *Natl. Bur. Stand. (U.S.), Spec. Publ.*, **415,** 37(1975); through *Chem. Abstr.*, **83,** 197770u(1975).

(793) Y. Sakurada, *Kobunshi*, **24,** 587(1975); through *Chem. Abstr.*, **83,** 197705b(1975).

(794) Y. Sakurai and T. Akaike, *ibid.*, **24,** 581(1975); through *Chem. Abstr.*, **83,** 197704a(1975).

(795) L. L. Hench, H. A. Paschall, W. C. Allen, and G. Piotrowski, *Natl. Bur. Stand. (U.S.), Spec. Publ.*, **415,** 19(1975); through *Chem. Abstr.*, **83,** 197715e(1975).

(796) N. D. Greene, C. Onkelinx, L. J. Richelle, and P. A. Ward, *ibid.*, **415,** 45(1975); through *Chem. Abstr.*, **83,** 197716f(1975).

(797) R. B. Beard, J. F. DeRosa, S. F. Dubin, L. Sturm, R. M. Koerner, and A. Miller, *ibid.*, **415,** 55(1975); through *Chem. Abstr.*, **83,** 197717g(1975).

(798) I. M. Zaikina, E. A. Sokolova, A. I. Krivonosov, L. A. Nikitina, and L. E. Ageeva, *Med. Tekh.*, **Apr. 1974,** 31; through *Chem. Abstr.*, **82,** 89991n(1975).

(799) J. M. Anderson and D. F. Gibbons, *Biomater., Med. Devices, Artif. Organs*, **2,** 235(1974); through *Chem. Abstr.*, **82,** 129190j(1975).

(800) P. Predecki, *J. Biomed. Mater. Res.*, **8,** 487(1974); through *Chem. Abstr.*, **82,** 129250d(1975).

(801) Y. Sukurai, *Purasuchikkusu*, **23,** 2(1974); through *Chem. Abstr.*, **82,** 34969f(1975).

(802) W. O. Statton, S. L. Cannon, and R. N. King, *U.S. NTIS, PB Rep. 240631*, 1975.

(803) E. J. Sutow, *Diss. Abstr. Int. B*, **36,** 340(1975); through *Chem. Abstr.*, **83,** 168440f(1975).

(804) S. H. Wu, *ibid.*, **36,** 360(1975); through *Chem. Abstr.*, **83,** 168439n(1975).

(805) S. J. Gourlay, R. M. Rice, A. F. Hegyeli, J. C. Eaton, Jr., J. W. Hodge, Jr., and C. W. R. Wade, *Trans., Am. Soc. Artif. Intern. Organs*, **21,** 28(1975); through *Chem. Abstr.*, **83,** 168422b(1975).

(806) Z. Ott, *Polim. Med.*, **5,** 167(1975); through *Chem. Abstr.*, **83,** 183380e(1975).

(807) E. S. Nuwayser, T. C. Wu, R. S. Hotchkiss, E. E. Arcon, J. J. Hulka, K. Mohr, and A. Poddar, *Trans., Am. Soc. Artif. Intern. Organs*, **21,** 523(1975); through *Chem. Abstr.*, **83,** 168427g(1975).

(808) K. Kamide and S. Manabe, *Nippon Gomu Kyokaishi*, **48,** 506(1975); through *Chem. Abstr.*, **83,** 168341z(1975).

(809) R. N. King and D. J. Lyman, *Environ. Health Perspect.*, **11,** 71(1975); through *Chem. Abstr.*, **83,** 168343b(1975).

(810) T. Miyata, M. Nishizawa, T. Sohde, A. L. Rubin, and K. H. Stenzel, *Kagaku No Ryoiki*, **28,** 469(1974); through *Chem. Abstr.*, **83,** 168357j(1975).

(811) P. W. R. Beaumont and R. J. Young, *J. Biomed. Mater. Res.*, **9,** 423(1975); through *Chem. Abstr.*, **83,** 183376h(1975).

(812) J. R. Parsons and A. W. Ruff, *Govt. Rep. Announce. (U.S.)*, **74,** 51(1974); through *Chem. Abstr.*, **82,** 116007e(1975).

(813) I. Le May, V. G. Lappi, and W. E. White, *Polym. Eng. Sci.*, **15,** 789(1975); through *Chem. Abstr.*, **83,** 197723f(1975).

(814) R. P. Kusy and D. T. Turner, *J. Biomed. Mater. Res.*, **9,** 89(1975); through *Chem. Abstr.*, **83,** 152310c(1975).

(815) R. P. Kusy and D. T. Turner, *Adv. Chem. Ser.*, **142,** 36(1975); through *Chem. Abstr.*, **83,** 183375g(1975).

(816) K. De Groot and A. C. De Visser, *Ned. Tijdschr. Geneeskd.*, **118,** 1153(1974); through *Chem. Abstr.*, **82,** 7568t(1975).

ACKNOWLEDGMENTS AND ADDRESSES

Received from the **Warner-Lambert Research Institute, Morris Plains, NJ 07950,* and *‡Stuart Pharmaceuticals, Wilmington, DE 19897*

ˣ To whom inquiries should be directed.

Stability of Vitamin C (Ascorbic Acid) in Tablets

S. H. RUBIN, E. DeRITTER, and J. B. JOHNSON ˣ

Abstract □ Stability of ascorbic acid (vitamin C) in various tablet formulations and the nature and extent of formation of decomposition products (dehydroascorbic acid, diketogulonic acid, and oxalic acid) were determined under normal conditions of storage and in simulated use tests. IR spectrophotometric, colorimetric, fluorometric, titrimetric, polarographic, and chromatographic methods were applied. Recent implications concerning the instability of ascorbic acid in tablets and the potentially harmful nature of the breakdown products are shown to be unfounded. Under normal storage conditions, commercial-type ascorbic acid tablets are stable for over 5 years (>95% potency retention). The amounts of all three breakdown products formed under the various storage conditions constitute a small percentage of the ascorbic acid content and pose no dietary hazard. IR spectroscopy was inadequate as a quantitative method for evaluating ascorbic acid potency in tablet formulations. The official titration methods and TLC, colorimetric, and polarographic determinations correlate well and define accurately the stability of ascorbic acid in these dosage forms.

Keyphrases □ Ascorbic acid—stability in various tablet formulations, nature and extent of formation of decomposition products □ Vitamins—ascorbic acid, stability in various tablet formulations, nature and extent of formation of decomposition products □ Stability—ascorbic acid in various tablet formulations, nature and extent of formation of decomposition products □ Decomposition products, ascorbic acid—various tablet formulations, nature and extent of formation

At the Second Conference on Vitamin C (1) in October 1974, international authorities in the fields of human biochemistry, physiology, pharmacology, and clinical medicine presented papers demonstrating that ascorbic acid (vitamin C) is essential not only to prevent scurvy but also to protect the body against drugs (2), environmental chemicals (3–7), and production of certain tumors (8, 9), to make energy available at the cellular level (10), to protect vascular systems, including protection against cholesterol (11, 12), to increase athletic performance (13), and to ameliorate the severity of the common cold (14–16). It was shown that the need for ascorbic acid is increased in women taking oral contraceptives (17), in smokers (18), and in persons with intestinal malabsorption (19). It was shown too that ascorbic acid supplements are safe (20). Tablets of ascorbic acid are the dosage form most commonly used.

Recently, Wilk (21) claimed, on the basis of very limited data, that extensive degradation of ascorbic acid occurred in tablets during "household storage." He alleged that existing analytical methodology is nonspecific and that IR spectroscopy is a better measure of ascorbic acid stability. It was also alleged that degradation products of ascorbic acid (I, Scheme I) in aged tablets, as well as normal tablet excipients, are potentially harmful to the consumer. These products include dehydroascorbic acid as an alleged diabetogenic agent, oxalate from aged tablets as a possible contributor to kidney stone formation, and the excipients sucrose, starch, and dextrin as weight-increasing substances and lactose as undesirable for individuals intolerant to that sugar. None of these was actually measured by Wilk (21).

The present paper provides more comprehensive data on the stability of ascorbic acid tablets under various storage conditions, as well as actual measurements of dehydroascorbic acid (II), diketogulonic acid (III), and oxalic acid (IV) (Scheme I) in various tablets. Diverse analytical methods are available for the determination of ascorbic acid. For tablets where ascorbic acid is the only reducing agent present, direct oxidimetric titration is classical. Official methods involve titration with iodine (22, 23) or 2,6-dichloroindophenol (23, 24). Chloramine-T (25) and *N*-bromosuccinimide (26, 27) also have been used as titrants.

Colorimetric or spectrophotometric methods for assay of ascorbic acid have been based on reactions with 2,6-dichloroindophenol (28–30), diazotized 2-nitroaniline (31, 32), diazotized 4-methoxy-2-nitroaniline (33, 34), 2,4-dinitrophenylhydrazine (35), 4-nitrobenzenediazonium fluoroborate (36), phosphomolybdate complex (37), 2,3,5-triphenyltetrazolium chloride (38), and phenylhydrazium chloride (39). A highly specific, microfluorometric assay for ascorbic acid, based on the reaction of dehydroascorbic acid with *o*-phenylenediamine plus a borate blank was described (40).

Other reported methods used for the assay of ascorbic acid include polarography (41, 42), GLC (43, 44), and thermometric measurement (45). Several chromatographic separation techniques, prior to titration or colorimetric assay of ascorbic acid, have been utilized to increase the specificity of the determination. These techniques include separations on paper (46–50), thin-layer plates (51, 52), and columns (53–58).

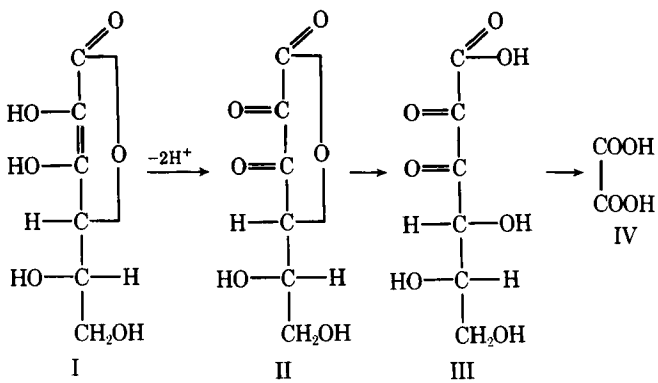

Scheme I

Table I—Analysis of Ascorbic Acid, 100-mg Tablets, after Long-Term Storage at 25°

Lot Number	Storage Time, Months	Assay, % of Claim[a]	Initial Assay, % of Claim[a]	Loss in Potency, %	Diketogulonic Acid, %	Oxalic Acid, %	Dehydroascorbic Acid, %
V-418	103	99	103	4	1	0.5	0.5
KRK-202-66-I	103	104	107	3	2	0.5	0.2
KRK-202-65-III	103	106	110	4	1	0.5	0.2
KRK-202-65-IV	103	106	110	4	1	0.5	0.4
KRK-202-66-II	103	105	111	6	2	1.0	2.4
DMS-289-II	90	104	102	—	0.5	0.5	0.3
Lot 2082	120	111	—	—	—	0.2	0.4
Lot 2694B	240	101	—	—	—	0.4	2.3
Lot 002-0B097A	96	98	—	—	—	—	1.3

[a] Assay by iodometric and 2,6-dichloroindophenol titrations.

EXPERIMENTAL

Stability Tests of Ascorbic Acid Tablets—Samples of commercial ascorbic acid tablets stored for many years at room temperature in closed bottles were assayed for ascorbic acid, dehydroascorbic acid, diketogulonic acid, and oxalic acid.

Commercial ascorbic acid tablets were stored under various test conditions as detailed later. The tablets contained 100 mg of ascorbic acid, dextrins, starch USP, lactose, talc, and magnesium stearate. Tablets were stored at room temperature (25°) and in the refrigerator (5°) in glass and in polyethylene bottles. The bottles were opened daily (five times per week) and returned to closed storage to simulate normal conditions of use. Tablets were also stored in an open dish at 25°.

Assays were run at monthly intervals for ascorbic acid, dehydroascorbic acid, diketogulonic acid, oxalic acid, and moisture, using whole tablets. Scrapings from the tablet surfaces, 15–20% of the total tablet weights, were assayed for intact ascorbic acid.

Analytical Methods—Ascorbic acid was determined by titration with iodine (22, 23) and 2,6-dichloroindophenol (23, 24) and by differential pulse polarography[1]. Dehydroascorbic acid was determined fluorometrically (40). Diketogulonic acid and oxalic acid were determined by TLC[2] (59). In addition to the TLC methods, oxalic acid was determined by a modification[3] of the fluorometric method of Zarembski and Hodgkinson (60). Moisture content of tablets was determined by drying at 105° for 3 hr. The specificity of these analytical methods for determining intact ascorbic acid in the presence of decomposition products was evaluated by assaying an aqueous solution of ascorbic acid at pH 4 which was heated at 45° for varying periods to induce graded levels of ascorbic acid decomposition up to 40%.

IR Spectroscopic Determination of Ascorbic Acid Stability—IR curves were determined for ascorbic acid, dehydroascorbic acid, 2-ketogulonic acid[4], oxalic acid, and tablet placebos to assess the utility of IR measurements as an indicator of the stability of ascorbic acid in tablets as suggested by Wilk (21). All measurements were made using potassium bromide pellets, since no suitable solvent is available for preparing solutions of ascorbic acid and its degradation products that is compatible with the commonly used IR cell (sodium chloride).

RESULTS

Long-Term Storage at Room Temperature—Table I shows the results of assays for ascorbic acid and potential breakdown products in various commercial tablets stored for many years in closed bottles at room temperature. The excellent stability of ascorbic acid in these formulations is evidenced by the fact that all maintained the claimed level for periods of 5 years and longer. The amounts of decomposition products of ascorbic acid found, namely, dehydroascorbic acid, diketogulonic acid, and oxalic acid, when detectable, represented only a very small percentage of the ascorbic acid content.

Short-Term Use Tests at 5 and 25°—The results of these tests for 20 weeks to date are summarized in Table II. Assays of whole tablets showed no measurable loss at 25° in open storage or in amber or polyethylene bottles opened daily five times per week; the retention of ascorbic acid by three assay methods averaged 100% of claim after 3 months. The surface scrapings (15–20% of the tablet weight) showed average retentions of 96.5 and 96% at 5 and 25°, respectively, after 20 weeks. These small losses of 3.5–4% in 15–20% of the tablet weight would be equivalent to losses of 0.7–0.8% in the whole tablets. It is clear that greater losses of ascorbic acid occur at the surface of the tablets, as expected.

The amounts of dehydroascorbic acid measured in these stored tablets after 20 weeks are equivalent to about 3% of the original ascorbic acid content. Dehydroascorbic acid is fully active as ascorbic acid and represents no loss in vitamin activity. No detectable amount of diketogulonic acid could be seen on the thin-layer chromatograms after any storage test. The maximum amount of oxalic acid found in these storage tests is equivalent to about 0.2% of the ascorbic acid content, a trivial amount.

The overall averages of all assays of ascorbic acid in the stability tests listed in Table II by iodometric titration, 2,6-dichloroindophenol, and polarographic measurements are 100, 101, and 100%, respectively. This agreement confirms the utility of all three methods for measuring ascorbic acid in these tablets.

DISCUSSION

Adequacy of Analytical Methods for Ascorbic Acid—The direct titration of ascorbic acid with iodine or 2,6-dichloroindophenol, as per the methods for tablets in the official compendia (23, 24), is eminently suitable for tablets, since neither the decomposition products of ascorbic acid nor the normal excipients in such tablets have reducing activity. Deutsch and Weeks (40) assayed tablets containing ascorbic acid, multivitamins, and multivitamins–minerals by titration with 2,6-dichloroindophenol and *N*-bromosuccinimide, by colorimetry with diazotized *p*-nitroaniline, and by fluorometry after oxidation to dehydroascorbic acid. They found excellent agreement by all four methods.

Differential pulse polarography, a newer technique, showed close agreement to titration with iodine or 2,6-dichloroindophenol in the present study. Although not necessary for simple ascorbic acid tablets, several chromatographic methods are available to provide specific assays for ascorbic acid in the presence of interfering substances (*e.g.*, multivitamin tablets, low-potency foods, and biological samples).

Assays by four different methods of deliberately decomposed solutions of ascorbic acid are summarized in Table III. It is evident from the agreement among results and correlation with specific determinations quantitating the level of degradation products found by the various methods that all four methods measure intact residual ascorbic acid after extensive degradation has occurred. Moreover, the methods designed to determine specific degradation products are capable of doing so when detectable amounts of these materials are present. Wilk's (21) contention that there are no specific assays for ascorbic acid is unfounded.

IR Spectroscopic Determination of Ascorbic Acid Stability—IR curves were determined for pure ascorbic acid, dehydroascorbic acid, diketogulonic acid, oxalic acid, and tablet placebos to assess the utility of IR measurements as an indicator of the stability of ascorbic acid in tablets as proposed by Wilk (21). The spectrum of ascorbic acid does vary from those of the degradation products, as expected, and the band assignments stated in the literature were substantiated (Figs. 1–5). However, a great deal of band overlap is observed with ascorbic

[1] J. B. Johnson, M. J. Frank, J. McCaffrey, and S. H. Rubin, to be published.
[2] Due to the instability of 2,3-diketogulonic acid, 2-ketogulonic acid was used as a reference standard.
[3] M. Osadca and M. Araujo, to be published.
[4] Due to the instability of 2,3-diketogulonic acid, the IR spectrum of 2-ketogulonic acid, which is of similar structure, is shown.

Table II—Analysis of Ascorbic Acid, 100-mg Tablets (Lot JG-4969-58-2A)

Storage Conditions	Assay, % of Claim: Iodometric Total	Iodometric Surface	2,6-Dichloroindophenol Total	2,6-Dichloroindophenol Surface	Polarographic Total	Polarographic Surface	Percent of Moisture Content	Average Weight, mg/Tablet	Degradation Products[a] (Fluorometric Analysis): Dehydroascorbic Acid, %	Oxalic Acid, %
Initial	102	97	103	96	100	97	1.23	401	—	—
4 weeks/5°										
Amber glass bottle	99	102	103	90	101	97	1.05	401	—	—
Polyethylene bottle	104	103	103	100	100	99	1.33	401	—	—
4 weeks/25°										
Amber glass bottle	102	98	100	99	99	103	1.20	404	1.3	0.04
Polyethylene bottle	105	100	98	101	99	98	1.20	398	1.1	N.D.[b]
Open dish	98	93	99	98	101	100	1.37	396	1.2	0.03
8 weeks/5°										
Amber glass bottle	104	102	99	94	100	92	1.21	403	3.1	N.D.
Polyethylene bottle	97	94	100	94	100	96	1.25	399	3.5	N.D.
8 weeks/25°										
Amber glass bottle	101	92	102	93	98	94	1.15	403	2.1	0.07
Polyethylene bottle	99	89	100	90	100	95	1.20	396	2.4	0.04
Open dish	100	85	101	91	98	91	1.45	397	3.1	0.03
12 weeks/5°										
Amber glass bottle	98	92	100	92	97	95	1.30	402	3.3	N.D.
Polyethylene bottle	98	92	99	95	98	98	1.21	400	2.9	N.D.
12 weeks/25°										
Amber glass bottle	101	92	100	96	100	95	1.16	400	3.1	0.03
Polyethylene bottle	98	97	101	96	103	94	1.22	398	2.8	N.D.
Open dish	100	95	101	93	103	95	1.16	397	2.9	N.D.
16 weeks/5°										
Amber glass bottle	97	94	98	95	99	92	1.16	403	3.6	—
Polyethylene bottle	103	100	103	101	103	98	1.38	400	3.5	—
16 weeks/25°										
Amber glass bottle	100	93	102	93	102	95	1.00	405	3.7	—
Polyethylene bottle	103	95	99	95	100	95	1.10	398	2.8	—
Open dish	98	89	99	91	100	88	0.94	395	4.6	—
20 weeks/5°										
Amber glass bottle	96	96	95	95	100	97	1.47	400	5.4	—
Polyethylene bottle	99	99	102	96	101	96	1.56	400	4.5	—
20 weeks/25°										
Amber glass bottle	100	96	100	94	100	96	1.16	401	5.8	—
Polyethylene bottle	98	98	99	97	99	98	1.27	396	5.8	—
Open dish	98	95	98	96	99	96	1.28	396	—	—

[a] No degradation products were found using TLC. Limits of detection were 0.02% for diketogulonic acid and 0.07% for oxalic acid. [b] N.D. = none detected.

acid, dehydroascorbic acid, diketogulonic acid, and oxalic acid, as well as a large baseline displacement from the placebo. The combined effect of overlapping bands, placebo interference, and the availability of only imprecise methods for sample preparation make the use of IR impractical as a quantitative tool for ascorbic acid.

Stability of Ascorbic Acid in Tablets—The data in Table I show clearly that commercial ascorbic acid tablets stored at room temperature in closed bottles retain full label potency over a shelflife period of many years. In the use tests reported in Table II, the stability of ascorbic acid in the 100-mg tablets was excellent throughout the 3-month storage period involving intermittent brief exposure at both the 5 and 25° storage conditions and in open storage at 25° for the entire period. The relative humidity of the laboratory atmosphere to which these tablets were exposed ranged from 55 to 65%.

In 3-week storage tests at 45° of simple powder mixtures of ascorbic acid with tablet excipients, it was demonstrated (61) that moisture content is a critical factor determining ascorbic acid stability. At moisture levels below 2%, the stability of ascorbic acid was excellent, but progressively higher levels of moisture caused increasing but limited losses of the vitamin. The data in Tables I and II show that ascorbic acid tablets manufactured with proper control of moisture content have excellent stability. The moisture content of the tablets in Table II was low initially and remained low throughout the exposure tests, indicating that the compressed tablets are strongly resistant to moisture uptake under the stated conditions.

Significance of Dehydroascorbic Acid Formation—Wilk (21) implied that dehydroascorbic acid formed by oxidation of ascorbic acid represented a potentially harmful substance due to alleged diabetogenic activity. Actually, the diabetogenic activity referred to was that reported by Patterson (62) following *massive, intravenous* in-

Table III—Validation of Assay Procedures (Solution: 100 mg/ml, pH 4.0)

Incubation Conditions	Iodometric (23) Titration, % of Claim	2,6-Dichloroindophenol (23) Titration, % of Claim	Colorimetric (33) Assay, % of Claim	Polarographic Assay, % of Claim	TLC Determination: Diketogulonic Acid, mg/ml	TLC Determination: Oxalic Acid, mg/ml	Fluorometric (40) Determination of Dehydroascorbic Acid, mg/ml	pH
Initial	100	100	100	100	N.D.[a]	N.D.	N.D.	4.0
3 days/45°	85	86	86	86	6	5	0.2	—
7 days/45°	71	72	72	71	10	15	3.6	—
11 days/45°	62	61	60	62	10	20	5.1	4.3

[a] N.D. = none detected.

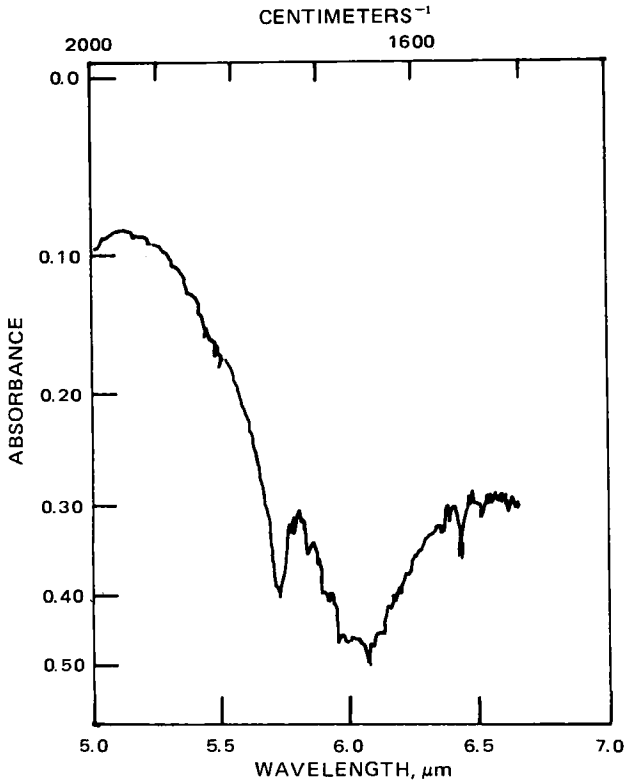

Figure 1—*IR spectrum of ascorbic acid standard (USP), 3.0 mg/350 mg (potassium bromide pellet).*

jection of dehydroascorbic acid into rats. The doses involved were close to lethal and were, in fact, lethal to many animals.

No diabetogenic activity of dehydroascorbic acid has been reported for oral dosage. On the contrary, a number of reports show that orally administered dehydroascorbic acid is quantitatively equal to ascorbic

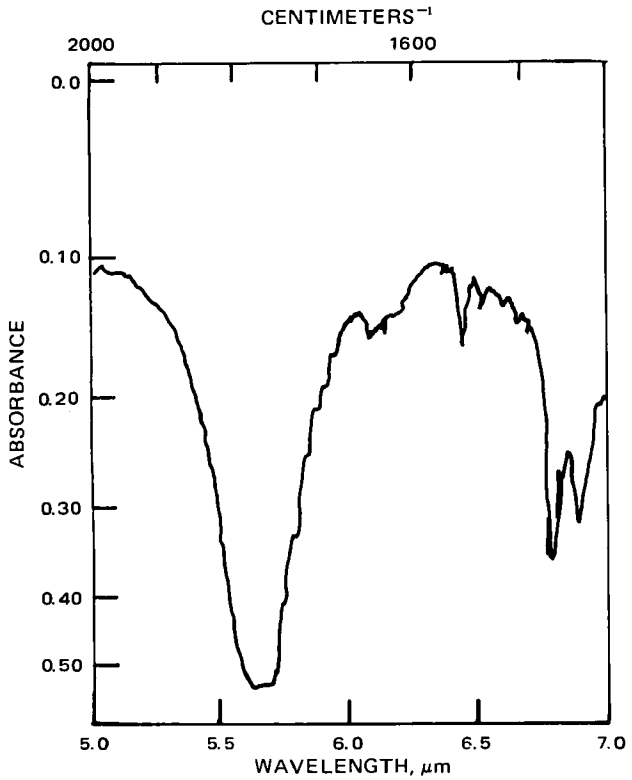

Figure 2—*IR spectrum of dehydroascorbic acid, 3.0 mg/350 mg (potassium bromide pellet).*

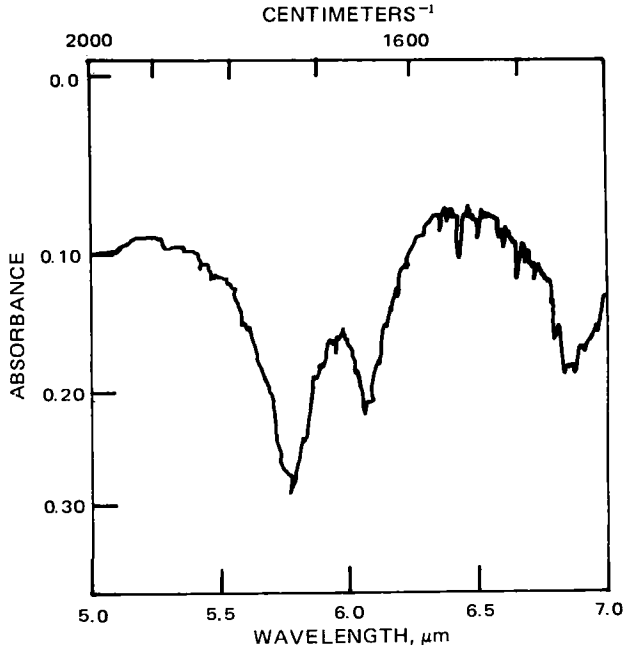

Figure 3—*IR spectrum of 2-ketogulonic acid, 3.0 mg/350 mg (potassium bromide pellet).*

acid for humans. This equivalence was demonstrated by measuring urinary excretion of ascorbic acid after comparable doses of dehydroascorbic acid and ascorbic acid in the 300–600-mg range (63, 64). Comparable blood levels and urinary excretion of ascorbic acid were found in young women following consumption of 65 mg of ascorbic acid from orange juice or 65 mg of dehydroascorbic acid from activated charcoal-treated orange juice (65). Oral intake of equal amounts of ascorbic acid or dehydroascorbic acid resulted in equivalent increases in both ascorbic acid and dehydroascorbic acid levels in the blood of human subjects (66, 67). Thus, the biological utility of doses of dehydroascorbic acid has been well documented. The small quantities of dehydroascorbic acid that may occur in aged ascorbic acid tablets represent full vitamin activity and present no dietary hazard.

Significance of Oxalic Acid Formation—Although Wilk (21) did not measure oxalic acid in aged ascorbic acid tablets, the possible occurrence of oxalic acid in such tablets was cited by him as being potentially harmful to the consumer. The actual amounts of oxalic acid found in aged tablets in the present study (Tables I and II) were small: only 1.0 mg or less in a 100-mg tablet.

These amounts of oxalic acid are negligible compared to amounts

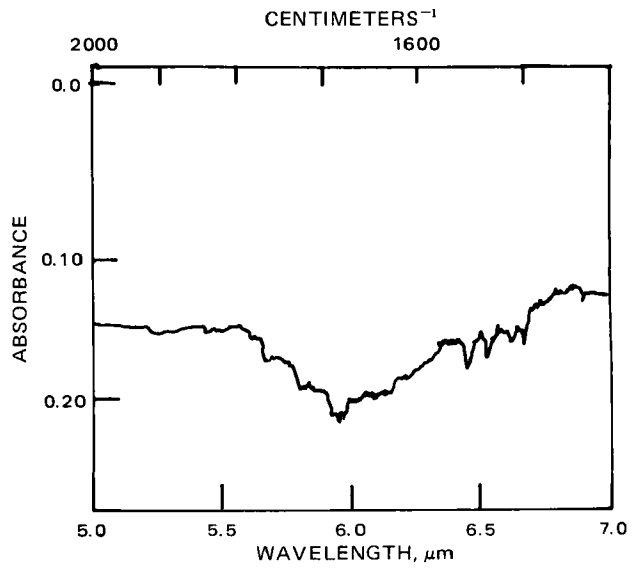

Figure 4—*IR spectrum of oxalic acid, 5.0 mg/350 mg (potassium bromide pellet).*

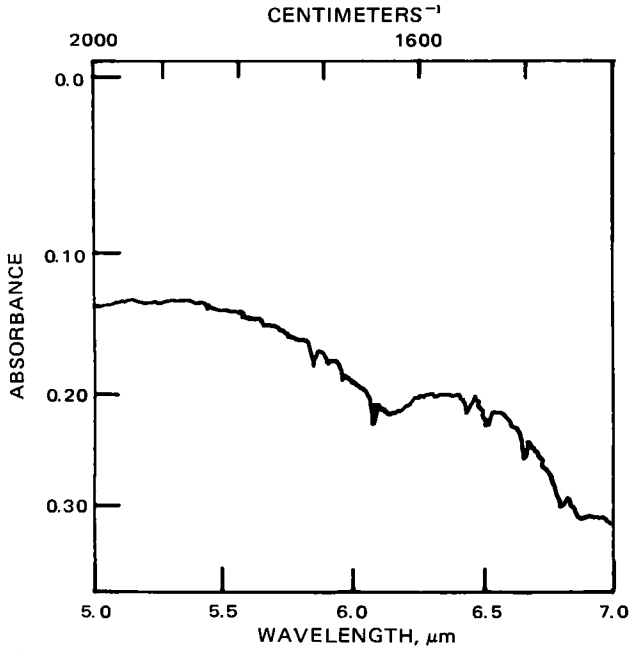

Figure 5—*IR spectrum of tablet placebo, 3.0 mg/350 mg (potassium bromide pellet).*

normally consumed by humans in the diet. For example, 82 and 150 mg of oxalic acid/100 g were found in two composite meals (68), and as much as 850–980 mg of anhydrous oxalic acid was found in 10 daily English diets from which high oxalate foods such as rhubarb and spinach were excluded (69). Obviously, the ingestion of even a number of aged tablets daily will cause practically no increase in the intake of oxalic acid.

The metabolic breakdown of ascorbic acid in human subjects has been studied (70). In a group of 10 subjects, the average excretion of a 1-g dose of ascorbic acid was approximately 65% as unchanged ascorbic acid, 6% as dehydroascorbic acid, and 2.3% as diketogulonic acid. After 90 days of dosing with 1 g of ascorbic acid/day or 2 g/day for 180 days, average increases in oxalic acid excretion were equivalent to less than 0.5% of the daily dose of ascorbic acid and were not statistically significant.

Lactose Intake from Ascorbic Acid Tablets—Wilk (21) cited the presence of lactose, commonly used as an excipient in ascorbic acid tablets, as a problem for lactose-intolerant individuals ingesting large numbers of such tablets, *e.g.*, 40 tablets to provide 4 g of vitamin. However, it is extremely unlikely that anyone wishing to take such a quantity would use 100-mg tablets, since 500-mg tablets are readily available and much more convenient. With the higher potency tablets, the intake of excipients is proportionately much less.

Even the theoretical consumption of 40 tablets containing 100 mg of ascorbic acid each would provide, with usual formulations, not more than 3.6 g of lactose. This quantity is relatively small compared to approximately 12 g in a glass of milk, which is tolerated by most people who are sensitive to a lactose tolerance test of 53–100 g.

Sodium Content of Chewable Ascorbic Acid Tablets—The question has been raised whether the amount of sodium from sodium ascorbate in chewable tablets is sufficient to be of concern to patients on a low-sodium diet. For taste reasons, a mixture of sodium ascorbate and ascorbic acid is sometimes used in such tablets. A typical formulation contains 60% of the ascorbic acid as the sodium salt, resulting in a sodium content of about 20 mg/tablet. The average daily dietary intake of sodium chloride of 6–18 g is equivalent to 120–360 times the amount of sodium in such a chewable vitamin tablet. Nonchewable tablets usually contain ascorbic acid in the free acid form only and contribute no sodium to the diet.

CONCLUSIONS

Contrary to allegations by Wilk (21), ascorbic acid tablets stored in closed bottles retain their claimed vitamin potency for 5 years or longer at room temperature. Storage of 100-mg tablets in an open dish at 25° or daily opening of glass or polyethylene bottles stored at room temperature or in the refrigerator for 20 weeks to date caused from 0 to 2% loss of ascorbic acid; slight losses occurred close to the surface of the tablets.

Analytical methods with high specificity are available, and have been for years, for determining the stability of ascorbic acid; IR spectroscopy is not suitable for quantitative assessment of ascorbic acid breakdown in tablets.

Very small amounts of dehydroascorbic acid are found in aged tablets. This oxidized form of the vitamin is fully active as ascorbic acid and is not diabetogenic.

Little or no oxalic acid has been found in aged tablets; the minute quantities found are insignificant in relation to normal levels in the diet. Similarly, tablet excipients such as lactose and sodium from sodium ascorbate are present in relatively small quantities, compared to the lactose content of milk and the normal sodium content of the diet, respectively.

REFERENCES

(1) *Ann. N.Y. Acad. Sci.*, **258**, 5(1974).
(2) V. G. Zannoni and P. H. Sato, *ibid.*, **258**, 119(1974).
(3) J. C. Street and R. W. Chadwick, *ibid.*, **258**, 132(1974).
(4) M. R. S. Fox, *ibid.*, **258**, 144(1974).
(5) J. J. Kamm, T. Dashman, A. H. Conney, and J. J. Burns, *ibid.*, **258**, 169(1974).
(6) S. S. Mirvish, *ibid.*, **258**, 175(1974).
(7) R. Ranieri and J. H. Weisburger, *ibid.*, **258**, 181(1974).
(8) C. W. M. Wilson, *ibid.*, **258**, 355(1974).
(9) J. U. Schlegel, *ibid.*, **258**, 432(1974).
(10) A. B. Robinson and S. L. Richheimer, *ibid.*, **258**, 314(1974).
(11) N. M. Sulkin and D. F. Sulkin, *ibid.*, **258**, 317(1974).
(12) E. Ginter, *ibid.*, **258**, 410(1974).
(13) H. Howald, B. Segesser, and W. F. Körner, *ibid.*, **258**, 458(1974).
(14) T. W. Anderson, *ibid.*, **258**, 498(1974).
(15) T. L. Lewis, T. R. Karlowski, A. Z. Kapikian, J. M. Lynch, G. W. Shaffer, and D. A. George, *ibid.*, **258**, 505(1974).
(16) C. W. M. Wilson, *ibid.*, **258**, 529(1974).
(17) J. M. Rivers and M. J. Devine, *ibid.*, **258**, 465(1974).
(18) O. Pelletier, *ibid.*, **258**, 156(1974).
(19) C. D. Gerson, *ibid.*, **258**, 483(1974).
(20) L. A. Barness, *ibid.*, **258**, 523(1974).
(21) I. J. Wilk, presented at the 169th National Meeting, American Chemical Society, Philadelphia, Pa., Apr. 1975.
(22) "Food Chemicals Codex," 2nd ed., National Academy of Sciences, Washington, D.C., 1972, pp. 66, 67.
(23) "The United States Pharmacopeia," 19th rev., Mack Publishing Co., Easton, Pa., 1975, pp. 36, 37.
(24) "Official Methods of Analysis of the AOAC," 12th ed., Association of Official Analytical Chemists, Washington, D.C., 1975, pp. 175, 176.
(25) H. Leonhardt and W. Moeser, *Z. Anal. Chem.*, **122**, 3(1941).
(26) M. Z. Barakat, M. F. A. El-Wahab, and M. M. El-Sadr, *Anal. Chem.*, **27**, 536(1955).
(27) D. F. Evered, *Analyst*, **85**, 515(1960).
(28) L. P. Pepkowitz, *J. Biol. Chem.*, **151**, 405(1943).
(29) W. B. Robinson and E. Stotz, *ibid.*, **160**, 217(1945).
(30) S. H. Rubin, F. W. Jahns, and J. C. Bauernfeind, *Fruit Prod. J. Am. Food Manuf.*, **24**, 327(1950).
(31) H. Mohr, *Mitt. Geb. Lebensmittelunters. Hyg.*, **47**, 20(1966).
(32) C. E. Weeks and M. J. Deutsch, *J. Assoc. Offic. Agr. Chem.*, **48**, 1245(1965).
(33) M. Schmall, C. W. Pifer, and E. G. Wollish, *Anal. Chem.*, **25**, 1486(1953).
(34) M. Schmall, C. W. Pifer, E. G. Wollish, R. Duschinsky, and H. Gainer, *ibid.*, **26**, 1521(1954).
(35) J. J. Roe and C. A. Kuether, *Science*, **95**, 77(1942); J. J. Roe and C. A. Kuether, *J. Biol. Chem.*, **147**, 399(1943).
(36) K. Istvan and F. Gusztave, *Acta Pharm. Hung.*, **37**, 127(1967).
(37) A. DeVleeschauwer, W. Deschacht, and H. Hendrickx, *Meded. Landbouwhogesch. Opzoekingsstn. Staat Gent*, **26**, 149(1961).
(38) H. M. Hashmi, A. S. Adil, A. Viegas, and I. Ahmad, *Mikrochim. Acta*, **1970**, 457.
(39) N. Wahba, D. A. Yassa, and R. S. Labib, *Analyst*, **99**, 397(1974).
(40) M. J. Deutsch and C. E. Weeks, *J. Assoc. Offic. Agr. Chem.*, **48**, 1248(1965).

(41) S. M. Deshpande and R. Natarajan, *Drug Stand.*, **26**, 181(1961).
(42) W. U. Malik and K. L. Singh, *Indian J. Technol.*, **6**, 344(1968).
(43) J. H. Allison and M. A. Stewart, *Anal. Biochem.*, **43**, 401(1971).
(44) J. E. Schlack, *J. Assoc. Offic. Anal. Chem.*, **57**, 1346(1974).
(45) L. S. Bark and J. K. Grime, *Analyst*, **99**, 38(1974).
(46) C. A. Patschky, *Angew. Chem.*, **62**, 50(1950).
(47) R. Strohecker, W. Heimann, and F. Matt, *Z. Anal. Chem.*, **145**, 401(1955).
(48) K. Szöke, *Nahrung*, **4**, 825(1960).
(49) L. W. Mapson, *Biochem. J.*, **80**, 459(1961).
(50) D. Hornig, *J. Chromatogr.*, **71**, 169(1972).
(51) R. Strohecker and H. Pies, *Z. Lebensm.-Unters.-Forsch.*, **118**, 394(1962).
(52) I. R. Villeumier and S. Nobile, "Proceedings, 12th World's Poultry Congress," Sydney, Australia, 1962, pp. 238–241.
(53) T. L. Parkinson, *Chem. Ind. (London)*, **1952**, 17.
(54) R. C. R. Barreto, *Rev. Quim. Ind.*, **25**, 14(1956).
(55) J. Gordon and I. Noble, *J. Am. Diet. Assoc.*, **35**, 241, 578(1959).
(56) I. Crossland, *Chem. Scand.*, **14**, 805(1960).
(57) J. Hegenaur and P. Saltman, *J. Chromatogr.*, **74**, 133(1972).
(58) C. F. Bourgeois and P. R. Mainguy, *Int. J. Vitam. Nutr. Res.*, **45**, 70(1975).
(59) E. Stahl, "Thin Layer Chromatography," 2nd ed., Springer-Verlag, New York, N.Y., 1969, p. 650.
(60) P. M. Zarembski and A. Hodgkinson, *Biochem. J.*, **96**, 717(1965).
(61) E. DeRitter, L. Magid, M. Osadca, and S. H. Rubin, *J. Pharm. Sci.*, **59**, 229(1970).
(62) J. W. Patterson, *J. Biol. Chem.*, **183**, 81(1950).
(63) E. DeRitter, N. Cohen, and S. H. Rubin, *Science*, **113**, 628(1951).
(64) B. E. Clayton, R. R. McSwiney, and R. T. G. Prunty, *Biochem. J.*, **58**, 542(1954).
(65) E. N. Todhunter, T. McMillan, and D. A. Ehmke, *J. Nutr.*, **42**, 297(1950).
(66) J. H. Sabry, K. H. Fisher, and M. L. Dodds, *ibid.*, **64**, 457(1958).
(67) H. Linkswiler, *ibid.*, **64**, 43(1958).
(68) P. M. Zarembski and A. Hodgkinson, *Analyst*, **87**, 698(1962).
(69) H. E. Archer, A. E. Dormer, E. F. Scowen, and R. W. E. Watts, *Clin. Sci.*, **16**, 405(1957).
(70) H. Takiguchi, S. Furuyama, and N. Shimazono, *J. Vitaminol.*, **12**, 307(1966).

ACKNOWLEDGMENTS AND ADDRESSES

Received November 6, 1975, from *Hoffmann-La Roche Inc., Nutley, NJ 07110*

Accepted for publication March 22, 1976.

* To whom inquiries should be directed.

Combined Assays for Vitamins A, D (Ergocalciferol), and E in Multivitamin Preparations with Separation by Reversed-Phase Partition Chromatography

JOHN W. STRONG

Abstract □ A rapid method was developed whereby vitamins A, D (ergocalciferol), and E in multivitamin products are measured in a common assay sample. The method depends on reversed-phase partition chromatography by which the vitamin alcohols are eluted in separate fractions from a column. Vitamins A and E are then determined by their UV absorption, while vitamin D is measured colorimetrically with an antimony trichloride reagent. The column consists of diatomaceous earth impregnated with dimethyl polysiloxane, with *n*-heptane as the immobile solvent, and 90% methanol followed by 95% methanol as the mobile solvents. Vitamins A and D elute in that order in the 90% methanol, and finally vitamin E elutes in the 95% methanol fraction. The method is widely applicable to various types of multivitamin and vitamin–mineral products including oil-based, water-based, and dry formulations.

Keyphrases □ Vitamins—combined analyses, vitamins A, D (ergocalciferol), and E in multivitamin preparations, reversed-phase partition chromatography □ Chromatography, reversed-phase partition—combined analyses, vitamins A, D, and E in multivitamin preparations □ Multivitamin preparations—combined analyses, vitamins A, D, and E, reversed-phase partition chromatography

The USP (1) provides assays for vitamins A and E in multivitamin preparations which utilize a common assay sample. However, duplication of procedure exists in that a similar assay step, depending on the selective degradation of vitamin A in the presence of vitamin E, is subsequently carried out in each of the two determinations. Duplication of assay steps is also involved with respect to the USP assay for vitamin D (ergocalciferol) (1). The procedure is similar to that for vitamins A and E through the initial steps of alkaline hydrolysis and extraction, but another sample is nevertheless taken and the complete analysis is carried out separately.

The USP vitamin D assay also is subject to the criticism that vitamin E, if present, carries through the analysis, causing high results for vitamin D. To correct for such interference, procedures have been proposed for the removal of vitamin E by adsorption on a column (2, 3); but this additional step lengthens what is already a rather long and tedious assay. Perhaps the main disadvantage is that the vitamin E fraction is lost, so a completely separate determination must be undertaken for vitamin E.

Incorporated in the USP vitamin D assay is a column step for the separation of vitamin D from vitamin A. This step depends on "conventional" partition chromatography; *i.e.*, the more polar solvent is the stationary phase and the less polar is the mobile phase. Conceivably such a system might also provide a separation between vitamins D and E, with vitamin E eluting first. The problem is that vitamins D and E both elute close to the solvent front, so their bands tend to overlap and a complete separation is difficult.

The reversed-phase partition column has been found

(41) S. M. Deshpande and R. Natarajan, *Drug Stand.*, **26**, 181(1961).
(42) W. U. Malik and K. L. Singh, *Indian J. Technol.*, **6**, 344(1968).
(43) J. H. Allison and M. A. Stewart, *Anal. Biochem.*, **43**, 401(1971).
(44) J. E. Schlack, *J. Assoc. Offic. Anal. Chem.*, **57**, 1346(1974).
(45) L. S. Bark and J. K. Grime, *Analyst*, **99**, 38(1974).
(46) C. A. Patschky, *Angew. Chem.*, **62**, 50(1950).
(47) R. Strohecker, W. Heimann, and F. Matt, *Z. Anal. Chem.*, **145**, 401(1955).
(48) K. Szöke, *Nahrung*, **4**, 825(1960).
(49) L. W. Mapson, *Biochem. J.*, **80**, 459(1961).
(50) D. Hornig, *J. Chromatogr.*, **71**, 169(1972).
(51) R. Strohecker and H. Pies, *Z. Lebensm.-Unters.-Forsch.*, **118**, 394(1962).
(52) I. R. Villeumier and S. Nobile, "Proceedings, 12th World's Poultry Congress," Sydney, Australia, 1962, pp. 238–241.
(53) T. L. Parkinson, *Chem. Ind. (London)*, **1952**, 17.
(54) R. C. R. Barreto, *Rev. Quim. Ind.*, **25**, 14(1956).
(55) J. Gordon and I. Noble, *J. Am. Diet. Assoc.*, **35**, 241, 578(1959).
(56) I. Crossland, *Chem. Scand.*, **14**, 805(1960).
(57) J. Hegenaur and P. Saltman, *J. Chromatogr.*, **74**, 133(1972).
(58) C. F. Bourgeois and P. R. Mainguy, *Int. J. Vitam. Nutr. Res.*, **45**, 70(1975).
(59) E. Stahl, "Thin Layer Chromatography," 2nd ed., Springer-Verlag, New York, N.Y., 1969, p. 650.
(60) P. M. Zarembski and A. Hodgkinson, *Biochem. J.*, **96**, 717(1965).
(61) E. DeRitter, L. Magid, M. Osadca, and S. H. Rubin, *J. Pharm. Sci.*, **59**, 229(1970).
(62) J. W. Patterson, *J. Biol. Chem.*, **183**, 81(1950).
(63) E. DeRitter, N. Cohen, and S. H. Rubin, *Science*, **113**, 628(1951).
(64) B. E. Clayton, R. R. McSwiney, and R. T. G. Prunty, *Biochem. J.*, **58**, 542(1954).
(65) E. N. Todhunter, T. McMillan, and D. A. Ehmke, *J. Nutr.*, **42**, 297(1950).
(66) J. H. Sabry, K. H. Fisher, and M. L. Dodds, *ibid.*, **64**, 457(1958).
(67) H. Linkswiler, *ibid.*, **64**, 43(1958).
(68) P. M. Zarembski and A. Hodgkinson, *Analyst*, **87**, 698(1962).
(69) H. E. Archer, A. E. Dormer, E. F. Scowen, and R. W. E. Watts, *Clin. Sci.*, **16**, 405(1957).
(70) H. Takiguchi, S. Furuyama, and N. Shimazono, *J. Vitaminol.*, **12**, 307(1966).

ACKNOWLEDGMENTS AND ADDRESSES

Received November 6, 1975, from *Hoffmann-La Roche Inc., Nutley, NJ 07110*

Accepted for publication March 22, 1976.

* To whom inquiries should be directed.

Combined Assays for Vitamins A, D (Ergocalciferol), and E in Multivitamin Preparations with Separation by Reversed-Phase Partition Chromatography

JOHN W. STRONG

Abstract □ A rapid method was developed whereby vitamins A, D (ergocalciferol), and E in multivitamin products are measured in a common assay sample. The method depends on reversed-phase partition chromatography by which the vitamin alcohols are eluted in separate fractions from a column. Vitamins A and E are then determined by their UV absorption, while vitamin D is measured colorimetrically with an antimony trichloride reagent. The column consists of diatomaceous earth impregnated with dimethyl polysiloxane, with *n*-heptane as the immobile solvent, and 90% methanol followed by 95% methanol as the mobile solvents. Vitamins A and D elute in that order in the 90% methanol, and finally vitamin E elutes in the 95% methanol fraction. The method is widely applicable to various types of multivitamin and vitamin–mineral products including oil-based, water-based, and dry formulations.

Keyphrases □ Vitamins—combined analyses, vitamins A, D (ergocalciferol), and E in multivitamin preparations, reversed-phase partition chromatography □ Chromatography, reversed-phase partition—combined analyses, vitamins A, D, and E in multivitamin preparations □ Multivitamin preparations—combined analyses, vitamins A, D, and E, reversed-phase partition chromatography

The USP (1) provides assays for vitamins A and E in multivitamin preparations which utilize a common assay sample. However, duplication of procedure exists in that a similar assay step, depending on the selective degradation of vitamin A in the presence of vitamin E, is subsequently carried out in each of the two determinations. Duplication of assay steps is also involved with respect to the USP assay for vitamin D (ergocalciferol) (1). The procedure is similar to that for vitamins A and E through the initial steps of alkaline hydrolysis and extraction, but another sample is nevertheless taken and the complete analysis is carried out separately.

The USP vitamin D assay also is subject to the criticism that vitamin E, if present, carries through the analysis, causing high results for vitamin D. To correct for such interference, procedures have been proposed for the removal of vitamin E by adsorption on a column (2, 3); but this additional step lengthens what is already a rather long and tedious assay. Perhaps the main disadvantage is that the vitamin E fraction is lost, so a completely separate determination must be undertaken for vitamin E.

Incorporated in the USP vitamin D assay is a column step for the separation of vitamin D from vitamin A. This step depends on "conventional" partition chromatography; *i.e.*, the more polar solvent is the stationary phase and the less polar is the mobile phase. Conceivably such a system might also provide a separation between vitamins D and E, with vitamin E eluting first. The problem is that vitamins D and E both elute close to the solvent front, so their bands tend to overlap and a complete separation is difficult.

The reversed-phase partition column has been found

advantageous for separating lipophilic substances (4). Although several reports described its application to oil-soluble vitamins (5–9), they have not dealt with multivitamin products or have not involved the determination of more than one vitamin at a time.

The present report describes a procedure for determining vitamins A, D, and E in multivitamin preparations. The three vitamins are separated from each other by reversed-phase partition chromatography on a column. There is no duplication of assay steps, and the presence of vitamin E is no longer a problem in the determination of vitamin D. The assays for vitamins A and D parallel those in the USP (1) in many respects, but an attempt has been made to simplify those steps that are similar wherever possible.

EXPERIMENTAL

Equipment—The following were used: hot plates with magnetic stirrers; glass chromatographic tubes, 2.5 cm i.d. × 25 cm long, with stopcocks; glass chromatographic tubes with upper sections 2.5 cm i.d. × 20 cm long and lower sections 1.5 cm i.d. × 15 cm long[1], with stopcocks; rotary evaporators[2] with controlled-temperature water baths and tubes for introducing nitrogen into the evaporating flasks; and a recording spectrophotometer[3] with 1- and 2-cm cells.

Reagents and Solutions—Reagent grades of the following were used: acetic anhydride, acetyl chloride, antimony trichloride, benzene[4], chloroform, ethylene dichloride[4], ether[5], *n*-heptane, methanol, petroleum ether, potassium hydroxide, and pyrogallol.

Other reagents were 95% ethanol, USP grade; anhydrous ethanol, pure; fuller's earth[6]; and light mineral oil, NF grade.

The reversed-phase column support was diatomaceous earth impregnated with 0.5% silicone. To prepare about 1.2 kg of final product, 1-kg portions of diatomaceous earth[7] were placed in each of two 18.9-liter (5-gallon) bottles and suspended in about 11.4 liters (3 gallons) of water at 25°. After 10 min, the supernatant portions were decanted and discarded to remove the fine-particle fraction from the diatomaceous earth. The sedimentation process was repeated three more times.

The residual diatomaceous earth was collected in a percolator, vacuum dried, rinsed with methanol, and then vacuum dried for a prolonged period. The dried diatomaceous earth was transferred to a suitable basin or tub and mixed with a solution of dimethyl polysiloxane[8], 1% (w/v) in chloroform, in the proportion 1 ml of solution for each 2 g of diatomaceous earth. The mixture was dried with occasional mixing under an air stream in a hood, then washed with several liters of methanol in a percolator, and vacuum dried.

To determine vitamin D, a solution of antimony trichloride in ethylene dichloride[4], 450 g/1000 ml[4] (Solution A), or acetyl chloride in ethylene dichloride[4], 1 + 4 (v/v) (Solution B), was used. A mixture of 9 volumes of Solution A with 1 volume of Solution B was used as the final color reagent.

Standard solutions of vitamin D were prepared from USP ergocalciferol reference standard[9] or from ergocalciferol USP purchased in sealed glass ampuls[10]. Ergocalciferol USP was found to be equivalent to the USP reference standard with respect to measurements by UV spectrophotometry and by colorimetry with antimony trichloride. Stock Solution I was made in 95% ethanol, USP grade, 50 mg/100 ml. Stock Solution II was prepared by evaporating 5.0 ml of Solution I and reconstituting in 100.0 ml of ethylene dichloride[4]. Working Solution III was prepared by diluting Solution II with ethylene dichloride[4] to a final concentration of 2.5 μg/ml.

All standard solutions were refrigerated during storage and were stable up to 1 week in the case of III, up to 3–4 weeks in the case of II, and up to several months in the case of I as measured colorimetrically with antimony trichloride. (Standard solutions in ethylene dichloride may be quite unstable unless the solvent is first purified as described.) Unused portions of ergocalciferol powder were refrigerated under a nitrogen atmosphere in a desiccator and were quite stable during such storage.

Procedure—Carry out the assays while avoiding bright daylight and allow only the minimum necessary exposure to artificial light, particularly with solutions containing vitamin A.

Alkaline Reflux—Place sample without pretreatment (*e.g.*, intact capsules or tablets), equivalent to 2000 I.U. (50 μg) of vitamin D, in a 250-ml low actinic conical flask containing a 5.1-cm (2-in.) stirring bar[11]. Add 48 ml of 95% ethanol, 2 ml of 5% pyrogallol in 95% ethanol, and 10 ml of ether. Mount under a condenser and heat to boiling using a hot plate with a magnetic stirrer.

Add 20 ml of 20% (w/v) aqueous potassium hydroxide through the condenser and reflux with stirring for 45 min for oil-based formulations, for 30 min for intact tablets or powder-filled capsules, or for 20 min for powder samples or water-based formulations. Cool and, without delay, rinse the condenser with 20 ml of water. Collect in the flask and add 40 ml of petroleum ether.

Extraction into Ether–Petroleum Ether (1 + 3)—Transfer the contents of the flask to a 250-ml separator. Add 40 ml of water, 15 ml of ether, and 35 ml of petroleum ether and shake vigorously. Drain the bottom aqueous–ethanol layer into a second separator and shake with 80 ml of ether–petroleum ether (1 + 3). Discard the bottom layer. Combine the extracts in the first separator and wash with 50 ml of 40% ethanol followed by 50 ml of water. Then discard the wash solutions.

If necessary, add a few drops of 15% (w/v) aqueous sodium sulfate solution to break emulsions. Filter the ether–petroleum ether extracts through cotton into a boiling flask containing 0.4 ml of light mineral oil. (*Note:* Apply technique of pouring through neck of separator, after completely draining bottom layer, to avoid possible contamination of extracts with traces of aqueous phase.)

Reversed-Phase Column Preparation—Thoroughly mix 10 g of silicone-treated diatomaceous earth with 7.0 ml of *n*-heptane in a 250-ml beaker. Avoid air currents and complete the mixing within about 1 min to avoid appreciable loss of solvent through evaporation. Without delay, transfer the mixture in divided portions (four portions) to a chromatographic tube, 2.5 cm i.d., with stopcock, containing a small pledget of cotton. Pack each portion evenly and firmly, applying sufficient pressure to eliminate visible air pockets.

Evaporate the ether–petroleum ether extracts under vacuum, warming to not over 40°. Take up the oily residue and transfer to a 150-ml beaker, using about 25 ml of petroleum ether. Evaporate to an oily residue on a steam bath under an air current, reducing the application of heat near the end. The evaporation should be carried out as rapidly as possible, but without allowing the temperature of the final residue to exceed about 40°.

Without delay, add 0.6 ml of *n*-heptane, cover with a watch glass, and mix by swirling. Warm slightly on a steam bath if necessary to effect complete dissolution of any congealed residue. Add 1.5 g of silicone-treated diatomaceous earth and mix thoroughly with a stirring rod.

Transfer to the chromatographic tube over the first layer, packing as before. Complete the transfer by scrubbing the beaker with 1.5 g of silicone-treated diatomaceous earth to which was added 1 ml of *n*-heptane and pack into the chromatographic tube as the top layer. Cap the column with a thin pledget of cotton. Proceed with the next step without delay.

Elution from Column—With the stopcock of the chromatographic tube in the open position, introduce over the column about 15 ml of exactly 90.0% (v/v) methanol in water, previously saturated with *n*-heptane[12]. When the solvent has just receded to the top of the column,

[1] Tube was similar to that used in the second column chromatography in the USP vitamin D assay (1) but with a larger diameter bottom section.
[2] Buchler model PTFE-1G.
[3] Cary model 15, equipped with 0–1 absorbance slide wire.
[4] Purified by filtration through aluminum oxide, Brockmann activity grade I, basic, for chromatography (J. T. Baker Chemical Co., Phillipsburg, N.J.), using 110 g/3.79 liters (1 gallon) of benzene and 220 g/3.79 liters (1 gallon) of ethylene dichloride in a 3.9-cm i.d. tube and 40 g/1000 ml of antimony trichloride in purified ethylene dichloride in a 2.5-cm i.d. tube.
[5] Kept in original metal containers for satisfactory storage.
[6] Florex AA-RVM, 60–90 mesh, Floridin Co., New York, N.Y.
[7] Celite 545, Johns-Manville Corp., New York, N.Y.
[8] Medical Fluid 360, 12,500 cSt., Dow Chemical Co., Midland, Mich.
[9] USP Reference Standards, Rockville, MD 20852
[10] ICN Nutritional Biochemicals, Cleveland, Ohio.
[11] Coated with Teflon (du Pont).
[12] The eluting solvents should be stored in stoppered containers under a layer of *n*-heptane and should be dispensed in such a way as to avoid evaporation. The solutions should be maintained at room temperature and should be freshly shaken with an excess of *n*-heptane before use. For satisfactory column operation, the procedure should be conducted at a room temperature, preferably 22–28°.

repeat the addition and maintain a little liquid over the top of the column until the effluent appears at the stem. Fill the chromatographic tube with the 90.0% methanol solvent and adjust the rate of flow with the stopcock to 3–5 ml/min. Collect the first 30 ml of effluent in a graduated cylinder and reserve, storing in the dark for the *Determination of Vitamin A*.

Collect the next 90 ml of effluent, introducing more 90.0% methanol solvent over the column as necessary, and reserve for the *Determination of Vitamin D*.

Continue passing the 90.0% methanol solvent through the column, collecting and discarding an additional 20 ml of effluent. Then pour off and discard any residual 90.0% methanol solvent remaining over the column and pass *n*-heptane-saturated 95.0% methanol[12] through the column; discard the next 20 ml of effluent and collect the following 90 ml at a flow rate of 3–5 ml/min. Reserve the collected effluent for the *Determination of Vitamin E*. If the sample taken contains more than 100 I.U. of vitamin E, collect 120 ml of effluent instead of 90 ml.

Determination of Vitamin A—Transfer the first fraction of column effluent, 30 ml, containing the vitamin A to a 100-ml volumetric flask. After completing the transfer, dilute to volume with methanol and then mix. Transfer an accurately measured volume of this solution, V_1, to a volumetric flask of suitable capacity, V_2, and dilute to volume with methanol to yield a solution containing 10–15 I.U. of vitamin A/ml. With a suitable spectrophotometer, determine the absorbance of this solution at the maximum at about 324 nm, using 1-cm cells, relative to methanol as the blank. Calculate the vitamin A content in the sample using:

$$0.549\,A_{max}/LC = \text{mg of vitamin A (alcohol)} \qquad \text{(Eq. 1)}$$

where A_{max} is the absorbance at the maximum at about 324 nm, L is the cell length in centimeters, and C is the amount of sample in terms of grams, milliliters, tablets, or capsules in each milliliter of final solution[13] [*cf.*, USP (1)]. Since C is equal to the amount of sample taken times V_1/V_2, where V_1 and V_2 are as previously defined, and L is equal to 1, the calculation formula then becomes:

$$(0.549)(V_2/V_1)(A_{max}) = \text{mg of vitamin A (alcohol) in sample} \qquad \text{(Eq. 2)}$$

To convert to international units of vitamin A, instead of milligrams, the factor 0.549 is divided by 0.0003 and the calculation formula is:

$$(1830)(V_2/V_1)(A_{max}) = \text{I.U. of vitamin A in sample} \qquad \text{(Eq. 3)}$$

Determination of Vitamin D—Combine the second fraction of column effluent, 90 ml, with 0.1 ml of light mineral oil mixed with a few milliliters of ether in a 500-ml boiling flask and evaporate to a clear oily residue under vacuum, using a rotary evaporator and water bath at about 40°. Remove residual water near the end of the evaporation by adding anhydrous ethanol and reevaporate. Introduce a slow stream of nitrogen to help prevent boiling or bumping and to remove the last traces of solvent. Finally, add 10 ml of *n*-heptane and evaporate again to an oily residue, thereby removing any residual traces of ethanol. Proceed with the next step without delay.

(At this point of the analysis, a purification step with fuller's earth is described for the purpose of removing degradation products of vitamin A. Where this interfering material is present in very small amounts, as is frequently the case with fresh samples, the fuller's earth treatment may be omitted. In such cases, the residue is then reconstituted directly in ethylene dichloride instead of in benzene and the colorimetric step is carried out as described next.)

Reconstitute the oily residue in 10 ml of purified benzene. Pass the benzene solution through a column of 10 g of fuller's earth contained in a 1.5-cm i.d. tube with stopcock, with thin layers of cotton at the bottom and the top, and previously rinsed with 40 ml of purified benzene. When the column is being prepared, the flow of benzene used as a rinse should be stopped by closing the stopcock so as to retain a thin layer of benzene over the top of the column before use and the rinsings should then be discarded.

Collect the effluent from the column in a 250-ml boiling flask, allowing unrestricted gravity flow. Use an additional 100 ml of purified benzene to complete the transfer to the tube and the elution of vitamin D from the column. Evaporate the collected effluent under vacuum to an oily residue, using a rotary evaporator with a water bath at not over 40°. Proceed with the next step without delay.

Reconstitute the oily residue in 20.0 ml of purified ethylene dichloride[14], stoppering the flask to prevent evaporation of the solvent. Transfer 3.0-ml portions of the solution into each of two suitable small stoppered containers (Solutions 1 and 2). Into each of two similar containers, transfer 3.0-ml portions of ergocalciferol working standard in purified ethylene dichloride, 2.5 μg/ml (Solutions 3 and 4). To Solutions 1 and 3, add 2.0 ml of purified ethylene dichloride; to Solutions 2 and 4, add 2.0 ml of acetic anhydride–ethylene dichloride (1:1) (color inhibitor solution). Mix.

Keep the containers stoppered. Apply the antimony trichloride color test successively to the contents of each container as follows. Add with a pipet 3.0 ml of antimony trichloride color reagent. Immediately mix and transfer to a 2-cm spectrophotometer cell. Exactly 1 min after completing the delivery of the color reagent, determine the absorbance, A, of the solution at 498 nm, using a suitable spectrophotometer, relative to ethylene dichloride as the blank. Calculate the vitamin D content in the sample using:

$$(800C)(A_u/A_s) = \text{I.U. of vitamin D} \qquad \text{(Eq. 4)}$$

where C is the concentration of the ergocalciferol working standard solution in micrograms per milliliter, A_u has the value A_{498} Solution 1 − A_{498} Solution 2, and A_s has the value A_{498} Solution 3 − A_{498} Solution 4.

Determination of Vitamin E—Transfer the last fraction of methanolic effluent from the reversed-phase column, containing the vitamin E, to a suitable volumetric flask of capacity V_1 in milliliters. Complete the transfer and dilute to volume with methanol; then mix. If necessary, prepare a second dilution by transferring an accurately measured volume of the first solution, V_2, to a volumetric flask of suitable capacity, V_3, and dilute to volume with methanol to obtain a solution containing 0.12–0.18 I.U. of *d*-alpha tocopherol/ml or 0.09–0.13 I.U. of *dl*-alpha tocopherol/ml.

With a suitable spectrophotometer, record the absorbance of the solution between 350 and 240 nm, using 1-cm cells, relative to a mixture of methanol and the eluting solvent as the blank in the same proportions. Construct a baseline by drawing a straight line tangent to the curve at two points, one in the region of the minimum at about 255 nm and the other in the longer wavelength region where the curve levels off, at about 317 nm. Draw a vertical line through the maximum at about 292 nm and intersecting the tangent baseline. The length of this vertical line from the maximum to the point of intersection with the tangent baseline represents the corrected absorbance at the maximum (corr. A_{max}). Calculate the vitamin E content in the sample taken if in the *d*-form (*d*-alpha tocopherol or its ester).

For single-step dilution:

$$(14.9V_1)(\text{corr. } A_{max}/72.4) = \text{I.U. of vitamin E} \qquad \text{(Eq. 5)}$$

For two-step dilution:

$$(14.9V_1)(V_3/V_2)(\text{corr. } A_{max}/72.4) = \text{I.U. of vitamin E} \qquad \text{(Eq. 6)}$$

If the vitamin E is present in the *dl*-form, the factor 14.9 is changed to 11. The number 72.4 represents the absorptivity (1%, 1 cm) of alpha tocopherol at the maximum at about 292 nm, with tangent baseline correction.

RESULTS AND DISCUSSION

Alkaline Hydrolysis or Saponification—The sample for assay requires no pretreatment, since even intact capsules and tablets disintegrate readily in the boiling medium used for alkaline hydrolysis with the aid of mechanical stirring. The stirring also helps to prevent overheating and bumping with vitamin–mineral formulations containing much insoluble material.

[13] The factor 0.549 is for solutions of vitamin A in 2-propanol; however, substitution of methanol as the solvent, as in the present analysis, results in practically no change of the value obtained for A_{max}, so that the calculation formula is still valid.

[14] Considerable difficulty with the vitamin D assay has been associated with the use of inadequately purified ethylene dichloride, resulting in unstable vitamin D solutions and low and variable readings in the colorimetric test with antimony trichloride. These results could be caused by a relatively high impurity content in the solvent before treatment or by the use of partially inactivated aluminum oxide for the purification. If necessary, the ethylene dichloride should be retreated with aluminum oxide that has been properly maintained in a well-sealed container in a dry atmosphere.

Table I—Exposure of Vitamin D Residues[a]

Container for Evaporation	Exposure of Residue after Evaporation	Recovery of Vitamin D, %	
		UV Method	Antimony Trichloride Method
	No Mineral Oil Present		
Volumetric flask	Nitrogen[b], 0 min	100.0	
Volumetric flask	Nitrogen[b], 30 min	99.4	
Volumetric flask	Nitrogen[b], 60 min	101.2	
Beaker	Nitrogen[b], 0 min	98.1	
Beaker	Nitrogen[b], 30 min	72.8	
Beaker	Nitrogen[b], 60 min	66.8	
Beaker	Nitrogen[b], 15 min	80.2	76.7
Beaker	Nitrogen[b], 60 min	66.5	55.8
	0.1 ml of Mineral Oil Present		
Beaker	Air, 15 min	99.3	
Extraction flask	Air, 15 min	99.9	

[a] At room temperature, after evaporation of petroleum ether solutions, using nitrogen. [b] Used nitrogen stream. In beaker or extraction flask, this procedure involves also exposure to admixed air.

The alkaline hydrolysis is needed for several additional reasons. First, oil vehicles, if present, should be removed by saponification and extraction as described; otherwise they may tend to overload the sample layer in the subsequent column step. Second, esters such as vitamin A acetate and vitamin E in the form of the acid succinate, if not first converted to the alcohols by hydrolysis, tend to overlap vitamin D in the elution from the column, so there is incomplete separation. Vitamin D itself is generally already present as the alcohol. Third, the differences in the solubility properties of the esters of vitamins A and E in general and also the differences in their absorption spectra can greatly complicate the problems of separation and measurement if they are allowed to remain in their esterified forms.

Ether in the hydrolysis mixture serves to lower the reflux temperature and helps to form a protective seal of solvent vapor over the solution when heated, thereby diminishing the effects of air oxidation. Vitamin E is particularly vulnerable with respect to air oxidation when hydrolyzed to the free alcohol form in alkaline media. Therefore, pyrogallol is added as a reducing agent which preferentially oxidizes on contact with the air. The oxidation of pyrogallol is characterized by a rapid darkening of the solution, but there is no interference with the analysis since pyrogallol and its oxidation product are readily removed in the subsequent extraction step. (Addition of a little ascorbic acid may also be desirable, but this step has not been performed routinely since ascorbic acid is generally present in the multivitamin formula.)

Finally, as precautionary measures, the mixture is heated to boiling to form the protective vapor seal before adding the aqueous potassium hydroxide solution. Immediately following reflux and cooling, some petroleum ether is added to provide a protective supernatant solvent layer. Hydrolysis of the esters of vitamins A and E is quite rapid, but an additional allowance of time is required for the disintegration of intact capsules and tablets and for the complete saponification of oil vehicles. Therefore, the total time for the alkaline reflux may be as much as 45 min, but usually it is less.

Extraction Step—Emulsions are no problem with the solvent system of 40% ethanol in aqueous potassium hydroxide solution with ether–petroleum ether (1 + 3) as the extracting solvent. Maintaining the proper ethanol concentration is important, as is the use of 40% ethanol instead of water for the first wash solution. If a little emulsion remains at the solvent interface, it may be broken up readily by introducing a few drops of a saturated aqueous solution of sodium sulfate [~15% (w/v) Na_2SO_4]. There are only four shaking operations and, when carried out in this manner, the overall extraction step is not time consuming.

The evaporation of the extracts can be an important part of the analysis, since losses may occur unless the evaporation is handled carefully. *The problem is rapid degradation of the dried residue if exposed to air, particularly when heated. For added protection, a little mineral oil is added to the extracts before evaporation.* The protective effect of mineral oil is demonstrated with vitamin D in Table I.

Reversed-Phase Column—The silicone-impregnated diatoma-

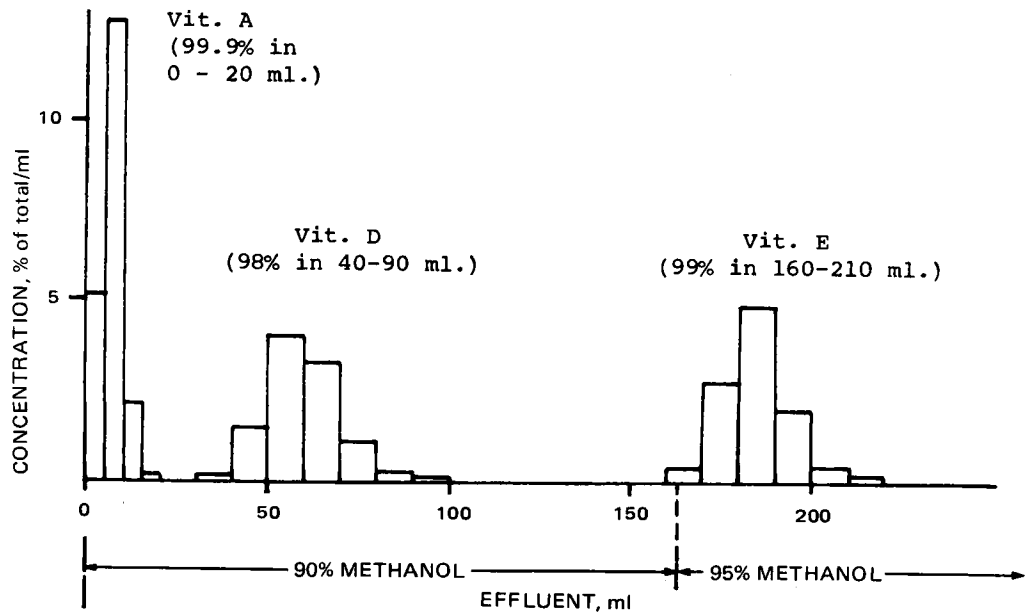

Figure 1—*Elution of vitamins A, D, and E from reversed-phase column.*

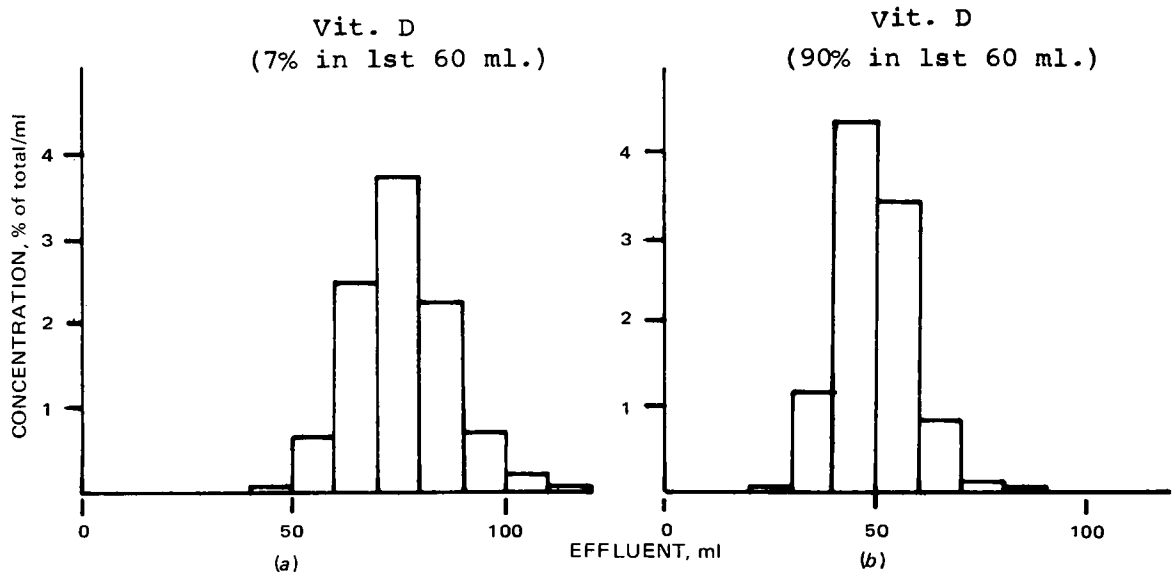

Figure 2—*Elution of vitamin D from reversed-phase column: effect of methanol concentration. Key:* (a), *89% methanol mobile solvent; and* (b), *91% methanol mobile solvent.*

ceous earth, from which the fine-particle fraction has been largely removed, has been found to be quite satisfactory as the column support. The silicone renders the diatomaceous earth readily wettable with the stationary hydrocarbon solvent but not with the mobile polar solvent, which is the desired condition in reversed-phase chromatography. Diatomaceous earth prepared in this manner is preferable to that silanized with dimethyldichlorosilane. Use of the latter results in more tailing, and the separations are not as sharp. Moreover, the silanized support is more difficult to handle during the column packing due to static charge, and it may also cause the stationary solvent to bleed from the column during the elution, a problem not encountered with the silicone-impregnated diatomaceous earth. Removal of the fine-particle fraction from the diatomaceous earth through a sedimentation process facilitates a rapid solvent flow.

Figure 1 shows the elution pattern for vitamins A, D, and E from the reversed-phase column, *i.e.*, the concentrations of the respective vitamins in successive fractions of the column effluent. According to the data from which this chart was prepared, 99.9% of the vitamin A present is eluted in the first 20 ml of effluent, 98% of the vitamin D is eluted in the portion of effluent between 40 and 90 ml, and 99% of the vitamin E is eluted in the portion between 160 and 210 ml. Larger fractions are actually collected to assure good recoveries.

To obtain consistent results, the stationary solvent (*n*-heptane) and the methanol content in the mobile solvent should be accurately measured. The importance of this step is demonstrated in Fig. 2, which depicts the effect on the elution of vitamin D if the concentration of methanol is allowed to deviate by a mere 1% from the intended 90.0% concentration. In this experiment, 7% of the vitamin D appeared in the first 60 ml of effluent with 89.0% methanol and 90% in the first 60 ml with 91.0% methanol.

To a lesser extent, variations in ambient temperature can affect the elution, with higher temperatures favoring early elution and lower temperatures favoring delayed elution. The column should be operated at 25 ± 3°.

Measurement of Vitamin A—The USP procedure for vitamin A makes use of the Morton–Stubbs (10) correction for background absorption in the spectrophotometric step of the assay. The big drawback with the method lies in the difficulty of obtaining accurate measurements on the slope of the curve at the designated wavelengths of 310 and 334 nm and the fact that any errors become greatly magnified in the final result.

The Morton–Stubbs correction has been omitted from the present procedure since the column provides added purification and removal of UV-absorbing impurities. However, the column does not serve to separate the geometric isomers of vitamin A from each other. In other words, as with the USP procedure for vitamin A, the absorbance that is finally measured represents the total amount due to all-*trans*-vitamin A, or retinol, plus any of the less active vitamin A isomers present. Although the latter are unlikely in fresh samples prepared with all-*trans*-synthetic vitamin A, they tend to form through isomerization of the all-*trans*-form in water-based formulations during aging (11). The spectrophotometric method then becomes subject to some positive error as a measure of biopotency, in which case corrective steps may be taken (12).

Measurement of Vitamin D—As with vitamin A, the measurement method is perhaps best discussed here by comparing it with the USP procedure. In several respects, the methods are similar. However, in the present method the color of the sample is compared directly with that of the standard instead of with that of a combination of sample and standard as in the USP method. Moreover, the correction based on readings of the solution at 550 nm has been dropped. These features of the USP colorimetric step appear to be unnecessary complications and may actually enhance any errors.

Other slight changes are as follows. The concentration of vitamin D in the final solution is slightly greater, and the solution is measured with 2- instead of 1-cm cells. The effect is to increase the absorbance reading. The corrected reading for the standard generally falls in the 0.360–0.400 range. The maximum for vitamin D has been observed to be at about 498 nm rather than at 500 nm as indicated in the USP.

Unfortunately, quite a few materials interfere with the antimony trichloride procedure for vitamin D, *i.e.*, materials that respond differently with and without the color inhibitor. Vitamin E is one of these, but it is removed by separation on the reversed-phase column. Degradation products of vitamin A would also interfere but are removed by the treatment with fuller's earth.

It was found advantageous to shorten the USP version of this step slightly by omitting the petroleum ether wash and by increasing the column diameter to permit a rapid flow rate by gravity flow. Furthermore, the capacity of the column for cleanup was improved by substitution of 10 g of fuller's earth for 3 g. The USP specifies 8.5–9.0% water content in the fuller's earth, and this amount was confirmed as being about optimum. A lower water content results in good

Table II—Recovery of Vitamin A in Extraction Step

Ether–Petroleum Ether Extracts	Vitamin A Found, UV Method	
	I.U. per Capsule[a]	Percent of Label Claim[a]
First two portions: 100 ml + 80 ml (usual extraction)	5597	139.9
Third portion (extra 80 ml)	3.1[b]	0.08

[a] Determinations were carried out with capsules having a high mineral content. [b] Result of 3.1 units, calculated as vitamin A, appeared to be due to extraneous background absorption rather than to actual vitamin A.

Table III—Recovery of Vitamin A through Reversed-Phase Column

Product	Type	Vitamin A Found	
		I.U. without Column	I.U. with Column
1	Capsules, with vitamins A and D	5698	5512
2	Tablets, with vitamins A, D, and E	5944	5807
3	Capsules, with vitamin A and minerals	2230	2196
4	Capsules, with vitamins A and E and minerals	6519	6353
5	Capsules, with vitamins A and E and minerals	6716	6569
5	Capsules, with vitamins A and E and minerals	6524	6313

cleanup of impurities but incomplete recovery of vitamin D from the column; a greater water content results in poor removal of impurities, although good recovery of vitamin D.

An important requirement is to use benzene free from water or contamination with polar solvents. Therefore, the benzene is treated before use by passing it through activated alumina. The USP specifies no pretreatment of the benzene.

Ergosterol and its irradiation products are not removed from the vitamin D fraction by the separation steps of either the present combined assay procedure or the USP assay for vitamin D. Ergosterol and lumisterol do not produce a significant amount of color with antimony trichloride color reagent, however, as observed by Shaw *et al.*

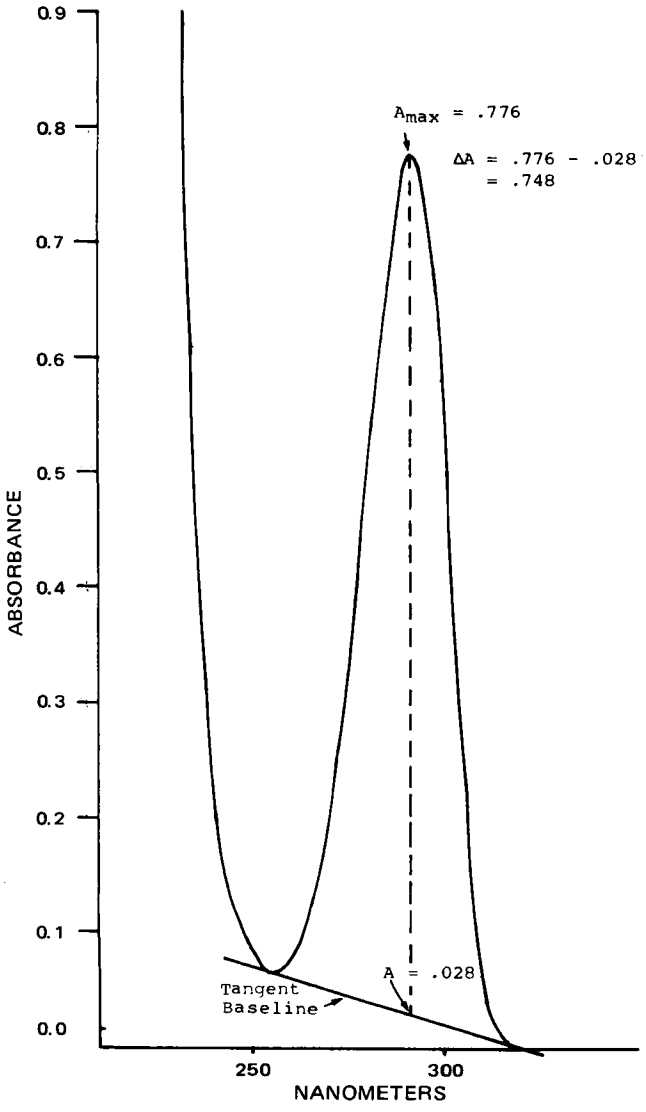

Figure 3—d-*Alpha tocopherol solution in methanol, 10.304 mg/100 ml. Absorptivity (1%, 1 cm) = 0.776/0.010304 = 75.3 (based on* A_{max}*) or 0.748/0.010304 = 72.6 (based on* ΔA_{max}*).*

(13). Precalciferol forms an equilibrium mixture with vitamin D, the rate of formation and final concentration being temperature dependent.

It has been contended that the total of vitamin D plus precalciferol, representing the potential biological activity, should be measured rather than the vitamin D content alone (14). Mixtures of the two would be typical in aged liquid preparations containing vitamin D. Fortunately in this regard, precalciferol produces the same response as vitamin D in the antimony trichloride test (13), so the assay procedure measures the total of the two.

Finally, tachysterol is not separated and would interfere if present in the original sample. Inactivation of tachysterol by reaction with maleic anhydride has been used to overcome the problem (15), but an extra step is needed. Preferably, the raw material used for the multivitamin product should be free from tachysterol. It might be monitored readily by the manufacturer by UV examination following reversed-phase column separation. As reported by Shaw *et al.* (13), tachysterol is a strong absorber in the UV region at wavelengths above 265 nm, the peak for vitamin D, so tachysterol would show up as a distortion of the vitamin D spectrum.

Some mention should be made here of material found in certain synthetic vitamin A concentrates that tends to cause extraneous color in the procedure for vitamin D. This material is not removed by the reversed-phase column, nor by the purification with fuller's earth. In the color test, the material has been observed to form a lavender background color. The absorbance is characterized by a maximum at about 580 nm, diminishing rapidly with time, and by a less pronounced maximum at about 475 nm which increases with time. Fortunately, the response is about the same with and without the color inhibitor at 498 nm, the point of measurement of vitamin D, so interference from this source has not been a serious problem.

Measurement of Vitamin E—Because of the cleanup on the reversed-phase column, it is possible to measure vitamin E by its UV absorption. Since a small amount of background absorption may still be present, a tangent baseline correction is used. The tangent baseline is illustrated in Fig. 3 as determined for a relatively pure sample of

Table IV—Recovery of Vitamin D

Product	Type	Recovery of Added Vitamin D, %
1	Water-based tablets, with vitamins A and D, Lot 1	101.1
	Lot 2	101.8
	Placebo	100.3
	Placebo	101.2
2	Capsules, with vitamins A, D, and E, Lot 1	92.5
	Lot 1	96.8
	Lot 2	93.4
3	Capsules, with vitamins A and D	98.3
4	Capsules, with vitamins A and D	101.6
5	Capsules, with vitamins A and D	100.0
6	Capsules, with vitamins A, D, and E and minerals	94.9
7	Tablets, with vitamins A, D, and E and minerals, Lot 1	96.0
	Lot 2	97.1
8	Tablets, with vitamins A, D, and E and minerals, Lot 2	92.6
9	Capsules, with vitamins A, D, and E and minerals; placebo	98.0
	Placebo	98.4

Table V—Determination of Vitamin E

Product	Type	Vitamin E, I.U. Label Claim	Found	
1	Capsules, with vitamins A, D, and E and minerals	30	31.4	
2	Capsules, with vitamins A, D, and E and minerals, Lot 1	15	15.41	
	Lot 2	15	15.66	
	Lot 3	15	16.07	
3	Tablets, with vitamins A, D, and E and minerals	30	11.12	
4	Tablets, with vitamins A, D, and E and minerals, Lot 1	10	11.12	32.6
	Lot 2	10	10.85	
	Lot 3	10	10.73	
5	Tablets, with vitamins A, D, and E and minerals	10	10.57	
6	Capsules, with vitamin E, Lot 1	400	398 (402 without column)	
	Lot 1	400	395 (404 without column)	
	Lot 2	400	406 (406 without column)	

d-alpha tocopherol[15]. This method is generally satisfactory for canceling out the effect of low levels of background.

For the calculations a standard value of 72.4 was determined, representing the absorptivity (1%, 1 cm) of alpha tocopherol (either *d* or *dl*) at 292 nm after tangent baseline correction. The standard value was obtained by collecting the middle portion of the vitamin E fraction from the reversed-phase column, with *dl*-alpha tocopherol as the starting material. The middle cut from the column was presumed to be quite pure. The collected effluent was then checked spectrophotometrically and by a gravimetric procedure to obtain the absorptivity value with tangent baseline correction for the isolated alpha tocopherol.

The average result of replicate determinations, 72.4, was in close agreement with the 72.6 value obtained with the pure sample (Fig. 3). The solvent used in this instance was methanol, but substitution of the 95% methanol eluting solvent resulted in practically no change of the absorptivity with tangent baseline correction.

The principal type of interference encountered in the UV determination of vitamin E has been background absorption due to degradation products of vitamin A. The background absorption from this source is typically characterized by a relatively broad peak near 290 nm. If not successfully removed, these impurities tend to produce a positive error for vitamin E. At low concentration, the vitamin A degradation products elute from the reversed-phase column ahead of vitamin E, largely in the vitamin D fraction but also in the discard fraction. At high concentration, as in certain aged samples, the column may become overloaded so that some of this degradation material tails into the vitamin E fraction. The answer is to reduce the amount of sample placed on the column to the point that overloading no longer occurs.

Although relatively little work was done with mixtures containing non-alpha tocopherols, they apparently also elute ahead of vitamin E (alpha tocopherol) and, consequently, do not interfere. Elution patterns obtained with such mixtures indicated little or no merging of the non-alpha tocopherols with the alpha tocopherols. Non-alpha tocopherols now may be largely phased out, however, with many newer multivitamin products being formulated to contain only the alpha form.

Recovery of Vitamin A—Good recovery of vitamin A in the extraction step is shown in Table II, *i.e.*, more than 99.9% recovery in the two portions of ether–petroleum ether normally used. The sample, a capsule formula high in mineral content, was used to demonstrate the absence of possible interference due to insoluble materials. These results for vitamin A are also indicative of good recoveries of vitamins D and E in the same extraction step, since they favor the nonpolar extracting solvent even more than does vitamin A.

In Table III, results are compared on assaying various formulations for vitamin A both with and without the column treatment. The indication is that about 2–3% of the vitamin A may be lost on the column, but the apparent loss can be greater with aged samples. In the latter case, the difference is probably due largely to purification on the column rather than to loss of vitamin A. The procedure without the column is similar to the USP vitamin A assay.

[15] Eastman Catalog No. 6340.

Recovery of Vitamin D—Percentage recoveries of known amounts of crystalline vitamin D were determined when added to placebo formulations or to the complete formulas themselves (Table IV). In each case, an accurately measured amount of vitamin D approximating the formula amount was added, the formula amount being 400 I.U. plus an excess. The average of the tabulated recoveries was 97.7%, and the standard deviation was 3.08.

Recovery of Vitamin E—Table V gives the assay results for vitamin E, comparing the amount found with the labeled amount in each case. The amount found is usually slightly more than the labeled amount, reflecting small formula excesses. With Product 6, which contains only vitamin E, assays were carried out both with and without the column separation and, as with vitamin A, the results indicate a slight loss on the column. The agreement is generally quite good, however, with apparent losses on the column usually not exceeding about 2%.

REFERENCES

(1) "The United States Pharmacopeia," 19th rev., Mack Publishing Co., Easton, Pa., 1975, pp. 631–634.

(2) F. J. Mulder, E. J. De Vries, and K. J. Keuning, *Pharm. Weekbl.*, **100**, 1457(1965).

(3) M. Osadca and E. DeRitter, *J. Pharm. Sci.*, **57**, 309(1968).

(4) G. A. Howard and A. J. P. Martin, *Biochem. J.*, **46**, 532(1950).

(5) J. Gillman, K. B. Norton, D. E. A. Rivett, and D. A. Sutton, *ibid.*, **63**, 458(1956).

(6) P. W. R. Eggitt and F. W. Norris, *J. Sci. Food Agr.*, **6**, 689(1955).

(7) P. S. Chen, Jr., A. R. Terepka, and N. Remsen, *Anal. Chem.*, **35**, 2030(1963).

(8) G. G. Dunckley and Y. J. MacFarlane, *J. Sci. Food Agr.*, **6**, 559(1955).

(9) M. Schmall, B. Senkowski, R. Colarusso, E. G. Wollish, and E. G. E. Shafer, *J. Am. Pharm. Assoc., Sci. Ed.*, **47**, 839(1958).

(10) R. A. Morton and A. L. Stubbs, *Biochem. J.*, **42**, 195(1948).

(11) R. W. Lehman, J. M. Dieterle, W. T. Fisher, and S. R. Ames, *J. Am. Pharm. Assoc., Sci. Ed.*, **49**, 363(1960).

(12) S. R. Ames and R. W. Lehman, *J. Assoc. Offic. Agr. Chem.*, **43**, 21(1960).

(13) W. H. C. Shaw, J. P. Jefferies, and T. E. Holt, *Analyst*, **82**, 2(1957).

(14) J. A. K. Buisman, K. H. Hanewald, F. J. Mulder, J. R. Roborgh, and K. J. Keuning, *J. Pharm. Sci.*, **57**, 1326(1968).

(15) F. J. Mulder, E. J. De Vries, and B. Borsje, *J. Assoc. Offic. Anal. Chem.*, **54**, 1168(1971).

ACKNOWLEDGMENTS AND ADDRESSES

Received March 24, 1975, from the *Quality Control and Government Regulations Division, Parke, Davis & Company, Detroit, MI 48232*

Accepted for publication September 29, 1975.

The author is grateful to Dr. S. A. Fusari for advice, Ida Semkus for technical assistance, and T. J. Korniski for discussions regarding normal testing applications.

Effect of Inorganic Additives on Solutions of Nonionic Surfactants III: CMC's and Surface Properties

HANS SCHOTT ˣ and SUK KYU HAN *

Abstract □ Continuing work on the interaction of inorganic additives with nonionic surfactants in aqueous solution dealt with their effect on the CMC and surface tension. The surfactants were octoxynol and polyoxyethylated oleyl alcohol, containing an average of 9.5 and 10 ethylene oxide units, respectively. Their CMC values were lowered by most electrolytes studied, representing salting out of the surfactants. The steepest reductions in the CMC were produced by the nitrates of sodium and potassium, which had been found to lower the cloud points of nonionic surfactants, salting them out because of the inability of their cations to form complexes with the ether oxygen linkages of the polyoxyethylene moieties. However, even electrolytes with cations such as hydrogen, lithium, calcium, nickel, lead, and aluminum capable of forming complexes with the ether oxygens, thereby increasing the cloud points of the surfactants, lowered their CMC values. In the presence of increasing concentrations of the latter electrolytes, the CMC values frequently went through minima and approached the CMC of the surfactant in the absence of additives. Increases in the CMC over the entire range of additive concentrations investigated were produced by cadmium nitrate for octoxynol, urea for polyoxyethylated oleyl alcohol, and magnesium nitrate for both. Net increases in the plateau or micellar surface tension of polyoxyethylated oleyl alcohol, *i.e.*, in the constant surface tension of surfactant solutions above the CMC, were brought about by the nitrates of cadmium, aluminum, and magnesium at low concentrations only and by urea at all concentrations. This increase is interpreted as salting in. The area per surfactant molecule adsorbed at the air–water interface was reduced by all added electrolytes. Urea caused no such reduction.

Keyphrases □ Surfactants, nonionic—effect of inorganic additives on CMC and surface properties □ Inorganic additives—effect on CMC and surface properties, nonionic surfactant solutions □ CMC—nonionic surfactant solutions, effect of inorganic additives □ Surface properties—nonionic surfactant solutions, effect of inorganic additives

Recent studies of the effect of electrolytes on the cloud points of nonionic polyoxyethylated surfactants (1, 2) showed that increases, representing salting in of the surfactants, are far more common than reductions in the cloud point, representing salting out. Two categories of additives caused sizable increases in cloud points: (*a*) urea and salts with anions known to break the structure of water, such as iodides, thiocyanates, and perchlorates (2, 3); and (*b*) salts with cations capable of forming complexes with model ethers such as dioxane (1, 2). Polyoxyethylated surfactants, which contain many ether linkages, acted as polydentate ligands for these cations. The resulting complexation increased the solubility of the surfactant molecules in such salt solutions above that in water, raising their cloud points.

Electrolytes in the second category included strong acids and salts of lithium and of all polyvalent cations tested, namely, lead, cadmium, magnesium, nickel(II), aluminum, and calcium (1, 2). In fact, the only salts that lowered cloud points were those of noncomplexing cations (sodium, potassium, ammonium, cesium, and, probably, rubidium) with anions of lyotropic numbers (4) below 11.7. The anions included nitrate (lyotropic number 11.6) but excluded perchlorate (lyotropic number 12.0) (1–3).

Most studies dealing with the effect of electrolytes on the critical micelle concentration (CMC) of polyoxyethylated nonionic surfactants reported a reduction in the CMC, corresponding to salting out (5). For instance, Hsiao *et al.* (6) found that all sodium salts examined depressed the CMC of nonoxynols (polyoxyethylated nonylphenols). The reduction in the CMC caused by the addition of 0.5 *N* sodium salts increased linearly with the decreasing lyotropic number of the anion; even sodium iodide lowered the CMC by nearly 30%. Becher (7, 8) found that 0.3 and 0.5 *N* sodium and calcium chloride, sodium citrate, and sodium sulfate lowered the CMC values of polyoxyethylated lauryl alcohol, tridecyl alcohol, and nonoxynol.

Schick and coworkers (3, 9) studied the effect of a variety of electrolytes, at the 0.86 *N* level, on the CMC of a nonoxynol. Only hydrochloric acid raised the CMC. The ability of the chlorides to lower the CMC increased in the order: lithium (41% reduction) < calcium < sodium < magnesium < potassium = strontium = barium < tetramethylammonium (59% reduction). For 0.86 *N* nitrates, the reduction in the CMC increased in the order: lithium < sodium < calcium = magnesium < potassium. For 0.86 *N* sodium salts with different anions, the reduction in the CMC increased in the order: thiocyanate (23% reduction) < iodide < nitrate = bromide < chloride < bromate < fluoride < citrate < sulfate (79% reduction).

While 0.5 *M* urea lowered the CMC of a nonoxynol by 18% (9), 3.0 and 6.0 *M* urea raised the CMC of that surfactant, as well as of polyoxyethylated lauryl and cetyl alcohols, by up to 200% at 25° (10, 11). The increases in the CMC were less pronounced at 45° than at 10°, because the structure of water is gradually disrupted by increasing temperatures even in the absence of urea. Guanidinium chloride and dioxane were even more effective than urea in raising the CMC of the nonoxynol (11), because they are even better structure breakers for water.

Measurements of sound velocity in solutions of polyoxyethylated octyl, nonyl, and decyl alcohols with added lithium chloride, bromide, or nitrate or potassium chloride revealed decreases in the CMC values as well as a narrowing in the concentration range over which micelles first appear (12).

Of the electrolytes of the second category (those with complex-forming cations), only hydrogen chloride has so far been found to increase the CMC of a polyoxyethylated surfactant. However, only three additional complexing cations have been studied, and only at single concentrations or over narrow concentration ranges. This prompted the investigation of the effect on the

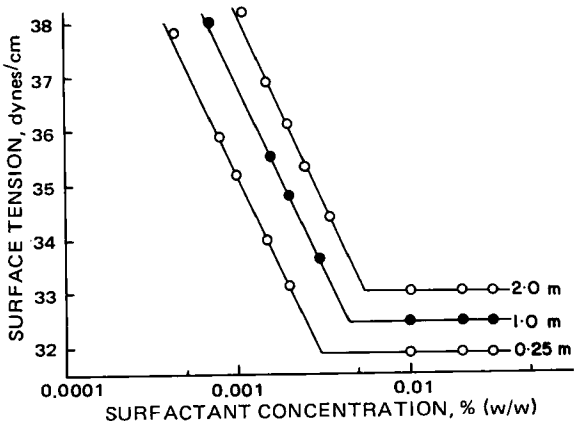

Figure 1—*Effect of cadmium nitrate on the surface tension of solutions of polyoxyethylated oleyl alcohol. Molalities (m) represent salt concentrations.*

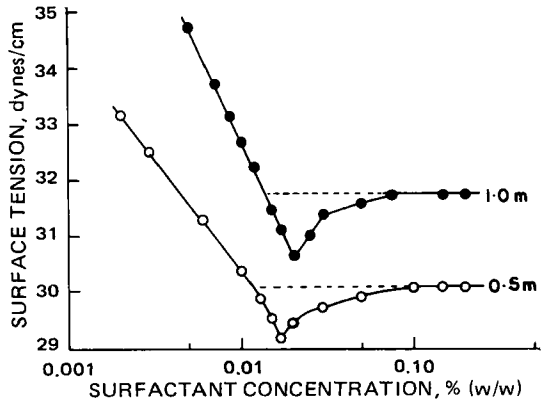

Figure 2—*Effect of magnesium nitrate on the surface tension of solutions of octoxynol. Molalities (m) represent salt concentrations.*

CMC of all those electrolytes of the second category that had demonstrated their ability to salt in polyoxyethylated surfactants by raising the cloud points. Relatively wide concentration ranges of added electrolytes were covered to spot trends in the variation of the CMC values.

EXPERIMENTAL

Two nonionic polyoxyethylated surfactants were studied, octoxynol NF[1] (branched octylphenol with 9–10 ethylene oxide units) and oleyl alcohol with an average of 10 ethylene oxide units[2]. These two surfactants were designated as I and IV, respectively, in Ref. 2, where their formulas and properties were tabulated. Surfactant I is a viscous, colorless liquid; Surfactant IV is a yellowish liquid and contains a solidified portion at 23°.

All chemicals were ACS reagent grade. The water was double distilled. The concentrations of all ternary mixtures are expressed as molality or as percent (w/w) based on the amount of water present. The preparation of ternary mixtures and the methods for assaying the electrolyte content of the concentrated stock solutions were described previously (1, 2).

Surface tensions were measured by means of a Wilhelmy balance[3] equipped with a thin rectangular sandblasted platinum blade which was cleaned by flaming. The receding contact angle was zero even in pure water. The solutions, stored in crystallizing dishes, had their surface cleaned by suction with a fine glass capillary. Surface tensions were measured after overnight storage at 25.0 ± 0.3°. The reproducibility of the measurements was within ±0.1 dyne/cm.

The surface tension *versus* log surfactant concentration plots for Surfactant IV in the vicinity of the CMC consisted of two straight lines, the one above the CMC being horizontal (*cf.*, Fig. 1). The CMC was taken as the intersection of these two lines, with a reproducibility of ±0.0002%. No minimum was observed down to the surfactant concentrations closest to the CMC at which surface tensions were measured, namely, 0.9 and 1.3 times the CMC of 0.055%.

The plots for Surfactant I exhibited a depression with a pronounced minimum. The flat branch rose beyond the CMC with increasing surfactant concentration and only gradually leveled off to become horizontal (*cf.*, Fig. 2). This behavior has been reported for most normally distributed polyoxyethylated octylphenols (13). The CMC was taken as the concentration corresponding to the minimum for the following reason.

The downward branch of the plots on approaching the minimum with increasing concentration was quite steep. This depression is produced by traces of highly surface-active impurities of low water solubility, presumably octylphenol molecules with zero or very few ethylene oxide units. Below the CMC, these impurities are preferentially adsorbed at the air–water interface, strongly depressing the surface tension. The subsequent rise of the curve above the minimum is due to the removal of the surface-active impurities from the air–water interface into the bulk of the surfactant solution by micellar solubilization. Since the minimum corresponds to the lowest surfactant concentration at which the impurities are first solubilized by micelles, it marks the onset of micelle formation. The surfactant concentration corresponding to the minimum is, therefore, the CMC[4].

While the absolute value of the CMC of Surfactant I as determined by surface tension is only approximate, relative shifts in the CMC caused by additives could be determined with a precision of about ±0.0005%.

RESULTS AND DISCUSSION

Effect of Additives on CMC—The effects of electrolytes on the CMC values of the two surfactants are shown in Tables I and II. The values are expressed as percent (w/w) based on the amount of water present. The most frequently observed trend is a reduction in the CMC, which deepens with increasing electrolyte concentration. Inasmuch as the electrolytes extend the surfactant concentration range over which micelles form at the expense of nonassociated surfactant molecules, lowering of the CMC represents salting out. From an alternative viewpoint, as its solubility is lowered through salting out, a surfactant becomes more surface active and accumulates more readily at the air–water interface. Therefore, saturation adsorption and plateau surface tension are reached at lower bulk concentrations, corresponding to a reduction in the CMC. Conversely, an increase in the CMC indicates salting in.

The electrolytes most effective in lowering the CMC of the two surfactants were the nitrates of sodium and potassium. These were also the most effective cations for depressing the cloud points (1, 2). Their salting-out effectiveness becomes even more apparent when comparing electrolytes at equal ionic strengths rather than at equal molalities, because at comparable molal concentrations the ionic strength of aluminum nitrate solutions is six times greater than that of sodium nitrate while that of nitrates of divalent cations is three times greater. Even at comparable molalities, the salts of most complexing cations depressed the CMC values less than did sodium or potassium nitrate.

The CMC of Surfactant I was nearly independent of the concentrations of lithium nitrate and hydrochloric acid in most of the range of concentrations covered. Also running counter to the general trend of monotonic decreases in the CMC with increasing electrolyte concentration, the CMC of Surfactant IV was increased somewhat by

[1] Triton X-100, Rohm & Haas Co.
[2] Brij 96, I.C.I. America (formerly Atlas Chemical Co.)
[3] Rosano surface tensiometer, V.W.R. Scientific.

[4] A lower value for the CMC of Surfactant I, namely, 0.010%, would have resulted if that concentration had been determined as the intersection between the extrapolated horizontal line obtained at concentrations beyond the minimum and the inclined straight line obtained at concentrations below the CMC. The order of the electrolytes ranked according to their effect on the CMC was the same according to both graphical methods of interpolation used for determining the CMC from the surface tension–concentration plots. The order of magnitude of the changes in CMC caused by these electrolytes was also the same for both methods of determining the CMC. The electrolytes did not substantially affect the depth of the minimum, which implies that no significant association between the former and the surface-active impurities of low water solubility took place.

Table I—Effect of Additives on the CMC of Octoxynol[a]

Additive	CMC, % (w/w), at Additive Molalities of 0.50	1.0	2.0	3.0
Sodium nitrate	0.015	0.013	0.009	0.006
Lithium nitrate	0.010	0.014	0.014	0.013
Hydrochloric acid	0.015	0.014	0.014	0.014
Sulfuric acid	0.014	0.013	0.013	0.011
Magnesium nitrate	0.017	0.018	0.016	0.012
Calcium nitrate	0.012	0.013	0.009	0.007
Aluminum nitrate	0.016	0.014	0.012	0.017[b]
Lead nitrate	0.015	0.013	0.010	
Nickel nitrate	0.016	0.014	0.013	0.009
Cadmium nitrate	0.021	0.020	0.022	
	0.10	0.25		
Cadmium nitrate	0.017	0.020		

[a] The CMC with no additive was 0.015–0.016% (w/w). [b] In 0.1 molal aluminum nitrate.

increasing concentrations of cadmium nitrate, following initial decreases at the lower salt concentrations.

Actual increases in the CMC values of both surfactants above their CMC values in the absence of additives were achieved by magnesium nitrate. Furthermore, cadmium nitrate increased the CMC of Surfactant I by one-third. Urea increased the CMC of Surfactant IV by as much as three-fourths above its CMC in pure water, in agreement with the observations of Schick (10) and Schick and Gilbert (11).

Lithium nitrate lowered the CMC of Surfactant IV more effectively than did sodium or potassium nitrate, in keeping with the order of the lyotropic series (4). In cloud point measurements, lithium was the only exception to the lyotropic series among the monovalent cations. Instead of lowering the cloud points more than did sodium and potassium, as expected from its position in that series, it raised them. This result was ascribed to the fact that lithium salts, unlike the salts of the other alkali metals and ammonia, form complexes with model ethers and with the ether groups of the nonionic surfactants (1, 2).

Cations bound to ether oxygens of nonionic surfactants by complexation confer a positive charge to the hydrophilic moiety. The resultant electrostatic repulsion between nonionic surfactant molecules turned cationic should increase their CMC (14). However, the very high ionic strength prevailing in the concentrated electrolyte solutions employed swamps this charge, restoring essentially nonionic conditions (15).

Most additives that depressed the CMC values brought about more extensive reductions in the CMC of Surfactant IV than in the CMC of Surfactant I, especially if the reductions are considered as a fraction of the CMC in water. This lesser salting out of Surfactant I compared to Surfactant IV may be due to the aromatic ring in the former, which, however, is unlikely to be an effective ligand in the presence of water

Table II—Effect of Additives on the CMC of Polyoxyethylated Oleyl Alcohol[a]

Additive	CMC, % (w/w), at Additive Molalities of 0.50	1.0	2.0	3.0
Sodium nitrate	0.0025	0.0025	0.0015	0.0015
Potassium nitrate	0.003	0.0015	0.0015	
Lithium nitrate	0.002	0.0015	0.001	0.0006
Hydrochloric acid	0.003	0.004	0.003	0.003
Sulfuric acid	0.005	0.004	0.003	0.003
Magnesium nitrate	0.009	0.006	0.007	0.010
Calcium nitrate	0.0065	0.004	0.005	0.004
Aluminum nitrate	0.0035	0.003	0.005	
Lead nitrate	0.0045	0.003		
Nickel nitrate	0.004	0.002	0.0025	
Urea	0.008	0.0095	0.010	0.010
Cadmium nitrate	0.0025	0.0045	0.0055	0.005
	0.10	0.25		
Cadmium nitrate	0.0025	0.003		

[a] The CMC with no additive was 0.0055–0.0060 % (w/w).

Table III—Net Effect of Additives on the Plateau Surface Tension of Polyoxyethylated Oleyl Alcohol

Additive	$\Delta\gamma P$[a], dynes/cm, at Additive Molalities of 0.50	1.0	2.0	3.0
Hydrochloric acid	0.6	0.8	1.9	4.1[b]
Sulfuric acid	0.1	−0.1	−0.5	−0.6
Magnesium nitrate	0.3	0.6	−1.7	−2.1
Calcium nitrate	0.4	−0.2	−2.3	−2.5
Aluminum nitrate	1.8	0.2	−1.9	
Nickel nitrate	0.0	−0.6	−0.6	−2.5
Urea	0.4	0.5	1.1	0.2
Cadmium nitrate	0.2	0.4	−1.0	−0.6
	0.10	0.25		
Cadmium nitrate	0.2	0.0		

[a] $\Delta\gamma P$ is defined by Eq. 1. [b] Concentration of hydrochloric acid is 4 molal.

and ether groups. A possible alternative explanation is that Surfactants I and IV may have different polyethylene oxide chain length distributions since they were prepared by different manufacturers.

While Schick (3) reported that 0.43 *M* magnesium nitrate depressed the CMC of a nonoxynol containing 15 ethylene oxide units by 30% at 25°, interpolation in Table I shows that the same salt concentration raised the CMC of Surfactant I (octoxynol with 10 ethylene oxide units) by approximately 8%.

Effect of Electrolytes on Plateau Surface Tension—Salts that depress the CMC of nonionic surfactants were reported to lower the plateau surface tension (3, 16) or to affect it little (6). The plateau, level-off, or micellar surface tension is the surface tension at surfactant concentrations above the CMC, represented by the nearly horizontal segments in Figs. 1 and 2.

In systems comprising only polyoxyethylated surfactants and water without additives, the following two trends have been reported. Both the CMC and plateau surface tension decrease as the number of ethylene oxide units per molecule is reduced (3, 13) and as the temperature of the solution of a given surfactant is raised (3, 17). In both instances, the solubility of the surfactants is lowered: in the first, by reducing the number of ether groups per molecule; in the second, by reducing the extent of hydration of each ether group. As the bulk solubility of the surfactants is lowered, their surface activity or tendency to accumulate at the air–water interface is enhanced. Salting out by additives also represents a reduction in solubility. As was seen in the previous section, it resulted in decreased CMC values. Lowering of the plateau or micellar surface tension is also indicative of salting out by added electrolytes, whereas increases in the CMC and/or plateau surface tension by additives are indicative of salting in.

The net change in plateau surface tension of the surfactant by an additive is defined as:

$$\Delta\gamma P = (\gamma_{PSA} - \gamma_{PS}) - (\gamma_A - \gamma^o) \qquad \text{(Eq. 1)}$$

where γ represents surface tension; the superscript o refers to pure water; and the subscripts P, S, and A refer to plateau, surfactant, and additive, respectively. The term in the first parentheses in Eq. 1 represents the effect of the additive on the surface tension of the surfactant solution. For Surfactant IV, $\gamma_{PS} = 31.5 \pm 0.2$ dynes/cm. The term in the second parentheses of Eq. 1 corrects the first term for increases in the surface tension of water by the additive in the absence of surfactant; γ_{PSA} and γ_A were measured at identical additive molalities. Among the additives used, only hydrochloric acid lowered the surface tension of water, as reported previously (18). Urea did not change the surface tension of water substantially.

The values of $\Delta\gamma P$ are listed in Table III. A positive value indicates that the additive raised the surface tension of the surfactant solution more than it raised the surface tension of water. A net increase in the plateau surface tension of the surfactant solution means that the additive made it more difficult to bring a surfactant molecule from the micellar solution to the air–water interface. This suggests salting in of the surfactant by the additive, paralleling an increase in the CMC. The only exception to the foregoing is hydrochloric acid, where the positive values of $\Delta\gamma P$ resulted from a lowering of the surface tension of water by the additive, *i.e.*, from negative values for $\gamma_A - \gamma^o$.

Effect of Additives on Molecular Area of Surfactant Adsorbed

at Air–Water Interface—The plots of surface tension *versus* the logarithm of the bulk surfactant concentration often became straight lines at concentrations as low as 10–30% of the CMC for Surfactant IV. Linear plots indicate that saturation adsorption has been reached: the surface excess concentration, Γ_2, of the surfactant has reached its limit and does not increase any further with increasing bulk surfactant concentration, C_2. Combining the Gibbs adsorption equation with the equation for the area, A, per surfactant molecule adsorbed at the air–water interface on the assumption of a monomolecular surfactant layer (17) gives the following expression at 25° (298°K):

$$A = -947\,(d \log C_2/d\gamma) \qquad \text{(Eq. 2)}$$

The constant 947 is obtained by multiplying 2.303 (the conversion factor of natural to common logarithms) by the gas constant (R = 8.314×10^7 ergs/mole °K), by the absolute temperature (298°K), and by the conversion factor of 10^{16} Å^2/cm^2 and dividing by Avogadro's number (6.023×10^{23}/mole). Solutions with a given additive level have surface tension values, γ, at surfactant concentrations, C_2.

The surface tension measurements were designed to determine the CMC as a function of additive concentration rather than the slope of the lines below the CMC. For most additives, the smallest number of compositions that afforded a precise determination of the CMC was studied. Despite the limited range and the paucity of C_2 values employed, the following observations could be made. All additives except urea increased the negative slope $-d\gamma/d \log C_2$ and, hence, decreased the A values. Urea produced no changes, or possibly small increases, in A. Cadmium nitrate and sulfuric acid produced the largest decreases in the area per molecule of Surfactant IV, as much as 30%, followed by hydrochloric acid and nickel nitrate. Calcium nitrate and potassium nitrate produced the smallest decreases.

These conclusions are qualitative, since the molecular areas were not always compared at saturation adsorption or at similar surface pressures. Furthermore, the area values are averages, because they depend on the chain length of the polyoxyethylene moiety (9) and the surfactant has a range of these. The average area is probably most strongly influenced by the surfactant molecules with the longest polyoxyethylene chains, which are also likely to be the most sensitive to the effect of the additives. However, the trend was general. The cross-sectional area per surfactant molecule adsorbed at the air–water interface at any specific value of surface pressure was reduced by the electrolytes; *i.e.*, the adsorbed surfactant monolayers became more closely packed. This finding is in agreement with the results of Schick (3) and Hsiao *et al.* (6). Based on a smaller number of electrolytes, which included few complexing cations, and on much more limited concentration ranges, they reported slight to moderate increases in $-d\gamma/d \log C_2$ for all systems investigated. According to Eq. 2, this corresponds to comparable reductions in A.

REFERENCES

(1) H. Schott, *J. Colloid Interface Sci.*, **43**, 150(1973).

(2) H. Schott and S. K. Han, *J. Pharm. Sci.*, **64**, 658(1975).

(3) M. J. Schick, *J. Colloid Sci.*, **17**, 801(1962).

(4) J. W. McBain, "Colloid Science," Heath, Boston, Mass., 1950, chap. 9.

(5) P. Mukerjee, *J. Phys. Chem.*, **69**, 4038(1965).

(6) L. Hsiao, H. N. Dunning, and P. B. Lorenz, *ibid.*, **60**, 657(1956).

(7) P. Becher, *J. Colloid Sci.*, **17**, 325(1962).

(8) *Ibid.*, **18**, 196(1963).

(9) M. J. Schick, S. M. Atlas, and F. R. Eirich, *J. Phys. Chem.*, **66**, 1326(1962).

(10) M. J. Schick, *ibid.*, **68**, 3585(1964).

(11) M. J. Schick and A. H. Gilbert, *J. Colloid Sci.*, **20**, 464 (1965).

(12) V. A. Volkov, N. G. Mikhailovskaya, and V. A. Kochetov, *Kolloidn. Zh.*, **35**, 960(1973).

(13) E. H. Crook, D. B. Fordyce, and G. F. Trebbi, *J. Phys. Chem.*, **67**, 1987(1963).

(14) C. R. Bury and J. Browning, *Trans. Faraday Soc.*, **49**, 209(1953).

(15) H. Schott, *J. Phys. Chem.*, **71**, 3611(1967).

(16) W. P. Evans, personal communication, cited in K. Durham, "Surface Activity and Detergency," Macmillan, London, England, 1961, chap. 1.

(17) H. Schott, *J. Pharm. Sci.*, **58**, 1521(1969).

(18) K. Schaefer, A. P. Masia, and H. Juentgen, *Z. Elektrochem.*, **59**, 425(1955).

ACKNOWLEDGMENTS AND ADDRESSES

Received April 28, 1975, from the *School of Pharmacy, Temple University, Philadelphia, PA 19140*

Accepted for publication August 27, 1975.

Presented at the Division of Colloid and Surface Chemistry, American Chemical Society, Philadelphia meeting, April 1975.

Adapted in part from a dissertation submitted by S. K. Han to Temple University in partial fulfillment of the Doctor of Philosophy degree requirements.

* Present address: College of Pharmacy, Busan National University, Busan, Korea.

ˣ To whom inquiries should be directed.

Effect of Inorganic Additives on Solutions of Nonionic Surfactants IV: Krafft Points

HANS SCHOTT ˣ and SUK KYU HAN *

Abstract □ Two polydisperse polyoxyethylated nonionic surfactants were found to possess Krafft points as well as cloud points. The significance of the Krafft point and the reason why it is rarely observed in nonionic surfactants are discussed. The values of the Krafft and cloud points of the two surfactants underwent only small changes as a function of surfactant concentration in the range of 0.5–7.5% (w/w). All electrolytes investigated, as well as urea, raised the Krafft points by between 1 and 4° in the concentration range of 0.5–4 molal. Included were salting-in electrolytes, which raised the cloud points, as well as salting-out electrolytes, which lowered them. Electrolytes that salt out nonionic surfactants strongly may depress the cloud point to the Krafft point temperature, rendering a water-soluble surfactant insoluble in salt solutions at all temperatures.

Keyphrases □ Surfactants, nonionic—aqueous solutions, effect of inorganic additives on Krafft and cloud points □ Electrolytes—effect on Krafft and cloud points of aqueous solutions of nonionic surfactants □ Inorganic additives—effect on Krafft and cloud points of aqueous solutions of nonionic surfactants □ Krafft point—aqueous solutions of nonionic surfactants, effect of inorganic additives □ Cloud point—aqueous solutions of nonionic surfactants, effect of inorganic additives □ Nonionic surfactants—Krafft and cloud points, effect of inorganic additives

During a study of the effect of electrolytes on the cloud points of four commercial polydisperse polyoxyethylated nonionic surfactants (1), two were found to possess Krafft points as well. These observations and the effect of electrolytes on the two Krafft points are reported.

SIGNIFICANCE OF KRAFFT POINT

The solubility–temperature relation of ionic surfactants in water follows a common pattern. At low temperatures, while the solubility remains below the critical micelle concentration (CMC), it is low and increases only slowly with rising temperature. A rapid increase in solubility takes place after the concentration limit reaches the CMC, at a temperature called the Krafft point. Above that temperature, the rate of increase of the solubility with temperature is high. Solubility–temperature plots consist of two segments. The one below the Krafft point has a small slope, while the one above it ascends steeply (2–5).

The temperature at which the sudden increase in solubility occurs has been interpreted as the melting point of the (hydrated) surfactant crystals or soap fibers (2, 6) or as the freezing point of the micelles (7, 8). The Krafft point increases regularly on ascending a homologous series of surfactants such as sodium alkyl sulfates (5, 9) or sodium soaps (5, 6) with even numbers of carbon atoms. In this respect, the Krafft point resembles the melting point, which undergoes regular increases on ascending the homologous series of normal paraffins or of normal fatty acids with even numbers of carbon atoms.

An alternative explanation for the sudden solubility increase is the necessity for a rapid increase in micellar concentration above the Krafft point (2). The aggregation of single surfactant molecules S into micelles S_n containing n surfactant molecules each is an equilibrium process: $nS \rightleftharpoons S_n$, for which the equilibrium constant is:

$$K = [S_n]/[S]^n \qquad \text{(Eq. 1)}$$

Brackets indicate concentration or, more exactly, activity. The equilibrium constant K and the CMC vary only gradually with temperature. At the Krafft point, the CMC curve crosses over the solubility curve in Fig. 1 and micelle formation begins. At that point, the micellar concentration $[S_n]$ has to increase fast to catch up with $[S]^n$ to maintain the ratio K constant or, rather, to allow for the increasing value of K with rising temperature. This requirement leads to an abrupt increase in surfactant solubility in the form of micelles, because the aggregation number n is fairly large, usually falling in the 30–200 range. Micelles have a much higher solubility in water than single surfactant molecules, because the hydrocarbon moieties in the former are largely shielded from contact with water by the polar headgroups (3).

Krafft point phenomena have been observed for soaps (5, 6) and most other anionic and cationic surfactants whose solubility–temperature relation was investigated (2–9). To the knowledge of the authors, only a single, homogeneous nonionic surfactant, cetyl alcohol with exactly seven ethylene oxide units, has been reported to possess a Krafft point (10). For homogeneous and polydisperse polyoxyethylated nonionic surfactants, an upper consolute temperature called the cloud point, above which they precipitate from aqueous solutions as relatively concentrated gels due to dehydration, is commonly observed (11).

A Krafft point or lower consolute temperature is rarely found because the CMC values of water-soluble nonionic surfactants are usually low and their solubility does not diminish appreciably with decreasing temperature. The Krafft point is the temperature at which the solubility of the surfactant equals its CMC. Thus, the solubility usually does not drop below the CMC before the freezing point of water is reached. Alternatively, most hydrated nonionic surfactants remain liquid down to temperatures in the vicinity of 0°; *i.e.*, their melting point is below the freezing point of water.

EXPERIMENTAL

The four surfactants employed are commercial polydisperse polyoxyethylated compounds. Surfactant I, octoxynol NF, is a branched octylphenol containing an average of nine to 10 ethylene oxide units[1]. Surfactants II, III, and IV consist of cetyl, stearyl, and oleyl alcohol with an average of 10 ethylene oxide units, respectively[2]. Their properties and formulas were given in Ref. 1. All other chemicals were ACS reagent grade; water was double distilled.

The assay methods for determining the electrolyte content of the concentrated stock solutions and the preparation of the ternary mixtures were described in Ref. 12. The electrolyte concentrations are given in molality, and the surfactant concentrations are expressed as percent weight to weight based on the amount of water present.

To measure its Krafft point, the 30-g portion of a solution was contained in a 60-ml (2-oz) bottle closed with a rubber stopper bearing a thermometer. The contents were first heated well above the Krafft point, but below the cloud point, to dissolve the surfactant and hydrate it completely. Cooling below the Krafft point caused the surfactant to separate as thin, needle-shaped crystals, which imparted a pearlescent appearance to the liquid. The suspensions of these crystals were heated at the rate of 1°/15 min.

The Krafft point was taken as the temperature at which the crystalline solid dissolved completely. The solutions often exhibited a slight turbidity above the Krafft point. Triplicate measurements were made on each system, which agreed within 0.5°. The few experiments in which the rate of heating was 1°/30 min gave the same values for the dissolution temperatures of the needles as were obtained at the faster heating rate.

[1] Triton X-100; supplied by Rohm and Haas Co.

[2] Brij 56, 76, and 96, respectively; supplied by Atlas Chemicals Division of ICI United States Inc.

Table I—Krafft Points and Cloud Points of Surfactants II and III as a Function of Concentration

Surfactant Concentration, % (w/w)	Consolute Temperatures of Surfactant II Krafft Point	Surfactant II Cloud Point	Surfactant III[a] Krafft Point	Surfactant III[a] Cloud Point
0.50	32.5°	67.0°	45.5°	64.0°
1.00	34.0°	64.0°	46.0°	63.0°
1.50	34.0°	63.5°	47.5°	62.0°
2.00	34.5°	62.5°	48.0°	62.0°
3.00	35.0°	62.0°	48.5°	63.5°
5.00	36.0°	61.0°	49.0°	64.0°
7.50	37.0°	—	49.0°	65.5°
10.00	37.5°	66.0°	—	—

[a] A different batch from that used for determining the data of Table III.

For cloud point determinations, the solutions were heated and cooled at rates from 1°/2 min to 1°/5 min. The cloud points were taken as the temperatures at which the solutions became turbid on heating and clear on cooling. The four cloud point values obtained from duplicate heating and cooling cycles agreed within 0.5°.

RESULTS AND DISCUSSION

The crystallization of Surfactants II and III upon cooling their solutions below the Krafft points was a slow process. It required about 0.5 hr after reaching that temperature without any additive or in the presence of the nitrates of lithium, sodium, potassium, or cesium or the bromide, iodide, or perchlorate of sodium. Crystallization required about 1 hr in the presence of the nitrates of calcium or lead or in the presence of sulfuric or hydrochloric acid. The nitrates of magnesium, aluminum, nickel, and cadmium delayed the crystallization of the two surfactants even more, requiring about 2 hr in the presence of low concentrations of these salts and overnight standing at high concentrations.

Very slow cooling of solutions containing surfactants, at rates of 1°/hr or 1°/2 hr, caused the crystals to separate about 10° below the temperature at which they cleared on heating. Because of this supercooling, attempts to determine Krafft points from above as well as from below were abandoned.

Only Surfactants II and III underwent phase separation on cooling. A cryoscopic study of Surfactant I indicated that micelles existed at the freezing point of its aqueous solutions (13), *i.e.*, its extrapolated Krafft point is below 0°. Aqueous solutions containing 2.00 and 3.00% (w/w) of Surfactant IV remained clear down to 2°. Therefore, the Krafft point of Surfactant IV is below that temperature.

The Krafft and cloud points of Surfactants II and III as a function of concentration are listed in Table I. The upper and lower consolute temperatures of the two surfactants did not increase appreciably with increasing surfactant concentration in the concentration range tested. This finding agrees with previous reports (10, 11). Hence, in Fig. 1, the main branches of the boundaries between phase fields I and II (labeled "cloud point curve") and between phase fields II and IV (labeled "solubility curve") are nearly horizontal. In this schematic figure, the Krafft point, defined by the intersection of the solubility curve and the CMC curve, resembles a triple point.

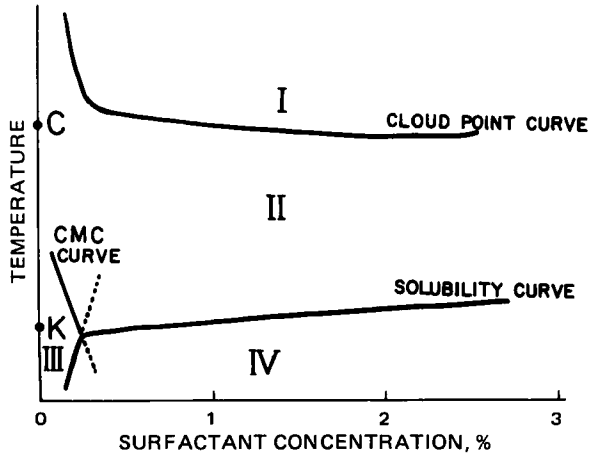

Figure 1—*Schematic phase diagram representing the binary system of nonionic surfactant–water. Key: C, cloud point; K, Krafft point; phase field I, isotropic solution plus gel; phase field II, isotropic undersaturated solution containing nonassociated molecules and micelles; phase field III, isotropic solution of nonassociated molecules; and phase field IV, isotropic solution of nonassociated molecules plus crystals.*

Phase field I corresponds to very dilute surfactant solutions plus relatively concentrated gels. Phase field II represents isotropic undersaturated solutions containing nonassociated surfactant molecules plus micelles. Dilute isotropic solutions of nonassociated surfactant molecules exist in phase field III, while such solutions coexist with solid surfactant crystals in phase field IV.

Surfactants II and III have the same number of ethylene oxide units per molecule. The Krafft point of Surfactant III, the stearyl alcohol adduct, exceeds that of Surfactant II, the cetyl alcohol adduct, by between 12.0 and 13.5°. This is due to the fact that the hydrocarbon moiety of the former is two methylene groups longer than that of the latter. The difference of 13° is comparable to the increase in Krafft point within a homologous series of ionic surfactants when the chain length is increased by two methylene groups (3, 5, 9). Replacement of a stearyl (Surfactant III) by an oleyl (Surfactant IV) group lowered the Krafft point from 47.5° to below 2°. This finding duplicates observations made with anionic surfactants (4) and parallels the drop in melting point when going from stearic to oleic acid.

The effect of additives on the Krafft points of Surfactants II and III was determined at the 1% surfactant level. The results are listed in Tables II and III. All additives in the 0.5–4 molal range raised the Krafft points of the two surfactants by between 1 and 4°. Inasmuch as increases in the lower consolute temperature

Table II—Effect of Additives on the Krafft Point of Surfactant II[a,b]

Additive	Krafft Point at Additive Molalities of 0.10	0.25	0.50	1.0	2.0	3.0	4.0	5.0
Sodium nitrate	37.2°	37.8°	37.8°	38.0°	37.2°	37.8°	—	—
Potassium nitrate	36.9°	37.3°	37.5°	37.8°	37.9°	38.0°	38.5°	—
Lithium nitrate	35.8°	—	37.2°	37.7°	38.3°	37.2°	36.9°	36.3°
Hydrochloric acid	—	—	37.2°	37.5°	37.7°	37.3°	36.9°	36.6°
Sulfuric acid	—	—	38.5°	38.3°	38.3°	38.8°	39.0°	—
Magnesium nitrate	—	—	38.3°	38.5°	38.5°	38.2°	—	—
Calcium nitrate	—	—	37.0°	37.3°	38.0°	37.5°	—	—
Cadmium nitrate	35.8°	36.4°	36.8°	36.8°	37.0°	36.5°	35.7°	—
Aluminum nitrate	—	—	38.4°	38.6°	38.6°	37.5°	—	—
Lead nitrate	36.5°	37.0°	37.5°	37.5°	37.8°	—	—	—
Urea	35.0°	—	35.5°	35.5°	35.5°	35.5°	—	—

[a] Surfactant concentration is 1.0%, based on weight of water. [b] Krafft point of Surfactant II without additive is 34.0–34.5° at 1.0%.

Table III—Effect of Additives on the Krafft Point of Surfactant III[a,b]

Additive	Krafft Point at Additive Molalities of							
	0.10	0.25	0.50	1.0	2.0	3.0	4.0	5.0
Sodium sulfate	50.0°	—	—	—	—	—	—	—
Sodium chloride	49.0°	—	49.5°	—	—	—	—	—
Sodium bromide	48.5°	49.2°	49.5°	49.8°	49.5°	48.8°	—	—
Sodium iodide	—	—	50.5°	50.5°	50.3°	50.0°	—	—
Sodium perchlorate	—	—	49.7°	49.8°	49.3°	49.0°	—	—
Sodium nitrate	—	—	48.8°	48.5°	48.3°	—	—	—
Potassium nitrate	47.6°	—	48.3°	48.7°	49.0°	—	—	—
Cesium nitrate	48.6°	—	48.5°	49.0°	49.3°	—	—	—
Lithium nitrate	—	—	49.3°	49.5°	50.5°	50.4°	—	—
Hydrochloric acid	48.8°	—	49.3°	49.6°	48.5°	48.3°	48.0°	47.6°
Sulfuric acid	—	—	48.8°	49.0°	49.3°	49.3°	49.5°	49.5°
Magnesium nitrate	—	—	50.3°	50.5°	51.5°	47.2°	—	—
Calcium nitrate	—	—	49.6°	49.4°	49.3°	48.7°	—	—
Cadmium nitrate	—	—	48.3°	49.3°	49.8°	49.3°	—	—
Aluminum nitrate	—	—	49.5°	49.5°	49.7°	48.8°	—	—
Lead nitrate	—	—	50.0°	50.3°	—	—	—	—
Nickel nitrate	—	—	50.5°	51.0°	51.0°	49.0°	—	—
Urea	—	—	48.8°	49.2°	49.0°	48.7°	48.0°	

[a] Surfactant concentration is 1.0%, based on weight of water. [b] Krafft point of Surfactant III without additive is 47.5° at 1.0%.

shrink the area on the phase diagram where undersaturated isotropic surfactant solutions prevail, this result represents a salting-out phenomenon. Even additives that raised the cloud points of Surfactants I–IV, salting them in (1, 12), raised the Krafft points of Surfactants II and III.

There were no major differences between the effects on the Krafft point of cloud point-raising and cloud point-lowering additives. Sodium iodide, which raised cloud points by destroying the structure of water, and the nitrates of lead and nickel, which raised them through complexation of the cations with the ether oxygens of the surfactants, raised the Krafft point of Surfactant III more than did sodium or potassium nitrate, which lowered the cloud points of polyoxyethylated surfactants by salting them out. Sulfuric acid and magnesium nitrate, which raised cloud points by complexation, and sodium or potassium nitrate, which lowered them through salting out, increased the Krafft point of Surfactant II to about the same extent.

Urea raised the Krafft points of both surfactants the least. While urea increased the cloud points of Surfactants II–IV only moderately (1), it increased the CMC of Surfactants I and IV more than did the salting-in electrolytes (14).

The limited effect of solution additives on the Krafft points of Surfactants II and III is not surprising when the Krafft point is considered as the melting point of the hydrated surfactant crystals. In that case, it involves primarily the hydrocarbon portion of the surfactant molecules in their crystalline lattice.

Even though the increases in Krafft point produced by the additives are limited to the narrow range of 1–4°, it can be seen from Tables II and III that the effect of additive concentration on the Krafft point follows one of three trends. As the concentration of the additive was progressively increased, the Krafft points increased monotonically, went through a maximum, or remained constant after an initial increase at low additive concentration. Even when the Krafft points went through a maximum and then decreased, they never dipped below the Krafft point of the surfactant in pure water. Generally, the nitrates of sodium, potassium, and cesium, which lowered the cloud points of the four surfactants through salting out (1), fell into the first category. Salting-in additives generally fell into the second or third category.

In the case of Surfactant II, the effect of the nitrates of sodium and potassium on the cloud point (1) as well as on the Krafft point was investigated over a wide concentration range. Increasing salt concentrations lowered the cloud point strongly and raised the Krafft point moderately. The two temperatures coincided in approximately 3 molal salt solutions and then overlapped. Thus, Surfactant II is practically insoluble in solutions having this or higher concentrations of sodium or potassium nitrate at all temperatures. A transition from crystalline solid to amorphous gel presumably occurs at the combined Krafft/cloud point.

REFERENCES

(1) H. Schott and S. K. Han, *J. Pharm. Sci.*, **64**, 658(1975).

(2) R. C. Murray and G. S. Hartley, *Trans. Faraday Soc.*, **31**, 183(1935).

(3) H. V. Tartar and K. W. Wright, *J. Amer. Chem. Soc.*, **61**, 539(1939).

(4) N. K. Adam and K. G. A. Pankhurst, *Trans. Faraday Soc.*, **42**, 523(1946).

(5) D. G. Dervichian, *Proc. Int. Congr. Surface Activity, 3rd*, **1**, 182(1960).

(6) F. Krafft and H. Wiglow, *Chem. Ber.*, **28**, 2566(1895).

(7) K. Shinoda and E. Hutchinson, *J. Phys. Chem.*, **66**, 577(1962).

(8) K. Shinoda and T. Soda, *ibid.*, **67**, 2072(1963).

(9) H. Lange and M. J. Schwuger, *Kolloid-Z. Z. Polym.*, **223**, 145(1968).

(10) D. Attwood, *J. Phys. Chem.*, **72**, 339(1968).

(11) H. Schott, *J. Pharm. Sci.*, **58**, 1443(1969).

(12) H. Schott, *J. Colloid Interface Sci.*, **43**, 150(1973).

(13) E. Gonick and J. W. McBain, *J. Amer. Chem. Soc.*, **69**, 334(1947).

(14) S. K. Han, Ph.D. thesis, Temple University, Philadelphia, Pa., 1974.

ACKNOWLEDGMENTS AND ADDRESSES

Received May 29, 1975, from the *School of Pharmacy, Temple University, Philadelphia, PA 19140*

Accepted for publication July 28, 1975.

Presented at the Division of Colloid and Surface Chemistry, American Chemical Society, Philadelphia meeting, April 1975.

Adapted in part from a dissertation submitted by S. K. Han to Temple University in partial fulfillment of the Doctor of Philosophy degree requirements.

* Present address: College of Pharmacy, Busan National University, Busan, Korea.

‡ To whom inquiries should be directed.

Interactions of Adenine, Thymine, and Uracil with Epinephrine: UV Studies

FAHAD A. AL-OBEIDI and HANNA N. BORAZAN ˣ

Abstract □ Based upon UV absorption studies, charge transfer complex formations by the nucleic acid bases adenine, thymine, and uracil with epinephrine were demonstrated. The pertinent equilibrium constants were calculated by assuming 1:1 complexes using the Benesi–Hildebrand equation and were found to decrease in the following order: uracil–epinephrine > thymine–epinephrine > adenine–epinephrine. The values of $\Delta G°$, $\Delta H°$, and $\Delta S°$ were calculated for the various interactions. Theoretical arguments are presented as to the possible stoichiometries of the various complexes existing in aqueous solutions. The electron-donating or electron-accepting abilities of the interacting molecular species are discussed.

Keyphrases □ Nucleic acid bases—adenine, thymine, and uracil, interaction with epinephrine, UV absorption studies □ Epinephrine—interaction with adenine, thymine, and uracil, UV absorption studies □ Complex formation—adenine, thymine, and uracil, with epinephrine, UV absorption studies □ UV spectrophotometry—absorption studies, interaction of adenine, thymine, and uracil with epinephrine

Catecholamines form a biologically important class of chemical compounds, called sympathomimetics, which mimic the action of the neurohumoral transmitters epinephrine and norepinephrine.

The receptors for catecholamines are considered to contain adenosine triphosphate (1). The common occurrence of phosphate and magnesium ions beside adenosine triphosphate at the adrenergic sites suggested that these amines form complexes with one or more of these ions during storage or the accompanying initiation of their biological actions. The existence of such compounds *in vivo* has not yet been established. Seifter *et al.* (2) synthesized the complex *in vitro*. The reaction among catecholamines, magnesium monophosphate ion, and the magnesium adenosine triphosphate complex was demonstrated by the formation of a water-soluble complex. This complex exhibits characteristic UV absorption and fluorescence spectra.

Kirshner *et al.* (3) investigated the uptake and storage of catecholamines and obtained further evidence for the storage of these biogenic amines in association with adenosine triphosphate and protein in the chromaffin granules. The presence of magnesium was not found to be essential for the uptake of catecholamines, indicating that an enzymatic system is not required to transfer these amines intracellularly.

The significance of nucleic acids for biological systems (4–6) has led to their being considered as possible targets for the action, directly or indirectly, of many drugs. The interactions between nucleic acids and some drugs were studied previously (7, 8). Indirect actions of drugs were attributed to interference with protein synthesis, either induction or inhibition (9, 10). For example, catecholamines affected the production of cyclic 3′,5′-adenosine monophosphate indirectly through their interferences with the enzymatic activity of adenyl cyclase (11). Cyclic 3′,5′-adenosine monophosphate was considered as the causative agent for the inhibitory responses.

Therefore, to gain a more basic understanding of: (*a*) the adrenergic receptors, (*b*) the mechanism of action of catecholamines at the molecular level, and (*c*) the possibility of adenosine triphosphate-like action of some other nucleoside triphosphates on the storage of catecholamines in the adrenal medulla and the splenic nerves, the nature of the complexes between nucleic acids, including synthetic polynucleotides and their derivatives, and catecholamines must be investigated.

The present work deals with the interactions of adenine, thymine, and uracil with epinephrine using a UV spectroscopic method.

EXPERIMENTAL

Epinephrine hydrogen tartrate[1], thymine[1], a standard solution of hydrochloric acid[1], adenine[2], and uracil[2] were obtained commercially.

Solutions for measurement were prepared by diluting concentrated stock solutions. All mixtures contained a fixed concentration of the nucleic acid base, 0.02 *M*, and the concentration of epinephrine was varied from 0.3 to 0.8 *M* in 0.1 *N* HCl. Solutions were freshly prepared each day, and their absorbances were measured within 12 hr.

An oxide film[3] was used to calibrate the spectrophotometer[4]. Constant temperatures were achieved throughout the measurement period by using a thermostated cell holder connected to a constant-temperature circulator and refrigerator[5]. The stoppered cells (1-cm path length) were flushed with nitrogen gas to avoid condensation of moisture at the cell surfaces when working at low temperatures.

The baseline was recorded before running each experiment, using the same solvent in the reference and sample compartments. Most work was done at 18–20° in a room with subdued light to avoid oxidations induced by light. At the beginning of the measurements of a set of solutions, the spectra of the pure components were taken at the working temperature to detect any decomposition.

RESULTS

The formation of a complex between a nucleic acid base and epinephrine was detected by observing the shift in the UV spectrum of the mixture toward longer wavelengths when the nucleic acid base solution in 0.1 *N* HCl was used as a reference (Fig. 1). The absorbance of a complex at a given wavelength was estimated by measuring the absorbance of the entire mixture and subtracting from it the sum of the absorbances, at the same wavelength, of equimolar solutions of the pure components. The experimental data used to calculate the various quantities (Table I) were actually measured in regions where the absorption of the free components was as small as possible and that of the complex was quite appreciable. The accuracy of the measurements was ±0.005 absorbance unit.

The absorbances of complexes obtained experimentally were used to calculate equilibrium constants using the Benesi–Hildebrand equation:

$$\frac{(A_0)}{A_\lambda^{AD}} = \frac{1}{\epsilon_\lambda^{AD}} + \frac{1}{K_c^{AD}\epsilon_\lambda^{AD}(D_0)} \qquad \text{(Eq. 1)}$$

[1] BDH Biochemicals, Ltd., Poole, England.
[2] Hopkin and Williams Chemical Co., Chadwell Heath, Essex, England.
[3] Holmium.
[4] Model 402 Perkin-Elmer UV–visible spectrophotometer.
[5] Model FK2, Haake Instrument Co.

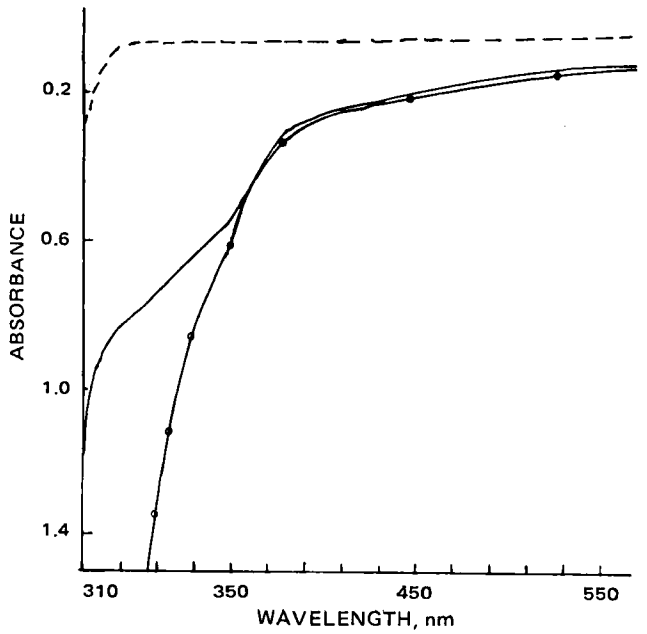

Figure 1—*Absorption spectra of 0.8 M epinephrine hydrogen tartrate (——), 2×10^{-2} M adenine (- - -), and 0.8 M epinephrine hydrogen tartrate plus 2×10^{-2} M adenine (O—O). All solutions were in 0.1 N HCl, and measurements were at 2°.*

where (A_0) and (D_0) are the total concentrations of the interacting species, A_λ^{AD} and ϵ_λ^{AD} are the absorbance and molar absorptivity of the complex at a given wavelength, and K_c^{AD} is the equilibrium constant.

The complex between cytosine and epinephrine showed a high degree of absorption in the region where the base itself absorbs. Because of this overlap, equilibrium constants could not be calculated.

Equation 1 is based on the assumptions that a 1:1 complex is formed:

$$A + D = AD \qquad \text{(Eq. 2)}$$

and that the total concentration of compound A, (A_0), is much less than the total concentration of compound D, (D_0), so that (D_0) can be approximated to the concentration of the free species, *i.e.*, $(D) \simeq (D_0)$.

The equilibrium constant and the molar absorptivity of Eq. 1 can

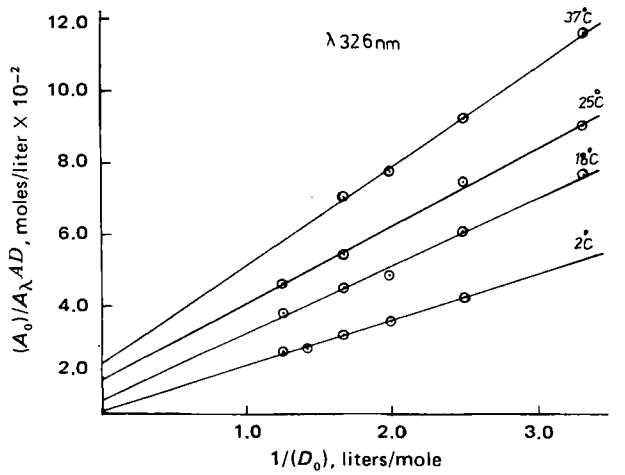

Figure 2—*Plots of $(A_0)/A_\lambda^{AD}$ versus $1/(D_0)$ of epinephrine hydrogen tartrate solutions containing adenine in 0.1 N HCl at different temperatures. The adenine total concentration, (A_0), = 2×10^{-2} M, and the epinephrine hydrogen tartrate total concentration, (D_0), = 0.3–0.8 M; A_λ^{AD} represents the absorbance of the complex at the wavelength. Curves have the same intercepts as that of 2°. They were separated to avoid crowding.*

Table I—Equilibrium Constants (K), Standard Free Energy ($\Delta G°$), Standard Enthalpy ($\Delta H°$), and Standard Entropy ($\Delta S°$) Changes Associated with the Interactions of Nucleic Acid Bases with Epinephrine Hydrogen Tartrate in Aqueous Solutions Containing 0.1 N HCl together with Molar Aborptivities (ϵ) at Different Wavelengths (λ)

Temperature ±0.5°	K, M^{-1} ±0.01	$\Delta G°$, kcal/mole	$\Delta H°$, kcal/mole	$\Delta S°$, cal/deg/mole ±0.1
		Adenine–Epinephrine		
2	0.79	0.129		
18	0.52	0.376		
			−3.857	−14.5
25	0.45	0.468		
37	0.35	0.635		
λ = 326 nm; ϵ = 103.1				
2	0.78	0.131		
18	0.55	0.348	−3.569	−13.5
25	0.48	0.438		
λ = 328 nm; ϵ = 79.4				
		Thymine–Epinephrine		
2	0.97	0.017		
18	0.73	0.183	−2.541	−9.3
37	0.57	0.347		
λ = 314 nm; ϵ = 51.8				
2	0.63	0.248		
18	0.53	0.369		
			−3.048	−11.8
25	0.44	0.487		
37	0.40	0.564		
λ = 316 nm; ϵ = 50.0				
		Uracil–Epinephrine		
3	1.04	−0.023		
18	0.69	0.209	−6.936	−24.5
37	0.49	0.433		
λ = 316 nm; ϵ = 31.3				

be obtained from the slope and intercept of a curve plotting $(A_0)/A_\lambda^{AD}$ *versus* $1/(D_0)$ when keeping (A_0) constant. Representative plots are shown in Fig. 2.

The standard enthalpy change, ΔH^0, of an interaction can be obtained graphically by plotting $\log K_c^{AD}$ *versus* $1/T$ of the following well-known equation:

$$\log K_c^{AD} = -\frac{\Delta H^0}{2.303RT} + \text{constant} \qquad \text{(Eq. 3)}$$

A plot of Eq. 3 is shown in Fig. 3. Linear slopes were also obtained for the other combinations.

The standard free energy change, ΔG^0, is calculated from:

$$\Delta G^0 = -RT \ln K_c^{AD} \qquad \text{(Eq. 4)}$$

The standard entropy change, ΔS^0, is calculated from:

$$\Delta G^0 = \Delta H^0 - T\,\Delta S^0 \qquad \text{(Eq. 5)}$$

All slopes and intercepts used to calculate the quantities in Table I and the figures were determined statistically by the method of least squares. The thermodynamic parameters together with the molar extinction coefficients are presented in Table I.

DISCUSSION

It has been demonstrated that catechols have strong tendencies for electron donation in forming complexes with many substances (12, 13), as evidenced by the appearance of new absorbing species.

Nucleic acid bases also have been shown to form charge transfer complexes with many compounds (14). Recently, the authors (15) demonstrated that catechol has the ability to form charge transfer complexes with nucleic acid bases (adenine, cytosine, thymine, and uracil) in aqueous solutions containing 0.1 N HCl. In that study,

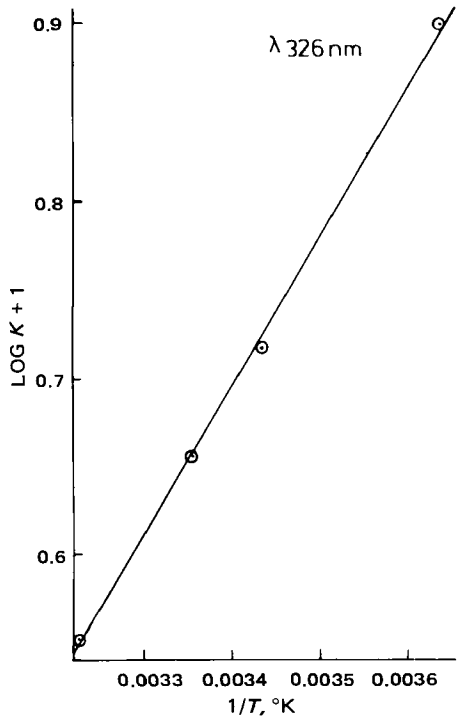

Figure 3—*Log* K *of the adenine–epinephrine interaction* versus *1*/T.

catechol was considered to be the electron donor and nucleic acid base the electron acceptor.

A simple general quantum mechanical theory of a 1:1 or *n*:1 interaction of the electron donor with the electron acceptor was proposed (16). In the ground state, the two molecules are held together when they are in close proximity by such forces as van der Waals, dispersion, London, and hydrogen bond forces. Additional forces are contributed by the transfer of a small amount of charge from the donor molecule to the acceptor one.

When a complex absorbs light of a suitable energy, it is raised from the ground to the excited state. In this state, an electron that was only slightly shifted toward the acceptor is almost wholly transferred. The transitions involved are called charge transfer transitions. Therefore, the transfer of an electron by light absorption is responsible for the characteristic colors of these complexes.

Based upon the reasoning previously pointed out for nucleic acid bases–catechol interactions, epinephrine is assumed to act as an electron donor while adenine, thymine, and uracil act as electron acceptors.

The molar absorptivities were discovered to be temperature independent; the slight change observed is attributable to experimental error. Therefore, the absorptivities presented in Table I represent essentially an average estimated from working at different temperatures. Furthermore, the molar absorptivity of the adenine–epinephrine complex changed rapidly with changes in wavelength.

The equilibrium constants of the reaction between adenine and epinephrine were wavelength independent (within the limits of accuracy), while the one between thymine and epinephrine was very sensitive to changes in the wavelengths used (Table I). Almost all equilibrium constants were less than unity. Hence, ΔG^0 values of all interactions were positive and small, even though the ΔH^0 values were generally high. The highest ΔH^0 values were those of the uracil–epinephrine interaction (approximately 7 kcal/mole); the lowest was for the reaction between thymine and epinephrine.

Another characteristic feature of the nucleic acid bases–epinephrine interactions was a high negative entropy change, which can account for the fact that ΔG^0 was small and positive even though the heat of formation of the complexes was high. A high $-\Delta S^0$ indicates a high degree of specificity of these reactions as well as a high degree of change in the structure of the solvent when the complex is formed. The order of decreasing $-\Delta S^0$ follows the same sequence as ΔH^0 (Table I).

Uracil–epinephrine interaction showed higher ΔH^0, ΔS^0, and even ΔG^0 values compared to those of other interactions (Table I). The uracil molecule is small and planar and has four centers forming hydrogen bonds with epinephrine in addition to the charge transfer forces arising from their π-system interactions. Although thymine has a similar structure to uracil, the structure of its mixed aggregate with epinephrine seems to be less ordered. For example, the number of molecules in these aggregates could be less than the corresponding uracil mixed aggregate. The presence of a methyl group in the thymine molecule changes both the electronic and steric properties. Changes in the electronic properties of a molecule obviously will change its electron-accepting or donating ability. It was found that the electron affinity of uracil is the same as that of thymine, while their ionization potentials differ considerably (17).

Recent quantum mechanical calculations on catechol derivatives (18) demonstrated that epinephrine has binding energies of -0.316 β and -1.114 β units for the highest occupied and the lowest empty molecular orbitals, respectively. These calculations also revealed high electron density at the aliphatic carbon carrying the hydroxyl group (1.148). A low binding energy of the highest occupied molecular orbital indicates a low ionization potential and a high electron-donating ability. Also, the fact that the binding energy of the lowest empty orbital is relatively low is in itself an indication of a low electron-accepting ability.

The apparent ΔH^0 values determined by experiments are actually functions of ΔH^0 values of different associated forms (19). This is evident in the case of thymine–epinephrine interaction and indicates the formation of more than one type of complex in solution.

A linear relationship between ΔH^0 and ΔS^0 was observed for many complexes between a given acceptor and related donors (20). Even though the situation was reversed in the present study, a similar relationship existed between ΔH^0 and ΔS^0.

Another interesting observation is that an inverse relationship seems to exist between molar absorptivities of thymine and uracil (at wavelength of 316 nm) and ΔH^0, ΔS^0, and ΔG^0. This finding is not in conflict with previous work (21) because the absorptivity does not always give an indication about the energy of the complex. The value of ΔH^0 is actually related to the total oscillator strength (22, 23). Moreover, the situation in the present study was more complicated because completely isolated bands were not formed.

The exact stoichiometry of the various complexes formed between nucleic acid bases and epinephrine is difficult to determine from UV absorption studies alone. Parallel stacking interactions between the nucleic acid bases and the aromatic nucleus of epinephrine can be invoked as they have been for similar systems (24–28). The presence of many sites on the interacting molecules that can be hydrogen bonded (whether acting as hydrogen bond donors or acceptors) could play a role in determining the size of mixed aggregates as well as their mode of aggregation (29–33).

The wavelength independence of association constants of weak interactions was interpreted (34) as being due to formations of 1:1 charge transfer complexes, isomeric forms (trimers in which one molecule of a compound is sandwiched between two molecules of a different compound), or contact charge transfer complexes.

Schellman (35) determined the heat of formation of the process of self-association of urea in aqueous solution and obtained a value of 1.5 kcal/mole/hydrogen bond. Although it is difficult to extrapolate these findings to the present case, using different systems in which hydrophobic as well as other types of interactions are operating, the concern is also with weakly bonded complexes and Schellman's findings could indicate a stoichiometry other than 1:1.

Johnson and Bowen (34) point out that linear slopes are obtained from the application of the Benesi–Hildebrand plots when 1:1 complexes are assumed to be the main contributors, while the wavelength dependence of the association constants indicates the presence of more than one molecular species. However, this is not always the case.

The dependence of ΔH^0 and the total oscillator strength on temperature was also demonstrated (34). This dependence does not always exist since straight lines were obtained in some cases when plotting log K *versus* $1/T$, log $K\epsilon_\lambda{}^{AD}$ *versus* $1/T$, and even log $\epsilon_\lambda{}^{AD}$ *versus* $1/T$ when the temperature range was not too high (36).

Person (37) proposed that the most accurate values for equilibrium constants of complexes may be obtained when the equilibrium concentrations of the complexes are of the same order of magnitude as the equilibrium concentrations of the more dilute pure components. Measurement of equilibrium constants of complexes by the Benesi–Hildebrand method or one of its modifications requires that the donor concentrations in the most concentrated solutions be greater than $0.1(1/K)$. It also was shown that K and $\epsilon_\lambda{}^{AD}$ of a complex depend on

concentration ratios (38). This dependence is significant only when the ratio of $(D_0)/(A_0)$ ranges from 1 to 10. In our studies, the ratios were between 15 and 40 and the donor concentrations were much greater than $0.1(1/K)$. All these facts indicate the validity of the results derived from the Benesi–Hildebrand equation.

The association constants of the interactions between nucleic acid bases and catechol were calculated and found to be higher generally than those for the interactions between nucleic acid bases and epinephrine. This was due to the facts that the amino group of the side chain of epinephrine is protonated and that epinephrine hydrogen tartrate was used instead of epinephrine free base.

CONCLUSION

Evidence was presented here for the formation of charge transfer complexes between nucleic acid bases (adenine, thymine, and uracil) and epinephrine in aqueous solutions containing 0.1 *N* HCl. The evidence was the appearance, in the UV region and at longer wavelengths from the absorptions of the pure components, of new absorption bands which can only be attributed to charge transfer transitions.

It was possible to calculate various thermodynamic parameters as well as molar extinction coefficients at different wavelengths. In general, equilibrium constants were found to be less than unity and heats of formation were relatively high. Wavelength dependence of equilibrium constants was observed in some cases.

Compared to catechol interactions with nucleic acid bases, the presence of an alkyl side chain in epinephrine leads to an additional heat of complex formation as well as to large changes in the specificity of these interactions, as reflected by changes in the entropy associated with the formation of these complexes. The presence of a protonated cationic group as well as an increase in ionic strength decreased the equilibrium constants.

It is proposed that parallel stacking interactions between the presumed donor molecule, epinephrine, and the acceptors, adenine, thymine, and uracil, exist in aqueous solutions. Hydrogen bonding possibilities were not excluded.

REFERENCES

(1) A. Korolkovas, "Essentials of Molecular Pharmacology," Wiley, New York, N.Y., 1970, p. 234.

(2) J. Seifter, E. Seifter, and G. Guideri, *Am. J. Med. Sci.*, **263,** 261(1972).

(3) N. Kirshner, C. Holloway, W. J. Smith, and A. G. Kirshner, *Biochim. Biophys. Acta*, **112,** 532(1966).

(4) J. D. Watson, "Molecular Biology of the Gene," 2nd ed., Benjamin, Menlo Park, Calif., 1970, p. 261.

(5) *Ibid.*, p. 327.

(6) *Ibid.*, p. 355.

(7) M. J. Waring, *Nature*, **219,** 1320(1968).

(8) M. J. Waring, *J. Mol. Biol.*, **54,** 247(1970).

(9) J. D. Watson, "Molecular Biology of the Gene," 2nd ed., Benjamin, Menlo Park, Calif., 1970, p. 553.

(10) V. M. Ingram, "Biosynthesis of Macromolecules," 2nd ed., Benjamin, Menlo Park, Calif., 1972, p. 212.

(11) E. W. Sutherland and G. A. Robison, "Second Symposium on Catecholamines," Williams & Wilkins, Baltimore, Md., 1966, p. 145.

(12) M. A. Slifkin, "Charge Transfer Interactions of Biomolecules," Academic, London, England, 1971, p. 214.

(13) G. Cilento and K. Zinner, *Biochim. Biophys. Acta*, **120,** 84(1966).

(14) M. A. Slifkin, "Charge Transfer Interactions of Biomolecules," Academic, London, England, 1971, p. 76.

(15) F. A. Al-Obeidi and H. N. Borazan, *J. Pharm. Sci.*, **65,** 892 (1976).

(16) R. S. Mulliken, *J. Am. Chem. Soc.*, **74,** 811(1952).

(17) B. Pullman, in "Molecular Biophysics," B. Pullman and M. Weissbluth, Eds., Academic, London, England, 1965, p. 150.

(18) M. Kumbar and D. V. S. Sankar, *Res. Commun. Chem. Pathol. Pharmacol.*, **5,** 45(1973).

(19) R. Foster, "Organic Charge Transfer Complexes," Academic, London, England, 1969, p. 174.

(20) *Ibid.*, p. 207.

(21) *Ibid.*, p. 73.

(22) *Ibid.*, p. 43.

(23) M. A. Slifkin, "Charge Transfer Interactions of Biomolecules," Academic, London, England, 1971, p. 5.

(24) P. O. P. Ts'o, I. S. Melvin, and A. C. Olson, *J. Am. Chem. Soc.*, **85,** 1289(1963).

(25) A. D. Broom, M. P. Schweizer, and P. O. P. Ts'o, *ibid.*, **89,** 3612(1967).

(26) J. L. Dimicoli and C. Helene, *ibid.*, **95,** 1036(1973).

(27) M. P. Schweizer, A. D. Broom, P. O. P. Ts'o, and D. P. Hollis, *ibid.*, **90,** 1042(1968).

(28) C. Helene, T. Montenay-Garestier, and J. L. Dimicoli, *Biochim. Biophys. Acta*, **254,** 349(1971).

(29) H. N. Borazan, *J. Pharm. Sci.*, **64,** 770(1975).

(30) F. M. Goyan and H. N. Borazan, *ibid.*, **57,** 861(1968).

(31) H. N. Borazan, Ph.D. thesis, University of California, San Francisco, Calif., 1969.

(32) H. N. Borazan and F. M. Goyan, *J. Pharm. Sci.*, **62,** 923(1973).

(33) H. N. Borazan, *ibid.*, **62,** 1982(1973).

(34) G. D. Johnson and R. E. Bowen, *J. Am. Chem. Soc.*, **87,** 1655(1965).

(35) J. A. Schellman, *C. R. Trav. Lab. Carlsberg, Ser. Chim.*, **29,** 223(1956).

(36) R. Foster, "Organic Charge Transfer Complexes," Academic, London, England, 1969, p. 163.

(37) W. B. Person, *J. Am. Chem. Soc.*, **87,** 167(1965).

(38) R. Foster, "Organic Charge Transfer Complexes," Academic, London, England, 1969, p. 158.

ACKNOWLEDGMENTS AND ADDRESSES

Received March 18, 1975, from the *Department of Pharmaceutical Chemistry, College of Pharmacy, University of Baghdad, Baghdad, Republic of Iraq.*

Accepted for publication September 4, 1975.

Abstracted in part from a dissertation submitted by F. A. Al-Obeidi to the University of Baghdad in partial fulfillment of the Master of Science degree requirements.

The authors thank Professor Hatif H. Al-Jalil for his encouragement during the investigation. They also thank the University of Baghdad for financial support.

[x] To whom inquiries should be directed.

Analysis of Alkaloid Mixtures by Charge-Transfer Complexation

ALY M. TAHA ˣ and CAMELIA S. GOMAA

Abstract □ Binary mixtures of weak and strong UV-absorbing alkaloids were analyzed by a charge-transfer spectrophotometric method, utilizing iodine in ethylene dichloride as the acceptor. In the uncomplexed form, the strong absorbing alkaloid (papaverine, quinine, ergotamine, or reserpine) was measured at a wavelength where there was no interference from weak absorbers (at 335, 332, 315, or 300 nm, respectively). The weak absorbing alkaloid (ephedrine, codeine, atropine, or homatropine methylbromide) was determined by computing its contribution to the total charge-transfer band at 295 nm where absorbance was linearly additive for mixtures. The greater increase in the original ϵ-values of the weak absorbers upon complexation with iodine relative to the corresponding increase in the ϵ-values of the strong absorbers led to good recoveries even at the low dose ratios of the weakly absorbing, and often more potent, alkaloids.

Keyphrases □ Alkaloids—weak and strong UV absorbing in binary mixtures, charge-transfer spectrophotometric analysis □ Spectrophotometry, charge transfer—analysis, weak and strong UV-absorbing alkaloids in binary mixtures □ UV-absorbing alkaloids, strong and weak—binary mixtures, charge-transfer spectrophotometric analysis

Alkaloids occupy a prominent position among extensively employed medicaments. They are frequently prescribed in admixture with each other. Among the convenient methods of analysis of such combinations is the direct UV assay (1, 2). However, the absorption bands of the various alkaloids differ greatly in intensity (1, 3), so the simultaneous analysis of binary systems containing weak and strong UV-absorbing alkaloids is challenging. The problem is made more difficult when the dose ratio of the two types in the mixture is not in favor of the weak absorbing alkaloid, which often happens to be the more potent [*e.g.*, ergotamine–hyoscyamine (4:1), papaverine–codeine (6:1), and papaverine–homatropine methylbromide (20:1)]. For these reasons, the assay of these combinations usually includes a separation procedure[1] (1, 2).

Although the separation of alkaloid mixtures into individual compounds is feasible, it is not always possible to obtain clearcut separations, particularly with alkaloids having close pKa values and similar solubility characteristics (1). Consequently, a method for the simultaneous determination of alkaloids in such combinations without prior separation may be of value.

Recent publications (4, 5) reported that a considerable increase in the band intensity of many alkaloids could be attained *via* charge-transfer complexation with σ-acceptors such as iodine in chlorinated solvents. Such an increase in the original ϵ-values was much greater for weak UV absorbers such as the tropine alkaloids, ephedrine, codeine, and sparteine (up to 100 times the value of the uncomplexed alkaloid) than for strong absorbers such as papaverine, quinine, reserpine, and strychnine (1.5–6 times the original value) (4). Subsequent examination of binary mixtures of the two types revealed a leveling of the maxima of the two components even at the low dose ratio of the weak absorber.

This finding constituted the basis of the present work, which was concerned with the simultaneous analyses of binary mixtures of ephedrine, tropine alkaloids, or codeine with the stronger absorbing papaverine, quinine, ergotamine, or reserpine in formulations. The method was also applied to the analogous combination of sparteine with benzyl alcohol.

EXPERIMENTAL[2]

Alkaloids—Pharmaceutical grade ephedrine base, ephedrine hydrochloride, papaverine hydrochloride, codeine phosphate, atropine sulfate, hyoscyamine hydrobromide, homatropine methylbromide, quinine sulfate, ergotamine tartrate, reserpine, and sparteine sulfate were utilized as working standards.

Alkaloid Dosage Forms—The following commercial preparations were analyzed: tablets of ephedrine hydrochloride with papaverine hydrochloride[3], tablets of ephedrine with reserpine[4], injection of homatropine methylbromide with papaverine hydrochloride[5], pulvules of codeine sulfate with papaverine hydrochloride[6], tablets of total belladonna alkaloids with ergotamine tartrate[7], and injection of sparteine sulfate[8].

Reagents—*Buffer*—Prepare 0.2 *M* pH 9.5 buffer, standardized against the glass electrode with a calomel reference electrode, by dissolving 34.8 g of dibasic potassium phosphate in 900 ml of water. Adjust to pH 9.5 and dilute to 1 liter with water.

Potassium Iodide Solution (*0.2* M)—Dissolve 3.32 g of analytical grade potassium iodide in water and dilute to volume in a 100-ml volumetric flask with water. Prepare fresh every 3 days.

Iodine Solution (10^{-3} M)—Dissolve 25.5 mg of resublimed iodine in spectrograde ethylene dichloride in a 100-ml volumetric flask. The solution is stable for 1 week at 4°.

Standard Solutions—*Alkaloidal Salts*—Dissolve an accurately weighed amount of the appropriate working standard in water and dilute the solution quantitatively and stepwise to obtain a concentration of the salt equivalent to 1.0 mg of base/ml. Pipet 1.0 ml of this solution into a 30-ml separator containing 5 ml of buffer. Extract with two 5-ml portions of ethylene dichloride, passing the separated organic layers through 2 g of anhydrous sodium sulfate supported by glass wool in a small funnel. Collect the filtrate in a 10-ml volumetric flask, wash the filter with a few drops of ethylene dichloride, and dilute to volume with the same solvent.

Ephedrine and Reserpine Bases—Dissolve an accurately weighed amount of the appropriate working standard in ethylene dichloride and dilute to obtain a concentration of 0.1 mg/ml.

[1] Manufacturer's Control Method, EL-Nile Co., Cairo, Egypt, personal communication with Dr. Z. Gad.

[2] Spectra were determined on a Spektromom-203 spectrophotometer, Mom, Budapest, Hungary.

[3] Asmasone (El-Nile Co., Cairo, Egypt) contains (per tablet): ephedrine hydrochloride, 10 mg; papaverine hydrochloride, 30 mg; phenobarbital sodium, 10 mg; and dexamethasone, 0.1 mg.

[4] Renir (Massengill, Bristol, Tenn.) contains (per tablet): reserpine, 0.25 mg; and ephedrine, 8 mg.

[5] Surparyl (Memphis Labs., Egypt) contains (per 2 ml): papaverine hydrochloride, 50 mg; and homatropine methylbromide, 2.5 mg.

[6] Copavin (Lilly, Indianapolis, Ind.) contains (per pulvule): codeine sulfate, 15 mg; and papaverine hydrochloride, 15 mg.

[7] Bellergal (Sandoz, Basel, Switzerland) contains (per tablet): total alkaloids of belladonna leaf as malates, 0.1 mg; ergotamine tartrate, 0.3 mg; and phenobarbital, 20 mg.

[8] Spartocin (Ayerst, New York, N.Y.) contains (per 1-ml ampul): sparteine sulfate, 150 mg; and benzyl alcohol, 0.5%.

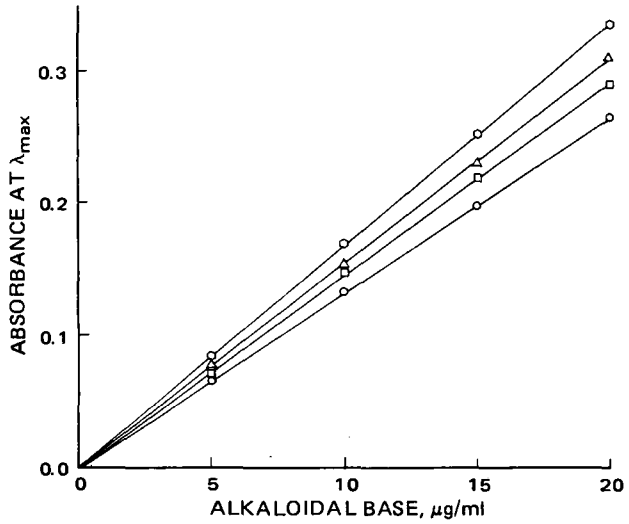

Figure 1—*Calibration curves of alkaloidal bases in ethylene dichloride. Key:* ○, *reserpine at 300 nm;* △, *quinine at 332 nm;* □, *papaverine at 335 nm; and* ○, *ergotamine at 315 nm.*

Homatropine Methylbromide—Proceed as directed under alkaloidal salts, substituting 2 ml of 0.2 *M* potassium iodide solution for the buffer.

Preparation of Samples—*Synthetic Mixtures*—Proceed as directed under alkaloidal salts, using the calculated amount of the proper salts to give the desired ratio of the component alkaloidal bases in the final dilution.

Tablets of Ephedrine Hydrochloride with Papaverine Hydrochloride—Place one powdered tablet, or its equivalent from a composite of 20 powdered tablets, in 2 ml of 0.1 *N* HCl in a 30-ml separator. Extract with 5 ml of freshly distilled ethyl acetate. Discard the organic layer and neutralize the aqueous phase with 0.1 *N* NaOH. Add 5 ml of buffer and extract with two 10-ml fractions of ethylene dichloride, passing the separated organic layers through 2 g of anhydrous sodium sulfate suitably supported in a small funnel. Wash the filter with about 3 ml of ethylene dichloride and collect the filtrate and washing in a 25-ml volumetric flask. Dilute to volume with the same solvent.

Tablets of Ephedrine with Reserpine—Place two powdered tablets, or the equivalent from a composite of 20 tablets, in a 30-ml beaker. Extract with two 4-ml portions of warm (40–50°) ethylene dichloride. Filter the fractions through a small piece of cotton wool, wash the powder in the beaker and the filter with a small amount of warm solvent, and collect the filtrate and washing in a 10-ml volumetric flask. Cool to room temperature and dilute to volume with ethylene dichloride.

Injection of Homatropine Methylbromide with Papaverine Hydrochloride—Pipet 1.0 ml, or the measured contents of a single-dose container of the injection, into a 30-ml separator containing 5 ml of buffer and 2 ml of 0.2 *M* potassium iodide solution. Continue as directed for the tablets of ephedrine hydrochloride with papaverine hydrochloride, beginning with: "extract with two 10-ml fractions of ethylene dichloride . . . ."

Pulvules of Codeine Sulfate with Papaverine Hydrochloride—Place the weighed contents of one capsule in 5 ml of buffer in a 30-ml separator. Continue as directed for the tablets of ephedrine hydrochloride with papaverine hydrochloride, beginning with: "extract with two 10-ml fractions of ethylene dichloride . . . ."

Tablets of Total Belladonna Alkaloids with Ergotamine Tartrate—Proceed as directed for the pulvules of codeine sulfate with papaverine hydrochloride, substituting 10 powdered tablets, or their equivalent from a composite of 20 tablets, for the capsule contents.

Sparteine Sulfate Injection—Proceed as directed for the standard solutions of alkaloidal salts, substituting 1.0 ml or the measured contents of a single-dose container of the injection, for the diluted solution of the alkaloidal salt.

General Procedure—Pipet a volume of the prepared sample equivalent to 0.1–0.2 mg of the strong absorbing alkaloid (papaverine, quinine, ergotamine, or reserpine) into a 10-ml volumetric flask. Dilute to volume with ethylene dichloride and determine the absorbance at the proper wavelength (335, 332, 315, or 300 nm, respectively).

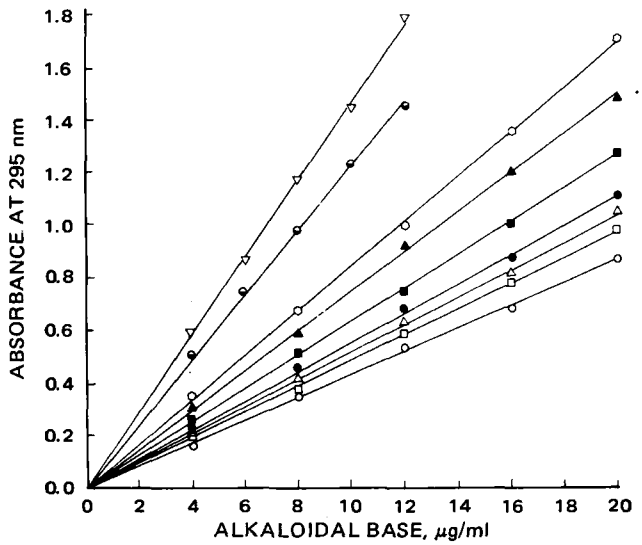

Figure 2—*Calibration curves of the charge-transfer band at 295 nm for ephedrine* (▽), *sparteine* (◒), *reserpine* (○), *homatropine methyliodide* (▲), *quinine* (■), *atropine* (●), *papaverine* (△), *ergotamine* (□), *and codeine* (○).

Pipet a second aliquot of the prepared sample equivalent to 0.05–0.1 mg of total alkaloids into a 10-ml volumetric flask. Add 1.0 ml of iodine reagent solution and dilute to volume with ethylene dichloride. Place the solution in a thermostated water bath at 25 ± 1° for 30 min and then transfer to a 1-cm quartz cell. Determine the absorbance at 295 nm *versus* a blank prepared from 1.0 ml of iodine reagent solution diluted to 10.0 ml with ethylene dichloride and treated similarly.

Calculate the amount of each alkaloid in the preparation by reference to the proper calibration curve and:

$$\text{concentration of strong absorbing alkaloid } (\mu g/ml) = \frac{A_u}{\alpha} \quad \text{(Eq. 1)}$$

$$\text{concentration of weak absorbing alkaloid } (\mu g/ml) = \frac{[A_{295} - (fA_u)]}{\beta} \quad \text{(Eq. 2)}$$

where:

A_u = absorbance of the solution containing the alkaloids in the uncomplexed form at the proper λ_{max} (335, 332, 315, or 300 nm for papaverine, quinine, ergotamine, or reserpine combinations, respectively)

α = slope of the calibration curve (Fig. 1) for the corresponding alkaloidal base in ethylene dichloride as determined by the method of least squares (0.0146, 0.0155, 0.0132, or 0.0168 for papaverine, quinine, ergotamine, or reserpine, respectively)

A_{295} = absorbance of the solution containing iodine-complexed alkaloids corrected to the same dilution as A_u

f = factor derived from the ratio of the slopes of the calibration curves of the strong absorbing alkaloid charge-transfer band at 295 nm (Fig. 2) and the same alkaloidal base at its λ_{max} in ethylene dichloride (Fig. 1) (3.56, 4.13, 3.70, or 5.06 for papaverine, quinine, ergotamine, or reserpine, respectively)

β = slope of the calibration curve for the weakly absorbing alkaloid present in the mixture (charge-transfer band at 295 nm, Fig. 2) as determined by the method of least squares (0.145, 0.123, 0.055, or 0.044 for ephedrine, sparteine, atropine, or codeine, respectively)

Sparteine Sulfate Injection—Pipet two equal aliquots of the prepared sample equivalent to 0.02–0.1 mg of sparteine into separate 10-ml volumetric flasks marked T and R. Add 1.0 ml of iodine reagent solution to Flask T and dilute each flask to volume with ethylene dichloride. Allow the flasks to stand in a thermostated water bath at 25 ± 1° for 30 min. Then determine the absorbance of the solution in Flask T *versus* the solution in Flask R at 295 nm.

Table I—Charge-Transfer Bands in Ethylene Dichloride

Alkaloid	295[a] nm	375[a] nm
Reserpine	46,200	32,000
Sparteine	28,800	14,700
Ergotamine	27,300	13,600
Quinine	24,500	—
Ephedrine	23,400	12,100
Papaverine	17,600	—
Atropine	15,900	6,200
Codeine	13,200	6,700

[a] Based on molecular weight of free base; average of three determinations.

Calculate the amount of sparteine in the preparation from:

$$\text{concentration of sparteine base } (\mu g/ml) = \frac{A}{0.123} \quad \text{(Eq. 3)}$$

where A = absorbance determined at 295 nm, and 0.123 = slope of the calibration curve of sparteine base at 295 nm (Fig. 2).

The conversion factor to convert sparteine base concentration into sparteine sulfate is 1.418.

RESULTS AND DISCUSSION

Charge-Transfer Spectra in Ethylene Dichloride—With iodine in ethylene dichloride, all alkaloids examined showed a major charge-transfer band at 295 nm with molar absorptivities of up to 46,200 (Table I). Most alkaloids also exhibited a second band of lower intensity at 375 nm. Typical charge-transfer spectra of the two types, exemplified by codeine and papaverine, are shown in Figs. 3 and 4, which also illustrate the spectra of uncomplexed alkaloids.

The consistency of the 295-nm band, in spite of the structural variations among the different alkaloids, is probably due to the common origin of the transition in n-electron transfer from the nitrogen of the alkaloid to the acceptor iodine. This is probably the case even for alkaloids having an aromatic heterocyclic nitrogen in addition to an alicyclic one, such as quinine and ergotamine, and for alkaloids containing only aromatic heterocyclic nitrogen, such as papaverine. The large association constants previously reported (4) and the high intensity of the charge-transfer bands (4, 5) (Table I) are common to complexes of n-donors with iodine (6, 7) and are much larger than those of typical aromatic π-donor complexes of iodine (6).

This consistency of the major band is used to advantage in the present assay of alkaloid mixtures, since its intensity is taken as a measure of the total alkaloids present.

Linearity of Beer's Plots of 295-nm Band—Absorbance values

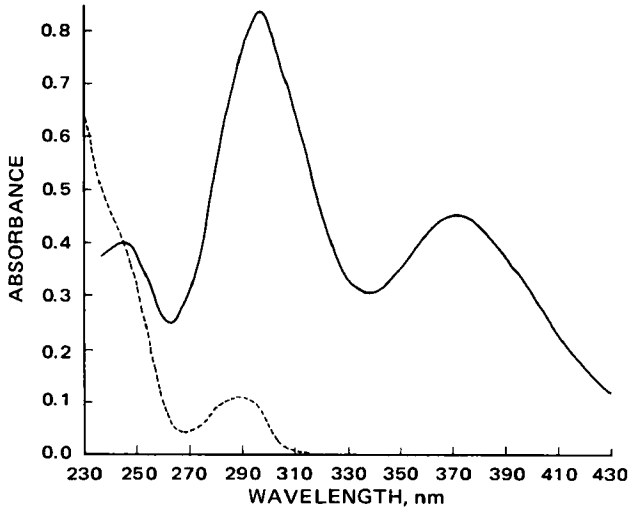

Figure 3—*Spectra of iodine-complexed and uncomplexed codeine in ethylene dichloride. Key: —, codeine (20 μg/ml) with iodine (25.5 μg/ml); and - - - -, codeine (20 μg/ml).*

of the charge-transfer band at 295 nm for each component alkaloid in a mixture were linearly additive, a feature that is imperative in the assay of mixtures (1), under certain conditions. First, the absorbance readings are to be taken after 30 min of equilibration in a constant-temperature water bath. Fixation of time and temperature is essential to minimize the changes in absorbance with time due to the conversion of outer charge-transfer complexes to inner complexes common to n-donor complexes of iodine (8).

Second, the ratio of the molar concentration of the acceptor iodine, [A], to the total alkaloid donor, [D], in the final dilution should not be less than 1.5:1. In the upper concentration ranges, this acceptor–donor ratio is within the stipulated range that is free from Beer's law deviations (4, 6, 8). Although anomalies are usually expected in lower concentration ranges where, in this case, [A] $\gg$ [D] (6, 8–11), no significant deviation from linearity was observed. This finding may be explained as follows.

Anomalies due to self-association (10) or the presence of termolecular complexes (11, 12) were apparently minimized due to the low concentrations employed in the assay (6) (2–20 μg of alkaloid/ml, corresponding to 6×10^{-6}–6×10^{-5} M for an alkaloid of an average molecular weight of 300, and iodine concentration of 10^{-4} M). These relatively low concentrations were attainable because of the large ϵ-values of the charge-transfer bands. Anomalies due to charge-transfer contact pairs with solvent (13, 14) were probably eliminated due to the low tendency of ethylene dichloride to form this type of

Table II—Analysis of Papaverine–Codeine Mixtures

			Recovery			
	Composition, mg %[a]		Papaverine		Codeine	
Mixture	Papaverine	Codeine	%[b]	± SD, %	%[b]	± SD, %
1	0	100	—	—	99.81	0.81
2	5	50	98.75	2.21	101.00	1.56
3	25	25	100.23	0.95	99.65	0.97
4	40	20	99.51	1.29	99.29	0.71
5	50	10	101.35	1.14	98.74	1.60
6	80	5	100.62	0.86	102.55	3.27
7	100	4	99.48	0.55	96.35	2.81
8	80	2	99.60	0.41	95.52	4.32
9	100	0	100.13	0.75	—	—
Mean recovery, %			99.934		99.114	
SE, %			0.326		0.811	
Pooled SD[c], ± S_p, %			0.815		2.137	

[a] Calculated as free bases. [b] Average of five determinations. [c] Calculated from the general formula:

$$S_p = \sqrt{\frac{\Sigma(x_i - \bar{x}_1)^2 + \Sigma(x_i - \bar{x}_2)^2 + \cdots + \Sigma(x_i - \bar{x}_n)^2}{f_1 + f_2 + \cdots + f_n}}$$

where $f_1 + f_2 + \cdots + f_n$ are the available degrees of freedom (16).

Table III—Analysis of Quinine–Atropine Mixtures

Mixture	Composition, mg %[a]		Recovery			
			Quinine		Atropine	
	Quinine	Atropine	%[a]	±SD, %	%[a]	±SD, %
1	0	75	—	—	100.35	0.88
2	10	50	101.25	1.68	99.58	0.63
3	30	30	100.08	0.79	99.61	0.43
4	50	10	99.64	0.97	100.72	0.58
5	80	5	100.55	1.04	99.00	1.02
6	50	2	98.73	1.54	103.7	2.61
7	80	2	100.61	0.82	96.70	4.05
8	50	1	99.48	1.26	93.88	5.34
9	75	0	100.38	0.86	—	—
Mean recovery, %			100.09		99.192	
SE, %			0.310		0.921	
Pooled SD^a, ± S_p, %			0.819		2.259	

[a] See footnotes to Table II.

complexes with alkaloids (5), especially when the species in excess was the acceptor, *i.e.* of the same electron type as the solvent.

These considerations were observed in the construction of calibration curves for the various alkaloids based on the 295-nm charge-transfer band (Fig. 2). Under these conditions, absorbances were linearly additive for mixtures over a reasonable range of the relative concentrations of the two components.

Wavelength Selection—In the assay of binary mixtures of weak and strong UV-absorbing alkaloids, the free bases, liberated by pH 9.5 buffer, were extracted into ethylene dichloride. The absorbance of one aliquot of the extract was read at a preselected wavelength to determine the strong absorbing component present in the uncomplexed form. Iodine was added to a second aliquot, and the absorbance of the total charge-transfer band was read at 295 nm.

The selection of the proper wavelength for measurement of uncomplexed strong absorbing alkaloid was based on the following observations. The alkaloids examined (papaverine, quinine, ergotamine, and reserpine) have very strong bands in ethylene dichloride at or below 270 nm (at 240, 236, 242, and 270 nm, respectively) and weaker, but still fairly strong, bands around or above 300 nm (at 335, 332, 315, and 300 nm, respectively). Maximum sensitivity may be attained by taking the measurements at the intense short wavelength bands. However, overlap with end absorption by many weak absorbers occurred at short wavelengths, leading to interference (Figs. 3 and 4). Accordingly, the long wavelength bands were used for the selective determination of the strong UV-absorbing alkaloids. At these wavelengths, none of the weakly absorbing alkaloids tested had any significant absorption (1, 2, 15), as was verified experimentally.

The amount of each alkaloid in the binary mixture may be calculated using Eqs. 1 and 2.

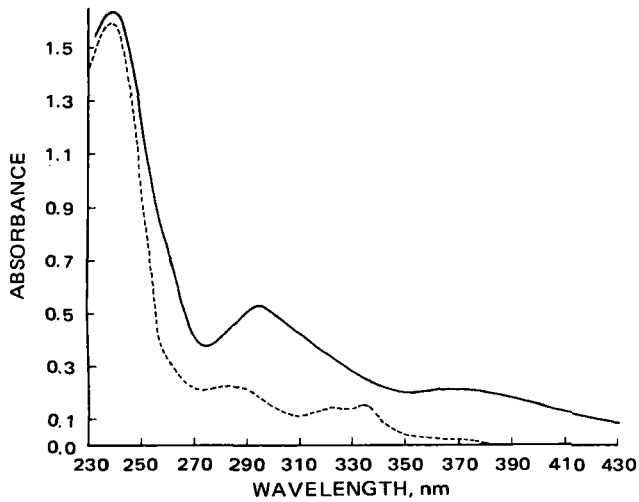

Figure 4—*Spectra of iodine-complexed and uncomplexed papaverine in ethylene dichloride. Key: —, papaverine (10 μg/ml) with iodine (25.5 μg/ml); and - - - -, papaverine (10 μg/ml).*

Application to Synthetic Mixtures—The validity of Eqs. 1 and 2 was tested by analyzing synthetic binary mixtures containing known amounts of alkaloids. Four mixtures were selected as typical examples of pharmaceutical preparations, namely, papaverine hydrochloride with codeine phosphate, quinine sulfate with atropine sulfate, ergotamine tartrate with hyoscyamine hydrobromide, and reserpine with ephedrine.

The results, illustrated in Tables II–V, show good recoveries and high precision in binary mixtures having the ratio of the two alkaloids in the general range of 1:10–10:1. Fairly good accuracy and precision were obtained in the wider range of 1:20–20:1. However, the method yielded progressively poorer results with more extreme ratios (Tables II–V). It failed on application to quinine–atropine mixtures in the ratio of 250:1 as exists in some commercial dosage forms[9].

The data in Tables II–V suggest the suitability of the charge-transfer spectrophotometric method for the analysis of binary mixtures of strong and weak UV-absorbing alkaloids when present in the ratio of their common doses.

Assay of Formulations—The charge-transfer spectrophotometric method was applied to assay a number of commercial preparations containing binary mixtures of alkaloids of the two types. The potential interference in the assay by other ingredients of some formulations was eliminated by adopting the proper extraction method. Thus, with tablets of ephedrine hydrochloride with papaverine hydrochloride, which also contain dexamethasone and phenobarbital sodium, the steroid was removed, together with most of the barbiturate, by preliminary extraction with ethyl acetate in an acidic medium. The second partition with ethylene dichloride in an alkaline medium effectively isolated the pure alkaloidal bases, retaining any remaining amounts of phenobarbital in the aqueous alkaline phase.

In tablets of total belladonna alkaloids, ergotamine tartrate, and phenobarbital, the single partition at the alkaline pH of the procedure was sufficient to separate the acidic barbiturate from the basic alkaloids.

In the case of sparteine sulfate injection, which contains no other alkaloid, the interference of benzyl alcohol present in the preparation was eliminated by a differential procedure. Placing the ethylene dichloride extract containing the uncomplexed alkaloid in the reference cell nullified any background absorption at 295 nm due to benzyl alcohol (λ_{max} of benzyl alcohol in ethylene dichloride at 256 nm, ϵ 468), which may be extracted with the alkaloidal base. Preliminary experiments on benzyl alcohol solutions in ethylene dichloride revealed no formation of charge-transfer bands with 10^{-4} *M* iodine.

The results of analyses (Table VI) confirm the suitability of the presented method for the analysis of these binary mixtures with an accuracy comparable to that obtained with synthetic mixtures.

Alkaloid Mixtures with Quaternary Salts—The quaternized salts of some tropine alkaloids such as atropine methylnitrate, homatropine methylbromide, and *N*-butylscopolammonium bromide are prescribed more often than the tertiary alkaloids, particularly in combination with papaverine. Their presence in the mixture creates a problem because, in spite of their high water solubility, they are

[9] Cold Caps with Quinine, Spencer-Mead, Valley Stream, N.Y.

Table IV—Analysis of Ergotamine–Hyoscyamine Mixtures

Mixture	Composition, mg %[a]		Recovery			
			Ergotamine		Hyoscyamine	
	Ergotamine	Hyoscyamine	%[a]	±SD, %	%[a]	±SD, %
1	0	75	—	—	99.60	0.16
2	5	50	101.88	1.42	100.91	1.47
3	20	20	99.44	0.48	100.45	1.01
4	40	15	98.65	0.80	100.83	1.39
5	60	10	99.89	0.73	98.90	0.50
6	80	5	101.06	0.65	98.60	1.78
7	100	5	101.54	1.32	96.7	3.77
8	100	0	100.68	0.52	—	—
Mean recovery, %			100.449		99.427	
SE, %			0.443		0.570	
Pooled *SD*[a], ± S_p, %			1.078		1.583	

[a] See footnotes to Table II.

Table V—Analysis of Reserpine–Ephedrine Mixtures

Mixture	Composition, mg %[a]		Recovery			
			Reserpine		Ephedrine	
	Reserpine	Ephedrine	%[a]	±SD, %	%[a]	±SD, %
1	0	75	—	—	100.68	0.74
2	5	60	101.65	1.93	99.75	1.02
3	10	80	98,34	1.07	99.74	0.52
4	10	50	99.49	0.80	100.32	1.39
5	40	40	100.81	0.44	99.61	0.78
6	50	15	99.55	0.74	101.05	1.47
7	80	10	101.09	0.95	100.96	1.79
8	80	0	99.86	0.94	—	—
Mean recovery, %			100.112		100.301	
SE, %			0.384		0.291	
Pooled *SD*[a], ± S_p, %			1.017		1.168	

[a] See footnotes to Table II.

partially extracted with halogenated solvents from neutral or basic media, especially when present as the halide salts. In this respect, they are similar to cationic surfactants and other quaternary ammonium compounds (17–19).

This situation resulted in their incomplete extraction into ethylene dichloride with the alkaloidal base and the partial formation of their trihalide charge-transfer band at 280 nm (4, 5), leading to interference. The problem was overcome by the addition of excess iodide ion to the alkaline buffer, which resulted in the quantitative recovery of the quaternized alkaloids as iodide salts into ethylene dichloride with the alkaloidal bases. This finding is in line with the reported facile extraction of many quaternary ammonium compounds into chloroform as their iodide salts (17, 20).

The charge-transfer spectrum of the quaternary iodide with iodine was different from the spectrum previously found for the quaternary bromide salt (4, 5). Instead of the single band at 280 nm and the shoulder at about 355 nm, two well-defined bands at 295 and 375 nm were found (Fig. 5). The spectrum of the quaternary iodide salt was practically identical with the common charge-transfer spectra of alkaloidal bases with iodine in ethylene dichloride (Table I and Fig. 3). This finding reflects the similar electron-donating ability of both the iodide ion and the *n*-electron lone pair of the nitrogen of the alkaloids and their difference from the bromide ion. This evidence also conforms with the spectra of precipitated triiodide salts of other quaternary ammonium compounds and betaines when dissolved in ethylene dichloride, with reported maxima at 295 and 365 nm (21). All of these spectra bear close resemblance to the spectrum of iodine in aqueous potassium iodide, with λ_{max} at 295 and 360 nm (22).

The appearance of the major band at 295 nm for the iodide salts simplified the analysis of mixtures of these weak UV-absorbing quaternary compounds with strong absorbing alkaloids by making possible the adoption of Eqs. 1 and 2 without any modifications. The slope β of the calibration curve of homatropine methylbromide was 0.075 (Fig. 2), determined by the method of least squares. The results

Table VI—Assay of Commercial Dosage Forms

Preparation[a]	Strong Absorbing Alkaloid				Weak Absorbing Alkaloid			
	Label Claim, mg/Unit	Found[b], mg	Added, mg	Recovered, mg	Label Claim, mg/Unit	Found[b], mg	Added, mg	Recovered, mg
Papaverine–ephedrine tablets	30	29.56	30	59.98	10	9.91	10	19.78
Reserpine–ephedrine tablets	0.25	0.261	0.50	0.776	8	8.13	8	16.06
Papaverine–homatropine methylbromide injection	50	49.41	25	75.14	2.5	2.68	5	7.65
Papaverine–codeine pulvules	15	15.33	15	30.51	15	14.73	15	30.0
Ergotamine–total belladonna alkaloids tablets	0.3	0.305	0.6	0.894	0.1	0.117	0.5	0.603
Sparteine sulfate injection	—	—	—	—	150	148.60	100	249.72

[a] Detailed composition is given in *Experimental* section. [b] Average of three determinations.

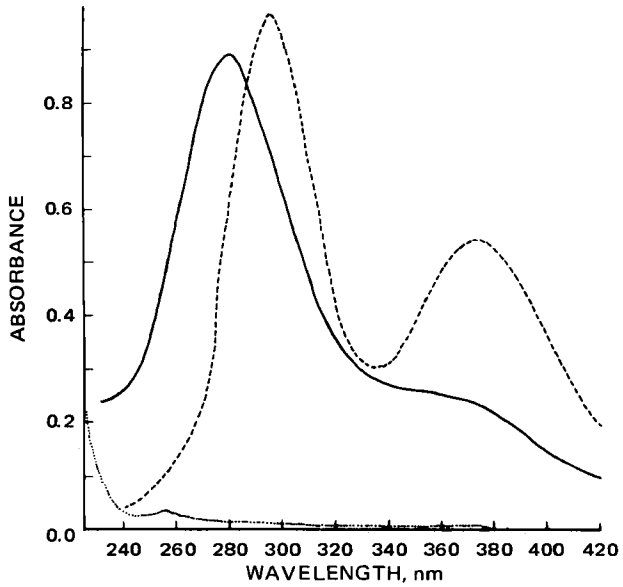

Figure 5—*Spectra of iodine-complexed and uncomplexed homatropine methylhalide salts in ethylene dichloride. Key: —, homatropine methylbromide (12.5 μg/ml) with iodine (25.5 μg/ml); - - - -, homatropine methyliodide (12.5 μg/ml) with iodine (25.5 μg/ml); and . . . . , homatropine methylbromide (12.5 μg/ml).*

of analysis of injection of papaverine hydrochloride with homatropine methylbromide are shown in Table VI.

Comments on Procedure—It is common practice in alkaloid analysis (1–3) first to isolate these basic nitrogenous compounds in one fraction by extracting the sample, buffered to alkaline pH, with suitable organic solvent. The extract is then subjected to further fractionation or directly to analysis. For extracts containing binary mixtures of weak and strong UV-absorbing alkaloids, the charge-transfer spectrophotometric procedure seems to represent a convenient method of analysis without prior separation. In view of the disproportionate amounts of alkaloids of the two types in dosage forms due to differences in potency and the difficulty in achieving clearcut separations of mixtures of alkaloids having close pKa values and solubility parameters, the method may be considered of practical value. Its applicability is not restricted to the specific examples analyzed, since the same technique could be applied to combinations of other strong UV-absorbing synthetic amines capable of charge-transfer formation with iodine such as many antihistamines in combination with weakly absorbing alkaloids or nonalkaloidal drugs[10].

The ratio of weak to strong absorber seems to be limited to the 1:10–1:20 range. More extreme ratios are expected to yield poor recoveries and unacceptable precision. This range, however, adequately covers many popular binary mixtures of alkaloids.

Since the different amines may vary in the rate of attaining maximum intensity of the charge-transfer band and also in the rate of change of absorbance due to the conversion of outer charge-transfer complexes to inner complexes (8), the proper temperature and time lapse before the UV measurement should be carefully controlled and investigated for each new system. Similarly, in the construction of calibration curves, care should be devoted to avoid possible anomalies from the presence of termolecular complexes or the formation of contact charge-transfer pairs in the different concentration ranges.

[10] A case in point is the combination of tripelennamine hydrochloride, 25 mg [λ_{max} 239 and 314 nm, ϵ 14,500 and 8100 (3)], with methylphenidate hydrochloride, 5 mg [λ_{max} 257 nm, ϵ 185 (3)], present in Plimasin (Ciba).

REFERENCES

(1) "Pharmaceutical Analysis," T. Higuchi and E. Brochmann-Hanssen, Eds., Interscience, New York, N.Y., 1961, pp. 313–543.

(2) "Official Methods of Analysis of the Association of Official Analytical Chemists," 11th ed., W. Horwitz, Ed., Association of Official Analytical Chemists, Washington, D.C., 1970, pp. 620–649.

(3) "Isolation and Identification of Drugs," E. G. C. Clarke, Ed., The Pharmaceutical Press, London, England, 1969.

(4) A. M. Taha, A. K. S. Ahmad, C. S. Gomaa, and H. El-Fatatry, *J. Pharm. Sci.*, **63**, 1853(1974).

(5) C. S. Gomaa and A. M. Taha, *ibid.*, **64**, 1398(1975).

(6) R. Foster, "Organic Charge-Transfer Complexes," Academic Press, London, England, 1969.

(7) H. Yada, J. Tanaka, and S. Nagakura, *Bull. Chem. Soc. Jpn.*, **33**, 1330(1960).

(8) C. N. R. Rao, S. N. Bhat, and P. C. Dwivedi, in "Applied Spectroscopy Reviews," vol. 5, E. G. Brame, Ed., Dekker, New York, N.Y., 1972, pp. 1–170.

(9) P. H. Emslie, R. Foster, C. A. Fyfe, and I. Horman, *Tetrahedron*, **21**, 2843(1965).

(10) D. W. Tanner and T. C. Bruice, *J. Phys. Chem.*, **70**, 3816(1966).

(11) G. D. Johnson and R. E. Bowen, *J. Am. Chem. Soc.*, **87**, 1655(1965).

(12) S. Carter, *J. Chem. Soc., A*, **1968**, 404.

(13) D. P. Stevenson and G. M. Koppinger, *J. Am. Chem. Soc.*, **84**, 149(1962).

(14) L. E. Sutton, *Arch. Pharm. Chem., Sci. Ed.*, **2**, 105(1974).

(15) A. L. Hayden, O. R. Sammul, G. B. Selzer, and J. Carol, *J. Assoc. Offic. Agr. Chem.*, **45**, 797(1962).

(16) P. D. Lark, B. R. Craven, and R. C. L. Bosworth, "The Handling of Chemical Data," Pergamon Press, Oxford, England, 1968, p. 107.

(17) "Cationic Surfactants," E. Jungermann, Ed., Dekker, New York, N.Y., 1970, pp. 420–422.

(18) P. A. Lincoln and C. C. T. Chinnick, *Analyst*, **81**, 100(1956).

(19) M. J. Rosen and H. A. Goldsmith, "Systematic Analysis of Surface Active Agents," 2nd ed., Wiley–Interscience, New York, N.Y., 1972, pp. 39–52.

(20) R. Reiss, *Arzneim.-Forsch.*, **6**, 77(1956).

(21) J. S. Wall, D. D. Christianson, R. J. Dimler, and F. R. Senti, *Anal. Chem.*, **32**, 870(1960).

(22) "Colorimetric Determination of Nonmetals," D. F. Boltz, Ed., Wiley–Interscience, New York, N.Y., 1958, pp. 218–220.

ACKNOWLEDGMENTS AND ADDRESSES

Received June 10, 1975, from the *Faculty of Pharmacy, University of Assiut, Assiut, Egypt.*

Accepted for publication September 29, 1975.

[x] To whom inquiries should be directed. Present address: Institut fur Pharmazeutische Chemie der Westfalischen Wilhelms-Universitat, 58-62 Hittorfstr., 4400 Munster (Westf.), West Germany.

Physical Aspects of Wet Granulations I: Distribution Kinetics of Water

J. T. CARSTENSEN *x, THOMAS LAI *, DONALD W. FLICKNER, H. E. HUBER, and M. A. ZOGLIO

Abstract □ The kinetics of wetting during the process of making tablet granulations were studied; the process progresses through an intermediate (overwetted) nonequilibrium granule to a final, equilibrated granule. In systematic formulation changes, there is an optimum composition from the point of view of hardness and content of equilibrium granules.

Keyphrases □ Kinetics, distribution—wetting during process of making tablet granulations □ Distribution kinetics—wetting during process of making tablet granulations □ Granulations, tablet—distribution kinetics of wetting during preparation □ Tablet granulations—distribution kinetics of wetting during preparation □ Dosage forms—tablet granulations, distribution kinetics of wetting during preparation

Granulation technology has been employed for close to a century in pharmacy (1), yet many aspects are still confined to what is considered art. The primary purposes of granulating material in general are to: (*a*) enlarge particle sizes to improve flow and uniformity of solid dosage forms, (*b*) make hydrophobic surfaces hydrophilic to improve bioavailability (2), (*c*) improve homogeneity of low dosage level dosage forms, (*d*) improve cohesion during and after compression of tablets, and (*e*) overcome adverse electrostatic properties of a powder blend (3).

In "wet" granulation operations, fine powders are agglomerated; the agglomerates attain their strength by formation of solid bridges (3–5). Improved binder distribution in the agglomerate improved the strength (5–8) when agglomerates were made by chemical reaction, hardened by melting, and hardened by crystallization of dissolved materials. In general, the agglomerate (ball) diameter, d, had a crushing strength, l, given by:

$$l = kd^n \qquad \text{(Eq. 1)}$$

where k and n are parameters particular to the solid and condition under study. When sodium chloride (or another inorganic salt) is the bridging (granulating) agent (9), then k increases with increasing drying temperature and depends on the concentration of salt in the granulating liquid since k reaches a maximum close to (but somewhat below) the saturation concentration. The value of n simply increased (from 1.5 to 2) with increasing temperature.

The quoted references concern the heavy and fine chemical industries. Unlike studies of this type, granulations in pharmacy are made either by adding the bridging agent to a mixture of finely subdivided pharmaceutical powders or by adding water to the powder containing the bridging agent in dry state. In both cases, the granulation goes through several stages:

1. At first, part of the mixture is wetted excessively and forms large aggregates. The remaining powder stays dry.
2. Distribution of water or the granulation liquid is then effected, and both large and small granules are present.
3. Finally, the granules equilibrate and attain a fairly uniform size (provided "proper" amounts of water or granulating fluid are present).
4. A granulation can be kept in a kneading mixer too long, and the equilibrium granular structure can be destroyed. Steps 1–3 are studied here.

EXPERIMENTAL

Powders of the following composition were used: $(29 - y)$ kg of lactose USP, y kg of sucrose USP, and 4 kg of starch USP (cornstarch). They were blended for 2 min in a chopper-ribbon mixer[1] with blades rotating at 140 rpm and chopper blades rotating at 3500 rpm. Four 750-ml portions of distilled water were added at 15-sec intervals, and the mixer was stopped at t min after addition of the first portion of water. Then the material was passed through an oscillating granulator[2] using a No. 6 screen. The material was then dried in a fluid bed drier[3] using air at an inlet velocity of 380 cfm and 42°. The drying end-point was about 20 min after the initial drying time, and the end-point was established by a rise in the outlet air temperature (35°).

The dried powders were subjected to sieve analysis with standard U.S. sieves; the density of the granulation was determined by pycnometry, using ethyl acetate as the displacement liquid. The hardness of the granules was estimated by the method of Harwood and Pilpel (10).

Experiments at mixing intensities lower than those obtained in the chopper-ribbon blender were performed in a planetary mixer[4]; 1150 g of lactose USP was mixed with 120 g of corn starch and granulated with 400 ml of a 1:10 starch paste (40 g of corn starch and 400 g of water) at low agitation speed (50 rpm), using a shield-type agitator blade in the following fashion. Forty grams of corn starch was suspended in 100 ml of water at 25° and added to 300 ml of boiling water, and the ensuing gel was cooled to 60°. The paste was placed in a plastic bag with a pinhole. When the temperature of the paste reached 50°, the paste was forced through the hole into the lactose–corn starch mix in the mixer. At the same time, a timer was started. The time for completion of addition was noted, and the mixing was stopped at a predetermined time.

The powder mass was poured out on a six-mesh screen, and the dry powder and/or the smaller wet granules were passed through by shaking. The retained and passed fractions were weighed, dried, and reweighed. The moisture balance was assured by checking the loss on drying, showing that the coarse fraction had the higher water content.

RESULTS AND DISCUSSION

The purposes of this study were to describe the initial granulation process and to follow the amount of granulation that is of a larger size than the equilibrium granule which eventually ensues. Therefore, granulations were mixed for the various times, t, indicated in Fig. 1 and subjected to screen analysis.

A convenient measure of the powder is its geometric surface area. Surface areas can, of course, be measured in many fashions (*e.g.*, gas

[1] Model FM-100 Littleford-Lodige, Cincinnati, Ohio.
[2] F. J. Stokes Machine Co., Philadelphia, Pa.
[3] Aeromatic A. G., Basel, Switzerland.
[4] Hobart Manufacturing Co., Troy, Ohio.

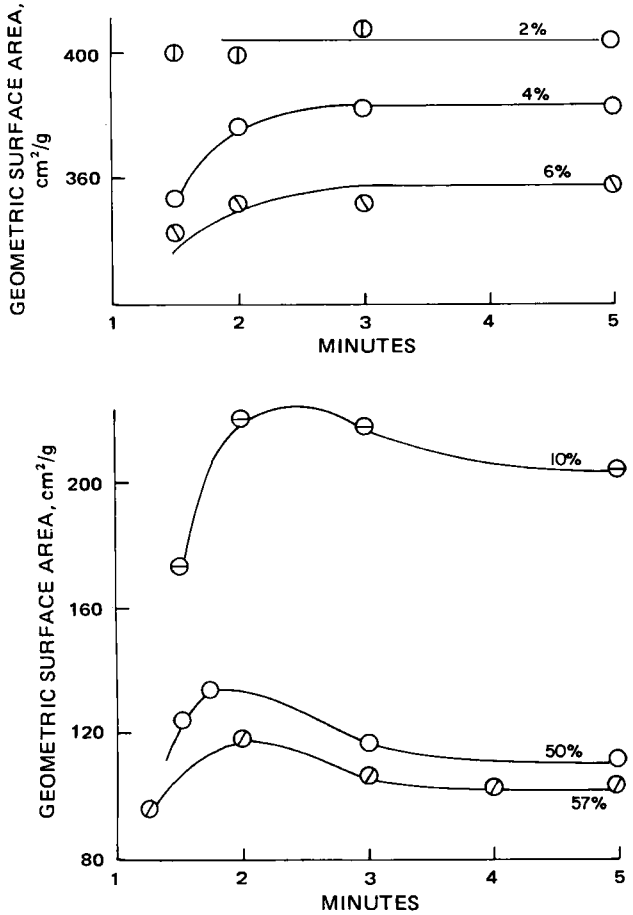

Figure 1—*Geometric surface areas as a function of kneading time for various* y *values.*

adsorption). In this study, however, the important characteristic was the external surface of agglomerates and not the internal surface of the pore space. For this reason, screen analysis was an appropriate tool.

The screen analysis data were converted to geometric surface areas in the following fashion. A mesh fraction is defined by a maximum size (the upper screen) and a minimum size (the lower screen). The particles are assumed to be spherical and of a size of the mean of the confining sieve openings; *e.g.*, a powder of fraction −20/+40 would be considered to consist of spheres of diameter (840 + 420)/2 = 630 μm = 0.063 cm, since the wire mesh openings of the two screens are

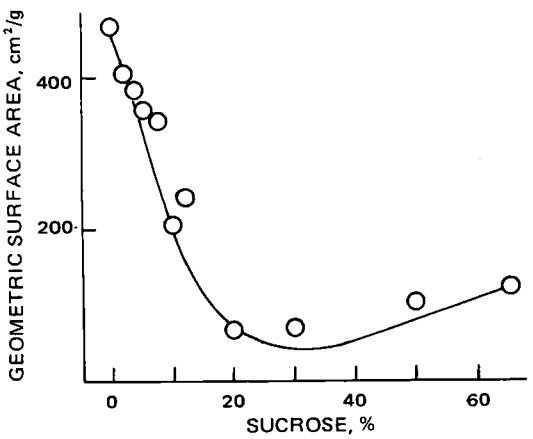

Figure 2—*Equilibrium geometric surface area as a function of the amount of sucrose.*

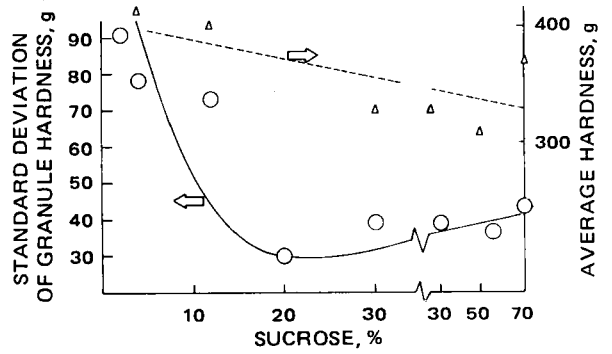

Figure 3—(Δ) *Average Pilpel hardness (grams) of final granules (right scale) as a function of percent sucrose in formulation. The final granulations were kneaded for 5 min. The points represent data set of 10.* (○) *Left scale represents standard deviation.*

840 and 420 μm, respectively[5].

If p g of density ρ (grams per milliliter) is retained by confining screens of q and s cm, then $d = (q + s)/2$ cm and the solid volume is p/ρ. Therefore, the number of particles in the mesh fraction is:

$$n = 6p/(\rho d^3\pi) \qquad \text{(Eq. 2)}$$

i.e., the surface area of the fraction is (11):

$$O' = \frac{6p}{\pi d^3 \rho}\pi d^2 = 6p/(\rho d) \qquad \text{(Eq. 3)}$$

The total area is $(6/\rho)$ $[\Sigma(p/d)]$ cm²/(Σp) g, so that the area (square centimeters) per gram is:

$$O = \frac{6\Sigma(p/d)}{\rho\Sigma p} \qquad \text{(Eq. 4)}$$

For −20/+40-mesh granules with 2% sucrose, ρ was found to be 1.50 ± 0.01. For −20/+40-mesh granules with 30% sucrose, it was 1.51 ± 0.01 g/ml. Therefore, ρ was estimated at 1.5 g/ml in all cases. There was a slight increase in density in the finer fractions (up to 1.53 g/ml), so the denominator in Eq. 4 more properly should be $\Sigma(\rho p)$. The error in factoring out ρ is, however, less than 2%.

Surface areas obtained *via* Eq. 4 are shown in Fig. 1. Equilibrium seems to be established after 5 min, and the surface areas at equilibrium were plotted *versus* the sucrose to lactose ratio (expressed in percent as 100*y*/29) in Fig. 2.

The hardness (Pilpel) of the granules estimated by the method of Harwood and Pilpel (10) is shown graphically in Fig. 3. The granule-to-granule variation decreased and became level at sugar concentrations above 20%.

The crushing strength of a granule as a function of its weight was determined by taking granules after 5 min of mixing (and subsequent drying), weighing various granules individually, and determining their Pilpel hardness (Fig. 4). There was a good correlation (r = 0.96) at granule weights of 4 mg or less. The effect of mixing time on Pilpel hardness is shown in Fig. 5.

A 10% sugar granulation was mixed for 1.5 min, dried granules were sampled randomly, and Pilpel hardness was checked (Fig. 6). The same procedure also was repeated for a granulation kneaded for 3 min.

It is apparent from Fig. 1 that O passes through a maximum in many cases and then approaches an equilibrium value. This finding is in accord with the introductory description of the granulation process (Steps 1–3). As shown schematically in Fig. 7, when the powder mass consisting of N particles of diameter d is "wetted," a fraction, f, of the particles is going to be overwet and a fraction, $(1 - f)$, is not wet at all[6]. Eventually the moisture distributes itself evenly over the powder mass. If it is assumed that a wet agglomerate can

[5] The rationale and limitations of this approach were described previously (12, 13); the validity of the approximations made here were tested with the larger screen sizes by weighing granules. The ensuing error in geometric surface area is about 5%. As opposed to crystalline solids, granules are fairly "spherical."

[6] This assumes that there is only one equilibrium size in the "equilibrium" granule. The more realistic case of several sizes present at the final stage is somewhat complex and is treated in the *Appendix*.

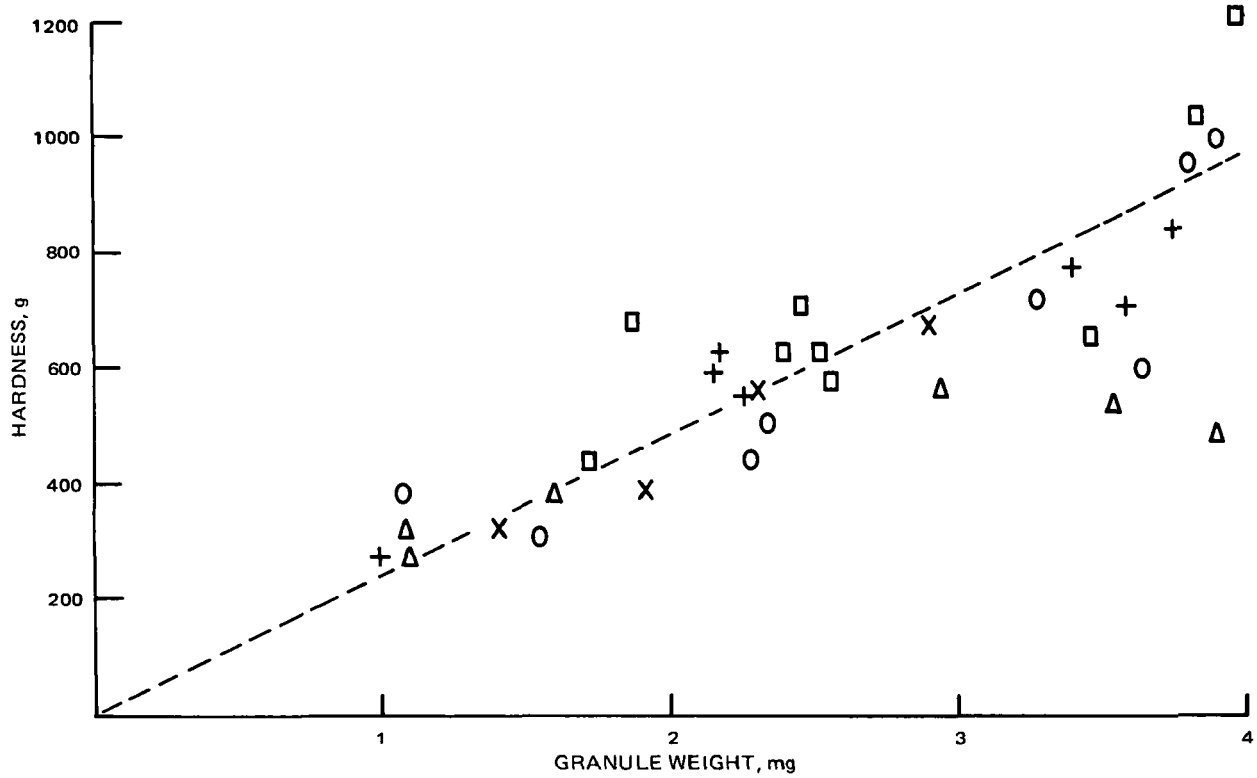

Figure 4—*Pilpel hardness (grams) as a function of granule weight. Key (percent sucrose): O, 2; +, 6; X, 12; □, 10; and Δ, 30.*

accommodate at most an amount of water w^* in an agglomerate of diameter d^* and at the end will accommodate an amount of water w' in an agglomerate of diameter d' and, furthermore, that a total of W g of water is added, then at first, there are W/w^* agglomerates with a total volume of $[W/w^*]\pi(d^*)^3/6$, which (in all) contain the Nf wetted particles.

If the amount of water in an agglomerate at time t is denoted w, then the geometric surface area, O, is a function of w and f, *i.e.*, $O = \phi[w,f]$. This function is defined for all values of w and f, where $w^* > w > w'$ and $0 < f < 1$. Not all of the w and f values occur in practice; *e.g.*, a high w value and a high f value will not occur simultaneously. A process, essentially, defines a set of w and f values as a function of time, so that the geometric surface area as a function of time is a *curve* defined by $O = \phi[w,f]$, $w = \psi_1(t)$, and $f = \psi_2(t)$.

For the sake of simplicity, it is assumed that $w = w^*$ until the entire mass is wetted (*i.e.*, $f = 1$). At higher time values, the nonequilibrium granule of diameter d^* containing w^* g of water decreases in size to a diameter of d' and a water content of w' g/granule.

If, as shown in Fig. 7, it is assumed that the individual particles in the agglomerates form cubic assemblages (14, 15), *i.e.*, that the spheres touch at the poles and at four points of their equator, then they have coordination number six and a porosity of 0.475[7]. Each particle occupies a virtual volume of d^3 in this configuration, so the volume of the agglomerates in total is Nfd^3. This leads to:

$$Nfd^3 = W(d^*)^3\pi/(6w^*) \qquad \text{(Eq. 5)}$$

and, therefore:

$$d^* = d[6w^*Nf/(\pi W)]^{1/3} \qquad \text{(Eq. 6)}$$

The geometric surface area, then, is:

$$O = N(1-f)\pi d^2 + \frac{W}{w^*}\pi(d^*)^2 \qquad \text{(Eq. 7)}$$

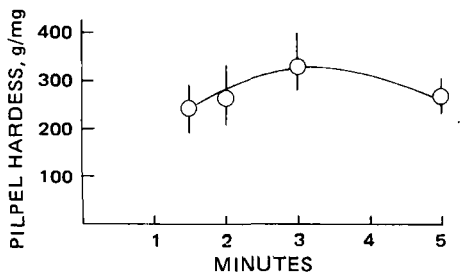

Figure 5—*Pilpel hardness of granules of less than 4 mg as a function of time (10% sucrose).*

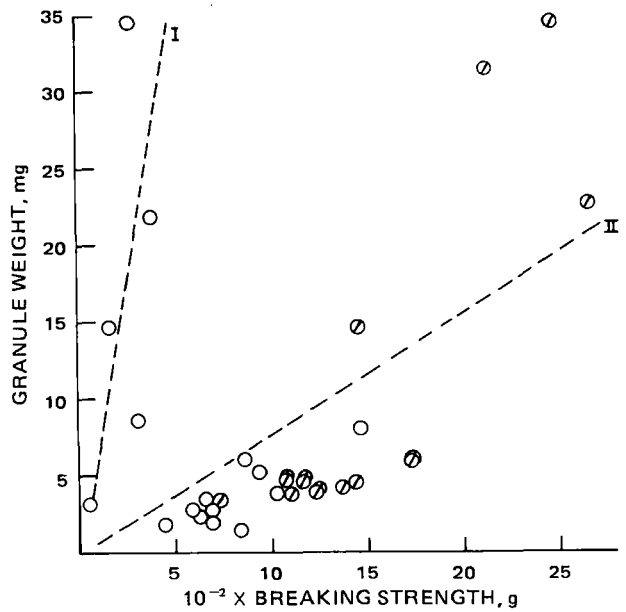

Figure 6—*Pilpel hardness and granule weights of a granulation kneaded for 1.5 min (⊘) and of a granulation kneaded for 3 min (O).*

[7] The volume of the sphere is $\pi d^3/6$ and that of the cube enclosing it is d^3, so the fraction of the void is $[1 - (\pi/6)] = 0.476$.

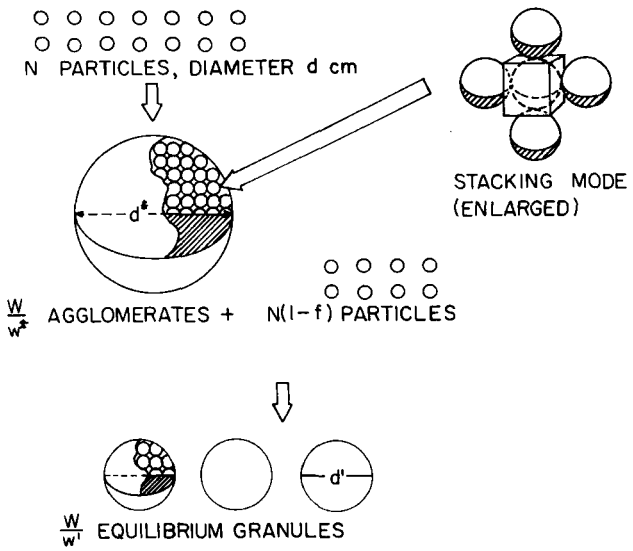

Figure 7—*Schematic drawing of the formation of agglomerates from prime particles plus water and the formation of equilibrium granules from the agglomerates. The curved lines indicate wedge-shaped cuts into spheres; the insert at the top right is an enlargement of the six-coordinated stacking within agglomerates and granules.*

From Eq. 6, it is seen that:

$$d^* = d\left(\frac{6w^*Nf}{\pi W}\right)^{1/3} \qquad \text{(Eq. 8)}$$

which, when inserted in Eq. 7, gives:

$$O = N(1-f)\pi d^2 + \frac{W}{w^*}\left(\frac{6w^*N}{W\pi}\right)^{2/3}(f^{2/3}\pi d^2) \qquad \text{(Eq. 9)}$$

It is seen that:

$$\partial O/\partial f = \pi d^2\left\{-N + \frac{2W}{3w^*}\left(\frac{6w^*N}{\pi W}\right)^{2/3}(f^{-1/3})\right\} = 0 \qquad \text{(Eq. 10)}$$

when:

$$f = 1.08\frac{1}{N}\frac{W}{w^*} \qquad \text{(Eq. 11)}$$

W/w^* is the number of particles wetted, and when $(W/w^*)/N < 0.93$ then $f < 1$; *i.e.*, under such conditions, there will be an extremum. This inequality is quite reasonable for "good" granulations.

The extremum is a maximum because:

$$\partial^2 O/\partial f^2 = -\frac{1}{3}\frac{2}{3}\frac{W}{w^*}\left(\frac{w^*N}{\pi W}\right)^{2/3}(f^{-4/3}) < 0 \qquad \text{(Eq. 12)}$$

for $0 < f < 1$.

The maximum refers to the initial stage where the powder is eventually all wetted at time t_1. The granule, at this point, contains w^* g of water/agglomerate of diameter $d[6w^*N/(\pi W)]^{1/3}$; this is obtained by inserting the value $f = 1$ in Eq. 8. Therefore the geometric surface area at time t_1 is:

$$O_1 = (w^*/W)(\pi)d^2[6w^*N/(\pi W)]^{2/3} \qquad \text{(Eq. 13)}$$

After time t_1, the agglomerate becomes smaller. At time t_2, it attains an equilibrium size of diameter d' containing w' g of water. Then w' and d' are related by an equation similar to Eqs. 8 and 13:

$$d' = d[6w'N/(\pi W)]^{1/3} \qquad \text{(Eq. 14)}$$

The geometric surface area at time t_2 is:

$$O_2 = (w'/W)(\pi)d^2[6w'N/(\pi W)]^{2/3} \qquad \text{(Eq. 15)}$$

The maximum referred to in the initial stage is an overall maximum if $O_1 > O_2$, *i.e.*, if:

$$(w^*/W)(\pi)d^2[6w^*N/(\pi W)]^{2/3} > (w'/W)(\pi)d^2[6w'N/(\pi W)]^{2/3} \qquad \text{(Eq. 16)}$$

i.e., if $w^* > w'$, which is true by definition. Therefore, with the assumptions made, the geometric surface area curve has a maximum in time under the conditions given by $[(W/w^*)/N] < 0.93$.

Table I—Amounts of Equilibrium and Nonequilibrium Granules as a Function of Kneading Time

Kneading Time, min	Number of Equilibrium Granules	Number of Nonequilibrium Granules
1.5	2[a]	14[a]
2	3	13
3	5[a]	11[a]
5	5	10

[a] These figures are shown in Fig. 6.

This relationship and Eqs. 5–16 are reflected in the final surface areas as well. A plot of O after 5 min is shown in Fig. 2. It is noted that O drops to a (fairly) constant value at the 20% sucrose concentration. In this respect[8], these experiments actually define an optimum formulation, *i.e.*, a sucrose concentration at or above 20%. Such optima have been reported in other systems under other circumstances (16).

Figure 4 shows that a −12/+20-sieve fraction shows consistent Pilpel hardness *versus* weight relations if one considers weights below 4 mg only. At higher weights, consistency disappears. Figure 6 shows the situation after 1.5 and 3 min of kneading; there seem to be two distinct lines in the graph. If there is a decrease in the hardness of the granule (through better distribution of water) as time progresses, more and more points should shift from line II to line I, *i.e.*, from nonequilibrium to equilibrium granules.

If one considers the points that have shifted away from the high load–weight ratio, this may, indeed, represent the fraction of granules that have acquired equilibrium conditions. The data in Table I are the fractions of equilibrium granules in randomly selected granules in a −12/+20-sieve fraction as a function of time. The slopes of the equilibrium load *versus* weight plots are shown in Fig. 5 and appear to be somewhat independent of time, since the slope of the line in Fig. 5 equals the slope of line II in Fig. 6.

The experiments in the planetary blender were performed to demonstrate the principle of equilibrium *versus* nonequilibrium granules and to test one step in the large-scale experimental procedure that might have affected the previous results. As a necessary step, the wet granulations from the ribbon-chopper mixer were processed through an oscillating granulator; the smaller scale experiments in the planetary blender did not include the oscillator step. The results (Fig. 8) demonstrate that the amount of wetted (nonequilibrium) material first increased (as the wetting progressed and more and more of the powder was wetted) and then decreased at the expense of

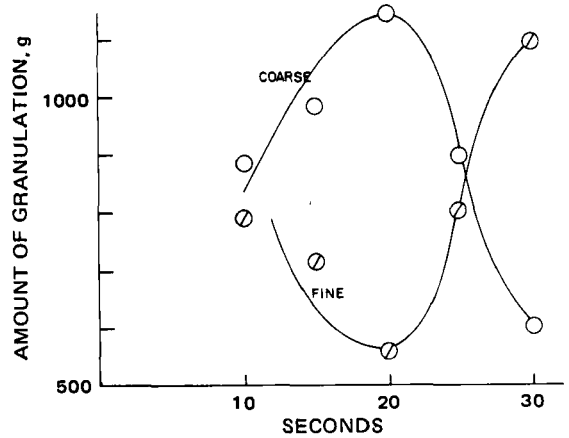

Figure 8—*Amount of wetted and nonwetted material of a corn starch–lactose granulation as a function of kneading time in a planetary mixer.*

[8] This is optimum with regard to hardness- and surface-area-related properties only. Other qualities (*e.g.*, disintegration) may not be optimum at this point.

Table II—Sieve Analysis Data[a] of a Granulation with $y = 16.57$ kg

Screen Cut	$t = 1.25$ min	$t = 2$ min	$t = 3$ min	$t = 4$ min	$t = 5$ min
+12	41	27.5	25	17.5	16
−12/+20	17	16	17.5	16	16.5
−20/+40	12.5	13	15.5	18.5	21
+40	70.5	56.5	58	52	53.5
−40/+60	11	17.5	22	31.5	31
−60/+80	8.5	15	13.5	12	11.5
−40/+80	19.5	32.5	35.5	43.5	42.5
−80/+100	4.5	6	4	3	2.5
−100/pan	6.5	7	5	3	3.5
−80/pan	11	13	9	6	6

[a] Values are in grams.

"finer" equilibrium granules. If one considers this process as $(p + w) \xrightarrow{k_1} n$ and $n \xrightarrow{k_2} m$, where p denotes the amount of powder, n is the amount of nonequilibrium granulation, w is the amount of water, and m is the amount of equilibrium granule, then:

$$n = Q\,(1 - e^{-k_1 t})e^{-k_2 t} \qquad \text{(Eq. 17)}$$

and:

$$m = p_0 - n \qquad \text{(Eq. 18)}$$

qualitatively describe the curves in Fig. 8. No attempts were made here to test k_1 and k_2 as a function of the operating conditions.

APPENDIX

Table II (and Fig. 9) lists the actual sieve mesh data ($y = 16.57$ kg) used in Fig. 1. It is obvious from the data that more than just one size granule was left after 5 min. The model suggested is, therefore, somewhat oversimplified. The following argument (although tedious) will show that a first-order improvement in the model considering three sizes will lead to maxima in the geometric surface area within certain limits.

The data in Table II show the amounts (per 100 g) retained by 12, 20, 40, 60, 80, and 100 mesh and pan. If it is assumed that the material above 40 mesh is nonequilibrium granules, the material between 40 and 80 mesh is equilibrium granules and the material below 80 mesh is prime particles (*i.e.*, nongranules), then the disappearance of the coarse and fine fractions at the expense of the middle fraction will have the appearance of the curves in Fig. 9.

This argument has the more realistic features, compared to the previous argument, that: (*a*) the equilibrium granules start being formed immediately and (*b*) some fine and some coarse fractions are always present.

In the terms of the established nomenclature, there are originally, prior to wetting, N particles of diameter d. After wetting, there are: n_1 large nonequilibrium granules of diameter d^*, and each granule contains P original particles; n_2 equilibrium granules of diameter d' and each granule contains q particles; and n_3 nonwetted particles of diameter d, and each particle contains one particle. It follows from the definitions that $P > q$.

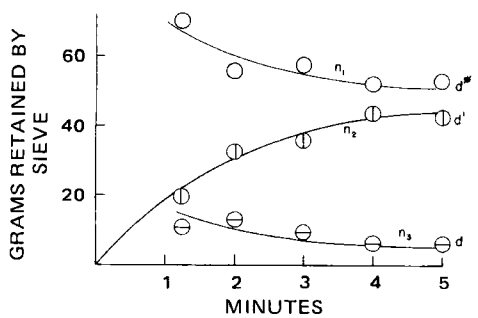

Figure 9—*Amounts of fractions larger than 40 mesh* (○), *between 80 and 40 mesh* (⊙), *and finer than 80 mesh* (⊖). *The data correspond to the cumulative figures in Table II.*

At any time t, the following number balance must hold:

$$N = n_1 P + n_2 q + n_3 \qquad \text{(Eq. A1)}$$

That is:

$$n_2 = \frac{1}{q}\,[N - n_1 P - n_3] \qquad \text{(Eq. A2)}$$

The curves in Fig. 9 suggest that n_1 and n_3 decrease by exponential decay; *i.e.*:

$$n_1 = n_\infty' + (n_0' - n_\infty')e^{-\alpha t} \qquad \text{(Eq. A3)}$$

and:

$$n_3 = n_\infty'' + (n_0'' - n_\infty'')e^{-\beta t} \qquad \text{(Eq. A4)}$$

The diameter of the overwet granule, d^*, is given by:

$$Pd^3 = (\pi/6)(d^*)^3 \qquad \text{(Eq. A5)}$$

so that the area of the overwet granule is:

$$O^* = \pi(6P/\pi)^{2/3}d^2 = \eta P^{2/3}d^2 \qquad \text{(Eq. A6)}$$

where:

$$\eta = \pi(6/\pi)^{2/3} \qquad \text{(Eq. A7)}$$

And d' and O' in a similar fashion give:

$$O' = \eta q^{2/3}d^2 \qquad \text{(Eq. A8)}$$

The total surface area at time t is given by:

$$O(t) = n_1\eta P^{2/3}d^2 + n_2\eta q^{2/3}d^2 + n_3\pi d^2 \qquad \text{(Eq. A9)}$$

Rearranging and introducing Eq. A2 then give:

$$O(t)/(\eta d^2) = P^{2/3}n_1 + q^{-1/3}[N - n_1 P - n_3] + n_3(\pi/\eta) =$$

$$n_1(P^{2/3} - Pq^{-1/3}) + n_3\left[\frac{\pi}{\eta} - q^{-1/3}\right] + Nq^{-1/3} \qquad \text{(Eq. A10)}$$

The surface area will have an extremum when the derivative with respect to time vanishes, *i.e.*, when:

$$\frac{1}{\eta d^2}\frac{\partial O}{\partial t} = [P^{2/3} - Pq^{-1/3}](\partial n_1/\partial t) + \left[\frac{\pi}{\eta} - q^{-1/3}\right](\partial n_3/\partial t) =$$

$$\alpha(Pq^{-1/3} - P^{2/3})(n_0' - n_\infty')e^{-\alpha t} -$$

$$\beta\left(\frac{\pi}{\eta} - q^{-1/3}\right)(n_0'' - n_\infty'')e^{-\beta t} = Ae^{-\alpha t} - Be^{-\beta t} \qquad \text{(Eq. A11)}$$

vanishes. It is noted that $(\pi/\eta) \sim (0.25)^{1/3}$, so the last preexponential term is positive when $q > 5$. Since $P > q$, $q^{-1/3} > P^{-1/3}$ or, by multiplying by P on both sides of the inequality sign, $Pq^{-1/3} > P^{2/3}$, so the first preexponential term is positive. Therefore, there is a solution to the equation:

$$Ae^{-\alpha t'} = Be^{-\beta t'} \qquad \text{(Eq. A12)}$$

when A and α are larger than B and β, respectively ($A > B$ *and* $\alpha > \beta$) or when A and α are smaller than B and β, respectively ($A < B$ *and* $\alpha < \beta$). The extremum occurs at $t = t'$. This extremum will be a maximum if the second derivative is smaller than zero:

$$\frac{1}{\eta d^2}\frac{\partial^2 O}{\partial t^2} = B\beta e^{-\beta t'} - A\alpha e^{-\alpha t'} < O \qquad \text{(Eq. A13)}$$

The time of extremum, t', is defined by Eq. A12. Introducing it into Eq. A13 gives:

$$\frac{1}{\eta d^2}\frac{\partial^2 O}{\partial t^2} = \beta Ae^{-\alpha t'} - A\alpha e^{-\alpha t'} = Ae^{-\alpha t'}(\beta - \alpha) \qquad \text{(Eq. A14)}$$

which is smaller than zero when $\alpha > \beta$; *i.e.*, when $\alpha > \beta$, there is a maximum in the O *versus* t curve with the assumptions made here.

REFERENCES

(1) J. T. Carstensen, "Theory of Pharmaceutical Systems," vol. 2, Academic, New York, N.Y., 1973.

(2) P. Finholt, in "Dissolution Technology," L. Leeson and J. T.

Carstensen, APhA Academy of Pharmaceutical Sciences, Washington, D.C., 1974.
(3) C. E. Capes, "Proceedings of Powtech 71," Harrgate, England, Powder Advisory Centre, London NW110GP, England, 1972, p. 149.
(4) H. Rumpf, in "Agglomeration," W. A. Knepper, Ed., Wiley, New York, N.Y., 1962, p. 379.
(5) C. E. Capes, *Powder Technol.*, **4**, 77(1971).
(6) W. B. Pietsch, *Can. J. Chem. Eng.*, **47**, 403(1971).
(7) W. B. Pietsch and H. Rumpf, *C. R. Colloq. Int. CHRS*, No. 160 2.3 (1966).
(8) D. M. Newitt and A. L. Papadopoulos, "Proceedings No. 55," The Fertilizer Society, London, England, 1959.
(9) V. C. Marshall, "Proceedings of Powtech 71," 1971, p. 123.
(10) C. F. Harwood and N. Pilpel, *J. Pharm. Sci.*, **57**, 478(1968).
(11) J. T. Carstensen, "Pharmaceutics of Solids," Badger Freund, Fond du Lac, Wis., 1974.
(12) D. Brooke, *J. Pharm. Sci.*, **64**, 1409(1975).
(13) G. Steiner, M. Patel, and J. T. Carstensen, *ibid.*, **63**, 1395(1974).
(14) J. T. Carstensen, "Pharmaceutics of Solids," Badger Freund, Fond du Lac, Wis., 1974, p. 93.
(15) W. A. Gray, "The Packing of Solid Particles," Chapman & Hall, London, England, 1968, p. 125.
(16) S. Toyoshima, S. Watanabe, K. Matsuo, and M. Kasai, *Yakugaku Zasshi*, **91**, 1088(1971).

ACKNOWLEDGMENTS AND ADDRESSES

Received January 28, 1975, from *Merrell-National Laboratories, Cincinnati, OH 45214*

Accepted for publication September 10, 1975.

* Present address: School of Pharmacy, University of Wisconsin, Madison, WI 53706

ˣ To whom inquiries should be directed.

Comparative Serum Prednisone and Prednisolone Concentrations following Prednisone or Prednisolone Administration to Beagle Dogs

W. A. COLBURN *, C. R. SIBLEY, and R. H. BULLER ˣ

Abstract □ The relative serum prednisone and prednisolone concentrations were determined following the administration of prednisone or prednisolone as 5-mg tablets to male beagle dogs. Serum prednisone concentrations were significantly greater following prednisone administration than they were following prednisolone administration. Serum prednisolone concentrations were significantly greater following treatment with prednisolone than with prednisone. The combined prednisone and prednisolone areas under the serum concentration–time curves were similar for the two treatments.

Keyphrases □ Prednisone—serum concentration after administration of prednisone or prednisolone, radioimmunoassay, dogs □ Prednisolone—serum concentration after administration of prednisolone or prednisone, radioimmunoassay, dogs □ Bioavailability—prednisone and prednisolone, serum radioimmunoassay, dogs □ Glucocorticoids—prednisone and prednisolone, serum radioimmunoassay, dogs

With the advent of radioimmunoassays for both prednisone and prednisolone (1, 2), a unique opportunity arose to investigate the interconversion of prednisone and prednisolone in many experimental animals and in humans. In the present study, male beagle dogs were chosen as the test animal.

Previously, the conversion and interconversion of prednisone and prednisolone had been studied by tedious, time-consuming, and often difficult methods (3–7). With radioimmunoassays, the analyses could be conducted in just days without chromatography or separation steps.

The present study was conducted to investigate the interconversion of prednisone and prednisolone following the administration of 5-mg compressed tablets of prednisone[1] or prednisolone[2] to male beagle dogs.

EXPERIMENTAL

Materials—The buffers used were: tromethamine, 0.2 *M* and pH 8.0 (I), and sodium phosphate (monobasic and dibasic), 0.2 *M* and pH 6.5 (II). The tritiated steroids[3] were 6,7-^{3}H-prednisone at 40.0 Ci/mmole and 6,7-^{3}H-prednisolone at 45.4 Ci/mmole. The primary antiserums were rabbit antiprednisolone 21-hemisuccinate–bovine serum albumin (III) and rabbit antiprednisone 21-hemisuccinate–bovine serum albumin (IV).

Goat antirabbit serum or ammonium sulfate solution (80% saturated) was used as the precipitant. Analytical grade toluene-based liquid scintillation counting solution[3,4] was used, and the high capacity liquid scintillation spectrophotometer had a 4° refrigeration unit[5]. Other materials consisted of 1-ml adjustable automatic pipets and 100-, 200-, and 500-μl pipets with disposable tips[6,7]; 7-ml glass disposable miniature liquid scintillation counting vials with glass minivial holders[8]; 10 × 75-mm disposable culture tubes[9]; and a moderate speed refrigerated centrifuge[10].

Methods—*Animal Study*—Sixteen male beagle dogs, 9.5–17.2 kg, were placed in a randomized two-way crossover design. Blood samples were withdrawn from the jugular vein immediately prior to drug ad-

[1] Deltasone, 5-mg compressed tablet, The Upjohn Co.
[2] Delta-Cortef, 5-mg compressed tablet, The Upjohn Co.
[3] Bio-Solv, Beckman Instrument Co.
[4] Liquifluor, New England Nuclear Corp.
[5] Model 2450 Tri-Carb liquid scintillation spectrophotometer, Packard Instrument Co.
[6] Biopette, Bioschwartz.
[7] Microliter pipets, Eppendorf.
[8] Miniature holder and vials, Demuth Glass Co.
[9] Disposable culture tubes, Kimble Glass Co.
[10] Refrigerated centrifuge, International Equipment Co.

Carstensen, APhA Academy of Pharmaceutical Sciences, Washington, D.C., 1974.
(3) C. E. Capes, "Proceedings of Powtech 71," Harrgate, England, Powder Advisory Centre, London NW110GP, England, 1972, p. 149.
(4) H. Rumpf, in "Agglomeration," W. A. Knepper, Ed., Wiley, New York, N.Y., 1962, p. 379.
(5) C. E. Capes, *Powder Technol.*, **4**, 77(1971).
(6) W. B. Pietsch, *Can. J. Chem. Eng.*, **47**, 403(1971).
(7) W. B. Pietsch and H. Rumpf, *C. R. Colloq. Int. CHRS*, No. 160 2.3 (1966).
(8) D. M. Newitt and A. L. Papadopoulos, "Proceedings No. 55," The Fertilizer Society, London, England, 1959.
(9) V. C. Marshall, "Proceedings of Powtech 71," 1971, p. 123.
(10) C. F. Harwood and N. Pilpel, *J. Pharm. Sci.*, **57**, 478(1968).
(11) J. T. Carstensen, "Pharmaceutics of Solids," Badger Freund, Fond du Lac, Wis., 1974.
(12) D. Brooke, *J. Pharm. Sci.*, **64**, 1409(1975).
(13) G. Steiner, M. Patel, and J. T. Carstensen, *ibid.*, **63**, 1395(1974).
(14) J. T. Carstensen, "Pharmaceutics of Solids," Badger Freund, Fond du Lac, Wis., 1974, p. 93.
(15) W. A. Gray, "The Packing of Solid Particles," Chapman & Hall, London, England, 1968, p. 125.
(16) S. Toyoshima, S. Watanabe, K. Matsuo, and M. Kasai, *Yakugaku Zasshi*, **91**, 1088(1971).

ACKNOWLEDGMENTS AND ADDRESSES

Received January 28, 1975, from *Merrell-National Laboratories, Cincinnati, OH 45214*

Accepted for publication September 10, 1975.

* Present address: School of Pharmacy, University of Wisconsin, Madison, WI 53706

ˣ To whom inquiries should be directed.

Comparative Serum Prednisone and Prednisolone Concentrations following Prednisone or Prednisolone Administration to Beagle Dogs

W. A. COLBURN *, C. R. SIBLEY, and R. H. BULLER ˣ

Abstract □ The relative serum prednisone and prednisolone concentrations were determined following the administration of prednisone or prednisolone as 5-mg tablets to male beagle dogs. Serum prednisone concentrations were significantly greater following prednisone administration than they were following prednisolone administration. Serum prednisolone concentrations were significantly greater following treatment with prednisolone than with prednisone. The combined prednisone and prednisolone areas under the serum concentration–time curves were similar for the two treatments.

Keyphrases □ Prednisone—serum concentration after administration of prednisone or prednisolone, radioimmunoassay, dogs □ Prednisolone—serum concentration after administration of prednisolone or prednisone, radioimmunoassay, dogs □ Bioavailability—prednisone and prednisolone, serum radioimmunoassay, dogs □ Glucocorticoids—prednisone and prednisolone, serum radioimmunoassay, dogs

With the advent of radioimmunoassays for both prednisone and prednisolone (1, 2), a unique opportunity arose to investigate the interconversion of prednisone and prednisolone in many experimental animals and in humans. In the present study, male beagle dogs were chosen as the test animal.

Previously, the conversion and interconversion of prednisone and prednisolone had been studied by tedious, time-consuming, and often difficult methods (3–7). With radioimmunoassays, the analyses could be conducted in just days without chromatography or separation steps.

The present study was conducted to investigate the interconversion of prednisone and prednisolone following the administration of 5-mg compressed tablets of prednisone[1] or prednisolone[2] to male beagle dogs.

EXPERIMENTAL

Materials—The buffers used were: tromethamine, 0.2 *M* and pH 8.0 (I), and sodium phosphate (monobasic and dibasic), 0.2 *M* and pH 6.5 (II). The tritiated steroids[3] were 6,7-^{3}H-prednisone at 40.0 Ci/mmole and 6,7-^{3}H-prednisolone at 45.4 Ci/mmole. The primary antiserums were rabbit antiprednisolone 21-hemisuccinate–bovine serum albumin (III) and rabbit antiprednisone 21-hemisuccinate–bovine serum albumin (IV).

Goat antirabbit serum or ammonium sulfate solution (80% saturated) was used as the precipitant. Analytical grade toluene-based liquid scintillation counting solution[3,4] was used, and the high capacity liquid scintillation spectrophotometer had a 4° refrigeration unit[5]. Other materials consisted of 1-ml adjustable automatic pipets and 100-, 200-, and 500-μl pipets with disposable tips[6,7]; 7-ml glass disposable miniature liquid scintillation counting vials with glass minivial holders[8]; 10 × 75-mm disposable culture tubes[9]; and a moderate speed refrigerated centrifuge[10].

Methods—*Animal Study*—Sixteen male beagle dogs, 9.5–17.2 kg, were placed in a randomized two-way crossover design. Blood samples were withdrawn from the jugular vein immediately prior to drug ad-

[1] Deltasone, 5-mg compressed tablet, The Upjohn Co.
[2] Delta-Cortef, 5-mg compressed tablet, The Upjohn Co.
[3] Bio-Solv, Beckman Instrument Co.
[4] Liquifluor, New England Nuclear Corp.
[5] Model 2450 Tri-Carb liquid scintillation spectrophotometer, Packard Instrument Co.
[6] Biopette, Bioschwartz.
[7] Microliter pipets, Eppendorf.
[8] Miniature holder and vials, Demuth Glass Co.
[9] Disposable culture tubes, Kimble Glass Co.
[10] Refrigerated centrifuge, International Equipment Co.

Table I—Quantity (Milliliters) of Solutions in Prednisolone Assay Tubes

	Total Count	Zero Control	Standard	Unknowns	References
Buffer	0.6	0.1	—	0.1	—
Standard in buffer	—	—	0.1	—	0.1
Antiprednisolone	—	0.5	0.5	0.5	0.5
^{3}H-Prednisolone	0.2	0.2	0.2	0.2	0.2
Blank dog serum	0.1	0.1	0.1	—	0.1
Unknown dog serum	—	—	—	0.1	—
Antirabbit serum	0.1	0.1	0.1	0.1	0.1
Totals	1.0	1.0	1.0	1.0	1.0

Table II—Quantity (Milliliters) of Solutions in Prednisone Assay Tubes

	Total Count	Zero Control	Standard	Unknowns	References
Buffer	0.2	0.1	—	0.1	—
Standard in buffer	—	—	0.1	—	0.1
Antiprednisone	—	0.1	0.1	0.1	0.1
^{3}H-Prednisone	0.2	0.2	0.2	0.2	0.2
Blank dog serum	0.1	0.1	0.1	—	0.1
Unknown dog serum	—	—	—	0.1	—
Ammonium sulfate	0.6	0.6	0.6	0.6	0.6
Totals	1.1	1.1	1.1	1.1	1.1

ministration and at 0.5, 1, 2, 3, 4, 6, 8, 12, and 24 hr after drug administration. Samples were allowed to clot for 45 min and then were centrifuged for 20 min. The serum layer was removed, placed in labeled tubes, and frozen at −20° until analysis.

The treatments used were designated: A, prednisolone, 5-mg tablet; and B, prednisone, 5-mg tablet. Eight dogs received prednisolone during the 1st week of the study and prednisone during the 2nd week. The eight dogs in the other group received the drugs in reverse order.

Prednisolone Assay—Prednisolone antiserum stock solution was stored frozen at 1:10 dilution in tromethamine buffer. A final dilution of 1:650 was used in the assay. Standard prednisolone[11] was used to prepare known concentrations of 0.5–128 ng/ml of the tromethamine buffer. The 12-ng/ml standard was used to maintain a reference control throughout the analyses. All standards were stored in screw-capped[12] vials at 4°. Goat antirabbit serum was used at a final dilution of 1:4 to precipitate the primary antibody. Dog serum samples were diluted 1:10 before analysis by radioimmunoassay.

In the specific analytical procedure, 10 × 75-mm glass disposable culture tubes were labeled for controls, standards, and unknown samples. One-half milliliter of the tromethamine buffer was added to the total radiation tubes while antiprednisolone was added to the standard, zero-control, reference, and unknown tubes. Then 0.1 ml of the tromethamine buffer was added to the total radiation, zero-control, and unknown sample tubes while 0.1 ml of diluted blank serum was added to the zero-control, total radiation, reference, and standard tubes.

The standard and reference tubes received 0.1 ml of the respective standard solutions ranging from 0.5 to 128 ng/ml. One-tenth-milliliter aliquots of the unknown samples were placed in the respective assay tubes. All assay tubes received 0.2 ml (5000 counts/min) of ^{3}H-prednisolone; then they were agitated and allowed to equilibrate for 2 hr at room temperature. One-tenth milliliter of appropriately diluted goat antirabbit serum was added to every assay tube. All tubes were again agitated and allowed to equilibrate overnight at 4°. The volumes of the solutions in each tube are listed in Table I.

Approximately 16 hr later, all tubes were centrifuged at 2000 rpm; 0.6 ml of the supernate (unbound fraction) was aspirated and placed in a minivial containing 5 ml of liquid scintillation counting solution. These samples were counted for 5 min in a suitable multiple-sample liquid scintillation spectrophotometer with the refrigeration unit set at 4°. Standard concentrations were plotted semilogarithmically, and the unknown concentrations were determined by interpolation from the maximum slope. The establishment of the standard curve and interpolation of results were accomplished by a computer program[13].

Prednisone Assay—Prednisone antiserum stock solution was stored at −20° at a dilution of 1:10 in the sodium phosphate buffer. A dilution of 1:100 was prepared immediately prior to use in the assay. Prednisone[14] was used to prepare standard concentrations ranging from 0.13 to 48 ng/ml in the sodium phosphate buffer. The 2-ng/ml standard was used as a reference standard throughout the analyses.

All standards were stored in screw-capped[12] vials at 4°. An 80% saturated ammonium sulfate solution was used to precipitate the primary antibody–antigen complex. The same dog serum samples that had been diluted 1:10 for the prednisolone assay were used in the prednisone assay.

Duplicate 10 × 75-mm glass disposable culture tubes were labeled for zero-control, reference standard, standard control, unknown sample, and total radiation tubes. Total radiation, zero-control, and unknown serum sample tubes received 0.1 ml of the sodium phosphate buffer, while the standard and reference tubes received 0.1 ml of their respective standard prednisone concentrations in this buffer. One-tenth-milliliter aliquots of diluted blank dog serum were added to all assay tubes except the unknown sample tubes; 0.1 ml of the diluted unknown dog serum was used in the unknown sample tubes. One-tenth milliliter of appropriately diluted antiprednisone serum was placed in all assay tubes except those labeled for total radiation, and the total radiation tubes received 0.1 ml of the sodium phosphate buffer.

All tubes received 0.2 ml of the sodium phosphate buffer containing 4000 cpm of ^{3}H-prednisone. All assay tubes were allowed to equilibrate for 2 hr at room temperature before 0.6 ml of 80% saturated ammonium sulfate solution was added. The tubes were allowed to incubate overnight at 4°. The total volumes of each solution in the tubes are given in Table II.

After about 16 hr, all tubes were centrifuged at 3000 rpm for 20 min at 4°. A 0.6-ml aliquot of the supernate (unbound fraction) was placed in a minivial containing 5 ml of counting solution. All vials were counted in a suitable liquid scintillation spectrophotometer for one 5-min period. Standard concentrations were plotted semilogarithmically, and the unknown serum sample concentrations were determined by interpolation from the standard curve. The plotting of the standard curve and interpolation of the unknown sample results were accomplished by a computer program[15].

RESULTS

All dog serum samples were collected and stored according to protocol. Prednisolone and prednisone assays were carried out on each

Table III—Physicochemical Parameters

Parameter	Prednisolone, 5-mg Compressed Tablet	Prednisone, 5-mg Compressed Tablet
Dissolution rate, T_{50}, min		
Mean	4.4	6.5
High	5.6	8.6
Low	3.8	5.5
Disintegration rate, T_{50}, min		
Mean	1.5	3.5
High	2.0	4.0
Low	1.0	2.3
Content uniformity, %		
Mean	99.2	99.5
High	103.8	102.4
Low	94.4	98.0

[11] Control reference standard prednisolone, The Upjohn Co.
[12] Lined with Teflon (du Pont).
[13] Curve-fitting and interpolating computer program, A. R. Lewis, The Upjohn Co.
[14] Control reference standard prednisone, The Upjohn Co.
[15] Computer program, A. R. Lewis, The Upjohn Co.

Table IV—Summary of Prednisolone Bioavailability Data

		Prednisolone, 5-mg Compressed Tablet (A)	Prednisone, 5-mg Compressed Tablet (B)	Statistically Significant Difference, Tukey's, $p < 0.05$
	Hours	Serum Levels, ng/ml		
Serum concentration, ng/ml, by hourly intervals	0.5	204	139	A > B
	1	242	205	N.S.[a]
	2	196	184	N.S.
	3	156	136	N.S.
	4	104	93	N.S.
	6	46	41	N.S.
	8	20	18	N.S.
	12	4	3	N.S.
	24	0	0	N.S.
Mean area under serum concentration–time curve, ng/ml × hr		986	855	A > B
Peak of mean serum concentration, ng/ml		242	205	N.S.
Mean individual peak serum concentration, ng/ml		273	234	N.S.
Mean peak time, hr		0.9	1.3	N.S.
Half-lives, hr		1.8	1.6	N.S.

[a] N.S. = not significant.

sample. The relative bioavailability of one lot of prednisolone and one lot of prednisone was determined by comparing mean areas under the serum concentration–time curves, mean peak serum concentrations, and mean times of the peak serum concentrations as well as other relevant parameters. The two lots were compared for prednisolone concentrations, prednisone concentrations, and combined concentrations. The physicochemical parameters of the two treatments, 5-mg prednisolone tablets and 5-mg prednisone tablets, are given in Table III.

Significantly different serum concentrations were observed in the early portions of the serum concentration–time curves. The prednisolone treatment was significantly greater than the prednisone treatment according to the prednisolone levels at 0.5 hr (Table IV). The prednisolone treatment was significantly less than the prednisone treatment at the 1- and 2-hr intervals according to the prednisone concentrations (Table V). The combined serum steroid levels were not statistically different throughout the blood level curves (Table VI).

The mean areas under the serum prednisolone concentration–time curves were 986 and 855 ng/ml × hr (Table IV and Fig. 1), the prednisone areas were 638 and 694 ng/ml × hr (Table V and Fig. 2), and the combined areas were 1624 and 1550 ng/ml × hr (Table VI and Fig. 3) for the prednisolone and prednisone treatments, respectively. There were statistically significant differences between the two treatments according to prednisone and prednisolone concentrations; but according to the combined areas, the two treatments were not statistically different.

Following prednisolone administration, the serum prednisolone levels were significantly greater than they were following prednisone administration. Serum prednisone levels were significantly greater following prednisone administration than they were following prednisolone administration. However, when comparing the combined areas under the serum concentration–time curves for the two steroids, no statistically significant differences were observed.

Mean peak serum prednisolone concentrations were 242 and 205 ng/ml (Table IV and Fig. 1) for the prednisolone and prednisone treatments, respectively. Mean peak concentrations were attained at 0.9 and 1.3 hr (Table IV) for the two treatments. Mean peak prednisone concentrations were 111 and 132 ng/ml for the prednisolone and prednisone treatments (Fig. 2), while peaks were attained

Table V—Summary of Prednisone Bioavailability Data

		Prednisolone, 5-mg Compressed Tablet (A)	Prednisone, 5-mg Compressed Tablet (B)	Statistically Significant Difference, Tukey's $p < 0.05$
	Hours	Serum Levels, ng/ml		
Serum concentration, ng/ml, by hourly intervals	0.5	53	74	N.S.[a]
	1	96	131	A < B
	2	111	132	A < B
	3	100	105	N.S.
	4	78	82	N.S.
	6	45	40	N.S.
	8	22	21	N.S.
	12	6	6	N.S.
	24	0	0	N.S.
Mean area under serum concentration–time curve, ng/ml × hr		638	694	A < B
Peak of mean serum concentration, ng/ml		111	132	A < B
Mean individual peak serum concentration, ng/ml		124	149	A < B
Mean peak time, hr		2.0	1.2	A > B
Half-lives, hr		2.2	2.3	N.S.

[a] N.S. = not significant.

Table VI—Combined Steroid Bioavailability Data Summary[a]

		Prednisolone, 5-mg Compressed Tablet	Prednisone, 5-mg Compressed Tablet
	Hours	Serum Levels, ng/ml	
Serum concentration, ng/ml, by hourly intervals	0.5	257	213
	1	338	336
	2	307	316
	3	256	241
	4	182	175
	6	91	81
	8	42	39
	12	10	9
	24	0	0
Mean area under serum concentration–time curve, ng/ml × hr		1624	1550
Peak of mean serum concentration, ng/ml		338	336
Mean individual peak serum concentration, ng/ml		397	383
Mean peak time, hr		1.5	1.3
Half-lives, hr		2.0	1.9

[a] Differences were not significantly different according to the Tukey test at the $p < 0.05$ level.

at 2.0 and 1.2 hr, respectively. Peak serum prednisone concentrations and times were significantly different according to Tukey's method of comparison. Mean peak combined concentrations were 338 and 336 ng/ml (Table VI) and peak times were 1.5 and 1.3 hr for the prednisolone and prednisone treatments, respectively.

The means of the individual peak concentrations were 273 and 234 ng/ml for prednisolone (Table IV), 124 and 149 ng/ml for prednisone (Table V), and 397 and 383 ng/ml for the combined levels for the prednisolone and prednisone treatments, respectively. The two values from the prednisone treatment were significantly different by Tukey's method of analysis.

No statistically significant differences for the half-lives were detected between the treatments. The half-lives were 1.8 and 1.6 hr for prednisolone (Table IV) and 2.2 and 2.3 hr for prednisone (Table V) for the prednisolone and prednisone treatments, respectively.

The areas under the serum prednisone concentration–time curves were only 65% as large as the serum prednisolone concentration–time curve areas for the prednisolone treatment. Concurrently, the serum prednisone concentration areas were 81% as large as the prednisolone areas under the curve for the prednisone treatment. The prednisone areas under the serum level curves were 87% as large for the prednisolone treatment as for the prednisone treatment. At the same time, the areas under the serum prednisolone concentration–time curves were 92% as great for the prednisone treatment as for the prednisolone treatment. The areas under the curves for prednisone were 28% less than the simultaneous prednisolone areas throughout the study. The combined steroid areas under the curves were 95% as large for the prednisone treatment as for the prednisolone treatment.

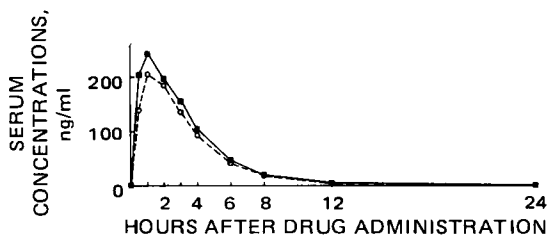

Figure 1—*Serum prednisolone concentration–time curves following oral administration of 5 mg of prednisolone (■) or prednisone (O) to 16 male beagle dogs.*

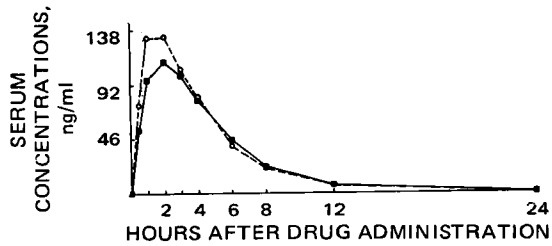

Figure 2—*Serum prednisone concentration–time curves following oral administration of 5 mg of prednisolone (■) or prednisone (O) to 16 male beagle dogs.*

DISCUSSION

The bioavailability, interconversion rates, and metabolism of prednisone and prednisolone have long intrigued the scientific community (9–11). With the recent advent of radioimmunoassays for the quantitation of these two compounds in biological fluids, a unique opportunity became available. The preceding results were obtained using these two assay methods to establish the simultaneous serum prednisone and prednisolone concentrations in male beagle dogs following treatment with prednisone or prednisolone.

It is apparent from the hourly serum concentrations that the immediate availability of the drugs depends only slightly on which drug is administered, indicating that the biological interconversion is very rapid. However, in both cases, *i.e.*, serum prednisone and prednisolone concentrations, the predominant drug in the serum is the administered drug. The drug being administered reaches the circulatory system more quickly than does the major metabolite, even though the interconversion is rapid.

The areas under the serum concentration–time curves followed an identical pattern. Prednisolone areas under the curves were always greater than the concomitant prednisone areas, but the prednisone areas were greater following prednisone administration than they were following prednisolone treatment, and prednisolone areas were larger following prednisolone than they were following prednisone. The differences were statistically significant in both cases; but when the combined prednisone–prednisolone areas under the curves were compared, the areas were not significantly different between the two treatments.

Peak serum concentrations were approximately two times as great for prednisolone as they were for prednisone regardless of the treatment. Peak serum prednisone concentrations were significantly higher following prednisone administration than they were following prednisolone administration. The differences in peak serum prednisolone concentrations were not statistically different with respect to treatment, and the combined prednisone–prednisolone peak serum concentrations were essentially equal.

Although the area under the serum concentration–time curve for prednisone was only 13% less for the prednisolone treatment than for the prednisone treatment, the areas were significantly different according to Tukey's method of analysis. This result was possible be-

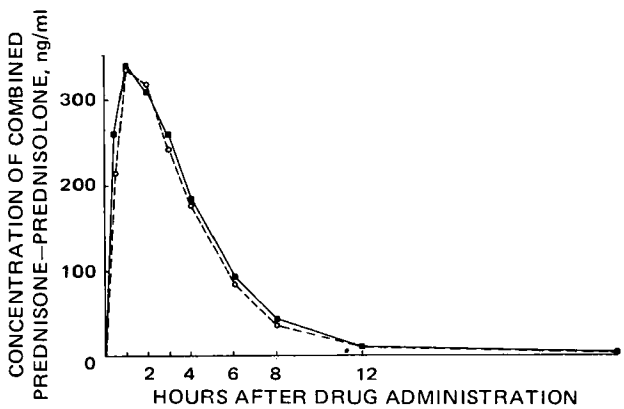

Figure 3—*Combined serum prednisolone and prednisone concentration–time curves. Key: ■, prednisolone treatment, and O prednisone treatment.*

cause of the extremely low overall coefficient of variation. The variation, including assay variation and intra- and intersubject variations, for the prednisone data was 15%. A statistically significant difference was found between the two treatments according to prednisolone data as well. Again, even though the observed difference was only 8% between the two treatments, significance was established and was attributed to the excessively low overall coefficient of variation (12%). The combined prednisone–prednisolone areas under the serum concentration–time curves were not different between the two treatments.

There was a consistent difference between treatments by both methods of analysis. However, the amount of synthetic steroid available following each treatment was essentially the same. Prednisolone was always present in larger quantities than was prednisone, regardless of the drug administered. The relative levels of prednisolone to prednisone, prednisolone to administered drug, and prednisone to administered drug in serum were dependent on which drug was administered. Contrary to previously published studies (8–11), prednisone areas under the serum concentration–time curves were greater following prednisone administration than they were after prednisolone administration, while prednisolone areas were greater following prednisolone treatment than they were following prednisone administration. The predominating steroid in serum was prednisolone, even though the relative serum levels were dependent on the administered drug.

Although there were statistically significant differences under the serum concentration–time curves between the two treatments, the therapeutic significance is difficult to assess. Both of these anti-inflammatory steroids are used on a chronic multiple-dose basis. The clinician establishes the dosing regimen by titrating the dose to a therapeutic end-point, *i.e.*, remission of symptoms. Even if these results were confirmed in humans, it would be difficult to establish that an 8 or 13% difference in total area under the serum concentration–time curve would actually be significant in the clinical situation.

REFERENCES

(1) W. A. Colburn and R. H. Buller, *Steroids*, **21**, 833(1973).

(2) W. A. Colburn, *ibid.*, **24**, 95(1974).

(3) D. H. Sandberg, C. Z. Bacallao, and W. W. Cleveland, *Biochem. Med.*, **4**, 383(1970).

(4) R. K. Sarim, G. M. Connel, and J. A. Linfoot, *Anal. Biochem.*, **41**, 265(1971).

(5) G. E. Bacon, *J. Lab. Clin. Med.*, **73**, 1030(1969).

(6) A. Vermeulen, *J. Clin. Endocrinol. Metab.*, **16**, 163(1956).

(7) L. W. Powell and E. Axelsen, *Gut*, **13**, 690(1972).

(8) I. E. Bush and V. B. Mahesh, *Biochem. J.*, **93**, 236(1964).

(9) E. Caspi and M. M. Pechet, *J. Biochem.*, **230**, 843(1958).

(10) C. H. Gray, M. A. S. Green, N. J. Holness, and J. B. Lunnon, *J. Endocrinol.*, **14**, 146(1956).

(11) A. Vermeulen, *ibid.*, **18**, 278(1959).

ACKNOWLEDGMENTS AND ADDRESSES

Received November 25, 1974, from *Control Analytical Research and Development, The Upjohn Company, Kalamazoo, MI 49001*

Accepted for publication September 24, 1975.

Presented at the APhA Academy of Pharmaceutical Sciences, New Orleans meeting, November 1974.

* Present address: Department of Pharmaceutics, School of Pharmacy, State University of New York at Buffalo, Buffalo, NY 14214

ˣ To whom inquiries should be directed.

Nonlinear Pharmacokinetic Model of Intravenous Anesthesia

PETER P. GILLIS *ˣ, ROBERT J. DeANGELIS *, and RICHARD L. WYNN ‡

Abstract □ A nonlinear pharmacokinetic model was constructed to describe the body distribution of intravenous anesthetics, using the physiological modeling approach for drug distribution kinetics. The model considers the physiological parameters of tissue volumes and blood flow rates for the standard four phases of blood, viscera, lean tissue, and adipose tissue and also the associated drug parameters known to influence drug distribution. A simple ramp function having a characteristic time (volume per flow rate) is used to describe the rate of approach to equilibrium conditions for each tissue phase. The model was evaluated for the distribution of methohexital and thiopental by comparing calculated values to experimental drug concentrations taken from the literature. The physiological alteration of obesity also was programmed into the model to evaluate its capability for predicting the influence of body alterations on drug distribution. The results indicated that a preliminary mathematical model of relatively simple design is capable of at least a semiquantitative prediction of intravenous anesthetic drug concentrations in body tissues and has the potential of accounting for differences in drug distribution in the presence of selected physiological alterations.

Keyphrases □ Anesthesia, intravenous—distribution, nonlinear pharmacokinetic model described, methohexital and thiopental □ Pharmacokinetic models, nonlinear—described for intravenous anesthetics methohexital and thiopental □ Distribution, drug—intravenous anesthesia, nonlinear pharmacokinetic model described

Induction, maintenance, and recovery during intravenous anesthesia are dependent upon the amounts of anesthetic agent within the brain tissues after dosing and are functions of the amounts of drug in the plasma. Alterations in body distribution processes controlling drug levels in the brain and plasma can influence the dosages required for anesthesia and may explain many ineffective dose regimens for these drugs.

Clinical use of methohexital and thiopental for anesthesia in dental patients has indicated some conditions that can alter the tissue levels of these anesthetics to result in enhanced potency or prolonged narcosis after normal induction doses. These conditions include dehydration (1), uremia (2), peripheral circulatory failure (2), increased cardiac output (2), electrolyte disturbances (2), hepatic failure (2), and chronic renal failure (3).

Attempts have been made to describe the pharma-

cause of the extremely low overall coefficient of variation. The variation, including assay variation and intra- and intersubject variations, for the prednisone data was 15%. A statistically significant difference was found between the two treatments according to prednisolone data as well. Again, even though the observed difference was only 8% between the two treatments, significance was established and was attributed to the excessively low overall coefficient of variation (12%). The combined prednisone–prednisolone areas under the serum concentration–time curves were not different between the two treatments.

There was a consistent difference between treatments by both methods of analysis. However, the amount of synthetic steroid available following each treatment was essentially the same. Prednisolone was always present in larger quantities than was prednisone, regardless of the drug administered. The relative levels of prednisolone to prednisone, prednisolone to administered drug, and prednisone to administered drug in serum were dependent on which drug was administered. Contrary to previously published studies (8–11), prednisone areas under the serum concentration–time curves were greater following prednisone administration than they were after prednisolone administration, while prednisolone areas were greater following prednisolone treatment than they were following prednisone administration. The predominating steroid in serum was prednisolone, even though the relative serum levels were dependent on the administered drug.

Although there were statistically significant differences under the serum concentration–time curves between the two treatments, the therapeutic significance is difficult to assess. Both of these anti-inflammatory steroids are used on a chronic multiple-dose basis. The clinician establishes the dosing regimen by titrating the dose to a therapeutic end-point, *i.e.*, remission of symptoms. Even if these results were confirmed in humans, it would be difficult to establish that an 8 or 13% difference in total area under the serum concentration–time curve would actually be significant in the clinical situation.

REFERENCES

(1) W. A. Colburn and R. H. Buller, *Steroids*, **21**, 833(1973).

(2) W. A. Colburn, *ibid.*, **24**, 95(1974).

(3) D. H. Sandberg, C. Z. Bacallao, and W. W. Cleveland, *Biochem. Med.*, **4**, 383(1970).

(4) R. K. Sarim, G. M. Connel, and J. A. Linfoot, *Anal. Biochem.*, **41**, 265(1971).

(5) G. E. Bacon, *J. Lab. Clin. Med.*, **73**, 1030(1969).

(6) A. Vermeulen, *J. Clin. Endocrinol. Metab.*, **16**, 163(1956).

(7) L. W. Powell and E. Axelsen, *Gut*, **13**, 690(1972).

(8) I. E. Bush and V. B. Mahesh, *Biochem. J.*, **93**, 236(1964).

(9) E. Caspi and M. M. Pechet, *J. Biochem.*, **230**, 843(1958).

(10) C. H. Gray, M. A. S. Green, N. J. Holness, and J. B. Lunnon, *J. Endocrinol.*, **14**, 146(1956).

(11) A. Vermeulen, *ibid.*, **18**, 278(1959).

ACKNOWLEDGMENTS AND ADDRESSES

Received November 25, 1974, from *Control Analytical Research and Development, The Upjohn Company, Kalamazoo, MI 49001*

Accepted for publication September 24, 1975.

Presented at the APhA Academy of Pharmaceutical Sciences, New Orleans meeting, November 1974.

* Present address: Department of Pharmaceutics, School of Pharmacy, State University of New York at Buffalo, Buffalo, NY 14214

ˣ To whom inquiries should be directed.

Nonlinear Pharmacokinetic Model of Intravenous Anesthesia

PETER P. GILLIS *ˣ, ROBERT J. DeANGELIS *, and RICHARD L. WYNN ‡

Abstract □ A nonlinear pharmacokinetic model was constructed to describe the body distribution of intravenous anesthetics, using the physiological modeling approach for drug distribution kinetics. The model considers the physiological parameters of tissue volumes and blood flow rates for the standard four phases of blood, viscera, lean tissue, and adipose tissue and also the associated drug parameters known to influence drug distribution. A simple ramp function having a characteristic time (volume per flow rate) is used to describe the rate of approach to equilibrium conditions for each tissue phase. The model was evaluated for the distribution of methohexital and thiopental by comparing calculated values to experimental drug concentrations taken from the literature. The physiological alteration of obesity also was programmed into the model to evaluate its capability for predicting the influence of body alterations on drug distribution. The results indicated that a preliminary mathematical model of relatively simple design is capable of at least a semiquantitative prediction of intravenous anesthetic drug concentrations in body tissues and has the potential of accounting for differences in drug distribution in the presence of selected physiological alterations.

Keyphrases □ Anesthesia, intravenous—distribution, nonlinear pharmacokinetic model described, methohexital and thiopental □ Pharmacokinetic models, nonlinear—described for intravenous anesthetics methohexital and thiopental □ Distribution, drug—intravenous anesthesia, nonlinear pharmacokinetic model described

Induction, maintenance, and recovery during intravenous anesthesia are dependent upon the amounts of anesthetic agent within the brain tissues after dosing and are functions of the amounts of drug in the plasma. Alterations in body distribution processes controlling drug levels in the brain and plasma can influence the dosages required for anesthesia and may explain many ineffective dose regimens for these drugs.

Clinical use of methohexital and thiopental for anesthesia in dental patients has indicated some conditions that can alter the tissue levels of these anesthetics to result in enhanced potency or prolonged narcosis after normal induction doses. These conditions include dehydration (1), uremia (2), peripheral circulatory failure (2), increased cardiac output (2), electrolyte disturbances (2), hepatic failure (2), and chronic renal failure (3).

Attempts have been made to describe the pharma-

cokinetics of intravenous anesthetics to predict the effects of altered body distribution processes on subsequent tissue levels. Gibaldi *et al.* (4) described the body distribution of thiamylal, ketamine, and phencyclidine according to the compartmental analysis presented by Wagner (5). Ketamine and phencyclidine were described according to a one-compartment open model and thiamylal according to a two-compartment open model.

Another model described thiopental pharmacokinetics according to blood flow rates and the relative mass for various tissues (6). The drug concentrations predicted by the model in blood and fat tissues 25 min after a single intravenous dose compared favorably with those measured directly in a patient. Quantitative predictions of the effect of liver metabolism of thiopental on its rate of disappearance from plasma were reported using a similar pharmacokinetic model (7). This model suggested that an inhibition of liver metabolism of the drug would prolong the duration of anesthesia. It was also used to suggest that an increase in hepatic drug clearance would simultaneously decrease brain concentrations (8).

Bischoff and Dedrick (9) devised a more elaborate model, which included flow limitations, lipid solubility, protein binding, and metabolism, to make *a priori* predictions of the distribution of thiopental in four body regions: blood, viscera, lean tissue, and adipose tissue. Absolute values were obtained for drug concentrations *versus* time and were compared with literature data of thiopental distribution in dogs and humans. Subsequently (10), they expanded their analysis, using additional body regions, to study the effects of intravenous injections of methotrexate in mice. Although certain discrepancies did exist, overall prediction of trends was correct.

These findings seem to be consistent with evidence that pharmacokinetic models can be used to predict dosage adjustments in various therapeutic situations (11–13). Also, much clinical evidence supports the belief that past dosing problems experienced with methohexital and thiopental can be anticipated with other drugs used in intravenous sedation techniques in dentistry. Therefore, sufficient justification exists to investigate the applicability of pharmacokinetic modeling of some of these drugs in predicting dosage adjustments and the time course of action in specific therapeutic situations. Of particular concern was the development of an appropriate model to predict the recovery time phase of drug action in view of the wide use of intravenous sedation and anesthesia in ambulant patients undergoing dental procedures.

The results indicate that a preliminary mathematical model of relatively simple design is capable of at least a semiquantitative prediction of drug concentrations in body tissues after intravenous dosing and can account for hypothetical differences in drug distribution in the presence of a select physiological alteration.

METHODS

Model Structure—The model can be thought of as an interactive blood–drug–tissue system. The body is assumed to consist of a single compartment having an aqueous phase, blood, and three tissue types (visceral, lean, and adipose) into which a drug can distribute. Features common to each type of tissue are a volume and a rate at which blood flows through it. These are denoted as V_sQ_s, V_lQ_l, and V_pQ_p for visceral, lean, and adipose tissues, respectively. The ratio of volume to rate establishes an estimate of the time required for equilibrium conditions to be achieved between the blood and the corresponding tissue.

The chief characteristic assigned to the blood is homogeneity; that is, the drug concentration in the blood is uniform throughout all blood vessels and tissues. Another feature assigned to the blood is the reversible binding of the drug to plasma protein. The fraction of drug in the blood that is not bound to protein is denoted by $f_1 = C_b{}^f/C_b$, where $C_b{}^f$ is the free concentration and C_b is the total concentration of drug in the blood. Of the free portion, some is ionized according to drug pKa and blood pH. The ionized fraction is denoted by $f_2 = C_b^{\text{ionized}}/C_b{}^f$. The effective free concentration is the nonionized free concentration, $(1 - f_2)C_b{}^f$, which is denoted by C^*. The fraction of drug reversibly bound to plasma protein at equilibrium is given by the nonlinear relationship:

$$C_b{}^b = C^*K_bB_b/(1 + C^*K_b) + C^*K_b'B_b'/(1 + C^*K_b') \quad \text{(Eq. 1)}$$

assuming two different families of binding sites as described by Gillette (14). Here the total concentration of drug in the blood is $C_b = C_b{}^f + C_b{}^b$, the sum of free and protein-bound drug; B_b and B_b' are the numbers of the two types of binding sites per liter of blood; and K_b and K_b' are the corresponding association constants, having the dimensions of inverse concentration.

A feature common to the lean and visceral tissues is that drug absorption from the blood follows a reversible protein binding relationship identical in form to Eq. 1. For lean tissue:

$$C_l = f_lC^*K_lB_l/(1 + C^*K_l) + f_lC^*K_l'B_l'/(1 + C^*K_l') \quad \text{(Eq. 2)}$$

where C_l is the drug concentration in the lean tissue, C^* is the effective free concentration of the drug in blood, B_l and B_l' are the numbers of binding sites per liter of tissue, and K_l and K_l' are the corresponding association constants. The fraction f_l describes the rate of approach to equilibrium. For this model, f_l is taken to be a simple ramp function of the characteristic time V_l/Q_l. The form of f_l is illustrated in Fig. 1. Similarly, in the visceral tissue:

$$C_s = f_sC^*K_sB_s/(1 + C^*K_s) + f_sC^*K_s'B_s'/(1 + C^*K_s') \quad \text{(Eq. 3)}$$

where the notation is as in Eq. 2 and f_s is a simple ramp function that reaches unity at time V_s/Q_s.

A feature unique to the visceral tissue is liver metabolism. This process is accounted for by assigning a separate flow rate, Q_r, through the liver. Obviously, Q_r is some fraction of Q_s. A reaction rate constant, K_r, is then assigned to describe what fraction of the available drug passing through the liver, *i.e.*, C^*Q_r, is metabolized. If the amount metabolized is denoted by A_r, then:

$$dA_r/dt = C^*Q_rK_r \quad \text{(Eq. 4)}$$

The adipose tissue absorbs drug from the blood according to the drug's lipid solubility. The average concentration of drug, C_p, in lipid cells at equilibrium is related to the free concentration in the blood through the lipid solubility, K_p, customarily defined as $K_p = C_p/C_b{}^f$. The concentration C_p at any time is assumed to be:

$$C_p = f_pK_pC_b{}^f \quad \text{(Eq. 5)}$$

where f_p is a ramp function of the type shown in Fig. 1 and has the characteristic time V_p/Q_p.

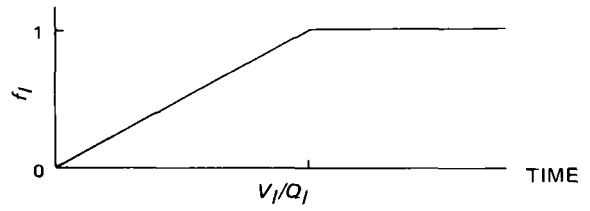

Figure 1—*Simple ramp function having a characteristic time (volume per flow rate) used to describe the rate of approach to equilibrium in the different tissue phases. The specific illustration is for the lean tissue, but similar ramp functions having correspondingly different characteristic times are used for visceral and adipose tissues.*

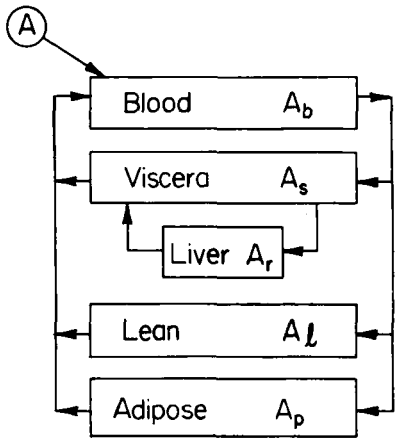

Figure 2—*Schematic representation of the present model: distribution of an initial amount of drug* (A) *to blood and tissue phases after initial dosing.*

For an initial drug dosage of amount A, the amount A_b remaining in the blood at any subsequent time is a function of the amounts of drug existing in the visceral tissues (A_s), lean tissues (A_l), and adipose tissues (A_p) and the amount metabolized by the liver (A_r) (Fig. 2).

The amount A_b at any time is found from the relationships describing amounts in other tissues:

$$A_s = C_s V_s \quad \text{(Eq. 6)}$$

$$A_r = \int_0^t (dA_r/dt)\, dt \quad \text{(Eq. 7)}$$

$$A_l = C_l V_l \quad \text{(Eq. 8)}$$

$$A_p = C_p V_p \quad \text{(Eq. 9)}$$

and the conservation relationship:

$$A_b = A - A_s - A_r - A_l - A_p \quad \text{(Eq. 10)}$$

Thus, the concentration of drug in the blood at any time is:

$$C_b = A_b/V_b \quad \text{(Eq. 11)}$$

Since Eq. 7 is merely a restatement of Eq. 4, it is clear that Eqs. 1–11 form a set of 10 simultaneous equations with the 10 variables C_b, $C_b f$, C_l, C_s, C_p, A_s, A_r, A_l, A_p, and A_b. These equations are fairly complex but can be easily handled by a computer.

The computer program[1] to solve this system of equations is written in CSMP (15, 16). This language is particularly convenient for investigating the time-dependent response of systems and has three built-in features useful in the present application. The special call LIMIT provides the ramps f_l, f_s, and f_p. The special call INTGRL integrates the differential Eq. 4 using a standard Runge–Kutta technique (17). The special call IMPL solves the simultaneous equations by a simple technique of successive approximations (17).

Parameters—Initial computer studies were performed on the distribution of methohexital and thiopental. Table I shows the physicochemical parameters and Table II shows values of tissue volumes, *etc.*, for a 70-kg man. The binding site concentrations and association constants are shown in Table III. Binding site concentrations are for the binding of thiopental by bovine albumin. It was assumed that these values, determined by Goldbaum and Smith (20), were appropriate for the binding of both thiopental and methohexital by plasma protein. These investigators also gave corresponding association constants for thiopental, but their values were somewhat at variance with the values of f_1 cited in Table I. Hence, the procedure adopted for determining the association constants shown in Table III was to: (*a*) select the first (K) on the basis of the results of Goldbaum and Smith and (*b*) calculate the second (K') using Eq. 1 and the corresponding values of f_1 from Table I for methohexital and thiopental.

Table I—Physicochemical Values for Methohexital and Thiopental (18)

Parameter	Methohexital	Thiopental
Protein binding, unbound fraction of drug in plasma, f_1	0.27	0.25
Ionization:		
pKa	7.9	7.6
Fraction of unbound drug ionized at pH 7.4, f_2	0.24	0.39
Lipid solubility, K_p	65	89

Table II—Values of Parameters Used to Describe the Four-Phase Model of the Blood–Tissue System for a 70-kg Man (19)

Tissue Volumes	Liters
Blood, V_b	5.4
Viscera, V_s	6.2
Lean, V_l	39.2
Adipose, V_p	12.2
Blood Flow Rates in Tissues	**Liters per Minute**
Viscera, Q_s	4.08
Lean, Q_l	1.28
Adipose, Q_p	0.26
Liver, Q_r	1.50

Since no corresponding data were available for visceral and lean tissues, the values B_s, B_s', . . . , K_l, K_l' remain as adjustable parameters in the model. In the calculations, these parameters are given the values listed in Table III. All remaining parameters are given in Table IV.

Results from a study of rats[2] indicated that the effective blood flow rate for adipose tissue may be similar to that for lean tissue in contrast to the value $Q_p = 0.26$ given in Table II. The plausibility of this postulate can be advocated from consideration of the usual interpenetrating configuration of adipose and lean tissues. The effective flow rate for the adipose tissue is the rate at which drug is made available for lipid dissolution. Thus, it may be that blood is brought to the lipid cells mainly through lean tissue "channels" so that the drug absorption rate is fixed by Q_l rather than by the flow rate Q_p. Consequently, two separate cases are treated in the initial calculations that follow; one is identified as $Q_p = 0.26$ (the Table II value) and the other is defined as $Q_p = Q_l$.

RESULTS

An initial goal of this study was to compare results calculated using the foregoing model to experimental drug concentrations, determined by Sunshine *et al.* (21), for methohexital. Such comparisons would be meaningful only at times for which the drug is relatively uniformly mixed in the blood. For example, the maximum blood concentration for the present model is A/V_b and occurs at time zero because of the assumed homogeneity of the blood compartment. Sunshine *et al.* (21), however, showed concentrations increasing from zero to values sub-

Table III—Values of Protein Binding Site Concentrations and Corresponding Association Constants[a]

Parameter	Value
B	870 mg/liter
B'	52 mg/liter
K	1.2×10^{-3} liters/mg
K' Methohexital	3.3×10^{-2} liters/mg
K' Thiopental	3.9×10^{-2} liters/mg

[a] From Ref. 20

[1] A listing of the program is available on request.

[2] To be published.

Table IV—Values of Remaining Parameters Used in the Present Calculations

Parameter	Value
Liver metabolism, K_r	1.0
Initial dose rate, A	2 mg/kg
Variations used in simulation of obesity:	
V_p	75.2 liters
Weight	140 kg
A (first computation)	1 mg/kg
A (second computation)	2 mg/kg

stantially larger than A/V_b during the 1st min after the start of injection. Therefore, it is conjectured that this elementary model is necessarily restricted to describing redistributions at times greater than the time in which the concentration of drug in the blood becomes relatively uniform. Based on the parameters, the calculations, and the cited experimental results, this restriction seems to be at times greater than approximately 1 min.

Figure 3 shows the calculated variations of methohexital concentration in the blood of a 70-kg man as a function of time for the two cases $Q_p = 0.26$ and $Q_p = Q_l$. The initial dosage was taken as 140 mg or 2 mg/kg. The values observed by Sunshine *et al.* (21), shifted (arbitrarily) by 1 min on the time scale, also are given. On this basis, calculated results are in fair agreement with the experimental observations.

The two sets of calculations, however, differ noticeably. The experimental data fall mainly between the two calculated curves and decidedly nearer the case $Q_p = Q_l$. The difference in drug concentration shown in Fig. 3 for the two cases is more predominant in the results for the visceral and adipose tissue concentrations (Figs. 4 and 5). Thus, a selection probably can ultimately be made between these two cases based upon experimental measurements of tissue concentrations.

Both the concentration and total amount of drug in lean tissue is never very large according to the model. Also, according to the calculations, the total amounts of methohexital metabolized during the 1st hr after injection are: (*a*) $Q_p = 0.26$, $A_r^{60} = 28$ mg or 20% of A, the administered dose; and (*b*) $Q_p = Q_l$, $A_r^{60} = 15$ mg or 11% of A.

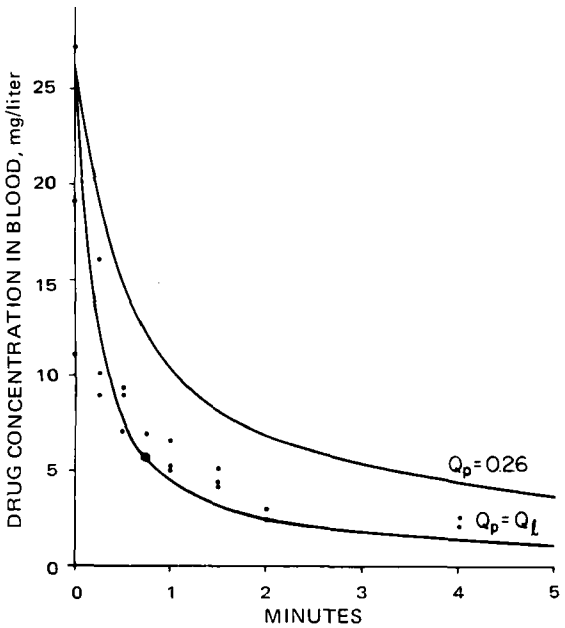

Figure 3—*Methohexital concentration in the blood* versus *time, calculated according to the model for the two cases* $Q_p = 0.26$ *and* $Q_p = Q_l$. *Curves denote calculated values; points are comparable experimental results (21).*

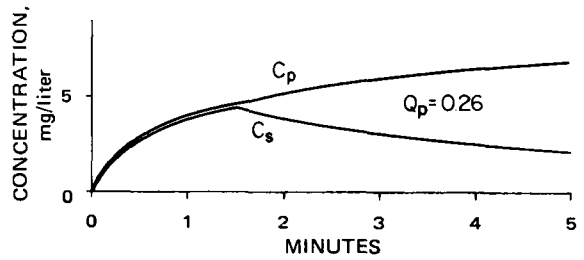

Figure 4—*Methohexital concentrations in adipose and visceral tissues* versus *time, calculated according to the model for the case* $Q_p = 0.26$.

In calculating the effect of liver metabolism, K_r was assumed to have the value of unity. Because the rate of metabolism is proportional to the nonionized free blood concentration, it varies as the blood concentration changes. Therefore, the rate in the model is greatest immediately following intravenous injection when the serum concentration is greatest. Subsequently, the metabolic rate decreases as drug is transferred from the blood to the tissue phases. Ultimately, most drug is stored in adipose tissue from which it slowly returns to the bloodstream and is metabolized by the liver. These calculated results for methohexital metabolism are in general agreement with the experimental observations of Brand *et al.* (18).

Figure 6 shows results calculated for thiopental using the parametric changes indicated in Tables I and III and restricted to the one case $Q_p = 0.26$. When comparing these results to the same case for methohexital, the differences to be noted are: the concentration of drug in the blood decays somewhat more rapidly for thiopental than for methohexital, the adipose tissue concentration is slightly higher for thiopental, and the peak visceral tissue concentration is 21% less for thiopental for the same initial dosage.

For the same liver reaction rate constant, $K_r = 1$, the amounts of thiopental metabolized are decidedly less than methohexital at corresponding times, *e.g.*, 14% of the administered dose during the 1st hr after injection with thiopental compared to 20% with methohexital. This finding also is in general agreement with the experimental observations of Brand *et al.* (18).

The effect of obesity was studied using the present model. In the absence of direct experimental data, it was decided to represent the hypothetical obese subject in the following way. The sum of phase volumes for the normal 70-kg man is 63 liters according to Table II. It was assumed that an obese subject had twice the normal weight—*viz.*, 140 kg, and twice the normal volume. It was further assumed that the entire added volume, 63 liters, was additional adipose tissue so that V_p has the value (12.2 + 63 =) 75.2 liters for the obese subject.

The effect on the obese subject of the same total initial dose of methohexital as used in the previous calculations for a normal subject, 140 mg, was computed. The peak value of drug concentration in the visceral tissue was the same in both calculations, but the subsequent decrease in visceral concentration was more rapid in the obese computation for both $Q_p = 0.26$ and $Q_p = Q_l$. Next the two subjects were compared on the basis of a total initial dose of 2 mg/kg, so the obese subject received 280 mg. This dose produced a peak concentration

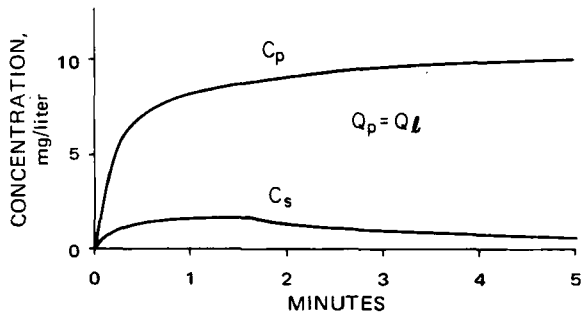

Figure 5—*Methohexital concentrations in adipose and visceral tissues* versus *time, calculated according to the model for the case* $Q_p = Q_l$.

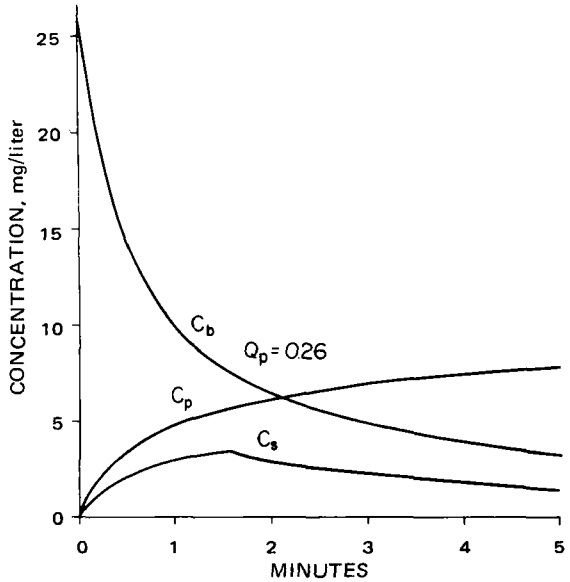

Figure 6—*Thiopental concentrations in blood, adipose tissue, and visceral tissue, calculated according to the model for the case* Q_p = *0.26.*

in the visceral tissue that was twice the previous value, again for the two cases of effective adipose tissue flow rates.

DISCUSSION

The described model is of the generalized nonlinear type discussed by Wagner (22), using the physiological modeling approach for drug distribution kinetics. The physiological parameters and the physicochemical drug parameters required by the model are similar to those used by Bischoff and Dedrick (9). Differences exist from their model, however, primarily in the fundamental assumptions made and in the manner of incorporating time dependence early in the analysis. Bischoff and Dedrick assumed an instantaneous equilibrium between blood and tissue in each body region, with redistributions resulting from the addition of drug to the blood phase during initial dosing and the mixing of blood of different drug concentrations from the different tissue phases. In the present model, it was assumed that equilibrium conditions in each tissue phase are approached in a simple, linear manner, with characteristic times determined by tissue volumes and blood flow rates. This model distinguishes between equilibrium drug concentrations in tissue phases and the volumes of blood associated with each phase.

The model was initially evaluated using methohexital as the prototype of other intravenous drugs to be considered for future analysis. The behavior of the model after intravenous injection is as follows. At time zero, the drug is wholly absorbed in the blood. Thereafter, rapid redistribution occurs in which most drug is dissolved by lipid cells, although a substantial amount becomes bound to visceral protein rather quickly. As the blood concentration decreases, reabsorption of drug from the visceral tissue is fairly rapid. The large amount of drug dissolved in adipose tissue is reabsorbed by the blood at a much slower rate and gradually removed from the blood by liver metabolism.

For the case treating the faster effective flow rate to adipose tissue ($Q_p = Q_l$), the effects of lipid solubility are more pronounced: blood concentration decreases more rapidly, visceral concentration does not reach as high a level, and the total amount of drug absorbed by lipid cells is much greater. According to the model, neither the concentration nor the total amount of drug in the lean tissue is ever very large. This condition results from the characteristic time for reaching equilibrium in lean tissue, V_l/Q_l, being relatively long (0.5 hr), so the blood flowing through the tissue has a very low drug concentration by that time. The same situation would occur in the visceral tissue were it not for the very short characteristic time, V_s/Q_s (1.5 min) for this tissue phase to equilibrate with the blood; at that time the blood is still fairly high in drug concentration.

The appropriateness of the model to describe the distribution of other intravenous drugs was tested by calculating the distribution kinetics of thiopental, using the values of the physicochemical parameters known for this drug. Two values of thiopental differed markedly from methohexital: the fraction of unbound drug ionized at pH 7.4 and the lipid solubility coefficient, K_p. The former value was 0.39 for thiopental compared to 0.24 for methohexital, and the latter value was 89 for thiopental and 65 for methohexital. These values for thiopental, along with the slightly different values for the unbound fraction of thiopental in plasma and protein binding site association constants, significantly influenced the calculated values of thiopental distribution. The results for thiopental showed a more rapid decrease in blood concentration, a higher concentration in adipose tissue, and a lower peak concentration in visceral tissue compared to methohexital for the same intravenous dose. These data support the suggestion by Brand *et al.* (18) that the greater potency and more rapid recovery from methohexital compared to thiopental were due to its slower decrease in blood levels and smaller accumulation in fat, allowing for more distribution to the brain tissue and subsequent faster elimination from the body.

By assuming K_r (the reaction rate constant describing what fraction of available drug passing through the liver is metabolized) to have a value of unity, the rate of liver metabolism was essentially a function of the changes in blood concentrations of the nonionized unbound drug fraction. Thus, the parametric changes for thiopental were expected to influence its calculated rate of metabolism. In fact, the calculated rates of thiopental and methohexital (14 and 20% of the administered dose, respectively, during the 1st hr) agreed favorably with experimental values (15 and 15–19%, respectively) reported by Brand *et al.* (18), a result providing confidence in the predictable nature of the model.

Obesity was selected as the physiological alteration for stressing the model because of the existence of accurate methods for obtaining values for this parameter in future studies (23, 24). In an obese subject of twice normal weight and volume, where the added volume was assumed to be all adipose tissue, the peak value of drug concentration in visceral tissue was the same after a 140-mg dose as that in the normal subject. If it is assumed that the visceral drug concentration reflects the same proportional brain concentration in both cases, the results indicate that an obese subject needs no additional increase in dose to provide similar brain levels. Thus, if the intravenous dose were based on the weight of the subject, more drug would be predicted to distribute in the viscera and, therefore, brain tissue.

This prediction was verified when the peak concentration of viscera of the obese subject was calculated to be twice that of the normal subject after 2 mg/kg iv. This observation is consistent with the fact that clinical induction doses of intravenous anesthetics are not derived on the basis of patient body weight but remain as established narrow dose ranges derived from the amounts of drug observed to produce clinical anesthesia.

The nonlinear pharmacokinetic model of intravenous anesthesia presented here seems capable of semiquantitative prediction of drug concentrations for times longer than about 1 min, using literature values for all parameters except the liver reaction rate constant. The two cases, $Q_p = 0.26$ and $Q_p = Q_l$, seem to provide lower and upper bounds, respectively, on the actual effective rate of drug delivery to adipose tissue within the framework of the present calculations. The strong points of this model are the simple ramp functions (Fig. 1) that provide an approximate description of the approach to equilibrium conditions in each tissue phase. The weak points are the oversimplifications incorporated in the simple ramp functions and the assumption of a single homogeneous phase to describe all of the blood throughout the body.

An improved model could easily be formulated by adding the gradual approach to equilibrium concept to the kinetics given by Bischoff and Dedrick (9) or to their more sophisticated, later analysis (10). However, it seems more reasonable at this stage to abandon the static law of mass action and to apply the elementary reaction rate theory to develop an improved model much in the spirit of Wagner (22).

Because the only easily controlled experimental variable besides total dosage is the rate at which the drug is administered, it is obviously important to develop an improved model in which the drug distribution at times less than 1 min can be adequately treated. Such a model can be studied and improved experimentally to develop values for its parameters that fit various actual situations. When this has been accomplished, one might justifiably assign some predictive capability to the model.

REFERENCES

(1) J. Waller, *Lancet*, **2**, 1129(1966).

(2) J. W. Dundee, *Br. J. Anaesth.*, **29**, 440(1957).

(3) F. G. Estafanous, J. K. Porter, M. Y. Tawil, and K. L. Popawniak, *Can. Anaesth. Soc. J.*, **20**, 769(1973).

(4) M. Gibaldi, G. Levy, and H. Weintraub, *Clin. Pharmacol. Ther.*, **12**, 734(1971).

(5) J. G. Wagner, *J. Mond. Pharm.*, **14**, 279(1971).

(6) H. L. Price, P. J. Kounat, J. N. Safer, E. H. Conner, and M. L. Price, *Clin. Pharmacol. Ther.*, **1**, 16(1960).

(7) L. J. Saidman and E. I. Eger, *Anesthesiology*, **27**, 118(1966).

(8) L. J. Saidman and E. I. Eger, *Clin. Pharmacol. Ther.*, **14**, 12(1973).

(9) K. B. Bischoff and R. L. Dedrick, *J. Pharm. Sci.*, **57**, 1346(1968).

(10) K. B. Bischoff, R. L. Dedrick, and D. S. Zaharko, *ibid.*, **59**, 149(1970).

(11) R. W. Jelliffe, *Ann. Intern. Med.*, **69**, 703(1968).

(12) K. B. Bischoff and R. L. Dedrick, *Proc. Ann. Cont. Eng. Med. Biol.*, **1967**, 86.

(13) R. L. Dedrick and K. B. Bischoff, *Chem. Eng. Prog. Symp. Ser. No. 84*, **64**, 32(1968).

(14) J. R. Gillette, *Proc. Int. Pharmacol. Mtg., 2nd*, **4**, 9(1963).

(15) IBM Publication H20-0307-2 System/360 Continuous System Modeling Program (300A-CS-16X) User's Manual, 1968.

(16) IBM Publication H20-0240-2 System/360 Continuous System Modeling Program (360A-CX-16X) Application Description, 1968.

(17) J. Walsh, "Numerical Analysis," Thompson Book Co., Washington, D.C., 1967.

(18) L. Brand, L. C. Mark, M. McM. Snell, P. Urindten, and P. G. Dayton, *Anesthesiology*, **24**, 331(1963).

(19) W. W. Mapelson, *J. Appl. Physiol.*, **18**, 197(1961).

(20) L. R. Goldbaum and P. K. Smith, *J. Pharmacol. Exp. Ther.*, **111**, 197(1954).

(21) I. Sunshine, J. G. Whitman, W. W. Fike, B. Finkle, and J. Lebeau, *Br. J. Anaesth.*, **38**, 23(1966).

(22) J. G. Wagner, *J. Pharmacokinet. Biopharm.*, **1**, 363(1973).

(23) J. Brozek, F. Grande, J. T. Anderson, and A. Keys, *Ann. N.Y. Acad. Sci.*, **110**, 113(1963).

(24) A. W. Sloan, *J. Appl. Physiol.*, **23**, 311(1967).

ACKNOWLEDGMENTS AND ADDRESSES

Received May 19, 1975, from the *Department of Metallurgical Engineering & Materials Science and the †Department of Oral Biology, University of Kentucky, Lexington, KY 40506

Accepted for publication September 24, 1975.

Supported by University of Kentucky General Research Grant A3W45.

[x] To whom inquiries should be directed.

CSTRIP, a Fortran IV Computer Program for Obtaining Initial Polyexponential Parameter Estimates

ALLEN J. SEDMAN * and JOHN G. WAGNER [x]

Abstract □ A new exponential stripping program, CSTRIP, has been developed. This program overcomes the problems associated with the use of previously published techniques and enables the rapid economical calculation of initial polyexponential parameter estimates. Values for the coefficients and exponents of the exponential terms are calculated as well as estimates of lag times. An exhaustive search procedure ensures that the results are comparable to, or better than, those obtained by manual residual methods.

Keyphrases □ Pharmacokinetic modeling—calculation of initial polyexponential parameter estimates by a Fortran computer program □ Polyexponential parameter estimates—pharmacokinetic modeling, calculation by a Fortran computer program □ Computer programs, Fortran—calculation of initial polyexponential estimates for use in pharmacokinetic modeling □ Automated computer analysis—initial polyexponential parameter estimates for use in pharmacokinetic modeling, Fortran program

Pharmacokinetic models have proven to be a succinct method of describing the behavior of drugs *in vivo*. Classical linear pharmacokinetic models are represented by systems of homogeneous linear differential equations with constant coefficients. Solutions of such systems are given by the sums of exponential terms. Calculation of the numerical values of the exponents and coefficients of the exponential terms is often laborious and time consuming. Fortunately, the operations involved in exponential stripping are generally systematic and lend themselves to computer programming and solution by machine.

Theoretical approaches to exponential stripping have been discussed (1–7). However, many procedures are difficult to adapt to automated computer analysis.

One technique (1) employed a modification of the standard residual method, where the concentration of drug, C, was plotted against its first derivative, $-\Delta C/\Delta t$. This procedure yielded more erratic results than conventional residual methods because of the extreme sensitivity of the derivative to experimental error. Other techniques (2, 3), based on the theory of difference equations, proved to be impractical due to computational difficulties; unreliable solutions were obtained in the presence of small experimental errors. These methods also required equally spaced time intervals and only resolved the sums of exponentials having *positive* coefficients. Implementation of other approaches (4, 5) was prevented by similar considerations.

A computer algorithm (7), based on the residual method, was reported to be suitable for fully automated data analysis. This procedure had the following desirable characteristics: (*a*) sums of exponentials having positive and/or negative coefficients were accurately analyzed, and numerical values of coefficients and exponents were computed; and (*b*) unequally spaced data were acceptable, and no numerical instability arose during computation. However, this program required a minimum of three points for each exponential, and its use gave results that were not in good agreement with

REFERENCES

(1) J. Waller, *Lancet*, **2**, 1129(1966).

(2) J. W. Dundee, *Br. J. Anaesth.*, **29**, 440(1957).

(3) F. G. Estafanous, J. K. Porter, M. Y. Tawil, and K. L. Popawniak, *Can. Anaesth. Soc. J.*, **20**, 769(1973).

(4) M. Gibaldi, G. Levy, and H. Weintraub, *Clin. Pharmacol. Ther.*, **12**, 734(1971).

(5) J. G. Wagner, *J. Mond. Pharm.*, **14**, 279(1971).

(6) H. L. Price, P. J. Kounat, J. N. Safer, E. H. Conner, and M. L. Price, *Clin. Pharmacol. Ther.*, **1**, 16(1960).

(7) L. J. Saidman and E. I. Eger, *Anesthesiology*, **27**, 118(1966).

(8) L. J. Saidman and E. I. Eger, *Clin. Pharmacol. Ther.*, **14**, 12(1973).

(9) K. B. Bischoff and R. L. Dedrick, *J. Pharm. Sci.*, **57**, 1346(1968).

(10) K. B. Bischoff, R. L. Dedrick, and D. S. Zaharko, *ibid.*, **59**, 149(1970).

(11) R. W. Jelliffe, *Ann. Intern. Med.*, **69**, 703(1968).

(12) K. B. Bischoff and R. L. Dedrick, *Proc. Ann. Cont. Eng. Med. Biol.*, **1967**, 86.

(13) R. L. Dedrick and K. B. Bischoff, *Chem. Eng. Prog. Symp. Ser. No. 84*, **64**, 32(1968).

(14) J. R. Gillette, *Proc. Int. Pharmacol. Mtg., 2nd*, **4**, 9(1963).

(15) IBM Publication H20-0307-2 System/360 Continuous System Modeling Program (300A-CS-16X) User's Manual, 1968.

(16) IBM Publication H20-0240-2 System/360 Continuous System Modeling Program (360A-CX-16X) Application Description, 1968.

(17) J. Walsh, "Numerical Analysis," Thompson Book Co., Washington, D.C., 1967.

(18) L. Brand, L. C. Mark, M. McM. Snell, P. Urindten, and P. G. Dayton, *Anesthesiology*, **24**, 331(1963).

(19) W. W. Mapelson, *J. Appl. Physiol.*, **18**, 197(1961).

(20) L. R. Goldbaum and P. K. Smith, *J. Pharmacol. Exp. Ther.*, **111**, 197(1954).

(21) I. Sunshine, J. G. Whitman, W. W. Fike, B. Finkle, and J. Lebeau, *Br. J. Anaesth.*, **38**, 23(1966).

(22) J. G. Wagner, *J. Pharmacokinet. Biopharm.*, **1**, 363(1973).

(23) J. Brozek, F. Grande, J. T. Anderson, and A. Keys, *Ann. N.Y. Acad. Sci.*, **110**, 113(1963).

(24) A. W. Sloan, *J. Appl. Physiol.*, **23**, 311(1967).

ACKNOWLEDGMENTS AND ADDRESSES

Received May 19, 1975, from the *Department of Metallurgical Engineering & Materials Science and the †Department of Oral Biology, University of Kentucky, Lexington, KY 40506

Accepted for publication September 24, 1975.

Supported by University of Kentucky General Research Grant A3W45.

[x] To whom inquiries should be directed.

CSTRIP, a Fortran IV Computer Program for Obtaining Initial Polyexponential Parameter Estimates

ALLEN J. SEDMAN * and JOHN G. WAGNER [x]

Abstract □ A new exponential stripping program, CSTRIP, has been developed. This program overcomes the problems associated with the use of previously published techniques and enables the rapid economical calculation of initial polyexponential parameter estimates. Values for the coefficients and exponents of the exponential terms are calculated as well as estimates of lag times. An exhaustive search procedure ensures that the results are comparable to, or better than, those obtained by manual residual methods.

Keyphrases □ Pharmacokinetic modeling—calculation of initial polyexponential parameter estimates by a Fortran computer program □ Polyexponential parameter estimates—pharmacokinetic modeling, calculation by a Fortran computer program □ Computer programs, Fortran—calculation of initial polyexponential estimates for use in pharmacokinetic modeling □ Automated computer analysis—initial polyexponential parameter estimates for use in pharmacokinetic modeling, Fortran program

Pharmacokinetic models have proven to be a succinct method of describing the behavior of drugs *in vivo*. Classical linear pharmacokinetic models are represented by systems of homogeneous linear differential equations with constant coefficients. Solutions of such systems are given by the sums of exponential terms. Calculation of the numerical values of the exponents and coefficients of the exponential terms is often laborious and time consuming. Fortunately, the operations involved in exponential stripping are generally systematic and lend themselves to computer programming and solution by machine.

Theoretical approaches to exponential stripping have been discussed (1–7). However, many procedures are difficult to adapt to automated computer analysis.

One technique (1) employed a modification of the standard residual method, where the concentration of drug, C, was plotted against its first derivative, $-\Delta C/\Delta t$. This procedure yielded more erratic results than conventional residual methods because of the extreme sensitivity of the derivative to experimental error. Other techniques (2, 3), based on the theory of difference equations, proved to be impractical due to computational difficulties; unreliable solutions were obtained in the presence of small experimental errors. These methods also required equally spaced time intervals and only resolved the sums of exponentials having *positive* coefficients. Implementation of other approaches (4, 5) was prevented by similar considerations.

A computer algorithm (7), based on the residual method, was reported to be suitable for fully automated data analysis. This procedure had the following desirable characteristics: (*a*) sums of exponentials having positive and/or negative coefficients were accurately analyzed, and numerical values of coefficients and exponents were computed; and (*b*) unequally spaced data were acceptable, and no numerical instability arose during computation. However, this program required a minimum of three points for each exponential, and its use gave results that were not in good agreement with

those obtained by noncomputerized methods.

A computer-oriented technique for obtaining initial estimates of the parameters in exponential fitting was reported (6). This method, based on the "peeling" technique, resolved only the sums of exponentials having positive coefficients and was particularly well adapted to decay-type data. A minimum of three points was required for each exponential to be determined.

The purposes of this paper are to describe a new computer program that overcomes the problems and restrictions associated with previously published exponential stripping methods and to illustrate the use of this program.

COMPUTER PROGRAM

CSTRIP, a Fortran IV computer program for obtaining initial polyexponential parameter estimates, is based on a computer adaptation of the classical residual, peeling-off technique. CSTRIP is composed of 12 separate subroutines, and the most important subroutines are discussed briefly here.

EXP2, EXP4, EXP6, EXP8, and EXP10—These five subroutines strip curves described by one to five exponentials. The number in the name of each subroutine refers to the number of parameters estimated.

A computer adaptation of the manual technique commonly used for exponential stripping was described previously (6). A modification of this technique is employed in these subroutines and the method is summarized below.

It is desired to fit a set of data to the equation:

$$C = \sum_{i=1}^{m} a_i e^{-b_i t} \qquad \text{(Eq. 1)}$$

where C is the concentration of drug at time t, m is the number of exponential terms, t is time, and a_i and b_i are the parameters to be determined.

At large times, a plot of log C against t can generally be approximated by a straight line. The straight-line portion for large t occurs because as t increases the exponentials with large exponents (b_i's) decay to zero, leaving only the exponential with the smallest exponent, $a_m e^{-b_m t}$. Use of the method of least squares enables a straight line to be fitted to the last few data points, so values of a_m and b_m can be obtained. Values for the C residuals can then be calculated by use of:

$$C_{\text{residual}} = C - a_m e^{-b_m t} \qquad \text{(Eq. 2)}$$

By repeating this process utilizing the C residual values at large times, values for a_{m-1} and b_{m-1} can be determined. The process of peeling-off is continued until all coefficients and exponents of the polyexponential equation are determined.

In CSTRIP, the minimum number of points for a computer calculation of a_i and b_i is described by:

$$NPE = L/(3 + M) \qquad \text{(Eq. 3)}$$

where NPE is the minimum number of points per exponential [rounded off to the smallest whole number (≥ 2)], L is the number of distinct time values, and M is the number of exponential terms. These principles are computer implemented as follows. To calculate a first set of initial values, the last NPE data points are used to obtain a_m and b_m, the next NPE points are used to obtain a_{m-1} and b_{m-1}, *etc.* Finally, the remaining $n - NPE(m-1)$ points are used to calculate a_1 and b_1, where n is the total number of data points.

Subroutine LTTEST is called for concentration–time data collected following the oral or intramuscular administration of a drug. An appropriate lag time is calculated, or the sum of the exponential terms is forced through zero.

The value F, the sum of squares of the deviations, is used to evaluate the goodness of fit of the estimates:

$$F = \sum_{i=1}^{n} (C_i - \hat{C}_i)^2 \qquad \text{(Eq. 4)}$$

where $\hat{C}_i$ is the estimated drug concentration.

A second set of initial estimates of the parameters is obtained by utilizing the last $NPE + 1$ to calculate a_m and b_m. The next NPE points are used to determine a_{m-1} and b_{m-1}, and the process is continued until only one exponential is left with $n - NPE(m-1) - 1$ points to calculate a_1 and b_1. The value of F is calculated for this set of parameters. The remaining sets of initial estimates are calculated by combining the data to keep NPE points as a minimum in calculating a_i and b_i.

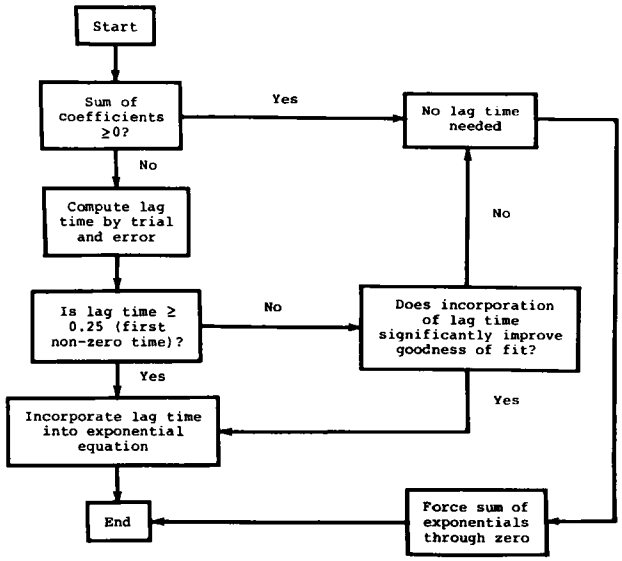

Figure 1—*Flowsheet for LTTEST subroutine.*

Every combination of data that meets these criteria is used to calculate initial estimates of the coefficients and exponents of the polyexponential equation. The set of parameters with the minimum F value is chosen as the best initial estimates. However, the following constraints also were imposed. Exponential terms describing intravenous or postinfusion data could not have negative coefficients. The value of b_{i-1} was required to be $\geq 1.33 b_i$, and exponents, b_i, could not assume values ≤ 0. Sums of exponentials that gave negative estimates at any time greater than zero were excluded.

CALC—Subroutine CALC computes the residual regression lines for the five curve-stripping subroutines discussed previously. Standard least-squares linear regression techniques are used.

FUN and RSQR—These subroutines calculate the goodness of fit for the curve-stripping subroutines. The sum of the squared deviations (Eq. 4) and the value of r^2:

$$r^2 = \left[\sum_{i=1}^{n} C_1^2 - \frac{\left(\sum_{i=1}^{n} C_i\right)^2}{n} - \sum_{i=1}^{n} (C_i - \hat{C}_i)^2 \right] \Bigg/ \left[\sum_{i=1}^{n} C_1^2 - \frac{\left(\sum_{i=1}^{n} C_i\right)^2}{n} \right] \qquad \text{(Eq. 5)}$$

are used as criteria for the goodness of fit.

LTTEST—This subroutine determines the suitability of a lag time for data collected following oral or intramuscular administration of a drug. A flowsheet for the LTTEST algorithm is given in Fig. 1. The lag time, t_1, is determined by trial-and-error solution of:

$$\sum_{i=1}^{m} a_i e^{-b_i t_1} = 0 \qquad \text{(Eq. 6)}$$

USE OF CSTRIP PROGRAM

Input of Data—Input to CSTRIP is specified in Table I. The following restrictions apply to the input of data. Abscissa (time) values must be ascendingly ordered. Although data collected during an intravenous infusion cannot be analyzed by CSTRIP, postinfusion values may be successfully analyzed.

For best results, a (0,0) data point should be used when data collected following oral or intramuscular administration are to be analyzed. The inclusion of the (0,0) point tends to minimize the importance of a lag time. However, if CSTRIP then indicates the presence

Table I—Input to CSTRIP

Format	Columns	Variable	Comments
		Card 1	
I2	1–2	NSET	Number of data sets
		Card 2[a]	
I1	1	MEX	Maximum number of exponential terms of interest
I3	2–4	N	Number of data points
I1	5	NROUTE	Route of administration NROUTE = 0, rapid intravenous injection or intravenous infusion NROUTE = 1, oral or intramuscular administration
		Card 3[a]	
8F10.0		Y(J), J = 1, N	Ordinate values; may take more than one card
		Card 4[a]	
8F10.0		T(J), J = 1, N	Abscissa values; may take more than one card

[a] Cards 2–4 are repeated for each set of data.

of a lag time, the data should be resubmitted without the (0,0) point to obtain a more accurate estimate of the lag time.

Replicate ordinate and/or abscissa values are permitted. Outliers should not be included in data sets.

Data Output—The CSTRIP output format is somewhat variable from one data set to another and is summarized in Fig. 2. The output parameters are defined in Table II.

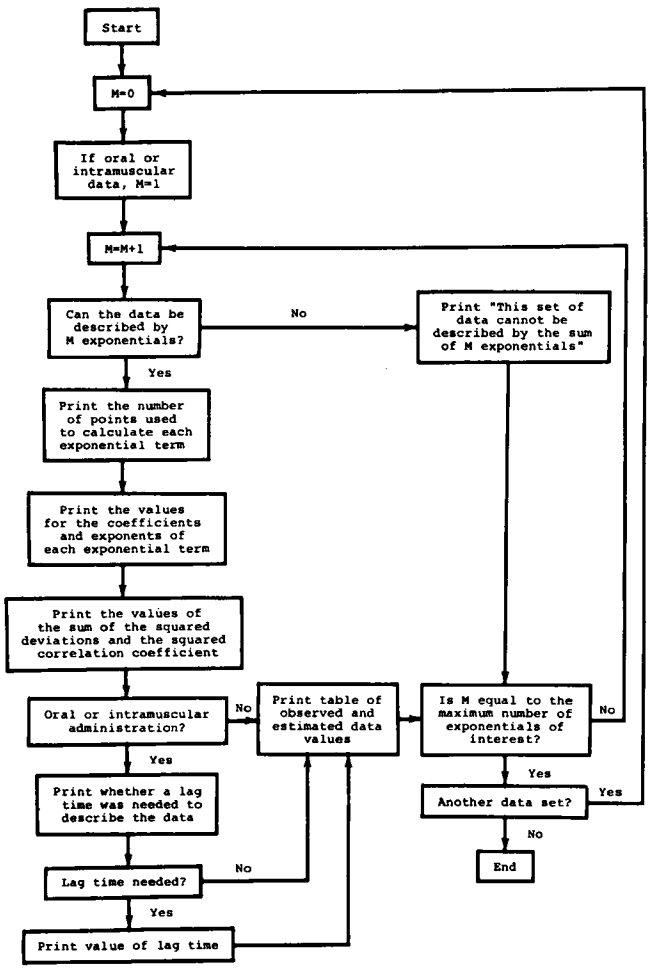

Figure 2—*Schematic diagram of CSTRIP output.*

Table II—CSTRIP Output Parameters

Parameter	Comments
L1, L2, *etc.*	Number of points used to calculate last exponential term (smallest exponent); next to last term; and so on
A1, A2, *etc.*	Coefficients of exponential terms of polyexponential equation
B1, B2, *etc.*	Exponents of polyexponential equation
F	Sum of squared deviations between observed data and values predicted by use of polyexponential equation
R SQUARE	Squared correlation coefficient
NO.	Data point number
TIME	Abscissa values
C(OBS)	Observed ordinate values
C(EST)	Ordinate values predicted by use of polyexponential equation
% DEV	Percent deviation of predicted from observed ordinate values

Table III—Tetracycline Data

Hours	Serum Concentration of Tetracycline Hydrochloride, μg/ml
1	0.7
2	1.2
3	1.4
4	1.4
6	1.1
8	0.8
10	0.6
12	0.5
16	0.3

Table IV—Intramuscular Spectinomycin Data

Hours	Serum Concentration of Spectinomycin, μg/ml
0.	0.
0.1667	15.7
0.3333	23.1
0.5	31.2
1.	31.6
2.	28.2
4.	12.8
6.	5.6
8.	2.4

Examples—Fifty sets of data, some simulated and the rest from the literature, were used to evaluate the capabilities of CSTRIP. Two representative data sets will be used to illustrate the performance of CSTRIP. Table III gives reported tetracycline data (8), and Table IV presents data collected after intramuscular injection of spectinomycin (9). These sets of data were submitted to CSTRIP for exponential analysis. The input format used is given in Table V.

RESULTS AND DISCUSSION

Tetracycline Data—The output resulting from the CSTRIP analysis of tetracycline[1] concentration–time data is given in Fig. 3. The analysis indicated that a biexponential equation:

$$C = -2.13e^{-1.03(t-0.610)} + 2.13e^{-0.129(t-0.610)} \qquad \text{(Eq. 7)}$$

with a lag time best described the concentration–time curve for tetracycline.

A reasonably high value for the goodness of fit parameter, r^2 = 0.979, indicated that the biexponential equation adequately described the data. Moreover, inclusion of an additional exponential term did not improve the goodness of fit.

Wagner (8) analyzed these data graphically and also determined that a biexponential equation was applicable. A comparison of

[1] Panmycin.

Table V—Input Format for Examples

```
02
30091
.7      1.2     1.4     1.4     1.1     .8      .6      .5
.3
1.      2.      3.      4.      6.      8.      10.     12.
16.
30091
0.      15.7    23.1    31.2    31.6    28.2    12.8    5.6
2.4
0.      .1667   .3333   .5      1.      2.      4.      6.
8.
```

graphical with CSTRIP curve stripping is made in Table VI. Although the reported graphical estimates are quite different than those obtained by use of CSTRIP, the goodness of fits, judged by sum of squared deviations, are comparable. Use of each set of parameters as initial parameter estimates for nonlinear least-squares analysis gave slightly different least-squares parameter values. However, each set of least-squares parameters seems to describe the data equally well.

Spectinomycin Data—The output resulting from the CSTRIP analysis of data collected after the administration of spectinomycin by intramuscular injection is given in Fig. 4. These data were described well by both a biexponential and triexponential equation. Wagner *et al.* (9) found that data collected after the intravenous administration

```
**********

DATA SET NUMBER  1


THE NUMBER OF EXPONENTIALS = 2
SUMMARY OF EXPONENTIAL STRIPPING

THE NUMBER OF POINTS IN THE EXPONENTIAL PHASES (LAST TO FIRST):
    L1=    6
    L2=    3


THE BEST ESTIMATES OF THE COEFFICIENTS AND EXPONENTS ARE:
A1= 0.213365E+01      B1= 0.128894E+00
A2=-0.213456E+01      B2= 0.103423E+01
F= 0.265306E-01



A LAG TIME WAS NEEDED TO DESCRIBE THESE DATA

THE LAG TIME =   0.610

R SQUARE(2) =   0.97942

 NO.          TIME          C(OBS)          C(EST)          % DEV
    1        1.0000          0.7000          0.6030          13.86
    2        2.0000          1.2000          1.2767          -6.39
    3        3.0000          1.4000          1.3877           0.88
    4        4.0000          1.4000          1.3143           6.12
    5        6.0000          1.1000          1.0570           3.91
    6        8.0000          0.8000          0.8221          -2.76
    7       10.0000          0.6000          0.6359          -5.99
    8       12.0000          0.5000          0.4915           1.70
    9       16.0000          0.3000          0.2935           2.16


THE NUMBER OF EXPONENTIALS = 3
SUMMARY OF EXPONENTIAL STRIPPING

THE NUMBER OF POINTS IN THE EXPONENTIAL PHASES (LAST TO FIRST):
    L1=    3
    L2=    3
    L3=    3


THE BEST ESTIMATES OF THE COEFFICIENTS AND EXPONENTS ARE:
A1= 0.184756E+01      B1= 0.117264E+00
A2= 0.969792E+00      B2= 0.462881E+00
A3=-0.282060E+01      B3= 0.896822E+00
F= 0.269580E-01



A LAG TIME WAS NEEDED TO DESCRIBE THESE DATA

THE LAG TIME =   0.587

R SQUARE(3) =   0.97908

 NO.          TIME          C(OBS)          C(EST)          % DEV
    1        1.0000          0.7000          0.6137          12.33
    2        2.0000          1.2000          1.2753          -6.28
    3        3.0000          1.4000          1.3856           1.03
    4        4.0000          1.4000          1.3058           6.73
    5        6.0000          1.1000          1.0365           5.77
    6        8.0000          0.8000          0.8023          -0.29
    7       10.0000          0.6000          0.6245          -4.08
    8       12.0000          0.5000          0.4894           2.12
    9       16.0000          0.3000          0.3039          -1.31
```

Figure 3—*CSTRIP analysis of tetracycline concentration and time data.*

Table VI—Comparison of Automated and Graphical Curve Stripping of Tetracycline Concentration and Time Data[a]

	Value of Parameter Estimate			
Parameter	Graphical[b]	CSTRIP	Nonlinear Least Squares	
A_1	2.30	2.13	2.65[c]	2.42[d]
B_1	0.130	0.129	0.149	0.139
A_2	−2.30	−2.13	−2.65	−2.42
B_2	0.810	1.03	0.716	0.794
t_1	0.328	0.610	0.421	0.436
Sum of squared deviations[e]	0.024	0.026	0.010	0.011

[a] Data fitted to a biexponential equation of the form $C = A_1e^{-B_1(t-t_1)} + A_2e^{-B_2(t-t_1)}$. [b] See Ref. 8 for method. [c] Graphical values used as initial least-squares estimates. [d] CSTRIP values used as initial least-squares estimates. [e] Sum of squared deviations between observed and model-predicted concentrations.

of spectinomycin were described by two exponential terms. They fitted data collected after intramuscular administration to a triexponential equation. Wagner *et al.* (9) did not report the values of their graphical (initial) estimates, but a comparison of final nonlinear

```
**********

DATA SET NUMBER  2


THE NUMBER OF EXPONENTIALS = 2
SUMMARY OF EXPONENTIAL STRIPPING

THE NUMBER OF POINTS IN THE EXPONENTIAL PHASES (LAST TO FIRST):
    L1=    3
    L2=    6


THE BEST ESTIMATES OF THE COEFFICIENTS AND EXPONENTS ARE:
A1= 0.685025E+02      B1= 0.418496E+00
A2=-0.685025E+02      B2= 0.187516E+01
F= 0.186380E+02



NO LAG TIME WAS NEEDED TO DESCRIBE THESE DATA
THEREFORE, THE SUM OF THE EXPONENTIAL TERMS WAS FORCED THROUGH ZERO

R SQUARE(2) =   0.98483

 NO.          TIME          C(OBS)          C(EST)          % DEV
    1        0.0             0.0             0.0             0.0
    2        0.1667         15.7000         13.7734          12.27
    3        0.3333         23.1000         22.9168           0.79
    4        0.5000         31.2000         28.7449           7.87
    5        1.0000         31.6000         34.5735          -9.41
    6        2.0000         28.2000         28.0518           0.53
    7        4.0000         12.8000         12.8062          -0.05
    8        6.0000          5.6000          5.5607           0.70
    9        8.0000          2.4000          2.4082          -0.34


THE NUMBER OF EXPONENTIALS = 3
SUMMARY OF EXPONENTIAL STRIPPING

THE NUMBER OF POINTS IN THE EXPONENTIAL PHASES (LAST TO FIRST):
    L1=    2
    L2=    5
    L3=    2


THE BEST ESTIMATES OF THE COEFFICIENTS AND EXPONENTS ARE:
A1= 0.711825E+02      B1= 0.423653E+00
A2=-0.526339E+02      B2= 0.136295E+01
A3=-0.185087E+02      B3= 0.455966E+01
F= 0.917597E+01



NO LAG TIME WAS NEEDED TO DESCRIBE THESE DATA
THEREFORE, THE SUM OF THE EXPONENTIAL TERMS WAS FORCED THROUGH ZERO

R SQUARE(3) =   0.99253

 NO.          TIME          C(OBS)          C(EST)          % DEV
    1        0.0             0.0             0.0             0.0
    2        0.1667         15.7000         15.7000          -0.00
    3        0.3333         23.1000         24.3070          -5.23
    4        0.5000         31.2000         29.0424           6.92
    5        1.0000         31.6000         32.9106          -4.15
    6        2.0000         28.2000         27.0405           4.11
    7        4.0000         12.8000         12.8411          -0.32
    8        6.0000          5.6000          5.5852           0.26
    9        8.0000          2.4000          2.3990           0.04
```

Figure 4—*CSTRIP analysis of spectinomycin concentration and time data.*

Table VII—Comparison of Automated and Least-Squares Parameter Estimates for Spectinomycin Concentration and Time Data[a]

Parameter	Value of Parameter Estimate	
	CSTRIP	Nonlinear Least Squares
A_1	71.1	70.5
B_1	0.424	0.422
A_2	-52.6	-54.7
B_2	1.36	1.46
A_3	-18.5	-15.8
B_3	4.56	4.61
Sum of squared deviations[b]	9.17	9.11

[a] Data fitted to a triexponential equation of the form $C = A_1e^{-B_1t} + A_2e^{-B_2t} + A_3e^{-B_3t}$. [b] Sum of squared deviations between observed and model-predicted concentrations.

least-squares parameter estimates with CSTRIP estimates is made in Table VII. There was excellent agreement between the CSTRIP and nonlinear least-squares parameter values.

CSTRIP generally gives results comparable to or better than those obtained by laborious graphical or other manual techniques.

CSTRIP not only provides accurate exponential parameter estimates but also is economical, and the input of data does not require excessive time. The total cost for the CSTRIP analyses of the two examples given was $0.51.

SUMMARY

The CSTRIP program provides for fully automated exponential stripping of pharmacokinetic data. This program enables the rapid, accurate, and economical computer analysis of data described by the sums of exponentials and gives results comparable to, or better than, those obtained by laborious manual techniques. Use of the CSTRIP program should greatly reduce the amount of time consumed in obtaining preliminary estimates of exponential parameters by graphical and/or electronic calculator methods and should result in least-squares parameter estimates having less variability and greater accuracy.

The program should prove suitable as an exponential stripping routine in other programs designed for fully automated data analysis.

REFERENCES

(1) W. Perl, *Int. J. Appl. Radiat. Isot.*, **8**, 211(1960).
(2) D. H. Parsons, *Math. Biosci.*, **2**, 123(1968).
(3) *Ibid.*, **9**, 37(1970).
(4) D. G. Gardner, *J. Chem. Phys.*, **31**, 978(1961).
(5) R. G. Cornell, *Biometrics*, **18**, 104(1962).
(6) S. D. Foss, *ibid.*, **25**, 580(1969).
(7) P. Mancini and A. Pilo, *Biomed. Res.*, **3**, 1(1970).
(8) J. G. Wagner, *Clin. Pharmacol. Ther.*, **8**, 20(1967).
(9) J. G. Wagner, E. Novak, L. G. Leslie, and C. M. Metzler, *Int. J. Clin. Pharmacol.*, **1**, 261(1968).

ACKNOWLEDGMENTS AND ADDRESSES

Received July 7, 1975, from the *College of Pharmacy and the Upjohn Center for Clinical Pharmacology, University of Michigan, Ann Arbor, MI 48109*

Accepted for publication September 24, 1975.

* Present address: Washington University School of Medicine, St. Louis, MO 63110

‡ To whom inquiries should be directed. (The computer program is not available on tape or cards. A complete microfilm source listing will be supplied upon request. No troubleshooting assistance will be provided.)

Anticonvulsant Activity and Inhibition of Cellular Respiratory Activity by Substituted Imidazolocarbamides

SUNIL K. CHAUDHARY *, SURENDRA S. PARMAR *‡x, MAHIMA CHAUDHARY *, and JAYANTI P. BARTHWAL *

Abstract □ Several 1-(1-aryl-2-mercaptoacetylimidazole)-3-alkylcarbamides were synthesized and characterized by their sharp melting points, elemental analyses, and IR spectra. These substituted imidazolocarbamides possessed anticonvulsant activity, which was reflected by the 20–80% protection observed with these compounds against pentylenetetrazol-induced convulsions in mice. These substituted imidazolocarbamides selectively inhibited the *in vitro* oxidation of nicotinamide adenine dinucleotide (NAD)-dependent oxidations of pyruvate, α-ketoglutarate, β-hydroxybutyrate, and NADH by rat brain homogenates. However, NAD-independent oxidation of succinate was not affected. The anticonvulsant activity possessed by 1-(1-aryl-2-mercaptoacetylimidazole)-3-alkylcarbamides had no relationship to their ability to inhibit cellular respiratory activity.

Keyphrases □ Imidazolocarbamides, substituted—synthesized, screened for anticonvulsant activity, effect on cellular respiratory activity □ Anticonvulsant activity—screened in series of substituted imidazolocarbamides, mice □ Cellular respiration—effect of series of substituted imidazolocarbamides on NAD-dependent and NAD-independent oxidations, rat brain homogenates □ Oxidations, NAD dependent and independent—effect of series of substituted imidazolocarbamides, rat brain homogenates □ Structure–activity relationships—series of imidazolocarbamides, anticonvulsant activity, cellular respiratory activity

Potentiation of pentobarbital-induced hypnosis and protection against pentylenetetrazol-induced convulsions indicated the central nervous system (CNS) depressant property of substituted carbamides (1–4). Certain derivatives of imidazoles also have been reported to possess anticonvulsant activity (5, 6). Earlier studies indicated significant degrees of muscle relaxant and anticonvulsant activities of 1-carbamoylpyrrolidines and 1-carbamoylpiperidines (7). Various aryloxyalkylcarbamides also have been shown to possess the CNS activity (8).

These observations led to the synthesis of 1-(1-aryl-

Table VII—Comparison of Automated and Least-Squares Parameter Estimates for Spectinomycin Concentration and Time Data[a]

Parameter	Value of Parameter Estimate	
	CSTRIP	Nonlinear Least Squares
A_1	71.1	70.5
B_1	0.424	0.422
A_2	-52.6	-54.7
B_2	1.36	1.46
A_3	-18.5	-15.8
B_3	4.56	4.61
Sum of squared deviations[b]	9.17	9.11

[a] Data fitted to a triexponential equation of the form $C = A_1e^{-B_1t} + A_2e^{-B_2t} + A_3e^{-B_3t}$. [b] Sum of squared deviations between observed and model-predicted concentrations.

least-squares parameter estimates with CSTRIP estimates is made in Table VII. There was excellent agreement between the CSTRIP and nonlinear least-squares parameter values.

CSTRIP generally gives results comparable to or better than those obtained by laborious graphical or other manual techniques.

CSTRIP not only provides accurate exponential parameter estimates but also is economical, and the input of data does not require excessive time. The total cost for the CSTRIP analyses of the two examples given was $0.51.

SUMMARY

The CSTRIP program provides for fully automated exponential stripping of pharmacokinetic data. This program enables the rapid, accurate, and economical computer analysis of data described by the sums of exponentials and gives results comparable to, or better than, those obtained by laborious manual techniques. Use of the CSTRIP program should greatly reduce the amount of time consumed in obtaining preliminary estimates of exponential parameters by graphical and/or electronic calculator methods and should result in least-squares parameter estimates having less variability and greater accuracy.

The program should prove suitable as an exponential stripping routine in other programs designed for fully automated data analysis.

REFERENCES

(1) W. Perl, *Int. J. Appl. Radiat. Isot.*, **8**, 211(1960).
(2) D. H. Parsons, *Math. Biosci.*, **2**, 123(1968).
(3) *Ibid.*, **9**, 37(1970).
(4) D. G. Gardner, *J. Chem. Phys.*, **31**, 978(1961).
(5) R. G. Cornell, *Biometrics*, **18**, 104(1962).
(6) S. D. Foss, *ibid.*, **25**, 580(1969).
(7) P. Mancini and A. Pilo, *Biomed. Res.*, **3**, 1(1970).
(8) J. G. Wagner, *Clin. Pharmacol. Ther.*, **8**, 20(1967).
(9) J. G. Wagner, E. Novak, L. G. Leslie, and C. M. Metzler, *Int. J. Clin. Pharmacol.*, **1**, 261(1968).

ACKNOWLEDGMENTS AND ADDRESSES

Received July 7, 1975, from the *College of Pharmacy and the Upjohn Center for Clinical Pharmacology, University of Michigan, Ann Arbor, MI 48109*

Accepted for publication September 24, 1975.

* Present address: Washington University School of Medicine, St. Louis, MO 63110

‡ To whom inquiries should be directed. (The computer program is not available on tape or cards. A complete microfilm source listing will be supplied upon request. No troubleshooting assistance will be provided.)

Anticonvulsant Activity and Inhibition of Cellular Respiratory Activity by Substituted Imidazolocarbamides

SUNIL K. CHAUDHARY *, SURENDRA S. PARMAR *‡x, MAHIMA CHAUDHARY *, and JAYANTI P. BARTHWAL *

Abstract □ Several 1-(1-aryl-2-mercaptoacetylimidazole)-3-alkylcarbamides were synthesized and characterized by their sharp melting points, elemental analyses, and IR spectra. These substituted imidazolocarbamides possessed anticonvulsant activity, which was reflected by the 20–80% protection observed with these compounds against pentylenetetrazol-induced convulsions in mice. These substituted imidazolocarbamides selectively inhibited the *in vitro* oxidation of nicotinamide adenine dinucleotide (NAD)-dependent oxidations of pyruvate, α-ketoglutarate, β-hydroxybutyrate, and NADH by rat brain homogenates. However, NAD-independent oxidation of succinate was not affected. The anticonvulsant activity possessed by 1-(1-aryl-2-mercaptoacetylimidazole)-3-alkylcarbamides had no relationship to their ability to inhibit cellular respiratory activity.

Keyphrases □ Imidazolocarbamides, substituted—synthesized, screened for anticonvulsant activity, effect on cellular respiratory activity □ Anticonvulsant activity—screened in series of substituted imidazolocarbamides, mice □ Cellular respiration—effect of series of substituted imidazolocarbamides on NAD-dependent and NAD-independent oxidations, rat brain homogenates □ Oxidations, NAD dependent and independent—effect of series of substituted imidazolocarbamides, rat brain homogenates □ Structure–activity relationships—series of imidazolocarbamides, anticonvulsant activity, cellular respiratory activity

Potentiation of pentobarbital-induced hypnosis and protection against pentylenetetrazol-induced convulsions indicated the central nervous system (CNS) depressant property of substituted carbamides (1–4). Certain derivatives of imidazoles also have been reported to possess anticonvulsant activity (5, 6). Earlier studies indicated significant degrees of muscle relaxant and anticonvulsant activities of 1-carbamoylpyrrolidines and 1-carbamoylpiperidines (7). Various aryloxyalkylcarbamides also have been shown to possess the CNS activity (8).

These observations led to the synthesis of 1-(1-aryl-

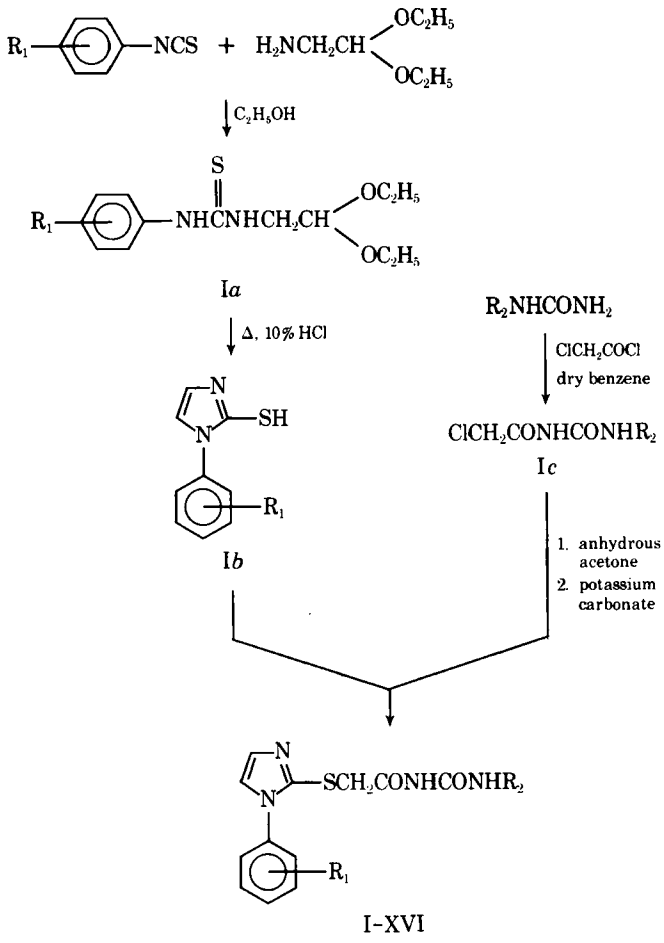

Scheme I

2-mercaptoacetylimidazole)-3-alkylcarbamides. In the present study, the anticonvulsant activity of these substituted imidazolocarbamides was determined against pentylenetetrazol-induced convulsions. The *in vitro* effects of these carbamides on the cellular respiratory activity of rat brain homogenates were investigated to study the biochemical mechanism of action for their anticonvulsant activity. The various substituted imidazolocarbamides were synthesized by following the methods outlined in Scheme I.

EXPERIMENTAL[1]

Aryldiethoxyethylthioureas (Ia)—An appropriate isothiocyanate (0.1 mole) was slowly added to the stirred solution of aminoacetaldehydehyde diethyl acetal (0.1 mole) in 100 ml of absolute ethanol at room temperature (9, 10). After the addition was complete, the mixture was refluxed on a steam bath for 30 min. Excess ethanol was removed by distillation and the crude thioureas, obtained as colorless oils, were used for the synthesis of 1-aryl-2-mercaptoimidazoles (*Ib*) without further purification.

1-Aryl-2-mercaptoimidazoles (Ib)—Crude *Ia* was stirred with 200 ml of 10% HCl, and the mixture was refluxed over a free flame for 30 min. Crystalline *Ib*, which separated on cooling, was collected by filtration, washed with water, and recrystallized from appropriate solvents. The melting points of these substituted mercaptoimidazoles corresponded with those reported in the literature (9, 10).

1-Chloroacetyl-3-alkylcarbamides (Ic)—A mixture of an appropriate alkylcarbamide (0.1 mole) and chloroacetyl chloride (0.11 mole) in 30 ml of dry benzene was refluxed on a steam bath for 4 hr. Excess benzene was removed by distillation; the crude products, which separated on cooling, were collected by filtration, washed with water, dried, and recrystallized from the appropriate solvents (11).

1-(1-Aryl-2-mercaptoacetylimidazole)-3-alkylcarbamides (I–XVI)—A mixture of *Ib* (0.01 mole), *Ic* (0.01 mole), and anhydrous potassium carbonate (0.015 mole) was added to 50 ml of anhydrous acetone and refluxed under anhydrous conditions on a steam bath for 6 hr. The reaction mixture was poured over cold water, and the separated crude products were collected by filtration, washed several times with water, dried, and recrystallized from ethanol.

The various 1-(1-aryl-2-mercaptoacetylimidazole)-3-alkylcarbamides (Table I) were characterized by their sharp melting points and elemental analyses. The presence of the characteristic bands of C=O attached to nitrogen (1710 cm^{-1}), C=N (1620 cm^{-1}), and NH (3300 cm^{-1}) in their IR spectra provided further confirmation of their molecular structure.

Determination of Anticonvulsant Activity—Anticonvulsant activity was determined in albino mice of either sex weighing 25–30 g. The mice were divided into groups of 10, keeping the group weights as near the same as possible. Each 1-(1-aryl-2-mercaptoacetylimidazole)-3-alkylcarbamide was suspended in 5% aqueous gum acacia to give a concentration of 1% (w/v). The test compounds were injected in a group of 10 mice at a dose of 100 mg/kg ip.

Four hours after the administration of the test compounds, the mice were injected with pentylenetetrazol (90 mg/kg sc). This dose of pentylenetetrazol has been shown to produce convulsions in almost all untreated mice and causes 100% mortality during 24 hr (1). However, no mortality was observed during 24 hr in animals treated with 100 mg/kg ip of the test compounds alone.

The mice were observed for 60 min for seizures. An episode of clonic spasm that persisted for at least 5 sec was considered a threshold convulsion. Transient intermittent jerks and tremulousness were not counted. Animals devoid of the threshold convulsions during 60 min were considered protected. The number of animals protected in each group was recorded, and the anticonvulsant activity of these 1-(1-aryl-2-mercaptoimidazole)-3-alkylcarbamides was represented as percent protection. In the present study, no anticonvulsant activity was observed in animals treated with 5% aqueous gum acacia solution alone. The animals were then observed for 24 hr, and their mortality was recorded.

Assay of Respiratory Activity of Rat Brain Homogenates[2]—Albino rats, 100–150 g, were kept on an *ad libitum* diet and were used in all experiments. Rat brains isolated from decapitated animals were immediately homogenized in ice-cold 0.25 *M* sucrose in a homogenizer[3] in a ratio of 1:9 (w/v). All incubations were carried out at 37°, and the oxygen uptake was measured by the conventional Warburg manometric technique, using air as the gas phase (12).

Fresh brain homogenates, equivalent to 100 mg wet weight, were added to chilled Warburg vessels containing 6.7 mmoles of magnesium sulfate, 20 mmoles of sodium hydrogen phosphate buffer solution (pH 7.4), 1 mmole of adenosine monophosphate (sodium salt), 33 mmoles of potassium chloride, and 500 μg of cytochrome c in a final volume of 3 ml, unless otherwise stated. The central well contained 0.2 ml of 20% KOH solution. Pyruvate, citrate, α-ketoglutarate, β-hydroxybutyrate, and succinate were used at a final concentration of 10 m*M*, while the concentration of NADH was 0.5 m*M*. It was presumed that the endogenous NAD, present in the homogenates, was sufficient for these oxidative processess.

All 1-(1-aryl-2-mercaptoacetylimidazole)-3-alkylcarbamides were dissolved in propylene glycol (100%) and were incubated with rat brain homogenates at 37° for 10 min prior to the addition of the various substrates. An equal volume of the solvent was added to the control vessels. The oxygen uptake was measured every 10 min for 60 min.

Determination of Approximate LD_{50}—The toxicity of the 1-(1-aryl-2-mercaptoacetylimidazole)-3-alkylcarbamides was evaluated by determination of the approximate 50% lethal dose (approximate LD_{50}) by following the method of Smith (13). All substituted imidazolocarbamides were suspended in aqueous gum acacia and were administered intraperitoneally to each group of 10 mice.

[1] All compounds were analyzed for their carbon, hydrogen, and nitrogen content. Melting points were taken in open capillary tubes with a partial immersion thermometer and are corrected. IR spectra were taken with a Perkin-Elmer Infracord spectrophotometer model 137 equipped with sodium chloride optics.

[2] Commercial chemicals were used in this study. Sodium pyruvate, trisodium citrate, monosodium α-ketoglutarate, sodium β-hydroxybutyrate, NADH, sodium succinate, adenosine monophosphate (sodium salt), and cytochrome c were obtained from Sigma Chemical Co., St. Louis, Mo.

[3] Potter–Elvehjem homogenizer.

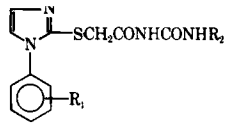

Table I—Physical Constants of 1-(1-Aryl-2-mercaptoacetylimidazole)-3-alkylcarbamides

Compound	R_1	R_2	Melting Point[a]	Yield, %	Molecular Formula		Analysis, % Calc.	Found
I	H	CH_3	164°	60	$C_{13}H_{14}N_4O_2S$	C	53.79	53.40
						H	4.82	4.65
						N	19.31	19.00
II	2-CH_3	CH_3	122°	55	$C_{14}H_{16}N_4O_2S$	C	55.26	55.00
						H	5.26	5.31
						N	18.42	18.40
III	4-CH_3	CH_3	120°	45	$C_{14}H_{16}N_4O_2S$	C	55.26	54.96
						H	5.26	5.37
						N	18.42	18.65
IV	2,4-$(CH_3)_2$	CH_3	170°	60	$C_{15}H_{18}N_4O_2S$	C	56.60	56.40
						H	5.66	5.26
						N	17.61	17.80
V	2,6-$(CH_3)_2$	CH_3	132°	68	$C_{15}H_{18}N_4O_2S$	C	56.60	56.20
						H	5.66	5.65
						N	17.61	17.40
VI	2-OCH_3	CH_3	160°	70	$C_{14}H_{16}N_4O_3S$	C	52.50	52.30
						H	5.00	4.82
						N	17.50	17.48
VII	4-OCH_3	CH_3	174°	56	$C_{14}H_{16}N_4O_3S$	C	52.50	52.46
						H	5.00	4.86
						N	17.50	17.48
VIII	4-Cl	CH_3	158°	62	$C_{13}H_{13}ClN_4O_2S$	C	48.07	48.35
						H	4.00	3.90
						N	17.25	17.56
IX	H	C_2H_5	118°	64	$C_{14}H_{16}N_4O_2S$	C	55.26	55.20
						H	5.26	5.65
						N	18.42	18.90
X	2-CH_3	C_2H_5	120°	48	$C_{15}H_{18}N_4O_2S$	C	56.60	56.20
						H	5.66	5.34
						N	17.61	17.40
XI	4-CH_3	C_2H_5	110°	40	$C_{15}H_{18}N_4O_2S$	C	56.60	56.56
						H	5.66	5.82
						N	17.61	17.30
XII	2,4-$(CH_3)_2$	C_2H_5	142°	38	$C_{16}H_{20}N_4O_2S$	C	57.83	57.46
						H	6.02	5.90
						N	16.86	16.39
XIII	2,6-$(CH_3)_2$	C_2H_5	130°	65	$C_{16}H_{20}N_4O_2S$	C	57.83	57.90
						H	6.02	6.25
						N	16.86	16.92
XIV	2-OCH_3	C_2H_5	152°	52	$C_{15}H_{18}N_4O_3S$	C	53.89	53.92
						H	5.38	5.60
						N	16.76	16.42
XV	4-OCH_3	C_2H_5	134°	50	$C_{15}H_{18}N_4O_3S$	C	53.89	53.40
						H	5.38	5.36
						N	16.76	16.90
XVI	4-Cl	C_2H_5	128°	56	$C_{14}H_{15}ClN_4O_2S$	C	49.63	49.50
						H	4.43	4.48
						N	16.54	16.76

[a] All compounds were recrystallized from ethanol. The melting points were taken in open capillary tubes with a partial immersion thermometer and are corrected.

RESULTS AND DISCUSSION

Results presented in Table II represent anticonvulsant activity possessed by 1-(1-aryl-2-mercaptoacetylimidazole)-3-alkylcarbamides against pentylenetetrazol-induced convulsions in mice. Anticonvulsant activity of these compounds ranged from 20 to 80%; 1-[1-(4-methylphenyl)-2-mercaptoacetylimidazole]-3-ethylcarbamide (XI) exhibited maximum protection in a dose of 100 mg/kg. The low toxicity of these substituted imidazolocarbamides was reflected by their low LD_{50} values, which ranged from 600 to >1000 mg/kg; most of these compounds exhibited values ≥1000 mg/kg.

Data on anticonvulsant activity of these substituted imidazolocarbamides and 24-hr pentylenetetrazol-induced mortality failed to indicate an association between increased protection from convulsions and decreased pentylenetetrazol mortality in experimental animals. None of these substituted imidazolocarbamides possessed any appreciable sedative or CNS depressant effect or 24-hr mortality in the dose of 100 mg/kg used in the present investigation.

The nature of the alkyl group attached to the carbamide moiety had some influence on the anticonvulsant activity of these compounds. Replacement of the methyl substituent with an ethyl substituent decreased the anticonvulsant activity of five compounds (X, XII, and XIV–XVI), increased the activity of two compounds (XI and XIII), and caused no change in the activity of one compound (IX). Attachment of a substituent at the phenyl nucleus attached to position 1 of the imidazole nucleus failed to provide any definite structure–activity relationship of these compounds with respect to their anticonvulsant activity.

All 1-(1-aryl-2-mercaptoacetylimidazole)-3-alkylcarbamides, in general, selectively inhibited NAD-dependent oxidation of pyruvate, citrate, α-ketoglutarate, β-hydroxybutyrate, and NADH by rat brain homogenates (Table III). NAD-independent oxidation of succinate remained unaltered. At present, it is difficult to explain the inability of I–III to inhibit the oxidation of citrate and of IX, X, and XIV–XVI to inhibit the oxidation of α-ketoglutarate. Higher concentrations of these compounds possibly may cause inhibition of the cellular respiratory activity during oxidation of citrate and α-ketoglutarate.

The inhibitory effects of these substituted imidazolocarbamides were not consistent with the nature of the substituent on the phenyl nucleus attached to position 1 of the imidazole moiety or the alkyl

Table II—Anticonvulsant Activity of 1-(1-Aryl-2-mercaptoacetylimidazole)-3-alkylcarbamides

Compound	Approximate LD_{50}, mg/kg	Anticonvulsant Activity[a], % Protection	Pentylenetetrazol Mortality[b], %	Compound	Approximate LD_{50}, mg/kg	Anticonvulsant Activity[a], % Protection	Pentylenetetrazol Mortality[b], %
I	600	50	30	IX	1000	50	Nil
II	1000	60	10	X	>1000	50	Nil
III	>1000	50	Nil	XI	>1000	80	Nil
IV	750	60	90	XII	>1000	30	50
V	750	30	30	XIII	1000	50	10
VI	>1000	50	50	XIV	>1000	30	50
VII	>1000	30	30	XV	>1000	20	70
VIII	750	60	80	XVI	1000	30	10

[a] Screening procedures for the determination of anticonvulsant activity are as described in the text. Substituted imidazolocarbamides were administered at a dose of 100 mg/kg ip 4 hr before the administration of pentylenetetrazol (90 mg/kg sc). [b] Represents mortality during 24 hr in each group of animals administered pentylenetetrazol.

Table III—Inhibition of Respiratory Activity of Rat Brain Homogenates by 1-(1-Aryl-2-mercaptoacetylimidazole)-3-alkylcarbamides

Compound	Inhibition of Substrate Oxidation[a], %					
	Pyruvate	Citrate	α-Ketoglutarate	β-Hydroxybutyrate	NADH	Succinate
I	29.2 ± 1.2	Nil	25.2 ± 1.0	21.7 ± 1.2	16.3 ± 1.5	Nil
II	38.7 ± 1.4	Nil	39.0 ± 1.2	19.2 ± 1.4	44.5 ± 1.4	Nil
III	72.8 ± 0.9	Nil	13.5 ± 1.3	56.8 ± 1.6	47.5 ± 1.0	Nil
IV	47.5 ± 1.5	15.6 ± 1.2	49.7 ± 0.6	28.7 ± 1.5	40.3 ± 1.2	Nil
V	54.0 ± 1.3	20.8 ± 1.4	26.2 ± 1.8	43.1 ± 1.8	31.9 ± 1.4	Nil
VI	20.5 ± 1.2	23.4 ± 0.8	18.7 ± 0.9	48.1 ± 1.2	22.2 ± 1.4	Nil
VII	20.9 ± 1.1	10.0 ± 1.0	16.5 ± 1.2	30.2 ± 1.5	14.7 ± 1.4	Nil
VIII	37.1 ± 1.0	10.0 ± 1.1	12.3 ± 1.3	36.5 ± 1.4	30.3 ± 1.3	Nil
IX	24.1 ± 0.8	29.7 ± 0.9	Nil	45.4 ± 1.3	38.3 ± 1.0	Nil
X	37.6 ± 0.6	52.9 ± 0.6	Nil	33.5 ± 1.0	49.5 ± 1.1	Nil
XI	57.6 ± 1.2	35.4 ± 1.2	47.8 ± 1.6	52.2 ± 1.1	57.6 ± 0.9	Nil
XII	38.4 ± 1.4	30.5 ± 1.4	20.5 ± 1.4	36.5 ± 1.5	29.1 ± 1.2	Nil
XIII	72.7 ± 1.8	74.8 ± 1.2	72.6 ± 1.0	56.7 ± 1.4	28.1 ± 1.2	Nil
XIV	20.0 ± 1.6	43.4 ± 1.3	Nil	40.2 ± 1.4	20.3 ± 1.5	Nil
XV	48.8 ± 1.2	39.2 ± 1.6	Nil	42.5 ± 1.3	46.3 ± 1.4	Nil
XVI	36.6 ± 1.4	61.9 ± 1.0	Nil	50.6 ± 1.2	30.4 ± 1.3	Nil

[a] Assay procedures and the contents of the reaction mixture are as indicated in the text. Each experiment was done in duplicate. All values represent mean values of percent inhibition with ±*SEM* calculated from three separate experiments. Inhibition was determined by the decrease in the oxygen uptake/100 mg wet brain weight/hr. All substituted imidazolocarbamides were used at a final concentration of 2 m*M*. Different substrates and NADH were used at a final concentration of 10 and 0.5 m*M*, respectively. The oxygen uptake (microliters) in control experiments during oxidation of pyruvate, citrate, α-ketoglutarate, β-hydroxybutyrate, NADH, and succinate was 86.2 ± 2.2, 77.6 ± 1.4, 66.1 ± 2.5, 61.5 ± 2.4, 78.4 ± 2.6, and 205.4 ± 2.8, respectively.

group attached to the carbamide moiety during oxidation of the various substrates. The selective inhibition of NAD-dependent oxidations by these imidazolocarbamides was thus unrelated to their structure, so a definite structure–activity relationship was not exhibited (Table III). The ability of these compounds to inhibit NAD-dependent oxidations provides evidence regarding the possible inactivation of the electron transfer process in the electron transport chain by acting presumably at a site of transfer of electrons from NADH to flavine adenine dinucleotide.

These results failed to provide any correlation between *in vitro* selective inhibition of NAD-dependent oxidations by these substituted imidazolocarbamides and their anticonvulsant activity. Detailed pharmacological and biochemical studies using other purified enzyme preparations possibly may reflect the cellular basis for the anticonvulsant activity of these 1-(1-aryl-2-mercaptoacetylimidazole)-3-alkylcarbamides.

REFERENCES

(1) A. K. Gupta, C. Dwivedi, T. K. Gupta, S. S. Parmar, and W. E. Cornatzer, *J. Pharm. Sci.*, **63**, 1227(1974).

(2) V. K. Agarwal, K. C. Sah, S. Nagar, and S. S. Parmar, *J. Prakt. Chem.*, **312**, 964(1970).

(3) S. Nagar and S. S. Parmar, *Indian J. Pharm.*, **34**, 45(1972).

(4) S. S. Parmar, C. Dwivedi, and B. Ali, *J. Pharm. Sci.*, **61**, 1366(1972).

(5) A. Almirante, L. Polo, A. Mugnaini, E. Provinciali, P. Rugarli, A. Biancotti, A. Gamba, and W. Murmann, *J. Med. Chem.*, **8**, 305(1965).

(6) A. Almirante, L. Polo, A. Mugnaini, E. Provinciali, P. Rugarli, A. Gamba, A. Olivi, and W. Murmann, *ibid.*, **9**, 29(1966).

(7) G. C. Helsley, R. L. Duncan, Jr., W. H. Funderburk, and D. N. Johnson, *ibid.*, **12**, 1098(1969).

(8) G. J. Durant, *ibid.*, **9**, 247(1966).

(9) A. Johnson, J. C. Kaner, D. C. Sharma, and R. I. Darfmann, *ibid.*, **12**, 1024(1969).

(10) P. Franchetti, M. Grifantini, and S. Martelli, *ibid.*, **17**, 19(1974).

(11) M. Verderame, *ibid.*, **9**, 153(1966).

(12) S. S. Parmar, P. C. Joshi, B. Ali, and W. E. Cornatzer, *J. Pharm. Sci.*, **63**, 872(1974).

(13) C. C. Smith, *J. Pharmacol. Exp. Ther.*, **100**, 408(1950).

ACKNOWLEDGMENTS AND ADDRESSES

Received June 16, 1975, from the **Department of Pharmacology and Therapeutics, King George's Medical College, Lucknow University, Lucknow 226003, India,* and the *[‡]Department of Physiology and Pharmacology, University of North Dakota School of Medicine, Grand Forks, ND 58202*

Accepted for publication September 17, 1975.

Supported in part by the Department of Atomic Energy, Government of India, Bombay, India, and by U.S. Public Health Service National Institutes of Health Grants 1 TO1 HL 05939 and 1 RO1 DA

0996-01.

The authors thank Professor K. P. Bhargava and Professor Stanley J. Brumleve for their advice and encouragement. Grateful acknowledgment is made to the Department of Atomic Energy, Government of India, Bombay, India, for providing a research fellowship to S. K. Chaudhary.

[x] To whom inquiries should be directed (at the University of North Dakota School of Medicine).

Quantum Chemical Studies on Drug Action V: Involvement of Structure–Activity, Quantum Chemical, and Hydrophobicity Factors in Thrombocyte Uptake of 5-Hydroxytryptamine

MAHADEVAPPA KUMBAR [x], VINCENT CUSIMANO, and D. V. SIVA SANKAR

Abstract □ Inhibition of the uptake of 5-hydroxytryptamine (serotonin) in the thrombocyte by various tryptamine derivatives was investigated. The activity depended on the nature and position of the substituent. This activity was correlated with the total orbital energy and hydrophobicity factors. Other quantum parameters, such as the highest occupied molecular orbital energy and the lowest empty molecular orbital energy, failed to correlate. The possible involvement of two receptor sites that are sterically and electronically dissimilar is postulated because compounds fell into two distinct groups. The hydrophobicity factor was important in only one group of compounds, while the electronic factor was important in both.

Keyphrases □ 5-Hydroxytryptamine—uptake by thrombocytes correlated with structure–activity, quantum chemical, and hydrophobicity factors, effect of various tryptamine derivatives □ Thrombocytes—uptake of 5-hydroxytryptamine correlated with structure–activity, quantum chemical, and hydrophobicity factors, effect of various tryptamine derivatives □ Structure–activity factors—correlated with 5-hydroxytryptamine uptake by thrombocytes □ Quantum chemical factors—correlated with 5-hydroxytryptamine uptake by thrombocytes □ Hydrophobicity—correlated with 5-hydroxytryptamine uptake by thrombocytes □ Tryptamine—derivatives, effect on 5-hydroxytryptamine uptake by thrombocytes

In the past decade, quantum chemistry has been widely applied in pharmacology and medicinal chemistry, mainly to investigate drug activity. Even though the limitations of molecular orbital calculations have been recognized for many years, the various quantum parameters such as the highest occupied molecular orbital energy, the lowest empty molecular orbital energy, frontier electron density, and superdelocalizability have been correlated with observed activities (1, 2).

The highest occupied molecular orbital energy has been studied extensively because of its relation to the electron-donating ability. However, recent work (3) in molecular pharmacology has begun to show the inadequacy of the application of this concept without other physicochemical parameters. Molecular structure, hydrophobicity, and conformational details are also important determinants.

Quantum chemical data on about 50 derivatives of catechol, indole, imidazole, and lysergamide was reported previously (4, 5). This paper reports the effect of several structural analogs (Table I) of 5-hydroxytryptamine (serotonin) on its uptake by rabbit platelets. These data are further analyzed in terms of quantum chemical indexes and the hydrophobicity of these analogs.

EXPERIMENTAL

New Zealand albino male rabbits, approximately 6–12 months old, were used. The incubation experiments were carried out as follows. Blood was drawn from the rabbits by cardiac puncture. Enough edetate disodium solution (adjusted to pH 7.4 with sodium hydroxide) was added to give a final concentration of 1 mg of edetate/ml of blood. Platelet-rich plasma was obtained by centrifuging the blood at $50\times g$ for approximately 30 min. All operations were carried out using siliconized vessels at 2°.

Two milliliters of platelet-rich plasma was incubated with ^{3}H-5-hydroxytryptamine creatinine sulfate[1] (0.1 mmole = 2.5 mCi of ^{3}H-5-hydroxytryptamine) and appropriate amounts of an analog. The mixture was incubated at 37° for 30 min. Then the incubates were centrifuged at $500\times g$ to sediment the platelets. The sedimented platelet pellet was washed two times with 5 ml of saline.

The final platelet pellet was frozen overnight. The following morning, enough water was added to the platelet preparation to yield a 1.0-ml suspension. The turbidity of the platelets was measured[2] at 660 nm. The radioactivity of the platelet preparation was counted in a liquid scintillation spectrometer. The ratio of the radioactivity to the turbidity is a relative measure of the uptake of 5-hydroxytryptamine per unit volume of the platelet.

All analogs studied had either no activity or had inhibitory activity on the uptake of 5-hydroxytryptamine by the rabbit platelets. The ED_{50} (effective dose producing 50% inhibition) values of these drugs were determined by varying the concentration of the analog used over a wide range. A curve was plotted for each drug as shown in Fig. 1. The ED_{50} and/or ED_{25} (effective dose producing 25% inhibition) values for the analogs were obtained from these plots. The ED_{50} values are (I/S) ratios.

The quantum parameters, the highest occupied molecular orbital energy, the lowest empty molecular orbital energy, the highest superdelocalizability, the total orbital energy[3] (calculated by summing the energies of the occupied orbitals and multiplying the sum by two to account for the double occupancy), and the π–π^* transition energy[4], were obtained using the Hückel method with the omega technique (6, 7) for the hyperconjugation model as described previously (3–5). The log P values, which measure the lipophilicity or the hydrophobicity, were calculated using the published values of Hansch *et al.* (8). The calculated quantum parameters, log P values, and experimental activities (ED_{50}) are listed in Table I.

[1] Amersham Searle.
[2] Beckman DU spectrophotometer.
[3] Total orbital energy is the same as the total π-electron energy.
[4] The π–π^* transition also has been referred to as "LEMO-HOMO" or $\Delta M\beta$.

0996-01.

The authors thank Professor K. P. Bhargava and Professor Stanley J. Brumleve for their advice and encouragement. Grateful acknowledgment is made to the Department of Atomic Energy, Government of India, Bombay, India, for providing a research fellowship to S. K. Chaudhary.

[x] To whom inquiries should be directed (at the University of North Dakota School of Medicine).

Quantum Chemical Studies on Drug Action V: Involvement of Structure–Activity, Quantum Chemical, and Hydrophobicity Factors in Thrombocyte Uptake of 5-Hydroxytryptamine

MAHADEVAPPA KUMBAR [x], VINCENT CUSIMANO, and D. V. SIVA SANKAR

Abstract □ Inhibition of the uptake of 5-hydroxytryptamine (serotonin) in the thrombocyte by various tryptamine derivatives was investigated. The activity depended on the nature and position of the substituent. This activity was correlated with the total orbital energy and hydrophobicity factors. Other quantum parameters, such as the highest occupied molecular orbital energy and the lowest empty molecular orbital energy, failed to correlate. The possible involvement of two receptor sites that are sterically and electronically dissimilar is postulated because compounds fell into two distinct groups. The hydrophobicity factor was important in only one group of compounds, while the electronic factor was important in both.

Keyphrases □ 5-Hydroxytryptamine—uptake by thrombocytes correlated with structure–activity, quantum chemical, and hydrophobicity factors, effect of various tryptamine derivatives □ Thrombocytes—uptake of 5-hydroxytryptamine correlated with structure–activity, quantum chemical, and hydrophobicity factors, effect of various tryptamine derivatives □ Structure–activity factors—correlated with 5-hydroxytryptamine uptake by thrombocytes □ Quantum chemical factors—correlated with 5-hydroxytryptamine uptake by thrombocytes □ Hydrophobicity—correlated with 5-hydroxytryptamine uptake by thrombocytes □ Tryptamine—derivatives, effect on 5-hydroxytryptamine uptake by thrombocytes

In the past decade, quantum chemistry has been widely applied in pharmacology and medicinal chemistry, mainly to investigate drug activity. Even though the limitations of molecular orbital calculations have been recognized for many years, the various quantum parameters such as the highest occupied molecular orbital energy, the lowest empty molecular orbital energy, frontier electron density, and superdelocalizability have been correlated with observed activities (1, 2).

The highest occupied molecular orbital energy has been studied extensively because of its relation to the electron-donating ability. However, recent work (3) in molecular pharmacology has begun to show the inadequacy of the application of this concept without other physicochemical parameters. Molecular structure, hydrophobicity, and conformational details are also important determinants.

Quantum chemical data on about 50 derivatives of catechol, indole, imidazole, and lysergamide was reported previously (4, 5). This paper reports the effect of several structural analogs (Table I) of 5-hydroxytryptamine (serotonin) on its uptake by rabbit platelets. These data are further analyzed in terms of quantum chemical indexes and the hydrophobicity of these analogs.

EXPERIMENTAL

New Zealand albino male rabbits, approximately 6–12 months old, were used. The incubation experiments were carried out as follows. Blood was drawn from the rabbits by cardiac puncture. Enough edetate disodium solution (adjusted to pH 7.4 with sodium hydroxide) was added to give a final concentration of 1 mg of edetate/ml of blood. Platelet-rich plasma was obtained by centrifuging the blood at $50\times g$ for approximately 30 min. All operations were carried out using siliconized vessels at 2°.

Two milliliters of platelet-rich plasma was incubated with ^{3}H-5-hydroxytryptamine creatinine sulfate[1] (0.1 mmole = 2.5 mCi of ^{3}H-5-hydroxytryptamine) and appropriate amounts of an analog. The mixture was incubated at 37° for 30 min. Then the incubates were centrifuged at $500\times g$ to sediment the platelets. The sedimented platelet pellet was washed two times with 5 ml of saline.

The final platelet pellet was frozen overnight. The following morning, enough water was added to the platelet preparation to yield a 1.0-ml suspension. The turbidity of the platelets was measured[2] at 660 nm. The radioactivity of the platelet preparation was counted in a liquid scintillation spectrometer. The ratio of the radioactivity to the turbidity is a relative measure of the uptake of 5-hydroxytryptamine per unit volume of the platelet.

All analogs studied had either no activity or had inhibitory activity on the uptake of 5-hydroxytryptamine by the rabbit platelets. The ED_{50} (effective dose producing 50% inhibition) values of these drugs were determined by varying the concentration of the analog used over a wide range. A curve was plotted for each drug as shown in Fig. 1. The ED_{50} and/or ED_{25} (effective dose producing 25% inhibition) values for the analogs were obtained from these plots. The ED_{50} values are (I/S) ratios.

The quantum parameters, the highest occupied molecular orbital energy, the lowest empty molecular orbital energy, the highest superdelocalizability, the total orbital energy[3] (calculated by summing the energies of the occupied orbitals and multiplying the sum by two to account for the double occupancy), and the π–π^* transition energy[4], were obtained using the Hückel method with the omega technique (6, 7) for the hyperconjugation model as described previously (3–5). The log P values, which measure the lipophilicity or the hydrophobicity, were calculated using the published values of Hansch *et al.* (8). The calculated quantum parameters, log P values, and experimental activities (ED_{50}) are listed in Table I.

[1] Amersham Searle.
[2] Beckman DU spectrophotometer.
[3] Total orbital energy is the same as the total π-electron energy.
[4] The π–π^* transition also has been referred to as "LEMO-HOMO" or $\Delta M\beta$.

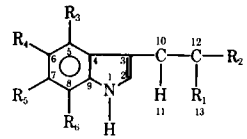

Table I—Structures and ED_{50}, log *P*, and Quantum Chemical Data for the Compounds Studied

Compound	R_1	R_2	R_3	R_4	R_5	R_6	HOMO β^{-1} [a]	LEMO β^{-1} [b]	HFED [c]	HSUP β [d]	TOE β^{-1} [e]	π–π^*	ED_{50}	log *P*
1	H_2	$N(C_2H_5)_2$	NH_2	H	H	H	0.318	−0.982	0.3198 at 2	2.0812 at R_3	42.480	1.300	7.5	2.27
2	H_2	$N(CH_3)_2$	NH_2	H	H	H	0.318	−0.982	0.3198 at 2	2.0812 at R_3	34.496	1.300	26.0	1.35
3	H_2	NH_2	NH_2	H	H	H	0.318	−0.982	0.3198 at 2	2.0812 at R_3	26.298	1.300	12.5	0.23
4	H_2	$N(C_2H_5)_2$	H	OH	H	OH	0.395	−0.969	0.4505 at 5	1.8962 at $N(R_2)$	48.620	1.364	84.0	2.83
5	H_2	$N(C_2H_5)_2$	H	OCH_3	H	OCH_3	0.392	−0.966	0.4554 at 5	1.8962 at $N(R_2)$	56.694	1.358	30.0	3.46
6	H_2	$N(C_2H_5)_2$	H	H	H	OH	0.423	−0.950	0.4378 at 3	1.8962 at $N(R_2)$	44.318	1.373	—	—
7	H_2	$N(C_2H_5)_2$	H	H	H	OCH_3	0.420	−0.947	0.4278 at 3	1.8967 at 15	48.356	1.367	18.0	3.48
8	H_2	NH_2	H	OH	OH	H	0.399	−0.962	0.464 at 2	1.948 at $N(R_2)$	32.422	1.361	22.5	0.72
9	H_2	NH_2	H	OH	H	OH	0.395	−0.969	0.4507 at 5	1.9482 at $N(R_2)$	32.426	1.364	48.5	0.12
10	H_2	NH_2	H	OCH_3	H	OCH_3	0.392	−0.966	0.4556 at −5	1.9485 at $N(R_2)$	40.510	1.358	9.5	1.42
11	H_2	$N(CH_3)_2$	H	OH	H	OH	0.395	−0.969	0.4505 at 5	1.8897 at $N(R_2)$	40.630	1.364	42.5	1.24
12	H_2	$N(CH_3)_2$	H	OCH_3	H	OCH_3	0.392	−0.966	0.4554 at 5	1.8897 at $N(R_2)$	48.704	1.358	9.3	2.54
13	H_2	$N(CH_3)_2$	H	H	H	OH	0.423	−0.950	0.4379 at 3	1.8897 at $N(R_2)$	36.330	1.373	46.0	1.91
14	H_2	$N(CH_3)_2$	H	H	H	OCH_3	0.420	−0.947	0.4278 at 3	1.8897 at $N(R_2)$	40.364	1.367	—	—
15	H_2	NHC_2H_5	H	OCH_3	H	OCH_3	0.392	−0.966	0.4555 at 5	1.916 at $N(R_2)$	48.612	1.358	9.0	1.98
16	H_2	NHC_2H_5	H	H	H	OH	0.423	−0.950	0.4380 at 3	1.9160 at $N(R_2)$	36.232	1.373	6.0	1.81
17	H_2	NHC_2H_5	H	H	H	OCH_3	0.420	−0.947	0.4280 at 3	1.9160 at $N(R_2)$	40.272	1.367	9.0	2.46
18	H_2	NH_2	OH	H	H	H	0.376	−0.966	0.430 at 3	1.670 at 3	28.806	1.342	12.0	0.79
19	H_2	NH_2	H	H	OH	H	0.388	−0.948	0.489 at 3	1.680 at 3	28.796	1.336	19.0	0.79
20	H_2	NH_2	H	H	H	OH	0.423	−0.950	0.438 at 3	1.948 at $N(R_2)$	28.128	1.373	18.0	0.79
21	H_2	$NHCH_3$	H	OCH_3	H	OCH_3	0.392	−0.966	0.4555 at 5	1.9122 at $N(R_2)$	44.614	1.358	8.0	2.44
22	H_2	$NHCH_3$	H	OH	H	H	0.454	−0.914	0.5151 at 3	1.9122 at $N(R_2)$	32.230	1.368	1.9	1.35
23	H_2	$NHCH_3$	H	H	H	OCH_3	0.420	−0.947	0.4280 at 3	1.9122 at $N(R_2)$	36.278	1.367	3.5	2.00
24	NH_2	COOH	H	OH	OH	H	−0.320	−0.964	1.109 at 12	1.6051 at 2	39.452	0.644	—	—
25	NH_2	COOH	OH	H	H	H	−0.320	−0.955	1.1009 at 12	1.5422 at 2	34.846	0.635	—	—
26	NH_2	COOH	H	H	OH	H	−0.320	−0.937	1.1009 at 12	1.5515 at 2	34.832	0.617	—	—
27	NH_2	COOH	H	H	H	OH	−0.320	−0.952	1.1009 at 12	1.5187 at 3	34.842	0.632	—	—
28	H_2	$NHCH_3$	NH_2	H	H	H	0.318	−0.982	0.3198 at 2	2.0812 at R_3	30.410	1.300	35.4	0.79
29	H_2	NH_2	H	OCH_3	H	H	0.453	−0.913	0.514 at 3	1.948 at R_2	32.156	1.366	36.0	1.44
30	DL-α-Methyl-*m*-tyrosine						−0.084	−1.010	0.7078 at 10	1.0220 at 7	31.708	0.926	—	—
31	COOH	NH_2	H	OCH_3	H	H	−0.320	−0.915	1.1009 at 12	1.5134 at 3	38.868	0.595	—	—
32	L-3-Methylhistidine						−0.319	−1.077	1.1002 at 10	1.4602 at 3	29.243	0.758	—	—
33	COOH	NH_2	H	OH	H	H	−0.286	−0.893	1.064 at 12	1.4480 at 3	34.912	0.607	—	—
34	L-Histidine						−0.319	−1.113	1.1003 at 8	1.4478 at 3	25.203	0.794	—	—
35	DL-Norepinephrine						−0.316	−1.114	1.148 at 7	1.932 at NH_2	27.824	0.798	—	—
36	H_2	NH_2	H	CH_3	H	H	0.470	−0.896	0.521 at 3	1.948 at R_2	27.656	1.366	—	—
37	Spermine						0.681	−1.504	0.505 at —NH— and —NH—	1.947 at —NH_2, —NH—, —NH—, and NH_2	49.624	2.185	—	—
38	Histamine						0.519	−1.103	0.670 at 5	1.948 at —NH_2	18.492	1.622	—	—
39	COOH	NH_2	H	H	H	H	−0.286	−0.893	1.064 at 12	1.465 at 3	30.60	0.607	—	—
40	H_2	NH_2	H	H	H	H	0.444	−0.903	0.514 at 3	1.531 at 3	24.482	1.347	—	—

[a] Highest occupied molecular orbital energy. [b] Lowest empty molecular orbital energy. [c] Highest frontier electron density. [d] Highest superdelocalizability. [e] Total orbital energy.

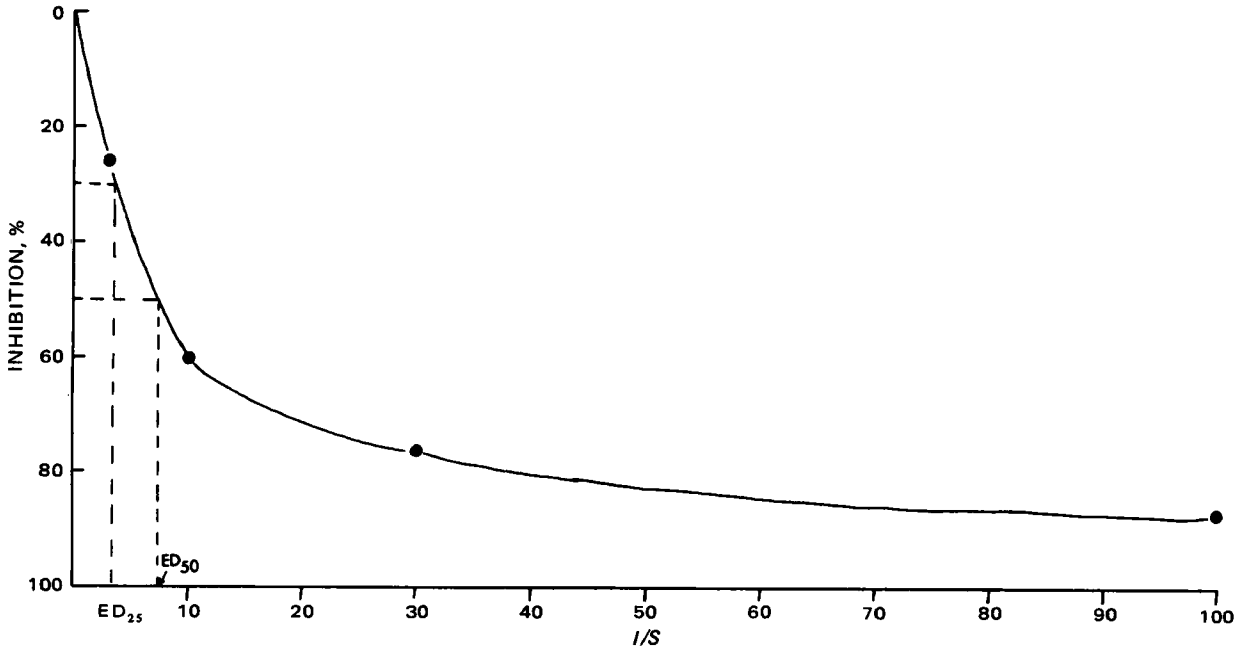

Figure 1—*Plot of percent inhibition* versus *the* I/S *ratio (*I = *concentration of inhibitor, and* S = *concentration of substrate). The* ED_{50} *and* ED_{25} *values are shown by the dotted lines. Only the* ED_{50} *values were calculated in the present investigation (Table I).*

RESULTS

The highest occupied molecular orbital energy, lowest empty molecular orbital energy, highest superdelocalizability, π–π^* transition energy, and highest frontier electron density did not correlate with the observed activity (ED_{50}). But the total orbital energy did correlate with the activity. Figure 2 shows the plot of log ED_{50} *versus* the total orbital energy. The data distinctly separated into upper and lower groups. Moreover, a linear relationship was observed between the points within each group and the total orbital energy, which might be attributed to the similar behavior of the compounds in each group.

A least-squares analysis of Fig. 2 yields the following equations. For the upper group:

$$\log ED_{50} = 0.1399 + 3.415 \times 10^{-2} \text{ total orbital energy} \qquad \begin{matrix} n & r & s \\ 12 & 0.832 & 0.141 \end{matrix} \qquad \text{(Eq. 1)}$$

For the lower group:

$$\log ED_{50} = -0.7982 + 3.947 \times 10^{-2} \text{ total orbital energy} \qquad \begin{matrix} n & r & s \\ 11 & 0.884 & 0.148 \end{matrix} \qquad \text{(Eq. 2)}$$

In addition, the log ED_{50} was correlated with the log (total orbital energy). The least-squares equation for the upper group is:

$$\log ED_{50} = -2.952 + 2.908 \log (\text{total orbital energy}) \qquad \begin{matrix} n & r & s \\ 12 & 0.851 & 0.134 \end{matrix} \qquad \text{(Eq. 3)}$$

For the lower group, it is:

$$\log ED_{50} = -5.539 + 3.954 \log (\text{total orbital energy}) \qquad \begin{matrix} n & r & s \\ 11 & 0.893 & 0.142 \end{matrix} \qquad \text{(Eq. 4)}$$

From the calculated correlation coefficients, it appears that the log–log plot yields a slightly better correlation. In any event, both methods lead to a separation of the data into two distinct groups.

Figure 3 shows the plot of the activity *versus* the log P or the hydrophobicity of the derivatives tested. Surprisingly, the data again separated into two distinct groups. And the compounds fell into the same groups as in the total orbital energy correlation (Fig. 2). Therefore, the separation is apparently not artificial. The least-squares equations for the lipophilicity relationship are as follow. For the upper group:

$$\log ED_{50} = 1.215 + 0.223 \log P \qquad \begin{matrix} n & r & s \\ 12 & 0.650 & 0.190 \end{matrix} \qquad \text{(Eq. 5)}$$

For the lower group:

$$\log ED_{50} = 7.899 \times 10^{-2} + 0.361 \log P \qquad \begin{matrix} n & r & s \\ 11 & 0.801 & 0.189 \end{matrix} \qquad \text{(Eq. 6)}$$

The poor correlation of the upper group may indicate that the hydrophobicity of these compounds plays a minor role in the drug activity mechanism. On the other hand, the hydrophobicity might be significant for the lower group of compounds as shown by the degree of correlation.

The experimental activity was further analyzed in terms of both total orbital energy and log P to assess the degree of electronic and hydrophobic interactions. Multiple regression analysis (9) of these data produced the following equations. For the upper group:

$$\log ED_{50} = \underset{(\pm 0.038)}{-3.581} + \underset{(\pm 0.939)}{3.363} \log (\text{total orbital energy}) - \underset{(\pm 0.094)}{0.0554} \log P \qquad \begin{matrix} n & r & s \\ 12 & 0.856 & 0.132 \end{matrix} \qquad \text{(Eq. 7)}$$

For the lower group:

$$\log ED_{50} = \underset{(\pm 0.033)}{-3.275} + \underset{(\pm 0.842)}{2.324} \log (\text{total orbital energy}) + \underset{(\pm 0.092)}{0.226} \log P \qquad \begin{matrix} n & r & s \\ 11 & 0.938 & 0.109 \end{matrix} \qquad \text{(Eq. 8)}$$

The numbers in the parentheses represent the standard error of the estimate for the respective coefficients. Thus, by comparing Eqs. 3 and 4 with Eqs. 7 and 8, respectively, it is clear that the inclusion of the hydrophobicity factor does not lead to an improvement for the upper group of compounds. However, a slight improvement is observed for the lower group of compounds, reconfirming that the hydrophobicity makes a lesser contribution to the activity of the upper group.

DISCUSSION

From the observed experimental activities (Table I), it is seen that both the side chain and ring substituents are important in deciding the inhibitory activity on the uptake of 5-hydroxytryptamine. If the side-chain substituents are bulky, for example, $R_2 = N(C_2H_5)_2$, the activity decreases. The higher the ED_{50} value, the lower is the inhibitory activity.

A further decrease in inhibitory activity occurs when two hydroxyl groups are substituted on the ring. That is, two hydroxyl groups are more effective in reducing the activity than a single hydroxyl, a single methoxy, or two methoxy groups. The activity also varies according to the position of the hydroxyl groups. For example, the ED_{50} values

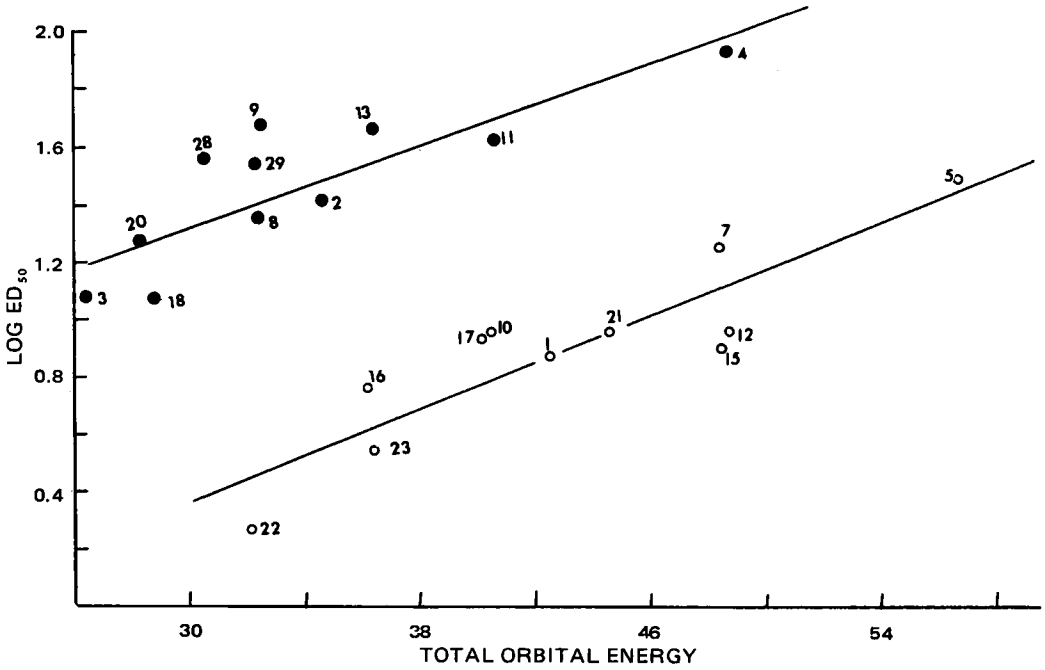

Figure 2—*Plot of log ED_{50}* versus *the total orbital energy. The numbers on the graph correspond to the compound numbers in Table I. The straight lines are the least-squares lines (Eqs. 1 and 2).*

of 6-hydroxytryptamine (Compound 19), 7-hydroxytryptamine (Compound 20), 5,6-dihydroxytryptamine (Compound 8), and 5,7-dihydroxytryptamine (Compound 9) are 19.0, 18.0, 22.5, and 48.5, respectively.

Various molecular orbital studies indicated extended (10) or folded (11) or extended and folded (12, 13) conformations to be the stable forms for 5-hydroxytryptamine. A recent empirical method study (14) also predicted two preferred (the most stable form) conformations (extended and folded, which are sterically different) for 5-hydroxytryptamine. These two stable conformations were also predicted by an NMR solution study (15). In the empirical study (14), it was suggested that these two stable conformations might correspond to two 5-hydroxytryptamine receptor sites. In the present study, the separation of compounds into two distinct groups (Figs. 2 and 3) may be a clear indication that two receptor sites of a sterically and electronically dissimilar nature are involved. Thus, one group of compounds might inhibit 5-hydroxytryptamine on the same site, so the correlation between them is possible.

It is generally accepted that anti-5-hydroxytryptamine activity is the result of the blocking of 5-hydroxytryptamine by a drug molecule at 5-hydroxytryptamine receptor sites. The drug molecule may bind to the receptor site(s) blocking the complexing of 5-hydroxytryptamine. However, this kind of drug–receptor binding may not be the only process that ultimately leads to inhibition.

Snyder (1) utilized the concept of structural resemblance to understand biological activities such as hallucinogenic activity. He tried to explain, with the help of this concept, the hallucinogenic activities of various indolealkylamine and amphetamine derivatives. He proposed that the latter derivatives achieve a conformation similar to a portion of the lysergic acid diethylamide (lysergide) molecule in order

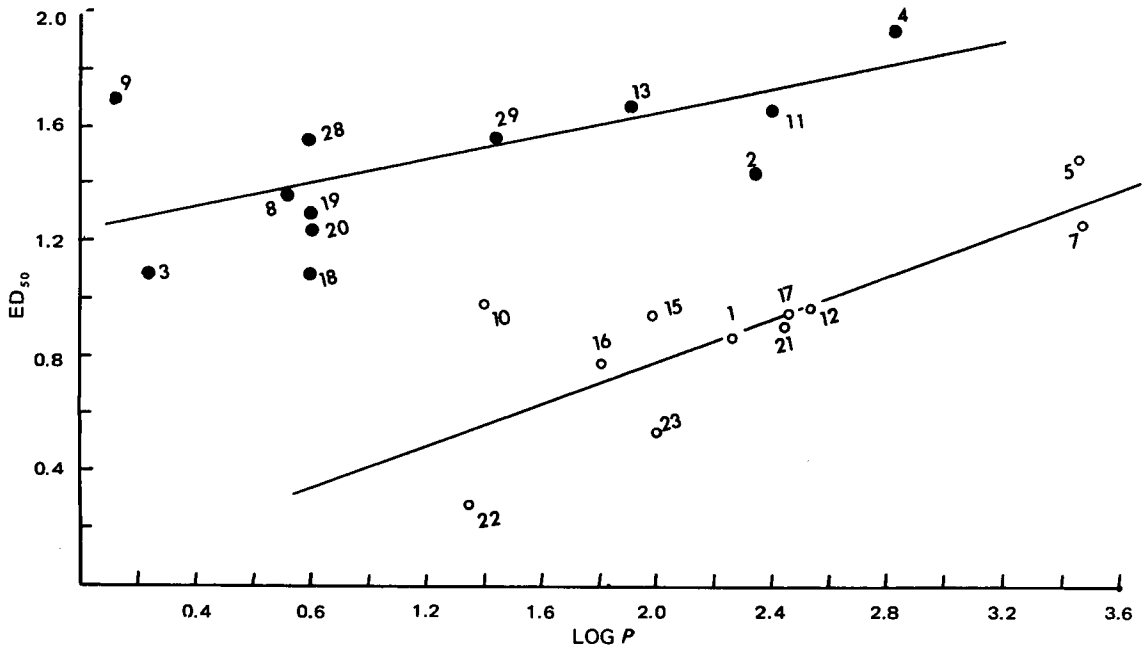

Figure 3—*Plot of log ED_{50}* versus *log* P. *The numbers on the graph correspond to the numbers in Table I. The straight lines are the least-squares lines (Eqs. 5 and 6).*

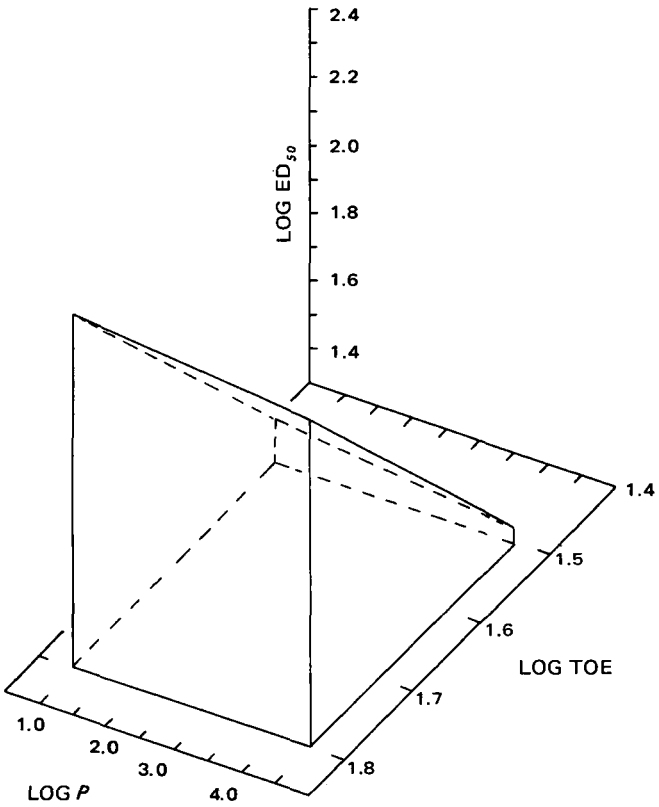

Figure 4—*Structure–activity surface generated by Eq. 7. (TOE = total orbital energy.)*

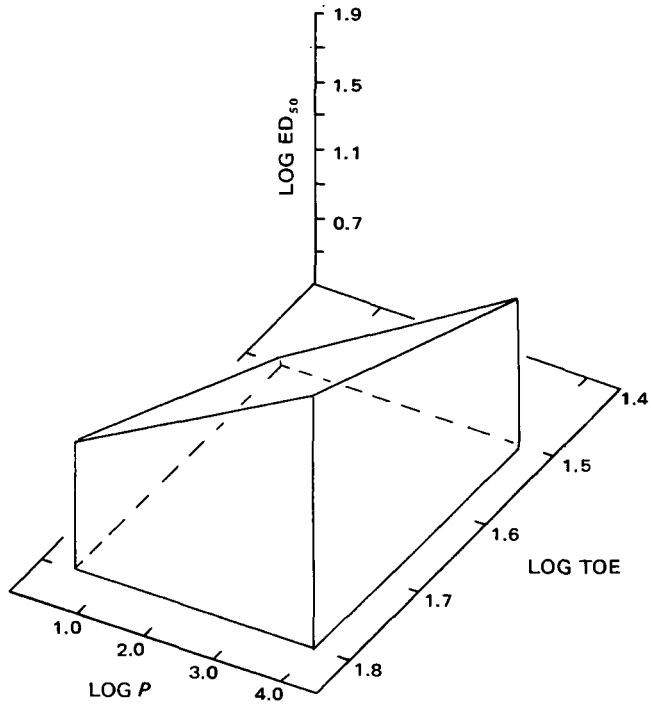

Figure 5—*Structure–activity surface generated by Eq. 8. (TOE = total orbital energy.)*

to elicit the hallucinogenic response. This hypothesis was supported by X-ray work (16).

The same idea also can be extended to the inhibitory activity of the tryptamine derivatives studied here. Furthermore, the conformational resemblance of a molecule can be related to its observed activity. Under biological conditions, the interaction of 5-hydroxytryptamine with the receptor site(s) may not occur in only the previously mentioned preferred conformations. Moreover, the minimum energy conformations, as determined by X-ray (16) and other methods (10–14), may not necessarily be the conformations at the receptor site (17). However, due to a lack of knowledge about the receptor site conformations, it is postulated that the two preferred conformations of 5-hydroxytryptamine are responsible for its action.

Evidence for an electronic dissimilarity of the previously mentioned two receptor sites may be obtained as follows. Cammarata (18) applied the Arrhenius equation to biological activity:

$$\log A = -\Delta E/2.303RT + c \qquad \text{(Eq. 9)}$$

where R is the gas constant, T is the absolute temperature, ΔE is the change in energy, and c is a constant. In Eq. 9, A reflects an equilibrium or a rate constant for the formation of a drug–receptor complex. The ΔE can be assumed to be the sum of the various contributions (18), such as:

$$\Delta E = \Delta E^e + \Delta E^d + \Delta E^s + \Delta E^p \qquad \text{(Eq. 10)}$$

where ΔE^e, ΔE^d, ΔE^s, and ΔE^p are the changes in electronic, solvation, steric, and conformational energies, respectively. More generally, Eq. 10 can be written as:

$$\Delta E = a_1 \Delta E^e + a_2 \Delta E^d + a_3 \Delta E^s + a_4 \Delta E^p \qquad \text{(Eq. 11)}$$

where a_1, a_2, a_3, and a_4 are coefficients. By substituting Eq. 11 into Eq. 9, the following equation is obtained:

$$\log A = -\frac{1}{2.303RT}(a_1 \Delta E^e + a_2 \Delta E^d + a_3 \Delta E^s + a_4 \Delta E^p) + c \qquad \text{(Eq. 12)}$$

Since the observed activity was correlated with the total orbital energy, ΔE^e can be represented by the total orbital energy. Thus, the final activity relationship takes the form:

$$\log A = -(2.303RT)^{-1}(a_1\beta)\,(\text{total orbital energy}) + (a_2' \Delta E^d + a_3' \Delta E^s + a_4' \Delta E^p + c') \qquad \text{(Eq. 13)}$$

where β is the resonance integral, and the constant $-(2.303RT)^{-1}$ has been absorbed in a_2', a_3', a_4', and c'.

Information on the electronic dissimilarity of both groups of compounds can be obtained by evaluating the coefficient a_1. To do so, it is necessary to have the information on the second term of Eq. 13. Since it is difficult to obtain such information, as a first approximation the second term is treated as constant. Moreover, it is assumed that the sum given in the second term remains constant even though each term in the sum might change. By comparing Eq. 13 with Eqs. 1 and 2, the first term in Eq. 13 is evaluated. For the upper group:

$$-\frac{a_1\beta}{2.303RT} = 3.415 \times 10^{-2} \qquad \text{(Eq. 14a)}$$

For the lower group:

$$-\frac{a_1\beta}{2.303RT} = 3.947 \times 10^{-2} \qquad \text{(Eq. 14b)}$$

And for the upper group:

$$a_2' \Delta E^d + a_3' \Delta E^s + a_4' \Delta E^p + c' = 0.1399 \qquad \text{(Eq. 15a)}$$

For the lower group:

$$a_2' \Delta E^d + a_3' \Delta E^s + a_4' \Delta E^p + c' = -0.7982 \qquad \text{(Eq. 15b)}$$

Since the experimental activities was derived at the physiological temperature of 37°, the values of R (2 cal/deg mole) and T (310°K) are substituted in Eqs. 14a and 14b. Then the value of $a_1\beta$ for the upper group is:

$$-a_1\beta = 48.761 \text{ cal/mole} \qquad \text{(Eq. 16a)}$$

For the lower group, it is:

$$-a_1\beta = 56.357 \text{ cal/mole} \qquad \text{(Eq. 16b)}$$

The value of the resonance integral, β, has frequently been taken as −18.0 kcal/mole for hydrocarbons (6). However, this value changes depending upon the chemical structure involved. A lengthy discussion regarding this parameter may be found in Ref. 6. As a first approximation, it is assumed that −18.0 kcal/mole is also applicable to indole systems. Then for the upper group:

$$a_1 = 27.089 \times 10^{-4} \qquad \text{(Eq. 17a)}$$

And for the lower group:

$$a_1 = 31.309 \times 10^{-4} \qquad \text{(Eq. 17}b\text{)}$$

The constant a_1, which is the coefficient of ΔE^e, might be related to an electronic factor associated with the change in the electronic energy. Hence, it is clear from the magnitude of a_1 (Eqs. 17*a* and 17*b*) or $-a_1\beta$ (Eqs. 16*a* and 16*b*) that both groups of compounds do not experience similar electronic interactions. Therefore, from this analysis, together with the apparent existence of two sterically different stable conformations, one can speculate that groups of compounds falling on the same line (upper or lower) might behave electronically and sterically similarly while acting on the same site.

The influence of electronic and hydrophobic interactions can be assessed by considering Eqs. 3–6. From the correlation coefficients of these equations, it is evident that the hydrophobic interactions are not significant in the upper group of compounds whereas they are important in the lower group. This difference can be explained in terms of the nature of the substituents. The lower group of compounds has one or two methoxy groups present on the ring portion (except Compounds 1, 16, and 22), and all of them (except Compound 10) carry a side-chain substituent. These groups (methyl, ethyl, and methoxy) present on the side chain as well as on the ring portion might engage in hydrophobic interactions.

On the other hand, the upper group of compounds carries hydroxyl and amino substituents (except Compound 29) on the ring portion, and only a few of them carry side-chain amino substituents. The hydroxyl and amino groups have much smaller hydrophobicity factors (8) compared to a methoxy group. Apart from that, the average lipophilicity of the upper and lower groups is 1.033 ± 0.756 and 2.292 ± 0.671, respectively. These values indicate that hydrophobicity does not play a large role in the upper group of compounds.

Figures 4 and 5 show the activity surface generated by Eqs. 7 and 8, respectively. For the upper group (Fig. 4), the influence of log P for a given total orbital energy is smaller, but it is larger for the lower group (Fig. 5).

REFERENCES

(1) S. H. Snyder, in "Molecular Orbital Studies in Chemical Pharmacology," L. B. Kier, Ed., Springer-Verlag, New York, N.Y., 1970, p. 238.

(2) J. P. Green and S. Kang, in *ibid.*, p. 105.

(3) M. Kumbar and D. V. S. Sankar, *Res. Commun. Chem. Pathol. Pharmacol.*, **7**, 259(1973).

(4) *Ibid.*, **5**, 45(1973).

(5) *Ibid.*, **6**, 65(1973).

(6) B. Pullman and A. Pullman, "Quantum Biochemistry," Interscience, New York, N.Y., 1963.

(7) A. Streitwieser, "Molecular Orbital Theory for Organic Chemists," Wiley, New York, N.Y., 1961.

(8) C. Hansch, A. Leo, S. H. Unger, K. H. Kim, D. Nikaitani, and E. J. Lien, *J. Med. Chem.*, **16**, 1207(1973).

(9) C. I. Bliss, "Statistics in Biology," vol. 2, McGraw Hill, New York, N.Y., 1970, p. 291.

(10) L. B. Kier, *J. Pharm. Sci.*, **57**, 1188(1968).

(11) G. N. J. Port and B. Pullman, *Theor. Chim. Acta*, **33**, 275(1974).

(12) S. Kang, C. L. Johnson, and J. P. Green, *J. Mol. Struct.*, **15**, 453(1973).

(13) S. Kang and M. H. Cho, *Theor. Chim. Acta*, **22**, 176(1971).

(14) M. Kumbar and D. V. S. Sankar, *Res. Commun. Chem. Pathol. Pharmacol.*, **10**, 433(1975).

(15) R. R. Ison, P. Partington, and G. C. K. Roberts, *J. Pharm. Pharmacol.*, **24**, 82(1972).

(16) R. W. Baker, C. Chothia, P. Pauling, and H. P. Weber, *Mol. Pharmacol.*, **9**, 23(1973).

(17) C. R. Ganellin, *J. Med. Chem.*, **16**, 620(1973).

(18) A. Cammarata, in "Molecular Orbital Studies in Chemical Pharmacology," L. B. Kier, Ed., Springer-Verlag, New York, N.Y., 1970, p. 156.

ACKNOWLEDGMENTS AND ADDRESSES

Received March 19, 1975, from the *Division of Research Laboratories, Queens Children's Psychiatric Center, Bellerose, NY 11426*

Accepted for publication September 17, 1975.

The authors thank Dr. Gloria Faretra for continued interest and support of this work.

[x] To whom inquiries should be directed.

Carbon-13 Magnetic Resonance Spectroscopy of Drugs II: Antihistamines

CHING-JER CHANG [*x] and GARNET E. PECK [‡]

Abstract □ The natural abundance carbon-13 magnetic resonance spectra of a series of antihistamines (pheniramine, chlorpheniramine, methapyrilene, tripelennamine, pyrilamine, and thonzylamine) were determined using the pulse Fourier transform technique. The chemical shifts were assigned with the aid of long-range carbon-13–hydrogen coupling constants.

Keyphrases □ Magnetic resonance spectroscopy, carbon-13—various antihistamines, spectra determined using pulse Fourier transform technique □ Antihistamines—carbon-13 magnetic resonance spectra determined using pulse Fourier transform technique □ Fourier transform technique—carbon-13 magnetic resonance spectra of various antihistamines

Histamine has continuously received great attention from chemists and biologists (1). This interest is stimulated by the variety and potency of its biological effects, *e.g.*, activities in the cardiovascular system, smooth muscle contraction, and gastric acid and other exocrine gland secretions. Numerous drugs antagonize the action of histamine at its cellular site of action.

According to the classical receptor theory, the biological effect of histamine and antihistamines is the result of physicochemical interactions with the receptor sites. Any successful attempt to correlate these receptor interactions with the configuration and conformation of the drug must rely on detailed studies of the structural chemistry of antihistamines. Great effort has been made recently to characterize these compounds by various physical techniques (2–7).

The development of the Fourier transform technique has added a new tool for the study of the structure and conformation of organic molecules in solution and, potentially, when bound to receptors. Carbon-13 magnetic resonance (CMR) spectroscopy (8–11) increasingly is being directed to the study of drugs (12–20). A detailed

And for the lower group:

$$a_1 = 31.309 \times 10^{-4} \qquad \text{(Eq. 17}b\text{)}$$

The constant a_1, which is the coefficient of ΔE^e, might be related to an electronic factor associated with the change in the electronic energy. Hence, it is clear from the magnitude of a_1 (Eqs. 17*a* and 17*b*) or $-a_1\beta$ (Eqs. 16*a* and 16*b*) that both groups of compounds do not experience similar electronic interactions. Therefore, from this analysis, together with the apparent existence of two sterically different stable conformations, one can speculate that groups of compounds falling on the same line (upper or lower) might behave electronically and sterically similarly while acting on the same site.

The influence of electronic and hydrophobic interactions can be assessed by considering Eqs. 3–6. From the correlation coefficients of these equations, it is evident that the hydrophobic interactions are not significant in the upper group of compounds whereas they are important in the lower group. This difference can be explained in terms of the nature of the substituents. The lower group of compounds has one or two methoxy groups present on the ring portion (except Compounds 1, 16, and 22), and all of them (except Compound 10) carry a side-chain substituent. These groups (methyl, ethyl, and methoxy) present on the side chain as well as on the ring portion might engage in hydrophobic interactions.

On the other hand, the upper group of compounds carries hydroxyl and amino substituents (except Compound 29) on the ring portion, and only a few of them carry side-chain amino substituents. The hydroxyl and amino groups have much smaller hydrophobicity factors (8) compared to a methoxy group. Apart from that, the average lipophilicity of the upper and lower groups is 1.033 ± 0.756 and 2.292 ± 0.671, respectively. These values indicate that hydrophobicity does not play a large role in the upper group of compounds.

Figures 4 and 5 show the activity surface generated by Eqs. 7 and 8, respectively. For the upper group (Fig. 4), the influence of log P for a given total orbital energy is smaller, but it is larger for the lower group (Fig. 5).

REFERENCES

(1) S. H. Snyder, in "Molecular Orbital Studies in Chemical Pharmacology," L. B. Kier, Ed., Springer-Verlag, New York, N.Y., 1970, p. 238.

(2) J. P. Green and S. Kang, in *ibid.*, p. 105.

(3) M. Kumbar and D. V. S. Sankar, *Res. Commun. Chem. Pathol. Pharmacol.*, **7**, 259(1973).

(4) *Ibid.*, **5**, 45(1973).

(5) *Ibid.*, **6**, 65(1973).

(6) B. Pullman and A. Pullman, "Quantum Biochemistry," Interscience, New York, N.Y., 1963.

(7) A. Streitwieser, "Molecular Orbital Theory for Organic Chemists," Wiley, New York, N.Y., 1961.

(8) C. Hansch, A. Leo, S. H. Unger, K. H. Kim, D. Nikaitani, and E. J. Lien, *J. Med. Chem.*, **16**, 1207(1973).

(9) C. I. Bliss, "Statistics in Biology," vol. 2, McGraw Hill, New York, N.Y., 1970, p. 291.

(10) L. B. Kier, *J. Pharm. Sci.*, **57**, 1188(1968).

(11) G. N. J. Port and B. Pullman, *Theor. Chim. Acta*, **33**, 275(1974).

(12) S. Kang, C. L. Johnson, and J. P. Green, *J. Mol. Struct.*, **15**, 453(1973).

(13) S. Kang and M. H. Cho, *Theor. Chim. Acta*, **22**, 176(1971).

(14) M. Kumbar and D. V. S. Sankar, *Res. Commun. Chem. Pathol. Pharmacol.*, **10**, 433(1975).

(15) R. R. Ison, P. Partington, and G. C. K. Roberts, *J. Pharm. Pharmacol.*, **24**, 82(1972).

(16) R. W. Baker, C. Chothia, P. Pauling, and H. P. Weber, *Mol. Pharmacol.*, **9**, 23(1973).

(17) C. R. Ganellin, *J. Med. Chem.*, **16**, 620(1973).

(18) A. Cammarata, in "Molecular Orbital Studies in Chemical Pharmacology," L. B. Kier, Ed., Springer-Verlag, New York, N.Y., 1970, p. 156.

ACKNOWLEDGMENTS AND ADDRESSES

Received March 19, 1975, from the *Division of Research Laboratories, Queens Children's Psychiatric Center, Bellerose, NY 11426*

Accepted for publication September 17, 1975.

The authors thank Dr. Gloria Faretra for continued interest and support of this work.

[x] To whom inquiries should be directed.

Carbon-13 Magnetic Resonance Spectroscopy of Drugs II: Antihistamines

CHING-JER CHANG [*x] and GARNET E. PECK [‡]

Abstract □ The natural abundance carbon-13 magnetic resonance spectra of a series of antihistamines (pheniramine, chlorpheniramine, methapyrilene, tripelennamine, pyrilamine, and thonzylamine) were determined using the pulse Fourier transform technique. The chemical shifts were assigned with the aid of long-range carbon-13–hydrogen coupling constants.

Keyphrases □ Magnetic resonance spectroscopy, carbon-13—various antihistamines, spectra determined using pulse Fourier transform technique □ Antihistamines—carbon-13 magnetic resonance spectra determined using pulse Fourier transform technique □ Fourier transform technique—carbon-13 magnetic resonance spectra of various antihistamines

Histamine has continuously received great attention from chemists and biologists (1). This interest is stimulated by the variety and potency of its biological effects, *e.g.*, activities in the cardiovascular system, smooth muscle contraction, and gastric acid and other exocrine gland secretions. Numerous drugs antagonize the action of histamine at its cellular site of action.

According to the classical receptor theory, the biological effect of histamine and antihistamines is the result of physicochemical interactions with the receptor sites. Any successful attempt to correlate these receptor interactions with the configuration and conformation of the drug must rely on detailed studies of the structural chemistry of antihistamines. Great effort has been made recently to characterize these compounds by various physical techniques (2–7).

The development of the Fourier transform technique has added a new tool for the study of the structure and conformation of organic molecules in solution and, potentially, when bound to receptors. Carbon-13 magnetic resonance (CMR) spectroscopy (8–11) increasingly is being directed to the study of drugs (12–20). A detailed

Table I—Carbon-13 NMR Chemical Shifts in Aqueous Solution

Carbon	I	II	III	IV	V	VI
α	56.3	56.2	56.9	56.6	57.2	56.2
β	28.6	28.6	44.3	44.8	44.8	50.0
γ	49.7	49.1	47.9	52.6	52.1	55.4
N-Methyl	42.8	42.9	43.4	43.6	43.0	43.8
2	160.9	160.4	157.1	157.7	157.6	161.3
3	122.9[a]	123.0[a]	108.0	107.7	108.0	—
4	138.7	138.8	138.9	138.6	138.9	158.6
5	123.4[a]	123.5[a]	114.0	113.6	113.6	111.4
6	148.3	148.4	147.2	147.6	146.7	158.6
1′	141.4	140.1	—	137.8	129.4	130.2
2′	127.8	129.3	140.5	126.9	128.1	129.2
3′	129.2	129.0	126.4	128.9	114.3	114.3
4′	127.5	132.4	127.3	127.4	158.3	158.6
5′	129.2	129.0	125.2	128.9	114.3	114.3
6′	127.8	129.3	—	126.9	128.1	129.2
C-Methyl	—	—	—	—	55.2	56.2

[a] These assignments might be reversed.

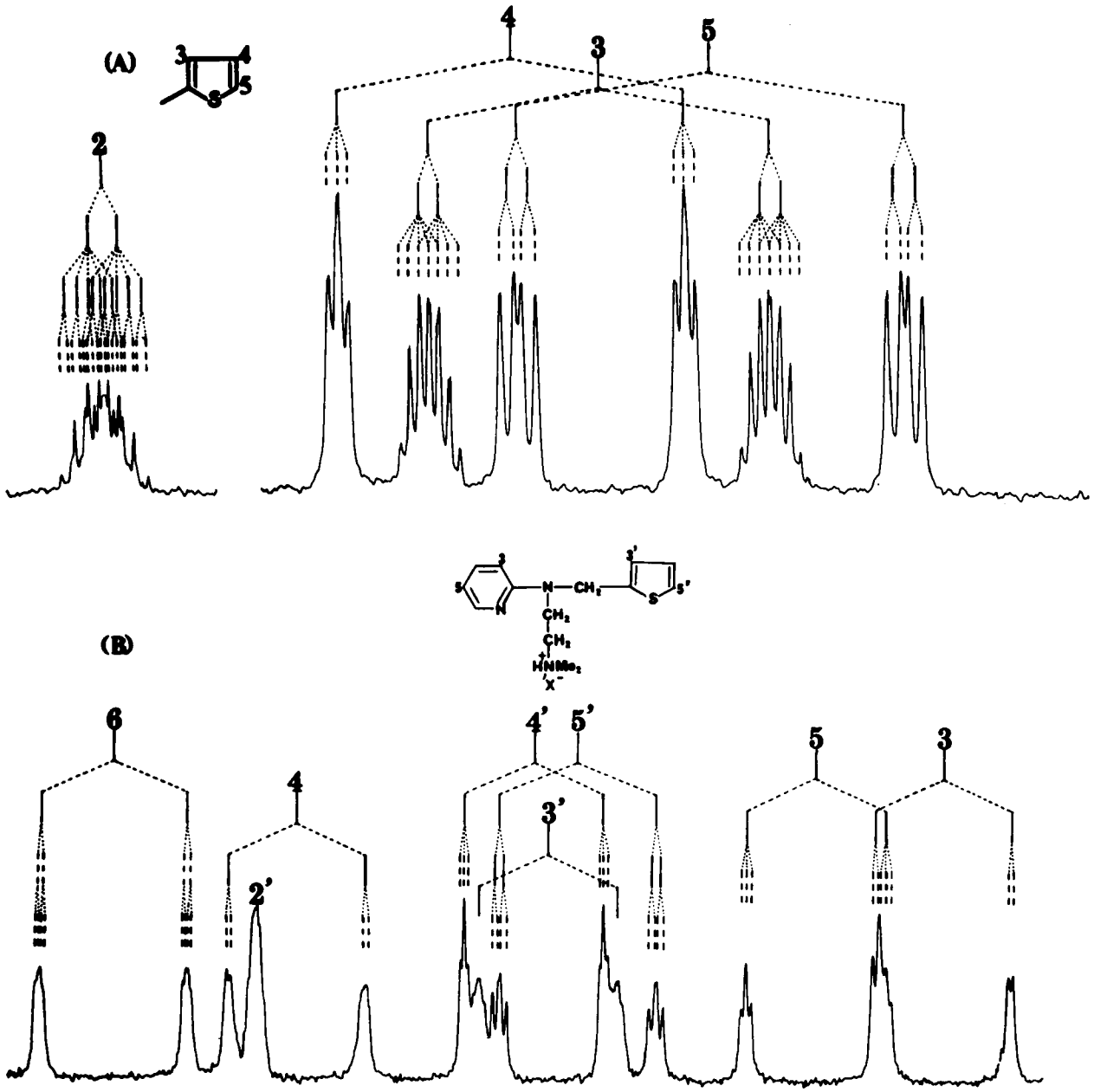

Figure 1—*High-resolution carbon-13 spectra of 2-methylthiophene (A) in deuterochloroform solution and methapyrilene hydrochloride (B). Only part of the aromatic carbon signals is shown.*

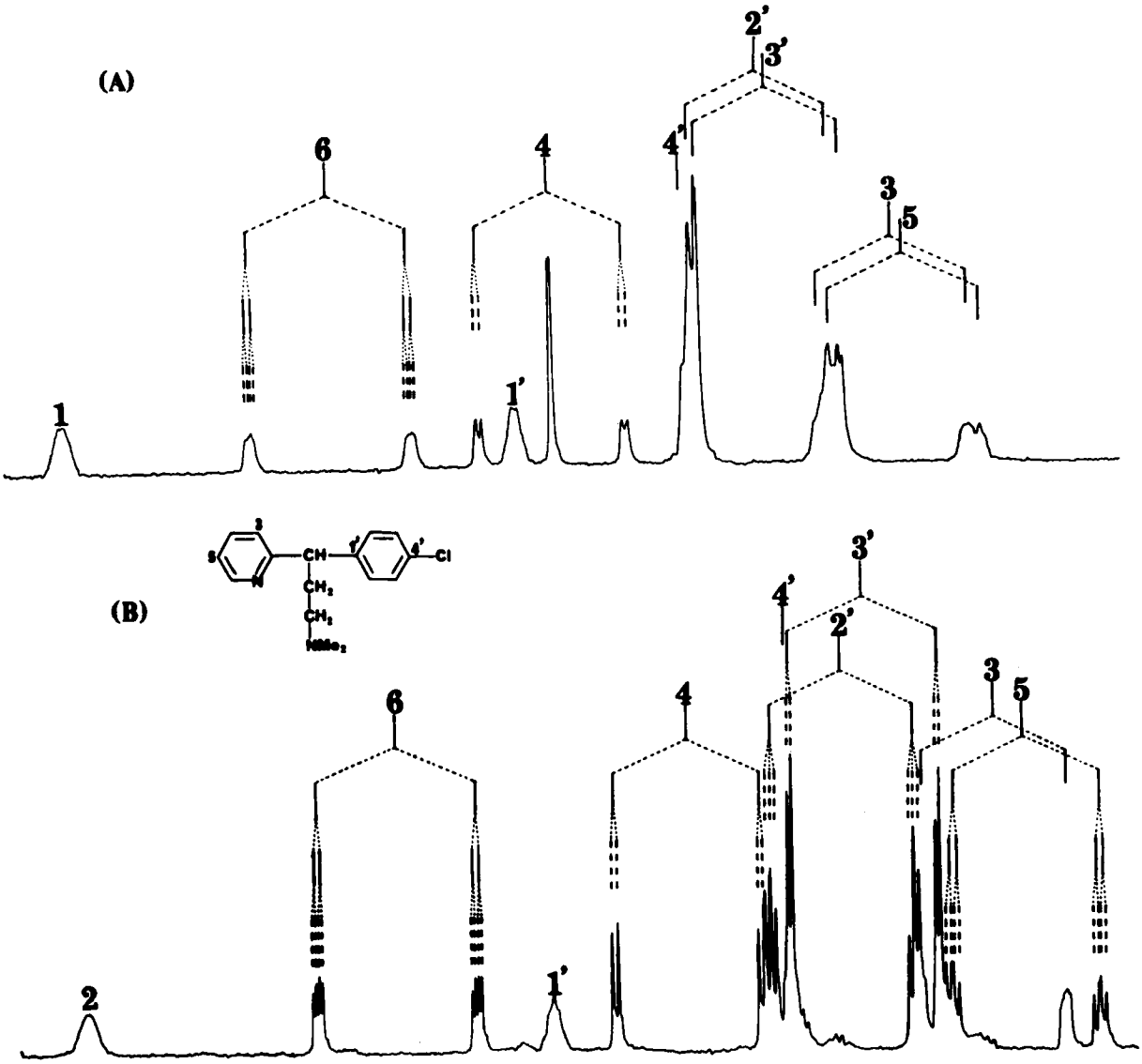

Figure 2—*High-resolution carbon-13 magnetic resonance spectra of chlorpheniramine maleate (A) and chlorpheniramine (B) in deuterochloroform solution. Only part of the aromatic carbon signals is shown.*

CMR spectral analysis of six antihistaminic drugs is reported here.

EXPERIMENTAL

The CMR spectra[1] of about 3 *M* solutions of the compounds in deuterium oxide and deuterochloroform solution were obtained in 10-mm spinning tubes. The carbon-13 resonances of methanol served as the internal reference, and chemical shift values were converted to the tetramethylsilane (I) scale using the following equation: δ (I) = δ (methanol) + 49.3 ppm.

The spectra were recorded at ambient temperature using a deuterium lock. All proton lines were decoupled by a broad band (2.5 kHz) irradiation from an incoherent 99.99-MHz source. The chemical shifts were measured for a 5000-Hz sweepwidth. The carbon-13–hydrogen coupling constants were measured from proton-coupled spectra. The typical pulse width was 12.25 μsec, and the repetition time between pulses was 3.0 sec.

All antihistaminic drugs were USP grade materials and were used without further purification.

[1] The instrument employed was a Jeol PFT-100 spectrometer, operating at 23.5 kG, interfaced with a Jeol EC-100 Fourier transform computer with 20 K memory (Jeol Inc., Cranford, NJ 07016).

RESULTS AND DISCUSSION

The spectral data of six antihistaminic drugs recorded in deuterium oxide solution are summarized in Table I. The carbon-13 resonances generally could be assigned through a combination of the following two methods: (*a*) use of chemical shift values expected for specific types of carbons from the carbon-13 chemical shift theory (8–11) and (*b*) determination of carbon-13–hydrogen coupling constants and the number of protons directly attached to each carbon atom from the proton-coupled spectrum. This system classifies all carbon atoms into four categories on the basis of the multiplicity. The γ-carbon atom and *N*-methyl carbons of pheniramine maleate (II) and chlorpheniramine maleate (III) can thus be designated directly. The α- and β-carbons can be distinguished since the α-carbon is directly attached to a nitrogen atom.

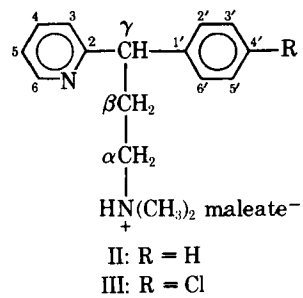

II: R = H
III: R = Cl

Table II—Carbon-13–Hydrogen Coupling Constants (Hertz)

2-Methylthiophene									
C-3′–H-3	C-3′–H-4′	C-3′–H-5′	C-3′–H-γ	C-4′–H-4′	C-4′–H-3′	C-4′–H-5′	C-5′–H-5′	C-5′–H-4′	C-5′–H-3′
164.2	4.7	9.2	4.7	166.6	4.6	4.6	185.3	6.7	10.1
Methapyrilene Maleate									
C-3′–H-3′	C-3′–H-4′	C-3′–H-5′	C-3′–H-γ	C-4′–H-4′	C-4–H-3′	C-4–H-5′	C-5′–H-5′	C-5′–H-4′	C-5′–H-3′
165.7	—[a]	—[a]	—[a]	168.4	4.3	4.3	187.1	7.9	9.9
C-3–H-3	C-3–H-5	C-4–H-4	C-4–H-6	C-5–H-5	C-5–H-3	C-5–H-6	C-6–H-6	C-6–H-4	C-6–H-5
164.3	5.5	163.0	—[a]	167.3	7.0	7.0	177.7	6.3	3.9
Tripelennamine Hydrochloride									
C-2′–H-2′	C-2′–H-6′	C-3′–H-3′	C-3′–H-5′	C-4′–H-4′	C-4′–H-2′				
158.1	—[a]	159.3	—[a]	~161	—[a]				
C-3–H-3	C-3–H-5	C-4–H-4	C-4–H-6	C-5–H-5	C-5–H-3	C-5–H-6	C-6–H-6	C-6–H-4	C-6–H-5
164.7	5.5	161.8	5.5	167.2	6.1	6.1	177.7	7.0	3.2
Thonzylamine Hydrochloride									
C-2′–H-2′	C-2′–H-6′	C-3′–H-3′	C-3′–H-5′						
159.6	—[a]	160.9	4.0						
C-2–H-4	C-2–H-6	C-4–H-4	C-4–H-6	C-4–H-5	C-5–H-5	C-5–H-4	C-5–H-6		
11.9	11.9	179.4	—[a]	—[a]	172.2	6.7	6.7		
Chlorpheniramine									
C-2′–H-2′	C-2′–H-6′	C-2′–H-γ	C-3′–H-3′	C-3′–H-5′					
160.0	6.0	6.0	165.5	4.3					
C-3–H-3	C-3–H-5	C-3–H-γ	C-4–H-4	C-4–H-6	C-5–H-5	C-5–H-6	C-5–H-3	C-6–H-6	C-6–H-4	C-6–H-5
~165	—[a]	—[a]	163.0	6.8	164.2	8.1	6.3	177.4	6.8	3.5

[a] Small splittings which could not be measured due to unresolved multiplicity.

The effects of individual substituents (shielding constants) of aromatic molecules appear to be additive for polysubstituted compounds (8–11, 21–24), particularly for *para*-disubstituted compounds as illustrated in the CMR spectral analysis of sulfonamide drugs (12). The pyridyl carbon signals are assigned according to the model study of 2-methylpyridine by Lauterbur (25) and this laboratory. The 141.4- and 127.5-ppm peaks are the resonance signals of C-1′ and C-4′ of pheniramine maleate. The assignment of the 127.8- and 129.2-ppm signals to C-2′ and C-3′ is based on the model study of isopropylbenzene (10). In addition, these assignments were confirmed by comparison with their corresponding one-bond carbon-13–hydrogen coupling constants (Hz).

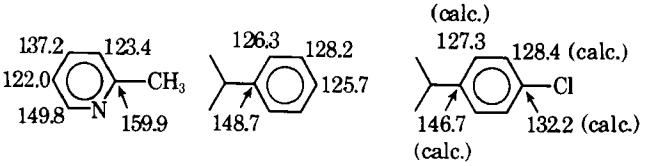

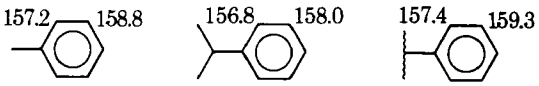

II

From the shielding constants of chloro and isopropyl groups, the chemical shifts of *p*-chloroisopropylbenzene can be calculated. Therefore, the observed signals at 140.1 and 132.4 ppm can be assigned to C-1′ and C-4′ of chlorpheniramine, respectively, and the signals at 129.3 and 129.0 ppm can be assigned to C-2′ and C-3′.

The aliphatic carbon resonance signals of diaminoethylene antihistamines are assigned by comparisons among them and with aminopropyl antihistamines, II and III. The interpretation of the aromatic carbon resonance signals of methapyrilene hydrochloride (IV) is based on the known chemical shift assignments of 2-aminopyridine (26) and 2-methylthiophene (27).

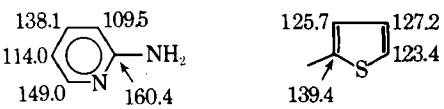

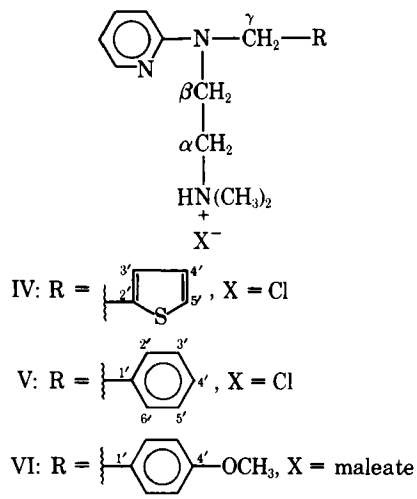

This interpretation was unambiguously confirmed by extensive analysis of the proton-coupled spectrum (Fig. 1). The carbon-13–hydrogen coupling constants of 2-methylthiophene and methapyrilene hydrochloride are summarized in Table II. The interpretation lies in the previous observations on aromatic compounds (28–33):

1. The ^3J (^{13}C-^1H) is normally in the range of 4–8 Hz.
2. The ^2J (^{13}C-^1H) is less than 4 Hz. The coupling between carbon-13 and the hydrogen adjacent to nitrogen is enhanced (14, 32–39). The ^2J (^{13}C-^1H) and ^3J (^{13}C-^1H) of five-membered heterocyclic compounds are almost the same (34–39).
3. The ^4J (^{13}C-^1H) is not larger than 2 Hz.

The chemical shifts of tripelennamine hydrochloride (V) can be assigned by analogy to methapyrilene hydochloride (IV) and pheniramine maleate (II). The intensive analysis of carbon-13–hydrogen coupling patterns of the aromatic carbon resonances further substantiates this conclusion (Table II). These results can then be applied to the spectral analysis of pyrilamine maleate (VI). The chemical shift assignments of the *p*-alkylanisole portion are made by the additivity rule of the shielding constants of aromatic substituents (21–24). Therefore, one can assign the corresponding moiety of thonzylamine hydrochloride (VII).

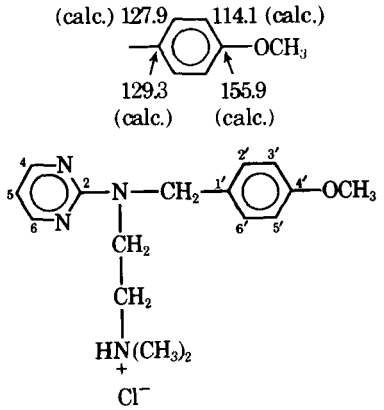

VII

The resonance signals of the pyrimidyl unit can be determined from their relative intensity and multiplicity. The C-3′ resonance signal appears as a doublet of doublets due to the ^1J (C-3′—H-3′) and ^3J (C-3′—H-5′), while the C-2′ signal appears as an unresolved multiple doublet. The unresolved multiplicity is due to the extra three-bond coupling between C-2′ and H-γ. This observation may be useful in distinguishing C-3′ from C-2′ of chlorpheniramine maleate. Unfortunately, these signals are not well resolved enough to yield unequivocal differentiation. The line-broadening effect is shown in all proton-coupled spectra of antihistaminic salts, which may be the result of intramolecular and/or intermolecular proton exchange among the nitrogen atoms. Thus, the spectrum of free chlorpheniramine in deuterochloroform solution was measured (Fig. 2) and clearly indicates that the more upfield peak at 127.7 ppm, doublet of doublets [^1J (C-3′—H-3′): 165.5 Hz, ^3J (C-3′—H-5′): 4.3 Hz], is the C-3′ resonance signal and that the peak at 128.7 ppm, triplet of doublets [^1J (C-2′—H-2′): 160.0 Hz, ^3J (C-2′—H-4′) = ^3J (C-2′—H-γ): 6.0 Hz], is the C-2′ signal.

The assignment of the carbon-13 resonance signals of substituted aromatic molecules usually has been accomplished on the basis of the additivity principle as already described. However, this approach often leaves some uncertainty in the assignment when the estimated chemical shifts are close. In fact, in the case of C-2′ and C-3′ of chlorpheniramine, the predicted values even provide incorrect relative chemical shifts. The assignment based on the long-range carbon-13–hydrogen coupling constants is unequivocal. We, therefore, believe that long-range carbon-13–hydrogen coupling constants can be a very valuable aid for structure determinations and spectral interpretations.

REFERENCES

(1) M. Schachter, "Histamine and Antihistamines," Pergamon, New York, N.Y., 1973.

(2) C. R. Ganellin, *J. Med. Chem.*, **16**, 620(1973).

(3) C. R. Ganellin, G. N. J. Port, and W. G. Richards, *ibid.*, **16**, 616(1973).

(4) C. R. Ganellin, E. S. Pepper, G. N. J. Port, and W. G. Richards, *ibid.*, **16**, 610(1973).

(5) N. S. Ham, A. F. Casy, and R. R. Ison, *ibid.*, **16**, 470(1973).

(6) M. V. Veidis, G. J. Palenik, R. Schaffrin, and J. Trotter, *J. Chem. Soc., A*, **1969**, 2659.

(7) L. B. Kier, *J. Med. Chem.*, **11**, 441(1968).

(8) J. B. Strothers, "Carbon-13 NMR Spectroscopy," Academic, New York, N.Y., 1972.

(9) G. C. Levy and G. L. Nelson, "Carbon-13 Nuclear Magnetic Resonance for Organic Chemists," Wiley–Interscience, New York, N.Y., 1972.

(10) L. F. Johnson and W. C. Jankowski, "Carbon-13 NMR Spectra," Wiley–Interscience, New York, N.Y., 1972.

(11) G. C. Levy, "Topics in Carbon-13 NMR Spectroscopy," vol. 1, Wiley–Interscience, New York, N.Y., 1974.

(12) C.-j. Chang, H. G. Floss, and G. E. Peck, *J. Med. Chem.*, **18**, 505(1975).

(13) N. J. Bach, H. E. Boaz, E. C. Kornfeld, C.-j. Chang, H. G. Floss, E. W. Hageman, and E. Wenkert, *J. Org. Chem.*, **39**, 1274(1974).

(14) E. Wenkert, J. S. Bindra, C.-j. Chang, D. W. Cochran, and F. M. Schell, *Acc. Chem. Res.*, **7**, 46(1974).

(15) J. W. Lown and A. Begleiter, *Can. J. Chem.*, **52**, 2331(1974).

(16) C. G. Moreland, A. Philip, and F. I. Carroll, *J. Org. Chem.*, **39**, 2413(1974).

(17) F. I. Carroll and C. G. Moreland, *J. Chem. Soc., Perkin Trans.*, **1**, 374(1974).

(18) J. E. Walker, H. P. C. Hogenkamp, J. E. Needham, and N. A. Matwiyoff, *J. Chem. Soc. Chem. Commun.*, **1974**, 85.

(19) A. A. Gallo and H. Z. Sable, *J. Biol. Chem.*, **249**, 1384(1974)

(20) L. Simeral and G. E. Maciel, *Org. Magn. Reson.*, **6**, 226(1974).

(21) P. Lazzeretti and F. Taddei, *ibid.*, **3**, 283(1971).

(22) G. Miyajima, Y. Sasaki, and M. Suzuki, *Chem. Pharm. Bull.*, **19**, 230(1971).

(23) *Ibid.*, **20**, 429(1972).

(24) Y. Sasaki, *Chem. Pharm. Bull.*, **21**, 1901(1973).

(25) P. C. Lauterbur, *J. Chem. Phys.*, **43**, 360(1965).

(26) H. L. Retcofsky and R. A. Friedel, *J. Phys. Chem.*, **72**, 2619(1968).

(27) J. F. Page, Jr., T. Alger, and D. M. Grant, *J. Am. Chem. Soc.*, **87**, 5333(1965).

(28) J. L. Marshall, D. E. Miiller, S. A. Conn, R. Seiwell, and A. M. Ihrig, *Acc. Chem. Res.*, **7**, 333(1974).

(29) J. L. Marshall and R. Seiwell, *J. Magn. Reson.*, **15**, 150(1974).

(30) A. R. Tarpley, Jr., and J. H. Goldstein, *J. Mol. Spectrosc.*, **39**, 275(1971).

(31) A. R. Tarpley, Jr., and J. H. Goldstein, *J. Am. Chem. Soc.*, **93**, 3573(1971).

(32) F. J. Weigert and J. D. Roberts, *ibid.*, **89**, 2967(1967).

(33) Y. Takeuchi and N. Dennis, *ibid.*, **96**, 3658(1974).

(34) M. Hansen, R. S. Hansen, and H. J. Jakobsen, *J. Magn. Reson.*, **13**, 386(1974).

(35) F. Fringuelli, S. Gronowitz, A. B. Hornfeldt, I. Johnson, and A. Taticchi, *Acta Chem. Scand. B*, **1974**, 175.

(36) M. Begtrup, *ibid.*, **1974**, 61.

(37) *Ibid.*, **27**, 3101(1973).

(38) J. M. Briggs, E. Rahkamaa, and E. W. Randall, *J. Magn. Reson.*, **12**, 40(1973).

(39) M. C. Thorpe and W. C. Coburn, Jr., *ibid.*, **12**, 225(1973).

ACKNOWLEDGMENTS AND ADDRESSES

Received July 7, 1975, from the *Department of Medicinal Chemistry and Pharmacognosy and the †Department of Industrial and Physical Pharmacy, School of Pharmacy and Pharmacal Sciences, Purdue University, West Lafayette, IN 47907

Accepted for publication September 24, 1975.

Supported by U.S. Public Health Service Research Grant AI 11728.

The authors are grateful to Mr. John W. Clevenger for technical assistance.

ˣ To whom inquiries should be directed.

High-Performance Liquid Chromatographic Analysis of Vitamins I: Quantitation of Cholecalciferol or Ergocalciferol in Presence of Photochemical Isomers of the Provitamin and Application to Cholecalciferol Resins

KATHLEEN A. TARTIVITA, JAMES P. SCIARELLO ˣ, and BRUCE C. RUDY *

Abstract □ A high-performance liquid chromatographic (HPLC) procedure was developed for the quantitative determination of cholecalciferol or ergocalciferol in the presence of the photochemical isomers of the provitamin. Separation is also achieved from various common reaction products encountered in the vitamin synthesis as well as other fat-soluble vitamins. The method was applied to the routine analysis of cholecalciferol resins, and experimental data are set forth. A comparison of the HPLC method to the AOAC biological and chemical procedures shows that the HPLC method most closely approximates the antirachitic activity of a cholecalciferol sample. The specificity, sensitivity, and reproducibility of the method make it applicable to various vitamin samples containing cholecalciferol or ergocalciferol.

Keyphrases □ Cholecalciferol—high-performance liquid chromatographic analysis and separation from photochemical isomers and reaction products of provitamin □ Ergocalciferol—high-performance liquid chromatographic analysis and separation from photochemical isomers and reaction products of provitamin □ Vitamins—ergocalciferol and cholecalciferol, high-performance liquid chromatographic analysis and separation from photochemical isomers and reaction products of provitamins □ High-performance liquid chromatography—analysis and separation, ergocalciferol or cholecalciferol

A method utilizing high-performance liquid chromatography (HPLC) was developed which quantifies ergocalciferol (vitamin D_2) or cholecalciferol (vitamin D_3) after separation from the previtamin and the photochemical isomers of the provitamin.

In the preparation of synthetic ergocalciferol or cholecalciferol, the specific provitamin, ergosterol or 7-dehydrocholesterol, respectively, is irradiated at low temperatures, and the resultant previtamin (precholecalciferol or preergocalciferol) is isolated and thermally converted to vitamin D[1] (1, 2). The irradiation sequence of the provitamins, Scheme I (3–5), was thoroughly investigated and results in a mixture of the previtamin, lumisterol, and tachysterol (6–17).

Any method for vitamin D analysis must be capable, therefore, of distinguishing the vitamin from these isomers as well as the provitamin. The HPLC method described in this paper accomplishes these goals. Vitamin D is also separated from the *trans*-isomers, isotachysterol, and dihydrotachysterol. However, this method does not separate ergocalciferol from cholecalciferol.

The biological activity of three of the photochemical isomers of the provitamin was established previously. Lumisterol has no antirachitic activity, tachysterol exhibits slight antirachitic activity, and the activity of precholecalciferol is 35% of that of cholecalciferol (18–21). Precholecalciferol in itself is inactive, and any biological activity exhibited by this isomer can be attributed to its *in vivo* conversion to cholecalciferol (18).

Since previtamin D and vitamin D are well separated in this system, the "actual" vitamin D content as well as the "potential" vitamin D content can be quantified. The actual vitamin D content of the sample is determined by measuring the area of the vitamin D peak; the potential vitamin D content is determined through measurement of both the previtamin D and the vitamin D peak areas. A correction factor is necessary for the calculation of previtamin D since its absorptivity at 254 nm is 40% of that of vitamin D (22). A further correction is needed to convert the amount of previtamin D present to potential vitamin D since, as already stated, it possesses only 35% of the activity of vitamin D.

In addition, the HPLC technique is carried out at room temperature, thereby reducing the possibility of thermal breakdown or of shifting of the vitamin D ⇄ previtamin D equilibrium.

EXPERIMENTAL

Equipment—A liquid chromatograph[2], operated at ambient temperature and equipped with a UV detector for monitoring the column effluent at 254 nm, was used. The column was a 30-cm × 4-mm (i.d.) commercially available microparticle silica column[3]. The liquid chromatographic detector was connected to a programmed digital computer-based system[4] for obtaining the areas of the chromatogram peaks.

Reagents—USP cholecalciferol reference standard and *p*-dimethylaminobenzaldehyde[5], 99+% pure, were the reference and internal standards, respectively. Spectroquality grade chloroform[6] and *n*-hexane[6], as well as analytical reagent grade tetrahydrofuran[7], were used for the preparation of the mobile phase. A GLC analysis of the chloroform was performed to assure that it was essentially free of ethanol and water.

Mobile Phase—A mixture of chloroform–*n*-hexane–tetrahydrofuran (70:30:1 v/v) was used.

Preparation of Internal Standard Solution—Accurately weigh approximately 30 mg of *p*-dimethylaminobenzaldehyde into a 100-ml volumetric flask and dissolve in and dilute to volume with the mobile phase.

Preparation of Standard Solution—Accurately weigh approximately 12 mg of cholecalciferol standard into a 50-ml amber volumetric flask and dissolve in and dilute to volume with the mobile phase. Prepare a mixture (1:1) of the cholecalciferol standard and the *p*-dimethylaminobenzaldehyde solution in a suitable amber vessel and mix well.

Preparation of Sample Solution—Accurately weigh a quantity

[1] The term vitamin D will be used throughout to mean either ergocalciferol or cholecalciferol.

[2] Dupont 830.
[3] μPorasil, Water's Associates.
[4] PACE, Electronic Associates.
[5] Aldrich Chemical Co.
[6] Matheson, Coleman and Bell.
[7] Fisher.

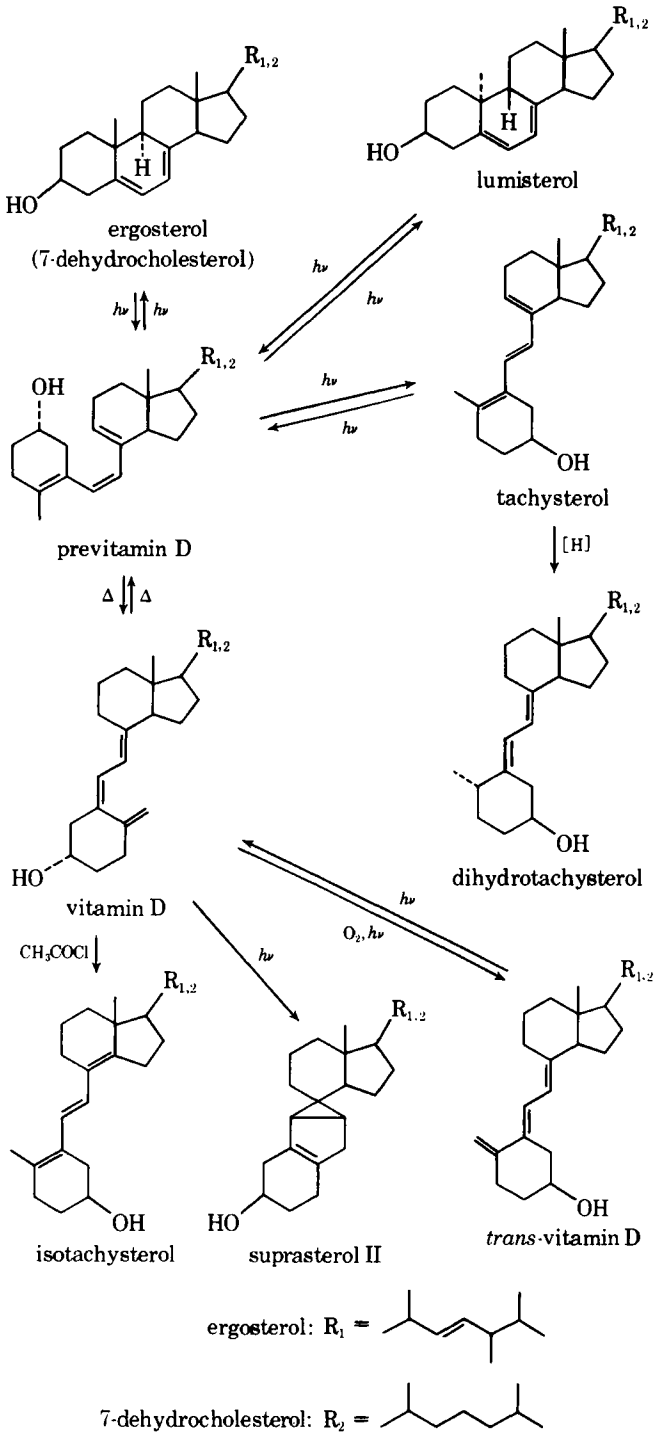

Scheme I—Effect of UV radiation and heat on the synthesis and isomerization of vitamin D. (The $R_{1,2}$ group signifies that the chain can be either R_1 or R_2. When the group is R_1, the chain for ergosterol is specified and the reaction scheme is for the synthesis of ergocalciferol. Similarly, when the group is R_2, the chain for 7-dehydrocholesterol is specified and the reaction scheme is for the synthesis of cholecalciferol.)

of the resin sample, equivalent to 30 mg of cholecalciferol, into a 25-ml amber volumetric flask and dissolve in and dilute to volume with mobile phase. Pipet 5 ml of the resultant solution into a 25-ml amber volumetric flask and dilute to volume with the mobile phase. Prepare a 1:1 mixture of the final sample solution and the *p*-dimethylaminobenzaldehyde solution in a suitable amber vessel and mix well.

Chromatography—Condition the column with the mobile phase at a flow rate of approximately 1.0 ml/min. Inject 5 µl of the standard solution and adjust the flow rate to give retention times of 13–15 and

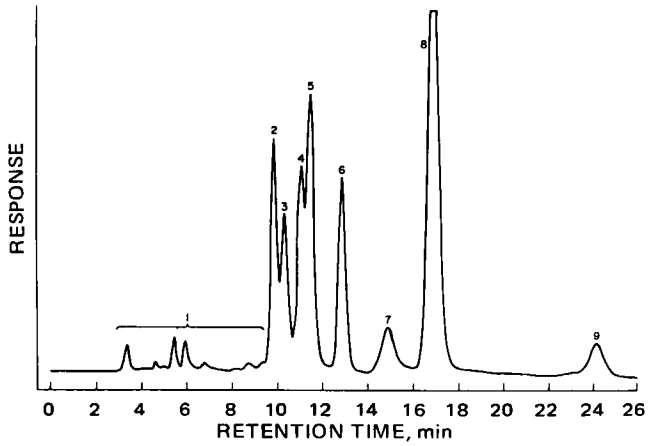

Figure 1—*Chromatogram of a synthetic mixture of photochemical isomers and reaction products of vitamin D_3. Key: 1, unknowns; 2, trans-vitamin D_3; 3, previtamin D_3; 4, lumisterol$_3$; 5, isotachysterol$_3$; 6, p-dimethylaminobenzaldehyde (internal standard); 7, tachysterol$_3$; 8, vitamin D_3; and 9, 7-dehydrocholesterol.*

16–18 min for *p*-dimethylaminobenzaldehyde and cholecalciferol, respectively. Determine the response ratio by replicate injections of the standard solution. When the deviation of the response ratio is less than 2%, make duplicate injections of the sample solution. Use the peak areas obtained to calculate the cholecalciferol content of the resin.

Calculations—Determine the areas of the peaks and calculate the ratio of the area of the cholecalciferol peak to the area of the *p*-dimethylaminobenzaldehyde peak for each chromatogram. Use the average ratio obtained for the standard replicates and the ratio for each sample duplicate for the calculation of cholecalciferol in the samples as shown in the following equations:

$$\text{response ratio (R.R.)} = \frac{A_D\ (\text{standard}) \times C_{IS}\ (\text{standard})}{A_{IS}\ (\text{standard}) \times C_D\ (\text{standard})} \quad \text{(Eq. 1)}$$

$$\text{IU of cholecalciferol/g} = \frac{A_D\ (\text{sample}) \times C_{IS}\ (\text{sample}) \times 250 \times 40{,}000}{A_{IS}\ (\text{sample}) \times \text{R.R.} \times \text{sample weight, g}} \quad \text{(Eq. 2)}$$

where:

A_D = area of cholecalciferol peak
A_{IS} = area of internal standard peak
C_D = concentration of cholecalciferol standard in milligrams per milliliter
C_{IS} = concentration of internal standard in milligrams per milliliter
250 = dilution factor
40,000 = number of International Units of cholecalciferol per milligram of USP reference standard

RESULTS AND DISCUSSION

Typical cholecalciferol resin samples contain various minor impurities. Although there is quantitative variation from different manufacturers, most impurities are photochemical isomers of 7-dehydrocholesterol and various reaction products such as *trans*-cholecalciferol and isotachysterol$_3$. The chromatographic system employed for the analysis of cholecalciferol resins must separate these impurities from cholecalciferol. A synthetic mixture of several interfering compounds plus cholecalciferol was prepared and well resolved by the HPLC procedure (Fig. 1). In addition, this system also separates dihydrotachysterol$_3$ from cholecalciferol. The retention time of this impurity, not shown in Fig. 1, was 10.5 min.

Figure 2 shows a chromatogram of a typical cholecalciferol resin. Again, separation of the resin impurities from cholecalciferol is well evidenced. There is also baseline separation of the internal standard, cholecalciferol, and tachysterol$_3$, one of the most difficult isomers to separate from cholecalciferol.

To evaluate the precision of this method, six replicate sample

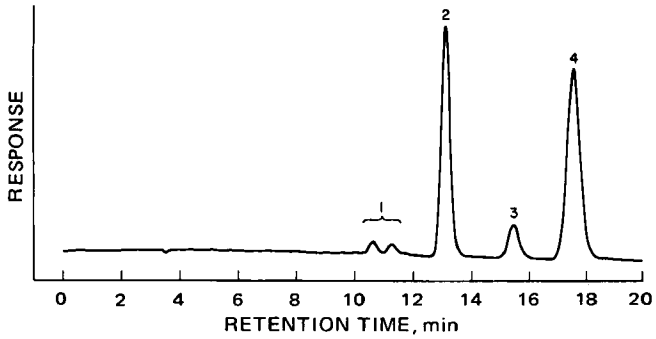

Figure 2—*Chromatogram of a typical vitamin D_3 resin. Key: 1, resin impurities; 2, p-dimethylaminobenzaldehyde (internal standard); 3, tachysterol$_3$; and 4, vitamin D_3.*

preparations of a cholecalciferol resin and six replicate injections of one sample solution were analyzed (Table I). The relative standard deviations for the replicate sample preparations and the replicate injections were 1.37 and 0.36%, respectively. These data indicate the low variability between test results.

In addition, the method was evaluated for linearity of the cholecalciferol response at concentrations ranging from 3 to 580 μg/ml. A plot of concentration *versus* absorbance was found to obey Beer's law. The sensitivity limit of this method was 3 μg/ml.

In an effort to establish the correlation between the HPLC method and biological activity, 10 samples of cholecalciferol resin were sent to two independent laboratories, A and B, for bioassay by the Association of Official Analytical Chemists (AOAC) three-level chick method (23). The data summarized in Table II show the large deviations in the bioassay results. Interlaboratory assays on the same sample differed by 1–41%, with most results differing by greater than 20%. This wide range in results attests to the lack of precision of the bioassay method.

The same samples were also assayed by the AOAC chemical (24) and HPLC methods. The results obtained by these two methods were compared to the average of the bioassay obtained by Laboratories A and B. As seen in Table III, both methods correlated well with the bioassay. However, the AOAC chemical method generally overestimated the biological activity and was found to be 114.3% of the mean of the bioassay. On the other hand, the HPLC assay closely approximated the biological activity and was 99.2% of the mean of the bioassay. The relative standard deviations of the AOAC and the HPLC methods, as compared to the bioassay, were essentially equal, 12.7 and 12.8%, respectively.

The current USP chemical method (25) for the analysis of cholecalciferol or ergocalciferol results in an overestimation of the amount of vitamin D present in a sample since it is not specific enough to distinguish between vitamin D and interfering sterols (24, 26, 27). With the USP method, the sample is pretreated and then reacted with Nield's reagent; vitamin D-type compounds produce a pink color measured at 500 nm. The amount of vitamin D is determined by comparison to a standard.

It has already been shown that vitamin D is not the only compound that produces color with Nield's reagent (24, 26, 27). Several photochemical isomers that may be present in a vitamin D sample, which have little or no antirachitic activity, are quantified as vitamin D. The AOAC chemical method of vitamin D analysis was subsequently developed to eliminate the interference of one of these isomers, tachysterol. With the AOAC chemical method, the sample is treated with maleic anhydride and a Diels–Alder adduct is formed with the tachysterol, thereby making it inactive toward Nield's reagent. Thus, the AOAC chemical method is more specific than the current USP method but still overestimates the amount of antirachitic activity present in a resin sample.

This result suggests that there may yet be another interfering substance present, such as isotachysterol, that is reacting with Nield's reagent to give measurable color at 500 nm. The HPLC method eliminates this problem since the method is specific for vitamin D and there is no interference from the various impurities. Because of the separation capability, only the desired compounds are measured and quantified. From the results, it was concluded that the HPLC method most closely relates the cholecalciferol content of a resin to its antirachitic activity.

Cholecalciferol and ergocalciferol are used in many products and are often found in combination with other fat-soluble vitamins. Therefore, mixtures of cholecalciferol and other fat-soluble vitamins were investigated (Fig. 3). The high efficiency of this HPLC system allows for the separation of cholecalciferol from vitamin A acetate, vitamin A palmitate, alpha tocopherol, and alpha tocopheryl acetate. Vitamin A alcohol, phytonadione, and antioxidants are also separated from cholecalciferol by this system (not shown in Fig. 3).

Table I—Precision Study of Cholecalciferol Analysis on Cholecalciferol Resin

Run Number	Cholecalciferol × 10^{-6}, IU/g: Replicate Sample Preparations	Cholecalciferol × 10^{-6}, IU/g: Replicate Injections of One Preparation
1	20.32	20.38
2	20.34	20.36
3	20.97	20.34
4	20.69	20.25
5	20.57	20.38
6	20.22	20.21
Mean	20.52	20.32
SD	±0.28	±0.07
RSD, %	±1.37	±0.36

Table II—Results of AOAC Bioassay[a] from Two Independent Laboratories for the Analysis of Cholecalciferol in Resin Samples

Sample	Cholecalciferol × 10^{-6}, ICU[b]/g: Laboratory A	Laboratory B	Average
1	21.8	21.6	21.7
2	23.5	19.9	21.7
3	20.3	12.0	16.2
4	18.8	24.1	21.5
5	26.6	16.5	21.6
6	22.8	17.6	20.2
7	29.4	20.6	25.0
8	22.2	18.3	20.3
9	19.0	25.9	22.5
10	22.6	24.3	23.5

[a] Three-level chick method. [b] International Chick Units.

Table III—Comparison of HPLC, AOAC Chemical, and AOAC Bioassay Results for the Determination of Cholecalciferol in Resins

Sample	Cholecalciferol × 10^{-6}, IU/g: HPLC[a] Method	AOAC[a] Chemical Method	HPLC as Percent of Mean of Bioassay[b]	AOAC as Percent of Mean of Bioassay[c]
1	21.0	22.6	96.8	104.1
2	20.6	22.0	94.9	101.4
3	20.9	23.7	129.0	146.3
4	19.9	22.9	92.6	106.5
5	21.3	23.1	98.6	106.9
6	22.2	25.7	109.9	127.2
7	21.8	26.0	87.2	104.0
8	21.3	25.8	104.9	127.1
9	19.6	24.4	87.1	108.4
10	21.4	26.1	91.1	111.1
Mean			99.2	114.3
SD			±12.7	±14.5
RSD, %			±12.8	±12.7

[a] Average of two sample weights. [b] The percentage was obtained by comparing the HPLC method to the average of the AOAC bioassay (Table II). [c] The percentage was obtained by comparing the AOAC chemical method to the average of the AOAC bioassay (Table II).

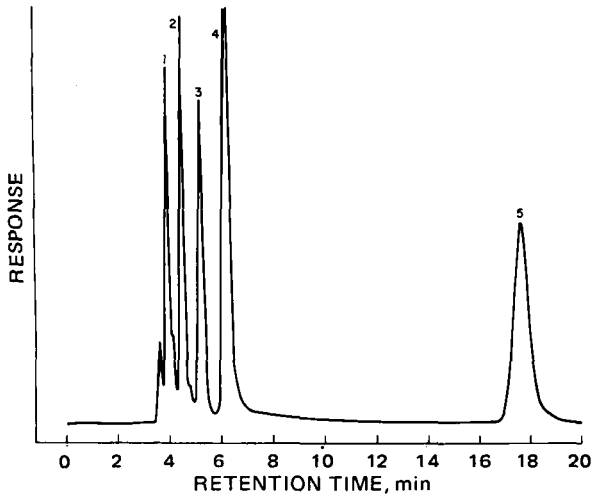

Figure 3—*Chromatogram of a synthetic mixture of fat-soluble vitamins. Key: 1, vitamin A palmitate; 2, vitamin E acetate; 3, vitamin A acetate; 4, vitamin E alcohol; and 5, vitamin D_3.*

Methodology also has been developed for the determination of ergocalciferol in vitamin A and D_2 gelatin-protected beadlets, cholecalciferol premix formulations, and commercial multivitamin formulations and will be published later.

REFERENCES

(1) L. F. Fieser and M. Fieser, "Steroids," Reinhold, New York, N.Y., 1959, p. 90–168.

(2) E. Abillon and R. Mermet-Bouvier, *J. Pharm. Sci.*, **62,** 1688(1973).

(3) E. Havinga, *Experientia*, **29,** 1181(1973).

(4) A. J. Sheppard, D. E. LaCroix, and A. R. Prosser, *J. Assoc. Offic. Anal. Chem.*, **51,** 834(1968).

(5) A. Verloop, A. L. Koevoet, and E. Havinga, *Rec. Trav. Chim. Pays-Bas*, **74,** 1125(1955).

(6) M. P. Rappoldt, P. Westerhof, K. H. Hanewald, and J. A. Keverling Buisman, *ibid.*, **77,** 241(1958).

(7) E. Havinga, A. Verloop, and A. L. Koevoet, *ibid.*, **75,** 371(1956).

(8) M. P. Rappoldt, J. A. Keverling Buisman, and E. Havinga, *ibid.*, **77,** 327(1958).

(9) P. Westerhof and J. A. Keverling Buisman, *ibid.*, **75,** 1243(1956).

(10) M. P. Rappoldt and E. Havinga, *ibid.*, **79,** 369(1960).

(11) E. Havinga, A. L. Koevoet, and A. Verloop, *ibid.*, **74,** 1230(1955).

(12) E. Havinga and J. L. M. A. Schlatmann, *Tetrahedron*, **16,** 146(1961).

(13) R. J. DeKock, G. van der Kuip, A. Verloop, and E. Havinga, *Rec. Trav. Chim. Pays-Bas*, **80,** 20(1961).

(14) G. M. Sanders and E. Havinga, *ibid.*, **86,** 665(1964).

(15) M. P. Rappoldt, *ibid.*, **79,** 1012(1960).

(16) *Ibid.*, **79,** 392(1960).

(17) A. Verloop, A. L. Koevoet, and E. Havinga, *Rec. Trav. Chim. Pays-Bas*, **76,** 689(1957).

(18) K. H. Hanewald, M. P. Rappoldt, and J. R. Roborgh, *ibid.*, **80,** 1003(1961).

(19) E. Heftman and E. Mosettig, "Biochemistry of Steroids," Reinhold, New York, N.Y., 1960, pp. 34–44.

(20) M. F. Holick, H. F. DeLuca, P. M. Kasten, and M. B. Korycka, *Science*, **180,** 964(1973).

(21) E. Heftman, "Steroid Biochemistry," Academic, New York, N.Y., 1970, pp. 31–36.

(22) E. Havinga, A. L. Koevoet, and A. Verloop, *Rec. Trav. Chim. Pays-Bas*, **74,** 1230(1955).

(23) "Official Methods of Analysis," 11th ed., Association of Official Analytical Chemists, Washington, D.C., 1970, pp. 799, 800.

(24) F. J. Mulder, E. J. deVries, and B. Borsje, *J. Assoc. Offic. Anal. Chem.*, **54,** 1168(1971).

(25) "The United States Pharmacopeia," 19th rev., Mack Publishing Co., Easton, Pa., 1974, pp. 633, 634.

(26) F. J. Mulder, E. J. deVries, and K. J. Keuning, *Pharm. Weekbl.*, **100,** 1457(1965).

(27) K. H. Hanewald, *Rec. Trav. Chim. Pays-Bas*, **78,** 604 (1959).

ACKNOWLEDGMENTS AND ADDRESSES

Received May 14, 1975, from the *Quality Control Department, Hoffmann-La Roche Inc., Nutley, NJ 07110*

Accepted for publication July 9, 1975.

Presented in part at the APhA Academy of Pharmaceutical Sciences, New Orleans meeting, November 1974.

The authors thank Dr. Enrico Baggiolini for the model compounds and Mrs. Doris Mianecki for technical assistance.

* Present address: Schering Corp., Bloomfield, NJ 07003

ˣ To whom inquiries should be directed.

Coumarins XIV: High-Resolution Mass Spectra of 3′,4′-Disubstituted 3′,4′-Dihydroseselins

NADIM A. SHAATH *, TAITO O. SOINE ˣ, and M. T. SHIPCHANDLER ‡

Abstract □ High-resolution mass spectra of 14 3′,4′-disubstituted 3′,4′-dihydroseselins were examined. The nature of the substituents determines the mode of fragmentation. Compounds having one or two acyloxy substituents fragment mainly by a pathway leading to the stable coumarinopyrilium ion. Coumarins with alkoxy or hydroxy substituents proceed by way of fission of the chroman ring, accompanied by the loss of two ring carbon atoms. Several generalizations are formulated which will aid in the interpretation of the mass spectra of this class of coumarins from a structural standpoint.

Keyphrases □ 3′,4′-Dihydroseselins, 3′,4′-disubstituted—high-resolution mass spectra, mode of fragmentation, structural interpretation □ Coumarins, substituted—high-resolution mass spectra, mode of fragmentation, structural interpretation □ Mass spectroscopy, high resolution—3′,4′-disubstituted 3′,4′-dihydroseselins, mode of fragmentation, structural interpretation

In earlier mass spectral studies, fragmentation patterns of several linear furano- (1), angular dihydrofurano-, and dihydropyranocoumarins (2–5) were examined. As an extension of these studies, high-resolution mass spectra of 14 3′,4′-disubstituted 3′,4′-dihydroseselins (I–XIV, Table I) were examined. The examples selected provide the data needed to give substance to certain general fragmentation pathways based on the structural types examined. These pathways are supported by exact mass measurements and provide some interesting generalizations which may be of value for the structural elucidation of coumarins.

DISCUSSION

Two major routes of fragmentation were evident.

Pathway A—This process involves loss of ROH in one or two steps, *i.e.*, loss of RO· followed by H·, to generate a chromene system followed by a ·CH_3 expulsion to provide a stable coumarinopyrilium ion (6) (Scheme I). Subsequent fragmentations take place without destruction of this stable ring system. This mode of fragmentation is of major consequence in the spectra of esters of lomatin but is of minor consequence for lomatin itself (4).

Pathway B—Fission of the chroman ring with the loss of two ring carbons (2′ and 3′) along with their respective substituents is an alternative mode of fragmentation (7) (Scheme II). This retro Diels–Alder-type fragmentation occurs with or without a hydrogen transfer and constitutes the principal mode of fragmentation (with one and/or two hydrogen transfers) in the spectrum of lomatin (4, 8).

The group behavior was as follows.

Group 1—Anomalin (I) and calipteryxin (II) exhibit similar spectra (Table I) with no molecular ion (M^+), presumably because the bulkiness of both substituents renders them unstable[1]. The base peak at *m/e* 83 is derived from the angeloyl and/or senecioyl groups. Pathway A is the major fragmentation route. Scheme III shows the major fragmentation routes of I as an example. Bohlmann and coworkers (9, 10) reported the mass spectra of several compounds that could be classified in Group 1, and their fragmentation conforms to pathway A expectations.

Groups 2–4—Compounds III–VII exhibit moderately intense molecular ion peaks and fragment predominantly *via* pathway A. Compounds III and IV exhibit base peaks at *m/e* 83 due to the relatively stable ion derived from the unsaturated five-carbon acid substituents. The base peak appears at *m/e* 229 when one substituent is a saturated five-carbon acyloxy group and the other is an acetoxy group, as in the spectra of V and VI. This is also true when both substituents are acetoxy groups, as in VII.

An M − 60 peak due to the loss of acetic acid is present in the spectrum of pteryxin (III) (Scheme IV) but not in the spectrum for isopteryxin (IV) (Scheme V); this difference indicates that the loss of the 3′-substituent (as the acid) is preferred over the loss of the 4′-substituent. In addition, the loss of five-carbon acids seems to be favored over the loss of acetic acid. Similar conclusions are reached when the spectra of suksdorfin (V) (Scheme VI) and visnadin (VI) (Scheme VII) are compared. These two observations permit differ-

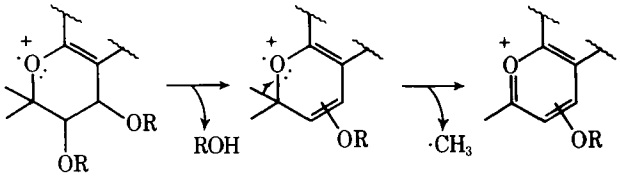

Scheme I—Pathway A

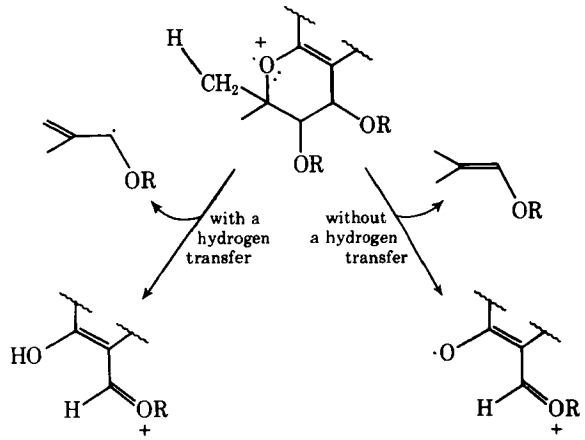

Scheme II—Pathway B

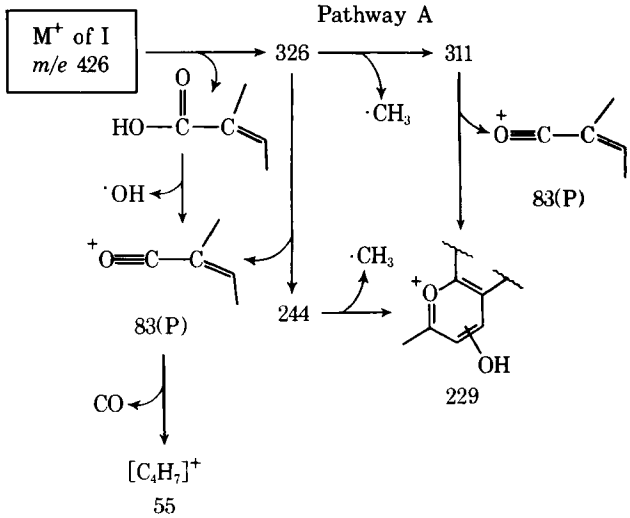

Scheme III

[1] These peaks were visible at 15 ev.

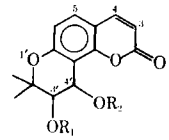

Table I—High-Resolution Mass Measurements of the Major Fragments for Compounds I–XIV[a]

Compound	R_1	R_2	m/e	Elemental Composition	Calculated Mass	Measured Mass	Relative Intensity, %
Anomalin[b] (I)			327	$C_{19}H_{19}O_5$	327.1232	327.1198	28
			326	$C_{19}H_{18}O_5$	326.1153	326.1157	12
			311	$C_{18}H_{15}O_5$	311.0918	311.0904	15
			244	$C_{14}H_{12}O_4$	244.0735	244.0741	9
			243	$C_{14}H_{11}O_4$	243.0657	243.0678	7
			229	$C_{13}H_9O_4$	229.0500	229.0449	32
			83 (P)	C_5H_7O	83.0496	83.0493	100
			55	C_4H_7	55.0546	55.0538	40
Calipteryxin[b] (II)			327	$C_{19}H_{19}O_5$	327.1232	327.1269	6
			326	$C_{19}H_{18}O_5$	326.1153	326.1150	16
			311	$C_{18}H_{15}O_5$	311.0918	311.0910	10
			244	$C_{14}H_{12}O_4$	244.0735	244.0728	8
			243	$C_{14}H_{11}O_4$	243.0657	243.0644	6
			229	$C_{13}H_9O_4$	229.0500	229.0505	28
			83 (P)	C_5H_7O	83.0496	83.0500	100
			55	C_4H_7	55.0546	55.0549	30
Pteryxin[c] (III)	CH_3CO		386 (M)	$C_{21}H_{22}O_7$	386.1364	386.1400	6
			326	$C_{19}H_{18}O_5$	326.1153	327.1200	14
			311	$C_{18}H_{15}O_5$	311.0918	311.0927	14
			287	$C_{16}H_{15}O_5$	287.0919	287.0879	42
			261	$C_{14}H_{13}O_5$	261.0762	261.0746	28
			245	$C_{14}H_{13}O_4$	245.0813	245.0751	46
			244	$C_{14}H_{12}O_4$	244.0735	244.0738	9
			229	$C_{13}H_9O_4$	229.0500	229.0467	38
			191	$C_{10}H_7O_4$	191.0343	191.0343	5
			83 (P)	C_5H_7O	83.0496	83.0502	100
			55	C_4H_7	55.0546	55.0547	40
			43	C_2H_3O	43.0284	43.0276	26
Isopteryxin[b] (IV)		CH_3CO	386 (M)	$C_{21}H_{22}O_7$	386.1364	386.1348	22
			326	$C_{19}H_{18}O_5$	326.1153	—	—
			311	$C_{18}H_{15}O_5$	311.0918	—	—
			287	$C_{16}H_{15}O_5$	287.0919	287.0869	6
			261	$C_{14}H_{13}O_5$	261.0762	261.0762	5
			245	$C_{14}H_{13}O_4$	245.0813	245.0688	24
			244	$C_{14}H_{12}O_4$	244.0735	244.0724	34
			229	$C_{13}H_9O_4$	229.0500	229.0532	72
			191	$C_{10}H_7O_4$	191.0343	191.0334	18
			83 (P)	C_5H_7O	83.0496	83.0487	100
			55	C_4H_7	55.0546	55.0539	44
			43	C_2H_3O	43.0284	43.0290	26
Suksdorfin[c] (V)	CH_3CO		388 (M)	$C_{21}H_{24}O_7$	388.1520	388.1524	22
			328	$C_{19}H_{20}O_5$	328.1309	328.1322	16
			313	$C_{18}H_{17}O_5$	313.1074	313.1067	12
			286	$C_{16}H_{14}O_5$	286.0840	286.0829	11
			261	$C_{14}H_{13}O_5$	261.0762	261.0756	21
			245	$C_{14}H_{13}O_4$	245.0813	245.0787	25
			244	$C_{14}H_{12}O_4$	244.0735	244.0731	48
			229 (P)	$C_{13}H_9O_4$	229.0500	229.0527	100
			191	$C_{10}H_7O_4$	191.0343	191.0325	18
			190	$C_{10}H_6O_4$	190.0265	190.0286	12
			85	C_5H_9O	85.0653	85.0654	22
			57	C_4H_9	57.0702	57.0704	26
			43	C_2H_3O	43.0284	43.0288	26
Visnadin (provismine)[d] (VI)		CH_3CO	388 (M)	$C_{21}H_{24}O_7$	388.1520	388.1540	12
			328	$C_{19}H_{20}O_5$	328.1309	—	—
			313	$C_{18}H_{17}O_5$	313.1074	—	—
			286	$C_{16}H_{14}O_5$	286.0840	286.0831	5
			261	$C_{14}H_{13}O_5$	261.0762	261.0746	13
			245	$C_{14}H_{13}O_4$	245.0813	245.0766	10
			244	$C_{14}H_{12}O_4$	244.0735	244.0720	65
			229 (P)	$C_{13}H_9O_4$	229.0500	229.0464	100
			191	$C_{10}H_7O_4$	191.0343	191.0329	25
			190	$C_{10}H_6O_4$	190.0265	190.0245	22
			85	C_5H_9O	85.0653	85.0653	26
			57	C_4H_9	57.0702	57.0701	28
			43	C_2H_3O	43.0284	43.0289	26
trans-Khellactone diacetate[d] (VII)	CH_3CO	CH_3CO	346 (M)	$C_{18}H_{18}O_7$	346.1052	346.1056	18
			286	$C_{16}H_{14}O_5$	286.0840	286.0847	5
			245	$C_{14}H_{13}O_4$	245.0813	245.0779	10
			244	$C_{14}H_{12}O_4$	244.0735	244.0708	36
			229 (P)	$C_{13}H_9O_4$	229.0500	229.0514	100
			213	$C_{13}H_9O_3$	213.0551	213.0547	20
			191	$C_{10}H_7O_4$	191.0343	191.0346	26
			190	$C_{10}H_6O_4$	190.0265	190.0272	14

(continued)

Table I—(*Continued*)

Compound	R_1	R_2	*m/e*	Elemental Composition	Calculated Mass	Measured Mass	Relative Intensity, %
			60	$C_2H_4O_2$	60.0300	60.0289	30
			43	C_2H_3O	43.0284	43.0282	35
cis-4′-*O*-Ethylkhellactone acetate[c] (VIII)	CH_3CO	CH_3CH_2	333 (M + 1)	$C_{18}H_{21}O_6$	333.1337	333.1358	7
			332 (M)	$C_{18}H_{20}O_6$	332.1259	332.1273	16
			258	$C_{15}H_{14}O_4$	258.0891	258.0854	12
			257 (P)	$C_{15}H_{13}O_4$	257.0813	257.0806	100
			245	$C_{14}H_{13}O_4$	245.0813	245.0835	5
			229	$C_{13}H_9O_4$	229.0500	229.0483	52
			219	$C_{12}H_{11}O_4$	219.0657	219.0663	26
			218	$C_{12}H_{10}O_4$	218.0579	218.0562	43
			213	$C_{13}H_9O_3$	213.0551	213.0578	14
			191	$C_{10}H_7O_4$	191.0343	191.0346	65
			190	$C_{10}H_6O_4$	190.0265	190.0248	48
			176	$C_{10}H_8O_3$	176.0473	176.0454	12
			162	$C_9H_6O_3$	162.0316	162.0307	57
			134	$C_8H_6O_2$	134.0367	134.0369	36
			43	C_2H_3O	43.0284	43.0292	35
trans-4′-*O*-Ethylkhellactone acetate[c] (IX)	CH_3CO	CH_3CH_2	333 (M + 1)	$C_{18}H_{21}O_6$	333.1337	333.1349	5
			332 (M)	$C_{18}H_{20}O_6$	332.1259	332.1252	30
			258	$C_{15}H_{14}O_4$	258.0891	258.0878	15
			257 (P)	$C_{15}H_{13}O_4$	257.0813	257.0852	100
			245	$C_{14}H_{13}O_4$	245.0813	245.0809	11
			229	$C_{13}H_9O_4$	229.0500	229.0495	66
			219	$C_{12}H_{11}O_4$	219.0657	219.0617	42
			218	$C_{12}H_{10}O_4$	218.0579	218.0584	82
			213	$C_{13}H_9O_3$	213.0551	213.0537	24
			191	$C_{10}H_7O_4$	191.0343	191.0334	72
			190	$C_{10}H_6O_4$	190.0265	190.0261	55
			176	$C_{10}H_8O_3$	176.0473	176.0485	21
			162	$C_9H_6O_3$	162.0316	162.0319	92
			134	$C_8H_6O_2$	134.0367	134.0361	40
			43	C_2H_3O	43.0284	43.0277	30
cis-4′-*O*-Methylkhellactone[c] (X)	H	CH_3	277 (M + 1)	$C_{15}H_{17}O_5$	277.1075	277.1044	8
			276 (M)	$C_{15}H_{16}O_5$	276.0997	276.1017	44
trans-4′-*O*-Methylkhellactone[c,e] (XI)	H	CH_3	229	$C_{13}H_9O_4$	229.0500	229.0448	9
			205 (P)	$C_{11}H_9O_4$	205.0500	205.0507	100
			204	$C_{11}H_8O_4$	204.0422	204.0424	66
			189	$C_{10}H_5O_4$	189.0187	189.0178	30
			176	$C_{10}H_8O_3$	176.0473	176.0443	20
			175	$C_{10}H_7O_3$	175.0394	175.0357	8
			161	$C_9H_5O_3$	161.0238	161.0254	16
			77	C_6H_5	77.0391	77.0393	8
			73	C_4H_9O	73.0653	73.0671	14
cis-4′-*O*-Ethylkhellactone[c] (XII)	H	CH_3CH_2	291 (M + 1)	$C_{16}H_{19}O_5$	291.1231	291.1218	10
			290 (M)	$C_{16}H_{18}O_5$	290.1153	290.1178	43
trans-4′-*O*-Ethylkhellactone[c,e] (XIII)	H	CH_3CH_2	219	$C_{12}H_{11}O_4$	219.0657	219.0660	56
			218 (P)	$C_{12}H_{10}O_4$	218.0579	218.0579	100
			203	$C_{13}H_9O_3$	203.0551	203.0562	8
			191	$C_{10}H_7O_4$	191.0343	191.0353	74
			190	$C_{10}H_6O_4$	190.0265	190.0273	41
			176	$C_{10}H_8O_3$	176.0473	176.0478	5
			175	$C_{10}H_7O_3$	175.0394	175.0379	5
			162	$C_9H_6O_3$	162.0316	162.0324	46
			134	$C_8H_6O_2$	134.0367	134.0378	15
trans-Khellactone[d] (XIV)	H	H	262 (M)	$C_{14}H_{14}O_5$	262.0840	262.0840	15
			192	$C_9{}^{13}CH_7O_4$	192.0377	192.0388	12
			191 (P)	$C_{10}H_7O_4$	191.0343	191.0347	100
			190	$C_{10}H_6O_4$	190.0265	190.0255	16
			162	$C_9H_6O_3$	162.0316	162.0311	17
			134	$C_8H_6O_2$	134.0367	134.0377	17
			107	C_7H_7O	107.0496	107.0492	7

[a] Fragments with a relative abundance of less than 5% of the parent peak were not considered. [b] Reference 12. [c] Reference 13. [d] Reference 14. [e] The accurate mass measurements for XI and XIII are not included. The relative intensities of the low-resolution peaks as compared to X and XII, respectively, were almost identical and, therefore, are not included.

entiation of positional isomers, a problem frequently encountered in this class of coumarins. Obviously, when the diacetate (VII) fragments (Scheme VIII), it is impossible to tell which acetoxy group is eliminated, although one would suggest loss of the 3′-moiety by analogy to V and VI.

It is also of interest to compare the spectra of Group 1 and 2 compounds with those of Group 3. In this case, peaks due to the loss of $C_4H_7COO\cdot$ are present in the spectra of I–IV but not in the spectra of V and VI. Das *et al.* (11) reported fragmentation patterns for visnadin (VI) that are in accord with the results of this study.

Group 5—Pathways A and B seem to be equally important in the spectra of VIII and IX. The presence of an acetoxy group apparently is necessary for the observation of Pathway A (Scheme IX). Only small differences in peak height are observed in the spectra of VIII and IX.

Groups 6 and 7—Compounds X–XIV exhibit sizable molecular ion peaks, although ethers X–XIII also exhibit $M^+ + 1$ peaks. Pathway A seems to be of little or no consequence (Schemes X–XII). A stepwise loss of carbon monoxide, characteristic of coumarins, was observed from Pathway B fragmentation.

The following generalizations will aid in the interpretation of the mass spectra of this class of coumarins and, hopefully, will lead to the effective use of these results in the structural elucidation of unknown coumarins.

1. All compounds exhibit M^+, except when R_1 and R_2 are both

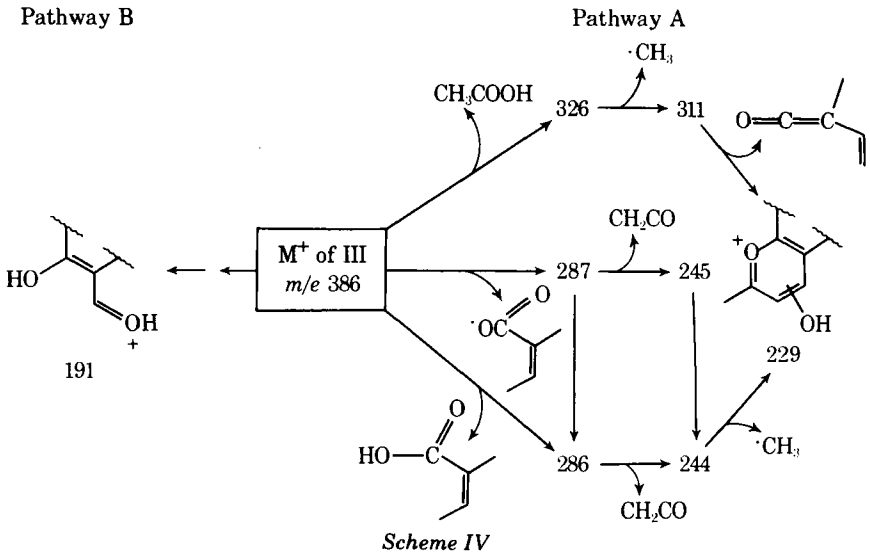

Scheme IV

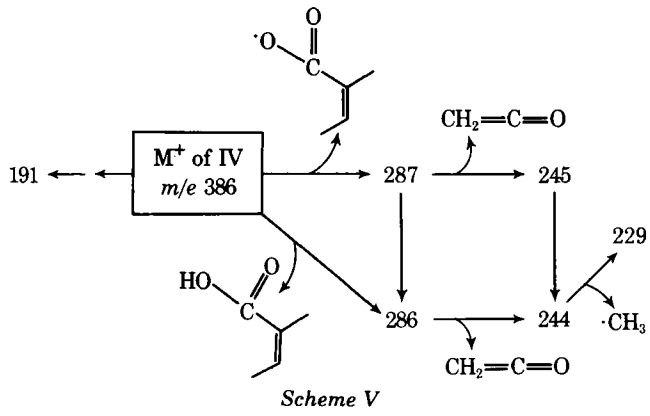

Scheme V

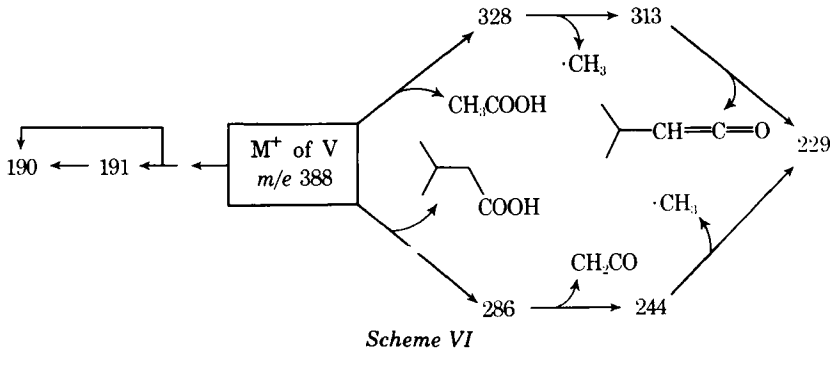

Scheme VI

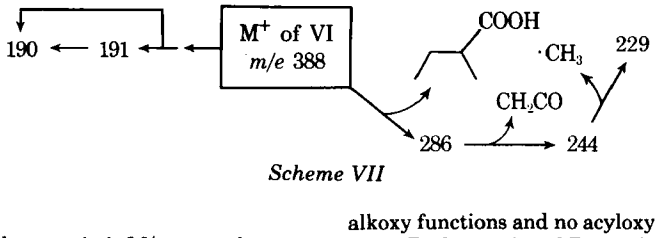

Scheme VII

bulky (Group 1).

2. When R_2 is an alkoxy group, characteristic $M^+ + 1$ peaks appear.

3. Pathway A predominates when both substituents are acyloxy groups (Groups 1–4).

4. Pathway B predominates in compounds with hydroxy and alkoxy functions and no acyloxy substituent.

5. Pathways A and B are of equal importance when one substituent is an acyloxy function (*e.g.*, Group 5).

6. Loss of a 3′-acyloxy substituent is preferred over loss of a 4′-acyloxy moiety.

7. Loss of five-carbon acids is more facile than loss of acetic acid.

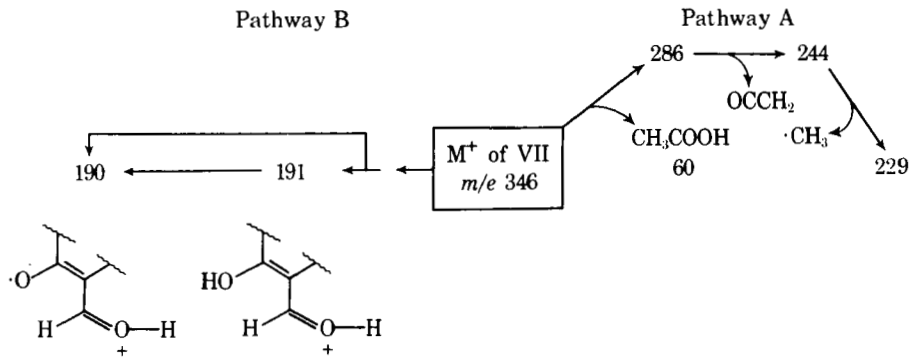

Scheme VIII

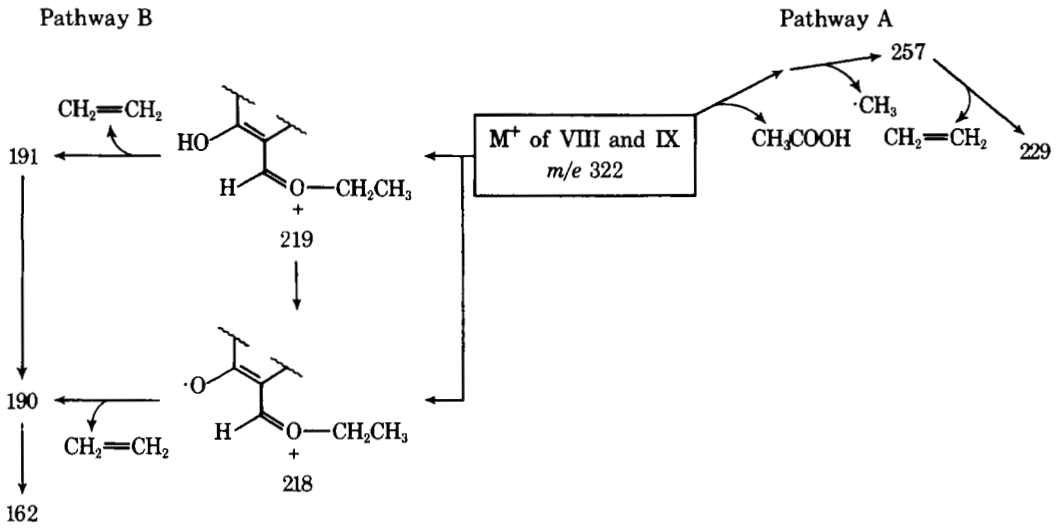

Scheme IX

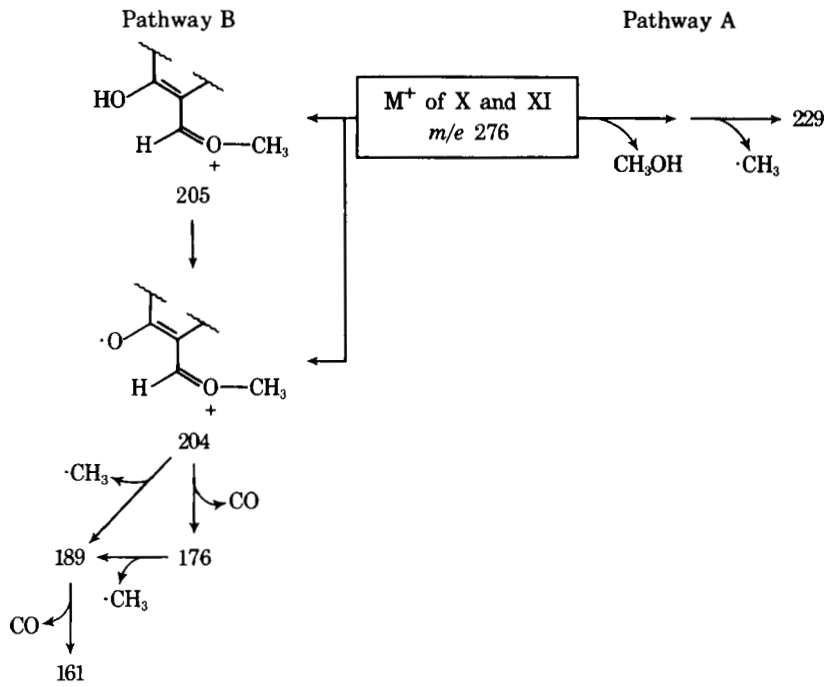

Scheme X

8. Loss of an unsaturated five-carbon acyloxy substituent occurs more readily than loss of a corresponding five-carbon saturated analog.

9. The acyloxy substituents give rise to their respective characteristic peaks. For example, angelates and/or senecioates show peaks at *m/e* 83 and 55, isovalerates and α-methylbutyrates show peaks at

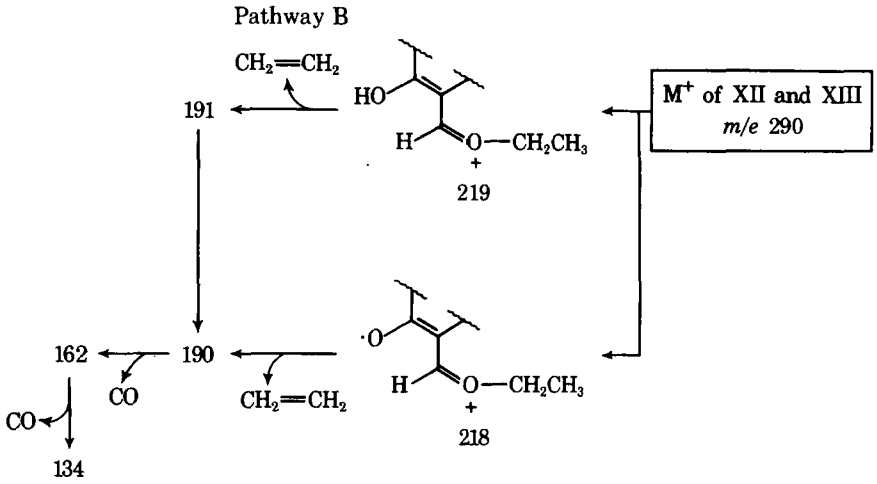

Scheme XI

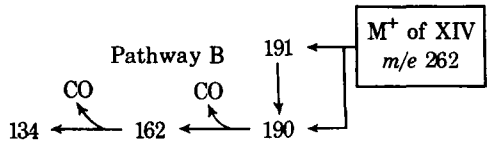

Scheme XII

m/e 85 and 57, and acetates show a peak at *m/e* 43.

10. No significant differences are observed in the spectra of *cis*- and *trans*-isomers.

EXPERIMENTAL

Materials—Compounds I–XIV were available from previous studies (12–14).

Mass Spectra[2]—The mass spectrometer was operated at an ionizing voltage of 70 ev, a source temperature of 200°, and an unheated direct inlet. Perfluorokerosene was used as the internal standard.

REFERENCES

(1) K. H. Lee and T. O. Soine, *J. Pharm. Sci.*, **57**, 865(1968).

(2) M. Shipchandler and T. O. Soine, *ibid.*, **57**, 741(1968).

(3) *Ibid.*, **57**, 747(1968).

(4) *Ibid.*, **57**, 2062(1968).

(5) M. Shipchandler, T. O. Soine, and P. K. Gupta, *J. Pharm. Sci.*, **59**, 67(1970).

(6) C. S. Barnes and J. L. Occolowitz, *Aust. J. Chem.*, **17**, 975(1964).

(7) B. Willhalm, A. F. Thomas, and F. Gautchi, *Tetrahedron*, **20**, 1185(1964).

(8) T. Seshadri, M. S. Sood, K. H. Handa, and Vishwapaul, *ibid.*, **23**, 1883(1967).

(9) F. Bohlmann and K. M. Rode, *Chem. Ber.*, **101**, 2741(1968).

(10) F. Bohlmann and W. Thefeld, *Tetrahedron Lett.*, **41**, 3577(1970).

(11) K. G. Das, A. Bose, C. Mesta, S. Shanbhag, M. Meheshwari, and S. C. Battacharyya, *Indian J. Chem.*, **7**, 132(1969).

(12) B. E. Nielsen and T. O. Soine, *J. Pharm. Sci.*, **56**, 184(1967).

(13) R. E. Willette and T. O. Soine, *ibid.*, **51**, 149(1962).

(14) E. Smith, N. Hosansky, W. G. Bywater, and E. E. Van Tamelen, *J. Am. Chem. Soc.*, **79**, 3534(1957).

ACKNOWLEDGMENTS AND ADDRESSES

Received July 17, 1975, from the *Department of Medicinal Chemistry, College of Pharmacy, University of Minnesota, Minneapolis, MN 55455*

Accepted for publication September 12, 1975.

* Present address: Division of Natural Sciences, State University of New York, College at Purchase, Purchase, NY 10577

‡ Present address: Research Department, Commercial Solvents Corporation, Terre Haute, IN 47802

x To whom inquiries should be directed.

[2] Determined by Dr. N. Shaath and Dr. R. Upham, Mass Spectrometry Laboratory, Department of Chemistry, University of Minnesota, employing an AEI MS30 high-resolution mass spectrometer. Preliminary mass spectral data were obtained using a Hitachi Perkin-Elmer RMU-6D mass spectrometer.

Ionization Constants of Cephalosporin Zwitterionic Compounds

WILLIAM H. STRENG ˣ, H. E. HUBER, JOYCE L. DeYOUNG, and M. A. ZOGLIO

Abstract □ The microionization constants for two zwitterionic compounds were determined by incorporating two experimental techniques. These compounds have chromophoric changes dependent upon the solution pH. By combining the spectrophotometric measurements with potentiometric measurements, all four microionization constants were calculated. The method used is completely general and is applicable to all diprotic compounds that exhibit this spectrophotometric behavior. The observed pKa's had differences of at most 1.2 units for either compound and were in the 1–4 range. A comparison of the results with each compound and similar compounds indicates that the values are reasonable.

Keyphrases □ Ionization constants—cephalosporin zwitterionic compounds, calculated by combining spectrophotometric and potentiometric measurements □ Cephalosporin zwitterionic compounds—ionization constants calculated by combining spectrophotometric and potentiometric measurements □ Zwitterionic compounds, cephalosporins—ionization constants calculated by combining spectrophotometric and potentiometric measurements

The ionization constants of acids and acid salts have been determined by several methods and investigators since the late 1800's. Albert and Serjeant (1) discussed the potentiometric, spectrophotometric, and conductometric methods. Compounds containing one acidic proton generally have uncomplicated calculations, and determination of the ionization constants is a simple matter using any of the three methods.

BACKGROUND

If two acidic protons are present, four equilibria need to be considered instead of two (Scheme I) and the determination becomes more complex. If HRH is a symmetrical molecule, K_1 and K_3 will be equal as will K_2 and K_4; this is not the case for unsymmetrical molecules, and elucidating the constants becomes a problem. Most methods result in the calculation of two constants instead of four (2). It is easy to show that these macroscopic constants are related to the microscopic constants as follows:

$$K_{13} = K_1 + K_3 \qquad \text{(Eq. 1)}$$

$$\frac{1}{K_{24}} = \frac{1}{K_2} + \frac{1}{K_4} \qquad \text{(Eq. 2)}$$

where K_{13} and K_{24} are the macroscopic constants and K_1, K_2, K_3, and K_4 are the microscopic constants. Obviously, if K_1 is much larger than K_3 or if K_2 is much smaller than K_4, the macroscopic constant K_{13} will equal K_1 and K_{24} will equal K_2. In this case, there will be little $[HR^-]$ in solution at any pH. However, if K_1 is of similar magnitude to K_3 and if K_2 is of similar magnitude to K_4, $[HR^-]$ and $[^-RH]$ will both be appreciable. Under these conditions, it is necessary to determine each microscopic constant to calculate individual species concentrations.

Included among the diacidic compounds represented by Scheme I are amphoteric compounds, *i.e.*, those that can behave as either a

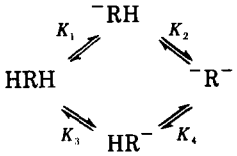

Scheme I

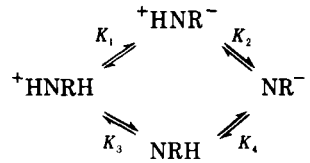

Scheme II

proton acceptor or donor. As depicted in Scheme II, these compounds can simultaneously contain positive and negative charges and are, as such, zwitterions. The relative concentrations of zwitterion and uncharged molecules will depend on the magnitudes of K_1 and K_3 or K_2 and K_4, *i.e.*, $[^+HNR^-]/[NRH] = (K_1/K_3) = (K_4/K_2)$.

Several methods have been reported for determining the microscopic constants of zwitterionic compounds utilizing spectrophotometric (3–5) and potentiometric (6) techniques. Each method has its own restrictions, from requiring accurate measurements over wide pH ranges to preparing esters and assuming that they will not influence other equilibria.

As a means of circumventing some undesirable limitations, a method has been developed that combines spectrophotometric and potentiometric measurements to calculate the constants. Two constants can be obtained directly from calculations while the remaining two can be determined by either graphical techniques or further calculations utilizing one of the first two constants.

Measurements were made on two compounds which form zwitterions, pyridoneacetic acid (I) and the sodium salt of 3-[(acetyloxy)-methyl] -8-oxo-7- [[(4-oxo-1(4*H*)-pyridinyl)acetyl]amino] -5-thia-1-azabicyclo[4.2.0]oct-2-ene-2-carboxylic acid (II). Compound II is a cephalosporin containing the pyridone moiety. Each behaves as an amphoteric compound for which the carboxylic acid group acts as a proton donor and the nitrogen in the pyridone ring acts as a proton acceptor.

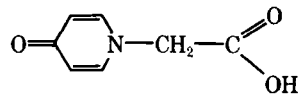

I

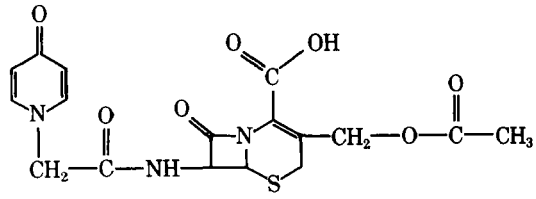

II

EXPERIMENTAL

Apparatus and Equipment—Potentiometric measurements were made using the system diagrammed in Fig. 1. Four holes were cut into a number 13½ rubber stopper to hold two electrodes, a 50-ml buret, and a nitrogen tube. The two electrodes[1], a standard calomel electrode and a glass electrode, were attached to a pH meter[2] which could be operated in expanded scale mode. A glass extension (12 cm) was fused to a 50-ml buret so that the tip of the buret would be below the surface of the solution. Water-saturated nitrogen was bubbled into the so-

[1] Beckman calomel internal with quartz junction reference electrode 39400 and Beckman pH (glass) electrode 39301.
[2] Beckman Century SS-1.

lution to stir it and to keep other gases from being dissolved. The stopper was fit into a 250-ml beaker.

Spectrophotometric measurements were made with a UV–visible spectrophotometer[3].

Solution Preparation and Measurement—Solutions were prepared for the spectrophotometric measurements using 0.05 *M* ionic strength buffers in the pH range of 1.72–2.97 for II and 0.05 and 0.2 *M* ionic strength buffers in the pH range of 2.56–3.93 for I. The concentrations of II and I were approximately 4×10^{-5} *M*.

Two chromophores were assigned to the pyridone ring. A peak at $\lambda = 262$ nm was attributed to the unprotonated nitrogen; that at $\lambda = 245$ nm was attributed to the protonated nitrogen. Spectra were obtained over the 350–225-nm range using the appropriate buffer solution as a reference. Other studies have shown that, over the pH range used, the compounds are stable for the duration of the experiment. Furthermore, measurements on 3-[(acetyloxy)methyl]-7-[[(2-methylpropoxy)carbonyl]amino] -8-oxo-5-thia-1-azabicyclo[4.2.0]oct-2-ene-2-carboxylic acid (III), which is similar to II but has only the β-lactam chromophore, indicated that the β-lactam ring absorbance at $\lambda = 262$ nm changes 3% at most over this pH range. Therefore, any absorbance changes can be considered to be due to changes in the concentration of the unprotonated nitrogen species.

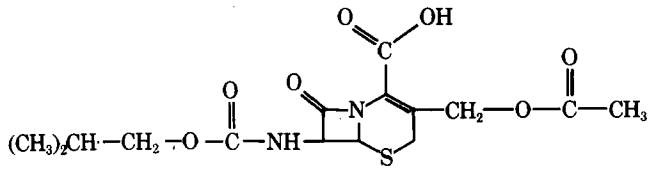

III

Solutions of the sodium salt of II were prepared in the $1–2.3 \times 10^{-2}$ *M* concentration range; solutions of I were prepared at a concentration of 2×10^{-3} *M*. These solutions were titrated with hydrochloric acid solution to doubly protonate the molecules and then back-titrated with potassium hydroxide solutions as diprotic compounds. The potassium hydroxide solutions were standardized with potassium acid phthalate, and the hydrochloric acid solutions were standardized with potassium hydroxide solutions. For the titration of I, the acid and base concentrations were 0.023 *N* hydrochloric acid and 0.003 *N* potassium hydroxide; for II, both titrant solutions were 0.15 *N*.

THEORETICAL

In the following derivations, {}, [], *Y*, and *K* represent activity, concentration, activity coefficient, and equilibrium constant on a molar scale, respectively. The total concentration of base added as titrant, halide, and acid being titrated are given by [B], [X], and [A].

Exact Solution to Scheme II—An expression can be derived that relates the individual equilibrium constants in Scheme II to the total acid concentration, base concentration, and pH. This exact solution is as follows.

The equilibrium constants are given by:

$$K_1 = \frac{\{^+HNR^-\}\{H^+\}}{\{^+HNRH\}} = \frac{[^+HNR^-]\{H^+\}}{[^+HNRH]}\frac{Y_{^+HNR^-}}{Y_{^+HNRH}} \quad \text{(Eq. 3a)}$$

$$K_2 = \frac{\{NR^-\}\{H^+\}}{\{^+HNR^-\}} = \frac{[NR^-]\{H^+\}}{[^+HNR^-]}\frac{Y_{NR^-}}{Y_{^+HNR^-}} \quad \text{(Eq. 3b)}$$

$$K_3 = \frac{\{NRH\}\{H^+\}}{\{^+HNRH\}} = \frac{[NRH]\{H^+\}}{[^+HNRH]}\frac{Y_{NRH}}{Y_{^+HNRH}} \quad \text{(Eq. 3c)}$$

$$K_4 = \frac{\{NR^-\}\{H^+\}}{\{NRH\}} = \frac{[NR^-]\{H^+\}}{[NRH]}\frac{Y_{NR^-}}{Y_{NRH}} \quad \text{(Eq. 3d)}$$

$$K_\omega = \{H^+\}\{OH^-\} \quad \text{(Eq. 3e)}$$

The material balance for the acid is:

$$[A] = [^+HNRH] + [^+HNR^-] + [NRH] + [NR^-] \quad \text{(Eq. 4)}$$

and the electrical balance is:

$$[B] + [H^+] + [^+HNRH] = [OH^-] + [X] + [NR^-] \quad \text{(Eq. 5)}$$

[3] Beckman Acta III or Cary 17.

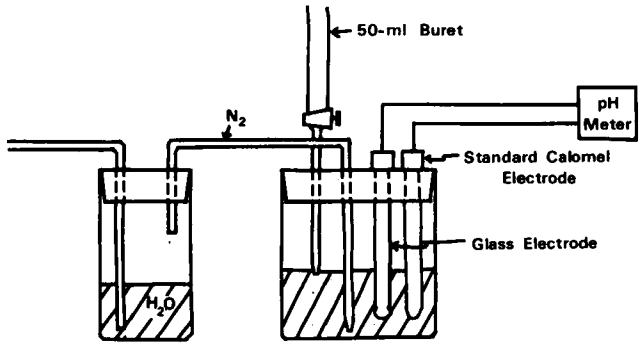

Figure 1—*Apparatus used for potentiometric measurements.*

By using the equilibrium constants, the material balance equation can be expressed in terms of $[NR^-]$:

$$[A] = \frac{[NR^-]\{H^+\}^2}{K_3K_4}\frac{Y_{NR^-}}{Y_{^+HNRH}} + \frac{[NR^-]\{H^+\}}{K_2}\frac{Y_{NR^-}}{Y_{^+HNR^-}} + \frac{[NR^-]\{H^+\}}{K_4}\frac{Y_{NR^-}}{Y_{NRH}} + [NR^-] \quad \text{(Eq. 6)}$$

In the same manner, the electrical balance equation can be solved for $[NR^-]$:

$$[NR^-] = \{[B] + [H^+] - [OH^-] - [X]\} \Big/ \left\{1 - \frac{\{H^+\}^2}{K_3K_4}\frac{Y_{NR^-}}{Y_{^+HNRH}}\right\} \quad \text{(Eq. 7)}$$

Substituting Eq. 7 into Eq. 6 for $[NR^-]$ and realizing that [X] will equal [A] for this type of compound result in:

$$[A] = \left\{\frac{[B] + [H^+] - [OH^-] - [A]}{K_3K_4 - \{H^+\}^2\frac{Y_{NR^-}}{Y_{^+HNR^-}}}\right\}\left\{K_3K_4 + K_3\{H^+\}\frac{Y_{NR^-}}{Y_{NRH}} + \frac{\{H^+\}}{K_2}\frac{Y_{NR^-}}{Y_{^+HNR^-}} + \frac{\{H^+\}^2}{K_3K_4}\frac{Y_{NR^-}}{Y_{^+HNRH}}\right\} \quad \text{(Eq. 8)}$$

Equation 8 can be rearranged to the form:

$$\alpha = K_1\frac{Y_{^+HNRH}}{Y_{^+HNR^-}}\beta + K_3\frac{Y_{^+HNRH}}{Y_{NRH}}\beta + K_3K_4\frac{Y_{^+HNRH}}{Y_{NR^-}}\gamma \quad \text{(Eq. 9)}$$

where:

$$\alpha = [B]\{H^+\}^3 + \frac{\{H^+\}^4}{Y_{H^+}} - \frac{K_\omega\{H^+\}^2}{Y_{OH^-}}$$

$$\beta = [A]\{H^+\}^2 - [B]\{H^+\}^2 - \frac{\{H^+\}^3}{Y_{H^+}} + \frac{K_\omega\{H^+\}}{Y_{OH^-}}$$

$$\gamma = 2[A]\{H^+\} - [B]\{H^+\} - \frac{\{H^+\}^2}{Y_{H^+}} + \frac{K_\omega}{Y_{OH^-}}$$

It is not possible to solve Eq. 9 directly for the equilibrium constants because the first two terms on the right have the same coefficient, β. If one equilibrium constant is known, it is then possible to use this equation to solve for the remaining constants.

Combining Measurements to Solve Scheme II—The individual constants (microconstants) in Scheme II can be determined if the compound has a chromophore dependent upon the pH. The spectrophotometric information can be combined with potentiometric data to obtain the constants. In this derivation, it is assumed that protonation or deprotonation of the nitrogen atom is responsible for the observed spectral changes. Therefore, from the spectrophotometric data, the total concentration of protonated nitrogen species, [Z], can be determined:

$$[Z] = [^+HNRH] + [^+HNR^-] \quad \text{(Eq. 10)}$$

Substituting Eq. 10 into the material balance equation, Eq. 4, and expressing [NRH] in terms of $[NR^-]$ result in:

$$[A] = [NR^-] + \frac{[NR^-]\{H^+\}}{K_4}\frac{Y_{NR^-}}{Y_{NRH}} + [Z] \quad \text{(Eq. 11)}$$

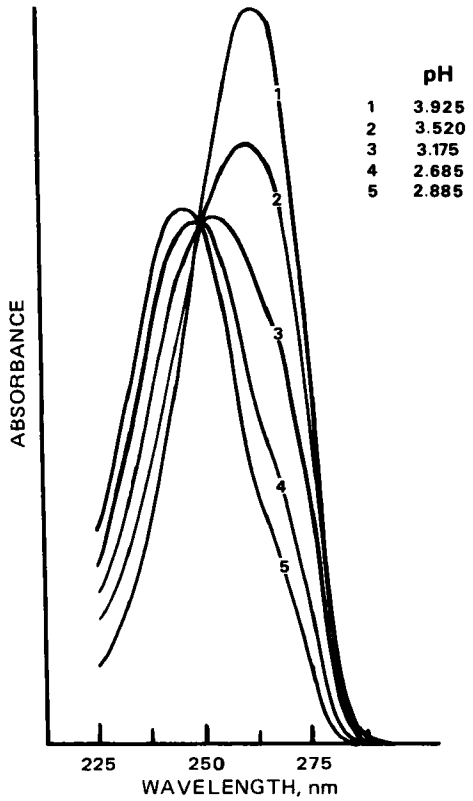

Figure 2—*Spectral curves for I.*

Inserting Eq. 7 into Eq. 11 for $[NR^-]$ gives:

$$[A] = \left\{ \frac{[B] + \{H^+\} - [OH^-] - [A]}{K_3K_4 - \{H^+\}^2 \frac{Y_{NR^-}}{Y_{+HNRH}}} \right\} \left\{ 1 + \frac{\{H^+\}Y_{NR^-}}{K_4 Y_{NRH}} \right\} + [Z] \qquad \text{(Eq. 12)}$$

Equation 12 can be rearranged as shown by Eq. 13 to obtain an expression that can be used to determine K_3 and K_4:

$$\{H^+\}^2 \frac{Y_{NR^-}}{Y_{+HNRH}} \{[Z] - [A]\} = K_4\{H^+\} \frac{Y_{NR^-}}{Y_{NRH}} \left\{ [B] + \frac{\{H^+\}}{Y_{H^+}} - \frac{K_\omega}{\{H^+\}Y_{OH^-}} - [A] \right\} + K_3K_4 \left\{ [B] + \frac{\{H^+\}}{Y_{H^+}} - \frac{K_\omega}{\{H^+\}Y_{OH^-}} - 2[A] + [Z] \right\} \qquad \text{(Eq. 13)}$$

Equation 13 can be solved either by graphical techniques or by simultaneous equations for K_3 and K_4. Therefore, Eq. 13 is expressed as follows:

$$\delta = K_4\epsilon + K_3K_4\xi \qquad \text{(Eq. 14)}$$

A plot of δ/ξ *versus* ϵ/ξ will be linear with a slope of K_4 and δ/ξ will equal K_3K_4 at $\epsilon/\xi = 0$. Also, the value of ϵ/ξ at $\delta/\xi = 0$ will equal $-K_3$.

Equation 14 may be solved using simultaneous equations by utilizing titrimetric and spectrophotometric data obtained at each of two pH values. By labeling the two sets of data as 1 and 2, K_4 and K_3 can be calculated according to:

$$K_4 = \frac{\frac{\delta_1}{\xi_1} - \frac{\delta_2}{\xi_2}}{\frac{\epsilon_1}{\xi_1} - \frac{\epsilon_2}{\xi_2}} \qquad \text{(Eq. 15)}$$

$$K_3 = \frac{\delta_1 - K_4\epsilon_1}{K_4\xi_1} \qquad \text{(Eq. 16)}$$

Substituting the value of K_3 or K_4, calculated from Eq. 13, into Eq. 9 will permit the determination of K_1 and K_2. Again, K_1 and K_2 can be determined using either graphical or simultaneous equation techniques. A plot of α/γ *versus* β/γ should be linear with an intercept at $\beta/\gamma = 0$ of K_3K_4 while the slope will equal $K_1 + K_3$. Combining K_4 with K_3K_4 will result in K_3, which can then be used to obtain K_1 from the slope.

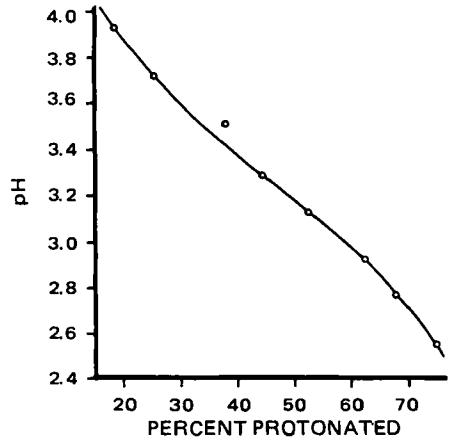

Figure 3—*Percentage of species containing a protonated nitrogen for I.*

There is a relationship between the four equilibrium constants, and it is easy to show that K_1K_2 must equal K_3K_4. Therefore, when knowing K_1, K_3, and K_4, it is possible to determine K_2 according to the relationship $K_2 = K_3K_4/K_1$. Solving Eq. 9 using simultaneous equations results in equations similar to Eqs. 15 and 16. The values calculated are the same as those obtained by the graphical method; *i.e.*, the product K_3K_4, the sum $K_1 + K_3$, and the individual constants can be determined as before.

RESULTS AND DISCUSSION

Since the results for both compounds are similar, only those for I will be used to demonstrate the procedure. In Fig. 2, the spectral curves as a function of pH are shown for the solution of 0.2 *M* ionic strength; these curves are not affected by ionic strength changes over the 0.05–0.2 *M* range. It can be seen that the chromophore occurring at $\lambda = 262$ nm is a basic form while that at $\lambda = 245$ nm is an acidic form. From these curves, the concentration of the protonated nitrogen species can be determined as a function of pH. A plot of the percent protonated nitrogen species *versus* pH is given in Fig. 3.

A typical potentiometric titration curve for I is given in Fig. 4. From this curve, it can be seen that there is no break at the first equivalence point and that there is a very large break at the second. An excess of hydrochloric acid was added to the solution prior to the titration with potassium hydroxide to assure that the I was entirely in its diprotic form. Therefore, an initial volume of base is needed to titrate the excess acid and the titration of I does not start until the volume at the mark indicated on the figure is reached.

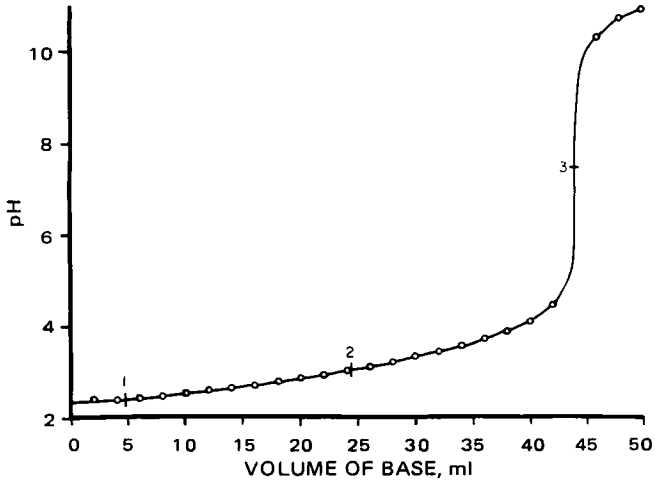

Figure 4—*Potentiometric titration curve for I. Key: 1, titration of I starts here (4.76 ml); 2, first equivalence point (24.38 ml); and 3, second equivalence point (43.99 ml).*

Table I—Ionization Constants of I and II

	$\frac{K_1}{Y_{+-}}$	$K_2\ Y_{+-}$	K_3	K_4
		I		
	1.065×10^{-2}	4.89×10^{-4}	4.57×10^{-3}	1.14×10^{-3}
pKa	1.97	3.31	2.34	2.94
		II		
	2.01×10^{-2}	1.45×10^{-3}	1.04×10^{-2}	2.79×10^{-3}
	2.00×10^{-2}	1.54×10^{-3}	9.96×10^{-3}	3.10×10^{-3}
	1.97×10^{-2}	1.76×10^{-3}	1.17×10^{-2}	2.97×10^{-3}
Average	1.99×10^{-2}	1.58×10^{-3}	1.07×10^{-2}	2.95×10^{-3}
pKa	1.70	2.80	1.97	2.53

	$[^+HNR^-]/[NRH]$
I	2.330
II	1.864

From the potentiometric titration, values of the pH for a given volume of base addition (taking account of the excess) were obtained and combined with the spectrophotometric data to calculate K_3 and K_4 using Eq. 14. The most consistent values using simultaneous equations were those for K_4. The remaining equilibrium constants could then be determined by Eq. 9. A plot of α/γ *versus* β/γ for I is shown in Fig. 5. It can be seen that the relationship is linear and can be treated as explained, resulting in values for K_1, K_2, and K_3.

In performing the calculations, an attempt was made to correct for activity effects by utilizing the Davies equation (7) to approximate the single ion activities:

$$-\log Y_i = AZ_i^2 \left\{ \frac{\sqrt{I}}{1+\sqrt{I}} - 0.2I \right\} \qquad \text{(Eq. 17)}$$

where Y_i is the single ion activity coefficient, A is a parameter whose value at 25° is 0.5092 on a molar scale, Z_i is the charge of ion i, and I is the molar ionic strength. The advantage of this equation over the extended Debye–Hückel law is that it does not require the use of any ion size parameters.

An approximation was not made for the activity of the zwitterionic species because there is no expression comparable to Eq. 17. It was not expected that Y_{+-}[4] would deviate greatly from the ideal value of 1. It also was assumed that the uncharged species had an activity coefficient of 1, a reasonable assumption within the limits of the experiment.

The calculated values for the equilibrium constants are listed in Table I. All calculations were performed on a computer[5]. A computer program was written which calculated δ, ϵ, and ξ in Eq. 14 and α, β, and γ in Eq. 9 for 10 sets of data. The values of δ, ϵ, and ξ were combined according to Eqs. 15 and 16 to determine K_4 and K_3; α, β, and γ were output to determine the remaining constants graphically. The consistency of the calculations for several concentrations can be seen in the data for II.

A comparison of the K's with literature values is not directly possible because there have been no ionization constants of comparable compounds determined in a manner resulting in the microscopic constants. It would appear that they are reasonable if the macroscopic constants for I, as given by Eqs. 1 and 2, are compared with those listed as proton gained and proton lost for the pyridinecarboxylic acids in Ref. 1[6]. This work, originally reported by Lumme (8), gave values of about 2 and 4.8 for these pKa's, whereas the pK_{13} and pK_{24} values for I are 1.8 and 3.5.

One review article gave a value of 1.75 for the carboxylic acid group on 7-aminocephalosporanic acid (9). This value is in good agreement with the carboxylic acid equilibrium constant, pK_1, for II, which is 1.70. From structural considerations, it would be expected that the pKa's associated with the deprotonation of the nitrogen should be nearly the same for I and II. As shown in Table I, the corresponding K_a values differ by only a factor of two, which is in agreement with this assumption.

By knowing the equilibrium constants, species profiles can be calculated:

$$\%[^+HNRH] = 100 \Big/ \left\{ 1 + \frac{K_1}{[H^+]} + \frac{K_3}{[H^+]} + \frac{K_3K_4}{[H^+]^2} \right\} \qquad \text{(Eq. 18a)}$$

$$\%[NRH] = 100 \Big/ \left\{ 1 + \frac{[H^+]}{K_3} + \frac{K_4}{[H^+]} + \frac{K_1}{K_3} \right\} \qquad \text{(Eq. 18b)}$$

$$\%[^+HNR^-] = 100 \Big/ \left\{ 1 + \frac{[H^+]}{K_1} + \frac{K_2}{[H^+]} + \frac{K_3}{K_1} \right\} \qquad \text{(Eq. 18c)}$$

$$\%[NR^-] = 100 \Big/ \left\{ 1 + \frac{[H^+]}{K_2} + \frac{[H^+]}{K_4} + \frac{[H^+]^2}{K_3K_4} \right\} \qquad \text{(Eq. 18d)}$$

The equations are written in their most general form. It is possible to express the percentages of one species as percentage functions of the other species (10) to simplify these equations.

The species profiles given in Figs. 6 and 7 were obtained using Eqs. 18a–18d to calculate the percent of species. According to the results in Table I, K_1 is larger than K_3 for both compounds. Consequently,

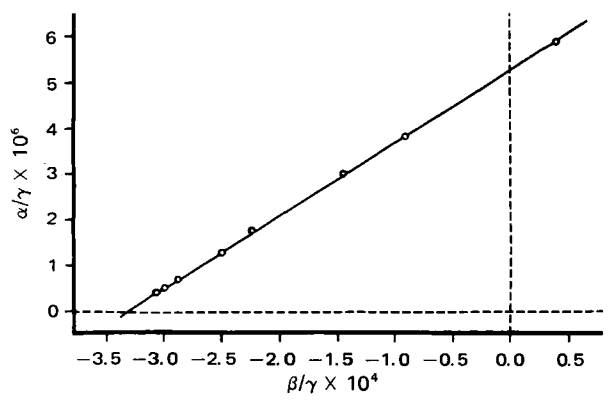

Figure 5—*Plot of* α/γ versus β/γ *for I.*

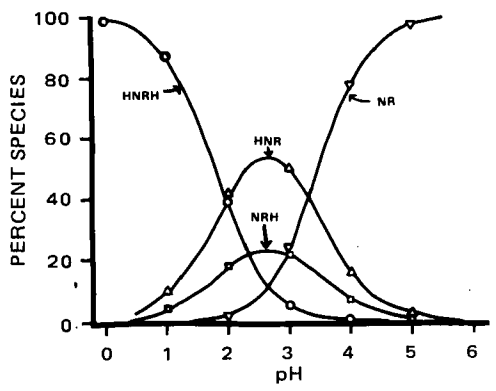

Figure 6—*Species profile for I.*

[4] The activity coefficient for the zwitterionic species.
[5] Digital Equipment Corp. RSTS-PDP-11.
[6] See Table 8.13.

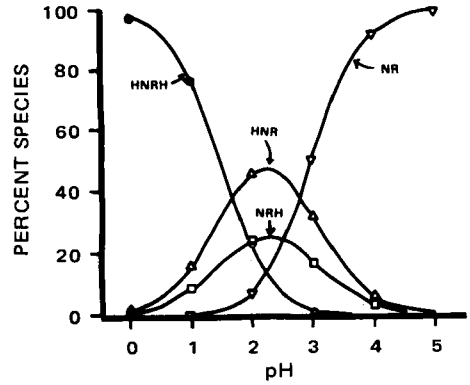

Figure 7—*Species profile for II.*

more zwitterions than unchanged molecules will be present in solution. This can be seen in the species profiles for I and II, for which the ratios of zwitterions to uncharged molecules are 2.33 and 1.864, respectively. The maximum concentration of zwitterionic species occurs at a pH equal to the average of pK_1 and pK_2 or pK_3 and pK_4, *i.e.*:

$$pH = \frac{pK_1 + pK_2}{2} = \frac{pK_3 + pK_4}{2} \qquad \text{(Eq. 19)}$$

For I, the maximum concentration occurs at pH 2.64; for II, it occurs at pH 2.25.

CONCLUSION

The ionization constants calculated for these compounds are reasonable when compared with each other and literature values for similar compounds. The approach used to calculate the individual equilibrium constants involves two methods, one that measures the total influence of all species upon the pH and one that measures only the sum of the concentrations of two species. Although neither method is suitable by itself, their combination enables one to calculate all four constants. Any two methods can be used provided that they are interrelated but not equivalent and one method gives the total influence of all species.

REFERENCES

(1) A. Albert and E. P. Serjeant, "Ionization Constants of Acids and Bases," Wiley, New York, N.Y., 1962.

(2) R. A. Robinson and R. H. Stokes, "Electrolyte Solutions," 2nd ed., 5th rev., Butterworth and Co., London, England, 1970, p. 348.

(3) D. E. Metzler and E. E. Snell, *J. Am. Chem. Soc.*, **71**, 2431(1955).

(4) J. T. Edsall, R. B. Martin, and B. R. Hollingworth, *Proc. Nat. Acad. Sci. USA*, **44**, 505(1958).

(5) S. Riegelman, L. A. Strait, and E. Z. Fischer, *J. Pharm. Sci.*, **51**, 129(1962).

(6) M. J. Nye and W. P. Tang, *Tetrahedron*, **28**, 463(1972).

(7) J. N. Butler, in "Ionic Equilibrium, a Mathematical Approach," Addison-Wesley, Reading, Mass., 1964, p. 437.

(8) P. O. Lumme, *Suom. Kemistil.*, **30B**, 173(1957).

(9) J. P. Hou and J. W. Poole, *J. Pharm. Sci.*, **60**, 503(1971).

(10) J. N. Butler, in "Ionic Equilibrium, a Mathematical Approach," Addison-Wesley, Reading, Mass., 1964, pp. 210–212.

ACKNOWLEDGMENTS AND ADDRESSES

Received June 24, 1975, from *Merrell-National Laboratories, Division of Richardson-Merrell Inc., Cincinnati, OH 45215*

Accepted for publication September 29, 1975.

[x] To whom inquiries should be directed.

Pharmacokinetic Studies of Pentylenetetrazol in Dogs

H. W. JUN

Abstract □ Pharmacokinetic profiles of pentylenetetrazol in the dog were studied following rapid intravenous and oral administrations of a convulsant dose (15–20 mg/kg). Plasma level–time curves after a rapid intravenous injection showed biexponential decline, indicating that the disposition of this drug in the dog follows a two-compartment body model. Pharmacokinetic parameters were calculated from the intravenous data. After oral administration of the solution dose, the peak plasma level appeared at about 30 min postdose, indicating that the absorption occurs rapidly. Areas under the oral plasma level–time curves showed that the drug was absorbed completely and that the first-pass metabolism effect was minimal. The ligation studies of the kidney and the liver suggested that the main elimination pathway of this drug was biotransformation in the liver. The average plasma half-life was 1.4 hr. At steady state, the volume of distribution was approximately equivalent to the volume of the total body water.

Keyphrases □ Pentylenetetrazol—pharmacokinetic studies following intravenous and oral administrations, dogs □ Pharmacokinetics—pentylenetetrazol, intravenous and oral administrations, dogs □ Stimulants—pentylenetetrazol, pharmacokinetic studies following intravenous and oral administrations, dogs

Pentylenetetrazol[1] is being used for various clinical purposes in humans and animals. The primary use of this drug in humans is as a central nervous system (CNS) stimulant for the therapeutic management of chronic depression and confusion in mental patients. In animals, this drug is also being used as a CNS stimulant for respiratory failure or collapse during surgical anesthesia.

Although the properties of biological disposition of pentylenetetrazol were studied (1, 2), pharmacokinetic profiles have not been reported. Recently, a sensitive and reproducible GLC determination of this compound in biological fluids was described (3); the method allowed the determination of pharmacokinetic properties of pentylenetetrazol in the dog as reported in this study.

EXPERIMENTAL

Conditions of Dogs—Seven healthy dogs (four beagle and three mongrel breeds), 8–13 kg, were used. Four dogs received a single pentylenetetrazol dose of 15 or 20 mg/kg iv and po on separate occasions. Three dogs were utilized in the liver and kidney ligation studies. When two or more blood level studies were performed on the same dog, at least 2 weeks was allowed between experiments. During the blood level studies, dogs were anesthetized with pentobarbital sodium.

Assay Procedures—Plasma concentrations of pentylenetetrazol were determined by the GLC technique recently developed (3). The

[1] Metrazol, Knoll Pharmaceutical Co., Whippany, N.J.

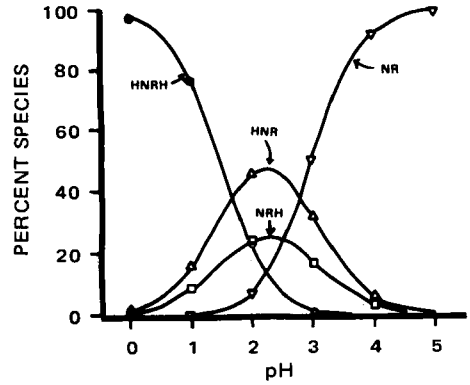

Figure 7—*Species profile for II.*

more zwitterions than unchanged molecules will be present in solution. This can be seen in the species profiles for I and II, for which the ratios of zwitterions to uncharged molecules are 2.33 and 1.864, respectively. The maximum concentration of zwitterionic species occurs at a pH equal to the average of pK_1 and pK_2 or pK_3 and pK_4, *i.e.*:

$$pH = \frac{pK_1 + pK_2}{2} = \frac{pK_3 + pK_4}{2} \qquad \text{(Eq. 19)}$$

For I, the maximum concentration occurs at pH 2.64; for II, it occurs at pH 2.25.

CONCLUSION

The ionization constants calculated for these compounds are reasonable when compared with each other and literature values for similar compounds. The approach used to calculate the individual equilibrium constants involves two methods, one that measures the total influence of all species upon the pH and one that measures only the sum of the concentrations of two species. Although neither method is suitable by itself, their combination enables one to calculate all four constants. Any two methods can be used provided that they are interrelated but not equivalent and one method gives the total influence of all species.

REFERENCES

(1) A. Albert and E. P. Serjeant, "Ionization Constants of Acids and Bases," Wiley, New York, N.Y., 1962.

(2) R. A. Robinson and R. H. Stokes, "Electrolyte Solutions," 2nd ed., 5th rev., Butterworth and Co., London, England, 1970, p. 348.

(3) D. E. Metzler and E. E. Snell, *J. Am. Chem. Soc.*, **71**, 2431(1955).

(4) J. T. Edsall, R. B. Martin, and B. R. Hollingworth, *Proc. Nat. Acad. Sci. USA*, **44**, 505(1958).

(5) S. Riegelman, L. A. Strait, and E. Z. Fischer, *J. Pharm. Sci.*, **51**, 129(1962).

(6) M. J. Nye and W. P. Tang, *Tetrahedron*, **28**, 463(1972).

(7) J. N. Butler, in "Ionic Equilibrium, a Mathematical Approach," Addison-Wesley, Reading, Mass., 1964, p. 437.

(8) P. O. Lumme, *Suom. Kemistil.*, **30B**, 173(1957).

(9) J. P. Hou and J. W. Poole, *J. Pharm. Sci.*, **60**, 503(1971).

(10) J. N. Butler, in "Ionic Equilibrium, a Mathematical Approach," Addison-Wesley, Reading, Mass., 1964, pp. 210–212.

ACKNOWLEDGMENTS AND ADDRESSES

Received June 24, 1975, from *Merrell-National Laboratories, Division of Richardson-Merrell Inc., Cincinnati, OH 45215*

Accepted for publication September 29, 1975.

[x] To whom inquiries should be directed.

Pharmacokinetic Studies of Pentylenetetrazol in Dogs

H. W. JUN

Abstract □ Pharmacokinetic profiles of pentylenetetrazol in the dog were studied following rapid intravenous and oral administrations of a convulsant dose (15–20 mg/kg). Plasma level–time curves after a rapid intravenous injection showed biexponential decline, indicating that the disposition of this drug in the dog follows a two-compartment body model. Pharmacokinetic parameters were calculated from the intravenous data. After oral administration of the solution dose, the peak plasma level appeared at about 30 min postdose, indicating that the absorption occurs rapidly. Areas under the oral plasma level–time curves showed that the drug was absorbed completely and that the first-pass metabolism effect was minimal. The ligation studies of the kidney and the liver suggested that the main elimination pathway of this drug was biotransformation in the liver. The average plasma half-life was 1.4 hr. At steady state, the volume of distribution was approximately equivalent to the volume of the total body water.

Keyphrases □ Pentylenetetrazol—pharmacokinetic studies following intravenous and oral administrations, dogs □ Pharmacokinetics—pentylenetetrazol, intravenous and oral administrations, dogs □ Stimulants—pentylenetetrazol, pharmacokinetic studies following intravenous and oral administrations, dogs

Pentylenetetrazol[1] is being used for various clinical purposes in humans and animals. The primary use of this drug in humans is as a central nervous system (CNS) stimulant for the therapeutic management of chronic depression and confusion in mental patients. In animals, this drug is also being used as a CNS stimulant for respiratory failure or collapse during surgical anesthesia.

Although the properties of biological disposition of pentylenetetrazol were studied (1, 2), pharmacokinetic profiles have not been reported. Recently, a sensitive and reproducible GLC determination of this compound in biological fluids was described (3); the method allowed the determination of pharmacokinetic properties of pentylenetetrazol in the dog as reported in this study.

EXPERIMENTAL

Conditions of Dogs—Seven healthy dogs (four beagle and three mongrel breeds), 8–13 kg, were used. Four dogs received a single pentylenetetrazol dose of 15 or 20 mg/kg iv and po on separate occasions. Three dogs were utilized in the liver and kidney ligation studies. When two or more blood level studies were performed on the same dog, at least 2 weeks was allowed between experiments. During the blood level studies, dogs were anesthetized with pentobarbital sodium.

Assay Procedures—Plasma concentrations of pentylenetetrazol were determined by the GLC technique recently developed (3). The

[1] Metrazol, Knoll Pharmaceutical Co., Whippany, N.J.

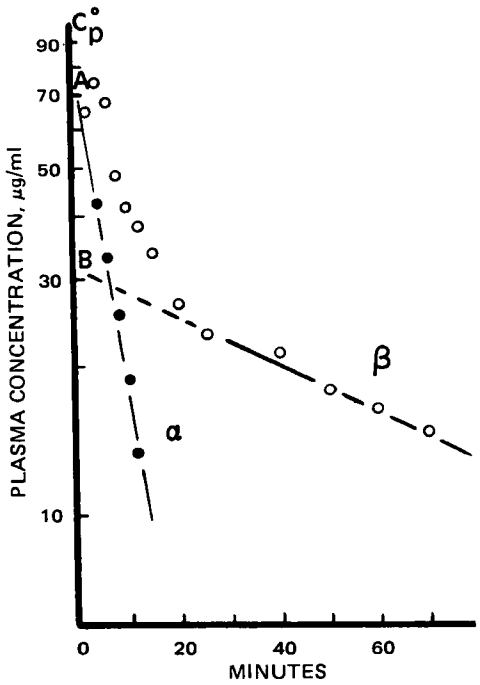

Figure 1—*Plasma concentrations of pentylenetetrazol at different times in a dog (11 kg) after a rapid intravenous injection of 20 mg/kg. Key:* O, *actual plasma concentrations;* ●, *points for the fast disposition phase by the feathering method; and* A *and* B, *extrapolated zero time intercepts of the α- and β-phases, respectively* (C_p^0 = A + B).

sensitivity limit of the assay is 0.5 μg of pentylenetetrazol/ml of plasma using a 2-ml sample. The method is sufficiently sensitive to determine plasma levels of the drug for three biological half-lives after administration of a 15-mg/kg dose.

Drug Administration—*Intravenous Injection*—The pentylenetetrazol dose (15 or 20 mg/kg) dissolved in 3 ml of normal saline was rapidly injected into the blood circulation through the front leg vein.

Oral Route—The oral dose (15 mg/kg) was dissolved in 25 ml of water and administered by stomach tube. Immediately after administration, the tube was flushed with 25 ml of water.

Blood Sampling—After drug administration, blood samples (4–8 ml) were withdrawn at various time intervals with a heparinized disposable syringe through an intravenous catheter inserted into the femoral vein. A three-way stopcock device was used during blood sampling. After each sample was taken, about 4 ml of lactated Ringer's solution was injected into the bloodstream to minimize the blood volume change.

Treatment of Blood Samples—Blood samples were placed in tubes[2] containing edetate sodium and were immediately centrifuged at 2000 rpm for 5 min. Pentylenetetrazol in the plasma portion was assayed by the GLC method (3).

Kidney Ligation Studies—To examine the role of the kidneys in the elimination of pentylenetetrazol in the dog, the following experiments were performed. A 13-kg dog received a rapid intravenous dose (15 mg/kg), and blood samples were withdrawn for 2 hr at various time intervals. After 2 hr (approximately one biological half-life in this dog), the kidneys of the dog were completely ligated; blood samples were withdrawn after ligation for drug analysis.

To ligate the kidneys, a surgical operation was made to place ligating threads around the renal blood vessels prior to drug administration. At the time of the kidney ligation, the threads were tied securely around the renal blood vessels to block the blood supply into the kidneys. Complete ligation was ascertained by the postmortem examination.

Liver Ligation Studies—The effect of liver ligation on the plasma level profiles of pentylenetetrazol was studied in a 12-kg dog. This dog received two intravenous doses of 15 mg/kg at zero time and 140 min after the first dose. The liver ligation was then made 140 min after the second dose by tying off the portal blood vessels with ligating threads placed surgically around the portal blood vessels.

Extreme care was taken to prevent internal bleeding during the liver ligation procedure. Following the first dose, blood samples were withdrawn frequently for 6 hr for analysis. The postmortem examination showed that the liver was completely ligated.

Kidney and Liver Ligation Studies—In this experiment, a 12-kg dog received three successive intravenous doses of pentylenetetrazol (15 mg/kg) at 0, 2, and 4 hr. The kidneys were first ligated 1 hr after the second dose, and the liver was ligated 1.75 hr after the third dose. To monitor the complete plasma level profile of the drug in this dog, blood samples were withdrawn frequently for about 7 hr.

Pharmacokinetic Analysis—The biexponential plasma level profiles of pentylenetetrazol after rapid intravenous injection indicate that the pharmacokinetics of the drug in the dog could be suitably evaluated on the basis of the two-compartment open model (Scheme I). The time course of biexponential decline of plasma levels for this model may be described by:

$$C_p^t = Ae^{-\alpha t} + Be^{-\beta t} \quad \text{(Eq. 1)}$$

$$C_p^0 = A + B \quad \text{(Eq. 2)}$$

where C_p^t and C_p^0 are the drug plasma concentrations at time t and time zero, respectively; A and B are the extrapolated concentrations at the zero time; and α and β are the first-order hybrid rate constants for the rapid and the slow disposition phases, respectively. The slopes of the log C_p *versus* time and log residual *versus* time plots are $-\beta/2.303$ and $-\alpha/2.303$, respectively. The biological half-life of the drug in a two-compartment open model is determined from the slope of the slow disposition phase. The estimates of the parameters A, B, α, and β are graphically obtained by the feathering method, using plasma data plotted on semilogarithmic scales. These values are used to calculate the model parameters such as k_{12}, k_{21}, and k_{el} by:

$$k_{el} = \frac{C_p^0}{\frac{A}{\alpha} + \frac{B}{\beta}} \quad \text{(Eq. 3)}$$

$$k_{21} = \frac{\alpha\beta}{k_{el}} \quad \text{(Eq. 4)}$$

$$k_{12} = (\alpha + \beta) - (k_{21} + k_{el}) \quad \text{(Eq. 5)}$$

The volume terms, V_p and $(V_d)_{ss}$, are calculated by the method previously described (4).

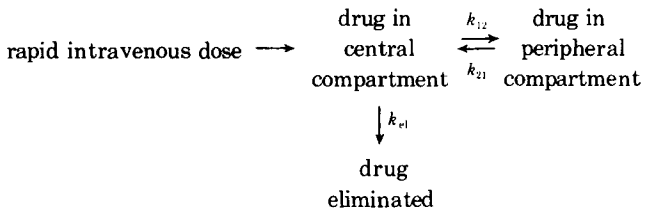

Scheme I—Two-compartment body model

RESULTS AND DISCUSSION

All plasma level–time curves (Figs. 1–5) of pentylenetetrazol in dogs after rapid intravenous administration exhibited typical biexponential decline. The duration and general shape of the rapid disposition phase were remarkably similar, whereas the slopes of the slow disposition phase varied among subjects (Table I). This result may have been due to more pronounced intersubject variation in the rate of metabolism than in the blood flow rate into tissues and the size of the peripheral compartment for the drug.

The biexponential plasma level profile of this drug indicates that a two-compartment body model can be used to describe adequately the pharmacokinetic properties of pentylenetetrazol in the dog. Several investigators (5, 6) discussed the use of a two-compartment model in pharmacokinetic studies. According to this model, pentylenetetrazol seems to be redistributed rapidly into a peripheral compartment after initial mixing in the central compartment. The slow distribution of this drug into the secondary compartment may be controlled primarily by the partition properties of the drug and different blood flow rates into various body tissues.

[2] Vacutainer, Becton-Dickinson, Rutherford, N.J.

Table I—Pharmacokinetic Parameters of Pentylenetetrazol in Dogs Based on the Two-Compartment Open Model

	Dog 1	Dog 2[a]		Dog 3	Dog 4	Dog 5
Dose, mg/kg	20	15	15	15	15	15
Weight, kg	11	12.5	12.5	9	10	13
A, μg/ml	73	17	24	10	34	23
B, μg/ml	31	19	18	29	28	17
α, hr^{-1}	8.56	6.9	7.92	9.6	12.5	10.2
β, hr^{-1}	0.67	0.54	0.53	0.59	0.784	0.32
Half-life[b], hr	1.03	1.28	1.3	1.17	0.88	2.17
C_p^0, μg/ml	104	36	42	39	62	40
V_p[c], liters	2.12	5.2	4.46	3.46	2.42	4.88
V_p, l/kg	0.19	0.42	0.36	0.39	0.242	0.38
$(V_d)_{ss}$[d], liters	5.1	8.68	8.81	5.1	4.70	10.6
$(V_d)_{ss}$, l/kg	0.46	0.69	0.71	0.59	0.47	0.81
k_{12}, hr^{-1}	4.29	2.6	3.61	3.01	5.61	5.29
k_{21}, hr^{-1}	3.05	3.88	3.7	6.4	6.05	4.53
k_{el}, hr^{-1}	1.89	0.96	1.14	0.78	1.62	0.72

[a] Plasma level data were obtained at two separate occasions in the same dog. [b] $T_{1/2} = 0.693/\beta$. [c] Volume of central compartment, V_p = dose/C_p^0. [d] Volume of distribution at steady state, $(V_d)_{ss} = V_p \times (k_{12} + k_{21})/k_{21}$.

Table I summarizes the pharmacokinetic data obtained after single rapid intravenous injections of pentylenetetrazol in five dogs. The data show that pentylenetetrazol was rapidly eliminated from the body with a mean half-life of 1.4 hr. The range of 0.88–2.2 hr indicates significant intersubject variation. Since pentylenetetrazol is metabolized completely in the dog, the variation in the rate of elimination was primarily due to different enzyme activities in the liver among different subjects. The volumes of the central compartment in these dogs (0.19–0.42 liter/kg) appeared to be approximately equivalent to the extracellular body water of the dog (0.190–0.350 liter/kg) (7), whereas the volumes of distribution at the steady state, $(V_d)_{ss}$ (0.46–0.810 liter/kg), seemed to be consistent with the physiological volume of the total body water of the dog (0.500–0.800 liter/kg) (7). These findings indicate that pentylenetetrazol initially mixes in the extracellular fluid (central compartment), including the blood, and then rapidly redistributes into the extracellular tissue fluid (peripheral compartment). In this model, the highly perfused tissue groups such as the liver and kidney are included in the central compartment.

Figure 1 shows a typical plasma level profile of pentylenetetrazol in Dog 1, 11 kg, after rapid intravenous injection of a 20-mg/kg dose. The profile was plotted on semilogarithmic graph paper with an expanded time scale. Frequent sampling during the first 20 min clearly indicated a biexponential decline of plasma levels. The first two samples at 3 and 5 min postdose showed that complete mixing of the drug in the central compartment occurred very rapidly, whereas the distribution of the drug into the tissue compartment appeared to be completed approximately 20 min after injection. The rapid initial decline in the plasma level indicated that the drug redistributed into the peripheral compartment. After completion of equilibrium in the tissues, the plasma level profile exhibited a linear decline (β-phase). Figure 1 also illustrates the graphical evaluation of the biexponential plasma level profile for the two-compartment open model. The pharmacokinetic parameters of the drug in this dog are listed in Table I.

Figure 2 compares two plasma level profiles in Dog 3, 9 kg, after rapid intravenous and oral administrations of a 15-mg/kg dose. The biexponential decline is shown clearly in the intravenous plasma level profile (curve A). Following oral administration of pentylenetetrazol in aqueous solution, the maximal peak concentration occurred about 30 min after administration (curve B), indicating that this drug is absorbed very rapidly and completely in the GI tract. This finding is in good agreement with the literature information on the absorption of this drug (8). The rapid absorption may be due to unusual physicochemical properties of the drug. Pentylenetetrazol does not include a strong acidic or basic functional group in the molecule and should remain primarily in the unionized form in the GI tract. Solubility also may be a factor for rapid and complete absorption, because this drug is freely soluble in both polar and nonpolar solvents (9).

The areas under the plasma level–time curves were almost the same

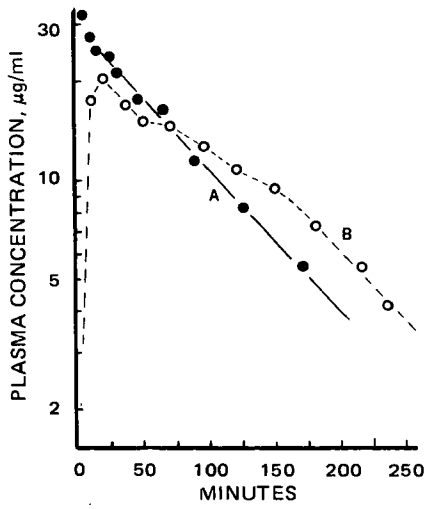

Figure 2—*Plasma concentrations of pentylenetetrazol in a dog (9 kg) after a rapid intravenous injection of 15 mg/kg (●) and oral administration of 15 mg/kg (○).*

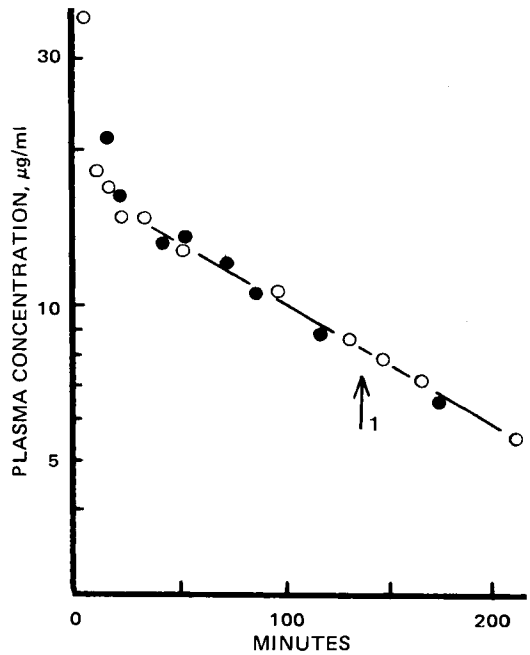

Figure 3—*Plasma concentrations of pentylenetetrazol in a dog (13 kg) after rapid intravenous administrations of 15 mg/kg at two separate times, about 2 weeks apart. Arrow 1 indicates the time at which the kidneys were completely ligated in one experiment (○).*

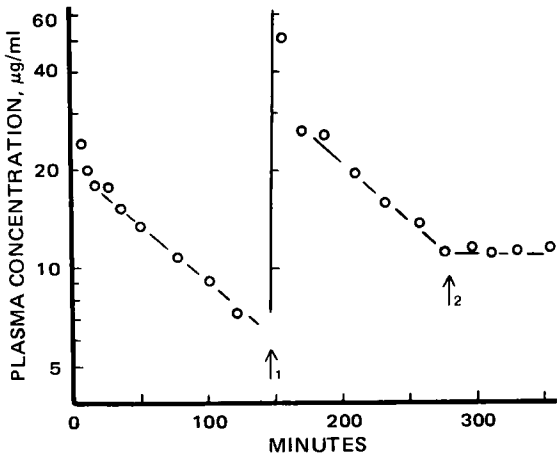

Figure 4—*Plasma concentrations of pentylenetetrazol in a dog (12 kg) after rapid intravenous administration of 15 mg/kg. Arrow 1 indicates the second intravenous dose (15 mg/kg). Arrow 2 shows the time at which the liver was completely ligated.*

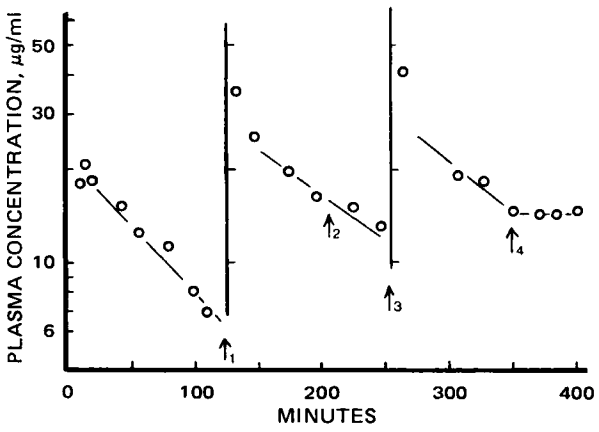

Figure 5—*Plasma concentrations of pentylenetetrazol in a dog (12 kg) after three successive intravenous administrations of equal doses of 15 mg/kg. Key: arrow 1, second intravenous dose; arrow 2, time at which the kidney was ligated; arrow 3, third intravenous dose; and arrow 4, time at which the liver was ligated.*

for the intravenous and oral plasma level–time curves, indicating the complete absorption after oral administration and the minimal first-pass metabolism effect. If the drug was significantly metabolized during the first passage through the liver, a reduced area under the curve would have been seen. The percent ratio of the area under the oral plasma level–time curve to that of the intravenous dose was about 98%. Figure 2 also shows similar biological half-lives of the drug for intravenous and oral routes (1.17 hr).

Figure 3 shows the intravenous plasma level profile of pentylenetetrazol in Dog 5 before and after kidney ligation. The arrow indicates the time of the kidney ligation. After the ligation, the apparent elimination phase remained virtually unchanged, indicating that the kidneys play a minimal role in the elimination of the intact drug. In a similar study, Esplin and Woodbury (1) found that the removal of the kidneys of rats did not affect blood level profiles of pentylenetetrazol. It is clear from this experiment that pentylenetetrazol itself is not excreted in urine in significant amounts, since the kidney ligation does not seem to alter the elimination rate of pentylenetetrazol. In this dog, almost identical plasma level profiles were obtained when an equal dose (15 mg/kg) of pentylenetetrazol was administered at two different times.

Figure 4 illustrates the effect of the liver ligation on the plasma level of pentylenetetrazol. After the first and second intravenous doses, the plasma level declined biexponentially. However, the ligation of the liver, at 2 hr after the second dose, seemed to block the elimination of the drug completely. This result indicates that the liver is probably mainly responsible for the elimination of pentylenetetrazol in the dog. These results are in agreement with the data reported by Esplin and Woodbury (1), who found that hepatectomy of the rat greatly decreased the rate of disappearance of intact pentylenetetrazol. Using rabbits, Tatum and Kozelka (10) showed that liver damage with carbon tetrachloride prevented the elimination of this drug. Therefore, the elimination rate constant for this drug represents the rate of biotransformation in the liver.

Figure 5 further supports the findings of the role of the kidney and liver in the elimination of pentylenetetrazol. In this experiment, when the kidney was first ligated during the second dose interval, no significant effect on the plasma level was observed. However, the liver ligation occurring after the third dose completely stopped the elimination of the drug. Arrows 2 and 4 indicate the times of the kidney and liver ligation, respectively. In this experiment, the dog was alive until the last blood sampling.

In summary, the two-compartment open model adequately describes the pharmacokinetic profiles of pentylenetetrazol in the dog. After oral administration, the drug enters the blood circulation rapidly and completely. The volume of the total body water appears to represent the distribution volume of the drug at the steady state. The elimination of pentylenetetrazol occurs rapidly in the dog. The liver and the kidney ligation studies indicate that the liver is primarily responsible for the elimination. In the clinical use of pentylenetetrazol, it may be important to be aware of the possible effects of administering this drug to patients with severe liver dysfunction. Accumulation of the drug in the body and subsequent toxic effects may occur in these patients.

REFERENCES

(1) D. W. Esplin and D. M. Woodbury, *J. Pharmacol. Exp. Ther.*, **118**, 129(1956).

(2) S. G. Rowles, G. S. Born, H. T. Russel, W. V. Kessler, and J. E. Christian, *J. Pharm. Sci.*, **60**, 725(1971).

(3) H. W. Jun, W. B. Iturrian, J. T. Stewart, and B. H. Lee, *ibid.*, **64**, 1843(1975).

(4) D. S. Riggs, "The Mathematical Approach to Physiological Problems," Williams & Wilkins, Baltimore, Md., 1963, pp. 193–217.

(5) S. Riegelman, J. C. K. Loo, and M. Rowland, *J. Pharm. Sci.*, **57**, 117(1968).

(6) S. A. Kaplan, K. Alexander, M. L. Jack, C. V. Puglisi, J. A. F. de Silva, T. H. Lee, and R. E. Weinfeld, *ibid.*, **63**, 527(1974).

(7) P. L. Altman and D. S. Dittmar, "Blood and Other Body Fluids," Biological Handbooks, American Societies for Experimental Biology, Washington, D.C., 1971, pp. 3, 352, 397.

(8) "The Pharmacological Basis of Therapeutics," L. S. Goodman and A. Gilman, Eds., Macmillan, New York, N.Y., 1970, p. 353.

(9) "The Merck Index," Merck and Co., Rahway, N.J., 1968, p. 796.

(10) H. J. Tatum and F. L. Kozelka, *J. Pharmacol. Exp. Ther.*, **72**, 284(1941).

ACKNOWLEDGMENTS AND ADDRESSES

Received April 23, 1975, from the *Department of Pharmacy, School of Pharmacy, University of Georgia, Athens, GA 30602*

Accepted for publication September 25, 1975.

The author thanks Knoll Pharmaceutical Co. for supplies of pentylenetetrazol.

Model Systems for Dissolution of Finely Divided (Multisized) Drug Powders

J. MAUGER ˣ and S. HOWARD

Abstract □ Several reports have dealt with model systems for the dissolution of log-normally distributed powders. A numerical solution is presented for the previously published Higuchi–Hiestand equations for a log-normal particle-size distribution. This solution was realized *via* an application of the System 360 Continuous System Modeling Program (CSMP). The resulting computer-aided calculations were utilized in the comparisons between the Higuchi–Hiestand model and other existing models. These comparisons provided a basis for the development of an adaptation of the Nielsen moving sphere model for log-normally distributed powders. The adaptation of the Nielsen equation for multisized particle systems is suggested as being potentially useful for treating experimental data where hydrodynamic effects must be considered.

Keyphrases □ Dissolution—model system, multisized drug powders, compared to other models □ Powders, multisized—model system for dissolution, compared to other models □ Particle-size distribution—numerical solution, multisized drug powders, model system for dissolution

Diffusional models for the description of the dissolution rate of a multisize particle population have been discussed previously (1–3). Higuchi and Hiestand (1) derived equations describing the dissolution rate of finely divided (multisized) particles in a diffusion-controlled dissolution process. The Higuchi–Hiestand treatment considered a limiting case, which is valid when hydrodynamic effects on the solute diffusion near the particles are minimal; *i.e.*, the treatment is valid for small particles. To integrate the complex equations, an approximation was assumed for a log-normal particle distribution.

In a later paper (4), the previously derived theoretical considerations were used to analyze data for the dissolution rate of a methylprednisolone suspension in water. The agreement of theory with the experimental data was reasonable in view of the fact that the theoretical values were calculated independently of the experimentally determined data.

Later papers (2, 3) noted that the original theoretical exposition of Higuchi and Hiestand had considered an approximate function for a log-normal distribution to reduce the complexity of the equations and to allow an analytical solution. Carstensen and Musa proposed a need for an analytical solution using the actual log-normal distribution rather than an approximation and accomplished the integration using numerical analysis techniques aided by a computer (2). Subsequent work (3) provided an exact treatment for the equations used by Carstensen and Musa (2).

These studies (2, 3) differed significantly from the original theoretical considerations (1). In particular, the distribution functions used for an analytical solution were different, one being an approximation and the other the actual function. In addition, an even more fundamental difference existed. Higuchi and Hiestand used a mathematical model that considered major assumptions surrounding a realistic diffusion-controlled case. But Carstensen and Musa (2) and Brooke (3) chose to use the Hixson–Crowell treatment as a basis for their analytical solutions. Although the Hixson–Crowell treatment has been tested under controlled experimental conditions for monosized particles (5), application of this model to multisized particles has not been experimentally justified. Furthermore, the Hixson–Crowell treatment anticipates significant hydrodynamic effects, and one is presumably dealing with large particles relative to those valid for use of the Higuchi–Hiestand model.

A further consideration of the differences between the Higuchi–Hiestand treatment and the Hixson–Crowell treatment centers about the diffusion layer. While the diffusion layer thickness is always the same for all particles of the same size and is comparable to or greater than the particle radius for the former, the latter ignores the effective diffusion layer or assumes that it is constant for all particles and remains constant throughout a particle's lifetime. The assumption that the effective diffusion layer is constant for all particles is particularly rigid for a multisized particle population, and the constancy throughout a particle's lifetime for any given particle has been questioned (5).

THEORY

With the limitations of the Hixson–Crowell treatment in mind, the Higuchi–Hiestand model provides a more rigorous approach but does not incorporate a quantitative consideration of the hydrodynamic effects. The Nielsen model (6) for a moving sphere is purposeful in this connection. The kinetic expression for the Nielsen model is:

$$-\frac{da}{dt} = \frac{DCF}{a(\rho_d)} \qquad \text{(Eq. 1)}$$

where a is the particle radius (centimeters), t is time (seconds), D is the diffusion coefficient (square centimeters per second), C is the saturation concentration (grams per milliliter), ρ_d is the particle density (grams per milliliter), $F = (1 + A)^{0.285}$, and A is given by:

$$A = \frac{2a^3G(\rho_d - \rho_m)}{9D\eta} \qquad \text{(Eq. 2)}$$

where $G = 981$ cm/sec^2, ρ_m is the density of the medium, and η is the viscosity of the medium (grams per centimeter per second).

The Nielsen model, as expressed by Eq. 1, considers a combined diffusion–convection-controlled dissolution rate of a particle. The model assumes that: (*a*) the dissolution rate of the particle is diffusion controlled and that convection is also contributing to the transport process, (*b*) the effective diffusion layer thickness is the same for all particles of the same size and is equal to or greater than the particle radius, (*c*) the particle is dissolving under sink conditions, and (*d*) the dissolving particle is spherical. As noted by Higuchi and Hiestand (1), the second assumption is important because it implies a quasi-steady-state condition in the diffusion layer.

The quantity A (Eq. 2) is derived from a theoretical consideration of the convection effect of a sphere moving through a liquid at a rate in keeping with Stokes' law. As the particle radius approaches zero, the quantity A also approaches zero and the parameter F in Eq. 1 approaches unity. Therefore, as F approaches unity, the Nielsen model relaxes to a pure diffusional model, *i.e.*, the Higuchi–Hiestand

Table I—Predicted Dissolution Profile for a Single Methylprednisolone Particle

Seconds	Higuchi–Hiestand Model Particle Radius, μm	Nielsen Model Particle Radius, μm
0	10.00	10.00
400	8.32	7.89
830	6.01	5.06
970	5.04	3.80

model, $-da/dt = DC/a\rho_d$. Nielsen noted that Eq. 2 is valid when the Reynolds number is less than one; under this constraint, the model becomes useful for pharmaceutical powders.

The authors applied Eq. 1 to a multisized powder population based on numbers. An expression for the weight fraction undissolved, W_f, at time t is:

$$W_f = \frac{\int_{a_{0t}}^{a_{l0}} \frac{4}{3}\pi\rho_d a_t^3 f(a_0)\, da_0}{\int_{a_{s0}}^{a_{l0}} \frac{4}{3}\pi\rho_d a_0^3 f(a_0)\, da_0} \qquad \text{(Eq. 3)}$$

The quantity $f(a_0)$ given in both the numerator and denominator of Eq. 3 is the density function for a specific number distribution of powders, with the particle radius as the random variable. The full quantity in the denominator of Eq. 3 expresses the fraction of total weight in a powder population at time zero. Therefore, integrating this quantity between the limits of the smallest particle radius at time zero, a_{s0}, and the largest particle radius of the powder at time zero, a_{l0}, gives the total weight at time zero.

The full quantity in the numerator of Eq. 3 expresses the fraction of the total weight in a powder population at time t, where a_t is the particle radius at time t and is found using either the Nielsen or Higuchi–Hiestand model *via* Eq. 1. The lower limit of integration in the numerator of Eq. 3 is the zero time radius of the particle that just dissolved, a_{0t}, and the upper limit remains set at a_{l0}. Integrating the numerator at time t yields the total weight of the powder population remaining at time t. Therefore, W_f in Eq. 3 represents the weight *fraction* undissolved at time t. The actual expressions associated with $f(a_0)$ are shown in Eqs. 4 and 5, where the approximation for the log-normal case as used by Higuchi and Hiestand is given by Eq. 4 and the approximation for the log-normal case is given by Eq. 5:

$$f(a_0) = \alpha \frac{1}{a_0^4} \qquad \text{(Eq. 4)}$$

$$f(\ln a_0) = \alpha \exp\left[-(\ln a_0 - \ln \bar{a}_0)^2/(2SDEV^2)\right] \qquad \text{(Eq. 5)}$$

where $\bar{a}_0$ in Eq. 5 is the mean of a log-normal population. Strictly speaking, the use of the log-normal case requires the integration limits in Eq. 3 to be changed to ln ( ) and $f(a_0)\, da_0$ becomes $f(\ln a_0)\, d \ln a_0$. Normalization constants associated with Eqs. 4 and 5 are not shown since they cancel to unity when $f(a_0)$ or $f(\ln a_0)$ is inserted into Eq. 3.

The purpose of this study was to use computer-generated data to compare the characteristics of the Nielsen moving sphere model with the Higuchi–Hiestand model for both mono- and multisized powder systems. These simulated data dissolution profiles should provide information concerning the use and limitations of the kinetic model as described by Eq. 1.

COMPUTATIONAL DETAILS

All solutions to Eqs. 1 and 3 were numerically obtained using System 360 Continuous System Modeling Program[1] (CSMP). Although CSMP is designed to handle time-variant problems, its usefulness is not limited to kinetic models where the limits of integration are typically zero to time t or zero to time infinity. The limits can be set to accommodate statistical populations where the limits are determined by the population under study, in this case, a particle-size population.

Table II—Predicted Dissolution Profile for a Single Methylprednisolone Particle

Seconds	Higuchi–Hiestand Model Particle Radius, μm	Nielsen Model Particle Radius, μm
0	25.0	25.0
2000	21.7	17.1
3100	19.7	12.4
4800	16.0	00.0
6100	12.5	00.0

Table III—Summary of Zero-Time Methylprednisolone Radii

Seconds	Higuchi–Hiestand Model Particle Radius, μm	Nielsen Model Particle Radius, μm
400	5.6	5.6
1500	10.7	11.6
3000	15.2	18.0
4500*	18.6	23.8

For the log-normal powder populations in the present experiment, the limits of integration were set initially to include ±10 standard deviation units, *SDEV*, of ln a_0. As the temporal behavior of a log-normal powder population is followed, the initial limits up to some critical time are $\int_{a_{s0}}^{a_{l0}}$ and later, when a_{s0} dissolves, the limits become $\int_{a_{0t}}^{a_{l0}}$, where a_{0t} is defined as the zero time radius of the particle that just dissolved[2]. The quantity a_{0t} is determined from the kinetic model given in Eq. 1.

CSMP offers a variety of routines to perform the integration operation. The routine chosen and used for all calculations was the fixed step Runge–Kutta, which provided the desired stability and accuracy. The integration step size was set by dividing the ±10 standard deviation interval into 500 intervals.

RESULTS AND DISCUSSION

An immediate purpose of this study was to conduct an analysis of the Nielsen moving sphere model and the Higuchi–Hiestand model for a single particle to demonstrate quantitatively the conditions where one may expect hydrodynamic effects to be significant.

The physical–chemical data for methylprednisolone are available[3], and computer-generated particle lifetimes *via* CSMP for the hypothetical, yet realistic, methylprednisolone example are shown in Table I. These data show that the Higuchi–Hiestand treatment is not substantially different from the Nielsen treatment for a particle with a zero time radius of 10 μm.

The half-life predicted by the Higuchi–Hiestand model is approximately 970 sec, whereas the Nielsen model predicts a half-life of about 830 sec. For larger particles, the difference is more striking (Table II). For a 25-μm particle, the Higuchi–Hiestand model predicts a half-life value of 6100 sec, while the Nielsen model predicts a value of 3100 sec. In other words, the effect of convection in addition to diffusion is contributing to the dissolution of the particle as the sphere falls through the medium at a rate in keeping with Stokes' law. Later in the particle's lifetime, when the radius approaches 10 μm, the process relaxes to a diffusion-controlled case.

The data in Table III summarize the quantitative difference between the two models. Notice in particular that the Higuchi–Hiestand model predicts that a methylprednisolone particle with a zero time radius of 18.6 μm will dissolve in 4500 sec, while the Nielsen model predicts that a methylprednisolone particle with a zero time radius of 23.8 μm will dissolve in the same time frame. Although the radius of the larger particle is only 1.28 times greater than that of the smaller, the weight of the larger particle is more than two times that of the smaller.

This single-particle example shows under what particle-size conditions one might expect the Nielsen model to be useful. In addition, the dynamic features of the Nielsen model are exemplified since the convection portion of the process will decay as the particle size diminishes.

For multisized powder populations, CSMP was used to solve nu-

[1] The system is discussed in IBM Application Program Manual 360 A-CX-16X.

[2] For the Higuchi–Hiestand model, $a_{0t} = [2DCt/\rho_d]^{1/2}$.

[3] Data were taken from Ref. 1. Saturation concentration, C, is 1.0×10^{-4} g/ml; diffusion coefficient, D, is 5.0×10^{-6} cm²/sec; and particle density, ρ_d, is 1.3 g/ml.

Table IV—Validation of the CSMP Program

Seconds	Weight Fraction Undissolved	
	CSMP	Closed Form
13	0.726	0.725
52	0.435	0.434
130	0.255	0.254
400	0.743×10^{-1}	0.741×10^{-1}

merically for the weight fraction remaining for the Higuchi–Hiestand or Nielsen moving sphere model with either the approximate log-normal or log-normal case. The program was validated by comparing the CSMP output for a multisized population against the closed form solution using the Higuchi–Hiestand model and the approximate log-normal case. The data used to generate the values in Table IV were for methylprednisolone particles where a_{s0} = 1 μm and a_{l0} = 10 μm.

The accuracy of the CSMP-generated data was consistently on the order of 0.2%. The consistency of the error is important, and these data show that the numerical process does not drift as a function of time. Other validation steps were taken and smaller programs were written to ensure the accuracy of the output.

The first log-normal population, by numbers, that was tested was assigned population parameters such that the geometric mean radius was 3.16 μm and the smallest and largest radii in the population were 1 and 10 μm, respectively. Again, methylprednisolone was used as an example of a pharmaceutical powder.

The weight fraction remaining *versus* time profile for this example is shown in Fig. 1. Note that W_f reaches zero in about 250 sec, although a methylprednisolone particle with an initial radius of 10 μm has a theoretical lifetime of 1300 sec. This finding has important experimental implications, because one cannot expect to assay the small weight that will dissolve between 250 and 1300 sec. The fact that the Nielsen model is superimposed on the Higuchi–Hiestand model is not surprising in view of the similarity of the data for the single methylprednisolone particle studies where the zero time radius equals 10 μm.

The second log-normal population studied was assigned the following population parameters: $\ln \bar{a}_0 = 2.7607$ and $SDEV = 0.04582$. Therefore, the quantity $\bar{a}_0$ corresponded to a radius of 15.8 μm, and the largest and smallest radii in the population were 25 and 10 μm, respectively. The dissolution profile for this methylprednisolone powder population (Fig. 2) shows that the particles are large enough to be sensitive to hydrodynamic effects. The W_f values for the Nielsen model are consistently smaller than those for the Higuchi–Hiestand model. This population was designed so that about 99% of the weight was within ±3 *SD* of the mean. Therefore, the standard deviation was small when compared to the mean, and approximately 75% of the total weight dissolved before the smallest particle dissolved.

The third log-normal methylprednisolone population studied was assigned the following population parameters: $\ln \bar{a}_0 = 2.7607$ and $SDEV = 0.12$. Therefore, the quantity $\bar{a}_0$ corresponded to a radius of 15.8 μm, and the largest and smallest radii in the population were

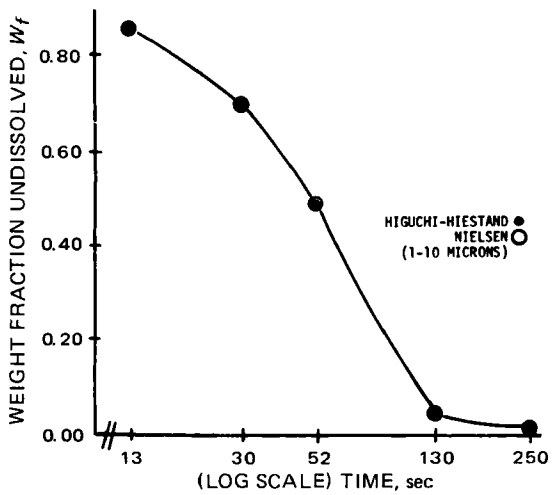

Figure 1—*Weight fraction remaining* versus *time profile.*

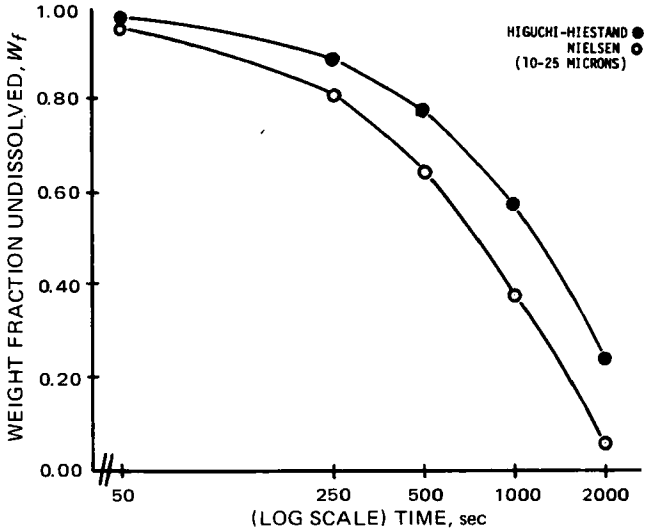

Figure 2—*Weight fraction remaining* versus *time profile.*

53 and 4.8 μm, respectively. The dissolution profile for this population is shown in Fig. 3 and is interesting because the population includes particles large enough to be very sensitive to hydrodynamic effects and particles small enough to be relatively insensitive to hydrodynamic effects. In other words, early in the dissolution profile, the large particles dissolve according to a model where both convection and diffusion are important. Later, the smaller particles have melted away and the larger particles reach a particle radius where the diffusion process predominates.

The results of this study confirm these expectations. At 500 sec, W_f for the Higuchi–Hiestand model is about 0.80; for the Nielsen model, it is 0.66. The difference between the models increases with time; at 2000 sec, W_f is 0.28 for the Higuchi–Hiestand model and 0.08 for the Nielsen model. The relative magnitude of difference between the two models shows the importance of the convection effect.

An interesting characteristic of this kinetic treatment is related to the difference between the particle and medium densities. According to Eq. 2, the difference between these two quantities is one determinant of the magnitude of *A*. Therefore, the kinetic model relies on a suspended particle population where the influence of gravity mimics stirring conditions. One might question this model when it is applied to experimental data. Experimental data are required to test this issue, but the discussion by Calderbank (7) is instructive. Calderbank argued that: "When the particles in a mixing vessel are just completely suspended, turbulence forces balance those due to gravity, and the mass-transfer rates are the same as for particles moving freely under gravity."

Calderbank also provided equations that could be used in place of

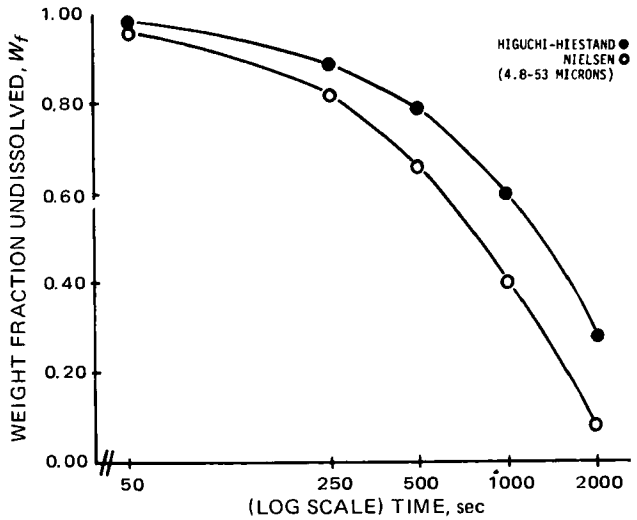

Figure 3—*Weight fraction remaining* versus *time profile.*

Stokes' law in the derivation of Eq. 2 and that account for the total shear stress which has to be generated in a mixing vessel to cause free suspension of particles. The derivation given by Goyan (8) for the Dankwerts model under laminar flow conditions of stirring relies on a physical model of a particle falling slowly in a liquid medium.

In summary, the multisized particle dissolution profiles point to actual experimental conditions where one may be dealing with a particle-size distribution broad enough to include large particles where $F > 1$ and small particles where $F = 1$. In these circumstances, a simple diffusion model would be inadequate and the Nielsen model in combination with the appropriate distribution function should more successfully predict the dissolution profile.

REFERENCES

(1) W. Higuchi and E. Hiestand, *J. Pharm. Sci.*, **52**, 67(1963).

(2) J. Carstensen and M. Musa, *ibid.*, **61**, 223(1972).

(3) D. Brooke, *ibid.*, **62**, 795(1973).

(4) W. Higuchi, E. Rowe, and E. Hiestand, *ibid.*, **52**, 162(1963).

(5) P. Niebergall, G. Milosovich, and J. Goyan, *ibid.*, **52**, 236(1963).

(6) A. Nielsen, *J. Phys. Chem.*, **65**, 46(1961).

(7) P. H. Calderbank, in "Mixing–Theory and Practice," vol. 2, V. Uhl and J. Gray, Eds., Academic, New York, N.Y., 1967, p. 2.

(8) J. E. Goyan, *J. Pharm. Sci.*, **54**, 645(1965).

ACKNOWLEDGMENTS AND ADDRESSES

Received March 10, 1975, from the *School of Pharmacy, West Virginia University, Morgantown, WV 26506*

Accepted for publication September 29, 1975.

Presented at the Basic Pharmaceutics Section, APhA Academy of Pharmaceutical Sciences, New Orleans meeting, November 1974.

[x] To whom inquiries should be directed.

Correlation of *In Vitro* and *In Vivo* Methodology for Evaluation of Antacids

R. D. SMYTH [x], T. HERCZEG, T. A. WHEATLEY, W. HAUSE, and N. H. REAVEY-CANTWELL

Abstract □ The rate and extent of acid consumption of an antacid suspension and tablet were evaluated by *in vitro* and *in vivo* techniques. Four different test procedures were used to estimate *in vitro* antacid reactivity. *In vivo* effects were determined in the fasted and postcibal states in normal human subjects by a radiotelemetry procedure. The duration of elevation of intragastric pH >3 was in agreement with *in vitro* estimates of total acid consumption of the antacid. There was also good correlation between onset, extent, and duration of *in vivo* antacid activity and a modified *in vitro* Beekman antacid test procedure. There was no significant difference in antacid activity of the tablet or suspension in either *in vitro* or *in vivo* test procedures. A wide variation in antacid activity was observed between subjects and also in the fasted *versus* postcibal states. These studies emphasize the requirements for standardization of antacid products by comparative *in vitro* and *in vivo* evaluations to facilitate individualized dose titration of the antacid in each patient and correlation of the acid secretion rate in various types of GI disease with the antacid dose.

Keyphrases □ Antacids—suspensions and tablets, rate and extent of acid consumption, *in vitro* and *in vivo* evaluations compared □ Acid consumption—rate and extent by antacid suspensions and tablets, *in vitro* and *in vivo* evaluations compared

The Food and Drug Administration (FDA) recently introduced an *in vitro* test (1) to determine the acid-neutralizing rate and acid-consuming capacity of over-the-counter antacid products. FDA also recommended that research be initiated to develop an *in vivo* model to assess antacid activity. Although an *in vitro* test can approximate *in vivo* conditions with respect to acid-consuming capacity, speed and duration of action, and maximum buffering capacity of the antacid, it cannot account for variations in antacid activity due to gastric emptying, changes in the acid secretion rate as seen in the fasting and postcibal states, interaction of antacids with glycoproteins and mucoproteins of gastric juice, coating of the gastric mucosa by antacids, and the effect of antacids on endogenous control of gastric acid secretion (2, 3).

The purpose of the present study was to compare the activity of an antacid tablet and suspension in both *in vitro* and *in vivo* models. Onset of action, maximum buffering capacity, and duration of antacid effect were compared in various *in vitro* systems and in normal human subjects in both the fasting and postcibal states.

EXPERIMENTAL

Methods—Each antacid tablet or 5 ml of suspension contained 200 mg of magnesium hydroxide, 225 mg of aluminum hydroxide, and 250 mg of calcium carbonate. The minimum recommended dose is two tablets (chewed) or 10 ml of suspension.

Total acid-consuming capacity was determined by the USP XVIII procedure (4) and by the OTC antacid test (1). A completely automated Bachrach procedure (5) was developed to determine the rate and extent of acid consumption.

A modified Beekman procedure (6, 7) was developed to determine the onset, duration, and buffering capacity of the antacid and to correlate *in vivo* and *in vitro* results. The modifications were as follows: antacid was added to 50 ml of 0.1 *N* hydrochloric acid at 37.5 ± 1° contained in a jacketed glass vessel provided with a combination pH electrode, agitator, and tubing to introduce the acid and to remove the antacid–acid mixture. The agitator was a paddle-type propeller[1] operated at approximately 400 rpm. Acid was continuously added, and the antacid–acid mixture was continuously removed at the rate of 270 ± 14 ml/hr with a positive displacement tubing pump. A glass reservoir of 0.1 *N* hydrochloric acid was maintained at 37.5 ± 1°. The pH was measured with a combination electrode and standardized pH meter connected to a recorder operating at a chart speed of 20.3 cm (8 in.)/hr.

The timer was activated, on addition of the test sample, and the pH values were recorded. The pump was then automatically started, adding 0.1 *N* hydrochloric acid and removing the antacid–acid reac-

[1] Coated with Teflon (du Pont).

Stokes' law in the derivation of Eq. 2 and that account for the total shear stress which has to be generated in a mixing vessel to cause free suspension of particles. The derivation given by Goyan (8) for the Dankwerts model under laminar flow conditions of stirring relies on a physical model of a particle falling slowly in a liquid medium.

In summary, the multisized particle dissolution profiles point to actual experimental conditions where one may be dealing with a particle-size distribution broad enough to include large particles where $F > 1$ and small particles where $F = 1$. In these circumstances, a simple diffusion model would be inadequate and the Nielsen model in combination with the appropriate distribution function should more successfully predict the dissolution profile.

REFERENCES

(1) W. Higuchi and E. Hiestand, *J. Pharm. Sci.*, **52**, 67(1963).

(2) J. Carstensen and M. Musa, *ibid.*, **61**, 223(1972).

(3) D. Brooke, *ibid.*, **62**, 795(1973).

(4) W. Higuchi, E. Rowe, and E. Hiestand, *ibid.*, **52**, 162(1963).

(5) P. Niebergall, G. Milosovich, and J. Goyan, *ibid.*, **52**, 236(1963).

(6) A. Nielsen, *J. Phys. Chem.*, **65**, 46(1961).

(7) P. H. Calderbank, in "Mixing–Theory and Practice," vol. 2, V. Uhl and J. Gray, Eds., Academic, New York, N.Y., 1967, p. 2.

(8) J. E. Goyan, *J. Pharm. Sci.*, **54**, 645(1965).

ACKNOWLEDGMENTS AND ADDRESSES

Received March 10, 1975, from the *School of Pharmacy, West Virginia University, Morgantown, WV 26506*

Accepted for publication September 29, 1975.

Presented at the Basic Pharmaceutics Section, APhA Academy of Pharmaceutical Sciences, New Orleans meeting, November 1974.

[x] To whom inquiries should be directed.

Correlation of *In Vitro* and *In Vivo* Methodology for Evaluation of Antacids

R. D. SMYTH [x], T. HERCZEG, T. A. WHEATLEY, W. HAUSE, and N. H. REAVEY-CANTWELL

Abstract □ The rate and extent of acid consumption of an antacid suspension and tablet were evaluated by *in vitro* and *in vivo* techniques. Four different test procedures were used to estimate *in vitro* antacid reactivity. *In vivo* effects were determined in the fasted and postcibal states in normal human subjects by a radiotelemetry procedure. The duration of elevation of intragastric pH >3 was in agreement with *in vitro* estimates of total acid consumption of the antacid. There was also good correlation between onset, extent, and duration of *in vivo* antacid activity and a modified *in vitro* Beekman antacid test procedure. There was no significant difference in antacid activity of the tablet or suspension in either *in vitro* or *in vivo* test procedures. A wide variation in antacid activity was observed between subjects and also in the fasted *versus* postcibal states. These studies emphasize the requirements for standardization of antacid products by comparative *in vitro* and *in vivo* evaluations to facilitate individualized dose titration of the antacid in each patient and correlation of the acid secretion rate in various types of GI disease with the antacid dose.

Keyphrases □ Antacids—suspensions and tablets, rate and extent of acid consumption, *in vitro* and *in vivo* evaluations compared □ Acid consumption—rate and extent by antacid suspensions and tablets, *in vitro* and *in vivo* evaluations compared

The Food and Drug Administration (FDA) recently introduced an *in vitro* test (1) to determine the acid-neutralizing rate and acid-consuming capacity of over-the-counter antacid products. FDA also recommended that research be initiated to develop an *in vivo* model to assess antacid activity. Although an *in vitro* test can approximate *in vivo* conditions with respect to acid-consuming capacity, speed and duration of action, and maximum buffering capacity of the antacid, it cannot account for variations in antacid activity due to gastric emptying, changes in the acid secretion rate as seen in the fasting and postcibal states, interaction of antacids with glycoproteins and mucoproteins of gastric juice, coating of the gastric mucosa by antacids, and the effect of antacids on endogenous control of gastric acid secretion (2, 3).

The purpose of the present study was to compare the activity of an antacid tablet and suspension in both *in vitro* and *in vivo* models. Onset of action, maximum buffering capacity, and duration of antacid effect were compared in various *in vitro* systems and in normal human subjects in both the fasting and postcibal states.

EXPERIMENTAL

Methods—Each antacid tablet or 5 ml of suspension contained 200 mg of magnesium hydroxide, 225 mg of aluminum hydroxide, and 250 mg of calcium carbonate. The minimum recommended dose is two tablets (chewed) or 10 ml of suspension.

Total acid-consuming capacity was determined by the USP XVIII procedure (4) and by the OTC antacid test (1). A completely automated Bachrach procedure (5) was developed to determine the rate and extent of acid consumption.

A modified Beekman procedure (6, 7) was developed to determine the onset, duration, and buffering capacity of the antacid and to correlate *in vivo* and *in vitro* results. The modifications were as follows: antacid was added to 50 ml of 0.1 *N* hydrochloric acid at 37.5 ± 1° contained in a jacketed glass vessel provided with a combination pH electrode, agitator, and tubing to introduce the acid and to remove the antacid–acid mixture. The agitator was a paddle-type propeller[1] operated at approximately 400 rpm. Acid was continuously added, and the antacid–acid mixture was continuously removed at the rate of 270 ± 14 ml/hr with a positive displacement tubing pump. A glass reservoir of 0.1 *N* hydrochloric acid was maintained at 37.5 ± 1°. The pH was measured with a combination electrode and standardized pH meter connected to a recorder operating at a chart speed of 20.3 cm (8 in.)/hr.

The timer was activated, on addition of the test sample, and the pH values were recorded. The pump was then automatically started, adding 0.1 *N* hydrochloric acid and removing the antacid–acid reac-

[1] Coated with Teflon (du Pont).

Table I—*In Vitro* Evaluation of Antacids by the Bachrach Procedure[a]

Antacid	Initial pH[b]	Initial Neutralization[c], ml of 0.800 *N* HCl in sec: ml	Initial Neutralization[c], ml of 0.800 *N* HCl in sec: sec	End-Point[d], ml of 0.800 *N* HCl in min: ml	End-Point[d], ml of 0.800 *N* HCl in min: min	Acid Consumed at 10 min, ml of 0.800 *N* HCl
Suspension	8.56 ± 0.21	1.80	~75	5.40 ± 0.10	9.3 ± 0.8	5.41 ± 0.11
Tablet	8.66 ± 0.20	1.10	~60	4.90 ± 0.09	13.8 ± 1.9	4.62 ± 0.21

[a] Data are based on samples from five lots of each antacid. Comparable sample sizes of antacids were used (1.20 ml of suspension or 12% of weight of two tablets). All results are expressed as mean ± *SD*. [b] The pH of the antacid. [c] Volume of acid to initially obtain pH 3.5. [d] The end-point was the volume of acid necessary to maintain a pH of 3.5 ± 0.1 for at least 30 sec.

tion mixture. With the automation provided, the apparatus required no further attention until the titration was completed (pH ≤ 3).

The suspension was introduced directly into the reaction vessel with a syringe. Tablets were crushed and handscreened through a No. 20 mesh screen. A three-tablet equivalent, mixed with 15 ml of distilled water to maintain a reaction volume equivalent to the suspension sample size (15 ml), was used.

***In Vivo* Studies**—About 70% of the subjects tested were admitted to the study. The normal male and female subjects had a steady baseline intragastric pH value of less than 1.8 for at least 60 min. This value was confirmed by a baseline test, which followed the same procedures as the studies but substituted 35 ml of water for the dose of antacid.

None of the subjects had active upper respiratory or GI infections, a history of malabsorption disease, milk–alkali syndrome, pernicious anema, achlorhydria, peptic ulcer disease, or liver or kidney dysfunction. Upon confirmation of a steady baseline pH of less than 1.8, subjects were assigned to treatment according to a randomized allocation schedule. Subjects did not recieve any medication known to affect GI secretion or motility for 72 hr prior to each test day.

In the fasting study, subjects did not receive any food or liquids, except water, for a minimum of 8 hr before each test day. In the postcibal study, subjects ate a standard breakfast of 1 cup of dry cereal, 240 ml (8 oz.) of whole milk, 180 ml (6 oz.) of orange juice, sugar to flavor the cereal, and 1 cup of coffee or tea. One hour prior to testing, subjects ate a standard meal of 180 g (6 oz.) of medium-cooked chopped sirloin steak, one lightly toasted bun, and 1 cup of coffee or tea.

At the start of the test, the Heidelberg capsule (8, 9) was activated by immersion in 0.15 *M* sodium chloride at 37° for 5 min. The capsule was standardized with 0.1 *M* glycine–hydrochloric acid buffer, pH 1.0, and 0.1 *M* tromethamine buffer, pH 7.0. The capsule was then attached to a nonwettable surgical string and swallowed with 100–150 ml of water. The position of the capsule was controlled by the thread.

When 10–15 cm of the thread had passed through the esophagogastric junction, as indicated by the appearance of a pH reading of below 3 in the stomach, the thread was taped to the cheek. The position of the capsule in the stomach was confirmed by observation of a continuous baseline pH of less than 1.8 for 30 min. Free movement of the capsule in the stomach was confirmed by moving the string 2–4 cm without a significant interruption in the pH recording signal.

The subject remained in an upright seated position during the test. The pH of the gastric content was telemetered continuously by a belt antenna positioned around the upper abdomen and connected to the receiver and recorder. A steady baseline pH of less than 1.8 for 30 min was required for the subject to continue the study on each test day. In a randomized, crossover design, subjects were given either three antacid tablets (which the subject chewed) followed by 20 ml of water or 15 ml of antacid suspension followed by 10 ml of water. Administration of a corresponding volume of water had no significant effect on intragastric pH.

The onset of antacid activity, maximum pH, and duration of antacid activity (pH >3) were determined by direct observation. Intragastric pH was monitored until it returned to a steady baseline value for at least 20 min. The capsule was then retrieved, checked for standardization, and discarded.

Each subject underwent 1 test day with the antacid suspension and 1 test day with the antacid tablets; test days were separated by 2–7 days. Analyses of variance for a crossover design (10) were performed to compare the duration of activity of the tablets to the suspension in the fasting and postcibal studies.

Table II—*In Vitro* Evaluation of Antacids by the Modified Beekman Procedure[a]

Antacid	Maximum pH Reached	Time to Maximum pH, min	Time to Reach pH 3 Initially, min	Time above pH 3, min
Suspension	5.62–5.70	5.0–7.5	Immediate	26.5–27.5
Tablet	5.72–6.10	2.5–5.0	Immediate	25.5–28.0

[a] Data are based on samples from five lots of each antacid. Comparable sample sizes of antacids were used (15 ml of suspension or three tablets).

RESULTS

***In Vitro* Tests**—The total acid-consuming capacity was 36.4 ± 0.6 mEq/0.1 *N* HCl with two tablets or 10 ml of suspension, as determined by the USP procedure (4). The acid-neutralizing capacity, as measured by the OTC procedure (1), at the minimum recommended dose of two tablets or 10 ml of suspension was 34.1–35.7 or 32.6–39.5 mEq, respectively. The results of the Bachrach titration are shown in Table I; the modified Beekman test results are listed in Table II.

***In Vivo* Tests**—The antacid activity of the suspension and tablets, as determined by the Heidelberg capsule telemetering technique in the fasting and postcibal states, is shown in Table III. Twenty-two normal male and female volunteers, 21–45 years old, completed the fasting study. All subjects had a baseline pH of less than 1.8 for 30 min prior to antacid administration.

On the 1st test day, subjects randomly received either three antacid tablets or 15 ml of antacid suspension (11 received tablets and 11 received suspension). The crossover was then completed on another test day. No statistically significant difference was observed between the tablet or the suspension for rate of onset, peak pH, and duration of antacid activity. The range of duration of antacid activity was 8–121 min in the fasting state.

Twenty-two normal male and female volunteers (20 of whom participated in the fasting study) completed the postcibal study. Just as in the fasting study, all of the subjects in the postcibal study had a baseline pH of less than 1.8 for 30 min prior to antacid administration. On the 1st test day, the subjects randomly received either three antacid tablets or 15 ml of antacid suspension (12 received suspension and 10 received tablets). The subjects then completed the crossover on another test day. No statistically significant difference was observed between the tablets or the suspension for rate of onset, peak pH, and duration of antacid activity. The range of duration of antacid activity was 2–48 min.

In contrast to a previous report (11), no significant problems were encountered in the standardization and performance of the Heidelberg capsules.

DISCUSSION

Fordtran *et al.* (3) recommended that the dose of an antacid should be determined by its neutralizing capacity. They showed direct correlation of an *in vitro* test and *in vivo* neutralization of gastric acid by antacid suspensions following a standard meal. The *in vitro* test measured the capacity of the antacid to neutralize acid over 2 hr; the *in vivo* evaluation was performed by following intragastric pH in intubated subjects who received the antacid 1 hr after a standard meal.

The results of Piper and Fenton (12) are also in agreement with the

Table III—Evaluation of the *In Vivo* Antacid Activity of Antacid Tablets and Suspension

State	Antacid[a]	Distribution of Peak pH[b]				Duration[c], min	
		≥7	6.0–6.9	5.0–5.9	3.0–4.9	pH >3	pH >1.8
Fasting	Tablet	15[d]	7	0	0	43 ± 6 (12–121)	49 ± 5 (19–127)
	Suspension	21	1	0	0	44 ± 5 (8–100)	56 ± 6 (14–114)
Postcibal	Tablet	8	6	7	1	28 ± 3 (6–45)	38 ± 3 (6–55)
	Suspension	7	7	6	2	29 ± 3 (2–48)	41 ± 3 (2–64)

[a] Onset of antacid effect (pH >3) was <1 min in all cases. [b] Maximum pH reached after antacid administration (number of subjects = 22). [c] Time of intragastric pH >3 or pH >1.8 (baseline value) (mean ± *SEM* with range of values in parentheses). [d] Number of subjects, *i.e.*, 15 of 22 subjects had pH ≥7.

Fordtran *et al.* (3) observation in that a standard dose of antacid does not exist due to the variable response of patients to antacids. Significant differences in the *in vitro* acid-consuming capacity of various antacid tablets and suspensions and the overall superiority of suspensions has been reported (3, 12, 13). The chewable antacid tablets utilized were formulated (14) to provide an equivalent rate, duration, and extent of *in vitro* acid neutralization as the suspension.

A definite correlation was shown between the total acid-consuming capacity, as measured by the USP or OTC procedures, and the duration of *in vivo* neutralization of gastric acid. The total acid-consuming capacity and *in vivo* neutralization of antacid tablets and suspension were equivalent. However, these *in vitro* tests do not provide any data on the onset, rate, or duration of acid neutralization. The Bachrach titration provides data on the rate of acid consumption and total antacid capacity. Although *in vitro* data from this titration predicted that the suspension would be slightly better than the tablet with respect to onset and neutralization capacity, this result was not observed *in vivo*.

The modified Beekman test provided an excellent correlation with *in vivo* observations in the postcibal state. This *in vitro* test predicted an immediate onset of action, maximum pH between 5.6 and 6.1 in 3–8 min, and a 25–27-min duration of antacid effect. *In vivo* tests showed an immediate onset of action, maximum pH between 5 and 7 in about 5 min, and a 28 ± 3-min duration of intragastric pH >3.

Fordtran and coworkers (3, 15) recommended that maximum neutralization of gastric acid could be accomplished by administering the antacid 1 hr after meals, in contrast to the fasting state. Their results were based on studies using a standard morning meal of 150 g of broiled ground meat, two pieces of toast, and 180 ml of water. They concluded that the combined buffer capacity of the meal and antacid and the increased retention of antacid in the stomach at this time accounted for a longer duration of acid neutralization in the postcibal (3 hr) than in the fasted (20–40 min) state in duodenal or gastric ulcer patients.

The protocol used in this study more closely paralleled normal eating habits and utilized a different test meal, inclusive of a standard morning breakfast, midmorning coffee, and coffee with the midday test meal in normal subjects. Antacid was administered about 1.5 hr after the meal, at which time the intragastric pH was less than 1.8 for 30 min. The longer duration of antacid activity in the fasting state than in the postcibal state is in agreement with the increased rate of postcibal gastric acid secretion (16). However, the combined buffering capacity of the meal and the antacid should result in a 2-hr interval with the intragastric pH greater than 1.8. There was also considerable subject-to-subject variation in antacid activity in both the fasting and postcibal states due to the normal variation in the rate of gastric acid secretion and gastric emptying time.

These results are in agreement with the conclusions of the OTC antacid review panel (1) and other investigators (3, 12, 13) in that: (*a*) the rate and extent of acid-consuming capacity of antacid products are not alike[2], (*b*) the required dose of antacid not only varies between subjects but during each subject's day, and (*c*) additional *in vivo* studies are required to substantiate and correlate *in vitro* acid neutralization results.

REFERENCES

(1) *Fed. Regist.*, **39**, 19862(1974).

(2) J. F. Morrissey, T. Honda, Y. Tanaka, and G. Perna, *Arch. Intern. Med.*, **119**, 510(1967).

(3) J. S. Fordtran, S. G. Morawski, and C. T. Richardson, *N. Engl. J. Med.*, **288**, 923(1973).

(4) "The United States Pharmacopeia" 18th rev., Mack Publishing Co., Easton, Pa., 1970, p. 26.

(5) W. H. Steinberg, H. H. Hutchins, P. G. Pick, and J. S. Lazar, *J. Pharm. Sci.*, **54**, 625(1965).

(6) J. M. Holbert, N. Noble, and I. Grote, *J. Am. Pharm. Assoc., Sci. Ed.*, **37**, 292(1948).

(7) S. M. Beekman, *ibid.*, **49**, 191(1960).

(8) E. Jóhannesson, P.-O. Magnusson, N.-O. Sjöberg, and A. Skov-Jensen, *Scand. J. Gastroenterol.*, **8**, 65(1973).

(9) J. C. McAlhany, Jr., D. R. Yarbrough, III, M. G. Weidner, Jr., and R. Ravenel, *Am. Surg.*, **35**, 836(1969).

(10) B. J. Winer, "Statistical Principles in Experimental Design," 7th ed., McGraw-Hill, New York, N.Y., 1971, p. 711.

(11) F. J. Goldstein and E. W. Packman, *J. Pharm. Sci.*, **59**, 425(1970).

(12) D. W. Piper and B. H. Fenton, *Gut*, **5**, 585(1964).

(13) R. S. Murphey, *J. Am. Pharm. Assoc., Sci. Ed.*, **41**, 361(1952).

(14) J. Diamond, R. Joslin, and J. Buehler, British pat. 1,336,373 (Nov. 1973).

(15) J. S. Fordtran and J. A. H. Collyns, *N. Engl. J. Med.*, **274**, 921(1966).

(16) J. S. Fordtran and J. H. Walsh, *J. Clin. Invest.*, **52**, 645(1973).

ACKNOWLEDGMENTS AND ADDRESSES

Received October 7, 1974, from the *Research Laboratories, William H. Rorer, Inc., Fort Washington, PA 19034*

Accepted for publication September 26, 1975.

[x] To whom inquiries should be directed.

[2] Data on file, William H. Rorer, Inc., Fort Washington, PA 19034 (available on request).

Effect of Solvent on Tetrazolium Reaction

R. E. GRAHAM*x, E. R. BIEHL ‡, and C. T. KENNER ‡

Abstract □ The rate of color development of a tetrazolium formazan is shown to be inversely proportional to the dielectric constant of the solvent medium and directly proportional to the hydrogen-bonding capability of solvent mixtures having the same dielectric constant. The geometric isomers of the formazans have different absorbance maxima, and the wavelength of maximum absorbance of a mixture of formazans in different solvents depends upon which isomer predominates in that solvent. The *trans-syn*-isomer (blue form) of blue tetrazolium has a maximum absorbance at 625 nm in dimethylformamide while the *trans-anti*-isomer (red form) absorbs at 517 nm in methanol. The absorbance maxima of the corresponding isomers of the formazans of triphenyltetrazolium occur at 535 and 485 nm, respectively. Water and/or methanol (to a lesser extent) are important in the stabilization of the *trans-anti*-isomer, since the small size of these two substances allows them to form strong intermolecular hydrogen bonds with one or both nitrogen atoms of the azo linkage, thereby preventing the formation of the intramolecular hydrogen bonding exhibited by the *trans-syn*-isomer. The formazan produced by the reaction of corticosteroids with tetrazolium in strongly basic media can lose a reduction unit and be reoxidized to the tetrazolium. This reaction is solvent dependent and occurs at a much faster rate in chloroform than in alcohol USP.

Keyphrases □ Tetrazolium reaction—effect of varying solvents and dielectric constants of solvents on rate of color development and wavelength of maximum absorption of formazan □ Solvent systems—effect on rate of color development and wavelength of maximum absorption of formazan, tetrazolium reaction □ Dielectric constants—solvents in tetrazolium reaction, effect on rate of color development and wavelength of maximum absorption □ Color development—tetrazolium reaction, effect of varying solvents and dielectric constants of solvents □ Absorption, spectrophotometric—maximum wavelength of tetrazolium formazan, effect of varying solvents and dielectric constants of solvents

The blue tetrazolium reaction is widely used for the analysis of corticosteroids. USP XIX (1) and NF XIV (2) use a slightly modified procedure of Mader and Buck (3) for corticosteroid analysis. Blue tetrazolium (I), 3,3′- (3,3′- dimethoxy-4,4′-biphenylylene)bis(2,5 -diphenyl-2*H*-tetrazolium chloride), oxidizes the α-keto moiety of the C-17 side chain of corticosteroids in strongly alkaline solution and is reduced quantitatively to a highly colored formazan whose concentration is measured spectrophotometrically.

The analytical procedure is subject to several variables such as temperature (4–6), solvent (1–3, 7–12), concentration of base (13), water (6, 13), and I (6), as well as the steric configuration of the corticosteroid molecule (14). The effect of these variables is minimized by analyzing the blank, standard, and samples concurrently.

Mechanistic studies (14) showed that the reaction of I with corticosteroids involves a bimolecular reaction in which a reduction unit is transferred from the α-keto moiety of the corticosteroid to I to produce a formazan. The nature of the reduction unit is not known.

The influence of solvent on the production of formazan in this reaction has not been studied extensively. The analysis of corticosteroids by I is generally conducted in alcohol USP (1, 2), although absolute alcohol (7–10) and mixtures of chloroform and alcohol USP (11) have been used. The rate and extent of formazan formation are dependent upon the apparent pH of the solvent medium and are inhibited by increasing concentrations of water (13).

The structure of formazans was reviewed previously (15). The interconversion of the formazan derived from triphenyltetrazolium (II) between different colored forms in the presence of visible light also was reported (16). Formazans contain a basic structure which allows the existence of four possible configurations due to geometric isomerization about the two double bonds.

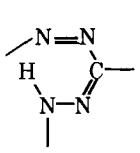

III: *cis-syn*

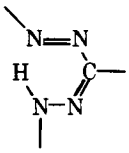

IV: *trans-syn*

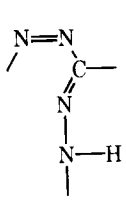

V: *cis-anti*

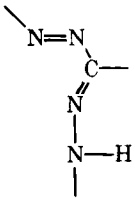

VI: *trans-anti*

A complete study of the influence of various solvents on the rate of formation and distribution of the various geometric forms of the formazan and their effect on the quantitation of corticosteroids has not been reported. The distribution of the formazan should be highly dependent upon the polarity of the solvent, since only III and IV can exist as intramolecular hydrogen-bonded structures. Consequently, any analytical method using the reduction of a tetrazolium should be solvent dependent.

This paper reports a study of the variation of absorbance with change of solvent in the II and I reaction with selected corticosteroids. Solvent effect on the rate of color development and the wavelength of maximum absorption of the respective formazans produced is discussed.

EXPERIMENTAL

Apparatus—The following were used: UV–visible recording spectrophotometers[1] with 1-cm stoppered quartz cells, glass chromatographic columns for partition chromatography (1.2 and 2.2 × 25 cm constricted at one end to 0.4 × 5 cm), IR spectrophotometers[2], an electrobalance[3], and TLC equipment[4].

Materials—Chloroform (distilled in glass), alcohol USP, and analytical reagent grade absolute ethanol, dimethylformamide, 1-pro-

[1] Cary models 15 and 17.
[2] Perkin-Elmer models 337 and 567.
[3] Cahn model G-2.
[4] Eastman No. 6060 silica gel with fluorescent indicator.

Table I—Solvent Mixtures and Dielectric Constant Range in Reaction of I with Hydrocortisone

Solvent Mixture	Range, %	Dielectric Constant Range
Methanol and 1-propanol	8.3–49.6 90.9–41.3	21.5–26.5
Methanol and methylene chloride	8.3–49.6 90.9–41.3	9.1–23.2
Ethanol and methylene chloride	16.1–98.8 82.6–0.0	9.1–24.8
Ethanol and water	99.6–82.3 0.4–17.7	24.5–33.5

panol, absolute methanol, and methylene chloride were used.

Sodium borohydride[5] [0.8-cm (10/32-in.) pellets], blue tetrazolium[6], 10% aqueous tetramethylammonium hydroxide[7] (VII), triphenyltetrazolium[7], and 70–230-mesh column chromatographic grade silica gel 60[8] were also used.

Reagents—A 1% solution of tetramethylammonium hydroxide was prepared by diluting 5.00 ml of the 10% aqueous solution to 50.0 ml with alcohol USP. Blue tetrazolium, 5 mg/ml, was prepared by dissolving 50.0 mg of I in 10.0 ml of alcohol USP. Corticosteroid standard solutions were prepared to contain 0.010 mg/ml in alcohol USP unless otherwise indicated. The source of each standard is listed in the tables.

General Procedure—The procedure followed, unless otherwise specified, is the official procedure given in USP XIX (1); a 20.00-ml volume of standard corticosteroid in alcohol USP is treated with 2.00 ml of I reagent (5 mg/ml) followed by 2.00 ml of 1% VII. The absorbance is measured against a reagent blank 90 min after the addition of VII.

Separation and Isolation of Formazan and Tetrazolium—An alcoholic solution of the reacted mixture containing the formazan and tetrazolium, diluted with four volumes of water in a separator, was extracted repeatedly with chloroform until colorless. The combined extracts were filtered through chloroform-washed cotton and taken to dryness to recover the formazan. The remaining alcoholic aqueous phase was taken to dryness on the steam bath after being scanned in the UV region.

The resulting residue was washed with cyclohexane to remove the blue formazan of I or the total formazan of II produced during the evaporation. The residue was dissolved in chloroform and filtered into a 100-ml beaker, and the solvent was evaporated under air on the steam bath to yield a crystalline residue.

Rate Studies—A 20.00-ml aliquot of a standard corticosteroid in the appropriate solvent (chloroform or methylene chloride) and a 20.00-ml blank of the same solvent were treated according to the *General Procedure*. Both solutions were transferred to cells as rapidly as possible and placed in the spectrophotometer, and absorbance readings were made each minute at 525 nm until the reaction reached essential completion or 90 min elapsed. This procedure was repeated for selected corticosteroids in various concentrations in other solvents. Rate constants were calculated as previously described (14).

Effect of Dielectric Constant on Rate—The rate of formation of the formazan by the reaction of I with aliquots containing 0.200 mg of hydrocortisone was studied in the solvent mixtures listed in Table I.

The capacitance of several pure liquids was measured according to the procedure of LeFevre (17). A calibration curve was prepared which related the dielectric constants (18) of these liquids to their capacitance. The capacitances of various mixtures of solvents were then measured, and the dielectric constants were obtained from the calibration curve. Fixed amounts of other solvents in these mixtures, such as water and ethanol, are not included in Table I but were used in the determination of the dielectric constants of the solutions. The dielectric constant values for ethanol and water mixtures were obtained from Ref. 19.

Formazan Isolation—*Formazan from I*—

1. One pellet of sodium borohydride was added to a solution containing 55 mg of I and 5 ml of 1% VII in 100 ml of absolute ethanol, and the solution was kept in the dark for 1 week. The blue precipitate which formed (85% of the expected amount) was filtered, washed with absolute ethanol, dissolved in chloroform, and evaporated to dryness.

2. Cortisone (0.5 μmole) and I (0.5 μmole) were allowed to react in chloroform. The resulting solution was placed on a silica gel column (1.2 × 23 cm) and eluted with 25 ml of chloroform. The red formazan remained on the column while the blue was eluted with the chloroform. The silica gel packing was extruded from the column and dampened with equal volumes of methanol and water, and the mixture was allowed to stand for 20 min. It was then mixed thoroughly with chloroform, and the solution containing the red formazan was decanted. Evaporation of both final solutions yielded blue and red formazans.

3. To obtain the formazan of triphenyltetrazolium, one pellet of sodium borohydride was added to a solution containing 100 mg of II in 20 ml of absolute ethanol; the solution was kept in the dark for 24 hr. A crystalline formazan was isolated by the method shown under *Separation and Isolation of Formazan and Tetrazolium.*

Reversibility of Formazan to Tetrazolium—

1. To obtain triphenyltetrazolium from its formazan, 4 drops of 10% VII were added to a solution of the formazan of II in alcohol USP (8 mg/15 ml); the solution was kept in the dark for 8 days. Crystalline II was isolated from the solution following the method described under *Separation and Isolation of Formazan and Tetrazolium.*

2. To obtain blue tetrazolium from its formazan, a solution containing 8.8 mg of the red formazan of I, 10.0 ml of alcohol USP, and 1 ml of 1% VII was kept in the dark for 24 days. The color of the solution changed from red to a brownish yellow. A brownish crystalline substance was obtained from the alcoholic aqueous phase by following the method described under *Separation and Isolation of Formazan and Tetrazolium.*

Effect of Hydrogen Bonding on Formazan Color—A solution of II in dimethylformamide plus 1 drop of 10% VII developed an intense red color, which was scanned in the visible region *versus* a dimethylformamide blank. Approximately 0.5 ml of alcohol USP was then added, and the solution was rescanned four more times at 5-min intervals. The experiment was repeated using I instead of II.

RESULTS AND DISCUSSION

Table II lists the values for the absorbance of the formazan per micromole of corticosteroid from the reaction of I with typical corticosteroid and corticosteroid esters in 83% methylene chloride and in 83% chloroform. The average value of 1.081 (*SD* 0.121) absorbance units/μmole obtained in 83% methylene chloride compares favorably with that [1.031 (*SD* 0.056)] obtained previously in alcohol USP (14), which indicates that one reduction unit is also transferred in the methylene chloride solvent.

The higher average value for absorbance per micromole obtained in methylene chloride was probably due to the increased speed of the reaction, which caused increased absorbance due to less base degradation of I by VII (14). However, the standard deviation was about twice as great in methylene chloride as in alcohol USP, which indicates that the I–corticosteroid reaction is less precise in the former solvent. The high value of 1.195 for flurandrenolide may have been due to slow hydrolysis of the acetonide group to produce a compound that can reduce I.

The formazan absorption band was more symmetric and its wavelength of maximum absorption was displaced to a higher wavelength (532 *versus* 525 nm) in spectra obtained in methylene chloride as compared to those in alcohol USP. In most cases, maximum absorption values were reached in less than 50 min, and the absorption then declined very slowly in methylene chloride. Since methylene chloride can be used to extract corticosteroids from certain pharmaceutical formulations, this solvent may be used advantageously for the direct determination of selected corticosteroids by I.

In contrast, the average value of 0.787 (*SD* 0.206) absorbance unit/μmole for the reaction of the corticosteroid alcohols and esters listed in Table II with I in 83% chloroform indicates that the amount of formazan produced per micromole of corticosteroid is less than that expected with the exception of hydrocortisone. Furthermore, the visible spectra of the formazans produced exhibited wavelengths of maximum absorption at 525 nm as in alcohol USP. In addition, the absorbance reached a maximum value rapidly and then decreased to a constant value within 40 min or more after initial scanning. During this time, the wavelength of maximum absorption gradually shifted

[5] Alpha Products.
[6] Dajac Laboratories.
[7] E. Merck Co.
[8] Eastman Organic Chemicals.

Table II—Absorbance per Micromole Values for Selected Corticosteroids with I in Chloroform and Methylene Chloride

Corticosteroid	Source[a]	83% Methylene Chloride[b] Minutes to A_{max}	Maximum Absorbance	Absorbance per Micromole	83% Chloroform[b] Minutes to A_{max}	Maximum Absorbance	Absorbance per Micromole
Betamethasone	1	30	0.571	1.113	19	0.370	0.726
Betamethasone 17-benzoate	2	50	0.386	0.958	55[c]	0.124	0.306
Betamethasone 21-benzoate	2	50	0.381	0.946	60[c]	0.196	0.491
Cortisone	3	30	0.582	1.049	3	0.524	0.945
Cortisone acetate	4	35	0.541	1.079	6	0.457	0.913
Corticosterone	5	45	0.629	1.056	32	0.410	0.705
Dexamethasone	1	46	0.542	1.056	6	0.438	0.859
11-Desoxycorticosterone	5	71	0.854	1.417	35[c]	0.360	0.583
11-Desoxycorticosterone acetate	4	69	0.664	1.231	40[c]	0.185	0.341
11-Desoxycortisone	5	17	0.576	1.008	11	0.514	0.887
Fluprednisolone	1	8	0.542	1.025	5	0.465	0.877
Flurandrenolide	6	90[c]	0.553	1.195	14	0.399	0.965
Hydrocortisone	4	90[c]	0.598	1.089	12	0.560	1.012
Hydrocortisone acetate	4	44	0.544	1.104	11	0.439	0.884
Methylprednisolone	1	13	0.539	0.988	7	0.435	0.806
19-Norhydrocortisone	7	90[c]	0.536	0.919	9	0.501	0.846
Prednisolone	4	90[c]	0.601	1.087	5	0.485	0.879
Prednisolone acetate	4	45	0.639	1.268	8	0.432	0.866
Prednisone	4	90[c]	0.568	1.020	3	0.528	0.944
Prednisone acetate	5	9	0.504	1.009	5	0.453	0.909
Triamcinolone	4	90[c]	1.497	2.938[d]	40[c]	1.237	2.425[d]
Average				1.081			0.787
SD[e]				0.121			0.206

[a] 1 = NF reference standard; 2 = Warner Lambert Co., Morris Plains, N.J.; 3 = K & K Laboratories, Plainview, N.Y.; 4 = USP reference standard; 5 = Schwarz/Mann, Orangeburg, N.Y.; 6 = Eli Lilly & Co., Indianapolis, Ind.; and 7 = Syntex Research, Palo Alto, Calif. [b] Also contains 8.3% absolute methanol, 7.1% alcohol, and 1.2% water. [c] Absorbance increases beyond the time shown are minimal. [d] Not included in average. [e] Standard deviation = $\sqrt{d^2/(n-1)}$.

to 532 nm, and the resulting formazan spectrum was similar to that obtained in methylene chloride. The bathochromic shift observed in 83% chloroform was probably due to the partial conversion of the red formazan to the blue formazan.

Although the reaction of corticosteroids with I was generally rapid (3 min required for prednisone and cortisone analysis) in 83% chloroform, the spectral shifts and low sensitivities observed indicate that this solvent is not suitable for quantitation of corticosteroids.

Table III shows rate constants and relative rate comparisons for reaction of I with selected corticosteroids in alcohol, methylene chloride, and chloroform. The median rate of the reaction in the less polar solvents, methylene chloride and chloroform, was 6.1 and 6.7 times as rapid for 19 different corticosteroids as it was in the more polar solvent, alcohol; the median rate in chloroform was about 1.2 times as fast as it was in methylene chloride. Hydrolysis of the ester is a prerequisite to the reaction of corticosteroids with I (14). Table III shows that the rates of formazan formation from corticosteroid esters and the corresponding corticosteroid alcohols were similar in methylene chloride and chloroform, indicating that ester hydrolysis occurs rapidly in these solvents.

The absorbance per micromole values and rate constants for six steroids and steroid esters in seven different solvent systems are reported in Table IV. With the exception of 83% methanol and 62.5% chloroform, the average absorbance per micromole values (1.030–

Table III—Rates and Relative Rate Comparisons for the Reaction of Selected Corticosteroids with I in Various Solvents

Corticosteroid	K_a[a]	K_m[b]	K_c[c]	K_m/K_a	K_c/K_a	K_c/K_m
Betamethasone 21-benzoate	0.017	0.113	0.202	6.6	11.9	1.8
Betamethasone	0.024	0.147	0.351	6.1	14.6	2.4
Flurandrenolide	0.056	0.340	0.375	6.1	6.7	1.1
19-Norhydrocortisone	0.072	0.614	0.625	8.5	8.7	1.0
Hydrocortisone acetate	0.081	0.588	0.550	7.3	6.8	1.0
Prednisolone acetate	0.086	0.535	0.610	6.2	7.1	1.1
Hydrocortisone	0.090	0.672	0.431	7.5	4.8	0.64
11-Desoxycorticosterone acetate	0.090	0.086	0.206	1.0	2.3	2.4
Prednisolone	0.092	1.658	1.105	18.0	12.0	0.67
Triamcinolone	0.093	0.206	0.741	2.2	8.0	3.6
11-Desoxycortisone	0.094	0.442	0.477	4.7	5.1	1.1
Methylprednisolone	0.096	0.615	0.746	6.4	7.8	1.2
Corticosterone	0.098	0.110	0.207	1.1	2.1	1.9
Dexamethasone	0.098	0.668	0.885	6.8	9.0	1.3
11-Desoxycorticosterone	0.109	0.072	0.208	0.7	1.9	2.9
Cortisone acetate	0.230	0.657	0.864	2.9	3.8	1.3
Cortisone	0.243	1.123	1.170	4.6	4.8	1.0
Prednisone	0.305	1.140	1.280	3.7	4.2	1.1
Prednisone acetate	0.307	0.745	1.100	2.4	3.6	1.5
Median				6.1	6.7	1.2
Steroid alcohols, median				6.1	6.7	1.1
Steroid esters, median				6.4	6.8	1.5

[a] K_a is the rate in alcohol USP; these solutions contain 86.3% ethanol, 8.3% methanol, and 5.4% water. [b] K_m is the rate in methylene chloride; these solutions contain 83.3% methylene chloride, 8.3% methanol, 7.1% ethanol, and 1.2% water. [c] K_c is the rate in chloroform; these solutions contain 83.3% chloroform, 8.3% methanol, 7.1% ethanol, and 1.2% water.

Table IV—Comparison of Rates of Reactivity and Absorbance per Micromole for Six Different Corticosteroids Reacted with Blue Tetrazolium in Seven Different Solvent Systems

Corticosteroid	Minutes to A_{max}	Absorbance per Micromole	Ethanol, %	Water, %	Average Absorbance per Micromole	Other Solvents
Dexamethasone	70	1.060	99.6	0.4		
11-Desoxycorticosterone acetate	80	1.141	99.6	0.4		
Hydrocortisone	90	1.065	99.6	0.4	1.073	None
Hydrocortisone acetate	80	1.079	99.6	0.4		
Prednisolone	30	1.056	99.6	0.4		
Prednisone	8	1.038	99.6	0.4		
Dexamethasone	50	1.020	90.2	9.8		
11-Desoxycorticosterone acetate	77	1.061	90.2	9.8		
Hydrocortisone	70	1.033	90.2	9.8	1.030	None
Hydrocortisone acetate	67	1.033	90.2	9.8		
Prednisolone	60	1.030	90.2	9.8		
Prednisone	16	0.999	90.2	9.8		
Dexamethasone[a]	70	1.050	91.7	None[b]		
11-Desoxycorticosterone acetate[a]	90	1.107	91.7	None[b]		
Hydrocortisone[a]	90	1.072	91.7	None[b]	1.070	8.3% methanol
Hydrocortisone acetate[a]	90	1.098	91.7	None[b]		
Prednisolone[a]	90	1.055	91.7	None[b]		
Prednisone[a]	70	1.035	91.7	None[b]		
Dexamethasone	ND[c]	0.163	15.1	1.6		
11-Desoxycorticosterone acetate	ND[c]	0.381	15.1	1.6		83.3% methanol
Hydrocortisone	ND[c]	0.127	15.1	1.6	0.190	
Hydrocortisone acetate	ND[c]	0.095	15.1	1.6		
Prednisolone	ND[c]	0.130	15.1	1.6		
Prednisone	ND[c]	0.242	15.1	1.6		
Dexamethasone	12	1.020	7.5	0.9		
11-Desoxycorticosterone acetate	60	1.046	7.5	0.9		83.3%
Hydrocortisone	13	1.086	7.5	0.9	1.039	methylene
Hydrocortisone acetate	14	1.050	7.5	0.9		chloride
Prednisolone	10	0.973	7.5	0.9		8.3%
Prednisone	11	1.061	7.5	0.9		methanol
Dexamethasone	60	1.004	15.1	1.6		
11-Desoxycorticosterone acetate	90	1.109	15.1	1.6		
Hydrocortisone	85	1.059	15.1	1.6	1.052	83.3%
Hydrocortisone acetate	80	1.087	15.1	1.6		1-propanol
Prednisolone	85	1.058	15.1	1.6		
Prednisone	5	0.992	15.1	1.6		
Dexamethasone	20	0.938	34.8	2.7		
11-Desoxycorticosterone acetate	55	0.292	34.8	2.7		
Hydrocortisone	15	0.959	34.8	2.7	0.830	62.5%
Hydrocortisone acetate	48	0.878	34.8	2.7		chloroform
Prednisolone	29	0.972	34.8	2.7		
Prednisone	5	0.943	34.8	2.7		

[a] Contains 5.0 mg of I. [b] Molar equivalent of sodium ethoxide substituted for VII. [c] Not determined.

1.073) indicate that these reactions go essentially to completion during the time required for analysis. In addition, the rate was particularly rapid (5–30 min) in 83% 1-propanol. The visible absorption spectra in most solvent systems were similar to those obtained in alcohol USP, with a maximum absorption at 525 nm (517 nm for 83% methanol).

The average absorbance per micromole in 62.5% chloroform (0.830) was similar to that determined for 83% chloroform (0.820). If it is assumed that the previously reported value of 1.031 absorbance units/μmole for alcohol USP (14) is correct, it appears that only 80% of the theoretical amount of formazan was formed in these solvent mixtures. The average absorbance per micromole value for the same six steroids in 83% methanol was 0.190 after 90 min, or about 18% of the value reported for alcohol USP. The average absorbance per micromole value had increased to 0.413 after 20 hr, which indicates that the reaction was greatly retarded in methanol. However, the absorbance per micromole value of a hydrocortisone solution in 83% methanol after 90 min was 0.498 when 10% VII was used instead of 1% VII. This change represents an approximate fourfold increase in the rate of reaction.

The influence of the dielectric constant of the medium on the rate of reaction of I with corticosteroids is shown in Fig. 1. This figure is a typical plot of the log of the rate constant for the reaction of hydrocortisone *versus* the dielectric constant for several solvent pairs. Two important relationships are exemplified. First, there is an inverse relationship between the log of the rate constant and the dielectric constant for a particular solvent pair; that is, reaction rates increase as the dielectric constant decreases. Second, rates are faster for those solvent mixtures having more hydrogen-bonding capability in media of the same dielectric constant. For example, reactions proceed faster in 1-propanol–methanol than in methylene chloride–methanol mixtures of the same dielectric constant.

Figure 1 also shows that the inhibition effect of water on the reaction rate of I previously noted (13) may in part be a dielectric constant effect. The very rapid reaction rate observed for corticosteroids with I in 1-propanol appears to be due to the low dielectric constant and the hydrogen-bonding properties of this solvent.

The two relationships obtained from Fig. 1, together with the dependence of the absorbance upon the apparent pH in strongly basic media (13) and the evidence that the reaction of corticosteroids with I is not a radical reaction (14), support a mechanism that involves initial enolization of the α-keto group of corticosteroids and subsequent enolate formation. The collision of the negative enolate ion and the positive tetrazolium ion which controls the reaction rate follows ion formation. Reactions involving oppositely charged ions are known to be favored in low dielectric media (20).

The influence of the solvent on the wavelength of the absorption

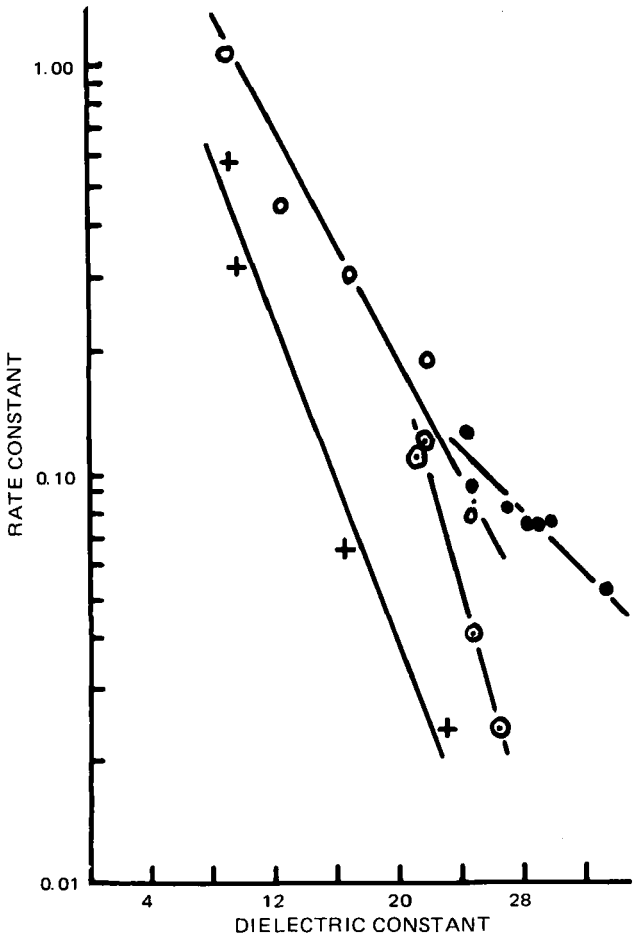

Figure 1—*Variation of rate constant with dielectric constant for the reaction of hydrocortisone with I. Key: ×, mixtures of methylene chloride and methanol; ○, mixtures of methylene chloride and ethanol; ⊙, mixtures of 1-propanol and methanol; and ●, mixtures of ethanol and water.*

maxima of the formazans derived from I and II also was studied. Formazans were prepared in high yield by the reduction of the corresponding tetrazolium with sodium borohydride and were purified by extraction and/or filtration techniques. TLC was used to confirm the absence of the unreacted tetrazolium in the corresponding purified formazan. The reversion of the formazan of II in alcohol USP solution containing 1% VII to II was 94.4% complete in 8 days, and the identity of II so formed was confirmed by UV, IR, and TLC comparison with an authentic sample.

When similarly treated, the formazan of I was also unstable but was converted at a slower rate (36% in 20 days) to a compound that appeared to be a derivative of I. Comparison of this compound with a standard of I showed that the UV curves and R_f values by TLC were similar while the IR spectra were slightly different. These results indicate that under the basic conditions employed in the *General Procedure*, the formazans derived from II and I lose a reduction unit and are oxidized fairly rapidly to II or slowly to a derivative of I.

A similar study of the formazan of II in chloroform (which greatly increases the rate of formazan formation) showed that the rate of reformation of the tetrazolium was much more rapid than in alcohol USP. For this reason, the use of chloroform in the II reaction with corticosteroids would be expected to lead to decreased sensitivity in the measurement of the resultant formazan.

The spectrum of the formazan produced by the corticosteroid reaction with I under the conditions of the *General Procedure* of the official compendia typically exhibit an absorption maximum at 525 nm. TLC analysis of this formazan on silica gel indicates that it is a mixture containing predominantly the red formazan plus a small amount of the blue formazan. The red form, being the more polar of the two, moves with methanol as the mobile solvent while the blue

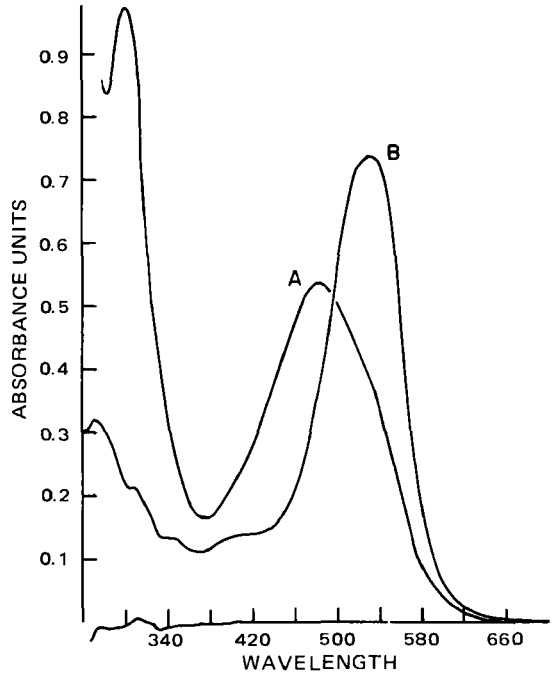

Figure 2—*Spectra of formazans of II. Key: A, spectrum of formazan of II with λ_{max} of 485 nm; and B, spectrum of formazan of II with λ_{max} of 535 nm.*

formazan remains at the point of origin. Conversely, the blue formazan of I moves readily with chloroform as the mobile solvent while the red formazan does not.

Dreiding stereomodels of the possible geometric isomers of the formazans of I indicate that steric interactions are at a minimum in the two *trans*-isomers. Of these, intramolecular hydrogen bonding is possible only in the *trans-syn*-form, which renders this form less polar than the *trans-anti*-form. On this basis, the red and blue formazans of I are assigned the *trans-anti*- and *trans-syn*-configurations, respectively.

The pure red and blue formazans were prepared by the corticosteroid reaction with I in the presence of VII in ethanol and by the action of I plus 1 drop of 10% VII in dimethylformamide. Spectral analysis of the reaction solutions revealed absorption maxima at 517 nm for the red form and 625 nm for the blue form. Furthermore, treatment of I with sodium borohydride in absolute ethanol and treatment of I with 1 drop of 10% VII in 2-propanol yielded the corresponding formazans, which exhibited wavelength maxima of 595 and 580 nm, respectively, indicating that mixtures of the two forms were produced by these reactions. Since the absorbance maximum values are closer to 625 nm than 517 nm, evidently the blue form is formed preferentially under essentially anhydrous conditions.

The addition of either water or methanol to a dimethylformamide solution of the blue formazan of I converts the blue color to purple because some red formazan is produced by reaction of the blue formazan with the added solvent. Thus, water and, to a lesser extent, methanol are important in the stabilization of the red formazan of I. Apparently, the small size of the molecules of water and methanol allows them to form strong intermolecular hydrogen bonds with one or both of the nitrogen atoms of the azo group of the formazan, which prevents the formation of the intramolecular hydrogen bonding exhibited by blue formazan.

Treatment of II dissolved in dimethylformamide with 1 drop of 10% VII produced formazans of intense red color. Immediate spectrophotometric scanning of this solution yielded a nontypical formazan spectrum with an absorption maximum at 535 nm, due to the *trans-syn*-formazan form. Figure 2 shows the effect of the addition of alcohol USP to this solution. Successive scans of the mixture showed that the absorption maximum decreased in absorbance and was shifted to lower wavelengths (from 535 to 485 nm). Also, a new absorption maximum appeared at 300 nm and increased in absorbance with time. Within 20 min, a spectrum was obtained that was similar to that of II formazan obtained in alcohol USP.

REFERENCES

(1) "The United States Pharmacopeia," 19th rev., Mack Publishing Co., Easton, Pa., 1975, p. 622.

(2) "The National Formulary," 14th ed., Mack Publishing Co., Easton, Pa., 1975, p. 976.

(3) W. J. Mader and R. R. Buck, *Anal. Chem.*, **24**, 666(1952).

(4) T. E. Weichselbaum and H. Margraf, *J. Clin. Endocrinol. Metab.*, **15**, 970(1955).

(5) W. Nowaczynski, M. Goldner, and J. Genest, *J. Lab. Clin. Med.*, **45**, 818(1955).

(6) R. O. Rechnagel and M. Litteria, *ibid.*, **48**, 463(1956).

(7) D. E. Guttman, *J. Pharm. Sci.*, **55**, 919(1966).

(8) P. E. Manni and J. E. Sinsheimer, *Anal. Chem.*, **33**, 1900(1961).

(9) J. E. Sinsheimer and E. F. Salim, *ibid.*, **37**, 29(1965).

(10) C. A. Johnson, R. King, and C. Vikers, *Analyst*, **85**, 714(1960).

(11) P. Ascione and C. Fogelin, *J. Pharm. Sci.*, **52**, 709(1963).

(12) J. J. Callahan, F. Litterio, E. Britt, B. D. Rosen, and J. Owens, *ibid.*, **51**, 333(1962).

(13) R. E. Graham and C. T. Kenner, *ibid.*, **62**, 103(1973).

(14) R. E. Graham, E. R. Biehl, C. T. Kenner, G. H. Luttrell, and D. L. Middleton, *ibid.*, **64**, 226(1975).

(15) A. W. Nineham, *Chem. Rev.*, **55**, 355(1955).

(16) R. Kuhn and H. M. Weitz, *Chem. Ber.*, **86**, 1199(1953).

(17) R. J. W. LeFevre, "Dipole Moments," Methusen and Co., Ltd., London, England, 1948, pp. 32, 33.

(18) N. A. Lange, "Handbook of Chemistry," 10th ed., McGraw-Hill, New York, N.Y., 1961, p. 1222.

(19) "International Critical Tables of Numerical Data, Physics, Chemistry and Technology," vol. 6, McGraw-Hill, New York, N.Y., 1929, p. 101.

(20) A. A. Frost and R. G. Pearson, "Kinetics and Mechanisms," Wiley, New York, N.Y., 1961, p. 145.

ACKNOWLEDGMENTS AND ADDRESSES

Received June 25, 1975, from the **Food and Drug Administration, Dallas District, Dallas, TX 75204,* and the *‡Department of Chemistry, Southern Methodist University, Dallas, TX 75275*

Accepted for publication October 10, 1975.

The authors thank Dr. G. H. Luttrell, Jr. (Wyeth Laboratories), for the computer program and for calculation of many rate constants.

[x] To whom inquiries should be directed.

Aggregation of Antihistamines in Aqueous Solution: Effect of Counterions on Self-Association of Pyridine Derivatives

D. ATTWOOD [x] and O. K. UDEALA

Abstract □ The effects of electrolytes on the self-association of the antihistaminic drugs, tripelennamine hydrochloride, thenyldiamine hydrochloride, pyrilamine maleate, pheniramine maleate, chlorpheniramine maleate, and brompheniramine maleate, in aqueous solution were examined by light-scattering methods. The concentration dependence of the light scattering from tripelennamine hydrochloride and thenyldiamine hydrochloride in 0.154 mole of sodium chloride/kg and 0.150 mole of sodium maleate/kg indicated a micellar pattern of aggregation. Higher aggregation numbers and lower CMC's were determined in the presence of the maleate ion. No significant discontinuity in the concentration dependence of the light scattering of the remaining compounds in either of the two electrolytes was evident, and the aggregation of these compounds was treated using a stepwise association model. Values of the association constants and the limiting number of associating species were, in general, increased by the addition of electrolyte in the order water < sodium chloride < sodium maleate. An apparently nonmicellar pattern of aggregation could be induced by chemically changing the counterion from chloride to maleate.

Keyphrases □ Antihistamines—pyridine derivatives, aggregation in aqueous solution, effect of counterions on self-association □ Aggregation—antihistaminic pyridine derivatives, aqueous solution, effect of counterions on self-association □ Counterions—effect on self-association of antihistaminic pyridine derivatives in aqueous solution □ Pyridine derivatives—antihistamines, aggregation in aqueous solution, effect of counterions on self-association □ Electrolytes—effect on self-association of antihistaminic pyridine derivatives in aqueous solution

The self-association in aqueous solution of some antihistamines containing a pyridine nucleus was investigated by light-scattering methods previously (1). No significant discontinuity in the concentration dependence of the light scattering, attributable to a critical micelle concentration (CMC), could be detected. In all cases, however, the scattering intensity exceeded that calculated for the unassociated monomer.

The scattering behavior of three of these compounds, [pyrilamine (mepyramine) maleate, brompheniramine maleate, and chlorpheniramine maleate] could be simulated using a nonmicellar model of association which assumed aggregate growth by stepwise addition of monomers. The intensity of the light scattered by the other compounds studied (pheniramine maleate, tripelennamine hydrochloride, and thenyldiamine chloride) was not of sufficient intensity to establish if association conformed to a micellar or nonmicellar pattern.

Other reports in this series (2–4) concerned antihistamines containing a diphenylmethane nucleus (diphenhydramine hydrochloride, bromodiphenhydramine hydrochloride, chlorcyclizine hydrochloride, and diphenylpyraline hydrochloride). Such compounds have been shown to exhibit typical colloidal behavior in aqueous solution.

This study examined the light scattering of the antihistamines containing a pyridine nucleus in the presence of sodium chloride and sodium maleate. The effect of chemically changing the counterion was investigated for tripelennamine and pyrilamine in an attempt to isolate the cause of their nonmicellar behavior.

REFERENCES

(1) "The United States Pharmacopeia," 19th rev., Mack Publishing Co., Easton, Pa., 1975, p. 622.

(2) "The National Formulary," 14th ed., Mack Publishing Co., Easton, Pa., 1975, p. 976.

(3) W. J. Mader and R. R. Buck, *Anal. Chem.*, **24**, 666(1952).

(4) T. E. Weichselbaum and H. Margraf, *J. Clin. Endocrinol. Metab.*, **15**, 970(1955).

(5) W. Nowaczynski, M. Goldner, and J. Genest, *J. Lab. Clin. Med.*, **45**, 818(1955).

(6) R. O. Rechnagel and M. Litteria, *ibid.*, **48**, 463(1956).

(7) D. E. Guttman, *J. Pharm. Sci.*, **55**, 919(1966).

(8) P. E. Manni and J. E. Sinsheimer, *Anal. Chem.*, **33**, 1900(1961).

(9) J. E. Sinsheimer and E. F. Salim, *ibid.*, **37**, 29(1965).

(10) C. A. Johnson, R. King, and C. Vikers, *Analyst*, **85**, 714(1960).

(11) P. Ascione and C. Fogelin, *J. Pharm. Sci.*, **52**, 709(1963).

(12) J. J. Callahan, F. Litterio, E. Britt, B. D. Rosen, and J. Owens, *ibid.*, **51**, 333(1962).

(13) R. E. Graham and C. T. Kenner, *ibid.*, **62**, 103(1973).

(14) R. E. Graham, E. R. Biehl, C. T. Kenner, G. H. Luttrell, and D. L. Middleton, *ibid.*, **64**, 226(1975).

(15) A. W. Nineham, *Chem. Rev.*, **55**, 355(1955).

(16) R. Kuhn and H. M. Weitz, *Chem. Ber.*, **86**, 1199(1953).

(17) R. J. W. LeFevre, "Dipole Moments," Methusen and Co., Ltd., London, England, 1948, pp. 32, 33.

(18) N. A. Lange, "Handbook of Chemistry," 10th ed., McGraw-Hill, New York, N.Y., 1961, p. 1222.

(19) "International Critical Tables of Numerical Data, Physics, Chemistry and Technology," vol. 6, McGraw-Hill, New York, N.Y., 1929, p. 101.

(20) A. A. Frost and R. G. Pearson, "Kinetics and Mechanisms," Wiley, New York, N.Y., 1961, p. 145.

ACKNOWLEDGMENTS AND ADDRESSES

Received June 25, 1975, from the **Food and Drug Administration, Dallas District, Dallas, TX 75204,* and the *‡Department of Chemistry, Southern Methodist University, Dallas, TX 75275*

Accepted for publication October 10, 1975.

The authors thank Dr. G. H. Luttrell, Jr. (Wyeth Laboratories), for the computer program and for calculation of many rate constants.

[x] To whom inquiries should be directed.

Aggregation of Antihistamines in Aqueous Solution: Effect of Counterions on Self-Association of Pyridine Derivatives

D. ATTWOOD [x] and O. K. UDEALA

Abstract □ The effects of electrolytes on the self-association of the antihistaminic drugs, tripelennamine hydrochloride, thenyldiamine hydrochloride, pyrilamine maleate, pheniramine maleate, chlorpheniramine maleate, and brompheniramine maleate, in aqueous solution were examined by light-scattering methods. The concentration dependence of the light scattering from tripelennamine hydrochloride and thenyldiamine hydrochloride in 0.154 mole of sodium chloride/kg and 0.150 mole of sodium maleate/kg indicated a micellar pattern of aggregation. Higher aggregation numbers and lower CMC's were determined in the presence of the maleate ion. No significant discontinuity in the concentration dependence of the light scattering of the remaining compounds in either of the two electrolytes was evident, and the aggregation of these compounds was treated using a stepwise association model. Values of the association constants and the limiting number of associating species were, in general, increased by the addition of electrolyte in the order water < sodium chloride < sodium maleate. An apparently nonmicellar pattern of aggregation could be induced by chemically changing the counterion from chloride to maleate.

Keyphrases □ Antihistamines—pyridine derivatives, aggregation in aqueous solution, effect of counterions on self-association □ Aggregation—antihistaminic pyridine derivatives, aqueous solution, effect of counterions on self-association □ Counterions—effect on self-association of antihistaminic pyridine derivatives in aqueous solution □ Pyridine derivatives—antihistamines, aggregation in aqueous solution, effect of counterions on self-association □ Electrolytes—effect on self-association of antihistaminic pyridine derivatives in aqueous solution

The self-association in aqueous solution of some antihistamines containing a pyridine nucleus was investigated by light-scattering methods previously (1). No significant discontinuity in the concentration dependence of the light scattering, attributable to a critical micelle concentration (CMC), could be detected. In all cases, however, the scattering intensity exceeded that calculated for the unassociated monomer.

The scattering behavior of three of these compounds, [pyrilamine (mepyramine) maleate, brompheniramine maleate, and chlorpheniramine maleate] could be simulated using a nonmicellar model of association which assumed aggregate growth by stepwise addition of monomers. The intensity of the light scattered by the other compounds studied (pheniramine maleate, tripelennamine hydrochloride, and thenyldiamine chloride) was not of sufficient intensity to establish if association conformed to a micellar or nonmicellar pattern.

Other reports in this series (2–4) concerned antihistamines containing a diphenylmethane nucleus (diphenhydramine hydrochloride, bromodiphenhydramine hydrochloride, chlorcyclizine hydrochloride, and diphenylpyraline hydrochloride). Such compounds have been shown to exhibit typical colloidal behavior in aqueous solution.

This study examined the light scattering of the antihistamines containing a pyridine nucleus in the presence of sodium chloride and sodium maleate. The effect of chemically changing the counterion was investigated for tripelennamine and pyrilamine in an attempt to isolate the cause of their nonmicellar behavior.

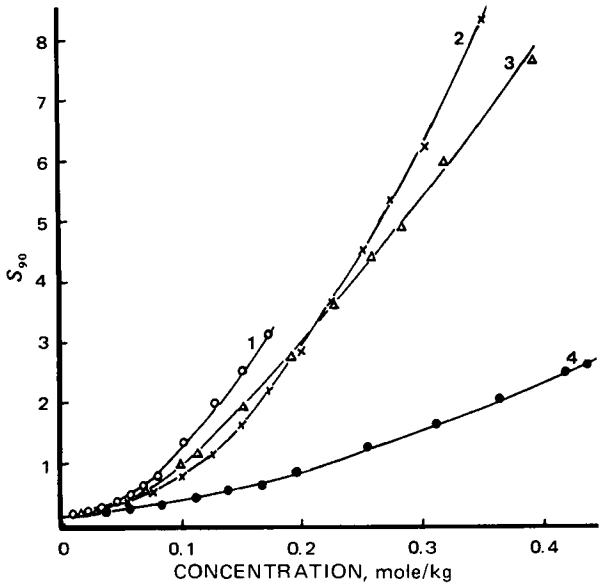

Figure 1—*Light-scattering plots in 0.154 mole of sodium chloride/kg at 303° K. Scattering at 90° to the incident beam, S_{90}, is plotted as a function of molal concentration. Key: 1, brompheniramine maleate; 2, pyrilamine maleate; 3, chlorpheniramine maleate; and 4, pheniramine maleate.*

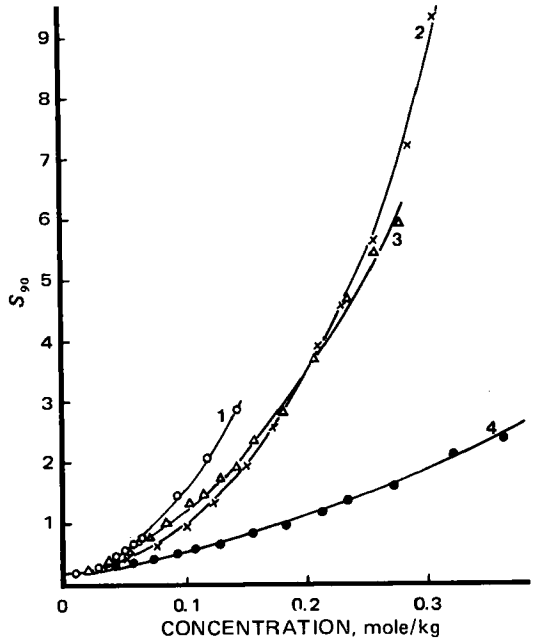

Figure 2—*Light-scattering plots in 0.150 mole of sodium maleate/kg at 303° K. Scattering at 90° to the incident beam, S_{90}, is plotted as a function of molal concentration. Key: 1, brompheniramine maleate; 2, pyrilamine maleate; 3, chlorpheniramine maleate; and 4, pheniramine maleate.*

EXPERIMENTAL

Materials—The following drugs were used as received: pyrilamine maleate[1] {*N*-[(4-methoxyphenyl)methyl]-*N'*,*N'*-dimethyl-*N*-2-pyridinyl-1,2-ethanediamine butenedioate}, tripelennamine hydrochloride[2] BP [*N*,*N*-dimethyl-*N'*-(phenylmethyl)-*N'*-2-pyridinyl-1,2-ethanediamine monohydrochloride], thenyldiamine hydrochloride[3] [*N*,*N*-dimethyl-*N'*-2-pyridinyl-*N'*-(3-methylthienyl)ethylenediamine hydrochloride], pheniramine maleate[4] [*N*,*N*-dimethyl-3-phenyl-3-(2-pyridinyl)propylamine butenedioate], chlorpheniramine maleate[5] [3-(4-chlorophenyl)-*N*,*N*-dimethyl-3-(2-pyridinyl)propylamine butenedioate], and brompheniramine maleate[6] [3-(4-bromophenyl)-*N*,*N*-dimethyl-3-(2-pyridinyl)propylamine butenedioate].

Tripelennamine maleate was prepared by the addition of maleic acid to tripelennamine base in anhydrous ether. The salt was recrystallized from methanol–ether and dried over phosphorus pentoxide under vacuum, mp 132°.

Anal.—Calc. for $C_{20}H_{25}N_3O_4$: C, 64.67; H, 6.78; N, 11.31. Found: C, 64.7; H, 7.1; N, 11.3.

Pyrilamine hydrochloride was prepared by passing dried hydrogen chloride gas into a solution of pyrilamine base in anhydrous ether. The salt was recrystallized from methanol–ether and dried over phosphorus pentoxide under vacuum, mp 138–140° [lit. (5) mp 143°].

Anal.—Calc. for $C_{17}H_{24}ClN_3O$; C, 63.44; H, 7.52; Cl, 11.02; N, 13.06. Found: C, 59.2; H, 7.2; Cl, 12.6; N, 12.2.

Sodium chloride was Analar grade, sodium maleate was reagent grade, and the water was double distilled from glass.

Light Scattering—The light-scattering instrument[7] was thermostated at 303° K, and measurements were made at a wavelength of 546 nm. Solutions were clarified by ultrafiltration[8] until the ratio of the light scattering at angles of 30 and 150° did not exceed 1.10. The refractive index increments of the micellar species were measured at 546 nm using a differential refractometer.

RESULTS

The light-scattering plots for pyrilamine maleate, chlorpheniramine maleate, brompheniramine maleate, and pheniramine maleate in 0.154 mole of sodium chloride/kg and 0.15 mole of sodium maleate/kg are shown in Figs. 1 and 2. The scattering curves are similar in appearance to those previously obtained in the absence of electrolyte (1). The scattering at 90°, S_{90}, increased continuously with concentration, with no apparent discontinuity normally associated with a CMC.

The scattering data were treated using a proposed nonmicellar model of association (6), which was previously applied to the aggregation of these systems in water. Aggregate growth was assumed to occur by a stepwise addition of monomers (Scheme I).

$$M_{N-1} + M_1 \rightleftharpoons M_N$$

Scheme I

The weight fraction, x, of compound existing as the monomer was determined by graphical integration of the light-scattering data according to:

$$\ln x = \int_0^c [(M/M_w) - 1]\, d \ln c \qquad \text{(Eq. 1)}$$

where M is the monomer molecular weight, M_w is the apparent weight-average aggregate weight, and c is the weight concentration (grams per cubic decimeter). Stepwise equilibrium constants, K_N, were estimated, as described previously, from:

$$[(M_w/xM) - 1]/(xc/M) = 4K_2 + 9K_2K_3\,(xc/M) \ldots + N^2 \left(\prod_2^N K_N\right) (xc/M)^{N-2} \qquad \text{(Eq. 2)}$$

This method was derived for ideal systems and does not take into account the interactions between charged aggregates. Such interactions are reduced in the presence of a swamping electrolyte. No corrections were applied to the refractive index increments measured in sodium chloride to allow for the presence of mixed counterions.

Errors in the calculation of K_N are cumulative, and only the lower values are quoted in Table I. Also included in Table I are approximate values of l, the degree of association of the highest molecular species existing in solution in significant amount, which were derived as described previously. The K_N and l values were, in general, increased by the addition of electrolyte in the order water < sodium chloride < sodium maleate.

The concentration dependence of the scattering from tripelennamine hydrochloride and thenyldiamine hydrochloride in the two electrolytes is shown in Fig. 3. The curves are typical of those normally

[1] May and Baker Ltd., Dagenham, Essex, United Kingdom.
[2] Ciba Labs., Horsham, Sussex, United Kingdom.
[3] Winthrop Labs., Surbiton-on-Thames, Surrey, United Kingdom.
[4] Hoechst Pharmaceuticals Ltd., Hounslow, Middlesex, United Kingdom.
[5] Allen & Hanburys Ltd., London, United Kingdom.
[6] A. H. Robins & Co., Horsham, Sussex, United Kingdom.
[7] Fica 42,000 photogoniodiffusometer.
[8] Millipore filters, 0.1 μm.

Table I—Self-Association of Antihistamines in Water, 0.154 Mole of Sodium Chloride/kg, and 0.150 Mole of Sodium Maleate/kg

Compound	Solvent	Stepwise Association Constants, dm³/mole K_2	K_3	Limiting Aggregation Number, l
Pheniramine maleate	Water[a]	1.61	5.2	7
	Sodium chloride	1.58	4.0	10
	Sodium maleate	1.58	5.1	8
Chlorpheniramine maleate	Water[a]	2.03	9.9	11
	Sodium chloride	5.00	35.3	22
	Sodium maleate	6.13	39.2	21
Brompheniramine maleate	Water[a]	3.50	21.0	15
	Sodium chloride	3.10	35.6	22
	Sodium maleate	6.30	62.2	>30
Pyrilamine maleate	Water[a]	2.00	7.2	10
	Sodium chloride	2.50	17.8	>30
	Sodium maleate	2.90	17.7	>30
Tripelennamine maleate	Water[a]	0.75	6.30	14

[a] Values from Ref. 1.

obtained for surfactant solutions, showing clearly defined inflections at the CMC. The scattering below the CMC could be represented by theoretical lines calculated for the scattering of unassociated monomers, and accurate values of the CMC (Table II) were determined from the intersection of these lines with those representing the scattering at higher concentrations.

Where systems involved mixed counterions, *e.g.*, tripelennamine hydrochloride in sodium maleate, the relative refractive index increments used in the calculation of the theoretical lines were determined as a function of the solution concentration using equations

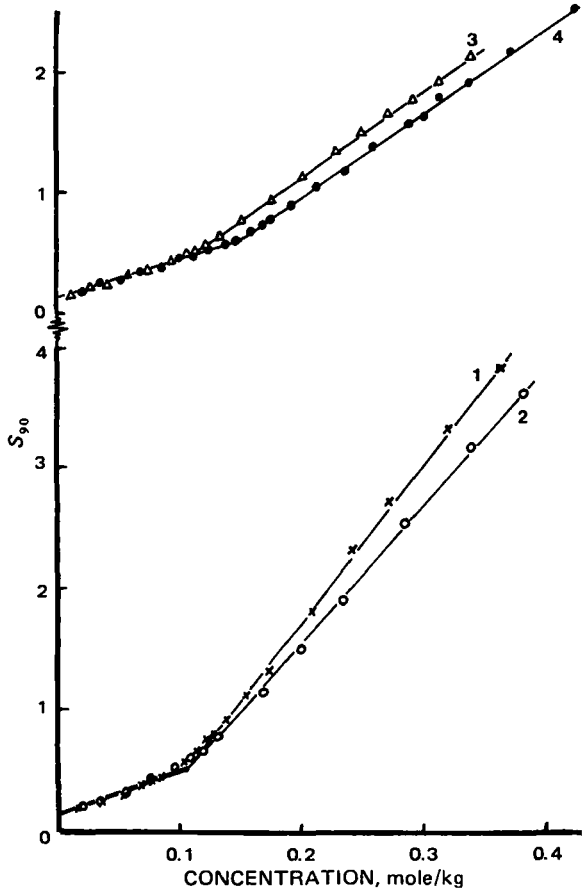

Figure 3—*Light scattering of tripelennamine and thenyldiamine hydrochloride in 0.154 mole of sodium chloride/kg and 0.150 mole of sodium maleate/kg at 303° K. Key: 1, tripelennamine hydrochloride in sodium maleate; 2, thenyldiamine hydrochloride in sodium maleate; 3, tripelennamine hydrochloride in sodium chloride; and 4, thenyldiamine hydrochloride in sodium chloride.*

proposed previously (7), in which the refractive index gradient of the solute, dn/dm_2, is given by

$$dn/dm_2 = (a + b)^{-1}\, a(dn/dm_{D\ \text{maleate}}) + b(dn/dm_{D\ \text{HCl}}) \quad \text{(Eq. 3)}$$

where a and b are the molalities of the sodium maleate and the hydrochloride salt of the drug, respectively; and $dn/dm_{D\text{maleate}}$ and $dn/dm_{D\ \text{HCl}}$ are the refractive index increments of the maleate and hydrochloride salts of the drug, respectively.

The refractive index increment of tripelennamine maleate could be determined experimentally. Since thenyldiamine maleate was not available, a value of $dn/dm_{D\ \text{maleate}}$ was calculated from the refractive index increment of thenyldiamine hydrochloride as suggested previously (7). A solution that was a molal in sodium maleate and b molal in thenyldiamine hydrochloride was regarded as being b molal in thenyldiamine maleate, b molal in sodium chloride, and $(a-b)$ molal in sodium maleate. The measured refractive index difference between a b molal solution of thenyldiamine hydrochloride and the sodium maleate solvent was corrected by adding the quantity b $(dn/dm_{\text{Na maleate}} - dn/dm_{\text{NaCl}})$ to give the corresponding refractive index difference for thenyldiamine maleate. A literature value (8) of 0.0104 kg/mole was used for the refractive index increment of sodium chloride, dn/dm_{NaCl}. A value of 0.0290 kg/mole was experimentally determined for the refractive index increment of sodium maleate.

The micellar aggregation numbers were calculated using equations proposed previously (9):

$$p = 2fm_3B \pm (8m_3B)^{1/2}A^{-1}(2 - fA)^{-1} \quad \text{(Eq. 4)}$$

$$N = p(p + 1)A(2m_3B + pA^2)^{-1} \quad \text{(Eq. 5)}$$

where A and B are the intercept and slope, respectively, of plots of Km_2/R_{90} against the molal concentration of micelles, m_2. The R_{90} is the Rayleigh ratio of the solution in excess of that of a solution at the CMC; $K = 2\pi^2 n_0^2 (dn/dm_2)_{m_3}^2 V^0/L\lambda^4$; n_0 is the refractive index of the solvent; V^0 is the volume of solution containing 1 kg of water; L is the Avogadro number; λ is the wavelength of the incident light; m_3 is the molality of supporting electrolyte; and $f = (dn/dm_3)_{m_2}/(dn/$

Table II—Properties of Micelles of Tripelennamine Hydrochloride and Thenyldiamine Hydrochloride in 0.154 Mole of Sodium Chloride/kg and 0.150 Mole of Sodium Maleate/kg

Compound	Solvent	CMC, mole/kg	Aggregation Number, N
Tripelennamine hydrochloride	Sodium chloride	0.11	3.3
	Sodium maleate	0.10	4.5
Thenyldiamine hydrochloride	Sodium chloride	0.13	2.9
	Sodium maleate	0.11	3.6

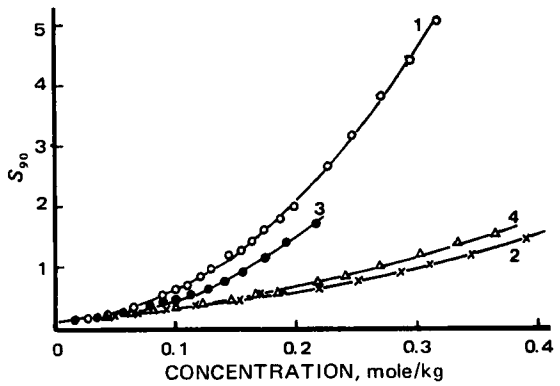

Figure 4—*Effect of change of counterion on the light scattering of pyrilamine and tripelennamine in water at 303° K. Key: 1, pyrilamine maleate; 2, pyrilamine hydrochloride; 3, tripelennamine maleate; and 4, tripelennamine hydrochloride. Light-scattering data for pyrilamine maleate and tripelennamine hydrochloride are from Ref. 1.*

$dm_2)_{m_3}$. Then $(dn/dm_2)_{m_3}$ and, hence, K vary with surfactant concentration according to Eq. 3.

To simplify the computational procedure, plots of m_2/R_{90} *versus* m_2 rather than Km_2/R_{90} *versus* m_2 were drawn, and the value of K appropriate at the CMC was applied to the intercept and slope to give values of A and B. Since the B values were too low to be determined accurately, N was equated with A^{-1}. Aggregation numbers are given in Table II.

A change of the counterion associated with tripelennamine, from hydrochloride to maleate, increased the intensity of scattering and gave a scattering curve similar in appearance to that observed with the other compounds with maleate counterions. The data were treated according to Eqs. 1 and 2 and Scheme I, and values of K_N and l are included in Table I. Changing the counterion of pyrilamine from maleate to chloride reduced the scattering intensity to a level similar to that of tripelennamine hydrochloride. Although the S_{90} value exceeded that calculated for unassociated monomers, it was not sufficiently high to indicate clearly the type of association.

DISCUSSION

The effect of the structure of the hydrophobic group on the pattern of aggregation was discussed previously (10). Hydrophobic groups containing aromatic ring structures are thought to aggregate by a continuous stepwise association process. Such ring structures are usually planar, and association involves a face-to-face stacking of monomers. Antihistamines with a diphenylmethane hydrophobic group have been shown (2–4) to aggregate by a micellar process rather than by stepwise association. The hydrophobic groups of such compounds, although aromatic, are neither planar nor rigid structures. Rotation around the central C atom of the diphenylmethane nucleus would clearly hinder the stacking process.

In contrast, the antihistamines under investigation have a single planar hydrophobic ring only. With the exception of thenyldiamine hydrochloride and tripelennamine hydrochloride, their aggregation may be adequately represented by a stepwise association model both in water (1) and in the presence of excess electrolyte (Figs. 1 and 2). The aggregation of thenyldiamine hydrochloride and tripelennamine hydrochloride in the presence of electrolyte is apparently a micellar process, as indicated by Fig. 3. Although it was not possible to establish by light-scattering methods the type of association for these two compounds in the absence of electrolyte (1), recent surface tension measurements (11) indicated that this process is also micellar.

The reason for the difference between the mode of aggregation of these two compounds and the remaining pyridine derivatives is not clear but may be associated with the nature of the counterion. Figure 4 shows that chemically changing the counterion of tripelennamine from chloride to maleate not only resulted in increased scattering but also in an apparently nonmicellar pattern of aggregation.

It is interesting to compare the effects of changing the counterions by addition of electrolyte with those of changing the counterions by chemical synthesis. The addition of a relatively high concentration of sodium maleate to tripelennamine hydrochloride and thenyldiamine hydrochloride, although increasing the scatter, did not result in the nonmicellar aggregation typical of the compounds with a maleate counterion. Similarly, the addition of sodium chloride to pyrilamine, chlorpheniramine, brompheniramine, and pheniramine maleates did not induce a micellar pattern of aggregation. A major difference between these two types of systems is that, in solutions with mixed counterions, the ratio of the chloride and maleate ions is continually changing as the solution concentration is altered; consequently, the two systems are not directly comparable.

Table III—Free Energies of Micelle Formation of Antihistamines (kJ/mole)

Compound	Water	0.154 Mole of Sodium Chloride/kg	0.150 Mole of Sodium Maleate/kg
Pheniramine maleate	−11.21	−11.95	−11.77
Chlorpheniramine maleate	−13.69	−16.15	−16.75
Brompheniramine maleate	−15.19	−16.42	−17.49
Pyrilamine maleate	−13.84	−15.31	−15.69
Tripelennamine maleate	−13.03	—	—

The average free energy change for the monomer, ΔG_m, for the formation of the N-mer is given by (10):

$$N\,\Delta G_m = -RT \ln \beta \qquad \text{(Eq. 6)}$$

where β is the product of all stepwise association constants K_2, K_3, . . . K_l, *i.e.*, $\beta = \Pi_2^l K_N$. Application of Eq. 6 to those antihistamines showing nonmicellar aggregation gave the ΔG_m values of Table III. Included in this table are ΔG_m values in the absence of electrolyte calculated from previously reported K_N and l values. For systems in which a complete analysis of the equilibrium constants was not possible, *i.e.*, brompheniramine maleate in sodium maleate and pyrilamine maleate in sodium chloride and sodium maleate, approximate ΔG_m values were calculated from available K_N values.

The value of ΔG_m may be considered to be composed of electrical and hydrocarbon contributions, designated ΔG_e and ΔG_h, respectively. In a rigorous examination of the thermodynamics of micellization of the cationic surfactant dodecyltrimethylammonium bromide, Anacker (12) noted an increase in $-\Delta G_m$ on the addition of electrolyte, which was shown to result from a reduction in ΔG_e. A similar increase in $-\Delta G_m$ is noted in Table III, the greater effect being produced by sodium maleate. From the data of Kauzmann (13), the free energy change, ΔG_h, associated with the formation of a micelle in which a phenyl ring is completely shielded from the aqueous environment would be −17kJ/mole.

The value of $-\Delta G_m$ is generally slightly less than $-\Delta G_h$ since the electrical contribution is small and positive. The approximate ΔG_m values calculated assuming the applicability of the stepwise association model are thus of a reasonable magnitude. If a similar ΔG_e is assumed for each compound, the ΔG_m values reflect an increased hydrophobicity in the order pheniramine $\ll$ chlorpheniramine $<$ brompheniramine, as might be expected. For pyrilamine maleate, ΔG_m in water is slightly larger than that of tripelennamine maleate, reflecting the increased hydrophobicity conferred by the methoxyl group on the phenyl ring of pyrilamine, the two compounds having otherwise identical structures.

The greater aggregating power of the maleate counterion as compared to that of the chloride ion is evident from the aggregation numbers of tripelennamine hydrochloride and thenyldiamine hydrochloride (Table II), from the magnitude of K_N and l values of Table I, and from a comparison of the scattering intensity of the hydrochlorides and maleates of tripelennamine and pyrilamine (Fig. 4). These observations are in agreement with previously reported investigations of the effect of organic counterions on the micellization of both anionic and cationic surfactants. In general, a greater depression of the CMC (14–16) and a greater increase in aggregation number (17) have been noted with organic counterions than with inorganic ions; these findings have been explained in terms of hydrophobic bonding between the micelle surface and the organic counterions.

REFERENCES

(1) D. Attwood and O. K. Udeala, *J. Phys. Chem.*, **79**, 889(1975).
(2) D. Attwood, *J. Pharm. Pharmacol.*, **24**, 751(1972).
(3) D. Attwood and O. K. Udeala, *ibid.* **26**, 854(1974).
(4) *Ibid.*, **27**, 395(1975).
(5) "The Merck Index," 8th ed., Merck and Co., Rahway, N.J., 1968.
(6) R. F. Steiner, *Arch. Biochem. Biophys.*, **39**, 333(1952).
(7) E. W. Anacker and H. M. Ghose, *J. Am. Chem. Soc.*, **90**, 3161(1968).
(8) A. Kruis, *Z. Phys. Chem.*, **B34**, 13(1936).
(9) E. W. Anacker and A. E. Westwell, *J. Phys. Chem.*, **68**, 3490(1964).
(10) P. Mukerjee, *J. Pharm. Sci.*, **63**, 972(1974).
(11) D. Attwood and O. K. Udeala, *J. Pharm. Pharmacol.*, **27**, 754(1975).
(12) E. W. Anacker, in "Cationic Surfactants," E. Jungermann, Ed., Dekker, New York, N.Y., 1970.
(13) W. Kauzmann, *Adv. Protein Chem.*, **14**, 1(1959).
(14) E. D. Goddard, O. Harva, and T. G. Jones, *Trans. Faraday Soc.*, **49**, 980(1953).
(15) K. Meguro and T. Kondo, *Nippon Kagaku Zasshi*, **80**, 818, 823(1959).
(16) P. Mukerjee, K. J. Mysels, and P. Kapauan, *J. Phys. Chem.*, **71**, 4166(1967).
(17) K. J. Mysels and L. H. Princen, *ibid.*, **63**, 1699(1959).

ACKNOWLEDGMENTS AND ADDRESSES

Received February 28, 1975, from the *Pharmacy Department, University of Manchester, Manchester, M13 9PL, United Kingdom.*

Accepted for publication October 1, 1975.

The authors thank Winthrop Labs., Surrey, United Kingdom; Hoechst Pharmaceuticals Ltd., Middlesex, United Kingdom, Allen and Hanburys Ltd., London, United Kingdom, and A. H. Robins & Co., Sussex, United Kingdom, for the gifts of antihistamines. They also acknowledge financial support from a British Technical Aid award to the University of Nigeria.

[x] To whom inquiries should be directed.

Binding Characteristics of Drugs to Synthetic Levodopa Melanin

K. SHIMADA, R. BAWEJA, T. SOKOLOSKI, and P. N. PATIL [x]

Abstract □ To define binding characteristics of drugs, levodopa melanin was prepared with the aid of mushroom tyrosinase. The binding of radiolabeled substances was studied with increasing concentrations of melanin in a fixed volume of potassium phosphate buffer (pH 7.4) at 37°. The affinity and capacity of the drug binding were calculated according to Langmuir's adsorption isotherm. The affinity constant of various sympathomimetic amines such as (−)-amphetamine, (+)-amphetamine, (−)-ephedrine, (±)-octopamine, and (+)-norepinephrine ranged from 1.1 to 2.8 × 10^5 M^{-1}. The binding capacity for the amines ranged from 1.4 to 3.2 × 10^{-9} mole/mg. Although the capacity of (±)-cocaine for binding was similar to that of the amines, the affinity was slightly higher, 8.9 × 10^5 M^{-1}. The binding of atropine to the synthetic melanin appeared to be a saturable process with the affinity and capacity values of 0.2 × 10^5 M^{-1} and 7.6 × 10^{-9} mole/mg, respectively. Although the binding lacks stereoselectivity, the drugs vary in their capacity and affinity to bind with melanin. The observed differential pharmacological and toxicological properties of drugs in the pigmented tissues may in part be related to their differential binding characteristics.

Keyphrases □ Melanin, synthetic—prepared by action of mushroom tyrosinase on levodopa, affinity and capacity of drug binding evaluated, various sympathomimetic amines □ Levodopa melanin—affinity and capacity of drug binding evaluated, various sympathomimetic amines □ Binding, drug-melanin—affinity and capacity evaluated, various sympathomimetic amines □ Sympathomimetic amines—binding to synthetic melanin, affinity and capacity evaluated □ Pigments—synthetic melanin, affinity and capacity of drug binding, various sympathomimetic amines

Several tissues such as iris, skin, hair, inner ear, and substantia nigra contain melanin. Many phenothiazines (1, 2), chloroquine (3), cocaine (4), antibiotics (5), and sympathomimetic drugs (6, 7) are markedly accumulated and retained for a long time by the pigmented tissue. The nonpigmented tissues from albino or nonalbino animals accumulate very little drug, and the accumulated substance is rapidly lost from the tissue (4, 6, 7).

In the pigmented tissue, the accumulation presumably occurs by the pigment cells and their constituent melanin granules. These granules consist of a lipoid membrane, a protein, and the melanin derived from levodopa (8). Since little is known about the binding characteristics of drugs by melanin, synthetic levodopa melanin was prepared and the affinity and capacity for drug binding were studied.

EXPERIMENTAL

Preparation of Synthetic Levodopa Melanin—Melanin was prepared by a modification of a reported method (2, 9). Ten grams of levodopa (L-dihydroxyphenylalanine)[1] and 66 mg of mushroom tyrosinase[2] (polyphenol oxidase) were placed in 3 liters of 0.1 *M* potassium phosphate buffer, pH 7.4, and stirred in a water bath at 37° for 4 hr. Buffers were prepared from reagent grade chemicals. Oxygen gas (95% oxygen–5% carbon dioxide) was bubbled through the preparation at room temperature for 90 min. The suspension was then stirred for an additional 4 hr. The mixture was then allowed to stand overnight (14 hr) with continual bubbling of oxygen.

The resultant precipitate of melanin was collected after centrifuging (19,000 rpm) at −2° and washed by resuspending in distilled water. The washings, followed by centrifugation, were performed until a clear supernatant solution was obtained. The washed precipitate thus obtained was freeze dried. The yield of melanin was approximately 1.41 g. The material exhibited a characteristic free radical signal in the electron spin resonance spectrometer[3] (like that seen in the natural melanins).

Methodology for Binding Studies—In all binding studies, the general procedure used was as follows. Aliquots of 1.0, 2.0, 4.0, 6.0, and 8.0 mg of synthetic melanin were placed in five 25-ml erlenmeyer flasks. Amounts of radiolabeled substances were added to each flask in the concentrations of 2 nCi/ml for ^{14}C-labeled materials and 6

[1] Merck Sharp & Dohme Research Laboratories, West Point, Pa.
[2] Sigma Chemical Co., St. Louis, Mo. (3690 units/mg).
[3] The spectra was supplied through the courtesy of Dr. L. Malspeis, College of Pharmacy, Ohio State University.

REFERENCES

(1) D. Attwood and O. K. Udeala, *J. Phys. Chem.*, **79**, 889(1975).
(2) D. Attwood, *J. Pharm. Pharmacol.*, **24**, 751(1972).
(3) D. Attwood and O. K. Udeala, *ibid.* **26**, 854(1974).
(4) *Ibid.*, **27**, 395(1975).
(5) "The Merck Index," 8th ed., Merck and Co., Rahway, N.J., 1968.
(6) R. F. Steiner, *Arch. Biochem. Biophys.*, **39**, 333(1952).
(7) E. W. Anacker and H. M. Ghose, *J. Am. Chem. Soc.*, **90**, 3161(1968).
(8) A. Kruis, *Z. Phys. Chem.*, **B34**, 13(1936).
(9) E. W. Anacker and A. E. Westwell, *J. Phys. Chem.*, **68**, 3490(1964).
(10) P. Mukerjee, *J. Pharm. Sci.*, **63**, 972(1974).
(11) D. Attwood and O. K. Udeala, *J. Pharm. Pharmacol.*, **27**, 754(1975).
(12) E. W. Anacker, in "Cationic Surfactants," E. Jungermann, Ed., Dekker, New York, N.Y., 1970.
(13) W. Kauzmann, *Adv. Protein Chem.*, **14**, 1(1959).
(14) E. D. Goddard, O. Harva, and T. G. Jones, *Trans. Faraday Soc.*, **49**, 980(1953).
(15) K. Meguro and T. Kondo, *Nippon Kagaku Zasshi*, **80**, 818, 823(1959).
(16) P. Mukerjee, K. J. Mysels, and P. Kapauan, *J. Phys. Chem.*, **71**, 4166(1967).
(17) K. J. Mysels and L. H. Princen, *ibid.*, **63**, 1699(1959).

ACKNOWLEDGMENTS AND ADDRESSES

Received February 28, 1975, from the *Pharmacy Department, University of Manchester, Manchester, M13 9PL, United Kingdom.*

Accepted for publication October 1, 1975.

The authors thank Winthrop Labs., Surrey, United Kingdom; Hoechst Pharmaceuticals Ltd., Middlesex, United Kingdom, Allen and Hanburys Ltd., London, United Kingdom, and A. H. Robins & Co., Sussex, United Kingdom, for the gifts of antihistamines. They also acknowledge financial support from a British Technical Aid award to the University of Nigeria.

[x] To whom inquiries should be directed.

Binding Characteristics of Drugs to Synthetic Levodopa Melanin

K. SHIMADA, R. BAWEJA, T. SOKOLOSKI, and P. N. PATIL [x]

Abstract □ To define binding characteristics of drugs, levodopa melanin was prepared with the aid of mushroom tyrosinase. The binding of radiolabeled substances was studied with increasing concentrations of melanin in a fixed volume of potassium phosphate buffer (pH 7.4) at 37°. The affinity and capacity of the drug binding were calculated according to Langmuir's adsorption isotherm. The affinity constant of various sympathomimetic amines such as (−)-amphetamine, (+)-amphetamine, (−)-ephedrine, (±)-octopamine, and (+)-norepinephrine ranged from 1.1 to 2.8 × 10^5 M^{-1}. The binding capacity for the amines ranged from 1.4 to 3.2 × 10^{-9} mole/mg. Although the capacity of (±)-cocaine for binding was similar to that of the amines, the affinity was slightly higher, 8.9 × 10^5 M^{-1}. The binding of atropine to the synthetic melanin appeared to be a saturable process with the affinity and capacity values of 0.2 × 10^5 M^{-1} and 7.6 × 10^{-9} mole/mg, respectively. Although the binding lacks stereoselectivity, the drugs vary in their capacity and affinity to bind with melanin. The observed differential pharmacological and toxicological properties of drugs in the pigmented tissues may in part be related to their differential binding characteristics.

Keyphrases □ Melanin, synthetic—prepared by action of mushroom tyrosinase on levodopa, affinity and capacity of drug binding evaluated, various sympathomimetic amines □ Levodopa melanin—affinity and capacity of drug binding evaluated, various sympathomimetic amines □ Binding, drug-melanin—affinity and capacity evaluated, various sympathomimetic amines □ Sympathomimetic amines—binding to synthetic melanin, affinity and capacity evaluated □ Pigments—synthetic melanin, affinity and capacity of drug binding, various sympathomimetic amines

Several tissues such as iris, skin, hair, inner ear, and substantia nigra contain melanin. Many phenothiazines (1, 2), chloroquine (3), cocaine (4), antibiotics (5), and sympathomimetic drugs (6, 7) are markedly accumulated and retained for a long time by the pigmented tissue. The nonpigmented tissues from albino or nonalbino animals accumulate very little drug, and the accumulated substance is rapidly lost from the tissue (4, 6, 7).

In the pigmented tissue, the accumulation presumably occurs by the pigment cells and their constituent melanin granules. These granules consist of a lipoid membrane, a protein, and the melanin derived from levodopa (8). Since little is known about the binding characteristics of drugs by melanin, synthetic levodopa melanin was prepared and the affinity and capacity for drug binding were studied.

EXPERIMENTAL

Preparation of Synthetic Levodopa Melanin—Melanin was prepared by a modification of a reported method (2, 9). Ten grams of levodopa (L-dihydroxyphenylalanine)[1] and 66 mg of mushroom tyrosinase[2] (polyphenol oxidase) were placed in 3 liters of 0.1 *M* potassium phosphate buffer, pH 7.4, and stirred in a water bath at 37° for 4 hr. Buffers were prepared from reagent grade chemicals. Oxygen gas (95% oxygen–5% carbon dioxide) was bubbled through the preparation at room temperature for 90 min. The suspension was then stirred for an additional 4 hr. The mixture was then allowed to stand overnight (14 hr) with continual bubbling of oxygen.

The resultant precipitate of melanin was collected after centrifuging (19,000 rpm) at −2° and washed by resuspending in distilled water. The washings, followed by centrifugation, were performed until a clear supernatant solution was obtained. The washed precipitate thus obtained was freeze dried. The yield of melanin was approximately 1.41 g. The material exhibited a characteristic free radical signal in the electron spin resonance spectrometer[3] (like that seen in the natural melanins).

Methodology for Binding Studies—In all binding studies, the general procedure used was as follows. Aliquots of 1.0, 2.0, 4.0, 6.0, and 8.0 mg of synthetic melanin were placed in five 25-ml erlenmeyer flasks. Amounts of radiolabeled substances were added to each flask in the concentrations of 2 nCi/ml for ^{14}C-labeled materials and 6

[1] Merck Sharp & Dohme Research Laboratories, West Point, Pa.
[2] Sigma Chemical Co., St. Louis, Mo. (3690 units/mg).
[3] The spectra was supplied through the courtesy of Dr. L. Malspeis, College of Pharmacy, Ohio State University.

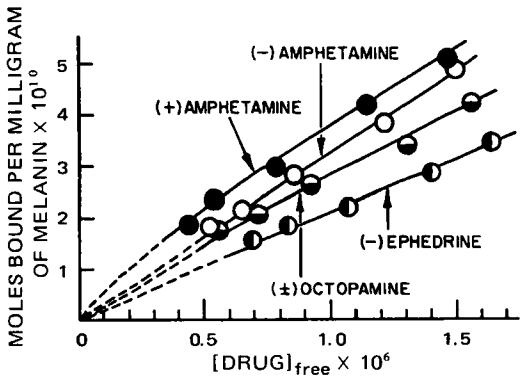

Figure 1—*Relationship between moles of drug bound per milligram of melanin for several different compounds and the molar concentration of free drug in equilibrium with amount bound.*

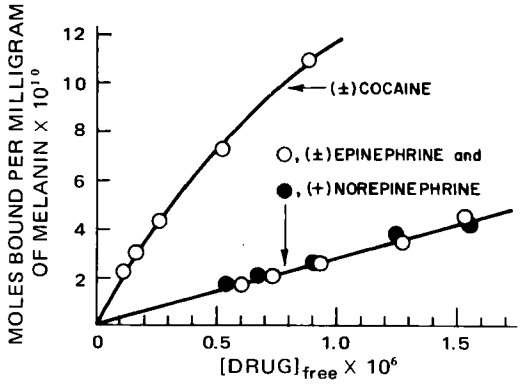

Figure 2—*Relationship between moles of cocaine, epinephrine, and norepinephrine bound per milligram of melanin and the molar concentration of free drug in equilibrium with amount bound.*

nCi/ml for ^{3}H-labeled compounds (2×10^{-6} *M*). The solutions were made with 0.1 *M* potassium phosphate buffer (pH 7.4); those containing epinephrine, norepinephrine, and octopamine contained sodium metabisulfite (0.1–1.9%) and edetic acid (0.001%) to minimize oxidation. In one study with (+)-amphetamine, 0.1 *M* sodium phosphate buffer (pH 7.4) was used.

The prepared suspensions were shaken in a water bath at 37° for 1 hr at 135 rpm. Then the mixture was centrifuged at 19,000 rpm for 30 min at −2°. One milliliter of the supernate was placed in a counting vial, and 1.0 ml of distilled water and 12.0 ml of liquid scintillation cocktail[4] were added. All samples were then counted[5] for 10 min. The counting efficiency was 86–87% for carbon-14 and 23–25% for tritium.

In studies with atropine, the same general procedure was followed. In one study, however, the concentration of atropine was three times that used for the other drugs. In another study using a constant amount of melanin (1 mg), cold atropine was added to the labeled compound in ratios of 10:1, 50:1, 100:1, 200:1, and 300:1 to determine the nature of binding at higher concentrations. All experiments were repeated five times.

The following drugs were used: (+)-[1-^{14}C-propyl]amphetamine sulfate[6], specific activity 1.99 mCi/mmole; (−)-^{14}C-amphetamine sulfate[7], specific activity 12.4 mCi/mmole; (±)-7-^{3}H(N)-epinephrine 1-bitartrate[8], specific activity 9.45 Ci/mmole; (−)-^{14}C-ephedrine hydrochloride[9], specific activity 2.8 mCi/mmole; (±)-2-^{3}H(N)-octopamine[8], specific activity 2.89 Ci/mmole; (±)-norepinephrine(methylene-^{14}C) *d*-bitartrate, specific activity 21.2 mCi/mmole; ^{3}H(G)-atropine[10], specific activity 407 mCi/mmole; and (±)-cocaine(methoxy-^{14}C)[8], specific activity 3.12 mCi/mmole. All radiolabeled substances were checked for purity. Only a single peak was observed by TLC in appropriate solvent systems.

All unlabeled drugs were used as obtained without further purification: (+)-amphetamine sulfate[11], (−)-amphetamine sulfate[12], (±)-epinephrine bitartrate[12], (−)-ephedrine hydrochloride[6], (±)-octopamine[13], (+)-norepinephrine bitartrate[14], atropine sulfate[1], and (−)-cocaine hydrochloride[1].

RESULTS

Binding of Drugs to Melanin—Centrifugation of the suspensions containing drug and melanin was a convenient means of separating free drug from drug bound to melanin. From the number of counts in the supernatant solution of the drug–melanin suspension, it was possible to determine the concentration of free drug. By knowing the amount of free drug and the total amount initially added, it was possible to determine by simple difference the amount of drug bound. The assumption is made that potential binding of drug to glass is not significant.

The number of moles of bound drug calculated as free base, for the five separate trials determined at each amount of melanin added, was averaged and the standard error of the mean was calculated. Treatment of the data obtained in this way showed that the standard error of the mean varied between only 1 and 5% of the amount of bound drug, indicating excellent reproducibility.

The average numbers of moles of the free base form of drug interacting per milligram of melanin in potassium phosphate buffer as a function of the free drug concentration in moles per liter are presented in Figs. 1–3. As the concentration of free drug increased, the amount of drug bound per milligram of melanin increased. For cocaine (Fig. 2) and atropine at high concentrations (Fig. 3), saturation of melanin possibly was approached.

When studies were made with (+)-amphetamine using a sodium phosphate buffer instead of a potassium phosphate buffer, slightly more drug was bound at approximately the same free drug concentration but the same almost linear relation as that presented in Fig. 1 was found. This observation emphasizes the need to make comparisons only in identical systems.

Treatment of Binding Data—The results obtained with cocaine (Fig. 2) and atropine (Fig. 3) suggested that the binding of the various drugs to melanin could be analyzed by assuming that the binding is analogous to the adsorption of a drug on a solid and follows a Type I Langmuir isotherm (10). Specifically, the amount of drug bound per milligram of melanin, r, should be related to the concentration of free drug, $[D]_{free}$, by:

$$r = \frac{r_{max} K [D]_{free}}{1 + K [D]_{free}} \qquad \text{(Eq. 1)}$$

where r_{max} is the maximum moles bound per milligram of melanin, that is, the amount needed to form a monolayer, and K is a constant related to the affinity or strength of the interaction. Rearrangement of Eq. 1 to:

$$\frac{1}{r} = \frac{1}{r_{max}} + \frac{1}{r_{max} K} \frac{1}{[D]_{free}} \qquad \text{(Eq. 2)}$$

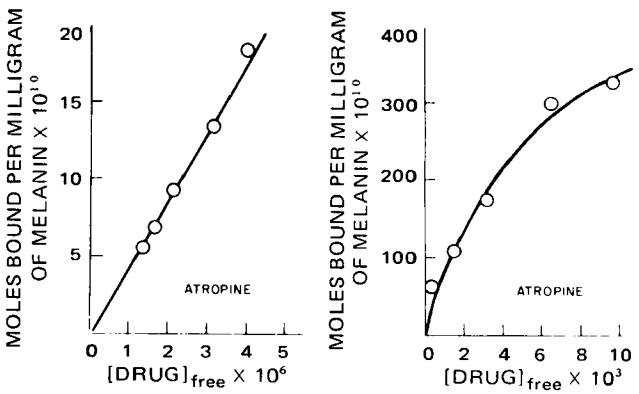

Figure 3—*Relationship between moles of atropine bound and the molar concentration of free atropine in equilibrium with the amount bound. Data show different concentration ranges.*

[4] Aquasol, New England Nuclear, Boston, Mass.
[5] Packard liquid scintillation spectrometer.
[6] Mallinckrodt (Nuclear), St. Louis, Mo.
[7] Schwarz/Mann, Orangeburg, N.Y.
[8] New England Nuclear, Boston, Mass.
[9] Supplied by Dr. Dennis Feller and Dr. L. Malspeis, College of Pharmacy, Ohio State University.
[10] Amersham/Searle, Arlington Heights, Ill.
[11] Smith Kline and French, Philadelphia, Pa.
[12] K & K Labs.
[13] Regis Chemicals, Chicago, Ill.
[14] Sterling-Winthrop Research Institute, Rensselaer, N.Y.

Table I—Linear Regression Parameters for the Langmuir Treatment of the Binding of Drugs to Melanin

Drug	Slope × 10^{-3} (Lower/Upper Limit)[a]	Intercept × 10^{-8} (Lower/Upper Limit)[a]	Maximum Moles Bound per Milligram of Melanin[b]	Affinity[c], M^{-1}
(−)-Amphetamine	2.7 (2.5/2.9)	3.1 (−0.4/6.6)	3.2×10^{-9}	1.1×10^{5}
(+)-Amphetamine	2.1 (1.7/2.4)	5.7 (1.0/10)	1.8×10^{-9}	2.8×10^{5}
(±)-Epinephrine	3.5 (3.1/3.9)	0.25 (−4.1/4.6)	39.7×10^{-9}	0.072×10^{5}
(−)-Ephedrine	4.0 (3.3/4.8)	5.6 (−0.6/11.7)	1.8×10^{-9}	1.4×10^{5}
(±)-Octopamine	2.8 (2.2/3.3)	7.2 (0.8/14)	1.4×10^{-9}	2.6×10^{5}
(+)-Norepinephrine	2.7 (2.4/3.1)	5.8 (1.4/10)	1.7×10^{-9}	2.1×10^{5}
Atropine	2.3 (2.1/2.4)	0.57 (0.07/1.1)	17.6×10^{-9}	0.25×10^{5}
(±)-Cocaine	0.48 (0.45/0.51)	4.2 (2.8/5.7)	2.4×10^{-9}	8.9×10^{5}

[a] 95% confidence intervals calculated at $p = 0.05$. [b] Calculated as the reciprocal of the y-intercept. [c] Calculated from intercept and slope.

shows that a linear relation should be obtained when $1/r$ is plotted as a function of $1/[D]_{free}$. The extrapolated y-axis intercept is $1/r_{max}$, and the slope is $1/r_{max}K$. Thus, such a treatment of the binding data would permit a calculation of r_{max} and K for each drug and provide a basis for comparisons of the binding of drugs to melanin.

When the data of Figs. 1–3 were plotted according to the treatment, linear relationships were obtained, thus providing some justification for the use of this method. If binding to glass complicated the treatment of data, such a linear relationship would not be expected. Typical results are presented in Figs. 4 and 5. Linear regression analyses of data were made for all drugs (Figs. 4 and 5), and the regression parameters thus generated are given in Table I together with the 95% confidence limits calculated at $p = 0.05$. Values for r_{max} and K, calculated from the slopes and intercepts, are also listed in this table.

DISCUSSION

The drug binding with melanin is of considerable interest in pharmacology and toxicology. Retinopathy, skin coloration, bleaching of hair, ototoxicity, and an extrapyramidal syndrome caused by some drugs can be correlated to drug accumulation by the pigment (2, 4, 11). The longer duration of atropine mydriasis in the pigmented rabbit is related to drug binding by melanin (12).

The data from the present study indicate that synthetic levodopa melanin does have a varying capacity and affinity for binding to the synthetic drugs. Among the substances examined, cocaine has the highest affinity for binding to synthetic levodopa melanin. Irrespective of the differences in the chemical structure of the sympathomimetic amines studied, the net binding was similar. The affinity of (±)-epinephrine appears to be low, but the capacity is high. The product of these two numbers, capacity and affinity, determines the net binding and is the same for all sympathomimetic amines. The binding of the amines to synthetic melanin does not parallel the binding by the pigmented iris.

The nonphenolic amines such as ephedrine and β-phenethylamine are accumulated more by the pigmented iris than are the phenolic amines such as tyramine, phenylephrine, epinephrine, and norepinephrine (6, 7). The high liposolubility of the nonphenolic amines may be responsible for their greater accumulation by the pigmented iris. In other words, these substances could easily be transported across the lipoid membrane of the melanin granules. Binding of drugs to natural melanin presumably occurs after the transport. If the drugs pass the lipoid membrane with difficulty, the low binding of nonphenolic amines to the pigmented tissue is understandable. Hence, a strict parallelism between the drug binding to synthetic melanin and that of the melanin granules or the pigmented tissue may not be observed.

The only drug binding property common to both synthetic melanin and the pigmented tissue is the lack of stereoselectivity. Pigmented guinea pig iris binds both (−)- and (+)-^{14}C-ephedrine to the same extent (7). In the present study, there was a lack of selectivity in the

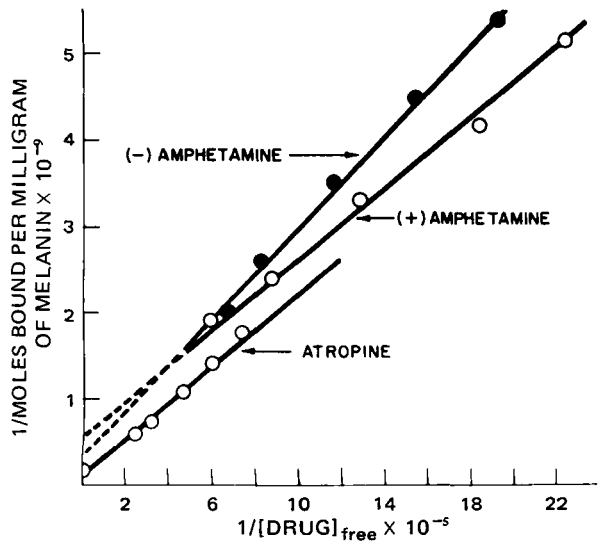

Figure 4—*Langmuir plots: reciprocal of amount of drug bound* versus *reciprocal of molar free drug concentration for amphetamines and atropine.*

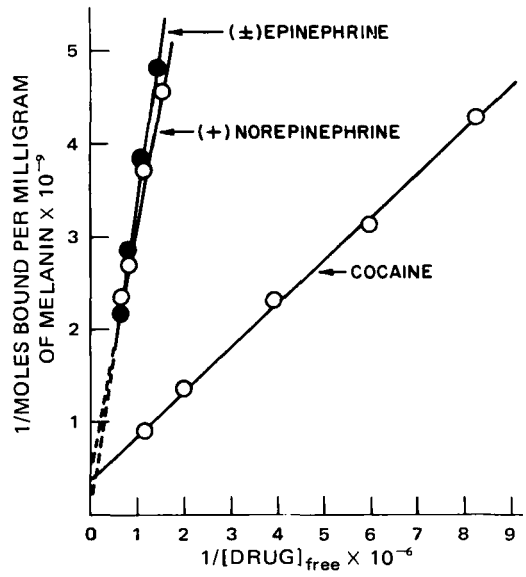

Figure 5—*Langmuir plots: reciprocal of amount of drug bound* versus *reciprocal of molar free drug concentration for epinephrine, norepinephrine, and cocaine.*

binding of (−)- or (+)-amphetamine by synthetic melanin. Data indicate that the α-methyl group is not involved in the binding of the amines, as evidenced by a comparison of the results found for amphetamine and ephedrine with those of norepinephrine and epinephrine (Table I).

Among several biopolymers examined, sepiomelanin showed outstanding affinity for binding certain drugs (13). The details of the molecular mechanism of binding of drugs to natural melanin have been the subject of much speculation (2, 14, 15). Under certain conditions, melanin can be considered as a free radical which can attract and bind some drugs with unshared electrons (2, 15, 16). As yet, there is no unanimity regarding the orientation of indole units of synthetic or natural melanin (17). Hence, the binding site or sites with which a drug interacts will be purely speculative.

A question emerges as to how drug binding to the synthetic melanin compares with the drug binding to the plasma proteins. In terms of affinity, the constants observed for the binding of drugs to melanin, 10^5–$10^6\ M^{-1}$, are comparable to the affinity constants for the binding of drugs to serum albumin. For example, thyroxine showing strong binding to albumins has a primary affinity constant of $1.6 \times 10^6\ M^{-1}$ for bovine serum albumin (18).

Since the molecular weight of melanin is unknown, comparisons of capacity between melanin and albumins should be based on the net binding of drug per unit mass of material. Drugs showing a capacity of about 2×10^{-9} mole/mg of melanin, as found for some drugs in this study, would be equivalent to approximately 0.1 mole bound/mg of serum albumin where a molecular weight of 70,000 is assumed for the albumin. This calculated equivalent value for serum albumin capacity is lower than that usually found for drugs, but surface area plays a significant role in determining capacity in the case of melanin. The surface area per unit mass of the synthetic melanin used in these studies may be considerably less than that found within naturally occurring melanosome, so the actual capacity found *in vivo* may be considerably greater.

The accumulation of atropine appears to be a saturable process, and presumably similar saturation occurs with other drugs. As stated earlier, the toxicity of several drugs could be correlated to their local accumulation by the pigment. However, drug binding to melanin may not necessarily mean toxicity; since drugs vary in their affinity for the binding, theoretically it should be possible to displace a toxic drug by a nontoxic drug. Such a study should be valuable in reducing the toxic effects of drugs related to the binding.

REFERENCES

(1) A. Potts, *Invest. Ophthalmol.*, **1**, 522(1962).

(2) *Ibid.*, **3**, 405(1964).

(3) H. N. Bernstein, *Survey Ophthalmol.*, **12**, 415(1967).

(4) P. N. Patil, *Invest. Ophthalmol.*, **11**, 739(1972a).

(5) N. G. Lindquist, *Acta Radiol., Suppl.*, **1973** 325.

(6) P. N. Patil and D. Jacobowitz, *Am. J. Ophthalmol.*, **78**, 470(1974).

(7) P. N. Patil, K. Shimada, D. R. Feller, and L. Malspeis, *J. Pharmacol. Exp. Ther.*, **188**, 342(1974).

(8) J. Duchôn, J. Borovansky, and P. Hach, *Pigm. Cell*, **1**, 165(1973).

(9) F. Binn, R. F. Chapman, N. C. Robson, G. A. Swan, and A. Waggott, *J. Chem. Soc., Sect. C, Org. Chem.*, **8**, 1128(1970).

(10) A. N. Martin, J. Swarbrick, and A. Camarata, "Physical Pharmacy," Lea & Febiger, Philadelphia, Pa., 1969, p. 434.

(11) N. G. Lindquist and S. Ullberg, *Acta Pharmacol. Toxicol., Suppl. II*, **31** (1972).

(12) M. M. Salazar, K. Shimada, and P. N. Patil, *J. Pharmacol. Exp. Ther.*, **197**, 79(1976).

(13) M. S. Blois and L. Taskovich, *Invest. Dermatol.*, **53**, 344(1969).

(14) G. Karreman, I. Isenberg, and A. Szent-Gyorgyi, *Science*, **130**, 1191(1959).

(15) M. S. Blois, Jr., in "Biology of Normal and Abnormal Melanocytes," T. Kawamura, T. B. Fitzpatrick, and M. Seiji, Eds., University Park Press, Baltimore, Md., 1971, p. 125.

(16) H. S. Mason, D. J. E. Ingram, and B. Allen, *Arch. Biochem. Biophys.*, **86**, 225(1960).

(17) G. A. Swan, *Pigm. Cell*, **1**, 151(1973).

(18) R. F. Steiner, J. Roth, and J. Robins, *J. Biol. Chem.*, **241**, 560(1966).

ACKNOWLEDGMENTS AND ADDRESSES

Received June 23, 1975, from the *Divisions of Pharmacology and Pharmaceutics, College of Pharmacy, Ohio State University, Columbus, OH 43210*

Accepted for publication October 1, 1975.

Supported in part by the U.S. Public Health Service, National Institutes of Health (Research Grant EY-01308).

[x] To whom inquiries should be directed.

Hermetic Packaging of Drugs: Optimized Sealing of Foil Pouches

D. E. AUSLANDER *x and S. G. GILBERT ‡

Abstract □ Factors affecting the sealing of foil packages were studied in three laboratories. The relationship of sealing temperature (with machine speed and pressure kept constant) to the incidence of defective packages was determined. The maximum acceptable limit for defective pouches was 1%. Three tests were employed to detect defects: vacuum–dye, seal strength, and pressurized ammonia vapor. Only the last was sensitive enough to determine the optimum sealing conditions. This test also was capable of detecting leakage sites. Replacement of the cellophane layer of the foil laminate with polyvinylidene chloride-coated polyester improved the barrier properties of the package.

Keyphrases □ Foil packages—heat seals, relationship of sealing temperature to incidence of defective packages, vacuum–dye, seal strength, and pressurized ammonia vapor tests for defects □ Seals, heat—foil packages, relationship of sealing temperature to incidence of defective packages, vacuum–dye, seal strength, and pressurized ammonia vapor tests for defects

The flexible pouch or foil package is assuming a major role in drug distribution, particularly in overseas markets, because of its ease of formation and strength. However, the lack of adequate methodology for evaluating package performance has become apparent. The technology used in testing packages generally is similar to that used for ampuls (1–3).

A typical foil package is a four-ply laminate. The outermost portion is generally cellophane, paper, or polyester. This portion is bonded to aluminum foil, usually with polyethylene or a similar adhesive material. The innermost film is a heat-sealable polymer, either colaminated or coextruded with the foil. The most commonly used heat-sealing polymer is polyethylene.

An important factor affecting the stability of drugs in foil packages is the effectiveness of the heat seal formed during commercial production. The need for an almost absolute barrier was shown previously with yeast products packaged in foil (4).

A fusion heat seal is formed by melting the thermoplastic polymer used as the inside sealing layer. Most polymers form seals at 90–200°. An optimum heat seal results from the correct interaction of three variables: (*a*) temperature of the sealer platens, (*b*) pressure applied to the seal area by the heated platens, and (*c*) dwell time (period for which the heated sealable surfaces are held under pressure to form an effective bond) (5).

The procedure most commonly used for assessing foil packages is the vacuum–dye test. Packages are submerged under vacuum in a dye solution, and discovery of the dye within the package is considered clear evidence of incomplete sealing. The advantages and disadvantages of this test were discussed previously (1–4). In particular, failure to standardize the test may lead to erroneous conclusions because of capillary resistance (2, 3).

Deficiencies in this test, particularly with respect to gas permeation, have been observed in this laboratory.

This article discusses the inadequacies of tests now employed for measuring package integrity, reports an improved test procedure, and demonstrates how the optimization of the sealing conditions for two foil laminates can be obtained.

EXPERIMENTAL

Materials—The following materials were used: nitrocellulose-coated cellophane–polyethylene–0.018-mm aluminum foil–0.043-mm polyethylene[1], polyvinylidene chloride-coated polyester[2]–polyethylene–0.018-mm aluminum foil–0.043-mm polyethylene[3], and nitrocellulose-coated cellophane–polyethylene–0.018-mm aluminum foil–0.030-mm polyethylene[4].

Vacuum–Dye Test—Foil packages were submerged in an aqueous solution of amaranth for 1 min at 38 cm (15 in.) of vacuum. After this treatment, packages were blotted dry. The package was considered a leaker if the contents or the inner lining revealed a red spot.

Seal Strength Test—The seal strength of end (shorter dimension) and side (longer dimension) foil packages was measured with a tensile tester[5]. Samples 1 cm wide were taken from the center end and center side positions.

Pressurized Ammonia Vapor Test—Approximately 200 packages were placed in a suitable pressure container evacuated for 5 min at 38 cm (15 in.) of vacuum. The vacuum was broken by the slow addition of 2 kg/cm^2 (2 atm) of ammonia vapor, and this pressure was maintained for 1 hr. Subsequently, the packages were rinsed with a 10% citric acid solution to remove residual surface ammonia and were then dried over an air current. A 1% phenolphthalein gel [water–ethanol (1:1) with 1% carboxypolymethylene[6]] was applied with slight pressure to the entire surface. The appearance of a pink color indicated that the foil package leaked.

Optimization Studies—Trials were conducted at three outside locations using sealing temperatures over approximately a 60° range (Table I).

About 50,000 placebo capsules (No. 0) were used per foil laminate per machine. Each run was performed at the operating pressure and dwell time (machine speed) normally used for that machine and foil laminate. All machines were of the rotary sealing type. The dwell time and pressure were kept constant, and the sealing temperature was varied to provide for a broad range of conditions. During the optimization trials, 100 and 25–50 packages were used for the pressurized ammonia and vacuum–dye tests, respectively, at 15-min intervals.

RESULTS AND DISCUSSION

Pressurized Ammonia Vapor Test—The number of defective

[1] Dow, Inc., Cleveland, Ohio
[2] Mylar, E. I. du Pont de Nemours and Co., Wilmington, Del.
[3] Standard Packaging, Clifton, N.J.
[4] *Champion Packaging*, Englewood Cliffs, N.J.
[5] Instron Universal testing instrument, Instron Corp., Canton, Mass.
[6] Carbopol 961, B. F. Goodrich, Cleveland, Ohio.

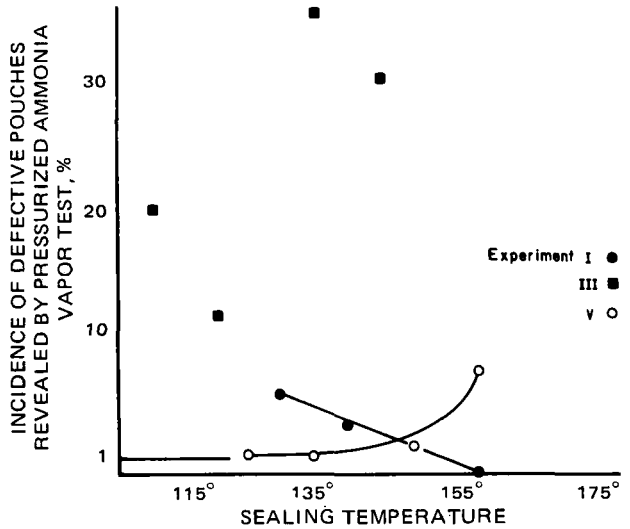

Figure 1—*Effect of sealing temperature on the incidence of defective pouches revealed by the pressurized ammonia vapor test.*

packages was plotted against the sealing temperature (Figs. 1 and 2). Arbitrarily, the maximum acceptable limit was set at 1%. In Experiment I, at 155–165°, this optimum point was achieved. Above 180°, under these experimental conditions, the exterior portion of the laminate started to "steam."

In Experiment III, the incidence of defective pouches was considerably over 1%. A clearly defined defect in the crimp area, as determined from the nature of the color reaction, was ascribed to excessive localized pressure arising from the design of the machine. With the pressurized ammonia vapor test, the use of an indicator dye revealed the site of permeation and subsequently provided insight into the reasons for the defect.

In Experiment V, the 1% limit was approached asymptotically. Hypothetically, the decreased thickness in the polyethylene heat sealing layer (Table I) was responsible for the inability of this foil laminate to achieve the 1% limit under these conditions.

The critical feature of Experiments II, IV, and VI was the replacement of cellophane with polyvinylidene chloride-coated polyester. The data (Fig. 2) show that this change afforded a significant improvement in the pouches.

Cellophane is a hydrophilic polymer that can become brittle when dried during sealing; in contrast, polyester is a thermoplastic and hydrophobic polymer which elongates under deforming stresses (6). In addition, the polyvinylidene chloride coating provides an excellent barrier to gases (6).

The effect of the polyvinylidene chloride-coated polyester was most evident in Experiment IV, where the incidence of defective pouches was reduced to zero. Apparently, the thermoplastic properties of polyester aid in reducing any damage to the laminate caused by the sealing dies.

That the pressurized ammonia vapor test is more sensitive than the vacuum–dye test is illustrated in Table II.

Seal Strength (Experiment I)—Samples taken from the shorter

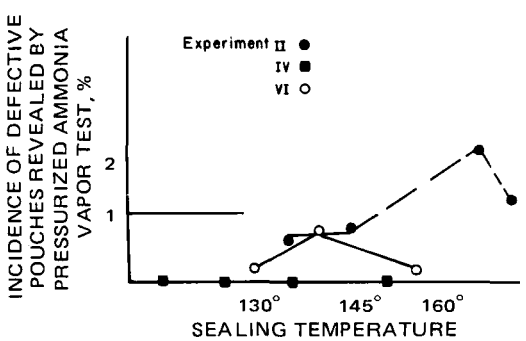

Figure 2—*Effect of sealing temperature on the incidence of defective pouches revealed by the pressurized ammonia vapor test.*

Table I—Conditions Used in the Optimization Studies

Experiment	Location	Foil Laminate	Machine Speed, rpm
I	A	Nitrocellulose-coated cellophane–polyethylene–0.018-mm aluminum foil–0.043-mm polyethylene	14
II	A	Polyvinylidene chloride-coated polyester–polyethylene–0.018-mm aluminum foil–0.043-mm polyethylene	14
III	B	Same as in Experiment I	45
IV	B	Same as in Experiment II	45
V	C	Nitrocellulose-coated cellophane–polyethylene–0.018-mm aluminum foil–0.030-mm polyethylene	14
VI	C	Same as in Experiment II	14

Table II—Comparison of the Pressurized Ammonia Vapor Test with the Vacuum–Dye Test

Experiment	Temperature	Incidence (%) of Leaking Pouches Revealed by: Pressurized Ammonia Vapor Test	Vacuum–Dye Test
I	135°	6.0	1.3
	145°	3.8	0.8
	165°	0.2	0.0
II	135°	0.6	0.3
	145°	0.8	0.0
	165°	2.0[a]	0.0
	175°	1.2[a]	0.0
III	115°	20.0	0.0
	125°	12.0	0.0
	140°	35.0	8.3
	150°	30.0	2.1
IV	115°	0.0	0.0
	125°	0.0	0.0
	140°	0.0	0.0
	150°	0.0	0.0
V	130°	1.5	0.5
	140°	1.5	1.0
	155°	2.0	0.0
	165°	8.5	1.6
VI	130°	0.2	0.0
	140°	0.8	0.0
	155°	0.2	0.0

[a] These defects were attributable to a specific machine error.

dimension showed that parting took place predominantly at the foil–cellophane laminate, with the polyethylene–polyethylene heat seal remaining intact. This finding suggests that the heat seal was stronger than the lamination and that the strength of the foil–cello-

Table III—Average Force Required to Separate Pouch at the Seal

Sealing Temperature	Force, kg
	End
135°	1.77 ± 0.10
145°	1.73 ± 0.18
165°	1.95 ± 0.24
175°	1.77 ± 0.20
	Side
135°	2.22 ± 0.20
145°	2.32 ± 0.15
165°	2.41 ± 0.10
175°	2.36 ± 0.22

phane bond was not affected by temperature.

Analysis of the data displayed in Table III by the Student–Newman–Keul's test (7) showed that none of the observed differences in separation force for both end and side samples was statistically significant.

Seal strength measurements of samples from the longer dimensions showed that parting took place at the polyethylene–polyethylene heat seal for all temperatures studied except 175°. At 175°, parting was at the foil–cellophane lamination. These data suggest that, except for the 175° treatment, the seal was less strong than the lamination. At 175°, the seal strength must surpass the lamination strength, causing parting at the latter site. This finding indicates that the seal strength increased as temperature increased. Miller (8) found a similar correlation.

The seal strength test was not pursued after Experiment I since a definitive discrimination among sealing temperatures was not shown.

REFERENCES

(1) I. G. Brizell and J. T. Shatwell, *Pharm. J.*, **211**, 73(1973).

(2) W. J. Artz, W. T. Gloor, Jr., and D. R. Reese, *J. Pharm. Sci.*, **50**, 258(1961).

(3) D. E. McVean, P. A. Tuerck, G. L. Christenson, and J. T. Carstensen, *ibid.*, **61**, 1609(1972).

(4) R. Dale, *Mod. Packag.*, **29**, 170(1956).

(5) B. Metz, *Package Dev.*, **3**, 16(1973).

(6) J. Heller, *ibid.*, **2**, 2(1972).

(7) R. Steele and J. Torrie, "Principles and Practices of Statistics," McGraw Hill, New York, N.Y., 1960, p. 110.

(8) D. Miller, in "Technical Advances in Packaging with Flexible Barrier Materials," American Society for Testing and Materials, Philadelphia, Pa., 1973, p. 3.

ACKNOWLEDGMENTS AND ADDRESSES

Received July 7, 1975, from the *Department of Pharmaceutical Research and Development, Squibb Institute for Medical Research, New Brunswick, NJ 08903, and the ‡Department of Food Sciences, Rutgers—the State University, New Brunswick, NJ 08903

Accepted for publication September 11, 1975.

Presented at the Industrial Pharmaceutical Technology Section, APhA Academy of Pharmaceutical Sciences, New Orleans meeting, November 1974.

The authors thank Dr. R. M. Cohn and Mr. M. L. Schwartz for their helpful advice and discussions and Dr. David Frost for his editorial assistance.

ˣ To whom inquiries should be directed.

Comparison of Observed and Predicted First-Pass Metabolism of Imipramine in Humans

SARFARAZ NIAZI

Abstract □ The first-pass metabolism of imipramine was calculated based on the dose, hepatic blood flow, and total area under the plasma–time curve after oral administration of 0.71 ± 0.03 mg/kg of imipramine to four individuals suffering from mild depression. The predicted values of first-pass metabolism ranged from 37 to 68%, consistent with experimentally derived estimates.

Keyphrases □ Imipramine—comparison of observed and predicted first-pass metabolism □ Metabolism, first pass—imipramine, comparison of observed and predicted values □ Antidepressants—imipramine, comparison of observed and predicted first-pass metabolism

The bioavailability of imipramine following oral administration in humans was recently reported (1). A comparison of the total metabolites excreted following intravenous and oral administration shows that the absorption of impramine from the solution dosage form was complete. The low bioavailability of imipramine following oral administration was attributed to the first-pass metabolism, mainly to desipramine, as evidenced by the higher levels of this metabolite following administration of an oral dose compared to an equal intravenous dose.

DISCUSSION

The following equation was proposed by Gibaldi and coworkers (2, 3) to predict the degree to which a drug is subject to first-pass metabolism:

$$f = \frac{\text{flow rate}}{\text{flow rate} + \left(\text{dose} \Big/ \int_0^\infty C_0\, dt\right)} \qquad \text{(Eq. 1)}$$

where f is the fraction of orally administered dose that actually reaches the systemic circulation, the flow rate is the hepatic blood flow rate, and $\int_0^\infty C_0\, dt$ is the total area under the plasma concentration–time curve after oral administration. This equation is applicable, however, only if the absorption is complete, as was evidenced for imipramine (1). A correction factor is needed(2) if the dose administered orally is not completely absorbed.

Therefore, the percentage of drug metabolized during the first pass can be expressed as:

$$\%\ \text{first pass} = \frac{\left(\text{dose} \Big/ \int_0^\infty C_0\, dt\right) \times 100}{\text{flow rate} + \left(\text{dose} \Big/ \int_0^\infty C_0\, dt\right)} \qquad \text{(Eq. 2)}$$

EXPERIMENTAL

The area under the plasma concentration–time curve following oral administration was calculated from reported (1) values of apparent hepatic blood flow and apparent clearance (Table I). A mean blood flow of 1.53 liters/min (3) was used for calculations using Eq. 2.

RESULTS

As reported in Table I, the predicted first-pass metabolism, 58.25 ± 14.38, correlated very well with the experimentally determined value, 52.75 ± 21.36, obtained by comparison with the intravenous data. Therefore, the reliability of Eq. 1 for the prediction of first-pass metabolism following oral administration was confirmed.

The variability of blood flow rates does not seem to affect the first-pass metabolism estimates significantly. For example, the reported apparent hepatic blood flow rates were 1.3–3.5 liters/min (1), whereas a constant value of 1.53 liters/min was used for the calculation of first-pass metabolism in all individuals; both values resulted in fairly good agreement.

phane bond was not affected by temperature.

Analysis of the data displayed in Table III by the Student–Newman–Keul's test (7) showed that none of the observed differences in separation force for both end and side samples was statistically significant.

Seal strength measurements of samples from the longer dimensions showed that parting took place at the polyethylene–polyethylene heat seal for all temperatures studied except 175°. At 175°, parting was at the foil–cellophane lamination. These data suggest that, except for the 175° treatment, the seal was less strong than the lamination. At 175°, the seal strength must surpass the lamination strength, causing parting at the latter site. This finding indicates that the seal strength increased as temperature increased. Miller (8) found a similar correlation.

The seal strength test was not pursued after Experiment I since a definitive discrimination among sealing temperatures was not shown.

REFERENCES

(1) I. G. Brizell and J. T. Shatwell, *Pharm. J.*, **211**, 73(1973).

(2) W. J. Artz, W. T. Gloor, Jr., and D. R. Reese, *J. Pharm. Sci.*, **50**, 258(1961).

(3) D. E. McVean, P. A. Tuerck, G. L. Christenson, and J. T. Carstensen, *ibid.*, **61**, 1609(1972).

(4) R. Dale, *Mod. Packag.*, **29**, 170(1956).

(5) B. Metz, *Package Dev.*, **3**, 16(1973).

(6) J. Heller, *ibid.*, **2**, 2(1972).

(7) R. Steele and J. Torrie, "Principles and Practices of Statistics," McGraw Hill, New York, N.Y., 1960, p. 110.

(8) D. Miller, in "Technical Advances in Packaging with Flexible Barrier Materials," American Society for Testing and Materials, Philadelphia, Pa., 1973, p. 3.

ACKNOWLEDGMENTS AND ADDRESSES

Received July 7, 1975, from the *Department of Pharmaceutical Research and Development, Squibb Institute for Medical Research, New Brunswick, NJ 08903, and the ‡Department of Food Sciences, Rutgers—the State University, New Brunswick, NJ 08903

Accepted for publication September 11, 1975.

Presented at the Industrial Pharmaceutical Technology Section, APhA Academy of Pharmaceutical Sciences, New Orleans meeting, November 1974.

The authors thank Dr. R. M. Cohn and Mr. M. L. Schwartz for their helpful advice and discussions and Dr. David Frost for his editorial assistance.

ˣ To whom inquiries should be directed.

Comparison of Observed and Predicted First-Pass Metabolism of Imipramine in Humans

SARFARAZ NIAZI

Abstract □ The first-pass metabolism of imipramine was calculated based on the dose, hepatic blood flow, and total area under the plasma–time curve after oral administration of 0.71 ± 0.03 mg/kg of imipramine to four individuals suffering from mild depression. The predicted values of first-pass metabolism ranged from 37 to 68%, consistent with experimentally derived estimates.

Keyphrases □ Imipramine—comparison of observed and predicted first-pass metabolism □ Metabolism, first pass—imipramine, comparison of observed and predicted values □ Antidepressants—imipramine, comparison of observed and predicted first-pass metabolism

The bioavailability of imipramine following oral administration in humans was recently reported (1). A comparison of the total metabolites excreted following intravenous and oral administration shows that the absorption of impramine from the solution dosage form was complete. The low bioavailability of imipramine following oral administration was attributed to the first-pass metabolism, mainly to desipramine, as evidenced by the higher levels of this metabolite following administration of an oral dose compared to an equal intravenous dose.

DISCUSSION

The following equation was proposed by Gibaldi and coworkers (2, 3) to predict the degree to which a drug is subject to first-pass metabolism:

$$f = \frac{\text{flow rate}}{\text{flow rate} + \left(\text{dose} \Big/ \int_0^\infty C_0\, dt\right)} \qquad \text{(Eq. 1)}$$

where f is the fraction of orally administered dose that actually reaches the systemic circulation, the flow rate is the hepatic blood flow rate, and $\int_0^\infty C_0\, dt$ is the total area under the plasma concentration–time curve after oral administration. This equation is applicable, however, only if the absorption is complete, as was evidenced for imipramine (1). A correction factor is needed(2) if the dose administered orally is not completely absorbed.

Therefore, the percentage of drug metabolized during the first pass can be expressed as:

$$\%\ \text{first pass} = \frac{\left(\text{dose} \Big/ \int_0^\infty C_0\, dt\right) \times 100}{\text{flow rate} + \left(\text{dose} \Big/ \int_0^\infty C_0\, dt\right)} \qquad \text{(Eq. 2)}$$

EXPERIMENTAL

The area under the plasma concentration–time curve following oral administration was calculated from reported (1) values of apparent hepatic blood flow and apparent clearance (Table I). A mean blood flow of 1.53 liters/min (3) was used for calculations using Eq. 2.

RESULTS

As reported in Table I, the predicted first-pass metabolism, 58.25 ± 14.38, correlated very well with the experimentally determined value, 52.75 ± 21.36, obtained by comparison with the intravenous data. Therefore, the reliability of Eq. 1 for the prediction of first-pass metabolism following oral administration was confirmed.

The variability of blood flow rates does not seem to affect the first-pass metabolism estimates significantly. For example, the reported apparent hepatic blood flow rates were 1.3–3.5 liters/min (1), whereas a constant value of 1.53 liters/min was used for the calculation of first-pass metabolism in all individuals; both values resulted in fairly good agreement.

Table I—Predicted and Observed First-Pass Metabolism of Imipramine in Four Subjects

Subject	Sex	Age	Dose, mg	Body Weight, kg	$\int_0^\infty C_0\,dt$, mg min/liter	First Pass Predicted, %	First Pass Observed[a], %
A.B.	f	28	35	52	11.97	66	71
G.A.	f	28	40	55	44.24	37	23
U.F.	m	25	50	68	15.13	68	52
P.L.B.	m	59	50	71	19.84	62	65
Mean ± *SD*						58.25 ± 14.38	52.75 ± 21.36

[a] Reference 1.

Another significant aspect of the correlations presented here is that the area under the plasma concentration–time curve described the first-pass metabolism adequately, signifying that red blood cell transport is not significant in the first-pass metabolism of imipramine. This result may be due either to almost equal partitioning between blood cells and plasma or to quick equilibrations between red blood cells and plasma.

REFERENCES

(1) L. F. Gram and J. Christiansen, *Clin. Pharmacol. Ther.*, **17**, 555(1975).

(2) M. Gibaldi, *J. Pharm. Sci.*, **64**, 1036(1975).

(3) M. Gibaldi, R. N. Boyes, and S. Feldman, *ibid.*, **60**, 1338(1971).

ACKNOWLEDGMENTS AND ADDRESSES

Received June 25, 1975, from the *Department of Pharmacy, College of Pharmacy, University of Illinois at the Medical Center, Chicago, IL 60612*

Accepted for publication September 4, 1975.

High-Pressure Liquid Chromatographic Determination of Acetaminophen in Biological Fluids

LAWRENCE T. WONG ˣ, GNANAPRAKASAM SOLOMONRAJ, and BARRY H. THOMAS

Abstract □ A method for the rapid estimation of free acetaminophen in biological fluids is described. The assay involves ether extraction and high-pressure liquid chromatographic analysis on a 10-μm particle-size silica gel column, using a mobile phase of 10% chloroform in tetrahydrofuran. The procedure was used to determine acetaminophen levels in urine from two healthy volunteers who ingested 650 mg of ^{14}C-acetaminophen (20 μCi), and the accuracy of the method was compared with the carbon-14 determination. The limit of detectability for acetaminophen is 1 μg/ml.

Keyphrases □ Acetaminophen—high-pressure liquid chromatographic analysis, biological fluids, compared to radioisotope method □ High-pressure liquid chromatography—analysis, acetaminophen, biological fluids, compared to radioisotope method □ Analgesics—acetaminophen, high-pressure liquid chromatographic analysis, biological fluids

For the determination of free acetaminophen [*N*-(4-hydroxyphenyl)acetamide] in biological fluids, a GLC procedure (1) has been used frequently (2–4). The method requires a silylation step to convert acetaminophen into a volatile disilyl derivative before it is suitable for GLC determination. Although GLC analysis of phenolic drugs (*e.g.*, acetaminophen) is possible by this technique, the silylation step often lengthens the analysis time and also introduces another variable. Liquid chromatography appears to be more suitable for the quantitation of these drugs. It usually requires no derivatization of samples, and nonvolatile compounds can be analyzed just as easily as volatile compounds. The main requirement is that the sample be soluble in the mobile solvent.

This paper describes a simple high-pressure liquid chromatography (HPLC) method for the rapid estimation of acetaminophen in biological fluids using a UV absorption detector. A high-performance liquid chromatographic method for the quantitation of acetaminophen was reported recently (5). The technique, which employs a less common but highly sensitive electrochemical detector, does not involve high pressure in its operation. Determination of acetaminophen in the picogram level using this technique has been reported. However, its sensitivity is limited when applied to the analysis of the drug in biological samples due to the interference of endogenous, electrochemically reactive materials.

EXPERIMENTAL

Reagents and Materials—Acetaminophen was obtained commercially[1]. ^{14}C-Acetaminophen (uniformly labeled), with a specific activity of 17.24 μCi/mg, was custom synthesized[2]. Chloroform[3], methanol[3], and acetic acid[2] were all reagent grade and were used as received. Tetrahydrofuran[4] was freshly distilled prior to use.

Instrumentation—A liquid chromatograph[5] equipped with a positive displacement pump capable of developing a pressure of 5000 psi, a stop-flow injection port, a variable wavelength UV absorbance detector operated at 247 nm, and an integrator[6] was employed. The

[1] McNeil Laboratories (Canada) Ltd., Don Mills, Ontario, Canada.
[2] Mallinckrodt, St. Louis, MO 63160
[3] Caledon Labs., Georgetown, Ontario, Canada.
[4] BDH (Canada) Ltd., Toronto, Canada.
[5] Varian model 4100, Varian Aerograph, Walnut Creek, Calif.
[6] Model 3370A, Hewlett-Packard, Avondale, PA 19311

Table I—Predicted and Observed First-Pass Metabolism of Imipramine in Four Subjects

Subject	Sex	Age	Dose, mg	Body Weight, kg	$\int_0^\infty C_0\,dt$, mg min/liter	First Pass Predicted, %	First Pass Observed[a], %
A.B.	f	28	35	52	11.97	66	71
G.A.	f	28	40	55	44.24	37	23
U.F.	m	25	50	68	15.13	68	52
P.L.B.	m	59	50	71	19.84	62	65
Mean ± *SD*						58.25 ± 14.38	52.75 ± 21.36

[a] Reference 1.

Another significant aspect of the correlations presented here is that the area under the plasma concentration–time curve described the first-pass metabolism adequately, signifying that red blood cell transport is not significant in the first-pass metabolism of imipramine. This result may be due either to almost equal partitioning between blood cells and plasma or to quick equilibrations between red blood cells and plasma.

REFERENCES

(1) L. F. Gram and J. Christiansen, *Clin. Pharmacol. Ther.*, **17**, 555(1975).

(2) M. Gibaldi, *J. Pharm. Sci.*, **64**, 1036(1975).

(3) M. Gibaldi, R. N. Boyes, and S. Feldman, *ibid.*, **60**, 1338(1971).

ACKNOWLEDGMENTS AND ADDRESSES

Received June 25, 1975, from the *Department of Pharmacy, College of Pharmacy, University of Illinois at the Medical Center, Chicago, IL 60612*

Accepted for publication September 4, 1975.

High-Pressure Liquid Chromatographic Determination of Acetaminophen in Biological Fluids

LAWRENCE T. WONG ˣ, GNANAPRAKASAM SOLOMONRAJ, and BARRY H. THOMAS

Abstract □ A method for the rapid estimation of free acetaminophen in biological fluids is described. The assay involves ether extraction and high-pressure liquid chromatographic analysis on a 10-μm particle-size silica gel column, using a mobile phase of 10% chloroform in tetrahydrofuran. The procedure was used to determine acetaminophen levels in urine from two healthy volunteers who ingested 650 mg of ^{14}C-acetaminophen (20 μCi), and the accuracy of the method was compared with the carbon-14 determination. The limit of detectability for acetaminophen is 1 μg/ml.

Keyphrases □ Acetaminophen—high-pressure liquid chromatographic analysis, biological fluids, compared to radioisotope method □ High-pressure liquid chromatography—analysis, acetaminophen, biological fluids, compared to radioisotope method □ Analgesics—acetaminophen, high-pressure liquid chromatographic analysis, biological fluids

For the determination of free acetaminophen [*N*-(4-hydroxyphenyl)acetamide] in biological fluids, a GLC procedure (1) has been used frequently (2–4). The method requires a silylation step to convert acetaminophen into a volatile disilyl derivative before it is suitable for GLC determination. Although GLC analysis of phenolic drugs (*e.g.*, acetaminophen) is possible by this technique, the silylation step often lengthens the analysis time and also introduces another variable. Liquid chromatography appears to be more suitable for the quantitation of these drugs. It usually requires no derivatization of samples, and nonvolatile compounds can be analyzed just as easily as volatile compounds. The main requirement is that the sample be soluble in the mobile solvent.

This paper describes a simple high-pressure liquid chromatography (HPLC) method for the rapid estimation of acetaminophen in biological fluids using a UV absorption detector. A high-performance liquid chromatographic method for the quantitation of acetaminophen was reported recently (5). The technique, which employs a less common but highly sensitive electrochemical detector, does not involve high pressure in its operation. Determination of acetaminophen in the picogram level using this technique has been reported. However, its sensitivity is limited when applied to the analysis of the drug in biological samples due to the interference of endogenous, electrochemically reactive materials.

EXPERIMENTAL

Reagents and Materials—Acetaminophen was obtained commercially[1]. ^{14}C-Acetaminophen (uniformly labeled), with a specific activity of 17.24 μCi/mg, was custom synthesized[2]. Chloroform[3], methanol[3], and acetic acid[2] were all reagent grade and were used as received. Tetrahydrofuran[4] was freshly distilled prior to use.

Instrumentation—A liquid chromatograph[5] equipped with a positive displacement pump capable of developing a pressure of 5000 psi, a stop-flow injection port, a variable wavelength UV absorbance detector operated at 247 nm, and an integrator[6] was employed. The

[1] McNeil Laboratories (Canada) Ltd., Don Mills, Ontario, Canada.
[2] Mallinckrodt, St. Louis, MO 63160
[3] Caledon Labs., Georgetown, Ontario, Canada.
[4] BDH (Canada) Ltd., Toronto, Canada.
[5] Varian model 4100, Varian Aerograph, Walnut Creek, Calif.
[6] Model 3370A, Hewlett-Packard, Avondale, PA 19311

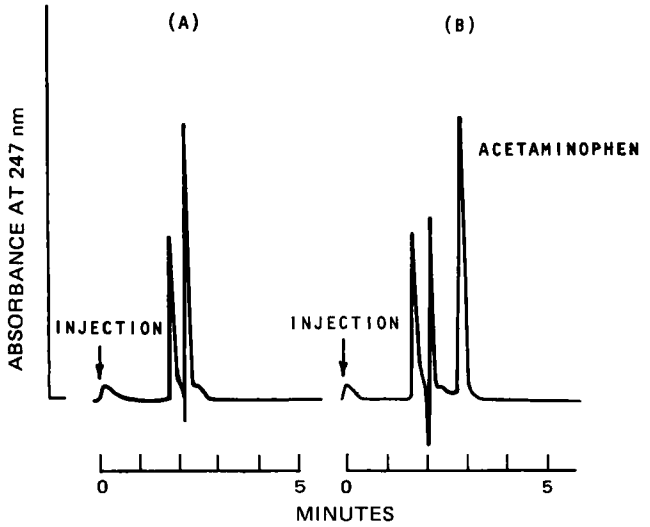

Figure 1—*High-pressure liquid chromatogram of human plasma extract from: (A) blank plasma and (B) plasma spiked with acetaminophen (7 μg/ml).*

column[7] (50 cm × 2.2 mm) was packed with silica gel with an average diameter of 10 μm.

Analyses were performed using a mobile phase of tetrahydrofuran–chloroform–5% acetic acid in methanol (90:10:0.04 v/v) at a flow rate of 40 ml/hr (1000 psi) and ambient temperature. The UV absorbance detector was set at 0.1–0.5 absorbance unit full scale (aufs), depending on the sample, to keep the acetaminophen signal on scale for proper integration of the peak. The mobile phase was degassed by applying vacuum to the solvent reservoir for 1 min before use.

Extraction and Analysis Procedure—Urine or plasma (1 ml) and 1 *M* phosphate buffer, pH 7.4 (1 ml), were saturated with sodium chloride and extracted two times with ether (2 ml each). The ether layer was removed and dried with a current of dry nitrogen. The inner wall of the tube was rinsed with tetrahydrofuran (1 ml), which also was evaporated. The resultant residue was redissolved in 50–250 μl of a chloroform–tetrahydrofuran (2:1 v/v) mixture to give an anticipated acetaminophen concentration of 1–10 μg/μl, and a 2-μl aliquot was injected into the liquid chromatograph.

Urinary Excretion of Free Acetaminophen—Two healthy human volunteers each took a single dose of ^{14}C-acetaminophen (650 mg, 20 μCi). Urine samples were collected at 3, 6, 9, and 12 hr. A working standard curve was prepared by adding known amounts of acetaminophen at five different concentrations to drug-free urine. The urine samples were worked up as already described.

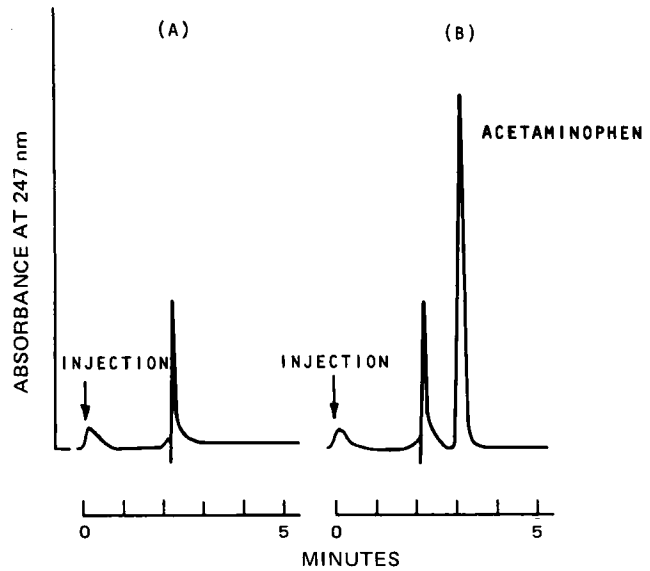

Figure 2—*High-pressure liquid chromatogram of human urine extract from: (A) blank urine and (B) urine spiked with acetaminophen (10 μg/ml).*

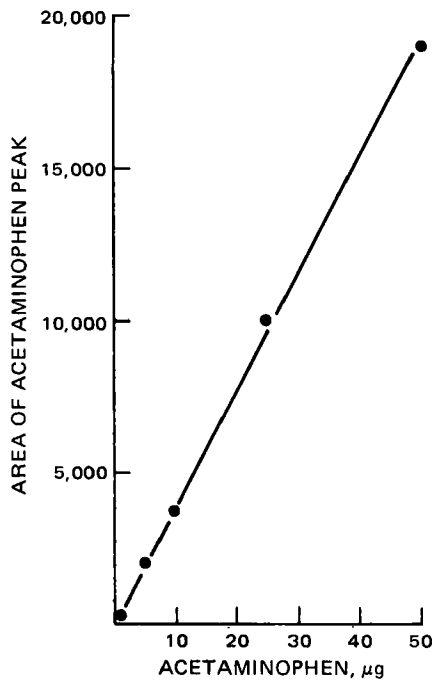

Figure 3—*Standard curve for acetaminophen.*

Determination of ^{14}C-Acetaminophen in Urine by Radioisotope Counts—Urine (25 μl) was applied as a band to strips of chromatography paper[8] and developed using the alkaline paper chromatography system described by Shahidi (6, System C). Radioactivity on the developed chromatograms was detected by serial sectioning into 1-cm strips and counting in a liquid scintillation counter. The peak corresponding to standard ^{14}C-acetaminophen was quantitated.

RESULTS AND DISCUSSION

The mobile phase used in the chromatograph was a simple solvent system of tetrahydrofuran modified with 10% chloroform. A small amount of acetic acid (0.002%) was added to reduce the slight tendency of acetaminophen to tail. The sample residues were redissolved in a chloroform–tetrahydrofuran (2:1) mixture to minimize the diffusion of the compound when injected into the mobile phase.

The extraction procedure using ether gave a cleaner extract with fewer extraneous peaks. The recoveries of processed standards of acetaminophen from plasma and urine were virtually complete, as reported previously (3). The chromatograms (Figs. 1 and 2) yielded an acetaminophen peak with a retention time (t_R) of 3 min. Chromatograms from control plasma (Fig. 1) and control urine (Fig. 2) also yielded an extraneous peak around 2.2 min, but it did not interfere with the acetaminophen peak. The plasma extract had an additional peak at 1.8 min. No other interfering compounds were extracted when ether was used as the solvent.

This method was used to study the urinary excretion of free acetaminophen in two healthy human volunteers. Figure 3 represents the standard curve obtained by plotting peak areas *versus* acetaminophen concentrations obtained from the analysis of spiked urine samples. The plot is a straight line over the concentration range of 1–50 μg/ml. The data obtained from duplicate analyses were reproducible to within 4%.

Figure 4 illustrates the cumulative urinary excretion of free acetaminophen by the two subjects after ingestion of 650 mg. The slopes of the curves tend to level off at about 6 hr. The total acetaminophen excreted at 12 hr was 19.12 mg in one subject and 29.08 mg in the other as determined by HPLC. These results were compared with those obtained from ^{14}C-radioisotope counts (Fig. 4). In the latter deter-

[7] Varian MicroPak Si-10, Varian Aerograph, Walnut Creek, Calif.

[8] Whatman No. 1.

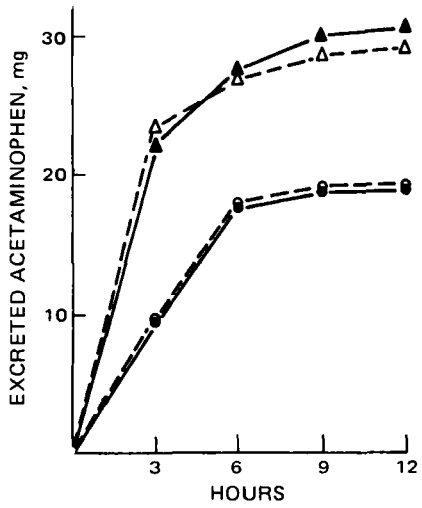

Figure 4—*Cumulative urinary excretion of free acetaminophen in two healthy subjects as determined by HPLC (○, △) and radioisotope (●, ▲) methods.*

mination, the paper chromatography system of Shahidi (6) was used to separate the ^{14}C-acetaminophen from its metabolites. The overall difference between the two methods was less than 6%.

This HPLC method is rapid and simple for the determination of acetaminophen in biological fluids. It involves no silylation of the compound as is required in GLC determinations. Because the extraction procedure is simple and complete, the use of an internal standard is not necessary; reproducible results to within 4% were achieved. The limit of detectability for acetaminophen by this method is 1 μg/ml. Below this concentration, the reproducibility of acetaminophen estimations is more variable.

This HPLC technique also could be used for the determination of acetaminophen metabolites. The estimation of the glucuronide and sulfate of acetaminophen is usually carried out by analyzing the free acetaminophen generated from enzymatic cleavage of these metabolites (7). Likewise, the cysteine and mercapturate metabolites could be estimated after chemical cleavage with Raney nickel (8).

REFERENCES

(1) L. F. Prescott, *J. Pharm. Pharmacol.*, **23**, 111(1971).

(2) G. Ramachander, F. D. Williams, and J. F. Emele, *J. Pharm. Sci.*, **62**, 1498(1973).

(3) B. H. Thomas and B. B. Coldwell, *J. Pharm. Pharmacol.*, **24**, 243(1972).

(4) R. P. Miller and L. J. Fischer, *J. Pharm. Sci.*, **63**, 969(1974).

(5) R. M. Riggin, A. L. Schmidt, and P. T. Kissinger, *ibid.*, **64**, 680(1975).

(6) N. J. Shahidi, *Ann. N.Y. Acad. Sci.*, **151**, 822(1968).

(7) G. Levy and H. Yamada, *J. Pharm. Sci.*, **60**, 215(1971).

(8) J. R. Mitchell, S. S. Thorgeirsson, W. Z. Potter, D. J. Jollow, and H. Keiser, *Clin. Pharmacol. Ther.*, **16**, 676(1974).

ACKNOWLEDGMENTS AND ADDRESSES

Received May 30, 1975, from the *Drug Research Laboratories, Health Protection Branch, Health and Welfare Canada, Tunney's Pasture, Ottawa, Ontario, Canada K1A 0L2*

Accepted for publication September 4, 1975.

[x] To whom inquiries should be directed.

Enthalpies of Hydrogen Bonding in Psychotropic Drugs

TIMOTHY B. PATRICK [x] and RANDALL R. BRESEE

Abstract □ The enthalpy of hydrogen bonding of some antipsychotic, antidepressant, anticonvulsant, and antianxiety agents with phenol, as determined from IR and NMR spectroscopic measurements, was shown not to be responsible for differences in activity within the drug classes. These results support a theoretical prediction advanced for anticonvulsant activity.

Keyphrases □ Enthalpy—hydrogen bonding between various psychotropic drugs with phenol, IR and NMR spectral measurement, related to differences in activity □ Hydrogen bonding—various psychotropic drugs with phenol, IR and NMR spectral measurement, related to differences in activity □ Psychotropic drugs—enthalpy of hydrogen bonding with phenol, IR and NMR spectral measurement, related to differences in activity

Hydrogen bonding is often mentioned when the mechanism of drug action is considered. However, little quantitative information concerning this subject has been reported (1, 2). Therefore, the enthalpy of hydrogen bonding of several psychotropic drugs with phenol was investigated to obtain factual information for testing the theoretically based conclusion that hydrogen bond acceptance is not responsible for variations in anticonvulsant activity (3). Furthermore, hydrogen bond strengths of some tranquilizing and anticonvulsant drugs were examined so that information regarding the importance of hydrogen bonding in diazepam (V), which acts as both a tranquilizer and an anticonvulsant (4), could be evaluated.

DISCUSSION

Hydrogen-bonding enthalpies with phenol were obtained using the IR and NMR spectral techniques developed by Drago and coworkers (5, 6). The IR technique relies on a linear relationship between the enthalpy of hydrogen bonding and the hydroxyl frequency difference of free phenol and hydrogen-bonded phenol. The NMR method is based on a linear relationship between hydrogen-bonding enthalpy and the chemical shift of a hydroxyl proton in a hydrogen-bonded phenol–base adduct. The IR procedure is better because measurements are straightforward and small sample concentrations are used; the NMR method requires many sample variations and an estimate of anisotropic corrections (6).

The IR–enthalpy relationship obtained was:

$$-\Delta H \text{ (kcal/mole)} = 0.010\,(\Delta\nu) + 3.67 \pm 0.04 \qquad r = 0.986 \quad \text{(Eq. 1)}$$

The NMR–enthalpy relationship is:

$$-\Delta H \text{ (kcal/mole)} = 1.89\,(\delta \text{ adduct}) - 9.14 \pm 0.52 \qquad r = 0.991 \quad \text{(Eq. 2)}$$

Errors are reported at the 99% confidence level (7).

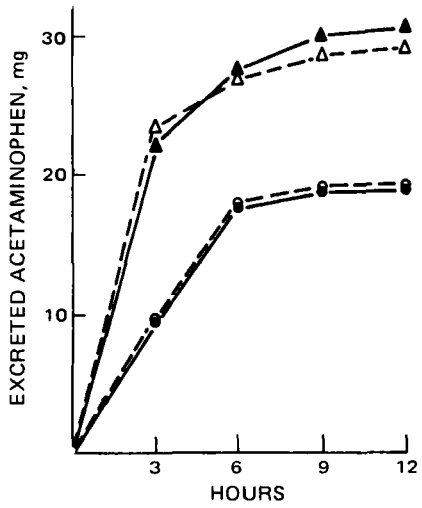

Figure 4—*Cumulative urinary excretion of free acetaminophen in two healthy subjects as determined by HPLC (○, △) and radioisotope (●, ▲) methods.*

mination, the paper chromatography system of Shahidi (6) was used to separate the ^{14}C-acetaminophen from its metabolites. The overall difference between the two methods was less than 6%.

This HPLC method is rapid and simple for the determination of acetaminophen in biological fluids. It involves no silylation of the compound as is required in GLC determinations. Because the extraction procedure is simple and complete, the use of an internal standard is not necessary; reproducible results to within 4% were achieved. The limit of detectability for acetaminophen by this method is 1 μg/ml. Below this concentration, the reproducibility of acetaminophen estimations is more variable.

This HPLC technique also could be used for the determination of acetaminophen metabolites. The estimation of the glucuronide and sulfate of acetaminophen is usually carried out by analyzing the free acetaminophen generated from enzymatic cleavage of these metabolites (7). Likewise, the cysteine and mercapturate metabolites could be estimated after chemical cleavage with Raney nickel (8).

REFERENCES

(1) L. F. Prescott, *J. Pharm. Pharmacol.*, **23**, 111(1971).

(2) G. Ramachander, F. D. Williams, and J. F. Emele, *J. Pharm. Sci.*, **62**, 1498(1973).

(3) B. H. Thomas and B. B. Coldwell, *J. Pharm. Pharmacol.*, **24**, 243(1972).

(4) R. P. Miller and L. J. Fischer, *J. Pharm. Sci.*, **63**, 969(1974).

(5) R. M. Riggin, A. L. Schmidt, and P. T. Kissinger, *ibid.*, **64**, 680(1975).

(6) N. J. Shahidi, *Ann. N.Y. Acad. Sci.*, **151**, 822(1968).

(7) G. Levy and H. Yamada, *J. Pharm. Sci.*, **60**, 215(1971).

(8) J. R. Mitchell, S. S. Thorgeirsson, W. Z. Potter, D. J. Jollow, and H. Keiser, *Clin. Pharmacol. Ther.*, **16**, 676(1974).

ACKNOWLEDGMENTS AND ADDRESSES

Received May 30, 1975, from the *Drug Research Laboratories, Health Protection Branch, Health and Welfare Canada, Tunney's Pasture, Ottawa, Ontario, Canada K1A 0L2*

Accepted for publication September 4, 1975.

[x] To whom inquiries should be directed.

Enthalpies of Hydrogen Bonding in Psychotropic Drugs

TIMOTHY B. PATRICK [x] and RANDALL R. BRESEE

Abstract □ The enthalpy of hydrogen bonding of some antipsychotic, antidepressant, anticonvulsant, and antianxiety agents with phenol, as determined from IR and NMR spectroscopic measurements, was shown not to be responsible for differences in activity within the drug classes. These results support a theoretical prediction advanced for anticonvulsant activity.

Keyphrases □ Enthalpy—hydrogen bonding between various psychotropic drugs with phenol, IR and NMR spectral measurement, related to differences in activity □ Hydrogen bonding—various psychotropic drugs with phenol, IR and NMR spectral measurement, related to differences in activity □ Psychotropic drugs—enthalpy of hydrogen bonding with phenol, IR and NMR spectral measurement, related to differences in activity

Hydrogen bonding is often mentioned when the mechanism of drug action is considered. However, little quantitative information concerning this subject has been reported (1, 2). Therefore, the enthalpy of hydrogen bonding of several psychotropic drugs with phenol was investigated to obtain factual information for testing the theoretically based conclusion that hydrogen bond acceptance is not responsible for variations in anticonvulsant activity (3). Furthermore, hydrogen bond strengths of some tranquilizing and anticonvulsant drugs were examined so that information regarding the importance of hydrogen bonding in diazepam (V), which acts as both a tranquilizer and an anticonvulsant (4), could be evaluated.

DISCUSSION

Hydrogen-bonding enthalpies with phenol were obtained using the IR and NMR spectral techniques developed by Drago and coworkers (5, 6). The IR technique relies on a linear relationship between the enthalpy of hydrogen bonding and the hydroxyl frequency difference of free phenol and hydrogen-bonded phenol. The NMR method is based on a linear relationship between hydrogen-bonding enthalpy and the chemical shift of a hydroxyl proton in a hydrogen-bonded phenol–base adduct. The IR procedure is better because measurements are straightforward and small sample concentrations are used; the NMR method requires many sample variations and an estimate of anisotropic corrections (6).

The IR–enthalpy relationship obtained was:

$$-\Delta H \text{ (kcal/mole)} = 0.010\,(\Delta\nu) + 3.67 \pm 0.04 \qquad r = 0.986 \quad \text{(Eq. 1)}$$

The NMR–enthalpy relationship is:

$$-\Delta H \text{ (kcal/mole)} = 1.89\,(\delta \text{ adduct}) - 9.14 \pm 0.52 \qquad r = 0.991 \quad \text{(Eq. 2)}$$

Errors are reported at the 99% confidence level (7).

Table I—Hydrogen-Bonding Enthalpies for Phenol–Drug Adducts

Compound	$\Delta\nu$, cm^{-1}	$-\Delta H$, kcal/mole	δ Adduct, ppm	$-\Delta H$, kcal/mole	Activity[a]
I: Promazine	367	6.91	8.97	7.81	—
II: Amitriptyline	336	6.63	8.94	7.76	—
III: Imipramine	308	6.35	8.80	7.49	—
IV: Chlorpromazine	262	5.89	8.25	6.45	—
V: Diazepam	154	5.72	7.32	4.69	0.04[b]
VI: Phenobarbital	207	5.34	7.23	4.52	0.10
VII: Dimethadione	194	5.21	7.30	4.66	2.6
VIII: Phenytoin	170	4.97	7.01	4.10	0.04
IX: Bemegride	137	4.62	7.19	4.45	Convulsant

[a] Supramaximal electroshock data. Activity is in dose (millimoles per kilogram) that protects 50% of mice from the tonic extensor phase (3). [b] L. H. Sternbach, L. O. Randall, and S. R. Gustafson, in "Psychopharmacological Agents," vol. I, M. Gorden, Ed., Academic, New York, N.Y., 1968, p. 138.

The data in Table I clearly show that the hydrogen-bonding enthalpies found by IR measurements for the anticonvulsant compounds (VI–IX) have a mean value of 5.04 kcal/mole; the spread of enthalpies is within the ±0.40-kcal/mole experimental error. Enthalpies measured by NMR spectroscopy for VI–IX show a mean value of 4.60 kcal/mole, with the enthalpy spread within the ±0.52-kcal/mole experimental error. According to these results, enthalpies of hydrogen bonding of phenol with the anticonvulsants studied are essentially the same and support the theoretical prediction that hydrogen bond acceptance alone cannot account for differences in anticonvulsant activity (3).

The antipsychotic and antidepressant agents (I–IV) exhibit enthalpy values of 1.41 (IR) and 2.77 (NMR) kcal/mole higher than the anticonvulsants V–IX. The enthalpy spread in this class is also within experimental error, suggesting that differences in activity are not the result of differences in hydrogen-bonding strength. Hydrogen bond acceptance has been suggested to be an important factor in chlorpromazine's activity (8).

Diazepam, which exhibits both tranquilizing and anticonvulsant activities (4) and belongs to both drug classes, displays an enthalpy of hydrogen bonding intermediate between that of the two classes. The significance of this observation is not apparent at present and must await further quantitative studies of other factors important for physiological activity.

In summary, the evidence presented shows that hydrogen bond acceptance alone is not responsible for the differences in activity within drug classes.

EXPERIMENTAL[1]

Materials—All solvents were spectrograde quality and were stored over 4A molecular sieves[2]. Phenol was distilled and then freshly sublimed before each run. Amitriptyline[3], chlorpromazine[4], promazine[5], and imipramine[6] were obtained as their hydrochloride salts. The free amines, obtained by neutralization of the salts with ammonia, were purified by sublimation. Diazepam[7] was obtained as the free amine. Phenytoin, dimethadione, bemegride, and phenobarbital were obtained commercially[8]. All compounds had melting points and spectral data consistent with reported properties. All materials were sublimed directly before use.

Procedures—*IR Spectroscopy*—To a 0.02 *M* solution of phenol in carbon tetrachloride was added the base until IR absorbances due to both free phenol and complexed phenol could be observed. This procedure was repeated at several concentrations, and the results were extrapolated to infinite dilution. The frequency difference between free phenol and complexed phenol ($\Delta\nu$) was correlated with the enthalpies for the compounds listed in Table II to give Eq. 1. The procedure was repeated with the drugs listed in Table I to obtain ($\Delta\nu$); Eq. 1 was used to determine ΔH.

[1] IR measurements were made in carbon tetrachloride solution using a Perkin-Elmer model 621 spectrophotometer. NMR spectra were run in methylene chloride solution at 35° employing a Varian T-60 instrument locked on tetramethylsilane (0.0 Hz).
[2] Linde.
[3] Merck Sharp and Dohme.
[4] Smith Kline and French.
[5] Wyeth.
[6] Geigy.
[7] Hoffmann-La Roche.
[8] Sigma Chemical Co.

Table II—Chemical Shifts and Frequency Differences for Phenol–Base Adducts

Base	$\Delta\nu$ (CCl_4), cm^{-1}[a]	δ (Adduct) (CH_2Cl_2), ppm[b]	$-\Delta H$, kcal/mole[c]
Triethylamine	592	9.41	9.1
Pyridine	484	9.10	8.0
Dimethyl sulfoxide	357	8.53	6.9
N-Methylpyrrolidinone	325	8.00	6.1
N,N-Dimethylacetamide	312	8.45	6.8
Acetamide	193	7.89	5.0
Ethyl acetate	149	7.15	4.8

[a] ±10 cm^{-1}. [b] Correction of −1.1 ppm included except for triethylamine and dimethyl sulfoxide. [c] Reference 5.

NMR Spectroscopy—A dilution study of phenol in methylene chloride showed that only monomeric phenol was present at concentrations below 0.05 *M*. Solutions containing 0.50–0.25 *M* base and 0.25 *M* phenol in methylene chloride were observed at 35°. The concentration of uncomplexed phenol under these conditions was less than 0.05 *M*. The base concentration was increased in 0.05 *M* increments.

Chemical shift dependence of the phenolic hydroxyl proton signal as a function of concentration was recorded. A previously described computerized method (9) was used to determine the chemical shift of the 1:1 phenol–base adduct (5). A plot of the chemical shift of adducts (δ adduct) for the compounds listed in Table II *versus* the known enthalpy values provided Eq. 2. The adduct chemical shift for the drugs listed in Table I was obtained in the same manner, and the hydrogen bonding enthalpy was determined from Eq. 2. Anisotropic corrections of −1.1 ppm were used for the compounds containing carbonyl groups (5).

REFERENCES

(1) A. Burger, "Medicinal Chemistry," 3rd ed., vols. I and II, Wiley-Interscience, New York, N.Y., 1970.
(2) L. B. Kier, "Molecular Orbital Theory in Drug Research," Academic, New York, N.Y., 1971.
(3) P. R. Andrews, *J. Med. Chem.*, **12**, 761(1969).
(4) R. A. Boyer, Jr., *Dis. Nerv. Syst.*, **27**, 35(1966).
(5) R. S. Drago, G. C. Vogel, and T. E. Needham, *J. Am. Chem. Soc.*, **93**, 6014(1971).
(6) D. P. Eyman and R. S. Drago, *ibid.*, **88**, 1617(1966).
(7) W. J. Youden, "Statistical Methods for Chemists," Wiley, New York, N.Y., 1951.
(8) T. Nash and A. C. Allison, *Biochem. Pharmacol.*, **12**, 601(1963).
(9) T. B. Patrick and P. H. Patrick, *J. Am. Chem. Soc.*, **95**, 5192(1973).

ACKNOWLEDGMENTS AND ADDRESSES

Received June 16, 1975, from the *Department of Chemistry, Southern Illinois University, Edwardsville, IL 62026*

Accepted for publication September 12, 1975.

[x] To whom inquiries should be directed.

GLC Determination of Doxepin Plasma Levels

J. E. O'BRIEN [x] **and O. N. HINSVARK**

Abstract □ A procedure is described for extracting doxepin, a tricyclic antidepressant, from plasma and subsequently measuring its concentration by GLC. The developed technique permits the resolution and quantitative determination of the *cis*- and *trans*-isomers of doxepin as well as its desmethyl metabolite. The method allows precise, reliable measurement of the drug and one of its metabolites in concentrations as low as 10 ng/ml of plasma.

Keyphrases □ Doxepin—GLC analysis of *cis*- and *trans*-isomers and desmethyl metabolite, plasma □ GLC—analysis, *cis*- and *trans*-isomers and desmethyl metabolite of doxepin, plasma □ Antidepressants—doxepin, GLC analysis, plasma

Doxepin, *N,N*-dimethyl-3-dibenz[*b,e*]oxepin-11(6*H*)ylidene-1-propanamine (I) hydrochloride, is a therapeutic agent used in the treatment of psychoneurotic anxiety and depression. It is a tricyclic dibenzoxepine derivative used as an isomeric mixture with a distribution of approximately 15% *cis* and 85% *trans*. Oral administration of an efficacious drug may result in a therapeutic failure unless it is sufficiently bioavailable. To compare the absorption of doxepin formulated in different dosage forms, a method was developed to measure plasma levels of doxepin (I) and its desmethyl metabolite (II) in humans who had received oral, therapeutic doses.

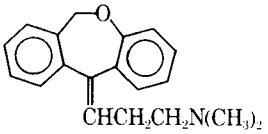

I

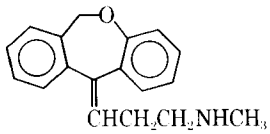

II

Previous efforts to produce a bioassay of doxepin by GC (1, 2) did not provide adequate sensitivity for the measurement of normal plasma drug levels. More recently, however, a technique for tricyclic antidepressants (3) demonstrated suitable sensitivity. The procedure described here provides not only sensitivity but also simultaneous resolution and measurement of the *cis*- and *trans*-isomers of doxepin as well as its desmethyl metabolite.

EXPERIMENTAL

Reagents—The following were used: 20% NaOH, *n*-hexane[1], 1 *N* HCl, and 0.02% triethanolamine in chloroform.

Instrumentation—A biomedical gas chromatograph[2] equipped with a flame-ionization detector was used. The glass column was 1.83 m × 2 mm i.d., packed with 3% OV-225 on 100–120-mesh Gas Chrom Q[3].

The column was operated isothermally at 215°; the detector temperature was 280°, and the injection port temperature was 200°. The helium flow rate was 40 ml/min with an inlet pressure of 40 psig, the hydrogen flow was 35 ml/min, and the air flow was 300 ml/min. The electrometer range was 1 with an attenuation of 16–64.

[1] Mallinckrodt Nanograde.
[2] Hewlett-Packard 7610A.
[3] Applied Science Laboratories.

Table I—Recovery of Doxepin from Human Plasma

cis-Isomer			*trans*-Isomer		
ng Spike/ml Plasma	Recovery, ng	%	ng Spike/ml Plasma	Recovery, ng	%
8	4.8	60	45	31	69
8	6.8	85	45	32	71
8	5.0	62	45	32	71
8	5.4	68	45	32	71
8	6.8	85	45	32	71
16	11	69	90	57	63
16	11	69	90	61	68
16	12	75	90	57	63
16	11	69	90	63	70
32	25	78	180	134	74
32	24	75	180	133	74
32	22	69	180	126	70
32	26	81	180	133	74
		$\bar{x}$ = 73			$\bar{x}$ = 70
		SD = 8			*SD* = 4

Extraction of Doxepin from Plasma—A 5-ml sample of plasma is pipetted into a 50-ml round-bottom test tube fitted with a plastic stopper. The plasma is made basic with 0.5 ml of 20% NaOH and then extracted twice with 5 ml of *n*-hexane by shaking the tube, in a horizontal position, on a wrist-action shaker for 20 min each time.

The sample is centrifuged after each extraction, and the organic layers are combined in a 15-ml centrifuge tube. Then 1.0 ml of 1 *N* HCl is added to the combined hexane fractions and mixed on a wrist-action shaker for 15 min to extract the drug into the acid aqueous phase.

The hexane containing lipid-soluble material is discarded. Then 0.3 ml of 20% NaOH is added to the 1-ml aqueous acid extract, and the sample is reextracted twice with 1-ml portions of *n*-hexane on a wrist-action shaker for 5 min each. The extracts in which the doxepin has been distributed are combined in a 13-ml centrifuge tube.

The overall purpose of this three-step extraction procedure is to provide a "chromatographically clean" sample with minimum background contamination.

Preparation of Sample for Chromatography—One milliliter of 0.02% (v/v) triethanolamine in chloroform is added to the sample extract. It acts as a "scavenger" and minimizes the adsorption of the doxepin on the glass surfaces during the concentration step. The extract is then evaporated to dryness at 50° in a heating block[4] under a gentle stream of dry nitrogen.

The residue is reconstituted with 100 μl of *n*-hexane containing 1 mg % promazine (III). (Promazine was chosen as an internal standard because of its structural similarity to doxepin and its chromatographic characteristics.) The tube and contents are mixed on a vortex mixer for approximately 20 sec, and then 5 μl is withdrawn and injected into the chromatograph.

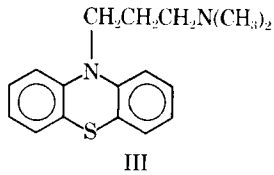

III

The feasibility and efficiency of the extraction and measurement were tested by adding known quantities of doxepin[5] to plasma and following the described procedure.

[4] Temp-Blok module heater, Lab Line Instruments.
[5] Adapin, Pennwalt Corp., Rochester, N.Y.

Table II—Doxepin Levels in Chronically Treated Subjects

Subject	Age, years	Sex	Doxepin or Placebo Regimen[a]	Patient Response	Plasma Level, ng/ml		
					cis	*trans*	Desmethyl
1	68	Female	25 mg tid–16 weeks	Moderately good	11	42	87
2	66	Female	25 mg qid–6 weeks	Good	9	43	Nil
3	68	Female	100 mg bid–37 weeks	Very good	10	141	100
4	31	Female	25 mg qd–5 weeks	No change	Nil	Nil	Nil
5	60	Female	50 mg qid–3 weeks	Moderately good	9	63	Nil
6	33	Female	50 mg tid–3 weeks 25 mg tid–4 days	No change	Nil	Nil	Nil
7	35	Male	50 mg tid–5 weeks	No change	11	46	Nil

[a] Double-blind study; not complete.

RESULTS AND DISCUSSION

Typical chromatograms of human plasma extracts are shown in Fig. 1. The blank plasma extract is from a subject receiving a placebo, while the patient plasma is from a chronically treated subject approximately 3 hr after a 25-mg dose (given three times daily). The chromatographic technique developed permits the resolution and quantitative determination of the *cis*- and *trans*-isomers of doxepin and its desmethyl metabolite.

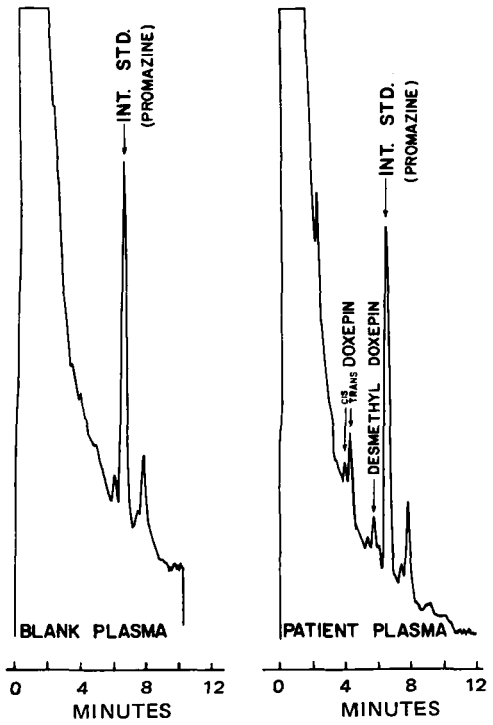

Figure 1—*Typical chromatograms of extracts of human plasma.*

To determine that the methodology provided a reliable measure of plasma drug levels, human plasma was spiked with varying concentrations of doxepin hydrochloride and assayed according to the procedure (Table I). As can be seen from the data, the technique allows precise and reliable measurement of the drug in concentrations as low as 10 ng/ml of plasma.

Table II shows the doxepin and metabolite levels in the plasma of chronically treated subjects undergoing therapy according to the indicated regimen. The values show that the method has adequate sensitivity for measuring drug levels in the blood of patients receiving therapeutic doses.

REFERENCES

(1) D. C. Hobbs, *Biochem. Pharmacol.*, **18**, 1941(1969).

(2) L. J. Dusci and L. P. Hackett, *J. Chromatogr.*, **61**, 231 (1971).

(3) L. A. Gifford, P. Turner, and C. M. B. Pare, *ibid.*, **105**, 107(1975).

ACKNOWLEDGMENTS AND ADDRESSES

Received July 18, 1975, from the *Analytical Chemistry Department, Pharmaceutical Division, Pennwalt Corporation, Rochester, NY 14623*

Accepted for publication September 24, 1975.

The authors thank Dr. Lino Covi, Johns Hopkins University, and Richard Lawlor, Medical Department, Pharmaceutical Division, Pennwalt Corp., for providing the clinical samples. They also thank Carolyn McClain, Analytical Chemistry Department, Pharmaceutical Division, Pennwalt Corp., for technical assistance.

[x] To whom inquiries should be directed.

Synthesis, Physicochemical Parameters, and *In Vitro* Evaluation of N^1-*p*-Chlorophenyl-N^5-alkylbiguanides

VICTOR D. WARNER ˣ, DONALD M. LYNCH, and ROSS S. AJEMIAN

Abstract □ A series of N^1-*p*-chlorophenyl-N^5-alkylbiguanides were synthesized as potential inhibitors of dental plaque. Partition coefficients and pKa values were determined by standard methods. Biological activity was evaluated against *Streptococcus mutans*, a pure strain of plaque-forming bacteria. All compounds were compared to chlorhexidine acetate.

Keyphrases □ Biguanides, substituted—synthesized, partition coefficients and pKa values determined, ability to inhibit dental plaque screened □ Partition coefficients—determined for series of substituted biguanides □ pKa values—determined for series of substituted biguanides □ Dental plaque inhibitors, potential—series of substituted biguanides synthesized and screened □ Plaque inhibitors, potential—series of substituted biguanides synthesized and screened □ Structure–activity relationships—series of substituted biguanides synthesized and screened for ability to inhibit dental plaque

The accumulation of dental deposits such as plaque shows strong positive correlation with caries formation and periodontal disease (1). Mechanical means for removing plaque are of limited effectiveness, since it can only be removed by vigorous use of abrasives. Chlorhexidine [1,6-bis-(N^5-*p*-chlorophenyl-N^1-biguanido)hexane] (I), an antibacterial bisbiguanide, has shown promise as an effective inhibitor of dental plaque (2).

The monobiguanide chloroguanide, III (R = isopropyl), produces no inhibition of plaque growth (3). This observation, coupled with an earlier report that a molecule carrying only one biguanide residue was only weakly antibacterial (4), indicated that two biguanide residues may be required in this type of molecule for antiplaque activity. In an attempt to test this hypothesis and determine physicochemical properties that may be correlated to antiplaque activity, Compounds IV–X were prepared and compared to chlorhexidine acetate.

EXPERIMENTAL

Synthesis[1]—The synthetic approach involved the method of Curd and Rose (5) as outlined in Scheme I.

N¹-p-*Chlorophenyl*-N³-*cyanoguanidine* (*II*)—*p*-Chloroaniline hydrochloride (27.33 g, 0.162 mole) and sodium dicyanamide (15.14 g, 0.17 mole) were dissolved in water (175 ml) and stirred at 25° for 12 hr. The reaction mixture was then filtered. The tan residue was recrystallized from ethanol, yielding white needles (25.18 g, 79.9%), mp 202–203° [lit. (5) mp 202.5–203°].

N¹-p-*Chlorophenyl*-N⁵-*alkylbiguanides* (*IV–X*)—Compound II (9.73 g, 0.05 mole), the appropriate alkylamine (0.2 mole), ethanol (80 ml), and copper sulfate pentahydrate (6.25 g, 0.025 mole) in water (30 ml) were refluxed with stirring for 16 hr. A semisolid precipitate of the copper–biguanide complex formed upon the addition of water (250 ml) to the purple solution. The copper complex was destroyed upon addition of acetic acid (15 g, 0.25 mole). Copper was removed by bubbling gaseous hydrogen sulfide through the solution and the resulting copper sulfide was removed by vacuum filtration. Adjustment of the filtrate pH to 8 using concentrated ammonium hydroxide and evaporation *in vacuo* to about one-third its volume resulted in precipitation of the alkylbiguanide acetate. The crude biguanide acetate was then recrystallized using the appropriate solvent. Details are given in Table I.

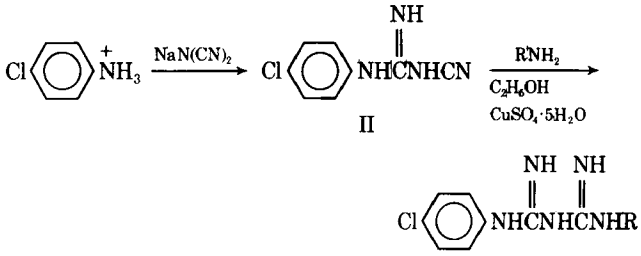

III: R = isopropyl
IV: R = methyl
V: R = ethyl
VI: R = *n*-propyl
VII: R = *n*-butyl
VIII: R = *n*-hexyl
IX: R = *n*-octyl
X: R = *n*-dodecyl

Scheme I

Determination of pKa—The pKa's of IV–VII were determined in duplicate by potentiometric titration. A water-jacketed 200-ml beaker connected to a circulating water bath held the temperature of the titrating vessel at 25°. Nitrogen was bubbled through the solution to be titrated, and the buret (10 ml) was fitted with a soda lime drying tube to exclude atmospheric carbon dioxide. At least 15 0.25-ml aliquots of carbonate-free 0.02 *N* KOH were added to 100 ml of a 10^{-3} *M* solution of the alkylbiguanide in deionized distilled water. For each addition of titrant, the pH was measured[2] and the pKa was calculated using the method of Albert and Serjeant (7).

Solubility problems for VIII–X and chlorhexidine acetate[3] were encountered. Therefore, a 10^{-3} *M* solution of IV–VII and chlorhexidine in water–ethanol (3:1) was used to determine relative pKa values (Table II).

Partition Coefficients—Compounds IV–VI were partitioned between a 0.05 *M* phosphate buffer (pH 11.5) saturated with octanol and octanol saturated with phosphate buffer. Usually, 50–150-ml portions of octanol and buffer were used. In partitioning these compounds, gentle shaking for 90 min was carried out at room temperature (25 ± 5°). The volume ratio of these two phases and the amount of sample were chosen so that the absorbance[4] of the sample from the buffered layer after partitioning had a value between 0.2 and 0.9, using a 1-cm cell and buffer solution as a blank. By working at a fixed pH and knowing the pKa for these compounds, the partition coefficient (P) of the free base could be determined using (8):

$$P = \frac{C_{\text{octanol}}}{C_{\text{buffer}}(1 - \alpha)} \qquad \text{(Eq. 1)}$$

where α = degree of ionization.

The higher homologs and chlorhexidine were insoluble at this pH, and their partition coefficients as free bases could not be experimentally determined. However, due to the additive nature of π (9), the log P of each homolog could be calculated by the addition of 0.5 for each methylene unit. Since chlorhexidine and V–X were highly lipid soluble, their protonated forms could be partitioned. To do this,

[1] Melting points were determined on a Thomas-Hoover capillary melting-point apparatus and are uncorrected. Microanalyses were performed by Midwest Microlab, Ltd., Indianapolis, Ind. NMR (Varian Associates model T-60 spectrometer) and IR (Perkin-Elmer model 700 spectrometer) spectral data were in accord with the assigned structures.

[2] Orion Research Ionanalizer model 801 digital pH meter with full range Corning combination electrode.

[3] Ayerst Laboratories, Inc.

[4] Spectra of all compounds were recorded at 253 nm using a Beckman DB-G spectrophotometer.

Table I—N^1-*p*-Chlorophenyl-N^5- alkylbiguanide Acetates

Compound	R	Yield, %	Melting Point (Solvent)	Formula	Analysis, % Calc.	Found
IV	Methyl	22	149° (ether)	$C_{11}H_{16}ClN_5O_2$	C 46.24	46.40
					H 5.65	5.41
					N 24.51	24.64
V	Ethyl	42	161°[a] (ether)	$C_{12}H_{18}ClN_5O_2$	C 48.08	48.08
					H 6.05	5.86
					N 23.36	23.15
VI	*n*-Propyl	31	165–166°[b] (acetone–ethanol)	$C_{13}H_{20}ClN_5O_2$	C 49.76	49.86
					H 6.42	6.48
					N 22.32	22.43
VII	*n*-Butyl	59	158–159°[c] (acetone–ethanol)	$C_{14}H_{22}ClN_5O_2$	C 51.30	51.18
					H 6.78	6.71
					N 21.36	21.52
VIII	*n*-Hexyl	35	137°[d] (ethanol–water)	$C_{16}H_{26}ClN_5O_2$	C 53.99	53.73
					H 7.36	7.38
					N 19.68	19.63
IX	*n*-Octyl	24	132°[e] (ethanol–water)	$C_{18}H_{30}ClN_5O_2$	C 56.42	56.25
					H 7.88	7.95
					N 18.28	18.33
X	*n*-Dodecyl	57	169° (ethanol–water)	$C_{22}H_{38}ClN_5O_2$	C 60.04	59.78
					H 8.70	8.82
					N 15.92	15.93

[a] Lit. (5) mp 160–161°. [b] Lit. (5) mp 164–165°, (6) 165–166°. [c] Lit. (5) mp 158°. [d] Lit. (6) mp 136–137°. [e] Lit. (6) mp 133.5–134°.

Table II—Physicochemical Parameters of N^1-*p*-Chlorophenyl-N^5-alkylbiguanides

Compound	Log *P*[a] Free Base[c]	Log *P*[a] Acetate[d]	pKa[b] Water	pKa[b] Water–Ethanol (3:1)
IV	1.58 (0.030)	−0.754[e]	10.95 ± 0.04	10.60 ± 0.04
V	2.14 (0.030)	−0.254 (0.043)	11.01 ± 0.03	10.82 ± 0.06
VI	2.63 (0.029)	0.208 (0.023)	11.02 ± 0.06	10.78 ± 0.06
VII	3.13[e]	0.783 (0.007)	10.83 ± 0.05	10.78 ± 0.04
VIII	4.13[e]	1.85 (0.013)	—	—
IX	5.13[e]	2.85[e]	—	—
X	7.13[e]	4.85[e]	—	—
Chlorhexidine	4.87[e]	0.081 (0.011)	—	10.78 ± 0.05

[a] All determinations were done in triplicate using different amounts of samples, and the average value for log *P* was determined. Values in parentheses indicate standard deviations. [b] All determinations were done in duplicate. [c] Aqueous phase, 0.05 *M* phosphate buffer (pH 11.5). [d] Aqueous phase, 0.05 *M* acetate buffer (pH 5.0). [e] Calculated log *P*.

Table III—Comparison of Log *P* and *In Vitro* Antibacterial Activity of N^1-*p*-Chlorophenyl-N^5-alkylbiguanides

Compound	Log *P*	Inhibition, % 10^{-3} *M*, 24 hr	10^{-4} *M*, 24 hr	10^{-5} *M* 24 hr	10^{-5} *M* 48 hr	10^{-6} *M*, 24 hr
IV	1.58	100	0	—	—	—
V	2.14	100	0	—	—	—
VI	2.63	100	0	—	—	—
VII	3.13	—	100	0	—	—
VIII	4.13	—	100	100	0	0
IX	5.13	—	100	100	100	0
X	7.13	—	100	100	0	0
Chlorhexidine	4.87	—	100	100	100	0

Compounds V–VIII and chlorhexidine were partitioned as their acetate salts between a 0.05 *M* acetate buffer (pH 5) and octanol.

The log *P* values for compounds determined either in both buffer systems or in one buffer system and the calculated log *P* of its conjugate differed by an average value of 2.35 ± 0.07. This average difference between the log *P* of the free base and its salt enabled the assignment of a π value of −2.35 for the protonation of nitrogen in this series. Since chlorhexidine is a dibasic compound, the log *P* of the free base could be calculated from the experimentally determined log *P* of the diacetate salt, yielding a value of 4.87 (Table II).

Antibacterial Activity—To 8.85 ml of sterile trypticase broth, 0.1 ml of an ethanolic solution of the test compound and 1 ml of 50% sterile sucrose solution were added. The medium was inoculated with 0.15 ml of a 24-hr culture of *Streptococcus mutans* (No. 6715), a pure strain of plaque-forming bacteria[5]. This mixture was incubated under anaerobic conditions[6] at 37°. After 24 and 48 hr, subjective estimates were made of adherent microbial growth on the test tube walls and of nonadherent growth in the broth using a scale of 0 (no growth) to 4 (maximum growth).

The total microbial accumulation was considered as *in vitro* plaque.

[5] Isolated and made available by the National Institute of Dental Research.
[6] BBL-Gaspack, BBL, Division of Bioquest, Cockeysville, Md.

For the results, growth ratings of 0 or 1 were scored as inhibition. Each compound was evaluated on five tubes, with percent inhibition values being reported. This procedure indicates the percentage of tubes that did not show plaque formation after the stated incubation period. The solvent served as the control (Table III).

RESULTS AND CONCLUSION

The biological results for VII–X (Table III), when compared to chlorhexidine acetate, indicate that two biguanide residues are not required for activity. The length of the alkyl chain need only be extended to achieve the higher lipid solubility required for activity. The two most active compounds tested, IX and chlorhexidine, have log *P* values near 5, suggesting an optimal log *P* for this series. This information will enable prediction, prior to synthesis, of the expected relative activity of biguanides based on lipophilic considerations.

REFERENCES

(1) H. Löe, in "Dental Plaque," W. D. McHugh, Ed., D. C. Thompson and Co., Dundee, Scotland, 1970, p. 259.

(2) H. Löe, *J. Periodont. Res., Suppl.*, **8**, 12, 93(1973).

(3) P. Gjermo, K. L. Baastad, and G. Rölla, *J. Periodont. Res.*, **5**, 102(1970).

(4) F. L. Rose and G. Swain, *J. Chem. Soc.*, **1956**, 4422.

(5) F. H. S. Curd and F. L. Rose, *ibid.*, **1946**, 729.

(6) R. G. Fisher, R. P. Quintana, and M. A. Boulware, *J. Dent. Res.*, **54**, 20(1975).

(7) A. Albert and E. P. Serjeant, in "Determination of Ionization and Stability Constants," Butler and Tanner Ltd., London, England, 1962.

(8) A. F. Yopel, in "Biological Correlations—The Hansch Approach," Advances in Chemistry Series vol. 114, R. F. Gould, Ed., American Chemical Society, Washington, D.C., 1972, p. 189.

(9) C. Hansch and S. M. Anderson, *J. Org. Chem.*, **32**, 2583(1967).

ACKNOWLEDGMENTS AND ADDRESSES

Received July 25, 1975, from the *Department of Medicinal Chemistry and Pharmacology, College of Pharmacy and Allied Health Professions, Northeastern University, Boston, MA 02115*

Accepted for publication September 17, 1975.

Presented in part at the Medicinal Chemistry Section, APhA Academy of Pharmaceutical Sciences, San Francisco meeting, April 1975.

The authors gratefully acknowledge the support of this work by the National Institute of Dental Research (Grant 1R01 DE03212-0-1A1).

[x] To whom inquiries should be directed.

Calibration of a Horizontal Pendulum-Type Tablet Breaking Strength Tester

FRANK W. GOODHART [x], J. RONALD DRAPER, MICHAEL J. KILLEEN, and FRED C. NINGER

Abstract □ A rapid, simplified method of checking the calibration of a new motorized pendulum type of tablet hardness tester and the accuracy and precision of three testers were determined. Two force gauges were calibrated, and both gauges were used by two operators to determine the accuracy of the new testers. This calibration method using the force gauge was reliable for checking the accuracy. The results show the various new testers to be in calibration and to give reproducible results.

Keyphrases □ Tablet hardness testers—motorized pendulum type, method for checking calibration and determining accuracy and precision, three testers compared □ Hardness testers, tablet—motorized pendulum type, method for checking calibration and determining accuracy and precision, three testers compared □ Strength, tablet—testers, motorized pendulum type, method for checking calibration and determining accuracy and precision, three testers compared

Certain deficiencies in the more popular tablet hardness testers have been reported previously (1–3). A new type of tablet hardness tester[1], which operates on the principle of a pendulum being displaced by consistent loading obtained by an electric motor-driven anvil, was made available in 1970 (4). The operation and merits of this tester were reported previously (1). Among its advantages compared to the more typical pneumatic type were: (*a*) more uniform force application, (*b*) less maintenance, and (*c*) the need for fewer calibration checks.

Since that report was completed, a new tablet breaking strength tester[2] became available. Its operating principle is the same as the original but the load scale readout is horizontal rather than circular. The overall size of the new tester is larger, and there are two anvil opening settings, 15 and 35 mm, to accommodate small and large size tablets. Also, the maximum scale values have been increased to 20 kg and 28 Strong-Cobb units to allow for the breakage of harder tablets such as troches and mints. A schematic diagram is shown in Fig. 1.

At the time the new tester was marketed, the manufacturer did not offer a method for checking the calibration. A persistent problem in the use of tablet breaking strength testers has been the lack of a suitable calibration checking device. The objectives of this study were to develop a rapid method for checking the calibration of the horizontal pendulum-type instrument and to determine the accuracy and reproducibility of this new tester.

EXPERIMENTAL

Two force gauges[3] (range of 0–25 kg in 0.25-kg increments) were calibrated against a tension compression testing machine[4] using the

[1] Heberlein.

[2] Heberlein model 2E, Dr. K. Scheuniger & Co., Zurich, Switzerland.

[3] Model U, W. C. Dillon & Co., Van Nuys, CA 92407

[4] Instron Corp., Canton, Mass.

For the results, growth ratings of 0 or 1 were scored as inhibition. Each compound was evaluated on five tubes, with percent inhibition values being reported. This procedure indicates the percentage of tubes that did not show plaque formation after the stated incubation period. The solvent served as the control (Table III).

RESULTS AND CONCLUSION

The biological results for VII–X (Table III), when compared to chlorhexidine acetate, indicate that two biguanide residues are not required for activity. The length of the alkyl chain need only be extended to achieve the higher lipid solubility required for activity. The two most active compounds tested, IX and chlorhexidine, have log *P* values near 5, suggesting an optimal log *P* for this series. This information will enable prediction, prior to synthesis, of the expected relative activity of biguanides based on lipophilic considerations.

REFERENCES

(1) H. Löe, in "Dental Plaque," W. D. McHugh, Ed., D. C. Thompson and Co., Dundee, Scotland, 1970, p. 259.

(2) H. Löe, *J. Periodont. Res., Suppl.*, **8**, 12, 93(1973).

(3) P. Gjermo, K. L. Baastad, and G. Rölla, *J. Periodont. Res.*, **5**, 102(1970).

(4) F. L. Rose and G. Swain, *J. Chem. Soc.*, **1956**, 4422.

(5) F. H. S. Curd and F. L. Rose, *ibid.*, **1946**, 729.

(6) R. G. Fisher, R. P. Quintana, and M. A. Boulware, *J. Dent. Res.*, **54**, 20(1975).

(7) A. Albert and E. P. Serjeant, in "Determination of Ionization and Stability Constants," Butler and Tanner Ltd., London, England, 1962.

(8) A. F. Yopel, in "Biological Correlations—The Hansch Approach," Advances in Chemistry Series vol. 114, R. F. Gould, Ed., American Chemical Society, Washington, D.C., 1972, p. 189.

(9) C. Hansch and S. M. Anderson, *J. Org. Chem.*, **32**, 2583(1967).

ACKNOWLEDGMENTS AND ADDRESSES

Received July 25, 1975, from the *Department of Medicinal Chemistry and Pharmacology, College of Pharmacy and Allied Health Professions, Northeastern University, Boston, MA 02115*

Accepted for publication September 17, 1975.

Presented in part at the Medicinal Chemistry Section, APhA Academy of Pharmaceutical Sciences, San Francisco meeting, April 1975.

The authors gratefully acknowledge the support of this work by the National Institute of Dental Research (Grant 1R01 DE03212-0-1A1).

[x] To whom inquiries should be directed.

Calibration of a Horizontal Pendulum-Type Tablet Breaking Strength Tester

FRANK W. GOODHART [x], J. RONALD DRAPER, MICHAEL J. KILLEEN, and FRED C. NINGER

Abstract □ A rapid, simplified method of checking the calibration of a new motorized pendulum type of tablet hardness tester and the accuracy and precision of three testers were determined. Two force gauges were calibrated, and both gauges were used by two operators to determine the accuracy of the new testers. This calibration method using the force gauge was reliable for checking the accuracy. The results show the various new testers to be in calibration and to give reproducible results.

Keyphrases □ Tablet hardness testers—motorized pendulum type, method for checking calibration and determining accuracy and precision, three testers compared □ Hardness testers, tablet—motorized pendulum type, method for checking calibration and determining accuracy and precision, three testers compared □ Strength, tablet—testers, motorized pendulum type, method for checking calibration and determining accuracy and precision, three testers compared

Certain deficiencies in the more popular tablet hardness testers have been reported previously (1–3). A new type of tablet hardness tester[1], which operates on the principle of a pendulum being displaced by consistent loading obtained by an electric motor-driven anvil, was made available in 1970 (4). The operation and merits of this tester were reported previously (1). Among its advantages compared to the more typical pneumatic type were: (*a*) more uniform force application, (*b*) less maintenance, and (*c*) the need for fewer calibration checks.

Since that report was completed, a new tablet breaking strength tester[2] became available. Its operating principle is the same as the original but the load scale readout is horizontal rather than circular. The overall size of the new tester is larger, and there are two anvil opening settings, 15 and 35 mm, to accommodate small and large size tablets. Also, the maximum scale values have been increased to 20 kg and 28 Strong-Cobb units to allow for the breakage of harder tablets such as troches and mints. A schematic diagram is shown in Fig. 1.

At the time the new tester was marketed, the manufacturer did not offer a method for checking the calibration. A persistent problem in the use of tablet breaking strength testers has been the lack of a suitable calibration checking device. The objectives of this study were to develop a rapid method for checking the calibration of the horizontal pendulum-type instrument and to determine the accuracy and reproducibility of this new tester.

EXPERIMENTAL

Two force gauges[3] (range of 0–25 kg in 0.25-kg increments) were calibrated against a tension compression testing machine[4] using the

[1] Heberlein.

[2] Heberlein model 2E, Dr. K. Scheuniger & Co., Zurich, Switzerland.

[3] Model U, W. C. Dillon & Co., Van Nuys, CA 92407

[4] Instron Corp., Canton, Mass.

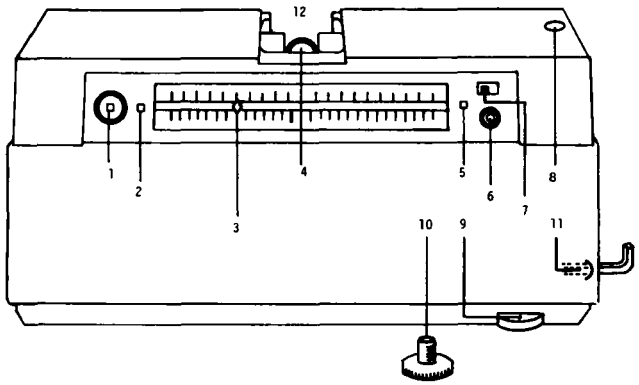

Figure 1—*Schematic diagram of new tester. Key: 1, main switch; 2, pilot lamp; 3, pointer; 4, tablet; 5, pilot lamp; 6, test button; 7, range switch (15 or 35 mm); 8, level; 9, leveling screws (front and back); 10, pendulum lock screw; 11, zero adjustment for pointer; and 12, milled portion of bridge.*

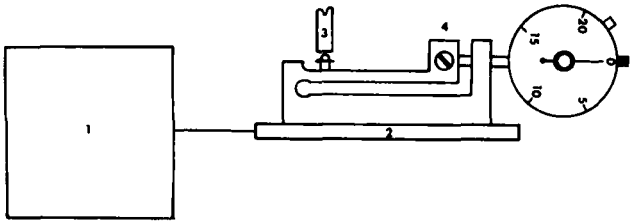

Figure 2—*Schematic view of the calibration method of the force gauge by the tension compression tester. Key: 1, tension compression tester recorder (kilograms); 2, tension compression load cell; 3, gear drive plunger (tension compression tester); and 4, calibration screw (force gauge).*

setup shown in Fig. 2. Recalibration of the force gauges, if necessary, was accomplished with an adjusting screw (Fig. 3) located on the beam just ahead of the dial and by rechecking at several load levels against the tension compression machine. With both force gauges in calibration, simultaneous load readings were obtained from the force gauge and the tension compression testing machine throughout the entire load range of the instrument.

Three pendulum-type testers were employed: Testers A and B (both new) and Tester C (in use for 12 months). To allow for the force gauge to be placed between the jaws of the tester horizontally, a 55-mm portion of the bridge was milled away at the back of the new tester (Fig. 1). The cut was made deep enough to provide a planar surface parallel to the surface supporting the tablet. The milled

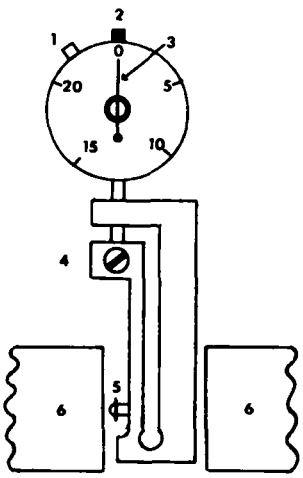

Figure 3—*Schematic view of force gauge. Key: 1, dial face zero adjustment; 2, dust cap; 3, measuring pointer; 4, calibration screw; 5, measuring point contact; and 6, tester anvils.*

Table I—Calibration of the Force Gauge Using the Tension Compression Testing Machine[a]

	Day 1	Day 2	Day 3	Day 4
Slopes				
Force gauge I	1.00	1.00	1.00	1.00
Force gauge II	0.99	0.99	1.00	1.00
Intercepts				
Force gauge I	0.079	−0.013	−0.051	−0.022
Force gauge II	0.117	−0.105	−0.054	0.032

[a] All data are based on nine readings ranging from 3 to 19 kg. The correlation coefficient for all data was >0.99.

portion of the bridge was polished to a smooth finish to reduce the effect of drag on the force gauge.

By using the setup shown in Fig. 3, simultaneous load readings were obtained from the force gauge and the new tester at random loadings throughout the entire load range of the tester. This procedure was repeated using both force gauges and all three of the new hardness testers. Ten random readings were taken for all testers on 3 separate days by two independent operators.

RESULTS AND DISCUSSION

Both force gauges were checked against the tension compression tester to ensure the accuracy of the manufacturer's specification of ±1% of full scale. Adjustments were made, if necessary, *via* the adjusting screw on the gauge. After both force gauges were within the specified accuracy, nine sets of readings ranging from 3 to 19 kg were obtained randomly from both force gauges and tension compression tester over 4 days. The data collected were evaluated statistically to determine the day-to-day reliability of the force gauges.

A typical calibration curve for the new tester, using a force gauge as the standard, is shown in Fig. 4; complete results are given in Table I. Variation between the two force gauges and the tension compression tester from day to day was well within the ±1% accuracy claimed by the manufacturer. The gauges exhibited good linearity and reproducibility over the 4 days. The intercept values did not differ appreciably from zero, and the regression coefficients were >0.99.

After the accuracy and dependability of the force gauges were determined, they were used as the standard in testing the calibration of the new motorized pendulum-type testers. Comparisons were obtained for the three new testers against the force gauge, using kilograms as the unit of measure. Random load readings, ranging from 2 to 18 kg, were simultaneously obtained from the force gauge and the new tester, and the data collected were evaluated statistically (Tables

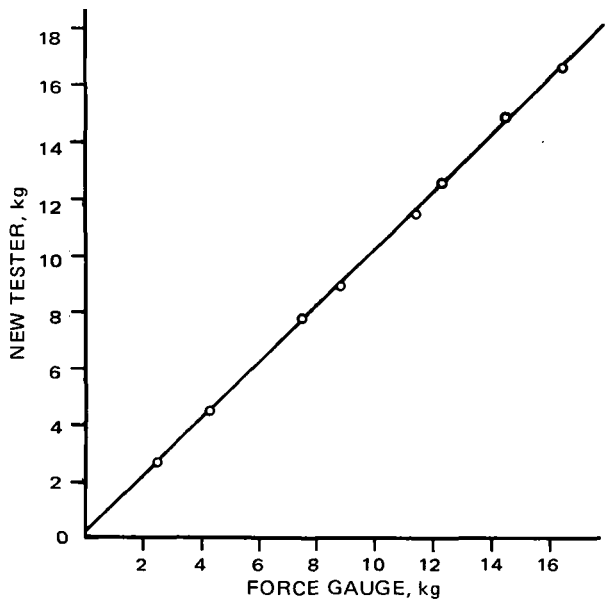

Figure 4—*Typical calibration curve for the new tester using the force gauge.*

Table II—Comparison of Force Gauge I[a] to Three New Testers[b] over 3 Days[c]

	Slope						Intercept					
	Operator 1			Operator 2			Operator 1			Operator 2		
Tester	Day 1	Day 2	Day 3	Day 1	Day 2	Day 3	Day 1	Day 2	Day 3	Day 1	Day 2	Day 3
A	1.03	1.02	1.01	1.01	1.02	1.02	0.061	0.068	0.118	0.103	−0.053	−0.043
B	1.00	0.994	0.988	0.995	0.992	0.990	−0.203	−0.185	−0.159	−0.171	−0.107	−0.091
C	1.00	1.00	1.00	0.999	0.993	0.998	−0.185	−0.168	−0.219	0.002	−0.035	0.017

[a] Dillon force gauge I was used. [b] Heberlein 2E tablet hardness tester. [c] Correlation coefficient for all data was >0.99.

Table III—Comparison of Force Gauge II[a] to Three New Testers[b] over 3 Days[c]

	Slope						Intercept					
	Operator 1			Operator 2			Operator 1			Operator 2		
Tester	Day 1	Day 2	Day 3	Day 1	Day 2	Day 3	Day 1	Day 2	Day 3	Day 1	Day 2	Day 3
A	1.05	1.03	1.02	1.04	1.01	1.03	0.087	0.059	0.040	−0.136	−0.017	−0.255
B	1.01	0.992	1.02	1.00	1.00	1.01	−0.031	0.003	−0.191	−0.157	−0.132	−0.143
C	1.01	0.995	1.01	1.01	0.985	0.980	−0.051	−0.142	−0.172	0.049	0.142	0.067

[a] Dillon force gauge II was used. [b] Heberlein 2E tablet hardness tester. [c] Correlation coefficient for all data was >0.99.

II and III). Tables II and III compare the two force gauges with the three new testers, using the kilogram scale, by two independent operators over 3 days. The slopes for all testers on all days were nearly one, and the intercepts did not differ appreciably from zero. The pendulum-type testers showed good day-to-day reproducibility, and there appeared to be no significant operator variability.

REFERENCES

(1) F. W. Goodhart, J. R. Draper, D. Dancz, and F. C. Ninger, *J. Pharm. Sci.*, **62**, 297(1973).

(2) D. B. Brook and K. Marshall, *ibid.*, **57**, 481(1968).

(3) W. A. Ritschel, F. S. Skinner, and R. Schlumpf, *Pharm. Acta Helv.*, **44**, 547(1969).

(4) K. A. Flury (Heberlein & Co., Switzerland), U.S. pat. 3,757,566 (1973).

ACKNOWLEDGMENTS AND ADDRESSES

Received June 23, 1975, from the *Pharmaceutical Research and Development Laboratories, Warner-Lambert Research Institute, Morris Plains, NJ 07950*

Accepted for publication September 12, 1975.

[x] To whom inquiries should be directed.

Antimicrobial Agents: Synthesis and Antimicrobial Activity of New Aryloxyalkyl Esters of *p*-Hydroxybenzoic Acid

D. R. SHRIDHAR *[x], C. V. REDDY SASTRY *, N. K. VAIDYA *, G. S. REDDI [‡], and G. S. THAPAR [‡]

Abstract □ Several new aryloxyalkyl esters of *p*-hydroxybenzoic acid were synthesized and screened for *in vitro* antimicrobial activity. Although a few compounds showed low antifungal activity, many possessed appreciable *in vitro* antibacterial activity. However, none of these compounds was active against *Mycobacterium tuberculosis* ($H_{37}Rv$).

Keyphrases □ *p*-Hydroxybenzoic acid—aryloxyalkyl esters synthesized and screened for antibacterial and antifungal activity *in vitro* □ Parabens—synthesized and screened for antibacterial and antifungal activity *in vitro* □ Antibacterial activity—aryloxyalkyl esters of *p*-hydroxybenzoic acid screened □ Antifungal activity—aryloxyalkyl esters of *p*-hydroxybenzoic acid screened

p-Hydroxybenzoic acid esters (parabens) are known to possess antibacterial and antifungal activities and have been used extensively as preservatives (1–3). Aryloxyalkanols such as *p*-chlorophenoxyethanol (*p*-chlorophenoxetol) and 1-phenoxypropan-2-ol (propylene phenoxetol) possess marked *in vitro* antifungal activity (4).

A literature survey showed that only two aryloxyalkyl esters of *p*-hydroxybenzoic acid, namely, 2-phenoxy- and 2-(*o*-chlorophenoxy)ethyl esters, have been synthesized (5). These two esters were used as plasticizers in making films, and no pharmacological activity was reported. Therefore, the continued search for antimicrobial agents (6) prompted the synthesis of compounds that would combine the characteristic features of the forementioned esters as well as aryloxyalkanols with a view to examining antimicrobial activity. These compounds also could possibly act as *p*-hydroxybenzoic acid

Table II—Comparison of Force Gauge I[a] to Three New Testers[b] over 3 Days[c]

	Slope						Intercept					
	Operator 1			Operator 2			Operator 1			Operator 2		
Tester	Day 1	Day 2	Day 3	Day 1	Day 2	Day 3	Day 1	Day 2	Day 3	Day 1	Day 2	Day 3
A	1.03	1.02	1.01	1.01	1.02	1.02	0.061	0.068	0.118	0.103	−0.053	−0.043
B	1.00	0.994	0.988	0.995	0.992	0.990	−0.203	−0.185	−0.159	−0.171	−0.107	−0.091
C	1.00	1.00	1.00	0.999	0.993	0.998	−0.185	−0.168	−0.219	0.002	−0.035	0.017

[a] Dillon force gauge I was used. [b] Heberlein 2E tablet hardness tester. [c] Correlation coefficient for all data was >0.99.

Table III—Comparison of Force Gauge II[a] to Three New Testers[b] over 3 Days[c]

	Slope						Intercept					
	Operator 1			Operator 2			Operator 1			Operator 2		
Tester	Day 1	Day 2	Day 3	Day 1	Day 2	Day 3	Day 1	Day 2	Day 3	Day 1	Day 2	Day 3
A	1.05	1.03	1.02	1.04	1.01	1.03	0.087	0.059	0.040	−0.136	−0.017	−0.255
B	1.01	0.992	1.02	1.00	1.00	1.01	−0.031	0.003	−0.191	−0.157	−0.132	−0.143
C	1.01	0.995	1.01	1.01	0.985	0.980	−0.051	−0.142	−0.172	0.049	0.142	0.067

[a] Dillon force gauge II was used. [b] Heberlein 2E tablet hardness tester. [c] Correlation coefficient for all data was >0.99.

II and III). Tables II and III compare the two force gauges with the three new testers, using the kilogram scale, by two independent operators over 3 days. The slopes for all testers on all days were nearly one, and the intercepts did not differ appreciably from zero. The pendulum-type testers showed good day-to-day reproducibility, and there appeared to be no significant operator variability.

REFERENCES

(1) F. W. Goodhart, J. R. Draper, D. Dancz, and F. C. Ninger, *J. Pharm. Sci.*, **62**, 297(1973).

(2) D. B. Brook and K. Marshall, *ibid.*, **57**, 481(1968).

(3) W. A. Ritschel, F. S. Skinner, and R. Schlumpf, *Pharm. Acta Helv.*, **44**, 547(1969).

(4) K. A. Flury (Heberlein & Co., Switzerland), U.S. pat. 3,757,566 (1973).

ACKNOWLEDGMENTS AND ADDRESSES

Received June 23, 1975, from the *Pharmaceutical Research and Development Laboratories, Warner-Lambert Research Institute, Morris Plains, NJ 07950*

Accepted for publication September 12, 1975.

[x] To whom inquiries should be directed.

Antimicrobial Agents: Synthesis and Antimicrobial Activity of New Aryloxyalkyl Esters of *p*-Hydroxybenzoic Acid

D. R. SHRIDHAR *[x], C. V. REDDY SASTRY *, N. K. VAIDYA *, G. S. REDDI [‡], and G. S. THAPAR [‡]

Abstract □ Several new aryloxyalkyl esters of *p*-hydroxybenzoic acid were synthesized and screened for *in vitro* antimicrobial activity. Although a few compounds showed low antifungal activity, many possessed appreciable *in vitro* antibacterial activity. However, none of these compounds was active against *Mycobacterium tuberculosis* ($H_{37}Rv$).

Keyphrases □ *p*-Hydroxybenzoic acid—aryloxyalkyl esters synthesized and screened for antibacterial and antifungal activity *in vitro* □ Parabens—synthesized and screened for antibacterial and antifungal activity *in vitro* □ Antibacterial activity—aryloxyalkyl esters of *p*-hydroxybenzoic acid screened □ Antifungal activity—aryloxyalkyl esters of *p*-hydroxybenzoic acid screened

p-Hydroxybenzoic acid esters (parabens) are known to possess antibacterial and antifungal activities and have been used extensively as preservatives (1–3). Aryloxyalkanols such as *p*-chlorophenoxyethanol (*p*-chlorophenoxetol) and 1-phenoxypropan-2-ol (propylene phenoxetol) possess marked *in vitro* antifungal activity (4).

A literature survey showed that only two aryloxyalkyl esters of *p*-hydroxybenzoic acid, namely, 2-phenoxy- and 2-(*o*-chlorophenoxy)ethyl esters, have been synthesized (5). These two esters were used as plasticizers in making films, and no pharmacological activity was reported. Therefore, the continued search for antimicrobial agents (6) prompted the synthesis of compounds that would combine the characteristic features of the forementioned esters as well as aryloxyalkanols with a view to examining antimicrobial activity. These compounds also could possibly act as *p*-hydroxybenzoic acid

and aryloxyalkanols as a result of biotransformations.

The synthesis and antimicrobial activity of several new aryloxyalkyl esters of *p*-hydroxybenzoic acid (Structure I, Scheme I) are reported in this article.

RESULTS AND DISCUSSION

Chemistry—The aryloxyalkyl esters of *p*-hydroxybenzoic acid listed in Table I were synthesized by treating *p*-hydroxybenzoic acid with different aryloxyalkanols at 140–160°, using *p*-toluenesulfonic acid as a catalyst (Scheme I). The intermediate aryloxyethanols were prepared by condensing different phenols with 2-chloroethanol according to the method of Nair and Peacock (7). The remaining aryloxyalkanols were made by converting the respective aryloxyalkyl bromides (8) into the corresponding acetates followed by hydrolysis with methanolic potassium hydroxide.

Fifty-six compounds with varying alkyl chain lengths (n = 2–6) and different aryl functions (Table I) were synthesized and tested *in vitro* for antifungal and antibacterial activities against various fungi and bacteria. All esters were characterized by elemental analyses; IR (mineral oil): 3450 (hydroxyl) and 1700 (ester carbonyl) cm^{-1}.

Biology—All esters were assayed *in vitro* for antibacterial activity against 11 bacteria and for antifungal activity against 10 fungi. The compounds that exhibited significant antibacterial and antifungal activities are listed in Tables II and III. From these data, it can be seen that nine compounds (VII, XX, XXV, XXVII, XXXII, XXXVI, XXXVII, XLII, and XLIV) differed from the rest in showing good activity only against the Gram-negative bacterium, namely, *Pseudomonas aeruginosa*. The *p*-chloro-*m*-tolyloxypentyl ester (XLII) possessed significant activity, inhibiting the growth of this microorganism at 2.5 μg/ml.

Among the compounds showing activity against both Gram-positive and Gram-negative bacteria, the *p*-chloro-*m*-tolyloxybutyl ester (XXIX), the *o*-chlorophenoxypentyl ester (XXXV), and the phenoxyhexyl ester (XLVII) exhibited appreciable activity by inhibiting the growth of five bacteria at 5–25 μg/ml. However, none of these compounds was active against *Escherichia coli, Salmonella typhi, Proteus vulgaris, Vibrio cholerae, Shigella dysenteriae,* or *Mycobacterium tuberculosis* ($H_{37}Rv$) at test concentrations (200 μg/ml).

Only a few compounds exhibited antifungal activity against nine

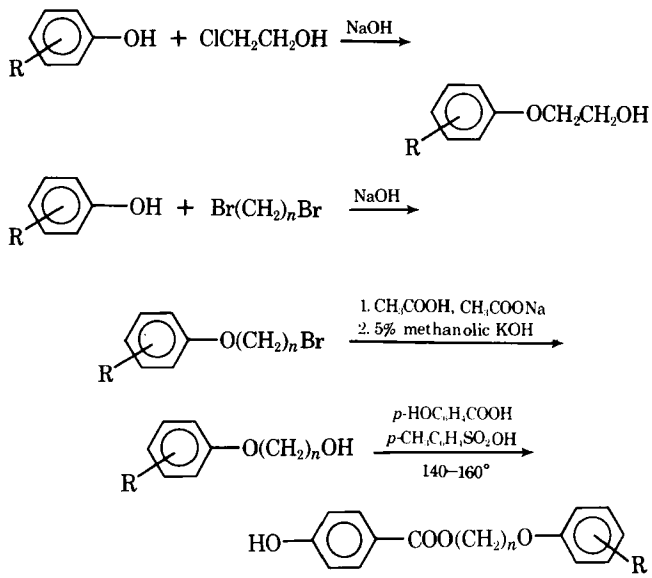

Scheme I

Table I—Physical Constants of Aryloxyalkyl Esters of *p*-Hydroxybenzoic Acid[a]

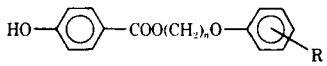

Compound	R	n	Melting Point[b,c]	Yield[d], %	Molecular Formula	Analysis, %	
						Calc.	Found
I[e]	H	2	109–111°	48	$C_{15}H_{14}O_4$	C 69.77 H 5.42	69.38 5.56
II	2-Cl	2	150–151°	35	$C_{15}H_{13}ClO_4$	C 61.54 H 4.44	61.40 4.80
III	4-Cl	2	152–154°	57	$C_{15}H_{13}ClO_4$	C 61.54 H 4.44	62.04 5.01
IV	2,4-Cl_2	2	123–125°	48	$C_{15}H_{12}Cl_2O_4$	C 55.05 H 3.67	54.50 4.00
V	4-Br	2	156–158°	34	$C_{15}H_{13}BrO_4$	C 53.55 H 3.86	53.90 4.00
VI	2-CH_3	2	115–117°	20	$C_{16}H_{16}O_4$	C 70.58 H 5.88	70.04 6.05
VII	4-CH_3	2	124–125°	21	$C_{16}H_{16}O_4$	C 70.58 H 5.88	70.31 6.36
VIII	3-CH_3, 6-Cl	2	140–142°	35	$C_{16}H_{15}ClO_4$	C 62.65 H 4.90	62.13 5.11
IX	3-CH_3, 6-$CH(CH_3)_2$	2	153–155°	53	$C_{19}H_{22}O_4$	C 72.61 H 7.00	72.40 6.80
X	3-CH_3, 4-Cl, 6-$CH(CH_3)_2$	2	180–181°	60	$C_{19}H_{21}ClO_4$	C 65.42 H 6.02	65.81 6.16
XI	3-NO_2	2	147–149°	27	$C_{15}H_{13}NO_6$	C 59.41 H 4.29	59.12 4.18
XII	4-NO_2	2	170–172°	35	$C_{15}H_{13}NO_6$	C 59.41 H 4.29	59.80 4.60
XIII	H	3	112–114°	26	$C_{16}H_{16}O_4$	C 70.58 H 5.88	70.14 6.05
XIV	2-Cl	3	124–125°	75	$C_{16}H_{15}ClO_4$	C 62.65 H 4.90	63.20 5.18
XV	4-Cl	3	129–130°	15	$C_{16}H_{15}ClO_4$	C 62.65 H 4.90	63.01 5.10
XVI	2,4-Cl_2	3	127–129°	48	$C_{16}H_{14}Cl_2O_4$	C 56.30 H 4.10	56.19 3.98
XVII	2-CH_3	3	113–114°	46	$C_{17}H_{18}O_4$	C 71.32 H 6.29	70.87 6.39
XVIII	3-CH_3	3	111–113°	58	$C_{17}H_{18}O_4$	C 71.32 H 6.29	71.03 6.25

(*continued*)

Table I—*(Continued)*

Compound	R	n	Melting Point[b,c]	Yield[d], %	Molecular Formula	Analysis, % Calc.	Found
XIX	4-CH_3	3	89–91°	69	$C_{17}H_{18}O_4$	C 71.32	70.88
						H 6.29	6.50
XX	3-CH_3, 6-Cl	3	117–118°	86	$C_{17}H_{17}ClO_4$	C 63.65	63.65
						H 5.30	5.42
XXI	3-CH_3, 6-$CH(CH_3)_2$	3	98–100°	62	$C_{20}H_{24}O_4$	C 73.16	73.62
						H 7.31	7.50
XXII	H	4	72–73°	50	$C_{17}H_{18}O_4$	C 71.32	71.20
						H 6.29	6.26
XXIII	2-Cl	4	122–124°	60	$C_{17}H_{17}ClO_4$	C 63.65	63.96
						H 5.30	5.72
XXIV	4-Cl	4	121–122°	60	$C_{17}H_{17}ClO_4$	C 63.65	63.86
						H 5.30	5.64
XXV	2,4-Cl_2	4	107–108°	83	$C_{17}H_{16}Cl_2O_4$	C 57.46	57.30
						H 4.50	5.00
XXVI	4-Br	4	112–114°	74	$C_{17}H_{17}BrO_4$	C 55.89	55.80
						H 4.65	4.94
XXVII	2-CH_3	4	120–121°	50	$C_{18}H_{20}O_4$	C 72.00	71.93
						H 6.66	6.62
XXVIII	4-CH_3	4	83–85°	82	$C_{18}H_{20}O_4$	C 72.00	71.64
						H 6.66	6.58
XXIX	3-CH_3, 6-Cl	4	93–94°	60	$C_{18}H_{19}ClO_4$	C 64.60	64.20
						H 5.68	5.88
XXX	3-CH_3, 6-$CH(CH_3)_2$	4	117–118°	30	$C_{21}H_{26}O_4$	C 73.69	73.33
						H 7.60	7.69
XXXI	3-CH_3, 4-Cl, 6-$CH(CH_3)_2$	4	133–134°	76	$C_{21}H_{25}ClO_4$	C 66.93	66.42
						H 6.16	6.63
XXXII	3-NO_2	4	100–101°	30	$C_{17}H_{17}NO_6$	C 61.63	61.18
						H 5.13	4.70
XXXIII	4-NO_2	4	143–144°	15	$C_{17}H_{17}NO_6$	C 61.63	62.00
						H 5.13	5.52
XXXIV	H	5	132–133°	72	$C_{18}H_{20}O_4$	C 72.00	72.60
						H 6.66	6.92
XXXV	2-Cl	5	114–116°	42	$C_{18}H_{19}ClO_4$	C 64.60	64.80
						H 5.68	5.80
XXXVI	4-Cl	5	113–114°	54	$C_{18}H_{19}ClO_4$	C 64.60	64.65
						H 5.68	5.65
XXXVII	2,4-Cl_2	5	109–110°	79	$C_{18}H_{18}Cl_2O_4$	C 58.55	58.40
						H 4.87	4.98
XXXVIII	4-Br	5	112–114°	55	$C_{18}H_{19}BrO_4$	C 57.01	56.90
						H 5.01	5.22
XXXIX	2-CH_3	5	86–88°	55	$C_{19}H_{22}O_4$	C 72.61	73.00
						H 7.00	7.10
XL	3-CH_3	5	75–77°	35	$C_{19}H_{22}O_4$	C 72.61	73.10
						H 7.00	7.24
XLI	4-CH_3	5	102–104°	41	$C_{19}H_{22}O_4$	C 72.61	72.34
						H 7.00	7.09
XLII	3-CH_3, 6-Cl	5	110–112°	70	$C_{19}H_{21}ClO_4$	C 65.42	65.51
						H 6.02	6.34
XLIII	3-CH_3, 6-$CH(CH_3)_2$	5	99–100°	64	$C_{22}H_{28}O_4$	C 74.15	74.40
						H 7.86	7.95
XLIV	3-CH_3, 4-Cl, 6-$CH(CH_3)_2$	5	104–106°	50	$C_{22}H_{27}ClO_4$	C 67.61	67.38
						H 6.92	6.97
XLV	3-NO_2	5	102–103°	76	$C_{18}H_{19}NO_6$	C 62.62	62.80
						H 5.50	5.77
XLVI	4-NO_2	5	114–116°	20	$C_{18}H_{19}NO_6$	C 62.62	62.32
						H 5.50	5.51
XLVII	H	6	89–90°	82	$C_{19}H_{22}O_4$	C 72.61	72.20
						H 7.00	7.03
XLVIII	2-Cl	6	80–82°	48	$C_{19}H_{21}ClO_4$	C 65.42	65.80
						H 6.02	6.42
XLIX	4-Cl	6	105–106°	70	$C_{19}H_{21}ClO_4$	C 65.42	65.90
						H 6.02	6.19
L	2,4-Cl_2	6	62–63°	72	$C_{19}H_{20}Cl_2O_4$	C 59.53	59.80
						H 5.22	5.48
LI	2-CH_3	6	59–61°	55	$C_{20}H_{24}O_4$	C 73.16	73.05
						H 7.31	7.31
LII	3-CH_3	6	84–86°	84	$C_{20}H_{24}O_4$	C 73.16	73.01
						H 7.31	7.44
LIII	4-CH_3	6	94–95°	92	$C_{20}H_{24}O_4$	C 73.16	72.85
						H 7.31	7.12
LIV	3-CH_3, 6-Cl	6	102–103°	51	$C_{20}H_{23}ClO_4$	C 66.21	66.65
						H 6.34	6.53
LV	3-CH_3, 6-$CH(CH_3)_2$	6	100–101°	83	$C_{23}H_{30}O_4$	C 74.59	74.16
						H 8.10	8.29
LVI	3-CH_3, 4-Cl, 6-$CH(CH_3)_2$	6	103–105°	58	$C_{23}H_{29}ClO_4$	C 68.23	68.73
						H 7.16	7.32

[a] These compounds were purified by chromatography over silica gel and eluting with benzene. Final recrystallizations were done with benzene–petroleum ether (bp 40–60°). [b] Analytical sample. [c] Melting points were determined in closed capillary tubes in a sulfuric acid bath and are uncorrected. [d] Based on material that melts within 5° of the analytical sample. [e] The reported melting point (5) is 118°, and it did not improve in this study even after repeated recrystallizations.

Table II—Antibacterial Activities[a] (Minimum Inhibitory Concentration, Micrograms per Milliliter)

Compound	Bacteria				
	Staphylococcus aureus	*Streptococcus faecalis*	*Klebsiella pneumoniae*	*Pseudomonas aeruginosa*	*Agrobacterium tumefaciens*
VII	n.a.	n.a.	n.a.	10	n.a.
XIV	n.a.	n.a.	25	10	25
XV	n.a.	n.a.	200	10	n.a.
XVI	100	25	25	5	200
XVIII	25	n.a.	50	10	25
XIX	25	25	25	25	25
XX	n.a.	n.a.	n.a.	5	n.a.
XXI	25	10	25	5	100
XXII	25	25	50	25	25
XXIII	25	10	25	10	25
XXV	n.a.	n.a.	n.a.	5	n.a.
XXVII	n.a.	n.a.	n.a.	5	n.a.
XXVIII	n.a.	25	n.a.	25	25
XXIX	10	10	25	5	10
XXXII	n.a.	n.a.	n.a.	25	n.a.
XXXV	25	5	5	5	5
XXXVI	n.a.	n.a.	n.a.	5	n.a.
XXXVII	n.a.	n.a.	n.a.	5	n.a.
XXXIX	25	25	25	5	25
XL	25	25	25	5	100
XLI	25	10	25	5	10
XLII	n.a.	n.a.	n.a.	2.5	n.a.
XLIII	n.a.	25	n.a.	5	n.a.
XLIV	n.a.	n.a.	n.a.	5	n.a.
XLV	200	50	25	10	25
XLVII	25	25	10	5	25
XLVIII	25	25	10	5	25
L	n.a.	10	10	5	200
LI	50	25	25	5	n.a.
LII	100	25	50	5	100
LIII	n.a.	200	n.a.	10	200
LIV	n.a.	25	50	25	n.a.
LV	n.a.	50	n.a.	25	n.a.

[a] n.a. = not active up to 200 μg/ml.

Table III—Antifungal Activities[a] (Minimum Inhibitory Concentration, Micrograms per Milliliter)

Compound	Fungi								
	Microsporum canis	*Microsporum gypseum*	*Trichophyton mentagrophytes*	*Trichophyton rubrum*	*Epidermophyton floccosum*	*Candida albicans*	*Cryptococcus neoformans*	*Sporotrichum schenkii*	*Histoplasma capsulatum*
I	50	50	25	50	—	n.a.	100	100	50
VIII	n.a.	n.a.	n.a.	n.a.	—	100	25	n.a.	100
XIV	n.a.	n.a.	n.a.	n.a.	—	n.a.	25	n.a.	n.a.
XV	25	25	n.a.	25	200	n.a.	200	n.a.	n.a.
XVI	n.a.	n.a.	n.a.	n.a.	—	n.a.	7.5	n.a.	n.a.
XVIII	n.a.	100	n.a.	100	—	n.a.	25	n.a.	25
XIX	25	50	50	50	200	n.a.	200	100	200
XXII	n.a.	n.a.	n.a.	n.a.	—	100	25	n.a.	100
XXIII	n.a.	n.a.	n.a.	n.a.	—	n.a.	10	n.a.	n.a.
XXVIII	10	25	50	25	n.a.	n.a.	n.a.	25	n.a.

[a] n.a. = not active up to 200 μg/ml; -- = not tested.

of the 10 fungi tested, while none was active against *Aspergillus fumigatus*. The 2-phenoxyethyl ester (I) showed the widest, albeit low, activity, ranging from 25 to 100 μg/ml against seven fungi.

EXPERIMENTAL[1]

3-(*o*-Chlorophenoxy)propyl *p*-Hydroxybenzoate (XIV, Table I)—A mixture of 3-(*o*-chlorophenoxy)propanol (4.1 g, 0.022 mole), *p*-hydroxybenzoic acid (2.75 g, 0.02 mole), and *p*-toluenesulfonic acid (0.1 g) was heated with stirring for 6 hr at 140–160° in an oil bath. The reaction mixture was cooled and extracted with ether (4 × 50 ml), and the ether extract was washed with 5% sodium bicarbonate solution to remove the unreacted acid. The ether layer was then thoroughly extracted with 5% cold sodium hydroxide solution.

The sodium hydroxide extract was neutralized with dilute hydrochloric acid and reextracted with ether (4 × 50 ml). The dried (sodium sulfate) ether extract, on evaporation, gave crude XIV as a brown solid. This solid was purified by chromatography over silica gel, eluting with benzene. An analytically pure sample was obtained as white shining needles by recrystallization from benzene–petroleum ether (bp 40–60°), mp 124–125°, 75% yield; IR[2] (mineral oil): 3450 (hydroxyl) and 1700 (ester carbonyl) cm^{-1}.

All aryloxyalkyl esters of *p*-hydroxybenzoic acid reported in Table I were similarly prepared and characterized by sharp melting points, elemental analyses, and IR spectra.

Biological Methods—The bacteria used were *Staphylococcus aureus*[3] (ATCC 6538), *Streptococcus faecalis*[3] (ATCC 10541),

[1] All compounds were analyzed for their carbon and hydrogen content.

[2] IR spectra were taken in Nujol on a Perkin-Elmer 237 grating IR spectrophotometer.

[3] Obtained from Central Drug Research Institute, Lucknow, India.

Escherichia coli[3] (114), *Salmonella typhi*[3] (115), *Klebsiella pneumoniae*[3] (ATCC 10031), *Pseudomonas aeruginosa*[3] (ATCC 10145), *Agrobacterium tumefaciens*[3] (NRRL B 36), *Proteus vulgaris*[4] (145), *Vibrio cholerae*[4] (ATCC 14033), *Shigella dysenteriae*[4] (ISRC 566/61), and *Mycobacterium tuberculosis*[5] ($H_{37}Rv$).

The fungi used were *Microsporum canis*[3] (VM 200-USPHS), *Microsporum gypseum*[3] (153 CSTM), *Trichophyton mentagrophytes*[3] (A 280-USPHS), *Trichophyton rubrum*[3] (252 CSTM), *Candida albicans*[3] (SKF 2270), *Cryptococcus neoformans*[3] (103), *Sporotrichum schenkii*[3] (107), *Aspergillus fumigatus*[3] (68 LI), *Histoplasma capsulatum*[3] (RNSH Hi 70½ Sydney), and *Epidermophyton floccosum*[5] (HM 300).

Antibacterial Activity—The *in vitro* antibacterial activity was determined by an agar dilution method (9). Twofold serial dilutions of the test compound were prepared in melted tryptone soya agar (oxoid), made into slopes in 18 × 150-mm test tubes. The slopes were streaked with one loopful of an overnight culture of each test organism in tryptone soya broth and incubated for 48 hr at 37°. *M. tuberculosis* was maintained on Lowenstein–Jensen medium.

Antituberculosis activity was tested in Youmans medium (10) following the serial dilution method. To 5 ml of Youmans medium containing the concentrations of the compound, one loopful (4 mm diameter) of 12–14-day-old culture was added. Cells were grown as stationary floating cultures, and growth of cells was followed visually at weekly intervals for 3 weeks.

Antifungal Activity—The compounds were tested for activity by the agar dilution assay method described by Robinson *et al.* (11). The compound under test was diluted in Sabouraud dextrose agar medium, maintained at 50°, in 18 × 150-mm test tubes and slanted. The fungi were streaked across the surface of the slants containing different concentrations of the test compound. The growth was observed visually after 3–14 days, depending upon the test organism.

In all cases, the minimum inhibitory concentration was expressed in terms of micrograms per milliliter at which the growth of the test culture was completely suppressed. A control tube containing the same medium without the test compound was included for each organism tested. Duplicates were maintained for all concentrations.

[4] Obtained from Indian Institute of Experimental Medicine, Calcutta, India.

[5] Obtained from Microbiology & Pharmacology Department, Indian Institute of Science, Bangalore, India.

REFERENCES

(1) E. P. Taylor and P. F. D'arcy, in "Progress in Medicinal Chemistry," vol. I, G. P. Ellis and G. B. West, Eds., Butterworths, London, England, 1961, p. 230.

(2) M. Huppert, *Antibiot. Chemother.*, **7**, 29(1957).

(3) T. R. Aalto, M. C. Firman, and N. E. Rigler, *J. Am. Pharm. Assoc., Sci. Ed.*, **42**, 449(1953).

(4) H. Berry, *Lancet*, **2**, 175(1944).

(5) E. F. Grether and R. B. Du Vall (to Dow Chemical Co.), U.S. pat. 2,198,582 (1940); through *Chem. Abstr.*, **34**, 5965(1940).

(6) N. K. Vaidya, C. V. Reddy Sastry, D. R. Shridhar, G. S. Thapar, and G. S. Reddi, *Curr. Sci.*, **44**, 48(1975).

(7) C. N. Nair and D. H. Peacock, *J. Indian Chem. Soc.*, **12**, 318(1935).

(8) C. S. Marvel and A. L. Tanenbaum, "Organic Syntheses," coll. vol. I, Wiley, New York, N.Y., 1944, p. 435.

(9) M. Nishida, Y. Mine, T. Matsubara, S. Goto, and S. Kawahara, *J. Antibiot.*, **25**, 582(1972).

(10) G. P. Youmans, *Proc. Soc. Exp. Biol. Med.*, **57**, 122(1944).

(11) R. C. V. Robinson, T. N. Ferciot, III, and H. M. Robinson, Jr., *Arch. Dermatol.*, **81**, 681(1960).

ACKNOWLEDGMENTS AND ADDRESSES

Received July 15, 1975, from the *[*]Chemistry Division and the [†]Microbiology Division, Research & Development Department, Synthetic Drugs Plant, Indian Drugs & Pharmaceuticals Limited, Hyderabad-500 037, India.

Accepted for publication September 24, 1975.

The authors thank Mr. R. Deshpande and Mr. H. Muralidhar Rao of this Department for microanalyses and spectral data, respectively, and Mr. N. Sridhara Rao and Mr. V. L. V. Ramana Rao for assistance.

[x] To whom inquiries should be directed.

Anti-Inflammatory and Antiproteolytic Properties of 1-(1-Naphthylacetyl)-3-substituted Carbamides

VIMAL KISHORE *[§], SUSHIL KUMAR *, SURENDRA S. PARMAR *[‡x], and VIRGIL I. STENBERG [§]

Abstract □ Several 1-(1-naphthylacetyl)-3-substituted carbamides were synthesized, characterized, and evaluated for anti-inflammatory and antiproteolytic activity. The protection afforded by most of these carbamides against carrageenan-induced edema in rats at a dose of 100 mg/kg ranged from 4.4 to 50%. Some of these carbamides, which showed higher protection against carrageenan-induced edema, were further evaluated for their antigranulation effect against cotton pellet-induced granuloma formation in rats. All carbamides showed a poor degree of protection against granuloma formation. The antiproteolytic activity of these carbamides, as reflected by their ability to inhibit trypsin-induced hydrolysis of the bovine serum albumin, was of a low order and was unrelated to their anti-inflammatory activity.

Keyphrases □ Carbamides, 1-(1-naphthylacetyl)-3-substituted—synthesized, evaluated for anti-inflammatory and antiproteolytic activity □ Anti-inflammatory activity—1-(1-naphthylacetyl)-3-substituted carbamides evaluated □ Antiproteolytic activity—1-(1-naphthylacetyl)-3-substituted carbamides evaluated □ Structure–activity relationships—1-(1-naphthylacetyl)-3-substituted carbamides synthesized and evaluated for anti-inflammatory and antiproteolytic activity

Several arylacetic acids and amides have been reported to be active anti-inflammatory agents (1–6). Earlier studies reported high anti-inflammatory activity for several derivatives of 1-naphthylacetic acid (7, 8) and substituted 1-naphthylacetamide (4, 9). Certain substituted ureas also have been reported to possess anti-inflammatory activity (10). These observations prompted the synthesis of a series of 1-(1-naphthylacetyl)-3-substituted carbamides, which were evaluated for anti-inflammatory activity against carrageenan-induced edema and cotton pellet-induced granuloma formation.

Escherichia coli[3] (114), *Salmonella typhi*[3] (115), *Klebsiella pneumoniae*[3] (ATCC 10031), *Pseudomonas aeruginosa*[3] (ATCC 10145), *Agrobacterium tumefaciens*[3] (NRRL B 36), *Proteus vulgaris*[4] (145), *Vibrio cholerae*[4] (ATCC 14033), *Shigella dysenteriae*[4] (ISRC 566/61), and *Mycobacterium tuberculosis*[5] ($H_{37}Rv$).

The fungi used were *Microsporum canis*[3] (VM 200-USPHS), *Microsporum gypseum*[3] (153 CSTM), *Trichophyton mentagrophytes*[3] (A 280-USPHS), *Trichophyton rubrum*[3] (252 CSTM), *Candida albicans*[3] (SKF 2270), *Cryptococcus neoformans*[3] (103), *Sporotrichum schenkii*[3] (107), *Aspergillus fumigatus*[3] (68 LI), *Histoplasma capsulatum*[3] (RNSH Hi 70½ Sydney), and *Epidermophyton floccosum*[5] (HM 300).

Antibacterial Activity—The *in vitro* antibacterial activity was determined by an agar dilution method (9). Twofold serial dilutions of the test compound were prepared in melted tryptone soya agar (oxoid), made into slopes in 18 × 150-mm test tubes. The slopes were streaked with one loopful of an overnight culture of each test organism in tryptone soya broth and incubated for 48 hr at 37°. *M. tuberculosis* was maintained on Lowenstein–Jensen medium.

Antituberculosis activity was tested in Youmans medium (10) following the serial dilution method. To 5 ml of Youmans medium containing the concentrations of the compound, one loopful (4 mm diameter) of 12–14-day-old culture was added. Cells were grown as stationary floating cultures, and growth of cells was followed visually at weekly intervals for 3 weeks.

Antifungal Activity—The compounds were tested for activity by the agar dilution assay method described by Robinson *et al.* (11). The compound under test was diluted in Sabouraud dextrose agar medium, maintained at 50°, in 18 × 150-mm test tubes and slanted. The fungi were streaked across the surface of the slants containing different concentrations of the test compound. The growth was observed visually after 3–14 days, depending upon the test organism.

In all cases, the minimum inhibitory concentration was expressed in terms of micrograms per milliliter at which the growth of the test culture was completely suppressed. A control tube containing the same medium without the test compound was included for each organism tested. Duplicates were maintained for all concentrations.

[4] Obtained from Indian Institute of Experimental Medicine, Calcutta, India.

[5] Obtained from Microbiology & Pharmacology Department, Indian Institute of Science, Bangalore, India.

REFERENCES

(1) E. P. Taylor and P. F. D'arcy, in "Progress in Medicinal Chemistry," vol. I, G. P. Ellis and G. B. West, Eds., Butterworths, London, England, 1961, p. 230.

(2) M. Huppert, *Antibiot. Chemother.*, **7**, 29(1957).

(3) T. R. Aalto, M. C. Firman, and N. E. Rigler, *J. Am. Pharm. Assoc., Sci. Ed.*, **42**, 449(1953).

(4) H. Berry, *Lancet*, **2**, 175(1944).

(5) E. F. Grether and R. B. Du Vall (to Dow Chemical Co.), U.S. pat. 2,198,582 (1940); through *Chem. Abstr.*, **34**, 5965(1940).

(6) N. K. Vaidya, C. V. Reddy Sastry, D. R. Shridhar, G. S. Thapar, and G. S. Reddi, *Curr. Sci.*, **44**, 48(1975).

(7) C. N. Nair and D. H. Peacock, *J. Indian Chem. Soc.*, **12**, 318(1935).

(8) C. S. Marvel and A. L. Tanenbaum, "Organic Syntheses," coll. vol. I, Wiley, New York, N.Y., 1944, p. 435.

(9) M. Nishida, Y. Mine, T. Matsubara, S. Goto, and S. Kawahara, *J. Antibiot.*, **25**, 582(1972).

(10) G. P. Youmans, *Proc. Soc. Exp. Biol. Med.*, **57**, 122(1944).

(11) R. C. V. Robinson, T. N. Ferciot, III, and H. M. Robinson, Jr., *Arch. Dermatol.*, **81**, 681(1960).

ACKNOWLEDGMENTS AND ADDRESSES

Received July 15, 1975, from the *[*]Chemistry Division and the [†]Microbiology Division, Research & Development Department, Synthetic Drugs Plant, Indian Drugs & Pharmaceuticals Limited, Hyderabad-500 037, India.

Accepted for publication September 24, 1975.

The authors thank Mr. R. Deshpande and Mr. H. Muralidhar Rao of this Department for microanalyses and spectral data, respectively, and Mr. N. Sridhara Rao and Mr. V. L. V. Ramana Rao for assistance.

[x] To whom inquiries should be directed.

Anti-Inflammatory and Antiproteolytic Properties of 1-(1-Naphthylacetyl)-3-substituted Carbamides

VIMAL KISHORE *[§], SUSHIL KUMAR *, SURENDRA S. PARMAR *[‡x], and VIRGIL I. STENBERG [§]

Abstract □ Several 1-(1-naphthylacetyl)-3-substituted carbamides were synthesized, characterized, and evaluated for anti-inflammatory and antiproteolytic activity. The protection afforded by most of these carbamides against carrageenan-induced edema in rats at a dose of 100 mg/kg ranged from 4.4 to 50%. Some of these carbamides, which showed higher protection against carrageenan-induced edema, were further evaluated for their antigranulation effect against cotton pellet-induced granuloma formation in rats. All carbamides showed a poor degree of protection against granuloma formation. The antiproteolytic activity of these carbamides, as reflected by their ability to inhibit trypsin-induced hydrolysis of the bovine serum albumin, was of a low order and was unrelated to their anti-inflammatory activity.

Keyphrases □ Carbamides, 1-(1-naphthylacetyl)-3-substituted—synthesized, evaluated for anti-inflammatory and antiproteolytic activity □ Anti-inflammatory activity—1-(1-naphthylacetyl)-3-substituted carbamides evaluated □ Antiproteolytic activity—1-(1-naphthylacetyl)-3-substituted carbamides evaluated □ Structure–activity relationships—1-(1-naphthylacetyl)-3-substituted carbamides synthesized and evaluated for anti-inflammatory and antiproteolytic activity

Several arylacetic acids and amides have been reported to be active anti-inflammatory agents (1–6). Earlier studies reported high anti-inflammatory activity for several derivatives of 1-naphthylacetic acid (7, 8) and substituted 1-naphthylacetamide (4, 9). Certain substituted ureas also have been reported to possess anti-inflammatory activity (10). These observations prompted the synthesis of a series of 1-(1-naphthylacetyl)-3-substituted carbamides, which were evaluated for anti-inflammatory activity against carrageenan-induced edema and cotton pellet-induced granuloma formation.

Table I—Physical Constants of 1-(1-Naphthylacetyl)-3-substituted Carbamides

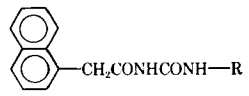

Compound	R	Melting Point[a]	Yield, %	Molecular Formula[b]	Analysis, %	
					Calc.	Found
I	CH_3	197°	45	$C_{14}H_{14}N_2O_2$	C 69.42	69.46
					H 5.78	5.62
					N 11.57	11.56
II	C_2H_5	172°	56	$C_{15}H_{16}N_2O_2$	C 70.35	70.31
					H 6.25	6.24
					N 10.94	10.93
III	n-C_3H_7	141°	51	$C_{16}H_{18}N_2O_2$	C 71.11	71.35
					H 6.66	6.61
					N 10.37	10.45
IV	n-C_4H_9	120°	75	$C_{17}H_{20}N_2O_2$	C 71.83	71.69
					H 7.04	7.12
					N 9.86	9.80
V	C_6H_5	202°	70	$C_{19}H_{16}N_2O_2$	C 74.99	74.78
					H 5.26	5.12
					N 9.21	9.40
VI	o-$CH_3C_6H_4$	202°	65	$C_{20}H_{18}N_2O_2$	C 75.48	75.51
					H 5.66	5.60
					N 8.80	8.81
VII	m-$CH_3C_6H_4$	197°	58	$C_{20}H_{18}N_2O_2$	C 75.48	75.56
					H 5.66	5.68
					N 8.80	8.86
VIII	p-$CH_3C_6H_4$	188°	50	$C_{20}H_{18}N_2O_2$	C 75.48	75.48
					H 5.66	5.61
					N 8.80	8.79
IX	3,4-$(CH_3)_2C_6H_3$	190°	55	$C_{21}H_{20}N_2O_2$	C 75.91	76.14
					H 6.02	6.31
					N 8.43	8.49
X	m-$OCH_3C_6H_4$	173°	65	$C_{20}H_{18}N_2O_3$	C 71.86	71.66
					H 5.39	5.42
					N 8.38	8.45
XI	m-ClC_6H_4	185°	61	$C_{19}H_{15}ClN_2O_2$	C 67.36	67.24
					H 4.42	4.41
					N 8.26	8.28

[a] Melting points were taken in open capillary tubes with a partial immersion thermometer and are corrected. [b] All substituted carbamides, except IX, were recrystallized from ethanol; IX was recrystallized from a benzene–ethanol mixture.

Furthermore, the role of proteolytic enzymes in the inflammatory process is well documented (11, 12). The antiprotease property of various anti-inflammatory compounds has been shown to reflect their ability to inhibit enzymes causing the formation of permeability-increasing factors (13, 14). These observations prompted the investigation of the effects of substituted carbamides on protein catabolism to elucidate the biochemical basis of their anti-inflammatory property.

EXPERIMENTAL[1]

1-Naphthylacetyl Chloride—A mixture of 1-naphthylacetic acid (0.25 mole) and thionyl chloride (0.3 mole) in 100 ml of dry benzene was refluxed on a steam bath for 2–4 hr. Excess benzene and thionyl chloride were removed by distillation under reduced pressure. 1-Naphthylacetyl chloride, obtained as a residue, was distilled under reduced pressure, bp 167°/10 mm [as reported earlier (15)].

Arylcarbamides—The appropriate aromatic amine (0.1 mole) was dissolved in warm acetic acid (10 ml) containing 50 ml of water. This solution was diluted with 150 ml of water, and a warm solution of potassium cyanate (0.1 mole) in 50 ml of water was added with stirring. The arylcarbamides, which precipitated almost immediately, were allowed to stand for several hours. Then they were collected by filtration, washed with water, dried, and recrystallized from the appropriate solvents (16).

1-(1-Naphthylacetyl)-3-substituted Carbamides—A mixture of 1-naphthylacetyl chloride (0.015 mole) and the appropriate alkyl-[2] or arylcarbamide (0.015 mole) in 30 ml of dry benzene was refluxed on a steam bath. As the reaction proceeded, the alkyl- or arylcarbamide dissolved into benzene solution. Finally, when the reaction was complete, a clear solution was obtained. Excess benzene was removed by distillation under reduced pressure, and the residual mass was first extracted with a dilute solution of sodium bicarbonate to remove any acid present in the compound; this procedure was followed by thorough washing with water.

The crude products were collected by filtration, dried, and recrystallized from the appropriate solvents. The various 1-(1-naphthylacetyl)-3-substituted carbamides (Table I) were characterized by their sharp melting points, elemental analyses, and IR spectra. The presence of a characteristic band for carbonyl (1884 cm^{-1}) and amino (3185 cm^{-1}) in the IR spectra provided further support for their molecular structure. However, the substituted carbamides formed during condensation of substituted ureas with 1-naphthylacetyl chloride will possess either Structure I or II; that is, acylation could occur at the 3-*N* (I) or 1-*N* (II) position of the urea molecule.

In the present study, NMR spectra[3] of three 1-(1-naphthylacetyl)-3-substituted carbamides possessing substituents of various sizes, *i.e.*, methyl, ethyl, and phenyl, established the exact position of the substituent group and provided evidence that acylation occurs at the 3-*N*-position (I) of the urea molecule rather than the 1-*N*-position (II). The NMR spectra showed two signals for amino protons (NH^a and NH^b). Because of its direct attachment to two carbonyl groups, the signal of NH^a was assigned at a lower field than NH^b. The NMR spectra obtained after shaking these three substituted carbamides with deuterium oxide showed the absence of two signals observed for NH^a and NH^b.

[1] All compounds were analyzed for their carbon, hydrogen, and nitrogen content. Melting points were taken in open capillary tubes with a partial immersion thermometer and are corrected. IR spectra were obtained with Perkin-Elmer Infracord spectrophotometer model 137, equipped with sodium chloride optics, in potassium bromide films in the 700–3500-cm^{-1} range.

[2] Aldrich Chemical Co., Milwaukee, Wis.

[3] Varian A-60 spectrometer.

Table II—Chemical Shifts of Some Protons of 1-(1-Naphthylacetyl)-3-substituted Carbamides

Compound	Chemical Shifts[a], ppm					
	$CDCl_3$			$CDCl_3 + D_2O$[b]		
	NH^a	NH^b	R	NH^a	NH^b	R
I ($R = CH_3$)	8.63 (1 H, broad)	8.1 (1 H, broad)	2.8 (3H, d, J = 5 Hz)	—	—	2.8 (3H, s)
II ($R = C_2H_5$)	9.58 (1H, broad)	8.41 (1H, broad)	1.12 (3H, t, J = 7Hz), 3.33 (2H, m)	—	—	1.12 (3H, t, J = 7 Hz), 3.30 (2H, q)
V ($R = C_6H_5$)	10.53 (1H, broad)	9.05 (1H, broad)	m (12H)	—	—	m (12H)

[a] Chemical shifts are expressed in δ units relative to tetramethylsilane as the internal standard. All spectra were taken in deuterochloroform solution; s = singlet, d = doublet, t = triplet, q = quartet, and m = multiplet. [b] In exchange experiments with deuterium oxide, a crystal of potassium carbonate was added to the solution to promote the exchange.

Structure I

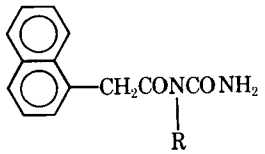

Structure II

To substantiate further the structural assignment of the methyl and ethyl carbamides, the effect of NH^b on the multiplicity of the substituent group was examined before and after deuterium exchange. As expected, the methyl signal of the carbamide changed from a doublet to a singlet; for the ethyl derivative, the methylene signal changed from a multiplet to a quartet. The chemical shifts of some protons presented in Table II clearly demonstrated that Structure I represents the substitution pattern and that acylation occurs at the 3-*N*-position rather than the 1-*N*-position of the urea molecule to form the 1-(1-naphthylacetyl)-3-substituted carbamides used in this study.

Determination of Anti-Inflammatory Activity—Albino rats, 100–120 g, were used for the evaluation of the anti-inflammatory activity of 1-(1-naphthylacetyl)-3-substituted carbamides. They were allowed food and water *ad libitum*.

Carrageenan-Induced Edema Method—The substituted carbamides, suspended in 5% aqueous gum acacia, were administered (100 mg/kg ip) to a group of six rats 1 hr before the injection of 0.05 ml of a suspension of freshly prepared carrageenan (1% in 0.91% NaCl) under the plantar aponeurosis of the right hindpaw (17). The control group of six rats received an equivalent amount of 5% aqueous gum acacia. The mean increase in paw volume, measured by the micropipet method (18) before and 4 hr after carrageenan treatment, was used to determine antiedema activity. Hydrocortisone (10 mg/kg ip) and oxyphenbutazone (40 mg/kg ip) were used as standard reference drugs.

Cotton Pellet-Induced Granuloma Formation Method—Sterilized cotton pellets (10 ± 1 mg each) were implanted into groups of four rats by making a small incision of about 2 mm on each axilla and each groin (19, 20), and the wound was stitched. One group served as the control while other groups were administered substituted carbamides (100 mg/kg ip) or oxyphenbutazone (100 mg/kg ip) every 24 hr for 6 days. On the 7th day, all implanted cotton pellets were carefully dissected out, dried for 2 hr at 150°, and weighed. The increase in weight due to granuloma formation was used to determine the anti-inflammatory activity.

Assay of Proteolytic Activity of Trypsin—The antiproteolytic activity of substituted carbamides at a final concentration of 1 m*M* was determined by evaluating their ability to inhibit trypsin-induced hydrolysis of bovine serum albumin (21). The reaction mixture consisted of 0.05 *M* tromethamine buffer (pH 8.2), 0.075 mg of crystalline trypsin (1 g is sufficient to hydrolyze 250 g of casein), 0.03 m*M* bovine serum albumin, appropriate substituted carbamide dissolved in dimethylformamide, and water in a total volume of 1 ml. An equivalent amount of dimethylformamide, added to the control tubes, had no effect on trypsin activity.

The test compounds were preincubated with trypsin for 10 min prior to the addition of bovine serum albumin, and the reaction mixture was incubated further for 5 min. The reaction was stopped by the addition of 5 ml of 15% (w/v) trichloroacetic acid solution. The

Table III—Antiedema and Antiproteolytic Activity of 1-(1-Naphthylacetyl)-3-substituted Carbamides

Compound[a]	Mean Increase in Paw Volume[b], ml ± *SE*	Antiedema Activity		Antiproteolytic Activity[c], % Inhibition
		% Protection	*p*	
Control	0.90 ± 0.02	—	—	
I	0.86 ± 0.02	4.4	>0.1	6.4 ± 0.3
II	0.60 ± 0.01	33.3	<0.001	11.0 ± 0.2
III	0.48 ± 0.03	46.6	<0.001	7.7 ± 0.2
IV	0.67 ± 0.01	30.0	<0.001	19.3 ± 0.3
V	0.45 ± 0.03	50.0	<0.001	13.5 ± 0.3
VI	0.59 ± 0.02	34.4	<0.001	4.9 ± 0.2
VII	0.69 ± 0.04	23.3	0.001	16.4 ± 0.3
VIII	0.89 ± 0.04	0.0	—	8.7 ± 0.2
IX	0.70 ± 0.02	22.2	<0.001	12.0 ± 0.2
X	0.56 ± 0.01	37.7	<0.001	14.8 ± 0.3
XI	0.91 ± 0.02	0.0	—	3.9 ± 0.2
Hydrocortisone	0.47 ± 0.02	47.7	<0.001	—
Oxyphenbutazone	0.45 ± 0.03	50.0	<0.001	—
Sodium salicylate	—	—	—	55.4 ± 0.3

[a] Substituent groups are as indicated in Table I. [b] Assay procedures are as indicated in the text. All substituted carbamides were used in a dose of 100 mg/kg, while hydrocortisone and oxyphenbutazone were used in a dose of 10 and 40 mg/kg, respectively. [c] Assay procedures are as indicated in the text. Each experiment was done in duplicate and the values are the mean values with ± *SEM* calculated from two separate experiments. All substituted carbamides and sodium salicylate were used at a final concentration of 1 m*M*.

Table IV—Antigranulation Effect of 1-(1-Naphthylacetyl)-3-substituted Carbamides

Compound[a]	Average Weight of Granulation Tissue, mg ± SE	Antigranulation Activity	
		% Protection	p
Control	17.6 ± 0.49	—	—
II	15.8 ± 0.44	10.2	0.01
III	16.6 ± 0.82	5.6	>0.1
IV	15.6 ± 0.61	11.3	0.02
V	14.8 ± 0.77	15.9	0.001–0.01
VI	16.9 ± 0.81	3.9	>0.1
X	16.2 ± 0.55	7.9	0.05
Oxyphenbutazone	9.0 ± 0.36	48.8	<0.001

[a] Substituent groups are as indicated in Table I. Assay procedures are as indicated in the text. All substituted carbamides and oxyphenbutazone were used in a dose of 100 mg/kg.

acid-soluble products of protein breakdown, obtained after centrifugation, were determined (22) as an index of the enzyme activity. Sodium salicylate also was used at a final concentration of 1 m*M* for comparative evaluation of antiproteolytic activity.

RESULTS AND DISCUSSION

The anti-inflammatory activity of these substituted carbamides against carrageenan-induced edema is recorded in Table III. Most of these carbamides afforded protection ranging from 4.5 to 50%. However, 1-(1-naphthylacetyl)-3-*p*-tolylcarbamide (VIII) and 3-*m*-chlorophenylcarbamide (XI) were devoid of anti-inflammatory activity. Hydrocortisone and oxyphenbutazone, under similar experimental conditions, provided protection of 47 and 50% in doses of 10 and 40 mg/kg, respectively, against carrageenan-induced edema as compared to substituted carbamides used in a dose of 100 mg/kg.

As is evident from Table III, an increase in the number of the carbon atoms in the alkyl chain attached to the nitrogen atom of these carbamides influenced their ability to protect against carrageenan-induced edema. The degree of protection was in the order of methyl < ethyl < *n*-propyl > *n*-butyl, and maximum anti-inflammatory activity was observed with the *n*-propyl-substituted carbamide (III).

Attachment of a methyl or methoxy substituent on the phenyl nucleus attached to the nitrogen atom of these aryl-substituted carbamides decreased their antiedema effectiveness. The introduction of a *p*-methyl or *m*-chloro substituent on the phenyl nucleus completely abolished the anti-inflammatory activity of the phenyl-substituted carbamide (V).

All substituted carbamides possessed low antiproteolytic activity, as reflected by only 3.9–19.3% inhibition of trypsin activity during hydrolysis of bovine serum albumin (Table III). Such an inhibition of trypsin-induced hydrolysis of bovine serum albumin was significantly higher (55.4%) with sodium salicylate, used as a reference drug for comparative evaluation. These results failed to provide any correlation between antiedema activity of these substituted carbamides and their ability to inhibit trypsin-induced hydrolysis of bovine serum albumin.

Some of the substituted carbamides possessing higher antiedema activity were evaluated also for their antigranulation activity. Their ability to protect against cotton pellet-induced granuloma formation in rats was of a low order (Table IV). The decrease in the weight of granuloma formation in implanted cotton pellets was 4–16% as compared to oxyphenbutazone, which showed 48.8% antigranulation activity at 100 mg/kg, a dose shown to exhibit 50% (ED_{50}) protection against cotton pellet-induced granuloma formation (23). In the present study, as in the case of antiedema activity, 1-(1-naphthylacetyl)-3-phenylcarbamide (V) exhibited maximum antigranulation activity of 15.9% against cotton pellet-induced granuloma formation.

These results indicated that 1-(1-naphthylacetyl)-3-substituted carbamides are active only against the acute phase of inflammation and provide poor protection against the chronic phase of inflammatory reactions. Failure to observe a relationship between antiedema and antigranulation activity of these substituted carbamides indicated that different mechanisms presumably are responsible for the acute and the chronic inflammatory reactions. In addition, the low antiproteolytic activity observed in the present study cannot account for the biochemical basis for the antiedema activity of these 1-(1-naphthylacetyl)-3-substituted carbamides.

REFERENCES

(1) S. S. Adams, E. E. Cliffe, B. Lessel, and J. S. Nicholson, *Nature (London)*, **200**, 271(1963).

(2) S. Cassadio, G. Pala, T. Bruzzese, E. Crescenzi, E. Marazzi-Uberti, and G. Coppi, *J. Med. Chem.*, **8**, 594(1965).

(3) C. W. Denko, E. A. Defelice, and J. Shaffer, *Curr. Ther. Res.*, **7**, 749(1965).

(4) T. Bruzzese and C. Turba, *J. Med. Chem.*, **9**, 264(1966).

(5) S. Cassadio, G. Pala, E. Marazzi-Uberti, and G. Coppi, *Experientia*, **20**, 457(1964).

(6) G. Pala, S. Cassadio, T. Bruzzese, E. Crescenzi, and E. Marazzi-Uberti, *J. Med. Chem.*, **8**, 698(1965).

(7) G. Pala, T. Bruzzese, E. Marazzi-Uberti, and G. Coppi, *ibid.*, **9**, 603(1966).

(8) E. Szarvasi and L. Fontaine, *Bull. Soc. Chim. Fr.*, **1964**, 3113.

(9) E. Marazzi-Uberti, C. Turba, and G. Erba, *Arch. Int. Pharmacodyn. Ther.*, **162**, 398(1966).

(10) F. K. Krichna and A. W. Zelay, U.S. pat. 3,429,911 (1969).

(11) M. I. Barnhart, C. Quintana, H. L. Lenon, G. B. Bluhm, and J. M. Riddle, *Ann. N.Y. Acad. Sci.*, **146**, 527(1968).

(12) A. Bertelli, *Biochem. Pharmacol., Suppl.*, **1968**, 229.

(13) A. Bertelli, L. Dontai, and M. A. Rossana, in "International Symposium on Nonsteroidal Antiinflammatory Drugs," S. Garattini and M. N. G. Dukes, Eds., Excerpta Medica, New York, N.Y., 1964, p. 98.

(14) W. G. Spector and D. A. Willoughby, *J. Pathol. Bacteriol.*, **79**, 21(1960).

(15) D. Libermann, J. Himbert, and L. Hengl, *Bull. Soc. Chim. Fr.*, **1950**, 486.

(16) F. Kurzer, in "Organic Synthesis," vol. 31, R. S. Schreiber, Ed., Wiley, New York, N.Y., 1951, p. 8.

(17) C. A. Winter, E. A. Risley, and G. W. Nuss, *Proc. Soc. Exp. Biol. Med.*, **111**, 544(1962).

(18) G. A. H. Buttle, P. F. D'Arcy, E. M. Howard, and D. N. Kellet, *Nature (London)*, **179**, 629(1957).

(19) R. Meier, W. Schuler, and P. Dessaules, *Experientia*, **6**, 469(1950).

(20) P. F. D'Arcy, E. M. Howard, D. W. Muggleton, and S. B. Townsent, *J. Pharm. Pharmacol.*, **12**, 659(1960).

(21) A. Chaudhari, A. K. Chaturvedi, S. S. Parmar, and S. J. Brumleve, *Res. Commun. Chem. Pathol. Pharmacol.*, **7**, 205(1974).

(22) O. H. Lowry, N. J. Rosenbrough, A. L. Farr, and R. J. Randall, *J. Biol. Chem.*, **193**, 265(1951).

(23) T. N. Bhalla, M.D. thesis, Lucknow University, Lucknow, India, 1967.

ACKNOWLEDGMENTS AND ADDRESSES

Received May 20, 1975, from the *Department of Pharmacology and Therapeutics, King George's Medical College, Lucknow University, Lucknow 226003, India, and the Departments of ‡Physiology and Pharmacology (School of Medicine) and §Chemistry, University of North Dakota, Grand Forks, ND 58202

Accepted for publication September 26, 1975.

Supported in part by the State Council of Scientific and Industrial Research, Lucknow, India, and U.S. Public Health Service National Institutes of Health Grants 1 TO1 HL 05939, 5-RO1-GM-21590, and 1 RO1 DA00996-01.

The authors thank Professor S. J. Brumleve and Professor Roland G. Severson for advice and encouragement. Grateful acknowledgment is made to the Council of Scientific and Industrial Research, New Delhi, India, and the State Council of Scientific and Industrial Research, Lucknow, India, for providing Research Fellowships to V. Kishore and S. Kumar, respectively.

x To whom inquiries should be directed (at the Department of Physiology and Pharmacology, University of North Dakota).

Vinyl Acetate Casts of Emphysematous Rat Lungs

CARMELO COLOMBO, SALVATORE COLOMBO, and BERNARD STEINETZ ˣ

Abstract □ Emphysema was induced in rats by chronic exposure to a papain aerosol according to established methods. The emphysematous changes were evaluated by previously described histological and biochemical parameters and by a new method employing infiltration of the lungs with vinyl acetate to make casts of the air spaces of the pulmonary tree. The weights and gross and microscopic appearance of the casts demonstrated the emphysematous changes in lungs of the papain-treated rats. Vinyl acetate casting may offer a new and useful tool in evaluating experimental induction of emphysema in rats.

Keyphrases □ Vinyl acetate—lung infiltration, casts formed, papain-induced emphysematous changes evaluated, rats □ Lung infiltration—vinyl acetate, casts formed, papain induced emphysematous changes evaluated, rats □ Emphysema, papain induced—lung changes evaluated by infiltration with vinyl acetate to form casts, rats

Pulmonary emphysema is a chronic respiratory disease characterized by a gradual destruction of alveolar walls, resulting in the formation of enlarged air spaces distal to the terminal bronchioles. Various substances have been used to induce an emphysema-like condition in laboratory animals. These substances include aerosols of papain, polymorphonuclear leukocyte homogenates, and other noxious substances (1–4) and intratracheally administered papain, phytohemagglutinin, and silica dust (5, 6).

The severity of the lung disease produced may be evaluated histologically, biochemically, or physiologically, but none of these parameters is entirely satisfactory (1, 3). Latex casts were used to study acinar changes in human emphysema (7). In the present investigation, the pulmonary trees of rats were infiltrated with vinyl acetate and the resulting casts were freed from tissue by digestion in mineral acid. The technique revealed distinct differences between control and emphysematous lungs.

EXPERIMENTAL

Male Charles River CD albino rats, ~100 g, were used in two major groups of 18 rats each. Each group was divided into three subgroups of six animals each. The subgroups were used for: (*a*) lung histology, (*b*) lung β-glucuronidase activity, and (*c*) vinyl acetate casts of lungs.

One major group of rats served as the control (water aerosol), and the other group was exposed to a 10% papain[1] aerosol in a Laskin chamber as previously described (3). The animals were exposed to the aerosol twice a week for 3 weeks, after which they were sacrificed and used for the various determinations. The lungs of six rats from each group were infused with 10% neutral buffered formalin by means of a tracheal cannula attached to a reservoir; the cannula delivered the fixative at a pressure of 10 cm water. When the flow of fixative ceased, the trachea was ligated and the thoracic cavity was opened. The entire chest contents were carefully removed and placed in additional formalin.

Following fixation, the lungs were routinely sectioned and stained with hematoxylin and eosin. The slides of right and left lungs of each rat were examined at 100× magnification with an ocular micrometer, and the alveoli falling on a line 0.2 mm long were counted. Ten fields per lung were randomly chosen, and 10 counts were made in each field. The average number of alveoli per linear millimeter was computed.

The lungs of six rats from each group were used for β-glucuronidase determination as previously described (3). The tracheas of the remaining six rats from each group were exposed and cannulated with 0.6-cm (0.25-in.) (i.d.) dimethicone tubing[2]. Vinyl acetate[3] (12% stock solution) was mixed 2:1 (v/v) with acetone and delivered into the lungs *via* the tracheal cannula from a calibrated reservoir at a height of 40 cm. The volume of vinyl acetate infused was recorded. The apparatus was washed with acetone immediately after infusion to prevent permanent clogging by the vinyl acetate.

After 1 hr, the lungs were carefully removed and immersed in 100 ml of concentrated hydrochloric acid in screw-capped jars. Twenty-four hours later, the remaining bits of tissue were removed by gentle washing. Then the casts were air dried and weighed prior to examination under a dissecting microscope at 40× magnification. By means of an ocular micrometer, the long and short axes of 20 alveoli were measured for each lung and the cross-sectional areas were calculated. The alveoli to be measured were picked at random in areas that could be clearly seen.

Table I—Comparison of Various Parameters in the Evaluation of Papain-Induced Emphysema

Parameter	Treatment: Control	Treatment: Papain Aerosol
Lung histology, alveoli/linear mm	92 ± 4	59 ± 4[a]
Lung β-glucuronidase, *E* at 450 nm	0.37 ± 0.02	0.73 ± 0.04[a]
Lung weight, g/100 g body weight	0.51 ± 0.02	0.87 ± 0.06
Vinyl acetate cast of lung		
Cross-sectional area, mm²	0.29 ± 0.02	0.48 ± 0.02[a]
Weight of cast, mg	420 ± 20	320 ± 30†
Lung capacity, vinyl acetate infused, ml	2.90 ± 0.14	2.03 ± 0.16[b]

[a] $p < 0.01$ *versus* control. [b] $p < 0.05$ *versus* control.

RESULTS AND DISCUSSION

The rats exposed to the papain aerosol developed unmistakable signs of emphysema as determined histologically and biochemically. The alveolar spaces were enlarged, leading to a 36% decrease in their number per linear millimeter (Table I). In agreement with previous findings (3), lung β-glucuronidase activity increased by 97% in the papain-treated rats (Table I). These results correlated well with observations made on the vinyl acetate casts.

Gross inspection of the casts revealed distinct differences between control and emphysematous lungs (Fig. 1). The terminal buds of lungs of exposed rats were coarser and sparser, and the bronchioles were more distended than those of the controls (Figs. 2 and 3). Fused and broken alveoli also were observed. The casts of alveolar spaces of the emphysematous lungs averaged 66% larger in cross-sectional area than those of controls (Table I). The casts of the emphysematous lungs also weighed less than the control casts. On the other hand, lung tissue weight increased by 71%.

Previous results showed that lungs of rats exposed chronically to papain demonstrated changes resembling those seen in lungs of human patients with diagnosed emphysema (1, 3, 6). In the present

[1] Papain–High Test, S. B. Penick and Co., New York, N.Y.

[2] Silastic tubing, Dow Corning Medical Products Division, Midland, Mich.

[3] Ward's Natural Science Establishment, Rochester, N.Y.

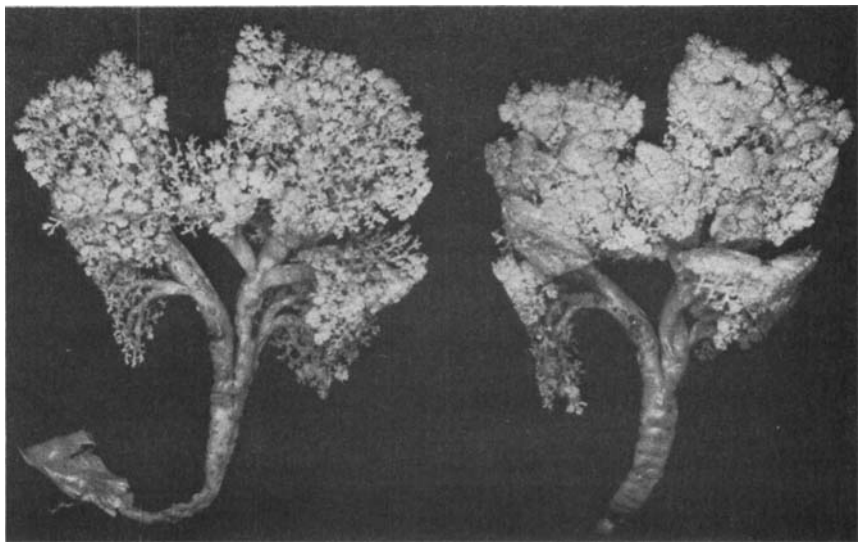

Figure 1—*Vinyl acetate casts of control (right) and emphysematous (left) rat lungs (approximately 2× natural size). Note "solid" appearance of control lungs (due to close spacing of alveoli) in comparison with lacy appearance of emphysematous lungs.*

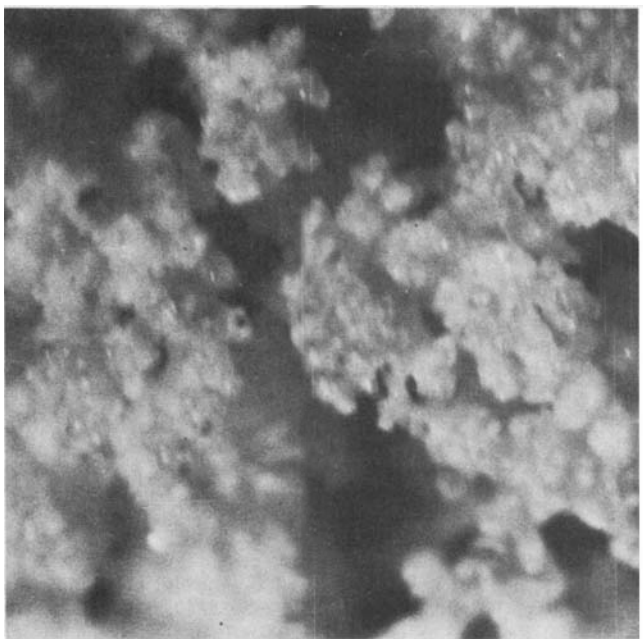

Figure 2—*Vinyl acetate cast of control lung (56× magnification). Note detail of alveoli.*

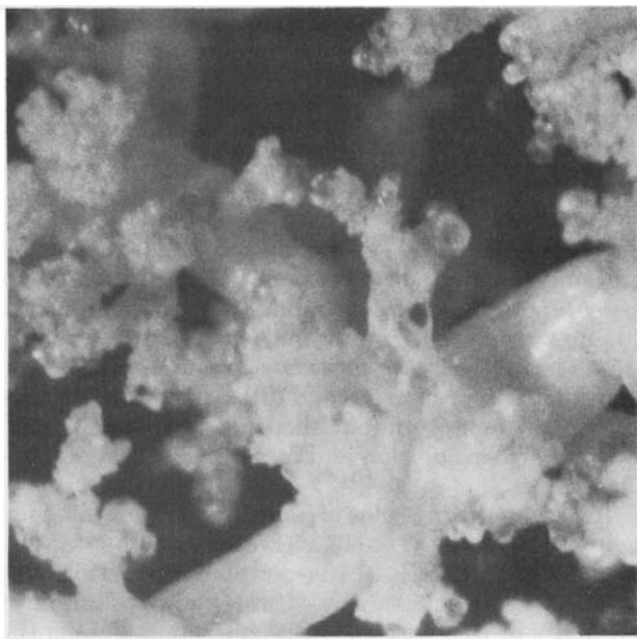

Figure 3—*Vinyl acetate cast of emphysematous lung (56× magnification). Note relative sparseness and coarseness of alveoli in comparison with Fig. 2.*

studies, the typical histological (dilation and depletion of alveoli) and biochemical (increased β-glucuronidase activity) changes were observed in papain-treated rats. The vinyl acetate casts accurately reflected the emphysematous changes. The terminal buds were grossly enlarged, presumably reflecting the breakdown and coalescence of smaller alveoli.

The distension of the bronchioles may have been due to a loss of elasticity together with a hyperplasia of nonfunctional parenchymal tissue, leading to obstruction of air passageways and enlargement and eventual destruction of alveoli. Emphysema has been reported to be due to loss of alveoli, resulting in enlargement of respiratory bronchioles, alveolar ducts, and lung distension (5). In corrosion models of emphysematous human lungs, a notable abnormality was a loss of alveoli on the respiratory bronchioles which appeared as smooth and bulging structures (7), similar to what was observed in the present study.

These phenomena were observable by gross inspection of the casts or by measurement of the alveolar cross-sectional area, which was increased by 66%. The decrease in functional alveolar capacity was also reflected in the 24% reduction in the weight of the lung casts and the decreased volume of vinyl acetate required to inflate the lungs of emphysematous rats. The reduction in these parameters probably was due to nonfunctional connective tissue hyperplasia, which resulted in obstruction of the respiratory bronchioles and broken or absent alveoli. The nonfunctional tissue was, of course, later removed during hydrochloric acid digestion.

Vinyl acetate casts of lungs, therefore, offer an effective, rapid, and relatively simple adjunct to histological and biochemical parameters in evaluating the severity of experimental emphysema in laboratory rats.

REFERENCES

(1) R. Giles, M. Finkel, and R. Leeds, *Proc. Soc. Exp. Biol. Med.*, **134**, 157(1970).

(2) B. Mass, T. Ikeda, D. Meranze, G. Weinbaum, and P. Kimbel, *Am. Rev. Resp. Dis.*, **103**, 907(1971).

(3) C. Colombo and B. Steinetz, *Arch. Int. Pharmacodyn. Ther.*, **216**, 86(1975).

(4) H. Boren, *Am. Rev. Resp. Dis.*, **92**, 1(1965).
(5) P. Gross, E. Pfitzer, E. Tolker, M. Babyak, and M. Kaschak, *Arch. Environ. Health*, **11**, 50(1965).
(6) H. Ito and D. Aviado, *J. Pharmacol. Exp. Ther.*, **161**, 197(1968).
(7) K. K. Pump, *Am. Rev. Resp. Dis.*, **108**, 610(1973).

ACKNOWLEDGMENTS AND ADDRESSES

Received August 18, 1975, from the *Research Department, Pharmaceutical Division, Ciba-Geigy Corporation, Ardsley, NY 10502*
Accepted for publication September 25, 1975.
[x] To whom inquiries should be directed.

Isolation of Cannabisativine, an Alkaloid, from *Cannabis sativa* L. Root

CARLTON E. TURNER [*], MEI-FENG H. HSU [§], JOSEPH E. KNAPP [‡], PAUL L. SCHIFF, Jr. [‡], and DAVID J. SLATKIN [‡x]

Abstract □ An ethanol extract of the root of a Mexican variant of *Cannabis sativa* L. (marijuana) afforded, after partitioning and chromatography, the new spermidine alkaloid cannabisativine.

Keyphrases □ *Cannabis sativa*—cannabisativine isolated from ethanol extract of roots □ Alkaloids—cannabisativine isolated from ethanol extract of roots of *Cannabis sativa* □ Cannabisativine—isolated from roots of *Cannabis sativa*

The occurrence of several low molecular weight, nitrogen-containing substances in *Cannabis sativa* L. has been reported including choline (1–4), trigonelline (2, 3), muscarine (5), piperidine (6), *N*-(*p*-hydroxy-β-phenylethyl)-*p*-hydroxy-*trans*-cinnamamide (7), neurine (8), L-proline (8), and L-(+)-isoleucine betaine (9). Small amounts of four alkaloids were isolated (10), but the high-resolution and mass spectra were inconclusive.

Recently, the presence of a new spermidine alkaloid, cannabisativine (I) [13-(1,2-dihydroxyheptanyl)-1,4,5,6,7,8,9,10,11,13,16,16a-dodecahydropyrido[2,1-*d*][1,5,9]triazacyclotridecin-2(3*H*)-one], was found in the roots of this species (11). This report details the procedure used in the isolation of this substance.

EXPERIMENTAL[1]

Plant Material—Roots of a Mexican variant of *C. sativa* L. were used[2].

Extraction—Air-dried ground roots of *C. sativa* (11.72 kg) were extracted by percolation with methanol (150 liters). The extract was evaporated *in vacuo* at 40° to leave a dark-brown syrup (323 g, 2.8%).

Isolation of Cannabisativine—The methanol extract (323 g) was partitioned between water (4 liters) and chloroform (4 liters) to give fractions of 266.0 g (2.3%) and 47.7 g (0.4%), respectively. The chloroform fraction was then partitioned between petroleum ether (bp 60–90°) (2 liters) and methanol–water (9:1) (2 liters) to yield fractions of 12.7 g (0.1%) and 33.4 g (0.3%), respectively.

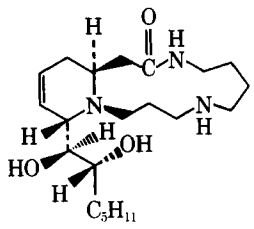

I

The aqueous methanol fraction was chromatographed on silicic acid[3] (450 g, 5 × 49 cm) packed in petroleum ether (bp 60–90°). Elution with 8% methanol–chloroform afforded a residue (3.0 g), which was dissolved in chloroform (25 ml) and partitioned with 1% hydrochloric acid (3 × 25 ml). The combined acid layers (75 ml) were basified to pH 8 with concentrated ammonium hydroxide and partitioned with chloroform (3 × 75 ml). The combined chloroform layers were dried over anhydrous sodium sulfate and evaporated, *in vacuo*, at 40° to yield a white residue (48 mg).

Crystallization from acetone afforded cannabisativine (29 mg), mp 167–168°; $[\alpha]_D^{25}$ + 55.1° (c 0.53, $CHCl_3$); UV: no maximum above 210 nm; IR: ν_{max} (KBr) 3300, 3020, 2960, 2920, 2850, 1628, 1580, 1470, 1250, 1130, 1045, and 707 cm^{-1}; NMR: δ 5.90 (2H, s, vinyl) and 9.6 (1H, s, broad, CONH); mass spectrum (M^+): *m/e* 381 (1%), 363 (1), 352 (1), 310 (2), 280 (3), 250 (64), 208 (100), 198 (6), 171 (12), 129 (5), 114 (5), 112 (6), 96 (4), 94 (6), 84 (8), 80 (6), 72 (7), 70 (8), and 55 (6). The structure of this compound was recently determined to be I (11).

REFERENCES

(1) E. Jahns, *Arch. Pharm.*, **225**, 479(1887).
(2) E. Schulze and S. Frankfurt, *Ber. Dtsch. Chem. Ges.*, **27**, 769(1894).
(3) K. W. Merz and K. B. Bergner, *Arch. Pharm.*, **278**, 49(1940).
(4) M. L. Mole, Jr., and C. E. Turner, *Acta Pharm. Jugosl.*, **23**, 203(1973).
(5) V. Kwasniewski, *Dtsch. Apothek.-Ztg.*, **94**, 1177(1954).
(6) Y. Obata, Y. Ishikawa, and R. Kitizawa, *Bull. Agr. Chem. Soc. Jpn.*, **24**, 670(1960).
(7) D. J. Slatkin, N. J. Doorenbos, L. S. Harris, A. N. Masoud, M. W. Quimby, and P. L. Schiff, Jr., *J. Pharm. Sci.*, **60**, 1891(1971).
(8) M. L. Mole, Jr., and C. E. Turner, *ibid.*, **63**, 154(1974).
(9) C. A. L. Bercht, R. J. J. C. Lousberg, F. J. E. M. Kuppers, and

[1] Melting points were determined on a Thomas-Hoover Uni-Melt melting-point apparatus and are corrected. IR spectra were run in potassium bromide using a Perkin-Elmer 257 spectrophotometer. Optical rotations were determined on a Perkin-Elmer 241 polarimeter. UV spectra were run on a Perkin-Elmer 202 spectrophotometer. NMR spectra were obtained in deuterated chloroform on a Hitachi Perkin-Elmer R-24 spectrometer, with tetramethylsilane as the internal standard. Mass spectra were recorded on a LKB-9000 spectrometer.

[2] Lot Me-A(2)-C-69 grown in 1971; voucher specimens were deposited in the herbarium of the School of Pharmacy, University of Mississippi.

[3] Mallinckrodt.

(4) H. Boren, *Am. Rev. Resp. Dis.*, **92**, 1(1965).
(5) P. Gross, E. Pfitzer, E. Tolker, M. Babyak, and M. Kaschak, *Arch. Environ. Health*, **11**, 50(1965).
(6) H. Ito and D. Aviado, *J. Pharmacol. Exp. Ther.*, **161**, 197(1968).
(7) K. K. Pump, *Am. Rev. Resp. Dis.*, **108**, 610(1973).

ACKNOWLEDGMENTS AND ADDRESSES

Received August 18, 1975, from the *Research Department, Pharmaceutical Division, Ciba-Geigy Corporation, Ardsley, NY 10502*
Accepted for publication September 25, 1975.
[x] To whom inquiries should be directed.

Isolation of Cannabisativine, an Alkaloid, from *Cannabis sativa* L. Root

CARLTON E. TURNER [*], MEI-FENG H. HSU [§], JOSEPH E. KNAPP [‡], PAUL L. SCHIFF, Jr. [‡], and DAVID J. SLATKIN [‡x]

Abstract □ An ethanol extract of the root of a Mexican variant of *Cannabis sativa* L. (marijuana) afforded, after partitioning and chromatography, the new spermidine alkaloid cannabisativine.

Keyphrases □ *Cannabis sativa*—cannabisativine isolated from ethanol extract of roots □ Alkaloids—cannabisativine isolated from ethanol extract of roots of *Cannabis sativa* □ Cannabisativine—isolated from roots of *Cannabis sativa*

The occurrence of several low molecular weight, nitrogen-containing substances in *Cannabis sativa* L. has been reported including choline (1–4), trigonelline (2, 3), muscarine (5), piperidine (6), *N*-(*p*-hydroxy-β-phenylethyl)-*p*-hydroxy-*trans*-cinnamamide (7), neurine (8), L-proline (8), and L-(+)-isoleucine betaine (9). Small amounts of four alkaloids were isolated (10), but the high-resolution and mass spectra were inconclusive.

Recently, the presence of a new spermidine alkaloid, cannabisativine (I) [13-(1,2-dihydroxyheptanyl)-1,4,5,6,7,8,9,10,11,13,16,16a-dodecahydropyrido[2,1-*d*][1,5,9]triazacyclotridecin-2(3*H*)-one], was found in the roots of this species (11). This report details the procedure used in the isolation of this substance.

EXPERIMENTAL[1]

Plant Material—Roots of a Mexican variant of *C. sativa* L. were used[2].

Extraction—Air-dried ground roots of *C. sativa* (11.72 kg) were extracted by percolation with methanol (150 liters). The extract was evaporated *in vacuo* at 40° to leave a dark-brown syrup (323 g, 2.8%).

Isolation of Cannabisativine—The methanol extract (323 g) was partitioned between water (4 liters) and chloroform (4 liters) to give fractions of 266.0 g (2.3%) and 47.7 g (0.4%), respectively. The chloroform fraction was then partitioned between petroleum ether (bp 60–90°) (2 liters) and methanol–water (9:1) (2 liters) to yield fractions of 12.7 g (0.1%) and 33.4 g (0.3%), respectively.

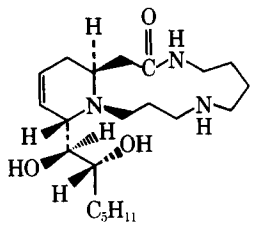

I

The aqueous methanol fraction was chromatographed on silicic acid[3] (450 g, 5 × 49 cm) packed in petroleum ether (bp 60–90°). Elution with 8% methanol–chloroform afforded a residue (3.0 g), which was dissolved in chloroform (25 ml) and partitioned with 1% hydrochloric acid (3 × 25 ml). The combined acid layers (75 ml) were basified to pH 8 with concentrated ammonium hydroxide and partitioned with chloroform (3 × 75 ml). The combined chloroform layers were dried over anhydrous sodium sulfate and evaporated, *in vacuo*, at 40° to yield a white residue (48 mg).

Crystallization from acetone afforded cannabisativine (29 mg), mp 167–168°; $[\alpha]_D^{25}$ + 55.1° (c 0.53, $CHCl_3$); UV: no maximum above 210 nm; IR: ν_{max} (KBr) 3300, 3020, 2960, 2920, 2850, 1628, 1580, 1470, 1250, 1130, 1045, and 707 cm^{-1}; NMR: δ 5.90 (2H, s, vinyl) and 9.6 (1H, s, broad, CONH); mass spectrum (M^+): *m/e* 381 (1%), 363 (1), 352 (1), 310 (2), 280 (3), 250 (64), 208 (100), 198 (6), 171 (12), 129 (5), 114 (5), 112 (6), 96 (4), 94 (6), 84 (8), 80 (6), 72 (7), 70 (8), and 55 (6). The structure of this compound was recently determined to be I (11).

[1] Melting points were determined on a Thomas-Hoover Uni-Melt melting-point apparatus and are corrected. IR spectra were run in potassium bromide using a Perkin-Elmer 257 spectrophotometer. Optical rotations were determined on a Perkin-Elmer 241 polarimeter. UV spectra were run on a Perkin-Elmer 202 spectrophotometer. NMR spectra were obtained in deuterated chloroform on a Hitachi Perkin-Elmer R-24 spectrometer, with tetramethylsilane as the internal standard. Mass spectra were recorded on a LKB-9000 spectrometer.

[2] Lot Me-A(2)-C-69 grown in 1971; voucher specimens were deposited in the herbarium of the School of Pharmacy, University of Mississippi.

[3] Mallinckrodt.

REFERENCES

(1) E. Jahns, *Arch. Pharm.*, **225**, 479(1887).
(2) E. Schulze and S. Frankfurt, *Ber. Dtsch. Chem. Ges.*, **27**, 769(1894).
(3) K. W. Merz and K. B. Bergner, *Arch. Pharm.*, **278**, 49(1940).
(4) M. L. Mole, Jr., and C. E. Turner, *Acta Pharm. Jugosl.*, **23**, 203(1973).
(5) V. Kwasniewski, *Dtsch. Apothek.-Ztg.*, **94**, 1177(1954).
(6) Y. Obata, Y. Ishikawa, and R. Kitizawa, *Bull. Agr. Chem. Soc. Jpn.*, **24**, 670(1960).
(7) D. J. Slatkin, N. J. Doorenbos, L. S. Harris, A. N. Masoud, M. W. Quimby, and P. L. Schiff, Jr., *J. Pharm. Sci.*, **60**, 1891(1971).
(8) M. L. Mole, Jr., and C. E. Turner, *ibid.*, **63**, 154(1974).
(9) C. A. L. Bercht, R. J. J. C. Lousberg, F. J. E. M. Kuppers, and

C. A. Salemink, *Phytochemistry*, **12**, 2459(1973).

(10) F. K. Klein, H. Rapoport, and H. W. Elliott, *Nature*, **232**, 258(1971).

(11) H. L. Lotter, D. J. Abraham, C. E. Turner, J. E. Knapp, P. L. Schiff, Jr., and D. J. Slatkin, *Tetrahedron Lett.*, **33**, 2815(1975).

ACKNOWLEDGMENTS AND ADDRESSES

Received July 16, 1975, from the *Research Institute of Pharmaceutical Sciences, School of Pharmacy, University of Mississippi, University, MS 38677, and the ‡Department of Pharmacognosy, School of Pharmacy, University of Pittsburgh, Pittsburgh, PA 15261

Accepted for publication September 26, 1975.

Supported in part by Research Grant 5S01RR05455-10 from the National Institutes of Health, Contract HSM-42-70-109 from the National Institute on Drug Abuse, and the Research Institute of Pharmaceutical Sciences, School of Pharmacy, University of Mississippi.

§ Present address: Harrison Department of Surgical Research, School of Medicine, University of Pennsylvania, Philadelphia, Pa.

xTo whom inquiries should be directed.

Synthesis and Antibacterial and Antifungal Activities of Alkyl and Polyhalophenyl Esters of Benzo[*b*]-3-methyl-2-furancarbamic Acid

F. GHABGHARAN, H. KOOSHKABADI, M. EMAMI, A. RASHIDBAIGI, and A. SHAFIEE x

Abstract □ Several alkyl and polyhalophenyl esters of benzo[*b*]-3-methyl-2-furancarbamic acid were prepared and tested for antifungal activity against *Candida albicans, Penicillium notatum*, and *Aspergillus niger*. The pentachlorophenyl ester was the most active substance and the only compound to show antibacterial activity against *Staphylococcus aureus*.

Keyphrases □ Carbamic acid esters—synthesized, screened for antifungal and antibacterial activities □ Furancarbamic acid esters—synthesized, screened for antifungal and antibacterial activities □ Antifungal activity—alkyl and polyhalophenyl esters of furancarbamic acid synthesized and screened □ Antibacterial activity—alkyl and polyhalophenyl esters of furancarbamic acid synthesized and screened

In continuing studies on the chemistry and antibacterial and antifungal activities of carbamic acid esters (1–3), alkyl and polyhalophenyl esters of benzo[*b*]-3-methyl-2-furancarbamic acid were synthesized from benzo[*b*]-3-methyl-2-furancarboxazide (III) and the appropriate alcohol or phenol (Scheme I). The physical data of the compounds prepared are summarized in Table I. All compounds listed in Table I were tested against *Candida albicans* (28012), *Penicillium notatum* (S-13), and *Aspergillus niger* (23171) *in vitro* using Sabouraud dextrose agar medium[1].

Each compound was dissolved in acetone to a concentration of 1 mg/ml. These solutions were diluted with hot culture medium to the desired concentrations and autoclaved at 120° for 2 hr. Five replicates of each concentration were prepared.

The antifungal activity of all compounds tested, except IV*n*, was insignificant at a concentration of 5 μg/ml. All compounds were active against *P. notatum* and *A. niger* but inactive against *C. albicans* at a concentration of 10 μg/ml. However, they were active against *C. albicans* at a concentration of 30 μg/ml. Griseofulvin was used as a control (Table II).

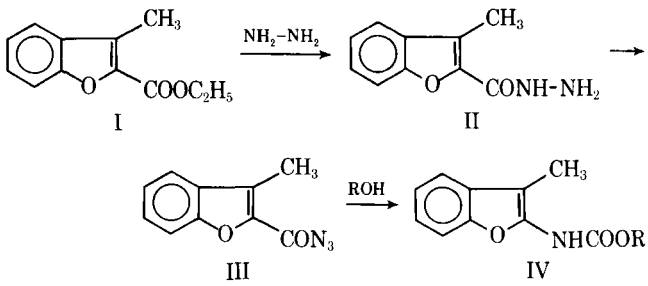

Scheme I

All compounds also were tested against *Bacillus subtilis* (NCTC 3610), *Staphylococcus aureus* (ATCC 6538), *Klebsiella pneumoniae* (ATCC 10031), and *Sarcina lutea* (ATCC 9341). Nitrofurazone was used as a control. Standard paper disks, 6 mm in diameter, were immersed in solution and placed on an inoculated assay medium surface[2].

The antibacterial activity of all compounds that dissolved in acetone at the 0.5% concentration was insignificant. However, IV*n* at the same concentration showed 12-mm inhibition zones against *S. aureus* and had no activity against other strains.

EXPERIMENTAL[3]

Benzo[*b*]-3-methyl-2-furancarboxyhydrazide (II)—To a stirring solution of 25 g (0.5 mole) of hydrazine hydrate in 150 ml of ethanol was added dropwise a solution of 20.4 g (0.1 mole) of ethyl benzo[*b*]-3-methyl-2-furancarboxylate (I) (5) in 50 ml of ethanol.

[1] These microorganisms were obtained from the Department of Parasitology, Public Health Institute, Tehran, Iran.

[2] Antibiotic assay medium, British Pharmacopoeia, 1968.

[3] Melting points were taken on a Kofler hot-stage microscope and are uncorrected. IR spectra were recorded using a Leitz model III spectrograph. NMR spectra were recorded on a Varian A60A instrument.

C. A. Salemink, *Phytochemistry*, **12**, 2459(1973).

(10) F. K. Klein, H. Rapoport, and H. W. Elliott, *Nature*, **232**, 258(1971).

(11) H. L. Lotter, D. J. Abraham, C. E. Turner, J. E. Knapp, P. L. Schiff, Jr., and D. J. Slatkin, *Tetrahedron Lett.*, **33**, 2815(1975).

ACKNOWLEDGMENTS AND ADDRESSES

Received July 16, 1975, from the *Research Institute of Pharmaceutical Sciences, School of Pharmacy, University of Mississippi, University, MS 38677, and the ‡Department of Pharmacognosy, School of Pharmacy, University of Pittsburgh, Pittsburgh, PA 15261

Accepted for publication September 26, 1975.

Supported in part by Research Grant 5S01RR05455-10 from the National Institutes of Health, Contract HSM-42-70-109 from the National Institute on Drug Abuse, and the Research Institute of Pharmaceutical Sciences, School of Pharmacy, University of Mississippi.

§ Present address: Harrison Department of Surgical Research, School of Medicine, University of Pennsylvania, Philadelphia, Pa.

xTo whom inquiries should be directed.

Synthesis and Antibacterial and Antifungal Activities of Alkyl and Polyhalophenyl Esters of Benzo[*b*]-3-methyl-2-furancarbamic Acid

F. GHABGHARAN, H. KOOSHKABADI, M. EMAMI, A. RASHIDBAIGI, and A. SHAFIEE x

Abstract □ Several alkyl and polyhalophenyl esters of benzo[*b*]-3-methyl-2-furancarbamic acid were prepared and tested for antifungal activity against *Candida albicans, Penicillium notatum*, and *Aspergillus niger*. The pentachlorophenyl ester was the most active substance and the only compound to show antibacterial activity against *Staphylococcus aureus*.

Keyphrases □ Carbamic acid esters—synthesized, screened for antifungal and antibacterial activities □ Furancarbamic acid esters—synthesized, screened for antifungal and antibacterial activities □ Antifungal activity—alkyl and polyhalophenyl esters of furancarbamic acid synthesized and screened □ Antibacterial activity—alkyl and polyhalophenyl esters of furancarbamic acid synthesized and screened

In continuing studies on the chemistry and antibacterial and antifungal activities of carbamic acid esters (1–3), alkyl and polyhalophenyl esters of benzo[*b*]-3-methyl-2-furancarbamic acid were synthesized from benzo[*b*]-3-methyl-2-furancarboxazide (III) and the appropriate alcohol or phenol (Scheme I). The physical data of the compounds prepared are summarized in Table I. All compounds listed in Table I were tested against *Candida albicans* (28012), *Penicillium notatum* (S-13), and *Aspergillus niger* (23171) *in vitro* using Sabouraud dextrose agar medium[1].

Each compound was dissolved in acetone to a concentration of 1 mg/ml. These solutions were diluted with hot culture medium to the desired concentrations and autoclaved at 120° for 2 hr. Five replicates of each concentration were prepared.

The antifungal activity of all compounds tested, except IV*n*, was insignificant at a concentration of 5 μg/ml. All compounds were active against *P. notatum* and *A. niger* but inactive against *C. albicans* at a concentration of 10 μg/ml. However, they were active against *C. albicans* at a concentration of 30 μg/ml. Griseofulvin was used as a control (Table II).

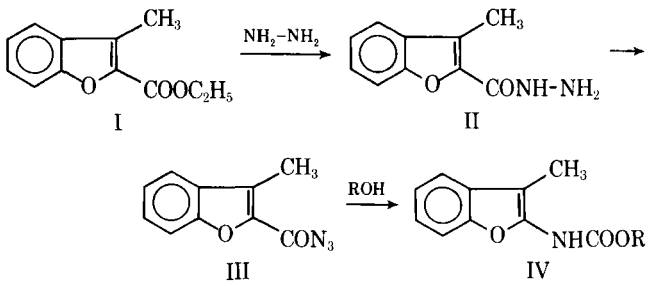

Scheme I

All compounds also were tested against *Bacillus subtilis* (NCTC 3610), *Staphylococcus aureus* (ATCC 6538), *Klebsiella pneumoniae* (ATCC 10031), and *Sarcina lutea* (ATCC 9341). Nitrofurazone was used as a control. Standard paper disks, 6 mm in diameter, were immersed in solution and placed on an inoculated assay medium surface[2].

The antibacterial activity of all compounds that dissolved in acetone at the 0.5% concentration was insignificant. However, IV*n* at the same concentration showed 12-mm inhibition zones against *S. aureus* and had no activity against other strains.

EXPERIMENTAL[3]

Benzo[*b*]-3-methyl-2-furancarboxyhydrazide (II)—To a stirring solution of 25 g (0.5 mole) of hydrazine hydrate in 150 ml of ethanol was added dropwise a solution of 20.4 g (0.1 mole) of ethyl benzo[*b*]-3-methyl-2-furancarboxylate (I) (5) in 50 ml of ethanol.

[1] These microorganisms were obtained from the Department of Parasitology, Public Health Institute, Tehran, Iran.

[2] Antibiotic assay medium, British Pharmacopoeia, 1968.

[3] Melting points were taken on a Kofler hot-stage microscope and are uncorrected. IR spectra were recorded using a Leitz model III spectrograph. NMR spectra were recorded on a Varian A60A instrument.

Table I—Physical Constants of Benzo[*b*]-3-methyl-2-furancarbamic Acid Esters

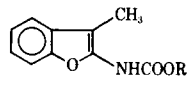

Compound	R	Yield, %	Melting Point[a]	Formula[b]	Analysis, %	
					Calc.	Found
IV*a*	CH_3	80	94°	$C_{11}H_{11}NO_3$	C 64.39 H 5.37 N 6.83	64.28 5.41 6.97
IV*b*	C_2H_5	75	80–81°[c]	—	—	—
IV*c*	n-C_3H_7	65	82–83°	$C_{13}H_{15}NO_3$	C 66.95 H 6.44 N 6.01	66.87 6.32 6.17
IV*d*	iso-C_3H_7	68	133–134°	$C_{13}H_{15}NO_3$	C 66.95 H 6.44 N 6.01	67.14 6.38 5.82
IV*e*	n-C_4H_9	50	78–79°	$C_{14}H_{17}NO_3$	C 68.02 H 6.88 N 5.67	68.14 6.72 5.52
IV*f*	C_6H_{11}	75	132–133°	$C_{16}H_{19}NO_3$	C 70.33 H 6.96 N 5.13	70.17 7.12 5.05
IV*g*	$CH_2C_6H_5$	70	104–105°	$C_{17}H_{15}NO_3$	C 72.60 H 5.34 N 4.98	72.75 5.51 4.99
IV*h*	*p*-Chlorophenyl	55	141–142°	$C_{16}H_{12}ClNO_3$	C 63.68 H 3.98 N 4.64	63.79 3.82 4.73
IV*i*	*p*-Bromophenyl	70	155–156°	$C_{16}H_{12}BrNO_3$	C 55.49 H 3.47 N 4.05	55.62 3.58 4.23
IV*j*	*o*-Chlorophenyl	55	130–131°	$C_{16}H_{12}ClNO_3$	C 63.68 H 3.98 N 4.64	63.53 3.99 4.75
IV*k*	2,4-Dichlorophenyl	45	155–156°	$C_{16}H_{11}Cl_2NO_3$	C 57.14 H 3.27 N 4.17	57.01 3.12 4.35
IV*l*	2,4,5-Trichlorophenyl	85	138–139°	$C_{16}H_{10}Cl_3NO_3$	C 51.82 H 2.70 N 3.78	52.03 2.85 3.85
IV*m*	2,4,6-Trichlorophenyl	83	162–163°	$C_{16}H_{10}Cl_3NO_3$	C 51.82 H 2.70 N 3.78	51.65 2.85 3.63
IV*n*	Pentachlorophenyl	90	169–170°	$C_{16}H_8Cl_5NO_3$	C 43.69 H 1.82 N 3.19	43.82 1.93 3.09

[a] Unless otherwise indicated, the recrystallization solvent was benzene or benzene–hexane. [b] IR and NMR spectra of all compounds were as expected. [c] Lit. (4) mp 81–82°.

After the addition was complete, the mixture was refluxed for 5 hr. The solvent was evaporated, and the residue was crystallized from ethanol to give 17 g (90%) of II, mp 139–140° [lit. (4) mp 139–141°].

Benzo[*b*]-3-methyl-2-furancarboxazide (III)—To a stirring solution of II (20.6 g, 0.1 mole) in 200 ml of 50% acetic acid at 0° was added dropwise a solution of sodium nitrite (6.9 g, 0.1 mole) in 100 ml of water. The reaction mixture was stirred for an additional 30 min. The precipitate was filtered, washed with water, and dried at room temperature under reduced pressure, mp 105–106° [lit. (4) mp 105–106.5°].

Methyl Benzo[*b*]-3-methyl-2-furancarbamate (IV*a*)—A solution of III (2.01 g, 0.01 mole) in 50 ml of absolute methanol was refluxed for 5 hr. The solvent was evaporated, and the residue was crystallized from benzene–hexane, mp 94–95°; IR (KBr): 3200 (NH),

Table II—Antifungal Activity[a] of Alkyl and Polyhalophenyl Esters of Benzo[*b*]-3-methyl-2-furancarbamic Acid

Compound	*P. notatum*			*C. albicans*			*A. niger*		
	5 μg/ml	10 μg/ml	30 μg/ml	5 μg/ml	10 μg/ml	30 μg/ml	5 μg/ml	10 μg/ml	30 μg/ml
IV*a*	—	+	+	—	—	+	—	+	+
IV*b*	—	+	+	—	—	+	—	+	+
IV*c*	—	+	+	—	—	+	—	+	+
IV*d*	—	+	+	—	—	+	—	+	+
IV*e*	—	+	+	—	—	+	—	+	+
IV*f*	—	+	+	—	—	+	—	+	+
IV*g*	—	+	+	—	—	+	—	+	+
IV*h*	—	+	+	—	—	+	—	+	+
IV*i*	—	+	+	—	—	+	—	+	+
IV*j*	—	+	+	—	—	+	—	+	+
IV*k*	—	+	+	—	—	+	—	+	+
IV*l*	—	+	+	—	—	+	—	+	+
IV*m*	—	+	+	—	—	+	—	+	+
IV*n*	+	+	+	+	+	+	+	+	+
Griseofulvin	—	—	+	—	—	+	—	—	+

[a] + = complete inhibition, and — = no inhibition.

3020 (aromatic), 2940, 2915, 1700 (CO), 1650, 1530, 1490, 1450, 1315, 1110, 1080, 1058, 860, and 748 cm^{-1}; NMR ($CDCl_3$): δ 7.1–7.42 (m, 4H, aromatic), 6.70–7.10 (broad s, 1H, NH), 3.66 (s, 3H, OCH_3), and 2.07 (s, 3H, CH_3) ppm.

Anal.—Calc. for $C_{11}H_{11}NO_3$: C, 64.39; H, 5.37; N, 6.83. Found: C, 64.28; H, 5.41; N, 6.97.

Compounds IV*b*–IV*g* were prepared similarly from III and the appropriate alcohols (Table I).

***p*-Chlorophenyl Benzo[*b*]-3-methyl-2-furancarbamate (IV*h*)**—A solution of III (2.01 g, 0.01 mole) and *p*-chlorophenol (1.28 g, 0.01 mole) in 30 ml of dry benzene was refluxed for 4 hr. The solvent was evaporated, and the residue was crystallized from benzene to give 1.65 g (55%) of the desired compound, mp 155–156°; IR (KBr): 3230 (NH), 1722 (CO), 1670, 1510, 1490, 1460, 1250, 1202, 1100, 1020, 1015, 855, and 752 cm^{-1}; NMR ($CDCl_3$): δ 7.7–7 (m, 8H, aromatic), 7–6.7 (broad s, 1H, NH), and 2.17 (s, 3H, CH_3) ppm.

Anal.—Calc. for $C_{16}H_{12}ClNO_3$: C, 63.68; H, 3.98; N, 4.64. Found: C, 63.79; H, 3.82; N, 4.73.

Compounds IV*i*–IV*n* were prepared similarly.

REFERENCES

(1) A. Shafiee, I. Lalezari, S. Yazdani, and A. Pournorouz, *J. Pharm. Sci.*, **62**, 839(1973).

(2) I. Lalezari, H. Golgolab, A. Shafiee, and M. Wossoughi, *ibid.*, **62**, 332(1973).

(3) A. Shafiee, I. Lalezari, S. Yazdani, F. M. Shahbazian, and T. Partovi, *ibid.*, **65**, 304(1976).

(4) S. Shibata, J. Shoji, N. Tokutake, Y. Kaneko, H. Shimizu, and H. H. Chiang, *Chem. Pharm. Bull.*, **10**, 477(1962).

(5) W. R. Boehme, *Org. Synth.*, **33**, 43(1953).

ACKNOWLEDGMENTS AND ADDRESSES

Received May 27, 1975, from the *Department of Chemistry, College of Pharmacy, Tehran University, Tehran, Iran.*

Accepted for publication September 26, 1975.

[x] To whom inquiries should be directed.

Simultaneous Analysis of Hydrocortisone and Hydrocortisone Phosphate by High-Pressure Liquid Chromatography: Reversed-Phase, Ion-Pairing Approach

J. KORPI [*], D. P. WITTMER [*], B. J. SANDMANN [‡], and W. G. HANEY, Jr. [‡x]

Abstract □ The reversed-phase, ion-pairing approach to high-pressure liquid chromatography was applied to the simultaneous analysis of hydrocortisone and its phosphate ester in laboratory-prepared samples and injectable solutions. Results of this technique were evaluated and compared with results of the official procedure.

Keyphrases □ Hydrocortisone—base and phosphate, simultaneous high-pressure liquid chromatographic analysis, prepared samples and injectable solutions □ High-pressure liquid chromatography—reversed-phase, ion-pairing approach, simultaneous analysis, hydrocortisone base and phosphate, prepared samples and injectable solutions □ Ion-pairing—application to high-pressure liquid chromatography, simultaneous analysis of hydrocortisone base and phosphate □ Glucocorticoids—hydrocortisone base and phosphate, simultaneous high-pressure liquid chromatographic analysis

For some time, these laboratories have been interested in the chromatographic applications of ion-pairing (1), and this interest has resulted in a unique approach to the rational separation of ionic compounds by high-pressure liquid chromatography (HPLC) (2). The technique involves the use of a lipophilic stationary phase and the addition of selected ionic compounds to the mobile phase. Ionic analytes injected into this chromatographic system are retained, apparently as a function of the lipophilicity of the ion-pair formed within the system. Therefore, the technique may be referred to as resulting from a reversed-phase, ion-pairing approach to HPLC.

The advantages of this technique over conventional ion-exchange HPLC were discussed previously, and the utility of the approach to the simultaneous analysis of several ionic substances was explored (2). In this investigation, the reversed-phase, ion-pairing approach was applied to the simultaneous analysis of nonionic and ionic compounds, as exemplified by hydrocortisone and hydrocortisone phosphate. These drugs were selected because they may be encountered together in commercial preparations (*e.g.*, injectable solutions) of the phosphate ester. Since free hydrocortisone is regarded as an impurity in these preparations and limited in concentration to less than 1%, procedures for the analysis of hydrocortisone and its ester are required.

Currently (3), the determination of hydrocortisone in the drug substance requires a number of manipulative steps prior to analysis and subsequent use of the enzyme alkaline phosphatase. Problems in the use of the enzyme were noted previously (4), and the complex workup makes the assay lengthy and the results subject to variation. Present methods for the analysis of hydrocortisone phosphate in injectable solutions (5) make no attempt to quantitate the free hydrocortisone present, so a procedure for the simultaneous analysis of the two drugs is of interest.

EXPERIMENTAL

Apparatus and Operating Conditions—A liquid chromatograph

3020 (aromatic), 2940, 2915, 1700 (CO), 1650, 1530, 1490, 1450, 1315, 1110, 1080, 1058, 860, and 748 cm^{-1}; NMR ($CDCl_3$): δ 7.1–7.42 (m, 4H, aromatic), 6.70–7.10 (broad s, 1H, NH), 3.66 (s, 3H, OCH_3), and 2.07 (s, 3H, CH_3) ppm.

Anal.—Calc. for $C_{11}H_{11}NO_3$: C, 64.39; H, 5.37; N, 6.83. Found: C, 64.28; H, 5.41; N, 6.97.

Compounds IV*b*–IV*g* were prepared similarly from III and the appropriate alcohols (Table I).

***p*-Chlorophenyl Benzo[*b*]-3-methyl-2-furancarbamate (IV*h*)**—A solution of III (2.01 g, 0.01 mole) and *p*-chlorophenol (1.28 g, 0.01 mole) in 30 ml of dry benzene was refluxed for 4 hr. The solvent was evaporated, and the residue was crystallized from benzene to give 1.65 g (55%) of the desired compound, mp 155–156°; IR (KBr): 3230 (NH), 1722 (CO), 1670, 1510, 1490, 1460, 1250, 1202, 1100, 1020, 1015, 855, and 752 cm^{-1}; NMR ($CDCl_3$): δ 7.7–7 (m, 8H, aromatic), 7–6.7 (broad s, 1H, NH), and 2.17 (s, 3H, CH_3) ppm.

Anal.—Calc. for $C_{16}H_{12}ClNO_3$: C, 63.68; H, 3.98; N, 4.64. Found: C, 63.79; H, 3.82; N, 4.73.

Compounds IV*i*–IV*n* were prepared similarly.

REFERENCES

(1) A. Shafiee, I. Lalezari, S. Yazdani, and A. Pournorouz, *J. Pharm. Sci.*, **62**, 839(1973).

(2) I. Lalezari, H. Golgolab, A. Shafiee, and M. Wossoughi, *ibid.*, **62**, 332(1973).

(3) A. Shafiee, I. Lalezari, S. Yazdani, F. M. Shahbazian, and T. Partovi, *ibid.*, **65**, 304(1976).

(4) S. Shibata, J. Shoji, N. Tokutake, Y. Kaneko, H. Shimizu, and H. H. Chiang, *Chem. Pharm. Bull.*, **10**, 477(1962).

(5) W. R. Boehme, *Org. Synth.*, **33**, 43(1953).

ACKNOWLEDGMENTS AND ADDRESSES

Received May 27, 1975, from the *Department of Chemistry, College of Pharmacy, Tehran University, Tehran, Iran.*

Accepted for publication September 26, 1975.

[x] To whom inquiries should be directed.

Simultaneous Analysis of Hydrocortisone and Hydrocortisone Phosphate by High-Pressure Liquid Chromatography: Reversed-Phase, Ion-Pairing Approach

J. KORPI [*], D. P. WITTMER [*], B. J. SANDMANN [‡], and W. G. HANEY, Jr. [‡x]

Abstract □ The reversed-phase, ion-pairing approach to high-pressure liquid chromatography was applied to the simultaneous analysis of hydrocortisone and its phosphate ester in laboratory-prepared samples and injectable solutions. Results of this technique were evaluated and compared with results of the official procedure.

Keyphrases □ Hydrocortisone—base and phosphate, simultaneous high-pressure liquid chromatographic analysis, prepared samples and injectable solutions □ High-pressure liquid chromatography—reversed-phase, ion-pairing approach, simultaneous analysis, hydrocortisone base and phosphate, prepared samples and injectable solutions □ Ion-pairing—application to high-pressure liquid chromatography, simultaneous analysis of hydrocortisone base and phosphate □ Glucocorticoids—hydrocortisone base and phosphate, simultaneous high-pressure liquid chromatographic analysis

For some time, these laboratories have been interested in the chromatographic applications of ion-pairing (1), and this interest has resulted in a unique approach to the rational separation of ionic compounds by high-pressure liquid chromatography (HPLC) (2). The technique involves the use of a lipophilic stationary phase and the addition of selected ionic compounds to the mobile phase. Ionic analytes injected into this chromatographic system are retained, apparently as a function of the lipophilicity of the ion-pair formed within the system. Therefore, the technique may be referred to as resulting from a reversed-phase, ion-pairing approach to HPLC.

The advantages of this technique over conventional ion-exchange HPLC were discussed previously, and the utility of the approach to the simultaneous analysis of several ionic substances was explored (2). In this investigation, the reversed-phase, ion-pairing approach was applied to the simultaneous analysis of nonionic and ionic compounds, as exemplified by hydrocortisone and hydrocortisone phosphate. These drugs were selected because they may be encountered together in commercial preparations (*e.g.*, injectable solutions) of the phosphate ester. Since free hydrocortisone is regarded as an impurity in these preparations and limited in concentration to less than 1%, procedures for the analysis of hydrocortisone and its ester are required.

Currently (3), the determination of hydrocortisone in the drug substance requires a number of manipulative steps prior to analysis and subsequent use of the enzyme alkaline phosphatase. Problems in the use of the enzyme were noted previously (4), and the complex workup makes the assay lengthy and the results subject to variation. Present methods for the analysis of hydrocortisone phosphate in injectable solutions (5) make no attempt to quantitate the free hydrocortisone present, so a procedure for the simultaneous analysis of the two drugs is of interest.

EXPERIMENTAL

Apparatus and Operating Conditions—A liquid chromatograph

Table I—Effect of Selected Salts on the Retention Volume of Hydrocortisone and Hydrocortisone Phosphate

Salt[a]	Hydrocortisone Phosphate Retention Volume, ml[b]	Hydrocortisone Retention Volume, ml
None	1.9	6.1
Tetramethylammonium hydroxide	4.5	6.1
Tetraethylammonium hydroxide	7.9	6.0
Tetrapropylammonium hydroxide	16.2	6.1
Tetrabutylammonium hydroxide	21.4	6.1
Tetrapentylammonium hydroxide	27.6	6.2
Tridecylammonium formate	39.4	6.0

[a] In a mobile phase of methanol–water (420:500). [b] Flow rate of 3.0 ml/min.

equipped with a 6000-psi pump, a high-pressure injector[1], and a 254-nm detector was used. Peak areas were determined with an electronic digital integrator[2].

Column—The column[3] (0.64 cm o.d. and 25 cm in length) was prepacked with a stationary phase of porous silica (average particle size of 10 μm) to which was bonded a monomolecular layer of octadecylsilane. The value of V_0 for the column was 1.9 ml.

Mobile Phase—A solution of tetrapentylammonium hydroxide (1×10^{-2} *M*) in methanol (100 ml) was prepared as described previously (6). An aliquot (20 ml) of this solution was mixed with distilled water (500 ml). The pH of the combined solution was adjusted to 7.5 with 1% formic acid solution, and the mixture was combined with methanol (400 ml). The flow rate used for the analysis was 3.0 ml/min.

Standard Solutions—Hydrocortisone phosphate[4] solutions in water were prepared to contain 4.0, 4.5, 5.0, 5.5, and 6.0 mg/ml (hydrocortisone equivalent); hydrocortisone[4] solutions in methanol contained 0.15, 0.10, 0.075, 0.05, and 0.025 mg/ml. Solutions of *p*-propenylanethole[5] in water (0.15 mg/ml) and benzophenone[6] in methanol (0.60 mg/ml) were prepared for use as internal standard solutions.

Calibration Curves—Aliquots (100 μl) of the hydrocortisone and hydrocortisone phosphate solutions were mixed with a like quantity of each internal standard solution, and a 15-μl portion of this mixture was injected into the chromatograph. The area ratio of each peak to its respective internal standard was determined, and calibration curves were constructed based on the area ratio of the drug peak to the concentration of drug in solution.

Analysis of Injectable Solutions—A portion of the solution was removed and diluted to a concentration of 5.0 mg/ml based on the labeled claim. An aliquot (100 μl) of this solution was mixed with 100 μl of each internal standard solution and of methanol, and 15 μl of this solution was injected. Peak area ratios were determined as already indicated, and the quantities of hydrocortisone and its phosphate ester were calculated by reference to the previously determined calibration curves.

RESULTS AND DISCUSSION

As noted in a recent discussion of the lineage of ion-pairing (7), the technique has been known since at least 1922. Analytical applications and other aspects of ion-pairing have been extensively reviewed (8, 9). However, the application of ion-pairing to HPLC has been of more recent origin; the approach has been to use cellulose as a support heavily loaded with aqueous solutions of the ion-pairing salt (10, 11). When using this approach, column lifetimes have been predictably short and the ability to use modern high-efficiency, small particle packings has been lost. These disadvantages are overcome by the addition of the ion-pairing agent to the mobile phase.

The process of selecting a mobile phase for an analysis using the ion-pairing approach may be divided into two stages. First, the customary procedures are employed to select a mobile phase in which the nonionic constituents are suitably separated. In this case, a solution of methanol–water (420:500) gave rapid separation of hydrocortisone from methylparaben and propylparaben. Second, quaternary ammonium compounds are added to the selected mobile phase, the retention characteristics of the ionic constituents are noted (Table I), and a single quaternary ammonium compound or a mixture is then chosen on the basis of the combined chromatographic characteristics of the ionic and nonionic constituents. Since the phosphate ester is normally present in quantities greatly in excess of free hydrocortisone, it was advisable to choose a reasonably lipophilic quaternary ammonium compound to retain the ester most strongly.

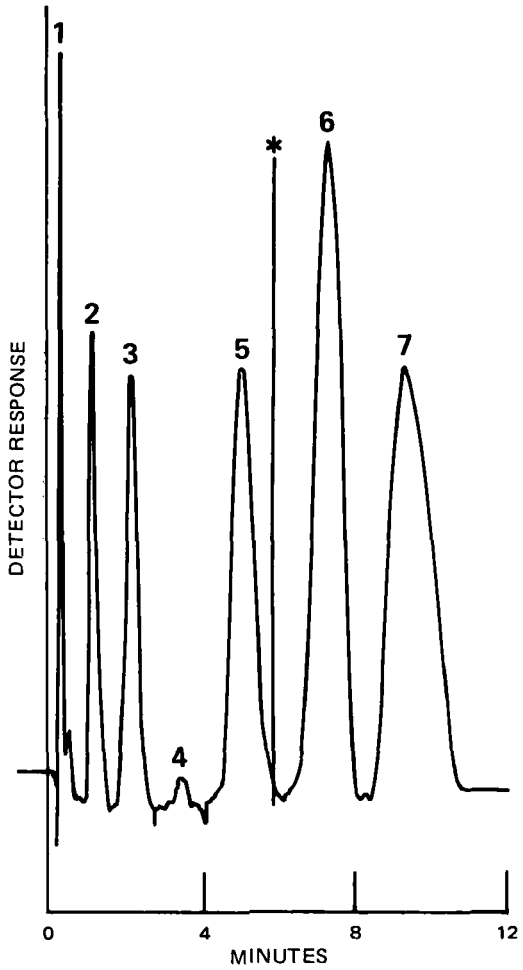

Figure 1—*Typical chromatographic trace of hydrocortisone phosphate injectable solution and internal standards. Key: 1, creatinine; 2, methylparaben; 3, hydrocortisone; 4, propylparaben; 5, benzophenone; 6, anethole; and 7, hydrocortisone phosphate.*

Figure 1 illustrates a typical chromatogram of constituents of the injectable hydrocortisone phosphate dosage form with internal standards. Since the amounts of hydrocortisone and its ester were quite different, it was deemed prudent to use a separate internal standard for each. The large difference in quantity also necessitated an attenuation change after elution of the first internal standard.

Standard curves were prepared daily for 10 days, and the standard deviation of slopes, average correlation coefficients, and average γ-intercept values were calculated. Values for hydrocortisone phosphate were 0.37%, 0.997, and −0.003, respectively; for hydrocortisone, they were 0.59%, 0.996, and 0.004, respectively. These values indicate that the procedure is amenable to use of a single-point standard for both compounds.

Data from laboratory-prepared samples (Table II) show close similarity between the currently official procedure and the HPLC procedure. Accuracy of the procedure in the analysis of hydrocortisone extends at least to the 0.5% level, and hydrocortisone is detectable at levels of 0.05%.

[1] ALC model 202 with model 6000 pump and U6K injector, Waters Associates, Milford, Mass.
[2] Model 450, Varian, Palo Alto, Calif.
[3] Microbondapak C_{18}, Waters Associates, Milford, Mass.
[4] USP reference standards.
[5] Baker Analyzed, J. T. Baker.
[6] Fisher Certified.

Table II—Results of the Analysis of Hydrocortisone and Hydrocortisone Phosphate in Laboratory-Prepared Samples

	Hydrocortisone Phosphate			Hydrocortisone		
		Found			Found	
Sample[a]	Added	UV[b]	HPLC	Added	UV	HPLC
1	50.0	49.45[c] (3.57)	49.64 (2.12)	5.0	4.54 (2.76)	4.68 (2.59)
2	50.0	49.57 (3.46)	49.76 (2.23)	0.25	0.23 (3.94)	0.24 (2.30)
3	60.0	57.56 (3.04)	58.31 (2.64)	0.5	0.47 (4.46)	0.47 (2.4)
4	40.0	39.89 (3.94)	40.44 (3.10)	5.0	4.62 (2.55)	4.74 (2.47)
5	40.0	39.46 (4.12)	40.16 (3.00)	0.25	0.24 (4.26)	0.25 (2.59)

[a] Expressed in milligrams per milliliter. [b] USP XIX. [c] Average (% *SD*), $n = 7$.

Table III—Analysis of Hydrocortisone and Hydrocortisone Phosphate in Injectable Solutions

	Hydrocortisone Phosphate Found[a]		Hydrocortisone Found[c]
Sample	Colorimetric[b]	HPLC	
1	103.42 (4.68)	102.94 (3.76)	0.76 (2.46)
2	98.50 (5.44)	97.64 (3.54)	1.18 (2.76)
3	96.64 (4.50)	97.76 (3.94)	2.02 (3.14)
4	105.74 (4.77)	104.68 (3.22)	0.46 (2.17)

[a] Expressed as percent of labeled claim (% *SD*). [b] USP XIX. [c] Expressed as percent of labeled claim of hydrocortisone phosphate (% *SD*).

Table III presents results of the analysis of these drugs in several lots of the injectable solution. Results of the two procedures are again comparable, and the standard deviations are again lower with the HPLC assay, reflecting the simplified sample workup procedure.

The HPLC procedure is simple in nature and easily mastered. Triplicate analyses of a sample require approximately 1 hr, and more than 400 injections were made with no discernible change in the characteristics of the chromatographic system. It appears, therefore, that the reversed-phase, ion-pairing approach is well suited to the simultaneous analysis of such nonionic and ionic drugs as hydrocortisone and its phosphate ester.

There is, however, a precaution regarding the use of this technique. The quaternary ammonium hydroxides are basic substances, and the pH of their aqueous solutions rapidly inactivates the permanently bonded, reversed-phase systems. As a result, it is necessary to adjust the pH of the aqueous solution of the salt to less than 8.0 prior to use.

In regard to other applications of the reversed-phase, ion-pairing approach, a corollary to the technique presented here is that the addition of lipophilic acid salts to the mobile phase would result in the retention of amines. Therefore, the technique should be of use in the analysis of amines. Also, it should not be necessary to restrict its use to the stationary phase used here. These additional aspects will be discussed later.

REFERENCES

(1) D. Wittmer, S. A. Atwell, and W. G. Haney, Jr., *J. Forensic Sci.*, **20**, 88(1975).

(2) D. P. Wittmer, N. O. Nuessle, and W. G. Haney, Jr., *Anal. Chem.*, **47**, 1422(1975).

(3) "The United States Pharmacopeia," 19th rev., Mack Publishing Co., Easton, Pa., 1975, p. 241.

(4) G. B. Kaplan and J. Levine, *J. Assoc. Offic. Anal. Chem.*, **57**, 735(1974).

(5) "The United States Pharmacopeia," 19th rev., Mack Publishing Co., Easton, Pa., 1975, p. 242.

(6) R. Osiewicz, V. Aggarwal, R. M. Young, and J. Sunshine, *J. Chromatogr.*, **88**, 157(1974).

(7) J. Levine, *J. Assoc. Offic. Anal. Chem.*, **57**, 237(1974).

(8) B. A. Persson, *Acta Pharm. Suec.*, **8**, 217(1971).

(9) R. Modin, *ibid.*, **9**, 157(1972).

(10) B. L. Karger and B. A. Persson, *J. Chromatogr. Sci.*, **12**, 521(1974).

(11) B. L. Karger, S. C. Su, S. Marchese, and B. A. Persson, *ibid.*, **12**, 678(1974).

ACKNOWLEDGMENTS AND ADDRESSES

Received June 13, 1975, from **Waters Associates, Milford, MA 01757*, and the *‡School of Pharmacy, University of Missouri-Kansas City, Kansas City, MO 64110*

Accepted for publication October 8, 1975.

The authors appreciate the technical assistance of Kathy Butler.

ˣ To whom inquiries should be directed.

High-Pressure Liquid Chromatographic Determination of Thiothixene in Pharmaceutical Formulations

C. K. WONG, D. M. COHEN, and K. P. MUNNELLY ˣ

Abstract □ A method was developed for the quantitative determination of thiothixene in pharmaceutical formulations by high-pressure liquid chromatography after dissolution of the sample in methanol.

Keyphrases □ Thiothixene—high-pressure liquid chromatographic analysis, pharmaceutical formulations □ High-pressure liquid chromatography—analysis, thiothixene, pharmaceutical formulations □ Tranquilizers—thiothixene, high-pressure liquid chromatographic analysis, pharmaceutical formulations

Thiothixene, a thioxanthene derivative, is the *cis*-isomer of *N,N*-dimethyl-9-[3-(4-methyl-1-piperazinyl)propylidene]thioxanthene-2-sulfonamide. The thioxanthenes differ from the phenothiazines by replacement of the nitrogen in the central ring with a carbon-linked side chain fixed in space in a rigid structural configuration and an *N,N*-dimethylsulfonamide functional group bonded to the thioxanthene nucleus. Thiothixene is supplied as a capsule, injection, and solution and is effective in the management of manifestations of psychotic disorders (1).

Some methods for the quantitative determination of thiothixene in pharmaceutical formulations have appeared in compendial monographs. Three basic methods exist: a spectrophotometric assay, a paper chromatographic assay, and a colorimetric assay involving the formation of a methyl orange complex (2). However, these methods do not have the rapidity, simplicity, sensitivity, and selectivity found in high-pressure liquid chromatographic (HPLC) methodology. The subject of this report is the development of a simple, direct, and extremely rapid HPLC procedure for the quantitation of thiothixene in several pharmaceutical formulations.

EXPERIMENTAL

Equipment—A liquid chromatograph[1], operated at ambient temperatures and equipped with a UV detector for monitoring the column effluent at 254 nm, was used. The column was 1-m × 2.1-mm (i.d.) stainless steel tubing, dry packed with Corasil II[2]. An electronic integrator[3] was used to obtain peak areas.

Reagents—NF thiothixene reference standard, dried *in vacuo* at 100° for 3 hr, was used. *N*-(1-Naphthyl)ethylenediamine dihydrochloride[4] was the internal standard. Analytical reagent grade methanol[5], 95% ethanolamine[6], and distilled water were used to prepare the mobile phase.

Preparation of Mobile Phase—Add 0.37 ml of ethanolamine and 400 ml of water to 2.8 liters of methanol and shake vigorously. Degas prior to use.

Preparation of Standard Solution—Dissolve approximately 350 mg of *N*-(1-naphthyl)ethylenediamine dihydrochloride in 100 ml of methanol. Accurately weigh approximately 25 mg of thiothixene standard, transfer quantitatively to a 25-ml volumetric flask, add 5 ml of the *N*-(1-naphthyl)ethylenediamine dihydrochloride solution, and dissolve in and dilute to volume with methanol.

Preparation of Sample Solution—For thiothixene capsules, transfer as completely as possible the contents of not less than 30 capsules to a tared beaker and weigh. Mix and transfer an accurately weighed portion of the powder, equivalent to 25 mg of thiothixene, to a glass-stoppered centrifuge tube. Add 5 ml of the *N*-(1-naphthyl)ethylenediamine dihydrochloride solution and 20 ml of methanol, shake for 2 min, centrifuge, and use the supernate for analysis. For the thiothixene injection or solution, accurately pipet an aliquot of sample equivalent to 25 mg of thiothixene into a 25-ml volumetric flask. Add 5 ml of the *N*-(1-naphthyl)ethylenediamine dihydrochloride solution and dissolve in and dilute to volume with methanol.

Chromatography—Condition the column for 24 hr with the mobile phase at a flow rate of 0.5 ml/min. This procedure is necessary for newly packed columns; conditioning is not required for previously used columns. Inject 4 μl of the standard solution and adjust either the pressure or flow rate so that the *N*-(1-naphthyl)ethylenediamine dihydrochloride exhibits a retention time of approximately 4–5 min. Repeat if necessary.

Inject 4 μl of the standard solution followed by two 4-μl injections of the sample solution and one 4-μl injection of the standard solution, allowing sufficient time between injections for development of the chromatograms and return to baseline. The peak areas obtained are used for the calculations.

Calculations—Calculate the quantity of thiothixene in milligrams

Table I—Percent Recovery of Thiothixene by HPLC from Spiked Placeboes

Product	Day	Weight	Injection Number 1	2	3
Capsule[a]	1	1	100.6	99.2	99.1
		2	96.9	98.6	97.7
		3	100.1	97.1	99.0
	2	1	98.8	96.8	95.8
		2	101.5	98.0	98.8
		3	98.1	99.5	98.7
	3	1	97.1	94.7	97.9
		2	96.9	94.5	96.7
		3	96.8	95.5	96.3
Injection[b]	1	1	97.5	98.5	98.2
		2	104.0	100.7	102.7
		3	104.0	101.2	105.1
	2	1	100.0	100.9	101.8
		2	100.8	102.6	102.3
		3	101.3	103.7	102.6
	3	1	99.7	101.2	103.8
		2	103.7	99.2	98.1
		3	101.4	101.0	102.6
Solution[c]	1	1	100.2	98.9	96.9
		2	100.2	97.3	100.1
		3	98.4	99.1	99.3
	2	1	100.1	98.0	101.3
		2	96.6	99.7	98.6
		3	97.0	98.3	99.1
	3	1	100.7	98.6	101.8
		2	101.1	101.8	98.2
		3	98.7	98.4	98.0

[a] The average percent recovery was 97.8 with 95% confidence limits of 97.1–98.5 [b] The average percent recovery was 101.4 with 95% confidence limits of 100.6–102.2. [c] The average percent recovery was 99.1 with 95% confidence limits of 98.5–99.7.

[1] DuPont 820.
[2] Waters Associates.
[3] Hewlett-Packard 3370A.
[4] Fisher Scientific Co.
[5] Mallinckrodt.
[6] Aldrich Chemical Co.

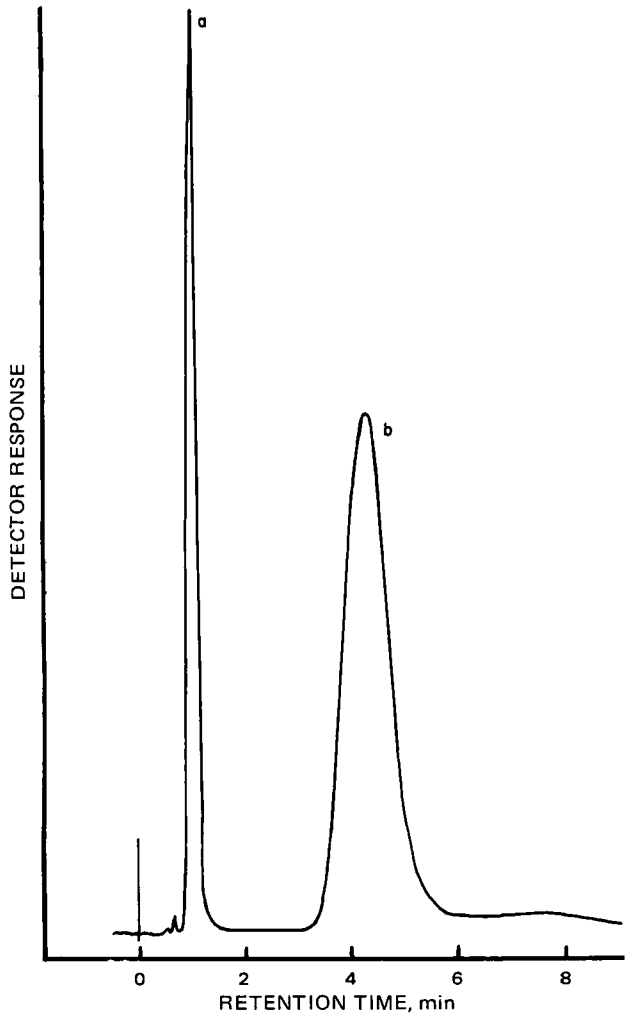

Figure 1—*Representative chromatogram. Key: a, thiothixene; and b, N-(1-naphthyl)ethylenediamine.*

per capsule or milliliter according to:

$$\text{mg/capsule} = \frac{R_{spl} \times W_{std}\ (\text{mg}) \times \text{average capsule weight (mg)}}{R_{std} \times W_{spl}\ (\text{mg})} \qquad \text{(Eq. 1)}$$

$$\text{mg/ml} = \frac{R_{spl} \times W_{std}\ (\text{mg})}{R_{std} \times W_{spl}\ (\text{ml})} \qquad \text{(Eq. 2)}$$

where R_{spl} is the ratio of the thiothixene peak area to the *N*-(1-naphthyl)ethylenediamine dihydrochloride peak area in a sample solution injection, R_{std} is the average ratio of the thiothixene peak area to the *N*-(1-naphthyl)ethylenediamine dihydrochloride peak area in the standard solution injections before and after the sample, W_{std} is the weight of the standard, and W_{spl} is the weight or volume of the sample.

RESULTS AND DISCUSSION

Initial studies were conducted utilizing methanol as the mobile phase, and acceptable peak symmetry and retention time were observed for thiothixene. *N*-(1-Naphthyl)ethylenediamine dihydrochloride appeared satisfactory as the internal standard, showing the greatest separation from thiothixene. However, its longer retention time (~30 min) resulted in a significant increase in the cycle time of an analysis. Further studies were initiated to modify the methanol mobile phase so as to decrease the retention time of the *N*-(1-naphthyl)ethylenediamine dihydrochloride without affecting the peak symmetry and retention of the thiothixene.

Modifiers for improving separation and retention in nonpolar mobile phases have been used for some time in liquid–solid chromatography (3). However, the use of modifiers in polar mobile phases, especially those containing large percentages of water, is unique in its application to HPLC. The addition of small amounts of ethanolamine to the methanol significantly decreased the retention of the *N*-(1-naphthyl)ethylenediamine dihydrochloride while only a minute decrease was observed for thiothixene. This decrease appears due to the conversion of the internal standard from the dihydrochloride to the free base. Excellent separation of the two components was maintained and the cycle time for an analysis decreased substantially when a mobile phase of methanol–ethanolamine (7560:1) was employed.

Although the resulting separation was considered optimum, the shape of the *N*-(1-naphthyl)ethylenediamine dihydrochloride peak required further improvement since the lack of a defined beginning and end presents considerable problems for quantitation by electronic integration. By the addition of water, the characteristic tailing for adsorption chromatography was eliminated (4). The mobile phase

Table II—Estimates of Precision for Determination of Thiothixene by HPLC in Pharmaceutical Formulations

Weights per Day	Injections per Weight	Estimates of Precision[a], % Capsule	Injection	Solution
1	1	±3.8	±4.3	±2.9
1	2	±3.3	±3.7	±2.1
1	3	±3.1	±3.5	±1.8
2	2	±2.9	±2.6	±1.5
2	3	±2.8	±2.4	±1.2
Injection to injection within a weight		±2.7	±3.2	±2.9

[a] Ninety-five percent of the individual results or averages of two, three, four, or six results will not vary from each other by more than the percentages quoted. These estimates include variability due to days, weights, and injections. The estimates of precision for injection to injection within a weight exclude variability due to days and weights.

Table III—Comparison of HPLC and Compendial Paper Chromatographic Methods for Determination of Thiothixene in Pharmaceutical Formulations

Product	Day	Sample	HPLC	Paper Chromatography
Capsule[a]	1	1	5.31	4.94
		2	5.13	4.99
		3	5.37	—
	2	4	5.26	5.18
		5	5.35	4.88
		6	5.16	—
	3	7	4.95	5.15
		8	5.08	5.05
		9	5.14	—
		Average	5.19	5.03
Injection[b]	1	1	2.01	2.01
		2	2.01	2.02
		3	1.99	—
	2	4	2.04	1.97
		5	2.03	2.04
		6	2.05	—
	3	7	2.02	2.01
		8	2.02	1.99
		9	2.00	—
		Average	2.02	2.01
Solution[c]	1	1	4.97	5.07
		2	5.05	4.92
		3	5.02	—
	2	4	5.00	5.06
		5	5.00	5.06
		6	5.02	—
	3	7	5.15	5.09
		8	5.13	5.09
		9	5.13	—
		Average	5.05	5.05

[a] Results are given in milligrams per capsule. [b] Results are given in milligrams per milliliter. [c] Results are given in milligrams per 5 ml.

reported in this study improved peak shape, with the resulting chromatogram resembling the characteristics of partition chromatography; all peaks were well defined and symmetrical (Fig. 1).

The accuracy and precision of the HPLC method were determined by the following experiments. Three weights of a placebo of each pharmaceutical formulation to which known quantities of thiothixene hydrochloride had been added were assayed per day for 3 consecutive days. The average percent recoveries of thiothixene were 97.8, 101.4, and 99.1 for the capsule, injection, and solution, respectively (Table I). The estimates of precision (Table II) were obtained using the analysis of variance statistical technique. Ninety-five percent of the individual results will not vary from each other (*i.e.*, from the mean) by more than ±3.8, ±4.3, and ±2.9% for the capsule, injection, and solution, respectively. The standard errors for the average of two injections per sample were ±1.6, ±1.8, and ±1.1% for the capsule, injection, and solution, respectively.

The proposed HPLC method was compared to the compendial paper chromatographic assays (2), and the results obtained (Table III) were in agreement. All samples were within the requirements of NF XIV for thiothixene formulations by the HPLC methodology (2). Because of the speed, accuracy, and precision of the proposed procedure, it represents a viable alternative to present compendial methodology.

REFERENCES

(1) "Physicians' Desk Reference," 29th ed., Medical Economics, Inc., Oradell, N.J., 1975, p. 1272.

(2) "The National Formulary," 14th ed., Mack Publishing Co., Easton, Pa., 1975, and 1st supplement, official July 1, 1975.

(3) "Modern Practice of Liquid Chromatography," J. J. Kirkland, Ed., Wiley–Interscience, New York, N.Y., 1971, p. 223.

(4) "Chromatography," E. Heftmann, Ed., Reinhold, New York, N.Y., 1964, p. 63.

ACKNOWLEDGMENTS AND ADDRESSES

Received July 21, 1975, from *Quality Control, Pfizer Inc., Brooklyn, NY 11206*

Accepted for publication September 26, 1975.

[x] To whom inquiries should be directed.

Structural Features and Protective Activity of Dexamethasone and Pregnenolone-16α-carbonitrile

A. TERZIS [*], P. KOUROUNAKIS [x], and T. THEOPHANIDES

Abstract □ Pretreatment with dexamethasone acetate or pregnenolone-16α-carbonitrile markedly diminished the pharmacological effect of zoxazolamine in rats. This prophylactic action was associated with significantly decreased plasma drug levels, which, in turn, were correlated with enhanced hepatic drug biotransformation, induced by the steroids. Dexamethasone proved to be more active than pregnenolone-16α-carbonitrile in this respect. The A-ring conformation as well as the distances of O-3–O-11, O-11–O-17, and the O-3–mean plane C-5–C-17 may be key factors in glucocorticoid activity, and the longer the distances, the greater the potency. These characteristics have no bearing on catatoxic activity for which the 16α-substituent appears to be a structural prerequisite.

Keyphrases □ Dexamethasone acetate—structural and conformational features, effect of pretreatment on pharmacological action, plasma concentrations, and liver homogenate metabolism of zoxazolamine, rats □ Pregnenolone-16α-carbonitrile—structural and conformational features, effect of pretreatment on pharmacological action, plasma concentrations, and liver homogenate metabolism of zoxazolamine, rats □ Structure–activity relationships—dexamethasone acetate and pregnenolone-16α-carbonitrile, structural features, prophylactic activity against zoxazolamine, rats □ Glucocorticoids—dexamethasone acetate and pregnenolone-16α-carbonitrile, structural features, prophylactic activity against zoxazolamine, rats □ Zoxazolamine—effect of pretreatment with dexamethasone acetate and pregnenolone-16α-carbonitrile on pharmacological action, plasma concentrations, and liver homogenate metabolism, rats

Numerous compounds induce liver microsomal enzymes and can be divided into three main classes: barbiturates, polycyclic aromatic hydrocarbons, and steroids (1–3). Pregnenolone-16α-carbonitrile (I), a synthetic "catatoxic" steroid devoid of any other known hormonal or pharmacological activity, and dexamethasone acetate, a synthetic glucocorticoid, are potent microsomal enzyme inducers (3). Pretreatment with I or dexamethasone protects experimental animals against numerous toxic agents, mainly *via* the induction of drug-metabolizing enzymes in liver microsomes (catatoxic mechanism). However, the protective effect of some steroids is attributed to their glucocorticoid activity (3, 4).

Because the mechanism of microsomal enzyme induction at the molecular level is still not known and little accurate structural information is available (5), an investigation was conducted on the structure–activity relationships of these and other similarly acting steroids. In this study, the prophylactic activity of I and dexamethasone against zoxazolamine was correlated with plasma drug concentrations and *in vitro* metabolism by the 9000×*g* liver homogenate fraction. Thus, the protective mechanism was demonstrated and the relative potency of these enzyme inducers was established.

In addition, the steroid structure was determined in an effort to elucidate the common structural and conformational prerequisites for their inductive properties. This information should prove useful in the continuing investigations of the structure–activity relationships of similarly acting steroids. Since information on the structure (6–8) and activity (9, 10) of fludrocortisone, cortisone, and 6α-methylprednisolone was available, it is also discussed.

reported in this study improved peak shape, with the resulting chromatogram resembling the characteristics of partition chromatography; all peaks were well defined and symmetrical (Fig. 1).

The accuracy and precision of the HPLC method were determined by the following experiments. Three weights of a placebo of each pharmaceutical formulation to which known quantities of thiothixene hydrochloride had been added were assayed per day for 3 consecutive days. The average percent recoveries of thiothixene were 97.8, 101.4, and 99.1 for the capsule, injection, and solution, respectively (Table I). The estimates of precision (Table II) were obtained using the analysis of variance statistical technique. Ninety-five percent of the individual results will not vary from each other (*i.e.*, from the mean) by more than ±3.8, ±4.3, and ±2.9% for the capsule, injection, and solution, respectively. The standard errors for the average of two injections per sample were ±1.6, ±1.8, and ±1.1% for the capsule, injection, and solution, respectively.

The proposed HPLC method was compared to the compendial paper chromatographic assays (2), and the results obtained (Table III) were in agreement. All samples were within the requirements of NF XIV for thiothixene formulations by the HPLC methodology (2). Because of the speed, accuracy, and precision of the proposed procedure, it represents a viable alternative to present compendial methodology.

REFERENCES

(1) "Physicians' Desk Reference," 29th ed., Medical Economics, Inc., Oradell, N.J., 1975, p. 1272.

(2) "The National Formulary," 14th ed., Mack Publishing Co., Easton, Pa., 1975, and 1st supplement, official July 1, 1975.

(3) "Modern Practice of Liquid Chromatography," J. J. Kirkland, Ed., Wiley–Interscience, New York, N.Y., 1971, p. 223.

(4) "Chromatography," E. Heftmann, Ed., Reinhold, New York, N.Y., 1964, p. 63.

ACKNOWLEDGMENTS AND ADDRESSES

Received July 21, 1975, from *Quality Control, Pfizer Inc., Brooklyn, NY 11206*

Accepted for publication September 26, 1975.

[x] To whom inquiries should be directed.

Structural Features and Protective Activity of Dexamethasone and Pregnenolone-16α-carbonitrile

A. TERZIS [*], P. KOUROUNAKIS [x], and T. THEOPHANIDES

Abstract □ Pretreatment with dexamethasone acetate or pregnenolone-16α-carbonitrile markedly diminished the pharmacological effect of zoxazolamine in rats. This prophylactic action was associated with significantly decreased plasma drug levels, which, in turn, were correlated with enhanced hepatic drug biotransformation, induced by the steroids. Dexamethasone proved to be more active than pregnenolone-16α-carbonitrile in this respect. The A-ring conformation as well as the distances of O-3–O-11, O-11–O-17, and the O-3–mean plane C-5–C-17 may be key factors in glucocorticoid activity, and the longer the distances, the greater the potency. These characteristics have no bearing on catatoxic activity for which the 16α-substituent appears to be a structural prerequisite.

Keyphrases □ Dexamethasone acetate—structural and conformational features, effect of pretreatment on pharmacological action, plasma concentrations, and liver homogenate metabolism of zoxazolamine, rats □ Pregnenolone-16α-carbonitrile—structural and conformational features, effect of pretreatment on pharmacological action, plasma concentrations, and liver homogenate metabolism of zoxazolamine, rats □ Structure–activity relationships—dexamethasone acetate and pregnenolone-16α-carbonitrile, structural features, prophylactic activity against zoxazolamine, rats □ Glucocorticoids—dexamethasone acetate and pregnenolone-16α-carbonitrile, structural features, prophylactic activity against zoxazolamine, rats □ Zoxazolamine—effect of pretreatment with dexamethasone acetate and pregnenolone-16α-carbonitrile on pharmacological action, plasma concentrations, and liver homogenate metabolism, rats

Numerous compounds induce liver microsomal enzymes and can be divided into three main classes: barbiturates, polycyclic aromatic hydrocarbons, and steroids (1–3). Pregnenolone-16α-carbonitrile (I), a synthetic "catatoxic" steroid devoid of any other known hormonal or pharmacological activity, and dexamethasone acetate, a synthetic glucocorticoid, are potent microsomal enzyme inducers (3). Pretreatment with I or dexamethasone protects experimental animals against numerous toxic agents, mainly *via* the induction of drug-metabolizing enzymes in liver microsomes (catatoxic mechanism). However, the protective effect of some steroids is attributed to their glucocorticoid activity (3, 4).

Because the mechanism of microsomal enzyme induction at the molecular level is still not known and little accurate structural information is available (5), an investigation was conducted on the structure–activity relationships of these and other similarly acting steroids. In this study, the prophylactic activity of I and dexamethasone against zoxazolamine was correlated with plasma drug concentrations and *in vitro* metabolism by the 9000×*g* liver homogenate fraction. Thus, the protective mechanism was demonstrated and the relative potency of these enzyme inducers was established.

In addition, the steroid structure was determined in an effort to elucidate the common structural and conformational prerequisites for their inductive properties. This information should prove useful in the continuing investigations of the structure–activity relationships of similarly acting steroids. Since information on the structure (6–8) and activity (9, 10) of fludrocortisone, cortisone, and 6α-methylprednisolone was available, it is also discussed.

Table I—Effect of Pregnenolone-16α-carbonitrile and Dexamethasone Acetate on Zoxazolamine Paralysis Time, Plasma Concentrations, and *In Vitro* Metabolism[a]

Pretreatment	Paralysis		Zoxazolamine Concentrations in Plasma, μg/ml	Zoxazolamine Hydroxylation	
	Time, min	Reduction, %		Rate, μmoles/g[b]/hr	Increase, %
Pregnenolone-16α-carbonitrile	52 ± 4***[c] (16)	65	25.8 ± 0.9 (6)	44.7 ± 1.8*** (6)	128
Water	150 ± 8 (10)		36.6 ± 1.2[d]*** (8)	19.6 ± 1.0 (6)	
			21.2 ± 0.6[e] NS (6)		
Dexamethasone acetate	32 ± 3*** (7)	71	20.4 ± 0.9 (7)	60.8 ± 4.3 (6)	210
Water	110 ± 2 (9)		28.8 ± 1.6[d]*** (9)	19.6 ± 1.0***	
			17.3 ± 0.6[e]** (10)		

[a] In the 9000×*g* supernatant fraction of the liver. [b] Of liver protein. [c] ** = $p < 0.025$. *** = $p < 0.001$. NS = not significant. Figures in parentheses indicate number of rats used. [d] Unrecovered controls. [e] Recovered controls. (The recovered and unrecovered controls are compared with the steroid-pretreated groups).

EXPERIMENTAL

Female Sprague–Dawley rats[1], averaging 100 g (range 95–105 g) and maintained *ad libitum* on food[2] and tap water, were used for the biochemical study.

Study 1—Compound I[3] or dexamethasone acetate[4] was given orally at a dose level of 20 μmoles in 1 ml of water (micronized with a trace of polysorbate 80) twice daily for 3 days. On the 4th day, 18 hr after the last steroid administration, all rats received 10 mg ip of zoxazolamine[5]. Blood was removed from the pretreated animals when they reacquired the righting reflex; it was also taken from an unrecovered control group killed at that moment as well as from a second control group sacrificed at spontaneous recovery (recovered controls). Drug-free plasma from all rats was used for preparing standards and blanks. The plasma zoxazolamine concentrations were determined by the method of Burns *et al.* (11).

Study 2—The rats were treated as in Study 1 and decapitated 18 hr after the last steroid administration. Their livers were immediately removed, weighed, and washed in an ice-cold 1.15% KCl solution. Liver samples of 3 g were homogenized in 9 ml of isotonic potassium chloride containing 0.02 *M* tromethamine (pH 7.4). The homogenate was centrifuged at 9000×*g* for 20 min, and the supernatant fraction was used for studying zoxazolamine metabolism. The entire procedure was conducted at 0–3°.

Zoxazolamine hydroxylation was determined by the method of Juchau *et al.* (12). The incubation medium contained: tromethamine buffer (pH 7.4), 5 m*M* $MgCl_2$, 5 m*M* glucose 6-phosphate[6], 0.4 m*M* NADP[6], homogenate corresponding to 0.220 g of liver, and 1.2 μmoles of zoxazolamine. The duration of incubation was 30 min. The protein content of the homogenate was determined according to a reported method (13).

Table I shows the effects of I and dexamethasone acetate on: (*a*) zoxazolamine-induced paralysis, (*b*) zoxazolamine concentrations in plasma, and (*c*) zoxazolamine hydroxylation *in vitro*.

The important features of the molecular structures of five steroids were compared. These structures were determined by X-ray analysis from three-dimensional diffraction data, and the nonhydrogen atoms were refined with anisotropic thermal parameters. In all cases, the hydrogen atoms were found by difference Fourier syntheses. The structures compared were: I (R = 3.0%) (14), dexamethasone (R = 2.8%) (14), fludrocortisone (R = 4.6%) (6), cortisone (R = 5.8%) (7), and 6α-methylprednisolone (R = 3.6%) (8). The crystallographic R values ($R = \Sigma||F_o| - |F_c|/F_o|$), which measure the agreement between the observed and calculated structure factors, showed that all these structures are good and that the standard deviations are of the order of 0.005 Å for carbon–carbon bond lengths.

[1] Canadian Breeding Farms and Laboratories Ltd., St. Constant, Quebec, Canada.
[2] Purina Laboratory Chow.
[3] The Upjohn Co.
[4] Schering Corp.
[5] K. and K. Laboratories.
[6] Sigma Chemical Co.

RESULTS AND DISCUSSION

Compound I or dexamethasone pretreatment significantly reduced zoxazolamine paralysis, which was accompanied by markedly lower plasma drug levels in the pretreated groups as compared with the unrecovered controls. This finding has been attributed to increased drug biotransformation. There were no differences between the plasma zoxazolamine concentrations in the recovered controls and I-pretreated animals, since both groups were in the same clinical state. However, dexamethasone-pretreated rats showed higher zoxazolamine levels than the recovered controls. The reason for this apparent discrepancy was explained earlier (9).

Both steroids greatly enhanced zoxazolamine hydroxylation *in vitro* (Table I). They appeared to protect against this toxicant *via* drug-metabolizing enzyme induction in hepatocytes. Dexamethasone seemed to be more active than I with respect to both *in vivo* prophylaxis and *in vitro* zoxazolamine hydroxylation.

Weeks *et al.* (15) postulated a relationship between glucocorticoid activity and A-ring conformation. They found that the more the ring deviates from the C-5–C-17 mean plane, the greater is the anti-inflammatory activity, for example, of cortisone, 6α-fluorocortisol, 6α-methylprednisolone, and fludrocortisone, the latter having the highest activity. It is known (10) that dexamethasone is considerably more potent than fludrocortisone. As shown in Fig. 1 and Table II, while dexamethasone follows the trend established by Weeks *et al.* (15), the great difference between its activity and that of fludrocortisone cannot be accounted for by the small divergence in the distance of O-3 from the mean plane for these compounds.

Although A-ring conformation may be an important determinant in glucocorticoid activity, other factors such as a C-16 substituent and

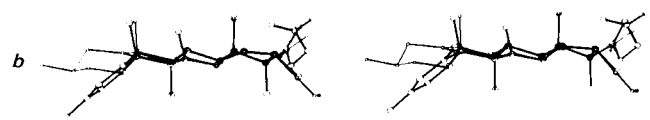

Figure 1—*Projections parallel to the least-squares plane passed through atoms C-5–C-17 inclusive. The molecules of fludrocortisone* (a) *and I* (b) *are successively imposed on those of dexamethasone acetate (large circles).*

Table II—Comparison of Glucocorticoid Activity with Some Features of Steroid Structure (10)

Treatment	Hepatic Glycogen, mg/g	Thymus Weight, g/100 g of Body Weight	O-3–O-11, Å	O-11–O-17, Å	O-3–Mean Plane C-5–C-17, Å
Cortisone	0.67 ± 0.24 NS[a]	0.44 ± 0.003 NS	6.551 (6)[b]	5.195 (6)	1.30
Control water	0.71 ± 0.10	0.48 ± 0.02			
6α-Methylprednisolone	12.30 ± 1.8*	0.24 ± 0.03*	6.593 (4)	5.219 (4)	1.95
Control water	0.71 ± 0.10	0.48 ± 0.02			
Fludrocortisone	11.53 ± 0.33*	0.11 ± 0.01*	6.816 (5)	5.210 (5)	2.43
Control water	0.59 ± 0.10	0.39 ± 0.02			
Dexamethasone acetate	61.99 ± 4.10*	0.08 ± 0.01*	6.822 (5)	5.321 (5)	2.57
Control water	0.59 ± 0.10	0.39 ± 0.02			

[a] NS = not significant. * = $p < 0.005$. [b] Standard deviation.

distances between oxygen functions must also play significant roles. It can be seen in Table II that the oxygen–oxygen distances also follow those of the O-3–mean plane (C-5–C-17). There is actually a better correlation between the O-11–O-17 distances and glucocorticoid activity than with the one just mentioned.

The effect of the oxygen–oxygen distances on the catatoxic activity of I and dexamethasone cannot be very significant since I, which does not have oxygen functions on either C-11 or C-17, is nonetheless a potent catatoxic steroid. Superimposition of the molecule of fludrocortisone on that of dexamethasone (Fig. 1*a*) indicates that C-16 substitution is a decisive factor for strong catatoxic activity. This is further supported by the fact that I (itself a potent agent) and dexamethasone have a C-16 substituent in the α-configuration. Removal of this substituent results in a loss of catatoxic potency.

The present findings established a relationship between A-ring conformation and distances between oxygen functions and glucocorticoid activity. However, such a correlation was not demonstrated for catatoxic activity. Compound I and dexamethasone, both potent catatoxic steroids, have widely differing A-ring conformations (Fig. 1); dexamethasone and fludrocortisone (Table I), with almost identical A-ring conformations, show great differences in catatoxic activity.

REFERENCES

(1) A. H. Conney, *Pharmacol. Rev.*, **19**, 317(1967).

(2) J. R. Gillette, *Prog. Drug Res.*, **6**, 11(1965).

(3) H. Selye, "Hormones and Resistance," Springer-Verlag, Heidelberg, Germany, 1971.

(4) P. Kourounakis, *Am. J. Pharm.*, **146**, 22(1974).

(5) A. Goldstein, L. Aronow, and S. M. Kalman, "Principles of Drug Action," Hoeber Medical Division, Harper & Row, New York, N.Y., 1969, pp. 206–279.

(6) L. Dupont, O. Didenberg, and H. Campsteyn, *Cryst. Struct. Commun.*, **1**, 177(1972).

(7) J. P. Declercq, G. Germain, and M. Van Meerssche, *ibid.*, **1**, 5(1972).

(8) *Ibid.*, **1**, 13(1972).

(9) P. Kourounakis, S. Szabo, and H. Selye, *Proc. Int. Congr. Pharm. Sci., 33rd*, **1973**, 251.

(10) H. Selye, S. Szabo, Y. Taché, P. Kourounakis, I. Mécs, and J. Taché, *Steroids Lipids Res.*, **5**, 10(1974).

(11) J. J. Burns, T. F. Yü, L. Berger, and A. B. Gutman, *Am. J. Med.*, **25**, 401(1958).

(12) M. R. Juchau, R. L. Cram, G. Plaa, and J. R. Fouts, *Biochem. Pharmacol.*, **14**, 473(1965).

(13) O. H. Lowry, N. J. Rosebrough, A. L. Farr, and R. J. Randall, *J. Biol. Chem.*, **193**, 265(1951).

(14) A. Terzis and T. Theophanides, *Acta Crystallogr.*, **B31**, 790(1975).

(15) C. M. Weeks, W. L. Duax, and M. E. Wolff, *J. Am. Chem. Soc.*, **95**, 2865(1973).

ACKNOWLEDGMENTS AND ADDRESSES

Received July 22, 1975, from the *Institute of Experimental Medicine and Surgery and the Department of Chemistry, University of Montreal, Montreal, Quebec, Canada.*

Accepted for publication October 8, 1975.

The technical assistance of Miss F. Dionne and Mrs. D. Papin is gratefully acknowledged.

* Department of Chemistry, Dalhousie University, Halifax, Nova Scotia.

ˣ To whom inquiries should be directed.

COMMUNICATIONS

Medazepam pKa Determined by Spectrophotometric and Solubility Methods

Keyphrases □ Medazepam—pKa determination, spectrophotometric and solubility methods compared □ UV spectrophotometry—pKa determination, medazepam, compared to solubility method □ Solubility—medazepam, pKa determination, compared to spectrophotometric method □ Tranquilizers—medazepam, pKa determination

To the Editor:

The spectral behavior of medazepam shows a marked pH dependence. The peak at 253 nm in acid solutions decreases above pH 3.5 while a new peak appears at 234 nm. The absorptivity and the maximum wavelength of medazepam shift with increasing pH. No variation with pH is observed at the isosbestic point at 243 nm.

All UV absorption spectra were taken at 37° using a spectrophotometer[1] with thermostated cell holders. The pKa was calculated from four series of spectra of pH-varied solutions according to the method of Albert and Serjeant (1) at the wavelengths of 233, 253, and 286 nm (Fig. 1) using:

$$\text{pKa} = \text{pH} - \log\frac{A-B}{B-C} \qquad \text{(Eq. 1)}$$

where A is the absorbance of a solution at pH 1.0, B is the absorbance in buffered solution, and C is the absorbance at pH 10.0. The distance $A - B$ is representative for the concentration of the unionized form of the base, whereas $B - C$ is representative for the ionized

[1] Unicam SP 800.

Table II—Comparison of Glucocorticoid Activity with Some Features of Steroid Structure (10)

Treatment	Hepatic Glycogen, mg/g	Thymus Weight, g/100 g of Body Weight	O-3–O-11, Å	O-11–O-17, Å	O-3–Mean Plane C-5–C-17, Å
Cortisone	0.67 ± 0.24 NS[a]	0.44 ± 0.003 NS	6.551 (6)[b]	5.195 (6)	1.30
Control water	0.71 ± 0.10	0.48 ± 0.02			
6α-Methylprednisolone	12.30 ± 1.8*	0.24 ± 0.03*	6.593 (4)	5.219 (4)	1.95
Control water	0.71 ± 0.10	0.48 ± 0.02			
Fludrocortisone	11.53 ± 0.33*	0.11 ± 0.01*	6.816 (5)	5.210 (5)	2.43
Control water	0.59 ± 0.10	0.39 ± 0.02			
Dexamethasone acetate	61.99 ± 4.10*	0.08 ± 0.01*	6.822 (5)	5.321 (5)	2.57
Control water	0.59 ± 0.10	0.39 ± 0.02			

[a] NS = not significant. * = $p < 0.005$. [b] Standard deviation.

distances between oxygen functions must also play significant roles. It can be seen in Table II that the oxygen–oxygen distances also follow those of the O-3–mean plane (C-5–C-17). There is actually a better correlation between the O-11–O-17 distances and glucocorticoid activity than with the one just mentioned.

The effect of the oxygen–oxygen distances on the catatoxic activity of I and dexamethasone cannot be very significant since I, which does not have oxygen functions on either C-11 or C-17, is nonetheless a potent catatoxic steroid. Superimposition of the molecule of fludrocortisone on that of dexamethasone (Fig. 1*a*) indicates that C-16 substitution is a decisive factor for strong catatoxic activity. This is further supported by the fact that I (itself a potent agent) and dexamethasone have a C-16 substituent in the α-configuration. Removal of this substituent results in a loss of catatoxic potency.

The present findings established a relationship between A-ring conformation and distances between oxygen functions and glucocorticoid activity. However, such a correlation was not demonstrated for catatoxic activity. Compound I and dexamethasone, both potent catatoxic steroids, have widely differing A-ring conformations (Fig. 1); dexamethasone and fludrocortisone (Table I), with almost identical A-ring conformations, show great differences in catatoxic activity.

REFERENCES

(1) A. H. Conney, *Pharmacol. Rev.*, **19**, 317(1967).

(2) J. R. Gillette, *Prog. Drug Res.*, **6**, 11(1965).

(3) H. Selye, "Hormones and Resistance," Springer-Verlag, Heidelberg, Germany, 1971.

(4) P. Kourounakis, *Am. J. Pharm.*, **146**, 22(1974).

(5) A. Goldstein, L. Aronow, and S. M. Kalman, "Principles of Drug Action," Hoeber Medical Division, Harper & Row, New York, N.Y., 1969, pp. 206–279.

(6) L. Dupont, O. Didenberg, and H. Campsteyn, *Cryst. Struct. Commun.*, **1**, 177(1972).

(7) J. P. Declercq, G. Germain, and M. Van Meerssche, *ibid.*, **1**, 5(1972).

(8) *Ibid.*, **1**, 13(1972).

(9) P. Kourounakis, S. Szabo, and H. Selye, *Proc. Int. Congr. Pharm. Sci., 33rd*, **1973**, 251.

(10) H. Selye, S. Szabo, Y. Taché, P. Kourounakis, I. Mécs, and J. Taché, *Steroids Lipids Res.*, **5**, 10(1974).

(11) J. J. Burns, T. F. Yü, L. Berger, and A. B. Gutman, *Am. J. Med.*, **25**, 401(1958).

(12) M. R. Juchau, R. L. Cram, G. Plaa, and J. R. Fouts, *Biochem. Pharmacol.*, **14**, 473(1965).

(13) O. H. Lowry, N. J. Rosebrough, A. L. Farr, and R. J. Randall, *J. Biol. Chem.*, **193**, 265(1951).

(14) A. Terzis and T. Theophanides, *Acta Crystallogr.*, **B31**, 790(1975).

(15) C. M. Weeks, W. L. Duax, and M. E. Wolff, *J. Am. Chem. Soc.*, **95**, 2865(1973).

ACKNOWLEDGMENTS AND ADDRESSES

Received July 22, 1975, from the *Institute of Experimental Medicine and Surgery and the Department of Chemistry, University of Montreal, Montreal, Quebec, Canada.*

Accepted for publication October 8, 1975.

The technical assistance of Miss F. Dionne and Mrs. D. Papin is gratefully acknowledged.

* Department of Chemistry, Dalhousie University, Halifax, Nova Scotia.

ˣ To whom inquiries should be directed.

COMMUNICATIONS

Medazepam pKa Determined by Spectrophotometric and Solubility Methods

Keyphrases □ Medazepam—pKa determination, spectrophotometric and solubility methods compared □ UV spectrophotometry—pKa determination, medazepam, compared to solubility method □ Solubility—medazepam, pKa determination, compared to spectrophotometric method □ Tranquilizers—medazepam, pKa determination

To the Editor:

The spectral behavior of medazepam shows a marked pH dependence. The peak at 253 nm in acid solutions decreases above pH 3.5 while a new peak appears at 234 nm. The absorptivity and the maximum wavelength of medazepam shift with increasing pH. No variation with pH is observed at the isosbestic point at 243 nm.

All UV absorption spectra were taken at 37° using a spectrophotometer[1] with thermostated cell holders. The pKa was calculated from four series of spectra of pH-varied solutions according to the method of Albert and Serjeant (1) at the wavelengths of 233, 253, and 286 nm (Fig. 1) using:

$$\text{pKa} = \text{pH} - \log\frac{A-B}{B-C} \qquad \text{(Eq. 1)}$$

where A is the absorbance of a solution at pH 1.0, B is the absorbance in buffered solution, and C is the absorbance at pH 10.0. The distance $A - B$ is representative for the concentration of the unionized form of the base, whereas $B - C$ is representative for the ionized

[1] Unicam SP 800.

Table I—Comparison of pKa Values of Medazepam

pKa	Determination by	Reference
4.4	Spectroscopy	2
8.7	Polarography, pK_1	3
4.4	Spectroscopy, pK_1	3
6.17	Spectroscopy	This study
6.19	Solubility	This study

form using the Henderson–Hasselbalch equation.

In the region where the pH approximates the pKa, buffer solutions differing by 0.5 pH unit were used. All pH values of the mixtures were measured potentiometrically with a glass electrode, calibrated with accurate standard buffer solutions. Calculation of all results yielded a pKa of 6.17 ± 0.02. The findings disagreed with previous results (2, 3) (Table I).

Further determinations of the pKa were carried out by the solubility method reported previously (4). The plot of the hydrogen-ion activity against solubility is shown in Fig. 2. The relationship yields an ordinate intercept of $-K$, which can be converted into pKa = $-\log K$. In the equation:

$$[H^+] = \frac{KS}{S_0} - K \qquad \text{(Eq. 2)}$$

K is the acid dissociation constant of the base, S_0 is the low solubility of the free base, and S is the total solubility at a particular pH.

Solubility determinations were carried out at 37° by incubating excess amounts of medazepam with buffer solutions in closed vials in a temperature-controlled water bath for 48 hr. The samples were intermittently shaken, the supernate was filtered at 37° and diluted with buffer solution, and the concentrations of medazepam were determined by UV spectrophotometry at 37°. The pH of the supernate was measured with a glass electrode at 37°.

All determinations were repeated, with a longer equilibrating time, without any deviation in the results. The ordinate intercept of K was 6.5×10^{-7} and yielded a pKa of 6.19. This finding was in good agreement with the value from the spectrophotometric determination.

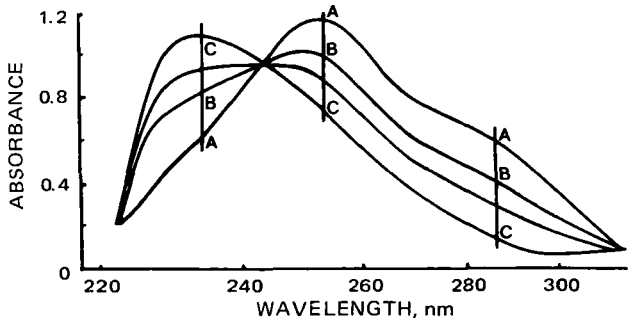

Figure 1—*UV spectra of medazepam in acid (pH 1, points A) and alkaline (pH 12, points C) solutions and at pH 6.0 (points B).*

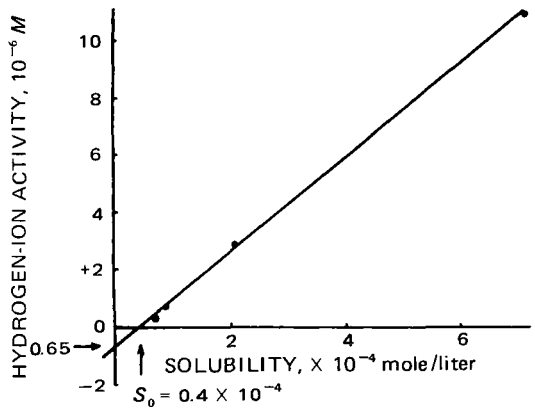

Figure 2—*Determination of* −K *by the method of Green (4) from the relationship between hydrogen-ion activity [H⁺] and solubility,* S, *of medazepam;* S_0 *is the low solubility of the free base.*

(1) A. Albert and E. P. Serjeant, "Ionization Constants of Acids and Bases," Wiley, New York, N.Y., 1962, pp. 62–91.

(2) J. Barrett, W. F. Smyth, and I. E. Davidson, *J. Pharm. Pharmacol.*, **25**, 387(1973).

(3) J. M. Clifford and W. F. Smyth, *Z. Anal. Chem.*, **264**, 149(1973).

(4) A. L. Green, *J. Pharm. Pharmacol.*, **19**, 10(1967).

G. F. le Petit
Institute of Clinical Pharmacology
Medical Academy "Carl Gustav Carus"
8019 Dresden
German Democratic Republic

Received August 26, 1975.
Accepted for publication April 5, 1976.

Differences in Ocular Penetration of Pilocarpine in Rabbits of Different Ages

Keyphrases □ Pilocarpine—differences in ocular penetration related to age, rabbits □ Ocular penetration—pilocarpine, related to differences in age, rabbits □ Age, rabbits—effects on ocular penetration of pilocarpine

To the Editor:

In topical ophthalmic drug therapy, generally no distinction is made between age groups. In most cases, from the neonate to the geriatric, the same dosage is administered. The potential hazards of such an approach were recognized by France and France (1), who observed toxic side effects when administering the usual adult dose of phenylephrine to neonates.

It has been our contention for some time that the administration of equal doses of topical ophthalmic drugs to widely varying age groups should result in substantial differences in the amount of drug reaching the aqueous humor. The theoretical aspects of these considerations were discussed recently (2). Such an approach involves both therapeutic and toxicity considerations.

The present communication demonstrates, for the first time, that differences do exist in the penetration of topically applied ophthalmic drugs as a function of age. Such differences may be due to size, weight, tear flow, rate of drainage, and/or structure and function of the various ocular tissues. A more detailed examination of such differences is warranted so that ophthalmic dosage regimens can be placed on a more rational basis.

Identical doses of 25 μl of 1×10^{-2} *M* tritiated pilocarpine solution were instilled into the eyes of 20- and

Table I—Comparison of pKa Values of Medazepam

pKa	Determination by	Reference
4.4	Spectroscopy	2
8.7	Polarography, pK_1	3
4.4	Spectroscopy, pK_1	3
6.17	Spectroscopy	This study
6.19	Solubility	This study

form using the Henderson–Hasselbalch equation.

In the region where the pH approximates the pKa, buffer solutions differing by 0.5 pH unit were used. All pH values of the mixtures were measured potentiometrically with a glass electrode, calibrated with accurate standard buffer solutions. Calculation of all results yielded a pKa of 6.17 ± 0.02. The findings disagreed with previous results (2, 3) (Table I).

Further determinations of the pKa were carried out by the solubility method reported previously (4). The plot of the hydrogen-ion activity against solubility is shown in Fig. 2. The relationship yields an ordinate intercept of $-K$, which can be converted into pKa = $-\log K$. In the equation:

$$[H^+] = \frac{KS}{S_0} - K \qquad \text{(Eq. 2)}$$

K is the acid dissociation constant of the base, S_0 is the low solubility of the free base, and S is the total solubility at a particular pH.

Solubility determinations were carried out at 37° by incubating excess amounts of medazepam with buffer solutions in closed vials in a temperature-controlled water bath for 48 hr. The samples were intermittently shaken, the supernate was filtered at 37° and diluted with buffer solution, and the concentrations of medazepam were determined by UV spectrophotometry at 37°. The pH of the supernate was measured with a glass electrode at 37°.

All determinations were repeated, with a longer equilibrating time, without any deviation in the results. The ordinate intercept of K was 6.5×10^{-7} and yielded a pKa of 6.19. This finding was in good agreement with the value from the spectrophotometric determination.

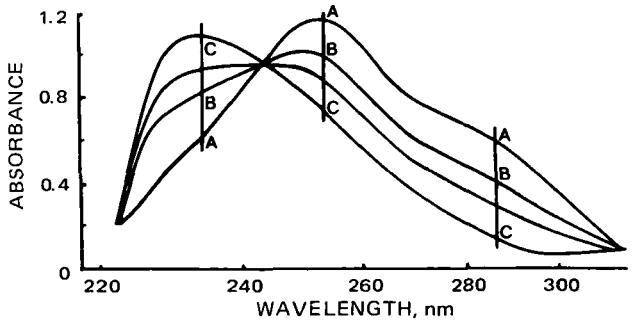

Figure 1—*UV spectra of medazepam in acid (pH 1, points A) and alkaline (pH 12, points C) solutions and at pH 6.0 (points B).*

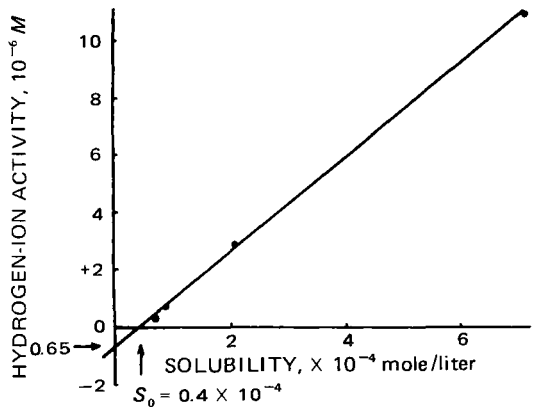

Figure 2—*Determination of* −K *by the method of Green (4) from the relationship between hydrogen-ion activity [H⁺] and solubility,* S, *of medazepam;* S_0 *is the low solubility of the free base.*

(1) A. Albert and E. P. Serjeant, "Ionization Constants of Acids and Bases," Wiley, New York, N.Y., 1962, pp. 62–91.

(2) J. Barrett, W. F. Smyth, and I. E. Davidson, *J. Pharm. Pharmacol.*, **25**, 387(1973).

(3) J. M. Clifford and W. F. Smyth, *Z. Anal. Chem.*, **264**, 149(1973).

(4) A. L. Green, *J. Pharm. Pharmacol.*, **19**, 10(1967).

G. F. le Petit
Institute of Clinical Pharmacology
Medical Academy "Carl Gustav Carus"
8019 Dresden
German Democratic Republic

Received August 26, 1975.
Accepted for publication April 5, 1976.

Differences in Ocular Penetration of Pilocarpine in Rabbits of Different Ages

Keyphrases □ Pilocarpine—differences in ocular penetration related to age, rabbits □ Ocular penetration—pilocarpine, related to differences in age, rabbits □ Age, rabbits—effects on ocular penetration of pilocarpine

To the Editor:

In topical ophthalmic drug therapy, generally no distinction is made between age groups. In most cases, from the neonate to the geriatric, the same dosage is administered. The potential hazards of such an approach were recognized by France and France (1), who observed toxic side effects when administering the usual adult dose of phenylephrine to neonates.

It has been our contention for some time that the administration of equal doses of topical ophthalmic drugs to widely varying age groups should result in substantial differences in the amount of drug reaching the aqueous humor. The theoretical aspects of these considerations were discussed recently (2). Such an approach involves both therapeutic and toxicity considerations.

The present communication demonstrates, for the first time, that differences do exist in the penetration of topically applied ophthalmic drugs as a function of age. Such differences may be due to size, weight, tear flow, rate of drainage, and/or structure and function of the various ocular tissues. A more detailed examination of such differences is warranted so that ophthalmic dosage regimens can be placed on a more rational basis.

Identical doses of 25 μl of 1×10^{-2} *M* tritiated pilocarpine solution were instilled into the eyes of 20- and

Table I— Concentration of Pilocarpine in the Aqueous Humor of 20- and 60-Day-Old Rabbits following Instillation of 25 μl of 1×10^{-2} *M* Pilocarpine

Minutes	Concentration[a], μg/ml	
	20-Day-Old Rabbits	60-Day-Old Rabbits
5	0.84 (0.03, 10)	0.55 (0.06, 8)
10	1.67 (0.05, 8)	1.03 (0.14, 11)
15	1.88 (0.17, 8)	1.11 (0.11, 8)
20	2.06 (0.10, 8)	0.98 (0.12, 10)
30	1.51 (0.18, 8)	0.93 (0.12, 9)
45	1.17 (0.12, 7)	0.42 (0.04, 8)
60	0.88 (0.12, 8)	0.44 (0.04, 7)
90	0.38 (0.03, 8)	0.19 (0.02, 7)
120	0.17 (0.01, 9)	0.11 (0.01, 8)

[a] Mean concentrations. The first number in parentheses refers to standard error, and the second number is the number of eyes sampled at that time point.

60-day-old male, New Zealand albino rabbits[1]. At various times postinstillation, rabbits were sacrificed and the aqueous humor was aspirated from the anterior chamber. Liquid scintillation counting allowed conversion of counts to micrograms of pilocarpine per milliliter of aqueous humor. All experimental procedures have been well established (3–5).

The aqueous humor concentration *versus* time profiles in the two categories of test animals are reported in Table I. At every time point, the concentration of pilocarpine was significantly higher in the 20-day-old rabbits as compared to the 60-day-old rabbits. The calculated areas under the curves were different by approximately a factor of two. The implication is that it should be possible to reduce substantially the dose administered to the 20-day-old rabbits while simultaneously maintaining aqueous humor concentrations equivalent to the 60-day-old rabbits. We make no comment, at this time, regarding the required concentration to produce a pharmacological effect.

Many studies currently appearing in the ophthalmic literature do not concern themselves to any extent with the age or size of animals used. These studies, although using relatively large differences in age, certainly point out the need for standardization of test animals. Also apparent are the inherent difficulties in comparing studies between laboratories without adequate knowledge concerning age and size of test subjects.

More importantly, further investigation into the development of ophthalmic pediatric dosage regimens is warranted. When one considers differences in the aqueous humor volume in the eye, as well as differences in the surface area available for absorption and the existence of immature membranes, it becomes apparent that some dosage adjustments may be in order, at least during the rapid growth phase of the eye (*i.e.*, birth to 3 years).

In addition, it is known that tear production and instilled volume drainage account for a large loss of drug from any topically applied dose (6, 7) and can affect the ocular bioavailability of drugs (8). No one to date has quantitatively considered these effects as applied to the bioavailability of topically administered drugs in children, nor have the potential toxic effects due to drainage been quantitated.

Also worthy of mention is the fact that numerous functional changes take place in the eyes of geriatrics. Decreased tear flow and volume are not uncommon with age and could cause differences in instilled drug concentration. One also might suspect changes to take place in the drainage of instilled solutions and, potentially, in the integrity of ocular membranes. All such changes have the potential to cause differences similar to those noted here and may warrant dosage adjustments.

Finally, one major problem in topical ophthalmic drug therapy of both infants and geriatrics is compliance with the medication dosage regimen. It is hoped that, by quantitating and maximizing dosage regimens, therapy can be simplified and the degree of compliance increased.

(1) T. D. France and N. K. France, *Am. J. Ophthalmol.*, **76,** 857(1973).

(2) T. F. Patton and J. R. Robinson, *J. Pediatr. Ophthalmol.*, in press.

(3) S. S. Chrai and J. R. Robinson, *Am. J. Ophthalmol.*, **77,** 735(1974).

(4) T. F. Patton, Ph.D. thesis, University of Wisconsin, Madison, Wis., 1975.

(5) T. F. Patton and J. R. Robinson, *J. Pharm. Sci.*, in press.

(6) S. S. Chrai, T. F. Patton, A. Mehta, and J. R. Robinson, *ibid.*, **62,** 1112(1973).

(7) T. F. Patton, M.S. thesis, University of Wisconsin, Madison, Wis., 1973.

(8) T. F. Patton and J. R. Robinson, *J. Pharm. Sci.*, **64,** 1312(1975).

Ted S. Friedman
Thomas F. Patton [x]
Department of Pharmaceutical Chemistry
School of Pharmacy
University of Kansas
Lawrence, KS 66044

Received March 12, 1976.
Accepted for publication April 19, 1976.
Supported by a grant from the University of Kansas General Research Fund (GRF 3081-5038).
[x] To whom inquiries should be directed.

[1] At the 20th postnatal day, the rabbit's globe is about two-thirds of adult size; at 60 days, the rabbit's globe attains 90% of adult size. The human eye is about two-thirds of adult size at birth and about 90% of adult size at 3 years of age.

Culture of Isotopically Substituted Plants of Pharmacological Importance: Conservation and Recycling of Stable Isotope Substrates

Keyphrases □ Isotopes, stable—^{2}H- and ^{13}C-substituted tobacco plants cultured, sealed growth chambers, isotope substrates conserved and recycled □ Plant culture—^{2}H- and ^{13}C-substituted tobacco plants cultured, sealed growth chambers, isotope substrates conserved and recycled □ Tobacco plants—*Nicotiana tabacum*, ^{2}H- and ^{13}C-substituted, cultured in sealed growth chambers, isotope substrates conserved and recycled

To the Editor:

We have successfully cultured algae, bacteria, protozoa, molds, yeasts, and fungi in fully deuterated form (1). Deuterated metabolites have been isolated from

Table I— Concentration of Pilocarpine in the Aqueous Humor of 20- and 60-Day-Old Rabbits following Instillation of 25 μl of 1×10^{-2} *M* Pilocarpine

Minutes	Concentration[a], μg/ml	
	20-Day-Old Rabbits	60-Day-Old Rabbits
5	0.84 (0.03, 10)	0.55 (0.06, 8)
10	1.67 (0.05, 8)	1.03 (0.14, 11)
15	1.88 (0.17, 8)	1.11 (0.11, 8)
20	2.06 (0.10, 8)	0.98 (0.12, 10)
30	1.51 (0.18, 8)	0.93 (0.12, 9)
45	1.17 (0.12, 7)	0.42 (0.04, 8)
60	0.88 (0.12, 8)	0.44 (0.04, 7)
90	0.38 (0.03, 8)	0.19 (0.02, 7)
120	0.17 (0.01, 9)	0.11 (0.01, 8)

[a] Mean concentrations. The first number in parentheses refers to standard error, and the second number is the number of eyes sampled at that time point.

60-day-old male, New Zealand albino rabbits[1]. At various times postinstillation, rabbits were sacrificed and the aqueous humor was aspirated from the anterior chamber. Liquid scintillation counting allowed conversion of counts to micrograms of pilocarpine per milliliter of aqueous humor. All experimental procedures have been well established (3–5).

The aqueous humor concentration *versus* time profiles in the two categories of test animals are reported in Table I. At every time point, the concentration of pilocarpine was significantly higher in the 20-day-old rabbits as compared to the 60-day-old rabbits. The calculated areas under the curves were different by approximately a factor of two. The implication is that it should be possible to reduce substantially the dose administered to the 20-day-old rabbits while simultaneously maintaining aqueous humor concentrations equivalent to the 60-day-old rabbits. We make no comment, at this time, regarding the required concentration to produce a pharmacological effect.

Many studies currently appearing in the ophthalmic literature do not concern themselves to any extent with the age or size of animals used. These studies, although using relatively large differences in age, certainly point out the need for standardization of test animals. Also apparent are the inherent difficulties in comparing studies between laboratories without adequate knowledge concerning age and size of test subjects.

More importantly, further investigation into the development of ophthalmic pediatric dosage regimens is warranted. When one considers differences in the aqueous humor volume in the eye, as well as differences in the surface area available for absorption and the existence of immature membranes, it becomes apparent that some dosage adjustments may be in order, at least during the rapid growth phase of the eye (*i.e.*, birth to 3 years).

In addition, it is known that tear production and instilled volume drainage account for a large loss of drug from any topically applied dose (6, 7) and can affect the ocular bioavailability of drugs (8). No one to date has quantitatively considered these effects as applied to the bioavailability of topically administered drugs in children, nor have the potential toxic effects due to drainage been quantitated.

Also worthy of mention is the fact that numerous functional changes take place in the eyes of geriatrics. Decreased tear flow and volume are not uncommon with age and could cause differences in instilled drug concentration. One also might suspect changes to take place in the drainage of instilled solutions and, potentially, in the integrity of ocular membranes. All such changes have the potential to cause differences similar to those noted here and may warrant dosage adjustments.

Finally, one major problem in topical ophthalmic drug therapy of both infants and geriatrics is compliance with the medication dosage regimen. It is hoped that, by quantitating and maximizing dosage regimens, therapy can be simplified and the degree of compliance increased.

(1) T. D. France and N. K. France, *Am. J. Ophthalmol.*, **76,** 857(1973).

(2) T. F. Patton and J. R. Robinson, *J. Pediatr. Ophthalmol.*, in press.

(3) S. S. Chrai and J. R. Robinson, *Am. J. Ophthalmol.*, **77,** 735(1974).

(4) T. F. Patton, Ph.D. thesis, University of Wisconsin, Madison, Wis., 1975.

(5) T. F. Patton and J. R. Robinson, *J. Pharm. Sci.*, in press.

(6) S. S. Chrai, T. F. Patton, A. Mehta, and J. R. Robinson, *ibid.*, **62,** 1112(1973).

(7) T. F. Patton, M.S. thesis, University of Wisconsin, Madison, Wis., 1973.

(8) T. F. Patton and J. R. Robinson, *J. Pharm. Sci.*, **64,** 1312(1975).

Ted S. Friedman
Thomas F. Patton [x]
Department of Pharmaceutical Chemistry
School of Pharmacy
University of Kansas
Lawrence, KS 66044

Received March 12, 1976.
Accepted for publication April 19, 1976.
Supported by a grant from the University of Kansas General Research Fund (GRF 3081-5038).
[x] To whom inquiries should be directed.

[1] At the 20th postnatal day, the rabbit's globe is about two-thirds of adult size; at 60 days, the rabbit's globe attains 90% of adult size. The human eye is about two-thirds of adult size at birth and about 90% of adult size at 3 years of age.

Culture of Isotopically Substituted Plants of Pharmacological Importance: Conservation and Recycling of Stable Isotope Substrates

Keyphrases □ Isotopes, stable—^{2}H- and ^{13}C-substituted tobacco plants cultured, sealed growth chambers, isotope substrates conserved and recycled □ Plant culture—^{2}H- and ^{13}C-substituted tobacco plants cultured, sealed growth chambers, isotope substrates conserved and recycled □ Tobacco plants—*Nicotiana tabacum*, ^{2}H- and ^{13}C-substituted, cultured in sealed growth chambers, isotope substrates conserved and recycled

To the Editor:

We have successfully cultured algae, bacteria, protozoa, molds, yeasts, and fungi in fully deuterated form (1). Deuterated metabolites have been isolated from

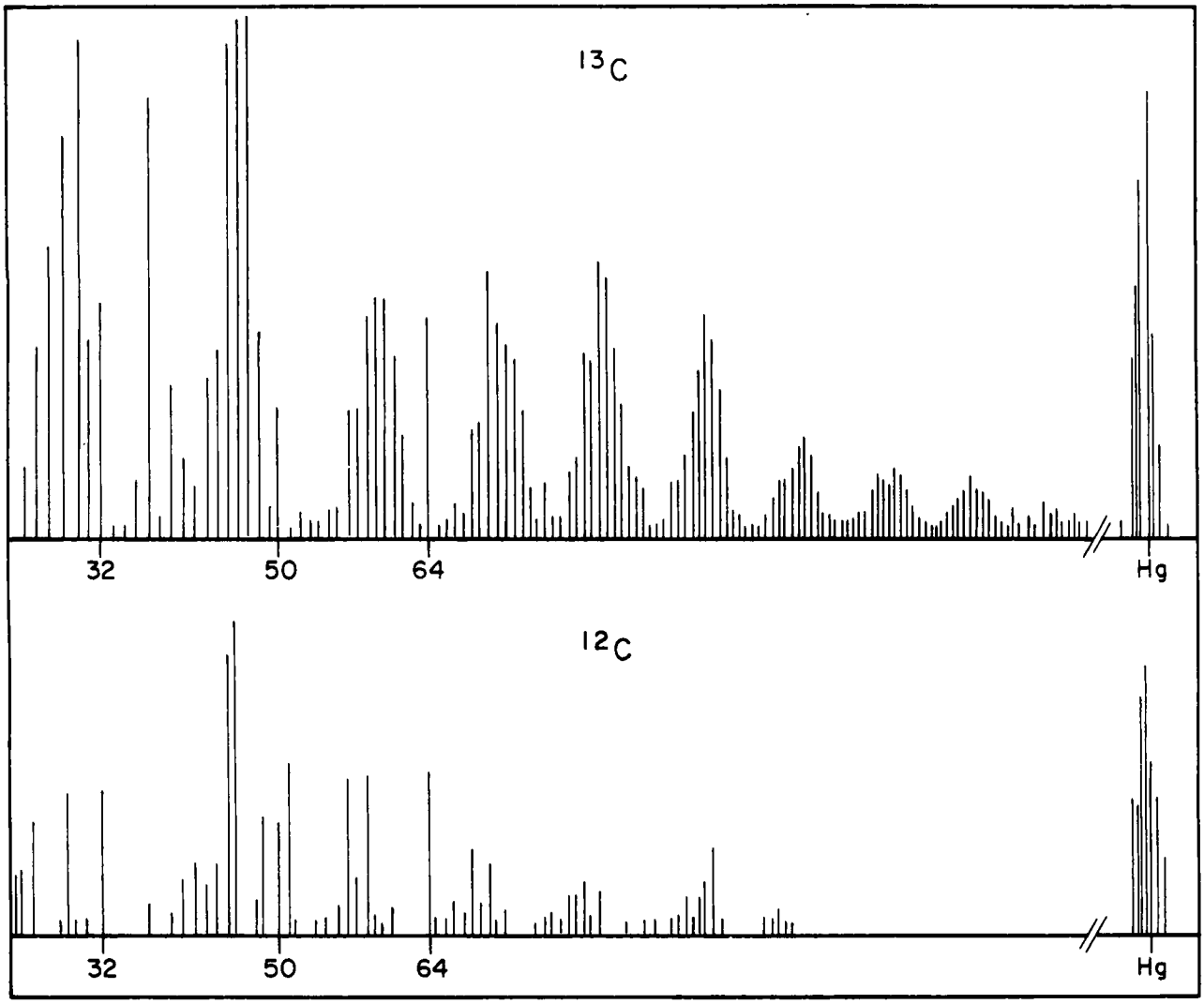

Figure 1—*Time-of-flight mass spectra of ordinary and carbon-13 white fly wing wax. The additional lines in the ^{13}C-spectrum arise from various combinations of carbon-12 and carbon-13 present in the wax hydrocarbons.*

these organisms and are being used in further studies. In culturing these organisms, deuterium oxide replaced the water in the usual nutrient medium. Where organic substrates were required, a serious effort was made to provide the deuterated analog to assure maximum deuteration.

Less successful have been attempts to culture higher plants in fully deuterated environments. Plant growth is severely inhibited when the deuterium oxide content of the growth medium exceeds 60%; at this time the possibility of obtaining more highly deuterated metabolites from higher plants seems remote. The cost of deuterium oxide is one limiting factor because large volumes of water must be used in such studies; with the facilities available, it has not been possible to recover and recycle the deuterium oxide from the spent nutrient medium or from the vapor transpired by the plants.

The results of our studies to date on pharmacologically significant substances were reported recently (2).

Our work in stable isotope biology has extended to studies of plant growth on highly enriched ^{13}C-carbon dioxide, the stable heavy isotopic form of carbon present in nature. The labile character of ^{13}C-carbon dioxide again makes for complications. The high cost of carbon-13 necessitates conservation in closed systems. We recently designed and tested completely sealed growth chambers suitable for culturing higher plants of pharmaceutical importance; rare isotopically substituted substrates (deuterium oxide and ^{13}C-carbon dioxide) are conserved during growth, and materials not utilized are recovered and recycled. Some features of the design and operation of these chambers were reported previously (3). We present here the results of experiments that illustrate the advantages of stable isotope studies with this type of growth chamber.

Three growth chambers are in operation in a climate-controlled greenhouse[1]. One chamber is always reserved for the growth of control plants using substrates of ordinary isotopic composition. These systems are of sufficient size (1 m high, 6 m^3 total volume) to accommodate large terrestrial plants. The chambers are completely sealed and leakproof, precluding loss of

[1] The authors are indebted to Dr. Norman R. Farnsworth and Dr. Harry H. S. Fong for permission to use the facilities of the University of Illinois Pharmacognosy and Horticulture Field Station, Lisle, Ill.

deuterium oxide or ^{13}C-carbon dioxide during the entire growth period (which may extend for several months or more) and assuring maximal and uniform incorporation of isotope.

The chambers are fabricated with an aluminum floor and structural elements and have a ceiling and walls of transparent acrylic sheets. A large circular port (covered by an O-ring sealed disk) located at one end of the chamber permits entry before and after a growth study. A bulkhead port is located at the opposite end of the chamber and provides for electrical power, gas, and liquid transport into or out of the chamber. Sets of glove ports, fitted with arm-length Neoprene dry box gloves, are located along both sides of the chamber and permit manipulations within the chamber during the period of plant growth.

Entry into the chamber and exposure to the external environment are completely avoided during the growth period of the plants under study. Temperature and humidity are controlled by continuous circulation of the chamber atmosphere over a heat exchanger. The heat exchanger is enclosed in a separate compartment extending into a plenum constructed along the ceiling. The highly humid atmosphere resulting from plant transpiration is directed from the growth area into the heat exchanger compartment, where it is cooled, and the dried gas is redistributed from the chamber top.

The condensed water is collected in a trough under the heat exchanger, passed through a mixed bed ion exchanger, stored in a reservoir, and conducted to a watering distribution system for recycling to the plant containers. Plants are watered periodically by means of a timer actuated by a solenoid valve, which permits water to be pumped to the distributor system at a predetermined rate. Soil moisture is monitored by conductivity probes embedded in the root support medium of each plant container.

In a typical growth study, seedlings are bedded in pots containing a vermiculite–sand mixture. For experiments with ^{13}C-carbon dioxide, this mixture ensured that there was no preformed carbon source available to the plants. In the deuterium oxide studies, the bed (*e.g.*, vermiculite or peat moss) was exchanged with the deuterium oxide solvent prior to the growth study to preclude dilution of the deuterium content of the solvent by the exogenous hydrogen of the potting material.

The carbon dioxide content of the atmosphere within the chamber was determined by measurement of the IR absorption of a 10-cm path length gas cell, calibrated for both ^{12}C-carbon dioxide and ^{13}C-carbon dioxide. In the deuterium studies, the deuterium oxide content of the nutrient was determined at the beginning and end of the study by comparing the density of the solvent with that of pure deuterium oxide (99.6%) and water (0% D_2O) at the same temperature.

Initial studies with these chambers involved the growth of tobacco[2] (*Nicotiana tabacum* L.) in an atmosphere of carbon dioxide highly enriched (90–92%) in ^{13}C-carbon dioxide. One objective was to observe any biological effects induced by incorporation of the heavy isotope of carbon by the plant during an entire life cycle of growth. Combustion of tobacco samples after harvest, followed by mass spectrometric determination of the carbon isotopes, indicated that the isotopic content of the plant material was essentially that of the carbon dioxide substrate employed during growth (about 90% ^{13}C).

A second objective of the study was to produce ^{13}C-enriched cured tobacco from the leaves. Reactive chemical species ("free radicals") are always present in tobacco smoke and are believed to be possible initiators of pathological conditions such as lung cancer. The presence of the heavy isotope of carbon in the free radical allows inferences to be made about the chemical nature of the molecular species from changes in the observed electron spin resonance spectrum. A study of the spectra of the smoke produced by the combustion of tobacco may aid in the identification of specific chemical species present in the smoke and possibly give insight into the nature of carcinogens present in tobacco smoke.

Other related studies involved the growth of tobacco in media containing 50 and 60% D_2O. In an earlier study (4), the effects of deuterium on tobacco plants were observed by growing the plants hydroponically and open to the air. This procedure required several hundred liters of deuterium oxide for only a few plants. For obvious economic reasons, it is generally not practical to grow plants in this manner on a large scale. Use of closed growth systems greatly reduces the amounts of deuterium oxide required for such an experiment.

We now have tobacco plants growing in deuterium oxide in two sealed growth chambers. The third chamber contains control plants. It is estimated that at maximum and complete utilization of growth space in one of these large chambers, using 70% D_2O levels of recycling solvent, the total volume of heavy water (99%) required for the entire experiment will be 30–35 liters. This amount is all that will be required to produce about 10 fully grown tobacco plants in a single chamber. Any residual deuterium oxide collected in the reservoir is, of course, available for recycling in other experiments. Another important consideration that recommends such closed systems is that very little attention to the plants is required after initial setup because of the complete automation of the system.

The growth chambers described here are, in effect, miniature ecosystems capable of supporting entire chains of isotopically substituted organisms that show metabolic dependence. One such relationship is that of host and parasite. In one series of ^{13}C-substituted tobacco experiments, after a growth period of several weeks, an infestation of white flies (*Trialeurodes vaporariorum*) was observed in the sealed chamber. This common greenhouse insect is parasitic on a wide range of plants and was evidently introduced adventitiously (as larvae or eggs) into the chamber at the outset of the experiment.

To prove conclusively that the mature insects had been using the isotopically substituted tobacco plants as their food source, the wing wax of the captured specimen was examined in a time-of-flight mass spec-

[2] A voucher specimen was deposited in the Chemistry Division, Argonne National Laboratory; the plants were identified by Mr. W. D. Atkinson, Department of Agronomy, University of Kentucky.

trometer[3]. The mass spectrum obtained (Fig. 1) contained additional mass peaks, one unit greater than the normal ^{12}C-containing peaks, in an abundance indicating massive carbon-13 incorporation into the constituents of the white fly tissue.

(1) J. J. Katz, R. A. Uphaus, H. L. Crespi, and M. I. Blake, in "Isotopes and Chemical Principles," P. A. Rock, Ed., ACS Symposium Series, American Chemical Society, Washington, D.C., 1975.

(2) M. I. Blake, H. L. Crespi, and J. J. Katz, *J. Pharm. Sci.*, **64**, 367(1975).

(3) R. A. Uphaus, "Proceedings of the First International Conference on Stable Isotopes in Chemistry, Biology and Medicine, May 9–11, 1973," Argonne National Laboratory, Argonne, Ill., 1973.

(4) R. A. Uphaus, M. I. Blake, and J. J. Katz, *Can. J. Bot.*, **56**, 352(1975).

Robert A. Uphaus
Joseph J. Katz
Chemistry Division
Argonne National Laboratory
Argonne, IL 60439

Martin I. Blake ˣ
Department of Pharmacy
College of Pharmacy
University of Illinois
Chicago, IL 60612

Received December 1, 1975.

Accepted for publication March 4, 1976.

Presented in part at the Pharmacognosy and Natural Products Section, APhA Academy of Pharmaceutical Sciences, Chicago meeting, August 1974.

Performed under the auspices of the Atomic Energy Commission with the aid of a grant from the American Medical Association Tobacco Research Fund.

Supported in part by AMA Tobacco Contract P-7146-C.

ˣ To whom inquiries should be directed.

[3] The authors are indebted to Dr. Martin Studier, Argonne National Laboratory, for the mass spectral data.

Biased Bioavailability Estimates

Keyphrases □ Bioavailability—griseofulvin, use of fractional urinary excretion data questioned □ Griseofulvin—bioavailability, use of fractional urinary excretion data questioned □ Urinary excretion data, fractional—value in griseofulvin bioavailability studies questioned □ Antifungal agents—griseofulvin bioavailability, use of fractional urinary excretion data questioned

To the Editor:

In a recent communication (1), followed by publication of the detailed data (2), Bates and Sequeira proposed that 24-hr urinary excretion data of total (free and glucuronide conjugated) 6-desmethylgriseofulvin, the main metabolite of griseofulvin, be used to determine the bioavailability of the parent drug. However, I wish to point out that this general practice (1, 3, 4) of using fractional urinary drug excretion data and/or areas under the plasma level–time curve without proper pharmacokinetic justification, even with apparent correlations with total urinary excretion and total area under the plasma level–time curve data, is dangerous.

Table I—Relative Bioavailability of Formulations I–IV of Griseofulvin Calculated from the Ratios of the Total Urinary Metabolite at 24 and 96 hr[a]

Formulation[b]	24 hr	96 hr
I:IV	0.32	0.43
II:IV	0.41	0.53
III:IV	0.52	0.60
I:III	0.61	0.71
II:III	0.78	0.87
I:II	0.79	0.81

[a] Data are from Fig. 1 and Table II of Ref. 2. The differences among the relative bioavailabilities calculated from the urinary excretion data of total metabolite at 24 and 96 hr are statistically significant; two-tailed paired *t*-test: t (0.002) = 5.89, t calc = 5.97. [b] I = aqueous suspension, II = commercial Tablet A, III = commercial Tablet B, and IV = corn oil-in-water emulsion.

Bates and Sequeira (1) stated that, while the plasma levels of the entirely metabolized griseofulvin are usually low after oral administration of different formulations, the measurement of 24-hr urinary excretion of the main metabolite, 6-desmethylgriseofulvin, could be more reliable and more convenient since the use of a 72–96-hr urinary collection period "increases the chances for a lack of compliance to the experimental protocol on the part of subjects . . . ." These investigators reported that a correlation existed between the dose percentages of total 6-desmethylgriseofulvin excreted within 24 and 96 hr after administration of various formulations of griseofulvin and concluded that: "These correlations . . . provide the basis for possible utilization of 24-hr cumulative total 6-desmethylgriseofulvin excretion data as an index of griseofulvin bioavailability in humans."

However, an accurate assessment of the relative bioavailability of a given griseofulvin formulation from metabolite cumulative recovery excretion data measured over a limited 24-hr time interval is only possible if the absorption process of griseofulvin is complete much sooner than 24 hr after drug administration. However, with some oral formulations of griseofulvin, the absorption process occurs for 30–40 hr and even up to 80 hr (5). The bioavailability of such formulations would be underestimated by the use of 24-hr cumulative metabolite excretion data, since the total fraction of the dose administered that will eventually be absorbed is not totally absorbed at 24 hr after administration.

Urinary excretion data of the metabolite (free and glucuronide conjugated) after oral administration permit only the calculation of relative bioavailabilities of different formulations given by the same route of administration. Since griseofulvin is entirely metabolized (6) [most likely in the liver (7)], a first-pass effect, although not large (8–19% of the dose absorbed), must be anticipated (8). The linearity of an existing first-pass effect needs to be experimentally challenged. The fact that ultimately the amounts of free 6-desmethylgriseofulvin excreted in the urine are constant fractions of dosages of formulations with widely differing absorption characteristics does not negate a possible nonlinearity of griseofulvin metabolism (2). Parent drug data ob-

trometer[3]. The mass spectrum obtained (Fig. 1) contained additional mass peaks, one unit greater than the normal ^{12}C-containing peaks, in an abundance indicating massive carbon-13 incorporation into the constituents of the white fly tissue.

(1) J. J. Katz, R. A. Uphaus, H. L. Crespi, and M. I. Blake, in "Isotopes and Chemical Principles," P. A. Rock, Ed., ACS Symposium Series, American Chemical Society, Washington, D.C., 1975.

(2) M. I. Blake, H. L. Crespi, and J. J. Katz, *J. Pharm. Sci.*, **64**, 367(1975).

(3) R. A. Uphaus, "Proceedings of the First International Conference on Stable Isotopes in Chemistry, Biology and Medicine, May 9–11, 1973," Argonne National Laboratory, Argonne, Ill., 1973.

(4) R. A. Uphaus, M. I. Blake, and J. J. Katz, *Can. J. Bot.*, **56**, 352(1975).

Robert A. Uphaus
Joseph J. Katz
Chemistry Division
Argonne National Laboratory
Argonne, IL 60439

Martin I. Blake ˣ
Department of Pharmacy
College of Pharmacy
University of Illinois
Chicago, IL 60612

Received December 1, 1975.

Accepted for publication March 4, 1976.

Presented in part at the Pharmacognosy and Natural Products Section, APhA Academy of Pharmaceutical Sciences, Chicago meeting, August 1974.

Performed under the auspices of the Atomic Energy Commission with the aid of a grant from the American Medical Association Tobacco Research Fund.

Supported in part by AMA Tobacco Contract P-7146-C.

ˣ To whom inquiries should be directed.

[3] The authors are indebted to Dr. Martin Studier, Argonne National Laboratory, for the mass spectral data.

Biased Bioavailability Estimates

Keyphrases □ Bioavailability—griseofulvin, use of fractional urinary excretion data questioned □ Griseofulvin—bioavailability, use of fractional urinary excretion data questioned □ Urinary excretion data, fractional—value in griseofulvin bioavailability studies questioned □ Antifungal agents—griseofulvin bioavailability, use of fractional urinary excretion data questioned

To the Editor:

In a recent communication (1), followed by publication of the detailed data (2), Bates and Sequeira proposed that 24-hr urinary excretion data of total (free and glucuronide conjugated) 6-desmethylgriseofulvin, the main metabolite of griseofulvin, be used to determine the bioavailability of the parent drug. However, I wish to point out that this general practice (1, 3, 4) of using fractional urinary drug excretion data and/or areas under the plasma level–time curve without proper pharmacokinetic justification, even with apparent correlations with total urinary excretion and total area under the plasma level–time curve data, is dangerous.

Table I—Relative Bioavailability of Formulations I–IV of Griseofulvin Calculated from the Ratios of the Total Urinary Metabolite at 24 and 96 hr[a]

Formulation[b]	24 hr	96 hr
I:IV	0.32	0.43
II:IV	0.41	0.53
III:IV	0.52	0.60
I:III	0.61	0.71
II:III	0.78	0.87
I:II	0.79	0.81

[a] Data are from Fig. 1 and Table II of Ref. 2. The differences among the relative bioavailabilities calculated from the urinary excretion data of total metabolite at 24 and 96 hr are statistically significant; two-tailed paired *t*-test: t (0.002) = 5.89, t calc = 5.97. [b] I = aqueous suspension, II = commercial Tablet A, III = commercial Tablet B, and IV = corn oil-in-water emulsion.

Bates and Sequeira (1) stated that, while the plasma levels of the entirely metabolized griseofulvin are usually low after oral administration of different formulations, the measurement of 24-hr urinary excretion of the main metabolite, 6-desmethylgriseofulvin, could be more reliable and more convenient since the use of a 72–96-hr urinary collection period "increases the chances for a lack of compliance to the experimental protocol on the part of subjects . . . ." These investigators reported that a correlation existed between the dose percentages of total 6-desmethylgriseofulvin excreted within 24 and 96 hr after administration of various formulations of griseofulvin and concluded that: "These correlations . . . provide the basis for possible utilization of 24-hr cumulative total 6-desmethylgriseofulvin excretion data as an index of griseofulvin bioavailability in humans."

However, an accurate assessment of the relative bioavailability of a given griseofulvin formulation from metabolite cumulative recovery excretion data measured over a limited 24-hr time interval is only possible if the absorption process of griseofulvin is complete much sooner than 24 hr after drug administration. However, with some oral formulations of griseofulvin, the absorption process occurs for 30–40 hr and even up to 80 hr (5). The bioavailability of such formulations would be underestimated by the use of 24-hr cumulative metabolite excretion data, since the total fraction of the dose administered that will eventually be absorbed is not totally absorbed at 24 hr after administration.

Urinary excretion data of the metabolite (free and glucuronide conjugated) after oral administration permit only the calculation of relative bioavailabilities of different formulations given by the same route of administration. Since griseofulvin is entirely metabolized (6) [most likely in the liver (7)], a first-pass effect, although not large (8–19% of the dose absorbed), must be anticipated (8). The linearity of an existing first-pass effect needs to be experimentally challenged. The fact that ultimately the amounts of free 6-desmethylgriseofulvin excreted in the urine are constant fractions of dosages of formulations with widely differing absorption characteristics does not negate a possible nonlinearity of griseofulvin metabolism (2). Parent drug data ob-

tained in intravenous and oral studies are indispensable for this purpose. Differences in the ratio of free to glucuronide-conjugated 6-desmethylgriseofulvin observed after different oral formulations (2) appear to be indicative of nonlinear kinetics for these metabolites.

The fact that highly significant statistical correlations apparently exist between 24- and 96-hr urinary metabolite excretions of a given formulation does not prove that 24-hr urinary metabolite excretion data are accurate and adequate for bioavailability assessments of griseofulvin. The existence of these correlations indicates only that a formulation with higher bioavailability will tend to give higher urinary metabolite levels at 24 and 96 hr than a formulation with lower bioavailability at these times.

Notwithstanding an apparent correlation, the bias in estimating relative bioavailabilities of different formulations using 24- rather than 96-hr urinary excretion total metabolite data can be demonstrated with the data reported by Bates and Sequeira (2). They investigated the cumulative urinary excretion of total 6-desmethylgriseofulvin after the administration of four different griseofulvin formulations to five individuals. On the assumption of first-order kinetics, the relative bioavailability of the four different griseofulvin formulations can be calculated from the ratios of the mean amounts of total metabolite excreted in urine at different times (Table I).

It is evident that the use of 24-hr urinary excretion data of total metabolite leads consistently to underestimations of derived relative bioavailabilities. The underestimation increases with the smaller bioavailabilities, consistent with the premise that delayed absorption is the primary reason for low bioavailability. Thus, underestimation will be greatest when the relative bioavailability of poorly absorbed formulations is studied[1].

The standard error of the mean, expressed as percent of the mean, was consistently larger for the total amount of urinary metabolite at 24 hr. At 24 hr, the values were: I, 11.5%; II, 18.3%; III, 15.6%; and IV, 4.6%. At 96 hr, they were: I, 5.4%; II, 12.2%; III, 10.6%; and IV, 4.2%. Thus, routine assessments of bioavailabilities of different griseofulvin formulations should not be based on 24-hr urinary excretion data of total 6-desmethylgriseofulvin even if first-order kinetics exist.

I feel strongly that this dangerous procedure of using fractional urinary excretion data and/or areas (1, 3, 4) for the assessment of bioavailability must be clearly recognized.

(1) T. R. Bates and J. A. Sequeira, *J. Pharm. Sci.*, **64**, 709(1975)
(2) *Ibid.*, **64**, 793(1975).
(3) D. J. Greenblatt, D. W. Duhme, J. Koch-Weser, and T. W. Smith, *Clin. Pharmacol. Ther.*, **16**, 813(1974).
(4) E. Steiness, V. Christensen, and H. Johansen, *ibid.*, **14**, 949(1973).
(5) W. L. Chiou and S. Riegelman, *J. Pharm. Sci.*, **60**, 1376 (1971).
(6) C.-C. Lin, J. Magat, R. Chang, J. McGlotten, and S. Simchowicz, *J. Pharmacol. Exp. Ther.*, **187**, 415(1973).
(7) M. Rowland, S. Riegelman, and W. L. Epstein, *J. Pharm. Sci.*, **57**, 984(1968).
(8) P. A. Harris and S. Riegelman, *ibid.*, **58**, 93(1969).

Peter H. Hinderling
Department of Pharmacology
Biozentrum der Universitae Basel
Basel CH-4056
Switzerland

Received July 14, 1975.
Accepted for publication March 30, 1976.

[1] The rank order for the bioavailability of products in Table I is the same at 24 as it is at 96 hr (IV > III > II > I).

BOOKS

REVIEWS

Aliphatic Chemistry, Volume 3, Specialist Periodical Report. Senior Reporter, A. McKILLOP. The Chemical Society, Burlington House, London WIV OBN, England, 1975. xii + 409 pp. 14.5 × 22 cm. Price £13.50.

The first volume of "Aliphatic Chemistry" was published as Part I of a three-part Specialist Periodical Report on aliphatic, alicyclic, and saturated heterocyclic chemistry. Subsequently, these areas have been reviewed in separate Specialist Periodical Reports. This Specialist Report is the third volume of the series, dealing with aliphatic chemistry and, except for one chapter, reviews the literature published during 1973. Chapter 1, by R. S. Atkinson, is devoted to acetylenes, alkanes, allenes, and alkenes; Chapter 2, by E. W. Colvin, surveys the literature on other functional groups (carboxylic acids, esters, lactones, anhydrides, amides, nitriles, aldehydes and ketones, alcohols, amines, alkyl halides, ethers, and sulfur compounds). These chapters are similar in format and style to analogous chapters by the same authors in the two preceding volumes.

This volume, like Volume 2, contains chapters that summarize progress in the area of naturally occurring polyolefinic and polyacetylenic compounds (Chapter 3) and in the chemistry of the prostaglandins (Chapter 4). Both chapters are authored by G. Pattenden, as were the corresponding chapters in Volume 2. The literature on fatty acids and related compounds was reviewed in Volume 1 but not in Volume 2. Developments in this area during both 1972 and 1973, therefore, comprise Chapter 5 by F. D. Gunstone. The specialized areas of Chapters 3–5 are exemplified by sections dealing with polyolefinic antibiotics and other microbial metabolites, insect pheromones, acetylenes and olefins of marine or plant origin, prostaglandin syntheses, the multifaceted aspects of studies of fatty acids, and others.

A cumulative set of volumes may serve as summaries of the literature for the specialist engaged in research in one of these areas; but, perhaps more importantly, these annual surveys will provide a means by which others may be introduced to, or become familiar with, developments in a specific area. The value of surveys of the annual literature devoted to specific areas, such as those of Chapters 3–5, is readily recognized. Reviews of the more general topics of the first two chapters are equally valuable, since much effort would be required for the individual to extract this type of information from the periodical or abstract literature. In giving comprehensive coverage of the significant literature, the authors maintain the high standards of the preceding volumes.

Reviewed by Y. Fulmer Shealy
Southern Research Institute
Birmingham, AL 35205

tained in intravenous and oral studies are indispensable for this purpose. Differences in the ratio of free to glucuronide-conjugated 6-desmethylgriseofulvin observed after different oral formulations (2) appear to be indicative of nonlinear kinetics for these metabolites.

The fact that highly significant statistical correlations apparently exist between 24- and 96-hr urinary metabolite excretions of a given formulation does not prove that 24-hr urinary metabolite excretion data are accurate and adequate for bioavailability assessments of griseofulvin. The existence of these correlations indicates only that a formulation with higher bioavailability will tend to give higher urinary metabolite levels at 24 and 96 hr than a formulation with lower bioavailability at these times.

Notwithstanding an apparent correlation, the bias in estimating relative bioavailabilities of different formulations using 24- rather than 96-hr urinary excretion total metabolite data can be demonstrated with the data reported by Bates and Sequeira (2). They investigated the cumulative urinary excretion of total 6-desmethylgriseofulvin after the administration of four different griseofulvin formulations to five individuals. On the assumption of first-order kinetics, the relative bioavailability of the four different griseofulvin formulations can be calculated from the ratios of the mean amounts of total metabolite excreted in urine at different times (Table I).

It is evident that the use of 24-hr urinary excretion data of total metabolite leads consistently to underestimations of derived relative bioavailabilities. The underestimation increases with the smaller bioavailabilities, consistent with the premise that delayed absorption is the primary reason for low bioavailability. Thus, underestimation will be greatest when the relative bioavailability of poorly absorbed formulations is studied[1].

The standard error of the mean, expressed as percent of the mean, was consistently larger for the total amount of urinary metabolite at 24 hr. At 24 hr, the values were: I, 11.5%; II, 18.3%; III, 15.6%; and IV, 4.6%. At 96 hr, they were: I, 5.4%; II, 12.2%; III, 10.6%; and IV, 4.2%. Thus, routine assessments of bioavailabilities of different griseofulvin formulations should not be based on 24-hr urinary excretion data of total 6-desmethylgriseofulvin even if first-order kinetics exist.

I feel strongly that this dangerous procedure of using fractional urinary excretion data and/or areas (1, 3, 4) for the assessment of bioavailability must be clearly recognized.

(1) T. R. Bates and J. A. Sequeira, *J. Pharm. Sci.*, **64**, 709(1975)
(2) *Ibid.*, **64**, 793(1975).
(3) D. J. Greenblatt, D. W. Duhme, J. Koch-Weser, and T. W. Smith, *Clin. Pharmacol. Ther.*, **16**, 813(1974).
(4) E. Steiness, V. Christensen, and H. Johansen, *ibid.*, **14**, 949(1973).
(5) W. L. Chiou and S. Riegelman, *J. Pharm. Sci.*, **60**, 1376 (1971).
(6) C.-C. Lin, J. Magat, R. Chang, J. McGlotten, and S. Simchowicz, *J. Pharmacol. Exp. Ther.*, **187**, 415(1973).
(7) M. Rowland, S. Riegelman, and W. L. Epstein, *J. Pharm. Sci.*, **57**, 984(1968).
(8) P. A. Harris and S. Riegelman, *ibid.*, **58**, 93(1969).

Peter H. Hinderling
Department of Pharmacology
Biozentrum der Universitae Basel
Basel CH-4056
Switzerland

Received July 14, 1975.
Accepted for publication March 30, 1976.

[1] The rank order for the bioavailability of products in Table I is the same at 24 as it is at 96 hr (IV > III > II > I).

BOOKS

REVIEWS

Aliphatic Chemistry, Volume 3, Specialist Periodical Report. Senior Reporter, A. McKILLOP. The Chemical Society, Burlington House, London WIV OBN, England, 1975. xii + 409 pp. 14.5 × 22 cm. Price £13.50.

The first volume of "Aliphatic Chemistry" was published as Part I of a three-part Specialist Periodical Report on aliphatic, alicyclic, and saturated heterocyclic chemistry. Subsequently, these areas have been reviewed in separate Specialist Periodical Reports. This Specialist Report is the third volume of the series, dealing with aliphatic chemistry and, except for one chapter, reviews the literature published during 1973. Chapter 1, by R. S. Atkinson, is devoted to acetylenes, alkanes, allenes, and alkenes; Chapter 2, by E. W. Colvin, surveys the literature on other functional groups (carboxylic acids, esters, lactones, anhydrides, amides, nitriles, aldehydes and ketones, alcohols, amines, alkyl halides, ethers, and sulfur compounds). These chapters are similar in format and style to analogous chapters by the same authors in the two preceding volumes.

This volume, like Volume 2, contains chapters that summarize progress in the area of naturally occurring polyolefinic and polyacetylenic compounds (Chapter 3) and in the chemistry of the prostaglandins (Chapter 4). Both chapters are authored by G. Pattenden, as were the corresponding chapters in Volume 2. The literature on fatty acids and related compounds was reviewed in Volume 1 but not in Volume 2. Developments in this area during both 1972 and 1973, therefore, comprise Chapter 5 by F. D. Gunstone. The specialized areas of Chapters 3–5 are exemplified by sections dealing with polyolefinic antibiotics and other microbial metabolites, insect pheromones, acetylenes and olefins of marine or plant origin, prostaglandin syntheses, the multifaceted aspects of studies of fatty acids, and others.

A cumulative set of volumes may serve as summaries of the literature for the specialist engaged in research in one of these areas; but, perhaps more importantly, these annual surveys will provide a means by which others may be introduced to, or become familiar with, developments in a specific area. The value of surveys of the annual literature devoted to specific areas, such as those of Chapters 3–5, is readily recognized. Reviews of the more general topics of the first two chapters are equally valuable, since much effort would be required for the individual to extract this type of information from the periodical or abstract literature. In giving comprehensive coverage of the significant literature, the authors maintain the high standards of the preceding volumes.

Reviewed by Y. Fulmer Shealy
Southern Research Institute
Birmingham, AL 35205

Absolute Configuration of Tetracycline

During the past years, in approaching research in the area of tetracycline chemistry and obtaining reviews on manuscripts, some question has been raised as to the absolute configuration of tetracycline. This letter simply is a review of the primary literature in this area and, hopefully, will settle this controversy.

The structures of oxytetracycline[1] and chlortetracycline[2,3] were elucidated by chemical degradation early in the history of these antibiotics. The relative configurations at the asymmetric carbons were established chemically[3–10]; for 7-chlorotetracycline hydrochloride[11–13], oxytetracycline hydrochloride[14,15], anhydrotetracycline hydrobromide[16], and 2,5a-diacetyloxytetracycline[17], the configurations were approached by X-ray crystallography. This work establishing the configuration of the asymmetric centers has led to considerable confusion in the literature as to the exact absolute configuration because tetracycline and its related derivatives have been variously drawn as stereoisomers.

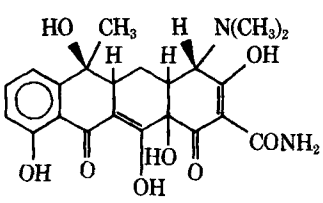

I

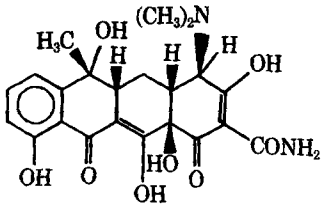

II

Some crystallographers have favored I[17] while others have favored II[11–16]. Since an anomalous scattering atom is not present in the tetracycline, the absolute configuration is indeterminate by X-ray crystallography. Furthermore, the apparent incongruities among the X-ray structures in the work done by NMR[18,19] and circular dichroism[20–24] have led to confusion among researchers.

The absolute configuration of the tetracyclines, however, was chemically determined[25] by degradation of chlortetracycline to a derivative that was comparable to a derivative prepared from atrolactinic acid, the absolute configuration of which is known. This work showed that I is, in fact, the correct absolute configuration of the tetracyclines.

It is hoped that this discussion will prevent further inconsistencies in the representation of the absolute configuration of the tetracyclines.

M. Erickson
N. Baenziger
C. W. Frank
Department of Chemistry
University of Iowa
Iowa City, IA 52242

Received March 5, 1976.

[1] F. A. Hochstein, C. R. Stephens, L. H. Conover, P. P. Regna, R. Pasternack, P. N. Cordeon, F. J. Pilgrim, K. J. Brunings, and R. B. Woodward, *J. Am. Chem. Soc.*, **75**, 5455(1953).
[2] C. R. Stephens, L. H. Conover, R. Pasternack, F. A. Hochstein, W. T. Moreland, P. P. Regna, F. J. Pilgrim, K. J. Brunings, and R. B. Woodward, *ibid.*, **76**, 3568(1954).
[3] C. W. Waller, B. L. Hutchings, R. W. Broschard, A. A. Goldman, W. J. Stein, C. F. Solfe, and J. H. Williams, *ibid.*, **74**, 4981(1952).
[4] L. H. Conover, Special Publication No. 5, The Chemical Society, London, England, 1956, p. 48.
[5] J. R. D. McCormick, P. A. Miller, J. A. Browich, N. O. Sjolander, and A. P. Doerschuk, *J. Am. Chem. Soc.*, **80**, 5572(1958).
[6] A. Green and J. H. Boothe, *ibid.*, **82**, 3590(1960).
[7] R. K. Blackwood, H. H. Rennhard, and C. R. Stephens, *ibid.*, **82**, 745(1960).
[8] R. K. Blackwood, J. J. Beereboom, H. H. Rennhard, M. Schach von Wittenau, and C. R. Stephens, *ibid.*, **83**, 2773(1961).
[9] H. H. Rennhard, R. K. Blackwood, and C. R. Stephens, *ibid.*, **83**, 2775(1961).
[10] M. Schach von Wittenau and R. K. Blackwood, *J. Org. Chem.*, **31**, 613(1966).
[11] S. Hirokawa, Y. Okaya, F. M. Lovell, and R. Pepinsky, *Acta Crystallogr.*, **12**, 84(1959).
[12] S. Hirokawa, Y. Okaya, F. M. Lovell, and R. Pepinsky, *Z. Kristallogr.*, **112**, 439(1959).
[13] J. Donohue, J. D. Dunitz, K. N. Trueblood, and M. S. Webster, *J. Am. Chem. Soc.*, **85**, 851(1963).
[14] Y. Takeuchi and M. J. Buerger, *Proc. Nat. Acad. Sci. USA*, **46**, 1366(1960).
[15] H. Cid-Dresdner, *Z. Kristallogr.*, **121**, 170(1965).
[16] R. Restivo and G. J. Palenik, *Biochem. Biophys. Res. Commun.*, **36**, 621(1969).
[17] R. B. Von Dreele and R. E. Hughes, *J. Am. Chem. Soc.*, **93**, 7290(1971).
[18] M. Schach von Wittenau, R. K. Blackwood, L. H. Conover, R. H. Glauert, and R. B. Woodward, *ibid.*, **87**, 134(1965).
[19] H. Muxfelt, H. Dopp, J. E. Kaufman, J. Schneider, P. E. Hansen, A. Sasaki, and T. Geiser, *Angew. Chem., Int. Ed.*, **12**, 497(1973).
[20] L. A. Mitscher, J. H. Martin, A. C. Dornbush, L. Leeson, and G. Redin, *Antimicrob. Ag. Chemother.*, **1968**, 78.
[21] L. A. Mitscher, A. C. Bonacci, and T. D. Sokolóski, *Tetrahedron Lett.*, **1968**, 5361.
[22] L. A. Mitscher, A. C. Bonacci, and T. D. Sokoloski, *Antimicrob. Ag. Chemother.*, **1968**, 78.
[23] L. A. Mitscher, A. C. Bonacci, B. Slater-Eng, A. K. Hacker, and T. D. Sokoloski, *ibid.*, **1969**, 111.
[24] L. A. Mitscher, B. Slater-Eng, and T. D. Sokoloski, *ibid.*, **1972**, 66.
[25] V. N. Dobrynin, A. J. Gurevich, M. G. Karapetyan, M. N. Kosolov, and M. M. Shemyakin, *Tetrahedron Lett.*, **1962**, 901.

The Bloomin' Blossoms Have to Bloom to Be of Any Value

Until the FDA came forth with their regulations dealing with over-the-counter antacid drug products, industry had almost as many variations to demonstrate their products' acid-neutralizing power as there were antacids on the market. The end result was that no one could readily correlate the reported values, and the consumer was completely mystified as to what an antacid really should be.

In another field, dissolution test methods have promulgated proliferously in every direction possible during the past 15–20 years. The major purpose was to show that more of a given drug under the stated conditions, using the appropriately described apparatus, goes into solution faster than any of the competitive ones. This, of course, is good business strategy but very confusing and trying to those who attempt to interpret results from the different techniques. Being one of the many verbally battle-scarred victims, I felt great relief, and almost disbelief, that the USP finally took a firm stand on the dire need for a standard dissolution test.

We all like to be unique and very individualistic in the introduction of new and different approaches to an analytical problem because that is what makes the analysis of pharmaceuticals so intriguing and even exciting. However, there comes a time when a uniform approach, such as a compendium procedure, is a complete and unconditional necessity for the benefit of the one who really counts—the patient. I believe that the time is now for all of us in quality assurance to smoke a peace pipe and join the USP in its tremendous undertaking in putting sound scientific backing into a standard dissolution test and apparatus. *It can be done!*

Epilog: If the USP does not succeed, you know who will!

Clark A. Kelly
22 Huntersfield Road
Westchester Woods
Delmar, NY 12054

Received May 10, 1976.

Absolute Configuration of Tetracycline

During the past years, in approaching research in the area of tetracycline chemistry and obtaining reviews on manuscripts, some question has been raised as to the absolute configuration of tetracycline. This letter simply is a review of the primary literature in this area and, hopefully, will settle this controversy.

The structures of oxytetracycline[1] and chlortetracycline[2,3] were elucidated by chemical degradation early in the history of these antibiotics. The relative configurations at the asymmetric carbons were established chemically[3–10]; for 7-chlorotetracycline hydrochloride[11–13], oxytetracycline hydrochloride[14,15], anhydrotetracycline hydrobromide[16], and 2,5a-diacetyloxytetracycline[17], the configurations were approached by X-ray crystallography. This work establishing the configuration of the asymmetric centers has led to considerable confusion in the literature as to the exact absolute configuration because tetracycline and its related derivatives have been variously drawn as stereoisomers.

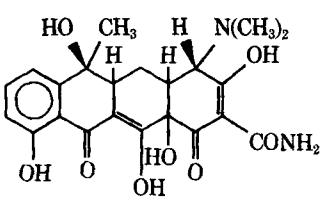

I

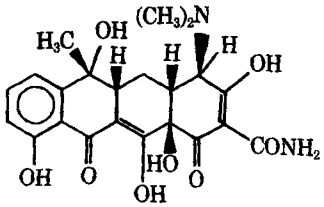

II

Some crystallographers have favored I[17] while others have favored II[11–16]. Since an anomalous scattering atom is not present in the tetracycline, the absolute configuration is indeterminate by X-ray crystallography. Furthermore, the apparent incongruities among the X-ray structures in the work done by NMR[18,19] and circular dichroism[20–24] have led to confusion among researchers.

The absolute configuration of the tetracyclines, however, was chemically determined[25] by degradation of chlortetracycline to a derivative that was comparable to a derivative prepared from atrolactinic acid, the absolute configuration of which is known. This work showed that I is, in fact, the correct absolute configuration of the tetracyclines.

It is hoped that this discussion will prevent further inconsistencies in the representation of the absolute configuration of the tetracyclines.

M. Erickson
N. Baenziger
C. W. Frank
Department of Chemistry
University of Iowa
Iowa City, IA 52242

Received March 5, 1976.

[1] F. A. Hochstein, C. R. Stephens, L. H. Conover, P. P. Regna, R. Pasternack, P. N. Cordeon, F. J. Pilgrim, K. J. Brunings, and R. B. Woodward, *J. Am. Chem. Soc.*, **75**, 5455(1953).
[2] C. R. Stephens, L. H. Conover, R. Pasternack, F. A. Hochstein, W. T. Moreland, P. P. Regna, F. J. Pilgrim, K. J. Brunings, and R. B. Woodward, *ibid.*, **76**, 3568(1954).
[3] C. W. Waller, B. L. Hutchings, R. W. Broschard, A. A. Goldman, W. J. Stein, C. F. Solfe, and J. H. Williams, *ibid.*, **74**, 4981(1952).
[4] L. H. Conover, Special Publication No. 5, The Chemical Society, London, England, 1956, p. 48.
[5] J. R. D. McCormick, P. A. Miller, J. A. Browich, N. O. Sjolander, and A. P. Doerschuk, *J. Am. Chem. Soc.*, **80**, 5572(1958).
[6] A. Green and J. H. Boothe, *ibid.*, **82**, 3590(1960).
[7] R. K. Blackwood, H. H. Rennhard, and C. R. Stephens, *ibid.*, **82**, 745(1960).
[8] R. K. Blackwood, J. J. Beereboom, H. H. Rennhard, M. Schach von Wittenau, and C. R. Stephens, *ibid.*, **83**, 2773(1961).
[9] H. H. Rennhard, R. K. Blackwood, and C. R. Stephens, *ibid.*, **83**, 2775(1961).
[10] M. Schach von Wittenau and R. K. Blackwood, *J. Org. Chem.*, **31**, 613(1966).
[11] S. Hirokawa, Y. Okaya, F. M. Lovell, and R. Pepinsky, *Acta Crystallogr.*, **12**, 84(1959).
[12] S. Hirokawa, Y. Okaya, F. M. Lovell, and R. Pepinsky, *Z. Kristallogr.*, **112**, 439(1959).
[13] J. Donohue, J. D. Dunitz, K. N. Trueblood, and M. S. Webster, *J. Am. Chem. Soc.*, **85**, 851(1963).
[14] Y. Takeuchi and M. J. Buerger, *Proc. Nat. Acad. Sci. USA*, **46**, 1366(1960).
[15] H. Cid-Dresdner, *Z. Kristallogr.*, **121**, 170(1965).
[16] R. Restivo and G. J. Palenik, *Biochem. Biophys. Res. Commun.*, **36**, 621(1969).
[17] R. B. Von Dreele and R. E. Hughes, *J. Am. Chem. Soc.*, **93**, 7290(1971).
[18] M. Schach von Wittenau, R. K. Blackwood, L. H. Conover, R. H. Glauert, and R. B. Woodward, *ibid.*, **87**, 134(1965).
[19] H. Muxfelt, H. Dopp, J. E. Kaufman, J. Schneider, P. E. Hansen, A. Sasaki, and T. Geiser, *Angew. Chem., Int. Ed.*, **12**, 497(1973).
[20] L. A. Mitscher, J. H. Martin, A. C. Dornbush, L. Leeson, and G. Redin, *Antimicrob. Ag. Chemother.*, **1968**, 78.
[21] L. A. Mitscher, A. C. Bonacci, and T. D. Sokolóski, *Tetrahedron Lett.*, **1968**, 5361.
[22] L. A. Mitscher, A. C. Bonacci, and T. D. Sokoloski, *Antimicrob. Ag. Chemother.*, **1968**, 78.
[23] L. A. Mitscher, A. C. Bonacci, B. Slater-Eng, A. K. Hacker, and T. D. Sokoloski, *ibid.*, **1969**, 111.
[24] L. A. Mitscher, B. Slater-Eng, and T. D. Sokoloski, *ibid.*, **1972**, 66.
[25] V. N. Dobrynin, A. J. Gurevich, M. G. Karapetyan, M. N. Kosolov, and M. M. Shemyakin, *Tetrahedron Lett.*, **1962**, 901.

The Bloomin' Blossoms Have to Bloom to Be of Any Value

Until the FDA came forth with their regulations dealing with over-the-counter antacid drug products, industry had almost as many variations to demonstrate their products' acid-neutralizing power as there were antacids on the market. The end result was that no one could readily correlate the reported values, and the consumer was completely mystified as to what an antacid really should be.

In another field, dissolution test methods have promulgated proliferously in every direction possible during the past 15–20 years. The major purpose was to show that more of a given drug under the stated conditions, using the appropriately described apparatus, goes into solution faster than any of the competitive ones. This, of course, is good business strategy but very confusing and trying to those who attempt to interpret results from the different techniques. Being one of the many verbally battle-scarred victims, I felt great relief, and almost disbelief, that the USP finally took a firm stand on the dire need for a standard dissolution test.

We all like to be unique and very individualistic in the introduction of new and different approaches to an analytical problem because that is what makes the analysis of pharmaceuticals so intriguing and even exciting. However, there comes a time when a uniform approach, such as a compendium procedure, is a complete and unconditional necessity for the benefit of the one who really counts—the patient. I believe that the time is now for all of us in quality assurance to smoke a peace pipe and join the USP in its tremendous undertaking in putting sound scientific backing into a standard dissolution test and apparatus. *It can be done!*

Epilog: If the USP does not succeed, you know who will!

Clark A. Kelly
22 Huntersfield Road
Westchester Woods
Delmar, NY 12054

Received May 10, 1976.

Official Microbiological Assays

Official methods such as those of AOAC are important; they are used by regulatory analysts and generally have preferred status in courts. They are considered to be reliable enough to be used by those too inexperienced to judge the reliability of a method. They are expected to give reliable and precise results. Thus, AOAC methods should represent the state of the art in high quality assaying. Advances in physical and chemical methods are incorporated into official methods reasonably soon after their reliability has been established. The situation with microbiological assays for antibiotics and vitamins is quite different; official methods are essentially those available in 1945.

All antibiotic assays in the 12th edition of "Official Methods of Analysis of AOAC," as in the earlier editions, are by diffusion methods in petri dishes. Current practice in the United States is to assay as many antibiotics as possible by nonofficial turbidimetric methods, preferably automated ones. These methods are inherently more precise than diffusion methods, and even manual ones require much less work to obtain a more precise answer. However, the legally important sample must be assayed by the less desirable official methods. Does the analytical microbiologist, unlike the analytical chemist, need two distinct qualities of assays depending upon the legal importance of the sample? Should not official methods also be suitable for precise routine assays?

Official methods, in theory, specify exactly those operations essential to proper assaying, deviation from which can be claimed to reduce accuracy. If the unstated assumptions about operations are not examined too closely and if fairly wide limits are put on the answers, the methods seem dependable. However, in reality, the microbiological assays are of low accuracy and precision and are obsolete in concept and design. Lack of adequate specification of details of critical operations is one cause of poor interlaboratory agreement. Too many of the details given are not important to success, whereas those likely to cause significant problems are not mentioned. Among the latter are: dilution procedures and equipment; form and extent of calibration lines; prediffusion time and time schedule for heating to incubation temperature in diffusion assays; qualitative and quantitative identity of composition of standards and samples in many antibiotic assays; standards and samples in different menstrua; inadequate extracting solvent; excessive manipulation of samples; inaccurate measurement of volumes during sample preparation; exposure of photolabile substances to strong light; use of decayed standards; and the idea that the methods being biological are inherently inaccurate and that, consequently, care need not be exercised. The last may be the most damaging to high quality assaying.

The inherent accuracy of microbiological assays can be achieved only after the listed factors are recognized as important and are properly controlled. When these changes are made, as they can be with little cost and effort, microbiological assays can be as accurate, precise, and reliable as many chemical ones. Until these changes are made, "Methods" will be of more value to lawyers engaged in adversary proceedings than to analysts needing good methods of general applicability.

Frederick Kavanagh
231 Blue Ridge Road
Indianapolis, IN 46208

Received May 14, 1976.

Authors please note:

Page charges for contributed articles published in the Journal of Pharmaceutical Sciences *are $70 per printed page, effective July 1976. Recognizing that publication of research reports is an integral part of research, page charge costs should be considered as a part of research funding.*

Acceptance of manuscripts for publication is not contingent upon payment of page charges. However, the continued viability of scientific journals is contingent upon the sponsors of research assuming some of the responsibility for publication of the results of research.

1976

July 18–22
American Association of Colleges of Pharmacy, Leamington Hotel, Minneapolis, Minn.

August 4–6
American Academy of Clinical Toxicology, American Association of Poison Control Centers, and Canadian Academy of Clinical Toxicology, Annual Meeting, Olympia Hotel, Seattle, Wash.

August 9–13
Gordon Research Conferences, Medicinal Chemistry, Colby-Sawyer College, New London, N.H. (Contact Dr. A. M. Cruickshank, Director, Gordon Research Conferences, Pastore Chemical Laboratory, University of Rhode Island, Kingston, RI 02881)

August 15–19
American Society for Pharmacology and Experimental Therapeutics, Tulane University, New Orleans, La.

August 27–29
The European Symposium of the International Association of Forensic Toxicologists, State University of Ghent, Belgium (Contact Department of Toxicology, State University of Ghent, Hospitaalstraat 13, 9000 Ghent, Belgium)

August 29–September 2
American Chemical Society, National Meeting, San Francisco, Calif. (Contact A. T. Winstead, American Chemical Society, 1155 16th St., N.W., Washington, DC 20036)

August 29–September 3
International Conference on Health Education, Ottawa, Canada

September 6–11
International Congress of Pharmaceutical Sciences, Warsaw, Poland

September 20–22
National Conference on Cancer Research and Clinical Investigation, American Cancer Society and National Cancer Institute, Regency Hyatt Atlanta Hotel, Atlanta, Ga. (Contact Dr. S. L. Arje, American Cancer Society, 777 3rd Ave., New York, NY 10017)

October 7–10
American College of Apothecaries, Annual Meeting, Bellevue Stratford, Philadelphia, Pa.

October 11–15
National Society for Histotechnology, Convention and Symposium, Radisson Hotel Downtown, Minneapolis, Minn. (Contact Registrar, P.O. Box 36, Lanham, MD 20801)

October 17–20
ASTM Committee E-19, Practice of Chromatography, North Shore Hilton Hotel, Chicago, Ill. (Contact Gerald Dupre, Biodynamics, Inc., Box 43, Mettlers Road, East Millstone, NJ 08874)

October 17–21
American Public Health Association, Annual Meeting, Miami Beach, Fla.

October 18
APhA Academy of Pharmaceutical Sciences, Annual Western Regional Meeting, Industrial Pharmaceutical Technology Section, D-Registry, Irvine, Calif. (Contact Dr. D. Swanson, ALZA Corp., Palo Alto, CA 94304)

October 18–21
Association of Official Analytical Chemists, Marriott Twin Bridges, Washington, D.C. (Contact L. G. Ensminger, AOAC, Box 540, Ben Franklin Station, Washington, DC 20044)

October 22
APhA Academy of Pharmaceutical Sciences, Annual Eastern Regional Meeting, Industrial Pharmaceutical Technology Section, Cherry Hill Inn, Cherry Hill, N.J. (Contact Dr. Arthur Goldberg, Applied Sciences, TDD, Hoffmann-La Roche Inc., Nutley, NJ 07110)

November 11–12
Health Care Delivery Systems in North America: The Changing Concepts, Canadian–American Seminar, University of Windsor, Windsor, Ontario, Canada N9B 3P4 (Contact Director, Canadian–American Seminar, University of Windsor, Windsor, Ontario, Canada N9B 3P4)

November 14–18
APhA Academy of Pharmaceutical Sciences, National Meeting, Carleton House Hotel, Orlando, Fla.

November 14–18
American Dental Association, Annual Meeting, Las Vegas, Nev.

November 14–19
International Symposium on Industrial Wastes and Environment, Caracas, Venezuela (Contact Dr. Richard Abbou, 115 rue de la Pompe, F 75116, Paris, France)

November 14–20
Federation of Analytical Chemistry and Spectroscopy Societies, Annual Meeting, American Chemical Society Division of Analytical Chemistry and others, Civic Center, Philadelphia, Pa. (Contact C. White, Analytical Chemistry Division, Oak Ridge National Laboratories, Oak Ridge, TN 37830)

December 4–8
American Medical Association, Clinical Meeting, Philadelphia, Pa.

December 5–10
American Society of Hospital Pharmacists, Midyear Meeting, Anaheim, Calif.

December 14–15
Food and Drug Law Institute, Annual Meeting, Washington Hilton, Washington, D.C.

1977

February 20–26
American Association for the Advancement of Science, Annual Meeting, Denver, Colo.

April 26–28
Pharmaceutical Manufacturers Association, Annual Convention, Boca Raton Hotel, Boca Raton, Fla.

May 14–19
APhA Annual Meeting, New York, N.Y.

May 15–18
Proprietary Association, Annual Meeting, The Greenbrier, White Sulphur Springs, W.Va.

June 18–23
American Medical Association, Annual Meeting, San Francisco, Calif.

Items to be considered for inclusion or corrections should be addressed to:

J. Pharm. Sci. Calendar
2215 Constitution Avenue, N.W.
Washington, DC 20037

Journal of Pharmaceutical Sciences

AUGUST 1976

VOLUME 65 NUMBER 8

MARY H. FERGUSON
Editor

LUAN CORRIGAN
Assistant Editor

SHELLY ELLIOTT
Production Editor

JANET D. SHOFF
Copy Editor

EDWARD G. FELDMANN
Contributing Editor

SAMUEL W. GOLDSTEIN
Contributing Editor

LELAND J. ARNEY
Publications Director

EDITORIAL ADVISORY BOARD

JOHN AUTIAN — HARRY B. KOSTENBAUDER

LYNN R. BRADY — CARL J. LINTNER, JR.

WILLIAM O. FOYE — DAVID E. MANN, JR.

WILLIAM J. JUSKO — GERALD J. PAPARIELLO

The *Journal of Pharmaceutical Sciences* is published monthly by the American Pharmaceutical Association at 2215 Constitution Ave., N.W., Washington, DC 20037. Second-class postage paid at Washington, D.C., and at additional mailing office.

All expressions of opinion and statements of supposed fact appearing in articles or editorials carried in this journal are published on the authority of the writer over whose name they appear and are not to be regarded as necessarily expressing the policies or views of the American Pharmaceutical Association.

Offices—Editorial, Advertising, and Subscription Offices: 2215 Constitution Ave., N.W., Washington, DC 20037. Printing Offices: 20th & Northampton Streets, Easton, PA 18042.

Annual Subscriptions—United States and foreign, industrial and government institutions $50, educational institutions $50, individuals *for personal use only* $30; single copies $5. All foreign subscriptions add $5 for postage. Subscription rates are subject to change without notice. Members of the American Pharmaceutical Association may elect to receive the *Journal of Pharmaceutical Sciences* as a part of their annual $60 (foreign $65) APhA membership dues.

Claims—Missing numbers will not be supplied if dues or subscriptions are in arrears for more than 60 days or if claims are received more than 60 days after the date of the issue, or if loss was due to failure to give notice of change of address. The Association cannot accept responsibility for foreign delivery when its records indicate shipment has been made.

Change of Address—Members and subscribers should notify at once both the Post Office and the American Pharmaceutical Association, 2215 Constitution Ave., N.W., Washington, DC 20037, of any change of address.

© Copyright 1976, American Pharmaceutical Association, 2215 Constitution Ave., N.W., Washington, DC 20037; all rights reserved.

IN THE NAME OF LIBERTY

A student of history, taking note of the crusades in the middle ages—as well as of the many other "holy wars" past and present—once observed that more wars are claimed to be waged and more blood is professed to be shed in the name of the Almighty than for all other causes combined.

We were recently reminded of this comment as we noted the many advertising stunts, promotional campaigns, and various other gimmicks which have been cloaked with some reference to the nation's Bicentennial celebration, in an effort to dignify them. The words "liberty," "freedom," and "self-determination," among others, have been widely used in association with all sorts of proposals, positions, and causes, most of which—when stripped of their Bicentennial puffery—are propositions of dubious value at best.

These comments are prompted by a recent request to us from a physician asking that we lend support to a bill (H.R. 12573) introduced this spring in the U.S. Congress. The bill is appealingly entitled the "Medical Freedom of Choice Act," and its descriptive summary states that it is intended: "*To expand the medical freedom of choice of consumers by amending the Federal Food, Drug, and Cosmetic Act to provide that drugs will be regulated under that Act solely to assure their safety.*" Specifically, the purpose of the bill is to revoke the provisions of the 1962 Drug Amendments which require that, as a condition of approval for marketing, a new drug must be demonstrated to be effective, as well as safe, for the claims made in its labeling. H.R. 12573 has the active support of at least two physician-members of the House of Representatives.

The proposition that the need to demonstrate effectiveness should no longer be required for new drugs appears to be gathering support, particularly from among those physicians and medical organizations with a politically conservative stance. The most notable example is the American Medical Association which, about a year ago, adopted a resolution in its House of Delegates calling for repeal of the effectiveness requirement in the Federal law.

We have already expressed our own view that the effectiveness requirement is a necessary provision if we are to avoid a return to the era of quackery and nostrums. The editorial in the October 1975 issue of this Journal specifically dealt with this point. These present comments are intended to review the subject from a slightly different perspective.

A sizable segment of the medical profession has been noted for its fiercely independent beliefs and attitudes. Any law or regulation which serves to establish boundaries or restrictions—no matter how logical and justifiable such limits may be—is met at least with suspicion, generally with hostility, and often with outright resistance by this segment of medicine. In the case at hand, such physicians feel that their bounds to prescribe and use drugs in the treatment of patients should be limitless and without restriction. In their view, this represents a "freedom" which physicians have a right to enjoy.

It strikes us that those who hold such views probably have not stopped to consider where the extension of such a line of thinking will ultimately lead. For example, is not the prescription legend category of drugs a comparable restriction on freedom for the general public? American citizens could readily argue the position that their personal freedom is restricted by the legal requirement that many drugs may be obtained only on the prescription of a duly authorized prescriber.

Moreover, are not the medical practice acts—which limit the practice of medicine to individuals who have fulfilled certain requirements pertaining to education, experience, examination, and licensure—restrictions on the liberty of other citizens who might wish to offer their services in the field of medicine without having fulfilled such requirements? As absurd as these questions may seem—particularly to the medical profession—they are directly equatable to the suggestion that the effectiveness requirement be eliminated for new drug approval.

If the Food and Drug Administration has been dragging its feet in processing new drug applications, or if the drug industry has been negligent in submitting adequate proof to demonstrate effectiveness, these are problems of mechanics for which other, more specific remedies should be sought and considered. It should be recognized that the basic system is sound, and this fact must be clearly distinguished from any faults in its implementation or operation. —EGF

Journal of Pharmaceutical Sciences

AUGUST 1976

VOLUME 65 NUMBER 8

MARY H. FERGUSON
Editor

LUAN CORRIGAN
Assistant Editor

SHELLY ELLIOTT
Production Editor

JANET D. SHOFF
Copy Editor

EDWARD G. FELDMANN
Contributing Editor

SAMUEL W. GOLDSTEIN
Contributing Editor

LELAND J. ARNEY
Publications Director

EDITORIAL ADVISORY BOARD

JOHN AUTIAN — HARRY B. KOSTENBAUDER

LYNN R. BRADY — CARL J. LINTNER, JR.

WILLIAM O. FOYE — DAVID E. MANN, JR.

WILLIAM J. JUSKO — GERALD J. PAPARIELLO

The *Journal of Pharmaceutical Sciences* is published monthly by the American Pharmaceutical Association at 2215 Constitution Ave., N.W., Washington, DC 20037. Second-class postage paid at Washington, D.C., and at additional mailing office.

All expressions of opinion and statements of supposed fact appearing in articles or editorials carried in this journal are published on the authority of the writer over whose name they appear and are not to be regarded as necessarily expressing the policies or views of the American Pharmaceutical Association.

Offices—Editorial, Advertising, and Subscription Offices: 2215 Constitution Ave., N.W., Washington, DC 20037. Printing Offices: 20th & Northampton Streets, Easton, PA 18042.

Annual Subscriptions—United States and foreign, industrial and government institutions $50, educational institutions $50, individuals *for personal use only* $30; single copies $5. All foreign subscriptions add $5 for postage. Subscription rates are subject to change without notice. Members of the American Pharmaceutical Association may elect to receive the *Journal of Pharmaceutical Sciences* as a part of their annual $60 (foreign $65) APhA membership dues.

Claims—Missing numbers will not be supplied if dues or subscriptions are in arrears for more than 60 days or if claims are received more than 60 days after the date of the issue, or if loss was due to failure to give notice of change of address. The Association cannot accept responsibility for foreign delivery when its records indicate shipment has been made.

Change of Address—Members and subscribers should notify at once both the Post Office and the American Pharmaceutical Association, 2215 Constitution Ave., N.W., Washington, DC 20037, of any change of address.

© Copyright 1976, American Pharmaceutical Association, 2215 Constitution Ave., N.W., Washington, DC 20037; all rights reserved.

IN THE NAME OF LIBERTY

A student of history, taking note of the crusades in the middle ages—as well as of the many other "holy wars" past and present—once observed that more wars are claimed to be waged and more blood is professed to be shed in the name of the Almighty than for all other causes combined.

We were recently reminded of this comment as we noted the many advertising stunts, promotional campaigns, and various other gimmicks which have been cloaked with some reference to the nation's Bicentennial celebration, in an effort to dignify them. The words "liberty," "freedom," and "self-determination," among others, have been widely used in association with all sorts of proposals, positions, and causes, most of which—when stripped of their Bicentennial puffery—are propositions of dubious value at best.

These comments are prompted by a recent request to us from a physician asking that we lend support to a bill (H.R. 12573) introduced this spring in the U.S. Congress. The bill is appealingly entitled the "Medical Freedom of Choice Act," and its descriptive summary states that it is intended: "*To expand the medical freedom of choice of consumers by amending the Federal Food, Drug, and Cosmetic Act to provide that drugs will be regulated under that Act solely to assure their safety.*" Specifically, the purpose of the bill is to revoke the provisions of the 1962 Drug Amendments which require that, as a condition of approval for marketing, a new drug must be demonstrated to be effective, as well as safe, for the claims made in its labeling. H.R. 12573 has the active support of at least two physician-members of the House of Representatives.

The proposition that the need to demonstrate effectiveness should no longer be required for new drugs appears to be gathering support, particularly from among those physicians and medical organizations with a politically conservative stance. The most notable example is the American Medical Association which, about a year ago, adopted a resolution in its House of Delegates calling for repeal of the effectiveness requirement in the Federal law.

We have already expressed our own view that the effectiveness requirement is a necessary provision if we are to avoid a return to the era of quackery and nostrums. The editorial in the October 1975 issue of this Journal specifically dealt with this point. These present comments are intended to review the subject from a slightly different perspective.

A sizable segment of the medical profession has been noted for its fiercely independent beliefs and attitudes. Any law or regulation which serves to establish boundaries or restrictions—no matter how logical and justifiable such limits may be—is met at least with suspicion, generally with hostility, and often with outright resistance by this segment of medicine. In the case at hand, such physicians feel that their bounds to prescribe and use drugs in the treatment of patients should be limitless and without restriction. In their view, this represents a "freedom" which physicians have a right to enjoy.

It strikes us that those who hold such views probably have not stopped to consider where the extension of such a line of thinking will ultimately lead. For example, is not the prescription legend category of drugs a comparable restriction on freedom for the general public? American citizens could readily argue the position that their personal freedom is restricted by the legal requirement that many drugs may be obtained only on the prescription of a duly authorized prescriber.

Moreover, are not the medical practice acts—which limit the practice of medicine to individuals who have fulfilled certain requirements pertaining to education, experience, examination, and licensure—restrictions on the liberty of other citizens who might wish to offer their services in the field of medicine without having fulfilled such requirements? As absurd as these questions may seem—particularly to the medical profession—they are directly equatable to the suggestion that the effectiveness requirement be eliminated for new drug approval.

If the Food and Drug Administration has been dragging its feet in processing new drug applications, or if the drug industry has been negligent in submitting adequate proof to demonstrate effectiveness, these are problems of mechanics for which other, more specific remedies should be sought and considered. It should be recognized that the basic system is sound, and this fact must be clearly distinguished from any faults in its implementation or operation. —EGF

Journal of Pharmaceutical Sciences

AUGUST 1976
VOLUME 65 NUMBER 8

REVIEW ARTICLE

Pharmaceutical Sciences—1975: Literature Review of Pharmaceutics II ▲

FRANK W. GOODHART *x **and MARTIN L. EICHMAN** ‡

Keyphrases □ Pharmaceutical sciences—1975 literature review of pharmaceutics □ Technology, pharmaceutical—sterility, dosage forms, cosmetics, packaging equipment, dental products, biomedical devices, 1975 literature review □ Stability—solids, solutions, injectable products, antibiotics, and vitamins, kinetics, 1975 literature review □ Dosage forms—tablets, suspensions, emulsions, suppositories, aerosols, controlled-release devices, 1975 literature review □ Cosmetics—formulation and technology, microbiological contamination, 1975 literature review □ Instrumentation—in pharmaceutical technology, 1975 literature review □ Literature review—pharmaceutical sciences, 1975

CONTENTS

Physical Pharmacy 1101
Dissolution 1102
Solubility-Solubilization Phenomena 1104
Membrane Permeation and Release 1104
Complexation 1106
Interactions of Drugs with Biological Substances 1106
Interactions of Drugs with Nonbiological Substances 1108
Surface Phenomena 1109
Interface Studies 1109
Adsorption Studies 1109
General Properties of Surfactants 1110
Micelle Studies 1111
Dispersion Stabilization and Rheology 1111
Pharmaceutical Aspects 1112
Antibiotics 1112
Radiopharmaceuticals 1113
Biopharmaceutics 1113
Bioavailability of Drug Substances 1113
Methodology 1113
Physicochemical Factors 1114
Formulation Factors 1114
Differing Administration Routes 1117
Physiological Factors 1118
Pharmacokinetics 1120
References 1126

▲ *Editor's note:* Part I of this article appeared in the July 1976 issue of the *Journal of Pharmaceutical Sciences.*

PHYSICAL PHARMACY

Several articles discussed the polymorphic characteristics of drugs. Of the two polymorphic forms of homatropine hydrochloride described, Form I was found to be metastable whereas Form II was stable at room temperature (817). Slow heating during melting-point determinations converted Form II to Form I. Polymorphs of testosterone were analyzed by IR spectroscopy, differential scanning calorimetry, and thermal analysis (818). Upon heating, all forms reverted to Form I. Differential scanning calorimetry was employed to describe the δ-form of chloramphenicol palmitate and to study its interconversion to other forms (819).

The physical properties of 20% gelatin gels prepared from Pharmagel A were investigated, and their behavior in electric fields was explored (820). A review of the literature dealing with the modification of crystalline structures of pharmaceutical solids and its application was published (821). The effect of various additives on the rate of transformation of metastable anhydrous succinylsulfathiazole Form I to the water-stable dihydrate Form II in aqueous suspension was reported (822, 823). Structurally related compounds, viscosity-imparting agents, surfactants, and colorants were used as possible retardants for the conversion. Methylcellulose, phthalylsulfathiazole, and polysorbate 80 were shown

to inhibit crystal growth of suspensions prepared from the metastable polymorph. Physical factors and additives that had accelerating or retarding effects on the transformation rate of Form I had similar effects on the crystal growth rate in aqueous suspension.

A review of the pharmaceutical aspects of crystallography was presented (824).

Electron microscopy was employed to determine the physical properties of dextran and polyvinyl alcohol in solutions (825). Formation of aggregates and the effect of time and concentration on aggregation were described. The relationship between the polymer structure and biocompatibility of hydrophilic gels was investigated (826). A method for preparing microcrystals of aspirin by pouring a hot solution with glycol into cold water was presented (827), and no evidence of polymorphism was found.

An X-ray diffraction method was employed to study the apparent velocity constant of the degradation of the crystalline network of an aspirin–aminophenazone (aminopyrine) mixture (828). Starch apparently retarded the decomposition. The kinetics of particle-size reduction was followed by investigating the time dependence of the average size (829). The physical properties of mixtures of oleic acid with tripalmitin and with fatty acid triglycerides were studied (830). Oleic acid appeared to retard the release of salicylic acid from a suppository formed from fatty acid triglycerides.

The role of principal component analysis in the selection of pharmaceutical formulations was discussed (831). The technique was successfully applied to a system consisting of 10 tablet variables. This methodology may be useful for achieving cost and time savings in measuring responses. A simple test was made to determine the importance of surfactants in the disintegration of tablets (832). The determining factors appeared to be the hydration of the bonding agent and the dissolution of binding bridges. The pK values for about 600 drugs were presented, and the importance of the dissociation constant and lipid solubility in determining the potential drug activity was discussed (833–835).

The uses and medical applications of polymer membranes and silicones were reviewed. Special emphasis was paid to medical grade silicone (836, 837). Size distribution of particles in solutions, suspensions, and ointments was studied using optical electronic imaging evaluation (838). The limitations of the method and the reproducibility of the results were discussed. Reviews of the physical properties, stability, and analysis of phenformin hydrochloride, norgestrel, norethindrone, and cephalexin were published (839–842).

Dissolution—A general equation was derived for the dissolution profile of powders under sink conditions (843), was used to develop an equation for the dissolution of log-normal powders, and was found to be more applicable than previous approaches. A biphasic cube-root dependence was found in the dissolution of oxalic acid dihydrate of log-normal particle-size distribution in 0.1 *N* HCl (844).

Dissolution profiles were calculated for sieve cuts of varying widths on the assumption of diffusion rate-limited dissolution under sink conditions from spherical particles (845). Even narrow sieve cuts varied from cube-root law expectations by as much as 3%, but the experimental data could be treated on the assumption that sieve cuts act like monosized powders to provide acceptable information, except in cases of critical tests of dissolution rate theory. Equations describing nonsink dissolution rates on the basis of simple film theory were shown to hold to 80–90% of the dissolution process for *p*-hydroxybenzoic acid and sodium chloride (846).

A critical review of drug dissolution focused upon methods for determining rates that could lead to realistic specification standards (847). A mathematical model based upon convective diffusion was developed to describe the rate of dissolution from the surface of a compressed compact (848, 849). Correlations between experimental results and theory were good for describing dissolution rates from rectangular and circular surfaces of a homologous series of *p*-aminobenzoate esters.

Dissolution rates of three polymorphs and two hydrates of phenobarbital were determined, and Form II dissolved most rapidly (850). On the basis of dissolution studies of chloramphenicol palmitate polymorphs in pancreatic solutions, it was determined that the first step of enzymatic hydrolysis could not be drug dissolution but rather appeared to be ester hydrolysis in the undissolved state (851). Linear multiple-regression analysis was used to assess the dependence of the dissolution rate on the diffusion coefficient and viscosity of the dissolution medium (852).

Dissolution profiles of aspirin from three dosage forms (microcapsule, powder, and enteric-coated granule) were examined at constant pH (853). The dissolution process of microencapsulated drug was zero order in the initial phase of the experiment. An irregularly shaped dissolution pattern was obtained with the enteric-coated granules. FD&C Violet No. 1 and Ext D&C Blue No. 1, at 50 μg/ml, inhibited the dissolution rate of sulfathiazole, diethylstilbestrol, and hexestrol in micellar bile solutions (854). The effect of the dissolution rates of drug solid dispersion systems on the GI absorption of drugs was reviewed (855). A model system, using a rotary disk technique, was developed to measure the dissolution rate and change of testosterone to testosterone monohydrate II (856).

Solid dispersions of several steroids, hydrochlorothiazide, and phenylbutazone in povidone (PVP) or polyethylene glycol 6000 exhibited more rapid dissolution than optimally wetted and dispersed pure drug powders (857). Formation of solid dispersions of indomethacin, however, did not increase the dissolution rate. Ball milling in the presence of povidone increased the solubility and dissolution rate of phenothiazine, vitamin K_3 (menadione), and other insoluble drugs (858). Low concentrations of povidone decreased the apparent solubility of hydroflumethiazide, whereas solubility was enhanced at high concentrations (859). Dissolution data were consistent with a model accounting for crystalline and amorphous drug together with complexing and crystal growth-inhibiting effects of povidone. The enhancing effect of povidone upon tolbutamide solubility was suggested to result from complex formation as demonstrated by TLC and IR measurements (860).

Stirring frequency had a greater effect upon the dissolution rate than did stirrer positioning in a study of factors affecting dissolution rates of benzoic acid from flat-faced disks (861). A system employing continuous extractions of drugs from the aqueous medium in a closed system was employed to determine the dissolution rate of slightly soluble drugs (862). The Sartorius solubility simulator was superior to the rotating-basket method and the disintegration apparatus method for determining dissolution rates of drugs from solid dosage forms (863).

An adaptation of the Langenbucher continuous-flow apparatus was used to determine dissolution rates of prednisolone tablets (864). The beaker and column methods for determining drug dissolution gave more reproducible results than the rotating-basket method in dissolution testing of acetaminophen (865). An automated dissolution test apparatus was proposed and evaluated with diazepam, methyldopa, phenylbutazone, and oxytetracycline tablets (866). A highly versatile, reliable, automated *in vitro* dissolution test apparatus for pharmaceutical solids, using a rotating filter–stationary basket was described (867). Tablet dissolution rates were determined with a relative standard deviation of 1.09 *versus* 16.6% with an automated USP–NF method.

A multichannel, continuous-flow apparatus for dissolution rate measurements was described (868). Typical data were presented to demonstrate its utility for drug powders as well as tablets and capsules. Column flow-through methods for tablet dissolution rate determinations were reviewed, and their superiority to beaker methods was suggested (869).

As in previous years, the assessment of digoxin dissolution from tablet dosage forms received attention. Single-tablet dissolution studies were performed with digoxin using the USP rotating-basket assembly (870, 871). Dissolution profiles for 11 samples of digoxin tablets revealed variations between samples from different manufacturers, different batches from a single manufacturer, and single tablets from a single batch. Samples from 105 production batches of digoxin tablets, produced in the United Kingdom, had 12-hr dissolution ranges of 43–100% of labeled strength (872). In another study, dissolution rates correlated closely with plasma levels found in the first 7 hr after an oral dose (873). It was suggested that the differences in dissolution rates between different brands is an important determinant of biological availability and that the measurement of the digoxin dissolution rate after 1 hr is a useful guide for assessing bioavailability.

Dissolution studies of enteric-coated tablets and granules of aspirin were performed using the USP rotating-flask method and the beaker method (874). Good correlation was shown between *in vivo* absorption with dissolution rates obtained with the rotating-flask procedure. Another study showed that for aspirin only the rotating-flask method at 50 rpm gave statistically correlatable results with *in vivo* data when 10-min dissolution rates were compared to 1-hr urinary excretion values (875). Several brands of enteric-coated sodium salicylate tablets were evaluated for *in vitro* dissolution characteristics and plasma levels (876). Although most tablets provided full availability, absorption rates were highly variable.

Table XXI—Additional References on Dissolution

Reference	Topic
886	Effect of aging on dissolution of phenylbutazone tablets
887	Eutectic mixtures of aspirin and urea
888	Size distribution effects in multiparticulate dissolution
889	Concept of dissolution efficiency
890	Transition temperature and heat of transition of barbital polymorphs
891	Transition temperatures of sulfanilamide polymorphs determined by dissolution rate measurements
892	Influence of processing and bile salts on the dissolution rate of flufenamic acid tablets
893	Review of dissolution rate of powders
894	Dissolution of aspirin–polyethylene glycol 6000 coprecipitates
895	Dissolution of acetaminophen solidified melts
896	Parameters in dissolution rate studies
897	Tablet dissolution apparatus
898	Variability in automated dissolution determinations
899	Disintegration and dissolution of tablets
900	Dissolution of propyromazine from directly compressed tablets
901	*In vitro* dissolution of digoxin from tablets
902	Dissolution testing of L-dopa (levodopa) tablets
903	Dissolution testing of glutathione tablets
904	Dissolution of caffeine and salicylamide tablets
905	Differences in USP disintegration test and *in vivo* behavior of enteric-coated tablets
906	Dissolution and stability of silicone-coated ascorbic acid tablets
907	Comparison of tablet dissolution and disintegration rates
908	Review of solubilization techniques
909	Solubilities of barbiturate polymorphs

The effect of hardness on disintegration and dissolution characteristics of uncoated caffeine tablets made at eight different pressure levels were studied (877). Tablet hardness affects dissolution from the tablets as well as from fully disintegrated granules and small particles. A continuous-flow column apparatus was used to study the dissolution rate of sulfamerazine sodium and was recommended for distinguishing between tablets of varying composition and for assessing batch-to-batch variation (878). A comparative study of the *in vitro* release of three brands of slow-release potassium chloride tablets was presented, and the data were critically examined in the light of dissolution rate equations (879). The time required for 50% dissolution of five brands of tetracycline capsules varied from 4.6 to 30.5 min under standardized conditions at pH 1.4 (880).

An apparatus utilizing liquid turbulence to simulate hydrodynamic conditions generated by GI peristalsis was designed to estimate drug release from solid oral dosage forms (881). A correlation was developed between dissolution rates and absorption patterns of two misformulated tablets. Great variation was observed in dissolution rates of 15 brands of quinidine sulfate capsules and tablets (882). The rank order of dissolution in 0.1 *N* HCl and in phosphate buffer was not the same. The release rates of quinine sulfate from time-released tablets prepared with various amounts of carbomer

934P and cellulose acetate phthalate at different compaction pressures were measured (883). Dissolution rates of commercially available chlorothiazide and hydrochlorothiazide tablets were determined (884). The time required for 100% dissolution was less than or equal to 100 min for all samples except one, which had a value of 190 min. Although differences in *in vitro* dissolution between anhydrous ampicillin and the trihydrate were recorded, *in vivo* availability of the two substances as determined from loosely filled hard gelatin capsules was the same (885).

Additional references on dissolution are listed in Table XXI.

Solubility–Solubilization Phenomena—A physical model approach was utilized to study cholesterol gallstone dissolution in simulated bile (910). Quaternary amines enhanced dissolution rates of gallstones in bile acid–lecithin solutions; in bile acid systems, cholesterol dissolution was sensitive to electrolyte concentrations (911). Sodium chloride increased cholesterol dissolution rates in sodium cholate solutions. In another study, various drug compounds excreted in bile were evaluated to determine their potential for increasing the solubility of cholesterol in bile (912). A viable *in vitro* screening method for identifying compounds that enhance biliary-holding capacity for cholesterol was proposed.

The pH–solubility profiles of tetracycline antibiotics in hydrochloric acid–sodium acetate buffer solutions were obtained at 37° (913). Chlortetracycline had a maximum solubility at pH 2.8, whereas tetracycline, demethylchlortetracycline (demeclocycline), and methacycline showed increases in solubility with decreasing pH. The solubility of oxytetracycline in double-distilled water at pH 6.5 and 20° was reported to be 195 μg/ml (914). Substituted ureas were studied for their solubilizing effect upon aminophenazone (aminopyrine), caffeine, sulfanilamide, and *N*-acetylsulfanilamide. In all cases, thiourea enhanced the solubility to a greater extent than urea did (915). Short chain aliphatic amine hydrochlorides were reported to depress the solubility of benzoic acid, aminophenazone, and caffeine in water (916). The effect decreased with increasing chain length. A study of the uptake of halothane and trichloroethylene in aqueous dispersions showed that coagulated systems appeared to absorb more vapor than did flocculated structures (917).

The aqueous solubility of steroids increased exponentially following the addition of a cosolvent (918). An equation was derived to describe the relationship between the amount of drug solubilized and the volume fraction of cosolvent incorporated. Both single and multiple cosolvent systems followed the derived relationship. Neglect of steroid absorption onto membrane or fiber filters was reported to be responsible for erroneous solubility values reported in the literature (919). This problem was uncovered in a solubility study which demonstrated the increase in solubility of estradiol in the presence of progesterone. Amino acid prodrugs of acetaminophen provided water-soluble forms of the drug (920). Although the lability of these esters precluded their use in liquid dosage forms, their use in solid products was recommended. The solubilization of water and water–amide solutions by bis(2-ethylhexyl) sodium sulfosuccinate in heptane was studied (921). A linear relationship was shown between moles of water solubilized per mole of surfactant and the surfactant concentration.

A mixed polysorbate–sorbitan surfactant system was employed to solubilize liquid paraffin (922). Incorporation of the solubilizate within the nonpolar environment created by the combined hydrophobic portions of the mixed surfactants was proposed as a possible mechanism. The influence of surfactant structure on, and distribution of salicylic acid in, micelles was reported (923); structurally related polysorbate and polyoxyl[14] surfactants were employed.

Spray-drying techniques were used to improve the solubility and dissolution rate of salicylic acid (924). Spray drying from acacia solutions resulted in as much as a 50% increase in solubility, and the dissolution rate was about 60 times faster than that of the drug alone. A study of the solubility of caffeine and aminophenazone (aminopyrine) in the presence of sodium salts of organic carboxylic acids showed that the solubility increased with increasing acid chain length (925). Determination of solubility of actinomycin D (dactinomycin) revealed that the solubility increased with a decrease in temperature (926). By a freeze-thaw technique, aqueous concentrations as high as 0.5 mg/ml were obtained at room temperature.

A study of the effect of pH, temperature, and electrolyte concentration on the solubilization of phenobarbital and barbital in nonionic surfactants showed that the degree of interaction increased as the temperature increased (927). This result was attributed to the improved solubility of the barbiturate in the micelles and not to alteration of the micellar structure. Alkyl esters of *p*-aminobenzoic acid were solubilized by lysophosphatidal choline (928). Solubilization increased in the following order: ethyl, *n*-propyl, and *n*-butyl esters. Sodium escinate dissolved more rapidly in artificial gastric juice than did amorphous escin (929). A literature review of the effect of compounds in enhancing riboflavin solubility in water and the mechanism of solubilization was provided (930).

Membrane Permeation and Release—Relative permeation constants for phenobarbital, salicylic acid, and nitrazepam through hexadecane–collodion membranes were determined (931). An equation independent of membrane area and volume of compartments was developed to describe drug permeation through artificial lipid membranes. Zero-order release kinetics were obtained when a film without drugs was laminated to the releasing side of a film containing dispersed drug (932). In this manner, the drug layer served as a reservoir to control the duration of drug release while the nondrug layer determined the rate of permeation. Hydroxypropyl cellulose was employed as the reservoir layer, and mixtures of hydroxypropyl cellulose and polyvinyl acetate were used as the inert layer. Inverse relationships between the release rate and membrane thickness and between the logarithm of the rate and the percentage of polyvinyl acetate in the membrane layer were observed.

[14] Myrj, ICI United States.

Dissolution rate studies of quinine sulfate from polyamide matrixes in simulated gastric and intestinal juice in the presence of surfactants revealed that the dissolution rate was dependent upon dissolution medium pH and the type and concentration of the surfactant employed (933). Pinhole-free silicone membranes were produced by removal of silica filler aggregates prior to casting of the dispersion (934, 935). A procedure for the preparation of fabric-reinforced membranes was also developed. Postcuring membranes with UV irradiation increased tensile strength by 30%. These defect-free membranes were more biocompatible than commercially available membranes.

Membranes consisting of the polyvinyl alcohol and oxystarch were described (936, 937). A cross-linking structure within the membranes was suggested, and the relationship between permeability and preparation conditions was studied. Lecithin–collodion membranes were employed to determine the permeability of various drugs (938, 939). A correlation was exhibited between membrane permeation and absorption from the GI tract. However, a direct relationship could not be established between membrane permeation and partition coefficients in octanol–water. The membrane permeability for lipid-soluble substances was temperature dependent and decreased when membranes were washed before use or were stored for long periods. The effect of lecithin–collodion ratios upon membrane properties was explored.

The permeability of drugs from ethylcellulose films containing up to 50% polyethylene glycol 4000 was determined (940). For salicylic acid and caffeine, steady-state constants were independent of film thickness and solute concentration but increased linearly and sharply with polyethylene glycol content. Mass transfer appeared to be controlled by a solubility diffusion process in the ethylcellulose of the membrane. Enhancement of permeability by polyethylene glycol appeared to be due to increased membrane porosity. Balancing of membrane porosity and thickness could be employed to control drug release. A review discussed ophthalmic applications of membrane-controlled drug delivery systems (941).

Low concentrations of dioctyl sodium sulfosuccinate increased the rate of pentobarbital absorption from the rat small intestine (942). Higher concentrations decreased drug penetration due to micellar effects.

A general equation was proposed to predict the diffusion coefficient of a drug in a polymeric gel from the molecular weight, the diffusion coefficient of the compound in solvent, and the polymer concentration of the gel (943). A logarithmic dependence of the diffusion coefficient on polymer concentration and solute molecular weight was observed in a study of the release of hormonal implants in hamsters. Membranes prepared by casting thin films of polyalkylsulfones onto porous polypropylene provided greater oxygen and carbon dioxide permeation than did silicone membranes (944). The potential application of these films for drug implants was suggested.

A homologous series of quaternary esters of benzilic acid was employed to study the partition behavior in a three-phase water–1-octanol–water system. The rate-determining step for interphase transport of hydrophilic compounds was diffusion through the organic layer (945). The rate constants for transfer from the aqueous to the organic phase increased linearly with the corresponding partition coefficient. As the chain length increased, diffusion through the aqueous diffusion layer became rate determining; thus, rate constants were independent of partition coefficients. The relationship of these studies to biological considerations was discussed.

An *in vitro* test apparatus was developed to measure release of ionic drugs from ointment bases (946), and the release of sodium salicylate from a petrolatum ointment base was studied using this apparatus. The permeation constants for a group of structurally related homologous heterocyclic compounds through lecithin membranes were directly related to their decanol–water partition coefficients (947). The effect of serum and membrane binding and intrinsic membrane permeability upon the uptake and release kinetics of drugs in living systems was studied using three cardiac glycosides in the Burkitt lymphoma cell system (948). The data conformed to a physical model of rapid solute equilibration within the cell after permeation through the rate-determining plasma membrane barrier. Transport of digitoxin was influenced by membrane and serum binding, while transport of digoxin was influenced by membrane binding only.

Increased rates of permeation of sulfaguanidine through the intestinal lumen of rats occurred when the drug was coadministered with chelating agents and surfactants (949). Except for poloxamer 188[15], all additives produced histological changes. It was suggested that changes in the rate of permeation with time be used as an indicator for the damaging effect of drugs on the intestinal mucosa.

A two-compartment diffusion cell employing a semipermeable cellophane membrane was used to determine diffusion rates of tetracycline at various pH values in the presence of metal ions (950). Tetracycline chelate formation was pH dependent. Chelation reduced diffusion even where water-soluble chelates were formed. Anomalies in the phase transfer of phenylbutazone were attributed to unusually slow protonation and deprotonation reactions (951). General physical models were derived for the diffusional transport of drugs across membranes of mammalian cells (952). The models were developed to represent different sets of possible physical processes that take place during drug transport. In these models, the assumption was made that the cell membrane is an integral part of the total barrier. This model was used to explain the kinetics of uptake and release of desmosterol, cholesterol, and β-sitosterol by Burkitt lymphoma cells (953). Effects of permeability and partition coefficients of the sterols were inversely proportional to the serum concentration in the external medium due to sterol–serum binding. The results were consistent with the mechanism in which only unbound solute participates in the membrane transport process.

The absorption of benorilate across the everted rat

[15] Pluronic F-68, Wyandotte.

intestine showed that the physicochemical form in which the drug was present was the primary factor in determining the rate of passage (954). The entry of intact drug into mucosal cells appeared to be the rate-determining step in the absorption process. Drug hydrolysis occurred during passage through the intestinal wall. An *in vitro* apparatus was employed to evaluate factors affecting the membrane permeation of dihydroergotoxin methanesulfonate, and the absorption rate from the small intestine was predicted (955). Carbomer 934P[16] was shown to delay membrane transport.

Incorporation of water, dimethyl sulfoxide, and alcohol at 1–5% concentrations accelerated the rate of release of atropine sulfate from various ointment bases as determined by an *in vitro* study (956). The diffusion of drug was zero order during the initial phase of the release. Procedures were developed for studying the release of fluocinonide and flucloronide from oleaginous ointment bases containing various adjuvants (957). Data obtained from model systems enabled rates from modified ointment bases to be predicted. The simple model did not provide correlation for ointments containing emulsifying agents.

The effects of interaction between drug and skin, drug and vehicle, and vehicle and skin on the penetration rate of a drug through the skin were evaluated by comparing penetration rates through excised skin and polyethylene (958). Dimethyl sulfoxide, dimethylformamide, ethanol, and water increased permeability of the skin, but they reduced penetration through the polyethylene membrane. Release rates of 8-hydroxyquinoline sulfate from hydrophilic and hydrophobic vehicles were determined (959). Release from aqueous vehicles was faster than from lipophilic preparations. Ointments containing zinc oxide prevented drug release.

Solubilization of chloramphenicol with dimethylacetamide resulted in markedly accelerated release rates of the drug from petrolatum vehicles (960). A study of the release of prednisolone from an oil-in-water emulsion showed that increasing the drug concentration by a factor of 4 resulted in an increased liberation rate of only 1.6 from the base (961). These results were supported by clinical findings. Release of hydrocortisone from a propylene glycol–alcohol–water gel did not agree with theory based upon Poulsen's hypothesis (962), but release of cortisone from similar gel systems conformed to this theory.

A mathematical model of the stratum corneum was proposed in which the tissue was described as a two-phase protein–lipid heterogeneous membrane with the lipid phase being continuous (963). In this model, the permeability of the membrane was correlated with the water solubility of the penetrants and with their lipid–protein partition coefficient. Experimentally measured permeabilities of human skin to various drugs conformed to the model. In another study, mathematical models were developed to simulate percutaneous drug absorption and drug transport within an ointment (964, 965). Ointment and skin were assumed to be homogeneous phases through which drug diffuses according to Fick's law. The percutaneous absorption of sodium iodide from the hydrophilic ointment agreed with calculations based upon the developed model. The effect of the ointment vehicle upon penetration of nicotinic acid and its esters into skin was studied (966). Water appeared to be the most suitable vehicle, whereas propylene glycol and olive oil were less satisfactory. Nicotinic acid penetrated skin more slowly than did the esters from all vehicles studied.

An apparatus consisting of a Lucite cell divided into two compartments by a clamped rabbit cornea was devised for studying formulation effects on drug transport through the cornea, and the reliability of the system was tested (967). The Resomat, an apparatus for *in vitro* absorption studies, was evaluated for correlation with *in vivo* results (968). Reproducible results were obtained when the same batch of membranes was employed, and absorption profiles for drugs gave good agreement with usual theories of drug absorption *in vivo*.

Additional references on membrane permeation and release are listed in Table XXII.

Table XXII—Additional References on Membrane Permeation and Release

Reference	Topic
969	*In vitro* transport of tetracyclines through everted rat intestine
970	*In vitro* release of vitamin A from ointment bases
971	Diffusion of ethylparaben in polyethylene glycol ointment
972	*In vitro* release of chloramphenicol from suppository bases
973	*In situ* transport of flavonoids across rat small intestines
974	Permeation of antidepressants and phenothiazines through cellulose membranes
975	Diffusion of penicillin G and ampicillin through phospholipid sols
976	Synthetic semipermeable membranes for biomedical processes
977	Review of use of membranes in pharmaceutical research
978	Biological fuel cell incorporating selective membranes
979	Mathematical analysis of membranes; solution–solubility dependency of controlled-release drugs from polymer matrixes
980	Controlled drug release from matrix systems
981	Penetration of water vapor through lipid monolayers
982	Effect of chemical modifications on transmembrane permeation in rats
983	Effect of tubular secretion inhibitor on organic anion transport
984	Release of resorcinol from ointment vehicles
985	Development of *in situ* vaginal drug absorption procedure
986	Method for studying release from ointment bases
987	Effect of experimental conditions on *in vitro* release from ointments
988	Transepidermal penetration of venoruton (troxerutin)
989	Effect of polyethylene glycol 300 on release of hydrocortisone from ointments

Complexation—Studies related to complexation phenomena are categorized into: (*a*) interactions of drugs with biological substances, and (*b*) interactions of drugs with nonbiological substances.

Interactions of Drugs with Biological Substances—An ultrafiltration procedure was employed to demon-

[16] Carbopol 934, Goodrich.

strate that, at a 20-μmole level, more than 98% of furosemide was bound to a 7.5% albumin solution (990). Studies with an isolated perfused rat kidney showed that albumin inhibited tubular clearance of the drug. Binding of thiopental to plasma proteins from healthy, cirrhotic, and uremic subjects, using equilibrium dialysis, showed that the greatest binding occurred in the healthy subjects (991). In human blood plasma, digitoxin, digoxin, and other cardiac glycosides were extensively bound to plasma proteins (992). One mole of glycoside appeared to bind per mole of albumin.

A fluorescence assay procedure was employed to study the displacement of warfarin from human serum albumin by other drugs (993). Dicumarol, phenylbutazone, rifampicin (rifampin), ethacrynic acid, tolbutamide, and salicylic acid displaced warfarin (in decreasing order). In the therapeutic range, about 35% of the serum morphine concentration was bound to human plasma, primarily to the albumin fraction, as shown by equilibrium dialysis experiments (994). The binding of furosemide to human albumin was studied by dialysis (995). Decreased binding occurred in the presence of aspirin, diazoxide, phenylbutazone, and sulfisoxazole. The interaction of phenothiazine and aminodibenzyl compounds with human serum albumin was demonstrated by spectrofluorometric quenching titration (996). Competition for binding sites and binding constants were determined.

Under *in vitro* conditions, six anticonvulsants and aspirin did not significantly displace carbamazepine from plasma protein binding sites (997). *In vivo* studies showed that only about 27% of the drug was unbound in serum. The stoichiometry and strength of binding of pamaquine to bovine serum albumin were monitored by a fluorometric technique (998). The results indicated that three singly protonated pamaquine molecules were bound per mole of albumin. Binding constants were calculated using the Bjerrum procedure.

The relationships among protein binding, distribution, and kinetics of elimination of warfarin were studied (999). The results showed excellent correlation between the fraction of free drug in rat plasma and the plasma clearance of the drug. Large intersubject variation in fraction bound was not related to variations in serum albumin or total protein concentration. These differences may reflect individual configuration differences of proteins or the presence of an endogenous displacing agent at different concentrations. Benzalkonium chloride reduced sulfaethidole binding to bovine serum albumin (1000). The concentration of ethambutol in human cerebrospinal fluid was a function of the nonprotein-bound drug fraction in serum (1001). Serum protein binding varied from 8.3 to 39.3%, depending upon serum level.

The elimination rate of bilirubin was reported to be proportional to the concentration of free bilirubin in plasma (1002). Protein binding decreased the excretion rate. The importance of using specific analytical procedures for a drug in the presence of its degradation products or metabolites was demonstrated during protein binding studies with warfarin, since anomalous results were obtained when nondiscriminatory procedures were employed (1003).

Table XXIII—Additional References on Interactions of Drugs with Biological Substances

Reference	Topic
1013	Serum binding of digoxin
1014	Model for modified drug absorption; effect of surfactant on chloramphenicol binding to an albumin–lecithin complex
1015	Effect of divalent cations on adsorption of prothrombin complex
1016	Stereospecific binding of D-lysergic acid diethylamide (lysergide) to brain membranes
1017	Binding site interaction of chlorthalidone and acetazolamide to red blood cells
1018	Binding of chlorpromazine and imipramine to blood components
1019	Binding site interaction of chlorthalidone and acetazolamide
1020	New fluorescence probes for drug–protein binding studies
1021	*In vitro* binding of bromophenol blue and amaranth to liver cytoplasmic binding proteins
1022	Decreased plasma protein binding to diazoxide in uremia
1023	Morphine and phenytoin binding to plasma proteins in renal and hepatic failure

The use of kanamycin to inhibit bacterial growth during plasma binding studies was recommended, since this agent did not appear to bind nor to interfere with the binding of other compounds under investigation (1004).

Quinidine was shown to bind at two sites on serum albumin (1005). Computations showed that 74–88% of the administered drug would be bound to albumin and that 71–74% of this fraction would be bound by the high affinity sites on the protein. Quantitative relationships between therapeutic levels of quinidine and its distribution in plasma were discussed.

Gelatin–acacia coacervate systems were employed as models for protein binding studies of drugs (1006). The protein binding characteristics of chloramphenicol and several other antimicrobial agents were described using this procedure. The fraction of methaqualone bound to human serum was determined, by equilibrium dialysis, to be 80% in the therapeutic range (1007). The drug concentration in cerebrospinal fluid correlated well with unbound drug levels in serum. The extent of plasma binding of 13 disopyramide derivatives was reported (1008). Structural variations influenced binding characteristics, with a linear correlation being exhibited between binding and drug lipophilicity.

Metronidazole and four derivatives were studied *in vitro* to determine the effect of structural differences upon binding to plasma proteins (1009). A linear correlation was found between the protein binding parameter and the frontier electron density on the hetero atom at the 3′-position on the alkyl side chain, as shown by NMR techniques. The administration of phenylbutazone together with warfarin to dogs produced an elevation of the free fraction of warfarin in plasma, with a resultant twofold decrease in the plasma half-life of the drug (1010). The antimicrobial activity of sulfadimethoxine in rabbit plasma was significantly increased by concomitant injection of phenylbutazone (1011). The binding of papaverine to plasma components of several animals was investigated to show that binding occurred in all species to an extent greater than 90% at physio-

logically active levels (1012).

Additional references on the interactions of drugs with biological substances are listed in Table XXIII.

Interactions of Drugs with Nonbiological Substances—A permeation rate technique was employed to study the interaction of methylparaben with polyvinylpyrrolidone (povidone) and polysorbate 80 (1024). The results obtained were in agreement with data reported by other techniques, and it was concluded that dynamic dialysis could be used to quantitate drug binding by macromolecules. The self-association of antihistaminic drugs was investigated by light scattering (1025). A CMC could not be detected. For a number of the compounds, the data were consistent with the model involving aggregate growth by the stepwise addition of monomers.

A study of the interactions of α-cyclodextrin and β-cyclodextrin with nonsteroidal anti-inflammatory drugs showed that β-cyclodextrin accelerated the degradation of azapropazone (apazone) but retarded the decomposition of phenylbutazone (1026). Addition of urea to the solution promoted inclusion of the drug within the β-cyclodextrin, while sodium chloride gave the opposite effect. A 1:1 stoichiometric ratio was found to exist for the complexes formed between β-cyclodextrin and fenamates, *trans*-cinnamic acid, or phenothiazines (1027–1029). Complex formation was studied using circular dichroism, UV absorption, and NMR spectroscopy. The binding mechanisms and the positioning of the small molecules within the β-cyclodextrin were postulated from the results. On the basis of IR spectral data, complex formation between barbiturates and polyethylene glycol 4000 was shown to occur through hydrogen bonding between the nitrogen hydrogens of the barbiturate ring and two oxygen atoms of the polyoxyethylene moiety (1030). The aqueous stability of these complexes as a function of varying barbiturate structure was discussed. A literature review described the interaction of iodine with solvents and surfactants (1031).

Differential thermal analysis was employed to determine the stoichiometry of complexes formed between aspirin and phenobarbital, chloramphenicol and methenamine, and other drug systems (1032). The effect of complexation with caffeine on the *in vitro* transport of salicylates was studied using a three-phase liquid barrier model (1033). Generally, the presence of caffeine decreased salicylate transport. By using a similar system, only slight retardation of chlorpromazine transport through a lipoidal barrier was observed in the presence of various xanthines (1034). On the other hand, the rate of chlorpromazine diffusion through a dimethicone[17] membrane in the presence of complexing agents was markedly decreased.

The types and structures of inclusion compounds of pharmaceutical importance were reviewed (1035). Solubility profiles for benzocaine–caffeine, menadione–desoxycholic acid, and other systems were obtained in mixed solvents of ethanol–water and propylene glycol–water (1036); the interactions were affected by the composition of the solvents. Menadione photodegradation was inhibited in the presence of solutions of cetylethylmorpholinium ethosulfate (1037). Complexation in this system was demonstrated by shifts in the UV absorption spectrum.

Evidence was presented for the formation of a phenobarbital–ephedrine complex in the solid state, and the physical properties of the complex were elucidated (1038). Coprecipitates of tolbutamide with povidone and fusion mixtures with polyethylene glycol 6000 were evaluated for dissolution rate enhancement (1039). Complexation was shown to occur between tolbutamide and povidone, but no binding could be detected with polyethylene glycol 6000. Complexation between menadione and hydrotropic salts was evaluated by solubility analysis (1040). Spectral studies indicated that molecular interactions occurred at low concentrations, whereas the hydrotropic effect predominated at high salt concentrations.

Anionic drugs such as benzoic acid and salicylic acid were shown to bind by ion exchange to hydroxyl groups on the amphoteric surface of titanium dioxide below pH 6.5, whereas cationic drugs bound to titanium dioxide

Table XXIV—Additional References on Interactions of Drugs with Nonbiological Substances

Reference	Topic
1045	Interaction of antipyrine and caffeine with sulfacetamide
1046	Review of principles of preservative inactivation by nonionic surfactants
1047	Dissolution and physical properties of the *p*-aminobenzoic acid–caffeine complex
1048	Inhibition of hydrolysis of acronycine (acronine) esters by complexation
1049	Interaction of sodium citrate with bivalent metal ions
1050	Binding of cationic drugs by carboxymethylcellulose
1051	Interaction of methylparaben with polysorbate surfactants determined by solubility studies
1052	Metal complexes of anhydrotetracycline
1053	Influence of cosolvents and substrate substituents on sorption of benzoic acid derivatives by polyamides
1054	Acetaminophen binding by a biocompatible polymer-coated charcoal
1055	Interaction between cortisone and arginine
1056	Interaction of vinyl acetate–vinylpyrrolidone copolymer with surfactants
1057	Interaction of sodium dodecyl (lauryl) sulfate with monoalkylolamides of aliphatic acids
1058	Determination of interactions between hydrocarbons and polyoxyethylene nonylphenyl ethers by GC
1059	Interaction of polyvinyl alcohol with benzoic acid and its monohydroxy derivatives
1060	Binding of quaternary surfactants by carboxymethylcellulose
1061	Interaction of sorbic acid and emulsifiers
1062	Interaction of a cationic substituted cellulose ether (Polymer JR) with surfactants
1063	Interactions of polyethylene glycol 6000 and povidone 40,000 with succinylsulfathiazole and chlorpropamide
1064	Properties of interaction products between ethyl gallate and surfactants
1065	Review of release of pharmaceuticals from macromolecular hydrophilic complexes
1066	Review of interactions between surface-active agents and polymers
1067	Distribution and antimicrobial activity of preservatives in solubilized and emulsified systems

[17] Silastic, Dow-Corning.

at alkaline pH values (1041). On the basis of X-ray diffraction measurements, the conclusion was reached that codeine cations bind to montmorillonite clays between the silicate layers (1042). The reaction was shown to depend upon the particle size and charge distribution of the clay as well as on the pH and ion concentration of the medium.

Complexation between morphine and divalent cations was demonstrated by spectrophotofluorometric analysis (1043). The fluorescence intensity of the magnesium complex was depressed in the presence of calcium. Formation constants for the interaction of iron(II) ions with ascorbate, fumarate, and succinate ligands were determined, and the results were employed in a computer model to predict absorption from the small intestine (1044). It was predicted that optimum absorption would occur with ligands having a divalent anionic charge that formed 1:1 complexes. The model also allowed for low molecular weight polymers.

Additional references related to interactions of drugs with nonbiological substances are listed in Table XXIV.

Surface Phenomena—The publications dealing with surface phenomena are divided into five major categories: (*a*) interface studies, (*b*) adsorption studies, (*c*) general properties of surfactants, (*d*) micelle studies, and (*e*) dispersion stabilization and rheology.

Because of overlap of subject material, the reader with special interest in this field should review the entire section.

Interface Studies—A thermodynamic study of the stability of microemulsions showed that spontaneous formation occurred only when the specific surface free energy was sufficiently small (1068). Phase inversion was predicted, and information on droplet size was derived. An approximate equation based on the average environment of each droplet was used to calculate the entropy of formation.

Light-scattering and depolarization measurements were employed to construct phase diagrams of microemulsion systems (1069). Settling rates for colloidal silicone dioxide dispersed in water and heptane were measured, and the results were interpreted on the basis of an equation for hindered settling (1070). Mean particle radii independent of particle concentration were determined in the system.

The interaction between water vapor and fully hydroxylated surfaces of silicon dioxide, alumina, and aluminum silicate was studied by measuring physisorption isotherms (1071). The strength of sites for physisorption of water increased with the decreasing content of aluminum. Various denture base polymers were evaluated to determine the amount and rate of water uptake (1072). The high diffusion coefficients within certain polymers were indicative of the faster uptake of water and may be related to the amount of cross-linking, the plasticizing effect of the free monomer in those polymers, or to molecular weight. All materials studied took up most of their water during the 1st day, and hydration was essentially complete after 1 week.

A study of the influence of raw materials and manufacturing methods on the surface properties of magnesium silicates showed that the addition of sodium silicate to magnesium compounds produced a silicate having a higher absorption capacity for methylene blue; other physical measurements such as specific surface area, specific gravity, and acidity were the same (1073). The volume of coacervate produced from gelatin–acacia systems varied with the starting and final pH and with the concentrations and ratios of the coacervate materials (1074).

Table XXV—Additional References on Interface Studies

Reference	Topic
1078	Influence of methylene blue and crystal (gentian) violet on emulsifying activity of methylcellulose
1079	Interaction of antihistamines in lecithin monolayers
1080	Factors affecting fibrinogen–fibrin conversion
1081	Surface area measurements by nitrogen and argon adsorption
1082	Review of determination of specific surface area and porosity of solids
1083	Surface activity of antihistamines at air–solution interface
1084	Evaluation of methods for determining antifoam activity
1085	Apparatus for recording change in surface tension with respect to time
1086	Theoretical considerations on mononuclear aggregation of nucleosides in dilute aqueous solutions
1087	Effect of acids and bases on viscosity of salicylic acid–cetrimide system

The wettability of hydroxyethyl methacrylate used for contact lens material was evaluated by sessile drop and captive air bubble techniques (1075). The water content of the gels did not appear to affect wettability in the hydration range investigated. Differences among the gels were most likely due to alterations of surface structure and variations in the methods of preparation. Viscosity, vapor pressure, and electron microscopy techniques were employed to study the molecular characteristics of povidone in solution (1076). It was determined that, with increasing concentration, molecules aggregate to form spheres of increasing size. A study of factors affecting wettability of human skin showed that approaches used to characterize contact angles of low energy solids are of limited value when applied to skin studies (1077).

Additional references on interface studies are listed in Table XXV.

Adsorption Studies—*In vitro* studies showed that uncoated carbon and carbon coated with an acrylic hydrogel were capable of adsorbing drugs from horse serum (1088). Although the polymer coating presented a barrier to the rate of adsorption, it did not affect total capacity. It was suggested that coating with a biocompatible polymer would enable carbon to be used during hemoperfusion in the treatment of drug overdoses. Distribution equilibration was reported to explain the sorption of sulfonamides by neutral, acidic, basic, and quaternary polymethacrylic acid derivatives (1089). Binding occurred primarily by hydrophobic reaction and hydrogen bridging, although ion exchange with the polyions also took place. Because of polymer swelling with increasing pH, maximum binding occurred in the pH region of the isoelectric point of the sulfonamides.

Table XXVI—Additional References on Adsorption Studies

Reference	Topic
1099	Adsorption layer structure during adsorption of nonionic surfactants onto charcoal
1100	Regulating drug binding onto colloidal silica by nonionic surfactants
1101	Adsorption kinetics and interior structure of activated carbon
1102	Adsorption of alkylarylpyridinium chloride by montmorillonite
1103, 1104	Adsorption of sulfanilamides by ion-exchange polymers
1105	Sorption of colored impurities in kanamycin by a cation-exchange resin
1106	Effect of surfactant adsorption on interfacial electrical properties and stability of clay dispersions

The viscosity, sedimentation, and adsorption properties of four aluminum hydroxides employed in the production of bacterial and viral preparations were evaluated (1090). Addition of sucrose prevented loss of stability and sorption properties resulting from freezing and thawing. Sonication produced gels with rapid settling characteristics. Adsorption of orthophosphate onto hydrous aluminum oxide was shown to follow a Langmuir isotherm (1091). Although the sorption capacity was similar to other aluminum oxides, the binding constant was much greater. Urethane-cured crosslinked polybutadiene polymers and polyethylene oxide polymers separately showed little tendency to adsorb bile lipids from micellar solutions (1092). However, polymers containing both types of chains homogeneously distributed were capable of adsorbing large amounts. It was suggested that mixed polymers could be used for regulating cholesterol uptake after oral administration. The kinetics of epinephrine adsorption from aqueous suspensions by fibrous polymeric materials were studied (1093). Complete extraction of the drug into the polymer was achieved by shaking for 15–20 min.

X-Ray diffraction and radioisotope desorption methods provided evidence for the adsorption of povidone onto the surface of montmorillonite (1094). Adsorption of the povidone to the tetrahedral sheets of the polymer was implicated. The adsorption of chlorpheniramine maleate onto kaolin followed a Langmuir isotherm (1095). Lack of discontinuity indicated that only monolayer binding occurred. The adsorption of chlorophyll from benzene solution onto colloidal silicon dioxide followed a stepwise isotherm (1096). This finding suggested the formation of molecular aggregates with increasing concentrations of the pigment in the adsorption layer. Codeine adsorbed onto bentonite or hectorite[18] was shown to be desorbed under physiological conditions of the GI tract (1097). Addition of mucin to the gastric juice increased the desorption. It was suggested that clays could be used in the preparation of oral pharmaceutical products containing cationic drugs. The adsorption of morphine by kaolin was found to obey a Langmuir isotherm (1098). Although washing did not remove the drug from the kaolin, decreased binding was observed in alkaline solutions.

Additional references on adsorption studies are found in Table XXVI.

General Properties of Surfactants—A study was made of the effect of additives on the cloud point of nonionic surfactants (1107). Additives that salted-out polyoxyethylene chains caused decreased stability of oil-in-water emulsions. Additives that salted-in nonionic surfactants increased the effective hydrophilic–lipophilic balance (HLB) of the system.

Nonionic and ionic surfactants had an appreciable effect on the transfer rate of drugs between cyclohexane and water (1108). Increasing concentrations of poloxamer 188[15] increased the rate of phenylbutazone transfer from water to solvent, whereas a decrease in the rate of transfer of alprenolol hydrochloride occurred in the same system.

Changes in the surface tension–concentration curves of cetomacrogol during autoxidation were observed (1109). Decreases in CMC values and cloud points were found. Autoxidation was shown to occur by degradation of the polyoxyethylene chains, with a resultant decrease in CMC values and cloud points. The significance of the findings in relation to the detection of decomposition in synthesized and commercial surfactants was discussed. Mixture of nonionic sucrose-based surfactants and quaternary surfactants produced mixtures having lower CMC values than were found in solutions of the individual surfactants (1110). Multichain nonionic surfactants derived from pentaerythritol were studied for the dependence upon structure of interfacial lowering, foaming, suspending, emulsifying, and detergency properties (1111). An optimum structure for each property was proposed.

Literature reviews were published discussing the use of surfactants in detergent formulations (1112), uses of quaternary ammonium compounds (1113), the synthesis and properties of surfactants (1114), the properties of surfactants in nonaqueous systems (1115), the colloidal behavior of surface-active agents (1116), manufacturing processes and properties of nonionic surfactants (1117), the use of sequestrants in detergent products (1118), and the physical properties of surfactants (1119–1121).

The hydrophobic groups in sodium dodecyl (lauryl) sulfate, ethoxylated dodecanol, and sulfate esters of ethoxylated dodecanol had the controlling effect upon surface activity and micelle formation (1122). The absorption of solids by the surfactants described was examined. Partial phosphorylation of pentaerythritol esters of fatty acids was reported to improve their surfactant properties (1123). The phosphates were found to be good dispersants for inorganic pigments.

The classification of surfactants and applications of the HLB concept were reviewed (1124–1127). HLB values were determined from conductivity measurements of surfactant-stabilized emulsion systems, and an equation was presented for predicting HLB values of a homologous series (1128). A linear relationship existed between the HLB value and the hydrophilic–oleophilic ratio (HOR) for a series of surfactants in water–benzene and water–heptane systems (1129). The

[18] Laporite, Laporte.

Table XXVII—Additional References on General Properties of Surfactants

Reference	Topic
1131	Determination of HLB of fatty alcohol polyoxyethylene ethers by GC
1132	Surface adsorption of *N*-dodecyl-β-alanine in aqueous solution
1133	Colloidal properties of nonionic surfactants in aqueous solution
1134	Interaction of monosubstituted phenols with a cationic surfactant
1135	Review of interactions between surfactants and polymers
1136	Colloidal properties of nonionic and phosphate ester surfactants
1137	Relationship of surfactant structure to efficiency in surface tension reduction
1138	Dependence of properties of mixed block ethylene and propylene oxide copolymers on composition and structure
1139	Determination of hydrophilic and hydrophobic ratios for polysorbate surfactants by proton magnetic resonance and mass spectrometry

minimum HOR values occurred at phase inversion from oil-in-water to water-in-oil emulsions. A thermodynamic definition was provided for the HLB ratio as a function of the chemical potential of a surfactant in the oil and water phases, respectively (1130).

Additional references on the general properties of surfactants are provided in Table XXVII.

Micelle Studies—Ionic equilibria in micellar solutions were discussed on the basis of micelle–monomer equilibrium, mass conservation, and electroneutrality (1140). A decreasing concentration of monomeric form was found to occur as the micellar concentration increased. The structure of lecithin micelles was shown to depend upon the length of apolar portions (1141). Micelle size increased with an increasing concentration of lecithin. CMC's for two-component and multicomponent mixtures of anionic surfactants were determined, and an equation was developed to explain the variation of the CMC with composition on the basis of micellar surface charge and an electrostatic contribution (1142).

The CMC's for the mixed micelles of an alkyl sulfate surfactant and an anionic surfactant were determined and found to be in agreement with theory (1143). Dialysis rates of benzoic acid and its derivatives in aqueous solutions of polysorbate 80 decreased as the surfactant concentration increased (1144). Experimental and theoretical dialysis rates were in good agreement. The dialysis rate constants were inversely related to the lipophilicity of the benzoic acid derivative.

The solubilization ratio of dyes to micelles and their flow dichroism were investigated to determine the mechanism of solubilization (1145). At saturation, one molecule of dye was solubilized per mole of surfactant. At surfactant concentrations above 10%, surfactant molecules were nonspherical and solubilized dyes were oriented within the micelle. The CMC's of surfactants increased with the addition of methyl alcohol to aqueous solutions (1146, 1147). However, when propyl, butyl, or pentyl alcohol was added, a decrease in the CMC occurred. The increasing effect was attributed to a

Table XXVIII—Additional References on Micelle Studies

Reference	Topic
1151	Review of electrokinetic phenomena and micellar structure
1152	Changes in UV absorption spectrum of 1-methylnaphthalene solubilized in micelles
1153	Entropy changes in micelle formation and solubilization
1154	Determination of aggregation numbers and solubilizate diffusion in cationic micelles
1155	Determination of CMC of potassium palmitate by electron spin-resonance spectroscopy
1156	Effect of temperature on CMC of sodium sulfoalkyl esters of aliphatic alcohols
1157	Determination of CMC values of polyoxyethylene glycerol fatty acid ester surfactants
1158	Multiple equilibrium model for micelle formation of ionic surfactants in nonaqueous solvents
1159	Effect of pressure on micelle formation in surfactant aqueous urea solutions
1160	Effect of urea on micelle formation of sodium sulfoalkyl esters of aliphatic alcohols
1161	Effects of inorganic salts and urea on micellar structure of a nonionic surfactant
1162	CMC of multicomponent mixtures of metal alkyl sulfates in solution
1163	Kinetic models for micelle formation
1164	Mechanism of micelle formation in sodium dodecyl (lauryl) sulfate solutions
1165	CMC of sucrose monostearate
1166	Dissociation of fatty acids in micellar systems

weakening of hydrophobic bonds, whereas the decreasing effect was explained by a reduction in the free energy of mixing due to solubilization of the alcohol within the micelle.

Nitrates of cations that form stable solid complexes with model ethers such as dioxane raised the cloud point of nonionic polyoxyethylated surfactants (1148). This increase occurred through salting-in of the surfactants through complexation with the ether oxygens. Nitrates of sodium, potassium, ammonium, and cesium, which do not form complexes with ether oxygens, had the opposite effect. The data demonstrated the need for revising current theories of the effect of salts on the solubility of nonelectrolytes in water, since current theories do not consider the interaction between electrolytes and nonelectrolytes, even though many nonelectrolytes compete with water as ligands for the cations.

Formation of micelles in aqueous solutions by antihistamines (1149) and 2-butyl-3-benzofuranyl-4-[2-(diethylamino)ethoxy]-3,5-diiodophenyl ketone hydrochloride was shown to occur (1150).

Additional references on micelle studies are given in Table XXVIII.

Dispersion Stabilization and Rheology—Addition of an anionic colloidal polyelectrolyte to an antacid suspension resulted in a change in the ζ-potential from positive to negative (1167). Maximum fluidization was confirmed by correlating viscosity measurements with the ζ-potential. Highly concentrated antacid suspensions could be formulated through the use of the procedures described. The physical stability of suspensions and emulsions were reviewed, and the origin and location of charges were related to particulate interaction and electrophoretic mobility (1168). The effect of aging

Table XXIX—Additional References on Dispersion Stabilization and Rheology

Reference	Topic
1178	Effect of size of silica particles on stability of suspensions containing polyethylene oxide
1179	Rheological behavior and effect of aging on soluble salts of cellulose acetate phthalate
1180	Influence of dextran on rheological properties of blood
1181	Relationship of viscosity of celnovocaine solutions to the solution pH
1182	Colloid and surface properties of clay suspensions
1183	Comparison of properties of two grades of tragacanth
1184	Flow properties of gums useful to food industry

at 4° on the viscoelastic properties of acid- and alkaline-processed gelatin gels was investigated (1169). Although a decrease in gel structure due to amide hydrolysis with aging was apparent, viscoelastic properties were not affected. The increased rigidity of alkaline gels was discussed in terms of differences in molecular weight, polydispersity, charge, and charge distribution.

Five petrolatums used in ointment vehicles were tested for rheological properties (1170). Differences in rheological properties were related to the content of cycloparaffins and lower hydrocarbons but not to the isoparaffin fraction. Mechanical treatment decreased the consistency of the petrolatums and petrolatum-containing ointments. The rheological properties of gelatin–glycerin bases were reported to vary with the concentration of components and temperature (1171). The absorption rate of aspirin from rectal suppositories prepared with these bases paralleled the elastic modules. The gelation of 8–30% solutions of gelatin was studied at 24–40° (1172). Transition from a Newtonian liquid to a gel system was detected by a method of deformation at constant shear rate.

Blending of acid and alkaline gelatins was shown to affect rheological properties (1173). Blending reduced rigidity of weak gels, but an increase occurred with stronger gels and more concentrated solutions. The results were explained on the basis of existing charges and intermolecular forces.

Good agreement resulted when apparent viscosity values for pseudoplastic fluids were obtained at the same shear rate on various types of viscometers (1174). Simplified treatment of data from concentric viscometers introduced a systematic error in comparisons with results from cone-plate systems. The magnitude of error increased with increasing ratio between radii of the outer and inner cylinders and with increasing structural viscosity of the solution. The viscosities of carrageenan solutions were compared to those of other commonly employed suspending agents (1175). Carrageenan solutions exhibited significant thixotropy, and an irreversible increase in apparent viscosity occurred at elevated temperature. A calcium carbonate suspension prepared with 0.5% carrageenan showed no sedimentation after 30 days at room temperature.

A concentric core and sphere compression rheometer was designed, and measurements of the rheological characteristics of methylcellulose and carboxymethylcellulose gel systems at low shear rates were obtained with this apparatus (1176). The rheological properties of colloidal silicon dioxide in liquid systems were examined as a function of concentration and the physical and chemical nature of the medium (1177). The colloidal silica exerted greater influence on the viscosity in apolar systems than in semipolar or polar ones. This result was attributed to the possible involvement of secondary valencies in diminishing the interstructure binding forces in the latter systems.

Additional references related to dispersion stabilization and rheology are listed in Table XXIX.

PHARMACEUTICAL ASPECTS

Antibiotics—The apparent rate of degradation of penicillin G in the micellar form existing at a concentration of 500,000 units/ml was compared to that of nonmicellar penicillin G at 8000 units/ml in the 5.0–9.5 pH range (1185). In the micellar solutions, the rate of hydrogen-catalyzed degradation was increased twofold but that of water- and hydroxyl-ion-catalyzed hydrolysis was decreased two- to threefold. Consequently, the pH–rate profile of the micellar solutions was shifted to higher pH values, and the pH of minimum degradation was 7.0 compared to 6.5 for the nonmicellar solutions at the same ionic strength. Compared at their respective pH–rate profile minima, micellar penicillin G was 2.5 times as stable as the nonmicellar solution.

The partition mechanism of tetracycline in an octanol–water system was studied by measuring the change in spectral properties of tetracycline in organic solvents (1186). Only the neutral form partitioned into the organic phase, and the amount transferred out of the aqueous solution was considered to be related to the concentration of the neutral species present. The relationship between partition coefficient and microscopic ionization constants of tetracycline was also clarified. Some carboxyl-containing ethylene copolymers were prepared and exhibited long-term antibacterial and antifungal properties (1187). These compounds contained antimicrobial agents bound to the copolymer backbone as carboxylate salts and were tested for self-sanitizing properties. Tests demonstrated that these materials, although not bactericidal, inhibited microbial growth.

The crystalline properties of epicillin and ampicillin and their hydrates were compared (1188). Amphotericin B was dissolved according to the manufacturer's directions to form colloidal solutions, which were filtered through membranes of different porosity (1189). Numerous particulates were observed in the unfiltered reconstituted commercial solution. Kinetic studies were carried out on the hydrolysis and photochemical degradation of the cytotoxic agent coralyne (1190). The photochemical reaction was reduced by protecting the drug from visible light or by increasing the concentration in solution, and it was reversed by lyophilization, heating, or increasing solution pH to above 12. Other factors affecting the degradation were explored, and the mechanisms involved were discussed. A salt formed from propionyl erythromycin and sulfamethoxypy-

ridazine showed more rapid dissolution and greater bioavailability than an admixture of the two components (1191). The use of the salt in pharmaceutical preparations was recommended.

Radiopharmaceuticals—Bleomycin was radiolabeled by iodine monochloride, chloramine-T, and lactoperoxidase methods (1192). The iodine monochloride technique was preferred and produced 80% radionuclide. Hydrolytic deiodination occurred at a rate of only 1.2%/day. Inulin modified by *o*-hydroxybenzaldehyde (salicylaldehyde) and *o*-hydroxybenzoic (salicylic) acid demonstrated increased ability to bind iodine-131 and demonstrated high hydrolytic stability (1193). Gel filtration demonstrated no differences between inulin and the labeled material. The quality control of radiopharmaceuticals was discussed, and the possibilities of new tests using isotopic materials for determination of sterility and endotoxin detection were presented (1194). Reviews were published concerning the quality control of radiopharmaceuticals (1195), the status and future of radiopharmaceuticals (1196 and 1197), the production of radioisotopes for medical use (1198), the detection of radioisotopes in living bodies (1199), and the biological properties of radiopharmaceuticals (1200 and 1201).

BIOPHARMACEUTICS

Publications on biopharmaceutics are subdivided according to areas of special interest. However, in view of the overlap in subject matter, anyone interested in this subject should consider a thorough reading of the entire section.

Bioavailability of Drug Substances—Complete uptake of radioactivity from the upper part of the GI tract occurred after oral administration of tritiated digitoxin (1202). A small fraction of the absorbed material was shown to represent hydrolysis products of the drug. In another study, only two-thirds of orally administered tritiated methyldigoxin (medigoxin) was absorbed from the upper GI tract (1203). Saliva was reported to offer a convenient means for monitoring the digoxin levels in blood serum (1204). The mean saliva–serum concentration ratio in 34 patients was 1.14.

The bioavailability of alprenolol was demonstrated to be dose dependent, apparently due to a limited capacity for biotransformation before entering the general circulation (1205). The half-life after a single dose was the same as that following four doses given in a single day. Labeled butylscopolamine was measured in bile and urine following oral administration (1206). Negligible absorption was found, leading to the hypothesis that the drug acts by a local effect in the GI tract. In contradiction, a review presented information that butylscopolamine was absorbed to a considerable degree (1207). The bioavailability of nortriptyline was predicted from the use of an equation estimating first-pass metabolism from the dose, hepatic blood flow, and total area under the plasma level–time curve (1208). The predicted values for bioavailability ranged from 45 to 75%, consistent with experimentally derived estimates.

Excellent agreement was obtained between the 24- and 96-hr urinary excretion data for griseofulvin products after oral administration of a single 500-mg dose (1209). It was proposed that 24-hr cumulative total 6-desmethylgriseofulvin excretion data be used an an index of griseofulvin bioavailability in humans.

A series of monographs was published describing the bioavailability of ampicillin (1210), nitrofurantoin (1211), phenytoin (1212), prednisone (1213), tetracycline (1214), oxytetracycline (1215), digoxin (1216), and indomethacin (1217).

Methodology—Two equations were developed for employing urinary excretion data to estimate drug bioavailability (1218). The equations were examined using simulated data for both one- and two-compartment open models and were tested with literature data with excellent results. A procedure to permit bioavailability estimations at quasi- and nonsteady states was proposed (1219). Necessary requirements for its application are that drug disposition obeys linear kinetics and that succeeding doses are administered during the log-linear phase, free from the influence of continuing absorption. A demonstration was provided that the use of a two-term Taylor expansion to simplify calculations of drug absorption rates in multicompartmental systems may lead to serious errors which can be avoided if the Taylor expansion is not employed (1220).

Methodology for calculating fast and slow release drug components in sustained-release dosage forms was described (1221 and 1222). If the pharmacokinetics of the sustained dosage form and the immediate release preparation are known, two equations, one describing the duration and the other the height of the plasma concentration–time curve, were proposed. Assessment of the *in vivo* quality of a sustained-release product during the initial stages of development through the application of this procedure was proposed. Administration of immediately released drug in divided doses over time along with the comparison of matching blood level curves obtained with a sustained-release formulation was presented as a method to demonstrate the achievement of controlled drug release (1223).

The use of incomplete block designs in determining comparative bioavailability was suggested where administration of all formulations to each subject would be impractical (1224). Statistical evaluation of data so obtained was illustrated by an actual trial comparing four formulations of lithium carbonate. Equations were developed to permit the estimation of biological availability after oral drug administration for drugs eliminated by urinary excretion and hepatic metabolism (1225), and the first-pass effect through the liver was estimated by this procedure.

Three *in situ* animal models were studied to determine the effect of intestinal pH upon bioavailability (1226). Data from the rat and dog correlated well with results in humans, but results from the rabbit did not. It was suggested that the rabbit would be a poor candidate for attempted animal–human bioavailability correlations. A dialysis apparatus was designed to measure the *in vitro* availability of drug from oral liquid preparations (1227). This methodology was employed to compare availability of phenethicillin from three commercially available oral pediatric preparations. An improved column-type dissolution apparatus was de-

scribed (1228). Procedures were incorporated to eliminate blockage of the filtration system by insoluble fragments. Results with uncoated and coated tablets were analyzed to discuss problems with column-type dissolution systems.

A correlation was shown to exist between saliva and plasma levels for quinidine (1229) and amobarbital (1230). Possible effects of pH and protein binding upon results were discussed.

A review discussing methodology and factors affecting percutaneous absorption was presented (1231). The validity of using *in vitro* human skin preparations to predict *in vivo* absorption was demonstrated with 12 organic compounds (1232). Although quantitative agreement was less than perfect, a rank-order correlation was achieved. An *in vivo* method for monitoring the rate of water desorption from human forearms using dry nitrogen gas passed over the skin was investigated (1233). Experimental results confirmed an earlier finding that polysorbate 85 increased epidermal permeability.

Methodology was developed for assessing the contribution of tear turnover, instilled solution drainage, and nonproductive absorption to the loss of drug from the precorneal area of the eye (1234). Experimental data obtained upon corneal application of pilocarpine nitrate in rabbits were used to develop these projections.

A linear correlation was found between the logarithm of the *in situ* gastric absorption rate constant of 14 barbiturates with the R_m values obtained in selected reverse-phase partition chromatographic systems (1235). Possible relationships between chromatographic parameters and absorption rate constants from sites other than the stomach were explored. On the basis of pharmacokinetic simulations and experimental data, it was shown that urinary excretion measurements should be made during the 1st hr to permit adequate evaluation of absorption of aspirin from different dosage products (1236). Measurements made after 3 hr were inadequate. Results from percutaneous absorption studies conducted with hydrocortisone, testosterone, and benzoic acid correlated with results obtained in monkeys and humans (1237). Therefore, the Rhesus monkey was suggested as a suitable animal model for percutaneous absorption studies of relevance to humans.

Physicochemical Factors—A study was made of factors affecting the bioavailability of tetracycline compounds (1238, 1239). Two polymorphs each of tetracycline, chlortetracycline, and oxytetracycline were demonstrated, and their solubilities were determined. The crystal form significantly influenced the bioavailability only of tetracycline as determined by a urinary excretion study in human subjects. Administration of the free base forms produced higher plasma levels as well as greater total cumulative absorption than were obtained with the hydrochloride salts.

Blood levels after injection of an ampicillin trihydrate aqueous suspension were compared with those produced by injection of an ampicillin sodium solution (1240). The suspension produced a longer duration of activity, although higher peak levels were obtained with the solution. The phthalidyl ester of ampicillin provided serum levels in humans 2.5 times as great as those produced by ampicillin (1241). Orally administered carbenicillin indanyl sodium was readily absorbed to produce a maximum serum level within 2 hr. Higher blood levels were achieved than with carbenicillin (1242). Tissue esterases were shown to convert the ester rapidly to carbenicillin, and *in vivo* activity was attributable to the latter compound. Oral administration of pivampicillin hydrochloride to normal human subjects resulted in higher peak levels and greater total availability than were obtained with ampicillin (1243, 1244). Similar results were obtained when suspensions of the free base forms were compared. In studies comparing the bioavailability of different ester forms of ampicillin, absorption rates correlated with the lipid solubility of the ester (1245).

Both particle size and vehicle viscosity affected the bioavailability of pentobarbital (1246). Particle size was also shown to influence significantly the absorption of digoxin (1247, 1248). The bioavailability of tablets prepared with drug of 7–13-μm particle size was 78–97% of that of the drug administered in solution. Tablets prepared from 102-μm material provided only 39% of the bioavailability of the reference solution.

The use of the prodrug approach to facilitate absorption was explored in several studies, and its application to antibiotics (1249) and cytotoxic agents (1250–1252) was discussed.

The activity of local anesthetics (as hydrochlorides) in producing overturn in goldfish, measured in pH 8.0 buffer solution, was shown to increase in the following order: procaine < lidocaine < tetracaine < dibucaine (1253). The results were explained on the basis of the drug partition coefficient and the minimum effective concentration in goldfish, with only the unionized fraction of drug being responsible for the observed effects. A two-compartment open model was used to describe the buccal absorption of steroids (1254). Rate constants were calculated using a feathering technique, and an analog computer was employed to project absorption values which agreed favorably with experimental data. On the basis of a crossover experimental design, the absorption profile of griseofulvin was assessed in humans following oral administration of a 500-mg dose in capsules of the anhydrous and monochloroform solvate forms (1255). Bioavailability was significantly higher with the solvated drug, and the results correlated well with solubility and dissolution rate studies in simulated intestinal fluid.

Several reviews discussed the effects of physical and chemical properties of the drug on bioavailability (1256–1265).

Formulation Factors—Bioavailability of digoxin from different commercial and experimental products continued to be of interest during the year. Bioavailability from four randomly selected lots of digoxin produced by a single manufacturer showed no greater variability than that obtained when one lot was administered twice (1266). Intersubject variation in areas under the serum concentration–time curve and in the 24-hr urinary measurements was more than twice that of intrasubject variations. Although four brands of digoxin tablets did not differ in total absorption or total

urinary excretion in humans and were equivalent for maintenance treatment, marked differences occurred in area and steepness of the absorption curves (1267). One brand was absorbed so slowly as to be unsuitable for rapid oral digitalization.

The bioavailability of digoxin from tablets compared to *in vitro* dissolution rates showed that tablets releasing a minimum of 90% of drug within 2 hr were likely to be bioequivalent (1268). In another study, digoxin tablets having different dissolution rates were administered at 0.5 mg/day for 9 days (1269). Products that showed differences after a single dose also produced significant variations in steady-state levels. Use of a 24-hr urinary excretion was proposed as the most reliable screening test to assess bioavailability.

Rapidly dissolving digoxin tablets were shown to provide complete absorption (1270, 1271). No significant differences in urinary excretion levels were shown when the rapidly dissolving tablets were compared to a digoxin elixir. A solution of digoxin in capsule form was demonstrated to provide greater bioavailability than rapidly dissolving tablets (1272), but no explanation was offered for the results. In a bioavailability study comparing digoxin tablets produced by two major manufacturers, cumulative urinary excretion data were recommended for assessing bioavailability rather than plasma data obtained after 2 hr (1273). Storage of tablets for 2 years did not affect bioavailability. No differences were seen in the bioavailability of digoxin administered as a rapidly dissolving tablet, capsule, or oral solution in water (1274). However, administration of a pediatric elixir provided consistently higher urinary excretion levels. In comparison with an intravenous injection, only 63% of the drug was absorbed from tablets and 75% from the elixir. Finally, experimental digoxin tablets, having a wide range of dissolution rates, were shown to produce gross variations in bioavailability as determined from peak plasma concentrations, areas under the 5-hr plasma concentration–time curve, and 10-day urinary excretion results following administration of single doses (1275). Determination of dissolution rate was the best method for predicting bioavailability, and the establishment of a minimal acceptance level was proposed.

Several studies were published in which bioavailability of commercial tetracycline products was assessed. In a Canadian study, significant differences were seen in commercial products (1276). The use of 6–8-hr blood or urine data was proposed to assess bioavailability. Statistical correlations were shown between T_{60} dissolution data and blood and urine results. Bioavailability differences in other commercial tetracycline products also were reported (1277, 1278). No significant differences in the bioavailability of different brands of doxycycline capsule products were found when compared to a suspension.

More rapid and complete absorption of phenethicillin occurred from the oral aqueous solution of the potassium salt than from an oil suspension of the same material (1279). Slow and incomplete absorption occurred after administration of a suspension of the benzathine salt. Significant differences in absorption rate, peak blood level, and blood level 4 hr after administration were demonstrated in a crossover study of 11 brands of phenoxymethyl penicillin (penicillin V) (1280).

Urinary excretion of acetaminophen after rectal administration of three suppository formulations was compared to that after oral administration of a tablet dosage form (1281). Rectal absorption showed extreme variability, and relative bioavailabilities of from 68 to 88% were obtained compared to the oral tablet. Differences in absorption rates from the suppository products were great, and in one case the clinical efficacy of the product would be questioned.

No significant differences were found in the bioavailability of three dexamethasone tablet products, and the results were essentially identical to those from an elixir formulation (1282). Statistical differences were shown in the rate of appearance of prednisolone in plasma but not in the total amount converted to prednisolone following administration of three commercial prednisone tablets to volunteers (1283, 1284). The results suggested that differences in *in vivo* rates of appearance of prednisone be employed to assess bioavailability and be compared to *in vitro* dissolution rates.

The influence of crystal size (macro or micro) and dosage form (capsule or tablet) on urinary excretion of nitrofurantoin was investigated in 20 subjects (1285). Higher urinary excretion levels were obtained from tablets. Differences in crystal size affected urinary excretion when the drug was administered in capsules. Side effects appeared equally with all preparations.

Blood levels determined following oral administration of single doses of three commercially available brands of chlorpropamide revealed significant differences between products (1286). Two tolbutamide products also differed markedly in the serum concentration–time curves produced following oral dosing (1287). Differences in serum levels were obtained with sulfadiazine tablets from different manufacturers, although *in vitro* release values of the products were comparable. The relationship between the bioavailability of fluorides and their anticaries effectiveness was discussed (1288). A comparison was made between two groups of studies, one in which sodium fluoride was reported to be effective and another in which it was reported to be ineffective.

The percutaneous absorption of hexachlorophene following daily whole body washings was employed to compare the bioavailability of two commercially available detergent-based skin-cleansing products (1289). Differences were demonstrated between the products, and blood level data demonstrated considerable absorption. There was no correlation between whole blood concentration, body surface area, or skin pigmentation.

The period following administration over which blood level measurements should be made to obtain a reliable bioavailability comparison of two or more formulations of the same drug was examined on the basis of literature data for a number of drugs (1290). For most drugs, ratios of areas under the curve changed little between the end of the absorption period and the time when blood sampling was terminated. It was suggested that reliable bioavailability comparisons among different brands

could be made by blood sampling over 24 hr or less.

The percutaneous absorption of anthralin and its triacetate was investigated through the use of tritium-labeled drugs (1291). Four ointment vehicles were evaluated, and depth of penetration was determined by stripping skin layers with cellophane tape. The best penetration occurred through hydrophobic ointments. Absorption of anthralin was superior to that of the triacetate compound. The depth of penetration of coal tar and ichthammol into rabbit skin also was determined by the stripping method (1292). The deepest penetration of the tar occurred from a water-in-oil low fat base, while the best absorption of ichthammol was from petrolatum.

In another study of percutaneous absorption, the penetration of salicylic acid with and without dimethyl sulfoxide decreased as the ointment vehicle pH was increased (1293). The topical absorption and retention of salicylic acid and carbinoxamine from four oil vehicles followed first-order kinetics after an initial lag phase (1294). The vehicle with the strongest affinity for the drug demonstrated the poorest absorption. Higher absorption rate constants were observed through excised skin than intact skin. Measurement of total radioactivity in the blood of rats for 5 hr following rectal administration of tritiated benzocaine in ointment vehicles demonstrated that the greatest release occurred from the water-soluble vehicle (1295).

The bioavailability of vitamin E administered intramuscularly was determined by comparing free tocopherol levels in blood after administration of aqueous micellar dispersions of tocopherol and tocopherol acetate (1296). The rate-limiting step in the bioavailability was shown to be the rate of hydrolysis of the acetate ester to the physiologically active free tocopherol, and vitamin E activity in blood was much greater when the free alcohol was administered. The use of lipids such as cholesterol, cholesteryl acetate, and β-sitosterol as carriers for oral and implantation therapy was investigated (1297). *In vitro* and *in vivo* studies demonstrated the usefulness of this approach. Naltrexone–poly(lactic acid) composites demonstrated effective blocking action to morphine in animals for 20–29 days (1298).

Effects of surfactants on the intramuscular absorption of a water-soluble drug were investigated (1299). Inhibitory effects were shown to occur in the presence of both ionic and nonionic surface-active agents. A morphine implantation pellet prepared by adsorbing morphine sulfate onto a molecular sieve induced physical dependence in mice (1300). The pellet was implanted subcutaneously, and the peak of physical dependence occurred within 24 hr after implantation.

An attempt was made to employ liposomes for prolonging intramuscular absorption of highly water-soluble drugs (1301). After injection in the form of liposomal suspensions, clearance of model drugs from the injection site was considerably delayed in comparison with the controlled aqueous buffer injections. The larger the amount of cholesterol incorporated into the liposomes, the slower the drug absorption became. Hydrolysis of liposomes at the injection site appeared to be responsible for the greater *in vivo* release than was predicted from *in vitro* results.

The influences of concentration and vehicle composition on corneal penetration of the steroid fluorometholone were studied in the albino rabbit (1302). A sustaining effect noted upon instillation of a micronized drug suspension was attributed to the retention of particles within the cul-de-sac of the eye. When an ointment preparation was employed, the peak aqueous humor concentration was not achieved until 3 hr after administration. Predosing with a saturated solution followed by application of the ointment was recommended to achieve an immediately effective concentration followed by a sustaining effect.

The influence of drainage and tear turnover was studied through the administration of radioactive technetium Tc 99m sulfur colloid in the presence of topical anesthetics (1303). Reduction in the tear turnover rate varied for different anesthetics and was dose dependent. Aqueous humor concentration–time profiles for radioactive pilocarpine nitrate in the presence and absence of topical anesthesia verified the importance of tear turnover and instilled solution drainage as the major routes of drug loss in the eye. The effect of methylcellulose and polyvinyl alcohol as viscosity enhancers in ophthalmic preparations was explored, and a viscosity range of 12–15 cps was reported as optimum for prolonging contact time (1304). A study of the ophthalmic efficacy of dexamethasone showed that a suspension of the alcohol was more effective in suppressing inflammation than an equal quantity of the phosphate solution, whereas the solution was more effective than the phosphate ointment (1305).

Soft contact lenses saturated with tritiated pilocarpine provided greater activity in the aqueous humor for up to 6 hr compared to a topically applied pilocarpine solution (1306). The application of drug bioavailability input and pharmacological response output results in designing drug delivery systems was discussed (1307), and this approach was exemplified with two antiglaucoma drugs.

Micronized griseofulvin administered in a corn oil-in-water emulsion demonstrated significantly enhanced bioavailability compared to an aqueous suspension and a commercial tablet dosage form (1308, 1309). A mechanism based on the ability of linoleic and oleic acids liberated during the digestion of corn oil to inhibit GI motility and stimulate gallbladder evacuation was proposed. Although the onset of absorption after administration of the corn oil emulsion was delayed, this difference in comparison with the aqueous suspension disappeared after multiple dosing of the two dosage forms.

Enhanced bioavailabilities of sulfisoxazole acetyl and dicumarol were found when the drugs were administered in lipids as compared to administration in water (1310). The absolute bioavailability of griseofulvin was increased by coadministration with polysorbate 80 in which the drug was quite soluble. An attempt was made to correlate polarity, micelle-forming properties, digestibility, and chylomicron-forming properties of lipid vehicles with their effect on drug bioavailability. Emulsifier effects upon the absorption of vitamin A acetate and phenylbutazone were studied (1311). Absorption of vitamin A acetate was found to occur *via* the

micellar phase, whereas the free concentration in the aqueous phase was the determining factor for phenylbutazone. The effect of surfactants, tetracycline, and edetic acid (EDTA) upon intestinal mucosal integrity was studied by intravenously administering sulfaguanidine to rats and monitoring the concentration of drug appearing in the intestinal lumen (1312). Except for poloxamer 188[15], all agents studied had a damaging effect upon the intestinal walls.

Administration of dioctyl sodium sulfosuccinate markedly enhanced the GI absorption of phenolsulfonphthalein in rats (1313). This result appeared to be due to altered permeability of the intestinal mucosa. In contrast, poloxamer 188 showed no potentiating activity. At higher concentrations, both surfactants decreased absorption, presumably due to micellar drug entrapment. Several nonionic and anionic surfactants increased thioridazine absorption in goldfish (1314). This effect occurred at or near the CMC. Above this level, the surfactants had a decreasing effect on absorption.

A study of the effect of alcohol upon theophylline absorption showed that, in contrast to results obtained in rats, ethanol produced no enhancing effect upon average plasma levels of theophylline in humans (1315, 1316). Other alcohols, namely methanol, 1-butanol, glycerin, propylene glycol, and, to a lesser extent, mannitol and sorbitol, increased net water flux from the small intestine of rats, thereby increasing the rate of theophylline absorption. Evaluation of the effects of normal alcohols on intestinal absorption of salicylic acid, sulfapyridine, and prednisolone in rats showed that the presence of alcohol produced dissimilar absorption rates for the drugs studied (1317). In view of the results, the absorption-altering effects of the alcohol could not be attributed solely to increased water flux. Although a 25–50-fold molar excess of trichloroacetate increased the disappearance of methantheline bromide from intestinal loops, the onset of mydriasis in animals appeared to be delayed in the presence of trichloroacetate (1318). Administration with sodium lauryl sulfate and methylcellulose increased the absorption of aspirin, salicylic acid, and sulfadimidine (sulfamethazine) in rats (1319). Absorption was greater from oral solutions than from suspensions.

Although a qualitative correlation was found between the *in vitro* dissolution rate and the calculated initial absorption rate constants for prednisone, *in vitro* dissolution rates were not predictive of the overall bioavailability of the tablets tested (1320). A sustained-release capsule containing 20 mg of isosorbide dinitrate produced blood levels similar to 5 mg of an immediate release dosage form administered four times at 3-hr intervals (1321). Peak nitrate serum levels were reached in the 9th hr. Administration of a slow release procainamide tablet every 8 hr produced about the same mean plasma level at steady state as ordinary tablets given every 4 hr (1322, 1323). Occasional high plasma concentration peaks observed after administration of nonsustained-release tablets did not occur when the slow release product was administered. When a 180-mg sustained-release pseudoephedrine hydrochloride tablet was administered twice daily, plateau plasma levels were reached after 3 days (1324). An initial increase in heart rate and insomnia disappeared within 3 days.

A prolonged-acting quinidine bisulfate tablet provided more stable serum levels and less GI reactions than immediate release tablet products (1325). A crossover study was conducted to compare the bioavailability of amitriptyline administered as a 25-mg tablet three times daily with a 75-mg sustained-release pelletized form (1326). Blood levels were essentially equivalent after 1 week. No difference was demonstrated between the absorption of ferrous sulfate from an immediate release tablet and a slow release form in normal subjects and anemic patients (1327). Ascorbic acid enhanced iron absorption, especially in anemic postgastrectomy patients. The duration of the neutralizing effect in human subjects of a slow release antacid tablet was demonstrated to be 300% greater than that of the simple antacid (1328). In the slow release product, calcium carbonate was incorporated into wax-containing granules.

Differing Administration Routes—In volunteers administered imipramine orally and parenterally, higher levels of the metabolite desipramine occurred after oral dosing (1329). The therapeutic consequence of this difference was discussed. Although intravenous propantheline lowered blood ethanol levels after ingestion of a standard ethanol load, oral doses were without significant effect (1330). The marked reduction in oral bioavailability should be considered in clinical situations. Absorption of naproxen from water-soluble and fat-based suppositories were comparable to absorption from an equivalent oral dose (1331). Indomethacin was well absorbed after oral dosing, and peak plasma concentrations were achieved within 2 hr (1332). Comparison with the area under the curve after intravenous dosing indicated that complete bioavailability was achieved by the oral route. Although complete absorption occurred following rectal administration, the rate was slower than after oral dosing.

Comparison of plasma phenytoin concentrations in an intravenous and intramuscular crossover study showed that the intramuscularly administered drug was absorbed over 5 days (1333). A model simulating precipitation and redissolution of the drug at the injection site provided a satisfactory fit for the observed plasma concentrations. Rectally administered proxyphylline was shown to fit a two-compartment open model, whereas oral administration conformed to a one-compartment model system (1334). The drug appeared to be well absorbed by both routes. The blood concentration of chlordiazepoxide hydrochloride was higher after oral administration of a 50-mg dose than after intramuscular injection of 100 mg (1335). Peak levels of the metabolite were similarly lower after injection. Oral and intramuscular administrations of nortriptyline hydrochloride provided equivalent blood levels (1336). These results demonstrated complete GI absorption.

Subcutaneous disappearance of lidocaine hydrochloride was followed as a function of time using a closed absorption cell affixed to anesthetized rats (1337). A shift of the solution to higher pH values within the cell suggested that precipitation of lidocaine base occurred in some experiments.

No measurable radioactivity was found in serum after dermal application of clotrimazole as a 1% cream or solution (1338). Less than 0.5 and 0.05% of the radioactivity applied to the skin in the cream and solution, respectively, were excreted in the urine within 4–5 days. Following vaginal application of the solution, serum concentrations of only 0.2% of those obtained after oral administration were observed. Factors influencing the bioavailability of drug products administered by different routes of administration were reviewed (1339).

Physiological Factors—Significant intersubject variability was observed in the cumulative excretion in urine after 7 days and in the area under the 24-hr serum concentration curve following single-dose administration of 0.5 mg of digoxin (1340). A significant correlation existed between cumulative digoxin excreted during the first 2 days compared to 7-day excretion data. Use of cumulative 2-day excretion data following single-dose administration was recommended to compare bioavailabilities of oral digoxin preparations. A review was published in which a magnesium trisilicate antacid product was found not to affect digoxin bioavailability in dogs (1341). These results contradicted previous findings in which the dissolution of digoxin was completely suppressed by the antacid. In contradiction to a previous study, one report indicated that phenylbutazone absorption was not adversely affected by antacids (1342).

Enhancement of *in situ* absorption of several drugs from the rat small intestine occurred upon perfusion of drug with hypotonic solutions, whereas hypertonic solutions diminished drug transfer (1343). The rate of intestinal blood flow also played an important role in the absorption of drugs that were lipid soluble and very rapidly absorbed. Ephedrine hydrochloride administered orally to mice was more rapidly absorbed from isotonic glucose than from isotonic sodium chloride (1344, 1345). This result was attributed to the effect of glucose in facilitating transmucosal fluid uptake. Reduction in mesenteric blood flow rates resulted in impairment of sulfaethidole absorption in an *in situ* canine intestinal preparation (1346). Haloperidol absorption also decreased with decreased intestinal perfusion but differed from sulfaethidole in that membrane storage of haloperidol appeared to take place during its absorption.

Absorption rates of salicylate and antipyrine across the rat gut intestine were reduced under the influence of fasting (1347). Mucosal cell viability, cell number, and mesenteric blood flow were considered to be major factors affecting drug absorption rates. In another study, the diminished volume of distribution induced by fasting was considered to be a major cause of the decrease of drug absorption from the intestines of fasted rats (1348). Reduced absorption rates in fasted rats were also demonstrated with salicylic acid and antipyrine (1349). In this study, the effect was attributed to inhibition of intestinal cell proliferation during fasting, resulting in a decreased absorptive surface.

Absorption of theophylline was more rapid when administered following a high protein meal than after a high fat or high carbohydrate meal (1350). Absorption from solution was faster than from a solid dosage form in all treatments studied. An increase in the bioavailability of nitrofurantoin coadministered with propantheline was attributed to a delay in gastric emptying (1351). Administration of atropine sulfate significantly increased the time necessary to achieve peak blood levels of lidocaine (1352). This delay was also attributed to a gastric emptying inhibition effect. Increased absorption of indomethacin occurred with coadministration of buffered aspirin in healthy volunteers (1353). Concomitant administration of aminosalicylic acid delayed peak blood serum levels of rifampicin (rifampin) and decreased by half the area under the absorption curve (1354). The conclusion was reached that this combination of drugs is not suitable for routine tuberculosis therapy.

Marked intersubject variability was found in the ratio of saliva to serum concentration of procainamide in 12 chronically medicated patients (1355). There was no correlation between the dose administered and the minimum serum or saliva concentration. The ratio of saliva to serum concentration increased with decreasing saliva pH. This result was largely explained by the pH-dependent ionization and distribution of the drug. Evaluation of serum concentrations and urinary excretion data indicated the occurrence of a sex difference in the rate and extent of cephradine absorption from three injection sites (1356). Smaller areas under the curve occurred in female patients. The proportion of a dose of meperidine excreted unchanged or as metabolite was found to depend upon the urinary pH and the route of administration (1357). Older people appeared to metabolize more of the drug and excrete less in unchanged form. Excretion of the drug in acid urine was directly proportional to the plasma concentration.

A widely used carbonated beverage and an antiemetic product containing carbohydrates and phosphoric acid, when administered together with riboflavin 5-phosphate or salicylamide, significantly increased the bioavailability of riboflavin and appreciably altered the metabolic fate of salicylamide by increased conversion to the sulfate and decreased formation of the glucuronide (1358). These effects were attributed to the decreased gastric emptying rate caused by the carbohydrates and phosphoric acid, consistent with the empirical use of these products as antinauseants and antiemetics. The results demonstrated that the choice of beverage taken with medication can affect the bioavailability and/or metabolic fate of the drug. In the presence of mucin, an approximately 50% reduction in the bioavailability of tetracycline was found in everted rat gut and diffusion cell studies (1359, 1360). The results suggested that the drug is bound to the mucin macromolecule.

Pretreatment of healthy subjects with metoclopramide, a stimulator of gastric and intestinal motility, increased L-dopa (levodopa) absorption (1361). This increase was attributed to rapid stomach emptying, facilitating absorption in the small intestine where an active transport mechanism takes place. A study of the variability of L-dopa absorption in healthy fasting subjects showed that peak plasma levels ranged from 0.25 to 2.42 mg/ml and occurred 0.5–4 hr after ingestion (1362).

Table XXX—Additional References on Bioavailability

Reference	Topic
1367	Bioavailability as an international problem with reference to digoxin
1368	Bioavailability and elimination of β-methyldigoxin (medigoxin)
1369	Absorption and biotransformation of topically applied adenosine monophosphate
1370	Bioavailability in humans of ICRF-159, an antineoplastic agent
1371	Bioavailability in humans of *N*-acetylprocainamide
1372	Review of corticosteroid bioavailability
1373	Review of *in vivo* laboratory techniques to assess bioavailability
1374	*In vitro* bioavailability testing
1375	Review of methods for bioavailability testing
1376	*In vitro* tests for determination of antacid activity
1377	*In vitro* antacid and antipepsin activity of hydrotalcite
1378	GI absorption of anticholinergic drugs
1379	Preparation, hydrolysis, and oral absorption of *d*-carboxy esters of carbenicillin
1380	Comparative release rates of depot fluphenazine injections
1381	Effect of probenecid on serum half-life of cefoxitin and cephalothin
1382	Biological availability and alteration of silybin (silymarin)
1383	Bioavailability of lysine salt of cephalexin after intramuscular injection
1384	Chemical significance of differing absorption rates of diazepam and oxazepam
1385	Bioavailability of digoxin preparations
1386	Comparative bioavailability of sustained-release quinidine preparations and quinidine bisulfate
1387	Comparative *in vitro* dissolution of quinidine tablets
1388	Comparative bioavailability of penicillin V pediatric products
1389	*In vivo* comparison of bioavailability of two ampicillin trihydrate products
1390	Bioavailability of two oral erythromycin stearate formulations
1391	Biopharmaceutical assessment of phenylbutazone and indomethacin preparations
1392	*In vitro* and *in vivo* evaluations of phenylbutazone tablets
1393	Comparative effectiveness of two brands of phenothiazine
1394	Comparative bioavailability of two oral diazepam products
1395	Comparative human bioavailability of three rifampicin (rifampin) products
1396	Evaluation of bioavailability of 13 hydrochlorothiazide products
1397	*In vivo* comparison of two lidocaine preparations
1398	Discussion of bioavailability comparisons between different manufacturers and different lots of product
1399	Bioavailability of meperidine using urinary excretion
1400	Urinary excretion studies of coated sulfamethazine
1401	Enhancement of skin absorption by poly[2-(methylsulfinyl)ethyl acrylate]
1402	Biopharmaceutical studies on nitrofurantoin
1403	Biopharmaceutical evaluation of calcium gluconate
1404	Dissolution and absorption of aspirin tablets
1405	Comparative absorption and pharmacokinetics of immediate and slow release proxyphylline tablets
1406	Effect of solution viscosity on ophthalmic activity of cocaine and pilocarpine
1407	Effect of formulation on ophthalmic activity of neomycin
1408	Formulation effects upon oral activity of indoprofen (K4277), a new nonsteroid anti-inflammatory agent
1409	Effect of microencapsulation of aspirin upon bioavailability and gastric irritation
1410	Correlation of aspirin dissolution from enteric-coated tablets on *in vivo* absorption
1411	Influence of base upon bioavailability of acetaminophen from suppositories
1412	Comparison of bioavailability of lithium carbonate and a slow release lithium sulfate preparation
1413	Influence of changes in formulation and urinary pH upon bioavailability and excretion of diethylpropion
1414	Comparative bioavailability of oral immediate and slow release iron preparations
1415	Bioavailability of fluoride
1416	Bioavailability of timed-release orciprenaline (metaproterenol) sulfate
1417	Bioavailability of isoniazid in a liquid dosage form
1418	Rectal absorption of a coated aspirin suppository
1419	Effect of formulation on absorption of naproxen suppositories
1420	Effect of lactose on increasing dissolution rate and absorption of a narcotic analgesic (Ro-03-4661) from capsules
1421	Mechanism of intestinal absorption of drugs from emulsions
1422	Enhanced intestinal absorption of methyl orange administered in emulsions
1423	Role of bile in lymphatic transport of lipid-soluble drugs
1424	Comparative bioavailability of cyanocobalamin from capsules and tablets
1425	Slow absorption of phenytoin after intramuscular injection
1426	Comparative bioavailability from tablets and capsules
1427	Effect of implantation on physical properties of silicone rubber
1428	Effect of muscle blood flow upon drug absorption
1429	Review of bioavailability of drugs administered in enteric-coated gelatin capsules
1430	Review of pharmacokinetic aspects of controlled drug delivery systems
1431	Review of rectal absorption of drugs from suppositories
1432	Effect of formulation on dissolution of aminosalicylic acid tablets
1433	Review of the role of biopharmaceutical studies in drug optimization
1434	Effect of suppository bases on antibiotic bioavailability
1435	Influence of vehicle on penetration of steroids through skin
1436	Effect of emulsions in enhancing transport of mitomycin C administered parenterally
1437	Serum levels of ampicillin and dicloxacillin after injection by intravenous and intramuscular routes
1438	Effects of different routes of administration of microencapsulated enzymes
1439	Pharmacokinetics of ascorbic acid administered rectally and intravenously
1440	Review of GI drug absorption
1441	Review of effect of food on drug absorption
1442	Effect of phenformin on calcium absorption
1443	Inhibition of rifampicin (rifampin) absorption by bentonite
1444	Effect of epinephrine in lowering blood concentrations and prolonging anesthesia of lidocaine administered by pudendal block
1445	Factors affecting absorption of drugs across rat intestines

(continued)

Table XXX—*(Continued)*

Reference	Topic	Reference	Topic
1446	Effect of fasting and antineoplastic agents on intestinal absorption of drugs in rats	1462	Review of bioavailability from pharmaceutical dosage forms
1447	Meal interference with orally administered antibiotics	1463	Comparative bioavailability of chlorpromazine oral dosage forms determined by pharmacological response data
1448	Increase in absorption of drugs in rats by exposure to light	1464	Subject variation in oral absorbability of ampicillin
1449	Increased absorption of L-dopa (levodopa) attributed to ion intestinal decarboxylation	1465	Effect of route of administration on chlordiazepoxide serum levels
1450	Biopharmaceutic influences on anticholinergic effects of propantheline	1466	Variation in bioavailability of two orally administered ampicillin trihydrate products
1451	Review of cutaneous absorption of pharmaceuticals	1467	Pharmacokinetics of five ampicillin preparations
1452	Review of pathological and physiological factors affecting bioavailability and pharmacokinetics	1468	Bioavailability of four doxycycline products
1453	Review of pharmacological modification of drug absorption processes	1469	Absorption and elimination of orally and parenterally administered tetracycline compounds
1454	Review of GI drug absorption	1470	Excretion of cephapirin after intramuscular administration
1455	Pitfalls in interpreting bioavailability data	1471	Effect of food type on absorption of zinc sulfate
1456	Review of effects of route, dosage regimen, and delivery system on drug activity	1472	Effect of cationic drugs on intestinal absorption of pralidoxime iodide
1457	Review of biopharmaceutical aspects of drug research	1473	Enhancing effect of rifampin on warfarin excretion
1458	Review of biopharmaceutics and pharmacokinetics in professional practice	1474	Pharmacokinetics of ampicillin in cirrhotic patients
1459	Review of problems in bioavailability assessment	1475	Effect of drugs and excipients on aspirin absorption
1460	Review of biological availability of drugs	1476	Review of factors affecting GI drug absorption
1461	Discussion of factors affecting bioavailability		

The importance of determining the biopharmaceutics and pharmacokinetics of new drug products to permit correlation with safety and activity was discussed (1363). Differences in individuals with respect to absorption, distribution, and elimination patterns were suggested to account for deviations from ideal dose–response relationships.

Blood concentrations of acetaminophen following oral administration of a short chain ester, *p*-acetamidophenyl acetate, were not significantly different from those found using acetaminophen (1364). Lower blood levels occurred when intermediate hydrocarbon chain-length compounds were administered. A direct relationship appeared to exist between *in vitro* hydrolysis rates and blood concentrations *in vivo*. Concomitant oral administration of acetaminophen derivatives, pancreatic lipase, and calcium salts resulted in an increase in the blood levels of acetaminophen as compared to administration of the esters alone. A combination of short chain and longer chain esters of the drug provided a prolonged release, which maintained therapeutic blood concentrations for 13 hr following a single administration in dogs.

Elevated free serum iodide levels were determined in burn patients treated topically with povidone-iodine (1365). Iodine absorption was suggested as a possible cause of unexplained abnormalities, including acidosis and renal failure, in patients so treated. Following a shower employing a whole body lather with soap containing 2% triclocarban, about 0.23% of the drug was recovered in the feces over 6 days and 0.15% in the urine over 2 days (1366). No detectable levels were found in the blood.

Additional references relating to bioavailability are found in Table XXX.

PHARMACOKINETICS

A general disposition equation for a linear mammillary model consisting of n compartments was derived and employed to develop models based upon drug administration into the central compartments and into a peripheral compartment (1477). Equations describing the time course of a drug in a particular compartment after administration by various routes were also presented. An empirical equation not based upon compartment modeling was developed to describe pharmacokinetic behavior (1478). The proposed method provided superior correlations to those obtained with a one-compartment model and could be employed to describe the time course behavior of a highly protein-bound drug for which a one-compartment model failed. An analog computer was employed to generate pharmacokinetic data, and the use of radiolabeled drugs and computers to obtain pharmacokinetic parameters was discussed (1479). Quinidine administration to rabbits was used to illustrate the application of analog computers to generate pharmacokinetic information (1480).

Novel hydrodynamic models for distribution of intravenously administered drugs was presented and compared to the conventional compartmental pharmacokinetic modeling systems currently employed (1481, 1482). The superiority of the new procedure was discussed. The application of the Loo–Riegelman absorption method was discussed by Wagner, who also reviewed problems encountered in attempting to develop pharmacokinetic models (1483, 1484). Lemberger, in discussing pharmacokinetic toxicity, recommended that the B/S level should be kept to a minimum (1485).

Table XXXI—Additional References on Pharmacokinetics of Digitalis Glycosides

Reference	Topic
1510	Serum and urine concentrations after oral administration of β-methyldigoxin (medigoxin)
1511	Physiological distribution of digoxin in the heart
1512	Influence of heart failure on serum digoxin levels
1513, 1514	Ratio between myocardial and plasma digoxin levels
1515	Effect of propantheline, metoclopramide, and L-dopa (levodopa) on serum digoxin levels
1516	Metabolism and body distribution of digoxin
1517	Review of digitoxin serum levels and elimination
1518	Digoxin levels in patients with atrial fibrillation
1519	Effect of cardiopulmonary bypass on plasma digoxin levels
1520	Ratio between myocardial and serum digoxin levels
1521	Digitalis pharmacokinetics and metabolism
1522	Formation and disposition of bis- and monoglycosides after 4‴-*O*-methyldigoxin (medigoxin) administration
1523	Renal excretion of digoxin
1524	Biliary excretion and enterohepatic circulation of digitoxin
1525	Review of digoxin pharmacokinetics and metabolism
1526	Review of digitoxin pharmacokinetics and metabolism
1527	Review of pharmacokinetics of ouabain and acetylstrophanthidin
1528	Review of pharmacokinetics of lanatoside C and methyldigoxin (medigoxin)
1529	Pharmacokinetics and metabolism of digitoxin
1530	Effect of intestinal blood flow on enterohepatic circulation of digitalis glycosides
1531	ECG changes and plasma digoxin levels
1532	Role of renal failure in digoxin pharmacokinetics
1533	Biliary excretion and enterohepatic circulation of digitoxin and metabolites
1534	Relationship between serum and saliva digoxin concentrations
1535	Pharmacokinetics of digoxin after intravenous bolus and infusion doses
1536	Pharmacokinetics and metabolism of digoxin in patients with hepatitis
1537	Determinants in renal clearance of digoxin
1538	Effects of antituberculosis drugs on digitoxin pharmacokinetics
1539	Plasma half-life following repeated administration of β-acetyldigoxin
1540	Plasma half-life following repeated administration of β-methyldigoxin (medigoxin)
1541	Serum concentrations of digoxin in infants following overdosing
1542	Influence of renal function on digitoxin pharmacokinetics
1543	Disposition and pharmacokinetics of digoxin after intravenous administration

A multicompartmental model was employed to predict organ and plasma concentrations of antileukemia drugs after administration to animals, and new therapeutic strategies based upon the results were suggested for therapy in humans (1486). A new method for multicompartment pharmacokinetic analysis was described in which a simple treatment of cumulation processes in the central compartment was performed to avoid full analysis of the system (1487). The method reduces complex accumulation calculations to the simplicity of single-compartment formulas. A one-compartment model designed to predict alterations in persistence of drugs in uremic patients was constructed using information obtained from normal subjects. For the drugs examined, the model was able to predict overall elimination rate constants in severe uremia with an error of 10% for 12 drugs and of 20% for seven additional drugs (1488). The model was proposed as a useful approach for predicting dosage adjustment in uremic patients for drugs for which data are not available.

Several articles reviewed the principles of pharmacokinetics and the applicability of pharmacokinetic data to drug therapy (1489–1509).

As in recent years, considerable attention was devoted to the uptake, metabolism, distribution, and excretion of digitalis glycosides. A listing of these studies is provided in Table XXXI.

Serum and urine data were employed to study the elimination of diphenylhydantoin (phenytoin) from children administered excessive doses of the drug (1544). Nonlinear regression analysis using a one-compartment pharmacokinetic model was employed. A trend toward relatively lower K_M and higher V_{max}/K_m values was seen in the patients. A computer program was developed to provide complete pharmacokinetic analysis of blood ethanol level data (1545). Lower peak blood levels and decreased areas under the concentration–time curve resulted when ethanol was administered with fats or carbohydrates (1546).

Plasma nortriptyline concentrations were assayed in four subjects after intravenous infusion (1547). Best-fitting curves were obtained using a two-compartment open model. A pharmacokinetic study of nortriptyline was performed using oral and intravenous dosing (1548). Only 46–59% of the orally administered drug was systemically available. This level was attributed to metabolism following administration. Quantitative measurements of first-pass metabolism also were obtained from urinary metabolite excretion data when the kinetics of metabolite formation and elimination were taken into account. Analysis of data from the intravenous test according to a two-compartment open model showed close correlation between the rate constant of distribution from the central to the peripheral compartment and the elimination rate constant in the central compartment.

A linear relationship was demonstrated between the elimination rate constant of sulfadiazine and the endogenous creatinine clearance in patients with normal and impaired kidney function (1549). The mean half-life of the drug was 10 hr in normal patients and 22 hr in anuric patients. The plasma phenytoin half-life following intravenous administration was 14.5 hr (1550). Following oral administration, peak plasma concentrations were reached in 4–12 hr. Steady-state plasma levels varied considerably among individuals after multiple oral doses and exceeded those predicted from a single intravenous dose by 29–77%. This discrepancy was attributed to transition to dose-dependent kinetics. The heparin half-life in blood was about 1.5 hr and did not increase with dose (1551). Differences in four methods used for measuring heparin pharmacokinetics were discussed. Treatment of healthy volunteers with allopurinol and clofibrate did not alter the plasma

warfarin elimination rate (1552). Enhancement of warfarin activity by clofibrate in humans was thus attributed to interaction at the receptor site. Treatment with allopurinol resulted in significant prolongation of the plasma dicumarol half-life.

To investigate the effect of end-stage renal insufficiency and hemodialysis on the serum procainamide half-life, 500 mg was administered orally to control subjects and dialysis patients (1553). The mean half-life in normal subjects was 3.2–3.5 hr *versus* 11.3–16 hr in the patients. Mean plasma acetaminophen and phenacetin half-lives were approximately 15% longer in normal male volunteers at 6 am than at 2 pm (1554). The apparent volume of distribution decreased by about 13% from 6 am to 12 pm, whereas the mean metabolic clearance rate did not change significantly. Although plasma half-lives at these hours were highly reproducible within a given subject, much individual variation occurred. Only a maximum of 10% orally administered acetaminophen was metabolized during the first pass through the liver (1555).

The pharmacokinetics of acetaminophen in 2–3-day-old full-term infants showed the half-life to be 3.5 hr compared with 1.9–2.2 hr observed in adults (1556). The rate constant for glucuronide formation in neonates was considerably smaller than in adults, whereas the rate for formation of sulfate was somewhat larger than in adults. The limited ability of neonates to conjugate phenolic drugs with glucuronic acid appears to be partially compensated for by a well-developed capability for sulfate conjugation.

Individual plateau serum salicylate levels correlated better with urinary excretion rates of the metabolite, salicylurate, than with total urinary excretion of salicylates (1557). This finding suggested that large intersubject variations in plateau serum salicylate levels may be attributable to differences in maximum rates of a capacity-limited metabolic reaction. For optimal therapeutic response, individualization of aspirin dosing by following serum salicylate levels was recommended. The use of 2-*p*-aminobenzoyloxybenzoic acid as a prodrug was suggested, since it is well absorbed from the GI tract and hydrolyzed to salicylic acid in blood and tissues (1558). However, 50% of the dose was excreted unchanged in urine.

The pharmacokinetics and metabolic fate of gentisic acid in humans were investigated (1559). The compound was excreted unchanged in urine with an elimination half-life of 1.4–2.6 hr. In normal male subjects, the half-lives of antipyrine, aminopyrine, and phenacetin were not significantly different from the half-lives of each drug in saliva (1560). Apparent volumes of distribution in plasma and saliva differed by the extent to which each drug is bound to serum protein. General equations were used to show the relationship between the half-life for elimination of the parent drug from the body and the rate of excretion of metabolites. The salivary half-life of antipyrine is used as a convenient procedure for estimating the relative rates of drug metabolism in humans (1561). The elimination of antipyrine from saliva was shown to be a useful index of drug metabolism in animals and humans.

A study of the biological disposition of methadone in acute and chronic administration suggested that both dispositional and pharmacological tolerance are involved in the development of tolerance following chronic administration (1562). In the acute study, a biexponential plasma methadone level decay was observed. The acute primary half-life of 14.3 hr in combination with the acute secondary half-life of 54.8 hr was longer than the single exponential product half-life of 22.2 hr determined in the same subjects. In six patients given increasing doses of methadone during a 1-month period, the ratio of the *N*-monomethylated metabolite to the parent drug increased and the urinary recovery of unchanged methadone decreased (1563). In addition to methadone, seven metabolites were isolated and identified in urine and three metabolites were found in feces.

The plasma concentration–time profiles of meperidine following intravenous injection were investigated by reference to a classical two-compartment open model (1564). When administration proceeded induction of anesthesia, induction was consistently followed by an increase in venous plasma concentration that prevented classical kinetic analysis. Increasing alcohol consumption by patients was associated with increasing volumes of distribution, and an increased fraction of drug unbound in plasma occurred with increasing patient age. The disposition of morphine following administration of 10 mg/kg was determined by a sensitive and specific radioimmunoassay in 31 anesthetized patients (1565). Following intravenous injection, 93% of the morphine disappeared from the serum within 5 min. The 2-min serum levels of the drug correlated directly with the patients' ages. The serum half-life between 10 and 240 min was independent of age and averaged about 2 hr. Following intramuscular administration, the drug was rapidly absorbed and peak levels occurred within 10–20 min. The decline in serum levels paralleled the decline in analgesia and was coincident with the appearance of morphine glucuronide in the serum.

The urinary excretion of free naltrexone and its major urinary metabolite was 1.2 and 26.3% of the administered dose, respectively (1566). The urinary excretion of conjugated drug and the metabolites was 9.7 and 16.4%, respectively. The half-life of naltrexone was determined to be 1.1 hr, whereas that of the metabolite was 14–18 hr. A multicompartment model was developed for the pharmacokinetics of adriamycin (doxorubicin) (1567). On this basis, human plasma levels were predicted and a comparison with patient data demonstrated reasonably good correlation.

A GC procedure was found to be more reliable than the UV procedure previously employed for pharmacokinetic studies of theophylline. By using this procedure, a half-life of 11 hr was determined and the pharmacokinetics were described by a two-compartment model (1568). Considerable individual variations in theophylline metabolism were found in five human subjects given 300 mg po (1569). For example, in two subjects, the concentration of drug plus metabolites excreted in the urine within 24 hr was 27.4 and 7.0 mg, respectively, while the 12-hr plasma levels were 10 and 2.3 mg/liter. Two major metabolites were identified as 1,3-dimethyluric acid and 3-methylxanthine. In a group

of hospitalized patients, most of whom smoked, the half-life of theophylline following 5 mg/kg iv was 3.6 hr (1570). In nonsmokers, the half-life was 7.2 hr; it was 4.1 hr for those who smoked. This difference was attributed to enzymatic induction in the smokers.

The serum half-life of propylthiouracil administered intravenously averaged 77 min in seven normal subjects (1571). The data conformed to a two-compartment model, and rate constants and elimination constants were calculated. The half-life of 200 mg of propylthiouracil administered orally was 1.1 hr (1572). Haloperidol was rapidly absorbed by normal subjects following intramuscular administration, with the maximum plasma level reached within 20 min (1573). The plasma level profile followed multicompartment model kinetics with a terminal elimination half-life of 20.7 hr. The prolonged elimination half-life suggested that a delay of 3–5 days occurred before equilibrium plasma levels are reestablished following a change in dosage regimen. Concomitant administration of vitamin C (ascorbic acid) was shown to alter the ratio of metabolic products of salicylamide excreted in the urine (1574). Although the sum of urinary excretion products was unaffected by vitamin C, glucuronide formation increased whereas sulfate conjugation decreased.

Antigen distribution and clearance were viewed as pharmacokinetic problems complicated by the intervention of the immune response (1575). A model characterizing the clearance of a simple antigen from the bloodstream of experimental animals, as well as the subsequent serum antibody response, was developed. Although it was envisioned that modification of the model would be required to explain more complex systems, early events in the immunological response were adequately accounted for in a consistent and quantitative manner. Blood levels and exhalation data from dogs and humans were used to elucidate a pharmacokinetic model describing the time course of trichloromonofluoromethane and dichlorodifluoromethane (1576). The model was used to estimate the percent of dose absorbed, which averaged 77% for trichloromonofluoromethane and 55% for dichlorodifluoromethane, and to predict their levels under various conditions simulating both short- and long-term exposure to maximum allowable concentrations.

Bioavailability of commercial carbamazepine tablets administered with and without meals was compared to that of a propylene glycol solution with respect to extent of absorption (1577). Although the drug was rapidly absorbed from the glycol solution, only 8% was absorbed from the commercial tablet. The data were consistent with dissolution rate-limited absorption. The fraction of dose absorbed and excreted in urine, the time of maximum serum concentration, and absorption and elimination half-lives appeared to be independent of dose.

In another study, an alcoholic solution of carbamazepine administered orally produced maximum plasma concentrations varying from 1 to 7 hr after dosing (1578, 1579). The half-life ranged from 24 to 46 hr and was dose independent. In patients subjected to multiple dosing, however, the plasma half-life decreased. The steady-state plasma concentration expected during multiple dosing was calculated from pharmacokinetic parameters obtained in single-dose studies. The results suggested that the drug induced its own metabolism.

In a comparative study of three penicillins, peak serum concentration and area under the serum concentration–time curve were greatest for amoxicillin followed by pivampicillin and then hetacillin (1580). The serum half-lives for amoxicillin and hetacillin were greater in nonfasting than in fasting subjects. Approximately 45% of the radioactivity given orally as ^{35}S-labeled phenoxymethyl penicillin (penicillin V) potassium was absorbed by the upper region of the GI tract (1581). In GI aspirates, ~10% of the drug was degraded to pencilloic acid. The cumulative recovery of intact drug in the urine was ~30% of the dose. The incomplete recovery was due to decomposition and poor absorption in the GI tract.

A two-compartment open model was developed to describe the absorption, distribution, metabolism, and excretion of cephapirin and its major metabolite, the desacetyl derivative, following intravenous and intramuscular administrations (1582). The model included metabolism in both plasma and the kidney. Clearance calculations and digital computer simulation supported the model.

The literature pertaining to the pharmacokinetics of cephalosporin antibiotics and their clinical use was reviewed (1583). Significant differences were shown to exist in the blood level–time profiles for the various dosage regimens of gentamicin recommended for patients with impaired renal function (1584). Although most methods achieved peak steady-state blood levels that exceeded the effective response concentration of 4 mg/ml, the percent duration of the dosing interval above and below minimal effective levels varied markedly for the various methods. Methods based on serum creatinine levels were considered to be less desirable than those using creatinine clearance as an index of renal function, since unduly long dosing intervals during moderate to severe renal impairment may be incorrectly employed. The recommendation was made that serum creatinine measurements be converted to creatinine clearance.

Clotrimazole was shown to be well absorbed orally and readily eliminated, mainly as an active metabolite in bile with only small quantities found in urine (1585). Peak plasma levels of sulfamethoxazole were reached in 2–4 hr by persons ingesting 800 mg alone or together with 160 mg of trimethoprim (1586). Simultaneous administration of trimethoprim did not affect the pharmacokinetics of sulfamethoxazole. An oral dose of 5 mg of isosorbide dinitrate was rapidly absorbed, biotransformed, and excreted in human subjects (1587). Peak whole blood concentrations of radioactivity were reached after 1.5–2 hr and declined relatively slowly. The radioactivity in whole blood was mainly represented by metabolic products. The metabolic products declined relatively slowly during 6 hr after oral dosing. Following oral administration of propoxyphene to children, peak blood levels were found after 2–3 hr with an apparent half-life of 4.8 hr (1588). A positive correlation was found between the plasma level of propoxyphene and norpropoxyphene, the major metabolic

Table XXXII—Additional References on Pharmacokinetics

Reference	Topic
1602	Absorption and metabolism of 7-chloro-3,3a-dihydro -2-methyl- 2*H*,9*H*-isoxazolo[3,2-*b*]-[1,3]benzoxazin-9-one
1603	Review of pharmacokinetics of flavinoids
1604	Pharmacokinetics of acetazolamide in glaucoma
1605	Plasma levels after single oral dose of proscillaridin
1606	Bioavailability of dioxidine and quinoxidine
1607	Review of metabolism of griseofulvin
1608	Review of pharmacokinetics of D-penicillamine
1609	Pharmacokinetics of haloperidol
1610	Review of pharmacokinetic function of pulmonary circulation
1611	Review of pharmacokinetics of inhalation anesthetic agents
1612	Absorption and elimination of clofazimine
1613	Bioavailability of clofazimine
1614	Pharmacokinetics of 1-(isopropylamino)-3-(2-methylindole-4-yloxy)-2-propanol (LF 17-895)
1615	Review of pharmacokinetics of pentazocine
1616	Review of pharmacokinetics of pentobarbital
1617	Pharmacokinetics of acetaminophen elimination in anephric patients
1618	Review of pharmacokinetics of frusemide (furosemide)
1619	Pharmacokinetics of indapamide
1620	Absorption, blood levels, and elimination of prothionamide
1621	Butylbiguanide concentrations in plasma, liver, and intestine after intravenous and oral administrations
1622	Review of pharmacokinetics of hypoglycemic agents
1623	Review of pharmacokinetics of tolbutamide
1624	Review of pharmacokinetics of sulfonylureas
1625	Pharmacokinetics of 4-amidinophenylpyruvic acid
1626	Influence of viral hepatitis on phenytoin pharmacokinetics
1627	Review of pharmacokinetics of heparin
1628	Effect of proadifen hydrochloride (SKF 525A) on pharmacokinetics of rifampicin (rifampin)
1629	Effect of phenobarbital on half-life of rifampicin
1630	Pharmacokinetics of cefoxitin and cephalothin
1631	Pharmacokinetics of cefazolin
1632	Review of pharmacokinetics of doxycycline
1633	Review of pharmacokinetics of minocycline
1634	Review of pharmacokinetics of amoxicillin
1635	Comparison of pharmacokinetics of a substituted penicillanic acid (BL-P1654) and ampicillin
1636	Pharmacokinetics of carbamazepine
1637	Pharmacokinetics of oxazepam and other benzodiazepines
1638	Pharmacokinetics of cytosine arabinoside (cytarabine) and pharmacokinetic simulation
1639	Blood digoxin levels
1640	Plasma concentrations of intravenous β-methyldigoxin (medigoxin)
1641	Plasma concentrations of diphenylhydantoin (phenytoin)
1642	Absorption and metabolism of pivampicillin
1643	Steady-state kinetics of penfluridol in psychiatric patients
1644	Absorption, metabolism, and excretion of naftidrofuryl (LS-121)
1645	Serum cephalosporin levels
1646	Review of pharmacokinetics of antineoplastic agents and immunosuppressants
1647	Blood levels in mother and child after oral administration of doxycycline antepartum
1648	Digoxin intoxication and plasma levels
1649	Review of pharmacokinetics of rifampicin
1650	Review of usefulness of blood levels of antiepileptic drugs
1651	Pharmacodynamics of 4-bromo-2,5-dimethoxyphenylisopropylamine
1652	Plasma half-life of cytosine arabinoside (cytarabine)
1653	Serum diazepam levels after repeated injections
1654	Distribution of labeled chlorpromazine
1655	Pharmacokinetics of maprotiline
1656	Pharmacokinetics of sulfaclomide and effect on *p*-aminohippuric acid clearance
1657, 1658	Review of pharmacokinetics of amoxicillin
1659	Disposition of acetylmethadol (methadyl acetate) in relation to pharmacological action
1660	Change in elimination half-life of aminophenazone (aminopyrine) in pregnancy
1661	Review of pathways of drug metabolism
1662	Review of drug distribution
1663	Review of drug metabolism
1664	Review of pharmacokinetic drug interactions
1665	Acetaminophen metabolism
1666	Metabolism of 2-(*p*-aminobenzoyloxy)benzoic acid
1667	Plasma levels and clinical effects of thioridazine and thiothixene
1668	Plasma levels and effects of antidepressants
1669	Relationship of clinical effect to digoxin concentration
1670	Disposition of *d*-propoxyphene
1671	Effect of diuretics on urinary excretion of cephalothin
1672	Acetanilide pharmacokinetics before and during diphenylhydantoin (phenytoin) administration
1673	Pharmacokinetics of amoxicillin
1674	Metabolism of cyproheptidine
1675	Comparison of blood levels with bupivacaine carbonate and hydrochloride
1676	Plasma levels of diftalone in rheumatoid arthritis
1677	Structural analysis of compartmental models for hepatic kinetics of drugs
1678	Review of pharmacokinetics of drug interactions
1679	Pharmacokinetic principles in chemical teratology
1680	Pharmacokinetic aspects of antibiotic therapy
1681	Pharmacokinetics of tranexamic acid
1682	Pharmacokinetics of radioiodine-labeled mercury compounds
1683	Pharmacokinetics of bucloxic acid
1684	Pharmacokinetics of methindione
1685	Blood trichloroethanol levels after oral administration of chloral hydrate
1686	Review of pharmacokinetics of nonsteroidal anti-inflammatory agents
1687	Pharmacokinetics of single oral dose of clofibrate
1688	Pharmacokinetics of ascorbic acid
1689	Pharmacokinetics in newborns and infants
1690	Plasma levels and urinary excretion of thiamphenicol in infants
1691	Review of absorption, metabolism, and excretion of drugs in geriatric patients
1692	Review of digoxin metabolism in geriatric patients
1693	Absorption, distribution, and excretion of labeled C-methyl ester of amphotericin B
1694	Blood levels and urinary excretion of *N*-(2-hydroxyethyl)cinnamamide
1695	Absorption and excretion of lactulose
1696	Review of pharmacokinetics of diphenylhydantoin (phenytoin)
1697	Review of pharmacokinetics of diphenylhydantoin in uremic patients
1698	Plasma concentrations of diphenylhydantoin and its metabolites
1699	Alteration of warfarin pharmacokinetics in an operating-room environment
1700	Pharmacokinetics of anticoagulant activity of coumarin drugs

(continued)

Table XXXII—*(Continued)*

Reference	Topic
1701	Pharmacokinetics of procainamide
1702	Pharmacokinetics of *N*-acetylated metabolite of procainamide
1703	Elimination of *N*-acetylprocainamide after intravenous dose of procainamide
1704	Influence of heart failure on blood levels of lidocaine and its monodeethylated metabolite
1705	Pharmacokinetic analysis of pharmacological effects and drug disposition of acetaminophen and 4-aminoantipyrine
1706	Pharmacokinetics of phenacetin
1707	Kinetics of salicylate elimination by anephric patients
1708	Kinetics of salicylates in blood and joint fluid
1709	Metabolism of secobarbital
1710	Pharmacokinetics of hexobarbital in humans after intravenous infusion
1711	Pharmacokinetics of hexobarbital in acute hepatitis
1712	Levels of morpethidine in maternal and fetal plasma following intramuscular administration of meperidine
1713	Pharmacokinetics of ^{3}H-4-acetylvinblastine
1714	Pharmacokinetics of guanazole
1715	Absorption, distribution, and excretion of alprenolol
1716	First-pass effect and dose-dependent availability of alprenolol
1717	Plasma concentrations and time course of β-adrenergic blockade due to propranolol
1718	Kinetics of propylthiouracil in hyperthyroidism
1719	Pharmacokinetics of disopyramide (Norpace)
1720	Pharmacokinetics of metronidazole
1721	Absorption and excretion of thioridazine and mesoridazine
1722	Pharmacokinetic determinants of response to single doses of chlordiazepoxide
1723	Effects of age and liver disease on disposition and elimination of diazepam
1724	Pharmacokinetics of chlorprothixene
1725	Pharmacokinetics of transfer of ampicillin to amniotic fluid
1726	Blood, urine, and bile levels of ampicillin after continuous infusion
1727	Pharmacokinetic studies with mecillinam and pivmecillinam
1728	Clinical pharmacokinetics of ticarcillin and carbenicillin
1729	Pharmacokinetics of sulbenicillin
1730	Pharmacokinetics of transfer of cephalothin into amniotic fluid
1731	Pharmacokinetics of cefazolin
1732	Adjustment of cephaloridine dosage according to its pharmacokinetics
1733	Gentamicin blood level–time profiles of various dosage regimens in renal impairment
1734	Unaltered metabolism of antipyrine and tolbutamide in fasting man
1735	Measurement of plasma concentrations of tolbutamide by GLC
1736	Pharmacokinetics of floctafenine
1737	Pharmacokinetics of flucytosine in cryptococcal meningitis
1738	Pharmacokinetics of clofibrate and chlorophenoxyisobutyric acid
1739	Monitoring of plasma levels of halofenate
1740	Pharmacokinetic studies with radioactive *N*-propylajmalinium hydrogen tartrate
1741	Comparative pharmacokinetic studies of ornidazole and metronidazole
1742	Fate of emepronium in humans in relation to its effect
1743	Pharmacokinetics of pindolol
1744	Pharmacokinetics of magnesium
1745	Pharmacokinetics of viloxazine
1746	Blood levels of bupivacaine in obstetric analgesia
1747	Cerebrospinal fluid concentrations of diazepam and its metabolites
1748	Methaqualone in serum and cerebrospinal fluid after oral intake
1749	Plasma concentrations and effects of methaqualone after single and multiple oral doses
1750	Relationship between behavioral effects and plasma levels of amantadine
1751	Pharmacokinetics of ifosfamide
1752	Pharmacokinetics of saralasin in hypertensive patients
1753	Pharmacokinetics and metabolism of glycinexylidide
1754	Effect of etiocholanolone-induced fever on plasma antipyrine half-life
1755	Pharmacokinetic data and drug monitoring: antibiotics and antiarrhythmics
1756	Pharmacokinetics rational for sulfadoxine–pyrimethamine mixture administered once monthly for malarial suppression
1757	Pharmacokinetics of bethanidine in hypertensive patients
1758	Pharmacokinetics of 5,6-*trans*-25-hydroxycholecalciferol
1759	Pharmacokinetics of tinidazole and metronidazole in women after single large oral doses
1760	Pharmacokinetics of rimiterol
1761	Pharmacokinetics of chlormethiazole
1762	Prediction of steady-state plasma levels of nortriptyline from single oral dose kinetics
1763	Pharmacokinetics of drugs in patients with nephrotic syndrome
1764	Carbenicillin therapy in patients with normal and impaired renal function
1765	Plasma concentrations of pancuronium bromide in patients with normal and impaired renal function
1766	Pharmacokinetics of doxycycline in patients with normal and diseased kidneys
1767	Minocycline excretion and distribution in relation to renal function
1768	Pharmacokinetics and dosage of dextran 40 in relation to renal function
1769	Disappearance of phenazone (antipyrine) from plasma in patients with obstructive jaundice
1770	Pharmacokinetics of thiamphenicol in normal and renal insufficiency subjects
1771	Changes in blood thiamphenicol levels in renal failure
1772	Serum levels of thiamphenicol in patients with impaired liver and kidney function
1773	Pharmacokinetics of terbuclomine in renal insufficiency
1774	Lithium elimination as a function of age in normal and renal insufficiency subjects
1775	Pharmacokinetics of clindamycin in normal subjects and renal failure patients
1776	Pharmacokinetics and metabolism of lidocaine in patients with renal failure
1777	Plasma levels of lidocaine during treatment with phenytoin and procainamide
1778	Pharmacokinetics of acetanilide and diphenylhydantoin (phenytoin)
1779	Metabolism and disposition of labeled hydralazine
1780	Pharmacokinetics of actinomycin D (dactinomycin) in patients with malignant melanoma
1781	Acetylation of procainamide and its relationship to isonicotinic acid hydrazide (isoniazid) acetylation phenotype
1782	Polymorphic acetylation of procainamide

product. The first-pass liver metabolism, as well as variation in the half-life, was suggested as being responsible for changes in the amount of available propoxyphene.

Plasma levels of dexamethasone phosphate and free alcohol were determined following intravenous ad-

ministration of the phosphate (1589). Areas under the plasma dexamethasone alcohol curves were a linear function of the phosphate dosage over a 40-fold range, and an overall conversion of phosphate to alcohol of 90% was indicated. A first-order rate conversion constant of 4.03 hr^{-1} was approximately 25 times that for hydrolysis in whole blood incubated *in vitro*. The results suggested that the major component of phosphate hydrolysis occurs within highly perfused organs comprising the central kinetic compartment. A large first-pass effect was evident, with about 50% of orally administered diphenhydramine being metabolized by the liver before reaching general circulation (1590). The drug administered in solution appeared to be fully available to the hepatoportal system. Cumulative amounts of unchanged drug excreted in the urine were less than 4% of the administered dose.

Theoretical equations were derived to estimate the extent of the hepatic and pulmonary first-pass effect after oral and intraperitoneal administrations (1591). Calculations using data from two normal adult subjects suggest that the fractions of chloroform metabolized in the liver and excreted intact from the lung in the first pass are maximally 0.38 and 0.172, respectively. Close agreement between predicted and experimental values for the pulmonary excretion clearance also was found. The pharmacokinetics of tolmetin studied after oral administration showed that the data were capable of being fitted to a one-compartment open model (1592). An overall mean elimination rate constant of 0.839 hr^{-1}, corresponding to a plasma half-life of 0.83 hr, was obtained in the 12 subjects studied. Similar results were seen after multiple dosing in arthritic patients.

Approximately one-third of a single therapeutic dose of phenformin administered to two healthy volunteers was excreted unchanged in the urine over a 4-day period subsequent to dosing (1593). Profiles were obtained for urinary excretion rates and plasma and saliva concentrations. The terminal exponential decline indicated a half-life of approximately 11 hr. A one-compartment model was proposed to describe the pharmacokinetics of creatinine in humans (1594). The average biological half-life in normal male adults between 20 and 39 years was 3.85 hr and was prolonged in patients with renal dysfunction to up to 77 hr when renal function decreased to 5% of normal. The use of a pharmacokinetic approach to interpret serum creatinine levels in patients suffering from renal failure was recommended. Plasma and saliva concentrations of isoniazid were determined following oral administration to two slow acetylator subjects (1595). The results indicated that salivary levels provide a useful approach for acetylation phenotyping. A report reviewed recent publications dealing with the study of pharmacokinetics in the aged population (1596). The rate and extent of drug absorption do not appear to be altered to an appreciable degree in elderly patients. However, drug disposition may be affected by a number of factors, including alterations in protein binding, apparent volumes of distribution, and renal and/or extrarenal clearance of drug.

The plasma half-life of diphenylhydantoin (phenytoin) in newborn infants of epileptic mothers treated with the drug was shown to be in the same range as the plasma half-life in adults (1597). Rapid metabolism and plasma disappearance of the drug were demonstrated. In newborn children whose mothers had been given phenobarbital, the blood plasma half-lives ranged from 77 to 404 hr and were inversely correlated with the extent of prenatal exposure to the drug (1598). In three infants, a biphasic plasma curve was found in which there was a sudden change from slow to fast disappearance of drug on the 5th–7th day of life.

A study of the distribution and elimination of lidocaine and mepivacaine in subjects after obstetric epidural anesthesia showed that epinephrine significantly lowered the concentrations of the anesthetics in the mothers' circulations (1599). However, epinephrine significantly increased the concentrations of the anesthetics found in the newborn's circulation at delivery. Of importance was the long persistence of the anesthetics in the infant's circulation.

Amoxicillin absorption was similar in normal subjects, pernicious anemia patients, and patients with renal failure (1600). Therapeutic levels were reached in the serum and urine of patients with creatinine clearance levels below 10 ml/min. The half-life was increased markedly in patients undergoing dialysis therapy. A one-compartment model designed to predict alterations in persistence of drugs in uremic patients was constructed using information obtained from normal subjects, and predictions were made for 22 drugs (1601). Terminal half-lives, percent excreted unchanged, and reported changes in half-life associated with decreased renal and hepatic functions were tabulated for 186 drugs studied in humans. References were obtained from 332 original articles which were critically evaluated in this study.

Additional references on pharmacokinetics are listed in Table XXXII.

REFERENCES

(817) M. Kuhnert-Brandstaetter and W. Heindl, *Sci. Pharm.*, **43**, 112(1975); through *Chem. Abstr.*, **83**, 168383q(1975).

(818) I. P. S. Kang, *Aust. J. Pharm. Sci.*, **3**, 55(1974); through *Chem. Abstr.*, **82**, 77037t(1975).

(819) M. A. Miyamoto and T. Maeda, *Chem. Pharm. Bull.*, **23**, 1866(1975).

(820) J. Winter and D. Shifler, *U.S. NTIS*, **75**, 105(1975); through *Chem. Abstr.*, **83**, 168399z(1975).

(821) J. K. Haleblian, *J. Pharm. Sci.*, **64**, 1269(1975).

(822) A. R. Ebian, M. A. Moustafa, S. A. Khalil, and M. M. Motawi, *ibid.*, **64**, 1481(1975).

(823) M. A. Moustafa, A. R. Ebian, S. A. Khalil, and M. M. Motawi, *ibid.*, **64**, 1485(1975).

(824) K. Nikolics, *Szerves Vegyuletek Krisztallogr. Vizsgalata*, **1973**, 267; through *Chem. Abstr.*, **83**, 32931j(1975).

(825) E. F. Titova, E. S. Obolonkova, and E. M. Belavtseva, *Farmatsiya*, **23**, 12(1974); through *Chem. Abstr.*, **82**, 64427v(1975).

(826) J. Kopecek and L. Sprincl, *Polim. Med.*, **4**, 109(1974); through *Chem. Abstr.*, **82**, 77018n(1975).

(827) Y. Kato, S. Togawa, and H. Watanabe, *Yakuzaigaku*, **34**, 135(1974); through *Chem. Abstr.*, **83**, 152267u(1975).

(828) S. Moisescu and M. Moisescu, *Farmacia*, **22**, 353(1974); through *Chem. Abstr.*, **82**, 64420n(1975).

(829) J. F. Yan, *J. Colloid Interface Sci.*, **52**, 504(1975).

(830) I. Lichnerova and M. Chalabala, *Cesk. Farm.*, **23**, 353(1974); through *Chem. Abstr.*, **83**, 48144r(1975).

(831) N. R. Bohidar, F. A. Restaino, and J. B. Schwartz, *J. Pharm. Sci.*, **64**, 966(1975).

(832) E. Huettenrauch, I. Keiner, and S. Fricke, *Pharmazie*, **29**, 715(1974); through *Chem. Abstr.*, **82**, 38316p(1975).

(833) W. A. Ritschel, *Perspect. Clin. Pharm.*, **1972**, 325; through *Chem. Abstr.*, **82**, 38316p(1975).

(834) G. Le Petit, *Zentralbl. Pharm. Pharmakother. Laboratoriumsdiagn.*, **114**, 565(1975); through *Chem. Abstr.*, **83**, 197710z(1975).

(835) W. Fuerst, *ibid.*, **114**, 571(1975); through *Chem. Abstr.*, **83**, 19771a(1975).

(836) N. Nakabayashi, *Kagaku Kogaku*, **38**, 402(1974); through *Chem. Abstr.*, **82**, 64361u(1975).

(837) J. Evans, *Polim. Med.*, **4**, 135(1974); through *Chem. Abstr.*, **82**, 64360t(1975).

(838) B. W. Mueller, *Seifen, Oele, Fette, Wachse*, **101**, 284(1975); through *Chem. Abstr.*, **83**, 103224u(1975).

(839) J. E. Moody, *Anal. Profiles Drug Subst.*, **4**, 319(1975); through *Chem. Abstr.*, **83**, 152221z(1975).

(840) A. P. Schroff and E. S. Moyer, *ibid.*, **4**, 324(1975); through *Chem. Abstr.*, **83**, 152219e(1975).

(841) A. M. Soptrak and L. F. Cullen, *ibid.*, **4**, 294(1975); through *Chem. Abstr.*, **83**, 152220y(1975).

(842) L. P. Marrelli, *ibid.*, **4**, 21(1975); through *Chem. Abstr.*, **83**, 152218d(1975).

(843) P. V. Pedersen and K. F. Brown, *J. Pharm. Sci.*, **64**, 1192(1975).

(844) J. T. Carstensen and M. Patel, *ibid.*, **64**, 1770(1975).

(845) D. Brooke, *ibid.*, **64**, 1409(1975).

(846) M. Patel and J. Carstensen, *ibid.*, **64**, 1651(1975).

(847) J. Hersey and J. Marty, *Manuf. Chem. Aerosol News*, **46**, 43(1975).

(848) K. G. Nelson and A. C. Shah, *J. Pharm. Sci.*, **64**, 610(1975).

(849) A. C. Shah and K. G. Nelson, *ibid.*, **64**, 1518(1975).

(850) H. M. El-Ba-na, A. R. Ebian, and A. A. Ismail, *Pharmazie*, **30**, 455(1975); through *Chem. Abstr.*, **83**, 136823s(1975).

(851) H. Andersgaard, P. Finholt, and R. Gjermundson, *Acta Pharm. Suec.*, **11**, 239(1974); through *Chem. Abstr.*, **82**, 7601y(1975).

(852) J. H. Collett and J. A. Rees, *J. Pharm. Pharmacol.*, **27**, 647(1975).

(853) S. Goto, J. Nakashima, T. Minoru, H. Sato, and T. Nakayanna, *Yakuzaigaku*, **34**, 160(1974); through *Chem. Abstr.*, **83**, 152268v(1975).

(854) S. Dubois and R. Tawashi, *Pharm. Acta Helv.*, **50**, 184(1975); through *Chem. Abstr.*, **83**, 120757n(1975).

(855) B. R. Hajratwala, *Aust. J. Pharm. Sci.*, **3**, 101(1974); through *Chem. Abstr.*, **82**, 103043p(1975).

(856) Sh. Froekjar and V. S. Andersen, *Arch. Pharm. Chemi, Sci. Ed.*, **2**, 79(1974); through *Chem. Abstr.*, **82**, 160159e(1975).

(857) A. Hoelgaard and N. Moeller, *ibid.*, **3**, 65(1975); through *Chem. Abstr.*, **83**, 152289c(1975).

(858) K. Nobuyoshi and A. Ikekawa, *Chem. Pharm. Bull.*, **23**, 2973(1975).

(859) O. I. Corrigan and R. F. Timoney, *J. Pharm. Pharmacol.*, **27**, 759(1975).

(860) S. A. Said, H. M. El-Fatatry, and A. S. Geneidi, *Aust. J. Pharm. Sci.*, **3**, 42(1974); through *Chem. Abstr.*, **82**, 90007c(1975).

(861) J. Riehl and H. Walz, *Arch. Pharm.*, **307**, 857(1974); through *Chem. Abstr.*, **82**, 90016e(1975).

(862) P. Schwarze and H. Hittinger, *Pharm. Ind.*, **36**, 732(1974); through *Chem. Abstr.*, **82**, 90035k(1975).

(863) T. Saito, S. Suzuki, N. Nambu, and T. Nagai, *Yakuzaigaku*, **34**, 143(1974); through *Chem. Abstr.*, **83**, 136819v(1975).

(864) G. G. Kwee and G. A. Ulex, *Pharm. Ind.*, **36**, 576(1974); through *Chem. Abstr.*, **82**, 47676h(1975).

(865) R. V. Bathe, O. Hafliger, F. Langenbucher, and D. Schonleber, *Pharm. Acta Helv.*, **50**, 3(1975); through *Chem. Abstr.*, **82**, 144902m(1975).

(866) N. Randall and J. A. Goldsmith, *Lab. Pract.*, **24**, 77(1975); through *Chem. Abstr.*, **82**, 175185j(1975).

(867) A. C. Shah, C. B. Peot, and J. F. Ochs, *Adv. Autom. Anal., Technicon Int. Congr.*, **9**, 35(1973); through *Chem. Abstr.*, **82**, 160185k(1975).

(868) C. Cakiryildiz, P. Mehta, W. Rahmen, and D. Schoenleber, *J. Pharm. Sci.*, **64**, 1692(1975).

(869) M. J. Groves and M. H. Alkan, *Manuf. Chem. Aerosol News*, **46**, 37(1975).

(870) K. Raymond, E. Shotton, and P. Patel, *Postgrad. Med. J. Suppl.*, **50**, 40(1974); through *Chem. Abstr.*, **82**, 175193k(1975).

(871) E. J. Fraser, R. H. Leach, and J. W. Poston, *ibid.*, **50**, 43(1974); through *Chem. Abstr.*, **83**, 15577f(1975).

(872) J. B. Stenlake and D. Watt, *J. Pharm.*, **214**, 56(1975).

(873) N. Kingsley and R. M. McCredie, *Med. J. Aust.*, **1**, 698(1974); through *Chem. Abstr.*, **82**, 64395h(1975).

(874) K. Matsunaga, E. Masai, I. Tsutomu, K. Furukawa, K. Miyai, Y. Hirano, and S. Tsuro, *Iryo*, **27**, 787(1973); through *Chem. Abstr.*, **82**, 175191h(1975).

(875) E. Doelker, H. Schwyter, and D. Mordier, *Pharm. Acta Helv.*, **50**, 24(1975); through *Chem. Abstr.*, **83**, 48125k(1975).

(876) M. A. Page, R. A. Anderson, K. F. Brown, and M. S. Roberts, *Aust. J. Pharm. Sci.*, **3**, 95(1974); through *Chem. Abstr.*, **83**, 32981a(1975).

(877) K. Shikifumi, I. Johno, I. Yoko, S. Teramura, and J. Okada, *J. Pharm. Pharmacol.*, **27**, 765(1975).

(878) H. Armand, J. M. Lemarie, G. P. Graham, C. Jeannin, and A. Verain, *Pharm. Belg.*, **30**, 150(1975); through *Chem. Abstr.*, **83**, 136811m(1975).

(879) W. H. Thomas and G. F. Cooney, *Aust. J. Pharm. Sci.*, **3**, 37(1974); through *Chem. Abstr.*, **82**, 90006b(1975).

(880) S. J. A. Bolman, *Pharm. Weekbl.*, **110**, 41(1975); through *Chem. Abstr.*, **83**, 48127n(1975).

(881) D. L. Simmons, A. A. Legor, P. Picotte, K. S. Lee, and J. Narendra, *J. Pharmacokinet. Biopharm.*, **3**, 39(1975).

(882) T. N. Huynh and G. Sirois, *Pharm. Acta Helv.*, **50**, 69(1975); through *Chem. Abstr.*, **83**, 15581c(1975).

(883) N. H. Choulis and H. Papadopoulos, *J. Pharm. Sci.*, **64**, 1033(1975).

(884) J. Sanchez-Morcillo, A. Cerezo, and J. Sune, *Cienc. Ind. Farm.*, **6**, 416(1974); through *Chem. Abstr.*, **83**, 15561w(1975).

(885) S. A. Hill, K. Jones, H. Seager, and C. Taskis, *J. Pharm. Pharmacol.*, **27**, 594(1975).

(886) D. Barrett and J. T. Fell, *J. Hosp. Pharm.*, **32**, 192(1974); through *Chem. Abstr.*, **82**, 12921t(1975).

(887) C. Cid and G. Moran, *An. R. Acad. Farm.*, **40**, 487(1974); through *Chem. Abstr.*, **83**, 15566b(1975).

(888) P. V. Pedersen and K. F. Brown, *J. Pharm. Sci.*, **64**, 1981(1975).

(889) K. A. Khan, *J. Pharm. Pharmacol.*, **27**, 48(1975).

(890) K. Sekiguchi, M. Kanke, N. Nakamura, and Y. Tsuda, *Chem. Pharm. Bull.*, **23**, 1347(1975).

(891) K. Sekiguchi, Y. Tsuda, and M. Kanke, *ibid.*, **23**, 1353(1975).

(892) I. Arias and R. Cadorniga, *Boll. Chim. Farm.*, **113**, 82(1974); through *Chem. Abstr.*, **82**, 34989n(1975).

(893) H. E. Tschakert, *Seifen, Oele, Fette, Wachse*, **100**, 499(1974); through *Chem. Abstr.*, **82**, 126892d(1975).

(894) A. F. Asker and C. W. Whitworth, *Pharmazie*, **30**, 530(1975); through *Chem. Abstr.*, **83**, 168447p(1975).

(895) H. El-Banna and A. A. Ismail, *ibid.*, **30**, 226(1975); through *Chem. Abstr.*, **83**, 15589m(1975).

(896) F. Langenbucher, *Pharm. Acta Helv.*, **49**, 187(1974); through *Chem. Abstr.*, **82**, 77060v(1975).

(897) W. Czarnecki and H. Nerlo, *Acta Pol. Pharm.*, **32**, 227(1975); through *Chem. Abstr.*, **83**, 183347z(1975).

(898) P. L. Madan, *J. Pharm. Sci.*, **64**, 1080(1975).

(899) S. Honma and S. Shirasaki, *Hokkaidoritsu Eisei Kenkyusho Ho*, **24**, 165(1974); through *Chem. Abstr.*, **83**, 136798n (1975).

(900) A. Stamm and C. Mathis, *J. Pharm. Belg.*, **29**, 375(1974); through *Chem. Abstr.*, **82**, 34993j(1975).

(901) L. Nyberg, L. Bratt, A. Forsgren, and S. Hugosson, *Acta Pharm. Suec.*, **11**, 447(1974); through *Chem. Abstr.*, **82**, 64431s(1975).

(902) K. Satake, N. Zaitsu, T. Shibuta, S. Maeno, M. Takahama, and K. Nakamura, *Kyushu Yakugakkai Kaiho*, **28**, 7(1974); through *Chem. Abstr.*, **83**, 103095g(1975).

(903) *Ibid.*, **28**, 13(1974); through *Chem. Abstr.*, **82**, 103094f(1975).

(904) H. Nerlo and W. Czarnecki, *Pol. J. Pharmacol. Pharm.*, **26**, 549(1974); through *Chem. Abstr.*, **82**, 175194m(1975).

(905) J. Coll, *Circ. Farm.*, **32**, 625(1974); through *Chem. Abstr.*, **82**, 160188p(1975).

(906) A. Kassem, S. Said, and S. El-Bassouni, *Manuf. Chem. Aerosol News*, **46**, 53(1975).

(907) J. Sanchez-Morcillo, A. Cerezo, and F. Aguilar, *Ars Pharm.*, **15**, 67(1974); through *Chem. Abstr.*, **83**, 15602k(1975).

(908) G. S. Bashura, G. I. Kabachnyi, and I. M. Pertsev, *Farm. Zh.*, **29**, 26(1974); through *Chem. Abstr.*, **82**, 77021h(1975).

(909) I. Grabowska, R. Kaliszan, and P. Zoga, *Acta Pol. Pharm.*, **31**, 189(1974); through *Chem. Abstr.*, **82**, 34988m(1975).

(910) S. Prakongpan, *Diss. Abstr. Int.*, **35**, 5350(1975).

(911) A. M. Molokhia and W. I. Higuchi, *J. Pharm. Sci.*, **64**, 2029(1975).

(912) D. Mufson, K. Triyanond, and L. J. Ravin, *ibid.*, **64**, 362(1975).

(913) S. Miyazaki, M. Nakano, and T. Arita, *Chem. Pharm. Bull.*, **23**, 1197(1975).

(914) G. I. Linkov and S. A. Zhukovskaya, *Antibiotiki*, **20**, 53(1975); through *Chem. Abstr.*, **82**, 160167f(1975).

(915) P. Rohdewald, *Pharmazie*, **30**, 460(1975); through *Chem. Abstr.*, **83**, 197725h(1975).

(916) *Ibid.*, **30**, 532(1975); through *Chem. Abstr.*, **83**, 183330p(1975).

(917) W. F. Stanaszek, B. Ecanow, and R. S. Levinson, *Proc. Okla. Acad. Sci.*, **54**, 80(1974); through *Chem. Abstr.*, **82**, 47684j(1975).

(918) Y. Chien and H. Lambert, *Chem. Pharm. Bull.*, **23**, 1085(1975).

(919) S. Batra, *J. Pharm. Pharmacol.*, **27**, 777(1975).

(920) I. B. Kovach, *Diss. Abstr. Int.*, **36**, 734-B(1975).

(921) D. Attwood, C. McDonald, and S. Perry, *J. Pharm. Pharmacol.*, **27**, 692(1975).

(922) L. S. Wan and P. F. S. Lee, *Can. J. Pharm. Sci.*, **10**, 69(1975).

(923) J. H. Collett, R. Withington, and L. Koo, *J. Pharm. Pharmacol.*, **27**, 46(1975).

(924) Y. Kawashima, M. Saito, and H. Takenaka, *ibid.*, **27**, 6(1975).

(925) P. Rohdewald, *Pharm. Ztg.*, **119**, 959(1974); through *Chem. Abstr.*, **82**, 21757k(1975).

(926) S. N. Giri and L. R. Kartt, *Experientia*, **31**, 482(1975); through *Chem. Abstr.*, **83**, 15576e(1975).

(927) A. A. Ismail, M. W. Goudah, and M. M. Motawi, *Pharm. Ind.*, **36**, 735(1974); through *Chem. Abstr.*, **82**, 116043p(1975).

(928) M. J. Hunt and L. Saunders, *J. Pharm. Pharmacol.*, **27**, 119(1975).

(929) W. Schlemmer, *Dtsch. Apoth.-Ztg.*, **114**, 2017(1974); through *Chem. Abstr.*, **82**, 129216x(1975).

(930) J. Knapczyk and K. Jarnot-Jurkiewicz, *Farm. Pol.*, **30**, 927(1974); through *Chem. Abstr.*, **82**, 175148z(1975).

(931) W. Kuerst, M. Falk, R. Neubert, and I. Klapper, *Pharmazie*, **30**, 614(1975); through *Chem. Abstr.*, **83**, 201777w(1975).

(932) S. Borodkin and F. E. Tucker, *J. Pharm. Sci.*, **64**, 1289(1975).

(933) N. H. Choulis and H. Papadopoulos, *Pharmazie*, **30**, 233(1975); through *Chem. Abstr.*, **83**, 48156w(1975).

(934) T. Kolobow, F. Hayano, and P. Weathersby, *Med. Instrum.*, **9**, 124(1975); through *Chem. Abstr.*, **83**, 197773x(1975).

(935) T. Kolobow and R. G. Spragg, *ibid.*, **7**, 268(1973); through *Chem. Abstr.*, **83**, 197774y(1975).

(936) Y. Nozawa, F. Higashide, and T. Kanakoto, *J. Polym. Sci.*, **13**, 433(1975).

(937) N. Yano, Y. Nozawa, and F. Higashide, *Yakuzaigaku*, **34**, 59(1974); through *Chem. Abstr.*, **83**, 136815r(1975).

(938) M. Falk and W. Fuerst, *Pharmazie*, **29**, 590(1974); through *Chem. Abstr.*, **82**, 34991g(1975).

(939) *Ibid.*, **29**, 715(1974); through *Chem. Abstr.*, **82**, 77053v(1975).

(940) M. Donbrow and M. Friedman, *J. Pharm. Pharmacol.*, **27**, 633(1975).

(941) K. T. Richardson, Jr., *Trans. New Orleans Acad. Ophthalmol.*, **23**, 50(1975); through *Chem. Abstr.*, **83**, 15226e(1975).

(942) M. W. Gouda, S. N. Malik, and S. A. Khalil, *Can. J. Pharm. Sci.*, **10**, 24(1975).

(943) B. K. Davis, *Proc. Nat. Acad. Sci. USA*, **71**, 3120(1974); through *Chem. Abstr.*, **82**, 21790r(1975).

(944) J. Ketteringham, W. Zapol, J. Birkett, L. Nelsen, A. Massucco, and C. Raith, *Trans. Am. Soc. Artif. Intern. Organs*, **21**, 224(1975); through *Chem. Abstr.*, **83**, 168423c(1975).

(945) B. C. Lippold and G. F. Schneider, *Arzneim-Forsch.*, **25**, 843(1975); through *Chem. Abstr.*, **83**, 197735m(1975).

(946) M. Bornschein, H. Bauer, and R. Voigt, *Pharmazie*, **30**, 304(1975); through *Chem. Abstr.*, **83**, 120737f(1975).

(947) M. Falk, W. Fuerst, E. Hannig, and R. Boehm, *ibid.*, **29**, 542(1974); through *Chem. Abstr.*, **82**, 11034h(1975).

(948) J. S. Turi, N. F. H. Ho, W. I. Higuchi, and C. Shipman, *J. Pharm. Sci.*, **64**, 631(1975).

(949) T. Nadai, M. Kume, A. Tatematsu, and H. Sezaki, *Chem. Pharm. Bull.*, **23**, 543(1975).

(950) T.-F. Chin and J. L. Lach, *Am. J. Hosp. Pharm.*, **32**, 625(1975).

(951) V. J. Stella, *J. Pharm. Sci.*, **64**, 706(1975).

(952) J. S. Turi, N. F. H. Ho, W. I. Higuchi, and C. Shipman, *ibid.*, **64**, 622(1975).

(953) J. S. Turi, W. I. Higuchi, N. F. H. Ho, and C. Shipman, *ibid.*, **64**, 627(1975).

(954) K. J. Humphreys and J. R. Smy, *J. Pharm. Pharmacol.*, **27**, 962(1975).

(955) V. Pasotti and L. Fleischmann, *Boll. Chim. Farm.*, **114**, 259(1975); through *Chem. Abstr.*, **83**, 152775v(1975).

(956) C. W. Whitworth and R. E. Stephenson, *Can. J. Pharm. Sci.*, **10**, 89(1975).

(957) Z. T. Chowhan and R. Pritchard, *J. Pharm. Sci.*, **64**, 754(1975).

(958) M. S. Roberts and R. A. Anderson, *J. Pharm. Pharmacol.*, **27**, 599(1975).

(959) W. Horsch and B. Mette, *Pharmazie*, **29**, 546(1974); through *Chem. Abstr.*, **82**, 7609g(1975).

(960) A. Kubis and Z. Olszewski, *Acta Pol. Pharm.*, **31**, 781(1974); through *Chem. Abstr.*, **83**, 48137r(1975).

(961) W. Horsch, J. Koegel, and U. Kretzschmann, *Pharmazie*, **30**, 56(1975); through *Chem. Abstr.*, **82**, 144895m(1975).

(962) M. Gillet-Vanderbruggen and M. Roland, *J. Pharm. Belg.*, **30**, 3(1975); through *Chem. Abstr.*, **83**, 183326s(1975).

(963) A. S. Michaels, S. K. Chandrasekaran, and J. E. Shaw, *AIChE J.*, **21**, 985(1975); through *Chem. Abstr.*, **83**, 188176c(1975).

(964) K. Kakemi, H. Kameda, M. Kakemi, M. Ueda, and T. Koizumi, *Chem. Pharm. Bull.*, **23**, 2109(1975).

(965) *Ibid.*, **23**, 2114(1975).

(966) M. Ishihara, *Dermatol. Proc. Int. Congr. 14th*, **1972**, 971; through *Chem. Abstr.*, **83**, 103221r(1975).

(967) J. Barrelet, M. Tsacopoulos, and P. Buri, *J. Pharm. Pharmacol.*, **27**, 919(1975).

(968) A. M. Guyot-Hermann, C. Bonnet, H. Robert, and P. Balatre, *J. Pharm. Belg.*, **29**, 297(1974); through *Chem. Abstr.*, **82**, 21803x(1975).

(969) M. L. Shih, *Diss. Abstr. Int.*, **35**, 5970-B(1975).

(970) H. Wardynska, *Acta Pol. Pharm.*, **32**, 95(1975); through *Chem. Abstr.*, **83**, 136809s(1975).

(971) V. Zecchi, L. Rodriguez, and M. Amorosa, *Farmaco, Ed. Prat.*, **29**, 714(1974); through *Chem. Abstr.*, **82**, 77057z(1975).

(972) A. A. Kassem, E. Nour El-Din, A. Abd El-Bary, and H. M. Fadel, *Pharmazie*, **30**, 472(1975).

(973) C. Crevoisier, P. Buri, and J. Boucherat, *Pharm. Acta Helv.*, **50**, 231(1975); through *Chem. Abstr.*, **83**, 188172y(1975).

(974) N. Nambu, S. Sakurai, and T. Nagai, *Chem. Pharm. Bull.*, **23**, 1404(1975).

(975) J. M. Padfield and I. Kellaway, *J. Pharm. Pharmacol.*, **27**, 348(1975).

(976) M. J. Lysaght and C. A. Ford, *Proc. Annu. Conf. Eng. Med. Biol.*, **15**, 137(1973); through *Chem. Abstr.*, **82**, 103035n(1975).

(977) P. Buri and C. Crevoisier, *Bull. Tech. Gattefosse SFPA*, **68**, 38(1974); through *Chem. Abstr.*, **83**, 152222a(1975).

(978) S. Affrossman, J. M. Courtney, T. Gilchrist, and I. Martin, *Med. Biol. Eng.*, **13**, 539(1975); through *Chem. Abstr.*, **83**, 168438m(1975).

(979) Y. Chien, H. Lambert, and T. Lin, *J. Pharm. Sci.*, **64**, 1643(1975).

(980) T. J. Roseman, *ibid.*, **64**, 1731(1975).

(981) S. R. Turner, M. Litt, W. S. Lynn, *J. Colloid Interface Sci.*, **50**, 181(1975).

(982) Y. M. Amin and J. B. Nagwekar, *J. Pharm. Sci.*, **64**, 1804(1975).

(983) *Ibid.*, **64**, 1813(1975).

(984) B. Richter, J. Kary, and R. Voigt, *Pharmazie*, **30**, 591(1975); through *Chem. Abstr.*, **83**, 197764v(1975).

(985) T. Yotsuyanagi, A. Molokhia, S. Hwang, N. F. H. Ho, G. L. Flynn, and W. I. Higuchi, *J. Pharm. Sci.*, **64**, 71 (1975).

(986) A. M. Josse-Auzelle and J. C. Chaumeil, *Ann. Pharm. Fr.*, **32**, 581(1974); through *Chem. Abstr.*, **83**, 48123h(1975).

(987) W. Horsch, J. Koegel, M. Schiefer, and I. Finke, *Pharmazie*,

29, 720(1974); through *Chem. Abstr.*, **83,** 90011z(1975).

(988) J. Horacek and M. Cernikova, *Cesk. Dermatol.*, **50,** 21(1975); through *Chem. Abstr.*, **83,** 108166m(1975).

(989) D. C. Horne, *J. Hosp. Pharm.*, **32,** 177(1974); through *Chem. Abstr.*, **82,** 47683h(1975).

(990) R. H. Bowman, *Am. J. Physiol.*, **229,** 93(1975).

(991) M. M. Ghoneim and H. Pandya, *Anesthesiology*, **42,** 545(1975); through *Chem. Abstr.*, **83,** 108134z(1975).

(992) D. S. Lukas, *Symp. Digitalis*, **1973,** 31; through *Chem. Abstr.*, **83,** 350c(1975).

(993) R. A. Henry and W. D. Wosilait, *Toxicol. Appl. Pharmacol.*, **33,** 267(1975).

(994) G. D. Olsen, *Clin. Pharmacol. Ther.*, **17,** 31(1975).

(995) J. Prandota and A. W. Pruitt, *ibid.*, **17,** 159(1975).

(996) D. Sharples, *J. Pharm. Pharmacol.*, **27,** 379(1975).

(997) W. D. Hooper, D. K. Dubetz, F. Bochner, L. M. Cotter, G. A. Smith, M. J. Eadle, and J. H. Tyrer, *Clin. Pharmacol. Ther.*, **17,** 433(1975).

(998) D. Naik, W. Paul, and S. Schulman, *J. Pharm. Sci.*, **64,** 1677(1975).

(999) A. Yacobi and G. Levy, *ibid.*, **64,** 1660(1975).

(1000) J. H. Perrin and D. A. Nelson, *ibid.*, **64,** 361(1975).

(1001) U. Gundert-Remy, M. Klett, and E. Weber, *Eur. J. Clin. Pharmacol.*, **6,** 133(1973); through *Chem. Abstr.*, **82,** 106122z(1975).

(1002) S. Øie and G. Levy, *J. Pharm. Sci.*, **64,** 1433(1975).

(1003) A. Yacobi and G. Levy, *J. Pharmacokinet. Biopharm.*, **3,** 439(1975).

(1004) K. F. Ilett, I. E. Hughes, and L. B. Jellett, *J. Pharm. Pharmacol.*, **27,** 861(1975).

(1005) W. D. Wosilait, *Res. Commun. Chem. Pathol. Pharmacol.*, **12,** 147(1975); through *Chem. Abstr.*, **83,** 201724b(1975).

(1006) S. Javidan and R. G. Mrtek, *J. Pharm. Sci.*, **64,** 420(1975).

(1007) J. M. Christensen and S. Holfort, *J. Pharm. Pharmacol.*, **27,** 538(1975).

(1008) Y. Chien, M. Akers, and P. Yonan, *J. Pharm. Sci.*, **64,** 1632(1975).

(1009) D. R. Sanvordeker, Y. W. Chien, T. K. Lin, and H. J. Lambert, *ibid.*, **64,** 1797(1975).

(1010) K. A. Bachmann and A. M. Burkman, *J. Pharm. Pharmacol.*, **27,** 832(1975).

(1011) Y. Imamura, K. Shigemori, and H. Ichibagase, *Chem. Pharm. Bull.*, **23,** 1377(1975).

(1012) F. M. Belpaire and M. G. Bogaert, *Xenobiotica*, **5,** 421(1975); through *Chem. Abstr.*, **83,** 188137r(1975).

(1013) J. E. Doherty, W. H. Hall, S. Joyce, D. Girkin, and J. Gammill, *Symp. Digitalis*, **1973,** 48; through *Chem. Abstr.*, **83,** 200d(1975).

(1014) F. Alhaique, D. Giacchetti, M. Marchetti, and F. M. Riccieri, *J. Pharm. Pharmacol.*, **27,** 811(1975).

(1015) R. Honorato, E. Novoa, and M. Ayala, *Acta Physiol. Lat. Am.*, **24,** 134(1974); through *Chem. Abstr.*, **82,** 64377d(1975).

(1016) J. P. Bennett and S. H. Snyder, *Brain Res.*, **94,** 523(1975); through *Chem. Abstr.*, **83,** 188152s(1975).

(1017) B. Beermann, K. Hellstrom, B. Linstrom, and A. Rosen, *Clin. Pharmacol. Ther.*, **17,** 424(1975).

(1018) M. H. Bickel, *J. Pharm. Pharmacol.*, **27,** 733(1975).

(1019) B. Beermann, K. Hellstrom, B. Lindstrom, and A. Rosen, *Clin. Pharmacol. Ther.*, **17,** 424(1975).

(1020) P. Hsu, *Diss. Abstr. Int.*, **36,** 2158-B(1975).

(1021) K. Takada, O. Narumiya, and S. Muranish, *Chem. Pharm. Bull.*, **23,** 729(1975).

(1022) K. O'Malley, M. Valasco, A. Puritt, and J. McNay, *Clin. Pharmacol Ther.*, **18,** 53(1975).

(1023) G. Olsen, W. Bennett, and G. Porter, *ibid.*, **17,** 677(1975).

(1024) F. Bottari, G. DiColo, E. Nannipieri, M. F. Saettone, and M. F. Serafini, *J. Pharm. Sci.*, **64,** 946(1975).

(1025) D. Attwood and O. K. Udeala, *J. Phys. Chem.*, **79,** 889(1975); through *Chem. Abstr.*, **83,** 15588k(1975).

(1026) Y. Hamada, N. Nambu, and T. Nagai, *Chem. Pharm. Bull.*, **23,** 1205(1975).

(1027) K. Ikeda, K. Uekama, and M. Otagiri, *ibid.*, **23,** 201(1975).

(1028) K. Uekama, M. Otagiri, Y. Kanie, S. Tanka, and K. Ikeda, *ibid.*, **23,** 1421(1975).

(1029) M. Otagiri, K. Uekama, and K. Ikeda, *ibid.*, **23,** 188(1975).

(1030) B. L. Chang, N. O. Nuessle, and W. G. Haney, Jr., *J. Pharm. Sci.*, **64,** 1787(1975).

(1031) K. J. Morgan and R. A. Anderson, *Aust. J. Pharm. Sci.*, **3,** 110(1974).

(1032) T. Goina, C. Rif, and G. Schmidt, *Rev. Med.*, **20,** 83(1974); through *Chem. Abstr.*, **82,** 21758m(1975).

(1033) S. Khalil, M. Moustafa, G. Ghaly, M. Gouda, and M. Motawi, *Can. J. Pharm. Sci.*, **10,** 83(1975).

(1034) G. Ghaly, S. Khalil, M. Moustafa, M. Gouda, and M. Motawi, *ibid.*, **10,** 79(1975).

(1035) S. G. Frank, *J. Pharm. Sci.*, **64,** 1585(1975).

(1036) M. K. Park, *Diss. Abstr. Int.*, **35,** 3425B(1975).

(1037) C. R. Kowarski and H. I. Ghandi, *J. Pharm. Sci.*, **64,** 696(1975).

(1038) M. B. M. Mrtek, *Diss. Abstr. Int.*, **36,** 2734-B(1975).

(1039) S. A. Said, H. M. El-Fatatry, and A. S. Geneidi, *Aust. J. Pharm. Sci.*, **3,** 42(1974); through *Chem. Abstr.*, **82,** 90007c(1975).

(1040) A. M. Saleh and N. A. Daabis, *Pharmazie*, **29,** 525(1974); through *Chem. Abstr.*, **82,** 47689q(1975).

(1041) H. Rupprecht and M. Biedermann, *Dtsch. Apoth.-Ztg.*, **115,** 1249(1975); through *Chem. Abstr.*, **83,** 183358d(1975).

(1042) H. Rupprecht, F. Stanislaus, and G. Lagaly, *Colloid Polym. Sci.*, **253,** 773(1975); through *Chem. Abstr.*, **83,** 197745q(1975).

(1043) S. C. Lin, V. C. Sutherland, and E. L. Way, *Proc. West Pharmacol. Soc.*, **18,** 181(1975); through *Chem. Abstr.*, **83,** 197733j(1975).

(1044) J. Cape, D. H. Cook, and D. R. Williams, *J. Chem. Soc., Dalton Trans.*, **17,** 1849(1974).

(1045) S. Alberola, J. Rambaud, J. Masse, and F. Sabon, *Trav. Soc. Pharm. Montpellier*, **34,** 275(1974); through *Chem. Abstr.*, **82,** 160179m(1975).

(1046) L. Marszall, *Zentralbl. Pharm. Pharmakother. Laboratoriumsdiagn.*, **113,** 959(1974); through *Chem. Abstr.*, **82,** 64355v(1975).

(1047) W. E. Brochu, *Diss. Abstr. Int.*, **36,** 659-B(1975).

(1048) D. Bourne, *ibid.*, **36,** 732-B(1975).

(1049) J. S. Sahai, *Labdev, Part A*, **11A,** 81(1973); through *Chem. Abstr.*, **83,** 197736n(1975).

(1050) H. Rupprecht, L. Mansel, and E. Ullmann, *Pharm. Ind.*, **37,** 22(1975); through *Chem. Abstr.*, **83,** 48131j(1975).

(1051) M. C. Poelman, J. C. Chameil, and F. Puisieux, *Ann. Pharm. Fr.*, **32,** 595(1974); through *Chem. Abstr.*, **83,** 3259B(1975).

(1052) L. J. Stoel, *Diss. Abstr.*, **35,** 3259B(1975).

(1053) N. E. Richardson and B. J. Meakin, *J. Pharm. Pharmacol.*, **27,** 145(1975).

(1054) B. G. Gazzard, P. G. Langley, M. J. Weston, E. H. Dunlop, and R. Williams, *Clin. Sci. Mol. Med.*, **47,** 97(1974); through *Chem. Abstr.*, **82,** 64417s(1975).

(1055) G. Porcelli, M. DiIorio, M. Ranier, and F. Menichini, *Farmaco, Ed. Sci.*, **29,** 548(1974); through *Chem. Abstr.*, **82,** 64412m(1975).

(1056) G. Popescu, M. Radu, and D. Anghel, *Chem. Phys. Chem. Anwendungstech. Grenzflaechenaktiven Stoffe, Ber. Int. Kongr. 6th*, **2,** 953(1973); through *Chem. Abstr.*, **82,** 60458h(1975).

(1057) P. A. Demchenko, T. P. Kudrya, and V. G. Roskolodko, *Kolloidn. Zh.*, **36,** 765(1974); through *Chem. Abstr.*, **82,** 5562n(1975).

(1058) K. Konno, M. Sakiyama, and A. Kitahara, *Yukagaku*, **23,** 501(1974); through *Chem. Abstr.*, **82,** 5565r(1975).

(1059) P. Kahela and J. Honkavaara, *Farm. Aikak.*, **83,** 201(1974); through *Chem. Abstr.*, **83,** 15586h(1975).

(1060) B. C. Lippold, L. Mansel, and E. Ullmann, *Pharm. Ind.*, **37,** 100(1975); through *Chem. Abstr.*, **83,** 168372k(1975).

(1061) D. I. Dmitrievskii, I. P. Pertsev, and G. S. Bashura, *Farm. Zh.*, **29,** 75(1974); through *Chem. Abstr.*, **82,** 116038r(1975).

(1062) E. D. Goddard, J. S. Phillips, and R. B. Hannon, *J. Soc. Cosmet. Chem.*, **26,** 461(1975).

(1063) S. A. Said. H. M. El-Fatatry, and M. S. El-Samaligy, *Aust. J. Pharm. Sci.*, **3,** 123(1974); through *Chem. Abstr.*, **82,** 116046s(1975).

(1064) L. Wan, *Can. J. Pharm. Sci.*, **10,** 29(1975).

(1065) E. Ellmann, *Dtsch. Apoth.-Ztg.*, **115,** 1240(1975).

(1066) K. Negoro, *Sen'i Kako*, **26,** 631(1974); through *Chem. Abstr.*, **82,** 88028s(1975).

(1067) S. J. A. Kazmi, *Diss. Abstr. Int.*, **35,** 5511-B(1975).

(1068) E. Ruckenstein and J. C. Chi, *J. Chem. Soc., Faraday Trans.*

2, **71**, 1690(1975); through *Chem. Abstr.*, **83**, 183967b(1975).

(1069) A. A. Giniger, *Diss. Abstr. Int.*, **36**, 2822-B(1975).

(1070) D. Dollimore, N. F. Owens, *Chem. Phys. Chem. Anwendungstech. Grenzflaechenaktiven Stoffe, Ber. Int. Kongr., 6th*, **2**, 631(1973); through *Chem. Abstr.*, **82**, 22210p(1975).

(1071) T. Morimoto, M. Nagao, and J. Imai, *Bull. Chem. Soc. Jpn.*, **47**, 2994(1974); through *Chem. Abstr.*, **83**, 90359u(1975).

(1072) G. D. Stafford and R. Huggett, *IRCS Libr. Compend.*, **1**, (1973); through *Chem. Abstr.*, **82**, 35005a(1975).

(1073) S. Tanada, K. Boki, T. Tamura, and K. Matsumoto, *Yakuzaigaku*, **34**, 128(1974); through *Chem. Abstr.*, **83**, 136818u(1975).

(1074) A. B. Dhruv, T. E. Needham, and L. A. Luzzi, *Can. J. Pharm. Sci.*, **10**, 33(1975).

(1075) F. J. Holly and M. F. Refojo, *J. Biomed. Mater. Res.*, **9**, 315(1975); through *Chem. Abstr.*, **83**, 48178e(1975).

(1076) M. H. Rubinstein, *J. Pharm. Pharmacol.*, **27**, 776(1975).

(1077) J. L. Zatz, *J. Pharm. Sci.*, **64**, 1080(1975).

(1078) A. Vaziri, *IRCS Libr. Compend.*, **2**, 1598(1974); through *Chem. Abstr.*, **82**, 47682g(1975).

(1079) D. Attwood and O. K. Udeala, *J. Pharm. Pharmacol.*, **27**, 806(1975).

(1080) B. M. Gupta, *Diss. Abstr. Int.*, **35**, 3424B(1975).

(1081) R. S. Mikhail and S. Brunauer, *J. Colloid Interface Sci.*, **52**, 572(1975).

(1082) E. Robens and G. Walter, *Method. Chim.*, **B**, 678(1974).

(1083) D. Attwood and O. K. Udeala, *J. Pharm. Pharmacol.*, **27**, 754(1975).

(1084) V. Veber and M. Paucek, *Acta Fac. Pharm. Univ. Comenianae*, **26**, 241(1974); through *Chem. Abstr.*, **82**, 144908t(1975).

(1085) V. P. Boiko and V. G. Chernenko, *Maslob.-Zhir. Prom.*, **11**, 20(1974); through *Chem. Abstr.*, **82**, 77377d(1975).

(1086) H. N. Borazan, *J. Pharm. Sci.*, **64**, 770(1975).

(1087) L. Wan, *ibid.*, **64**, 1037(1975).

(1088) J. Kolthammer, *J. Pharm. Pharmacol.*, **27**, 801(1975).

(1089) B. C. Lippold and B. H. Lippold, *Pharmazie*, **29**, 534(1974); through *Chem. Abstr.*, **82**, 47690h(1975).

(1090) I. B. Ishkil'din, *Vaktsiny Syvorotki*, **20**, 175(1973); through *Chem. Abstr.*, **82**, 90042k(1975).

(1091) C. P. Huang, *J. Colloid Interface Sci.*, **53**, 178(1975).

(1092) H. E. Marsh, Jr., G. C. Hsu, C. J. Wallace, and D. H. Blankenhorn, *Am. Chem. Soc. Div. Org. Coat. Plast. Chem. Pap.*, **33**, 327(1973); through *Chem. Abstr.*, **83**, 15572a(1975).

(1093) L. V. Emets, V. V. Kotetski, I. M. Strukova, A. M. Maksimov, and L. A. Vol'f, *Zh. Obsch. Khim.*, **44**, 2041(1974); through *Chem. Abstr.*, **82**, 77048x(1975).

(1094) R. Levy and C. Francis, *J. Colloid Interface Sci.*, **50**, 442(1975).

(1095) J. J. V. De Souza, A. K. Mitra, and B. K. Gupta, *East. Pharm.*, **17**, 117(1974); through *Chem. Abstr.*, **82**, 21764k(1975).

(1096) N. A. Mamleeva and L. I. Nekrasov, *Zh. Fiz. Khim.*, **48**, 1874(1974); through *Chem. Abstr.*, **82**, 22175f(1975).

(1097) H. Rupprecht and F. Stanislaus, *Pharm. Ind.*, **36**, 797(1974); through *Chem. Abstr.*, **82**, 90040h(1975).

(1098) A. N. Armstrong and A. Johns, *J. Hosp. Pharm.*, **32**, 185(1974); through *Chem. Abstr.*, **82**, 129211s(1975).

(1099) N. A. Klimenko, A. A. Premilovskays, and A. M. Koganovskii, *Kolloidn. Zh.*, **36**, 788(1974); through *Chem. Abstr.*, **82**, 5564q(1975).

(1100) H. Rupprecht and H. Liebl, *Pharm. Ztg.*, **120**, 179(1975); through *Chem. Abstr.*, **83**, 48133m(1975).

(1101) W. Huhn, *Fortschr. Wasserchem. Ihrer Grenzgeb.*, **15**, 167(1973); through *Chem. Abstr.*, **82**, 22127s(1975).

(1102) D. A. Tadzhieva, N. K. Khadzhikhanov, E. A. Aripov, and T. M. Makhmudov, *Tr. Taskk. i Fegan. Politekh, in-tou*, **5**, 82(1973); through *Chem. Abstr.*, **83**, 16219c(1975).

(1103) G. N. Al'tshuler and A. I. Fomchenkova, *Zh. Fiz. Khim.*, **49**, 1591(1975); through *Chem. Abstr.*, **83**, 168377r(1975).

(1104) G. N. Al'tshuler and A. I. Fomchenkova, *Zh. Fiz. Khim.*, **49**, 1589(1975); through *Chem. Abstr.*, **83**, 168376q(1975).

(1105) A. V. Uzhegov, L. M. Cyueva, and G. A. Tishchenko, *Khim.-Farm. Zh.*, **8**, 43(1974); through *Chem. Abstr.*, **82**, 64379f(1975).

(1106) I. B. Petkanchin, S. Sokerov, and S. P. Stoilov, *Chem. Phys. Chem. Anwendungstech. Grenzflaechenaktiven Stoffe Ber. Int. Kongr. 6th*, **2**, 671(1972); through *Chem. Abstr.*, **82**, 22212r(1975).

(1107) A. T. Florence, F. Madsen, and F. Puisieux, *J. Pharm. Pharmacol.*, **27**, 385(1975).

(1108) A. Brodin, *Acta Pharm. Suec.*, **12**, 41(1975); through *Chem. Abstr.*, **83**, 32970w(1975).

(1109) M. Donbrow, R. Hamburger, and E. Azaz, *J. Pharm. Pharmacol.*, **27**, 160(1975).

(1110) V. A. Lutsenko, R. M. Panich, O. P. Koren'kova, and L. I. Chebotaeva, *Kolloidn. Zh.*, **37**, 181(1975).

(1111) T. Kuwamura, H. Takahashi, Y. Umezu, and H. Ohkawa, *Yukagaku*, **24**, 176(1975); through *Chem. Abstr.*, **83**, 45138f(1975).

(1112) H. Andree and P. Krings, *Chem.-Ztg.*, **99**, 168(1975); through *Chem. Abstr.*, **83**, 30294e(1975).

(1113) H. Hein, *Seifen, Oele, Fette, Wachse*, **101**, 443(1975); through *Chem. Abstr.*, **83**, 195641d(1975).

(1114) T. Kuwamura, *Yukagaku*, **23**, 703(1974); through *Chem. Abstr.*, **82**, 88025p(1975).

(1115) Y. K. Jeon, *Sumyu Konghak Hoeji*, **11**, 43(1974); through *Chem. Abstr.*, **82**, 32751e(1975).

(1116) S. Kuroiwa, *Yukagaku*, **23**, 521(1974); through *Chem. Abstr.*, **82**, 32753g(1975).

(1117) W. Wirth, *Tenside Deterg.*, **12**, 245(1975).

(1118) W. W. Morgenthaler, *Surfactant Sci. Ser., Part 2*, **5**, 453(1975); through *Chem. Abstr.*, **83**, 149496N(1975).

(1119) G. Lang, *Inf. Chim.*, **146**, 119(1975); through *Chem. Abstr.*, **83**, 149495m(1975).

(1120) H. Lange, *Chem.-Ztg.*, **99**, 161(1975); through *Chem. Abstr.*, **83**, 30293d(1975).

(1121) T. Sasaki, *Yukagaku*, **24**, 207(1975); through *Chem. Abstr.*, **83**, 45130x(1975).

(1122) H. Lange, *Tenside Deterg.*, **12**, 27(1975); through *Chem. Abstr.*, **82**, 158123v(1975).

(1123) J. Perka and S. Ropuszynski, *Pr. Nauk Inst. Technol.*, **18**, 31(1975); through *Chem. Abstr.*, **83**, 12727u(1975).

(1124) J. Micic, *Hem. Ind.*, **29**, 337(1975); through *Chem.Abstr.*, **83**, 166164v(1975).

(1125) G. Proserpio and V. Mariotti, *Riv. Ital. Essenze, Profumi, Piante Off., Aromi, Saponi, Cosmet., Aerosol*, **55**, 820(1973); through *Chem. Abstr.*, **82**, 21697r(1975).

(1126) A. Radecki and L. Marszall, *Rozpr. Wydz., 3*, **9**, 5(1973); through *Chem. Abstr.*, **82**, 45575a(1975).

(1127) *Ibid.*, **9**, 25(1973); through *Chem. Abstr.*, **82**, 60416t(1975).

(1128) R. Runac, *Hem. Ind.*, **29**, 351(1975); through *Chem. Abstr.*, **83**, 152747a(1975).

(1129) P. M. Kruglyakov, T. V. Mikina, and A. F. Foretskii, *Izv. Sib., Otd. Akad, Nauk SSSR, Ser. Khim. Nauk*, **1**, 3(1974); through *Chem. Abstr.*, **82**, 88032p(1975).

(1130) P. M. Kruglikov and A. F. Koretskii, *Opyt Primen. Nov. Moyushch. Sredstv*, **1973**, 76; through *Chem. Abstr.*, **83**, 99681w(1975).

(1131) M. E. Bottini and I. Bonadeo, *Riv. Ital. Essenze, Profumi, Piante Off., Aromi, Saponi, Cosmet., Aerosol*, **56**, 707(1974); through *Chem. Abstr.*, **83**, 15563y(1975).

(1132) T. Okumura, A. Nakamura, K. Tajima, and T. Sasaki, *Bull. Chem. Soc. Jpn.*, **47**, 2986(1974); through *Chem. Abstr.*, **83**, 90337k(1975).

(1133) T. A Lyubova, T. S. Solov'eva, S. A. Kovaleva, L. G. Tokareva, and S. G. Serebryakova, *Zh. Prikl. Khim.*, **48**, 1608(1975); through *Chem. Abstr.*, **83**, 195645h(1975).

(1134) A. J. Hyde, D. H. Maguire, and D. M. Stevenson, *Chem. Phys. Chem. Anwendungstech. Grenzflaechenaktiven Stoffe, Ber. Int. Kongr.*, **2**, 813(1972); through *Chem. Abstr.*, **82**, 35290q(1975).

(1135) K. Negoro, *Sen'i Kato*, **26**, 631(1974); through *Chem. Abstr.*, **82**, 88028s(1975).

(1136) A. A. Petrov and Y. S. Smirnov, *Kollodn. Zh.*, **37**, 187(1975); through *Chem. Abstr.*, **82**, 158129b(1975).

(1137) M. J. Rosen, *J. Am. Oil Chem. Soc.*, **51**, 461(1974); through *Chem. Abstr.*, **82**, 60429z(1975).

(1138) D. N. Levchenko and N. M. Nikolaeva, *Chem. Phys. Chem. Anwendungstech. Grenzflaechenaktiven Stoffe, Bar. Int. Kongr.*, **2**, 157(1972); through *Chem. Abstr.*, **82**, 60488t(1975).

(1139) P. A. Crooks, J. H. Collett, and R. Withington, *Pharm. Acta Helv.*, **49**, 274(1974); through *Chem. Abstr.*, **82**, 129229d(1975).

(1140) K. Shirahama, *Bull. Chem. Soc. Jpn.*, **47**, 3165(1974); through *Chem. Abstr.*, **83**, 90345m(1975).

(1141) J. T. G. Overbeek, *Versl. Gewone Vergad. Afd. Natuurkd. K. Ned. Akad. Wet.*, **84**, 73(1975); through *Chem. Abstr.*, **83**, 181439g(1975).

(1142) Y. Moroi, N. Nishikido, and R. Matuura, *J. Colloid Interface Sci.*, **50**, 344(1975).
(1143) Y. Moroi, N. Nishikido, M. Saito, and R. Matuura, *ibid.*, **52**, 356(1975).
(1144) J. H. Collett and L. Koo, *Acta Pharm. Suec.*, **12**, 81(1975); through *Chem. Abstr.*, **83**, 15587j(1975).
(1145) S. Kuroiwa, S. Ogasawara, T. Kawasaki, and M. Yamazaki, *Yukagaku*, **23**, 567(1974); through *Chem. Abstr.*, **82**, 77386f(1975).
(1146) S. Kaneshina, M. Tanaka, and R. Matuura, *Mem. Fac. Sci. Kyushu Univ. Ser. C*, **9**, 71(1974); through *Chem. Abstr.*, **82**, 60443z(1975).
(1147) N. Nishikido, Y. Moroi, H. Uehara, and R. Matura, *Bull. Chem. Soc. Jpn.*, **47**, 2634(1974); through *Chem. Abstr.*, **82**, 60443z(1975).
(1148) H. Schott and S. Kyuhan, *J. Pharm. Sci.*, **64**, 658(1975).
(1149) D. Attwood and O. K. Udeala, *J. Pharm. Pharmacol.*, **27**, 395(1975).
(1150) L. J. Ravin, E. G. Shami, and E. S. Rattie, *J. Pharm. Sci.*, **64**, 1830(1975).
(1151) S. S. Dukhin, *Surf. Colloid Sci.*, **7**, 1(1974); through *Chem. Abstr.*, **82**, 47909I(1975).
(1152) S. Gravsholt, *Chem. Phys. Chem. Anwendungstech. Grenzflaechenaktiven Stoffe, Ber. Int. Kongr.*, **2**, 805(1973); through *Chem. Abstr.*, **82**, 35289w(1975).
(1153) S. N. Markina, O. P. Bovkun, and V. V. Levin, *ibid.*, **2**, 1001(1973); through *Chem. Abstr.*, **82**, 35292s(1975).
(1154) R. C. Dorrance and T. F. Hunter, *J. Chem. Soc., Faraday Trans.*, **70**, 1572(1974); through *Chem. Abstr.*, **82**, 35254f(1975).
(1155) P. Tormala and J. Brotherus, *Finn. Chem. Lett.*, **4**, 127(1974); through *Chem. Abstr.*, **82**, 48021c(1975).
(1156) T. Hikota and K. Meguro, *Yukagaku*, **23**, 563(1974); through *Chem. Abstr.*, **82**, 77385e(1975).
(1157) K. Thoma, *Pharm. Ind.*, **37**, 552(1975); through *Chem. Abstr.*, **83**, 168396w(1975).
(1158) N. Muller, *J. Phys. Chem.*, **79**, 287(1975); through *Chem. Abstr.*, **82**, 88030m(1975).
(1159) M. Tanaka, S. Kaneshina, S. Kuramoto, and R. Matuura, *Bull. Chem. Soc. Jpn.*, **48**, 432(1975); through *Chem. Abstr.*, **82**, 126896h(1975).
(1160) T. Hikota and K. Meguro, *Yukagaku*, **23**, 560(1974), through *Chem. Abstr.*, **82**, 77384d(1975).
(1161) K. Deguchi and K. Meguro, *J. Colloid Interface Sci.*, **50**, 223(1975).
(1162) Y. Moroi, N. Nishikido, and R. Matuura, *ibid.*, **50**, 344(1975).
(1163) J. E. Rassing and E. Wyn-Jones, *Ber. Bunsenges, Phys. Chem.*, **78**, 651(1974); through *Chem. Abstr.*, **82**, 60428t(1975).
(1164) R. Folger, H. Hoffman, and W. Ulbricht, *ibid.*, **78**, 980(1974); through *Chem. Abstr.*, **83**, 90340f(1975).
(1165) J. S. Noh, K. S. Lee, S. H. Chang, and W. Ahn, *Taehan Hwahak Hoechi*, **18**, 354(1974); through *Chem. Abstr.*, **82**, 3527n(1975).
(1166) A. O. Den and J. Koning, *Chem. Phys. Chem. Anwendungstech. Grenzflaechenaktiven Stoffe, Ber. Int. Kongr.*, **2**, 909(1973); through *Chem. Abstr.*, **82**, 35291r(1975).
(1167) A. Heyd and D. Dhabhar, *J. Pharm. Sci.*, **64**, 1697(1975).
(1168) R. Schwarz and P. Speiser, *Inform. Arbeitsgem. Pharm. Verfahrenstech.*, **20**, 210(1974); through *Chem. Abstr.*, **82**, 145483n(1975).
(1169) J. Robinson, I. Kellaway, and C. Marriott, *J. Pharm. Pharmacol.*, **27**, 653(1975).
(1170) G. S. Bashura, G. V. Tsagaereishvili, A. S. Lekham, and I. P. Kovalev, *Tr. Inst. Farmakokhim., Akad. Nauk Gruz. SSR*, **12**, 218(1973); through *Chem. Abstr.*, **83**, 103214r(1975).
(1171) M. S. Mohamed, I. Y. Gurevich, and A. A. Abramzon, *Farmatsiya*, **24**, 29(1975); through *Chem. Abstr.*, **83**, 168407a(1975).
(1172) A. A. Trapeznikov, A. T. Pylaeva, and Y. A. Bureev, *Kolloidn. Zh.*, **37**, 716(1975); through *Chem. Abstr.*, **83**, 184049r (1975).
(1173) J. A. J. Robinson, I. W. Kellaway, and C. Marriott, *J. Pharm. Pharmacol.*, **27**, 818(1975).
(1174) H. Asche, *Pharm. Acta Helv.*, **49**, 277(1974); through *Chem. Abstr.*, **82**, 129230x(1975).
(1175) T. Abe, T. Komatsu, and H. Fukuchi, *Yakuzaigaku*, **34**, 105(1974); through *Chem. Abstr.*, **83**, 136817t(1975).
(1176) A. J. Cutie, *Diss. Abstr. Int.*, **36**, 2234-B(1975).
(1177) I. Eros, E. Toricht, and I. Bacsi, *Gyogyszereszet.*, **19**, 290(1975); through *Chem. Abstr.*, **83**, 18331q(1975).
(1178) I. I. Kocherga, A. A. Baran, and O. D. Kurilevko, *Dopov. Akad. Nauk Ukr. RSR*, **5**, 438(1975); through *Chem. Abstr.*, **83**, 137322q(1975).
(1179) A. F. Asker and O. R. Jerbina, *Pharmazie*, **30**, 186(1975); through *Chem. Abstr.*, **83**, 152260m(1975).
(1180) M. Singh and N. A. Coulter, Jr., *Biorheology*, **11**, 217(1974).
(1181) M. Pormale, N. A. Kashkina, E. Simsone, and D. Adamone, *Khim. Drev.*, **3**, 108(1975); through *Chem. Abstr.*, **83**, 103219w(1975).
(1182) S. L. Swarzen-Allan and E. Matijevic, *J. Colloid Interface Sci.*, **50**, 143(1975).
(1183) K. R. Stauffer and S. A. Andon, *Food Technol.*, **29**, 46(1975).
(1184) K. L. Krumel and N. Sarkar, *ibid.*, **29**, 36(1975).
(1185) J. T. H. Ong and H. B. Kostenbauder, *J. Pharm. Sci.*, **64**, 1378(1975).
(1186) H. Terada and T. Inagi, *Chem. Pharm. Bull.*, **23**, 1960(1975).
(1187) W. B. Ackart, R. L. Camp, W. L. Wheelwright, and J. S. Byck, *J. Biomed. Mater. Res.*, **9**, 55(1975); through *Chem. Abstr.*, **82**, 144928z(1975).
(1188) J. P. Hou and A. Restivo, *J. Pharm. Sci.*, **64**, 710(1975).
(1189) J. J. Piecoro, N. L. Goodman, W. E. Wheeler, P. R. Gwilt, and R. P. Rapp, *Am. J. Hosp. Pharm.*, **32**, 381(1975).
(1190) M. J. Cho, A. J. Repta, C. C. Cheng, K. Y. Zee-Cheng, T. Higuchi, and I. H. Pitman, *J. Pharm. Sci.*, **64**, 1825(1975).
(1191) M. Roig, L. Castells, P. Mestres, M. Jordi, and A. De la Chica, *Cienc. Ind. Farm.*, **7**, 173(1975); through *Chem. Abstr.*, **83**, 183352x(1975).
(1192) J. Meyers, K. Kroan, and G. DeNardo, *J. Nucl. Med.*, **16**, 835(1975); through *Chem. Abstr.*, **83**, 197776a(1975).
(1193) V. I. Stanko, V. K. Shavratskii, T. G. Malinina, and V. N. Kulakov, *Isotopenpraxis*, **10**, 259(1974); through *Chem. Abstr.*, **82**, 77065a(1975).
(1194) Y. Cohne, *Radioanal. Chem.*, **26**, 317(1975); through *Chem. Abstr.*, **83**, 168358k(1975).
(1195) H. Stelmach and J. L. Quinn, *Semin. Nucl. Med.*, **4**, 295(1974); through *Chem. Abstr.*, **82**, 21739f(1975).
(1196) Y. Murakami, *Genshiryoku Kogyo*, **20**, 9(1974); through *Chem. Abstr.*, **82**, 34970z(1975).
(1197) K. Hisada, *ibid.*, **20**, 14(1974); through *Chem. Abstr.*, **82**, 34971a(1975).
(1198) R. S. Tilbury, *Semin. Nucl. Med.*, **4**, 245(1974); through *Chem. Abstr.*, **82**, 21738e(1975).
(1199) T. Kobayashi, *Oyo Butsuri*, **43**, 845(1974); through *Chem. Abstr.*, **82**, 116008f(1975).
(1200) H. B. Hupf, *Study Guide Nucl. Med.*, **1972**, 36; through *Chem. Abstr.*, **83**, 103185g(1975).
(1201) A. E. A. Mitta, *Bioquim. Clin.* **8**, 165(1974); through *Chem. Abstr.*, **83**, 15519p(1975).
(1202) B. Beermann, K. Hellstrom, and A. Rosen, *Symp. Digitalis*, **1973**, 213; through *Chem. Abstr.*, **82**, 132750x(1975).
(1203) B. Beermann, *Eur. J. Clin. Pharmacol.*, **5**, 28(1972); through *Chem. Abstr.*, **83**, 92871d(1975).
(1204) W. J. Jusko, L. Gerbracht, L. H. Golden, and J. R. Koup, *Res. Commun. Chem.*, **10**, 189(1975); through *Chem. Abstr.*, **82**, 13695h(1975).
(1205) B. Ablad, M. Ervik, J. Hallgren, G. Johnsson, and L. Solvell, *Eur. J. Clin. Pharmacol.*, **5**, 44(1972); through *Chem. Abstr.*, **83**, 93301e(1975).
(1206) H. Vapaatalo, A. Penttila, and E. Ka'tiala, *J. Pharm. Pharmacol.*, **27**, 538(1975).
(1207) F. Waldeck, *Drugs Made Ger.*, **15**, 10(1972); through *Chem. Abstr.*, **82**, 25509d(1975).
(1208) M. Gibaldi, *J. Pharm. Sci.*, **64**, 1036(1975).
(1209) T. R. Bates and J. A. L. Sequeira, *ibid.*, **64**, 709(1975).
(1210) W. J. Jusko, L. W. Dittert, and J. T. Doluisio, *J. Am. Pharm. Assoc.*, **15**, 591(1975).
(1211) D. E. Cadwallader and J. Swarbrick, *ibid.*, **15**, 409(1975).
(1212) S. Feldman, H. B. Kostenbauder, and S. Riegelman, *ibid.*, **15**, 647(1975).
(1213) E. T. Sugita, P. J. Niebergall, J. A. Seitz, and P. G. Welling, *ibid.*, **15**, 529(1975).
(1214) T. D. Sokoloski, M. R. Blum, L. J. Leeson, and K. S. Lin, *ibid.*, **15**, 709(1975).

(1215) W. G. Crouthamel, J. W. Poole, and T. Sokoloski, *ibid.*, **15,** 461(1975).
(1216) J. L. Colaizzi and J. G. Wagner, *ibid.*, **15,** 43(1975).
(1217) M. E. Baer, H. B. Hucker, and D. E. Duggan, *Ann. Clin. Res. Suppl.*, **6,** 44(1974); through *Chem. Abstr.*, **82,** 10919p(1975).
(1218) P. Niebergall, E. Sugita, and R. Schnaare, *J. Pharm. Sci.*, **64,** 1721(1975).
(1219) K. Kwan, J. Bondi, and K. Yeh, *ibid.*, **64,** 1639(1975).
(1220) H. Boxenbaum and S. Kaplan, *J. Pharmacokinet. Biopharm.*, **3,** 257(1975).
(1221) M. Dobrinska and P. Welling, *J. Pharm. Sci.*, **64,** 1728(1975).
(1222) J. Meier, E. Nuesch, and R. Schmidt, *Eur. J. Clin. Pharmacol.*, **7,** 429(1974).
(1223) W. J. Westlake, *J. Pharm. Sci.*, **64,** 1075(1975).
(1224) W. J. Westlake, *Biometrics*, **30,** 319(1974); through *Chem. Abstr.*, **82,** 106088t(1975).
(1225) D. P. Vaughan, *J. Pharm. Pharmacol.*, **27,** 458(1975).
(1226) W. Crouthamel, C. Abolin, J. Hsieh, and J. Lim, *J. Pharm. Sci.*, **64,** 1726(1975).
(1227) J. J. Marty and J. A. Hersey, *J. Pharm. Pharmacol.*, **27,** 437(1975).
(1228) M. J. Groves, M. H. Alkan, and M. A. Deer, *ibid.*, **27,** 400(1975).
(1229) J. M. Jaffe, J. D. Strum, P. C. Martineau, and J. L. Colaizzi, *J. Pharm. Sci.*, **64,** 2028(1975).
(1230) T. Inaba and W. Kalow, *Clin. Pharmacol. Ther.*, **18,** 558(1975).
(1231) B. Idson, *J. Pharm. Sci.*, **64,** 901(1975).
(1232) T. J. Franz, *J. Invest. Dermatol.*, **64,** 190(1975).
(1233) K. J. Ryan and M. Mezei, *J. Pharm. Sci.*, **64,** 671(1975).
(1234) T. F. Patton, *Diss. Abstr. Int.*, **36,** 1158-B(1975).
(1235) J. M. Pla-Delfina, J. Moreno, J. Duran, and A. Del Pozo, *J. Pharmacokinet. Biopharm.*, **3,** 115(1975).
(1236) G. Levy and A. Yacobi, *J. Clin. Pharmacol. New Drugs*, **15,** 525(1975).
(1237) R. C. Wester and H. I. Maibach, *Toxicol. Appl. Pharmacol.*, **32,** 394(1975).
(1238) S. Miyazaki, M. Nakano, and T. Arita, *Chem. Pharm. Bull.*, **23,** 552(1975).
(1239) *Ibid.*, **23,** 2151(1975).
(1240) K. Matsumoto, Y. Uzuka, I. Umezawa, K. Komiyama, T. Morino, and H. Takeshima, *Jpn. J. Antibiot.*, **27,** 481(1974); through *Chem. Abstr.*, **82,** 16016z(1975).
(1241) J. P. Clayton, M. Cole, S. W. Elson, and H. Ferres, *Antimicrob. Ag. Chemother.*, **5,** 670(1974); through *Chem. Abstr.*, **82,** 64391d(1975).
(1242) Y. Kimura, H. Kano, Y. Noguchi, T. Tanaka, and K. Shimooka, *Chemotherapy*, **23,** 591(1975); through *Chem. Abstr.*, **83,** 108129b(1975).
(1243) K. Roholt, B. Nielsen, and E. Kristensen, *Antimicrob. Ag. Chemother.*, **6,** 563(1974); through *Chem. Abstr.*, **82,** 68042p(1975).
(1244) L. Verbist, *ibid.*, **6,** 588(1974); through *Chem. Abstr.*, **82,** 68043q(1975).
(1245) H. Matsui, N. Sakamotb, H. Sasaki, F. Kumagai, S. Kawahara, and M. Murakami, *Yamanouchi Seiyaku Kenkyu Hokoku*, **2,** 109(1974); through *Chem. Abstr.*, **83,** 157679q(1975).
(1246) W. A. Ritschel, P. E. Ring, and E. G. Siegel, *Arzneim.-Forsch.*, **25,** 853(1975); through *Chem. Abstr.*, **83,** 152282v(1975).
(1247) T. R. D. Shaw and J. E. Carless, *Eur. J. Clin. Pharmacol.*, **7,** 269(1974); through *Chem. Abstr.*, **83,** 32954u(1975).
(1248) A. J. Jounela, P. J. Pentikainen, and A. Sothmann, *ibid.*, **8,** 365(1975); through *Chem. Abstr.*, **83,** 152284x(1975).
(1249) A. A. Sinkula, *ACS Symp. Ser.*, **14,** 116(1974); through *Chem. Abstr.*, **83,** 71318j(1975).
(1250) A. J. Repta, *ibid.*, **14,** 196(1974); through *Chem. Abstr.*, **83,** 71319k(1975).
(1251) V. Stella, *ibid.*, **14,** 1(1975); through *Chem. Abstr.*, **83,** 71317h(1975).
(1252) D. W. Bourne, *Diss. Abstr. Int.*, **36,** 732-B(1975).
(1253) S. Feldman, M. Defrancisco, and P. Cascella, *J. Pharm. Sci.*, **64,** 1713(1975).
(1254) A. H. Beckett and M. E. Pickup, *J. Pharm. Pharmacol.*, **27,** 226(1975).
(1255) T. R. Bates, H. Fung, H. Lee, and A. V. Tembo, *Res. Commun. Chem. Pathol. Pharmacol.*, **11,** 233(1975); through *Chem. Abstr.*, **83,** 120749m(1975).
(1256) E. J. Lien, *Med. Chem., Ser. Monogr.*, **5,** 81(1975); through *Chem. Abstr.*, **83,** 152237j(1975).
(1257) E. J. Lien, *Med. Chem. Proc. Int. Symp. Main Lect., 4th,* **1974,** 319; through *Chem. Abstr.*, **83,** 157721x(1975).
(1258) R. E. Notari, *Pharm. Weekbl.*, **110,** 577(1975); through *Chem. Abstr.*, **83,** 103182d(1975).
(1259) E. J. Ariens and A. M. Simonis, *Fed. Eur. Biochem. Soc. Meet.*, **30,** 725(1974); through *Chem. Abstr.*, **82,** 118665s(1975).
(1260) J. K. Kim, *Hwahak Kwa Kongop Ui Chinbo*, **15,** 28(1975); through *Chem. Abstr.*, **83,** 71236f(1975).
(1261) Y. Topaloglu, *Eczancilik Bul.*, **17,** 8(1975); through *Chem. Abstr.*, **83,** 103174c(1975).
(1262) K. Kuroda and T. Nomura, *Kobe J. Med. Sci.*, **20,** 47(1974); through *Chem. Abstr.*, **82,** 77039v(1975).
(1263) G. Ross and D. Hiller, *Pharm. Unserer Zeit*, **3,** 152(1974); through *Chem. Abstr.*, **82,** 7574s(1973).
(1264) S. A. Kaplan, *Adv. Autom. Anal., Technicon Int. Congr.*, **9,** 61(1972); through *Chem. Abstr.*, **82,** 149079h(1975).
(1265) E. Cid, *Pharm. Acta Helv.*, **49,** 285(1974); through *Chem. Abstr.*, **83,** 48106c(1975).
(1266) J. Lindenbaum, *Clin. Pharmacol. Ther.*, **17,** 296(1975).
(1267) C. Michalopoulos and C. Loutoulidis, *IRCS Libr. Compend.*, **2,** 1127(1974); through *Chem. Abstr.*, **82,** 64396j(1975).
(1268) L. Nyberg, K. E. Andersson, and A. Bertler, *Acta Pharm. Suec.*, **11,** 471(1974); through *Chem. Abstr.*, **82,** 77056y(1975).
(1269) J. J. Preibisz, V. P. Butler, and J. Lindenbaum, *Ann. Intern. Med.*, **81,** 469(1974); through *Chem Abstr.*, **82,** 77049y(1975).
(1270) D. J. Greenblatt, D. W. Duhme, J. Koch-Weser, and T. W. Smith, *J. Am Med. Assoc.*, **229,** 1774(1974); through *Chem. Abstr.*, **82,** 103096h(1975).
(1271) T. R. D. Shaw, K. Raymond, and H. Greenwood, *Postgrad. Med. J. Suppl.*, **50,** 55(1974); through *Chem. Abstr.*, **83,** 48155v(1975).
(1272) G. I. Mallis, D. H. Schmidt, and J. Lindenbaum, *Clin. Pharmacol. Ther.*, **18,** 761(1975).
(1273) T. Beveridge, F. Kalberger, E. Nueesch, and R. Schmidt, *Eur. J. Clin. Pharmacol.*, **8,** 371(1975); through *Chem. Abstr.*, **83,** 152285y(1975).
(1274) B. F. Johnson, C. Bye, and S. Lader, *Postgrad. Med. J. Suppl.*, **50,** 62(1974); through *Chem. Abstr.*, **83,** 15604n(1975).
(1275) B. Johnson, H. Greer, J. A. McGrerie, C. Bye, and A. S. E. Fowle, *ibid.*, **50,** 48(1974); through *Chem. Abstr.*, **83,** 120727c(1975).
(1276) E. G. Lovering, I. J. McGilveray, I. McMillan, W. Tostowaryk, T. Matula, and G. Marier, *Can. J. Pharm. Sci.*, **10,** 36(1975).
(1277) J. Tuomisto and P. Mannisto, *Eur. J. Clin. Pharmacol.*, **6,** 64(1973); through *Chem. Abstr.*, **82,** 900034j(1975).
(1278) V. F. Okhotnikova, I. Y. Geitman, V. D. Yakh'yaev, L. K. Grakovskaya, and G. Y. Kivman, *Antibiotiki*, **19,** 843(1974); through *Chem. Abstr.*, **82,** 26140p(1975).
(1279) J. J. Marty and J. A. Hersey, *Med. J. Aust.*, **1,** 382(1975); through *Chem. Abstr.*, **83,** 168405y(1975).
(1280) C. Simon, V. Malerczyk, and J. Grothkopp, *Med. Klin.*, **70,** 1637(1975); through *Chem. Abstr.*, **83,** 197763u(1975).
(1281) S. Feldman, *Am. J. Hosp. Pharm.*, **32,** 1173(1975).
(1282) D. Duggan, K. Yeh, N. Matalia, C. Ditzler, and F. McMahon, *Clin. Pharmacol. Ther.*, **18,** 205(1975).
(1283) T. Sullivan, E. Sakmar, K. Albert, D. Blair, and J. Wagner, *J. Pharm. Sci.*, **64,** 1723(1975).
(1284) T. J. Sullivan, *Diss. Abstr. Int.*, **35,** 5513(1975).
(1285) S. Pittlich, L. Cohen, and J. Rosenfeld, *Isr. Pharm. J.*, **17,** 73(1974); through *Chem. Abstr.*, **82,** 90036m(1975).
(1286) A. M. Monro and P. G. Welling, *Eur. J. Clin. Pharmacol.*, **7,** 47(1974); through *Chem. Abstr.*, **83,** 15594j(1975).
(1287) W. Rupp, H. W. Dibbern, P. Hajdu, G. Ross, and E. E. Vander, *Dtsch. Med. Wochenschr.*, **100,** 690(1975); through *Chem. Abstr.*, **83,** 230p(1975).
(1288) S. D. Gershon, *Cosmet. Perfum.*, **90,** 45(1975).
(1289) B. Calesnick, C. H. Costello, J. P. Ryan, and G. J. DiGregorio, *Toxicol. Appl. Pharmacol.*, **32,** 204(1975).
(1290) E. G. Lovering, I. J. McGilveray, I. McMillan, and W. Tostowaryk, *J. Pharm. Sci.*, **64,** 1521(1975).
(1291) B. Kammerau, A. Zesch, and H. Schaefer, *J. Invest. Dermatol.*, **64,** 145(1975).
(1292) W. A. Ritschel, E. G. Siegel, and P. E. Ring, *Sci. Pharm.*, **43,** 11(1975); through *Chem. Abstr.*, **83,** 103203m(1975).

(1293) F. Marcus, *Diss. Abstr. Int.*, **35,** 4974-B(1975).
(1294) M. Washitake, T. Anmo, I. Tanaka, T. Arita, and M. Nakano, *J. Pharm. Sci.*, **64,** 397(1975).
(1295) J. W. Ayres, D. Lorskulsint, and A. Lock, *ibid.*, **64,** 1958(1975).
(1296) H. L. Newmark, W. Pool, J. C. Bauernfeind, and E. DeRitter, *ibid.*, **64,** 655(1975).
(1297) S. P. Patel, *Diss. Abstr. Int.*, **35,** 4013-B(1975).
(1298) S. Yolles, T. D. Leafe, J. H. R. Woodland, and F. J. Meyer, *J. Pharm. Sci.*, **64,** 348(1975).
(1299) H. Kobayashi, T. Peng, A. Kagayama, K. Okumura, S. Muranishi, and H. Sezaki, *Chem. Pharm. Bull.*, **23,** 42(1975).
(1300) K. S. Hui and M. B. Roberts, *J. Pharm. Pharmacol.*, **27,** 569(1975).
(1301) E. Arakawa, Y. Imai, H. Kobayashi, K. Okumura, and H. Sezaki, *Chem. Pharm. Bull.*, **23,** 2218(1975).
(1302) J. W. Sieg and J. R. Robinson, *J. Pharm. Sci.*, **64,** 931(1975).
(1303) T. F. Patton and J. R. Robinson, *ibid.*, **64,** 267(1975).
(1304) *Ibid.*, **64,** 1312(1975).
(1305) H. M. Leibowitz and A. Kupferman, *Am. Acad. Ophthalmol. Otolaryngol.*, **78,** OP856(1974); through *Chem. Abstr.*, **83,** 183360y(1975).
(1306) R. M. Ramer and A. R. Gasset, *Ann. Ophthalmol.*, **6,** 1325(1974); through *Chem. Abstr.*, **83,** 15557z(1975).
(1307) V. F. Smolen, P. B. Kuehn, and E. J. Williams, *Drug. Dev. Commun.*, **1,** 231(1974); through *Chem. Abstr.*, **83,** 15585g(1975).
(1308) T. R. Bates and J. A. Sequeira, *J. Pharm. Sci.*, **64,** 793(1975).
(1309) T. R. Bates and P. J. Carrigan, *ibid.*, **64,** 1475(1975).
(1310) D. C. Bloedow, *Diss. Abstr. Int.*, **35,** 4973-B(1975).
(1311) H. Ogata, K. Kakemi, S. Muranishi, and H. Sezaki, *Chem. Pharm. Bull.*, **23,** 707(1975).
(1312) T. Nadai, M. Kume, A. Tatematsu, and H. Sezaki, *ibid.*, **23,** 543(1975).
(1313) S. N. Malik, D. H. Canaham, and M. W. Gouda, *J. Pharm. Sci.*, **64,** 987(1975).
(1314) A. T. Florence and J. M. N. Gillan, *J. Pharm. Pharmacol.*, **27,** 152(1975).
(1315) R. Koysooko, E. F. Ellis, and G. Levy, *J. Pharm. Sci.*, **64,** 299(1975).
(1316) J. B. Houston and G. Levy, *ibid.*, **64,** 607(1975).
(1317) W. L. Hayton, *ibid.*, **64,** 1450(1975).
(1318) J. Newburger, *Diss. Abstr. Int.*, **36,** 1157-B(1975).
(1319) G. Kedvessy, H. I. Abdel, and J. Morvay, *Pharmazie*, **30,** 476(1975); through *Chem. Abstr.*, **83,** 1975(1975).
(1320) A. R. DiSanto and K. A. DeSante, *J. Pharm. Sci.*, **64,** 109(1975).
(1321) H. Spatz and N. Spatz, *Therapiewoche*, **25,** 71(1975); through *Chem. Abstr.*, **82,** 144870z(1975).
(1322) C. Graffner, G. Johnsson, and J. Sjogren, *Clin. Pharmacol. Ther.*, **17,** 414(1975).
(1323) E. Karlsson, *Eur. J. Clin. Pharmacol.*, **6,** 245(1973); through *Chem. Abstr.*, **82,** 102075a(1975).
(1324) C. Bye, H. M. Hill, D. T. D. Hughes, and A. W. Peck, *ibid.*, **8,** 47(1974).
(1325) A. M. Soeterboek and M. Van Thiel, *Pharm. Weekbl.*, **110,** 129(1975); through *Chem. Abstr.*, **82,** 118754v(1975).
(1326) H. B. Hucker, S. C. Stauffer, F. G. Clayton, B. R. S. Nakra, and R. Gaind, *J. Clin. Pharmacol. New Drugs*, **15,** 168(1975).
(1327) I. McL. Baird, R. L. Waters, and D. R. Sutton, *Br. Med. J.*, **4,** 505(1974); through *Chem. Abstr.*, **82,** 77045u(1975).
(1328) W. Madee and K. Mueller-Wieland, *Arzneim-Forsch.*, **25,** 122(1975); through *Chem. Abstr.*, **83,** 48148v(1975).
(1329) A. Nagy and R. Johansson, *Naunyn-Schmiedeberg's Arch. Pharmacol.*, **290,** 145(1975); through *Chem. Abstr.*, **83,** 188185e(1975).
(1330) D. Gibbons and A. Lant, *Clin. Pharmacol. Ther.*, **17,** 578(1975).
(1331) H. Sevelius, R. Runkel, A. Pardo, E. Ortega, J. Varady, and E. Segre, *Eur. J. Clin. Pharmacol.*, **6,** 22(1973); through *Chem. Abstr.*, **82,** 90033h(1975).
(1332) G. Alvan, M. Orme, L. Bertilsson, R. Ekstrand, and L. Palmer, *Clin. Pharmacol. Ther.*, **18,** 364(1975).
(1333) H. B. Kostenbauder, R. P. Rapp, J. P. McGovren, T. S. Foster, D. G. Perrier, H. M. Blacker, W. C. Hulon, and A. W. Kinkel, *ibid.*, **18,** 449(1975).
(1334) M. Banarer and W. A. Ritschel, *Bull. Tech., Gattefoss SFPA*, **68,** 56(1974); through *Chem. Abstr.*, **83,** 157682k(1975).
(1335) D. J. Greenblatt, R. I. Shader, J. Koch-Weser, and K. Franke, *N. Engl. J. Med.*, **291,** 1116(1974); through *Chem. Abstr.*, **83,** 92899u(1975).
(1336) B. Alexanderson, O. Borga, and G. Alvan, *Eur. J. Clin. Pharmacol.*, **5,** 181(1973); through *Chem. Abstr.*, **82,** 68050q(1975).
(1337) B. E. Ballard, *J. Pharm. Sci.*, **64,** 781(1975).
(1338) B. Duhm and W. Maul, *Drugs Made Ger.*, **15,** 99(1972); through *Chem. Abstr.*, **82,** 10996m(1975).
(1339) S. Riegelman and M. Rowland, *Pharmacol. Pharmacokinet.*, **1972,** 87; through *Chem. Abstr.*, **83,** 15521h(1975).
(1340) D. H. Huffman, C. V. Manion, and D. L. Azarnoff, *J. Pharm. Sci.*, **64,** 433(1975).
(1341) J. Loo, M. Rowe, and I. McGilveray, *ibid.*, **64,** 1727 (1975).
(1342) A. T. Florence, *Pharm. J.*, **214,** 364(1975).
(1343) S. Kojima and J. Miyake, *Chem. Pharm. Bull.*, **23,** 1247(1975).
(1344) S. Kitazawa, H. Ito, and M. Iinuma, *ibid.*, **23,** 2128 (1975).
(1345) S. Kitazawa, I. Hajime, and H. Sezaki, *ibid.*, **23,** 1856(1975).
(1346) W. G. Crouthamel, L. Diamond, L. W. Dittert, and J. T. Doluisio, *J. Pharm. Sci.*, **64,** 664(1975).
(1347) J. M. Orr, *Diss. Abstr. Int.*, **36,** 252-B(1975).
(1348) T. Komuro, S. Kitazawa, and H. Sezaki, *Chem. Pharm. Bull.*, **23,** 909(1975).
(1349) J. M. Orr and L. Z. Benet, *Am. J. Dig. Dis.*, **20,** 858(1975); through *Chem. Abstr.*, **83,** 201729g(1975).
(1350) P. G. Welling, L. L. Lyons, W. A. Craig, and B. S. Trochta, *Clin. Pharmacol. Ther.*, **17,** 475(1975).
(1351) J. Jaffe, *J. Pharm. Sci.*, **64,** 1729(1975).
(1352) K. K. Adjepon-Yamoah, D. B. Scott, and L. F. Prescott, *Eur. J. Clin. Pharmacol.*, **7,** 397(1974); through *Chem. Abstr.*, **83,** 855w(1975).
(1353) J. C. Garnham, K. Raymon, E. Shotton, and P. Turner, *ibid.*, **8,** 107(1975); through *Chem. Abstr.*, **83,** 48159z(1975).
(1354) G. Boman, *ibid.*, **7,** 217(1974); through *Chem. Abstr.*, **82,** 16498y(1975).
(1355) J. R. Koup, W. J. Jusko, and A. L. Goldfarb, *J. Pharm. Sci.*, **64,** 2008(1975).
(1356) R. Vukovich, L. Brannick, A. Sugerman, and E. Neiss, *Clin. Pharmacol. Ther.*, **18,** 218(1975).
(1357) K. Chan, M. Kendall, W. Wells, and M. Mitchard, *J. Pharm. Pharmacol.*, **27,** 235(1975).
(1358) J. B. Houston and G. Levy, *J. Pharm. Sci.*, **64,** 1504(1975).
(1359) M. P. Braybooks, B. W. Barry, and E. T. Abbs, *J. Pharm. Pharmacol.*, **27,** 508(1975).
(1360) K. W. Kellaway and C. Marriott, *ibid.*, **27,** 283(1975).
(1361) P. T. Mearrick, D. N. Wade, D. J. Birkett, and J. Morris, *Aust. N. Z. J. Med.*, **4,** 144(1974); through *Chem. Abstr.*, **82,** 38402p(1975).
(1362) D. N. Wade, P. T. Mearrick, D. J. Birkett, and J. Morris, *ibid.*, **4,** 138(1974).
(1363) B. E. Cabana and L. W. Dittert, *J. Pharmacokinet. Biopharm.*, **3,** 143(1975).
(1364) C. T. Bauguess, J. H. Fincher, F. Sadik, and C. W. Hartman, *J. Pharm. Sci.*, **64,** 1489(1975).
(1365) K. J. Lavelle, D. J. Doedens, S. A. Kleit, and R. B. Forney, *Clin. Pharmacol. Ther.*, **17,** 355(1975).
(1366) L. G. Scharpf, I. D. Hill, and H. I. Maibach, *Arch. Environ. Health*, **30,** 7(1975); through *Chem. Abstr.*, **82,** 106147m(1975).
(1367) A. D. Munro-Faure, S. E. Arthur, J. Fox, B. F. Johnson, and S. Lader, *Postgrad. Med. J. Suppl.*, **50,** 14(1974); through *Chem. Abstr.*, **83,** 32930h(1975).
(1368) R. Haasis, D. Larbig, and K. O. Klenk, *Klin. Wochenschr.*, **53,** 529(1975); through *Chem. Abstr.*, **83,** 108123v(1975).
(1369) J. Dreyfuss, T. Mischler, E. S. Neiss, J. M. Shaw, and E. C. Schreiber, *Br. J. Dermatol.*, **93,** 379(1975); through *Chem. Abstr.*, **83,** 201727e(1975).
(1370) P. J. Creaven, L. M. Allen, and D. A. Alford, *J. Pharm. Pharmacol.*, **27,** 914(1975).
(1371) J. Strong, J. Dutcher, W. Lee, and A. Atkinson, *Clin. Pharmacol. Ther.*, **18,** 613(1975).
(1372) S. S. Stubbs, *Transplant. Proc.*, **7,** 11(1975); through *Chem.*

Abstr., **83,** 48103b(1975).

(1373) R. Revilla de Granda, *Cienc. Ind. Farm.*, **5,** 210(1973); through *Chem. Abstr.*, **83,** 1511e(1975).

(1374) T. P. Michaels, *Anal. Technicon Int. Congr.*, **9,** 29(1972); through *Chem. Abstr.*, **82,** 12934b(1975).

(1375) J. G. Wagner, *Relevant Pharmacokinet.* **1971,** 180; through *Chem. Abstr.*, **82,** 47642u(1975).

(1376) J. R. B. J. Brouwers, *Pharm. Weekbl.*, **110,** 337(1975); through *Chem. Abstr.*, **83,** 48139t(1975).

(1377) A. C. Playle, S. R. Gunning, and A. F. Llewellyn, *Pharm. Acta Helv.*, **49,** 298(1974); through *Chem. Abstr.*, **83,** 103232v(1975).

(1378) B. Beermann, K. Hillstrom, and A. Rosen, *Eur. J. Clin. Pharmacol.*, **5,** 87(1972).

(1379) J. Clayton, M. Cole, S. Elson, K. Hardy, L. Mizen, and R. Sutherland, *J. Med. Chem.*, **18,** 172(1975).

(1380) J. Dreyfuss, J. J. Ross, J. M. Shaw, I. Miller, and E. C. Shreiber, *J. Pharm. Pharmacol.*, **27,** 791(1975).

(1381) S. Goodwin, E. B. Raftery, A. D. Goldbert, H. Skeegs, A. E. Till, and C. M. Martin, *Antimicrob. Ag. Chemother.*, **6,** 388(1974); through *Chem. Abstr.*, **82,** 68403g(1975).

(1382) W. H. Mennicke, *Dtsch. Apoth.-Ztg.*, **115,** 1205(1975); through *Chem. Abstr.*, **83,** 172368f(1975).

(1383) S. Barrios, J. Sorensen, and R. Spickett, *J. Pharm. Pharmacol.*, **27,** 711(1975).

(1384) A. Bliding, *Eur. J. Clin. Pharmacol.*, **7,** 201(1974); through *Chem. Abstr.*, **82,** 164987w(1975).

(1385) H. Ochs, G. Bodem, and H. J. Dengler, *Klin. Wochenschr.*, **13,** 637(1974); through *Chem. Abstr.*, **82,** 47675g(1975).

(1386) R. Henning and G. Nyberg, *Eur. J. Clin. Pharmacol.*, **6,** 239(1973); through *Chem. Abstr.*, **82,** 116033k(1975).

(1387) E. Krstoffersson and L. Niemi, *Farm. Aikak.*, **83,** 19(1974); through *Chem. Abstr.*, **82,** 21763j(1975).

(1388) H. Rollag, T. Midtvedt, and S. Wetterhus, *Acta Paediatr. Scand.*, **64,** 421(1975); through *Chem. Abstr.*, **83,** 168385s(1975).

(1389) J. Pijck, H. Soep, and J. L. Fraux, *Chemotherapy*, **21,** 11(1974); through *Chem. Abstr.*, **82,** 116056v(1975).

(1390) J. Da Silva, J. A. Rosemberg, O. P. J. Capaccia, A. O. Barbosa, J. M. Araujo, and O. G. Dias, *Rev. Bras. Clin. Ter.*, **4,** 107(1975); through *Chem. Abstr.*, **83,** 103225v(1975).

(1391) H. Turakka and M. Airakinsen, *Clin. Res. Suppl.*, **6,** 34(1974); through *Chem. Abstr.*, **82,** 21769r(1975).

(1392) H. Turakka, V. E. Krogerus, and V. Vallinkoski, *Farm. Aikak.*, **83,** 43(1974); through *Chem. Abstr.*, **82,** 64407p(1975).

(1393) G. N. Tanasov and T. P. Vesselova, *Veterinariya*, **10,** 85(1974); through *Chem. Abstr.*, **83,** 15542r(1975).

(1394) R. Dugal, G. Caille, J. Brodeur, S. Cooper, and J. G. Besner, *Union Med. Can.*, **102,** 1744(1973); through *Chem. Abstr.*, **83,** 92858e(1975).

(1395) H. Rollag, S. Wetterhus, and T. Midtvedt, *Medd. Nor. Farm. Selsk.*, **37,** 123(1975); through *Chem. Abstr.*, **83,** 120787x(1975).

(1396) M. C. Meyer, A. P. Melikian, P. L. Whyatt, and W. A. G. Slywka, *Curr. Ther. Res. Clin.*, **17,** 570(1975); through *Chem. Abstr.*, **83,** 120751f(1975).

(1397) J. M. Mishler, C. A. Jackson, R. W. Nicora, and R. M. Julien, *Am. J. Hosp. Pharm.*, **32,** 489(1975).

(1398) K. Ilver, *Arch. Pharm. Chemi*, **81,** 725(1974); through *Chem. Abstr.*, **82,** 47651w(1975).

(1399) J. E. Stambaugh and I. W. Wainer, *J. Clin. Pharmacol.*, **15,** 269(1975).

(1400) C. R. Kowarski, R. M. Schachere, C. T. Agostini, and A. L. Friedman, *Pharm. Acta Helv.*, **50,** 91(1975); through *Chem. Abstr.*, **83,** 15608s(1975).

(1401) V. Hofmann, H. Ringsdorf, and G. Muacevic, *Makromol. Chem.*, **176,** 1929(1975); through *Chem. Abstr.*, **83,** 197731g(1975).

(1402) H. A. Rosenberg, *Diss. Abstr. Int.*, **36,** 1158-B(1975).

(1403) V. I. Ishchenko and L. V. Zharkov, *Farmatsiya*, **23,** 26(1974); through *Chem. Abstr.*, **82,** 47705s(1975).

(1404) I. Wiik, K. Svenn, T. Renaa, and L. Dramsrud, *Medd. Nor. Farm. Selsk.*, **37,** 21(1975); through *Chem. Abstr.*, **83,** 120739h(1975).

(1405) C. Graffner, G. Johnsson, and J. Sjogren, *Acta Pharm. Suec.*, **11,** 125(1974); through *Chem. Abstr.*, **82,** 21754g(1975).

(1406) B. Pankowska and J. Felczak, *Klin. Oczna*, **45,** 795(1975); through *Chem. Abstr.*, **83,** 18334lt(1975).

(1407) A. A. Verzin, *Antibiotiki*, **20,** 842(1975); through *Chem. Abstr.*, **83,** 201884d(1975).

(1408) L. Simioni, A. Buttinoni, and V. Tamassia, *Boll. Chim. Farm.*, **110,** 232(1974); through *Chem. Abstr.*, **83,** 103106m(1975).

(1409) H. Sato, M. Tsuruta, and T. Nakanishi, *Rakuno Kagaku No Kenkyu*, **24,** A139(1975); through *Chem. Abstr.* **83,** 183342u(1975).

(1410) J. P. Delporte and F. Jaminet, *J. Pharm. Belg.*, **30,** 99(1975); through *Chem. Abstr.*, **83,** 183329v(1975).

(1411) O. P. Lukash, V. A. Golovkin, S. F. Slivko, and N. G. Ribalka, **30,** 81(1975); through *Chem. Abstr.*, **83,** 136804m(1975).

(1412) G. Persson, *Acta Psychiatr. Scand.*, **50,** 174(1974); through *Chem. Abstr.*, **82,** 21770j(1975).

(1413) B. Testa and A. H. Beckett, *Pharm. Acta Helv.*, **49,** 21(1974); through *Chem. Abstr.*, **82,** 21772m(1975).

(1414) H. Kilchling, *Arzneim.-Forsch.*, **25,** 105(1975); through *Chem. Abstr.*, **83,** 22574f(1975).

(1415) D. Henschler, W. Buettner, and J. Patz, *Germ. Calcium Metab., Bone Metab. Bone Dis.*, **1975,** 111.

(1416) H. J. Gilfrich, K. F. Ober, and K. L. Rominger, *Verh. Dtsch. Ges. Inn. Med.*, **80,** 1095(1974); through *Chem. Abstr.*, **82,** 118756x(1975).

(1417) S. R. Chavan, S. T. Nikam, D. V. Pradhan, M. Bhide, and B. B. Gaitonde, *Indian J. Physiol. Pharmacol.*, **18,** 120(1974); through *Chem. Abstr.*, **82,** 77034q(1975).

(1418) T. Stozek, *Pol. J. Pharmacol. Pharm.*, **27,** 227(1975); through *Chem. Abstr.*, **83,** 168398y(1975).

(1419) H. Sevelius, R. Runkel, A. Pardo, E. Ortega, J. Varady, and E. Serge, *Eur. J. Clin. Pharmacol.*, **6,** 22(1973); through *Chem. Abstr.*, **82,** 90033h(1975).

(1420) J. G. Allen and C. A. Davies, *J. Pharm. Pharmacol.*, **27,** 50(1975).

(1421) T. Noguchi, C. Takahash, T. Kimura, S. Muranishi, and H. Sezaki, *Chem. Pharm. Bull.*, **23,** 775(1975).

(1422) H. Ogata, K. Kakemi, A. Furuya, F. Michiko, S. Muranishi, and H. Sezaki, *ibid.*, **23,** 716(1975).

(1423) T. Noguchi, Y. Jinguji, T. Kimura, S. Muranishi, and H. Sezaki, *ibid.*, **23,** 782(1975).

(1424) D. Baun, B. Bowen, and D. Wood, *Am. J. Hosp. Pharm.*, **32,** 1047(1975).

(1425) J. D. Cameron and D. W. Hedley, *Lancet*, **7908,** 700(1975).

(1426) C. Cardini, F. Mazzaracchio, and V. Querica, *Boll. Chim. Farm.*, **113,** 455(1974); through *Chem. Abstr.*, **83,** 1552u(1975).

(1427) J. W. Swanson and J. E. Lebeau, *J. Biomed. Mater. Res.*, **8,** 357(1974); through *Chem. Abstr.*, **82,** 116066y(1975).

(1428) E. F. Evans, J. D. Proctor, M. J. Fratkin, J. Velandia, and A. J. Wasserman, *Clin. Pharmacol. Ther.*, **17,** 44(1975).

(1429) J. M. Aiache, J. L. Vidal, S. Aiache, A. Jeanneret, and F. Cornat, *Labo-Pharma-Probl. Tech.*, **22,** 457(1974); through *Chem. Abstr.*, **82,** 21759n(1975).

(1430) G. Levy, *Alza Conf. Ser.*, **2,** 107(1973); through *Chem. Abstr.*, **82,** 57656b(1975).

(1431) J. G. Wagner, *Biopharm. Relevant Pharmacokinet.*, **1971,** 214; through *Chem. Abstr.*, **82,** 47643v(1975).

(1432) D. Bustos and E. Cid, *Farmaco, Ed. Prat.*, **30,** 388(1975); through *Chem. Abstr.*, **83,** 120759q(1975).

(1433) P. Finholt, *Informationsdienst, Arbeitsgem. Pharm. Verfahrenstech.*, **20,** 279(1974); through *Chem. Abstr.*, **83,** 32933m(1975).

(1434) A. Zaremba and L. Krowczynski, *Acta Pol. Pharm.*, **32,** 89(1975); through *Chem. Abstr.*, **83,** 183328u(1975).

(1435) W. D. Hoffman, A. Zesch, and H. Schaefer, *Dermatol. Forsch.*, **250,** 295(1974); through *Chem. Abstr.*, **82,** 47685k(1975).

(1436) Y. Nakamoto, M. Fujiwara, T. Noguchi, T. Kimura, S. Muranishi, and H. Sezaki, *Chem. Pharm. Bull.*, **23,** 2232(1975).

(1437) M. Girola, F. C. de Jamundo, *G. Mal. Infett. Parassit.*, **26,** 747(1974); through *Chem. Abstr.*, **82,** 10619v(1975).

(1438) M. S. T. Chang, *Enzyme Eng.*, **1974,** 419; through *Chem. Abstr.*, **83,** 32936q(1975).

(1439) S. P. Gladkikh, A. Tentsova, V. M. Avakumov, and I. V. Klement'eva, *Farmatsiya*, **23,** 22(1974); through *Chem. Abstr.*, **82,** 2599p(1975).

(1440) A. Hurwitz, *Drug Interact.*, **1974,** 21; through *Chem. Abstr.*, **82,** 38320k(1975).

(1441) A. N. Kudrin and O. N. Davydova, *Klin. Med.*, **53,** 13(1975); through *Chem. Abstr.*, **82,** 118648p(1975).

(1442) A. Czyzyk, J. Szymendera, E. Jozwicka, and M. Radwan,

IRCS Libr. Compend., **2**, 1171(1974); through *Chem. Abstr.*, **82**, 133127m(1975).

(1443) G. Boman, P. Lundgren, and G. Stjernstrom, *Eur. J. Clin. Pharmacol.*, **8**, 293(1975); through *Chem. Abstr.*, **83**, 152283w(1975).

(1444) G. Zador, G. Lindmark, and B. A. Nilsson, *Obstet. Gynecol. Scand., Suppl.*, **34**, 51(1974); through *Chem. Abstr.*, **82**, 149490k(1975).

(1445) J. M. Orr, *Diss. Abstr. Int.*, **36**, 252-B(1975).

(1446) T. Komuro, S. Kitazawa, and H. Sezaki, *Chem. Pharm. Bull.*, **23**, 400(1975).

(1447) R. Petrick and K. Kleinmann, *Am. J. Hosp. Pharm.*, **32**, 1008(1975).

(1448) F. Ghazy, T. Kimura, S. Muranishi, and H. Sezaki, *J. Pharm. Pharmacol.*, **27**, 268(1975).

(1449) A. K. Granerus, R. Jagenburg, S. Rodjer, and A. Svanborg, *Acta Med. Scand.*, **196**, 459(1974); through *Chem. Abstr.*, **82**, 106153k(1975).

(1450) M. Gibaldi and B. Grundhofer, *Clin. Pharmacol. Ther.*, **18**, 457(1975).

(1451) F. Meyer and J. Ziegenmeyer, *Dtsch. Apoth.-Ztg.* **114**, 1407(1974); through *Chem. Abstr.*, **82**, 25564t(1975).

(1452) L. F. Prescott, *Handb. Exp. Pharmakol.*, **28**, 234(1975); through *Chem. Abstr.*, **83**, 141605b(1975).

(1453) M. Bartolome, *Av. Ter.* **6**, 119(1975), through *Chem. Abstr.*, **83**, 197722e(1975).

(1454) L. F. Prescott, *Clin. North Am.*, **58**, 907(1974); through *Chem. Abstr.*, **82**, 10934q(1975).

(1455) G. E. Schumacher, *Am. J. Hosp. Pharm.*, **32**, 839(1975).

(1456) L. Z. Benet, *Princ. Tech. Hum. Res. Ther.*, **3**, 9(1974); through *Chem. Abstr.*, **82**, 149072a(1975).

(1457) A. Danek, *Farm. Pol.*, **31**, 267(1975); through *Chem. Abstr.*, **83**, 108009n(1975).

(1458) R. E. Notari, *Pharm. Weekbl.*, **110**, 625(1975); through *Chem. Abstr.*, **83**, 108056a(1975).

(1459) W. J. O'Reilly, *Aust. J. Pharm. Sci.*, **3**, 46(1974); through *Chem. Abstr.*, **82**, 51167k(1975).

(1460) D. H. Sorby, *Rev. Mex. Cienc. Farm.*, **5**, 49(1974); through *Chem. Abstr.*, **82**, 132676c(1975).

(1461) V. Vibhuti, *Pharmastudent*, **16**, 46(1972).

(1462) J. B. Stenlake, *Analyst(London)*, **99**, 824(1974); through *Chem. Abstr.*, **82**, 129187p(1975).

(1463) V. F. Smolen, H. K. Murdock, W. P. Stoltman, J. W. Clevenger, L. W. Combs, and F. J. Williams, *J. Clin. Pharmacol.*, **15**, 734(1975).

(1464) C. MacLeod, H. Rabin, R. Ogilvie, J. Ruedy, M. Caron, D. Zarowny, and R. Q. Davies, *Can. Med. Assoc. J.*, **111**, 341(1974); through *Chem. Abstr.*, **82**, 51743v(1975).

(1465) L. Gottschalk, R. Biener, and E. Dinova, *Res. Commun. Chem. Pathol. Pharmacol.*, **8**, 697(1974); through *Chem. Abstr.*, **82**, 68w(1975).

(1466) I. Arias, M. Llabres, and R. Cadorniga, *Cienc. Ind. Farm.*, **7**, 94(1975); through *Chem. Abstr.*, **83**, 103212p(1975).

(1467) P. Mannisto and J. Tuomisto, *Farm. Aikak.*, **84**, 15(1975); through *Chem. Abstr.*, **83**, 168391r(1975).

(1468) P. Mannisto, J. Tomisto, and I. Saario, *ibid.*, **84**, 9(1975); through *Chem. Abstr.*, **83**, 168390q(1975).

(1469) T. Dimmling and O. Vanderbeke, *Med. Klin.*, **70**, 27(1975); through *Chem. Abstr.*, **82**, 132755c(1975).

(1470) S. Ishiyama, I. Nakayama, H. Iwamoto, S. Iwai, M. Takatori, T. Kawabe, H. Kawamura, H. Mizutari, and K. Shibata, *Chemotherapy*, **22**, 1301(1974); through *Chem. Abstr.*, **83**, 92910r(1975).

(1471) A. Pecoud, P. Donzel, and J. L. Schelling, *Clin. Pharmacol. Ther.*, **17**, 469(1975).

(1472) E. Suzuki, K. Doi, T. Kondo, H. Matsui, and H. Sezaki, *Chem. Pharm. Bull.*, **23**, 899(1975).

(1473) R. A. O'Reilly, *Ann. Intern. Med.*, **81**, 337(1974); through *Chem. Abstr.*, **82**, 389b(1975).

(1474) G. P. Lewis and W. J. Jusko, *Clin. Pharmacol. Ther.*, **18**, 475(1975).

(1475) M. Preti, U. Cornelli, and C. Carpi, *Boll. Chim. Farm.*, **113**, 645(1974); through *Chem. Abstr.*, **83**, 48132k(1975).

(1476) J. Adir, *Isr. Pharm. J.*, **17**, 19(1974); through *Chem. Abstr.*, **82**, 103041m(1975).

(1477) D. Vaughan and A. Trainor, *J. Pharmacokinet. Biopharm.*, **3**, 203(1975).

(1478) H. Engberg-Pedersen, *Antimicrob. Ag. Chemother.*, **6**, 554(1974); through *Chem. Abstr.*, **82**, 51301z(1975).

(1479) Y. Dormard and J. C. Levron, *Therapie*, **30**, 21(1975); through *Chem. Abstr.*, **83**, 71421n(1975).

(1480) J. P. Devissaguet and R. Le Verge, *ibid.*, **30**, 7(1975); through *Chem. Abstr.*, **83**, 22228w(1975).

(1481) V. S. Vaidhyanathan, *J. Pharm. Sci.*, **64**, 88(1975).

(1482) *Ibid.*, **64**, 92(1975).

(1483) J. G. Wagner, *J. Pharmacokinet. Biopharm.* **3**, 51(1975).

(1484) *Ibid.*, **3**, 457(1975).

(1485) A. P. Lemberger, *J. Pharmacokinet. Biopharm.*, **3**, 219(1975).

(1486) T. L. Lincoln, J. F. Gross, and P. A. Harris, *Proc. Annu. Conf. Eng. Med. Biol.*, **16**, 254(1974); through *Chem. Abstr.*, **82**, 68016h(1975).

(1487) W. Mueller-Schauuenburg, *Eur. J. Clin. Pharmacol.*, **6**, 203(1973); through *Chem. Abstr.*, **82**, 68020e(1975).

(1488) P. G. Welling, W. A. Craig, and C. M. Kunin, *Clin. Pharmacol. Ther.*, **18**, 45(1975).

(1489) D. H. Sorby, *Rev. Mex. Cienc. Farm.*, **5**, 33(1974); through *Chem. Abstr.*, **82**, 132674a(1975).

(1490) S. Lindgren, *Sven. Farm. Tidskr.*, **78**, 813(1974); through *Chem. Abstr.*, **82**, 11867w(1975).

(1491) C. Regamey and F. A. Waldvogel, *Pathol.-Biol.*, **22**, 795(1974); through *Chem. Abstr.*, **82**, 118466m(1975).

(1492) B. E. Cabana and L. W. Dittert, *J. Pharmacokinet. Biopharm.*, **3**, 143(1975).

(1493) H. M. Von Hattingberg, *Arzneim.-Forsch.*, **25**, 1126(1975); through *Chem. Abstr.*, **83**, 157612n(1975).

(1494) D. G. Shand, J. R. Mitchell, and J. A. Oates, *Handb. Exp. Pharmakol.*, **28**, 272(1975); through *Chem. Abstr.*, **83**, 157587h(1975).

(1495) V. A. Filov, *Farmakol. Toksikol.*, **37**, 490(1974); through *Chem. Abstr.*, **83**, 157575c(1975).

(1496) B. R. Hajratwala, *Pharm. J. N. Z.*, **36**, 19(1974); through *Chem. Abstr.*, **82**, 67963c(1975).

(1497) R. E. Notari, *Pharm. Weekbl.*, **110**, 625(1975); through *Chem. Abstr.*, **83**, 108056a(1975).

(1498) C. Heusghem and P. A. Delwaide, *Med. Hyg.*, **32**, 1276(1974); through *Chem. Abstr.*, **82**, 67975h(1975).

(1499) W. J. O'Reilly, *Aust. J. Pharm.*, **55**, 297(1974); through *Chem. Abstr.*, **82**, 17d(1975).

(1500) S. Riegelman, *Princ. Tech. Hum. Res. Ther.*, **3**, 25(1974); through *Chem. Abstr.*, **82**, 149073b(1975).

(1501) N. Matussek and W. Greil, *Arzneim.-Forsch.*, **25**, 1178(1975); through *Chem. Abstr.*, **83**, 141647s(1975).

(1502) W. Rupp, *ibid.*, **25**, 1148(1975); through *Chem. Abstr.*, **83**, 141645q(1975).

(1503) G. R. Bourne and T. Taylor, *Proc. Soc. Anal. Chem.*, **11**, 225(1974); through *Chem. Abstr.*, **82**, 164559h(1975).

(1504) L. Dettli, *Pharmacol. Pharmacokinet.*, **1974**, 69.

(1505) D. D. Breimer and R. F. Rekker, *Chem. Weekbl.*, **70**, F10(1974); through *Chem. Abstr.*, **82**, 38357c(1975).

(1506) H. Koch, *Oesterr. Apoth.-Ztg.*, **27**, 510(1973); through *Chem. Abstr.*, **82**, 106084p(1975).

(1507) *Ibid.*, **27**, 853(1973); through *Chem. Abstr.*, **82**, 106083n(1975).

(1508) V. A. Filov, *Itogi Nauki Tekh. Farmakol., Khimioter., Sredstva Toksikol.*, **5**, 9(1973); through *Chem. Abstr.*, **82**, 67973f(1975).

(1509) V. N. Solov'ev, *ibid.*, **5**, 81(1973); through *Chem. Abstr.*, **82**, 51210u(1975).

(1510) R. Haasis, D. Larbig, and K. O. Klenk, *Klin. Wochenschr.*, **53**, 529(1975); through *Chem. Abstr.*, **83**, 108123v(1975).

(1511) J. D. Coltart, H. G. Gullner, M. Billingham, R. H. Goldman, E. B. Stinson, M. S. Kalman, and D. C. Harrison, *Br. Med. J.*, **4**, 733(1974); through *Chem. Abstr.*, **83**, 207m(1975).

(1512) C. G. Oliver, R. Taxman, and R. Frederickson, *Symp. Digitalis*, **1973**, 336; through *Chem. Abstr.*, **83**, 203g(1975).

(1513) A. Redfors, A. Bertler, and H. Schueller, *ibid.*, **1973**, 265; through *Chem. Abstr.*, **83**, 835q(1975).

(1514) L. Storstein, *ibid.*, **1973**, 249; through *Chem. Abstr.*, **82**, 132751y(1975).

(1515) V. Manninen, A. Eisalo, A. Apajalahti, and A. Heino, *ibid.*, **1973**, 329; through *Chem. Abstr.*, **82**, 132752z(1975).

(1516) F. I. Marcus, *ibid.*, **1973**, 112; through *Chem. Abstr.*, **83**, 31z(1975).

(1517) K. Gjerdrum, *ibid.*, **1973**, 103; through *Chem. Abstr.*, **83**,

30y(1975).
(1518) D. A. Chamberlain, *ibid.*, **1973,** 361, through *Chem. Abstr.*, **83,** 37f(1975).
(1519) *Ibid.*, **1973,** 277; through *Chem. Abstr.*, **83,** 36e(1975).
(1520) *Ibid.*, **1973,** 262; through *Chem. Abstr.*, **83,** 35d(1975).
(1521) F. I. Marcus, *Am. J. Med.*, **58,** 452(1975); through *Chem. Abstr.*, **83,** 83t(1975).
(1522) U. Abshagen, H. Rennekamp, R. Kuechler, and N. Reitbrock, *Eur. J. Clin. Pharmacol.*, **7,** 177(1974); through *Chem. Abstr.*, **83,** 211h(1975).
(1523) E. Steiness, *Symp. Digitalis,* **1973,** 178; through *Chem. Abstr.*, **83,** 201e(1975).
(1524) L. Storstein, *Clin. Pharmacol. Ther.*, **17,** 313(1975); through *Chem. Abstr.*, **83,** 90589q(1975).
(1525) J. E. Doherty, *Symp. Digitalis,* **1973,** 419; through *Chem. Abstr.*, **82,** 149070y(1975).
(1526) O. Storstein, *ibid.*, **1973,** 410; through *Chem. Abstr.*, **83,** 40b(1975).
(1527) R. Selden and T. W. Smith, *ibid.*, **1973,** 396; through *Chem. Abstr.*, **83,** 38g(1975).
(1528) B. Beermann, *ibid.*, **1973,** 404; through *Chem. Abstr.*, **83,** 39h(1975).
(1529) D. S. Lukas, *ibid.*, **1973,** 84; through *Chem. Abstr.*, **83,** 833n(1975).
(1530) H. Luellman and T. Peters, *ibid.*, **1973,** 210; through *Chem. Abstr.*, **83,** 33b(1975).
(1531) P. F. Binnion and M. McDermott, *ibid.*, **1973,** 366; through *Chem. Abstr.*, **82,** 132754b(1975).
(1532) J. Koup, W. Jusko, C. Elwood, and R. Kohli, *Clin. Pharmacol. Ther.*, **18,** 9(1975).
(1533) L. Storstein, *ibid.*, **17,** 313(1975).
(1534) D. H. Huffman, *ibid.*, **17,** 310(1975).
(1535) J. Koup, D. Greenblatt, W. Jusko, T. Smith, and J. Koch-Weser, *J. Pharmacokinet. Biopharm.*, **3,** 181(1975).
(1536) W. Zilly, E. Richter, and N. Rietbrock, *Clin. Pharmacol. Ther.*, **17,** 302(1975).
(1537) H. Halkin, L. B. Sheiner, C. C. Peck, and K. L. Melmon, *ibid.*, **17,** 385(1975).
(1538) U. Peters, T. U. Hausamen, and F. Grosse-Brockhoff, *Dtsch. Med. Wochenschr.*, **99,** 2381(1974); through *Chem. Abstr.*, **83,** 37892g(1975).
(1539) G. G. Belz and H. Nuebling, *Klin. Wochenschr.*, **53,** 543(1975); through *Chem. Abstr.*, **83,** 108124w(1975).
(1540) G. G. Belz and U. R. Kleeberg, *ibid.*, **53,** 491(1975); through *Chem. Abstr.*, **83,** 108131w(1975).
(1541) A. J. Windorfer, W. Pringsheim, R. Gaedeke, and G. Schumacher, *Kinderhelikunde,* **118,** 207(1974); through *Chem. Abstr.*, **83,** 92916x(1975).
(1542) L. Storstein, *Symp. Digitalis,* **1973,** 158; through *Chem. Abstr.*, **83,** 834p(1975).
(1543) L. Nyberg, K. E. Andersson, and A. Bertler, *Acta Pharm. Suec.*, **11,** 459(1974); through *Chem. Abstr.*, **83,** 92883j(1975).
(1544) L. K. Garrettson and W. J. Jusko, *Clin. Pharmacol. Ther.*, **17,** 481(1975).
(1545) A. J. Sedman, *Diss. Abstr. Int.*, **35,** 5351-B(1975).
(1546) P. K. Wilkinson, *ibid.*, **36,** 2735-B(1975).
(1547) K. Overoe, L. F. Gram, and V. Hansen, *Eur. J. Clin. Pharmacol.*, **8,** 343(1975); through *Chem. Abstr.*, **83,** 141738x(1975).
(1548) L. F. Gram and K. F. Overo, *Clin. Pharmacol. Ther.*, **18,** 305(1975).
(1549) E. Ohnhaus and P. Spring, *J. Pharmacokinet. Biopharm.*, **3,** 171(1975).
(1550) L. Lund, G. Alvan, A. Berlin, and B. Alexanderson, *Eur. J. Clin. Pharmacol.*, **7,** 81(1974); through *Chem. Abstr.*, **82,** 164667s(1975).
(1551) J. W. Estes, *Curr. Ther. Res., Clin. Exp.*, **18,** 45(1975); through *Chem. Abstr.*, **83,** 108128a(1975)
(1552) S. M. Pond, G. G. Graham, D. N. Wade, and G. Sudlow, *Aust. N. Z. J. Med.*, **5,** 324(1975); through *Chem. Abstr.*, **83,** 188168b(1975).
(1553) T. P. Gibson, D. T. Lowenthal, H. A. Nelson, and W. A. Briggs, *Clin. Pharmacol. Ther.*, **17,** 321(1975).
(1554) C. A. Shively and E. S. Vesell, *ibid.*, **18,** 413(1975).
(1555) W. L. Chiou, *J. Pharm. Sci.*, **64,** 1734(1975).
(1556) G. Levy, N. Khana, D. M. Soda, O. Tsuzuki and L. Stern, *Pediatrics,* **55,** 818(1975); through *Chem. Abstr.*, **83,** 90638e(1975).
(1557) N. Gupta, E. Sarkissian, and H. E. Paulus, *Clin. Pharmacol. Ther.*, **18,** 350(1975).
(1558) R. D. Smith, A. Polk, J. Diamond, B. J. Burns, and T. Herczeg, *Xenobiotica,* **4,** 383(1974); through *Chem. Abstr.*, **82,** 252629t(1975).
(1559) B. L. Kamath, *Diss. Abstr. Int.*, **36,** 1156-B(1975).
(1560) B. H. Dvorchik, *Clin. Pharmacol. Ther.*, **18,** 259(1975).
(1561) R. M. Welch, R. L. DeAngelis, M. Wingfield, and T. W. Farmer, *ibid.*, **18,** 249(1975).
(1562) R. Resnick, *ibid.*, **18,** 180(1975).
(1563) E. Anggard, L. M. Gunne, J. Holmstrand, R. E. McMahon, C. G. Sandberg, and H. Sullivan, *ibid.*, **17,** 258(1975).
(1564) A. E. Pflug, M. E. Lindop, and C. Wilkerson, *ibid.*, **17,** 21(1975).
(1565) B. Berkowitz, S. Ngai, J. Yang, J. Hempstead, and S. Spector, *ibid.*, **7,** 629(1975).
(1566) E. J. Cone, C. Gorodetzky, and S. Y. Yeh, *Drug. Metab. Dispos.*, **2,** 506(1974); through *Chem. Abstr.*, **82,** 118747v(1975).
(1567) P. A. Harris and J. F. Gross, *Cancer Chemother. Rep., Part I,* **59,** 819(1975); through *Chem. Abstr.*, **83,** 141709p(1975).
(1568) F. A. Chrzanowski, *Diss. Abstr. Int.*, **36,** 1658-B (1975).
(1569) F. Quattrocchi, G. Bressard, C. Advenier, J. Fourneret, and P. Fabiani, *Ann. Falsif. Expert. Chim.*, **67,** 11(1974); through *Chem. Abstr.*, **83,** 71399m(1975).
(1570) J. Jenne, H. Nagasawa, R. McHugh, F. MacDonald, and E. Wyse, *Life Sci.*, **17,** 195(1975); through *Chem. Abstr.*, **83,** 15766q(1975).
(1571) J. Kampmann and L. Skovsted, *Acta Pharmacol. Toxicol.*, **35,** 361(1974); through *Chem. Abstr.*, **82,** 51326m(1975).
(1572) D. S. Sitar and D. B. Hunninghake, *J. Clin. Endocrinol. Metab.*, **40,** 26(1975); through *Chem. Abstr.*, **83,** 92848b(1975).
(1573) W. A. Cressman, J. R. J. Bianchine, V. B. Slotnick, P. C. Johnson, and J. Plostnieks, *Eur. J. Clin. Pharmacol.*, **7,** 99(1974); through *Chem. Abstr.*, 164669u(1975).
(1574) J. Houston and G. Levy, *Nature,* **255,** 78(1975); through *Chem. Abstr.*, **83,** 126010k(1975).
(1575) A. Cammarata, J. Smith, and N. P. Willett, *J. Pharm. Sci.*, **64,** 1325(1975).
(1576) J. Ader, D. A. Blake, and G. M. Mergner, *J. Clin. Pharmacol.*, **15,** 760(1975).
(1577) R. Levy, W. Pitlick, A. Troupin, J. Green, and J. Neal, *Clin. Pharmacol. Ther.*, **17,** 657(1975).
(1578) M. D. Rawlins, P. Collste, I. Bertilsson, and L. Palmer, *Eur. J. Clin. Pharmacol.*, **8,** 91(1975); through *Chem. Abstr.*, **83,** 37455s(1975).
(1579) M. Eichelbaum, K. Ekbom, L. Bertilsson, V. A. Ringberger, and A. Rane, *ibid.*, **8,** 337(1975); through *Chem. Abstr.*, **83,** 141740s(1975).
(1580) M. F. Michel, *Ned. Tijdschr. Geneeskd.*, **118,** 1508(1974); through *Chem. Abstr.*, **82,** 51302a(1975).
(1581) K. Hellstrom, A. Rosen, and A. Swahn, *Clin. Pharmacol. Ther.*, **16,** 826(1974); through *Chem. Abstr.*, **82,** 68064x(1975).
(1582) B. E Cabana, D. R. Van Harken, G. H. Hottendorf, J. T. Doluisio, W. O. Griffen, Jr., D. W. A. Bourne, and L. W. Dittert, *J. Pharmacokinet. Biopharm.*, **3,** 419(1975).
(1583) C. H. Nightingale, D. S. Greene, and R. Quintiliana, *J. Pharm. Sci.*, **64,** 1899(1975).
(1584) G. E. Schumacher, *J. Clin. Pharmacol.*, **15,** 656(1975).
(1585) B. Duhm, W. Maul, H. Medenwald, K. Patzschke, J. Puetter, and L. A. Wegner, *Postgrad. Med. J. Suppl.*, **500,** 13(1974); through *Chem. Abstr.*, **82,** 25601c(1975).
(1586) H. Notle and H. Buettner, *Chemotherapy,* **20,** 321(1974); through *Chem. Abstr.*, **82,** 51282u(1975).
(1587) L. F. Chasseaud, W. H. Down, and R. K. Grundy, *Eur. J. Clin. Pharmacol.*, **8,** 157(1975); through *Chem. Abstr.*, **83,** 71433t(1975).
(1588) J. T. Wilson, *Acta Pharm. Suec.*, **11,** 651(1974); through *Chem. Abstr.*, **83,** 193d(1975).
(1589) L. E. Hare, K. C. Yeh, C. A. Ditzler, F. G. McMahon, and D. E. Duggan, *Clin. Pharmacol. Ther.*, **18,** 330(1975).
(1590) K. Albert, M. Hallmark, E. Sakmar, D. Weidler, and J. Wagner, *J. Pharmacokinet. Biopharm.*, **3,** 159(1975).
(1591) W. L. Chiou, *ibid.*, **3,** 193(1975).
(1592) M. Selley, J. Glass, E. Triggs, and J. Thomas, *Clin. Pharmacol. Ther.*, **17,** 599(1975).
(1593) D. Alkalay, L. Khemani, W. E. Wagner, Jr., and M. F. Bartlett, *J. Clin. Pharmacol.*, **15,** 446(1975).
(1594) W. L. Chiou, *ibid.*, **15,** 427(1975).

(1595) H. G. Boxenbaum, I. Bekersky, V. Mattaliano, and S. A. Kaplan, *J. Pharmacokinet. Biopharm.*, **3**, 443(1975).
(1596) E. J. Triggs and R. L. Nation, *ibid.*, **3**, 387(1975).
(1597) A. Rane, *J. Pediatr.*, **85**, 543(1974).
(1598) B. Jalling, L. O. Boreus, N. Kallberg, and S. Agurell, *Eur. J. Clin. Pharmacol.*, **6**, 234(1973); through *Chem. Abstr.*, **82**, 98272e(1975).
(1599) W. U. Brown, G. C. Bell, A. O. Luire, J. B. Weiss, J. W. Scanlon, and M. H. Alper, *Anesthesiology*, **42**, 698(1975); through *Chem. Abstr.*, **83**, 108122u(1975).
(1600) D. H. Lawson, A. K. Henderson, and R. R. McGeachy, *Postgrad. Med. J.*, **50**, 500(1974); through *Chem. Abstr.*, **82**, 72t(1975).
(1601) P. Welling, W. Craig, and C. Kunin, *Clin. Pharmacol. Ther.*, **18**, 45(1975).
(1602) J. Edelson, J. F. Douglas, B. J. Ludwig, E. B. Schuster, and S. Shahinian, *J. Pharm. Sci.*, **64**, 1316(1975).
(1603) J. Mosser, M. Trouilloud, V. Vergely, and F. Fauran, *Bull. Liaison, Groupe Polyphenols*, **5**, 12(1974); through *Chem. Abstr.*, **83**, 37307v(1975).
(1604) J. P. Wistrand, *Pharmacol. Pharmacokinet.*, **1974**, 191; through *Chem. Abstr.*, **82**, 164592p(1975).
(1605) G. G. Belz, M. Stauch, and G. Rudofsky, *Eur. J. Clin. Pharmacol.*, **7**, 95(1974); through *Chem. Abstr.*, **82**, 164668t(1975).
(1606) E. A. Rudzit, A. M. Bespalov, L. I. Lisitsa, and R. F. Tagirov, *Nov. Antibakterinal'nye Prep.*, **1974**, 9; through *Chem. Abstr.*, **83**, 141725r(1975).
(1607) C. Lin and S. Symchowicz, *Drug Metab. Rev.*, **4**, 75(1975); through *Chem. Abstr.*, **83**, 141624g(1975).
(1608) L. Friedrich, *Therapiewoche*, **25**, 3720(1975); through *Chem. Abstr.*, **83**, 141574r(1975).
(1609) A. Forsman, E. Martensson, G. Nyberg, and R. Oehman, *Naunyn-Schmiedeberg's Arch. Pharmacol.*, **286**, 113(1974); through *Chem. Abstr.*, **82**, 132701g(1975).
(1610) Y. S. Bakhle and J. R. Vane, *Physiol. Rev.*, **54**, 1007(1974); through *Chem. Abstr.*, **82**, 10932n(1975).
(1611) A. Feingold, *Introd. Pract. Anesth.*, **1974**, 122; through *Chem. Abstr.*, **82**, 118658s(1975).
(1612) D. K. Banerjee, G. A. Ellard, P. T. Gammon, and M. F. R. Waters, *Am. J. Trop. Med. Hyg.*, **23**, 1110(1974); through *Chem. Abstr.*, **82**, 25605g(1975).
(1613) L. Levy, *ibid.*, **23**, 1097(1974); through *Chem. Abstr.*, **82**, 25604f(1975).
(1614) R. Gugler, L. Kreis, and H. J. Dengler, *Arzneim.-Forsch.*, **25**, 1067(1975); through *Chem. Abstr.*, **83**, 126039b(1975).
(1615) F. Jane and E. Puigdellivol, *Cienc. Ind. Farm.*, **5**, 224(1973); through *Chem. Abstr.*, **82**, 106079r(1975).
(1616) M. Ehrnebo, *Acta Pharm. Suec.*, **11**, 655(1974); through *Chem. Abstr.*, **83**, 11t(1975).
(1617) S. Øie, D. T. Lowenthal, W. A. Briggs, and G. Levy, *Clin. Pharmacol. Ther.*, **18**, 680(1975).
(1618) W. Rupp, *Scott. Med. J.*, **19**, 5(1975); through *Chem. Abstr.*, **82**, 106023t(1975).
(1619) D. B. Campbell and E. M. Phillips, *Eur. J. Clin. Pharmacol.*, **7**, 407(1974); through *Chem. Abstr.*, **82**, 14949q(1975).
(1620) H. Franz, R. Urbanczik, K. Stoll, and U. Mueller, *Prax. Pneumol.*, **28**, 605(1974); through *Chem. Abstr.*, **82**, 149148e(1975).
(1621) W. Lintz, W. Berger, W. Aenishaenslin, V. Kutova, C. Baerlocher, J. P. Kapp, and R. Bechmann, *Eur. J. Clin. Pharmacol.*, **7**, 433(1974); through *Chem. Abstr.*, **82**, 149157g(1975).
(1622) N. L. Chabria, *Proc. Asia Oceania Congr. Endocrinol., 5th*, **2**, 432(1974); through *Chem. Abstr.*, **83**, 125928d(1975).
(1623) M. Rowland, S. B. Matin, J. Thiessen, and J. Karam, *Drug. Interact.*, **1974**, 199; through *Chem. Abstr.*, **82**, 38325r(1975).
(1624) H. Sauer, *Therapiewoche*, **25**, 767(1975); through *Chem. Abstr.*, **83**, 65p(1975).
(1625) F. Markwardt, M. Richter, and G. Vogel, *Zentralbl. Pharm. Pharmakother. Laboratoriumdsiagn.*, **113**, 787(1974); through *Chem. Abstr.*, **82**, 26115j(1975).
(1626) T. Blaschke, P. Meffin, K. Melmon, and M. Rowland, *Clin. Pharmacol. Ther.*, **17**, 685(1975).
(1627) J. W. Estes and P. F. Poulin, *Thromb. Diath. Haemorrh.*, **33**, 26(1975); through *Chem. Abstr.*, **83**, 71218b(1975).
(1628) G. Pepe and N. Frascolla, *Rass. Med. Sper.*, **21**, 49(1974); through *Chem. Abstr.*, **83**, 212j(1974).
(1629) G. Acocella, L. Bonollo, M. Mainardi, P. Margaroli, and F. B. Nicolis, *Tijdschr. Gastro-Enterol.*, **17**, 151(1974); through *Chem. Abstr.*, **82**, 106582d(1975).
(1630) W. Brumfitt, J. Kosmidis, J. M. T. Hamilton-Miller, and J. N. G. Gilchrist, *Antimicrob. Ag. Chemother.*, **6**, 290(1974); through *Chem. Abstr.*, **82**, 68402f(1975).
(1631) H. Lode, S. Gerbert, and A. Hendrischk, *Chemotherapy*, **21**, 19(1974); through *Chem. Abstr.*, **83**, 93345x(1975).
(1632) M. W. von Schach, *Opusc. Med., Suppl.*, **33**, 5(1974); through *Chem. Abstr.*, **82**, 67941u(1975).
(1633) R. N. Brogden, T. M. Speight, and G. S. Avery, *Drugs*, **9**, 251(1975); through *Chem. Abstr.*, **83**, 108015m(1975).
(1634) *Ibid.*, **7**, 326(1974); through *Chem. Abstr.*, **82**, 51181k(1975).
(1635) J. T. Clarke, R. D. Libke, E. D. Ralph, R. P. Luthy, and W. M. Kirby, *Antimicrob. Ag. Chemother.*, **6**, 729(1974); through *Chem. Abstr.*, **82**, 118742q(1975).
(1636) W. H. Pitlick, *Diss. Abstr. Int.*, **36**, 2734-B(1975).
(1637) D. J. Greenblatt, R. I. Shader, and J. Koch-Weser, *Dis. Nerv. Syst.*, **36**, 6(1975); through *Chem. Abstr.*, **83**, 7132f(1975).
(1638) T. Lincoln and E. J. Freireich, *Recent Results Cancer Res.*, **49**, 103(1974); through *Chem. Abstr.*, **82**, 11851z(1975).
(1639) K. Hiramori, S. Takahashi, Y. Matsumoto, T. Honda, M. Kondo, T. Hosoda, and K. Kirosawa, *Horumon To Rinsho*, **23**, 489(1975); through *Chem. Abstr.*, **83**, 108087m(1975).
(1640) G. G. Belz, *Klin. Wochenschr.*, **52**, 749(1974); through *Chem. Abstr.*, **82**, 380s(1975).
(1641) R. A. Ouvrier, *Aust. N. Z. J. Med.*, **4**, 524(1974); through *Chem. Abstr.*, **82**, 67946z(1975).
(1642) H. Shindo, K. Kawai, K. Fukuda, M. Matsumura, K. Tanaka, M. Tanaka, and T. Yokota, *Proc. Symp. Drug Metab. Action, 5th*, **1973**, 49; through *Chem. Abstr.*, **83**, 90593m(1975).
(1643) S. F. Cooper, R. Dugal, J. M. Albert, and M. Bertrand, *Clin. Pharmacol. Ther.*, **18**, 325(1975).
(1644) A. Tatematsu, T. Nadai, M. Kume, and S. Hoshika, *Oyo, Yakuri*, **9**, 195(1975); through *Chem. Abstr.*, **83**, 108106s(1975).
(1645) L. R. Fare, P. Actor, C. Sachs, L. Phillips, M. Joloza, J. F. Pauls, and J. A. Weisbach, *Antimicrob. Ag. Chemother.*, **6**, 150(1974); through *Chem. Abstr.*, **82**, 25603e(1975).
(1646) V. T. Oliverio, *Handb. Exp. Pharmakol.*, **38**, 229(1974); through *Chem. Abstr.*, **83**, 19b(1975).
(1647) H. J. Wallner and A. Schmiedel, *Muench. Med. Wochenschr.*, **117**, 349(1975); through *Chem. Abstr.*, **83**, 222n(1975).
(1648) A. Bertler, A. Gustafson, P. Ohlin, M. Monti, and A. Refors, *Symp. Digitalis*, **1973**, 300; through *Chem. Abstr.*, **83**, 836r(1975).
(1649) S. Tsutsumi, Y. Sakamoto, and S. Digoh, *Repura*, **43**, 1(1974); through *Chem. Abstr.*, **82**, 51151a(1975).
(1650) H. Kutt and J. K. Penry, *Arch. Neurol.*, **31**, 283(1974); through *Chem. Abstr.*, **82**, 51185q(1975).
(1651) T. Sargent, D. A. Kalbhen, A. T. Shuigin, G. Braum, H. Stauffer, and N. Kusubov, *Neuropharmacology*, **14**, 165(1975); through *Chem. Abstr.*, **83**, 22224s(1975).
(1652) B. Baguley and E. M. Falkenhaug, *Eur. J. Cancer*, **11**, 43(1975); through *Chem. Abstr.*, **83**, 2203j(1975).
(1653) M. Linnoila, K. Korttila, and M. J. Mattila, *Acta Pharmacol. Toxicol.*, **36**, 181(1975); through *Chem. Abstr.*, **83**, 22184d(1975).
(1654) D. Comar, M. Maziere, and C. Raynaud, *Report*, **1974**, 2680; through *Chem. Abstr.*, **83**, 108100k(1975).
(1655) W. Riess, L. Dubey, E. W. Fuenfgeld, P. Imhof, H. Huerzeler, N. Matussek, T. G. Rajagopalan, F. Raschdorf, and G. Schmid, *J. Int. Med. Res.*, **3**, 16(1975); through *Chem. Abstr.*, **83**, 108126y(1975).
(1656) G. Peiker, A. Traeger, H. Hoeschel, A. Bonow, and U. Hertel, *Zentralbl. Gyanekol.*, **97**, 612(1975); through *Chem. Abstr.*, **83**, 108133y(1975).
(1657) R. N. Brogden, T. M. Speight, and G. S. Avery, *Drugs*, **9**, 88(1975); through *Chem. Abstr.*, **83**, 10795u(1975).
(1658) G. Motta and R. Malberti, *Farmaco, Ed. Prat.*, **30**, 357(1975); through *Chem. Abstr.*, **83**, 108007k(1975).
(1659) R. Kaiko and C. Inturrisi, *Clin. Pharmacol. Ther.*, **18**, 96(1975).
(1660) B. Mueller and H. Noeschel, *Zentralbl. Gynaekol.*, **97**, 601(1975); through *Chem. Abstr.*, **83**, 108132x(1975).
(1661) D. E. Drayer, *Med. Clin. North Am.*, **58**, 927(1974); through *Chem. Abstr.*, **82**, 10936s(1975).
(1662) S. Feldman, *ibid.*, **58**, 917(1974); through *Chem. Abstr.*, **82**, 10935r(1975).
(1663) S. C. Glauser, *ibid.*, **58**, 945(1974); through *Chem. Abstr.*,

82, 10937t(1975).

(1664) A. S. Nies, *ibid.*, **58,** 965(1974); through *Chem. Abstr.*, **82,** 10939v(1975).

(1665) J. E. Mrochek, S. Katz, W. H. Christie, and S. R. Dinsmore, *Clin. Chem.*, **20,** 1086(1974); through *Chem. Abstr.*, **82,** 25624n(1974).

(1666) R. D. Smyth, A. Polk, J. Diamond, B. J. Burns, and T. Herczeg, *Xenobiotica,* **4,** 383(1974); through *Chem. Abstr.*, **82,** 25629t(1975).

(1667) R. Bergling, T. M. Jorndal, L. Oreland, W. Rapp, and S. Wold, *J. Clin. Pharmacol.*, **15,** 178(1975).

(1668) F. Sjoqvist, *Acta Pharm. Suec.*, **11,** 661(1974); through *Chem. Abstr.* **83,** 12u(1975).

(1669) D. A. Chamberlain, *Postgrad. Med. J. Suppl.* **50,** 29(1974); through *Chem. Abstr.*, **83,** 89z(1975).

(1670) R. E. McMahon, H. R. Sullivan, and S. I. Due, *Acta Pharm. Suec.*, **11,** 639(1974); through *Chem. Abstr.*, **83,** 19a(1975).

(1671) A. D. Tice, M. Barba, M. G. Bergeron, J. L. Brusch, and L. Weinstein, *Antimicrob. Ag. Chemother.*, **7,** 168(1975); through *Chem. Abstr.*, **83,** 189g(1975).

(1672) J. L. Chuningham and D. A. Price Evans, *Eur. J. Clin. Pharmacol.*, **7,** 387(1974); through *Chem. Abstr.*, **83,** 853u(1975).

(1673) G. Motta and R. Malberti, *Farmaco, Ed. Prat.*, **30,** 357(1975); through *Chem. Abstr.*, **83,** 108007k(1975).

(1674) C. C. Porter, B. H. Arison, V. F. Gruber, D. C. Titus, and W. J. A. Vandenheuvel, *Drug Metab. Dispos.*, **3,** 189(1975); through *Chem. Abstr.*, **83,** 71465e(1975).

(1675) T. N. Appleyard, A. Witt, R. E. Atkinson, and A. D. G. Nicholas, *Br. J. Anaesth.*, **46,** 530(1974); through *Chem. Abstr.*, **83,** 90590h(1975).

(1676) F. B. Nicolis, G. Vuniva, L. Bonollo, L. Tenconi, and L. Schiavetti, *Int. J. Clin. Pharmacol, Ther. Toxicol.*, **10,** 255(1974); through *Chem. Abstr.*, **82,** 106586d(1975).

(1677) G. Molino and M. Milanese, *J. Lab. Clin. Med.*, **85,** 865(1975).

(1678) L. F. Prescott, *Proc. Eur. Soc. Study Drug Toxic.*, **14,** 49(1973); through *Chem. Abstr.*, **83,** 90516p(1975).

(1679) W. J. Jusko, *ibid.*, **14,** 9(1973); through *Chem. Abstr.*, **83,** 90488f(1975).

(1680) P. Pomarelli, *Farmaco, Ed. Prat.*, **30,** 257(1975); through *Chem. Abstr.*, **83,** 90488f(1975).

(1681) O. Eriksson, H. Kjellman, A. Pibrant, and M. Schannong, *Eur. J. Clin. Pharmacol.*, **7,** 375(1974); through *Chem. Abstr.*, **83,** 22193f(1975).

(1682) H. Deckart, H. Herzmann, H. Flentje, A. Blottner, and K. D. Schwartz, *Strahlentherapie, Sonderb.*, **74,** 134(1975); through *Chem. Abstr.*, **83,** 22213n(1975).

(1683) P. M. Gros, H. J. Davi, L. F. Chasseaud, and D. R. Hawking, *Arzneim.-Forsch.*, **24,** 1385(1974); through *Chem. Abstr.*, **82,** 38451d(1975).

(1684) A. P. Gilve, M. N. Koptelova, and E. A. Shafro, *Byull. Eksp. Biol. Med.*, **78,** 59(1974); through *Chem. Abstr.*, **82,** 25649z(1975).

(1685) D. D. Breimer, H. L. M. Cox, and J. M. Van Rossum, *Pharm. Weekbl.*, **109,** 1041(1974); through *Chem. Abstr.*, **82,** 64404k (1975).

(1686) E. H. Wiseman, *Med. Chem. Ser. Monogr.*, **13,** 235(1974); through *Chem. Abstr.*, **82,** 67982h(1975).

(1687) G. Houin, J. J. Thebault, P.D'Athis, J. P. Tillement, and J. L. Beamont, *Eur. J. Clin. Pharmacol.*, **8,** 433(1975); through *Chem. Abstr.*, **83,** 188127n(1975).

(1688) S. P. Gladkikh, I. A. Tentsova, V. M. Avakumov, and I. V. Lement'eva, *Farmatsiya,* **23,** 22(1974); through *Chem. Abstr.*, **82,** 2599p(1975).

(1689) H. M. Von Hattingberg, *Monatsschr. Kinderheilkd.*, **123,** 23(1975); through *Chem. Abstr.*, **83,** 22131j(1975).

(1690) J. M. Albores, H. E. Cammarota, J. M. Cosin, A. F. Gandolti, M. S. Casares, O. J. Senet, and E. Correa de Araujo, *Postgrad. Med. J. Suppl.*, **50,** 46(1974); through *Chem. Abstr.*, **83,** 71453z(1975).

(1691) J. W. Gorrod, *Gerontol. Clin.*, **16,** 30(1974); through *Chem. Abstr.*, **82,** 23c(1975).

(1692) F. I. Caird, *ibid.*, **16,** 68(1975); through *Chem. Abstr.*, **82,** 10933p(1975).

(1693) N. Monji, D. P. Bonner, Y. Hashimoto, and C. P. Schaffner, *J. Antibiot. (Tokyo),* **28,** 317(1975).

(1694) M. Belleville, J. C. Lechevin, A. Meynaud, M. Grand, and L. Fontaine, *Eur. J. Med. Chem.-Chim. Ther.*, **9,** 543(1974); through *Chem. Abstr.*, **82,** 132749d(1975).

(1695) Y. Hinohara and S. Shigeo, *Oyo Yakuri,* **8,** 417(1974); through *Chem. Abstr.*, **82,** 68031j(1975).

(1696) N. Rietbrock, *Bibl. Psychiatr.*, **151,** 15(1975); through *Chem. Abstr.*, **83,** 125966q(1975).

(1697) O. Borga and I. Odar-Cederlof, *Acta Pharm. Suec.*, **11,** 653(1974); through *Chem. Abstr.*, **83,** 10s(1975).

(1698) K. S. Albert, M. R. Hallmark, E. Sakmar, D. J. Weidler, and J. G. Wagner, *Res. Commun. Chem. Pathol. Pharmacol.*, **9,** 463(1974); through *Chem. Abstr.*, **82,** 149121r(1975).

(1699) M. M. Ghoneim, M. Delle, W. R. Wilson, and J. J. Ambre, *Anesthesiology,* **43,** 333(1975); through *Chem. Abstr.*, **83,** 188495f(1975).

(1700) G. Levy, *Pharmacol. Pharmacokinet.*, **1974,** 339; through *Chem. Abstr.*, **82,** 164601r(1975).

(1701) K. J. Simons, R. H. Levy, R. E. Cutler, G. T. Christopher, and A. Lindner, *Res. Commun. Chem. Pathol. Pharmacol.*, **11,** 173(1975); through *Chem. Abstr.*, **83,** 90640z(1975).

(1702) J. Strong, J. Dutcher, W. Lee, and A. Atkinson, *J. Pharmacokinet. Biopharm.*, **3,** 223(1975).

(1703) C. Graffner, *ibid.*, **3,** 69(1975).

(1704) H. Halkin, P. Meffin, K. Melmon, and M. Rowland, *Clin. Pharmacol. Ther.*, **17,** 669(1975).

(1705) M. Kakemi, K. Masuda, M. Ueda, and T. Koizumi, *Chem. Pharm. Bull.*, **23,** 736(1975).

(1706) J. Raaflaub and U. C. Dubach, *Eur. J. Clin. Pharmacol.*, **8,** 261(1975); through *Chem. Abstr.*, **83,** 71435v(1975).

(1707) D. T. Lowenthal, W. A. Briggs, and G. Levy, *J. Clin. Invest.*, **54,** 1221(1974); through *Chem. Abstr.*, **82,** 25648y(1975).

(1708) A. Soren, *J. Clin. Pharmacol.*, **15,** 173(1975).

(1709) J. N. T. Gilbert, J. W. Powell, and J. Templeton, *J. Pharm. Pharmacol.*, **27,** 923(1975).

(1710) D. D. Breimer, C. Honhoff, W. Zilly, E. Richter, and J. M. van Rossum, *J. Pharmacokinet. Biopharm.*, **3,** 1(1975).

(1711) D. D. Breimer, W. Zilly, and E. Richter, *Clin. Pharmacol. Ther.*, **18,** 433(1975).

(1712) S. E. O'Donoghur-Ryan, *IRCS Med. Sci.*, **3,** 395(1975); through *Chem. Abstr.*, **83,** 157688s(1975).

(1713) R. J. Owellen and C. A. Hartke, *Cancer Res.*, **35,** 975(1975); through *Chem. Abstr.*, **83,** 22208q(1975).

(1714) D. Chandrakant, D. Higby, J. Mattern, D. O. Halland, and J. F. Grace, *Clin. Pharmacol. Ther.*, **17,** 36(1975).

(1715) N. O. Bodin, K. O. Borg, R. Johannson, H. Obianwu, and R. Svenson, *Acta Pharmacol. Toxicol.*, **35,** 261(1974); through *Chem. Abstr.*, **82,** 25647x(1975).

(1716) C. Von Bahr, G. Alvan, M. Lind, B. Mellstrom, and F. Sjoqvist, *Acta Pharm. Suec.*, **11,** 649(1974); through *Chem. Abstr.*, **83,** 192c(1975).

(1717) D. G. McDevitt and D. G. Shand, *Clin. Pharmacol. Ther.*, **18,** 708(1975).

(1718) J. Kampmann and L. Skovsted, *Acta Pharmacol. Toxicol.*, **37,** 201(1975); through *Chem. Abstr.*, **83,** 172361y(1975).

(1719) A. Karim, *Angiology,* **26,** 85(1975); through *Chem. Abstr.*, **83,** 37434j(1975).

(1720) E. D. Ralph, J. T. Clarke, R. D. Libke, R. P. Luthy, and M. M. William, *Antimicrob. Ag. Chemother.*, **6,** 691(1974); through *Chem. Abstr.*, **83,** 92905t(1975).

(1721) K. D. Charalampous, P. Johnson, and V. Estevez, *Mesoridazine,* **35,** 494(1974); through *Chem. Abstr.*, **82,** 132715q(1975).

(1722) D. J. Greenblatt, R. I. Shader, and J. Koch-Weser, *Am. J. Psychiatry,* **131,** 1395(1974); through *Chem. Abstr.*, **82,** 10166s(1975).

(1723) U. Klotz, G. R. Avant, A. Hoyumpa, S. Schenker, and G. R. Wilkinson, *J. Clin. Invest.*, **55,** 347(1975); through *Chem. Abstr.*, **83,** 92893n(1975).

(1724) J. Raaflaub, *Experientia,* **31,** 557(1975); through *Chem. Abstr.*, **83,** 71427u(1975).

(1725) G. Bastert, K. H. Wallhaeuser, K. Wernicke, and W. G. Mueller, *Z. Gerburtshilfe Perinatol.*, **177,** 330(1973); through *Chem. Abstr.*, **83,** 188166z(1975).

(1726) C. Simon, V. Malerczyk, G. Zierott, K. Lehmann, and U. Thiesen, *Arzneim.-Forsch.*, **25,** 654(1975); through *Chem. Abstr.*, **83,** 22227v(1975).

(1727) K. Roholt, B. Nielsen, and E. Kristensen, *Chemotherapy,* **21,** 146(1975); through *Chem. Abstr.*, **83,** 90644d(1975).

(1728) R. D. Libke, J. T. Clarke, E. D. Ralph, R. P. Luthy, and W. M. M. Kirby, *Clin. Pharmacol. Ther.*, **17,** 441(1975).

(1729) I. Hansen, E. Jacobsen, and J. Weis, *ibid.*, **17,** 339(1975).

(1730) G. Bastert, K. Wernicke, W. G. Mueller, and H. Hebauf, *Z. Geburtshilfe Perinatol.*, **178**, 164(1974); through *Chem. Abstr.*, **83**, 188164x(1975).

(1731) H. Lode, A. Hendrischk, and S. Gebert, *Verh. Dtsch. Ges. Inn. Med.*, **80**, 1541(1974); through *Chem. Abstr.*, **83**, 875c(1975).

(1732) J. M. Brogard, C. Brandt, M. Dorner, and A. Dammron, *Chemotherapy*, **22**, 1(1976); through *Chem Abstr.*, **83**, 172384h(1975).

(1733) G. E. Schumacher, *Am. J. Hosp. Pharm.*, **32**, 299(1975).

(1734) M. Reidenberg and E. Vesell, *Clin. Pharmacol. Ther.*, **17**, 650(1975).

(1735) F. J. E. Vajda, F. Williams, and D. S. Davies, *Med. J. Aust.*, **2**, 64(1974); through *Chem. Abstr.*, **82**, 106089u(1975).

(1736) J. Pottier, M. Busigny, and J. P. Raynaud, *Drug Metab. Dispos.*, **3**, 133(1975); through *Chem. Abstr.*, **83**, 71462b(1975).

(1737) J. R. Horn and D. L. Giusti, *Drug. Intel. Clin. Pharm.*, **9**, 180(1975).

(1738) P. T. Mannisto, J. Tuomisto, A. Jounela, and O. Penttila, *Acta Pharmacol. Toxicol.*, **36**, 353(1975); through *Chem. Abstr.*, **83**, 15554w(1975).

(1739) J. E. Baer, *Clin. Pharmacol. Ther.*, **16**, 272(1974); through *Chem. Abstr.*, **82**, 25615k(1975).

(1740) E. Schaumloeffel, *Med. Welt*, **25**, 2008(1974); through *Chem. Abstr.*, **83**, 92919a(1975).

(1741) D. E. Schwartz and F. Jeunet, *Chemotherapy*, **22**, 19(1976); through *Chem. Abstr.*, **83**, 188161u(1975).

(1742) A. Sundwall, J. Vessman, and B. Strindberg, *Eur. J. Clin. Pharmacol.*, **6**, 191(1973); through *Chem. Abstr.*, **82**, 149123t(1975).

(1743) R. Gugler, W. Herold, and H. J. Dengler, *ibid.*, **7**, 17(1974); through *Chem. Abstr.*, **82**, 149155e(1975).

(1744) H. Ebel, H. G. Classen, P. Marquardt, and M. Spaeth, *Muench. Med. Wochenschr.*, **117**, 1243(1975); through *Chem. Abstr.*, **83**, 126366f(1975).

(1745) D. E. Case and P. R. Reeves, *Xenobiotica*, **5**, 113(1975); through *Chem. Abstr.*, **83**, 108097q(1975).

(1746) A. Berlin, P. Belfrage, and R. Magno, *Acta Pharm. Suec.*, **11**, 646(1974); through *Chem. Abstr.*, **83**, 191b(1975).

(1747) J. Kanto, L. Kangas, and T. Sirtola, *Acta Pharmacol. Toxicol.*, **36**, 328(1975); through *Chem. Abstr.* **83**, 194e(1975).

(1748) J. M. Christensen and S. Holfort, *J. Pharm. Pharmacol.*, **27**, 538(1975); through *Chem. Abstr.*, **83**, 172791p(1975).

(1749) G. Alvan, O. Ericsson, S. Levander, and J. E. Lindgren, *Eur. J. Clin. Pharmacol.*, **7**, 449(1974); through *Chem. Abstr.*, **83**, 847v(1975).

(1750) M. Rizzo, P. Biandrate, G. Tognoni, and P. L. Morselli, *ibid.*, **5**, 226(1973); through *Chem. Abstr.*, **82**, 106564v(1975).

(1751) L. M. Allen and P. J. Creaven, *Clin. Pharmacol. Ther.*, **17**, 492(1975).

(1752) W. A. Pettinger, K. Keeton, M. Phil, and K. Tanaka, *ibid.*, **17**, 146(1975).

(1753) J. M. Strong, D. E. Mayfield, A. J. Atkinson, C. B. Burris, F. Raymond, and L. T. Lesile, *ibid.*, **17**, 184(1975).

(1754) R. J. Elin, E. S. Vesell, and S. M. Wolff, *ibid.*, **17**, 447(1975).

(1755) M. S. S. Chow and R. A. Ronfeld, *J. Clin. Pharmacol.*, **15**, 405(1975).

(1756) C. C. Peck, A. N. Lewis, and B. E. Joyce, *Ann. Trop. Med. Parasitol.*, **69**, 141(1975); through *Chem. Abstr.*, **83**, 90609w(1975).

(1757) D. Shen, M. Gibaldi, M. Throne, G. Bellward, R. Cunningham, Z. Israili, P. Dayton, and J. McNay, *Clin. Pharmacol. Ther.*, **17**, 363(1975).

(1758) G. Offermann, K. Schaefer, H. G. Grigoleit, and F. Dittmar, *Eur. J. Clin. Pharmacol.*, **8**, 255(1975); through *Chem. Abstr.*, **83**, 71434u(1975).

(1759) B. A. Wood and A. M. Monro, *Br. J. Vener. Dis.*, **51**, 51(1975); through *Chem. Abstr.*, **83**, 71415p(1975).

(1760) M. E. Evans, G. M. Shenfield, N. Thomas, S. R. Walker, and J. W. Paterson, *Xenobiotica*, **4**, 681(1974); through *Chem. Abstr.*, **82**, 132728w(1975).

(1761) R. G. Moore, E. J. Triggs, C. A. Shanks, and J. Thomas, *Eur. J. Clin. Pharmacol.*, **8**, 353(1975); through *Chem. Abstr.*, **83**, 141739y(1975).

(1762) B. Alexanderson, *ibid.*, **6**, 44(1973); through *Chem. Abstr.*, **83**, 92895q(1975).

(1763) R. Gugler, D. W. Shoeman, D. H. Huffman, J. B. Cohlmia, and D. L. Azarnoff, *J. Clin. Invest.*, **55**, 1182(1975); through *Chem. Abstr.*, **83**, 37469z(1975).

(1764) D. Latos, C. Bryan, and W. Stone, *Clin. Pharmacol. Ther.*, **17**, 692(1975).

(1765) K. McLeod, M. J. Watson, and M. D. Rawling, *Br. J. Anaesth.*, **47**, 902(1975); through *Chem. Abstr.*, **83**, 201732c(1975).

(1766) A. Whelton, S. D. Nightingale, G. G. Carter, L. S. Gordon, H. H. Bryant, and W. G. Gordon, *J. Infect. Dis.*, **132**, 467(1975); through *Chem. Abstr.*, **83**, 201715z(1975).

(1767) S. Carney, R. A. Butcher, J. K. Dawborn, and G. Pattison, *Clin. Exp. Pharmacol. Physiol.*, **1**, 299(1974); through *Chem. Abstr.*, **83**, 93342u(1975).

(1768) H. Koehler, W. Kirch, D. Hoeffler, and P. Koeppe, *Klin. Wochenschr.*, **52**, 1111(1974); through *Chem. Abstr.*, **83**, 92923x(1975).

(1769) J. Elfstrom and S. Lindgren, *Eur. J. Clin. Pharmacol.*, **7**, 467(1974); through *Chem. Abstr.*, **83**, 210g(1975).

(1770) A. Tacquet, B. Devulder, D. Cuvelier, J. Legros, M. G. Gobert, and M. Franque, *Postgrad. Med. J. Suppl.*, **50**, 36(1974); through *Chem. Abstr.*, **83**, 71450w(1975).

(1771) J. Traeger, J. Moskovchenko, J. C. Monier, and P. Zech, *ibid.*, **50**, 39(1974); through *Chem. Abstr.*, **83**, 71451x(1975).

(1772) H. F. Von Oldershausen, H. P. Menz, I. Hartmann, H. J. Bezler, R. Ilg, and G. C. Burck, *ibid.*, **50**, 44(1974); through *Chem. Abstr.*, **83**, 71452y(1975).

(1773) J. Schweiger and D. Renner, *Verh. Dtsch. Ges. Inn. Med.*, **80**, 667(1974); through *Chem. Abstr.*, **83**, 869d(1975).

(1774) K. Lehmann and K. Merten, *Int. J. Clin. Pharmacol., Ther. Toxicol.*, **10**, 292(1974); through *Chem. Abstr.*, **83**, 92921v(1975).

(1775) J. B. Eastwood and P. E. Gower, *Postgrad. Med. J.*, **50**, 710(1974); through *Chem. Abstr.*, **82**, 11871k(1975).

(1776) K. Collinsworth, J. Strong, A. Atkinson, R. Winkle, F. Periroth, and D. Harrison, *Clin. Pharmacol. Ther.*, **18**, 59(1975).

(1777) E. Karlsson, P. Collste, and M. D. Rawlins, *Eur. J. Clin. Pharmacol.*, **7**, 455(1974); through *Chem. Abstr.*, **82**, 149496s(1975).

(1778) J. L. Cunningham, M. F. Bullen, and D. A. P. Evans, *ibid.*, **7**, 461(1974); through *Chem. Abstr.*, **82**, 149158h(1975).

(1779) J. M. Lesser, Z. H. Israili, D. C. Davis, and P. G. Dayton, *Drug Metab. Dispos.*, **2**, 351(1974); through *Chem. Abstr.*, **82**, 64s(1975).

(1780) M. H. N. Tattersall, J. E. Sodergren, S. K. Sengupta, D. H. Trites, E. J. Modest, and E. Frei, *Clin. Pharmacol. Ther.*, **17**, 701(1975); through *Chem. Abstr.*, **83**, 71471d(1975).

(1781) T. P. Gibson, J. Matusi, E. Matusik, H. A. Nelson, J. Wilkinson, and W. A. Briggs, *ibid.*, **17**, 395(1975); through *Chem. Abstr.*, **83**, 71454a(1975).

(1782) M. M. Reidenberg, D. E. Drayer, M. Levy, and H. Warner, *ibid.*, **17**, 722(1975); through *Chem. Abstr.*, **83**, 90619z(1975).

ACKNOWLEDGMENTS AND ADDRESSES

Received from the **Warner-Lambert Research Institute, Morris Plains, NJ 07950,* and *‡Stuart Pharmaceuticals, Wilmington, DE 19897*

ˣ To whom inquiries should be directed.

Critical Analysis of "Flip-Flop" Phenomenon in Two-Compartment Pharmacokinetic Model

PETER R. BYRON and ROBERT E. NOTARI ˣ

Abstract □ Computer simulations were used to examine the effect of first-order absorption on the disposition of one- and two-compartment model drugs. Two-compartment systems that attain a clinically acceptable β-phase after rapid intravenous injection were perturbed by introduction of drug *via* first-order absorption. The validity of perceiving such a system as a potential "flip-flop" model was tested by comparing the negative slopes of log-linear plasma–time profiles to known values for k_a and β for various values of k_a, k_{12}, k_{21}, and k_{10}. Although most log-linear plots showed excellent correlation coefficients ($r^2 > 0.996$), their negative slopes (S) did not represent either k_a or β under various combinations. A similar consideration of the one-compartment model enabled a comparison to be made between the two systems. Maximum negative errors were observed for both one- and two-compartment drugs as $k_a \rightarrow k_2$ or β, respectively. The value for S provided a good estimate of the absorption rate constant, k_a, when $k_2 \geq 2k_a$ (one compartment) or $\beta \geq 2k_a$. The elimination rate constant (k_2 or β) could be obtained from S for all one-compartment and some two-compartment drugs when the value of k_a was approximately twice that of k_2 or β. Large positive errors also were observed with certain two-compartment drugs where the ratio of the four rate constants apparently linearized a nonlinear plasma profile. Conditions wherein S may be expected to approach β wherein S approaches k_a are clearly defined.

Keyphrases □ Pharmacokinetic models, two compartment—equation derived for time required for constancy of drug fraction in Compartment 1, effect of absorption and elimination rate constants □ Models, pharmacokinetic—equation derived for the time required for constancy of drug fraction in Compartment 1, effect of absorption and elimination rate constants □ Drug disposition—two-compartment open model, equation derived for time required for constancy of drug fraction in Compartment 1

Distribution and elimination kinetics of a number of drugs can be described by the two-compartment open model shown in Scheme I. Methods were discussed previously (1) for calculating the first-order rate constants, k_{12}, k_{21}, and k_{10}, from blood level data after rapid intravenous injection. Biological half-life, $t_{0.5}$, is commonly estimated from the terminal negative slope (β_{app}) of a first-order plot of plasma concentration using:

$$t_{0.5} = 0.693/\beta_{app} \qquad \text{(Eq. 1)}$$

Reliable estimates are obtained if the fraction of drug in Compartment 1:

$$f_1 = \{(\text{amount})_1/[(\text{amount})_2 + (\text{amount})_1]\}_t \qquad \text{(Eq. 2)}$$

achieves a relatively constant value following intravenous bolus administration. It can easily be shown that f_1 approaches a constant value at its limit, $t \rightarrow \infty$, where:

$$\lim (f_1)_{t \rightarrow \infty} = \beta/k_{10} \qquad \text{(Eq. 3)}$$

and that certain combinations of values of k_{12}, k_{21}, and k_{10} can prolong the time to approach the β-phase.

In this study, an equation was derived to estimate the time required to achieve a "clinically acceptable" degree of constancy for f_1 wherein the value for β_{app} approaches the theoretical value for β. The influence of the relative values of the first-order rate constants upon this time was investigated.

Several reviews (2–4) tabulating $t_{0.5}$ values for numerous commonly used drugs included estimates obtained after extravascular drug administration. Scheme I may be modified to include first-order input to Compartment 1 at a rate described by a first-order absorption rate constant, k_a. In this model, the calculation of half-lives from the terminal log-linear negative slope (S) assumes that $S \rightarrow \beta$.

If absorption is rate limiting, then S is purported to approach k_a (5), a phenomenon commonly known as "flip-flop." This impression is based on the behavior of consecutive first-order reactions ($A \rightarrow B \rightarrow C$), where log-linear plots for the concentration of B can be used to determine the rate constant for the rate-determining step (6). This investigation was designed to determine the errors that could be incurred when β or k_a was estimated by linear regression after extravascular drug administration, using the flip-flop assumption.

EXPERIMENTAL

Time to Reach β-Phase after Intravenous Administration—A typical time profile for a drug administered by rapid intravenous injection and described by Scheme I is illustrated in Fig. 1*a*. The time profile for the fraction of *dose* in Compartment 1, F_1, is seen to parallel that in Compartment 2, F_2, after time, t_d, at which time the total body content, $F_1 + F_2$, also becomes linear and parallel. That fraction of *drug in the body* that is contained in Compartment 1, f_1, approaches a constant value at t_d.

Data for drug in the central compartment may be described by:

$$F_1 = F_A e^{-\alpha t} + F_B e^{-\beta t} \qquad \text{(Eq. 4)}$$

where the estimation of values for F_A, α, F_B, and β by the feathering method is illustrated in Fig. 1*b*. Since the time course representing F_1 is the sum of two exponentials, it is possible to estimate the distribution time, t_d, by choosing some arbitrary minimum contribution by the first term, $F_A e^{-\alpha t}$. Therefore, it is possible to solve for the time, t_d, at which the contribution of $F_A e^{-\alpha t}$ becomes equal to some small fraction, P, of $F_B e^{-\beta t}$. When P is sufficiently small, then $F_1 \rightarrow F_B e^{-\beta t}$. Thus, to calculate the time where $F_A e^{-\alpha t}$ is 1% of $F_B e^{-\beta t}$ or:

$$P = F_A e^{-\alpha t}/F_B e^{-\beta t} = 0.01 \qquad \text{(Eq. 5)}$$

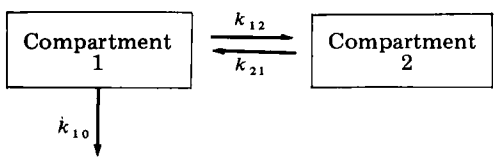

Scheme I

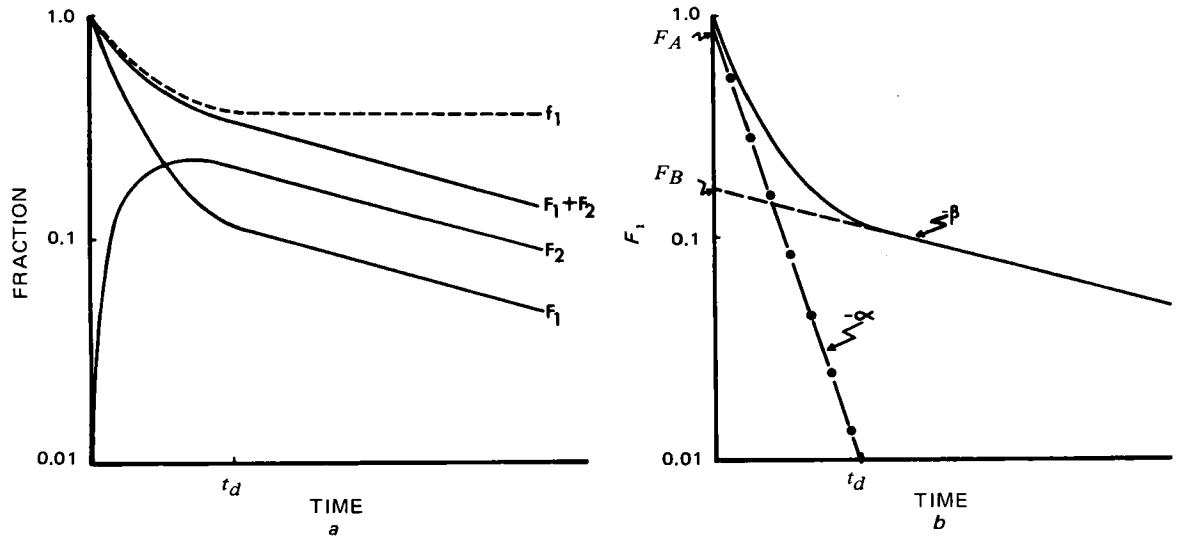

Figure 1—(a) *Dose fraction* (F)*–time profiles for a two-compartment drug after intravenous administration. Dashed line shows* $f_1 = [F_1/(F_1 + F_2)]$ *approaching a constant value at time* t_d. (b) *Graphical estimation of* F_A, α, F_B, *and* β *for a two-compartment drug.*

it is necessary only to rearrange and solve for t_d according to:

$$t_d = [\ln P - \ln (F_A/F_B)]/(\beta - \alpha) \quad \text{(Eq. 6)}$$

This equation may also be rewritten in terms of the first-order rate constants since the ratio, F_A/F_B, may be defined:

$$R = F_A/F_B = (k_{21} - \alpha)/(\beta - k_{21}) \quad \text{(Eq. 7)}$$

Equation 6 may then be simplified to:

$$t_d = [\ln (P/R)]/(\beta - \alpha) \quad \text{(Eq. 8)}$$

which, for the case where $P = 0.01$, may be written:

$$t_d = (4.6 + \ln R)/(\alpha - \beta) \quad \text{(Eq. 9)}$$

Negative Slope of Plasma Level Curve with First-Order Input—The negative slope of the log-linear plasma profile was calculated for values of the constants k_a, k_{12}, k_{21}, and k_{10} by iterative digital computer simulation using Eq. 10 (two-compartment model) and Eq. 11 ($A \xrightarrow{k_a} B \xrightarrow{k_2} C$), which can be found in many texts:

$$F_1 = k_a \{[(k_{21} - k_a)/(\alpha - k_a)(\beta - k_a)]e^{-k_a t} + [(k_{21} - \alpha)/(k_a - \alpha)(\beta - \alpha)]e^{-\alpha t} + [(k_{21} - \beta)/(k_a - \beta)(\alpha - \beta)]e^{-\beta t}\} \quad \text{(Eq. 10)}$$

$$F_1 = \{k_a/(k_2 - k_a)\}[e^{-k_a t} - e^{-k_2 t}] \quad \text{(Eq. 11)}$$

The program was designed to simulate plasma analysis as it is commonly practiced. It begins by finding $(F_1)_{max}$, t_{max}, and t_2, where t_2 corresponds to $0.1(F_1)_{max}$. Subsequently, three sets of eight data points were calculated beginning at $(t_{max} + I)$, $(t_{max} + 2I)$, or $(t_{max} + 3I)$ and separated by a time increment I, where $I = (t_2 - t_{max})/8.0$. Linear regressions of ln F_1 *versus* time enabled an assessment of the correlation coefficients and a comparison of the slopes with theoretical values for β and the absorption rate constant, k_a.

In many cases, obvious nonlinearity was apparent when F_1 values calculated for $t < (t_{max} + 3I)$ were included in the regression analyses. To maintain uniformity, therefore, the negative log-linear slopes quoted throughout this paper are those beginning at $t_1 = (t_{max} + 3I)$ and ending at $t_3 = (t_2 + 2I)$. Simultaneous use of Eq. 9 enabled the prediction of t_d after intravenous administration. The values of k_a, k_{12}, and k_{21} were varied from 0 to 40. In the case of k_{10}, values ranged from 0 to 100.

RESULTS AND DISCUSSION

Time to Reach β-Phase after Intravenous Administration—To evaluate the effect of first-order absorption on drug disposition, it was necessary first to determine the time, t_d, to achieve distribution following rapid intravenous injection (Eq. 9). Very large values for t_d may preclude the clinical assessment of terminal blood level data since the plasma concentration will fall below assayable limits.

The effect of variation of the constants k_{12}, k_{21}, and k_{10} on the time (t_d in half-lives) taken to approach an acceptable β-phase after intravenous administration is summarized in Fig. 2. It is readily apparent that t_d is extremely sensitive to changes in k_{12} as compared to the other constants. As k_{12} decreases relative to k_{21} and k_{10}, t_d increases dramatically. For example, Eq. 9 may be used to predict a t_d value when the ratio k_{12}:k_{21}:k_{10} is 1:40:40. Let us assume that the actual values (in hours^{-1}) are 0.01:0.40:0.40. The calculated value for t_d ($P = 0.01$) would be 37.5 hr (or 18.75 half-lives).

Plasma level data under clinical conditions probably would be assumed to be monoexponential for such a case. In actual fact, the data would be nonlinear, but it would be very difficult to detect this due to biological variation. The apparent value for $t_{0.5}$ might be estimated as 1.78 hr whereas the value calculated from β is 2.0 hr. The reason for this near agreement follows. The fraction of the *dose* in Compartment 2, F_2, at its maximum (where $dF_2/dt = 0$) is described by:

$$(F_2)_{max} = F_1' k_{12}/k_{21} \quad \text{(Eq. 12)}$$

where F_1' = the value for F_1 at the time when $F_2 = (F_2)_{max}$.

The fraction of the *total body content* contained in Compartment 2 when $F_2 = (F_2)_{max}$ may be defined as:

$$(f_2)_{(F_2)_{max}} = (F_2)_{max}/[F_1' + (F_2)_{max}] = k_{12}/(k_{12} + k_{21}) \quad \text{(Eq. 13)}$$

The inset in Fig. 2 illustrates the effect of k_{12} on three parameters, t_d, $(f_2)_{(F_2)_{max}}$, and $(f_2)_\infty$, where:

$$(f_2)_\infty = 1 - (\beta/k_{10}) \quad \text{(Eq. 14)}$$

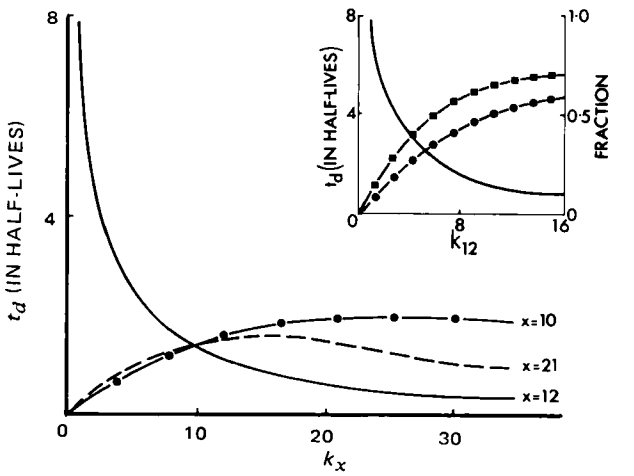

Figure 2—*Effect of* k_{12}, k_{21}, *and* k_{10} *on the distribution time,* t_d *(*x = *12,* $k_{21} = k_{10} = 10$; x= *21,* $k_{12} = k_{10} = 10$; x = *10,* $k_{12} = k_{21} = 10$*). The inset shows the effect of* k_{12} *on: (—)* t_d, *(●)* $(f_2)_{(F_2)_{max}}$, *and (■)* $(f_2)_\infty$.

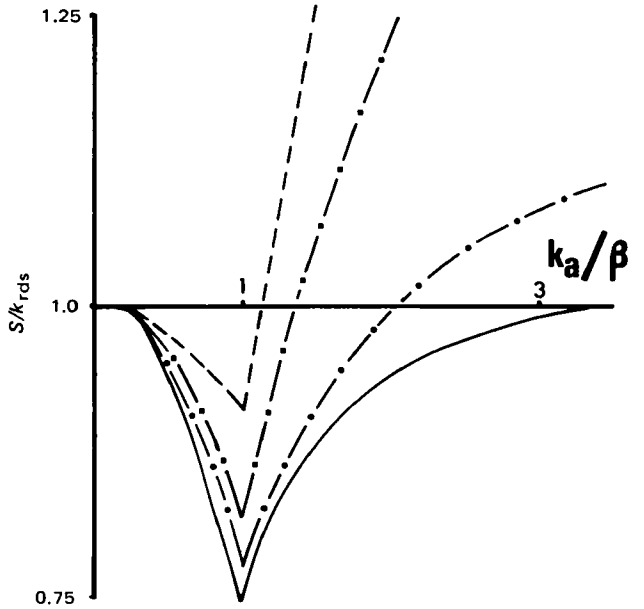

Figure 3—*Ratios of* S/k_a, $(k_a/\beta) < 1$, *and* S/β, $(k_a/\beta) > 1$, *for the cases:* (—) $[k_{10}/(k_{12} = k_{21})] = 0.5$, (●) $[k_{10}/(k_{12} = k_{21})] = 1.5$, (■) $[k_{10}/(k_{12} = k_{21})] = 3.5$, *and* (- -) $[k_{10}/(k_{12} = k_{21})] = 10$.

The inset shows that as the time to approach the β-phase, t_d, increases due to $k_{12} \rightarrow 0$, the fraction in Compartment 2 also approaches zero. Thus, the error incurred in regarding the data as monoexponential decreases at t_d increases. In the limiting case, as $k_{12} \rightarrow 0$, $(f_2)_t \rightarrow 0$ and $\beta \rightarrow k_{10}$, so that monoexponential data result.

Negative Slope (S) of Log-Linear Plasma Level Curve with First-Order Input—Estimating $t_{0.5}$ from plasma level data requires the negative slope of the log-linear plot to approach the value for the first-order rate constant for whole body elimination, *i.e.*, $S \rightarrow \beta$. The phenomenon of flip-flop, a well-recognized occurrence in pharmacokinetics, is assumed due to the absorption rate becoming the rate-determining step (rds) in drug elimination. The value of S was compared to k_a when $(k_a/\beta) < 1$ and to β when $(k_a/\beta) > 1$ for some 2000 computer-generated log-linear plasma profiles defined by the values of k_a, k_{12}, k_{21}, and k_{10}.

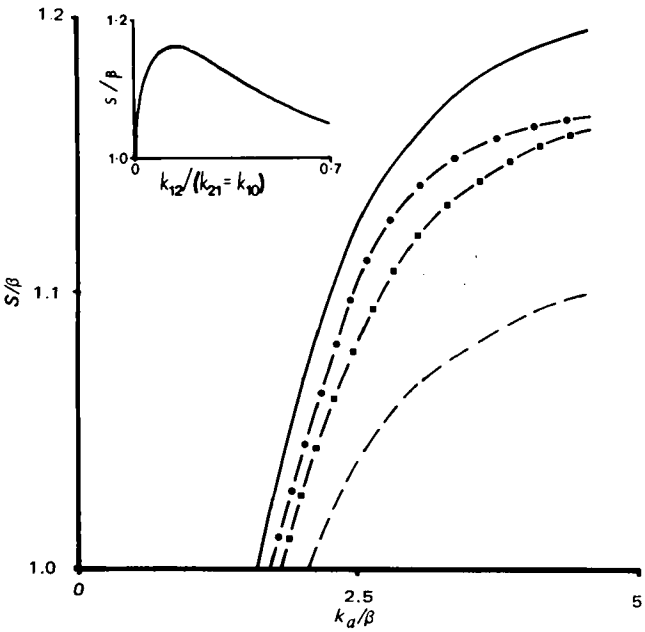

Figure 4—*Relationship of* S *to* β *for the cases:* (●) $[k_{12}/(k_{21} = k_{10})] = 0.05$, (—) $[k_{12}/(k_{21} = k_{10})] = 0.1$, (■) $[k_{12}/(k_{21} = k_{10})] = 0.3$, *and* (- -) $[k_{12}/(k_{21} = k_{10})] = 0.5$. *Inset shows* S/β versus $k_{12}/(k_{21} = k_{10})$ *when* $k_a/\beta = 3$.

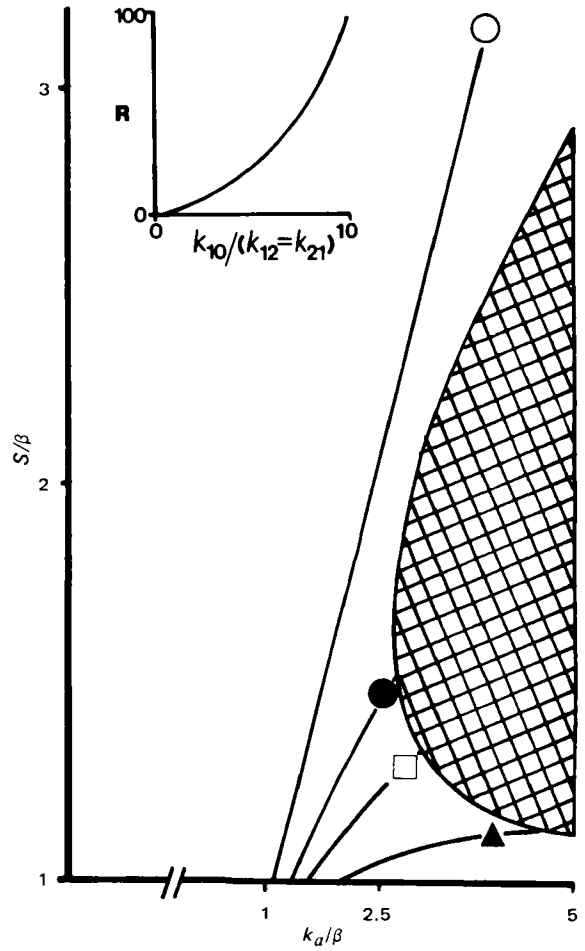

Figure 5—S/β versus k_a/β *for the cases:* (○) $[k_{10}/(k_{12} = k_{21})] = 10$, (●) $[k_{10}/(k_{12} = k_{21})] = 3.5$, (■) $[k_{10}/(k_{12} = k_{21})] = 2.5$, *and* (▲) $[k_{10}/(k_{12} = k_{21})] = 1.5$. *Cross-hatched area represents a zone of nonlinearity where* $r > -0.998$. *Inset plot shows the relationship between* $R = (F_A/F_B)$ *and* $[k_{10}/(k_{12} = k_{21})]$.

Figure 3 shows typical examples of S/k_{rds} ratios for the cases where $k_{12} = k_{21}$ and k_a and k_{10} are varied. The concept of flip-flop was rigorously examined in terms of such diagrams by varying k_a, k_{12}, k_{21}, and k_{10}. In Fig. 3, maximum negative errors are defined by the k_a/β ratio of unity where neither absorption nor elimination is rate limiting. When $(k_a/\beta) < 1$, then $S/k_{rds} \rightarrow 1$ and $S \rightarrow k_a$. Conversely, if $(k_a/\beta) > 1$, elimination may become rate determining and $S \rightarrow \beta$. If $k_{10} > (k_{12} = k_{21})$, however, then S/k_{rds} may become greater than unity at some point defined by the relative values of k_{10} and k_a to k_{12} and k_{21}. In these cases where $(S/k_{rds}) > 1$, a positive error would be made when estimating β from the value of the terminal slope (S).

In all cases discussed, least-squares regression analyses of ln F_1 *versus* t yielded correlation coefficients of $r < -0.998$ ($r^2 > 0.996$).

Negative Errors—The solid line of Fig. 3 represents the negative errors, $(S/k_{rds}) < 1$, incurred in the estimation of β or k_a from the negative slope of log-linear plasma profiles. Purely negative errors were observed only when $k_{12} > (k_{21} = k_{10})$, $k_{21} > (k_{12} = k_{10})$, or $k_{10} < (k_{21} = k_{12})$. The point of the minimum S/k_{rds} ratio is defined by a k_a/β ratio of unity since both k_a and β have the same percentage error when compared to S. At this point, neither absorption nor elimination is rate limiting. The percentage error becomes smaller as the k_a/β ratio is increased from unity ($S \rightarrow \beta$ as $S/k_{rds} \rightarrow 1$). Calculation of S for a one-compartment model using Eq. 11 for a variety of k_a/k_2 ratios yields a plot of S/k_{rds} *versus* k_a/k_2, which is identical to the solid line plot of Fig. 3. The terminal slope, S, may be used to estimate the values of k_a or β (or k_2) within 5% of their true values when $[0.5 > (k_a/\beta) > 2.1]$ or $[0.5 > (k_a/k_2) > 2.1]$.

The dashed lines in Fig. 3, however, show typical effects of variation in the k_{12}:k_{21}:k_{10} ratio outside the conditions of purely negative error defined previously. If the k_a/β ratio is increased still further, then S/β also increases to values well above unity. In these cases, which will be

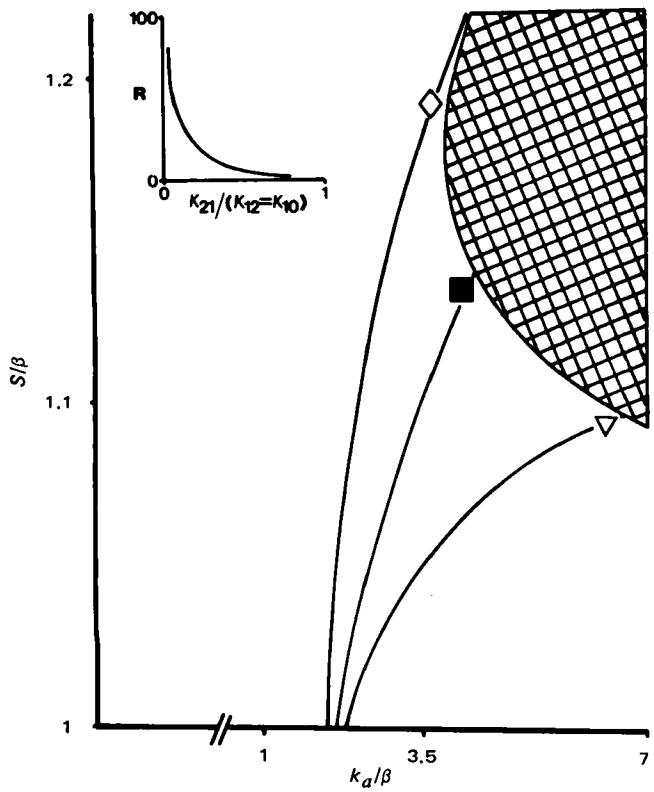

Figure 6—S/β versus k_a/β *for the cases:* (◇) $[k_{21}/(k_{12} = k_{10})] = 0.05$, (□) $[k_{21}/(k_{12} = k_{10})] = 0.2$, *and* (▽) $[k_{21}/(k_{12} = k_{10})] = 0.5$. *Cross-hatching represents nonlinearity* ($r > -0.998$). *Inset shows* R = (F_A/F_B) versus $[k_{21}/(k_{12} = k_{10})]$.

discussed more fully in the following section, a k_a/β ratio exists at which the correct value for β may be obtained from S for entirely fortuitous reasons.

Positive Errors Due to Effect of t_d—Positive errors in the estimates for $\beta(S > \beta)$ are observed in cases where k_{12} approaches relatively small values. Figure 4 shows examples of typical S/β ratios when $k_{21} = k_{10} = 10$ while k_{12} and k_a/β are varied from 0.5 to 5. The inset plot of Fig. 4 demonstrates that when the k_a/β ratio is held constant, $(k_a/\beta) = 3.0$, and $k_{12} = 1.5$, a position of maximum positive error occurs at $(S/\beta) = 1.16$. This effect can be attributed to slow distribution.

Following intravenous administration (Fig. 2), the distribution time, t_d, is greater than 3.8 half-lives when $[k_{12}/(k_{21} = k_{10})] < 0.3$. Thus, when $[k_{12}/(k_{21} = k_{10})] = 0.15$ and $k_a/\beta = 3$ at the position of maximum positive error (Fig. 4 inset), a similar overestimate of β would probably be made from intravenous data.

Positive Errors Due to Effect of F_A/F_B Ratio—Figures 5 and 6 show the relationship between S/β and k_a/β for the cases $k_{10} > (k_{12} = k_{21})$ and $k_{21} < (k_{12} = k_{10})$. It is readily apparent from the inset plots of F_A/F_B *versus* $[k_{10}/(k_{21} = k_{12})]$ and $[k_{21}/(k_{12} = k_{10})]$ that the S/β ratio increases with either decreasing k_{21} or increasing k_{10} if k_a/β is held constant. In cases where $[k_{10}/(k_{12} = k_{21})] > 8$, plots always appeared linear ($r < -0.998$) irrespective of the k_a/β ratio.

Intravenous and oral plots are shown for $[k_{10}/(k_{12} = k_{21})] = 10$ in Fig. 7*a*. After intravenous bolus administration, the α-slope might mistakenly be used to calculate the $t_{0.5}$ of the drug unless the plasma was sampled through at least 2.5 log cycles. However, administration by first-order absorption ($k_a/\beta = 3.9$) shows how k_a can apparently linearize plasma decay. This negative slope, S, approaches neither the α nor β value between t_1 and t_3. If linearity were accepted as the criterion for $S \rightarrow \beta$, then the $t_{0.5}$ estimate would be less than half the theoretical value.

In contrast to the previous case, Fig. 7*b* shows an example where it is more likely that a correct estimate for β would be made after intravenous administration ($F_A/F_B = 10.9$). Administration by first-order absorption, however, shows the pronounced influence of k_a upon the negative slope, S, $(k_a/\beta) = 2.65$. A 39% overestimate can be made in β by accepting linearity as an indication that $S \rightarrow \beta$. The cross-

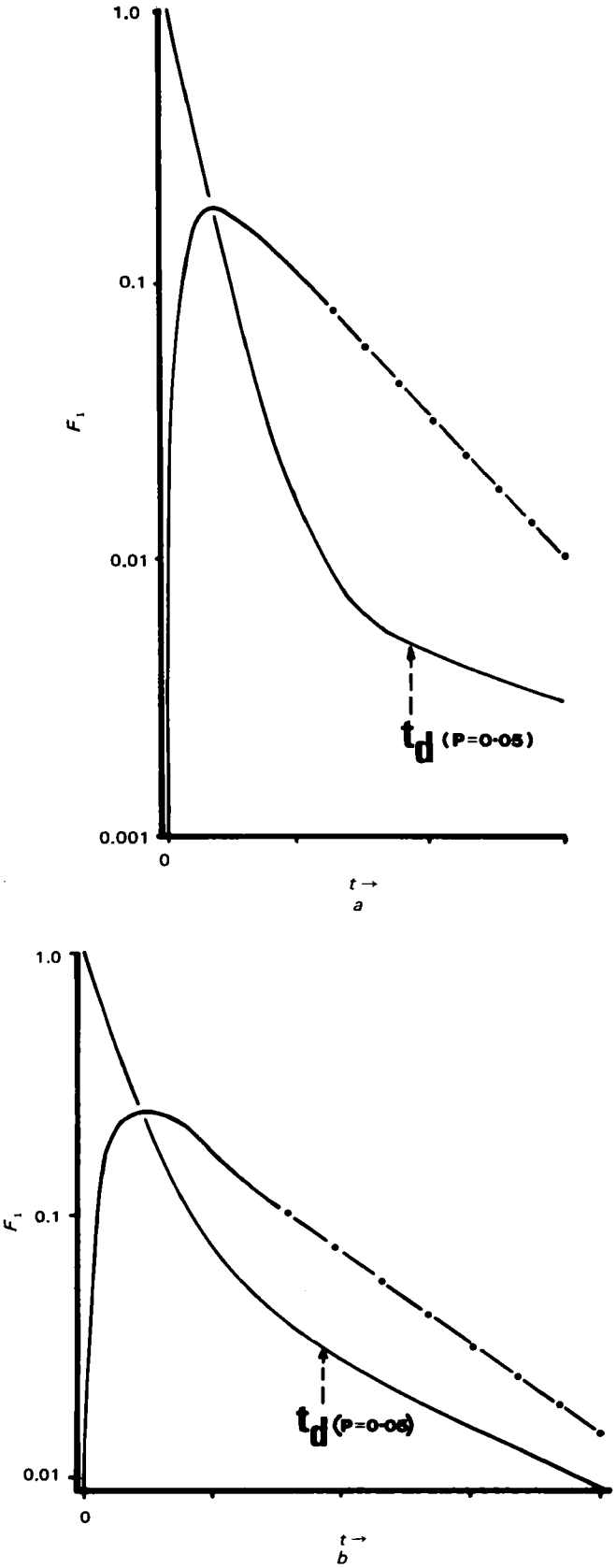

Figure 7—*Comparison of intravenous and oral log-linear plasma profiles for the cases:* (a) $[k_{10}/(k_{12} = k_{21})] = 10$, $k_a/\beta = 3.9$; *and* (b) $[k_{10}/(k_{12} = k_{21})] = 3$, $k_a/\beta = 2.65$.

hatched area in Fig. 5, where $[k_{10}/(k_{12} = k_{21})] = 3$, clearly demonstrates that as k_a/β is increased still further, the t_1–t_3 portion of the oral plot approaches obvious nonlinearity ($r > -0.998$).

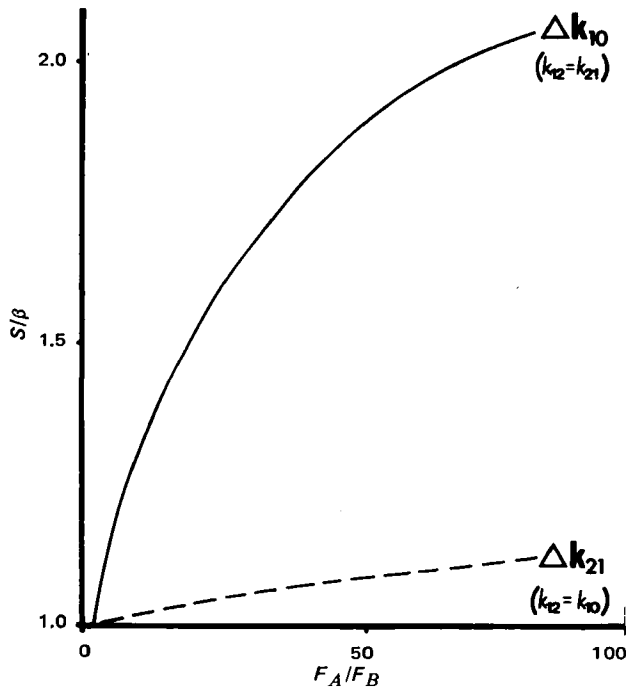

Figure 8—*Relationship between* S/β *and* F_A/F_B *shown at a constant* k_a/β (= 2.5) *by variation of* k_{10} *and* k_{21} (*solid and dashed lines, respectively*).

The errors shown in Figs. 5 and 6, therefore, were attributed directly to the observation of α-phase data which can be apparently linearized during the time period t_1–t_3 over a wide range of k_a/β values. Figure 8 shows that F_A/F_B ratios alone do not predict the positive errors in estimating β from S values. Thus, positive errors in β estimates are, in fact, specific to the k_a:k_{12}:k_{21}:k_{10} ratio and are not predictable solely by consideration of F_A/F_B.

CONCLUSIONS

It is well recognized that the negative terminal slopes of log-linear plots of plasma drug concentration following oral administration may not represent reasonable estimates for the first-order elimination constant, β. In cases where the value of the slope is less than the intravenous estimate for β, it generally has been concluded that absorption is rate limiting and that the slope reflects the absorption rate constant. The results clearly demonstrate the frailty of this assumption for both one- and two-compartmental model drugs. In fact, β (or k_2) must have at least twice the value of the absorption rate constant before a reasonable estimate of k_a can be made from the negative slope, S.

It also was reported in the literature that in certain cases the value for S is apparently too large following oral administration. The significant decrease of estimates made from slopes during the steady state as compared to values from single oral doses (7) is perhaps the most widely discussed example (4, 6–8). It was suggested that the single oral dose values represent the influence of distribution (4). The present study demonstrates that S following oral administration can indeed be larger than β due to the apparent linearization of α-phase data at certain k_a/β ratios.

Thus, it is possible to obtain all of the following: good estimates for k_a or β; negative errors in the estimates for k_a; and both negative and positive errors in the estimates for β depending on the relative values for k_a, k_{12}, k_{21}, and k_{10}.

REFERENCES

(1) S. Riegelman, J. C. K. Loo, and M. Rowland, *J. Pharm. Sci.*, **57**, 117(1968).

(2) T. R. Simpson and J. P. Juergens, *Hosp. Pharm.*, **8**, 68(1973).

(3) W. A. Ritschel, *Drug Intel. Clin. Pharm.*, **4**, 332(1970).

(4) J. M. Van Rossum, in "Drug Design," vol. 1, E. J. Ariens, Ed., Academic, New York, N.Y., 1971, pp. 472, 509.

(5) J. T. Doluisio, J. C. La Piana, and L. W. Dittert, *J. Pharm. Sci.*, **60**, 715(1971).

(6) R. E. Notari, "Biopharmaceutics and Pharmacokinetics, An Introduction," 2nd ed., Dekker, New York, N.Y., 1975, pp. 86, 200.

(7) J. T. Doluisio and L. W. Dittert, *Clin. Pharmacol. Ther.*, **10**, 690(1969).

(8) M. Gibaldi and H. Weintraub, *J. Pharm. Sci.*, **60**, 624(1971).

ACKNOWLEDGMENTS AND ADDRESSES

Received August 20, 1975, from the *Pharmaceutics Research Group, University of Aston in Birmingham, Gosta Green, Birmingham, B4 7ET, England.*

Accepted for publication October 8, 1975.

[x] To whom inquiries should be directed. Present address: College of Pharmacy, Ohio State University, Columbus, OH 43210

Wettability of Pharmaceutical Solids: Estimates of Solid Surface Polarity

GEORGE ZOGRAFI [x] and STANLEY S. TAM

Abstract □ Contact angle measurements of water and methylene iodide with various organic solids were used to estimate the surface free energy per square centimeter, γ_S, and the contributions of nonpolar and polar forces, γ_S^d and γ_S^p, respectively. The ratio of γ_S^p to γ_S was used as an estimate of solid surface polarity, and values ranging from 0 to 42% polarity were calculated for materials of pharmaceutical interest. Surface free energies per mole were calculated to compare the influence of different substituent groups on wettability. This approach offers a convenient means to quantitate the polarity of organic pharmaceutical solid surfaces.

Keyphrases □ Solids, pharmaceutical—wettability evaluated by measurement of surface free energy and contributions of polar and nonpolar forces, effect of substituent groups □ Wettability—pharmaceutical solids, evaluated by measurement of surface free energy and contributions of polar and nonpolar forces, effect of substituent groups □ Polarity, solid surface—quantitated by measurement of surface free energy and contributions of polar and nonpolar forces, effect of substituent groups

The nature of solid surfaces plays an important role in various pharmaceutical processes (1, 2). Such processes include crystal nucleation and growth, fracture mechanics, powder flow, powder dispersion in liquids, powder compaction, and the coating of solids. For situations where powder dispersion of drugs in water or water penetration into solid compacts is required, a lack of wetting due to unfavorable surface energetics leads to significant difficulty in disintegration and/or dissolution (3). Solid drugs exhibiting such behavior have been termed "hydrophobic," and the use of surfactants to overcome such problems is well established (3).

Some general questions one can ask at this point are:

1. How hydrophobic are the surfaces of various drugs and related solids?
2. What methodology can be used to measure hydrophobicity on a quantitative basis?
3. What factors contribute to the hydrophobic behavior?

Answers to such questions could be useful in any situation where solid surfaces are involved in interactions with other phases.

A rational approach to this problem involves determining the energy of molecules residing at the surface, as well as the contributions to surface energy from various forces, *e.g.*, dispersion forces or hydrogen bonding. For pure liquids, surface energies and entropies can be determined from surface tension measurement at various temperatures since their surface free energy per square centimeter is their surface tension (4).

Surface free energy per square centimeter can be determined for solids, but the problem is both theoretically and experimentally difficult due to the immobility of the molecules and to the heterogeneity of the surface caused by the presence of different crystal faces, imperfections, impurities, and surface roughness (2, 5, 6). Approaches using spectroscopy, calorimetry, solubility, and vapor adsorption have been used to estimate an overall surface free energy per square centimeter or a distribution of energies. However, these techniques are generally more applicable to metals and inorganic compounds than to organic solids such as drugs (6) because of the temperatures and pressures to which solids must be subjected as well as the very high specific surface area generally required for accurate measurements.

Measurement of contact angles exhibited by liquids on solid surfaces has been used to estimate the average surface free energy per square centimeter for many polymers of relatively low surface energy, *i.e.*, polyethylene or nylon (7, 8). Despite many uncertainties when applied to more polar solids, this technique, when properly utilized and interpreted, allows some understanding of organic solid surface energetics in a relatively convenient manner. Consequently, the following report presents estimates of solid surface free energy from contact angle data for a number of drugs and related organic solids. Estimates of the contributions of polar and nonpolar forces to this term also are presented.

THEORETICAL

The basis for using contact angles to estimate surface free energies of solids rests on the relationships between solid surface free energy per square centimeter, γ_S, liquid surface free energy per square centimeter, γ_L, and their interfacial free energy per square centimeter, γ_{SL}, as developed in the Young equation (5, 7):

$$\gamma_S - \gamma_{SL} = \gamma_L \cos\theta + \pi_e \qquad \text{(Eq. 1)}$$

where θ is the contact angle, and π_e is the change in surface free energy per square centimeter due to any adsorption of vapor from the liquid to the solid surface:

$$\pi_e = \gamma_S - \gamma_{SV} \qquad \text{(Eq. 2)}$$

where γ_{SV} is the surface free energy per square centimeter of the solid after vapor adsorption.

For systems where wetting is poor and at room temperature, it is assumed the π_e is zero; for systems with a greater tendency for wetting, the possibility of vapor adsorption at room temperature is enhanced. The significance of this term recently was evaluated theoretically, and it was concluded the π_e is negligible for relatively nonpolar solids at room temperature when high boiling-point liquids are used (9). Consequently, a contribution from this term is considered to be negligible in the present case.

To obtain γ_S from Eq. 1, γ_L and θ can be measured, but no direct estimate of γ_{SL} can be made experimentally. The interfacial free energy between any two phases, γ_{12}, can be estimated by knowing the individual surface free energies, γ_1 and γ_2, and the energies associated with the interactions taking place across the interface (8, 10). This relationship can be written in the general form (11):

$$\gamma_{12} = \gamma_1 + \gamma_2 - 2\phi^d - 2\phi^p \qquad \text{(Eq. 3)}$$

where ϕ^d and ϕ^p are terms reflecting nonpolar and polar interactions, respectively. The further assumption (8) that the surface free energy

Table I—Contact Angles and Surface Free Energy Terms for Various Liquids Using Paraffin at 25°

Liquid	γ_L, ergs/cm²	Contact Angle	γ_L^d	γ_L^p
Water	72.0	109°	23.2	48.8
Glycerin	63.7	96°	32.0	31.7
Formamide	58.3	91°	32.3	26.0
Ethylene glycol	48.9	79°	33.4	15.5
1,3-Butanediol	39.1	62°	32.5	6.6
Methylene iodide	50.4	65°	50.4	0

of a solid or liquid contains contributions from polar and nonpolar forces gives:

$$\gamma_i = \gamma_i^d + \gamma_i^p \quad \text{(Eq. 4)}$$

Although a number of forces can contribute to γ_i^d and γ_i^p, the methods used to determine these values give γ_i^d primarily due to London dispersion forces and γ_i^p due to all other forces, with hydrogen bonding predominating. To estimate ϕ^d and ϕ^p, Fowkes (8) suggested taking the geometric mean of the surface free energy components for each phase such that:

$$\phi^d = (\gamma_1^d \gamma_2^d)^{1/2} \quad \text{(Eq. 5)}$$

$$\phi^p = (\gamma_1^p \gamma_2^p)^{1/2} \quad \text{(Eq. 6)}$$

Wu (11) suggested using a reciprocal mean such that:

$$\phi^d = \frac{2\gamma_1^d \gamma_2^d}{\gamma_1^d + \gamma_2^d} \quad \text{(Eq. 7)}$$

and:

$$\phi^p = \frac{2\gamma_1^p \gamma_2^p}{\gamma_1^p + \gamma_2^p} \quad \text{(Eq. 8)}$$

Either pair of terms can then be used in Eq. 3 to give the expressions:

$$\gamma_{12} = \gamma_1 + \gamma_2 - 2(\gamma_1^d \gamma_2^d)^{1/2} - 2(\gamma_1^p \gamma_2^p)^{1/2} \quad \text{(Eq. 9)}$$

$$\gamma_{12} = \gamma_1 + \gamma_2 - \frac{4\gamma_1^d \gamma_2^d}{\gamma_1^d + \gamma_2^d} - \frac{4\gamma_1^p \gamma_2^p}{\gamma_1^p + \gamma_2^p} \quad \text{(Eq. 10)}$$

Calculations (11) of interfacial tension for a series of immiscible liquid polymers, using either Eq. 9 or 10, reveal good agreement with experimental values in both cases if one or both of the polymers are relatively nonpolar. However, Eq. 10 gives better agreement for systems containing two relatively polar polymers (11).

To measure γ_S^d and γ_S^p, Eqs. 1 and 9 were combined to give Eq. 11 (12), and Eqs. 1 and 10 were combined to give Eq. 12 (11). These equations are:

$$\gamma_L(1 + \cos\theta) = 2[(\gamma_L^d \gamma_S^d)^{1/2} + (\gamma_L^p \gamma_S^p)^{1/2}] \quad \text{(Eq. 11)}$$

and:

$$(b + c - a)\gamma_S^d \gamma_S^p + c(b - a)\gamma_S^d + b(c - a)\gamma_S^p - abc = 0 \quad \text{(Eq. 12)}$$

where a is $(\gamma_L/4)(1 + \cos\theta)$, b is γ_L^d, and c is γ_L^p.

In Eqs. 11 and 12 there are two unknowns, γ_S^d and γ_S^p, so it is necessary to obtain contact angles on a particular solid with two liquids of known γ_L^d and γ_L^p. Then the best fit of γ_S^d and γ_S^p for both sets of contact angle data can be determined by computer analysis.

Table II—Contact Angles for Various Liquids on Nylon 11 and β-Sitosterol at 25°

Liquid	Contact Angle	
	Nylon	β-Sitosterol
Water	76°	94°
Glycerin	65°	83°
Formamide	61°	69°
Ethylene glycol	51°	54°
1,3-Butanediol	36°	48°
Methylene iodide	40°	58°

In most reported cases (11–13), only water and methylene iodide were used, except in one study (14) where glycerin, formamide, and trichlorophenol were used in addition to water and methylene iodide. Comparison of data obtained for the same low energy solids indicates that Eq. 11 results in slightly different answers than Eq. 12.

Since Wu (11) had shown that the reciprocal mean approach (Eq. 10) provides better agreement between calculated and experimental interfacial tensions in liquid polar–polar systems, it was decided to utilize Eq. 12 to estimate γ_S^d and γ_S^p for the solids of pharmaceutical interest. Most studies were conducted using methylene iodide and water only, but the specific effects exerted by the liquid were considered in a few cases by comparing results with other liquids.

EXPERIMENTAL

Contact Angle Measurement—Measurements were made using a telemicroscope[1] attached to a high precision protractor eyepiece. The sample was contained in a thermostated closed chamber at 25° in an atmosphere saturated with the test liquid. Liquid drops of about 0.03 ml were placed on the solid surface using a microliter syringe[2]. Preliminary measurements revealed this drop size to be convenient, although increasing or decreasing the drop volume did not affect the results.

The advancing angles (7) measured in this manner were independent of time after 5 min. Readings, therefore, generally were made from 5 to 10 min after placement of the drop on the surface. Measurements were repeated at least three times with new samples of solid and liquid. The reproducibility of contact angle values generally was better than 2° and no worse than 3°.

Generally, any nonidealized solid surface will exhibit differences in advancing and receding contact angles (7). Consequently, no contact angle in most studies such as this one is an exact thermodynamic value. However, the excellent reproducibility in the measurements for various conditions and the use of the advancing angle for the standard, paraffin, as well as all other solids provide confidence that the surface energies calculated represent the best estimates possible in systems of practical interest.

In all cases where contact angles are reported, no dissolution of the solid by the liquid was noted over the 5–10-min period of measurement. On more extended exposure of some solids to various liquids, some etching of the surface was noticed. To minimize the possibility of dissolution, it is possible to work with saturated solutions of the drug in each liquid. This approach suffers, however, from the fact that liquids with different surface tensions are being used and constants must be determined for each test liquid. Since dissolution did not seem to be a problem, particularly with those hydrophobic drugs of major interest, it was decided that saturated solutions would not be used. In cases where organic acids were used, 0.1 *N* HCl was substituted for water; a random check of values for some of these solids with 0.1 *N* HCl and water, however, revealed no significant differences in contact angle.

Materials[3]—The various solids used in this study are listed in Tables I–V. They were used as received, after initial drying to remove adsorbed water vapor. Densities for the various solids not reported in the literature were measured pycnometrically (15). In some cases, it was necessary to use dilute surfactant solutions to ensure wetting of the solid in the pycnometer. The solids whose densities were measured were griseofulvin, phenacetin, benzocaine, indomethacin, β-sitosterol, sebacic acid, dodecanedioic acid, thopsic acid, salicylic acid, and *p*-hydroxybenzoic acid. All other values were taken from the literature (16, 17) (Table VI).

The liquids used were: water, triple distilled from permanganate; methyl iodide[4]; and ethylene glycol, glycerin, 1,3-butanediol, and

[1] Gaertner Scientific Corp., Chicago, Ill.

[2] Agla, Wellcome Reagents, Ltd., Kent, England.

[3] Magnesium stearate and β-sitosterol were provided by Dr. E. N. Hiestand, The Upjohn Co.; ethinamate was provided by Dr. James Boylan, Eli Lilly Co.; griseofulvin was provided by Dr. Hal Wolkoff, Schering Corp.; indomethacin was provided by Mr. John Allegrehetti, Merck Sharp and Dohme. Benzocaine, phenacetin, aspirin, and salicylic acid were obtained from Ruger Chemical Co., Hillside, N.J. Benzoic, *p*-fluorobenzoic, *p*-chlorobenzoic, and *p*-bromobenzoic acids were obtained from Eastman Organic Chemicals, Rochester, N.Y. Hydrocortisone and hydrocortisone acetate were obtained from The Upjohn Co., Kalamazoo, Mich.; the various dicarboxylic acids came from Aldrich Chemical Co., Milwaukee, Wis. The *p*-hydroxybenzoic acid was provided by Dr. J. T. Carstensen, University of Wisconsin.

[4] Aldrich Chemical Co.

Table III—Estimated Values for Surface Free Energy (Ergs per Square Centimeter) Using Various Combinations of Liquids

Paired Liquids	Nylon 11			β-Sitosterol		
	γ_S^d	γ_S^p	γ_S	γ_S^d	γ_S^p	γ_S
Water–glycerin	20.4	15.1	35.5	19.3	7.2	36.5
Water–formamide	18.0	16.4	34.4	38.5	2.4	40.9
Water–ethylene glycol	18.8	15.9	34.7	33.1	3.3	36.4
Water–1,3-butanediol	22.2	14.3	36.5	—	—	—
Water–methylene iodide	40.0	9.2	49.2	31.2	3.7	34.9
Ethylene glycol–1,3-butanediol	23.9	9.7	33.6	18.4	14.7	33.1

Table IV—Contact Angles and Surface Free Energies per Square Centimeter for Various Solids Using Water and Methylene Iodide

Solid	Contact Angle		γ_S^d	γ_S^p	γ_S	P_0[a]
	Water	Methylene Iodide				
Magnesium stearate	118°	65°	23.0	0	23.0	0
Phenacetin	66°	25°	45.8	12.5	58.3	21
Indomethacin	61°	20°	47.3	14.5	61.8	24
Griseofulvin	57°	26°	45.5	16.7	62.2	27
Hydrocortisone acetate	57°	22°	46.9	16.5	63.4	26
Hydrocortisone	43°	28°	45.1	23.6	68.7	34
Ethinamate	35°	32°	43.3	27.6	70.0	39
Aspirin	37°	41°	39.4	28.1	67.5	42

[a] P_0 is the percent polarity; see Eq. 13.

Table V—Contact Angles and Surface Free Energies per Square Centimeter for Various Solids Using 0.1 *N* HCl and Methylene Iodide

Solid	Contact Angle		γ_S^d	γ_S^p	γ_S	P_0[a]
	0.1 *N* HCl	Methylene Iodide				
Benzoic acid	48°	42°	39.0	22.7	61.7	37
p-Hydroxybenzoic acid	37°	38°	40.6	27.7	68.3	41
o-Hydroxybenzoic acid	39°	34°	42.3	26.2	68.5	38
p-Fluorobenzoic acid	57°	48°	36.0	19.1	54.1	35
p-Chlorobenzoic acid	83°	32°	43.3	5.7	49.0	12
p-Bromobenzoic acid	88°	23°	46.5	3.4	49.9	7
p-Aminobenzoic acid	42°	33°	40.6	25.3	65.9	38
Benzocaine	51°	17°	48.1	19.0	67.1	28
Adipic acid (C_6)	25°	Spreads	—	—	—	—
Pimelic acid (C_7)	29°	26°	45.5	29.5	75.0	39
Suberic acid (C_8)	27°	17°	48.4	29.7	78.1	38
Sebacic acid (C_{10})	56°	39°	40.3	18.1	58.4	31
Dodecanedioic acid (C_{12})	54°	26°	45.5	18.0	63.5	28
Thopsic acid (C_{16})	62°	26°	45.5	14.5	60.0	24

[a] P_0 is the percent polarity; see Eq. 13.

formamide, described previously (18). The surface tensions of these liquids were measured using the Wilhelmy plate technique.

Solid Sample Preparation—The paraffin samples used were sheets of Parafilm[5]. These sheets were quite convenient and gave results with water and methylene iodide that were in excellent agreement with previous studies using blocks of paraffin (19). Nylon 11 was used in the form of smooth sheets and gave contact angles for water and methylene iodide that were in good agreement with previous studies (13).

All solids used, except for β-sitosterol, magnesium stearate, *p*-aminobenzoic acid, and three dicarboxylic acids, were prepared for study by compaction against a flat surface[6]. The size of the tablet and the force used [up to 4540 kg (10,000 lb)] allowed for pressures of about 90,000 psi. The appearance of the tablets compressed at these pressures was quite smooth when the tablets were kept in the die during the contact angle measurement. Preliminary checks at higher or lower pressures indicated no significant dependence of contact angle on pressure in the range studied. Magnesium stearate and β-sitosterol were received as compacts compressed at about 16,000 psi.

Another approach used for sample preparation was to melt the solid on a smooth glass plate and then allow it to resolidify. This approach is unsatisfactory if decomposition or crystal structure changes occur. An advantage of this approach, however, is the lack of any pores between compacted solid particles. Comparison of contact angles with a compact and a melt of *p*-hydroxybenzoic acid, *p*-chlorobenzoic acid, and pimelic acid produced excellent agreement, whereas *p*-fluorobenzoic acid and *p*-bromobenzoic acid exhibited changes in surface appearance after melting and solidification. Thus, melted samples were used only when the compact did not appear suitable, *i.e.*, poor cohesion or high porosity, and when no physical changes after melting were apparent. This was found to be the case for *p*-aminobenzoic acid and the 10-, 12-, and 16-carbon dicarboxylic acids.

RESULTS

Earlier studies showed that one can determine γ_L^d and γ_L^p for pure liquids either by measuring interfacial tensions against liquid hy-

[5] American Can Co., Neenah, Wis.
[6] Carver Press, Fred S. Carver, Inc., Summit, N.J.

Table VI—Molar Area, A_m, of Molecules at the Surface

Solid	A_m, (cm^2/mole) × 10^{-9}	Molecular Weight	ρ, g/cm^3
p-Aminobenzoic acid	1.83	137	1.39
p-Hydroxybenzoic acid	1.80	138	1.40
o-Hydroxybenzoic acid	1.80	138	1.40
Benzoic acid	1.75	122	1.32
p-Fluorobenzoic acid	1.77	140	1.48
p-Chlorobenzoic acid	1.86	157	1.54
p-Bromobenzoic acid	1.95	201	1.86
Hydrocortisone	3.59	345	1.28
Hydrocortisone acetate	3.96	403	1.29
Phenacetin	2.32	179	1.25
Benzocaine	2.24	165	1.21
β-Sitosterol	4.64	415	1.02
Griseofulvin	3.22	341	1.44
Indomethacin	3.46	358	1.35
Pimelic acid	2.05	160	1.33
Suberic acid	2.25	175	1.26
Sebacic acid	2.48	202	1.27
Dodecanedioic acid	2.88	230	1.16
Thopsic acid	3.45	286	1.10

drocarbons having a γ_L^p of zero or by measuring contact angles against a nonpolar solid such as paraffin with a γ_S^p equal to zero (8, 18). Equations 9 and 10, respectively, together with Eq. 4 would be applied. An earlier study (18) showed that the choice of nonpolar phase determines the exact values of γ_L^d and γ_L^p obtained. It was suggested that for consistency these values should be determined from wetting experiments using paraffin when such values are to be applied to subsequent wetting data.

Since paraffin was used in this study, all values of γ_S^d and γ_S^p reported are fixed to one standard nonpolar substance, paraffin. To calculate γ_L^d from the paraffin data, a value of γ_S^d for paraffin was taken as 25.5 ergs/cm^2 (8). Table I lists contact angles for various liquids on paraffin along with values of γ_L^d, γ_L^p, and γ_L for each liquid. Table II lists contact angles of these liquids on nylon 11 and β-sitosterol, while Table III contains calculated values of γ_S^d, γ_S^p, and γ_S for nylon 11 and β-sitosterol using the data in Tables I and II. These values were calculated by solving Eq. 12 simultaneously for each pair of liquids listed. The two nonlinear equations were solved using a zero-finding routine[7] based upon Brown's (20) method.

Table IV lists the contact angles of water and methylene iodide obtained from different solids of pharmaceutical interest, while Table V contains such values for various dicarboxylic and benzoic acid derivatives where 0.1 *N* HCl was used instead of water. The values of γ_S^d, γ_S^p, and γ_S for each solid, calculated as indicated earlier, also are found in these tables. Along with these values is given an index of polarity, P_0, where:

$$P_0 = \frac{\gamma_S^p}{\gamma_S} \times 100 \qquad \text{(Eq. 13)}$$

DISCUSSION

Basic to the use of contact angle measurements for estimating solid surface energetics is the assumption that no highly specific interaction and orientation of molecules occur at the solid–liquid interface. If so, using different liquid pairs should lead to the same values of γ_S^d and γ_S^p for a particular solid. The results in Table III for nylon 11 and β-sitosterol clearly indicate the lack of liquid independence, as do the data of Kaeble (14) before he averaged his results.

Molecular orientation might be expected for semipolar molecules such as glycerin, formamide, or ethylene glycol, but it would be expected less for the more symmetrical methylene iodide and water molecules. Indeed, it has been shown that values of critical surface tension, γ_C, for various solids, *i.e.*, surface tension of a liquid required to produce zero contact angle, depend on the type of semipolar liquid used for the determination (15, 21). In addition, mixtures of semipolar solvents and water result in adsorption of the semipolar solvent and a lower value of γ_C as compared to that obtained using liquid hydrocarbons (21).

Indeed, in Table III it can be noted that γ_S values obtained with the various semipolar liquids generally are lower than those obtained with methylene iodide and water. Consequently, it was decided to utilize only methylene iodide and water data, assuming that the values which are highest are most likely closest to the correct value. At worst, the surface energies are standardized with methylene iodide and water against paraffin but are still characteristic of the solid surface under consideration.

[7] Available at the Academic Computing Center, University of Wisconsin.

Table VII—Comparison of Surface Energy per Square Centimeter Obtained from Contact Angle and from the Parachor Method

Solid	Surface Free Energy, ergs/cm^2: Wu (11) Equation	Surface Free Energy, ergs/cm^2: Parachor
Benzoic acid	61.7	45.6
p-Fluorobenzoic acid	54.1	67.8
p-Chlorobenzoic acid	49.0	95.9
p-Bromobenzoic acid	49.9	88.9

Wu and Brzozowski (22) used methylene iodide and water contact angle data to calculate γ_S^d and γ_S^p for some organic pigments and showed that there was reasonably good agreement between γ_S values estimated in this way and those obtained by the parachor method (23). In the parachor method, parachor values, *P*, are obtained by adding atomic and group contributions previously estimated with pure liquids. Surface tension, γ, is calculated using ρ (the density), *M* (the molecular weight), and the equation:

$$\gamma = (P\rho/M)^4 \qquad \text{(Eq. 14)}$$

Extrapolation of this concept to solids is certainly not as dependable as with liquids, particularly when one considers that errors are amplified by the fourth-power dependence. However, in Table VII are listed calculated and experimental values for four benzoic acid derivatives which are certainly of the right order of magnitude. Thus, it is assumed that these numbers are indeed reflecting the solids under study.

The estimates of surface free energy per unit area, as given in Tables IV and V, are useful in providing some idea of the total energy change that will occur when a given area of contact between phases is increased or decreased. Thus, these are the values of interest when one is concerned with interactions taking place across various interfaces as during powder dispersion. However, the value of γ_S reflects not only the chemical composition of those molecules at the surface but also the number of such molecules per square centimeter.

Thus, to assess further the significance of the values obtained in molecular terms, it is necessary to account for differences in surface density or the number of molecules occupying a unit area of surface. A convenient parameter for comparisons on the molecular level would be the surface free energy per mole, γ_{Sm}:

$$\gamma_{Sm} = A_m\gamma_S \qquad \text{(Eq. 15)}$$

where A_m is the area in square centimeters occupied by Avogadro's number of molecules. In the absence of any direct method of determining A_m, some estimate may be made by assuming the molecules to be spheres with a molar surface area that is merely the two-thirds power of the molar volume (24). Thus:

$$A_m = fN^{1/3}(M/\rho)^{2/3} \qquad \text{(Eq. 16)}$$

where *N* is Avogadro's number, and *f* is a packing factor generally close to one (24). Table VI lists values of A_m calculated from Eq. 16 for a group of compounds; Table VIII lists the values of γ_{Sm}, γ_{Sm}^d, and γ_{Sm}^p calculated from Eq. 15.

From Table VIII, it is possible to compare values of γ_{Sm}^d and γ_{Sm}^p with changing chemical structure and to see if the calculated values are consistent with expected behavior. This, in turn, would support the fact that the wetting results are, in part, reflecting the chemical structure of the molecules in the solid state. In the benzoic acid series, it is apparent that the absence of a *para*-substituted group of high polarity such as hydroxyl and amino and the introduction of increasingly nonpolar halogens produce a reduction in the γ_{Sm}^p term in the rank order expected. Addition of *para*-substituents on benzoic acid does increase γ_{Sm}^d, which is what is expected on the basis of

Table VIII—Surface Free Energy per Mole[a]

Solid	γ_{Sm}	γ_{Sm}^d	γ_{Sm}^p
p-Aminobenzoic acid	121	74	47
p-Hydroxybenzoic acid	123	73	50
o-Hydroxybenzoic acid	123	76	47
Benzoic acid	108	68	40
p-Fluorobenzoic acid	96	64	32
p-Chlorobenzoic acid	91	81	10
p-Bromobenzoic acid	97	91	6
Hydrocortisone	246	162	84
Hydrocortisone acetate	251	185	65
Phenacetin	135	106	29
Benzocaine	150	107	43
β-Sitosterol	162	144	18
Griseofulvin	200	147	53
Indomethacin	214	164	50
Pimelic acid	154	93	61
Suberic acid	176	109	67
Sebacic acid	145	100	45
Dodecanedioic acid	183	131	52
Thopsic acid	207	157	50

[a] Values are (ergs per mole) × 10^{-9}

increased polarizability. Esterification of a normally polar alcohol or carboxyl group as in benzocaine *versus* *p*-aminobenzoic acid and hydrocortisone *versus* hydrocortisone acetate likewise can be seen to reduce polar contributions while increasing the dispersion force component.

In the dicarboxylic acid series, the general trend is that the dispersion component increases as the number of methylene groups per mole increases whereas the value of γ_{Sm}^p remains fairly constant, as does the number of polar groups per mole. Sebacic acid seems somewhat of an exception in this regard, which could indicate that the calculation of area per mole, as in Eq. 16, may not always be correct.

At this point, if it is assumed that the values of γ_S, γ_S^d, and γ_S^p do reflect properties unique to the solid surface, one can make generalizations concerning the overall surface properties of the pharmaceutical solids studied here. It is clear, for instance, that except for magnesium stearate and β-sitosterol on a per square centimeter basis, all of these solids can be considered moderate in their surface energy as compared to paraffin, a low energy substance, and metals, on the other end of the scale. It is clear also that the fatty acid chains dominate the surface properties of magnesium stearate, thus making it a good lubricant and a good waterproofing agent.

In Tables IV and V, it is interesting to note the rather constant value for γ_S^d and the large variation in γ_S^p. This finding suggests that comparison of P_0 values for such a diverse series of compounds is a valid means of comparing the expected level of polarity on a per square centimeter basis. It is clear from a comparison of P_0 values and contact angles that even 42% polarity can lead to a nonwetting solid. It is difficult to assess at what point the hydrophobicity becomes significant enough to influence a particular process without knowing all factors influencing that process. However, with these numbers as an index of polarity and the various surface free energy terms, it should be possible to see whether a meaningful correlation with various surface-controlled phenomena does exist. Such studies involving the dispersion and dissolution of low energy pharmaceutical solids are now being performed.

CONCLUSIONS

The contact angle obtained with water and methylene iodide on various organic solids was used to calculate surface free energies for these solids. The overall free energy term, when expressed on a molar basis, appears to reflect the chemical structure of the molecule; however, on a per square centimeter basis, the results also reflect the number of molecules occupying a unit area. From such measurements, an index of polarity was determined which indicates that, per square centimeter, drug molecules that present wetting problems may be as high as 40% polar. Although some theoretical uncertainties still exist as to the surface free energy per square centimeter of a solid, as determined from contact angle, the numbers estimated here provide systemic standard parameters which reflect solid surface properties.

REFERENCES

(1) E. N. Hiestand, *J. Pharm. Sci.*, **55**, 1325(1966).

(2) G. Zografi, "Compilation of Symposium Papers, 5th National Meeting," APhA Academy of Pharmaceutical Sciences, Washington, D.C., 1968, p. 190.

(3) P. Finholt, in "Dissolution Technology," L. J. Leeson and J. T. Carstensen, Eds., Industrial Pharmaceutical Technology Section, APhA Academy of Pharmaceutical Sciences, Washington, D.C., 1974, p. 106.

(4) A. W. Adamson, "Physical Chemistry of Surfaces," 2nd ed., Wiley–Interscience, New York, N.Y., 1967, p. 53.

(5) *Ibid.*, p. 281.

(6) H. Mykura, "Solid Surfaces and Interfaces," Dover, New York, N.Y., 1966, p. 14.

(7) W. A. Zisman, "Contact Angle, Wettability and Adhesion," Advances in Chemistry Series 43, American Chemical Society, Washington, D.C., 1964, p. 1.

(8) F. M. Fowkes, *Ind. Eng. Chem.*, **56**, 40(1964).

(9) R. J. Good, in "Adsorption At Interfaces," ACS Symposium Series 8, K. L. Mittal, Ed., American Chemical Society, Washington, D.C., 1975, p. 28.

(10) R. J. Good and L. A. Girafalco, *J. Phys. Chem.*, **64**, 561 (1960).

(11) S. Wu, *J. Polym. Sci.: Part C*, **34**, 19(1971).

(12) D. K. Owens and R. C. Wendt, *J. Appl. Polym. Sci.*, **13**, 1741(1969).

(13) A. El-Shimi and E. D. Goddard, *J. Colloid Interface Sci.*, **48**, 242(1974).

(14) D. H. Kaeble, *J. Adhes.*, **32**, 66(1970).

(15) N. Bauer and S. Z. Lewin, in "Weissberger's Techniques of Organic Chemistry," 3rd ed., vol. 1, part 1, Interscience, New York, N.Y., 1959, p. 175.

(16) "Handbook of Chemistry and Physics," 54th ed., CRC Press, Cleveland, Ohio, 1973–1974.

(17) J. D. H. Donnay and H. M. Ondik, "Crystal Data," 3rd ed., U.S. Department of Commerce, National Bureau of Standards, and Joint Committee on Powder Diffraction, Washington, D.C., 1972.

(18) G. Zografi and S. H. Yalkowsky, *J. Pharm. Sci.*, **63**, 1533(1974).

(19) J. R. Dann, *J. Adhes.*, **32**, 321(1970).

(20) K. M. Brown, *SIAM, J. Numerical Anal.*, **6**, 560(1969).

(21) W. J. Murphy, M. W. Roberts, and R. H. Ross, *J. Chem. Soc., Faraday Trans. 1*, **68**, 1190(1972).

(22) S. Wu and K. H. Brzozowski, *J. Colloid Interface Sci.*, **37**, 686(1971).

(23) O. R. Quayle, *Chem. Rev.*, **53**, 439(1953).

(24) A. S. Skapski, *J. Chem. Phys.*, **16**, 389(1948).

ACKNOWLEDGMENTS AND ADDRESSES

Received July 25, 1975, from the *School of Pharmacy, University of Wisconsin, Madison, WI 53706*

Accepted for publication October 8, 1975.

Presented at the Basic Pharmaceutics Section, APhA Academy of Pharmaceutical Sciences, San Francisco meeting, April 1975.

Supported by a grant from Pfizer Co., Groton, Conn.

The authors acknowledge the interest of Dr. Armando Aguiar, Pfizer Co., and the assistance of Mr. Mahendra Patel and Mr. Richard Pyter, University of Wisconsin.

[x] To whom inquiries should be directed.

Oxidation of Selected Pteridine Derivatives by Mammalian Liver Xanthine Oxidase and Aldehyde Oxidase

C. N. HODNETT, J. J. McCORMACK ˣ, and J. A. SABEAN

Abstract □ Considerable information is available concerning the oxidation of pteridine derivatives by bovine milk xanthine oxidase, but few investigations have been carried out on the oxidation of such compounds by mammalian liver xanthine oxidase and the related aldehyde oxidase. Xanthine oxidase, obtained from rat liver, oxidizes a variety of substituted amino- and hydroxypteridines in a manner identical to that previously observed for milk xanthine oxidase. For example, 2-aminopteridine and its 4- and 7-hydroxy derivatives were oxidized efficiently to 2-amino-4,7-dihydroxypteridine (isoxanthopterin) by the rat liver enzyme, and 4-aminopteridine and its 2- and 7-hydroxy derivatives were oxidized to 4-amino-2,7-dihydroxypteridine. 4-Hydroxypteridine and the isomeric 2- and 7-hydroxypteridines were oxidized by rat liver xanthine oxidase to 2,4,7-trihydroxypteridine. Rabbit liver aldehyde oxidase, but not rat liver xanthine oxidase, was able to catalyze the oxidation in position 7 of 2,4-diaminopteridine and its 6-methyl and 6-hydroxymethyl derivatives. 2-Aminopteridine and 4-aminopteridine were both oxidized to the corresponding 7-hydroxy derivatives in the aldehyde oxidase system; 2-amino-4-hydroxypteridine appeared to be a minor product in the oxidation of 2-aminopteridine by rabbit liver aldehyde oxidase. Both aldehyde oxidase and xanthine oxidase were able to catalyze the oxidation of 2-amino-6,7-disubstituted pteridines to the corresponding 4-hydroxy derivatives; 4-hydroxy-6,7-disubstituted pteridines were oxidized in position 2 by both enzymes. 4-Amino-6,7-disubstituted pteridines were not oxidized by either enzyme. 2-Amino-4-methylpteridine was oxidized in position 7 by aldehyde oxidase but was not an effective substrate for xanthine oxidase; 2-hydroxypteridine and 7-hydroxypteridine were not oxidized to a detectable extent by aldehyde oxidase. All oxidations mediated by xanthine oxidase were strongly inhibited by allopurinol (4-hydroxypyrazolo[3,4-*d*]pyrimidine), and all oxidations mediated by aldehyde oxidase were inhibited by menadione (2-methyl-1,4-naphthoquinone). Rat liver xanthine oxidase and, to a lesser extent, rabbit liver aldehyde oxidase were inhibited by 4-chloro-6,7-dimethylpteridine; 2-amino-3-pyrazinecarboxylic acid inhibited xanthine oxidase but not aldehyde oxidase. The oxidations of 2- and 4-aminopteridines by aldehyde oxidase resulted in concomitant reduction of cytochrome c.

Keyphrases □ Pteridine derivatives—oxidation by mammalian liver xanthine oxidase and aldehyde oxidase □ Xanthine oxidase—mammalian liver, oxidation of pteridine derivatives □ Aldehyde oxidase—mammalian liver, oxidation of pteridine derivatives □ Enzymes—mammalian liver xanthine oxidase and aldehyde oxidase, oxidation of pteridine derivatives □ Oxidation—pteridine derivatives by mammalian liver xanthine oxidase and aldehyde oxidase

Xanthine oxidase (xanthine:oxygen oxidoreductase, EC 1.2.3.2) and aldehyde oxidase (aldehyde:oxygen oxidoreductase, EC 1.2.3.1) have a number of common characteristics (1), *e.g.*, similar molecular weights, the ability to utilize a variety of electron acceptors, and the presence of a nonheme iron, molybdenum, and flavin adenine dinucleotide. The presence of a quinone of the coenzyme Q type has been demonstrated (2) in aldehyde oxidase but not in xanthine oxidase; however, recent studies (3) called into question the significance of a coenzyme Q type of factor in the function of aldehyde oxidase.

Both enzymes are found in mammalian liver and both are capable of oxidizing various substrates including heterocyclic compounds of the purine (4), pteridine, and azapteridine (5–11) types and aldehydes (12, 13). Both enzymes are capable of oxidizing important pharmacological agents; for example, xanthine oxidase oxidizes the antineoplastic agent mercaptopurine (14), and aldehyde oxidase oxidizes methotrexate (15), an agent used extensively in antineoplastic therapy, and the immunosuppressive agent azathioprine (16). The xanthine oxidase system also has been demonstrated (17) to be capable of participating indirectly in oxidative reactions (*via* generation of superoxide radicals), and both xanthine oxidase and aldehyde oxidase mediate reductive reactions of the nitro group of important drugs (18–20).

Certain pteridine derivatives are used clinically (21–23) and have been implicated as important participants in biochemical functions (24–27). Because of these considerations, the chemistry and biochemistry of pteridine derivatives and the behavior of pteridines were investigated in several enzyme systems.

Previously (7), the behavior of aminopteridines in the milk xanthine oxidase system was described. It was of interest to determine whether the same reaction patterns observed in oxidations catalyzed by the milk enzyme would be observed with rat liver xanthine oxidase and whether the oxidation patterns determined for xanthine oxidase were similar to those observed with the analogous enzyme, aldehyde oxidase.

Since studies of the abilities of heterocyclic compounds to serve as substrates and/or inhibitors of xanthine oxidase frequently are carried out with the enzyme obtained from milk, it was important to investigate whether the substrate specificity for pteridine oxidation mediated by liver xanthine oxidase was the same as that observed with the "standard" milk enzyme and whether the same products were formed in the two enzyme systems. Information about the relative susceptibilities of pteridine derivatives to liver xanthine oxidase and aldehyde oxidase *in vitro* can be of value in predicting patterns of oxidation *in vivo* and also in the design of new inhibitors of these enzymes.

This report presents the results of studies carried out to ascertain the behavior of pteridines in the xanthine oxidase system obtained from rat liver and the aldehyde oxidase system obtained from rabbit liver.

EXPERIMENTAL

The oxidation of pteridine derivatives by xanthine oxidase and aldehyde oxidase was investigated by spectrophotometric and chromatographic techniques. For spectrophotometric studies, reaction solutions were scanned in the 270–390-nm region using a recording spectrophotometer[1] equipped with a thermostated sample chamber at 34 ± 1°. Rat liver xanthine oxidase was prepared by the method of Kielley (28) up to the fifth ammonium sulfate step. Aldehyde oxi-

[1] Perkin-Elmer model 202.

dase was prepared from rabbit liver using a modification of the method of Rajagopalan *et al.* (2). In agreement with recent studies (18), aldehyde oxidase that was substantially free from xanthine oxidase activity was obtained using appropriate ammonium sulfate fractionations without chromatographic procedures. Bovine milk xanthine oxidase was a commercial product[2].

Studies with xanthine oxidase were carried out using a trometh-amine buffer system (0.05 *M*, pH 7.8, containing 0.005% ethylenediaminetetraacetic acid), the pteridine derivative (1×10^{-4} *M*), and sufficient xanthine oxidase to give an absorbance change of 0.50 unit/10 min at 290 nm, evaluated with hypoxanthine (1×10^{-4} *M*) as the standard substrate. Catalase[2] (151 units/ml) was added routinely to the xanthine oxidase system even though, as found previously (8) for milk xanthine oxidase, catalase did not affect the rate of pteridine oxidation by liver xanthine oxidase. Catalase was added to the xanthine oxidase system simply to ensure that this system resembled as closely as possible the aldehyde oxidase system described here.

All pteridine derivative substrates for rat liver xanthine oxidase were examined in a system containing a high concentration (1×10^{-4} *M*) of allopurinol (4-hydroxypyrazolo[3,4-*d*]pyrimidine)[3] to establish the susceptibility of the xanthine oxidase-mediated reaction to this inhibitor. The classification of compounds as ineffective substrates for xanthine oxidase was based on the failure to demonstrate a detectable alteration in the absorption spectrum of the compound over 3–4 hr in the presence of the enzyme.

Essentially the same procedure as already outlined was used for spectrophotometric studies with rabbit liver aldehyde oxidase; the composition of the reaction solution was identical except that xanthine oxidase was replaced by aldehyde oxidase in an amount sufficient to produce an absorbance change of 0.50 unit/10 min at 300 nm, using the standard substrate N^1-methylnicotinamide (3×10^{-3} *M*). Catalase addition was required for maximal activity with aldehyde oxidase. For inhibition studies with aldehyde oxidase, menadione (2-methyl-1,4-naphthoquinone[4], 1×10^{-5} *M*) was added to the reaction vessel.

All but two pteridine derivatives used were synthesized by published procedures. 2-Amino-4-hydroxy-6,7-cyclohexenopteridine was prepared in the following manner. 6-Hydroxy-2,4,5-triaminopyrimidine sulfate[3] (0.40 g) was suspended in water (10 ml), and sodium bicarbonate was added carefully to the mixture until pH 7 was attained. Cyclohexane-1,2-dione[3] (0.20 g) and ethanol (1 ml) then were added, and the mixture was refluxed on a water bath for 4 hr. The precipitate that formed upon chilling the reaction mixture was isolated by suction filtration and washed with successive portions of water and ethanol. The UV absorption characteristics of the compound were identical to material obtained by acid hydrolysis of 2,4-diamino-6,7-cyclohexenopteridine[5], and the substance migrated as a single spot in several chromatographic systems.

The identities of reaction products formed when various pteridines were incubated with xanthine oxidase or aldehyde oxidase, initially assigned by spectroscopic methods, were confirmed by TLC. Reaction solutions identical with those already described, except that the pteridine concentration was 3×10^{-4} *M*, were incubated overnight at 37° to ensure complete conversion of the substrate to hydroxylated derivatives. The reaction solutions were heated at 90° for 5 min to inactivate the enzymes, and the mixtures were centrifuged to remove precipitated protein.

Aliquots (10 and 20 μl) of the supernatant solutions were applied to analytical TLC plates[6] along with pertinent standard pteridines, and the chromatograms were developed in the appropriate solvent systems. Pteridine spots were visualized using both short (256 nm) and long (360 nm) wavelength UV light in a chromatogram-viewing cabinet equipped with a transilluminator[7]. Identification of reaction products was made on the basis of comparison of the chromatographic mobility and fluorescence properties with those of standard compounds.

The reduction of cytochrome c was investigated by adding cytochrome c[8] (1×10^{-5} *M*) to the described aldehyde oxidase reaction solutions and observing the appearance of the characteristic absorption maximum of reduced cytochrome c at 550 nm.

RESULTS

Pteridine (7) itself was oxidized readily by both rat liver xanthine oxidase and by aldehyde oxidase; however, the pattern of spectral change observed during the reaction was different for the two enzymes. For example, while both reactions were characterized by the appearance of a new absorption maximum at 328 nm, the intensity of the new peak in the xanthine oxidase reaction was approximately twice that for the aldehyde oxidase reaction, and a prominent shoulder was observed at 338 nm in the xanthine oxidase reaction but not in the aldehyde oxidase reaction.

Comparison of the UV absorption maxima observed for the product of the xanthine oxidase-catalyzed reaction with those of 2,4,7-trihydroxypteridine (7) (Table I) suggested that pteridine is converted, in the rat liver system, to the latter compound. TLC analysis also indicated that the product of this reaction was 2,4,7-trihydroxypteridine. On the other hand, the aldehyde oxidase-mediated conversion of pteridine did not yield the trihydroxylated derivative but gave a product identified as 2,4-dihydroxypteridine (7) (lumazine) on the basis of its spectroscopic properties. Chromatographic analysis of the aldehyde oxidase mixture revealed a major spot corresponding to 2,4-dihydroxypteridine and a minor spot corresponding to 4-hydroxypteridine (7). The presence of the 4-hydroxypteridine spot suggests that this compound may be an intermediate in the aldehyde oxidase-catalyzed oxidation of pteridine.

When these studies were completed on the oxidation of pteridine by aldehyde oxidase, a report by Krenitsky *et al.* (5) described their studies of the same reaction. Our results are in agreement with their studies with regard to the formation of 2,4-dihydroxypteridine as the major ultimate product of the reaction of pteridine with aldehyde oxidase.

When 2-hydroxy- (7), 4-hydroxy-, 7-hydroxy- (7), and 2,4-dihydroxypteridines were incubated with xanthine oxidase, the final absorption spectrum of each reaction mixture was identical with that of 2,4,7-trihydroxypteridine, and the chromatographic properties of the products also were those of the trihydroxy derivative. It was reported previously (9) that 4-hydroxypteridine is oxidized by rabbit liver aldehyde oxidase only in position 2, and Krenitsky *et al.* (5) confirmed this observation.

The spectroscopic and chromatographic properties of the product of the reaction of 4-hydroxypteridine with aldehyde oxidase are summarized in Table I. The 6,7-dimethyl derivative (29) and the 6,7-cyclohexeno derivative (30) of 4-hydroxypteridine were oxidized in position 2 by aldehyde oxidase, and the same products (30, 31) were obtained when these substrates were treated with rat liver xanthine oxidase. Incubation of 2-hydroxy-, 2,4-dihydroxy-, or 7-hydroxypteridine with aldehyde oxidase did not result in detectable spectroscopic changes over a 4-hr period.

Aminopteridines—2-Amino-, 2-amino-4-hydroxy-, and 2-amino-7-hydroxypteridines (8) were oxidized readily by rat liver xanthine oxidase to a common product, exhibiting spectral maxima at 282 and 333 nm. This product was identified as 2-amino-4,7-dihydroxypteridine (isoxanthopterin) (8) on the basis of its spectral characteristics and its behavior on TLC. Neither 2-amino-4-hydroxypteridine nor its 7-hydroxy isomer was oxidized by aldehyde oxidase. Indeed, both substances were products of the reaction of 2-aminopteridine with this enzyme; chromatographic analysis of the reaction mixture as well as spectroscopic studies indicated that oxidation of 2-aminopteridines by aldehyde oxidase occurs mainly in position 7. Oxidation of 2-amino-6,7-dimethylpteridine (8) and its 6,7-diphenyl and 6,7-cyclohexeno derivatives (32) was mediated by both rat liver xanthine oxidase and rabbit liver aldehyde oxidase; in all cases, oxidation was observed at position 4.

2,4-Diaminopteridine (33) and 2-amino-4-methylpteridine (8) are not oxidized by milk xanthine oxidase (8, 34); these compounds also do not serve as substrates for hepatic xanthine oxidase. On the other hand, both 2,4-diaminopteridine and 2-amino-4-methylpteridine were oxidized by aldehyde oxidase to products identified spectroscopically as the respective 7-hydroxy derivatives[9] (35). 2,4-Diamino-6-meth-

[2] Worthington Biochemical Co., Freehold, N.J.
[3] Aldrich Chemical Co., Milwaukee, Wis.
[4] Merck and Co., Rahway, N.J.
[5] Provided by Professor E. C. Taylor, Princeton University.
[6] MN cellulose and Avicel, Analtech, Newark, Del.
[7] Ultraviolet Products, Inc., San Gabriel, Calif.
[8] Sigma Chemical Co., St. Louis, Mo.

[9] The assignment of the 7-hydroxy structure to the product of oxidation of 2-amino-4-methylpteridine was done on the basis of the similarity of the spectral characteristics of this product to those of 2-amino-7-hydroxypteridine.

Table I—Spectroscopic and Chromatographic Properties of Pteridines and Pteridine Products of Oxidation by Rat Liver Xanthine Oxidase and Rabbit Liver Aldehyde Oxidase[a]

Pteridine Derivative	UV Maxima	R_f	Solvent System
Pteridine	300, 310	Streak	A
2-Hydroxypteridine	308	0.57	A
4-Hydroxypteridine	328	0.39	A
7-Hydroxypteridine	261, 328	0.65	A
2,4-Dihydroxypteridine	270, 328	0.51	A
2,4,7-Trihydroxypteridine	275, 328, 338[b]	0.22	A
Product of pteridine and its 2-, 4-, and 7-hydroxy- and 2,4-dihydroxy derivatives and xanthine oxidase	275, 328, 338[b]	0.22	A
Product of pteridine and 4-hydroxypteridine and aldehyde oxidase	270, 328	0.51	A
2-Aminopteridine	370	0.40	B
2-Amino-4-hydroxypteridine	270, 346	0.19	B
2-Amino-7-hydroxypteridine	270, 341, 353[b]	0.30	B
2-Amino-4,7-dihydroxypteridine	282, 333	0.01	B
Product of 2-aminopteridine and its 4- and 7-hydroxy derivatives and xanthine oxidase	282, 333	0.01	B
Product of 2-aminopteridine and aldehyde oxidase	270, 341, 353[b]	0.30, 0.19[c]	B
2-Amino-6,7-dimethylpteridine	368	0.72	B
2-Amino-4-hydroxy-6,7-dimethylpteridine	346	0.35	B
Product with xanthine and aldehyde oxidase	346	0.35	B
2-Amino-6,7-diphenylpteridine	281[d]	0.92	B
2-Amino-4-hydroxy-6,7-diphenylpteridine	301[d]	0.44	B
Product with xanthine and aldehyde oxidase	301[d]	0.44	B
2-Amino-6,7-cyclohexenopteridine	265, 372	0.55	B
2-Amino-4-hydroxy-6,7-cyclohexenopteridine	275, 350	0.34	B
Product with xanthine and aldehyde oxidase	275, 350	0.34	B
2,4-Diaminopteridine	365	0.17	D
2,4-Diamino-7-hydroxypteridine	353	0.22	D
Product with aldehyde oxidase	353	0.22	D
2,4-Diamino-6-methylpteridine	367	0.29	B
2,4-Diamino-6-methyl-7-hydroxypteridine	353	0.17	B
Product with aldehyde oxidase	353	0.17	B
2,4-Diamino-6-hydroxymethylpteridine	371	0.29	B
Product with aldehyde oxidase	350	0.14	B
2-Amino-4-methylpteridine	367	—	B
Product with aldehyde oxidase	345, 353[b]	—	B
4-Aminopteridine	337	0.48	B
4-Amino-2-hydroxypteridine	285, 337, 351[b]	0.18	B
4-Amino-7-hydroxypteridine	332, 344	0.33	B
4-Amino-2,7-dihydroxypteridine	276, 335, 350[b]	0.24	B
Product of 4-aminopteridine and its 2- and 7-hydroxy derivatives with xanthine oxidase	276, 335, 350[b]	0.24	B
Product of 4-aminopteridine and aldehyde oxidase	332, 344	0.33	B
4-Hydroxy-6,7-dimethylpteridine	275, 316	0.39	B
2,4-Dihydroxy-6,7-dimethylpteridine	270, 332	0.31	B
Product with xanthine and aldehyde oxidase	270, 332	0.31	B
4-Hydroxy-6,7-cyclohexenopteridine	321	0.26	C
2,4-Dihydroxy-6,7-cyclohexenopteridine	340	0.24	C
Product with xanthine and aldehyde oxidase	340	0.24	C

[a] Spectra were recorded in the 270–390-nm range in tromethamine buffer (0.05 *M*, pH 7.8) containing enzyme as described under *Experimental*. Pteridine derivatives were spotted 2.5 cm from the bottom of prepared plates, the spots were dried with warm forced air, the solvent was allowed to ascend the plate for a distance of 15 cm, and the spots were visualized with UV light. TLC solvent systems used were the following: A, 2-methyl-1-propanol–dimethylformamide–water (65:25:10); B, ethanol–ammonia–water (80:10:10); C, 2-propanol–dimethylformamide–ammonia (65:25:10); and D, water. [b] Shoulder. [c] Minor component. [d] Maximum observed also >400 nm.

ylpteridine and its 6-hydroxymethyl analog (36) also were oxidized by aldehyde oxidase to products formulated as 7-hydroxy derivatives (37) based on their spectroscopic properties. 2,4-Diamino-6-hydroxymethylpteridine was not oxidized by liver xanthine oxidase.

4-Aminopteridine, as well as its 2-hydroxy and 7-hydroxy derivatives (8), were oxidized by rat liver xanthine oxidase to 4-amino-2,7-dihydroxypteridine (8). 4-Aminopteridine was oxidized by aldehyde oxidase to a product exhibiting spectroscopic and chromatographic properties identical with those of 4-amino-7-hydroxypteridine. Neither 4-amino-7-hydroxypteridine nor its 2-hydroxy isomer was an effective substrate for aldehyde oxidase under the reaction conditions employed. It was reported previously (8, 30) that 4-amino-6,7-dimethylpteridine and 4-amino-6,7-cyclohexenopteridine were not oxidized by bovine milk oxidase, and these compounds were not oxidized by either rat liver xanthine oxidase or by aldehyde oxidase. When 4-amino-6,7-diphenylpteridine (32) was incubated with aldehyde oxidase, no spectroscopic evidence was obtained for oxidation.

Inhibition Studies—The oxidation of various substrates, including pteridines (8), by milk xanthine oxidase is susceptible to inhibition by allopurinol. All oxidations of pteridine derivatives catalyzed by rat liver xanthine oxidase are inhibited strongly by this agent. Thus, in the presence of a relatively high concentration (1×10^{-4} *M*) of allopurinol in the various reaction mixtures, inhibition of oxidation of more than 95% was observed. Menadione is a potent inhibitor of many oxidations catalyzed by aldehyde oxidase (38). Inclusion of menadione (1×10^{-5} *M*) in reaction mixtures containing pteridine derivatives and aldehyde oxidase resulted in virtually complete (greater than 90%) inhibition of pteridine oxidation. Thus, oxidation of pteridine derivatives by both mammalian liver enzyme systems studied exhibited conventional sensitivity to standard inhibitory agents.

It was observed previously that 2-amino-3-pyrazinecarboxylic acid (30), a substance that can be formed by chemical degradation (39) of 4-hydroxypteridine, is a moderately potent inhibitor of milk xanthine oxidase. 2-Amino-3-pyrazinecarboxylic acid also inhibited rat liver xanthine oxidase; no significant inhibition by 2-amino-3-pyrazinecarboxylic acid was observed (at 1×10^{-4} *M*) against aldehyde oxidase. No evidence for detectable oxidation of this pyrazine derivative was obtained in either enzyme system.

4-Chloro-6,7-dimethylpteridine was found (30) to inhibit milk

xanthine oxidase, and an apparent K_I value of 5×10^{-7} M was estimated for it. This chloropteridine did inhibit rat liver xanthine oxidase to an extent comparable with that observed with the enzyme obtained from milk. 4-Chloro-6,7-dimethylpteridine inhibited aldehyde oxidase, but the degree of inhibition was modest. For example, the chloropteridine (1×10^{-4} M) inhibited the oxidation of N^1-methylnicotinamide by only 30% whereas the same concentration of chloropteridine completely inhibited the oxidation of hypoxanthine by both milk and rat liver xanthine oxidase.

When investigating the effect of 4-chloro-6,7-dimethylpteridine on the hepatic oxidases, the use of tromethamine buffer was unsuitable. Therefore, a phosphate buffer was employed in these inhibition studies. 4-Chloro-6,7-dimethylpteridine underwent a transformation in tromethamine buffer, as evidenced by a gradual disappearance of the spectral maxima at 306 and 318 nm with the concomitant appearance of a new peak at 346 nm. Daley and Christensen (40) reported that 4-chloro-6,7-dimethylpteridine is very susceptible to nucleophilic displacement reactions at position 4 and can be readily hydrolyzed to the 4-hydroxy derivative and aminated to the 4-amino derivative. The final absorption spectrum of the product of the reaction of 4-chloro-6,7-dimethylpteridine in the tromethamine system resembled the spectrum of 4-amino-6,7-dimethylpteridine, suggesting that a product is formed in this buffer by attack of the pteridine nucleus by the amino function of tromethamine.

Cytochrome c Reduction—Both milk xanthine oxidase and aldehyde oxidase mediate a concomitant reduction of cytochrome c (2, 41) when these enzymes catalyze oxidation of a suitable substrate. Oxidations of 2-amino- and 4-aminopteridines in the aldehyde oxidase system were accompanied by reduction of cytochrome c, as evidenced by the appearance of a characteristic peak at 550 nm. The rates of appearance of reduced cytochrome c during the oxidation of the two substrates correlated well with the rate of oxidation of the substrates determined in the absence of cytochrome c.

DISCUSSION

Various pteridine derivatives are oxidized in an identical manner by rat liver xanthine oxidase and milk xanthine oxidase. Pteridines found previously to be effective substrates for the milk enzyme were found to be good substrates for the liver enzyme, and pteridines that were not oxidized by the milk enzyme also proved to be ineffective substrates for the rat liver enzyme. The relative rates of oxidation of pteridine substrates by rat liver xanthine oxidase paralleled the rates observed with the milk enzyme, and allopurinol exhibited approximately the same activity as an inhibitor of pteridine oxidation catalyzed by xanthine oxidase from either source.

The results demonstrate that pteridine oxidation reactions are closely similar whether catalyzed by milk xanthine oxidase or catalyzed by rat liver xanthine oxidase. The observations concerning the correspondence of characteristics of pteridine oxidation carried out by both enzymes parallel observations made by Bergmann and Dikstein (4) concerning purine oxidation by xanthine oxidase obtained from milk and from mammalian liver. However, at least one purine substrate appears to exhibit markedly different susceptibilities (42) to xanthine oxidase from bovine milk and that from mammalian liver.

Although aldehyde oxidase resembles xanthine oxidase, the two enzymes do not share a uniform pattern of substrate specificity. 4-Amino-6,7-dimethylpteridine and 4-amino-6,7-cyclohexenopteridine are substrates for neither aldehyde oxidase nor rat liver xanthine oxidase; this observation is in agreement with previously reported studies which described the inability of milk xanthine oxidase to oxidize these compounds. Both rat liver xanthine oxidase and rabbit liver aldehyde oxidase catalyzed the oxidation of various pteridines, resulting in the introduction of hydroxyl functions at positions 2, 4, and 7 of the pteridine ring. However, rather large differences were noted in the abilities of the two enzymes to oxidize several substrates. For example, 2,4-dihydroxypteridine was readily oxidized by the rat liver xanthine oxidase but not altered by treatment with aldehyde oxidase under comparable conditions. Similarly, 2-hydroxypteridine and 7-hydroxypteridine were oxidized by xanthine oxidase but not by aldehyde oxidase; the 4-hydroxy isomer was oxidized by both enzymes.

Presumably, hydroxyl substitution at position 2 or 7 but not at position 4 inhibits effective interaction of the pteridine ring with the catalytic site of aldehyde oxidase. Observations concerning the oxidation of pteridine at positions 2 and 4 catalyzed by aldehyde oxidase and at positions 2, 4, and 7 catalyzed by rat liver xanthine oxidase confirm those findings of Krenitsky *et al.* (5). They studied pteridine oxidation in the rabbit liver aldehyde oxidase and milk xanthine oxidase systems. Chromatographic evidence was obtained suggesting that the aldehyde oxidase-mediated oxidation of pteridine to 2,4-dihydroxypteridine proceeds through the intermediacy of 4-hydroxypteridine, and this evidence is consistent with the finding that 4-hydroxypteridine is converted to 2,4-dihydroxypteridine when incubated with aldehyde oxidase but that 2-hydroxypteridine is not oxidized in this system.

2-Amino- and 4-aminopteridines are converted to monohydroxy derivatives by aldehyde oxidase, whereas xanthine oxidase oxidizes these compounds in two positions; this observation parallels that made concerning the degree of hydroxylation produced by the two enzymes with 4-hydroxypteridine and other heterocyclic substrates as well. Xanthine oxidase can oxidize readily pteridine derivatives such as 2-amino-4-hydroxypteridine, 2-amino-7-hydroxypteridine, and 2,4-dihydroxypteridine, while aldehyde oxidase is unable to oxidize these substrates effectively. Such observations may indicate that there are subtle differences in the binding sites of the two enzymes for various substrates and/or inhibitors.

It is of interest in this regard that the 4,6-dihydroxy derivative of pyrazolo[3,4-*d*]pyrimidine is the "active metabolite" involved in the inhibition of xanthine oxidase by allopurinol and is bound (43) extremely effectively to this enzyme, whereas this compound is not a useful inhibitor of aldehyde oxidase. Thus, the dihydroxypteridine is a good substrate for xanthine oxidase and the dihydroxypyrazolopyrimidine is an excellent inhibitor of this enzyme, whereas the dihydroxypteridine is not a substrate and the dihydroxypyrazolopyrimidine is not an inhibitor of aldehyde oxidase. While both 4-aminopteridine and 2-aminopteridine were oxidized in position 7 by aldehyde oxidase, only the 2-amino derivative was found to undergo oxidation (albeit to a minor extent) in the pyrimidine portion of the molecule. The ability of 2-aminopteridine, but not its 4-amino isomer, to undergo oxidation in the pyrimidine portion when incubated with aldehyde oxidase might be related to the observation (44) that 2-aminopteridine, but not 4-aminopteridine, readily undergoes nucleophilic addition reactions (*e.g.*, covalent hydration) under appropriate conditions.

Introduction of substituents (*e.g.*, methyl groups or a cyclohexane ring) at positions 6 and 7 of the 4-aminopteridine nucleus was associated with a loss of substrate activity in both the xanthine oxidase and aldehyde oxidase systems, while the same substituents in the 2-aminopteridine nucleus did not result in a loss of substrate activity. These observations may, of course, simply indicate that the 2-position of the 6,7-disubstituted 4-aminopteridines does not effectively interact with the catalytic site of these flavoproteins, whereas the 4-position in the isomeric compounds is capable of effective interaction.

The antineoplastic agent methotrexate is a 2,4-diaminopteridine to which is attached, at position 6, a *p*-methylaminobenzoylglutamic acid function; methotrexate is oxidized readily by rabbit liver aldehyde oxidase *in vitro*, and the extent to which this agent is hydroxylated *in vivo* has been correlated with the level of aldehyde oxidase present in the liver of several mammalian species (15, 45). It was of interest to determine whether the large 6-substituent was essential for the oxidation of the 2,4-diaminopteridine nucleus by aldehyde oxidase. 2,4-Diaminopteridine and its 6-methyl and 6-hydroxymethyl derivatives were oxidized in position 7 by aldehyde oxidase; accordingly, the large *p*-aminobenzoylglutamic acid substituent is not required for oxidation of the diaminopteridine nucleus to occur. It should be stressed, however, that recent studies in this laboratory indicated that methotrexate is oxidized much more rapidly under comparable conditions than are the simpler 2,4-diaminopteridines.

The 2,4-diaminopteridine derivatives and 2-amino-4-methylpteridine proved to be unique among the pteridines investigated in that they were oxidized by aldehyde oxidase but not by xanthine oxidase. The differences between the abilities of aldehyde oxidase and xanthine oxidase to oxidize various pteridine substrates are of particular interest in view of the similarity of the internal electron-transport systems of the two enzymes (46, 47), and such differences probably are best related to subtle differences in the environment of the catalytic site of these enzymes. Differences in the abilities of these enzymes to oxidize pteridine substrates are especially striking when comparisons are made of hydroxylated pteridines; xanthine oxidase appears to have a broader pattern of catalytic specificity with respect to oxidation of hydroxypteridines than does aldehyde oxidase. A

similar situation exists in the purine series where 8-hydroxypurine and 2,6-dihydroxypurine are oxidized readily by xanthine oxidase but not by aldehyde oxidase (5).

Cytochrome c reduction mediated by xanthine oxidase and, presumably, by aldehyde oxidase is associated with generation of superoxide free radicals by the flavoprotein enzyme system as a consequence of enzyme-catalyzed oxidation of a suitable substrate (48). Pteridine oxidations are conventional in the sense that the concomitant reduction of cytochrome c can be demonstrated to occur during enzymatic oxidation of 4-amino- and 2-aminopteridines, and these findings parallel those made in studies of analogous oxidations.

In summary, this study demonstrated that various pteridine derivatives are capable of being oxidized efficiently by mammalian liver xanthine oxidase and aldehyde oxidase; oxidations of pteridines mediated by liver xanthine oxidase follow reaction pathways essentially similar to those observed previously for the milk enzyme. Substantial differences exist between the susceptibilities of pteridines to oxidation by rat liver xanthine and rabbit liver aldehyde oxidase.

These studies have important implications for studies of pteridine metabolism *in vivo*; in fact, recent studies in this laboratory demonstrated extensive oxidation of pteridines *in vivo*, apparently mediated by both xanthine oxidase and aldehyde oxidase (49). It should be stressed that xanthine oxidase from various sources can be shown, under appropriate circumstances, to behave as an NAD^+-dependent dehydrogenase (50); the patterns of oxidation of pteridines by the "dehydrogenase" system may differ substantially from those observed for the "oxidase," and exploration of this possibility is planned.

REFERENCES

(1) R. C. Bray and J. C. Swann, in "Structure and Bonding," J. B. Dunitz, P. Hemmerich, J. A. Ibers, C. K. Jorgensen, J. B. Neilands, R. S. Nyholm, D. Reinen, and R. J. P. Williams, Eds., Springer-Verlag, New York, N.Y., 1972, p. 107.

(2) K. V. Rajagopalan, I. Fridovich, and P. Handler, *J. Biol. Chem.*, **237**, 922(1962).

(3) J. Romeo, V. Pinphanichakarn, Y. Iwamoto, and K. Folkers, *Biochem. Biophys. Res. Commun.*, **59**, 1286(1974).

(4) F. Bergmann and S. Dikstein, *J. Biol. Chem.*, **223**, 765(1956).

(5) T. A. Krenitsky, S. M. Neil, G. B. Elion, and G. H. Hitchings, *Arch. Biochem. Biophys.*, **150**, 585(1972).

(6) F. Bergmann and H. Kwietny, *Biochim. Biophys. Acta*, **28**, 613(1958).

(7) *Ibid.*, **33**, 29(1959).

(8) D. M. Valerino and J. J. McCormack, *Biochim. Biophys. Acta*, **184**, 154(1969).

(9) J. J. McCormack, J. A. Sabean, and C. N. Hodnett, *Pharmacologist*, **12**, 562(1970).

(10) H. Rembold, M. Metzger, and W. Gutensohn, *Biochim. Biophys. Acta*, **230**, 117(1971).

(11) F. Bergmann, L. Levene, Z. Neiman, and D. J. Brown, *ibid.*, **222**, 191(1970).

(12) K. V. Rajagopalan and P. Handler, *J. Biol. Chem.*, **239**, 2027(1964).

(13) L. Greenlee and P. Handler, *ibid.*, **239**, 1090(1964).

(14) G. B. Elion, S. Callahan, R. W. Rundles, and G. H. Hitchings, *Cancer Res.*, **23**, 1207(1963).

(15) D. G. Johns, A. T. Iannotti, A. C. Sartorelli, B. A. Booth, and J. R. Bertino, *Biochim. Biophys. Acta*, **105**, 380(1965).

(16) A. H. Chalmers, P. R. Knight, and M. R. Atkinson, *Aust. J. Exp. Biol. Med. Sci.*, **47**, 263(1969).

(17) H. W. Strobel and M. J. Coon, *J. Biol. Chem.*, **246**, 7826(1971).

(18) M. K. Wolpert, J. R. Althaus, and D. G. Johns, *J. Pharmacol. Exp. Ther.*, **185**, 202(1973).

(19) M. Morita, D. R. Feller, and J. R. Gillette, *Biochem. Pharmacol.*, **20**, 217(1971).

(20) C. Y. Wang, B. C. Behrens, M. Ichikawa, and G. T. Bryan, *ibid.*, **23**, 3395(1974).

(21) G. F. Ross, D. Goldstein, R. Hertz, M. B. Lipsett, and W. D. Odell, *Am. J. Obstet. Gynecol.*, **93**, 223(1965).

(22) P. D. Condit, *Ann. N. Y. Acad. Sci.*, **186**, 475(1971).

(23) K. B. Hausen and A. D. Bender, *Clin. Pharmacol. Ther.*, **8**, 392(1967).

(24) R. L. Blakley, in "The Biochemistry of Folic Acid and Related Pteridines," Frontiers of Biology, vol. 13, A. Neuberger and E. L. Tatum, Eds., Wiley, New York, N.Y., 1969.

(25) S. Kaufman and D. B. Fisher, *J. Biol. Chem.*, **245**, 4745(1970).

(26) T. Lloyd and N. Weiner, *Mol. Pharmacol.*, **7**, 569(1971).

(27) J. G. Lehoux, A. G. Fazekas, H. Leblanc, A. Chapdelaine, and T. Sandor, *J. Steroid Biochem.*, **3**, 773(1972).

(28) R. K. Kielley, *J. Biol. Chem.*, **216**, 405(1955).

(29) A. Albert, D. J. Brown, and G. W. H. Cheeseman, *J. Chem. Soc.*, **1951**, 474.

(30) J. J. McCormack and D. M. Valerino, in "Chemistry and Biology of Pteridines," Proceedings of the 4th International Symposium on Pteridines, K. Iwai *et al.*, Eds., International Academic, Tokyo, Japan, pp. 381–389.

(31) J. B. Bicking, C. M. Robb, S. F. Kwong, and E. J. Cragoe, *J. Med. Chem.*, **10**, 598(1967).

(32) M. D. Potter and T. Henshall, *J. Chem. Soc.*, **1956**, 2000.

(33) M. F. Mallette, E. C. Taylor, and C. K. Cain, *J. Am. Chem. Soc.*, **69**, 1814(1947).

(34) D. M. Valerino, Ph.D. dissertation, University of Vermont, Burlington, Vt., 1970.

(35) G. B. Elion and G. H. Hitchings, *J. Am. Chem. Soc.*, **74**, 3877 (1952).

(36) C. M. Baugh and E. Shaw, *J. Org. Chem.*, **29**, 3610(1964).

(37) G. B. Elion, G. H. Hitchings, and P. B. Russell, *J. Am. Chem. Soc.*, **72**, 78(1950).

(38) K. V. Rajagopalan and P. Handler, *J. Biol. Chem.*, **239**, 2022(1964).

(39) J. Clark and G. Neath, *J. Chem. Soc.*, **1966**, 1113.

(40) J. W. Daly and B. E. Christensen, *J. Am. Chem. Soc.*, **78**, 225(1956).

(41) J. Hurwitz, *J. Biol. Chem.*, **212**, 757(1955).

(42) S. Skupp and J. Ayvazian, *J. Lab. Clin. Med.*, **73**, 909(1969).

(43) T. Spector and D. G. Johns, *J. Biol. Chem.*, **245**, 5079 (1970).

(44) A. Albert, T. J. Batterham, and J. J. McCormack, *J. Chem. Soc. B*, **1966**, 1105.

(45) D. G. Johns and T. L. Loo, *J. Pharm. Sci.*, **56**, 356(1967).

(46) G. Palmer, R. C. Bray, and H. Beinert, *J. Biol. Chem.*, **239**, 2657(1964).

(47) P. Handler, K. V. Rajagopalan, and V. Aleman, *Fed. Proc.*, **23**, 30(1964).

(48) J. M. McCord and I. Fridovich, *J. Biol. Chem.*, **243**, 5753(1968).

(49) J. O. Knipe and J. J. McCormack, *Fed. Proc.*, **34**, 738 (1975).

(50) M. G. Battelli, E. Lorenzoni, and F. Stirpe, *Biochem. J.*, **131**, 191(1973).

ACKNOWLEDGMENTS AND ADDRESSES

Received June 11, 1975, from the *Department of Pharmacology, College of Medicine, University of Vermont, Burlington, VT 05401*

Accepted for publication October 3, 1975.

Adapted in part from a dissertation submitted by C. N. Hodnett to the Graduate College, University of Vermont, in partial fulfillment of the Doctor of Philosophy degree requirements.

Supported in part by a U.S. Public Health Service Research Grant (CA 12876) from the National Cancer Institute, by a grant from the Vermont Division of the American Cancer Society, and by a predoctoral fellowship (NDEA Title IV) awarded to C. N. Hodnett.

* To whom inquiries should be directed.

Comparative Evaluation of Tablet Lubricants: Effect of Application Method on Tablet Hardness and Ejectability after Compression

YOSHIHISA MATSUDA ˣ, YUHKO MINAMIDA, and SHIN-ICHI HAYASHI *

Abstract □ The effect of four lubricants (stearic acid, magnesium stearate, calcium stearate, and talc) on the ejectability and hardness of statically compressed tablets of a lactose granulation was examined. Two methods of application of these lubricants, incorporation into the granulation and mixing with the granulation, were compared. In both methods, the energy consumption curves during ejection and the hardness curves with lubricant concentration were similar and showed complicated behavior at a lower concentration. The mixing method gave better results for ejectability and hardness than the incorporation method.

Keyphrases □ Tablet lubricants—effect on ejectability and tablet hardness, comparison of mixing and incorporation methods of formulation □ Lubricants, tablet—effect on ejectability and tablet hardness, comparison of mixing and incorporation methods of formulation □ Dosage forms—tablet lubricants, effect on ejectability and tablet hardness, comparison of mixing and incorporation methods of formulation

It is customary to add lubricants as the last step in tablet formulation before compression, because they must be present on the surface of the granules and between them and the parts of the tableting machine. Nevertheless, in some formulas, the lubricants are added before wet granulating (1). One reason for this approach is that the intragranular addition (incorporation into the granulation) of the lubricants guarantees their uniform distribution within the granulation. Consequently, stable physical properties may be expected for the compressed tablets. This approach also has the advantages of eliminating the process of dry blending granulations and lubricants before compression and of preventing subsequent generation of "fines."

However, most reports concerning the addition of a lubricant to a granulation were about extragranular addition (mixing with the granulation) (2–12); little work has been reported on the behavior and effect of the lubricant added into the granulation *via* the binder solution (13).

The purpose of the present investigation was to evaluate the behavior and effect of four widely used lubricants, added by means of the described application methods, from the points of ejection force and tablet hardness, which are dynamic and static factors respectively, relating to compression in tablet formation.

EXPERIMENTAL

Preparation of Granulations and Application of Lubricants—Four kilograms of spray-dried lactose JP, under 100 mesh in size, and 600 g of 13% (w/w) ethanol solution of hydroxypropylcellulose[1] as a binding agent were kneaded thoroughly in a kneading machine[2] and then extruded through a 0.5-mm screen on a rotary-type granulator[3]. The granulations were dried for 30 min at 40° in a fluidized bed-type dryer[4], and the 24–48-mesh fraction was used.

These samples were blended for 20 min in a given mix ratio in a twin-shell-type mixer[5] with each lubricant, stearic acid, magnesium stearate, calcium stearate, and talc JP. The concentrations of the lubricant added were 0.1, 0.2, 0.5, 1.0, 2.0, and 5.0% (w/w) in every test granulation (mixing method).

Each lubricant was added beforehand to the same binder solution in a given concentration and dispersed thoroughly using a homogenizer[6]. In this case, stearic acid clarified the binder solution at a lower concentration due to its solubility in ethanol, while the other lubricants did not dissolve and remained dispersed. These binder solutions were kneaded with lactose in the same manner as in the mixing method and then granulated (incorporation method).

The concentrations of each lubricant contained in each test granulation were the same as in the mixing method. A granulation without any lubricant also was prepared as a control. These samples were stored in tightly stoppered containers until weighed for compression tests. The micromeritic characteristics of the powders are shown in Table I.

Compression of Granulations and Ejection—To control the compression operation closely, an accurate compression/tension testing machine[7], with rates of compression many times slower than those of commercial units, was used. Prior to each compression, the die wall and punches were cleaned with water and acetone and then dried to equalize experimental conditions.

Each 260 ± 0.7 mg of test granulation was filled into a single set of 8-mm flat-faced punches and die and compressed under the compression rate of 25 mm/min. The upper and lower punch forces during compression were detected by load cells and recorded by an electromagnetic oscillograph[8]. The displacement of the upper punch was followed by a differential transformer.

The effect of the lubricants during compression will be reported in a separate paper. According to the described procedures, 980 tablets were compressed in random order to reduce systematic errors. For a single concentration of one lubricant, the compression force ranged from 200 kg (400 kg/cm²) to 2000 kg (4000 kg/cm²); 20 tablets were made at every 100 kg within this range.

After compression, the lower punch was taken down, the die was inverted, and the compressed tablet was ejected downward at the same rate as during compression using the upper punch. The ejection force curve during ejection also was recorded by the electromagnetic oscillograph. The energy consumption for ejection was calculated by integrating the area beneath the force–displacement curve with a planimeter.

The thickness of these compressed tablets was individually measured with a micrometer; it ranged from 4.509 mm for the compression force of 200 kg to 3.631 mm for 2000 kg. The tablets were stored in a desiccator over silica gel until used for hardness tests. To examine the compression state of tablets, porosity (ϵ) was calculated using the apparent volume obtained from the geometric dimensions of the tablets and the particle density of the ingredients given in Table I. The porosity of a tablet composed of more than two ingredients is expressed by (16):

$$\epsilon = 1 - \rho_B \sum \frac{x_i}{\rho_i} \qquad \text{(Eq. 1)}$$

[1] Nisso HPC, Type L, Nihon Soda Co., Niigata, Japan.
[2] Dalton model 5DM, San-ei Manufacturing Co., Tokyo, Japan.
[3] Model RG-5, Kikusui Seisakusho Co., Kyoto, Japan.
[4] Midget dryer model MD-A-200, Fuji Pawdal Co., Osaka, Japan.
[5] Model V-1, Tokuju Kosakusho Co., Tokyo, Japan.
[6] Universal homogenizer (capacity 300 ml, impeller speed 7950 rpm), Nihon Seiki Seisakusho Co., Tokyo, Japan.
[7] Autograph model IS-5000, Shimadzu Co., Kyoto, Japan.
[8] Visigraph model FR-301, San-ei Instrument Co., Tokyo, Japan.

Table I—Micromeritic Characteristics of Sample Powders

Parameter	Lactose	Stearic Acid	Magnesium Stearate	Calcium Stearate	Talc	Hydroxypropylcellulose
Particle density, g/cm^3[a]	1.545	0.998	1.086	1.074	2.703	1.203
Specific surface area, cm^2/g[b]	1.8×10^4	4.0×10^4	6.3×10^4	4.6×10^4	9.2×10^3	—

[a] Measured by Beckmann air comparison pycnometer. [b] This value was calculated from the Kozeny–Carman equation (14) using the air permeability apparatus (15). Each value is the mean of five determinations.

where ρ_B is the bulk density (grams per cubic centimeter) of a compressed tablet, ρ_i is the particle density (grams per cubic centimeter) of the ith ingredient, and x_i is the weight fraction of the ith ingredient.

Tablet Hardness—The diametrical crushing strength of tablets was measured on a hardness tester[9] to the nearest one-fourth of a scale reading. The loading speed was 27.7 kg/min. All measured values fell within the maximum scale reading of this tester.

RESULTS AND DISCUSSION

Ejection Properties—In the compression of a tablet, the lubricant is expected (4) to prevent sticking and binding to the punch faces and die wall and to reduce friction at the tablet–die wall interface during compression and ejection. The latter has usually been considered the true property of a lubricant and has been evaluated in the compression process by the R-value, *etc.* (2, 4, 5, 9, 10, 17–20). When commercial tableting machines were used, a few examples of ejection force curves were presented (2, 3, 21), but these curves did not refer to the relationship between the kind of lubricant used and the shape of the curves or to the energy consumption for ejection.

Accurate ejection force curves can be recorded under a relatively low paper speed (100 mm/min) when the ejection speed is as slow as in the present work. Three ejection force curves recorded for the same kind of test granulation under the same compression conditions are shown in Fig. 1. These curves are close to each other throughout the whole ejection process and show good reproducibility, similar to the results obtained previously (22, 23). Consequently, it was confirmed that energy consumption also could be one useful means for evaluating ejectability besides the maximum ejection force.

As shown in Fig. 2, there appears to be a good linear correlation between the energy consumption and the maximum ejection force under the same condition of the addition of one lubricant over the whole range of ejection force measured. However, as is evident from Fig. 3, even in the same maximum ejection force, the shape of the curves changes with a close relation with lubricity, depending on the kind of lubricant and the application condition. Figure 3 shows representative examples of the ejection force curves, among those obtained from the control and eight kinds of lubricated samples, in which the maximum ejection force fell within the range of 40–50 kg. For every chart, the peak was at around 500 μm (incorporation method) or 250 μm (mixing method) from the starting point of the upper punch. This finding demonstrates that the intimacy of a tablet and die wall is completed within 1 sec and that the maximum ejection force is produced just before it.

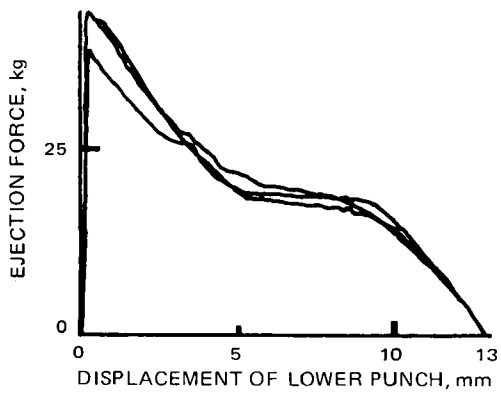

Figure 1—*Reproducibility of ejection force curves [lubricated by 0.2% stearic acid (incorporation method)]. Compression force = 1100 kg.*

In the control, the time lag until the tablet took to the die wall was longer than with the lubricated samples. For stearic acid, magnesium stearate, and calcium stearate, the peaks were sharp with both methods of application; they were rounded and somewhat irregular for the control. After passing the peak, the ejection force tended to decrease rapidly with the moving of the upper punch and then showed a plateau or a second peak inside the outlet for stearic acid, magnesium stearate, and calcium stearate; it decreased monotonously to the outlet for the control and talc.

The outlet of a die cavity is usually tapered due to the manufacturing technique and to prevent capping of the compressed tablets. Table II gives the geometric dimensions of the die cavity used in the present work. The position of a tablet moving in the die cavity, calculated from the paper speed and the position of the second peak on each chart, agreed with that of the diameter of the die wall shown in Table II. This finding suggests that the second peak shows the elastic recovery of a tablet inside the tapered outlet and is closely related to the lubricity of a tablet. Thus, it became clear that, even with the same maximum ejection force, differences in the shape of curves gave the different energy consumption. Therefore, the correct evaluation of ejectability should be made using energy consumption rather than ejection force.

The correlation between the compression force and energy consumption of tablets lubricated with 1% of calcium stearate is shown in Fig. 4 (mixing method). It appears that both parameters are directly and linearly related on the double-log scale over the whole range of compression forces used. The same result was also obtained for this lubricant with the incorporation method. The regression lines and the confidence limits of estimated values at the compression force of 1000 kg are summarized in Fig. 5 and Table III for the incorporation method using magnesium stearate. As shown in Fig. 5, these lines did not intersect. Therefore, the lubricant efficiency may be compared by the value of energy consumption interpolated into the compression force of, for example, 1000 kg.

Changes in energy consumption with the concentration of lubricant addition are shown in Fig. 6. With the incorporation method, the energy consumption (W_I) decreased rapidly at a very low lubricant concentration and then recovered immediately before decreasing again for three of the lubricants but not stearic acid. No minimum

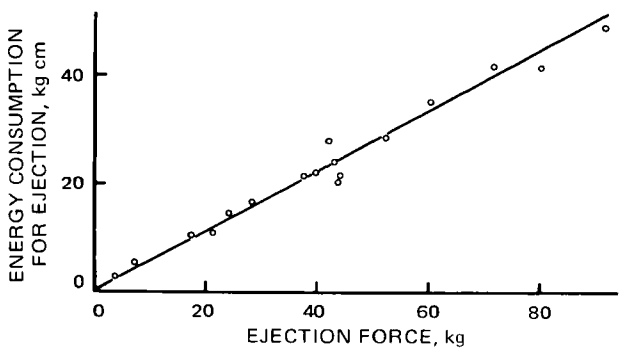

Figure 2—*Relationship between energy consumption for ejection and maximum ejection force [lubricated by 0.5% stearic acid (mixing method)].*

[9] Erweka model TBT/S, Erweka-Apparatebau, Offenbach/Main, West Germany.

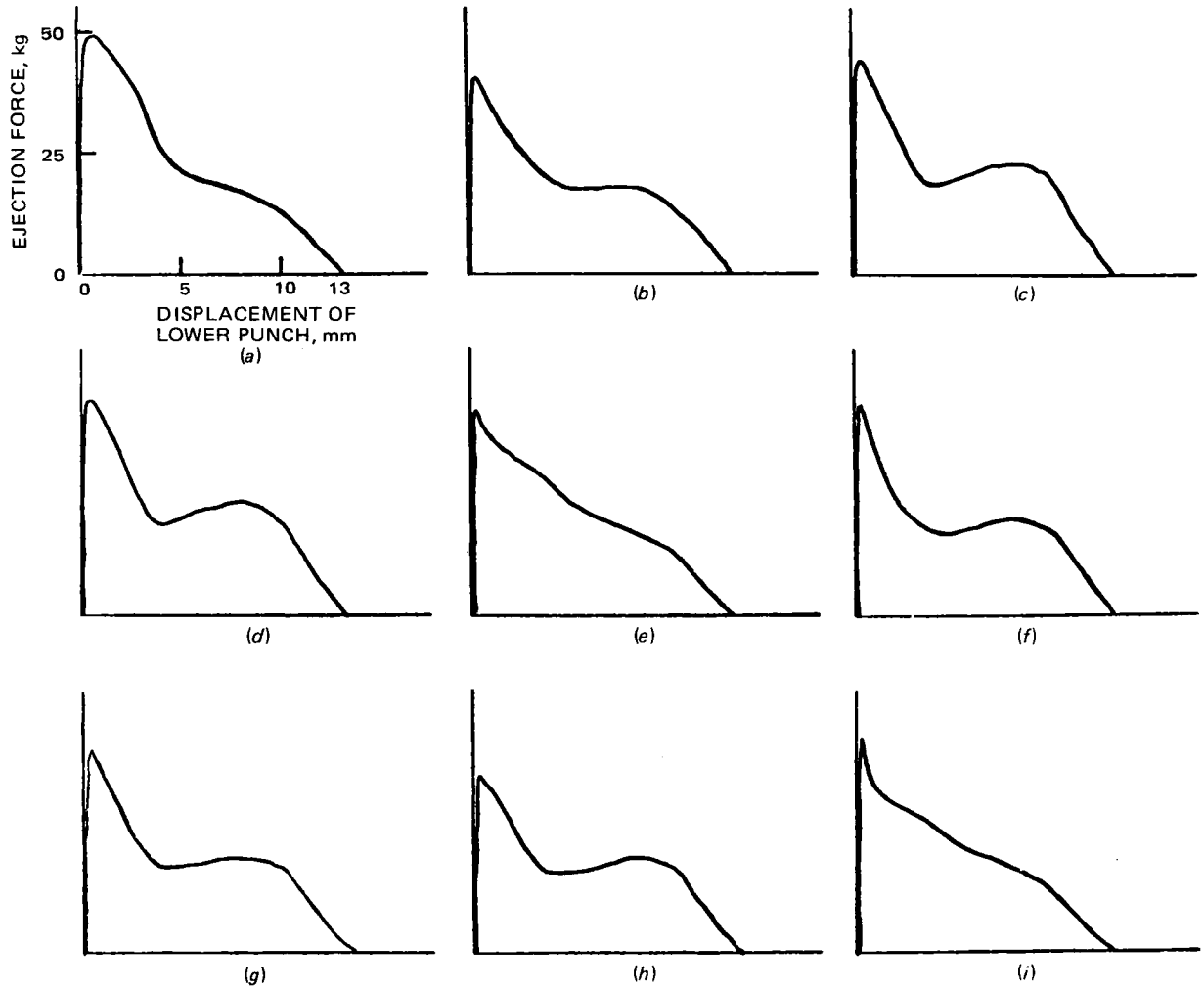

Figure 3—*Representative examples of ejection force curves lubricated by (a) nothing (compression force = 1020 kg), (b) 0.2% stearic acid (960 kg, incorporated), (c) 1% calcium stearate (1440 kg, incorporated), (d) 1% magnesium stearate (1410 kg, incorporated), (e) 1% talc (690 kg, incorporated), (f) 0.5% stearic acid (1140 kg, mixed), (g) 0.2% magnesium stearate (1430 kg, mixed), (h) 0.2% calcium stearate (1940 kg, mixed), and (i) 0.5% talc (410 kg, mixed).*

value was shown for stearic acid at the same region of concentration.

This result was probably due to the difference in the dispersion state of the ethanol-soluble stearic acid and of the ethanol-insoluble other lubricants in the binding agent. There were practically no significant differences in ejectability among stearic acid, magnesium stearate, and calcium stearate. With the mixing method, the energy consumption (W_M) decreased rapidly up to about 0.5% addition without showing either the minimum or the maximum, except for talc, and lubricity was saturated at the higher concentration.

It is, therefore, evident that stearates exhibit sufficient effectiveness at a concentration of less than 1% addition. Both magnesium stearate and calcium stearate exhibited similarly shaped curves over the whole range of addition concentration and showed better ejection properties than stearic acid. Talc showed a complicated behavior of two maxima and minima, and the concentrations of addition giving these values were almost the same for both methods of application. Talc also required far greater energy consumption at any one concentration than the other three lubricants. Moreover, especially for the incorporation method, the effect of addition of talc was hardly recognized, while the lubricity was less than that of the control at a concentration of 0.5%.

Table II—Geometric Dimensions of Die Cavity

Depth from Outlet of Die Cavity, mm	Diameter of Die Cavity, mm
0	8.050
1	8.009
2	8.006
3	8.005
4	8.005
—	—
20	8.005

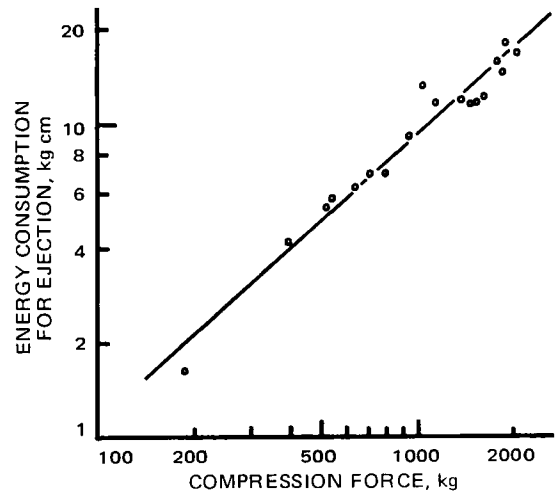

Figure 4—*Relationship between energy consumption and compression force [lubricated by 1% calcium stearate (mixing method)].*

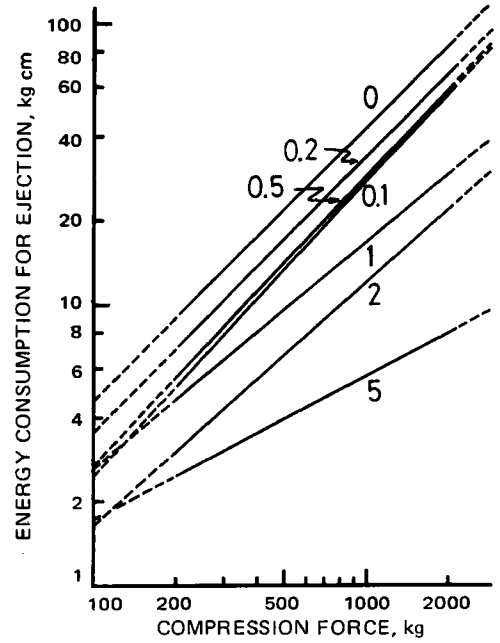

Figure 5—*Regression lines of energy consumption–compression force plots [lubricated by magnesium stearate (incorporation method)]. Numbers on curves are the lubricant concentrations in percent.*

The values of the transmission ratio (the ratio of the upper punch force to the lower punch force at the finished state of compression) interpolated into the compression force of 1000 kg on the transmission ratio–compression force curves (not presented in this paper) are given in Table IV. The tendency of energy consumption shown in Fig. 6 and that of the transmission ratio shown in Table IV are almost in agreement except for talc. This comparison makes the correlation between the lubricant properties during and after compression much clearer (2).

Energy consumption for the incorporation and mixing method is compared in Fig. 7, which indicates that the difference in lubricity according to the application method was most marked for magnesium stearate and calcium stearate; their ratio was about 2.6 times at 0.5% of lubricant present. This concentration agrees with those at which the lubricating effectiveness of magnesium stearate and calcium stearate almost reached the equilibrium state for the mixing method shown in Fig. 6. Above 0.5%, it decreased gradually with increasing

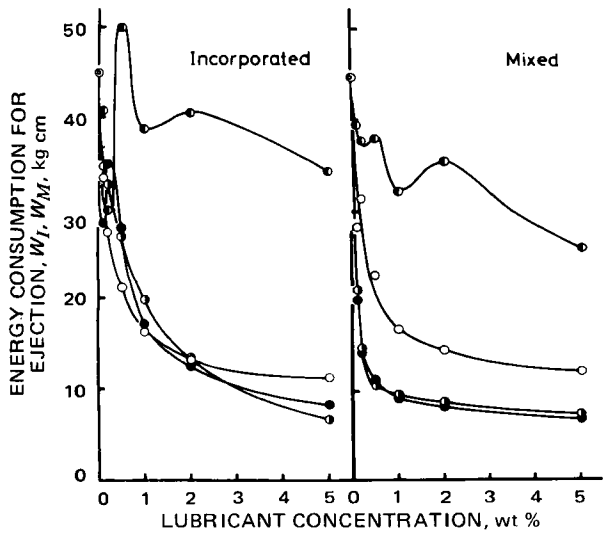

Figure 6—*Regressed energy consumption at compression force of 1000 kg. Key: ◎, control; ○, stearic acid; ●, magnesium stearate; ◑, calcium stearate; and ◐, talc.*

Table III—Estimated Values at the Compression Force of 1000 kg and Their Confidence Limits in Fig. 5

Lubricant Concentration, %	U.C.L., kg cm[a]	$\overline{W}$, kg cm[b]	L.C.L., kg cm[c]
0	54.0	44.6	37.2
0.1	38.6	28.2	21.1
0.2	49.6	34.7	24.1
0.5	35.7	28.7	23.4
1.0	22.0	17.2	14.5
2.0	16.9	12.4	9.1
5.0	13.3	8.3	5.4

[a] Upper confidence limit at 95% probability. [b] The estimated value interpolated in each regression line. [c] Lower confidence limit at 95% probability.

concentration, and no significant difference was obtained at a 5% concentration. On the other hand, the incorporation method gave somewhat better lubricity for stearic acid, but it did not show such a marked effectiveness as the other three. It may be concluded from these facts that the mixing method is better than the incorporation method in regard to ejectability at the common range of lubricant addition.

The lubricants applied in dry powder form (mixing method in the present work) were shown previously (4) to be present on the surface and extragranular regions of compressed tablets and not to mix intimately with the contents of granules. In the incorporation method, they would be captured at a lower concentration in the binding agent, which exists as the coating films in the intragranular region or over the surface of granulation. Consequently, the mobility of lubricant particles in the tablet and their frequency of contact with the die wall during compression would be lower than in the mixing method.

A definite difference in the ejectability of the two methods is likely to be due to the distribution state of the lubricant particles with newly exposed surface existing between the compressed tablet and die wall. From observations of direct compression tablets containing magnesium stearate, stearic acid, or talc, using the scanning electron microscope, it was confirmed that magnesium stearate was spread most completely. Stearic acid also was spread, but talc was not spread in spite of a partial crushing (24). The reason for the complicated phenomena shown in Fig. 6 is, however, unaccountable at present; work is in progress to clarify this point.

Tablet Hardness—The crushing strength of tablets has been reported in connection with compression force (6–8, 18, 19, 25–29). However, it is desirable that the relationship between hardness and porosity rather than that between hardness and compression force is presented to examine the mechanical strength of tablets, because the volume of tablets changes owing to the elastic recovery during the removal of compression.

A typical example of the relationship between the porosity of a

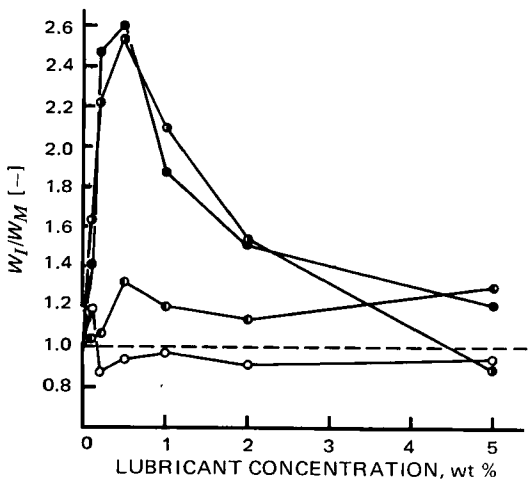

Figure 7—*Comparison of ejectability of two methods of application at compression force of 1000 kg. Key: ○, stearic acid; ●, magnesium stearate; ◑, calcium stearate; and ◐, talc.*

Table IV—Transmission Ratios under Compression Force of 1000 kg[a]

Lubricant Concentration, %	Stearic Acid		Magnesium Stearate		Calcium Stearate		Talc	
	I[b]	M[c]	I	M	I	M	I	M
0	0.678	0.678	0.678	0.678	0.678	0.678	0.678	0.678
0.1	0.685	0.692	0.726	0.750	0.689	0.741	0.687	0.695
0.2	0.710	0.700	0.690	0.801	0.677	0.787	0.687	0.693
0.5	0.736	0.727	0.705	0.860	0.713	0.859	0.685	0.714
1.0	0.778	0.776	0.750	0.883	0.743	0.881	0.706	0.733
2.0	0.802	0.801	0.814	0.904	0.802	0.897	0.709	0.746
5.0	0.846	0.869	0.860	0.916	0.867	0.914	0.741	0.778

[a] Each value was obtained by interpolating on the transmission ratio–compression force curves (not presented in this paper). [b] Incorporation method. [c] Mixing method.

finished tablet and hardness is shown in Fig. 8. The rate of decrease in hardness with increasing porosity was constant in semilogarithmic fashion, in the same manner as reported previously (30). This finding suggests that the following empirical equation by Duckworth (31) can be applied to the crushing of the compact containing such components as in this work:

$$H = H_0 \exp(-k\epsilon) \qquad \text{(Eq. 2)}$$

where H is the tablet hardness, H_0 is an imaginary maximum hardness of a tablet when completely compressed ($\epsilon = 0$), and k is the empirical constant. The values of H_0 and the slope, k, calculated from the regression lines of hardness–porosity data are plotted against the concentration of lubricant addition in Figs. 9 and 10. For a single method of application of one lubricant, these regression lines did not intersect each other within and below the range of porosity measured (ϵ = 0.07–0.20). Therefore, the tendency of H_0 in Figs. 9 and 10 corresponds with that of the hardness measured.

The curves of H_0 and k were similar in shape and closely related. From this fact, it may be said that the harder the tablet, the more dependent the hardness is on the compression state, ϵ, and, therefore, the more structure sensitive is the tablet. The values of k fell within the range of 4–9 calculated by Knudsen (32) for porous materials like ceramics. This finding suggests that the mechanism of crushing of tablets does not differ from those of the above-mentioned compacts. As shown in Fig. 9, hardness decreased once remarkably at a very low concentration of every lubricant and then increased again with an increasing concentration of the addition. The occurrence of such a minimum in hardness values is in qualitative agreement with the behavior of energy consumption (Fig. 6).

In the case of the mixing method, the hardness curves were more complicated than those of the incorporation method; they gave two maxima for stearic acid and calcium stearate. For calcium stearate, an erratic result, showing H_0 = 96.0 kg at a 0.2% concentration, was obtained. This result was not accidental, and its confidence is supported by the fact that the hardness value at a 0.1% concentration did not give such a marked drop off as in the other three cases.

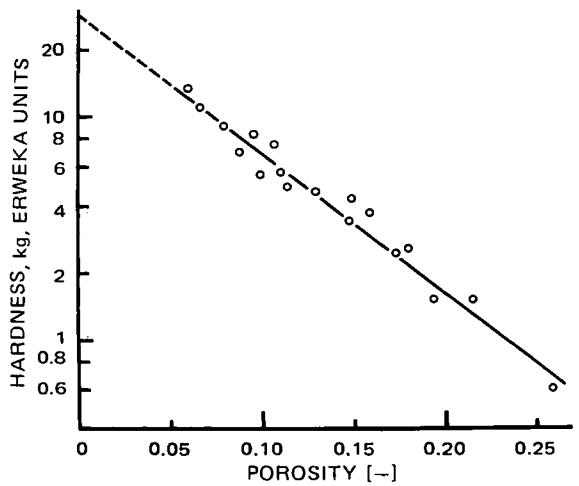

Figure 8—*Semilog plots of hardness and porosity [lubricated by 0.5% talc (incorporation method)].*

Strickland *et al.* (4) explained the effect of the concentration of addition of stearic acid and magnesium stearate as the smoothed curves (dotted lines in Fig. 10) in the hardness tests (Strong-Cobb unit) of sulfathiazole tablets. They stated that the addition of lubricants did not appear to have significant effects at concentrations less than 1%, which were effective for lubricant purposes. The shapes of curves connecting the plots of measured values were similar to the results of Shotton and Lewis (8) and the present work, and the complicated behavior of the addition was increased at lower concentrations.

The relation between good ejectability and a decrease in hardness may be accounted for as follows. For tablets containing magnesium stearate or calcium stearate, the film of lubricant particles over the lactose granulation decreases the area of actual binding and causes elastic recovery along with partial separation of the surface in contact when compression is removed. A more detailed explanation is not obvious at present, and additional information is necessary before any conclusion can be drawn.

The mixing method produced harder tablets than the incorporation method for all of the lubricants. In this respect, it is concluded that the mixing method is better than the incorporation method. However, the incorporation method gave a higher coefficient of correlation in the relationship between hardness and porosity than did the mixing method, and this result fulfilled some of the expectations described earlier.

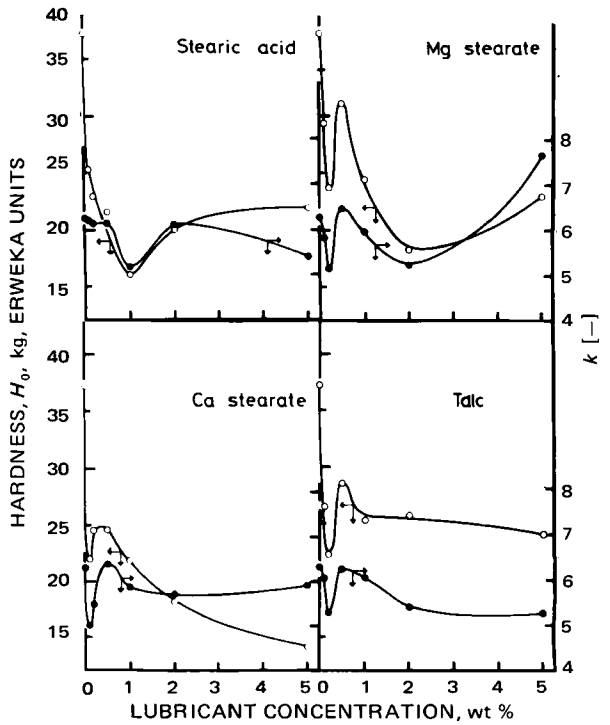

Figure 9—*Effect of lubricant concentrations on hardness (incorporation method). Key: ○, imaginary maximum hardness extrapolated to $\epsilon = 0$ on hardness–porosity plots; and ●, constant, k, in Eq. 2.*

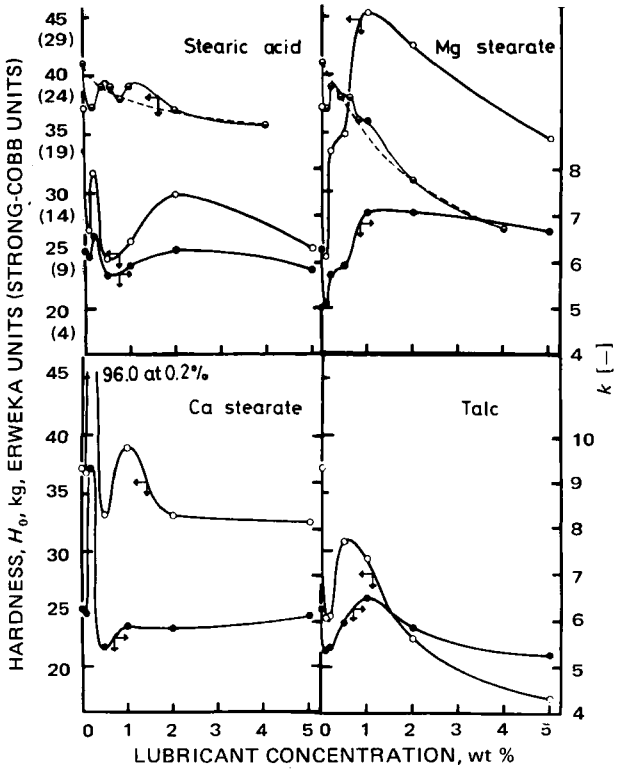

Figure 10—*Effect of lubricant concentrations on hardness (mixing method). Key:* ○, *imaginary maximum hardness extrapolated to* $\epsilon = 0$ *on hardness–porosity plots;* ●, *constant,* k, *in Eq. 2; and* ⊖, *hardness (Strong-Cobb units) measured by Strickland* et al. *(4).*

SUMMARY

The effect of lubricants on the ejectability and crushing strength of tablets of lactose granulation made by static compression was investigated. Formulations were prepared by incorporating such lubricants as stearic acid, magnesium stearate, calcium stearate, or talc into the granulation or by mixing each of them with it.

The ejection force curves of tablets compressed under the same condition showed good reproducibility but had different shapes for different lubricants and methods of application. The ejectability was evaluated by the energy consumption for ejection. In the incorporation method, ejectability was generally improved once at a very low additive concentration of lubricants and became worse again with increasing concentrations; ejectability generally improved progressively in the mixing method. The mixing method was better than the incorporation method for ejectability at any concentration of any lubricant.

Hardness was evaluated by the imaginary maximum value extrapolated to $\epsilon = 0$ on hardness–porosity curves. Hardness curves also decreased markedly at the same concentration as in ejectability, and hardness apparently was closely related to the lubricity of tablets. The mixing method was more useful with regard to hardness than was the incorporation method.

REFERENCES

(1) "The Theory and Practice of Industrial Pharmacy," L. Lachman, H. A. Lieberman, and J. L. Kanig, Eds., Lea & Febiger, Philadelphia, Pa., 1970, p. 314.

(2) E. Nelson, S. M. Naqvi, L. W. Busse, and T. Higuchi, *J. Am. Pharm. Assoc., Sci. Ed.*, **43**, 596(1954).

(3) E. Nelson, L. W. Busse, and T. Higuchi, *ibid.*, **44**, 223 (1955).

(4) W. A. Strickland, E. Nelson, L. W. Busse, and T. Higuchi, *ibid.*, **45**, 51(1956).

(5) W. A. Strickland, T. Higuchi, and L. W. Busse, *ibid.*, **49**, 35(1960).

(6) E. Yumioka, Y. Imasato, and N. Nakajima, *Arch. Pract. Pharm.*, **23**, 55(1963).

(7) E. Yumioka, Y. Imasato, and H. Sagara, *ibid.*, **24**, 106 (1964).

(8) E. Shotton and C. J. Lewis, *J. Pharm. Pharmacol.*, **16**, 111T(1964).

(9) C. J. Lewis and E. Shotton, *ibid.*, **17**, 71S(1965).

(10) *Ibid.*, **17**, 82S(1965).

(11) J. A. Seitz and G. M. Flessland, *J. Pharm. Sci.*, **54**, 1353(1965).

(12) A. M. Salpekar and L. L. Augsburger, *ibid.*, **63**, 289(1974).

(13) J. B. Appino, G. S. Banker, and H. G. DeKay, *Drug. Stand.*, **27**, 193(1959).

(14) P. C. Carman, *J. Soc. Chem. Ind. (London)*, **57**, 225(1938).

(15) E. Suito, M. Arakawa, and M. Takahashi, *Kogyokagaku Zasshi*, **59**, 307(1956).

(16) J. Okada, Y. Matsuda, and Y. Wada, *J. Pharm. Soc. Jpn.*, **88**, 647(1968).

(17) T. Higuchi, T. Shimamoto, S. P. Eriksen, and T. Yashiki, *J. Pharm. Sci.*, **54**, 111(1965).

(18) F. W. Goodhart, G. Mayorga, M. N. Milles, and F. C. Ninger, *ibid.*, **57**, 1770(1968).

(19) O. Alpar, J. J. Deer, J. A. Hersey, and E. Shotton, *J. Pharm. Pharmacol.*, **21**, 6S(1969).

(20) I. Sinozaki, M. Sugihara, T. Nagai, and H. Nogami, *Arch. Pract. Pharm.*, **31**, 232(1971).

(21) T. Higuchi, E. Nelson, and L. W. Busse, *J. Am. Pharm. Assoc., Sci. Ed.*, **43**, 344(1954).

(22) C. J. De Blaey and J. Polderman, *Pharm. Weekbl.*, **105**, 241(1970).

(23) C. J. De Blaey and J. Polderman, *Farm. Aikak.*, **80**, 111(1971).

(24) H. Maekawa, T. Sakamoto, and H. Takeda, Preprints of the 94th Annual Meeting of the Pharmaceutical Society of Japan, Sendai, 1974, Part IV, p. 162.

(25) T. Higuchi, L. N. Elowe, and L. W. Busse, *J. Am. Pharm. Assoc., Sci. Ed.*, **43**, 685(1954).

(26) L. N. Elowe, T. Higuchi, and L. W. Busse, *ibid.*, **43**, 718(1954).

(27) E. Nelson, *ibid.*, **45**, 354(1956).

(28) K. C. Kwan, F. O. Swart, and A. M. Mattocks, *ibid.*, **46**, 236(1957).

(29) H. Yamada, *Arch. Pract. Pharm.*, **20**, 115(1960).

(30) E. Shotton and D. Ganderton, *J. Pharm. Pharmacol.*, **12**, 87T(1960).

(31) W. Duckworth, *J. Am. Ceram. Soc.*, **36**, 68(1953).

(32) F. P. Knudsen, *ibid.*, **42**, 376(1959).

ACKNOWLEDGMENTS AND ADDRESSES

Received June 23, 1975, from *Kobe Women's College of Pharmacy, Higashinada, Kobe 658, Japan.*

Accepted for publication October 9, 1975.

Presented at the Pharmaceutical Technology Section, 95th Annual Meeting of the Pharmaceutical Society of Japan, Nishinomiya, Japan, April 1975.

* Present address: Rohto Pharmaceuticals Co., Osaka, Japan.

ˣ To whom inquiries should be directed.

Phenylbutazone Ionization Kinetics

V. J. STELLA ˣ and J. D. PIPKIN

Abstract □ Phenylbutazone has been associated with bioavailability problems and has shown nonclassical behavior in phase-transport studies. This nonclassical behavior has been attributed, in part, to the fact that phenylbutazone, as a carbon acid, undergoes noninstantaneous ionization kinetics. Instantaneous reaction is an assumption made in many diffusion-limited transport models involving a simultaneous ionization reaction. The ionization kinetics of phenylbutazone were determined at an ionic strength of 0.1 and 25° using a stopped-flow spectrophotometer. A log k_{obs} *versus* pH profile for the approach to the ionization equilibrium was determined, and a mechanism consistent with the profile was postulated. The percent enol *versus* the diketo form of phenylbutazone acid as well as pKa_{enol} and pKa_{diketo} was kinetically calculated. The protonation reaction was highly catalyzed by general acids while the deprotonation reaction was highly catalyzed by general bases. The general acid, water, was a poor proton donor to the anionic form (the so-called mesomeric anion) of phenylbutazone.

Keyphrases □ Phenylbutazone—ionization kinetics, relative concentrations and pKa's of enol and diketo forms calculated, effect of acids and bases □ Ionization kinetics—phenylbutazone, relative concentrations and pKa's of enol and diketo forms calculated, effect of acids and bases □ Anti-inflammatory agents—phenylbutazone, ionization kinetics

The anti-inflammatory phenylbutazone (I) has demonstrated nonclassical phase-transport characteristics (1–7). It was recently postulated that this nonclassical behavior of the carbon acid phenylbutazone might be accounted for by its relatively slow ionization rate (7). Noninstantaneous ionization is a characteristic of most carbon acids (8–10). In the design of any model involving phase-transport phenomena with simultaneous ionization, the assumption often is made that all ionizations are rapid (instantaneous) relative to diffusion processes, and the role of buffer components is often neglected. However, it is uncertain at this time what constitutes instantaneous ionization.

The ionization kinetics of phenylbutazone have not been studied previously, although the ionization kinetics of other carbon acids have been well documented (8–18). The immediate objective of this study was to determine the ionization kinetics of phenylbutazone. The ultimate objective is to use this information to help define when an ionization can be considered instantaneous or noninstantaneous in relation to phase-transport phenomena.

EXPERIMENTAL

Materials—Phenylbutazone[1] was used as supplied. All reactions and pKa determinations were carried out in glass-distilled water. The buffer components and sodium chloride used to adjust the ionic strength were of reagent or analytical reagent quality and were used without further purification.

pKa Determination—The pKa of phenylbutazone was determined spectrophotometrically[2] (19) at 265 nm and the same conditions of temperature and ionic strength as the kinetic studies, *i.e.*, 25 ± 0.2° and $\mu = 0.1$.

Kinetic Studies—The ionization kinetics of phenylbutazone were

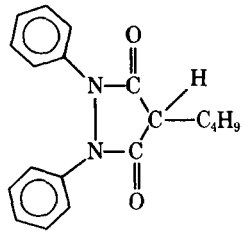

I

determined at 25 ± 0.2° and $\mu = 0.1$ with sodium chloride using a stopped-flow spectrophotometer[3] at 265 nm and a pH jump technique (18). For example, when the ionization kinetics of phenylbutazone acid to phenylbutazone mesomeric anion were studied, phenylbutazone at 6×10^{-5} *M* and $\mu = 0.1$ in water, with the pH lowered to approximately 4 with very dilute hydrochloric acid, was placed in one syringe of the stopped-flow spectrophotometer. The desired buffer at double the desired final concentration ($\mu = 0.1$) was stored in the second syringe.

On activation, equal volumes of the two syringes were mixed and the change in transmission at 265 nm was recorded on the calibrated oscilloscope of the stopped-flow spectrophotometer. A permanent recording of the transmission change with time was recorded by photography[4]. Plots of log $(A_{eq} - A)$ *versus* t, where A_{eq} and A are the absorbances (calculated from the transmission data) at time infinity (or at equilibrium) and time t, respectively, were constructed to determine the observed rate constant. Least-squares analysis of the data was performed.

Because the system under study represents a reversible reaction, the observed rate constant, k_{obs}, is the sum of both the forward and reverse rate constants. Buffer concentrations were varied to allow for the calculation of k_{obs} at zero buffer concentration. At pH's where the primary reaction was the protonation of the mesomeric anion to phenylbutazone acid, phenylbutazone at pH ~7 was jumped to acid pH with the transmission as a function of time again being recorded at 265 nm.

RESULTS

Figure 1 shows the UV spectrum of phenylbutazone under basic

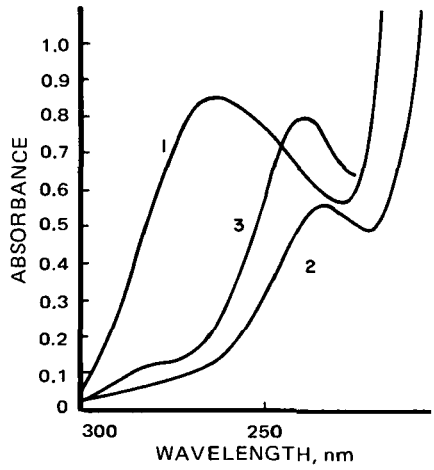

Figure 1—*UV spectrum of phenylbutazone (5.00×10^{-5} M) in 0.1 M NaOH (curve 1), 0.1 M HCl (curve 2), and dichloromethane (curve 3).*

[1] Ciba Geigy Corp.
[2] Perkin-Elmer 356 dual-beam spectrophotometer.
[3] Durrum, with a thermostated cell and syringes maintained at 25 ± 0.2°.
[4] Tetronix C-27 oscilloscope camera.

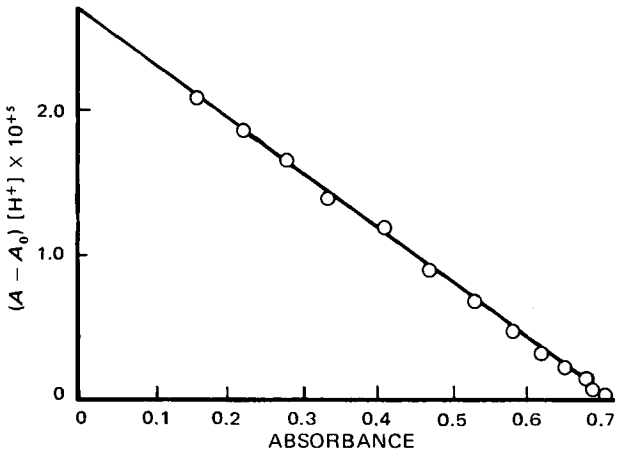

Figure 2—*Plot used to determine the macroscopic ionization constant of phenylbutazone at 25° and μ = 0.1 with sodium chloride.*

as well as acidic conditions. The equilibrium ionization constant of phenylbutazone could be determined by observing the change in absorbance at 265 nm as a function of pH using:

$$K_a = \frac{(A - A_0)[H^+]}{(A_\infty - A)} \qquad \text{(Eq. 1)}$$

where K_a is the macroscopic or observed ionization constant at 25° and μ = 0.1; A is the absorbance of phenylbutazone at a given hydrogen-ion concentration, $[H^+]$; A_0 is the absorbance of the phenylbutazone under acidic conditions, *i.e.*, the ionization completely suppressed (pH = 1.0 or 0.1 *M* HCl); and A_∞ is the absorbance of the phenylbutazone at pH's $\gg$ pKa (pH = 13 in 0.1 *M* NaOH).

Rearranging Eq. 1 allows the determination of K_a:

$$(A - A_0)[H^+] = K_a A_\infty - K_a A \qquad \text{(Eq. 2)}$$

from a plot of $(A - A_0)[H^+]$ *versus* A, with the ionization constant K_a being calculated from the slope. This approach is useful when an exact value of A_∞ is difficult to obtain. Figure 2 gives such a plot for a 4×10^{-5} *M* solution of phenylbutazone. The value of K_a under the experimental conditions was 3.71×10^{-5} (average of three determinations) with pKa calculated as 4.43.

Table I gives the observed rate constants for the ionization kinetics of phenylbutazone under various pH and buffer concentrations. All observed rate constants are the mean of at least three or more determinations. Also included in this table are the observed rate constants extrapolated to zero buffer concentration obtained from plots of k_{obs} *versus* total buffer concentration. Figure 3 is a plot of $\log k'_{obs}$ *versus* pH for the ionization of phenylbutazone where k'_{obs} is the buffer-independent observed rate constant.

DISCUSSION

A model for the ionization and ionization kinetics of relatively strong carbon acids is defined in Scheme I. The three possible species of phenylbutazone that can exist in solution are the diketo form of phenylbutazone, K, the enol form of phenylbutazone, E, and the so-called mesomeric anion or E^- (9). Therefore, the macroscopic ionization constant for phenylbutazone would be defined by:

$$K_a = \frac{[E^-][H^+]}{[K] + [E]} \qquad \text{(Eq. 3)}$$

Rearranging gives:

$$\frac{1}{K_a} = \frac{1}{K_{a,\text{diketo}}} + \frac{1}{K_{a,\text{enol}}} \qquad \text{(Eq. 4)}$$

which shows the relationship of this macroscopic constant to the microscopic constants, $K_{a,\text{diketo}}$ and $K_{a,\text{enol}}$, which are the ionization constants for the diketo and enol forms of phenylbutazone, respectively.

In Scheme I, the assumption is made that the equilibrium defined by $K_{a,\text{enol}}$ is rapid and instantaneous[5]. This assumption appears valid

[5] The word instantaneous is used to describe phenomena taking place at rates near the diffusion-controlled limit of $\sim 2 \times 10^{10}\ M^{-1}\ \text{sec}^{-1}$.

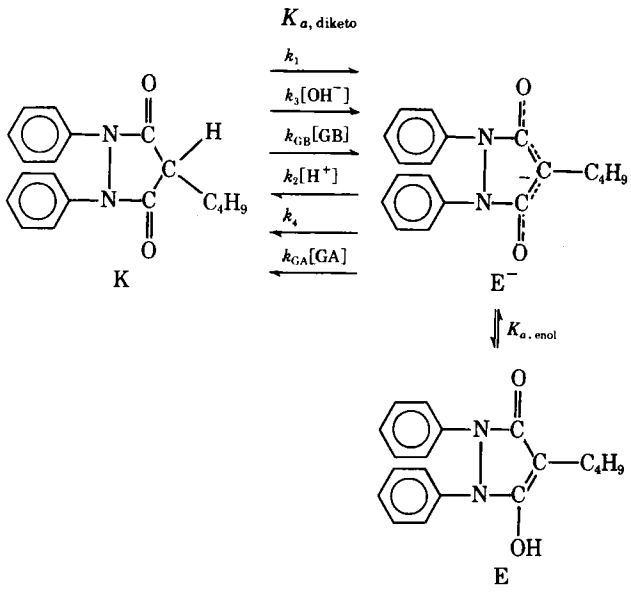

Scheme I

in light of Eigen's studies (9) of the ionization rates of enolic compounds. The equilibrium represented by $K_{a,\text{diketo}}$ is considered to be the slow step (9). The rate constant k_1 represents the water-catalyzed deprotonation of phenylbutazone, k_3 is the hydroxide-ion-catalyzed deprotonation rate constant, and k_{GB} is the general base-catalyzed deprotonation rate constant. The constant k_2 represents the specific acid-catalyzed protonation constant of the mesomeric anion, k_4 is the water or spontaneous rate constant for the protonation of the mesomeric anion, and k_{GA} is the general acid-catalyzed protonation of the mesomeric anion.

Deriving the equation for the equilibrium ionization kinetics of phenylbutazone, assuming Scheme I and neglecting the buffer contribution to the kinetics, leads to:

$$k'_{obs} = k_1 + k_3[OH^-] + \frac{k_2[H^+]K_{a,\text{enol}}}{K_{a,\text{enol}} + [H^+]} + \frac{k_4 K_{a,\text{enol}}}{K_{a,\text{enol}} + [H^+]} \qquad \text{(Eq. 5)}$$

By referring to Fig. 1, it is obvious from the poor UV absorption of phenylbutazone under acid conditions in the 250–270-nm range that phenylbutazone exists primarily in the diketo form. This was confirmed by measuring the UV absorption spectrum of phenylbutazone

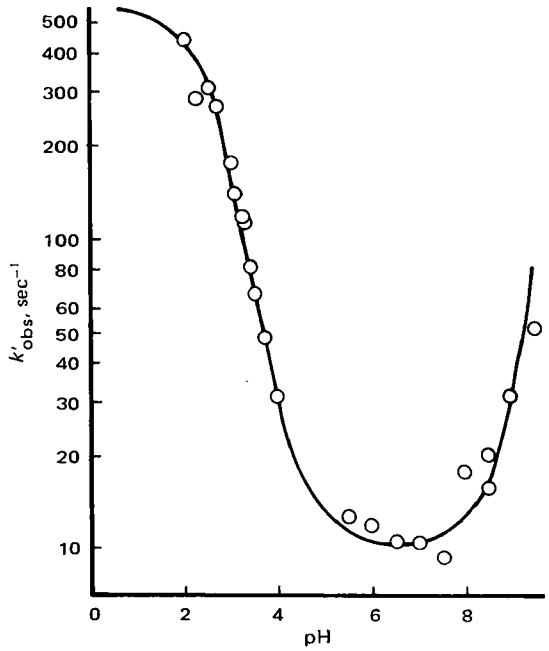

Figure 3—*Plot of log* k'_{obs} versus *pH for the establishment of an ionization equilibrium for phenylbutazone.*

Table I—Effect of pH and Buffer Concentrations on the Ionization Kinetics of Phenylbutazone at 25° and μ = 0.1 with Sodium Chloride

pH	Buffer	Buffer Concentration, *M*	k_{obs}, sec^{-1}	k'_{obs}, sec^{-1}
2.00	Hydrochloric acid	—	440 ± 56[a]	440 ± 56[a]
2.30	Hydrochloric acid	—	281 ± 18	281 ± 18
2.52	Hydrochloric acid	—	309 ± 23	309 ± 23
2.70	Hydrochloric acid	—	269 ± 10	269 ± 10
3.00	Hydrochloric acid	—	178 ± 7	178 ± 7
3.00	Hydrochloric acid	—	172 ± 4	172 ± 4
3.00	Hydrochloric acid	—	140 ± 6	140 ± 6
3.22	Hydrochloric acid	—	117 ± 3	47 ± 3
3.30	Hydrochloric acid	—	112 ± 7	112 ± 7
3.40	Hydrochloric acid	—	79.9 ± 1.1	79.9 ± 1.0
3.50	Acetate	0.02	81.6 ± 2.1	—
3.50	Acetate	0.03	93.6 ± 1.4	—
3.50	Acetate	0.04	100 ± 2	—
3.50	Acetate	0.05	107 ± 3	—
3.50	Acetate	0.00 (calc.)	—	66.6
3.70	Hydrochloric acid	—	47 ± 2	47 ± 2
4.00	Acetate	0.02	47.6 ± 1.1	—
4.00	Acetate	0.03	55.4 ± 0.5	—
4.00	Acetate	0.04	61.3 ± 2.9	—
4.00	Acetate	0.05	72.9 ± 0.1	—
4.00	Acetate	0.00 (calc.)	—	30.7
5.50	Acetate	0.005	16.4 ± 1.0	—
5.50	Acetate	0.02	33.4 ± 0.3	—
5.50	Acetate	0.03	45.1 ± 2.2	—
5.50	Acetate	0.04	51.9 ± 1.6	—
5.50	Acetate	0.05	62.6 ± 0.6	—
5.50	Acetate	0.00 (calc.)	—	12.5
6.00	Acetate	0.02	32.5 ± 1.0	—
6.00	Acetate	0.03	44.9 ± 1.4	—
6.00	Acetate	0.04	52.4 ± 1.2	—
6.00	Acetate	0.05	65.8 ± 0.8	—
6.00	Acetate	0.00 (calc.)	—	11.6
6.50	Succinate	0.0075	23.7 ± 0.9	—
6.50	Succinate	0.009	25.6 ± 0.8	—
6.50	Succinate	0.012	31.9 ± 1.0	—
6.50	Succinate	0.015	36.5 ± 1.4	—
6.50	Succinate	0.00 (calc.)	—	10.3
7.00	Succinate	0.0075	23.7 ± 0.5	—
7.00	Succinate	0.009	26.2 ± 0.8	—
7.00	Succinate	0.012	32.2 ± 1.8	—
7.00	Succinate	0.015	37.0 ± 0.5	—
7.00	Succinate	0.00 (calc.)	—	10.2
7.50	Phosphate	0.0075	39.5 ± 1.4	—
7.50	Phosphate	0.009	46.0 ± 2.0	—
7.50	Phosphate	0.012	59.4 ± 1.2	—
7.50	Phosphate	0.015	70.0 ± 4.0	—
7.50	Phosphate	0.00 (calc.)	—	9.2
8.00	Phosphate	0.0075	46.8 ± 1.6	—
8.00	Phosphate	0.009	54.2 ± 1.7	—
8.00	Phosphate	0.012	67.0 ± 2.1	—
8.00	Phosphate	0.015	77.4 ± 3.0	—
8.00	Phosphate	0.00 (calc.)	—	17.1
8.50	Phosphate	0.0075	50.5 ± 1.2	—
8.50	Phosphate	0.009	57.5 ± 1.7	—
8.50	Phosphate	0.012	69.4 ± 3.1	—
8.50	Phosphate	0.015	81.9 ± 2.1	—
8.50	Phosphate	0.00 (calc.)	0.00	19.7
8.50	Borate	0.02	23.7 ± 0.5	—
8.50	Borate	0.03	29.3 ± 0.2	—
8.50	Borate	0.04	32.6 ±	
8.50	Borate	0.05	37.2 ± 0.3	—
8.50	Borate	0.00 (calc.)	—	15.4
9.00	Borate	0.00	42.8 ± 0.9	—
9.00	Borate	0.03	50.2 ± 1.1	—
9.00	Borate	0.04	55.7 ± 0.7	—
9.00	Borate	0.05	61.9 ± 0.9	—
9.00	Borate	0.00 (calc.)	—	30.7
9.50	Borate	0.02	75.6 ± 5.4	—
9.50	Borate	0.03	91.0 ± 4.6	—
9.50	Borate	0.04	103.0 ± 1.6	—
9.50	Borate	0.05	114.0 ± 7.2	—
9.50	Borate	0.00 (calc.)	—	51.4

[a] Mean ± *SD*.

in an inert solvent such as dichloromethane where the formation of the more polar enol form of phenylbutazone would be suppressed [curve 3 of Fig. 1 (20)]. This means that $pKa_{diketo} \gg pKa_{enol}$ or that $K_{a,enol} \gg K_{a,diketo}$. Because of this observation, it can be concluded that $pKa_{diketo} \approx$ pKa and that $pKa_{enol} < 4.43$.

At pH's where the primary observed reaction is the *ionization of*

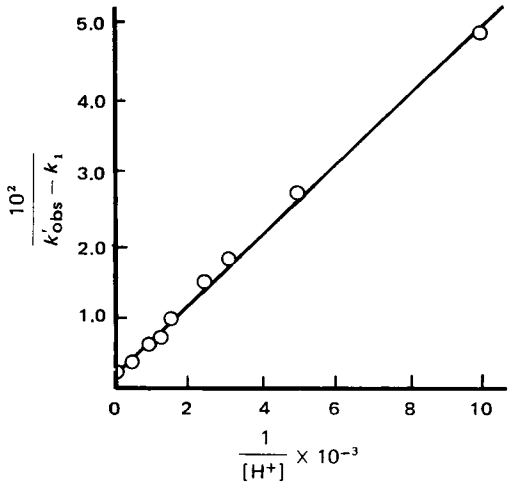

Figure 4—*Plot used to determine* k_2 *and* $K_{a,enol}$ *for the ionization of phenylbutazone. (Refer to Eq. 14 and Scheme I.)*

phenylbutazone acid to the mesomeric anion, *i.e.*, at pH ≫ pKa_{diketo}, the observed rate constant can be approximated to:

$$k'_{obs} = k_1 + k_3[OH^-] + \frac{k_4 K_{a,enol}}{K_{a,enol} + [H^+]} \quad \text{(Eq. 6)}$$

and since $K_{a,enol} \gg [H^+]$ at this pH:

$$k'_{obs} = (k_1 + k_4) + k_3[OH^-] \quad \text{(Eq. 7)}$$

$$k'_{obs} = k_0 + k_3[OH^-] \quad \text{(Eq. 8)}$$

where:

$$k_0 = k_1 + k_4 \quad \text{(Eq. 9)}$$

Equation 8 predicts that a plot of k'_{obs} *versus* $[OH^-]$ should give a straight line. However, as can be noted in Fig. 3, there was much scatter in the data in this pH range. Therefore, only an estimate could be made of k_3 ($\sim 2 \times 10^6\ M^{-1}\ sec^{-1}$), although a reasonably accurate estimate could be made of k_0 ($10.1\ sec^{-1}$).

Since $pKa_{diketo} \approx$ pKa, Eq. 10 can be derived:

$$\frac{K_{a,diketo}}{K_w} = \frac{k_3}{k_4} \sim \frac{K_a}{K_w} \quad \text{(Eq. 10)}$$

allowing an estimation of k_4 by knowing k_3, K_a, and K_w under the experimental conditions. This approach gives a value of k_4 of $5.4 \times 10^{-4}\ sec^{-1}$. It is obvious, therefore, that the constant k_0 is approximately equal to k_1:

$$k_0 = k_1 + k_4 \sim k_1 = 10.1\ sec^{-1} \quad \text{(Eq. 11)}$$

From Fig. 1, it can be noted that at pH < 8, $k_3[OH^-]$ can be neglected. Therefore:

$$k'_{obs} = k_1 + \frac{k_2[H^+]K_{a,enol}}{K_{a,enol} + [H^+]} + \frac{k_4 K_{a,enol}}{K_{a,enol} + [H^+]} \quad \text{(Eq. 12)}$$

and since $K_{a,enol}/(K_{a,enol} + [H^+])$ is always < 1 and k_4 is small, Eq. 12 collapses to:

$$k'_{obs} = k_1 + \frac{k_2[H^+]K_{a,enol}}{K_{a,enol} + [H^+]} \quad \text{(Eq. 13)}$$

which can be rearranged to:

$$\frac{1}{k'_{obs} - k_1} = \frac{1}{k_2[H^+]} + \frac{1}{k_2 K_{a,enol}} \quad \text{(Eq. 14)}$$

Equation 14 predicts that a plot of $1/(k'_{obs} - k_1)$ *versus* $1/[H^+]$ will give a straight line of slope $= 1/k_2$ and intercept $1/k_2 K_{a,enol}$, thus allowing the estimation of k_2 and $K_{a,enol}$. Such a plot is shown in Fig. 4. The rate constant k_2 was estimated to be $2.11 \times 10^5\ M^{-1}\ sec^{-1}$, and $K_{a,enol}$ was estimated to be 2.62×10^{-3} (pKa_{enol} 2.58).

The equilibrium ionization constant of the diketo form of phenylbutazone is defined as:

$$K_{a,diketo} = \frac{k_1}{k_2} = \frac{10.1}{2.11 \times 10^5} = 4.78 \times 10^{-5} \quad \text{(Eq. 15)}$$

Table II—Kinetic and Equilibrium Constants for the Ionization of Phenylbutazone at 25° and μ = 0.1 with Sodium Chloride

Parameter	Value
k_1	$10.1\ sec^{-1}$
k_2	$2.11 \times 10^5\ M^{-1}\ sec^{-1}$
k_3	$\sim 2 \times 10^6\ M^{-1}\ sec^{-1}$
k_4	$\sim 4.2 \times 10^{-4}\ sec^{-1}$
$K_{a,enol}$	2.62×10^{-3} ($pKa_{enol} = 2.58$)
$K_{a,diketo}$	4.78×10^{-5} ($pKa_{diketo} = 4.32$)
K_a	4.67×10^{-5} or pKa = 4.33 (kinetically determined) 3.71×10^{-5} or pKa = 4.43 (determined spectrophotometrically)
% enol	1.8

or $pKa_{diketo} = 4.32$. A value for K_a can be calculated (Eq. 4) from the kinetic data to be 4.67×10^{-5} or pKa can be kinetically calculated to be 4.33. This value compares favorably with the experimentally determined value of 4.43. Determination of $K_{a,diketo}$ specifically allows a reestimation of the value of k_4 ($4.2 \times 10^{-4}\ sec^{-1}$).

Table II is a summary of the kinetic and equilibrium constants. Included in this table is the percent enol present in phenylbutazone acid dissolved in solution. It can be shown that the percent enol can be calculated from Eqs. 16 and 17:

$$\% \text{ enol} = \frac{[E]}{[E] + [K]} \times \frac{100}{1} \quad \text{(Eq. 16)}$$

$$\% \text{ enol} = \frac{K_{a,diketo}}{K_{a,diketo} + K_{a,enol}} \times \frac{100}{1} \quad \text{(Eq. 17)}$$

The rate constants from Table II were placed back into Eq. 5 to help generate a theoretical curve for the ionization behavior of phenylbutazone, assuming the mechanism shown in Scheme I. The solid line drawn through the experimental points in Fig. 3 is the line generated by Eq. 5 using the constants summarized in Table II. As can be seen from the fit of these data, Eq. 5 and subsequently Scheme I do appear to define the ionization kinetics of phenylbutazone adequately.

Alternative mechanisms might be postulated to describe the ionization of phenylbutazone. For example, it might be postulated that a pathway exists that allows the direct conversion of the diketo phenylbutazone to the enol in a concerted acid–base mechanism. This mechanism appears unlikely because the plots of k_{obs} *versus* total buffer concentration were linear for a range of buffer species; *i.e.*, no second-order term in buffer concentration was noted. It is becoming increasingly evident that few, if any, concerted acid–base mechanisms exist in aqueous solvents (21).

A second mechanism that might be postulated is the conversion of the diketo phenylbutazone to the enolic form of phenylbutazone *via* an acid-catalyzed mechanism. But such a mechanism would not predict the type of curve given in Fig. 3. Moreover, protonation of the diketo phenylbutazone [estimated pKa of the diketone, acetylacetone, is −5 to −6 (22)] is so unfavorable that it would represent a case of an intermediate for which heightened reactivity fails to compensate for inferior concentration (23).

This discussion is not to say that alternative mechanisms such as these two do not exist. The point can be made, however, that Scheme I does appear to describe the ionization of phenylbutazone adequately.

As a result of the choice of buffers used in this study, accurate and meaningful values of k_{GA} and k_{GB} could not be determined from these data because species such as the monoanion of succinic acid, $H_2PO_4^-$, and HPO_4^{-2} could act both as acids or bases. The general acid–general base catalysis of phenylbutazone ionization is currently under investigation. The objective of this extended study is to define mechanistically the ionization kinetics of phenylbutazone. However, two observations can be made from the buffer data:

1. Relative to its pKa, water is a very weak proton donor to a carbanion [an observation consistent with other recent work (24)].

2. Relative to its pKa, borate ion is a very weak proton acceptor [an observation also consistent with earlier findings (25)].

In an earlier study (7), it was demonstrated that the phenylbutazone dissolution rate and phase-transport phenomena in general may be affected by the relatively slow ionization of phenylbutazone.

Constants k_1 through k_4 of Table II are substantially slower than the diffusion-limited constants for the ionization of normal or classical acids such as carboxylic, phenolic, and nitrogen acids (8, 9). The ionization kinetics generated in this work will be used to determine whether, in fact, the nonclassical phase-transport behavior of phenylbutazone (1–7) can be traced to this relatively slow ionization rate.

REFERENCES

(1) E. G. Lovering and D. B. Black, *J. Pharm. Sci.*, **63**, 671(1974).

(2) *Ibid.*, **63**, 1399(1974).

(3) A. Brodin and A. Agren, *Acta Pharm. Suec.*, **8**, 609(1971).

(4) A. Brodin and M. Nilsson, *ibid.*, **10**, 187(1973).

(5) A. Brodin, *ibid.*, **11**, 141(1974).

(6) *Ibid.*, **12**, 41(1975).

(7) V. Stella, *J. Pharm. Sci.*, **64**, 706(1975).

(8) M. L. Bender, "Mechanisms of Homogeneous Catalysis from Protons to Proteins," Wiley–Interscience, New York, N.Y., 1971, chap. 2.

(9) M. Eigen, *Angew. Chem. Int. Ed.*, **3**, 1(1964).

(10) J. R. Jones, *Prog. Phys. Org. Chem.*, **9**, 241(1972).

(11) T. Riley and F. A. Long, *J. Am. Chem. Soc.*, **84**, 522(1962).

(12) R. F. Pratt and T. P. Bruice, *J. Org. Chem.*, **37**, 3563(1972).

(13) F. G. Bordwell and W. J. Boyle, Jr., *J. Am. Chem. Soc.*, **97**, 3447(1975).

(14) *Ibid.*, **93**, 512(1971).

(15) F. G. Bordwell, W. J. Boyle, Jr., J. A. Hautala, and K. C. Yee, *J. Am. Chem. Soc.*, **91**, 4002(1969).

(16) F. G. Bordwell, W. J. Boyle, Jr., and K. C. Yee, *ibid.*, **92**, 5926(1970).

(17) F. G. Bordwell and W. J. Boyle, Jr., *ibid.*, **93**, 511(1971).

(18) *Ibid.*, **94**, 3907(1972).

(19) A. Albert and E. P. Serjeant, "Ionization Constants of Acids and Bases," Methuen and Co., London, England, 1962, chap. 4.

(20) Y. Linaberg, O. Neiland, A. Veis, A. N. Latv, and G. Vanag, *Dokl. Akad. SSSR*, **154**, 1385(1964); *Engl. Transl.*, **154**, 184(1964).

(21) F. G. Bordwell, *Acc. Chem. Res.*, **3**, 281(1970).

(22) D. D. Perrin, "Dissociation Constants of Organic Bases in Aqueous Solutions," Butterworths, London, England, 1965, p. 418.

(23) D. S. Kemp, *J. Am. Chem. Soc.*, **90**, 7153(1968).

(24) G. S. Rork and I. H. Pitman, *ibid.*, **96**, 4654(1974).

(25) W. P. Jencks, "Catalysis in Chemistry and Enzymology," McGraw-Hill, New York, N.Y., 1969, chap. 3.

ACKNOWLEDGMENTS AND ADDRESSES

Received August 11, 1975, from the *Department of Pharmaceutical Chemistry, University of Kansas, Lawrence, KS 66045*

Accepted for publication October 8, 1975.

Presented at the Basic Pharmaceutics Section, APhA Academy of Pharmaceutical Sciences, San Francisco meeting, April 1975.

Supported by University of Kansas General Research Funds and a HSAA award to V. Stella. Supported in part by National Institute of Health Grant GM 22 357.

[x] To whom inquiries should be directed.

Kinetic Analysis of Penicillin Degradation in Acidic Media

JEAN M. BLAHA*[¶], ADELBERT M. KNEVEL[‡], DAVID P. KESSLER[§], JEROME W. MINCY*, and STANLEY L. HEM*[x]

Abstract □ Degradation of penicillin in acidic media (pH 2.7) was monitored by high-pressure liquid chromatography and UV spectroscopy. The effects of temperature, buffer concentration, and ionic strength were examined. A degradation pathway is proposed, and the apparent first-order rate constant and energy of activation were calculated for each reaction. One or more degradation products containing a sulfhydryl group, a functional group often suggested as having a major role in eliciting allergic responses to penicillin therapy, were present throughout the degradation scheme.

Keyphrases ◻ Penicillin—degradation in acidic media, kinetic analysis, monitored by high-pressure liquid chromatography and UV spectroscopy, effect of temperature, buffer concentration, and ionic strength ◻ Degradation—penicillin in acidic media, kinetic analysis, monitored by high-pressure liquid chromatography and UV spectroscopy, effect of temperature, buffer concentration, and ionic strength □ High-pressure liquid chromatography—used to monitor degradation of penicillin in acidic media, kinetic analysis □ UV spectroscopy—used to monitor degradation of penicillin in acidic media, kinetic analysis □ Antibacterial agents—penicillin, degradation in acidic media, kinetic analysis

It is estimated that between 1 and 10% of the population experiences allergic response after penicillin therapy, with 300 fatalities in the United States each year (1). Research on penicillin allergy has considered four factors which may be of importance: (*a*) direct reactions of the drug with protein *in vivo*, (*b*) degradation products of penicillin that can react with protein, (*c*) impurities other than degradation products that may be in the dosage form with penicillin, and (*d*) metabolites of penicillin that can react with protein (2).

One approach to the problem of penicillin allergy would be to determine the role of specific penicillin degradation products in producing an allergic response and, through dosage form design, to minimize the formation of degradation products showing significant potential as allergenic determinants. To use this approach, the time sequence for the presence of penicillin degradation products in aqueous media needs to be established.

Several reviews (2, 3) suggested schemes for the degradation of penicillin. It was proposed that penillic and penicilloic acids are the major degradation products when penicillin is aged in acidic solutions (4). The mechanism of penicillin degradation was studied in acidic solution, and it was proposed that penicillenic acid forms from the reaction of the penicillin ion with a proton or from the spontaneous rearrangement of undissociated penicillin (5). It was suggested also that penillic acid forms from penicillenic acid and that penilloic acid is the product from the acid catalysis of

Constants k_1 through k_4 of Table II are substantially slower than the diffusion-limited constants for the ionization of normal or classical acids such as carboxylic, phenolic, and nitrogen acids (8, 9). The ionization kinetics generated in this work will be used to determine whether, in fact, the nonclassical phase-transport behavior of phenylbutazone (1–7) can be traced to this relatively slow ionization rate.

REFERENCES

(1) E. G. Lovering and D. B. Black, *J. Pharm. Sci.*, **63**, 671(1974).

(2) *Ibid.*, **63**, 1399(1974).

(3) A. Brodin and A. Agren, *Acta Pharm. Suec.*, **8**, 609(1971).

(4) A. Brodin and M. Nilsson, *ibid.*, **10**, 187(1973).

(5) A. Brodin, *ibid.*, **11**, 141(1974).

(6) *Ibid.*, **12**, 41(1975).

(7) V. Stella, *J. Pharm. Sci.*, **64**, 706(1975).

(8) M. L. Bender, "Mechanisms of Homogeneous Catalysis from Protons to Proteins," Wiley–Interscience, New York, N.Y., 1971, chap. 2.

(9) M. Eigen, *Angew. Chem. Int. Ed.*, **3**, 1(1964).

(10) J. R. Jones, *Prog. Phys. Org. Chem.*, **9**, 241(1972).

(11) T. Riley and F. A. Long, *J. Am. Chem. Soc.*, **84**, 522(1962).

(12) R. F. Pratt and T. P. Bruice, *J. Org. Chem.*, **37**, 3563(1972).

(13) F. G. Bordwell and W. J. Boyle, Jr., *J. Am. Chem. Soc.*, **97**, 3447(1975).

(14) *Ibid.*, **93**, 512(1971).

(15) F. G. Bordwell, W. J. Boyle, Jr., J. A. Hautala, and K. C. Yee, *J. Am. Chem. Soc.*, **91**, 4002(1969).

(16) F. G. Bordwell, W. J. Boyle, Jr., and K. C. Yee, *ibid.*, **92**, 5926(1970).

(17) F. G. Bordwell and W. J. Boyle, Jr., *ibid.*, **93**, 511(1971).

(18) *Ibid.*, **94**, 3907(1972).

(19) A. Albert and E. P. Serjeant, "Ionization Constants of Acids and Bases," Methuen and Co., London, England, 1962, chap. 4.

(20) Y. Linaberg, O. Neiland, A. Veis, A. N. Latv, and G. Vanag, *Dokl. Akad. SSSR*, **154**, 1385(1964); *Engl. Transl.*, **154**, 184(1964).

(21) F. G. Bordwell, *Acc. Chem. Res.*, **3**, 281(1970).

(22) D. D. Perrin, "Dissociation Constants of Organic Bases in Aqueous Solutions," Butterworths, London, England, 1965, p. 418.

(23) D. S. Kemp, *J. Am. Chem. Soc.*, **90**, 7153(1968).

(24) G. S. Rork and I. H. Pitman, *ibid.*, **96**, 4654(1974).

(25) W. P. Jencks, "Catalysis in Chemistry and Enzymology," McGraw-Hill, New York, N.Y., 1969, chap. 3.

ACKNOWLEDGMENTS AND ADDRESSES

Received August 11, 1975, from the *Department of Pharmaceutical Chemistry, University of Kansas, Lawrence, KS 66045*

Accepted for publication October 8, 1975.

Presented at the Basic Pharmaceutics Section, APhA Academy of Pharmaceutical Sciences, San Francisco meeting, April 1975.

Supported by University of Kansas General Research Funds and a HSAA award to V. Stella. Supported in part by National Institute of Health Grant GM 22 357.

[x] To whom inquiries should be directed.

Kinetic Analysis of Penicillin Degradation in Acidic Media

JEAN M. BLAHA*[¶], ADELBERT M. KNEVEL[‡], DAVID P. KESSLER[§], JEROME W. MINCY*, and STANLEY L. HEM*[x]

Abstract □ Degradation of penicillin in acidic media (pH 2.7) was monitored by high-pressure liquid chromatography and UV spectroscopy. The effects of temperature, buffer concentration, and ionic strength were examined. A degradation pathway is proposed, and the apparent first-order rate constant and energy of activation were calculated for each reaction. One or more degradation products containing a sulfhydryl group, a functional group often suggested as having a major role in eliciting allergic responses to penicillin therapy, were present throughout the degradation scheme.

Keyphrases ◻ Penicillin—degradation in acidic media, kinetic analysis, monitored by high-pressure liquid chromatography and UV spectroscopy, effect of temperature, buffer concentration, and ionic strength ◻ Degradation—penicillin in acidic media, kinetic analysis, monitored by high-pressure liquid chromatography and UV spectroscopy, effect of temperature, buffer concentration, and ionic strength □ High-pressure liquid chromatography—used to monitor degradation of penicillin in acidic media, kinetic analysis □ UV spectroscopy—used to monitor degradation of penicillin in acidic media, kinetic analysis □ Antibacterial agents—penicillin, degradation in acidic media, kinetic analysis

It is estimated that between 1 and 10% of the population experiences allergic response after penicillin therapy, with 300 fatalities in the United States each year (1). Research on penicillin allergy has considered four factors which may be of importance: (*a*) direct reactions of the drug with protein *in vivo*, (*b*) degradation products of penicillin that can react with protein, (*c*) impurities other than degradation products that may be in the dosage form with penicillin, and (*d*) metabolites of penicillin that can react with protein (2).

One approach to the problem of penicillin allergy would be to determine the role of specific penicillin degradation products in producing an allergic response and, through dosage form design, to minimize the formation of degradation products showing significant potential as allergenic determinants. To use this approach, the time sequence for the presence of penicillin degradation products in aqueous media needs to be established.

Several reviews (2, 3) suggested schemes for the degradation of penicillin. It was proposed that penillic and penicilloic acids are the major degradation products when penicillin is aged in acidic solutions (4). The mechanism of penicillin degradation was studied in acidic solution, and it was proposed that penicillenic acid forms from the reaction of the penicillin ion with a proton or from the spontaneous rearrangement of undissociated penicillin (5). It was suggested also that penillic acid forms from penicillenic acid and that penilloic acid is the product from the acid catalysis of

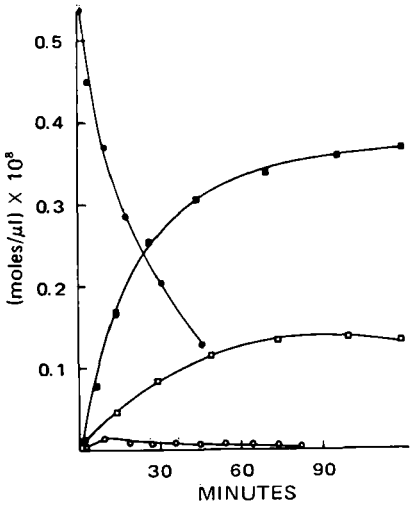

Figure 1—*Occurrence of penicillin G potassium degradation products at pH 2.70 (Condition I). Key: ●, penicillin G potassium; ○, benzylpenicillenic acid; □, benzylpenamaldic acid; and ■, benzylpenillic acid.*

undissociated penicillin, with penicilloic acid as the intermediate (5). Other investigators hypothesized the presence of an oxazolone–thiazolidine intermediate in the formation of penicillenic acid (6) or the formation of penicillamine and penaldic acid (7) as degradation pathways for penicillin in acidic media.

Because of its high reactivity and its suggested role in penicillin allergy, added attention has been given to the fate of benzylpenicillenic acid after it forms in aqueous solution. It was speculated that four reaction products could form from benzylpenicillenic acid, and their theoretical yields if penicillenic acid was aged at pH 0.5–14 were calculated (8). The investigators concluded that only penillic and penamaldic acids were formed at pH 2.0 and 2.9, with no indication of penicilloic acid being present in the solution.

The objective of this study was to use a combination of high-pressure liquid chromatography (HPLC) and UV spectroscopy to identify and quantify the degradation products that form during the aging of penicillin in acid media (pH 2.70). These data permitted the development of a pathway for the acidic degradation of penicillin. By using the scheme, the rate constant and the energy of activation of each degradation product were calculated. The presence of degradation products

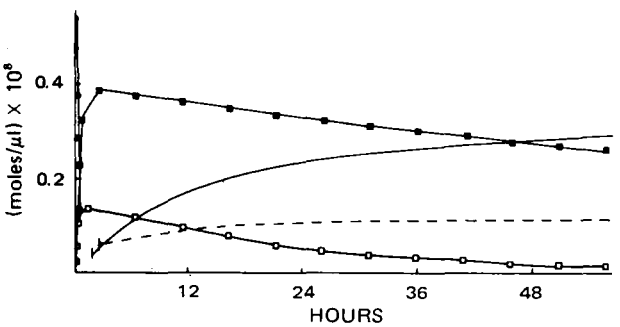

Figure 2—*Occurrence of penicillin G potassium degradation products at pH 2.70 (Condition I). Key: -●-, penicillin G potassium; -□-, benzylpenamaldic acid; -■-, benzylpenillic acid; —, benzylpenilloic acid; and – –, penicillamine.*

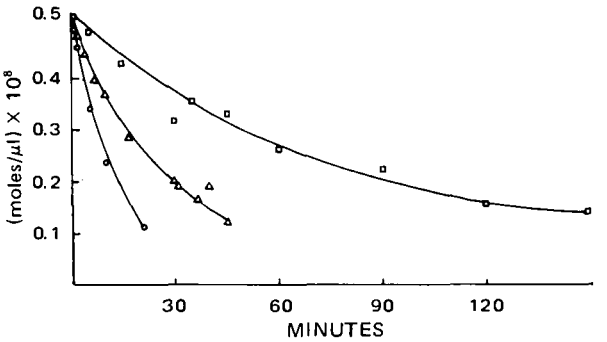

Figure 3—*Loss of penicillin G potassium with time at pH 2.70. Key: ○, 45°; △, 37°; and □, 25°.*

that could be responsible for eliciting an allergic response is especially noted.

EXPERIMENTAL

Materials—All chemicals used were official or reagent grade. Penicillin G potassium[1], benzylpenicillenic acid, and penicillamine[2] were obtained commercially.

Benzylpenillic acid, benzylpenilloic acid, and benzylpenicilloic acid were synthesized by standard methods (9–11). Their identities were confirmed using combinations of UV spectroscopy, IR spectroscopy, mass spectrometry, NMR spectroscopy, potentiometric titration, and elemental analysis.

Benzylpenamaldic acid was obtained using HPLC. Penicillin G potassium (0.05 *M*) was dissolved in 0.03 *M* citric acid–0.0067 *M* disodium phosphate buffer, pH 2.70, and aged at 37° for 2 hr. Ten-microliter samples were withdrawn and injected onto an anion-exchange[3] column in a high-pressure liquid chromatograph[4]. The compounds were eluted with a mobile phase of 15.4 ml of 0.1 *M* citric acid and 7.0 ml of 0.2 *M* disodium phosphate diluted to 650 ml with double-distilled water. The fraction of eluant containing the compound with a retention time of 13 min was collected immediately after it had passed through a refractive index detector and was then lyophilized[5].

Instrumentation—The liquid chromatograph was equipped with a UV detector operating at 254 nm. The refractive index detector was double beamed, referenced against a cell filled with mobile phase.

The stationary phase was an anion-exchange resin prepacked into a pair of coupled 0.61-m stainless steel columns, 2.3 mm i.d. The mobile phase was 15.4 ml of 0.1 *M* citric acid and 7.0 ml of 0.2 *M* disodium phosphate diluted to 650 ml with double-distilled water, giving a 0.0045 *M* buffer solution at pH 3.80.

All injections were made on-stream with a 25-μl high-pressure syringe[6].

Operating parameters for the instrument were as follows: flow rate, 0.7 ml/min (pressure 1000–1200 psi); temperature, ambient; and UV attenuation, 0.04 absorbance unit full scale, except for the assay of benzylpenillic acid which was at 0.08 unit full scale.

An analog computer was used to fit the data to potential degradation schemes. A digital computer was used to confirm the scheme selected and to perform statistical analysis.

Assay Methods—Benzylpenicillenic acid was determined by measuring the UV absorbance[7] of the aqueous solutions at 322 nm (12). By using ϵ max of 31,500 (13) and Beer's law, the molar concentration of penicillenic acid was calculated.

Penicillin, benzylpenillic acid, benzylpenamaldic acid, benzylpenilloic acid, and penicillamine were monitored using HPLC (14). Linear calibration curves were obtained for each compound, and their equations were used to convert UV peak areas into solution concentrations.

[1] Chas. Pfizer and Co., New York, N.Y.
[2] Sigma Chemical Co., St. Louis, Mo.
[3] Bondapak AX/Corasil, Waters Associates, Framingham, Mass.
[4] Model ALC 202, Waters Associates, Framingham, Mass.
[5] Model USM-15, Virtis Co., Gardiner, N.Y.
[6] Series B-110 Pressure-LOK liquid syringe, Precision Sampling Corp., Baton Rouge, La.
[7] Cary model 17 spectrophotometer, Cary Instruments, Monrovia, Calif.

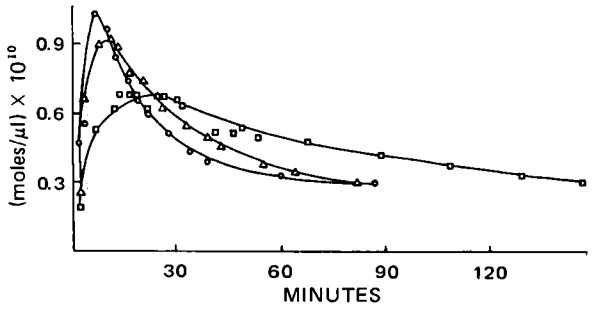

Figure 4—*Kinetic behavior of benzylpenicillenic acid at pH 2.70. Key:* O, *45°;* Δ, *37°; and* □, *25°.*

Kinetic Studies—*Condition I*—The solvent was a 0.03 *M* citric acid–0.0067 *M* disodium phosphate buffer, pH 2.70 and ionic strength 0.028. The temperature was maintained at 37 ± 0.01° in a constant-temperature water bath[8].

Conditions II and III—All conditions were similar to those described for I, except that the solvent temperatures were 25 and 45°, respectively.

Condition IV—Sodium chloride was added to the solvent described for I, 0.977 g/100 ml, to adjust the ionic strength to 0.195.

Condition V—The solvent was a 0.11 *M* buffer at pH 2.7, prepared from 90 ml of 0.1 *M* citric acid and 10 ml of 0.2 *M* disodium phosphate. The ionic strength was adjusted to 0.195 by adding sodium chloride, 0.649 g/100 ml. The temperature of the solvent was maintained at 37°.

Penicillin G potassium, 2 mg/ml, was added to the described solvents. Injections of the aging solutions, ranging in size from 4 to 15 μl, were made into the HPLC system. The UV absorbance of each solution at 322 nm was also monitored for the initial 2.5 hr.

RESULTS AND DISCUSSION

Monitoring Penicillin Solutions—Five degradation products were detected and quantified in penicillin solutions aged at pH 2.70. The results at 37° are presented in Figs. 1 and 2. After 45 min, penicillin was no longer present in amounts detectable by the HPLC system. Benzylpenicillenic acid reached its point of maximum concentration in solution at 10 min. At 2 hr, benzylpenillic acid and benzylpenamaldic acid were the only two degradation products detected.

Benzylpenilloic acid and penicillamine were detected after 4 hr. Four degradation products, benzylpenillic acid, benzylpenamaldic acid, benzylpenilloic acid, and penicillamine, were still present after 48 hr.

Benzylpenicilloic acid (retention time of 19.5 min) was not detected in the reaction mixture, as anticipated (4). It is believed that the five degradation products detected represent the compounds that form

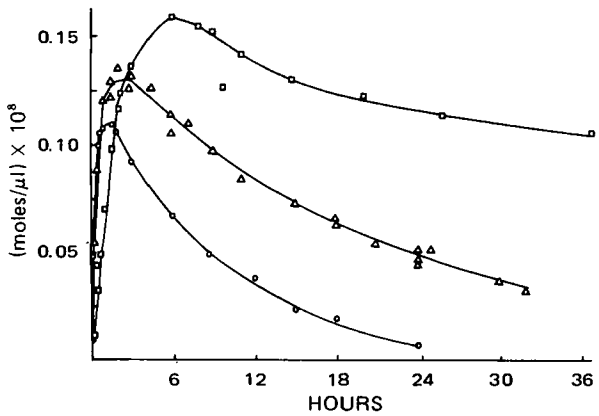

Figure 5—*Kinetic behavior of benzylpenamaldic acid at pH 2.70. Key:* O, *45°;* Δ, *37°; and* □, *25°.*

[8] Model ST Sargent-Welch Thermonitor, Sargent-Welch Scientific Co., Skokie, Ill.

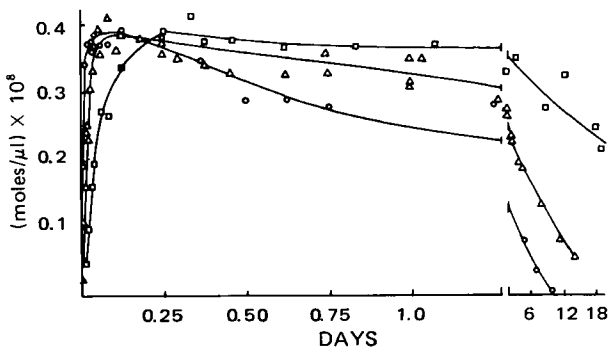

Figure 6—*Kinetic behavior of benzylpenillic acid at pH 2.70. Key:* O, *45°;* Δ, *37°; and* □, *25°.*

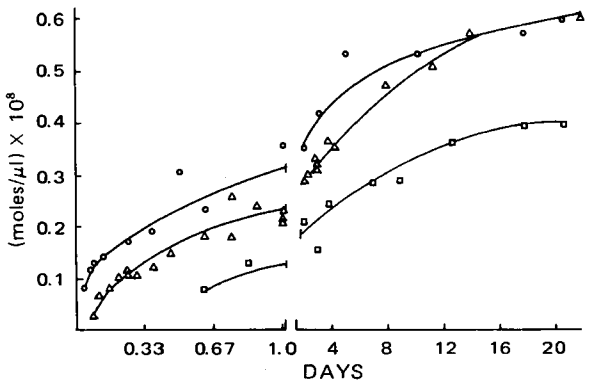

Figure 7—*Kinetic behavior of benzylpenilloic acid at pH 2.70. Key:* O, *45°;* Δ, *37°; and* □, *25°.*

in significant amounts, since the average mass balance during the first 12 hr was 101.8% of theory with a range of 96–108% of theory.

Increased temperature accelerated the rate of degradation of penicillin (Fig. 3). The rates of formation and loss of benzylpenicillenic acid (Fig. 4), benzylpenamaldic acid (Fig. 5), and benzylpenillic acid (Fig. 6) were also directly related to temperature. Benzylpenilloic acid appeared most rapidly in solutions aged at 45° (Fig. 7). No difference in the number or identity of the compounds formed was seen at the temperatures studied.

The rate of degradation of penicillin was directly related to buffer concentration. This relationship is seen by comparing the degradation profiles at Conditions IV (37°, 0.0367 *M* buffer, 0.195 ionic strength) and V (37°, 0.110 *M* buffer, 0.195 ionic strength). The increased buffer concentration increased the rate of penicillin degradation (Fig. 8). Figure 9 shows that there was a small increase in both the rates of formation and loss of benzylpenicillenic acid when the buffer concentration was increased. A similar effect was noted for benzylpenamaldic acid (Fig. 10) and benzylpenillic acid (Fig. 11). As with temperature, there was no change in the number or identity of degradation products due to the buffer effect.

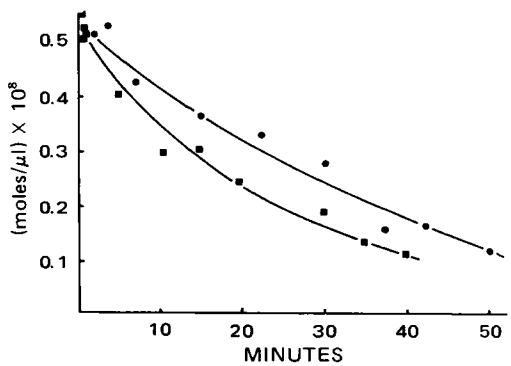

Figure 8—*Loss of penicillin with time at pH 2.70 and 37°. Key:* ●, *0.0367* M *buffer; and* ■, *0.11* M *buffer.*

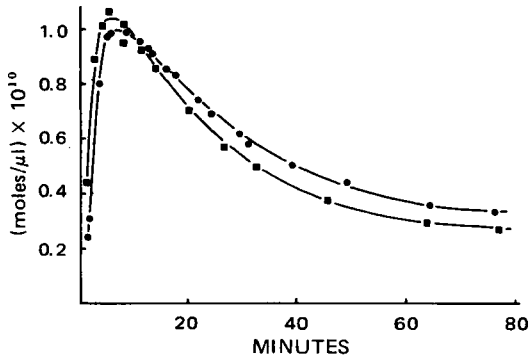

Figure 9—*Kinetic behavior of benzylpenicillenic acid at pH 2.70 and 37°. Key: ●, 0.0367 M buffer; and ■, 0.11 M buffer.*

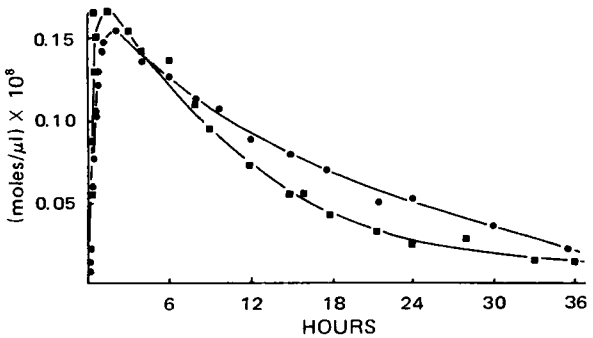

Figure 10—*Kinetic behavior of benzylpenamaldic acid at pH 2.70 and 37°. Key: ●, 0.0367 M buffer; and ■, 0.11 M buffer.*

The catalytic effect of the buffer was not unexpected; at pH 2.7, the citric acid in the buffer is present as dihydrogen citrate anion, which is known to have a catalytic effect on the degradation of penicillin in aqueous solution (15, 16).

The effect of ionic strength on the degradation of penicillin was examined by comparing the degradation profiles at Conditions I (37°, 0.0367 *M* buffer, 0.028 ionic strength) and IV (37°, 0.0367 *M* buffer, 0.195 ionic strength). The increase in ionic strength had no significant effect on the degradation of penicillin at pH 2.7, as illustrated by benzylpenicillenic acid (Fig. 12) and benzylpenamaldic acid (Fig. 13). There was also no change in the number or identity of the compounds formed in the 3-week aging period of the solutions.

Proposed Degradation Scheme—Based on the order of appearance and peak times for the degradation products (Figs. 1 and 2), it appears that benzylpenicillenic acid forms from penicillin. Benzylpenamaldic acid (peak at 1.5 hr) and benzylpenillic acid (peak at 2 hr) appear to form next. The final products are penicillamine and benzylpenilloic acid, which were still increasing after 92 hr at 37°.

To establish the role of benzylpenicillenic acid in the scheme, the decomposition of benzylpenicillenic acid in 0.0367 *M* buffer, pH 2.70, was monitored by HPLC. Ten milligrams of benzylpenicillenic acid was dissolved in 1 ml of absolute methanol and diluted to 5 ml with

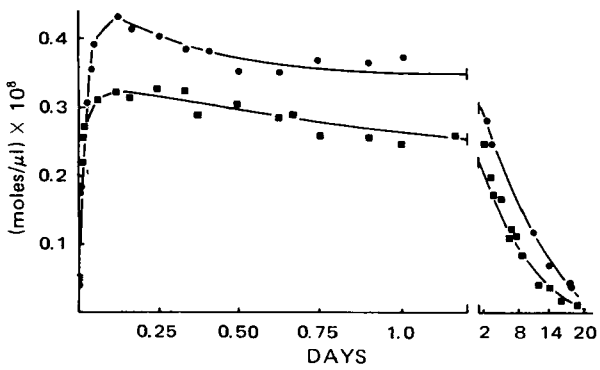

Figure 11—*Kinetic behavior of benzylpenillic acid at pH 2.70 and 37°. Key: ●, 0.0367 M buffer; and ■, 0.11 M buffer.*

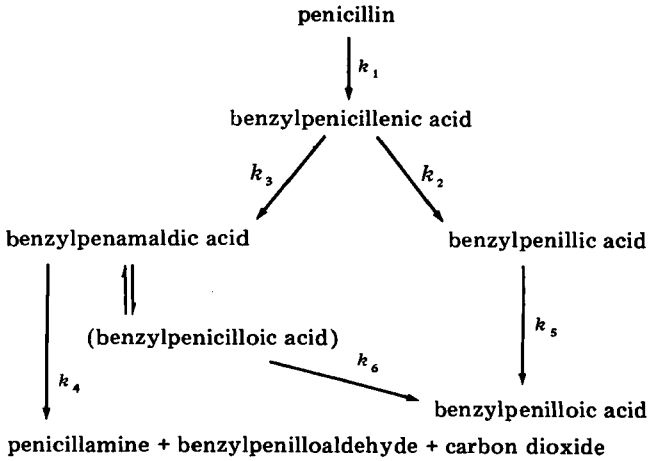

Scheme I—Proposed degradation pathway for penicillin in acidic media

pH 2.7 buffer. The solution was aged at 25° and monitored by HPLC at 0, 37, 90, 130, and 200 min. A peak with a retention time corresponding to benzylpenamaldic acid was seen to increase in height from the 0- to the 37-min sample and then decrease at 90, 130, and 200 min. A peak with a retention time equal to benzylpenillic acid followed the same pattern. Peaks corresponding to penicillamine and benzylpenilloic acid steadily increased during the 190-min sampling period.

Based on this observation of the degradation of benzylpenicillenic acid and Longridge and Timms' (8) study of the hydrolysis of benzylpenicillenic acid in which they found both benzylpenamaldic acid and benzylpenillic acid in benzylpenicillenic acid solutions aged at pH 2.9, the sequence illustrated in Scheme I is proposed for the degradation of penicillin in acidic aqueous media.

Benzylpenicilloic acid was not detected in the study, but it is known to exist in equilibrium with benzylpenamaldic acid (3) and it is probably quickly decarboxylated to produce benzylpenilloic acid. Benzylpenilloaldehyde and penicillamine form upon the degradation of benzylpenamaldic acid. Benzylpenilloaldehyde was probably not

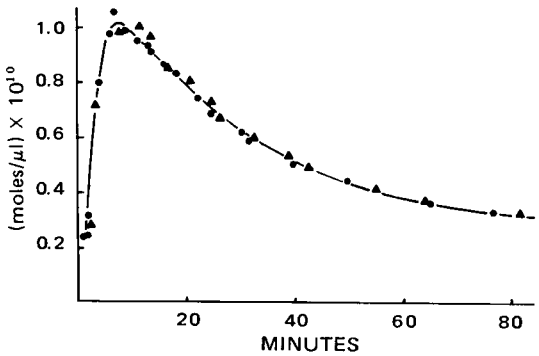

Figure 12—*Kinetic behavior of benzylpenicillenic acid at pH 2.70 and 37°. Key: ▲, 0.028 ionic strength; and ●, 0.195 ionic strength.*

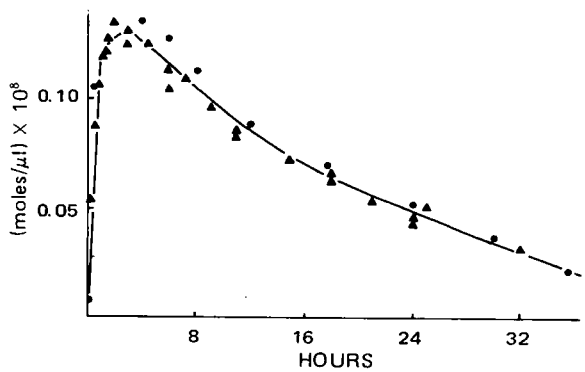

Figure 13—*Kinetic behavior of benzylpenamaldic acid at pH 2.70 and 37°. Key: ▲, 0.028 ionic strength; and ●, 0.195 ionic strength.*

Table I—Apparent First-Order Rate Constants and Energy of Activation

Constant	25°, 0.0367 *M* Buffer	37°, 0.0367 *M* Buffer	37°, 0.11 *M* Buffer	45°, 0.0367 *M* Buffer	E_a, kcal mole^{-1} deg^{-1}	R^2 for E_a
k_1, min^{-1}	9.0×10^{-3}	3.1×10^{-2}	3.7×10^{-2}	7.9×10^{-2}	20.3	0.998
k_2, min^{-1}	2.5×10^{-1}	5.0×10^{-1}	7.0×10^{-1}	1.0	12.8	0.992
k_3, min^{-1}	8.0×10^{-2}	2.0×10^{-1}	4.0×10^{-1}	3.3×10^{-1}	13.2	0.999
k_4, min^{-1}	3.8×10^{-5}	2.3×10^{-4}	3.5×10^{-4}	6.4×10^{-4}	26.8	0.999
k_5, min^{-1}	4.9×10^{-5}	1.2×10^{-4}	2.0×10^{-4}	2.1×10^{-4}	13.8	0.999
k_6, min^{-1}	1.8×10^{-4}	5.0×10^{-4}	8.5×10^{-4}	8.1×10^{-4}	14.6	0.996

Table II—Mean Square Relative Deviations

Conditions	Penicillin	Benzylpenicillenic Acid	Benzylpenillic Acid	Benzylpenamaldic Acid	Penicillamine	Benzylpenilloic Acid
25°, 0.0367 *M* buffer	0.13 (8)[a]	0.17 (7)	6.2 (21)	348.7 (20)	—	1875 (8)
37°, 0.0367 *M* buffer	0.005 (10)	0.25 (7)	0.68 (24)	0.25 (24)	2.42 (10)	0.85 (13)
37°, 0.11 *M* buffer	0.002 (9)	0.21 (7)	0.43 (24)	0.25 (23)	—	1.59 (15)
45°, 0.0367 *M* buffer	0.011 (5)	0.04 (6)	6.5 (20)	0.17 (14)	—	0.19 (15)

[a] Parenthetical values denote the number of experimental points.

separated from the solvent and, therefore, was not detected by the HPLC system. It is included in Scheme I.

Benzylpenicillenic acid, benzylpenamaldic acid, and penicillamine each contain a free sulfhydryl group which is the functional group often suggested as having a major role in eliciting allergic responses to penicillin therapy. One or more of these free sulfhydryl-containing compounds are present during the entire degradation scheme.

Kinetics—The apparent first-order rate constants k_1, k_2, and k_3 were initially determined by fitting the data by eye to the proposed reaction sequence using an analog computer. Figure 14 shows the fit obtained at 37° and is typical of results at other conditions.

The apparent first-order rate constant k_5 was determined by plotting the logarithm of benzylpenillic acid concentration *versus* time and assuming that the exponential term in k_5 dominated during an observed linear region of the semilogarithmic plot. This assumption was shown to be true by the analytical solution.

Similar treatment of a graph of the logarithm of benzylpenamaldic acid concentration *versus* time yielded $k_4 + k_6$. A graph of the logarithm of the concentration of benzylpenilloic acid *versus* time produced $k_5 + k_6$. Since k_5 was known from the direct data on the degradation of benzylpenillic acid, it was possible to determine k_6 and, hence, k_4. In all cases, the assumption that the term of interest dominated during the linear portion of the graphs was confirmed by the analytical solution.

The apparent first-order rate constants and the energy of activation for each reaction are given in Table I. The square of the correlation coefficient (R^2) approaches 1 for each energy of activation. Minimal literature values are available for comparison. However, the energy of activation for the hydrolysis of penicillin agrees well with Brodersen (3), and the sum of k_2 and k_3 at 25° agrees with Longridge and Timms' (8) rate constant for the hydrolysis of benzylpenicillenic acid.

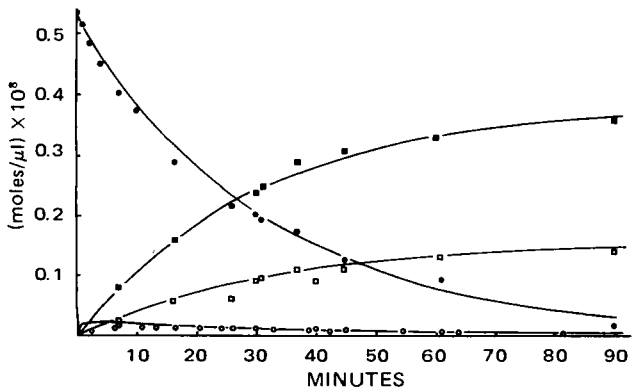

Figure 14—*Analog fit of penicillin degradation at pH 2.70 and 37° in 0.0367* M *buffer using Scheme I and rate constants from Table I. Key: ●, penicillin; ○, benzylpenicillenic acid; □, benzylpenamaldic acid; and ■, benzylpenillic acid.*

The system of equations describing the proposed scheme was integrated analytically, and the solution was programmed for a digital computer. No single criterion can be used to determine the best set of values for the reaction rate constants. The best set of values will depend, among other things, on the use to which the information will be put. For example, if one compound is known to cause the allergic response and normal storage is at one temperature, one would wish to fit the data to minimize deviations for that compound at the storage temperature. If two or more compounds are important, one would wish to fit each compound in a best sense. Similarly, if two or more temperatures are involved, one would fit one or more compounds over the pertinent range. Finally, one must decide whether relative or absolute deviations are more important.

Since so many possible criteria for a best fit exist, no attempt was made to optimize the fit by any of the criteria. Instead, a reasonable fit was obtained. The mean square relative deviations (relative deviation equals observed value minus predicted value divided by predicted value) are shown in Table II. Penicillamine was only monitored at 37°, 0.0367 *M* buffer. As can be noted from Table II, an appreciable mean square relative deviation only occurred for the later appearing compounds at 25°. At the lower temperature, these compounds only appeared in small concentrations, so a small absolute deviation resulted in a large relative deviation. The proposed degradation scheme and rate constants accurately describe the observed degradation of penicillin G potassium at pH 2.70.

REFERENCES

(1) J. P. McGovern, C. E. Roberson, and G. T. Stewart, in "Penicillin Allergy," G. T. Stewart and J. P. McGovern, Eds., Charles C Thomas, Springfield, Ill., 1970, chap. 1.

(2) M. A. Schwartz, *J. Pharm. Sci.*, **58**, 643(1969).

(3) J. P. Hou and J. W. Poole, *ibid.*, **60**, 503(1971).

(4) D. W. Dennen and W. W. Davis, *Antimicrob. Ag. Chemother.*, **1961**, 531.

(5) M. A. Schwartz, *J. Pharm. Sci.*, **54**, 472(1965).

(6) H. Bundgaard, *ibid.*, **60**, 1273(1971).

(7) P. P. Regna, in "Antibiotics, Their Chemistry and Non-Medical Uses," H. S. Goldberg, Ed., Van Nostrand, Princeton, N.J., 1959, p. 61.

(8) J. L. Longridge and D. Timms, *J. Chem. Soc. B*, **1971**, 852.

(9) A. H. Cook, in "The Chemistry of Penicillin," H. T. Clarke, J. R. Johnson, and B. Robinson, Eds., Princeton University Press, Princeton, N.J., 1949, chap. 6.

(10) R. Mozingo and K. Folkers, *ibid.*, chap. 8.
(11) H. W. Florey, E. Chain, N. G. Heatley, M. A. Jennings, A. G. Sanders, E. P. Abraham, and M. E. Florey, "Antibiotics," vol. II, Oxford University Press, London, England, 1949, pp. 839–870.
(12) B. B. Levine, *Arch. Biochem. Biophys.*, **93**, 50(1961).
(13) K. H. Dudley, T. C. Butler, and D. Johnson, *J. Pharmacol. Exp. Ther.*, **179**, 505(1971).
(14) J. M. Blaha, A. M. Knevel, and S. L. Hem, *J. Pharm. Sci.*, **64**, 1384(1975).
(15) P. Finholt, G. Jurgensen, and H. Kristiansen, *ibid.*, **54**, 387(1965).
(16) R. E. Lindsay and S. L. Hem, *ibid.*, **61**, 202(1972).

ACKNOWLEDGMENTS AND ADDRESSES

Received July 5, 1974, from the *Department of Industrial and Physical Pharmacy and the ‡Department of Medicinal Chemistry and Pharmacognosy, School of Pharmacy and Pharmacal Sciences, and the §School of Chemical Engineering, Purdue University, West Lafayette, IN 47907

Accepted for publication October 9, 1975.

Abstracted from a dissertation submitted by J. M. Blaha to the Graduate School, Purdue University, in partial fulfillment of the Doctor of Philosophy degree requirements.

Supported in part by a National Defense Educational Act Fellowship and an American Foundation for Pharmaceutical Education Fellowship (J. M. Blaha).

The authors are grateful to Pfizer, Inc., for generously providing penicillin G potassium.

¶Present address: Squibb Institute for Medical Research, New Brunswick, N.J.

xTo whom inquiries should be directed.

Effect of Intragranular and Extragranular Disintegrating Agents on Particle Size of Disintegrated Tablets

E. SHOTTON x and G. S. LEONARD *

Abstract □ Five materials were compared for their effectiveness as disintegrating agents: maize starch, sodium calcium alginate, alginic acid, microcrystalline cellulose, and a colloidal aluminum silicate. The effect of the proportion of the agent present and the position with respect to the granule, intra- and extragranular, was examined. The extragranular formulations disintegrated much more rapidly than the intragranular ones, but the latter gave a much finer dispersion of particles. A combination of intra- and extragranular disintegrating agents gave the best compromise; of those tested, the alginates appeared to effect the breakdown to the smallest particles when placed intragranularly. A method of assessing the effectiveness of disintegrating agents for uncoated tablets is suggested, but the resulting weight mean particle size is the more important criterion for tablets complying with a pharmacopoeial disintegration test. The porosity and crushing strength of tablets are useful as guides to disintegration only when a given formulation is used.

Keyphrases □ Disintegrating agents—intra- and extragranular, effect on particle size of disintegrated tablets □ Particle size—disintegrated tablets, effect of intra- and extragranular disintegrating agents □ Tablets—effect of intra- and extragranular disintegrating agents on particle size □ Dosage forms—tablets, effect of intra- and extragranular disintegrating agents on particle size

The disintegration test described in the British Pharmacopoeia ensures that the tablet will break down to pass a 1.70-mm sieve aperture. This size is larger than the granule size used for most tablets and has been criticized (1). A few attempts have been made to assess the particle sizes formed on disintegration.

A nest of three sieves with apertures of 0.81, 0.54, and 0.27 mm was used in the USP disintegration test apparatus instead of the tube described (2). An automated particle counter[1] was used to determine particle-size frequencies for tablets prepared from aspirin and starch mixtures (3). Sandell (4) used a method similar to that of Sanders (2), but the sieves had apertures of 0.1, 0.5, and 2.0 mm.

Previous work on the sizing of the disintegrant has been reviewed (5). To obtain rapid dissolution, disintegration should release drug as near as possible to its original particle size.

EXPERIMENTAL

Materials—Sulfadiazine BP was used as the active drug. The solubility was determined as 14.4 mg in 100 ml of water at 37°, and the density was 1.505 g/ml at 21°.

The size distribution of the sulfadiazine powder was determined using an automated particle counter[1] with 0.9% (w/v) solution of sodium chloride saturated with sulfadiazine as the electrolyte. The average mean weight diameter was approximately 9 μm (6).

The following disintegrating agents were used: maize starch BP, microcrystalline cellulose[2], sodium calcium alginate[3], alginic acid, and a synthetic colloidal aluminum silicate[4]. Povidone was used as a binder to form the granules.

Preparation—Wet granulation was accomplished by moistening sulfadiazine with a sufficient quantity of 10% povidone solution to give a final content of 3% (w/w) followed by additional distilled water. The moistened mass was pushed through a granulator[5], the granules were then dried, and a sieve fraction of 355–500-μm particles was used. Extragranular agents were added to the dried granules.

Intragranular disintegrating agents were mixed with the sulfadiazine powder before granulating with the povidone solution.

Granulation by precompression was used only for the sodium calcium alginate, since this method was recommended by the suppliers. One gram of the mixed powders was compressed in a 15.35-mm diameter die to form a weak tablet. Such tablets were then broken to form granules, and a 355–500-μm fraction was selected. Before precompression, povidone powder (3%) was incorporated in one batch of powder but not in a second batch. The tablets produced from these granules were thus comparable with the intragranular tablets containing sodium calcium alginate from the wet granulation method.

The proportions of these agents are shown in Table I.

[1] Coulter.
[2] Avicel PH.
[3] Alginate F417, Alginate Industries Ltd.
[4] Laponite CP, Laporte Industries Ltd.
[5] Erweka F.A.G.

(10) R. Mozingo and K. Folkers, *ibid.*, chap. 8.
(11) H. W. Florey, E. Chain, N. G. Heatley, M. A. Jennings, A. G. Sanders, E. P. Abraham, and M. E. Florey, "Antibiotics," vol. II, Oxford University Press, London, England, 1949, pp. 839–870.
(12) B. B. Levine, *Arch. Biochem. Biophys.*, **93**, 50(1961).
(13) K. H. Dudley, T. C. Butler, and D. Johnson, *J. Pharmacol. Exp. Ther.*, **179**, 505(1971).
(14) J. M. Blaha, A. M. Knevel, and S. L. Hem, *J. Pharm. Sci.*, **64**, 1384(1975).
(15) P. Finholt, G. Jurgensen, and H. Kristiansen, *ibid.*, **54**, 387(1965).
(16) R. E. Lindsay and S. L. Hem, *ibid.*, **61**, 202(1972).

ACKNOWLEDGMENTS AND ADDRESSES

Received July 5, 1974, from the *Department of Industrial and Physical Pharmacy and the ‡Department of Medicinal Chemistry and Pharmacognosy, School of Pharmacy and Pharmacal Sciences, and the §School of Chemical Engineering, Purdue University, West Lafayette, IN 47907

Accepted for publication October 9, 1975.

Abstracted from a dissertation submitted by J. M. Blaha to the Graduate School, Purdue University, in partial fulfillment of the Doctor of Philosophy degree requirements.

Supported in part by a National Defense Educational Act Fellowship and an American Foundation for Pharmaceutical Education Fellowship (J. M. Blaha).

The authors are grateful to Pfizer, Inc., for generously providing penicillin G potassium.

¶Present address: Squibb Institute for Medical Research, New Brunswick, N.J.

xTo whom inquiries should be directed.

Effect of Intragranular and Extragranular Disintegrating Agents on Particle Size of Disintegrated Tablets

E. SHOTTON x and G. S. LEONARD *

Abstract □ Five materials were compared for their effectiveness as disintegrating agents: maize starch, sodium calcium alginate, alginic acid, microcrystalline cellulose, and a colloidal aluminum silicate. The effect of the proportion of the agent present and the position with respect to the granule, intra- and extragranular, was examined. The extragranular formulations disintegrated much more rapidly than the intragranular ones, but the latter gave a much finer dispersion of particles. A combination of intra- and extragranular disintegrating agents gave the best compromise; of those tested, the alginates appeared to effect the breakdown to the smallest particles when placed intragranularly. A method of assessing the effectiveness of disintegrating agents for uncoated tablets is suggested, but the resulting weight mean particle size is the more important criterion for tablets complying with a pharmacopoeial disintegration test. The porosity and crushing strength of tablets are useful as guides to disintegration only when a given formulation is used.

Keyphrases □ Disintegrating agents—intra- and extragranular, effect on particle size of disintegrated tablets □ Particle size—disintegrated tablets, effect of intra- and extragranular disintegrating agents □ Tablets—effect of intra- and extragranular disintegrating agents on particle size □ Dosage forms—tablets, effect of intra- and extragranular disintegrating agents on particle size

The disintegration test described in the British Pharmacopoeia ensures that the tablet will break down to pass a 1.70-mm sieve aperture. This size is larger than the granule size used for most tablets and has been criticized (1). A few attempts have been made to assess the particle sizes formed on disintegration.

A nest of three sieves with apertures of 0.81, 0.54, and 0.27 mm was used in the USP disintegration test apparatus instead of the tube described (2). An automated particle counter[1] was used to determine particle-size frequencies for tablets prepared from aspirin and starch mixtures (3). Sandell (4) used a method similar to that of Sanders (2), but the sieves had apertures of 0.1, 0.5, and 2.0 mm.

Previous work on the sizing of the disintegrant has been reviewed (5). To obtain rapid dissolution, disintegration should release drug as near as possible to its original particle size.

EXPERIMENTAL

Materials—Sulfadiazine BP was used as the active drug. The solubility was determined as 14.4 mg in 100 ml of water at 37°, and the density was 1.505 g/ml at 21°.

The size distribution of the sulfadiazine powder was determined using an automated particle counter[1] with 0.9% (w/v) solution of sodium chloride saturated with sulfadiazine as the electrolyte. The average mean weight diameter was approximately 9 μm (6).

The following disintegrating agents were used: maize starch BP, microcrystalline cellulose[2], sodium calcium alginate[3], alginic acid, and a synthetic colloidal aluminum silicate[4]. Povidone was used as a binder to form the granules.

Preparation—Wet granulation was accomplished by moistening sulfadiazine with a sufficient quantity of 10% povidone solution to give a final content of 3% (w/w) followed by additional distilled water. The moistened mass was pushed through a granulator[5], the granules were then dried, and a sieve fraction of 355–500-μm particles was used. Extragranular agents were added to the dried granules.

Intragranular disintegrating agents were mixed with the sulfadiazine powder before granulating with the povidone solution.

Granulation by precompression was used only for the sodium calcium alginate, since this method was recommended by the suppliers. One gram of the mixed powders was compressed in a 15.35-mm diameter die to form a weak tablet. Such tablets were then broken to form granules, and a 355–500-μm fraction was selected. Before precompression, povidone powder (3%) was incorporated in one batch of powder but not in a second batch. The tablets produced from these granules were thus comparable with the intragranular tablets containing sodium calcium alginate from the wet granulation method.

The proportions of these agents are shown in Table I.

[1] Coulter.
[2] Avicel PH.
[3] Alginate F417, Alginate Industries Ltd.
[4] Laponite CP, Laporte Industries Ltd.
[5] Erweka F.A.G.

Table I—Disintegration Times, Crushing Strengths, and Mean Particle Sizes of the Disintegrated Tablets Made with Five Disintegrating Agents

Disintegrating Agent and Siting	Percentage Disintegrant															
	2.5				5.0				10.0				20.0			
	T_d	S_m	F_c	ϵ	T_d	S_m	F_c	ϵ	T_d	S_m	F_c	ϵ	T_d	S_m	F_c	ϵ
Maize starch:																
Intragranular	2939	540	16.6	16.8	748	372	16.5	16.7	212	46	15.4	17.0	—	—	—	—
Extragranular	736	616	15.8	14.7	106	295	15.0	15.3	30	181	10.7	17.1	—	—	—	—
5% intragranular and 5% extragranular	—	—	—	—	—	—	—	—	79	84	12.8	17.7	—	—	—	—
Microcrystalline cellulose:																
Intragranular	>1 hr	—	18.2	17.1	>1 hr	—	18.4	17.1	2959	322	18.3	17.3	331	182	19.1	17.5
Extragranular	>1 hr	—	18.2	16.7	>1 hr	—	17.7	16.7	2659	425	17.4	17.3	550	428	17.2	17.9
Percent intragranular and percent extragranular		2.5i and 7.5e				5.0i and 5.0e				10.0i and 10.0e				20.0i and 10.0e		
	847	451	17.9	17.5	1952	479	17.7	17.6	184	222	16.8	17.9	98	118	16.3	17.9
Sodium calcium alginate:																
Percent disintegrant		1				2				4				8		
Intragranular SP	>1 hr	—	7.1	15.6	369	745	8.0	16.3	75	478	7.2	15.5	—	—	—	—
Intragranular S	>1 hr	—	8.4	15.1	639	806	7.8	15.3	59	500	8.2	15.1	—	—	—	—
Intragranular	1984	82	18.5	17.2	1754	37	19.7	17.1	1490	26	19.9	16.9	1258	18	19.3	17.5
Extragranular	367	514	16.9	16.3	237	390	17.4	16.1	93	292	15.0	16.4	84	267	14.9	16.8
Alginic acid:																
Intragranular	2034	406	18.6	16.7	635	215	18.3	16.9	243	127	17.6	17.2	156	48	17.2	17.4
Extragranular	2147	516	17.6	16.6	556	336	17.3	16.3	195	255	15.9	16.6	97	253	13.0	17.0
Colloidal aluminum silicate:																
Extragranular	>1 hr	—	19.2	15.9	1242	462	17.4	16.0	151	233	16.5	16.6	57	149	14.7	17.6

[a] All tablets were prepared from granules 355–500 μm in diameter and were compressed at approximately 1000 kg (F_a). Key: i = intragranular, e = extragranular, T_d = disintegration time (seconds), S_m = mean particle-size disintegrated tablet (micrometers), F_c = crushing strength (kilograms), ϵ = porosity expressed as a percent of the tablet volume, S = granulation by precompression without povidone, and SP = granulation by precompression with povidone.

Table II—Tablet Crushing Strengths for Different Maize Starch Formulations[a]

Disintegrating Agent, % and Siting	Mean Applied Compression Force, kg											
	750			1000			1500			1800		
	T_d	F_c	S_m	T_d	F_c	S_m	T_d	F_c	S_m	T_d	F_c	S_m
2.5i	268	13.1	186	2939	16.6	540	>1 hr	21.8	n.d.	>1 hr	23.4	n.d.
5.0i	146	12.6	168	748	16.5	372	>1 hr	21.2	n.d.	>1 hr	23.1	n.d.
10.0i	124	12.5	34	212	15.4	46	4530	21.6	258	>1 hr	22.5	n.d.
2.5e	125	13.2	359	736	15.8	616	>1 hr	21.5	n.d.	>1 hr	24.5	n.d.
5.0e	54	10.1	131	106	15.0	295	2182	20.4	646	>1 hr	22.7	n.d.
10.0e	32	8.2	89	30	10.7	181	79	14.0	310	147	14.9	387
5.0i and 5.0e	69	10.8	53	79	12.8	84	269	18.8	216	695	20.9	316

[a] All tablets were prepared from granules 355–500 μm in diameter. Key: e = extragranular, i = intragranular, n.d. = not done, F_c = tablet crushing strength (kilograms), T_d = disintegration time (seconds), and S_m = mean particle size of the disintegrated tablet (micrometers).

Table III—Disintegration Factors for Some Disintegrating Agents[a]

Disintegrating Agent, % and Siting		Disintegration Factor	Disintegration Time, sec	Mean Particle Size, μm
Starch	10e	161	30	181
Starch	5i and 5e	131	79	84
Alginic acid	8i	117	156	48
Colloidal aluminum silicate	8e	103	57	149
Starch	10i	89	212	46
Microcrystalline cellulose	20i and 10e	75	98	118
Sodium calcium alginate	8e	39	84	267
Sodium calcium alginate	8i	39	1258	18
Alginic acid	8e	36	97	253
Sodium calcium alginate	4e	32	93	292
Sodium calcium alginate	4iS	30	59	500
Alginic acid	4i	28	243	127
Starch	5e	28	106	295
Colloidal aluminum silicate	4e	25	151	233
Sodium calcium alginate	4iSP	24	75	478
Sodium calcium alginate	4i	23	1490	26
Microcrystalline cellulose	10i and 10e	21	184	222
Alginic acid	4e	18	195	255
Microcrystalline cellulose	20i	15	331	182
Microcrystalline cellulose	20e	4	550	322
Starch	5i	3	748	372
Microcrystalline cellulose	10i	0.9	2959	428
Microcrystalline cellulose	10e	0.8	2659	425

[a] All tablets were prepared from granules 355–500 μm and were compressed at approximately 1000 kg. Key: i = intragranular, wet granulation; e = extragranular, wet granulation; S = granulation by precompression without povidone; and SP = granulation by precompression with povidone.

Compression of the granules was carried out on a single-punch, hand-driven tablet machine with both top and bottom punches instrumented with strain gauges. The die wall and punch faces were dusted lightly with magnesium stearate as a lubricant, the excess being wiped away with a paper tissue. A total dry weight of granules of 500 ± 5 mg was hand filled into the die for each compression, and 12 tablets were prepared from each granulation. The flat-faced punches used for the final tablet were 12 mm in diameter, and the machine was driven at a rate equivalent to 20 compression cycles/min.

A series of experiments in which the applied force was kept roughly constant at 1000 kg was carried out using a sieve fraction of the granules with a diameter in the 355–500-μm range.

Tablet Crushing Strength—A diametral crushing strength tester, as described by Shotton and Ganderton (7) and modified by Leonard (8), was used to determine the force applied diametrically to break the tablets. The results given in this report are the mean figures from five tablets.

Disintegration Time—The method described in the British Pharmacopoeia was used; the five tablets were timed individually. The internal diameter of the reservoir tube was 44 mm, and the aqueous medium was 0.9% sodium chloride saturated with sulfadiazine. This medium was chosen to act as the electrolyte in the counter and to prevent dissolution of the sulfadiazine particles. A guided disk was not used.

For very slowly disintegrating tablets, the test was stopped after 1 hr.

Size Analysis of Disintegrated Tablets—The suspensions from three of the five tablets, which had intermediate disintegration times, were passed through a nest of 3.8-cm diameter sieves with the following apertures: 1400, 1000, 710, 500, 355, 250, 180, 125, 90, and 75 μm. The apparatus was described previously (6).

The liquid, with particles less than 75 μm, was collected in a flask, and the particles in a sample of 0.5 ml were sized with an automated particle counter using a 200-μm diameter sampling tube. The wide range of particle sizes imposed limitations on the orifice size of the counting tube that could be used with the counter. In addition, to count the high proportion of particles present below 20 μm would involve considerable dilution. Further stirring and dilution would break down more aggregates above 20 μm. Therefore, in each case, the particles below 20 μm were assumed to be the original sulfadiazine powder with a mean particle size of 9 μm (6). This value was used in calculating the mean size of particles obtained from the disintegrated tablet (Tables I–III) to give comparative values.

Tablet Porosity—The mass, diameter, and thickness of the tablets were measured before subjecting them to further tests, and the porosity was calculated from these values. The volume of the powder used was obtained from the mass and density of each constituent present, and the porosity was the difference between this value and the volume of the tablet. The porosity is expressed as a percentage of the tablet volume.

RESULTS

The porosity of the tablets from all wet granulation formulations was within 17 ± 1%, except for 2.5 and 5.0% extragranular starch which was between 14.5 and 15.5%. Tablets prepared from granules formed by precompression were between 15 and 16.3% porosity (Table I).

The crushing strength, the time taken for the tablets to disintegrate, and the mean particle size of the disintegrated tablets are also given in Table I for disintegrants incorporated both intra- and extragranularly. Table II gives the mean disintegration time, crushing force, and particle size for tablets containing maize starch and compressed at four pressure levels.

Examples of particle-size distributions obtained from disintegrated tablets, from which the mean size was calculated, are given in Fig. 1 for sodium calcium alginate; similar curves for maize starch and the sulfadiazine powder were published previously (6).

DISCUSSION

The disintegration of oral tablets in the GI tract is desired to facilitate the dissolution of the drug and thus its absorption. The effectiveness of a disintegrating agent could be assessed based on the time taken for the wet tablet to break up and on the size of the recovered particles. The size of the disintegrated particles should be compared with the particle size of the original powdered drug. The effect of the proportion of the disintegration agent on the disintegration time is well known, and this work examines the effect of the position, intra- and extragranular, and concentration of the agent upon the particle size of the disintegrated tablets. Previous work (6) showed the effect of 2.5, 5.0, and 10% maize starch upon the disintegration time and the recovered mean particle size of sulfadiazine tablets, and some results are included for comparison with the other disintegrating agents.

A more rapid disintegration of the tablets was found at all concentrations with extragranular agents than with intragranular agents (Fig. 2). This result may be explained by the local concentrations of these substances around the granules. Hydrophilic channels are formed which are rapidly penetrated by water, as shown by placing a drop of dilute iodine solution on the tablet (6). With tablets having intragranular agents, the particles of the agent are isolated and sur-

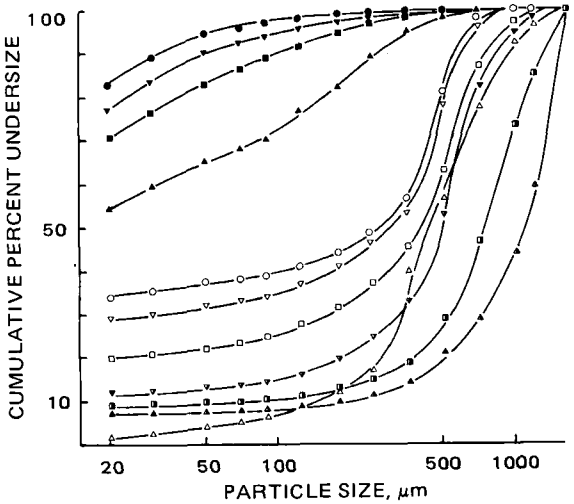

Figure 1—*Effect of formulation and granulation on the particle-size distribution of disintegrated tablets containing sodium calcium alginate. Disintegrating agent was 1% (△), 2% (□), 4% (▽), or 8% (○). Open symbols represent extracellular agents; solid symbols represent intragranular agents by wet granulation; half-open symbols represent intragranular agents by precompression. Granules were 355–500 μm, and applied compression force was 1000 kg.*

rounded by sulfadiazine particles which are not so readily wetted. Thus, although the porosities of comparable formulations are similar (Table I), the disintegration times are very different.

Similar results were obtained at the four compression forces used, as shown in Table II for maize starch as the disintegrating agent. From Fig. 2, the most effective agent would appear to be extragranular maize starch at the greater proportions, with alginic acid, colloidal aluminum silicate, and sodium calcium alginate being slightly less effective. At low concentrations, 1 and 2% sodium calcium alginate was superior to the other agents used.

The crushing force required to break the tablets was affected very little by the concentration of disintegrating agent placed intragranularly. With extragranular agents, however, weaker tablets were formed, which also contributed to the shorter disintegration time.

The disintegration patterns of the two formulation types were

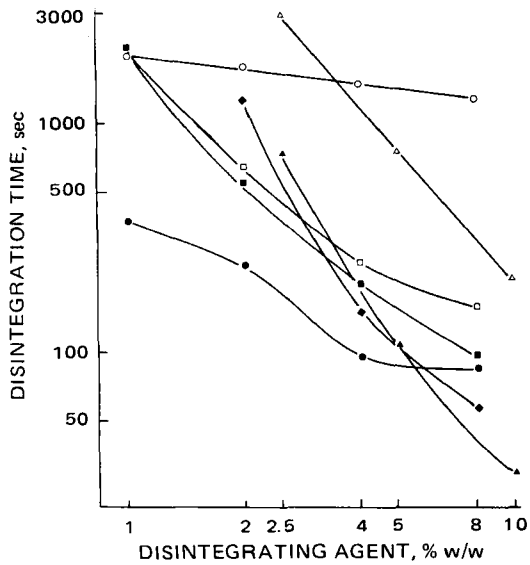

Figure 2—*Effect of concentration of disintegrating agent on tablet disintegration time. Key: ● ○, sodium calcium alginate; ■ □, alginic acid; ♦, colloidal aluminum silicate; and ▲ △, maize starch. Open symbols represent intragranular agents; solid symbols represent extragranular agents. Granules were 355–500 μm, and applied compression force was 1000 kg.*

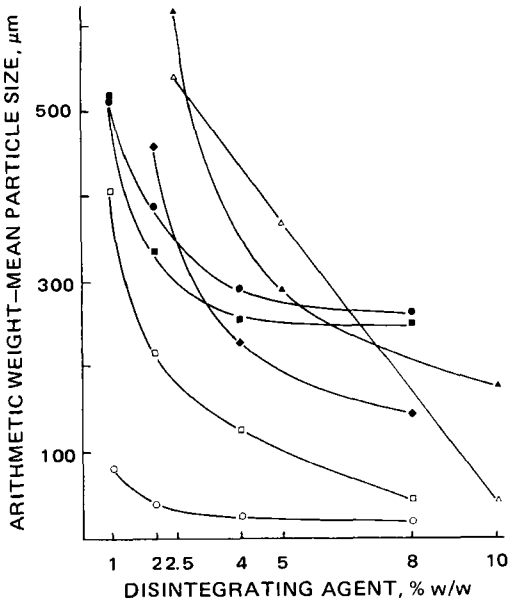

Figure 3—*Effect of concentration on the arithmetic weight-mean particle size of disintegrated tablets. Key: see Fig. 2.*

different in that the extragranular disintegrant caused the tablet to break up rapidly to aggregates, many of which corresponded in size to the original granule. In contrast, the intragranular disintegrant caused erosion of the tablet from the outside since penetration was slow, but the mean aggregate size was much smaller (Table I), with only few aggregates corresponding to the granule size.

Figure 1, concerning sodium calcium alginate, shows that a high proportion of particles and aggregates fell below 20 μm for all intragranular proportions of this agent and that very few were greater than 100 μm. With 4 and 8% of sodium calcium alginate, a mean particle size of 26 and 18 μm, respectively, was obtained so that a high proportion of the sulfadiazine must have been released as original particles. These granules had a mean particle size of about 9 μm and 80% below 20 μm (6).

The effect of the proportion of the agent upon the weight-mean particle size of the disintegrated tablet is shown in Fig. 3. The effectiveness of the intragranular agent compared with the extragranular formulation is clearly indicated. The alginic acid and sodium calcium alginate were much more effective as intragranular agents even at proportions as low as 1 and 2%.

Again, at this compression force, the weight-mean particle size of the intragranular formulations is affected by the proportion of the agent but not by the breaking strength of the tablet or the porosity, which are nearly constant. No allowance for the particle size of the disintegrating agent was made since the sodium calcium alginate, alginic acid, and colloidal aluminum silicate all swell considerably in water to form a gel. Since the maize starch size range was between 5 and 30 μm, correcting for its presence would have increased the weight-mean particle size with all proportions of starch and the comparison with the alginate would have been less favorable. Only comparative values have meaning in this context, because the results are greatly influenced by the compression force and materials being compressed.

The tablets formed from granules prepared by precompression (Table I) gave weaker tablets than those from the wet granulations. These contained intragranular sodium calcium alginate, and the porosity was only a little less than for tablets from wet granulations. Although the disintegration time was greatly reduced, the size of aggregates after disintegration of the tablet was of the same order as the original granules. It may be assumed that the second compression consolidated the granules further so that penetration of water into the granule was resisted.

Microcrystalline cellulose was not very effective, either intra- or extragranularly, and it is used principally as a direct compression diluent (Table I). Its binding properties are good.

When using a mixture of 5% intragranular and 5% extragranular maize starch, intermediate values for disintegration time and weight-mean particle size were obtained.

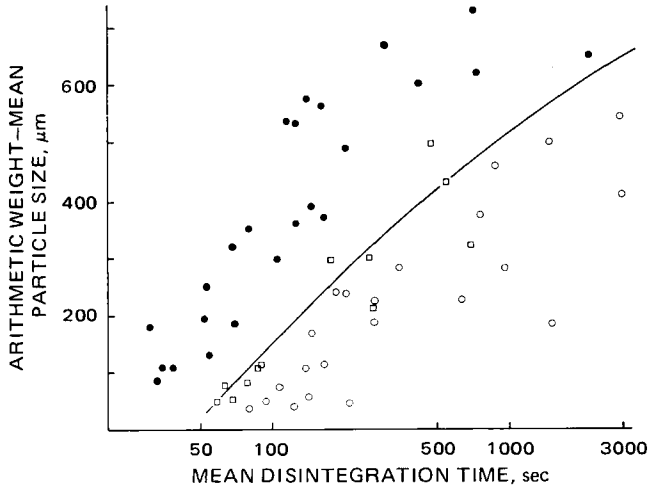

Figure 4—*Relationship between the disintegration time and the mean particle size recovered on disintegration for maize starch formulations. Key: ●, extragranular formulations; ○, intragranular formulations; and □, mixed formulations.*

When all values for mean particle size were plotted against the mean disintegration time for maize starch formulations, Fig. 4 was obtained. This figure shows that, for a given disintegration time, the intragranular agent gave a smaller particle size than the extragranular formulations; the mixed formulations were intermediate. These results do not discriminate between different concentrations of maize starch or the effect of compression pressure. Figure 5 shows a similar plot for alginic acid and sodium calcium alginate.

When comparing disintegrating agents, both the disintegration time and the mean particle size should be considered together. For uncoated tablets, a factor comparing the disintegration time with the official limit for uncoated tablets (15 min in the British Pharmacopoeia) and the particle size of the drug should be useful initially:

$$\text{disintegration factor} = \frac{15\text{ min}}{\text{actual disintegration time}} \times \frac{\text{arithmetic mean size of drug}}{\text{arithmetic mean size from tablet}} \times 100 \quad \text{(Eq. 1)}$$

The larger the factor, the more effective is the disintegrating agent. Examples of values of this factor for the materials examined are shown in Table III together with the approximate disintegration times and the mean particle sizes of disintegrated tablets. By using different ratios of intra- and extragranular agents, or different agents intra- and extragranularly, a tablet with improved properties can be formulated, particularly if sodium calcium alginate or alginic acid is incorporated intragranularly.

For drugs absorbed from the GI tract, the particle size of the disintegrated tablet and the disintegration time are both important for obtaining the desired dissolution characteristics.

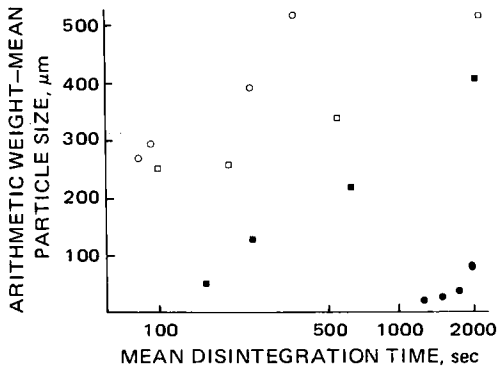

Figure 5—*Disintegration time and mean particle size recovered on disintegration for alginic acid and sodium calcium alginate formulations. Key: ■, intragranular alginic acid; ●, sodium calcium alginate; □, extragranular alginic acid; and ○, sodium calcium alginate.*

REFERENCES

(1) A. D. Nair and V. N. Bhatia, *J. Am. Pharm. Assoc., Sci. Ed.*, **46**, 131(1957).

(2) J. C. Sanders, *Pharm. Weekbl.*, **104**, 485(1969).

(3) M. Van Ootghem, R. Boni, and H. Herbots, *Cesk. Farm.*, **18**, 122(1969).

(4) E. Sandell, *Acta Pharm. Suec.*, **7**, 55(1970).

(5) W. Lowenthal, *J. Pharm. Sci.*, **61**, 1695(1972).

(6) E. Shotton and G. S. Leonard, *J. Pharm. Pharmacol.*, **24**, 798(1972).

(7) E. Shotton and D. Ganderton, *ibid.*, **12**, 877(1960).

(8) G. S. Leonard, Ph.D. thesis, University of London, London, England, 1971.

ACKNOWLEDGMENTS AND ADDRESSES

Received May 23, 1975, from the *Department of Pharmaceutics, School of Pharmacy, University of London, Brunswick Square, London, WC1N 1AX, England.*

Accepted for publication October 9, 1975.

Adapted in part from a thesis submitted by G. S. Leonard to the University of London in partial fulfillment of the Doctor of Philosophy degree requirements.

The authors thank the School of Pharmacy for the financial support of G. S. Leonard which enabled this work to be undertaken.

* Present address: Smith Kline and French Ltd., Welwyn Garden City, Herts., England.

ˣ To whom inquiries should be directed.

Conversion of Cefamandole Nafate to Cefamandole Sodium

JOSEPH M. INDELICATO ˣ, WILLIAM L. WILHAM, and BENITO J. CERIMELE

Abstract □ The rate of hydrolysis of the formyl moiety of cefamandole nafate was determined as a function of pH, temperature, and concentration of added sodium carbonate or tromethamine. The reaction rate was sensitive to hydroxide ion in the pH 5.5–8.0 range with half-life values of hours to minutes. Hydrolysis was rapid upon the addition of sodium carbonate or tromethamine. Chirality in the 7-D-mandelamido side chain was unaffected by hydrolysis.

Keyphrases □ Cefamandole nafate—hydrolysis of formyl moiety, effect of pH, temperature, and carbonate or tromethamine concentration □ Hydrolysis—cefamandole nafate formyl moiety, effect of pH, temperature, and carbonate or tromethamine concentration □ Antibacterial agents—cefamandole nafate, hydrolysis of formyl moiety, effect of pH, temperature, and carbonate or tromethamine concentration

The antibiotic cefamandole (I*a*), 7-D-mandelamido-3-[[(1-methyl-1*H*-tetrazol-5-yl)thio]methyl]-3-cephem-4-carboxylic acid, sodium salt, is active *in vitro* against a wide variety of Gram-positive and Gram-negative bacteria (1, 2). Attempts to prepare cefamandole sodium in crystalline form suitable for commercial use with respect to purity and long-term stability were unsuccessful. Since cefamandole nafate (I*b*), the formyl ester of cefamandole sodium, has the desired pharmaceutical characteristics, it is used in the clinical formulation of the antibiotic. Cefamandole nafate is indistinguishable from cefamandole microbiologically in routine clinical assay procedures (3) and is rapidly converted to cefamandole *in vivo* (4).

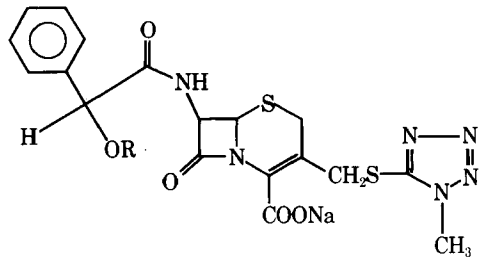

I*a*: R = H

I*b*: R = CH(=O)

During the development of the cefamandole nafate dosage form, it was found necessary to add sodium carbonate or tromethamine powder to the vial[1] to prevent turbidity when the drug is reconstituted with intravenous fluids. Turbidity is due to the precipitation of cefamandole nafate and cefamandole free acids when the pH of the solution slowly drops as a result of aqueous ester hydrolysis.

The purpose in this study was to determine the rate of hydrolysis of the formyl moiety as a function of pH, temperature, and the concentration of added sodium carbonate or tromethamine.

EXPERIMENTAL

Materials—D-6-Formylmandelamidopenicillanic acid (II), D- and L-cefamandole nafate[2], and D-formylmandelyl chloride[2] were used as supplied. The pH-stat[3] was calibrated with pH 7.00 buffer[4]. Sodium hydroxide solutions[4] (0.1 or 0.02 *N*) were employed in the constant pH titrations. All other chemicals were reagent grade and were used as received.

Kinetic Methods—The hydrolysis rates were followed by constant pH titration. The formic acid produced in the hydrolysis was titrated automatically with a pH-stat[3] fitted with a combination electrode[5]. Rate determinations were conducted at 25.0, 37.0, 45.0, and 55.0 ± 0.1°. Constant ionic strength (0.102 *N* ± 0.003) was established by prior addition of potassium chloride.

The formyl ester concentrations varied between 0.001 and 0.005 *M*. Carbon dioxide was excluded from the system with an argon blanket. Because methyl formate is volatile, a closed titration vessel (without argon) was used to measure its hydrolysis rate. From the recorded volume of standard sodium hydroxide solution consumed as a function of time, plots of log [ester] *versus* time were constructed. From these plots the pesudo-first-order rate constants were calculated. The fast reactions were followed for two half-lives, while the slow reactions were followed to 25% completion. In all cases, straight-line plots were obtained when one assumed that 1 mole of formic acid was produced for each mole of ester hydrolyzed.

The formation of any cephalosporic acids from the hydrolysis of the cephalosporin β-lactams would interfere in the constant pH titration of the formic acid produced by the ester hydrolysis. Such an interference is insignificant since the rate of base consumption due to β-lactam hydrolysis of cefamandole is ≤1/100 the rate of base consumption due to ester hydrolysis of cefamandole nafate. The rate of β-lactam hydrolysis of cefamandole nafate is assumed to be similar to that for cefamandole, because previous studies showed that side-chain alterations have little effect upon β-lactam reactivity (5).

Ester hydrolysis as the result of the addition of sodium carbonate or amines was also determined by NMR[6] at 25 ± 1°. Cefamandole nafate, 100 mg, and 18.6 mg (0.90 molar equivalent), 12.4 mg (0.60 molar equivalent), or 5.7 mg (0.275 molar equivalent) of sodium carbonate were dissolved in 1 ml of deuterium oxide immediately prior to insertion into the probe. Percent hydrolysis was calculated from the integrated peak intensities. The disappearance of the formyl proton at δ 8.2 and the appearance of the formate anion proton at δ 8.5 were monitored as a function of time. [These changes could also be monitored when water was substituted for deuterium oxide since the water peak (δ 4.8) does not interfere with the measurement.] The disappearance of the α-phenylmethine proton of cefamandole nafate at δ 6.2 and the appearance of the α-phenylmethine proton of cefamandole at δ 5.3 also could be followed, but monitoring this region was inconvenient since the δ 5.3 peak is located between the β-lactam peaks.

Similarly, cefamandole nafate and 1.0 molar equivalent of tromethamine or ethanolamine were dissolved in the appropriate volume of deuterium oxide to obtain an approximately 10% solution of the nafate. In these cases, it was necessary to monitor the disappearance

[1] Vials equal to 1 g of cefamandole (free acid) contain 1.11 g of cefamandole nafate and 0.063 g (0.28 mole equivalent) of sodium carbonate.

[2] Received from Dr. J. M. Greene, Lilly Research Laboratories. Synthesis of these antibiotics will be reported by Dr. Greene at a later date.

[3] Radiometer (TTT2), Copenhagen, Denmark.

[4] Fisher Scientific Co., Fair Lawn, N.J.

[5] A. H. Thomas (4049-L15), Philadelphia, Pa.

[6] A-60 or HA-100 spectrometers, Varian Associates, Palo Alto, Calif.

Table I—Apparent Pseudo-First-Order Rate Constants of Formate Ester Hydrolysis of Cefamandole Nafate

pH	Temperature	Number of Observations	$k \times 10^5$ sec^{-1} Mean	SE
5.5	37°	4	1.65	0.06
5.5	45°	4	3.99	0.32
5.5	55°	4	14.18	0.52
6.0	37°	4	3.54	0.20
6.0	45°	4	9.03	0.92
6.0	55°	4	30.70	3.18
6.5	25°	4	2.11	0.07
6.5	37°	4	8.24	0.25
6.5	45°	4	18.60	1.92
6.5	55°	4	52.25	3.89
7.0	25°	5	4.91	0.63
7.0	37°	4	19.40	0.69
7.0	45°	4	33.85	5.70
7.0	55°	4	133.25	10.37
7.4	25°	5	9.39	1.37
7.4	37°	5	40.40	2.53
7.4	45°	4	66.95	7.97
8.0	25°	8	29.00	1.83
8.0	37°	5	119.82	6.44
8.0	45°	4	174.88	8.16

of the α-phenylmethine proton of cefamandole nafate and the appearance of the α-phenylmethine proton of cefamandole. Peaks from *N*-formyl tromethamine made monitoring of the formyl proton impossible.

Retention of Chirality in 7-Mandelamido Side Chain of Cefamandole—D-Cefamandole nafate (0.513 g, 1 mmole) and sodium carbonate (0.106 g, 1 mmole) were dissolved in 25 ml of water and allowed to react for 30 min. At that time, the solution was layered with ethyl acetate, and the pH of the aqueous layer was adjusted to 2 with 1 *N* HCl. The ethyl acetate layer was collected and dried with anhydrous sodium sulfate, and the solvent was removed *in vacuo*. The 100-MHz NMR spectrum of the resulting foam was obtained in pyridine-d_5.

The pertinent features of the D-cefamandole free acid spectrum were δ 4.08 (d, $J_{H\text{-}H}$ = 5.0 Hz, C-6 proton), 4.46 (s, α-phenylmethine), and 8.41 (d, $J_{H\text{-}H}$ = 9.6 Hz, NH). The pertinent features of L-cefamandole free acid, obtained from L-cefamandole nafate by a procedure identical to the described one, were δ 3.96 (d, $J_{H\text{-}H}$ = 5.0 Hz, C-6 proton), 4.40 (s, α-phenylmethine), and 8.30 (d, $J_{H\text{-}H}$ = 9.6 Hz, NH). Each of these NMR spectra was free of the other isomer (>95% pure, the limit of this instrumental method).

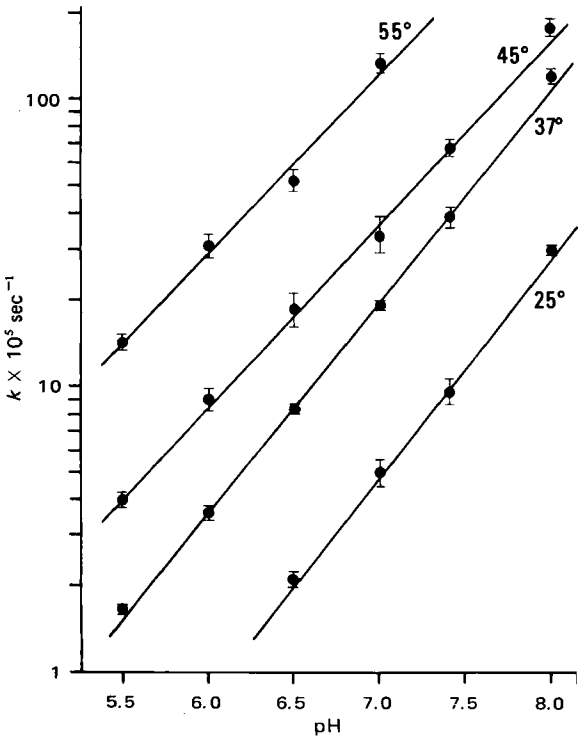

Figure 1—*The pH–rate profile of formate ester hydrolysis of cefamandole nafate. Coefficients of determination are 0.953 (25°), 0.995 (37°), 0.974 (45°), and 0.963 (55°).*

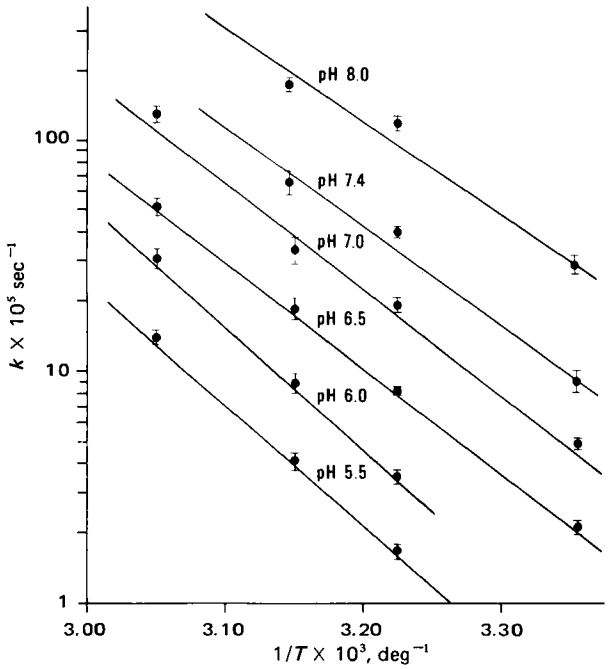

Figure 2—*Arrhenius plots of formate ester hydrolysis of cefamandole nafate. Key (E_a in kcal/mole): pH 5.5, 24.3; pH 6.0, 24.2; pH 6.5, 20.7; pH 7.0, 20.8; pH 7.4, 19.3; and pH 8.0, 18.0.*

***N*-Formyl Tromethamine**—Tromethamine (12.1 g, 0.1 mole) was allowed to react with methyl formate (6 g, 0.1 mole) in 120 ml of water at 25° for 24 hr, and the reaction mixture was lyophilized. The resulting solids were triturated with several 500-ml portions of hot acetone. Crystals were collected from the acetone solutions after cooling. Recrystallization from acetone yielded 4 g of *N*-formyl tromethamine, mp 104°; NMR (D_2O): 74% *trans*-configuration δ 3.27 (s, 6, CH_2OH) and 8.04 [s, 1, HC(=O)], 26% *cis*-configuration δ 3.23 (s, 6, CH_2OH) and 8.15 [s, 1, HC(=O)]; mass spectrum: M^+ 150; IR (mull): 1650 (amide) cm^{-1}.

Anal.—Calc. for $C_5H_{11}NO_4$: C, 40.27; H, 7.43; N, 9.39. Found: C, 40.17; H, 7.21; N, 9.52.

D-Isopropylmandelamide, Formate Ester—D-Formylmandelyl chloride (3.72 g, 20 mmoles), was dissolved in 50 ml of dichloromethane. Sodium bicarbonate, 4 g, was added to this solution, and the resulting suspension was cooled to 0°. Isopropylamine (1.18 g, 20 mmoles) dissolved in 25 ml of dichloromethane, was added dropwise to this suspension. The mixture was allowed to warm to room temperature, and the sodium bicarbonate was filtered after 2 hr. Dichloromethane was removed *in vacuo*, and the resulting solids recrystallized from hexane to yield 2.4 g (55%), mp 90°; NMR ($CDCl_3$): δ 1.18 (d, $J_{H\text{-}H}$ = 7 Hz, 6, CH_3CH), 4.40 [m, J = 7 Hz, 1, $(CH_3)_2CH$], 6.16 (s, 1, α-phenylmethine), 7.42 (m, 5, aromatic), and 8.16 [s, 1, $HC(=O)OR$]; IR (CCl_4): 1729 (ester), 1673, and 3420 (amide) cm^{-1}; mass spectrum: M^+ 221.

Anal.—Calc. for $C_{12}H_{15}NO_3$: C, 65.14; H, 6.83; N, 6.33. Found: C, 65.07; H, 6.76; N, 6.23.

RESULTS AND DISCUSSION

At a constant pH between 5.5 and 8.0, the formyl moiety of cefamandole nafate hydrolyzes by an apparent pseudo-first-order process. The effects of pH and temperature on the rate of hydrolysis are shown in Table I. The effect of the hydroxide ion in the pH 5.5–8.0 range is large, with the half-life at 37° decreasing from ~290 to ~7 min. The pH–rate profile for the hydrolysis at 25, 37, 45, and 55° (Fig. 1) is linear with coefficients of determination of 0.953 or better. The Arrhenius activation energy increases (Fig. 2) with a decrease in pH because nucleophilic attack at the formate carbonyl by a neutral water molecule is more difficult than nucleophilic attack by a negatively charged hydroxide ion.

Table II—Apparent Pseudo-First-Order Rate Constants of Formate Hydrolysis (pH 8.0, 25°) of Related Formate Esters

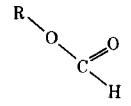

Compound	R	Number of Observations	$k \times 10^5$ sec^{-1} Mean	$k \times 10^5$ sec^{-1} SE	k_{obs} (D-Cefamandole) / k_{obs} (R—O—COH)
D-Cefamandole	—	8	29.0	1.83	—
L-Cefamandole	—	3	24.0	0.90	1.2
II	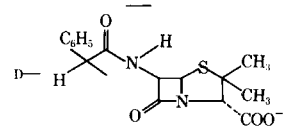	3	15.0	2.14	1.9
III	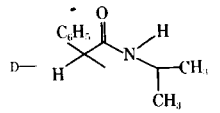	3	19.3	2.31	1.5
IV	CH_3	3	4.48	0.05	6.5

The rate of hydrolysis of cefamandole nafate (pH 8 and 25°) is 6.5 times greater than that of methyl formate (Table II). To determine if the increase in reactivity is the result of the effect of the mandelic moiety or of some interaction of it with the β-lactam-containing portion of the cephalosporin, several formylmandelic acid derivatives were prepared and their rates of hydrolysis were determined. It is apparent from the relative rates of formate hydrolysis (Table II) of the β-lactam-containing molecules, D- and L-cefamandole nafates, of II and of the non-β-lactam, III, that the increase in reactivity over that observed for methyl formate is merely the substituent effect of the mandelic moiety.

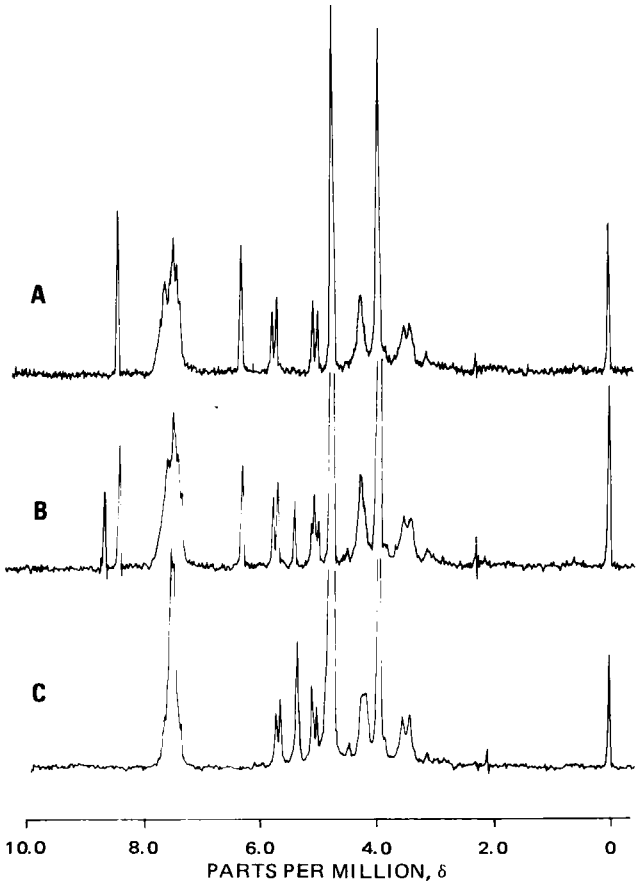

Figure 3—*NMR spectra (D_2O). Key: A, cefamandole nafate; B, cefamandole nafate hydrolyzed to ~28% cefamandole by the addition of 0.28 molar equivalent of sodium carbonate; and C, cefamandole.*

The hydrolysis of the formylmandelic derivatives may involve bond breakage at two possible sites, cleavage at the acyl—oxygen bond or cleavage at the alkyl—oxygen bond. Most esters hydrolyze by an acyl—oxygen cleavage, but alkyl—oxygen cleavage may occur in the hydrolysis of esters that yield stable carbonium ions, such as benzhydryl esters (6). In the case of cefamandole nafate, acyl—oxygen bond cleavage would result in the retention of chirality in the mandelic side chain; alkyl—oxygen cleavage would result first in a benzylic cation intermediate which, upon reaction with water, would yield a mixture of D- and L-cefamandoles. Because L-cefamandole possesses significantly lower microbiological activity than D-cefamandole[7], it is fortunate that D-cefamandole nafate hydrolyzes by acyl—oxygen cleavage to D-cefamandole. The D- and L-cefamandoles may be differentiated by their 100-MHz NMR spectra in pyridine-d_5[8].

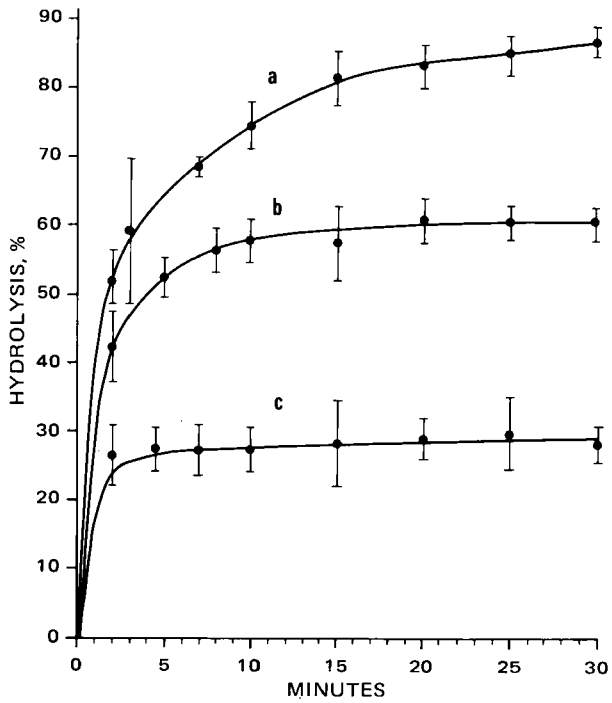

Figure 4—*Effect of 0.90 (a), 0.60 (b), and 0.28 (c) mole equivalent of sodium carbonate on the percent hydrolysis of cefamandole nafate to cefamandole at 25 ± 1°. Without the addition of sodium carbonate, no detectable hydrolysis was observed in 30 min and only ~10% hydrolysis was observed in 24 hr.*

[7] D. A. Preston, Lilly Research Laboratories, personal communication.
[8] G. W. Huffman, Lilly Research Laboratories, personal communication.

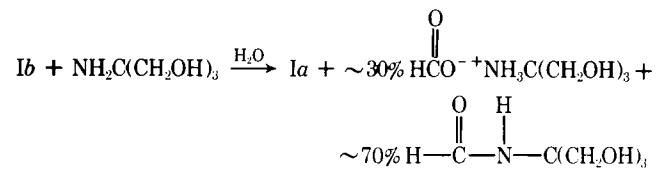

Scheme I

The rate of hydrolysis of cefamandole nafate to cefamandole upon the addition of sodium carbonate may be studied conveniently by NMR. The NMR spectrum of cefamandole nafate (Fig. 3A) differs from that of cefamandole (Fig. 3C) in the position of the α-phenylmethine proton peaks, at δ 6.2 and 5.3, respectively, and in the presence of a formyl proton peak at δ 8.2 in the ester. In cefamandole, the formyl proton is absent but occurs as a formate anion peak, δ 8.5 (Fig. 3B). By determining either the ratio of the cefamandole nafate methine peak (δ 6.2) to the cefamandole methine peak (δ 5.3) or, more conveniently, the ratio of the formyl peak (δ 8.2) to the formate anion peak (δ 8.5), one may calculate the percent hydrolysis at a given time. Figure 3B represents ~28% hydrolysis upon the addition of 0.28 mole of sodium carbonate.

Figure 4 shows the percent conversion of cefamandole nafate to cefamandole by 0.28, 0.60, and 0.90 molar equivalents of sodium carbonate at 25 ± 1°. The error indicated represents the 95% confidence interval determined from five experiments.

The aqueous hydrolysis of cefamandole nafate with tromethamine (Scheme I) and ethanolamine was also examined by NMR. In each case, upon the addition of 1.0 molar equivalent of amine, hydrolysis was complete within the time necessary to obtain the NMR spectrum. The NMR spectrum of the products of the tromethamine reaction indicated two new kinds of formyl peaks at δ 8.04 and 8.15 in addition to ~30% formate anion at δ 8.5. These new formyl peaks were identified as the formyl proton of *N*-formyl tromethamine in the *trans*- and *cis*-configurations of the amide bond (7). An authentic sample of *N*-formyl tromethamine was prepared by the reaction of methyl formate and tromethamine.

REFERENCES

(1) W. E. Wick and D. A. Preston, *Antimicrob. Ag. Chemother.*, **1**, 221(1972).

(2) H. C. Neu, *ibid.*, **6**, 177(1974).

(3) R. B. Kammer, D. A. Preston, and J. R. Turner, "Abstracts, 9th International Congress of Chemotherapy," London, England, 1975.

(4) J. S. Wold, R. R. Joost, H. R. Black, and K. E. Briscoe, *ibid.*

(5) J. M. Indelicato, T. T. Norvilas, R. R. Pfeiffer, W. J. Wheeler, and W. L. Wilham, *J. Med. Chem.*, **17**, 523(1974).

(6) E. S. Gould, "Mechanism and Structure in Organic Chemistry," Holt, Rinehart, and Winston, New York, N.Y., 1959, p. 316.

(7) L. A. LaPlanche and M. T. Rogers, *J. Am. Chem. Soc.*, **86**, 337(1964).

ACKNOWLEDGMENTS AND ADDRESSES

Received June 4, 1975, from the *Lilly Research Laboratories, Indianapolis, IN 46206*

Accepted for publication August 6, 1975.

Presented in part at the 15th Interscience Conference on Antimicrobial Agents and Chemotherapy, September 1975.

The authors thank Dr. James M. Greene for samples of D- and L-cefamandole nafates, D-6-formylmandelamidopenicillanic acid, and D-formylmandelyl chloride. They also thank Mr. George Fraction for computer programming assistance.

[x] To whom inquiries should be directed.

Quantitative Determination of Theophylline in Pharmaceutical Dosage Forms by Differential Spectrophotometry

YOUNG SOON CHAE and WILLIAM H. SHELVER [x]

Abstract □ Theophylline was determined with good precision in tablets and capsules by differential spectrophotometry. Xanthines such as caffeine and theobromine did not interfere providing the total xanthine concentration was kept below 100 μg/ml. At a higher total xanthine concentration, nonlinearity occurred, presumably due to complex formation. This interference could be minimized by proper selection of the analytical wavelength.

Keyphrases □ Theophylline—analysis, differential spectrophotometry, pharmaceutical formulations □ Spectrophotometry, differential—analysis, theophylline in pharmaceutical formulations □ Aminophylline tablets and capsules—theophylline content analyzed by differential spectrophotometry

An argentimetric titration is described in the USP for the analysis of aminophylline and tablets containing aminophylline. The reactive component in the analysis is the theophylline (I) portion of aminophylline. The silver salt titration was compared with a spectrophotometric method, and some difficulties of the official method were discussed, particularly the effect of materials obscuring the end-point or interfering with filtration prior to titration (1). In addition, compounds with a structure similar to theophylline, such as theobromine (II), were reported (2) to interfere with the official method of analysis.

The direct spectrophotometric method, measuring the absorption peak in either acid (1) or base (3), is convenient and precise. However, it suffers from interference from other substances, such as theobromine and caffeine (III), absorbing in the same spectral region. Differential spectrophotometry offers the convenience and most of the precision of spectrophotometric

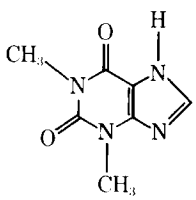

I

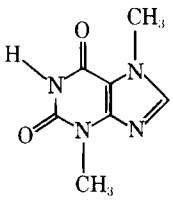

II

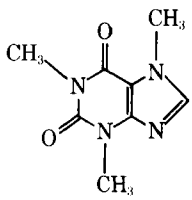

III

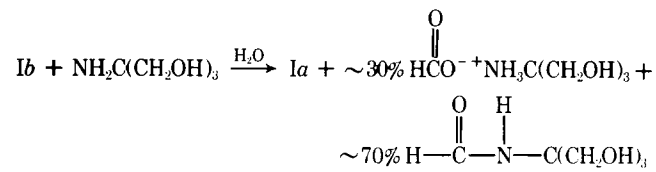

Scheme I

The rate of hydrolysis of cefamandole nafate to cefamandole upon the addition of sodium carbonate may be studied conveniently by NMR. The NMR spectrum of cefamandole nafate (Fig. 3A) differs from that of cefamandole (Fig. 3C) in the position of the α-phenylmethine proton peaks, at δ 6.2 and 5.3, respectively, and in the presence of a formyl proton peak at δ 8.2 in the ester. In cefamandole, the formyl proton is absent but occurs as a formate anion peak, δ 8.5 (Fig. 3B). By determining either the ratio of the cefamandole nafate methine peak (δ 6.2) to the cefamandole methine peak (δ 5.3) or, more conveniently, the ratio of the formyl peak (δ 8.2) to the formate anion peak (δ 8.5), one may calculate the percent hydrolysis at a given time. Figure 3B represents ~28% hydrolysis upon the addition of 0.28 mole of sodium carbonate.

Figure 4 shows the percent conversion of cefamandole nafate to cefamandole by 0.28, 0.60, and 0.90 molar equivalents of sodium carbonate at 25 ± 1°. The error indicated represents the 95% confidence interval determined from five experiments.

The aqueous hydrolysis of cefamandole nafate with tromethamine (Scheme I) and ethanolamine was also examined by NMR. In each case, upon the addition of 1.0 molar equivalent of amine, hydrolysis was complete within the time necessary to obtain the NMR spectrum. The NMR spectrum of the products of the tromethamine reaction indicated two new kinds of formyl peaks at δ 8.04 and 8.15 in addition to ~30% formate anion at δ 8.5. These new formyl peaks were identified as the formyl proton of *N*-formyl tromethamine in the *trans*- and *cis*-configurations of the amide bond (7). An authentic sample of *N*-formyl tromethamine was prepared by the reaction of methyl formate and tromethamine.

REFERENCES

(1) W. E. Wick and D. A. Preston, *Antimicrob. Ag. Chemother.*, **1**, 221(1972).

(2) H. C. Neu, *ibid.*, **6**, 177(1974).

(3) R. B. Kammer, D. A. Preston, and J. R. Turner, "Abstracts, 9th International Congress of Chemotherapy," London, England, 1975.

(4) J. S. Wold, R. R. Joost, H. R. Black, and K. E. Briscoe, *ibid.*

(5) J. M. Indelicato, T. T. Norvilas, R. R. Pfeiffer, W. J. Wheeler, and W. L. Wilham, *J. Med. Chem.*, **17**, 523(1974).

(6) E. S. Gould, "Mechanism and Structure in Organic Chemistry," Holt, Rinehart, and Winston, New York, N.Y., 1959, p. 316.

(7) L. A. LaPlanche and M. T. Rogers, *J. Am. Chem. Soc.*, **86**, 337(1964).

ACKNOWLEDGMENTS AND ADDRESSES

Received June 4, 1975, from the *Lilly Research Laboratories, Indianapolis, IN 46206*

Accepted for publication August 6, 1975.

Presented in part at the 15th Interscience Conference on Antimicrobial Agents and Chemotherapy, September 1975.

The authors thank Dr. James M. Greene for samples of D- and L-cefamandole nafates, D-6-formylmandelamidopenicillanic acid, and D-formylmandelyl chloride. They also thank Mr. George Fraction for computer programming assistance.

[x] To whom inquiries should be directed.

Quantitative Determination of Theophylline in Pharmaceutical Dosage Forms by Differential Spectrophotometry

YOUNG SOON CHAE and WILLIAM H. SHELVER [x]

Abstract □ Theophylline was determined with good precision in tablets and capsules by differential spectrophotometry. Xanthines such as caffeine and theobromine did not interfere providing the total xanthine concentration was kept below 100 μg/ml. At a higher total xanthine concentration, nonlinearity occurred, presumably due to complex formation. This interference could be minimized by proper selection of the analytical wavelength.

Keyphrases □ Theophylline—analysis, differential spectrophotometry, pharmaceutical formulations □ Spectrophotometry, differential—analysis, theophylline in pharmaceutical formulations □ Aminophylline tablets and capsules—theophylline content analyzed by differential spectrophotometry

An argentimetric titration is described in the USP for the analysis of aminophylline and tablets containing aminophylline. The reactive component in the analysis is the theophylline (I) portion of aminophylline. The silver salt titration was compared with a spectrophotometric method, and some difficulties of the official method were discussed, particularly the effect of materials obscuring the end-point or interfering with filtration prior to titration (1). In addition, compounds with a structure similar to theophylline, such as theobromine (II), were reported (2) to interfere with the official method of analysis.

The direct spectrophotometric method, measuring the absorption peak in either acid (1) or base (3), is convenient and precise. However, it suffers from interference from other substances, such as theobromine and caffeine (III), absorbing in the same spectral region. Differential spectrophotometry offers the convenience and most of the precision of spectrophotometric

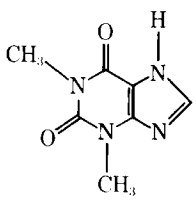

I

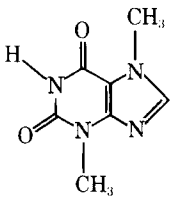

II

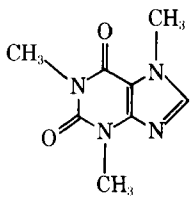

III

Table I—Percentage Recovery of Theophylline from Theophylline–Xanthine Mixtures Containing 50 μg of Total Xanthine/ml

Components	Analytical Wavelength of Differential Spectrophotometry[a] 281–290 nm	285 nm	290 nm	USP Method[b]	Direct UV Method[c]
Theophylline[a], 25 μg/ml	102.39 ± 2.32	102.73 ± 2.32	101.73 ± 2.14	99.18 ± 0.37	102.40 ± 4.44
Theophylline[a], 25 μg/ml, plus caffeine, 25 μg/ml	96.22 ± 0.74	96.04 ± 0.67	96.89 ± 0.64	81.99 ± 1.47	100.25 ± 3.40
Theophylline[a], 25 μg/ml, plus theobromine, 25 μg/ml	100.06 ± 1.85	99.56 ± 1.98	100.51 ± 2.49	197.88 ± 0.38	168.98 ± 2.99

[a] The values represent the mean of four determinations, two independent weighings with duplicate determinations from each. The error is the standard deviation of the four determinations. [b] The analyses were carried out utilizing the procedure described in USP XVIII. [c] The analyses were carried out using the Schack and Waxler method as described under *Experimental.*

methods and is much more specific (4). This report compares results from the application of the differential spectrophotometric method with those from the official analysis.

EXPERIMENTAL

Instrument—A double-beam spectrophotometer[1] was used for differential UV analysis, and incident radiation was maintained constant by utilizing the automatic slit programs for all determinations.

Reagents—Tromethamine buffer solutions of pH 7 and 9 were prepared according to the formula given in Ref. 5. All dosage forms were obtained commercially. Theophylline[2], caffeine[3], and theobromine[3] were the best quality commercially available. All other chemicals employed were analytical reagent grade and were used without further purification.

The dosage forms[4] analyzed were aminophylline tablets[5], 100 mg; aminophylline tablets[5], 200 mg; and capsules[6] containing 130 mg of aminophylline, 25 mg of ephedrine, and 25 mg of amobarbital.

USP Method—*Aminophylline Tablets*—The USP XVIII (6) method was followed.

Aminophylline Capsules—The contents of 12 capsules were removed as completely as possible and mixed with 50 ml of distilled water and 10 ml of ammonia TS in a 125-ml beaker. This mixture, including the capsules, was stirred on a magnetic stirrer for 30 min and then filtered by suction. The beaker and residue were washed with five 10-ml portions of distilled water. The filtrate was transferred into a 250-ml volumetric flask, the suction flask was washed with six 15-ml portions of distilled water, and the combined solution was diluted to volume. A 50.0-ml aliquot was used for the USP XVIII method (6).

Theophylline and Xanthine Mixtures—Two hundred milligrams of theophylline alone or mixed with 200.0 mg of caffeine or theobromine was used for the USP XVIII method.

Schack and Waxler Method—A procedure adopted from the original Schack and Waxler (3) method and utilized for the determination of theophylline in blood was used to test for potential interference of xanthine derivatives in the theophylline analysis. Theophylline, 30 μg, or theophylline, 30 μg, and either caffeine, 30 μg, or theobromine, 30 μg, in 1 ml of water were extracted with 15 ml of chloroform. After centrifuging, a 10-ml aliquot of the chloroform was removed and extracted with 5 ml of 0.1 *N* sodium hydroxide.

After centrifuging again, approximately 4 ml of the sodium hydroxide solution was heated in a boiling water bath for 30 min, cooled, and then read in a spectrophotometer at 310 and 274 nm. A set of theophylline standards at 15, 30, and 60 μg/ml was carried through the same procedure. The percent recovery of the theophylline is reported in Table I.

Differential UV Method—*Standard Curve*—Standard stock solutions of theophylline were prepared by dissolving 50.0 mg of anhydrous theophylline in sufficient tromethamine buffer solutions of pH 7 and 9 to make 500.0 ml. The stock solutions were diluted with each buffer solution to obtain the concentrations of 10, 20, 40, 50, and 60 μg/ml. The pH 7 solution was placed in the reference side, and the pH 9 solution was placed in the sample side.

All solutions were prepared in duplicate, and duplicate readings were obtained for all concentrations. The absorbances of the standard solutions were determined at 10 wavelengths (281–290 nm). The regression line of the absorbance–concentration curves through zero was determined with standard statistical procedures, calculated and plotted with a programmable calculator[7]. The regression analysis for the absorbance–concentration curves are shown in Table II.

Tablets—Twenty tablets of each preparation were accurately weighed to determine the average tablet weight. Then the tablets were crushed and ground to a fine powder with a mortar and pestle. A portion of each tablet powder, equivalent to 500.0 mg of theophylline, was accurately weighed in a 150-ml beaker, dissolved in 100 ml of distilled water, filtered through filter paper[8] into a 250-ml volumetric flask, and diluted to volume with distilled water through the filter paper. An aliquot of the filtrate was diluted to 100.0 ml with each buffer solution to obtain a theophylline concentration of 50 μg/ml. The absorbances were determined at 10 wavelengths (281–290 nm). Four different lots of 20 tablets were subjected to this procedure.

Capsules—The contents of 20 capsules (as one batch) were removed as completely as possible and mixed with 250 ml of distilled water. The mixture, including the capsules, was stirred on a magnetic stirrer for 30 min, filtered through filter paper into a 500-ml volumetric flask, and diluted to volume with distilled water passed through the filter paper. An aliquot of the filtrate was diluted to 100.0 ml with each buffer solution. The filtrates of four different batches of capsules were prepared, each with two separate aliquots, and the absorbances were determined at 10 wavelengths (281–290 nm).

Theophylline and Xanthine Mixtures—Five hundred milligrams of theophylline alone or with either caffeine or theobromine was accurately weighed and dissolved in distilled water to make 100.0 ml of each solution. Heating was necessary to dissolve theobromine. An aliquot of each solution was combined and diluted to 100.0 ml with each buffer solution to obtain a theophylline concentration of 25 or 50 μg/ml, mixed either with the same volume of distilled water or with the same concentration of caffeine or theobromine.

The aliquots of theobromine solution were taken while the solution was warm to prevent precipitation. Two separate weighings of each xanthine were subjected to this procedure, each with two dilutions. The absorbances were determined at 10 wavelengths (281–290 nm) and the percent recovery was calculated. The means and standard deviations were calculated with a programmable calculator[7].

RESULTS AND DISCUSSION

Differential spectrophotometry offers the convenience and most of the precision of direct spectrophotometric methods but is more specific. The method requires the component to exist in two forms that differ in their absorptivity. Most frequently, the forms are different ionization states; the ionization must affect the absorptivity so the two forms have different absorption spectra.

[1] Cary model 118C.
[2] Mann Research Laboratories.
[3] Eastman.
[4] Obtained from the proprietary laboratory, College of Pharmacy, North Dakota State University.
[5] Searle.
[6] Lilly Amsec.
[7] Hewlett-Packard model 10.
[8] Whatman No. 40.

Table II—Regression Analysis of Concentration–Absorbance Data for Theophylline[a]

Wavelength, nm	Slope[b]	95% Confidence Limits	SE of Slope
281	0.01063	0.01042–0.01083	0.000089
282	0.01069	0.01049–0.01089	0.000086
283	0.01075	0.01053–0.01096	0.000093
284	0.01078	0.01055–0.01102	0.000101
285	0.01079	0.01022–0.01055	0.000101
286	0.01073	0.01050–0.01097	0.000102
287	0.01061	0.01039–0.01082	0.000095
288	0.01035	0.01015–0.01055	0.000087
289	0.00968	0.00978–0.01015	0.000078
290	0.00948	0.00934–0.00961	0.000059

[a] The regression analysis was carried out utilizing a computer program, WHSR, written by W. H. Shelver. [b] The slopes are in terms of absorbance *versus* concentration in micrograms per milliliter. The slope was determined by utilizing duplicate measurements at 10, 20, 40, and 50 μg/ml.

Theophylline, with a pKa of 8.79 (7), undergoes a bathochromic shift (8) upon ionization and is well suited to analysis by differential spectrophotometry. After initiation of this study, Gupta and Lundberg (9) reported a method for the determination of theophylline in blood by differential spectrophotometry. These investigators utilized an acid solution prepared from 3 ml of 0.2 *N* sodium hydroxide and 0.5 ml of 2.5 *M* monobasic sodium phosphate in the reference cell and 0.2 *N* sodium hydroxide in the sample cell. To eliminate interference from either caffeine or theobromine, pH 7 tromethamine buffer was used in the reference cell and the pH 9 buffer was used in the sample cell.

Caffeine decomposes rapidly in strongly alkaline solutions, and the products differ in their absorption spectra, possibly causing changes in the difference spectra if a strongly alkaline solution is used in the sample cell. The rate of decomposition at pH 9 is slow enough so no noticeable effects are observed in the analysis. Theobromine, with a pKa of 9.95, is not appreciably ionized at pH 9 and produced little absorption under the analysis conditions. To obtain this specificity, some sensitivity is given up since the theophylline is not fully ionized under the analysis conditions.

Recovery experiments for theophylline alone and for mixtures of theophylline and caffeine and theophylline and theobromine are shown in Tables I and III. Observation of the spectral curves (Figs. 1 and 2) obtained from runs with relatively high total xanthine concentrations indicated the development of a strong peak at 274 nm and a slight decrease in the analytical peak at 285 nm, presumably from the formation of a complex (10). Consequently, two recovery experiments were run, one at high total xanthine concentrations and the other at low total xanthine concentrations. Observation of the spectral curves indicated that there was little interference at wavelengths above 290 nm, so the data were processed three ways: (*a*) averaging results from 10 wavelengths from 281 to 290 nm, (*b*) measurement at the peak at 285 nm, and (*c*) measurement at 290 nm where interference was at a minimum.

The USP method was also used to analyze the theophylline and theophylline–xanthine mixtures. The Schack and Waxler method utilized in many clinical laboratories for the determination of theophylline was applied to the analysis of theophylline and theophylline–xanthine mixtures. The recovery experiments run at low total xanthine concentrations (Table I) showed no appreciable difference between the methods of calculation utilized in the differential spectrophotometric method but demonstrated the superiority of this method to the USP method. As previously mentioned, theobromine interferes; the recovery experiment demonstrated that the USP method analyzes theobromine as if it were theophylline. Caffeine demonstrated a different type of interference in the USP method, lowering the recovery of theophylline by nearly 20%. The Schack and Waxler method also showed interference from theophylline but the caffeine removed both by extraction and heating in alkali showed no interference.

The recovery experiments run at high total xanthine concentrations

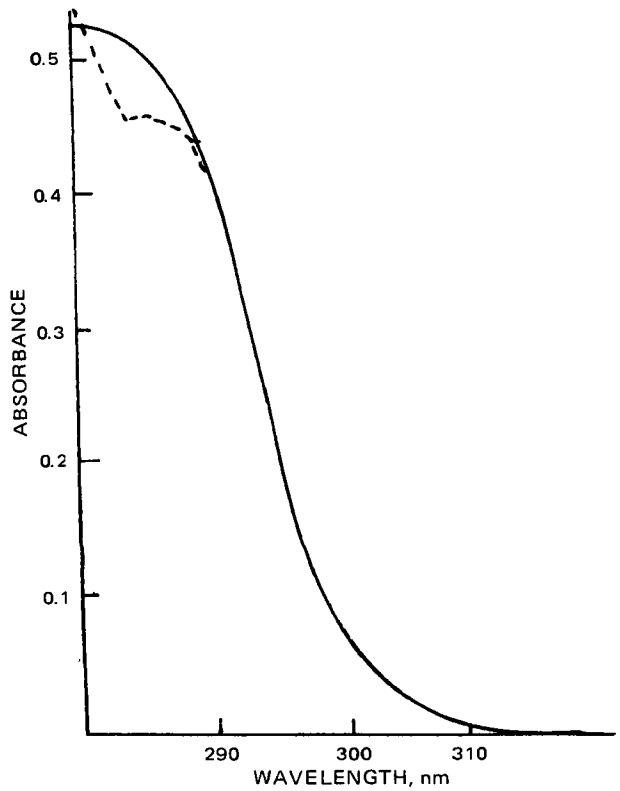

Figure 1—*Effect of increased nonabsorbing xanthine on the difference absorption spectrum of theophylline (pH 7 reference and pH 9 sample). Key: ——, 50 μg of theophylline/ml; and – – –, 50 μg of theophylline/ml plus 50 μg of caffeine/ml.*

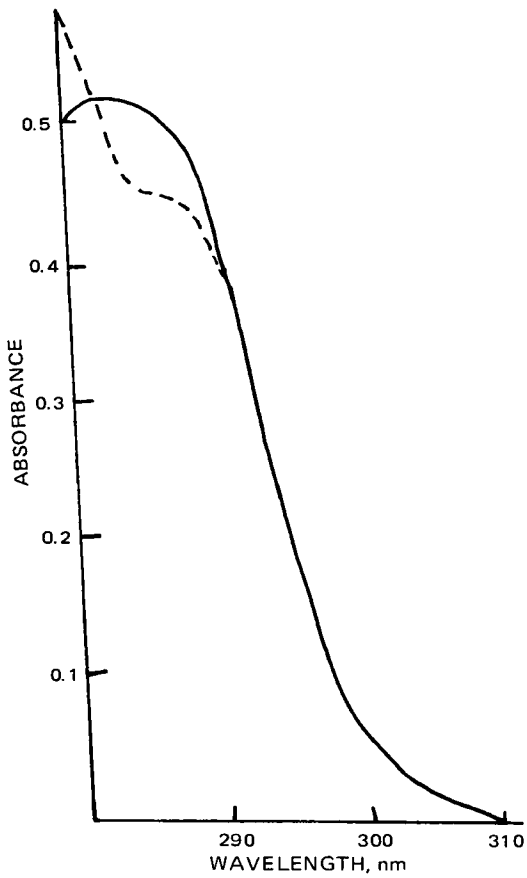

Figure 2—*Effect of increased nonabsorbing xanthine on the difference absorption spectrum of theophylline (pH 7 reference and pH 9 sample). Key: ——, 50 μg of theophylline/ml; and – – –, 50 μg of theophylline/ml plus 50 μg of theobromine/ml.*

Table III—Percentage Recovery of Theophylline from Theophylline–Xanthine Mixtures Containing 100 μg of Total Xanthine/ml

Components	Analytical Wavelengths of Differential Spectrophotometry[a]		
	281–290 nm	285 nm	290 nm
Theophylline, 50 μg/ml	98.50 ± 2.53	98.62 ± 2.55	97.99 ± 2.24
Theophylline, 50 μg/ml, plus caffeine, 50 μg/ml	89.83 ± 1.96	84.49 ± 2.21	91.87 ± 1.78
Theophylline, 50 μg/ml, plus theobromine, 50 μg/ml	93.00 ± 1.04	86.23 ± 1.27	95.01 ± 0.77

[a] The values represent the mean of eight determinations, four independent weighings with duplicate determinations for each. The error is the standard deviation of the eight determinations.

Table IV—Analysis of Theophylline in Dosage Forms

Dosage Form	281–290 nm	285 nm	290 nm	USP Method[b]
Tablet, 100 mg[a]	101.44 ± 1.27	101.55 ± 1.29	102.53 ± 0.69	—[c]
Tablet, 200 mg[a]	101.23 ± 0.71	101.89 ± 1.03	101.79 ± 0.89	100.54 ± 1.36
Capsule, 130 mg[a], plus ephedrine, 25 mg, plus amobarbital, 25 mg	98.35 ± 0.72	98.67 ± 0.77	99.05 ± 0.50	96.47 ± 1.31

[a] Each value represents the mean of four determinations and is expressed as the percent of the labeled amount. [b] The analyses were carried out utilizing the procedure described in USP XVIII. [c] The presence of coloring matter obscured the end-point of the USP method.

(Table III) demonstrated the interference observed in the spectral curves shown in Figs. 1 and 2. Calculation of the results in the high xanthine recovery experiments demonstrated the advantage of calculating results at 290 nm compared to using either an average of 10 wavelengths or the peak at 285 nm. The results from Tables I and III also indicate the desirability of keeping the concentration of total xanthine in the solutions being read below 50 μg/ml.

The results obtained in the analysis of pharmaceutical dosage forms are shown in Table IV. Three dosage forms were analyzed: a tablet containing 100 mg of aminophylline, a tablet containing 200 mg of aminophylline, and a capsule containing 130 mg of aminophylline, 25 mg of ephedrine, and 25 mg of amobarbital. The results were calculated by the same three methods already described and show no appreciable differences. The precision of the differential spectrophotometric method was comparable with the USP method. The USP analysis of the 100-mg tablets failed to give acceptable results, presumably because color change made observation of the end-point difficult. The 100- and 200-mg tablets were of obviously different formulations, even though produced by the same company, and no difficulty was observed in analyzing the 200-mg tablets by the USP method.

The results from the analyses of the capsule indicated no interference from either ephedrine or amobarbital. An attempt was also made to analyze a syrup containing theophylline without prior extraction of the theophylline. The analysis of this product showed obvious spectral interference when differential spectrophotometry was employed. The direct application of the USP method also failed to give satisfactory results because of the colored material in the syrup.

REFERENCES

(1) J. P. Comer and W. W. Hilty, *J. Am. Pharm. Assoc., Sci. Ed.*, **43**, 287(1954).

(2) K. A. Connors, in "Pharmaceutical Analysis," T. Higuchi and E. Brochmann-Hanssen, Eds., Interscience, New York, N.Y., 1961.

(3) J. A. Schack and S. H. Waxler, *J. Pharmacol. Exp. Ther.*, **97**, 283(1949).

(4) T. D. Doyle and F. R. Fazzari, *J. Pharm. Sci.*, **63**, 1921(1974).

(5) "Handbook of Chemistry and Physics," 50th ed., Chemical Rubber Co., Cleveland, Ohio, 1969.

(6) "The United States Pharmacopeia," 18th rev., Mack Publishing Co., Easton, Pa., 1970, pp. 33, 35.

(7) "Dictionary of Organic Compounds," vol. 5, 4th ed., Oxford University Press, New York, N.Y., 1965, p. 3041.

(8) F. Bergmann, D. Lictenberg, and Z. Nieman, in "The Jerusalem Symposia on Quantum Chemistry and Biochemistry, Vol. 4, The Purines Theory and Experiment," E. D. Bergmann and B. Pullman, Eds., Jerusalem Academic Press, Jerusalem, Israel, 1972, pp. 264, 265.

(9) R. C. Gupta and G. D. Lundberg, *Anal. Chem.*, **45**, 2403(1973).

(10) J. Kirschbaum, *J. Pharm. Sci.*, **62**, 168(1973).

ACKNOWLEDGMENTS AND ADDRESSES

Received November 8, 1974, from the *Department of Pharmaceutical Chemistry, College of Pharmacy, North Dakota State University, Fargo, ND 58102*

Accepted for publication October 10, 1975.

The authors thank Dr. Lloyd E. Matheson, Jr., and Dr. Fred F. Farris for helpful discussions.

[x] To whom inquiries should be directed.

Comparison of Graphical and Computerized Methods for Calculating Binding Parameters for Two Strongly Bound Drugs to Human Serum Albumin

J. J. VALLNER [x], J. H. PERRIN *, and S. WOLD [‡]

Abstract □ The determination of drug–protein binding parameters (n's and K's) can lead to important information on the required therapeutic dosage regimen and possible clinical complications associated with competitive displacement of one drug by a concurrently administered agent. Graphical and computer estimates of the data are often incorrectly formulated, and seldom are adequate data obtained at low binding ratios. Commonly used graphical procedures, inadequately formulated computer methods, and a statistically correct computer method were used to compare results obtained from a circular dichroic examination of dicumarol–human serum albumin and fenoprofen–human serum albumin interactions. Literature binding constants for dicumarol–albumin range from 1×10^5 to 30 times that figure, and it is shown here that a wide range in parameter estimates may be obtained depending on the method of data analysis. The parameter estimates in the case of fenoprofen–albumin are even more variable.

Keyphrases □ Binding parameters—dicumarol and fenoprofen to human serum albumin, comparison of graphical and computerized methods of calculation □ Dicumarol—binding to human serum albumin, comparison of graphical and computerized methods of calculation of binding parameters □ Fenoprofen—binding to human serum albumin, comparison of graphical and computerized methods of calculation of binding parameters □ Albumin, human serum—binding of dicumarol and fenoprofen, comparison of graphical and computerized methods of calculation of binding parameters

The importance of the determination of small molecule–macromolecule binding parameters is seen from the voluminous literature on the subject (1–5). The determination of numbers of the binding sites (n) and the corresponding association constants (K) led to information concerning the conformational nature of the active sites of enzymes, the nature of the binding forces, and possible clinical complications associated with competitive displacement of one drug by a concurrently administered second drug.

Protein binding data can be included in the pharmacokinetic compartmentalized description of a drug's distribution and action in the body (6, 7) and, consequently, used to determine therapeutic dosage regimens.

Most work done to elucidate binding parameters (n's and K's) for drug–albumin or ligand–macromolecule interactions has used graphical representation of the data. However, several shortcomings exist with this approach:

1. Measured quantities, *i.e.*, terms with significant errors, are almost always plotted against each other.
2. The slopes and intercepts are frequently incorrectly designated and represented mathematically.
3. Low binding ratios (*i.e.*, small r values) are seldom used, causing hazardous extrapolation to the various axes.
4. More weight is often (unknowingly) given to data obtained at high binding ratios, thus negating the possibility for clinically significant primary binding constants to be obtained.

Some of these obvious deficiencies were discussed recently (8, 9).

Computerized treatment of binding data also has become prevalent in recent years; however, it suffers from some of the same drawbacks as graphical representations. Frequently the data existing in the Scatchard or Klotz (double-reciprocal) format, which is subject to the plotting of error-containing terms against one another, are simply programmed into a computer to give the best curve through the points. This approach gives few improvements over the graphical method of determination by eye.

An attempt is made here to unify some graphical and computer methods for the analysis of binding data; often the relationship of graphical parameters to binding constants is not what seems to be taken for granted. Recently, a new computerized treatment of drug–albumin binding data for a noncooperative process appeared (10), and this method is used to compare the results for dicumarol–human serum albumin and fenoprofen–albumin interactions with the more standard graphical and computer techniques.

EXPERIMENTAL

Graphical Procedures—It has long been known that the primary step in a pharmacological action is the combination of one or several small molecules with a macromolecule. The equilibrium aspects of such interactions have been correlated through the mass law to yield the familiar equation:

$$r = \frac{nK[A]}{1 + K[A]} \qquad \text{(Eq. 1)}$$

where r represents the moles of ligand bound per mole of macromolecule, n is the number of similar binding sites available on the macromolecule, K is the association (binding) constant, and $[A]$ is the concentration of unbound (free) ligand. Equation 1 applies when the binding site is a single site or is a single class of sites with the assumed same intrinsic binding constant. When multiple classes of sites exist on the protein, the representation becomes:

$$r = \sum_{i=1}^{m} \frac{n_i K_i [A]}{1 + K_i [A]} \qquad \text{(Eq. 2)}$$

where m represents the number of classes of independent sites such that each class, i, has n_i sites with binding affinity K_i.

Scatchard (11), Klotz (12), and Scott (13) have all been responsible for transformation of these equations to equations suitable for graphical representation of binding data. The Scatchard plot results from graphing the data in the form:

$$\frac{r}{A} = Kn - Kr \qquad \text{(Eq. 3)}$$

The Klotz or double-reciprocal plot results from a representation given as:

$$\frac{1}{r} = \frac{1}{nK}\frac{1}{A} + \frac{1}{n} \qquad \text{(Eq. 4)}$$

and the Scott or half-reciprocal plot is given by:

$$\frac{A}{r} = \frac{1}{n}A + \frac{1}{nK} \qquad \text{(Eq. 5)}$$

All of these plots are linear equations and yield straight lines when only one single class of site exists on the macromolecule; however, when multiple classes are present, marked curvature of the plot is observed. Since one class of sites existing for the small molecule–macromolecule interaction occurs only rarely and since such data are easily handled, giving unequivocal values of n and K in this instance, only the determination of binding parameters when two or more classes of sites are present is considered here.

To obtain values for n and K from a set of binding data, appropriate extrapolations to the axes must be made for all plots according to Eqs. 3–5. However, such extrapolations frequently tend to be hazardous since, as in the case of the Scatchard and Klotz plots, r/A or $1/A$ approach zero as A gets very large; in the Scott plot, the intercept A/r when A is very small is a difficult experimental quantity to approach since r is small when A is small. When such circumstances exist, the error in r increases greatly since r is usually obtained from the difference between the initial concentration of A and that of free A, in most cases the difference between two large numbers.

Both the double-reciprocal and Scott representations of binding data suffer from the fact that an inverse function of A is being used, which results in a great compression of the concentration range as the concentration of A is increased. In practice, experimental data covering a range of A more than 10-fold is uncommon. Therefore, uncertainty exists as to whether a linear representation is exhibited with larger ranges of A values. Extrapolations to various intercepts are usually quite uncertain unless broad ranges in concentration are used or unless saturation of the protein is approached. Moreover, since r occurs on both the ordinate and abscissa of Scatchard plots and A occurs on both the ordinate and abscissa of the Scott representation, extrapolations should be viewed with some skepsis.

The graphical representations of the Klotz, Scatchard, and Scott plots are shown in Fig. 1 when multiple independent classes of sites exist on the macromolecule. In Table I, the limiting slope and intercept values are given for the situation in which two independent binding classes are displayed by the protein, each having one or more sites involved (14, 15). In the case of the much abused Scatchard plot, it can be seen from the table that slope 1 and intercept 3 are not equivalent to the frequently assumed values of K_1 and n_1, respectively. The situation is somewhat improved if K_1 is much larger than K_2, in which case the equations simplify to K_1 and n_1, respectively. If the binding constant of the second class of sites is not separated from the first by at least a power of 10, or if the number of binding sites in the second class far outweighs the number in the first, then, at best, only a hazardous prediction of the parameters can be made. The commonly used values for the slopes and intercepts are shown in parentheses in Table I.

Other graphical treatments have been suggested (16–19) but, in all instances, error terms are again plotted against one another. With the semilogarithmic plot (r *versus* log A), one can quite reliably determine the total number of sites on the macromolecule provided that saturation can be reached (19). Although the total number of sites (Σn_i) displayed by a protein for a particular ligand may be of interest from a physical standpoint, it is not an important quantity clinically or in pharmacokinetics. In other graphical methods, the fraction bound (usually given the symbol β) is used on the ordinate axis; this approach is fruitful when more than one binding protein exists in the mixture (16) but is of little value in the determination of quantitative binding constants.

Computer Procedures—Computerized treatment of protein binding data results in parameter fitting procedures generally regarded as more quantitative than graphical techniques. However, most of these analyses determine the parameters through a least-squares fit of the data based on the Scatchard model. In effect then, minimization of the square of the deviations from the "best" curve is carried out on data plotted in such a manner that substantial errors exist in both the ordinate and abscissa.

Fletcher and coworkers (20–22) described a computer technique designed to determine stepwise association constants in ligand–macromolecule interactions which may undergo cooperative binding and conformational changes. Their model is not constrained in that sites do not have to bind independently. Again, however, a least-squares fit of the data in the Scatchard model is used.

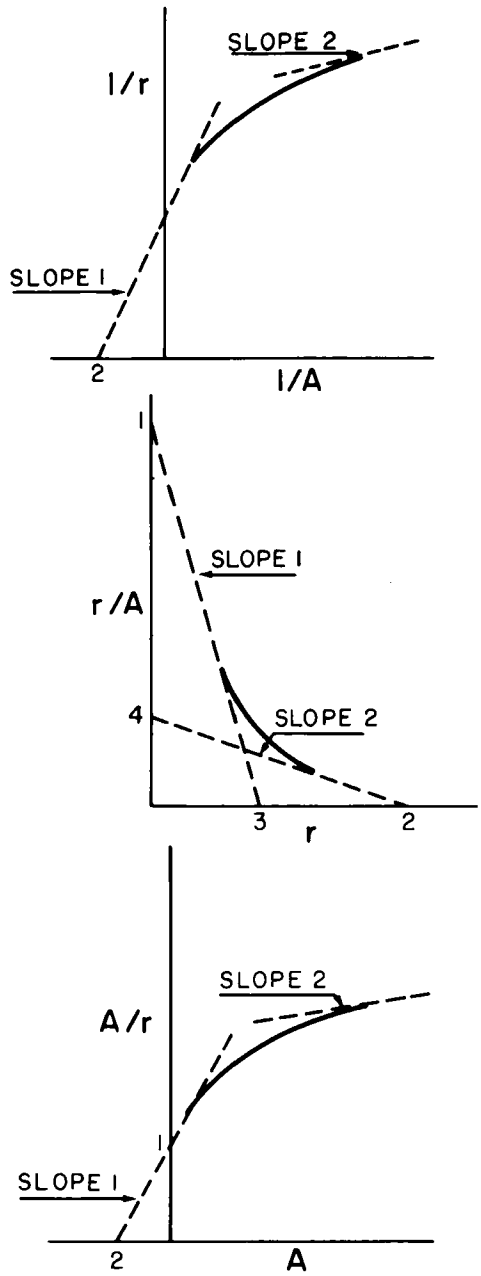

Figure 1—*Graphical representation of the Klotz, Scatchard, and Scott plots (in descending order) when multiple independent classes of sites exist on the macromolecule.*

Other computerized methods have been suggested (23–25), and parameter estimations are also based on either the minimization of Σ (errors)^2, which corresponds to the assumption that the free concentration is measured accurately compared to the bound concentration, or the assumption that errors in the bound concentration are not correlated with the free. When r/A is plotted against r (Scatchard plot), the assumption is adopted that the errors in r/A are much larger than the errors in r and independent of r.

Recently, a new method of binding data analysis appeared which circumvents the biased results obtained with other techniques (10). This method is based on a number of well-known statistical assumptions (26), the violation of which can cause serious errors in the parameter values estimated.

DISCUSSION

To illustrate more clearly some problems involved with the various procedures for handling drug binding data, the results of a dicumarol–human serum albumin and fenoprofen–albumin study will be

Table I—Values for Limiting Slopes and Intercepts when Two Independent Binding Classes, Each with One or More Sites, Exist on the Macromolecule[a]

Plot	Slope 1	Slope 2	Intercept 1	Intercept 2	Intercept 3	Intercept 4
$1/r$ *versus* $1/A$ (Klotz plot)	$\frac{\frac{n_1}{K_1}+\frac{n_2}{K_2}}{(n_1+n_2)^2}$	$\frac{1}{n_1K_1+n_2K_2}\left(\frac{1}{n_1K_1}\right)$	$\frac{1}{n_1+n_2}$	$\frac{2K_1K_2}{K_1+K_2}$	—	—
r/A *versus* r (Scatchard plot)	$\frac{n_1K_1^2+n_2K_2^2}{n_1K_1+n_2K_2}(-K_1)$	$\frac{n_1+n_2}{\frac{n_1}{K_1}+\frac{n_2}{K_2}}(-K_2)$	$n_1K_1+n_2K_2(n_1K_1)$	n_1+n_2	$\frac{(n_1K_1+n_2K_2)^2}{n_1K_1^2+n_2K_2^2}(n_1)$	$\frac{(n_1+n_2)^2}{\frac{n_2}{K_2}+\frac{n_2}{K_2}}$
A/r *versus* A (Scott plot)	$\frac{n_1K_1^2+n_2K_2^2}{(n_1K_1+n_2K_2)^2}\left(\frac{1}{n_1}\right)$	$\frac{1}{n_1+n_2}$	$\frac{1}{n_1K_1+n_2K_2}\left(\frac{1}{n_1K_1}\right)$	$\frac{n_1K_1+n_2K_2}{n_1K_1^2+n_2K_2^2}\left(\frac{1}{K_1}\right)$	—	—

[a] Values in parentheses result when K_1 is much larger than K_2 and n_2 is of the same order as n_1.

Table II—Summary of Literature Binding Affinities and Number of Sites for the Dicumarol–Albumin Interaction

Reference	n_1	K_1	n_2	K_2
23	2.1	$2.1 \times 10^6\ M^{-1}$	7.3	$1.4 \times 10^4\ M^{-1}$
27	1.0	$2.9 \pm 10\% \times 10^6\ M^{-1}$	1.0	$1.8 \pm 5\% \times 10^5\ M^{-1}$
28	2	$1.0 \times 10^5\ M^{-1}$	—	—
29	1	$2 \times 10^5\ M^{-1}$	—	—
30	3	$2–5.2 \times 10^5\ M^{-1}$	—	—

examined (15, 27). The dicumarol–albumin data presented (27) are considered precise quantitative information, so the variation in binding parameters, depending on the method of analysis, should not be overly significant. However, the fenoprofen–albumin interaction has led to less precise data (15). Since many techniques for studying drug–albumin interactions may lead to even less precision and quality of data, the variation in the parameters estimated can be of an extremely significant magnitude.

Dicumarol–Albumin Interaction—Table II summarizes literature binding parameter results for the anticoagulant–albumin interaction. These results indicate that various inadequacies must exist in either the experimental design or the compilation of data. A possibility for the results for K_1 being in the 10^5 range is that most experimental techniques used to measure free and bound drugs do not allow the investigator to obtain results at low binding ratios (*i.e.*, $r < 1$), particularly with this drug of very limited solubility. Therefore, obtaining a clinically significant binding constant becomes hazardous because the tangent (Scatchard plot, slope 1) drawn is usually less steep, giving a smaller binding constant, and intersects the r axis at larger r values, giving a greater number of equivalent binding sites than exists.

Examination of the data of Ref. 27 by the three graphical methods (invoking the assumptions that $K_1 > K_2$ and $n_1 \approx n_2$ allows these parameters to be obtained) and the newly developed computer technique (10) as well as the common Σ (errors)^2 gives the results shown in Figs. 2–5 and Table III. These data were considered to be accurate and reproducible and contained 66 data points obtained by a circular dichroic technique, which allowed for the accumulation of a large amount of data at low binding ratios. The accumulation of sufficient data at low binding ratios (*i.e.*, r values <1) is extremely important to the determination of a primary binding constant having clinical and pharmacokinetic application. Only these low ratios are usually reached with therapeutic dosages of a drug.

Figure 2 presents the Klotz plot, and it can be determined that two binding sites exist. Heterogeneity in the binding process is clearly indicated, so logic implies two classes of binding sites, each containing a single site. Making this assumption allows the binding constants for each class to be determined (Table III). The data show that slope 2 can, at best, be drawn only with large inaccuracy, and the calculation of binding parameters from it would be meaningless. The value of K_1 from the Klotz plot is approximately 50% higher than the value estimated by the newly developed computer technique; however, such discrepancies are common and inherent to binding analyses.

Figure 3 contains the data plotted in the Scatchard format. The

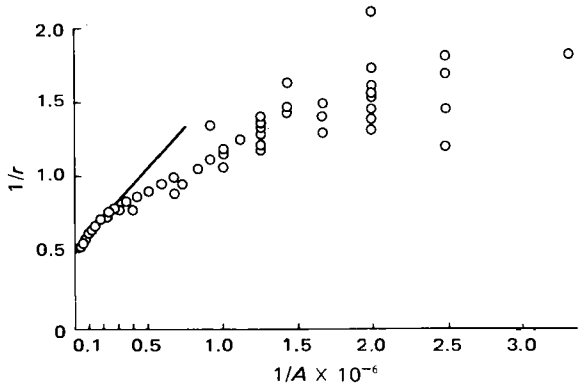

Figure 2—*Klotz (double-reciprocal) plot for the dicumarol–albumin interaction. (More points exist at low 1/A values than can be shown in the figure.)*

Table III—Dicumarol–Albumin Data[a]

Parameter	Graphical Value	Parameter Estimates			
		K_1	n_1	K_2	n_2
1/*r versus* 1/*A* (Klotz)					
Intercept 1	0.50				
Slope 1	1.14×10^{-6}				
Intercept 2	-4.38×10^{5}	5.4×10^{6}	—[b]	2.3×10^{5}	—[b]
Slope 2	1.79×10^{-7}				
r/A versus r (Scatchard)					
Intercept 1	3.36×10^{6}				
Slope 1	-3.30×10^{6}				
Intercept 3	1.00				
Intercept 4	4.37×10^{5}	3.61×10^{6}	1.0	4.1×10^{5}	1.0
Slope 2	-2.15×10^{5}				
Intercept 2	2.00				
A/r versus A (Scott)					
Intercept 1	1.11×10^{-7}				
Slope 1	1.12				
Intercept 2	-0.99×10^{-7}	4.45×10^{6}	—[c]	3.1×10^{5}	—[c]
Slope 2	—				
Σ(errors)^2 (computer)		1.4×10^{6}	0.53	3.3×10^{5}	1.45
New computer (Ref. 10)		$2.9 \pm (10\%) \times 10^{6}$	1.0	$1.8 \pm (5\%) \times 10^{5}$	1.0

[a] Values are for the slopes and intercepts of the three graphical procedures for binding estimation as well as the common and newly developed (10) computer techniques. Parameter estimates are given from all five techniques using the data from Ref. 27. [b] It was determined unequivocally that two classes of sites existed, but the number in each cannot be determined by this method. [c] Separation of terms in order to determine n_1 and n_2 is not possible with this method.

slopes and intercept values are presented in Table III. Good agreement for the numbers of sites present in each of the two classes from the Scatchard graphical procedure and the new computer treatment is seen. Moreover, the primary binding affinity is in excellent agreement with that of the unbiased computer method. It should be recalled, however, that these data for the dicumarol–albumin data are of a high quality, in direct contrast to those to be presented for the fenoprofen–albumin interaction.

Figure 4 represents the low free dicumarol data plotted in the manner of Scott. In common with the Klotz procedure, the n's cannot be determined; slope 2 is at best only grossly obtained.

Figure 5 presents the data plotted in the Scatchard manner but analyzed according to the newly developed computer technique (10, 27). The solid line in the figure is the result of holding $n_1 = n_2 = 1$ in the program; the dashed line allows n_1 and n_2, as well as K_1 and K_2, to be free floating. As can be seen from the figure, little difference results from fixed or free-floating n values, probably due to the quality of the data in this instance.

As seen from Table III, the results for K_1 and K_2 contain 95% confidence intervals, a feature of few other methods of binding analysis. Weights were incorporated in the program to allow for differing regions of error in the circular dichroic method. The fact that most methods of measuring free and bound ligand concentrations vary widely over the amount of ligand present in the system makes this an attractive inclusion in the minimization. Consequently, the parameters were minimized using the weighted form (26):

$$U = \sum_k W_k (G/G^1)^2 \qquad \text{(Eq. 6)}$$

The weights are inversely proportional to the variance of $Y_{obs,k}$. That is, when little drug exists as free drug or as saturation of the protein is approached, differences in the accuracy of measurement are inherent in almost all methods. In this case, relative error (*i.e.*, weight) of R_k is 4% if $0.9 \leq C_k \leq 1.3$, 11% if $C_k < 0.8$ or $1.5 < C_k$, and 7% if $0.8 \leq C_k < 0.9$ or $1.3 < C_k \leq 1.5$. For the 66 data points of the dicumarol–albumin study, the residuals ranged from -0.15×10^{-7} to 0.45×10^{-8} when the method of Ref. 10 was employed.

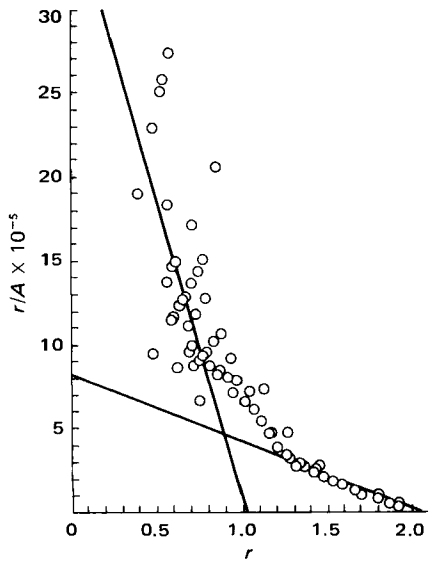

Figure 3—*Scatchard plot of the 66 data points obtained for the dicumarol–albumin interaction. Good agreement is seen between the graphical procedure and the newly developed computer method.*

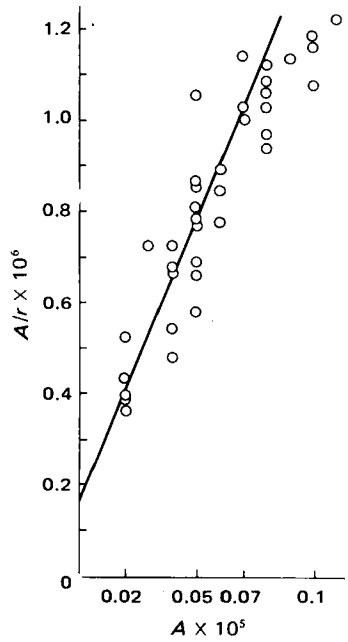

Figure 4—*Scott (half-reciprocal) plot of the data at low concentrations of unbound dicumarol (i.e., slope 1 of the Scott plot). When more free drug is present, the points become more separated and do not allow for slope 2 to be drawn with any degree of accuracy.*

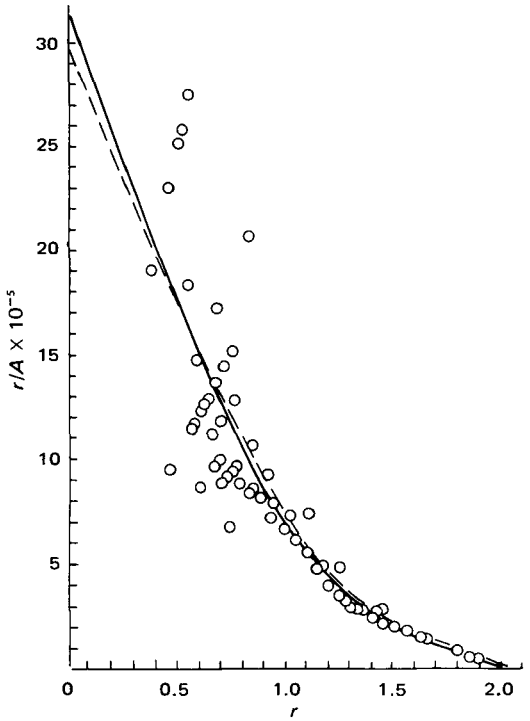

Figure 5—*Data analyzed according to the newly developed computer technique (10) and the resultant estimates for* n_1, n_2, K_1, *and* K_2 *represented in the Scatchard manner. (See text for explanation of solid and dashed curves.)*

Table III also contains parameter estimates for n_1, n_2, K_1, and K_2 of the dicumarol–albumin interaction based on minimization of the sum of squares of the errors, a common technique of computerized analyses. This procedure gives values for K_1 and n_1 far different from graphical analysis or the newly developed computer method. Perhaps the implied assumptions in such a technique, that the free concentration is measured accurately compared to the bound concentration and that the errors in the bound concentration are not correlated with the free (10), are somewhat less than adequate.

Fenoprofen–Albumin Interaction—Fenoprofen[1] [2-(3-phenoxyphenyl)propionic acid] is a nonsteroidal anti-inflammatory and analgesic drug. It has been shown to exhibit extrinsic optical activity following the binding to protein (31). Again the circular dichroic technique was chosen to assess the binding constants and numbers of sites displayed by albumin for this drug (15).

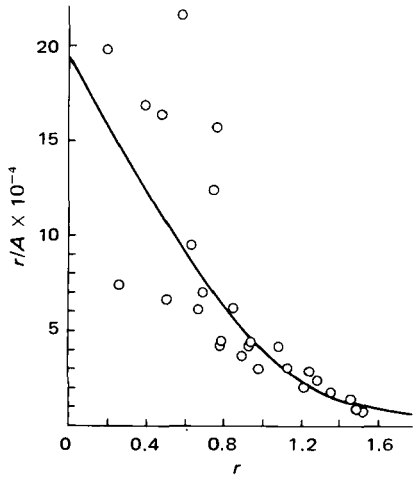

Figure 6—*Data for the fenoprofen–albumin interaction plotted according to the Scatchard technique, showing that considerable variability is present. The curve drawn is the result of the parameter estimates obtained according to the newly developed computer technique. If slopes 1 and 2 were drawn through the data, it would be expected that slope 1 would be much greater, resulting in an overestimated primary binding constant.*

[1] Eli Lilly and Co., Indianapolis, Ind.

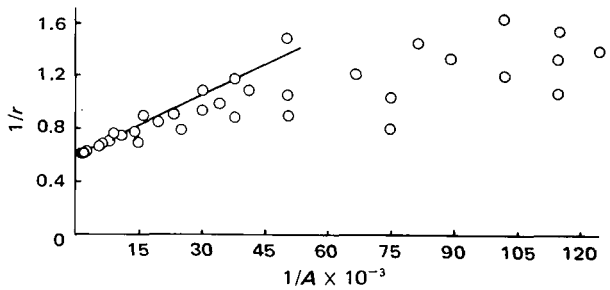

Figure 7—*Klotz plot of the fenoprofen–albumin data.*

Considerable variation in the fenoprofen binding data existed because of low signal-to-noise ratios (approximately 10:1) with this drug; it exhibited a rather small circular dichroic signal and had a relatively high absorbance. The circular dichroic peak was at 282 nm, a wavelength at which albumin has significant absorption, making quantitative measurements more difficult. Nevertheless, considerable data were obtained at low r values, certainly more than are possible with other more classical techniques. Overall, a total of 43 data points was obtained. However, the quality of the data and the reproducibility were not nearly so great as with the dicumarol data.

Table IV presents the results of the fenoprofen–albumin interactions when the graphical procedures and the unbiased computer techniques were used for data analysis. The graphical procedures (Figs. 6–8) overemphasize somewhat the slope used in the determination of the K_1 value; this fact can be seen readily upon examination of the Scatchard results in that the best slope through the points (using a linear least-squares fitting procedure) results in a large value for K_1 and an n_1 of 0.68. The significance of two-thirds of a binding site is somewhat obscure.

In applying the new computer technique, the values of all parameters (n_1, K_1, n_2, and K_2) were allowed to be free floating. Furthermore, in an attempt to assess the validity of the program to arrive at sensible estimates, the values for n_1 and n_2 were constrained to certain values. The results in Table IV for the computer technique are given when $n_1 = 1$ and $n_2 = 1$, which seemingly were the best estimates obtainable. In constraining n_1 from values of 0.6–2.0 (by increments of 0.1) while fixing n_2 at 1.0, it was observed that K_2 was negligible if K_1 was estimated with n_1 greater than 1.0. Also, when n_1 was greater than 1.0, the standard error for the K_1 value was high and the variance was large.

The estimates of K_1 and K_2 when $n_1 = 1$ and $n_2 = 1$ seem to make sense both from the standpoint of sensibility of the K_2 value (the Scatchard plot was curved, indicating a heterogeneity in binding sites so the data were analyzed on the basis of two classes of sites) and the standard errors for each value. Lending credibility to the likelihood of the correctness of $n_1 = 1$ and $n_2 = 1$ are the parameter estimates when no constraints are imposed on the system: $n_1 = 0.98 \pm 0.02$, $K_1 = 2.12 \pm 0.29 \times 10^5$, $n_2 = 0.81 \pm 0.11$, and $K_2 = 8.24 \pm 1.24 \times 10^3$.

Figure 6 presents some data points plotted according to the Scatchard procedure. The line through these points is the result obtained

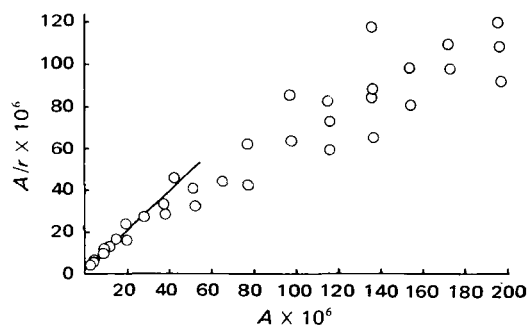

Figure 8—*Scott plot of the fenoprofen–albumin data.*

Table IV—Binding Parameters for the Fenoprofen–Albumin Interaction

Method of Analysis	K_1	K_2	n_1	n_2
Klotz	7.5×10^6	3.3×10^4	—	—
Scott	3.0×10^6	3.5×10^4	—	—
Scatchard	6.3×10^6	6.9×10^4	0.68	1.70
New computer	$1.86 \pm 0.21 \times 10^5$	$7.94 \pm 1.03 \times 10^3$	1.0	1.0

by the unbiased computer method ($K_1 = 1.8 \times 10^5$ and $K_2 = 7.94 \times 10^3$); the residuals ranged from -0.31×10^{-7} to 0.62×10^{-6}. It is readily apparent that had the data been analyzed by any of the graphical procedures alone, a much larger primary binding constant would have resulted.

Seemingly a good estimate of K_1 for the fenoprofen–albumin interaction was obtained. Supporting evidence for the assignment arises when one considers the only other work published (to date) measuring the binding of fenoprofen to albumin (32). In this work, the investigators stated that concentrations of 40 μg of fenoprofen/ml (which implies a 1.515×10^{-4} *M* solution) and 4.9 μg of albumin/ml (which is 7.10×10^{-5} *M*) were used in equilibrium dialysis experiments at pH 7.4. It was stated that 99% of the drug was bound at these concentrations and that the affinity constant was 3×10^4 at a saturation (total *n*) level of 4–5 moles of fenoprofen/mole of albumin. If one assumes that the binding affinity of all these sites is equal and applies simple mass law analysis, an affinity constant greater than 10^5 is obtained.

In the same work, data were presented on attempts to displace some drug from its albumin binding sites; however, in ratios greater than 3:1 of competitor to fenoprofen, various competitors were unable to act as antagonists. However, when phenylbutazone was used in a 10-fold excess [$K_1 = 2.37 \times 10^5$ (33)], it was able to displace fenoprofen. These data imply that either competitors do not compete for the same sites as fenoprofen or that fenoprofen has a binding constant greater than 3×10^4. It seems likely, therefore, that fenoprofen has a binding affinity for albumin greater than 10^5.

CONCLUSION

Obvious deficiencies are inherent in the various graphical methods of analyzing binding data. Computer techniques also exist; however, most fall into the same type of pitfalls; *i.e.*, the analysis is based on minimizing the error in terms of measured (error-containing) quantities. More statistically and, therefore, more clinically correct binding parameters may be obtained if one represents the problem in terms of independent and dependent variables. It can be seen from these analyses that merely fitting the data may result in parameter estimates widely different than those in which the situation is correctly treated by known statistical methods. It is also extremely important to have a fair number of data at low binding ratios ($r < 1$) if drug binding parameters with clinical significance are to be obtained.

REFERENCES

(1) A. Goldstein, *Pharmacol. Rev.*, **1**, 102(1949).

(2) B. K. Martin, *Nature*, **207**, 274(1965).

(3) I. Moriguchi, *Chem. Pharm. Bull.*, **16**, 597(1968).

(4) J. H. Perrin and D. A. Nelson, *J. Pharm. Pharmacol.*, **25**, 125(1973).

(5) M. C. Meyer and D. E. Guttman, *J. Pharm. Sci.*, **57**, 895(1968).

(6) W. A. Craig and C. M. Kunin, *Ann. Intern. Med.*, **78**, 491(1973).

(7) G. Evans and D. Shand, *Clin. Pharmacol. Ther.*, **14**, 494(1973).

(8) B. W. Madsen and J. S. Robertson, *J. Pharm. Pharmacol.*, **28**, 807(1974).

(9) H. G. Weder, J. Schildknecht, R. A. Lutz, and P. Kesselring, *Eur. J. Biochem.*, **42**, 475(1974).

(10) J. H. Perrin, J. J. Vallner, and S. Wold, *Biochim. Biophys. Acta*, **371**, 482(1974).

(11) G. F. Scatchard, *Ann. N.Y. Acad. Sci.*, **51**, 660(1949).

(12) I. M. Klotz, *Arch. Biochem.*, **9**, 109(1946).

(13) R. L. Scott, *Rec. Trav. Chim.*, **75**, 787(1956).

(14) I. M. Klotz and D. L. Hunston, *Biochemistry*, **10**, 3065(1971).

(15) J. J. Vallner, Ph.D. thesis, University of Wisconsin, Madison, Wis., 1974.

(16) H. E. Rosenthal, *Anal. Biochem.*, **20**, 525(1967).

(17) C. J. Thompson and I. M. Klotz, *Arch. Biochem. Biophys.*, **147**, 178(1974).

(18) A. Danchin and M. Gueron, *Eur. J. Biochem.*, **16**, 532(1970).

(19) H. A. Feldman, *Anal. Biochem.*, **48**, 317(1972).

(20) J. E. Fletcher and A. A. Spector, *Comput. Biomed. Res.*, **2**, 164(1968).

(21) J. E. Fletcher, A. A. Spector, and J. D. Ashbrook, *Biochemistry*, **9**, 4580(1970).

(22) J. E. Fletcher, J. D. Ashbrook, and A. A. Spector, *Ann. N.Y. Acad. Sci.*, **226**, 69(1973).

(23) S. Garten and W. D. Wosilart, *Comput. Programs Biomed.*, **1**, 281(1971).

(24) *Ibid.*, **2**, 61(1972).

(25) J. P. Raynaud, *Comput. Programs Biomed.*, **3**, 63(1973).

(26) G. Wahba and S. Wold, Tech. Rep. 275, Dept. of Statistics, University of Wisconsin, Madison, Wis., June 1974.

(27) J. H. Perrin, J. J. Vallner, and D. A. Nelson, *Biochem. Pharmacol.*, **24**, 769(1975).

(28) R. A. O'Reilly, *Mol. Pharmacol.*, **7**, 209(1971).

(29) M. J. Cho, A. G. Mitchell, and M. Pernarowski, *J. Pharm. Sci.*, **60**, 196(1971).

(30) C. F. Chignell, *Mol. Pharmacol.*, **6**, 1(1970).

(31) J. H. Perrin, *J. Pharm. Pharmacol.*, **25**, 208(1973).

(32) A. Rubin, P. Warrick, R. Wolen, S. Chernish, A. Ridolfo, and C. Gruber, *J. Pharmacol. Exp. Ther.*, **183**, 449(1972).

(33) A. Rosen, *Biochem. Pharmacol.*, **6**, 1(1970).

ACKNOWLEDGMENTS AND ADDRESSES

Received January 20, 1975, from the *School of Pharmacy and the Department of Statistics, University of Wisconsin, Madison, WI 53706*

Accepted for publication October 21, 1975.

* Present address: School of Pharmacy, University of Utrecht, Catharijnesingel 60, Utrecht, The Netherlands.

‡ Present address: Research Group for Chemometrics, Institute of Chemistry, Umea University, Umea, Sweden.

x To whom inquiries should be directed. Present address: School of Pharmacy, University of Georgia, Athens, GA 30602

Structure of Aluminum Hydroxide Gel I: Initial Precipitate

STEVEN L. NAIL *, JOE L. WHITE ‡, and STANLEY L. HEM *x

Abstract □ The initial aluminum hydroxide gel precipitate resulting from the reaction of aluminum chloride or aluminum sulfate with ammonium hydroxide is shown by potentiometric titration, chemical analysis, and the ratio of bound hydroxide to aluminum to fit a polymer model described previously. The formation of polynuclear hydroxyaluminum particles is treated as a stepwise process involving a deprotonation–dehydration mechanism, which results in the formation of six-membered rings; these rings may further coalesce by the same mechanism. The aluminum hydroxide gel precipitated from aluminum chloride can be represented by the formula $Al(OH)_{2.55}(Cl)_{0.45}$ and probably exists as a polymer of 10 fused six-membered rings. The aluminum hydroxide gel precipitated from aluminum sulfate can be represented by the formula $Al(OH)_{2.30}(SO_4)_{0.35}$. This species probably exists as a polymer of three fused six-membered rings.

Keyphrases □ Aluminum hydroxide gel—polymer structure of initial precipitate from reaction of aluminum chloride or sulfate with ammonium hydroxide □ Gels—aluminum hydroxide, polymer structure of initial precipitate from reaction of aluminum chloride or sulfate with ammonium hydroxide □ Polymer structure—aluminum hydroxide gel, initial precipitate from reaction of aluminum chloride or sulfate with ammonium hydroxide □ Antacids—aluminum hydroxide gel, polymer structure of initial precipitate from reaction of aluminum chloride or sulfate with ammonium hydroxide

Aluminum hydroxide gel is an effective antacid, although many aspects of its structure and acid reactivity are not well understood. Aluminum hydroxide gel is often represented by the formula $Al(OH)_3$. This representation is somewhat misleading, since the crystalline polymorphs of aluminum hydroxide, gibbsite, bayerite, and nordstrandite, are resistant to attack even by concentrated acid. In addition, acid-reactive aluminum hydroxide gels, useful as pharmaceutical antacids, contain anions associated with the gel structure (1–9).

The purposes of this investigation were to study the initial precipitate resulting from the reaction of solutions of aluminum chloride or aluminum sulfate with dilute ammonium hydroxide to a final pH of 7.0 and to propose a structure as the basis for explaining the antacid properties of aluminum hydroxide gel and the changes in antacid properties that occur upon aging. The proposed structure is based on potentiometric titration, chemical analysis, and reaction with sodium fluoride to determine the molar ratio of bound hydroxide to aluminum in the aluminum hydroxide gel.

EXPERIMENTAL

Materials—All chemicals used were either reagent or analytical grade.

Potentiometric Titrations—The ratio of hydroxyl to aluminum in the initial precipitate was determined by potentiometric titration of 0.294 *M* $AlCl_3 \cdot 6H_2O$ and 0.145 *M* $Al_2(SO_4)_3 \cdot 16H_2O$ with standard 1.0 *N* NaOH and 13% strong ammonia solution. The pH was measured[1] after the addition of each 5 ml of base, allowing the system to equilibrate until the pH was stable for 30 sec. The graphical method of Matijević *et al.* (10) was used to calculate the hydroxyl to aluminum ratio.

Sodium hydroxide was used as the titrant because it is a strong base and, therefore, gives an accurate value of the hydroxyl to aluminum ratio. Ammonium hydroxide was used because it is a common reactant in the precipitation of aluminum hydroxide gel.

Aluminum Hydroxide Gel Preparation—To make 1 liter of chloride-containing gel, 71.8 g of aluminum chloride hexahydrate was dissolved in 835 ml of distilled water. To make 1 liter of sulfate-containing gel, 92.6 g of aluminum sulfate hexadecahydrate was dissolved in 835 ml of distilled water. Ammonium hydroxide solution was then added at a rate of 120 ml/min.

The gel system was stirred[2] throughout the precipitation, and a combination electrode[3] was placed in the system for continuous monitoring of the pH. When the pH reached 4.5–5, there was a sharp increase in viscosity and a sharp rise in the rate of pH increase with further addition of base. At this point, base was added dropwise until pH 7.00 was reached. The system was maintained at this pH, with continuous stirring, for 30 min.

While being stirred continuously, the gels were washed with various amounts of deionized water by draining through a canvas bag. After washing, the volume of each gel was adjusted to 1 liter with distilled water.

Analytical Procedures—The equivalent aluminum oxide content was determined by the ethylenediaminetetraacetic acid titration (11).

The total chloride content was determined by the Volhard titration (12) after 3 g of gel was dissolved in 15 ml of 6 *N* nitric acid.

A procedure similar to that reported by Hsu and Bates (13) was used to determine the molar ratio of bound hydroxide to aluminum in the aluminum hydroxide gel samples. The procedure is as follows:

1. Place 50 ml of 0.5 *N* NaF in a 100-ml beaker. Add 2 drops of phenolphthalein indicator and measure the pH of the solution. If necessary, adjust the pH to about 7.4 with 0.10 *N* HCl.
2. Using a syringe, accurately weigh about 1.0 g of gel and add it to the sodium fluoride solution. Agitate thoroughly. Prepare a 50-ml aliquot of sodium fluoride solution as a blank.
3. Immerse the pH electrode in the sample and titrate to the original pH of the sodium fluoride solution (about 7.4) with standard 0.10 *N* HCl.
4. Cover the beaker containing the sample with aluminum foil or plastic wrap and place on a steam bath for 1 hr.
5. Allow the sample to cool and again titrate to the original pH. Repeat this heat-and-titrate operation until no more than 1 drop of 0.10 *N* HCl is required. The phenolphthalein serves as a visual indicator of the extent of reaction taking place with each heat-and-titrate step.
6. Record the total milliequivalents of acid used and subtract from this value the number of milliequivalents consumed by the blank. The net milliequivalents of acid consumed equals the milliequivalents of hydroxide liberated from the sample.
7. Calculate the molar ratio of bound hydroxide to aluminum from the milliequivalents of hydroxide liberated and the millimoles of aluminum present in the sample.

RESULTS AND DISCUSSION

Potentiometric Titrations—A plot of pH *versus* milliliters of base added is shown in Fig. 1 for the titration of 0.29 *M* $AlCl_3 \cdot 6H_2O$ with 1.0 *N* NaOH. The hydroxide to aluminum molar ratio is also shown on the *x*-axis. A very small increase in pH with addition of base was

[1] Model NX, Sargent-Welch Scientific Co., Skokie, Ill.

[2] "Stedi-Speed" stirrer, Fisher Scientific, Pittsburgh, Pa.

[3] Model S-30072-15, Sargent-Welch Scientific Co., Skokie, Ill.

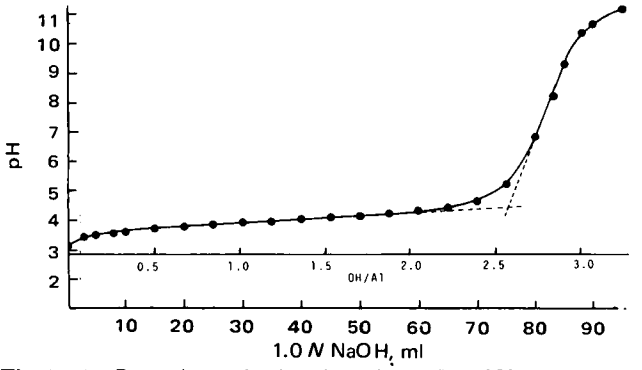

Figure 1—*Potentiometric titration of 0.29 M $AlCl_3$ with 1.0 N NaOH.*

observed for hydroxide to aluminum ratios in the 0–2 range. This finding indicates that the added hydroxide ions were immediately bound by aluminum ions. Little change in the appearance or viscosity of the precipitate occurred during this phase of the titration. At a ratio of about 2.5, there was a sharp increase in pH. At this point, the viscosity also sharply increased and the system changed in appearance from a dilute suspension to a gel.

Sodium hydroxide added beyond the break point of the curve caused a rapid increase in pH, which indicates that the hydroxide ions were not included in the hydroxyaluminum structure but were in solution. The ratio of hydroxyl to aluminum in the initial precipitate was taken as the point where added sodium hydroxide caused a sharp increase in pH (10), reflecting the appearance of hydroxide ions in solution. Hydroxide ions added prior to this point had little effect on pH, because they were bound by aluminum and were not free to affect the pH. As seen in Fig. 1, the hydroxyl to aluminum ratio in the initial precipitate formed from the reaction of aluminum chloride and sodium hydroxide was 2.55. A duplicate titration gave a value of 2.49.

The titration curve of a 0.29 *M* $AlCl_3 \cdot 6H_2O$ with 13% strong ammonia solution had an initial region in which the pH was nearly constant, indicating that the added hydroxide ions were bound by aluminum ions. A point was reached where the added hydroxide was not incorporated into the hydroxyaluminum structure, as evidenced by a rapid increase in pH. The rapid rise in pH began at pH 4.5, corresponding to the pH at the break point for the aluminum chloride–sodium hydroxide system. In addition, this gel increased in viscosity and changed in appearance at this point. These observations suggest that the initial aluminum hydroxide gel precipitated with ammonium hydroxide is equivalent to that precipitated with sodium hydroxide.

The potentiometric titration of 0.145 *M* $Al_2(SO_4)_3 \cdot 16H_2O$ with 1.0 *N* NaOH was similar to the titration shown in Fig. 1. In this case, the hydroxyl to aluminum ratio of the initial precipitate was 2.30.

Titration of a similar aluminum sulfate solution with 13% strong ammonia solution gave the same titration curve as was obtained for aluminum sulfate–sodium hydroxide.

The fact that the titration curves for aluminum chloride and aluminum sulfate gave different inflection points must be attributed to the different aluminum salt anion present. The hydroxyl to aluminum ratio taken from the titration curve of the aluminum chloride system suggests the formation of a hydroxyaluminum complex of approximate composition $Al(OH)_{2.50-2.55}Cl_{0.50-0.45}$. The titration curve of the sulfate system suggests a composition of approximately $Al(OH)_{2.30}(SO_4)_{0.35}$. These formulas represent average values, because the slow attainment of equilibria in these systems prevents the precise determination of the hydroxyl to aluminum ratio (14). In addition, there is evidence that hydrolyzed aluminum species are polynuclear (10, 14, 15).

Reaction with Fluoride—When aluminum hydroxide gels are treated with sodium fluoride solution, the fluoride ion displaces hydroxide ions from the gel structure (13, 16). The hydroxide ions released into solution are then titrated, which allows calculation of the hydroxide to aluminum ratio.

Duplicate determinations of the hydroxide to aluminum ratio of seven different chloride-containing gels precipitated at pH 7.0 gave an average value of 2.55 ± 0.03 (*SD*). The results of both the potentiometric titration experiment and hydroxide to aluminum ratio determinations by reaction with fluoride led to the postulation of an

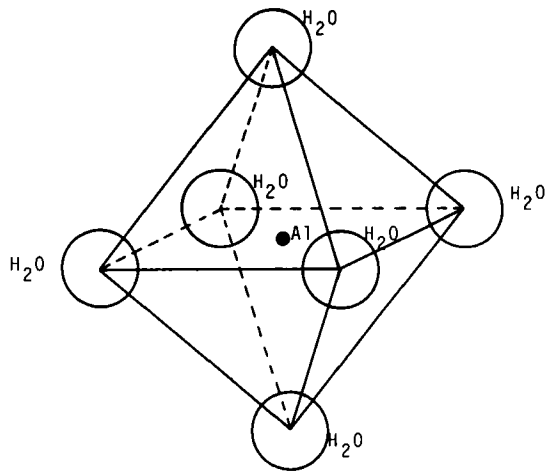

Figure 2—*Hydrolyzed aluminum ion $Al(OH_2)_6^{+3}$. (Reprinted, with permission, from Ref. 15.)*

empirical formula for the fresh precipitate of $Al(OH)_{2.55}Cl_{0.45}$. This ratio of hydroxide to aluminum is a numerical average. The fresh precipitate is probably a highly random structure (17, 18) containing polynuclear hydroxyaluminum species with a wide range of values of bound hydroxide to aluminum.

Duplicate determinations of the hydroxide to aluminum ratio of a gel precipitated from aluminum sulfate–ammonium hydroxide gave a value of 2.38, which is in reasonable agreement with the value of 2.30 obtained from the titration curve.

Based on these data, it is not possible to specify the number of aluminum atoms contained in the average polymeric particle. However, a theory that provides a structural picture of the formation of polynuclear hydroxyaluminum complexes by the neutralization of aqueous aluminum salt solutions has evolved in the mineralogy literature. This model, discussed in detail by Hem and Roberson (15), makes possible an estimate of the polymer size based on the hydroxide to aluminum molar ratio.

The formation of polynuclear hydroxyaluminum complexes in dilute solution was treated by Hem and Roberson (15) as a stepwise process involving a deprotonation–dehydration mechanism. In aqueous aluminum salt solutions below pH 4, aluminum exists primarily as the trivalent cation with six water molecules in octahedral coordination, $Al(H_2O)_6^{+3}$ (Fig. 2). The coordinated water molecules are oriented with the oxygen toward the aluminum ion. The high charge of the aluminum ion tends to weaken the oxygen—hydrogen bond of the coordinated water, which facilitates the removal of a proton and accounts for the initial low pH of aluminum salt solutions.

The first step in the conversion of hydrated aluminum ions to polymerized species involves deprotonation of one of the coordinated water molecules of the aluminum cation (Scheme I).

$$Al(OH_2)_6^{+3} \rightleftharpoons Al(OH)(OH_2)_5^{+2} + H^+$$

Scheme I

Two deprotonated octahedra can then join to form a dimer (Scheme II).

$$2Al(OH)(OH_2)_5^{+2} \rightleftharpoons Al_2(OH)_2(OH_2)_8^{+4} + 2H_2O$$

Scheme II

This unit contains the characteristic double hydroxide bridge between aluminum ions (Fig. 3).

Dimers then can join to form either a chain structure or a ring structure by the same deprotonation–dehydration mechanism. The general formula for a chain structure would be: $Al_m(OH)_{2m-2}(OH_2)_{2m+4}^{+(m+2)}$. The upper limit of the hydroxide to aluminum ratio for a chain structure is 2. This structure is not consistent with the experimental values of 2.55 and 2.38, nor would it allow the formation of bayerite, gibbsite, or nordstrandite, all having hydroxide to aluminum ratios of 3.0.

A ring structure can be formed by joining dimers (Fig. 4). These six-membered rings may then coalesce further by continued polymerization, resulting in a higher ratio of structural hydroxyl to alu-

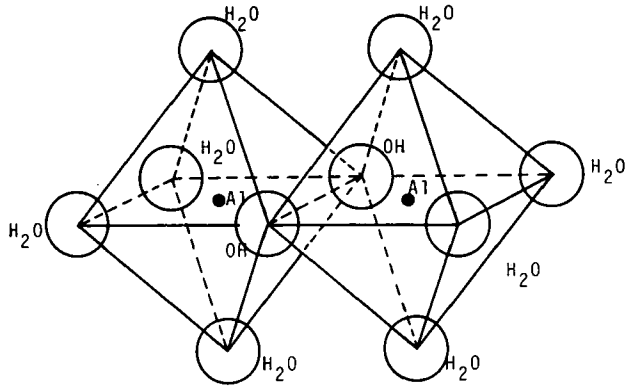

Figure 3—*Dimeric cation $Al_2(OH)_2(OH_2)_8^{+4}$. (Reprinted, with permission, from Ref. 15.)*

minum. The hydroxide to aluminum ratio approaches 3 as the structure increases in size.

The growth of a hydroxyaluminum particle by formation of six-membered rings and multiples thereof is shown in Scheme III. As the number of fused rings in a complex increases, there is a corresponding

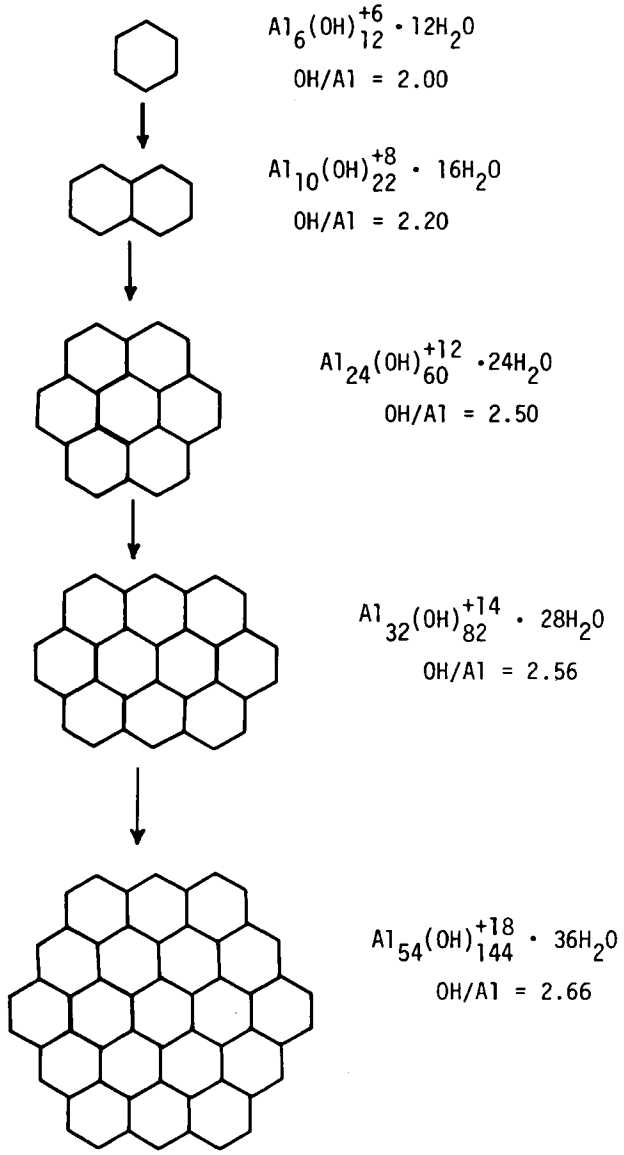

Scheme III—Proposed development of crystalline aluminum hydroxide. (Adapted from Ref. 13.)

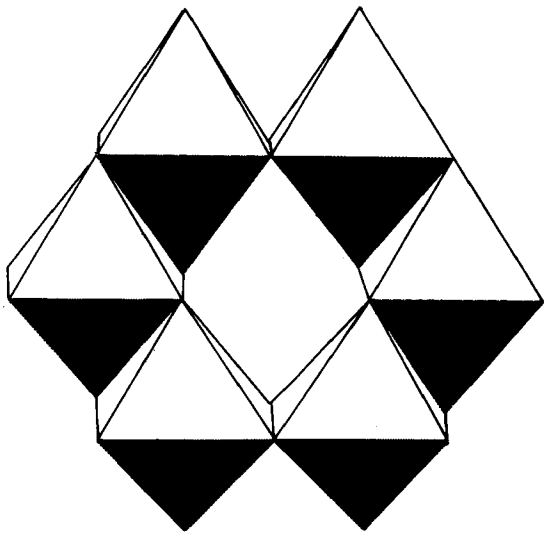

Figure 4—*Ring structure formed by six aluminum hydroxide octahedra. (Reprinted, with permission, from Ref. 15.)*

increase in the ratio of bound hydroxide to aluminum. For a gel precipitated from aluminum chloride and ammonium hydroxide at pH 7.0, this model would suggest that the predominant structure is a polymer of 10 fused rings, $Al_{32}(OH)_{82}^{+14} \cdot 28H_2O$. This species has a bound hydroxide to aluminum ratio of 2.56, which is in close agreement with the experimental data.

To propose a structure containing 32 aluminum atoms, it must be assumed that all hydroxide groups are present as double hydroxide bridges between aluminum atoms. It is possible that some hydroxide is bound to the polymer by single bonds to edge aluminum. For example, Brosset *et al.* (19) proposed a structure, $Al_6(OH)_{15}^{+3}$, consisting of a six-membered ring with the extra hydroxide groups attached by single bonds to alternate aluminum atoms in the ring. For a given number of aluminum atoms in the complex, the presence of these "nonstructural" hydroxide groups causes larger values of hydroxide to aluminum than those predicted from Scheme III. Therefore, the complex containing 32 aluminum atoms is the maximum size of the polymer that can be postulated from the available data.

It is apparent that the average polymer size resulting from the neutralization of aluminum sulfate solution is smaller than that of the corresponding chloride system. Based on a hydroxide to aluminum ratio of 2.30, a maximum polymer size of three rings containing 13 aluminum atoms is predicted.

Effect of Washing on Initial Precipitate—Several chloride-containing gels were precipitated at pH 7.0 and washed with various amounts of distilled water. Chloride concentrations were determined by the Volhard method (12), and the molar ratio of chloride to aluminum was calculated. These chloride to aluminum ratios varied from 0.78 for gels washed with 1 liter of water/liter of gel to 0.23 for gels washed with 5 liters of water/liter of gel. This range of values is in general agreement with a chloride to aluminum ratio of 0.45, which would be predicted from the hydroxide to aluminum ratio.

A direct relationship was observed between the chloride concentration in the gel after washing and the pH of the gel immediately after washing (Fig. 5). As chloride is removed from the gel by washing, the pH decreases. The chloride ions probably occupy edge position of the hydroxyaluminum particles (13). Removal of chloride by washing results in attraction of water molecules to the positive edge positions. Protons are released due to the polarization of these water molecules, resulting in the observed pH decrease.

Another mechanism contributing to the observed decrease in pH is that any hydroxide added after the inflection point of the titration curve is not bound. It follows that this extra hydroxide should be readily removed from the system by washing. These mechanisms explain the observed relationship between the amount of washing, or chloride content, and the pH after the washing operation.

It also was observed that addition of sodium chloride solution to a gel after washing caused a significant increase in the pH of the gel. A gel was precipitated, washed, and divided into two portions. One portion was diluted to final volume with distilled water, the other with 1 *N* NaCl. The pH of the gel diluted with water was 6.87, compared

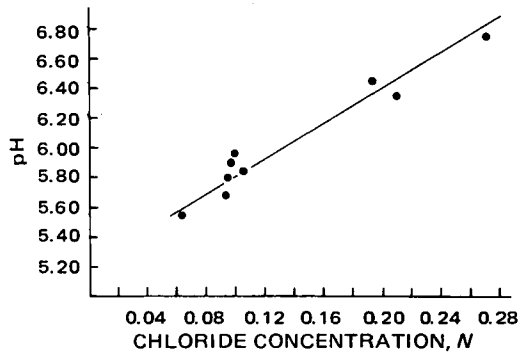

Figure 5—*Gel pH* versus *chloride concentration for gels precipitated at pH 7.0.*

to 8.28 for the gel diluted with 1 *N* NaCl. This finding suggests that the chloride ion displaced some hydroxide ion from the gel structure. Although the displacement of structural hydroxide cannot be ruled out, it seems more probable that chloride ions would displace the nonstructural hydroxyl groups from the edge of the hydroxyaluminum particles. The displacement of hydroxide by chloride would result in an increase in pH upon the addition of sodium chloride, as was observed. The direct relationship between chloride concentration in the gel and gel pH shown in Fig. 5 also supports this mechanism.

It was noted during washing studies that a direct relationship existed between the rate at which water drained from the gel during washing and the pH at which a gel was precipitated. For example, a gel precipitated at pH 5.5 drained quite slowly relative to a gel precipitated at pH 8.5. This observation could be explained by the fact that at pH 5.5, where the hydroxide to aluminum ratio is about 2.5, the positive charge per aluminum atom would be considerably greater than at pH 8.5, where the hydroxide to aluminum ratio is about 2.85 (Fig. 1). The higher charge at low pH means that more water would be polarized, or immobilized, at the lower pH. The higher charge also would result in a more dispersed system, which could produce a lower porosity cake and contribute to a slower draining rate.

SUMMARY

Based on potentiometric titrations and chemical analysis of the precipitate, the freshly precipitated chloride-containing gel can be represented by the empirical formula $Al(OH)_{2.55}Cl_{0.45}$. The empirical formula of the sulfate-containing gel prepared under the same conditions is $Al(OH)_{2.30}(SO_4)_{0.35}$. Polymerization by the formation of six-membered rings and multiples thereof would result in polymeric particles containing a maximum of 32 aluminum atoms per structure in the chloride-containing gel and a maximum of 13 aluminum atoms in the sulfate-containing gel.

The relationship between chloride concentration and gel pH suggests that the chloride ion may be weakly bound to positive sites at the edge of the hydroxyaluminum particles. Washing apparently removes chloride ions from these sites, resulting in an increase in the polarization of water by the edge aluminum ions and a concomitant decrease in pH.

REFERENCES

(1) R. I. Barnhisel and C. I. Rich, *Soil Sci. Soc. Am. Proc.*, **29,** 531(1965).

(2) R. C. Turner and G. J. Ross, *Can. J. Soil Sci.*, **49,** 389 (1969).

(3) R. C. Turner and G. J. Ross, *Can. J. Chem.*, **48,** 723(1970).

(4) S. L. Hem, E. J. Russo, S. M. Bahal, and R. S. Levi, *J. Pharm. Sci.*, **59,** 317(1970).

(5) G. J. Ross and R. C. Turner, *Soil Sci. Soc. Am. Proc.*, **35,** 389(1971).

(6) P. H. Hsu, *Int. Comm. Study Bauxites Aluminum Oxides-Hydroxides, 3rd,* **1973,** 613.

(7) J. L. White and S. L. Hem, *J. Pharm. Sci.*, **64,** 468(1975).

(8) P. H. Hsu, *Soil Sci. Soc. Am. Proc.*, **30,** 173(1966).

(9) P. H. Hsu, *Soil Sci.*, **103,** 101(1967).

(10) E. Matijević, K. G. Mathai, R. H. Ottewill, and M. Kerker, *J. Phys. Chem.*, **65,** 826(1961).

(11) "The United States Pharmacopeia," 18th rev., Mack Publishing Co., Easton, Pa., 1970, p. 26.

(12) I. M. Kolthoff, E. B. Sandell, E. J. Meehan, and S. Bruckenstein, "Quantitative Chemical Analysis," 4th ed., Macmillan, New York, N.Y., 1969, p. 799.

(13) P. H. Hsu and T. F. Bates, *Miner. Mag.*, **33,** 749(1964).

(14) J. Aveston, *J. Chem. Soc.*, **1965,** 4438.

(15) J. D. Hem and C. E. Roberson, "Form and Stability of Aluminum Hydroxide Complexes in Aqueous Solution," U.S. Geological Survey Water-Supply Paper 1827-A, U.S. Government Printing Office, Washington, D.C., 1967.

(16) J. M. Bracewell, A. S. Campbell, and B. D. Mitchell, *Clay Miner.*, **8,** 325(1970).

(17) S. L. Nail, J. L. White, and S. L. Hem, *J. Pharm. Sci.*, **64,** 1166(1975).

(18) *Ibid.*, **65,** 231(1976).

(19) C. Brosset, G. Biedermann, and L. G. Sillén, *Acta Chem. Scand.*, **8,** 1917(1954).

ACKNOWLEDGMENTS AND ADDRESSES

Received July 2, 1975, from the **Industrial and Physical Pharmacy Department, School of Pharmacy and Pharmacal Sciences, and the ‡Department of Agronomy, Purdue University, West Lafayette, IN 47907*

Accepted for publication February 19, 1976.

Supported in part by an American Foundation for Pharmaceutical Education Fellowship (S. L. Nail).

This report is Journal Paper 5934, Purdue University Agricultural Experiment Station, West Lafayette, IN 47907

ˣ To whom inquiries should be directed.

Structure of Aluminum Hydroxide Gel II: Aging Mechanism

STEVEN L. NAIL *, JOE L. WHITE ‡, and STANLEY L. HEM *x

Abstract □ The aging of aluminum hydroxide gel prepared by the reaction of aluminum chloride and ammonium hydroxide was studied by measurement of pH, acid-consuming capacity, hydroxide to aluminum ratio, chloride activity, and X-ray line broadening. The results were consistent with a polymer model involving particle growth by a deprotonation–dehydration mechanism. Anions inhibit this reaction by binding to the positively charged edges of the hydroxyaluminum polymers.

Keyphrases □ Aluminum hydroxide gel—aging mechanism studied, effect of anions □ Gels—aluminum hydroxide, aging mechanism studied, effect of anions □ Aging mechanism—aluminum hydroxide gel, effect of anions □ Antacids—aluminum hydroxide gel, aging mechanism studied

A polymer model based on a six-membered ring was found to describe the properties of an aluminum hydroxide gel precipitated by the reaction of aluminum chloride or aluminum sulfate solutions with sodium hydroxide or ammonium hydroxide to a final pH of 7.0 (1). The purpose of this investigation was to determine whether this polymer model can be applied to explain the loss of acid reactivity observed as the gel ages.

A series of aluminum hydroxide gels was prepared from aluminum chloride and ammonium hydroxide at a final pH of 7.0. The washing process was controlled to produce gels with different chloride concentrations. The aging process was then monitored by determination of the pH of the gel, acid-consuming capacity, hydroxide to aluminum molar ratio, and chloride activity in the gel. Crystallite size of the (*hkl*) dimensions of two different gels was measured by X-ray line broadening.

EXPERIMENTAL

Materials—All chemicals used were either reagent or analytical grade.

Aluminum Hydroxide Gel Preparation—Gels were prepared by the addition of 13% (v/v) strong ammonia solution to 0.29 *M* $AlCl_3 \cdot 6H_2O$ at a rate of 120 ml/min to a final pH of 7.0. Since this study involved the effect of washing on the aging characteristics of the gel, a large batch was precipitated (1) and subsequently divided into 1-liter portions to eliminate the effects of batch-to-batch variation. Each portion was washed individually with 1, 3, or 5 liters of distilled water, as previously described (1), and adjusted to 1 liter with distilled water.

The gels were stored in tightly capped 1-liter glass bottles.

Another gel was prepared in an identical manner except that aluminum sulfate replaced the aluminum chloride. To make 1 liter of gel, 92.6 g of aluminum sulfate hexadecahydrate was dissolved in 835 ml of distilled water.

Analytical Procedures—The equivalent aluminum oxide content was determined by the ethylenediaminetetraacetic acid titration (2). The prepared gels contained between 1.40 and 1.50% equivalent aluminum oxide.

The total chloride content was determined by the Volhard titration (3) after 3 g of gel was dissolved in 15 ml of 6 *N* nitric acid.

The molar ratio of bound hydroxide to aluminum was determined by reaction of a 1-g sample of gel with sodium fluoride solution (1). As the gel aged, several heat-and-titrate steps were required to drive the reaction to completion. The reported values are the averages of four determinations. The standard deviation ranged from 0.15 to 1.6%.

The pH of each gel was measured at approximately 5-day intervals. The pH meter[1] was calibrated prior to each measurement.

The acid-consuming capacity of each gel was determined as a function of age by a modification of the USP test (4). Samples were back-titrated to an end-point of pH 3.5 rather than using bromophenol blue TS as given in the USP.

The chloride activity of each gel was measured periodically by means of a chloride-selective electrode[2] and a pH meter[1] adjusted for millivolt measurement. Solutions of 1.0, 0.75, 0.50, 0.25, 0.10, and 0.05 *N* NaCl were standardized by the Volhard titration (3). The activity of these samples was calculated (5), and a calibration curve of millivolts *versus* the log of the chloride activity was prepared. The potential of the aluminum hydroxide gel samples was then measured, and the chloride activity was calculated from the calibration curve.

The total chloride content of each gel was determined by the Volhard titration periodically during aging to assure that changes in chloride activity were not due to changes in chloride concentration.

X-Ray Line-Broadening Measurements—The line widths of the (002) and (110) reflections were measured using a technique described by Klug and Alexander (6). Samples were prepared by the McCreery technique (7). The 4.27-Å peak of novaculite was used to determine the amount of broadening due to instrumental factors. Since instrumental broadening is a function of the diffraction angle, this peak was chosen because it lies close to the sample peaks of interest: 4.82 and 4.35 Å. The following conditions were used in recording the diffractogram: Cu K_α radiation, 40 kV, 20 mamp, 500 Hz sensitivity, and 0.2°/min scan speed.

RESULTS AND DISCUSSION

The aging of three portions of a gel, washed with 1, 3, or 5 liters of distilled water, was compared. The milliequivalents of chloride per millimole of aluminum in these gels were 0.80 (Gel I, wash volume of 1 liter), 0.37 (Gel II, wash volume of 3 liters), and 0.35 (Gel III, wash volume of 5 liters).

pH Measurement and Acid-Consuming Capacity—Plots of gel pH and the log of the acid-consuming capacity *versus* aging time for each of the three gels are shown in Figs. 1–3. By plotting the two parameters together, the relationship between the decrease in pH and a loss of acid reactivity is apparent.

The decrease in pH of the gel with age is consistent with a deprotonation–dehydration condensation polymerization reaction between adjacent hydroxyaluminum particles (8). This type of reaction results in the two particles being joined by one or more double hydroxide bridges. The formation of each double hydroxide bridge results in the release of two protons and two water molecules.

The pH *versus* time curves in Figs. 1–3 can be divided into four different parts. A relatively rapid decrease was seen during the first 1–10 days. A linear decrease was then seen until the gel pH reached about 5, at which time the pH decreased at a considerably faster rate. When the pH reached a value of 3.8–3.9, it remained nearly constant.

The initial decrease in pH was consistent with the incorporation of unbound hydroxide ions into the gel structure as double hydroxide bridges. During the first 20 days, the pH of Gel I (Fig. 1) decreased more rapidly than the other gels, probably because it had more "free" hydroxyl groups as evidenced by the highest initial pH. After the first 20 days, the rate of decrease in pH of this gel was slower than Gels II and III.

The reason for the break in the pH *versus* time curve at about pH 5 is not well understood; however, the physical appearance of the gel changed at a time corresponding to this break. Prior to this inflection point, the gel appeared as a milky dispersion which partially settled

[1] Model NX, Sargent-Welch Scientific Co., Skokie, Ill.
[2] Orion Research, Cambridge, Mass.

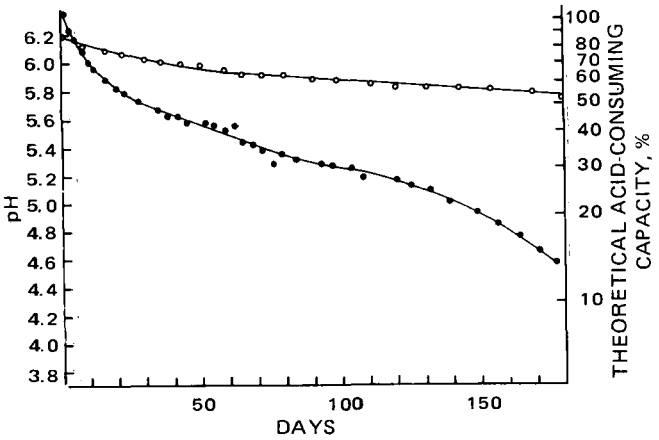

Figure 1—*Change in pH and acid-consuming capacity of Gel I during aging at 25°. Key: O, acid-consuming capacity; and ●, pH.*

when allowed to stand overnight. However, when a time was reached that apparently corresponded to the inflection point of the pH *versus* time curve, the gel became more translucent. No sediment was observed even when the gel was allowed to stand for prolonged periods; *i.e.*, the gel appeared to be completely dispersed.

The rate of interparticular condensation (and, therefore, the rate of decrease in pH of the gel) would be expected to be determined by the fraction of the total number of collisions due to Brownian motion between the particles that are of sufficient energy for a reaction to occur. This fraction would be affected by the interaction of van der Waals forces of attraction and electrical double-layer repulsion between the charged colloidal particles. Figure 4 is a typical potential energy curve showing the sum of the attractive and repulsive forces between particles.

The behavior of the gels might be explained by flocculation of the fresh gel due to the secondary minimum, *M*. The character of this type of flocculation is unique in that it is completely reversible and equilibrium distances between particles are of the order of several times the thickness of the double layer (9). Because of the potential energy barrier between particles, the rate of the deprotonation–dehydration reaction between particles would be expected to be relatively slow. However, each collision that does result in a reaction also results in a lower surface potential due to the neutralization of a positively charged edge aluminum ion. As this process continues and the surface potential approaches zero, the potential energy maximum, *S*, and secondary minimum, *M*, disappear (Fig. 4). The removal of the potential energy barrier, *S*, should increase the rate of the deprotonation–dehydration reaction, while removal of the secondary minimum, *M*, should result in deflocculation or dispersion of the system. Both of these phenomena, dispersion and an increased rate of change of pH, are observed experimentally at nearly the same time during aging.

Figures 1–3 show that the mechanism responsible for the decrease

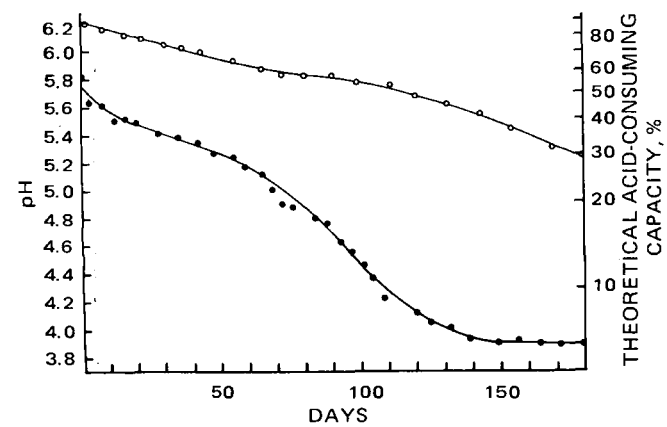

Figure 2—*Change in pH and acid-consuming capacity of Gel II during aging at 25°. Key: O, acid-consuming capacity; and ●, pH.*

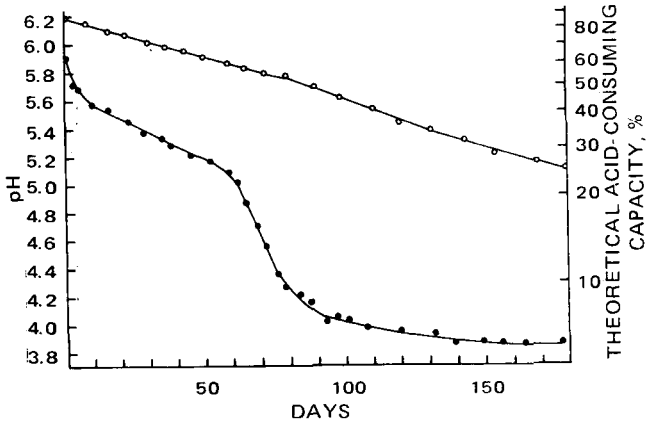

Figure 3—*Change in pH and acid-consuming capacity of Gel III during aging at 25°. Key: O, acid-consuming capacity; and ●, pH.*

in the pH of the gel with time also causes a decrease in acid-consuming capacity. Polymerization would result in a system in which the hydroxyaluminum particles are larger and more highly ordered; therefore, they should be less susceptible to attack by acid. Therefore, the relationship between acid-consuming capacity and pH decrease is strong evidence for the proposed deprotonation–dehydration reaction.

Based on this mechanism, it would be expected that once the pH reaches a constant value, the acid-consuming capacity should do the same. Figures 2 and 3 clearly indicate that this is not the case. There is, however, a mechanism by which the system could become more resistant to acid which involves no change in pH. According to Hsu (10), the crystallization of aluminum hydroxide involves the combination of small hydroxyaluminum particles vertically and horizontally. Vertical combination of particles, or stacking, involves hydrogen bonding between layers and would not affect the pH of the system. This explanation is feasible for the fact that acid-consuming capacity continues to decrease after the pH reaches a stable value.

Since the gels represented in Figs. 1–3 were precipitated as one batch, the observed differences in the rate of loss of reactivity must be attributed to differences in the amount of washing. The gels lost reactivity in the order III > II > I. There was an inverse relationship between the chloride concentration and the rate of decrease in pH and loss of acid-consuming capacity. This relationship could be accounted for by inhibition of a deprotonation–dehydration reaction by the chloride ion.

Aging of Gels Containing Sulfate—A gel was precipitated from aluminum sulfate with ammonium hydroxide solution to a final pH of 7.0. As seen in Fig. 5, the acid-consuming capacity and the pH remained nearly constant throughout the aging period studied. It is clear

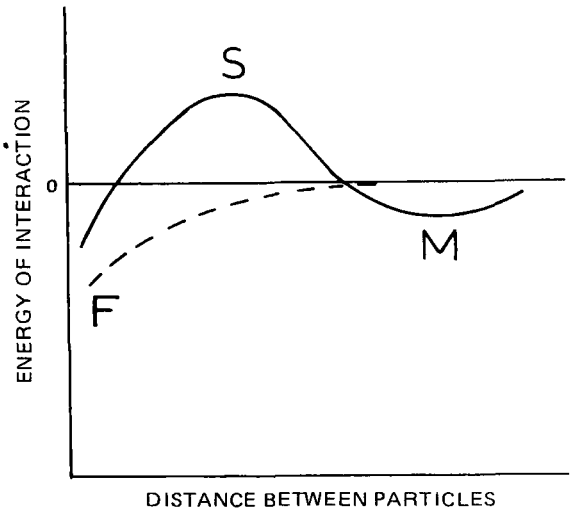

Figure 4—*Potential energy curve showing primary minimum, F, maximum, S, and secondary minimum, M. Key: —, charged surface; and - - -, uncharged surface. (Adapted from Ref. 9.)*

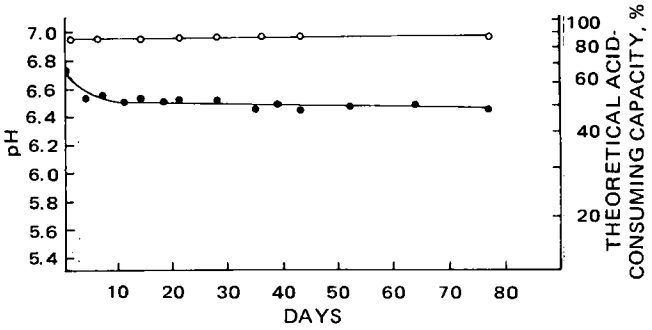

Figure 5—*Change in pH and acid-consuming capacity of sulfate-containing gel during aging at 25°. Key: ○, acid-consuming capacity; and ●, pH.*

that the gel containing sulfate was more stable than the corresponding chloride-containing gel.

Hydroxide to Aluminum Ratio—Plots of the molar ratio of bound hydroxide to aluminum for Gels I–III are shown in Fig. 6. The hydroxide to aluminum ratio increased as the gels aged. The change in hydroxide to aluminum ratio was greatest for Gel III, which was most thoroughly washed and therefore had the lowest chloride content. The hydroxide to aluminum ratio was increasing toward 3.0, which is the hydroxide to aluminum ratio that would be predicted by the polymer model as the *ab* dimension approaches infinity. As the hydroxide to aluminum ratio approaches 3, the system should develop the characteristics of a crystalline aluminum hydroxide.

Chloride Activity—The chloride activity, expressed as normality, was determined at several intermediate times during aging for Gels I–III (Fig. 7). The total chloride concentration, as determined by the Volhard titration, and the corresponding activity coefficients expected in aqueous solution are shown in Table I. The fourth column in Table I should represent the maximum value of the chloride activity in the respective gels. If, on the other hand, chloride is being bound by any component of the gel, the measured activity would be expected to be less than the value predicted by Table I.

As seen in Fig. 7, this was exactly what was observed experimentally. In Gels II and III, the chloride activity increased in the order III > II, corresponding to the rates of loss of acid reactivity, decrease in pH, and increase in hydroxide to aluminum ratio. The chloride activity of the gels ultimately reached a constant value which, as shown in Table I, was the activity expected if all chloride in the gels was in solution. These data indicate that chloride ions are being bound in the fresh gel and released gradually as the gel ages. This is consistent with a structural scheme in which anions are bound to the positively charged edge aluminum atoms of the hydroxyaluminum particles. Binding with sufficient strength would prohibit secondary hydrolysis of the edge aluminum, which leads to the formation of a double hydroxide bridge between particles. Although the presence of chloride inhibits this process, the bonding is apparently not strong enough to prevent it entirely.

This picture of the role of the anion is consistent with the fact that gels prepared from aluminum sulfate are more stable than those

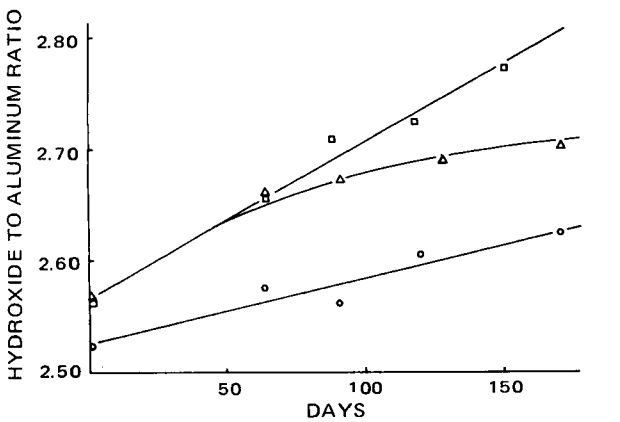

Figure 6—*Change in hydroxide to aluminum ratio during aging at 25°. Key: ○, Gel I; △, Gel II; and □, Gel III.*

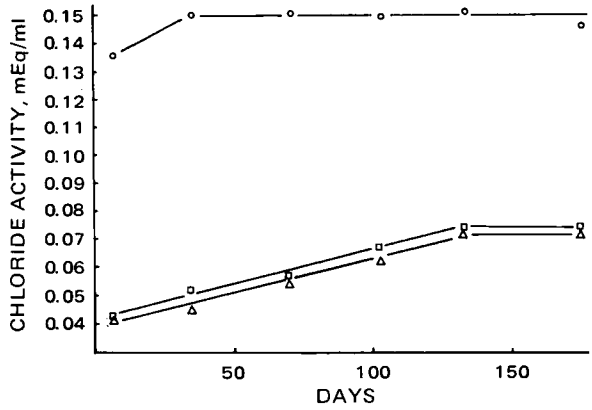

Figure 7—*Change in chloride activity during aging at 25°. Key: ○, Gel I; △, Gel II; and □, Gel III.*

prepared from aluminum chloride. The doubly charged sulfate ion would be expected to be more strongly attracted to the positive sites on the hydroxyaluminum particles than the singly charged chloride ion. The small change in pH with age of the sulfate gel (Fig. 5) compared to a chloride gel indicates that interparticular condensation is inhibited to a greater extent in the sulfate gel.

Before the deprotonation–dehydration reaction between particles can occur, the anion must be excluded from the gel structure. Hsu (11) proposed Scheme I for the aging of partially neutralized dilute hydroxyaluminum solutions.

$$(\text{initial polymer})^{+}\text{Cl}^{-} \xrightarrow{\text{rate-determining step}} (\text{initial polymer})^{+} + \text{Cl}^{-}$$

$$(\text{initial polymer})^{+} + \text{H}_2\text{O} \rightarrow (\text{initial polymer})\text{—OH} + \text{H}^{+}$$

$$\text{X(initial polymer)—OH} \rightarrow \text{larger polymer}$$

Scheme I

The first step of this scheme would account for the observed increase in chloride activity with age.

Crystallite Dimensions—It was shown previously (1) that the relative intensities of the 4.82- and 4.35-Å peaks of poorly crystalline aluminum hydroxide gels are reversed in comparison to highly crystalline gibbsite. The more rapid development of the (110) reflection (4.35 Å) is consistent with horizontal alignment of particles resulting from the deprotonation–dehydration reaction.

Two chloride-containing gels prepared under the same conditions were studied by X-ray diffraction. One had been aged for 1 year, the other for 6 months. The acid-consuming capacities were 9 and 22% of theory, respectively. The pH of both gels was between 3.8 and 3.9. The results for the two gels in terms of crystallite dimensions are D_{002} (Å) = 31.5 at 6 months and 37.3 at 1 year, D_{110} (Å) = 246.0 at 6 months and 238.0 at 1 year.

The dimension of the *ab* plane was nearly the same for the two gels. If crystal growth in the *ab* plane takes place by deprotonation–dehydration between smaller particles, the pH values of the gels would be expected to be nearly the same, which was the case.

The gel aged 1 year had a significantly larger dimension in the *c* direction than the 6-month sample. This finding indicates that stacking of structural units, involving no pH change, was more developed in the older gel. This mechanism could account for the observed difference in acid-consuming capacity.

These findings are consistent with the polymer model discussed previously (1). The initial reaction consists of polymerization of hy-

Table I—Chloride Concentration of Gels and Corresponding Activity Coefficients in Aqueous Solution

Gel	(Cl), *N*	γ^a	a_{Cl}, *N*	Final Activity Value (Experimental)
I	0.211	0.67	0.142	0.145
II	0.105	0.77	0.081	0.072
III	0.099	0.77	0.076	0.074

[a] From G. M. Barrow, "Physical Chemistry," 2nd ed., McGraw-Hill, New York, N.Y., 1961, p. 706.

droxyaluminum ions into stable six-membered rings or multiples thereof. According to Hsu and Bates (12), the inclusion of aluminum ions into rings is complete at a hydroxide to aluminum ratio of about 2. Additional base transforms these rings into larger units. Hsu (11) proposed that the difference between the initial precipitation process and the aging process is the source of hydroxide. Hydroxide added during precipitation is taken up rapidly, whereas the spontaneous hydrolysis is slow, especially in the presence of high salt concentrations (11). This secondary hydrolysis results in the formation of larger particles, which are more highly ordered and resistant to attack by acid, and leads ultimately to the formation of gibbsite (13, 14).

SUMMARY

The aging of aluminum hydroxide gels precipitated at pH 7.0 from aluminum chloride solution and strong ammonia solution was studied by determination of the hydroxide to aluminum ratio as a function of the age of the gel, measurement of gel pH and acid-consuming capacity, determination of the chloride activity of the gel, and X-ray line-broadening measurements. The results are consistent with a deprotonation–dehydration polymerization reaction in which positively charged hydroxyaluminum particles are joined at their edges by double hydroxide bridges. This process results in larger particles, which are more highly ordered and resistant to attack by acid. This reaction leads to the eventual formation of microcrystalline gibbsite.

Chloride was found to inhibit the loss of reactivity of aluminum hydroxide gel. The chloride activity increases as the gel ages until it reaches the activity of chloride in aqueous solution. It was concluded that chloride inhibits the loss of reactivity by binding at the positively charged edge of the hydroxyaluminum particles. This inhibits further polymerization of the particles.

A sulfate-containing gel precipitated at pH 7.0 was more stable than a chloride-containing gel precipitated at the same pH. This finding was attributed to stronger binding of the doubly charged sulfate ion by the polymers than the singly charged chloride ion.

REFERENCES

(1) S. L. Nail, J. L. White, and S. L. Hem, *J. Pharm. Sci.*, **65**, 1188(1976).

(2) "The United States Pharmacopeia," 18th rev., Mack Publishing Co., Easton, Pa., 1970, p. 27.

(3) I. M. Kolthoff, E. B. Sandell, E. J. Meehan, and S. Bruckenstein, "Quantitative Chemical Analysis," 4th ed., Macmillan, New York, N.Y., 1969, p. 799.

(4) "The United States Pharmacopeia," 18th rev., Mack Publishing Co., Easton, Pa., 1970, p. 26.

(5) Instruction Manual, Halide Ion Electrodes, Orion Research, Cambridge, Mass., 1971.

(6) H. P. Klug and L. E. Alexander, "X-ray Diffraction Procedures for Polycrystalline and Amorphous Materials," Wiley, New York, N.Y., 1954, chap. 9.

(7) *Ibid.*, p. 300.

(8) J. D. Hem and C. E. Roberson, "Form and Stability of Aluminum Hydroxide Complexes in Aqueous Solution," U.S. Geological Survey Water-Supply Paper 1827-A, U.S. Government Printing Office, Washington, D.C., 1967.

(9) L. I. Osipow, "Surface Chemistry," Kreiger, Huntington, N.Y., 1972, p. 95.

(10) P. H. Hsu, *Int. Comm. Study Bauxites Aluminum Oxides-Hydroxides, 3rd*, **1973**, p. 613.

(11) P. H. Hsu, *Soil. Sci. Soc. Am. Proc.*, **30**, 173(1966).

(12) P. H. Hsu and T. F. Bates, *Miner. Mag.*, **33**, 749(1964).

(13) S. L. Nail, J. L. White, and S. L. Hem, *J. Pharm. Sci.*, **64**, 1166(1975).

(14) *Ibid.*, **65**, 231(1976).

ACKNOWLEDGMENTS AND ADDRESSES

Received July 2, 1975, from the **Industrial and Physical Pharmacy Department, School of Pharmacy and Pharmacal Sciences, and the ‡Department of Agronomy, Purdue University, West Lafayette, IN 47907*

Accepted for publication October 23, 1975.

Supported in part by an American Foundation for Pharmaceutical Education Fellowship (S. L. Nail).

This report is Journal Paper 5944, Purdue University Agricultural Experiment Station, West Lafayette, IN 47907

ˣ To whom inquiries should be directed.

Structure of Aluminum Hydroxide Gel III: Mechanism of Stabilization by Sorbitol

STEVEN L. NAIL *, JOE L. WHITE ‡, and STANLEY L. HEM *ˣ

Abstract □ The effect of sorbitol on the aging of aluminum hydroxide gel, prepared by the reaction of aluminum chloride solution with strong ammonia solution to a final pH of 7.0, was studied by potentiometric titration, acid-consuming capacity, pH, hydroxide to aluminum ratio, chloride activity, X-ray diffraction, and IR spectroscopy. Gels containing sorbitol lost less than 10% of their acid-consuming capacity during a 6-month aging period compared with a loss of more than 60% for an identical gel without sorbitol. The mechanism by which sorbitol stabilizes the gel appears to be inhibition of the secondary polymerization reaction which takes place upon aging. Another polyhydroxy compound, quercetin, also stabilizes aluminum hydroxide gel.

Keyphrases □ Aluminum hydroxide gel—aging mechanism studied, effect of sorbitol □ Gels—aluminum hydroxide, aging mechanism studied, effect of sorbitol □ Aging mechanism—aluminum hydroxide gel, effect of sorbitol □ Antacids—aluminum hydroxide gel, aging mechanism studied, effect of sorbitol □ Sorbitol—effect on aging mechanism of aluminum hydroxide gel

Previous investigations (1, 2) demonstrated that a polymer model can be used to describe the structure and aging characteristics of aluminum hydroxide gel precipitated by the reaction of aluminum chloride or aluminum sulfate solution with sodium hydroxide or strong ammonia solution to a final pH of 7.0. The purpose of this investigation was to study the effect of sorbitol on the initial precipitate and on the aging characteristics of a gel prepared from aluminum chloride solution and strong ammonia solution at pH 7.0.

droxyaluminum ions into stable six-membered rings or multiples thereof. According to Hsu and Bates (12), the inclusion of aluminum ions into rings is complete at a hydroxide to aluminum ratio of about 2. Additional base transforms these rings into larger units. Hsu (11) proposed that the difference between the initial precipitation process and the aging process is the source of hydroxide. Hydroxide added during precipitation is taken up rapidly, whereas the spontaneous hydrolysis is slow, especially in the presence of high salt concentrations (11). This secondary hydrolysis results in the formation of larger particles, which are more highly ordered and resistant to attack by acid, and leads ultimately to the formation of gibbsite (13, 14).

SUMMARY

The aging of aluminum hydroxide gels precipitated at pH 7.0 from aluminum chloride solution and strong ammonia solution was studied by determination of the hydroxide to aluminum ratio as a function of the age of the gel, measurement of gel pH and acid-consuming capacity, determination of the chloride activity of the gel, and X-ray line-broadening measurements. The results are consistent with a deprotonation–dehydration polymerization reaction in which positively charged hydroxyaluminum particles are joined at their edges by double hydroxide bridges. This process results in larger particles, which are more highly ordered and resistant to attack by acid. This reaction leads to the eventual formation of microcrystalline gibbsite.

Chloride was found to inhibit the loss of reactivity of aluminum hydroxide gel. The chloride activity increases as the gel ages until it reaches the activity of chloride in aqueous solution. It was concluded that chloride inhibits the loss of reactivity by binding at the positively charged edge of the hydroxyaluminum particles. This inhibits further polymerization of the particles.

A sulfate-containing gel precipitated at pH 7.0 was more stable than a chloride-containing gel precipitated at the same pH. This finding was attributed to stronger binding of the doubly charged sulfate ion by the polymers than the singly charged chloride ion.

REFERENCES

(1) S. L. Nail, J. L. White, and S. L. Hem, *J. Pharm. Sci.*, **65**, 1188(1976).

(2) "The United States Pharmacopeia," 18th rev., Mack Publishing Co., Easton, Pa., 1970, p. 27.

(3) I. M. Kolthoff, E. B. Sandell, E. J. Meehan, and S. Bruckenstein, "Quantitative Chemical Analysis," 4th ed., Macmillan, New York, N.Y., 1969, p. 799.

(4) "The United States Pharmacopeia," 18th rev., Mack Publishing Co., Easton, Pa., 1970, p. 26.

(5) Instruction Manual, Halide Ion Electrodes, Orion Research, Cambridge, Mass., 1971.

(6) H. P. Klug and L. E. Alexander, "X-ray Diffraction Procedures for Polycrystalline and Amorphous Materials," Wiley, New York, N.Y., 1954, chap. 9.

(7) *Ibid.*, p. 300.

(8) J. D. Hem and C. E. Roberson, "Form and Stability of Aluminum Hydroxide Complexes in Aqueous Solution," U.S. Geological Survey Water-Supply Paper 1827-A, U.S. Government Printing Office, Washington, D.C., 1967.

(9) L. I. Osipow, "Surface Chemistry," Kreiger, Huntington, N.Y., 1972, p. 95.

(10) P. H. Hsu, *Int. Comm. Study Bauxites Aluminum Oxides-Hydroxides, 3rd*, **1973**, p. 613.

(11) P. H. Hsu, *Soil. Sci. Soc. Am. Proc.*, **30**, 173(1966).

(12) P. H. Hsu and T. F. Bates, *Miner. Mag.*, **33**, 749(1964).

(13) S. L. Nail, J. L. White, and S. L. Hem, *J. Pharm. Sci.*, **64**, 1166(1975).

(14) *Ibid.*, **65**, 231(1976).

ACKNOWLEDGMENTS AND ADDRESSES

Received July 2, 1975, from the **Industrial and Physical Pharmacy Department, School of Pharmacy and Pharmacal Sciences, and the ‡Department of Agronomy, Purdue University, West Lafayette, IN 47907*

Accepted for publication October 23, 1975.

Supported in part by an American Foundation for Pharmaceutical Education Fellowship (S. L. Nail).

This report is Journal Paper 5944, Purdue University Agricultural Experiment Station, West Lafayette, IN 47907

ˣ To whom inquiries should be directed.

Structure of Aluminum Hydroxide Gel III: Mechanism of Stabilization by Sorbitol

STEVEN L. NAIL *, JOE L. WHITE ‡, and STANLEY L. HEM *ˣ

Abstract □ The effect of sorbitol on the aging of aluminum hydroxide gel, prepared by the reaction of aluminum chloride solution with strong ammonia solution to a final pH of 7.0, was studied by potentiometric titration, acid-consuming capacity, pH, hydroxide to aluminum ratio, chloride activity, X-ray diffraction, and IR spectroscopy. Gels containing sorbitol lost less than 10% of their acid-consuming capacity during a 6-month aging period compared with a loss of more than 60% for an identical gel without sorbitol. The mechanism by which sorbitol stabilizes the gel appears to be inhibition of the secondary polymerization reaction which takes place upon aging. Another polyhydroxy compound, quercetin, also stabilizes aluminum hydroxide gel.

Keyphrases □ Aluminum hydroxide gel—aging mechanism studied, effect of sorbitol □ Gels—aluminum hydroxide, aging mechanism studied, effect of sorbitol □ Aging mechanism—aluminum hydroxide gel, effect of sorbitol □ Antacids—aluminum hydroxide gel, aging mechanism studied, effect of sorbitol □ Sorbitol—effect on aging mechanism of aluminum hydroxide gel

Previous investigations (1, 2) demonstrated that a polymer model can be used to describe the structure and aging characteristics of aluminum hydroxide gel precipitated by the reaction of aluminum chloride or aluminum sulfate solution with sodium hydroxide or strong ammonia solution to a final pH of 7.0. The purpose of this investigation was to study the effect of sorbitol on the initial precipitate and on the aging characteristics of a gel prepared from aluminum chloride solution and strong ammonia solution at pH 7.0.

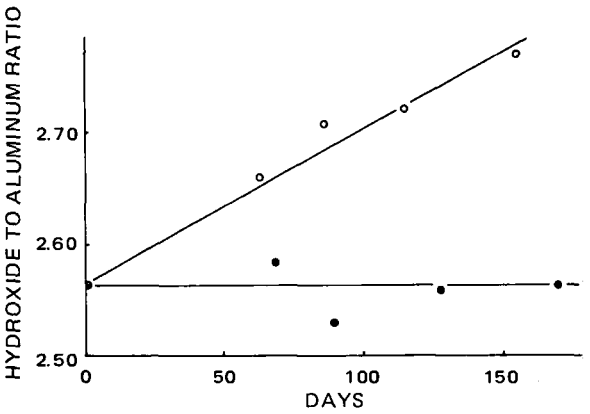

Figure 1—*Change in hydroxide to aluminum ratio during aging at 25°. Key: ○, Gel I; and ●, Gel II.*

EXPERIMENTAL

Materials—All chemicals used were either reagent or analytical grade.

Potentiometric Titrations—One hundred milliliters of a solution of 0.29 *M* $AlCl_3 \cdot 6H_2O$ and an identical solution containing 1 g of sorbitol were titrated potentiometrically with standard 1.0 *N* NaOH. The system was allowed to equilibrate after the addition of each aliquot of base until the pH[1] was stable for 30 sec.

Aluminum Hydroxide Gel Preparation—Two liters of gel was prepared by the addition of 13% (v/v) strong ammonia solution to a solution of 143.6 g of aluminum chloride hexahydrate in 1670 ml of distilled water at a rate of 120 ml/min. The gel system was stirred throughout the precipitation, and a combination electrode[2] was placed in the system for continuous monitoring of pH. Strong ammonia solution was added until pH 7.0 was reached, and the system was maintained at this pH for 30 min. The gel was then washed with 10 liters of distilled water by draining through a canvas bag. The gel was stirred throughout the washing operation.

After washing, the gel was divided into equal portions, and the volume of each portion was adjusted to 1 liter. For the first portion (I), the final volume adjustment was made with distilled water. For the second portion (II), 10 g of sorbitol was dissolved in distilled water and added to the gel with stirring, and the gel was diluted to 1 liter with distilled water. The gels were prepared in this manner to eliminate any effects of batch-to-batch variation.

Analytical Procedures—The equivalent aluminum oxide content, total chloride content, molar ratio of bound hydroxide to aluminum, pH, acid-consuming capacity, chloride activity, and X-ray diffraction pattern of the gels were determined as previously described (2). The hydroxyl-stretching region of the IR spectrum was recorded using a commercial IR spectrophotometer[3]. Samples were prepared by air drying a 0.10-ml sample on a silver chloride window[4]. The concentration on the window was 0.3 mg of aluminum oxide/cm^2.

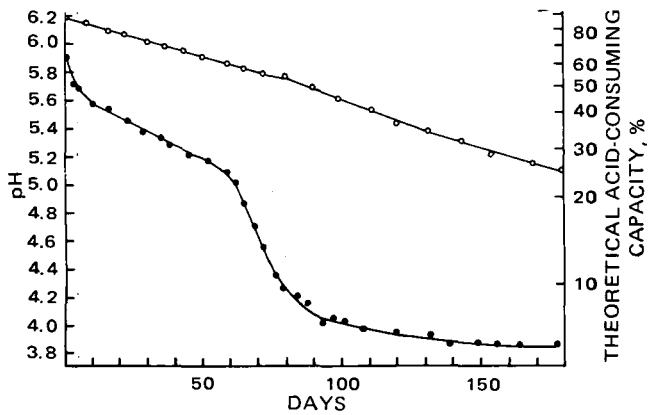

Figure 2—*Change in pH and acid-consuming capacity of Gel I during aging at 25°. Key: ○, acid-consuming capacity; and ●, pH.*

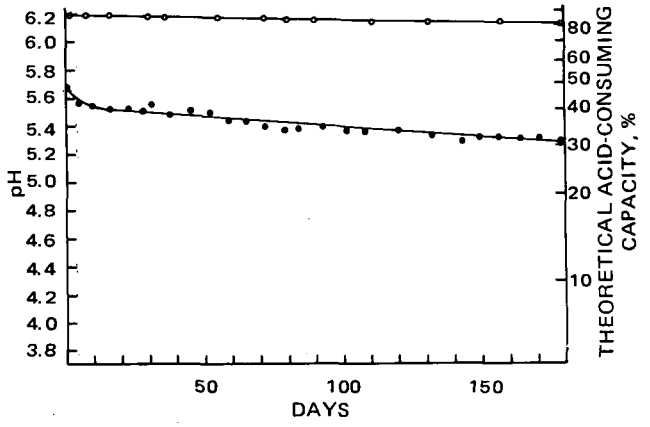

Figure 3—*Change in pH and acid-consuming capacity of Gel II during aging at 25°. Key: ○, acid-consuming capacity; and ●, pH.*

RESULTS AND DISCUSSION

Potentiometric Titrations—Potentiometric titrations of 0.29 *M* $AlCl_3 \cdot 6H_2O$ and a similar solution containing 1% (w/v) sorbitol with 1.0 *N* NaOH were performed. The purpose of these titrations was to determine whether any interaction takes place between sorbitol and the hydroxyaluminum complex during gel formation. The two curves were nearly parallel, with the inflection point occurring at a hydroxide to aluminum ratio of 2.51 for both titrations. This result indicates that the primary polymerization reaction is not affected by the presence of sorbitol.

Hydroxide to Aluminum Ratio—The change in the molar ratio of bound hydroxide to aluminum with time is shown in Fig. 1 for Gels I and II. For Gel I, the ratio increased from 2.57 to 2.75 after 150 days. After the same aging time, the ratio for Gel II was between 2.55 and 2.60.

The increase in the hydroxide to aluminum ratio of Gel I indicates that further polymerization occurred during aging (2). The fact that the ratio for Gel II remained relatively constant indicates that secondary polymerization did not take place. Since the gels were precipitated and washed as one batch, the observed difference must be attributed to the presence of sorbitol in Gel II. Sorbitol apparently inhibits the secondary polymerization reaction.

pH and Acid-Consuming Capacity—Plots of the change in pH and acid-consuming capacity with time are shown in Figs. 2 and 3 for Gels I and II, respectively. During 180 days of aging, the pH of Gel I decreased from 5.70 to 3.85 while the acid-consuming capacity decreased from 88 to 25% of the theoretical capacity (Fig. 2). During the

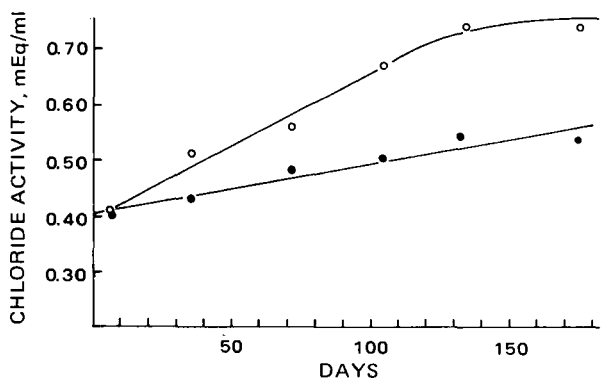

Figure 4—*Change in chloride activity during aging at 25°. Key: ○, Gel I; and ●, Gel II.*

[1] Model NX, Sargent-Welch Scientific Co., Skokie, Ill.
[2] Sargent-Welch Scientific Co., Skokie, Ill.
[3] Model 421, Perkin-Elmer Corp., Norwalk, Conn.
[4] Harshaw Chemical Co., Cleveland, Ohio.

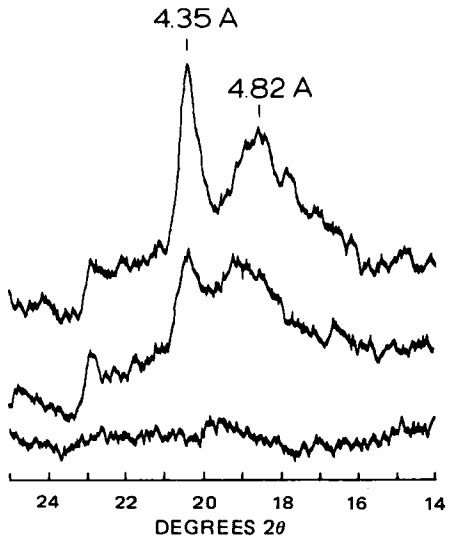

Figure 5—*Change in X-ray diffraction pattern of Gel I during aging at 25°. Key: bottom, 38 days; middle, 94 days; and top, 143 days.*

same period, the pH of Gel II decreased from 5.67 to 5.38 and the acid-consuming capacity decreased from 87 to 81% of the theoretical capacity.

The pH decrease with age is predicted by the deprotonation–dehydration reaction (2) leading to larger, more ordered particles. Increased order with age is consistent with lower acid reactivity. The stability of the pH of Gel II relative to that of Gel I is strong evidence for inhibition of the deprotonation–dehydration reaction by sorbitol.

Chloride Activity—Changes in chloride activity for the two gels (Fig. 4) are also consistent with inhibition of the secondary polymerization reaction by sorbitol. Increased activity of chloride with age indicates that the anion is initially bound by the gel (2) and released during aging. Therefore, the rate of increase in the activity should correspond with the rate of change in the other indicators of secondary polymerization, *i.e.*, pH, acid-consuming capacity, and hydroxide to aluminum ratio. The rate of chloride activity increase in the sorbitol-containing gel was significantly less than for the control gel, which had released virtually all bound chloride after 150 days.

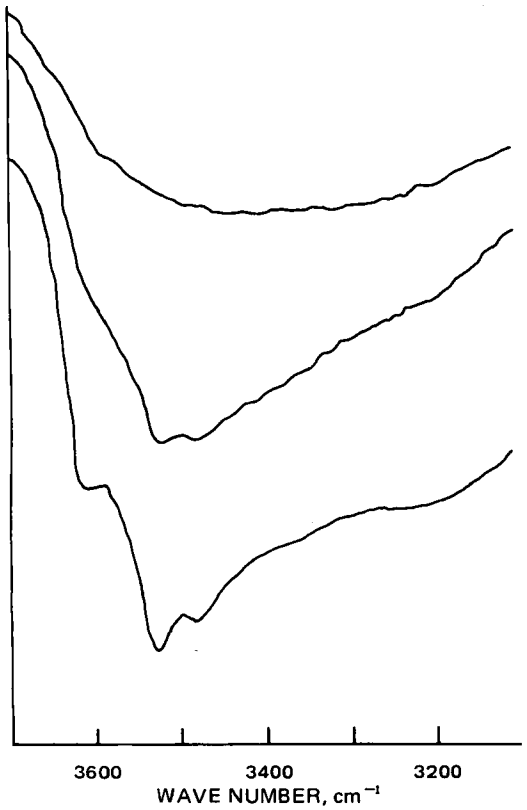

Figure 6—*Change in hydroxyl-stretching region of Gel I during aging at 25°. Key: top, fresh precipitate; middle, 89 days; and bottom, 147 days.*

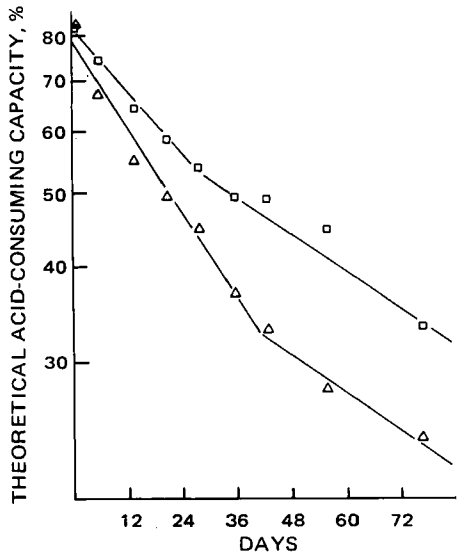

Figure 7—*Change in acid-consuming capacity during aging at 25°. Key: □, gel containing quercetin; and △, gel without quercetin.*

X-Ray Diffraction and IR Spectroscopy—In previous studies (3, 4), X-ray diffraction and IR spectroscopy were employed to detect the formation of microcrystalline gibbsite in aluminum hydroxide gel. Figures 5 and 6 show the change in the X-ray diffractogram and IR spectrum with age for Gel I. Crystalline material is readily detected by both techniques after about 100 days. No significant changes occurred in either the X-ray diffractogram or the IR spectrum of Gel II, which contained sorbitol. This retention of its original amorphous nature is in sharp contrast to the behavior of Gel I.

Other Polyhydroxy Compounds—Various other polyhydroxy compounds such as glycine (5), sucrose (6), disaccharides (7), hydroxypropylcellulose (8), and polyethylene glycol (9) have been reported to stabilize the reactivity of aluminum hydroxide gel.

Another study was carried out under the same conditions of gel preparation with quercetin (3,3′,4′,5,7-pentahydroxyflavone) in solution during precipitation. Since quercetin is only slightly soluble (0.5 g/liter), the aluminum chloride was dissolved in a saturated solution of quercetin. The change in acid-consuming capacity with age was then compared with that of a control gel prepared under the same conditions without quercetin (Fig. 7). The quercetin-containing gel was more stable than the control gel. Some quercetin probably was removed from the gel during washing. A more significant stabilizing effect would probably occur if quercetin was added after the gel was prepared, as is the usual practice with sorbitol.

SUMMARY

Comparison of changes in the hydroxide to aluminum ratio, chloride activity, pH, acid-consuming capacity, X-ray diffractogram, and IR spectrum of an aluminum hydroxide gel with an identical gel containing 1% (w/v) sorbitol showed that the mechanism responsible for aging is strongly inhibited by sorbitol. Potentiometric titration curves indicate that sorbitol is not incorporated into the hydroxyaluminum structure during gel precipitation.

The observed behavior can be explained by hydrogen bonding between the hydroxyl groups of sorbitol and the edge of the hydroxyaluminum particles, thus inhibiting further polymerization with age. It is believed that the stabilizing effect of other polyhydroxy compounds involves a similar mechanism.

REFERENCES

(1) S. L. Nail, J. L. White, and S. L. Hem, *J. Pharm. Sci.*, **65**, 1188(1976).

(2) *Ibid.*, **65**, 1192(1976).

(3) *Ibid.*, **64**, 1166(1975).
(4) *Ibid.*, **65**, 231(1976).
(5) S. M. Beekman, U.S. pat. 3,208,906 (1965); through *Chem. Abstr.*, **63**, 17809a(1965).
(6) B. K. Davison and R. E. Schaffer, *J. Pharm. Pharmacol.*, **13**, 95T(1961).
(7) Y. Ideguchi and K. Shibata, Japanese pat. 7,005,659 (1970); through *Chem. Abstr.*, **72**, P103769y(1970).
(8) L. C. Greene, A. Misher, and W. E. Smith, U.S. pat. 3,591,680 (1971); through *Chem. Abstr.*, **75**, P80265b(1971).
(9) R. Persson and J. Sjoergren, German pat. 1,467,767 (1968); through *Chem. Abstr.*, **73**, P38544a(1970).

ACKNOWLEDGMENTS AND ADDRESSES

Received July 2, 1975, from the **Industrial and Physical Pharmacy Department, School of Pharmacy and Pharmacal Sciences, and the ‡Department of Agronomy, Purdue University, West Lafayette, IN 47907*

Accepted for publication October 23, 1975.

Supported in part by an American Foundation for Pharmaceutical Education Fellowship (S. L. Nail).

This report is Journal Paper 5945, Purdue University Agricultural Experiment Station, West Lafayette, IN 47907

ˣ To whom inquiries should be directed.

Kinetics and Mechanisms of Hydrolysis of 1,4-Benzodiazepines I: Chlordiazepoxide and Demoxepam

WESLEY W. HAN *, GERALD J. YAKATAN, and DALE D. MANESS ˣ

Abstract □ Differential absorbance spectroscopy was successfully used to follow the hydrolysis kinetics of chlordiazepoxide and demoxepam from pH 1 to 11. Loss of the methylamino group from chlordiazepoxide produced demoxepam. Demoxepam degraded by a parallel consecutive reaction to 2-amino-5-chlorobenzophenone and a glycine derivative. Two intermediates were observed by TLC for demoxepam hydrolysis. One was assigned the open-ring structure, resulting from amide hydrolysis, which kinetically appears to be the major mechanistic route leading to the benzophenone product. The other intermediate, representing an alternative but minor pathway, presumably results from initial scission of the azomethine linkage. Protonation of the *N*-oxide slightly alters the importance of these two pathways. Recyclization of the carboxylic acid intermediate was facile at pH values below the pKa of this intermediate. The stability parameters involving buffer catalysis, ionic strength effects, and temperature dependence of rate constants are reported.

Keyphrases □ 1,4-Benzodiazepines—kinetics and mechanisms of hydrolysis evaluated by differential absorbance spectroscopy □ Chlordiazepoxide—kinetics and mechanisms of hydrolysis evaluated by differential absorbance spectroscopy □ Demoxepam—kinetics and mechanisms of hydrolysis evaluated by differential absorbance spectroscopy □ Hydrolysis—chlordiazepoxide and demoxepam, kinetics and mechanisms, evaluated by differential absorbance spectroscopy □ Differential absorbance spectroscopy—evaluation of kinetics and mechanisms of hydrolysis of chlordiazepoxide and demoxepam

Little kinetic information is available on the solution stability and mechanisms of hydrolytic reactions of the 1,4-benzodiazepines. This class of nitrogen heterocycles is susceptible to acid–base-catalyzed hydrolysis at two potential sites of scission: the 1,2-amide linkage and the 4,5-azomethine bond. Both bonds undergo heterolysis under appropriate solvolytic conditions, forming a substituted benzophenone product and a glycine derivative (1–3).

Chlordiazepoxide (I) was reported (4) to degrade sequentially in aqueous solution, yielding 2-amino-5-chlorobenzophenone as the final product. An isolated intermediate in the reaction is the corresponding lactam, demoxepam (II); II is formed by hydrolytic cleavage of the methylamino substituent at the 2-position of chlordiazepoxide. That study (4) described kinetically the hydrolysis of chlordiazepoxide to the intermediate lactam. The purpose of the present study is to describe completely the kinetics and mechanism of hydrolysis from the parent molecule to the product benzophenone. This paper is the first of a series that will describe quantitatively the kinetics and mechanisms of hydrolysis of 1,4-benzodiazepines.

EXPERIMENTAL

Materials—The purity of the compounds was verified by TLC. Chlordiazepoxide[1], demoxepam[1], and 2-amino-5-chlorobenzophenone[1] were used without further purification. All other chemicals were of reagent grade quality. Distilled, deionized water was used for preparing aqueous solutions.

The buffer systems used were: pH 1.0–3.0, hydrochloric acid; pH 3.2–5.6, acetate; pH 4.7–7.4, phosphate; pH 6.9–9.5, borate; and pH 10.1–11, sodium hydroxide. The ionic strength was adjusted to 1.0 with sodium chloride, except for the ionic strength effect studies. The pH values were determined with a digital pH meter[2] at the temperature of the kinetic run.

Kinetic Measurements—The compound to be studied was dissolved in ethanol to make a 10^{-3} *M* stock solution. It was stored in the refrigerator in a light-protected flask to eliminate reported photolytic reactions (5). A light-protected reaction flask containing appropriate buffer solution was equilibrated at reaction temperature in a constant-temperature oil bath[3]. Less than ±0.05° variation was measured with an iron–constantan thermocouple.

An appropriate amount of stock solution was pipetted into the reaction flask so that the final concentration was about 10^{-5} *M*. An aliquot was withdrawn and quenched immediately in a light-protected ice water bath. The UV spectrum of the aliquot was measured as the zero-time sample on a recording spectrophotometer[4]. Subsequent aliquots were analyzed similarly at suitable time intervals for at least three half-lives of the slowest reaction. The final measurement, ab-

[1] Hoffmann–La Roche, Nutley, N.J.
[2] Orion model 701 equipped with a high temperature electrode, Cambridge, Mass.
[3] Sargent model SW equipped with a Sargent thermonitor (model ST), Dallas, Tex.
[4] Coleman model 124, Maywood, Ill.

(3) *Ibid.*, **64**, 1166(1975).
(4) *Ibid.*, **65**, 231(1976).
(5) S. M. Beekman, U.S. pat. 3,208,906 (1965); through *Chem. Abstr.*, **63**, 17809a(1965).
(6) B. K. Davison and R. E. Schaffer, *J. Pharm. Pharmacol.*, **13**, 95T(1961).
(7) Y. Ideguchi and K. Shibata, Japanese pat. 7,005,659 (1970); through *Chem. Abstr.*, **72**, P103769y(1970).
(8) L. C. Greene, A. Misher, and W. E. Smith, U.S. pat. 3,591,680 (1971); through *Chem. Abstr.*, **75**, P80265b(1971).
(9) R. Persson and J. Sjoergren, German pat. 1,467,767 (1968); through *Chem. Abstr.*, **73**, P38544a(1970).

ACKNOWLEDGMENTS AND ADDRESSES

Received July 2, 1975, from the **Industrial and Physical Pharmacy Department, School of Pharmacy and Pharmacal Sciences, and the ‡Department of Agronomy, Purdue University, West Lafayette, IN 47907*

Accepted for publication October 23, 1975.

Supported in part by an American Foundation for Pharmaceutical Education Fellowship (S. L. Nail).

This report is Journal Paper 5945, Purdue University Agricultural Experiment Station, West Lafayette, IN 47907

ˣ To whom inquiries should be directed.

Kinetics and Mechanisms of Hydrolysis of 1,4-Benzodiazepines I: Chlordiazepoxide and Demoxepam

WESLEY W. HAN *, GERALD J. YAKATAN, and DALE D. MANESS ˣ

Abstract □ Differential absorbance spectroscopy was successfully used to follow the hydrolysis kinetics of chlordiazepoxide and demoxepam from pH 1 to 11. Loss of the methylamino group from chlordiazepoxide produced demoxepam. Demoxepam degraded by a parallel consecutive reaction to 2-amino-5-chlorobenzophenone and a glycine derivative. Two intermediates were observed by TLC for demoxepam hydrolysis. One was assigned the open-ring structure, resulting from amide hydrolysis, which kinetically appears to be the major mechanistic route leading to the benzophenone product. The other intermediate, representing an alternative but minor pathway, presumably results from initial scission of the azomethine linkage. Protonation of the *N*-oxide slightly alters the importance of these two pathways. Recyclization of the carboxylic acid intermediate was facile at pH values below the pKa of this intermediate. The stability parameters involving buffer catalysis, ionic strength effects, and temperature dependence of rate constants are reported.

Keyphrases □ 1,4-Benzodiazepines—kinetics and mechanisms of hydrolysis evaluated by differential absorbance spectroscopy □ Chlordiazepoxide—kinetics and mechanisms of hydrolysis evaluated by differential absorbance spectroscopy □ Demoxepam—kinetics and mechanisms of hydrolysis evaluated by differential absorbance spectroscopy □ Hydrolysis—chlordiazepoxide and demoxepam, kinetics and mechanisms, evaluated by differential absorbance spectroscopy □ Differential absorbance spectroscopy—evaluation of kinetics and mechanisms of hydrolysis of chlordiazepoxide and demoxepam

Little kinetic information is available on the solution stability and mechanisms of hydrolytic reactions of the 1,4-benzodiazepines. This class of nitrogen heterocycles is susceptible to acid–base-catalyzed hydrolysis at two potential sites of scission: the 1,2-amide linkage and the 4,5-azomethine bond. Both bonds undergo heterolysis under appropriate solvolytic conditions, forming a substituted benzophenone product and a glycine derivative (1–3).

Chlordiazepoxide (I) was reported (4) to degrade sequentially in aqueous solution, yielding 2-amino-5-chlorobenzophenone as the final product. An isolated intermediate in the reaction is the corresponding lactam, demoxepam (II); II is formed by hydrolytic cleavage of the methylamino substituent at the 2-position of chlordiazepoxide. That study (4) described kinetically the hydrolysis of chlordiazepoxide to the intermediate lactam. The purpose of the present study is to describe completely the kinetics and mechanism of hydrolysis from the parent molecule to the product benzophenone. This paper is the first of a series that will describe quantitatively the kinetics and mechanisms of hydrolysis of 1,4-benzodiazepines.

EXPERIMENTAL

Materials—The purity of the compounds was verified by TLC. Chlordiazepoxide[1], demoxepam[1], and 2-amino-5-chlorobenzophenone[1] were used without further purification. All other chemicals were of reagent grade quality. Distilled, deionized water was used for preparing aqueous solutions.

The buffer systems used were: pH 1.0–3.0, hydrochloric acid; pH 3.2–5.6, acetate; pH 4.7–7.4, phosphate; pH 6.9–9.5, borate; and pH 10.1–11, sodium hydroxide. The ionic strength was adjusted to 1.0 with sodium chloride, except for the ionic strength effect studies. The pH values were determined with a digital pH meter[2] at the temperature of the kinetic run.

Kinetic Measurements—The compound to be studied was dissolved in ethanol to make a 10^{-3} *M* stock solution. It was stored in the refrigerator in a light-protected flask to eliminate reported photolytic reactions (5). A light-protected reaction flask containing appropriate buffer solution was equilibrated at reaction temperature in a constant-temperature oil bath[3]. Less than ±0.05° variation was measured with an iron–constantan thermocouple.

An appropriate amount of stock solution was pipetted into the reaction flask so that the final concentration was about 10^{-5} *M*. An aliquot was withdrawn and quenched immediately in a light-protected ice water bath. The UV spectrum of the aliquot was measured as the zero-time sample on a recording spectrophotometer[4]. Subsequent aliquots were analyzed similarly at suitable time intervals for at least three half-lives of the slowest reaction. The final measurement, ab-

[1] Hoffmann–La Roche, Nutley, N.J.
[2] Orion model 701 equipped with a high temperature electrode, Cambridge, Mass.
[3] Sargent model SW equipped with a Sargent thermonitor (model ST), Dallas, Tex.
[4] Coleman model 124, Maywood, Ill.

sorbance at infinite time, was made after 10 half-lives. Beer's law plots were constructed to ensure that absorbance was directly proportional to concentration.

Product and Intermediate Identification—For isolation and identification studies, the solutions were prepared to be 10^{-3} *M*. Samples were withdrawn at various times, lyophilized, and redissolved in chloroform for TLC analysis. The chloroform solutions were spotted on silica gel GF plates, 250 μm, and eluted for about 50 min, using the solvent system of dioxane–benzene–hexane–7.4 *M* NH_4OH (45:50:70:5).

The chromatograms, after air drying, were visualized under UV light or developed with ninhydrin aerosol spray reagent. Reference standards, when available, were spotted directly on TLC plates. When possible, intermediates were isolated by preparative TLC (1000-μm plates). IR[5], NMR[6], and high-resolution mass[7] spectra were obtained on the isolated compound.

RESULTS AND DISCUSSION

Kinetically, the hydrolysis of 1,4-benzodiazepines may be expected to proceed as depicted in Scheme I. In this scheme, I represents chlordiazepoxide, II represents the 1,4-benzodiazepin-2-one, III is the intermediate resulting from hydrolysis of the 1,2-amide bond, IV is the intermediate derived from rupture of the 4,5-azomethine linkage, and V and VI are the products, benzophenone and the glycine derivative.

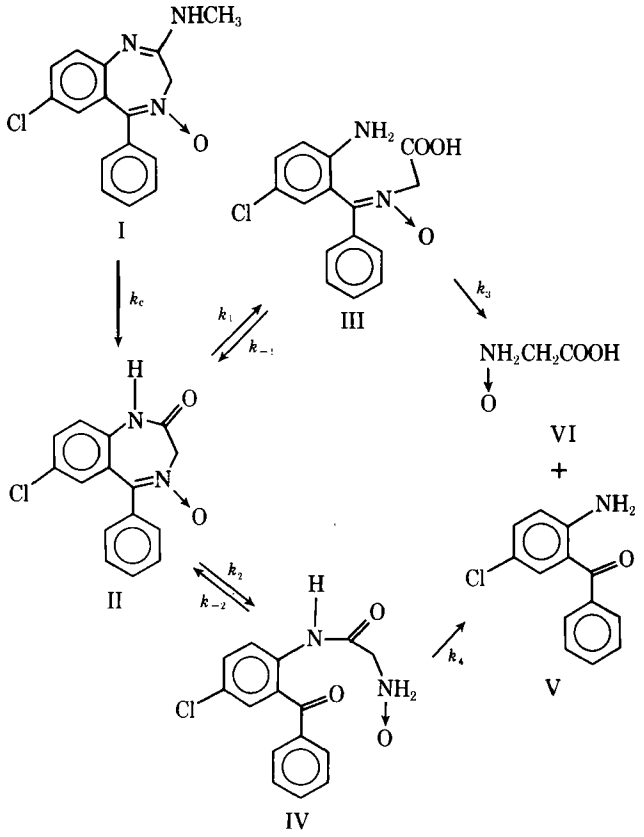

Scheme I

Chlordiazepoxide represents a special case of 1,4-benzodiazepine hydrolysis, since cleavage of the methylamino group is required to form II. Inclusion of this step adds an exponential term into a general integrated rate expression, but it can be experimentally eliminated by studying demoxepam hydrolysis. The two steps leading to intermediates III and IV are shown as reversible steps, since, under appropriate conditions, the reversion for III was experimentally observed (6). From entropy considerations, reversibility from final products to intermediates is not expected to be as favorable as the initial steps.

By solving the differential equations for Scheme I by using Laplace transforms and determinants, unique expressions for the concentration–time dependence of each species may be obtained:

$$[II]/[II]_0 = A_{11}\exp(-b_1t) + A_{12}\exp(-b_2t) + A_{13}\exp(-b_3t) + A_{14}\exp(-b_4t) \quad \text{(Eq. 1)}$$

$$[III]/[II]_0 = A_{21}\exp(-b_1t) + A_{22}\exp(-b_2t) + A_{23}\exp(-b_3t) + A_{24}\exp(-b_4t) \quad \text{(Eq. 2)}$$

$$[IV]/[II]_0 = A_{31}\exp(-b_1t) + A_{32}\exp(-b_2t) + A_{33}\exp(-b_3t) + A_{34}\exp(-b_4t) \quad \text{(Eq. 3)}$$

$$[V]/[II]_0 = A_{41}\exp(-b_1t) + A_{42}\exp(-b_2t) + A_{43}\exp(-b_3t) + A_{44}\exp(-b_4t) \quad \text{(Eq. 4)}$$

where [II], [III], [IV], and [V] are the molar concentrations of the species in Scheme I; $[II]_0$ is the initial concentration of II; and A_j and b_k are constants, which are related to combinations of the six rate constants given in Scheme I.

The absorbance at any wavelength and any time for the four-component system may be written as:

$$A = \epsilon_{II}[II] + \epsilon_{III}[III] + \epsilon_{IV}[IV] + \epsilon_{V}[V] \quad \text{(Eq. 5)}$$

where A is the absorbance, and ϵ_j is the absorptivity for species j. By combining Eqs. 1–5 and rearranging the terms, one obtains:

$$A_t - A_\infty = M\exp(-b_1t) + N\exp(-b_2t) + P\exp(-b_3t) + Q\exp(-b_4t) \quad \text{(Eq. 6)}$$

where A_t is the absorbance at any time; A_∞ is the absorbance at infinite time; and M, N, P, and Q are constants. Thus, ideally, a plot of logarithm of $A_t - A_\infty$ *versus* time should yield a tetraexponential curve with the slope of the last linear segment equal to the negative of the slowest rate constant. All other rate constants can be obtained by the feathering technique or by computer methods. Actually, the kinetics may be simplified by the competitive nature of the parallel sequential reactions. Thus, a tetraexponential curve may become a monoexponential, biexponential, or triexponential curve, depending on the magnitude of the rate constants and on the potential for reversibility of each reaction step.

For example, if the steps leading to intermediates are not reversible, Eq. 6 simplifies to:

$$A_t - A_\infty = M'\exp -(k_1 + k_2)t + N'\exp(-k_3t) + P'\exp(-k_4t) \quad \text{(Eq. 7)}$$

where the exponential factors are expressed in terms of the observed rate constants of Scheme I.

Spectral Changes and Rate Constant Determination—Spectral characteristics of the 1,4-benzodiazepines were described as superimposed spectra of two substituted benzene chromophores (7). This same report gave a pKa of 4.6 for chlordiazepoxide attributed to protonation of the *N*-oxide. Chlordiazepoxide spectral changes upon hydrolysis at pH values below the pKa showed two apparent reaction steps (Fig. 1). The first reaction step was characterized by an absorbance loss at 245 nm with a hypsochromic shift of λ_{max} from 245 to 236 nm. The second reaction was characterized by a loss in absorbance of both chromophoric absorption bands. Two new absorption bands with λ_{max} of 253 and 261 nm were observed.

The spectral changes for demoxepam in the same pH region were identical to the second reaction step of the hydrolysis of chlordiazepoxide. This finding indicated that the first observable reaction step of chlordiazepoxide was the formation of demoxepam, and the second reaction step was attributed to the ring-opening processes. The final product observed had the same spectrum as 2-amino-5-chlorobenzophenone. The benzophenone also exhibited an acid–base behavior, and its UV spectrum was dependent on the pH values. The end spectra of the hydrolysis of chlordiazepoxide at pH values close to the pKa of the benzophenone varied according to the spectral shifts observed with the benzophenone alone. The kinetic data were amenable to treatment according to the biexponential equation:

$$A_t - A_\infty = M\exp(-b_1t) + N\exp(-b_2t) \quad \text{(Eq. 8)}$$

Plots of the logarithm of $A_t - A_\infty$ *versus* time consisted of two linear segments. An isosbestic point at 270 nm was observed during the hydrolysis of demoxepam to benzophenone. By plotting absorbance

[5] Beckman model IR8, Fullerton, Calif.
[6] Joel model C60HL, Medford, Mass.
[7] Du Pont, CEC-21-110.

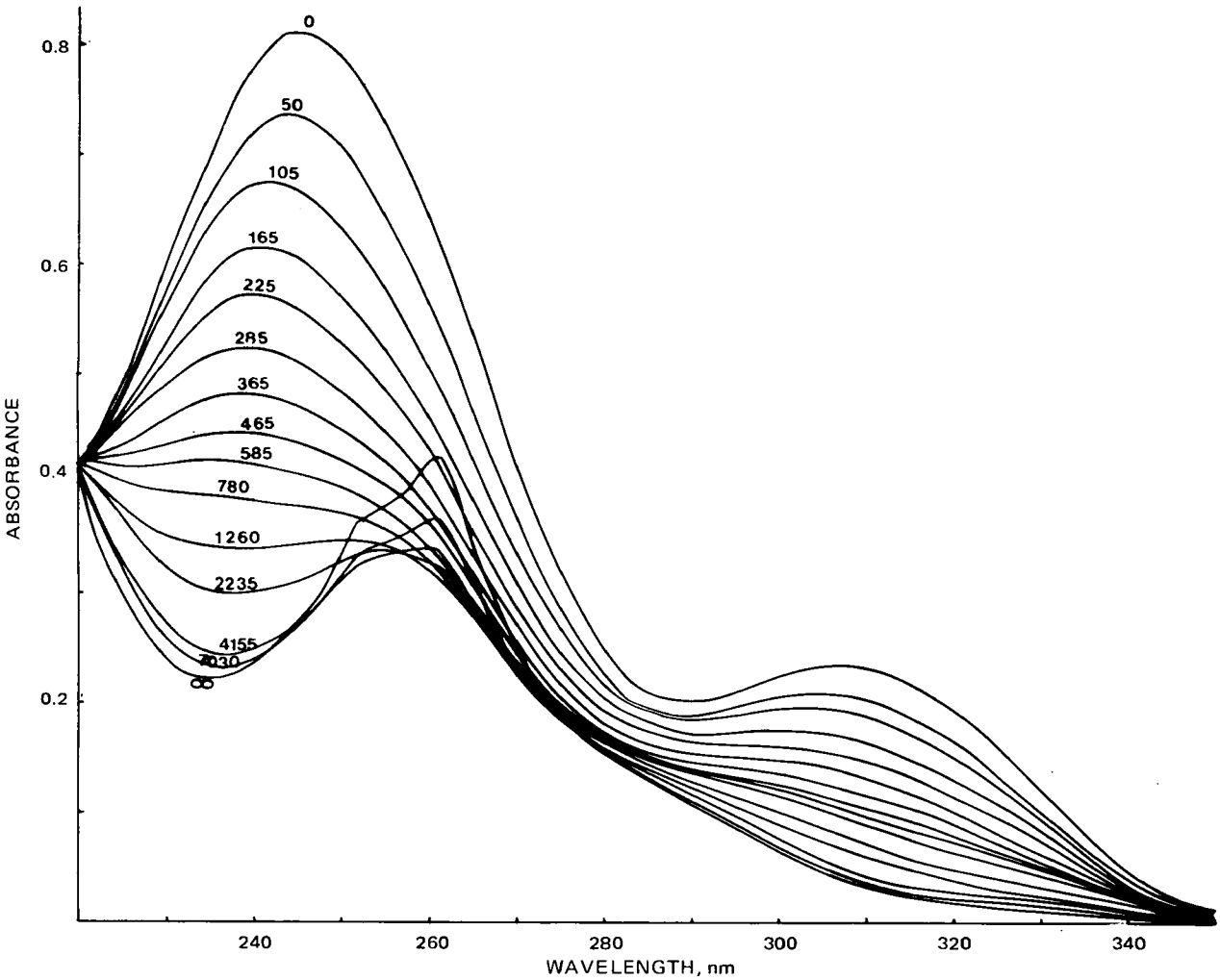

Figure 1—*Typical spectral changes for the hydrolysis of 10^{-5} M chlordiazepoxide in 0.1 N HCl, μ = 1.0, at 80°. Curves are labeled as to minutes after the start of the reaction.*

values at this wavelength, feathering to obtain the larger rate constant was unnecessary. Figure 2 shows a typical kinetic plot for the hydrolysis of chlordiazepoxide in 0.1 *N* HCl. Identical rate constants were obtained for the larger rate constant by employing either feathering or the isosbestic point plot. Both reaction steps demonstrated apparent first-order kinetics.

Table I—Apparent First-Order Rate Constants, $10^4 k$ (in Minutes^{-1}), for Chlordiazepoxide at 80°, μ = 1.0

pH	Buffer, *M*		k_c	k_1	k_3	r_c	r_1	r_3
		[HCl]						
0.93		0.1000	49.0	—	6.19	0.99	—	0.98
1.24		0.0398	20.6	—	—	0.99	—	—
1.70		0.0158	23.1	—	3.47	0.98	—	0.99
2.13		0.0063	23.9	—	—	0.90	—	—
2.60		0.0025	17.8	—	1.69	0.99	—	0.98
3.03		0.0010	22.7	—	—	0.99	—	—
	[CH_3COOH]	[CH_3COO^-]						
3.24	0.0957	0.0043	34.2	—	1.57	0.99	—	0.99
4.00	0.0761	0.0239	40.1	—	1.01	0.99	—	0.99
4.85	0.0322	0.0678	43.0	—	0.42	0.99	—	0.99
5.64	0.0081	0.0919	43.5	—	0.40	0.99	—	0.99
	[$H_2PO_4^-$]	[HPO_4^{-2}]						
4.73	0.0648	0.0018	43.0	—	0.52	0.99	—	0.99
5.58	0.0553	0.0011	47.7	—	0.28	0.99	—	0.99
6.47	0.0275	0.0391	48.2	11.80	0.20	0.99	0.97	0.97
7.40	0.0049	0.0617	44.3	21.00	0.24	0.99	0.99	0.99
	[H_3BO_3]	[$H_2BO_3^-$]						
6.96	0.103	0.003	31.0	—	—	0.97	—	—
7.93	0.103	0.029	41.4	2.70	0.32	0.99	0.98	0.99
8.52	0.061	0.112	39.9	5.88	—	0.99	0.98	—
9.53	0.003	0.100	39.9	31.32	0.31	0.99	0.99	0.99
		[NaOH]						
10.18		0.010	33.0	—	0.29	0.99	—	0.97
10.90		0.050	49.9	—	2.59	0.99	—	0.84

Table II—Apparent First-Order Rate Constants, $10^4\ k$ (in Minutes^{-1}), for Demoxepam at 80°, $\mu = 1.0$

pH	Buffer, *M*		k_1	k_3	r_1	r_3
		[HCl]	—	—	—	—
0.93		0.100	—	8.91	—	0.99
	[CH_3COOH]	[CH_3COO^-]	—	—	—	—
3.24	0.0957	0.0043	—	2.26	—	0.97
4.85	0.0322	0.0678	—	4.75	—	0.99
	[$H_2PO_4^-$]	[HPO_4^{-2}]	—	—	—	—
5.58	0.0553	0.0011	7.23	0.26	0.99	0.86
7.40	0.0049	0.0617	23.79	—	0.99	—
7.40	0.0049	0.0617	25.98	0.22	0.99	0.99
	[H_3BO_3]	[$H_2BO_3^-$]	—	—	—	—
6.96	0.103	0.003	—	0.25	—	0.98
7.93	0.103	0.029	2.96	0.28	0.99	0.99
8.52	0.061	0.112	7.60	—	0.99	—
9.53	0.003	0.100	49.60	0.34	0.99	0.99
		[NaOH]	—	—	—	—
10.18		0.010	250.16	0.30	0.99	0.95
10.90		0.05	>1000.00	3.60	—	0.98

The rate constants were calculated from least-squares analysis of slopes and are listed in Tables I and II for chlordiazepoxide and demoxepam, respectively. There was good agreement between the rate constants for demoxepam hydrolysis and the comparable rate constant for hydrolysis of the demoxepam derived from degradation of chlordiazepoxide, confirming that the first reaction step observed for chlordiazepoxide resulted in demoxepam formation. The last columns of each table give the correlation coefficients for the linear segments and suggest excellent linearity.

The spectral changes for chlordiazepoxide at pH values above the pKa of chlordiazepoxide and below pH 10 showed three apparent reaction steps. The initial spectral changes corresponded to the hydrolysis of the methylamino group at position 2. Spectral changes for hydrolysis of demoxepam in the same pH region were identical with the last two reaction steps of the hydrolysis of chlordiazepoxide. Above pH 10, the apparent first-order rate constant for the first step of hydrolysis of demoxepam was larger in magnitude than the apparent first step of the hydrolysis of chlordiazepoxide leading to demoxepam. Therefore, above pH 10, the reaction of demoxepam to the intermediate was not kinetically observed.

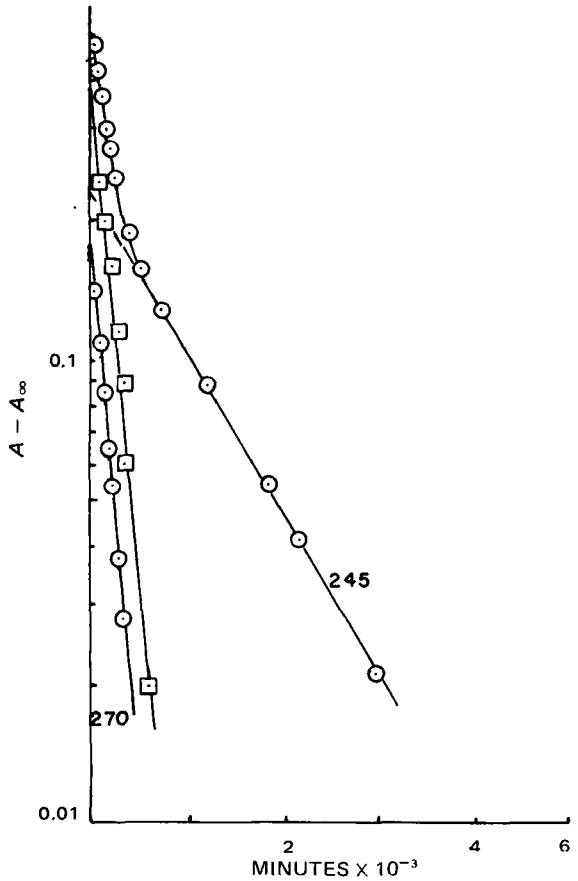

Figure 2—*Typical apparent first-order plots for hydrolysis of* 10^{-5} M *chlordiazepoxide in 0.1 N HCl, at 80°,* $\mu = 1.0$. *Plots are labeled as to wavelength;* □ *represents feathered data.*

Rate–pH Profiles—The log k–pH profile for hydrolysis of chlordiazepoxide to demoxepam (Fig. 3) was constructed from the logarithm of the apparent first-order rate constant, k_c, and pH values at 80° for ionic strength 1.0. In the acidic pH region, the rate–pH profile indicated hydrogen-ion catalysis on the protonated species. As the pH approached the pKa for chlordiazepoxide and more chlordiazepoxide existed in the neutral form, the observed rate constant became relatively independent of pH. This phase was attributed to water attack on the neutral species or hydroxide-ion attack on the protonated species as the kinetic equivalent.

As the pH values approached 2.5, the rate–pH profile indicated water attack on the protonated species or hydrogen-ion attack on the neutral species as the kinetic equivalent. This contribution to the overall log k–pH profile may be accounted for by:

$$k_{obs} = (k_H[H^+] + k_{H_2O} + k_{OH}[OH^-])f_{HS} \qquad \text{(Eq. 9)}$$

with the kinetic equivalents:

$$k_{H_2O}f_{HS} = k_{H'}[H^+]f_S \qquad \text{(Eq. 10)}$$

$$k_{OH}[OH^-]f_{HS} = k'_{H_2O}f_S \qquad \text{(Eq. 11)}$$

where f_{HS} and f_S are the fractions protonated and unprotonated, respectively.

The bimolecular rate constants were calculated according to Eq. 9 from the experimental data (Table III); the data were corrected for buffer catalysis. Based on these calculated values and the reported pKa at 80° for chlordiazepoxide, the fit of the theoretical curve to the experimental points is shown in Fig. 3. A reasonable fit was obtained, in good agreement with the data reported previously (4). This agreement suggests that the complex quantitative TLC method of analysis used in that study (4) is unnecessary.

The log k–pH profile for the second and third reaction steps for hydrolysis of chlordiazepoxide was constructed from the apparent

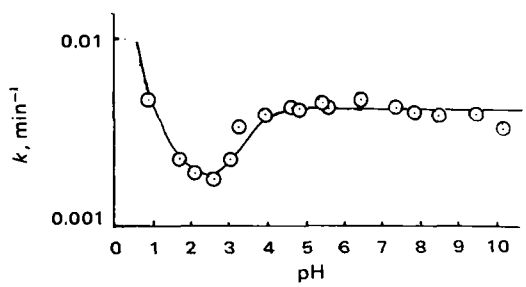

Figure 3—*Log* k–*pH profile for the hydrolysis of chlordiazepoxide at 80°,* $\mu = 1.0$, *first reaction step.*

Table III—Bimolecular Rate Constants (Minutes^{-1} M^{-1}) for Hydrolysis of Chlordiazepoxide and Demoxepam at 80°

k_H	k'_H	k_{H_2O}	k'_{H_2O}	k_{OH}	k'_{OH}	pKa
		Chlordiazepoxide, k_c				
0.03	—	0.0016	0.0045 (0.0036)[a]	—	—	4.6
		Chlordiazepoxide, Demoxepam, k_1				
—	—	—	—	6.1	—	—
		Chlordiazepoxide, Demoxepam, k_3				
0.0065	5.37	0.00017	0.000027	3640	0.014	4.2

[a] Corrected for buffer catalysis.

first-order rate constants, corrected for buffer catalysis, at 80° (Fig. 4). The data for hydrolysis of demoxepam also were plotted on the same graph. The two sets of data are in excellent agreement. The profile in the alkaline region indicates a two-step sequential reaction, both catalyzed by hydroxide ion on the neutral species. The log k–pH profiles in the acid region indicate hydrogen-ion catalysis on the positively charged ion, followed by water attack on the same species as the pH values increase. The observed apparent first-order rate constant for the acidic pH region can be described by:

$$k_{obs} = (k_H[H^+] + k_{H_2O} + k_{OH}[OH^-])f_{HS} \quad \text{(Eq. 12)}$$

The two possible kinetic equivalents are:

$$k_{H_2O}f_{HS} = k_H'[H^+]f_S \quad \text{(Eq. 13)}$$

$$k_{OH}[OH^-]f_{HS} = k_{H_2O}f_S \quad \text{(Eq. 14)}$$

Upon substitution of the dissociation constant, K_a, Eq. 11 becomes:

$$k_{obs} = (k_H[H^+] + k_{H_2O} + k_{OH}[OH^-])\frac{H^+}{H^+ + K_a} \quad \text{(Eq. 15)}$$

The values that produced the best fit are given in Table III. The kinetic pKa for the intermediate was calculated to be 4.2. The log k–pH profiles for the basic pH region can be represented for the first reaction step as:

$$k_{obs} = k_{OH}'[OH^-]f_S \quad \text{(Eq. 16)}$$

and for the second reaction step:

$$k_{obs} = k_{OH}[OH^-]f_S \quad \text{(Eq. 17)}$$

The values that provided the best fit are also given in Table III.

This interpretation of the rate–pH profiles for the second and third reaction steps provides a reasonably good fit to the experimental data over the 1–11 pH range. In spite of the possible complexity of the mechanistic scheme, the observed kinetic expressions are surprisingly simple. The specific rate constants calculated according to the profiles cannot be attributed to a unique kinetic step in Scheme I from these data alone. Therefore, examination by TLC of the reaction solution at reaction times when intermediates should be present was conducted.

Isolation and Identification—Samples withdrawn at appropriate times were subjected to TLC analysis as described under *Experimental.* Demoxepam (R_f 0.07) formation was observed from the hydrolysis of chlordiazepoxide throughout the entire pH range studied. The final products from hydrolysis of either chlordiazepoxide or demoxepam were 2-amino-5-chlorobenzophenone (visualized by short UV wavelength excitation) and the *N*-oxide glycine (purple spot produced at the origin upon spraying with 0.5% ninhydrin aerosol).

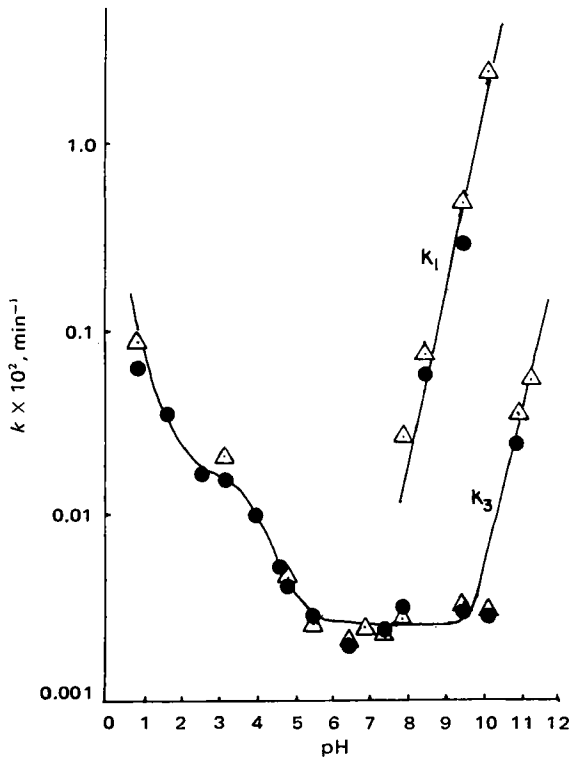

Figure 4—*Log* k–*pH profile for the hydrolysis of chlordiazepoxide and demoxepam at 80°, μ = 1.0. Key: ●, chlordiazepoxide; and △, demoxepam, second and third reaction steps.*

Subsequent to the appearance of demoxepam and prior to product formation, two other compounds were observed by TLC (R_f 0.27 and 0.43) and tentatively attributed to reaction intermediates IV and III, respectively. Visually, the intensity of these spots appeared to be similar at pH <5.0, although much less intense than the demoxepam spot. Above pH 5.0, the chromatograms showed two spots (R_f 0.0 and 0.27). The compound at the origin, upon acidification in pH 4.0 buffer and immediate TLC analysis, resulted in movement on the plate to an R_f value of 0.40. This finding implied that the compound at the origin is the conjugate base of intermediate III. In the basic region, the relative intensities of spots attributed to intermediates III and IV indicate that intermediate III formation is favored over the formation of IV. In fact, preparative TLC above pH 5.0 was successful in the isolation of III, whereas the small amount of IV formed precluded isolation.

Analysis by NMR and mass spectrometry did not prove useful in structure identification. Compound decomposition in the ionization chamber of the mass spectrometer was indicated by a color change in the compound from yellow to gray. The NMR spectrum showed only aromatic and methylene absorption, which would not differentiate between 1,2- and 4,5-bond scission. The IR spectrum of the potassium bromide disk did show a characteristic absorption peak for a carboxylic anion at 1610 cm^{-1}. Compound III was tentatively assigned the structure that would result from 1,2-bond cleavage. Sternbach and Reeder (2) and Bell *et al.* (6) reported the formation of the sodium salt of the carboxylic acid resulting from hydrolysis of the 1,2-amide linkage of demoxepam in alkaline solution, which supports this assignment.

Table IV—Apparent First-Order Rate Constants, 10^4 k (in Minutes^{-1}), for Hydrolysis of Chlordiazepoxide at Various Buffer Concentrations, μ = 1.0

pH	Buffer	Total Buffer Concentration as 1X	k_c 1X	2X	3X	4X	k_o	S[a]
4.74	$[CH_3COOH][CH_3COO^-]$	0.100	44.5	48.4	61.8	78.7	29	110
6.37	$[H_2PO_4^-][HPO_4^{-2}]$	0.066	44.4	50.5	51.3	55.4	38	51
8.55	$[H_3BO_3][H_2BO_3^-]$	0.173	38.3	37.1	35.6	—	—	—

[a] $S = k_{HA}[H^+]/K_a + k_A$.

Table V—Buffer Catalytic Constants for Hydrolysis of Chlordiazepoxide at 80°, $\mu = 1.0$

Buffer and pH	$10^4 k_{obs}$	$10^4 k_0$	$[A^-]$	$\frac{[k_{obs} - k_0]}{[A^-]}$	$\frac{[H^+]}{K_a}$	$10^4 k_{HA}$	$10^4 k_A$
$[CH_3COOH][CH_3COO^-]$							
3.24	34.2	18.0	0.00256	0.632	38.33	160	70
4.00	40.1	20.0	0.0133	0.153	6.66	—	—
4.85	43.0	30.1	0.0517	0.025	0.93	—	—
5.64	43.5	34.1	0.0868	0.012	0.14	—	—
$[H_2PO_4^-][HPO_4^{-2}]$							
4.73	43.0	28.0	0.000238	6.302	275.86	220	60
5.85	47.7	34.1	0.0030	0.456	20.92	—	—
6.47	48.2	36.0	0.011	0.110	5.01	—	—
7.40	44.3	36.0	0.041	0.019	0.58	—	—

Attempts to isolate sufficient quantities of III and IV below pH 5.0 were unsuccessful due to the small amounts present. It seems likely that IV is the ring-opened compound resulting from azomethine hydrolysis, although no confirming evidence is available to support this assignment.

Recyclization of Intermediate III—Subsequent to hydrolysis of demoxepam in basic solution leading to III, the reaction solution was acidified to pH 1. Maintenance of this solution at 24° resulted in spectral changes indicative of demoxepam formation. The apparent first-order rate constant for cyclization was 0.013 min^{-1}. This facile recyclization was not observed above pH 5.0, that is, in the pH region where III exists as the conjugate base. As the carboxylate anion, the carbonyl carbon would possess a smaller net positive charge, decreasing the possibility of nucleophilic attack of the aromatic amine. No recyclization above pH 5.0 was observed. Recyclization of IV was neither indicated nor discounted based on the experimental data.

Hydrolytic Mechanism—The preceding kinetic and TLC data are mechanistically interpretable in two separate pH regions: above and below the pKa values for demoxepam and the corresponding intermediates. Below pH 5.0, a monophasic first-order system is observed kinetically, even though TLC evidence demonstrated the presence of two intermediates, III and, presumably, IV. The observation of two intermediates implicates a parallel consecutive reaction, as depicted in Scheme I, with recyclization occurring for III (step k_1 reversible). At these pH values, the *N*-oxide would be protonated with strong resonance contribution from Structure VII.

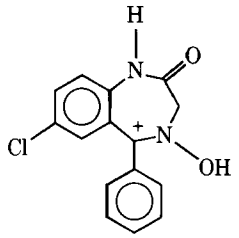

VII

Although models show that position 5 should be sterically hindered from nucleophilic attack, the resident positive charge due to protonation of the *N*-oxide must make attack at this position sufficiently competitive with nucleophilic attack on the carbonyl carbon so that IV is observable by TLC. The facile recyclization of III suggests that the 1,2-bond breakage is favored more than the TLC data would indicate. The monophasic behavior of the kinetic system infers that the predominant pathway for hydrolysis in this pH region proceeds through III as follows: II $\rightleftarrows$ III $\rightarrow$ V. Prior equilibrium for this system would result in:

$$\frac{A_t - A_\infty}{A_0 - A_\infty} = e^{-Kk_3 t} \qquad \text{(Eq. 18)}$$

with $K = k_1/k_{-1}$.

Table VI—Apparent First-Order Rate Constants, $10^4 k$ (in Minutes^{-1}), for Hydrolysis of Chlordiazepoxide at Various Ionic Strengths, 80°

pH	k_i	0.1	0.2	0.4	0.8	2Q
0.80	k_C	42.3	49.6	50.8	68.5	0.83
—	k_3	3.49	3.55	4.84	5.87	1.05

Other kinetic schemes with the inclusion of the relevant contribution from IV could be invoked but would necessitate numerous assumptions to transform the resulting tri- or tetraexponential equations into the observed monoexponential expression fitting the experimental data.

Above pH 5.0, the TLC data clearly indicate that formation of III is favored over IV. This preference is expected since the conjugate base of the protonated *N*-oxide group would not electronically favor nucleophilic attack at position 5. Additionally, since the complicating contribution from recyclization is absent, the simplified kinetic sequence in this pH region is: II $\rightarrow$ III $\rightarrow$ V. The operable equation for the biphasic system is:

$$A_t - A_\infty = Me^{-k_1 t} + Pe^{-k_3 t} \qquad \text{(Eq. 19)}$$

Thus, a simple nucleophilic attack on the amide linkage is followed by a similar nucleophilic reaction involving the azomethine linkage.

Stability Parameters—To provide a complete profile of the kinetic stability of chlordiazepoxide, hydrolysis kinetics as a function of buffer concentration, ionic strength, and temperature were investigated. Buffer catalysis was studied according to the relationship:

$$k_{obs} = k_0 + [k_{HA}[H^+]/K_a + k_A][A^-] \qquad \text{(Eq. 20)}$$

where K_a is the dissociation constant for the buffer species, k_0 is the hydrolysis rate constant in the absence of buffer catalysis, and k_{HA} and k_A are the rate constants for buffer catalysis of the acid buffer species and its conjugate base, respectively. Buffer effects were investigated by changing the original buffer concentration fourfold in a gradient manner. Table IV gives the results of these studies on the rate constant for transformation of chlordiazepoxide to demoxepam. Acetate and phosphate buffers catalyzed the hydrolysis, while borate had no effect. Table V presents the rate constants for the general catalysis observed with the acid and base species of both of these buffer systems. These values agree with those reported previously (4). Only phosphate catalysis was observed for the reaction of demoxepam to intermediate III. The buffer effect problem was avoided by changing to a different buffer system.

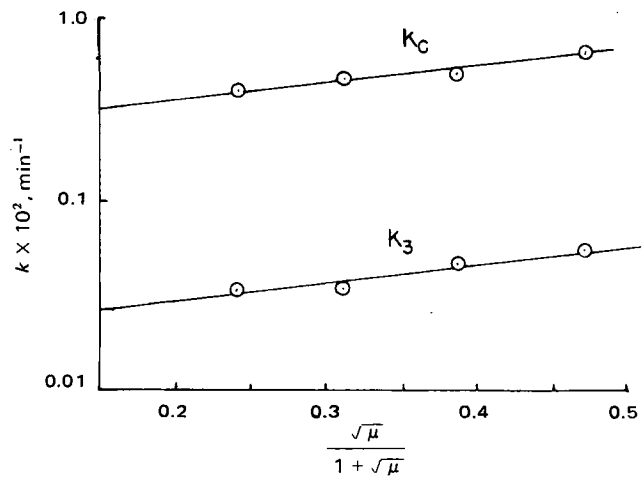

Figure 5—*Effect of varying ionic strength on apparent first-order rate constant for hydrolysis of chlordiazepoxide.*

Table VII—Apparent First-Order Rate Constants, 10^4k (in Minutes^{-1}), and Thermodynamic Parameters for Hydrolysis of Chlordiazepoxide

pH	k_i	85°	80°	75°	70°	E_a, kcal/mole	ln P	ΔH_a, kcal/mole	ΔS_a, cal/°K-mole
0.93	k_C	—	49.0	28.0	15.0	28.4	35.3	27.3	9.3
—	k_3	—	6.16	3.95	2.97	17.6	17.7	16.9	−25.6
11.23	k_3	8.01	—	5.47	2.37	18.4	18.8	17.5	−23.4

Ionic strength effects were observed for the biphasic hydrolysis of chlordiazepoxide at pH 0.80 (Table VI). Use of the Bronsted–Bjerrum equation together with the extended Debye–Huckel equation yields:

$$\log k = \log k_0 + 2QZ_AZ_B \sqrt{\mu}/(1 + \sqrt{\mu}) \qquad \text{(Eq. 21)}$$

where k is the apparent first-order rate constant, k_0 is the rate constant at zero ionic strength, Q is the constant equal to 0.55 at 80° (8), Z_A and Z_B are the charges of reaction molecules, and μ is the ionic strength. The positive slope values close to unity for the plots of log $k - \sqrt{\mu}/(1 + \sqrt{\mu})$ (Fig. 5) indicate that the reaction involves molecules of like univalent charge.

The apparent first-order rate constants were determined as a function of temperature in the strong acid and strong base regions. These values are given in Table VII along with the thermodynamic parameters obtained from slope and intercept values of the Arrhenius plots shown in Fig. 6. These values will allow stability prediction in the pH regions showing rapid degradation profiles.

CONCLUSIONS

A multicomponent solution resulting from a complex hydrolysis is often assumed not to be amenable to kinetic analysis by using absorbance spectroscopy. The present study demonstrated that this is not the case. Successful employment of absorbance spectroscopy yielded reasonably good kinetic data for the previously reported chlordiazepoxide to demoxepam reaction. Additionally, the parallel consecutive transformation of demoxepam to the benzophenone product was determined in the same manner without additional experimental workups such as extraction or TLC.

The hydrolysis of chlordiazepoxide to demoxepam may proceed uncatalyzed or by specific acid and base catalysis. This reaction step is subject to buffer catalysis with acetate and phosphate buffer systems. Ordinary ionic strength effects for bimolecular reactions involving like-charged molecules were observed only in the strong acid region.

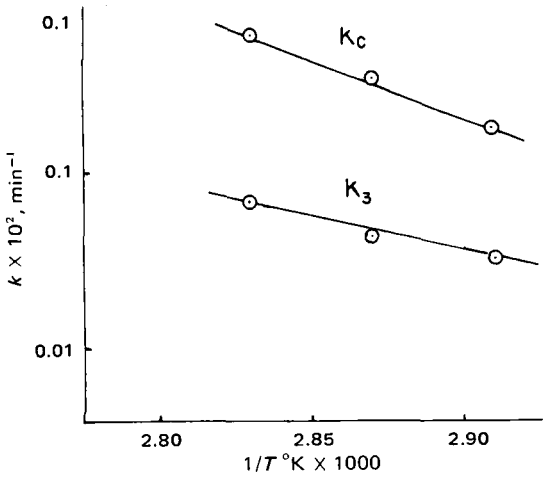

Figure 6—*Typical Arrhenius plots for apparent first-order rate constant for chlordiazepoxide, μ = 1.0.*

Further degradation of demoxepam involves ring opening to yield two intermediates, which subsequently are transformed into 2-amino-5-chlorobenzophenone and a glycine derivative. Throughout the pH region, the kinetically predominant intermediate is the one resulting from hydrolysis of the amide linkage. Initial hydrolysis of the azomethine bond is more competitive with the amide hydrolysis below pH 5.0. *N*-Oxide protonation below this pH electronically favors nucleophilic attack to compensate for adverse steric hindrance.

However, recyclization of the intermediate resulting from amide hydrolysis and the monophasic kinetics suggests that azomethine hydrolysis is still a minor pathway in the acid pH region. The log k–pH profile for demoxepam hydrolysis showed a specific base-catalyzed reaction. The transformation of the intermediate to the benzophenone product demonstrated specific acid- and base-catalyzed regions as well as an uncatalyzed hydrolysis. A kinetic pKa of 4.2 was calculated for intermediate III. Phosphate catalysis was observed for hydrolysis of III.

REFERENCES

(1) J. A. F. de Silva, *Anal. Chem.*, **36**, 2099(1964).

(2) L. H. Sternbach and E. Reeder, *J. Org. Chem.*, **26**, 4936(1961).

(3) J. T. Carstensen, K. S. E. Su, P. Madrell, J. B. Johnson, and H. N. Newmark, *Bull. Parenteral Drug Assoc.*, **25**, 193(1971).

(4) H. V. Maulding, J. P. Nazareno, J. E. Pearson, and A. F. Michaelis, *J. Pharm. Sci.*, **64**, 279(1975).

(5) L. H. Sternbach, B. A. Koechlin, and E. Reeder, *J. Org. Chem.*, **27**, 4671(1962).

(6) S. C. Bell, T. S. Sulrowski, C. Gochman, and S. T. Childress, *ibid.*, **27**, 562(1962).

(7) J. Barrett, W. F. Smyth, and I. E. Davidson, *J. Pharm. Pharmacol.*, **25**, 387(1973).

(8) J. T. Carstensen, *J. Pharm. Sci.*, **59**, 1140(1970).

ACKNOWLEDGMENTS AND ADDRESSES

Received September 2, 1975, from the *College of Pharmacy, University of Texas at Austin, Austin, TX 78712*

Accepted for publication October 29, 1975.

Presented in part at the Basic Pharmaceutics Section, APhA Academy of Pharmaceutical Sciences, San Francisco meeting, April 1975.

Abstracted in part from a dissertation submitted by W. W. Han to the University of Texas at Austin in partial fulfillment of the Doctor of Philosophy degree requirements.

Supported in part by a grant from the University Research Institute, University of Texas at Austin.

The authors express their gratitude to Dr. W. E. Scott of Hoffmann-La Roche Inc. for samples supplied and to Dr. Jay Nematollahi for helpful discussions.

* Present address: Searle Laboratories, Chicago, IL 60680

ˣ To whom inquiries should be directed.

Physical Aspects of Wet Granulations II: Factors Involved in Prolonged and Excessive Mixing

MICHAEL A. ZOGLIO ˣ, H. E. HUBER, GERALD KOEHNE, PING LING CHAN *, and J. T. CARSTENSEN *

Abstract □ Evidence is presented that excessive blending in a wet granulation process shifts the packing arrangement of the wet granule, causing it to become dense and nonporous. With prolonged kneading, a larger amount of the water-soluble excipients dissolves in the granulating fluid, and these two factors make the drying slower. This result, coupled with the previous finding that a certain time is required to attain an equilibrium size granule, explains why there exists an optimum kneading time for a wet granulation from a mechanical performance point of view.

Keyphrases □ Granulations, wet—physical aspects, effect of prolonged and excessive mixing □ Hardness, granule—effect of prolonged and excessive mixing □ Dissolution rate—wet granulations, effect of prolonged and excessive mixing

It has been shown (1) that the initial steps in wet granulation processes are (*a*) moisture distribution and (*b*) formation of an equilibrium size granule. It has also been pointed out (1) that kneading (mixing) beyond a certain time point decreases the quality of the ensuing granule. The purpose of this study was to elaborate this latter point.

EXPERIMENTAL

A wet granulation was made of the composition denoted A in Table I. This formula is identical to the optimal formula described previously (1); other lactose–sucrose ratios cause less uniformity in granule hardness and lower overall granule hardness per granule weight.

The granulation procedure was as described elsewhere (1), except that the kneading times were varied; *i.e.*, granulations were kneaded 3, 5, 7, 9, 11, and 13 min. The wet granulation mass was processed through an oscillating granulator[1] with a No. 6 screen and then dried in a fluid bed drier[2] with an incoming air stream at a velocity of 380 ft^3/min and a temperature of 42°.

The dried granulations were subjected to sieve analysis and Karl Fischer moisture determinations. Pilpel hardness determinations (1–3) of the +20 and the −6/+14-mesh fractions were performed. The drying rates of Formulation A kneaded for 2 and 10 min were determined by checking the weight of the granulations as a function of time.

A starch–lactose granulation was made[3] with the following composition: 1150 g of lactose USP, 160 g of starch USP, and 6 g of FD&C Yellow No. 5. A premix of the dye and 100 g of lactose was made, and this premix was blended[3] with the remaining lactose and 80 g of starch. It was then granulated with a paste made with the remaining starch in 300 ml of water. The granulation was passed through a No. 6 hand screen and dried in a forced air oven for 3 hr at 65°. The dried granulation was sieved, and the −20/+40 and −40/+60 fractions were isolated.

Ten tablets, each weighing 300 mg, were made by hand on a single-punch tablet machine[4] using a 0.9-cm (0.37-in.) standard concave punch. Six tablets were subjected to thickness and hardness determinations; the remaining four tablets were subjected to the USP dissolution rate test at 27.5°, using 0.1 *N* HCl as the dissolution medium. Each mesh fraction was then made into 500 tablets with the machine run at the same punch levels. The fill weights were recorded, which show the flow rates of each fraction under actual running conditions.

[1] F. J. Stokes Machine Co., Philadelphia, Pa.
[2] Aeromatic A.G., Basel, Switzerland.
[3] Hobart mixer, Hobart Manufacturing Co., Troy, Ohio.
[4] Stokes model E, F. J. Stokes Co., Philadelphia, Pa.

Table I—Formulas of Granulations Used[a]

Ingredient	Formulation A	Formulation B
Lactose USP (dry mix)	23.2	22.6
Sucrose USP (dry mix)	5.8	—
Starch USP (dry mix)	4.05	4.05
Starch USP (dissolved)	0.15	0.15
Sucrose USP (dissolved)	—	5.8
Lactose USP (dissolved)	—	0.6
Water	3.0	3.0

[a] Amounts are in kilograms or liters.

RESULTS AND DISCUSSION

It was shown previously (1) that, at kneading times less than 5 min in a chopper-ribbon mixer, the wet screening through a No. 6 mesh screen does not affect the granulation. At higher kneading times, it is obvious from visual observation that the screen starts acting as an extruder. The mesh analyses are shown in Table II, and the distribution eventually (13 min) reaches one dictated by a 6-mesh extruate.

Table III shows the Karl Fischer moisture contents and the Pilpel hardnesses of the granulation as a function of kneading time. As seen from Fig. 1, the hardness *versus* weight curves are of the type described earlier (1, 4). Capes's equation (4) states that $L = qd^n$, where L is the crushing strength, d is the diameter of the granule, and q and n are characteristics for the material crushed. Values of n for sodium chloride are 1.7–2.6. Since mass, m, is proportional to d^3, it follows that L is proportional to $m^{n/3}$, where $n/3 = 0.6$–0.9 for sodium chloride. It is apparent in this study that $n/3 = 1$, since the L *versus* m plots (Fig. 1) are linear.

Figure 2 shows that the hardness to weight ratio increases with drying time. It is seen from Table III that the ratio goes through a maximum at 7 min. With the −6/+14-mesh fraction, the moisture values vary and the hardness–weight ratios are not actually directly comparable; with the −14/+20-mesh fraction, however, the moisture contents are close and the maximum at 7 min is quite apparent.

The drying curves of Formulation A, kneaded for 2 and 10 min, are shown in Fig. 3. The drying is strictly monophasic as opposed to the

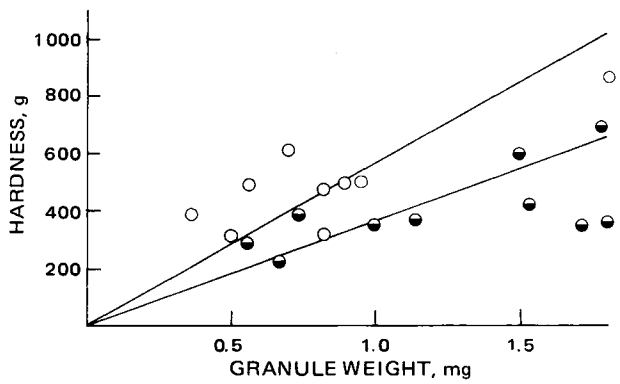

Figure 1—*Pilpel hardness as a function of granule weight for 14/20-mesh granules produced by 5 min of kneading and 45 min of drying (○) and by 11 min of kneading and 25 min of drying (◒).*

Table II—Amounts of Material[a] on the Indicated Mesh after Various Kneading Times

Screen	Minutes					
	3	5	7	9	11	13
14	19	10	10	19	40	73
20	16	18	25	44	37	12
40	25	43	42	31	19	13
60	27	25	19	6	4	2
80	10	3	3	—	—	—
100	2	1	1	—	—	—
Pan	1	—	—	—	—	—

[a] Values are percentages.

Table III—Moisture Contents and Hardness to Weight Ratios (x) of Granulations Kneaded for Different Lengths of Time (t)

t, min	x, 10^{-5}, g/g, −6/+14	SD of x	Moisture, % by Weight	x, 10^{-5}, g/g, +20	SD of x	Moisture, % by Weight
3	0.18	0.04	4.9	2.18	1.15	5.3
5	0.83	0.65	5.1	3.22	1.27	5.7
7	1.02	0.68	5.3	2.75	1.40	5.9
9	0.62	0.25	6.2	1.34	0.27	5.4
11	0.49	0.21	6.8	0.73	0.15	6.6

granulations reported by Opankunkle *et al.*[5] (5); this finding signifies that no surface moisture is present and that the drying is not carried past the point of bound moisture. As shown in Fig. 3, the drying follows the conventional relationship (6):

$$\ln\frac{W - W_\infty}{W_0 - W_\infty} = -\Gamma t \qquad \text{(Eq. 1)}$$

where W is the moisture retained, the subscripts denote initial and final time, Γ is a drying rate constant, and t is time. The drying rate constants are 0.12 and 0.06 min^{-1} for the material kneaded 2 and 10 min, respectively. It is, therefore, apparent that drying becomes slower at increased kneading times. The effect of kneading time described up to this point suggests a mechanism of wet granulation such as is outlined in Fig. 4. It was shown previously (1) that the initial granule is a loosely stacked arrangement of particles; these data imply that, as kneading continues, the configuration changes to a more closely packed arrangement and this change, in turn, means that the proportion of fine capillary pores in the granule increases, causing the

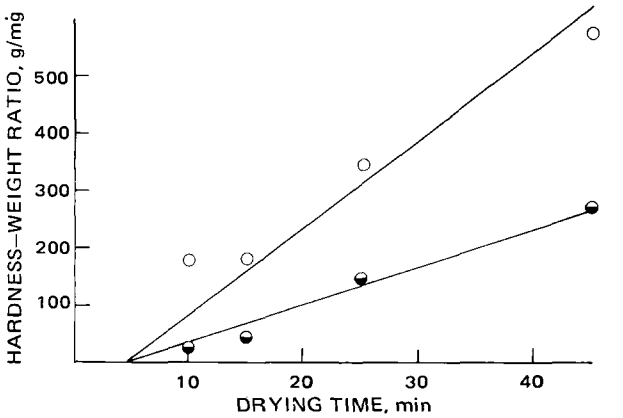

Figure 2—*Hardness to weight ratio of granules produced by 5 min of kneading as a function of drying time of 14/20- (○) and 6/14- (◒) mesh fractions.*

[5] In the data reported by Opankunkle *et al.*, surface (unbound) moisture gives rise to linear drying curves, whereas diffusional drying phases are log-linear (as in Eq. 1). There is no conflict between the views stated here and those reported by Opankunkle *et al.* (5).

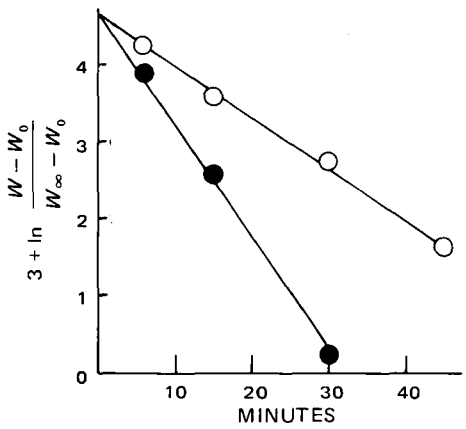

Figure 3—*The σ^--drying plot of tray drying of granules produced by 2 (●) and 10 (○) min of kneading.*

granule to dry more slowly. The Kelvin equation (7) states that:

$$\ln(P/P_0) = \frac{2M\gamma}{RT\rho}\frac{1}{r} \qquad \text{(Eq. 2)}$$

where P is the vapor pressure over a capillary of radius r, P_0 is the equilibrium vapor pressure, M is the molecular weight, γ is the interfacial tension, R is the gas constant, T is the absolute temperature, and ρ is the density of the liquid. According to Eq. 2, the vapor pressure is lower over the smaller pores in the granule produced by the longer kneading time, explaining why it dries more slowly; it also may explain why a larger granule may not equilibrate with a smaller granule, as reported (8).

To test further the concept of dissolution contributing to the mechanical structure of the granule in excessive kneading, Formulation B (Table I) was made. The sucrose was dissolved in the starch gel; the results from this experiment are shown in Table IV and show that the hardness to weight ratio did not change much as a function of kneading time. The granules have hardness to weight ratios and particle-size distributions that are fairly close to the results obtained from granulations kneaded for 13 min (Table III). It appears, therefore, that the end result of progressively longer kneading times can be simulated to some extent by first dissolving the solubles in the granulating liquid.

Results from the studies in the planetary blender are shown in Table V and in Fig. 5. The dissolution is by a σ^--curve, showing that the diffusion of liquid into the granule and diffusion of drug out of the granule are the rate-limiting steps[6] (9). At low kneading times, the dissolution rates are high and they decrease with increased kneading time. This result can be due to the granule becoming more

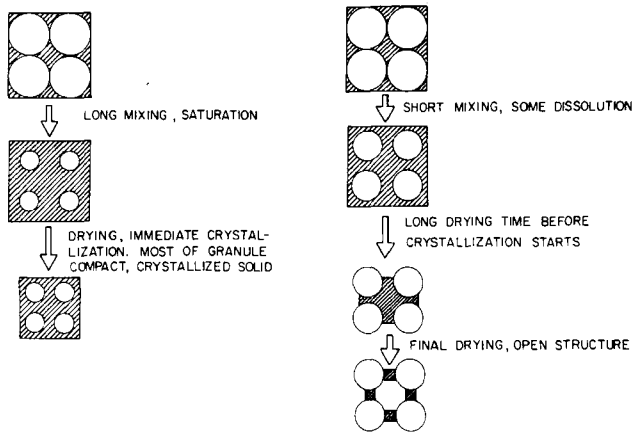

Figure 4—*Schematic diagram of the steps in drying of a granule kneaded for a long (left) and a short (right) time.*

[6] The lag times, t_i, of all five curves in Fig. 5 are of comparable magnitude (0.7 min). This length of time represents disintegration plus penetration times. The former values are of the order of 0.5 min.

Table IV—Characteristics of Granules Made by First Dissolving the Sucrose

Kneading Time, min	Hardness–Weight		Sieve Analysis				
	x, 10^{-5}, g/g, −6/+14	x, 10^{-5}, g/g, −14/+20	6/14	14/20	20/40	40/60	60/Pan
2	0.23 ± 0.1	1.14 ± 0.2	—	—	—	—	—
3	0.40 ± 0.15	0.86 ± 0.2	—	—	—	—	—
4	0.20 ± 0.1	1.05 ± 0.2	—	—	—	—	—
5	0.17 ± 0.1	0.93 ± 0.2	—	—	—	—	—
10	0.25 ± 0.1	1.01 ± 0.2	81	10	5	2	1
15	—	—	78	14	6	1	1

Table V—Characteristics of Tablets Made from Starch–Lactose Granulations Prepared in a Planetary Mixer

Kneading Time, min	20/40-Mesh				40/60-Mesh			
	Hardness, kg	Thickness, mm	k^a, min^{-1}	Weight[b], mg	Hardness, kg	Thickness, mm	k^a, min^{-1}	Weight[b], mg
3	6.7	4.05	0.28	293 ± 0.5	6.5	4.04	1.2	292 ± 0.5
5	8.1	4.04	0.10	307 ± 2.0	6.5	4.03	0.30	308 ± 1.5
8	8.1	4.04	0.06	330 ± 0.5	7.2	4.03	0.15	332 ± 1.0
10	8.1	4.03	0.07	332 ± 0.8	6.5	4.03	0.20	328 ± 1.5

[a] Based on (9): $\ln_e[(C-C_\infty)/(C_0-C_\infty)] = -k[t-t_i]$, where C is the concentration at time t, k is the dissolution constant in $minutes^{-1}$, and t_i is the lag time in minutes. [b] Weights are from the sustained run. The other figures correspond to 300.0-mg tablets made by hand on the tablet machine. Figures are averages of 15 measurements, and limits are 95% confidence limits of the averages.

homogeneous (in the sense that less and less dye is found on the outside of the granule). This assumption was substantiated by experiments where the dye was dissolved in the starch paste (Fig. 5). Here the dissolution rate constant was $k = 0.07 \pm 0.005\ min^{-1}$ for tablets made with a 20/40-mesh cut of a granulation kneaded for 5 min as compared to $k = 0.072 \pm 0.008\ min^{-1}$ for a granulation kneaded for 10 min where the dye (as in the remaining experiments) had been added to the dry powders prior to addition of paste.

In Table V, the column denoted "Weight" (which is the only figure relating to the tablets not run by hand) reflects the flow rates and consolidating rates of the granules in the die. The test was conducted by having one particular punch setting on the tablet machine; *i.e.*, the tablets were made with a fixed die volume. From the first two lines, it is obvious that a granulation kneaded for 5 min will flow into the die in larger amounts (*i.e.*, have better flow) than one kneaded for 3 min, since, *e.g.*, 307 ± 2 mg is significantly larger than 293 ± 0.5 mg (on the 99% level). The tablet hardness in this case increases with tablet weight since the volume is fixed. The granulations kneaded for 8 and 10 min, however, flowed so well that the tablets were too hard to make in the volume used.

Tablets could be made by increasing the height of the upper punch (*i.e.*, keeping the *die* volume constant but increasing the tablet volume and decreasing the tablet hardness), and the fill weights after 8 and 10 min of kneading (330 ± 0.5 and 332 ± 0.8 mg) are comparable, but higher, than after the shorter kneading times. Hence, the flow characteristics under actual tableting conditions increased with increasing kneading time. The model outlined in Fig. 4 is consistent with this finding, since the granule surface is smoother and the shape is closer to spherical the longer the kneading time; both these qualities aid in flow and consolidation of the granules.

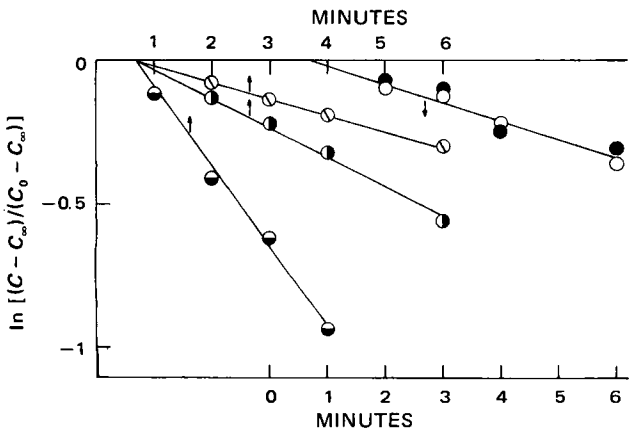

Figure 5—*USP dissolution rate test (27°, 50 rpm) of lactose–starch tablets of FD&C Yellow No. 5. Kneading times were 3 (◒), 5 (◑), 8 (◔), and 10 (○) min. The solid circles (●) indicate the sample where dye was dissolved in the starch paste.*

SUMMARY

1. In a wet granulation process, there appears to be an optimum kneading time for mechanical properties (here 5–7 min). This time appears to be a function of (*a*) the time required to attain the equilibrium granule size and (*b*) the amount of solid (here sucrose and lactose) dissolved. With longer kneading times, the granules are more consolidated in structure and smoother because more material dissolves at the time of drying. This causes a finer pore structure, which, in turn, makes the granule dry more slowly.

2. The optimum in mechanical performance criteria is not the optimum point for some other important parameters. Dissolution rates, for instance, are higher the lower the kneading time. Flow and consolidation characteristics are associated with smoothness of granule surface and optimize at high kneading times and at points where large-scale manufacture would not be feasible. At the point of optimum granule hardness, however, drying rates, flow rates, and dissolution rates are in acceptable ranges in the formulas studied here. Prudent process design should make possible the best possible combination of all important variables in wet granulation in general.

REFERENCES

(1) J. T. Carstensen, T. Lai, D. W. Flickner, H. E. Huber, and M. A. Zoglio, *J. Pharm. Sci.*, **65**, 992(1976).

(2) J. T. Carstensen, "Theory of Pharmaceutical Systems, II–Heterogeneous Systems," Academic, New York, N.Y., 1973, p. 239.

(3) C. F. Harwood and N. Pilpel, *J. Pharm. Sci.*, **57**, 478(1968).

(4) C. E. Capes, in "Proceedings of Powtech '71," A. S. Goldberg, Ed., Powder Advisory Centre, London, England, 1971, p. 151.

(5) W. O. Opankunkle, B. R. Bhutani, and V. N. Bhatia, *J. Pharm. Sci.*, **64**, 1023(1975).

(6) J. T. Carstensen, "Theory of Pharmaceutical Systems, II–Heterogeneous Systems," Academic, New York, N.Y., 1973, p. 228.

(7) P. W. M. Jacobs and F. C. Tompkins, in "Chemistry of the Solid State," W. E. Garner, Ed., Butterworths, London, England, 1955, p. 100.

(8) C. Pitkin and J. T. Carstensen, *J. Pharm. Sci.*, **62**, 1215(1973).

(9) J. T. Carstensen, "Pharmaceutics of Solids," Badger-Freund, Fond du Lac, Wis., 1974, p. 136.

ACKNOWLEDGMENTS AND ADDRESSES

Received August 25, 1975, from *Merrell-National Laboratories, Cincinnati, OH 45215*

Accepted for publication October 21, 1975.

Presented at the Basic Pharmaceutics Section, APhA Academy of Pharmaceutical Sciences, Atlanta meeting, November 1975.

* School of Pharmacy, University of Wisconsin, Madison, WI 53706

x To whom inquiries should be directed.

Spectrofluorometric Determination of Hydroflumethiazide in Plasma and Urine

RANDALL B. SMITH *, ROBERT V. SMITH, and GERALD J. YAKATAN x

Abstract □ A rapid, accurate, sensitive, and reproducible assay for hydroflumethiazide in plasma and urine was developed after studies of its UV and fluorescence spectral properties and partitioning behavior. The assay is based on initial extraction from acidified plasma or urine into ether, back-extraction into basic solution followed by acidification to about pH 1, and measurement of the fluorescence derived from the unionized molecule. Analysis of variance indicated no significant differences in assays performed on the same day. The mean recovery was 98.8 ± 7.4% for plasma over a concentration range of 0.2–2.0 μg/ml. The method is convenient for routine clinical use and has sufficient sensitivity to quantify hydroflumethiazide levels after administration of therapeutic doses.

Keyphrases □ Hydroflumethiazide—spectrofluorometric analysis, plasma and urine □ Spectrofluorometry—analysis, hydroflumethiazide, in plasma and urine □ Diuretics—hydroflumethiazide, spectrofluorometric analysis, plasma and urine

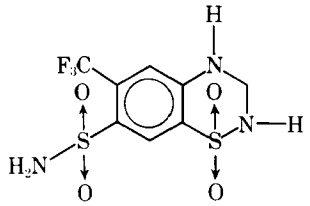

I

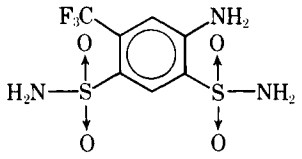

II

Attempts to describe the comparative pharmacokinetics of diuretic agents in various species of animals and in humans have comprised a major research effort in these laboratories. The paucity of pharmacokinetic information on this class of compounds is due in part to the lack of sensitive analytical methods for their determination in biological fluids. Generally, diuretics are given at relatively low doses and have short half-lives; thus, the blood levels obtained are relatively low a short time after administration.

A proposed study of the pharmacokinetics of the diuretic hydroflumethiazide (I) prompted interest in analytical methodology for this compound. A fluorometric TLC procedure was reported for the quantitative analysis of hydroflumethiazide in urine and plasma (1). This method involved extraction and TLC followed by fluorometric determination of hydroflumethiazide utilizing a scanning spectrodensitometer; hydroflumethiazide fluoresced below 400 nm, but no specific emission or excitation maxima were given. Other quantitative or qualitative procedures for benzothiadiazine diuretics in urine or dosage forms principally involved hydrolysis and colorimetric determination of the diazotized amino degradation products (2, 3).

Since hydroflumethiazide fluoresces strongly, it was proposed that a direct fluorometric determination in biological fluids might prove possible. This technique would decrease assay time and markedly simplify routine clinical determination by eliminating the necessity for TLC and scanning spectrodensitometry. Based on the fluorescence and partitioning properties of hydroflumethiazide, the present work reports the development of a sensitive, accurate, precise, and convenient procedure for its determination in both plasma and urine.

EXPERIMENTAL

Equipment—A scanning spectrofluorometer[1] and a recording UV–visible spectrophotometer[2] were utilized for spectral measurements.

Materials—Hydroflumethiazide[3] powder was used in the analytical procedures without further purification. All chemicals and solvents were of analytical reagent grade. Standard solutions were prepared by dissolving hydroflumethiazide in enough methanol to solubilize the drug and then diluting to the desired volume with pH 7.0 phosphate buffer.

UV Spectral Measurements—The UV spectra of 2.53×10^{-5} *M* hydroflumethiazide solutions were recorded at various pH values in the 1–12 range. The following buffer solutions (4) were used: potassium chloride–hydrochloric acid (pH 1.0–2.0), glycine buffers (pH 2.4–3.4), acetate buffers (pH 4.0–5.4), phosphate buffers (pH 6.0–7.2), borate buffers (pH 8.0–9.0), carbonate buffers (pH 9.4–10.4), and potassium chloride–sodium hydroxide (pH 11.0–12.0).

Fluorescence Spectral Measurements—The fluorescence spectra of 2.53×10^{-6} *M* hydroflumethiazide solutions were recorded

[1] Turner model 430, G. K. Turner Associates, Palo Alto, Calif.
[2] Coleman model 124, Perkin-Elmer Corp., Maywood, Ill.
[3] Bristol Laboratories, Syracuse, N.Y.

ACKNOWLEDGMENTS AND ADDRESSES

Received August 25, 1975, from *Merrell-National Laboratories, Cincinnati, OH 45215*

Accepted for publication October 21, 1975.

Presented at the Basic Pharmaceutics Section, APhA Academy of Pharmaceutical Sciences, Atlanta meeting, November 1975.

* School of Pharmacy, University of Wisconsin, Madison, WI 53706

x To whom inquiries should be directed.

Spectrofluorometric Determination of Hydroflumethiazide in Plasma and Urine

RANDALL B. SMITH *, ROBERT V. SMITH, and GERALD J. YAKATAN x

Abstract □ A rapid, accurate, sensitive, and reproducible assay for hydroflumethiazide in plasma and urine was developed after studies of its UV and fluorescence spectral properties and partitioning behavior. The assay is based on initial extraction from acidified plasma or urine into ether, back-extraction into basic solution followed by acidification to about pH 1, and measurement of the fluorescence derived from the unionized molecule. Analysis of variance indicated no significant differences in assays performed on the same day. The mean recovery was 98.8 ± 7.4% for plasma over a concentration range of 0.2–2.0 μg/ml. The method is convenient for routine clinical use and has sufficient sensitivity to quantify hydroflumethiazide levels after administration of therapeutic doses.

Keyphrases □ Hydroflumethiazide—spectrofluorometric analysis, plasma and urine □ Spectrofluorometry—analysis, hydroflumethiazide, in plasma and urine □ Diuretics—hydroflumethiazide, spectrofluorometric analysis, plasma and urine

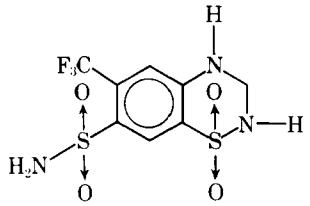

I

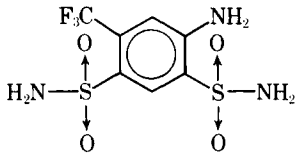

II

Attempts to describe the comparative pharmacokinetics of diuretic agents in various species of animals and in humans have comprised a major research effort in these laboratories. The paucity of pharmacokinetic information on this class of compounds is due in part to the lack of sensitive analytical methods for their determination in biological fluids. Generally, diuretics are given at relatively low doses and have short half-lives; thus, the blood levels obtained are relatively low a short time after administration.

A proposed study of the pharmacokinetics of the diuretic hydroflumethiazide (I) prompted interest in analytical methodology for this compound. A fluorometric TLC procedure was reported for the quantitative analysis of hydroflumethiazide in urine and plasma (1). This method involved extraction and TLC followed by fluorometric determination of hydroflumethiazide utilizing a scanning spectrodensitometer; hydroflumethiazide fluoresced below 400 nm, but no specific emission or excitation maxima were given. Other quantitative or qualitative procedures for benzothiadiazine diuretics in urine or dosage forms principally involved hydrolysis and colorimetric determination of the diazotized amino degradation products (2, 3).

Since hydroflumethiazide fluoresces strongly, it was proposed that a direct fluorometric determination in biological fluids might prove possible. This technique would decrease assay time and markedly simplify routine clinical determination by eliminating the necessity for TLC and scanning spectrodensitometry. Based on the fluorescence and partitioning properties of hydroflumethiazide, the present work reports the development of a sensitive, accurate, precise, and convenient procedure for its determination in both plasma and urine.

EXPERIMENTAL

Equipment—A scanning spectrofluorometer[1] and a recording UV–visible spectrophotometer[2] were utilized for spectral measurements.

Materials—Hydroflumethiazide[3] powder was used in the analytical procedures without further purification. All chemicals and solvents were of analytical reagent grade. Standard solutions were prepared by dissolving hydroflumethiazide in enough methanol to solubilize the drug and then diluting to the desired volume with pH 7.0 phosphate buffer.

UV Spectral Measurements—The UV spectra of 2.53×10^{-5} *M* hydroflumethiazide solutions were recorded at various pH values in the 1–12 range. The following buffer solutions (4) were used: potassium chloride–hydrochloric acid (pH 1.0–2.0), glycine buffers (pH 2.4–3.4), acetate buffers (pH 4.0–5.4), phosphate buffers (pH 6.0–7.2), borate buffers (pH 8.0–9.0), carbonate buffers (pH 9.4–10.4), and potassium chloride–sodium hydroxide (pH 11.0–12.0).

Fluorescence Spectral Measurements—The fluorescence spectra of 2.53×10^{-6} *M* hydroflumethiazide solutions were recorded

[1] Turner model 430, G. K. Turner Associates, Palo Alto, Calif.
[2] Coleman model 124, Perkin-Elmer Corp., Maywood, Ill.
[3] Bristol Laboratories, Syracuse, N.Y.

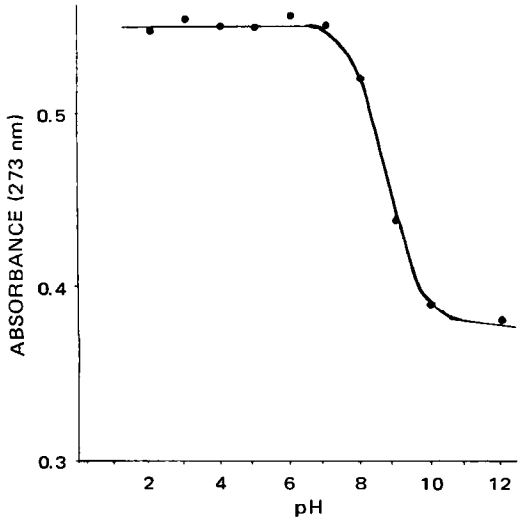

Figure 1—*Absorbance (273 nm) of hydroflumethiazide (2.53×10^{-5} M) as a function of pH. The curve is generated from the equation $pKa = pH - log\ [(A - A_u)/(A_I - A)]$, where A_I and A_u are the asymptotic absorbances in basic and acid solutions, respectively. The points are the experimentally measured values.*

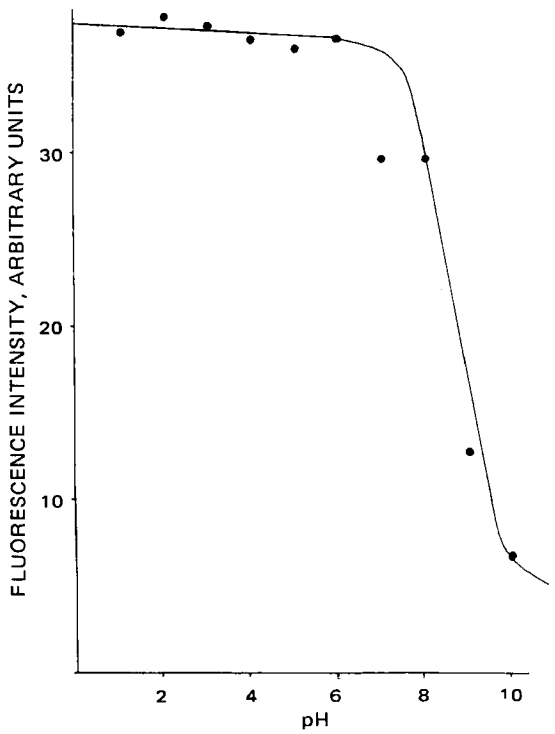

Figure 2—*Fluorescence intensity of hydroflumethiazide (2.53×10^{-6} M) as a function of pH at 333 and 393 nm.*

at various pH values in the 1–12 range using the described buffers. The fluorescence spectra in the Hammett acidity region were also obtained by preparing 2.53×10^{-6} *M* solutions in 10, 20, 30, 40, 50, 70, 80, 90, and 100% (v/v) sulfuric acid.

Partitioning Studies—Hydroflumethiazide (2.53×10^{-6} *M*) in pH 4 acetate buffer was analyzed spectrofluorometrically before and after extraction with an organic solvent. The following solvents were screened for use: ether, ethyl acetate, methylene chloride, chloroform, hexane, and heptane.

Procedure for Assay of Plasma—A stock plasma solution of hydroflumethiazide (2 μg/ml) was prepared by adding a concentrated aqueous solution of hydroflumethiazide to fresh human plasma. This stock plasma solution was further diluted with plasma to prepare hydroflumethiazide solutions containing 0.05, 0.5, 1.0, 1.5, and 2.0 μg/ml. One milliliter of pH 4 acetate buffer was added to 1 ml of diluted plasma solutions in 115 × 13-mm screw-capped culture tubes. Five-milliliter portions of ether were added, and the contents were agitated for 30 sec[4].

The samples then were centrifuged (3000 rpm) for 2 min, and 4 ml of the ether layers was transferred to a second similar screw-capped culture tube. One milliliter of 0.01 *N* sodium hydroxide ($\mu = 0.2$, adjusted with potassium chloride) was added to the ether, and the mixture was agitated for 30 sec. After centrifugation (1–2 min, 3000 rpm), the ether layer was removed and discarded. Residual ether in the aqueous phase was evaporated under a stream of nitrogen. One milliliter of 1 *N* hydrochloric acid was added and the fluorescence was measured at λ_{exc} of 333 nm and λ_{em} of 393 nm. The instrument settings were: blank, high; sensitivity, low; meter damp, −1; range, minimum sensitivity; and attenuation, ×3 or ×10.

Determination of Hydroflumethiazide in Urine—Fresh human urine was collected, and a stock urine solution containing 37.5 μg/ml of hydroflumethiazide was prepared. The stock urine solution was diluted with blank urine to prepare solutions containing 37.5, 28.1, 18.8, and 9.4 μg/ml. Then 0.1-ml aliquots of these solutions were diluted with 3 ml of distilled water. One milliliter of the diluted solutions and 1 ml of pH 4 acetate buffer were placed in a 115 × 13-mm culture tube, and 5 ml of ether was added. The same procedure as for plasma was then followed.

Hydrolysis of Hydroflumethiazide—Hydroflumethiazide solutions (10 μg/ml) were prepared in 0.01 *N* sodium hydroxide, 10% (v/v) sulfuric acid, and 1 *N* hydrochloric acid. These solutions were heated in a boiling water bath for 8 hr. The basic solution was made acidic by the addition of 1 *N* hydrochloric acid, and all three solutions were extracted twice with 10 ml of ether. The combined ether extracts from each solution were evaporated to dryness at 50° in 115 × 13-mm culture tubes. The sides of the tubes were washed with 1 ml of ether and again evaporated to dryness.

The residue in each tube was dissolved in 100 μl of methanol and subjected to TLC using a system described previously (1). The bands on the TLC plate were visualized under a short wavelength UV lamp. The band corresponding to the known degradation product, 2,4-disulfamyl-5-(trifluoromethyl)aniline (II), was scraped from the plate and shaken with two 5-ml aliquots of methanol. The mixture was centrifuged (4 min, 3000 rpm), and the supernate was transferred to a second culture tube.

After evaporation of the methanol, the residue was taken up in 1 ml of 0.01 *N* sodium hydroxide and made acidic by the addition of 2 ml of hydrochloric acid. Then the UV spectra were determined. After a 1:10 dilution with 1 *N* hydrochloric acid, the fluorescence spectrum also was determined.

Instrument Calibration—Prior to initiating a series of readings, the spectrofluorometer was adjusted to maximum sensitivity and a quinine bisulfate standard solution (0.05 μg/ml in 0.1 *N* sulfuric acid) was utilized to standardize to a meter reading of 35 at range ×10 at 333 and 393 nm. The standard was checked periodically thereafter to adjust for any drift.

Validation of Method—A beagle dog was given 15 mg of hydroflumethiazide intravenously in the same manner as described by Garceau *et al.* (1). Heparinized blood samples were collected prior to and at 5, 10, 15, 20, 30, 45, 60, and 90 min after injection. The samples were centrifuged, and the plasma was separated and assayed as already described.

RESULTS AND DISCUSSION

Hydroflumethiazide is a weak acid with reported pKa's of 8.9 and 10.5 (5). The UV spectrum of hydroflumethiazide contained two maxima. In solutions with a pH less than the first pKa, the maxima occurred at 273 ($\epsilon = 22{,}750$) and 325 ($\epsilon = 4340$) nm. When the pH of the solution was greater than the first pKa, a hypochromic and bathochromic shift of the latter maximum to 333 nm was observed. There was no change in the spectra of solutions with pH's greater than the reported second pKa. The absorbance of hydroflumethiazide at 273 nm, as a function of pH, is shown in Fig. 1. The pKa calculated from these data (pKa = 8.73) is in good agreement with the appropriate literature value (5).

Fluorometric spectra of hydroflumethiazide demonstrated an excitation maximum at 333 nm and an emission maximum at 393 nm

[4] Micro-mixer, Lab-lines Inc.

Table I—Results[a] of Repetitive Assays of Drug Spiked in Extraction Blanks and Extracted from Plasma and Urine

Concentration, μg/ml	Assay 1	2	3	4	Mean	±SD
			Drug Added to Acidic Extraction Blanks			
0.00	0.2	0.4	0.1	0.6	0.325	0.221
0.05	1.6	1.85	1.5	1.9	1.713	0.193
0.5	10.2	10.5	9.6	9.3	9.90	0.548
1.0	19.0	19.4	19.0	20.0	19.35	0.472
1.5	28.5	29.0	27.9	28.8	28.55	0.479
2.0	37.5	38.0	37.8	40.9	38.55	1.58
			Drug Extracted from Plasma			
0.00	1.1	0.9	1.5	1.0	1.13	0.263
0.05	1.6	1.4	1.9	1.7	1.65	0.208
0.50	6.8	5.4	6.2	6.1	6.13	0.574
1.00	11.5	11.5	12.5	10.5	11.5	0.816
1.5	17.6	17.5	17.5	16.8	17.35	0.369
2.0	22.0	22.0	23.0	21.0	22.0	0.816
			Drug Extracted from Urine[b]			
0.0	1.1	1.51	2.1	1.0	1.427	0.499
0.31	4.5	4.33	4.3	3.55	4.17	0.422
0.615	6.9	6.83	7.66	7.00	7.097	0.381
0.915	9.7	9.63	10.33	9.35	9.752	0.413
1.219	13.8	12.0	12.6	11.7	12.525	0.919

[a] Results are given in the arbitrary fluorescence units of the spectrofluorometer. [b] Concentration after dilution.

when determined at pH's between 1 and 12. The fluorescence intensity of hydroflumethiazide as a function of pH (333 and 393 nm) is shown in Fig. 2. The apparent pKa calculated from these data is 8.79, which is in very close agreement to the value calculated from the absorbance data and indicates that the fluorescence is a function of the ground-state pKa.

The fluorometric titration in the Hammett acidity region (333 and 393 nm) is depicted in Fig. 3 and shows that fluorescence intensity decreases with increasing sulfuric acid concentration. The apparent pKa is approximately −4.3, which probably corresponds to the protonation of the anilino nitrogen. The data from the Hammett acidity region and pH 1–12 indicate that the observed fluorescence of hydroflumethiazide in aqueous solution is due to the unionized molecule.

Of the solvents screened for extraction of hydroflumethiazide from aqueous solution, ether provided the highest recovery for a single extraction. As would be anticipated from the pKa's, the maximum extraction was obtained when the pH was less than 5.

The UV spectrum of 2,4-disulfamyl-5-(trifluoromethyl)aniline, the hydrolytic degradation product of hydroflumethiazide, showed absorbance maxima at 260 and 325 nm (pH 1.0). This compound fluoresces at the same wavelength as hydroflumethiazide and thus may potentially interfere with the spectrofluorometric determination of hydroflumethiazide. However, hydrolytic degradation is not known to occur *in vivo*, and interference due to the degradation product is not anticipated. To prevent hydrolysis during the analytical procedure, the drug should not be allowed to stand in acidic or basic solu-

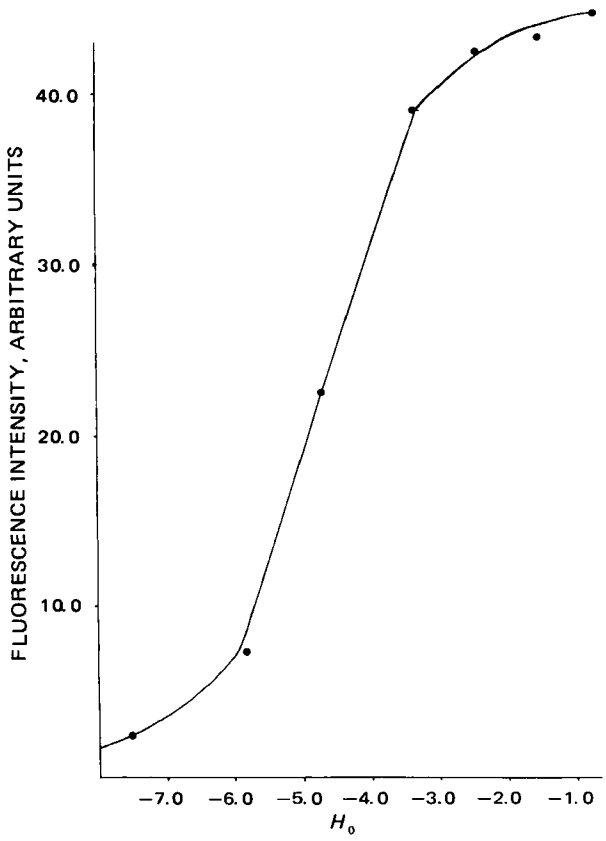

Figure 3—*Fluorescence intensity of hydroflumethiazide (2.53 × 10^{-6} M) as a function of Hammett acidity.*

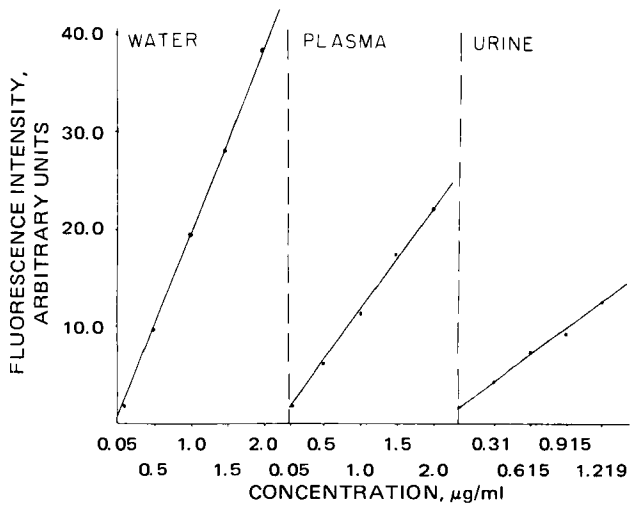

Figure 4—*Calibration curves for hydroflumethiazide added to aqueous extraction blanks and added to and extracted from plasma and urine. The lines are the least-squares linear regression fits of the data.*

Table II—Two-Way Analysis[a] of Variance for Data in Table I

Source	*df*	Sum of Squares	Mean Squares
		Extraction Blanks	
Concentration	5	4656.2422	931.24
Replication	3	2.8644	0.9548
Residual	15	7.1248	0.4749
Total	23	4666.2316	
		Plasma	
Concentration	5	1455.0633	291.0126
Replication	3	2.8283	0.9428
Residual	15	2.9066	0.1938
Total	23	1460.7983	
		Urine	
Concentration	4	308.691	77.172
Replication	3	2.241	0.747
Residual	12	2.582	0.215
Total	19	313.514	

[a] Not significant at the $p < 0.01$ level.

tions for lengthy periods and the analysis should be carried out without interruption.

Calibration curves for hydroflumethiazide extracted from plasma and urine and for hydroflumethiazide added to extraction blanks are shown in Fig. 4. Each point represents the mean of four replications for plasma, urine, and water. The data on which the curves are based are shown in Table I. The curves were fit by the method of least squares.

The slopes of the curves were 18.91 (spectrofluorometric response units per micrograms per milliliter at 333 and 396 nm at range setting of minimum sensitivity) for direct analysis of drug added to extraction blanks, 10.86 for drug extracted from plasma, and 9.13 for drug extracted from urine (after 1:31 dilution). The average fraction of the drug extracted could be determined from the ratio of the slopes of the urine and plasma curves to the slope of drug in extraction blanks. The mean percent of drug extracted was 57.4% from plasma or 48.3% from urine.

A blind analysis of hydroflumethiazide in spiked human plasma samples was performed. Recoveries ranged from 87.0 to 114.5%, and the mean was 98.8 ± 7.4% (*SD*) for 10 samples over the 0.2–2.0-μg/ml range.

The analysis of variance for the data in Table I is shown in Table II. These data demonstrate that there were no significant variations between extractions performed on the same day for urine, plasma, or drug added to extraction blanks. These results indicate the high reproducibility of the procedure.

An *in vivo* study was conducted similar to that of Garceau *et al.* (1) in which hydroflumethiazide was administered to a beagle dog by intravenous injection. A plot of plasma levels of hydroflumethiazide following a single intravenous injection of 15 mg is shown in Fig. 5. The determined plasma levels parallel those reported previously (1) and demonstrate the validity of the assay method.

The developed methodology appears to have sufficient sensitivity to determine hydroflumethiazide levels following the administration of therapeutic doses. The method is more convenient for routine clinical determinations of hydroflumethiazide than any previously reported methods with equivalent sensitivity.

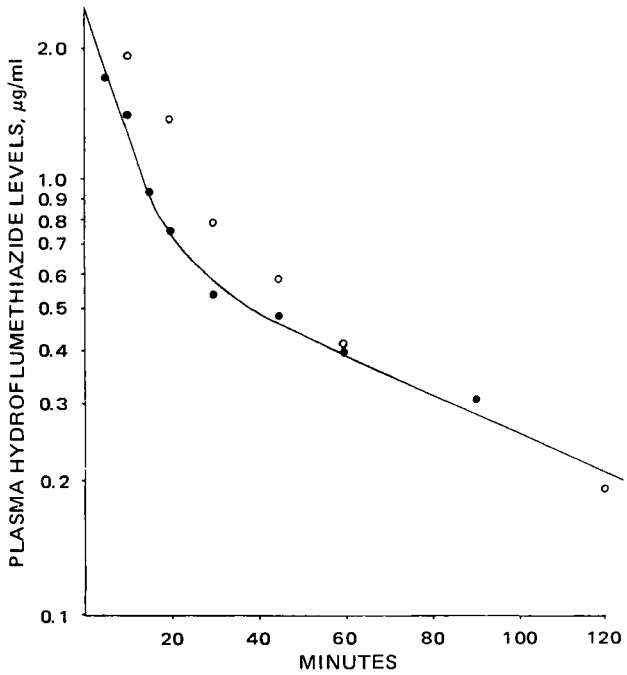

Figure 5—*Plasma levels of hydroflumethiazide following a single intravenous injection of 15 mg to a beagle dog. Key: ●, data from the present study; and ○, data from Ref. 1.*

REFERENCES

(1) Y. Garceau, I. Davis, and J. Hasegawa, *J. Pharm. Sci.*, **63**, 1793(1974).

(2) H. Sheppard, T. F. Mowles, and A. J. Plummer, *J. Am. Pharm. Assoc., Sci. Ed.*, **49**, 722(1960).

(3) V. B. Pilsbury and J. V. Jackson, *J. Pharm. Pharmacol.*, **18**, 713(1966).

(4) "Scientific Tables," 7th ed., K. Diem and C. Lentner, Eds., Geigy Pharmaceuticals, Ardsley, N.Y., 1974, pp. 280–282.

(5) "Handbook of Analytical Toxicology," I. Sunshine, Ed., Chemical Rubber Co., Cleveland, Ohio, 1969, p. 58.

ACKNOWLEDGMENTS AND ADDRESSES

Received August 20, 1975, from the *Drug Dynamics Institute, College of Pharmacy, University of Texas at Austin, Austin, TX 78712*

Accepted for publication October 23, 1975.

Presented in part at the Pharmaceutical Analysis Section, APhA Academy of Pharmaceutical Sciences, Atlanta meeting, November 1975.

The authors gratefully acknowledge support of this study from Bristol Laboratories, Syracuse, N.Y., and the American Heart Association, Texas Affiliate, Inc.

* Fellow of the American Foundation for Pharmaceutical Education.

[x] To whom inquiries should be directed.

Pharmaceutical Applications of Solid Dispersion Systems: Dissolution of Griseofulvin–Succinic Acid Eutectic Mixture

WIN L. CHIOU ˣ and SARFARAZ NIAZI

Abstract □ The dissolution profile of the griseofulvin–succinic acid eutectic mixture system was evaluated using the powder and constant-surface area tablet methods. Factors contributing to the enhancement of griseofulvin dissolution from the dispersion in succinic acid are discussed. Contrary to the original proposal of Sekiguchi and coworkers, dissolution rates of griseofulvin from solid dispersions were found to be markedly affected by the particle size of solid dispersions.

Keyphrases □ Dispersion systems, solid—evaluation of dissolution profile of griseofulvin–succinic acid eutectic mixture system, effect of particle size □ Dissolution—griseofulvin from dispersion in succinic acid, profile evaluated, effect of particle size □ Griseofulvin—dissolution from dispersion in succinic acid, profile evaluated, effect of particle size □ Antifungal agents—griseofulvin, dissolution from dispersion in succinic acid, profile evaluated

Pharmaceutical applications of solid dispersion systems were extensively reviewed by Chiou and Riegelman (1). In the past, these systems were primarily used to increase the dissolution and absorption rates of poorly water-soluble or insoluble solid drugs by dispersing them in a water-soluble carrier. More recently, they have also been employed to formulate liquid drugs in solid dosage forms (2) and to prepare sustained-release dosage forms by dispersing a drug in a water-insoluble carrier (3).

The dissolution rate of griseofulvin, a water-insoluble antifungal antibiotic, was enhanced significantly by solid dispersion in water-soluble succinic acid (4); the investigators attributed this result to the extensive formation of a solid solution of griseofulvin in succinic acid (4). Later, it was shown by X-ray diffraction and differential thermal analysis methods that the solid solubility of griseofulvin in succinic acid was negligible and such a binary system could more adequately be classified as a simple eutectic mixture (5).

In light of these findings, additional dissolution studies using constant surface area and powder methods were undertaken to explore the dissolution profile for certain compositions of the binary system. Results of these studies and their implications in using the solid dispersion method for dissolution and absorption enhancement are discussed in this paper.

EXPERIMENTAL

Sample Preparation—Solid dispersions containing 2.5, 5, 10, 25, and 55% (eutectic composition) of griseofulvin[1] in the griseofulvin–succinic acid[2] system were prepared by the fusion method (5). They were pulverized with a mortar and pestle, and the 60–100-mesh fraction was collected. For the 10% griseofulvin solid dispersion, the following mesh sizes of powder were also collected: 10–20, 20–40, 40–60, 60–80, and 80–100. The same mesh sizes of succinic acid were prepared after fusion and resolidification.

Tablets (1.3 cm in diameter) for use in constant surface area dissolution studies were prepared by compressing 300 mg of fine powder at 50,000 psi pressure in a press[3]. The tablets prepared included pure griseofulvin, 10% griseofulvin solid dispersion, 10% griseofulvin–90% succinic acid physical mixture, and 10% griseofulvin–90% succinic anhydride[4] physical mixture.

Dissolution Rate Studies—The powder dissolution method used was identical to that reported previously (6). The solid-dispersed samples containing 5 mg of griseofulvin were used in each study in 500 ml of distilled water at 37°. The amount of griseofulvin dissolved was monitored spectrophotometrically at 295 nm. The dissolution rate of succinic acid (45 mg) from various sizes of powder was measured spectrophotometrically at 195 nm based on the established Beer's law plot.

Dissolution rates of griseofulvin from constant surface area tablets were also studied in 500 ml of distilled water at 37°. The tablet was mounted into a tablet holder with only one surface area exposed to the dissolution medium. The tablet contained in the holder was placed vertically against the wall of the beaker in the middle of the dissolution medium.

The griseofulvin concentration was determined using a spectrophotofluorometer[5] with excitation at 298 nm (uncorrected) and fluorescence at 440 nm (uncorrected). Both succinic acid and succinic anhydride were found not to interfere with the griseofulvin measurement. The sample (1 ml) was returned immediately to the dissolution medium after measurement. This fluorometric assay was employed because of its high sensitivity, since griseofulvin concentrations obtained from the tablet study were too low to be measured by the UV spectrophotometric method.

All dissolution studies were conducted at least in duplicate, and highly reproducible results were always achieved. Only the average values are reported.

RESULTS AND DISCUSSION

Goldberg *et al.* (4) reported the dissolution properties of only two compositions of the solid-dispersed system and found that the dissolution rate from the 20% griseofulvin powder was much higher than that from the 55% griseofulvin powder due to the presence of the entire griseofulvin in the form of a solid solution in the former composition. In the present study, five different compositions with the same particle size were evaluated. Their dissolution profiles are shown in Fig. 1.

The dissolution rate of griseofulvin was inversely proportional to the concentration of griseofulvin in the dispersed system. Since such a binary system was shown to be a simple eutectic mixture, one can conclude that the faster dissolution rate observed with a lower concentration of griseofulvin dispersion was primarily due to the finer crystals formed in a low concentration dispersion system (1). Furthermore, Fig. 1 shows that the 55% solid dispersion dissolved somewhat more slowly than the micronized griseofulvin. This finding indicates that the average particle size of griseofulvin crystals formed in the solid dispersion was larger than that of the micronized griseofulvin.

The similar dissolution rate observed between the 25% solid dispersion and the 10% physical mixture made of 60–100-mesh succinic acid and micronized griseofulvin also indicated that the griseofulvin

[1] Griseofulvin USP (micronized), McNeil Laboratories, Fort Washington, Pa.

[2] Succinic acid, Merck & Co., Rahway, N.J.

[3] Carver Press, Fred S. Carver Co., Summit, N.J.

[4] Succinic anhydride, Merck & Co., Rahway, N.J.

[5] Aminco-Bowman spectrophotofluorometer, American Instrument Co., Silver Spring, Md.

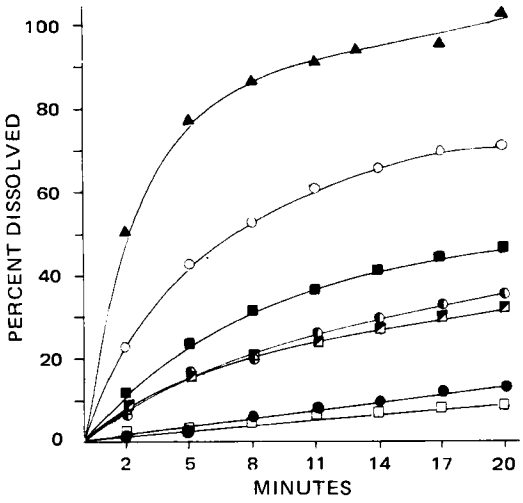

Figure 1—*Dissolution rates of griseofulvin from micronized griseofulvin, physical mixture, and 60–100-mesh fraction of various solid dispersions. Key: ▲, 2.5% solid dispersion; ○, 5% solid dispersion; ■, 10% solid dispersion; ◐, 25% solid dispersion; ◩, 10% physical mixture; ●, pure griseofulvin (micronized); and □, 55% solid dispersion.*

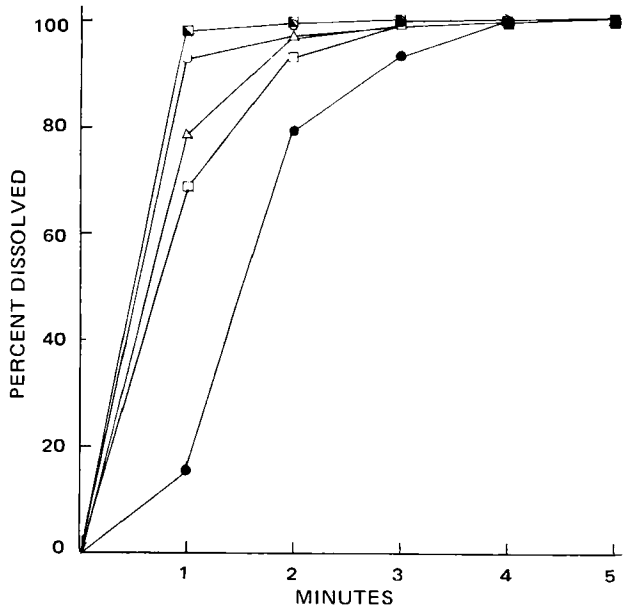

Figure 3—*Dissolution rates of various mesh sizes of succinic acid. Key: ◙, 80–100; ○, 60–80; △, 40–60; □, 20–40; and ●, 10–20.*

crystals in that dispersion were similar in size to the micronized powder. These findings are supportive of the previous study on the limited solid solubility of griseofulvin in succinic acid (5).

If the solid solubility of griseofulvin in succinic acid is as high (up to 25%) as reported by Goldberg *et al.* (4), one probably should not observe the marked difference in dissolution rate from dispersed systems containing 25% or less griseofulvin because the griseofulvin molecules should all be present in the same molecular form. The dissolution rates of sulfathiazole from the solid solutions of 5% sulfathiazole–95% urea and 10% sulfathiazole–90% urea systems were shown to be the same and to approach instantaneousness. The dissolution rate at 2 min from the 2.5% solid dispersion was about 30 times faster than from the micronized griseofulvin, indicating an extremely fine dispersion of griseofulvin in such a low concentration dispersed system. In the previous study (4), the dissolution of griseofulvin from the 25% "solid solution" was only about twice as fast as that of the micronized griseofulvin.

Although solid dispersion methods for increasing dissolution rates of drugs have been used for more than a decade, no comparison of the dissolution rates of various particle sizes of the same composition of solid dispersions apparently has been reported. According to the theory of Sekiguchi *et al.* (7), the eutectic mixture composed of intimately mixed fine crystals of each component will quickly disintegrate in water or GI fluids into finely divided particles of the drug because the water-soluble carrier will dissolve rapidly into the medium. Accordingly, one would expect that the particle size of solid dispersions should have little effect on the dissolution rate of the drug.

Surprisingly, opposite results were obtained even for the 10% griseofulvin solid dispersion where an excess amount of the soluble carrier was available (Fig. 2). The particles of the solid dispersion

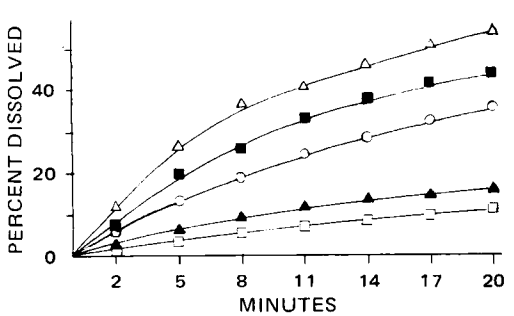

Figure 2—*Dissolution of various sizes of 10% griseofulvin solid dispersion particles. Key: △, 80–100 mesh; ■, 60–80 mesh; ○, 40–60 mesh; ▲, 20–40 mesh; and □, 10–20 mesh.*

powder, especially in the 10–20- and 20–40-mesh ranges, appeared not to decrease in size or disintegrate even after 20 min. Subsequently, the dissolution characteristics of succinic acid alone in various particle sizes were investigated (Fig. 3). Particles of all sizes were found to dissolve within 1–4 min. This finding indicates that the soluble carrier in the dispersed system might dissolve rapidly into the dissolution medium, leaving a strong, cohesive, and dissolution rate-limiting layer of griseofulvin at the outer surface of the particle. This assumption was substantiated by the following experiment.

One gram of the 10–20-mesh size of the 10% solid dispersion was stirred in 100 ml of water at 37° in the dissolution apparatus. After 10 min of stirring, the suspended particles were removed, dried, and analyzed. They were found to contain 79% of griseofulvin, indicating that most succinic acid had already dissolved. A 100% griseofulvin content was found after 20 min. No disintegration or reduction in particle size of the granules was observed.

These results clearly indicate that the unique feature of the ultrafine crystals of griseofulvin in the eutectic mixture might be lost if large particles are used. However, it remains to be investigated whether this will significantly affect the bioavailability of the drug in humans. The results of the present study did not contradict the previous findings that showed disintegration of solid dispersion particles under observation with a microscope.

The constant surface area tablet technique often has been used to study dissolution mechanisms of various systems. Only the 10% griseofulvin composition was selected for evaluation in the present study (Fig. 4).

As expected, a zero-order dissolution rate of griseofulvin from the pure griseofulvin tablet was found. The dissolution rate of griseofulvin from the 10% griseofulvin–90% succinic acid physical mixture at the early stage (less than 30 min) was faster than that from the pure compound. This result can be explained by the solubilizing effect of succinic acid (4). As succinic acid was depleted, the effect disappeared and the dissolution rate became identical to that from a pure griseofulvin tablet (8).

Such a dissolution enhancement was not observed in the previous study using the powder method, probably due to the lack of intimate contact between the two components in the physical mixture of powder. Therefore, one can postulate that the solubilizing effect of succinic acid can contribute partially to the observed dissolution enhancement in the solid dispersion system. The increased wettability of the hydrophobic griseofulvin by the intimate contact of the polar succinic acid also may play a role in the enhancement of the dissolution rate (1).

The dissolution profile from the 10% solid dispersion was interesting. A constant release of griseofulvin was observed for up to about 24 min. This rate was about 2.6 times higher than that of the physical mixture and about 4 times higher than that of pure griseofulvin. Such

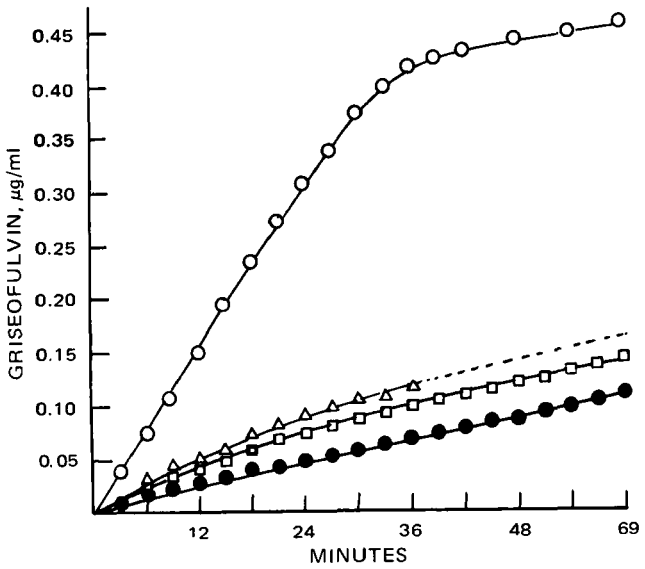

Figure 4—*Release of griseofulvin from constant surface tablets. Key: ○, 10% solid dispersion; △, 10% griseofulvin–90% succinic anhydride physical mixture; □, 10% griseofulvin–90% succinic acid physical mixture; and ●, pure griseofulvin.*

a marked increase in dissolution rate cannot be explained by the presence of a higher energy polymorphic form because the X-ray diffraction study showed that the identical crystalline form was present in the dispersed system as the pure griseofulvin used in the present study (5).

Since some succinic anhydride (about 7% w/w) was formed during the preparation of solid dispersions (5), it was thought that such an impurity might enhance the dissolution rate. The fact that the dissolution rate of griseofulvin was only moderately increased in the presence of 90% succinic anhydride (Fig. 4), however, rules out the important role of this decomposition product. Based on these results and analyses, it is postulated that the major factor in the increasing dissolution rate in the 10% griseofulvin dispersion was the presence of extremely fine crystals of griseofulvin. Crystalline size alone has been shown to affect the solubility of drugs (9).

After about 42 min, the cumulative plot curve of the 10% griseofulvin solid dispersion became parallel with that of pure griseofulvin. This result probably was due to the presence of negligible concentrations of the solubilizers, succinic acid and succinic anhydride, at the outer controlling layer of the tablet and to the presence of a coarser particle size of griseofulvin at the dissolution surface; this coarser particle size was formed as a result of the aggregation and/or crystal growth of ultrafine crystals. It must be noted that these tablet dissolution studies were carried out under essentially sink conditions (the solubility of griseofulvin at 37° is about 12.5 µg/ml).

REFERENCES

(1) W. L. Chiou and S. Riegelman, *J. Pharm. Sci.*, **60**, 1231(1971).

(2) W. L. Chiou and L. D. Smith, *ibid.*, **60**, 125(1971).

(3) N. Athanikar and W. L. Chiou, Abstract 22, presented at the Basic Pharmaceutics Section, APhA Academy of Pharmaceutical Sciences, San Francisco meeting, April 1975.

(4) A. H. Goldberg, M. Gibaldi, and J. L. Kanig, *J. Pharm. Sci.*, **55**, 487(1966).

(5) W. L. Chiou and S. Niazi, *ibid.*, **62**, 498(1973).

(6) *Ibid.*, **60**, 1333(1971).

(7) K. Sekiguchi, N. Obi, and Y. Ueda, *Chem. Pharm. Bull.*, **9**, 866(1961).

(8) W. I. Higuchi, *J. Pharm. Sci.*, **56**, 315(1967).

(9) A. N. Martin, J. Swarbrick, and A. Cammarata, "Physical Pharmacy," 2nd ed., Lea & Febiger, Philadelphia, Pa., 1969, p. 313.

ACKNOWLEDGMENTS AND ADDRESSES

Received August 29, 1975, from the *Clinical Pharmacokinetics Laboratory and Department of Pharmacy, College of Pharmacy, University of Illinois at the Medical Center, Chicago, IL 60680* and the *College of Pharmacy, Washington State University, Pullman, WA 99163*

Accepted for publication October 23, 1975.

Presented in part at the Basic Pharmaceutics Section, APhA Academy of Pharmaceutical Sciences, Houston meeting, April 1972.

Supported in part by funds provided for biological and medical research by State of Washington Initiative Measure 171 and Graduate School Research Funds, Washington State University.

[x] To whom inquiries should be directed. Present address for both authors: College of Pharmacy, University of Illinois at the Medical Center, Chicago, IL 60680

Application of Trichloroacetyl Isocyanate to NMR Analysis of Steroids of Pharmaceutical Interest I: Corticosteroids and Chemically Related Compounds

MONIQUE LANOUETTE, DONALD LEGAULT, and BRUCE A. LODGE [x]

Abstract □ The trichloroacetyl carbamates of 38 corticosteroids and chemically related compounds were prepared, and their NMR spectra in deuterochloroform were obtained. The effects of the introduction of a number of functional groups on the chemical shift of the carbamate proton signals were determined.

Keyphrases □ Trichloroacetyl isocyanate—reaction with corticosteroids to form carbamates, application to NMR analysis □ NMR—analysis, carbamates of corticosteroids formed by reaction with trichloroacetyl isocyanate □ Corticosteroids—NMR analysis of carbamates formed by reaction with trichloroacetyl isocyanate □ Carbamates—formed by reaction of trichloroacetyl isocyanate with corticosteroids, NMR analysis

Over the past several years, trichloroacetyl isocyanate has been used as a synthetic (1–6) and as a diagnostic (7–10) reagent. It reacts with hydroxyl groups to form carbamates of type I. Such derivatives are usually much more soluble in deuterochloroform than are the parent compounds; indeed, many underivatized corticosteroids

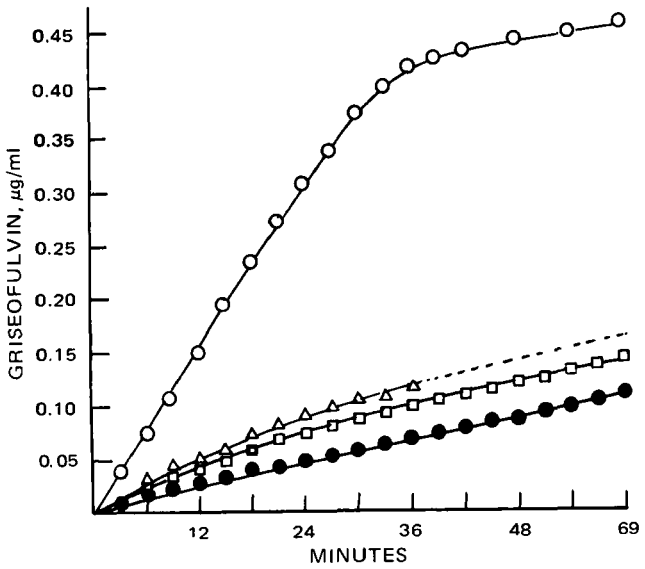

Figure 4—*Release of griseofulvin from constant surface tablets. Key: ○, 10% solid dispersion; △, 10% griseofulvin–90% succinic anhydride physical mixture; □, 10% griseofulvin–90% succinic acid physical mixture; and ●, pure griseofulvin.*

a marked increase in dissolution rate cannot be explained by the presence of a higher energy polymorphic form because the X-ray diffraction study showed that the identical crystalline form was present in the dispersed system as the pure griseofulvin used in the present study (5).

Since some succinic anhydride (about 7% w/w) was formed during the preparation of solid dispersions (5), it was thought that such an impurity might enhance the dissolution rate. The fact that the dissolution rate of griseofulvin was only moderately increased in the presence of 90% succinic anhydride (Fig. 4), however, rules out the important role of this decomposition product. Based on these results and analyses, it is postulated that the major factor in the increasing dissolution rate in the 10% griseofulvin dispersion was the presence of extremely fine crystals of griseofulvin. Crystalline size alone has been shown to affect the solubility of drugs (9).

After about 42 min, the cumulative plot curve of the 10% griseofulvin solid dispersion became parallel with that of pure griseofulvin. This result probably was due to the presence of negligible concentrations of the solubilizers, succinic acid and succinic anhydride, at the outer controlling layer of the tablet and to the presence of a coarser particle size of griseofulvin at the dissolution surface; this coarser particle size was formed as a result of the aggregation and/or crystal growth of ultrafine crystals. It must be noted that these tablet dissolution studies were carried out under essentially sink conditions (the solubility of griseofulvin at 37° is about 12.5 µg/ml).

REFERENCES

(1) W. L. Chiou and S. Riegelman, *J. Pharm. Sci.*, **60**, 1231(1971).

(2) W. L. Chiou and L. D. Smith, *ibid.*, **60**, 125(1971).

(3) N. Athanikar and W. L. Chiou, Abstract 22, presented at the Basic Pharmaceutics Section, APhA Academy of Pharmaceutical Sciences, San Francisco meeting, April 1975.

(4) A. H. Goldberg, M. Gibaldi, and J. L. Kanig, *J. Pharm. Sci.*, **55**, 487(1966).

(5) W. L. Chiou and S. Niazi, *ibid.*, **62**, 498(1973).

(6) *Ibid.*, **60**, 1333(1971).

(7) K. Sekiguchi, N. Obi, and Y. Ueda, *Chem. Pharm. Bull.*, **9**, 866(1961).

(8) W. I. Higuchi, *J. Pharm. Sci.*, **56**, 315(1967).

(9) A. N. Martin, J. Swarbrick, and A. Cammarata, "Physical Pharmacy," 2nd ed., Lea & Febiger, Philadelphia, Pa., 1969, p. 313.

ACKNOWLEDGMENTS AND ADDRESSES

Received August 29, 1975, from the *Clinical Pharmacokinetics Laboratory and Department of Pharmacy, College of Pharmacy, University of Illinois at the Medical Center, Chicago, IL 60680* and the *College of Pharmacy, Washington State University, Pullman, WA 99163*

Accepted for publication October 23, 1975.

Presented in part at the Basic Pharmaceutics Section, APhA Academy of Pharmaceutical Sciences, Houston meeting, April 1972.

Supported in part by funds provided for biological and medical research by State of Washington Initiative Measure 171 and Graduate School Research Funds, Washington State University.

[x] To whom inquiries should be directed. Present address for both authors: College of Pharmacy, University of Illinois at the Medical Center, Chicago, IL 60680

Application of Trichloroacetyl Isocyanate to NMR Analysis of Steroids of Pharmaceutical Interest I: Corticosteroids and Chemically Related Compounds

MONIQUE LANOUETTE, DONALD LEGAULT, and BRUCE A. LODGE [x]

Abstract □ The trichloroacetyl carbamates of 38 corticosteroids and chemically related compounds were prepared, and their NMR spectra in deuterochloroform were obtained. The effects of the introduction of a number of functional groups on the chemical shift of the carbamate proton signals were determined.

Keyphrases □ Trichloroacetyl isocyanate—reaction with corticosteroids to form carbamates, application to NMR analysis □ NMR—analysis, carbamates of corticosteroids formed by reaction with trichloroacetyl isocyanate □ Corticosteroids—NMR analysis of carbamates formed by reaction with trichloroacetyl isocyanate □ Carbamates—formed by reaction of trichloroacetyl isocyanate with corticosteroids, NMR analysis

Over the past several years, trichloroacetyl isocyanate has been used as a synthetic (1–6) and as a diagnostic (7–10) reagent. It reacts with hydroxyl groups to form carbamates of type I. Such derivatives are usually much more soluble in deuterochloroform than are the parent compounds; indeed, many underivatized corticosteroids

Table I—Chemical Shifts[a] (Hertz) of the Proton Signals in the NMR Spectra[b] of the Trichloroacetyl Carbamate Derivatives of Corticosteroids and Chemically Related Compounds

		Carbamate Protons						Carbinol Protons				Methyl Protons			Vinylic Protons			
	Compound	11β	17α	21	17β	11α	3β	11α	21	11β	3α	18	19	(Other)	1	2	4	6
I	11α-Hydroxypregn-4-ene-3,20-dione	—	—	—	—	523	—	—	—	323	—	46	80	128 (21)	—	—	346	—
II	11β-Hydroxypregn-4-ene-3,20-dione	508	—	—	—	—	—	336	—	—	—	52	79	128 (21)	—	—	343	—
III	11β-Hydroxyandrost-4-ene-3,17-dione	512	—	—	—	—	—	338	—	—	—	68	80	—	—	—	344	—
IV	11β-Hydroxyandrosta-1,4-diene-3,17-dione	520	—	—	—	—	—	342	—	—	—	67	78	—	421	377	364	—
V	17α-Hydroxypregn-4-ene-3,20-dione	—	562	—	—	—	—	—	—	—	—	44	72	131 (21)	—	—	345	—
VI	17α-Hydroxypregn-4-ene-3,11,20-trione	—	544	—	—	—	—	—	—	—	—	40	85	129 (21)	—	—	344	—
VII	21-Hydroxypregn-4-ene-3,20-dione	—	—	526	—	—	—	—	286	—	—	44	71	—	—	—	344	—
VIII	21-Hydroxypregn-4-ene-3,11,20-trione	—	—	528	—	—	—	—	285	—	—	43	85	—	—	—	344	—
IX	Pregnenolone	—	—	—	—	—	503	—	—	—	282	40	64	128 (21)	—	—	—	326
X	11β,21-Dihydroxypregn-4-ene-3,20-dione	510	—	529	—	—	—	336	287	—	—	56	79	—	—	—	344	—
XI	11β,21-Dihydroxypregn-4-ene-3,20-dione 21-acetate	503	—	—	—	—	—	335	285	—	—	54	79	—	—	—	343	—
XII	17α,21-Dihydroxypregn-4-ene-3,20-dione	—	594	547	—	—	—	—	302	—	—	50	72	—	—	—	344	—
XIII	17α,21-Dihydroxypregn-4-ene-3,20-dione 21-acetate	—	574	—	—	—	—	—	293	—	—	48	72	—	—	—	344	—
XIV	Cortisone[c]	—	583	549	—	—	—	—	302	—	—	47	85	—	—	—	345	—
XV	Cortisone acetate[d]	—	563	—	—	—	—	—	291	—	—	46	86	—	—	—	344	—
XVI	Prednisone[e]	—	590	550	—	—	—	—	301	—	—	49	86	—	465	367	364	—
XVII	Prednisone 21-acetate	—	576	—	—	—	—	—	291	—	—	48	86	—	465	368	364	—
XVIII	Hydrocortisone[d]	512	563	547	—	—	—	342	305	—	—	62	78	—	—	—	342	—
XIX	Prednisolone	520	566	548	—	—	—	344	304	—	—	64	77	—	424	374	361	—
XX	Prednisolone 21-acetate	513	547	—	—	—	—	344	292	—	—	62	78	—	424	377	363	—
XXI	Betamethasone[d]	522	606	545	—	—	—	333	290	—	—	59	87	62 (16β)	418	380	367	—
XXII	Betamethasone 21-acetate[d]	517	586	—	—	—	—	334	280	—	—	58	85	60 (16β)	416	378	366	—
XXIII	Betamethasone 21-valerate[d]	514	586	—	—	—	—	333	281	—	—	58	86	60 (16β)	416	378	366	—
XXIV	Betamethasone 17-valerate	520	—	528	—	—	—	340	280	—	—	59	88	60 (16β)	417	382	371	—
XXV	Beclomethasone 17-propionate	520	—	530	530	—	—	346	280	—	—	60	93	61 (16β)	418	382	369	—
XXVI	Beclomethasone 21-propionate[d]	520	581	—	—	—	—	344	282	—	—	59	92	71 (16β)	416	380	367	—
XXVII	Beclomethasone dipropionate	514	—	—	—	—	—	344	272	—	—	57	92	61 (16β)	416	381	368	—
XXVIII	Dexamethasone[f]	531	611	547	—	—	—	331	306	—	—	69	80	57 (16α)	412	375	365	—
XXIX	Dexamethasone 21-acetate[f]	529	576	—	—	—	—	331	295	—	—	69	82	57 (16α)	413	377	366	—
XXX	Methylprednisolone 21-acetate	514	548	—	—	—	—	345	291	—	—	61	77	68 (6α)	423	375	363	—
XXXI	Fluprednisolone	516	553	540	—	—	—	345	304	—	—	64	76	—	422	378	381	—
XXXII	Fludrocortisone acetate[d]	509	594	—	—	—	—	338	292	—	—	59	86	—	—	—	346	—
XXXIII	Fluperolone acetate[c]	520	582	—	—	—	—	344	281	—	—	60	92	—	417	380	367	—
XXXIV	Paramethasone 21-acetate[f]	519	553	—	—	—	—	346	296	—	—	69	75	56 (16α)	422	377	381	—
XXXV	Triamcinolone acetonide	524	—	527	—	—	—	337	302	—	—	55	74	—	416	382	370	—
XXXVI	Triamcinolone 16α,21-diacetate[f]	533	587	—	—	—	—	334	299	—	—	67	84	—	415	381	368	—
XXXVII	Triamcinolone hexacetonide	517	—	—	—	—	—	334	291	—	—	54	74	—	415	382	370	—
XXXVIII	Fluocinonide	519	—	—	—	—	—	336	292	—	—	52	73	—	413	383	388	—

[a] Chemical shifts downfield from tetramethylsilane (0 Hz). [b] All spectra obtained at a concentration of 40 mg/ml. [c] Sample required 1 hr to react completely. [d] Sample required 30 min to react completely. [e] Sample required 24 hr to dissolve. [f] Spectrum obtained after 24 hr.

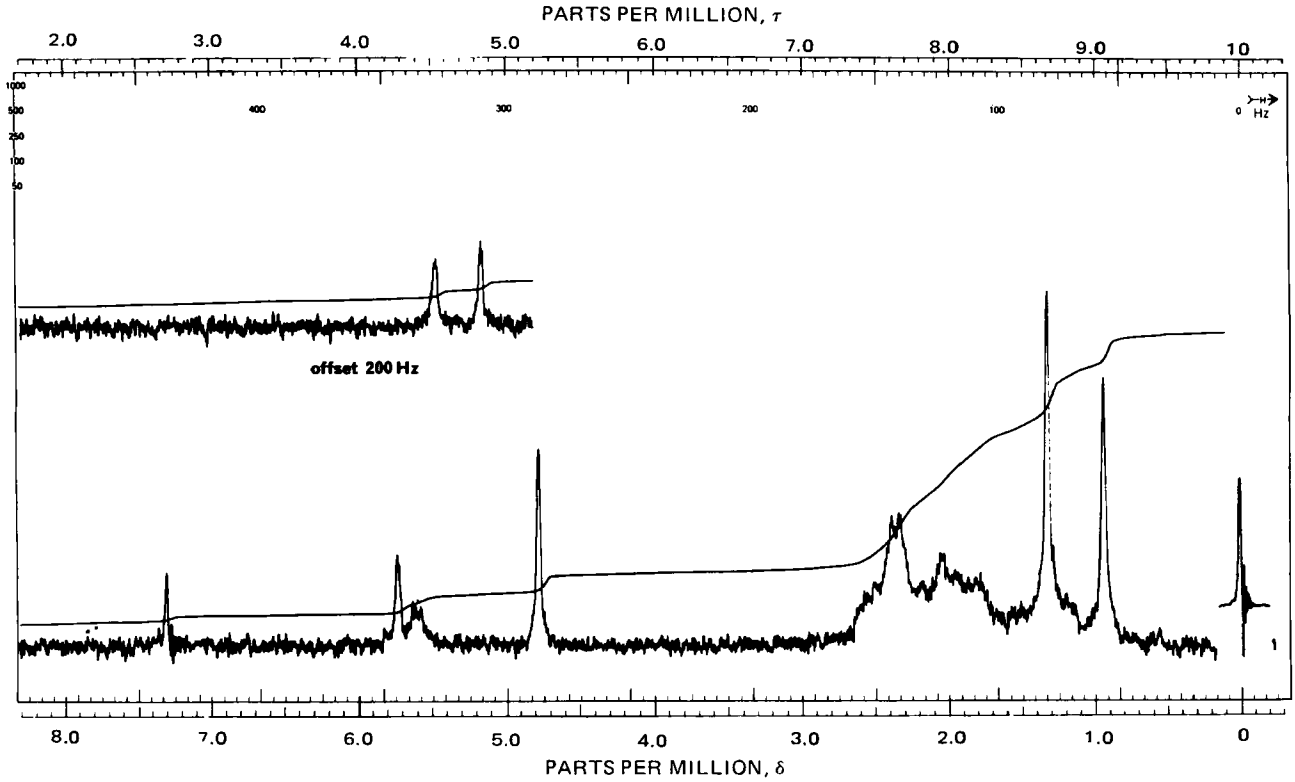

Figure 1—*The 60-MHz NMR spectrum of the trichloroacetyl isocyanate derivative of 11β,21-dihydroxypregn-4-ene-3,20-dione in deuterochloroform.*

are not sufficiently soluble in deuterochloroform for the determination of their NMR spectra.

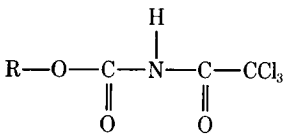

type I

A note by Trehan *et al.* (7) led to a detailed study of the NMR spectroscopy of the trichloroacetyl carbamate derivatives of numerous corticosteroids and chemically related compounds of pharmaceutical interest. Polyhydroxy compounds should react at each hydroxyl group, with the carbamate proton signal in the NMR spectrum for each such hydroxyl appearing as a distinct singlet in a region of the spectrum isolated from all other signals.

EXPERIMENTAL

Approximately 40 mg of a hydroxysteroid[1] was accurately weighed into a 1-ml volumetric flask. Approximately 0.5 ml of deuterochloroform was added to the flask, followed by trichloroacetyl isocyanate[2] (~20 μl/hydroxyl group). Deuterochloroform was added to volume, and the flask was shaken until dissolution occurred.

The NMR spectrum was obtained[3] in the usual manner at 40 ± 2°, with tetramethylsilane added as the internal standard. Chemical shifts are reported as hertz downfield from tetramethylsilane (0 Hz).

[1] Steroids were obtained from the Pharmaceutical Chemistry Division collection of reference materials.

[2] Eastman Kodak Co., Rochester, N.Y.

[3] Varian A60A NMR spectrometer, Varian Associates, Georgetown, Ontario, Canada.

Table II—Concentration Effect on the Chemical Shift[a] (Hertz) of the Three Carbamate Proton Signals in the NMR Spectrum of the Reaction Product of Prednisolone with Trichloroacetyl Isocyanate

Origin of Proton	Concentration, *M*			
	0.07	0.14	0.21	0.28
11β	513	520	525	527
17α	551	566	572	575
21	538	548	554	556

[a] Chemical shifts downfield from tetramethylsilane (0 Hz).

Some samples (dexamethasone, dexamethasone acetate, paramethasone acetate, and triamcinolone diacetate) were left for 24 hr at room temperature after being made up to volume because of the very slow reaction to the severely hindered 17α-hydroxyl group with the reagent. Other slow reactions are noted in Table I.

The concentration dependence of the signal from the carbamate proton was determined by accurately weighing 10, 20, 30, and 40 mg of prednisolone and making up to 0.4 ml after adding 15, 30, 45, and 60 μl, respectively, of trichloroacetyl isocyanate.

Table III—Effect of Each 11β, 17α-, and 21-Hydroxyl Group Carbamate on the Chemical Shift[a] (Hertz) of the Carbamate Proton Signal of the Others

Compound	Hydroxyl		
	11β	17α	21
II	508	—	—
XI	510	—	529
VII	—	—	526
V	—	562	—
XII	—	594	547
XVIII	512	563	547
XIX	520	566	547

[a] Chemical shifts downfield from tetramethylsilane (0 Hz).

Table IV—Effect of Introducing an 11-Carbonyl Group on the Chemical Shift[a] (Hertz) of the Carbamate Proton Signals from 17α- and 21-Hydroxyl Groups

Compound	Hydroxyl	
	17α	21
XII	594	547
XIV	583	549
XIII	574	—
XV	563	—
V	562	—
VI	554	—
VII	—	526
VIII	—	528

[a] Chemical shifts downfield from tetramethylsilane (0 Hz).

RESULTS AND DISCUSSION

Chemical shifts are reported in Table I for the carbamate proton signals and also for the signals from the carbinol protons, the tertiary methyl protons (C-18 and C-19), and the vinylic protons. All spectra were obtained at a concentration of 40 mg/ml, because, as shown in Table II, there is a marked concentration effect on the position of the carbamate proton signals. A typical spectrum is shown in Fig. 1 (Compound X).

Table III shows the effect of each 11β-, 17α-, and 21-hydroxyl group on the chemical shift of the others (in terms of the respective carbamate NH signals). From Table III, the following conclusions may be drawn: (*a*) the chemical shifts of the 11β- and 21-hydroxyl group derivatives are independent of each other and (*b*) the 17α- and 21-hydroxyl group derivatives are mutually deshielding.

Introducing a 17α-hydroxyl into the parent molecule deshields the 21-carbamate proton signal by approximately 20 Hz; likewise, introducing a 21-hydroxyl deshields the 17α-carbamate proton signal by approximately 30 Hz. However, an 11β-hydroxyl counteracts the effect of the 21-hydroxyl on the 17α-carbamate proton signal (XII *versus* XVIII). Comparison of XVIII with XIX shows that the Δ^1-function has a minimal effect on the chemical shift of the 17α- and 21-carbamate NH signals but deshields the 11β-carbamate signal by 8 Hz.

Table IV shows the effects of introducing an 11-carbonyl group on the chemical shift of the 17α- and 21-carbamate proton signals. The compounds are grouped in pairs, with the 11-carbonyl derivative appearing below the corresponding unoxygenated compound. From these results, it can be seen that the 17α-carbamate proton signal is shielded by approximately 10 Hz, whereas the 21-carbamate proton signal is deshielded by only 2 Hz, which is not significant.

Table V shows the effect of acetylation of the 21-hydroxyl group on the chemical shift of the carbamate proton signals at 11β and 17α. Some general comments may be made about these results, noting that there is one significant exception (XXVIII/XXIX). The 17α-carbamate proton signal is shielded by approximately 20 Hz, and the 11β-carbamate proton signal is shielded by 5–7 Hz upon acetylation of the 21-hydroxyl.

Table V—Effect of 21-Acetylation on the Chemical Shift[a] (Hertz) of the 11- and 17-Carbamate Proton Signals

Compound	Proton		
	11β	17α	21
XII	—	594	547
XIII	—	574	—
XIV	—	583	549
XV	—	563	—
XVI	—	590	550
XVII	—	576	—
XIX	520	566	548
XX	513	547	—
XXI	522	606	545
XXII	517	586	—
X	510	—	529
XI	503	—	—
XXVIII	531	611	547
XXIX	529	576	—

[a] Chemical shifts downfield from tetramethylsilane (0 Hz).

Table VI—Predictions of Major Signals (Hertz) in the NMR Spectra of the Carbamates of XV and XX[a]

Compound	Protons	Predicted	Observed
XV	C-18 Methyl	48	46
	C-19 Methyl	85	86
	21	293	291
	C-4 Vinylic	344	344
	17α-Carbamate	563	563
XX	C-18 Methyl	63	63
	C-19 Methyl	78	78
	21	291	292
	11α	342	344
	C-4 Vinylic	361	363
	C-2 Vinylic	374	377
	C-1 Vinylic	424	424
	11β-Carbamate	520	513
	17α-Carbamate	545	547

[a] Chemical shifts downfield from tetramethylsilane (0 Hz).

Compound XXVIII has a 16α-methyl substituent, which sterically interacts with the 17α-hydroxyl group. The best evidence for this hindrance is the fact that XXVIII, together with XXIX, XXXIV, and XXXVI, all of which possess 16α-substituents, requires 24 hr for the 17α-carbamate derivative to form. The distortion created by the 16α-substituent in XXVIII has the effect that, when a 21-acetyl group is introduced (XXIX), the 17α-carbamate proton signal is shielded by 35 Hz, whereas the shielding of the 11α-carbamate proton signal is reduced to 2 Hz.

For two of the compounds studied, XV and XX, predictions were made, based on accumulated results, of the major signals in their NMR spectra. These results are shown in Table VI. Some signals, such as the vinylic protons, are easy to predict. The tertiary methyl signals are also relatively easy to predict since tables are available to assist in the prediction (11). As more compounds are studied, further rules may be discovered to assist in more accurate predictions of the carbamate proton signals.

The reverse situation is immediately obvious: that given such an NMR spectrum, one can deduce the structure and stereochemistry of functional groups. Therefore, the technique is of value in the structure determination in unknown compounds, thereby extending its analytical applications.

REFERENCES

(1) J. L. Chitwood, J. C. Martin, and P. G. Gott, *J. Org. Chem.*, **36**, 2228(1971).

(2) N. N. Arbuzov, G. N. Rusanov, and B. A. Arbuzov, *Izv. Akad. Nauk SSSR, Ser. Khim.*, **1972**, 2016.

(3) B. A. Arbuzov, N. N. Zobova, and F. B. Balabanova, *ibid.*, **1972**, 2086.

(4) B. A. Arbuzov, N. N. Zobova, F. B. Balabanova, and M. F. Tarasova, *ibid.*, **1972**, 2324.

(5) Z. Sanek and L. Novotny, *Tetrahedron Lett.*, **1972**, 5167.

(6) B. A. Arbuzov, N. N. Zobova, F. B. Balabanova, and N. F. Tarasova, *Izv. Akad. Nauk SSSR, Ser. Khim.*, **1973**, 456.

(7) I. R. Trehan, C. Monder, and A. K. Bose, *Tetrahedron Lett.*, **1968**, 67.

(8) F. Will and C. Varsel, *Anal. Chim. Acta*, **44**, 233(1969).

(9) D. H. Mak and M. G. Rogers, *Anal. Chem.*, **44**, 837(1972).

(10) V. Goodlett, *ibid.*, **37**, 431(1965).

(11) N. S. Bhacca and D. H. Williams, "Applications of NMR Spectroscopy in Organic Chemistry," Holden-Day, San Francisco, Calif., 1964, p. 19.

ACKNOWLEDGMENTS AND ADDRESSES

Received June 30, 1975, from the *Drug Research Laboratories, Health Protection Branch, Tunney's Pasture, Ottawa, Ontario, Canada K1A 0L2.*

Accepted for publication October 24, 1975.

[x] To whom inquiries should be directed.

Drug Biotransformation Interactions in Man VI: Acetaminophen and Ascorbic Acid

J. BRIAN HOUSTON and GERHARD LEVY ×

Abstract □ Oral administration of 3 g of ascorbic acid 1.5 hr after an oral dose of 1 g of acetaminophen caused a rapid and pronounced decrease in the excretion rate of acetaminophen sulfate in five healthy adult volunteers. There was a statistically significant increase in the fractions of the dose of acetaminophen excreted as such and as acetaminophen glucuronide but a decrease in the fraction excreted as acetaminophen sulfate. The apparent biological half-life of acetaminophen increased from 2.3 ± 0.2 (mean ± *SD*) to 3.1 ± 0.5 hr. Concomitant administration of sodium sulfate prevented these effects. Ascorbic acid, which itself is metabolized in part to the sulfate, inhibits the conjugation of acetaminophen with sulfate by competing for available sulfate in the body.

Keyphrases □ Drug biotransformation interactions—effect of ascorbic acid on half-life and excretion rate of acetaminophen, humans □ Interactions, drug biotransformation—effect of ascorbic acid on half-life and excretion rate of acetaminophen, humans □ Biotransformation—effect of ascorbic acid on half-life and excretion rate of acetaminophen, humans □ Acetaminophen—half-life and excretion rate, effect of ascorbic acid, humans □ Ascorbic acid—effect on half-life and excretion rate of acetaminophen, humans

Conjugation with sulfate is an important biotransformation pathway for phenolic drugs (1). Humans have a limited capacity for sulfate formation, so drugs subject to this metabolic process tend to exhibit nonlinear (saturable) elimination kinetics (2, 3) and competitive inhibitory effects. For example, acetaminophen and salicylamide interact in humans by mutual inhibition of their respective conjugation with sulfate (3). This inhibitory effect can be prevented by concomitant administration of sulfate or a sulfate donor such as L-cysteine (3, 4).

It was found recently that ascorbic acid (vitamin C) is converted partly to ascorbic acid sulfate in humans (5). Since this vitamin is often taken in relatively large doses, it is desirable to explore the possible effect of ascorbic acid on the conjugation of phenolic drugs with sulfate. In a preliminary study, ascorbic acid caused a decrease in the fraction of an oral dose of salicylamide excreted as salicylamide sulfate (6). This interaction probably occurred mainly during absorption, since salicylamide is extensively metabolized in the first pass, probably largely in the intestinal wall (7).

Unlike salicylamide, acetaminophen is not subject to a pronounced first-pass effect (8, 9). It can be used, therefore, to determine if ascorbic acid can inhibit systemically the conjugation of a drug with sulfate. The investigation described here was designed to determine the effect of ascorbic acid on the biotransformation of acetaminophen under postabsorptive conditions in order to assess the effect of the vitamin on the elimination kinetics of acetaminophen and to elucidate the mechanism of the interaction.

EXPERIMENTAL

Five healthy male volunteers, 27–40 years old and capable by education and experience to give their informed consent (research assistants and associates), were instructed not to take any drugs or vitamin preparations for 1 week before and during the study. They fasted overnight, emptied their bladders in the morning, and took 1 g of acetaminophen[1] followed by 50 ml of water.

Urine was collected every 0.5 hr for 4 hr, every hour for the next 4 hr, and then at convenient intervals for a total of 24 hr. Water (100 ml) was ingested after each urine collection to assure an adequate flow rate. Food intake was permitted after the first 4 hr. Three grams of ascorbic acid in 200 ml of water, or 200 ml of water only, was administered at 1.5 hr. The experiments were carried out in random order at least 1 week apart.

Two subjects repeated the acetaminophen–ascorbic acid experiment twice, once with sodium sulfate (1 g in 100 ml of water at 0.5, 1.5, and 2.5 hr) and once with L-cysteine (2 g in 100 ml of water at 0.5, 1.5, and 2.5 hr).

The urine samples were analyzed colorimetrically for acetaminophen, acetaminophen glucuronide, and acetaminophen sulfate after selective extraction and enzymatic hydrolysis, as described previously (3, 10).

RESULTS

To determine a possible effect of ascorbic acid and its metabolites on the assay of acetaminophen and its conjugates, urine obtained after acetaminophen administration was assayed as such and after addition of urine obtained after ascorbic acid administration. There was no interference in the assay of acetaminophen and its major metabolites.

Ascorbic acid caused a significant decrease in the fraction of acetaminophen excreted as the sulfate and a significant increase in the fractions excreted as acetaminophen and acetaminophen glucuronide, but it had no effect on the recovery of total acetaminophen (*i.e.*, the sum of acetaminophen, its glucuronide, and its sulfate) (Table I).

A rapid and pronounced decrease in the excretion rate of acetaminophen sulfate occurred after ascorbic acid administration (Figs. 1 and 2, left panels). This effect lasted for about 4 hr on the average. Concomitant administration of sodium sulfate prevented this inhibition, while administration of L-cysteine had no apparent effect (Figs. 1 and 2, right panels). Sodium sulfate, but not L-cysteine, prevented the change in the metabolic fate of acetaminophen produced by ascorbic acid (Table II).

Ascorbic acid had no significant effect on the pH or flow rate of urine. The control and ascorbic acid experiment values (mean ± *SD*) from 1.5 to 5.5 hr (the period when the effect of ascorbic acid on acetaminophen biotransformation was most apparent) were 5.90 ± 0.46 and 5.81 ± 0.66 pH units and 174 ± 152 and 220 ± 153 ml/hr, respectively.

Examples of the excretion rate profiles of acetaminophen and acetaminophen glucuronide were reported previously (3, 10), and similar results were observed in this investigation. Figure 3 shows the excretion rate profiles for acetaminophen in Subject H during concomitant administration of sodium sulfate or L-cysteine. The excretion rate profile in these and other experiments had a terminal, apparently exponential phase, which may be characterized by an apparent half-life value[2]. The half-life of acetaminophen determined by this method was significantly increased by concomitant administration of ascorbic acid (Table III). Sodium sulfate, but not L-cysteine, prevented this effect.

There was a strong ($r = -0.95$) and statistically significant ($p < 0.01$) negative correlation between the change in the half-life of acetaminophen and the change in the fraction of acetaminophen

[1] Tylenol Elixir, McNeil Laboratories, Fort Washington, Pa.

[2] The elimination kinetics of acetaminophen are obviously not truly first order following administration of a competitive inhibitor of one biotransformation pathway, but this is not apparent in the excretion rate profile of acetaminophen. The term "apparent half-life" is used because of these considerations.

Table I—Effect of Ascorbic Acid on the Metabolic Fate of Acetaminophen in Humans

Subject	Excreted in Urine, % of Dose							
	Acetaminophen		Acetaminophen Glucuronide		Acetaminophen Sulfate		Total Acetaminophen	
	Control	With Ascorbic Acid	Control	With Ascorbic Acid	Control	With Ascorbic Acid	Control	With Ascorbic Acid
H	4.1	5.2	47.7	57.8	29.4	19.6	81.2	82.6
L	4.3	6.3	34.0	44.9	41.8	20.8	80.1	72.0
O	5.4	6.6	40.9	47.6	36.1	26.0	82.4	80.2
S	5.0	6.2	54.7	62.2	26.7	24.8	86.4	93.2
Y	3.9	5.0	53.5	62.0	32.3	23.6	89.7	90.6
Mean	4.5	5.9	46.2	54.9	33.3	23.0	84.0	83.7
SD	0.6	0.7	8.7	8.2	5.9	2.7	8.4	8.4
Statistical difference from control[a]		$p < 0.005$		$p < 0.001$		$p < 0.05$		N.S.

[a] Paired *t*-test.

Table II—Effect of Sodium Sulfate and L-Cysteine on the Biotransformation Interaction between Acetaminophen and Ascorbic Acid[a]

Subject	Sulfate Donor	Excreted in Urine, % of Dose			
		Acetaminophen	Acetaminophen Glucuronide	Acetaminophen Sulfate	Total Acetaminophen
H	None	5.2	57.8	19.6	82.6
H	L-Cysteine[b]	5.8	56.7	20.5	83.0
H	Sodium sulfate[c]	4.5	53.8	32.7	91.0
Y	None	5.0	62.0	23.6	90.6
Y	L-Cysteine[b]	6.3	59.1	23.8	89.2
Y	Sodium sulfate[c]	4.5	52.1	31.8	88.4

[a] One gram of acetaminophen followed by 3 g of ascorbic acid 1.5 hr later. [b] Two grams at 0.5, 1.5, and 2.5 hr after acetaminophen administration. [c] One gram at 0.5, 1.5, and 2.5 hr after acetaminophen administration.

sulfate produced by ascorbic acid (Fig. 4). Conversely, there was a positive correlation between the change in the half-life of acetaminophen and the change in the fractions of unmetabolized acetaminophen ($r = 0.86$, $p < 0.05$) and acetaminophen glucuronide ($r = 0.88$, $p < 0.05$) caused by ascorbic acid administration (Fig. 4).

DISCUSSION

This study shows that ascorbic acid can inhibit the systemic conjugation of acetaminophen with sulfate by competing for available sulfate in the body. The results of this study and of previous investi-

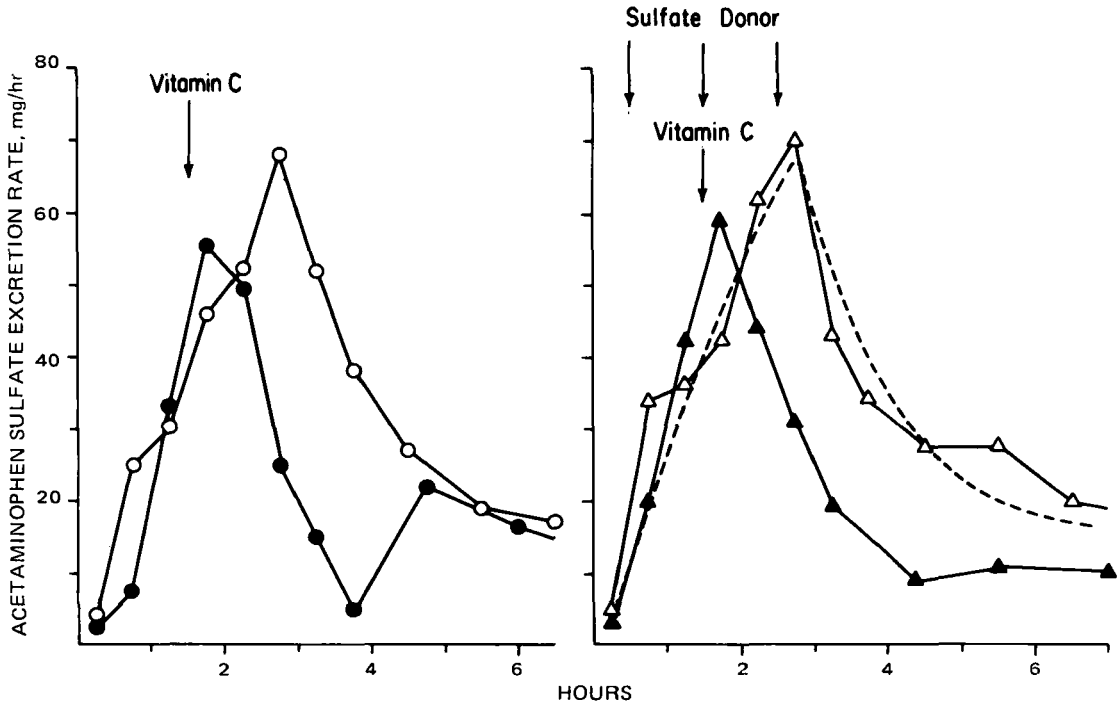

Figure 1—*Urinary excretion rate of acetaminophen sulfate after oral administration of 1 g of acetaminophen, Subject H. Key: ○ and - - -, control; ●, with 3 g of ascorbic acid at 1.5 hr; △, with 3 g of ascorbic acid at 1.5 hr and 1 g of sodium sulfate at 0.5, 1.5, and 2.5 hr; and ▲, with 3 g of ascorbic acid at 1.5 hr and 2 g of L-cysteine at 0.5, 1.5, and 2.5 hr.*

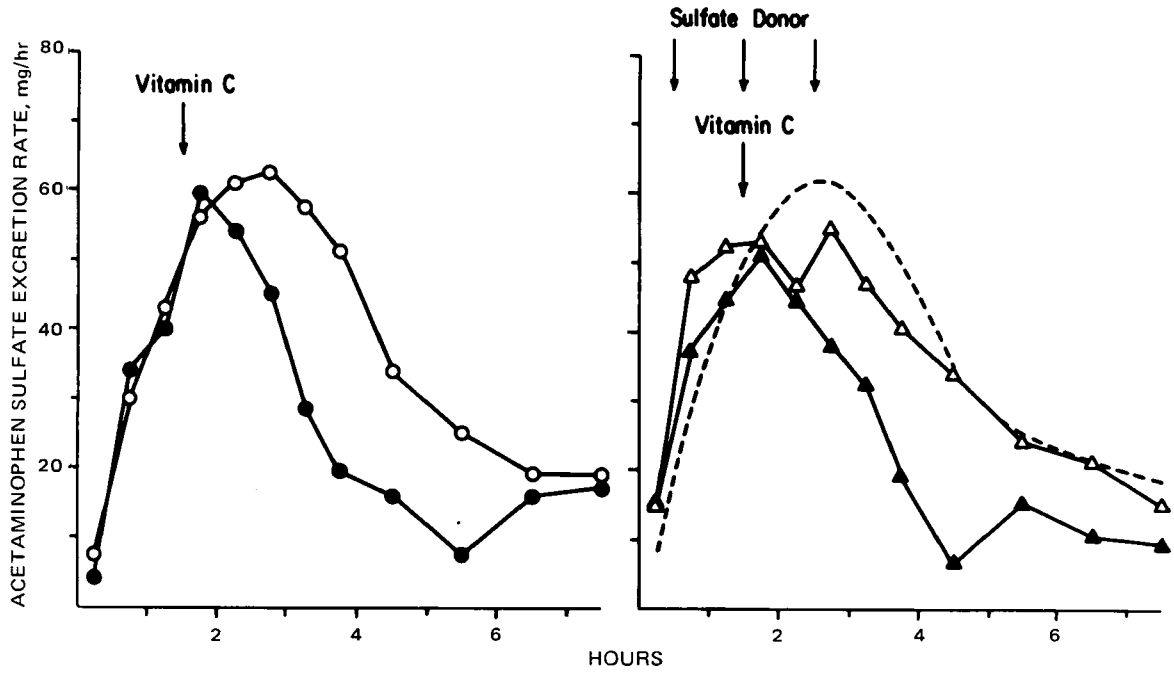

Figure 2—*Same experiment as in Fig. 1, Subject Y.*

gations in humans (3) and animals (4) lead to the conclusion that the availability of sulfate, rather than its activation to 3′-phosphoadenosine 5′-phosphosulfate or the subsequent transfer of activated sulfate to the acceptor molecule, is the rate-limiting step in phenolic sulfate formation. The limited availability of sulfate in the body causes the sulfate conjugation process to be easily saturated and subject to competitive inhibition.

Ascorbic acid is itself partly metabolized to the sulfate and will compete with phenolic drugs such as acetaminophen and salicylamide for available sulfate. It is not unreasonable to expect similar interactions between ascorbic acid and steroids or other compounds whose conjugation with sulfate is mediated by different sulfokinases. Of particular concern is the possibility of an interaction between ascorbic acid and drugs subject to pronounced first-pass biotransformation such as isoproterenol (6). Competitive inhibition of sulfate formation can increase the systemic availability of such a drug and, thereby, enhance its pharmacological effect (11). The wide use of large doses of ascorbic acid makes it necessary to be concerned about the possibility and consequences of such interactions.

The specific interaction between acetaminophen and ascorbic acid described here is important in demonstrating a principle but is probably of little clinical significance under the usual conditions, *i.e.*, when acetaminophen is taken in single recommended doses as an analgesic or antipyretic. The somewhat slower elimination of acetaminophen when taken with ascorbic acid may result in a slightly more pronounced and protracted effect of the former, but this result

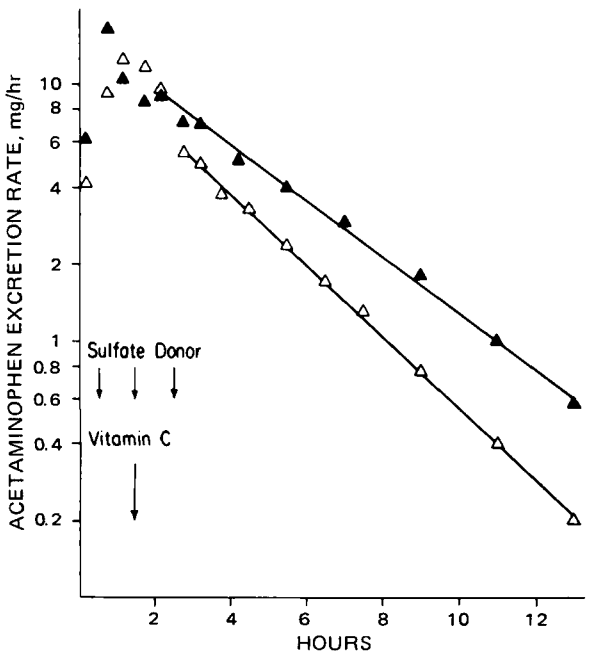

Figure 3—*Urinary excretion rate of acetaminophen after oral administration of 1 g of acetaminophen and 3 g of ascorbic acid 1.5 hr later, Subject H. Key: Δ, with sodium sulfate; and ▲, with L-cysteine.*

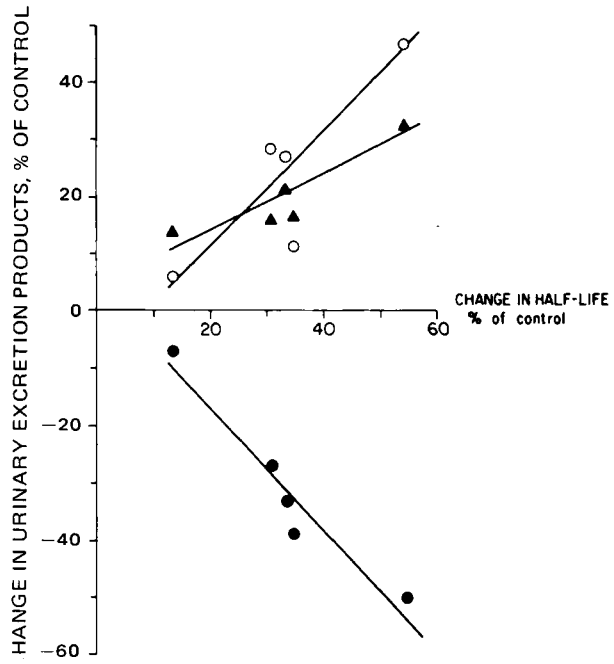

Figure 4—*Relationship between the change in the apparent half-life of acetaminophen produced by ascorbic acid and the change in the amount of excreted acetaminophen (○), acetaminophen glucuronide (▲), and acetaminophen sulfate (●) in five subjects.*

Table III—Effect of Ascorbic Acid and Sulfate Donors on the Apparent Terminal Half-Life of Acetaminophen

Subject	Apparent Half-Life, hr			
	Control	Ascorbic Acid	Ascorbic Acid and L-Cysteine	Ascorbic Acid and Sodium Sulfate
H	2.1	2.8	2.8	2.2
L	2.2	3.4	—	—
S	2.6	3.5	—	—
O	2.2	2.5	—	—
Y	2.6	3.4	3.2	2.6
Mean	2.3	3.1	3.0	2.4
SD	0.2	0.5		
Statistical difference from control[a]		$p < 0.01$		

[a] Paired *t*-test.

will be difficult to establish under clinical conditions.

It is interesting that sodium sulfate prevented the inhibition of acetaminophen sulfate formation by ascorbic acid while L-cysteine had no such effect. L-Cysteine is a source of inorganic sulfate (12). It was used as a sulfate donor in a previous study because it was thought that inorganic sulfate would not be well absorbed from the GI tract (3). More recently, oral administration of sodium sulfate was found to increase the amount of available sulfate in the body (13). The results of this investigation confirm that orally administered sodium sulfate is an adequate source of sulfate. Its effectiveness in preventing the inhibition of acetaminophen sulfate formation by ascorbic acid shows that the mechanism of the interaction is the competition for available sulfate.

L-Cysteine is oxidized in the body to cysteine sulfinate which, in turn, is converted to sulfinyl pyruvate; sulfinyl pyruvate then decomposes into sulfite and pyruvate. The sulfite is then oxidized to sulfate by sulfite oxidase (12). Orally administered L-cysteine reduces or prevents the mutual competitive inhibition of sulfate formation by acetaminophen and salicylamide in humans (3). The reason for its lack of effectiveness in preventing the acetaminophen–ascorbic acid interaction is not readily apparent. The amount of L-cysteine administered was the same as in the previous study and represents almost five times the dose of inorganic sulfate used, on a molar basis.

Ascorbic acid may be able to inhibit the conversion of L-cysteine to sulfate. It is also possible that the effectiveness of L-cysteine with salicylamide is related to the likelihood that the biotransformation of salicylamide occurs largely in the intestinal wall. Irrespective of these speculations, this study demonstrated that ascorbic acid can inhibit the conjugation of a drug with sulfate, a type of interaction that assumes particular significance because of the wide use of large doses of the vitamin.

REFERENCES

(1) R. T. Williams, "Detoxification Mechanisms," 2nd ed., Chapman and Hall, London, England, 1959, pp. 279–282.

(2) G. Levy and T. Matsuzawa, *J. Pharmacol. Exp. Ther.*, **156,** 285(1967).

(3) G. Levy and H. Yamada, *J. Pharm. Sci.*, **60,** 215(1971).

(4) H. Büch, C. H. Eschrick, and K. Pfleger, *Arch. Exp. Pathol. Pharmakol.*, **225,** 6(1966).

(5) E. M. Baker, D. C. Hammer, S. C. March, B. M. Tolbert, and J. E. Canham, *Science*, **173,** 826(1971).

(6) J. B. Houston and G. Levy, *Nature*, **255,** 78(1975).

(7) W. H. Barr, T. Aceto, Jr., M. Chung, and M. Shukur, *Rev. Can. Biol., Suppl.*, **32,** 31(1973).

(8) G. Levy, *J. Pharm. Sci.*, **60,** 499(1971).

(9) D. T. Lowenthal, S. Øie, J. C. Van Stone, W. A. Briggs, and G. Levy, *J. Pharmacol. Exp. Ther.*, **196,** 570(1976).

(10) G. Levy and C.-G. Regårdh, *J. Pharm. Sci.*, **60,** 608(1971).

(11) C. F. George, E. W. Blackwell, and D. S. Davies, *J. Pharm. Pharmacol.*, **26,** 265(1974).

(12) B. Sörbo, *Scand. J. Clin. Lab. Invest., Suppl. 86,* **17,** 21(1965).

(13) I. Smith and P. D. Mitchell, *Biochem. J.*, **112,** 189(1974).

ACKNOWLEDGMENTS AND ADDRESSES

Received August 8, 1975, from the *Department of Pharmaceutics, School of Pharmacy, State University of New York at Buffalo, Buffalo, NY 14214*

Accepted for publication October 23, 1975.

Supported in part by Grant GM 20852 from the National Institutes of Health.

[x] To whom inquiries should be directed.

Structural Functions of Taste in the Sugar Series VII: Taste Properties of Ketoses

CHEANG KUAN LEE [x] and GORDON G. BIRCH

Abstract □ The preferable structural feature for sweetness is a lipophilic moiety, *e.g.*, a five- or six-membered ring with a polar substituent containing an A–H/B system outside the ring. In ketoses, this unit is probably the 1,2-glycol. If a third feature (the lipophilic, γ, site) is required for the attainment of optimum sweetness and if it is C-6 in ketoses, then this site can accommodate quite a large constituent, both above and below the plane of the ring. The removal of the hydroxyl group from the C-6 hydroxymethyl substituent to yield the 7-deoxy derivatives causes bitterness, thus implicating the primary hydroxymethyl group with bitterness. Therefore, the creation of lipophilic site(s) in the sugar ring causes the realignment of the sugar molecule on the taste receptor surface. The disturbance of the proposed A–H/B system, *e.g.*, the removal of the C-2 hydroxyl group, causes the ring α-glycol unit (most likely the ring C-3 and C-4 hydroxyl groups) to function as the A–H/B system.

Keyphrases □ Structure–activity relationships—sweetness of ketoses related to structural functions □ Ketoses—structural functions related to sweetness □ Sweetness—related to structural functions of ketoses □ Taste physiology—structural functions of ketoses related to sweetness

In considering the chemical characteristics of a biologically active compound, it is necessary to know at how many points in the molecule significant interaction can occur and also the nature of the molecules to which the compound may attach itself. Even with simple molecules, a study of the behavior of analogs is often necessary to determine which groupings are responsible for union with the receptor sites and which are responsible for the reactions concerned with function.

In studying the phenomenon of sweetness, evidence already published (1–3) suggests that a direct binding of saporific molecule with taste bud protein is the criterion of magnitude. Molecular patterns have been educed (1, 4–6) to account for the sweet taste of such a diverse group of chemical compounds as sugars, amino acids, synthetic sweetening compounds such as saccharin, cyclamates, dulcin, and 2-amino-4-nitrobenzenes, salts of beryllium, *etc.*

Although these patterns can explain the varying sweetness of sugars, it is nonetheless remarkable that such a vast difference in sweetness of sugars exists at all. Sucrose and fructose, the two sweetest simple sugars known, are not very sweet when compared with artificial sweeteners like saccharin and cyclamates, despite possessing several α-glycol groups, each satisfying Shallenberger's requirement of a geometrically suitable A–H/B system. Only one such system is present in the artificial sweeteners.

In previous publications (7, 8), it was suggested that although a high anionic character or the ability to form hydrogen bonds is an important prerequisite for sweetness, the preferable structural feature may be a five- or six-membered ring with a polar substituent including an A–H/B system outside the ring. Most sugars studied are aldoses and as such do not have this structure. Ketoses, on the other hand, would be ideal molecular models for such studies. Pentuloses, hexuloses, and various octuloses are found in various naturally occurring materials, *e.g.*, honey (9), passion fruits, avocado pears, and dried roots of primrose (*Primula officinalis* Jacq.) (10–12). Therefore, it is of particular fundamental interest that their sensory properties should be evaluated. Accordingly, this paper describes the structural functions of taste in a number of ketoses.

EXPERIMENTAL

Materials—The following sugars were used as received: D-*gluco*-heptulose[1], D-*manno*-heptulose[1], D-*talo*-heptulose[1], L-*gluco*-heptulose[1], L-*galacto*-heptulose[1], L-*allo*-heptulose[1], D-glycero-D-*gulo*-octulose[1], D-glycero-L-*gluco*-octulose[1], sedoheptulose hexaacetate[1], D-*altro*-3-heptulose[2] (coriose), D-*gluco*-heptulose[2], 7-deoxy-D-*altro*-heptulose[3], and 7-deoxy-L-*galacto*-heptulose[3]. All other parent sugars used were crystalline materials[4] (99% pure).

Tasting of Crystalline Substances—Panelists were selected and

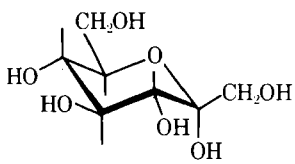
α-D-*gluco*-heptulose

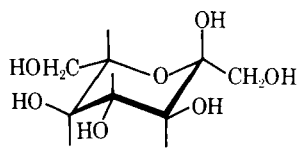
α-L-*gluco*-heptulose

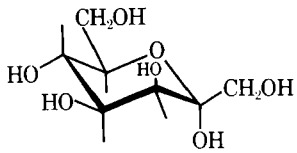
α-D-*manno*-heptulose

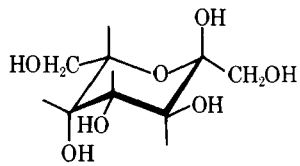
α-L-*galacto*-heptulose

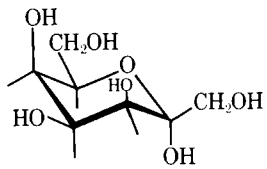
α-D-*talo*-heptulose

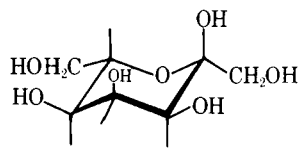
α-L-*allo*-heptulose

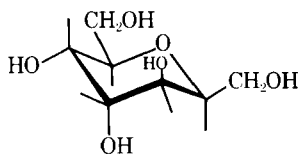
α-D-*altro*-heptulose (sedoheptulose)

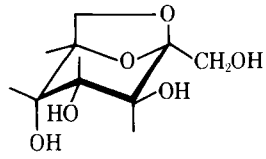
sedoheptulosan

[1] Gift of Dr. Emmanuel Zissis, National Institutes of Health, Bethesda, Md.
[2] Gift of Professor T. Okuda, Okayama University, Japan.
[3] Gift of Dr. T. Ito, Meiji Seika Kaishi Ltd. Research Laboratories, Japan.
[4] Obtained from British Drug Houses, Chemicals, Poole, Dorset, England; Koch-Light Laboratories, Colnbrook, Berks, England; Pfanstiehl Laboratories, Ill.; Senn Chemicals, Switzerland; and T. I. Sas and Son Ltd., England.

trained from College personnel according to a previous publication (13). Each panelist was asked to place a few milligrams of each substance (finely powdered crystals) on the tongue and to comment whether it was trace sweet (tr. S), sweet (S), intensely sweet (SS), trace bitter (tr. B), bitter (B), or intensely bitter (BB). Tastelessness was designated zero (0). Panelists were presented with standards for comparison: *myo*-inositol, trace sweet, rating 0–0.35; methyl-α-D-glucopyranoside, sweet, rating 0.35–0.70; and sucrose, intensely sweet, rating 0.70 and above[5].

The decisions listed in Tables I and II are those obtained in at least 75% of the total judgments, with each panelist carrying out duplicate tasting sessions. Eight subjects formed the panel. Each panelist was asked to taste all substances once at each session, rinsing with distilled water between substances and pausing for a short interval (usually about 1 min) before passing on to the following substance.

Difference Testing—For comparing the intensity of sweetness, the two-sample difference testing method was used; each taster was asked to select the sweeter sample. At each sitting, the two possible orders of presentation, AB and BA, were presented, the tasting being carried out in duplicate. No retasting was allowed.

The number of correct selections of the sweeter sample within a pair in excess of chance expectation is defined in terms of standard deviations, σ, where:

$$\sigma = \frac{n - Np}{\sqrt{Npq}} \qquad \text{(Eq. 1)}$$

where N = total number of judgments, n = number of correct selections, p = probability of "correct" selection by chance, and q = probability of "incorrect" selection by chance. The level of significance was then obtained by referring to the table compiled by Yule and Kendall (14).

Rinsing with distilled water between substances and pausing 1 min before passing on to the following substances were required. Swallowing was permitted.

RESULTS AND DISCUSSION

The use of equilibrated solutions of reducing sugars in taste–structure studies has been criticized since, at equilibrium, solutions of such substances consist of a complex mixture of anomers. Therefore, it is not possible to relate taste with a particular structure (15). However, if such sugars are tasted in the crystalline state, the sweet taste appears to be perceived prior to any appreciable conformational change due to mutarotation. Electrophysiological studies (16) showed that the interval between initial stimulation of the receptors and the report of a reaction was 0.02–0.06 sec, and Kiesow (17) reported that oral response for sweet taste was about 0.5 sec. Thus, it could be reasonably assumed that the structure of the sugar (when tasted in the "solid" form) would be in its preferred conformation when stimulation occurred.

Dihydroxyacetone, like glyceraldehyde and glycolic aldehyde, exists as a crystalline dimeric compound (Schemes I–III) but gradually dissociates to the monomer in dilute aqueous solution (18). This fact was confirmed recently (19) using GC, NMR, and mass spectrometric analyses. Glyceraldehyde in its monomeric form is tasteless (20), but

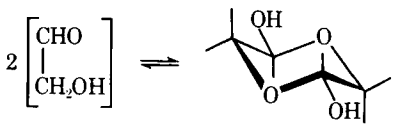

Scheme I—Glycolic aldehyde

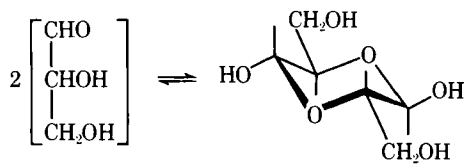

Scheme II—Glyceraldehyde

[5] Sucrose has a sweetness of SS (intensely sweet on this scale), but it is two or three orders of magnitude of sweetness lower than perillaldehyde *anti*-oxime and P-4000 and artificial sweeteners such as saccharin and cyclamates.

Table I—Taste Properties of Ketoses[a]

Sugar	Sweetness	Bitterness
Hexulose		
L-Sorbopyranose	S	0
D-Fructopyranose	SS	0
D-Tagatose	S	0
2-Deoxy-D-fructopyranose	S	0
Heptulose		
D-*gluco*-Heptulose	S	0
D-*manno*-Heptulose	S	0
D-*talo*-Heptulose	S	0
D-*altro*-Heptulose (sedoheptulose)	SS	0
Sedoheptulosan	SS	0
L-*gluco*-Heptulose	S	0
L-*galacto*-Heptulose	S	0
L-*allo*-Heptulose	S	0
1-Deoxy-D-*manno*-heptulose	S	0
D-*altro*-3-Heptulose	0-tr	0
7-Deoxy-D-*altro*-heptulose	S	B
7-Deoxy-L-*galacto*-heptulose	S	B
Octulose		
D-Glycero-L-*gluco*-octulose	S	0
D-Glycero-D-*gulo*-octulose	S	0
Disaccharide		
Maltulose (4-*O*-α-D-glucopyranosyl D-fructofuranose)	S	0
Lactulose (4-*O*-β-D-galactopyranosyl D-fructofuranose)	S	0
Palatinose (6-*O*-α-D-glucopyranosyl D-fructofuranose)	S	0
Turanose (3-*O*-α-D-glucopyranosyl D-fructopyranose)	SS	0

[a] Sucrose has a sweetness of SS (intensely sweet on this scale), but all of these values are two or three orders of magnitude of sweetness lower than perillaldehyde *anti*-oxime and P-4000 and artificial sweeteners such as saccharin and cyclamates.

the dimer is reported to be sweet (21). In the solid form, dihydroxyacetone was observed to be much sweeter than glyceraldehyde (which had only trace sweetness). This result, however, is not surprising since the dimeric form of dihydroxyacetone has an α-glycol system outside the ring (whereas glyceraldehyde does not), a structural feature we have maintained to be the preferable structure for sweetness and a feature found in β-D-fructopyranose and artificial sweeteners like saccharin and cyclamates.

The results in Table I give further proof of this hypothesis. All ketoses tested were consistently sweeter or of about the same sweetness as the corresponding aldoses and were never bitter. That they were consistently not bitter strongly suggests that binding to the taste receptor could be analogous to that in β-D-fructopyranose, *i.e.*, the 1,2-glycol unit functioning as the A–H/B system. Whether or not this 1,2-glycol unit does constitute the A–H/B system could, however, depend on the overall conformation concerned. Possibly, for molecules in the $_4C^1$ conformation, which are true analogs of an identical system in β-D-fructopyranose, the 1,2-glycol functions as the A–H/B, but this may not be the case in the $^4C_1$ conformation since, for example, 1-deoxy-D-*manno*-heptulose is only very slightly less sweet than D-*manno*-heptulose.

It was proposed previously (7, 22) that the hydrophilic–lipophilic ratio of a compound governs its binding behavior. A lipophilic moiety, *e.g.*, a five- or six-membered ring, with a polar substituent containing an A–H/B system outside the ring seems the preferable structural

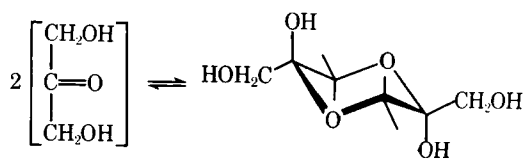

Scheme III—Dihydroxyacetone

Table II—Comparison of Sweetness by Paired Comparison Test

Sugar	Number Correct	Number Incorrect	Total	Percent Correct		Number Correct in Excess of Expectancy in σ Values	Significance Designation
				Obtained	Expected		
D-*manno*-Heptulose *versus* 1-deoxy-D-*manno*-heptulose—D-*manno*-heptulose sweeter	10	0	10	100	50	3.16	Very highly significant, $p < 0.001$
Palatinose *versus* isomaltose—palatinose sweeter	10	0	10	100	50	3.16	Very highly significant, $p < 0.001$
Maltulose *versus* maltose—maltulose sweeter	8	2	10	80	50	1.89	Significant, $p < 0.05$
Lactulose *versus* lactose—lactulose sweeter	9	1	10	90	10	2.53	Highly significant, $p < 0.01$

feature. Thus, for the attainment of optimum sweetness, a third binding site (as a lipophilic center) probably is required (23–25). Kier (4) proposed a dispersion or hydrophobic site, γ, located at about 3.5 Å from atom A of AH and about 5.5 Å from B, while Shallenberger[6] suggested that the "stereochemistry of this 'greasy' (γ) site, in relation to AH and B is defined by D-glucose where AH is the C-4 hydroxyl group, B the C-3 oxygen atom and γ is C-6." The center of the orbital A is quoted to be 2.9 Å from the center of B and 3.1 Å from γ, while the center of B is 5.13 Å from γ. These values are not very different from those of Kier (4).

The intense sweetness of β-D-fructopyranose is significant because it possesses a ring methylene grouping, thus giving the sugar an element of lipoid character not present in all other sugars tested (except in tagatose, which exists in the stable $^4C_1$ conformation). The sweetness of heptuloses coupled with the pure sweet taste of octuloses clearly suggests that this greasy γ site, as proposed by Shallenberger and Kier, can accommodate quite a large substituent, both above and below the plane of the sugar ring. A greater insight into the molecular basis of the pharmacophore now appears to be available from the work of Holtje and Kier (26).

However, the removal of the hydroxyl group from the C-6 hydroxymethyl substituent to give the 7-deoxy derivatives (Table I) causes the development of bitterness, thus implicating the primary hydroxymethyl group with bitterness. This finding is in agreement with an earlier prediction (7), and it supports the contention that the presence of freshly available lipophilic sites causes the alignment of the sugar differently from the parent sugar, thus eliciting bitterness (8). Also, the slightly lower sweetness intensity of 1-deoxy-D-*manno*-heptulose compared to D-*manno*-heptulose (using paired comparison testing) (Table II) could be rationalized on this basis; *i.e.*, the removal of the C-1 hydroxyl group of *manno*-heptulose possibly causes the ring C-3 and C-4 (C-4 and C-5, respectively, in the normal carbohydrate nomenclature) hydroxyl groups to act as the A–H/B system, as in aldoses.

The sweetness intensity of 1-deoxy-D-*manno*-heptulose and β-D-arabinose (analogs of β-D-fructopyranose) demonstrate the importance of the C-1 hydroxyl group. This finding, coupled with the results of Birch and Lindley (27) on the importance of the C-2 hy-

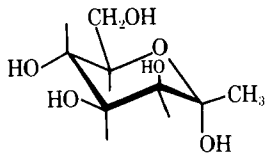

1-deoxy-α-D-*manno*-heptulose

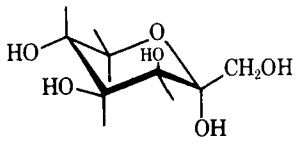

α-D-tagatose

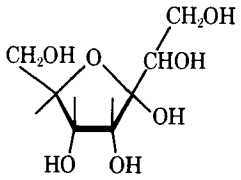

α-D-*altro*-3-heptulose

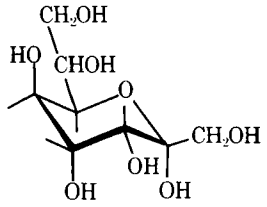

D-glycero-α-D-*gulo*-octulose

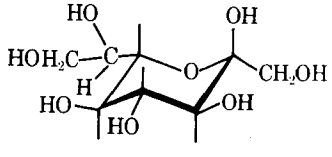

D-glycero-α-L-*gluco*-octulose

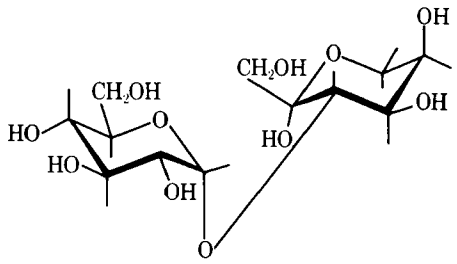

turanose (3-*O*-α-D-glucopyranosyl β-D-fructopyranose)

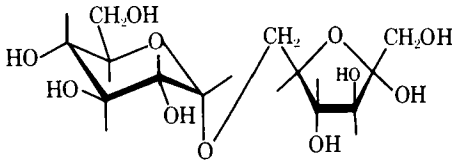

palatinose (6-*O*-α-D-glucopyranosyl α-D-fructofuranose)

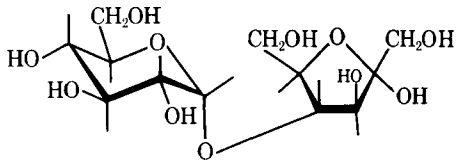

maltulose (4-*O*-α-D-glucopyranosyl α-D-fructofuranose)

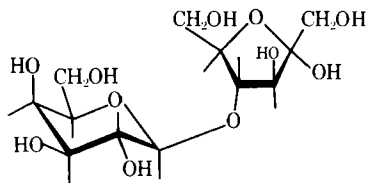

lactulose (4-*O*-β-D-galactopyranosyl α-D-fructofuranose)

[6] R. S. Shallenberger, New York State Agriculture Experimental Station, Cornell University, Geneva, N.Y., personal communication, 1975.

droxyl group in ketoses, thus offers an unequivocal support for the validity of the proposed A–H/B system for intense sweetness. The virtual tastelessness of D-*altro*-3-heptulose is not very surprising, being due to the free rotation of the primary hydroxyethyl grouping.

The sensory evaluation of β-D-fructopyranose and α-L-sorbopyranose implicated the configuration of the C-5 hydroxyl group as being of unique importance in sweetness. In fructose, the participation of this (axial) hydroxyl group with the ring oxygen in hydrogen bonding leaves the C-2 hydroxyl group free (this being also sterically disposed to hydrogen bond the ring oxygen) to exert the maximum effect on sweetness intensity (27). The intense sweetness of sedoheptulose could similarly be due to the availability of the C-3 axial hydroxyl group to hydrogen bond with the ring oxygen, a situation analogous to mannose (1).

A recent study on the binding behavior of reducing disaccharides (28) showed that the nonreducing glycosyl residue was involved in the binding to the taste receptor site. In disaccharides containing a terminal ketose, the presence of a 1,2-glycol unit in the ketose residue changes the binding behavior. Just as in the monosaccharide ketoses, this glycol unit preferentially becomes the A–H/B system. Thus, lactulose, turanose, palatinose, and maltulose are considerably sweeter than their corresponding aldose analogs (using the paired comparison test ($p < 0.05$) (Table II). Furthermore, the exceptional sweetness of turanose (3-*O*-α-D-glucopyranosyl D-fructopyranose) (judged to be nearly as sweet as sucrose) suggests that the C-3 hydroxyl group is not critical in eliciting sweetness. This finding, together with the lower sweetness intensity of maltulose and lactulose (both having 1 → 4 linkages), seems to suggest that the C-4 hydroxyl group (*i.e.*, ring C-3) is more critical than the C-3 hydroxyl group (*i.e.*, ring C-2 of the fructose ring) as regards sweetness.

REFERENCES

(1) R. S. Shallenberger, in "Handbook of Physiology, IV. Chemical Senses 2. Taste," L. M. Beidler, Ed., Springer-Verlag, Berlin, Germany, 1971, pp. 221–227, and previous papers cited.

(2) F. R. Dastoli and S. Price, *Science*, **154**, 905(1966).

(3) L. M. Beidler, in "Progress in Biophysics and Biophysical Chemistry," J. A. V. Butler, H. E. Huxley, and R. E. Zirkle, Eds., Pergamon, New York, N.Y., 1962, pp. 109–151.

(4) L. B. Kier, *J. Pharm. Sci.*, **61**, 1394(1972).

(5) J. A. Deutsch and C. Hansch, *Nature*, **211**, 75(1966).

(6) J. E. Hodge and G. E. Inglett, in "Symposium: Sweeteners," G. E. Inglett, Ed., AVI Publishing, Westport, Conn., 1974, pp. 216–234.

(7) G. G. Birch and M. G. Lindley, *J. Food Sci.*, **38**, 1179 (1973).

(8) G. G. Birch and C. K. Lee, *ibid.*, **39**, 947(1974).

(9) I. R. Siddiqui, *Adv. Carbohydr. Chem. Biochem.*, **25**, 285(1970).

(10) C. M. Martin and F. H. Reuter, *Nature*, **164**, 407(1949).

(11) R. Begbie and N. K. Richtmyer, *Carbohydr. Res.*, **2**, 272(1966).

(12) I. Johansson and N. K. Richtmyer, *ibid.*, **13**, 461(1970).

(13) G. G. Birch, N. D. Cowell, and R. H. Young, *J. Sci. Food Agr.*, **23**, 1207(1972).

(14) G. U. Yule and M. G. Kendall, "An Introduction to the Theory of Statistics," Hafner, New York, N.Y., 1950.

(15) G. G. Birch, C. K. Lee, and E. J. Rolfe, *J. Sci. Food Agr.*, **21**, 650(1970).

(16) C. Pfaffmann, *J. Neurophysiol.*, **18**, 429(1955).

(17) F. Kiesow, in "The Sense of Taste," H. L. Hollingworth and A. T. Poffenberger, Jr., Eds., Moffat, Yard and Co., New York, N.Y., 1911.

(18) H. O. L. Fischer and Milbrand, *Ber.*, **57**, 707(1924).

(19) B. Arrequin and J. Taboada, *J. Chromatogr. Sci.*, **8**, 187(1970).

(20) "The Merck Index," 8th ed., Merck & Co., Rahway, N.J., 1968, p. 498.

(21) H. J. H. Fenton and H. Jackson, *J. Chem. Soc.*, **75**, 575(1899).

(22) C. K. Lee, Ph.D. thesis, University of Reading, Surrey, England, 1973.

(23) G. G. Birch, C. K. Lee, and M. G. Lindley, *Starke*, **27**, 51(1975).

(24) G. G. Birch and R. S. Shallenberger, in "Molecular Structure and Function of Food Carbohydrate," G. G. Birch and L. F. Green, Eds., Applied Science Publishers, London, England, 1973, pp. 9–20.

(25) R. S. Shallenberger and G. G. Birch, "Sugar Chemistry," AVI Publishing, Westport, Conn., 1975, p. 115.

(26) H. D. Holtje and L. B. Kier, *J. Pharm. Sci.*, **63**, 1722(1974).

(27) G. G. Birch and M. G. Lindley, *J. Sci. Food Agr.*, **26**, 117(1975).

(28) C. K. Lee and G. G. Birch, *ibid.*, **26**, 1513(1975).

ACKNOWLEDGMENTS AND ADDRESSES

Received August 16, 1975, from the *National College of Food Technology, University of Reading, St. George's Avenue, Weybridge, Surrey, England.*

Accepted for publication October 24, 1975.

The authors acknowledge J. Sainsbury Ltd. for a Postdoctoral Research Fellowship for this research. They also thank Professor N. K. Richtmyer, Dr. Emmanuel Zissis, Professor T. Okuda, and Dr. T. Ito for their generous gifts of the various sugars. Finally, they express their gratitude to the late Miss Sundrawattee Elizabeth Mattai for her inspiration and constant encouragement.

[x] To whom inquiries should be directed.

Molecular Connectivity V: Connectivity Series Concept Applied to Density

LEMONT B. KIER *x, WALLACE J. MURRAY *, MILAN RANDIĆ ‡, and LOWELL H. HALL §

Abstract □ The concept of the expanded series of the connectivity index, χ, is introduced and applied to a consideration of the density of three classes of molecules. Correlations are found using two terms in the expanded series. A preliminary reflection on the extended series terms is made. It is noted that the regression equation constant in the three studies is close to the phase volume, 0.7402, and the possible significance of this fact is discussed.

Keyphrases □ Molecular connectivity—expanded series, correlated with densities of alkanes, aliphatic alcohols, and carboxylic acids □ Densities—alkanes, aliphatic alcohols, and carboxylic acids correlated with molecular connectivity

Density is a property of a molecule in the bulk phase, defined as the mass in a unit volume. Density can be viewed as both an additive and constitutive property. The additive nature relates to the volume of the molecule, while the constitutive nature relates to the intermolecular alignments governed by surface area and other superficial features.

Recent studies examined various surface area and volume-related physicochemical and biological properties (1–4). Fundamental to both the volume and surface area of a molecule is a structural property defined as molecular connectivity (1). This property was expressed in numerical form with an index first devised by Randić (5) for hydrocarbons.

The index, χ, has been shown to relate to molecular cavity surface area, polarizability, nonspecific local anesthetic activity (1), water solubility, boiling point (2), oil–water partition coefficient, barnacle larvae narcosis, tadpole inhibition (3), and enzyme inhibition (4). The fundamental nature of χ can be seen from these studies in that it closely relates to properties with molecular volume or surface area, as well as to properties of the bulk phase or of individual molecules.

To explore further the fundamental nature and general applicability of χ, this study begins with the hypothesis that the density of a molecule should be related in some way to a physical property or properties governed by molecular connectivity. In view of experience with χ relating to properties associated with molecular volume (1), the relationship $\rho = a(1/\chi) + b$, where ρ is the density and a and b are constants, should obtain. A test of this relationship with 82 aliphatic hydrocarbons (Table I) proved to be encouraging; the correlation amounted to $r = 0.9029$. The density probably is more complex, involving more than just a simple volume relationship.

In the initial paper in this series, it was stated that any function of a molecule can be represented by a combination of terms representing various bond contributions (1). The previous studies in this series dealt with only the first-order term, *i.e.*, the value of χ for each bond. In the case of density, it is apparently necessary to include additional terms in a molecular connectivity function.

CONNECTIVITY SERIES

The first term in the connectivity series is the index χ, derived from a summation of values describing each bond in the molecule. The second term is a summation of values describing each adjacent pair of bonds. This term can be symbolized as ${}^2\chi$. The calculation follows the presciption previously described (1, 2, 5). The δ values are assigned to each first row atom according to the connectivity or branching. The product of the three adjacent δ values (i, j, and k) for each pair of adjacent bonds is obtained. The square root of the reciprocal of the product of the δ values give a bond pair term, C_{ijk}. The value of ${}^2\chi = \Sigma C_{ijk}$.

The calculation of ${}^2\chi$ for isopentane illustrates the procedure.

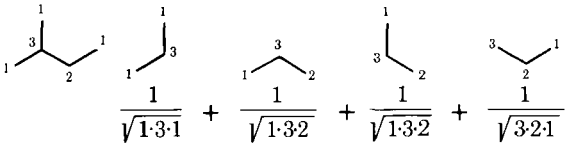

$$\frac{1}{\sqrt{1\cdot3\cdot1}} + \frac{1}{\sqrt{1\cdot3\cdot2}} + \frac{1}{\sqrt{1\cdot3\cdot2}} + \frac{1}{\sqrt{3\cdot2\cdot1}} = 1.558$$

The third term in the χ series is an index derived from three linear adjacent bonds, designated as ${}^3\chi$. The C_{ijkl} terms are calculated as square root reciprocals of products of four first-row atoms i, j, k, and l comprising three linearly adjacent bonds. For isopentane, the value of ${}^3\chi$ is obtained as follows:

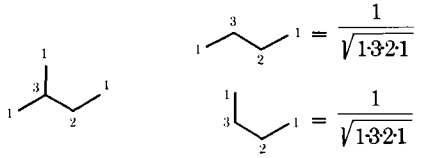

$$= \frac{1}{\sqrt{1\cdot3\cdot2\cdot1}}$$

$$= \frac{1}{\sqrt{1\cdot3\cdot2\cdot1}}$$

$${}^3\chi = 0.816$$

Subsequent terms in the series are calculated similarly.

Where double bonds occur, including carbonyl groups, the χ terms are computed with valence δ as described previously (3).

Analysis of Hydrocarbon Densities with χ Series—The question is, which terms in the expansion series of χ adequately describe structural features that are manifest in influencing the experimentally observed value of the density. The answer is not obvious, since one has no developed intuition as to the significance of each term in the expanded series of χ. As an approach to the answer, 82 aliphatic liquid hydrocarbons were analyzed. Each term in the χ expansion series, as well as combinations of terms, was tested for correlation with density. The results clearly show that $1/\chi$ and ${}^3\chi$ give excellent correlation with the density. The statistical analysis and regression equation are:

$$D_4^{20}(\text{aliphatic liquid hydrocarbons}) = 0.0030\,{}^3\chi - \frac{0.2927}{\chi} + 0.7348$$

$$r = 0.9889 \quad s = 0.0046 \quad n = 82 \qquad \text{(Eq. 1)}$$

Analysis of Aliphatic Alcohol Densities with χ Series—An analysis of 42 alcohols (Table II) also demonstrated the contribution of ${}^3\chi$ to the χ term in correlations with density. The statistical analysis and regression equation are:

$$D_4^{20}(\text{aliphatic monoalcohols}) = 0.0183\,{}^3\chi - \frac{0.0043}{\chi} + 0.7933$$

$$r = 0.9305 \quad s = 0.0045 \quad n = 42 \qquad \text{(Eq. 2)}$$

Based upon the regression equation, the density of two alcohols was predicted. For heptanol, $d_{obs} = 0.8224$; the predicted value was 0.8189. For decanol, $d_{obs} = 0.8292$; the predicted value was 0.8364. The residual for both was less than the standard error.

Analysis of Aliphatic Acid Densities with χ Series—The acids present a third test of the role of χ and ${}^3\chi$ in the density of a molecule. Twenty acids (Table III) were analyzed. The best relationship was

Table I—Densities (Specific Gravities) of Alkanes Predicted from Functions of χ

Alkane	$^3\chi$	$\frac{1}{\chi}$	D_4^{20} (obs)[a]	D_4^{20} (calc)[a]
Pentane	0.70700	0.41425	0.62620	0.63481
2-Methylbutane	0.81600	0.44053	0.61970	0.63040
2,2-Dimethylpropane	0.00000	0.50000	0.59100	0.58846
Hexane	0.50000	0.34317	0.65940	0.64940
2-Methylpentane	0.86600	0.36101	0.65320	0.65518
3-Methylpentane	1.39400	0.35613	0.66430	0.67248
2,2-Dimethylbutane	1.06100	0.39047	0.64920	0.65241
2,3-Dimethylbutane	1.33300	0.37836	0.66160	0.66414
2,4-Dimethylpentane	0.94300	0.31990	0.67270	0.66953
2,2-Dimethylpentane	1.00000	0.32669	0.67380	0.66925
2-Methylhexane	1.13300	0.30581	0.67860	0.67936
Heptane	1.20700	0.29291	0.68380	0.68536
3-Methylhexane	1.47800	0.30230	0.68710	0.69076
2,2,3-Trimethylbutane	1.73200	0.33979	0.69010	0.68742
3,3-Dimethylpentane	1.66400	0.32041	0.69330	0.69105
2,3-Dimethylpentane	1.78200	0.31447	0.69510	0.69634
3-Ethylpentane	1.73200	0.29886	0.69820	0.69940
Octane	1.45700	0.25549	0.70250	0.70383
2-Methylheptane	1.38500	0.26525	0.69790	0.69881
3-Methylheptane	1.45800	0.26261	0.70580	0.70178
4-Methylheptane	1.56300	0.26261	0.70460	0.70493
2,2-Dimethylhexane	1.28000	0.28082	0.69530	0.69110
3,3-Dimethylhexane	1.88400	0.27617	0.71000	0.71061
2,3-Dimethylhexane	2.00200	0.27167	0.71710	0.71548
2,4-Dimethylhexane	1.57100	0.27293	0.70040	0.70215
2,2,3-Trimethylpentane	2.09100	0.28727	0.71600	0.71358
2,2,4-Trimethylpentane	1.02100	0.29265	0.69190	0.67985
2,3,4-Trimethylpentane	2.10300	0.28145	0.71910	0.71565
2,3,3-Trimethylpentane	2.34500	0.28539	0.72620	0.72177
2-Methyl-3-ethylpentane	1.99200	0.26889	0.71930	0.71599
3,4-Dimethylhexane	2.18400	0.26889	0.71920	0.72176
3-Methyl-3-ethylpentane	2.56100	0.27159	0.72740	0.73230
3-Ethylhexane	1.85200	0.26001	0.71360	0.71438
Nonane	1.70700	0.22655	0.71760	0.71982
2-Methyloctane	1.63500	0.23419	0.71340	0.71542
3-Methyloctane	1.70900	0.23213	0.72070	0.71825
2,2-Dimethylheptane	1.53000	0.24624	0.71050	0.70873
2,3-Dimethylheptane	2.09800	0.23918	0.72600	0.72787
2,4-Dimethylheptane	1.65500	0.24015	0.71600	0.71427
2,2,3-Trimethylhexane	2.20000	0.25119	0.72920	0.72742
3-Ethylheptane	2.12100	0.23010	0.72700	0.73122
3,3-Dimethylheptane	2.16400	0.24266	0.72500	0.72884
Decane	1.95700	0.20350	0.73010	0.73408
2,2,6-Trimethylheptane	1.83800	0.22640	0.71950	0.72380
2,2,5-Trimethylhexane	1.47200	0.25530	0.70720	0.70434
2,2,4-Trimethylhexane	1.65800	0.25290	0.71560	0.71063
2,3,4-Trimethylhexane	2.32600	0.25140	0.72380	0.73115
2,3,5-Trimethylhexane	2.01200	0.24770	0.72190	0.72279
2,2,3,4-Tetramethylpentane	2.33600	0.25950	0.73900	0.72908
2-Methyl-4-ethylhexane	1.95900	0.23800	0.72300	0.72404
2,2-Dimethyl-3-ethylpentane	2.21000	0.24880	0.73480	0.72842
4,4-Dimethylheptane	1.85400	0.24260	0.72500	0.71954
2,6-Dimethylheptane	1.56300	0.24240	0.70890	0.71085
2,5-Dimethylheptane	1.93400	0.24020	0.71500	0.72265
3,4-Dimethylheptane	2.19900	0.23800	0.72300	0.73126
2,4-Dimethyl-3-ethylpentane	2.53500	0.24440	0.73790	0.73948
2,2,5-Trimethylhexane	1.62500	0.23770	0.71880	0.71409
2,3,3-Trimethylhexane	2.45700	0.24970	0.73800	0.73559
2-Methyl-3-ethylhexane	2.12700	0.23700	0.73100	0.72938
2,3,4-Trimethylhexane	2.35700	0.24440	0.73920	0.73413
2,2,3,3-Tetramethylpentane	2.91400	0.25980	0.75670	0.74637
3-Methyl-4-ethylhexane	2.49700	0.23490	0.74200	0.74112
3,3,4-Trimethylhexane	2.65400	0.24740	0.74540	0.74218
4-Ethylheptane	1.97100	0.23010	0.73000	0.72671
2,3,3,4-Tetramethylpentane	2.97600	0.25730	0.75470	0.74896
2,3-Dimethyl-3-ethylpentane	3.00900	0.24600	0.75400	0.75326
4-Methyloctane	1.83200	0.23210	0.71990	0.72195
2,4,6-Trimethylheptane	1.74800	0.22130	0.72250	0.72259
3,3-Diethylpentane	3.00000	0.23570	0.75360	0.75601
2,2-Dimethyl-4-ethylhexane	2.05600	0.22260	0.73300	0.73146
3,4-Dimethylheptane	2.12400	0.23700	0.73140	0.72929
3-Methyl-3-ethylhexane	2.56100	0.23910	0.74100	0.74182
2,2,4-Trimethylheptane	1.74200	0.22450	0.72750	0.72147
2,2,5-Trimethylheptane	2.08400	0.22450	0.72600	0.73175
2,2-Dimethyloctane	1.78000	0.21930	0.72450	0.72413
2,4-Dimethyloctane	1.92400	0.22440	0.72590	0.72697
2,7-Dimethyloctane	1.81300	0.21620	0.72420	0.72603
4-Isopropylheptane	2.26200	0.21190	0.74100	0.74079
4-Propylheptane	2.19100	0.20640	0.73640	0.74027
5-Methylnonane	2.07700	0.20800	0.73260	0.73637
Undecane	2.18300	0.18470	0.74020	0.74638
Dodecane	2.45700	0.16910	0.74870	0.75918

[a] Values from "Handbook of Tables for Organic Compound Identification," 3rd ed., CRC Press, Cleveland, Ohio, 1974.

Table II—Densities (Specific Gravities) of Aliphatic Alcohols Predicted from Functions of χ

Alcohol	$^3\chi$	$\frac{1}{\chi}$	D_4^{20} (obs)[a]	D_4^{20} (calc)[a]
Methanol	0.00000	1.00000	0.79150	0.78902
Ethanol	0.00000	0.70721	0.78140	0.79027
2-Propanol	0.00000	0.57737	0.78510	0.79083
1-Propanol	0.50000	0.52247	0.80360	0.80022
2-Butanol	0.81600	0.44053	0.80690	0.80636
2-Methyl-2-butanol	1.22500	0.39047	0.80890	0.81407
2-Methylpropanol	0.81600	0.44053	0.80200	0.80636
3-Methyl-2-butanol	1.33300	0.37850	0.81800	0.81610
3-Pentanol	1.47800	0.35625	0.82040	0.81885
1-Butanol	0.70700	0.41425	0.80960	0.80448
2-Pentanol	0.86600	0.36101	0.80920	0.80762
3,3-Dimethyl-2-butanol	1.73200	0.33979	0.81850	0.82357
2,3-Dimethyl-2-butanol	1.73200	0.33979	0.82080	0.82357
3-Methyl-3-pentanol	1.41400	0.32041	0.82330	0.81783
2-Methyl-2-pentanol	1.00000	0.32669	0.81340	0.81022
2-Methyl-3-pentanol	1.70700	0.31447	0.82490	0.82322
2-Methylbutanol	1.39400	0.35625	0.81930	0.81731
4-Methyl-2-pentanol	0.94300	0.31990	0.80710	0.80920
3-Methylbutanol	0.86600	0.36101	0.80920	0.80762
3-Hexanol	1.47800	0.30239	0.81850	0.81908
2,2-Dimethylbutanol	1.91400	0.32041	0.82830	0.82699
1-Pentanol	0.93300	0.34317	0.81480	0.80892
2-Hexanol	1.13500	0.30581	0.80980	0.81278
2,4-Dimethyl-3-pentanol	2.10300	0.28145	0.82880	0.83062
3-Ethyl-3-pentanol	2.56100	0.27624	0.83890	0.83903
2,3-Dimethylbutanol	1.70700	0.31437	0.82970	0.82322
2-Methylpentanol	1.47800	0.30230	0.82080	0.81908
2-Ethylbutanol	1.73200	0.29886	0.83350	0.82375
3-Methylpentanol	1.47800	0.30230	0.82420	0.81908
4-Methylpentanol	1.13500	0.30581	0.81310	0.81278
4-Heptanol	1.53600	0.26261	0.81830	0.82031
1-Hexanol	1.20700	0.29291	0.81890	0.81416
2-Heptanol	1.38500	0.26525	0.81670	0.81753
2-Methylhexanol	1.74700	0.26261	0.82700	0.82418
4-Methylhexanol	1.74700	0.26261	0.82390	0.82418
2,6-Dimethyl-4-heptanol	1.74800	0.22124	0.81290	0.82437
2-Octanol	1.63500	0.23419	0.82050	0.82225
2-Ethylhexanol	2.12100	0.23010	0.83280	0.83117
1-Octanol	1.70700	0.22655	0.82490	0.82360
2-Nonanol	1.88500	0.20964	0.81910	0.82693
2-Decanol	2.13500	0.18975	0.82500	0.83160
1-Nonanol	1.95700	0.20350	0.82710	0.82828

[a] Values from "Handbook of Tables for Organic Compound Identification," 3rd ed., CRC Press, Cleveland, Ohio, 1974.

again revealed with χ and $^3\chi$. The statistical analysis and regression equation are:

$$D_4^{20}(\text{aliphatic acids}) = 0.0252\ ^3\chi + \frac{0.4358}{\chi} + 0.7546$$

$$r = 0.9831 \qquad s = 0.0137 \qquad n = 20 \qquad \text{(Eq. 3)}$$

Predictions of densities for two acids, nonanoic (d_{obs} = 0.9055) and oleic (d_{obs} = 0.8935), yielded the values 0.8913 and 0.8966, respectively.

DISCUSSION

Relationship of χ Terms to Density—The analyses of three series of compound classes using χ and $^3\chi$ reveal good correlations with the densities of these molecules. With the hydrocarbons and acids, the correlation is excellent. In these two cases, the value of the densities increases in an opposite direction with increasing molecular weight. The same terms of the connectivity expansion, χ and $^3\chi$, still predict the densities rather well.

The correlation with the alcohol densities is good with χ and $^3\chi$ but not of the quality of the other two. One explanation lies in the failure of χ and $^3\chi$ to distinguish between isomers such as 2-pentanol and 3-methylbutanol and 3-methyl-3-pentanol and 2,2-dimethylbutanol. Each pair has the same χ and $^3\chi$ value. The first pair of isomers has exactly the same density. The second pair has a density difference of 0.005. This duplication exists in seven cases in the list of alcohols studied. A more definitive index must be developed to characterize uniquely these molecules.

Nature of $^3\chi$—At this time, one can only make a preliminary analysis of the nature of the structural features defined by χ and $^3\chi$ that influence density. The authors have already observed a relationship between χ and the volume of a molecule (1). The reciprocal of χ would, therefore, be expected to contribute to the density definition.

The nature of $^3\chi$ becomes more apparent on closer inspection. The value of $^3\chi$ is really a summation of C_k values for pairs of alternate bonds. For example, in the case of hexane, the $^3\chi$ value is a summation of the molecular fragments shown here:

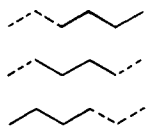

Each bond type is counted a different number of times in the total summation: terminal bonds once, the central bond three times, and others twice.

In contrast, the $^3\chi$ value for the hexane isomer 2,3-dimethylbutane is a summation of the fragments shown here:

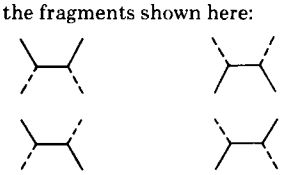

The four terminal bonds are each counted twice, while the central bond is not implicitly counted at all. This pattern of weighting of bonds in different molecules emphasizes certain structural features that bear a significance to density along with the χ term. In-depth studies of this kind are currently underway in this laboratory.

Regression Equation Constant—An interesting observation from the regression equation deserves comment. The three equation con-

Table III—Densities (Specific Gravities) of Aliphatic Acids Predicted from Functions of χ

Acid	$^3\chi$	$\frac{1}{\chi}$	D_4^{20} (obs)[a]	D_4^{20} (calc)[a]
Formic	0.00000	1.01420	1.22030	1.19654
Acetic	0.00000	0.73746	1.04930	1.07595
Propionic	0.60400	0.52247	0.99390	0.99751
2-Methylpropionic	0.98600	0.43535	0.94790	0.96919
Butanoic	0.67700	0.41425	0.95790	0.95219
2-Methylbutanoic	1.53800	0.35273	0.93800	0.94712
3-Methylbutanoic	0.75700	0.36101	0.92620	0.93101
3,3-Dimethylbutanoic	0.83200	0.32669	0.91240	0.91795
Pentanoic	0.95700	0.34317	0.93920	0.92829
2,2-Dimethylbutanoic	2.03900	0.31596	0.92760	0.94374
2,3-Dimethylbutanoic	1.79600	0.31172	0.92750	0.93576
2-Ethylbutanoic	1.70500	0.29647	0.92390	0.92682
2-Methylpentanoic	1.58500	0.29985	0.92300	0.92526
3-Methylpentanoic	1.39400	0.30221	0.92620	0.92147
4-Methylpentanoic	1.14800	0.30572	0.92250	0.91679
Hexanoic	1.20700	0.29291	0.93570	0.91270
4-Methylhexanoic	1.76100	0.26518	0.91940	0.91460
4-Ethyl-4-methylbutanoic	1.76100	0.26254	0.91490	0.91345
Heptanoic	1.63400	0.25549	0.91980	0.90717
Octanoic	1.88400	0.22655	0.90880	0.90087

[a] Values from "Handbook of Tables for Organic Compound Identification," 3rd ed., CRC Press, Cleveland, Ohio, 1974.

stants for the hydrocarbons, alcohols, and acids are 0.7348, 0.7933, and 0.7546, respectively. These values are close enough to cause one to suspect that this term may have some fundamental significance, particularly if one considers the different values of the densities in the three series and the fact that one set of densities decreases with increasing molecular weight.

The density (expressed as specific gravity) of a hypothetical hydrocarbon is predicted to be 0.7348 if $^3\chi$ is zero and χ is infinite in spite of the fact that the density values of the hydrocarbons in Table I range above and below this value. This number cannot be a limiting value of the density. For the acids, the constant is 0.7546, a value well below the range of values of the densities.

If only the hydrocarbons and acids are considered, in view of the quality of these two equations, the two constants are seen to be very close to the phase volume of 0.7402. This is the fraction of space occupied by spheres of identical size. Therefore, the derived equations may be of such a fundamental quality that the geometrical constant of phase volume is the limiting value when $^3\chi$ is zero and χ is infinite.

If this interpretation of the constant is true, it is possible to describe the influences of the χ terms on the experimental value of the density. In a hypothetical primary state, a molecule with $\chi = \infty$ and $^3\chi = 0$ would be a perfect sphere. This would describe an infinite number of bonds radiating from a single central atom; this is the connectivity definition of a perfect sphere. It would pack into a unit space, filling 0.7402 part of that space. In an actual molecule, the χ terms may be viewed as modifiers of the perfect sphericity that gave a density (specific gravity) of 0.7402. The χ terms reflect modifications in the sphericity that may increase or decrease the packing ability of the molecules in the bulk phase. Thus, an experimental density may be higher or lower than the phase volume of 0.7402.

CONCLUSIONS

Once again, the fundamental molecular property of connectivity is seen to have a close relationship to a physical property. In this case, the density is seen to be a function of two terms in a series expansion of χ.

The equations relating χ and $^3\chi$ to the densities of three groups of molecules results in a constant term quite close to the phase volume. This finding suggests a fundamental quality of the equations and, in turn, the roles of the χ terms. It also permits an interpretation of the contributions of the χ terms to the experimental value of the density, at least in a general sense.

Finally, the quality of the correlations of χ with density has a very practical consequence to the pharmaceutical scientist. Acids and alcohols are classes of molecules frequently used in formulation as solvents and buffers for their physical properties, such as osmotic influence, and in their own right as active agents. With this simple approach, other classes of molecules of equal interest in pharmacy may be treated and physical properties such as density may be predicted.

APPENDIX

An alternate formulation of the extended series arises from a consideration of powers of the connectivity matrix of the graph. When using isopentane as an example and numbering the skeleton in any manner, the matrix is:

$$\begin{pmatrix} 0 & 1 & 0 & 0 & 0 \\ 1 & 0 & 1 & 0 & 1 \\ 0 & 1 & 0 & 1 & 0 \\ 0 & 0 & 1 & 0 & 0 \\ 0 & 1 & 0 & 0 & 0 \end{pmatrix}$$

In the upper triangle, there are four unit entries corresponding to the four C_{ij} bond terms in the calculation of χ.

The square of the matrix is:

$$\begin{pmatrix} 1 & 0 & 1 & 0 & 1 \\ 0 & 3 & 0 & 1 & 0 \\ 1 & 0 & 2 & 0 & 1 \\ 0 & 1 & 0 & 1 & 0 \\ 1 & 0 & 1 & 0 & 1 \end{pmatrix}$$

In the upper triangle, there are four unit entries corresponding to each C_{ijk} term in the calculation of $^2\chi$. The diagonal of the matrix contains the δ_i values of the graph.

The cube of the matrix is:

$$\begin{pmatrix} 0 & 3 & 0 & 1 & 0 \\ 3 & 0 & 4 & 0 & 3 \\ 0 & 4 & 0 & 2 & 0 \\ 1 & 0 & 2 & 0 & 1 \\ 0 & 3 & 0 & 1 & 0 \end{pmatrix}$$

Again, the number of unit entries in the upper triangle corresponds to the C_{ijkl} terms used in computing $^3\chi$. The fourth power of the matrix has no unit terms and there are no C_{ijklm} terms; hence, $^4\chi$ is zero.

Studies on the matrix formulation of the extended series are in progress in this laboratory.

REFERENCES

(1) L. B. Kier, L. H. Hall, W. J. Murray, and M. Randić, *J. Pharm. Sci.*, **64**, 1971(1975).

(2) L. H. Hall, L. B. Kier, and W. J. Murray, *ibid.*, **64**, 1974(1975).

(3) W. J. Murray, L. H. Hall, and L. B. Kier, *ibid.*, **64**, 1978(1975).

(4) L. B. Kier, W. J. Murray, and L. H. Hall, *J. Med. Chem.*, 18, 1272(1975).
(5) M. Randić, *J. Am. Chem. Soc.*, 97, 6609(1975).

ACKNOWLEDGMENTS AND ADDRESSES

Received May 27, 1975, from the *Massachusetts College of Pharmacy, Boston, Mass., ‡Tufts University, Medford, Mass., and §Eastern Nazarene College, Quincy, Mass.

Accepted for publication October 24, 1975.

The authors acknowledge technical assistance from Mr. F. Savageau and computer and statistical assistance from Dr. F. Parmenter.

x To whom inquiries should be directed.

Spectrofluorometric Determination of Bufuralol in Blood and Urine

J. ARTHUR F. de SILVA x, JOHN C. MEYER, and CARL V. PUGLISI

Abstract □ The benzofuran analog bufuralol, a β-adrenergic blocker, was determined in blood and urine by a specific and sensitive spectrofluorometric assay. The compound was extracted into ether from blood or urine adjusted to pH 10. The ether extract was separated by TLC to resolve the parent drug from any basic metabolites present, and the spots were eluted off the silica gel and quantitated fluorometrically in 0.1 *N* HCl. The overall recovery of the assay was 85 ± 3.0%; the sensitivity limit was 2–4 ng/ml of blood or urine, using a 2.5-ml specimen/analysis. The method was applied to the determination of blood levels in a dog following a single 10-mg/kg oral dose and in two human subjects administered a single 20-mg oral dose.

Keyphrases □ Bufuralol—spectrofluorometric analysis in blood and urine □ Spectrofluorometry—analysis, bufuralol in blood and urine □ β-Adrenergic blocking agents—bufuralol, spectrofluorometric analysis in blood and urine

Several phenethanolamines, polycyclic aromatic alkanolamines, and naphthyloxyethanolamines, possessing β-adrenergic blocking activity in humans, have been investigated as therapeutic agents in cardiovascular disorders such as angina pectoris, tachyarrhythmias, and essential hypertension (1–3). All of these compounds contain an *N*-isopropyl side chain similar to that in isoproterenol and propranolol. A spectrofluorometric method for the determination of plasma propranolol levels (4) and a clinical evaluation of plasma propranolol levels and β-adrenergic blockade in humans (5) were reported.

β-Adrenergic activity was noted in a series of benzofuran derivatives, and the pharmacology of 6,7-dimethyl-α-[(isopropylamino)methyl]-2-benzofuranmethanol hydrochloride (I) was reported (6). The clinical evaluation of this compound against propranolol was also reported (7), and a spectrofluorometric assay for I was developed and used in pharmacokinetic studies in normal volunteers (8).

Another member of the benzofuran series, bufuralol [7-ethyl-α-[(*tert*-butylamino)methyl]-2-benzofuranmethanol hydrochloride] (II) (9), is under clinical investigation as a β-adrenergic blocking agent in the treatment of cardiac arrhythmias (10). A spectrofluorometric assay was developed for the determination of II in blood and urine by a modification of a procedure published for I (8). The modified procedure includes a

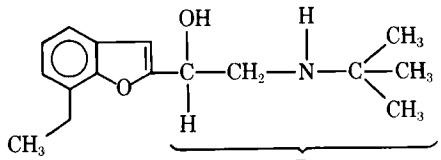

II

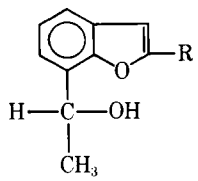

III

Scheme I

TLC separation step to resolve the parent drug (II) from its major metabolite (III) in blood and urine (Scheme I), thereby imparting specificity to the assay. Compounds II and III fluoresce in 0.1 *N* HCl with excitation at 250 nm and emission at 300–305 nm (Fig. 1). The sensitivity limit of the assay is 2 ng of compound/ml of blood, using a 2.5-ml specimen/analysis and specially selected instrumental conditions.

The method was used to determine blood levels of II in a dog given a 10-mg/kg oral dose and in two human subjects following administration of a single 20-mg oral dose.

EXPERIMENTAL

Standard Solutions—Compound II, $C_{16}H_{23}NO_2$·HCl (mol. wt. 297.82, mp 145–146°), of pharmaceutical grade purity (>99%) was used. Weigh out 11.40 mg of the hydrochloride salt equivalent to 10.0 mg of the free base. Transfer it into a 10-ml volumetric flask, dissolve in 5 ml of acetone, and dilute to volume with *n*-hexane. This stock solution (A) contains 1.0 mg of free base/ml. Prepare working solutions containing 0.25, 0.50, 0.75, or 1.0 μg/ml by making serial dilutions of Solution A with acetone–*n*-hexane (50:50).

Similarly, prepare standard solutions of Metabolite III, $C_{16}H_{23}O_3N(COOH)_2$ (mol. wt. 367.39, mp 115°), by weighing out 13.26 mg of the oxalate salt equivalent to 10 mg of the free base and proceeding as described for II. These solutions are used as external

(4) L. B. Kier, W. J. Murray, and L. H. Hall, *J. Med. Chem.*, 18, 1272(1975).
(5) M. Randić, *J. Am. Chem. Soc.*, 97, 6609(1975).

ACKNOWLEDGMENTS AND ADDRESSES

Received May 27, 1975, from the *Massachusetts College of Pharmacy, Boston, Mass., ‡Tufts University, Medford, Mass., and §Eastern Nazarene College, Quincy, Mass.

Accepted for publication October 24, 1975.

The authors acknowledge technical assistance from Mr. F. Savageau and computer and statistical assistance from Dr. F. Parmenter.

x To whom inquiries should be directed.

Spectrofluorometric Determination of Bufuralol in Blood and Urine

J. ARTHUR F. de SILVA x, JOHN C. MEYER, and CARL V. PUGLISI

Abstract □ The benzofuran analog bufuralol, a β-adrenergic blocker, was determined in blood and urine by a specific and sensitive spectrofluorometric assay. The compound was extracted into ether from blood or urine adjusted to pH 10. The ether extract was separated by TLC to resolve the parent drug from any basic metabolites present, and the spots were eluted off the silica gel and quantitated fluorometrically in 0.1 *N* HCl. The overall recovery of the assay was 85 ± 3.0%; the sensitivity limit was 2–4 ng/ml of blood or urine, using a 2.5-ml specimen/analysis. The method was applied to the determination of blood levels in a dog following a single 10-mg/kg oral dose and in two human subjects administered a single 20-mg oral dose.

Keyphrases □ Bufuralol—spectrofluorometric analysis in blood and urine □ Spectrofluorometry—analysis, bufuralol in blood and urine □ β-Adrenergic blocking agents—bufuralol, spectrofluorometric analysis in blood and urine

Several phenethanolamines, polycyclic aromatic alkanolamines, and naphthyloxyethanolamines, possessing β-adrenergic blocking activity in humans, have been investigated as therapeutic agents in cardiovascular disorders such as angina pectoris, tachyarrhythmias, and essential hypertension (1–3). All of these compounds contain an *N*-isopropyl side chain similar to that in isoproterenol and propranolol. A spectrofluorometric method for the determination of plasma propranolol levels (4) and a clinical evaluation of plasma propranolol levels and β-adrenergic blockade in humans (5) were reported.

β-Adrenergic activity was noted in a series of benzofuran derivatives, and the pharmacology of 6,7-dimethyl-α-[(isopropylamino)methyl]-2-benzofuranmethanol hydrochloride (I) was reported (6). The clinical evaluation of this compound against propranolol was also reported (7), and a spectrofluorometric assay for I was developed and used in pharmacokinetic studies in normal volunteers (8).

Another member of the benzofuran series, bufuralol [7-ethyl-α-[(*tert*-butylamino)methyl]-2-benzofuranmethanol hydrochloride] (II) (9), is under clinical investigation as a β-adrenergic blocking agent in the treatment of cardiac arrhythmias (10). A spectrofluorometric assay was developed for the determination of II in blood and urine by a modification of a procedure published for I (8). The modified procedure includes a

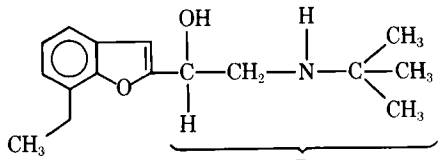

II

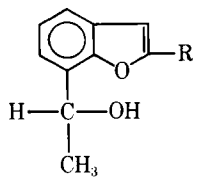

III

Scheme I

TLC separation step to resolve the parent drug (II) from its major metabolite (III) in blood and urine (Scheme I), thereby imparting specificity to the assay. Compounds II and III fluoresce in 0.1 *N* HCl with excitation at 250 nm and emission at 300–305 nm (Fig. 1). The sensitivity limit of the assay is 2 ng of compound/ml of blood, using a 2.5-ml specimen/analysis and specially selected instrumental conditions.

The method was used to determine blood levels of II in a dog given a 10-mg/kg oral dose and in two human subjects following administration of a single 20-mg oral dose.

EXPERIMENTAL

Standard Solutions—Compound II, $C_{16}H_{23}NO_2$·HCl (mol. wt. 297.82, mp 145–146°), of pharmaceutical grade purity (>99%) was used. Weigh out 11.40 mg of the hydrochloride salt equivalent to 10.0 mg of the free base. Transfer it into a 10-ml volumetric flask, dissolve in 5 ml of acetone, and dilute to volume with *n*-hexane. This stock solution (A) contains 1.0 mg of free base/ml. Prepare working solutions containing 0.25, 0.50, 0.75, or 1.0 μg/ml by making serial dilutions of Solution A with acetone–*n*-hexane (50:50).

Similarly, prepare standard solutions of Metabolite III, $C_{16}H_{23}O_3N(COOH)_2$ (mol. wt. 367.39, mp 115°), by weighing out 13.26 mg of the oxalate salt equivalent to 10 mg of the free base and proceeding as described for II. These solutions are used as external

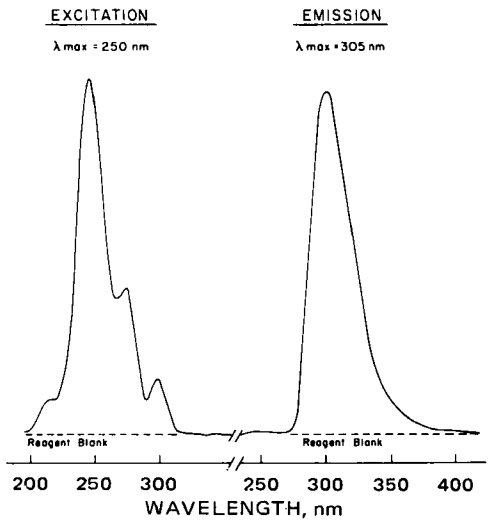

Figure 1—*Excitation–emission spectra of II in 0.1 N HCl.*

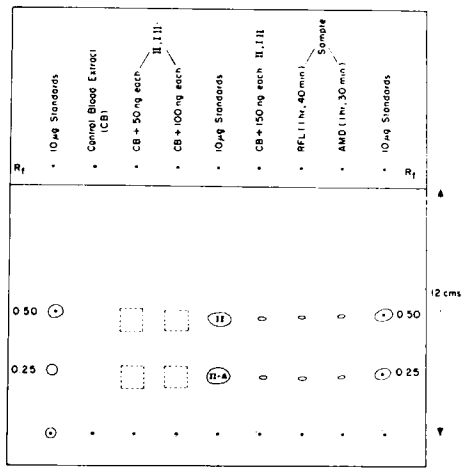

Figure 2—*One-dimensional thin-layer chromatogram of human blood extracts following oral administration of 20 mg of II in a tablet formulation. System 1 = methylene chloride–methanol–concentrated ammonium hydroxide (90:10:1).*

standards for preparing a calibration curve of the compound and are added to blood or urine as internal standards for the determination of percent recovery and of unknowns.

The spectrofluorometer[1] used was equipped with double grating monochromators, a specially selected xenon lamp[2] of high energy output in the UV region, and a selected photomultiplier tube[3] (lumen rating >10). A xenon–mercury vapor lamp[4] may also be used, because of its high UV energy output at 250 nm, but at the expense of higher control (blank) readings. The entrance windows to the excitation and emission monochromators had 5-nm slits in position, whereas the exit windows had 10-nm slits in position. The energy of the lamp was adjusted (focused through the excitation monochromator with the off-axis elipsoidal mirror) for maximum sensitivity, using a Pyrex rod having excitation–emission maxima at 310/360 nm in the sample chamber as the reference standard.

Reagents—All reagents[5] were of analytical reagent grade purity (>99%) and were used without further purification. All inorganic solutions were made up in distilled, deionized water. The inorganic reagents used in the assay were 1.0 *M* (pH 9.0) borate–sodium carbonate–potassium chloride buffer solution, prepared as previously described (11); hydrochloric acid (0.1 *N*), freshly prepared from ultrahigh purity acid[6]; 0.1 and 1.0 *N* NaOH; and a 0.1% solution of bromthymol blue indicator in ethanol–water (1:1). Ether[7] (absolute), of peroxide content <0.00005% and residue after evaporation <0.0005%, from a can opened fresh daily was used as the solvent for extraction.

Glassware Pretreatment—All glassware (volumetric flasks, centrifuge tubes, pipets, *etc.*) used in the assay were acid washed in a cleaning solution[8] (potassium dichromate in concentrated sulfuric acid) by soaking overnight in an acid bath. The glassware was rinsed with distilled water and oven dried. The inner surfaces of the glassware were then deactivated by soaking for 10 min in a freshly prepared 1% aqueous solution of a siliconizing agent[9]. The glassware was then rinsed thoroughly with distilled water and oven dried at 105° for 30 min prior to use.

Glassware so treated can be used five or six times with regular detergent washing in a commercial glassware washing machine before adsorption losses become appreciable and retreatment is necessary.

Assay in Blood or Urine—In a 50-ml glass-stoppered centrifuge tube, add either 2.5 ml of whole blood and 1.3 ml of 0.1 *N* NaOH or 2.5 ml of urine and 1.5 ml of 1 *M* borate–sodium carbonate–potassium chloride buffer (pH 9.0). Along with the unknowns, process a 2.5-ml specimen of control blood or urine and four separate 2.5-ml specimens of control blood or urine to which 25, 50, 75, or 100 ng of II and III are added as internal standards.

Add 10 ml of ether to all specimens, stopper the tubes with stoppers[10], and extract by shaking for 10 min on a reciprocating shaker. Centrifuge at 2000 rpm for 5 min (preferably at 0–4°) and transfer the ether layer to another 50-ml centrifuge tube. Repeat the extraction with another 10-ml portion of ether, combine the ether extracts, and add 5 ml of 0.1 *N* HCl. Shake the tubes for 10 min, centrifuge for 3 min, and remove the ether by aspiration.

Add 1 drop (0.1 ml) of bromthymol blue indicator to the acid extract and titrate to a permanent blue end-point with 1 *N* NaOH added dropwise. Extract this alkaline solution with 2 × 10 ml of ether by shaking and centrifuging as described and combine the ether extracts in a 15-ml centrifuge tube by serial evaporation at 45° in a rotary evaporator[11]. If the samples have to be left overnight, they must be vacuum dried for 15 min and left in a desiccator.

Add 100 μl of ether–methanol (90:10) to dissolve the residues and transfer quantitatively onto a 20 × 20-cm plate[12] of silica gel G of 250-μm bed thickness and 60-μm particle size. Rinse the tubes with 50 μl of ether–methanol (90:10) and combine with the original. Develop the plate for 12 cm ascending in a vapor-saturated chamber containing methylene chloride–methanol–concentrated ammonium hydroxide (90:10:1). Authentic standards of 10 μg of II and III are run alongside the sample extracts as reference standards (Fig. 2).

Scrape silica gel areas (1.5 cm^2) corresponding to II ($R_f \simeq 0.50$) and III ($R_f \simeq 0.25$) off the TLC plate into separate 15-ml centrifuge tubes. Add 1 ml of borate–sodium carbonate–potassium chloride buffer (pH 9.0) to the tubes and slurry the silica gel on a mixer[13] for 30 sec. Extract the slurry with 2 × 4 ml of ether by shaking and centrifuging as before.

Combine the ether extracts in a 15-ml centrifuge tube and extract into 2.5 ml of 0.1 *N* HCl[6]. Remove the ether layer by aspiration and determine the fluorescence of the parent drug (II) at 305 nm in a 1-cm path quartz cell[14], with excitation at 250 nm. Determine the fluorescence of the metabolite (III) at 300 nm with excitation at 250 nm.

Calculations—The fluorescence readings[15] of the unknowns and the internal standards are corrected for the control (blank) reading. The concentration of II in the unknowns is determined by interpolation from a calibration curve of the internal standards processed along with the samples. The concentration of III is determined similarly.

Determination of Percent Recovery—The overall percent recovery of the added internal standards of II and III is determined by

[1] Model Mark I, Farrand Optical Co., Valhalla, N.Y.
[2] Hanovia lamp, Englehardt Industries, Newark, N.J.
[3] RCA 1-P-28 photomultiplier tube.
[4] Hanovia or Osram.
[5] ACS certified reagents.
[6] Ultrex, J. T. Baker and Co.
[7] Mallinckrodt Chemical Co., St. Louis, Mo.
[8] Chromerge, Monostat, New York, N.Y.
[9] Siliclad, Clay Adams Co., New York, N.Y.
[10] Teflon (du Pont).
[11] Buchler Evapomix, Buchler Instruments, Fort Lee, N.J.
[12] E. Merck F_{254}, Brinkmann Instruments, Westbury, N.Y.
[13] Vortex supermixer, Labline Industries, N.Y.
[14] Quarasil, Precision Cells Inc., New York, N.Y.
[15] [*TM*] = transmission (*T*) × meter multiplier factor (*M*).

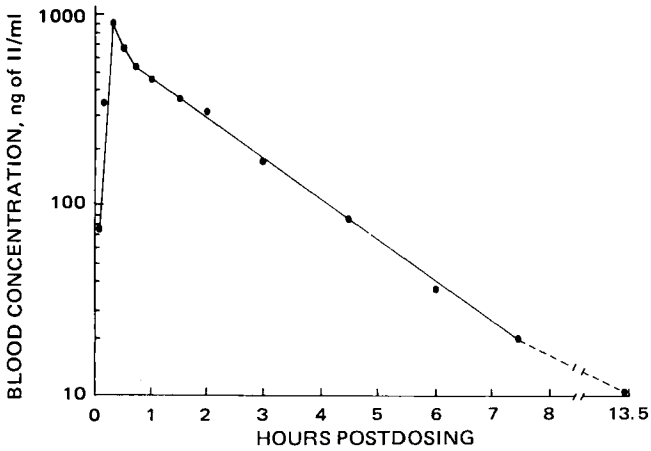

Figure 3—*Blood level fall-off curve of II in a dog following oral administration of a 10-mg/kg dose of the clinically used tablet formulation.*

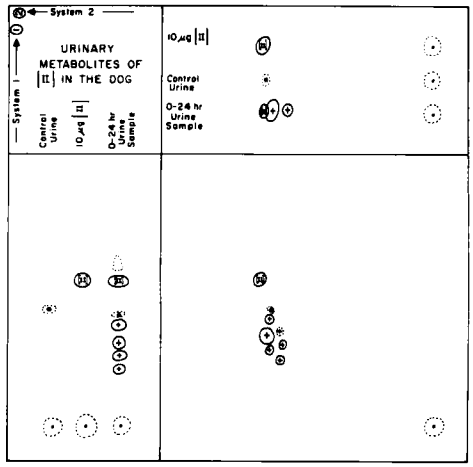

Figure 4—*Two-dimensional thin-layer chromatogram of an extract of dog urine postdosing. System 1 = methylene chloride–methanol–concentrated ammonium hydroxide (90:10:1). System 2 = acetone–methyl ethyl ketone–concentrated ammonium hydroxide (89:10:1). Key: *, longwave UV fluorescence; and +, urinary metabolites of II.*

direct comparison of the slope of the internal standard curve to that of the external standard curve, prepared with 25, 50, 75, or 100 ng of II/2.5 ml of 0.1 *N* HCl[6], prewashed with 4 ml of ether, by shaking for 5 min before the fluorescence is determined. Overall percent recovery should be determined routinely as a check on precision and reproducibility.

RESULTS AND DISCUSSION

The benzofuran analogs I and II exhibited analytically usable UV absorption and fluorescence in acidic media. Both compounds exhibited weak phosphorescence in ether–isopentane–ethanol (5:5:2) at 77° K (liquid nitrogen), with excitation at 255 and emission at 445 nm, with a decay half-life of 2.8 sec. Their potential sensitivity, however, was not sufficient for quantitation in the nanogram range.

Although II and III exhibited weak UV absorbance at 250 nm in 0.1 *N* HCl [$A^{1\%}_{1cm} = 650$], their fluorescence behavior in the same medium was sufficiently intense for their quantitation with nanogram sensitivity. Both compounds exhibited the same excitation maximum at 250 nm. Their emission spectra differed in their maxima by only 5 nm, with II at 305 nm and III at 300 nm. The relative fluorescence intensity of the two compounds measured at their respective excitation–emission maxima was similar.

The linear range of fluorescence covered a sufficiently wide concentration range, from 10 to 3000 ng/ml of 0.1 *N* HCl. The ability to measure less than 10 ng recovered from blood required extensive sample cleanup, which was effected by back-extraction into acid, reextraction at pH 9.0, and a TLC separation step, which also imparted specificity to the assay.

Compounds II and III were quantitatively extracted into ether from blood or urine buffered to pH 10.0 and were also back-extracted quantitatively (>95%) into 0.1 *N* HCl. This fact was used as an effective cleanup step to reduce the amount of endogenous impurities carried through the procedure. Following TLC separation, the area of silica gel corresponding in R_f to that of 10 μg of authentic standards of II and III was carefully scraped off and extracted into ether after slurrying with pH 9.0 buffer. Concentrations less than 100 ng of compound could not be visualized on the TLC plate; however, the areas on the plate of similar R_f were located mainly by comparison to the R_f of the authentic reference standards run alongside the sample extracts.

The overall recovery of internal standards of 25, 50, 75, and 100 ng of II added per milliliter of blood or urine taken through the entire assay was about 86 ± 3.0%, while that of III was about 88 ± 7.4%. The limit of detection was approximately 2–4 ng of each compound/2.5 ml of 0.1 *N* HCl[6] or 2.5 ml of blood or urine extracted. These low sensitivity limits can be realized if certain essential precautions are meticulously observed. These precautions include the pretreatment of all glassware used with a siliconizing agent[9] to minimize adsorption losses and the use of spectrofluorometer[1] equipped with a specially selected high UV energy (250 nm) xenon energy source[2] and a specially selected high lumen output (>10) photomultiplier tube[3].

Since the excitation–emission wavelengths (250/305 nm) used are in the UV spectral range, monochromator gratings of high spectral resolution (<15 nm) in the UV are necessary. The spectrofluorometer[1] used in this study met these specifications. The use of a high purity 1-cm path quartz cell[14] of very low fluorescence background and high UV transmission characteristics (>90% at 200 nm) is also essential. The use of high purity 0.1 *N* HCl made from high purity hydrochloric acid[6], using distilled deionized water as the solvent, for fluorescence measurement further ensured very low background in the determination of II and its metabolite in biological specimens.

Application to Biological Specimens—*Dog Studies*—Blood levels of II were determined in a dog (in a pilot study) following a single 10-mg/kg oral dose of the clinically used 20-mg tablet formulation. Blood specimens were taken at suitable time intervals up to 24 hr (Fig. 3). The data indicate rapid absorption of the drug, with a measurable level seen at 15 min and a peak blood level of 940 ng/ml seen at 30 min postdosing. The blood level declined thereafter to a nonmeasurable amount at 24 hr, with an "apparent" half-life of elimination of about 80 min.

The urinary excretion of II in the 0–24-hr excretion period accounted for only 1.0% of the dose as intact drug in both the unconjugated and conjugated forms. The urine extract was analyzed by two-dimensional TLC (Fig. 4) and showed the presence of one major and three minor metabolites in the extract, indicating extensive biotransformation of the drug. In the blood assay, Solvent System I, consisting of methylene chloride–methanol–concentrated ammonium hydroxide (90:10:1), was capable of resolving the parent drug (II) and four basic metabolites from each other, thereby ensuring the specificity of the fluorometric assay.

The characterization of the major metabolites of II in the dog and in humans using GLC–mass fragmentography will be reported elsewhere[16]. The major basic metabolite in humans and in the dog results from the oxidation of the 7-ethyl group in the molecule, wherein the methylene group is oxidized to a secondary alcohol (Metabolite III). Several phenolic metabolites formed due to hydroxylation of the phenyl ring were also identified as minor urinary metabolites. The *tert*-butylaminomethyl side chain is apparently unaltered.

Human Studies—In a pilot study, blood levels were determined in two healthy normal volunteers to test the clinical utility of the assay. Two subjects (AMD and RFL) were each given a single 20-mg oral dose (tablet), and blood samples were taken at the time intervals shown in Table I. Blood levels of the intact drug (II) and its major metabolite, the alcohol (III), are summarized in Table I and plotted semilogarithmically *versus* time in Fig. 5. In both subjects, the intact drug was measurable up to 9 hr postdosing.

[16] R. J. Francis and R. F. Long, Roche Products Ltd., Welwyn Garden City, Hertfordshire, England, unpublished data on file.

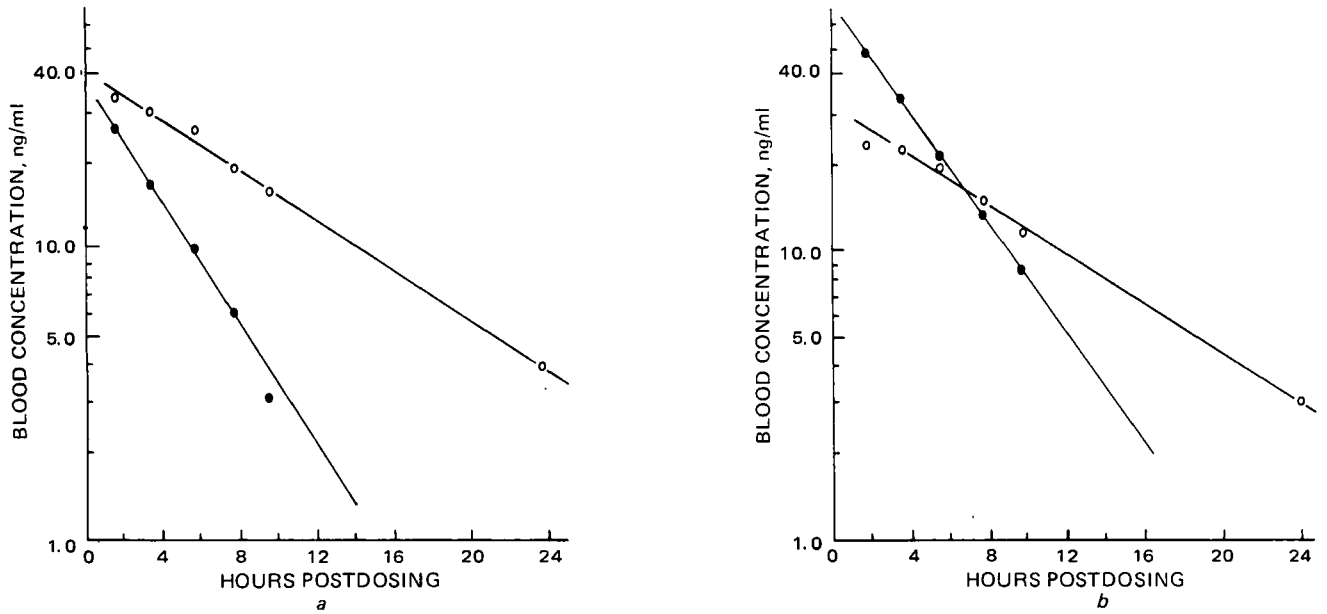

Figure 5—*Blood level fall-off curves of II (●) and its major metabolite, III (○), in humans following a single 20-mg oral dose of the drug. Key:* a, *Patient AMD, weight of 84.1 kg, dose of 20 mg = 0.24 mg/kg; and* b, *Patient RFL, weight of 87.3 kg, dose of 20 mg = 0.23 mg/kg.*

These data were further verified by GLC–mass fragmentography and showed excellent correlation in most cases (Table I), attesting to the accuracy and specificity of the spectrofluorometric assay. The blood levels of II declined monoexponentially, with an apparent half-life of elimination of about 3 hr in both subjects. The levels of III were measurable up to 24 hr postdosing and declined monoexponentially, with an apparent half-life of elimination of about 7 hr in both subjects.

Specificity of Blood Assay—The chromatographic purity and homogeneity of the bands having the same R_f as authentic II and III from the human blood extracts (Fig. 2) were further verified following elution. They were characterized by the similarities of their respective luminescence spectra compared to the authentic standards and also by cochromatography with the respective authentic standards by TLC analysis in a different solvent system, in which no separation of the cochromatographed compounds was evident. Electron-capture GLC analysis of II and III as either the *N*-heptafluorobutyryl or *N*-heptafluorobutyryl-*O*-trimethylsilyl ether derivative was inconclusive due to the formation of mixed products with multiple peaks, especially for the alcohol (III). Nevertheless, electron-capture GLC analysis of these derivatives showed excellent sensitivity and has worthwhile potential as an alternative means of analysis.

These data substantiate the clinical utility of the spectrofluorometric assay for the determination of the parent drug, II, and its major metabolite, III, in blood.

Table I—Blood Levels of II in Humans following a Single 20-mg Oral Dose Determined by a TLC–Spectrofluorometric Assay

Sample	Hours Postdosing	II[a], ng/ml of Blood		Metabolite[b] III, ng/ml of Blood
		Patient AMD[c]		
1	0 hr	—		—
2	1 hr, 30 min	26	(25.9)[d]	34
3	3 hr, 20 min	17	(14.1)	30
4	5 hr, 40 min	10	(10.1)	26
5	7 hr, 40 min	6	(5.4)	19
6	9 hr, 35 min	3	(4.2)	16
7	23 hr, 45 min	N.M.[e]	(1.1)	4
		Patient RFL[f]		
1	0 hr	—		—
2	1 hr, 40 min	48	(48.7)[d]	23
3	3 hr, 30 min	34	(28.3)	22
4	5 hr, 35 min	21	(21.7)	19
5	7 hr, 45 min	13	(14.7)	15
6	9 hr, 40 min	9	(12.1)	12
7	23 hr, 55 min	N.M.	(2.5)	3

[a] Calculated as free base equivalent of hydrochloride salt. [b] Calculated as free base equivalent of hemioxalate salt. [c] Weight of 84.1 kg; dose of 20 mg = 0.24 mg/kg. [d] Determined by GLC–mass fragmentography. [e] N.M. = not measurable, <2 ng/ml of blood. [f] Weight of 87.3 kg; dose of 20 mg = 0.23 mg/kg.

REFERENCES

(1) B. N. C. Pritchard, *Angiologica*, **3**, 318(1966).

(2) *Am. J. Cardiol.*, **18**, 303(1966).

(3) J. H. Biel and B. K. B. Lum, in "Progress in Drug Research," vol. 10, E. Jucker, Ed., Birkhauser Publishers, Basel, Switzerland, 1966, pp. 46–89.

(4) D. G. Shand, E. M. Nuckolls, and J. A. Oates, *Clin. Pharmacol. Ther.*, **11**, 112(1970).

(5) D. J. Coltart and D. G. Shand, *Br. Med. J.*, **3**, 731(1970).

(6) W. Haefely, A. Hurlimann, and H. Thoenen, *Angiologica*, **4**, 203(1967).

(7) R. C. Hill and P. Turner, *Br. J. Pharmacol. Chemother.*, **32**, 663(1968).

(8) E. M. Phillips and D. Hicks, *Eur. J. Clin. Pharmacol.*, **5**, 158(1973).

(9) G. A. Fothergill, R. J. Francis, T. C. Hamilton, J. M. Osbond, and M. W. Parkes, *Experientia*, **31**, 1322(1975).

(10) J. R. Kilborn and P. Turner, *Br. J. Clin. Pharmacol.*, **1**, 143(1974).

(11) J. A. F. de Silva and J. Kaplan, *J. Pharm. Sci.*, **55**, 1278(1966).

ACKNOWLEDGMENTS AND ADDRESSES

Received July 11, 1975, from the *Department of Biochemistry and Drug Metabolism, Hoffmann-La Roche Inc., Nutley, NJ 07110*

Accepted for publication October 31, 1975.

The authors are deeply indebted to Dr. R. F. Long and Dr. R. J. Francis of Roche Products Ltd., Welwyn Garden City, Hertfordshire, England, for their interest in this study, for supplying the clinical blood specimens and the authentic reference standard of Metabolite III (alcohol), for their permission to use unpublished data on the metabolism of II, and for the GLC–mass spectral data on the analysis of II. The authors also thank Mr. R. McGlynn for the drawings of the figures.

[x] To whom inquiries should be directed.

Computerized Automated System for Determining Dissolution Rate Profiles for Solid Dosage Forms

F. J. CIOFFI ˣ, H. M. ABDOU, and A. T. WARREN

Abstract □ A unique automated system was developed for the measurement of dissolution rates of tablets and capsules. This system, which adheres to principles set forth in the compendia, can test six dosage forms simultaneously. It is modular in form and capable of maintaining sink conditions, and it can handle any type of chemistry amenable to an automatic analyzer. In addition to the usual dissolution apparatus, the system includes a 12-channel combination sampling and solvent addition pump, a sequence control module, pertinent automated analyzer components, a spectrophotometer or fluorometer, an optional recorder, a specially designed digitizing system, and a teletype equipped with a paper tape punch reader and acoustic coupler. Each dissolution flask is automatically sampled every 6 min. Standards may be run either before or after the samples. Since dissolution, sampling, chemistry, and readout are all accomplished simultaneously, the complete test time is essentially reduced to the dissolution time itself. At the completion of sample dissolution, raw dissolution profile data are on the punched paper tape ready for computer processing *via* a time-sharing system. Developed software provides for the printout of a complete test report in less than 15 min.

Keyphrases □ Dissolution—solid dosage forms, rate profiles determined using computerized automated system □ Computerized automated system—utilized for determining dissolution rate profiles of solid dosage forms □ Automated computer system—utilized for determining dissolution rate profiles of solid dosage forms □ Dosage forms, solid—tablets and capsules, dissolution rate profiles determined using computerized automated system

In recent years, the dissolution rates of solid dosage forms such as tablets and capsules have become of prime importance in pharmaceutical studies, as reflected by the inclusion in the compendia of monographs requiring the dissolution test. Once clinical correlations have been established, *in vitro* dissolution measurements can serve as a reliable, rapid, and economical technique to indicate the *in vivo* rate and extent of drug release and, hence, bioavailability (1–3). Dissolution testing also can serve as an important criterion in evaluating the effects of different constituents in drug formulations; in manufacturing, it can be an important method for determining uniformity both within and between different production batches.

BACKGROUND

Automation in dissolution rate testing has evolved in various ways and to different degrees. Three main approaches have been taken:

1. *Continuous flow* of dissolution fluid with the solid dosage form agitated by means of a motor-driven propeller, a rotating wire mesh basket containing the tablet[1], or some sort of rocking device (4–6).
2. Methods based on *mass transfer* between the solid dosage form and the dissolution fluid, with the tablet being held in a fixed position and traversed by a continuous flow of solvent. This concept may be referred to as the "flow-through" or "column" technique (7–9).
3. Methods based on *dialysis* (10).

In all three approaches, a constant volume is normally maintained in the dissolution flask throughout the test by techniques ranging from simply replacing manually the volume of the sample withdrawn by pure solvent to continuous dilution with pure solvent. In the former case, the dissolution curve is an integral function of the rate itself; the latter techniques can permit the maintenance of the sink condition, with the curve being a differential function of the rate.

Multiple automated dissolution testing systems were developed by a few investigators to relieve the ever increasing workload. Castello *et al.* (11) introduced an apparatus having multiple testing stations and capable of testing up to 20 tablets simultaneously. This apparatus, however, is really only a discrete sampling device, with the actual analysis being performed separately. Ferrari and Khoury (12) described a system capable of testing more than one tablet at a time. It uses a dialysis technique with the diffusate being fed into an automatic analyzer. This system, however, does not incorporate the official compendia dissolution apparatus, which has been generally accepted by the pharmaceutical industry.

Beyer and Smith (13) introduced a six-tablet apparatus in 1971 which does conform to compendia criteria. It consists of a dissolution apparatus in which seven flowcells[2] can be alternately positioned in the light beam of the spectrophotometer at programmed intervals. A single, seven-channel pump continually circulates the fluid from each of the six dissolution flasks through its respective cell and back again; the seventh cell is used for standardization with air. Absorbances are recorded on a strip-chart recorder in the form of bar graphs. Two limitations of this apparatus are that: (*a*) only direct spectrophotometric measurement of the "pure" dissolution fluid is possible, since the concept of this apparatus precludes sample dilution or reagent addition; and (*b*) sink conditions are not maintained.

The system developed in this laboratory also incorporates the USP–NF dissolution apparatus and can test six tablets simultaneously. Unlike other systems, however, it is completely automated from the point of tablet introduction to final readout of the raw data on punched paper tape. In addition, the system maintains sink conditions[3] at all times and performs any type of chemistry amenable to an automatic analyzer. The raw data are computer analyzed in minutes, and final results are presented in the form of a complete tabular report, a graphical dissolution profile, or both.

EXPERIMENTAL

Equipment—The system is modular, with the components being arranged as shown in Fig. 1. From left to right these components are:

Six-Spindle Dissolution Tester—It has a variable speed motor (25–250 rpm) and indicating tachometer[4]. This unit is shown in position over a 76.2 × 30.5 × 19.1-cm (30 × 12 × 7.5-in.) constant-temperature water bath[5] containing the six dissolution flasks[6]. The six shafts that hold the stainless steel wire mesh dissolution baskets[7] are shown extending from the chucks into the dissolution flasks.

12-Channel Peristaltic Pump[8]—The flow range is between 0.08 and 85 ml/min. Six channels pump sample continuously from each respective dissolution flask, while the other six channels return pure solvent to the dissolution flasks at the same flow rate. For standard measurements, only six channels are used. The six three-way stopcocks shown positioned above this pump allow solution to be sampled either from the dissolution flasks or from six standard containers.

Sequence Control Module (SCM)—This specially designed unit controls both the sampling sequence and the modified digital voltmeter (DDA) which, in turn, controls the electronic data acquisition

[1] From this point on, "tablet" will be used synonymously with "solid dosage form."

[2] Beckman Kintrac VII.

[3] Defined as never allowing the drug concentration in the dissolution flask to exceed 10–20% of saturation.

[4] Hansen model T-1044-20X, available from Scientific Glass Apparatus Co.

[5] Model 1064, Cole-Parmer.

[6] Corning No. 6947 1000-ml resin reaction flasks.

[7] Described in USP XVIII.

[8] Model 7555X Servodyne power drive system, Cole-Parmer, Chicago, Ill.

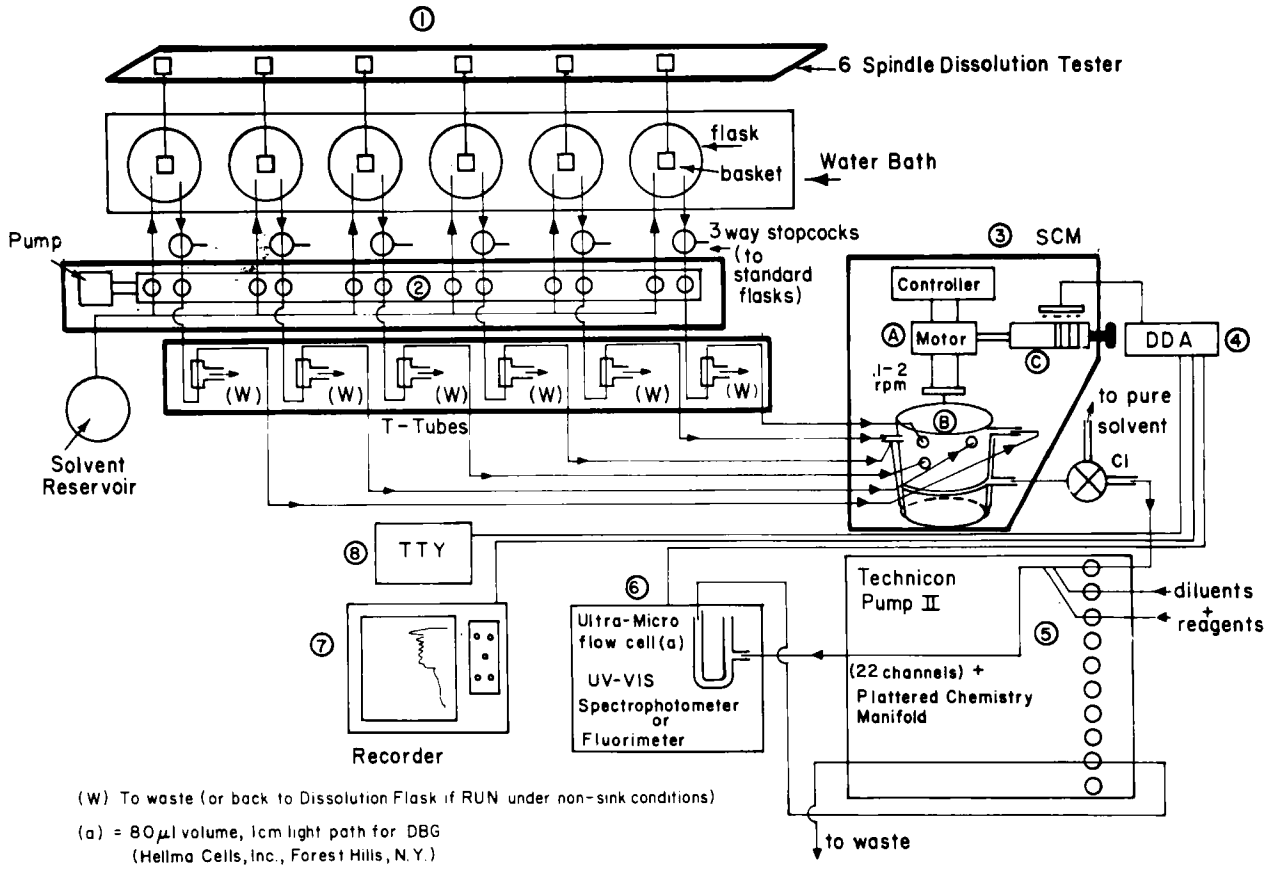

Figure 1—*Schematic of system (pat. 3,846,075).*

operations and the optional recorder. The sequence control module consists of a constant-speed 1/150 hp motor[9], which can be very accurately controlled over a range of 0–2 rpm by means of a controller[10] built into the front panel of the sequence control module. The double shaft of the motor is connected at one end to the sampling valve and at the other end, *via* a magnetic clutch[11], to a revolving plastic drum[12] having 60 equally spaced slots cut lengthwise along its outer cylindrical surface. Thus, sequence programming for the modified digital voltmeter unit is accomplished by placing small plastic actuators in the slots such that any of a number of microswitches may be contacted at desired intervals.

The sampling valve is a specially designed seven-port stopcock with a glass outer barrel and plug[13]. It is housed in the small compartment at the left side of the sequence control module. Figure 2 gives an operational diagram of the valve, showing the six equally spaced inlet ports (numbered 1–6), each connected to a separate dissolution flask *via* the sampling pump, and the single exit port (E). All glass ports attached to the outer barrel and the grooves shown on the plug are 1 mm i.d.

The length of the upper groove on the plug is 14/15 of the distance between the equally spaced inlet ports so that no two inlet ports can be opened at the same time as the plug rotates. The lower annular groove in the plug is connected to the upper groove by the vertical groove and is always open to the exit port. Thus, as the valve rotates, each dissolution flask is sampled in sequence, with the sample aliquot entering the automated chemistry system *via* the single exit port (E).

Digital Data Acquisition Module (DDA)—This modified unit[14] receives the raw analog data signal from the spectrophotometer and converts it to digital form for the teletypewriter printout while preserving the analog signal for input to the recorder, which it also controls. In addition, the digital data acquisition module controls the data output format on the teletypewriter. The "digitize period" wheel on the module sets the time in seconds over which the signal is averaged before it digitizes. This time should always be set to 4 sec or less to

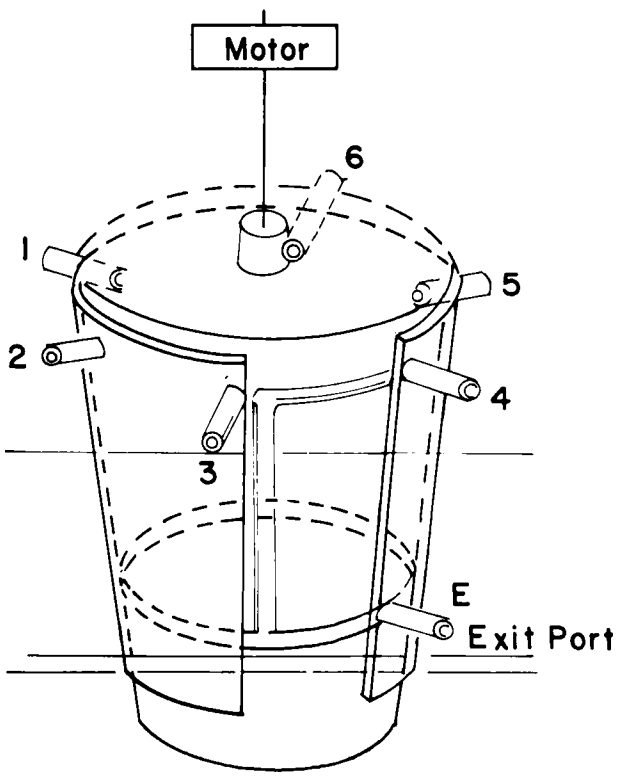

Figure 2—*Diagram of sampling valve (pat. 3,814,129).*

[9] Catalog No. B7096C-1080G, B&B Motor & Control Corp., New York, N.Y.
[10] Model MR-05, B&B Motor & Control Corp., New York, N.Y.
[11] Model SBEC clutch coupling, Electroid Co., Union, NJ 07083
[12] Model 091-1061-501 programming switch, Selectro Corp., Mamaroneck, NY 10543
[13] Teflon (du Pont).
[14] Infotronics model CRS-230 digitizer system.

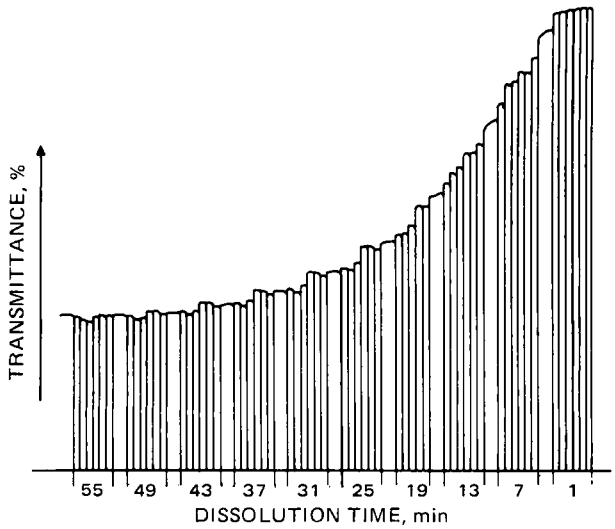

Figure 3—*Typical recorder chart.*

prevent any overlap between the signal averaging interval and the next digitize command.

The different control functions of this unit are activated by closure of four microswitches by the rotating drum of the sequence control module in a desired preprogrammed sequence. These functions are as follows:

1. Stand-By Mode—It resets the sample counter to 1 (Tablets 1–6 are numbered as such in the data printout).

2. Repetitive Mode—This microswitch returns the teletypewriter carriage, advances the line feed, and causes the next consecutive line number to printout.

3. Digitize Mode—The unit digitizes whenever this microswitch is closed.

4. Single Mode—Closure of this microswitch takes the unit out of the digitize mode, but manual digitization is still possible after this microswitch has been closed.

In addition to these functions, the digital data acquisition module also controls the recorder, which remains off most of the time. Before a run, the operator can set a selectable switch on the digital data acquisition module to any digitizing interval. The digital data acquisition module then automatically turns on the recorder only during this period for each tablet, the result being a series of bar graphs. Each set of six bar graphs corresponds to the degree of dissolution of Tablets 1–6, respectively, at the particular dissolution times noted and is separated by an elongated line for the sixth tablet value. An example of a typical recorder chart is shown as Fig. 3.

Since the sink condition is normally maintained by continuous dilution of the sample, as described earlier, the recorder bar graphs reflect only the actual concentration of drug in the dissolution flask at any time—not true amount dissolved. The recorder, therefore, usually serves only as an optional visual guide to the approach and maintenance of the sink condition. The same data, of course, are available in numerical form on the teletypewriter printout. However, with very soluble substances where it is not necessary to dilute the sample continually to maintain sink conditions, the system may be adjusted so that the recorder gives the actual percent dissolved directly.

The other modules shown in Fig. 1 include the proportioning pump (5), the spectrophotometer (6), the recorder (7), and the teletypewriter (8). Since the entire system is modular, it is quite simple to substitute different modules, *e.g.*, a fluorometer for the spectrophotometer.

The raw data output is obtained on the teletypewriter in both printed form and on punched paper tape. Each line represents a single tablet. Thus, under the usual preset conditions of 1-min sampling times for each flask (motor set to speed of ⅛ rpm) and a 6-sec digitizing interval program set on the drum, each tablet solution passes through the spectrophotometer flowcell for 1 min at 6-min intervals. Readings are taken automatically at 6-sec intervals for each tablet solution as it passes through the flowcell, beginning with 18 sec after the solution enters the cell. Since the standards are usually run at half this sampling rate to ensure steady state in the flowcell, readings are taken every 12 sec for each standard level, beginning 36 sec after the respective standard solution enters the cell.

Table I—Typical Standard and Sample Raw Data (on Punched Paper Tape)

				Standard Data				
	1	9802	9919	9992	9992	9992	6482	9448
	2	7879	7744	7621	7520	7390	7153	6848
	3	6024	5947	5913	5875	5816	5735	5649
	1	5383	5348	5332	5332	5344	5403	5522
	2	6126	6219	6298	6345	6387	6482	6731
	3	7823	7988	8123	8258	8411	5735	8815
1E25								
				Sample Data				
	1	4981	4975	5003	5002	4999	5003	5000
	2	4997	5000	5001	5005	5006	5002	5004
	3	4996	5001	5000	5009	5013	5005	5005
	4	4997	4998	5000	5002	5004	5009	5011
	5	5002	5000	5000	5000	5001	5005	5005
	6	5002	5006	5000	4998	5003	5001	5000
	1	5009	5027	5020	5021	5016	5012	5014
	2	5026	5023	5025	5021	5020	5015	5022
	3	5017	5018	5013	5015	5022	5019	5015
	4	5013	5007	5010	5008	5013	5012	5010
	5	5014	5012	5007	5019	5013	5006	5008
	6	5017	5015	5011	5016	5016	5016	5021
	1	6325	6283	6248	6210	6156	6107	6076
	2	6008	6010	6018	6020	6020	6034	6051
	3	6123	6133	6149	6178	6201	6217	6225
	4	6212	6188	6172	6175	6167	6152	6133
	5	6155	6177	6198	6250	6272	6279	6292
	6	6366	6371	6354	6352	6345	6335	6331
	1	6239	6199	6161	6122	6077	6046	6008
	2	5938	5941	5959	5982	6010	6020	6031
	3	6105	6120	6126	6151	6173	6188	6198
	4	6162	6147	6142	6052	6125	6126	6125
	5	6152	6150	6173	6186	6209	6221	6238
	6	6261	6271	6273	6259	6257	6254	6260
	1	6192	6153	6113	6072	6036	6004	5974
	1	5898	5903	5905	5917	5946	5975	6005
	2	6107	6125	6131	6116	6121	6133	6133
	3	6114	6098	6090	6082	6083	6095	6105
	4	6133	6133	6144	6149	6155	6160	6167
	5	6172	6167	6175	6174	6168	6167	6172
	1	6130	6093	6059	6019	5986	5940	5898
	1	5824	5829	5843	5868	5902	5920	5949
	2	6061	6082	6087	6093	6089	6078	6054
	3	6020	6022	6018	6024	6028	6043	6055
	4	6074	6078	6082	6087	6093	6090	6089
	5	6053	6045	6044	6043	6048	6056	6069
	1	6060	6019	5964	5929	5883	5841	5802
	2	5770	5782	5801	5838	5874	5913	5950
	3	6050	6042	6040	6037	6020	6017	6007
	4	5991	5969	5968	5977	5996	5993	6018
	5	6070	6069	6053	6050	6054	6057	6032
	6	5967	5964	5957	5957	5965	5968	5966
1E25								

Therefore, under the conditions specified, sample data printouts occur at 18, 24, 30, 36, 42, 48, and 54 sec after the sample enters the flowcell and standard data printouts occur at 36, 48, 60, 72, 84, 96, and 108 sec after the standard solutions enter the cell. An example of typical raw data output is shown as Table I. The columns of standard and sample data that most closely represent steady-state readings are easily noted by visual inspection. These columns (usually numbers 4 or 5 for the standards and 5 or 6 for the samples) are used in the computer calculations.

Operation—After setting up the appropriate automated chemistry platter on the proportioning pump[15], the teletype is switched to "DATA SYSTEM." The procedure for starting the system running automatically is as follows.

Standards

1. Turn stopcock C1 (Fig. 1) to the solvent position. This three-way stopcock is positioned to take solution from the sampling valve exit port during the sample run and standard measurements. It is positioned toward a flask containing pure solvent when rapid flushing of the system is desired to obtain a pure solvent baseline reading.

2. The six three-way stopcocks attached to the six alternate sampling channels of the 12-channel pump are positioned toward the six flasks containing the standard solutions; the remaining six solvent return channels are not used.

[15] Technicon.

AUTOMATED DISSOLUTION TEST

Product: An Antibiotic Tablet Formulation
Code: None
Lot Number: Red Oval
Control: KDN-140-UJB1

Date Tested: 3-15-73
Analyst: HA

Solvent: Simulated Intestinal Fluid W.O. Pancreatin
Volume: 1000ml
Basket Rotation Rate: 150RPM

F = 19.3 ml/minute
T = 37 deg.c

Percent Dissolved (Corrected to Sink Conditions)
(Basis-Label)

Time (Min)	Tablet Number 1	2	3	4	5	6	Min.	Max.	Avg.
1	3.46	4.72	4.52	5.27	5.40	9.06	3.46	9.06	5.41
7	10.46	10.88	11.66	12.96	15.44	21.84	10.46	21.84	13.88
13	22.13	23.11	24.29	24.21	27.33	31.66	22.13	31.66	25.45
19	32.55	33.39	33.67	35.58	37.33	41.77	32.55	41.77	35.71
25	41.21	41.12	43.27	44.59	47.61	48.33	41.12	48.33	44.35
31	48.34	48.92	52.01	53.87	54.25	53.46	48.34	54.25	51.81
37	53.29	52.87	56.58	58.37	60.43	57.62	52.87	60.43	56.53
43	55.72	57.33	58.97	61.53	64.63	61.10	55.72	64.63	59.88
49	58.86	60.71	62.46	66.42	67.77	63.48	58.86	67.77	63.28
55	62.55	63.15	66.71	68.10	69.18	65.22	62.55	69.18	65.82
61	64.21	64.26	69.00	70.95	72.15	68.06	64.21	72.15	68.10
67	66.66	66.87	70.95	73.83	75.47	70.74	66.66	75.47	70.75
73	69.14	69.89	74.63	76.84	76.87	74.31	69.14	76.87	73.61
79	73.63	73.10	79.03	79.97	79.42	77.15	73.10	79.97	77.05
85	77.55	76.37	82.51	83.92	83.40	80.10	76.37	83.92	80.64
91	81.11	80.70	86.91	86.64	86.05	83.43	80.70	86.91	84.14
97	84.07	83.19	90.09	89.55	88.05	86.08	83.19	90.09	86.84
103	86.27	86.19	92.54	91.67	91.87	87.98	86.19	92.54	89.42
109	89.76	89.13	95.26	96.07	93.09	90.80	89.13	95.26	92.08
115	90.79	90.12	96.45	96.83	95.67	92.59	90.12	96.83	93.74
121	93.09	92.16	100.33	99.37	98.20	93.77	92.15	100.33	96.15
127	96.02	95.43	103.64	102.54	101.17	98.07	95.43	103.64	99.48
133	97.45	96.46	106.37	103.69	103.34	98.73	96.46	106.37	101.01

DT (50) = 29.5 minutes
DT (85) = 92.9 minutes

Figure 4—*Typical computer printout of final dissolution test report.*

3. The 12-channel pump is then set to a relatively fast speed for about 2 min to make sure that the six tubes leading to the sampling valve are filled with their standard solutions. Then, by using a preconstructed calibration curve, the speed is reduced to about twice the sampling speed of the proportioning pump; the excess standard solution exits *via* the overflow T-tubes either to waste or back to its standard flask.

4. The program drum is set manually by means of a position-indicating wheel attached to the drum through the sequence control module case such that the "STAND-BY" microswitch is just closed as indicated by the "STAND-BY" light on the digital data acquisition module. The magnetic clutch is not yet engaged.

5. The sequence control module motor (A in Fig. 1) speed is set to 12 min/revolution, equivalent to a 2-min sampling time for each standard solution.

6. When the buzzer sounds, indicating that the sampling valve has just reached the Sample 1 position, stopcock C1 (Fig. 1) is turned to sample from the exit port of the sampling valve and a stopwatch is started. Standard 1 is now being drawn into the automated chemistry system, and all six standard levels will be sampled automatically, sequentially, and repetitively for 2-min intervals. The relative concentration of the standard levels decreases from 1 to 6, with the range in terms of percent of label being from about 110 to 20% of the maximum concentration of drug in the dissolution flask at the sink condition maintained. This reduced absolute concentration range is used to improve the linearity of the standard curve.

To minimize any cumulative effect of carryover in the flowcell, the sampling order used for the standards is 1, 3, 5, 6, 4, 2. When the first (and most concentrated) standard reaches the flowcell, as indicated by the first deflection of the spectrophotometer needle, the stopwatch is stopped and the switch engaging the programming drum is thrown. The time for the solution to move from the sampling valve to the flowcell is noted as $T1$. As the standards are automatically run, the raw data (transmittance or absorbance) are recorded on the teletype and on punched paper tape.

Samples—Except for a few obvious differences, the procedure for

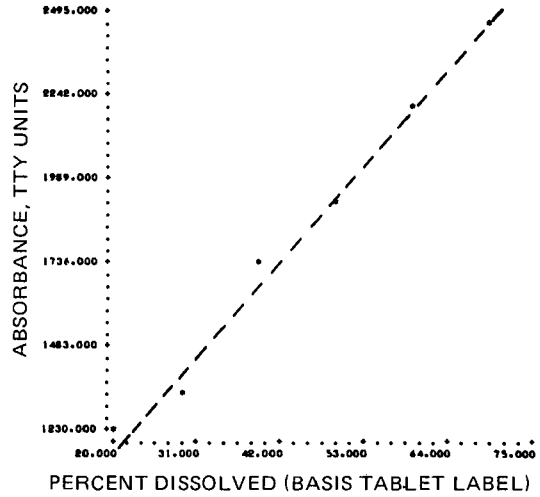

Figure 5—*Computer-drawn standard curve.*

running the samples is similar to that for the standards.

1. All channels of the 12-channel peristaltic pump are used. The six channels not used for the standard run are used to add pure solvent to the tablet dissolution flasks.

2. The six baskets containing the test tablets are positioned above their respective dissolution flasks. At exactly $(6 - x)$ min[16] from the first sound of the buzzer after a satisfactory baseline has been obtained, the basket containing Tablet 1 is lowered into its dissolution flask and rotation is begun. Tablets 2–6 are then started at 1-min intervals.

3. At exactly $(T1 + x)$ min after Tablet 1 was started, the program drum is engaged and the tape punch is turned on. At this point, Sample 1 is just entering the flowcell. The run now proceeds automatically until complete dissolution is obtained and the system is manually stopped.

Data Handling—The data tape is fed into a time-share computer system, and all calculations are done *via* software developed in this laboratory. The standard data are fit to six possible equations, and the equation that best fits the data is chosen by the computer for further calculations. The percent dissolved (uncorrected for dilution) is then calculated for each tablet at 6-min intervals up to complete dissolution. In addition, the high, low, and average results of the six tablets are also calculated for each time interval. At this point, the results are corrected for dilution based on the method of Richter *et al.* (6) as follows.

The rate of elimination of dissolved drug under constant volume conditions may be expressed as:

$$E = F/V \qquad \text{(Eq. 1)}$$

where F = flow rate in milliliters per minute, and V = constant volume in dissolution flask in milliliters.

The rate of change of concentration in the solution (neglecting continued dissolution of undissolved drug) can be expressed as:

$$-\frac{dc}{dt} = (E)(c) \qquad \text{(Eq. 2)}$$

where c = concentration in milligrams per milliliter.

Integrating between the limits c_0 and c_t gives:

$$\int_{c_0}^{c_t} \frac{dc}{c} = -E \int_0^t dt \qquad \text{(Eq. 3)}$$

or:

$$c_t = c_0 e^{-Et} \qquad \text{(Eq. 4)}$$

where c_t = concentration of dissolved drug at any time, t, in milligrams per milliliter, and c_0 = concentration of dissolved drug at time zero. Thus, the rate of change of the drug concentration in solution under constant volume conditions is first-order kinetic.

As the tablet dissolves, the concentration of drug in the dissolution flask builds up to a peak value after which, because of continuous dilution, it begins to decrease. Thus, before the peak, the amount of drug dissolved may be calculated as follows. During the first interval, Δt, the amount of drug released is given by:

$$C_1 = c_1 + c_t \qquad \text{(Eq. 5)}$$

where c_1 = amount of drug *observed* in solution, and $c_t = c_0 e^{-Et}$, the amount of drug *eliminated* from solution (Eq. 4).

If the sampling time interval is small[17], then Eq. 4 may be simplified to:

$$c_t = c_1 \, \Delta t E \qquad \text{(Eq. 6)}$$

and Eq. 5 becomes:

$$C_1 = c_1 + c_1 \, \Delta t E \qquad \text{(Eq. 7)}$$

For the next interval, Δt, the amount of drug released is calculated in a similar manner:

$$C_2 = c_2 + c_1 \, \Delta t E + c_2 \, \Delta t E = c_2 + \Delta t E(c_1 + c_2) \qquad \text{(Eq. 8)}$$

This calculation is done for every time interval up to the peak in the curve, where the amount of drug released is given by:

$$C_p = c_p + E \, \Delta t(c_1 + c_2 \ldots c_p) \qquad \text{(Eq. 9)}$$

or:

$$C_p = c_p + E \, \Delta t \sum_{t=1}^{t=p} c_t \qquad \text{(Eq. 10)}$$

After the peak, if there is no further release of drug from the solid dosage form, the elimination of the dissolved drug will follow Eq. 4. However, if the amount of drug observed in solution after the next time interval is higher than that calculated by Eq. 4, then the solid dosage form is still dissolving and releasing drug into solution. Hence, during the first time interval after the peak, the amount of drug released is given by:

$$C_{p+1} = c_{p+1} - c_p e^{-E \, \Delta t} \qquad \text{(Eq. 11)}$$

where C_{p+1} = amount of drug released during the first time interval after the peak, c_{p+1} = amount of drug observed in solution, and $c_p e^{-E \, \Delta t}$ = amount of drug expected in solution due to pure dilution after the first interval (by Eq. 4).

For the second time interval after the peak, the amount of drug released from the solid dosage form will be:

$$C_{p+2} = c_{p+2} - (c_{p+1})e^{-E \, \Delta t} \qquad \text{(Eq. 12)}$$

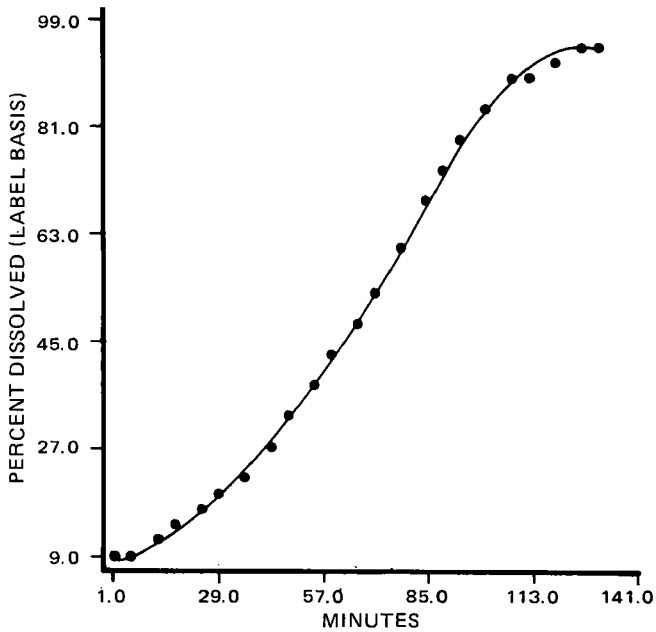

Figure 6—*Computer-drawn dissolution profile curve.*

[16] The x is the time required for the solution to be pumped from the dissolution flasks to the sampling valve at the particular flow rate being used. Since the length of tubing is the same from each flask, x is the same from each flask and is known from a calibration table constructed beforehand for any flow rate setting of the peristaltic pump.

[17] Satisfactory results were obtained for sampling intervals of up to 10 min.

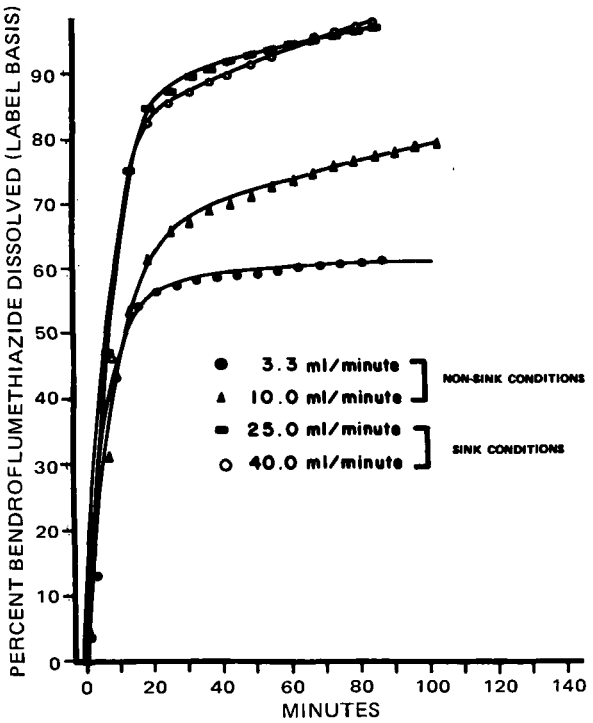

Figure 7—*Effect of flow rate on approach to sink conditions.*

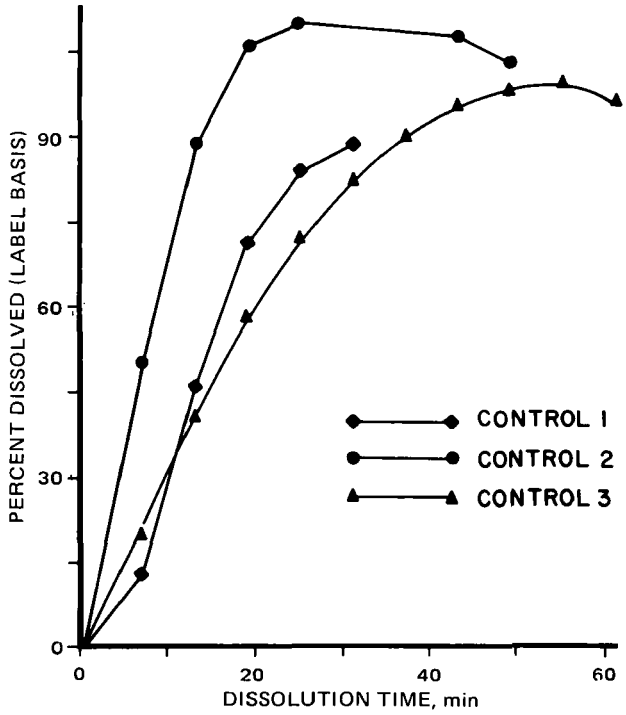

Figure 8—*Computer-drawn series of dissolution profiles.*

In general form, then:

$$C_{p+n} = c_{p+n} - (c_{p+(n-1)})e^{-E\,\Delta t} \qquad \text{(Eq. 13)}$$

where C_{p+n} = amount of drug released during any time interval, n; c_{p+n} = amount of drug observed in solution after n − time intervals after the peak; and $(c_{p+(n-1)})e^{-E\,\Delta t}$ = amount of drug expected in solution after $(n - 1)$ time intervals after the peak (by Eq. 4). When:

$$c_{p+n} = (c_{p+(n-1)})e^{-E\,\Delta t} \qquad \text{(Eq. 14)}$$

Eq. 13 becomes:

$$C_{p+n} = 0 \qquad \text{(Eq. 15)}$$

and there is no further release of drug. Therefore, the total amount of drug released (or dissolved) from the solid dosage form is obtained by combining Eqs. 10 and 13, *i.e.*:

$$C_T = C_p + \sum_{q=p+1}^{q=p+n} C_q \qquad \text{(Eq. 16)}$$

where C_T = total amount of drug released (dissolved from solid dosage form), C_p = amount of drug released before peak, and C_q = amount of drug released after peak. After the dilution correction is applied, the final results are presented in a tabular report format.

RESULTS AND DISCUSSION

An example of a typical computer-generated dissolution test report is shown in Fig. 4[18]. In this case, the product was an antibiotic tablet formulation. Figure 5 shows an optional printout of the standard curve, and Fig. 6 shows an optional printout of the dissolution profile curve for these tablets.

The importance of maintaining sink conditions by using an ample flow rate is clearly demonstrated in Fig. 7, which shows the effect of the flow rate on the dissolution profiles of the very insoluble bendroflumethiazide in a tablet formulation. NF XIV gives the solubility as "practically insoluble in water" (1 part in > 10,000 parts of water). Laboratory measurement showed a solubility of only 37.3 mg of bendroflumethiazide/liter of 0.1 *N* HCl, the dissolution fluid used. As Fig. 7 shows, a flow rate of 25 ml/min was necessary to maintain the calculated sink condition of +3.7–7.5 mg/ml in the dissolution flask.

Figure 8 shows an example of a computer-drawn set of dissolution profiles for three controls of the same product. In this case, the profile data for each control are stored in the computer as they are calculated and later combined into the single graph shown by using a commercial[19] package. Graphs such as these provide rapid visual observation of differences in the dissolution characteristics between different batches and thus provide an excellent technique for monitoring uniformity in product manufacture.

In addition to the drugs mentioned in the figures, the system described has been used to determine the dissolution profiles of more than 70 other tablet and capsule formulations. These include various antibiotics, steroids, vitamins, sedatives, diuretics, antituberculins, and antifilarial drugs and utilize UV, colorimetric, and fluorescence assays. Some results will be reported in forthcoming articles, along with *in vitro–in vivo* comparison studies.

CONCLUSION

A computerized automated dissolution testing system has been described which conforms to the basic requirements of the USP and NF dissolution test. The system, which can accommodate almost any type of tablet agitation technique, can test six dosage forms simultaneously under sink or nonsink conditions and can test products requiring any type of chemistry amenable to an automatic analyzer. The total run time is reduced essentially to the sample dissolution time. Finally, a complete dissolution profile report, with or without graphs, is obtained within minutes after the required sample dissolution time.

REFERENCES

(1) R. A. Nash and A. D. Marcus, *Drug Stand.*, **28**, 1(1960).

(2) D. Wurster and P. Taylor, *J. Pharm. Sci.*, **54**, 169(1965).

(3) J. G. Wagner, *Drug Intell. Clin. Pharm.*, **4**, 77(1970).

(4) L. Schroeter and W. Hamlin, *J. Pharm. Sci.*, **52**, 811 (1963).

(5) M. Pernarowski, W. Woo, and R. Searl, *ibid.*, **57**, 1419(1968).

(6) A. Richter, B. Myhre, and S. C. Khanna, *J. Pharm. Pharmacol.*, **21**, 409(1969).

[18] The computer input parameters and calculation procedure may be obtained from the authors on request.

[19] EASYPLOT, Tymshare Corp.

(7) D. C. Baun and G. C. Walker, *J. Pharm. Sci.*, **58**, 611 (1969).
(8) J. Tingstad and S. Riegelman, *ibid.*, **59**, 692(1970).
(9) F. Langenbucher, *ibid.*, **58**, 1265(1969).
(10) R. B. Barzilay and J. A. Hersey, *J. Pharm. Pharmacol., Suppl.*, **20**, 232S(1968).
(11) R. A. Castello, G. Jellinek, J. Konieczny, K. C. Kwan, and R. O. Toberman, *J. Pharm. Sci.*, **57**, 485(1968).
(12) A. Ferrari and A. Khoury, *Ann. N.Y. Acad. Sci.*, **153**, 660(1968).
(13) W. F. Beyer and E. W. Smith, *J. Pharm. Sci.*, **60**, 1556(1971).

ACKNOWLEDGMENTS AND ADDRESSES

Received March 25, 1974, from *E. R. Squibb & Sons, Inc., New Brunswick, NJ 08903*

Accepted for publication November 7, 1975.

The authors thank Len Solimene, Harvey Hendler, and William Glasofer of Tymshare, Inc., for their invaluable assistance in developing the computer software used in the data analysis, and C. H. Newman of Squibb for continued support and encouragement during the development of the total system.

[x] To whom inquiries should be directed.

Sensitive GLC Procedure for Simultaneous Determination of Phenytoin and Its Major Metabolite from Plasma following Single Doses of Phenytoin

K. K. MIDHA [x], I. J. McGILVERAY, and D. L. WILSON

Abstract □ An improved GLC procedure was developed for the simultaneous determination of phenytoin and its metabolite, 5-(*p*-hydroxyphenyl)-5-phenylhydantoin, in plasma and urine following enzyme hydrolysis. After extraction, the drug, the metabolite, and the internal standard, 5-(*p*-methylphenyl)-5-phenylhydantoin, are measured by GLC with flame-ionization detection as their respective methyl derivatives following flash-heater methylation with trimethylanilinium hydroxide. The drug and metabolite give well-resolved symmetrical peaks on a phenyl methyl silicone column, and the method has a sensitivity of 150 ng/ml of phenytoin and 125 ng/ml of the metabolite. GLC–mass spectral evidence is presented for the formation and intact determination of methyl derivatives of the drug, its metabolite, and the internal standard.

Keyphrases □ Phenytoin and major metabolite—simultaneous GLC analysis, plasma □ GLC—simultaneous analysis, phenytoin and major metabolite, plasma □ Anticonvulsant agents—phenytoin, GLC analysis, plasma

Phenytoin is a commonly prescribed anticonvulsant drug. The various procedures used for drug level measurements were reviewed (1). It is one of the few drugs for which plasma concentrations are routinely monitored, and many GLC methods (2–14) are suitable for the assay of steady-state levels. The dose-dependent biotransformation of phenytoin and variations in its metabolism in treated subjects require that assay methods for determining plasma concentrations of the unchanged drug and its principal metabolite, 5-(*p*-hydroxyphenyl)-5-phenylhydantoin (15), suitable for single-dose pharmacokinetic studies be developed.

Chang and Glazko (8) reported the preparation of trimethylsilyl derivatives applied to the GLC assay of phenytoin in plasma and 5-(*p*-hydroxyphenyl)-5-phenylhydantoin in urine. However, when this procedure is used routinely, traces of moisture cause problems and the sensitivity is limited. Derivatization with diazomethane was applied in procedures based on GLC estimation of 3-*N*-methyl derivatives (2, 4).

The safer tetramethylammonium hydroxide reagent also was used in a flash-heater methylation procedure (6), while trimethylanilinium hydroxide was described as a methylating agent for analysis of phenytoin and its metabolite (13). However, in the assay procedure for the latter, acid hydrolysis was used to degrade the conjugate and the method required two internal standards. Although the unconjugated metabolite could be measured (13), the plasma levels were not given for the metabolite and no variation or sensitivity limit was reported.

Recently, tetramethylammonium hydroxide was used for methylating phenytoin and its metabolite along with subsequent quantitative estimation by GLC with temperature programming (14). This reported procedure is cumbersome and is only applicable when plasma concentrations of phenytoin and the metabolite are around 1 μg or more. In this report, a modified method is described for the GLC analysis of plasma phenytoin and total 5-(*p*-hydroxyphenyl)-5-phenylhydantoin by formation of methyl derivatives with trimethylanilinium hydroxide. The procedure is of sufficient sensitivity to allow the quantitation of 0.15 μg/ml of phenytoin and 0.125 μg/ml of the metabolite. In addition, GLC–mass spectral evidence is presented for the formation and determination of methyl derivatives of the drug and the metabolite used in the quantitation.

EXPERIMENTAL

Reagents—Ether[1] was glass distilled prior to use. Stock solutions containing 100 μg/ml of phenytoin were prepared by dissolving appropriate amounts of the sodium salt of phenytoin[2] in distilled water. Stock solutions containing 100 μg/ml of 5-(*p*-hydroxyphenyl)-5-phenylhydantoin[3] were prepared by dissolving the appropriate amount in 0.01 *N* NaOH. Appropriate dilutions of the drug (0.15–8.0 μg/ml) and the metabolite (0.125–4.0 μg/ml) were prepared as required.

Aqueous solutions (100 μg/ml) of the internal standard, 5-(*p*-methylphenyl)-5-phenylhydantoin[3], were prepared by dissolving an appropriate amount of the internal standard in 0.01 *N* NaOH and

[1] Ether (anhydrous), Mallinckrodt Chemical Works Ltd., Montreal, Canada.
[2] Diphenylhydantoin-Na, Parke-Davis & Co., Brockville, Ontario, Canada.
[3] Aldrich Chemical Co., Milwaukee, Wis.

(7) D. C. Baun and G. C. Walker, *J. Pharm. Sci.*, **58**, 611 (1969).
(8) J. Tingstad and S. Riegelman, *ibid.*, **59**, 692(1970).
(9) F. Langenbucher, *ibid.*, **58**, 1265(1969).
(10) R. B. Barzilay and J. A. Hersey, *J. Pharm. Pharmacol., Suppl.*, **20**, 232S(1968).
(11) R. A. Castello, G. Jellinek, J. Konieczny, K. C. Kwan, and R. O. Toberman, *J. Pharm. Sci.*, **57**, 485(1968).
(12) A. Ferrari and A. Khoury, *Ann. N.Y. Acad. Sci.*, **153**, 660(1968).
(13) W. F. Beyer and E. W. Smith, *J. Pharm. Sci.*, **60**, 1556(1971).

ACKNOWLEDGMENTS AND ADDRESSES

Received March 25, 1974, from *E. R. Squibb & Sons, Inc., New Brunswick, NJ 08903*

Accepted for publication November 7, 1975.

The authors thank Len Solimene, Harvey Hendler, and William Glasofer of Tymshare, Inc., for their invaluable assistance in developing the computer software used in the data analysis, and C. H. Newman of Squibb for continued support and encouragement during the development of the total system.

[x] To whom inquiries should be directed.

Sensitive GLC Procedure for Simultaneous Determination of Phenytoin and Its Major Metabolite from Plasma following Single Doses of Phenytoin

K. K. MIDHA [x], I. J. McGILVERAY, and D. L. WILSON

Abstract □ An improved GLC procedure was developed for the simultaneous determination of phenytoin and its metabolite, 5-(*p*-hydroxyphenyl)-5-phenylhydantoin, in plasma and urine following enzyme hydrolysis. After extraction, the drug, the metabolite, and the internal standard, 5-(*p*-methylphenyl)-5-phenylhydantoin, are measured by GLC with flame-ionization detection as their respective methyl derivatives following flash-heater methylation with trimethylanilinium hydroxide. The drug and metabolite give well-resolved symmetrical peaks on a phenyl methyl silicone column, and the method has a sensitivity of 150 ng/ml of phenytoin and 125 ng/ml of the metabolite. GLC–mass spectral evidence is presented for the formation and intact determination of methyl derivatives of the drug, its metabolite, and the internal standard.

Keyphrases □ Phenytoin and major metabolite—simultaneous GLC analysis, plasma □ GLC—simultaneous analysis, phenytoin and major metabolite, plasma □ Anticonvulsant agents—phenytoin, GLC analysis, plasma

Phenytoin is a commonly prescribed anticonvulsant drug. The various procedures used for drug level measurements were reviewed (1). It is one of the few drugs for which plasma concentrations are routinely monitored, and many GLC methods (2–14) are suitable for the assay of steady-state levels. The dose-dependent biotransformation of phenytoin and variations in its metabolism in treated subjects require that assay methods for determining plasma concentrations of the unchanged drug and its principal metabolite, 5-(*p*-hydroxyphenyl)-5-phenylhydantoin (15), suitable for single-dose pharmacokinetic studies be developed.

Chang and Glazko (8) reported the preparation of trimethylsilyl derivatives applied to the GLC assay of phenytoin in plasma and 5-(*p*-hydroxyphenyl)-5-phenylhydantoin in urine. However, when this procedure is used routinely, traces of moisture cause problems and the sensitivity is limited. Derivatization with diazomethane was applied in procedures based on GLC estimation of 3-*N*-methyl derivatives (2, 4).

The safer tetramethylammonium hydroxide reagent also was used in a flash-heater methylation procedure (6), while trimethylanilinium hydroxide was described as a methylating agent for analysis of phenytoin and its metabolite (13). However, in the assay procedure for the latter, acid hydrolysis was used to degrade the conjugate and the method required two internal standards. Although the unconjugated metabolite could be measured (13), the plasma levels were not given for the metabolite and no variation or sensitivity limit was reported.

Recently, tetramethylammonium hydroxide was used for methylating phenytoin and its metabolite along with subsequent quantitative estimation by GLC with temperature programming (14). This reported procedure is cumbersome and is only applicable when plasma concentrations of phenytoin and the metabolite are around 1 μg or more. In this report, a modified method is described for the GLC analysis of plasma phenytoin and total 5-(*p*-hydroxyphenyl)-5-phenylhydantoin by formation of methyl derivatives with trimethylanilinium hydroxide. The procedure is of sufficient sensitivity to allow the quantitation of 0.15 μg/ml of phenytoin and 0.125 μg/ml of the metabolite. In addition, GLC–mass spectral evidence is presented for the formation and determination of methyl derivatives of the drug and the metabolite used in the quantitation.

EXPERIMENTAL

Reagents—Ether[1] was glass distilled prior to use. Stock solutions containing 100 μg/ml of phenytoin were prepared by dissolving appropriate amounts of the sodium salt of phenytoin[2] in distilled water. Stock solutions containing 100 μg/ml of 5-(*p*-hydroxyphenyl)-5-phenylhydantoin[3] were prepared by dissolving the appropriate amount in 0.01 *N* NaOH. Appropriate dilutions of the drug (0.15–8.0 μg/ml) and the metabolite (0.125–4.0 μg/ml) were prepared as required.

Aqueous solutions (100 μg/ml) of the internal standard, 5-(*p*-methylphenyl)-5-phenylhydantoin[3], were prepared by dissolving an appropriate amount of the internal standard in 0.01 *N* NaOH and

[1] Ether (anhydrous), Mallinckrodt Chemical Works Ltd., Montreal, Canada.
[2] Diphenylhydantoin-Na, Parke-Davis & Co., Brockville, Ontario, Canada.
[3] Aldrich Chemical Co., Milwaukee, Wis.

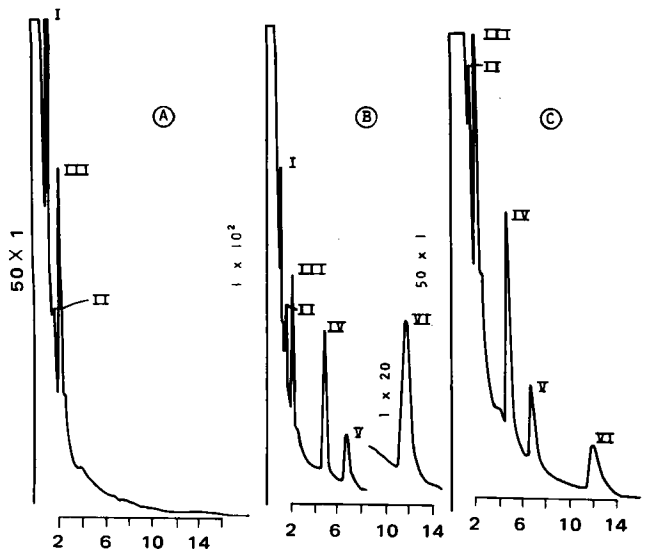

Figure 1—*Typical chromatograms of human plasma. Key: A, control plasma; B, plasma containing 2.0 μg/ml of phenytoin, 1.0 μg/ml of the metabolite, and 2.5 μg/ml of internal standard; C, plasma from a human volunteer who has been given 200 mg of phenytoin containing 2.04 μg of phenytoin and 1.03 μg of the metabolite; peak IV, methylated phenytoin; peak V, methylated internal standard; and peak VI, methylated metabolite. Peaks I–III are due to endogenous materials in plasma.*

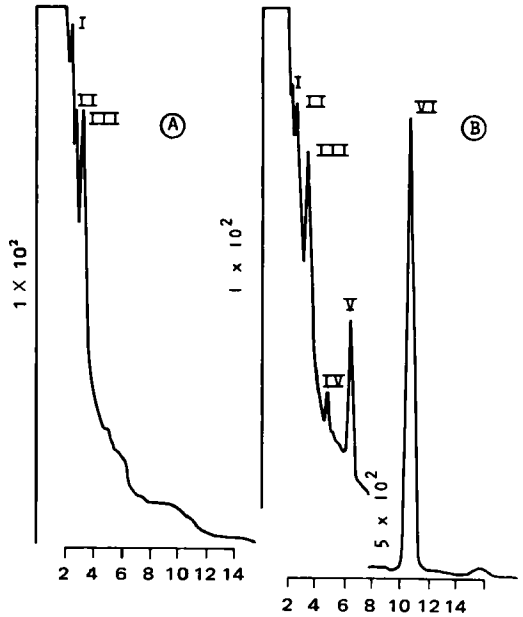

Figure 2—*Typical chromatograms of human urine. Key: A, control urine; B, urine (2 ml) from a total 48-hr collection from a human volunteer who has been given 300 mg of phenytoin containing 0.8 μg of phenytoin, 10.0 μg of internal standard, and 88.4 μg of the metabolite; peak IV, methylated phenytoin; peak V, methylated internal standard; and peak VI, methylated metabolite. Peaks I–III are due to endogenous materials in urine.*

diluting to 2.5 μg/ml with distilled water before use. Methanolic trimethylanilinium hydroxide was synthesized according to the method of Barrett (12). Plasma and blood were obtained from the Red Cross Blood Bank. All other chemicals were of the purest grade commercially available.

GLC—A gas chromatograph[4], equipped with a metal sleeve injection port and a flame-ionization detector, was employed. The column was of coiled glass tubing, 1.83 m (6 ft) long by 3.0 mm i.d., packed with a 5% phenyl methyl silicone fluid[5] (OV-7) on acid-washed, dimethylchlorosilane-treated, high performance Chromosorb W[5] support, 80–100 mesh. The column was conditioned by maintaining the oven at 340° for 18 hr with a low nitrogen flow. Operating conditions were: injection port, 310°; column oven, 215°; and detector, 280°. The flow rate of nitrogen was 60 ml/min. Hydrogen and compressed air flow rates were adjusted to give maximum response.

Procedure—To 2-ml plasma or urine samples in screw-capped[6] centrifuge tubes (15 ml) were added 0.2 ml of 1 *M* acetate buffer (pH 5.0) and 50 μl of β-glucuronidase[7]. Then the samples were incubated for 4 hr at 37°. To the hydrolyzed samples were added 1 ml of the internal standard (2.5 μg/ml) and 2 ml of 1 *N* HCl. The samples were then extracted with 5 ml of ether by shaking[8] for 10 min at 50 rpm followed by centrifugation at 2500 rpm for 10 min.

Four-milliliter portions of the ether layer were transferred into a centrifuge tube (20 ml) containing 5 ml of 0.2 *M* phosphate buffer (pH 11.2). The tubes were mixed for 10 min followed by centrifugation for 10 min, and the organic extracts were then discarded. The remaining aqueous phosphate solution was acidified with 2 ml of 2 *N* HCl and extracted twice with 5-ml portions of ether (mixed for 10 min and centrifuged for 10 min).

Four milliliters of the first extract and 5 ml of the second extract were transferred into an evaporating tube[9] (16), and the combined ether extracts were evaporated to dryness at 50° under a stream of dry nitrogen. The dried extracts were dissolved by mixing[10] with 25 μl of methanolic trimethylanilinium hydroxide (0.2 *M*), and aliquots (1–2 μl) were injected into the gas chromatograph.

Calibration Curves—Peak height ratios were calculated by dividing the height of the peak from the drug or the metabolite by the height of the peak from the internal standard. Calibration curves were assembled from the results of spiked control plasma or urine by plotting the peak height ratios against the concentrations of the drug or the metabolite.

RESULTS AND DISCUSSION

Flash-heater methylation of phenytoin, the internal standard, and the metabolite with trimethylanilinium hydroxide gave sharp peaks with retention times of 4.9, 6.9, and 11.9, respectively (peaks IV–VI, Fig. 1B), under the described conditions. The structures of the methyl derivatives of the drug, the internal standard, and the metabolite formed under these conditions were established by combined GLC–mass spectrometry[11].

The mass spectrum of methylated phenytoin (peak IV, Fig. 1B) suggested the dimethylated derivative, namely, 1,3-dimethyl-5,5-diphenylhydantoin. The mass spectrum gave a molecular ion at *m/e* 280 and other diagnostic ions at *m/e* 251, 223, 203, 194, 165, 152, 146, and 118. This observation was in agreement with literature reports (6, 14), except that flash-heater methylation was carried out by means of tetramethylammonium hydroxide in previous studies.

The GLC–mass spectrum of the internal standard (peak V, Fig. 1B) showed a molecular ion at *m/e* 294 and other major ions at *m/e* 279, 265, 251, 237, 217, 208, 203, 194, 165, 132, 118, and 91. These ions suggested that the methylated 5-(*p*-methylphenyl)-5-phenylhydantoin had the structure 1,3-dimethyl-5-(*p*-methylphenyl)-5-phenylhydantoin, *i.e.*, methylation taking place at 1-*N* and 3-*N* atoms of the hydantoin ring.

GLC–mass spectrometry of the metabolite 5-(*p*-hydroxyphenyl)-5-phenylhydantoin (peak VI, Fig. 1B) indicated that three methyl groups had been introduced in the molecule. It had a molecular ion at *m/e* 310 and other characteristic ions at *m/e* 280, 233, 224, 203, 148, and 118. These ions suggested that the methylated metabolite had the structure 1,3-dimethyl-5-(*p*-methoxyphenyl)-5-phenylhydantoin. This observation was in agreement with those of previous investigators (13, 14).

Figure 1A shows a typical chromatogram obtained by processing control blank plasma as already described but with the internal standard omitted. Extraneous peaks I, II, and III at retention times

[4] Model F-11, Perkin-Elmer, Montreal, Quebec, Canada.
[5] Chromatographic Specialties, Brockville, Ontario, Canada.
[6] Lined with Teflon (du Pont).
[7] Glusulase, Endo Laboratories, Garden City, N.Y.
[8] Roto-Rack, Fisher Scientific Co., Montreal, Quebec, Canada.
[9] Custom-made by Canadian Laboratory Supplies Ltd., Montreal, Quebec, Canada.
[10] Vortex Genie mixer, Fisher Scientific Co., Montreal, Quebec, Canada.
[11] Hitachi Perkin-Elmer model RMSU mass spectrometer coupled to a Perkin-Elmer model 990 gas chromatograph through a two-stage jet separator.

Table I—GLC Estimation of Phenytoin Added to 1 ml of Plasma

Phenytoin Added, μg	Mean Peak Height Ratio[a]	CV, %[b]
0.15	0.305	3.6
0.25	0.406	0.86
0.50	0.609	1.38
1.00	1.34	2.2
2.00	2.70	0.8
4.00	5.67	0.55
6.00	8.62	2.79
8.00	12.07	0.86

[a] $n = 9$. [b] Mean $CV = 1.63\%$ and $y = mx$, where $m = 1.4840$; $r^2 = 1.0$.

Table II—GLC Estimation of the Metabolite Added to 1 ml of Plasma

Metabolite Added, μg	n	Mean Peak Height Ratio	CV, %[a]
0.125	6	0.07	7.04
0.25	7	0.13	3.98
0.50	3	0.31	1.88
1.0	6	0.58	1.29
2.0	4	1.24	1.98
4.0	4	2.38	1.22

[a] Mean $CV = 2.90\%$ and $y = mx$, where $m = 0.599$; $r^2 = 1.0$.

Table III—Recovery of Phenytoin, the Metabolite, and the Internal Standard from Plasma Determined by GLC Assay

Micrograms Added	Mean Micrograms Recovered[a]	Mean Percent Recovery	CV, %
Phenytoin, 2	1.52	76	3.8
Metabolite, 1	0.64	64	3.5
Internal standard, 5	2.95	59	1.0

[a] $n = 3$.

1.2, 1.6, and 2.2 min, respectively, were observed in the chromatograms of all human plasma samples. A chromatogram obtained when the method was applied to spiked plasma containing 2.0 μg of phenytoin and 1.0 μg of the metabolite is shown in Fig. 1B, where it is clear that extraneous peaks I, II, and III do not interfere with the peaks due to the methylated drug (peak IV), the internal standard (peak V), and the metabolite (peak VI).

Figure 1C shows a chromatogram obtained from the plasma sample (2 ml) from blood withdrawn from a male volunteer (84 kg) at 8 hr after administration of 200 mg (two 100-mg tablets)[12] of phenytoin. An analysis time of 14 min was achieved.

Figure 2A shows a typical chromatogram obtained by processing control blank urine without the internal standard. The flow rate of the carrier gas was 65 ml/min. Extraneous peaks I, II, and III (Fig. 2A) were observed in the chromatograms of all human urine samples. A chromatogram obtained when the method was applied to a urine sample (2 ml) from total urine collected over 48 hr from a volunteer who received 300 mg (three 100-mg tablets)[11] of phenytoin is shown in Fig. 2B, where it is clear that extraneous peaks I, II, and III before 4 min do not interfere with the peaks due to methylated phenytoin (peak IV), the internal standard (peak V), and the metabolite (peak VI). By increasing the flow rate of the carrier gas, an analysis time of 12 min was achieved.

The response of the flame-ionization detector to phenytoin was linear with concentrations over the 0.15–8.00-μg/ml range. The ratio of peak height of phenytoin and the internal standard plotted against concentration in the 0.15–8.00-μg/ml range gave a straight line passing through the origin ($r^2 = 0.9989$). A mean slope value of 1.4840 was obtained for phenytoin. Similarly, the response of the flame-ionization detector to the metabolite was linear with concentrations over the 0.125–4.00-μg/ml range.

The ratio of peak height of the metabolite and the internal standard plotted against concentration in the 0.125–4.00-μg/ml range gave a straight line passing through the origin ($r^2 = 0.9995$). A mean slope value of 0.599 was obtained for the metabolite assay. The overall coefficients of variation for phenytoin and 5-(*p*-hydroxyphenyl)-5-phenylhydantoin were 1.63% (Table I) and 2.90% (Table II), respectively. The overall recoveries of the drug, the metabolite, and the internal standard from plasma were 76 ± 3.8, 64 ± 3.5, and 59 ± 1.0%, respectively (Table III).

[12] Commercial phenytoin (diphenylhydantoin) product.

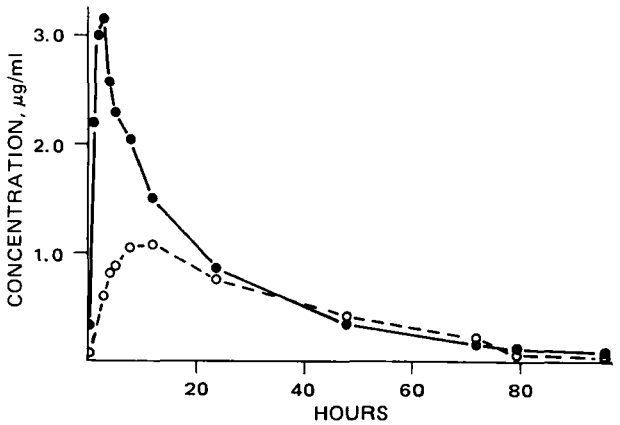

Figure 3—*Phenytoin (●) and the metabolite (○) concentrations in the plasma of a human volunteer (84 kg) following a single oral dose of 200 mg of phenytoin.*

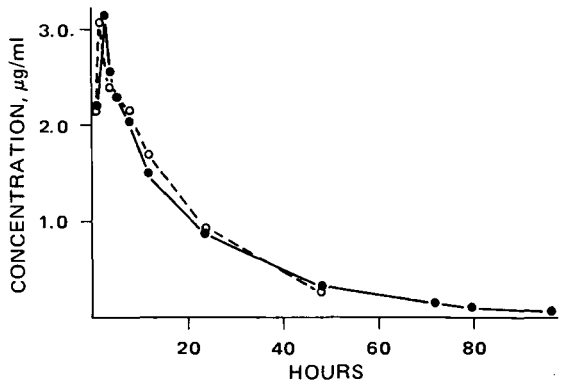

Figure 4—*Comparison of phenytoin plasma concentrations by the GLC method (●) and a UV method (○) following a single oral dose of two 100-mg tablets of phenytoin to a human volunteer (84 kg).*

The application of the present method to the plasma level determination of phenytoin and the metabolite is shown in Fig. 3. A 200-mg dose of phenytoin (two 100-mg tablets) was given to a healthy male volunteer (84 kg), blood was withdrawn at different time intervals over 96 hr, and aliquots of the plasma were assayed for phenytoin and the metabolite by GLC.

Figure 4 illustrates the comparison of the GLC assay for phenytoin with that of a UV procedure (17), as modified previously (18, 19), over 48 hr in the same volunteer (84 kg). The UV methods, which lacked sensitivity below 0.5 μg/ml, compared favorably for phenytoin. The slope of the line, two-variable linear regression, between the GLC plasma concentration (X) and the modified UV method (Y) was 0.927. This line did not include zero slope within the 95% confidence limits ($p = 0.05$, two tailed) and had a correlation coefficient of 0.987. The intercept was 0.176. When areas under the curves to 96 hr were compared, a difference of 1.80% was obtained.

In conclusion, the described GLC method is simple, sensitive, and specific for phenytoin and the metabolite 5-(*p*-hydroxyphenyl)-5-phenylhydantoin. It can be employed for single- as well as multiple-dose pharmacokinetic studies. It has the advantage that it measures the drug and its major metabolite simultaneously.

REFERENCES

(1) A. J. Glazko, in "Antiepileptic Drugs," D. M. Woodbury, J. Kiffin, Penry, and R. P. Schmidt, Eds., Raven, New York, N.Y., 1972.

(2) D. H. Sandberg, G. L. Resnick, and C. Z. Bacallao, *Anal.*

Chem., 40, 736(1968).
(3) C. E. Pippenger and H. W. Gillen, *Clin. Chem.*, **15**, 582(1969).
(4) G. Grimmer, J. Jacob, and H. Schafer, *Arzneim.-Forsch.*, **19**, 1287(1959).
(5) K. Sabih and K. Sabih, *Anal. Chem.*, **41**, 1452(1969).
(6) J. MacGee, *ibid.*, **42**, 421(1970).
(7) M. A. Evenson, P. Jones, and B. Darcey, *Clin. Chem.*, **16**, 107(1970).
(8) T. Chang and A. J. Glazko, *J. Lab. Clin. Med.*, **75**, 145(1970).
(9) H. J. Kupferberg, *Clin. Chim. Acta*, **29**, 283(1970).
(10) K. Sabih and K. Sabih, *J. Pharm. Sci.*, **60**, 1216(1971).
(11) D. Sampson, I. Harasymiv, and W. J. Hensley, *Clin. Chem.*, **17**, 382(1971).
(12) M. J. Barrett, *Clin. Chem. Newsl.*, **3**, 16(1971).
(13) R. H. Hammer, B. J. Wilder, R. R. Streiff, and A. Mayersdorf, *J. Pharm. Sci.*, **60**, 327(1971).
(14) A. Estas and P. A. Dumont, *J. Chromatogr.*, **82**, 307(1973).
(15) A. J. Glazko, T. Chang, J. Baukema, W. A. Dill, J. R. Goulet, and R. A. Buchanan, *Clin. Pharmacol. Ther.*, **10**, 498(1969).
(16) A. H. Beckett, *Dan. Tidsskr. Farm.*, **40**, 197(1966).
(17) W. A. Dill, L. Chucot, T. Chang, and A. J. Glazko, *Clin. Chem.*, **17**, 1200(1971).
(18) Y. Saitoh, K. Nishihara, F. Nakagawa, and T. Suzuki, *J. Pharm. Sci.*, **62**, 206(1973).
(19) K. S. Albert, E. Sakimar, M. Hallmark, D. Weidler, and J. G. Wagner, *Clin. Pharmacol. Ther.*, **16**, 727(1974).

ACKNOWLEDGMENTS AND ADDRESSES

Received August 25, 1975, from the *Drug Research Laboratories, Health Protection Branch, Health and Welfare Canada, Ottawa, Ontario K1A 0L2, Canada.*

Accepted for publication November 6, 1975.

Presented in part at the APhA Academy of Pharmaceutical Sciences, New Orleans meeting, November 1974.

Helpful discussions with Dr. S. Sved are gratefully acknowledged. The authors express their appreciation to Mrs. N. Beaudoin for technical assistance and to Dr. A. By and Mr. J. C. Ethier for running the mass spectra.

[x] To whom inquiries should be directed.

NOTES

Synthesis of 1,2-Dioleoyl-3-(α-^{14}C-1-adamantoyl)-*sn*-glycerol and 1-^{14}C-Adamantanecarboxylic Acid

ANTHONY J. VILLANI [x] and FRANCIS R. PFEIFFER

Abstract □ The pancreatic lipase inhibitor 1,2-dioleoyl-3-(α-^{14}C-1-adamantoyl)-*sn*-glycerol, with a specific activity of 8 mCi/mmole, was prepared by consecutive acylation of 1,2-isopropylidene-*sn*-glycerol with 1-^{14}C-adamantanecarboxylic acid chloride and oleoyl chloride. The ^{14}C-labeled acid was conveniently prepared by carboxylation of 1-adamantanol using ^{14}C-sodium formate in concentrated sulfuric acid.

Keyphrases □ 1,2-Dioleoyl-3-(α-^{14}C-1-adamantoyl)-*sn*-glycerol—pancreatic lipase inhibitor, synthesized □ 1-^{14}C-Adamantanecarboxylic acid—synthesized by carboxylation of 1-adamantanol using ^{14}C-sodium formate in sulfuric acid □ Pancreatic lipase inhibitor—1,2-dioleoyl-3-(α-^{14}C-1-adamantoyl)-*sn*-glycerol synthesized □ Inhibitors, pancreatic lipase—1,2-dioleoyl-3-(α-^{14}C-1-adamantoyl)-*sn*-glycerol synthesized

The investigation of biological applications of novel synthetic lipids has led to the study of pancreatic lipase inhibitors (1). The triglyceride 1,2-dioleoyl-3-(α-^{14}C-1-adamantoyl)-*sn*-glycerol (I) was found to be an inhibitor of pancreatic lipase when tested *in vitro* with isolated enzyme.

The mode of inhibition may involve covalent bonding of the 1-adamantoyl group of I to the enzyme. If the acylated enzyme could be isolated, then the role of the sterically hindered adamantoyl group in the mechanism of inhibition might be delineated.

The carbonyl carbon of the adamantoyl moiety of I was labeled with carbon-14 to test this theory. The synthesis of I is shown in Scheme I. *In vivo* biological data of I in rats will be reported elsewhere.

DISCUSSION

Since the literature procedure (2) for the carboxylation of 1-adamantanol was not readily adaptable to the semimicro radiosynthetic preparation, a modification was developed. In the present procedure, ^{14}C-carbon monoxide was generated *in situ* from ^{14}C-sodium formate and concentrated sulfuric acid. When this reaction was run in the presence of the adamantane cation, generated *in situ* from 1-adamantanol (II), the desired carboxylation was achieved and adamantanecarboxylic acid (III) was obtained in 82% yield. This procedure and the alternative method of Majerski *et al.* (3) provide convenient routes for the introduction of a carbon label in adamantane.

The carboxylic acid III was readily converted (4) to the acid chloride (IV) with thionyl chloride in refluxing benzene. The esterification of IV with 1,2-isopropylidene-*sn*-glycerol (5, 6) in the presence of pyridine was attended by the formation of the anhydride of adamantanecarboxylic acid (VI). The ratio of the ester V to the anhydride VI was identified (Fig. 1) as approximately 2:1 after 20 hr of refluxing in methylene chloride. The maximum yield of V could be obtained by the addition of excess isopropylideneglycerol and an increased reaction time.

Compound VI was also isolated and identified in cold runs and compared to an authentic sample of adamantanecarboxylic anhydride prepared by the procedure of Stetter and Rauscher (7).

The isopropylidene protective group was cleaved by mild acid to give the diol VII, which was used without purification. The acylation of VII with oleoyl chloride (8, 9) in the presence of pyridine gave crude I as a clear oil. After purification by magnesium silicate[1] column

[1] Florisil.

Chem., 40, 736(1968).
(3) C. E. Pippenger and H. W. Gillen, *Clin. Chem.*, **15**, 582(1969).
(4) G. Grimmer, J. Jacob, and H. Schafer, *Arzneim.-Forsch.*, **19**, 1287(1959).
(5) K. Sabih and K. Sabih, *Anal. Chem.*, **41**, 1452(1969).
(6) J. MacGee, *ibid.*, **42**, 421(1970).
(7) M. A. Evenson, P. Jones, and B. Darcey, *Clin. Chem.*, **16**, 107(1970).
(8) T. Chang and A. J. Glazko, *J. Lab. Clin. Med.*, **75**, 145(1970).
(9) H. J. Kupferberg, *Clin. Chim. Acta*, **29**, 283(1970).
(10) K. Sabih and K. Sabih, *J. Pharm. Sci.*, **60**, 1216(1971).
(11) D. Sampson, I. Harasymiv, and W. J. Hensley, *Clin. Chem.*, **17**, 382(1971).
(12) M. J. Barrett, *Clin. Chem. Newsl.*, **3**, 16(1971).
(13) R. H. Hammer, B. J. Wilder, R. R. Streiff, and A. Mayersdorf, *J. Pharm. Sci.*, **60**, 327(1971).
(14) A. Estas and P. A. Dumont, *J. Chromatogr.*, **82**, 307(1973).
(15) A. J. Glazko, T. Chang, J. Baukema, W. A. Dill, J. R. Goulet, and R. A. Buchanan, *Clin. Pharmacol. Ther.*, **10**, 498(1969).
(16) A. H. Beckett, *Dan. Tidsskr. Farm.*, **40**, 197(1966).
(17) W. A. Dill, L. Chucot, T. Chang, and A. J. Glazko, *Clin. Chem.*, **17**, 1200(1971).
(18) Y. Saitoh, K. Nishihara, F. Nakagawa, and T. Suzuki, *J. Pharm. Sci.*, **62**, 206(1973).
(19) K. S. Albert, E. Sakimar, M. Hallmark, D. Weidler, and J. G. Wagner, *Clin. Pharmacol. Ther.*, **16**, 727(1974).

ACKNOWLEDGMENTS AND ADDRESSES

Received August 25, 1975, from the *Drug Research Laboratories, Health Protection Branch, Health and Welfare Canada, Ottawa, Ontario K1A 0L2, Canada.*

Accepted for publication November 6, 1975.

Presented in part at the APhA Academy of Pharmaceutical Sciences, New Orleans meeting, November 1974.

Helpful discussions with Dr. S. Sved are gratefully acknowledged. The authors express their appreciation to Mrs. N. Beaudoin for technical assistance and to Dr. A. By and Mr. J. C. Ethier for running the mass spectra.

[x] To whom inquiries should be directed.

NOTES

Synthesis of 1,2-Dioleoyl-3-(α-^{14}C-1-adamantoyl)-*sn*-glycerol and 1-^{14}C-Adamantanecarboxylic Acid

ANTHONY J. VILLANI [x] and FRANCIS R. PFEIFFER

Abstract □ The pancreatic lipase inhibitor 1,2-dioleoyl-3-(α-^{14}C-1-adamantoyl)-*sn*-glycerol, with a specific activity of 8 mCi/mmole, was prepared by consecutive acylation of 1,2-isopropylidene-*sn*-glycerol with 1-^{14}C-adamantanecarboxylic acid chloride and oleoyl chloride. The ^{14}C-labeled acid was conveniently prepared by carboxylation of 1-adamantanol using ^{14}C-sodium formate in concentrated sulfuric acid.

Keyphrases □ 1,2-Dioleoyl-3-(α-^{14}C-1-adamantoyl)-*sn*-glycerol—pancreatic lipase inhibitor, synthesized □ 1-^{14}C-Adamantanecarboxylic acid—synthesized by carboxylation of 1-adamantanol using ^{14}C-sodium formate in sulfuric acid □ Pancreatic lipase inhibitor—1,2-dioleoyl-3-(α-^{14}C-1-adamantoyl)-*sn*-glycerol synthesized □ Inhibitors, pancreatic lipase—1,2-dioleoyl-3-(α-^{14}C-1-adamantoyl)-*sn*-glycerol synthesized

The investigation of biological applications of novel synthetic lipids has led to the study of pancreatic lipase inhibitors (1). The triglyceride 1,2-dioleoyl-3-(α-^{14}C-1-adamantoyl)-*sn*-glycerol (I) was found to be an inhibitor of pancreatic lipase when tested *in vitro* with isolated enzyme.

The mode of inhibition may involve covalent bonding of the 1-adamantoyl group of I to the enzyme. If the acylated enzyme could be isolated, then the role of the sterically hindered adamantoyl group in the mechanism of inhibition might be delineated.

The carbonyl carbon of the adamantoyl moiety of I was labeled with carbon-14 to test this theory. The synthesis of I is shown in Scheme I. *In vivo* biological data of I in rats will be reported elsewhere.

DISCUSSION

Since the literature procedure (2) for the carboxylation of 1-adamantanol was not readily adaptable to the semimicro radiosynthetic preparation, a modification was developed. In the present procedure, ^{14}C-carbon monoxide was generated *in situ* from ^{14}C-sodium formate and concentrated sulfuric acid. When this reaction was run in the presence of the adamantane cation, generated *in situ* from 1-adamantanol (II), the desired carboxylation was achieved and adamantanecarboxylic acid (III) was obtained in 82% yield. This procedure and the alternative method of Majerski *et al.* (3) provide convenient routes for the introduction of a carbon label in adamantane.

The carboxylic acid III was readily converted (4) to the acid chloride (IV) with thionyl chloride in refluxing benzene. The esterification of IV with 1,2-isopropylidene-*sn*-glycerol (5, 6) in the presence of pyridine was attended by the formation of the anhydride of adamantanecarboxylic acid (VI). The ratio of the ester V to the anhydride VI was identified (Fig. 1) as approximately 2:1 after 20 hr of refluxing in methylene chloride. The maximum yield of V could be obtained by the addition of excess isopropylideneglycerol and an increased reaction time.

Compound VI was also isolated and identified in cold runs and compared to an authentic sample of adamantanecarboxylic anhydride prepared by the procedure of Stetter and Rauscher (7).

The isopropylidene protective group was cleaved by mild acid to give the diol VII, which was used without purification. The acylation of VII with oleoyl chloride (8, 9) in the presence of pyridine gave crude I as a clear oil. After purification by magnesium silicate[1] column

[1] Florisil.

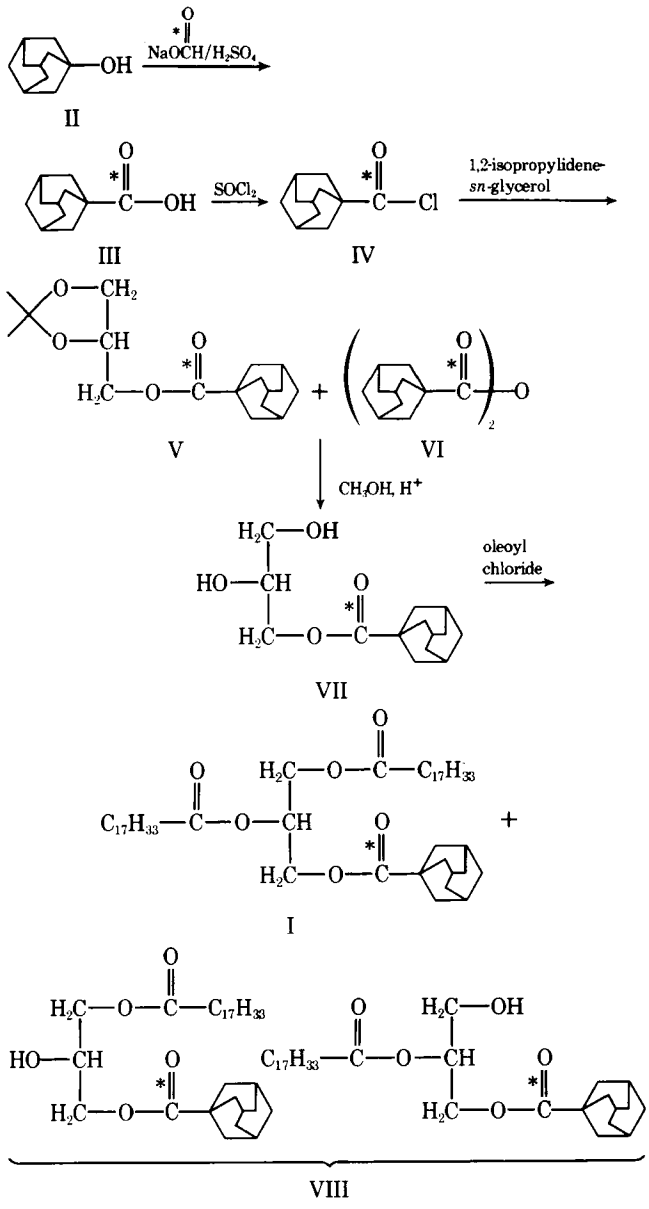

Scheme I

chromatography, I was isolated as an oil and had a radiopurity of 94.3% (Fig. 2) and a specific activity of 8 mCi/mmole. The only radioactive impurity was the diglyceride VIII, which amounted to 5.5%.

The labeled triglyceride was stored at −10° without desiccant. Reassay after 4 years showed a drop in radiopurity to 70.4%. The poor shelflife of the triglyceride was attributed to the formation of di- and monoglycerides by slow hydrolysis (10) under storage conditions and not to self-radiolytic decomposition.

EXPERIMENTAL[2]

1-^{14}C-Adamantanecarboxylic Acid (III)—To a mixture of 1-adamantanol (1.06 g, 7 mmoles) and ^{14}C-sodium formate (0.4 g, 6 mmoles, 40 mCi) in a 25-ml flask, fitted with a magnetic stirring bar and cooled in an ice–water bath, was added concentrated sulfuric acid

[2] ^{14}C-Sodium formate (6.8 mCi/mmole), purchased from New England Nuclear Corp., Boston, Mass., had a radiopurity of 99%. The specific activities were determined with a Packard Tri-Carb scintillation spectrometer (model 3003), which had a carbon-14 counting efficiency of 80%. The radiopurity of the labeled compounds was determined by thin-layer scanning, using the Berthold radioscanner/integrater (model 6000-10). Methylene chloride solvent was distilled over phosphorus pentoxide, and pyridine base was distilled over barium oxide. A thin-layer system of 3:1 (v/v) cyclohexane–ethyl acetate on silica GF was used throughout except where noted. 1,2-Isopropylidene-*sn*-glycerol was 95% pure by vapor phase chromatography.

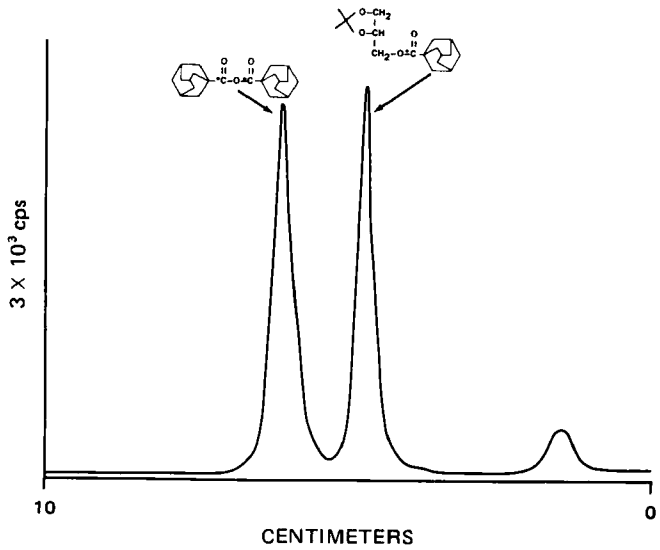

Figure 1—*Radiochromatogram of V (after 20 hr of refluxing in methylene chloride) using silica gel GF and a solvent system of cyclohexane–ethyl acetate (3:1 v/v).*

(40 ml) in one portion. The flask was quickly stoppered and allowed to reach room temperature gradually. The clear reaction mixture was then stirred at room temperature for 22 hr, warmed at 50° for 3 hr, and then poured over ice. The white solid precipitate was collected and dried under aspirator vacuum at 50°. The solid weighed 1.203 g (113% based on ^{14}C-sodium formate).

Purification was effected by dissolving the solid in freshly prepared 5% sodium bicarbonate solution, filtering, and acidifying with 3 *N* hydrochloric acid to pH 1. The solid was filtered and dried under aspirator vacuum at 50°. The product (0.866 g, 33 mCi, mp 170.5–175°) had a radiochromatographic purity of 98.8% as determined by TLC on silica gel GF, using a solvent system of ethyl acetate–acetic acid (99.5:0.5 v/v). The radiochemical yield was 82% (based on ^{14}C-sodium formate) with a specific activity of 7.2 mCi/mmole.

1-^{14}C-Adamantanecarboxylic Acid Chloride (IV)—A mixture of 1-^{14}C-adamantanecarboxylic acid (0.55 g, 3.1 mmoles, 22 mCi) and thionyl chloride (1 ml, 13.8 mmoles) was heated at reflux for 30 min. The reaction mixture was cooled and evaporated to dryness under aspirator vacuum. The residual white solid was used directly in the next step. Total chloride assays of 100% were routinely obtained in cold runs.

1,2-Isopropylidene-3-(α-^{14}C-1-adamantoyl)-*sn*-glycerol (V)—To a solution of 1,2-isopropylidene-*sn*-glycerol (0.79 g, 6 mmoles) and pyridine (0.475 g, 6 mmoles) in methylene chloride (6 ml) was

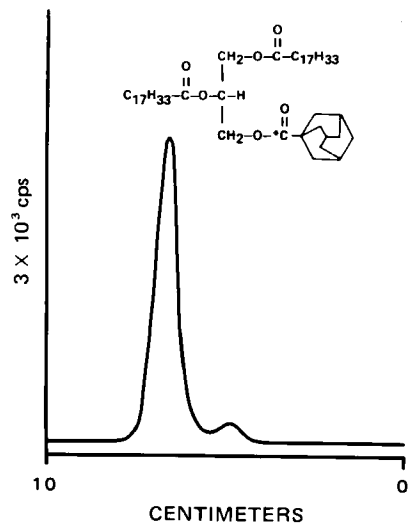

Figure 2—*Radiochromatogram of I using 0.4* N *boric acid–silica gel GF and a solvent system of chloroform–acetone–formic acid (96:4:0.4).*

added dropwise, at 0° and under nitrogen, a solution of IV in methylene chloride (5 ml). The addition took 10 min. The reaction was allowed to reach room temperature and then refluxed for 24 hr. At that time, a 30% excess of isopropylidene-*sn*-glycerol was added and the reaction was refluxed for an additional 16 hr or until TLC indicated maximum conversion.

The reaction mixture was diluted with ether and washed successively with 3 *N* hydrochloric acid, 5% sodium bicarbonate, and water. The bicarbonate extract was acidified with concentrated hydrochloric acid to give 1.92 mCi of 1-^{14}C-adamantanecarboxylic acid. The organic layer was dried over magnesium sulfate, filtered, and concentrated to dryness under aspirator vacuum. The residual oil was used directly in the next step. The radiochromatographic purity of the product was 95% as determined by TLC.

In a typical cold run, the reaction was stopped after 24 hr of refluxing in methylene chloride. After workup in the usual manner, the residual clear oil was stored in a stoppered glass vial at 4°. After a few days, a white solid crystallized out of the oil. The solid was triturated with cold acetonitrile and vacuum filtered to give 0.060 g, mp 204–205°; IR (KBr): 1810 and 1730 cm^{-1}; NMR ($CDCl_3$): 1.9 (m, 18H) and 1.7 (m, 12H) ppm; mass spectrum *m/e* 168, 135; identical to an authentic sample of adamantanecarboxylic anhydride prepared by the method of Stetter and Rauscher (7).

3-(α-^{14}C-1-Adamantoyl)-*sn*-glycerol (VII)—A solution of V in ether (2.5 ml), methanol (1 ml), and 3 *N* hydrochloric acid (0.4 ml) was stirred magnetically at room temperature for 16 hr. An additional 0.2 ml of 3 *N* hydrochloric acid was added, and the mixture was stirred for 15 hr or until TLC indicated complete conversion. The reaction mixture was diluted with ether and washed successively with water, 5% sodium bicarbonate, and saturated sodium chloride solution. The organic layer was dried over sodium sulfate, filtered, and concentrated to dryness under aspirator vacuum. The residual oil was used directly in the next step. The radiochromatographic purity of the product was 98.5% as determined by TLC.

1,2-Dioleoyl-3-(α-^{14}C-1-adamantoyl)-*sn*-glycerol (I)—To a solution of VII in methylene chloride (2 ml) was added pyridine (0.48 g, 6 mmoles) in methylene chloride (1 ml). The solution was cooled to 0–5° in an ice–water bath. To this magnetically stirred solution under nitrogen atmosphere was added dropwise oleoyl chloride (1.8 g, 6 mmoles) in methylene chloride (3 ml) over 5 min. The reaction was allowed to reach room temperature, stirred magnetically for 15 hr, diluted with ether, and washed successively with water, 3 *N* hydrochloric acid, 5% sodium bicarbonate, and saturated sodium chloride solution.

The ether solution was dried over sodium sulfate, filtered, and concentrated under aspirator vacuum to an oil. The oil was dissolved in 2 ml of petroleum ether–ether (1:1 v/v) and applied to a glass column packed with 50 g of magnesium silicate. The column was eluted with five 30-ml volumes of petroleum ether–ether (1:1 v/v). Fractions 4 and 5, which contained the desired product, were combined and evaporated to an oil under a vacuum of 5 μm. The residual oil weighed 1.35 g (13.8 mCi). The radiochemical yield was 63.8% (based on III), and the radiochromatographic purity was 94.3% as determined by TLC (Fig. 2); the specific activity was 8 mCi/mmole.

REFERENCES

(1) F. R. Pfeiffer, C. K. Miao, S. C. Hoke, and J. A. Weisbach, *J. Med. Chem.*, **15**, 58(1972).

(2) H. Koch and W. Haaf, *Angew. Chem.*, **72**, 628(1960).

(3) Z. Majerski, A. P. Wolf, and P. v. R. Schleyer, *J. Labelled Compd.*, **6**, 179(1970).

(4) H. Stetter and M. Schwarz, *Angew. Chem.*, **71**, 429(1959).

(5) E. Baer, *Biochem. Prep.*, **2**, 31(1952).

(6) J. LeCocq and C. E. Ballow, *Biochemistry*, **3**, 976(1964).

(7) H. Stetter and E. Rauscher, *Ber.*, **93**, 1161(1960).

(8) C. F. H. Allen, J. R. Byers, and W. J. Humphlett, "Organic Syntheses," coll. vol. IV, Wiley, New York, N.Y., 1963, p. 739.

(9) F. H. Mattson and R. A. Volpenhein, *J. Lipid Res.*, **3**, 281(1962).

(10) B. Serdorevich, *J. Am. Oil Chem. Soc.*, **44**, 381(1967).

ACKNOWLEDGMENTS AND ADDRESSES

Received July 21, 1975, from the *Research and Development Division, Smith Kline & French Laboratories, Philadelphia, PA 19101*

Accepted for publication October 24, 1975.

The authors are indebted to Mr. Alex Post and his coworkers of the Analytical and Physical Chemistry Section for providing analytical data and to Mr. Louis Petka and Mr. Peter Begosh for technical assistance.

ˣ To whom inquiries should be directed.

Anticonvulsant Activity of Enzyme Inhibitors in Rats

K. RAMABADRAN *, M. BANSINATH, and M. N. GURUSWAMI ˣ

Abstract □ Three liver microsomal enzyme inhibitors, proadifen, 2,4-dichloro-6-phenylphenoxyethyldiethylamine, and 2,4-dichloro-6-phenylphenoxyethylamine, and a hepatotoxic agent, carbon tetrachloride, were tested for anticonvulsant activity in adult male albino rats using the maximal electroshock seizure technique. All four substances exhibited significant anticonvulsant activity 1 hr after intraperitoneal administration. This protection was absent when tested 24 hr later.

Keyphrases □ Enzyme inhibitors, liver microsomal—proadifen and two substituted ethylamines screened for anticonvulsant activity, rats □ Hepatotoxic agents—carbon tetrachloride, screened for anticonvulsant activity, rats □ Anticonvulsant activity—evaluation of liver microsomal enzyme inhibitors proadifen and substituted ethylamines, rats

Several reports indicated that enzyme inhibitors, when combined with antiepileptic drugs, increased the therapeutic effects of antiepileptic drugs (1–3). These results suggested the need to study the effect of enzyme inhibitors *per se* for anticonvulsant activity. Preliminary results are reported now.

EXPERIMENTAL

Adult male albino rats, 100–200 g, were allowed free access to food and water prior to testing. Anticonvulsant potency was determined by the maximal electroshock seizure test (150 mamp for 0.2 sec through ear clip electrodes) (4). Abolition of the hindlimb tonic extensor phase of the maximal electroshock seizure test was taken as the end-point for measuring anticonvulsant activity (5).

Five groups of animals (20–37/group) were used, one group each for proadifen[1] (β-diethylaminoethyl diphenylpropylacetate) (I), 2,4-dichloro-6-phenylphenoxyethyldiethylamine[2] (II), 2,4-di-

[1] Also designated by the code number SKF-525A; courtesy of Smith Kline and French Laboratories, Welwyn Garden City, Herts., England.

[2] Also designated by the code number Lilly 18947; courtesy of Eli Lilly.

added dropwise, at 0° and under nitrogen, a solution of IV in methylene chloride (5 ml). The addition took 10 min. The reaction was allowed to reach room temperature and then refluxed for 24 hr. At that time, a 30% excess of isopropylidene-*sn*-glycerol was added and the reaction was refluxed for an additional 16 hr or until TLC indicated maximum conversion.

The reaction mixture was diluted with ether and washed successively with 3 *N* hydrochloric acid, 5% sodium bicarbonate, and water. The bicarbonate extract was acidified with concentrated hydrochloric acid to give 1.92 mCi of 1-^{14}C-adamantanecarboxylic acid. The organic layer was dried over magnesium sulfate, filtered, and concentrated to dryness under aspirator vacuum. The residual oil was used directly in the next step. The radiochromatographic purity of the product was 95% as determined by TLC.

In a typical cold run, the reaction was stopped after 24 hr of refluxing in methylene chloride. After workup in the usual manner, the residual clear oil was stored in a stoppered glass vial at 4°. After a few days, a white solid crystallized out of the oil. The solid was triturated with cold acetonitrile and vacuum filtered to give 0.060 g, mp 204–205°; IR (KBr): 1810 and 1730 cm^{-1}; NMR ($CDCl_3$): 1.9 (m, 18H) and 1.7 (m, 12H) ppm; mass spectrum *m/e* 168, 135; identical to an authentic sample of adamantanecarboxylic anhydride prepared by the method of Stetter and Rauscher (7).

3-(α-^{14}C-1-Adamantoyl)-*sn*-glycerol (VII)—A solution of V in ether (2.5 ml), methanol (1 ml), and 3 *N* hydrochloric acid (0.4 ml) was stirred magnetically at room temperature for 16 hr. An additional 0.2 ml of 3 *N* hydrochloric acid was added, and the mixture was stirred for 15 hr or until TLC indicated complete conversion. The reaction mixture was diluted with ether and washed successively with water, 5% sodium bicarbonate, and saturated sodium chloride solution. The organic layer was dried over sodium sulfate, filtered, and concentrated to dryness under aspirator vacuum. The residual oil was used directly in the next step. The radiochromatographic purity of the product was 98.5% as determined by TLC.

1,2-Dioleoyl-3-(α-^{14}C-1-adamantoyl)-*sn*-glycerol (I)—To a solution of VII in methylene chloride (2 ml) was added pyridine (0.48 g, 6 mmoles) in methylene chloride (1 ml). The solution was cooled to 0–5° in an ice–water bath. To this magnetically stirred solution under nitrogen atmosphere was added dropwise oleoyl chloride (1.8 g, 6 mmoles) in methylene chloride (3 ml) over 5 min. The reaction was allowed to reach room temperature, stirred magnetically for 15 hr, diluted with ether, and washed successively with water, 3 *N* hydrochloric acid, 5% sodium bicarbonate, and saturated sodium chloride solution.

The ether solution was dried over sodium sulfate, filtered, and concentrated under aspirator vacuum to an oil. The oil was dissolved in 2 ml of petroleum ether–ether (1:1 v/v) and applied to a glass column packed with 50 g of magnesium silicate. The column was eluted with five 30-ml volumes of petroleum ether–ether (1:1 v/v). Fractions 4 and 5, which contained the desired product, were combined and evaporated to an oil under a vacuum of 5 μm. The residual oil weighed 1.35 g (13.8 mCi). The radiochemical yield was 63.8% (based on III), and the radiochromatographic purity was 94.3% as determined by TLC (Fig. 2); the specific activity was 8 mCi/mmole.

REFERENCES

(1) F. R. Pfeiffer, C. K. Miao, S. C. Hoke, and J. A. Weisbach, *J. Med. Chem.*, **15**, 58(1972).

(2) H. Koch and W. Haaf, *Angew. Chem.*, **72**, 628(1960).

(3) Z. Majerski, A. P. Wolf, and P. v. R. Schleyer, *J. Labelled Compd.*, **6**, 179(1970).

(4) H. Stetter and M. Schwarz, *Angew. Chem.*, **71**, 429(1959).

(5) E. Baer, *Biochem. Prep.*, **2**, 31(1952).

(6) J. LeCocq and C. E. Ballow, *Biochemistry*, **3**, 976(1964).

(7) H. Stetter and E. Rauscher, *Ber.*, **93**, 1161(1960).

(8) C. F. H. Allen, J. R. Byers, and W. J. Humphlett, "Organic Syntheses," coll. vol. IV, Wiley, New York, N.Y., 1963, p. 739.

(9) F. H. Mattson and R. A. Volpenhein, *J. Lipid Res.*, **3**, 281(1962).

(10) B. Serdorevich, *J. Am. Oil Chem. Soc.*, **44**, 381(1967).

ACKNOWLEDGMENTS AND ADDRESSES

Received July 21, 1975, from the *Research and Development Division, Smith Kline & French Laboratories, Philadelphia, PA 19101*

Accepted for publication October 24, 1975.

The authors are indebted to Mr. Alex Post and his coworkers of the Analytical and Physical Chemistry Section for providing analytical data and to Mr. Louis Petka and Mr. Peter Begosh for technical assistance.

ˣ To whom inquiries should be directed.

Anticonvulsant Activity of Enzyme Inhibitors in Rats

K. RAMABADRAN *, M. BANSINATH, and M. N. GURUSWAMI ˣ

Abstract □ Three liver microsomal enzyme inhibitors, proadifen, 2,4-dichloro-6-phenylphenoxyethyldiethylamine, and 2,4-dichloro-6-phenylphenoxyethylamine, and a hepatotoxic agent, carbon tetrachloride, were tested for anticonvulsant activity in adult male albino rats using the maximal electroshock seizure technique. All four substances exhibited significant anticonvulsant activity 1 hr after intraperitoneal administration. This protection was absent when tested 24 hr later.

Keyphrases □ Enzyme inhibitors, liver microsomal—proadifen and two substituted ethylamines screened for anticonvulsant activity, rats □ Hepatotoxic agents—carbon tetrachloride, screened for anticonvulsant activity, rats □ Anticonvulsant activity—evaluation of liver microsomal enzyme inhibitors proadifen and substituted ethylamines, rats

Several reports indicated that enzyme inhibitors, when combined with antiepileptic drugs, increased the therapeutic effects of antiepileptic drugs (1–3). These results suggested the need to study the effect of enzyme inhibitors *per se* for anticonvulsant activity. Preliminary results are reported now.

EXPERIMENTAL

Adult male albino rats, 100–200 g, were allowed free access to food and water prior to testing. Anticonvulsant potency was determined by the maximal electroshock seizure test (150 mamp for 0.2 sec through ear clip electrodes) (4). Abolition of the hindlimb tonic extensor phase of the maximal electroshock seizure test was taken as the end-point for measuring anticonvulsant activity (5).

Five groups of animals (20–37/group) were used, one group each for proadifen[1] (β-diethylaminoethyl diphenylpropylacetate) (I), 2,4-dichloro-6-phenylphenoxyethyldiethylamine[2] (II), 2,4-di-

[1] Also designated by the code number SKF-525A; courtesy of Smith Kline and French Laboratories, Welwyn Garden City, Herts., England.

[2] Also designated by the code number Lilly 18947; courtesy of Eli Lilly.

Table I—Effects of Enzyme Inhibitors on Maximal Electroshock Seizure

Group	Drug	Dose, per 100 g	Number of Animals Protected / Number of Animals Used: After 1 hr	After 24 hr	Percentage of Animals Showing Abolition of Extensor Phase: After 1 hr	After 24 hr	Statistical Significance[a]: After 1 hr	After 24 hr
1	Sodium chloride (0.9%)	0.1 ml	2/20	0/20	10	0	N.S.[b]	—
2	Carbon tetrachloride (95%)	0.1 ml	27/37	1/37	73	3	<0.001	N.S.
3	I	5 mg	24/35	2/35	69	6	<0.001	N.S.
4	II	1 mg	20/20	6/20	100	30	<0.001	N.S.
5	III	1 mg	15/20	1/20	75	5	<0.001	N.S.

[a] Determined by the χ-square test. [b] N.S. = not significant.

chloro-6-phenylphenoxyethylamine[3] (III), and carbon tetrachloride. One group served as a control.

Rats previously shown to produce a positive hindlimb extensor phase for maximal electroshock when tested 1 hr before the actual study were injected intraperitoneally with the drug. For the control group, 0.9% sodium chloride was injected intraperitoneally. All animals were subjected to maximal electroshock 1 and 24 hr after injection, and the number of animals showing absence of the extensor phase was noted.

RESULTS

A summary of the results obtained is given in Table I. The control group did not show any apparent change.

All three enzyme inhibitors and the hepatotoxic agent showed significant anticonvulsant activity 1 hr after administration. The protection afforded was gone when tested 24 hr later.

DISCUSSION

Of the agents used, anticonvulsant activity was reported previously only for I (1). In that study, 129–141 mg/kg administered orally to mice produced anticonvulsant activity within 1–2 hr, reached a peak effect after 3 hr, and entirely disappeared within 10 hr. It also was reported that 50 mg/kg had no observable effect on the pattern of maximal electroshock seizures. In the present study, 50 mg/kg ip of I in rats produced significant anticonvulsant activity. Absence of such activity 24 hr later is in agreement with previous results (1).

A comparative time course study of the duration of anticonvulsant activity in rats for I, II, III, and carbon tetrachloride is currently underway. Compound I was reported (6) to have a membrane-stabilizing activity, which may be one possible mechanism for its anticonvulsant action.

To date, except for liver enzyme-inhibiting activity (7–9), no pharmacological data are available for II and III[4]. Hence, a detailed study of these agents, particularly for their membrane-stabilizing activity, is in progress.

Peak enzyme inhibition after the intraperitoneal injection of I, reported to be 1–2 hr (10), correlates with the time of its peak anticonvulsant effect. Since both enzyme inhibitors and the hepatotoxic agent have been shown to have anticonvulsant activity, the possible role of biochemical changes produced by these agents (including alteration in functional enzymic level) in affording protection against maximal electroshock warrants further study.

[3] Also designated by the code name DPEA; courtesy of Eli Lilly.

[4] Robert E. McMahon, Eli Lilly Research Laboratories, Indianapolis, Ind., personal communication.

REFERENCES

(1) E. A. Swinyard, J. A. Madsen, and L. S. Goodman, *J. Pharmacol. Exp. Ther.*, **111**, 54(1954).

(2) J. M. Maxwell, L. Cook, G. J. Navis, J. J. Toner, and E. J. Fellows, *Fed. Proc.*, **12**, 349(1953).

(3) J. J. Toner, L. Cook, and E. J. Fellows, *ibid.*, **12**, 373(1953).

(4) J. G. Millchap, "Physiological Pharmacology," vol. II, Academic Press, London, England, 1965, p. 106.

(5) J. E. P. Toman and G. M. Everett, "Evaluation of Drug Activities—Pharmacometrics," vol. I, Academic Press, London, England, 1964, p. 291.

(6) A. P. Viana and W. Osswald, *Arzneim.-Forsch.*, **20**, 851(1970).

(7) R. E. McMahon, J. Mills, H. W. Culp, W. R. Gibson, W. M. Miller, and F. J. Marshall, *J. Med. Chem.*, **12**, 207(1969).

(8) C. J. Parli, N. Wang, and R. E. McMahon, *J. Pharmacol. Exp. Ther.*, **180**, 791(1972).

(9) C. J. Parli, N. W. Lee, and R. E. McMahon, *ibid.*, **1**, 628 (1973).

(10) A. W. Lessin, *J. Pharmacol.*, **14**, 251(1959).

ACKNOWLEDGMENTS AND ADDRESSES

Received July 21, 1975, from the *Department of Pharmacology, Kasturba Medical College, Manipal, Karnataka, India 576 119.*

Accepted for publication October 10, 1975.

The authors are grateful to Professor E. A. Swinyard, College of Pharmacy, University of Utah, Salt Lake City, Utah, for suggestions and criticism during this study and for reviewing the manuscript.

The authors thank Smith Kline and French Laboratories, Welwyn Garden City, Herts., England, for their generous gift of proadifen and Eli Lilly Research Laboratories, Indianapolis, Ind., for 2,4-dichloro-6-phenylphenoxyethyldiethylamine and 2,4-dichloro-6-phenylphenoxyethylamine.

* Present address: Department of Pharmacology, Pasteur Institute, 25, Rue du Docteur Roux, 75015 Paris, France.

^{x} To whom inquiries should be directed.

Antiradiation Compounds XVI: *N*-Heterocyclic Aminoethyl Disulfides and Aminoethanethiosulfuric Acids

WILLIAM O. FOYE ˣ, YOUNG HEE LOWE, and JOSEPH J. LANZILLO

Abstract □ A series of *N*-heterocyclic and *N*-heterocyclic alkyl derivatives of bis(2-aminoethyl) disulfide and aminoethanethiosulfuric acid was synthesized as potential antiradiation and anticancer agents. The compounds were prepared by the reactions of the heterocyclic halides with bis(2-aminoethyl) disulfide and aminoethanethiosulfuric acid. A dithio acid derivative, 3,3-dimercapto-2-cyanoacryloylpyrrolidide, was also prepared. Several compounds, including the dithio acid derivative, provided good radiation protection to mice. None of the compounds screened showed appreciable anticancer activities in two leukemia systems.

Keyphrases □ Antiradiation compounds, potential—series of *N*-heterocyclic aminoethyl disulfides and aminoethanethiosulfuric acids synthesized and screened □ Nitrogen heterocycles—series of *N*-heterocyclic aminoethyl disulfides synthesized and screened for antiradiation activity □ Disulfides, *N*-heterocyclic aminoethyl—series synthesized and screened for antiradiation activity □ Thiosulfuric acids, aminoethane—series synthesized and screened for antiradiation activity □ Radioprotective agents, potential—series of *N*-heterocyclic aminoethyl disulfides and aminoethanethiosulfuric acids synthesized and screened

Perhaps the most important single cellular event leading to radiation protection is the repair of DNA along with prevention of its breakdown. In the case of the radioprotective aminothiols, the ability of their disulfides to bind reversibly to DNA is known (1). This ability, according to Brown (2), can result in two restorative effects:

1. The loose ends of the helix resulting from single-strand rupture are held in place so that shortening or alteration of the chain is prevented.
2. The replication rate of DNA is diminished or halted so that repair can take place before radiation-induced alterations are replicated.

With the possibility that the presence of nitrogen heterocycles in the aminoalkylthiol structure might provide stronger binding to DNA, and hence increase radiation protective ability, a series of heterocyclic aminoethyl disulfides $(HetNHCH_2CH_2S)_2$ and thiosulfates $(HetNHCH_2CH_2S_2O_3H)$ was synthesized as potential radiation protective agents.

It is also possible that such compounds, with sufficiently strong binding to DNA, may have anticancer or antimalarial activities. Some evidence of the latter activity from compounds of this general type has been found (3).

DISCUSSION

Chemistry—Mercaptoethylation of the aromatic heterocyclic amines employed, using ethylene sulfide or ethylene monothiocarbonate, as a means of obtaining the desired heterocyclic aminoethyl disulfides and thiosulfates was unsuccessful. The disulfides were obtained by heating the heterocyclic halides with cystamine [bis(2-aminoethyl)disulfide, free base] in 1-propanol with a slight excess of base until the reaction was complete (one spot on TLC) or showed evidence of disulfide cleavage by a positive nitroprusside test for thiol. This procedure was superior to the use of cystamine dihydrochloride in the presence of a base, such as potassium carbonate or triethylamine, where appreciable cleavage of the disulfide was observed. However, the latter procedure was successful in several instances. Reaction of a chloromethyl heterocycle, 2-chloromethylpyridine, gave the bis(*N,N*-disubstituted) cystamine derivative. The synthesis of 2-(2-quinolylmethylamino)ethyl disulfide could not be obtained by direct reaction with cystamine.

Synthesis of the heterocyclic aminoethanethiosulfuric acids was accomplished by reaction of the heterocyclic halides with 2-aminoethanethiosulfuric acid in the presence of alkali. Yields ranged from 30 to 57%. Reaction with 2-chloromethyl-1,4-benzodioxane gave the bis(*N,N*-disubstituted) aminoethanethiosulfuric acid. One thiosulfuric acid derivative, 2-(2-quinoxalinyl)aminoethanethiosulfuric acid, was prepared from the corresponding disulfide by the method of Lecher and Hardy (4), using potassium metabisulfite and dimethyl sulfoxide. Characteristic IR peaks for $S_2O_3^-$ absorption near 1180 and 1240 cm^{-1} were shown by all of the thiosulfuric acids.

Several dithio acid dianions were prepared (3) from the condensation of substituted acetonitriles with carbon disulfide and isolated as the dipotassium salts using a literature procedure (5). Compounds of this type have shown some radiation protective properties and could act similarly to the aminothiols or possibly as thiolating agents. These compounds are stable on storage when dry but cannot be recrystallized or even reprecipitated without decomposition. Reaction of carbon disulfide with cyanoacetylpyrrolidine gave a product for which a satisfactory carbon analysis could not be obtained, as was the case with previous compounds of this type (5). Conversion of the product to the 1,3-dithiolane and 1,3-dithiole derivatives, however, gave products with satisfactory analyses.

These dimercaptoacrylonitriles (see also Ref. 3) were converted to the corresponding 1,3-dithiole derivatives, using bromoacetophenone, according to a reported procedure (6). Attempts to oxidize the 1,3-dithioles to the corresponding dithiolium salts led to decomposition, apparently due to the presence of the cyano groups.

Biological Testing Results—Testing data[1] were reported for several dosage levels of the test compounds administered by intraperitoneal and oral routes in mice. Dosage levels giving some protection and the highest dosage levels for inactive compounds are reported here (Table I). The following compounds provided good protection against ionizing radiation, conferring better than 45% survival of treated mice over a 30-day observation period: 2-(4-methyl-1-piperazinyl)ethyl disulfide (V), 2-(*N*-morpholinyl)ethyl disulfide (VI), 2-(2-quinoxalinylamino)ethanethiosulfuric acid (IX), and 3,3-dimercapto-2-cyanoacryloylpyrrolidide (XVIII).

The disulfide of the quinoxalinylcysteamine (II) and the thiosulfate of the morpholinylcysteamine (XVI) gave either slight or no protection. This finding indicates that corresponding disulfides and thiosulfates do not necessarily protect against radiation damage in similar fashions, although thiosulfates are known to be readily converted to disulfides (7). One compound that gave good protection, XVIII, provides another example of a radiation protective compound lacking a basic nitrogen atom but containing a thiol anion in conjunction with an electron-rich heterocycle (8).

In antitumor tests[2], only small differences between mean survival times of treated and control animals or weight differences were found, none being large enough to warrant further testing (Table II).

[1] Tests of radiation protective properties of several of these and structurally related compounds, previously reported (3), were carried out at the Walter Reed Army Institute of Research.

[2] Antitumor tests, using two leukemia systems, were carried out for some of these compounds by the Division of Cancer Treatment, National Cancer Institute, in accordance with their protocol (9).

Table I—Radiation Protective Activities in Mice[a]

Number	Compound	LD_{50}[b], mg/kg	Route[c]	Drug Dose, mg/kg	Minutes[d]	Survival, %[e]
I	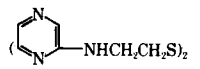	150 600+	ip po	100 600	30 30	0 0
II	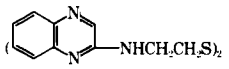	600+ 600+	ip ip po	200 600 600	30 30 30	20 10 10
III	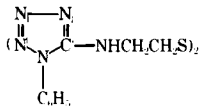	125 600+	ip po	50 600	30 30	10 0
V	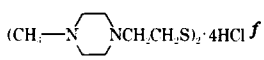 [f]	140 600+	ip po	80 600	15 30	60 0
VI	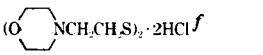 [f]	300 900+	ip ip po po	20 100 300 600	30 30 30 30	50 20 20 40
VII	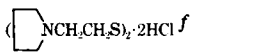 [f]	80 350	ip ip po po	20 20 100 200	15 30 30 30	0 10 10 20
VIII	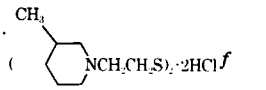 [f]	80 300+	ip ip po po po	30 60 50 100 300	30 30 30 30 30	10 10 10 20 22[g]
IX	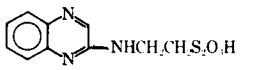	400+ 600+	ip ip po	200 400 600	30 30 30	30 70 0
X	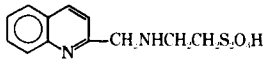 [f]	130 200	ip ip po	50 100 100	30 30 30	20 0 0
XI	[f]	80 75	ip po	50 100	30 30	0 0
XII	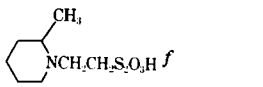 [f]	80 300	ip ip po	50 50 200	15 30 30	0 0 10
XIII	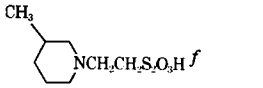 [f]	230 600	ip ip po po	50 100 150 300	30 30 30 30	20 10 20 10
XIV	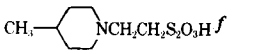 [f]	150 550	ip po	65 200	15 30	20 20
XV	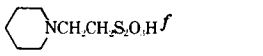 [f]	115 300+	ip po	60 180	15 30	20 0
XVI	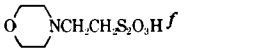 [f]	500 400+	ip po	100 400	15 30	0 0
XVII	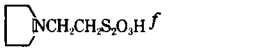 [f]	100 300	ip po	70 300	15 30	0 0
XVIII	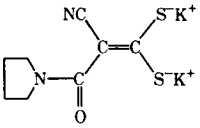	600+ 600+	ip ip po	300 600 600	30 30 30	10 80 30
XIX	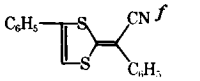 [f]	280	ip ip	25 50	30 30	10 0

[a] Radiation dosage was 849 rads (a lethal dose to mice) from a cesium-137 γ-irradiator given at a rate of 141.5 rads/min. For each drug screened, 10 mice were used at each dosage level; 10 mice were used for the vehicle controls. [b] Mortality was determined 10 days after a single dose. [c] Compounds were administered by the indicated route in either water, physiological saline, or 0.3% methylcellulose–0.1% polysorbate (Tween 80) vehicle. Solutions ranged from 0.2 to 3.0%, and the pH was generally 3.5–5.5. [d] The number of minutes preirradiation at which the drug was administered. [e] Calculated from the number of surviving mice at 30 days postirradiation. Good protection was considered with >45% survival, fair protection with 25–44% survival, and slight protection at 1–24% survival. [f] Reference 3. [g] Nine mice were used.

Table II—Antitumor Activities in Mice

Number	Compound[a]	Tumor[b]	Dose, mg/kg	Animal Weight Difference (T − C), g[c]	Survival (T/C), %[d]
II	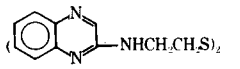	LE PS	400 200	−2.9 −1.4	87 86
IV		LE	200	−0.8	97
V	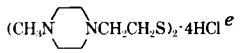 [e]	LE PS	100 200	−0.9 −1.3	105 109
VI	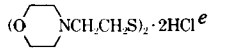 [e]	LE PS	200 100	−3.1 −0.3	104 113
VIII	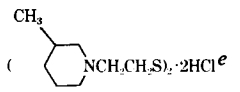 [e]	LE PS	12.5 25	−2.1 −0.7	104 113
XI	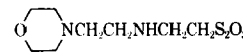 [e]	LE PS	25 12.5	−0.2 −0.2	107 110
XV	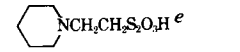 [e]	LE PS	50 12.5	−2.0 −0.8	104 110
XVI	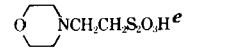 [e]	LE PS	200 200	−0.9 −0.9	106 115
XVII	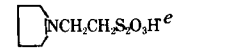 [e]	LE PS	12.5 50	−0.4 −0.4	107 110
XVIII	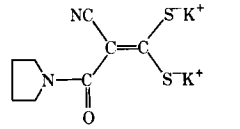	LE PS	400 200	−0.1 −0.2	103 100
XX	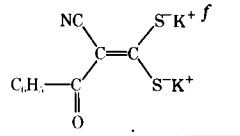 [f]	LE PS	100 50	−0.5 −1.1	102 109

[a] Compounds were administered intraperitoneally every 4th day for the LE tumor system, for a total of three injections, and every day for the PS tumor system, for a total of nine injections, beginning on the 1st day after tumor implantation. The vehicle used was either saline or saline with polysorbate (Tween 80). Six mice were used at each dosage level. [b] LE refers to L-1210 lymphoid leukemia; PS refers to P-388 lymphocytic leukemia. [c] Average weight change of test group minus average weight change of control animals as determined on Day 5. [d] Ratio of mean survival time of treated animals to that of control animals. Observations were made for 20 days. [e] Reference 3. [f] Reference 5.

EXPERIMENTAL[3]

2-Aminoethyl Disulfide—2-Aminoethyl disulfide dihydrochloride was prepared by the procedure of Johnston and Gallagher (10). The free base was obtained by neutralization with 10% aqueous sodium hydroxide followed by evaporation to dryness *in vacuo* at 50°. The residue was extracted several times with chloroform, and the combined extracts were evaporated to dryness under reduced pressure, giving 92–95% of straw-colored oil; NMR (CF_3CO_2H): 2.45 (t, CH_2S) and 3.50 (t, CH_2N).

2-(2-Pyrazinylamino)ethyl Disulfide (I)—2-Chloropyrazine (17.2 g, 0.15 mole) in 1-propanol (25 ml) was added to a stirred mixture of 2-aminoethyl disulfide (14.1 g, 0.092 mole), anhydrous potassium carbonate (24.5 g, 0.17 mole), and 1-propanol (70 ml). The mixture was refluxed overnight and evaporated to dryness under reduced pressure. The residue was suspended in water (100 ml) and brought to pH 7 with 1 *N* hydrochloric acid. The oil that separated was extracted with benzene (4 × 50 ml), and the benzene extract was washed with water, treated with activated carbon[4], and dried over sodium sulfate.

The solution was evaporated to dryness under reduced pressure, the residue was triturated with small amounts of ethanol and water, and the triturate was chilled. A yellow crystalline product was obtained, and a second crop resulted on adding water to the concentrated filtrate, giving 9.65 g (31%), mp 154–155°; R_f [ethyl acetate–chloroform–ethanol (5:4:1)] 0.37; IR (KBr): 3290 (NH), 1585, 1340 (pyrazine ring), and 1220 (CH_2S) cm^{-1}; NMR (CH_3SOCH_2D): δ 2.55 (t, CH_2S) and 3.58 (t, CH_2N).

Anal.—Calc. for $C_{12}H_{16}N_6S_2$: C, 46.73; H, 5.23; N, 27.25; S, 20.79. Found: C, 47.00; H, 5.09; N, 26.93; S, 20.51.

2-(2-Quinoxalinylamino)ethyl Disulfide (II)—2-Chloroquinoxaline (24.7 g, 0.15 mole) in 1-propanol (20 ml) was added to a stirred mixture of 2-aminoethyl disulfide (14.5 g, 0.095 mole) and anhydrous potassium carbonate (24.5 g, 0.17 mole) in 1-propanol (80 ml). The reaction was carried out as in the preceding preparation, and 30.7 g (50%) of yellow crystals were obtained, mp 156–158°; R_f [chloroform–ethyl acetate (2:3)] 0.2; IR (KBr): 3300 (NH), 1590, 1240 (CH_2S), and 750–760 (quinoxaline ring) cm^{-1}.

Anal.—Calc. for $C_{20}H_{20}N_6S_2$: C, 58.80; H, 4.93; N, 20.57; S, 15.70. Found: C, 58.69; H, 4.80; N, 20.33; S, 16.20.

2-[5-(1-Phenyl-1*H*-tetrazolyl)amino]ethyl Disulfide (III)—To a stirred mixture of 2-aminoethyl disulfide (9.18 g, 0.06 mole) and anhydrous potassium carbonate (13.82 g, 0.1 mole) in 1-propanol (100 ml) was added 5-chloro-1-phenyl-1*H*-tetrazole (16.26 g, 0.09 mole) in 1-propanol (60 ml), and the resulting mixture was refluxed overnight. The cooled reaction mixture was diluted with water, and a crude product separated. The filtered product was dissolved in dimethyl sulfoxide and treated with activated carbon. Addition of water precipitated a white solid, mp 236–237°; IR (KBr): 3300 (NH), 1585, 1235 (CH_2S), and 1090 (tetrazole ring) cm^{-1}.

[3] Melting points were determined with a Mel-Temp capillary melting-point block and are uncorrected. IR spectra were measured using a Perkin-Elmer model 137B or 237B spectrophotometer. NMR spectra were obtained with a Varian A-60 spectrometer, using tetramethylsilane as the external or internal standard. TLC was carried out using silica gel, and products were detected by exposure to iodine vapor. Elemental analyses were done by F. B. Strauss, Oxford, England, or by Carol K. Fitz, Carlisle, Mass. Heterocyclic amines and other reagents were purchased from Aldrich Chemical Co., Eastman Organic Chemicals, and Fisher Scientific Co.

[4] Norite.

Anal.—Calc. for $C_{18}H_{20}N_{10}S_2$: C, 49.07; H, 4.58; N, 31.79; S, 14.56. Found: C, 48.8; H, 4.6; N, 31.5; S, 14.9.

2-(2-Pyrimidinylamino)ethyl Disulfide (IV)—To a stirred mixture of 2-aminoethyl disulfide (14.65 g, 0.096 mole), anhydrous potassium carbonate (24.5 g, 0.170 mole), and 1-propanol (75 ml) was added 2-bromopyrimidine (23.85 g, 0.15 mole), and the resulting suspension was refluxed for 6 hr. The reaction mixture was cooled and diluted with water (750 ml) to give a crude product which was vacuum dried over phosphorus pentoxide. Recrystallization from ethanol and activated carbon gave yellow crystals (71% yield), mp 166–167°; R_f [ethyl acetate–chloroform–methanol (5:4:1)] 0.45; IR (KBr): 3270 (NH), 1595, 1220 (CH_2S), 1010, and 800 (pyrimidine ring) cm^{-1}.

Anal.—Calc. for $C_{12}H_{16}N_6S_2$: C, 46.73; H, 5.23; N, 27.25; S, 20.79. Found: C, 46.48; H, 5.03; N, 26.98; S, 20.50.

2-[Bis(2-pyridylmethyl)amino]ethyl Disulfide—To a stirred mixture of 2-aminoethyl disulfide (1.5 g, 0.010 mole), anhydrous potassium carbonate (3.25 g, 0.020 mole), and 1-propanol (40 ml) was added 2-chloromethylpyridine (2.59 g, 0.020 mole), and the mixture was refluxed for 5 hr. The reaction mixture was cooled to 0° and filtered, and the filtrate was evaporated to 15 ml and diluted with water. A solid product resulted after standing at room temperature for 3 days. It was recrystallized from ethanol and water and dried *in vacuo* over phosphorus pentoxide, giving 0.94 g (9%) of tan solid, mp 76–77°; R_f [ethyl acetate–chloroform (3:2)] 0.1; IR (KBr): 1585, 1370, 1250 (CH_2S), and 780 (pyridine ring) cm^{-1}.

Anal.—Calc. for $C_{16}H_{22}N_4S_2$: C, 65.08; H, 6.25; N, 16.26. Found: C, 65.0; H, 6.6; N, 16.4.

2-Aminoethanethiosulfuric Acid—A mixture of 2-bromoethylamine hydrobromide (20.49 g, 0.1 mole) and thallous thiosulfate (11) (52.08 g, 0.1 mole) in water (100 ml) was stirred vigorously for 24 hr. The precipitated thallous bromide was filtered and washed with water, and the filtrate was evaporated under reduced pressure at 50°. The resulting syrup was dissolved in a small amount of water and crystallized by addition of methanol to give 12.5 g (80%) of white crystals, mp 196–198° [lit. (4) mp 195–196°]; R_f [1-butanol–ethanol–water (3:1:1)] 0.5; NMR (CH_3SOCH_2D): δ 3.33 (m, NCH_2CH_2S).

2-[Bis(2-benzimidazolylmethyl)amino]ethanethiosulfuric Acid—To a warm solution of sodium hydroxide (4 g, 0.1 mole) in 95% ethanol (50 ml) was added rapidly, with stirring, a hot solution of 2-aminoethanethiosulfuric acid (15.7 g, 0.1 mole) in water (10 ml). To the refluxing mixture was added dropwise 2-chloromethylbenzimidazole (13.7 g, 0.08 mole) in 60 ml of ethanol during 2 hr. Heating and stirring were continued for 48 hr, and the reaction mixture was evaporated. The residue was washed with ether and then acidified to pH 5 with acetic acid. The resulting organic layer was separated from the aqueous phase, and addition of a small amount of ethanol followed by water precipitated a solid.

The product was collected after standing at room temperature for a day, yielding 6.4 g (46%) of crude material. This material was dissolved in ethanol and treated with activated carbon. Addition of water and chilling overnight gave white crystals which were dried over phosphorus pentoxide, mp 128–129°; R_f [1-butanol–ethanol–water (3:1:1)] 0.6; IR (KBr): 3400 (NH), 1620, 1235, 1175 (S_2O_3), 1020, and 750 (benzimidazole ring) cm^{-1}.

Anal.—Calc. for $C_{18}H_{19}N_5O_3S_2$: C, 51.78; H, 4.59; N, 16.77. Found: C, 51.6; H, 5.0; N, 16.3.

2-[2-(1,4-Benzodioxanyl)methylamino]ethanethiosulfuric Acid—To a warm solution of sodium hydroxide (1 g, 0.025 mole) in 95% ethanol (30 ml) was added rapidly, with stirring, a hot solution of 2-aminoethanethiosulfuric acid (3.8 g, 0.025 mole) in water (3 ml). To the refluxing mixture was added dropwise 2-chloromethyl-1,4-benzodioxane (2.8 g, 0.015 mole) in ethanol (15 ml), and heating and stirring were continued for 24 hr. After removal of the solvent, 30 ml of water was added; this solution was neutralized with acetic acid and extracted with ether to remove unreacted starting material.

The resulting mixture was stored at 0° for 2 days, and a solid was collected. A second crop was obtained from the mother liquor by evaporation, addition of methanol to the residue, removal of unreacted 2-aminoethanethiosulfuric acid, concentration of the solution, and addition of water. A combined yield of 1.35 g (30%) was obtained which was recrystallized from aqueous ethanol, mp 227–229°; R_f [1-butanol–ethanol–water (3:1:1)] 0.6; IR (KBr): 3450 (NH), 1575, 1180–1240 (S_2O_3), 1025, and 755 (benzodioxane ring) cm^{-1}.

Anal.—Calc. for $C_{11}H_{15}NO_5S_2$: C, 43.26; H, 4.95; N, 4.58. Found: C, 43.2; H, 4.9; N, 4.5.

2-(2-Quinoxalinylamino)ethanethiosulfuric Acid (IX)—A solution of potassium metabisulfite (4 g, 0.036 mole) in hot water (3 ml) was added to a solution of 2-(2-quinoxalinylamino)ethyl disulfide (3.68 g, 0.009 mole) in methanol (75 ml) and dimethyl sulfoxide (15 ml). The mixture was refluxed overnight under nitrogen, and potassium hydroxide (0.51 g, 0.009 mole) in methanol (5 ml) was added to convert excess metabisulfite to sulfite. The mixture was filtered while hot, and the residue was washed with hot methanol. The filtrate was evaporated under reduced pressure and neutralized with sulfuric acid.

After removal of potassium sulfate, the methanol solution was concentrated *in vacuo*, and addition of water gave a solid product. Recrystallization from methanol–water produced yellow crystals, 0.85 g (35%), mp 192–194°; R_f [ethyl acetate–chloroform–ethanol (5:4:1)] 0.75; IR (KBr): 3500 (NH), 1600, 1160–1210 (S_2O_3), 1025, and 765 (quinoxaline ring) cm^{-1}.

Anal.—Calc. for $C_{10}H_{11}N_3O_3S_2$: C, 42.09; H, 3.89; N, 14.73. Found: C, 42.0; H, 4.2; N, 14.4.

3,3-Dimercapto-2-cyanoacryloylpyrrolidide (XVIII)—Metallic potassium (3.9 g, 0.1 mole) was dissolved in 2-methyl-2-propanol (85 ml) under dry nitrogen, with stirring, at 100° during 4 hr. 1-Cyanoacetylpyrrolidine (6.9 g, 0.05 mole) in absolute ethanol (30 ml) was added in one portion at 25°, and carbon disulfide (3.8 g, 0.05 mole) in anhydrous ether (30 ml) was added dropwise at 5–7° during 30 min. Stirring was continued for 15 hr at room temperature, and the yellow precipitate was filtered, washed with anhydrous ether, and dried over phosphorus pentoxide to give 14.7 g (90%), mp ~140°.

Anal.—Calc. for $C_8H_8K_2N_2OS_2 \cdot \frac{1}{2}C_4H_9OH$: N, 8.52; S, 19.58. Found: N, 8.5; S, 19.98.

2 - (2 - Cyanoacetopyrrolidide - 2 - ylidene)-4-phenyl-4-hydroxy-1,3-dithiolane—To a solution of XVIII (3.25 g, 0.010 mole) in ethanol (100 ml) and dimethylformamide (10 ml), a solution of sodium bicarbonate (1.6 g) and bromoacetophenone (1.99 g, 0.010 mole) in ethanol (20 ml) was added. After the mixture was stirred for 24 hr at room temperature, a precipitate was removed. The filtrate was evaporated to dryness under reduced pressure, and the gummy residue was triturated with ether to remove unreacted bromoacetophenone. The residue was dissolved in a small amount of ethanol, and addition of water precipitated a bright-yellow solid (1.3 g). An additional 0.2 g was obtained from the mother liquor, giving a yield of 45%. Recrystallization was accomplished from 1-propanol and 2-propanol after treatment with activated carbon, and the product was dried *in vacuo* over phosphorus pentoxide, mp 217–219°; IR (KBr): 3400–3500 (OH), 2200 (C≡N), and 1590 (C=O) cm^{-1}.

Anal.—Calc. for $C_{16}H_{16}N_2O_2S_2$: C, 57.81; H, 4.85; N, 8.46; S, 19.25. Found: C, 57.6; H, 5.0; N, 8.70; S, 19.41.

2-(2-Cyanoacetopyrrolidide-2-ylidene)-4-phenyl-1,3-dithiole—A solution of 2-(2-cyanoacetopyrrolidide-2-ylidene)-4-phenyl-4-hydroxy-1,3-dithiolane (1 g) in concentrated sulfuric acid (15 ml) was poured into chilled ethanol (50 ml) at a rate that did not allow the temperature to exceed 20°. After the solution stood at room temperature for a few hours, water was added and a yellow solid precipitated. The crude product was filtered, washed with water, and dried *in vacuo* over phosphorus pentoxide. It was dissolved in 1-propanol, treated with activated carbon, and concentrated to give yellow plates (0.54 g, 55%), mp 217–218°; R_f [ethyl acetate–chloroform–ethanol (6:3:1)] 0.7; NMR (CH_3SOCH_2D): δ 7.5 (m, 5H, aromatic H).

Anal.—Calc. for $C_{16}H_{14}N_2OS_2$: C, 61.12; H, 4.49; N, 8.91. Found: C, 60.7; H, 4.9; N, 8.6.

REFERENCES

(1) E. Jellum, *Int. J. Radiat. Biol.*, **9**, 185(1965).

(2) P. E. Brown, *Nature*, **213**, 363(1967).

(3) W. O. Foye, J. J. Lanzillo, Y. H. Lowe, and J. M. Kauffman, *J. Pharm. Sci.*, **64**, 211(1975).

(4) H. Z. Lecher and E. M. Hardy, *J. Org. Chem.*, **20**, 475(1955).

(5) W. O. Foye and J. M. Kauffman, *J. Pharm. Sci.*, **57**, 1611(1968).

(6) E. Campaigne and F. Haaf, *J. Org. Chem.*, **30**, 732(1965).

(7) B. Milligan and J. M. Swan, *J. Chem. Soc.*, **1962**, 2172.

(8) W. O. Foye, J. M. Kauffman, J. J. Lanzillo, and E. F. LaSala, *J. Pharm. Sci.*, **64**, 1371(1975).

(9) R. I. Geran, N. H. Greenberg, M. M. MacDonald, A. M. Schumacher, and B. J. Abbott, *Cancer Chemother. Rep., Part 3*, **3**, 1(1972).

(10) T. P. Johnston and A. Gallagher, *J. Org. Chem.*, **27**, 2452(1962).

(11) D. H. Ball, J. M. Williams, and L. Long, Jr., *ibid.*, **28**, 1589(1963).

ACKNOWLEDGMENTS AND ADDRESSES

Received September 5, 1975, from the *Samuel M. Best Research Laboratory, Massachusetts College of Pharmacy, Boston, MA 02115*

Accepted for publication October 23, 1975.

Abstracted from a thesis submitted by Y. H. Lowe to the Massachusetts College of Pharmacy in partial fulfillment of the Doctor of Philosophy degree requirements.

The authors express their appreciation to the Gillette Co. for financial assistance.

[x] To whom inquiries should be directed.

Gravimetric Determination of Chlorhexidine Using Tetraphenylborate Ion

SERGIO PINZAUTI [x], VITTORIO DAL PIAZ, and ENZO LA PORTA

Abstract □ A precise and accurate gravimetric procedure was developed for the determination of chlorhexidine diacetate, digluconate, or dihydrochloride. Sodium tetraphenylborate solution was the precipitant in an acidic medium (pH 1). Tablets containing both chlorhexidine diacetate and benzocaine also were assayed.

Keyphrases □ Chlorhexidine—gravimetric analysis, tetraphenylborate as precipitant, pharmaceutical formulations □ Gravimetry—analysis, chlorhexidine in pharmaceutical formulations, tetraphenylborate as precipitant □ Tetraphenylborate—use as precipitant in gravimetric analysis of chlorhexidine □ Bactericidals, topical—chlorhexidine, gravimetric analysis, pharmaceutical formulations

Chlorhexidine is a potent topical bactericidal, effective in high dilutions (1). Presently, it is the most efficient drug for the inhibition of dental bacterial plaque (2–4). Chlorhexidine is employed as the digluconate (5), dihydrochloride (6), and diacetate (7), alone and in combinations with neomycin, cetrimide, or benzocaine in liquid and solid pharmaceutical dosage forms.

A literature review showed that few analytical methods (colorimetry and high-pressure liquid chromatography) were used to determine chlorhexidine quantitatively (8–10). The British Pharmacopoeia offers a nonaqueous method, with glacial acetic acid as the solvent system for the analysis of chlorhexidine digluconate aqueous solution (20% w/v) and chlorhexidine dihydrochloride (5, 6). The procedure for the digluconate involves preliminary evaporation to low bulk of a weighed aliquot of the solution; no monograph is provided for pharmaceutical dosage forms.

This report describes the gravimetric analysis of chlorhexidine salts (gluconate, hydrochloride, and acetate) in aqueous acid solution. Sodium tetraphenylborate, a compound that has found extensive application as a reagent for potassium as well as for the identification and determination of organic bases (11), is used as a precipitant. The method also was applied to tablets containing chlorhexidine diacetate and benzocaine in combination.

EXPERIMENTAL

Reagents—The chlorhexidine salt samples were the highest grades of commercially available materials and were used without further purification. Tablets were prepared in house, and their composition was similar to a product[1] marketed in Italy.

For the sodium tetraphenylborate[2] solution (0.6% w/v), an appropriate amount (purity of 99.5%) was dissolved in water and stabilized according to Cooper (12) at pH 8–9.

Procedures—*Chlorhexidine Diacetate or Digluconate*—Weigh accurately about 30–60 mg of chlorhexidine diacetate, or pipet 2 ml of 2% (w/v) chlorhexidine digluconate solution. Transfer into a 150-ml beaker and dissolve with 20 ml of 0.2 *N* HCl. Slowly add, with stirring, 20 ml of 0.6% sodium tetraphenylborate solution and then allow the mixture to stand for 10–15 min.

Filter the precipitate under suction through a previously dried and tared sintered-glass crucible (porosity 4); then wash the residue with three 5-ml portions of water. Dry the crucible and contents to constant weight (4 hr) at 40–45° at a pressure not exceeding 0.2 mm Hg. Each milligram of the dried chlorhexidine tetraphenylborate is equivalent to 0.5459 mg of chlorhexidine diacetate or 0.7834 mg of chlorhexidine digluconate.

Anal.—Calc. for $C_{70}H_{72}B_2Cl_2N_{10}$: C, 73.37; H, 6.33; N, 12.22. Found: C, 73.69; H, 6.46; N, 11.95.

Chlorhexidine Dihydrochloride—Weigh accurately about 20–60 mg of chlorhexidine dihydrochloride and transfer it into a 150-ml beaker. Dissolve with 20 ml of water by warming gently at 80–85° and cool; then add 0.3 ml of 37% (w/w) HCl. Complete the assay as described for chlorhexidine diacetate or digluconate, beginning with: "Slowly add, ..." Each milligram of the dried chlorhexidine tetraphenylborate is equivalent to 0.5047 mg of chlorhexidine dihydrochloride.

Tablets—The declared amounts, in milligrams per tablet, were: chlorhexidine diacetate, 5; benzocaine, 2; magnesium stearate, 15; mannitol, 300; lactose, 100; and sucrose, 578.

Weigh and powder 25 tablets. Weigh accurately, into a previously tared sintered-glass crucible (porosity 4), a quantity of the powder calculated to contain approximately 100 mg of chlorhexidine diacetate. Then add, under suction, three 20-ml portions of ether and discard the filtrate. Dry the crucible and contents at 50° for 10 min and then dissolve, under suction, chlorhexidine diacetate with 70 ml of 0.2 *N* HCl.

Transfer the combined filtrate and washings of the büchner flask (20 ml of water) into a 100-ml volumetric flask and dilute to volume with water. Pipet an accurately measured aliquot (50 ml) of the solution into a 150-ml beaker. Complete the assay as described for chlorhexidine diacetate or digluconate, beginning with: "Slowly add, ..." Each milligram of the dried chlorhexidine tetraphenylborate is equivalent to 0.5459 mg of chlorhexidine diacetate.

Estimation of Maximum Value for K_{sp}—The apparent solubility product value of chlorhexidine tetraphenylborate was determined in an aqueous hydrochloric acid solution (pH 1) by measurement of the molar detection limit for chlorhexidinium ion in the presence of

[1] Visan, Angiolini S.p.A., Milan, Italy.
[2] E. Merck, Darmstadt, Germany.

(11) D. H. Ball, J. M. Williams, and L. Long, Jr., *ibid.*, **28**, 1589(1963).

ACKNOWLEDGMENTS AND ADDRESSES

Received September 5, 1975, from the *Samuel M. Best Research Laboratory, Massachusetts College of Pharmacy, Boston, MA 02115*

Accepted for publication October 23, 1975.

Abstracted from a thesis submitted by Y. H. Lowe to the Massachusetts College of Pharmacy in partial fulfillment of the Doctor of Philosophy degree requirements.

The authors express their appreciation to the Gillette Co. for financial assistance.

[x] To whom inquiries should be directed.

Gravimetric Determination of Chlorhexidine Using Tetraphenylborate Ion

SERGIO PINZAUTI [x], VITTORIO DAL PIAZ, and ENZO LA PORTA

Abstract □ A precise and accurate gravimetric procedure was developed for the determination of chlorhexidine diacetate, digluconate, or dihydrochloride. Sodium tetraphenylborate solution was the precipitant in an acidic medium (pH 1). Tablets containing both chlorhexidine diacetate and benzocaine also were assayed.

Keyphrases □ Chlorhexidine—gravimetric analysis, tetraphenylborate as precipitant, pharmaceutical formulations □ Gravimetry—analysis, chlorhexidine in pharmaceutical formulations, tetraphenylborate as precipitant □ Tetraphenylborate—use as precipitant in gravimetric analysis of chlorhexidine □ Bactericidals, topical—chlorhexidine, gravimetric analysis, pharmaceutical formulations

Chlorhexidine is a potent topical bactericidal, effective in high dilutions (1). Presently, it is the most efficient drug for the inhibition of dental bacterial plaque (2–4). Chlorhexidine is employed as the digluconate (5), dihydrochloride (6), and diacetate (7), alone and in combinations with neomycin, cetrimide, or benzocaine in liquid and solid pharmaceutical dosage forms.

A literature review showed that few analytical methods (colorimetry and high-pressure liquid chromatography) were used to determine chlorhexidine quantitatively (8–10). The British Pharmacopoeia offers a nonaqueous method, with glacial acetic acid as the solvent system for the analysis of chlorhexidine digluconate aqueous solution (20% w/v) and chlorhexidine dihydrochloride (5, 6). The procedure for the digluconate involves preliminary evaporation to low bulk of a weighed aliquot of the solution; no monograph is provided for pharmaceutical dosage forms.

This report describes the gravimetric analysis of chlorhexidine salts (gluconate, hydrochloride, and acetate) in aqueous acid solution. Sodium tetraphenylborate, a compound that has found extensive application as a reagent for potassium as well as for the identification and determination of organic bases (11), is used as a precipitant. The method also was applied to tablets containing chlorhexidine diacetate and benzocaine in combination.

EXPERIMENTAL

Reagents—The chlorhexidine salt samples were the highest grades of commercially available materials and were used without further purification. Tablets were prepared in house, and their composition was similar to a product[1] marketed in Italy.

For the sodium tetraphenylborate[2] solution (0.6% w/v), an appropriate amount (purity of 99.5%) was dissolved in water and stabilized according to Cooper (12) at pH 8–9.

Procedures—*Chlorhexidine Diacetate or Digluconate*—Weigh accurately about 30–60 mg of chlorhexidine diacetate, or pipet 2 ml of 2% (w/v) chlorhexidine digluconate solution. Transfer into a 150-ml beaker and dissolve with 20 ml of 0.2 *N* HCl. Slowly add, with stirring, 20 ml of 0.6% sodium tetraphenylborate solution and then allow the mixture to stand for 10–15 min.

Filter the precipitate under suction through a previously dried and tared sintered-glass crucible (porosity 4); then wash the residue with three 5-ml portions of water. Dry the crucible and contents to constant weight (4 hr) at 40–45° at a pressure not exceeding 0.2 mm Hg. Each milligram of the dried chlorhexidine tetraphenylborate is equivalent to 0.5459 mg of chlorhexidine diacetate or 0.7834 mg of chlorhexidine digluconate.

Anal.—Calc. for $C_{70}H_{72}B_2Cl_2N_{10}$: C, 73.37; H, 6.33; N, 12.22. Found: C, 73.69; H, 6.46; N, 11.95.

Chlorhexidine Dihydrochloride—Weigh accurately about 20–60 mg of chlorhexidine dihydrochloride and transfer it into a 150-ml beaker. Dissolve with 20 ml of water by warming gently at 80–85° and cool; then add 0.3 ml of 37% (w/w) HCl. Complete the assay as described for chlorhexidine diacetate or digluconate, beginning with: "Slowly add, ..." Each milligram of the dried chlorhexidine tetraphenylborate is equivalent to 0.5047 mg of chlorhexidine dihydrochloride.

Tablets—The declared amounts, in milligrams per tablet, were: chlorhexidine diacetate, 5; benzocaine, 2; magnesium stearate, 15; mannitol, 300; lactose, 100; and sucrose, 578.

Weigh and powder 25 tablets. Weigh accurately, into a previously tared sintered-glass crucible (porosity 4), a quantity of the powder calculated to contain approximately 100 mg of chlorhexidine diacetate. Then add, under suction, three 20-ml portions of ether and discard the filtrate. Dry the crucible and contents at 50° for 10 min and then dissolve, under suction, chlorhexidine diacetate with 70 ml of 0.2 *N* HCl.

Transfer the combined filtrate and washings of the büchner flask (20 ml of water) into a 100-ml volumetric flask and dilute to volume with water. Pipet an accurately measured aliquot (50 ml) of the solution into a 150-ml beaker. Complete the assay as described for chlorhexidine diacetate or digluconate, beginning with: "Slowly add, ..." Each milligram of the dried chlorhexidine tetraphenylborate is equivalent to 0.5459 mg of chlorhexidine diacetate.

Estimation of Maximum Value for K_{sp}—The apparent solubility product value of chlorhexidine tetraphenylborate was determined in an aqueous hydrochloric acid solution (pH 1) by measurement of the molar detection limit for chlorhexidinium ion in the presence of

[1] Visan, Angiolini S.p.A., Milan, Italy.
[2] E. Merck, Darmstadt, Germany.

Table I—Gravimetric Assays of Chlorhexidine Salts with Tetraphenylborate Solution

Drug	Amount Taken, mg	Recovery, %	*SD* on 15 Analyses, %
Chlorhexidine digluconate	40.0	99.69	±0.42
Chlorhexidine diacetate	28.6–59.6	100.11	±0.46
Chlorhexidine dihydrochloride	22.3–59.3	100.34	±0.31
Tablet (chlorhexidine diacetate)	5.0	97.66	±0.69[a]

[a] Based on six analyses.

a known excess of tetraphenylborate ion. The method is similar to one described by Loach (13).

The apparent solubility product value was calculated from the product of the nominal tetraphenylborate-ion concentration (1×10^{-3} *M*) and the nominal chlorhexidinium-ion concentration (1×10^{-3}–1×10^{-7} *M*) at the detection limit. By using this technique, the solubility product was estimated to be less than 6.5×10^{-13}. While the result could only be regarded as a crude approximation, it provided guidelines for the design of experimental conditions for gravimetric procedures.

RESULTS AND DISCUSSION

As shown in Table I, gravimetric procedures for chlorhexidine salts gave precise and accurate results. The experimental conditions were chosen on the basis of preliminary investigations. The precipitate is only sparingly soluble in water ($K_{sp} = 6.5 \times 10^{-13}$), and it has a definite and reproducible composition corresponding to the formula $C_{70}H_{72}B_2Cl_2N_{10}$. The compound must be dried at a temperature lower than 50° to avoid decomposition. Gravimetric factors of 0.5459 for chlorhexidine diacetate, 0.7834 for chlorhexidine digluconate, and 0.5047 for chlorhexidine dihydrochloride are favorable.

The effect of acidity on the stability of tetraphenylborate and on the filtration properties of tetraphenylborate salts was tested by other workers (14–17), and published information often contained contradictory statements on the optimum conditions for the precipitation. In general, the precipitate formed under alkaline conditions is poorly filterable; however, excessive acidity promotes decomposition of the precipitant (18).

For the determination of the chlorhexidine salts, the final acidity of the reaction solution must be about 0.1 *N* (at 15–25°) to obtain precipitates that are easily separable by filtration. Under these conditions, 1 mole of chlorhexidine salt reacts with 2 moles of sodium tetraphenylborate. Between pH 2 and 5.5, colloidal precipitates which were difficult to filter were obtained; filter aids (19) were not helpful. Because of the tendency for the tetraphenylborate to decompose slowly at this proposed acid concentration (pH 1) (14), standing times up to 60 min did not vitiate the determinations, but the precipitate can be filtered off after standing for 10 min.

When assaying tablets containing chlorhexidine diacetate and benzocaine, benzocaine is dissolved out from the powder mass with ether. 4-Chloroaniline, a possible degradation product of chlorhexidine (10), also is eliminated by ether. Specificity experiments for other interfering products were not conducted. Excipients such as agar and povidone interfere with the proposed method by acting as peptizing agents.

The present method appears to offer a convenient alternative to the few existing methods for the determinations of chlorhexidine salts.

REFERENCES

(1) C. A. Lawrence, *J. Am. Pharm. Assoc., Sci. Ed.*, **49**, 731(1960).

(2) P. Gjermo and H. Erisson, *Caries Res.*, **6**, 1(1973).

(3) B. Regolati, R. Schmid, and H. R. Muhlemann, *Helv. Odontol. Acta*, **18**, 12(1974).

(4) B. R. Cumming and H. Loe, *J. Periodontal Res.*, **8**, 57(1973).

(5) "British Pharmacopoeia 1973," Her Majesty's Stationery Office, London, England, 1973, p. 97.

(6) *Ibid.*, p. 98.

(7) "Martindale, The Extra Pharmacopoeia," 26th ed., The Pharmaceutical Press, London, England, 1973, p. 175.

(8) A. Holbrook, *J. Pharm. Pharmacol.*, **10**, 370(1958).

(9) M. Aoki and Y. Kusaka, *Yakuzaigaku*, **26**, 58(1966).

(10) F. Bailey, P. N. Brittain, and B. F. Williamson, *J. Chromatogr.*, **109**, 305(1975).

(11) J. Bonnard, *Farmaco, Ed. Prat.*, **22**, 305(1967).

(12) S. S. Cooper, *Anal. Chem.*, **29**, 446(1957).

(13) K. W. Loach, *ibid.*, **47**, 315(1969).

(14) M. Kohler, *Z. Anal. Chem.*, **138**, 9(1953).

(15) W. Geilmann and W. Gebauhr, *ibid.*, **139**, 161(1953).

(16) K. Sporek and A. F. Williams, *Analyst*, **80**, 347(1955).

(17) H. J. Cluley, *ibid.*, **80**, 354(1955).

(18) H. A. Laitinen, "Chemical Analysis," McGraw-Hill, New York, N.Y., 1960, p. 258.

(19) H. W. Berkhout and G. H. Iongen, *Chemist-Analyst*, **45**, 6(1956).

ACKNOWLEDGMENTS AND ADDRESSES

Received March 3, 1975, from the *Istituto di Chimica Farmaceutica dell'Università di Firenze, Via G. Capponi 9, 50121 Firenze, Italy.*

Accepted for publication August 26, 1975.

The authors thank Dr. G. Pisaturo for his assistance.

[x] To whom inquiries should be directed.

GLC Determination of Cyclobenzaprine in Plasma and Urine

HOWARD B. HUCKER ˣ and SUSAN C. STAUFFER

Abstract □ A GLC determination of cyclobenzaprine in human plasma and urine is described. After extraction from alkalinized samples with heptane–isopentyl alcohol (97:3), the drug and internal standard were back-extracted into 0.1 *N* HCl and then reextracted into ether. Use of a lower homolog of the drug as an internal standard was effective in reducing variability. Drug concentrations as low as 25 ng/ml could be assayed with high precision. Plasma levels in humans given 40 mg po or iv ranged from 5 to 51 ng/ml; little unchanged cyclobenzaprine was present in the urine. The *N*-desmethyl analog of the drug was detected as a metabolite in urine.

Keyphrases □ Cyclobenzaprine—GLC analysis, plasma and urine □ GLC—analysis, cyclobenzaprine, plasma and urine □ Sedatives—cyclobenzaprine, GLC analysis, plasma and urine

Cyclobenzaprine, *N,N*-dimethyl-5*H*-dibenzo[*a,d*]-cycloheptene-Δ^5,γ-propylamine, is a unique, centrally acting, skeletal muscle relaxant currently in clinical trial (1, 2). Since knowledge of plasma concentrations is often of value in adjusting dosage and dosage schedules to obtain optimal therapeutic response, a GLC method for the drug in plasma was developed. The procedure used is similar to that previously described for the analysis of amitriptyline (3). The method is also applicable to the analysis of the drug in urine and may be an attractive alternative in this case to a previously proposed assay (4), based on quantitative TLC, which requires careful control of several parameters.

EXPERIMENTAL

Reagents—*n*-Heptane[1] was used without further purification. Isopentyl alcohol[2] was washed successively with 1 *N* NaOH, 1 *N* HCl, and water before use. Ether[3] was redistilled immediately before use, and ethyl acetate[4] was redistilled before use. Double-distilled water was used to prepare 0.5 *N* NaOH (from the solid reagent[5]) and 0.1 *N* HCl (by dilution of the concentrated acid[6]).

Cyclobenzaprine and desmethylcyclobenzaprine were used as their hydrochloride salts[7]; the internal standard, *N,N*-dimethyl-5*H*-dibenzo[*a,d*]cycloheptene-Δ^5,γ-ethylamine, was used as the hydrogen maleate salt[7]. Concentrations of each drug are expressed as the free base. Solutions of drug and internal standard were prepared in double-distilled water.

Apparatus—A gas chromatograph[8] with a hydrogen flame-ionization detector was used. A glass column, 1.8 × 4 mm i.d., packed with 1.5% OV-17 on 80–100-mesh Gas Chrom Q[9], was conditioned before use by heating at 250° overnight under helium flow. Analyses were performed under the following conditions: injection port temperature, 260°; column temperature, 218°; and detector temperature, 285°. The gas flows were: hydrogen, 50 ml/min; air, 450 ml/min; and helium carrier gas, 100 ml/min. The recorder was used on range 1 (4×10^{-12} amp) and attenuation 16.

Disposable glass tubes with constricted tips[10] were used for evaporation of the final ether extract and were cleaned by washing with detergent, rinsing thoroughly with double-distilled water, draining, and drying in a vacuum oven at 100°.

Procedure—Two milliliters of plasma or urine, 200 ng of internal standard (in 0.1 ml of water), 1 ml of 0.5 *N* NaOH, and 25 ml of *n*-heptane–isopentyl alcohol (97:3) were shaken for 20 min in a 45-ml glass-stoppered centrifuge tube. The tube was centrifuged, and as much of the organic phase as possible was transferred to a similar tube containing 5 ml of 0.1 *N* HCl. The tube was shaken for 10 min and centrifuged, and the organic (upper) phase was discarded by aspiration.

The aqueous phase was washed three times with *n*-heptane (25 ml each) to remove any residual isopentyl alcohol, the washings being discarded each time by aspiration. Then the aqueous phase was transferred to a clean 13-ml glass-stoppered centrifuge tube. Five milliliters of freshly distilled ether and 1.5 ml of 0.5 *N* NaOH were added, and the tube was shaken for 10 min. After centrifuging, the ether layer was transferred with a Pasteur pipet to a glass tube with a constricted tip.

The solvent was removed in a warm water bath (40°), with periodic chilling in ice water to rinse down the sides. The residue was dissolved in 25 μl of ethyl acetate, and a 5-μl aliquot was injected into the chromatograph. All samples were assayed in duplicate.

Following chromatography, a baseline was drawn and peak heights of cyclobenzaprine and the internal standard were measured. The ratio of cyclobenzaprine and internal standard peak heights was calculated, and the concentration of drug was obtained by reference to the standard curve.

A standard curve was constructed by analysis of samples to which known amounts of cyclobenzaprine and internal standard had been added. After plotting the peak height ratios of drug to internal standard *versus* cyclobenzaprine concentration, the best-fit straight line was drawn that passed through the experimental points and the origin.

RESULTS AND DISCUSSION

Cyclobenzaprine and the internal standard were adequately separated under these conditions (Fig. 1) with retention times of 2.8 and 2.2 min, respectively. Possible metabolites of the drug, the mono- and didesmethyl analogs, had retention times of 3.2 and 3.1 min, respectively, and thus would not interfere in the analysis. Further evidence of the specificity of the method may be inferred from the fact that the drug was well separated from the internal standard, which, in this case, was the closely related homologous compound containing a two-, rather than three-, carbon side chain.

The precision and accuracy of the method are demonstrated in Tables I and II. The mean relative standard deviations were 9.0% for plasma and 6.7% for urine[11]. The limit of detection of the method was approximately 4 ng/ml of plasma, but the practical limit of sensitivity was about 10 ng/ml. Sensitivity could be increased by using larger plasma volumes since plasma extracts showed negligible interfering peaks.

The plasma levels and urinary excretion of cyclobenzaprine in two

[1] Pesticide grade, Matheson, Coleman and Bell, East Rutherford, N.J.
[2] Reagent grade, J. T. Baker Co., Phillipsburg, N.J.
[3] Anhydrous, analytical reagent ACS grade, Fisher Scientific Co., King of Prussia, Pa.
[4] Fisher certified ACS grade.
[5] Fisher certified grade.
[6] Analytical reagent grade, J. T. Baker Co.
[7] Synthesized in the Merck Sharp and Dohme Research Laboratories.
[8] Hewlett-Packard model 810 equipped with a model 7123A recorder.
[9] Applied Science Laboratories, State College, Pa.
[10] Laboratory Research Co., Los Angeles, Calif.

[11] The following formula was used to estimate the mean relative standard deviation:

$$\text{mean } RSD = \frac{\text{pooled } SD}{\text{overall average}}$$

where pooled *SD* (*Sp*) is estimated as

$$Sp = \left[\frac{(n_1 - 1)S_1^2 + \ldots + (n_k - 1)S_k^2}{(n_1 - 1) + \ldots + (n_k - 1)}\right]^{1/2}$$

and:

$$\text{overall average} = \frac{n_1\bar{X}_1 + \ldots + n_k\bar{X}_k}{n_1 + \ldots + n_k}$$

for k groups with $n_1, n_2 \ldots, n_k$ observations/group.

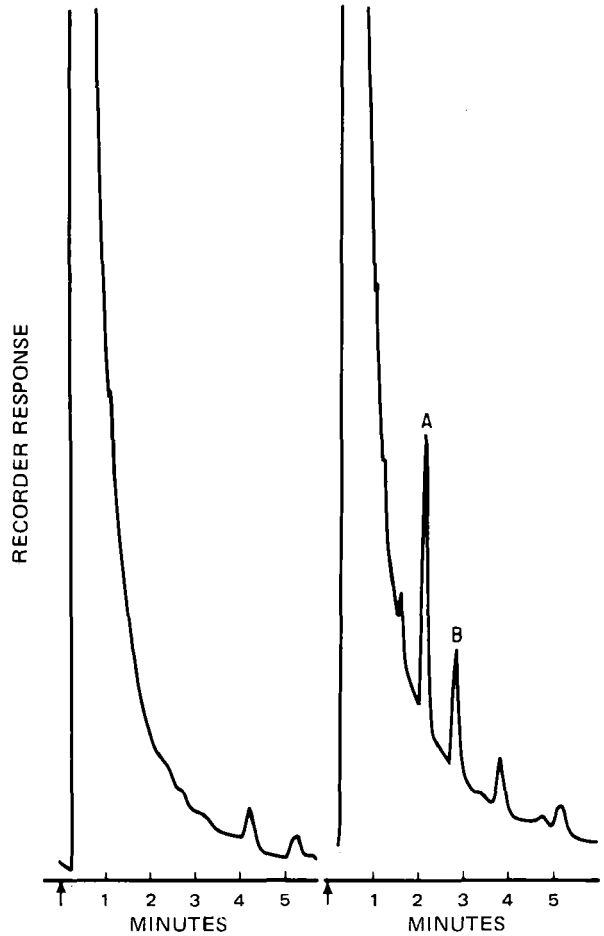

Figure 1—*Gas chromatogram of an extract of 2 ml of control human plasma containing no drugs (left) and of an extract of 2 ml of human plasma containing 50 ng/ml of cyclobenzaprine and 100 ng/ml of internal standard (right). Key: arrow, time of injection; A, internal standard peak; and B, cyclobenzaprine peak.*

human subjects after oral and intravenous administration of a 40-mg dose are shown in Tables III and IV. These preliminary results suggested that the drug is somewhat slowly absorbed, since peak plasma levels of 29.6 ng/ml were observed after 4–6 hr. Intravenous administration of the drug gave plasma levels that were somewhat unusual in that the sample taken after 15 min was no higher than the samples taken over the following 2 hr.

Table I—Accuracy and Precision of GLC Analysis of Cyclobenzaprine Added to Human Plasma[a]

Added, ng/ml	Found, Mean (Range)	*SD*	*RSD*, %
250	228 (210–262)	16.2	7.1
100	100 (92–105)	7.0	7.0
50	50 (46–54)	2.8	5.6
25	24 (22–30)	3.2	13.1

[a] Number of analyses was eight in all cases.

Table II—Accuracy and Precision of GLC Analysis of Cyclobenzaprine Added to Human Urine[a]

Added, ng/ml	Found, Mean (Range)	*SD*	*RSD*, %
250	244 (228–258)	12.5	5.1
100	99 (95–105)	5.1	5.1
50	47 (45–50)	2.2	4.6
25	24 (20–25)	2.4	10.2

[a] Number of analyses was four in all cases.

Table III—Plasma Levels of Cyclobenzaprine in Human Subjects after Oral and Intravenous Doses[a]

Hours	Drug Concentration, ng/ml	
	Oral Dose	Intravenous Dose
0.25	6.4 ± 3.1	48.2 ± 11.7
0.5	10.5 ± 2.1	51.1 ± 9.2
0.75	5.1 ± 1.6	46.7 ± 3.8
1	11.6 ± 9.2	45.0 ± 0.3
2	15.4 ± 8.0	51.0 ± 19.2
3	17.6 ± 1.7	38.8 ± 2.7
4	28.8 ± 0.4	43.0 ± 12.8
6	29.6 ± 13.1	39.4 ± 6.7
8	24.3 ± 6.9	26.6 ± 0.6

[a] The subjects received a 40-mg single dose of the drug by one route followed 7 days later with the same dose by the second route. The figures represent the mean ± *SD* of two subjects.

Table IV—Urinary Excretion of Cyclobenzaprine in Human Subjects after Oral and Intravenous Doses[a]

Hours	Cyclobenzaprine in Urine	
	Oral Dose	Intravenous Dose
0–2	0.01 ± 0.00	0.21 ± 0.05
2–3	0.03 ± 0.01	0.27 ± 0.35
3–4	0.02 ± 0.01	0.09 ± 0.10
4–8	0.04 ± 0.01	0.28 ± 0.21
8–24	0.10 ± 0.01	0.67 ± 0.78
Total	0.20 ± 0.01	1.52 ± 1.39

[a] Dosage was as described for the same two subjects in Table III. Results are expressed as the mean percent of dose excreted ± *SD*.

This finding suggests, as does an estimate of the apparent volume of distribution, that cyclobenzaprine is rapidly taken up by tissues from which sites the drug is slowly and relatively constantly released into the blood. Levels after the intravenous dose were considerably

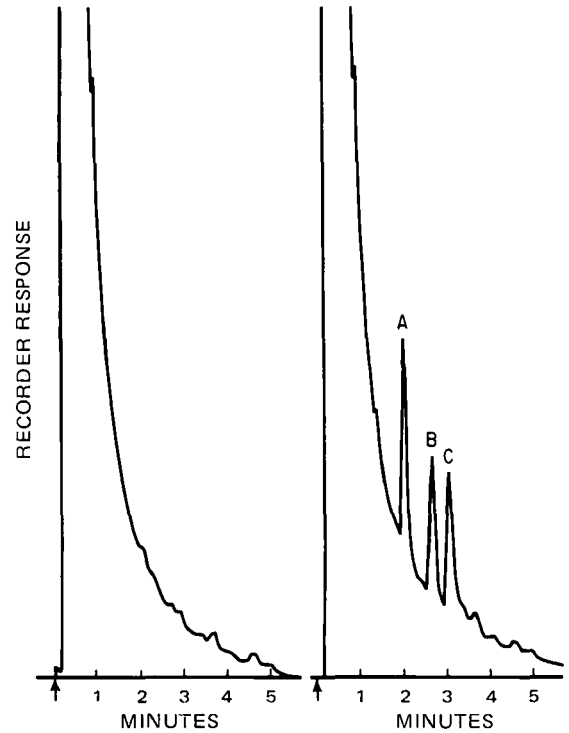

Figure 2—*Gas chromatogram of an extract of 2 ml of control human urine containing no drugs (left) and of an extract of 2 ml of human urine collected 8–24 hr after oral administration of 40 mg of cyclobenzaprine (right). Key: arrow, time of injection; A, internal standard peak; B, cyclobenzaprine peak; and C, desmethylcyclobenzaprine peak.*

higher during the first 4 hr than those attained following the oral dose, suggesting also that first-pass hepatic metabolism is important and that this phenomenon may be involved in the pharmacokinetics of cyclobenzaprine absorption in humans.

The presence of only a relatively small amount of unchanged drug in the urine (0.2–1.5% of the administered doses) would suggest that the drug was virtually completely metabolized in humans. The extent of metabolism may not be quite this complete since, after administration of ^{14}C-labeled drug[12], only 6.3% of a 10-mg po dose and 7.1% of a 10-mg iv dose were excreted in the 24-hr urine.

No peaks attributable to metabolites of cyclobenzaprine in plasma were observed during assay of the human samples. Norcyclobenzaprine was presumably present in the plasma, since it was found in the urine, but the detection limit for the desmethyl derivative was much higher than for cyclobenzaprine because of less favorable GLC and extraction properties[12]. In contrast, nortriptyline is readily detected in plasma after administration of amitriptyline, a drug having a structure very similar to that of cyclobenzaprine (3, 5, 6).

GLC analysis of the urine samples revealed the presence of an additional peak at 3.2 min, the same retention time as that of *N*-desmethylcyclobenzaprine (Fig. 2). Treatment of the final ethyl acetate extract with trifluoroacetic anhydride before GLC analysis caused the disappearance of the 3.2-min peak and the appearance of a new peak at 5.0 min, the same retention time as that of the trifluoroacetyl derivative of authentic *N*-desmethylcyclobenzaprine. The possibility that the metabolite was didesmethylcyclobenzaprine was ruled out by the fact that, although the retention time of the free amine was similar to that of the metabolite, the retention time of its trifluoroacetyl derivative was 4.0 min.

The desmethyl metabolite was most predominant in the 8–24-hr urine samples and appeared to be present in equal or higher concentrations compared to unchanged cyclobenzaprine. Evidently, the *N*-desmethyl metabolite was present in plasma in concentrations too low to be detected, but urinary levels were sufficiently high for identification.

The present GLC method is suitable for the quantitative assay of cyclobenzaprine in human plasma and urine samples after administration of a single 40-mg dose. Greater sensitivity may be necessary when a smaller dose is administered and can be achieved by using a larger plasma sample for assay.

[12] Unpublished work.

REFERENCES

(1) P. Molina-Negro and R. A. Illingworth, *Union Med. Can.*, **100**, 1947(1971).

(2) N. N. Share and C. S. McFarlane, *Neuropharmacology*, **14**, 9(1975).

(3) H. B. Hucker and S. C. Stauffer, *J. Pharm. Sci.*, **63**, 296(1974).

(4) D. B. Faber, *J. Chromatogr.*, **74**, 85(1972).

(5) H. B. Hucker, S. C. Stauffer, F. G. Clayton, B. R. S. Nakra, and R. Gaind, *J. Clin. Pharmacol.*, **15**, 168(1975).

(6) R. A. Braithwaite and B. Widdop, *Clin. Chim. Acta*, **35**, 461(1971).

ACKNOWLEDGMENTS AND ADDRESSES

Received July 30, 1975, from the *Merck Institute for Therapeutic Research, West Point, PA 19486*

Accepted for publication October 8, 1975.

The authors thank Dr. F. G. McMahon for making the human samples available and Dr. N. R. Bohidar for assistance with statistical analyses.

[x] To whom inquiries should be directed.

Kinetics of Acid Neutralization by Aluminum Hydroxide Gel

STEVEN L. NAIL [*], JOE L. WHITE [‡], and STANLEY L. HEM [*x]

Abstract □ The rate of acid neutralization by an aluminum hydroxide gel prepared by the reaction of aluminum chloride solution and strong ammonia solution was studied. The decrease in acid-consuming capacity during aging as measured by the USP test is due to a decrease in the rate of reaction rather than to a decrease in equilibrium reactivity. The reactivity profile has three phases, which are shown to be related to the structure of the gel. The rate of loss of reactivity is directly related to the extent of washing.

Keyphrases □ Aluminum hydroxide gel—kinetics of acid neutralization, effect of aging, reactivity related to gel structure □ Acid neutralization—by aluminum hydroxide gel, effect of aging, reactivity related to gel structure □ Gels—aluminum hydroxide, kinetics of acid neutralization, reactivity related to gel structure □ Antacids—aluminum hydroxide gel, kinetics of acid neutralization, effect of aging

Aluminum hydroxide gel is known to lose acid reactivity on aging (1–3). The purposes of this investigation were: (*a*) to study this neutralization reaction for an aluminum hydroxide gel prepared by the reaction of aluminum chloride solution with strong ammonia solution; and (*b*) to determine whether the decrease in acid reactivity, as determined by a modification of the USP acid-consuming capacity test (4), was attributable to a decreased rate of reaction or to a decrease in equilibrium reactivity.

EXPERIMENTAL

Materials—All chemicals used were either reagent or analytical grade.

Aluminum Hydroxide Gel Preparation—A 4-liter batch of gel was prepared by the addition of 13% (v/v) strong ammonia solution to a solution of 287.2 g of aluminum chloride hexahydrate in 3340 ml of distilled water. Strong ammonia solution was added with agitation at a rate of approximately 120 ml/min to a final pH of 7.0. After precipitation, the gel was divided into four equal portions. The first portion (I) was washed with 1 liter of distilled water by draining through a canvas bag, and a second portion (II) was washed with 5 liters of distilled water. The gels were diluted to 1 liter with distilled water, stored in tightly closed glass containers, and aged at 25°.

Analytical Procedures—The equivalent aluminum oxide content was determined by the ethylenediaminetetraacetic acid titration (4). The gels contained between 1.40 and 1.50% equivalent of aluminum oxide.

The total chloride content was determined by the Volhard titration (5) after 3 g of gel was dissolved in 15 ml of 6 *N* nitric acid.

The rate of reaction of the gel with acid was studied by preparing a series of 5-g samples of gel in 125-ml glass-stoppered flasks and adding 50 ml of 0.1 *N* HCl. Samples were then placed in a water bath[1]

[1] Thermo-Shake incubator shaker, Forma Scientific, Pittsburgh, Pa.

higher during the first 4 hr than those attained following the oral dose, suggesting also that first-pass hepatic metabolism is important and that this phenomenon may be involved in the pharmacokinetics of cyclobenzaprine absorption in humans.

The presence of only a relatively small amount of unchanged drug in the urine (0.2–1.5% of the administered doses) would suggest that the drug was virtually completely metabolized in humans. The extent of metabolism may not be quite this complete since, after administration of ^{14}C-labeled drug[12], only 6.3% of a 10-mg po dose and 7.1% of a 10-mg iv dose were excreted in the 24-hr urine.

No peaks attributable to metabolites of cyclobenzaprine in plasma were observed during assay of the human samples. Norcyclobenzaprine was presumably present in the plasma, since it was found in the urine, but the detection limit for the desmethyl derivative was much higher than for cyclobenzaprine because of less favorable GLC and extraction properties[12]. In contrast, nortriptyline is readily detected in plasma after administration of amitriptyline, a drug having a structure very similar to that of cyclobenzaprine (3, 5, 6).

GLC analysis of the urine samples revealed the presence of an additional peak at 3.2 min, the same retention time as that of *N*-desmethylcyclobenzaprine (Fig. 2). Treatment of the final ethyl acetate extract with trifluoroacetic anhydride before GLC analysis caused the disappearance of the 3.2-min peak and the appearance of a new peak at 5.0 min, the same retention time as that of the trifluoroacetyl derivative of authentic *N*-desmethylcyclobenzaprine. The possibility that the metabolite was didesmethylcyclobenzaprine was ruled out by the fact that, although the retention time of the free amine was similar to that of the metabolite, the retention time of its trifluoroacetyl derivative was 4.0 min.

The desmethyl metabolite was most predominant in the 8–24-hr urine samples and appeared to be present in equal or higher concentrations compared to unchanged cyclobenzaprine. Evidently, the *N*-desmethyl metabolite was present in plasma in concentrations too low to be detected, but urinary levels were sufficiently high for identification.

The present GLC method is suitable for the quantitative assay of cyclobenzaprine in human plasma and urine samples after administration of a single 40-mg dose. Greater sensitivity may be necessary when a smaller dose is administered and can be achieved by using a larger plasma sample for assay.

[12] Unpublished work.

REFERENCES

(1) P. Molina-Negro and R. A. Illingworth, *Union Med. Can.*, **100**, 1947(1971).

(2) N. N. Share and C. S. McFarlane, *Neuropharmacology*, **14**, 9(1975).

(3) H. B. Hucker and S. C. Stauffer, *J. Pharm. Sci.*, **63**, 296(1974).

(4) D. B. Faber, *J. Chromatogr.*, **74**, 85(1972).

(5) H. B. Hucker, S. C. Stauffer, F. G. Clayton, B. R. S. Nakra, and R. Gaind, *J. Clin. Pharmacol.*, **15**, 168(1975).

(6) R. A. Braithwaite and B. Widdop, *Clin. Chim. Acta*, **35**, 461(1971).

ACKNOWLEDGMENTS AND ADDRESSES

Received July 30, 1975, from the *Merck Institute for Therapeutic Research, West Point, PA 19486*

Accepted for publication October 8, 1975.

The authors thank Dr. F. G. McMahon for making the human samples available and Dr. N. R. Bohidar for assistance with statistical analyses.

[x] To whom inquiries should be directed.

Kinetics of Acid Neutralization by Aluminum Hydroxide Gel

STEVEN L. NAIL [*], JOE L. WHITE [‡], and STANLEY L. HEM [*x]

Abstract □ The rate of acid neutralization by an aluminum hydroxide gel prepared by the reaction of aluminum chloride solution and strong ammonia solution was studied. The decrease in acid-consuming capacity during aging as measured by the USP test is due to a decrease in the rate of reaction rather than to a decrease in equilibrium reactivity. The reactivity profile has three phases, which are shown to be related to the structure of the gel. The rate of loss of reactivity is directly related to the extent of washing.

Keyphrases □ Aluminum hydroxide gel—kinetics of acid neutralization, effect of aging, reactivity related to gel structure □ Acid neutralization—by aluminum hydroxide gel, effect of aging, reactivity related to gel structure □ Gels—aluminum hydroxide, kinetics of acid neutralization, reactivity related to gel structure □ Antacids—aluminum hydroxide gel, kinetics of acid neutralization, effect of aging

Aluminum hydroxide gel is known to lose acid reactivity on aging (1–3). The purposes of this investigation were: (*a*) to study this neutralization reaction for an aluminum hydroxide gel prepared by the reaction of aluminum chloride solution with strong ammonia solution; and (*b*) to determine whether the decrease in acid reactivity, as determined by a modification of the USP acid-consuming capacity test (4), was attributable to a decreased rate of reaction or to a decrease in equilibrium reactivity.

EXPERIMENTAL

Materials—All chemicals used were either reagent or analytical grade.

Aluminum Hydroxide Gel Preparation—A 4-liter batch of gel was prepared by the addition of 13% (v/v) strong ammonia solution to a solution of 287.2 g of aluminum chloride hexahydrate in 3340 ml of distilled water. Strong ammonia solution was added with agitation at a rate of approximately 120 ml/min to a final pH of 7.0. After precipitation, the gel was divided into four equal portions. The first portion (I) was washed with 1 liter of distilled water by draining through a canvas bag, and a second portion (II) was washed with 5 liters of distilled water. The gels were diluted to 1 liter with distilled water, stored in tightly closed glass containers, and aged at 25°.

Analytical Procedures—The equivalent aluminum oxide content was determined by the ethylenediaminetetraacetic acid titration (4). The gels contained between 1.40 and 1.50% equivalent of aluminum oxide.

The total chloride content was determined by the Volhard titration (5) after 3 g of gel was dissolved in 15 ml of 6 *N* nitric acid.

The rate of reaction of the gel with acid was studied by preparing a series of 5-g samples of gel in 125-ml glass-stoppered flasks and adding 50 ml of 0.1 *N* HCl. Samples were then placed in a water bath[1]

[1] Thermo-Shake incubator shaker, Forma Scientific, Pittsburgh, Pa.

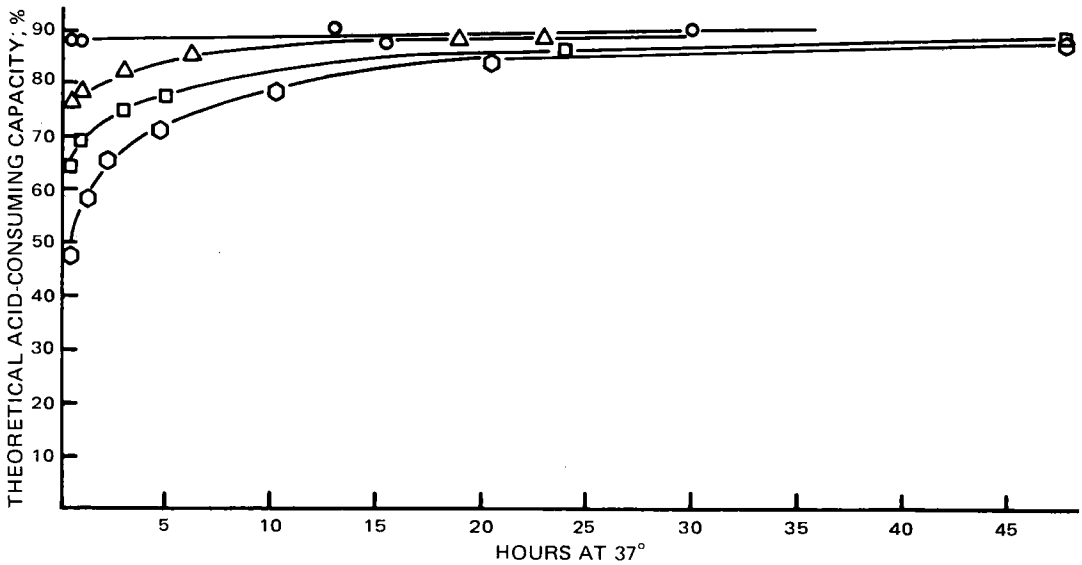

Figure 1—*Change in rate of reaction of Gel I with acid during aging. Key:* ○, *1 day;* △, *30 days;* □, *50 days; and* ○, *163 days.*

at 37° with agitation. Samples were removed from the bath after periods ranging from 0.5 hr to 1 week, and the amount of acid neutralized was determined by back-titrating the sample to pH 3.5 with standard 0.1 *N* NaOH. The acid reactivity of each gel was expressed as the percent of the theoretical acid-consuming capacity (TACC):

$$\text{TACC} = \frac{W \times A \times 60}{10.2} \qquad \text{(Eq. 1)}$$

where W = weight of gel sample in grams, and A = assay of gel as percent aluminum oxide.

This procedure was repeated for each gel at various times during aging.

RESULTS AND DISCUSSION

The rate of reaction of each gel with acid is shown in Figs. 1 and 2. The general features of the reaction rate curve for Gels I and II are similar. Equilibrium reactivity is reached within 0.5 hr for the gel aged 1 day. After further aging, three types of kinetic behavior become apparent. A portion of each gel reacts almost immediately, and the amount of this fast reacting portion decreases with age. The gel then reacts at a slower rate until the equilibrium reactivity is reached, the rate during this period becoming slower as the gel ages (curved portions of Figs. 1 and 2). However, the gels appear to reach the same end-point reactivity if sufficient time is allowed for the reaction to proceed. The slope is nearly zero in all cases after about 20 hr, indicating a final period represented by a slow zero-order reaction.

For the intermediate rate portion of the reaction curve, the essentially straight portion of the curve is extrapolated to time zero, and the difference between the percent of the theoretical acid-consuming capacity from the extrapolated zero-order line (TACC_∞) and the percent of the theoretical acid-consuming capacity at time t (TACC_t) is calculated. When the negative log of this value is plotted against time, a straight line results, indicating that the reaction follows apparent first-order kinetics during this period.

If similar plots are made for each aging time studied, a series of straight lines is obtained (Figs. 3 and 4). The slopes of these lines decrease with increasing age, indicating a slower reaction rate. The y-intercept of these plots provides an accurate determination of the amount of immediately reacting material present at each aging period. Plotting the log of the amount of immediately reacting material determined in this manner against aging time also gives a straight line, indicating a first-order decrease in this quantity (Fig. 5). The rate of decrease in the fast reacting portion follows the order II > I.

Smith (6) also observed three types of kinetic behavior in the reaction of dilute hydroxyaluminum systems with 8-hydroxy-7-iodo-5-quinolinesulfonic acid (III). The slow zero-order portion was attributed to reaction of microcrystalline material with III. It seems reasonable that the slow portions of Figs. 1 and 2 would result from acid attack on the surface of highly ordered material.

The first-order portion of the reaction curve is believed to result from acid attack on material that is less ordered; *i.e.*, protons can penetrate the gel structure more readily than in the zero-order portion.

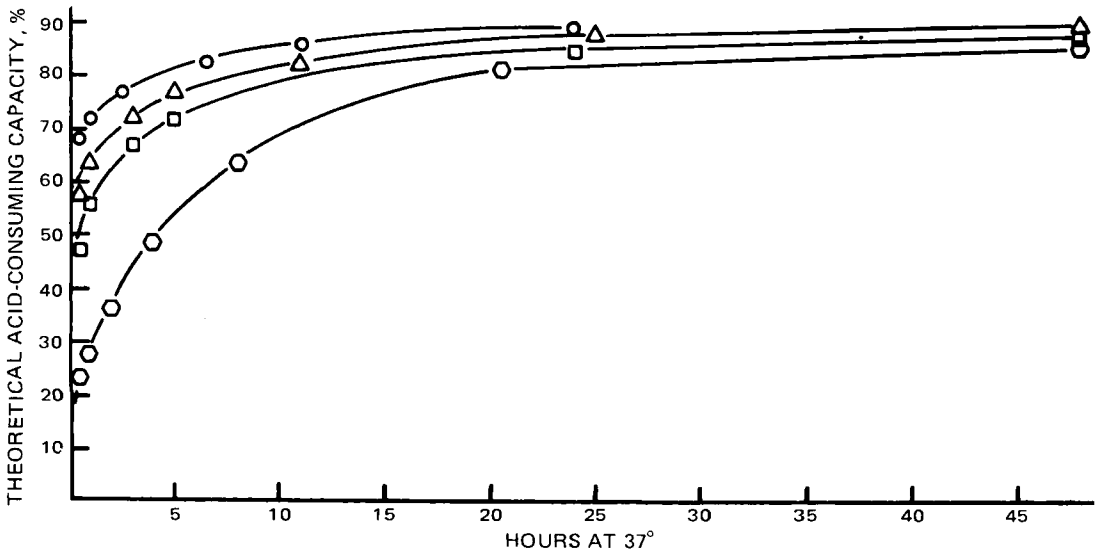

Figure 2—*Change in rate of reaction of Gel II with acid during aging. Key:* ○, *30 days;* △, *50 days;* □, *72 days; and* ○, *157 days.*

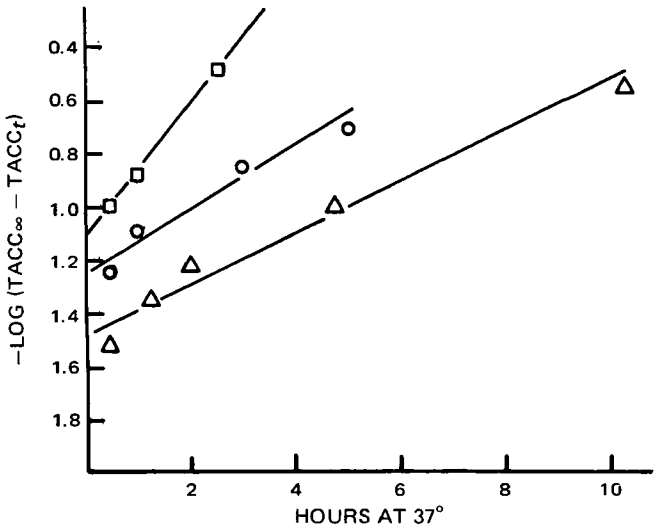

Figure 3—*Change in rate of first-order portion of Gel I during aging. Key: □, 30 days; ○, 50 days; and △, 163 days.*

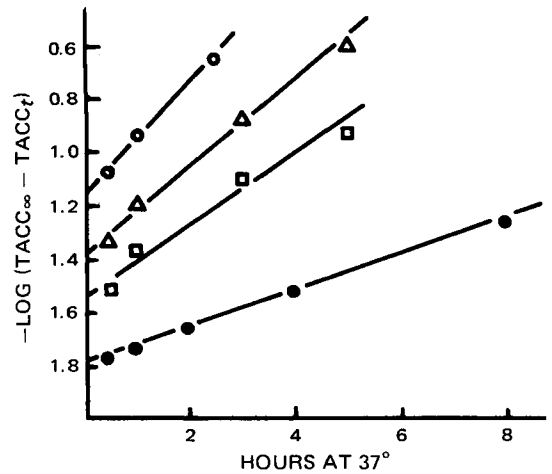

Figure 4—*Change in rate of first-order portion of Gel II during aging. Key: ○, 30 days; △, 50 days; □, 72 days; and ●, 157 days.*

The initial fast reacting portion of Figs. 1 and 2 probably results from acid attack on easily accessible hydroxyl groups. Hydroxyl groups on the edge of the hydroxyaluminum particles would be readily accessible, and neutralization of these hydroxyl groups might explain the initial fast reaction rate. Particle growth by formation of double hydroxide bridges between the edges of adjacent particles (6) would decrease the relative number of edge hydroxyls, thus explaining the observed decrease in the fast reacting portion of the gel during aging.

The direct relationship between the degree of washing and the decreased rate of acid neutralization is consistent with the inhibition of secondary polymerization by the chloride ion (7). Chloride ions can occupy edge positions on the hydroxyaluminum polymers and thereby block further polymerization at these sites. Gel I, which was washed with 1 liter of distilled water, contains 0.80 mEq of chloride/mmole of aluminum and changes more slowly than Gel II, which was washed with 5 liters of distilled water and contains 0.35 mEq of chloride/mmole of aluminum. Inhibition of this reaction retards particle growth and the subsequent development of crystalline forms of aluminum hydroxide.

Calculation of the theoretical acid-consuming capacity of a gel is based on the reaction of 6 equivalents of hydrochloric acid with 1 mole of aluminum oxide or of 3 equivalents of acid with 1 mole of aluminum hydroxide. In other words, calculation of the theoretical acid-consuming capacity is based on a bound hydroxide to aluminum ratio of 3. Previous investigations (7, 8) showed that this is not always the case. The gels studied, resulting from the reaction of aluminum chloride solution with strong ammonia solution to a final pH of 7.0, were shown to have an average ratio of bound hydroxide to aluminum of 2.55 (7). This ratio increases with age due to secondary polymerization of the hydroxyaluminum particles (7). This explains why the equilibrium reactivity of these gels is less than 100% of theoretical capacity. Complete reaction of a gel with a bound hydroxide to aluminum ratio of 2.55 would consume 85% of the theoretical amount. The gels in this study initially consumed about 90% of the theoretical capacity at equilibrium, somewhat higher than the value predicted by the hydroxide to aluminum ratio but in reasonable agreement with theory.

SUMMARY

Aluminum hydroxide gel prepared from aluminum chloride and ammonium hydroxide at a final pH of 7.0 has an acid reactivity profile with three phases: (*a*) an initial fast reacting portion whose contribution decreases as the gel ages; (*b*) a portion that reacts with acid according to apparent first-order kinetics at a rate that decreases with age; and (*c*) a slow, zero-order reacting portion believed to be highly ordered material.

The decrease in USP acid-consuming capacity is due to a decreased

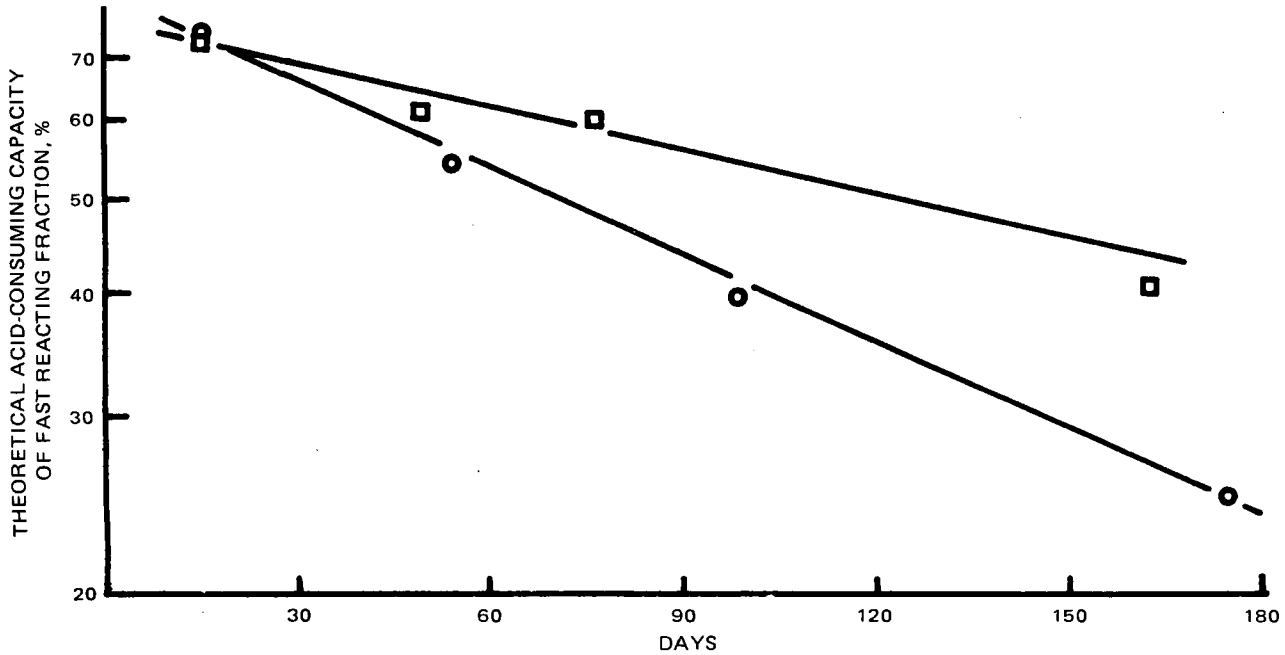

Figure 5—*Change in fast reacting portion of gels during aging. Key: □, Gel I; and ○, Gel II.*

rate of reactivity rather than to a change in equilibrium reactivity. The USP acid-consuming capacity test is based on the amount of acid neutralized by the gel in 1 hr. Thus, the acid reactivity measured by the USP test decreased during aging, although the equilibrium reactivity of the gels was unchanged.

REFERENCES

(1) S. L. Hem, E. J. Russo, S. M. Bahal, and R. S. Levi, *J. Pharm. Sci.*, **59,** 317(1970).

(2) S. L. Nail, J. L. White, and S. L. Hem, *ibid.*, **64,** 1166(1975).

(3) *Ibid.*, **65,** 231(1976).

(4) "The United States Pharmacopeia," 18th rev., Mack Publishing Co., Easton, Pa., 1970, p. 26.

(5) I. M. Kolthoff, E. B. Sandell, E. J. Meehan, and S. Bruckenstein, "Quantitative Analysis," 4th ed., Macmillan, London, England, 1969, p. 799.

(6) R. W. Smith, *Adv. Chem.*, **106,** 250(1971).

(7) S. L. Nail, J. L. White, and S. L. Hem, *J. Pharm. Sci.*, **65,** 1192(1976).

(8) *Ibid.*, **65,** 1188(1976).

ACKNOWLEDGMENTS AND ADDRESSES

Received July 2, 1975, from the *Industrial and Physical Pharmacy Department, School of Pharmacy and Pharmacal Sciences, and the ‡Department of Agronomy, Purdue University, West Lafayette, IN 47907

Accepted for publication September 4, 1975.

Supported in part by an American Foundation for Pharmaceutical Education Fellowship (S. L. Nail).

This report is Journal Paper 5947, Purdue University Agricultural Experiment Station, West Lafayette, IN 47907

ˣ To whom inquiries should be directed.

IR Spectroscopic Characterization of 2-Thiohydantoins and 2-Thiobarbiturates

J. POUPAERT and R. BOUCHE ˣ

Abstract □ A characterization of 2-thiohydantoins and 2-thiobarbiturates by IR spectra is proposed, using three characteristic group frequencies: the "thioureide band" around 1500 cm^{-1} and the antisymmetric-symmetric stretching modes of NCS bonds around 1400 and 1200 cm^{-1}. The general characteristic absorption areas are found by comparison with *N*-phenylthioureas and thioanilides.

Keyphrases □ Thiohydantoins—characterization by IR spectroscopy □ Thiobarbiturates—characterization by IR spectroscopy □ IR spectroscopy—characterization of thiohydantoins and thiobarbiturates

Whereas the origin and localization of the characteristic group frequencies of the carbonyl in hydantoins (1) and barbiturates (2) have been thoroughly studied, the question is still open for the corresponding thio compounds because of difficulties in assignments. Strong coupling occurs between the C–S and C–N vibrations, resulting in numerous bands in the 1550–1200-cm^{-1} region, each of which contains a significant contribution from the C=S stretching mode (3).

The identification in the literature is often based on the "thioureide band," as defined previously (4, 5), in spite of the absence of a C=S contribution to this mode[1].

A new characterization of the thiohydantoins and thiobarbiturates series by IR spectra, involving the antisymmetric and symmetric stretching modes of NCS bonds, is now reported.

EXPERIMENTAL

IR spectra were recorded[2] using the potassium bromide pellets technique (1 mg/200 mg) after the compounds were dried overnight under vacuum (0.2 mm Hg at 60°). The structures of utilized compounds were confirmed by comparison with literature data or by mass spectrometry[3] (ionization potential of 70 ev).

N-Phenylthioureas (I–VII) were obtained by interaction of phenyl isothiocyanate and amines in ether and subsequent recrystallization in methanol (6). The properties of I–IV (6) and VII (7) were in agreement with the literature.

Compound V had a melting point of 104–107°; *m/e* 270 (M^+), 236 (—H_2S), 145 [$C_6H_5CH_2CH(CH_3)NC$], 135 (C_6H_5NCS), 91 ($C_6H_5CH_2$), and 77 (C_6H_5). Compound VI had a melting point of 114–117°; *m/e* 282 (—H_2O), 264 (—H_2S), 207 ($C_6H_5NH_2$), 145

Table I—Characteristic Bands (Centimeters^{-1}) of *N*-Phenylthioureas

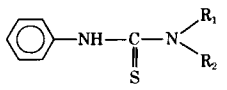

Compound		$\nu_{thioureide}$	ν_{as} NCS/ ν_{s} NCS[a]
I	R_1 = H, R_2 = H	1530	1450/1232
II	R_1 = H, R_2 = C_6H_5	1555	1452/1245
III	R_1 = C_6H_5, R_2 = C_6H_4—OCH_3	1550	1450/1240
IV	R_1 = R_2 = cyclo-$(CH_2)_5$	1540	1440/1230
V	R_1 = H, R_2 = C_6H_5—CH_2—CH(—CH_3)	1538	1450/1245
VI	R_1 = CH_3, R_2 = C_6H_5—CH(OH)—CH(—CH_3)	1538	1450/1260
VII	R_1 = H, R_2 = cyclo C_6H_{11}—CH(—COOH)	1515	1410/1230

[a] ν_{as} NCS and ν_{s} NCS designate the antisymmetric and symmetric stretching modes of the NCS function.

[1] The "thioureide band" is due to a νC–N mode; coupling between νC–N and δ NH may occur in suitable cases. This band is designated as the B band in the classification of Jensen and Nielsen (5).

[2] Perkin-Elmer model 621.

[3] LKB 900 S.

rate of reactivity rather than to a change in equilibrium reactivity. The USP acid-consuming capacity test is based on the amount of acid neutralized by the gel in 1 hr. Thus, the acid reactivity measured by the USP test decreased during aging, although the equilibrium reactivity of the gels was unchanged.

REFERENCES

(1) S. L. Hem, E. J. Russo, S. M. Bahal, and R. S. Levi, *J. Pharm. Sci.*, **59,** 317(1970).

(2) S. L. Nail, J. L. White, and S. L. Hem, *ibid.*, **64,** 1166(1975).

(3) *Ibid.*, **65,** 231(1976).

(4) "The United States Pharmacopeia," 18th rev., Mack Publishing Co., Easton, Pa., 1970, p. 26.

(5) I. M. Kolthoff, E. B. Sandell, E. J. Meehan, and S. Bruckenstein, "Quantitative Analysis," 4th ed., Macmillan, London, England, 1969, p. 799.

(6) R. W. Smith, *Adv. Chem.*, **106,** 250(1971).

(7) S. L. Nail, J. L. White, and S. L. Hem, *J. Pharm. Sci.*, **65,** 1192(1976).

(8) *Ibid.*, **65,** 1188(1976).

ACKNOWLEDGMENTS AND ADDRESSES

Received July 2, 1975, from the *Industrial and Physical Pharmacy Department, School of Pharmacy and Pharmacal Sciences, and the ‡Department of Agronomy, Purdue University, West Lafayette, IN 47907

Accepted for publication September 4, 1975.

Supported in part by an American Foundation for Pharmaceutical Education Fellowship (S. L. Nail).

This report is Journal Paper 5947, Purdue University Agricultural Experiment Station, West Lafayette, IN 47907

ˣ To whom inquiries should be directed.

IR Spectroscopic Characterization of 2-Thiohydantoins and 2-Thiobarbiturates

J. POUPAERT and R. BOUCHE ˣ

Abstract □ A characterization of 2-thiohydantoins and 2-thiobarbiturates by IR spectra is proposed, using three characteristic group frequencies: the "thioureide band" around 1500 cm^{-1} and the antisymmetric-symmetric stretching modes of NCS bonds around 1400 and 1200 cm^{-1}. The general characteristic absorption areas are found by comparison with *N*-phenylthioureas and thioanilides.

Keyphrases □ Thiohydantoins—characterization by IR spectroscopy □ Thiobarbiturates—characterization by IR spectroscopy □ IR spectroscopy—characterization of thiohydantoins and thiobarbiturates

Whereas the origin and localization of the characteristic group frequencies of the carbonyl in hydantoins (1) and barbiturates (2) have been thoroughly studied, the question is still open for the corresponding thio compounds because of difficulties in assignments. Strong coupling occurs between the C–S and C–N vibrations, resulting in numerous bands in the 1550–1200-cm^{-1} region, each of which contains a significant contribution from the C=S stretching mode (3).

The identification in the literature is often based on the "thioureide band," as defined previously (4, 5), in spite of the absence of a C=S contribution to this mode[1].

A new characterization of the thiohydantoins and thiobarbiturates series by IR spectra, involving the antisymmetric and symmetric stretching modes of NCS bonds, is now reported.

EXPERIMENTAL

IR spectra were recorded[2] using the potassium bromide pellets technique (1 mg/200 mg) after the compounds were dried overnight under vacuum (0.2 mm Hg at 60°). The structures of utilized compounds were confirmed by comparison with literature data or by mass spectrometry[3] (ionization potential of 70 ev).

N-Phenylthioureas (I–VII) were obtained by interaction of phenyl isothiocyanate and amines in ether and subsequent recrystallization in methanol (6). The properties of I–IV (6) and VII (7) were in agreement with the literature.

Compound V had a melting point of 104–107°; *m/e* 270 (M^+), 236 (—H_2S), 145 [$C_6H_5CH_2CH(CH_3)NC$], 135 (C_6H_5NCS), 91 ($C_6H_5CH_2$), and 77 (C_6H_5). Compound VI had a melting point of 114–117°; *m/e* 282 (—H_2O), 264 (—H_2S), 207 ($C_6H_5NH_2$), 145

Table I—Characteristic Bands (Centimeters^{-1}) of *N*-Phenylthioureas

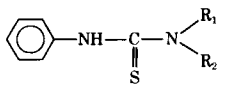

Compound		$\nu_{thioureide}$	ν_{as} NCS/ ν_{s} NCS[a]
I	R_1 = H, R_2 = H	1530	1450/1232
II	R_1 = H, R_2 = C_6H_5	1555	1452/1245
III	R_1 = C_6H_5, R_2 = C_6H_4—OCH_3	1550	1450/1240
IV	R_1 = R_2 = cyclo-$(CH_2)_5$	1540	1440/1230
V	R_1 = H, R_2 = C_6H_5—CH_2—CH(—CH_3)	1538	1450/1245
VI	R_1 = CH_3, R_2 = C_6H_5—CH(OH)—CH(—CH_3)	1538	1450/1260
VII	R_1 = H, R_2 = cyclo C_6H_{11}—CH(—COOH)	1515	1410/1230

[a] ν_{as} NCS and ν_{s} NCS designate the antisymmetric and symmetric stretching modes of the NCS function.

[1] The "thioureide band" is due to a νC–N mode; coupling between νC–N and δ NH may occur in suitable cases. This band is designated as the B band in the classification of Jensen and Nielsen (5).

[2] Perkin-Elmer model 621.

[3] LKB 900 S.

Table II—Characteristic Bands (Centimeters^{-1}) of 2-Thiohydantoins

Compound			$\nu_{C=O}$	$\nu_{thioureide}$	ν_{as} NCS/ν_{s} NCS[a]
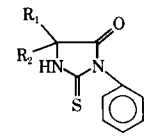	VIII	$R_1 = CH_3$, $R_2 = H$	1740	1510	1430/1250
	IX	$R_1 = CH_2—C_6H_5$, $R_2 = H$	1735	1500	1440/1240
	X	R_1 = cyclo C_6H_{11}, $R_2 = H$	1745	1490	1430/1245
	XI	$R_1 = C_6H_5$, $R_2 = H$	1755	1510	1445/1240
	XII	$R_1 = R_2 = C_6H_5$	1750	1485	1445/1230
	XIII	$R_1 = C_6H_5$, R_2 = cyclo C_6H_{11}	1730	1500	1445/1245
	XIV	$R_1 = CH_3$, $R_2 = C_2H_5$	1760	1520	1445/1240
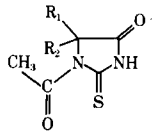	XV	$R_1 = C_6H_5$, $R_2 = H$	1770	1470	1410/1210
	XVI	$R_1 = CH_3$, $R_2 = C_2H_5$	1765	1470	1410/1210
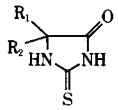	XVII	$R_1 = R_2 = C_6H_5$	1750	1530	1445/1220
	XVIII	$R_1 = C_6H_5$, R_2 = cyclo C_6H_{11}	1740	1512	1445/1225
	XIX	$R_1 = CH_3$, $R_2 = C_2H_5$	1730	1530	1450/1220

[a] ν_{as} NCS and ν_{S} NCS designate the antisymmetric and symmetric stretching modes of the NCS function.

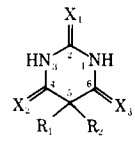

Table III—Characteristic Bands (Centimeters^{-1}) of Thiobarbiturates

Compound		$\nu_{thioureide}$	ν_{as} NCS/ν_{s} NCS[a]
XX	$R_1 = R_2 = C_2H_5$, $X_1 = S$, $X_2 = X_3 = O$	1545	1425/1225 (2-thio)
XXI	$R_1 = —CH(CH_3)—C_3H_7$, $R_2 = C_2H_5$, $X_1 = S$, $X_2 = X_3 = O$	1535	1420/1215 (2-thio)
XXII	$R_1 = —CH(CH_3)—C_2H_5$, $R_2 = C_2H_5$, $X_1 = S$, $X_2 = X_3 = O$	1535	1418/1215 (2-thio)
XXIII	$R_1 = —CH(C_2H_5)—C_3H_7$, $R_2 = C_2H_5$, $X_1 = S$, $X_2 = X_3 = O$	1530	1420/1210 (2-thio)
XXIV	$R_1 = —CH_2—CH=CH_2$, $R_2 =$, $X_1 = S$, $X_2 = X_3 = O$	1510	1410/1200 (2-thio)
XXV	$R_1 = R_2 = C_2H_5$, $X_2 = S$, $X_1 = X_3 = O$	—	1455/1248 (4-thio)
XXVI	$R_1 = R_2 = C_2H_5$, $X_1 = X_2 = S$, $X_3 = O$	1545	1432/1225 (2-thio) 1448/1240 (4-thio)
XXVII	$R_1 = R_2 = C_2H_5$, $X_2 = X_3 = S$, $X_1 = O$		1445/1225 (4,6-dithio) 1442/1175 (4,6-dithio)
XXVIII	$R_1 = R_2 = C_2H_5$, $X_1 = X_2 = X_3 = S$	1540	1440/1225 (2-thio) 1460/1245 (4,6-dithio) 1435/1190 (4,6-dithio)

[a] ν_{as} NCS and ν_{S} NCS designate the antisymmetric and symmetric stretching modes of the NCS function.

$[C_6H_5CH_2CH(CH_3)NC]$, 135 (C_6H_5NCS), 91 ($C_6H_5CH_2$), and 77 (C_6H_5).

2-Thiohydantoins were prepared according to standard procedures from the literature. Compounds VIII–XII and XIV were synthesized by Edman's (8) method; XII and XIII were prepared according to the procedure of Elmore (4); XV, XVI, and XIX were obtained by Carrington's (9) procedures. Compound XVIII was obtained by thionation of the corresponding hydantoin with phosphorus hemipentasulfide in refluxing dioxane. Compound XVII was the commercial product[4]. Properties of VIII, IX (7), XII (10), and XIV (11) were in agreement with the literature.

Compound X had a melting point of 245–246°; *m/e* 274 (M^+), 245 (—COH), 192 (C_6H_{10}), 135 (C_6H_5NCS), 104 (C_6H_5CNH), and 77 (C_6H_5). Compound XI had a melting point of 229–231° dec.; *m/e* 268 (M^+), 239 (—COH), 149 ($C_6H_5CH_2NCS$), 135 (C_6H_5NCS), 104 (C_6H_5CNH), and 77 (C_6H_5). Compound XIII had a melting point of 251–253°; *m/e* 350 (M^+), 268 (C_6H_{10}), 135 (C_6H_5NCS), 104 (C_6H_5CNH), and 77 (C_6H_5).

Compound XV had a melting point of 195–196° dec.; *m/e* 234 (M^+), 206 (—CO), 163 ($C_6H_5CHNCSNH$), 105 (C_6H_5CHNH), and 77 (C_6H_5). Compound XVIII had a melting point of 290–292°; *m/e* 274 (M^+), 245 (—CHO), 240 (—H_2S), 192 (C_6H_{10}), 84 (C_6H_{10}, C_6H_5), and

[4] Aldrich D 21, 425-6.

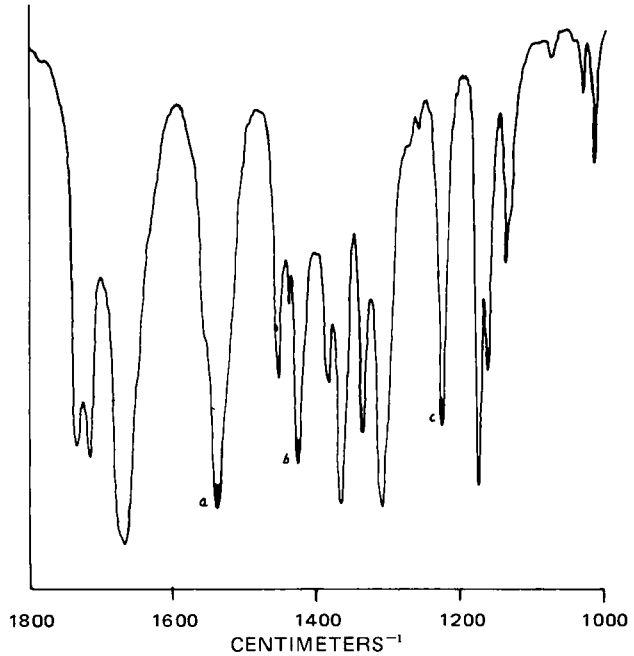

Figure 1—*IR spectrum of 2-thiobarbital in potassium bromide pellet. Key: a, thioureide band; b, antisymmetric stretching mode of NCS; and c, symmetric stretching mode of NCS.*

77 (C_6H_5).

2-Thiobarbiturates XX[5], XXI[6], XXII[7], XXIII[8], and XXIV[9] were commercial products. Thiobarbiturates XXV–XXVIII were described previously (2).

RESULTS AND DISCUSSION

On the assumption that similar structures of thiourea derivatives, including the NC(=S)N sequence in different surroundings, would present only slight modifications in their NCS antisymmetric and stretching modes, 2-thiohydantoins can be regarded as cyclic monoacylthioureas and 2-thiobarbiturates can be regarded as cyclic diacylthioureas.

According to the study of Davies and Jones (12), the NCS antisymmetric and symmetric stretching modes were tentatively assigned at 1452–1410 and 1260–1230 cm^{-1}, respectively, in a series of *N*-phenylthioureas (I–VII) (Table I). This value was in good agreement with the observed C and D bands[10] in the extensive work of Jensen and Nielsen (5).

In a series of seven 3-phenyl-2-thiohydantoins (VIII–XIV), ranges of 1445–1430 and 1250–1230 cm^{-1} were found for ν_{as} and ν_s NCS, respectively. 2-Thiohydantoins (XVII–XIX) showed the ν_{as} NCS mode centered at 1445 cm^{-1} and the ν_s NCS mode at 1220 cm^{-1}. 1-Acetyl-2-thiohydantoins (XV and XVI), which are structurally related to 2-thiobarbiturates, had bands at 1410 and 1210 cm^{-1} (Table II). 2-Thiobarbiturates (XX–XXIV) (Table III) showed bands at 1425–1410 and 1225–1200 cm^{-1}, in good agreement with 1-acetyl-2-thiohydantoins (XV and XVI) (Table II).

In 2,4-dithiobarbital (XXVI) and 2,4,6-trithiobarbital (XXVIII), the position of characteristic bands of the 2-thiocarbonyl group seemed to be rather independent and showed only slight deviations, which probably arose from electronic density modifications in the barbiturate nucleus by introducing a second and a third thiocarbonyl group. In 4-thiobarbital (XXV) and 2,4-dithiobarbital (XXVI), the values of 1455/1248 and 1448/1240 cm^{-2} were somewhat higher than the observed range for 2-thiobarbiturates; this fact is in agreement with the "more thioamide character" of the 4-thiocarbonyl group (Table III).

In the thiobarbiturate series, coupling between the 4- and 6-thiocarbonyl groups can be expected, as was demonstrated in the barbiturate series (2). In this type of coupling, the vibrators are not directly linked; in consequence, the higher characteristic frequency is assigned to ν_s. Owing to the coupling strength (about 200 cm^{-1}) and the symmetry of the barbiturate nucleus, the NCS antisymmetric and symmetric stretching modes of the 4- and 6-thiocarbonyl groups are coupled two by two; four signals result, two around 1400 cm^{-1} and two around 1200 cm^{-1}. This prediction agrees with the observed values (Table III).

The use of ν_{as} and ν_s NCS completes the characterization by the thioureide band. Whereas the phenyl nucleus bands around 1600 and 1500 cm^{-1} are generally of moderate absorption, the thioureide band can be easily located as a strong band in *N*-phenylthioureas (I–VII) at 1555–1515, in 3-phenyl-2-thiohydantoins (VIII–XIV) at 1520–1485, in 2-thiohydantoins (XVII–XIX) at 1530–1512, and in 1-acetyl-2-thiohydantoins (XV and XVI) at 1470 cm^{-1}. 2-Thiobarbiturates (XX–XXIV), 2,4-dithiobarbital (XXVI), and 2,4,6-trithiobarbital (XXVIII) present thioureide bands at 1545–1510 cm^{-1}. Figure 1 shows one representative IR spectrum of this series of compounds.

4-Thiobarbital (XXV) and 4,6-dithiobarbital (XXVII) do not show thioureide bands. This fact reflects the "more thioamide character" of the 4-thiocarbonyl group in agreement with above results. Bands were found at 1480 cm^{-1} for XXV and at 1460 cm^{-1} for XXVII in the observed range for *N*-acetylthioamides (13).

[5] Thyreosedine, Kela.
[6] Pentothal, Abbott.
[7] Inactin, Promonta.
[8] Thionarcex, Crinex Uve.
[9] Kemithal, Imperial Chemical.
[10] In this appellation, C and D bands can be regarded as the antisymmetric and symmetric stretching modes of NCS, respectively.

REFERENCES

(1) W. A. S. Paul and P. J. A. Demoen, *Bull. Soc. Chim. Belg.*, **75**, 524(1966).

(2) R. Bouche, *Chim. Ther.*, **1973**, 676.

(3) L. J. Bellamy, "Advances in Infrared Group Frequencies," Methuen, London, England, 1968, p. 212.

(4) T. D. Elmore, *J. Chem. Soc.*, **1958**, 3489.

(5) K. A. Jensen and P. H. Nielsen, *Acta Chem. Scand.*, **20**, 597(1966).

(6) A. I. Vogel, "Practical Organic Chemistry," 3rd ed., Longmans, London, England, 1962, p. 422.

(7) V. H. Stepanov, N. S. Vul'fson, V. A. Puchkov, and A. M. Zyakun, *Zh. Obshch. Khim.*, **34**, 3822(1964).

(8) P. Edman, *Acta Chem. Scand.*, **4**, 277(1950).

(9) H. C. Carrington, *J. Chem. Soc.*, **1947**, 684.

(10) G. Simig, K. Lempert, and J. Tamas, *Tetrahedron*, **29**, 3571(1973).

(11) H. Auterhoff and J. G. Hansen, *Pharmazie*, **250**, 336(1970).

(12) M. Davies and W. J. Jones, *J. Chem. Soc.*, **1958**, 955.

(13) J. Goerdeler and K. Stadelbauer, *Ber.*, **98**, 1557(1965).

ACKNOWLEDGMENTS AND ADDRESSES

Received March 31, 1975, from the *Laboratory for Pharmaceutical Analysis, Medicinal Chemistry Department, Catholic University of Louvain, Van Evenstraat, 4, B–3000 Leuven, Belgium.*

Accepted for publication October 10, 1975.

J. Poupaert is indebted to IRSIA (Institut pour l'encouragement de la recherche scientifique dans l'industrie et l'agriculture) for financial support.

[x] To whom inquiries should be directed.

In Vivo Loss of Tritium from Labeled Drugs: Determinations in Urine and Plasma

Keyphrases □ Tritium-labeled drugs—*in vivo* loss of tritium, urine and plasma analyses compared □ Radioactive labels—*in vivo* loss of tritium, urine and plasma levels compared □ Benzazocines, substituted—tritium labeled, used in study of *in vivo* loss of tritium, urine and plasma levels compared

To the Editor:

We wish to report an interesting observation that occurred during metabolic studies with tritium-labeled compounds.

Frequently, tritiated compounds can be prepared more economically and with a higher specific activity than carbon-14-labeled compounds. The main disadvantage of using tritium is that the tracer can be lost from the molecule by exchange with the hydrogen atoms of the solvent, whereas a similar exchange between carbon-14 and carbon-12 is not possible. Even where no *in vitro* exchange is observed in water, urine, or plasma, an *in vivo* loss of label leading to problems of interpretation is still possible.

The *in vivo* stability of a tritium label is usually tested by distillation of urine specimens (1). Our results indicate that the distillation of plasma specimens provides an earlier and more apparent indication regarding the *in vivo* stability of the tritium label in an organic molecule.

During studies on the biological disposition of several tritium-labeled drugs, we found a considerably greater percentage of volatile radioactivity in plasma than in urine. The following example is illustrative.

The analgesic *l*-6,11α-diethyl-1,2,3,4,5,6-hexahydro-3-methyl-2,6-methano-3-benzazocin-8-ol hydrochloride (I)(2) was labeled by adding 3.0 g of tritiated water (3.0 Ci) to 3.4 g of I and 4.8 g of phosphorus pentoxide at −70°. The mixture was allowed to warm, and the resulting solution was heated at 100° for 4 hr. The reaction mixture was poured onto a mixture of ice and concentrated ammonium hydroxide, and the resulting precipitate was collected by filtration.

The solid was dissolved in ether, and the solution was washed with water, dried over sodium sulfate, and acidified with hydrogen chloride gas. Then the product was collected and recrystallized from 2-propanol to give 2.4 g of analytically pure (C, H, Cl, N) prisms. The NMR spectrum of the product of a similar experiment using

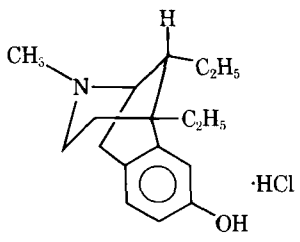

I

Table I—Urinary Excretion of Radioactivity in a Monkey Given 2 mg/kg ip of ^{3}H-I

Interval, hr	Excreted Radioactivity, % of Dose		Distillable / Total × 100
	Total	Distillable	
0–6	48.8	0.05	0.1
6–24	14.5	0.35	2.4
24–48	3.2	0.84	26.3

deuterium oxide showed the deuterium to be in both positions *ortho* to the phenolic hydroxyl group of I. A similar acid-catalyzed exchange reaction also was reported (3).

A 2-mg/kg ip dose of tritiated I (specific activity 34 μCi/mg) was given to a Rhesus monkey, and the total radioactivity content of plasma and urine specimens was measured by direct counting[1] in Bray's solution (4) using the external standard method of quench correction. Volatile radioactivity was determined by lyophilization and counting. Two consecutive lyophilizations were performed to avoid contamination by mechanical carryover of nonvolatile material. The *in vitro* stability of the tritium label was demonstrated in control experiments by incubation at 37° in urine and plasma.

Urinary excretion of radioactivity is summarized in Table I. These results might suggest that the initial *in vivo* loss of label was not sufficiently fast to affect the validity of the experiment, at least during the first 24 hr after administration of I. However, a considerably greater proportion of distillable radioactivity was found in the plasma of the animal during that time interval (Table II).

Further analysis revealed that the discrepancy between urine and plasma could be resolved in terms of the concentrations of tritiated water. Since the weight of the monkey was approximately 3 kg, it received approximately 204 μCi of radioactivity. During the first 6 hr after dosing, the urine (volume of 25 ml) contained 0.05% of the dose or 0.1 μCi as distillable radioactivity. Thus, the concentration of distillable urinary radioactivity amounted to 4×10^{-3} μCi/ml.

Since some time was necessary for absorption to occur from the injection site, the 4-hr time point was an acceptable approximation for the true midpoint of the interval between 0 and 6 hr. Distillable plasma radioactivity at 4 hr attained 0.102 μg/ml, expressed as unchanged I. This value corresponds to 3.4×10^{-3} μCi/ml of distillable radioactivity.

Thus, at the early time interval, the results show good agreement between the concentrations of tritiated water in urine and plasma. The agreement was found in spite of the apparently large differences between the ratios of distillable to total radioactivity in urine and plasma (Tables I and II). One can rationalize the findings by assuming that the glomerular filtration and tubular

[1] Packard Tri-Carb model 3380 scintillation spectrophotometer.

Table II—Plasma Concentrations of Radioactivity in a Monkey Given 2 mg/kg ip of ^{3}H-I

Hours	Plasma Radioactivity[a], μg/ml		Distillable / Total × 100
	Total	Distillable	
0.5	2.48	0.060	2.4
1	2.11	0.076	3.6
2	1.34	0.043	3.2
4	0.61	0.102	16.7
7	0.19	0.057	29.9
24	0.11	0.093	84.5
48	0.08	0.076	94.7

[a] Each value is the amount of administered drug that would give rise to the observed radioactivity.

reabsorption processes of the kidney could not distinguish tritiated water from unlabeled water. Therefore, tritiated water would have comparable concentrations in urine and plasma and would be excreted at the same rate as unlabeled water. The exact value for the half-life of water in the monkey is not known, but corresponding values of 3.5, 3.9, and 5.1 days have been reported for the rat, rabbit, and dog, respectively (5).

In contrast, I and/or its metabolites were rapidly excreted and their plasma levels fell below their concentration in urine. The result of these differences in the excretion rates of tritiated water and I was a greater ratio of distillable to total radioactivity in plasma than in urine.

The observed *in vivo* loss of the tritium label might be attributed to a tritium–hydrogen exchange, perhaps facilitated by some biological mechanism, or to a specific metabolic alteration of the molecule at the site of tritium substitution. To distinguish between these two mechanisms of *in vivo* instability, one must isolate the unchanged drug from urine or plasma and compare its specific activity with that of the administered drug. Comparable specific activities would suggest that the loss of label occurred in conjunction with metabolism at the site of tritium substitution. In contrast, a decrease of specific activity would indicate that the loss of label was caused partly or entirely by exchange.

The findings reported in this communication may have general applicability and serve as a warning to the uninitiated user of tritium. One must be careful in drawing conclusions from urinary data regarding the *in vivo* stability of the tritium label in a compound. Furthermore, our results strengthen the argument that when a substantial fraction of the label is lost, tritium should not be used as a tracer for the parent molecule.

(1) L. E. Feinendegen, "Tritium-Labeled Molecules in Biology and Medicine," Academic, New York, N.Y., 1967, pp. 26–48.

(2) J. H. Ager and E. L. May, *J. Org. Chem.*, **27**, 245(1962).

(3) R. Schoenheimer, D. Rittenberg, and A. S. Keaton, *J. Am. Chem. Soc.*, **59**, 1765(1937).

(4) A. Bray, *Anal. Biochem.*, **1**, 279(1960).

(5) C. R. Richmond, W. H. Laugham, and T. T. Trujillo, *J. Cell. Comp. Physiol.*, **59**, 45(1962).

George Lukas [x]
Elliot Redalieu
Research Department
Pharmaceuticals Division
Ciba-Geigy Corporation
Ardsley, NY 10502

Received January 16, 1975.
Accepted for publication June 7, 1976.
The authors are indebted to Dr. Frank H. Clarke, Dr. Naokata Yokoyama, and Mr. Walter Munch, Ciba-Geigy Corp., for the preparation of tritiated I. The technical assistance of Mrs. Judith Zagarella is gratefully acknowledged.

[x] To whom inquiries should be directed.

GLC Determination of Pilocarpine

Keyphrases □ Pilocarpine—GLC analysis, rabbit aqueous humor □ GLC—analysis, pilocarpine, rabbit aqueous humor □ Ophthalmic cholinergic agents—pilocarpine, GLC analysis, rabbit aqueous humor

To the Editor:

Measurement of the transport of pilocarpine into the internal eye as well as information concerning its distribution and inactivation within individual intraocular structures depends on accurate determination of small quantities of this drug in biological fluids. Although many procedures have been used for this purpose, including those involving polarimetric, polarographic, volumetric, colorimetric, and kinetic techniques (1–6), all have been associated with problems of complexity, lack of specificity, or lack of sensitivity.

GLC coupled with electron-capture detection has been employed during the past 10 years for the determination of nanogram amounts of organic compounds exhibiting certain similarities to pilocarpine (7–9). A similar technique provided an ideal system for a sensitive new procedure for the reliable assay of pilocarpine.

Heptafluorobutyric anhydride[1], trimethylamine, and pesticide grade benzene[2] were utilized in the formation of the derivative of pilocarpine[3]. Heptafluorobutyric anhydride (10 μl) and 0.1 ml of trimethylamine (0.05 *M* in benzene) were added to 500 μg of pilocarpine hydrochloride in benzene (10). The reaction was performed in screw-capped vials[4]. After the sample was heated for 15 min at 50°, 1 ml of water was added and the vial was shaken for 1 min. One milliliter of aqueous ammonia (5%) was added, and the reaction mixture was shaken for an additional 5 min.

After centrifugation, the benzene layer was diluted to give a derivative concentration of 100 ng/ml. Then 1 μl (equal to 0.1 ng) was injected into a 1.2-m × 4-mm i.d. U-shaped column packed with 2% XF-1105[5] on Gas Chrom Q[6] (80–100 mesh) for GLC analysis. Separation of the derivative was achieved using a gas chromatograph[7] equipped with two electron-capture detectors, each containing a 150-mCi tritium foil.

The oven temperature was kept at 190°; the detector, inlet, and outlet temperatures were maintained at 200°.

[1] Pierce Chemical Co., Rockford, Ill.
[2] Fisher Scientific Co.
[3] Mallinckrodt Chemical Co.
[4] Lined with Teflon (du Pont).
[5] Now called OV-105.
[6] Ohio Valley Specialty Chemical, Marietta, Ohio.
[7] Packard model 7400.

Table II—Plasma Concentrations of Radioactivity in a Monkey Given 2 mg/kg ip of ^{3}H-I

Hours	Plasma Radioactivity[a], μg/ml		Distillable / Total × 100
	Total	Distillable	
0.5	2.48	0.060	2.4
1	2.11	0.076	3.6
2	1.34	0.043	3.2
4	0.61	0.102	16.7
7	0.19	0.057	29.9
24	0.11	0.093	84.5
48	0.08	0.076	94.7

[a] Each value is the amount of administered drug that would give rise to the observed radioactivity.

reabsorption processes of the kidney could not distinguish tritiated water from unlabeled water. Therefore, tritiated water would have comparable concentrations in urine and plasma and would be excreted at the same rate as unlabeled water. The exact value for the half-life of water in the monkey is not known, but corresponding values of 3.5, 3.9, and 5.1 days have been reported for the rat, rabbit, and dog, respectively (5).

In contrast, I and/or its metabolites were rapidly excreted and their plasma levels fell below their concentration in urine. The result of these differences in the excretion rates of tritiated water and I was a greater ratio of distillable to total radioactivity in plasma than in urine.

The observed *in vivo* loss of the tritium label might be attributed to a tritium–hydrogen exchange, perhaps facilitated by some biological mechanism, or to a specific metabolic alteration of the molecule at the site of tritium substitution. To distinguish between these two mechanisms of *in vivo* instability, one must isolate the unchanged drug from urine or plasma and compare its specific activity with that of the administered drug. Comparable specific activities would suggest that the loss of label occurred in conjunction with metabolism at the site of tritium substitution. In contrast, a decrease of specific activity would indicate that the loss of label was caused partly or entirely by exchange.

The findings reported in this communication may have general applicability and serve as a warning to the uninitiated user of tritium. One must be careful in drawing conclusions from urinary data regarding the *in vivo* stability of the tritium label in a compound. Furthermore, our results strengthen the argument that when a substantial fraction of the label is lost, tritium should not be used as a tracer for the parent molecule.

(1) L. E. Feinendegen, "Tritium-Labeled Molecules in Biology and Medicine," Academic, New York, N.Y., 1967, pp. 26–48.

(2) J. H. Ager and E. L. May, *J. Org. Chem.*, **27**, 245(1962).

(3) R. Schoenheimer, D. Rittenberg, and A. S. Keaton, *J. Am. Chem. Soc.*, **59**, 1765(1937).

(4) A. Bray, *Anal. Biochem.*, **1**, 279(1960).

(5) C. R. Richmond, W. H. Laugham, and T. T. Trujillo, *J. Cell. Comp. Physiol.*, **59**, 45(1962).

George Lukas [x]
Elliot Redalieu
Research Department
Pharmaceuticals Division
Ciba-Geigy Corporation
Ardsley, NY 10502

Received January 16, 1975.
Accepted for publication June 7, 1976.
The authors are indebted to Dr. Frank H. Clarke, Dr. Naokata Yokoyama, and Mr. Walter Munch, Ciba-Geigy Corp., for the preparation of tritiated I. The technical assistance of Mrs. Judith Zagarella is gratefully acknowledged.

[x] To whom inquiries should be directed.

GLC Determination of Pilocarpine

Keyphrases □ Pilocarpine—GLC analysis, rabbit aqueous humor □ GLC—analysis, pilocarpine, rabbit aqueous humor □ Ophthalmic cholinergic agents—pilocarpine, GLC analysis, rabbit aqueous humor

To the Editor:

Measurement of the transport of pilocarpine into the internal eye as well as information concerning its distribution and inactivation within individual intraocular structures depends on accurate determination of small quantities of this drug in biological fluids. Although many procedures have been used for this purpose, including those involving polarimetric, polarographic, volumetric, colorimetric, and kinetic techniques (1–6), all have been associated with problems of complexity, lack of specificity, or lack of sensitivity.

GLC coupled with electron-capture detection has been employed during the past 10 years for the determination of nanogram amounts of organic compounds exhibiting certain similarities to pilocarpine (7–9). A similar technique provided an ideal system for a sensitive new procedure for the reliable assay of pilocarpine.

Heptafluorobutyric anhydride[1], trimethylamine, and pesticide grade benzene[2] were utilized in the formation of the derivative of pilocarpine[3]. Heptafluorobutyric anhydride (10 μl) and 0.1 ml of trimethylamine (0.05 *M* in benzene) were added to 500 μg of pilocarpine hydrochloride in benzene (10). The reaction was performed in screw-capped vials[4]. After the sample was heated for 15 min at 50°, 1 ml of water was added and the vial was shaken for 1 min. One milliliter of aqueous ammonia (5%) was added, and the reaction mixture was shaken for an additional 5 min.

After centrifugation, the benzene layer was diluted to give a derivative concentration of 100 ng/ml. Then 1 μl (equal to 0.1 ng) was injected into a 1.2-m × 4-mm i.d. U-shaped column packed with 2% XF-1105[5] on Gas Chrom Q[6] (80–100 mesh) for GLC analysis. Separation of the derivative was achieved using a gas chromatograph[7] equipped with two electron-capture detectors, each containing a 150-mCi tritium foil.

The oven temperature was kept at 190°; the detector, inlet, and outlet temperatures were maintained at 200°.

[1] Pierce Chemical Co., Rockford, Ill.
[2] Fisher Scientific Co.
[3] Mallinckrodt Chemical Co.
[4] Lined with Teflon (du Pont).
[5] Now called OV-105.
[6] Ohio Valley Specialty Chemical, Marietta, Ohio.
[7] Packard model 7400.

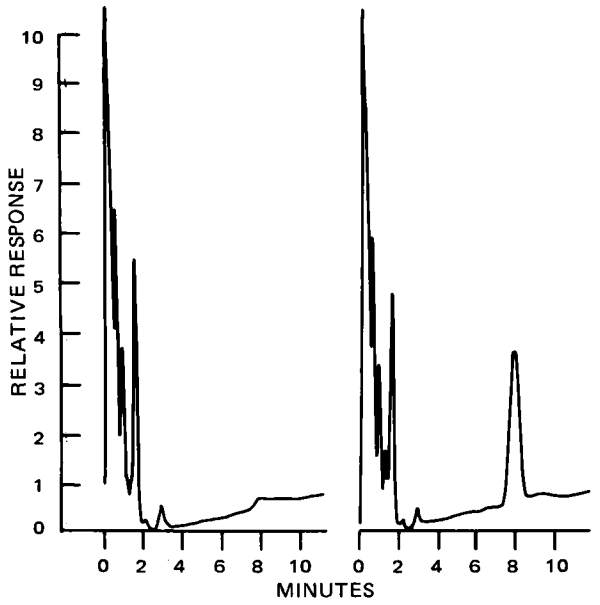

Figure 1—*Chromatogram of rabbit aqueous humor as the control and after the addition of pilocarpine. Chart speed was 0.5 cm/min.*

The flow rate of prepurified nitrogen was 70 ml/min, and the high voltage was set at 20 v. The full-scale deflection used on the 1-mv recorder was 1×10^{-9} amp.

The determination of retention time and linearity was done on dilutions of the standard. The standard curve was obtained by adding known amounts of pilocarpine hydrochloride to rabbit aqueous humor and isolating the drug as follows. Twenty-five microliters of rabbit aqueous humor was added to a 5-ml ground-glass centrifuge tube and diluted to 1 ml with a saturated solution of sodium chloride. The sample was acidified with 6 *N* hydrochloric acid to pH <1 and extracted with 3 ml of ethyl acetate by shaking for 1 min.

The ethyl acetate layer was discarded, and the aqueous layer was made basic (pH > 8) with 2 *M* potassium carbonate and reextracted with ethyl acetate (3, 3, and 2 ml) by shaking for 1 min. Then the ethyl acetate extracts were combined and evaporated in a 40° water bath. The sample was then transferred to a 3-ml screw-capped vial[4] with 0.5 ml of methanol followed by 0.5 ml of ethyl acetate. The specimen was again evaporated under a stream of dry nitrogen and derivatized as previously described.

The heptafluorobutyramide derivative of pilocarpine gave a single, sensitive, symmetrical peak with a retention time of 8 min. A linear response with respect to peak height was demonstrated by injection of 10–150 pg. The derivatized samples were stable for more than 1 week, and the recovery of pilocarpine added to samples was quantitative (95 ± 2%). The standard curve, obtained by addition of 25–200 ng of pilocarpine to 25 μl of rabbit aqueous humor, was described by the equation $y = 0.29x - 0.18$ ($r = 0.998$). No substances interfering with pilocarpine were noted in physiological saline, Ringer's solution, or rabbit aqueous fluid (Fig. 1).

Addition of serum to aqueous fluid caused no significant changes in the standard curve. The method thus obviates the analytical problem of serum binding of pilocarpine (11). The use of tritiated pilocarpine to test the reproducibility of the method was unsuitable because of the instability of the label in acidic and basic solutions. The minimum detectable quantity of this substance under the conditions of this study is 1 pg.

A comparably sensitive and specific method for the assay of small amounts of pilocarpine has not been described previously. Use of an apparently similar technique was alluded to recently (12), but details of the methodology are not available.

Assays in the past have been sensitive only to microgram quantities. Those employing tritiation have been limited by problems of purification (13), uncertainty of labeling position in the molecule, and tritium exchange when in solution. Those involving colorimetry required extreme care in excluding interfering compounds. The many potential pitfalls of UV spectrophotometry rendered such analyses complex and time consuming because of the requirement for elaborate controls (14, 15). Preparation of ^{14}C-pilocarpine, currently unavailable commercially, is complex and expensive (16).

The GLC procedure described here is reliable, easily performed, and more than three orders more sensitive than previously used methods. It is ideally suited to determinations of small quantities of pilocarpine (1 ng) in small amounts of biological fluid (such as 25 μl of aqueous humor).

(1) O. Hockwin, H. K. Muller, and U. Blaser, *Graefes Arch. Ophthalmol.*, **167**, 459(1964).

(2) I. S. Gibbs and M. M. Tuckerman, *J. Pharm. Sci.*, **59**, 395(1970).

(3) A. Repta and T. Higuchi, *ibid.*, **60**, 1465(1971).

(4) P. Chung, T. Chin, and J. L. Lach, *ibid.*, **59**, 1300(1970).

(5) E. Brochmann-Hanssen, P. Schmid, and J. D. Benmaman, *ibid.*, **54**, 783(1965).

(6) M. S. Karawya and M. G. Ghourab, *J. Assoc. Offic. Anal. Chem.*, **55**, 1180(1972).

(7) L. M. Bertani, S. W. Dziedzic, D. D. Clarke, and S. E. Gitlow, *Clin. Chim. Acta*, **30**, 227(1970).

(8) S. Wilk, S. E. Gitlow, and L. M. Bertani, in "Methods in Diagnostic and Investigative Endocrinology," S. A. Berson and I. J. Kopin, Eds., Elsevier, New York, N.Y., 1972, pp. 452–473.

(9) S. W. Dziedzic and S. E. Gitlow, *J. Neurochem.*, **22**, 333(1974).

(10) T. Walle and H. Ehrsson, *Acta Pharm. Suec.*, **7**, 389(1970).

(11) D. A. Newsome and R. Stern, *Am. J. Ophthalmol.*, **77**, 918(1974).

(12) W. F. Bayne, F. T. Tao, L. C. Chu, and J. Urquhart, presented at the Association for Research in Vision and Ophthalmology, Sarasota, Fla., May 1, 1975.

(13) J. J. Chrai and J. R. Robinson, *Am. J. Ophthalmol.*, **77**, 735(1974).

(14) D. L. Krohn and J. M. Breitfeller, *Invest. Ophthalmol.*, **13**, 312(1974).

(15) *Ibid.*, **14**, 152(1975).

(16) L. Sendelbeck, D. Moore, and J. Urquhart, *Am. J. Ophthalmol.*, **80**, 274(1975).

Stanley W. Dziedzic
Stanley E. Gitlow
Department of Medicine
Mount Sinai School of Medicine
New York, NY 10029

David L. Krohn [x]
Department of Ophthalmology
New York University Medical Center
New York, NY 10016

Received January 27, 1976.
Accepted for publication May 26, 1976.
Supported in part by Grant HL 12648 from the National Heart and Lung Institute and Grant CA 18705 from the National Cancer Institute, National Institutes of Health.
* To whom inquiries should be directed.

Effect of Plasma Protein Binding of Drugs on Duration and Intensity of Pharmacological Activity

Keyphrases □ Plasma protein binding—effect on duration and intensity of pharmacological activity of drugs □ Binding, plasma protein—effect on duration and intensity of pharmacological activity of drugs □ Pharmacological activity—duration and intensity, effect of plasma protein binding of drugs

To the Editor:

There is increasing evidence that the pharmacological activity of drugs is a function of their free (not protein bound) concentration (1–4). It has also become apparent that the total clearance of drugs by the body is affected by the extent to which they are plasma protein bound (5–7). It is informative, therefore, to consider the effect of a change in plasma protein binding of a drug on the duration and intensity of its pharmacological activity, particularly since these indicators have been used to study drug interactions involving competitive displacement from plasma protein binding sites (8, 9).

It will be assumed as a matter of convenience that the free fraction of drug in plasma (f) is essentially constant over a wide concentration range (5, 6, 10), that the elimination of the drug is by apparent first-order kinetics and not affected by organ perfusion rate, that the drug is distributed in the body so rapidly as to justify the use of a one-compartment pharmacokinetic model, and that the only *direct* perturbation of the biological system is a change in f. Under these conditions:

$$\text{total clearance} = k''f \qquad \text{(Eq. 1)}$$

where k'' is the intrinsic clearance of the drug (5, 6). Also:

$$\text{total clearance} = V_d k_{app} \qquad \text{(Eq. 2)}$$

where V_d is the apparent volume of distribution of total (free and bound) drug, and k_{app} is the apparent first-order elimination rate constant. It is evident that an increase in f results in a corresponding increase in total clearance or $V_d k_{app}$. The quantitative effect of an increase in f on V_d is difficult to predict, but it appears to be smaller than the effect on k_{app} (6).

Figure 1 shows the effect of an increase in f from 0.01 to 0.03 on the time course of free and total drug concentrations after intravenous injection of 100 mg/kg of a drug with V_d = 0.20 liter/kg and k_{app} = 0.05776 hr^{-1} (equivalent to $t_{1/2}$ = 12 hr) under conditions where: (*a*) V_d increases to 0.25 liter/kg or (*b*) V_d is unaffected. In either case, it is evident that the increase in f causes an

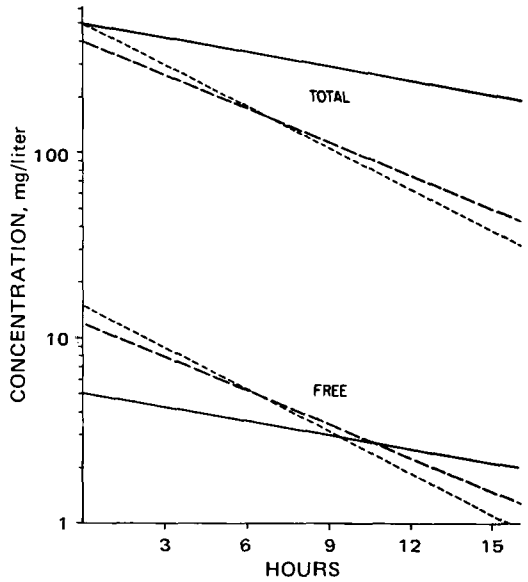

Figure 1—*Effect of a change in free fraction in plasma (f) on the time course of total and free drug concentrations in plasma after intravenous injection of 100 mg/kg. Key: continuous line, V_d = 0.20 liter/kg, $t_{1/2}$ = 12 hr, and f = 0.01; short stippled line, f increased to 0.03, and V_d unchanged; and long stippled line, f increased to 0.03, and V_d increased to 0.25 liter/kg. These simulations are based on the assumption that the total clearance increases proportionally with f.*

increase in the initial concentration of free drug but also a more rapid decline so that the free concentration when f = 0.03 will eventually be lower than when f = 0.01. This means that an increase in f will cause an increase in the intensity of the initial (maximum) pharmacological effect but that the duration of action may be increased *or* decreased, depending on the dose and the minimum effective concentration of free drug. For any one drug, an increase in f under the stated conditions may be expected to prolong the duration of pharmacological activity of small doses and to shorten the duration of action of large single doses.

It has been observed that the incidence of adverse

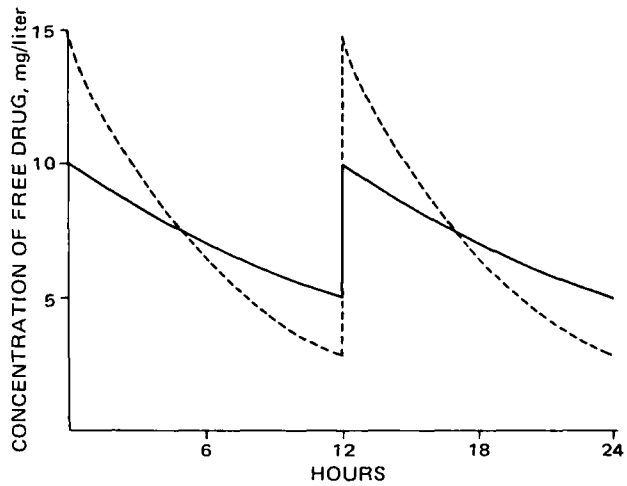

Figure 2—*Effect of a change in f on the time course of free drug concentrations in plasma at the steady state when 100 mg of drug/kg is administered intravenously every 12 hr. Key: continuous line, V_d = 0.20 liter/kg, $t_{1/2}$ = 12 hr, and f = 0.01; and stippled line, f increased to 0.03, V_d increased to 0.25 liter/kg, and $t_{1/2}$ decreased, therefore, to 5 hr.*

Received January 27, 1976.
Accepted for publication May 26, 1976.
Supported in part by Grant HL 12648 from the National Heart and Lung Institute and Grant CA 18705 from the National Cancer Institute, National Institutes of Health.
* To whom inquiries should be directed.

Effect of Plasma Protein Binding of Drugs on Duration and Intensity of Pharmacological Activity

Keyphrases □ Plasma protein binding—effect on duration and intensity of pharmacological activity of drugs □ Binding, plasma protein—effect on duration and intensity of pharmacological activity of drugs □ Pharmacological activity—duration and intensity, effect of plasma protein binding of drugs

To the Editor:

There is increasing evidence that the pharmacological activity of drugs is a function of their free (not protein bound) concentration (1–4). It has also become apparent that the total clearance of drugs by the body is affected by the extent to which they are plasma protein bound (5–7). It is informative, therefore, to consider the effect of a change in plasma protein binding of a drug on the duration and intensity of its pharmacological activity, particularly since these indicators have been used to study drug interactions involving competitive displacement from plasma protein binding sites (8, 9).

It will be assumed as a matter of convenience that the free fraction of drug in plasma (f) is essentially constant over a wide concentration range (5, 6, 10), that the elimination of the drug is by apparent first-order kinetics and not affected by organ perfusion rate, that the drug is distributed in the body so rapidly as to justify the use of a one-compartment pharmacokinetic model, and that the only *direct* perturbation of the biological system is a change in f. Under these conditions:

$$\text{total clearance} = k''f \qquad \text{(Eq. 1)}$$

where k'' is the intrinsic clearance of the drug (5, 6). Also:

$$\text{total clearance} = V_d k_{app} \qquad \text{(Eq. 2)}$$

where V_d is the apparent volume of distribution of total (free and bound) drug, and k_{app} is the apparent first-order elimination rate constant. It is evident that an increase in f results in a corresponding increase in total clearance or $V_d k_{app}$. The quantitative effect of an increase in f on V_d is difficult to predict, but it appears to be smaller than the effect on k_{app} (6).

Figure 1 shows the effect of an increase in f from 0.01 to 0.03 on the time course of free and total drug concentrations after intravenous injection of 100 mg/kg of a drug with V_d = 0.20 liter/kg and k_{app} = 0.05776 hr^{-1} (equivalent to $t_{1/2}$ = 12 hr) under conditions where: (*a*) V_d increases to 0.25 liter/kg or (*b*) V_d is unaffected. In either case, it is evident that the increase in f causes an

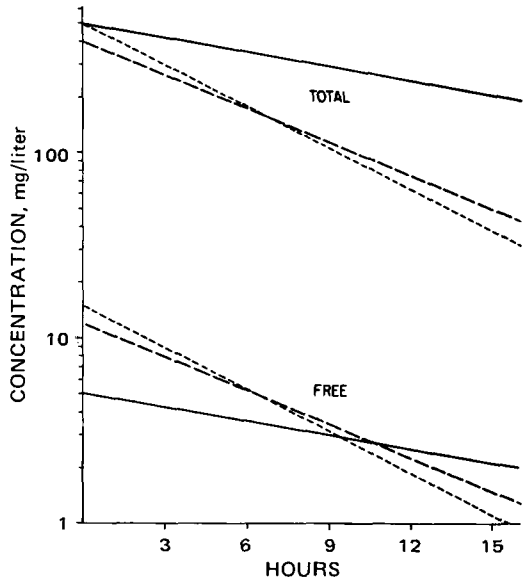

Figure 1—*Effect of a change in free fraction in plasma (f) on the time course of total and free drug concentrations in plasma after intravenous injection of 100 mg/kg. Key: continuous line, V_d = 0.20 liter/kg, $t_{1/2}$ = 12 hr, and f = 0.01; short stippled line, f increased to 0.03, and V_d unchanged; and long stippled line, f increased to 0.03, and V_d increased to 0.25 liter/kg. These simulations are based on the assumption that the total clearance increases proportionally with f.*

increase in the initial concentration of free drug but also a more rapid decline so that the free concentration when f = 0.03 will eventually be lower than when f = 0.01. This means that an increase in f will cause an increase in the intensity of the initial (maximum) pharmacological effect but that the duration of action may be increased *or* decreased, depending on the dose and the minimum effective concentration of free drug. For any one drug, an increase in f under the stated conditions may be expected to prolong the duration of pharmacological activity of small doses and to shorten the duration of action of large single doses.

It has been observed that the incidence of adverse

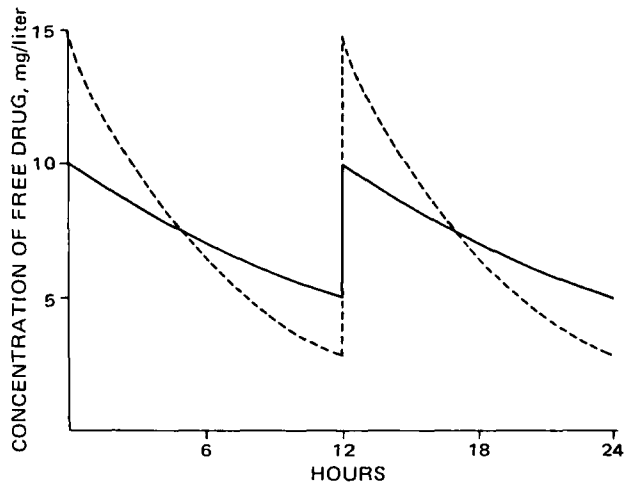

Figure 2—*Effect of a change in f on the time course of free drug concentrations in plasma at the steady state when 100 mg of drug/kg is administered intravenously every 12 hr. Key: continuous line, V_d = 0.20 liter/kg, $t_{1/2}$ = 12 hr, and f = 0.01; and stippled line, f increased to 0.03, V_d increased to 0.25 liter/kg, and $t_{1/2}$ decreased, therefore, to 5 hr.*

effects of certain drugs increases with a decrease in the concentration of albumin in plasma (11, 12). Since f increases with decreasing albumin concentration, it has been suggested that the increased incidence of adverse effects of drugs in patients with hypoalbuminemia may be due to decreased binding of such drugs to plasma proteins, among other factors (11, 12). The "average" steady-state concentration of total drug in plasma ($\bar{C}_p$) is:

$$\bar{C}_p = R/\text{total clearance} \qquad \text{(Eq. 3)}$$

where R is the dosing rate (13). Therefore, according to Eq. 1:

$$f\bar{C}_p = R/k'' \qquad \text{(Eq. 4)}$$

which shows that the average steady-state concentration of free drug should be unaffected by a change in f. This effect was demonstrated experimentally (14, 15). Based on these considerations, it has been stated that a change in f should not affect the intensity of pharmacological activity of a drug during the steady state. However, this conclusion is not necessarily correct.

Figure 2 shows the time course of steady-state free drug concentrations for the hypothetical drug described in Fig. 1 under conditions when $f = 0.01$ or 0.03 and V_d is 0.20 or 0.25 liter/kg. While the average concentration of free drug (area under the curve divided by dosing interval) is equal under both conditions, its maximum concentration is substantially higher when $f = 0.03$. Consequently, it is entirely feasible that an increase in f results in an increased incidence of adverse effects[1].

(1) A. H. Anton, *J. Pharmacol. Exp. Ther.*, **129**, 282(1960).

(2) H. E. Booker and B. Darcey, *Epilepsia*, **14**, 177(1973).

(3) A. Yacobi and G. Levy, *Res. Commun. Chem. Pathol. Pharmacol.*, **12**, 405(1975).

(4) D. W. Shoeman and D. L. Azarnoff, *J. Pharmacol. Exp. Ther.*, **195**, 84(1975).

(5) G. Levy and A. Yacobi, *J. Pharm. Sci.*, **63**, 805(1974).

(6) A. Yacobi and G. Levy, *ibid.*, **64**, 1660(1975).

(7) G. R. Wilkinson and D. G. Shand, *Clin. Pharmacol. Ther.*, **18**, 377(1975).

(8) G. Pagnini, R. DiCarlo, F. DiCarlo, and E. Genazzani, *Biochem. Pharmacol.*, **20**, 3247(1971).

(9) M. D. Chaplin, A. P. Roszkowski, and R. K. Richards, *Proc. Soc. Exp. Biol. Med.*, **143**, 667(1973).

(10) W. J. Jusko and G. Levy, *J. Pharm. Sci.*, **58**, 58(1969).

(11) G. P. Lewis, W. J. Jusko, C. W. Burke, and L. Graves, *Lancet*, **2**, 778(1971).

(12) Boston Collaborative Drug Surveillance Program, *Clin. Pharmacol. Ther.*, **14**, 529(1973).

(13) J. G. Wagner, J. I. Northam, C. D. Alway, and O. S. Carpenter, *Nature*, **207**, 1301(1965).

(14) S. Øie and G. Levy, *J. Pharm. Sci.*, **64**, 1433(1975).

(15) R. Gugler, D. W. Shoeman, D. H. Huffman, J. B. Cohlmia, and D. L. Azarnoff, *J. Clin. Invest.*, **55**, 1182(1975).

Gerhard Levy

Department of Pharmaceutics
School of Pharmacy
State University of New York at Buffalo
Buffalo, NY 14214

[1] *Note added in proof:* Consistent with the theoretical predictions in this communication, it was recently reported [R. Gugler and D. L. Azarnoff, *Clin. Pharmacokinet.*, **1**, 25(1976)] that the maximum plasma concentration of free phenytoin is higher and the minimum plasma concentration is lower in nephrotic patients with hypoalbuminemia (phenytoin free fraction = 0.19) than in normal subjects (phenytoin free fraction = 0.10) at the steady state during multiple dosing of phenytoin. The incidence of adverse effects of phenytoin is increased in patients with hypoalbuminemia (12).

Received March 1, 1976.

Accepted for publication April 23, 1976.

Supported in part by Grants GM 19568 and GM 20852 from the National Institute of General Medical Sciences, National Institutes of Health, Bethesda, MD 20014

Appearance of Myelin Forms in Rheopexic Dispersions of Dioctyl Sodium Sulfosuccinate

Keyphrases ☐ Dioctyl sodium sulfosuccinate—rheopexic dispersions, formation of micelles ☐ Micelles—formation in rheopexic dispersions of dioctyl sodium sulfosuccinate ☐ Dispersions, rheopexic—dioctyl sodium sulfosuccinate, formation of micelles ☐ Rheopexic dispersions—dioctyl sodium sulfosuccinate, formation of micelles ☐ Surfactants—dioctyl sodium sulfosuccinate, rheopexic dispersions, formation of micelles

To the Editor:

The detection of long tubular structures visible under the electron microscope has been reported for aqueous dispersions of many phospholipids (1). These observable structural units have been described variously as "myelin forms" and "micelles." Stoeckenius (2) and Fernandez-Moran (3) detected, identified, and described myelin forms of phospholipids under the electron microscope at magnifications of 400,000–1,250,000×.

During work on the development of rheopexy in dispersions of dioctyl sodium sulfosuccinate in normal saline (4), the pronounced development of myelin forms was observed under the light microscope at 430× after a shear stress was applied. The dispersion consisting of

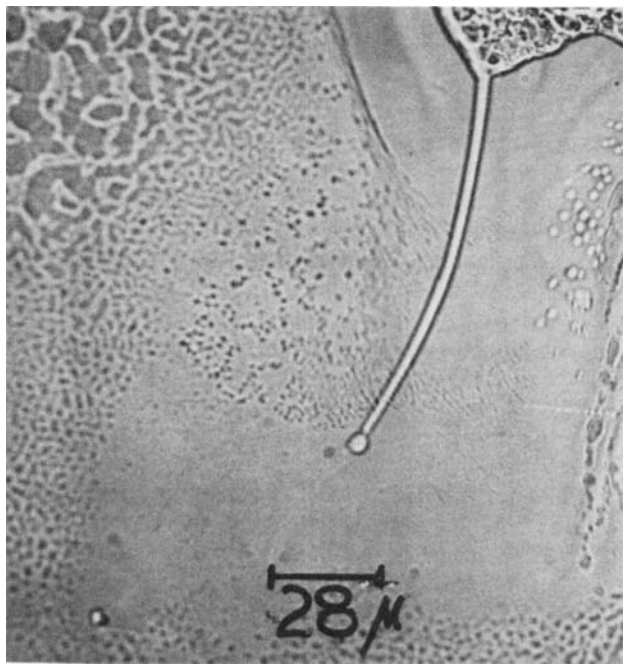

Figure 1—*Single tubular body thought to be a myelin form or micelle (430×).*

effects of certain drugs increases with a decrease in the concentration of albumin in plasma (11, 12). Since f increases with decreasing albumin concentration, it has been suggested that the increased incidence of adverse effects of drugs in patients with hypoalbuminemia may be due to decreased binding of such drugs to plasma proteins, among other factors (11, 12). The "average" steady-state concentration of total drug in plasma ($\bar{C}_p$) is:

$$\bar{C}_p = R/\text{total clearance} \qquad \text{(Eq. 3)}$$

where R is the dosing rate (13). Therefore, according to Eq. 1:

$$f\bar{C}_p = R/k'' \qquad \text{(Eq. 4)}$$

which shows that the average steady-state concentration of free drug should be unaffected by a change in f. This effect was demonstrated experimentally (14, 15). Based on these considerations, it has been stated that a change in f should not affect the intensity of pharmacological activity of a drug during the steady state. However, this conclusion is not necessarily correct.

Figure 2 shows the time course of steady-state free drug concentrations for the hypothetical drug described in Fig. 1 under conditions when $f = 0.01$ or 0.03 and V_d is 0.20 or 0.25 liter/kg. While the average concentration of free drug (area under the curve divided by dosing interval) is equal under both conditions, its maximum concentration is substantially higher when $f = 0.03$. Consequently, it is entirely feasible that an increase in f results in an increased incidence of adverse effects[1].

(1) A. H. Anton, *J. Pharmacol. Exp. Ther.*, **129**, 282(1960).

(2) H. E. Booker and B. Darcey, *Epilepsia*, **14**, 177(1973).

(3) A. Yacobi and G. Levy, *Res. Commun. Chem. Pathol. Pharmacol.*, **12**, 405(1975).

(4) D. W. Shoeman and D. L. Azarnoff, *J. Pharmacol. Exp. Ther.*, **195**, 84(1975).

(5) G. Levy and A. Yacobi, *J. Pharm. Sci.*, **63**, 805(1974).

(6) A. Yacobi and G. Levy, *ibid.*, **64**, 1660(1975).

(7) G. R. Wilkinson and D. G. Shand, *Clin. Pharmacol. Ther.*, **18**, 377(1975).

(8) G. Pagnini, R. DiCarlo, F. DiCarlo, and E. Genazzani, *Biochem. Pharmacol.*, **20**, 3247(1971).

(9) M. D. Chaplin, A. P. Roszkowski, and R. K. Richards, *Proc. Soc. Exp. Biol. Med.*, **143**, 667(1973).

(10) W. J. Jusko and G. Levy, *J. Pharm. Sci.*, **58**, 58(1969).

(11) G. P. Lewis, W. J. Jusko, C. W. Burke, and L. Graves, *Lancet*, **2**, 778(1971).

(12) Boston Collaborative Drug Surveillance Program, *Clin. Pharmacol. Ther.*, **14**, 529(1973).

(13) J. G. Wagner, J. I. Northam, C. D. Alway, and O. S. Carpenter, *Nature*, **207**, 1301(1965).

(14) S. Øie and G. Levy, *J. Pharm. Sci.*, **64**, 1433(1975).

(15) R. Gugler, D. W. Shoeman, D. H. Huffman, J. B. Cohlmia, and D. L. Azarnoff, *J. Clin. Invest.*, **55**, 1182(1975).

Gerhard Levy

Department of Pharmaceutics
School of Pharmacy
State University of New York at Buffalo
Buffalo, NY 14214

[1] *Note added in proof:* Consistent with the theoretical predictions in this communication, it was recently reported [R. Gugler and D. L. Azarnoff, *Clin. Pharmacokinet.*, **1**, 25(1976)] that the maximum plasma concentration of free phenytoin is higher and the minimum plasma concentration is lower in nephrotic patients with hypoalbuminemia (phenytoin free fraction = 0.19) than in normal subjects (phenytoin free fraction = 0.10) at the steady state during multiple dosing of phenytoin. The incidence of adverse effects of phenytoin is increased in patients with hypoalbuminemia (12).

Received March 1, 1976.

Accepted for publication April 23, 1976.

Supported in part by Grants GM 19568 and GM 20852 from the National Institute of General Medical Sciences, National Institutes of Health, Bethesda, MD 20014

Appearance of Myelin Forms in Rheopexic Dispersions of Dioctyl Sodium Sulfosuccinate

Keyphrases ☐ Dioctyl sodium sulfosuccinate—rheopexic dispersions, formation of micelles ☐ Micelles—formation in rheopexic dispersions of dioctyl sodium sulfosuccinate ☐ Dispersions, rheopexic—dioctyl sodium sulfosuccinate, formation of micelles ☐ Rheopexic dispersions—dioctyl sodium sulfosuccinate, formation of micelles ☐ Surfactants—dioctyl sodium sulfosuccinate, rheopexic dispersions, formation of micelles

To the Editor:

The detection of long tubular structures visible under the electron microscope has been reported for aqueous dispersions of many phospholipids (1). These observable structural units have been described variously as "myelin forms" and "micelles." Stoeckenius (2) and Fernandez-Moran (3) detected, identified, and described myelin forms of phospholipids under the electron microscope at magnifications of 400,000–1,250,000×.

During work on the development of rheopexy in dispersions of dioctyl sodium sulfosuccinate in normal saline (4), the pronounced development of myelin forms was observed under the light microscope at 430× after a shear stress was applied. The dispersion consisting of

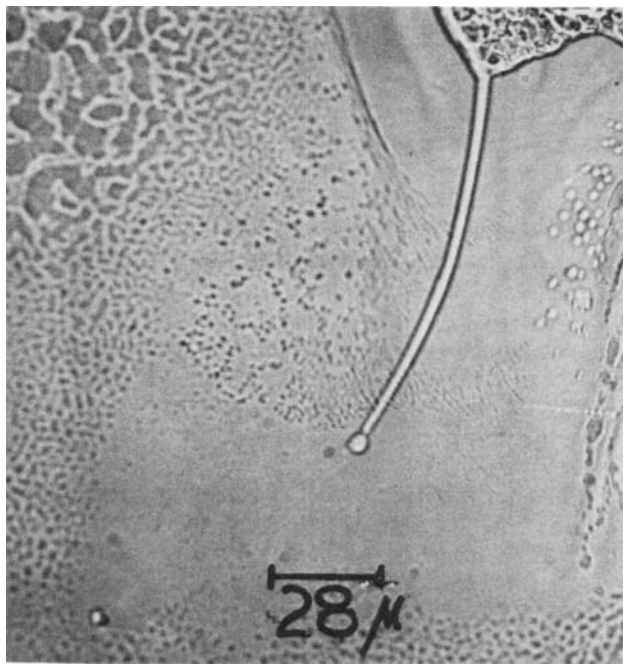

Figure 1—*Single tubular body thought to be a myelin form or micelle (430×).*

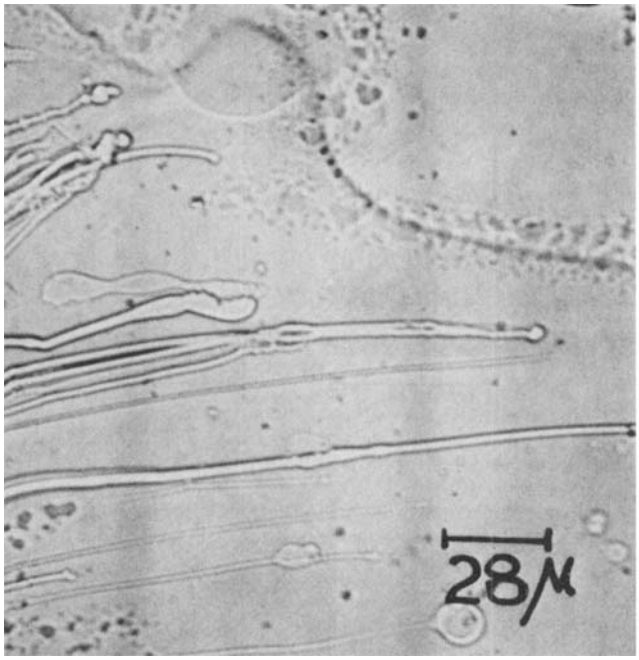

Figure 2—*Elongated and multiple myelin forms (430×).*

Figure 3—*Myelin forms exhibiting optical birefringence (430×).*

10% (w/v) dioctyl sodium sulfosuccinate in 0.9% NaCl developed the greatest degree of rheopexy as well as a large number of observable myelin forms. Similar concentrations of the surfactant in distilled water failed to produce the rheopexic quality or the myelin forms. Figures 1–3 illustrate the morphology of the structural units observed in the 10% (w/v) dioctyl sodium sulfosuccinate dispersion in normal saline.

From a purely speculative consideration, we felt that the development of the rheopexic character (*i.e.*, the increase in viscosity under shear stress without a concomitant volume dilation) in dispersions of dioctyl sodium sulfosuccinate in saline was due to a shear stress-induced aggregation of small micelles into large micellar units. The detection of long "strand-like" tubular bodies in rheopexic dispersions of dioctyl sodium sulfosuccinate in saline gives credence to this speculation.

Figure 3 illustrates myelin forms exhibiting optical birefringence. The observed phenomenon of optical anisotropy, which occurred only after a shear stress was applied, indicates the formation of a spontaneously oriented, highly structured system which develops with the shear stress and/or saline environment (5). This optical phenomenon has been described in the literature (5, 6) for some colloidal dispersions which exhibit structuring upon stirring, such as in the formation of "tactoids" of ferric hydroxide and tungsten trioxide.

The significance of the formation of such large micellar units or myelin forms is far reaching from a thermodynamic view. From an entropy consideration alone, the spontaneous structuring of surfactant molecules into the observed large structural units, due ostensibly to a favorable saline concentration and shear stress, escapes traditional explanation.

Furthermore, as Stein (7) suggested, and we concur, the structure of these myelin forms may have an important bearing on an understanding of animal cell membrane origin and structure.

Our observation that a nonphospholipid surfactant can spontaneously form large structural units, under proper conditions of shear stress and salinity, gives apparent credence to the supposition that there exists a chemical nonspecificity in the formation of myelin forms. The formation of such structural bodies may be an indication of a previously unknown general physical characteristic of surface-active agents under the influence of salinity and shear stress.

(1) W. D. Stein, "The Movement of Molecules Across Cell Membranes," Academic, New York, N.Y., 1967, p. 12.

(2) W. Stoeckenius, in "Symposia of the International Society for Cell Biology," vol. I, R. J. C. Harris, Ed., Academic, New York, N.Y., 1962, pp. 349–368.

(3) H. Fernandez-Moran, in *ibid.*, pp. 411–428.

(4) R. S. Levinson, L. V. Allen, and J. Daigle, *J. Colloid Interface Sci.*, in press.

(5) B. Jirgensons and M. E. Straumanis, "A Short Textbook of Colloid Chemistry," 2nd ed., Macmillan, New York, N.Y., 1962, p. 125.

(6) *Ibid.*, pp. 220, 221.

(7) W. D. Stein, "The Movement of Molecules Across Cell Membranes," Academic, New York, N.Y., 1967, p. 15.

R. Saul Levinson [x]
Loyd V. Allen, Jr.
Krishna S. Vishnupad
College of Pharmacy
University of Oklahoma
Norman, OK 73069

Bernard Ecanow
College of Pharmacy
University of Illinois
Chicago, IL 60612

Received February 17, 1976.
Accepted for publication April 23, 1976.
Supported by the University of Oklahoma Faculty Research Council.

[x] To whom inquiries should be directed.

REVIEWS

Microbiology–1974. Edited by David Schlessinger. American Society for Microbiology, Washington, DC 20006, 1975. 314 pp. 16 × 26.5 cm. Price $16.00.

David Schlessinger has gathered together, from several symposia, topics of interest to a wide range of microbiologists. The first two-thirds of the book is devoted to the first ASM Conference on Extrachromosomal Elements in Bacteria held in New Orleans in January 1974. A comprehensive coverage of plasmid developments is presented.

The last third of the book is shared by two topical symposia held in the National ASM meetings in 1974. The first topic is a discussion of *Vibrio parahaemolyticus*, presenting the occurrence, identification and clinical significance of this little known but important cause of human bacterial gastroenteritis. This section can be of value to laboratories conducting tests for this organism because of the background information included. The second topic presents the roles of iron in host–parasite interactions and covers the decided need for more information on this subject. These relationships can be of critical importance in the treatment of the disease.

I believe that the book is of value to microbiologists so that they may keep current with some developments in the many fields of their specialty. However, I feel uncomfortable with the title. "Microbiology–1974" implies a far broader coverage of the subject than is found. A more appropriate title could have been used to lessen the all encompassing sweep of this title.

Reviewed by M. A. Garth
Chief, Microbiological Assay Branch
National Center for Antibiotic Analysis
Food and Drug Administration
Washington, DC 20204

The Theory and Practice of Industrial Pharmacy. Second Ed. L. LACHMAN, H. A. LIEBERMAN, and J. L. KANIG. Lea & Febiger, 600 Washington Square, Philadelphia, PA 19106, 1976. 787 pp. 18.5 x 26.5 cm. Price $38.50.

The second edition of this book improves upon the worthwhile original. This improvement, apart from the usual updating of chapters, results primarily from the addition of a knowledgeable and much needed chapter on preformulation. The new section on packaging materials science is also welcome, although it is somewhat superficial and suffers by comparison with the preformulation chapter. The new organization of the book, whereby theory and practice are juxtapositioned for each dosage form, adds clarity.

The elimination of the sections on heat and momentum transfer and fluid flow is an improvement, primarily because it is difficult to deal adequately with these highly technical subjects in a few pages of a book of this type. The demise of the chapters on law and the structure of pharmaceutical companies can only be applauded, not because of any serious flaws in prose or content but rather because these subjects seem out of phase with the general thrust of the book.

Unfortunately, valuable space in the new edition is unnecessarily and unwisely taken up by new chapters on drug regulatory affairs and production management. The former suffers from the fact that such a complicated, rapidly changing subject cannot be dealt with effectively in 30 pages of a book that is updated every 6 years, especially when questionable subjects, *e.g.*, patents, copyrights, and unfair competition, are included. The latter (production management) is in a more critical state of suffering because, in the main, the subject matter is either redundant or irrelevant. This is not a criticism of the authors, who have done a creditable job, but of the editors, who are, as they say in the preface, responsible for "the choices of subject matter."

One more chapter, present in both editions, must be added to a list of extraneous material—that on pilot plant scale-up techniques. Most of this information is redundant with that in the chapters on dosage forms; instead, pertinent comments on scale-up problems should be added to the dosage form chapters. The editors should seriously consider eliminating these three chapters from the third edition and use that space for a more thorough and enlarged updating of the many necessary and worthwhile sections of the book. One gets the feeling that these three chapters are included for students, and this perhaps best illustrates the difficulty of trying to prepare a text for such a wide range of readers, from undergraduate students to industrial scientists to regulatory personnel.

One last critical comment: while the chapter on "Quality Control: Process and Dosage Form" is adequate, for the third edition the editors might do well to assign that subject to practicing experts in the field.

The overall high quality of this book demands that any reviewer end on a positive note. The editors are to be applauded for enlisting the help of many recognized experts in the various technical fields represented in the text. The book is an ambitious undertaking, and the editors and authors can take justifiable pride in the fact that they have essentially succeeded. The above critical comments are only intended to suggest how even more excellence might be attained.

Reviewed by James E. Tingstad
Riker Laboratories, Inc.
Subsidiary of 3M Company
St. Paul, MN 55101

Quantitative Thin Layer Chromatography. Edited by JOSEPH TOUCHSTONE. Wiley, New York, New York, 10016, 1973. 330 pp. 16 × 24 cm. Price $14.95.

The title of this book is misleading. It is not a text designed to tell you everything you ever wanted to know about quantitative TLC. It is a collection of papers presented by various authors describing how they use densitometry and TLC to solve a particular problem. The text assumes that the reader is familiar with the techniques of quantitative determination by visual comparison and elution followed by instrumentation. The major objective of this text, as stated by the editor, is to delineate the parameters and requirements of densitometry.

Some of the chromatographic procedural problems discussed, which are associated with adsorbants, sample application and development, apply to other methods as well as densitometry. However, densitometry is further complicated by background and nonuniformity of the plate, external light, and measurement at a single wavelength. One must decide whether to use a single- or double-beam instrument, reflectance, or transmittance. The general conclusion reached upon completion of the book is that one must try changing all of the variables to suit a particular situation.

The selection of articles for the book does illustrate the versatility and scope of TLC and densitometry. After the introduction, there are 15 chapters, each dealing with a different field such as amino acids, air pollutants, pharmaceuticals, and polymers.

Data are presented to show densitometry to be superior to other methods such as GC, paper chromatography, and direct fluorescence assay. One chapter contains data to show the superiority of densitometry over the more subjective visual inspection of the plate.

REVIEWS

Microbiology–1974. Edited by David Schlessinger. American Society for Microbiology, Washington, DC 20006, 1975. 314 pp. 16 × 26.5 cm. Price $16.00.

David Schlessinger has gathered together, from several symposia, topics of interest to a wide range of microbiologists. The first two-thirds of the book is devoted to the first ASM Conference on Extrachromosomal Elements in Bacteria held in New Orleans in January 1974. A comprehensive coverage of plasmid developments is presented.

The last third of the book is shared by two topical symposia held in the National ASM meetings in 1974. The first topic is a discussion of *Vibrio parahaemolyticus*, presenting the occurrence, identification and clinical significance of this little known but important cause of human bacterial gastroenteritis. This section can be of value to laboratories conducting tests for this organism because of the background information included. The second topic presents the roles of iron in host–parasite interactions and covers the decided need for more information on this subject. These relationships can be of critical importance in the treatment of the disease.

I believe that the book is of value to microbiologists so that they may keep current with some developments in the many fields of their specialty. However, I feel uncomfortable with the title. "Microbiology–1974" implies a far broader coverage of the subject than is found. A more appropriate title could have been used to lessen the all encompassing sweep of this title.

Reviewed by M. A. Garth
Chief, Microbiological Assay Branch
National Center for Antibiotic Analysis
Food and Drug Administration
Washington, DC 20204

The Theory and Practice of Industrial Pharmacy. Second Ed. L. LACHMAN, H. A. LIEBERMAN, and J. L. KANIG. Lea & Febiger, 600 Washington Square, Philadelphia, PA 19106, 1976. 787 pp. 18.5 x 26.5 cm. Price $38.50.

The second edition of this book improves upon the worthwhile original. This improvement, apart from the usual updating of chapters, results primarily from the addition of a knowledgeable and much needed chapter on preformulation. The new section on packaging materials science is also welcome, although it is somewhat superficial and suffers by comparison with the preformulation chapter. The new organization of the book, whereby theory and practice are juxtapositioned for each dosage form, adds clarity.

The elimination of the sections on heat and momentum transfer and fluid flow is an improvement, primarily because it is difficult to deal adequately with these highly technical subjects in a few pages of a book of this type. The demise of the chapters on law and the structure of pharmaceutical companies can only be applauded, not because of any serious flaws in prose or content but rather because these subjects seem out of phase with the general thrust of the book.

Unfortunately, valuable space in the new edition is unnecessarily and unwisely taken up by new chapters on drug regulatory affairs and production management. The former suffers from the fact that such a complicated, rapidly changing subject cannot be dealt with effectively in 30 pages of a book that is updated every 6 years, especially when questionable subjects, *e.g.*, patents, copyrights, and unfair competition, are included. The latter (production management) is in a more critical state of suffering because, in the main, the subject matter is either redundant or irrelevant. This is not a criticism of the authors, who have done a creditable job, but of the editors, who are, as they say in the preface, responsible for "the choices of subject matter."

One more chapter, present in both editions, must be added to a list of extraneous material—that on pilot plant scale-up techniques. Most of this information is redundant with that in the chapters on dosage forms; instead, pertinent comments on scale-up problems should be added to the dosage form chapters. The editors should seriously consider eliminating these three chapters from the third edition and use that space for a more thorough and enlarged updating of the many necessary and worthwhile sections of the book. One gets the feeling that these three chapters are included for students, and this perhaps best illustrates the difficulty of trying to prepare a text for such a wide range of readers, from undergraduate students to industrial scientists to regulatory personnel.

One last critical comment: while the chapter on "Quality Control: Process and Dosage Form" is adequate, for the third edition the editors might do well to assign that subject to practicing experts in the field.

The overall high quality of this book demands that any reviewer end on a positive note. The editors are to be applauded for enlisting the help of many recognized experts in the various technical fields represented in the text. The book is an ambitious undertaking, and the editors and authors can take justifiable pride in the fact that they have essentially succeeded. The above critical comments are only intended to suggest how even more excellence might be attained.

Reviewed by James E. Tingstad
Riker Laboratories, Inc.
Subsidiary of 3M Company
St. Paul, MN 55101

Quantitative Thin Layer Chromatography. Edited by JOSEPH TOUCHSTONE. Wiley, New York, New York, 10016, 1973. 330 pp. 16 × 24 cm. Price $14.95.

The title of this book is misleading. It is not a text designed to tell you everything you ever wanted to know about quantitative TLC. It is a collection of papers presented by various authors describing how they use densitometry and TLC to solve a particular problem. The text assumes that the reader is familiar with the techniques of quantitative determination by visual comparison and elution followed by instrumentation. The major objective of this text, as stated by the editor, is to delineate the parameters and requirements of densitometry.

Some of the chromatographic procedural problems discussed, which are associated with adsorbants, sample application and development, apply to other methods as well as densitometry. However, densitometry is further complicated by background and nonuniformity of the plate, external light, and measurement at a single wavelength. One must decide whether to use a single- or double-beam instrument, reflectance, or transmittance. The general conclusion reached upon completion of the book is that one must try changing all of the variables to suit a particular situation.

The selection of articles for the book does illustrate the versatility and scope of TLC and densitometry. After the introduction, there are 15 chapters, each dealing with a different field such as amino acids, air pollutants, pharmaceuticals, and polymers.

Data are presented to show densitometry to be superior to other methods such as GC, paper chromatography, and direct fluorescence assay. One chapter contains data to show the superiority of densitometry over the more subjective visual inspection of the plate.

REVIEWS

Microbiology–1974. Edited by David Schlessinger. American Society for Microbiology, Washington, DC 20006, 1975. 314 pp. 16 × 26.5 cm. Price $16.00.

David Schlessinger has gathered together, from several symposia, topics of interest to a wide range of microbiologists. The first two-thirds of the book is devoted to the first ASM Conference on Extrachromosomal Elements in Bacteria held in New Orleans in January 1974. A comprehensive coverage of plasmid developments is presented.

The last third of the book is shared by two topical symposia held in the National ASM meetings in 1974. The first topic is a discussion of *Vibrio parahaemolyticus*, presenting the occurrence, identification and clinical significance of this little known but important cause of human bacterial gastroenteritis. This section can be of value to laboratories conducting tests for this organism because of the background information included. The second topic presents the roles of iron in host–parasite interactions and covers the decided need for more information on this subject. These relationships can be of critical importance in the treatment of the disease.

I believe that the book is of value to microbiologists so that they may keep current with some developments in the many fields of their specialty. However, I feel uncomfortable with the title. "Microbiology–1974" implies a far broader coverage of the subject than is found. A more appropriate title could have been used to lessen the all encompassing sweep of this title.

Reviewed by M. A. Garth
Chief, Microbiological Assay Branch
National Center for Antibiotic Analysis
Food and Drug Administration
Washington, DC 20204

The Theory and Practice of Industrial Pharmacy. Second Ed. L. LACHMAN, H. A. LIEBERMAN, and J. L. KANIG. Lea & Febiger, 600 Washington Square, Philadelphia, PA 19106, 1976. 787 pp. 18.5 x 26.5 cm. Price $38.50.

The second edition of this book improves upon the worthwhile original. This improvement, apart from the usual updating of chapters, results primarily from the addition of a knowledgeable and much needed chapter on preformulation. The new section on packaging materials science is also welcome, although it is somewhat superficial and suffers by comparison with the preformulation chapter. The new organization of the book, whereby theory and practice are juxtapositioned for each dosage form, adds clarity.

The elimination of the sections on heat and momentum transfer and fluid flow is an improvement, primarily because it is difficult to deal adequately with these highly technical subjects in a few pages of a book of this type. The demise of the chapters on law and the structure of pharmaceutical companies can only be applauded, not because of any serious flaws in prose or content but rather because these subjects seem out of phase with the general thrust of the book.

Unfortunately, valuable space in the new edition is unnecessarily and unwisely taken up by new chapters on drug regulatory affairs and production management. The former suffers from the fact that such a complicated, rapidly changing subject cannot be dealt with effectively in 30 pages of a book that is updated every 6 years, especially when questionable subjects, *e.g.*, patents, copyrights, and unfair competition, are included. The latter (production management) is in a more critical state of suffering because, in the main, the subject matter is either redundant or irrelevant. This is not a criticism of the authors, who have done a creditable job, but of the editors, who are, as they say in the preface, responsible for "the choices of subject matter."

One more chapter, present in both editions, must be added to a list of extraneous material—that on pilot plant scale-up techniques. Most of this information is redundant with that in the chapters on dosage forms; instead, pertinent comments on scale-up problems should be added to the dosage form chapters. The editors should seriously consider eliminating these three chapters from the third edition and use that space for a more thorough and enlarged updating of the many necessary and worthwhile sections of the book. One gets the feeling that these three chapters are included for students, and this perhaps best illustrates the difficulty of trying to prepare a text for such a wide range of readers, from undergraduate students to industrial scientists to regulatory personnel.

One last critical comment: while the chapter on "Quality Control: Process and Dosage Form" is adequate, for the third edition the editors might do well to assign that subject to practicing experts in the field.

The overall high quality of this book demands that any reviewer end on a positive note. The editors are to be applauded for enlisting the help of many recognized experts in the various technical fields represented in the text. The book is an ambitious undertaking, and the editors and authors can take justifiable pride in the fact that they have essentially succeeded. The above critical comments are only intended to suggest how even more excellence might be attained.

Reviewed by James E. Tingstad
Riker Laboratories, Inc.
Subsidiary of 3M Company
St. Paul, MN 55101

Quantitative Thin Layer Chromatography. Edited by JOSEPH TOUCHSTONE. Wiley, New York, New York, 10016, 1973. 330 pp. 16 × 24 cm. Price $14.95.

The title of this book is misleading. It is not a text designed to tell you everything you ever wanted to know about quantitative TLC. It is a collection of papers presented by various authors describing how they use densitometry and TLC to solve a particular problem. The text assumes that the reader is familiar with the techniques of quantitative determination by visual comparison and elution followed by instrumentation. The major objective of this text, as stated by the editor, is to delineate the parameters and requirements of densitometry.

Some of the chromatographic procedural problems discussed, which are associated with adsorbants, sample application and development, apply to other methods as well as densitometry. However, densitometry is further complicated by background and nonuniformity of the plate, external light, and measurement at a single wavelength. One must decide whether to use a single- or double-beam instrument, reflectance, or transmittance. The general conclusion reached upon completion of the book is that one must try changing all of the variables to suit a particular situation.

The selection of articles for the book does illustrate the versatility and scope of TLC and densitometry. After the introduction, there are 15 chapters, each dealing with a different field such as amino acids, air pollutants, pharmaceuticals, and polymers.

Data are presented to show densitometry to be superior to other methods such as GC, paper chromatography, and direct fluorescence assay. One chapter contains data to show the superiority of densitometry over the more subjective visual inspection of the plate.

The chapters are well written, concise, and include adequate diagrams, graphs, and pictures of plates. However, this text in no way covers the complete scope of quantitative TLC. And although it is instructive reading, it is not written to be used as a reference text.

Reviewed by Jeanne T. Reamer
United States Pharmacopeia
Drug Research and Testing Laboratory
Rockville, MD 20852

USAN and the USP Dictionary of Drug Names. Edited by MARY C. GRIFFITHS, MARIE J. DICKERMAN, and LLOYD C. MILLER. U.S. Pharmacopeial Convention, Inc., 12601 Twinbrook Parkway, Rockville, MD 20852, 1975. 352 pp. 21 × 28 cm. Price $18.50.

This is the 13th edition of "USAN and the USP Dictionary of Drug Names," one of the most comprehensive compilations of its kind. It is an alphabetical list of USAN and many other names for both marketed and investigational drugs. Its more than 10,000 entries include 1403 USAN (all U.S. Adopted Names selected and released from June 1961 through June 1975), more than 1700 investigational drug code designations, USP XIX and NF XIV official names, FDA established names, brand names, and trivial names. Also included are a pronunciation guide, the pharmacological category, and reference to sources of additional information for each entry.

The book contains three appendixes: Guiding Principles for Coining U.S. Adopted Names, Molecular Formulas Corresponding to USAN, and Names and Addresses of Domestic Firms, as well as a cross-index of names by pharmacological category.

This publication is a most valuable reference work for all those involved with pharmaceuticals.

Staff Review

Webster's Medical Speller. Published by G. & C. Merriam Company, 47 Federal Street, Springfield, MA 01101, 1975. 400 pp. 10.8 × 14.6 cm. Price $3.95.

"Webster's Medical Speller" is a pocket-sized reference book containing an alphabetical list of 35,000 medical words and technical terms. The book covers the broad field of medicine as well as related fields such as pharmacology, biochemistry, and microbiology. It indicates the correct word division, use of hyphens in compound words, and the most widely used plurals.

Special features include a list of Latin abbreviations used in writing prescriptions, with their full Latin forms and English equivalents; 1500 medical abbreviations; and a list of medical symbols.

This book appears to be a valuable reference aid to everyone communicating in the health-care fields.

Staff Review

NEW JOURNALS

Journal of Toxicology and Environmental Health. MYRON A. MEHLMAN, Editor. Hemisphere Publishing Corp., 1025 Vermont Ave., N.W., Washington, DC 20005, 1975. 17.5 × 25.5 cm.

Pharmacology and Therapeutics. Part B: General and Systemic Pharmacology. J. M. WALKER, Exec. Editor. Sponsored by the International Union of Pharmacology. Pergamon Press Ltd., Maxwell House, Fairview Park, Elmsford, NY 10523, 1975. 19 × 27 cm. Price $100.00 annual subscription (4 issues).

Cancer Therapy Abstracts. C. M. SOUTHAM, Editor. Franklin Institute Press, Benjamin Franklin Parkway, Philadelphia, PA 19103, 1975.18.5 × 25.5 cm. Price $45.00 U.S., $55.00 abroad (12 issues).

The chapters are well written, concise, and include adequate diagrams, graphs, and pictures of plates. However, this text in no way covers the complete scope of quantitative TLC. And although it is instructive reading, it is not written to be used as a reference text.

Reviewed by Jeanne T. Reamer
United States Pharmacopeia
Drug Research and Testing Laboratory
Rockville, MD 20852

USAN and the USP Dictionary of Drug Names. Edited by MARY C. GRIFFITHS, MARIE J. DICKERMAN, and LLOYD C. MILLER. U.S. Pharmacopeial Convention, Inc., 12601 Twinbrook Parkway, Rockville, MD 20852, 1975. 352 pp. 21 × 28 cm. Price $18.50.

This is the 13th edition of "USAN and the USP Dictionary of Drug Names," one of the most comprehensive compilations of its kind. It is an alphabetical list of USAN and many other names for both marketed and investigational drugs. Its more than 10,000 entries include 1403 USAN (all U.S. Adopted Names selected and released from June 1961 through June 1975), more than 1700 investigational drug code designations, USP XIX and NF XIV official names, FDA established names, brand names, and trivial names. Also included are a pronunciation guide, the pharmacological category, and reference to sources of additional information for each entry.

The book contains three appendixes: Guiding Principles for Coining U.S. Adopted Names, Molecular Formulas Corresponding to USAN, and Names and Addresses of Domestic Firms, as well as a cross-index of names by pharmacological category.

This publication is a most valuable reference work for all those involved with pharmaceuticals.

Staff Review

Webster's Medical Speller. Published by G. & C. Merriam Company, 47 Federal Street, Springfield, MA 01101, 1975. 400 pp. 10.8 × 14.6 cm. Price $3.95.

"Webster's Medical Speller" is a pocket-sized reference book containing an alphabetical list of 35,000 medical words and technical terms. The book covers the broad field of medicine as well as related fields such as pharmacology, biochemistry, and microbiology. It indicates the correct word division, use of hyphens in compound words, and the most widely used plurals.

Special features include a list of Latin abbreviations used in writing prescriptions, with their full Latin forms and English equivalents; 1500 medical abbreviations; and a list of medical symbols.

This book appears to be a valuable reference aid to everyone communicating in the health-care fields.

Staff Review

NEW JOURNALS

Journal of Toxicology and Environmental Health. MYRON A. MEHLMAN, Editor. Hemisphere Publishing Corp., 1025 Vermont Ave., N.W., Washington, DC 20005, 1975. 17.5 × 25.5 cm.

Pharmacology and Therapeutics. Part B: General and Systemic Pharmacology. J. M. WALKER, Exec. Editor. Sponsored by the International Union of Pharmacology. Pergamon Press Ltd., Maxwell House, Fairview Park, Elmsford, NY 10523, 1975. 19 × 27 cm. Price $100.00 annual subscription (4 issues).

Cancer Therapy Abstracts. C. M. SOUTHAM, Editor. Franklin Institute Press, Benjamin Franklin Parkway, Philadelphia, PA 19103, 1975.18.5 × 25.5 cm. Price $45.00 U.S., $55.00 abroad (12 issues).

The chapters are well written, concise, and include adequate diagrams, graphs, and pictures of plates. However, this text in no way covers the complete scope of quantitative TLC. And although it is instructive reading, it is not written to be used as a reference text.

Reviewed by Jeanne T. Reamer
United States Pharmacopeia
Drug Research and Testing Laboratory
Rockville, MD 20852

USAN and the USP Dictionary of Drug Names. Edited by MARY C. GRIFFITHS, MARIE J. DICKERMAN, and LLOYD C. MILLER. U.S. Pharmacopeial Convention, Inc., 12601 Twinbrook Parkway, Rockville, MD 20852, 1975. 352 pp. 21 × 28 cm. Price $18.50.

This is the 13th edition of "USAN and the USP Dictionary of Drug Names," one of the most comprehensive compilations of its kind. It is an alphabetical list of USAN and many other names for both marketed and investigational drugs. Its more than 10,000 entries include 1403 USAN (all U.S. Adopted Names selected and released from June 1961 through June 1975), more than 1700 investigational drug code designations, USP XIX and NF XIV official names, FDA established names, brand names, and trivial names. Also included are a pronunciation guide, the pharmacological category, and reference to sources of additional information for each entry.

The book contains three appendixes: Guiding Principles for Coining U.S. Adopted Names, Molecular Formulas Corresponding to USAN, and Names and Addresses of Domestic Firms, as well as a cross-index of names by pharmacological category.

This publication is a most valuable reference work for all those involved with pharmaceuticals.

Staff Review

Webster's Medical Speller. Published by G. & C. Merriam Company, 47 Federal Street, Springfield, MA 01101, 1975. 400 pp. 10.8 × 14.6 cm. Price $3.95.

"Webster's Medical Speller" is a pocket-sized reference book containing an alphabetical list of 35,000 medical words and technical terms. The book covers the broad field of medicine as well as related fields such as pharmacology, biochemistry, and microbiology. It indicates the correct word division, use of hyphens in compound words, and the most widely used plurals.

Special features include a list of Latin abbreviations used in writing prescriptions, with their full Latin forms and English equivalents; 1500 medical abbreviations; and a list of medical symbols.

This book appears to be a valuable reference aid to everyone communicating in the health-care fields.

Staff Review

NEW JOURNALS

Journal of Toxicology and Environmental Health. MYRON A. MEHLMAN, Editor. Hemisphere Publishing Corp., 1025 Vermont Ave., N.W., Washington, DC 20005, 1975. 17.5 × 25.5 cm.

Pharmacology and Therapeutics. Part B: General and Systemic Pharmacology. J. M. WALKER, Exec. Editor. Sponsored by the International Union of Pharmacology. Pergamon Press Ltd., Maxwell House, Fairview Park, Elmsford, NY 10523, 1975. 19 × 27 cm. Price $100.00 annual subscription (4 issues).

Cancer Therapy Abstracts. C. M. SOUTHAM, Editor. Franklin Institute Press, Benjamin Franklin Parkway, Philadelphia, PA 19103, 1975.18.5 × 25.5 cm. Price $45.00 U.S., $55.00 abroad (12 issues).

The chapters are well written, concise, and include adequate diagrams, graphs, and pictures of plates. However, this text in no way covers the complete scope of quantitative TLC. And although it is instructive reading, it is not written to be used as a reference text.

Reviewed by Jeanne T. Reamer
United States Pharmacopeia
Drug Research and Testing Laboratory
Rockville, MD 20852

USAN and the USP Dictionary of Drug Names. Edited by MARY C. GRIFFITHS, MARIE J. DICKERMAN, and LLOYD C. MILLER. U.S. Pharmacopeial Convention, Inc., 12601 Twinbrook Parkway, Rockville, MD 20852, 1975. 352 pp. 21 × 28 cm. Price $18.50.

This is the 13th edition of "USAN and the USP Dictionary of Drug Names," one of the most comprehensive compilations of its kind. It is an alphabetical list of USAN and many other names for both marketed and investigational drugs. Its more than 10,000 entries include 1403 USAN (all U.S. Adopted Names selected and released from June 1961 through June 1975), more than 1700 investigational drug code designations, USP XIX and NF XIV official names, FDA established names, brand names, and trivial names. Also included are a pronunciation guide, the pharmacological category, and reference to sources of additional information for each entry.

The book contains three appendixes: Guiding Principles for Coining U.S. Adopted Names, Molecular Formulas Corresponding to USAN, and Names and Addresses of Domestic Firms, as well as a cross-index of names by pharmacological category.

This publication is a most valuable reference work for all those involved with pharmaceuticals.

Staff Review

Webster's Medical Speller. Published by G. & C. Merriam Company, 47 Federal Street, Springfield, MA 01101, 1975. 400 pp. 10.8 × 14.6 cm. Price $3.95.

"Webster's Medical Speller" is a pocket-sized reference book containing an alphabetical list of 35,000 medical words and technical terms. The book covers the broad field of medicine as well as related fields such as pharmacology, biochemistry, and microbiology. It indicates the correct word division, use of hyphens in compound words, and the most widely used plurals.

Special features include a list of Latin abbreviations used in writing prescriptions, with their full Latin forms and English equivalents; 1500 medical abbreviations; and a list of medical symbols.

This book appears to be a valuable reference aid to everyone communicating in the health-care fields.

Staff Review

NEW JOURNALS

Journal of Toxicology and Environmental Health. MYRON A. MEHLMAN, Editor. Hemisphere Publishing Corp., 1025 Vermont Ave., N.W., Washington, DC 20005, 1975. 17.5 × 25.5 cm.

Pharmacology and Therapeutics. Part B: General and Systemic Pharmacology. J. M. WALKER, Exec. Editor. Sponsored by the International Union of Pharmacology. Pergamon Press Ltd., Maxwell House, Fairview Park, Elmsford, NY 10523, 1975. 19 × 27 cm. Price $100.00 annual subscription (4 issues).

Cancer Therapy Abstracts. C. M. SOUTHAM, Editor. Franklin Institute Press, Benjamin Franklin Parkway, Philadelphia, PA 19103, 1975.18.5 × 25.5 cm. Price $45.00 U.S., $55.00 abroad (12 issues).

Cyanocobalamin Degradation

In the May 1976 issue of the Journal, Yazdany and Badii[1] reported on the degradation of cyanocobalamin when autoclaved in the presence of 0.1% methylparaben sodium. This observation is not surprising since cyanocobalamin is known to be inactivated in alkaline solutions[2] and methylparaben sodium (a sodium phenolate) gives an alkaline pH in solution. Thus, we are dealing here simply with a base-catalyzed degradation. The authors of the paper seem uncognizant of this and suggest instead some undefined direct interaction between the paraben moiety and cyanocobalamin.

The relatively isolated situation of the authors may explain their unawareness of the nature of the reported reaction. It is surprising, however, that the Journal's reviewer failed to call it to their attention.

Stanley Scheindlin
Lemmon Pharmacal Company
Sellersville, PA 18960

Received June 1, 1976.

[1] S. Yazdany and F. Badii, *J. Pharm. Sci.*, **65**, 745(1976).
[2] A. Osol, "United States Dispensatory," 27th ed., Lippincott, Philadelphia, Pa., 1973, p. 359.

Equations for Bolus Intravenous Injection in Linear Pharmacokinetics

S. Niazi[1] recently stated that in a linear pharmacokinetic model where instantaneous input is assumed (*i.e.*, bolus intravenous injection), the assumption embodied in Eq. 1 is made:

$$\frac{1 - e^{-b_i\theta}}{b_i\theta} = 1 \qquad \text{(Eq. 1)}$$

He suggested that the coefficients of the bolus intravenous equation should be corrected by multiplying by the reciprocal of the left-hand side of Eq. 1. I would like to caution readers *not* to make such "corrections," since Eq. 1 is incorrect.

The equations for bolus intravenous injection, during a constant rate intravenous infusion, and after constant rate infusion are shown below. They are derived for different initial conditions but are consistent, and the coefficients may be interconverted by means of Eqs. 5 and 6.

For bolus intravenous injection:

$$C_p = \sum_{i=1}^{n} C_i e^{-b_i t} \qquad \text{(Eq. 2)}$$

During an infusion:

$$C_p = \sum_{i=1}^{n} X_i(1 - e^{-b_i t}) = \sum_{i=1}^{n} \frac{C_i}{b_i\theta}(1 - e^{-b_i t}) \qquad \text{(Eq. 3)}$$

After infusion:

$$C_p = \sum_{i=1}^{n} Y_i e^{-b_i t} = \sum_{i=1}^{n} C_i \left(\frac{e^{+b_i\theta} - 1}{b_i\theta}\right) e^{-b_i t} \qquad \text{(Eq. 4)}$$

From Eq. 3:

$$C_i = X_i b_i \theta \qquad \text{(Eq. 5)}$$

From Eq. 4:

$$C_i = \frac{b_i\theta Y_i}{e^{+b_i\theta} - 1} \qquad \text{(Eq. 6)}$$

In Eqs. 1–6, θ is the infusion time, t is time from the start of administration, and the b_i's are eigenvalues. For the two-compartment open model, $n = 2$; for the three-compartment open model, $n = 3$.

John G. Wagner
College of Pharmacy and Upjohn Center for Clinical Pharmacology
University of Michigan
Ann Arbor, MI 48109

Received May 28, 1976.

[1] S. Niazi, *J. Pharm. Sci.*, **65**, 750(1976).

Drug Delivery Systems versus *Dosage Forms*

The phrase "drug delivery system" is becoming increasingly prominent in professional communications. It would be well to consider the distinction between this phrase and the classic term "dosage form."

As currently used, a drug delivery system is really a dosage form delivery system. It delivers the physical–chemical system, *i.e.*, the solution or suspension, *etc.*, that contains the drug (*e.g.*, a drug in solution contained within a polymeric matrix). Thus, in the case of Ocusert, the polymeric plastic material contains the solution which is the dosage form and which, in turn, contains the dissolved drug, pilocarpine.

By way of illustrating possible confusion, a capsule that is recognized as a dosage form is really a dosage form delivery system. The gelatin capsule itself can deliver any of a variety of physical–chemical systems (dosage forms) such as suspensions, solutions, or powders. A further illustration exists with intravenous injectables. Here the syringe is the dosage form delivery system; the solution, suspension, *etc.*, are the dosage forms containing the drug.

We suggest that the term "drug delivery system" be used to refer to the dosage form. The pharmaceutical community would do well to consider the confusions that are developing through ill-defined terminology.

Bernard Ecanow
Bernard H. Gold
College of Pharmacy
University of Illinois at the Medical Center
Chicago, IL 60680

Received June 7, 1976.

Cyanocobalamin Degradation

In the May 1976 issue of the Journal, Yazdany and Badii[1] reported on the degradation of cyanocobalamin when autoclaved in the presence of 0.1% methylparaben sodium. This observation is not surprising since cyanocobalamin is known to be inactivated in alkaline solutions[2] and methylparaben sodium (a sodium phenolate) gives an alkaline pH in solution. Thus, we are dealing here simply with a base-catalyzed degradation. The authors of the paper seem uncognizant of this and suggest instead some undefined direct interaction between the paraben moiety and cyanocobalamin.

The relatively isolated situation of the authors may explain their unawareness of the nature of the reported reaction. It is surprising, however, that the Journal's reviewer failed to call it to their attention.

Stanley Scheindlin
Lemmon Pharmacal Company
Sellersville, PA 18960

Received June 1, 1976.

[1] S. Yazdany and F. Badii, *J. Pharm. Sci.*, **65**, 745(1976).
[2] A. Osol, "United States Dispensatory," 27th ed., Lippincott, Philadelphia, Pa., 1973, p. 359.

Equations for Bolus Intravenous Injection in Linear Pharmacokinetics

S. Niazi[1] recently stated that in a linear pharmacokinetic model where instantaneous input is assumed (*i.e.*, bolus intravenous injection), the assumption embodied in Eq. 1 is made:

$$\frac{1 - e^{-b_i\theta}}{b_i\theta} = 1 \qquad \text{(Eq. 1)}$$

He suggested that the coefficients of the bolus intravenous equation should be corrected by multiplying by the reciprocal of the left-hand side of Eq. 1. I would like to caution readers *not* to make such "corrections," since Eq. 1 is incorrect.

The equations for bolus intravenous injection, during a constant rate intravenous infusion, and after constant rate infusion are shown below. They are derived for different initial conditions but are consistent, and the coefficients may be interconverted by means of Eqs. 5 and 6.

For bolus intravenous injection:

$$C_p = \sum_{i=1}^{n} C_i e^{-b_i t} \qquad \text{(Eq. 2)}$$

During an infusion:

$$C_p = \sum_{i=1}^{n} X_i(1 - e^{-b_i t}) = \sum_{i=1}^{n} \frac{C_i}{b_i\theta}(1 - e^{-b_i t}) \qquad \text{(Eq. 3)}$$

After infusion:

$$C_p = \sum_{i=1}^{n} Y_i e^{-b_i t} = \sum_{i=1}^{n} C_i \left(\frac{e^{+b_i\theta} - 1}{b_i\theta}\right) e^{-b_i t} \qquad \text{(Eq. 4)}$$

From Eq. 3:

$$C_i = X_i b_i \theta \qquad \text{(Eq. 5)}$$

From Eq. 4:

$$C_i = \frac{b_i\theta Y_i}{e^{+b_i\theta} - 1} \qquad \text{(Eq. 6)}$$

In Eqs. 1–6, θ is the infusion time, t is time from the start of administration, and the b_i's are eigenvalues. For the two-compartment open model, $n = 2$; for the three-compartment open model, $n = 3$.

John G. Wagner
College of Pharmacy and Upjohn Center for Clinical Pharmacology
University of Michigan
Ann Arbor, MI 48109

Received May 28, 1976.

[1] S. Niazi, *J. Pharm. Sci.*, **65**, 750(1976).

Drug Delivery Systems versus *Dosage Forms*

The phrase "drug delivery system" is becoming increasingly prominent in professional communications. It would be well to consider the distinction between this phrase and the classic term "dosage form."

As currently used, a drug delivery system is really a dosage form delivery system. It delivers the physical–chemical system, *i.e.*, the solution or suspension, *etc.*, that contains the drug (*e.g.*, a drug in solution contained within a polymeric matrix). Thus, in the case of Ocusert, the polymeric plastic material contains the solution which is the dosage form and which, in turn, contains the dissolved drug, pilocarpine.

By way of illustrating possible confusion, a capsule that is recognized as a dosage form is really a dosage form delivery system. The gelatin capsule itself can deliver any of a variety of physical–chemical systems (dosage forms) such as suspensions, solutions, or powders. A further illustration exists with intravenous injectables. Here the syringe is the dosage form delivery system; the solution, suspension, *etc.*, are the dosage forms containing the drug.

We suggest that the term "drug delivery system" be used to refer to the dosage form. The pharmaceutical community would do well to consider the confusions that are developing through ill-defined terminology.

Bernard Ecanow
Bernard H. Gold
College of Pharmacy
University of Illinois at the Medical Center
Chicago, IL 60680

Received June 7, 1976.

Cyanocobalamin Degradation

In the May 1976 issue of the Journal, Yazdany and Badii[1] reported on the degradation of cyanocobalamin when autoclaved in the presence of 0.1% methylparaben sodium. This observation is not surprising since cyanocobalamin is known to be inactivated in alkaline solutions[2] and methylparaben sodium (a sodium phenolate) gives an alkaline pH in solution. Thus, we are dealing here simply with a base-catalyzed degradation. The authors of the paper seem uncognizant of this and suggest instead some undefined direct interaction between the paraben moiety and cyanocobalamin.

The relatively isolated situation of the authors may explain their unawareness of the nature of the reported reaction. It is surprising, however, that the Journal's reviewer failed to call it to their attention.

Stanley Scheindlin
Lemmon Pharmacal Company
Sellersville, PA 18960

Received June 1, 1976.

[1] S. Yazdany and F. Badii, *J. Pharm. Sci.*, **65**, 745(1976).
[2] A. Osol, "United States Dispensatory," 27th ed., Lippincott, Philadelphia, Pa., 1973, p. 359.

Equations for Bolus Intravenous Injection in Linear Pharmacokinetics

S. Niazi[1] recently stated that in a linear pharmacokinetic model where instantaneous input is assumed (*i.e.*, bolus intravenous injection), the assumption embodied in Eq. 1 is made:

$$\frac{1 - e^{-b_i\theta}}{b_i\theta} = 1 \qquad \text{(Eq. 1)}$$

He suggested that the coefficients of the bolus intravenous equation should be corrected by multiplying by the reciprocal of the left-hand side of Eq. 1. I would like to caution readers *not* to make such "corrections," since Eq. 1 is incorrect.

The equations for bolus intravenous injection, during a constant rate intravenous infusion, and after constant rate infusion are shown below. They are derived for different initial conditions but are consistent, and the coefficients may be interconverted by means of Eqs. 5 and 6.

For bolus intravenous injection:

$$C_p = \sum_{i=1}^{n} C_i e^{-b_i t} \qquad \text{(Eq. 2)}$$

During an infusion:

$$C_p = \sum_{i=1}^{n} X_i(1 - e^{-b_i t}) = \sum_{i=1}^{n} \frac{C_i}{b_i\theta}(1 - e^{-b_i t}) \qquad \text{(Eq. 3)}$$

After infusion:

$$C_p = \sum_{i=1}^{n} Y_i e^{-b_i t} = \sum_{i=1}^{n} C_i \left(\frac{e^{+b_i\theta} - 1}{b_i\theta}\right) e^{-b_i t} \qquad \text{(Eq. 4)}$$

From Eq. 3:

$$C_i = X_i b_i \theta \qquad \text{(Eq. 5)}$$

From Eq. 4:

$$C_i = \frac{b_i\theta Y_i}{e^{+b_i\theta} - 1} \qquad \text{(Eq. 6)}$$

In Eqs. 1–6, θ is the infusion time, t is time from the start of administration, and the b_i's are eigenvalues. For the two-compartment open model, $n = 2$; for the three-compartment open model, $n = 3$.

John G. Wagner
College of Pharmacy and Upjohn Center for Clinical Pharmacology
University of Michigan
Ann Arbor, MI 48109

Received May 28, 1976.

[1] S. Niazi, *J. Pharm. Sci.*, **65**, 750(1976).

Drug Delivery Systems versus *Dosage Forms*

The phrase "drug delivery system" is becoming increasingly prominent in professional communications. It would be well to consider the distinction between this phrase and the classic term "dosage form."

As currently used, a drug delivery system is really a dosage form delivery system. It delivers the physical–chemical system, *i.e.*, the solution or suspension, *etc.*, that contains the drug (*e.g.*, a drug in solution contained within a polymeric matrix). Thus, in the case of Ocusert, the polymeric plastic material contains the solution which is the dosage form and which, in turn, contains the dissolved drug, pilocarpine.

By way of illustrating possible confusion, a capsule that is recognized as a dosage form is really a dosage form delivery system. The gelatin capsule itself can deliver any of a variety of physical–chemical systems (dosage forms) such as suspensions, solutions, or powders. A further illustration exists with intravenous injectables. Here the syringe is the dosage form delivery system; the solution, suspension, *etc.*, are the dosage forms containing the drug.

We suggest that the term "drug delivery system" be used to refer to the dosage form. The pharmaceutical community would do well to consider the confusions that are developing through ill-defined terminology.

Bernard Ecanow
Bernard H. Gold
College of Pharmacy
University of Illinois at the Medical Center
Chicago, IL 60680

Received June 7, 1976.

Journal of Pharmaceutical Sciences

SEPTEMBER 1976

VOLUME 65 NUMBER 9

MARY H. FERGUSON
Editor

L. LUAN CORRIGAN
Assistant Editor

SHELLY ELLIOTT
Production Editor

JANET D. SHOFF
Copy Editor

EDWARD G. FELDMANN
Contributing Editor

SAMUEL W. GOLDSTEIN
Contributing Editor

LELAND J. ARNEY
Publications Director

EDITORIAL ADVISORY BOARD

JOHN AUTIAN	HARRY B. KOSTENBAUDER
LYNN R. BRADY	CARL J. LINTNER, JR.
WILLIAM O. FOYE	DAVID E. MANN, JR.
WILLIAM J. JUSKO	GERALD J. PAPARIELLO

The *Journal of Pharmaceutical Sciences* is published monthly by the American Pharmaceutical Association at 2215 Constitution Ave., N.W., Washington, DC 20037. Second-class postage paid at Washington, D.C., and at additional mailing office.

All expressions of opinion and statements of supposed fact appearing in articles or editorials carried in this journal are published on the authority of the writer over whose name they appear and are not to be regarded as necessarily expressing the policies or views of the American Pharmaceutical Association.

Offices—Editorial, Advertising, and Subscription Offices: 2215 Constitution Ave., N.W., Washington, DC 20037. Printing Offices: 20th & Northampton Streets, Easton, PA 18042.

Annual Subscriptions—United States and foreign, industrial and government institutions $50, educational institutions $50, individuals *for personal use only* $30; single copies $5. All foreign subscriptions add $5 for postage. Subscription rates are subject to change without notice. Members of the American Pharmaceutical Association may elect to receive the *Journal of Pharmaceutical Sciences* as a part of their annual $60 (foreign $65) APhA membership dues.

Claims—Missing numbers will not be supplied if dues or subscriptions are in arrears for more than 60 days or if claims are received more than 60 days after the date of the issue, or if loss was due to failure to give notice of change of address. The Association cannot accept responsibility for foreign delivery when its records indicate shipment has been made.

Change of Address—Members and subscribers should notify at once both the Post Office and the American Pharmaceutical Association, 2215 Constitution Ave., N.W., Washington, DC 20037, of any change of address.

© Copyright 1976, American Pharmaceutical Association, 2215 Constitution Ave., N.W., Washington, DC 20037; all rights reserved.

DISSECTING THE LABYRINTH

"There's got to be a better way!"

How many times all of us have exclaimed our irritation in those or similar words when we encountered obstructions, obstacles, and assorted roadblocks which have frustrated us in our efforts to accomplish what ought to be some seemingly simple objective.

From various press reports, it appears that HEW Secretary David Mathews reached such a conclusion this summer with respect to the manner in which his Department develops and issues its regulations. That appears to be the basis for his announcement on July 25 that, effective immediately, he was instituting "sweeping reforms" in the HEW regulations process.

The Secretary stated, in part, that: *"For far too long HEW has gone to the public in these (controversial) situations only to tell them what it intends to do. From now on our first step will be to ask the people of this country what they think we should do."* The announcement further explained that one of the extreme new reforms is a *"requirement for HEW to consult broad segments of the public before it puts pen to paper in preparing controversial regulations mandated by congressional action or compelling administrative need."*

A detailed, ten-step process was described as the specific procedure that is to be followed in the future in promulgating new regulations.

Beyond this step-wise procedure, the Secretary included several other features in his reform package. One of these—which in our view is sorely needed and long overdue—reflects Secretary Mathews' academic background. We refer to the part calling for *"training sessions for Department regulations writers so that regulations are written in clear, concise English."*

Washington bureaucrats have developed a well-deserved reputation for having a facility for translating simple concepts and ideas into the most confusing and complex messages. A Washington daily newspaper for some time has made sport of this penchant by publishing a daily feature titled "Gobbledygook," in which a choice piece of unintelligible federal government jargon is reprinted for the amusement of the newspaper readership.

Another ancillary feature of the Secretary's directive calls for *"modification of (existing) regulations which impose too numerous or needlessly complex requirements on program administrators; for example, a special task force is now at work in HEW simplifying the Medicaid regulations."*

It may seem absurd that such a dictate needs to be spelled out for a gigantic department within the federal government. But few of us fully appreciate the awesome influence of this single agency.

HEW alone has 135,000 employees—enough to constitute a fair sized city. In our personal lives, most of us would be impressed by the fact that a given person is responsible for managing the annual expenditure of a million dollars. Yet, in light of HEW's current budget of $128 billion, this translates into an average disbursement or expenditure figure of almost that amount (actually, over $948,000) for each and every one of those 135,000 employees!

But the real basis for public unhappiness with HEW seems to stem from the fact that the regulations the agency has created over the years have often been confusing, contradictory, and controversial. The perceived result has been inefficiency and unfairness at best, and waste and illegality at worst. Although Congress may enact legislation, it is through regulations that broad, general laws are applied and put into practice. Consequently, the regulation writers exert about as much influence—and sometimes more—within the government processes that affect our lives as do all our elected representatives!

Therefore, a reexamination of how this system is operating—and a serious effort to improve its operation—seem to us to be long overdue. Preliminary to the July 25 announcement from HEW, the Secretary's office had written to APhA, as well as to a number of other organizations, soliciting our views on what is wrong with the present system and what might be done to improve it. We don't know how the others responded, but APhA was not the least bit shy—as evidenced by its five-page reply—in telling HEW in plain and simple language just what the Association thought about the current process!

We wish Secretary Mathews well in his program and hope that the magnitude of reform needed does not prompt him to despair in seeing it through to completion.

—EGF

Journal of Pharmaceutical Sciences

SEPTEMBER 1976

VOLUME 65 NUMBER 9

MARY H. FERGUSON
Editor

L. LUAN CORRIGAN
Assistant Editor

SHELLY ELLIOTT
Production Editor

JANET D. SHOFF
Copy Editor

EDWARD G. FELDMANN
Contributing Editor

SAMUEL W. GOLDSTEIN
Contributing Editor

LELAND J. ARNEY
Publications Director

EDITORIAL ADVISORY BOARD

JOHN AUTIAN	HARRY B. KOSTENBAUDER
LYNN R. BRADY	CARL J. LINTNER, JR.
WILLIAM O. FOYE	DAVID E. MANN, JR.
WILLIAM J. JUSKO	GERALD J. PAPARIELLO

The *Journal of Pharmaceutical Sciences* is published monthly by the American Pharmaceutical Association at 2215 Constitution Ave., N.W., Washington, DC 20037. Second-class postage paid at Washington, D.C., and at additional mailing office.

All expressions of opinion and statements of supposed fact appearing in articles or editorials carried in this journal are published on the authority of the writer over whose name they appear and are not to be regarded as necessarily expressing the policies or views of the American Pharmaceutical Association.

Offices—Editorial, Advertising, and Subscription Offices: 2215 Constitution Ave., N.W., Washington, DC 20037. Printing Offices: 20th & Northampton Streets, Easton, PA 18042.

Annual Subscriptions—United States and foreign, industrial and government institutions $50, educational institutions $50, individuals *for personal use only* $30; single copies $5. All foreign subscriptions add $5 for postage. Subscription rates are subject to change without notice. Members of the American Pharmaceutical Association may elect to receive the *Journal of Pharmaceutical Sciences* as a part of their annual $60 (foreign $65) APhA membership dues.

Claims—Missing numbers will not be supplied if dues or subscriptions are in arrears for more than 60 days or if claims are received more than 60 days after the date of the issue, or if loss was due to failure to give notice of change of address. The Association cannot accept responsibility for foreign delivery when its records indicate shipment has been made.

Change of Address—Members and subscribers should notify at once both the Post Office and the American Pharmaceutical Association, 2215 Constitution Ave., N.W., Washington, DC 20037, of any change of address.

© Copyright 1976, American Pharmaceutical Association, 2215 Constitution Ave., N.W., Washington, DC 20037; all rights reserved.

DISSECTING THE LABYRINTH

"There's got to be a better way!"

How many times all of us have exclaimed our irritation in those or similar words when we encountered obstructions, obstacles, and assorted roadblocks which have frustrated us in our efforts to accomplish what ought to be some seemingly simple objective.

From various press reports, it appears that HEW Secretary David Mathews reached such a conclusion this summer with respect to the manner in which his Department develops and issues its regulations. That appears to be the basis for his announcement on July 25 that, effective immediately, he was instituting "sweeping reforms" in the HEW regulations process.

The Secretary stated, in part, that: *"For far too long HEW has gone to the public in these (controversial) situations only to tell them what it intends to do. From now on our first step will be to ask the people of this country what they think we should do."* The announcement further explained that one of the extreme new reforms is a *"requirement for HEW to consult broad segments of the public before it puts pen to paper in preparing controversial regulations mandated by congressional action or compelling administrative need."*

A detailed, ten-step process was described as the specific procedure that is to be followed in the future in promulgating new regulations.

Beyond this step-wise procedure, the Secretary included several other features in his reform package. One of these—which in our view is sorely needed and long overdue—reflects Secretary Mathews' academic background. We refer to the part calling for *"training sessions for Department regulations writers so that regulations are written in clear, concise English."*

Washington bureaucrats have developed a well-deserved reputation for having a facility for translating simple concepts and ideas into the most confusing and complex messages. A Washington daily newspaper for some time has made sport of this penchant by publishing a daily feature titled "Gobbledygook," in which a choice piece of unintelligible federal government jargon is reprinted for the amusement of the newspaper readership.

Another ancillary feature of the Secretary's directive calls for *"modification of (existing) regulations which impose too numerous or needlessly complex requirements on program administrators; for example, a special task force is now at work in HEW simplifying the Medicaid regulations."*

It may seem absurd that such a dictate needs to be spelled out for a gigantic department within the federal government. But few of us fully appreciate the awesome influence of this single agency.

HEW alone has 135,000 employees—enough to constitute a fair sized city. In our personal lives, most of us would be impressed by the fact that a given person is responsible for managing the annual expenditure of a million dollars. Yet, in light of HEW's current budget of $128 billion, this translates into an average disbursement or expenditure figure of almost that amount (actually, over $948,000) for each and every one of those 135,000 employees!

But the real basis for public unhappiness with HEW seems to stem from the fact that the regulations the agency has created over the years have often been confusing, contradictory, and controversial. The perceived result has been inefficiency and unfairness at best, and waste and illegality at worst. Although Congress may enact legislation, it is through regulations that broad, general laws are applied and put into practice. Consequently, the regulation writers exert about as much influence—and sometimes more—within the government processes that affect our lives as do all our elected representatives!

Therefore, a reexamination of how this system is operating—and a serious effort to improve its operation—seem to us to be long overdue. Preliminary to the July 25 announcement from HEW, the Secretary's office had written to APhA, as well as to a number of other organizations, soliciting our views on what is wrong with the present system and what might be done to improve it. We don't know how the others responded, but APhA was not the least bit shy—as evidenced by its five-page reply—in telling HEW in plain and simple language just what the Association thought about the current process!

We wish Secretary Mathews well in his program and hope that the magnitude of reform needed does not prompt him to despair in seeing it through to completion.

—EGF

Self-Serving Trade Secrets: A Response

I welcome the opportunity to comment on your proposed editorial[1] for the *Journal of Pharmaceutical Sciences.*

The quotes from PMA testimony are accurate, but I do not agree with your interpretation of them in implying that "data critical to the informed use of a new drug" is being withheld by the current system or that health care practitioners are denied ready and convenient access to "information which may either save lives or prevent needless deaths." As you know, the review process for New Drug Applications leading to required labeling for a new drug product, which is followed by the FDA, takes the following points into consideration. The package insert must contain full disclosure and list all pertinent indications and contraindications for the proper use of the product. Also, FDA now releases a summary of the clinical data establishing safety and efficacy for approved new drugs. For drugs not subject to NDA procedures, and for all antibiotic drugs, all of this data is available.

The "purely economic profit considerations" which you refer to should not be dismissed so cavalierly, since they represent a most important incentive for continued research support. If indeed you agree, as you seem to indicate in your editorial, that the control of drug testing and related research should remain with the private industry, rather than with government, you should also be concerned with how the research-based pharmaceutical industry will maintain the initiative and wherewithal to continue its innovative work.

We would agree that the patent system has worked successfully to foster innovation and we do not want it to be discontinued or altered to discriminate against pharmaceutical protection. Patent protection, however, in and by itself is not always sufficient, either because such protection is not available or it is of limited scope. Also, on the average, the effective life of a patented new drug discovery is diminished (currently about nine years) because of the time delays associated with obtaining new drug approval from the FDA.

The incentive to conduct research and development of new therapeutic entities should be provided by a plurality of systems, including the patent laws, trademark laws, trade secret concepts, and, with respect to new drugs, government protection of raw clinical data supporting product safety and efficacy. This plurality of systems is available to other industries and we see no reason to prejudice new drug research incentive by eliminating any one mechanism.

Finally, we think it is somewhat inflammatory to imply that needless deaths may be occurring under the present system and that data critical to the informed use of a new drug is being denied practitioners. The FDA approval process is basically sound, although refinements certainly could be made. FDA approved labeling is detailed and precise and apparently health professionals have not been clamoring for additional information. The data in question would primarily be of value to a drug manufacturer to support a second NDA and thereby avoid adding to the scientific knowledge.

Ed, I appreciate the opportunity to comment on your proposed editorial, and would ask that, if possible, this letter be printed along with it.

C. Joseph Stetler
Pharmaceutical Manufacturers Association
1155 Fifteenth Street, N.W.
Washington, DC 20005

Received July 19, 1976.

[1] E. G. Feldmann, *J. Pharm. Sci.*, 65 (7), i(1976).

Editor's note: An advance copy of Dr. Feldmann's editorial for the July 1976 issue was sent to Mr. C. Joseph Stetler, President of the Pharmaceutical Manufacturers Association, with an invitation to comment. Unfortunately, the Journal publication schedule did not permit this response from Mr. Stetler to be published in that same issue in which the editorial appeared.

1976

September 20–22
National Conference on Cancer Research and Clinical Investigation, American Cancer Society and National Cancer Institute, Regency Hyatt Atlanta Hotel, Atlanta, Ga. (Contact Dr. S. L. Arje, American Cancer Society, 777 3rd Ave., New York, NY 10017)

September 23–24
Annual Conference on New Advances in Separation Technology, Sheraton Poste Inn, Cherry Hill, N.J. (Contact W. F. Heneghan, 289 Greenwich Ave., Greenwich, CT 06930)

October 3–8
Congress of International Technology, Pittsburgh Hilton, Pittsburgh, Pa. (Contact International Technology Institute, 7125 Saltsburg Rd., Pittsburgh, PA 15235)

October 7–10
American College of Apothecaries, Annual Meeting, Bellevue Stratford, Philadelphia, Pa.

October 11–15
National Society for Histotechnology, Convention and Symposium, Radisson Hotel Downtown, Minneapolis, Minn. (Contact Registrar, P.O. Box 36, Lanham, MD 20801)

October 17–20
ASTM Committee E-19, Practice of Chromatography, North Shore Hilton Hotel, Chicago, Ill. (Contact Gerald Dupre, Biodynamics, Inc., Box 43, Mettlers Road, East Millstone, NJ 08874)

October 17–21
American Public Health Association, Annual Meeting, Miami Beach, Fla.

October 18
APhA Academy of Pharmaceutical Sciences, Annual Western Regional Meeting, Industrial Pharmaceutical Technology Section, D-Registry, Irvine, Calif. (Contact Dr. D. Swanson, ALZA Corp., Palo Alto, CA 94304)

October 18–20
International Symposium on Platinum Coordination Complexes in Cancer Chemotherapy, Dallas, Tex. (Contact Dr. Amanullah Khan, Wadley Institutes of Molecular Medicine, 9000 Harry Hines, Dallas, TX 75235)

October 18–21
Association of Official Analytical Chemists, Marriott Twin Bridges, Washington, D.C. (Contact L. G. Ensminger, AOAC, Box 540, Ben Franklin Station, Washington, DC 20044)

October 22
APhA Academy of Pharmaceutical Sciences, Annual Eastern Regional Meeting, Industrial Pharmaceutical Technology Section, Cherry Hill Inn, Cherry Hill, N.J. (Contact Dr. Arthur Goldberg, Applied Sciences, TDD, Hoffmann-La Roche Inc., Nutley, NJ 07110)

October 25–29
International Symposium on Medical Radionuclide Imaging, Los Angeles, Calif. (Contact John H. Kane, Energy Research and Development Administration, Washington, DC 20545)

November 1–4
International Symposium on Advances in Chromatography, Houston, Tex. (Contact Dr. A. Zlatkis, Chemistry Department, University of Houston, Houston, TX 77004)

November 11–12
Health Care Delivery Systems in North America: The Changing Concepts, Canadian–American Seminar, University of Windsor, Windsor, Ontario, Canada N9B 3P4 (Contact Director, Canadian–American Seminar, University of Windsor, Windsor, Ontario, Canada N9B 3P4)

November 14–18
APhA Academy of Pharmaceutical Sciences, National Meeting, Carleton House Hotel, Orlando, Fla.

November 14–18
American Dental Association, Annual Meeting, Las Vegas, Nev.

November 14–19
International Symposium on Industrial Wastes and Environment, Caracas, Venezuela (Contact Dr. Richard Abbou, 115 rue de la Pompe, F 75116, Paris, France)

November 14–20
Federation of Analytical Chemistry and Spectroscopy Societies, Annual Meeting, American Chemical Society Division of Analytical Chemistry and others, Civic Center, Philadelphia, Pa. (Contact C. White, Analytical Chemistry Division, Oak Ridge National Laboratories, Oak Ridge, TN 37830)

December 1–3
Symposium on New Biochemical Aspects of Prostaglandins and Thromboxanes, Los Angeles, Calif. (Contact Marilyn Cheung, Intra-Science Research Foundation, P.O. Box 18589, Los Angeles, CA 90018)

December 4–8
American Medical Association, Clinical Meeting, Philadelphia, Pa.

December 5–10
American Society of Hospital Pharmacists, Midyear Meeting, Anaheim, Calif.

December 6–10
International Symposium on Biological Applications of Stable Isotopes, Leipzig, West Germany (Contact John H. Kane, Energy Research and Development Administration, Washington, DC 20545)

December 9–10
Toxic Substances Seminar, Washington, D.C. (Contact Nancy McNerney, Government Institutes, 4733 Bethesda Ave., Washington, DC 20014)

December 13–15
International Congress on Advances in Automated Analysis and Information Systems, New York, N.Y. (Contact Michele Barth, Technicon Corp., Tarrytown, NY 10591)

December 14–15
Food and Drug Law Institute, Annual Meeting, Washington Hilton, Washington, D.C.

1977

January 9–12
Symposium on Quantum Biology and Quantum Pharmacology, Sanibel Island, Fla. (Contact John R. Sabin, Williamson Hall, University of Florida, Gainesville, FL 32611)

February 15–19
The American Academy of Forensic Sciences, San Diego, Calif. (Contact Dr. Naresh C. Jain, Rancho Los Amigos Hospital, 7601 E. Imperial Highway, Downey, CA 90242)

February 20–26
American Association for the Advancement of Science, Annual Meeting, Denver, Colo.

February 28–March 4
Pittsburgh Conference on Analytical Chemistry and Applied Spectroscopy, Cleveland, Ohio (Contact John E. Graham, Koppers Co., 440 College Park Dr., Monroeville, PA 15146)

March 7–11
Symposium on Biologically Active Polypeptides, Le Chateau Montebello, Montebello, Quebec, Canada (Contact Chemical Institute of Canada, 151 Slater St., Suite 906, Ottawa, Ontario K1P 5H3, Canada)

March 20–25
American Chemical Society National Meeting, New Orleans, La. (Contact A. T. Winstead, American Chemical Society, 1155 16th St., N.W., Washington, DC 20036)

Items to be considered for inclusion or corrections should be addressed to:

J. Pharm. Sci. Calendar
2215 Constitution Avenue, N.W.
Washington, DC 20037

Journal of Pharmaceutical Sciences

SEPTEMBER 1976
VOLUME 65 NUMBER 9

RESEARCH ARTICLES

Knudsen Vapor Pressure Measurements on Pure Materials and Solutions Dispersed in Porous Media: Molded Nitroglycerin Tablets

M. J. PIKAL ˣ and A. L. LUKES

Abstract □ The gravimetric Knudsen method for vapor pressure measurement may be subject to serious systematic errors when the sample: (*a*) consists of the volatile component dispersed in an inert porous matrix and/or (*b*) contains a dissolved polymeric solute. Vaporization of water present as an impurity in the matrix may result in an appreciable "background" mass loss, and "nonequilibrium effects" may be present; *i.e.*, the vapor of interest may be unable to escape from the sample rapidly enough to maintain the equilibrium vapor pressure in the Knudsen cell. Methods for eliminating the interference due to background effects are described, and a theoretical analysis of nonequilibrium effects is presented. The essential validity of the theories for nonequilibrium effects and the effectiveness of the methods for circumventing background effects were verified by experimental studies with molded nitroglycerin tablets. With nitroglycerin tablets, accurate Knudsen vapor pressure data may be obtained using the modified procedures and data analysis presented in this report.

Keyphrases □ Vapor pressure—gravimetric measurement, pure materials and solutions dispersed in porous media, analysis of nonequilibrium and background effects □ Dispersions—solutions in porous media, gravimetric vapor pressure measurement, analysis of nonequilibrium and background effects □ Nitroglycerin—tablets, gravimetric vapor pressure measurement, analysis of nonequilibrium and background effects □ Dosage forms—nitroglycerin tablets, solutions dispersed in porous media, gravimetric vapor pressure measurement

The gravimetric Knudsen effusion technique is a convenient and accurate method for measuring vapor pressures of pure materials having low volatility (1–5). The rate of vapor loss through a small orifice is measured gravimetrically under conditions of free molecule flow (*i.e.*, large mean free path), and the vapor pressure is calculated directly from the proportionality between the rate of mass loss and vapor pressure. However, when the volatile material of interest is dispersed at trace levels in a porous nonvolatile matrix and/or contains a polymeric solute, several major problems may arise which are not discussed in the literature.

First, the amount of volatile water in the sample (*i.e.*, nitroglycerin tablet) may be of the same order of magnitude as the volatile material of interest (*i.e.*, nitroglycerin), and the measured rate of mass loss contains a "background" due to water evaporation.

Second, nonequilibrium effects may be present. That is, if the vapor of interest cannot leave the sample rapidly enough to maintain the equilibrium vapor pressure in the Knudsen cell, the measured vapor pressure will be lower than the equilibrium value.

Extension of the gravimetric Knudsen method of vapor pressure measurement to complex systems is described in this report. Specifically, a theoretical–experimental analysis of nonequilibrium effects is given, and the procedures required to circumvent errors due to nonequilibrium effects and background effects are described.

Although the theoretical results and most of the procedures are of general application, the discussion is presented in terms of molded nitroglycerin tablets as a specific example, and the experimental studies were limited to nitroglycerin tablets. The tablets were mostly α-lactose, containing 1–2% nitroglycerin (0.3–0.6 mg). "Stabilized" tablets also contained 1% povidone dissolved in the nitroglycerin.

EXPERIMENTAL

Materials—Reagent grade benzoic acid was recrystalled twice from warm water; reagent grade benzophenone was recrystallized once from water–ethanol. The crystals were dried overnight *in vacuo* (10 Torr) at 35°. The nitroglycerin samples were prepared and assayed as described elsewhere (6).

Apparatus—The Knudsen cells (*i.e.*, sample containers) used were similar to those described previously (2–4). The cell was basically an aluminum pot with a flanged screw-on lid, allowing a platinum foil cover to fit inside the lid. A small orifice was drilled in the foil, and a vaportight seal between the bottom of the pot and the platinum foil was achieved using a small "O" ring[1]. Three cells were used; they all had the same weight (1 g) and dimensions (height, 1 cm; diameter, 1 cm) and differed only in the orifice size.

The effusion rate was measured by suspending the cell from one arm of an electronic vacuum microbalance[2]. The noise level (due to building vibrations) was generally low enough to allow small mass changes to be measured with an accuracy of about ±0.5 μg. The original tubes on both the sample and tare sides of the balance were replaced by a combination sample tube–cold finger, which joined with the balance through an "O" ring joint. The cold finger was a 20-mm Pyrex tube, which joined the main sample tube about 10 cm above the Knudsen cell. The output of the balance was connected to a strip-chart recorder[3], thereby providing a curve of mass (m) *versus* time.

The pumping system was an oil diffusion pump backed by a rotary pump. During an experiment, the system was evacuated to less than 0.5 Torr with the rotary pump (within 1–2 min). The cold fingers were placed in liquid nitrogen, and the system was opened to the diffusion pump–rotary pump combination. The air pressure at the sample site was in the 10^{-5}-Torr range within 20 sec after the diffusion pump was placed in line. The ultimate air pressure was about 5×10^{-6} Torr. Temperature control was maintained within ±0.05° by a water thermostat.

Calibrations—With the vapor pressure, P (in Torr), and the effusion rate, R_0 (in micrograms per minute), the Knudsen equation may be written (4, 7):

$$10^4 P\,(\text{Torr}) = \frac{2.854}{10^3 A_0}\sqrt{\frac{T}{M}}R_0 \qquad \text{(Eq. 1)}$$

where A_0 is the "effective orifice area" in square centimeters and includes, in addition to the orifice area, several correction terms near unity (4, 7); T is the absolute temperature; and M is the molecular weight.

Measurements of R_0 for benzoic acid at 25° and the literature vapor pressure (4) were used to calibrate A_0 for Cells 1 and 2. The vapor pressure of nitroglycerin (10% trituration on lactose) was evaluated at 25° using Cells 1 and 2, and nitroglycerin at 25° was used to calibrate A_0 for Cell 3. The values of $10^3 A_0$ determined, in square centimeters, were 2.18 (Cell 1), 0.96 (Cell 2), and 27.4 (Cell 3). These data are in satisfactory agreement with the (less accurate) values determined by microscopic examination.

By using Cell 2 and the calibrated A_0 value, vapor pressures were measured for benzoic acid at 35° and for benzophenone at 25°. Agreement with the literature data (2, 4) was within 5%.

Origin of Background—The value of dm/dt computed (by numerical differentiation) directly from the recorder mass *versus* time curve contains significant contributions from several "background" effects, *i.e.*, mass loss other than effusion of nitroglycerin:

1. Presumably due to diffusion-limited loss of absorbed water, the balance system itself gives an apparent loss in mass with time, denoted "balance background."
2. The Knudsen cell loses mass, presumably adsorbed water, denoted "empty cell background."
3. In general, the samples of interest contain a small, although significant, quantity of volatile water[4], thereby producing a "water background."

Background effects were noted by other investigators (4). Background effects decrease in importance as time, t, increases, and the usual practice (4) is to wait until the background effects are small before calculating vapor pressure. However, for the samples studied, one cannot assume that vapor pressure is independent of time, and data as near time zero as possible must be obtained. Time zero is defined as the start of effusion, which to good approximation is when the diffusion pump is placed in line.

Table I—Experimental Test of the Placebo Background Approximation at 25°

Experiment	t, min	dm/dt, μg/min, Placebo at $t/2$	Δm (nitro)/t, μg/min: Gravimetric	Assay
One-Half Cut Commercial Tablets (1% Povidone)				
4-1	96	0.12	0.73	0.72
6-1	108	0.12	1.20	1.21
6-2	112	0.12	0.99	0.99
4-2	112	0.12	0.53	0.39
3-1	158	0.10	0.18	0.21
3-2	258	0.08	0.08_1	0.10_5
		Mean, gravimetric − assay =		$+0.01_5$
One-Half Crushed 0.4-mg Commercial Tablets (1% Povidone)				
4-2-A	92	0.22	0.66	0.75
4-2-B	97	0.22	0.49	0.64
4-2-C	98	0.22	0.46	0.57
		Mean, gravimetric − assay =		−0.12

Correction for Instrument Background—The sum of the balance background and the empty cell background, denoted "instrument background," is easily measured by performing the appropriate blank runs. All three cells gave nearly the same empty cell background, and another Knudsen cell was suspended from the tare arm of the balance to cancel most, if not all, of the empty cell background. Thus, the instrument background was determined for a given "configuration" (*e.g.*, Cell 2 tare arm, Cell 1 sample arm) by blank runs, and the total rate of mass loss for a given sample was corrected by subtraction of the blank.

Plots of instrument background *versus* time were roughly linear on a log–log plot and varied from about 1.0 μg/min at t = 2.5 min to about 0.07 μg/min at t = 90 min. Reproducibility at small t was rather poor, only about ±0.2 μg/min at t = 2.5 min; but for t > 10 min, reproducibility was good, about ±0.04 μg/min.

Correction for Water Background—*Placebo Method*—In this method, the water background for a given sample is assumed identical to that for a "placebo" sample, where the placebo contains no nitroglycerin but is identical in all other respects. In short, the presence of nitroglycerin is assumed to have no effect on the rate of water loss from a sample. Placebo water backgrounds were determined for a number of sample types where the water content was of the same order of magnitude, or less, than the nitroglycerin content. For the samples studied, the water background was independent of orifice area and directly proportional to the sample weight[5] (for a given type of sample).

As a check on the validity of the placebo background approximation, the loss in mass of nitroglycerin, Δm(nitro), in time t was determined gravimetrically (using the appropriate placebo background) and by chemical analysis. The procedure, illustrated for cut tablets, is as follows. A tablet is cut into four wedge-shaped pieces. Two pieces are assayed to obtain an "initial" nitroglycerin concentration. The remaining two pieces are placed in a Knudsen cell, and an effusion experiment is allowed to proceed for time t, after which the tablet pieces are assayed to obtain a "final" nitroglycerin concentration.

The loss of nitroglycerin is computed both from the mass *versus* time trace using the placebo background (gravimetric value) and from the assay results (Table I). The experiment number indicates the conditions of the experiment; *i.e.*, Experiment 4-1 refers to a 400-μg

[1] The first attempt was with a butyl rubber "O" ring, but it failed due to sorption of nitroglycerin in the rubber. Teflon (du Pont) "O" rings did not sorb significant quantities of nitroglycerin.

[2] Sartorius model 4102, Brinkmann Instruments, Westbury, NY 11590

[3] Omniscribe model 5121-5, Houston Instruments, Bellaire, TX 77401

[4] In the case of nitroglycerin tablets, the water of hydration in α-lactose is rather firmly bound and contributes little or nothing to the water background at temperatures near 25°.

[5] Some additional observations are: (*a*) plots of water background *versus* time are roughly linear on a log–log plot; (*b*) backgrounds are higher for samples containing povidone; (*c*) backgrounds are higher for crushed tablets than for tablets cut into four wedge-shaped pieces; (*d*) the background for tablets is independent of drying time for drying times between 0.5 and 2 hr and is also independent of sucrose level in the 0.1–0.5% range; and (*e*) the reproducibility of the water background is within ±20%.

tablet run in Cell 1, and 6-2 refers to a 600-μg tablet run in Cell 2. Comparison of the gravimetric and assay results for a given experiment with cut tablets shows that differences between the gravimetric and assay results are random in sign and generally small. Thus, at least as a first approximation, the placebo background approximation is valid for cut tablets. For the crushed tablets, the agreement is less satisfactory; it appears that the placebo background may be too high by about a factor of 2. Clearly, an alternative method for eliminating the water background would be useful.

Differential Method—As indicated earlier, the placebo background is independent of orifice size. By assuming that the water background for a sample is independent of orifice size, regardless of the accuracy of the placebo background approximation, the effects of volatile water may be canceled by the following differential experiment. Identical samples are placed in Cells 1 and 2. Cell 1 ($10^3 A_0 = 2.18$) is suspended from the sample arm of the balance, and Cell 2 ($10^3 A_0 = 0.96$) is suspended from the tare arm. During the effusion experiment, water evaporates from both samples *at the same rate*, thereby canceling, and nitroglycerin effuses from each cell at a rate proportional to the effective area of that cell's orifice. If the vapor pressure is independent of time t, the vapor pressure at any time is given by P_D:

$$10^4 P_D \text{ (Torr)} = \frac{2.854}{10^3 A_D}\sqrt{\frac{T}{M}} R_D \qquad \text{(Eq. 2)}$$

where P_D is the "differential vapor pressure," $A_D = A_0$ (Cell 1) $- A_0$ (Cell 2)[6], and R_D is the observed "net" effusion rate in the differential experiment.

In general, the vapor pressure decreases with time and P_D is equal to the vapor pressure only at $t = 0$. The physical interpretation of the variation of P_D with time will be given later. Empirically, observed P_D data are linear in time from the lowest time where data are taken[7] to a time corresponding to a 30–50% reduction in P_D. Similarly, data taken with either Cell 1 or 2 (using placebo backgrounds) are linear on a *P versus t* plot (one-component nitroglycerin phase) or on a ln *P versus t* plot (multicomponent nitroglycerin phase). Linearity begins at small times[7] and often extends over a fivefold reduction in P for multicomponent nitroglycerin systems.

Assuming that the linear plots remain valid in the small time regions where data are not obtained[8], data extrapolated to $t = 0$ yield the vapor pressure at $t = 0$. Therefore, a comparison of extrapolated differential results with the corresponding results obtained with Cells 1 and 2 (placebo background) is a test of the validity of the placebo background approximation. Several measurements were made on crushed 0.4-mg tablets containing povidone at 25° using Cell 1, Cell 2, and the differential technique.

Qualitatively, the results agree with those in Table I in that, for crushed tablets (1% povidone), the placebo background appears too high. However, the magnitude of the background error is much less, ~20%, rather than a factor of 2. The 20% figure is probably more accurate. Similar comparisons were made for a number of other additive–nitroglycerin–lactose systems. In all cases, good agreement was obtained between Cell 1, Cell 2, and differential measurements.

THEORETICAL

The equation relating mass loss from a Knudsen cell with equilibrium vapor pressure is derived assuming that all rate processes are sufficiently rapid to maintain the equilibrium vapor pressure within the Knudsen cell. While this "equilibrium" assumption is nearly always valid for homogeneous one-component systems, for the systems of interest to this research, there are two "mechanisms" by which the equilibrium assumption may be invalidated.

First, even if the maximum rate of evaporation of nitroglycerin is effectively infinite, as it would be if the nitroglycerin phase is pure nitroglycerin, the vapor cannot leave the sample at an infinite rate due to collisions with the tablet matrix. Thus, the vapor pressure maintained in steady state within the Knudsen cell, which is the vapor pressure measured in the experiment, is less than the equilibrium vapor pressure. This type of nonequilibrium effect is referred to as the "matrix effect."

The second type of nonequilibrium effect may arise when the nitroglycerin phase is a multicomponent system, as is the case in tablets containing stabilizing additives. Here, even if the matrix effect is negligibly small, a nonequilibrium effect can arise due to composition nonhomogeneities developing at the surface of the nitroglycerin phase as nitroglycerin is removed from the sample. If diffusion of nitroglycerin within the nitroglycerin phase is not sufficiently rapid to maintain approximate homogeneity, the vapor pressure measured in the Knudsen experiment corresponds to the composition at the surface layer, which is deficient in nitroglycerin, and not to the mean composition. Thus, this nonequilibrium effect, denoted the "diffusion effect," causes the measured vapor pressure to be lower than the equilibrium value.

The objective in this section is to develop mathematical models for the time dependence of the nonequilibrium effects discussed that are, upon parameterization, useful for a semiquantitative evaluation of nonequilibrium effects for a given set of experimental conditions.

Matrix Effect—The matrix effect will be approximated using a capillary pore model, defined by the following assumptions:

1. The tablet pore structure relevant to nonequilibrium effects is approximated as a network of cylindrical capillary tubes oriented normal to each surface. The capillaries are characterized by a "mean effective radius," a.

2. The number of capillary openings of area πa^2 per unit area of surface, denoted by $\hat{N}$, is taken to be a parameter characteristic of pore structure and, therefore, independent of gross sample geometry. Note that the total number of capillary tubes in the sample is then $\hat{N}A/2$, where A is the surface area. The factor of 1/2 arises since each tube intersects the surface at two points.

3. Nitroglycerin is assumed to exist in a phase that is (initially) homogeneously distributed on the interior surfaces of the capillary tubes. The fraction of capillary volume occupied by nitroglycerin is assumed small. For 0.6-mg tablets, about 95% of the total capillary volume is void.

4. The total area of capillary openings to the surface, $\hat{N}A\pi a^2$, is assumed large compared to the effective area of the Knudsen cell orifice, A_0.

One-Component Nitroglycerin Phase (Conventional Tablets)—Since, in this case, nitroglycerin is in the pure state, the vapor pressure in any volume element containing liquid nitroglycerin at distance or "depth" d from the surface is equal to the equilibrium vapor pressure P^0. Thus, all nitroglycerin is removed from a given volume element at depth d before any nitroglycerin is removed at depth $d + \delta d$. The concentration of *liquid* nitroglycerin is zero between the surface and depth d and is equal to the concentration at time zero at d. The vapor pressure outside the tablet, but within the Knudsen cell, is the apparent vapor pressure, P_a.

Consider a sample of undefined gross geometry but having volume V and surface area A and containing m^0 μg of nitroglycerin at time zero. At time t, evaporation has proceeded to depth d, removing $\Delta m(t)$ μg of nitroglycerin, where $\Delta m(t)/m^0 = \Delta V(t)/V$. Here, $\Delta V(t)$ is the volume of sample that has been "emptied" of liquid nitroglycerin. To first order in time, $\Delta V(t) = Ad$, and:

$$\frac{\Delta m(t)}{m^0} = \frac{Ad}{V} \qquad \text{(Eq. 3)}$$

Under conditions of free molecule flow (*i.e.*, large mean free path), conservation of mass requires that the flow through the Knudsen cell orifice, R_0, is equal to the net flow through the capillary openings, R_c. The flow rate, R_0, is given by the Knudsen relationship (8):

$$R_0 = \beta P_a \equiv \kappa A_0 P_a \qquad \text{(Eq. 4)}$$

where κ is a constant for the present purpose. Consistent with Assumption 4, R_c may be written (8):

$$R_c = \hat{N}A\pi a^3 \frac{8}{3}\kappa\left(\frac{P^0 - P_a}{d}\right) \qquad \text{(Eq. 5)}$$

The number of capillary openings per unit surface area, $\hat{N}$, may be related to the pore volume fraction, ϵ, by the following argument. In the volume element, δV, the total pore volume, V_p, is given by $V_p = \epsilon\delta V = \epsilon Ad$. However, the capillary model demands that the total pore volume is also given by $V_p = \hat{N}A\pi a^2 d$. Combination of the two ex-

[6] Although A_D may be evaluated from the calibrated orifice areas of Cells 1 and 2, it was determined by calibration with benzoic acid at 25° to avoid propagation of errors, yielding $10^3 A_D = 1.31 \pm 0.03$ cm^2.

[7] Because of background variability, reproducibility is poor at times where the background becomes comparable in magnitude to the effusion rate. Therefore, data are taken only for $t > 15$ min for Cell 2; for Cell 1 and differential measurements, data are taken for $t > 7$ min.

[8] Justification for this assumption as a good approximation will be given in the next section, where it is established that nonequilibrium effects for Cells 1 and 2 are negligible with crushed tablets.

pressions for pore volume yields:

$$\epsilon = \pi a^2 \hat{N} \qquad \text{(Eq. 6)}$$

By noting that, to first order in time, $\Delta m(t) = \beta P^0 t$, combination of Eqs. 3–6 yields the desired relationship between the observed vapor pressure, P_a, and the equilibrium vapor pressure, P^0:

$$\frac{P_a}{P^0} = 1 \sim \frac{\gamma \beta P^0}{m^0} t + 0(t^2, \ldots) \qquad \text{(Eq. 7)}$$

$$\beta = 10^4 \sqrt{\frac{M}{T}} \left(\frac{10^8 A_0}{2.854}\right) \qquad \text{(Eq. 8)}$$

where the nonequilibrium parameter, γ, is given by:

$$\gamma = \frac{3}{8}\left(\frac{A_0}{A}\right)\left(\frac{V}{A}\right)\frac{1}{\epsilon a} \qquad \text{(Eq. 9)}$$

The notation $0(t^2, \ldots)$ refers to higher order terms, which cannot be consistently evaluated using this simple capillary model. The result that all geometries behave alike to first order in time is a consequence of the model. The model essentially assumes that, at small times, flow from the sample surface is equal to flow from a slab of the same volume and area.

According to theory, the apparent vapor pressure, P_a, should decrease linearly with time, at least at small times, and the value of P_a extrapolated to $t = 0$ yields the equilibrium vapor pressure at time zero. Moreover, the magnitude of the nonequilibrium effect increases with the ratio A_0/A. To minimize nonequilibrium effects, effusion cells with small orifice areas, A_0, should be employed. Furthermore, a procedure found useful in this laboratory is to cut a given tablet into four equal wedge-shaped pieces, thus maximizing the area while still preserving the tablet character of the sample[9].

The "differential vapor pressure" analog for Eq. 7 may be developed by combination of Eqs. 2 and 7:

$$\frac{P_D}{P^0} = 1 - \left[1 - \frac{A_0(2)/A_0(1)}{[1 + A_0(2)/A_0(1)]^2}\right]\frac{\gamma_{12}\beta_{12}P^0}{m^0} t \qquad \text{(Eq. 10)}$$

$$\gamma_{12} = \frac{3}{8}\left[\frac{A_0(1) + A_0(2)}{A}\right]\frac{V}{A}\frac{1}{\epsilon a} \qquad \text{(Eq. 11)}$$

$$\beta_{12} = \frac{10^7}{2.854}\sqrt{\frac{M}{T}}\,[A_0(1) + A_0(2)] \qquad \text{(Eq. 12)}$$

where $A_0(1)$ and $A_0(2)$ are the effective orifice areas for Cells 1 and 2, respectively. The remaining symbols are as previously defined.

Multicomponent Nitroglycerin Phase (Tablets with Additives)—The diffusion effect is assumed negligible, and the same basic capillary model is used for both single- and multicomponent nitroglycerin phases. However, in the latter case, a significant variation of *equilibrium* vapor pressure with time may occur as the composition changes during a Knudsen experiment. For most additive–nitroglycerin systems studied, the nitroglycerin vapor pressure varied approximately linearly with concentration of nitroglycerin in the sample over a considerable concentration range. Thus, as a first approximation in general and as a rather good approximation[10] for the systems studied:

$$P = \frac{P^0}{c^0}\alpha_1 c + P^0(1 - \alpha_1) \qquad \text{(Eq. 13)}$$

Here, P is the equilibrium vapor pressure at concentration c, and P^0 is the equilibrium vapor pressure at time zero when $c = c^0$. For convenience, c is defined as micrograms of nitroglycerin per unit volume of capillary tubes, or $c = m/\epsilon V$, where ϵ is the pore volume fraction, V is the total volume of the sample, and m is the mass of nitroglycerin. The symbol α_1 denotes a unitless constant, reflecting the magnitude of the dependence of vapor pressure on concentration[10]. In the absence of nonequilibrium effects, use of Eq. 13 and the relationship $dm/dt = \beta P$ yields the equilibrium time dependence:

$$\ln P = \ln P^0 - \frac{\beta P^0 \alpha_1}{m^0} t \qquad \text{(Eq. 14)}$$

where P is the measured equilibrium vapor pressure at time t in the Knudsen experiment.

Nonequilibrium effects will now be estimated using the model defined by Assumptions 1–4 and Eq. 13. Consistent with the assumptions and the result for conventional tablets, at small times all geometries are assumed equivalent to a slab of thickness 2ι, with $\iota = V/A$; the calculations are based on such a slab model. This methodology is motivated largely by the difficulty in obtaining a solution to the problem for any geometry more complex than a slab.

Consider a small volume element of a given capillary tube. Consistent with Assumption 4, the flow past any plane normal to the tube axis is given by:

$$J = -\frac{8}{3} a\kappa \frac{\partial P}{\partial x} \qquad \text{(Eq. 15)}$$

where J is the vapor flux. Conservation of mass requires:

$$\frac{\partial c}{\partial t} = -\frac{\partial J}{\partial x} = \frac{8}{3} a\kappa \frac{\partial^2 P}{\partial x^2} \qquad \text{(Eq. 16)}$$

"Local equilibrium" is assumed in the following sense. At each point in (x, t) space, the vapor phase and the immediately adjacent liquid (or solid) nitroglycerin phase are in thermodynamic equilibrium. Thus, vaporization of nitroglycerin is assumed rapid. With the local equilibrium assumption, the vapor pressure $P(x, t)$ may be directly related to concentration $c(x, t)$ through Eq. 13, and the variable, P, in Eq. 16 may be eliminated to give:

$$\frac{\partial c}{\partial t} = D\frac{\partial^2 c}{\partial x^2} \qquad \text{(Eq. 17)}$$

$$D = \frac{8}{3} a\kappa \frac{P^0}{c^0}\alpha_1 \qquad \text{(Eq. 18)}$$

Equation 17 is of the same form as Fick's second law with a constant diffusion coefficient. However, in this case, D is not a diffusion coefficient but rather is a "conductance" coefficient for free molecule flow in a capillary tube.

Local equilibrium is likewise assumed at the tablet surface. At the surface, the vapor space adjacent to the liquid (or solid) nitroglycerin phase is the vapor space outside the tablet but within the Knudsen cell. Since the vapor pressure in this region is P_a, the vapor pressure measured in the Knudsen experiment, Eq. 13 implies that:

$$P_a = \frac{P^0}{c^0}\alpha_1 c(\iota, t) + P^0(1 - \alpha_1) \qquad \text{(Eq. 19)}$$

Therefore, if $c(x, t)$ is known from a solution of Eq. 17 subject to the appropriate boundary conditions, P_a may be calculated using Eq. 19.

The first boundary condition is:

$$c(x, 0) = c^0 \qquad \text{(Eq. 20)}$$

where c^0 is the concentration of nitroglycerin in the capillary tubes at $t = 0$. The second boundary condition may be determined by noting that the surface concentration, $c(\iota, t)$, must allow the evaporation rate from the tablet sample, R_c, to equal the rate of effusion through the Knudsen cell orifice, R_0. The total rate of nitroglycerin loss from a tablet containing $\hat{N}/2$ capillary tubes is twice the rate from one surface or:

$$R_c = \hat{N} A \pi a^2 D \left|\frac{\partial c(x, t)}{\partial x}\right| \qquad x = \iota \qquad \text{(Eq. 21)}$$

With R_0 given by Eq. 4 and R_c given by Eq. 21, the equality $R_0 = R_c$ yields:

$$D\left|\frac{\partial c}{\partial x}\right| = \frac{\alpha_1 \beta P^0 \iota}{m^0}(c - \hat{c}) \qquad x = \iota \qquad \text{(Eq. 22)}$$

$$\hat{c} = \left(\frac{\alpha_1 - 1}{\alpha_1}\right) c^0 \qquad \text{(Eq. 23)}$$

The differential equation, Eq. 17, subject to boundary conditions Eqs. 20 and 22 is readily solved using Fourier series. Evaluating $c(\iota, t)$ from the solution given by Crank (9) and using Eq. 19 yield the desired relationship:

$$P_a = P^0 \sum_{n=1} \frac{2\gamma}{\beta_n^2 + \gamma^2 + \gamma} \exp\left(-\beta_n^2 \frac{Dt}{\iota^2}\right) \qquad \text{(Eq. 24)}$$

where γ is the same nonequilibrium parameter defined by Eq. 9, and β_n's are the positive roots of:

$$\beta_n \tan \beta_n = \gamma \qquad \text{(Eq. 25)}$$

[9] The area for a single whole tablet is 0.56 cm^2; for a tablet cut into four equal wedge-shaped pieces (denoted cut tablet), $A = 0.96$ cm^2.

[10] It is readily demonstrated that Eq. 13 should be valid at small times. Assuming $(m^0 - m)/m^0$ is small and adopting a simple model for the polymer additive–nitroglycerin interaction (G. N. Lewis and M. Randall, in "Thermodynamics," revised by K. S. Pitzer and L. Brewer, McGraw-Hill, New York, N.Y., 1961, Eqs. 21–36), one may demonstrate that α_1 is $\alpha_1 = \Phi_2^2[1 - 2(W_\iota/RT)\Phi_1]$, where Φ_2 and Φ_1 are the volume fractions of additive and nitroglycerin, respectively, at time zero; and W_ι is an energy parameter reflecting the interaction between additive and nitroglycerin. When $(m^0 - m)/m^0$ is of order of magnitude of unity, Eq. 13 has no fundamental basis.

Combining Eqs. 9 and 18 and making the substitutions, $\beta = \kappa A_0$ and $c = m/\epsilon V$, give:

$$\frac{D}{\iota^2} = \frac{1}{\gamma}\frac{\alpha_1 \beta P^0}{m^0} \qquad \text{(Eq. 26)}$$

The evaluation of γ from data on conventional tablets, using Eq. 7, indicates that γ is small for the usual nitroglycerin experimental conditions. Furthermore, scatter in background data at small t limits reliable data to $t > 7$ min. Therefore, the form of Eq. 24 for small γ and $t > 7$ min is of particular importance. For $\gamma \sim 1$ or less, solution of Eq. 25 yields:

$$\beta_1^2 \simeq \frac{\gamma}{1 + \gamma/3} \qquad \text{(Eq. 27)}$$

$$\beta_n^2 \simeq (n-1)^2\pi^2 + 2\gamma \qquad n \geq 2 \qquad \text{(Eq. 28)}$$

When γ is nonzero but small (*i.e.*, $\gamma \ll \pi^2$), the terms corresponding to $n \geq 2$ are negligible except at very small times. Specifically, consider a tablet sample, having a mean pore radius, a, of 4 μm (6), which is cut into four wedge-shaped pieces. Here, numerical calculations show that at times greater than 7 min, the $n \geq 2$ terms are less than 3% of the $n = 1$ term. Combination of Eqs. 24–28 yields:

$$\ln P_a = \ln P_a{}^0 - \frac{\alpha_1 \beta P_a{}^0}{m^0} t \qquad \gamma \lesssim 1 \qquad t > \tau \qquad \text{(Eq. 29)}$$

$$P_a{}^0 = \frac{P^0}{1 + \gamma/3} \qquad \text{(Eq. 30)}$$

where $\tau \sim 5$–10 min for cut nitroglycerin tablets. Thus, when nonequilibrium effects are small to moderate in magnitude, the observed vapor pressure, P_a, decreases sharply at very small times to a value slightly less than the equilibrium vapor pressure and thereafter follows a simple exponential decrease with time. Numerical calculations show that Eqs. 29 and 30 are fair approximations even when $\gamma \sim 5$.

For γ_{12} small and $A_0(2)/A_0(1) < 0.5$, the differential vapor pressure analog for Eqs. 29 and 30 may be written:

$$P_D = P_D{}^0 - \frac{\alpha_1 \beta_{12} (P_D{}^0)^2}{m^0} t \qquad \text{(Eq. 31)}$$

$$P_D{}^0 = \frac{P^0}{1 + \gamma_{12}/3} \qquad \text{(Eq. 32)}$$

where pressure is in Torr. All symbols are as previously defined.

In summary, except at very small times, linearity (*i.e.*, $\ln P_a$ *versus* t or P_D *versus* t) is predicted. Extrapolation of vapor pressure data to $t = 0$ does *not* yield directly the equilibrium vapor pressure. However, with a small orifice area and $a \sim 4$ μm, the matrix effect is small. For example, for a sample of one cut nitroglycerin tablet, the matrix effect causes the extrapolated vapor pressure to be lower than the equilibrium vapor pressure by 9% for Cell 1 and 4% for Cell 2.

Critique of Capillary Model—The model assumes that nitroglycerin exists *only* on the interior surface of the capillary tubes and thereby ignores the presence of nitroglycerin on any surface that is not part of a capillary tube. It may be more reasonable to assume that nitroglycerin is uniformly distributed over the *entire* sample surface. The theoretical analysis for *conventional tablets* may be carried out with this modification of the basic model. The results may be summarized as follows. The amount of nitroglycerin outside the capillary tubes, *ms*, is given by:

$$\frac{ms}{m^0} = \frac{1}{1 + 2\epsilon\iota/a} \qquad \text{(Eq. 33)}$$

where the other symbols are as previously defined. The measured vapor pressure, P_a, is constant and equal to P^0 until *ms* μg of nitroglycerin are removed from the surface. Then Eq. 7 applies if t is replaced by $t - t_0$, where:

$$t_0 = \frac{ms/m^0}{\beta P^0/m^0} \qquad \text{(Eq. 34)}$$

In this research, all experimental (P_a, t) data pairs correspond to $t > t_0$. From these considerations, it then follows that the $t = 0$ intercept of a plot of P_a *versus* t will be *higher* than P^0 by the amount δP (surface error), where:

$$\delta P \text{ (surface error)} = +P^0 \frac{3}{16}\frac{1}{\epsilon^2}\frac{A_0}{A} \qquad \text{(Eq. 35)}$$

With $A_0 \sim 2 \times 10^{-3}$ cm^2, the "surface error" is on the order of 0.5% for nitroglycerin tablets, which is negligible. Equation 35 applies only to a one-component nitroglycerin phase. For the multicomponent case, the surface error will be of the same sign but smaller in magnitude.

The error introduced by Assumption 4 may be evaluated by considering each capillary opening as an orifice and thereby offering "resistance" to flow. The resistance to free molecule flow offered by a tube of length L and radius a may, with good approximation, be taken as proportional to the sum (8):

$$\frac{1}{\pi a^2} + \frac{1}{\pi a^2}\frac{3}{8}\frac{L}{a}$$

The first term is due to the end of the tube acting as an orifice (8) and may be termed an "end effect." Assumption 4 is equivalent to neglecting end effects, thereby assuming that when nonequilibrium effects are significant, the resistance to flow is due mainly to the second term, *i.e.*, $L \gg a$.

End effects may be included in the basic model, and the calculations may be performed without the restrictions imposed by Assumption 4. The vapor pressure extrapolated to $t = 0$ is found to be in error by the amount δP (end effect):

$$\delta P \text{ (end effect)} = -P^0 \frac{A_0}{A\epsilon} \qquad \text{(Eq. 36)}$$

In general, the end effect error is small compared to the calculated nonequilibrium effect and, in part, cancels with the error introduced by assuming all nitroglycerin is within the capillary tubes. Comparison of Eqs. 35 and 36 reveals that the cancellation is nearly complete with conventional tablets.

The model ignores capillary condensation of nitroglycerin. It may be more realistic to postulate that a portion of the nitroglycerin is condensed in small short capillaries (or cracks) which empty into either the larger capillaries or the sample surface. Consider the special case of a one-component nitroglycerin phase. If the amount condensed is less than the total amount present, the equilibrium vapor pressure is constant until enough nitroglycerin is evaporated to reach the point where all remaining nitroglycerin is in a "capillary" state.

For this time period, the only factor causing a decrease in vapor pressure with time is the nonequilibrium effect, which should be well approximated by the model. The only correction is due to the amount of nitroglycerin remaining between depth d and the surface. This correction was estimated for nitroglycerin tablets and found to be negligible to first order in time. However, if *all* the nitroglycerin is condensed, the *equilibrium* vapor pressure varies with time from time zero. Assuming a Fruendlich-type isotherm:

$$\frac{m}{\bar{m}} = \left(\frac{P}{P^0}\right)^n \qquad \text{(Eq. 37)}$$

where $\bar{m}$ is the amount of "capillary" nitroglycerin at $t = 0$ and $P = P^0$:

$$\frac{P}{P^0} = 1 - \frac{\beta P^0}{n\bar{m}} t + 0(t^2, \ldots) \qquad \text{(Eq. 38)}$$

The data for nitroglycerin tablets (6) suggest that $n \sim 8$ and $\bar{m} \sim 300$ μg. Thus, comparison of Eq. 38 with Eq. 7 shows that, when γ is small, the variation of equilibrium vapor pressure with time is comparable in magnitude to the calculated nonequilibrium effect. Under these conditions, the matrix effect model is probably a poor approximation. However, when γ is small, nonequilibrium effects are small and even a crude approximation suffices.

In summary, while these model deficiencies may be significant for some types of porous systems, these deficiencies do not introduce serious error for molded nitroglycerin tablets. The poorest approximation made in the theoretical analysis is the assumption that a porous body with flow in three dimensions is equivalent to a capillary impregnated slab of equivalent volume and area with flow in one dimension. While this is a plausible model for small distances from the sample surface, the calculated nonequilibrium effect may be seriously in error at times when flow from the "core" of the sample becomes important.

Thus, for conventional tablets, deviations from the theoretical result (Eq. 7) may be expected when $\beta P^0 t/m^0$ is greater than about 0.5. For tablets with additives, concentration profiles calculated from the slab theory (9) show that flow from the core of the sample becomes significant at about the same time that $\ln P_a$ becomes linear in time. In short, the $t = 0$ intercept in Eq. 29 is probably a good approximation, but the real dependence of the slope on γ may not correspond well with Eqs. 29 and 30. However, since the calculated effect of γ on the slope is quite small for moderate γ, it does not appear likely that a better model would result in a slope dramatically different.

Diffusion Effect—The diffusion effect is assumed to be the only *significant nonequilibrium effect.* The *nitroglycerin–additive phase* is approximated as a "slab" of constant thickness ι and area A_s. Area A_s refers to the total area of the nitroglycerin–additive phase exposed to the vapor phase. At the slab surface ($x = 0$), evaporation of nitroglycerin occurs, resulting in a lower nitroglycerin concentration, C, where C is concentration in *micrograms of nitroglycerin per cubic centimeter of nitroglycerin–additive phase.*

Evaporation at the surface is assumed to be sufficiently rapid to maintain an equilibrium between nitroglycerin *at the surface* and nitroglycerin in the vapor phase. However, in general, the surface concentration, C_s, is less than the mean concentration due to a finite *diffusion rate of nitroglycerin in the nitroglycerin–additive phase.* A relationship between concentration and vapor pressure equivalent to Eq. 13 is assumed. Thus, the measured vapor pressure, P_a, is related to the surface concentration, C_s, by:

$$P_a = \frac{P^0}{C^0}\alpha_1 C_s + P^0(1 - \alpha_1) \qquad \text{(Eq. 39)}$$

To evaluate C_s as a function of time, Fickian diffusion with a concentration-dependent diffusion coefficient is assumed:

$$\frac{\partial C}{\partial t} = \frac{\partial}{\partial x}\left(D\frac{\partial C}{\partial x}\right) \qquad \text{(Eq. 40)}$$

The zero-time boundary condition is:

$$C(x, 0) = C^0 \qquad \text{(Eq. 41)}$$

where C^0 is the initial concentration. The second boundary condition follows from the requirement that the rate of evaporation from the sample, $A_s\,(D\partial C/\partial x)$, $x = 0$, is equal to the rate of effusion from the Knudsen cell, βP_a. By using Eq. 39 to relate P_a to C_s:

$$D\frac{\partial C}{\partial x} = \frac{\alpha_1 \beta P^0 \iota}{m^0}[C_s - \hat{C}] \qquad x = 0 \qquad \text{(Eq. 42)}$$

$$\hat{C} = \left(\frac{\alpha_1 - 1}{\alpha_1}\right) C_0 \qquad \text{(Eq. 43)}$$

For the special case of a constant diffusion coefficient, Eqs. 40–43 are exactly the same in form as the corresponding equations used to evaluate the matrix effect for tablets with additives. Thus, for constant D, the solution of Eqs. 40–43 is given by Eqs. 24–26, provided γ in Eqs. 24–26 is replaced by γ_D where:

$$\gamma_D = \frac{\alpha_1 \beta P^0}{m^0}\frac{\iota^2}{D} \qquad \text{(Eq. 44)}$$

The assumption of a constant diffusion coefficient is realistic if the additive is a liquid that does not interact strongly with nitroglycerin. For this case, $D \sim 10^{-5}$ cm^2/sec. For the usual nitroglycerin experiments (6), $\alpha_1\beta P^0/m^0 \sim 10^{-4}$ sec^{-1} and $\iota \ll 10^{-1}$ cm. Thus, with constant D, $\gamma_D \ll 0.1$, and the diffusion effect is negligible.

If the additive is an amorphous solid "miscible" with nitroglycerin over a wide composition range (*i.e., such as povidone*), the assumption of constant D is a poor approximation for high levels of additive. As a first approximation, D is assumed to vary with concentration exponentially during a Knudsen experiment:

$$D = D_0 \exp(kC/C_0) \qquad \text{(Eq. 45)}$$

where D_0 and k are constants. The constant D_0 is, in effect, the tracer diffusion coefficient of nitroglycerin in the pure additive. While the exponential form is often used to relate D to concentration (9) and is a plausible relationship (10, 11), there is no firm evidence to support this choice of function for systems of interest to this research. Therefore, results based on Eq. 45 must be regarded as semiquantitative, with perhaps only an order of magnitude accuracy in predicting nonequilibrium effects for a given real system.

With D given by Eq. 45, the differential equation cannot be solved analytically; the solution must be obtained numerically. To facilitate numerical calculations, the following dimensionless variables are introduced:

$$X = \frac{x}{\iota} \qquad \text{(Eq. 46)}$$

$$T = \frac{D_0 t}{\iota^2}\exp\left[\frac{k(\alpha_1 - 1)}{\alpha_1}\right] \qquad \text{(Eq. 47)}$$

$$Y = \alpha_1\left(\frac{C}{C^0}\right) - (\alpha_1 - 1) \qquad \text{(Eq. 48)}$$

In terms of X, Y, and T, the differential equation and boundary conditions become:

$$\frac{\partial Y}{\partial T} = \frac{\partial}{\partial X}\left(e^{kY}\frac{\partial Y}{\partial X}\right) \qquad \text{(Eq. 49)}$$

$$Y(X, 0) = 1 \qquad \text{(Eq. 50)}$$

$$e^{kY}\left(\frac{\partial Y}{\partial X}\right) = e^{k\bar{\gamma}Y} \qquad X = 0 \qquad \text{(Eq. 51)}$$

$$Y(0, T) = P_a/P^0 \qquad \text{(Eq. 52)}$$

$$\hat{k} = \frac{1}{\alpha_1}\ln\left(\frac{D^0}{D_0}\right) \qquad \text{(Eq. 53)}$$

$$D^0 = D(t = 0) \qquad D_0 = D(t \to \infty) \qquad \text{(Eq. 54)}$$

$$\bar{\gamma} = \left(\frac{\alpha_1 \beta P^0}{m^0}\right)\frac{\iota^2}{D^0} \qquad \text{(Eq. 55)}$$

Using standard finite difference methods (9), solutions of Eqs. 49–51, were obtained with a computer. Specifically, values of P_a/P^0 were calculated as a function of $(\alpha_1\beta P^0/m^0)t$ for $\bar{\gamma}$ and $\hat{k}$ in the range $0.05 \le \bar{\gamma} \le 10$; $0 \le \hat{k} \le 8$. Agreement between the numerical solutions and the analytical results, Eq. 24, for $\hat{k} = 0$ is within 2% in P_a/P^0.

A selection of the results obtained are shown in Figs. 1 and 2. The equilibrium case, $\bar{\gamma} = 0$, is shown in Fig. 2 as a dashed line. Within the resolution of the graphs, the $\hat{k} = 0$ curves represent the equilibrium case in Fig. 1. The magnitude of the nonequilibrium effect depends strongly on both $\hat{k}$ and $\bar{\gamma}$; even for small (but nonzero) $\bar{\gamma}$, the nonequilibrium effect can be large.

When $\bar{\gamma}$ is small and $\hat{k}$ is large, nonequilibrium effects are small at small t, and the slope of ln P_a *versus* t *increases* as t increases from zero. However, when $\bar{\gamma}$ is large and $\hat{k}$ is small, nonequilibrium effects are large even at very small (but nonzero) times, and the ln P_a *versus* t slope *decreases* as t increases from zero.

Now consider the estimation of $\bar{\gamma}$ and $\hat{k}$ for a typical experiment. As a concrete example, consider the case of a 0.4-mg nitroglycerin tablet containing 0.36 mg of povidone where the Knudsen experiment is performed at 25° using Cell 1. For a sample of this composition, the povidone–nitroglycerin phase is a very viscous gel-like system. As a *rough* guess, the diffusion coefficient of nitroglycerin in this system, D^0, is estimated at $\sim 10^{-7}$ cm^2/sec. The diffusion coefficient of nitroglycerin in low density polyethylene was determined (in this research) to be $\sim 10^{-12}$ cm^2/sec, a value rather typical for large molecules diffusing in amorphous polymers (10–12). Thus, D_0 is estimated as $D_0 \sim 10^{-12}$ cm^2/sec. From Eq. 53 and these estimates of D_0 and D^0, $k \sim 11$. Experimentally, $\alpha_1 \sim 2$, so $\hat{k} \sim 5.5$. Of course, this estimate is very crude and may well be in error by as much as 50%.

Now consider the estimation of $\bar{\gamma}$. For a tablet, scanning electron microscope studies (6) suggest that much of the nitroglycerin–povidone phase is coated on the lactose surface. To evaluate ι, where $\iota = V/A_s$, the surface area must be estimated. The surface area determined by nitrogen adsorption (6) is probably too high for this purpose since much of the surface roughness is "lost" when the crystals are coated with a semiliquid phase. As a better approximation, the surface area is evaluated from the particle-size distribution curve for a sample of the lactose powder used in tablet preparation. The mean particle diameter is 60 μm, and the calculated surface area per tablet (35.6 mg) is 32 cm^2. By assuming that volumes are additive, $\iota \sim 2 \times 10^{-5}$ cm. For this example, $\beta P^0 = 0.033$ μg/sec. Thus, from Eq. 55 and the above estimates, $\bar{\gamma} \sim 10^{-6}$. Even if this estimate is in error by one or two orders of magnitude, the trends shown in Figs. 1 and 2 suggest that with $\hat{k} \sim 6$, the diffusion effect is not even close to being significant *for nitroglycerin tablet samples.*

The theory developed for the diffusion effect is only a rough approximation. The assumed relationship between diffusion coefficient and concentration is probably a reasonable approximation but is not likely to be quantitative. Moreover, the model assumes that the nitroglycerin phase is characterized by a constant thickness. While this is a good approximation for small times, the nonequilibrium effect will probably be overestimated at large times (*i.e.*, when $\Delta m/m^0$ approaches unity). In short, as nitroglycerin is removed from the sample, the effective thickness of the nitroglycerin phase is reduced, thereby decreasing the magnitude of the nonequilibrium effect.

RESULTS

Matrix Effect—*One-Component Nitroglycerin Phase*—As a test of the theory (Eq. 7), several effusion experiments were carried out

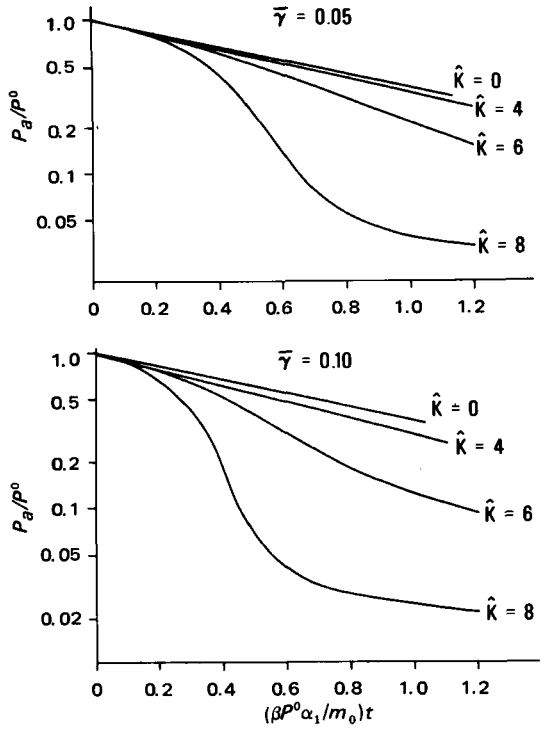

Figure 1—*Numerical solutions of Eqs. 49–51 for selected values of* $\bar{\gamma}$ *and* $\hat{k}$.

at 25° using well aged (6) 0.6-mg conventional commercial tablets (Lot A) from the same bottle. Being well aged, all tablets were assumed to have the same equilibrium vapor pressure at time zero. However, due to intertablet variations, the pore radii evaluated from the data using Eqs. 7–9 may not be identical.

As an example of the observed time dependence of P_a, a portion of the data obtained is illustrated in Fig. 3. As required by theory, P_a *versus* t is linear; in spite of a large variation in slope, all data ex-

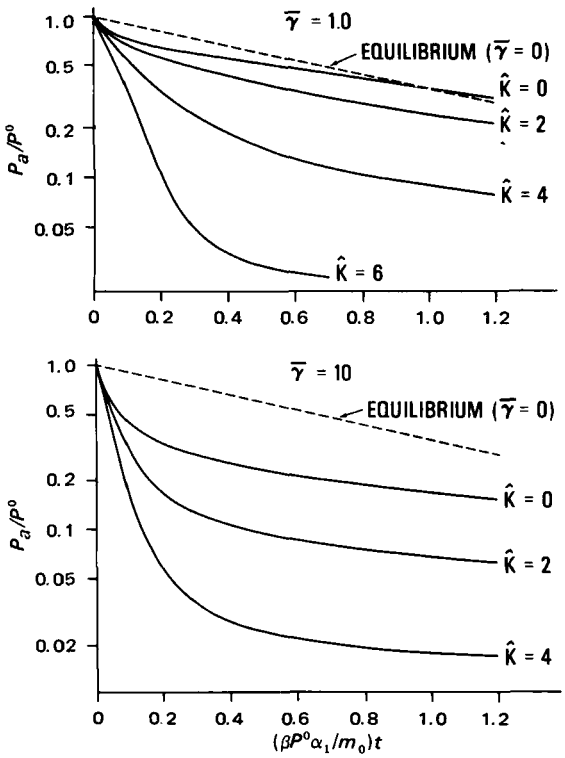

Figure 2—*Numerical solutions of Eqs. 49–51 for selected values of* $\bar{\gamma}$ *and* $\hat{k}$.

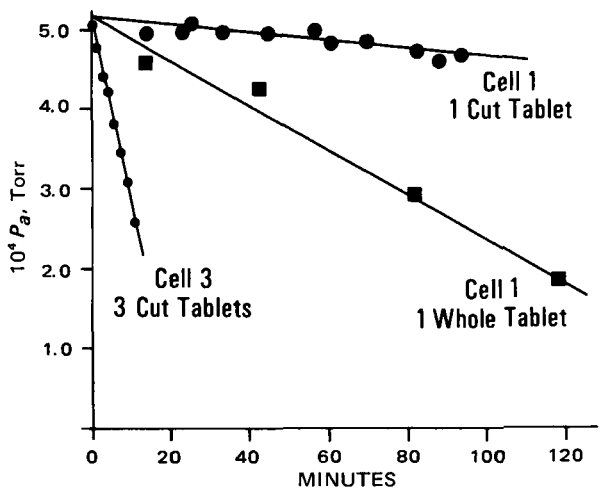

Figure 3—*Observed time dependence of apparent vapor pressure for nitroglycerin in conventional tablets at 25°.*

trapolate to a common value at $t = 0$. For each experiment performed with Lot A, the intercept and slope of the P_a *versus* t curve were evaluated by least-squares analysis; the corresponding value of the pore radius, a, was evaluated using Eqs. 7–9 (Table II). Within the precision of the data, the intercept does not depend on the magnitude of the nonequilibrium effect. While the pore radii calculated from Cell 1 data are in agreement within the precision of the data, the mean pore radius evaluated from the Cell 3 data (large nonequilibrium effect) appears significantly low relative to the other data.

A similar, although less extensive, analysis was carried out with a laboratory lot (0.5 mg) of aged conventional tablets. Three experiments with single tablets in Cell 1 at 25° yielded a mean pore radius of 2.9 ± 0.5 μm. Thus, it is not obvious whether the trend in a values shown in Table II represents a general defect in the theory or a phenomenon peculiar to Lot A. In any case, the data support the following conclusions:

1. The time dependence given by Eq. 7 is a good approximation.
2. The $t = 0$ intercept of Eq. 7 does represent the equilibrium vapor pressure.
3. The slope of P_a *versus* t is semiquantitatively represented by Eqs. 7–9 with $a \sim 4$ μm. Other experimental measures of the pore radius for molded tablets (6) give $a \sim 2$–5 μm.

Multicomponent Nitroglycerin Phase—Numerous data accumulated with Cells 1 and 2 support the theoretical predictions of Eq. 29. Specifically, plots of ln P_a *versus* t are linear. The extrapolated vapor pressures, $P_a{}^0$, obtained with Cell 1 ($A_0 = 2.18 \times 10^{-3}$ cm^2) are, on the average, slightly lower than those found with Cell 2 ($A_0 = 0.96 \times 10^{-3}$ cm^2) on the same sample. However, the uncertainty of the $P_a{}^0$ data is of the same magnitude as the nonequilibrium effect, so a more sensitive test of the theory is required. To this end, a number of experiments with Cell 3 ($A_0 = 27.4 \times 10^{-3}$ cm^2), designed to magnify the nonequilibrium effect, were performed on a single lot of 0.6-mg "stabilized" commercial tablets containing 1% povidone (Fig. 4 and Table III).

Because of the large effusion rate with Cell 3, background uncertainties are not a problem; measurements are possible at very small t. Thus, the data in Fig. 4 reveal not only the linear ln P_a *versus* t plot predicted for $t \gtrsim 7$ min but also show the sharp drop in P_a at very small times required by theory. Also, as predicted from theory, the (linear) intercept at $t = 0$ is smaller for the case of two tablets. Therefore, the theoretical results have at least qualitative validity.

As a quantitative check of the theory, the pore size parameter, a, was evaluated from the Cell 3 data by the following iterative procedure. To obtain a first approximation for P^0, differential data ($P_D{}^0$) are corrected for the small nonequilibrium effect using $a = 4$ μm. Next, this value of P^0 is used to obtain a first approximation for a from the Cell 3 data and Eq. 24. By using the value of a obtained, the calculations are repeated. Since the value of P^0 calculated from $P_D{}^0$ is not particularly sensitive to the choice of a, the iteration converges after several cycles (Table III).

The values of a obtained are of the correct order of magnitude and are, *as a first approximation*, independent of γ. In particular, the

Table II—Effective Pore Radius, a, Calculated from Vapor Pressures for Conventional Tablets at 25°[a]

Cell Used/ Sample	Number of Experiments	Mean $10^4 P^0$	Mean Slope $10^4 P$ *versus* t, min	Mean γ	Mean $a_{\mu m}$
Cell 1/one cut tablet	3	$5.3_7 \pm 0.1_8$[b]	−0.005	0.1_7	$7._2 \pm 1._2$[b]
Cell 1/one whole tablet	3	$5.3_6 \pm 0.1_0$	-0.02_1	0.6_4	5.5 ± 1.0
Cell 3/three cut tablets	2	$5.1_7 \pm 0.0_4$	-0.22_7	1.8_1	2.6 ± 0.01
Mean: all experiments		5.3_0			5

[a] All tablets were 0.6-mg commercial tablets, Lot A; units of pressure are Torr. The vapor pressure of pure nitroglycerin (bulk liquid) at 25° is 5.5×10^{-4} Torr (6). [b] The "uncertainty" given is the standard deviation of the mean and is significant only as a measure of the precision obtained.

agreement between the three-tablet sample in Table III (3.0 μm) is in excellent agreement with the Cell 3 result in Table II (2.6 μm). However, several features of the data suggest that the correspondence between theory and experiment is only semiquantitative.

Consistent with the trend shown in Table II, the data in Table III suggest that values of the a parameter determined from data at large γ are less than a values determined at small γ. Moreover, the slopes of the linear ln P_a *versus* t region are larger than predicted from theory. The theoretical slopes, as calculated from Eqs. 24–26 for the values of γ in Table III, are −0.020 for both three- and two-tablet samples, about 40% lower than the observed slopes.

Although the lack of quantitative agreement between theory and experiment may reflect defects in the theory, experimental error may also be a factor. Small systematic errors in background corrections have a significant effect on a values determined from data where γ is small. Furthermore, measurements with Cell 3 may be subject to small, but detectable, errors arising from the cooling effect of rapidly vaporizing nitroglycerin. The cooling effect would reduce the measured value of the a parameter.

Diffusion Effect—Nearly all experiments in this laboratory have been with samples where $\bar{\gamma}$ (Eq. 55) is expected to be very small, due to either small ι (as in the case of tablets) or large D^0 (as with liquid additives or small amounts of solid additive). For these sample classes, the diffusion effect should be negligible, and the data support this prediction. However, clear indications of a significant diffusion effect were observed for "dry mix" povidone–nitroglycerin samples at povidone–nitroglycerin weight ratios of 1.0 and higher.

Dry mix samples were prepared by dry blending appropriate quantities of povidone and a 10% nitroglycerin trituration on β-lactose. For example, one sample, denoted Dry Mix 3, consisted of aggregates of lactose crystals fused together by a "glue" of povidone–nitroglycerin. Microscopic examination indicated $\iota \sim 10^{-2}$ cm. Following the estimation procedure outlined in the theory section for m^0 = 900 μg (the value corresponding to the experiments), $\bar{\gamma}$ = 0.3 and 4 for measurements with Cells 1 and 3, respectively, at 25°. The parameter $\hat{k}$ is estimated at $\hat{k} \sim 5$. As indicated in the *Theoretical* section, the estimation procedure is very crude. It is clear, however, that a significant nonequilibrium effect is expected, particularly with Cell 3.

Table III—Effective Pore Radius from Vapor Pressure Data on Tablets with Povidone as Calculated from Eqs. 24–26[a]

Experiment	Number of Tablets in Sample	$10^4 P_a{}^0$	Slope[b], Linear ln P_a *versus* t, min	γ[c]	$a_{\mu m}$
1	3	2.9	−0.032	1.7_4	2.7
2	3	3.1	−0.036	1.4_8	3.2
3	2	1.9	−0.039	3.7	1.9
4	2	2.1	−0.035	3.2	2.2

[a] All tablets were from the same lot of commercial 0.6-mg tablets and were cut into four wedge-shaped pieces. All experiments were at 25° with Cell 3. [b] When using α_1 = 1.5, as evaluated from differential data (Cells 1 and 2), the theoretical slopes are −0.021 for three tablets and −0.019 for two tablets. [c] The value of γ is calculated by an iterative procedure using the experimental value (for one cut tablet), $10^4 P_D{}^0 = 4.06$; see text for more detail.

The data obtained with Dry Mix 3 are shown in Fig. 5 as solid symbols. The open symbols correspond to Cell 3 data for one crushed 0.4-mg commercial tablet with povidone. Each crushed tablet point is the mean of two experiments, and vertical lines reflect the uncertainty in the data. The equilibrium curve (solid line) was calculated from Eq. 14. The broken lines are theoretical curves for the indicated values of $\hat{k}$ and $\bar{\gamma}$. Figure 5 is not intended as a quantitative check of theory. Neither the theory nor the data are of sufficient accuracy to warrant such a comparison. However, a very significant nonequilibrium effect does exist with the Dry Mix 3 data. Moreover, the theoretical curves are a reasonable, although far from exact, representation of the data. In particular, at the point where both Cell 3 and Cell 1 data are available, the experimental ratio of Cell 1–Cell 3 P_a data is 3. The theoretical ratio at this point is 4.

Although there appears to be a small nonequilibrium effect for the crushed tablet data, the effect is much smaller than the corresponding effect with Dry Mix 3. This result is due, for the most part, to the smaller ι value for tablets. In fact, the nonequilibrium effect shown for crushed tablets is probably not due to the diffusion effect. Even crushed conventional tablets (one-component nitroglycerin phase) show a small nonequilibrium effect. These nonequilibrium effects are probably due to the powder bed behaving as a matrix. A good fit to the crushed tablet data in Fig. 5 can be obtained with the matrix effect theory using γ = 1.3. For measurements with Cell 1 or 2 on crushed nitroglycerin tablets, the "powder matrix" effect is small (less than ~3%) and may be ignored.

SUMMARY AND CONCLUSIONS

Theoretical and experimental evidence demonstrate that the Knudsen vapor pressure method may yield erroneous results when the sample consists of a small quantity of volatile material dispersed in an inert porous matrix or when the volatile component contains a dissolved polymer. However, with proper experimental design and suitable data analysis, reliable vapor pressure data may be obtained for the special case of molded nitroglycerin tablets and, presumably, for other porous systems as well. Errors due to background effects may

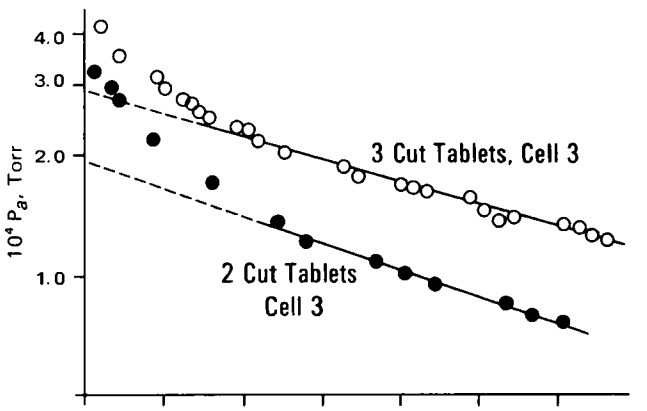

Figure 4—*Observed time dependence of apparent vapor pressure for nitroglycerin in tablets with povidone at 25°.*

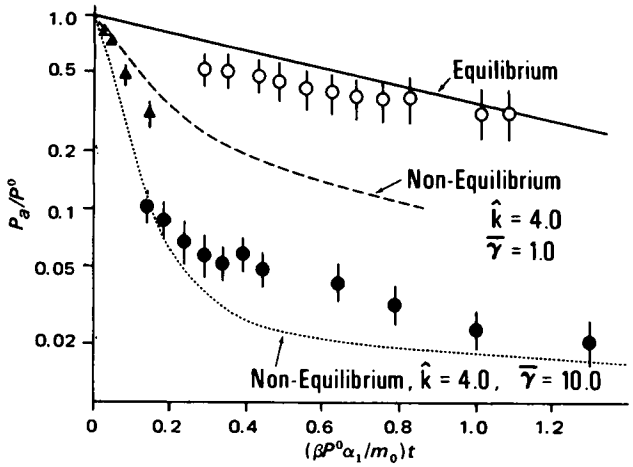

Figure 5—*Experimental evidence for the diffusion effect in povidone–nitroglycerin systems at 25°. Dry Mix 3 is 8.7% nitroglycerin, 9.0% povidone, 0.6% water, and 81.7% β-lactose. The crushed tablet contains 1.1% nitroglycerin and 1.0% povidone. Key: ○, one crushed tablet (0.4 mg), Cell 3; ▲, 10 mg of Dry Mix 3, Cell 1; and ●, 10 mg of Dry Mix 3, Cell 3.*

be minimized by performing blank placebo runs or by the differential technique.

While the numerical data in this report refer only to molded nitroglycerin tablets, the general procedures are probably valid for any porous system where the amount of highly volatile impurity, such as water, is of the same order of magnitude, or less, than the amount of the material under investigation. Nonequilibrium effects are minimized by using Knudsen cells with small orifice areas and (with tablet samples) by cutting the tablet to increase the exterior surface area while maintaining the tablet character of the sample.

When the volatile component is present in the pure state (not a solution), apparent vapor pressures decrease linearly with time due to the matrix effect, and the extrapolated ($t = 0$) value is the equilibrium vapor pressure of the sample (*cf.*, Eqs. 7 and 10). However, if the volatile component is present in a solution phase, the matrix effect cannot be removed by extrapolation; even data extrapolated according to the appropriate equation (*cf.*, Eqs. 29 and 31) are subject to a residual nonequilibrium effect which, if significant, necessitates a correction to the data. Provided a Knudsen cell with a small orifice ($\sim 10^{-3}$ cm^2) is used, the correction is small for molded nitroglycerin tablets.

The diffusion effect may result in the measured vapor pressure being significantly lower than the equilibrium value when the volatile component (solvent) is in solution form. Although negligible for the special case of nitroglycerin tablets, this type of nonequilibrium effect may be sizable when the solute is a highly soluble polymer and the thickness of the solution phase approaches 10^{-2} cm in order of magnitude.

Increasing the Knudsen cell orifice area *decreases* errors arising from background variability but *increases* the magnitude of nonequilibrium effects. The optimum orifice area and the corresponding accuracy of the vapor pressure data depend on the nature of the sample. For cut nitroglycerin tablets containing povidone, the observed precision at 25° was $\sim \pm 0.1$ in $10^4 P$ (Torr) for Cell 1 and differential measurements and $\sim \pm 0.2$ for measurements with Cell 2. Provided the data are corrected for the small matrix effect (using 4 μm for the pore size parameter, a), systematic errors in $10^4 P$ (Torr) from all sources are probably less than $\sim \pm 0.2$.

REFERENCES

(1) M. Knudsen, *Ann. Phys.*, **28**, 999(1909).

(2) G. W. Thomson, in "Physical Methods of Organic Chemistry," A. Weissberger, Ed., Interscience, New York, N.Y., 1959, chap. IX, part 1.

(3) M. Davies, A. H. Jones, and G. H. Thomas, *Trans. Faraday Soc.*, **55**, 1100(1959).

(4) M. Davies and B. Kybett, *ibid.*, **61**, 1608(1965).

(5) D. Bonderman, E. Cater, and W. Bennett, *J. Chem. Eng. Data*, **15**, 396(1970).

(6) M. J. Pikal, A. L. Lukes, and L. F. Ellis, *J. Pharm. Sci.*, **65**, 1278(1976).

(7) T. W. Edwards and G. L. Kington, *Trans. Faraday Soc.*, **58**, 1323(1962).

(8) S. Dushman, in "Scientific Foundations of Vacuum Technique," 2nd ed., revised by Members of the Research Staff, General Electric Research Laboratory, J. M. Lafferty, Ed., Wiley, New York, N.Y., 1962.

(9) J. Crank, "The Mathematics of Diffusion," Oxford University Press, London, England, 1956.

(10) R. J. Kokes and F. A. Long, *J. Am. Chem. Soc.*, **75**, 6142(1953).

(11) T. T. Wang and T. K. Kwei, *Macromolecules*, **6**, 919(1973).

(12) D. O. Jordan and A. E. Polack, *Aust. J. Pharm. Sci.*, **NS1**, 82(1972).

ACKNOWLEDGMENTS AND ADDRESSES

Received March 3, 1975, from *Eli Lilly and Company, Indianapolis, IN 46206*

Accepted for publication October 16, 1975.

The authors acknowledge the assistance of Dr. B. Cerimele and Mr. L. Simms in the numerical solution of differential equations.

[x] To whom inquiries should be directed.

Vapor Pressure of Nitroglycerin in Sublingual Molded Tablets: Implications for Stability

M. J. PIKAL ˣ, A. L. LUKES, and L. F. ELLIS

Abstract □ To understand nitroglycerin intertablet migration, vapor pressures of nitroglycerin in tablets were measured using a modified gravimetric Knudsen effusion technique. To supplement the vapor pressure data, adsorption isotherms at 296°K were determined, and tablets were studied by scanning electron microscopy. For conventional tablets (*i.e.*, tablets without stabilizing additives such as polyethylene glycol 400), the nitroglycerin vapor pressure in a tablet is within about 10% of that for pure liquid nitroglycerin, provided the potency is greater than 0.3 mg. Significant capillary condensation in tablets at relative vapor pressures close to unity is demonstrated. Stabilizing additives lower the vapor pressure of nitroglycerin, the magnitude of the effect depending on both the nature of the additive and the additive–nitroglycerin weight ratio. The mechanism of intertablet migration involves capillary condensation. Vapor pressure reduction of about 15%, achieved through the use of an additive, appears sufficient to prevent significant intertablet migration.

Keyphrases □ Nitroglycerin—vapor pressure in sublingual molded tablets, intertablet migration, effect of additives □ Vapor pressure—nitroglycerin, sublingual molded tablets, effect of additives □ Stability—nitroglycerin sublingual molded tablets, vapor pressure, intertablet migration, effect of additives □ Tablets, sublingual molded—nitroglycerin, vapor pressure, intertablet migration, effect of additives □ Dosage forms—nitroglycerin tablets, vapor pressure, intertablet migration, effect of additives

Several recent studies concerned the stability of molded sublingual nitroglycerin tablets (1–7). Although nitroglycerin undergoes thermal decomposition at elevated temperature (8) and may undergo basic hydrolysis (9), chemical decomposition does not appear to be a serious problem for nitroglycerin tablets (2). The major problem is physical instability. Nitroglycerin volatilizes and readily dissolves in, or adsorbs on, many types of packaging materials (2, 5). Moreover, a "migration effect" was demonstrated recently (2). That is, when nitroglycerin tablets are in a container for several months, nitroglycerin undergoes *permanent intertablet transfer* among a set of nominally equivalent tablets, resulting in decreased content uniformity. The mean potency, however, remains essentially constant.

The migration effect may be nearly eliminated by incorporating a stabilizing additive in the tablet (1). Povidone, polyethylene glycol 400, and polyethylene glycol 4000 have been used commercially[1]. However, both the mechanism responsible for the migration effect and the role of the "stabilizing" additive remain obscure. Nitroglycerin migration probably proceeds *via* the vapor phase (1, 2). If spontaneous transfer of nitroglycerin between two tablets does occur, thermodynamics require that gradients in the nitroglycerin chemical potential exist that do not time average to zero. The cause of the chemical potential gradients (*i.e.*, the driving force) has not been identified.

Fusari (1) suggested that the role of the stabilizing additive is to lower the vapor pressure of nitroglycerin to a point where vaporization is too slow to result in significant nitroglycerin migration. Vapor pressure data are available for liquid nitroglycerin (10–12). No data are available for nitroglycerin in tablets, and the effect of povidone or polyethylene glycol 400 on the vapor pressure of nitroglycerin has not been investigated.

To understand the migration effect and the role of stabilizing additives, vapor pressures of nitroglycerin were measured as a function of: (*a*) nitroglycerin environment (*i.e.*, nitroglycerin in molded sublingual tablets compared to nitroglycerin coated on lactose powder), (*b*) temperature, and (*c*) the nature of the stabilizing additive at selected additive–nitroglycerin ratios. To supplement the vapor pressure data, nitroglycerin adsorption isotherms at 23° were measured for placebo tablets and lactose powder, and scanning electron microscopy studies were carried out with molded tablets.

EXPERIMENTAL

Materials—Commercial tablets[2] were used as received.

Laboratory nitroglycerin samples were all prepared from the same lot of 10% nitroglycerin trituration on β-lactose. Contamination of the nitroglycerin by mono- and dinitrate esters of glycerin, as estimated by TLC, was less than 1%. Acid contamination, as nitric acid, was ~0.02% (w/w nitroglycerin), and the water content (Karl Fischer) of the trituration was ~0.23% (w/w 10% trituration). The solubility of water in nitroglycerin at 25° is only ~0.3% (w/w) (13), so most of the water is external to the nitroglycerin.

Povidone NF, polyethylene glycol USP, and bis(2-ethylhexyl) phthalate[3] samples were used as received except for vacuum drying to remove volatiles. The water used was deionized.

Preparation of Nitroglycerin Samples and Assay—Blending was done with a glass mortar and pestle, and laboratory lots of molded tablets were prepared by the usual procedure (1). The molded tablets were dried in a forced-air oven at 43°, normally for 2 hr. The α-lactose (−120 mesh) used as the diluent had the same specifications as the diluent used in the manufacture of commercial tablets[4]. Samples denoted "powder" were prepared using essentially the same procedure. Samples denoted "dry mix" were nitroglycerin–povidone samples prepared by dry blending appropriate quantities of povidone and the 10% nitroglycerin trituration on β-lactose.

The bis(2-ethylhexyl) phthalate–nitroglycerin samples were prepared by blending appropriate quantities of bis(2-ethylhexyl) phthalate and the 10% nitroglycerin trituration. At lower levels of bis(2-ethylhexyl) phthalate, acetone was added to form a slurry to achieve better mixing. All samples were forced-air dried at 43° for 2 hr.

Unless indicated otherwise, vapor pressure measurements were made only on "aged" samples, *i.e.*, tablets more than 4 months old and powder or dry mix samples more than 2 weeks old.

Nitroglycerin was assayed by a modified Bell (7) procedure.

Vapor Pressure Measurements—Vapor pressures were deter-

[1] Since December 1972, Lilly sublingual nitroglycerin tablets have contained povidone, present as 1% of the total tablet weight. Initially, Nitrostat, the Parke-Davis brand of stabilized nitroglycerin tablets, contained polyethylene glycol 400 at a level of 85% (w/w) of the nitroglycerin content (1). Recently, polyethylene glycol 4000 has replaced polyethylene glycol 400.

[2] All commercial tablets were Lilly molded sublingual nitroglycerin tablets except when noted otherwise.

[3] Bendix Corp.; purified bis(2-ethylhexyl) phthalate was used to prepare solutions of selected nitroglycerin vapor pressures for adsorption studies.

[4] Lilly.

mined by the modified Knudsen effusion method (14). Background and effusion rate data were obtained from the appropriate mass *versus* time curve by numerical differentiation. To minimize nonequilibrium effects (14), all vapor pressure data were determined with Cell 1 (orifice area 2.18×10^{-3} cm^2), Cell 2 (area 0.96×10^{-3} cm^2), or the differential method (14), and most of the tablet data were taken on tablets cut with a razor blade into four equal wedge-shaped pieces (14). The data for tablets with additives were corrected for the small nonequilibrium effect using 4 μm for the pore size parameter, a (14).

As a guard against unexpected nonequilibrium effects, one or both of the following procedures were followed:

1. Replicate measurements were made on each sample using both Cells 1 and 2.
2. For measurements with the differential method, the amount of sample was varied by at least a factor of 2.

Within the expected uncertainty of the data, equilibrium vapor pressures were independent of measurement conditions.

When nonequilibrium effects are negligible, vapor pressure data for additive–nitroglycerin systems may be obtained over a considerable composition range from a single effusion experiment. The loss of nitroglycerin, $\Delta m(t)$, at time t is given by:

$$\Delta m(t) = m^0 - m(t) = \beta \int_0^t P(t)\, dt \qquad \text{(Eq. 1)}$$

where $m(t)$ and m^0 are the masses of nitroglycerin at time t and time zero, respectively; and β is a constant for a given Knudsen cell as defined elsewhere (14). Thus, at any time t, both the vapor pressure and the corresponding composition may be calculated from the effusion experiment. Vapor pressures determined through the use of Eq. 1 are denoted "real time" data.

To eliminate systematic calibration errors, data are reported in the form $P/P^\cdot$, where $P^\cdot$ is the vapor pressure of pure nitroglycerin measured with the same procedure as is used to measure vapor pressure P. The $P/P^\cdot$ data are estimated to be accurate within ± 0.05 in general and within ± 0.02 for the nitroglycerin–bis(2-ethylhexyl) phthalate systems.

Adsorption Isotherms—Nitroglycerin adsorption isotherms for placebo tablets and lactose powder at $23 \pm 2°$ were determined by the following procedure. The placebo tablets, lactose powder, and a given bis(2-ethylhexyl) phthalate–nitroglycerin system of known vapor pressure were all placed in separate cups inside a small chamber[5]. A moderate vacuum (10 Torr) was applied, and the system was sealed. After an equilibration time of 1 month, the placebo tablets and powder were assayed for nitroglycerin.

Preliminary experiments with the 10% nitroglycerin trituration on lactose showed that about 50% of the nitroglycerin transfer to placebo tablets observed after 1 month had occurred within 1 week. Theoretical considerations[6] suggest that equilibrium is reached within about 2 weeks and, at least within the precision of the data, the data obtained at 1 month are assumed to be equilibrium data.

Since bis(2-ethylhexyl) phthalate has a very low vapor pressure, about 10^{-7} Torr (15), essentially no transfer of bis(2-ethylhexyl) phthalate occurs. The quantity of nitroglycerin in the nitroglycerin source was large compared to the amount transferred, and Knudsen vapor pressure measurements before and after the adsorption experiments verified that no significant changes in vapor pressure occurred during the experiment.

Scanning Electron Microscopy—The studies were carried out with a scanning electron microscope equipped with a hot–cold stage[7]. To prevent volatilization during coating and scanning electron microscopic examination, the tablet sample was maintained at low temperatures using procedures similar (but not identical) to those described by Echlin and Moreton (16). A cut tablet was mounted on a specimen stub. A holder[7] (which encloses the sample) was placed on the specimen stub, and the sample was quenched in liquid nitrogen. Nitroglycerin coated on lactose readily supercools[8] so the physical state of nitroglycerin at this point was either a supercooled liquid or a glass, probably the latter.

In preparation for coating, the sample was transferred *via* the holder to a precooled (liquid nitrogen temperature) cold table in a vacuum evaporator. The sample stub was ejected from the holder onto the cold table, and the vacuum chamber was quickly closed and evacuated. After coating with gold and carbon, the vacuum chamber was vented with dry air, the chamber was opened, and the precooled stub holder was immediately placed on the specimen stub. The sample was transferred *via* the holder to the cold stage ($-150°$) of the scanning electron microscope, and the cold stage chamber was immediately evacuated.

Because of the brief exposures of the sample to the atmosphere during the transfer procedures, this technique carries the risk of frost contamination. However, blank experiments carried out with tablets devoid of nitroglycerin (*i.e.*, removed in high vacuum at ambient temperature) showed that frost contamination was slight. The frost that did form was removed by sublimation within 5–10 min at $-100°$ under the high vacuum conditions of the scanning electron microscopic experiment. For samples containing nitroglycerin, frost contamination was not detectable; pictures obtained at $-150°$ were identical, within the resolution obtained, to those of the same area at $-100°$

RESULTS AND DISCUSSION

Physical Characteristics of Molded Tablets (Table I)—The porosity, ϵ, or pore volume fraction is somewhat specific for a given tablet but normally is within the range indicated. Hexagonal closest packing of uniform spheres would give $\epsilon = 0.26$ (18). Since the pore radius data are based upon rather different methods of measurement, only a very rough correspondence may be expected. The pore radii data appear consistent with mercury porosimetry measurements on lactose tablets prepared by direct compression of crystalline lactose (19). The specific surface area [Brunauer, Emmett, and Teller (BET)] is 0.57 m^2/g, a value consistent with a crystalline material having a significant fraction of particles in the micrometer range.

Since the tablets contain 90% α-lactose (monohydrate), the total water content is about 5%. The term "free water," as used in Table I, refers to water in excess of that needed for a monohydrate. The quantity of free water is comparable in magnitude to the nitroglycerin content. However, the solubility of water in the nitroglycerin–povidone phase is small[9], so most of the water is external to this phase and probably forms a film of aqueous lactose on the crystalline surface.

To determine if the distribution of nitroglycerin is uniform in a given tablet, about 0.5 mm of a tablet's surface was removed with a razor blade. This "surface" portion and the remaining "core" portion were assayed for nitroglycerin. For aged 0.6-mg tablets, the surface concentration of nitroglycerin (w/w) was about 25% higher than the corresponding core concentration. *No difference* between conventional and stabilized (1% povidone) tablets was detected. Thus, in

---

[5] The chamber was fashioned from inner and outer standard taper vented ground-glass joints (24/40). The total assembly was essentially a tube 15 cm long and 2 cm in diameter. The joints were *lightly* greased with high vacuum silicone grease.

[6] As demonstrated later, when significant quantities of nitroglycerin are adsorbed, most of it is condensed in the smaller tablet pores or "capillaries." Thus, equilibrium is reached when all pores small enough to condense nitroglycerin at vapor pressure P^0 are filled. If it is assumed that the rate of this process is controlled by the rate of gas phase diffusion from the nitroglycerin–bis(2-ethylhexyl) phthalate system to the sample, the rate of mass transfer is independent of time until equilibrium is reached (*i.e.*, the pores are filled). Furthermore, when assuming a Gaussian pore-size distribution with a mean pore size of ~ 4 μm, a first approximation for the equilibration time, τ, may be written:

$$\tau = B \frac{P_T}{P^\cdot} \left(\frac{P^\cdot}{P^0}\right)^2 \frac{1}{\ln (P^\cdot/P^0)}$$

when $(P^\cdot/P^0) - 1 > 0.02$. Here, B is a constant, P_T is the total pressure (~ 10 Torr for these experiments), $P^\cdot$ is the vapor pressure of pure liquid state nitroglycerin, and P^0 is the vapor pressure of nitroglycerin in the bis(2-ethylhexyl) phthalate–nitroglycerin phase. Over the range of $P^\cdot/P^0$ values where capillary condensation occurs, τ calculated from this equation increases as P^0 increases. Although the equation for τ is not defined for $P^0 = P^\cdot$, it is reasonable to assume that, for $0.98P^\cdot \leq P^0 \leq P^\cdot$, τ either remains constant or increases as P^0 increases. The latter is most likely.

Due to a finite nitroglycerin source, impurities, and multilayer condensation on all surfaces within the chamber, the nitroglycerin vapor pressure in the chamber at equilibrium will be slightly less than $P^\cdot$, even when no bis(2-ethylhexyl) phthalate is present. Thus, the equilibration time will always be finite. In particular, for the case of a 10% trituration of nitroglycerin on lactose as the nitroglycerin source, the observed rate is consistent with P^0 being 1 or 2% lower than the vapor pressure of pure liquid nitroglycerin and $\tau \sim 2$ weeks. When the nitroglycerin source is a bis(2-ethylhexyl) phthalate–nitroglycerin solution, $P^\cdot/P^0$ is greater and less time is required to reach equilibrium.

[7] ETEC Inc., Hayward, Calif.

[8] Differential thermal analysis studies did not show any evidence for a first-order phase transition near the melting point on samples of 10% nitroglycerin–90% α-lactose that were quenched in liquid nitrogen.

[9] That is, while the povidone–nitroglycerin system is a single phase, addition of water at about a 1:1 volume ratio produces a two-phase system of roughly the same volume ratio as before mixing.

Table I—Physical Characteristics of Molded Nitroglycerin Tablets

Property	Value
Weight	35 mg
Volume	0.032 cm^3
Pore volume fraction[a], ϵ	0.2–0.3
Effective pore radius; Poiseuille's law gas flow[b]	2 μm
Maximum pore radius; ASTM Test E128-61[c]	5 μm
Effective pore radius; nonequilibrium vapor pressure effects[d]	4 μm
Free water (*i.e.*, nonhydrate water)[e]; tablet with 1% povidone	0.18 mg
Surface area; BET nitrogen adsorption	200 cm^2

[a] Evaluated from the tablet weight and volume and the density of α-lactose. Measurements of the volume of ethanol "absorbed" by tablets gave essentially the same results. [b] Evaluated from experimental data for the volume of nitrogen flow at various pressures (17). A capillary model was used for the tablet pores, and Poiseuille's law was employed to develop the equation used to evaluate the pore radius from the experimental data. The value obtained may be slightly low due to turbulent flow. [c] This test is the standard ASTM test for the maximum pore size of porous filters. The porous body (*i.e.*, tablet) is immersed in a liquid (ethanol), and air pressure is applied until the first bubble of air passes through the porous body. The effective maximum pore radius is then calculated from the surface tension of the liquid and the applied pressure. The tablet was sealed with wax in a holder to eliminate leakage around the tablet sides. Numerous pores near the maximum pore size were observed. [d] From Ref. 14. [e] Determined from loss on drying placebo tablets under high vacuum. Karl Fischer water assays gave essentially the same results.

agreement with earlier speculation (2), some flow of nitroglycerin toward the surface appears to occur during the drying process, presumably due to capillary action.

Scanning Electron Microscopy—Scanning electron microscopy was undertaken to gain information concerning the physical state of nitroglycerin in a tablet. Fresh (*i.e.*, 1 month old) 0.3-mg tablets were used. The areas investigated were freshly cut surfaces located near one of the original tablet surfaces.

Representative scanning electron microscopy results are given in Fig. 1. Figure 1A is a photograph of a conventional tablet (no stabilizing additive) which was taken at −150°. A photograph of the area covered by the top portion of Fig. 1A was taken at −100° and, within the resolution obtained, the photographs were identical. Several areas were scanned at −100° over about 30 min, and all had the same general appearance.

Figure 1B is an example of the surface structure observed for a conventional tablet that had been subjected to high vacuum at ambient temperature prior to the scanning electron microscopic experiment. This procedure removed all nitroglycerin, so the surface structure in Fig. 1B is due to lactose and the small amounts of sucrose (0.1%) and impurities present. Thus, the difference between Figs. 1A and 1B is due to nitroglycerin. Figures 1C and 1D are representative photographs of a tablet containing povidone at temperatures of −100 and −10°, respectively.

To determine the temperature dependence of the surface structure, the temperature of a sample was increased from −100 to +35°, and the surface was monitored on the scanning electron microscope screen. The lactose surface (Fig. 1B) showed no changes in the temperature range investigated. The tablet containing nitroglycerin without povidone (Fig. 1A) yielded several dramatic effects. At a temperature around −80°, the sphere-like structure seen in Fig. 1A started to disappear; within about 1 min, the sample surface was essentially the same as that observed for a sample devoid of nitroglycerin (Fig. 1B).

At this point, several small patches of liquid-like material were observed on the surface. These patches grew in size, diminished in size, and finally disappeared, all within 10–20 sec. These phenomena ceased within 1–2 min; but before a photograph could be made, resolution was lost due to excessive surface charging. Evidently, the dynamic phenomena observed had badly eroded the conductive coating. All of the sample changes referred to occurred within about 5 min at temperatures between −80 and −50°.

With the tablet containing povidone, changes were not obvious until around −10°, where the vacuum gauge indicated a significant loss of volatiles from the sample and some of the surface features appeared to shrink. The changes ceased after 5–10 min; no further changes were obvious up to +35°, where the experiment was terminated. Figure 1D is representative of the "stable" surface structure from −10 to +35°.

The lactose surface is characterized by three main features, which are all illustrated in Fig. 1B:

1. Numerous examples of sharp angles characteristic of a crystalline sample are observed, and some of the larger crystals contain cracks. These features are particularly evident in the lower left quadrant of Fig. 1B.
2. A large number of fines are distributed on the surface.
3. A minor fraction of the surface has the appearance of an amorphous solid containing numerous craters. A few of these craters are visible in the center area of Fig. 1B. The straight horizontal lines, particularly evident in the top half of Fig. 1B, are charging artifacts due to the sample.

As a first approximation, nitroglycerin is absent from Fig. 1D, and the difference between Figs. 1B and 1D represents the contribution of povidone to the surface structure. Except for several crystal faces in the center of Fig. 1D, povidone obscures the crystalline character of the lactose and appears to be present in two forms: (*a*) a coating on the lactose fines and surface irregularities, as is evident in the upper and lower left quadrants of Fig. 1D; and (*b*) a nonuniform "spider web" form covering some of the crystalline surface. This form is particularly evident in the center of Fig. 1D. Presumably, the areas covered by povidone in Fig. 1D also contained nitroglycerin in the original tablet.

For tablets containing nitroglycerin (Figs. 1A and 1C), the tablet surface appears as an aggregate of sphere-like particles ranging in diameter from the limit of resolution, about 0.1 μm, up to about 3 μm. In particular, there was an obvious lack of sharp angles which are characteristic of a crystalline sample. Both stabilized (Fig. 1C) and conventional (Fig. 1A) tablets have the same general appearance when allowance is made for the difference in magnification. The main difference is that the sphere-like particles are less well defined in the case of the tablet with povidone, an observation consistent with a larger volume of liquid phase. Povidone and nitroglycerin are mutually soluble at 25° and form a viscous, gel-like liquid at a 1:1 weight ratio. Thus, a larger volume of liquid phase for a tablet containing povidone is expected. The temperature dependence of the sphere-like structure is undoubtedly due to evaporation of nitroglycerin under high vacuum. The interpretation of the observations regarding appearance and disappearance of liquid-like material is less obvious. Perhaps supercooled liquid nitroglycerin was being forced out of small pores by thermal expansion, forming pools of liquid which then evaporated.

In view of the aggregate nature of the structure, the sphere-like particles are most likely *not* completely liquid; that is, a system of liquid droplets would be mechanically stable only if the droplets were not in contact. Moreover, most of the sphere-like particles are not *perfect* spheres. Thus, the sphere-like structure probably represents nitroglycerin (Fig. 1A) or nitroglycerin–povidone (Fig. 1C) coated on the fines and surface irregularities characteristic of the lactose surface. The coating is sufficiently thick and uniform to obscure the "sharp angles" characteristic of a crystalline surface but, at least in some areas, sufficiently thin to allow surface irregularities on the order of 0.2 μm to be observed, suggesting that at least the larger sphere-like objects are mostly lactose.

If it is assumed that the Kelvin equation (20) may be applied to the sphere-like state for nitroglycerin, the vapor pressure for this state would be slightly greater than for bulk phase nitroglycerin (due to the convex liquid–vapor interface). However, the vapor pressure elevation would be quite small, about 1%, for spheres 1 μm in diameter[10].

Adsorption Isotherms—To investigate the surface properties of a molded tablet, in particular the pore structure, adsorption isotherms for nitroglycerin were determined. The multilayer condensation curve is approximated by the adsorption isotherm for the lactose powder used in tablet preparation, and the difference between the tablet and powder isotherms represents "capillary" condensation in the tablet. The tablet sample in most cases was five tablets. Two independent experiments were performed at 23°, using different batches of nom-

[10] Based on the Kelvin equation and the data for nitroglycerin (21) at 25°, $\bar{V}$ = 143 cm^3/mole, surface tension = 50 dynes/cm^2, and density = 1.59 g/cm^3.

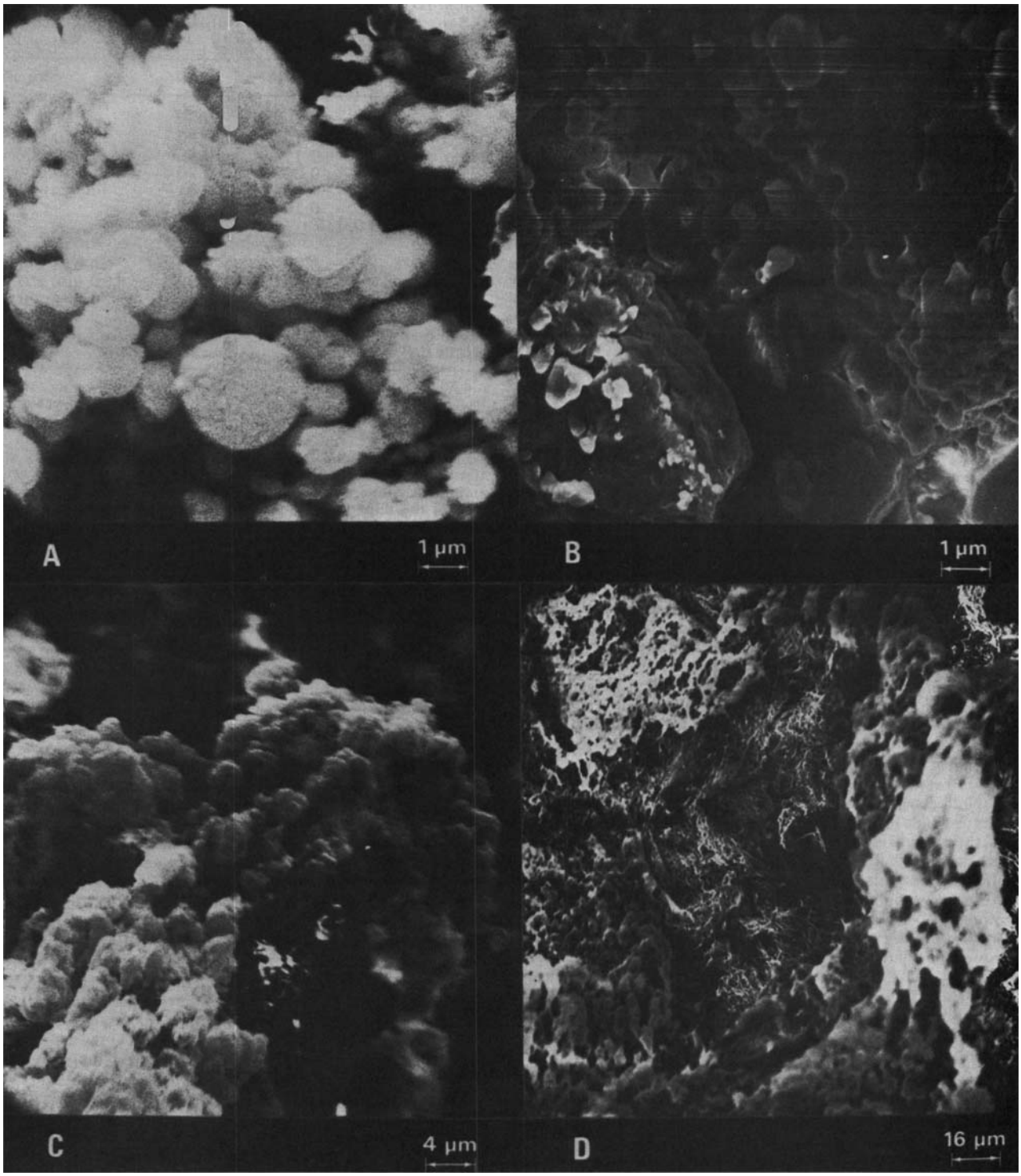

Figure 1—*Scanning electron micrographs of molded sublingual nitroglycerin tablets. Key: A, 0.3-mg conventional tablet, from −150 to −100° (both temperatures gave identical results); B, 0.3-mg conventional tablet with nitroglycerin removed prior to experiment, −100°; C, 0.3-mg stabilized tablet (1% povidone), −100°; and D, 0.3-mg stabilized tablet (1% povidone), −10°.*

inally equivalent "laboratory" placebo tablets without stabilizing additives. The estimated uncertainty is ±10% for the tablet data and ±20% for the powder data.

A given relative vapor pressure of nitroglycerin was maintained through the use of bis(2-ethylhexyl) phthalate–nitroglycerin solutions. Vapor pressure data for these solutions are given in Table II. The adsorption data are shown in Fig. 2, where nitroglycerin adsorbed, in micrograms per 35.6-mg sample, is plotted as a function of relative pressure, $P/P^{\cdot}$, where $P^{\cdot}$ is the vapor pressure of pure "bulk phase" nitroglycerin. The uncertainty in $P/P^{\cdot}$ is ±0.02 at all pressure values. The insert in the upper left quadrant of Fig. 2 gives the low pressure data on an expanded scale.

At relative pressures of 0.6 and lower, the multilayer (*i.e.*, powder) data and the tablet data are in agreement within experimental error. Thus, capillary condensation of nitroglycerin is undetectable (less than ~2 μg) below $P/P^{\cdot} = 0.6$. However, tablets show much greater adsorption at higher pressures. At relative pressures of 0.9 and higher, large quantities of nitroglycerin (~200 μg) are condensed in the pore structure of the tablet.

In general, the tablets were assayed as composite samples and no

Table II—Vapor Pressures of Nitroglycerin in Nitroglycerin–Bis(2-ethylhexyl) Phthalate Solutions at 25.0°

Nominal Mole Fraction Bis(2-ethylhexyl) Phthalate[a]	Measured Weight Ratio: Bis(2-ethylhexyl) Phthalate–Nitroglycerin[b]	P/P°[c] (±0.02)
0.0	0.00	1.0
0.3	0.82	0.97_5
0.4	1.26	0.91
0.5	1.91	0.79
0.55	2.33	0.70
0.60	2.86	0.60
0.65	3.5	0.50
0.70	4.4	0.39
0.75	5.7	0.29
0.80	7.6	0.22
0.90	17	0.11

[a] Mole fraction of bis(2-ethylhexyl) phthalate before drying at 43° in forced air for 2 hr. [b] Determined by nitroglycerin assay on dried samples. [c] P° ≡ vapor pressure of pure nitroglycerin.

information concerning variability of adsorption between tablets was obtained. However, for one group of six tablets at equilibrium (in the same experiment) with $P/P^{\circ} = 1.00 \pm 0.02$, single-tablet assays were performed. The results, in micrograms of nitroglycerin per 35.6-mg tablet sample, are 413, 338, 329, 326, 286, and 260. The standard deviation for these six assay results is ±15%. Thus, nitroglycerin adsorption is quite variable, indicating that the volume of *small* pores varies considerably among nominally equivalent tablets. It is interesting, and probably significant, that the standard deviation of 15% is of the same magnitude as the average standard deviation (12%) for assays on single, aged, conventional 0.3-mg tablets (2).

Nitrogen adsorption–desorption isotherms at 79°K were also determined for molded tablet samples (free of nitroglycerin). The nitrogen isotherms are in qualitative agreement with the nitroglycerin isotherms; that is, condensation of nitrogen in tablet pores is indicated by the data at high relative pressures.

Vapor Pressure Measurements—*Liquid Phase Nitroglycerin*—Since the thickness of the nitroglycerin coating on lactose at a 10% level corresponds to a multilayer thickness of several thousand molecules, the physical state of nitroglycerin in a 10% trituration on lactose is essentially that of bulk phase nitroglycerin, and vapor pressure data for such a sample refer to pure liquid nitroglycerin. Consistent with this conclusion, vapor pressures for samples of the 10% trituration were independent of the amount of nitroglycerin remaining in the sample until essentially all nitroglycerin was removed. At 25°, the vapor pressure of liquid nitroglycerin is, in units of 10^4 P (Torr), 5.4_9 (Cell 1), 5.3_8 (Cell 2), and 5.6_0 [differential method (14)]. The mean of these data, 5.5×10^{-4} Torr, is in excellent agreement with the mean of the best literature data (10–12), 5.0×10^{-4} Torr. At 37°, $P = 22.0 \times 10^{-4}$ Torr.

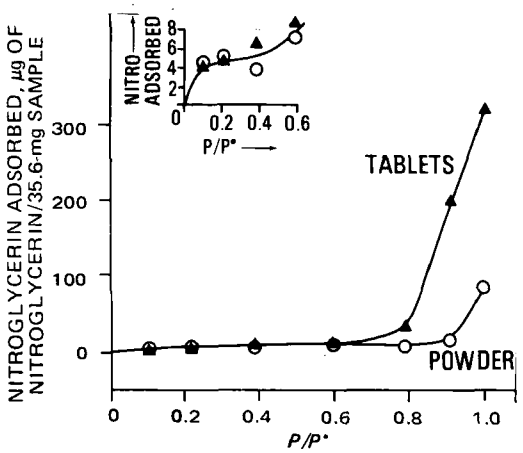

Figure 2—*Nitroglycerin adsorption isotherm at 23° for conventional molded sublingual tablets and α-lactose powder.*

Table III—Vapor Pressure Data for Conventional 0.3-mg Sublingual Tablets: Comparison of Aged and Fresh Tablets at 25°[a]

Tablet	$\sigma(10^4 P)$[b]	P/P°	−Slope[c]
	Aged Tablets		
1	±0.10	0.83	0.000
2	±0.17	0.89	0.000
3	±0.09	0.90	0.000
4	±0.05	0.91	$0.001_7 \pm 0.000_9$
Mean 1–4	0.10	0.88	
SD in $P/P^{\circ} = \pm 0.035$			
	Fresh Tablets		
5	±0.13	1.00	0.014 ± 0.003
6	±0.09	0.90	0.003 ± 0.002
7	±0.13	0.92	0.004 ± 0.002
8	±0.18	1.09	0.027 ± 0.004
Mean 5–8	±0.13	0.98	0.012
SD in $P/P^{\circ} = \pm 0.08_4$			

[a] Aged tablets are Lot C: mean potency is 262 μg, standard deviation for assay of 30 tablets is 19%, and age is 2 years. Fresh tablets are Lot D: mean potency is 316 μg, standard deviation is 9%, and age is 1 month. All measurements were with Cell 2 on tablets cut into four equal wedge-shaped pieces. [b] Standard deviation of fit for 10^4 P (Torr) *versus* t. [c] Slope for 10^4 P (Torr) *versus* t (minutes). Slope is assigned a value of zero when the standard deviation of the slope is larger than the slope. When using $a = 4$ μm, the theoretical slope (14) for nonequilibrium effects is −0.0006. The uncertainty given for a slope is the standard deviation of the slope.

Fresh Conventional Tablets—If the migration effect is real, a lack of equilibrium must exist in freshly prepared tablets, and differences in vapor pressure should exist. In an attempt to observe anomalous behavior in vapor pressure data that could be attributed to a lack of equilibrium, vapor pressure measurements were made on two lots of conventional 0.3-mg tablets using identical experimental procedures and data analysis. One lot (Lot C) was aged 2 years, and the fresh lot (Lot D) was 1 month old.

The only factor affecting the *precision* of vapor pressure data is the reproducibility of the background corrections (14), which is known from experiment. Thus, the expected standard deviation in a set of measurements of P/P° is calculated to be $\pm 0.04_1$ for the conditions of this experiment. Moreover, theoretical considerations (14) indicate that the observed vapor pressure should be essentially independent of time over the time range of this experiment; *i.e.*, the theoretical slope (14) of 10^4 P (Torr) *versus* t (minutes) is calculated as -0.000_6.

The data obtained are summarized in Table III. The second column gives the standard deviations in 10^4 P (Torr) for the linear fit. The observed scatter is typical for measurements with Cell 2 and is roughly the same for both aged and fresh tablets. The third column gives the apparent relative vapor pressure at zero time, which is the equilibrium relative vapor pressure for the tablet if the tablet is initially in internal equilibrium. For aged tablets, the precision (*i.e.*, standard deviations in P/P°) is consistent with the expected precision of the measurement. However, the standard deviation in P/P° for fresh tablets is about a factor of 2 larger than expected.

The time dependence is given in the last column in Table III in the form of the slope of the linear 10^4 P (Torr) *versus* time (minutes) curve. For aged tablets, the time dependence is too small to be consistently observed above the scatter in the data, as expected. However, fresh tablets show a decrease in vapor pressure with time that is much larger than can be accounted for by theory (14). Moreover, at least for Tablets 5 and 8, the slope appears far too large to be rationalized in terms of experimental error. Thus, the vapor pressure results for fresh tablets are anomalous, and the anomaly has physical meaning.

These results may be interpreted as evidence for a lack of equilibrium in fresh tablets. If a given tablet is not in internal equilibrium, the tablet approaches equilibrium at some finite rate upon aging. Transfer of nitroglycerin occurs from a state of higher chemical potential to a state of lower chemical potential. Data presented earlier in this report suggest that the state of low chemical potential is nitroglycerin condensed in small capillary pores which, by virtue of the concave liquid–vapor interface, has a relative vapor pressure less than unity (20). The state of higher chemical potential is probably that of nitroglycerin coated on lactose fines (Fig. 1A).

As the sample ages and equilibrium is approached, the "average"

Table IV—Vapor Pressures of Nitroglycerin in Conventional Sublingual Tablets

Tablet Sample	Mean Tablet Potency, μg	Relative Vapor Pressure[a], $P/P^{\cdot}$ Uncertainty, ±0.05	
		25.0°	36.9°
0.6 mg, aged (Lot A)	625	0.97[b]	0.88
0.4 mg, aged (Lot B)	400	1.01	0.88
0.3 mg, aged (Lot C)	262	0.90	0.88
0.3 mg, fresh (Lot D)	316	0.98	—

[a] $P^{\cdot}$ ≡ vapor pressure of liquid state nitroglycerin at temperature t. At 25°, $P^{\cdot} = 5.5 \times 10^{-4}$ Torr; at 36.9°, $P^{\cdot} = 21.9 \times 10^{-4}$ Torr. [b] Crushed tablets yielded $P/P^{\cdot} = 0.97$.

nitroglycerin vapor pressure decreases. The rate of approach to equilibrium is slow under ambient conditions and probably is limited by gas phase diffusion. However, at low pressure (~5×10^{-4} Torr), diffusion can no longer be rate limiting, and the sample approaches equilibrium at a significant rate during the effusion experiment, resulting in a decrease in apparent vapor pressure with time. The wide range of slopes for fresh tablets suggests that the tablets are not uniform in their displacement from equilibrium. Thus, a larger standard deviation in $P/P^{\cdot}$ is expected for fresh tablets than for tablets at equilibrium, as observed.

Aged Conventional Tablets—Vapor pressure data for aged conventional tablets of varying potency are given in Table IV. The fresh tablet (Lot D) data from Table III are included for comparison. At 36.9°, each entry represents the mean of two tablets; at 25°, each entry is the mean of at least four tablets.

The nitroglycerin adsorption isotherm (Fig. 2) indicates that a conventional molded tablet containing more than 0.3 mg of nitroglycerin at equilibrium should have a relative vapor pressure, $P/P^{\cdot}$, of unity within the accuracy of the Knudsen experiment. This conclusion is rigorous only near 25°, but it should also be a good approximation at other temperatures. In general, the vapor pressure data are consistent with the adsorption data. The relative vapor pressures at 25° for Lots A and B are unity well within experimental error, and the value for Lot C is slightly less than unity. The vapor pressures at 36.9° show no evidence of a dependence on tablet potency. However, the deviation from unity is somewhat larger than expected, an observation for which no explanation is obvious.

Stabilized Tablets—The effects of sample form (tablet *versus* powder) and "free water" content were investigated for nitroglycerin–povidone systems[11] (Fig. 3). Each experimental point is a mean of at least two, and normally more than four, replicate measurements. The data for crushed 0.4-mg tablets at povidone–nitroglycerin weight ratios higher than 0.87 are real time data (see *Experimental*). The solid curve represents the mean of all nontablet samples. The estimated uncertainty in relative vapor pressure is indicated by vertical lines.

As an excellent first approximation, the vapor pressure of a sample depends only on the povidone–nitroglycerin weight ratio. An order of magnitude increase in the ratio of free water to nitroglycerin does not significantly affect the vapor pressure. Moreover, the differences between tablet samples and nontablet samples are small and probably not significant. In particular, while the point for 0.3-mg tablets (weight ratio 1.15) appears somewhat lower than the solid curve, the vapor pressure for the same lot of tablets, when crushed, is also lower by nearly the same amount.

The effects of different additives on nitroglycerin vapor pressure are compared in Fig. 4. The povidone data refer to the smoothed nontablet data taken from Fig. 3. Although bis(2-ethylhexyl) phthalate is not used as a stabilizer, bis(2-ethylhexyl) phthalate–nitroglycerin data are included for purposes of comparison. Within experimental error, the two polyethylene glycols are identical in their

[11] The level of sucrose was varied between 0 and 1.4% for several tablet and powder samples with no apparent effect on the vapor pressure. Since sucrose is not soluble either in nitroglycerin or in the additives considered here, this result was expected.

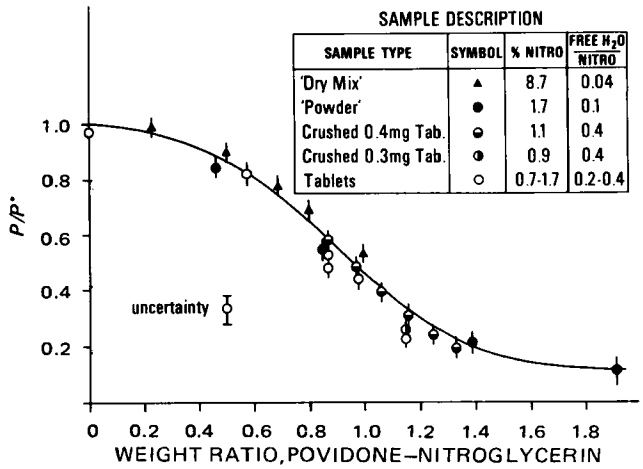

Figure 3—*Effects of sample type and free water on vapor pressure for nitroglycerin–povidone systems at 25°. P· ≡ vapor pressure of pure nitroglycerin.*

effects on the vapor pressure of nitroglycerin. The vapor pressure of a polyethylene glycol 400 stabilized tablet[12] is in excellent agreement with the powder curve. Both povidone and the polyethylene glycols significantly reduce the vapor pressure of nitroglycerin at weight ratios higher than 0.5. At high weight ratios, povidone is more effective in reducing the vapor pressure of nitroglycerin. Crude solubility measurements on microscopic samples indicate that all additives considered in Fig. 4 are soluble in nitroglycerin at weight ratios below ~1. Thus, the differences between bis(2-ethylhexyl) phthalate and the other additives are due to differences in the effective nitroglycerin–additive interaction in solution.

Vapor pressures at 37° were measured for povidone–nitroglycerin systems over a weight ratio range of 0.2–1.0. When the data are expressed in terms of relative pressure, $P/P^{\cdot}$, where $P^{\cdot}$ is the vapor pressure of pure nitroglycerin at 37°, the 37° data fall on the povidone curve in Fig. 4 (25° data) within the uncertainty of the data. Thus, the heat of vaporization of nitroglycerin is not greatly changed by the presence of povidone, indicating that the magnitude of the enthalpy change for the transfer process, nitroglycerin (pure liquid) → nitroglycerin (povidone–nitroglycerin system), is about 1 kcal/mole or less.

MIGRATION MECHANISMS

On the basis of the data, the following mechanism for the migration effect is proposed. Freshly prepared tablets exhibit significant and variable deviations from equilibrium due to a number of empty or partially filled small pores. As the tablet system (*e.g.*, 100 tablets in a bottle) approaches equilibrium, nitroglycerin is transferred from

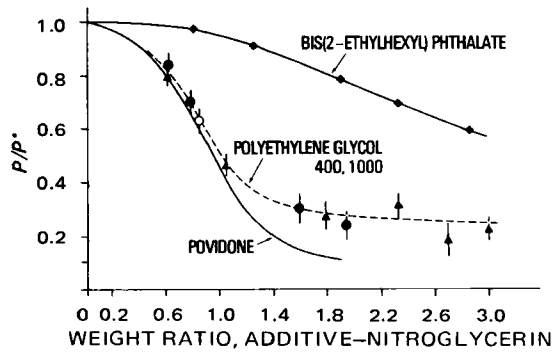

Figure 4—*Nitroglycerin vapor pressure reduction by additives at 25°: comparison of povidone, polyethylene glycols, and bis(2-ethylhexyl) phthalate. Key: ●, polyethylene glycol 400 powder sample; ○, polyethylene glycol 400 tablet; and ▲, polyethylene glycol 1000 powder sample.*

[12] Nitrostat, Parke-Davis and Co.

regions of high chemical potential (*i.e.*, coated on the lactose surface as shown in Fig. 1A) to the empty or partially filled small pores, which are states of lower chemical potential. When all pores small enough to condense nitroglycerin at the prevailing vapor pressure are filled, the surface-to-pore transfer stops. Since a given tablet is not an isolated system, intertablet as well as intratablet transfer takes place, resulting in potency variations of the same order of magnitude as variations in the volume of small pores.

The role of the stabilizing additive is *not* to minimize the migration effect by slowing the *rate* of volatilization. First, although the reduction in vapor pressure achieved in commercial formulations slows the rate of volatilization, the magnitude of the reduction is not sufficient to delay the development of poor content uniformity by more than a few months. For commercial polyethylene glycol 400 tablets[12], the reduction is about 35%; these stabilized tablets would be stable (*i.e.*, maintain good content uniformity) only about 35% longer than conventional tablets. Thus, an additive would not minimize the migration effect but would only moderately slow its development.

Second, if the additive minimized the migration effect by slowing the rate of volatilization, the formulation that produced the lowest vapor pressure would be superior. However, in spite of a higher vapor pressure (a factor of 2.5), 0.3-mg tablets stabilized with polyethylene glycol 400[12] appear equivalent to 0.3-mg tablets stabilized with povidone.

The role of the additive is clearly to lower the vapor pressure. However, the vapor pressure must be lowered *only enough to make it thermodynamically impossible for a significant quantity of nitroglycerin to be transferred from the lactose surface to a small pore.* Thus, for thermodynamic reasons, most of the permanent intertablet nitroglycerin migration occurring with conventional tablets will never occur in a closed system of stabilized tablets.

Reduction of the rate of volatilization is not particularly important within the context of the migration effect. Adsorption data imply that if the vapor pressure is reduced by more than about 15%, pore condensation is negligibly small. Thus, an additive prevents transfer to an empty pore if P/P° is less than about 0.85 in the additive–nitroglycerin phase. If the potential transfer is to a pore *partially filled* with the nitroglycerin–additive phase, transfer takes place until the composition changes are sufficient to result in about a 15% decrease in vapor pressure. Here, the parameters for nitroglycerin in the Kelvin equation (20) are assumed to be not greatly changed by the additive.

Thus, for povidone and polyethylene glycol 400 systems, transfer takes place until the concentration differences between the surface and pore are about 5%. With no additive present, this type of transfer takes place until either the small pore is filled or the surface is essentially devoid of nitroglycerin. The effectiveness of the additive in reducing this type of transfer depends on the slope of the vapor pressure *versus* weight ratio curve. For both povidone and polyethylene glycol 400, this slope becomes particularly large in the region where $P/P^{\circ} < 0.85$. Therefore, the use of these additives to achieve a vapor pressure reduction of about 15% is sufficient to prevent significant intertablet migration.

Finally, it should be emphasized that stabilized formulations are stabilized only with respect to intertablet nitroglycerin migration. The volatility is decreased, not eliminated, and losses of nitroglycerin arising from improper storage are decreased but not, in general, eliminated. At 25°, the air space above nitroglycerin tablets contains less than 7 μg of nitroglycerin/liter. Consequently, losses to the atmosphere are small, even if the container is not tightly closed or is repeatedly opened. Nitroglycerin sorption by polymeric packaging materials is a more serious problem[13]. Even stabilized tablets suffer severe sorption losses when in vapor contact with some polymers.

REFERENCES

(1) S. Fusari, *J. Pharm. Sci.*, **62,** 2012(1973).

(2) *Ibid.*, **62,** 122(1973).

(3) R. F. Shangraw and A. M. Contractor, *J. Am. Pharm. Assoc.*, **NS12,** 633(1972).

(4) B. A. Edelman, A. M. Contractor, and R. M. Shangraw, *ibid.*, **NS11,** 30(1971).

(5) D. Banes, *J. Pharm. Sci.*, **57,** 893(1968).

(6) M. D. Richman, C. D. Fox, and R. F. Shangraw, *ibid.*, **54,** 447(1965).

(7) F. J. Bell, *ibid.*, **53,** 752(1964).

(8) J. B. Segur, in "Glycerol," C. S. Miner and N. N. Dalton, Eds., American Chemical Society Monograph Series, Reinhold, New York, N.Y., 1953.

(9) R. T. M. Fraser, *Chem. Ind. (London)*, **1968,** 1117.

(10) A. Marshall, *J. Soc. Chem. Ind.*, **49,** 34T(1930).

(11) F. M. Ernsberger, J. G. Wyllie, and A. L. Olson, NAVORD Report No. 1184, Part I, U.S. Naval Ordnance Test Station, Sept. 28, 1949.

(12) M. D. Kemp, S. Goldhagen, and F. A. Zihlman, *J. Phys. Chem.*, **61,** 240(1957).

(13) V. V. Gorbunov, *Teor. Vzryuchatykh Veshchestv.*, **1963,** 219; through *Chem. Abstr.*, **59,** 9728b.

(14) M. J. Pikal and A. L. Lukes, *J. Pharm. Sci.*, **65,** 1269(1976).

(15) S. Dushman, in "Scientific Foundations of Vacuum Technique," 2nd ed., J. M. Lafferty, Ed., revised by Members of the Research Staff, General Electric Research Laboratory, Wiley, New York, N.Y., 1962.

(16) P. Echlin and R. Moreton, in "Scanning Electron Microscopy/1973 (Part III)," Proceedings of the Workshop on Scanning Electron Microscopy in Pathology, O. Johari and I. Corvin, Eds., IIT Research Institute, Chicago, Ill., Apr. 1973, p. 325.

(17) D. Ganderton and A. B. Selkirk, *J. Pharm. Pharmacol.*, **22,** 345(1970).

(18) R. G. Avery and J. D. F. Ramsay, *J. Colloid Interface Sci.*, **42,** 597(1973).

(19) A. B. Selkirk, *Powder Technol.*, **10,** 37(1974).

(20) A. W. Adamson, "Physical Chemistry of Surfaces," 2nd ed., Interscience, New York, N.Y., 1967.

(21) T. C. Sutton and H. L. Harden, *J. Phys. Chem.*, **38,** 779(1934).

ACKNOWLEDGMENTS AND ADDRESSES

Received March 3, 1975, from *Eli Lilly and Company, Indianapolis, IN 46206*

Accepted for publication November 12, 1975.

Presented in part at the APhA Academy of Pharmaceutical Sciences, New Orleans meeting, November 1974.

The authors thank Dr. J. Becker, Dr. G. Kaiser, Dr. R. Pfeiffer, and Dr. A. Thakkar for critical reviews of this manuscript.

[x] To whom inquiries should be directed.

[13] A study of nitroglycerin sorption by polymers will be the subject of a future report.

Effects of Colestipol Hydrochloride on Drug Absorption in the Rat II

WILLIAM A. PHILLIPS ˣ, JOHN M. RATCHFORD, and JOHN R. SCHULTZ

Abstract □ The effects of colestipol hydrochloride, a hypocholesterolemic bile acid-binding anion-exchange polymer, on the GI absorption of drugs commonly used in humans were studied in the rat. Colestipol hydrochloride was given by gavage in single doses of 71.5 or 214.5 mg/kg, equivalent to 5 or 15 g, respectively, in a 70-kg human; controls received equivalent amounts of microcrystalline cellulose. Single oral doses of labeled drugs were given concurrently with colestipol hydrochloride or microcrystalline cellulose at the human therapeutic dose range on a milligrams per kilogram basis. Subsequent changes in serum drug levels were measured at several time periods, and absorption was evaluated as the total area under the time–concentration curve. Colestipol hydrochloride at either dose did not significantly alter the absorption of 6-^{14}C-nicotinic acid, 7-^{3}H-tetracycline, ^{35}S-chlorpromazine, 12α-^{3}H-digoxin, warfarin (α-^{14}C-benzyl), or clofibrate (^{14}C-carboxyl). In addition, the effects of 214.5 mg/kg of colestipol hydrochloride were compared with the same dose of cholestyramine with respect to the absorption of 3-^{14}C-hydrochlorothiazide, 2-^{14}C-phenobarbital, and ^{3}H-digitoxin. Cholestyramine reduced absorption of hydrochlorothiazide by 42%, but colestipol hydrochloride had no significant effect. Neither resin altered phenobarbital or digitoxin absorption when compared with the control, but a significant difference occurred between the two resins with digitoxin; areas under the time–concentration curve [in (dpm/0.1 ml serum) × hr] were: colestipol hydrochloride, 2001; cholestyramine, 16,300; and cellulose, 17,067. These results indicate that colestipol hydrochloride and cholestyramine can differ in their effects on the absorption of certain drugs from the GI tract of the rat.

Keyphrases □ Colestipol hydrochloride—effect on GI absorption of various drugs, rats □ Absorption, GI—various drugs, effect of colestipol hydrochloride, rats □ Anion-exchange polymers—colestipol hydrochloride, effect on GI absorption of various drugs, rats

Colestipol hydrochloride[1] is a high molecular weight anion-exchange polymer, prepared by reacting polyethylenepolyamine and 1-chloro-2,3-epoxypropane. It contains approximately one of five amine nitrogens protonated as the chloride salt. Oral administration of the bile acid-binding colestipol hydrochloride increases the fecal excretion of bile acids by reducing their intestinal reabsorption, thereby reducing cholesterol levels in experimental animals (1–3) and in humans (4–7). Since colestipol hydrochloride may bind other substances, including drugs that might be used as concurrent therapy in hypercholesterolemic subjects, studies of possible drug–polymer interactions have been continued in the rat.

Previous results with aspirin, levothyroxine, cortisone acetate, phenobarbital, and sulfadiazine indicated that both aspirin and levothyroxine absorption were inhibited by the polymer when administered concurrently to the rat (8). It was suggested that the primary interaction with aspirin and levothyroxine was electrostatic between the negatively charged carboxyl groups of the adsorbates and the positively charged groups on the adsorbent. A reinforcement by a nonelectrostatic force (9) existing between the hydrophobic portion of levothyroxine and the polymer molecules could explain the marked reduction of levothyroxine by colestipol hydrochloride in comparison to the other drugs tested.

Cholestyramine is an insoluble quaternary ammonium anion-exchange resin that binds bile acids and possesses the same potential as colestipol hydrochloride for interactions with other therapeutic agents (10). Although cholestyramine has been reported to retard absorption of radioactive drugs (*e.g.*, aspirin and phenobarbital), differences in experimental conditions made it impossible to compare the drug-binding capacities of the two polymers. To study this relationship, *in vivo* experiments were conducted on the effects of the two resins, administered under identical conditions, on the absorption of 3-^{14}C-hydrochlorothiazide, 2-^{14}C-phenobarbital, and ^{3}H-digitoxin.

EXPERIMENTAL

Ten male rats[2], with an average weight of approximately 240 g (less than 20-g range), were used in each treatment group. The rats were fasted for 18 hr prior to and during each experiment, except in the warfarin and tetracycline tests in which food was returned at 1 and 3 days, respectively; water was allowed *ad libitum*. Colestipol hydrochloride was suspended in 0.25% aqueous methylcellulose and administered by stomach tube at 71.5 and 214.5 mg/kg. Controls received equal amounts of a bulk material, microcrystalline cellulose[3], suspended and dosed similarly to colestipol hydrochloride. These levels correspond on a weight basis to 5 and 15 g of material, respectively, in a 70-kg man.

In the comparison studies, colestipol hydrochloride, cholestyramine[4], or microcrystalline cellulose was suspended in sterile water and administered at 214.5 mg/kg. Water alone served as the fourth treatment group. Within 10 sec after treatment, radioactive drug, dissolved or suspended in 0.25% methylcellulose vehicle or sterile water, was administered by stomach tube. The radioactive drugs, found by TLC on silica gel and scanning with a radiochromatogram scanner[5] to be radiochemically pure, were 6-^{14}C-nicotinic acid, warfarin (α-^{14}C-benzyl), ^{35}S-chlorpromazine[6], 7-^{3}H-tetracycline hydrochloride, 12α-^{3}H-digoxin, 2-^{14}C-phenobarbital, 7-^{3}H-digitoxin[7], clofibrate (^{14}C-carboxyl)[8], and 3-^{14}C-hydrochlorothiazide[9].

In the experiments, the microcuries given per 100 g of body weight were: nicotinic acid or warfarin, 0.45; digoxin or digitoxin, 2.0; chlorpromazine, 3.6; tetracycline, 9.5; clofibrate, 0.1; phenobarbital, 0.65; and hydrochlorothiazide, 0.91. The total doses of the drugs, as milligrams per kilogram, after addition of nonradioactive compound[10]

[1] Colestid, The Upjohn Co., Kalamazoo, Mich.

[2] Upj:TUC(SD)spf.

[3] Avicel, PH-102, FMC Corp., American Viscose Division, Marcus Hook, Pa.

[4] Cuemid, No. 3300, Merck Sharp and Dohme, Division of Merck and Co., West Point, Pa. Administered at 234.4 mg/kg to allow for 8.5% inert material.

[5] Model 885, Vanguard Instrument Corp., La Grange, Ill.

[6] Amersham/Searle, Arlington Heights, Ill.

[7] New England Nuclear, Boston, Mass.

[8] From Dr. D. M. Foulkes, Imperial Chemical Industries Limited, England.

[9] From Dr. N. Chaudhuri, Ciba-Geigy Corp., Summit, N.J.

[10] Niacin NF; tetracycline hydrochloride and phenobarbital USP; digoxin and digitoxin, Mann Research Laboratories, Division of Becton, Dickinson & Co., New York, N.Y.; and warfarin and clofibrate, synthesized at The Upjohn Co. Supplementations with chlorpromazine and hydrochlorothiazide were not necessary.

Table I—Area under Time–Serum Drug Concentration Curves for Several Drugs with Concurrent Administration of Colestipol Hydrochloride or Cellulose Control[a]

Drug[b]	Dose, 71.5 mg/kg		Dose, 214.5 mg/kg		SD, %[d]
	Control	Colestipol Hydrochloride[c]	Control	Colestipol Hydrochloride	
Nicotinic acid	1,354	1,469	1,184	1,004	30.3
Tetracycline	10,445	10,583	11,239	9,679	23.3
Chlorpromazine	14,843	14,101	15,285	14,514	17.6
Digoxin	8,410	8,256[e]	8,350	8,633[e]	15.5
Warfarin	99,879	92,118	92,045	89,821	11.7
Clofibrate	9,039[a]	10,035	—	10,567[e]	24.3

[a] Except clofibrate control group given 0.25% aqueous methylcellulose vehicle (see text). [b] Mean areas for tetracycline expressed as (dpm/0.1 ml) × day; all other values expressed as (dpm/0.1 ml) × hr. [c] Within each dosage level, none of the means between control and colestipol hydrochloride group was statistically significant. [d] Obtained from analysis of variance over all four groups. [e] Represents mean of nine animals; all other values represent mean of 10 animals.

Table II—Peak Serum Radioactivities for Several Drugs with Concurrent Administration of Colestipol Hydrochloride or Cellulose Control[a]

Drug	Dose, 71.5 mg/kg		Dose, 214.5 mg/kg		SD, %
	Control	Colestipol Hydrochloride	Control	Colestipol Hydrochloride	
Nicotinic acid	1510	1423	1389	990[b]	14.1
Tetracycline	3823	4034	3851	3751	27.1
Chlorpromazine	638	610	679	670	25.4
Digoxin	528	454[c]	568	493[c]	24.1
Warfarin	3648	3461	3271	2821	23.7
Clofibrate	653[d]	734	—	776[c]	20.6

[a] Mean values expressed as dpm/0.1 ml serum. [b] Significant difference between colestipol hydrochloride mean and mean of corresponding cellulose control: $p < 0.01$. [c] Represents mean of nine animals; all other values represent mean of 10 animals. [d] Control group given 0.25% aqueous methylcellulose vehicle (see text).

were: nicotinic acid, 14.3; tetracycline, 3.6; chlorpromazine, 0.7; digoxin, 0.065; warfarin, 0.19; clofibrate, 7.6; hydrochlorothiazide, 1.8; phenobarbital, 1.34; and digitoxin, 0.004. The doses were generally within the range given to humans on a weight basis.

The rats were then bled from the jugular vein (0.25 ml) at various time periods (11). The scintillation fluid contained 8.8% serum solubilizer[11], 0.4% 2,5-diphenyloxazole, and 0.005% 1,4-bis[2-(5-phenyloxazolyl)]benzene in toluene. Radioassay of 0.1 ml of serum was accomplished in a liquid scintillation spectrometer[12], and quenching was determined using the automatic external standard and a prepared efficiency correlation curve. Correction for sulfur-35 decay was also made in the chlorpromazine experiment.

The data for each drug were analyzed statistically for specific activity (dpm/0.1 ml) at each sampling period, peak radioactivity was obtained from the observed curve, and the area under the time–concentration curve [(dpm/0.1 ml) × hr] was calculated with the trapezoidal rule. For each parameter, a one-way analysis of variance (12) was performed on the values from the four groups of animals; comparisons were made between each colestipol hydrochloride mean and the mean of the corresponding control. In the comparison study with colestipol hydrochloride and cholestyramine, the polymers were compared with cellulose and with each other; cellulose was compared with the water treatment group.

Of the drugs tested, the one-compartment open model was appropriate only for the data obtained with phenobarbital (8). When more than two samples were lost during centrifugation or when the rat died from the bleeding procedure, the data from that animal were not included in the analyses.

RESULTS AND DISCUSSION

The results obtained with colestipol hydrochloride at 71.5 and 214.5 mg/kg and corresponding levels of cellulose on areas under the time–concentration curves and peak serum radioactivities are summarized in Tables I and II. The serum drug levels for each drug at various sampling periods are presented in the figures.

6-^{14}C-Nicotinic Acid—The results obtained with 6-^{14}C-nicotinic acid administered at 14.3 mg/kg are presented in Fig. 1. The low level of colestipol hydrochloride significantly decreased the serum drug level at 15 min and increased the radioactivity at the 4-hr period. The high level of colestipol hydrochloride significantly decreased the appearance of the ^{14}C-label in the serum at 15 and 30 min; other changes did not differ from the control. Although peak radioactivity at the high dose of the polymer was significantly reduced by 29%, total drug availability, as measured under the time–concentration curve, was reduced 15% but did not differ significantly from the control.

It was previously reported that colestipol hydrochloride can in-

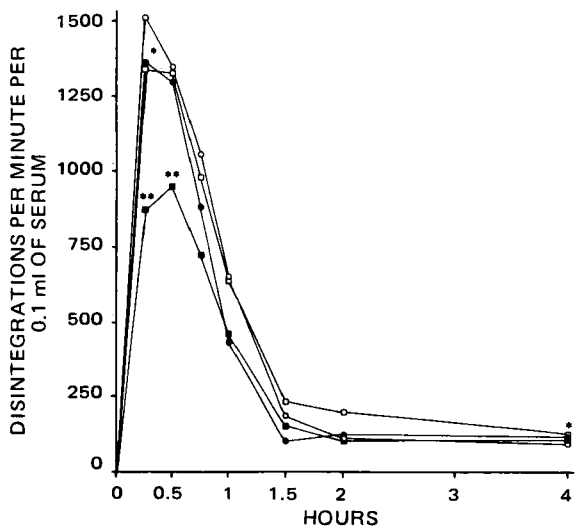

Figure 1—*Effect of colestipol hydrochloride on absorption of 6-^{14}C-nicotinic acid. Key: cellulose control at 71.5 (○) and 214.5 (●) mg/kg; colestipol hydrochloride at 71.5 (□) and 214.5 (■) mg/kg; and significant difference between colestipol hydrochloride mean and mean of corresponding control at* $p < 0.05$ (*) *and* $p < 0.01$ (**).

[11] Bio-Solv BBS-3, Beckman Instruments, Inc., Fullerton, Calif.
[12] Model 3375, Packard Instrument Co., Downers Grove, Ill.

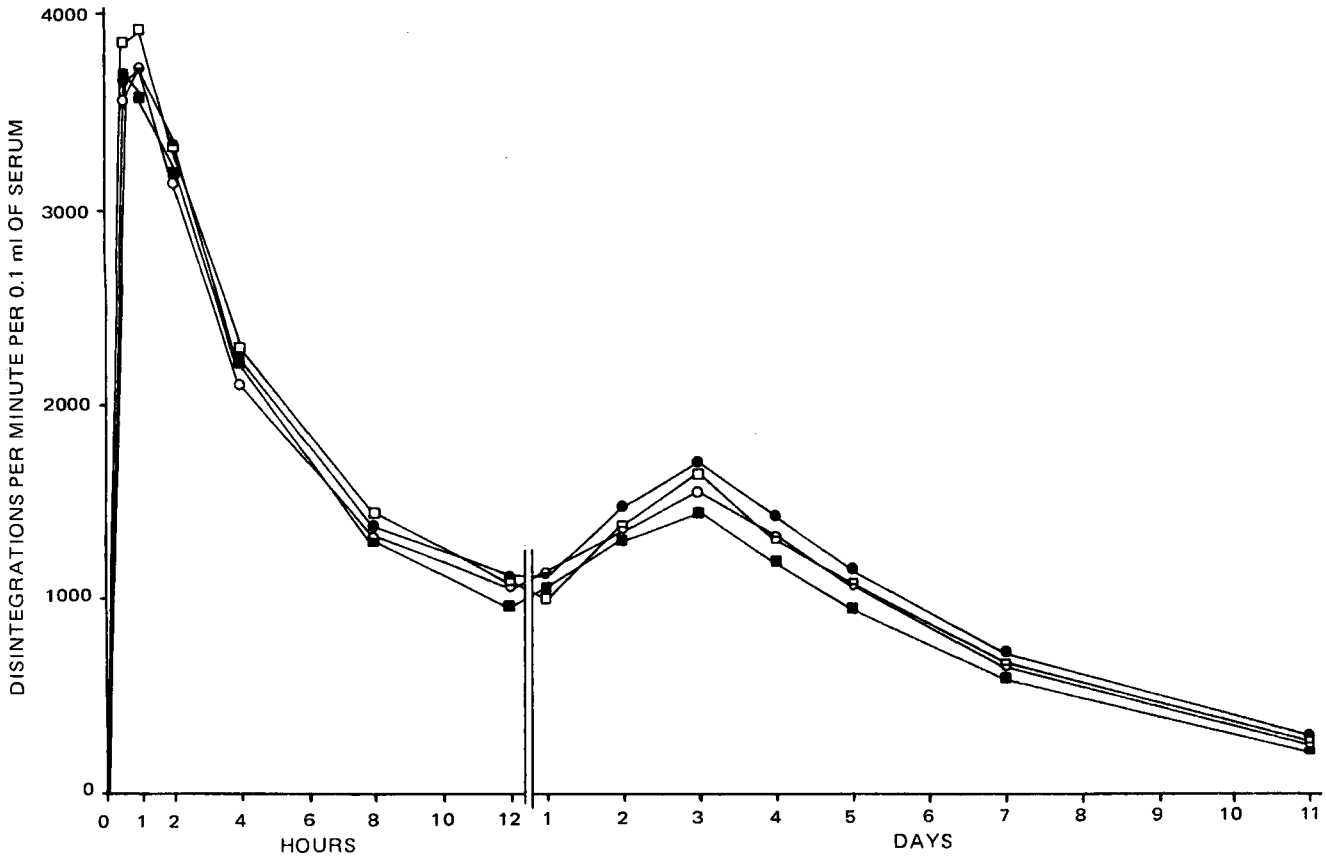

Figure 2—*Effect of colestipol hydrochloride on absorption of 7-^{3}H-tetracycline. Key: cellulose control at 71.5 (○) and 214.5 (●) mg/kg; and colestipol hydrochloride at 71.5 (□) and 214.5 (■) mg/kg.*

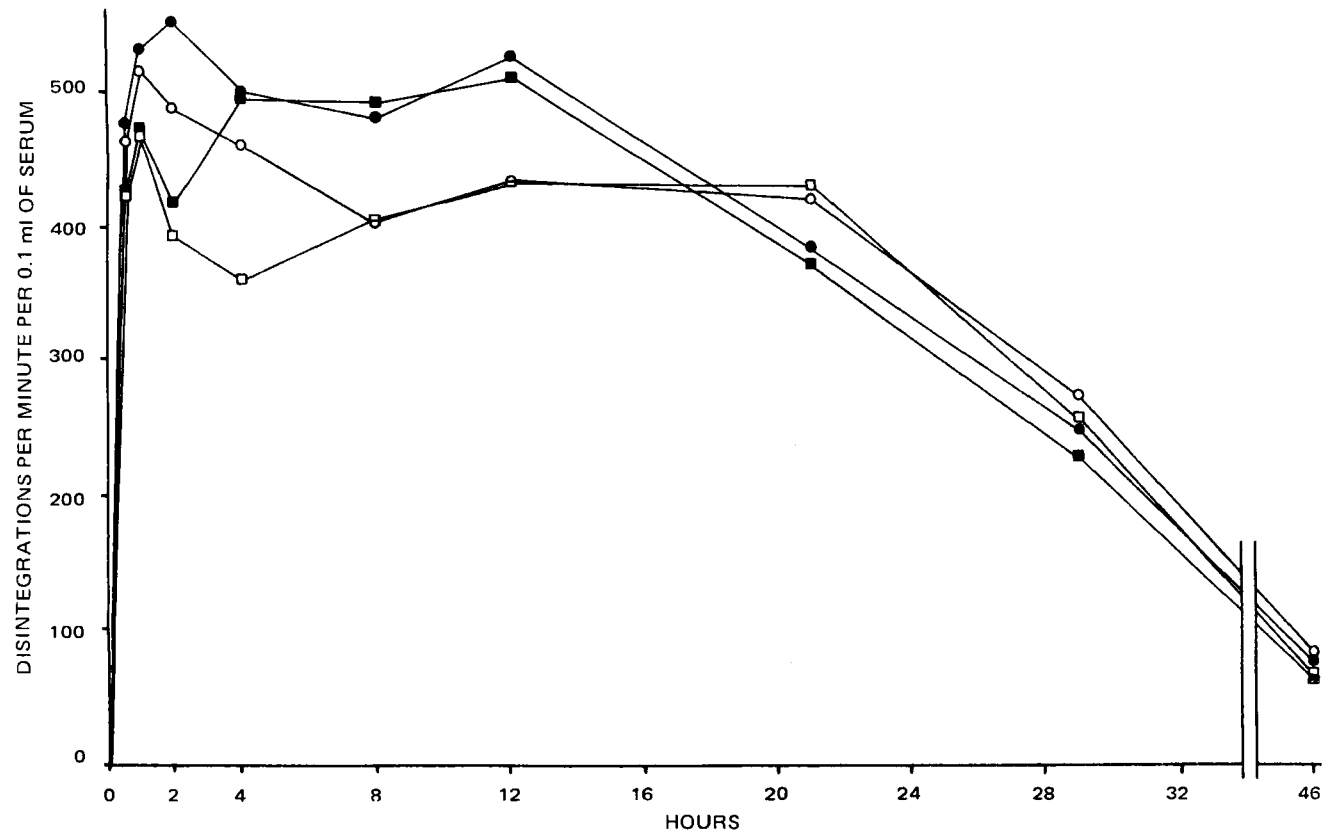

Figure 3—*Effect of colestipol hydrochloride on absorption of ^{35}S-chlorpromazine. Key: cellulose control at 71.5 (○) and 214.5 (●) mg/kg; and colestipol hydrochloride at 71.5 (□) and 214.5 (■) mg/kg.*

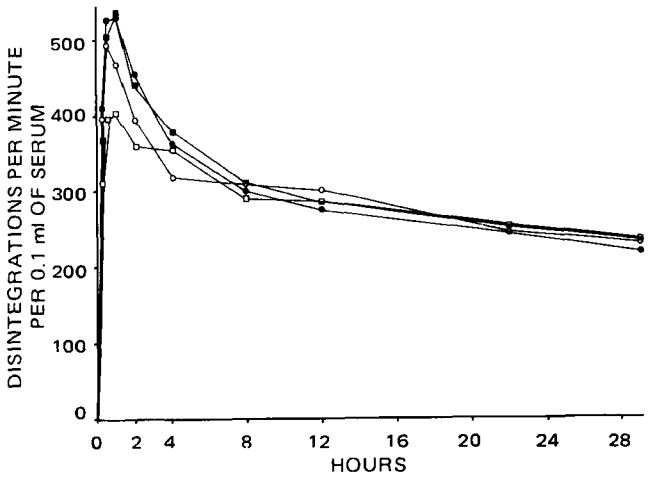

Figure 4—*Effect of colestipol hydrochloride on absorption of 12α-^{3}H-digoxin. Key: cellulose control at 71.5 (○) and 214.5 (●) mg/kg; and colestipol hydrochloride at 71.5 (□) and 214.5 (■) mg/kg.*

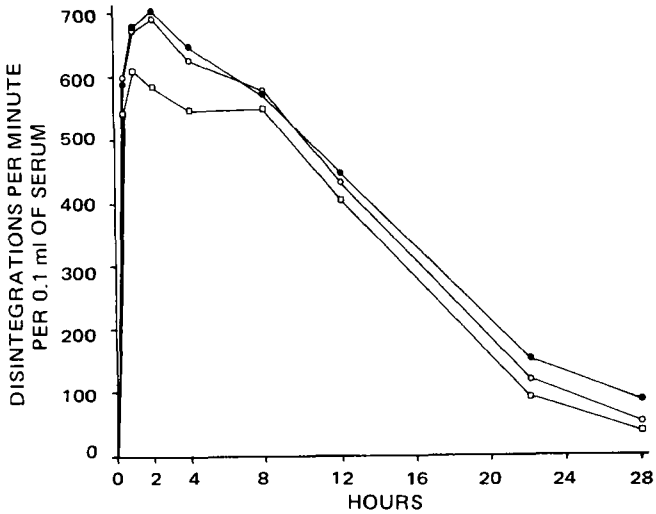

Figure 6—*Effect of colestipol hydrochloride on absorption of clofibrate (^{14}C-carboxyl). Key: methylcellulose vehicle control (□); and colestipol hydrochloride at 71.5 (○) and 214.5 (●) mg/kg.*

terfere with the absorption of aspirin (pKa 3.4) but not with phenobarbital (pKa 7.2) absorption (8). The stability of the drug–polymer interaction may be related to the pKa of these drugs. Nicotinic acid, with an intermediate pKa of 4.8, was bound less than aspirin, as evidenced by the delay of absorption or the reduction of peak radioactivity with little effect on the total amount absorbed. Electrolytes present in the GI tract could reduce the charge density on the charged adsorbate and adsorbent, thus weakening the electrostatic interaction between the polymer and nicotinic acid. Evidence for the inhibitory effect of electrolytes on the interaction of bile salt anions with cholestyramine was reported previously (13).

7-^{3}H-Tetracycline—Serum levels of 7-^{3}H-tetracycline after oral administration at 3.6 mg/kg were measured at various intervals over 11 days (Fig. 2). Serum radioactivities at various sampling periods, the amount of drug absorbed, and the peak radioactivity were not influenced at either level of colestipol hydrochloride. The unusual formation of a second peak of serum radioactivity after 24 hr may be related to the continued fasting of the animals for 3 days. The appearance of the second peak is not an artifact, since this effect was observed in all 40 animals. The explanation of this phenomenon is not clear at present, but double peaks were observed in rat blood levels with other antibiotics (14).

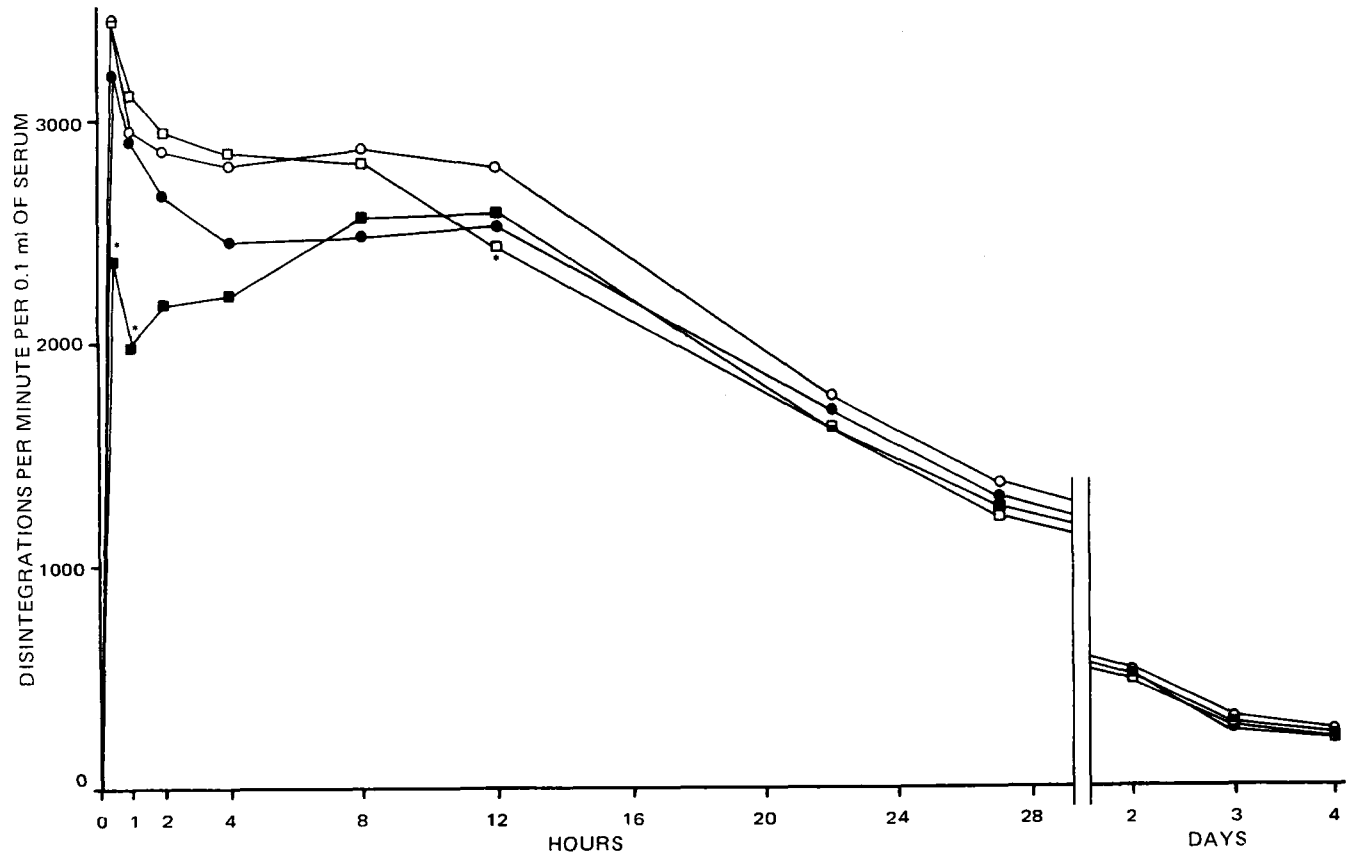

Figure 5—*Effect of colestipol hydrochloride on absorption of warfarin (α-^{14}C-benzyl). Key: cellulose control at 71.5 (○) and 214.5 (●) mg/kg; colestipol hydrochloride at 71.5 (□) and 214.5 (■) mg/kg; and significant difference between colestipol hydrochloride means and mean of corresponding control at $p < 0.05$ (*).*

Table III—Areas and Peak Radioactivities for 3-^{14}C-Hydrochlorothiazide with Concurrent Administration of Cellulose, Colestipol Hydrochloride, Cholestyramine, or Water[a]

Treatment	Area (0–11 hr)	Peak Radioactivity
Cellulose[b]	2478	486
Colestipol hydrochloride	2260	424
Cholestyramine[b]	1428	192
Water	2481	468
SD, %[c]	12.1	15.1

[a] Area under the time–concentration curve is in (dpm/0.1 ml) × hr; peak radioactivity is in dpm/0.1 ml serum. [b] Represents mean of nine animals; all other values represent mean of 10 animals. [c] Obtained from analysis of variance over all four groups.

^{35}S-Chlorpromazine and 12α-^{3}H-Digoxin—The results obtained with ^{35}S-chlorpromazine administered at 0.7 mg/kg and with 12α-^{3}H-digoxin administered at 0.065 mg/kg are shown in Figs. 3 and 4. The differences between serum radioactivity at both levels of colestipol hydrochloride and corresponding controls were not significant at any sampling period in both experiments.

Warfarin (α-^{14}C-Benzyl)—Warfarin (α-^{14}C-benzyl) was administered at 0.19 mg/kg to each rat (Fig. 5). Colestipol hydrochloride at 71.5 mg/kg reduced serum radioactivity at the 12-hr sampling period; other values did not differ significantly from the control. At 214.5 mg/kg, colestipol hydrochloride caused a significant decrease in serum drug levels at 0.5- and 1-hr sampling periods only. The early binding of warfarin may be due to the weakly acidic functional enol group of the drug. Values for drug availabilities and peak radioactivities at both levels of the polymer did not differ significantly from the corresponding controls, indicating that electrolytes present in the GI tract could weaken the electrostatic attraction of colestipol hydrochloride and warfarin.

Clofibrate (^{14}C-Carboxyl)—The results obtained with the hypocholesterolemic agent clofibrate administered at 7.6 mg/kg appear in Fig. 6. Due to the limited amount of radioactive compound, the control groups did not receive cellulose. The differences in serum radioactivities after the concurrent administration of the drug at both levels of colestipol hydrochloride and the control were not significant at any sampling period. Colestipol hydrochloride could delay or interfere with the absorption of clofibrate if the free acid was liberated in the GI tract of the animal; however, the ester after GI absorption is rapidly hydrolyzed by tissue and serum esterases to the free acid (15).

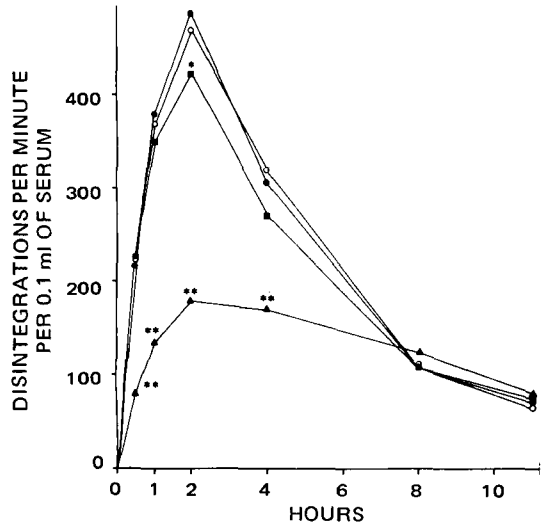

Figure 7—*Effect of colestipol hydrochloride or cholestyramine on absorption of 3-^{14}C-hydrochlorothiazide. Key: cellulose control at 214.5 (●) mg/kg; colestipol hydrochloride at 214.5 (■) mg/kg; cholestyramine at 214.5 (▲) mg/kg; water (○); and significant difference between colestipol hydrochloride or cholestyramine means and mean of corresponding cellulose control at p < 0.05 (*) or p < 0.01 (**).*

Table IV—Statistical Comparisons for Data Shown in Table III[a]

Comparison	Area (0–11 hr)	Peak Radioactivity
Cellulose *versus* colestipol hydrochloride	N.S.	$p < 0.05$
Cellulose *versus* cholestyramine	$p < 0.01$	$p < 0.01$
Colestipol hydrochloride *versus* cholestyramine	$p < 0.01$	$p < 0.01$
Cellulose *versus* water	N.S.	N.S.

[a] *The p values indicate level of significance; N.S. indicates not significant.*

The following results were obtained in comparison studies with colestipol hydrochloride and cholestyramine at 214.5 mg/kg.

3-^{14}C-Hydrochlorothiazide—The results obtained with 3-^{14}C-hydrochlorothiazide administered at 1.8 mg/kg are presented in Table III and Fig. 7. Colestipol hydrochloride significantly reduced the serum drug level at 2 hr by 13%; other values did not vary significantly from the cellulose control. Cholestyramine significantly reduced drug levels at 0.5, 1, 2, and 4 hr by 47–65%; values were significantly less than those obtained with colestipol hydrochloride. Colestipol hydrochloride and cholestyramine reduced peak radioactivity by 13 and 60%, respectively; cholestyramine reduced absorption by 42%, whereas drug availability with colestipol hydrochloride did not significantly vary from the control. There were no significant differences between cellulose and water treatments in this test (Table IV).

Cholestyramine is a relatively nonpolar resin, with the basic quaternary ammonium exchange groups attached to a styrene–divinylbenzene copolymer skeleton. Colestipol hydrochloride is a relatively polar hydroxyl aliphatic amino resin. Since both are anion-exchange resins, they would be expected to bind the acidic drug hydrochlorothiazide by electrostatic attraction. The increased binding efficiency of cholestyramine for the drug may be due to the greater lipophilic character of the phenyl rings of the resin. No information is available

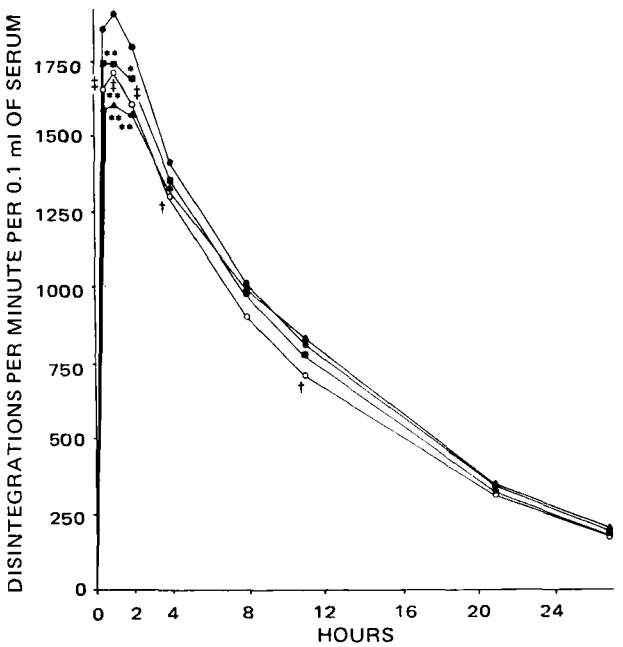

Figure 8—*Effect of colestipol hydrochloride or cholestyramine on absorption of 2-^{14}C-phenobarbital. Key: cellulose control at 214.5 (●) mg/kg; colestipol hydrochloride at 214.5 (■) mg/kg; cholestyramine at 214.5 (▲) mg/kg; water (○); significant difference between colestipol hydrochloride or cholestyramine and corresponding cellulose control at p < 0.05 (*) and p < 0.01 (**); and significant difference between water and cellulose means at p < 0.05 (†) and p < 0.01 (††).*

Table V—Kinetic Parameters for Phenobarbital with Concurrent Administration of Colestipol Hydrochloride, Cholestyramine, Cellulose, or Water

Model Parameters[a]	Dose, 214.5 mg/kg				
	Cellulose	Colestipol Hydrochloride[b]	Cholestyramine[b,c]	Water[c]	*SD*, %
K_A	5.88	5.82	5.64	4.84	37.7
$A^{1/2}$	0.130	0.124	0.136	0.145	28.1
K_E	0.091	0.087	0.076*	0.090	16.2
$E^{1/2}$	7.82	8.11	9.31*	7.87	15.4
Area	23,300	22,470	23,750	20,910	14.5
Observed area	20,932	19,853	20,139	18,729*	10.8
Peak radioactivity	1,925	1,780*	1,619**	1,705**	7.0

[a] K_A (hours^{-1}) = rate of absorption, $A^{1/2}$ (hours) = absorption half-life, K_E (hours^{-1}) = rate of elimination, $E^{1/2}$ (hours) = elimination half-life, area under the time–concentration curve is in (dpm/0.1 ml) × hr, and peak radioactivity is in dpm/0.1 ml serum (8). [b] Significant difference between colestipol hydrochloride, cholestyramine, or water means and cellulose control at (*) $p < 0.05$ and (**) $p < 0.01$. [c] Represents mean of eight animals; all other values represent mean of 10 animals.

comparing the influence of cholestyramine and colestipol hydrochloride on the absorption of this drug. However, differences between the polymers with the coumarin anticoagulant phenprocoumon in humans were reported (16, 17). Absorption of the phenprocoumon given concurrently with cholestyramine was significantly reduced; colestipol hydrochloride did not influence GI absorption of the coumarin anticoagulant.

2-^{14}C-Phenobarbital—The results obtained with 1.34 mg of 2-^{14}C-phenobarbital/kg appear in Table V and Fig. 8. Estimations of model parameters were made with phenobarbital, since the values were applicable to first-order kinetics (8). Colestipol hydrochloride significantly delayed the absorption of drug at 1 and 2 hr and cholestyramine at 0.5, 1, and 2 hr; the other values did not differ significantly from the cellulose control. Colestipol hydrochloride and cholestyramine significantly reduced peak radioactivity by 8 and 16%, respectively; drug availability with both polymers did not differ from the control. Therefore, neither polymer interfered with total absorption of the drug in the rat. Cholestyramine was reported to interfere with GI absorption of phenobarbital during a 2-hr test (10); evaluation of drug availability was not made due to insufficient data.

Estimated model parameters for absorption and elimination of phenobarbital with colestipol hydrochloride did not vary significantly from the cellulose control. Cholestyramine significantly reduced the rate of elimination (from 0.091 to 0.076 hr^{-1}) and increased the elimination half-life (from 7.82 to 9.31 hr) of the drug. The apparent reduction in the rate of elimination may reflect the latent absorption of loosely bound drug which dissociated from the drug–polymer molecule.

In this experiment, cellulose increased phenobarbital availability and serum drug levels at most time periods when compared to the water-treated group. These results may reflect the bulk effect of cellulose, which would increase stomach emptying time and delay entrance of drug into the intestine. Phenobarbital exists in the stomach almost totally in the absorbable nonionized form, becoming more ionized in the intestinal tract. Water alone has no influence on stomach emptying time (18) and permits more rapid entry of drug into a less favorable medium for absorption.

G-^{3}H-Digitoxin—The results obtained with ^{3}H-digitoxin administered at 0.004 mg/kg are presented in Table VI and Fig. 9. Colestipol hydrochloride caused significant increases in serum radioactivity at 21 and 27 hr; none of the other values varied significantly from the cellulose control. Values for observed peak radioactivity and the area under the curve were not altered significantly. Cholestyramine reduced significantly the serum radioactivity at 0.5, 1, and 2 hr and increased the serum radioactivity at 27 hr; observed peak radioactivity was reduced significantly (from 1489 to 1150 dpm), but the area under the curve did not differ significantly from the cellulose control (Table VII). Drug availability with cholestyramine was significantly less than with colestipol hydrochloride [16,300 *versus* 20,001 (dpm/0.1 ml) × hr], as was peak radioactivity (1150 *versus* 1524 dpm).

Studies in animals demonstrated that digitoxin participates in enterohepatic circulation (19). The reason for the significant elevation of serum drug levels with both polymers at the end of the test is not known, but it is reasonable to speculate that it is due to the appearance of newly synthesized bile acids, stimulated by administration of the polymers, which may aid in the reabsorption of digitoxin and its metabolites (20). When compared to the water-treated group, drug availability [17,067 *versus* 20,668 (dpm/0.1 ml) × hr], peak radioac-

Table VI—Areas and Peak Radioactivities for G-^{3}H-Digitoxin with Concurrent Administration of Cellulose, Colestipol Hydrochloride, Cholestyramine, or Water[a]

Treatment	Area (0–27 hr)	Peak Radioactivity
Cellulose	17,067	1,489
Colestipol hydrochloride[b]	20,001	1,524
Cholestyramine	16,300	1,150
Water	20,668	1,877
SD, %	20.2	21.2

[a] Area under the time–concentration curve is in (dpm/0.1 ml) × hr; peak radioactivity is in dpm/0.1 ml serum. [b] Represents mean of nine animals; all other values represent mean of 10 animals.

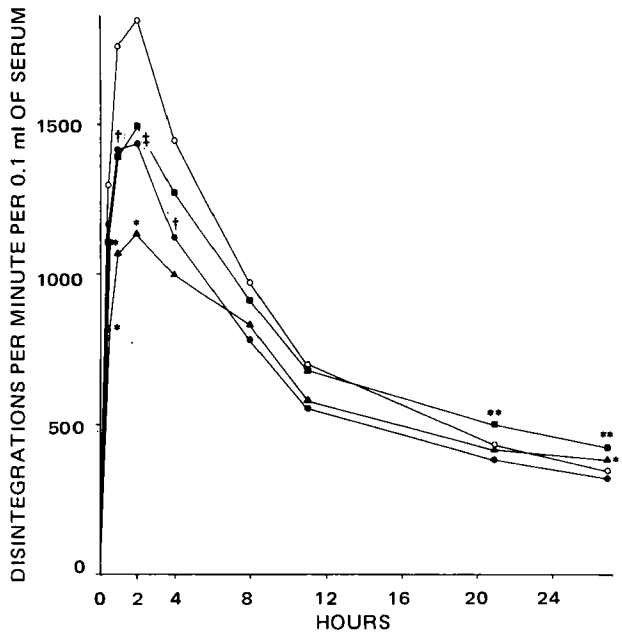

Figure 9—*Effect of colestipol hydrochloride or cholestyramine on absorption of ^{3}H-digitoxin. Key: cellulose control at 214.5 (●) mg/kg; colestipol hydrochloride at 214.5 (■) mg/kg; cholestyramine at 214.5 (▲) mg/kg; water (○); significant difference between colestipol hydrochloride or cholestyramine means and mean of corresponding cellulose control at* $p < 0.05$ *(*) and* $p < 0.01$ *(**); and significant difference between water and cellulose control at* $p < 0.05$ *(†) and* $p < 0.01$ *(††).*

Table VII—Statistical Comparison for Data Shown in Table VI[a]

Comparison	Area (0–27 hr)	Peak Radioactivity
Cellulose *versus* colestipol hydrochloride	N.S.	N.S.
Cellulose *versus* cholestyramine	N.S.	$p < 0.05$
Colestipol hydrochloride *versus* cholestyramine	$p < 0.05$	$p < 0.05$
Water *versus* cellulose	$p < 0.05$	$p < 0.05$

[a] The p values indicate level of significance; N.S. indicates not significant.

tivity (1489 *versus* 1877 dpm), and serum radioactivity at 1, 2, and 4 hr were significantly reduced by cellulose treatment. These results may reflect the bulk effect of cellulose, which would increase stomach emptying time and delay entrance of the drug into the intestine, where presumably the major portion of digitoxin is absorbed.

Colestipol hydrochloride is an anion-exchange polymer that would be expected to bind with ionized drugs by electrostatic forces, although other forces such as hydrogen bonding, dipole–dipole interactions, van der Waals forces, nonelectrostatic interactions, and intermolecular attractions of like molecules may be important factors in the binding process. The concurrent administration of nicotinic acid and colestipol hydrochloride reduced peak radioactivity at the high dose of the polymer; total drug availability, as measured under the time–concentration curve, was reduced but did not vary significantly from the control. Competition for binding sites on the polymer with bile acid anions and inorganic physiological anions (*e.g.*, phosphate, chloride, and bicarbonate) present in the GI tract could possibly explain these results.

The early binding of warfarin and the subsequent release from the drug–polymer interaction by these competing forces could weaken the electrostatic attraction of colestipol hydrochloride and the drug. Similarly, cholestyramine (357.5 mg/kg) in rats significantly depressed the plasma warfarin levels at all time intervals during a 4-hr test (10). Further tests on plasma prothrombin times used to calculate the relative clot index, at time intervals for 4 days, indicated that, although cholestyramine may delay early absorption of warfarin, the pharmacological effect was not significantly altered by a single dose of the drug and the polymer.

However, significant differences were noted between cholestyramine and colestipol hydrochloride in interfering with hydrochlorothiazide or digitoxin absorption from the GI tract of the rat. Whether results in rats are predictive of results in humans remains to be determined.

REFERENCES

(1) T. M. Parkinson, K. Gundersen, and N. A. Nelson, *Atherosclerosis*, **11**, 531(1970).

(2) T. M. Parkinson, J. C. Schneider, Jr., and W. A. Phillips, *ibid.*, **17**, 167(1973).

(3) J. R. Ryan and A. Jain, *J. Clin. Pharmacol.*, **12**, 268(1972).

(4) E. Marmo, A. P. Caputi, S. Cataldi, and A. Amelio, *G. Arterioscler.*, **8**, 229(1970).

(5) C. J. Glueck, S. Ford, Jr., D. Scheel, and P. Steiner, *J. Am. Med. Assoc.*, **222**, 676(1972).

(6) E. R. Nye, D. Jackson, and J. D. Hunter, *N. Z. Med. J.*, **76**, 12(1972).

(7) D. S. Goodman, R. P. Noble, and R. B. Dale, *J. Clin. Invest.*, **52**, 2646(1973).

(8) W. A. Phillips, J. R. Schultz, and W. W. Stafford, *J. Pharm. Sci.*, **63**, 1097(1974).

(9) W. H. Johns and T. R. Bates, *ibid.*, **59**, 329(1970).

(10) D. G. Gallo, K. R. Bailey, and A. L. Scheffner, *Proc. Soc. Exp. Biol. Med.*, **120**, 60(1965).

(11) W. A. Phillips, W. W. Stafford, and J. Stuut, Jr., *ibid.*, **143**, 733(1973).

(12) G. W. Snedecor and W. G. Cochran, "Statistical Methods," 6th ed., Iowa State University Press, Ames, Iowa, 1967, p. 258.

(13) W. H. Johns and T. R. Bates, *J. Pharm Sci.*, **59**, 788(1970).

(14) A. A. Sinkula, *ibid.*, **63**, 842(1974).

(15) J. M. Thorp, *Lancet*, **1**, 1323(1962).

(16) H. J. Hahn, W. Eiden, M. Schettle, M. Hahn, E. Walter, and E. Weber, *Eur. J. Clin. Pharmacol.*, **4**, 142(1972).

(17) C. Harvengt and J. P. Desager, *ibid.*, **6**, 19(1973).

(18) D. F. Magee, "Gastro-intestinal Physiology," Charles C Thomas, Springfield, Ill., 1962, p. 144.

(19) G. T. Okita, *Fed. Proc.*, **26**, 1125(1967).

(20) N. J. Greenberger and F. B. Thomas, *J. Lab. Clin. Med.*, **81**, 241(1973).

ACKNOWLEDGMENTS AND ADDRESSES

Received May 22, 1975, from *Diabetes and Atherosclerosis Research, The Upjohn Company, Kalamazoo, MI 49001*

Accepted for publication November 4, 1975.

[x] To whom inquiries should be directed.

Effects of Film Coatings on Tablet Hardness

PHILIP W. STERN

Abstract □ The effects of five conventional film-coating materials on tablet hardness were studied. Placebos showed apparently linear increases in hardness as coatings were applied. Completely coated samples exhibited hardness increases from 50 to 140%, with a corresponding 3% increase in tablet weight. Equations were derived relating hardness changes to the "breaking strength" of the film on the tablet. Findings indicate that the coatings exert their influence primarily along the diameter of the tablet in a direction perpendicular to an applied compressional force. Furthermore, the coating process itself did not alter core hardness since tablets from which the film could be stripped showed original values.

Keyphrases □ Film coatings—five different, effects on tablet hardness □ Hardness, tablet—effects of five different film coatings □ Tablet hardness—effects of five different film coatings □ Dosage forms—tablets, effects of five different film coatings on tablet hardness

The term "tablet hardness" is widely used today in a nonspecific or generic manner as an all-inclusive description of several important tablet parameters. Included among these parameters are bending or attrition resistance and impact or crushing strength (1–4). Of the four, measurement of crushing strength is probably the

Table VII—Statistical Comparison for Data Shown in Table VI[a]

Comparison	Area (0–27 hr)	Peak Radioactivity
Cellulose *versus* colestipol hydrochloride	N.S.	N.S.
Cellulose *versus* cholestyramine	N.S.	$p < 0.05$
Colestipol hydrochloride *versus* cholestyramine	$p < 0.05$	$p < 0.05$
Water *versus* cellulose	$p < 0.05$	$p < 0.05$

[a] The p values indicate level of significance; N.S. indicates not significant.

tivity (1489 *versus* 1877 dpm), and serum radioactivity at 1, 2, and 4 hr were significantly reduced by cellulose treatment. These results may reflect the bulk effect of cellulose, which would increase stomach emptying time and delay entrance of the drug into the intestine, where presumably the major portion of digitoxin is absorbed.

Colestipol hydrochloride is an anion-exchange polymer that would be expected to bind with ionized drugs by electrostatic forces, although other forces such as hydrogen bonding, dipole–dipole interactions, van der Waals forces, nonelectrostatic interactions, and intermolecular attractions of like molecules may be important factors in the binding process. The concurrent administration of nicotinic acid and colestipol hydrochloride reduced peak radioactivity at the high dose of the polymer; total drug availability, as measured under the time–concentration curve, was reduced but did not vary significantly from the control. Competition for binding sites on the polymer with bile acid anions and inorganic physiological anions (*e.g.*, phosphate, chloride, and bicarbonate) present in the GI tract could possibly explain these results.

The early binding of warfarin and the subsequent release from the drug–polymer interaction by these competing forces could weaken the electrostatic attraction of colestipol hydrochloride and the drug. Similarly, cholestyramine (357.5 mg/kg) in rats significantly depressed the plasma warfarin levels at all time intervals during a 4-hr test (10). Further tests on plasma prothrombin times used to calculate the relative clot index, at time intervals for 4 days, indicated that, although cholestyramine may delay early absorption of warfarin, the pharmacological effect was not significantly altered by a single dose of the drug and the polymer.

However, significant differences were noted between cholestyramine and colestipol hydrochloride in interfering with hydrochlorothiazide or digitoxin absorption from the GI tract of the rat. Whether results in rats are predictive of results in humans remains to be determined.

REFERENCES

(1) T. M. Parkinson, K. Gundersen, and N. A. Nelson, *Atherosclerosis*, **11**, 531(1970).

(2) T. M. Parkinson, J. C. Schneider, Jr., and W. A. Phillips, *ibid.*, **17**, 167(1973).

(3) J. R. Ryan and A. Jain, *J. Clin. Pharmacol.*, **12**, 268(1972).

(4) E. Marmo, A. P. Caputi, S. Cataldi, and A. Amelio, *G. Arterioscler.*, **8**, 229(1970).

(5) C. J. Glueck, S. Ford, Jr., D. Scheel, and P. Steiner, *J. Am. Med. Assoc.*, **222**, 676(1972).

(6) E. R. Nye, D. Jackson, and J. D. Hunter, *N. Z. Med. J.*, **76**, 12(1972).

(7) D. S. Goodman, R. P. Noble, and R. B. Dale, *J. Clin. Invest.*, **52**, 2646(1973).

(8) W. A. Phillips, J. R. Schultz, and W. W. Stafford, *J. Pharm. Sci.*, **63**, 1097(1974).

(9) W. H. Johns and T. R. Bates, *ibid.*, **59**, 329(1970).

(10) D. G. Gallo, K. R. Bailey, and A. L. Scheffner, *Proc. Soc. Exp. Biol. Med.*, **120**, 60(1965).

(11) W. A. Phillips, W. W. Stafford, and J. Stuut, Jr., *ibid.*, **143**, 733(1973).

(12) G. W. Snedecor and W. G. Cochran, "Statistical Methods," 6th ed., Iowa State University Press, Ames, Iowa, 1967, p. 258.

(13) W. H. Johns and T. R. Bates, *J. Pharm Sci.*, **59**, 788(1970).

(14) A. A. Sinkula, *ibid.*, **63**, 842(1974).

(15) J. M. Thorp, *Lancet*, **1**, 1323(1962).

(16) H. J. Hahn, W. Eiden, M. Schettle, M. Hahn, E. Walter, and E. Weber, *Eur. J. Clin. Pharmacol.*, **4**, 142(1972).

(17) C. Harvengt and J. P. Desager, *ibid.*, **6**, 19(1973).

(18) D. F. Magee, "Gastro-intestinal Physiology," Charles C Thomas, Springfield, Ill., 1962, p. 144.

(19) G. T. Okita, *Fed. Proc.*, **26**, 1125(1967).

(20) N. J. Greenberger and F. B. Thomas, *J. Lab. Clin. Med.*, **81**, 241(1973).

ACKNOWLEDGMENTS AND ADDRESSES

Received May 22, 1975, from *Diabetes and Atherosclerosis Research, The Upjohn Company, Kalamazoo, MI 49001*

Accepted for publication November 4, 1975.

[x] To whom inquiries should be directed.

Effects of Film Coatings on Tablet Hardness

PHILIP W. STERN

Abstract □ The effects of five conventional film-coating materials on tablet hardness were studied. Placebos showed apparently linear increases in hardness as coatings were applied. Completely coated samples exhibited hardness increases from 50 to 140%, with a corresponding 3% increase in tablet weight. Equations were derived relating hardness changes to the "breaking strength" of the film on the tablet. Findings indicate that the coatings exert their influence primarily along the diameter of the tablet in a direction perpendicular to an applied compressional force. Furthermore, the coating process itself did not alter core hardness since tablets from which the film could be stripped showed original values.

Keyphrases □ Film coatings—five different, effects on tablet hardness □ Hardness, tablet—effects of five different film coatings □ Tablet hardness—effects of five different film coatings □ Dosage forms—tablets, effects of five different film coatings on tablet hardness

The term "tablet hardness" is widely used today in a nonspecific or generic manner as an all-inclusive description of several important tablet parameters. Included among these parameters are bending or attrition resistance and impact or crushing strength (1–4). Of the four, measurement of crushing strength is probably the

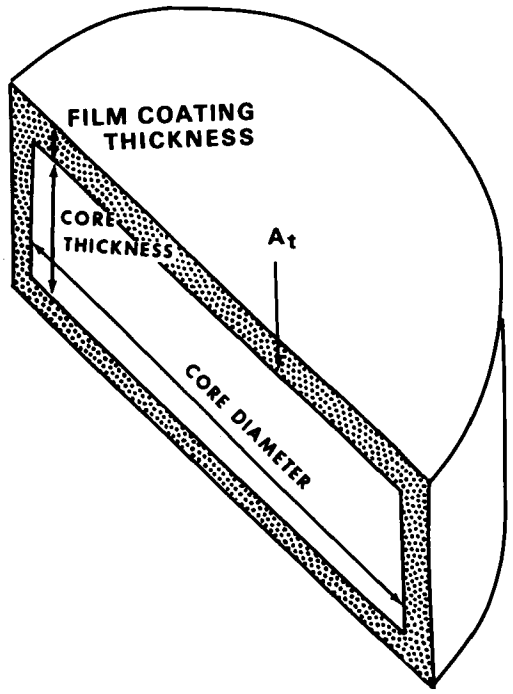

Figure 1—*Idealized cross-sectional view of film-coated tablet detailing the area of the film, A_t, subjected to tensile stress under transverse compression testing.*

most widely used to assess tablet integrity. Crushing strength may be defined as the minimal compressional force that, when diametrically applied to a tablet, causes it to fracture (4). Under exacting experimental conditions, the values associated with crushing strength may be interpreted as an indication of the tablet's tensile strength. Detailed studies have reported the use of transverse compression testing as a means of assessing tensile strength (5–7), but commercial products often possess shapes or heterogeneities that make quantification difficult.

Tablet hardness is known to be influenced by manufacturing methods, environmental conditions, and internal constituents. However, at a time when film-coated tablets have proliferated, comparatively little has been reported regarding the effects of thin film coatings on tablet hardness. Therefore, this study was undertaken to gain a mechanistic insight into the relationship between various film-coating materials and changes in tablet hardness that occur as a result of their application.

THEORY

Consider an uncoated round tablet core having an original hardness, H_o, with H_o determined by tensile failure along the tablet diameter. The hardness at any later time, t, then equals the original value plus the increase in hardness imparted by the film coat after a coating time of t. Therefore, the change in hardness at time t, ΔH_t, is the difference between two directly measurable quantities:

$$\Delta H_t = H_t - H_o \qquad \text{(Eq. 1)}$$

If one initially assumes that the tablet core is unaffected by the coating process, which will be verified, then any change in hardness is attributable to the film coat. Furthermore, from basic physical considerations, it is not unreasonable to assume that ΔH_t can be linearly related to the tensile strength, σ, of the film. In this case, the term A_t, the cross-sectional area of the film along the tablet diameter at time t over which a compressive testing force will manifest itself as tensile stress, can be introduced as the proportionality factor in:

$$\Delta H_t = \sigma A_t \qquad \text{(Eq. 2)}$$

Recently, Hiestand and Peot (7) detailed the difficulties in experimentally measuring true tensile strength values of tablets by diametral compression. Due to unequal stress distribution along a tablet's diameter and the possibility of brittle fracture or crack propagation, tablet failure may occur at values of applied stress below the true tensile strength. In addition to these considerations, three possible time sequences should be considered in the fracturing of a film-coated tablet: (*a*) concomitant fracture of the film and tablet at equal strain levels; (*b*) fracture of the tablet first, which immediately distributes the load to the film and breaks it; and (*c*) rupture of the film first, followed by tablet failure.

Under the experimental conditions reported in this study, discrimination among these three sequences was not possible, although the second seems most reasonable. In that case, the load at the instant of fracture produces enough tensile stress to fracture the core and

Table I—Solvent Systems for Coating Materials

Formula	Material	Percent (w/w)
1[a]	Hydroxypropyl methylcellulose[b]	5.0
	Methanol	30.0
	Methylene chloride	65.0
2	Ethylcellulose[c]	4.75
	Acetylated monoglyceride[d]	0.25
	Acetone	25.0
	Methylene chloride	70.0
3	Cellulose acetate phthalate[e]	4.75
	Triacetin[e]	0.25
	Methanol	20.0
	Acetone	75.0

[a] Formula 1 is used for hydroxypropyl cellulose (Klucel LF, Hercules Inc., Wilmington, Del.) and zein (Zein CG, Amcon Industries Inc., Buena Park, Calif.) also. [b] Methocel E-15 Premium, Dow Chemical Co., Midland, Mich. [c] Ethocel-10 cps, Dow Chemical Co., Midland, Mich. [d] Myvacet 9-40, DPI, Rochester, N.Y. [e] Eastman Kodak, Rochester, N.Y.

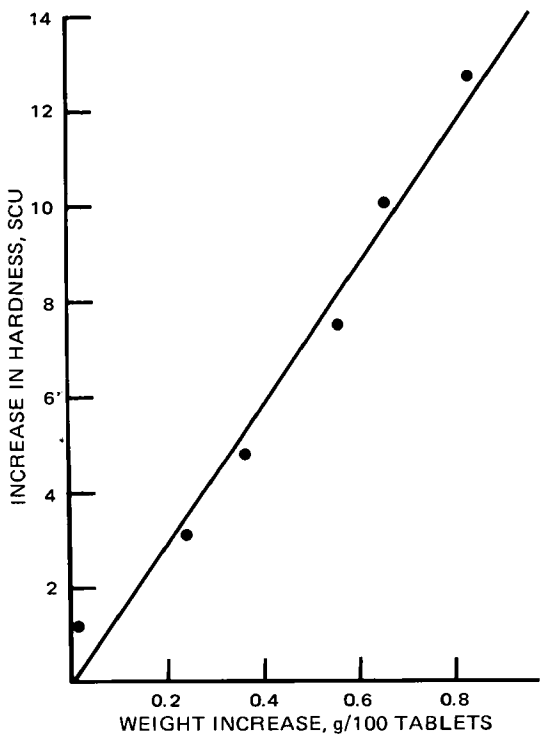

Figure 2—*Effect of hydroxypropyl methylcellulose film deposition on hardness values based on the measured increases in tablet weights.*

Table II—Hardness of Coated and Stripped Tablets

Material	Time after Coating	Average Hardness (±SD), SCU		
		Uncoated	Coated	Stripped
Hydroxypropyl methylcellulose	0.5 hr	9.1 (1.0)	22.4 (0.6)	7.7 (1.1)
	24 hr	8.1 (0.7)	22.5 (0.5)	7.0 (0.7)
	1 month	7.7 (0.9)	21.8 (1.6)	7.3 (1.1)
Ethylcellulose	0.5 hr	9.4 (1.0)	16.0 (2.0)	9.5 (0.9)
	24 hr	7.8 (0.6)	16.0 (1.5)	8.3 (0.9)
	1 month	7.5 (0.6)	14.6 (1.2)	7.6 (1.2)
Cellulose acetate phthalate	0.5 hr	9.4 (0.9)	15.4 (1.2)	9.1 (0.9)
	24 hr	8.4 (0.9)	17.5 (1.6)	8.1 (0.8)

partially stress the film. As the core breaks, the entire load must be absorbed by the film which then ruptures.

Because of the foregoing considerations, attempts to correlate measured hardness values quantitatively with the true tensile strength values of the film while on the tablet would be most difficult. Therefore, an effective "breaking strength" constant, k, was selected to serve as a measure of the stress to which the film was subjected. Substituting k for σ in Eq. 2 gives:

$$\Delta H_t = kA_t \qquad \text{(Eq. 3)}$$

An idealized graphic representation of A_t is given in Fig. 1. Combining Eqs. 1 and 3 gives a simple linear equation relating tablet hardness at any time to the breaking strength of the applied film:

$$H_t = kA_t + H_o \qquad \text{(Eq. 4)}$$

The term A_t can be calculated using Eq. 5:

$$A_t = \frac{RPt}{SD} \qquad \text{(Eq. 5)}$$

where R = gravimetric rate of film solids application per tablet, P = perimeter of the tablet along the breaking diameter, t = coating time, D = density of free dry film, and S = surface area per tablet. The term A_t can be further verified in some cases by directly measuring the thickness of the film coat when removed from a tablet. Substituting the right-hand side of Eq. 5 for A_t in Eq. 4 gives:

$$H_t = \frac{kRPt}{SD} + H_o \qquad \text{(Eq. 6)}$$

Equation 6 predicts that a plot of H_t *versus* coating time will be linear, with a slope proportional to k and intercept H_o. On the basis of this discussion, studies were designed and conducted to verify the applicability of these postulates to pharmaceutical coating systems.

EXPERIMENTAL

Materials—Five film-forming materials were selected for evaluation. Each was individually formulated in a compatible solvent system to produce a high quality film (Table I). A plasticizer was added to the formulation when the film former was too brittle for use alone. In all cases, the solids content of the solution was 5% (w/w).

Placebo tablets were made from a dicalcium phosphate (74%)–microcrystalline cellulose (20%)–starch (5%)–magnesium stearate (1%) direct compression mix and compressed on 0.874-cm diameter by 1.11-cm radius of curvature punches. Uncoated as well as coated cores prepared from this formulation consistently fractured cleanly along the diameter, indicating tensile failure during hardness testing.

Table III—Comparison of Tensile and Breaking Strength of Coating Materials

Coating Material	Tensile Strength of Free Film, kg/cm² (±SD)	Calculated Breaking Strength of Film on Tablet, kg/cm²
Hydroxypropyl methylcellulose	650 (65)	740
Zein	525 (80)	480
Cellulose acetate phthalate	505 (40)	410
Ethylcellulose	210 (55)	370
Hydroxypropyl cellulose	165 (15)	350

Fracture in this manner was necessary for applicability of the developed theory.

Free Films—Solutions described in Table I were spread on glass plates with an adjustable film-casting knife[1] to obtain free film samples for tensile strength measurements. The plates were allowed to air dry for 1 hr, after which film samples were cut with a scalpel and template designed such that the portion of the film at which the break was to occur was 0.5 cm wide. Typical samples were 0.02–0.08 mm thick, corresponding to the experimental film thickness on the coated placebo tablets. Tensile strength measurements[2] were made and values were calculated by dividing the force necessary to rupture the film by the original measured cross-sectional area of the film.

Film Coating—Coating experiments were carried out in a 61-cm baffled coating pan[3] rotating at 24 rpm and containing 15 kg of placebos. An automated airless spray system was used to control coating solution application from a pressure tank at approximately 85 psi through a 0.28-mm stainless steel nozzle orifice. The hydraulic pressure was adjusted slightly to equalize the delivery rates of the various coating solutions.

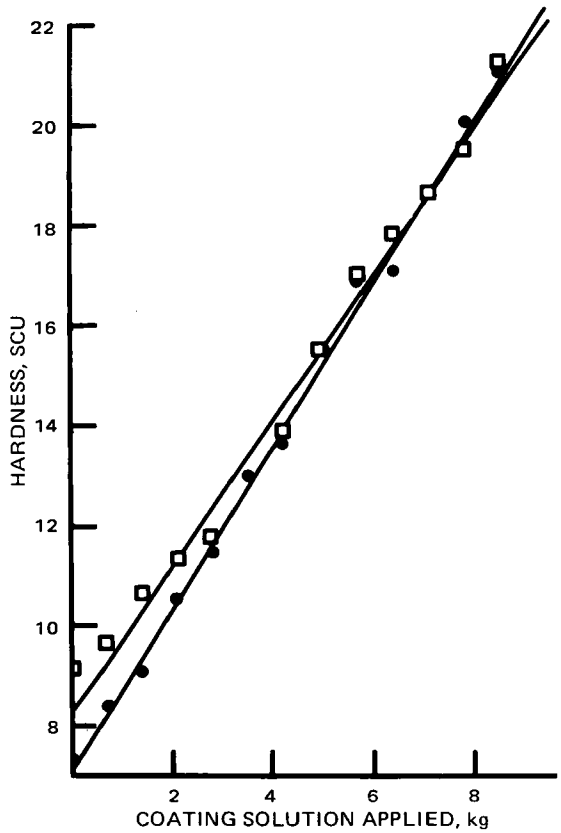

Figure 3—*Effect of time on hardness values of hydroxypropyl methylcellulose-coated tablets. Determinations were made 0.5 (□) and 24 (●) hr after coating.*

[1] Model AG-3820, Gardner Laboratory, Inc., Bethesda, Md.
[2] Instrom model TM, Instrom Corp., Canton, Mass.
[3] C. Skerman & Sons Ltd., London, England.

Table IV—Effects of Film-Coat Integrity and Orientation on Tablet Hardness

Material	Average Hardness (±*SD*), SCU				
	Uncoated Tablet	Coated Tablet	Film Cut Perpendicular to Applied Force	Film Cut Parallel to Applied Force	Film Cut Around Outside Edge
Hydroxypropyl methylcellulose	7.2 (0.4)	19.1 (2.1)	19.5 (1.7)	10.2 (1.0)	16.6 (0.6)
Cellulose acetate phthalate	7.2 (0.4)	16.8 (1.9)	14.9 (1.0)	8.3 (0.6)	15.5 (1.6)
Zein	7.2 (0.4)	14.8 (0.7)	14.8 (1.0)	8.0 (0.8)	14.3 (0.8)

Spraying operations were specifically performed in this low pressure region to minimize loss of material from spray drying and at the same time to promote uniform spreading of the solution on the tablet surface. Ten kilograms of each coating solution was applied over 130 min following a 10-sec spray–5-sec dry cycle. At appropriately selected times, samples were withdrawn and the hardness values of 10 tablets were measured[4].

RESULTS AND DISCUSSION

The increase in measured hardness values of the placebos due to hydroxypropyl methylcellulose film deposition is shown in Fig. 2. The maximum increase in tablet weight encountered in this study was approximately 3% of the original 0.292-g core weight, while the corresponding increase in hardness was 13 Strong-Cobb units (SCU) or 140% (1 SCU = 1.4 kg). From this result, it is apparent that a small amount of film-coating material on the tablet surface produced increases in hardness far exceeding estimates based on weight increases alone. To appreciate this finding, one should know that although the cross-sectional area of the tablet core along the diameter was approximately 0.2 cm^2 while the cross-sectional area of the film, A_t, at the same position on a fully coated tablet was approximately 0.013 cm^2, the film clearly dominated the hardness profile.

The effect of time on hardness measurements is shown in Fig. 3. The initial hardness determinations were made 0.5 hr after coating; another sample with the same amount of coating was evaluated after 24 hr of storage at coating room conditions of 24° and 40% relative humidity. It was generally observed that the hardness was slightly lower for the stored samples with low percentages of coating; those with greater coverage showed no changes with time. Overall, these time-dependent changes were considered to be of minimal importance, indicating that the films assume their final physical characteristics soon after coating ceases. Solvent penetration or entrapment appears to be insignificant.

In developing the theory, an initial assumption was made that any increase in measured hardness values was attributable to the film coat. This assumption directly implied that the tablet core was unaffected by the coating solvents or process. The data in Table II show the close agreement in hardness values between uncoated cores and coated cores from which the hydroxypropyl methylcellulose, ethylcellulose, or cellulose acetate phthalate coating had been carefully stripped. Hydroxypropyl cellulose and zein adhered tenaciously to the tablet surface and could not be removed without ruining the tablet. This observation that cores from which the film coat has been stripped exhibit hardness values equivalent to uncoated cores lends credence to the belief that the film alone is responsible for hardness changes.

The experimental data for hydroxypropyl methylcellulose, ethylcellulose, and hydroxypropyl cellulose coatings plotted in accordance with Eq. 6, *i.e.*, hardness *versus* time, are shown in Fig. 4. Here one can see the apparently linear increases in tablet hardness with coating time for each material. The standard deviations are shown only for hydroxypropyl methylcellulose but are representative of all five materials. The data for cellulose acetate phthalate and zein were separated from the other three sets for clarity (Fig. 5). Hydroxypropyl methylcellulose produced the most pronounced increase in hardness for a given amount of applied coating.

From the slopes of the least-squares regression lines, the breaking strength, k, of each film on the tablets was calculated using Eq. 6. These results are summarized in Table III and compared to the tensile strength values of the free films. Although significant quantitative differences exist between the breaking strength and tensile strength of a given film in some cases, which are not unexpected, the data do show rank-order correlation.

In all cases observed, when a coated or uncoated tablet fractured,

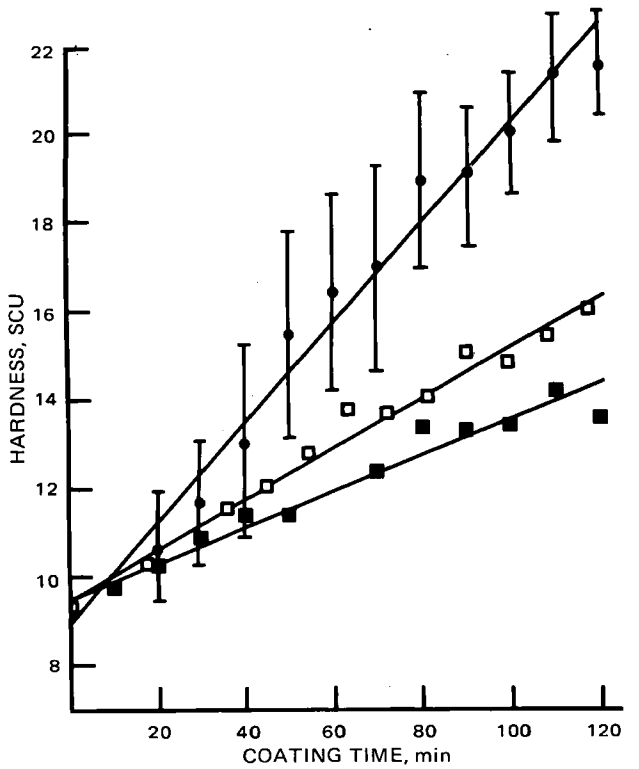

Figure 4—*Comparison of the increases in hardness for tablets coated with three cellulose-based coating materials. Key: ●, hydroxypropyl methylcellulose; □, ethylcellulose; and ■, hydroxypropyl cellulose.*

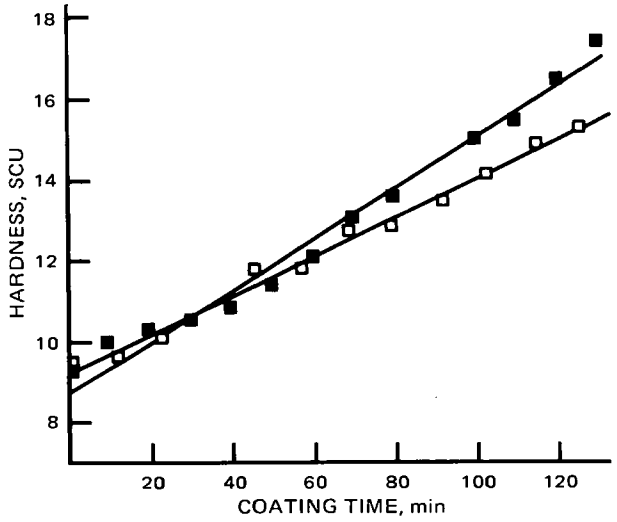

Figure 5—*Observed increases in tablet hardness for samples coated with zein (■) and cellulose acetate phthalate (□).*

[4] Heberlein tester, Cherry-Burrell Corp., Park Ridge, Ill.

it did so diametrically along a sharp line parallel to the direction of the applied force. It appears then that the film exerted its primary influence along this line under the test conditions employed. To verify this observation, cuts were carefully made with a scalpel through the coating along the diameter while other samples had cuts made around the circumference. The tablets with the cuts along the diameter were placed in the hardness tester such that the cut was either parallel or perpendicular to the applied force. Hardness measurements were made on these tablets (Table IV).

In cases where the cut was perpendicular to the applied force or the cut was around the outside edge, only minimal changes in hardness from intact coated tablets were observed. However, when the cut was aligned parallel to the applied force where normal tensile failure occurs, the film was unable to absorb any tensile stress and hardness values fell close to those for uncoated cores. These data support the use of the term A_t as the proportionality factor introduced in Eq. 2.

REFERENCES

(1) C. J. Endicott, W. Lowenthal, and H. M. Gross, *J. Pharm. Sci.*, **50**, 343(1961).

(2) H. J. Fairchield and F. Michel, *ibid.*, **50**, 966(1961).

(3) J. A. Seitz and G. M. Flessland, *ibid.*, **54**, 1353(1965).

(4) D. B. Brook and K. Marshall, *ibid.*, **57**, 481(1968).

(5) J. T. Fell and J. M. Newton, *J. Pharm. Pharmacol.*, **20**, 657(1968).

(6) J. T. Fell and J. M. Newton, *J. Pharm. Sci.*, **59**; 688(1970).

(7) E. N. Hiestand and C. B. Peot, *ibid.*, **63**, 605(1974).

ACKNOWLEDGMENTS AND ADDRESSES

Received August 18, 1975, from *Pharmaceutical Chemistry, Smith Kline & French Laboratories, Philadelphia, PA 19101*

Accepted for publication November 10, 1975.

The author thanks Mr. Robert Dolan for technical assistance.

Quantitative Precorneal Disposition of Topically Applied Pilocarpine Nitrate in Rabbit Eyes

THOMAS F. PATTON * and JOSEPH R. ROBINSON ˣ

Abstract □ The present study was designed to quantitate the influence of several precorneal factors on the disposition of topically applied ophthalmic drugs. With tritiated pilocarpine nitrate, methodology was developed for *in vivo* assessment of the relative contribution of tear turnover, instilled solution drainage, and nonproductive absorption to the loss of drug from the precorneal area. Studies were conducted in both awake and anesthetized rabbits whose drainage ducts were either unobstructed or plugged, and the loss of drug was monitored directly from the precorneal area or as appearance in the aqueous humor. By selective variation in experimental conditions, the influence of tear turnover, instilled solution drainage, and nonproductive absorption on ocular drug bioavailability was separately studied and quantitated. Instilled solution drainage was by far the largest contributing factor in the loss of drug from the precorneal area of the eye and, in the range of instilled volumes normally employed, tear turnover played a relatively minor role in drug loss. Compared to the cornea, precorneal tissue other than the cornea has a considerably greater surface area and thus is a potentially significant route for drug loss. However, under normal circumstances, loss by this route was minimal as compared to loss *via* instilled solution drainage.

Keyphrases □ Pilocarpine nitrate—topically applied, precorneal disposition, effect of tear turnover, instilled solution drainage, and nonproductive absorption □ Precorneal disposition—pilocarpine nitrate, topically applied, effect of tear turnover, instilled solution drainage, and nonproductive absorption □ Bioavailability—pilocarpine nitrate, topically applied, effect of tear turnover, instilled solution drainage, and nonproductive absorption □ Topically applied drugs—pilocarpine nitrate, precorneal disposition □ Ophthalmic drugs—pilocarpine nitrate, topically applied, precorneal disposition

Topical application of drugs to the eye is the most frequently employed route of administration for the treatment of various eye disorders. Unfortunately, the disposition of drugs administered by this route is not well understood, although it is generally agreed that the bioavailability of topically applied drugs is extremely poor. The present study was designed to provide a quantitative accounting of the precorneal distribution of pilocarpine nitrate and to generate some mechanistic insight into its relatively poor bioavailability.

Many factors can affect the bioavailability of topically applied ophthalmic drugs. The presence of tears in the cul-de-sac dilutes any instilled drug, and the continual addition and removal of tears can cause a significant loss of applied drug. In addition, the efficient drainage apparatus, used for removal of tears, also serves as a conduit through which instilled drug solutions can be lost from the precorneal area. Moreover, substances normally present in tear fluid can bind and/or degrade instilled drugs. Finally, topically applied drugs may be absorbed into a variety of ocular tissues, most notably the cornea and conjunctiva. To maximize therapy with topically applied ocular drugs, it is necessary to know the amounts and rates at which drugs are lost to these various precorneal routes and the relative contribution of each to the bioavailability question.

Numerous studies over the years were directed toward an understanding of tear properties, production, and drainage (1–20). However, only recently has attention been focused on the role of tear turnover and instilled solution drainage on ocular drug bioavailability (21). Studies describing some interactions of drugs with the components of tears also were reported (22, 23).

Topically applied drugs in the eye that are not lost to the drainage apparatus nor absorbed by the cornea are potentially available to be absorbed by the conjunctiva and, ultimately, the sclera or to be absorbed onto the lids. These routes are referred to as nonproductive, since it is unlikely that much or any drug from these areas will penetrate the interior portions of the eye due to rapid removal by local circulation (24–29).

The present study attempted to evaluate individually these routes of drug loss and to quantitate drug move-

it did so diametrically along a sharp line parallel to the direction of the applied force. It appears then that the film exerted its primary influence along this line under the test conditions employed. To verify this observation, cuts were carefully made with a scalpel through the coating along the diameter while other samples had cuts made around the circumference. The tablets with the cuts along the diameter were placed in the hardness tester such that the cut was either parallel or perpendicular to the applied force. Hardness measurements were made on these tablets (Table IV).

In cases where the cut was perpendicular to the applied force or the cut was around the outside edge, only minimal changes in hardness from intact coated tablets were observed. However, when the cut was aligned parallel to the applied force where normal tensile failure occurs, the film was unable to absorb any tensile stress and hardness values fell close to those for uncoated cores. These data support the use of the term A_t as the proportionality factor introduced in Eq. 2.

REFERENCES

(1) C. J. Endicott, W. Lowenthal, and H. M. Gross, *J. Pharm. Sci.*, **50**, 343(1961).

(2) H. J. Fairchield and F. Michel, *ibid.*, **50**, 966(1961).

(3) J. A. Seitz and G. M. Flessland, *ibid.*, **54**, 1353(1965).

(4) D. B. Brook and K. Marshall, *ibid.*, **57**, 481(1968).

(5) J. T. Fell and J. M. Newton, *J. Pharm. Pharmacol.*, **20**, 657(1968).

(6) J. T. Fell and J. M. Newton, *J. Pharm. Sci.*, **59**; 688(1970).

(7) E. N. Hiestand and C. B. Peot, *ibid.*, **63**, 605(1974).

ACKNOWLEDGMENTS AND ADDRESSES

Received August 18, 1975, from *Pharmaceutical Chemistry, Smith Kline & French Laboratories, Philadelphia, PA 19101*

Accepted for publication November 10, 1975.

The author thanks Mr. Robert Dolan for technical assistance.

Quantitative Precorneal Disposition of Topically Applied Pilocarpine Nitrate in Rabbit Eyes

THOMAS F. PATTON * and JOSEPH R. ROBINSON ˣ

Abstract □ The present study was designed to quantitate the influence of several precorneal factors on the disposition of topically applied ophthalmic drugs. With tritiated pilocarpine nitrate, methodology was developed for *in vivo* assessment of the relative contribution of tear turnover, instilled solution drainage, and nonproductive absorption to the loss of drug from the precorneal area. Studies were conducted in both awake and anesthetized rabbits whose drainage ducts were either unobstructed or plugged, and the loss of drug was monitored directly from the precorneal area or as appearance in the aqueous humor. By selective variation in experimental conditions, the influence of tear turnover, instilled solution drainage, and nonproductive absorption on ocular drug bioavailability was separately studied and quantitated. Instilled solution drainage was by far the largest contributing factor in the loss of drug from the precorneal area of the eye and, in the range of instilled volumes normally employed, tear turnover played a relatively minor role in drug loss. Compared to the cornea, precorneal tissue other than the cornea has a considerably greater surface area and thus is a potentially significant route for drug loss. However, under normal circumstances, loss by this route was minimal as compared to loss *via* instilled solution drainage.

Keyphrases □ Pilocarpine nitrate—topically applied, precorneal disposition, effect of tear turnover, instilled solution drainage, and nonproductive absorption □ Precorneal disposition—pilocarpine nitrate, topically applied, effect of tear turnover, instilled solution drainage, and nonproductive absorption □ Bioavailability—pilocarpine nitrate, topically applied, effect of tear turnover, instilled solution drainage, and nonproductive absorption □ Topically applied drugs—pilocarpine nitrate, precorneal disposition □ Ophthalmic drugs—pilocarpine nitrate, topically applied, precorneal disposition

Topical application of drugs to the eye is the most frequently employed route of administration for the treatment of various eye disorders. Unfortunately, the disposition of drugs administered by this route is not well understood, although it is generally agreed that the bioavailability of topically applied drugs is extremely poor. The present study was designed to provide a quantitative accounting of the precorneal distribution of pilocarpine nitrate and to generate some mechanistic insight into its relatively poor bioavailability.

Many factors can affect the bioavailability of topically applied ophthalmic drugs. The presence of tears in the cul-de-sac dilutes any instilled drug, and the continual addition and removal of tears can cause a significant loss of applied drug. In addition, the efficient drainage apparatus, used for removal of tears, also serves as a conduit through which instilled drug solutions can be lost from the precorneal area. Moreover, substances normally present in tear fluid can bind and/or degrade instilled drugs. Finally, topically applied drugs may be absorbed into a variety of ocular tissues, most notably the cornea and conjunctiva. To maximize therapy with topically applied ocular drugs, it is necessary to know the amounts and rates at which drugs are lost to these various precorneal routes and the relative contribution of each to the bioavailability question.

Numerous studies over the years were directed toward an understanding of tear properties, production, and drainage (1–20). However, only recently has attention been focused on the role of tear turnover and instilled solution drainage on ocular drug bioavailability (21). Studies describing some interactions of drugs with the components of tears also were reported (22, 23).

Topically applied drugs in the eye that are not lost to the drainage apparatus nor absorbed by the cornea are potentially available to be absorbed by the conjunctiva and, ultimately, the sclera or to be absorbed onto the lids. These routes are referred to as nonproductive, since it is unlikely that much or any drug from these areas will penetrate the interior portions of the eye due to rapid removal by local circulation (24–29).

The present study attempted to evaluate individually these routes of drug loss and to quantitate drug move-

ment and distribution in the precorneal portion of the eye.

EXPERIMENTAL

Materials—Pilocarpine nitrate USP was obtained commercially[1] and used without further purification. Tritiated pilocarpine[2] (specific activity 6.95 Ci/mmole) was purified by vacuum evaporation as previously described (30, 31). All other chemicals were either reagent or analytical grade and were used as received.

Male albino rabbits[3], 1.8–2.4 kg, were maintained on a normal diet, and no restrictions were placed on the amount of food or water consumed.

Methods—*Solution Preparation*—Pilocarpine nitrate solutions were prepared in isotonic Sorensen's phosphate buffer, pH 6.24 (32). In all studies, the concentration of pilocarpine nitrate employed was 1×10^{-2} *M*. No attempt was made to maintain the sterility of the solutions, but they were filtered for clarity. Solutions were prepared fresh and kept for a maximum of 48 hr. For each milliliter of 1×10^{-2} *M* pilocarpine nitrate to be prepared, 0.25 mCi of tritiated pilocarpine provided a final activity of 125,000–150,000 counts/min/μl. The small amount of isotopic material present did not affect the molarity of the final solution.

Anesthesia—Procedures for inducing and maintaining the desired level of general anesthesia were reported previously (21).

Blockage of Lacrimal and Instilled Fluid Drainage—In certain experiments, it was necessary to prevent instilled drug solution drainage through blockage of the drainage duct. While humans possess two puncta for drainage, rabbits have only one punctum, located deep in the inner surface of the lower lid near the medial canthus (33). Access to this punctum is difficult, and several methods of sealing it were attempted before the following procedure was adopted.

Polyethylene tubing[4] (PE 50), 0.61 mm i.d. and 0.96 mm o.d., was cut into sections approximately 5 mm in length. One end was cut into a bevel, and the other end was heat sealed. The beveled end was inserted into the punctum and threaded into the duct. The small cap which results from heat sealing serves to prevent the plug from slipping down into the duct and rests just at the surface of the punctum.

Care must be taken to ensure that the plug is inserted far enough so that the head does not protrude and scratch the cornea or conjunctiva. It was determined by the use of dye solutions that the plugs were effective in completely preventing any instilled solution drainage from the eye. It was also established that no drug was absorbed into the plugs.

Pilocarpine Nitrate Aqueous Humor Concentration–Time Profiles—In this series of experiments, four different categories of test animals were used: (*a*) normal unanesthetized rabbits, (*b*) unanesthetized rabbits whose drainage ducts had been plugged, (*c*) normal anesthetized rabbits, and (*d*) anesthetized rabbits whose drainage ducts had been plugged.

During the experiments, all test animals were kept in restraining boxes in the normal upright position. Twenty-five microliters of drug solution was instilled[5] onto the cornea of the test animal and collected in the lower cul-de-sac. In animals whose drainage ducts had been plugged, drug instillation was made 1 min after insertion of the plug. During instillation, the lower lid was pulled slightly away from the globe but was returned to its normal position immediately after instillation.

At various times postinstillation, rabbits were sacrificed by rapid injection of an overdose of pentobarbital sodium into a marginal ear vein. Eyes were immediately rinsed with distilled water and blotted with tissues to remove any residual radioactivity in the precorneal area. A single puncture then was made at the corneo-scleral junction, and 100–200 μl of aqueous humor was aspirated from the anterior chamber. One hundred microliters of aqueous humor was transferred[6] to a scintillation counting vial[7] containing 5 ml of liquid scintillation cocktail[8]. Vials containing the cocktail were refrigerated for 24 hr prior to addition of the samples; after addition of the samples, they were stored in the dark at room temperature for at least 24 hr prior to counting to minimize chemiluminescence.

Two consecutive 1-min counts were made[9] on each sample. Since quenching of radioactivity by aqueous humor was relatively constant from animal to animal, blank corrections were made on the basis of an aqueous humor sample from a single animal in each experiment. After suitable corrections, the counts were converted to micrograms per milliliter of aqueous humor.

The data were fit to a one-compartment open model, and graphical estimates of the parameters were obtained. The estimates were then subjected to computer analysis[10] to obtain final parameter values.

Loss of Pilocarpine Nitrate from Precorneal Area—Loss of drug directly from the precorneal area was determined by periodic sampling of the tear film following instillation of 25 μl of pilocarpine solution. Methodology for monitoring the loss of drug from the precorneal area of the eye had been developed previously (21), but such experiments had not been carried out for a drug that is absorbed into tissues.

Both awake and anesthetized animals were prepared in exactly the same manner as just described. In this series of experiments, however, only animals with drainage ducts plugged were employed. One minute after insertion of the plugs, pilocarpine solution was instilled. Fifteen seconds postinstillation, a 1-μl sample was withdrawn[11] from the tear film and assayed for drug content. The 15-sec time point was chosen to allow for mixing of the drug solution with the resident tear fluid and was designated as time zero. Additional samples were withdrawn at 5, 15, 30, 45, 60, and 90 min postinstillation. All samples were withdrawn from the center of the marginal tear strip.

Glass capillaries containing the 1-μl samples were dropped into 5 ml of scintillation cocktail and counted after 24 hr of storage. Procedures and preparation for liquid scintillation counting were identical to those previously described.

Data were converted to micrograms per milliliter of lacrimal fluid and analyzed *via* linear regression analysis. In so doing, it was possible to obtain first-order rate constants for the disappearance of drug from the precorneal area of the eye in both anesthetized and unanesthetized rabbits.

RESULTS

Aqueous Humor Concentration–Time Profiles—The concentrations of pilocarpine found in aqueous humor at various times postinstillation are compiled in Table I for the various categories of test animals. Examination of these data reveals that both anesthesia and the absence of drainage appear to result in more or less of an increase in the bioavailability of instilled pilocarpine solutions over that seen in unanesthetized animals with normal drainage function. Anesthesia significantly reduces or eliminates tear production in rabbits (21), so this experiment is a direct measure of the influence of lacrimation on ocular drug bioavailability. The purpose of the blocked drainage duct experiment is self-evident.

Analysis of the data in Table I produced the pharmacokinetic values shown in Table II. Two points are immediately evident when these data are inspected, specifically with regard to k_{abs}, FD/V, area, and peak time. Data for the duct open case show significant differences from those with the duct plugged, and, within a given category, either duct open or duct plugged, there is only a marginal, if any, difference in the parameter values. Areas under the aqueous humor drug concentration–time profiles reflect the differences in pilocarpine bioavailability for these experimental variations.

Measurement of Pilocarpine Nitrate Loss from Precorneal Pocket—An alternative approach to measuring drug appearance in aqueous humor is to measure its disappearance from the precorneal area of the eye. Since aqueous humor sampling presumably only measures drug that has penetrated the cornea, sampling of drug in the precorneal pocket should provide a measure of the loss of drug to other precorneal routes as well. This sampling procedure has the inherent disadvantage that, since the normal resident volume in the precorneal area is small, removal of even the smallest usable sample appreciably disturbs the system unless it is replaced. However, replacing the withdrawn volume can change the fluid dynamics in this area and is therefore undesirable. In addition, since the volume is so

[1] Merck and Co., Rahway, N.J.
[2] New England Nuclear, Boston, Mass.
[3] Klubertanz, Edgerton, Wis.
[4] Intramedic, Clay Adams Division of Becton Dickinson Co., Parsippany, N.J.
[5] Hamilton Co., Reno, Nev.
[6] Biopette, Schwarz/Mann, Orangeburg, N.Y.
[7] Mini vials, ICN, Irvine, Calif.
[8] Aquasol, New England Nuclear, Boston, Mass.
[9] Packard model 2002, Packard Instruments Co., Downers Grove, Ill.
[10] Madison Academic Computing Center Subroutine NREG.
[11] Microcap, Drummond Scientific Co., Bloomfield, N.J.

Table I—Aqueous Humor Concentration–Time Profiles following Instillation of 25 μl of a 1 × 10^{-2} *M* Solution of Pilocarpine Nitrate

Minutes	Micrograms of Pilocarpine per Milliliter of Aqueous Humor			
	Unanesthetized Duct Open	Unanesthetized Duct Plugged	Anesthetized Duct Open	Anesthetized Duct Plugged
5	0.34 (0.02)[a] [18][b]	0.38 (0.06) [8]	0.36 (0.05) [6]	0.70 (0.07) [6]
10	0.72 (0.09) [15]	0.82 (0.07) [8]	1.15 (0.22) [8]	1.53 (0.09) [7]
15	0.73 (0.06) [17]	1.33 (0.12) [8]	0.97 (0.10) [7]	1.81 (0.15) [6]
20	1.03 (0.08) [19]	1.66 (0.14) [7]	1.05 (0.14) [8]	1.79 (0.11) [7]
30	0.72 (0.07) [19]	2.16 (0.12) [7]	1.45 (0.30) [6]	2.40 (0.29) [6]
45		1.88 (0.18) [8]	0.70 (0.17) [7]	2.04 (0.33) [7]
60	0.62 (0.06) [15]	2.58 (0.38) [11]	0.51 (0.13) [5]	1.57 (0.24) [5]
75		1.70 (0.21) [6]		
90	0.26 (0.02) [14]	1.22 (0.22) [11]	0.65 (0.13) [10]	1.10 (0.17) [8]
105		1.00 (0.24) [6]		
120	0.12 (0.01) [7]	0.77 (0.23) [8]	0.19 (0.02) [6]	1.01 (0.22) [5]

[a] Numbers in parentheses refer to standard error of the mean. [b] Numbers in brackets refer to the number of determinations at that time point.

small and diffuse, withdrawing samples is quite difficult and can result in substantial irritation to the eye with subsequent lacrimation.

Due to these considerations, samples were withdrawn following the instillation of pilocarpine nitrate solutions only in rabbits whose drainage ducts had been plugged. Blockage of the drainage duct causes the instilled solution, after mixing with the resident tear fluid, to form a "pool" on the lower marginal tear strip. This makes withdrawal of 1-μl samples a relatively easy procedure and does not result in irritation to the eye. Also, the removal of several 1-μl samples over 90 min does not appreciably change the volume present, especially in awake animals whose normal tear production more than compensates for the withdrawal rate.

Withdrawal of 1-μl fluid samples from the precorneal area of rabbits with occluded drainage ducts at various times postinstillation revealed a first-order decline in drug concentration. Drug concentrations were plotted semilogarithmically *versus* time and subjected to linear regression analysis, and first-order rate constants were determined. Tables III and IV show the results of these studies. The data show good reproducibility both within and among rabbits and no significant variations due to either the eye used or the weight of the animal.

The first-order loss of drug from the precorneal area in the absence of drainage accounts for the loss of drug to all routes including conjunctival and corneal except drainage. It is necessary, however, to account for the difference in the observed rate constants between awake and anesthetized rabbits. Rabbits under systemic anesthesia of the type employed here do not produce tears (21). It is suggested that the larger rate constant for the decline in precorneal drug concentration in awake rabbits can be attributed to the dilution effect of incoming tears.

The rate of tear production in normal unanesthetized rabbits was determined (21) to be 0.66 μl/min. Using this rate enables one to calculate the dilution effect of tears for a given initial concentration of drug in the precorneal area in the absence of drainage. Table V illustrates the calculated dilution effect of tears on precorneal drug concentration following instillation of 25 μl of drug solution in rabbits whose drainage apparatus has been blocked.

This first-order decline in drug concentration has an associated rate constant of 1.16 × 10^{-2} min^{-1}. If this rate constant is added to that obtained for the decline in drug concentration in anesthetized rabbits with drainage ducts plugged (2.17 × 10^{-2} min^{-1}), the sum is 3.33 × 10^{-2} min^{-1}. This number is virtually identical to that obtained in awake rabbits where both absorption and dilution by tears are operable. Similarly, if one calculates the theoretical decline in precorneal drug concentration as a result of both absorption and tear production,

Table II—Pharmacokinetic Parameters for Topically Applied Pilocarpine Nitrate Solution[a]

Parameter	Unanesthetized Duct Open	Unanesthetized Duct Plugged	Anesthetized Duct Open	Anesthetized Duct Plugged
k_{abs}, min^{-1} [b]	7.80 × 10^{-2} (4.75 × 10^{-2}–1.08 × 10^{-1})	2.83 × 10^{-2} (2.00 × 10^{-2}–3.66 × 10^{-2})	8.31 × 10^{-2} (3.41 × 10^{-2}–1.32 × 10^{-1})	4.44 × 10^{-2} (3.38 × 10^{-2}–5.50 × 10^{-2})
K_{el}, min^{-1}	2.00 × 10^{-2}	2.00 × 10^{-2}	2.00 × 10^{-2}	2.00 × 10^{-2}
$\frac{FD}{V}$ [b]	1.39 (1.15–1.62)	4.81 (4.10–5.52)	1.81 (1.38–2.24)	4.23 (3.74–4.73)
Area[c]	69.5	240.5	90.5	211.5
Peak time[d], min	20–25	35–40	20–25	35
r-squared for function[e]	0.978	0.973	0.943	0.988
Correlation coefficient for function	0.963	0.952	0.889	0.968

[a] Obtained by fitting the data to the one-compartment open model *via* the computer program NREG. In all cases, the program was modified by fixing K_{el} prior to computer analysis. This procedure was necessary due to the closeness of k_{abs} to K_{el} in cases where drainage ducts were plugged. In these cases, the program was not able to distinguish between k_{abs} and K_{el} and continually set them equal. This approach was justified since extensive prior experience had confirmed that the value for K_{el} was about 2 × 10^{-2} min^{-1}. [b] Numbers in parentheses refer to the 95% confidence limits of the computer-generated values. [c] Area = FD/VK_{el}. [d] Approximate values read from the graphical printout of the computer-generated fit of the model. [e] r^2 = (Σ squared observations − Σ squared derivations)/Σ squared observations.

Table III—First-Order Rate Constants for the Decline in Drug Concentration in the Precorneal Area of Awake Rabbits with Drainage Ducts Plugged

Rabbit	Weight[a], kg	Eye	k, min^{-1}[b]	Correlation Coefficient for Line
1	1.9	Right	2.64×10^{-2}	0.968
	2.0	Right	3.61×10^{-2}	0.985
	1.9	Left	5.36×10^{-2}	0.957
	2.0	Left	2.94×10^{-2}	0.934
2	1.7	Right	2.66×10^{-2}	0.869
	2.1	Right	3.09×10^{-2}	0.914
	1.7	Left	4.82×10^{-2}	0.946
	2.1	Left	3.26×10^{-2}	0.942
3	2.1	Right	2.30×10^{-2}	0.974
	2.1	Right	2.64×10^{-2}	0.886
	2.1	Left	3.10×10^{-2}	0.978
	2.1	Left	3.42×10^{-2}	0.975
Mean k(min^{-1}) = 3.32×10^{-2} (2.64×10^{-3})[c]				

[a] Weights may vary for the same animal due to the time interval between reuse. [b] Calculated from the slope of the line determined *via* linear regression analysis. [c] Number in parentheses refers to the standard error of the mean.

the resulting first-order rate constant is in exact agreement with that found experimentally in Table III. This result is illustrated in Table VI. It is, therefore, confirmed that the larger rate constant for the decline in precorneal drug concentration in unanesthetized rabbits can be attributed to tear production.

In interpreting the results of the tear sampling studies, two other problems deserve comment. The first problem involves separating the observed drug loss into its component parts. In other words, absorption can occur *via* the cornea and into the anterior chamber, *i.e.*, productive absorption, or *via* the conjunctiva from where drug may enter the general circulation, *i.e.*, nonproductive absorption. The tear sampling studies demonstrated the overall loss of drug due to absorption from the precorneal area. To gain a complete quantitative picture, it is necessary to discuss these absorptive routes separately.

The second problem is that of extrapolating the results of the precorneal drug concentration decline in animals with plugged drainage ducts to the precorneal drug loss in normal rabbits. An independent measurement of precorneal drug concentrations in animals with normally functioning lacrimal drainage systems was not possible for reasons mentioned previously; therefore, the extension of these results to normal rabbits is of concern. However, both problems can be resolved with available data.

The first problem appears easily resolved by simply considering the amount of drug reaching the aqueous humor *via* corneal absorption. Table VII shows a summary of calculations for the amount of drug absorbed into the anterior chamber based on the parameters of Table II. Even in the largest case, only 1.44 μg or 2.12% of the instilled dose reaches the anterior chamber *via* corneal absorption. If one refers to the tear sampling studies and specifically to Table VI, it can be seen that absorption can account for a substantial loss of drug from the precorneal area. In fact, the amount of drug absorbed by the corneal (productive) route is insignificant when compared with the overall absorptive loss of drug. This finding indicates that, for all practical

Table IV—First-Order Rate Constants for the Decline in Drug Concentration in the Precorneal Area of Anesthetized Rabbits with Drainage Ducts Plugged

Rabbit	Weight, kg	Eye	k, min^{-1}[a]	Correlation Coefficient for Line
4	2.4	Right	2.19×10^{-2}	0.988
		Left	1.87×10^{-2}	0.973
5	2.0	Right	2.24×10^{-2}	0.913
		Left	2.12×10^{-2}	0.903
6	2.2	Right	2.96×10^{-2}	0.922
		Left	1.64×10^{-2}	0.882
Mean k(min^{-1}) = 2.17×10^{-2} (1.83×10^{-3})[b]				

[a] Calculated from the slope of the line determined *via* linear regression analysis. [b] Number in parentheses refers to the standard error of the mean.

Table V—Calculated Dilution Effect of Tears on Precorneal Drug Concentration following Instillation of 25 μl of a 1×10^{-2} *M* Pilocarpine Nitrate Solution into Eyes of Rabbits Whose Drainage Apparatus Has Been Blocked

Minutes	Amount of Drug Present, μg[a]	Volume of Fluid Present, ml[b,c]	Concentration of Drug, μg/ml
0	67.82	0.0325	2087
5	67.82	0.0358	1894
15	67.82	0.0424	1600
30	67.82	0.0523	1297
45	67.82	0.0622	1090
60	67.82	0.0721	941
90	67.82	0.0919	738
k(min^{-1})[d] = 1.16×10^{-2}			

[a] No drug is lost *via* drainage, and it is assumed that no absorption takes place in this case. [b] Initial volume is based on the normal resident volume of the rabbit eye, 7.5 μl, plus the instilled volume of 25 μl. Subsequent volumes are calculated on a rate of tear production of 0.66 μl/min. [c] It is assumed that no volume is lost due to evaporation. [d] Calculated from the slope of the line obtained by linear regression analysis.

purposes, the tear sampling studies measured only the loss of drug to the nonproductive route with an absorption rate constant of 2.17×10^{-2} min^{-1}. An implicit assumption is that drug penetrates to the anterior chamber only by corneal absorption.

Extrapolation of the results of the tear sampling studies to rabbits with unobstructed drainage ducts can be accomplished if the kinetics of the absorptive process are considered. If normal instilled solution drainage had been a factor in the tear sampling studies, large amounts of instilled drug would be lost to the drainage apparatus, leaving much less drug available for absorption. However, this would not affect the rate constant for nonproductive absorption—only the amount absorbed.

In addition to decreasing the amount of drug available for absorption, drainage reduces the volume present in the eye. Therefore, incoming tears have a more substantial effect on the concentration of drug in the precorneal area. The effect of the decreased concentration caused by the dilution by tears is a decreased rate of nonproductive absorption but an unchanged rate constant. Thus, the rate constant of 2.17×10^{-2} min^{-1} for nonproductive absorption is applicable to normal rabbits as well as to those with their drainage ducts plugged provided that the mechanism of pilocarpine absorption does not change.

DISCUSSION

Precorneal Drug Distribution in Normal Unanesthetized Rabbits—Instilled drug solution may be lost from the precorneal area

Table VI—Calculated Concentrations of Pilocarpine Nitrate in the Precorneal Area of the Eye following Instillation of 25 μl of a 1×10^{-2} *M* Solution which is Both Absorbed and Diluted by Tears in Rabbits Whose Drainage Apparatus Has Been Blocked

Minutes	Amount of Drug Present, μg[a]	Volume of Fluid Present, ml[b,c]	Concentration of Drug, μg/ml
0	67.82	0.0325	2087
5	60.85	0.0358	1700
15	48.98	0.0424	1155
30	35.37	0.0523	676
45	25.54	0.0622	411
60	18.45	0.0721	256
90	9.62	0.0919	105
k(min^{-1})[d] = 3.32×10^{-2}			

[a] No drug is lost *via* drainage, but loss occurs by a first-order absorption process with a rate constant of 2.17×10^{-2} min^{-1}. [b] Initial volume is based on the normal resident volume of the rabbit eye, 7.5 μl, plus the instilled volume of 25 μl. Subsequent volumes are calculated on a rate of tear production of 0.66 μl/min. [c] It is assumed that no volume is lost due to evaporation. [d] Calculated from the slope of the line obtained by linear regression analysis.

Table VII—Total Amount of Drug Appearing in the Aqueous Humor of Rabbits following Instillation of 25 μl of a 1×10^{-2} *M* Pilocarpine Nitrate Solution

Parameter	Unanesthetized Duct Open	Unanesthetized Duct Plugged	Anesthetized Duct Open	Anesthetized Duct Plugged
$\frac{FD}{V}$	1.39	4.81	1.81	4.23
F^a	6.15×10^{-3}	2.13×10^{-2}	8.01×10^{-3}	1.87×10^{-2}
Amount of drug absorbed[b], μg	0.42	1.44	0.54	1.27
Percent of instilled dose absorbed	0.62	2.12	0.80	1.87

[a] Calculated based on an instilled dose (D) of 67.82 μg and an aqueous humor volume (V) of 0.30 ml. [b] Amount = FD.

of the eye by any of several routes, *e.g.*, instilled solution drainage, tear turnover, corneal absorption, and nonproductive absorption. Following instillation, fluid is lost by drainage until the volume returns to the normal resident volume of 7.5 μl (21). Instilled solution drainage does not affect the concentration of drug present—only the amount—whereas absorption affects both the concentration and amount.

Instilled solution drainage is only operative until the volume in the eye returns to its normal resident volume. After this time, the volume remaining in the eye is constant and drug is lost *via* absorption and by the removal of 0.66 μl of solution/min. Drug concentration will be affected by absorption and by the dilution effect of incoming tears, with the net result that both the amount and concentration of pilocarpine nitrate in the precorneal area will decline in a biphasic fashion. Initially, the amount of drug decreases very rapidly due to drainage, while concentration declines more slowly, influenced only by absorption and tear turnover. As the volume in the eye returns to its normal level, the amount of drug present declines more slowly since drainage is no longer a factor. On the other hand, concentration now declines more rapidly due to the dilution effect of incoming tears.

When using these arguments, it is possible to comment on the effects of changing the volume or the concentration of the instilled drug solution. Varying the concentration of instilled drug solution changes the absolute values of both the concentration and amount of drug in the precorneal area at any time but probably does not change the pattern in which they decline. The more important consideration is the variation of instilled solution drainage with the variation in the instilled volume. This information is available (21), and it is known that the drainage rate varies linearly with the instilled volume over a wide range of instilled volumes. Thus, the initial decline in the amount of drug in the precorneal area is greater than the larger instilled volume. Once the volume returns to normal, however, the decline should be identical, regardless of the instilled volume.

Precorneal Drug Distribution in Unanesthetized Rabbits with Drainage Ducts Plugged—Blockage of the drainage canal eliminates instilled solution drainage as a source of drug loss from the precorneal area. Thus, solution volume in the eye, rather than decreasing to the normal resident tear volume, increases at a constant rate of 0.66 μl/min. Also, in contrast to unanesthetized normal rabbits, both the amount and concentration of drug decrease in a monophasic rather than biphasic fashion. In this case, the decline in concentration occurs at a faster rate than does the decline in amount due to the dilution effect of incoming tears.

Changing either the concentration or the volume instilled has no effect on the rate constant for nonproductive absorption. Likewise, simply changing the concentration of the instilled drug solution changes the absolute values of the concentration at any time but not the rate constant for the decline in concentration. However, the rate constant for the decline in concentration becomes larger as the instilled volume is decreased due to the greater dilution effect of the incoming tears on smaller volumes. Theoretically, if the instilled volume were large enough, limited, of course, by the capacity of the precorneal area to hold a given dose, incoming tears would have no effect on the concentration of drug, and the rate constant for the decline in concentration would be identical to that for the decline in amount, namely, $k_n = 2.17 \times 10^{-2}$ min^{-1}.

Precorneal Drug Distribution in Anesthetized Rabbits with Drainage Ducts Obstructed—There exist two distinct differences between rabbits under general anesthesia and awake rabbits with regard to the movement and distribution of instilled drug solutions. First, anesthetized rabbits do not produce tears (21); second, although instilled solution drainage does occur, it occurs at a considerably reduced rate.

In addition to the fact that the drainage of an instilled solution is considerably different in anesthetized and unanesthetized rabbits, it is important to note that there is no instilled volume dependency in drainage of fluid from the eye of anesthetized animals (21). Thus, the drainage rate constant, $k_d = 1.77 \times 10^{-1}$ min^{-1}, for anesthetized animals remains constant regardless of instilled volume. Moreover, the normal lacrimal volume is considerably larger in anesthetized than in unanesthetized rabbits. This higher value is probably due to relaxation of the eye muscles under anesthesia to accommodate a larger volume (21).

The volume remaining, amount remaining, and concentration at any time postinstillation in anesthetized rabbits should be considered. As was the case with unanesthetized rabbits, the amount decreases in a biphasic fashion. The initial decline in amount is considerably slower than that observed in unanesthetized rabbits but still greater than the initial decline in concentration. Concentration can only be changed by absorption of drug and, therefore, declines at a single rate governed by k_n. As such, the terminal decline in amount has the same slope as that for concentration. The rate constant for the decline in concentration is unaffected by changes in either the concentration or the volume instilled. Since k_d remains invariant with the volume instilled, the decline in amount also is unaffected by changing the volume; only the magnitude of the amounts varies by altering the concentration of the instilled solution.

Precorneal Drug Distribution in Anesthetized Rabbits with Drainage Ducts Plugged—The final category of rabbits employed in these studies consisted of rabbits under general anesthesia whose drainage ducts had been blocked. Neither tear production nor instilled solution drainage is operative in this case; therefore, they do not contribute to precorneal drug loss.

As noted previously with awake animals whose drainage ducts had been plugged, since there is no instilled solution drainage, both concentration and amount decline in first-order fashion and do not exhibit the biphasic decline observed when drainage is operative. Since, in addition to no drainage, there is also no tear production, the volume in the eye remains constant throughout. The result is that both concentration and amount decline with the same rate constant. This rate constant is simply the rate constant for absorption, $k_n = 2.17 \times 10^{-2}$ min^{-1}. Finally, the rate constants for the decline in both concentration and amount are unaffected by changing either the concentration or the volume of the instilled solution.

Precorneal Effects on Ocular Drug Bioavailability—If one examines the areas under the aqueous humor concentration–time profiles shown in Table II for the four categories of rabbits studied, some general comments can be made on the relative influence of precorneal factors on ocular drug bioavailability. Drainage apparently is the overwhelming factor in causing bioavailability differences for instilled drug solutions. In both anesthetized and unanesthetized rabbits, blocking the drainage duct results in considerable increases in bioavailability over cases in which instilled solution drainage is operative.

In animals whose drainage ducts were plugged, the unanesthetized animals gave bioavailabilities slightly higher than the anesthetized rabbits. At first this may seem surprising because no tears are being produced in the anesthetized rabbits. If the dilution effect of tears were a controlling factor in determining bioavailability, one would expect more drug to reach the aqueous humor of anesthetized rabbits. This is not the case, however, which seems to minimize the influence of tear production on ocular drug bioavailability. The difference in

the amount of drug reaching the anterior chamber can be explained by the fact that the initial drug concentration is smaller in anesthetized rabbits due to their larger resident tear volume.

Consider also that anesthetized rabbits show only a slight increase in bioavailability over unanesthetized rabbits in spite of a large difference in the drainage rate constant, k_d, and the fact that tear production is absent. It is already known that for a constant initial concentration and a normal rate of tear production (compare unanesthetized rabbits with drainage duct open and plugged), elimination of drainage significantly increases bioavailability. The small magnitude of the bioavailability increase observed in anesthetized rabbits over unanesthetized rabbits can be attributed to the decreased initial concentration in anesthetized animals. What appears to be happening is that the increase expected from decreasing drainage is being minimized by the lower initial concentration. This finding illustrates the important role played by the initial concentration of drug in the precorneal tear film in determining ocular drug bioavailability.

It is also confirmed that tear production appears to have a minimal influence on ocular drug bioavailability. Tear production would probably become a controlling influence only if its rate were significantly increased, by irritating the eye, for example, or if the instilled volume were very small. In the absence of these special circumstances, instilled solution drainage and the initial concentration of drug in the precorneal tear film appear to be the most important precorneal influences on ocular drug bioavailability.

In addition to these observations, some correlations can be made which, within limits, have predictive capabilities for determining the amount of an instilled dose of pilocarpine expected to reach the aqueous humor under various conditions. These correlations were reported elsewhere.

Several complicating factors make a mechanistic understanding of pilocarpine transport in the eye much more difficult than it initially appears. For example, in normal, unanesthetized rabbits, drainage accounts for the loss of as much as 75% of the instilled drug within 5 min after instillation of a 25-μl dose. One would intuitively expect that inhibiting this drainage loss would dramatically improve aqueous humor levels of drug simply by virtue of the improved contact time of the drug with the corneal membrane. That this is not the case can be illustrated as follows.

In normal, unanesthetized rabbits, instillation of 25 μl of 1×10^{-2} M pilocarpine, 67.82 μg, results in a total of 0.42 μg of drug being recovered in the aqueous humor. If drainage is inhibited, only 1.44 μg of drug reaches the aqueous humor. This unexpectedly small bioavailability increase was observed repeatedly in cases where viscous solutions were used to improve contact time of drug in the precorneal area (31, 34–36). At least as far as pilocarpine is concerned, for a given concentration, ocular contact time has only a very limited role in influencing the amount of drug reaching the anterior chamber unless the drug can be restricted to essentially the corneal area such as might occur with contact lenses impregnated with drug. This finding emphasizes the limited utility of viscous polymer solutions, which is common practice in ophthalmic formulations. Although the use of such formulations has some effect on ocular drug bioavailability, the ultimate solution to the problem is much more complicated than simply delaying drainage.

A second unexpected result that indicates a more complicated picture than would be expected is the variation in the absorption rate constants determined from the aqueous humor concentration–time profiles. As discussed previously, this rate constant is taken to represent the rate constant for the penetration of drug into the aqueous humor from the cornea. In both unanesthetized and anesthetized rabbits where the drainage ducts are plugged, the value of this rate constant is approximately one-half of that observed in those two cases where drainage is not obstructed.

When assuming that the rate constant remains first order, which it does, there are only two kinetic explanations for this shift in peak time and the resultant decrease in the rate constant. The first is that the larger rate constant is not a single rate constant but a sum of rate constants, indicating that drug is entering the aqueous humor by one or more additional routes in animals with open drainage ducts. This would have to be accounted for by drug reaching the anterior chamber from systemic circulation. Unpublished results from this laboratory showed that with the concentration and amounts of drug employed here, no drug that reaches the systemic circulation *via* drainage loss can be detected in the aqueous humor, at least within the time course of these studies.

The alternative explanation for the decrease in the rate constant is a change in the mechanism of the absorptive process, either by some alteration of the membrane or by another unknown process. It is this latter case that must be responsible for the shift in the peak aqueous humor concentration to later times in rabbits whose drainage ducts are plugged.

Some seemingly anomalous results of these studies can now be accounted for in light of some current work being conducted in this laboratory. Studies involving rinsing of the drug solution from the precorneal area of the eye at various times postinstillation have been conducted. Preliminary results indicate that if 25 μl of 1×10^{-2} M pilocarpine is instilled into the eyes of normal rabbits and then rinsed from the eye at anywhere from 2 to 5 min postinstillation, the aqueous humor concentration–time profile remains virtually identical to that reported here for unanesthetized, normal rabbits. There are two important implications of these findings for discussion purposes:

1. In rabbits with normal drainage function, the first few minutes postinstillation represent the critical period for drug uptake by the cornea.
2. A very rapid binding or equilibrium of pilocarpine with either the cornea or possibly the protein-rich mucin layer, which forms a protective film over the cornea, is indicated.

There is also preliminary evidence to indicate that a kinetic explanation for the observed peak shift can be made by considering a rapid parallel elimination step from the absorption depot.

Quantitation of corneal drug uptake is under study and will be reported later. Further speculation on the mechanism of the uptake and transport of pilocarpine by the cornea would be premature.

The observations reported here apply only to one drug, pilocarpine. In some respects, precorneal movement, for example, instilled solution drainage is not necessarily a function of the drug involved. However, with other factors such as absorption rate constants and mechanisms of transport, the specific drug obviously will be critical.

SUMMARY

Instilled solution drainage, tear production, and absorption have all been shown to be contributing factors in the movement and distribution of drugs in the precorneal area of the eye. The relative magnitude of each of these effects has been isolated and quantitated for the drug pilocarpine nitrate, and *in vivo* methodology has been established so that other drugs may also be investigated. In examining the effects of these precorneal factors on ocular drug movement and distribution, it is necessary to be mindful of the way in which both the amount and concentration of drug in the precorneal area are affected.

Despite the fact that loss of an instilled drug solution from the precorneal area is rapid and of considerable magnitude, the contact time of pilocarpine nitrate in this area has only modest effects on the amount of drug reaching the anterior chamber. Complete elimination of drainage of an instilled pilocarpine nitrate solution resulted in less than a 3.5-fold increase of drug reaching the aqueous humor. However, the initial concentration of drug in the tear film can have a tremendous effect on the amount of drug reaching the anterior chamber.

From studies in which the initial concentration, the drainage rate, and the rate of tear production were varied, either independently or simultaneously, it was possible to make some correlations as to the relative influence of their effects. Within limits, these correlations appear to have predictive capabilities for determining the relative bioavailability of pilocarpine nitrate in different concentrations and volumes of solutions.

By considering that instilled solution drainage is volume dependent, it becomes obvious that tremendous quantities of drug are wasted when large volumes, as are used commercially, are instilled into the eye. In fact, these large volumes are not only wasted but are potentially harmful, since drug lost to the drainage apparatus is potentially available to act systemically. On this basis, a much more rational approach to topical ophthalmic drug therapy would be a smaller instilled volume and a somewhat larger drug concentration. For example, 5 μl of 1.92×10^{-2} M pilocarpine nitrate provides the same initial concentration of drug in the tear film as 25 μl of 1×10^{-2} M. The 5-μl dose, however, contains more than 2.5 times less drug. Since the drainage of the 5-μl dose is considerably less than the 25-μl dose, the bioavailability is expected to be somewhat greater, while the amount of drug available to act systemically is dramatically reduced.

REFERENCES

(1) S. Mishima, A. Gasset, S. D. Klyce, Jr., and J. L. Baum, *Invest. Ophthalmol.*, **5**, 264(1966).

(2) O. Schirmer, *Graefes Arch. Ophthalmol.*, **56**, 197(1903).

(3) N. Ehlers, S. V. Kessing, and M. S. Norn, *Acta Ophthalmol.*, **50**, 210(1972).

(4) J. W. Henderson and W. A. Prough, *Arch. Ophthalmol.*, **43**, 224(1950).

(5) A. de Roetth, Sr., *ibid.*, **49**, 185(1953).

(6) J. C. Wright and G. E. Meger, *ibid.*, **67**, 564(1962).

(7) M. S. Norn, *Acta Ophthalmol.*, **43**, 567(1965).

(8) J. A. Brienen and C. A. R. D. Snell, *Ophthalmology*, **159**, 223(1969).

(9) L. T. Jones and M. L. Linn, *Am. J. Ophthalmol.*, **67**, 75(1969).

(10) S. Mishima, Z. Kubota, and R. L. Farris, *Excerpta Med. Found. Int. Congr., Ser. n222*, **1970**, 1801.

(11) D. M. Maurice, *Exp. Eye Res.*, **11**, 30(1971).

(12) J. Francois and A. Neetens, *Am. J. Ophthalmol.*, **76**, 351(1973).

(13) W. W. O'Nan, J. D. Wirtschafter, and D. F. Preston, *Arch. Ophthalmol.*, **91**, 187(1974).

(14) G. F. Rochat and C. E. Benjamins, *Graefes Arch. Ophthalmol.*, **91**, 66(1916).

(15) L. T. Jones, *Arch. Ophthalmol.*, **66**, 137(1961).

(16) M. S. Norn, *Acta Ophthalmol.*, **43**, 557(1965).

(17) L. T. Jones, M. M. Marquis, and N. J. Vincent, *Am. J. Ophthalmol.*, **73**, 658(1972).

(18) B. Rosengren, *Ophthalmology*, **164**, 409(1972).

(19) B. Rosengren, *Inaug. Diss.*, **1917**, 71.

(20) R. M. Rossomondo, W. H. Carlton, J. H. Trueblood, and R. P. Thomas, *Arch. Ophthalmol.*, **88**, 523(1972).

(21) S. S. Chrai, T. F. Patton, A. Mehta, and J. R. Robinson, *J. Pharm. Sci.*, **62**, 1112(1973).

(22) T. J. Mikkelson, S. S. Chrai, and J. R. Robinson, *ibid.*, **62**, 1648(1973).

(23) *Ibid.*, **62**, 1942(1973).

(24) L. Bellarminoff, *Arch. Ophthalmol.*, **39**, 38(1893).

(25) E. Ubry and M. Frezals, *Arch. Ophthalmol.*, **19**, 159(1899).

(26) T. Leber, "Graefe Saemische: Handbuch d. ges Augenhk.," 2:2.2 Aufl., Leipzig, Germany, 1903.

(27) J. Ursing, "On the Disappearance of Radiosodium Ions from Conjunctival and Subconjunctival Deposits in the Rabbit," Berlinska Boktryckeriet Lund, Malmö, Sweden, 1967.

(28) A. Sorsby and J. Ungar, *Br. Med. J.*, **2**, 723(1946).

(29) R. G. Janes and J. F. Stiles, *Arch. Ophthalmol.*, **62**, 69(1959).

(30) S. S. Chrai and J. R. Robinson, *Am. J. Ophthalmol.*, **77**, 735(1974).

(31) S. S. Chrai, Ph.D. thesis, University of Wisconsin, Madison, Wis., 1973.

(32) D. L. Deardorff, in "Remington's Pharmaceutical Sciences," 13th ed., Mack Publishing Co., Easton, Pa., 1965, p. 468.

(33) "The Rabbit in Eye Research," J. H. Prince, Ed., Charles C Thomas, Springfield, Ill., 1964.

(34) S. S. Chrai and J. R. Robinson, *J. Pharm. Sci.*, **63**, 1218(1974).

(35) T. F. Patton and J. R. Robinson, *ibid.*, **64**, 267(1975).

(36) *Ibid.*, **64**, 1312(1975).

ACKNOWLEDGMENTS AND ADDRESSES

Received September 8, 1975, from the *School of Pharmacy, University of Wisconsin, Madison, WI 53706*

Accepted for publication November 10, 1975.

Abstracted in part from a thesis submitted by T. F. Patton to the Graduate School, University of Wisconsin, Madison, Wis., in partial fulfillment of the Doctor of Philosophy degree requirements.

Supported by Allergan Pharmaceuticals, Irvine, CA 92664, and by a grant from the Graduate School, University of Wisconsin, Madison, WI 53706.

* Present address: Department of Pharmaceutical Chemistry, School of Pharmacy, University of Kansas, Lawrence, KS 66044

ˣ To whom inquiries should be directed.

Substituted 5-Nitro-1,3-dioxanes: Correlation of Chemical Structure and Antimicrobial Activity

LEWIS C. LAPPAS ˣ, CLARENCE A. HIRSCH, and CARL L. WINELY

Abstract □ Various derivatives of 5-nitro-1,3-dioxane were synthesized to determine the relative effect of chemical substitution in the 2- and 5-positions on broad spectrum antimicrobial activity. Each compound was evaluated quantitatively by calculation of a microbiocidal index, which measured the time to kill several different microorganisms. This test system indicated that 5-bromo-5-nitro substitution was essential for significant activity. Optimal activity was effected by 2-methyl substitution in the alkyl series and 2-hydroxyphenyl substitution in the aryl series. The antimicrobial activity of the substituted dioxanes was not related directly to water solubility or hydrolysis to microbiocidal diols or aldehydes.

Keyphrases □ Dioxanes, substituted—series synthesized, effect of substituents on antimicrobial activity □ Antimicrobial activity—series of substituted dioxanes synthesized, effect of substituents evaluated □ Structure–activity relationships—substituted dioxanes synthesized, effect of substituents on antimicrobial activity

Chemical agents that prevent microbial growth are essential ingredients for various topical products (1–3). The recent increased awareness of the potential health hazard of microbiologically contaminated pharmaceutical and cosmetic preparations (4–6) initiated a trend toward greater regulatory requirements for these products (7, 8). This turn of events emphasized the urgent need for more effective preservatives.

Several reviews described the significant factors contributing to the optimal efficacy of antimicrobial agents (9–11). Ideally, a preservative for topical preparations should be effective over a wide pH range (pH 5–9) and be physically and chemically compatible with the formulation ingredients. Furthermore, this agent should not be irritating, sensitizing, or absorbed to toxic levels after application.

To satisfy these requirements, chemical modification of the antimicrobial agent is often necessary. The design of the microbial test system to reflect significant differences in the activity of these modified compounds becomes a critical factor in their evaluation (12–14).

REFERENCES

(1) S. Mishima, A. Gasset, S. D. Klyce, Jr., and J. L. Baum, *Invest. Ophthalmol.*, **5**, 264(1966).

(2) O. Schirmer, *Graefes Arch. Ophthalmol.*, **56**, 197(1903).

(3) N. Ehlers, S. V. Kessing, and M. S. Norn, *Acta Ophthalmol.*, **50**, 210(1972).

(4) J. W. Henderson and W. A. Prough, *Arch. Ophthalmol.*, **43**, 224(1950).

(5) A. de Roetth, Sr., *ibid.*, **49**, 185(1953).

(6) J. C. Wright and G. E. Meger, *ibid.*, **67**, 564(1962).

(7) M. S. Norn, *Acta Ophthalmol.*, **43**, 567(1965).

(8) J. A. Brienen and C. A. R. D. Snell, *Ophthalmology*, **159**, 223(1969).

(9) L. T. Jones and M. L. Linn, *Am. J. Ophthalmol.*, **67**, 75(1969).

(10) S. Mishima, Z. Kubota, and R. L. Farris, *Excerpta Med. Found. Int. Congr., Ser. n222*, **1970**, 1801.

(11) D. M. Maurice, *Exp. Eye Res.*, **11**, 30(1971).

(12) J. Francois and A. Neetens, *Am. J. Ophthalmol.*, **76**, 351(1973).

(13) W. W. O'Nan, J. D. Wirtschafter, and D. F. Preston, *Arch. Ophthalmol.*, **91**, 187(1974).

(14) G. F. Rochat and C. E. Benjamins, *Graefes Arch. Ophthalmol.*, **91**, 66(1916).

(15) L. T. Jones, *Arch. Ophthalmol.*, **66**, 137(1961).

(16) M. S. Norn, *Acta Ophthalmol.*, **43**, 557(1965).

(17) L. T. Jones, M. M. Marquis, and N. J. Vincent, *Am. J. Ophthalmol.*, **73**, 658(1972).

(18) B. Rosengren, *Ophthalmology*, **164**, 409(1972).

(19) B. Rosengren, *Inaug. Diss.*, **1917**, 71.

(20) R. M. Rossomondo, W. H. Carlton, J. H. Trueblood, and R. P. Thomas, *Arch. Ophthalmol.*, **88**, 523(1972).

(21) S. S. Chrai, T. F. Patton, A. Mehta, and J. R. Robinson, *J. Pharm. Sci.*, **62**, 1112(1973).

(22) T. J. Mikkelson, S. S. Chrai, and J. R. Robinson, *ibid.*, **62**, 1648(1973).

(23) *Ibid.*, **62**, 1942(1973).

(24) L. Bellarminoff, *Arch. Ophthalmol.*, **39**, 38(1893).

(25) E. Ubry and M. Frezals, *Arch. Ophthalmol.*, **19**, 159(1899).

(26) T. Leber, "Graefe Saemische: Handbuch d. ges Augenhk.," 2:2.2 Aufl., Leipzig, Germany, 1903.

(27) J. Ursing, "On the Disappearance of Radiosodium Ions from Conjunctival and Subconjunctival Deposits in the Rabbit," Berlinska Boktryckeriet Lund, Malmö, Sweden, 1967.

(28) A. Sorsby and J. Ungar, *Br. Med. J.*, **2**, 723(1946).

(29) R. G. Janes and J. F. Stiles, *Arch. Ophthalmol.*, **62**, 69(1959).

(30) S. S. Chrai and J. R. Robinson, *Am. J. Ophthalmol.*, **77**, 735(1974).

(31) S. S. Chrai, Ph.D. thesis, University of Wisconsin, Madison, Wis., 1973.

(32) D. L. Deardorff, in "Remington's Pharmaceutical Sciences," 13th ed., Mack Publishing Co., Easton, Pa., 1965, p. 468.

(33) "The Rabbit in Eye Research," J. H. Prince, Ed., Charles C Thomas, Springfield, Ill., 1964.

(34) S. S. Chrai and J. R. Robinson, *J. Pharm. Sci.*, **63**, 1218(1974).

(35) T. F. Patton and J. R. Robinson, *ibid.*, **64**, 267(1975).

(36) *Ibid.*, **64**, 1312(1975).

ACKNOWLEDGMENTS AND ADDRESSES

Received September 8, 1975, from the *School of Pharmacy, University of Wisconsin, Madison, WI 53706*

Accepted for publication November 10, 1975.

Abstracted in part from a thesis submitted by T. F. Patton to the Graduate School, University of Wisconsin, Madison, Wis., in partial fulfillment of the Doctor of Philosophy degree requirements.

Supported by Allergan Pharmaceuticals, Irvine, CA 92664, and by a grant from the Graduate School, University of Wisconsin, Madison, WI 53706.

* Present address: Department of Pharmaceutical Chemistry, School of Pharmacy, University of Kansas, Lawrence, KS 66044

ˣ To whom inquiries should be directed.

Substituted 5-Nitro-1,3-dioxanes: Correlation of Chemical Structure and Antimicrobial Activity

LEWIS C. LAPPAS ˣ, CLARENCE A. HIRSCH, and CARL L. WINELY

Abstract □ Various derivatives of 5-nitro-1,3-dioxane were synthesized to determine the relative effect of chemical substitution in the 2- and 5-positions on broad spectrum antimicrobial activity. Each compound was evaluated quantitatively by calculation of a microbiocidal index, which measured the time to kill several different microorganisms. This test system indicated that 5-bromo-5-nitro substitution was essential for significant activity. Optimal activity was effected by 2-methyl substitution in the alkyl series and 2-hydroxyphenyl substitution in the aryl series. The antimicrobial activity of the substituted dioxanes was not related directly to water solubility or hydrolysis to microbiocidal diols or aldehydes.

Keyphrases □ Dioxanes, substituted—series synthesized, effect of substituents on antimicrobial activity □ Antimicrobial activity—series of substituted dioxanes synthesized, effect of substituents evaluated □ Structure–activity relationships—substituted dioxanes synthesized, effect of substituents on antimicrobial activity

Chemical agents that prevent microbial growth are essential ingredients for various topical products (1–3). The recent increased awareness of the potential health hazard of microbiologically contaminated pharmaceutical and cosmetic preparations (4–6) initiated a trend toward greater regulatory requirements for these products (7, 8). This turn of events emphasized the urgent need for more effective preservatives.

Several reviews described the significant factors contributing to the optimal efficacy of antimicrobial agents (9–11). Ideally, a preservative for topical preparations should be effective over a wide pH range (pH 5–9) and be physically and chemically compatible with the formulation ingredients. Furthermore, this agent should not be irritating, sensitizing, or absorbed to toxic levels after application.

To satisfy these requirements, chemical modification of the antimicrobial agent is often necessary. The design of the microbial test system to reflect significant differences in the activity of these modified compounds becomes a critical factor in their evaluation (12–14).

Various nitro and halonitro aliphatic alcohols exhibit antimicrobial activity and synergism (15–23). In particular, 2-bromo-2-nitro-1,3-propanediol is highly effective at low concentrations against many bacteria, yeasts, and molds. However, its inhibitory activity decreases as the pH increases from 5.3 to 7–8 (24). Its utility as a preservative was demonstrated in cosmetic formulations (25).

Various substituted 1,3-dioxanes also had antifungal and antibacterial properties. In some instances, this activity was attributed to ring cleavage and subsequent release of the antimicrobial aldehyde or alkane diol (26–28). However, many interesting dioxanes, including nitro and halonitro derivatives, are stable in the 5–9 pH range (29–35). Most notable is 5-bromo-5-nitro-1,3-dioxane, which exhibits broad spectrum antimicrobial activity and is an effective preservative in topical formulations (36).

In this study, derivatives of 5-nitro-1,3-dioxane were synthesized to determine the relative effect of various substituents in the 2- and 5-positions on broad spectrum antimicrobial activity.

EXPERIMENTAL

The chemical structures, physical constants, methods of preparation, and microbiocidal index for the compounds used are listed and referenced in Table I.

Chemical Synthesis—*Method A: 5-Bromo-5-nitro-1,3-dioxane (I)*—In accordance with the procedure of Wessendorf and Bellinger (36), a mixture of 50.5 g (0.25 mole) of 2-bromo-2-nitropropane-1,3-diol, 7.5 g of paraformaldehyde (equivalent to 0.25 mole of formaldehyde), and 12.5 g of polyphosphoric acid was heated at 100° for 3 hr. Then the mixture was cooled and extracted with methylene chloride. This extract was washed with 5% sodium bicarbonate solution, dried over anhydrous sodium sulfate, and evaporated to dryness, yielding 36 g of I, mp 49–50°.

Method B: 5-Bromo-2-methyl-5-nitro-1,3-dioxane (II)—Forty grams (0.2 mole) of 2-bromo-2-nitropropane-1,3-diol was slurried with 0.3 g of *p*-toluenesulfonic acid and 200 ml of benzene. Acetaldehyde (13.5 g, 0.3 mole) was added gradually and stirred for 30 min at room temperature. Then the mixture was refluxed until 4 ml of water was collected in a Dean–Stark trap during 1.5 hr.

The reaction mixture was cooled and subsequently washed with 5% sodium bicarbonate solution. The washed residue was dried over anhydrous sodium sulfate, and the solvent was removed *in vacuo*. The residual oil was distilled at 72°/0.2 mm to yield 37 g (85%) of colorless liquid (II).

Method C: 5-Bromo-2,2-dimethyl-5-nitro-1,3-dioxane (VII)—A solution of 100 g (0.5 mole) of 2-bromo-2-nitropropane-1,3-diol was prepared in 110 ml (1.5 moles) of acetone. To this solution, 65 ml (0.5 mole) of boron fluoride etherate was added rapidly with stirring. After being stirred for 10 min, the clear solution was poured into a mixture of 550 ml of a saturated solution of sodium bicarbonate and ice. The resultant crude product was isolated by filtration, dried, and recrystallized with water from ethanol solution, yielding 62 g (51%) of VII, mp 79–81°.

Method D: 5-Bromo-2-(m-hydroxyphenyl)-5-nitro-1,3-dioxane (XII)—A suspension containing 50 g (0.25 mole) of 2-bromo-2-nitropropane-1,3-diol and 0.4 g of *p*-toluenesulfonic acid in 200 ml of dry benzene was stirred and refluxed with heat through a Dean–Stark trap. A solution of 24.4 g (0.20 mole) of *m*-hydroxybenzaldehyde in 50 ml of dioxane was added dropwise to the refluxing mixture during 1 hr. After collection of 3.4 ml of water, the reaction mixture was cooled and the benzene was evaporated at reduced pressure.

The residue was dissolved in 200 ml of ethyl acetate and washed with two 100-ml portions of 10% sodium bisulfite solution. The ethyl acetate layer was separated, dried over anhydrous sodium sulfate, and evaporated to dryness *in vacuo*. The crude product was crystallized from hot benzene to yield 35 g (57%) of crystalline XII, mp 118–119°.

Method E: 5-Bromo-2-methoxy-5-nitro-1,3-dioxane (XV)—A suspension of 40 g (0.2 mole) of 2-bromo-2-nitropropane-1,3-diol in

Table I—Chemical and Microbiocidal Properties

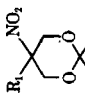

Compound	R_1	R_2	R_3	Melting Point (Boiling Point)	Empirical Formula	Analysis, %	Calc.	Found	Method[a] of Preparation	Microbiocidal[b] Index
I	Br	H	H	49–50°C	—	—	—	—	A	1275
II	Br	H	CH_3	(72°/0.25 mm)	$C_5H_8BrNO_4$	C	26.57	26.47	B	1375
						H	3.57	3.74		
						Br	35.35	35.31		
						N	6.20	6.13		
III	Br	H	C_2H_5	58–59°	$C_6H_{10}BrNO_4$	C	30.02	30.11	B	1350
						H	4.20	4.08		
						Br	33.29	33.39		
						N	5.83	5.60		
IV	Br	H	C_3H_7	(73–75°/0.005 mm)	$C_7H_{12}BrNO_4$	C	33.10	33.32	B	1275
						H	4.76	4.63		
						Br	31.45	31.64		
						N	5.50	5.66		

V	Br	H	$CH(CH_3)_2$	42–44°	$C_7H_{12}BrNO_4$	C	33.10	32.87	B	1300
						H	4.76	4.63		
						Br	31.45	31.66		
						N	5.50	5.24		
VI	Br	H	$C_{10}H_{21}$	55–58°	$C_{14}H_{26}BrNO_4$	C	47.73	47.98	B	75
						H	7.44	7.67		
						Br	22.68	22.48		
						N	3.98	4.15		
VII	Br	CH_3	CH_3	79–81°[d]	—		—	—	C	1175
VIII	Br	R_2R_3	$(CH_2)_5$	86–89°	$C_9H_{14}BrNO_4$	C	38.55	38.61	C	0
						H	5.00	4.80		
						Br	28.60	28.59		
						N	5.00	4.92		
IX	Br	H	C_6H_5	82–84°[e]	—		—	—	B	825
X	Br	CH_3	C_6H_5	87°	$C_{11}H_{12}BrNO_4$	C	43.73	43.48	C	950
						H	4.00	3.92		
						Br	26.45	26.83		
						N	4.64	4.66		
XI	Br	H	p-ClC_6H_4	103°[f]	—		—	—	B	0
XII	Br	H	m-HOC_6H_4	118–119°	$C_{10}H_{10}BrNO_5$	C	39.50	39.72	D	1300
						H	3.31	3.43		
						Br	26.28	26.06		
						N	4.61	4.55		
XIII	Br	H	p-HOC_6H_4	142–144°[g]	—		—	—	D	1375
XIV	Br	H	$CH{=}CHC_6H_5$	105–112°	$C_{12}H_{12}BrNO_4$	C	45.88	45.72	B	0
						H	3.85	3.86		
						Br	25.44	25.48		
						N	4.46	4.56		
XV	Br	H	OCH_3	88–90°	$C_5H_8BrNO_5$	C	24.81	24.64	E	1150[l]
						H	3.33	3.22		
						Br	33.01	33.26		
						N	5.79	5.59		
XVI	Br	R_2R_3	=O	142°	$C_4H_4BrNO_5$	C	21.26	21.47	F	1325[l]
						H	1.78	1.84		
						Br	35.36	35.20		
						N	6.20	6.41		
XVII	Cl	H	CH_3	Liquid	$C_5H_8ClNO_4$	C	33.07	33.31	G	150
						H	4.44	4.50		
						Cl	19.53	19.26		
						N	7.71	7.90		
XVIII	Cl	CH_3	CH_3	72–73°[h]	—		—	—	G	0
XIX	CH_3	H	H	67–69°[i]	—		—	—	C	0
XX	H	H	CH_3	73–74°	$C_5H_9NO_4$	C	41.10	40.92	H	0
						H	5.52	5.47		
						N	9.59	9.42		
XXI	CH_2OH	H	CH_3	(92–94°/0.025 mm)	$C_6H_{11}NO_5$	C	40.68	40.56	B	0
						H	6.26	5.96		
						N	7.91	7.92		
XXII	CH_2OH	CH_3	CH_2Cl	114–116°[j]	—		—	—	C	0
XXIII	$CH_2N(CH_3)_2$	CH_3	CH_3	81–83°[k]	—		—	—	I	225
XXIV	2-Bromo-2-nitropropane-1,3-diol			—	—		—	—		1200[m]

[a]Methods under *Experimental*. Elemental and NMR analyses for all compounds were consistent for their chemical structures. [b]Maximum score is 1400. [c]Lit. (36) mp 49°. [d]Lit. (39) mp 81°. [e]Lit. (34) mp 87°. [f]Lit. (34) mp 105–106°. [g]Lit. (34) mp 137–139°. [h]Lit. (39) mp 73–74°. [i]Lit. (40) mp 71°. [j]Lit. (32) mp 114.5°. [k]Lit. (37) mp 87°. [l]Significant activity attributed to hydrolysis to XXIV. [m]Obtained commercially from Goldschmidt Chemical Co.

Table II—Water Solubility *versus* Microbiocidal Activity

Compound	Solubility (25°), %	Microbiocidal Index
II	0.613	1375
I	0.577	1275
VII	0.105	1175
III	0.077	1350
XIII	0.043	1375
IX	0.046	825
IV	0.028	1275

250 ml of benzene was treated with 0.3 g of *p*-toluenesulfonic acid and 21.2 g (0.2 mole) of trimethyl formate. The agitated mixture was refluxed through a Dean–Stark trap until 120 ml of distillate was collected. The reaction mixture was evaporated to dryness, and the solid mass was recrystallized from absolute methanol, yielding 20 g (41%) of XV as dense acicular crystals, mp 88–90°.

Method F: 5-Bromo-5-nitro-1,3-dioxan-2-one (XVI)—A solution of 40 g (0.2 mole) of 2-bromo-2-nitropropane-1,3-diol was prepared in 100 ml of pyridine and cooled to 0°. Phosgene was bubbled slowly into the vigorously stirred reaction mixture for 45 min. The resultant viscous mixture was diluted with 600 ml of ether, and a tacky solid mass was produced. This residue was removed by decanting the liquid phase and then slurried in 200 ml of water. The crude product was filtered, air dried, and recrystallized twice from hot ethyl acetate, producing 10 g (22% yield) of XVI, mp 132°.

Method G: 5-Chloro-2-methyl-5-nitro-1,3-dioxane (XVII)—A solution containing 13.5 g (0.25 mole) of sodium methylate in 75 ml of absolute methanol was added slowly at room temperature to a stirred solution containing 35.4 g (0.20 mole) of 5-hydroxymethyl-2-methyl-5-nitro-1,3-dioxane in 75 ml of absolute methanol. After standing overnight, the mixture was diluted with 400 ml of ether. The sodium salt of 2-methyl-5-nitro-1,3-dioxane was precipitated, isolated by filtration, and dissolved in 150 ml of water. This solution was cooled to 0° in an ice bath and then saturated with chlorine gas.

The resultant oil layer was isolated using a separator and dissolved in 50 ml of chloroform. This solution was washed with water and subsequently dried over anhydrous sodium sulfate. The residue from the evaporation of chloroform yielded 10 g (55%) of pure XVII as a pale-green liquid.

Method H: 2-Methyl-5-nitro-1,3-dioxane (XX)—A solution of 20 g (0.12 mole) of L-cysteine hydrochloride in 200 ml of water was buffered to pH 6.0 with sodium bicarbonate. To this solution was added 11.3 g (0.05 mole) of 5-bromo-2-methyl-5-nitro-1,3-dioxane with vigorous stirring. L-Cystine precipitated, and the pH decreased rapidly to 2.3. Sodium bicarbonate was added to increase the pH to 7.5, and stirring was continued for 12 hr.

L-Cystine was removed by filtration and washed with 200 ml of chloroform; the wash solution was used to extract the filtrate. After drying over anhydrous sodium sulfate, the chloroform extract was evaporated to dryness. Recrystallization of the residue from benzene–heptane produced 5.5 g (75% yield) of XX as colorless needles, mp 73–74°.

Method I: 2,2-Dimethyl-5-dimethylaminomethyl-5-nitro-1,3-dioxane (XXIII)—In accordance with the procedure of Malinowski and Urbanski (37), 10.0 g (0.05 mole) of 2,2-dimethyl-5-hydroxymethyl-5-nitro-1,3-dioxane was stored in a closed container for 9 days with 35 ml of 40% aqueous dimethylamine. The resultant crystalline product (XXIII) was isolated by filtration and recrystallized from ethanol as dense prisms, yielding 5.0 g (45%), mp 81–83°.

Microbiological Methods—A preliminary challenge test was used to determine the antimicrobial potential of the test compounds. Since concentration gradients of antimicrobial suspensions can exhibit a dose response (38), each compound was prepared for testing as a solution or suspension at 0.1 and 0.5% (w/v) in sterile distilled water. Ten milliliters of each concentration was inoculated separately in test tubes with 0.1 ml of a suspension of *Pseudomonas aeruginosa* (ATCC 9027) and *Asperigillus niger* (ATCC 16404) containing 10^8 organisms/ml.

Plate counts were made initially and at 1, 7, 14, 21, and 28 days using a modified USP procedure (8) for efficacy testing. The incubation temperature of the test solution was reduced from 30 to 25°, and Sabouraud dextrose agar was substituted for soybean–casein digest agar for plating of *A. niger*. Compounds that reduced the counts for both organisms to less than 100 within 14 days at 0.1 and 0.5% concentrations were retested similarly at 0.05 and 0.1%, using the following microorganisms: *Staphylococcus aureus* (ATCC 6538), *Escherichia coli* (ATCC 4352), *Pseudomonas aeruginosa* (ATCC 9027), *Candida albicans* (ATCC 16231), *Aspergillus niger* (ATCC 16404), *Aspergillus flavus*[1], and *Streptococcus faecalis* (ATCC 8043).

The previous test regimen was followed. The Sabouraud dextrose agar was used only for *A. niger, A. flavus,* and *C. albicans;* all other organisms were cultured in the soybean–casein agar.

RESULTS AND DISCUSSION

Some substituted dioxanes were prepared from known antimicrobial alcohols and aldehydes. To evaluate the antimicrobial activity of the intact dioxane, all compounds were studied by conventional analytical methods for potential hydrolysis of the dioxane ring in water at 25°. Compound XV was hydrolyzed immediately to the antimicrobial diol (XXIV). Similarly, XVI was hydrolyzed to XXIV but at a slower rate. The percentage decomposition ($t_{\%}$) with time at 25° was t_{20} = 2 hr, t_{50} = 8 hr, and t_{90} = 32 hr. All other compounds revealed no significant hydrolysis of the dioxane ring.

The antimicrobial effectiveness of each compound was quantitated by calculation of the microbiocidal index from the challenge test data using seven organisms at 0.1 and 0.05% (w/v) concentrations. A value of 100, 75, 50, or 25 was assigned to any compound that reduced each organism to a count of less than 100/ml within 1, 7, 14, or 28 days, respectively. The maximum score possible was 1400. Compounds that were ineffective in the initial challenge test at 0.1 and 0.5% (w/v) against *P. aeruginosa* and *A. niger* were scored zero in the microbiocidal index.

The data in Table I indicate that II and XIII were the most active antimicrobials, with scores of 1375. Compounds I, III–V, XII, XIII, and XVI also were highly effective, since all organisms were reduced to less than 100/ml within 7 days. Compounds VII and XV were effective against all organisms within 14 days.

The presence of bromine in the 5-position appears to be essential to significant antimicrobial activity, as noted with I–V, VII, IX, X, XII, and XIII. Replacement of bromine with chlorine (XVII and XVIII) produced a marked reduction of activity; however, hydrogen (XX) or methyl (XIX) in the 5-position resulted in a greater loss of activity. Similar substitutions with the hydroxymethyl group (XXI) did not induce efficacy, and a tertiary amine (XXIII) had only slight antimicrobial action.

In conjunction with 5-bromo substitution, the highest activity for alkyl additions in the 2-position was noted with monosubstituted, minimal chain length (II); the activity decreased with an increase in molecular weight (III–VI). Dialkyl substitution with minimal chain length (dimethyl, VII) was slightly more effective than the 2-phenyl (IX) or 2-phenyl-2-methyl (X) derivatives. However, 2-hydroxyphenyl derivatives (XII and XIII) possessed activity equivalent to the most active alkyl-substituted compound (II). The introduction of 2-*p*-chlorophenyl (XI) and 2-styryl (XIV), which were substituents in certain antifungal dioxanes (34), resulted in marked reductions of antimicrobial properties.

Hydrolysis of XV (2-methoxy) and XVI (2-one) yielded the antimicrobial agent 2-bromo-2-nitropropane-1,3-diol (XXIV). As noted in Table I, the microbiocidal index of this diol was 1200; the values for XV and XVI were 1150 and 1325, respectively. No evidence of synergism was observed for these compounds and their hydrolysates when tested for zone inhibition against *Bacillus subtilis* (ATCC 6633). These data indicate that XVI contributes significantly to the microbiocidal action prior to its hydrolysis. Any contribution by XV to activity was not evident, since it hydrolyzed considerably faster than XVI.

GC analysis was used to determine the water solubility at 25° for some active compounds to determine the relationship of this parameter to microbiocidal activity. These data are given in decreasing order of solubility in Table II. Although it is generally accepted that some degree of water solubility is essential to activity, this comparison with substituted 5-bromo-5-nitro-1,3-dioxanes indicates that no direct relationship exists between the percent water solubility and the degree of antimicrobial activity.

This structure–activity relationship reveals a wide range in antimicrobial action due to chemical modification of the 5-nitrodioxane moiety. The introduction of bromine in the 5-position produced a high

[1] Laboratory culture.

degree of activity. The significance of further substitution in this comparative study is realized since some 2-monoalkyl and 2-hydroxyphenyl derivatives of the active 5-bromo-5-nitro-1,3-dioxane showed increased efficacy. These compounds offer some degree of selectivity to satisfy the multitude of antimicrobial requirements set forth for cosmetic and topical pharmaceutical products.

REFERENCES

(1) E. Sagarin, H. D. Goulden, E. G. Klarmann, and D. H. Powers, "Cosmetics Science and Technology," 3rd ed., Interscience, New York, N.Y., 1966, p. 1034.

(2) D. L. Wedderburn, "Advances in Pharmaceutical Sciences," Academic, New York, N.Y., 1964, p. 195.

(3) G. Sykes, *J. Mond. Pharm.*, **14**, 8(1971).

(4) M. T. Parker, *J. Soc. Cosmet. Chem.*, **23**, 415(1972).

(5) C. W. Bruch, *Drug Cosmet. Ind.*, **111**(4), 51(1972).

(6) *Ibid.*, **109**(1), 26(1971).

(7) C. W. Bruch, *Am. Perfum. Cosmet.*, **86**(4), 45(1971).

(8) "The United States Pharmacopeia," 18th rev., Mack Publishing Co., Easton, Pa., 1970, pp. 800, 845.

(9) C. A. Lawrence and S. S. Block, "Disinfection, Sterilization and Preservation," Lea & Febiger, Philadelphia, Pa., 1968, p. 555.

(10) D. L. Wedderburn, *Am. Perfum. Cosmet.*, **85**(3), 49(1970).

(11) H. S. Bean, G. H. Konning, and J. Thomas, *ibid.*, **85**(3), 61(1970).

(12) H. J. Van Abbé, *J. Soc. Cosmet. Chem.*, **21**, 719(1970).

(13) F. E. Halleck, *TGA Cosmet. J.*, **2**, 20(1970).

(14) C. W. Bruch, *Drug Cosmet. Ind.*, **110**(6), 32(1972).

(15) E. O. Bennett and H. N. Futch, *Lubr. Eng.*, **16**, 228(1960).

(16) E. O. Bennett, C. L. Adamson, and V. E. Feisal, *Appl. Microbiol.*, **7**, 368(1959).

(17) J. W. Ryder, U.S. pat. 3,044,864 (1972).

(18) Z. Eckstein, E. Grochowski, R. Kowalik, and T. Urbanski, *Bull. Acad. Pol. Sci., Ser. Sci. Chim.*, **11**, 687(1963); through *Chem. Abstr.*, **60**, 10529d(1964).

(19) H. G. Noesler, H. Bellinger, and R. Wessendorf, German pat. 1,297,813 (1969).

(20) *Ibid.*, German pat. 1,287,259 (1969).

(21) E. O. Bennett and E. B. Hodge, U.S. pat. 3,024,190 (1962).

(22) *Ibid.*, U.S. pat. 3,001,934–6 (1962).

(23) W. R. Bowman and R. J. Stretton, *Antimicrob. Ag. Chemother.*, **2**, 504(1972).

(24) B. Croshaw, J. J. Groves, and B. Lessel, *J. Pharm. Pharmacol. Suppl.*, **16**, 127(1964).

(25) N. G. Clark, B. Croshaw, and D. F. Spooner, British pat. 1,057,131 (1967).

(26) W. J. Houlihan, U.S. pat. 3,621,033 (1971).

(27) J. G. Horsfall and R. J. Lukens, *Conn. Agri. Exp. Stn., New Haven, Bull. No. 673*, **5** (1965).

(28) W. S. Gump and G. R. Walter, German pat. 1,171,110 (1964).

(29) Y. V. Baskov, V. V. Perekalin, H. Piotrowska, and T. Urbanski, *Bull. Acad. Pol. Sci., Ser. Sci. Chim.*, **19**, 681(1971); through *Chem. Abstr.*, **76**, 99578y(1972).

(30) J. Apjok, M. Bartok, R. A. Karakhanov, and N. I. Shuikin, *Usp. Khim.*, **38**, 72(1969); through *Chem. Abstr.*, **71**, 96657p(1969).

(31) M. Senkus, *J. Am. Chem. Soc.*, **63**, 2635(1941).

(32) M. Senkus, U.S. pat. 2,370,586 (1945).

(33) Z. Eckstein and T. Urbanski, *Rocz. Chem.*, **26**, 571(1952).

(34) Z. Eckstein, *ibid.*, **27**, 246(1953).

(35) L. W. Kissinger, T. M. Benziger, and R. K. Rohwer, *Nitro Compd., Proc. Int. Symp.*, **1963**, 317; through *Chem. Abstr.*, **64**, 731c(1966).

(36) R. Wessendorf and H. Bellinger, German pat. 1,920,298 (1970).

(37) S. Malinowski and T. Urbanski, *Rocz. Chem.*, **25**, 183(1951).

(38) D. C. Torgeson, "Fungicides, An Advanced Treatise," vol. II, Academic, New York, N.Y., 1969, p. 49.

(39) Z. Eckstein, *Rocz. Chem.*, **30**, 1151(1956).

(40) K. G. Shipp and M. E. Hill, *J. Org. Chem.*, **31**, 853(1966).

ACKNOWLEDGMENTS AND ADDRESSES

Received September 11, 1975, from the *Pharmaceutical Development Division, Lilly Research Laboratories, Eli Lilly and Company, Indianapolis, IN 46206*

Accepted for publication November 10, 1975.

The authors acknowledge E. Massey, M. L. Roy, J. W. Poole, R. J. Messenger, G. G. Cooke, and J. V. Dietz for their contributions to this work.

[x] To whom inquiries should be directed.

GLC and NMR Analysis of Isomeric Impurities in the New Anti-Inflammatory Agent Benoxaprofen

STELLA M. BROWNER *§, ANTHONY F. COCKERILL ‡, ROSEMARY J. MAIDMENT *, DAVID M. RACKHAM ‡x, and GORDON F. SNOOK *

Abstract □ GLC and NMR methods are described for the determination of four possible isomeric impurities in the novel anti-inflammatory agent benoxaprofen. The 2- and 3-chlorophenyl isomers were determined by GLC after alkaline hydrolysis and subsequent methylation. A rapid NMR procedure, using the lanthanide shift reagent tris- (1,1,1,2,2,3,3-heptafluoro- 7,7-dimethyl- 4,6-octanedionato)-europium, was developed for the 6- and 7-(α-methylacetic acid) isomers. Similar methodology, with tris-(3-heptafluorobutyryl-*d*-camphorato)europium, enabled the determination of the enantiomer ratio for benoxaprofen. For the positional isomers, the limits of detection were 0.05% by GLC and 0.2% by NMR.

Keyphrases □ Benoxaprofen—with four isomeric impurities, GLC and NMR analyses □ GLC—analysis, benoxaprofen and isomeric impurities □ NMR—analysis, benoxaprofen and isomeric impurities □ Anti-inflammatory agents—benoxaprofen and four isomeric impurities, GLC and NMR analyses

Recently, the syntheses and anti-inflammatory activity of a number of 2-aryl-5-benzoxazoleacetic acids were described (1). The most active member of the series, 2-(4-chlorophenyl)-α-methyl-5-benzoxazoleacetic acid (benoxaprofen, I), is several times more potent than phenylbutazone in the rat paw edema test and is currently under clinical evaluation.

The material for toxicology and clinical requirements was prepared in a 10-step synthesis (Scheme I).

Isomeric impurities, which can arise at Steps 3 and

degree of activity. The significance of further substitution in this comparative study is realized since some 2-monoalkyl and 2-hydroxyphenyl derivatives of the active 5-bromo-5-nitro-1,3-dioxane showed increased efficacy. These compounds offer some degree of selectivity to satisfy the multitude of antimicrobial requirements set forth for cosmetic and topical pharmaceutical products.

REFERENCES

(1) E. Sagarin, H. D. Goulden, E. G. Klarmann, and D. H. Powers, "Cosmetics Science and Technology," 3rd ed., Interscience, New York, N.Y., 1966, p. 1034.

(2) D. L. Wedderburn, "Advances in Pharmaceutical Sciences," Academic, New York, N.Y., 1964, p. 195.

(3) G. Sykes, *J. Mond. Pharm.*, **14**, 8(1971).

(4) M. T. Parker, *J. Soc. Cosmet. Chem.*, **23**, 415(1972).

(5) C. W. Bruch, *Drug Cosmet. Ind.*, **111**(4), 51(1972).

(6) *Ibid.*, **109**(1), 26(1971).

(7) C. W. Bruch, *Am. Perfum. Cosmet.*, **86**(4), 45(1971).

(8) "The United States Pharmacopeia," 18th rev., Mack Publishing Co., Easton, Pa., 1970, pp. 800, 845.

(9) C. A. Lawrence and S. S. Block, "Disinfection, Sterilization and Preservation," Lea & Febiger, Philadelphia, Pa., 1968, p. 555.

(10) D. L. Wedderburn, *Am. Perfum. Cosmet.*, **85**(3), 49(1970).

(11) H. S. Bean, G. H. Konning, and J. Thomas, *ibid.*, **85**(3), 61(1970).

(12) H. J. Van Abbé, *J. Soc. Cosmet. Chem.*, **21**, 719(1970).

(13) F. E. Halleck, *TGA Cosmet. J.*, **2**, 20(1970).

(14) C. W. Bruch, *Drug Cosmet. Ind.*, **110**(6), 32(1972).

(15) E. O. Bennett and H. N. Futch, *Lubr. Eng.*, **16**, 228(1960).

(16) E. O. Bennett, C. L. Adamson, and V. E. Feisal, *Appl. Microbiol.*, **7**, 368(1959).

(17) J. W. Ryder, U.S. pat. 3,044,864 (1972).

(18) Z. Eckstein, E. Grochowski, R. Kowalik, and T. Urbanski, *Bull. Acad. Pol. Sci., Ser. Sci. Chim.*, **11**, 687(1963); through *Chem. Abstr.*, **60**, 10529d(1964).

(19) H. G. Noesler, H. Bellinger, and R. Wessendorf, German pat. 1,297,813 (1969).

(20) *Ibid.*, German pat. 1,287,259 (1969).

(21) E. O. Bennett and E. B. Hodge, U.S. pat. 3,024,190 (1962).

(22) *Ibid.*, U.S. pat. 3,001,934–6 (1962).

(23) W. R. Bowman and R. J. Stretton, *Antimicrob. Ag. Chemother.*, **2**, 504(1972).

(24) B. Croshaw, J. J. Groves, and B. Lessel, *J. Pharm. Pharmacol. Suppl.*, **16**, 127(1964).

(25) N. G. Clark, B. Croshaw, and D. F. Spooner, British pat. 1,057,131 (1967).

(26) W. J. Houlihan, U.S. pat. 3,621,033 (1971).

(27) J. G. Horsfall and R. J. Lukens, *Conn. Agri. Exp. Stn., New Haven, Bull. No. 673*, **5** (1965).

(28) W. S. Gump and G. R. Walter, German pat. 1,171,110 (1964).

(29) Y. V. Baskov, V. V. Perekalin, H. Piotrowska, and T. Urbanski, *Bull. Acad. Pol. Sci., Ser. Sci. Chim.*, **19**, 681(1971); through *Chem. Abstr.*, **76**, 99578y(1972).

(30) J. Apjok, M. Bartok, R. A. Karakhanov, and N. I. Shuikin, *Usp. Khim.*, **38**, 72(1969); through *Chem. Abstr.*, **71**, 96657p(1969).

(31) M. Senkus, *J. Am. Chem. Soc.*, **63**, 2635(1941).

(32) M. Senkus, U.S. pat. 2,370,586 (1945).

(33) Z. Eckstein and T. Urbanski, *Rocz. Chem.*, **26**, 571(1952).

(34) Z. Eckstein, *ibid.*, **27**, 246(1953).

(35) L. W. Kissinger, T. M. Benziger, and R. K. Rohwer, *Nitro Compd., Proc. Int. Symp.*, **1963**, 317; through *Chem. Abstr.*, **64**, 731c(1966).

(36) R. Wessendorf and H. Bellinger, German pat. 1,920,298 (1970).

(37) S. Malinowski and T. Urbanski, *Rocz. Chem.*, **25**, 183(1951).

(38) D. C. Torgeson, "Fungicides, An Advanced Treatise," vol. II, Academic, New York, N.Y., 1969, p. 49.

(39) Z. Eckstein, *Rocz. Chem.*, **30**, 1151(1956).

(40) K. G. Shipp and M. E. Hill, *J. Org. Chem.*, **31**, 853(1966).

ACKNOWLEDGMENTS AND ADDRESSES

Received September 11, 1975, from the *Pharmaceutical Development Division, Lilly Research Laboratories, Eli Lilly and Company, Indianapolis, IN 46206*

Accepted for publication November 10, 1975.

The authors acknowledge E. Massey, M. L. Roy, J. W. Poole, R. J. Messenger, G. G. Cooke, and J. V. Dietz for their contributions to this work.

[x] To whom inquiries should be directed.

GLC and NMR Analysis of Isomeric Impurities in the New Anti-Inflammatory Agent Benoxaprofen

STELLA M. BROWNER *§, ANTHONY F. COCKERILL ‡, ROSEMARY J. MAIDMENT *, DAVID M. RACKHAM ‡x, and GORDON F. SNOOK *

Abstract □ GLC and NMR methods are described for the determination of four possible isomeric impurities in the novel anti-inflammatory agent benoxaprofen. The 2- and 3-chlorophenyl isomers were determined by GLC after alkaline hydrolysis and subsequent methylation. A rapid NMR procedure, using the lanthanide shift reagent tris- (1,1,1,2,2,3,3-heptafluoro- 7,7-dimethyl- 4,6-octanedionato)-europium, was developed for the 6- and 7-(α-methylacetic acid) isomers. Similar methodology, with tris-(3-heptafluorobutyryl-*d*-camphorato)europium, enabled the determination of the enantiomer ratio for benoxaprofen. For the positional isomers, the limits of detection were 0.05% by GLC and 0.2% by NMR.

Keyphrases □ Benoxaprofen—with four isomeric impurities, GLC and NMR analyses □ GLC—analysis, benoxaprofen and isomeric impurities □ NMR—analysis, benoxaprofen and isomeric impurities □ Anti-inflammatory agents—benoxaprofen and four isomeric impurities, GLC and NMR analyses

Recently, the syntheses and anti-inflammatory activity of a number of 2-aryl-5-benzoxazoleacetic acids were described (1). The most active member of the series, 2-(4-chlorophenyl)-α-methyl-5-benzoxazoleacetic acid (benoxaprofen, I), is several times more potent than phenylbutazone in the rat paw edema test and is currently under clinical evaluation.

The material for toxicology and clinical requirements was prepared in a 10-step synthesis (Scheme I).

Isomeric impurities, which can arise at Steps 3 and

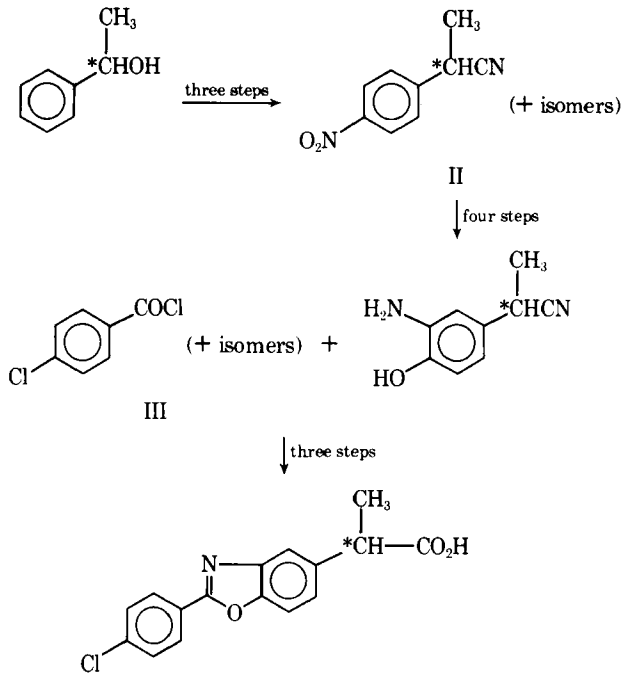

Scheme I— Asymmetric center*

8, might carry through to the final product and be very difficult to remove. Therefore, the isomer levels in II and III were carefully controlled. This paper describes the analytical procedures developed to estimate these four possible isomeric impurities, the 6- and 7-(α-methylacetic acid) and 2- and 3-chlorophenyl isomers (IV–VII), in the final product.

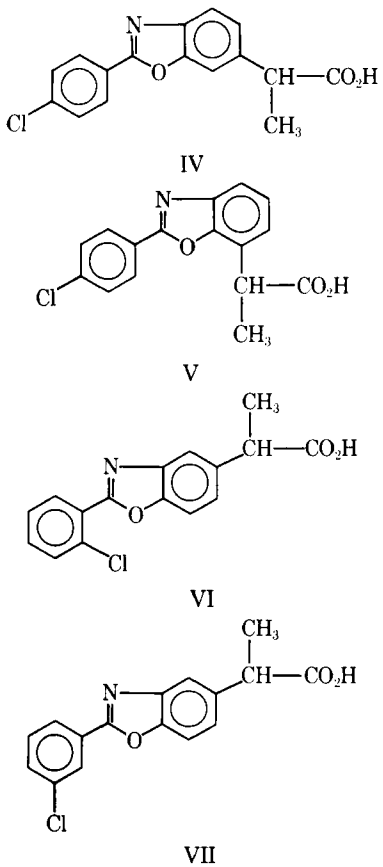

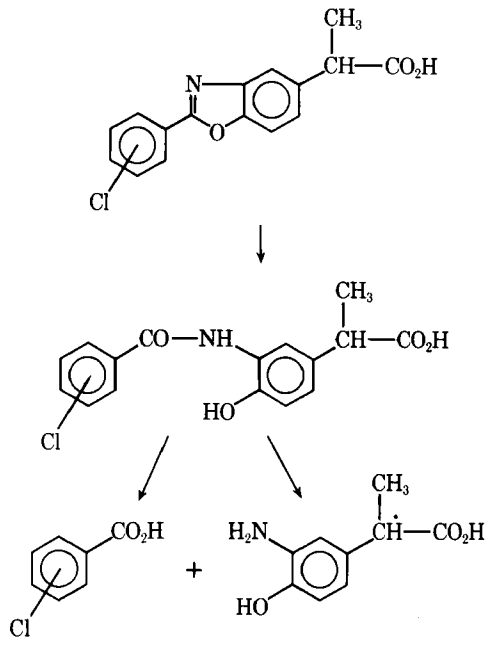

Scheme II

Attempts to achieve a separation of low concentrations of all four isomers of I by GLC using standard packed columns proved unsuccessful. These compounds, derivatized as their methyl esters, were not resolved on a number of different columns. However, hydrolytic ring fragmentation of I, VI, and VII yielded the corresponding chlorobenzoic acids (Scheme II), which were separated and determined as their methyl esters.

In the absence of a suitable GLC method for determining IV and V, a rapid NMR procedure was developed using the fluorinated europium shift reagent, tris-(1,1,1,2,2,3,3-heptafluoro-7,7-dimethyl-4,6-octanedionato)europium (VIII) (2). An optically active analog of this reagent also separates the NMR signals for the optical isomers of I, allowing their determination.

EXPERIMENTAL

Determination of Low Concentrations of 2- and 3-Chlorophenyl Isomers of I—*Reagents*—Compounds IV–VII were of at least 95% purity[1].

Acetone[2] and ether[3] were analytical reagent grade. Sodium hydroxide[2], hydrochloric acid[3], 4-chloroacetophenone[2], 4-chlorobenzoic acid[4], 3-chlorobenzoic acid[2], and 2-chlorobenzoic acid[2] were used as purchased. While the 4- and 2-chlorobenzoic acid samples showed <0.1% of the other isomers, the 3-chlorobenzoic acid contained 2.4% of the 4-isomer and 1.7% of the 2-isomer; an overall purity of 96% 3-isomer was assumed.

The diazomethane solution was prepared from *N*-methyl-*N*-nitroso-*p*-toluenesulfonamide[5] according to the manufacturer's recommended procedure. All operations with this reagent were carried out in a fume cupboard.

GLC—For the GLC determinations, a gas chromatograph[6] equipped with a hydrogen flame-ionization detector (hydrogen 30 ml/min and air 300 ml/min) was used. The glass column [1.8 m × 0.6

[1] Chemistry Department, Lilly Research Centre Ltd., Erl Wood Manor, Windlesham, Surrey, England.
[2] British Drug House Chemicals Ltd.
[3] May & Baker Ltd.
[4] Koch-Light Laboratories Ltd.
[5] Aldrich Chemical Co.
[6] Pye Unicam, model GCV.

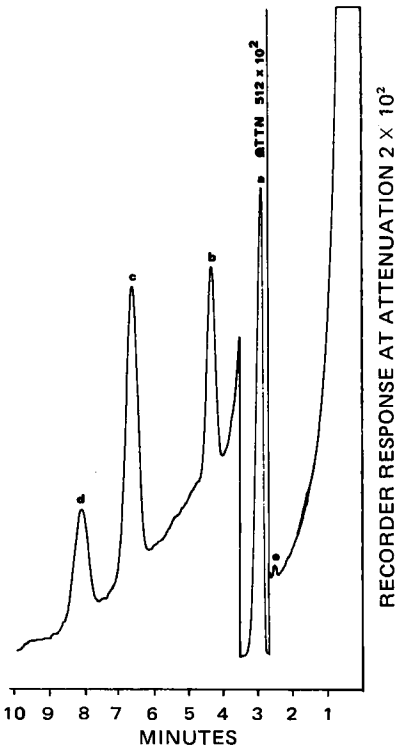

Figure 1—*Gas chromatogram from a sample containing 0.5% of VI and VII in I. Key: a, main component, methyl 4-chlorobenzoate; b, methyl 3-chlorobenzoate; c, internal standard, 4-chloroacetophenone; d, methyl 2-chlorobenzoate; and e, peak present in blank. The conditions were: 5% IX–4% diisooctyl phthalate on 80–100-mesh Gas Chrom Q, nitrogen flow rate of 30 ml/min, and column temperature of 180°.*

cm (3 ft × 0.25 in.) o.d.] was packed with 5% dimethyldioctadecylammonium bentonite[7] (IX) and 4% diisooctyl phthalate[2] on 80–100-mesh Gas Chrom Q[8]. The stationary phases were simultaneously coated on the solid support by the slurry technique. Nitrogen was used as carrier gas at 30 ml/min. The temperatures were as follows: column, 180°; injection port, 190°; and detector, 230°. The samples were injected on column.

Under these conditions, the retention times were: methyl 4-chlorobenzoate, 3.1 min; methyl 3-chlorobenzoate, 4.5 min; 4-chloroacetophenone, 6.8 min; and methyl 2-chlorobenzoate, 8.1 min.

A chromatogram obtained from a sample containing 0.5% of VI and VII in I is shown in Fig. 1. Quantitation was done using peak height ratios.

Calibration Graphs—The following reference compound solutions were prepared. The internal standard solution was 4-chloroacetophenone, 0.03 mg/ml, dissolved in acetone.

For stock solution of 2- and 3-chlorobenzoic acids, 50 mg of each acid was dissolved in ether and diluted to 50.0 ml. Then 1.0 ml of this solution was pipetted into a 50-ml volumetric flask and diluted to volume with ether.

For the working solutions, aliquots of 0.5, 1.0, 1.5, 2.0, and 2.5 ml of the stock solution were pipetted into 10-ml glass vials, and the solvent was evaporated to dryness in a fume cupboard under a stream of nitrogen. Several drops of diazomethane solution were carefully added, and the vial was lightly capped and left for about 10 min. If the solution was colorless, more diazomethane was added, and the procedure was repeated. If the solution was yellow, excess diazomethane was present, and the solution was then evaporated to dryness under a fume hood.

The residues were each dissolved in 1.0 ml of the internal standard solution. These solutions then contained approximately 0.01, 0.02, 0.03, 0.04, and 0.05 mg/ml of both 2- and 3-chlorobenzoic acid methyl esters. A 5-μl sample of each solution was injected into the chromatograph, and a peak height of each component was measured. Calibration graphs were obtained by plotting the peak height ratios of each methyl ester to the internal standard as a function of the concentration of the methyl ester. These were linear and passed through the origin.

Hydrolysis—About 50 mg of accurately weighed sample was placed in a 100-ml round-bottom flask, and 10 ml of 2 *N* sodium hydroxide was added. The solution was heated under reflux for 4 hr, cooled, and transferred to a 50-ml separator with water. Hydrochloric acid (5 ml of 5 *N*) was added, and the solution was extracted with two 10-ml aliquots of ether.

The ether extracts were combined, transferred to a 25-ml volumetric flask, and diluted to volume with ether. A 5.0-ml aliquot of this solution was pipetted into a 10-ml glass vial and evaporated to dryness under a stream of nitrogen in a fume cupboard. The residue was dissolved in excess diazomethane, lightly capped, and left for about 10 min. The excess diazomethane was evaporated to dryness, and the residue was dissolved in 1.0 ml of internal standard solution.

Then 5 μl of the solution was injected into the gas chromatograph. The peak heights of the methyl esters of 3- and 2-chlorobenzoic acids and of the internal standard were measured, and the appropriate ratios were calculated. Their concentrations were then determined from the calibration graph, and the concentrations of VI and VII present in the sample were calculated.

Recovery Experiments—Samples of about 50 mg of I, VI, and VII were weighed into 100-ml round-bottom flasks, 10 ml of 2 *N* sodium hydroxide was added, and the solutions were heated under reflux for 4 hr. These solutions were then cooled, acidified, and extracted as described for the hydrolysis procedure. A 5.0-ml aliquot of each ether extract was pipetted into 100-ml volumetric flasks and diluted to volume with ether. One-milliliter aliquots of each solution were pipetted into 10-ml glass vials and methylated as in the hydrolysis procedure.

Recovery calculations on VI and VII were determined using the calibration graphs, while those on I were obtained by plotting a similar calibration graph using 4-chlorobenzoic acid. Synthetic mixtures of VI and VII at the 0.1, 0.2, 0.5, and 1.0% levels in I were prepared and taken through the hydrolysis procedure. The recovery figures are shown in Table I.

Determination of VI and VII in I—Accurate weighings of about 50 mg of sample were taken through the hydrolysis procedure, and concentrations of VI and VII were determined by means of the standard calibration curves as follows:

$$\text{percentage of VII} = \frac{(\text{mg of methyl 3-chlorobenzoate produced}) \times 301.7 \times 100 \times 5}{(\text{sample weight, mg}) \times 170.5} \quad \text{(Eq. 1)}$$

$$\text{percentage of VI} = \frac{(\text{mg of methyl 2-chlorobenzoate produced}) \times 301.7 \times 5 \times 100 \times 1.22}{(\text{sample weight, mg}) \times 170.5} \quad \text{(Eq. 2)}$$

where 1.22 is a correction factor for 82% recovery.

Determination of Low Concentrations of 6- and 7-(α-Methylacetic Acid) Isomers of I—*Instruments and Reagents*—NMR spectra were obtained as 250 accumulations on a 90-MHz Fourier transform NMR spectrometer[9] or on a 60-MHz continuous-wave spectrometer[10]. Deuterochloroform[11], containing 1% (v/v) tetramethylsilane[11], was used as the solvent. Spectral scans (δ 0–13) were referred to the singlet due to tetramethylsilane set on the chart at δ = 0.00.

Deuterochloroform (99.8%) was dried over molecular sieve 4A[2] before use. Tetramethylsilane, VIII[11], and tris-(3-heptafluorobutyryl-*d*-camphorato)europium[12] were used as purchased.

Determination of IV and V in I—A 10.0-mg sample of the appropriate acid was treated with 1 ml of a 0.25 *M* ethereal diazomethane solution for 5 min at room temperature. The unreacted reagent and solvent were evaporated in a stream of nitrogen, and the resulting methyl ester was dissolved in 0.35 ml of deuterochloroform. Com-

[7] Bentone 34, Phase Separations Ltd.
[8] Applied Science Laboratories.
[9] Bruker WH90.
[10] Varian A-60A.
[11] Ryvan Chemical Co. Ltd.
[12] Willow Brook Laboratories Ltd.

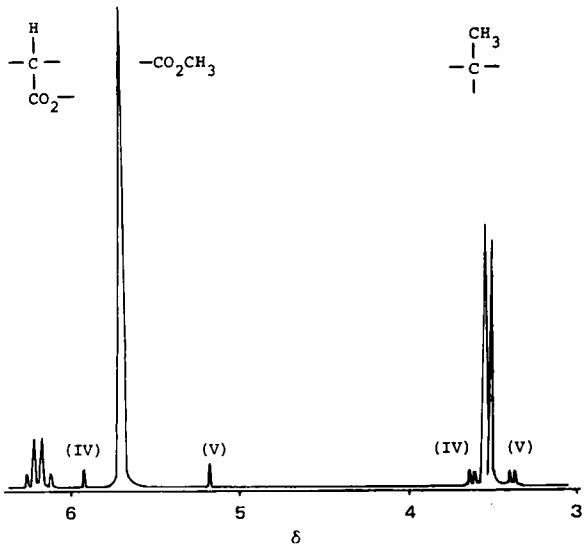

Figure 2—*Part spectrum of I (containing ~3% added IV and V) treated with 0.38 equivalent of VIII. Peaks due to the methyl groups of IV and V are indicated in parentheses.*

pound VIII (13 mg, 0.38 equivalent) was added, and the NMR spectrum was examined in the δ 2.5–6.5 region (Fig. 2). The peaks occurring in the δ 5–6 region in the lanthanide-shifted spectrum were due to the methyl ester protons of I or its 6- or 7-isomer (I = δ 5.69, IV = δ 5.90, and V = δ 5.14). Quantitation of the isomeric impurities followed from the duplicate measurement of the ratio of peak heights for the relevant methyl ester protons. Ordinate expansion by a factor of 8 was used to amplify the small peaks due to IV or V.

Determination of Enantiomers of I—Compound I (10.0 mg) was treated with diazomethane as already described, and the resulting methyl ester was dissolved in 0.35 ml of deuterochloroform. To this solution, 11.0 mg (0.28 equivalent) of tris-(3-heptafluorobutyryl-*d*-camphorato)europium was added, and the NMR spectrum was recorded in the δ 2–6 region (Fig. 3). The enantiomer ratio was determined by measuring the relative heights of the low field peaks for the side-chain methyl doublets (at δ 2.55 and 2.61).

RESULTS AND DISCUSSION

Column—Raley and Kaufman (3) reported the separation of the isomeric monochlorostyrenes using an organo clay[7] (IX) modified with

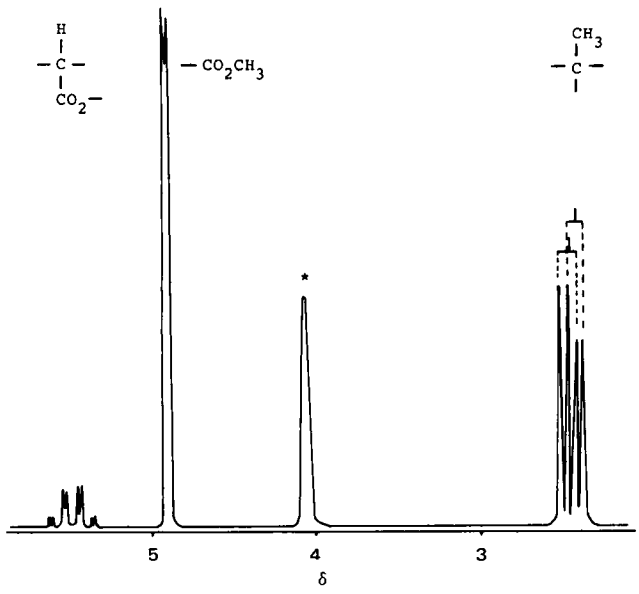

Figure 3—*Part spectrum of I treated with 0.28 equivalent of tris-(3-heptafluorobutyryl-*d*-camphorato)europium. Starred peak is due to europium reagent.*

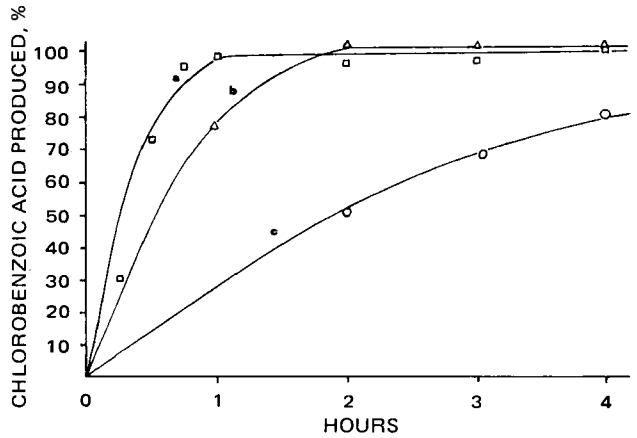

Figure 4—*Amounts of chlorobenzoic acids produced from I, VI, and VII with varying hydrolysis times. Key: a, 4-chlorobenzoic acid produced by hydrolysis of I; b, 3-chlorobenzoic acid produced by hydrolysis of VII; and c, 2-chlorobenzoic acid produced by hydrolysis of VI.*

other stationary phases. Compound IX modified with diisooctyl phthalate also has been used to separate the isomers of benzoyl chloride. Although the temperature limit of IX is too low to be of use for separating VI and VII, the methyl esters of the chlorobenzoic acids produced after hydrolysis can be separated with this phase. The most suitable column was a 1.8-m × 0.6-cm (3-ft × 0.25-in.) o.d. glass column packed with 5% IX–4% diisooctyl phthalate on 80–100-mesh Gas Chrom Q. It gave good resolution of the isomeric methyl chlorobenzoates with good peak shapes and minimum retention times (Fig. 1).

Hydrolysis Conditions—Preliminary studies showed that alkaline hydrolysis proceeded more rapidly than acid hydrolysis. Figure 4 shows the effect of varying hydrolysis time on the amount of chlorobenzoic acids produced from I, VI, and VII. Although hydrolysis of the main component, I, was complete in about 1 hr and hydrolysis of VII was complete in about 2 hr, VI required a longer time. And even after 4 hr, only 82% of the 2-chlorobenzoic acid had been produced. Consequently, a hydrolysis time of 4 hr was chosen, and the figures obtained from 2-chlorobenzoic acid were corrected accordingly.

Recovery Data—Table I shows the recovery figures obtained on samples of I, VI, VII, and several mixtures: approximately 100% for I and VII and 80% for VI. Recoveries were significantly lower in the 0.1% mixture, as the limit of detection was approached.

Analytical Performance—With the described method, VI and VII can be determined in the 0.1–1.0% range in I with a precision of ±10%. Higher levels can be easily determined by appropriate reduction of the size of aliquot taken in the hydrolysis procedure. Blank determinations show no interference. The limit of detection is about 0.05% of either isomer in a 50-mg sample.

NMR Conditions—NMR spectroscopy, with the aid of a lanthanide shift reagent (2, 4), provides a facile separation of signals from the 5-, 6-, and 7-isomers, enabling their quantitation. A sample of I, containing added amounts of IV and V, showed no separation of methyl ester peaks in the 90-MHz NMR spectrum after methylation. However, treatment with 0.38 equivalent of VIII caused the methyl ester signal of all three components to separate clearly (Fig. 2).

Further addition of shift reagent was not advantageous because of overlap of the methyl ester resonance of IV with the methine resonance of I. As shown in Fig. 2, the doublet signals for the methyl groups in the α-methylacetic acid side chain were separately resolved in the presence of VIII. The smaller separations and split nature of these signals make them an unattractive alternative to the procedure using the singlet of the methyl ester group.

Quantitation and Detection Limits—Quantitation was undertaken using peak height measurements rather than integrated areas to avoid problems of integral drift at low signal levels. Results obtained on standard mixtures are given in Table II. For the solution containing 0.31% of IV, the signal height for the methyl ester group of IV was four times the average noise excursion. Hence, the detection limit for IV and V is about 0.2%. On the continuous-wave instrument, the practical limit of detection was an order of magnitude poorer (3–4%), demonstrating the sensitivity advantages of the Fourier technique.

Table I—Recovery Data Obtained by Hydrolyzing Standard Mixtures of I, VI, and VII[a]

Sample	I			VI			VII		
	Milligrams Present	Milligrams Found	Average Recovery, %	Milligrams Present	Milligrams Found	Average Recovery, %	Milligrams Present	Milligrams Found	Average Recovery, %
Pure compound	51.4	49.5 ± 1.9	96	48.5	39.3 ± 0.3	81	49.3	48.0 ± 0.3	97
1% of VI and VII in reaction product	52.4	56.6 ± 0.6	108	0.564	0.467 ± 0.03	83	0.495	0.535 ± 0.06	108
0.5% of VI and VII in reaction product	50.7	55.3 ± 0.3	109	0.282	0.241 ± 0.013	85	0.248	0.281 ± 0.011	113
0.2% of VI and VII in reaction product	54.3	52.4 ± 4.9	97	0.113	0.092	81	0.099	0.093 ± 0.005	94
0.1% of VI and VII in reaction product	53.0	45.7 ± 2.1	86	0.056	0.040 ± 0.001	70	0.050	0.038 ± 0.001	76

[a] Individual figures quoted are usually the mean of two determinations.

Table II—Analyses of IV and V in I by NMR

Component	Added, % (w/w)	Found, % (w/w)
IV	2.9	2.2, 2.8
IV	0.31	0.38, 0.32
V	3.1	3.0, 3.5
	3.0	2.9, 3.5

Determination of Enantiomeric Ratio for I—Optically active lanthanide shift reagents have been applied successfully in the resolution of NMR signals of enantiomers (5). Addition of 0.28 equivalent of tris-(3-heptafluorobutyryl-*d*-camphorato)europium caused a useful δ 0.06 separation of the side-chain methyl doublets in the two enantiomers of the methyl ester of I (Fig. 3).

Addition of further shift reagent caused first an overlap of the middle peaks as the methyl doublets crossed and then excessive line broadening. It was possible to estimate the enantiomeric ratio to an accuracy of approximately ±3%. As expected from the mode of synthesis, the compound was racemic. This rapid procedure may prove valuable in the evaluation of the enantiomeric content of other anti-inflammatory acids, *e.g.*, for raw materials or in metabolic studies (6, 7).

CONCLUSION

A number of samples of I synthesized from different batches of intermediates, II and III, with isomeric impurities controlled to less than 0.5% in each, were examined for traces of IV–VII. None of the samples showed any detectable quantities of these compounds, indicating that adequate control of intermediate purity had been achieved and that impurities were not concentrated during the synthesis.

REFERENCES

(1) D. W. Dunwell, D. Evans, T. A. Hicks, C. H. Cashin, and E. A. Kitchen, *J. Med. Chem.*, **18**, 53(1975).

(2) A. F. Cockerill, G. L. O. Davies, R. C. Harden, and D. M. Rackham, *Chem. Rev.*, **73**, 553(1973).

(3) C. F. Raley and J. W. Kaufman, *Anal. Chem.*, **40**, 1371(1968).

(4) P. Reisberg, I. A. Brenner, and J. I. Bodin, *J. Pharm. Sci.*, **63**, 1586(1974).

(5) H. L. Goering, J. N. Eikenberry, G. S. Koermer, and C. J. Lattimer, *J. Am. Chem. Soc.*, **96**, 1493(1974).

(6) A. F. Cockerill, G. L. O. Davies, R. G. Harrison, and D. M. Rackham, *Org. Magn. Reson.*, **6**, 669(1974).

(7) R. F. Mills, S. S. Adams, E. E. Cliffe, W. Dickinson, and J. S. Nicholson, *Xenobiotica*, **3**, 589(1973).

ACKNOWLEDGMENTS AND ADDRESSES

Received April 7, 1975, from the **Analytical Development and Control Department and the ‡ Physical Organic Chemical Research Department, Lilly Research Centre Ltd., Erl Wood Manor, Windlesham, Surrey, GU20 6PH, England.*

Accepted for publication November 6, 1975.

The University of Surrey is thanked for the use of the Bruker NMR instrument.

§ Present address: Corporate Quality Standards Laboratory, Coca-Cola Co., Atlanta, GA 30301

ˣ To whom inquiries should be directed.

Fluphenazine Enanthate and Fluphenazine Decanoate: Intramuscular Injection and Esterification as Requirements for Slow-Release Characteristics in Dogs

JACQUES DREYFUSS ˣ, JAMES M. SHAW, and JOHN J. ROSS, Jr.

Abstract □ ^{14}C-Fluphenazine base was administered intramuscularly in sesame oil to five male beagles (2 mg/kg). The concentration of radioactivity in plasma and the excretion of radioactivity in urine and feces were measured for 14 days. Maximum concentrations of radioactivity were found in plasma 2 hr after administration. These levels declined with elimination half-lives of 3.20 hr during the 2–12-hr interval after dosing and of 4.02 days during the 2–14-day interval. Most administered radioactivity was excreted during the first 2 days after dosing, predominantly in the feces. An average of 0.43% of the dose was present at the injection site 14 days after dosing; some residual radioactivity was found in the liver and in the ocular portion consisting of the combined retina, choroid, and sclera. ^{14}C-Fluphenazine and its enanthate and decanoate esters were each administered intravenously to three different groups of intact dogs at doses of 1 mg/kg. Regardless of which compound was administered, concentrations of radioactivity in the plasma of these dogs were comparable. Thirty minutes after these dogs had been dosed with ^{14}C-fluphenazine enanthate or ^{14}C-fluphenazine decanoate, most radioactivity in the plasma was present as ^{14}C-fluphenazine base and other unidentified metabolites; at this time, at least 79% of either of the two ^{14}C-fluphenazine esters had been biotransformed. The excretion of radioactivity by these same three groups of dogs was very similar, regardless of which of the three compounds was given. In 7 days, an average of only 3–4% of the dose was excreted in urine; the remainder was excreted in feces. ^{14}C-Fluphenazine and its enanthate and decanoate esters (1 mg/kg) were administered intravenously to dogs whose bile ducts had been cannulated. The amounts of radioactivity excreted in the urine and bile in 8 hr were very similar, as were the residual amounts of radioactivity present in selected tissues. Comparison of the data obtained from dogs given these three compounds intravenously (unformulated) or intramuscularly in sesame oil points to the following conclusions: (*a*) fluphenazine base *per se* does not provide slow-release characteristics unless it has been esterified, for example, with heptanoic or decanoic acid, and (*b*) intramuscular rather than intravenous administration of these two esters is responsible for producing their slow-release characteristics.

Keyphrases □ Fluphenazine—base, enanthate, and decanoate esters, comparison of slow-release characteristics, effect of route of administration, dogs □ Pharmacokinetics—fluphenazine base, enanthate, and decanoate, comparison of slow-release characteristics, effect of route of administration, dogs □ Excretion—fluphenazine base, enanthate, and decanoate, comparison of slow-release characteristics, effect of route of administration, dogs □ Tranquilizers—fluphenazine base, enanthate, and decanoate esters, comparison of slow-release characteristics, effect of route of administration, dogs

The administration to dogs of the long-acting esters of fluphenazine base (I), the enanthate (II) and the decanoate (III), was studied to reveal the conditions necessary for producing slow-release characteristics. An earlier study (1) compared the relative rates of release of ^{14}C-fluphenazine enanthate and ^{14}C-fluphenazine decanoate (1) when each compound was administered intramuscularly in sesame oil to dogs. After that study, it became apparent that the data, which had been based only on measurements of radioactivity, could not be fully interpreted without additional supporting studies in which ^{14}C-fluphenazine and the enanthate and decanoate esters were administered intravenously in the unformulated state. Thus, it was recognized that some

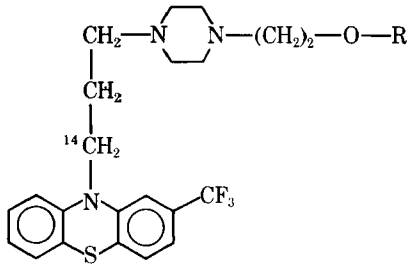

I: R = H

II: R = $C(CH_2)_5CH_3$ (=O)

III: R = $C(CH_2)_8CH_3$ (=O)

information regarding the nature of the radioactivity present in the circulation after the administration of each compound was needed. An additional objective was to determine to what extent ^{14}C-fluphenazine base, administered intramuscularly in sesame oil in the unesterified state, produced slow-release characteristics.

EXPERIMENTAL

Purity and Specific Activity—^{14}C-Fluphenazine hydrochloride and ^{14}C-fluphenazine base had specific activities of 5.8 and 5.5 μCi/mg, respectively, in their undiluted states. The compounds were not less than 98% chemically and radiochemically pure.

^{14}C-Fluphenazine enanthate had a specific activity of 4.6 μCi/mg in the undiluted state. The compound was not less than 97% chemically and radiochemically pure.

^{14}C-Fluphenazine decanoate had a specific activity of 4.4 μCi/mg. The compound was not less than 98% chemically and radiochemically pure.

Design of Intramuscular Studies with ^{14}C-Fluphenazine Base—Unesterified ^{14}C-fluphenazine base was dissolved in sesame oil at a concentration of 40.7 mg/ml. The sesame oil also contained 1.5% benzyl alcohol. Five purebred male beagles each received an intramuscular injection into the biceps femoris of formulated ^{14}C-fluphenazine base (0.5 ml of sesame oil preparation/10 kg of body weight). The dogs weighed 9.8 ± 0.4 kg (±*SE*); each was given a dose of 2.04 ± 0.02 mg/kg, containing 110 ± 5 μCi of total radioactivity.

The dogs were housed in metabolism cages that permitted the separate collection of urine and feces. Blood samples were drawn into heparinized syringes periodically for 14 days. The total urinary and fecal excretions were collected daily for 14 days; then the dogs were anesthetized with pentobarbital (30 mg/kg iv) and sacrificed by the intravenous injection of 5 ml of a saturated solution of potassium chloride.

The dogs were necropsied, and selected tissues were analyzed for residual radioactivity. In addition, the entire musculature of the left and right thighs was removed and analyzed so that the amount of radioactivity remaining in the injection site could be determined.

Analysis of Plasma—A 0.8-ml plasma sample was dissolved in 4 ml of solubilizer[1]. The sample was counted with 15 ml of toluene

[1] NCS solubilizer, Amersham/Searle Corp., Des Plaines, Ill.

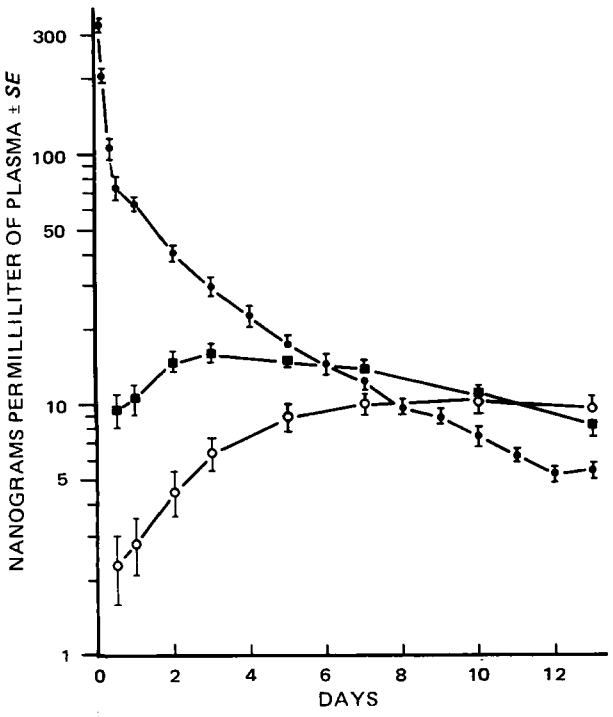

Figure 1—*Average concentrations of radioactivity in the plasma of male dogs after the intramuscular administration of 2-mg/kg doses of ^{14}C-fluphenazine base (●), ^{14}C-fluphenazine enanthate (■), or ^{14}C-fluphenazine decanoate (○) (n = 5/group). All three compounds were administered in sesame oil. The dogs ranged in weight from 9.2 to 11.6 kg. To facilitate comparison among the three compounds, the data were truncated at 13 days.*

scintillation fluid containing 5 g of 2,5-diphenyloxazole and 300 mg of 1,4-bis[2-(4-methyl-5-phenyloxazolyl)]benzene/liter of toluene.

Extraction Procedure for Plasma—Plasma (9–12 ml) from dogs was mixed with four volumes of methanol (40 ml) and shaken for 20 min. The samples were centrifuged at 200×*g* (10°), and the supernatant fluid was recovered and saved. The pellet that remained was extracted by shaking it with the same volume of methanol (40 ml) originally added to the plasma and centrifuging. The combined supernatant fluids were concentrated almost to dryness under reduced pressure at 40–50°. This extraction procedure removed the following average amounts of radioactivity from the plasma of dogs after intravenous treatment with the indicated drug: 77%, ^{14}C-fluphenazine; 68%, ^{14}C-fluphenazine enanthate; and 84%, ^{14}C-fluphenazine decanoate.

Analysis of Urine, Bile, and Feces—Samples of feces (200 g) were homogenized with 400 ml of methanol; 790–825 mg of homogenate was combusted[2]. Samples of urine (0.2 ml) and bile (50 μl) were counted directly in 15 ml of scintillation fluid (2).

Analysis of Tissues—Brain samples (80 g) were homogenized in water (100 ml), using an all-glass homogenizer[3]; 790–810 mg of homogenate was combusted. Certain portions of the eye (lens, cornea, aqueous and vitreous humors, and combined retina, choroid, and sclera) and blood were combusted. Similarly, representative portions of omental fat (180–220 mg) and skin without hair (280–320 mg) were combusted. Samples of kidney, liver, and thigh muscle were ground in a meat grinder; then 780–820 mg of the well-mixed sample was combusted.

Bile Collection—Purebred male beagles (8.8–15.8 kg) were anesthetized with pentobarbital (30 mg/kg iv). The radial vein of each dog was cannulated, and a buffered solution of mannitol and pentobarbital was infused throughout the 8-hr experiments at a rate of about 3 ml/min. The solution contained: mannitol, 100 g; monobasic potassium phosphate, 0.2 g; dibasic potassium phosphate, 0.9 g; pentobarbital, 25.5 mg/kg; and sufficient water to make a final volume of 2 liters.

A catheter was inserted into the urinary bladder of each dog. Then a midline incision was made, the entrance to the gallbladder from the bile duct was clamped, and the common bile duct was cannulated with polyethylene tubing (No. 100) near its point of entry into the duodenum. The midline incision was closed with wound clips. At the conclusion of the experiment, each dog was sacrificed by the intravenous administration of 5 ml of a saturated solution of potassium chloride.

Chromatography—Samples of bile (25–50 μl) and extracts of plasma (50–100 μl) were applied onto thin-layer plates coated with silica gel[4] and developed in benzene–28% ammonia–dioxane (60:5:35). This solvent system resolved fluphenazine base from its enanthate and decanoate esters and also from some of the unidentified metabolites (R_f values of 0.00, 0.06, and 0.23) of these three compounds.

The utility of this chromatographic system for separating fluphenazine base from its enanthate and decanoate esters was demonstrated by the following experiment. Solutions (5 ml, 80 μg/ml) of the dihydrochloride salts of the enanthate and decanoate esters of ^{14}C-fluphenazine were prepared in dog plasma, which had been denatured by heating for 30 min in a boiling water bath. These solutions were made strongly alkaline (pH 12–13) by the addition of 1 drop of 50% sodium hydroxide and incubated in a boiling water bath for 90 min. After incubation, the pH was adjusted to 6.5–7.5 and the samples were chromatographed. None of the radioactivity was now present at the R_f value of either ester; instead, all of it had been transformed to unesterified ^{14}C-fluphenazine base, as judged by the coincidence of the radioactive peak and the authentic reference compound.

Counting of Samples—Radioactivity in each sample was measured by a liquid scintillation spectrometer[5]. Counting efficiency was determined with automatic external standardization and the use of previously prepared quench curves. Chromatograms were scanned[6] for the presence of radioactivity, and the area under each curve was integrated in duplicate by using a planimeter. The average areas were accepted if the duplicate measurements agreed within 1.5%.

RESULTS

Intramuscular Studies with Unesterified ^{14}C-Fluphenazine Base—Average concentrations of radioactivity in the plasma of dogs dosed with 2 mg/kg im of unesterified ^{14}C-fluphenazine base in sesame oil are shown in Fig. 1. For comparison, plasma concentrations from an earlier study (1) are shown; the enanthate and decanoate esters had been given to dogs at 2 mg/kg under identical conditions. Even though ^{14}C-fluphenazine base was administered intramuscularly in sesame oil, no sustained-release effect was found for any of the five dogs, as was the case for the enanthate and decanoate esters.

Concentrations of radioactivity, already at a maximum 2 hr after the dogs were dosed, declined rapidly at first (2–12 hr) and then more slowly during the remainder of the test. Half-lives of elimination of radioactivity from the plasma were calculated for each dog based on a linear regression analysis. The regression lines for the concentrations of radioactivity in the plasma of each dog were calculated for the 2–12-hr and 2–14-day intervals. The pooled average values, considered to represent the most accurate analysis of regression, indicate an elimination half-life of radioactivity from plasma of 3.20 hr for the 2–12-hr interval after dosing (by the method of residuals). This portion of the plasma curve may represent a combination of distribution of radioactivity into tissues and excretion, but this point has not been verified experimentally. The elimination half-life of radioactivity from plasma during the 2–14-day interval is a pooled average of 4.02 days.

The average daily excretion of radioactivity in the urine and feces by the five dogs is shown in Table I. No more than 6% of the dose was excreted in urine by any individual dog, with the remainder appearing in the feces. Most of the radioactivity (102.3% of the dose) was excreted during the first 4 days, particularly during the first 2 days after dosing (90.1% of the dose). Four days after the dogs were dosed, they excreted only an additional 1.7–5.8% of the dose. This rapid excretion during the first 2 days after dosing also indicates a general lack of slow-release characteristics in dogs dosed with ^{14}C-fluphenazine base.

Fourteen days after the dogs were dosed, they were necropsied;

[2] Biological material oxidizer, R. J. Harvey Instrument Corp., Hillsdale, N.J.

[3] Potter-Elvehjem, Fisher Scientific Co., Springfield, N.J.

[4] QIF, Quantum Industries, Fairfield, N.J.

[5] Packard Tri-Carb model 3380, Packard Instrument Co., Downers Grove, Ill.

[6] Nuclear-Chicago Actigraph III, Amersham/Searle Corp., Des Plaines, Ill.

Table I—Average Daily Excretion of Radioactivity by Five Male Dogs after Intramuscular Administration of ^{14}C-Fluphenazine Base in Sesame Oil (2 mg/kg)

Days	Average[a] Percent of Dose ± *SE*		
	Urine	Feces	Total
1	2.30 ± 0.24	25.53 ± 10.63	27.84 ± 10.79
2	1.19 ± 0.26	61.09 ± 9.98	62.27 ± 10.07
3	0.40 ± 0.07	2.36 ± 0.23	2.76 ± 0.25
4	0.21 ± 0.04	9.18 ± 1.84	9.39 ± 1.85
5	0.13 ± 0.02	1.30 ± 0.35	1.44 ± 0.35
6	0.080 ± 0.014	0.70 ± 0.18	0.78 ± 0.18
7	0.047 ± 0.009	0.33 ± 0.07	0.38 ± 0.07
8	0.044 ± 0.006	0.26 ± 0.03	0.30 ± 0.03
9	0.028 ± 0.004	0.20 ± 0.01	0.23 ± 0.01
10	0.018 ± 0.001	0.15 ± 0.01	0.17 ± 0.01
11	0.014 ± 0.001	0.094 ± 0.009	0.11 ± 0.01
12	0.017 ± 0.003	0.10 ± 0.01	0.12 ± 0.01
13	0.019 ± 0.002	0.093 ± 0.004	0.11 ± 0.01
14	0.013 ± 0.002	0.067 ± 0.018	0.080 ± 0.019
Pan rinse	0.11 ± 0.02	—	0.11 ± 0.02
	4.64 ± 0.48	101.47 ± 0.92	106.08 ± 0.92

[a] All average values were rounded to two significant figures.

Table II—Average Residual Radioactivity in Selected Tissues of Five Male Dogs 14 Days after Intramuscular Administration of ^{14}C-Fluphenazine Base in Sesame Oil (2 mg/kg)

Tissue	Average ± *SE*	
	μg/g	% of Dose
Brain	0.000	0.000
Combined retina, choroid, and sclera	0.83 ± 0.13	—
Cornea	0.021 ± 0.003	—
Aqueous humor	0.013 ± 0.006	—
Vitreous humor	0.015 ± 0.006	—
Lens	0.006 ± 0.003	—
Kidneys	0.043 ± 0.004	0.010 ± 0.001
Liver	0.37 ± 0.03	0.54 ± 0.04
Omental fat	0.006 ± 0.003	—
Skin	0.024 ± 0.003	—
Left thigh muscle (contains injection site)	0.18 ± 0.02	0.44[a] ± 0.06
Right thigh muscle	0.003 ± 0.001	0.006 ± 0.001
Blood, μg/ml	0.004 ± 0.001	—

[a] The radioactivity remaining at each injection site, as presented in the text, was determined by subtracting the total amount of radioactivity present in the right thigh muscle from that present in the left thigh muscle.

selected tissues were removed for the analysis of residual radioactivity, including the thigh muscle containing the site of injection (Table II). The small amounts of radioactivity remaining at the sites of injection, an average of 0.43% (range of 0.29–0.55% of the dose), were consistent with the finding of essentially complete excretion of radioactivity by each dog. Of the other tissues analyzed, only the liver and the portion of the eye consisting of the combined retina, choroid, and sclera contained any appreciable quantities of radioactivity. The binding of phenothiazines to melanin is a well-documented phenomenon (3).

The excretion of ^{14}C-fluphenazine, its metabolites, or both in bile probably accounts for the relatively greater amounts of residual radioactivity found in liver than in the other tissues. Interestingly, no radioactivity could be detected in a homogenate of whole brain from any of the dogs, even though small amounts of radioactivity were still detectable in plasma 14 days after dosing. This finding is in contrast to the intramuscular injection of the enanthate and decanoate esters. In those cases, small amounts of radioactivity were present in the brain and blood 35 days after the dogs were dosed (1).

Intravenous Studies in Intact Dogs—^{14}C-Fluphenazine and the dihydrochloride salts of the enanthate and decanoate esters were administered to intact dogs at doses of 1 mg/kg iv. Regardless of which compound was administered, concentrations of radioactivity in the plasma of these dogs were quite comparable, except during the first 30 min after drug administration (Fig. 2). During this early time, radioactivity from each compound was being distributed to the various tissues of the body. Thereafter, the rates of elimination of total radioactivity from plasma were similar for each of the three compounds. Therefore, no slow-release characteristics were found when the enanthate and decanoate esters of fluphenazine were administered intravenously; such an effect was found previously when the esters were administered intramuscularly in sesame oil to dogs (1).

A large sample of blood (25–30 ml) was taken from each dog 30 min after it was dosed intravenously with either ^{14}C-fluphenazine or its enanthate or decanoate ester. The plasma (9–12 ml) from each blood sample was recovered, extracted, and chromatographed (Fig. 3). For two of the three dogs given ^{14}C-fluphenazine (upper portion of Fig. 3), there were detectable amounts of unchanged ^{14}C-fluphenazine in plasma, amounting to 28 and 72% of the radioactivity applied to the chromatograms. For both of these dogs, an unidentified metabolite with an R_f value of about 0.20 was also present, and there were additional unidentified metabolites present at (R_f value of 0.00) or just

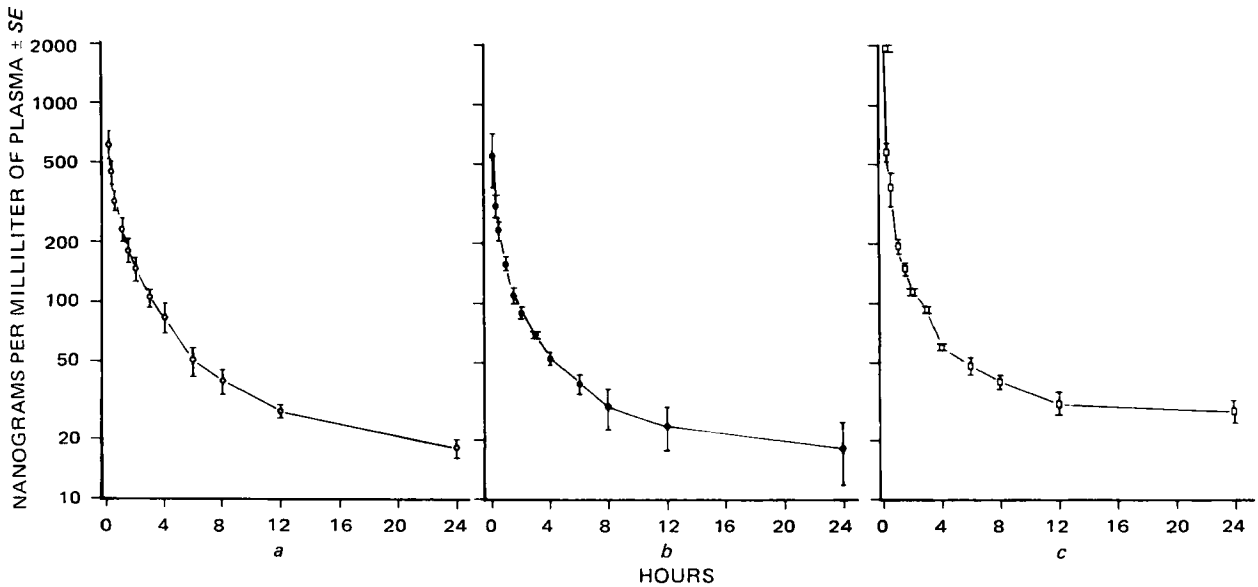

Figure 2—*Average concentrations of radioactivity in the plasma of intact male dogs after the intravenous administration of 1-mg/kg doses of ^{14}C-fluphenazine* (n = 3) (a), *^{14}C-fluphenazine enanthate dihydrochloride* (n = 2) (b), *or ^{14}C-fluphenazine decanoate dihydrochloride* (n = 2) (c). *All three compounds were dissolved in 1.5 ml of water containing either 25 or 50% ethanol and injected during 2-min periods.*

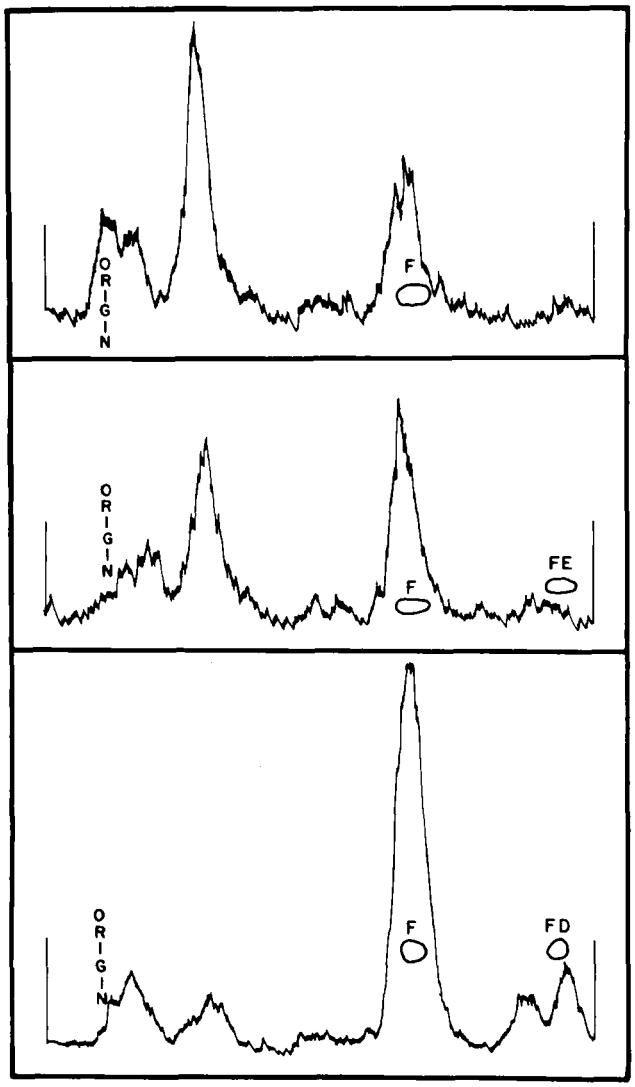

Figure 3—*Typical thin-layer chromatograms of extracts obtained from the plasma of dogs after the intravenous administration of 1-mg/kg doses of ^{14}C-fluphenazine (top), ^{14}C-fluphenazine enanthate dihydrochloride (middle), or ^{14}C-fluphenazine decanoate dihydrochloride (bottom). The circled areas represent material visible under UV light (254 nm). F is ^{14}C-fluphenazine base, FE is ^{14}C-fluphenazine enanthate, and FD is ^{14}C-fluphenazine decanoate.*

ahead of (R_f values of 0.06 and 0.23) the origin of this chromatogram.

Chromatograms of the extracts of plasma prepared 30 min after the dogs had been dosed intravenously with the enanthate ester are shown in the middle portion of Fig. 3. Virtually no unchanged ^{14}C-fluphenazine enanthate was present in these plasma samples (about 6%); however, significant amounts of ^{14}C-fluphenazine base (15 and 44%) were found, as well as the other metabolites that had been found previously in the plasma of dogs dosed with ^{14}C-fluphenazine. Chromatograms of plasma extracts of the dogs dosed intravenously with the decanoate ester (lower portion of Fig. 3) generally resembled those for dogs dosed with the enanthate ester: 9 and 21% of the radioactivity were unchanged ^{14}C-fluphenazine decanoate, 11 and 57% were unchanged ^{14}C-fluphenazine base, and the same additional metabolites were present as had been found in the plasma of dogs dosed with ^{14}C-fluphenazine.

The excretion of radioactivity in the urine and feces of each intact dog dosed intravenously with either ^{14}C-fluphenazine or its enanthate or decanoate ester is shown in the appropriate columns of Tables III and IV, respectively. Regardless of whether ^{14}C-fluphenazine or its enanthate or decanoate ester was administered intravenously, the excretion of radioactivity in urine and feces was similar as a function of time, and the total amounts of radioactivity excreted in the urine and feces in 7 days were essentially the same. Significantly, based on data for excretion, no slow-release characteristics were produced after the intravenous administration of either of the two esters.

Intravenous Studies in Bile-Cannulated Dogs—Since most of the radioactivity after an intravenous dose of ^{14}C-fluphenazine or its enanthate or decanoate ester was excreted in feces, it was difficult to follow the rates of excretion and biotransformation of any of these three compounds unless the bile was collected continuously. Accordingly, a comparison was made of excretion and biotransformation after administration of each of the three compounds to dogs whose bile ducts had been cannulated for the continuous collection of bile.

Single dogs prepared surgically in this manner were given 1-mg/kg doses of either ^{14}C-fluphenazine or the dihydrochloride salts of the enanthate or decanoate esters. As shown in Table V, approximately the same amounts of total radioactivity were excreted in urine and bile during an 8-hr test (58–75% of the dose). In addition, the approximate rates at which these total amounts of radioactivity were excreted as a function of time were comparable, and no unchanged ^{14}C-fluphenazine base or either of its esters was detectable in the earliest bile samples (0–1 hr) collected from the dogs given any of the three compounds.

An earlier study (4) showed that the nature of the radioactivity excreted in the bile of dogs dosed with ^{14}C-fluphenazine enanthate consisted primarily of the glucuronide conjugate of 7-hydroxyfluphenazine.

Eight hours after they were dosed, these three bile-cannulated dogs had similar amounts of radioactivity remaining in selected tissues (Table VI). No matter which of the three compounds was administered, radioactivity was most concentrated in the liver and lungs and less concentrated in the blood and other tissues examined.

DISCUSSION

Additional data summarizing the comparative rates of excretion of radioactivity in the urine and feces of intact dogs after intramus-

Table III—Average Excretion of Radioactivity in the Urine of Dogs after Intravenous (1 mg/kg) or Intramuscular (2 mg/kg in Sesame Oil) Administration of ^{14}C-Fluphenazine, ^{14}C-Fluphenazine Enanthate, or ^{14}C-Fluphenazine Decanoate

	Average Percent of Dose ± *SE*					
	^{14}C-Fluphenazine		^{14}C-Fluphenazine Enanthate		^{14}C-Fluphenazine Decanoate	
Days	Intravenously[a]	Intramuscularly[b]	Intravenously[a]	Intramuscularly[b]	Intravenously[a]	Intramuscularly[b]
1	2.22 ± 0.29	2.30 ± 0.24	1.86 ± 0.04	0.20 ± 0.04	—[c]	0.04 ± 0.00
2	0.80 ± 0.10	1.19 ± 0.26	0.76 ± 0.31	0.29 ± 0.03	2.98 ± 0.09	0.07 ± 0.02
3	0.43 ± 0.06	0.40 ± 0.07	0.26 ± 0.01	0.36 ± 0.07	0.41 ± 0.23	0.10 ± 0.02
4	0.36 ± 0.24	0.21 ± 0.04	0.18 ± 0.05	0.43 ± 0.03	0.22 ± 0.06	0.14 ± 0.03
5	0.16 ± 0.09	0.13 ± 0.02	0.07 ± 0.01	0.35 ± 0.05	0.12 ± 0.02	0.13 ± 0.03
6	0.06 ± 0.02	0.08 ± 0.01	0.05 ± 0.01	0.33 ± 0.01	0.11 ± 0.06	0.16 ± 0.02
7	0.05 ± 0.02	0.05 ± 0.01	0.05 ± 0.01	0.27 ± 0.02	0.03 ± 0.01	0.17 ± 0.03
	4.08[d] ± 0.06	4.35[d] ± 0.45	3.23[d] ± 0.41	2.18[d] ± 0.10	3.87[d] ± 0.28	0.81[d] ± 0.07

[a] Dihydrochloride salt. [b] Base. [c] None excreted. [d] The average weekly totals (±*SE*) for each treatment group were calculated based on the total amount of radioactivity excreted during the first 7 days by *each* dog. The average amounts (±*SE*) excreted per day for each treatment group were calculated based only on those dogs that actually excreted a sample on that particular day.

Table IV—Average Excretion of Radioactivity in the Feces of Dogs after Intravenous (1 mg/kg) or Intramuscular (2 mg/kg in Sesame Oil) Administration of ^{14}C-Fluphenazine, ^{14}C-Fluphenazine Enanthate, or ^{14}C-Fluphenazine Decanoate

	Average Percent of Dose ± *SE*					
	^{14}C-Fluphenazine		^{14}C-Fluphenazine Enanthate		^{14}C-Fluphenazine Decanoate	
Days	Intravenously[a]	Intramuscularly[b]	Intravenously[a]	Intramuscularly[b]	Intravenously[a]	Intramuscularly[b]
1	48.67 ± 15.51	31.92 ± 10.97	42.31 ± 36.35	1.23 ± 0.98	—[c]	0.50 ± 0.15
2	29.73 ± 14.43	61.09 ± 9.98	51.70 ± 30.77	10.57 ± 1.88	60.99 ± 21.30	1.29 ± 0.20
3	18.50 ± 9.54	2.36 ± 0.23	5.73 ± 2.30	7.17 ± 1.66	22.77 ± 17.50	2.98 ± 0.62
4	17.27 ± 15.12	9.18 ± 1.84	1.57 ± 0.01	8.16 ± 0.60	4.56 ± 1.39	2.63 ± 0.41
5	4.14 ± 3.24	1.30 ± 0.35	0.59 ± 0.05	9.20 ± 0.90	2.32 ± 1.33	3.22 ± 0.53
6	1.00 ± 0.60	0.70 ± 0.18	0.24 ± 0.05	5.18 ± 0.96	0.65 ± 0.09	3.60 ± 0.61
7	0.32 ± 0.15	0.33 ± 0.07	0.32 ± 0.02	5.90 ± 1.46	0.58 ± 0.46	2.84 ± 0.43
	103.40[d] ± 2.81	100.49[d] ± 0.92	102.46[d] ± 3.36	44.80[d] ± 2.58	91.87[d] ± 0.55	16.26[d] ± 2.34

[a] Dihydrochloride salt. [b] Base. [c] None excreted. [d] The average weekly totals (±*SE*) for each treatment group were calculated based on the total amount of radioactivity excreted during the first 7 days by *each* dog. The average amounts (±*SE*) excreted per day for each treatment group were calculated based only on those dogs that actually excreted a sample on that particular day.

Table V—Excretion of Radioactivity in the Urine and Bile of Dogs after Intravenous Administration of ^{14}C-Fluphenazine, ^{14}C-Fluphenazine Enanthate, or ^{14}C-Fluphenazine Decanoate (1 mg/kg)

	Percent of Dose		
Hours	^{14}C-Fluphenazine[a]	^{14}C-Fluphenazine Enanthate[a]	^{14}C-Fluphenazine Decanoate[a]
0–1	17.60	18.37	23.46
1–2	19.93	19.33	21.36
2–3	10.21	6.81	6.83
3–4	7.34	4.08	4.32
4–5	5.44	3.16	3.77
5–6	4.98	2.29	2.69
6–7	4.57	2.00	2.42
7–8	4.55	2.31	1.81
	74.62	58.35	66.66

[a] Dihydrochloride salt.

cular doses of ^{14}C-fluphenazine base or of its enanthate or decanoate ester (2 mg/kg) are shown in Tables III and IV. Although the intramuscular studies were for longer periods (14–35 days) than the intravenous studies (7 days), the data for both routes of administration were truncated at 7 days to permit direct comparison.

After intact dogs were dosed either intravenously or intramuscularly with ^{14}C-fluphenazine, similar amounts of radioactivity (intravenously, 107.5% of the dose; intramuscularly, 104.8% of the dose) were excreted in 7 days in urine and feces. After the administration of ^{14}C-fluphenazine by either route, most of the dose was excreted during the first 2 days (intravenously, 65.2% of the dose; intramuscularly, 90.1% of the dose). Thus, the administration of unesterified ^{14}C-fluphenazine base, either intravenously or intramuscularly, does not produce slow-release characteristics.

After the dosing of intact dogs with ^{14}C-fluphenazine enanthate, the excretion of radioactivity within 7 days was almost complete for dogs dosed intravenously but was only about half completed for dogs dosed intramuscularly. The results for intact dogs that were dosed either intravenously or intramuscularly with ^{14}C-fluphenazine decanoate were similar to those after dosing of such animals with the enanthate ester; however, for the decanoate ester, the rate of excretion of radioactivity was still slower than it was for the enanthate ester after the latter was administered intramuscularly. Thus, the intravenous administration of ^{14}C-fluphenazine or of its enanthate or decanoate ester to intact or bile-cannulated dogs produced no slow-release characteristics. In addition, the intramuscular administration of ^{14}C-fluphenazine base in sesame oil produced no slow-release characteristics, unless the parent molecule was esterified with heptanoic or decanoic acid.

An earlier study (1) compared the relative rates of release of ^{14}C-fluphenazine enanthate and ^{14}C-fluphenazine decanoate when these drugs were given intramuscularly (2 mg/kg) in sesame oil to dogs under the same conditions used in the present study with ^{14}C-fluphenazine base. ^{14}C-Fluphenazine decanoate was released from the site of injection more slowly than was the enanthate ester. By contrast, the administration of ^{14}C-fluphenazine base did not produce any slow-release characteristics; a large fraction of the dose was released from the site of injection during the first 12 hr after dosing.

Since, after the intramuscular administration of ^{14}C-fluphenazine base, most of the radioactivity was released from the site of injection

Table VI—Residual Radioactivity in Selected Tissues of Dogs 8 hr after Intravenous Administration of ^{14}C-Fluphenazine, ^{14}C-Fluphenazine Enanthate, or ^{14}C-Fluphenazine Decanoate (1 mg/kg)

	^{14}C-Fluphenazine[a,b]		^{14}C-Fluphenazine Enanthate[a,c]		^{14}C-Fluphenazine Decanoate[a,d]	
Tissue	Amount in Tissue, μg/g	Amount in Entire Organ, % of Dose	Amount in Tissue, μg/g	Amount in Entire Organ, % of Dose	Amount in Tissue, μg/g	Amount in Entire Organ, % of Dose
Brain cortex and subcortex	0.56	—	0.43	—	0.37	—
Brain stem	0.67	—	0.40	—	0.34	—
Cerebellum	0.27	—	0.52	—	0.26	—
Dorsal and hypothalamus	0.58	—	0.75	—	0.35	—
Heart	0.38	0.30	0.42	0.38	0.26	0.25
Kidneys	0.55	0.37	0.69	0.39	0.44	0.30
Liver	3.31	9.62	3.69	8.00	2.79	7.02
Lungs	2.91	2.52	2.73	1.71	2.67	2.07
Skeletal muscle	0.19	—	0.63	—	0.18	—
Omental fat	0.15	—	0.24	—	0.15	—
Skin	0.27	—	0.15	—	0.096	—
Blood, μg/ml	0.050	—	0.031	—	0.050	—

[a] Dihydrochloride salt. [b] A male dog was given 1 mg/kg of ^{14}C-fluphenazine dissolved in 3.4 ml of water as an intravenous injection lasting 2 min. [c] A male dog was given 1 mg/kg of ^{14}C-fluphenazine enanthate dissolved in 6.2 ml of water containing 28% ethanol as an intravenous injection lasting 2 min. [d] A male dog was given 1 mg/kg of ^{14}C-fluphenazine decanoate dissolved in 4.6 ml of water as an intravenous injection lasting 2 min.

and excreted from the body during the first 2–4 days after dosing, the concentrations of radioactivity remaining in the plasma during the 2–14-day interval after dosing are assumed to represent largely metabolites of fluphenazine rather than the parent compound. However, this point could not be established experimentally. On the other hand, in the case of the esters of fluphenazine base, because of their slow-release characteristics, the esters themselves, or fluphenazine base, the product of their hydrolysis, may be released continuously into the circulation for a much longer period.

For all intact dogs given intravenous doses (1 mg/kg) of ^{14}C-fluphenazine or of its enanthate or decanoate ester, virtually identical concentrations of radioactivity were present in the circulation. In addition, the enanthate and decanoate esters of ^{14}C-fluphenazine were rapidly converted to ^{14}C-fluphenazine base and other unidentified metabolites. Thus, slow-release characteristics were not produced by the intravenous administration of the esters of ^{14}C-fluphenazine base.

A number of other lines of evidence point to the fact that the slow-release characteristics produced by the esterified fluphenazine base are a function both of esterification *per se* and of intramuscular administration. In an earlier study (1), a comparison was made, during a 35-day period, of the relative rates of release of ^{14}C-fluphenazine enanthate and ^{14}C-fluphenazine decanoate. The rates of excretion of total radioactivity in urine and feces after administration of either of these two esters intramuscularly in sesame oil were dissimilar; however, the radioactivity was excreted at the same rate in *both* urine and feces for each ester but more slowly for the decanoate ester than for the enanthate ester. This finding is consistent with the idea that the rate-limiting step for the release of either ester is its diffusion into the circulation from the injection site.

Yet another experimental situation points to the necessity of administering ^{14}C-fluphenazine enanthate intramuscularly, although not necessarily in the presence of sesame oil, to produce slow-release characteristics. In that situation, a dog whose bile duct had been cannulated was given a 1-mg/kg im dose of ^{14}C-fluphenazine enanthate in absolute ethanol (4). During the 8-hr test, concentrations of radioactivity in the plasma increased consistently. Only about 0.55% of the dose was excreted during the 8 hr, the major portion of the dose (88%) remaining at the site of injection. Thus, the administration of ^{14}C-fluphenazine enanthate intramuscularly, but not necessarily in sesame oil, was capable of producing slow-release characteristics.

Studies *in vitro* have shown that ^{14}C-fluphenazine enanthate (4) and ^{14}C-fluphenazine decanoate[7] can be hydrolyzed slowly by plasma esterases of the dog. The rates of hydrolysis of these two esters in plasma, however, appeared to be much slower than those occurring in intact dogs when the compounds were injected intravenously. This observation suggests that other organs, such as the liver, may have a much greater enzymatic capacity than does the plasma to cleave these esters. The observation that most of an intravenous dose of ^{14}C-fluphenazine enanthate or ^{14}C-fluphenazine decanoate (1 mg/kg) can be hydrolyzed within 30 min suggests that the hydrolytic capabilities of the dog are much greater than the rates at which these two esters, formulated in sesame oil, are usually released from their intramuscular injection sites.

All of these observations point to the conclusions that:

1. The slow-release characteristics produced by the enanthate and decanoate esters of fluphenazine base are a consequence of their relative rates of diffusion into the circulation from an injection site.
2. Cleavage of these esters in the circulation occurs rapidly and plays little, if any, role in the observed differences between their relative rates of release.

Once either of these two esters is released into the circulation of dogs, it is rapidly hydrolyzed to fluphenazine base and further metabolized according to the metabolic pathways previously described for ^{14}C-fluphenazine (5).

[7] J. Dreyfuss and J. M. Shaw, unpublished data.

REFERENCES

(1) J. Dreyfuss, J. J. Ross, Jr., J. M. Shaw, I. Miller, and E. C. Schreiber, *J. Pharm. Sci.*, **65**, 502(1976).

(2) G. A. Bray, *Anal. Biochem.*, **1**, 279(1960).

(3) A. M. Potts, *Invest. Ophthalmol.*, **3**, 406(1964).

(4) J. Dreyfuss, J. J. Ross, Jr., and E. C. Schreiber, *J. Pharm. Sci.*, **60**, 829(1971).

(5) *Ibid.*, **60**, 821(1971).

ACKNOWLEDGMENTS AND ADDRESSES

Received August 16, 1975, from the *Department of Drug Metabolism, Squibb Institute for Medical Research, New Brunswick, NJ 08903*

Accepted for publication November 13, 1975.

The authors thank Mr. F. Dondzila for the synthesis of ^{14}C-fluphenazine; Mr. Peter Egli for the synthesis of ^{14}C-fluphenazine base, ^{14}C-fluphenazine enanthate, and ^{14}C-fluphenazine decanoate; Mrs. Louise Woodson and Mr. Carmen Mondi for excellent technical assistance; Dr. Sampat Singhvi for helpful discussions; Mr. Sal Meloni for preparing the illustrations; and Dr. David Frost for editing the manuscript.

[x] To whom inquiries should be directed.

dc Polarographic Assay of Tetracyclines

L. G. CHATTEN [x], R. E. MOSKALYK, R. A. LOCOCK, and K-S. HUANG

Abstract □ The optimum conditions for the polarographic reduction of some tetracycline antibiotics were studied. A boric acid–sodium borate buffer provided the best conditions for the electroreduction of tetracycline, oxytetracycline, chlortetracycline, and demeclocycline. Conditions are described for the quantitative determination of these tetracyclines in various dosage forms.

Keyphrases □ Tetracycline—polarographic analysis, pharmaceutical formulations □ Oxytetracycline—polarographic analysis, pharmaceutical formulations □ Chlortetracycline—polarographic analysis, pharmaceutical formulations □ Demeclocycline—polarographic analysis, pharmaceutical formulations □ Polarography—analysis, tetracycline, oxytetracycline, chlortetracycline, and demeclocycline in pharmaceutical formulations □ Antibiotics—tetracycline, oxytetracycline, chlortetracycline, demeclocycline, polarographic analysis in pharmaceutical formulations

Despite their well-known disadvantages, microbiological assays remain as the official methods of analysis for the tetracyclines (1, 2). However, the search for more accurate alternatives continues. Recently, two reviews (3, 4) dealt with the many methods reported for this important class of antibiotics.

Polarographic analyses of tetracyclines were first reported in the early 1950's (5, 6), and numerous studies

and excreted from the body during the first 2–4 days after dosing, the concentrations of radioactivity remaining in the plasma during the 2–14-day interval after dosing are assumed to represent largely metabolites of fluphenazine rather than the parent compound. However, this point could not be established experimentally. On the other hand, in the case of the esters of fluphenazine base, because of their slow-release characteristics, the esters themselves, or fluphenazine base, the product of their hydrolysis, may be released continuously into the circulation for a much longer period.

For all intact dogs given intravenous doses (1 mg/kg) of ^{14}C-fluphenazine or of its enanthate or decanoate ester, virtually identical concentrations of radioactivity were present in the circulation. In addition, the enanthate and decanoate esters of ^{14}C-fluphenazine were rapidly converted to ^{14}C-fluphenazine base and other unidentified metabolites. Thus, slow-release characteristics were not produced by the intravenous administration of the esters of ^{14}C-fluphenazine base.

A number of other lines of evidence point to the fact that the slow-release characteristics produced by the esterified fluphenazine base are a function both of esterification *per se* and of intramuscular administration. In an earlier study (1), a comparison was made, during a 35-day period, of the relative rates of release of ^{14}C-fluphenazine enanthate and ^{14}C-fluphenazine decanoate. The rates of excretion of total radioactivity in urine and feces after administration of either of these two esters intramuscularly in sesame oil were dissimilar; however, the radioactivity was excreted at the same rate in *both* urine and feces for each ester but more slowly for the decanoate ester than for the enanthate ester. This finding is consistent with the idea that the rate-limiting step for the release of either ester is its diffusion into the circulation from the injection site.

Yet another experimental situation points to the necessity of administering ^{14}C-fluphenazine enanthate intramuscularly, although not necessarily in the presence of sesame oil, to produce slow-release characteristics. In that situation, a dog whose bile duct had been cannulated was given a 1-mg/kg im dose of ^{14}C-fluphenazine enanthate in absolute ethanol (4). During the 8-hr test, concentrations of radioactivity in the plasma increased consistently. Only about 0.55% of the dose was excreted during the 8 hr, the major portion of the dose (88%) remaining at the site of injection. Thus, the administration of ^{14}C-fluphenazine enanthate intramuscularly, but not necessarily in sesame oil, was capable of producing slow-release characteristics.

Studies *in vitro* have shown that ^{14}C-fluphenazine enanthate (4) and ^{14}C-fluphenazine decanoate[7] can be hydrolyzed slowly by plasma esterases of the dog. The rates of hydrolysis of these two esters in plasma, however, appeared to be much slower than those occurring in intact dogs when the compounds were injected intravenously. This observation suggests that other organs, such as the liver, may have a much greater enzymatic capacity than does the plasma to cleave these esters. The observation that most of an intravenous dose of ^{14}C-fluphenazine enanthate or ^{14}C-fluphenazine decanoate (1 mg/kg) can be hydrolyzed within 30 min suggests that the hydrolytic capabilities of the dog are much greater than the rates at which these two esters, formulated in sesame oil, are usually released from their intramuscular injection sites.

All of these observations point to the conclusions that:

1. The slow-release characteristics produced by the enanthate and decanoate esters of fluphenazine base are a consequence of their relative rates of diffusion into the circulation from an injection site.
2. Cleavage of these esters in the circulation occurs rapidly and plays little, if any, role in the observed differences between their relative rates of release.

Once either of these two esters is released into the circulation of dogs, it is rapidly hydrolyzed to fluphenazine base and further metabolized according to the metabolic pathways previously described for ^{14}C-fluphenazine (5).

[7] J. Dreyfuss and J. M. Shaw, unpublished data.

REFERENCES

(1) J. Dreyfuss, J. J. Ross, Jr., J. M. Shaw, I. Miller, and E. C. Schreiber, *J. Pharm. Sci.*, **65**, 502(1976).

(2) G. A. Bray, *Anal. Biochem.*, **1**, 279(1960).

(3) A. M. Potts, *Invest. Ophthalmol.*, **3**, 406(1964).

(4) J. Dreyfuss, J. J. Ross, Jr., and E. C. Schreiber, *J. Pharm. Sci.*, **60**, 829(1971).

(5) *Ibid.*, **60**, 821(1971).

ACKNOWLEDGMENTS AND ADDRESSES

Received August 16, 1975, from the *Department of Drug Metabolism, Squibb Institute for Medical Research, New Brunswick, NJ 08903*

Accepted for publication November 13, 1975.

The authors thank Mr. F. Dondzila for the synthesis of ^{14}C-fluphenazine; Mr. Peter Egli for the synthesis of ^{14}C-fluphenazine base, ^{14}C-fluphenazine enanthate, and ^{14}C-fluphenazine decanoate; Mrs. Louise Woodson and Mr. Carmen Mondi for excellent technical assistance; Dr. Sampat Singhvi for helpful discussions; Mr. Sal Meloni for preparing the illustrations; and Dr. David Frost for editing the manuscript.

[x] To whom inquiries should be directed.

dc Polarographic Assay of Tetracyclines

L. G. CHATTEN [x], R. E. MOSKALYK, R. A. LOCOCK, and K-S. HUANG

Abstract □ The optimum conditions for the polarographic reduction of some tetracycline antibiotics were studied. A boric acid–sodium borate buffer provided the best conditions for the electroreduction of tetracycline, oxytetracycline, chlortetracycline, and demeclocycline. Conditions are described for the quantitative determination of these tetracyclines in various dosage forms.

Keyphrases □ Tetracycline—polarographic analysis, pharmaceutical formulations □ Oxytetracycline—polarographic analysis, pharmaceutical formulations □ Chlortetracycline—polarographic analysis, pharmaceutical formulations □ Demeclocycline—polarographic analysis, pharmaceutical formulations □ Polarography—analysis, tetracycline, oxytetracycline, chlortetracycline, and demeclocycline in pharmaceutical formulations □ Antibiotics—tetracycline, oxytetracycline, chlortetracycline, demeclocycline, polarographic analysis in pharmaceutical formulations

Despite their well-known disadvantages, microbiological assays remain as the official methods of analysis for the tetracyclines (1, 2). However, the search for more accurate alternatives continues. Recently, two reviews (3, 4) dealt with the many methods reported for this important class of antibiotics.

Polarographic analyses of tetracyclines were first reported in the early 1950's (5, 6), and numerous studies

Table I—Selected pH and Applied Potential at Which Total Diffusion Current is Read

Antibiotic	pH	Applied Voltage
Tetracycline hydrochloride	7.75	−1.70
Oxytetracycline hydrochloride	8.20	−1.60
Chlortetracycline hydrochloride	7.95	−1.66
Demeclocycline hydrochloride[a]	7.75	−1.70

[a] A 1% gelatin solution (0.13 ml) was added with a calibrated dropper.

on this subject have appeared since then (3). However, none of these studies has been concerned specifically with the potential of this technique for the quantitative analysis of the various tetracyclines in pharmaceutical dosage forms. Furthermore, although considerable work has been reported on the elucidation of the mechanism of reduction at the dropping mercury electrode (7–9), the exact nature and sites of reduction for these drugs remain in doubt.

The purposes of this present study were to systematically investigate the effect of pH and buffer systems on the reduction of these antibiotics at the dropping mercury electrode and then to apply the optimum conditions to their quantitative determination in pharmaceutical dosage forms. The results on the mechanism of reduction of the tetracyclines at the dropping mercury electrode will be the subject of a subsequent publication.

EXPERIMENTAL

Apparatus—All polarograms were recorded on a polarograph[1] equipped with a 30-ml H-type cell, maintained at 25 ± 0.2°, a saturated calomel electrode, and a dropping mercury electrode. A pH meter[2] fitted with a glass–calomel electrode system was used for all pH measurements and for the potentiometric titrations. Titration lamps and a magnetic stirring apparatus were also used.

Reagents and Solutions—All chemicals were either ACS or reagent grade. The following were used: acetic acid; 0.05 *N* perchloric acid in dioxane, standardized against primary standard potassium acid phthalate; 0.5% gentian violet in acetic acid; 6% mercuric acetate in acetic acid; 0.2 *M* boric acid stock solution; 0.05 *M* sodium borate stock solution; freshly prepared 1% gelatin solution; hydrochloric acid; and disodium ethylenediaminetetraacetic acid.

Reference Materials—Tetracycline hydrochloride (100.1%), oxytetracycline hydrochloride (96.8%), chlortetracycline hydrochloride (97.9%), and demeclocycline hydrochloride (100.6%) were used without further purification. Their purity was determined by the method of Sideri and Osol (10).

Optimum Buffer System and Optimum pH—The following buffer systems were examined: Britton–Robinson (pH 2.6–11.8), glycine–hydrochloric acid (pH 2.2–3.6), lithium acetate–acetic acid (pH 3.6–5.6), phthalate–sodium hydroxide (pH 4.2–6.0), barbital (pH 6.8–9.2), phosphate (pH 5.7–8.0), boric acid–sodium borate (pH 7.6–9.2), and sodium borate–sodium hydroxide (pH 9.3–10.0). All buffers were approximately 0.05 *M* (final dilution). Solutions of each buffer were prepared at intervals of 0.2 pH unit. After a 10-min deaeration with nitrogen, each buffer solution was scanned over an applied potential range of from 0 to −2.0 v.

Solutions of approximately 1×10^{-4} *M* for each tetracycline salt were prepared in each individual buffer solution, and a polarogram was obtained. The optimum buffer system was then selected, and a further study of the influence of pH was conducted at intervals of 0.1 pH unit. The pH was determined for all solutions before and after electrolysis.

Solution stability was determined for each tetracycline by obtaining polarograms on each solution at 0.5-hr intervals after preparation.

Calibration Curves—All calibration curves were made by averaging five determinations, and all current readings were corrected to account for the percent purity of the reference material.

A quantity of the tetracycline hydrochloride equivalent to about 50 mg of the antibiotic was accurately weighed, dissolved in boric acid–sodium borate buffer of optimum pH, transferred to a 100-ml volumetric flask, and diluted to volume with buffer (0.5 mg/ml). Working standard solutions were prepared to contain 0.010, 0.025, 0.0375, 0.050, 0.075, 0.100, and 0.125 mg/ml by appropriately diluting the stock solution with the buffer. A 25-ml aliquot of a standard solution was pipetted into the polarographic cell already equilibrated at 25° and then deaerated.

The applied potential range was from 0.00 to −2.00 v, and the sensitivity scale was set at 0.15 μamp/mm. The rate of mercury flow at the applied potential at which the diffusion current was measured was 2.95 mg/sec; the drop time, *t*, was 2.5 sec; and the mercury column height was 65.0 cm. Optimum conditions of pH and applied potential are presented in Table I.

Procedures for Dosage Forms—*Tablets and Capsules*—A suitable quantity of the powdered material was accurately weighed into a 150-ml beaker, 90 ml of the specified buffer solution was added, and the mixture was stirred for 10 min. The slurry was filtered under suction through a medium-porosity sintered-glass filter. The clear filtrate was quantitatively transferred to a 100-ml volumetric flask and diluted to volume with the specified buffer (concentration of stock solution ~0.5 mg/ml).

A 15-ml aliquot of the stock solution was quantitatively transferred to a 100-ml volumetric flask and diluted to volume with the buffer solution. A 25-ml aliquot of this solution was transferred to the polarographic cell. Deaeration was carried out, and the polarogram was obtained as previously described.

Ointments—The following modification was required. A stock solution was prepared by successively heating, stirring, cooling, and filtering an accurate weight of ointment with four separate portions of specified buffer (90, 50, 30, and 20 ml). The accumulated filtrate was transferred to a 200-ml volumetric flask and made up to volume with buffer. The procedure for tablets and capsules was then followed, beginning with: "A 15-ml aliquot of the stock solution . . . ."

Syrups, Suspensions, and Pediatric Drops—The liquid preparation was thoroughly mixed, and then a suitable quantity was pipetted into a 100-ml volumetric flask and diluted to volume with the optimum buffer (concentration of stock solution ~0.5 mg/ml). If the tetracycline existed as an insoluble form such as the free base or complex, an appropriate amount of 3 *M* HCl was added to ensure dissolution. The procedure for tablets and capsules was then followed, beginning with: "A 15-ml aliquot of the stock solution . . . ."

In the presence of a calcium–oxytetracycline complex, it was necessary to add 3 moles of disodium ethylenediaminetetraacetic acid/mole of complex.

RESULTS AND DISCUSSION

Doskočil and Vondrácek (5) examined the polarographic behavior of chlortetracycline in phosphate buffer from pH 5.0 to 8.2. They stated that the optimum condition for quantitative work was pH 6.0. The behavior of tetracycline, chlortetracycline, and oxytetracycline in phosphate buffers was investigated (11), and the optimum pH was 5.91 for tetracycline, 5.70 for chlortetracycline, and 6.0 for oxytetracycline. The author showed well-resolved second waves for each of these antibiotics and a good relationship between concentration in micrograms per milliliter and diffusion current. A reasonably well-resolved second wave for tetracycline hydrochloride in phosphate buffer at pH 6.2 was reported (12), and a plot of diffusion current *versus* concentration was linear. However, there was no reported attempt to apply the method to the analysis of pharmaceutical products.

In the present investigation into the use of phosphate buffers as media for the polarographic reduction of the tetracyclines, the results reported previously (5, 11, 12) could not be reproduced.

Maxima appeared in the polarograms for all antibiotics over the entire range studied in the phosphate buffer. Figure 1 illustrates the polarograms obtained for tetracycline in this buffer system and is representative for the other substances used. Only a small maximum occurred at pH 5.86; but when 1 drop of 1% gelatin (0.13 ml) was added, a poorly resolved wave resulted. In one study, Doskočil (6)

[1] Sargent model XV.
[2] Corning model 10.

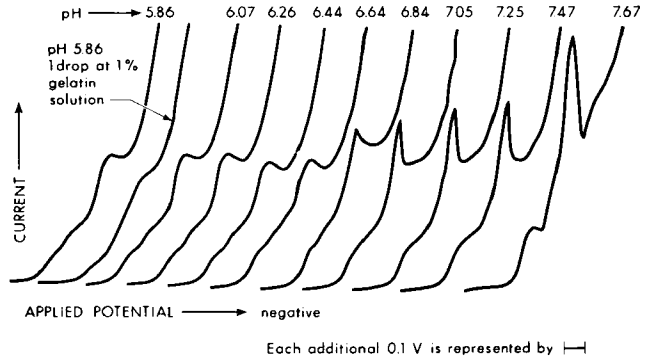

Figure 1—*Current–voltage curves of tetracycline hydrochloride in phosphate buffer. Each segment begins at −0.8 v. Concentration = 1.0 × 10⁻⁴ M.*

obtained poorly resolved waves at pH 8.3 with 0.2 *M* phosphate buffer. Silvestri (13) reported the behavior of doxycycline in phosphate buffer at pH 6, and his figures show that the two doxycycline waves were poorly resolved and could not be used quantitatively.

A method involving ac polarography was reported (14), and Hetman (15, 16) utilized differential cathode ray polarography with a twin-cell technique. While considerable advances have been made recently in ac polarography, the equipment for these two aspects is not so common that either can be employed on a routine analytical basis.

As outlined under *Experimental*, the suitability of a number of buffer systems for dc polarography was investigated. Polarograms were obtained at 0.2 pH intervals for each buffer over its entire operating range. Then solutions of the four tetracycline salts were prepared with each individual buffer solution. Only a few polarograms were found to be of analytical value.

In the Britton–Robinson buffer, the second wave for all tetracyclines was obscured by the reduction of hydrogen ion at pH values below 6. This result was generally true for all buffers studied. The glycine–hydrochloric acid buffer (pH 2.2–3.6) gave very poorly resolved polarograms for this reason. The same situation was observed with the lithium acetate–acetic acid buffer (pH 3.6–5.6) and potassium acid phthalate–sodium hydroxide buffer (pH 4.2–6.0). In the latter buffer, however, tetracycline hydrochloride gave three poorly resolved waves (pH 5.8–6.0), which were of no analytical value. Maxima were readily apparent over the entire range of the barbital sodium–hydrochloric acid buffer (pH 6.8–9.2). In the sodium borate–sodium hydroxide buffer (pH 9.3–10.0), a series of poorly resolved waves occurred for the tetracyclines.

Only in the boric acid–sodium borate buffer (pH 7.6–9.2) was it possible to achieve a well-resolved limiting current plateau for the tetracyclines (Fig. 2). The optimum pH for tetracycline hydrochloride was chosen to be 7.75, while 8.20 and 7.95 were the values for oxytetracycline and chlortetracycline, respectively. Figure 3 shows that demeclocycline gave either maxima or poorly resolved waves over the entire range of this buffer. However, the addition of 0.13 ml of 1% gelatin solution at pH 7.75 resulted in a satisfactory polarogram.

Solutions of 1×10^{-4} *M* were employed for all tetracyclines to determine diffusion dependency in the selected buffer system and at the optimum pH. The height of the mercury column was set at arbitrary intervals between 56.0 and 90.0 cm, and a polarogram was ob-

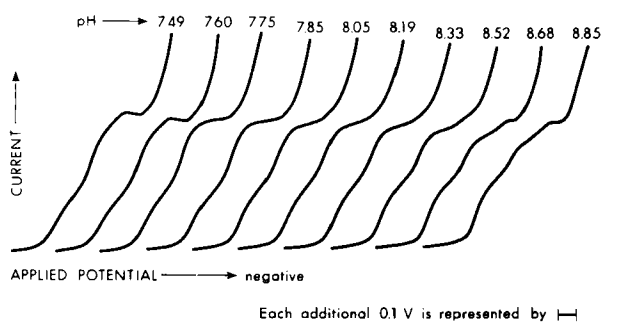

Figure 2—*Current–voltage curves of tetracycline hydrochloride in boric acid–sodium borate buffer. Each segment begins at −0.9 v. Concentration = 1.17 × 10⁻⁴ M.*

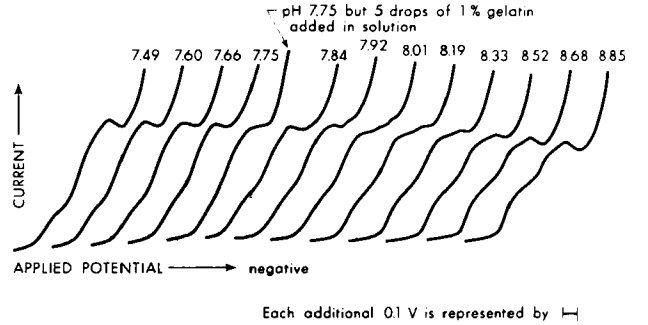

Figure 3—*Current–voltage curves of demeclocycline hydrochloride in boric acid–sodium borate buffer. Each segment begins at −0.9 v. Concentration = 1.05 × 10⁻⁴ M.*

tained at each interval. A plot was made of the current against the square root of the corrected mercury column height. The result was a straight line which, upon extrapolation, did not pass through the origin. Based upon Zuman's (17) report, it was concluded that, although the reduction process is largely diffusion dependent, kinetic factors also play a part. However, plots of total diffusion current *versus* concentration were linear for tetracycline hydrochloride and chlortetracycline hydrochloride from 0.01 to 0.125 mg/ml. For oxytetracycline hydrochloride and demeclocycline hydrochloride, linearity extended from 0.01 to 0.1 mg/ml; thereafter, the plot began to flatten.

The slopes of the respective calibration curves were as follows: tetracycline hydrochloride, 2.58; chlortetracycline hydrochloride, 2.20; oxytetracycline hydrochloride, 1.96; and demeclocycline hydrochloride, 2.96. Total diffusion current for the two waves was read in all instances, because the first wave was not sufficiently well resolved to permit separate measurements of either wave.

Tablets and Capsules—The general procedure was used without exception, even for products containing tetracycline phosphate complex (see Samples 15–18 in Table II). No calibration curve was developed for the complex because of batch-to-batch differences in the stoichiometry. Since the label of these products also declared a tetracycline hydrochloride equivalent, it was feasible to use the calibration curve for that antibiotic.

As a further check, tetracycline waves were determined in the presence of disodium as well as monosodium phosphate. No influence was observed until the phosphates were present in a quantity greatly exceeding the amount in the pharmaceutical product. Analytical results for all commercial preparations are given in Table II. As outlined under *Experimental*, 0.13 ml of 1% gelatin solution was employed for each demeclocycline hydrochloride sample.

Syrups, Suspensions, and Pediatric Drops—When the dosage form existed as the free base or as an insoluble complex, an appropriate amount of 3 *M* HCl was added to bring the antibiotic into solution. The acid would split any complex, with the resulting formation of calcium chloride. Before polarographing, this latter substance must be sequestered by the further addition of disodium ethylenediaminetetraacetic acid. In all instances, after the addition of hydrochloric acid, it was necessary to readjust the pH carefully to the optimum value by the addition of sodium borate powder. The general procedure was then followed.

Interferences—Nystatin was present in one capsule (Sample 18) and interfered with the tetracycline wave. Its presence was compensated for by running a polarogram on the amount of nystatin and subtracting its current from the total current obtained with the combined tetracycline–nystatin wave.

Polymyxin B sulfate interfered with the assay of ointments, and products containing that antibiotic could not be analyzed for their tetracycline content.

None of the commercial powders for injection could be assayed because of the presence of one or more of the following: procaine hydrochloride, magnesium chloride, and ascorbic acid. All interfered with the reduction of tetracycline, but magnesium chloride could be removed by chelating with disodium ethylenediaminetetraacetic acid.

The high values obtained with several liquid dosage forms can be attributed to undeclared, reducible preservatives, solubilizers, and stabilizers in the syrups and suspensions. If the nature and quantity of these substances were known to the analyst, it would be a simple

Table II—Analysis of Tetracycline Antibiotics

Sample	Dosage Form	Labeled Strength, %	
		Polarographic[a]	Manufacturer Assay
	Tetracycline Hydrochloride		
1	250-mg capsule	108.9 ± 0.6	Not available
2	250-mg capsule	107.2 ± 0.5	112.0
3	250-mg capsule	107.4 ± 0.7	109.0[b] 107.5[c]
4	250-mg capsule	101.3 ± 0.5	103.2[b]
5	250-mg capsule	99.9 ± 1.0	98.2[b] 101.0[c]
6	250-mg tablet	104.2 ± 0.2	106.0[b]
7	250-mg tablet	96.7 ± 0.5	102.5[b] 97.0[c]
8	1% ophthalmic ointment	110.2 ± 0.2	106.6[b] 115.8[c]
9	3% topical ointment	108.8 ± 0.2	103.5[d]
10	125-mg/5 ml suspension	134.7 ± 0.9	Not available
11	25-mg/ml syrup	110.7 ± 0.5	102.9[b] 116.0[c]
12	25-mg/ml suspension	124.5 ± 0.2	Not available
13	25-mg/ml syrup	107.3 ± 0.4	112.8[b]
14[e]	25-mg/ml suspension	134.6 ± 0.1	113.1
15[f]	100-mg capsule	109.6 ± 0.3	108.0[b]
16[f]	250-mg capsule	102.1 ± 0.1	106.4[b]
17[f]	500-mg capsule	100.8 ± 0.8	102.0[b]
18[f]	250-mg capsule	100.2 ± 0.2	108.8[b]
	Chlortetracycline Hydrochloride		
19	3% topical ointment	100.7 ± 1.1	107.8[b] 112.8[c]
20	1% ophthalmic ointment	89.6 ± 0.4	94.8[b] 106.8[c]
21	250-mg capsule	106.7 ± 0.8	108.0[b] 108.9[c]
	Demeclocycline Hydrochloride		
22	300-mg tablet	106.4 ± 0.2	110.0[b] 103.7[c]
23	150-mg capsule	104.8 ± 0.4	110.0[b] 105.9[c]
	Oxytetracycline		
24[g]	25-mg/ml syrup	127.2 ± 0.7	114.0[b]
25[g]	100-mg/ml drops	96.5 ± 0.4	113.0
26[h]	250-mg capsule	103.4 ± 0.8	103.9
27[h]	250-mg capsule	98.3 ± 0.3	99.4[b] 98.3[c]

[a] Average of five determinations ± *SD*. [b] Microbiological assay. [c] Spectrophotometric assay. [d] Chromatographic assay. [e] Tetracycline base. [f] Tetracycline phosphate. [g] Calcium salt. [h] Oxytetracycline hydrochloride.

matter to compensate for them by performing an appropriate blank.

Table II also contains the assay values provided by the manufacturers. In many instances, two methods of assay were employed, a spectrophotometric and a microbiological, and frequently their values agreed only moderately well. For most capsules and tablets, the proposed method agreed within 2% with one result or the other. Since the lack of accuracy by the microbiological method is well documented, it is not surprising to find more frequent agreement between the results of the polarographic and spectrophotometric methods.

CONCLUSION

The technique of dc polarography was applied to the analyses of a number of pharmaceutical products containing one of four tetracyclines. In general, satisfactory results were obtained with most dosage forms. However, interference resulted from the presence of certain other antibiotics as well as other electroreducible substances such as procaine hydrochloride and ascorbic acid. Optimum results for the tetracyclines were obtained with a boric acid–sodium borate buffer system.

REFERENCES

(1) "The United States Pharmacopeia," 18th rev., Mack Publishing Co., Easton, Pa., 1970, p. 857.

(2) "British Pharmacopoeia 1973," British Pharmacopoeia Commission, London, England, 1973, p. A102.

(3) D. W. Hughes and W. L. Wilson, *Can. J. Pharm. Sci.*, **8**, 67(1973).

(4) H. W. Unterman and S. Weissbuch, *Pharmazie*, **29**, 752(1974).

(5) J. Doskočil and M. Vondrácek, *Chem. Listy*, **46**, 564(1952); through *Chem. Abstr.*, **47**, 4947i(1953).

(6) J. Doskočil, *Pharmazie*, **9**, 394(1954).

(7) O. Krestýnova-Tělupilova, V. Măcák, and F. Santavý, *Chem. Listy*, **47**, 636(1953); through *Chem. Abstr.*, **48**, 3816f(1954).

(8) V. Cieleszky and L. Sebessy, *Abh. Dtsch. Akad. Wiss. Berlin, Kl. Chem., Geol., Biol.*, **1964**, 941; through *Chem. Abstr.*, **62**, 8675g(1965).

(9) M. E. Caplis, *Diss. Abstr. Int. B*, **51**, 1774(1970).

(10) C. N. Sideri and A. Osol, *J. Am. Pharm. Assoc., Sci. Ed.*, **42**, 688(1953).

(11) D. Doskacilová, *Pharmazie*, **13**, 548(1958).

(12) L. Doan and B. E. Riedel, *Can. Pharm. J. Sci. Sect.*, **96**, 109(1963).

(13) S. Silvestri, *Pharm. Acta Helv.*, **47**, 209(1972).

(14) M. E. Caplis, H. S. Ragheb, and E. D. Schall, *J. Pharm. Sci.*, **54**, 694(1965).

(15) J. S. Hetman, *Lab. Pract.*, **12**, 727, 740(1963).

(16) J. S. Hetman, *Abh. Dtsch. Akad. Wiss. Berlin, Kl. Chem., Geol., Biol.*, **1964**, 174; through *Chem. Abstr.*, **62**, 6788g(1965).

(17) P. Zuman, "The Elucidation of Organic Electrode Processes," Academic, New York, N.Y., 1969.

ACKNOWLEDGMENTS AND ADDRESSES

Received May 29, 1975, from the *Faculty of Pharmacy and Pharmaceutical Science, University of Alberta, Edmonton, Canada T6G 2H7*

Accepted for publication November 10, 1975.

The authors gratefully acknowledge the gifts of antibiotics and pharmaceutical dosage forms as well as analytical information from the following Canadian drug manufacturing houses: Bristol Laboratories of Canada, Candiac, Quebec; Cyanamid of Canada (Lederle), Montreal, Quebec; Empire Laboratories, Toronto, Ontario; MTC Pharmaceuticals, Hamilton, Ontario; Novopharm Ltd., Scarborough, Ontario; Pfizer Company Ltd., Arnprior, Ontario; and E.R. Squibb & Sons, Ltd., Montreal, Quebec.

[x] To whom inquiries should be directed.

Inhibitory Effect of Dioctyl Sodium Sulfosuccinate on Pepsin Activity

GURCHARAN S. JODHKA, SAID A. KHALIL [x], and M. WAFIK GOUDA [x]

Abstract □ The inhibitory effect of dioctyl sodium sulfosuccinate on hog pepsin activity was investigated over the pH 1.5–3.0 range. The inhibitory effect was studied using a natural substrate, hemoglobin, and a synthetic substrate, *N*-acetyl-L-phenylalanyl-L-diiodotyrosine. The mechanistic studies revealed that a substrate–inhibitor interaction was the major mechanism of inhibition with hemoglobin. However, some direct enzyme inhibition also was involved. With the synthetic substrate, the inhibition was due to a competition between the substrate and the inhibitor molecules for the enzyme. The possible therapeutic significance of the inhibitory effect of the medicinal surfactant is discussed.

Keyphrases □ Dioctyl sodium sulfosuccinate—mechanism of inhibition of pepsin activity □ Pepsin activity—mechanism of inhibition by dioctyl sodium sulfosuccinate □ Digestive enzymes—pepsin, mechanism of inhibition by dioctyl sodium sulfosuccinate □ Surfactants—dioctyl sodium sulfosuccinate, mechanism of inhibition of pepsin activity

Peptic ulcers can be defined as acute or chronic ulcerations of the digestive tract, occurring in an area accessible to gastric secretions. In spite of much recent effort, this disease continues to be an incompletely understood and a rather common disorder. Although little is known about the definite etiology of the disease, the interrelationship of a number of mucosal defensive and aggressive factors seems to determine an individual's susceptibility to ulcers (1, 2). Whatever the causative factors, it has now been unequivocally established that, through some unknown mechanism, the normal resistance of the gastric mucosa to acid and pepsin is compromised in all peptic ulcers (1).

Much experimental evidence is available indicating the importance of pepsin in the pathogenesis of the disease (3–6). In humans, the role of this enzyme in gastroduodenal ulceration was indirectly evidenced by the antiulcer activity shown by some macroanions, which inhibited peptic hydrolysis (7, 8). Oral administration of pepsin inhibitors such as degraded carrageenan, amylopectin sulfate, and a sulfated glycopeptide resulted in significant prevention and treatment of peptic ulcers in humans (9, 10). It was reported that the antipeptic effect of these sulfated macromolecules is related to the negative charge of the sulfate group and their high molecular weight (11–14).

Dioctyl sodium sulfosuccinate, an anionic surfactant that is widely used medicinally as a fecal softener, is a molecule with a relatively high molecular weight. Its inhibitory effect on tryptic activity was reported previously (15), and it strongly suppressed ulcer formation in restrained rats when given intraduodenally (16). These findings led to the present investigation, which dealt with the inhibitory effect of dioctyl sodium sulfosuccinate on the peptic activity of pepsin from hog stomach mucosa.

EXPERIMENTAL

Materials—Pepsin[1], hemoglobin[2], *N*-acetyl-L-phenylalanyl-L-diiodotyrosine[3], dioctyl sodium sulfosuccinate[4], and ninhydrin[5] were used as received. All other chemicals were either USP or reagent grade.

Methods for Antipeptic Activity—Two different methods for determining the antipeptic activity were used.

Method I—In this method, denatured hemoglobin was digested under standard conditions. The undigested hemoglobin was precipitated with trichloroacetic acid, and the amount of unprecipitated protein was estimated spectrophotometrically. The method used was a modification of Rajgopalan *et al.* (17).

The substrate (0.4–1.0 mg/ml), enzyme (10–60 μg/ml), and inhibitor (50–400 μg/ml) were prepared in hydrochloric acid (pH 1.8) or distilled water. All solutions were freshly prepared, adjusted to pH 1.8 immediately after preparation, and brought to 37° before mixing. One milliliter of the enzyme (pepsin) solution (I) was pipetted into each flask, already maintained at 37° in a metabolic water bath shaker[6]. Then 1 ml of the inhibitor (dioctyl sodium sulfosuccinate) solution (II) was added to each flask, followed by 2 ml of the substrate (hemoglobin) solution (III).

[1] From hog stomach mucosa, 3× crystallized and lyophilized, Nutritional Biochemicals Corp., Cleveland, Ohio.

[2] Denatured, standardized for protease assay, Nutritional Biochemicals Corp., Cleveland, Ohio.

[3] Sigma Chemical Co., St. Louis, Mo.

[4] Aerosol O. T. 100%, Sargent-Welch Scientific Co., Skokie, Ill.

[5] J. T. Baker Chemical Co., Philipsburg, N.J.

[6] Model G-77, New Brunswick Scientific Co., New Brunswick, N.J.

(17) P. Zuman, "The Elucidation of Organic Electrode Processes," Academic, New York, N.Y., 1969.

ACKNOWLEDGMENTS AND ADDRESSES

Received May 29, 1975, from the *Faculty of Pharmacy and Pharmaceutical Science, University of Alberta, Edmonton, Canada T6G 2H7*

Accepted for publication November 10, 1975.

The authors gratefully acknowledge the gifts of antibiotics and pharmaceutical dosage forms as well as analytical information from the following Canadian drug manufacturing houses: Bristol Laboratories of Canada, Candiac, Quebec; Cyanamid of Canada (Lederle), Montreal, Quebec; Empire Laboratories, Toronto, Ontario; MTC Pharmaceuticals, Hamilton, Ontario; Novopharm Ltd., Scarborough, Ontario; Pfizer Company Ltd., Arnprior, Ontario; and E.R. Squibb & Sons, Ltd., Montreal, Quebec.

[x] To whom inquiries should be directed.

Inhibitory Effect of Dioctyl Sodium Sulfosuccinate on Pepsin Activity

GURCHARAN S. JODHKA, SAID A. KHALIL [x], and M. WAFIK GOUDA [x]

Abstract □ The inhibitory effect of dioctyl sodium sulfosuccinate on hog pepsin activity was investigated over the pH 1.5–3.0 range. The inhibitory effect was studied using a natural substrate, hemoglobin, and a synthetic substrate, *N*-acetyl-L-phenylalanyl-L-diiodotyrosine. The mechanistic studies revealed that a substrate–inhibitor interaction was the major mechanism of inhibition with hemoglobin. However, some direct enzyme inhibition also was involved. With the synthetic substrate, the inhibition was due to a competition between the substrate and the inhibitor molecules for the enzyme. The possible therapeutic significance of the inhibitory effect of the medicinal surfactant is discussed.

Keyphrases □ Dioctyl sodium sulfosuccinate—mechanism of inhibition of pepsin activity □ Pepsin activity—mechanism of inhibition by dioctyl sodium sulfosuccinate □ Digestive enzymes—pepsin, mechanism of inhibition by dioctyl sodium sulfosuccinate □ Surfactants—dioctyl sodium sulfosuccinate, mechanism of inhibition of pepsin activity

Peptic ulcers can be defined as acute or chronic ulcerations of the digestive tract, occurring in an area accessible to gastric secretions. In spite of much recent effort, this disease continues to be an incompletely understood and a rather common disorder. Although little is known about the definite etiology of the disease, the interrelationship of a number of mucosal defensive and aggressive factors seems to determine an individual's susceptibility to ulcers (1, 2). Whatever the causative factors, it has now been unequivocally established that, through some unknown mechanism, the normal resistance of the gastric mucosa to acid and pepsin is compromised in all peptic ulcers (1).

Much experimental evidence is available indicating the importance of pepsin in the pathogenesis of the disease (3–6). In humans, the role of this enzyme in gastroduodenal ulceration was indirectly evidenced by the antiulcer activity shown by some macroanions, which inhibited peptic hydrolysis (7, 8). Oral administration of pepsin inhibitors such as degraded carrageenan, amylopectin sulfate, and a sulfated glycopeptide resulted in significant prevention and treatment of peptic ulcers in humans (9, 10). It was reported that the antipeptic effect of these sulfated macromolecules is related to the negative charge of the sulfate group and their high molecular weight (11–14).

Dioctyl sodium sulfosuccinate, an anionic surfactant that is widely used medicinally as a fecal softener, is a molecule with a relatively high molecular weight. Its inhibitory effect on tryptic activity was reported previously (15), and it strongly suppressed ulcer formation in restrained rats when given intraduodenally (16). These findings led to the present investigation, which dealt with the inhibitory effect of dioctyl sodium sulfosuccinate on the peptic activity of pepsin from hog stomach mucosa.

EXPERIMENTAL

Materials—Pepsin[1], hemoglobin[2], *N*-acetyl-L-phenylalanyl-L-diiodotyrosine[3], dioctyl sodium sulfosuccinate[4], and ninhydrin[5] were used as received. All other chemicals were either USP or reagent grade.

Methods for Antipeptic Activity—Two different methods for determining the antipeptic activity were used.

Method I—In this method, denatured hemoglobin was digested under standard conditions. The undigested hemoglobin was precipitated with trichloroacetic acid, and the amount of unprecipitated protein was estimated spectrophotometrically. The method used was a modification of Rajgopalan *et al.* (17).

The substrate (0.4–1.0 mg/ml), enzyme (10–60 μg/ml), and inhibitor (50–400 μg/ml) were prepared in hydrochloric acid (pH 1.8) or distilled water. All solutions were freshly prepared, adjusted to pH 1.8 immediately after preparation, and brought to 37° before mixing. One milliliter of the enzyme (pepsin) solution (I) was pipetted into each flask, already maintained at 37° in a metabolic water bath shaker[6]. Then 1 ml of the inhibitor (dioctyl sodium sulfosuccinate) solution (II) was added to each flask, followed by 2 ml of the substrate (hemoglobin) solution (III).

[1] From hog stomach mucosa, 3× crystallized and lyophilized, Nutritional Biochemicals Corp., Cleveland, Ohio.

[2] Denatured, standardized for protease assay, Nutritional Biochemicals Corp., Cleveland, Ohio.

[3] Sigma Chemical Co., St. Louis, Mo.

[4] Aerosol O. T. 100%, Sargent-Welch Scientific Co., Skokie, Ill.

[5] J. T. Baker Chemical Co., Philipsburg, N.J.

[6] Model G-77, New Brunswick Scientific Co., New Brunswick, N.J.

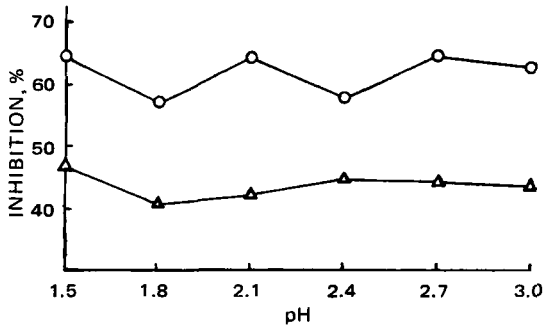

Figure 1—*Effect of pH and mixing orders on percentage inhibition of pepsin. Eight milliliters of digest contained 10 μg of enzyme, 2 mg of substrate (hemoglobin), and 200 μg of inhibitor. Key: ○, inhibitor added to enzyme first; and △, inhibitor added to substrate first. Each point represents the average of at least four determinations.*

All samples were incubated for 5 min with no shaking. At the end of the incubation period, 4 ml of 5% trichloroacetic acid was added to each sample in the same order and thoroughly mixed. The incubation mixtures were allowed to remain at 37° for 3 min and were then filtered[7]. The final volume of the incubation mixture was kept at 8 ml in all cases.

Blank determinations were carried out in exactly the same way as samples except that the substrate solution was added after trichloroacetic acid. The absorbance of all filtrates was determined spectrophotometrically[8] at 277 nm against distilled water. Controls were simultaneously run for every inhibition experiment. The controls differed from the samples in having the inhibitor solution replaced by an equivalent volume of hydrochloric acid (pH 1.8).

Differences between the absorbance of samples and their respective blanks represent the peptic activities and were used as measures of reaction velocities in all kinetic studies. The inhibition value, i, equals $1 - (v_i/v)$, where v_i and v represent reaction velocities with and without the inhibitor, respectively. Percentage inhibition values were calculated from the respective i values (15).

Method II—In this method, *N*-acetyl-L-phenylalanyl-L-diiodotyrosine (IV) was used as the substrate. Compound IV is a low molecular weight synthetic peptide which is easily hydrolyzed by pepsin. The extent of hydrolysis is determined by measuring the ninhydrin color given by the newly formed L-diiodotyrosine. The procedure used was that of Jackson *et al.* (18) with slight modifications.

A solution (20×10^{-5} *M*) of the substrate (IV) was prepared as described by Jackson *et al.* (18). Various concentrations of the enzyme (I) and the inhibitor (II) solutions were prepared as in Method I. The final volume of the reaction mixture was 9 ml in each case. Incubation of all samples was carried out at 37° for 10 min, and the reaction was stopped by adding 0.5 ml of 0.5 *N* sodium hydroxide into each test tube.

All controls and blanks were prepared as described for Method I. The absorbance of the reaction mixtures of both samples and blanks was read spectrophotometrically[8] at 570 nm against distilled water. All peptic activities, reaction velocities, and inhibition values were determined as indicated in Method I.

Various Orders of Mixing—Two different orders of mixing were used as described previously (15). The inhibitor was added to either the enzyme (Mixing Order A) or the substrate (Mixing Order B) before starting peptic hydrolysis. Mixing Order A was used in all studies except for the data of Fig. 1.

All experiments were performed at least in duplicate.

RESULTS AND DISCUSSION

The inhibitory effect of dioctyl sodium sulfosuccinate on pepsin activity was studied at various inhibitor concentrations using Method I. Data presented in Table I show a significant inhibitory effect at all concentrations. The effect of pH and mixing orders on the percentage inhibition was also studied using Method I (Fig. 1). Figure 1 shows

[7] Whatman No. 2 filter paper.

[8] Beckman ACTA CIII spectrophotometer, Beckman Instruments, Fullerton, Calif.

Table I—Effect of Various Concentrations of Dioctyl Sodium Sulfosuccinate on the Percentage Inhibition of Pepsin Activity at pH 1.8

Amounts of Components in 8 ml of Digest			Inhibition[b] of Control Activity, %
Enzyme, μg	Substrate[a], mg	Inhibitor, μg	
10	2	80	28.0
10	2	160	45.1
10	2	240	54.9
10	2	320	64.8
10	2	400	74.1

[a] Hemoglobin. [b] Average of at least two determinations.

a higher percentage inhibition with Mixing Order A (inhibitor added to the enzyme first) as compared to Mixing Order B (inhibitor added to the substrate first). Moreover, this increase in inhibition seemed to be almost constant over the pH 1.5–3.0 range. The marked difference in the inhibition pattern over the pH 1.5–3.0 range suggests that an enzyme–inhibitor interaction was taking place.

At pH 1.8, using hemoglobin as the substrate, a plot of $1/v_i$ against 1/III (Fig. 2) and a plot of $1/v_i$ against II (Fig. 3) were made. Both plots are indicative of a substrate–inhibitor interaction as the major mechanism of inhibition (19). When using the data of Figs. 2 and 3, plots of III/v_i against III, v_i against v_i/III, and $1/i$ against 1/II also yielded curves typical of a substrate–inhibitor interaction (20). Further characterization of this mechanism was done by making a plot of II against $i/(1 - i)$ (Fig. 4), which shows substrate depletion to be the basic mechanism involved (21).

With the data of Fig. 2, a plot of i against III was also made, which indicates that an enzyme–inhibitor interaction seems to be involved in addition to a substrate–inhibitor interaction in the overall mechanism of inhibition (15). This finding explains the increased percentage inhibition observed with Mixing Order A (Fig. 1). Such an additional enzyme–inhibitor interaction could have been confirmed further through preincubation studies (15). However, such studies were not feasible due to the autodigestion of pepsin under the experimental conditions, as reported earlier (22) and found in the present investigation.

A double reciprocal plot (Fig. 5) was made using the synthetic substrate (Method II). Figure 5 is typical of a true competitive inhibition due to a competition between the substrate and the inhibitor molecules for the same site at the enzyme surface (23). Such a mechanism was further confirmed by making a plot of $1/v_i$ against II (Fig. 6). The value of the inhibitor constant, K_i, was also determined from this plot (19).

From the foregoing discussion, it is apparent that dioctyl sodium sulfosuccinate interacts with both the substrate and the enzyme when the substrate used is natural protein (hemoglobin). When the sub-

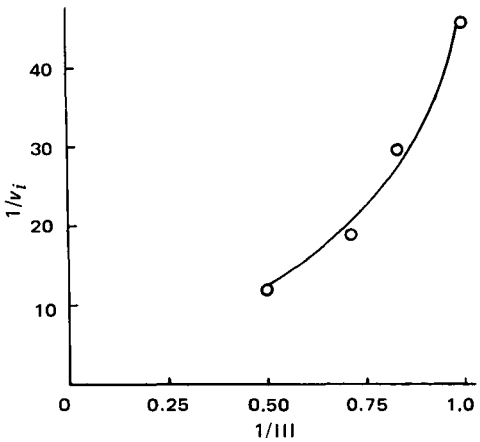

Figure 2—*Plot of $1/v_i$ (reciprocal reaction velocity) against 1/III (reciprocal substrate concentration) for antipeptic activity of dioctyl sodium sulfosuccinate at pH 1.8. Eight milliliters of digest contained 10 μg of enzyme, 200 μg of inhibitor, and 0.8–2.0 mg of substrate (hemoglobin).*

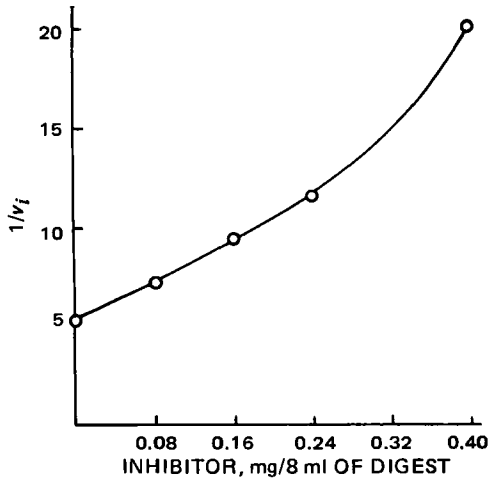

Figure 3—*Plot of* $1/v_i$ *(reciprocal reaction velocity) against II (inhibitor concentration) for antipeptic activity of dioctyl sodium sulfosuccinate at pH 1.8. Eight milliliters of digest contained 10 μg of enzyme and 2 mg of substrate (hemoglobin).*

strate is a synthetic dipeptide (IV), the inhibitor binds the enzyme molecule exclusively and shows no affinity for the substrate. This finding may indicate that the inhibitor probably alters the conformation of hemoglobin and that no involvement of the primary structure takes place. The lack of an interaction between the synthetic substrate and dioctyl sodium sulfosuccinate and its significant interacting capacity with hemoglobin are some of the typical inhibitory characteristics of the sulfated macroanion inhibitors of pepsin reported earlier (9).

These similarities in the inhibitory characteristics between dioctyl sodium sulfosuccinate and macroanion inhibitors may be a consequence of their structural similarities. However, the interaction between dioctyl sodium sulfosuccinate and pepsin in the presence of both a natural and a synthetic substrate is an additional inhibitory feature of this surfactant and is not exhibited by macroanion inhibitors (9). Such an enzyme-inhibiting property may be due to a higher water solubility, surface-active properties, or the lower molecular weight of dioctyl sodium sulfosuccinate. It is also possible that dioctyl

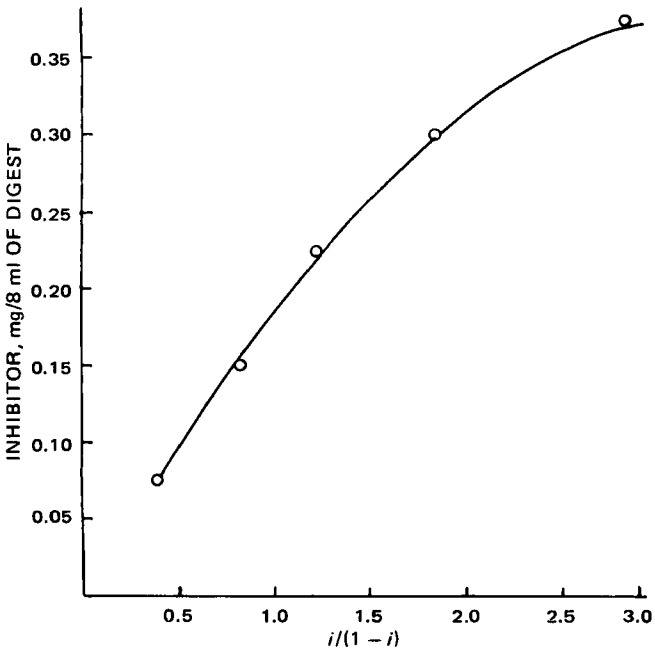

Figure 4—*Plot of II (inhibitor concentration) against* $i/(1-i)$ *for antipeptic activity of dioctyl sodium sulfosuccinate at pH 1.8. Eight milliliters of digest contained 10 μg of enzyme and 2 mg of substrate (hemoglobin).*

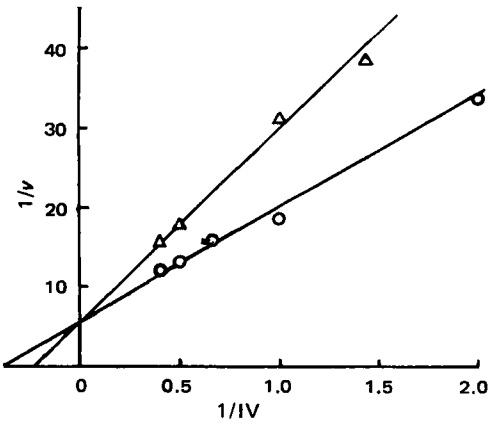

Figure 5—*Plot of 1/v (reciprocal reaction velocity) against 1/IV (reciprocal substrate concentration) for antipeptic activity of dioctyl sodium sulfosuccinate at pH 2.0. Nine milliliters of incubation mixture contained 60 μg of enzyme and* 10×10^{-8}–50×10^{-8} *mole of substrate (IV). Key: ○, no inhibitor added; and △, inhibitor = 50 μg. Both lines were drawn by the method of least squares: △,* $y = 22.94x + 6.55$ ($r = 0.990$); *and ○,* $y = 13.358x + 6.2712$ ($r = 0.9972$).

sodium sulfosuccinate has a molecular size and shape that favor the hydrophobic and steric considerations so important in the orientation and proximity effects necessary for its binding to the enzyme molecule.

The mechanistic studies also reveal that dioctyl sodium sulfosuccinate seems to possess a lower affinity for pepsin than for hemoglobin in the presence of the two. Such behavior was reported for some macroanion inhibitors (24).

Weiss and Serfontein (25) indicated some of the qualitative and quantitative biochemical differences between ulcerated tissues and surrounding normal tissues. Compounds like hexosamines, hyaluronic acid, mucopolysaccharides, and the glycoproteins are present at higher concentrations and in more reactive forms at the ulcerated tissues. The antipeptic activity of most macroanion sulfated polysaccharides as well as certain other antiulcer agents has been shown to be due to their ability to form insoluble complexes with these tissue degradation products or other proteins present at the ulcerated surface (26). An ulcerated site covered with such a complex is believed to be shielded from further exposure to the damaging effects of the acidic gastric juice and pepsin, thus facilitating healing of the ulcer. In view of the mechanistic evidence presented, dioctyl sodium sulfosuccinate may provide possible antiulcer action through such an indirect mechanism.

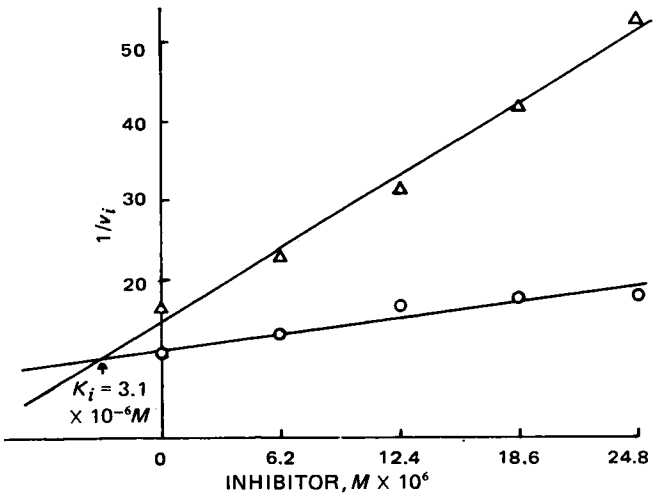

Figure 6—*Plot of* $1/v_i$ *(reciprocal reaction velocity) against II (inhibitor concentration) for antipeptic activity of dioctyl sodium sulfosuccinate at pH 2.0. Nine milliliters of incubation mixture contained: △,* 20×10^{-8} *mole of substrate (IV) and 60 μg of enzyme; and ○,* 40×10^{-8} *mole of substrate (IV) and 60 μg of enzyme. Both lines were drawn by the method of least squares: △,* $y = 1.4729x + 14.694$ ($r = 0.9948$); *and ○,* $y = 0.3166x + 11.1520$ ($r = 0.9415$).

It may also exert some additional healing effect due to its direct inhibitory effect against pepsin. Pepstatin, an antiulcer agent, has been shown to act through this direct inactivation of pepsin (26).

The results of the present studies strongly suggest a significant inhibition of gastric peptic activity by the surfactant at concentrations well below the dosages of dioctyl sodium sulfosuccinate presently used in laxative therapy. Such an inhibition of pepsin may explain the antiulcerogenic effect of dioctyl sodium sulfosuccinate already observed in rats (16). An additional antiulcer effect of this medicinal surfactant may be due to its potent ability to decrease the volume of secretions and the amount of acid secreted as indicated by Lish (16).

Although dioctyl sodium sulfosuccinate may provide an antiulcer action, a reduction in the digestive capacity of the gastric juice for dietary proteins and possibly certain drug interactions (15) must be considered when evaluating this agent for possible therapy of peptic ulcer patients.

REFERENCES

(1) J. L. Hirchman and E. T. Herfindal, *J. Am. Pharm. Assoc.*, **NS11**, 445(1971).

(2) C. Rowley, *Can. Pharm. J.*, **May**, 2/128(1971).

(3) M. J. Schiffein, *Proc. Soc. Exp. Biol. Med.*, **45**, 592(1940).

(4) M. J. Schiffrin and A. S. Warren, *Am. J. Dig. Dis.*, **9**, 205(1942).

(5) J. A. Vocac, R. S. Alphin, and P. J. Bolton, *Gastroenterology*, **56**, 1266(1969).

(6) A. Lietti and G. Prino, *Life Sci. II*, **10**, 541(1971).

(7) M. D. Turner, L. Miller, and H. L. Segal, *Gastroenterology*, **53**, 967(1967).

(8) I. M. Samloff, *ibid.*, **60**, 586(1971).

(9) G. Prino, A. Lietti, and G. Allegra, *Am. J. Dig. Dis.*, **17**, 863(1972).

(10) D. Cook and V. A. Drill, *Ann. N.Y. Acad. Sci.*, **140**, 724(1967).

(11) W. Anderson and A. J. Baillie, *J. Pharm. Pharmacol.*, **19**, 720(1967).

(12) W. Anderson, A. J. Baillie, and J. E. Harthill, *ibid.*, **20**, 715(1968).

(13) D. L. Cook, S. Eich, and P. S. Cammarata, *Arch. Int. Pharmacodyn. Ther.*, **144**, 1(1963).

(14) J. A. Vocac and R. S. Alphin, *Eur. J. Pharmacol.*, **4**, 99(1968).

(15) G. S. Jodhka, M. W. Gouda, R. S. Medora, and S. A. Khalil, *J. Pharm. Sci.*, in press.

(16) P. M. Lish, *Gastroenterology*, **41**, 580(1961).

(17) T. Rajgopalan, S. Moore, and W. Stein, *J. Biol. Chem.*, **241**, 4940(1966).

(18) W. Jackson, M. Schlamowitz, and A. Shaw, *Biochemistry*, **4**, 1537(1965).

(19) M. Dixon, *Biochem. J.*, **55**, 170(1953).

(20) J. M. Reiner, "Behavior of Enzyme Systems," 2nd ed., Van Nostrand Reinhold, New York, N.Y., 1969, pp. 192–199.

(21) J. L. Webb, "Enzyme and Metabolic Inhibitors," vol. 1, Academic, London, England, 1963, p. 85.

(22) G. E. Perlmann, *Nature*, **173**, 406(1954).

(23) K. M. Plowman, "Enzyme Kinetics," McGraw-Hill, New York, N.Y., 1972, p. 56.

(24) W. Anderson, *J. Pharm. Pharmacol.*, **13**, 139(1961).

(25) G. Weiss and W. J. Serfontein, *S. Afr. Med. J.*, **24**, 467(1971).

(26) M. H. McDoo, A. M. Dannenberg, Jr., J. Hayes, S. P. James, and J. H. Sanner, *Infect. Immun.*, **7**, 655(1973).

ACKNOWLEDGMENTS AND ADDRESSES

Received August 4, 1975, from the *School of Pharmacy, University of Montana, Missoula, MT 59801*

Accepted for publication November 13, 1975.

Presented at the Pharmacology and Biochemistry Division, 35th International Congress of Pharmaceutical Sciences, Dublin, Ireland, September 1975.

Supported in part by the U.S. National Science Foundation SFC program, Grants GF 38851 and GF 39207.

The authors express appreciation to Dr. Galen P. Mell, Department of Chemistry, University of Montana, for valuable suggestions.

* Faculty of Pharmacy, University of Alexandria, Alexandria, Egypt.

ˣ To whom inquiries should be directed.

GLC Determination of Aprindine: Quantitation and Stability Measurement

BONNIE S. RUTHERFORD ˣ and RAFIK H. BISHARA

Abstract □ A GLC method of analysis of a new antiarrhythmic agent, aprindine, is described. The raw material of the new drug substance, supplied as the hydrochloride salt, is dissolved in deionized water, and the base is liberated by a 10% aqueous solution of sodium carbonate. Aprindine is extracted with chloroform and mixed with the internal standard, 5α-cholestane. GLC is performed on a glass column packed with 3.8% W-98 on Chromosorb W-HP. Quantitation is achieved by computer calculation of the peak area ratios. GLC–mass spectral analysis indicates that the observed peak is that of aprindine, with a molecular ion at *m/e* 322. The retention times of aprindine and the internal standard are 2.0 and 5.8 min, respectively. All synthetic precursors show a shorter retention time than aprindine. This GLC method is applied to the quantitative determination of aprindine as raw material and in capsule and ampul formulations. The method is also used to measure the stability of aprindine to acid, base, dry heat, refluxing, and UV light and to pH variations.

Keyphrases □ Aprindine—GLC analysis in pharmaceutical formulations, effect of dry heat, refluxing, UV light, and varying pH on stability □ GLC—analysis, aprindine in pharmaceutical formulations □ Stability—aprindine in pharmaceutical formulations, effect of dry heat, refluxing, UV light, and varying pH □ Antiarrhythmic agents—aprindine, GLC analysis in pharmaceutical formulations, effect of dry heat, refluxing, UV light, and varying pH on stability

Aprindine (I), *N,N*-diethyl-*N'*-(2-indanyl)-*N'*-phenyl-1,3-propanediamine, is a new potent antiarrhythmic agent (1) which can be administered both orally and intravenously. The drug is presently being used in humans (1, 2) and has a long-lasting action when taken orally (1, 3).

It may also exert some additional healing effect due to its direct inhibitory effect against pepsin. Pepstatin, an antiulcer agent, has been shown to act through this direct inactivation of pepsin (26).

The results of the present studies strongly suggest a significant inhibition of gastric peptic activity by the surfactant at concentrations well below the dosages of dioctyl sodium sulfosuccinate presently used in laxative therapy. Such an inhibition of pepsin may explain the antiulcerogenic effect of dioctyl sodium sulfosuccinate already observed in rats (16). An additional antiulcer effect of this medicinal surfactant may be due to its potent ability to decrease the volume of secretions and the amount of acid secreted as indicated by Lish (16).

Although dioctyl sodium sulfosuccinate may provide an antiulcer action, a reduction in the digestive capacity of the gastric juice for dietary proteins and possibly certain drug interactions (15) must be considered when evaluating this agent for possible therapy of peptic ulcer patients.

REFERENCES

(1) J. L. Hirchman and E. T. Herfindal, *J. Am. Pharm. Assoc.*, **NS11**, 445(1971).

(2) C. Rowley, *Can. Pharm. J.*, **May**, 2/128(1971).

(3) M. J. Schiffein, *Proc. Soc. Exp. Biol. Med.*, **45**, 592(1940).

(4) M. J. Schiffrin and A. S. Warren, *Am. J. Dig. Dis.*, **9**, 205(1942).

(5) J. A. Vocac, R. S. Alphin, and P. J. Bolton, *Gastroenterology*, **56**, 1266(1969).

(6) A. Lietti and G. Prino, *Life Sci. II*, **10**, 541(1971).

(7) M. D. Turner, L. Miller, and H. L. Segal, *Gastroenterology*, **53**, 967(1967).

(8) I. M. Samloff, *ibid.*, **60**, 586(1971).

(9) G. Prino, A. Lietti, and G. Allegra, *Am. J. Dig. Dis.*, **17**, 863(1972).

(10) D. Cook and V. A. Drill, *Ann. N.Y. Acad. Sci.*, **140**, 724(1967).

(11) W. Anderson and A. J. Baillie, *J. Pharm. Pharmacol.*, **19**, 720(1967).

(12) W. Anderson, A. J. Baillie, and J. E. Harthill, *ibid.*, **20**, 715(1968).

(13) D. L. Cook, S. Eich, and P. S. Cammarata, *Arch. Int. Pharmacodyn. Ther.*, **144**, 1(1963).

(14) J. A. Vocac and R. S. Alphin, *Eur. J. Pharmacol.*, **4**, 99(1968).

(15) G. S. Jodhka, M. W. Gouda, R. S. Medora, and S. A. Khalil, *J. Pharm. Sci.*, in press.

(16) P. M. Lish, *Gastroenterology*, **41**, 580(1961).

(17) T. Rajgopalan, S. Moore, and W. Stein, *J. Biol. Chem.*, **241**, 4940(1966).

(18) W. Jackson, M. Schlamowitz, and A. Shaw, *Biochemistry*, **4**, 1537(1965).

(19) M. Dixon, *Biochem. J.*, **55**, 170(1953).

(20) J. M. Reiner, "Behavior of Enzyme Systems," 2nd ed., Van Nostrand Reinhold, New York, N.Y., 1969, pp. 192–199.

(21) J. L. Webb, "Enzyme and Metabolic Inhibitors," vol. 1, Academic, London, England, 1963, p. 85.

(22) G. E. Perlmann, *Nature*, **173**, 406(1954).

(23) K. M. Plowman, "Enzyme Kinetics," McGraw-Hill, New York, N.Y., 1972, p. 56.

(24) W. Anderson, *J. Pharm. Pharmacol.*, **13**, 139(1961).

(25) G. Weiss and W. J. Serfontein, *S. Afr. Med. J.*, **24**, 467(1971).

(26) M. H. McDoo, A. M. Dannenberg, Jr., J. Hayes, S. P. James, and J. H. Sanner, *Infect. Immun.*, **7**, 655(1973).

ACKNOWLEDGMENTS AND ADDRESSES

Received August 4, 1975, from the *School of Pharmacy, University of Montana, Missoula, MT 59801*

Accepted for publication November 13, 1975.

Presented at the Pharmacology and Biochemistry Division, 35th International Congress of Pharmaceutical Sciences, Dublin, Ireland, September 1975.

Supported in part by the U.S. National Science Foundation SFC program, Grants GF 38851 and GF 39207.

The authors express appreciation to Dr. Galen P. Mell, Department of Chemistry, University of Montana, for valuable suggestions.

* Faculty of Pharmacy, University of Alexandria, Alexandria, Egypt.

ˣ To whom inquiries should be directed.

GLC Determination of Aprindine: Quantitation and Stability Measurement

BONNIE S. RUTHERFORD ˣ and RAFIK H. BISHARA

Abstract □ A GLC method of analysis of a new antiarrhythmic agent, aprindine, is described. The raw material of the new drug substance, supplied as the hydrochloride salt, is dissolved in deionized water, and the base is liberated by a 10% aqueous solution of sodium carbonate. Aprindine is extracted with chloroform and mixed with the internal standard, 5α-cholestane. GLC is performed on a glass column packed with 3.8% W-98 on Chromosorb W-HP. Quantitation is achieved by computer calculation of the peak area ratios. GLC–mass spectral analysis indicates that the observed peak is that of aprindine, with a molecular ion at *m/e* 322. The retention times of aprindine and the internal standard are 2.0 and 5.8 min, respectively. All synthetic precursors show a shorter retention time than aprindine. This GLC method is applied to the quantitative determination of aprindine as raw material and in capsule and ampul formulations. The method is also used to measure the stability of aprindine to acid, base, dry heat, refluxing, and UV light and to pH variations.

Keyphrases □ Aprindine—GLC analysis in pharmaceutical formulations, effect of dry heat, refluxing, UV light, and varying pH on stability □ GLC—analysis, aprindine in pharmaceutical formulations □ Stability—aprindine in pharmaceutical formulations, effect of dry heat, refluxing, UV light, and varying pH □ Antiarrhythmic agents—aprindine, GLC analysis in pharmaceutical formulations, effect of dry heat, refluxing, UV light, and varying pH on stability

Aprindine (I), *N,N*-diethyl-*N'*-(2-indanyl)-*N'*-phenyl-1,3-propanediamine, is a new potent antiarrhythmic agent (1) which can be administered both orally and intravenously. The drug is presently being used in humans (1, 2) and has a long-lasting action when taken orally (1, 3).

Table I—Relative Retention Times (RRT) of Compounds Related to Aprindine

Identity[a]	Chemical Name	RRT[b]
P	Indene	N.D.
P	2-Indanone	N.D.
P	2-Indanol	N.D.
P	2-Indanol methanesulfonate	0.07
P	*N*-Phenyl-2-indanamine	0.17
Aprindine	*N,N*-Diethyl-*N'*-(2-indanyl)-*N'*-phenyl-1,3-propanediamine	1.00
PDP	*N,N*-Diethyl-*N'*-phenyl-1,3-propanediamine	0.07
PDP	*N*-Ethyl-*N'*-(2-indanyl)-*N'*-phenyl-1,3-propanediamine	0.81
PDP	*N*-2-Indanyl-*N*-phenyl-1,3-propanediamine	0.66

[a] P = synthetic precursor, and PDP = possible degradation product. [b] Retention times were measured relative to aprindine (RRT = 1.00). N.D. = compound not detected at the conditions used.

TLC (4), GLC (1, 5, 6), and radioactive scintillation counting of tritium (1, 3, 4) or ^{14}C-labeled aprindine (7) have been used to assay the drug in biological studies. Since all published GLC methods were used for biological experimentation, a wide range of accuracy up to 10% (1) was tolerated. The validation of the methods in regard to precision, accuracy, and specificity was not demonstrated. Furthermore, the methods were not designed to quantitate aprindine as a raw material or in pharmaceutical preparations.

This paper presents a precise analytical procedure for the quantitation of aprindine with no interference from precursors or degradation products. The method also measures the stability of the new drug substance and some pharmaceutical preparations containing it.

EXPERIMENTAL

Equipment—A gas chromatograph[1] equipped with a flame-ionization detector was used. The detected signals were fed to a computer[2] for peak area integration and to a 1-mv recorder[3]. A U-shaped glass column (122 cm × 3 mm i.d.) was packed with 3.8% methyl vinyl silicone gum (W-98) on 80–100-mesh Chromosorb W-HP[4].

The following conditions were used: oven temperature, 230°; injection port temperature, 255°; detector temperature, 255°; helium carrier gas flow rate, 60 ml/min; hydrogen flow rate, 40 ml/min; and oxygen flow rate, 300 ml/min. Injections were made using a 10-μl syringe[5].

Reagents and Chemicals—The sodium carbonate[6] and chloroform[6] used were analytical reagent grade.

Internal Standard Solution—A solution of 60 mg of 5α-cholestane[7]/50 ml of chloroform was used.

Diluted Internal Standard Solution—The internal standard solution was diluted 1 to 10 with chloroform.

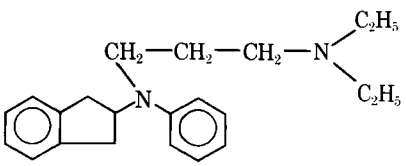

aprindine

[1] Hewlett-Packard model 402, Avondale, Pa.
[2] Hewlett-Packard 2100.
[3] Honeywell Electronik-16, Honeywell, Philadelphia, Pa.
[4] Custom-made nontested packing, Ohio Valley Specialty Chemical, Inc., Marietta, Ohio.
[5] Hamilton No. 701, Reno, Nev.
[6] Mallinckrodt, St. Louis, Mo.
[7] Aldrich, Milwaukee, Wis.

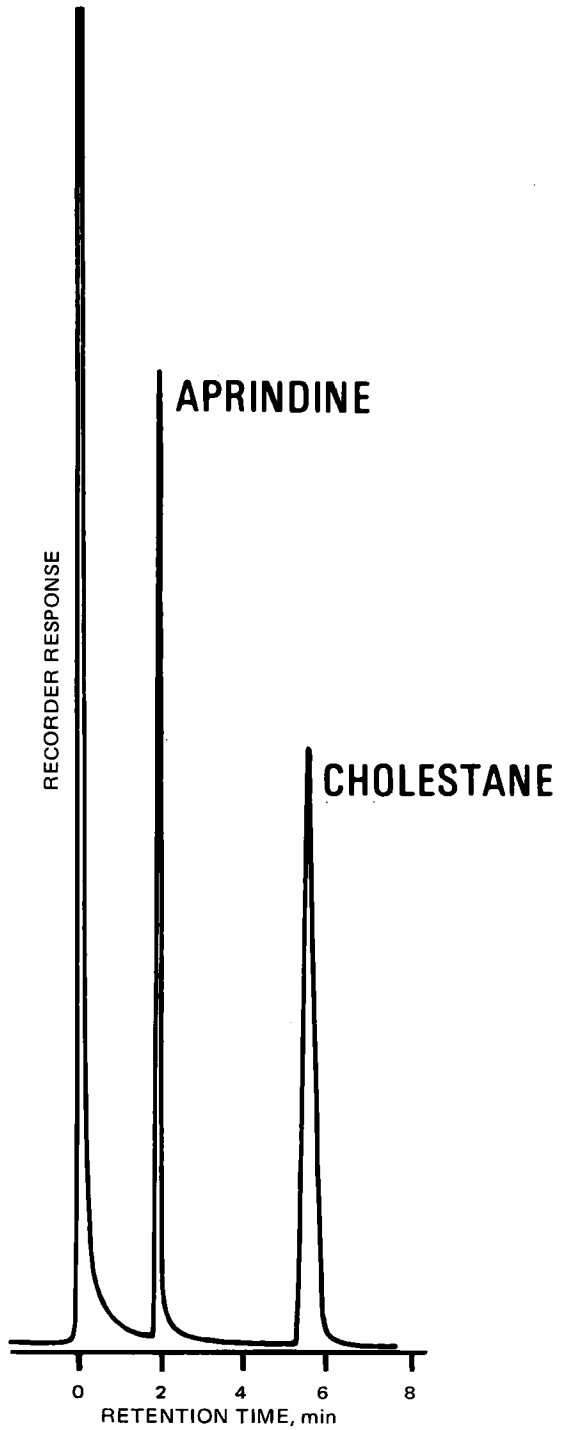

Figure 1—*Typical gas–liquid chromatogram of aprindine.*

Preparation of Raw Material—*Sample Solution*—Twenty-five milliliters of 10% sodium carbonate solution was added to 50 mg of the raw material dissolved in 5 ml of water in a separator, and the sample was extracted with three 10-ml portions of chloroform. The chloroform extracts were filtered through anhydrous sodium sulfate into a 50-ml volumetric flask. After dilution to volume with chloroform, the sample was mixed 1:1 with the internal standard solution.

Standard Solution—Fifty milligrams of reference standard aprindine hydrochloride was prepared in the same manner as the sample.

Preparation of Capsule Formulations—*Sample Solution*—The average fill weight of 10 capsules was determined. A portion of the capsule contents equivalent to 100 mg of aprindine hydrochloride was extracted from 15 ml of 10% sodium carbonate solution with three

Table II—Degradation Studies: Percent Recovery of Aprindine Determined by GLC

Treatment	Hours							
	0	2	6	12	24	48	72	144
Reflux in 1 *N* methanolic hydrochloric acid	100.6	—	—	—	100.4	—	99.5	99.0
Reflux in 1 *N* methanolic potassium hydroxide	102.0	—	—	—	102.5	—	101.1	101.5
Reflux in methanol	101.1	—	101.4	100.3	99.2	—	—	—
Irradiation with UV light	99.7	57.4	27.0	21.0	15.6	7.6	—	—
Heat at 110°	100.0	—	100.5	100.5	99.7	—	—	—
Solution in 5% dextrose in water at 50°	100.5	—	100.9	100.4	99.8	—	—	—
pH Profile at 50°								
pH 1.0	101.0	—	100.5	99.4	100.4	—	—	—
pH 4.0	101.7	—	101.5	101.5	100.9	—	—	—
pH 7.0	101.5	—	102.0	101.2	100.5	—	—	—

30-ml portions of chloroform. After dilution to 100 ml with chloroform, the sample was mixed 1:1 with the internal standard solution.

Standard Solution—One hundred milligrams of reference standard aprindine hydrochloride was extracted in the same manner as the capsule sample.

Preparation of Lyophilized Ampul Formulations—*Sample Solution*—The contents of one ampul (100 or 200 mg of aprindine hydrochloride) dissolved in 10 ml of water were extracted from 25 ml of 10% sodium carbonate solution with three 30-ml portions of chloroform. After dilution with chloroform to a concentration of 1 mg/ml, the sample solution was mixed 1:1 with the internal standard solution.

Standard Solution—One hundred milligrams of reference standard aprindine hydrochloride was extracted in the same manner as the ampul sample.

Preparation of Solution Formulations (1 mg/ml)—*Sample Solution*—A 5-ml aliquot was extracted from 20 ml of 10% sodium carbonate solution with three 10-ml portions of chloroform. After dilution to 50 ml with chloroform, the sample solution was mixed 1:1 with the diluted internal standard solution.

Standard Solution—A 1-mg/ml solution of reference standard aprindine hydrochloride in water was prepared. A 5-ml aliquot was extracted in the same manner as the solution formulation sample.

GLC—Two-microliter portions of the sample and standard solutions were injected, and the instrument parameters were adjusted to obtain the optimum response of the two peaks. The retention times were approximately 2.0 and 5.8 min for aprindine and cholestane, respectively.

GLC–Mass Spectrometry—A 70-ev electron-impact mass spectrum of the observed GLC aprindine peak was obtained using a gas chromatograph–mass spectrometer[8].

Calculations—For each chromatogram, the ratio (R) of the area of the aprindine peak to that of the internal standard was determined. The purity of the raw material is given by:

$$\text{milligrams of aprindine hydrochloride per gram} = \frac{R_{\text{sample}}}{R_{\text{standard}}} \times \frac{\text{milligrams of standard}}{\text{milligrams of sample}} \times \text{standard purity} \times 1000 \quad \text{(Eq. 1)}$$

The potency of the formulations is given by:

$$\text{milligrams of aprindine hydrochloride per capsule} = \frac{R_{\text{sample}}}{R_{\text{standard}}} \times \frac{\text{milligrams of standard}}{\text{grams of sample}} \times \text{average fill weight (grams)} \times \text{standard purity} \quad \text{(Eq. 2)}$$

$$\text{milligrams of aprindine hydrochloride per ampul} = \frac{R_{\text{sample}}}{R_{\text{standard}}} \times \frac{\text{milligrams of standard}}{\text{milliliters of standard solution}} \times \frac{\text{milliliters of sample solution}}{1 \text{ ampul}} \times \text{standard purity} \quad \text{(Eq. 3)}$$

[8] LKB 9000S, Produkter AB, Bromma, Sweden.

$$\text{milligrams of aprindine hydrochloride per milliliter of solution} = \frac{R_{\text{sample}}}{R_{\text{standard}}} \times \frac{\text{milligrams of standard}}{\text{milliliters of standard solution}} \times \text{standard purity} \quad \text{(Eq. 4)}$$

Degradation Studies—*Reflux in Acid, Base, and Methanol*—Solutions containing 1 mg of aprindine hydrochloride/ml in methanol, methanolic 1 *N* HCl, and methanolic 1 *N* KOH were prepared. Twenty-five-milliliter aliquots of each were refluxed for 24, 72, and 144 hr.

UV Irradiation of Solution—A solution containing 1 mg of aprindine hydrochloride/ml in water was prepared. Ten-milliliter aliquots were placed in quartz test tubes[9] and irradiated with UV light[10] for 2, 6, 12, 24, and 48 hr.

Heat: Solid—Twenty-five-milligram samples of aprindine hydrochloride were accurately weighed and placed in an oven at 110°. Samples were removed at 6, 12, and 24 hr.

Heat: Solution—Solutions containing 1 mg of aprindine hydrochloride/ml in 5% dextrose in water[11] and in buffers at pH 1, 4, and 7 were prepared. Twenty-five-milliliter aliquots were heated at 50° for 6, 12, and 24 hr.

All treated aqueous solutions were assayed by the addition of sodium carbonate solution and extraction into chloroform. The methanolic solutions were evaporated to dryness under vacuum and then extracted from sodium carbonate solution into chloroform. The oven-heated samples were dissolved in water, treated with sodium carbonate solution, and extracted into chloroform.

Appropriate aliquots (equivalent to 1 mg of aprindine hydrochloride) were evaporated to dryness with mild heat and an air stream and then redissolved in 1 ml of chloroform and 1 ml of internal standard solution. These solutions were assayed by GLC, using a standard solution prepared according to the raw material preparation.

RESULTS AND DISCUSSION

Hydrochloride salts generally give chromatographic peaks of the same retention time as the base, but nonreproducible results and tailing peaks are frequently encountered. For this reason, aprindine base is chromatographed instead of the salt. A typical gas chromatogram is shown in Fig. 1. The first peak is aprindine, which was confirmed by GLC–mass spectrometry. The mass spectrum showed the expected molecular ion at m/e 322. A linear response to aprindine raw material was obtained from 0.5 to 1.5 mg/ml.

To test the specificity of this GLC method for assaying aprindine, several related compounds, including its synthetic precursors, were chromatographed (Table I). All tested compounds had a retention time less than that of aprindine. To measure the retention times accurately, the column temperature was reduced to 200°. At this temperature, all compounds except indene, 2-indanone, and 2-indanol were detected. These three compounds were not resolved from the solvent front. Further lowering of the column temperature was not convenient for the assay due to the resulting increase in the retention

[9] 150 × 18 mm, MISCO Scientific, Berkeley, Calif.

[10] Hanovia lamp analytic model 7420, equipped with a high-pressure 325-w mercury vapor quartz lamp, Hanovia Lamp Division, Canrad Precision Industries, Newark, N.J. The tubes were about 15 cm from the lamp.

[11] D5W, Abbott Laboratories, North Chicago, Ill.

time of aprindine. None of the eight compounds tested interfered with the aprindine peak (Table I).

Duplicate injections of five 50-mg raw material samples, extracted by a single analyst, gave a standard deviation (*SD*) of 0.01 and a relative standard deviation [*RSD* = (*SD* × 100)/mean] of 1.48%. Duplicate injections of five capsule samples containing 25 mg/capsule gave a relative standard deviation of 1.04%. The relative error calculated for this formulation was +0.2%. Duplicate injections of five solution samples (1 mg/ml) gave a relative standard deviation of 0.79%.

No extra peaks were observed in the chromatograms of the refluxed or heated samples. Table II summarizes the results of the various degradation studies. With the exception of samples irradiated with UV light, the data indicate that aprindine is stable to these artificial degradation conditions. Analysis of the UV-irradiated solution showed detectable extra peaks. These were identified on the basis of their retention times to be *N*-phenyl-2-indanamine (II) and *N,N*-diethyl-*N'*-phenyl-1,3-propanediamine (III).

The formation of II and III may be due to a UV light-catalyzed homolytic cleavage of the appropriate carbon–nitrogen bond. Compounds II and III were reported previously as metabolites of aprindine (1, 4). None of the degraded solutions showed any interference with the assay of aprindine. Due to the light sensitivity of aprindine, ampul formulations must be protected from light. Natural shelflife stability data on raw material and capsule formulations for 2 years and on ampuls for 1 year indicate that the material is stable.

REFERENCES

(1) *Acta Cardiol., Suppl.*, **18**, 131, 177, 195, 233(1974).

(2) H. Kesteloot, W. Van Mieghem, and H. De Geest, *Acta Cardiol.*, **28**, 145(1973).

(3) M. F. Rousseau, L. A. Brasseur, and J. M. Detry, *ibid.*, **28**, 456(1973).

(4) L. Dodion, J. M. De Suray, M. Deblecker, and A. Georges, *Therapie*, **29**, 221(1974).

(5) J. P. Van Durme, M. G. Bogaert, and M. T. Rosseel, *Br. J. Clin. Pharmacol.*, **1**, 461(1974).

(6) J. P. Van Durme, M. G. Bogaert, and M. T. Rosseel, *Eur. J. Clin. Pharmacol.*, **7**, 343(1974).

(7) F. Verdonck, J. Vereecke, and A. Vleugels, *Eur. J. Pharmacol.*, **26**, 338(1974).

ACKNOWLEDGMENTS AND ADDRESSES

Received July 9, 1975, from the *Lilly Research Laboratories, Eli Lilly and Company, Indianapolis, IN 46206*

Accepted for publication November 12, 1975.

Presented at the Pharmaceutical Analysis and Control Section, APhA Academy of Pharmaceutical Sciences, San Francisco meeting, April 1975.

[x] To whom inquiries should be directed.

Comparative Plasma Concentrations of Quinidine following Administration of One Intramuscular and Three Oral Formulations to 13 Human Subjects

WILLIAM D. MASON [x], JOEL O. COVINSKY, JIMMIE L. VALENTINE, KIM L. KELLY, ORVILLE H. WEDDLE, and BILL L. MARTZ *

Abstract □ Three oral dosage forms of quinidine sulfate (*i.e.*, tablet, capsule, and solution) and one intramuscular formulation of quinidine gluconate were administered to 13 healthy volunteers in a randomized complete crossover design. The plasma concentration of quinidine following each dose (equivalent to 167 mg of quinidine) was determined at 0.25, 0.50, 1, 1.5, 2, 3, 4, 6, 8, 12, and 24 hr following dosing. Three conclusions were derived from analysis of the plasma concentration *versus* time data. First, the intersubject and intrasubject variability in the half-life of quinidine is large and should be considered in evaluating the bioavailability of quinidine. Second, the intramuscular quinidine gluconate gives a greater bioavailability than the quinidine sulfate tablet. And finally, the relative bioavailability of the quinidine sulfate capsule and solution administered orally as compared with the intramuscular quinidine gluconate depends on the methods employed to evaluate the plasma concentration *versus* time data.

Keyphrases □ Quinidine—pharmacokinetics and bioavailability of different dosage forms compared □ Pharmacokinetics—quinidine, different dosage forms compared □ Bioavailability—quinidine, different dosage forms compared □ Dosage forms—tablets, capsules, solutions, and intramuscular quinidine, pharmacokinetics and bioavailability compared □ Antiarrhythmic agents—quinidine, pharmacokinetics and bioavailability of different dosage forms compared

Quinidine is widely recognized as a clinically useful antiarrhythmic agent (1, 2). The plasma concentration *versus* time plots following both single and multiple doses were studied in several species of laboratory animals (3, 4) and in a relatively small number of humans (5–8). Intravenously administered quinidine hydrochloride gave varying plasma half-life values, depending on the species of laboratory animal (3).

Three different salts of quinidine (*i.e.*, sulfate, gluconate, and polygalacturonate) and dihydroquinidine gluconate were administered by mouth to 11 patients in both single- and multiple-dose studies (5). Following a single dose of quinidine sulfate, the maximum mean plasma concentration was 4.02 ± 0.74 (*SD*) μg/ml 2 hr after dosing. With multiple dosing, the gluconate and sulfate salts (in doses equivalent to 400 mg of quinidine sulfate every 8 hr) were most effective and gave steady-state plasma levels between 4 and 7 μg/ml.

The serum quinidine concentrations were determined in 17 patients taking 1–3 g of quinidine sulfate/day (6). The serum quinidine concentration following a single 664-mg dose of quinidine sulfate was measured at frequent intervals over 24 hr. The maximum serum concentration ranged from about 4 to 6 μg/ml, and the time to reach the maximum serum concentration ranged from 2 to 5 hr.

Three different oral quinidine preparations were administered to seven healthy volunteers in a comparative bioavailability study (7). The mean steady-state

time of aprindine. None of the eight compounds tested interfered with the aprindine peak (Table I).

Duplicate injections of five 50-mg raw material samples, extracted by a single analyst, gave a standard deviation (*SD*) of 0.01 and a relative standard deviation [*RSD* = (*SD* × 100)/mean] of 1.48%. Duplicate injections of five capsule samples containing 25 mg/capsule gave a relative standard deviation of 1.04%. The relative error calculated for this formulation was +0.2%. Duplicate injections of five solution samples (1 mg/ml) gave a relative standard deviation of 0.79%.

No extra peaks were observed in the chromatograms of the refluxed or heated samples. Table II summarizes the results of the various degradation studies. With the exception of samples irradiated with UV light, the data indicate that aprindine is stable to these artificial degradation conditions. Analysis of the UV-irradiated solution showed detectable extra peaks. These were identified on the basis of their retention times to be *N*-phenyl-2-indanamine (II) and *N,N*-diethyl-*N'*-phenyl-1,3-propanediamine (III).

The formation of II and III may be due to a UV light-catalyzed homolytic cleavage of the appropriate carbon–nitrogen bond. Compounds II and III were reported previously as metabolites of aprindine (1, 4). None of the degraded solutions showed any interference with the assay of aprindine. Due to the light sensitivity of aprindine, ampul formulations must be protected from light. Natural shelflife stability data on raw material and capsule formulations for 2 years and on ampuls for 1 year indicate that the material is stable.

REFERENCES

(1) *Acta Cardiol., Suppl.*, **18**, 131, 177, 195, 233(1974).

(2) H. Kesteloot, W. Van Mieghem, and H. De Geest, *Acta Cardiol.*, **28**, 145(1973).

(3) M. F. Rousseau, L. A. Brasseur, and J. M. Detry, *ibid.*, **28**, 456(1973).

(4) L. Dodion, J. M. De Suray, M. Deblecker, and A. Georges, *Therapie*, **29**, 221(1974).

(5) J. P. Van Durme, M. G. Bogaert, and M. T. Rosseel, *Br. J. Clin. Pharmacol.*, **1**, 461(1974).

(6) J. P. Van Durme, M. G. Bogaert, and M. T. Rosseel, *Eur. J. Clin. Pharmacol.*, **7**, 343(1974).

(7) F. Verdonck, J. Vereecke, and A. Vleugels, *Eur. J. Pharmacol.*, **26**, 338(1974).

ACKNOWLEDGMENTS AND ADDRESSES

Received July 9, 1975, from the *Lilly Research Laboratories, Eli Lilly and Company, Indianapolis, IN 46206*

Accepted for publication November 12, 1975.

Presented at the Pharmaceutical Analysis and Control Section, APhA Academy of Pharmaceutical Sciences, San Francisco meeting, April 1975.

[x] To whom inquiries should be directed.

Comparative Plasma Concentrations of Quinidine following Administration of One Intramuscular and Three Oral Formulations to 13 Human Subjects

WILLIAM D. MASON [x], JOEL O. COVINSKY, JIMMIE L. VALENTINE, KIM L. KELLY, ORVILLE H. WEDDLE, and BILL L. MARTZ *

Abstract □ Three oral dosage forms of quinidine sulfate (*i.e.*, tablet, capsule, and solution) and one intramuscular formulation of quinidine gluconate were administered to 13 healthy volunteers in a randomized complete crossover design. The plasma concentration of quinidine following each dose (equivalent to 167 mg of quinidine) was determined at 0.25, 0.50, 1, 1.5, 2, 3, 4, 6, 8, 12, and 24 hr following dosing. Three conclusions were derived from analysis of the plasma concentration *versus* time data. First, the intersubject and intrasubject variability in the half-life of quinidine is large and should be considered in evaluating the bioavailability of quinidine. Second, the intramuscular quinidine gluconate gives a greater bioavailability than the quinidine sulfate tablet. And finally, the relative bioavailability of the quinidine sulfate capsule and solution administered orally as compared with the intramuscular quinidine gluconate depends on the methods employed to evaluate the plasma concentration *versus* time data.

Keyphrases □ Quinidine—pharmacokinetics and bioavailability of different dosage forms compared □ Pharmacokinetics—quinidine, different dosage forms compared □ Bioavailability—quinidine, different dosage forms compared □ Dosage forms—tablets, capsules, solutions, and intramuscular quinidine, pharmacokinetics and bioavailability compared □ Antiarrhythmic agents—quinidine, pharmacokinetics and bioavailability of different dosage forms compared

Quinidine is widely recognized as a clinically useful antiarrhythmic agent (1, 2). The plasma concentration *versus* time plots following both single and multiple doses were studied in several species of laboratory animals (3, 4) and in a relatively small number of humans (5–8). Intravenously administered quinidine hydrochloride gave varying plasma half-life values, depending on the species of laboratory animal (3).

Three different salts of quinidine (*i.e.*, sulfate, gluconate, and polygalacturonate) and dihydroquinidine gluconate were administered by mouth to 11 patients in both single- and multiple-dose studies (5). Following a single dose of quinidine sulfate, the maximum mean plasma concentration was 4.02 ± 0.74 (*SD*) μg/ml 2 hr after dosing. With multiple dosing, the gluconate and sulfate salts (in doses equivalent to 400 mg of quinidine sulfate every 8 hr) were most effective and gave steady-state plasma levels between 4 and 7 μg/ml.

The serum quinidine concentrations were determined in 17 patients taking 1–3 g of quinidine sulfate/day (6). The serum quinidine concentration following a single 664-mg dose of quinidine sulfate was measured at frequent intervals over 24 hr. The maximum serum concentration ranged from about 4 to 6 μg/ml, and the time to reach the maximum serum concentration ranged from 2 to 5 hr.

Three different oral quinidine preparations were administered to seven healthy volunteers in a comparative bioavailability study (7). The mean steady-state

Table I—Treatment Schedule

Subject	Time Period 1	2	3	4
1	Capsule	Tablet	Injection[a]	Solution[b]
2	Capsule	Solution	Injection	Tablet
3	Capsule	Injection	Tablet	Solution
4	Tablet	Capsule	Solution	Injection
5	Tablet	Solution	Capsule	Injection
6	Tablet	Injection	Solution	Capsule
7	Injection	Tablet	Solution	Capsule
8	Injection	Capsule	Tablet	Solution
9	Solution	Injection	Capsule	Tablet
10	Solution	Tablet	Capsule	Injection
11	Solution	Capsule	Injection	Tablet
12	Tablet	Capsule	Solution	Injection
13	Tablet	Capsule	Solution	Injection

[a] Intramuscular injection. [b] Orally administered solution.

serum concentrations of quinidine were determined following a dosage regimen of 330 mg of quinidine base as the bisulfate salt in rapidly dissolving tablets, in a slowly dissolving form, and in a slowly dissolving arabogalactone sulfate form. A higher mean serum level was found for the more rapidly dissolving form than for the slow dissolving sustained-release forms.

Serum quinidine concentrations also were determined following a single 600-mg quinidine sulfate dose to each of 10 healthy subjects, 10 patients with congestive heart failure, and 10 patients with renal insufficiency (8). This study demonstrated the great variability of serum quinidine levels among subjects within each group as well as the differences between serum levels of the normal subjects and those with one of the diseases.

In the present study, the plasma quinidine concentration following administration of single doses of four different preparations was measured in a randomized complete crossover design. Three preparations contained quinidine sulfate and were administered by mouth; the fourth was an intramuscular injection of quinidine gluconate. In addition to comparing the bioavailability of the four dosage forms, two other objectives were designed into the study. First, numerous blood samples were drawn to describe the plasma concentration–time plot more accurately than had been done in previous studies while clearly defining the plasma quinidine half-life. Second, because of the large number of subjects being dosed at four different times, the intersubject and intrasubject variabilities can be assessed accurately.

EXPERIMENTAL

Subjects—Sixteen male and two female healthy adult volunteers between the ages of 22 and 40 were admitted to the study. All subjects were within 10% of ideal body weight. Each subject gave a medical history and received a medical examination. Values for the following tests were determined prior to the study and were required to be within the normal range: ECG, chest X-ray, creatinine, blood urea nitrogen, lactic dehydrogenase, alkaline phosphatase, serum glutamic oxalacetic transaminase, blood sugar, calcium, phosphorus, bilirubin, total protein, albumin, cholesterol, uric acid, urinalysis, hematocrit, hemoglobin, platelet count, and prothrombin time. In addition, the following tests were run during each treatment period and were required to be normal: white blood cell count, differential, platelet count, and urinalysis.

Dosage Forms—Four different dosage forms were administered, three by mouth and one by injection into the gluteus maximus. The three oral dosage forms were a tablet[1], capsule[1], and solution[1], each containing 200 mg of quinidine sulfate USP (equal to 167 mg of quinidine base). The oral solution was 1% quinidine sulfate, 1.3% sucrose, and 25% glycerin in water. Quinidine gluconate injection USP[1] was used for the intramuscular injections. All four dosage forms were assayed for potency by USP XVIII methods.

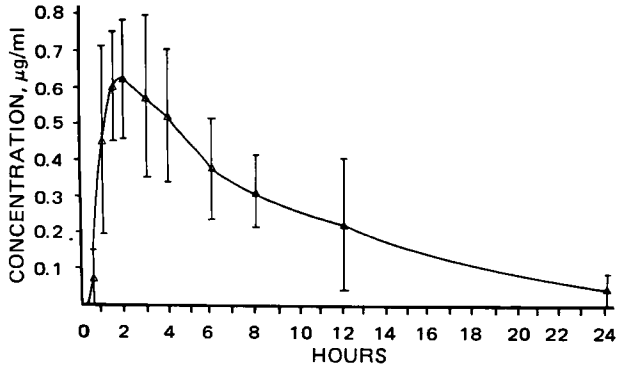

Figure 1—*Plasma concentration (mean ± SD) for 13 subjects following administration of a single capsule containing 200 mg of quinidine sulfate.*

Protocol—Subjects were permitted no food or drink for 10 hr prior to dosing and then were given only 100 ml of water with the quinidine and 100 ml of water each hour for 4 hr. A uniform lunch was provided 4 hr after dosing; after lunch, water was permitted *ad libitum*. All subjects were required to remain upright (standing, sitting, or walking) during the observation period (*i.e.*, 12 hr after dosing).

Blood (10 ml) was taken from the forearm vein *via* a heparin lock immediately prior to dosing and then at 0.25, 0.50, 1, 1.5, 2, 3, 4, 6, 8, 12, and 24 hr following dosing. The blood samples were drawn into heparin-containing vacutainer tubes and centrifuged at 2500 rpm within a few minutes of collection. The plasma samples were immediately frozen (−20°), and they remained frozen until analyzed.

Treatments and Schedules—The study was originally designed to contain four replications of a basic 4 × 4 Latin square with two extra subjects. A single dose (equal to 167 mg of quinidine) was to be administered to each subject each week over 4 successive weeks. However, only 13 of the original 18 subjects completed the schedule[2]. The resulting randomized complete crossover design is shown in Table I.

Because two subjects experienced chills, fever, arthralgia, and mild tachycardia 12 hr after the third treatment, the fourth treatment period was delayed 2 weeks so that the possible adverse drug reaction could be investigated. Therefore, the first three treatments were separated by 7-day intervals while the fourth was separated by a 21-day interval.

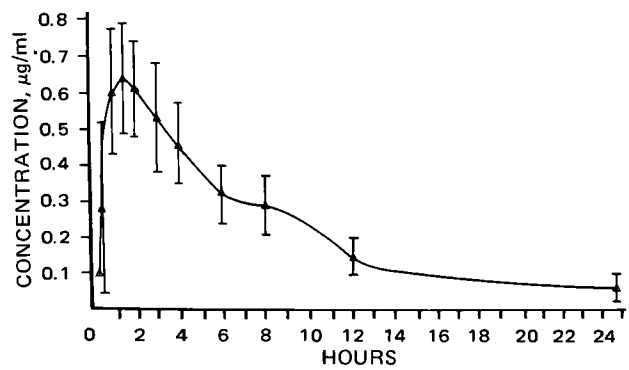

Figure 2—*Plasma concentration (mean ± SD) for 13 subjects following administration of a single tablet containing 200 mg of quinidine sulfate.*

[1] Supplied by Eli Lilly Co.

[2] The five subjects did not complete the study for the following reasons: two experienced chills, fever, arthralgia, and mild tachycardia after the third dose; the platelet count of one subject fell to 169,000; and two others developed conflicts with their work schedules.

Table II—Analysis of Variance for All Four Treatments (Randomized Complete Block, Two-Way Analysis)[a]

Parameter	Mean[b] Injection	Solution	Capsule	Tablet	df[c]	SS[d]	MS[e]	F Ratio
AUC_0^{24}, $\frac{\mu g \times min}{ml}$	472.6	305.4	337.9	318.7	3	231,986	77,328	16.05+
Subject					12	409,236.5	34,103	7.08+
Error					36	173,370	4,816	
Total					51	814,592.7		
C_p^{max}, $\frac{\mu g}{ml}$	0.908	0.673	0.721	0.692	3	0.455	0.1515	7.81+
Subject					12	0.959	0.0798	4.114+
Error					36	0.699	0.0194	
Total					51	2.11		
t_{max}, min	101	84.8	97.3	88.4	3	2,279	759.9	0.43 ns
Subject					12	44,129	3,677	2.12*
Error					36	62,299	1,730	
Total					51	108,707		
$(AUC_0^{\infty})(\beta)$, $\frac{\mu g}{ml}$	0.846	0.774	0.721	0.598	3	0.426	0.142	3.732*
Subject					12	2.010	0.168	4.401+
Error					36	1.370	0.038	
Total					51	3.807		

[a] ns = not significant at 0.05 level, * = significant at 0.05 level, and + = significant at 0.01 level. [b] Underlined values are not significantly different from each other when using Duncan's new multiple range test ($p < 0.05$). [c] Degrees of freedom. [d] Sums of squares. [e] Means squares.

Plasma Quinidine Analysis—The plasma concentration of quinidine was determined by the fluorometric method of Cramer and Isaksson (9). Each plasma sample was assayed in triplicate, and the mean value was used in the data treatment.

Treatment of Data and Statistical Analysis—The plasma concentration, C_p, *versus* time, t, was plotted for each dose administered. The maximum plasma concentration, C_p^{max}, and the time required to reach the maximum plasma concentration, t_{max}, were determined directly from the graphs. By using the trapezoidal method, the area under each plasma concentration–time plot for the first 24 hr following dosing, AUC_0^{24}, was calculated. For each dose, a plot of ln C_p *versus* t was made using the data at 6, 8, 12, and 24 hr.

The least-squares value of the slope, β, and the correlation coefficient, r, was calculated for each semilog plot. The biological half-life, $t_{1/2}$, for each dose was calculated using the equation $t_{1/2} = 0.693/\beta$. An adjustment of the area under the curve to add the area beyond 24 hr was calculated as:

$$AUC_0^{\infty} = AUC_0^{24} + (C_p{}^{24}/\beta) \qquad \text{(Eq. 1)}$$

where $C_p{}^{24}$ is the plasma concentration at 24 hr. Due to the relatively large variability in the biological half-lives among and within subjects, a "normalized area under the curve," $(AUC_0^{\infty})(\beta)$, was computed for each dose in each subject. The rationale and equations for correcting the area under the curve data for variability in the biological half-life were described by Wagner (10).

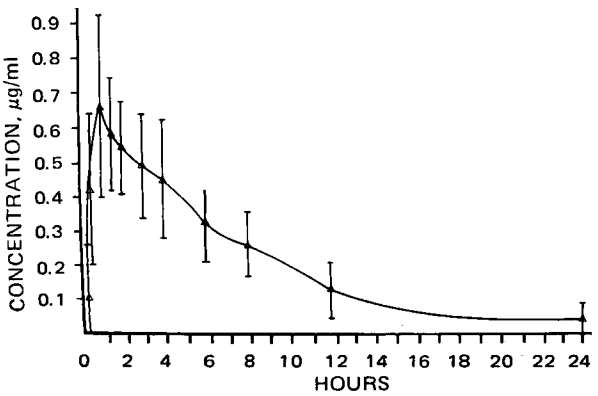

Figure 3—*Plasma concentration (mean ± SD) for 13 subjects following administration of a single oral solution containing 200 mg of quinidine sulfate.*

Each parameter [*i.e.*, C_p^{max}, t_{max}, AUC_0^{24}, and $(AUC_0^{\infty})(\beta)$] was evaluated for statistical significance using a two-way analysis of variance[3] and Duncan's new multiple range test. The sources of variation in the analysis included treatments, subjects, and residual.

RESULTS

Figures 1–4 present the mean plasma concentration–time plots for each treatment in 13 subjects. The standard deviation for the plasma concentration at each sampling time is indicated. Figure 5 presents the mean plasma concentration–time plots for comparison of all four treatments. An analysis of variance among the parameters determined [*i.e.*, C_p^{max}, t_{max}, AUC_0^{24}, and (AUC_0^{∞}) (β)] for all four treatments is shown in Table II. Table III presents the biological half-lives, $t_{1/2}$, and the least-squares values for the slopes, (β), of the ln C_p *versus* t plots along with their correlation coefficients, r.

DISCUSSION

The relatively large standard deviations shown in Figs. 1–4, the variability in the biological half-lives of Table III, and the large F-values for subject variability in Table II indicate a substantial vari-

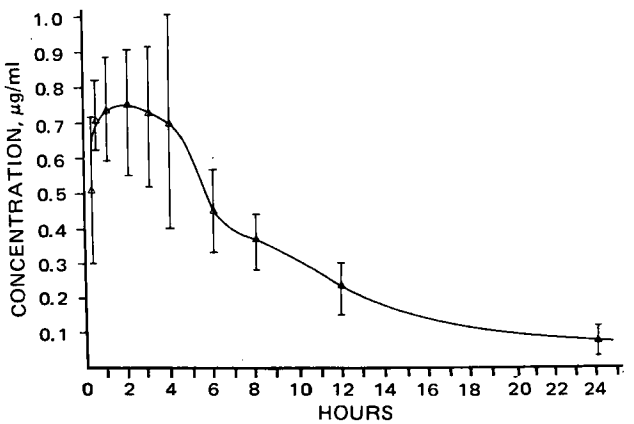

Figure 4—*Plasma concentration (mean ± SD) for 13 subjects following intramuscular injection of 321 mg of quinidine gluconate.*

[3] Monroe calculator program 2001-B.

Table III—Elimination Rate Constants[a] and Biological Half-Lives

	Treatment Period											
	1			2			3			4		
Subject	β, hr^{-1}	$t_{1/2}$, hr	r^b	β, hr^{-1}	$t_{1/2}$, hr	r^b	β, hr^{-1}	$t_{1/2}$, hr	r^b	β, hr^{-1}	$t_{1/2}$, hr	r^b
1	0.104	6.66	0.980	0.163	4.25	0.997	0.105	6.60	0.980	0.131	5.29	0.999
2	0.120	5.78	1.00	0.155	4.47	0.997	0.126	5.50	1.00	0.163	4.25	0.997
3	0.083	8.35	0.990	0.112	6.19	0.990	0.097	7.14	0.985	0.205	3.38	0.979
4	0.059	11.75	0.983	0.082	8.45	1.00	0.131	5.29	0.990	0.076	9.12	1.00
5	0.044	15.75	0.966	0.046	15.1	0.977	0.083	8.35	0.980	0.057	12.16	0.980
6	0.068	10.19	0.993	0.090	7.70	1.00	0.150	4.62	0.920	0.220	3.15	0.980
7	0.091	7.14	0.980	0.146	4.75	0.999	0.217	3.19	0.990	0.115	6.03	0.980
8	0.084	8.25	0.970	0.099	7.00	1.00	0.073	9.49	0.970	0.284	2.44	0.996
9	0.067	10.34	0.970	0.071	9.76	1.00	0.161	4.30	0.939	0.086	8.06	0.995
10	0.085	8.15	0.957	0.153	4.53	0.995	0.135	5.13	0.990	0.123	5.63	1.00
11	0.096	7.22	0.934	0.173	4.01	0.956	0.211	3.28	0.990	0.142	4.88	0.988
12	0.134	5.17	0.998	0.154	4.50	0.972	0.213	3.25	0.985	0.137	5.06	1.00
13	0.129	5.37	0.991	0.239	2.90	0.990	0.596	1.16	0.950	0.177	3.92	0.990

[a] Determined by least-squares fit of the natural logarithm of the plasma concentration plotted against time for the 6-, 8-, 12-, and 24-hr points. [b] Correlation coefficient.

ability in plasma levels attained for quinidine within and among subjects receiving the same dose. Specifically, the range in the biological half-life was 15.75–1.16 hr. Although the variability within a single subject was less than the variability among subjects, it was still considerable. With such significant intrasubject and intersubject variability, utilization of pharmacokinetic methods to "normalize" the data and the use of a complete crossover design become quite important (10).

From the statistical data in Table II, it is apparent that the parameters determined directly from the data (*i.e.*, C_p^{max}, AUC_0^{24}, and t_{max}) show the differences among the three oral dosage forms not to be significant ($p < 0.05$). These data also indicate that the relative amount of quinidine reaching the general circulation is greater from the intramuscular route than from the oral route. However, when the areas under the curve are corrected for the variability in the biological half-life [*i.e.*, (AUC_0^{∞}) (β)], the F-values decrease substantially for both the treatments and the subject variance. This result indicates that the bias produced by the variability in the half-life accentuated any differences among the four dosage forms.

Data from Duncan's new multiple range test support the assertion that the intramuscular route results in greater quinidine availability when only the C_p^{max} and AUC_0^{24} parameters are considered. However, the difference between oral and intramuscular routes decreases greatly when compensation is made for the variability in the biological half-life. Indeed, for the parameter $(AUC_0^{\infty})(\beta)$, only the oral tablet differs significantly from the intramuscular injection ($p < 0.05$).

The statistical analysis indicates that there is no difference ($p < 0.05$) in the time required to reach the maximal plasma concentration among the four treatments. Thus, the rate of absorption is not different for the three oral and one intramuscular preparations.

CONCLUSIONS

The plasma concentration of quinidine following a single dose may differ significantly from person to person and within the same person at different times. Much of this variability is due to the intersubject and intrasubject variabilities in biological half-life. This information points to the importance of individualization of dosage regimens for patients taking quinidine and the possible use of plasma levels in assessing quinidine therapy.

The data presented in this study show no significant differences ($p < 0.05$) in the bioavailability of quinidine from the three oral dosage forms tested. However, depending upon the treatment of the plasma level data, one may or may not conclude that the relative amount of quinidine available from an intramuscular injection is greater than from an equimolar oral dose in the capsule or solution dosage form. This possible difference between the oral and intramuscular routes of administration requires further study. The intramuscular quinidine gluconate does give a greater bioavailability than the quinidine sulfate tablet administered by mouth.

An important conclusion one can draw from these data on quinidine is the necessity for careful evaluation of bioavailability data. In this study, the variability in the biological half-life is sufficient to bias the data and lead one to conclude that the intramuscular route gives a greater bioavailability than any of the oral dosage forms tested; however, if the data are corrected for the variability in the half-life, only the tablet is significantly ($p < 0.05$) less bioavailable than the intramuscular injection.

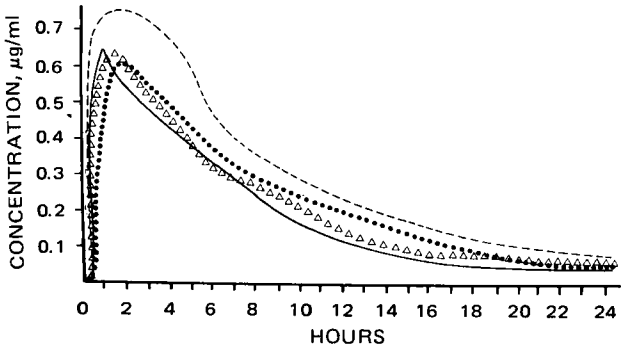

Figure 5—*Comparison of the mean plasma concentration–time curves for the four dosage forms of quinidine administered to 13 subjects. Key: △, tablet; - - -, intramuscular injection; . . ., capsule; and —, oral solution.*

REFERENCES

(1) S. S. Bloomfield, D. W. Romhilt, T. Chou, and N. O. Fowler, *Circulation*, **47**, 967(1973) and *N. Engl. J. Med.*, **285**, 979(1971).

(2) J. Koch-Weser, *N. Engl. J. Med.*, **285**, 1024(1971).

(3) C. A. Neff, L. E. Davis, and J. D. Baggot, *Am. J. Vet. Res.*, **33**, 1521(1972).

(4) J. Nakano and R. B. McCloy, Jr., *Arch. Int. Pharmacodyn. Ther.*, **168**, 400(1967).

(5) W. M. Goldberg and S. G. Chakrabarti, *Can. Med. Assoc. J.*, **91**, 991(1964).

(6) H. E. Archer, D. Weitzman, and H. L. Kay, *Br. Heart J.*, **17**, 534(1955).

(7) R. Henning and G. Nyberg, *Eur. J. Clin. Pharmacol.*, **6**, 239(1973).

(8) S. Bellet, L. R. Roman, and A. Boza, *Am. J. Cardiol.*, **27**, 368(1971).

(9) B. Cramer and B. Isaksson, *Scand. J. Clin. Lab. Invest.*, **15**, 553(1963).

(10) J. G. Wagner, "Biopharmaceutics and Relevant Pharmacokinetics," 1st ed., Drug Intelligence Publications, Hamilton, Ill., 1971, chap. 25.

ACKNOWLEDGMENTS AND ADDRESSES

Received April 21, 1975, from the *School of Medicine and the*

School of Pharmacy, University of Missouri–Kansas City, and the *Kansas City General Hospital and Medical Center, Kansas City, MO 64108*

Accepted for publication November 14, 1975.
* Present address: Dow Chemical Corp., Indianapolis, IN 46268
ˣ To whom inquiries should be directed.

GLC Determination of Methotrimeprazine and Its Sulfoxide in Plasma

SVEIN G. DAHL ˣ and STEN JACOBSEN

Abstract □ A GLC method, based on flame-ionization detection, was developed for the assay of methotrimeprazine and its sulfoxide in plasma. For a 6-ml aliquot, the sensitivity was 2–3 ng/ml for the unchanged drug and 4–5 ng/ml for the sulfoxide. The coefficient of variation, calculated from duplicate analyses of plasma samples, was 8–15% for concentrations between 10 and 100 ng/ml. Patients treated with orally administered methotrimeprazine had higher plasma levels of the sulfoxide than of unmetabolized drug. The method also was applied to the analysis of promazine and chlorpromazine in patient plasma.

Keyphrases □ Methotrimeprazine—base and sulfoxide, GLC analysis, plasma □ GLC—analysis, methotrimeprazine base and sulfoxide, plasma □ Analgesic agents—methotrimeprazine base and sulfoxide, GLC analysis in plasma

Methotrimeprazine[1] (I) has been widely used in Europe as a neuroleptic for the past 15 years. It is usually administered orally as tablets or syrup but occasionally is given intramuscularly. In the United States, the drug is mainly used as an analgesic and only is recognized for intramuscular use. The molecular formula resembles that of chlorpromazine (III), but unmetabolized methotrimeprazine has no electron-capturing groups or positions suitable for introduction of such groups. No sufficiently sensitive and specific assay for the drug in plasma is available, and information about the biological half-life and plasma levels was lacking when this study was undertaken.

Three metabolites have been identified and quantitated in urine from psychiatric patients after oral doses of methotrimeprazine: methotrimeprazine sulfoxide (II), monodesmethyl methotrimeprazine, and monodesmethyl methotrimeprazine sulfoxide (1). The urine contained II in considerably higher concentrations than the other two metabolites.

The pharmacological effects of methotrimeprazine are similar to those of chlorpromazine. A fall in the sitting systolic and diastolic blood pressure produced by chlorpromazine has been correlated with the plasma drug level (2). Sedation and orthostatic hypotension are the most important side effects of methotrimeprazine (3, 4). A method for analysis of this drug in plasma provides an opportunity to examine whether these and other adverse reactions are related to plasma drug concentrations and perhaps to establish a more rational dosage scheme.

[1] Known as levomepromazine in Europe.

A sensitive and specific method for quantitation of chlorpromazine and some of its metabolites in plasma was reported by Curry (5) and has since been modified to improve its sensitivity and accuracy (6–9). The method is based on GLC with electron-capture detection, which permits quantitation of absolute amounts down to 2 ng of chlorpromazine/sample. The method described in this report is based on a modification of the extraction procedure described by Curry (5). By a more extensive purification and concentration of the extract, absolute amounts down to 10–15 ng of methotrimeprazine and 20–25 ng of its sulfoxide/sample can be quantitated by GLC with flame-ionization detection.

By a check on whether other phenothiazines could interfere with the analysis, it became apparent that the method could be used for chlorpromazine and its sulfoxide (IV) in plasma and, by a slight reduction of the column temperature, for promazine (V) in plasma.

Sulfoxidation and *N*-demethylation are two of the known pathways of promazine metabolism in humans (10, 11). Peak concentrations of unchanged promazine in blood shortly after an intravenous injection were measured by a spectrophotometric method (12), but the

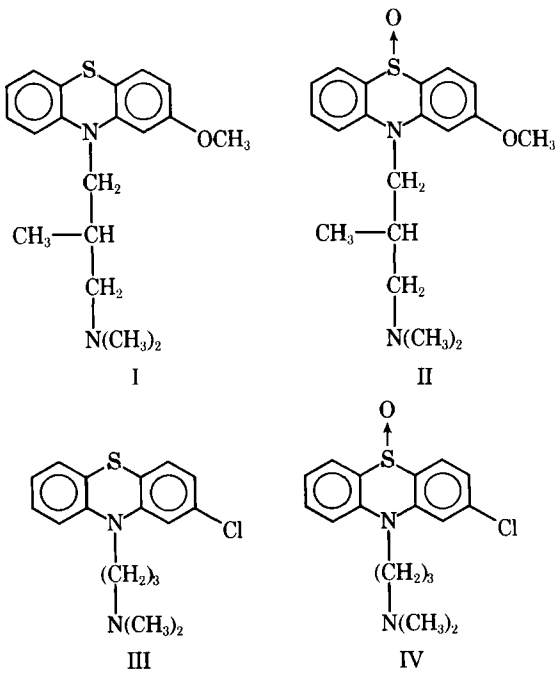

School of Pharmacy, University of Missouri–Kansas City, and the *Kansas City General Hospital and Medical Center, Kansas City, MO 64108*

Accepted for publication November 14, 1975.
* Present address: Dow Chemical Corp., Indianapolis, IN 46268
ˣ To whom inquiries should be directed.

GLC Determination of Methotrimeprazine and Its Sulfoxide in Plasma

SVEIN G. DAHL ˣ and STEN JACOBSEN

Abstract □ A GLC method, based on flame-ionization detection, was developed for the assay of methotrimeprazine and its sulfoxide in plasma. For a 6-ml aliquot, the sensitivity was 2–3 ng/ml for the unchanged drug and 4–5 ng/ml for the sulfoxide. The coefficient of variation, calculated from duplicate analyses of plasma samples, was 8–15% for concentrations between 10 and 100 ng/ml. Patients treated with orally administered methotrimeprazine had higher plasma levels of the sulfoxide than of unmetabolized drug. The method also was applied to the analysis of promazine and chlorpromazine in patient plasma.

Keyphrases □ Methotrimeprazine—base and sulfoxide, GLC analysis, plasma □ GLC—analysis, methotrimeprazine base and sulfoxide, plasma □ Analgesic agents—methotrimeprazine base and sulfoxide, GLC analysis in plasma

Methotrimeprazine[1] (I) has been widely used in Europe as a neuroleptic for the past 15 years. It is usually administered orally as tablets or syrup but occasionally is given intramuscularly. In the United States, the drug is mainly used as an analgesic and only is recognized for intramuscular use. The molecular formula resembles that of chlorpromazine (III), but unmetabolized methotrimeprazine has no electron-capturing groups or positions suitable for introduction of such groups. No sufficiently sensitive and specific assay for the drug in plasma is available, and information about the biological half-life and plasma levels was lacking when this study was undertaken.

Three metabolites have been identified and quantitated in urine from psychiatric patients after oral doses of methotrimeprazine: methotrimeprazine sulfoxide (II), monodesmethyl methotrimeprazine, and monodesmethyl methotrimeprazine sulfoxide (1). The urine contained II in considerably higher concentrations than the other two metabolites.

The pharmacological effects of methotrimeprazine are similar to those of chlorpromazine. A fall in the sitting systolic and diastolic blood pressure produced by chlorpromazine has been correlated with the plasma drug level (2). Sedation and orthostatic hypotension are the most important side effects of methotrimeprazine (3, 4). A method for analysis of this drug in plasma provides an opportunity to examine whether these and other adverse reactions are related to plasma drug concentrations and perhaps to establish a more rational dosage scheme.

[1] Known as levomepromazine in Europe.

A sensitive and specific method for quantitation of chlorpromazine and some of its metabolites in plasma was reported by Curry (5) and has since been modified to improve its sensitivity and accuracy (6–9). The method is based on GLC with electron-capture detection, which permits quantitation of absolute amounts down to 2 ng of chlorpromazine/sample. The method described in this report is based on a modification of the extraction procedure described by Curry (5). By a more extensive purification and concentration of the extract, absolute amounts down to 10–15 ng of methotrimeprazine and 20–25 ng of its sulfoxide/sample can be quantitated by GLC with flame-ionization detection.

By a check on whether other phenothiazines could interfere with the analysis, it became apparent that the method could be used for chlorpromazine and its sulfoxide (IV) in plasma and, by a slight reduction of the column temperature, for promazine (V) in plasma.

Sulfoxidation and *N*-demethylation are two of the known pathways of promazine metabolism in humans (10, 11). Peak concentrations of unchanged promazine in blood shortly after an intravenous injection were measured by a spectrophotometric method (12), but the

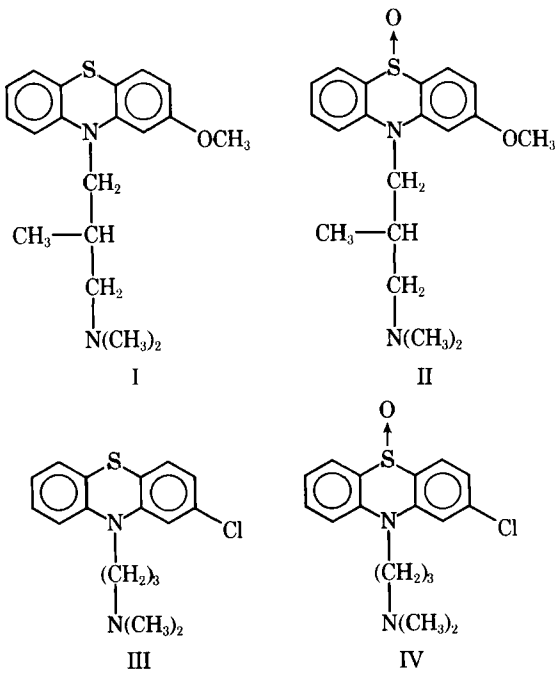

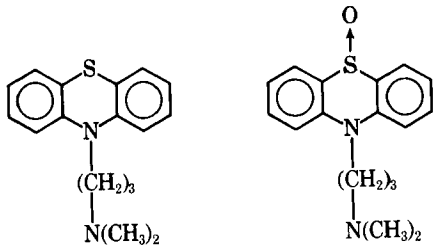

V

VI

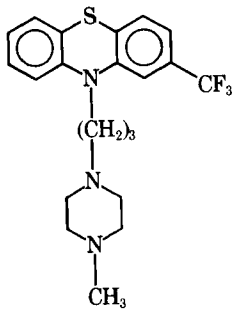

VII

method lacks satisfactory sensitivity and precision for a pharmacokinetic study.

EXPERIMENTAL

Glassware—The glassware was cleaned by standing overnight in chromic acid, 5% NaOH, and ethanol on consecutive nights and was rinsed with water after each cleaning step. It then was silylated with 5% dichlorodimethylsilane in toluene and rinsed with toluene.

Small pointed test tubes for evaporation of samples were made from Pasteur pipets by melting off the capillary at the neck of the pipet. The 14- and 20-ml centrifuge tubes used for extractions were tapered (4 mm i.d. near the bottom) to allow the complete aspiration of the lower aqueous phase without losing any of the upper organic layer.

Reagents and Standard Solutions—Heptane, analyzed grade[2], toluene[3], and isoamyl alcohol[4] were used without prior distillation. Hydrochloric acid[4] was diluted to 0.05 *N* and washed once with heptane containing 1.5% isoamyl alcohol and once with toluene containing 15% isoamyl alcohol. Analyzed grade sodium hydroxide, 50%[2], was diluted to 5 or 1%, washed twice with heptane containing 1.5% isoamyl alcohol, and kept in bottles[5]. Concentrated ammonium hydroxide[4] was diluted to 3 *N* and washed twice with toluene containing 15% isoamyl alcohol. The aqueous solutions were diluted with distilled water and washed by shaking for 10 min with a 20% volume of organic solvent.

The following reference compounds[6] were used: mono- and didesmethyl chlorpromazine, chlorpromazine sulfoxide, monodesmethyl chlorpromazine sulfoxide, trifluoperazine (VII), mono- and didesmethyl methotrimeprazine, monodesmethyl methotrimeprazine sulfoxide, didesmethyl promazine, promazine sulfoxide (VI), monodesmethyl promazine sulfoxide, chlorpromazine hydrochloride, methotrimeprazine hydrochloride, methotrimeprazine sulfoxide, promazine hydrochloride, monodesmethyl promazine, and chlorpromazine base.

The reference compounds were dissolved in heptane containing 1.5% isoamyl alcohol, for direct injection into the gas chromatograph, or in water, for addition to blank plasma to obtain standard curves. An amount equivalent to 10 mg of free base was dissolved in 10 ml and diluted further to 0.5 ng/μl. Aqueous solutions of reference compounds obtained as free bases were made by dissolving in 0.05 *N* HCl and diluting with distilled water. Organic solutions of compounds obtained as water-soluble salts were made by extraction from 0.5 ml of 5% NaOH into 10 ml of heptane–isoamyl alcohol.

Standard solutions were stored in the dark at 5° in silylated screw-capped glass counting vials. The aqueous solutions were stable for 3–4 months under these conditions, while the organic standard solutions remained unchanged for more than 1 year.

Preparation of Samples—Blood samples of 5–10 ml were collected in heparinized polyethylene tubes. After immediate centrifugation, the plasma was divided into two aliquots and stored at −24°. The two aliquots from each sample were analyzed on different days within 6 weeks after sampling.

Extraction Procedure—All extractions were performed with a mechanical shaker[7] at its maximum speed. The samples were centrifuged at 500×*g*[8].

A 1–6-ml aliquot of plasma was transferred to a 20-ml glass-stoppered centrifuge tube, and 100 μl of a 10-ng/μl aqueous solution of trifluoperazine hydrochloride was added as the internal standard. The plasma was made alkaline with a 20% volume of 5% NaOH and shaken for 60 min with 10 ml of heptane containing 1.5% isoamyl alcohol. The sample was centrifuged for 5 min, and the aqueous phase was removed by suction.

To the heptane phase was added 1 ml of 1% NaOH. The sample was shaken for 10 min, and the aqueous phase was aspirated before the tube was centrifuged for 2 min. The heptane phase was then transferred with a glass pipet to a 14-ml glass-stoppered centrifuge tube and shaken for 15 min with 1.5 ml of 0.05 *N* HCl. After 2 min of centrifugation, the heptane phase was discarded and 2.5 ml of heptane with 1.5% isoamyl alcohol was added. The sample was shaken for 10 min and centrifuged for 2 min, and the heptane phase was discarded.

The aqueous phase was made alkaline with 0.1 ml of 3 *N* NH_4OH, and the sample was extracted into 0.25 ml of toluene with 15% isoamyl alcohol by shaking for 15 min. Following 2 min of centrifugation, the aqueous phase was carefully removed with a Pasteur pipet, and the organic phase was transferred from the tip of the tube to a tapered 45-mm glass tube (5 mm i.d.).

The organic phase was evaporated to dryness at 45° under a stream of nitrogen, and the tubes were kept in a vacuum desiccator at room temperature, protected from light, until the GLC runs were made—usually on the following day but sometimes as much as 3 days later.

GLC—A gas chromatograph[9], equipped with two flame-ionization detectors and 180-cm glass columns (2 mm i.d.), was used. The columns were packed with 3% OV-17 on 80–100-mesh Supelcoport[10] and conditioned overnight at 315°. Purified nitrogen, 25 ml/min, was used as carrier gas. The injector and detector temperatures were 270°, and the column temperature was 245 or 255°.

At the beginning of each day, the columns were conditioned by an injection of 20 μl of a silylating reagent[11] and then saturated by an injection of 2 μg of each substance to be analyzed during the day.

Ten microliters of heptane containing 20% isoamyl alcohol was added to the small test tubes with evaporated samples. The opening of the tube was covered with aluminum foil, and the tube was stirred for 1 min on a mixer[12]. From 10–20% of the solvent evaporated during the stirring, and the residual 8–9 μl was injected into the gas chromatograph in two aliquots.

Standard Curves and Analysis of Samples—Standard curves for each drug and its sulfoxide were obtained by adding 50–300 μl of aqueous standard solutions (0.5 or 5.0 ng/μl) to 2.5 ml of blank plasma. The internal standard was added after 15 min of incubation, and the extraction and GLC were performed as already described. The ratio of the peak heights of the analyzed compound and the internal standard was determined for the drug and for the sulfoxide and used as a measure of the amount in the samples.

Standard curves of peak height ratios as a function of the amount of compound added were determined from four or five samples each time patient plasma was analyzed. The least-squares regression line of the standard curve was calculated using reciprocal weighting.

[2] J. T. Baker Chemicals N.V., Deventer, Holland.
[3] Fluka AG, Buchs, Switzerland.
[4] E. Merck, 61 Darmstadt, West Germany.
[5] Teflon (du Pont).
[6] All reference compounds were obtained from one of the following companies: Pharma Rhodia, Birkerod, Denmark; Société des Usines Chimiques Rhône-Poulenc, 94, Vitry-sur-Seine, France; AB Mekos, Helsingborg, Sweden; A/S Ferrosan, Copenhagen, Denmark; or May & Baker Ltd., Dagenham, England.
[7] C. Desaga, GmbH, Heidelberg, West Germany.
[8] IEC model UV centrifuge, International Equipment, Needham Heights, Mass.
[9] Varian model 2100, Varian-Aerograph, Walnut Creek, Calif.
[10] Supelco Inc., Bellefonte, PA 16823
[11] Silyl-8, Pierce Chemical Co., Rockford, IL 61105
[12] Vortex-Genie model K-550-GE, Scientific Industries Inc., Springfield, MA 01103

Table I—Absolute Recovery of Added Reference Compounds after Extraction from Plasma, Evaporation, and Solution in 10 μl of Organic Solvent

Compound	Recovery, % Nanograms Added 25	50	100	250	500	1000	1500	Mean ± SD
I	—	67 (5)[a]	68 (6)	63 (5)	62 (5)	65 (6)	65 (3)	65 ± 7 (30)
II	—	63 (5)	67 (6)	72 (6)	63 (4)	72 (5)	73 (5)	68 ± 6 (31)
III	70 (1)	66 (4)	58 (4)	65 (5)	68 (5)	65 (2)	64 (2)	65 ± 11 (24)
IV	87 (4)	82 (5)	81 (4)	90 (4)	89 (4)	—	—	86 ± 8 (21)
V	53 (1)	76 (4)	74 (5)	64 (3)	76 (5)	65 (3)	67 (3)	71 ± 12 (24)
VI	30 (1)	35 (1)	32 (2)	26 (3)	32 (3)	27 (1)	26 (1)	30 ± 4 (12)

[a] Number in parentheses is the number of determinations.

RESULTS

Extraction Procedure—The absolute recoveries of compounds added to blank plasma (Table I) were calculated from the peak heights after extraction and GLC *versus* the peak heights obtained when known amounts were injected from organic standard solutions. The recoveries varied considerably from sample to sample but were generally 60–70%, except for promazine sulfoxide where the recovery was as low as 30%.

The recovery was also determined by the addition of 250 ng of ^{35}S-labeled chlorpromazine[13] to blank plasma samples. After extraction, evaporation, and solution in 10 μl of heptane–isoamyl alcohol, the recovery in six samples was 68 ± 7%.

GLC—Figure 1 shows a chromatogram of a patient plasma sample containing I and II in concentrations close to the lower detection limit of the method. The sample was taken, 36 hr after administration of the last dose of methotrimeprazine, from a patient who had received 25 mg orally twice daily for 21 days.

Absolute amounts down to 10–15 ng/sample of I, III, and V and 20–25 ng of the sulfoxides gave measurable peaks in the chromatograms. Since as much as 6 ml of plasma could be used without the appearance of interfering peaks from plasma constituents, concentrations down to 2–3 ng/ml of I, III, and V and 4–5 ng/ml of the sulfoxides could be measured.

Column temperatures and retention times are given in Table II. To obtain satisfactory separation from the solvent peak, it was necessary to analyze V at a column temperature 10° lower than for I and III. The monodesmethyl analogs of Compounds I–VI had 20–27% longer retention times, and the didemethylated analogs of I, III, and V had 37, 31, and 26% longer retention times, respectively. The peaks of desmethyl methotrimeprazine, didesmethyl methotrimeprazine, and didesmethyl chlorpromazine overlapped partially with the peak of the internal standard.

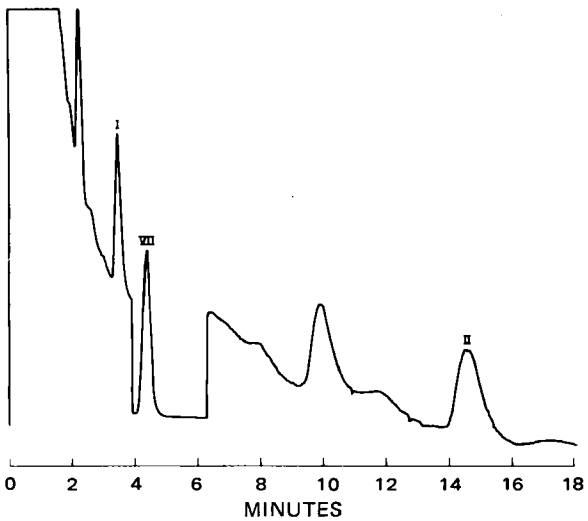

Figure 1—*Gas chromatogram from 6 ml of patient plasma containing I, 4.4 ng/ml, and II, 8 ng/ml. Trifluoperazine (VII) was the internal standard. Electrometer settings were: range, 10^{-12} for all peaks; and attenuation, 16 for I, 128 for VII, and 4 for II.*

[13] Radiochemical Centre, Amersham, England.

Standard Curves—Each standard curve was determined from two GLC runs of four or five known samples. The standard curves were linear within the range indicated in Table I, and the intersections with the *y*-axis were not significantly different from the origin.

The slopes of the standard curves showed some variation from column to column and sometimes also during the lifespan of each column (Table III). The relative standard deviation of the slope of the regression line for each standard curve was an average of 2–3% for I, III, and V and 3–5% for the sulfoxides (Table III).

Patient Plasma Samples—Figure 2 shows plasma concentration curves for three male patients following oral maintenance doses of either methotrimeprazine, chlorpromazine, or promazine. The biological half-lives (in hours), determined from the regression line through the points at 12–36 hr, were: 22.5 (I), 16.6 (II), 11.8 (III), 12.2 (IV), and 8.0 (V). The patient treated with methotrimeprazine showed plasma concentrations of the sulfoxide approximately double those of the unmetabolized drug. About the same ratio was found in plasma from two other male patients who had been treated for several months with methotrimeprazine tablets, 125 mg/day. Before the morning dose was given, plasma concentrations of I were 46 and 56 ng/ml, and the concentrations of II were 4.1 and 1.7 times higher, respectively.

The method has since been used to analyze plasma from five patients after single and multiple doses of methotrimeprazine (13). Chromatograms from blank plasma, taken before administration of the first dose, never contained peaks showing retention times similar to I–VII; all samples taken 2–12 hr after the first oral dose gave peaks with the same retention times as I and II.

The coefficients of variation of the overall method, calculated from duplicate analyses of patient plasma samples, are given in Table IV. Duplicate analyses were performed on different days, within 6 weeks after sampling. For methotrimeprazine in concentrations of 10–100 ng/ml, the coefficient of variation was 10–15%.

DISCUSSION

Endogenous substances with partitioning properties similar to the phenothiazines might theoretically interfere in this analysis, because of the general response of the flame-ionization detector to organic compounds. However, no interfering peaks were seen in chromatograms of blank plasma from healthy volunteers or of plasma taken from psychiatric patients who had received no drugs for 4 weeks or longer.

The recovery by extraction from plasma, evaporation to dryness, and solution in 10 μl of heptane–isoamyl alcohol was variable, but

Table II—Column Temperature and Retention Times

Compound	Column Temperature	Retention Time, min
I	255°	3.50
II	255°	14.50
III	255°	3.25
IV	255°	11.75
VII	255°	4.50
V	245°	2.75
VI	245°	11.50
VII	245°	6.30

Table III—Range of Slopes and Average Standard Deviation of Each Slope for Standard Curves Obtained on Different Days from Four or Five Known Samples Each Day

Compound	Number of Standard Curves	Slope of Regression Lines	
		Range	Average SD^a
I	8	$1.40–1.70 \times 10^{-3}$	0.03×10^{-3}
II	7	$2.75–3.80 \times 10^{-4}$	0.09×10^{-4}
III	5	$1.40–1.50 \times 10^{-3}$	0.03×10^{-3}
IV	6	$4.20–4.90 \times 10^{-4}$	0.16×10^{-4}
V	3	$2.75–3.25 \times 10^{-3}$	0.08×10^{-3}
VI	2	$2.50–2.75 \times 10^{-4}$	0.12×10^{-4}

[a] Calculated by the formula $\sqrt{\Sigma_{i=1}^{n} s_i^2/n}$, where s_i is the standard deviation of the slope of the regression line for the ith standard curve, and n is the number of standard curves.

these variations were generally not reflected in the ratio of the peak heights of the analyzed compound and the internal standard, which had very similar chemical properties. Christoph *et al.* (7) reported that a significant and irreproducible portion of ^{35}S-labeled chlorpromazine was lost when the sample was evaporated to dryness, presumably by adsorption to the glass walls. As indicated by the overall precision (Tables III and IV), this problem was overcome by the present method.

Adsorption to the GLC column was previously a problem, especially with nanogram amounts of the sulfoxides. However, on-column silylation improved the column performance sufficiently to quantitate injected amounts down to about 10 ng. Even with this treatment, adsorption to the column seemed to be the main source of variation in analysis of samples containing less than 100 ng; triplicate analyses of each sample might have improved the accuracy.

The plasma samples were sufficiently purified by the extraction procedure to permit the injection of the whole sample into the gas chromatograph, which is one reason for the relatively high sensitivity of the method, considering that flame-ionization detection was used. To obtain maximum sensitivity, the GLC conditions were adjusted so that the peaks of I, III, and V came at the base of the solvent peak and could be detected at $1/16$ of the maximum sensitivity of the instrument. Because of the relatively long retention times of the sulfoxides, the baseline was usually sufficiently stable to run the gas chromatograph at one-fourth of its maximum sensitivity when they eluted from the column.

Contamination from the glassware could disturb the analysis of samples containing less than 100 ng, and great care in washing and

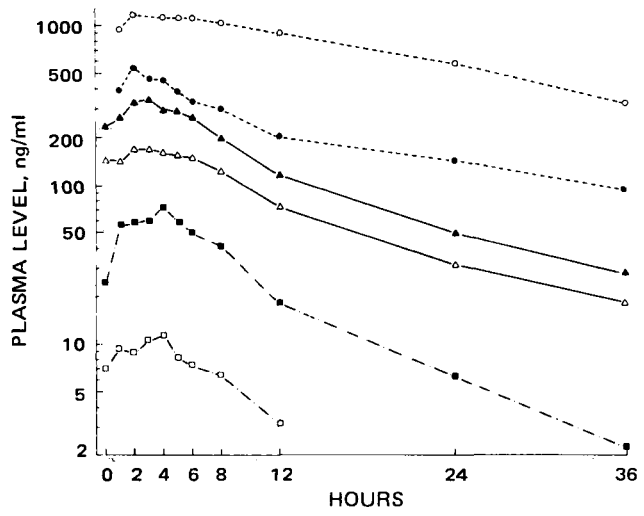

Figure 2—*Plasma concentrations in three adult male patients who had been treated for at least 4 weeks with oral doses of I (2 × 300 mg), III (4 × 400 mg), or V (2 × 150 mg). Each patient received only one drug. The usual morning dose was given at time 0 hr, and no medication was given during the 36 hr when the blood samples were drawn. Each point represents the mean value of two determinations, except for VI which was only determined once. Key: ●, I; ○, II; ▲, III; △, IV; ■, V; and □, VI.*

Table IV—Mean Coefficient of Variation Calculated from Duplicate Analyses of Patient Plasma Samples

Compound	Number of Samples	Concentration Range, ng/ml	Mean Coefficient of Variation[a], %
I	15	2–10	16.1
	56	10–25	14.7
	38	25–50	10.2
	18	50–100	10.3
II	4	5–10	12.1
	18	10–25	9.9
	30	25–50	7.6
	51	50–100	8.8
III	8	200–350	3.6
IV	7	100–175	6.7
V	6	40–75	5.9

[a] Calculated by the formula $(100/n)\sqrt{2}\,\Sigma_{i=1}^{n}[|A_i - B_i|/(A_i + B_i)]$ where A_i and B_i are the results from duplicate analyses of the same plasma, and n is the number of different plasma samples.

handling was necessary. Peaks from two unidentified substances appeared in the chromatograms of plasma samples (Fig. 1), but neither overlapped with any analyzed drug or metabolite. One had a retention time of 2 min at 255° and seemed to come from the heptane. The other, with a retention time of 10 min at 255°, was not seen when a buffer solution was analyzed in the same way as plasma.

Demethylated metabolites that would overlap with the peak of the internal standard did not disturb the analysis of plasma from patients, since as much as 1 μg of internal standard was used per sample. Even with another internal standard with a longer retention time, the present method is probably less accurate for the direct quantitation of the demethylated metabolites in plasma due to a stronger tendency to column adsorption of these compounds.

Within the concentration range indicated in Fig. 2, the method was used without changing the amount of heptane solution injected into the gas chromatograph or the amount of internal standard per sample. The method was successfully applied to samples from *in vitro* studies containing several micrograms simply by increasing the amount of internal standard.

The sensitivity of the method seems to be sufficient for plasma concentrations of I–V after single or multiple therapeutic doses of the drugs. The method is less suitable for promazine sulfoxide (VI) due to the low recovery from the extraction procedure. The extraction procedure is more elaborate than the procedures previously described for chlorpromazine, while this method has the advantage of the simpler operation of the flame-ionization detector, compared to the electron-capture detector.

As is evident from Table IV, the method has been used so far mainly to analyze I and II in plasma from patients receiving I, and it is well suited for this purpose.

REFERENCES

(1) A. De Leenheer and A. Heyndrickx, *J. Pharm. Sci.*, **61**, 914(1972).

(2) G. Sakalis, S. H. Curry, G. P. Mould, and M. H. Lader, *Clin. Pharmacol. Ther.*, **13**, 931(1972).

(3) V. M. Blanco, *Southwest. Med.*, **49**, 170(1968).

(4) *J. Am. Med. Assoc.*, **204**, 159(1968).

(5) S. H. Curry, *Anal. Chem.*, **40**, 1251(1968).

(6) D. R. Flint, C. R. Ferullo, P. Levandoski, and B. Hwang, *Clin. Chem.*, **17**, 830(1971).

(7) G. W. Christoph, D. E. Schmidt, and J. M. Davis, *Clin. Chim. Acta*, **38**, 265(1972).

(8) L. Rivera-Calimlim, L. Castaneda, and L. Lasagna, *Clin. Pharmacol. Ther.*, **14**, 978(1973).

(9) A. V. P. Mackay, A. F. Healey, and J. Baker, *Br. J. Clin. Pharmacol.*, **1**, 425(1974).

(10) H. Goldenberg, V. Fishman, A. Heaton, and R. Burnett, *Proc. Soc. Exp. Biol. Med.*, **115**, 1044(1964).

(11) V. Fishman and H. Goldenberg, *J. Pharmacol. Exp. Ther.*, **150**, 122(1965).

(12) J. S. Crawford and S. Rudofsky, *Br. J. Anaesth.*, **37**, 303(1965).

(13) S. G. Dahl, *Clin. Pharmacol. Ther.*, **19**, 435(1976).

ACKNOWLEDGMENTS AND ADDRESSES

Received July 9, 1975, from the *Institute of Pharmacology, University of Oslo, Oslo 3, Norway.*

Accepted for publication November 14, 1975.

Supported by Grant B 0106.4033 from the Royal Norwegian Council for Scientific and Industrial Research and by grants from the Norwegian Drug Monopoly and the Godfred Lies Foundation.

The authors thank Miss T. Morsund for technical assistance in the analysis of plasma samples. Plasma samples were obtained at Dikemark Hospital with the approval of Dr. B. Gunby. The authors also thank Mr. A. Birkenes for assistance in taking and preparing blood samples and Rhône-Poulenc, Pharma Rhodia, Mekos, Ferrosan, and May & Baker for providing reference compounds.

[x] To whom inquiries should be directed. Present address: Institute of Medical Biology, University of Tromsö, N-9001 Tromsö, Norway.

Drug Release from Methyl Acrylate–Methyl Methacrylate Copolymer Matrix III: Simultaneous Release of Noninteracting Drug–Excipient Mixtures

B. FARHADIEH

Abstract □ The simultaneous release of mixtures of noninteracting chemicals incorporated in a methyl acrylate–methyl methacrylate copolymer was studied. Different mixtures of dextrose–methapyrilene hydrochloride and sodium chloride–methapyrilene hydrochloride in the plastic were compressed into tablets, and single-surface release was obtained in 0.1 *N* HCl at 37°. The amounts of both drug and excipients released per unit surface area were linearly dependent on the square root of time. The release rate constants were analyzed in terms of the solubility, diffusion coefficient, concentration of each chemical, and porosity and tortuosity of the tablets. It was concluded that for each tablet system the individual solid–liquid boundaries of the incorporated chemicals had merged together, and the release could be explained by Higuchi's square root of time relationship.

Keyphrases □ Methyl acrylate–methyl methacrylate copolymer—tablets, simultaneous release of noninteracting drug–excipient mixtures □ Copolymers—methyl acrylate–methyl methacrylate copolymer tablets, simultaneous release of noninteracting drug–excipient mixtures □ Drug release—from methyl acrylate–methyl methacrylate copolymer tablets, effect of water-soluble excipients □ Tablets—water-soluble drug in methyl acrylate–methyl methacrylate copolymer tablets, effect of water-soluble excipients □ Methapyrilene hydrochloride—release from methyl acrylate–methyl methacrylate copolymer tablets, effect of water-soluble excipients

It was shown previously (1) that drug release from tablets compressed directly from mixtures of a single drug and a methyl acrylate–methyl methacrylate copolymer follows the time dependency suggested by Higuchi's (2) theoretical relationship. The magnitude of the release rate constant was dependent on the solubility, diffusivity, and concentration of the drug as well as the matrix porosity and tortuosity.

BACKGROUND

Singh *et al.* (3) considered the simultaneous release of a mixture of two noninteracting drugs dispersed in an inert insoluble matrix composed of a polyethylene–polyvinyl chloride mixture. The developed relationships expressed the diffusion-controlled rate of release of both drugs as functions of solubilities, diffusivities, and concentrations of each drug in the matrix and the porosities and tortuosities of the matrix. Thus, the release of drug a, which had the slower moving solid–liquid boundary, was described by (2):

$$\frac{dQ_a}{d(t^{1/2})} = \left[D_a \frac{\epsilon_1}{\tau_1} (2A_a - \epsilon_1 C_a{}^s) C_a{}^s \right]^{1/2} \qquad \text{(Eq. 1)}$$

where subscript 1 refers to that region of the tablet matrix bounded on one side by the solvent front and on the other side by the solid–liquid boundary of drug a. This part of the tablet will be described as region 1 in subsequent discussions. The release of drug b, with the faster moving solid–liquid boundary, was described by the following, more complex, expression:

$$\frac{dQ_b}{d(t^{1/2})} = \frac{2D_b\epsilon_1}{\tau_1 \dfrac{k_a}{A_a}} \left[\frac{\dfrac{\epsilon_2}{\tau_2} C_b{}^s}{\dfrac{\epsilon_2}{\tau_2} + \dfrac{\epsilon_1}{\tau_1} \left[\dfrac{\dfrac{k_b}{A_b} - \dfrac{k_a}{A_a}}{\dfrac{k_a}{A_a}} \right]} \right] \qquad \text{(Eq. 2)}$$

where subscript 1 is the same as in Eq. 1, and subscript 2 refers to region 2 in the tablet bounded on one side by the solid–liquid boundary for drug a and on the other side by the solid–liquid boundary for drug b. Other symbols used in Eqs. 1 and 2 are defined as follows:

- Q_i = grams of drug i released per unit area of exposed tablet surface at time t
- D_i = diffusion coefficient of drug i in the release medium
- A_i = concentration of drug i in the tablet
- $C_i{}^s$ = solubility of drug i in the release medium
- ϵ_j = porosity of region j of the tablet
- τ_j = tortuosity of region j of the tablet
- k_i = slope of Q_i *versus* $t^{1/2}$ plot for release of drug i from the tablet

The methyl acrylate–methyl methacrylate copolymer has been used to control and regulate the release of highly water-soluble drugs. The purpose of this investigation was to investigate the effect of two common, highly water-soluble excipients on the release of a model of a highly water-soluble drug from matrixes of this copolymer. Methapyrilene hydrochloride was selected as the model drug. It was also proposed to determine whether the mathematical model developed by Singh *et al.* (3) and tested with salicylic and benzoic acid combinations was valid for simultaneous release of highly water-soluble noninteracting chemicals.

EXPERIMENTAL

Chemicals—The plastic used in all tablets was a powdered methyl acrylate–methyl methacrylate copolymer[1]. This polymer is insoluble and inert in aqueous media at all pH values. The drug employed was methapyrilene hydrochloride NF. Anhydrous dextrose USP and

[1] Rohm and Haas Co., Philadelphia, Pa.

ACKNOWLEDGMENTS AND ADDRESSES

Received July 9, 1975, from the *Institute of Pharmacology, University of Oslo, Oslo 3, Norway.*

Accepted for publication November 14, 1975.

Supported by Grant B 0106.4033 from the Royal Norwegian Council for Scientific and Industrial Research and by grants from the Norwegian Drug Monopoly and the Godfred Lies Foundation.

The authors thank Miss T. Morsund for technical assistance in the analysis of plasma samples. Plasma samples were obtained at Dikemark Hospital with the approval of Dr. B. Gunby. The authors also thank Mr. A. Birkenes for assistance in taking and preparing blood samples and Rhône-Poulenc, Pharma Rhodia, Mekos, Ferrosan, and May & Baker for providing reference compounds.

[x] To whom inquiries should be directed. Present address: Institute of Medical Biology, University of Tromsö, N-9001 Tromsö, Norway.

Drug Release from Methyl Acrylate–Methyl Methacrylate Copolymer Matrix III: Simultaneous Release of Noninteracting Drug–Excipient Mixtures

B. FARHADIEH

Abstract □ The simultaneous release of mixtures of noninteracting chemicals incorporated in a methyl acrylate–methyl methacrylate copolymer was studied. Different mixtures of dextrose–methapyrilene hydrochloride and sodium chloride–methapyrilene hydrochloride in the plastic were compressed into tablets, and single-surface release was obtained in 0.1 *N* HCl at 37°. The amounts of both drug and excipients released per unit surface area were linearly dependent on the square root of time. The release rate constants were analyzed in terms of the solubility, diffusion coefficient, concentration of each chemical, and porosity and tortuosity of the tablets. It was concluded that for each tablet system the individual solid–liquid boundaries of the incorporated chemicals had merged together, and the release could be explained by Higuchi's square root of time relationship.

Keyphrases □ Methyl acrylate–methyl methacrylate copolymer—tablets, simultaneous release of noninteracting drug–excipient mixtures □ Copolymers—methyl acrylate–methyl methacrylate copolymer tablets, simultaneous release of noninteracting drug–excipient mixtures □ Drug release—from methyl acrylate–methyl methacrylate copolymer tablets, effect of water-soluble excipients □ Tablets—water-soluble drug in methyl acrylate–methyl methacrylate copolymer tablets, effect of water-soluble excipients □ Methapyrilene hydrochloride—release from methyl acrylate–methyl methacrylate copolymer tablets, effect of water-soluble excipients

It was shown previously (1) that drug release from tablets compressed directly from mixtures of a single drug and a methyl acrylate–methyl methacrylate copolymer follows the time dependency suggested by Higuchi's (2) theoretical relationship. The magnitude of the release rate constant was dependent on the solubility, diffusivity, and concentration of the drug as well as the matrix porosity and tortuosity.

BACKGROUND

Singh *et al.* (3) considered the simultaneous release of a mixture of two noninteracting drugs dispersed in an inert insoluble matrix composed of a polyethylene–polyvinyl chloride mixture. The developed relationships expressed the diffusion-controlled rate of release of both drugs as functions of solubilities, diffusivities, and concentrations of each drug in the matrix and the porosities and tortuosities of the matrix. Thus, the release of drug a, which had the slower moving solid–liquid boundary, was described by (2):

$$\frac{dQ_a}{d(t^{1/2})} = \left[D_a \frac{\epsilon_1}{\tau_1} (2A_a - \epsilon_1 C_a{}^s) C_a{}^s \right]^{1/2} \qquad \text{(Eq. 1)}$$

where subscript 1 refers to that region of the tablet matrix bounded on one side by the solvent front and on the other side by the solid–liquid boundary of drug a. This part of the tablet will be described as region 1 in subsequent discussions. The release of drug b, with the faster moving solid–liquid boundary, was described by the following, more complex, expression:

$$\frac{dQ_b}{d(t^{1/2})} = \frac{2D_b\epsilon_1}{\tau_1 \dfrac{k_a}{A_a}} \left[\frac{\dfrac{\epsilon_2}{\tau_2} C_b{}^s}{\dfrac{\epsilon_2}{\tau_2} + \dfrac{\epsilon_1}{\tau_1} \left[\dfrac{\dfrac{k_b}{A_b} - \dfrac{k_a}{A_a}}{\dfrac{k_a}{A_a}} \right]} \right] \qquad \text{(Eq. 2)}$$

where subscript 1 is the same as in Eq. 1, and subscript 2 refers to region 2 in the tablet bounded on one side by the solid–liquid boundary for drug a and on the other side by the solid–liquid boundary for drug b. Other symbols used in Eqs. 1 and 2 are defined as follows:

- Q_i = grams of drug i released per unit area of exposed tablet surface at time t
- D_i = diffusion coefficient of drug i in the release medium
- A_i = concentration of drug i in the tablet
- $C_i{}^s$ = solubility of drug i in the release medium
- ϵ_j = porosity of region j of the tablet
- τ_j = tortuosity of region j of the tablet
- k_i = slope of Q_i *versus* $t^{1/2}$ plot for release of drug i from the tablet

The methyl acrylate–methyl methacrylate copolymer has been used to control and regulate the release of highly water-soluble drugs. The purpose of this investigation was to investigate the effect of two common, highly water-soluble excipients on the release of a model of a highly water-soluble drug from matrixes of this copolymer. Methapyrilene hydrochloride was selected as the model drug. It was also proposed to determine whether the mathematical model developed by Singh *et al.* (3) and tested with salicylic and benzoic acid combinations was valid for simultaneous release of highly water-soluble noninteracting chemicals.

EXPERIMENTAL

Chemicals—The plastic used in all tablets was a powdered methyl acrylate–methyl methacrylate copolymer[1]. This polymer is insoluble and inert in aqueous media at all pH values. The drug employed was methapyrilene hydrochloride NF. Anhydrous dextrose USP and

[1] Rohm and Haas Co., Philadelphia, Pa.

Table I—Physical Constants of Chemicals Used

Chemical	Wavelength of Maximum Absorption, nm	Density, g/cm³	Solubility at 37°, g/ml	Diffusion Coefficient, $D \times 10^6$ cm²/sec
Plastic[a]	—	1.275	—	—
Methapyrilene hydrochloride	312[b]	1.295	0.676	19.2
Dextrose	425	1.513	0.766	9.22
Sodium chloride	589[c]	2.164	0.317	21.04

[a] Methyl acrylate–methyl methacrylate copolymer. [b] In 0.1 *N* HCl. [c] Atomic absorption method.

200-mesh sodium chloride powder (CP) were used as the other noninteracting soluble constituents of the tablets.

Physical Constants (Table I)—The pertinent physical constants of methapyrilene hydrochloride and the plastic were determined previously (1). The solubility of sodium chloride in water at 37° was determined by phase solubility analysis (4). Saturated aqueous solutions of dextrose, prepared at 37°, were assayed to obtain dextrose solubility. Densities of sodium chloride and dextrose were measured by the method described previously (1). The procedure described by Desai *et al.* (5) was used to obtain the diffusion coefficient of sodium chloride. The diffusion coefficient of dextrose at 37° was estimated by the method of Wilke (6).

The following complexation–solubility studies were carried out to see whether the drug–excipient mixtures were noninteracting. An excess of methapyrilene hydrochloride (8.0 g) was weighed into several 50-ml glass-stoppered erlenmeyer flasks, and 2 ml of 0.1 *N* hydrochloric acid solution was added to each. Known, but varying, quantities of either sodium chloride or dextrose were then added to these flasks. The stoppered flasks were equilibrated for 24 hr in a 25° constant-temperature shaking water bath. The content of each flask was centrifuged and an aliquot of the clear supernatant liquid was taken, diluted with 0.1 *N* hydrochloric acid solution, and assayed for the methapyrilene content.

Tablet Compression and Treatment—All tablets were compressed on a modified laboratory press[2], using 1.03-cm ($^{13}/_{32}$-in.) flat-faced punches and die. Different weight-to-weight ratios of sodium chloride and methapyrilene hydrochloride or dextrose and methapyrilene hydrochloride were homogeneously dispersed in the plastic and compressed. The total weight of the drug and inert chemical was maintained at 56.6% of tablet weight. For each mixture, compressional force was adjusted to yield tablets with hardnesses ranging from 12 to 14 Strong-Cobb hardness units[3].

In all cases, tablets weighing approximately 300 mg were made. Exact thickness and weight measurements were obtained on 10 tablets to establish the average for each lot. All individual values were within 1.0% of the mean. To prevent possible tablet breakage during release rate studies, all tablets were heat treated at 60° for 24 hr.

Release Rate Determinations—The apparatus and procedure used in the determination of release rates from a single tablet surface were described previously (1). Release data are based on a single experiment with three tablets used in each experiment. The solvent was 0.1 *N* HCl; it was kept at a constant temperature of 37° and agitated constantly at 100 rpm. Samples were withdrawn periodically and assayed for methapyrilene hydrochloride, sodium chloride, or dextrose.

Due to the high solubilities of methapyrilene hydrochloride and the two inert chemicals used, release studies were limited to tablets in which the ratios of inert soluble chemical to methapyrilene were 2:1, 1:1, and 1:2. At extreme ratios ($\geq$3:1 or $\leq$1:3), $\epsilon_1 C_s > 2A$ and Eq. 1 cannot be applied.

Assay Procedures—Methapyrilene hydrochloride was assayed by UV spectrophotometry at 312 nm. An atomic absorption spectrophotometer[4] was used for the determination of sodium chloride. In this method, samples diluted with 0.1 *N* hydrochloric acid were atomized into an air–acetylene flame and the sodium content was measured at 589 nm. Dextrose was assayed colorimetrically at 425 nm using the method of Keston (7) and Teller (8). The accuracy of the individual assay methods was better than 1.0%.

RESULTS AND DISCUSSION

The results of complexation–solubility experiments show that the drug excipients used in this study can be considered noninteracting in the sense that they do not interact to produce a new species with completely different physicochemical properties. Due to its high solubility, the saturated solution of methapyrilene hydrochloride could be considered nonideal. Addition of other soluble chemicals to such a system could cause a drop in the saturation solubility of the drug through salting out or the common ion effect. Thus, in solutions

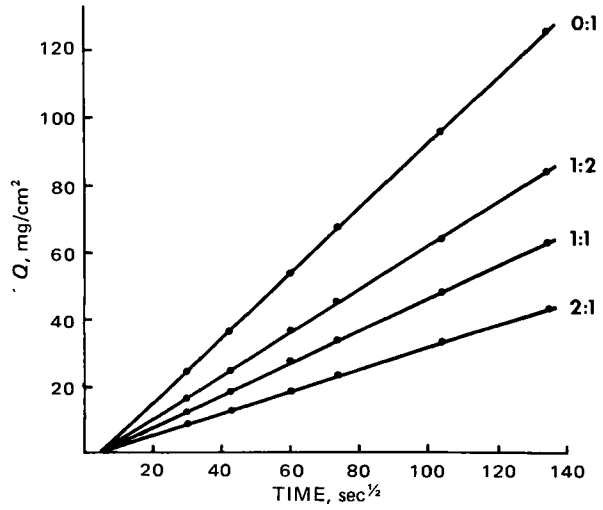

Figure 1—*Release of methapyrilene hydrochloride from tablets containing different ratios of dextrose to methapyrilene hydrochloride.*

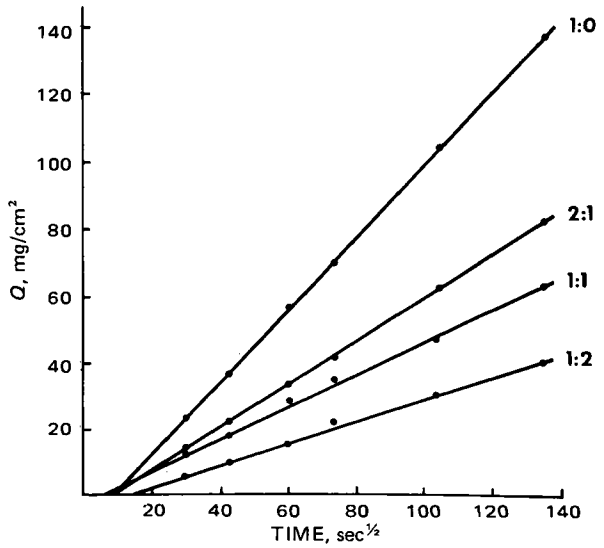

Figure 2—*Release of dextrose from tablets containing different ratios of dextrose to methapyrilene hydrochloride.*

[2] Model B, Carver laboratory press, Fred S. Carver, Inc., Menomonee Falls, WI 53051

[3] Abbott modified Strong-Cobb hardness unit.

[4] Model 303, Perkin-Elmer Corp., Norwalk, Conn.

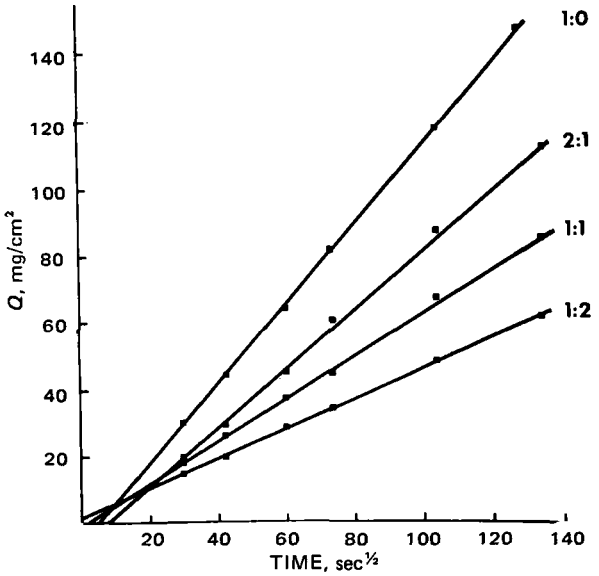

Figure 3—*Release of sodium chloride from tablets containing different ratios of sodium chloride to methapyrilene hydrochloride.*

containing 0.3 and 0.6 *M* sodium chloride, the methapyrilene solubility decreased by 6 and 19%, respectively. Similarly, in solutions containing 0.1 and 0.5 *M* dextrose, the solubility decreased by 7 and 11%, respectively.

The individual release profiles of methapyrilene hydrochloride and dextrose for tablets containing various ratios of these two chemicals are presented in Figs. 1 and 2, respectively. Similarly, Figs. 3 and 4 summarize the results of release studies for tablets containing different ratios of sodium chloride and methapyrilene hydrochloride. In each release study, dissolution was followed until at least 80% of each soluble component of the tablets had been released.

The total amounts released from dextrose–methapyrilene hydrochloride tablets and from sodium chloride–methapyrilene hydrochloride tablets are displayed in Figs. 5 and 6, respectively. These curves were prepared by the method of least squares (9). The good linearity of these lines, as evidenced by their statistically high correlation coefficient (Tables II and III), indicates that the amount released per unit tablet surface area is a linear function of the square root of time for both the total and the individual soluble components of the tablets studied. These linear fits also confirm that release of the soluble components of the tablets is diffusion controlled and adheres to either Eq. 1 or 2, depending on the magnitude of the inert soluble chemical to methapyrilene hydrochloride ratio.

The longest lag time observed (Figs. 1–6) was about 1.5 min (9.5

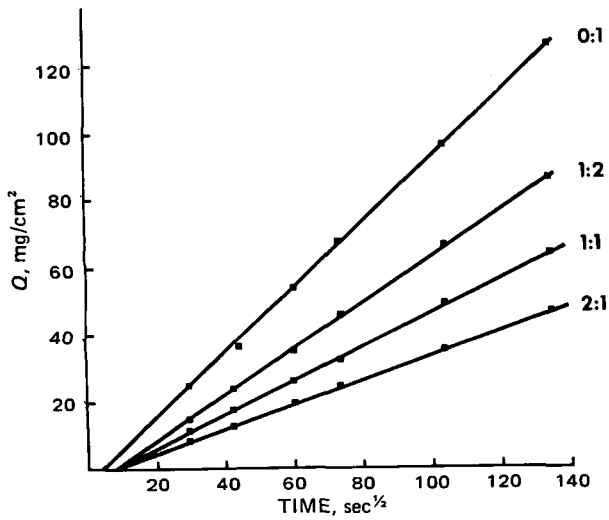

Figure 4—*Release of methapyrilene hydrochloride from tablets containing different ratios of sodium chloride to methapyrilene hydrochloride.*

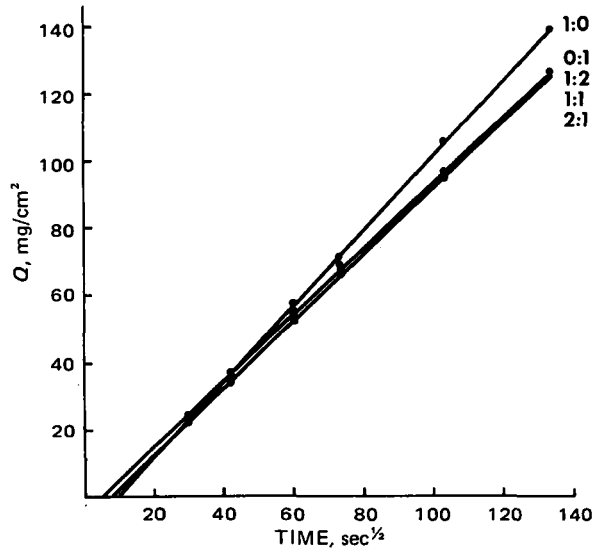

Figure 5—*Sum of methapyrilene hydrochloride and dextrose release in the same experiments as in Figs. 1 and 2.*

sec$^{1/2}$) and was probably due to initial wetting of the tablet surface and establishment of the pseudo-steady-state condition required by the model (2, 3). The observed lag time, however, was very short in comparison to the total depletion time (approximately 5 hr) and can, therefore, be ignored (10). For the same reason, its inclusion or exclusion in computation of the release rate constant should have an insignificant effect on the magnitude of the rate constant.

The release rate constants for tablets containing dextrose and methapyrilene hydrochloride are given in Table II. Similar data for tablets containing sodium chloride and methapyrilene hydrochloride are given in Table III. The condition of an equal boundary movement rate for dextrose–methapyrilene hydrochloride is satisfied when the ratio of their respective concentrations in the tablet matrix (A_{dex}/A_{meth}) equals 1:1.95. For tablets containing sodium chloride–methapyrilene hydrochloride, that condition exists when (A_{NaCl}/A_{meth}) equals 1:1.80.

According to Singh *et al.* (3), Eq. 1 is valid for release of the chemical whose boundary is moving at a lower rate. Thus, for dextrose–methapyrilene hydrochloride tablets, this equation can be used to describe methapyrilene hydrochloride release at ratios lower than 1:1.95 and dextrose release at higher ratios. Similarly, for sodium

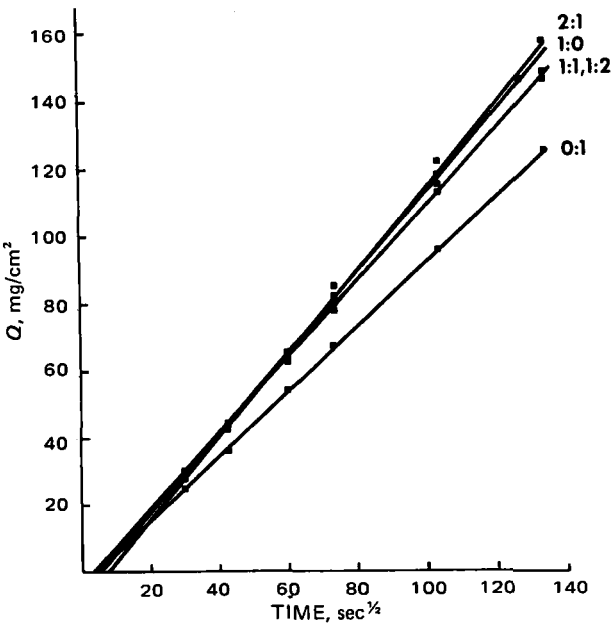

Figure 6—*Sum of sodium chloride and methapyrilene hydrochloride release in the same experiments as in Figs. 3 and 4.*

Table II—Release Rate Constants for Dextrose–Methapyrilene Hydrochloride Tablets

A_{dex}/A_{meth} Ratio	A_{dex}, g/cm³	A_{meth}, g/cm³	$k_{dex} \times 10^4$[a], g/cm² sec½	$k_{meth} \times 10^4$[a], g/cm² sec½
1:0	0.699	—	10.9 (0.996)	—
2:1	0.461	0.230	6.6 (0.999)	3.3 (0.999)
1:1	0.339	0.339	4.9 (0.999)	4.7 (0.999)
1:2	0.222	0.445	3.3 (0.999)	6.4 (0.999)
0:1	—	0.607	—	9.6 (0.999)

[a] Values in parentheses are the correlation coefficients for plot of amount released per unit tablet surface area *versus* square root of time.

Table III—Release Rate Constants for Sodium Chloride–Methapyrilene Hydrochloride Tablets

A_{NaCl}/A_{meth} Ratio	A_{NaCl}, g/cm³	A_{meth}, g/cm³	$k_{NaCl} \times 10^4$[a], g/cm² sec½	$k_{meth} \times 10^4$[a], g/cm² sec½
1:0	0.739	—	11.9 (0.999)	—
2:1	0.458	0.228	8.6 (0.998)	3.5 (0.999)
1:1	0.339	0.339	6.5 (0.999)	5.0 (0.999)
1:2	0.207	0.416	4.47 (0.999)	6.7 (0.999)
0:1	—	0.607	—	9.6 (0.999)

[a] Values in parentheses are the correlation coefficients for plot of amount released per unit tablet surface area *versus* square root of time.

chloride–methapyrilene hydrochloride tablets, sodium chloride release can be explained by Eq. 1 when the ratio is higher than 1:1.80, and it can be used for methapyrilene hydrochloride release at lower ratios.

The total porosity of the matrix, the diffusion coefficient, the solubility, and the concentration in the matrix of the predicted slower moving component of each tablet studied were substituted in Eq. 1, and the apparent tortuosity values, τ_1, for region 1 were calculated (Tables IV and V). The values listed in parentheses in Tables IV and V were obtained by using the parameters of the faster moving chemicals in these calculations. Although these values are incorrect (3), they are listed for comparison purposes.

The tortuosity values for each component of the two tablet systems studied are practically the same and are not greatly affected by the ratios of soluble excipient to drug. An explanation for these results would be to assume that region 2 has practically disappeared in each tablet system and that the boundaries of both soluble components of each tablet have merged to a single boundary moving at a fixed rate.

According to the theory (3) for the simultaneous release of a mixture of two noninteracting drugs dispersed in an inert plastic matrix, the position of the solid–liquid boundary, s_i, for drug i at time t is given by:

$$s_i = (k_i/A_i)t^{1/2} \qquad \text{(Eq. 3)}$$

where k_i and A_i are as defined previously. The s values for both soluble components of dextrose–methapyrilene hydrochloride tablets were calculated at the time period when 50% of each soluble component of the tablets was released (Table VI). The time required for 50% release was determined by the method discussed previously (1).

Table IV—Tortuosity of Region 1 for Tablets Containing Dextrose and Methapyrilene Hydrochloride

A_{dex}/A_{meth} Ratio	ϵ[a] Total	τ_1 Dextrose	τ_1 Methapyrilene
1:0	0.580	3.30	—
2:1	0.585	4.48	(4.56)[b]
1:1	0.596	3.97	(9.47)[b]
1:2	0.598	—[c]	9.10
0:1	0.634	—	7.10

[a] $\epsilon_{total} = \epsilon_{dex} + \epsilon_{meth} + \epsilon_{air}$; Ref. 1. [b] Incorrect value, included for comparison purposes. [c] The value of $(2A - \epsilon_1 C_s)$ is negative.

Table V—Tortuosity of Region 1 for Tablets Containing Sodium Chloride and Methapyrilene Hydrochloride

A_{NaCl}/A_{meth} Ratio	ϵ[a] Total	τ_1 Sodium Chloride	τ_1 Methapyrilene
1:0	0.552	3.33	—
2:1	0.589	3.86	(3.54)[b]
1:1	0.594	4.62	(8.44)[b]
1:2	0.626	(4.51)[b]	7.29
0:1	0.636	—	7.10

[a] $\epsilon_{total} = \epsilon_{NaCl} + \epsilon_{meth} + \epsilon_{air}$. [b] Incorrect value, included for comparison purposes.

Table VI—Solid–Liquid Boundary Position(s) at $t_{50\%}$ Release for Tablets Containing Dextrose–Methapyrilene Hydrochloride

A_{dex}/A_{meth} Ratio	$t_{50\%}$ Release, hr, for Dextrose	$t_{50\%}$ Release, hr, for Methapyrilene Hydrochloride	$s \times 10^2$, cm, at $t_{50\%}$ Release for Dextrose	$s \times 10^2$, cm, at $t_{50\%}$ Release for Methapyrilene Hydrochloride
2:1	2.88	2.91	14.5	14.6
1:1	3.01	3.15	14.9	14.9
1:2	2.88	3.04	15.2	15.1

Table VII—Solid–Liquid Boundary Position(s) at $t_{50\%}$ Release for Tablets Containing Sodium Chloride–Methapyrilene Hydrochloride

A_{NaCl}/A_{meth} Ratio	$t_{50\%}$ Release, hr, for Sodium Chloride	$t_{50\%}$ Release, hr, for Methapyrilene Hydrochloride	$s \times 10^2$, cm, at $t_{50\%}$ Release for Sodium Chloride	$s \times 10^2$, cm, at $t_{50\%}$ Release for Methapyrilene Hydrochloride
2:1	1.73	2.53	14.8	14.7
1:1	1.68	2.81	14.9	14.9
1:2	1.57	2.78	16.1	16.2

The $\dot{s}$ values for both soluble components of sodium chloride–methapyrilene hydrochloride tablets are summarized in Table VII. These data are in accord with the assumption made and again indicate that region 2 apparently did not exist in each tablet system for the ratios studied. The merger of boundaries at these ratios could be expected. The high solubilities of soluble components of each tablet system, plus the restriction imposed by Eq. 1 where $2A > \epsilon C_s$, necessitate the use of A values that are not greatly different from those calculated for the equal boundary movement condition (Tables II and III). Differences of these magnitudes in A values of the soluble components of the tablets investigated apparently are not enough to cause a separation of boundaries of the respective chemicals.

The methyl acrylate–methyl methacrylate copolymer sample used in this study contained octylphenoxyethanol[5], a nonionic surfactant. The concentration of this surfactant in the copolymer was 0.82% (w/w), as measured by the spectrophotometric determination of a 2% (w/v) solution of the copolymer in acetonitrile at 276 nm.

It has been shown (3, 5, 11) that incorporation of the surfactant in the tablet matrix or the release medium increased the release rates of the incorporated drugs and greatly reduced the dependence of the matrix tortuosities on the ratios of the drug mixtures. These effects have been attributed to the enhanced penetration of the release medium into the tablet matrix and elimination of air pockets through the surface tension-lowering effect of the surfactant.

The critical micelle concentration (CMC) of octylphenoxyethanol in water at 25°, as measured by the surface tension method, was 0.016

[5] Triton X-405, Rohm and Haas Co., Philadelphia, Pa.

g/100 ml. Separate solubility studies at concentrations above the surfactant's CMC did not reveal any change in the solubility of soluble chemicals used in this investigation. The concentration of the surfactant in the tablets probably was enough to cause an increase in their porosities and, consequently, to minimize the dependence of tablet tortuosities on the ratios of the soluble components of the tablets.

REFERENCES

(1) B. Farhadieh, S. Borodkin, and J. D. Buddenhagen, *J. Pharm. Sci.*, **60**, 209(1971).

(2) T. Higuchi, *ibid.*, **52**, 1145(1963).

(3) P. Singh, S. J. Desai, A. P. Simonelli, and W. I. Higuchi, *ibid.*, **56**, 1542(1967).

(4) R. M. Herriott, *Chem. Rev.*, **30**, 413(1942).

(5) S. J. Desai, P. Singh, A. P. Simonelli, and W. I. Higuchi, *J. Pharm. Sci.*, **55**, 1224(1966).

(6) C. R. Wilke, *Chem. Eng. Progr.*, **45**, 218(1949).

(7) A. S. Keston, "Abstract of Papers, 129th Meeting," American Chemical Society, Washington, D.C., 1956, p. 31-c.

(8) J. D. Teller, "Abstract of Papers, 130th Meeting," American Chemical Society, Washington, D.C., 1957, p. 69-c.

(9) A. Goldstein, "Biostatistics, An Introductory Text," Macmillan, New York, N.Y., 1967.

(10) T. Higuchi, *J. Pharm. Sci.*, **50**, 874(1961).

(11) S. J. Desai, A. P. Simonelli, and W. I. Higuchi, *ibid.*, **54**, 1459(1965).

ACKNOWLEDGMENTS AND ADDRESSES

Received September 30, 1974, from the *Pharmaceutical Products Division, Abbott Laboratories, North Chicago, IL 60064*

Accepted for publication November 14, 1975.

Binding of Spirolactones to Human Plasma Proteins

Y. W. CHIEN *x, L. M. HOFMANN ‡, H. J. LAMBERT *, and L. C. TAO §

Abstract □ The lipophilicity and plasma binding of 16 spirolactones and 4 hydroxy acid analogs were determined. Mathematical expressions were derived to correlate quantitatively the extent of plasma binding to the lipophilicity of the drugs. The nonspecific binding of these spirolactones and their hydroxy acid analogs was also analyzed using purified serum albumin. A computer program was developed to examine the mechanism of drug–serum protein interactions. One class of binding sites was observed for the range of concentrations used. The number of binding sites and the equilibrium binding constant were computed and were sensitive to substitution at the C-6 and C-7 positions. Hydrolysis of the C-17 lactone ring in spirolactones to form hydroxy acid analogs resulted in a decrease in the lipophilicity and, hence, the equilibrium constant for binding.

Keyphrases □ Spirolactones—lipophilicity and plasma protein binding determined and correlated quantitatively □ Lipophilicity—spirolactones, correlated quantitatively with plasma protein binding □ Plasma protein binding—spirolactones, quantitatively correlated with lipophilicity □ Binding, plasma protein—spirolactones, quantitatively correlated with lipophilicity

Spironolactone[1] has been used clinically to manage refractory edema and found to have the greatest selectivity of the competitive antagonists of aldosterone (1, 2).

The interaction of organic molecules with plasma proteins has been recognized for many years as an important parameter of tissue permeation and clinical efficacy of a drug (3, 4). Recently, this laboratory demonstrated that modifying the molecular structure of disopyramide significantly influenced both the antiarrhythmic activity (5) and the extent of plasma protein–drug interactions (6). Quantitative correlation was observed between the extent of drug–plasma protein interactions and the physicochemical parameters of disopyramide derivatives (6–8). Furthermore, a linear correlation was established between the extent of plasma protein binding and the frontier electron density, estimated by molecular orbital calculations, on the alkyl side chain of trichomonicidal metronidazole[2] derivatives (9).

Biopharmaceutical studies of spironolactone and its derivatives revealed that they were extensively bound to human plasma and that the strength of the plasma binding was sensitive to structural variation. The results are reported and analyzed in this paper.

EXPERIMENTAL

The procedure for measuring the lipophilicity and the membrane ultrafiltration technique for determining the binding of spirolactones to plasma protein and serum albumin[3] (1.4056×10^{-4} *M*) are essen-

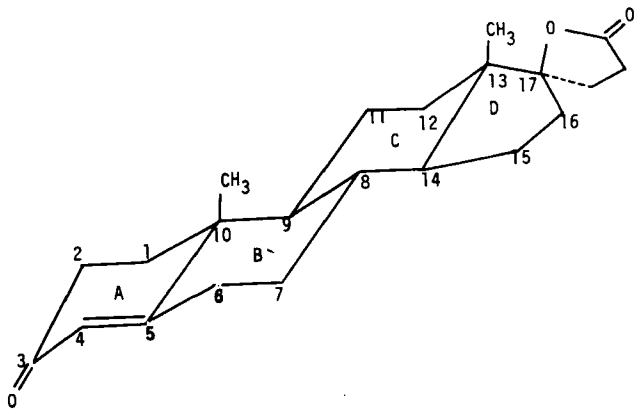

I

[1] Searle Laboratories, Division of G.D. Searle & Co., Chicago, IL 60680

[2] Flagyl, Searle Laboratories, Division of G.D. Searle & Co., Chicago, IL 60680

[3] Fraction V, fatty acid poor, Nutritional Biochemical Corp., Cleveland, Ohio.

g/100 ml. Separate solubility studies at concentrations above the surfactant's CMC did not reveal any change in the solubility of soluble chemicals used in this investigation. The concentration of the surfactant in the tablets probably was enough to cause an increase in their porosities and, consequently, to minimize the dependence of tablet tortuosities on the ratios of the soluble components of the tablets.

REFERENCES

(1) B. Farhadieh, S. Borodkin, and J. D. Buddenhagen, *J. Pharm. Sci.*, **60**, 209(1971).

(2) T. Higuchi, *ibid.*, **52**, 1145(1963).

(3) P. Singh, S. J. Desai, A. P. Simonelli, and W. I. Higuchi, *ibid.*, **56**, 1542(1967).

(4) R. M. Herriott, *Chem. Rev.*, **30**, 413(1942).

(5) S. J. Desai, P. Singh, A. P. Simonelli, and W. I. Higuchi, *J. Pharm. Sci.*, **55**, 1224(1966).

(6) C. R. Wilke, *Chem. Eng. Progr.*, **45**, 218(1949).

(7) A. S. Keston, "Abstract of Papers, 129th Meeting," American Chemical Society, Washington, D.C., 1956, p. 31-c.

(8) J. D. Teller, "Abstract of Papers, 130th Meeting," American Chemical Society, Washington, D.C., 1957, p. 69-c.

(9) A. Goldstein, "Biostatistics, An Introductory Text," Macmillan, New York, N.Y., 1967.

(10) T. Higuchi, *J. Pharm. Sci.*, **50**, 874(1961).

(11) S. J. Desai, A. P. Simonelli, and W. I. Higuchi, *ibid.*, **54**, 1459(1965).

ACKNOWLEDGMENTS AND ADDRESSES

Received September 30, 1974, from the *Pharmaceutical Products Division, Abbott Laboratories, North Chicago, IL 60064*

Accepted for publication November 14, 1975.

Binding of Spirolactones to Human Plasma Proteins

Y. W. CHIEN *x, L. M. HOFMANN ‡, H. J. LAMBERT *, and L. C. TAO §

Abstract □ The lipophilicity and plasma binding of 16 spirolactones and 4 hydroxy acid analogs were determined. Mathematical expressions were derived to correlate quantitatively the extent of plasma binding to the lipophilicity of the drugs. The nonspecific binding of these spirolactones and their hydroxy acid analogs was also analyzed using purified serum albumin. A computer program was developed to examine the mechanism of drug–serum protein interactions. One class of binding sites was observed for the range of concentrations used. The number of binding sites and the equilibrium binding constant were computed and were sensitive to substitution at the C-6 and C-7 positions. Hydrolysis of the C-17 lactone ring in spirolactones to form hydroxy acid analogs resulted in a decrease in the lipophilicity and, hence, the equilibrium constant for binding.

Keyphrases □ Spirolactones—lipophilicity and plasma protein binding determined and correlated quantitatively □ Lipophilicity—spirolactones, correlated quantitatively with plasma protein binding □ Plasma protein binding—spirolactones, quantitatively correlated with lipophilicity □ Binding, plasma protein—spirolactones, quantitatively correlated with lipophilicity

Spironolactone[1] has been used clinically to manage refractory edema and found to have the greatest selectivity of the competitive antagonists of aldosterone (1, 2).

The interaction of organic molecules with plasma proteins has been recognized for many years as an important parameter of tissue permeation and clinical efficacy of a drug (3, 4). Recently, this laboratory demonstrated that modifying the molecular structure of disopyramide significantly influenced both the antiarrhythmic activity (5) and the extent of plasma protein–drug interactions (6). Quantitative correlation was observed between the extent of drug–plasma protein interactions and the physicochemical parameters of disopyramide derivatives (6–8). Furthermore, a linear correlation was established between the extent of plasma protein binding and the frontier electron density, estimated by molecular orbital calculations, on the alkyl side chain of trichomonicidal metronidazole[2] derivatives (9).

Biopharmaceutical studies of spironolactone and its derivatives revealed that they were extensively bound to human plasma and that the strength of the plasma binding was sensitive to structural variation. The results are reported and analyzed in this paper.

EXPERIMENTAL

The procedure for measuring the lipophilicity and the membrane ultrafiltration technique for determining the binding of spirolactones to plasma protein and serum albumin[3] (1.4056×10^{-4} *M*) are essen-

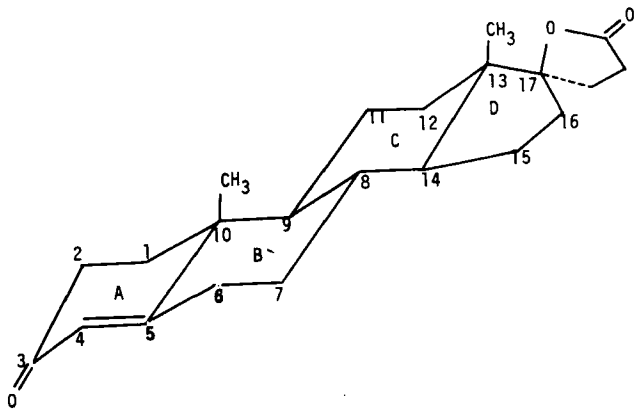

I

[1] Searle Laboratories, Division of G.D. Searle & Co., Chicago, IL 60680

[2] Flagyl, Searle Laboratories, Division of G.D. Searle & Co., Chicago, IL 60680

[3] Fraction V, fatty acid poor, Nutritional Biochemical Corp., Cleveland, Ohio.

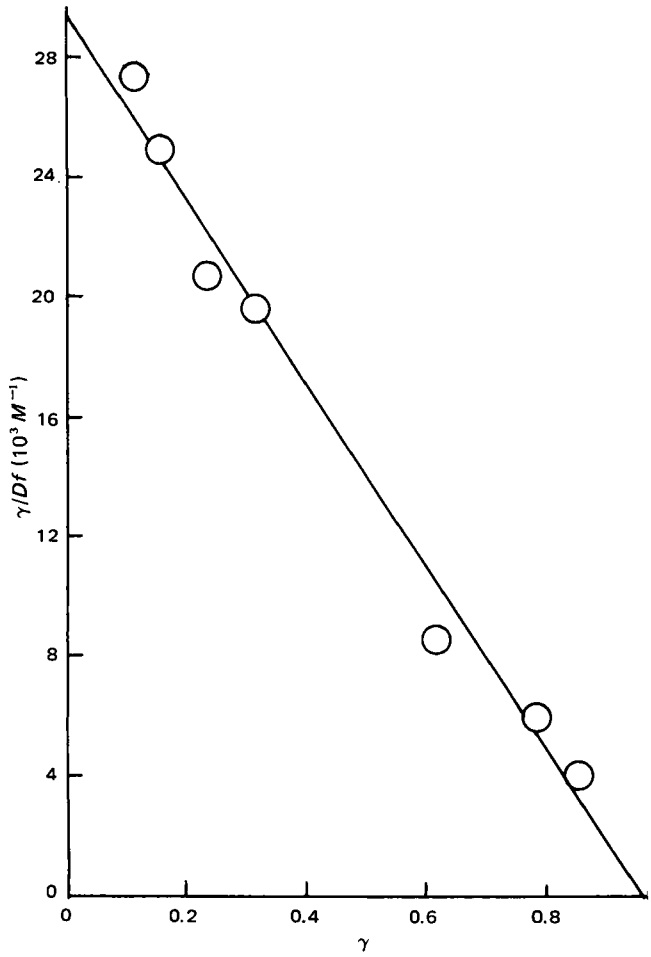

Figure 1—*Linear Scatchard plot for III, spirolactone derivative (Table I), using a representative set of data measured at pH 7.4 with a drug concentration range of 1.6–40 × 10^{-5} M and a human serum albumin concentration of 3.514 × 10^{-4} M. Key:* ○, *experimental observations; and —, computer-fitted theoretical line following Eq. 1. From the intercept and slope, the values of* n̄ *and* K *were calculated to be 0.986 and 30,457.6* M^{-1}, *respectively.*

tially the same as reported (6, 8) previously, except that 20% (v/v) 1,3-butylene glycol and 4% methanol were added to the phosphate buffer system as cosolvents to enhance the aqueous solubility of spirolactones (10). The addition of this cosolvent pair was compatible with plasma proteins and yielded no precipitation of plasma proteinaceous material.

RESULTS AND DISCUSSION

Mechanisms of Spirolactone–Plasma Protein Interaction—The mechanisms of the interaction between spirolactones and plasma proteins were analyzed using purified human serum albumin, the protein constituent in plasma responsible for most drug–plasma interactions. The binding of spirolactones to human serum albumin was observed to follow a linear Scatchard (11) relationship (Fig. 1) when the binding data were plotted in the following manner:

$$\frac{\gamma}{Df} = \bar{n}K - \gamma K \qquad \text{(Eq. 1)}$$

where γ is the ratio of the concentration of drug bound, Db, to a protein over the total concentration of serum protein, P, used; Df is the concentration of free (unbound) drug at equilibrium; $\bar{n}$ is the number of binding sites in a binding class available for drug–protein interactions; and K is the equilibrium binding constant. A computer program was developed to estimate the value of the binding ratio, γ, for each drug concentration investigated from the observed Df measured at equilibrium. The data obtained were then plotted following Eq. 1, and the magnitudes of $\bar{n}$ and K also were computed. Figure 1 is a typical example of this computer printout.

Both the number of binding sites, $\bar{n}$, and the equilibrium binding constant, K, for the spirolactones were observed to be influenced by structural modification of the B ring (Table I), although they all bind with only one class of binding sites in human serum albumin. This structural dependency was also illustrated in the corresponding hydroxy acid analogs with molecular structures similar to those of spirolactones, except that the lactone ring at the 17-position was hydrolyzed to form a potassium salt (Table II). Apparently, the hydrolysis process results in no significant variation in the number of binding sites, $\bar{n}$, but a substantial reduction (1.4–4.3-fold) in the strength, K, of the drug–serum protein interaction (Tables I and II).

For example, the hydrolysis of Compounds III–VII did not reduce the value of $\bar{n}$, but the magnitude of K was decreased more than twofold, from 3.09 × 10^4 to 1.29 × 10^4 M^{-1}. The effect of hydrolysis on the strength of the drug–protein interaction, K, was attributable, as expected, from the following relationship (Eq. 2) derived previously

Table I—Effect of Structural Modification on Binding Characteristics of Spirolactone Derivatives to Human Serum Albumin

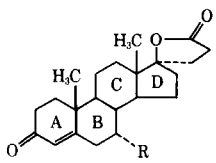

Compound	R	Human Serum Albumin Binding Characteristics[a] $\bar{n}$	K, 10^4 M^{-1}	$\bar{n}K$, 10^4 M^{-1}
I (spironolactone)	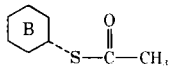	0.47	4.23	2.00
II[b]		0.94	3.64	3.41
III[c]		0.99	3.09	3.05
IV[d]	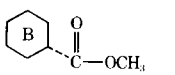	0.35	1.57	0.55
V[e]	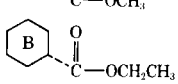	0.65	2.08	1.36

[a] Each value is the mean of three determinations. [b] SC-9376. [c] SC-23133. [d] SC-25152. [e] SC-26163.

Table II—Effect of Structural Modification on the Binding Characteristics of Hydroxy Acid Analogs to Human Serum Albumin

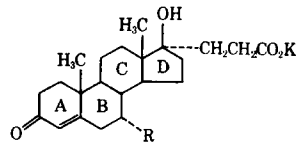

Compound	R	Human Serum Albumin Binding Characteristics[a] $\bar{n}$	K, $10^4\ M^{-1}$	$\bar{n}K$, $10^4\ M^{-1}$	Relative[b] K
VI[c] (canrenoate potassium)		0.84	2.64	2.22	1.4
VII[d] (prorenoate potassium)		1.03	1.29	1.32	2.4
VIII[e] (mexrenoate potassium)	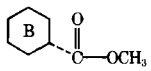	0.30	0.52	0.16	3.0
IX[f]	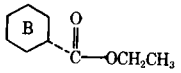	0.47	0.49	0.23	4.3

[a] Each value is the mean of three determinations. [b] Ratio of K (spirolactone) to K (hydroxy acid analog). [c] SC-14266. [d] SC-23992. [e] SC-26714. [f] SC-27719.

Table III—Correlation of the Strength (K) of Drug–Protein Interaction with the Lipophilicity, Log (p.c.), of Spirolactones and Hydroxy Acid Analogs

Compound	Log K[a]	Log (p.c.)[b]
I	4.626	2.777
II	4.561	2.680
III	4.490	2.536
IV	4.197	1.941
V	4.318	2.543
VI	4.422	0.449
VII	4.109	0.665
VIII	3.714	−0.379
IX	3.690	−0.220

[a] Each value is the mean of three determinations. [b] Determined in 1-octanol–pH 7.4 phosphate buffer. Each value is the mean of six determinations.

(6), to the reduction in the lipophilicity, log (p.c.), of drugs (Table III) due to the hydrolysis of 17-lactone:

$$\log K = \frac{\mu_0^0 - \mu_p^0}{2.303RT} + \log (\text{p.c.}) \qquad \text{(Eq. 2)}$$

where (p.c.) is the partition coefficient of the drug measured in a 1-octanol–pH 7.4 phosphate buffer system, and μ_p^0 and μ_0^0 are the standard chemical potentials for a drug species bound to a protein molecule and in an organic solvent system, respectively (6).

Equation 2 indicates that, for the interaction of spirolactones and their hydroxy acid analogs to serum protein, K is directly proportional to the magnitude of log (p.c.), the lipophilicity of the drug molecules. The validity of Eq. 2 in expressing the linear correlation between the strength of the drug–protein interaction (log K) and the lipophilicity of spirolactones and their hydroxy acid analogs was verified by submitting the data in Table III to a multiple regression analysis. The result of the correlation of log K with log (p.c.) is described by the following relationship:

$$\log K = 3.914 + 0.223 \log (\text{p.c.}) \qquad \text{(Eq. 3)}$$

n	r	s^2
9	0.845	0.030

The relatively high multiple correlation coefficient ($r = 0.845$) and the low residual variance ($s^2 = 0.030$) indicated that the strength of serum protein binding of spirolactones and their hydroxy acid analogs was highly dependent on the lipophilicity of the drugs. This observation agreed with results reported earlier for disopyramide derivatives (6).

Binding of Spirolactones to Plasma Proteins—To investigate further the lipophilicity dependency of spirolactones and the validity

Table IV—Lipophilicity, Log (p.c.), and Extent of Plasma Binding, Log (Db/Df), of Spirolactones (Structure I)

Compound	Structural Modification	Log (p.c.)[l]	Fraction of Drug Bound, %	Log (Db/Df)[m]
I	7α-$SCOCH_3$	2.777	94.21	1.211
X[a]	7β-$SCOCH_3$	2.262	92.08	1.065
XI[b]	—	2.978	92.91	1.117
II	6,7-Ene	2.680	98.22	1.742
XII[c]	9α-F,11β-OH	2.404	74.81	0.473
XIII[d]	9,11β-Oxide	1.962	74.22	0.459
XIV[e]	9,11α-Oxide	1.889	80.90	0.627
XV[f]	6-Spirocyclopropyl	3.149	89.69	0.940
III	6,7β-Methylene	2.536	90.59	0.984
XVI[g]	6,7α-Methylene	3.083	88.93	0.905
IV	7α-$COOCH_3$	1.941	73.52	0.444
XVII[h]	7α-COOH	−0.520	19.10	−0.627
V	7α-$COOC_2H_5$	2.543	82.66	0.678
XVIII[i]	7α-$CO_2CH(CH_3)_2$	2.818	93.66	1.170
XIX[j]	7α-CN	1.666	76.76	0.519
XX[k]	7β-$COOCH_3$	2.181	81.09	0.632

[a] SC-11940. [b] SC-5233. [c] SC-9837. [d] SC-9848. [e] SC-12950. [f] SC-17127. [g] SC-24441. [h] SC-25914. [i] SC-26304. [j] SC-26493. [k] SC-26704. [l] Each value is the mean of six determinations. [m] Each value is the mean of three determinations. The Db and Df values are the concentrations of drug bound and unbound to plasma protein at equilibrium, respectively. Data of this column were calculated from the fractions of drug bound shown in the fourth column of this table.

of Eq. 2 in defining the effect of lipophilicity on the extent and strength of binding of spirolactones to plasma proteins, more spirolactones with various structural modifications were examined (Table IV). Apparently both the lipophilicity and the fraction of spirolactone bound were sensitive to the structural modifications in the neighborhood of the B and C rings of the spirolactone molecule.

The combination of Eqs. 1 and 2 resulted in Eq. 4, a simplified mathematical expression (6) for the linear relationship between the extent of plasma binding, log (*Db/Df*), and the lipophilicity, log (p.c.), of a series of drugs:

$$\log \frac{Db}{Df} = \text{intercept} + \log (\text{p.c.}) \qquad \text{(Eq. 4)}$$

where:

$$\text{intercept} = \text{constant} + \frac{\mu_0{}^0 - \mu_p{}^0}{2.303RT} \qquad \text{(Eq. 5)}$$

The development of Eq. 4 permitted the calculation of the extent of plasma binding (*Db/Df*) directly from a binding measurement without requiring a Scatchard analysis to compute the magnitude of the equilibrium binding constant, *K*. The application of Eq. 4 in place of Eq. 2 should not only save a substantial workload when dealing with a large number of drugs but still preserve the equivalent theoretical validity (6).

The validity of Eq. 4 was demonstrated by submitting the data in Table IV to a multiple regression analysis. The correlation of log (*Db/Df*) with log (p.c.) is expressed by the following relationship:

$$\log \left(\frac{Db}{Df}\right) = -0.352 + 0.497 \log (\text{p.c.}) \qquad \text{(Eq. 6)}$$

n	r	s^2
16	0.846	0.069

Again, both the multiple correlation coefficient ($r = 0.846$) and the residual variance ($s^2 = 0.069$) demonstrate that the degree of plasma binding of spirolactones is apparently correlated to their lipophilicity. The results of Eqs. 3 and 6 suggest that the interactions of spirolactones with serum albumin and plasma protein are both nonspecific in nature. This observation agrees with results reported earlier for disopyramide derivatives (6) and other drugs (12).

In summary, the results demonstrated that the interactions of spirolactones and their hydroxy acid analogs with human plasma proteins are nonspecific in nature; any modification in their molecular structures that leads to a higher lipophilicity will result in an enhanced plasma binding.

REFERENCES

(1) "The Pharmacological Basis of Therapeutics," 4th ed., L. S. Goodman and A. Gilman, Eds., Macmillan, New York, N.Y., 1970, pp. 861, 862, 1612.

(2) L. M. Hofmann, in "Recent Advances in Renal Physiology and Pharmacology," L. G. Wesson and G. M. Fanelli, Jr., Eds., University Park Press, Baltimore, Md., 1974, pp. 305–315.

(3) R. D. Birkenmeyer, The 5th International Conference on Anti-microbial Agents and Chemotherapy and the 4th International Congress of Chemotherapy, Washington, D.C., Oct. 17–21, 1965, No. 37, p. 18.

(4) B. B. Brodie and C. A. M. Hogben, *J. Pharm. Pharmacol.*, **9**, 345(1957).

(5) T. K. Lin, Y. W. Chien, R. R. Dean, J. E. Dutt, H. W. Sause, C. H. Yen, and P. K. Yonan, *J. Med. Chem.*, **17**, 751(1974).

(6) Y. W. Chien, H. J. Lambert, and T. K. Lin, *J. Pharm. Sci.*, **64**, 961(1975).

(7) Y. W. Chien, M. J. Akers, and P. K. Yonan, *ibid.*, **64**, 1632(1975).

(8) Y. W. Chien, H. J. Lambert, and A. Karim, *ibid.*, **63**, 1877(1974).

(9) D. R. Sanvordeker, Y. W. Chien, T. K. Lin, and H. J. Lambert, *ibid.*, **64**, 1797(1975).

(10) Y. W. Chien and H. J. Lambert, *Chem. Pharm. Bull.*, **23**, 1085(1975).

(11) J. T. Edsall and J. Wyman, "Biophysical Chemistry," vol. 1, Academic, New York, N.Y., 1958, chap. 11.

(12) J. M. Vandenbelt, C. Hansch, and C. Church, *J. Med. Chem.*, **15**, 787(1973).

ACKNOWLEDGMENTS AND ADDRESSES

Received September 15, 1975, from the **Biopharmaceutics Section, Development Department, Searle Laboratories, the ‡Renal Pharmacology Section, Biological Research Department, Searle Laboratories, and the §Corporate Math/Stat. Department, G.D. Searle and Co., Chicago, IL 60680*

Accepted for publication November 19, 1975.

Appreciation is expressed to many organic chemists in the Chemical Research Department of these laboratories, especially Dr. L. J. Chinn, Dr. F. B. Colton, Dr. H. S. Lowrie, Dr. R. M. Weier, Mr. E. A. Brown, Jr., and Mr. R. T. Nicholson for making the spirolactones available. The authors also thank Ms. D. M. Jefferson for technical assistance and Miss S. Sering for manuscript preparation.

ˣ To whom inquiries should be directed (Biopharmaceutics Section, Development Department, Searle Laboratories, Skokie, IL 60076).

Rationale for Apparent Differences in Pharmacokinetic Aspects of Model Compounds Determined from Blood Level Data and Urinary Excretion Data in Rats

YASHWANT M. AMIN * and JANARDAN B. NAGWEKAR ˣ

Abstract □ Results of studies carried out in rats for model compounds, D-(−)-mandelic acid, benzoylformic acid, and some of their *para*-alkylated homologs, showed that their biological half-lives determined from the elimination phase of urinary excretion data were longer than those determined from the elimination phase of blood level data. With compounds that followed multicompartment open models, the initial distributive phase (α-phase) noted from the blood level data was not detected from the urinary excretion data. Based on the analysis of half-life data obtained in the absence and presence of DL-tropic acid (a competitive renal tubular secretion inhibitor of these compounds), it is proposed that, besides the shortness of the α-phase period, the factor accounting for these striking differences in the pharmacokinetic aspects of these compounds is their retention and/or detention in the renal tubular membranes during their tubular secretion. Furthermore, it is proposed that the renal tubular membranes do not constitute a part of the central or peripheral compartment. Examples are cited to show that, where studies are reported for the same drugs in the same human subjects in the same laboratory, drugs usually exhibit longer biological half-lives when urinary excretion data rather than blood level data are used.

Keyphrases □ Pharmacokinetics—model compounds, urinary excretion and blood level data compared, rats □ Elimination phase data—model compounds, urinary and blood level data compared, rats □ Biological half-lives—model compounds, determined from urinary excretion and blood level data and compared, rats

Upon comparing blood level data (1) with urinary excretion data (2–4) reported for the model compounds D-(−)-mandelic acid (I), D-(−)-*p*-methylmandelic acid (II), D-(−)-*p*-ethylmandelic acid (III), and D-(−)-*p*-isopropylmandelic acid (IV) in rats, striking differences became apparent with respect to two pharmacokinetic aspects.

1. The distributive phase noted from semilogarithmic plots of the blood concentration of the compound against time remained undetected in semilogarithmic plots of the urinary excretion rate of the compound against time. Accordingly, the two-compartment open model noted from blood level data reduced to a one-compartment open model when urinary excretion data were used.

2. The half-lives of the compounds, as determined from the elimination phase, were generally longer when determined from urinary excretion data rather than blood level data (Table I). Such apparent differences in these pharmacokinetic aspects were also observed for each compound in the presence of DL-tropic acid (V), a competitive inhibitor of renal tubular secretion of the compounds (2–6).

One purpose of this paper is to present the urinary excretion studies carried out in rats for additional model compounds, namely, benzoylformic acid (VI), *p*-methylbenzoylformic acid (VII), and *p*-ethylbenzoylformic acid (VIII). Their half-lives, as determined from the elimination phase, also were longer when calculated from urinary data rather than blood level data (1, 6), both in the absence and presence of V. Furthermore, the pharmacokinetics of VI, which were describable according to a three-compartment open model as evidenced from blood level studies (1, 6), reduced to a two-compartment open model when urinary excretion data were used. The pharmacokinetics of VII or VIII were describable according to a one-compartment open model (1, 6).

Another purpose of this report is to provide rationalization for the apparent differences noted in these pharmacokinetic aspects of I–IV and VI–VIII.

EXPERIMENTAL

Materials—The following were used: benzoylformic acid[1], mp 62–64°; *p*-methylbenzoylformic acid, mp 97–99°, synthesized by the method of Kindler *et al.* (7); *p*-ethylbenzoylformic acid, mp 65–67°, synthesized by the method of Kindler *et al.* (7); and DL-tropic acid, mp 118–120°.

Apparatus and Analytical Procedure—The GC procedure used for the quantitative determination of VI–VIII in rat urine was the same as described previously for mandelic acid and its *para*-alkylated homologs (2–4).

Methodology—The procedures for preparing rats and for urine collection following intravenous administration of VI–VIII were the same as described previously for I (2). Approximately 60 Sprague–Dawley male rats, 180–230 g (average, 200 g), were used repeatedly in all urinary excretion studies. The aqueous solution of the sodium salt of each compound used for intravenous administration was made isotonic, and the volume of the intravenous solution injected was 2 ml.

To determine the glomerular filtration rates[2] of the compound, the appropriate dose of the substrate compound (VI, VII, or VIII) and 3012 μmoles/kg of V as a renal tubular secretion inhibitor, both as their sodium salts contained in 2 ml, were injected intravenously to the rat. The intravenous dosage ranges used for VI, VII, and VIII were 166.65–333.3, 61.0–208.57, and 24.54–28.1 μmoles/kg, respectively[3].

RESULTS AND DISCUSSION

Ideal Properties—As reported previously (1, 6), VI–VIII are neither significantly bound to plasma proteins, metabolized, nor expected to be reabsorbed from the renal tubules; additionally, virtually 100% of the administered dose of each compound was recovered in the urine in the unchanged form. These properties of the compounds are considered ideal properties, since they facilitate interpretation of the data. Therefore, these compounds (pKa 3.2–3.3) are also referred to as "model" organic anions in view of the objective of the study.

Treatment of Urinary Excretion Data—Semilogarithmic plots of the excretion rate *versus* the midpoint time of the urine collection period were prepared for data obtained for each compound. The biological half-lives reported in this paper are referred to as the elimination phase half-lives, because these values were determined from the slopes of the straight lines (least squares) based on the data points obtained in the elimination phase noted in the urinary excretion or

[1] Aldrich Chemical Co., Milwaukee, Wis.

[2] The purpose of this determination will be discussed in a separate paper.

[3] The reason for employing a lower dosage range for VIII than that used for VI or VII will be dealt with in a separate paper.

Table I—Biological Half-Lives Calculated from the Elimination Phase for the Compounds Using Urinary Excretion Data and Blood Level Data Obtained in the Absence and Presence[a] of V in Rats

Compound	Biological Half-Life (DL-Tropic Acid Absent), min		Biological Half-Life (DL-Tropic Acid Present), min	
	Urinary	Blood	Urinary	Blood
I	30.0[b]	34.7[c]	46.0[b]	36.1[c]
II	17.0[d]	10.6[c]	30.0[d]	14.9[c]
III	13.0[d]	13.8[c]	26.0[d]	16.8[c]
IV	23.0[e]	20.4[c]	35.0[e]	22.7[c]
VI	42.0	33.7[c]	47.1	43.5[c]
VII	16.7	14.1[c]	21.0	16.9[c]
VIII	13.4	5.2[c]	25.6	9.4[c]

[a] A fixed dose of 3012 μmoles/kg iv of V was administered simultaneously with the appropriate smaller doses of each compound. [b] From Ref. 2. [c] From Refs. 1 and 6. [d] From Ref. 3. [e] From Ref. 4.

blood level studies. Of course, for compounds that showed a monoexponential decline in their blood levels or urinary excretion rates, all data points were in the elimination phase.

Urinary Excretion Kinetics—*Compound VI*—The kinetics of urinary excretion of VI were studied using three different intravenous doses, namely 166.65, 249.8, and 333.33 μmoles/kg, and the numbers of individual rat studies carried out at these dosage levels were 7, 6, and 14, respectively. Semilogarithmic plots of excretion rates *versus* time for each study indicated a multiexponential decline in the excretion rate, as expected from the blood level studies where the disappearance of the compound from the blood occurred triexponentially. However, the data points obtained (which ranged from three to six points) in an individual study were not sufficient to characterize the triexponential nature of the curve. Therefore, composite semilogarithmic plots were prepared for the data obtained at each dose; such plots are shown for two doses in Fig. 1.

Since, from the blood level data (1), the α-, β-, and γ-phases were identified for the time periods of 0–8, 12–20, and 20 min onward, respectively, the urinary excretion rate data obtained at each dose were feathered on the basis of these time periods. However, as illustrated in Fig. 1 for one dose, the existence of the α-phase was not revealed nor was the β-phase well characterized at any dose. However, the elimination phase was well defined, which facilitated calculation of the elimination phase half-life. The values of the biological half-lives thus obtained at three intravenous doses were similar (41–43.7 min), with the average value being 42 min (Table I). The half-life determined from the urinary excretion data was longer than that determined from the blood level data.

Compound VII—The kinetics of urinary excretion of VII were studied at intravenous doses ranging from 61.0 to 208.6 μmoles/kg, and 33 individual rat studies were performed. Semilogarithmic plots prepared for the data of each study indicated a monoexponential decline in the excretion rates of the compound, as expected from the blood level studies where the disappearance of the compound from the blood occurred monoexponentially (1). The typical apparent first-order plots obtained for the compound in this dosage range are presented in Fig. 2. The average biological half-life of the compound determined from the 33 studies was 16.7 ± 1.8 min, which was longer than that determined previously (1) from blood level data.

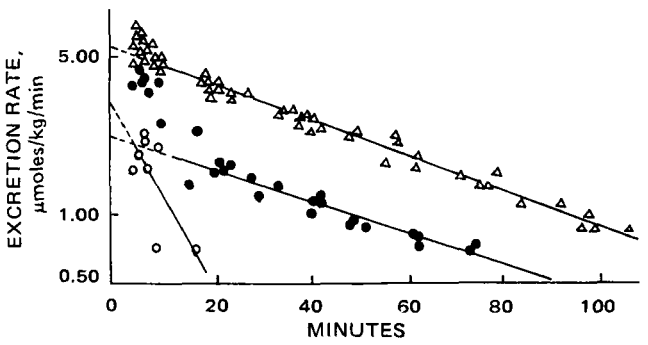

Figure 1—*Composite semilogarithmic plots of urinary excretion rate* versus *time constructed for data obtained for VI following fixed doses of 166.65 (●) and 333.33 (△) μmoles/kg iv to rats. The data points (○) obtained upon feathering are shown for the 166.65-μmoles/kg dose only.*

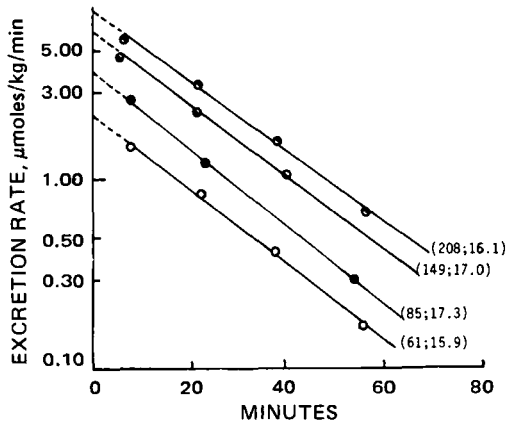

Figure 2—*Typical apparent first-order plots of log urinary excretion rate* versus *time obtained for VII following intravenous administration of various doses to rats. The numbers in parentheses refer to the intravenous dose of VII in micromoles per kilogram and its biological half-life in minutes, respectively.*

Compound VIII—The kinetics of urinary excretion of VIII were studied at the intravenous dose of 1 mg/rat. Depending on the body weight of the rats, this dose ranged from 25.54 to 28.1 μmoles/kg; only four individual rat studies were performed. Semilogarithmic plots prepared for the data of each study also indicated a monoexponential decline in the excretion rates of the compound, as expected from the blood level studies where the disappearance of the compound from the blood occurred monoexponentially even at an intravenous dose as high as 140.5 μmoles/kg (1). The typical apparent first-order plots obtained for the compound are shown in Fig. 3. The average biological half-life was 13.4 ± 1.6 min, which was longer than that determined previously (1) from blood level data.

Urinary Excretion Kinetics of VI–VIII in Presence of V—The original purpose of studying the kinetics of urinary excretion of VI, VII, or VIII in the presence of a simultaneously administered large intravenous dose (3012 μmoles/kg) of V was to determine the initial glomerular filtration rates of these compounds, which were necessary in the determination of the Michaelis–Menten kinetic parameters of renal tubular secretion of the compounds according to the methodology described previously (2–4). This objective was achieved for VII but not for VI and VIII.

Compound VII—The kinetics of urinary excretion of VII were studied following its intravenous administration at 55–192 μmoles/kg in the presence of 3012 μmoles/kg iv of V. This dose of V was employed because it was sufficient to inhibit the renal tubular secretion of I and its *para*-alkylated homologs (3, 4); 25 individual rat studies were carried out in this dosage range. As expected, the semilogarithmic plots prepared for the data of each study also indicated a monoexponential decline in the excretion rates of the compound; the typical apparent first-order plots obtained in this dosage range are presented in Fig. 4.

The apparent initial excretion rates obtained (from intercept values obtained upon extrapolating the least-squares straight lines such as those shown in Fig. 4) were plotted against the corresponding intravenous doses of the compound (Fig. 5). As seen in this figure, the ap-

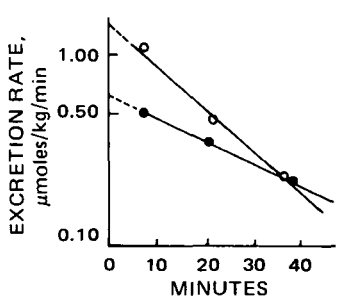

Figure 3—*Typical apparent first-order plots of log urinary excretion rate* versus *time obtained in rats for VIII following administration of 27.4 μmoles/kg iv in the absence of V (○) and 32.11 μmoles/kg iv in the presence of simultaneously administered 3012 μmoles/kg iv of V (●).*

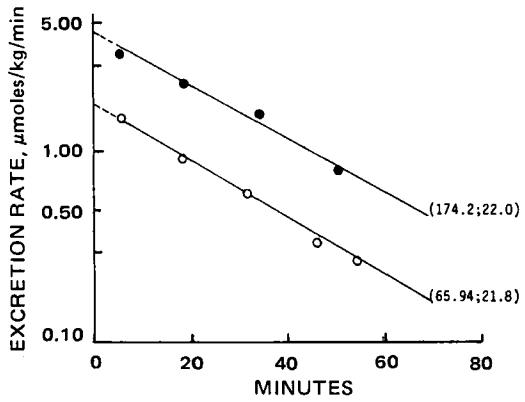

Figure 4—*Typical apparent first-order plots of log urinary excretion rate* versus *time obtained in rats for VII in the presence of simultaneously administered 3012 μmoles/kg iv of V. The numbers in parentheses refer to the intravenous dose of VII in micromoles per kilogram and its biological half-life in minutes, respectively.*

parent initial excretion rate of VII was directly proportional to its intravenous dose, indicating that the administered dose of V practically completely inhibited the renal tubular secretion of VII and that the apparent initial excretion rates of VII were due to its glomerular filtration rates, as shown for other compounds (3–5). On the basis of these data as well as the Michaelis–Menten kinetic parameters of renal tubular secretion[4] determined for VII, it was concluded that VII and V share the same pathway for their renal tubular secretion (3–5). The mean biological half-life of VII, owing to its elimination occurring by only the glomerular filtration process, was 21 min. In the presence of V, the half-life of the compound determined from urinary excretion data was indeed longer than that determined from blood level data (Table I).

Compound VI—The kinetics of urinary excretion of VI were studied at 166.65-, 249.8-, and 333.33-μmoles/kg doses, each in the presence of simultaneously administered 3012 μmoles/kg iv of V (six individual rat studies at each dose). For the reason stated previously, composite semilogarithmic plots were prepared for the data obtained at each dose; such plots are shown for two doses in Fig. 6. As can be seen upon feathering the data, as illustrated for one dose, the α-phase noted from the blood level data (5) remained undetected and the decline in the excretion rate appeared to occur biexponentially.

In contrast to the data obtained in the absence of V (Fig. 1), the distributive phase (Fig. 6) appeared to be fairly well defined in these studies. Since the initial excretion rates of the compound in the absence of V (Fig. 1) could not be determined, there was no interest or concern to determine the initial excretion rates of the compound in the presence of V (which actually are the initial glomerular filtration rates of the compound). The half-life values of the compound determined from the elimination phase at various doses were similar (average of 47.14 min). Since the half-life obtained in the presence of V was longer than that obtained in the absence of V, V probably inhibited the renal tubular secretion of VI and probably shared the same renal tubular secretion mechanism available for V (2). The half-life of the compound determined from the urinary excretion data was longer than that determined from the blood level data.

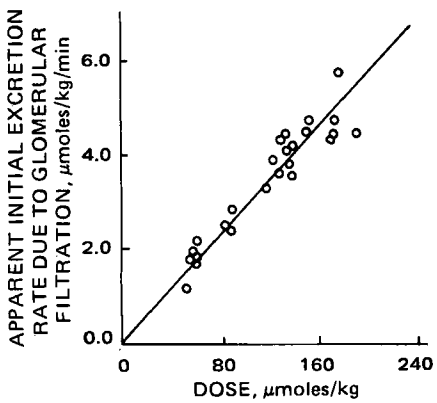

Figure 5—*Linear relationship between the apparent initial excretion rate due to glomerular filtration and the intravenous dose of VII.*

[4] To be discussed in a separate paper.

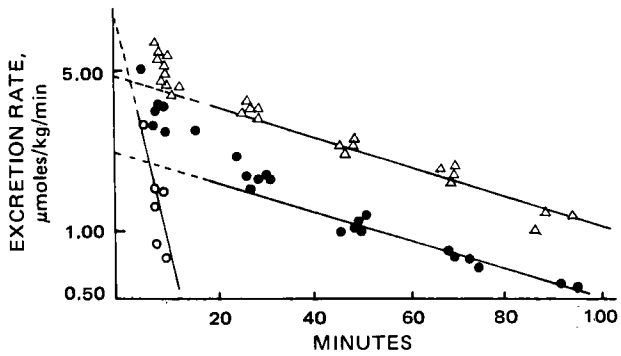

Figure 6—*Composite semilogarithmic plots of urinary excretion* versus *time for the data obtained in rats for VI following fixed doses of 166.65 (●) and 333.33 (△) μmoles/kg iv in the presence of simultaneously administered 3012 μmoles/kg iv of V. The data points (○) obtained upon feathering are shown for the 166.65-μmoles/kg dose of VI only.*

Compound VIII—The kinetics of urinary excretion of VIII were studied in the presence of V (3012 μmoles/kg) at one intravenous dose (1 mg/rat) only; three individual rat studies were performed. As expected, the decline in the excretion rate occurred monoexponentially (Fig. 3), and the half-life (25.6 min) was longer than that observed in the absence of V. This finding indicated that the compound probably shared the same renal tubular secretion mechanism that was available for V. Furthermore, the half-life of the compound determined from urinary excretion data was longer than that determined from blood level data.

Rationale for Apparent Differences Observed in Pharmacokinetic Aspects—The most probable reasons for the distributive phases to remain undetected in the urinary excretion studies are as follows.

First, as determined from the blood level data (1), the distributive phases for I–IV (which follow a two-compartment open system) lasted for 4–8 min. Therefore, unless at least three or four urine samples are collected during this period, the distributive phase cannot be characterized. Since the first urine samples that can be conveniently obtained from the rats without catheterizing their ureters are generally 10–12 min after the intravenous administration of the compounds, only one urine sample can be obtained from each rat to reflect partly the excretion rate during the distributive phase. Consequently, such a data point is likely to be equally influenced by elimination phase kinetics of the compound; subsequent urine samples would undoubtedly represent the data points due to the elimination phase. Therefore, it was not surprising that Nagwekar and coworkers (2–5) did not detect the distributive phase from the urinary excretion rate studies of I–IV in rats and treated urinary excretion data according to a one-compartment open model.

If urine samples are obtained at 1-min intervals by catheterizing the ureter of a rat, it might be possible to characterize the distributive phase. But this may not be possible if there is a delay time up to 4 min from glomerular filtration to the appearance of drug in the collecting vessel, as demonstrated (8) in rats for inulin and urea. When urine samples were collected from catheterized rats at 2-min intervals following the administration of inulin or urea, the peak rates of excretion of these compounds were noted in the third urine sample (at the 6th min) (8). In view of this observation made by Bourne and Barber (8), the distributive phase for a compound probably cannot be characterized from urinary excretion rate studies, especially when the duration of the distributive phase is 4–8 min as observed for I–IV from the blood level data.

For the case following a three-compartment open model, the duration of the α-phase was up to 8 min and the duration of the β-phase was noticeable from 12 to 20 min following the intravenous administration of the compound. Since the α-phase lasted for only 8 min, this phase, as explained for I–IV, could not be detected from the urinary excretion studies. Therefore, as seen in Figs. 1 and 6, the

Table II—Ratios of Elimination Phase Biological Half-Lives ($t_{1/2}$) of the Compounds Based on Data Presented in Table I

Compound	Urinary $t_{1/2}$ / Blood $t_{1/2}$ (V Present)	Urinary $t_{1/2}$ / Blood $t_{1/2}$ (V Absent)	(Urinary $t_{1/2}$) V Present / (Urinary $t_{1/2}$) V Absent	(Blood $t_{1/2}$) V Present / (Blood $t_{1/2}$) V Absent
I	1.27	0.90	1.35	1.04
II	2.01	1.60	1.76	1.40
III	1.54	0.94	2.00	1.21
IV	1.54	1.13	1.52	1.11
VI	1.08	1.25	1.12	1.29
VII	1.24	1.18	1.25	1.20
VIII	2.72	2.57	1.92	1.80

urinary excretion data appear to be describable by a two-compartment open model.

The second possible reason that may explain the absence of the distributive phase with I–IV and VI, as noted from urinary excretion data, is that there might be detention and/or retention of the compounds in the renal tubular membrane during their renal tubular secretion. The renal tubular secretion process mediated by the component of the tubular membrane that serves as a secretion carrier may be described by Scheme I, where D^- is the negatively charged compound, and C^+ is a positively charged carrier of the renal tubular membrane which complexes with the drug within the membrane to yield the complex D^-C^+. This complex diffuses across the membrane to the inner surface of the membrane.

The molecules of all compounds are expected to remain in the biological fluid in the ionic form, D^-, because their pKa values are low (3.2–3.7). In the transmembrane transport of the compounds, the role of proteins and/or phospholipids has been implicated (4, 5, 9, 10). Since the outer surface of the membrane is covered by proteins, the permeant molecules possibly could be adsorbed by the proteins, followed by desorption into the renal tubular membrane where the permeant molecules could complex with the positively charged carrier, possibly the phospholipids. The drug–carrier complex then diffuses to the inner surface of the membrane where the dissociation of the complex occurs. The permeant molecules thus released are adsorbed by the inner layer of protein and eventually desorbed into the tubular lumen fluid. The rate-determining step assumed in this scheme is the formation of the D^-C^+ complex.

The retention of the compounds in the renal tubular membrane, in the presence of an inhibitor (V), can be explained by Scheme II, where I^- is the competitive inhibitor of D^-, and I^-C^+ is the inhibitor–carrier complex. According to this scheme, the presence of a large concentration of the inhibitor (V) competitively inhibits the renal tubular secretion of the substrate compound, D^-.

As noted in Table I, in studies involving V, the biological half-lives of the substrate compounds determined from urinary excretion data were longer than those determined from blood level data. Similarly, in studies carried out in the absence of V, the biological half-lives of the compounds, except I and III, determined from urinary excretion data were longer than those determined from blood level data. These effects can be explained also in terms of the two factors discussed previously to account for the disappearance of the distributive phases of these compounds.

Schemes I and II lead to the assumption that, for these compounds, the renal tubular membranes are part of neither the central compartment nor the peripheral compartment(s) of the body. However, this statement does not imply that the rest of the kidney organ is also not a part of the central or peripheral compartments. This situation is analogous to the fact that drug present in the GI fluid is considered neither a part of the central compartment nor the peripheral compartment of the body. Therefore, the molecules of the compounds, appearing in the renal tubular membranes after desorption from the proteins of the outer surface of the membranes, are considered to be lost from the body. Furthermore, since these molecules are retained and/or detained temporarily within the membrane as a result of their relatively slower rates of entering the lumen of the tubules, the biological half-life of the compound can be expected to be shorter when determined from blood level data rather than urinary excretion data. This hypothesis gains support from the fact that the ratios of "urinary" biological half-life to "blood" half-life of the compounds calculated on the basis of data obtained in the presence of V are, for all practical purposes, greater than such ratios calculated for the compounds on the basis of data obtained in the absence of V (Table II).

Furthermore, for these compounds, the ratios of urinary biological half-life in the presence of V to that in the absence of V are, for all practical purposes, greater than the ratios of blood biological half-life in the presence of V to that in the absence of V (Table II). This observation also may be explained in light of the proposed theory that the competition of V with the substrate compounds for the carrier molecules within the renal tubular membrane can be expected to be greater than for the adsorption sites at the outer surface of the renal tubular membrane, since the number of carrier molecules is much more limited than that of the adsorption sites. The inherent suggestions made here are that: (*a*) the competition offered by V (because of its higher concentration) to the substrate compounds for gaining access from the central compartment to the renal tubular membrane is probably much less (and for some compounds insignificant) than to their association with the renal tubular secretion carrier molecules present within the tubular membrane, and (*b*) the substrate compound accumulated within the membrane does not readily diffuse back into the central compartment to reflect prolongation in the half-life of the compound when determined from blood level data to the same degree as when determined from urinary excretion data.

Examples from Literature—Although scientific literature is deluged with reports of pharmacokinetic studies of drugs in humans and animals, the half-lives of drugs usually were determined from either blood level data or urinary excretion data. However, in some studies the half-lives of the same drugs were determined in the same subjects in the same laboratory from both urinary excretion data and blood level data and, therefore, allow comparison of the biological half-lives determined from these two kinds of data (Table III). These data for the drugs were, of course, obtained in the absence of other drugs.

According to Table III, the biological half-lives (elimination phase) of these drugs tend to be longer when determined from urinary excretion data than from blood level data. Because these drugs do not

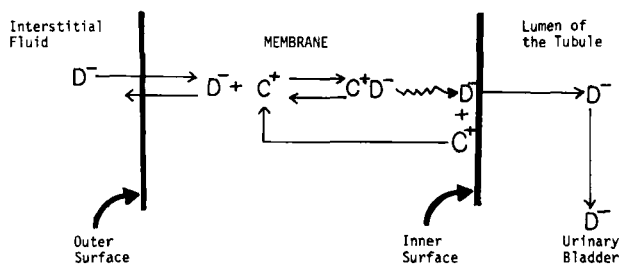

Scheme I

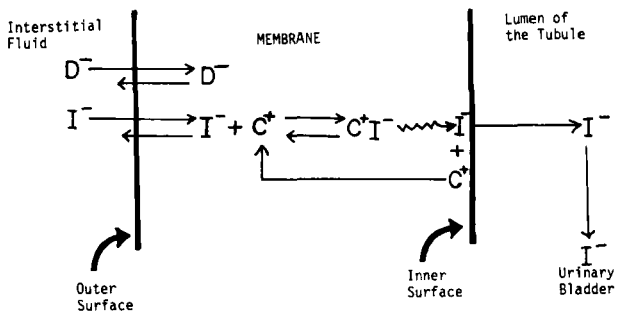

Scheme II

Table III—Ratios of Urinary Biological Half-Life to Blood Biological Half-Life Calculated for Drugs Based on Human Data[a] Reported in the Literature

Drug	Urinary $t_{1/2}$ / Blood $t_{1/2}$	Reference
Oxacillin	1.42	11
Ampicillin	1.10	11
Penicillin G	1.14	11
Methicillin	1.16	11
Dicloxacillin	1.07	11
Chlorpropamide	1.08	12
Acetylstrophanthidin	1.08	13
Pindolol	1.17	14
Pindolol (oral)	1.48	14
Dextroamphetamine (oral)	1.1	15

[a] Unless indicated otherwise, the route for drug administration used in these studies was intravenous.

possess the "ideal properties" described previously, one or several factors might contribute to yield longer biological half-lives when determined from urinary excretion data. However, since most of these drugs are secreted by renal tubules, the differences noted in the biological half-lives for these drugs may be explained in terms of the theory proposed here.

Significance of the Study—Other investigators have pointed out that pharmacokinetic analyses of drugs based on their urinary excretion data may not necessarily reflect their time course in the blood, especially at the initial time period, due to such factors as the metabolism of drugs in the kidney (16), insufficient frequency of collecting urine samples at the initial period following intravenous drug administration (17), overlooking of an important anatomical fact concerning the kidney with regards to kinetics of renal tubular secretion of drugs (18), and significant "lag time" for drug to appear in the urine (16, 19). The additional factor proposed from the analysis of the data presented in this paper is that, for drugs secreted by renal tubules, the accumulation of the drug may occur in the renal tubular membrane (which may not constitute a part of the central compartment or the peripheral compartment) and thereby cause the biological half-lives to be longer than those determined from blood level data. This interpretation is facilitated primarily because the compounds used in the study possess ideal properties, as described previously.

This study also shows that, if accumulation of drugs secreted by renal tubules occurs in the renal tubular membrane, especially in the presence of a renal tubular secretion inhibitor of the drugs, their chronic use in patients might result in nephrotoxicity due to interference by drug molecules in the integrity of the membrane structure (in terms of membrane porosity, *etc.*) and normal metabolic functions of tubular cells. Therefore, the optimum dosage regimen for certain drugs known or suspected to be nephrotoxic should be designed by considering their half-lives determined from urinary excretion data as well as blood level data in addition to other pharmacokinetic parameters.

REFERENCES

(1) Y. M. Amin and J. B. Nagwekar, *J. Pharm. Sci.*, **64**, 1804(1975).

(2) E. J. Randinitis, M. Barr, H. C. Wormser, and J. B. Nagwekar, *ibid.*, **59**, 806(1970).

(3) J. B. Nagwekar and A. Unnikrishnan, *ibid.*, **60**, 375(1971).

(4) J. B. Nagwekar, P. M. Patel, and M. A. Khambati, *ibid.*, **62**, 1093(1973).

(5) E. J. Randinitis, M. Barr, and J. B. Nagwekar, *ibid.*, **59**, 813(1970).

(6) Y. M. Amin and J. B. Nagwekar, *ibid.*, **64**, 1813(1975).

(7) K. Kindler, W. Metzendorf, and D.-Y. Kevok, *Ber.*, **76B**, 308(1943).

(8) G. R. Bourne and H. E. Barber, *J. Pharm. Pharmacol.*, **24**, 532(1972).

(9) W. Wilbrandt and T. Rosenberg, *Pharmacol. Rev.*, **13**, 109(1961).

(10) W. D. Stein, *Biochem. Biophys. Acta*, **59**, 47(1962).

(11) L. W. Dittert, W. O. Griffen, J. C. LaPiana, F. J. Shainfeld, and J. T. Doluisio, *Antimicrob. Ag. Chemother.*, **1969**, 42.

(12) J. A. Taylor, *Clin. Pharmacol. Ther.*, **13**, 710(1972).

(13) R. Selden, M. D. Klein, and T. W. Smith, *Circulation*, **47**, 744 (1973).

(14) R. Gugler, W. Herold, and H. J. Dengler, *Eur. J. Clin. Pharmacol.*, **7**, 17(1974).

(15) M. Rowland, *J. Pharm. Sci.*, **58**, 508(1969).

(16) S. H. Wan and S. Riegelman, *ibid.*, **61**, 1278(1972).

(17) I. Janku and V. Krebs, *Eur. J. Pharmacol.*, **14**, 286(1971).

(18) R. B. Conn., A. J. Sabo, D. Landes, and J. Y. L. Ho, *Nature*, **203**, 143(1964).

(19) N. G. Heatley, *Antibiot. Med. Clin. Ther.*, **2**, 33(1956).

ACKNOWLEDGMENTS AND ADDRESSES

Received August 11, 1975, from the *Pharmaceutics Division, College of Pharmacy and Allied Health Professions, Wayne State University, Detroit, MI 48202*

Accepted for publication November 21, 1975.

Abstracted in part from a dissertation submitted by Y. M. Amin to the Graduate Division, Wayne State University, in partial fulfillment of the Doctor of Philosophy degree requirements.

* Recipient of a Wayne State University Graduate Fellowship, 1973–1974.

[x] To whom inquiries should be directed.

Influence of Cholestasis on Drug Elimination: Pharmacokinetics

LESTER I. HARRISON and MILO GIBALDI ˣ

Abstract □ A two-compartment model representing the body and the GI tract, with elimination occurring in each compartment, was used to study, in theory, the influence of impaired biliary excretion on drug disposition. The results suggest that cholestasis can either increase or decrease a drug's half-life, depending upon the relative values of the two elimination rate constants. In all cases, however, impaired biliary excretion reduced the initial elimination of drug from the body and increased the half-life of the α-phase of drug disposition.

Keyphrases □ Pharmacokinetics—effect of cholestasis on drug half-life and elimination, two-compartment model studied □ Biliary excretion, impaired—effect on drug half-life and elimination, two-compartment pharmacokinetic model studied □ Elimination, drug—effect of cholestasis, two-compartment pharmacokinetic model studied

A rigorous description of the time course of elimination from the body of drugs subject to biliary excretion and enterohepatic cycling is among the most formidable challenges in pharmacokinetics. A general solution to the problem remains elusive, because of the discontinuous nature of bile flow in animals with a gallbladder. Failure of the liver to secrete bile into the duodenum can be due to a multiplicity of causes and can be of intrahepatic or extrahepatic origin (1). The syndrome can be developed experimentally in various laboratory animals by ligation of the common bile duct.

The results of several investigations suggest that cholestasis, like renal failure, can reduce the elimination of certain drugs. The disappearance of diethylstilbestrol from the plasma was markedly faster in control rats than in bile duct-ligated rats (2). The half-lives of ^{131}I-rose bengal were about 20 hr in a normal child, 41 and 61 hr in two children with partial biliary excretory defects, and 118–156 hr in four children with complete cholestasis (3). The average half-life of rifampin was 5.7 hr in five patients with obstructive jaundice (4). This value is about twice as long as in patients without biliary obstruction.

On the other hand, plasma clearance studies in the dog, 1 week after ligation of the common bile duct, revealed an increased clearance of colloidal gold Au 198 (5). Another example of the presumably anomalous effects of cholestasis was observed in this laboratory recently. After intravenous injection of ^{3}H-digoxin, the apparent half-life of elimination of total tritium from the plasma was shorter in bile duct-ligated rats than in control rats (Fig. 1).

The apparently unpredictable effects of cholestasis on drug half-life stimulated the development and examination of hypothetical pharmacokinetic models for enterohepatic cycling to rationalize the phenomenon. One such model is the subject of this report.

THEORETICAL

The model shown in Scheme I is probably the simplest schematic representation of the elimination of a drug subject to enterohepatic circulation. The tacit assumption that bile flow may be described by a continuous function is reasonable in the rat but oversimplifies the situation in most other species.

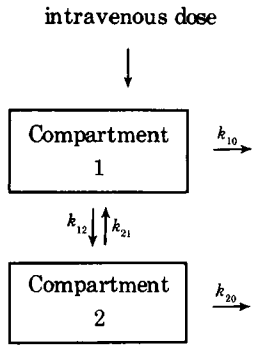

Scheme I—Pharmacokinetic model used to describe biliary excretion and enterohepatic circulation. Compartment 1 represents the body while Compartment 2 represents the GI tract.

The drug is administered as a bolus by intravenous injection, and the body is envisioned as a one-compartment system (Compartment 1). The GI tract is represented by the additional compartment (Compartment 2). The rate constant k_{10} represents the sum of all rate constants associated with nonbiliary elimination, *i.e.*, renal excretion and biotransformation. The rate constant k_{20} is associated with the removal of drug from the "reabsorption site" due to biotransformation by the intestine or intestinal bacteria and/or eventual fecal excretion.

At the simplest level, k_{12} and k_{21} are the rate constants describing biliary excretion and reabsorption of the drug, respectively. Functionally, k_{12} also may be an apparent rate constant describing the consecutive process of hepatic conjugation and biliary excretion of the metabolite where one step is rate limiting. In this case, k_{21} would be an apparent rate constant describing the consecutive processes of deconjugation and subsequent absorption of parent drug, provided that one step is rate limiting. Cholestasis is simulated by decreasing k_{12}.

The amount of drug in the body, A, as a function of time after administration of the dose, D, is given by:

$$A = \frac{(\alpha - k_{21} - k_{20})D}{(\alpha - \beta)} \exp(-\alpha t) + \frac{(k_{21} + k_{20} - \beta)D}{(\alpha - \beta)} \exp(-\beta t) \quad \text{(Eq. 1)}$$

where:

$$\alpha = \tfrac{1}{2}[k_{21} + k_{20} + k_{12} + k_{10} + \sqrt{(k_{21} + k_{20} + k_{12} + k_{10})^2 - 4(k_{12}k_{20} + k_{10}k_{21} + k_{10}k_{20})}] \quad \text{(Eq. 2)}$$

and:

$$\beta = \tfrac{1}{2}[k_{21} + k_{20} + k_{12} + k_{10} - \sqrt{(k_{21} + k_{20} + k_{12} + k_{10})^2 - 4(k_{12}k_{20} + k_{10}k_{21} + k_{10}k_{20})}] \quad \text{(Eq. 3)}$$

If enterohepatic cycling is maximally efficient, *i.e.*, $k_{20} \to 0$, then Eq. 3 reduces to:

$$\beta = \tfrac{1}{2}[k_{21} + k_{12} + k_{10} - \sqrt{(k_{21} + k_{12} + k_{10})^2 - 4k_{10}k_{21}}] \quad \text{(Eq. 4)}$$

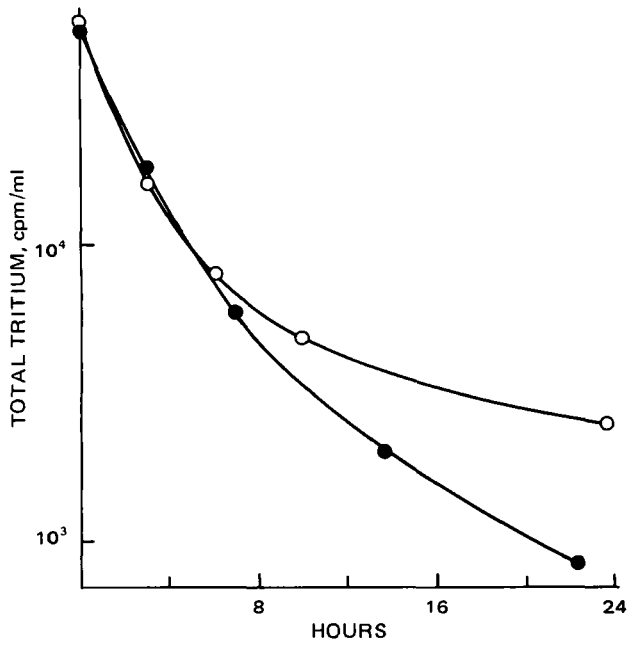

Figure 1—*Time course of total radioactivity in the plasma after intravenous administration of 1 mg of ^{3}H-digoxin/kg to a control rat (○) and a bile duct-ligated rat (●). Experimental details are given in Ref. 9.*

The half-life of the drug is given by:

$$t_{1/2} = 0.693/\beta \qquad \text{(Eq. 5)}$$

The half-life of the drug in complete cholestasis is given by:

$$t^*_{1/2} = 0.693/k_{10} \qquad \text{(Eq. 6)}$$

since the system then reduces to a one-compartment model.

EXPERIMENTAL

Numerical analyses were carried out with Eqs. 2 and 3, using values of k_{10}/k_{20} from 0.1 to 10 while k_{12}/k_{21} varied from 0.01 to 100 and k_{12}/k_{10} varied from 0.1 to 10. Simulated drug levels in the body were obtained by using the appropriate differential equations to describe the model in Scheme I, a unit dose, and various sets of rate constants as input data for the MIMED digital computer analog simulation program (6).

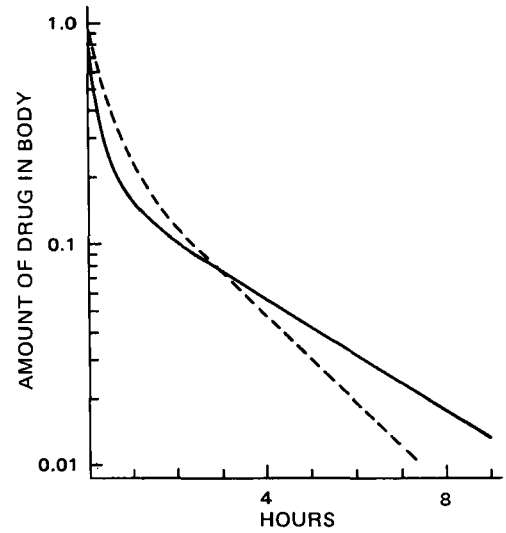

Figure 3—*Effect of reduced biliary excretion on biological half-life when $k_{10}/k_{20} > 1$. Key: —, control, $k_{12} = 3.0$, $k_{21} = 1.0$, $k_{10} = 1.0$, and $k_{20} = 0.1\ hr^{-1}$; and - - -, partial cholestasis, $k_{12} = 1.0$, $k_{21} = 1.0$, $k_{10} = 1.0$, and $k_{20} = 0.1\ hr^{-1}$.*

RESULTS AND DISCUSSION

If one considers the limiting case of maximal enterohepatic cycling (*i.e.*, $k_{20} \to 0$), the model shown in Scheme I reduces to a form identical to the customary two-compartment open model. It has been shown (7) that:

$$\beta = f_c^* k_{10} \qquad \text{(Eq. 7)}$$

where f_c^* is the fraction of drug in the system in Compartment 1 in the postdistributive phase. At any given values of k_{21} and k_{10}, a decrease in k_{12} results in an increase in f_c^*; in fact, as $k_{12} \to 0$, $f_c^* \to 1$. It follows that a decrease in k_{12} produces an increase in β. The model, therefore, predicts that cholestasis will actually decrease the biological half-life for drugs simply subject to biliary secretion and enterohepatic circulation but not to "gut elimination." A simulated example is shown in Fig. 2.

In cases where k_{20} was finite, an unambiguous relationship between β and k_{10} was not apparent and it was necessary to evaluate Eq. 3 by

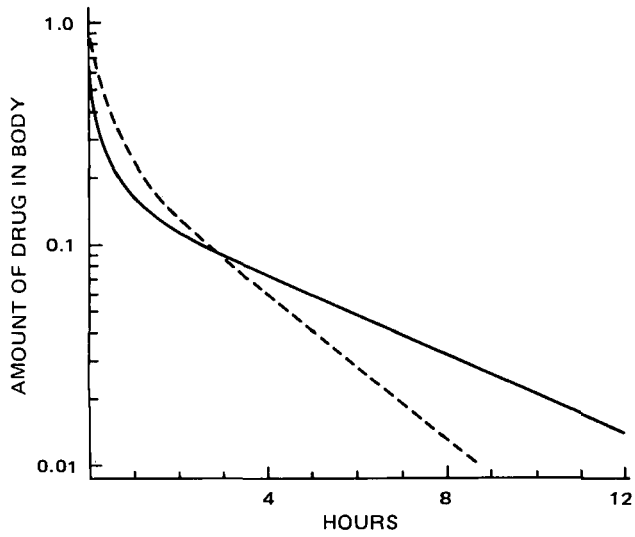

Figure 2—*Effect of reduced biliary excretion on biological half-life when $k_{20} = 0$. Key: —, control, $k_{12} = 3.0$, $k_{21} = 1.0$, and $k_{10} = 1.0\ hr^{-1}$; and - - -, partial cholestasis, $k_{12} = 1.0$, $k_{21} = 1.0$, and $k_{10} = 1.0\ hr^{-1}$.*

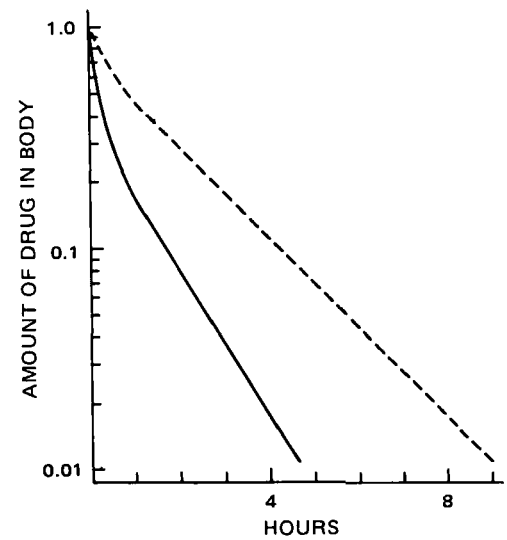

Figure 4—*Effect of reduced biliary excretion on biological half-life when $k_{10}/k_{20} < 1$. Key: —, control, $k_{12} = 3.0$, $k_{21} = 1.0$, $k_{10} = 0.1$, and $k_{20} = 1.0\ hr^{-1}$; and - - -, partial cholestasis, $k_{12} = 1.0$, $k_{21} = 1.0$, $k_{10} = 0.1$, and $k_{20} = 1.0\ hr^{-1}$.*

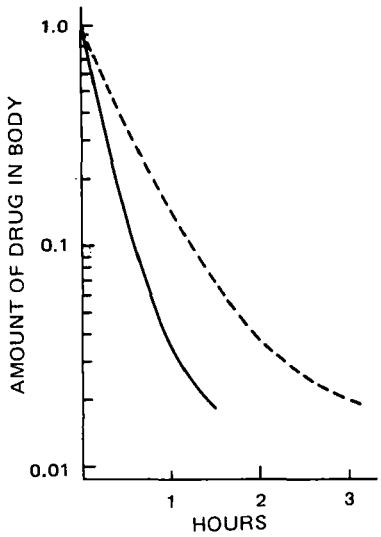

Figure 5—*Effect of reduced biliary excretion on the α-phase when* $k_{10}/k_{20} > 1$. *Key: —, control,* $k_{12} = 3.0$, $k_{21} = 0.1$, $k_{10} = 1.0$, *and* $k_{20} = 0.1\ hr^{-1}$; *and - - -, partial cholestasis,* $k_{12} = 1.0$, $k_{21} = 0.1$, $k_{10} = 1.0$, *and* $k_{20} = 0.1\ hr^{-1}$.

numerical analysis. The results of this analysis were quite clear over a wide range of rate constants. When $k_{10}/k_{20} > 1$, regardless of the value of k_{12}/k_{21}, a decrease in k_{12} produces an increase in β and a decrease in the half-life of the drug (Fig. 3). On the other hand, when $k_{10}/k_{20} < 1$, a decrease in k_{12} results in a decrease in β and an increased biological half-life (Fig. 4). Hence, the model in Scheme I suggests that cholestasis can either increase or decrease the biological half-life; the effect one observes depends on the relationship between the rate constants associated with nonbiliary elimination of the drug from the body and with "elimination" of the drug in the gut.

An interesting finding, made during the simulation and confirmed by numerical analysis of Eq. 2, suggests that an apparent decrease in drug elimination would be the most common observation in cholestasis. Regardless of the value of k_{10}/k_{20}, a decrease in k_{12} produces a decrease in α for any given set of rate constants. In other words, the half-life of the α-phase for a given drug will always be longer in cholestasis than under normal conditions. Limited computer studies suggest that this will also be the case when a multicompartment model is required to represent the body.

If, because of experimental design or assay limitations, the time course of drug concentrations in the plasma is followed for a period shorter than the time required to attain distribution equilibrium, *i.e.*, the time at which the β-phase becomes evident, one would conclude that the reduced biliary excretion increases the half-life of the drug, even if k_{10}/k_{20} were greater than 1 (Fig. 5). Although this conclusion is mathematically incorrect, it is realistic from a clinical and toxicological point of view. For example, it is highly likely that the LD_{50} of any drug subject to biliary excretion in the test species would be decreased in the bile duct-ligated animal compared to that observed in the control animal (8).

REFERENCES

(1) S. Sherlock, "Diseases of the Liver and Biliary System," 3rd ed., Blackwell Scientific Publications, Oxford, England, 1963.

(2) C. D. Klaassen, *Toxicol. Appl. Pharmacol.*, **24**, 142(1973).

(3) M. M. Thaler, *Pediat. Res.*, **6**, 100(1972).

(4) P. Spring, in "A Symposium on Rimactane," Ciba Ltd., Basel, Switzerland, 1968, pp. 32–34.

(5) E. G. Ohlsson, R. B. Rutherford, M. M. P. Haalebos, H. N. Wagner, Jr., and G. D. Zuidema, *J. Surg. Res.*, **10**, 201(1970).

(6) "MIMED, State University of New York at Buffalo Computer Center adaptation of MIMIC," Publication No. 44610400, Control Data Corp., St. Paul, Minn., 1968.

(7) M. Gibaldi, R. Nagashima, and G. Levy, *J. Pharm. Sci.*, **58**, 193(1969).

(8) C. D. Klaasen, *Toxicol. Appl. Pharmacol.*, **24**, 37(1973).

(9) L. I. Harrison and M. Gibaldi, *Drug Metab. Dispos.*, **4**, 88(1976).

ACKNOWLEDGMENTS AND ADDRESSES

Received September 22, 1975, from the *Department of Pharmaceutics, School of Pharmacy, State University of New York at Buffalo, Buffalo, NY 14214*

Accepted for publication November 21, 1975.

Supported in part by Grant GM-20852 from the National Institute of General Medical Sciences, National Institutes of Health.

ˣ To whom inquiries should be directed.

Biliary Secretion of Methotrexate in Rats and Its Inhibition by Probenecid

R. E. KATES ˣ **and T. N. TOZER**

Abstract □ The biliary secretion of methotrexate was investigated in rats under steady-state conditions. The transport system involved was saturable and displayed Michaelis–Menten-type kinetics. Values for the maximal rate of transport and a transport constant analogous to the Michaelis constant were 12 mg/hr and 32 mg/liter ($7 \times 10^{-5}\ M$), respectively. The inhibition of this transport mechanism by probenecid also was investigated, and the relationship between the plasma concentration of probenecid and the biliary clearance of methotrexate was elucidated. The value of K_i, the dissociation constant for the transport carrier–inhibitor complex, was 23 μg/ml ($8 \times 10^{-5}\ M$).

Keyphrases □ Methotrexate—biliary secretion, effect of coadministration of probenecid, rats □ Probenecid—effect on biliary secretion of methotrexate, rats □ Biliary secretion—methotrexate, effect of coadministration of probenecid, rats □ Antineoplastic agents—methotrexate, biliary secretion, effect of probenecid, rats □ Uricosuric agents—probenecid, effect on biliary secretion of methotrexate, rats

The effectiveness of methotrexate as an anticancer drug was first reported 25 years ago. Since then, its mechanisms of action have been studied extensively to determine how it can be utilized effectively in treating neoplastic diseases. As with other anticancer drugs, methotrexate is a nonspecific agent which arrests cell

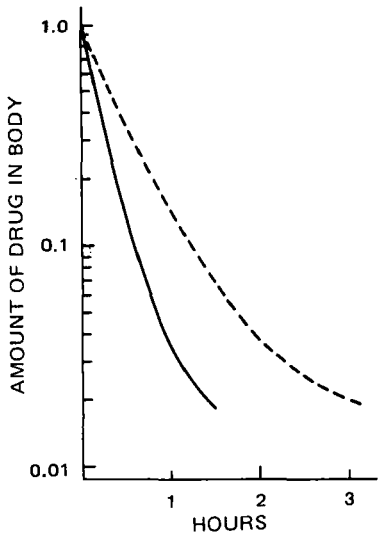

Figure 5—*Effect of reduced biliary excretion on the α-phase when* $k_{10}/k_{20} > 1$. *Key: —, control,* $k_{12} = 3.0$, $k_{21} = 0.1$, $k_{10} = 1.0$, *and* $k_{20} = 0.1\ hr^{-1}$; *and - - -, partial cholestasis,* $k_{12} = 1.0$, $k_{21} = 0.1$, $k_{10} = 1.0$, *and* $k_{20} = 0.1\ hr^{-1}$.

numerical analysis. The results of this analysis were quite clear over a wide range of rate constants. When $k_{10}/k_{20} > 1$, regardless of the value of k_{12}/k_{21}, a decrease in k_{12} produces an increase in β and a decrease in the half-life of the drug (Fig. 3). On the other hand, when $k_{10}/k_{20} < 1$, a decrease in k_{12} results in a decrease in β and an increased biological half-life (Fig. 4). Hence, the model in Scheme I suggests that cholestasis can either increase or decrease the biological half-life; the effect one observes depends on the relationship between the rate constants associated with nonbiliary elimination of the drug from the body and with "elimination" of the drug in the gut.

An interesting finding, made during the simulation and confirmed by numerical analysis of Eq. 2, suggests that an apparent decrease in drug elimination would be the most common observation in cholestasis. Regardless of the value of k_{10}/k_{20}, a decrease in k_{12} produces a decrease in α for any given set of rate constants. In other words, the half-life of the α-phase for a given drug will always be longer in cholestasis than under normal conditions. Limited computer studies suggest that this will also be the case when a multicompartment model is required to represent the body.

If, because of experimental design or assay limitations, the time course of drug concentrations in the plasma is followed for a period shorter than the time required to attain distribution equilibrium, *i.e.*, the time at which the β-phase becomes evident, one would conclude that the reduced biliary excretion increases the half-life of the drug, even if k_{10}/k_{20} were greater than 1 (Fig. 5). Although this conclusion is mathematically incorrect, it is realistic from a clinical and toxicological point of view. For example, it is highly likely that the LD_{50} of any drug subject to biliary excretion in the test species would be decreased in the bile duct-ligated animal compared to that observed in the control animal (8).

REFERENCES

(1) S. Sherlock, "Diseases of the Liver and Biliary System," 3rd ed., Blackwell Scientific Publications, Oxford, England, 1963.

(2) C. D. Klaassen, *Toxicol. Appl. Pharmacol.*, **24**, 142(1973).

(3) M. M. Thaler, *Pediat. Res.*, **6**, 100(1972).

(4) P. Spring, in "A Symposium on Rimactane," Ciba Ltd., Basel, Switzerland, 1968, pp. 32–34.

(5) E. G. Ohlsson, R. B. Rutherford, M. M. P. Haalebos, H. N. Wagner, Jr., and G. D. Zuidema, *J. Surg. Res.*, **10**, 201(1970).

(6) "MIMED, State University of New York at Buffalo Computer Center adaptation of MIMIC," Publication No. 44610400, Control Data Corp., St. Paul, Minn., 1968.

(7) M. Gibaldi, R. Nagashima, and G. Levy, *J. Pharm. Sci.*, **58**, 193(1969).

(8) C. D. Klaasen, *Toxicol. Appl. Pharmacol.*, **24**, 37(1973).

(9) L. I. Harrison and M. Gibaldi, *Drug Metab. Dispos.*, **4**, 88(1976).

ACKNOWLEDGMENTS AND ADDRESSES

Received September 22, 1975, from the *Department of Pharmaceutics, School of Pharmacy, State University of New York at Buffalo, Buffalo, NY 14214*

Accepted for publication November 21, 1975.

Supported in part by Grant GM-20852 from the National Institute of General Medical Sciences, National Institutes of Health.

ˣ To whom inquiries should be directed.

Biliary Secretion of Methotrexate in Rats and Its Inhibition by Probenecid

R. E. KATES ˣ **and T. N. TOZER**

Abstract □ The biliary secretion of methotrexate was investigated in rats under steady-state conditions. The transport system involved was saturable and displayed Michaelis–Menten-type kinetics. Values for the maximal rate of transport and a transport constant analogous to the Michaelis constant were 12 mg/hr and 32 mg/liter ($7 \times 10^{-5}\ M$), respectively. The inhibition of this transport mechanism by probenecid also was investigated, and the relationship between the plasma concentration of probenecid and the biliary clearance of methotrexate was elucidated. The value of K_i, the dissociation constant for the transport carrier–inhibitor complex, was 23 μg/ml ($8 \times 10^{-5}\ M$).

Keyphrases □ Methotrexate—biliary secretion, effect of coadministration of probenecid, rats □ Probenecid—effect on biliary secretion of methotrexate, rats □ Biliary secretion—methotrexate, effect of coadministration of probenecid, rats □ Antineoplastic agents—methotrexate, biliary secretion, effect of probenecid, rats □ Uricosuric agents—probenecid, effect on biliary secretion of methotrexate, rats

The effectiveness of methotrexate as an anticancer drug was first reported 25 years ago. Since then, its mechanisms of action have been studied extensively to determine how it can be utilized effectively in treating neoplastic diseases. As with other anticancer drugs, methotrexate is a nonspecific agent which arrests cell

growth in normal and malignant tissues. For optimal effectiveness, the therapeutic effect (malignant cell kill) must be maximized while the effect on normal, nonmalignant tissues is minimized.

Numerous empirical dosage regimens have been suggested, but only a few have proven advantageous (1). Methotrexate has been used most effectively with an intermittent administration schedule, with each dose followed by leucovorin rescue (2). To design a better dosage scheme, the total body and individual tissue disposition kinetics of methotrexate have been studied (3–5). Attention has been focused both on the role of disposition phenomona in the delivery of drug to target tissues and on how drug disposition influences the incidence and severity of toxic side effects.

The pharmacokinetics of methotrexate were first investigated by Henderson *et al.* (6), and later an extensive pharmacokinetic model of the kinetics of distribution and elimination of methotrexate in several species was presented by Bischoff *et al.* (3). Both reports clearly demonstrated that biliary secretion plays an important role in the disposition kinetics of methotrexate in some species. Henderson *et al.* (6) reported that about 55% of an intravenous dose in rats was secreted into the bile. They found that biliary secretion played a smaller role in the mouse and monkey. In the monkey, about 15% of an intravenous dose was secreted into the bile. Although bile was not collected from mice, 20–40% of an intravenous dose was excreted in the feces. Whether methotrexate is substantially secreted into the bile of humans is currently unresolved. However, only about 5% of an intravenously administered dose is eliminated in the feces of humans.

The relationship between enterohepatic cycling of drugs and their toxicity was reviewed (7). For a drug like methotrexate, where the length of tissue exposure is a major factor determining the severity of toxicity, enterohepatic cycling can be important. With methotrexate, biliary secretion puts the drug in direct contact with the tissue that is a primary site of toxicity, the intestinal mucosa.

A main concern of the present study was the possible role of biliary cycling as a contributing factor to the toxicity of methotrexate. The kinetics of the biliary secretion of methotrexate and its inhibition by probenecid were investigated in rats.

THEORETICAL

The processes involved in the transport of drugs into the bile have been studied (8, 9). Although a passive filtration component may play a part in the transport of drugs into the bile, it is generally believed that active transport is the primary process (8).

For a drug to be transported into the bile, it must travel from the liver sinusoid through the space of Disse and then through the hepatic parenchymal cell before entering the bile canaliculus. The process by which a drug molecule travels from the sinusoid into the space of Disse is one of simple diffusion. Although the transport from the parenchymal cell into the bile canaliculus is generally believed to be an active transport process, the mechanisms involved in the uptake of drugs from the space of Disse by the parenchymal cell are not clearly understood. While some investigators reported that the uptake is due to physiological binding of drugs to cellular proteins (10), more recent studies suggested an active transport mechanism for drug uptake by the hepatic parenchymal cell (11). Although the nature of the uptake mechanism(s) is currently an unsettled issue, at least one active transport process is involved in the secretion of drugs into the bile.

Irrespective of location, the transport process that is rate limiting should be characterizable. For the purpose of simplifying this discussion, the rate-limiting step is assumed to be the transport of drug from the parenchymal cell into the bile canaliculus; however, no physiological identification of the actual site of transport is implied. One could, with equal justification, assume that the rate-limiting transport step occurs between the space of Disse and the hepatic parenchymal cell.

Since active transport processes are subject to saturation, the rate of transport is expected to be described by a relationship analogous to the equation of Michaelis and Menten:

$$T = \frac{T_{max}[D]}{K_t + [D]} \qquad \text{(Eq. 1)}$$

where T = rate of transport, T_{max} = maximal rate of transport, K_t = transport constant (concentration of drug resulting in a rate of transport equal to one-half of the maximal rate), and $[D]$ = concentration of drug at the site where transport occurs.

This model assumes the formation of a complex, CD, between a transport carrier, C, and the drug, D. This complex is assumed to form in the hepatic parenchymal cell or in the cell membrane, and this complex crosses the membrane to deposit the drug into the bile canaliculus. The carrier then returns to the interior of the cell, where it complexes with more drug (Scheme I).

hepatic parenchymal cell | bile canaliculus

$$D + C \rightleftarrows CD \rightarrow D$$

Scheme I

The rate-limiting step is neither the association nor the dissociation of the complex but the translational event between them (12).

To characterize this transport mechanism adequately, it is necessary to determine both the value of the maximal rate of transport and the value of the transport constant. These values can be determined by measuring the rate of methotrexate transport into the bile as a function of the drug concentration at the transport site. Since this concentration cannot be determined directly, the blood methotrexate concentration is assumed to be representative of, or proportional to, the concentration at the transport site.

Furthermore, the rate at which methotrexate appears in the bile duct may not be equal to the transport rate into the bile if there is a significant lag between the time methotrexate is secreted into the bile and the time it can be detected in the bile duct. The studies reported here were carried out under conditions of steady state, thereby obviating the effect of a lag time. The methotrexate concentrations at the transport site and in the blood also were assumed to be at steady state. Since it is not possible to determine whether the concentration at the actual transport site is different than the blood concentration, the K_t for this system is defined relative to the concentration of drug in the blood.

To determine the values of the transport maximum, T_{max}, and the transport constant, K_t, the data obtained by measuring the rate of biliary secretion of methotrexate as a function of its concentration in the blood can be treated in three ways:

$$\frac{1}{T} = \frac{K_t}{T_{max}[D]} + \frac{1}{T_{max}} \qquad \text{(Eq. 2)}$$

$$T = \frac{-K_t T}{[D]} + T_{max} \qquad \text{(Eq. 3)}$$

$$\frac{[D]}{T} = \frac{K_t}{T_{max}} + \frac{[D]}{T_{max}} \qquad \text{(Eq. 4)}$$

Equations 2–4 are linearized rearrangements of the Michaelis–Menten equation.

Dowd and Riggs (13) analyzed these three linear transformations of the Michaelis–Menten equation and reported that they were not equivalent when used to estimate values of K_t and T_{max}. In Eqs. 2 and 4, the reciprocal of T tends to give unwarranted emphasis to the smallest values of T, and these values are most likely to have the greatest percent error in their measurement. According to Dowd and Riggs (13), the plot using Eq. 2 is by far the least reliable method. Furthermore, the plot using Eq. 4 is superior to the plot using Eq. 3 when the error in T is small; the reverse is true when the error in T is large. The data obtained in this study were analyzed by each of these treatments to facilitate comparison of the values.

Inhibition of active transport is generally classified as being com-

petitive or noncompetitive. In competitive inhibition, the inhibitor forms a reversible complex with the transport carrier and essentially competes with the substrate, in this case methotrexate, for the transport carrier. The actual rate at which a drug or substrate is transported depends on the relative concentrations of both the substrate and the inhibitor. In noncompetitive inhibition, there is no relationship between the degree of inhibition and the substrate concentration. Inhibition depends only on the inhibitor concentration (14).

The two relationships that describe systems subject to competitive and noncompetitive inhibition are:

$$T = \frac{T_{max}[D]}{K_t(1 + [I]/K_i) + [D]} \quad \text{(Eq. 5)}$$

and:

$$T = \frac{T_{max}[D]}{(K_t + [D])(1 + [I]/K_i)} \quad \text{(Eq. 6)}$$

respectively, where $[I]$ = inhibitor concentration, K_i = dissociation constant of the enzyme–inhibitor complex, and the other symbols are as previously described.

In competitive inhibition (Eq. 5), the maximal transport rate is unaffected by the inhibitor, but the apparent transport constant is increased by a factor of $(1 + [I]/K_i)$. The anticipated effect of a noncompetitive inhibitor (Eq. 6) is to decrease the maximal transport rate by a factor equal to the reciprocal of $(1 + [I]/K_i)$.

Probenecid was chosen as a potential inhibitor of the biliary secretion of methotrexate. Probenecid inhibits the active transport of organic acids at several sites in the body. To measure the inhibition of an active transport system, it is usually necessary to determine the transport rate of the substrate at several different concentrations while maintaining the inhibitor concentration at a constant level.

The elimination rate of probenecid, however, is subject to large intersubject variability. This variability makes it impractical to produce the same steady-state plasma probenecid concentration in different experimental animals. This problem was overcome by using methotrexate concentrations that were well below the value of K_t. If the methotrexate concentration, $[D]$, is much less than K_t, then the drug concentration term can be dropped from the denominator of both Eqs. 5 and 6, giving:

$$T = \frac{T_{max}[D]}{K_t(1 + [I]/K_i)} \quad \text{(Eq. 7)}$$

Dividing by $[D]$ and taking the reciprocal of both sides of Eq. 7 give:

$$[D]/T = K_t/T_{max} + [K_t/(T_{max}K_i)][I] \quad \text{(Eq. 8)}$$

The reciprocal of clearance is $[D]/T$. A plot of the reciprocal of the biliary clearance of methotrexate *versus* probenecid concentration theoretically should give a straight line with an intercept on the reciprocal clearance axis of K_t/T_{max} and a slope of $K_t/(T_{max}K_i)$. From this plot, the value of K_i for probenecid as an inhibitor of the biliary transport of methotrexate can be determined.

EXPERIMENTAL

Materials—Tritiated methotrexate[1] was diluted with the nonradioactive drug[2] and purified by the method of Oliverio (15). Probenecid was obtained as a powder[3]. A methotrexate solution for injection was prepared by dissolving a weighed amount of the purified drug in a few drops of 0.1 *M*, pH 8.2 ammonium bicarbonate buffer, and diluting to the desired volume with normal saline. A probenecid solution for injection was prepared similarly. A weighed amount of powder was dissolved in a few drops of 1.0 *N* NaOH, and the pH was then adjusted to 7.4 with a pH 7.0 phosphate buffer. This solution was diluted to the desired volume with normal saline.

All studies were conducted on male Sprague-Dawley rats, 400–500 g.

Analytical Procedures—Liquid scintillation counting techniques were used for the determination of the methotrexate concentration in blood and bile samples. Samples were collected in sacks prepared from sections of dialysis tubing. Nine centimeter lengths of 0.63-cm diameter cellulose dialysis tubing were tied at one end and used for the collection of blood samples; 10-cm lengths of 1.88-cm tubing were used for bile collection. The casings used for blood collection were weighed before and after being filled with approximately 0.5 ml of blood. The exact volume of the blood was determined by dividing the net weight of the blood sample by 1.05, the average specific gravity of rat blood (16).

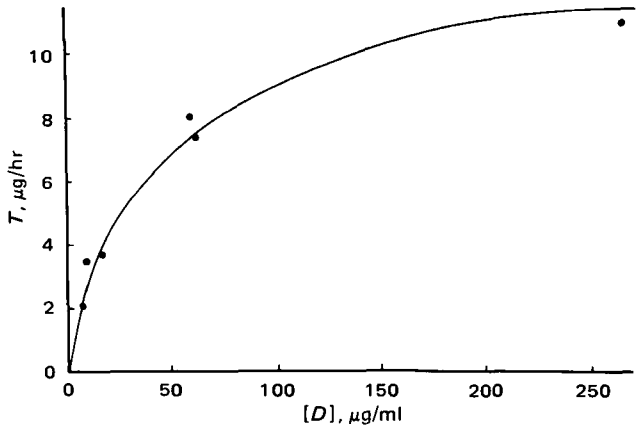

Figure 1—*Plot of the biliary secretion rate,* T, *against the blood concentration of methotrexate,* [D].

The samples were dried prior to being combusted on a sample oxidizer[4] in preparation for scintillation counting. A commercially prepared scintillation cocktail[5] was used.

All samples were counted on a liquid scintillation spectrometer[6]. Quenching was corrected for by means of an automatic internal standard. Since the total radiolabel in blood and bile samples was measured, a few selected samples were chromatographed by a previously reported procedure (17) to determine if a significant fraction of the radiolabel was associated with nonmethotrexate species.

The concentration of probenecid in plasma samples were determined by the spectrophotometric method of Dayton *et al.* (18).

Animal Preparation—To facilitate frequent sampling of blood and bile, the bile duct and the vena cava of each rat were cannulated. A cannula also was inserted into the aorta *via* the left carotid artery, and both methotrexate and probenecid were infused through this site. The carotid and vena cava cannulas were exteriorized through a small subcutaneous incision on the dorsal side of the head, between the ears. This procedure prevented the rat from pulling at or chewing on the cannulas and also permitted the study to be conducted without disturbing the rat each time a blood sample was drawn.

The rats were anesthesized with pentobarbital in preparation for surgery but were allowed to recover following surgery before a study was begun. During the study period, the rats were kept in restraining cages and allowed water *ad libitum*.

Procedures—Two studies were conducted. In one, the rats were infused with methotrexate alone; in the other, the rats were infused with both methotrexate and probenecid. The drugs were infused into the aorta by a constant infusion pump[7] connected to the carotid cannula. When both methotrexate and probenecid were infused, the carotid cannula was connected to two pumps by a four-way stopcock.

At the beginning of each study, loading doses were administered and constant infusions were then maintained for 6–8 hr. Each rat was infused at a different rate to produce a range of blood methotrexate concentrations. Bile was collected over 1-hr intervals, and a blood sample was obtained at the midpoint of each collection period. At 1.5, 4, and 7 hr after initiation of the infusion, plasma samples were obtained from rats receiving probenecid for the purpose of determining the probenecid concentration.

RESULTS AND DISCUSSION

The blood methotrexate concentration in the rats approached a steady state during the infusion period. The values of the blood con-

[1] Amersham/Searle.
[2] Nutritional Biochemicals Corp.
[3] Merck Sharp and Dohme Research Laboratories.
[4] Packard model 305.
[5] Insta Gel, Packard Corp.
[6] Packard Tri-Carb model 3775.
[7] Harvard model 975.

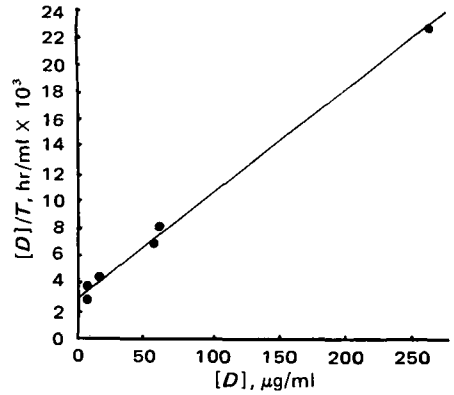

Figure 2—*Plot of the reciprocal of biliary clearance,* ([D]/T), *against the blood concentration of methotrexate,* [D].

centration and biliary excretion rate of methotrexate during the final 3 hr of each study were sufficiently constant to be averaged. In these studies, the total radioactivity in the blood was used to calculate the methotrexate concentration.

In a previous report (17), a fraction of the radioactivity in the blood was associated with nonmethotrexate species following a bolus injection of methotrexate to rats. The fraction of total label representing this nonmethotrexate component increased with time. In this study, however, the fraction of nonmethotrexate radiolabel in both blood and bile was undetectable.

There are two possible explanations for a significant nonmethotrexate fraction of the radiolabel in rat blood following a bolus injection but not when methotrexate is administered by constant infusion. Following a bolus injection, methotrexate is rapidly eliminated from the blood; the nonmethotrexate component, being very slowly removed, becomes the increasingly dominant species present. The nonmethotrexate component after a single bolus gains significance with time due to its retention in the blood. Under conditions in which a constant blood level is maintained, the concentration of the nonmethotrexate component is insignificant in relation to the concentration of the unchanged drug.

Another possible explanation arises from the fact that methotrexate has been shown to be metabolized by the bacteria of the lower intestine (19, 20). The nonmethotrexate species present in the blood could be an absorbed bacterial metabolite. In the current studies, however, the bile ducts of the rats were cannulated, preventing access of the drug to the intestinal lumen for bacterial metabolism. Whatever the actual reason, in these studies total radiolabel measurements adequately reflected levels of unchanged methotrexate.

A plot of the biliary secretion rate, T, of methotrexate as a function of blood concentration, $[D]$, is shown in Fig. 1. The biliary secretion rate approached saturation when blood levels were increased to over 250 μg/ml. The data obtained were treated by each of the three linear transformations of the Michaelis–Menten equation; each point represented the average of three sampling times from each individual rat study. The data were fit to each of the three equations using a nonweighted least-squares fitting program.

The plot resulting from Eq. 4 is shown in Fig. 2. A summary of the values obtained for the transport constant and the maximal transport rate is given in Table I, along with the correlation coefficient for each plot. The averages of the values obtained for K_i and T_{max} from the two "more reliable" plots (Eqs. 3 and 4) are 32 mg/liter or 7×10^{-5} M and 12 mg/hr, respectively. These values are surprisingly close to those obtained from the reportedly "less reliable" plot of Eq. 2.

The value of the biliary clearance for blood methotrexate concentrations, which are well below the value of the transport constant, is obtained by dividing T_{max} by K_t. When using the average values for T_{max} and K_t, respectively, a value for biliary clearance of 6.33 ml/min is obtained. A value of 3 ml/min was reported previously (3), but the average size of the rats used in that study was 200 g. In this study, the average weight was 420 g. If these values are normalized for body weight, they are in good agreement: 15 ml/min/kg from Ref. 3 and 15.1 ml/min/kg from this study.

Table I—Values of T_{max} and K_t for the Biliary Secretion of Methotrexate

Parameter	Equation 2, $1/T$ *versus* $1/[D]$	Equation 3, $[D]/T$ *versus* $[D]$	Equation 4, T *versus* $T/[D]$
K_t, mg/ml	0.0325	0.0376	0.0254
T_{max}, mg/hr	12.09	12.97	10.96
Correlation coefficient	0.940	0.997	0.858

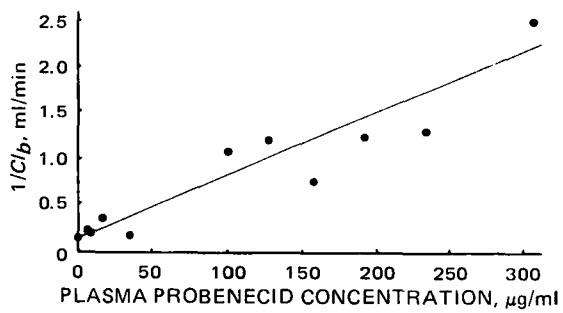

Figure 3—*Plot of the reciprocal of biliary clearance of methotrexate* Cl_b, *as a function of the plasma probenecid concentration.*

The efficiency of removal of methotrexate from the blood by the liver can be evaluated by relating the biliary clearance of methotrexate to the liver blood flow. In the adult rat, the blood flow to the liver is reported to be 79 ml/min/100 g of tissue, and the weight of the liver is reported to represent 3.35% of the total body weight (21). From these parameters, a value of 26.5 ml/min/kg can be calculated for the blood flow to the liver. The value of the biliary clearance of methotrexate divided by the liver blood flow gives an extraction ratio of 0.53. Therefore, the efficiency of removal of methotrexate from the blood by the liver is 53%. At high blood methotrexate concentrations, where saturation of the biliary secretion mechanism is approached, the extraction efficiency decreases.

The effect of probenecid on the biliary secretion of methotrexate was significant. Figure 3 is a plot of the reciprocal of the biliary clearance of methotrexate as a function of the plasma concentration of probenecid. With the exception of the point on the reciprocal clearance axis, each point represents the average of steady-state data obtained from individual rats. The value for the reciprocal of clearance when the probenecid concentration was zero is the average of four different studies. This value was weighted (times four) for purposes of fitting the data with a least-squares program.

As discussed previously, to utilize this simplified treatment of the data, the blood concentration of methotrexate in all rats was maintained at a level (<1 μg/ml) substantially lower than the value of K_t (30 μg/ml). The value of K_i obtained from this plot was 22.7 μg/ml or 8.1×10^{-5} M. The data were fit to Eq. 8 using a least-squares fitting program. The correlation coefficient was 0.95.

Qualitatively, it can be seen from Fig. 3 that the biliary secretion of methotrexate is sensitive to inhibition by probenecid. A plasma probenecid concentration of 50 μg/ml reduced the biliary clearance of methotrexate to about 4.4 ml/min/kg. This rate represents a significant reduction in the efficiency of the biliary extraction of methotrexate from the blood. At this low plasma probenecid concentration, the extraction efficiency was 17% or a reduction of 70%.

The value of the Y-intercept in Fig. 3 is equal to the reciprocal of biliary clearance in the absence of an inhibitor and should be equal to K_t/T_{max}. When using the values of 12 mg/hr and 32 mg/liter for T_{max} and K_t, respectively, a value for K_t/T_{max} of 0.158 min/ml was calculated. The actual intercept was 0.14 min/ml, in close agreement with the calculated value.

CONCLUSIONS

The biliary secretion of methotrexate in the rat is mediated by an active transport process which can be characterized by Michaelis–Menten kinetics, and this process is inhibited by the coadministration of probenecid. Whether accumulation of methotrexate in the intestinal lumen due to biliary secretion is a contributing factor to GI toxicity of methotrexate and whether the inhibition of this secretory process can be utilized to design a safer therapeutic dosage regimen remain to be determined.

REFERENCES

(1) P. T. Condit, *Ann. N.Y. Acad. Sci.*, **186**, 475(1971).

(2) E. Frei, N. Jaffe, M. H. N. Tattersall, S. Pitman, and L. Parker, *N. Engl. J. Med.*, **292**, 846(1975).

(3) K. B. Bischoff, R. L. Dedrick, D. S. Zaharko, and J. A. Longstreth, *J. Pharm. Sci.*, **60**, 1129(1971).

(4) R. L. Dedrick, D. S. Zaharko, and R. J. Lutz, *ibid.*, **62**, 882(1973).

(5) J. A. Straw, M. M. Hart, P. Klukes, D. S. Zaharko, and R. L. Dedrick, *J. Nat. Cancer Inst.*, **52**, 1327(1974).

(6) E. S. Henderson, R. H. Adamson, and V. T. Oliverio, *Cancer Res.*, **25**, 1018(1965).

(7) R. T. Williams, P. Millburn, and R. L. Smith, *Ann. N.Y. Acad. Sci.*, **123**, 110(1965).

(8) C. T. Ashworth and E. Sanders, *Am. J. Pathol.*, **37**, 343(1960).

(9) L. S. Schanker, in "Handbook of Physiology, Alimentary Canal," American Physiology Society, Washington, D.C., 1968, p. 2433.

(10) A. J. Levi, Z. Gatmanton, and I. M. Arias, *J. Clin. Invest.*, **48**, 2156(1969).

(11) S. Kenwright and A. J. Levi, *Lancet*, **2**, 1401(1973).

(12) H. N. Christensen, "Biological Transport," Benjamin, New York, N.Y., 1962.

(13) J. E. Dowd and D. S. Riggs, *J. Biol. Chem.*, **240**, 863(1965).

(14) A. White, P. Handler, and E. L. Smith, "Principles of Biochemistry," 3rd ed., McGraw-Hill, New York, N.Y., 1964.

(15) V. T. Oliverio, *Anal. Chem.*, **33**, 263(1961).

(16) W. S. Spector, "Handbook of Biological Data," Saunders, Philadelphia, Pa., 1964, p. 51.

(17) R. E. Kates and T. N. Tozer, *J. Pharm. Sci.*, **62**, 2056 (1973).

(18) P. G. Dayton, T. F. Yu, W. Chen, L. Berger, L. A. West, and A. B. Gutman, *J. Pharmacol. Exp. Ther.*, **140**, 278(1963).

(19) D. S. Zaharko, H. Burckner, and V. T. Oliverio, *Science*, **166**, 887(1969).

(20) D. M. Valerinio, D. G. Johns, D. S. Zaharko, and V. T. Oliverio, *Biochem. Pharmacol.*, **21**, 821(1972).

(21) W. S. Spector, "Handbook of Biological Data," Saunders, Philadelphia, Pa., 1964, p. 283.

ACKNOWLEDGMENTS AND ADDRESSES

Received September 12, 1975, from the *School of Pharmacy, University of California Medical Center, San Francisco, CA 94143*

Accepted for publication November 21, 1975.

Supported in part by Public Health Service Training Grant GM-00728-13.

[x] To whom inquiries should be directed. Present address: College of Pharmacy, Ohio State University, Columbus, OH 43210

GLC Determination of Nylidrin in Human Urine Samples

HERSCHEL LI and PETER CERVONI [x]

Abstract □ A method for the detection of nanogram quantities of nylidrin in human urine is described. The method involves β-glucuronidase hydrolysis, extraction with chloroform, derivatization by silylation, and GLC determination. The suitability of the method was tested by analysis of urine samples of subjects after oral ingestion of nylidrin hydrochloride.

Keyphrases □ Nylidrin—GLC analysis, urine □ GLC—analysis, nylidrin in urine □ Vasodilators, peripheral—nylidrin, GLC analysis in urine

Nylidrin hydrochloride[1], 1-(*p*-hydroxyphenyl)-2-(1′-methyl-3′-phenylpropylamino)-1-propanol hydrochloride, is a sympathomimetic agent that acts predominantly by β-adrenergic receptor stimulation (1–3). It is a vasodilator used in the treatment of some peripheral vascular disorders (4, 5). The recommended human oral dose of nylidrin hydrochloride is 3–12 mg three or four times a day.

Two colorimetric analytical methods for measurement of nylidrin have been reported (6, 7), but they do not provide specificity or sufficient sensitivity for the determination of nylidrin in biological fluids.

Walle and Ehrsson (8, 9) developed a GC procedure for various alcoholic and amino compounds, using heptafluorobutyric anhydride and trimethylamine to prepare suitable derivatives for electron-capture detection. However, application of their method in this laboratory for the derivatization of nylidrin was only partially successful, since two peaks were observed in the chromatogram. Mass spectral analysis revealed that the major peak was the triheptafluorobutyryl derivative and the minor peak was the diheptafluorobutyryl derivative of nylidrin. Whether the diheptafluorobutyryl derivative was due to incomplete reaction of nylidrin with heptafluorobutyric anhydride as a result of steric hindrance at the secondary amino group of nylidrin or due to reverse hydrolysis of the triheptafluorobutyryl derivative is not clear at this time. An alternative approach was taken to provide a suitable method of determining urinary nylidrin in human subjects.

Preliminary studies performed on dogs in this laboratory showed that nylidrin is excreted in the urine as the free base and its glucuronide. The present method was designed to measure the total amount of nylidrin in urine after the urine was subjected to β-glucuronidase hydrolysis.

EXPERIMENTAL

Reagents—An aqueous standard stock solution was prepared by dissolving 5.00 mg of nylidrin hydrochloride[2] (equivalent to 89%

[1] Nylidrin hydrochloride is marketed by the USV Pharmaceutical Corp. under the trade name of Arlidin as 6- and 12-mg tablets. Subjects in this study received the 6-mg tablet orally.

[2] Nylidrin hydrochloride and nylidrin base were prepared in the Organic Chemistry Laboratories, USV Pharmaceutical Corp., Tuckahoe, NY 10707

REFERENCES

(1) P. T. Condit, *Ann. N.Y. Acad. Sci.*, **186**, 475(1971).

(2) E. Frei, N. Jaffe, M. H. N. Tattersall, S. Pitman, and L. Parker, *N. Engl. J. Med.*, **292**, 846(1975).

(3) K. B. Bischoff, R. L. Dedrick, D. S. Zaharko, and J. A. Longstreth, *J. Pharm. Sci.*, **60**, 1129(1971).

(4) R. L. Dedrick, D. S. Zaharko, and R. J. Lutz, *ibid.*, **62**, 882(1973).

(5) J. A. Straw, M. M. Hart, P. Klukes, D. S. Zaharko, and R. L. Dedrick, *J. Nat. Cancer Inst.*, **52**, 1327(1974).

(6) E. S. Henderson, R. H. Adamson, and V. T. Oliverio, *Cancer Res.*, **25**, 1018(1965).

(7) R. T. Williams, P. Millburn, and R. L. Smith, *Ann. N.Y. Acad. Sci.*, **123**, 110(1965).

(8) C. T. Ashworth and E. Sanders, *Am. J. Pathol.*, **37**, 343(1960).

(9) L. S. Schanker, in "Handbook of Physiology, Alimentary Canal," American Physiology Society, Washington, D.C., 1968, p. 2433.

(10) A. J. Levi, Z. Gatmanton, and I. M. Arias, *J. Clin. Invest.*, **48**, 2156(1969).

(11) S. Kenwright and A. J. Levi, *Lancet*, **2**, 1401(1973).

(12) H. N. Christensen, "Biological Transport," Benjamin, New York, N.Y., 1962.

(13) J. E. Dowd and D. S. Riggs, *J. Biol. Chem.*, **240**, 863(1965).

(14) A. White, P. Handler, and E. L. Smith, "Principles of Biochemistry," 3rd ed., McGraw-Hill, New York, N.Y., 1964.

(15) V. T. Oliverio, *Anal. Chem.*, **33**, 263(1961).

(16) W. S. Spector, "Handbook of Biological Data," Saunders, Philadelphia, Pa., 1964, p. 51.

(17) R. E. Kates and T. N. Tozer, *J. Pharm. Sci.*, **62**, 2056 (1973).

(18) P. G. Dayton, T. F. Yu, W. Chen, L. Berger, L. A. West, and A. B. Gutman, *J. Pharmacol. Exp. Ther.*, **140**, 278(1963).

(19) D. S. Zaharko, H. Burckner, and V. T. Oliverio, *Science*, **166**, 887(1969).

(20) D. M. Valerinio, D. G. Johns, D. S. Zaharko, and V. T. Oliverio, *Biochem. Pharmacol.*, **21**, 821(1972).

(21) W. S. Spector, "Handbook of Biological Data," Saunders, Philadelphia, Pa., 1964, p. 283.

ACKNOWLEDGMENTS AND ADDRESSES

Received September 12, 1975, from the *School of Pharmacy, University of California Medical Center, San Francisco, CA 94143*

Accepted for publication November 21, 1975.

Supported in part by Public Health Service Training Grant GM-00728-13.

[x] To whom inquiries should be directed. Present address: College of Pharmacy, Ohio State University, Columbus, OH 43210

GLC Determination of Nylidrin in Human Urine Samples

HERSCHEL LI and PETER CERVONI [x]

Abstract □ A method for the detection of nanogram quantities of nylidrin in human urine is described. The method involves β-glucuronidase hydrolysis, extraction with chloroform, derivatization by silylation, and GLC determination. The suitability of the method was tested by analysis of urine samples of subjects after oral ingestion of nylidrin hydrochloride.

Keyphrases □ Nylidrin—GLC analysis, urine □ GLC—analysis, nylidrin in urine □ Vasodilators, peripheral—nylidrin, GLC analysis in urine

Nylidrin hydrochloride[1], 1-(*p*-hydroxyphenyl)-2-(1′-methyl-3′-phenylpropylamino)-1-propanol hydrochloride, is a sympathomimetic agent that acts predominantly by β-adrenergic receptor stimulation (1–3). It is a vasodilator used in the treatment of some peripheral vascular disorders (4, 5). The recommended human oral dose of nylidrin hydrochloride is 3–12 mg three or four times a day.

Two colorimetric analytical methods for measurement of nylidrin have been reported (6, 7), but they do not provide specificity or sufficient sensitivity for the determination of nylidrin in biological fluids.

Walle and Ehrsson (8, 9) developed a GC procedure for various alcoholic and amino compounds, using heptafluorobutyric anhydride and trimethylamine to prepare suitable derivatives for electron-capture detection. However, application of their method in this laboratory for the derivatization of nylidrin was only partially successful, since two peaks were observed in the chromatogram. Mass spectral analysis revealed that the major peak was the triheptafluorobutyryl derivative and the minor peak was the diheptafluorobutyryl derivative of nylidrin. Whether the diheptafluorobutyryl derivative was due to incomplete reaction of nylidrin with heptafluorobutyric anhydride as a result of steric hindrance at the secondary amino group of nylidrin or due to reverse hydrolysis of the triheptafluorobutyryl derivative is not clear at this time. An alternative approach was taken to provide a suitable method of determining urinary nylidrin in human subjects.

Preliminary studies performed on dogs in this laboratory showed that nylidrin is excreted in the urine as the free base and its glucuronide. The present method was designed to measure the total amount of nylidrin in urine after the urine was subjected to β-glucuronidase hydrolysis.

EXPERIMENTAL

Reagents—An aqueous standard stock solution was prepared by dissolving 5.00 mg of nylidrin hydrochloride[2] (equivalent to 89%

[1] Nylidrin hydrochloride is marketed by the USV Pharmaceutical Corp. under the trade name of Arlidin as 6- and 12-mg tablets. Subjects in this study received the 6-mg tablet orally.

[2] Nylidrin hydrochloride and nylidrin base were prepared in the Organic Chemistry Laboratories, USV Pharmaceutical Corp., Tuckahoe, NY 10707

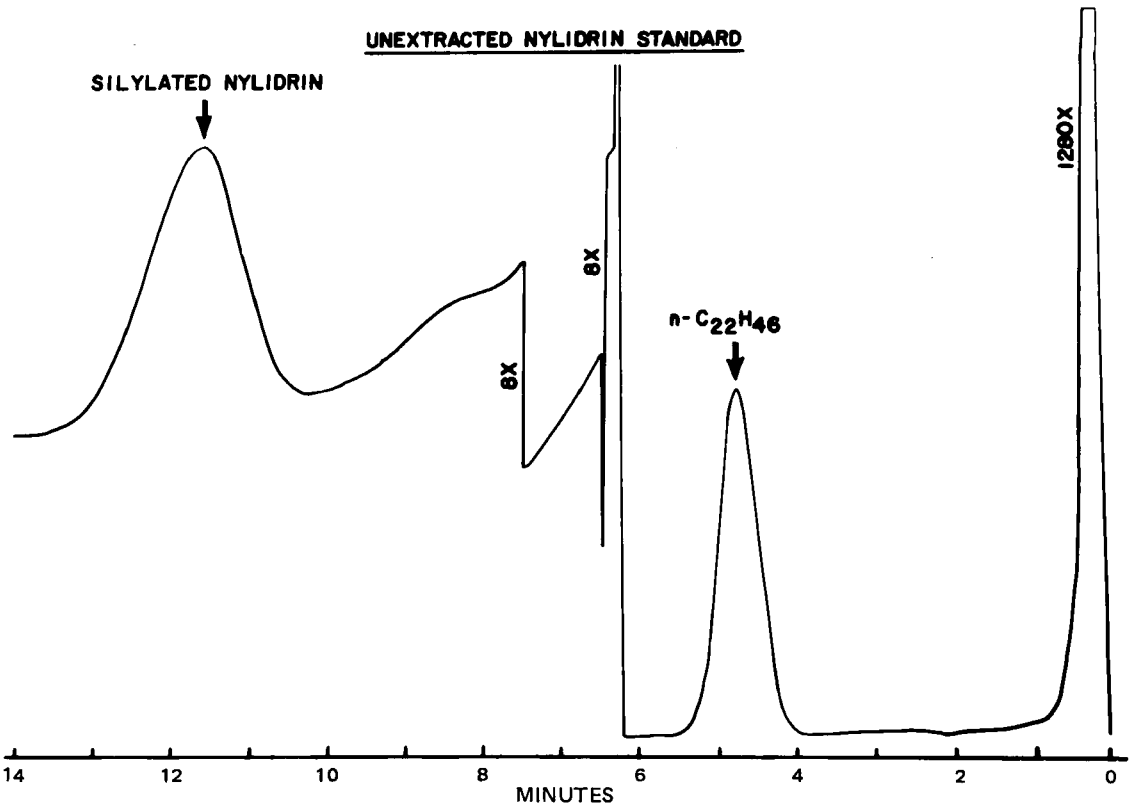

Figure 1—*Gas chromatogram of unextracted nylidrin standard after silylation* (*see* Experimental).

nylidrin free base moiety) in 1000 ml of distilled water. This solution was used in the preparation of a standard curve for nylidrin in urine from which nylidrin in the unknown urine samples was calculated.

Another standard stock solution containing 55.7 ng/μl was prepared by dissolving nylidrin as the free base[2] in spectral grade chloroform[3]. This solution was used in recovery experiments and for establishing the reference retention time for GLC analysis. A 0.2% solution of normal docosane[4] in spectral grade chloroform was used as the internal standard.

Urine Sample Collections—Normal male subjects were fasted overnight, and urine voided and collected just before oral administration of nylidrin hydrochloride tablets[1] served as the 0-hr control urine samples. Thereafter, the urine was voided *ad libitum* and the total volume was collected and stored in a freezer. Sample collection continued for as long as 30 hr after ingestion of nylidrin hydrochloride tablets.

β-Glucuronidase Hydrolysis—After adjustment of the urine to pH 5 with acetic acid[3], the volume was measured. A 5.0-ml aliquot was then pipetted into a 100-ml glass-stoppered bottle, and 5 ml of 0.1 *M* acetate buffer solution (pH 5.0) containing 5000 units of β-glucuronidase[5] was added. The samples were then kept in a Dubnoff metabolic shaking incubator[6] at 37° for 18 hr in the presence of air.

The hydrolyzed urine mixture was saturated with sodium carbonate and extracted three times with 25 ml of spectral grade chloroform. The chloroform extracts were pooled and dried over anhydrous sodium sulfate and condensed to a small volume. The drug was then back-extracted two times with 2.5 ml of 0.1 *N* HCl.

A 4.0-ml aliquot of the pooled acid extract was transferred to a glass-stoppered conical tube, and the acid was evaporated to dryness in a freeze-drying unit[7]. The side of the tube was washed with a small volume of methanol, and the methanol solution was evaporated to complete dryness under a stream of dry nitrogen for derivatization.

Preparation of Derivative—The trimethylsilyl derivative of nylidrin was prepared by adding 30 μl of bis(trimethylsilyl)trifluoroacetamide[8] and 20 μl of a 0.2% chloroform solution of docosane into conical tubes containing the dried acid extracts. The reactants were then thoroughly mixed using a vortex agitator. Silylation was carried out in an oil bath at 55–60° for 1 hr. Five microliters of the reaction mixture was injected directly into the chromatograph for analysis.

GLC—GLC separations were performed on a gas chromatograph[9] equipped with a flame-ionization detector. The 1.8-m × 0.63-cm (6-ft × 0.25-in.) o.d. glass column was packed with 0.2% OV-1 on 80–100-mesh Corning GLC-110 dimethylchlorosilane-treated glass beads[4]. The chromatographic conditions used were: injector and manifold temperature, 230°; column temperature, initially 170° and programmed at the rate of 0.5°/min; helium flow rate, 50 ml/min; hydrogen pressure, 27 psi; and air pressure, 30 psi. The recorder chart speed was 152.4 cm (60 in.)/hr.

RESULTS AND DISCUSSION

Derivatization—The derivative of nylidrin, when chromatographed under various column temperature conditions both with isothermal and temperature-programmed modes, showed only one derivative peak as compared to the reagent blank sample. The reaction was rapid and complete. Comparison of relative areas using a constant amount of nylidrin and internal standard at reaction times of 5, 20, 30, 45, 60, 90, and 120 min showed no further increase after 30 min.

The derivative was stable at room temperature in a tightly sealed reaction tube. However, upon exposure to moisture, reversible hydrolysis of the trimethylsilyl groups apparently took place. The following observation supports this postulate. If a reaction tube is opened for sampling on the 1st day and the same sample is reinjected into the chromatograph on a subsequent day, an occasional decrease in the relative peak area is observed. This loss in peak area can be restored upon resilylation with a fresh portion of bis(trimethylsilyl)trifluoroacetamide[8].

To assure a quantitative yield in derivative preparation and to prevent hydrolysis of the derivative, the following measures were

[3] Mallinckrodt Chemical Works, St. Louis, Mo.
[4] Applied Science Laboratories, State College, Pa.
[5] Sigma Chemical Co., St. Louis, Mo.
[6] Precision Scientific Co., Chicago, Ill.
[7] Thermovac model FDC-2-MH-CT-Mod., Thermovac Industries Corp., Copiague, N.Y.
[8] Regisil, Regis Chemical Co., Chicago, Ill.
[9] Model 900, Perkin-Elmer Corp., Norwalk, Conn.

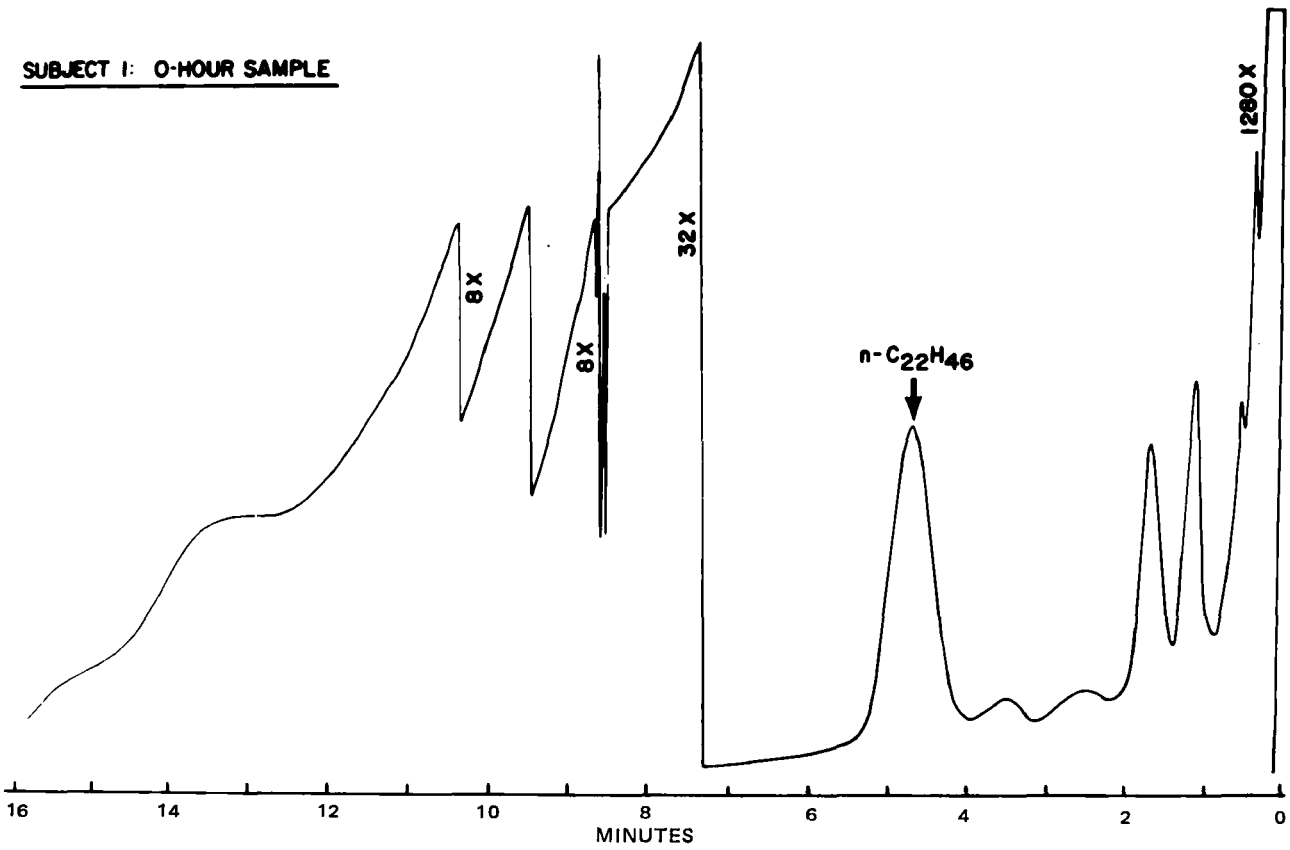

Figure 2—*Gas chromatogram obtained from the extract of a 5-ml 0-hr urine sample of Subject 1 after silylation.*

employed: (*a*) excess reaction time; (*b*) excess silylating reagent, which increases the protective capacity against moisture; (*c*) analysis of samples on the same day as the samples are derivatized; and (*d*) running of all samples in duplicate.

GLC–Mass Spectrometry—The derivative of nylidrin employed in this method was subsequently studied by GLC–mass spectrometry[10]. The electron-impact mass spectrum showed a strong peak at *m/e* 176. The molecular ion peak was not observed. However, the chemical ionization mass spectrum, using isobutane as the reactant gas, showed a strong quasimolecular ion at *m/e* 444 and a base peak at *m/e* 176.

The peak at *m/e* 444 was postulated to be the M + 1 ion of di(trimethylsilyl)nylidrin, the molecular weight of which is 443. The peak at *m/e* 176 probably was obtained after the cleavage between the α- and β-carbons. This result indicates that silylation took place at the phenolic and β-hydroxyl groups and that the sterically hindered nitrogen was not derivatized.

Chromatography—Under the described chromatographic conditions, the retention times of trimethylsilylnylidrin and docosane were approximately 11.7 and 4.7 min, respectively. The relative retention time of trimethylsilylnylidrin was 2.46–2.49.

Figure 1 shows the chromatogram obtained from a standard solution of nylidrin in chloroform. Figure 2 represents the chromatogram from an extract of a 5.0-ml 0-hr urine sample of Subject 1. No interfering peaks were observed in the region of the trimethylsilylnylidrin peak. Figure 3 shows the chromatogram obtained from the extract of a 5.0-ml 0-hr urine sample from Subject 1 with 1 μg of nylidrin hydrochloride standard added. The trimethylsilylnylidrin peak appears in the same region as the trimethylsilylnylidrin peak for the unextracted nylidrin standard shown in Fig. 1.

Standard Curve and Sensitivity—The areas of the trimethylsilylnylidrin and docosane peaks were measured by the method of triangulation. The relative area was determined by the ratio of the area of the trimethylsilylnylidrin peak to that of the docosane peak.

A standard curve was prepared for each experiment by adding aqueous stock solutions of nylidrin hydrochloride to 5.0 ml of the 0-hr urines, and these samples were carried through the same procedure as the unknown urine samples. Both the urine standards and unknown urine samples were extracted and derivatized by the same procedure and injected into the chromatograph under the same conditions.

The standard curve was obtained by plotting the relative area of the trimethylsilylnylidrin peaks against the nylidrin concentration, expressed as the free base equivalent. The slope and intercept of the standard curve were determined by the method of least squares. The total urinary nylidrin excreted during each time interval was calculated:

$$\text{total urinary nylidrin} = \text{ng/injection} \times \frac{\text{adjusted total urine volume (ml)}}{\text{5-ml aliquot}} \times \text{dilution factor} \quad \text{(Eq. 1)}$$

To examine the variabilities in the eight experiments when the unknown samples were being assayed, the values for the relative areas obtained from the same nylidrin concentrations used in determining the urine standard curves in these experiments were grouped together as replicates. These values were then applied to regression analysis. The equation for the regression line thus obtained was (n = 49, r = 0.82):

$$Y = -0.00354 + 0.00013X \quad \text{(Eq. 2)}$$

when $Y = 0$, and $X_0 = 68$ ng/ml of urine. The X intercept is interpreted as the average lower limit of detection of urinary nylidrin in

Table I—Recovery of Nylidrin from Urine[a]

Nylidrin in Urine, ng/ml		
Theoretical	Experimental	Recovery, %
178	106.75 ± 14.25	60 ± 8
356	206.75 ± 8.75	58 ± 2
534	358.0 ± 24.0	67 ± 4
712	477.75 ± 44.0	67 ± 6
890	639.0 ± 9.5	72 ± 1
1068	850.0 ± 27.0	80 ± 2

[a] Mean of three runs ± *SE* of the mean.

[10] Dupont 491 gas chromatograph–mass spectrometer, Dupont Instruments, Wilmington, Del.

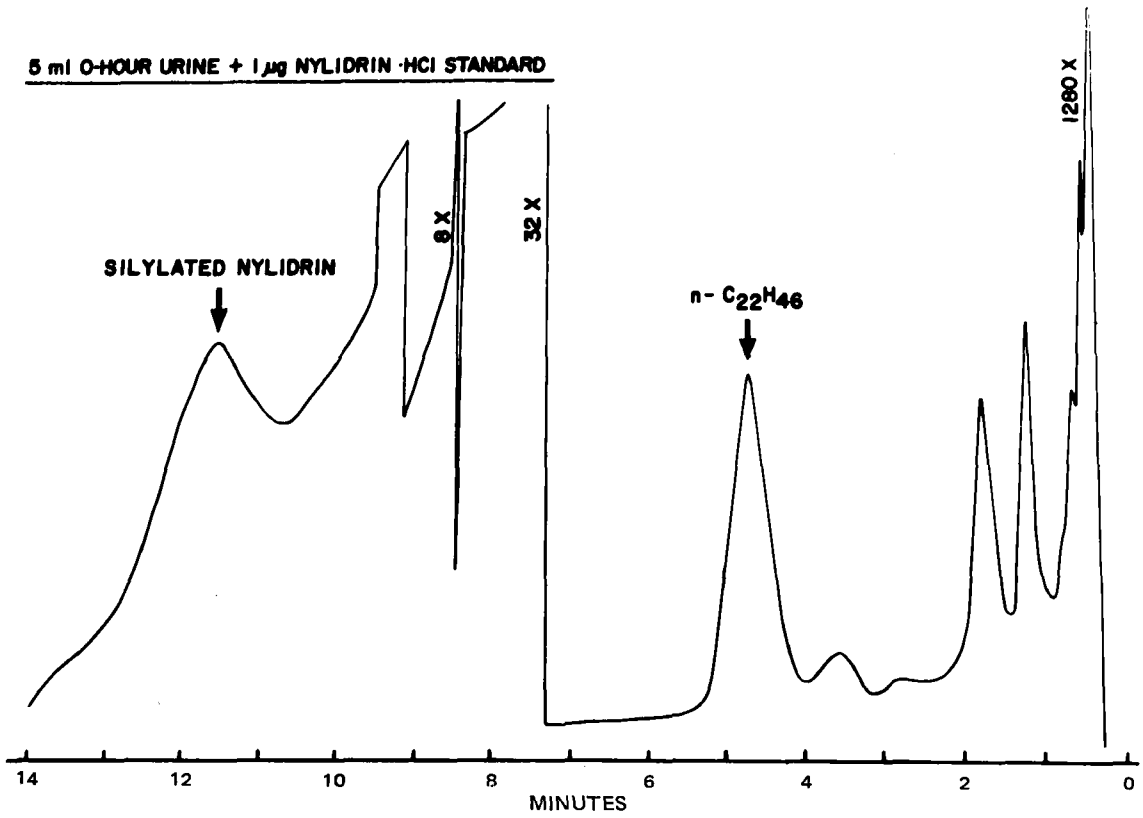

Figure 3—*Gas chromatogram obtained from the silylated extract of a 5-ml 0-hr urine sample of Subject 1 with 1 μg of nylidrin hydrochloride standard added.*

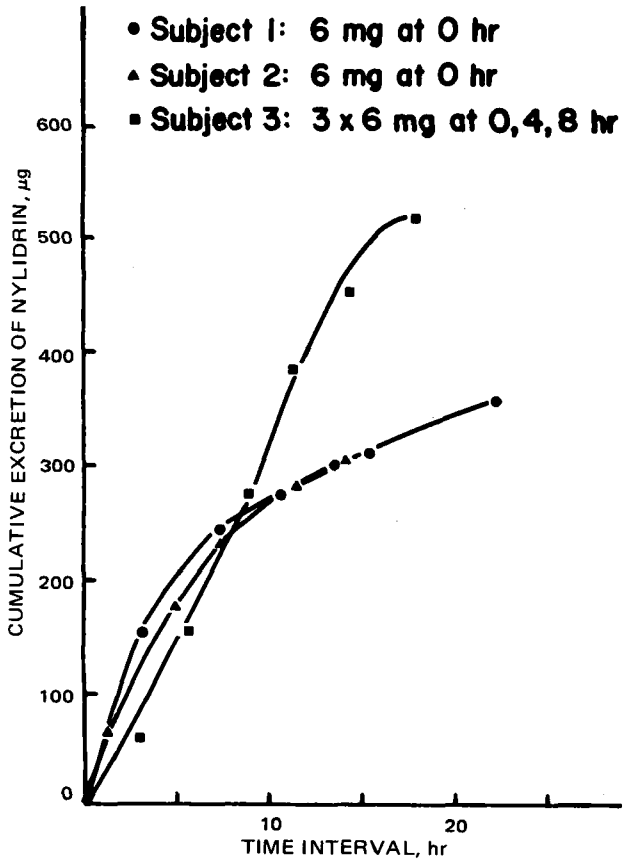

Figure 4—*Cumulative urinary excretion curves of nylidrin in three subjects after different oral dosage regimens of nylidrin hydrochloride tablets* (see Results and Discussion).

eight experiments.

Extraction Efficiency—To assure that nylidrin was adequately extracted from urine, a recovery experiment was conducted. The amount of nylidrin recovered from the urine after β-glucuronidase treatment was calculated on the basis of the values obtained from the unextracted standard samples.

Table I shows the recovery with different nylidrin concentrations. It is apparent that greater loss (lower recovery) was experienced in urine samples with low nylidrin concentrations. Therefore, unknown urine samples were calculated from the urine standard curve and not the unextracted standard curve to account for the differences in the extraction efficiency over the range of concentrations studied.

Application—The described assay method was applied to the analysis of urine samples of human subjects who received different oral dosage regimens of nylidrin hydrochloride tablets. Subjects 1 and 2 received one 6-mg tablet at 0 hr; Subject 3 received one 6-mg tablet at 0, 4, and 8 hr. Figure 4 shows the nylidrin cumulative excretion patterns in these subjects. The nylidrin excretion curves for Subjects 1 and 2 were identical. Excretion was rapid up to 8 hr and slowed thereafter throughout the remainder of the study. The excretion curve for Subject 3 was almost linear throughout the entire study.

Summary—The described GLC method, using flame-ionization detection, is capable of determining nylidrin in urine of human subjects given a single therapeutic dose. As reported for two subjects, varying oral doses of nylidrin hydrochloride tablets can be shown to result in a varied excretion pattern (Fig. 4). This method will be used in studies concerning the pharmacodynamic aspects of nylidrin.

REFERENCES

(1) B. Levy, *J. Pharmacol. Exp. Ther.*, **127**, 150(1959).

(2) E. J. Ariens, M. J. G. A. Waelen, P. F. Sonneville, and A. J. Simonis, *Arzneim.-Forsch.*, **13**, 541(1963).

(3) S. J. Manley and J. W. Lawson, *Arch. Int. Pharmacodyn. Ther.*, **175**, 239(1968).

(4) F. S. Caliva, R. Eich, H. L. Taylor, and R. H. Lyons, *Am. J. Med. Sci.*, **238**, 175(1959).

(5) E. D. Frohlich and H. W. Schraper, *Clin. Pharmacol. Ther.*, **5**, 569(1964).

(6) Internal communication, Troponwerke Köln, Biochem. Bericht.

No. 32, *Biochem. Forsch.* (Dec. 1968).
(7) J. H. Weikel, Jr., A. G. Wheeler, and P. D. Joiner, *Toxicol. Appl. Pharmacol.*, 1, 579(1959).
(8) T. Walle and H. Ehrsson, *Acta Pharm. Suec.*, 7, 389(1970).
(9) *Ibid.*, 8, 27(1971).

ACKNOWLEDGMENTS AND ADDRESSES

Received June 23, 1975, from the *Biological Research and Development Laboratories, USV Pharmaceutical Corporation, Tuckahoe, NY 10707*

Accepted for publication December 1, 1975.

The authors thank Dr. Newton Birkhead, Medical Department, USV Pharmaceutical Corp., for monitoring the human oral dosing study and Dr. Micheal O'Hare for carrying out the GLC–mass spectrometry analysis.

[x] To whom inquiries should be directed.

Assay of Sulfonylureas in Human Plasma by High-Performance Liquid Chromatography

S. SVED [x], I. J. McGILVERAY, and NICOLE BEAUDOIN

Abstract □ A sensitive and specific high-performance liquid chromatographic procedure for the determination of chlorpropamide or tolbutamide in plasma in the presence of their metabolites is described. The ether extract of acidified plasma is redissolved in the mobile phase, 17% acetonitrile in 0.05 *M* aqueous ammonium formate, and chromatographed on a reverse-phase column on a high-performance liquid chromatograph fitted with a UV absorbance detector. Quantitation of plasma samples containing less than 0.5 μg/ml of chlorpropamide and 5 μg/ml of tolbutamide is reported, using these drugs as mutual internal standards. The retention times of the metabolites are such that they do not interfere in the procedure. The assay method was tested in a human volunteer with both drugs and found suitable for single-dose pharmacokinetic studies.

Keyphrases □ Chlorpropamide—high-performance liquid chromatographic analysis in presence of metabolites, plasma □ Tolbutamide—high-performance liquid chromatographic analysis in presence of metabolites, plasma □ High-performance liquid chromatography—analysis, chlorpropamide or tolbutamide in presence of metabolites, plasma □ Sulfonylureas—chlorpropamide or tolbutamide, high-performance liquid chromatographic analyses in presence of metabolites, plasma □ Antidiabetic agents—chlorpropamide and tolbutamide, high-performance liquid chromatographic analysis in presence of metabolites, plasma

The two oral hypoglycemic drugs tolbutamide and chlorpropamide are widely used in the management of certain types of maturity-onset diabetes. Specific assay methods capable of measuring the unchanged drugs in plasma are desirable for monitoring clinical blood levels and for studies in pharmacokinetics (1) and drug interactions (2).

Early methods of estimation, based on UV absorbance, were neither specific nor sensitive. More recently, colorimetric procedures were introduced based on the method of Spingler (3) and modified (4, 5). They depend on the reaction of chlorpropamide or tolbutamide with 2,4-dinitrofluorobenzene, followed by measurement of the absorbance of the resultant *N*-propyl- or *N*-butyldinitroaniline at the appropriate wavelength. The sensitivity of these methods is limited, however, by the high and variable blanks from endogenous substances in the plasma. Furthermore, positive color is also obtained with some metabolites of the drugs. Attempts have been made to separate the metabolites by differential extraction prior to spectrophotometry (6, 7), but these methods are lengthy and the separation is incomplete[1].

A number of GC procedures were reported recently, involving methylation of the drugs with dimethyl sulfate (8) or diazomethane (9) or after reaction with 2,4-dinitrofluorobenzene (10). Most of these methods, however, suffer from the inability to distinguish between the parent drug and its metabolites (11), although this problem may have been overcome (12).

A TLC method employing a UV densitometer was described recently for the assay of chlorpropamide in serum (13).

High-performance liquid chromatography (HPLC) apparently has not been used for determining chlorpropamide and tolbutamide levels in the human plasma. Beyer (14) used a reverse-phase system for the determination of these drugs in pharmaceutical preparations, while Molins *et al.* (15) used an improved extraction method with a forward-phase HPLC system for the same purpose.

This work describes the use of a fast extraction procedure and reverse-phase HPLC for the estimation of chlorpropamide and tolbutamide in plasma at sufficiently high sensitivity and specificity to be used for single-dose bioavailability studies.

EXPERIMENTAL

Materials—Chlorpropamide[2], 2-hydroxychlorpropamide[2], 3-hydroxychlorpropamide[2], carboxytolbutamide[3], 4-hydroxytolbutamide[3], *p*-toluenesulfonamide[4], *p*-toluenesulfonylurea[4], *p*-chlorobenzenesulfonylurea[4], *p*-chlorobenzenesulfonamide[5], and tolbutamide[6] were used without further purification. Ether, anhydrous[7], was freshly redistilled before use. Acetonitrile[8] (UV grade)

[1] K. K. Midha and C. Charette of these Laboratories, personal communication.
[2] Supplied by Pfizer, Montreal, Quebec, Canada.
[3] Gift of Dr. J. Thiessen, University of Toronto, Toronto, Ontario, Canada.
[4] Synthesized in this laboratory.
[5] Baker, supplied by Canlab, Ottawa, Ontario, Canada.
[6] Strong-Cobb-Arner of Canada, Fort Erie, Ontario, Canada.
[7] Mallinckrodt Canada Ltd., Montreal, Quebec, Canada.
[8] Burdick & Jackson Laboratories Inc., Muskegon, Mich.

No. 32, *Biochem. Forsch.* (Dec. 1968).
(7) J. H. Weikel, Jr., A. G. Wheeler, and P. D. Joiner, *Toxicol. Appl. Pharmacol.*, 1, 579(1959).
(8) T. Walle and H. Ehrsson, *Acta Pharm. Suec.*, 7, 389(1970).
(9) *Ibid.*, 8, 27(1971).

ACKNOWLEDGMENTS AND ADDRESSES

Received June 23, 1975, from the *Biological Research and Development Laboratories, USV Pharmaceutical Corporation, Tuckahoe, NY 10707*

Accepted for publication December 1, 1975.

The authors thank Dr. Newton Birkhead, Medical Department, USV Pharmaceutical Corp., for monitoring the human oral dosing study and Dr. Micheal O'Hare for carrying out the GLC–mass spectrometry analysis.

[x] To whom inquiries should be directed.

Assay of Sulfonylureas in Human Plasma by High-Performance Liquid Chromatography

S. SVED [x], I. J. McGILVERAY, and NICOLE BEAUDOIN

Abstract □ A sensitive and specific high-performance liquid chromatographic procedure for the determination of chlorpropamide or tolbutamide in plasma in the presence of their metabolites is described. The ether extract of acidified plasma is redissolved in the mobile phase, 17% acetonitrile in 0.05 *M* aqueous ammonium formate, and chromatographed on a reverse-phase column on a high-performance liquid chromatograph fitted with a UV absorbance detector. Quantitation of plasma samples containing less than 0.5 μg/ml of chlorpropamide and 5 μg/ml of tolbutamide is reported, using these drugs as mutual internal standards. The retention times of the metabolites are such that they do not interfere in the procedure. The assay method was tested in a human volunteer with both drugs and found suitable for single-dose pharmacokinetic studies.

Keyphrases □ Chlorpropamide—high-performance liquid chromatographic analysis in presence of metabolites, plasma □ Tolbutamide—high-performance liquid chromatographic analysis in presence of metabolites, plasma □ High-performance liquid chromatography—analysis, chlorpropamide or tolbutamide in presence of metabolites, plasma □ Sulfonylureas—chlorpropamide or tolbutamide, high-performance liquid chromatographic analyses in presence of metabolites, plasma □ Antidiabetic agents—chlorpropamide and tolbutamide, high-performance liquid chromatographic analysis in presence of metabolites, plasma

The two oral hypoglycemic drugs tolbutamide and chlorpropamide are widely used in the management of certain types of maturity-onset diabetes. Specific assay methods capable of measuring the unchanged drugs in plasma are desirable for monitoring clinical blood levels and for studies in pharmacokinetics (1) and drug interactions (2).

Early methods of estimation, based on UV absorbance, were neither specific nor sensitive. More recently, colorimetric procedures were introduced based on the method of Spingler (3) and modified (4, 5). They depend on the reaction of chlorpropamide or tolbutamide with 2,4-dinitrofluorobenzene, followed by measurement of the absorbance of the resultant *N*-propyl- or *N*-butyldinitroaniline at the appropriate wavelength. The sensitivity of these methods is limited, however, by the high and variable blanks from endogenous substances in the plasma. Furthermore, positive color is also obtained with some metabolites of the drugs. Attempts have been made to separate the metabolites by differential extraction prior to spectrophotometry (6, 7), but these methods are lengthy and the separation is incomplete[1].

A number of GC procedures were reported recently, involving methylation of the drugs with dimethyl sulfate (8) or diazomethane (9) or after reaction with 2,4-dinitrofluorobenzene (10). Most of these methods, however, suffer from the inability to distinguish between the parent drug and its metabolites (11), although this problem may have been overcome (12).

A TLC method employing a UV densitometer was described recently for the assay of chlorpropamide in serum (13).

High-performance liquid chromatography (HPLC) apparently has not been used for determining chlorpropamide and tolbutamide levels in the human plasma. Beyer (14) used a reverse-phase system for the determination of these drugs in pharmaceutical preparations, while Molins *et al.* (15) used an improved extraction method with a forward-phase HPLC system for the same purpose.

This work describes the use of a fast extraction procedure and reverse-phase HPLC for the estimation of chlorpropamide and tolbutamide in plasma at sufficiently high sensitivity and specificity to be used for single-dose bioavailability studies.

EXPERIMENTAL

Materials—Chlorpropamide[2], 2-hydroxychlorpropamide[2], 3-hydroxychlorpropamide[2], carboxytolbutamide[3], 4-hydroxytolbutamide[3], *p*-toluenesulfonamide[4], *p*-toluenesulfonylurea[4], *p*-chlorobenzenesulfonylurea[4], *p*-chlorobenzenesulfonamide[5], and tolbutamide[6] were used without further purification. Ether, anhydrous[7], was freshly redistilled before use. Acetonitrile[8] (UV grade)

[1] K. K. Midha and C. Charette of these Laboratories, personal communication.
[2] Supplied by Pfizer, Montreal, Quebec, Canada.
[3] Gift of Dr. J. Thiessen, University of Toronto, Toronto, Ontario, Canada.
[4] Synthesized in this laboratory.
[5] Baker, supplied by Canlab, Ottawa, Ontario, Canada.
[6] Strong-Cobb-Arner of Canada, Fort Erie, Ontario, Canada.
[7] Mallinckrodt Canada Ltd., Montreal, Quebec, Canada.
[8] Burdick & Jackson Laboratories Inc., Muskegon, Mich.

Table I—Retention Characteristics of Chlorpropamide, Tolbutamide, and Their Metabolites

Substance	k'[a,b]	t[c]
Solvent front (t_0)	0	1.1
Chlorpropamide	1.0	2.2
p-Chlorobenzenesulfonylurea	0.2	1.3
p-Chlorobenzenesulfonamide	1.4	2.6
2-Hydroxychlorpropamide	0.3	1.4
3-Hydroxychlorpropamide	0.4	1.5
Tolbutamide	3.0	4.4
Carboxytolbutamide	0.1	1.2
4-Hydroxytolbutamide	0.4	1.5
p-Toluenesulfonylurea	0.2	1.3
p-Toluenesulfonamide	1.7	3.0

[a] Chromatographic conditions were: column, silica gel–octadecylsilane; mobile phase, 17% acetonitrile in 0.05 *M* aqueous ammonium formate; flow rate, 2.5 ml/min; and temperature, 50°. [b] $k' = (t - t_0)/t_0$. [c] Retention time in minutes.

and ammonium formate[9] were used without further purification. All other chemicals were reagent grade. The chromatographic mobile phase was filtered by passing through a 0.2-μm pore size membrane filter[10]. Plasma was obtained from fresh heparinized blood of normal human volunteers. The plasma was pooled and stored at 4° in glass containers.

Apparatus—The chromatographic apparatus[11] was fitted with a UV absorbance detector at a fixed wavelength of 254 nm. The column[12] was a bonded octadecylsilane–silica gel type, 10-μm particle size, 4 × 300 mm internal dimensions. This column was used at room temperature or heated to 50° by means of a glass jacket through which water from a constant-temperature water bath was circulated.

Columns were also prepared in-house[13] by reacting silica gel with trichlorooctadecylsilane (16) and packing the product into stainless steel tubing, using a balanced density slurry method similar to that of Cassidy *et al.* (17).

Preparation of Internal Standard Solutions—Chlorpropamide, 4 mg, or tolbutamide, 20 mg, was dissolved in 1 ml of 0.1 *N* NaOH and diluted to 50 ml with water. These solutions were used without further dilution as internal standards by adding the chlorpropamide solution to the tolbutamide determinations and vice versa. Appropriate dilutions of these same standard solutions were made with blank plasma for the calibration curves.

Extraction of Plasma—*Method 1*—Plasma, 1 ml, in a capped culture tube[14] was mixed with 0.25 ml of the internal standard solution and acidified to pH 3 by the addition of 1 ml of 0.15 *M* phosphoric acid. The drugs were extracted[15] (30 min at 50 rpm) with 10 ml of ether. The mixture was centrifuged, and the ether layer was separated and evaporated to dryness in a conical centrifuge tube, using a dry bath[16] at 45–50° with a gentle stream of dry filtered nitrogen. The residue was redissolved in 0.2 ml of 0.1 *M* ammonium carbonate and 0.2 ml of ethylene dichloride by mixing[17]. Aliquots of 0.02 ml[18] of the aqueous phase were chromatographed.

Method 2—This method was identical to that described by Midha *et al.* (12). It consisted of extracting the acidified plasma with toluene, back-extracting the drugs into phosphate buffer (pH 11.2), acidifying the buffer, reextracting with toluene, and evaporating the toluene phase with nitrogen. The dried extract was redissolved in the chromatographic mobile phase and chromatographed as described.

Method 3—This method, used in an earlier series of experiments[19], was for the determination of tolbutamide only. Plasma, 0.2 ml, in a capped culture tube[14], was mixed with 0.05 ml of internal standard solution and with 0.2 ml of 0.05 *M* phosphate buffer (pH 9.8) and extracted[15] twice with 2 ml of ether. After centrifugation, the ether extract was discarded. The remaining plasma in the tube was acidified with 0.15 ml of 0.05 *M* phosphoric acid and extracted as before with 2 ml of ether.

The separated ether layer was evaporated to dryness in a dry bath[16] at 45–50° with a gentle stream of dry filtered nitrogen. The residue was redissolved in 0.025 ml of the mobile phase, and the entire solution was chromatographed as already described.

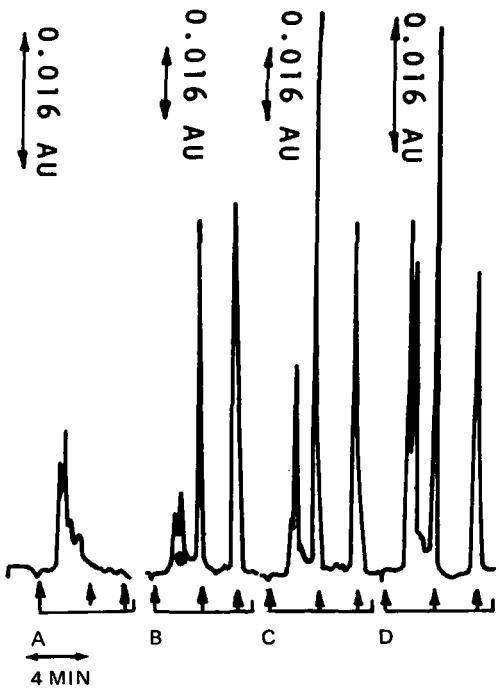

Figure 1—*Chromatograms of chlorpropamide and tolbutamide extracted from plasma by Method 1. Conditions for HPLC were as given in Table I. Key: A, blank plasma; B, blank plasma spiked with 20 μg of chlorpropamide/ml and 100 μg of tolbutamide/ml; C, plasma from an individual medicated with chlorpropamide (estimated value 31.1 μg/ml; internal standard, tolbutamide, 100 μg/ml); and D, plasma from an individual medicated with tolbutamide (estimated value 56.7 μg/ml; internal standard, chlorpropamide, 20 μg/ml).*

Chromatographic Conditions—HPLC was performed[11] on silica gel–octadecylsilane support, using 17% acetonitrile in 0.05 *M* aqueous ammonium formate as the mobile phase. At a flow rate of 2.5 ml/min, the back pressure for the column[12] at room temperature was approximately 2500 psi.

Recovery Experiments—The amounts of the drugs recovered after the extraction of the plasma by the different methods were estimated by comparing the peak heights obtained on chromatographing a known aliquot of the extract with the peak heights obtained from a known volume of a standard solution of the same drug.

Blood Profile Experiments—One volunteer (80 kg) was given orally, after fasting overnight, a 500-mg tolbutamide tablet[20] with 100 ml of water. Blood was withdrawn into heparinized vacuum tubes[21] at 0, 0.5, 1, 1.5, 2, 3, 4, 7, 24, and 28 hr. The samples were centrifuged immediately, and the plasma was kept at −20° until analysis by Method 1. After 1 week, the same subject received 250 mg of chlorpropamide[20]; the blood, sampled at 0, 1, 2, 3, 4, 5, 7, 24, 28, and 48 hr, was treated as described.

RESULTS AND DISCUSSION

To achieve good separation of chlorpropamide and tolbutamide from each other and from their metabolites, alternative chromatographic conditions were tried. The conditions finally chosen utilized a microparticulate bonded reverse-phase packing with a mobile phase consisting of 17% acetonitrile and 83% 0.05 *M* aqueous ammonium

[9] Catalog No. 15 6264, Aldrich Chemical Co. (Canada) Ltd., Montreal, Quebec, Canada.
[10] Millipore Teflon membrane filter, Catalog No. FGLP02500, Millipore Ltd., Mississauga, Ontario, Canada.
[11] Model ALC 202, consisting of a model 6000 pump, model U6K injector, and UV detector, Waters Associates Inc., Milford, Mass.
[12] MicroBondapak-C_{18}, Waters Associates Inc., Milford, Mass.
[13] By A. Butterfield and L. Wilson of this laboratory.
[14] Catalog No. T1356-1, Canlab, Ottawa, Ontario, Canada.
[15] Roto-Rack, Fisher Scientific, Ottawa, Ontario, Canada.
[16] Model SC/48, Brinkmann Instruments (Canada) Ltd., Rexdale, Ontario, Canada.
[17] Vortex Genie, Scientific Instruments, Springfield, Mass.
[18] Catalog No. 702N microliter syringe, Hamilton Co., Reno, Nev.
[19] Presented by S. Sved, N. Beaudoin, and I. J. McGilveray at the Twenty-Second Canadian Conference on Pharmaceutical Research, Montreal, Canada, 1975.
[20] Obtained commercially.
[21] Vacutainer, Becton, Dickinson & Co., Canada, Ltd., Mississauga, Ontario, Canada.

Table II—Recoveries and Statistical Parameters of the Calibration Curves for the Assay of Chlorpropamide and Tolbutamide

Drug	Correlation Coefficient (r^2)	Coefficient of Variation		Regression		Recovery[a], %
		Minimum	Maximum	Intercept	Slope	
Chlorpropamide[b,c]	0.998	3.23	6.08	−0.0032	0.0476	95.7 ± 2.9
Tolbutamide[b,c]	0.989	3.46	8.80	+0.0031	0.0095	93.3 ± 4.8
Tolbutamide[c,d]	0.980	3.78	5.95	−0.0049	0.0140	50.3 ± 2.9

[a] Mean ± *SD*. [b] Extraction by Method 1. [c] Conditions for HPLC as in Table I. [d] Extraction by Method 3.

formate. The retention times and capacity factors, k', for chlorpropamide, tolbutamide, and some of their metabolites are shown in Table I. All metabolites tested have retention times different from chlorpropamide and tolbutamide and thus do not interfere.

The column routinely used was commercially prepared, but similar results were obtained using other columns, including two that were bonded and packed in this laboratory. (The exact proportion of acetonitrile in the mobile phase had to be adjusted to the retentivity of each column.) An increase in temperature from ambient (~25°) to 50° made little difference in the resolution but markedly decreased the back pressure as well as the retention time. These reduced retention times (~4 min for the most retained drug, tolbutamide) permitted up to 12 analyses/hr.

Chromatograms of fresh human plasma extracts are shown in Fig. 1. In these experiments, control blank plasma was either extracted as such (trace A) or spiked with 20 μg of chlorpropamide/ml together with 100 μg of tolbutamide/ml and then extracted (trace B). The last two traces were obtained from a volunteer after the administration of chlorpropamide (Fig. 1C) or tolbutamide (Fig. 1D) and using the other drug as the internal standard. All extractions were done by Method 1.

No interfering peaks appeared in the blank plasma with a retention time similar to that of chlorpropamide, and only a very small peak appeared with a retention time similar to that of tolbutamide. However, dated plasma from the blood bank[22] contained substantial amounts of interfering materials having long retention times (23–28 min, $k' \simeq 20$–25), possibly leached out from the plastic bags used for storage (18).

Figure 2 shows the calibration curves for chlorpropamide and tolbutamide using blank plasma spiked with the appropriate amounts of the drugs, extracted, and chromatographed according to Method 1. The concentration range for chlorpropamide was 0.5–40 μg/ml with 100 μg of tolbutamide/ml as the internal standard. The concentration range for tolbutamide was 5–100 μg/ml with 20 μg of chlorpropamide/ml as the internal standard. The ratios of peak heights of the drug to internal standard plotted against drug concentration fell on a straight line. All points were within 1 *SE* of the means of five determinations from the curves. The statistical parameters of the calibration curves, as well as recoveries, are summarized in the first two lines of Table II. The overall extraction efficiencies were between 93 and 97%; the correlation coefficients, r^2, were 0.99 or better; and the intercepts were negligible.

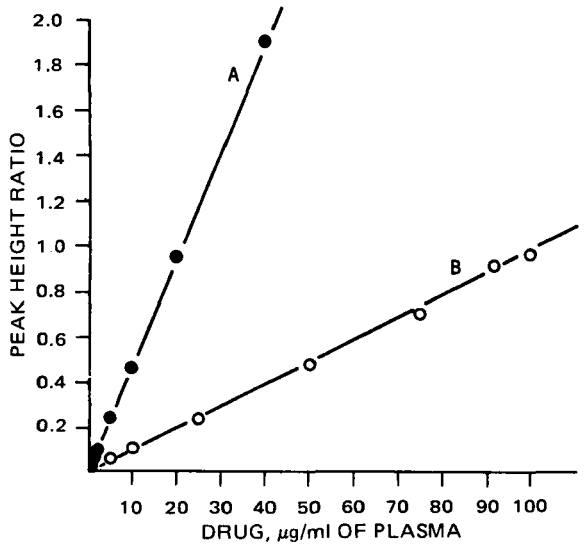

Figure 2—*Calibration curves for chlorpropamide and tolbutamide in plasma. Key: A (●), 0.5–40 μg of chlorpropamide/ml plus 100 μg of internal standard/ml (tolbutamide); and B (○), 5–100 μg of tolbutamide/ml plus 20 μg of internal standard/ml (chlorpropamide). Extraction was by Method 1. Conditions for HPLC were as given in Table I.*

[22] Canadian Red Cross, Ottawa, Ontario, Canada.

These results show that a single extraction with ether at pH ~3 quantitatively separated the drugs from most substances that could interfere in this study. After evaporation of the extract, the drug could be redissolved in aqueous ammonium carbonate buffer. However, it was desirable to add a small amount of ethylene dichloride at this stage to ensure dissolution of any drug that might be occluded inside some neutral lipids.

Use of this method allowed the preparation of all extracts for 1 day's analysis in less than 2 hr; dried extracts could be kept indefinitely in the deep freeze. Figure 3 shows the application of Method 1 to the plasma concentration of chlorpropamide (Fig. 3A) over 48 hr and tolbutamide (Fig. 3B) over 28 hr in a human volunteer following single doses of each drug at different time intervals.

In an earlier study[19], HPLC was compared with GLC in the analysis of samples obtained from a human volunteer treated successively with 125 mg of chlorpropamide or 500 mg of tolbutamide. In these experiments, the chlorpropamide profile was obtained using the extraction procedure of Midha *et al.* (12) (Method 2) while the tolbutamide profile was obtained using Method 3. In both cases, HPLC was performed as described. The parameters for the calibration curve using Method 3 are given in the last line of Table II.

The results of these experiments, published recently (12), show that the profiles are essentially the same whether assayed by GLC or high-speed liquid chromatography. The close similarity between the two methods is demonstrated in Table III. Differences between the drug levels found by GLC and HPLC amount to 4–7% average (means of absolute differences). None of the differences between the individual values exceeded 8 or 14% for chlorpropamide or tolbutamide, respectively, and the areas under the curve agreed within 2%. While the extraction procedures used in this series of experiments are not strictly equivalent to Method 1, the latter, with its improved recovery, should give similar results.

In conclusion, the HPLC procedure using extraction Method 1 is

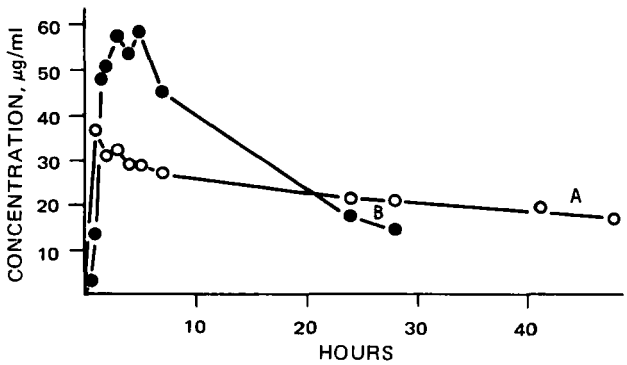

Figure 3—*Plasma profile of absorption and elimination of chlorpropamide and tolbutamide. The drugs were administered orally to a normal human volunteer after overnight fasting. Analysis was done by Method 1. Key: A (○), 250 mg of chlorpropamide; and B (●), 500 mg of tolbutamide. Conditions for HPLC were as given in Table I.*

Table III—Observed Differences between GLC and HPLC Assay of Drug Blood Profiles

Drug	Percent Difference: Maximum Observed	Percent Difference: Average[a]	AUC[b], % Difference
Chlorpropamide[c,d]	8.60	4.25	1.13
Tolbutamide[d,e]	14.10	7.41	1.90

[a] Mean of absolute differences. [b] Area under the plasma concentration–time curve (chlorpropamide, 0–168 hr; and tolbutamide, 0–28 hr). [c] Chlorpropamide was extracted by Method 2 for both HPLC and GLC. [d] Conditions for HPLC as in Table I. [e] Tolbutamide was extracted by Method 2 for GLC and by Method 3 for HPLC.

fast, sensitive, and specific for the determination of chlorpropamide and tolbutamide. Application of the method to plasma profiles in human volunteers showed that it can be used in single- and multiple-dose pharmacokinetic studies.

REFERENCES

(1) M. Rowland, S. B. Matin, J. Thiessen, and J. Karam, in "Drug Interactions," P. L. Morselli, S. Garattini, and S. N. Cohen, Eds., Raven, New York, N.Y., 1974.

(2) P. B. Andreasen and E. S. Vesell, *Clin. Pharmacol. Ther.*, **16**, 1059(1974).

(3) H. Spingler, *Klin. Wochenschr.*, **35**, 533(1957).

(4) R. H. Carmichael, *Clin. Chem.*, **5**, 597(1959).

(5) S. B. Matin and M. Rowland, *J. Pharm. Pharmacol.*, **25**, 186(1973).

(6) J. Shibasaki, R. Konishi, T. Ueki, and T. Morishita, *Chem. Pharm. Bull.*, **21**, 1747(1973).

(7) J. Shibasaki, R. Konishi, T. Morishita, and T. Ueki, *ibid.*, **21**, 1754(1973).

(8) K. Sabih and K. Sabih, *J. Pharm. Sci.*, **59**, 782(1970).

(9) J. A. Taylor, *Clin. Pharmacol. Ther.*, **13**, 710(1972).

(10) T. J. Toolan and R. L. Wagner, Jr., *Ann. N.Y. Acad. Sci.*, **74**, 449(1959).

(11) D. L. Simmons, R. J. Ranz, and P. Picotte, *J. Chromatogr.*, **71**, 421(1972).

(12) K. K. Midha, I. J. McGilveray, and C. Charette, *J. Pharm. Sci.*, **65**, 576(1976).

(13) A. M. Monro and P. G. Welling, *Eur. J. Clin. Pharmacol.*, **7**, 47(1974).

(14) W. F. Beyer, *Anal. Chem.*, **44**, 1312(1972).

(15) D. Molins, C. K. Wong, D. M. Cohen, and K. P. Munnelly, *J. Pharm. Sci.*, **64**, 123(1975).

(16) R. K. Gilpin, J. A. Korpi, and C. A. Janicki, *Anal. Chem.*, **46**, 1314(1974).

(17) R. M. Cassidy, D. S. LeGay, and R. W. Frei, *ibid.*, **46**, 340(1974).

(18) R. A. DeZeeuw, J. H. G. Jonkman, and F. J. W. van Mansvelt, *Anal. Biochem.*, **67**, 339(1975).

ACKNOWLEDGMENTS AND ADDRESSES

Received October 20, 1975, from the *Drug Research Laboratories, Health Protection Branch, Health and Welfare Canada, Ottawa, Ontario K1A OL2, Canada.*

Accepted for publication December 2, 1975.

The authors thank Dr. K. K. Midha and Mr. A. Butterfield for invaluable discussions and Mrs. F. Matsui and Mr. C. Charette for providing some sulfonylurea derivatives.

[x] To whom inquiries should be directed.

Effects of Intravenous Dantrolene Sodium on Respiratory and Cardiovascular Functions

K. O. ELLIS [x], F. L. WESSELS, and J. F. CARPENTER

Abstract □ Dantrolene sodium, a peripherally acting skeletal muscle relaxant, at doses up to 30 mg/kg iv had no effect on respiratory volume, respiratory rate, blood pressure, or heart rate in anesthetized dogs. The ED_{50} for inhibition of skeletal muscle contractions was 4.5 mg/kg in anesthetized dogs. In anesthetized sheep, the ED_{50} for skeletal muscle relaxation was 3.2 mg/kg under methoxyflurane anesthesia and 1.7 mg/kg under pentobarbital anesthesia. Unanesthetized sheep administered doses up to 30 mg/kg iv evidenced no dose-related cardiovascular effects. Respiratory volume decreased and respiratory rate increased, with the net result that the respiratory minute volume was not affected by dantrolene sodium. The results indicate that dantrolene sodium has no effect on the cardiovascular or respiratory systems that would preclude its use intravenously in acute conditions where direct relaxation of skeletal muscle is required, as in the management of malignant hyperthermia.

Keyphrases □ Dantrolene sodium—effects on respiratory and cardiovascular functions, dogs and sheep □ Respiratory functions—effects of dantrolene sodium, dogs and sheep □ Cardiovascular functions—effects of dantrolene sodium, dogs and sheep □ Relaxants, skeletal muscle—dantrolene sodium, effects on respiratory and cardiovascular functions, dogs and sheep

Dantrolene sodium[1], a new skeletal muscle relaxant, has therapeutic utility in chronic spasticity (1–4). The primary site of action of dantrolene sodium is outside the central nervous system (CNS) (5–8). It does not alter neuromuscular transmission or affect the electrical excitability of the muscle membrane (9, 10) but acts by uncoupling excitation–contraction mechanisms (11, 12). The hypothesized mechanism of dantrolene sodium's action is a decrease in release of Ca^{+2} from the sarcoplasmic reticulum (9, 13, 14).

The unique pharmacological action of dantrolene sodium suggests that it might be useful in the treatment of a condition characterized by muscle rigidity and elevated myoplasmic calcium (*i.e.*, malignant hyperthermia) (15). Recently, in the established syndrome of malignant hyperthermia in susceptible (MHS) swine, dantrolene sodium caused a rapid loss of muscle rigor commencing within 5 min, an immediate cessation of the increase in deep muscle temperature followed by a

[1] Dantrium, Eaton Laboratories, a subsidiary of Norwich Pharmacal Co., Division of Morton-Norwich Products, Norwich, N.Y.

Table III—Observed Differences between GLC and HPLC Assay of Drug Blood Profiles

Drug	Percent Difference: Maximum Observed	Percent Difference: Average[a]	AUC[b], % Difference
Chlorpropamide[c,d]	8.60	4.25	1.13
Tolbutamide[d,e]	14.10	7.41	1.90

[a] Mean of absolute differences. [b] Area under the plasma concentration–time curve (chlorpropamide, 0–168 hr; and tolbutamide, 0–28 hr). [c] Chlorpropamide was extracted by Method 2 for both HPLC and GLC. [d] Conditions for HPLC as in Table I. [e] Tolbutamide was extracted by Method 2 for GLC and by Method 3 for HPLC.

fast, sensitive, and specific for the determination of chlorpropamide and tolbutamide. Application of the method to plasma profiles in human volunteers showed that it can be used in single- and multiple-dose pharmacokinetic studies.

REFERENCES

(1) M. Rowland, S. B. Matin, J. Thiessen, and J. Karam, in "Drug Interactions," P. L. Morselli, S. Garattini, and S. N. Cohen, Eds., Raven, New York, N.Y., 1974.

(2) P. B. Andreasen and E. S. Vesell, *Clin. Pharmacol. Ther.*, **16**, 1059(1974).

(3) H. Spingler, *Klin. Wochenschr.*, **35**, 533(1957).

(4) R. H. Carmichael, *Clin. Chem.*, **5**, 597(1959).

(5) S. B. Matin and M. Rowland, *J. Pharm. Pharmacol.*, **25**, 186(1973).

(6) J. Shibasaki, R. Konishi, T. Ueki, and T. Morishita, *Chem. Pharm. Bull.*, **21**, 1747(1973).

(7) J. Shibasaki, R. Konishi, T. Morishita, and T. Ueki, *ibid.*, **21**, 1754(1973).

(8) K. Sabih and K. Sabih, *J. Pharm. Sci.*, **59**, 782(1970).

(9) J. A. Taylor, *Clin. Pharmacol. Ther.*, **13**, 710(1972).

(10) T. J. Toolan and R. L. Wagner, Jr., *Ann. N.Y. Acad. Sci.*, **74**, 449(1959).

(11) D. L. Simmons, R. J. Ranz, and P. Picotte, *J. Chromatogr.*, **71**, 421(1972).

(12) K. K. Midha, I. J. McGilveray, and C. Charette, *J. Pharm. Sci.*, **65**, 576(1976).

(13) A. M. Monro and P. G. Welling, *Eur. J. Clin. Pharmacol.*, **7**, 47(1974).

(14) W. F. Beyer, *Anal. Chem.*, **44**, 1312(1972).

(15) D. Molins, C. K. Wong, D. M. Cohen, and K. P. Munnelly, *J. Pharm. Sci.*, **64**, 123(1975).

(16) R. K. Gilpin, J. A. Korpi, and C. A. Janicki, *Anal. Chem.*, **46**, 1314(1974).

(17) R. M. Cassidy, D. S. LeGay, and R. W. Frei, *ibid.*, **46**, 340(1974).

(18) R. A. DeZeeuw, J. H. G. Jonkman, and F. J. W. van Mansvelt, *Anal. Biochem.*, **67**, 339(1975).

ACKNOWLEDGMENTS AND ADDRESSES

Received October 20, 1975, from the *Drug Research Laboratories, Health Protection Branch, Health and Welfare Canada, Ottawa, Ontario K1A OL2, Canada.*

Accepted for publication December 2, 1975.

The authors thank Dr. K. K. Midha and Mr. A. Butterfield for invaluable discussions and Mrs. F. Matsui and Mr. C. Charette for providing some sulfonylurea derivatives.

[x] To whom inquiries should be directed.

Effects of Intravenous Dantrolene Sodium on Respiratory and Cardiovascular Functions

K. O. ELLIS [x], F. L. WESSELS, and J. F. CARPENTER

Abstract □ Dantrolene sodium, a peripherally acting skeletal muscle relaxant, at doses up to 30 mg/kg iv had no effect on respiratory volume, respiratory rate, blood pressure, or heart rate in anesthetized dogs. The ED_{50} for inhibition of skeletal muscle contractions was 4.5 mg/kg in anesthetized dogs. In anesthetized sheep, the ED_{50} for skeletal muscle relaxation was 3.2 mg/kg under methoxyflurane anesthesia and 1.7 mg/kg under pentobarbital anesthesia. Unanesthetized sheep administered doses up to 30 mg/kg iv evidenced no dose-related cardiovascular effects. Respiratory volume decreased and respiratory rate increased, with the net result that the respiratory minute volume was not affected by dantrolene sodium. The results indicate that dantrolene sodium has no effect on the cardiovascular or respiratory systems that would preclude its use intravenously in acute conditions where direct relaxation of skeletal muscle is required, as in the management of malignant hyperthermia.

Keyphrases □ Dantrolene sodium—effects on respiratory and cardiovascular functions, dogs and sheep □ Respiratory functions—effects of dantrolene sodium, dogs and sheep □ Cardiovascular functions—effects of dantrolene sodium, dogs and sheep □ Relaxants, skeletal muscle—dantrolene sodium, effects on respiratory and cardiovascular functions, dogs and sheep

Dantrolene sodium[1], a new skeletal muscle relaxant, has therapeutic utility in chronic spasticity (1–4). The primary site of action of dantrolene sodium is outside the central nervous system (CNS) (5–8). It does not alter neuromuscular transmission or affect the electrical excitability of the muscle membrane (9, 10) but acts by uncoupling excitation–contraction mechanisms (11, 12). The hypothesized mechanism of dantrolene sodium's action is a decrease in release of Ca^{+2} from the sarcoplasmic reticulum (9, 13, 14).

The unique pharmacological action of dantrolene sodium suggests that it might be useful in the treatment of a condition characterized by muscle rigidity and elevated myoplasmic calcium (*i.e.*, malignant hyperthermia) (15). Recently, in the established syndrome of malignant hyperthermia in susceptible (MHS) swine, dantrolene sodium caused a rapid loss of muscle rigor commencing within 5 min, an immediate cessation of the increase in deep muscle temperature followed by a

[1] Dantrium, Eaton Laboratories, a subsidiary of Norwich Pharmacal Co., Division of Morton-Norwich Products, Norwich, N.Y.

Table I—Effect of Dantrolene Sodium on Cardiovascular and Respiratory Functions in Anesthetized Dogs[a]

Experiment	Treatment	Arterial Blood Pressure[b], mm Hg	Mean Arterial Blood Pressure[c], mm Hg	Heart Rate, beats/min	Gastrocnemius Muscle Twitch Tension, g	Rectal Body Temperature	Respiratory Rate per Minute[d]	Respiratory Volume[e]	Minute Volume[f]
1	Control (prior to drug administration)	150/100	117	170	920	36.0°	11	142	1562
2		175/125	142	160	1280	37.0°	11	170	1870
3		155/110	125	140	1020	36.2°	14	185	2590
4		155/120	132	170	1440	37.0°	11	143	1573
5		170/115	133	150	1220	36.9°	15	99	1485
$\bar{X}$		161/114	129.8	158	1176	36.6°	12.4	147.8	1816
±*SE*		4.8/4.3	4.2	5.8	92.8	0.2°	0.9	14.7	204
1	Dantrolene sodium, 0.1 mg/kg iv	150/100	117	150	880	—	11	150	1650
2		175/125	142	150	1240	—	11	160	1760
3		160/110	127	140	990	—	14	170	2380
4		160/120	133	170	1390	37.0°	10	163	1630
5		175/115	135	150	1180	36.9°	13	118	1534
$\bar{X}$		164/114	130.8	152	1136	37.0	11.8	152.2	1790
±*SE*		4.8/4.3	4.2	4.9	90.6	0.1°	0.7	9.1	151
Percent change		+1.8/0	+0.8	−3.8	−3.4	+0.8°	−4.8	+3.0	−1.4
1	Dantrolene sodium, 0.4 mg/kg iv	150/100	117	150	720	—	11	125	1375
2		180/130	147	150	1060	37.0°	11	163	1793
3		160/110	127	130	840	36.2°	13	175	2275
4		160/120	133	170	1200	37.0°	11	160	1760
5		175/115	135	150	1020	36.8°	15	118	1770
$\bar{X}$		165/115	131.8	150	968	36.8°	12.2	148.2	1795
±*SE*		5.5/5.0	4.9	6.3	84.5	0.2°	0.8	11.2	143
Percent change		+2.5/+0.9	+1.5	−5.1	−17.7	+0.5°	−1.6	+0.3	−1.2
1	Dantrolene sodium, 1.4 mg/kg iv	150/95	113	150	510	35.5°	12	150	1800
2		185/135	152	150	840	—	11	171	1881
3		170/110	130	130	650	36.1°	11	160	1760
4		165/120	135	170	980	36.9°	11	143	1573
5		175/115	135	140	840	36.2°	16	112	1792
$\bar{X}$		169/115	133.0	148	764	36.2°	12.2	147.2	1761
±*SE*		5.8/6.5	6.2	6.6	82.4	0.3°	1.0	10.0	51
Percent change		+4.9/+0.9	+2.5	−6.3	−35.0	−1.1°	−1.6	−0.4	−3.0
1	Dantrolene sodium, 4.4 mg/kg iv	145/90	107	140	320	35.0°	14	119	1666
2		180/130	147	140	620	36.3°	12	141	1692
3		170/110	130	140	440	36.0°	14	181	2534
4		170/120	137	160	770	36.8°	12	125	1500
5		175/115	135	140	620	36.0°	16	118	1888
$\bar{X}$		168/113	131.2	144	554	36.0°	13.6	136.8	1856
±*SE*		6.0/6.6	6.7	4.0	78.5	0.3°	0.8	11.8	180
Percent change		+4.3/−0.9	+1.1	−8.9	−52.9	−1.6°	+9.7	−7.4	+2.2
1	Dantrolene sodium, 14.4 mg/kg iv	150/80	103	120	235	34.5°	12	125	1500
2		185/130	148	130	470	36.0°	12	144	1728
3		175/115	135	180	390	36.0°	16	170	2720
4		170/120	137	150	600	36.2°	10	153	1530
5		175/110	132	130	580	35.1°	13	112	1456
$\bar{X}$		171/111	131.0	142	455	35.6°	12.6	140.8	1787
±*SE*		5.8/8.4	7.5	10.7	66.9	0.3°	1.0	10.2	238
Percent change		+6.2/−2.6	+0.9	−10.1	−61.3	−2.7°	+1.6	−4.7	−1.6
1	Dantrolene sodium, 30.4 mg/kg iv	155/95	118	110	300	33.8°	10	135	1350
2		175/125	142	130	620	35.8°	11	175	1925
3		160/110	127	170	400	37.0°	15	170	2550
4		175/125	142	150	640	36.2°	8	194	1552
5		160/100	120	110	620	34.2°	10	180	1800
$\bar{X}$		165/111	129.8	134	516	35.4°	10.8	170.8	1835
±*SE*		4.2/6.2	5.2	11.7	69.7	0.6°	1.2	9.8	204
Percent change		+2.5/−2.6	0	−15.2	−56.1	−3.3°	−12.9	+15.6	+0.5
6	Control (prior to solvent administration)	115/85	95	140	1400	37.0°	13	138	1794
7		155/120	132	180	1800	36.8°	5	365	1825
$\bar{X}$		135/103	113.5	160	1600	36.9°	9	251.5	1810
±*SE*		20/18	18.5	20	200	0.1°	4	113.5	16
6	Control solvent, 0.1 mg/kg[g]	115/85	95	140	1380	37.0°	12	135	1620
7		155/120	132	180	1800	36.8°	4	390	1560
$\bar{X}$		135/103	113.5	160	1590	36.9°	8	262.5	1590
±*SE*		20/18	18.5	20	210	0.1°	4	127.5	30
Percent change		0/0	0	0	−0.6	0	−11.1	+4.4	−12.1
6	Control solvent, 0.4 mg/kg[g]	115/85	95	140	1380	36.9°	11	138	1518
7		155/120	132	170	1800	36.8°	4	343	1372
$\bar{X}$		135/103	113.5	155	1590	36.9°	7.5	240.5	1445
±*SE*		20/18	18.5	15	210	0.1°	3.5	102.5	73

Table I—(*Continued*)

Experiment	Treatment	Arterial Blood Pressure[b], mm Hg	Mean Arterial Blood Pressure[c], mm Hg	Heart Rate, beats/min	Gastrocnemius Muscle Twitch Tension, g	Rectal Body Temperature	Respiratory Rate per Minute[d]	Respiratory Volume[e]	Minute Volume[f]
Percent change		0/0	0	−3.1	−0.6	0	−16.7	−4.4	−20.1
6	Control solvent, 1.4 mg/kg iv[g]	120/90	100	140	1380	36.5°	13	132	1716
7		155/120	132	170	1800	36.5°	5	415	2075
$\bar{X}$		137.5/105	116	155	1590	36.5°	9	273.5	1896
±*SE*		17.5/15	16	15	210	0	4	141.5	180
Percent change		+1.9/+1.9	+2.2	−3.1	−0.6	−1.1°	0	+8.7	+4.8
6	Control solvent, 4.4 mg/kg[g]	115/85	95	130	1380	36.2°	12	132	1584
7		155/115	128	160	1800	36.1°	5	390	1950
$\bar{X}$		135/100	111.5	145	1590	36.2°	8.5	261	1767
±*SE*		20/15	16.5	15	210	0.1°	3.5	129	183
Percent change		0/−2.9	−1.8	−9.4	−0.6	−1.9°	−5.6	+3.8	−2.3
6	Control solvent, 14.4 mg/kg[g]	120/90	100	120	1380	35.6°	12	150	1800
7		155/115	128	140	1800	35.2°	4	480	1920
$\bar{X}$		137.5/102.5	114	130	1590	35.4°	8	315	1860
±*SE*		17.5/12.5	14	10	210	0.2°	4	165	60
Percent change		+1.9/−0.5	+0.4	−18.8	−0.6	−4.1°	−11.1	+25.2	+2.8
6	Control solvent, 30.4 mg/kg iv[g]	115/85	95	110	1220	34.9°	8	170	1360
7		145/100	115	100	1620	34.5°	5	488	2440
$\bar{X}$		130/92.5	105	105	1420	34.7°	6.5	329	1900
±*SE*		15/7.5	10	5	200	0.2°	1.5	159	540
Percent change		−3.7/−10	−7.5	−34.4	−11.3	−6.0°	−27.8	+30.8	+5.0

[a] Pentobarbital sodium (35 mg/kg iv). [b] Systolic/diastolic. [c] Diastolic + (systolic − diastolic)/3. [d] Normal values are 15.5 ± 12.38. See Ref. 32. [e] Expired air per minute. Normal values are 198.88 ± 81.6. See Ref. 32. [f] Minute volume = $RV \times RR$. Normal values are 2923.2 ± 2585.7. See Ref. 32. [g] Control solvent at volumes necessary to deliver dantrolene sodium at these doses.

rapid decrease, and termination of the progressive acidosis characteristic of the syndrome (16). "A survival rate of 100 per cent was achieved in the last 7 of 8 experiments," with dantrolene sodium at doses ranging from 1 to 10 mg/kg iv (16).

This report presents the results of studies on the effects of intravenous administration of dantrolene sodium on cardiovascular and respiratory functions in anesthetized dogs and sheep and unanesthetized sheep.

EXPERIMENTAL

Anesthetized Dogs—Beagle dogs[2] (n = 7) of either sex, 9.3–15.3 kg, were anesthetized with 35 mg/kg iv of pentobarbital sodium. Arterial blood pressure was monitored from a catheter passed *via* the right femoral artery into the abdominal aorta. The catheter was connected to a pressure transducer[3] attached to a polygraph[4] for recording blood pressure and heart rate. The ipsilateral femoral vein was cannulated for drug administration. A tracheotomy was performed, and a trachea cannula was connected to a pneumotachograph[5] attached to a differential pressure transducer[6], which was coupled to the polygraph[4] for recording respiration.

The left gastrocnemius muscle was used to evaluate the contractility of skeletal muscle. The femur was fixed, and the dissected Achilles tendon was attached to a force displacement transducer[7] connected to the polygraph[4] for recording gastrocnemius muscle twitch tension. Resting tension of the muscle was set at 100 g. Monodirectional square-wave pulses from a stimulator[8] were conducted through an isolation unit[9] to electrodes placed in the tendon and muscle. Stimuli were supramaximal, 150 v for 5 msec at 0.1 Hz. Rectal temperature was monitored in these experiments with a telethermometer[10]. Experimentation was initiated after all recorded parameters had stabilized (about 30 min).

Anesthetized Sheep—Dorset sheep (n = 7) of either sex, 42–45 kg, were anesthetized with either 35 mg/kg iv of pentobarbital sodium or 12.5 mg/kg iv of thiamylal sodium. Sheep in which anesthesia was induced with thiamylal sodium were attached to a closed-circuit anesthesia machine[11], and anesthesia was maintained through inhalation of methoxyflurane (2%).

Experimental procedures similar to those described for dogs were conducted in the anesthetized sheep, except that the right extensor digitorum longus muscle under 50 g of resting tension and supramaximal stimuli of 90–120 v for 5 msec at 0.1 Hz were used for evaluation of skeletal muscle contractility.

Unanesthetized Sheep—Cheviot, Dorset, and Southdown rams and wethers (n = 11), 20.5–29.5 kg, were fasted overnight. Atropine sulfate, 10 mg, was administered intramuscularly, and the sheep were prepared for surgery. Anesthesia was induced with 12.5 mg/kg iv of thiamylal sodium followed by inhalation of methoxyflurane using the method already described for maintenance anesthesia.

The placement of indwelling cannulas in the femoral artery and vein was similar to that reported previously (17, 18). The exteriorized cannula ends were connected to plastic stopcocks[12] and fixed to the surface of the skin between the iliac crests with adhesive tape and branding cement[13]. The cannulas were kept filled with a 0.9% NaCl solution made up to contain approximately 500 units of heparin/ml and flushed every 1–3 days with saline to test for patency.

Four to 5 days after surgery, training of the sheep to accept the face

[2] Raised at Norwich Pharmacal Co. Animal Research Center.
[3] Statham P23DC.
[4] Grass model 7C.
[5] Fleisch 1/a 7318 No. 0.
[6] Statham PM15.
[7] Grass FT-10.
[8] Grass S88.
[9] Grass SIU-5A.
[10] Yellow Springs Instruments.
[11] Heidbrink–Ohio Medical Products.
[12] Tomac.
[13] Brand-Rite.

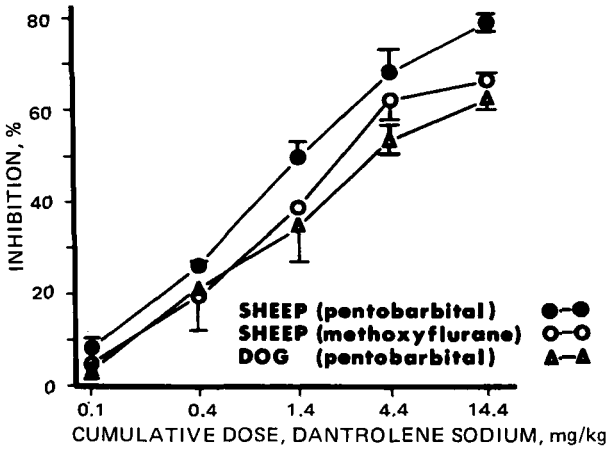

Figure 1—*Effects of intravenous dantrolene sodium on the twitch contraction of the gastrocnemius muscle in anesthetized dogs and the extensor digitorum longus muscle in anesthetized sheep. See* Experimental *for muscle stimulation parameters, techniques of anesthesia, and drug administration.*

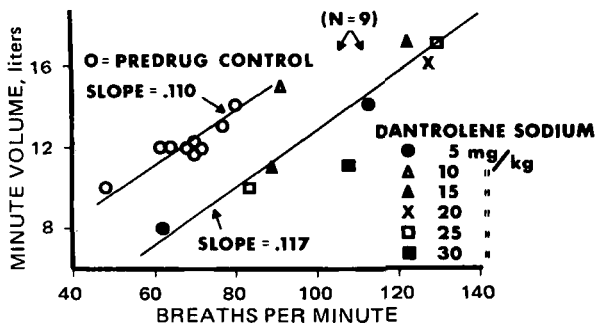

Figure 2—*Effects of dantrolene sodium, intravenously, on respiration (estimated relative respiration rate; see text for details) in unanesthetized sheep. Each symbol represents a single dose studied in one animal.*

mask (19) and to obtain baseline control values was started; this training required approximately 2 weeks before drug administration was initiated. Abdominal–aortic blood pressure and heart rate were monitored *via* a pressure transducer[3] connected to a polygraph[14].

Respiratory volumes were measured using a spirometer[15] attached to the face mask held by the investigator. The volumes of expired air were recorded for 15-sec intervals, and the rate of respiration was recorded by counting the audible closings of the air intake valve. During training and experimentation, the animals were confined in a goat milking stanchion for up to 6 hr in a warm room (22–28°).

Drugs—Dantrolene sodium was administered in a mannitol–sodium hydroxide solvent (dantrolene sodium, 0.5 mg/ml; mannitol, 44 mg/ml; sodium hydroxide, 0.08 mg/ml; and water for injection, pH ≈10.5). Dantrolene sodium, or the solvent, was administered in a cumulative dose manner through the venous cannula with an infusion pump[16] at a rate of 3.82 mg/min in sheep and 2.49 mg/min in dogs.

RESULTS

Skeletal Muscle Function under Anesthesia—In anesthetized dogs and sheep, dantrolene sodium produced dose-related inhibition of the muscle twitch responses (Fig. 1). The minimum effective dose was 0.4 mg/kg; peak effect was evident at 14.4 mg/kg in both species. Measurements of twitch tension were made after muscle contractions had stabilized following drug administration. The sodium hydroxide–mannitol solvent alone had no effect on the muscle contractions. In dogs, the ED_{50} (20) for gastrocnemius twitch tension inhibition was 4.5 mg/kg (2.0–10.3); in sheep, the ED_{50} for inhibition of the extensor digitorum longus muscle was 3.2 mg/kg (0.75–14.5) under methoxyflurane anesthesia and 1.7 mg/kg (0.72–3.9) under pentobarbital anesthesia.

Effects of dantrolene sodium and the solvent vehicle on respiratory and cardiovascular functions and the gastrocnemius muscle twitch tension in anesthetized dogs are shown in Table I. Dantrolene sodium had no significant effect from the control solvent on blood pressure ($p = 0.12$), heart rate ($p = 0.67$), or respiratory volume ($p = 0.09$) or rate ($p = 0.24$). The small changes in diastolic pressure and heart rate seen with the drug and vehicle appeared to be inconsistent and not related to dose or volume. No drug-related effects were noted on the body temperature, because the temperature of control animals decreased the same degree as dantrolene sodium-treated animals. This decrease in body temperature most likely was due to the barbiturate anesthetic (21).

Unanesthetized Sheep—In unanesthetized sheep, the estimated respiration rate was a count of the audible closings of the air intake valve and did not distinguish between panting and normal breathing. (Drug-treated and control animals were studied under the same conditions.) Treatment with dantrolene sodium caused a decrease in the tidal volume, but there was a concomitant increase in the rate of respiration. The slopes of the lines for the predrug control and dantrolene sodium data were not significantly different ($p > 0.3$) (Fig. 2).

Skeletal muscle relaxation was evident (by gross observation) at all doses of dantrolene sodium tested (5–30 mg/kg), and the effects on cardiovascular function noted in the unanesthetized sheep were inconsistent and not dose related (nonsignificant regression function) (Table II). Prior to drug administration, the animals were alert and bleated normally; however, bleating was weak following administration of dantrolene sodium, and the weakness appeared to be dose related. The ability for foot placement was affected; the relaxed animals dragged their hooves as they walked, a behavior not seen in control animals.

Head droop was observed, with the animals resting their heads on the stanchion during experimentation; again this behavior was not observed in the control animals. Dantrolene sodium-treated animals could be pushed down to a kneeling position with little or no resistance; however, when this force was removed, the animals regained normal posture, walked in a slow wobbly manner, and exhibited head droop. No loss of motor coordination or alertness was observed; the sheep were able to negotiate an inclined ramp and a winding route back to the housing area.

DISCUSSION

The effective intravenous dose of dantrolene sodium noted in this study with directly stimulated muscles of the dog and sheep is consistent with what other investigators have reported for other species (7, 16, 22–24). In all instances, the peak of the dose–response curve was approximately 4.4–14.4 mg/kg iv. A significant reduction in twitch tension was observed in the dose range of 1.2–5 mg/kg iv. Increasing the dose beyond 14.4 mg/kg iv did not produce any further significant increase in the twitch inhibition. Maximum inhibition of twitch appears species dependent [*e.g.*, dog, 50–54% (21); and cat, 80–98% (22)], with some variation probably attributable to differences in vehicles and rates of administration.

Dantrolene sodium's lack of significant effect on the cardiovascular measurements and its specificity for skeletal muscle are also in agreement with previously reported studies (21, 22). Harrison (16) reported that dantrolene sodium, contrary to procaine as presently used in treatment of malignant hyperthermia, had no effect on the myocardium. Nott and Bowman (10) reported that, in the absence of a neuromuscular blocker, spontaneous breathing in cats continued even after administration of dantrolene sodium sufficient to produce a 90% reduction of skeletal muscle twitch. The present results show that dantrolene sodium (up to 30 mg/kg iv) did not cause respiratory abnormality in unanesthetized sheep and anesthetized dogs. Other skeletal muscle relaxants depress respiratory function at doses that produce muscle relaxation through CNS depression or peripheral muscular paralysis. The lack of CNS depression (5–8) with dantrolene sodium would seem to allow for a compensatory increase in the rate, so that the minute volume is not changed.

Anesthetic-induced malignant hyperthermia, a phenomenon that has a reported fatality rate of over 70% (25), appears to result from some intrinsic abnormality of muscle (26); some evidence indicates

[14] Beckman-Type RS dynograph.
[15] Collins-Vitalometer.
[16] Harvard Apparatus.

Table II—Effect of Dantrolene Sodium on Cardiovascular Functions in Unanesthetized Sheep

Experiment[a]	Treatment	Arterial Blood Pressure[b], mm Hg	Mean Arterial Blood Pressure[c], mm Hg	Heart Rate, beats/min
1	Control	78/56	63	144
	Dantrolene sodium, 5 mg/kg iv	88/66	73	124
	Percent change	+13/+18	+16	−14
2	Control	82/56	65	156
	Dantrolene sodium, 5 mg/kg iv	82/60	67	118
	Percent change	0/+7	+3	−24
3	Control	80/62	68	126
	Dantrolene sodium, 10 mg/kg iv	75/59	64	128
	Percent change	−6/−5	−6	+2
4	Control	100/90	93	108
	Dantrolene sodium, 15 mg/kg iv	97/76	89	114
	Percent change	−3/−16	−4	+6
5	Control	112/106	108	96
	Dantrolene sodium, 15 mg/kg iv	80/70	73	102
	Percent change	−29/−34	−32	+6
6	Control	93/70	78	132
	Dantrolene sodium, 20 mg/kg iv	89/81	86	117
	Percent change	−4/+16	+10	−12
7	Control	118/60	79	114
	Dantrolene sodium, 25 mg/kg iv	106/70	82	97
	Percent change	−10/+17	+4	−15
8	Control	110/86	94	99
	Dantrolene sodium, 30 mg/kg iv	109/92	98	97
	Percent change	−1/+7	+4	−2
9	Control	80/64	69	114
	Solvent control, 10 mg/kg[d]	81/69	73	126
	Percent change	+1/+8	+6	+11
10	Control	106/70	82	96
	Solvent control, 25 mg/kg[d]	103/72	82	108
	Percent change	−3/+3	0	+13

[a] Each experiment consisted of one animal at each dose. [b] Systolic/diastolic. [c] Diastolic + (systolic − diastolic)/3. [d] Control solvent at volumes necessary to deliver dantrolene sodium at these doses.

that this defect is in the sarcoplasmic reticulum (27). Schwartz and Gracia (28) reported that among the clinical signs of malignant hyperthermia, that may develop during the initial general anesthetic procedure or not until the patient has been given a general anesthetic, are temperature elevation (as high as 45°), rigidity of skeletal muscle, ventricular arrhythmias, tachycardia, tachypnea, and mottled cyanosis. Among the drugs suggested as a treatment for this condition is procainamide (29). Procaine and procainamide lower myoplasmic calcium by transporting calcium out of the myoplasm into the sarcoplasmic reticulum. Their value in the treatment of malignant hyperthermia has been demonstrated in laboratory and clinical use (15). However, intravenous procainamide depresses cardiac contractility and causes a fall in blood pressure (30). Neuromuscular blocking agents can cause respiratory paralysis (30), and centrally acting drugs (*e.g.*, diazepam) can produce CNS depression and cardiorespiratory arrest (31).

The results of these animal studies with intravenous dantrolene sodium demonstrated its lack of cardiovascular and respiratory complications as well as a significant reduction in muscle contractile responses with doses of 2–5 mg/kg. Those results, in conjunction with the reported unique mechanism of action (5) and Harrison's reported (16) success in MHS swine, suggest that dantrolene sodium may be useful in the treatment of conditions where prompt relaxation of skeletal muscle is required (*e.g.*, in management of malignant hyperthermia).

CONCLUSIONS

The results of this study indicate that dantrolene sodium has no effect on the cardiovascular or respiratory systems that would preclude its use intravenously in acute conditions where direct relaxation of skeletal muscle is required, as in the management of malignant hyperthermia.

REFERENCES

(1) S. B. Chyatte and J. H. Birdsong, *South. Med. J.*, **64**, 830(1971).

(2) M. Chipman and S. Kaul, *Neurology*, **22**, 401(1972).

(3) J. V. Basmajian, *J. Rehabil.*, **39**, 7(1973).

(4) A. W. Monster, *Arch. Phys. Med. Rehabil.*, **55**, 373(1974).

(5) L. J. Honkomp, R. P. Halliday, and F. L. Wessels, *Pharmacologist*, **12**(2), 301(1970).

(6) K. O. Ellis and J. F. Carpenter, *Fed. Proc.*, **30**(3), 670 (1971).

(7) K. O. Ellis, A. W. Castellion, L. J. Honkomp, F. L. Wessels, J. F. Carpenter, and R. P. Halliday, *J. Pharm. Sci.*, **62**, 948(1973).

(8) D. E. Heald and Y. Matsumoto, *Pharmacologist*, **13**(2), 264(1971).

(9) K. O. Ellis and J. F. Carpenter, *Naunyn-Schmiedebergs Arch. Pharmakol.*, **275**, 83(1972).

(10) M. W. Nott and W. C. Bowman, *ibid.*, **279**(Suppl.), R30(1973).

(11) K. O. Ellis and S. H. Bryant, *ibid.*, **274**, 107(1972).

(12) J. W. Putney, Jr., and C. P. Bianchi, *Fed. Proc.*, **32**(3), 772(1973).

(13) K. O. Ellis and J. F. Carpenter, *Arch. Phys. Med. Rehabil.*, **55**, 362(1974).

(14) J. W. Putney, Jr., and C. P. Bianchi, *J. Pharmacol. Exp. Ther.*, **189**, 202(1974).

(15) B. A. Britt, *N. Engl. J. Med.*, **290**, 1140(1974).

(16) G. G. Harrison, *Br. J. Anesth.*, **47**, 62(1975).

(17) M. L. Katz and E. N. Bergman, *Am. J. Vet. Res.*, **30**(4), 655(1969).

(18) C. F. Kaufman and E. N. Bergman, *ibid.*, **32**(7), 1103 (1971).

(19) S. D. Dubin and G. Morrison, *J. Appl. Physiol.*, **27**, 104(1969).

(20) G. W. Snedecor and G. W. Cochran, "Statistical Methods," 6th ed., University of Iowa Press, Ames, Iowa, 1967, pp. 432–436.

(21) "Drill's Pharmacology in Medicine," 3rd ed., McGraw-Hill, New York, N.Y., 1965, pp. 193–194.

(22) J. L. Butterfield and K. O. Ellis, *Fed. Proc.*, **32**(3), 772(1973).

(23) M. W. Nott and W. C. Bowman, *Clin. Exp. Pharmacol. Physiol.*, **1**, 113(1974).

(24) A. W. Monster, Y. Tamai, and J. McHenry, *Arch. Phys. Med. Rehabil.*, **55**, 355(1974).

(25) G. G. Harrison, *Br. Med. J.*, **3**, 454(1971).

(26) J. H. Satnick, *Anesthesiology*, **30**, 472(1969).
(27) W. Kalow, B. A. Britt, and M. E. Terreau, *Lancet*, **2**, 895(1970).
(28) H. C. Schwartz and R. M. Gracia, *J. Oral Surg.*, **33**, 57(1975).
(29) T. H. Pan, A. R. Wollack, and J. A. DeMarco, *Curr. Res.*, **54**(1) (1973).
(30) "The Pharmacological Basis of Therapeutics," L. S. Goodman and A. Gilman, Eds., Macmillan, New York, N.Y., 1965, pp. 603, 711.
(31) *Med. Lett.*, **15**, 57(1973).
(32) "Biological Handbooks, Respiration and Circulation," P. L. Altman and D. S. Diltmer, Eds., Federation of American Societies of Experimental Biology, Bethesda, Md., 1971, p. 57.

ACKNOWLEDGMENTS AND ADDRESSES

Received August 16, 1975, from the *Research and Development Department, Eaton Laboratories, a Subsidiary of Norwich Pharmacal Company, Division of Morton-Norwich Products, Inc., Norwich, NY 13815*

Accepted for publication December 2, 1975.

The technical assistance of Ruth Turrell and Walton Dauchy is gratefully acknowledged. Suggestions and criticisms from Dr. A. W. Castellion during the preparation of this manuscript are also appreciated.

[x] To whom inquiries should be directed.

Spectrophotometric Study of Complex Formation between Oxovanadium(IV) and Antiamebic Drugs

R. ABU-EITTAH [x] and M. S. EL-NASR

Abstract □ Complex formation between oxovanadium(IV) and the antiamebic drugs 5,7-dibromo-8-quinolinol and 5,7-dichloro-8-quinolinol was studied in the pH 1.5–2.0 range, using ethanol, dioxane–water, and dimethylformamide as solvents. The composition of the formed complexes was determined by more than one procedure. In ethanol and dioxane–water, the 1:1 and 1:2 complexes were formed; in dimethylformamide, the 1:1, 1:2, and 1:3 complexes were formed. The stability constants were computed using two procedures: the molar ratio method and the extrapolation method. The reproducibility of results is satisfactory.

Keyphrases □ Complex formation—oxovanadium(IV) and substituted 8-quinolinols, spectrophotometric study in various solvents □ Oxovanadium(IV)—complex formation with substituted 8-quinolinols, spectrophotometric study in various solvents □ 8-Quinolinols, substituted—complex formation with oxovanadium(IV), spectrophotometric study in various solvents □ Spectrophotometry—determination of composition of complexes of oxovanadium(IV) and substituted 8-quinolinols in various solvents □ Antiamebic drugs—5,7-dibromo- and 5,7-dichloro-8-quinolinols, complex formation with oxovanadium(IV)

Quinoline derivatives, especially the iodinated ones, are active in amebiasis. Early work on these drugs was reviewed previously (1). Drugs such as 5,7-dibromo-8-quinolinol, 5,7-dichloro-8-quinolinol, and other 8-quinolinol derivatives were effective only in intestinal amebiasis (2). The chelating properties, ionization potential, and oil–water partition are predominant structure–activity factors (3).

The antibacterial action of the 8-quinolinol drugs, but not their efficiency as amebicides, is dependent on their chelating properties (4). The metal chelates of the studied drugs have tuberculostatic and fungitoxic activities (5, 6).

The chemistry of vanadium(IV) is almost entirely that of oxovanadium or vanadyl compounds. Selbin (7, 8) showed that VO^{+2} is probably the most stable diatomic ion known. The mixed ligand complexes of VO^{+2} with 8-quinolinol and thiocyanate were studied (9). The formation constant and free energy of formation of $[VOL(NCS)_2]HL$, where HL is 8-quinolinol and L is its anion, have been computed.

The chemistry of some 8-quinolinol complexes of vanadium, iron, and nickel was studied (10, 11). The use of 5,7-dibromo-8-quinolinol in the detection of vanadium was recommended (12, 13). Vanadium complexes of 8-quinolinol and its derivatives were used as sensitive indicators for the colorimetric determination of phenols and alcohols (14).

In this work, the complex formation between VO^{+2} and some 8-quinolinols was investigated in several organic solvents. The composition and formation constants of the formed complexes were found to be solvent dependent. Vanadyl quinolinolates may have tuberculostatic and fungitoxic activities similar to those of the copper derivatives (5).

EXPERIMENTAL

Materials—5,7-Dibromo-8-quinolinol (I) and 6,7-dichloro-8-quinolinol (II) were prepared by direct halogenation of 8-quinolinol[1] in acetic acid (15, 16). Vanadyl sulfate[2] solution was standardized potentiometrically (17). Ethanol (96%), dioxane, and dimethylformamide were purified by conventional methods (18).

Apparatus and Method—Electronic absorption spectra were determined[3] using 1.0-cm fused silica cells. To determine the composition and stability constant of the complexes, solutions of the metal ion and ligands were mixed just before scanning the spectra.

The solution pH was measured on a precision pH meter[4] by using the millivolt scale, and the corresponding pH values were calculated.

[1] British Drug Houses grade reagent.
[2] Prolabograde reagent.
[3] Unicam SP 8000 spectrophotometer.
[4] Radelkis type OP-205.

(26) J. H. Satnick, *Anesthesiology*, **30**, 472(1969).
(27) W. Kalow, B. A. Britt, and M. E. Terreau, *Lancet*, **2**, 895(1970).
(28) H. C. Schwartz and R. M. Gracia, *J. Oral Surg.*, **33**, 57(1975).
(29) T. H. Pan, A. R. Wollack, and J. A. DeMarco, *Curr. Res.*, **54**(1) (1973).
(30) "The Pharmacological Basis of Therapeutics," L. S. Goodman and A. Gilman, Eds., Macmillan, New York, N.Y., 1965, pp. 603, 711.
(31) *Med. Lett.*, **15**, 57(1973).
(32) "Biological Handbooks, Respiration and Circulation," P. L. Altman and D. S. Diltmer, Eds., Federation of American Societies of Experimental Biology, Bethesda, Md., 1971, p. 57.

ACKNOWLEDGMENTS AND ADDRESSES

Received August 16, 1975, from the *Research and Development Department, Eaton Laboratories, a Subsidiary of Norwich Pharmacal Company, Division of Morton-Norwich Products, Inc., Norwich, NY 13815*

Accepted for publication December 2, 1975.

The technical assistance of Ruth Turrell and Walton Dauchy is gratefully acknowledged. Suggestions and criticisms from Dr. A. W. Castellion during the preparation of this manuscript are also appreciated.

[x] To whom inquiries should be directed.

Spectrophotometric Study of Complex Formation between Oxovanadium(IV) and Antiamebic Drugs

R. ABU-EITTAH [x] and M. S. EL-NASR

Abstract □ Complex formation between oxovanadium(IV) and the antiamebic drugs 5,7-dibromo-8-quinolinol and 5,7-dichloro-8-quinolinol was studied in the pH 1.5–2.0 range, using ethanol, dioxane–water, and dimethylformamide as solvents. The composition of the formed complexes was determined by more than one procedure. In ethanol and dioxane–water, the 1:1 and 1:2 complexes were formed; in dimethylformamide, the 1:1, 1:2, and 1:3 complexes were formed. The stability constants were computed using two procedures: the molar ratio method and the extrapolation method. The reproducibility of results is satisfactory.

Keyphrases □ Complex formation—oxovanadium(IV) and substituted 8-quinolinols, spectrophotometric study in various solvents □ Oxovanadium(IV)—complex formation with substituted 8-quinolinols, spectrophotometric study in various solvents □ 8-Quinolinols, substituted—complex formation with oxovanadium(IV), spectrophotometric study in various solvents □ Spectrophotometry—determination of composition of complexes of oxovanadium(IV) and substituted 8-quinolinols in various solvents □ Antiamebic drugs—5,7-dibromo- and 5,7-dichloro-8-quinolinols, complex formation with oxovanadium(IV)

Quinoline derivatives, especially the iodinated ones, are active in amebiasis. Early work on these drugs was reviewed previously (1). Drugs such as 5,7-dibromo-8-quinolinol, 5,7-dichloro-8-quinolinol, and other 8-quinolinol derivatives were effective only in intestinal amebiasis (2). The chelating properties, ionization potential, and oil–water partition are predominant structure–activity factors (3).

The antibacterial action of the 8-quinolinol drugs, but not their efficiency as amebicides, is dependent on their chelating properties (4). The metal chelates of the studied drugs have tuberculostatic and fungitoxic activities (5, 6).

The chemistry of vanadium(IV) is almost entirely that of oxovanadium or vanadyl compounds. Selbin (7, 8) showed that VO^{+2} is probably the most stable diatomic ion known. The mixed ligand complexes of VO^{+2} with 8-quinolinol and thiocyanate were studied (9). The formation constant and free energy of formation of $[VOL(NCS)_2]HL$, where HL is 8-quinolinol and L is its anion, have been computed.

The chemistry of some 8-quinolinol complexes of vanadium, iron, and nickel was studied (10, 11). The use of 5,7-dibromo-8-quinolinol in the detection of vanadium was recommended (12, 13). Vanadium complexes of 8-quinolinol and its derivatives were used as sensitive indicators for the colorimetric determination of phenols and alcohols (14).

In this work, the complex formation between VO^{+2} and some 8-quinolinols was investigated in several organic solvents. The composition and formation constants of the formed complexes were found to be solvent dependent. Vanadyl quinolinolates may have tuberculostatic and fungitoxic activities similar to those of the copper derivatives (5).

EXPERIMENTAL

Materials—5,7-Dibromo-8-quinolinol (I) and 6,7-dichloro-8-quinolinol (II) were prepared by direct halogenation of 8-quinolinol[1] in acetic acid (15, 16). Vanadyl sulfate[2] solution was standardized potentiometrically (17). Ethanol (96%), dioxane, and dimethylformamide were purified by conventional methods (18).

Apparatus and Method—Electronic absorption spectra were determined[3] using 1.0-cm fused silica cells. To determine the composition and stability constant of the complexes, solutions of the metal ion and ligands were mixed just before scanning the spectra.

The solution pH was measured on a precision pH meter[4] by using the millivolt scale, and the corresponding pH values were calculated.

[1] British Drug Houses grade reagent.
[2] Prolabograde reagent.
[3] Unicam SP 8000 spectrophotometer.
[4] Radelkis type OP-205.

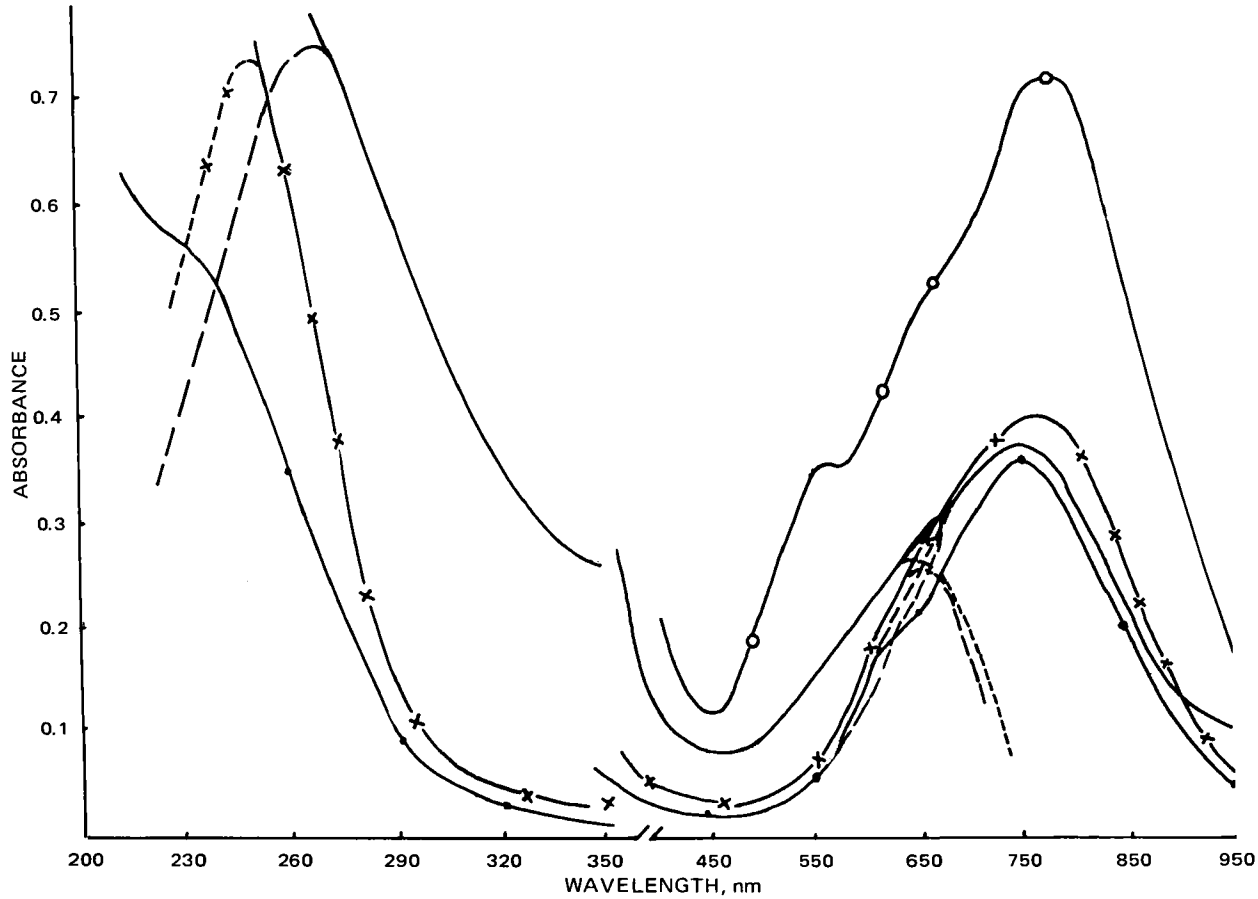

Figure 1—*Electronic absorption spectra of vanadyl sulfate. Key: —, in dioxane–water; ○, in dimethylformamide; ×, in ethanol; and ●, in water.*

RESULTS AND DISCUSSION

Absorption Spectra of Oxovanadium(IV) Solutions—The electronic absorption spectra of oxovanadium(IV) complexes consist of three *d–d* transitions in the 8000–32,000-cm^{-1} range in addition to a strong charge transfer transition in the near UV region (42,000 cm^{-1}). The three transitions are designated band 1 ($b_2 \rightarrow e$, 11,000–14,700 cm^{-1}), band 2 ($b_2 \rightarrow b_1$, $10D_q$, 14,800–20,400 cm^{-1}), and band 3 ($b_2 \rightarrow a_1$, 21,000–31,250 cm^{-1}). In many cases, band 3 is obscured by the long wavelength tail of the more intense charge transfer band.

The spectra of the species $[VO(H_2O)_5]^{+2}$ have been extensively studied (19–21), and it was recommended (19) to treat the ion as a tetragonally distorted octahedron. Figure 1 shows the absorption spectra of vanadyl sulfate in water, ethanol (96%), 90% (v/v) dioxane–water, and dimethylformamide. All solutions were acidified with sulfuric acid to pH 1.5–2.0.

Table I—Band Maxima, Molar Absorptivity, and *f* Values for Vanadyl Sulfate in Different Solvents

Solvent	Band	λ_{max}, nm	ϵ	$f^a \times 10^3$	Δ^b, cm^{-1}
Water	1	768	17.0	0.3	
	2	630	9.1	0.2	15,873
	3	—	—	—	
	4	240	275.0	0.1	
96% Ethanol	1	768	19.5	0.4	
	2	640	12.5	0.2	15,620
	3	—	—	—	
	4	245	—	—	
90% Dioxane–water	1	740	17.25	0.4	
	2	650	12.0	0.3	15,380
	3	—	—	—	
	4	266	—	—	
Dimethylformamide	1	775	35.75	0.8	
	2	650	24.00	0.5	15,150
	3	550	17.00	0.3	
	4	—	—	—	

[a] Oscillator strength. [b] $10D_q$.

The absorbing species can be considered to be $[VO(A_xB_y)]^{+2}$, where A and B are solvent molecules. These molecules are of the same type when vanadyl sulfate is dissolved in water and may be different when it is dissolved in an organic solvent, $x + y = 5$. Band maxima are given in Table I.

The water molecules in the inner coordination sphere of VO^{+2} ions are replaced partially or completely by other solvent molecules when vanadyl sulfate pentahydrate is dissolved in an organic solvent. With water as the solvent, the $b_2 \rightarrow b_1$ transition occurs at 15,873 cm^{-1}, giving a value of 1587 cm^{-1} for D_q. The value of Δ is appreciably below that expected by extrapolation of the $10D_q$ values of $V(H_2O)_6^{+2}$ (11,800 cm^{-1}) and $V(H_2O)_6^{+3}$ (18,500 cm^{-1}). Consequently, the crystal field description of the VO^{+2} ion is not the best, and π-bonding is significant.

With ethanol as the solvent, the numerical value of D_q and the energy of the charge transfer transition are less than the corresponding values with water. This finding indicates that alcohol molecules replace some water molecules in the inner coordination sphere. The ligand field strength is in the order water > ethanol. Also, the ionization potential of ethanol (10.5 ev) is less than that of water (12.6 ev), which accounts for the decrease of the energy of the charge transfer transition. Similar results were observed with dioxane–water.

The spectrum of vanadyl sulfate pentahydrate differs significantly in dimethylformamide. All of the *d–d* transitions are red shifted, and band 3 appears clearly (not obscured). On the other hand, the charge transfer transition is not observed, since it occurs in the region where the solvent absorbs. The results indicate that the ligand field strength is in the order water > ethanol > dioxane > dimethylformamide.

Complex Formation between Oxovanadium(IV) and I in Ethanol—*Absorption Spectra*—When the alcoholic solution of I (pale yellow) is mixed with the alcoholic solution of vanadyl sulfate (blue), the mixture becomes red. The formed complex has an ab-

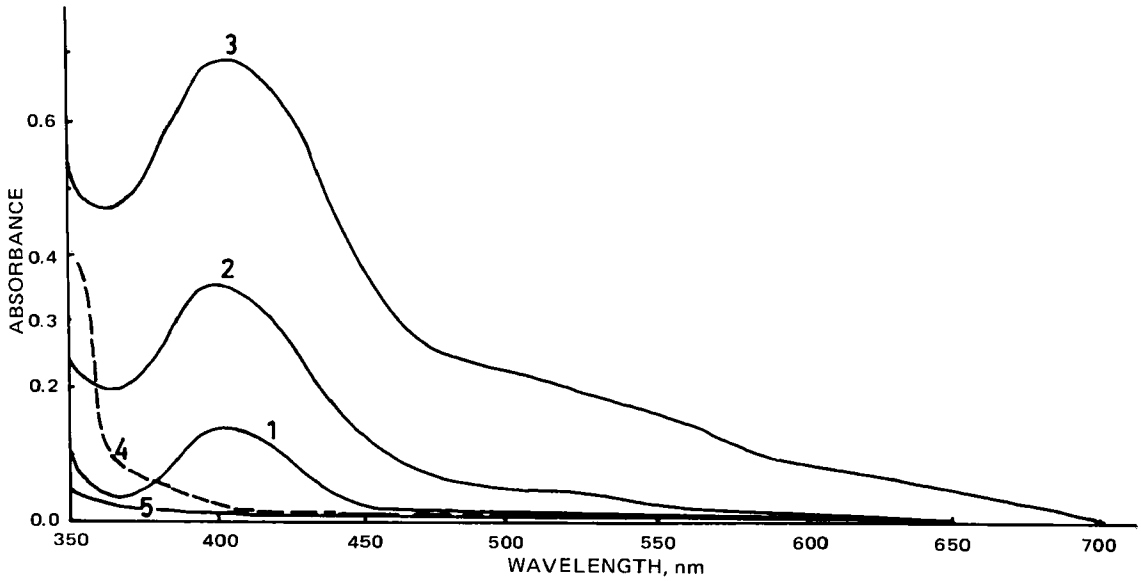

Figure 2—*Absorption spectra of vanadyl sulfate–I in ethanol. Total concentration was 5 × 10^{-4} M. The ratios of [VO^{+2}]–I were: 1, 5:1; 2, 1:9; and 3, 3:7. Curve 4 shows I at 4.5 × 10^{-4} M, and curve 5 is VO^{+2} at 4.5 × 10^{-4} M.*

sorption band of its own, with λ_{max} 396 nm (Fig. 2); this band is used to investigate its properties.

When applying Job's (22) method of continuous variations and the slope ratio and molar ratio methods (23, 24), the predominant complex proved to be the 1:2 vanadyl–I complex (Fig. 3).

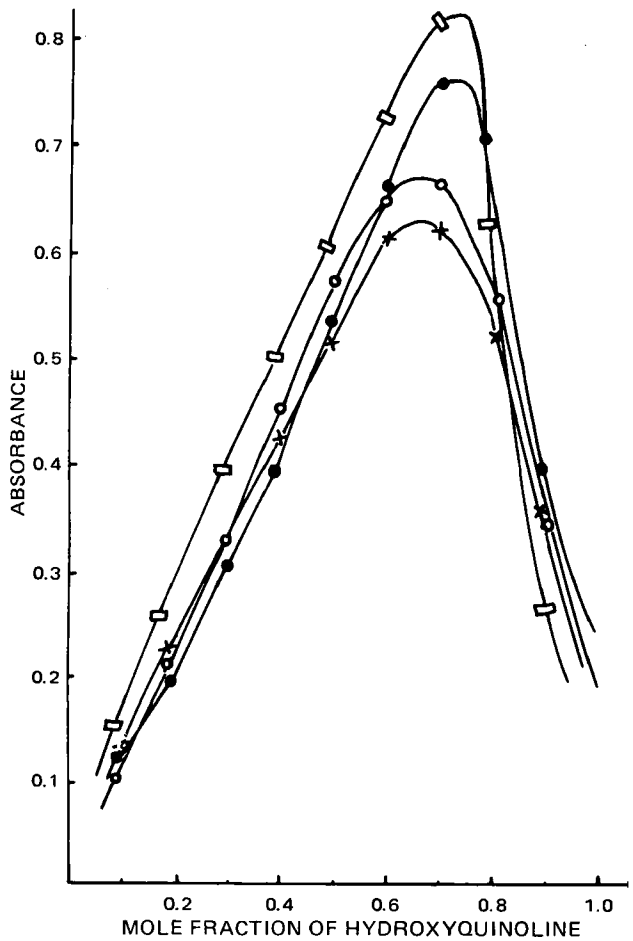

Figure 3—*Composition of vanadyl–8-quinolinol complexes using the continuous variation method. Key:* ○, *I in ethanol;* ×, *II in ethanol;* □, *I in demethylformamide; and* ●, *II in dimethylformamide.*

The acid dissociation constant of I in 96% ethanol was determined potentiometrically (25). The quinolinol solution in ethanol (2.0 × 10^{-3} *M*) was titrated against a 2 × 10^{-2} *M* alcoholic solution of standardized potassium hydroxide; the average value of pKa was 9.79. Since complexation of VO^{+2} with I was studied in the pH 1.5–2.0 range, the concentration of the 8-quinolinol anion was negligible and the ligating species was considered to be 8-quinolinol itself.

Stability Constant of Formed Complexes—The stability constant of the 1:2 vanadyl–I complex was computed using the simple molar ratio method. The spectra of mixtures of VO^{+2} and I, in which the ratio of [VO^{+2}]/[I] varied from 1:1 to 1:25, were determined. The relationship between the absorbance at 396 nm and the ratio of [I]/[VO^{+2}] is shown in Fig. 4. By using the simple known relationship (25), a value of 9.11 was computed for log β_2.

Yatsimiriskii's method for computing $\beta_1, \beta_2, \ldots, \beta_n$ for the first, second, and nth complex is applicable to spectrophotometric data. Details of the procedure and mathematical formalism are found elsewhere (26). The equations needed for computation are:

$$f_1 = (E - \epsilon_0)/a \qquad \lim_{a \to 0} f_1 = \Delta\epsilon_1\beta_1 = X \qquad \text{(Eq. 1)}$$

$$f_t = (f_{t-1} - X)/a \qquad \lim_{a \to 0} f_t = \Delta\epsilon_t\beta_t - \Delta\epsilon_1\beta_1^t \qquad \text{(Eq. 2)}$$

$$f_1' = f_1 a \qquad \lim_{a \to \infty} f_1' = \Delta\epsilon_N = Y \qquad \text{(Eq. 3)}$$

$$f_t' = (f_{t-1}' - Y) \qquad \lim_{a \to \infty} f_2' = (\Delta\epsilon_1 - \Delta\epsilon_2)\beta_1/\beta_2 \qquad \text{(Eq. 4)}$$

Table II—Data Needed for Yatsimiriskii's Method to Compute β_1 and β_2[a]

Ligand Concentration [A] × 10^4	$[A]^{-1} \times 10^{-3}$	E	$f_1 \times 10^{-6}$	$-f_2 \times 10^{10}$
0.2	50.00	1350	67.5	17.5
0.4	25.00	2600	65.6	13.8
0.5	20.00	3200	64.0	14.0
0.6	16.00	3750	62.5	14.1
0.8	12.50	4800	60.0	13.75
1.0	10.00	5575	55.7	15.3
1.2	8.30	6075	50.6	17.0[b]
1.6	6.25	6525	40.8	18.8[b]
4.0	2.50	7325	18.3	13.2
6.0	1.66	7625	12.7	9.7
8.0	1.25	7750	9.7	7.6
10.0	1.00	7975	8.0	6.3
12.0	0.83	8225	6.8	5.3

[a] [VO^{+2}] = 4 × 10^{-5} *M*. [b] Neglected.

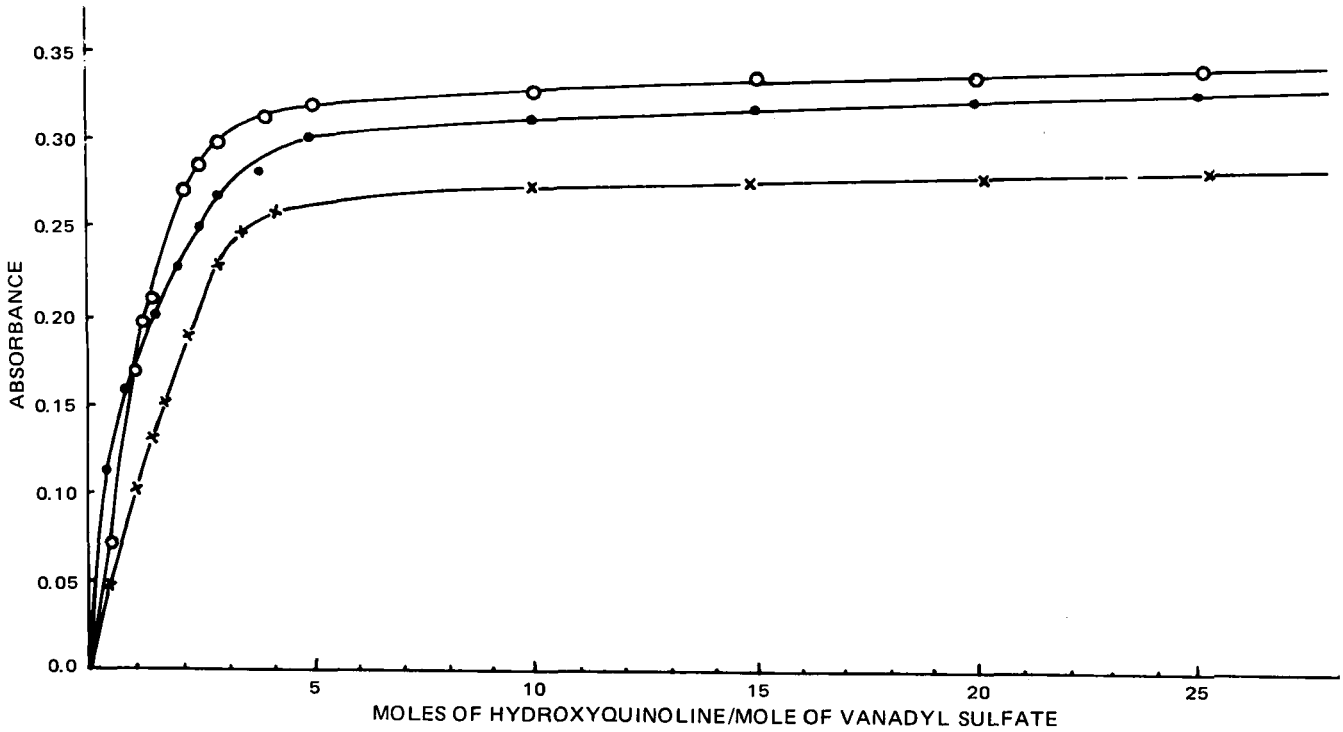

Figure 4—*Variation of absorbance of vanadyl sulfate–8-quinolinol solutions with 8-quinolinol concentration. Key: ×, I in ethanol, λ = 396 nm; ●, II in dimethylformamide, λ = 388 nm; and ○, I in dimethylformamide, λ = 386 nm.*

The spectra of solutions containing constant $[VO^{+2}]$ and increasing ligand concentrations were determined, and the value of E is given by:

$$E = (A_s - l\epsilon_A a)/Bl \qquad \text{(Eq. 5)}$$

where A_s = absorbance of the mixture at 396 nm, ϵ_A = molar absorptivity of the ligand at 396 nm, B = total metal concentration, and a = free ligand concentration.

The necessary data are given in Table II, and the values calculated for $\Delta\epsilon_1$, $\Delta\epsilon_2$, β_1, β_2 are given in Table III.

Complexes of Oxovanadium(IV) and II—To confirm these results, complex formation between VO^{+2} and II in 96% ethanol was investigated. The compositions of the formed complexes were similarly determined and proved to be 1:1 and 1:2. The acid dissociation constant of II was investigated, and a value of 9.83 was computed for the pKa. Consequently, the complexing species was thought to be 8-quinolinol at pH 1.5–2.0. In the kinetic study of complex formation of 8-quinolinol and 8-quinolinol 5-sulfonate (27) with nickel(II), the complexing species was considered to be 8-quinolinol.

The stability constants of the formed vanadyl–II complexes were computed as previously described. The molar ratio method gave 8.3 for log β_2, and results of Yatsimiriskii's procedures are given in Table III.

Comparison of the results in Table III indicates that vanadyl–I complexes are more stable than vanadyl–II complexes. This finding was expected on the basis of the stronger electron-donating properties of I compared to II.

Table III—Molar Absorptivities and Stability Constants of Vanadyl–I and Vanadyl–II Complexes

	I				II			
$[VO^{+2}] \times 10^5$	$\Delta\epsilon_1$	$\Delta\epsilon_2$	Log β_1	Log β_2	$\Delta\epsilon_1$	$\Delta\epsilon_2$	Log β_1	Log β_2
4.0	6870	7650	4.01	7.76	8000	8900	3.80	7.01
5.0	6600	7500	3.86	7.28	—	—	—	—
6.0	7000	7200	3.75	6.4[a]	7800	8500	3.65	6.81
8.0	—	—	—	—	7500	8300	3.64	6.87
Average	6820	7420	3.67	7.52	7800	8600	3.69	6.93

[a] Neglected.

Effect of Solvent on Complex Formation—The complex formation between VO^{+2} and I and II in dioxane–water or dimethylformamide was investigated spectrophotometrically. If the inner coordination sphere of the metal ion contains one or more solvent molecules, then the composition of the complex, band maxima of its absorption, molar absorptivity, and stability constant depend on the solvent. The compositions of the formed complexes were determined following the same procedures as before.

In dioxane–water, the main complexes between vanadyl ion and the studied 8-quinolinols were the 1:1 and 1:2 complexes. The 1:1, 1:2, and 1:3 complexes were formed when dimethylformamide was the solvent. The computed stability constants of the formed complexes using Yatsimiriskii's procedure are given in Table IV. With dimethylformamide, β_3 was calculated using the molar ratio method (Table IV).

CONCLUSIONS

Oxovanadium(IV) and 5,7-dibromo-8-quinolinol or 5,7-dichloro-8-quinolinol complex in the ratios of 1:1 and 1:2 when ethanol or dioxane–water is the solvent. The 1:1, 1:2, and 1:3 complexes are formed when dimethylformamide is the solvent. In all cases, complex formation was studied in the pH 1.5–2.0 range. If a distorted octahedron is assumed for the formed complex, the suggested composition for the 1:2 complex is $[VO(R)_2S]^{+2}$, where S stands for a solvent molecule; $[VO(R)_3]^{+2}$ stands for the 1:3 complex. In this case, two ligand molecules act as bidentate and the third acts as a unidentate ligand. It

Table IV—Band Maxima, Molar Absorptivities and Stability Constants of Vanadyl–8-Quinolinol Complexes in Different Solvents

Solvent	Ligand	Band Maximum, nm	Log β_1	Log β_2	Log β_3	$\Delta\epsilon \times 10^{-3}$ $\Delta\epsilon_1$	$\Delta\epsilon_2$	$\Delta\epsilon_3$
Dioxane–water (90% v/v)	I	394	3.92	7.25	—	6.45	6.7	—
	II	392	3.88	7.25	—	4.6	6.5	—
Dimethylformamide	I	386	—	—	15.87	—	—	8.5
	II	388	—	—	15.36	—	—	8.2

is suggested that the complexing species is the 8-quinolinol molecule and not its anion. This conclusion is based on the fact that, in the pH 1.5–2.0 range, the anion concentration is negligible as computed from the acid dissociation constant of the 8-quinolinol in the specific solvent.

Variation of the solvent affected significantly the composition, stability, and *d*-orbital splitting of the metal ion in the formed complex. Due to steric factors, no dimethylformamide molecules appear to coordinate in the inner coordination sphere of metal ion; as a result, the 1:3 vanadyl–8-quinolinol complexes are predominant. In 96% ethanol and dioxane–water, one solvent molecule coordinates in the inner coordination sphere and 1:2 complexes are formed.

REFERENCES

(1) H. H. Anderson and E. L. Hansem, *Pharmacol. Rev.*, **2**, 399(1950).

(2) "The Pharmacological Basis of Therapeutics", 4th ed., L. S. Goodman and A. Gilman, Eds., Macmillan, London, England, 1972, p. 1137.

(3) P. Thompson, J. Reinetson, A. Bayles, D. McCarthy, and E. Elslager, *Am. J. Trop. Med. Hyg.*, **4**, 224(1958).

(4) A. Albert, A. Hampton, F. Sebie, and R. Simon, *Br. J. Exp. Pathol.*, **35**, 75(1954).

(5) M. Georgol and G. Herman, *Residue Rev.*, **25**, 107(1969).

(6) P. Raisinghani, B. Murty, and M. Khorana, *Indian J. Pharm.*, **32**, 34(1970).

(7) J. Selbin, *Coord. Chem. Rev.*, **1**, 293(1966).

(8) J. Selbin, *Chem. Rev.*, **65**, 153(1965).

(9) V. Rao and Y. Anjaneyulu, *J. Inorg. Nucl. Chem.*, **33**, 3567(1971).

(10) A. Blair, D. Pantony, and G. Minkoff, *ibid.*, **5**, 316(1958).

(11) E. Sudo, *J. Chem. Soc. Jpn.*, **72**, 871(1951).

(12) G. Gutzeit and R. Monnier, *Helv. Chim. Acta*, **16**, 239(1933).

(13) J. Gillis, *Mikrochemie*, **31**, 273(1944).

(14) M. Pesez and J. Bartos, *Bull. Soc. Chim. Fr.*, **1**, 304 (1969).

(15) A. Claus and H. Howtiz, *J. Prakt. Chem.*, **46**, 444(1891).

(16) R. Berg, *Z. Anorg. Chem.*, **204**, 208(1932).

(17) H. Khalifa and A. El-Sirafy, *Z. Anal. Chem.*, **227**, 109(1967).

(18) A. Weissberger, E. Proskauer, J. Raddick, and E. Toops, "Organic Solvents," 2nd ed., Interscience, New York, N.Y., 1960.

(19) C. K. Jorgenson, *Acta Chem. Scand.*, **11**, 73(1957).

(20) S. C. Forman and C. S. Grauer, *J. Am. Chem. Soc.*, **72**, 1785(1955).

(21) F. Rossotti and H. Rossotti, *Acta Chem. Scand.*, **9**, 1177(1955).

(22) P. Job, *C.R.*, **180**, 228(1925).

(23) H. E. Harvey and D. L. Manning, *J. Am. Chem. Soc.*, **72**, 4488(1950).

(24) J. A. Joe and A. I. Jones, *Ind. Eng. Chem. Anal. Ed.*, **16**, 11(1944).

(25) A. Albert and E. P. Serjeant, "Ionization Constants," Wiley, New York, N.Y., 1962.

(26) F. Rossotti and H. Rossotti, "The Determination of Stability Constants," McGraw-Hill, New York, N.Y., 1962, p. 260.

(27) W. Johnson and R. Wilkins, *Inorg. Chem.*, **9**, 1917(1970).

ACKNOWLEDGMENTS AND ADDRESSES

Received July 21, 1975, from the *Department of Analytical Chemistry, Faculty of Pharmacy, University of Cairo, Cairo, Egypt.*

Accepted for publication December 4, 1975.

The authors express their gratitude to Professor M. M. Amer for assistance.

[x] To whom inquiries should be directed. Present address: Chemistry Department, Faculty of Science, Kuwait University, Kuwait.

Isolation and Characterization of the Cardiotonic Polypeptide Anthopleurin-A from the Sea Anemone *Anthopleura xanthogrammica*

TED R. NORTON [x], S. SHIBATA, M. KASHIWAGI, and JAMES BENTLEY

Abstract □ A highly potent cardiotonic polypeptide, anthopleurin-A, was isolated from the sea anemone, *Anthopleura xanthogrammica* (Brandt), using solvent partition, gel permeation chromatography, and cation-exchange chromatography. It is a pure basic polypeptide with a molecular weight of about 5500.

Keyphrases □ Anthopleurin-A—isolated from sea anemone *Anthopleura xanthogrammica* extract □ *Anthopleura xanthogrammica*—sea anemone extract, cardiotonic polypeptide anthopleurin-A isolated □ Cardiotonic polypeptide—anthopleurin-A isolated from sea anemone □ Sea anemone—extract, cardiotonic polypeptide anthopleurin-A isolated

Several extracts of coelenterates have been examined in this laboratory for antitumor activity (1–4) and, more recently, for a positive inotropic effect (4, 5). Interest was first stimulated in *Anthopleura xanthogrammica* when the crude extract was found to be highly toxic when administered intravenously to an anesthetized rat[1]. Later, the crude extract at much higher dilutions exhibited a strong positive inotropic effect on isolated rat atria; pretreatment with adrenergic receptor blocking agents, 6-hydroxydopamine or reserpine, did not affect the response, indicating that the extract acts by a nonadrenergic mechanism (5).

Many investigators have examined the chemical nature and pharmacology of toxins from coelenterates (6). An extract of the tentacles of *Calliactus polypus* (a sea anemone) caused a brief lowering of coronary outflow, heart rate, and amplitude of cardiac contractions in the isolated rabbit heart, and higher doses produced irregular cardiac contractions, usually resulting in cardiac

[1] Dr. George W. Read and Ms. Charlotte Oda, Department of Pharmacology, University of Hawaii, personal communication.

is suggested that the complexing species is the 8-quinolinol molecule and not its anion. This conclusion is based on the fact that, in the pH 1.5–2.0 range, the anion concentration is negligible as computed from the acid dissociation constant of the 8-quinolinol in the specific solvent.

Variation of the solvent affected significantly the composition, stability, and *d*-orbital splitting of the metal ion in the formed complex. Due to steric factors, no dimethylformamide molecules appear to coordinate in the inner coordination sphere of metal ion; as a result, the 1:3 vanadyl–8-quinolinol complexes are predominant. In 96% ethanol and dioxane–water, one solvent molecule coordinates in the inner coordination sphere and 1:2 complexes are formed.

REFERENCES

(1) H. H. Anderson and E. L. Hansem, *Pharmacol. Rev.*, **2**, 399(1950).

(2) "The Pharmacological Basis of Therapeutics", 4th ed., L. S. Goodman and A. Gilman, Eds., Macmillan, London, England, 1972, p. 1137.

(3) P. Thompson, J. Reinetson, A. Bayles, D. McCarthy, and E. Elslager, *Am. J. Trop. Med. Hyg.*, **4**, 224(1958).

(4) A. Albert, A. Hampton, F. Sebie, and R. Simon, *Br. J. Exp. Pathol.*, **35**, 75(1954).

(5) M. Georgol and G. Herman, *Residue Rev.*, **25**, 107(1969).

(6) P. Raisinghani, B. Murty, and M. Khorana, *Indian J. Pharm.*, **32**, 34(1970).

(7) J. Selbin, *Coord. Chem. Rev.*, **1**, 293(1966).

(8) J. Selbin, *Chem. Rev.*, **65**, 153(1965).

(9) V. Rao and Y. Anjaneyulu, *J. Inorg. Nucl. Chem.*, **33**, 3567(1971).

(10) A. Blair, D. Pantony, and G. Minkoff, *ibid.*, **5**, 316(1958).

(11) E. Sudo, *J. Chem. Soc. Jpn.*, **72**, 871(1951).

(12) G. Gutzeit and R. Monnier, *Helv. Chim. Acta*, **16**, 239(1933).

(13) J. Gillis, *Mikrochemie*, **31**, 273(1944).

(14) M. Pesez and J. Bartos, *Bull. Soc. Chim. Fr.*, **1**, 304 (1969).

(15) A. Claus and H. Howtiz, *J. Prakt. Chem.*, **46**, 444(1891).

(16) R. Berg, *Z. Anorg. Chem.*, **204**, 208(1932).

(17) H. Khalifa and A. El-Sirafy, *Z. Anal. Chem.*, **227**, 109(1967).

(18) A. Weissberger, E. Proskauer, J. Raddick, and E. Toops, "Organic Solvents," 2nd ed., Interscience, New York, N.Y., 1960.

(19) C. K. Jorgenson, *Acta Chem. Scand.*, **11**, 73(1957).

(20) S. C. Forman and C. S. Grauer, *J. Am. Chem. Soc.*, **72**, 1785(1955).

(21) F. Rossotti and H. Rossotti, *Acta Chem. Scand.*, **9**, 1177(1955).

(22) P. Job, *C.R.*, **180**, 228(1925).

(23) H. E. Harvey and D. L. Manning, *J. Am. Chem. Soc.*, **72**, 4488(1950).

(24) J. A. Joe and A. I. Jones, *Ind. Eng. Chem. Anal. Ed.*, **16**, 11(1944).

(25) A. Albert and E. P. Serjeant, "Ionization Constants," Wiley, New York, N.Y., 1962.

(26) F. Rossotti and H. Rossotti, "The Determination of Stability Constants," McGraw-Hill, New York, N.Y., 1962, p. 260.

(27) W. Johnson and R. Wilkins, *Inorg. Chem.*, **9**, 1917(1970).

ACKNOWLEDGMENTS AND ADDRESSES

Received July 21, 1975, from the *Department of Analytical Chemistry, Faculty of Pharmacy, University of Cairo, Cairo, Egypt.*

Accepted for publication December 4, 1975.

The authors express their gratitude to Professor M. M. Amer for assistance.

[x] To whom inquiries should be directed. Present address: Chemistry Department, Faculty of Science, Kuwait University, Kuwait.

Isolation and Characterization of the Cardiotonic Polypeptide Anthopleurin-A from the Sea Anemone *Anthopleura xanthogrammica*

TED R. NORTON [x], S. SHIBATA, M. KASHIWAGI, and JAMES BENTLEY

Abstract □ A highly potent cardiotonic polypeptide, anthopleurin-A, was isolated from the sea anemone, *Anthopleura xanthogrammica* (Brandt), using solvent partition, gel permeation chromatography, and cation-exchange chromatography. It is a pure basic polypeptide with a molecular weight of about 5500.

Keyphrases □ Anthopleurin-A—isolated from sea anemone *Anthopleura xanthogrammica* extract □ *Anthopleura xanthogrammica*—sea anemone extract, cardiotonic polypeptide anthopleurin-A isolated □ Cardiotonic polypeptide—anthopleurin-A isolated from sea anemone □ Sea anemone—extract, cardiotonic polypeptide anthopleurin-A isolated

Several extracts of coelenterates have been examined in this laboratory for antitumor activity (1–4) and, more recently, for a positive inotropic effect (4, 5). Interest was first stimulated in *Anthopleura xanthogrammica* when the crude extract was found to be highly toxic when administered intravenously to an anesthetized rat[1]. Later, the crude extract at much higher dilutions exhibited a strong positive inotropic effect on isolated rat atria; pretreatment with adrenergic receptor blocking agents, 6-hydroxydopamine or reserpine, did not affect the response, indicating that the extract acts by a nonadrenergic mechanism (5).

Many investigators have examined the chemical nature and pharmacology of toxins from coelenterates (6). An extract of the tentacles of *Calliactus polypus* (a sea anemone) caused a brief lowering of coronary outflow, heart rate, and amplitude of cardiac contractions in the isolated rabbit heart, and higher doses produced irregular cardiac contractions, usually resulting in cardiac

[1] Dr. George W. Read and Ms. Charlotte Oda, Department of Pharmacology, University of Hawaii, personal communication.

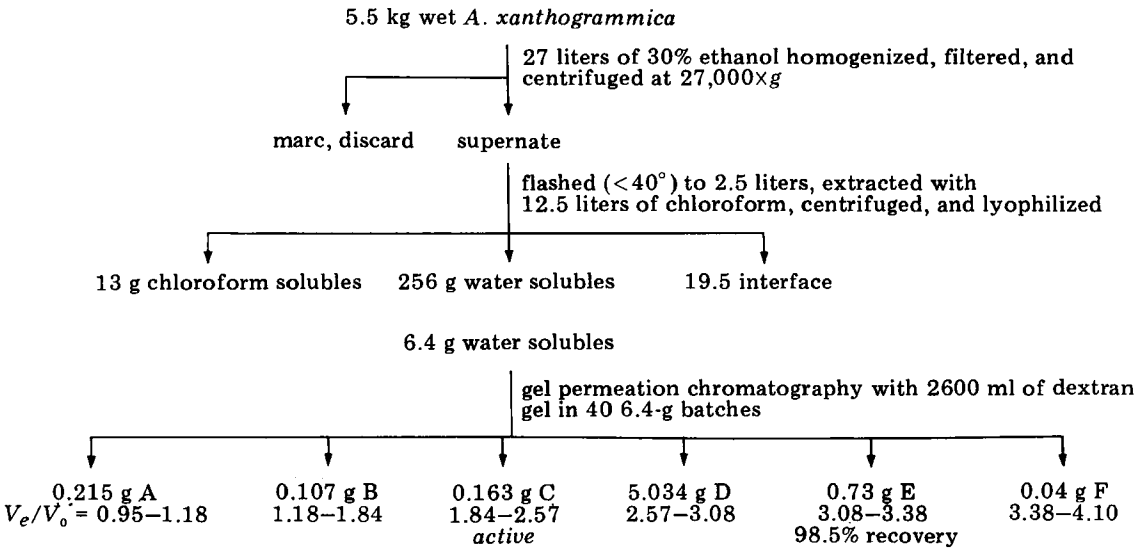

Scheme I—Extraction and initial purification scheme from A. xanthogrammica *to Fraction C*

arrest (7). It was reported[2] that extracts of about 15% of the species from five phyla of marine animals showed an increase in contractile force in the Langendorf guinea pig heart preparation and that a compound isolated from the polar fraction of the sponge, *Dasychalina cyathina,* is capable of reversible cessation of mechanical activity in the same preparation.

Low molecular weight polypeptides such as bradykinin and its congeners have been studied with respect to their cardioactivity (8). The question of whether these agents increase the heart rate and myocardial contractile force directly or indirectly through reflex is still moot (8). Recently, an inotropically active peptide from dog blood plasma was partially identified (9) as an "intact molecule" attached to an octapeptide (seven isoleucine and one glycine residues) and had activity parallel to that of epinephrine on the dog heart papillary muscle.

Although the cardiac glycosides have long been recognized as effective cardiotonic agents, they all have caused serious side effects such as arrhythmias and cardiac arrest. It, therefore, seemed advisable to pursue the isolation and pharmacological study of the cardiotonic substance(s) in *A. xanthogrammica.*

EXPERIMENTAL

Extraction—*A. xanthogrammica* (Brandt) specimens were collected from Bodega Bay, Calif.[3], preserved in 95% ethanol, and stored at 4° prior to extraction. Five different collections, made at different times of the year, contained a consistent amount of the cardiotonic substance.

Wet, drained anemones (5.5 kg) were cut into <2-cm pieces and homogenized in batches in a blender for 5 min with 27 liters of 30% ethanol; this volume included the ethanol used to preserve the specimens. The mixture was allowed to stand for 1 week at 20° with occasional stirring and was then filtered through six layers of cheesecloth. The filtrate was flash evaporated at ≤40° to about 2.5 liters and partitioned with 12.5 liters of chloroform, in batches, by thorough agitation followed by centrifugation at 27,000×*g* for 30 min. This procedure produced 13 g of chloroform solubles, 10 g of interface solids, and 256 g (lyophilized weight) of water solubles (contractile force in the isolated rat atria increased 240% in 20 min at 12 ppm in the atria bath; see Ref. 5 for details of the assay method).

Gel Permeation Chromatography—The crude extract was split into 40 equal portions for chromatographic separation on cross-linked dextran gel[4] (Fig. 1). A column, 53 × 8.3 cm, containing 2600 ml of wet gel (V_0 = 825 ml) was equilibrated with 0.1 *M* NH_4HCO_3 saturated with chloroform (to prevent microorganism growth). Fifty milliliters of water containing 6.4 g of crude extract was placed on the column and eluted with the 0.1 *M* NH_4HCO_3 at 8–9 ml/min at room temperature. Scheme I gives the weights and V_e/V_0 values for the lyophilized fraction. The bioassays for contractile force of the isolated rat atria, carried out as in Ref. 5, showed no activity in Fractions A, E, and F. The bioassays of Fractions B, C, and D were as follows:

fraction	concentration, ppm	increase in contractile force (time to maximum), %
B	4	0
	40	100 (6 min)
C	0.4	120 (5 min)
D	4	0
	40	30 (4 min)

Fraction C contained ~99% of the cardiotonic activity; 6.4 g of Fraction C was produced.

Ion-Exchange Chromatography—Fraction C, 610 mg, in 5 ml of 0.03 *M* phosphate buffer at pH 7.5, was put on a cation-exchange column[5], 48 × 4 cm. The column contained 600 ml of wet resin equilibrated with the same buffer saturated with chloroform (V_0 = 205 ml). A stirred reservoir of 1500 ml of the buffer was connected to the column. After 110 ml of buffer had flowed through the column, the reservoir volume was maintained constant by feeding with a 0.03 *M* phosphate buffer in 0.5 *M* NaCl adjusted to pH 7.5 for gradient elution. Both solutions were saturated with chloroform. The flow rate was about 3 ml/min, and the run was made at room temperature.

The effluent was monitored using UV absorbance at 280 nm[6]. Only two cuts contained activity: Compound I, V_e/V_0 2.99–3.39; and Compound II, V_e/V_0 6.30–7.01 (Fig. 2). The I cut (Fraction G) was immediately lyophilized (610 mg, including the salts), and the II cuts were frozen and accumulated for future work. Immediately following the II fraction, 25 ml of 10% NaCl was put on the column followed by the 0.03 *M* phosphate buffer (no sodium chloride) to clean the column and reequilibrate it for the next run. Fraction G was kept at −20° and was used for all pharmacological studies.

[2] S. G. Zelenski, A. J. Weinheimer, and P. N. Kaul, Fourth Food-Drugs from the Sea Conference, University of Puerto Rico, Mayaguez, Puerto Rico, Nov. 17–21, 1974.

[3] The authors thank Dr. Cadet Hand, Director, Bodega Marine Laboratory, University of California, Bodega Bay, Calif., for supplying the collections of the sea anemones.

[4] Sephadex G-50, Pharmacia Fine Chemicals.

[5] CM-Sephadex C-25, Pharmacia Fine Chemicals.

[6] Model UA-5 absorbance monitor, Instrument Specialties Co., Lincoln, NE 68505

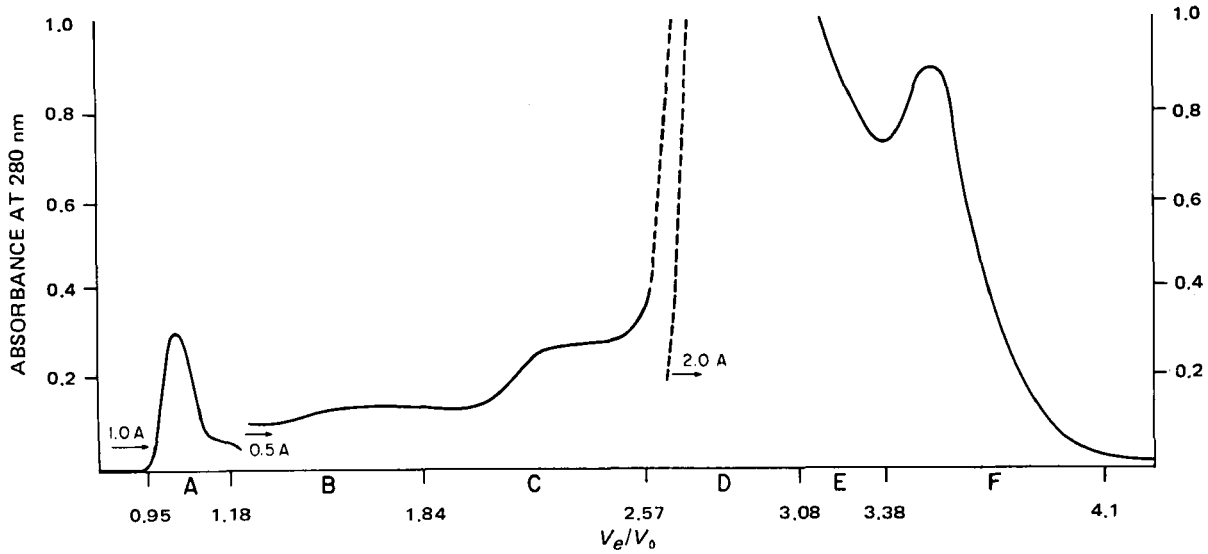

Figure 1—*Gel permeation chromatography of the crude extract of* A. xanthogrammica. *The notations 1.0A, 0.5A, and 2.0A indicate the points at which full-scale sensitivity on the chart was switched to these absorbance values.*

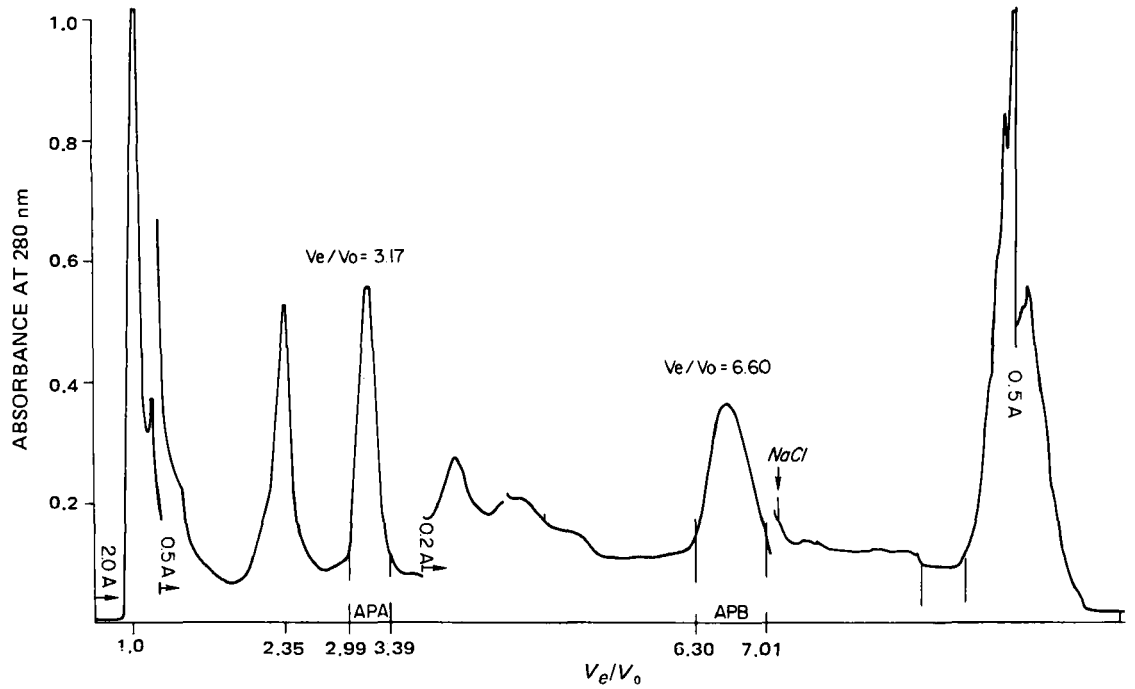

Figure 2—*Cation-exchange of Fraction C to give Fraction G [anthopleurin-A (APA)] and anthopleurin-B (APB). The notations 2.0A, 0.5A, and 0.2A indicate the points at which full-scale sensitivity on the chart was switched to these absorbance values.*

Compound I showed no signs of deterioration when kept at −20° for 1 year as lyophilized Fraction C or as lyophilized Fraction G. As Fraction G, it is stable for at least 24 hr at 20.5° in 10^{-7} *M* solutions at pH 4.55–7.80 but shows about 90% decomposition at pH above 11 (Table I).

Purification—A 50-ml buret (54 × 1.2 cm) containing 52 ml of wet dextran gel[4] was equilibrated with 0.017 *M* acetic acid in 0.03 *M* NaCl saturated with chloroform (V_0 = 21.1 ml). A solution of 102.6 mg of Fraction G was dissolved in 0.4 ml of water, put on the column, and eluted at room temperature with the equilibrating solution. Fraction H was collected at V_e/V_0 1.66–2.16. No UV-absorbing material appeared before Fraction H and only a trace appeared thereafter (Fig. 3). Fraction H was lyophilized and weighed 20 mg (including the sodium chloride).

The salt was removed using a dextran gel[7] column. If water alone was used for elution, only part of I eluted and in an erratic pattern. The 20 mg of Fraction H was dissolved in 0.3 ml of 10% NaCl and put on a 59 × 1.2-cm column of 54 ml of wet dextran gel[7] equilibrated with 0.017 *M* acetic acid saturated with chloroform. The sample was followed by 0.5 ml of 10% NaCl and then the equilibrating solution. Compound I emerged completely and sharply at void volume (V_e/V_0 0.93–1.12) and was salt free. It was immediately lyophilized to give 1.4 mg of pure anthopleurin-A (Fraction I).

For electrophoretic studies and amino acid analysis, the ion-exchange elution on both dextran gel columns was repeated (with about 60% overall recovery) starting with Fraction I. The column reruns were carried out in a fashion identical to the preparation of Fractions H and I to give the doubly purified Compound I (Fraction J). Figure 4 shows that the second scan[4] lacked extraneous material. Compound I as Fraction J did not crystallize from evaporation of a water solution in which it was very soluble, possibly due to a mixture of hydrates, but gave a colorless amorphous powder when an aqueous solution was lyophilized. If a molecular weight of 5500 is assumed, Fraction J has an ED_{50} for positive inotropic effect (isolated guinea pig atria) at 10^{-9} *M* in the atria bath (see Ref. 5 for method).

[7] Sephadex G-10, Pharmacia Fine Chemicals.

Table I—Effect of pH on Cardiotonic Activity of 10^{-7} *M* Anthopleurin-A

Sample	pH[a]	Incubation Period at 20.5°, hr	Concentration to Give Positive Inotropic Effect, *M*	
			Threshold	Maximum
1	4.55	2	5×10^{-10}	10^{-9}
2	4.55	24	5×10^{-10}	10^{-9}
3	6.78	2	5×10^{-10}	10^{-9}
4	6.78	24	5×10^{-10}	10^{-9}
5	7.8	2	10^{-9}	5×10^{-9}
6	7.8	24	10^{-9}	5×10^{-9}
7	11.15	2	10^{-9}	5×10^{-9}
8	11.15	24	5×10^{-9}	10^{-8}
9	11.15	2	5×10^{-9}	10^{-8}
10	11.75	24	5×10^{-9}	10^{-8}

[a] Using 0.1 *M* NaH_2PO_4 with incremental sodium hydroxide additions.

Electrophoretic Studies—For the acidic, basic, and sodium lauryl sulfate gel electrophoresis, commercial precast 12% acrylamide gels[8] and matched buffer systems were used.

Acid Disc Gel Electrophoresis—For the gel labeled AP-A + DTE, the sample was prepared by mixing 5 μl (containing 25 μg) of Compound I aqueous solution with 5 μl of 0.5 *M* dithioerythritol (adjusted to pH 8.7 with ethylenediamine) and allowing the mixture to stand for 2 hr. The mixture was then acidified with 2 μl of 1% acetic acid, and 3 μl of the tracking dye (0.5% methyl green in 30% sucrose, 0.4 *M* glycine–acetic acid at pH 3.6) was added. The total volume was 15 μl.

For the gel labeled AP-A + NH_3, 10 μl (containing 25 μg) of Compound I aqueous solution was mixed with 10 μl of 1 *M* NH_3 and heated at 60° for 1 hr. The sample was evaporated to dryness (nitrogen), and 10 μl of 0.1% acetic acid and 5 μl of the methyl green tracking dye were added. Ten microliters of the mixture was used.

The prepared samples were each carefully layered on top of the buffered gel under the buffer (0.188 *M* in both glycine and acetic acid, pH 3.5) in an electrophoresis bath[9] with 1500 ml of buffer in the bottom cathode compartment and 500 ml of buffer in the top anode compartment. The power was turned on without delay and set at 100 v (1 mamp/tube) until the samples had entered the gel completely (about 5 min). The voltage was then increased to 200 v (2 mamp/tube) until the tracking dye was within about 5 mm of the cathode end (bottom) of the tube (about 90 min).

The gel tubes were quickly pulverized using a "gel tube eliminator"[8], the end of the gel was cut off directly through the center of the dye, and each gel was placed in 50 ml of a 10% acetic acid–40% 2-propanol–50% water solution and gently swirled for 5 hr to fix the polypeptide. The shrunken gels were then placed in 1.5 × 10-cm test tubes with 22 ml of 0.25% anazolene sodium[10] in 7% acetic acid for 12 hr. The gels were transferred to the destainer[9] and washed with 7% acetic acid for 72 hr. The results are shown in Fig. 5.

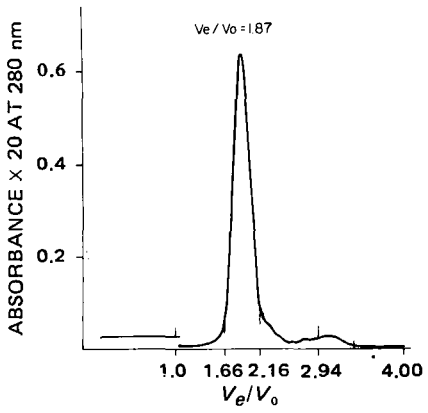

Figure 3—*Gel permeation chromatography of Fraction G to give Fraction H.*

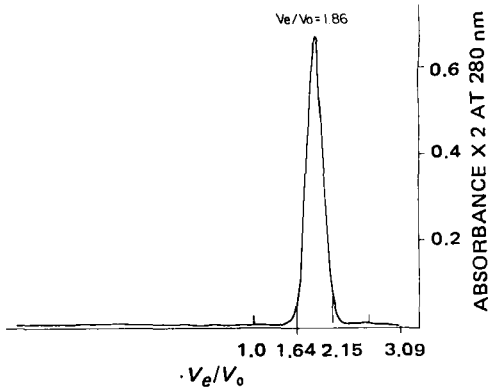

Figure 4—*Gel permeation chromatography of repurified Fraction H.*

Basic Disc Gel Electrophoresis—For basic gels, the procedure was the same as already described except that the anode was the bottom compartment, the buffer was pH 8.9 (0.188 *M* in both glycine and tromethamine), and the tracking dye was 0.5% bromphenol blue in 30% sucrose (0.05 *M* in both tromethamine and glycine[8]). A sample of 15 μl (containing 15 μg) of Compound I aqueous solution plus 3 μl of tracking dye was placed on the equilibrated gel and run as with the acid gel. The gel showed no bands.

Sodium Lauryl Sulfate Electrophoresis—For sodium lauryl sulfate-treated polypeptides and proteins, the procedure was as described previously[8]. The buffer was 0.205 *M* in both tromethamine and acetic acid and contained 0.1% (w/v) sodium lauryl sulfate, pH 6.4 in buffer and 6.1 in the gel. The buffer was introduced into the prepared gel at 100 v (constant voltage) and required about 6 hr. The buffer in the cathode compartment (top) was then replaced with fresh buffer. The samples were then introduced at 60 v (4 mamp/tube) and run at 105 v (7.5 mamp/tube). The incubating sodium lauryl sulfate solution was 0.04 *M* in both tromethamine and acetic acid, 0.04 *M* in dithioerythritol, and 0.001 *M* in edetic acid and contained 1% (w/v) sodium lauryl sulfate.

The samples for all three gels shown in Fig. 6 were prepared by incubating 10 μl of the protein or polypeptide solution with 10 μl of the incubating sodium lauryl sulfate solution at 65° for 30 min. Then 4 μl of the bromphenol blue tracking dye was added, and the run was carried out as already described. Fixing, staining, and destaining were performed as with the acid gel. The Compound I solution concen-

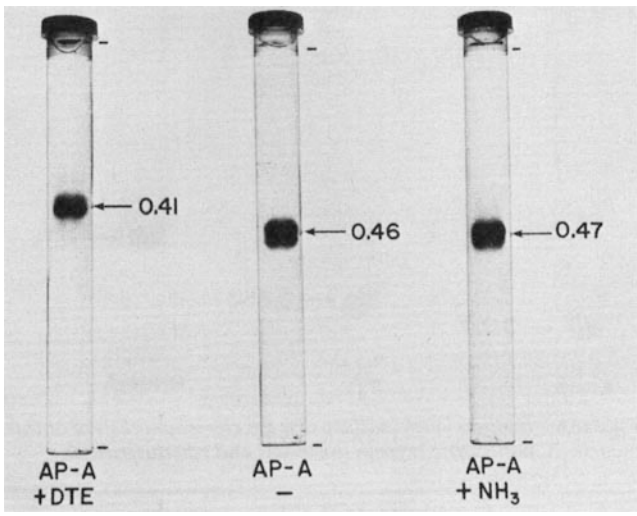

Figure 5—*Disc gel electrophoresis at pH 3.6. (Bottom was the cathode.)*

[8] Bio-phore precast gels, matched buffer systems, and other supplies from Bio-Rad Laboratories, Richmond, Calif. The buffers were introduced as described in their Bulletin 1024, with SDS addendum, Apr. 1974.

[9] Hoefer Scientific Instruments, San Francisco, CA 94107

[10] Coomassie Brilliant Blue R-250, Bio-Rad Laboratories, Richmond, Calif.

Table II—Amino Acid Analysis of Anthopleurin-A[a]

Amino Acid	Micromoles × 10			Average[b] or Extrapolation[c]	Micromoles[a] ÷ 0.0227	Closest Integer
	At 8 hr	At 12 hr	At 16 hr			
Aspartic acid	1.07	1.07	1.07	1.07[b]	4.71	5
Threonine	0.67	0.70	0.70	0.69[b]	3.04	3
Serine	1.17	1.12	1.10	1.18[c]	5.19	5
Glutamic acid	0.73	0.73	0.74	0.73[b]	3.21	3
Proline	1.12	1.12	1.11	1.12[b]	4.93	5
Glycine	1.89	1.88	1.87	1.88[b]	8.27	8
Alanine	0.44	0.44	0.44	0.44[b]	1.94	2
Cystine/2	1.10	1.11	1.03	1.35[c]	5.94	6
Valine	0.49	0.48	0.48	0.48[b]	2.11	2
Methionine	0.03	0.01	0.01	0.03[d]	0.13	0
Isoleucine	0.23	0.23	0.24	0.23[b]	1.01	1
Leucine	0.83	0.83	0.82	0.83[b]	3.65	4
Tyrosine	0.35	0.33	0.30	0.42[c]	1.85	2
Phenylalanine	0.19	0.21	0.19	0.20[b]	0.88	1
Lysine	0.51	0.49	0.50	0.50[b]	2.20	2
Histidine	0.34	0.35	0.35	0.35[b]	1.54	2
Ammonia	1.42	—[e]	1.58	1.26[f]	5.54	6
Arginine	—[e]	0.40	0.40	0.40[b]	1.76	2
Tryptophan	0.05	(24-hr barium hydroxide hydrolysis)		0.05	0.22	0

[a] Anthopleurin-A, 125 μg (0.0227 μmole), was used. [b] Average of the three values. [c] Extrapolated from 12- and 16-hr values. [d] Eight-hour value. [e] Spurious result. [f] Extrapolated from 8- and 16-hr values.

tration was 1 μg/μl (10 μg total), the pancreatic trypsin inhibitor[11] concentration was 2 μg/μl (20 μg total), and the ribonuclease A[11] concentration was 2 μg/μl (20 μg total), all in water.

When I was run by adding the sodium lauryl sulfate incubating solution and immediately putting it on the gel (0 incubation time), an intense single band at R_f 0.86 was seen. With 1 hr of incubation, the gel appeared the same as shown in Fig. 6 with a trace at R_f 0.86 and the dense band at 0.91.

Electrofocusing—To determine the isoelectric point and as a check of purity by electrofocusing, a modification of the procedure described by Wrigley (10) was employed. The 10% gels were prepared in 6.0 (i.d.) × 77-mm silica tubes using the following solutions: 1.16 ml of water, 0.67 ml of 30% acrylamide[12], 0.033 ml of ampholytic surfactant[13], 0.022 ml of ampholytic surfactant[14], and 0.11 ml of potassium persulfate (1% $K_2S_2O_8$ in water).

All solutions except the surfactants were deaerated by vacuum boiling and handled under nitrogen. The potassium persulfate was added last, and the well-mixed solution was placed in the tubes. About 200 μl of deaerated water was immediately layered on top of the solution. Polymerization was complete in 10–15 min, and gels were used within 30 min. The presence of oxygen may completely inhibit the polymerization.

The 5% sucrose solution for the top of the gel consisted of 0.10 ml of 40% ampholytic surfactant[13], 0.50 ml of 40% sucrose, and 3.40 ml of water.

The anode compartment (top) contained 500 ml of 0.2% H_2SO_4, and the cathode compartment (bottom) contained 1500 ml of 0.4% ethylene diamine.

The bottom compartment was filled, the gels were put in place, and the 5% sucrose solution was put on top of the gel. The sample containing 50 μg of I in 10 μl of 0.1% acetic acid was mixed with 3.3 μl of 40% sucrose and layered under the 5% sucrose and onto the gel. The power was immediately turned on at 75 v (2.5 mamp/tube) and allowed to rise to 400 v, where it was kept at constant voltage until the end of the run (1.0 mamp/tube at the end of the run) (85 min). The UV detector[6] was coupled with a gel scanner[15], and the gel was immediately scanned (solid line in Fig. 7).

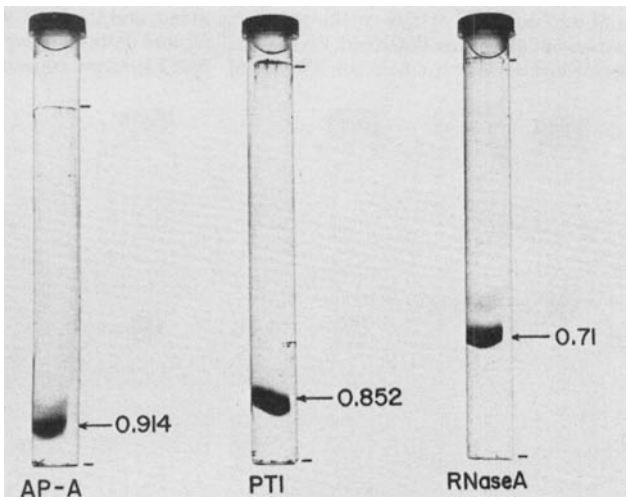

Figure 6—*Sodium lauryl sulfate disc gel electrophoresis of anthopleurin-A, pancreatic trypsin inhibitor, and ribonuclease A.*

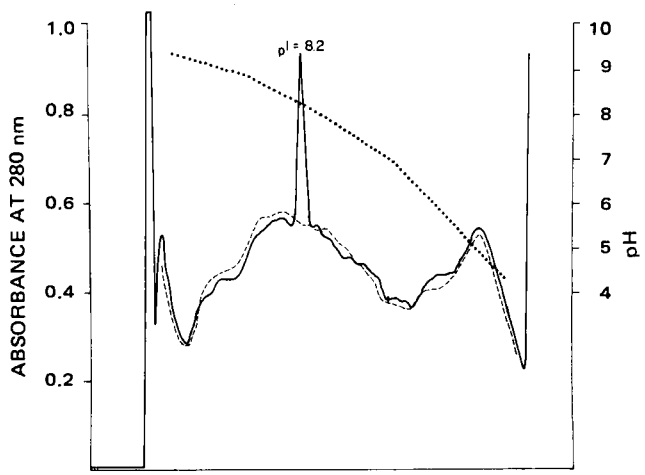

Figure 7—*Gel scan of gel isoelectric focusing of anthopleurin-A* (—), *blank ampholytes* (- - - -), *and pH of the gel* (. . . .).

[11] The authors are indebted to Dr. J. F. Lenney of the Pharmacology Department, University of Hawaii, for the pancreatic trypsin inhibitor and ribonuclease A (RNase A) samples.

[12] Nine grams of acrylamide, 0.03 g of *N,N'*-methylenebis(acrylamide) in 30 ml of solution.

[13] Ampholine carrier 3-10 ampholytes, 40%, pH 3-10, LKB Produkter AB, S 161 25 Bromma 1 Sweden.

[14] Bio-Rad 9-10 ampholytes, 40%, pH 9–10, Bio-Rad Laboratories, Richmond, Calif.

[15] Isco model 659 gel scanner, Instrument Specialties Co., Lincoln, NE 68505

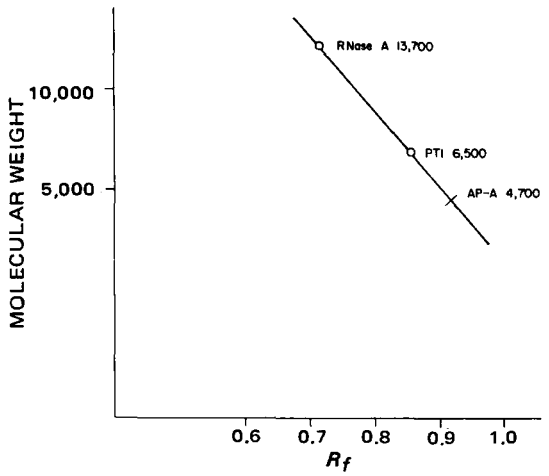

Figure 8—*Semilog plot of* R_f *values from Fig. 5* versus *molecular weight.*

A second gel was prepared similarly, except that no I was put on it. This gel was chilled (0°) and then scanned immediately after the I gel as a control (dashed line in Fig. 7). The gel with the I samples was then sliced into 10 equal length cylinders. Each slice was placed in 1.5 ml of water and allowed to stand for 2 hr. The pH of each tube was then measured: first (anode end), 4.35; second, 5.1; third, 6.0; fourth, 6.83; fifth, 7.35; sixth, 8.02; seventh, 8.40; eighth, 8.85, ninth, 9.13; and 10th (cathode end), 9.35. These results were plotted directly on the UV absorbance monitor readout (dotted line in Fig. 7) at 5, 15, 25, *etc.* to 95% of the duration of the gel scan (abscissa). Compound I gave a sharp peak at pH 8.2 (Fig. 7).

Amino Acid Analyses—A 1.0-mg sample of Compound I (Fraction J) was dissolved in 200 μl of water. Fifty-microliter samples of this solution were quantitatively transferred to four 3-ml ampuls. One milliliter of redistilled 6 *N* HCl was put in three of these ampuls, and 1 ml of 0.2 *M* $Ba(OH)_2$ was placed in the fourth (for tryptophan analysis). All of the ampuls were fire sealed under vacuum.

The three acid samples were placed in an oven at 112 ± 1.0°. One sample at a time was removed after 8, 12, and 16 hr; they were opened and placed over sodium hydroxide pellets in a vacuum. It had previously been determined that hydrolysis was almost complete at 6 hr. The barium hydroxide sample was heated at 128 ± 1.0° for 24 hr for the tryptophan analysis. The contents were then neutralized to pH 6.5 with 0.2 *M* H_2SO_4, centrifuged to remove barium sulfate, and then placed in a vacuum over sodium hydroxide pellets. The samples were dry in 48 hr.

Amino acid analyses[16] were carried out on an automatic amino acid analyzer[17] with acid hydrolysates split for first the acid and neutral amino acids and then the basic amino acid analyses (Table II). Standards containing 0.100 μmole of each amino acid were run just prior to the Compound I hydrolysates.

RESULTS AND DISCUSSION

Gel filtration of the crude extract from *A. xanthogrammica* gave a 40-fold increase in purity in the V_e/V_0 1.84–2.57 Fraction C (Scheme I). Cation exchange, using phosphate buffer at pH 7.5 and gradient elution with 0.5 *N* NaCl, provided an excellent separation of anthopleurin-A (I) in a purity of about 95% (based on UV absorbance areas of impurities seen in preparation of analytically pure material) (Fig. 2). When Fraction G was lyophilized, it contained 1–1.4 mg of polypeptide/100 mg total weight, the balance being sodium chloride and phosphate salts. This material was used for all pharmacological studies, details of which are reported elsewhere (11).

As shown in Fig. 2, there was a second active substance, anthopleurin-B (II) at V_e/V_0 6.30–7.01. This substance also showed a strong positive inotropic effect and no chronotropic effect at concentrations equivalent to I based on UV absorbance, assuming equal molar absorptivities. The characteristics of II have yet to be examined.

All trial separation procedures were monitored by bioassay, using the isolated rat atria for the determination of positive inotropic effects (5). Over 700 such bioassays were carried out during the development of this procedure. About 90% of the activity in the crude extract was recovered in Fraction G.

Qualitative tests of Fraction I indicated the presence of the polypeptide based on ninhydrin-positive spots, using paper chromatography of a hydrolysate, and the absence of sugars by the α-naphthol–sulfuric acid method.

Isoelectric focusing of Fraction J indicated a pI = 8.2 and the absence of any UV-absorbing impurities (Fig. 7). Disk gel electrophoresis at pH 3.6 gave an R_f value of 0.46 based on methyl green as the tracking dye and indicated lack of anazolene sodium dyeable impurities (Fig. 5). Compound I would not enter a basic gel at pH 8.9, indicating a possible lack of free carboxyl groups. By using sodium lauryl sulfate and incubation with dithioerythritol, gel electrophoresis indicated a molecular weight of about 4700 based on R_f values determined for ribonuclease A and pancreatic trypsin inhibitor. With the same solution, but zero incubation time, the R_f value corresponded to a molecular weight of about 6500, indicating the possible loss of a portion of the molecule by disulfide linkage splitting. No dyeable impurities were seen in either case.

Molecular weight determinations of polypeptides with molecular weights below 10,000–15,000 using the sodium lauryl sulfate technique are not considered reliable (12). However, the molecular weights based on the amino acid analysis (5500) and the zero incubation time sodium lauryl sulfate technique (6500) were not grossly disparate. Incubation with dithioerythritol changed the pH 3.6 gel electrophoresis R_f value from 0.46 to 0.41, again indicating that a segment of the molecule was lost and that the remaining residue was less basic than the original I; incubation with 1 *M* NH_3 did not change the R_f value (Fig. 8). Splitting of I by dithioerythritol incubation alone at pH 8.7 completely destroyed the activity.

The amino acid analyses showed that there were traces of methionine and tryptophan, apparently from impurities. However the other amino acids were recovered in good yields and with a reasonable integer fit. Histidine was a notable exception, with persistent 1.5-mole values. The moles of amino acids were based on the actual weight of I (125 μg) and a molecular weight of 5500, rather than the closest integer fit. Compound I was not retarded on G-10[7] (exclusion limit 700), was slightly retarded (peak $V_e/V_0 = 1.14$) on G-25[18] (exclusion limit 5000), and was markedly retarded (peak $V_e/V_0 = 1.87$) on G-50[4] (exclusion limit 30,000); also the molecular weight from incubated sodium lauryl sulfate electrophoresis was about 4700. Because of these data, the value of 5500 rather than 11,000 was chosen as the probable molecular weight. Compound I has 53 amino acids, with an excess of four basic groups over the number of acidic groups (Table II). The amino acid analysis can only be considered tentative until sequencing is done[19].

At this time it appears that I is a basic polypeptide containing 53 amino acids, with two segments (both inactive) separable by disulfide (cystine) splitting, and possibly containing no free carboxyl groups. It is relatively stable at neutral and lower pH values and is very soluble in deionized water.

The pharmacological data, appearing elsewhere in detail (11), indicate that I is about 200–1000 times as potent as ouabain in positive inotropic effect, having an ED_{50} at 10^{-9} *M* on isolated guinea pig atria. The LD_{50} in mice (intraperitoneal) is about 0.3–0.4 mg/kg. It does not show any chronotropic effect when pure (as Fraction G). It will reverse completely ouabain-induced cardiac arrest. At 5×10^{-7} *M* concentrations of Compound I, none of the following enzymes is inhibited: sodium or potassium adenosine triphosphatase, monoamine oxidase, catechol *O*-methyltransferase, and cyclic 3′,5′-nucleotide phosphodiesterase; nor does I affect the 3′,5′-cyclic adenosine monophosphate content of the guinea pig heart. Compound I is not nearly as sensitive to the Ca^{+2} concentration as is ouabain, and lowered external K^+ does not alter drug toxicity as with ouabain. Compound I has been shown

[16] The authors thank Dr. Suresh S. Patil, Plant Pathology Department, University of Hawaii, for the use of the instrument and Mr. Phillip D. Youngblood for running the analyses.

[17] Beckman model 116 amino acid analyzer, Beckman Instruments, Spinco Division, Palo Alto, CA 94304

[18] Sephadex G-25, Pharmacia Fine Chemicals.

[19] *Note added in proof:* The sequencing of I has been completed by M. Tanaka *et al.* (Department of Biochemistry, University of Hawaii), and a manuscript is in preparation. The sequence indicates the following amino acid composition: ASP_4 THR_3 SER_6 GLU PRO_4 GLY_8 ALA CYS_6 VAL_2 ILE LEU_4 TYR LYS_2 HIS_2 ARG TRP_3 $(NH_3)_3$.

to be effective in the isolated heart in rats, guinea pigs, rabbits, cats, and dogs and in the *in situ* heart in dogs and cats.

REFERENCES

(1) F. L. Tabrah, M. Kashiwagi, and T. R. Norton, *Int. J. Clin. Pharmacol., Ther. Toxicol.*, **5**, 420(1972).

(2) T. R. Norton and M. Kashiwagi, *J. Pharm. Sci.*, **61**, 1814(1972).

(3) R. J. Quinn, M. Kashiwagi, R. E. Moore, and T. R. Norton, *ibid.*, **63**, 257(1974).

(4) R. J. Quinn, M. Kashiwagi, T. R. Norton, S. Shibata, M. Kuchii, and R. E. Moore, *ibid.*, **63**, 1798(1974).

(5) S. Shibata, D. F. Dunn, M. Kuchii, M. Kashiwagi, and T. R. Norton, *ibid.*, **63**, 1332(1974).

(6) M. H. Baslow, "Marine Pharmacology," Williams & Wilkins, Baltimore, Md., 1969, pp. 100–115.

(7) C. L. Huang and G. N. Mir, *J. Pharm. Sci.*, **61**, 66(1972).

(8) H. Beaulnes and C. Beebe, in "Bradykinen and Related Kinens, Comparative Cardiac Effects of Angiotensin, Eledoisin, and Physalamein," F. Sicuteri, M. R. e Silva, and N. Back, Eds., Plenum, New York, N.Y., 1970, pp. 140–147; J. Nakano, in *ibid.*, pp. 157–170.

(9) P. Mäsiar, E. Mäsiar, and D. G. Oakley, *Biochem. Biophys. Res. Commun.*, **50**, 914(1973).

(10) C. W. Wrigley, in "New Techniques in Amino Acid, Peptide, and Protein Analysis," A. Niederwieser and G. Pataki, Eds., Ann Arbor Science Publishers, Ann Arbor, Mich., 1971, pp. 316–332.

(11) S. Shibata, T. R. Norton, T. Izumi, T. Matsuo, and S. Katsuki, *Pharmacologist*, **17**, 218(1975).

(12) K. Weber, J. R. Pringle, and M. Osborne, *Methods Enzymol.*, **26**, 20(1972).

ACKNOWLEDGMENTS AND ADDRESSES

Received February 21, 1975, from the *Department of Pharmacology, University of Hawaii, Leahi Hospital, Honolulu, HI 96816*

Accepted for publication December 5, 1975.

Supported by National Institutes of Health Research Grant HL 15991 from the National Heart and Lung Institute.

[x] To whom inquiries should be directed.

Hypocholesterolemic Agents V: Inhibition of β-Hydroxy-β-methylglutaryl Coenzyme A Reductase by Substituted 4-Biphenylylalkyl Carboxylic Acids and Methyl Esters

SHARON G. BOOTS [*], MARVIN R. BOOTS [*x], KENNETH E. GUYER [‡§], and PAUL E. MARECKI [*]

Abstract □ Eleven substituted 4-biphenylylalkyl carboxylic acids and three methyl esters were synthesized and assayed for inhibition of rat liver β-hydroxy-β-methylglutaryl coenzyme A reductase. Five of the acids were analogs, resulting from various isosteric replacements of the carbonyl and ether oxygens of the previously described reversible inhibitor 1-(4-biphenylyl)pentyl hydrogen succinate. No significant change in activity was noted, except upon introduction of an amide linkage where a decrease in inhibition was found. Six carboxylic acids and three methyl esters, all containing the 4-biphenylyl radical but lacking the *n*-butyl side chain found in 1-(4-biphenylyl)pentyl hydrogen succinate, also were inhibitors of the reductase.

Keyphrases □ β-Hydroxy-β-methylglutaryl coenzyme A reductase—effect of 4-biphenylylalkyl carboxylic acids, rat liver microsomes □ 4-Biphenylylalkyl carboxylic acids—synthesis, effect on β-hydroxy-β-methylglutaryl coenzyme A reductase, rat liver microsomes □ Enzymes—β-hydroxy-β-methylglutaryl coenzyme A reductase, effect of 4-biphenylylalkyl carboxylic acids, rat liver microsomes □ Hypocholesterolemic agents, potential—4-biphenylylalkyl carboxylic acids synthesized, effect on β-hydroxy-β-methylglutaryl coenzyme A reductase, rat liver microsomes □ Structure–activity relationships—4-biphenylylalkyl carboxylic acids synthesized, effect on β-hydroxy-β-methylglutaryl coenzyme A reductase

In previous reports (1, 2), an approach to the design of inhibitors of cholesterol biosynthesis as potential hypocholesterolemic agents was discussed. The rationale for the inhibition of the enzyme, β-hydroxy-β-methylglutaryl coenzyme A reductase, was presented (1). These studies led to the discovery that maximum inhibition was obtained in a series of arylalkyl hydrogen alkanedioates (I), where R_1 = biphenyl, R_2 = *n*-butyl, and m = 1–4.

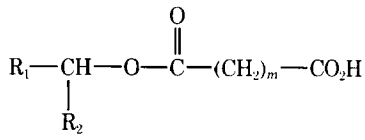

I

Modification of the acid portion of the glutarate analog of I by the incorporation of a β-hydroxy-β-methyl moiety provided II. Analog II, which closely resembles the acid portion of the substrate, β-hydroxy-β-methylglutaryl coenzyme A, was seven times more active than the glutarate analog of I and is the most active inhibitor found thus far.

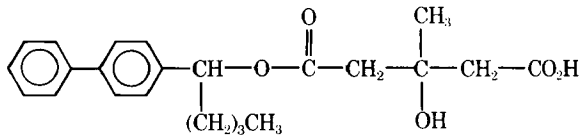

II

This paper describes the synthesis and assay of compounds where isosteric replacements of the various atoms of the ester function of I were made. In addition, reports by Eades *et al.* (3, 4) indicated that a series of 4-substituted biphenyl derivatives inhibited the incorporation of 1-^{14}C-acetate into cholesterol in the *in vitro* rat liver homogenate system and decreased serum

to be effective in the isolated heart in rats, guinea pigs, rabbits, cats, and dogs and in the *in situ* heart in dogs and cats.

REFERENCES

(1) F. L. Tabrah, M. Kashiwagi, and T. R. Norton, *Int. J. Clin. Pharmacol., Ther. Toxicol.*, **5**, 420(1972).

(2) T. R. Norton and M. Kashiwagi, *J. Pharm. Sci.*, **61**, 1814(1972).

(3) R. J. Quinn, M. Kashiwagi, R. E. Moore, and T. R. Norton, *ibid.*, **63**, 257(1974).

(4) R. J. Quinn, M. Kashiwagi, T. R. Norton, S. Shibata, M. Kuchii, and R. E. Moore, *ibid.*, **63**, 1798(1974).

(5) S. Shibata, D. F. Dunn, M. Kuchii, M. Kashiwagi, and T. R. Norton, *ibid.*, **63**, 1332(1974).

(6) M. H. Baslow, "Marine Pharmacology," Williams & Wilkins, Baltimore, Md., 1969, pp. 100–115.

(7) C. L. Huang and G. N. Mir, *J. Pharm. Sci.*, **61**, 66(1972).

(8) H. Beaulnes and C. Beebe, in "Bradykinen and Related Kinens, Comparative Cardiac Effects of Angiotensin, Eledoisin, and Physalamein," F. Sicuteri, M. R. e Silva, and N. Back, Eds., Plenum, New York, N.Y., 1970, pp. 140–147; J. Nakano, in *ibid.*, pp. 157–170.

(9) P. Mäsiar, E. Mäsiar, and D. G. Oakley, *Biochem. Biophys. Res. Commun.*, **50**, 914(1973).

(10) C. W. Wrigley, in "New Techniques in Amino Acid, Peptide, and Protein Analysis," A. Niederwieser and G. Pataki, Eds., Ann Arbor Science Publishers, Ann Arbor, Mich., 1971, pp. 316–332.

(11) S. Shibata, T. R. Norton, T. Izumi, T. Matsuo, and S. Katsuki, *Pharmacologist*, **17**, 218(1975).

(12) K. Weber, J. R. Pringle, and M. Osborne, *Methods Enzymol.*, **26**, 20(1972).

ACKNOWLEDGMENTS AND ADDRESSES

Received February 21, 1975, from the *Department of Pharmacology, University of Hawaii, Leahi Hospital, Honolulu, HI 96816*

Accepted for publication December 5, 1975.

Supported by National Institutes of Health Research Grant HL 15991 from the National Heart and Lung Institute.

[x] To whom inquiries should be directed.

Hypocholesterolemic Agents V: Inhibition of β-Hydroxy-β-methylglutaryl Coenzyme A Reductase by Substituted 4-Biphenylylalkyl Carboxylic Acids and Methyl Esters

SHARON G. BOOTS [*], MARVIN R. BOOTS [*x], KENNETH E. GUYER [‡§], and PAUL E. MARECKI [*]

Abstract □ Eleven substituted 4-biphenylylalkyl carboxylic acids and three methyl esters were synthesized and assayed for inhibition of rat liver β-hydroxy-β-methylglutaryl coenzyme A reductase. Five of the acids were analogs, resulting from various isosteric replacements of the carbonyl and ether oxygens of the previously described reversible inhibitor 1-(4-biphenylyl)pentyl hydrogen succinate. No significant change in activity was noted, except upon introduction of an amide linkage where a decrease in inhibition was found. Six carboxylic acids and three methyl esters, all containing the 4-biphenylyl radical but lacking the *n*-butyl side chain found in 1-(4-biphenylyl)pentyl hydrogen succinate, also were inhibitors of the reductase.

Keyphrases □ β-Hydroxy-β-methylglutaryl coenzyme A reductase—effect of 4-biphenylylalkyl carboxylic acids, rat liver microsomes □ 4-Biphenylylalkyl carboxylic acids—synthesis, effect on β-hydroxy-β-methylglutaryl coenzyme A reductase, rat liver microsomes □ Enzymes—β-hydroxy-β-methylglutaryl coenzyme A reductase, effect of 4-biphenylylalkyl carboxylic acids, rat liver microsomes □ Hypocholesterolemic agents, potential—4-biphenylylalkyl carboxylic acids synthesized, effect on β-hydroxy-β-methylglutaryl coenzyme A reductase, rat liver microsomes □ Structure–activity relationships—4-biphenylylalkyl carboxylic acids synthesized, effect on β-hydroxy-β-methylglutaryl coenzyme A reductase

In previous reports (1, 2), an approach to the design of inhibitors of cholesterol biosynthesis as potential hypocholesterolemic agents was discussed. The rationale for the inhibition of the enzyme, β-hydroxy-β-methylglutaryl coenzyme A reductase, was presented (1). These studies led to the discovery that maximum inhibition was obtained in a series of arylalkyl hydrogen alkanedioates (I), where R_1 = biphenyl, R_2 = *n*-butyl, and m = 1–4.

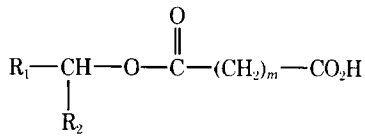

I

Modification of the acid portion of the glutarate analog of I by the incorporation of a β-hydroxy-β-methyl moiety provided II. Analog II, which closely resembles the acid portion of the substrate, β-hydroxy-β-methylglutaryl coenzyme A, was seven times more active than the glutarate analog of I and is the most active inhibitor found thus far.

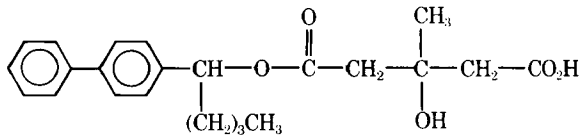

II

This paper describes the synthesis and assay of compounds where isosteric replacements of the various atoms of the ester function of I were made. In addition, reports by Eades *et al.* (3, 4) indicated that a series of 4-substituted biphenyl derivatives inhibited the incorporation of 1-^{14}C-acetate into cholesterol in the *in vitro* rat liver homogenate system and decreased serum

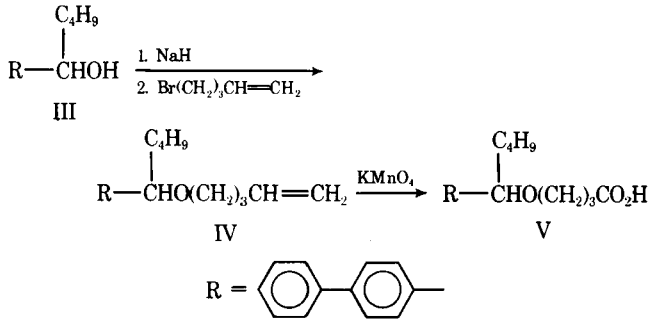

Scheme I

cholesterol levels in rats. These compounds were interesting in that they did not possess either an *n*-butyl group or an ester function situated positionally as in I. Therefore, several of these compounds (as well as similar compounds) were synthesized and assayed as inhibitors of rat liver β-hydroxy-β-methylglutaryl coenzyme A reductase.

DISCUSSION

4-[1-(4-Biphenylyl)pentyloxy]butanoic acid (V) was prepared *via* a two-step synthesis (Scheme I). Conversion of the substituted pentanol (III) to the ether olefin (IV) was readily effected in high yield by treatment of III with sodium hydride, followed by the addition of 5-bromo-1-pentene. The oxidation of the terminal olefin to the desired carboxylic acid (V) proved to be an extremely capricious reaction. Ozonolysis, followed by an oxidative workup, provided only high melting acidic material, which appeared to result from concomitant oxidation of the aromatic ring system. Potassium permanganate (using standard procedures) provided V in low and nonreproducible yields.

Fortunately, an article appeared (5) describing the use of tricaprylylmethylammonium chloride[1] as a phase-transfer agent. The presence of the phase-transfer catalyst allowed one to carry out the oxidation of IV to V with potassium permanganate in a 54% yield.

6-(4-Biphenylyl)decanoic acid (IX) was prepared *via* a two-step synthesis (Scheme II). Treatment of the known keto acid (VI) with *n*-butylmagnesium bromide afforded the desired addition product (VII) in a 70% yield. Also, the abnormal reaction occurred, affording the reduction product (VIII) in a yield of 22%. Hydrogenolysis of the hydroxyl group in VII occurred readily to afford IX.

Synthesis of *N*-[1-(4-biphenylyl)pentyl]succinamic acid (XIII) was performed *via* the pathway illustrated in Scheme III. Jones oxidation

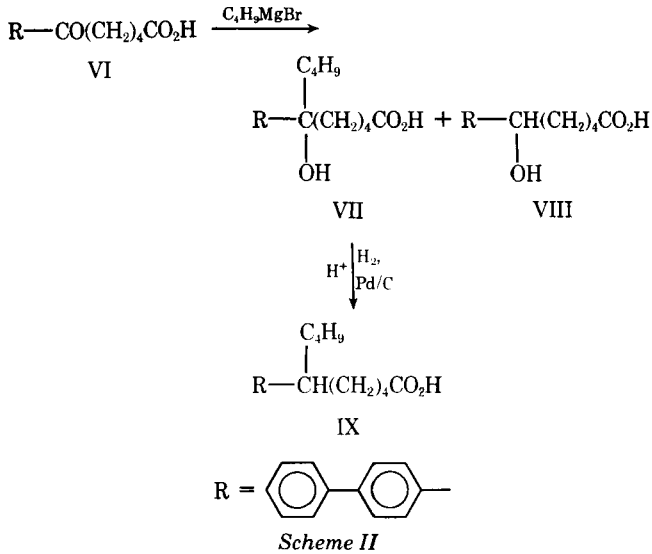

Scheme II

[1] Aliquat 336, General Mills Chemicals.

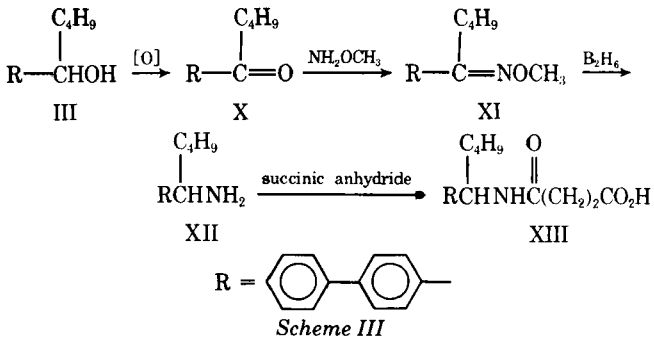

Scheme III

of the alcohol (III) readily afforded the ketone (X), which was subsequently converted to the *O*-methyloxime (XI) in an overall yield of 78%. Reduction of XI with diborane yielded the amine (XII), which was isolated and purified as the hydrochloride salt. Treatment of XII with succinic anhydride readily yielded XIII.

Synthesis of the amino acid (XVII) (Scheme IV) was effected by condensation of the ketone (X) with methyl 4-aminobutanoate hydrochloride (XIV) in the presence of sodium cyanoborohydride in methanol. Initially, the reaction was attempted in the absence of sodium acetate, which afforded an "apparent pH" of 5–6; X was recovered in essentially quantitative yield. When sufficient sodium acetate was added to raise the apparent pH to 6–7, the desired condensation–reduction occurred. A mixture of the ester (XV) and the lactam (XVI) was produced as well as some recovered X. No attempts were made to optimize the yield of this reaction. Saponification of the mixture of XV and XVI led to XVII.

5-Oxo-5-(4-biphenylyl)-3-methylpentanoic acid (XIX) was prepared using the method of Goldschmidt (6) from 3-methylglutaric anhydride and biphenyl in the presence of aluminum chloride (Scheme V). Hydrogenolysis occurred readily, using a palladium-

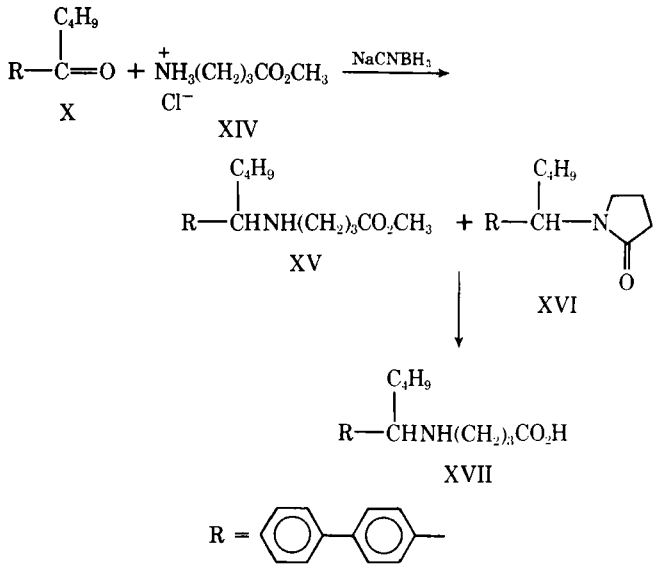

Scheme IV

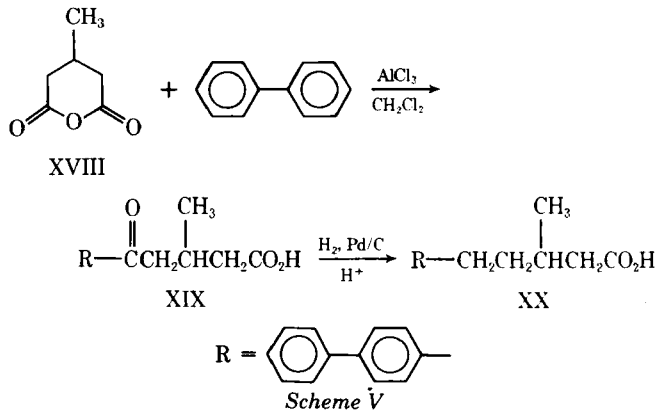

Scheme V

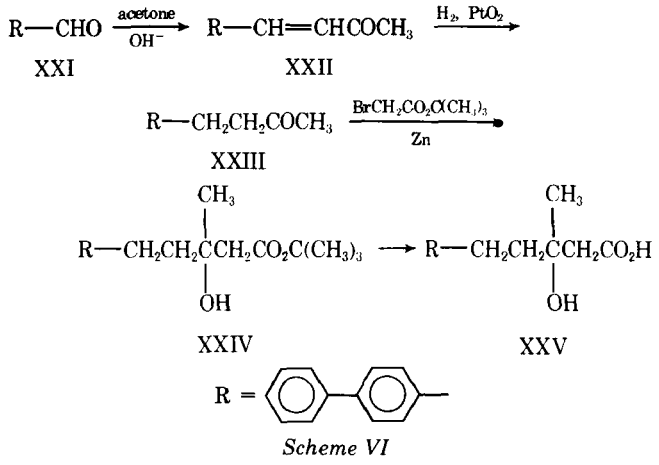

Scheme VI

on-charcoal catalyst in the presence of hydrochloric acid, to afford the desired deoxy acid (XX).

5-(4-Biphenylyl)-3-hydroxy-3-methylpentanoic acid (XXV) was prepared *via* a four-step synthesis (Scheme VI). The initial condensation of 4-biphenylcarboxaldehyde (XXI) and acetone, to yield the α,β-unsaturated ketone (XXII), was described previously (7). The subsequent catalytic hydrogenation of XXII to the saturated ketone (XXIII) was effected as described previously (8). The Reformatsky reaction of the ketone with *tert*-butyl bromoacetate and zinc proceeded readily to afford the β-hydroxy ester (XXIV). The ester was not purified but was hydrolyzed directly with *p*-toluenesulfonic acid monohydrate in benzene to yield XXV.

The keto ester (XXVI) (Scheme VII) and the corresponding keto acid (VI) were prepared by the method of Morand *et al.* (9). The hydroxy ester (XXVII) was readily prepared from XXVI by reduction of the keto group with pyridinylborane in acetic acid. The corresponding hydroxy acid (VIII) was obtained in a quantitative yield from XXVII using a standard saponification procedure.

Compound XXVII also was used to prepare the ester, methyl 6-(4-biphenylyl)hexanoate (XXVIII), and the corresponding acid

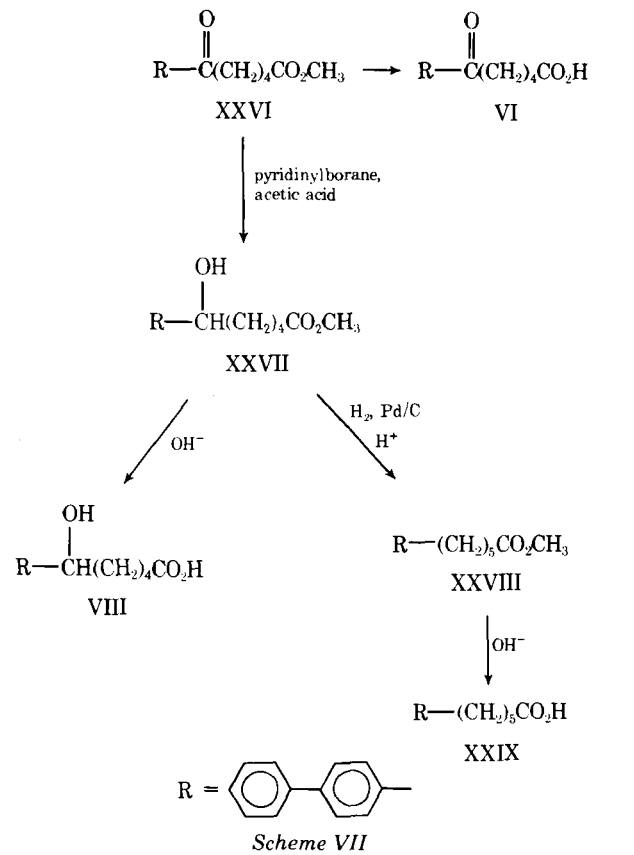

Scheme VII

(XXIX). Hydrogenolysis of the hydroxyl group, as already described, readily afforded XXVIII, which, upon saponification, yielded XXIX.

EXPERIMENTAL[2]

5-[1-(4-Biphenylyl)pentyloxy]-1-pentene (IV)—Sodium hydride (50% dispersion in oil), 1.2 g (0.025 mole), was rinsed thoroughly with dry benzene. Dry dimethylformamide (25 ml) was added. To this suspension was added dropwise, with stirring and cooling, a solution of 2.4 g (0.01 mole) of 1-(4-biphenylyl)pentanol (III) (1) in 25 ml of dry dimethylformamide. The resulting yellow suspension was stirred for 2 hr at 25° after the addition was completed.

A solution of 7.1 g (0.05 mole) of 5-bromo-1-pentene[3] in 10 ml of dry dimethylformamide then was added with stirring and cooling over 5 min. The mixture was stirred at 0–5° for an additional 1 hr and then at 25° for 24 hr. The resulting yellow solution was poured onto an ice–water mixture and extracted with ether. The organic phase was washed with water and with saturated sodium chloride solution, dried over anhydrous sodium sulfate, and concentrated under reduced pressure to a yellow liquid (2.94 g). Petroleum ether (bp 60–68°) was added (~10 ml), and the mixture was stored at 5° for 4 days.

The resulting white precipitate (identified by spectral and physical properties as the starting alcohol) was removed by filtration. The petroleum ether was then removed under reduced pressure to afford 2.44 g (80%) of IV as a yellow liquid. Since attempted distillation led to extensive decomposition, no analytical specimen could be prepared; NMR ($CDCl_3$): δ 0.70–2.30 (m, 13H, C_4H_9, CH_2CH_2), 3.30 (t, J = 6 Hz, 2H, OCH_2), 4.25 (t, J = 7 Hz, 1H, HCO), 4.80–5.20 (m, 2H, $=CH_2$), 5.48–6.17 (m, 1H, HC=C), and 7.20–7.80 (m, 9H, aromatic) ppm.

4-[1-(4-Biphenylyl)pentyloxy]butanoic Acid (V)—The procedure of Starks (5) was used. To a solution of 1.8 g (0.0056 mole) of IV in 30 ml of benzene containing 0.280 g (0.56 mmole) of tricaprylylmethylammonium chloride[1] was added dropwise, over 45 min with stirring and cooling, a solution of 3.5 g (0.022 mole) of potassium permanganate in 60 ml of water. The mixture was stirred at 26° for an additional 2 hr and then was added to 60 ml of a freshly prepared 10% sodium sulfite solution.

Sulfuric acid (55 ml, 3 *N*) was added and a colorless two-phase system resulted. Ether was added, and then the organic phase was washed with water and with saturated sodium chloride solution, dried over anhydrous sodium sulfate, and concentrated under reduced pressure to a yellow oil (2.2 g). This oil was chromatographed on 100 g of silicic acid.

Elution with 10% ether–petroleum ether (bp 60–68°) afforded 0.990 g (54%) of V as a colorless viscous oil. The oil was characterized analytically as the white *S*-benzylthiuronium salt (1), mp 116–118°; IR ($CHCl_3$): 1710 (acid C=O) cm^{-1}; NMR ($CDCl_3$): δ 0.65–2.55 (m, 13H, C_4H_9, CH_2CH_2), 3.30 (t, J = 6 Hz, 2H, OCH_2), 4.22 (t, J = 7 Hz, 1H, HCO), 7.20–7.70 (m, 9H, aromatic), and 8.76 (s, 1H, CO_2H) ppm.

Anal.—Calc. for $C_{21}H_{26}O_3 \cdot C_8H_{10}N_2S$: C, 70.7; H, 7.3; N, 5.7. Found: C, 70.6; H, 7.4; N, 5.5.

Treatment of 6-Oxo-6-(4-biphenylyl)hexanoic Acid (VI) with *n*-Butylmagnesium Bromide—The method of Morand *et al.* (9) was used for the preparation of VI, mp 160–161° [lit. (9) mp 162–163°]. To a mixture of 0.246 g (0.01 mole) of magnesium turnings and 2 ml of dry tetrahydrofuran was added dropwise, with stirring, 1.2 ml (0.011 mole) of *n*-butyl bromide in 5 ml of dry tetrahydrofuran. To this solution was added dropwise, with stirring, 1.06 g (0.0375 mole) of VI in 17 ml of dry tetrahydrofuran. The addition rate was regulated so that a gentle reflux was maintained without the necessity of warming or cooling.

After the addition was complete, the mixture was stirred at 25° for 17 hr. The reaction mixture was then poured onto an ice–water mixture, and concentrated hydrochloric acid was added until a pH of 2 was reached. The mixture was then extracted with ether. The organic phase was washed with water and with saturated sodium chloride

[2] Melting points were determined with a Thomas-Hoover capillary melting-point apparatus and are uncorrected. Elemental analyses were carried out by P. Marecki and by Galbraith Laboratories, Knoxville, Tenn. IR spectra were determined using a Perkin-Elmer model 237 spectrophotometer. NMR spectra were determined using a Perkin-Elmer model R-24 spectrometer or a Varian Associates A-60 spectrometer in the solvent specified, with tetramethylsilane as the internal reference.

[3] Chemical Samples Co.

solution, dried over anhydrous sodium sulfate, and concentrated under reduced pressure to a viscous yellow oil (1.24 g).

Chromatography on silicic acid afforded 0.900 g (70%) of the hydroxy acid VII as a viscous yellow oil (eluted with 50% ether–petroleum ether, bp 60–68°). Compound VII was characterized analytically as the white *S*-benzylthiuronium salt (1), mp 147–148°; IR ($CHCl_3$): 1708 (acid C=O) cm^{-1}; NMR ($CDCl_3$): δ 0.60–2.50 [m, 18H, C_4H_9, $(CH_2)_4$, ⩾CH], 6.45 (s broad, 2H, CO_2H, OH), and 7.20–7.70 (m, 9H, aromatic) ppm.

Anal.—Calc. for $C_{22}H_{28}O_3 \cdot C_8H_{10}N_2S$: C, 71.2; H, 7.5; N, 5.5. Found: C, 70.9; H, 7.6; N, 5.5.

Further elution with the same solvent mixture afforded 0.231 g (22%) of the hydroxy acid VIII as a white solid, mp 130–133°. A different route (described later) was used to synthesize VIII on a preparative scale. The physical and spectral properties are described under the method used to prepare it quantitatively.

6-(4-Biphenylyl)decanoic Acid (IX)—A mixture of 0.420 g (0.00124 mole) of VII, 0.100 g of a 10% palladium-on-charcoal catalyst, 0.1 ml of concentrated hydrochloric acid, and 50 ml of absolute ethanol was hydrogenated in a Parr apparatus at 25° and 40 psi for 6 hr. The mixture was filtered, the solvent was removed under reduced pressure, and the residue was dissolved in ether.

The mixture was washed with water, with 5% sodium hydroxide solution, with water, and with saturated sodium chloride solution. It was then dried over anhydrous sodium sulfate and concentrated under reduced pressure to a colorless oil (0.277 g). This oil was the ethyl ester of IX. The resulting ester was saponified by treatment with a mixture of 6 ml of methanol and 6 ml of a 5% sodium hydroxide solution at 25° for 17 hr. The colorless solution was added to ether and water. The basic, aqueous extract was acidified to pH 2 with an ice–concentrated hydrochloric acid mixture and then extracted with ether.

The organic phase was washed with water and with saturated sodium chloride solution, dried over anhydrous sodium sulfate, and concentrated under reduced pressure to 0.195 g (76%) of IX as a colorless oil, which crystallized slowly on standing. Two recrystallizations from petroleum ether (bp 38–52°) afforded an analytical specimen of IX as white prisms, mp 50–50.5°; IR ($CHCl_3$): 1710 (acid C=O) cm^{-1}; NMR ($CDCl_3$): δ 0.65–2.75 (m, 18H, aliphatic), 7.10–7.70 (m, 9H, aromatic), and 10.68 (s, 1H, CO_2H) ppm.

Anal.—Calc. for $C_{22}H_{28}O_2$: C, 81.5; H, 8.6. Found: C, 81.9; H, 8.6.

1-(4-Biphenylyl)-1-pentanone (X)—The procedure of Bowers *et al.* (10) was used. To a solution of 2.5 g (0.0104 mole) of 1-(4-biphenylyl)pentanol (III) (1) in 20 ml of acetone was added dropwise, with stirring and cooling, 15 ml (0.0210 mole) of Jones reagent (11). The temperature was maintained below 10° during the addition. The resulting brown mixture was stirred at 0° for 0.5 hr. Isopropyl alcohol (20 ml) was added, the mixture was stirred at 25° for 1 hr, and then ether was added.

The organic phase was washed with water and with saturated sodium chloride solution, dried over anhydrous sodium sulfate, and concentrated under reduced pressure to 2.2 g (87%) of the ketone X as a white solid, mp 75–77°. An analytical specimen was prepared by recrystallization from absolute ethanol, mp 79.5–80.5°; IR ($CHCl_3$): 1669 (aromatic ketone C=O) cm^{-1}; NMR ($CDCl_3$): δ 0.80–1.96 (m, 7H, C_3H_7), 2.81 (t, J = 7 Hz, 2H, CH_2CO), and 7.40–8.06 (m, 9H aromatic) ppm.

Anal.—Calc. for $C_{17}H_{18}O$: C, 85.7; H, 7.6. Found: C, 85.6; H, 7.5.

***O*-Methyloxime of 1-(4-Biphenylyl)-1-pentanone (XI)**—The method of Feuer and Braunstein (12) was used. To a solution of 2.15 g (0.009 mole) of X in 50 ml of absolute ethanol and 50 ml of dry pyridine was added 0.751 g (0.009 mole) of methoxylamine hydrochloride. The solution was heated at reflux for 24 hr and then cooled to 25°. The reaction mixture was poured onto a slurry of ice and 5% hydrochloric acid and then was extracted with ether. The organic phase was washed with water and with saturated sodium chloride solution, dried over anhydrous sodium sulfate, and concentrated under reduced pressure to a viscous yellow oil, which crystallized on standing.

This procedure afforded 2.12 g (88%) of XI as a white solid, mp 42–44°. An analytical specimen was prepared by recrystallization from ether–petroleum ether (bp 60–68°), mp 43.5–44.5°; IR ($CHCl_3$): 1610 (C=N) cm^{-1}; NMR ($CDCl_3$): δ 0.67–1.67 (m, 7H, C_3H_7), 2.75 (t, J = 7 Hz, 2H, N=CCH_2), 3.97 (s, 3H, OCH_3), and 7.23–7.90 (m, 9H, aromatic) ppm.

Anal.—Calc. for $C_{18}H_{21}NO$: C, 80.9; H, 7.9; N, 5.2. Found: C, 80.7; H, 8.1; N, 5.4.

1-(4-Biphenylyl)-1-aminopentane Hydrochloride (XII)—The method of Boots *et al.* (13) was modified. To a mixture of 1.83 g (0.0068 mole) of XI and 0.660 g (0.017 mole) of sodium borohydride in 25 ml of dry dimethoxyethane was added dropwise, with stirring and cooling, 3.2 g (0.023 mole) of boron trifluoride etherate in 20 ml of dimethoxyethane. The mixture was stirred an additional hour at 25° and then heated at reflux for 2 hr. The mixture was cooled, and then 3 ml of water was added slowly, followed by 15 ml of a 5% hydrochloric acid solution.

The resulting solution was heated at reflux for 1 hr and then stirred at 25° for 14 hr. The dimethoxyethane was removed under reduced pressure, and the residue was adjusted to pH 12 with a 5% sodium hydroxide solution and extracted with ether. The organic phase was washed with water and with saturated sodium chloride solution, dried over anhydrous sodium sulfate, and concentrated under reduced pressure to the amine as a viscous oil, which was characterized as the amine hydrochloride.

Addition of an ethereal hydrogen chloride solution to the amine afforded a white solid, 1.60 g (85%), mp 250–253°. Recrystallization from ethyl acetate afforded an analytical specimen of XII, mp 252–253.5°; IR (KBr): 3400 ($^+NH_3$) cm^{-1}; NMR (dimethyl sulfoxide-d_6): δ 0.62–1.53 (m, 9H, C_4H_9), 4.72 (s, 3H, $^+NH_3$), and 7.35–7.92 (m, 9H, aromatic) ppm.

Anal.—Calc. for $C_{17}H_{22}ClN$: C, 74.0; H, 8.0; N, 5.1. Found: C, 74.4; H, 8.2; N, 5.4.

***N*-[1-(4-Biphenylyl)pentyl]succinamic Acid (XIII)**—The method described by Vogel (14) was used. A solution of 0.50 g (0.0018 mole) of XII in 18 ml of an ice-cold 5% sodium hydroxide solution was extracted with 50 ml of benzene. The organic phase was washed with water and with saturated sodium chloride solution and dried over anhydrous sodium sulfate. To the benzene solution of the amine was added 0.200 g (0.002 mole) of succinic anhydride. The solution was stirred at 25° for 3 hr and then was extracted with a 5% sodium hydroxide solution. The basic aqueous phase was adjusted to pH 2 with an ice-cold 5% hydrochloric acid solution and then extracted with ether.

The organic phase was washed with water and with saturated sodium chloride solution, dried over anhydrous sodium sulfate, and concentrated under reduced pressure to 0.573 g of a white solid, mp 165–170°. Recrystallization from ethyl acetate–petroleum ether (bp 60–68°) afforded 0.259 g (40%) of XIII, mp 176.5–178°; IR (KBr): 3250 (NH), 1725 (acid C=O), and 1640 (amide C=O) cm^{-1}; NMR (dimethyl sulfoxide-d_6): δ 0.67–2.00 (m, 9H, C_4H_9), 2.54 (s, 4H, CH_2CH_2), and 7.34–7.84 (m, 9H, aromatic) ppm.

Anal.—Calc. for $C_{21}H_{25}NO_3$: C, 74.3; H, 7.4; N, 4.1. Found: C, 74.1; H, 7.4; N, 4.2.

4-[1-(4-Biphenylyl)pentylamino]butanoic Acid (XVII)—To a solution of 1.23 g (0.008 mole) of methyl 4-aminobutanoate hydrochloride (XIV), mp 119–120° [lit. (15) mp 121.5–122.5°], in 20 ml of methanol was added 1.0 g (0.012 mole) of sodium acetate. A cloudy solution resulted with an apparent pH of 6–7. To this solution was added a solution of 0.476 g (0.002 mole) of X in 15 ml of ether and 5 ml of methanol. To this mixture were added 2 g of anhydrous sodium sulfate and 0.112 g (0.0018 mole) of sodium cyanoborohydride[4].

The mixture was stirred at 25° for 72 hr and then poured into ether and water. The organic phase was washed with water and with saturated sodium chloride solution, dried over anhydrous sodium sulfate, and concentrated under reduced pressure to 530 mg of a pale-yellow semisolid, which was chromatographed on 30 g of magnesium silicate[5] (60–100 mesh). Elution with 5% ether–petroleum ether (bp 60–68°) afforded 0.149 g of X. Elution with 50% ether–petroleum ether (bp 60–68°) through 100% ether afforded 0.233 g of a mixture of the amino ester XV and the lactam XVI as a viscous colorless liquid; IR ($CHCl_3$): 1758 (ester C=O) and 1665 (lactam C=O) cm^{-1}. The mixture was hydrolyzed directly as described later.

To a solution of XV and XVI (0.230 g) in 5 ml of 95% ethanol and 15 ml of a 50% *tert*-butyl alcohol–water mixture was added 0.700 g (0.011 mole) of 85% potassium hydroxide pellets. The colorless solution was heated at reflux for 21 hr. Then the solvent was removed under reduced pressure, and the residue was made up to a total volume of 10 ml with water. The mixture was chilled (5°) and filtered, and the solid was rinsed with 10 ml of water (5°). The filtrate was adjusted to pH 6 with acetic acid, and the resulting white viscous oil was extracted with ethyl acetate.

[4] Aldrich Chemical Co.
[5] Florisil.

The organic phase was washed with water and with saturated sodium chloride solution, dried over anhydrous sodium sulfate, and concentrated under reduced pressure to 0.183 g of a pale-yellow viscous oil, which was triturated with ether and then allowed to stand at 5° for 6 days. A white solid resulted, which proved to be hygroscopic, so no melting point could be obtained. An analytical specimen of XVII was prepared by recrystallization from ethyl acetate–ether; IR ($CHCl_3$): 1715 (broad, acid C=O, unionized) and 1600–1560 (broad, acid C=O, ionized) cm^{-1}; NMR ($CDCl_3$): δ 0.65–3.00 (m, 16H, C_4H_9, $CH_2CH_2CH_2CH$), 7.30–7.80 (m, 9H, aromatic), and 8.15 (s, broad, 2H, NH, CO_2H) ppm.

Anal.—Calc. for $C_{21}H_{27}NO_2 \cdot 2H_2O$: C, 69.8; H, 8.6; N, 3.9. Found: C, 70.0; H, 7.9; N, 3.6.

5-Oxo-5-(4-biphenylyl)-3-methylpentanoic Acid (XIX)—The procedure of Goldschmidt (6) was used. To a suspension of 6.5 g (0.049 mole) of aluminum chloride in 60 ml of dry methylene chloride was added dropwise, with stirring at 25°, a solution of 2.49 g (0.02 mole) of 3-methylglutaric anhydride[4] in 20 ml of methylene chloride, followed by a solution of 3.08 g (0.02 mole) of biphenyl in 20 ml of methylene chloride. The reaction mixture was stirred at 25° for 23 hr and then poured onto an ice–concentrated hydrochloric acid mixture. Chloroform was added until a clear two-phase system was obtained, and then the chloroform was removed under reduced pressure. The residue was added to ether and water.

The organic phase was washed with water and with a 5% sodium hydroxide solution. The basic, aqueous extract was acidified to pH 2 with a 5% hydrochloric acid solution and extracted with ether. The organic phase was washed with water and with saturated sodium chloride solution, dried over anhydrous sodium sulfate, and concentrated under reduced pressure to 1.7 g (30%) of XIX as an orange oil, which crystallized on standing. Repeated recrystallization from ethyl acetate–petroleum ether (bp 60–68°) afforded an analytical specimen of XIX as cream plates, mp 119–120°; IR ($CHCl_3$): 1708 (acid C=O) and 1676 (ketone C=O) cm^{-1}; NMR ($CDCl_3$): δ 1.05 (d, J = 6 Hz, 3H, CH_3), 2.30–3.15 (m, 5H, CH_2CHCH_2), 7.20–8.18 (m, 9H, aromatic), and 10.05 (s, 1H, CO_2H) ppm.

Anal.—Calc. for $C_{18}H_{18}O_3$: C, 76.6; H, 6.4. Found: C, 76.6; H, 6.3.

5-(4-Biphenylyl)-3-methylpentanoic Acid (XX)—A mixture of 0.500 g (0.0018 mole) of XIX, 0.100 g of a 10% palladium-on-charcoal catalyst, 0.1 ml of concentrated hydrochloric acid, and 50 ml of absolute ethanol was hydrogenated on a Parr apparatus at 25° and 40 psi for 5 hr. The mixture was filtered, and the solvent was removed under reduced pressure to give 0.420 g of a colorless liquid. This mixture of the acid and ethyl ester was treated with a mixture of 10 ml of methanol and 10 ml of a 5% sodium hydroxide solution at 25° for 48 hr. The colorless solution was added to ether and water. The basic, aqueous extract was acidified to pH 2 with an ice–concentrated hydrochloric acid mixture and then extracted with ether.

The organic phase was washed with water and with saturated sodium chloride solution, dried over anhydrous sodium sulfate, and concentrated under reduced pressure to 0.370 g (78%) of XX as a pale-yellow solid. Recrystallization from petroleum ether (bp 60–68°) afforded 0.253 g of white needles, mp 89–91° [lit. (6) mp 92–93°]; IR ($CHCl_3$): 1708 (acid C=O) cm^{-1}; NMR ($CDCl_3$): δ 1.03 (d, J = 6 Hz, 3H, CH_3), 1.27–2.80 (m, 7H, $CH_2CH_2CHCH_2$), 7.14–7.58 (m, 9H, aromatic), and 10.15 (s, 1H, CO_2H) ppm.

4-Phenylbenzylideneacetone (XXII)—The procedure of Ayling *et al.* (7) was used for the synthesis of this α,β-unsaturated ketone, mp 126–129° [lit. (7) mp 137°].

4-(4-Biphenylyl)-2-butanone (XXIII)—The method of Cromwell and Cahoy (8) was used for the synthesis of this ketone, mp 71–73° [lit. (8) mp 75–77°].

***tert*-Butyl 5-(4-Biphenylyl)-3-hydroxy-3-methylpentanoate (XXIV)**—The procedure of Cornforth *et al.* (16) was used. To a mixture of 0.295 g (0.0045 mole) of zinc (20 mesh, unactivated) in 5 ml of dry tetrahydrofuran (heated at reflux and maintained under a nitrogen atmosphere) was added dropwise, over 15 min, a solution of 1.00 g (0.0045 mole) of XXIII and 0.7 ml (0.0045 mole) of *tert*-butyl bromoacetate in 7 ml of dry tetrahydrofuran. The mixture was heated at reflux for 3 hr after the addition was completed. Then the mixture was cooled, poured onto ice–5% hydrochloric acid, and rapidly extracted with ether.

The organic phase was washed with a 5% sodium hydroxide solution, with water, and with saturated sodium chloride solution, dried over anhydrous sodium sulfate, and concentrated under reduced pressure to 1.42 g (93%) of a colorless liquid. Attempts to purify XXIV resulted in extensive decomposition, so it was hydrolyzed directly to the free acid (XXV).

5-(4-Biphenylyl)-3-hydroxy-3-methylpentanoic Acid (XXV)—A mixture of 0.454 g (0.0013 mole) of the ester XXIV, 0.060 g of *p*-toluenesulfonic acid monohydrate, and 10 ml of benzene was heated at reflux for 30 min. The solution was added to ether and water. The organic phase was washed with water and with a 5% sodium hydroxide solution. The basic, aqueous extract was acidified to pH 2 with a 5% hydrochloric acid solution and then extracted with ether.

The organic phase was washed with water and with saturated sodium chloride solution, dried over anhydrous sodium sulfate, and concentrated under reduced pressure to 0.164 g (45%) of XXV as a white solid. Recrystallization from ethyl acetate–petroleum ether (bp 60–68°) afforded an analytical specimen as white needles, mp 91–91.5°; NMR ($CDCl_3$): δ 1.37 (s, 3H, CH_3), 1.70–2.03 (m, 2H, CH_2 at C-4), 2.60–3.12 (m, 4H, CH_2, CH_2 at C-2 and C-5), and 7.05–8.20 (m, 11H, aromatic, OH, CO_2H) ppm.

Anal.—Calc. for $C_{18}H_{20}O_3$: C, 76.0; H, 7.1. Found: C, 76.2; H, 6.9.

Methyl 6-Oxo-6-(4-biphenylyl)hexanoate (XXVI)—The method of Morand *et al.* (9) was used for the preparation of this ester, mp 109–110° [lit. (9) mp 108–109°].

6-Oxo-6-(4-biphenylyl)hexanoic Acid (VI)—The method of Morand *et al.* (9) was used for the preparation of this acid, mp 160–161° [lit. (9) mp 162–163°]. This keto acid was also used as an intermediate in the synthesis of IX.

Methyl 6-Hydroxy-6-(4-biphenylyl)hexanoate (XXVII)—The method of Boots[6] was used. To a solution of 1.81 g (0.0061 mole) of XXVI in 15 ml of acetic acid was added dropwise, with stirring at 25°, a solution of 2 ml (0.019 mole) of pyridinylborane[7] in 5 ml of acetic acid. The mixture was stirred at 25° for 4 hr and then poured onto an ice (100 g)–concentrated hydrochloric acid (6 ml) mixture. This mixture was stirred for 30 min and then extracted with ether.

The organic phase was washed with water, with 5% sodium hydroxide solution, with water, and with saturated sodium chloride solution. Then it was dried over anhydrous sodium sulfate and concentrated under reduced pressure to 1.44 g (79%) of a pale-pink oil, which crystallized upon trituration with ether–petroleum ether (bp 60–68°), mp 46–48°. An analytical specimen of XXVII as white prisms was prepared by recrystallization from ether–petroleum ether (bp 60–68°), mp 49–50°; IR ($CHCl_3$): 3450–3600 (broad, OH) and 1725 (ester C=O) cm^{-1}; NMR ($CDCl_3$): δ 1.2–2.5 [m, 9H, $(CH_2)_4$, OH], 3.62 (s, 3H, OCH_3), 4.72 (t, J = 6 Hz, 1H, CH), and 7.22–7.72 (m, 9H, aromatic) ppm.

Anal.—Calc. for $C_{19}H_{22}O_3$: C, 76.5; H, 7.4. Found: C, 76.8; H, 7.4.

6-Hydroxy-6-(4-biphenylyl)hexanoic Acid (VIII)—A solution of 0.330 g (0.0011 mole) of the hydroxy ester XXVII, 7.5 ml of methanol, and 5 ml of a 5% sodium hydroxide solution was heated at reflux for 1 hr. The solvent was removed under reduced pressure, and then the residue was added to ether and water. The basic, aqueous extract was acidified to pH 2 with an ice-cold 5% hydrochloric acid solution and then extracted with ethyl acetate.

The organic phase was washed with water and with saturated sodium chloride solution, dried over anhydrous sodium sulfate, and concentrated under reduced pressure to a quantitative yield (0.316 g) of the hydroxy acid VIII as a beige solid, mp 130–131°. Recrystallization from ethyl acetate–petroleum ether (bp 60–68°) afforded an analytical specimen as white prisms, mp 132–133°; IR (mineral oil): 1725 (acid C=O) cm^{-1}; NMR (acetone-d_6): δ 1.10–2.50 [m, 8H, $(CH_2)_4$], 4.71 (t, J = 6 Hz, 1H, CH), 6.25 (s, 2H, OH, CO_2H), and 7.30–7.75 (m, 9H, aromatic) ppm.

Anal.—Calc. for $C_{18}H_{20}O_3$: C, 76.0; H, 7.1. Found: C, 75.7; H, 7.4.

Methyl 6-(4-Biphenylyl)hexanoate (XXVIII)—A mixture of 0.600 g (0.002 mole) of XXVII, 0.100 g of a 10% palladium-on-charcoal catalyst, 0.1 ml of concentrated hydrochloric acid, and 50 ml of absolute ethanol was hydrogenated on a Parr apparatus at 25° and 40 psi for 6 hr. The mixture was filtered, and the solvent was removed under reduced pressure. The residue was added to ether and water.

The organic phase was washed with water and with saturated sodium chloride solution, dried over anhydrous sodium sulfate, and concentrated under reduced pressure to 0.490 g (85%) of a cream solid,

[6] Manuscript in preparation.
[7] Callery Chemical Co.

mp 35–38°. Recrystallization from petroleum ether (bp 60–68°) afforded an analytical specimen of XXVIII as white prisms, mp 37–39°; IR ($CHCl_3$): 1728 (ester C=O) cm^{-1}; NMR ($CDCl_3$): δ 1.15–2.85 [m, 10H, $(CH_2)_5$], 3.67 (s, 3H, OCH_3), and 7.20–7.72 (m, 9H, aromatic) ppm.

Anal.—Calc. for $C_{19}H_{22}O_2$: C, 80.8; H, 7.8. Found: C, 80.9; H, 7.8.

6-(4-Biphenylyl)hexanoic Acid (XXIX)—A solution of 0.215 g (0.00076 mole) of the ester XXVIII, 7 ml of methanol, and 5 ml of a 5% sodium hydroxide solution was heated at reflux for 1 hr. The solvent was removed under reduced pressure, and then the residue was added to ether and water. The basic, aqueous extract was acidified to pH 2 with 5% hydrochloric acid and then extracted with ethyl acetate.

The organic phase was washed with water and with saturated sodium chloride solution, dried over anhydrous sodium sulfate, and concentrated under reduced pressure to 0.184 g (91%) of a white solid, mp 95–97°. Recrystallization from ether–petroleum ether (bp 60–68°) afforded an analytical specimen of XXIX as white needles, mp 98–99° [lit. (17) mp 103–105°]; IR ($CHCl_3$): 1705 (acid C=O) cm^{-1}; NMR ($CDCl_3$): δ 1.2–2.85 [m, 10H, $(CH_2)_5$] and 7.15–7.65 (m, 9H, aromatic) ppm.

Assay of Enzyme Activity and Inhibition—Rat liver microsomes containing β-hydroxy-β-methylglutaryl coenzyme A reductase activity were prepared according to Shapiro and Rodwell (18). The assay procedure used was described previously (2). The enzyme incubation mixture consisted of $NADP^+$ (9.7 μmoles)[8], glucose 6-phosphate (59.7 μmoles)[8], torula yeast glucose 6-phosphate dehydrogenase (5 units)[8], microsomal protein (2 mg) as determined by a modification of the method of Lowry *et al.* (2, 19), 0.1 ml of ethylene glycol monoethyl ether containing the inhibitor, and sufficient assay buffer (30 m*M* ethylenediaminetetraacetic acid, 70 m*M* sodium chloride, and 10 m*M* β-mercaptoethanol, pH 6.8) to produce a total volume of 2.9 ml.

Enzymatic activity was initiated by the addition of 0.1 ml of a solution containing 94 nmoles (31 μ*M*) of 3-^{14}C-*dl*-β-hydroxy-β-methylglutaryl coenzyme A prepared (20) from 3-^{14}C-β-hydroxy-β-methylglutaric acid[9]. After 30 min of incubation, the reaction was stopped by the addition of 0.2 ml of concentrated hydrochloric acid, and 5-^{3}H-*dl*-mevalonolactone[9] was added. Mevalonolactone was extracted into ether and isolated by TLC, and the radioactivity was determined[10].

RESULTS

Various isosteric replacements of the ester group were made in an effort to determine if the ester function was critical for activity. Also, replacements were made to find compounds that would not contain the acid-labile ester group found in I. A recent review article (21) described a 2-(4-biphenylyl)propyl group as a "super-sensitive, acid-labile protecting group" of carboxylic acids. The close similarity between the alcoholic portion of the ester analogs I and II and this group suggested that the esters could be highly susceptible to acid hydrolysis (which could be important upon oral administration).

Thus, the ether analog V, the carbo analog IX, the amido analog XIII, and the amino analog XVII were evaluated as inhibitors of rat liver β-hydroxy-β-methylglutaryl coenzyme A reductase (Table I). Both V and IX had essentially the same inhibitory activity as I. However, XIII definitely showed less inhibitory activity than I, even though solubility problems were encountered. On the other hand, XVII was about one-half as active as I.

These data show that the ester function is not necessary for significant inhibitory activity. The isosteric replacements involved which afforded the ether and carbo analogs provided compounds with essentially equal inhibitory activity when compared to the ester I.

In 1966, Eades *et al.* (3, 4) reported the evaluation of 36 compounds as inhibitors of the incorporation of 1-^{14}C-acetate into cholesterol by rat liver homogenates. The close similarity in structure of these compounds to those described here led to the investigation as to whether three of these compounds (XIX, XX, and XXV) were inhibitors of β-hydroxy-β-methylglutaryl coenzyme A reductase. Analog XXV was selected on the basis of its close similarity in structure to our most active inhibitor, the ester II. Compound XX was also evaluated because it was the most active and extensively studied compound by Eades *et al.* Analogs XIX, XX, and XXV exhibited the same degree of inhibition shown by the ester analog I. Comparison of the substituted 3-hydroxy-3-methyl ester (II) with the similar analog XXV showed remarkable dissimilarities in their inhibitory activities. This finding suggests that XXV is binding to the enzyme at a different site or in a different mode than II.

Analogs VI and XXVI–XXIX could not be evaluated quantitatively because of their limited solubility in the test system. Analogs VII and VIII exhibited essentially the same inhibitory activity, demonstrating that the *n*-butyl side chain was not required for activity in this particular series.

Table I—Inhibition of β-Hydroxy-β-methylglutaryl Coenzyme A Reductase

Compound	Activity, $(I/S)_{50\%}$[a]
I, $m = 2$[b]	11
II[c]	1.5
V	10
VII	11
IX	16
XIII	30[d] (18%)
XVII	20
XIX	12
XX	12
XXV	15
VI	3[d] (30%)
XXVI	5[d] (16%)
VIII	15
XXVII	8[d] (26%)
XXIX	3[d] (40%)
XXVIII	3[d] (26%)

[a] The inhibition index, $(I/S)_{50\%}$, equals the ratio of the micromolar concentration of the inhibitor to the micromolar concentration of the substrate required to give 50% inhibition. At least two sets of duplicate determinations were used. [b] A standard inhibitor used routinely to provide comparability of each assay set (2). [c] Described previously (2). [d] The *I/S* ratio reported produced the parenthetical percentage of inhibition. The inhibitor was insoluble at higher concentrations.

REFERENCES

(1) M. R. Boots, S. G. Boots, C. M. Noble, and K. E. Guyer, *J. Pharm. Sci.*, **62**, 952(1973).

(2) K. E. Guyer, S. G. Boots, P. E. Marecki, and M. R. Boots, *ibid.*, **65**, 548(1976).

(3) C. H. Eades, Jr., C. M. Weiss, V. B. Solberg, and G. E. Phillips, *Med. Pharmacol. Exp.*, **14**, 225(1966).

(4) C. H. Eades, Jr., and V. B. Solberg, *ibid.*, **14**, 234(1966).

(5) C. M. Starks, *J. Am. Chem. Soc.*, **93**, 195(1971).

(6) E. N. Goldschmidt, U.S. pat. 3,120,551 (1964); through *Chem. Abstr.*, **60**, 9203h(1964). E. N. Goldschmidt, U.S. pat. 3,182,061 (1965); through *Chem. Abstr.*, **63**, 1740d(1965).

(7) E. E. Ayling, J. Hodges, and R. F. K. Meredith, *J. Chem. Soc.*, **1956**, 2679.

(8) N. H. Cromwell and R. P. Cahoy, *J. Am. Chem. Soc.*, **80**, 5524(1958).

(9) P. Morand, J. F. Bagli, M. Kraml, and J. Dubuc, *J. Med. Chem.*, **7**, 504(1964).

(10) A. Bowers, T. G. Halsall, E. R. H. Jones, and A. J. Lemin, *J. Chem. Soc.*, **1953**, 2548.

(11) K. Bowden, I. M. Heilbron, E. R. H. Jones, and B. C. L. Weedon, *ibid.*, **1946**, 39.

(12) H. Feuer and D. M. Braunstein, *J. Org. Chem.*, **34**, 1817(1969).

(13) M. R. Boots, S. G. Boots, and D. E. Moreland, *J. Med. Chem.*, **13**, 144(1970).

(14) A. I. Vogel, "A Textbook of Practical Organic Chemistry," 3rd ed., Longmans, Green and Co., London, England, 1957, p. 377.

(15) D. L. Garmaise, R. Schwartz, and A. F. McKay, *J. Am. Chem. Soc.*, **80**, 3332(1958).

(16) D. A. Cornforth, A. E. Opara, and G. Read, *J. Chem. Soc., C*, **1969**, 2799.

(17) French pat. 5737 (1968); through *Chem. Abstr.*, **70**, 114837d(1969).

[8] Sigma Chemical Co.
[9] New England Nuclear.
[10] Nuclear Chicago Mark I liquid scintillation counter.

(18) D. J. Shapiro and V. M. Rodwell, *J. Biol. Chem.*, **246**, 3210(1971).
(19) O. H. Lowry, N. J. Rosenbrough, A. L. Farr, and R. J. Randall, *ibid.*, **193**, 265(1951).
(20) S. G. Boots, M. R. Boots, and K. E. Guyer, *J. Pharm. Sci.*, **60**, 614(1971).
(21) L. A. Carpino, *Acc. Chem. Res.*, **6**, 191(1973).

ACKNOWLEDGMENTS AND ADDRESSES

Received September 8, 1975, from the *Departments of *Pharmaceutical Chemistry and ‡ Biochemistry, Medical College of Virginia Health Sciences Division, Virginia Commonwealth University, Richmond, VA 23298*

Accepted for publication December 8, 1975.

Abstracted in part from a dissertation submitted by P. E. Marecki to Virginia Commonwealth University in partial fulfillment of the Doctor of Philosophy degree requirements.

Supported by a grant from the U.S. Public Health Service (HL-11768, National Heart and Lung Institute).

P. E. Marecki thanks the following for their generous support: National Institutes of Health, Traineeship GM484, 1970–1972; and the American Foundation for Pharmaceutical Education, 1972–1974 (Sydnor Barksdale Penick Memorial Fellow, 1973–1974).

Excellent technical assistance by Ms. Bonnie Frazier is gratefully acknowledged.

§ Present address: Department of Biochemistry, Marshall University School of Medicine, Huntington, WV 25701

ˣ To whom inquiries should be directed.

Physical Characterization and Activity *In Vivo* of Polymorphic Forms of 7-Chloro-5,11-dihydrodibenz[*b,e*][1,4]oxazepine-5-carboxamide, a Potential Tricyclic Antidepressant

IRWIN S. GIBBS ˣ, ANTHONY HEALD, HAROLD JACOBSON, DEODATT WADKE, and IRVING WELIKY

Abstract □ The biological availability in dogs and humans of 7-chloro-5,11-dihydrodibenz[*b,e*][1,4]oxazepine-5-carboxamide, a potential antidepressant drug, was increased when the compound was administered in capsule formulations as micronized drug coated with 1% sodium lauryl sulfate or as a lyophilate with poloxamer 407. This increase with these two formulations had been predicted by dissolution tests *in vitro*. The lyophilized combination with poloxamer 407 was more soluble in 0.1 *N* HCl than was the untreated compound. Characterization of the lyophilate by differential thermal analysis, X-ray diffraction, and IR spectroscopy indicated that the increase in solubility was attributable to the formation of a polymorphic form. A polymorph of the compound, designated Form B, was prepared. The solubility and dissolution characteristics of the two polymorphic forms, A and B, as well as of the lyophilized combination with poloxamer 407, were determined.

Keyphrases □ Dibenz[*b,e*][1,4]oxazepine, substituted—solubility, dissolution rate, and bioavailability, micronized and surfactant coated compared to lyophilate with copolymer formulation □ Bioavailability—substituted dibenz[*b,e*][1,4]oxazepine, micronized and surfactant coated compared to lyophilate with copolymer formulation □ Polymorphic forms—substituted dibenz[*b,e*][1,4]oxazepine, solid dispersion, solubility, dissolution rate, and bioavailability □ Antidepressants, tricyclic—substituted dibenz[*b,e*][1,4]oxazepine, solubility, dissolution rate, and bioavailability

In preclinical studies for the development of a new drug, its biological availability should be assessed (1). If a drug is incompletely absorbed, efforts are usually made to increase its biological availability.

The common causes of biological unavailability of a drug include poor solubility and slow dissolution in aqueous media, specifically GI fluids (1). When synthesis of a more soluble chemical derivative is not feasible, diminution of the particle size (2, 3) or utilization of another polymorphic form (4–7) or solid dispersions of the drug (8–12) may increase its biological availability.

In preformulation studies of a potential tricyclic antidepressant, 7-chloro-5,11-dihydrodibenz[*b,e*][1,4]-oxazepine-5-carboxamide[1] (I), synthesized by Yale (13), the drug was more readily and more completely absorbed when given to dogs orally as capsules containing a fine powder rather than a coarse powder[2].

The equilibrium solubility of I in aqueous solution at 37° is 0.04 mg/ml, irrespective of pH.

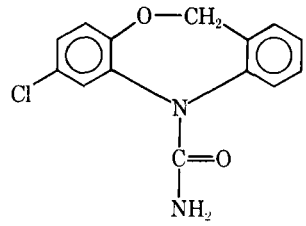

I

This report describes the methods evolved for increasing the bioavailability of this drug by increasing its dissolution rate and/or solubility. To accomplish these effects, the material was either micronized and combined with a wetting agent or prepared as a solid dispersion. During the preparation of the latter, the existence of a polymorphic form was discovered.

EXPERIMENTAL

Materials—The following was used: poloxamer 407[3], I polymorph Form A[4], sodium lauryl sulfate USP, magnesium stearate USP, an-

[1] SQ 10, 966.
[2] J. Dreyfuss, Department of Drug Metabolism, Squibb Institute for Medical Research, New Brunswick, N.J., unpublished data.
[3] Pluronic F-127, BASF Wyandotte Corp., Wyandotte, Mich.
[4] Squibb lot RR002RC (see Ref. 13).

(18) D. J. Shapiro and V. M. Rodwell, *J. Biol. Chem.*, **246**, 3210(1971).
(19) O. H. Lowry, N. J. Rosenbrough, A. L. Farr, and R. J. Randall, *ibid.*, **193**, 265(1951).
(20) S. G. Boots, M. R. Boots, and K. E. Guyer, *J. Pharm. Sci.*, **60**, 614(1971).
(21) L. A. Carpino, *Acc. Chem. Res.*, **6**, 191(1973).

ACKNOWLEDGMENTS AND ADDRESSES

Received September 8, 1975, from the *Departments of *Pharmaceutical Chemistry and ‡ Biochemistry, Medical College of Virginia Health Sciences Division, Virginia Commonwealth University, Richmond, VA 23298*

Accepted for publication December 8, 1975.

Abstracted in part from a dissertation submitted by P. E. Marecki to Virginia Commonwealth University in partial fulfillment of the Doctor of Philosophy degree requirements.

Supported by a grant from the U.S. Public Health Service (HL-11768, National Heart and Lung Institute).

P. E. Marecki thanks the following for their generous support: National Institutes of Health, Traineeship GM484, 1970–1972; and the American Foundation for Pharmaceutical Education, 1972–1974 (Sydnor Barksdale Penick Memorial Fellow, 1973–1974).

Excellent technical assistance by Ms. Bonnie Frazier is gratefully acknowledged.

§ Present address: Department of Biochemistry, Marshall University School of Medicine, Huntington, WV 25701

ˣ To whom inquiries should be directed.

Physical Characterization and Activity *In Vivo* of Polymorphic Forms of 7-Chloro-5,11-dihydrodibenz[*b,e*][1,4]oxazepine-5-carboxamide, a Potential Tricyclic Antidepressant

IRWIN S. GIBBS ˣ, ANTHONY HEALD, HAROLD JACOBSON, DEODATT WADKE, and IRVING WELIKY

Abstract □ The biological availability in dogs and humans of 7-chloro-5,11-dihydrodibenz[*b,e*][1,4]oxazepine-5-carboxamide, a potential antidepressant drug, was increased when the compound was administered in capsule formulations as micronized drug coated with 1% sodium lauryl sulfate or as a lyophilate with poloxamer 407. This increase with these two formulations had been predicted by dissolution tests *in vitro*. The lyophilized combination with poloxamer 407 was more soluble in 0.1 *N* HCl than was the untreated compound. Characterization of the lyophilate by differential thermal analysis, X-ray diffraction, and IR spectroscopy indicated that the increase in solubility was attributable to the formation of a polymorphic form. A polymorph of the compound, designated Form B, was prepared. The solubility and dissolution characteristics of the two polymorphic forms, A and B, as well as of the lyophilized combination with poloxamer 407, were determined.

Keyphrases □ Dibenz[*b,e*][1,4]oxazepine, substituted—solubility, dissolution rate, and bioavailability, micronized and surfactant coated compared to lyophilate with copolymer formulation □ Bioavailability—substituted dibenz[*b,e*][1,4]oxazepine, micronized and surfactant coated compared to lyophilate with copolymer formulation □ Polymorphic forms—substituted dibenz[*b,e*][1,4]oxazepine, solid dispersion, solubility, dissolution rate, and bioavailability □ Antidepressants, tricyclic—substituted dibenz[*b,e*][1,4]oxazepine, solubility, dissolution rate, and bioavailability

In preclinical studies for the development of a new drug, its biological availability should be assessed (1). If a drug is incompletely absorbed, efforts are usually made to increase its biological availability.

The common causes of biological unavailability of a drug include poor solubility and slow dissolution in aqueous media, specifically GI fluids (1). When synthesis of a more soluble chemical derivative is not feasible, diminution of the particle size (2, 3) or utilization of another polymorphic form (4–7) or solid dispersions of the drug (8–12) may increase its biological availability.

In preformulation studies of a potential tricyclic antidepressant, 7-chloro-5,11-dihydrodibenz[*b,e*][1,4]-oxazepine-5-carboxamide[1] (I), synthesized by Yale (13), the drug was more readily and more completely absorbed when given to dogs orally as capsules containing a fine powder rather than a coarse powder[2].

The equilibrium solubility of I in aqueous solution at 37° is 0.04 mg/ml, irrespective of pH.

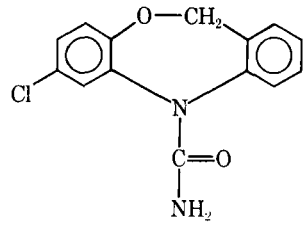

I

This report describes the methods evolved for increasing the bioavailability of this drug by increasing its dissolution rate and/or solubility. To accomplish these effects, the material was either micronized and combined with a wetting agent or prepared as a solid dispersion. During the preparation of the latter, the existence of a polymorphic form was discovered.

EXPERIMENTAL

Materials—The following was used: poloxamer 407[3], I polymorph Form A[4], sodium lauryl sulfate USP, magnesium stearate USP, an-

[1] SQ 10, 966.
[2] J. Dreyfuss, Department of Drug Metabolism, Squibb Institute for Medical Research, New Brunswick, N.J., unpublished data.
[3] Pluronic F-127, BASF Wyandotte Corp., Wyandotte, Mich.
[4] Squibb lot RR002RC (see Ref. 13).

hydrous lactose USP, starch USP, directly compressible starch[5], sodium glycine carbonate[6], and dioxane[7].

Dosage Forms—Bulk Formulation 1 was prepared by simple admixture of the ingredients. Microscopic examination showed a wide range of particle sizes for I, the largest being about 60 × 120 μm with variable thickness. Each unit dose, filled into a No. 3 gelatin capsule, consisted of: I, 100 mg; sodium lauryl sulfate, 1 mg; directly compressible starch, 20 mg; anhydrous lactose, 77 mg; and magnesium stearate, 2 mg.

For bulk Formulation 2, I was micronized[8] to yield particles smaller than 25 μm as determined by an automated particle counter[9]. The micronized powder was granulated with an aqueous solution of sodium lauryl sulfate. The damp granulation was dried under vacuum at room temperature until the total volatiles content was 0%, as determined by thermogravimetric analysis. After the dried granulation was passed through a No. 100 mesh screen, the remaining excipients were introduced by simple admixture. The final dosage unit was quantitatively identical to that of Formulation 1.

For Formulation 3, a lyophilized combination of I and poloxamer 407 was first prepared as a 1:1 (w/w) combination. Equal amounts of I and poloxamer 407 were dissolved separately in dioxane to yield a 3.3% solution of each material. The solution was poured into shallow glass dishes, frozen solid at −20°, and then lyophilized in a laboratory model freeze dryer[10]. Residual dioxane was removed by fluid bed drying at room temperature for approximately 30 hr[11]. The final product contained less than 1% dioxane.

Lyophilized I Form B Alone—Compound I was dissolved in dioxane to yield a 3.3% solution. The solution was placed into a shallow glass dish, frozen solid at −20°, and lyophilized. Residual dioxane was removed by fluid bed drying for 5 hr at room temperature and 2 hr at 40°; the residual dioxane content was 0%.

Lyophilized Poloxamer 407 Alone—A 6.6% solution of poloxamer 407 in dioxane was frozen solid at −20° in a shallow glass dish and then lyophilized. Residual dioxane was reduced to 0% by fluid bed drying at room temperature for 5 hr.

Dissolution—The dissolution test was a modification of the NF XIII method (14), *i.e.*, 300 ml of 0.1 *N* HCl at 37° and 60 rpm. Ten-milliliter samples of solution were removed from each resin flask periodically during 1 hr. Sample solution was replaced with an equal volume of 0.1 *N* HCl after each sampling. Removed samples were filtered through a 0.45-μm filter, and absorbance values were measured[12] at 290 nm.

Differential Thermal Analysis—Thermograms were obtained on a thermal analyzer[13] fitted with 2-mm microsample tubes. The heating rate was 15°/min, and the differential sensitivity was 1°/2.54 cm. The thermograms were obtained in the presence of static air.

X-Ray Diffraction—Powder X-ray diffraction patterns were obtained[14] employing nickel-filtered copper K_α X-radiation collimated by a 1° divergence slit, a 0.3° receiving slit, and a 1° antiscatter slit. Detection was mediated by a transistorized scintillation detector, and the output was eventually monitored by a recorder. A scan speed of 1° (2θ) was utilized at 30 kv and 10 mamp.

Before measurement, each sample was ground for about 12 sec by means of a glass ball in a plastic vial mounted on a dental amalgam shaker[15].

IR Absorbance Spectroscopy—IR spectra were determined[16] with the drug as a mineral oil mull or dissolved in deuterated chloroform.

Comparative Bioavailability in Dogs—The three formulations were administered orally to 9-month-old male beagle dogs, 11–15 kg, as capsules containing 100 mg of drug in a 3 × 3 Latin-square study, with a 1-week rest between treatments. The dogs were deprived of food for 12 hr before and throughout the study, with water available *ad libitum*. Each dog was weighed before the administration of each dose.

After a control plasma sample was obtained, each dog was dosed orally with one capsule, washed down with water given by gavage, 20 ml/kg. Plasma samples were obtained at 0.5, 1, 1.5, 2, 3, and 4 hr after the dose. The second and third doses were given (crossover arrangement) at 8 and 15 days after the initial dose. Plasma samples were assayed for intact I by GC (15).

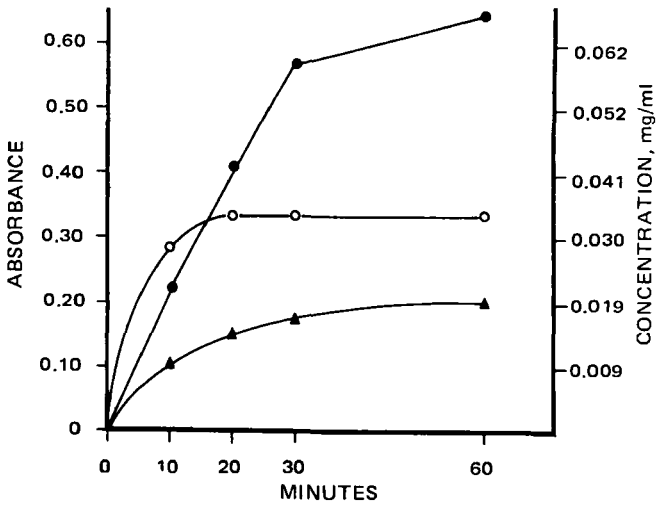

Figure 1—*Dissolution profiles (absorbance and concentration versus time) for three capsule formulations of I. Key: ▲, Formulation 1; ○, Formulation 2; and ●, Formulation 3.*

Comparative Bioavailability in Humans—The three capsule formulations were administered orally to two groups of six healthy male volunteers. The subjects ranged in age from 19 to 28 years (mean 23.2 years) and weighed between 68 and 96 kg (mean 79.6 kg). Each formulation was administered once to each subject before breakfast with 180 ml of water: Group I, single oral dose of 200 mg of I (two 100-mg capsules); and Group II, single oral dose of 400 mg of I (four 100-mg capsules).

Each group of six subjects was subdivided into groups of two, and each pair received a particular formulation on a given day. They were then crossed over at intervals of 7 days, so that each subject had received one dose of each formulation by the end of the study.

Individual 10-ml samples of venous blood were drawn from each subject and collected into nonheparinized tubes at 0 (pretreatment), 1, 2, 4, 6, 8, 12, 24, 48, and 72 hr after drug administration. Samples were permitted to clot and were then centrifuged. Serum samples were transferred to sterile tubes and frozen until assayed by a GC method specific for I (15).

RESULTS

Dissolution—The dissolution profiles of the three capsule formulations are shown in Fig. 1. Each point represents the average value obtained for three capsules of a formulation at a given sampling time. Formulation 1 yielded the slowest initial rate of solution for I. The concentration of drug in solution after 1 hr of study was approximately half of the equilibrium solubility of the drug (0.04 mg/ml).

Formulation 2, containing micronized I granulated with sodium lauryl sulfate, showed a faster initial rate of solution, and the concentration of I in solution after 1 hr of testing approached the equilibrium solubility of the drug. Formulation 3 showed an intermediate initial dissolution rate, similar to that of Formulation 2, but the solubility attained after 1 hr of study exceeded the equilibrium solubility of I by more than 60%.

Characterization of I Form in Lyophilate with Poloxamer 407—*Differential Thermograms*—Figure 2 shows the differential thermograms for I, lyophilized poloxamer 407, and the combination lyophilate of I and poloxamer 407. Compound I showed a melting endotherm at approximately 195°, followed by a decomposition exotherm at 250–300°. Lyophilized poloxamer 407 showed a melting endotherm at 48–50°, with no other thermal events of interest. The combination lyophilate product showed the characteristic melting endotherm for poloxamer 407, followed by a very small endotherm near 180°. The characteristic melting endotherm for I was not seen with the combination lyophilate, but the decomposition exotherm was apparent at 250–300°.

[5] StaRx 1500, A. E. Staley Manufacturing Co., Decatur, Ill.
[6] Edward Mendell Co., Carmel, N.Y.
[7] Spectroquality, Matheson, Coleman & Bell.
[8] Gem T research model pulverizer, Trost Equipment Corp.
[9] Coulter.
[10] No. 10-D1-SM, Virtis Co., Gardiner, N.Y.
[11] Model FBD/L72, Pfaltz and Bauer, Flushing, N.Y.
[12] Beckman model DU spectrophotometer.
[13] DuPont model 900.
[14] Philips X-ray diffractometer.
[15] Wig-L-Bug, Crescent Dental Manufacturing Co., Chicago, Ill.
[16] Perkin-Elmer 621 IR spectrophotometer.

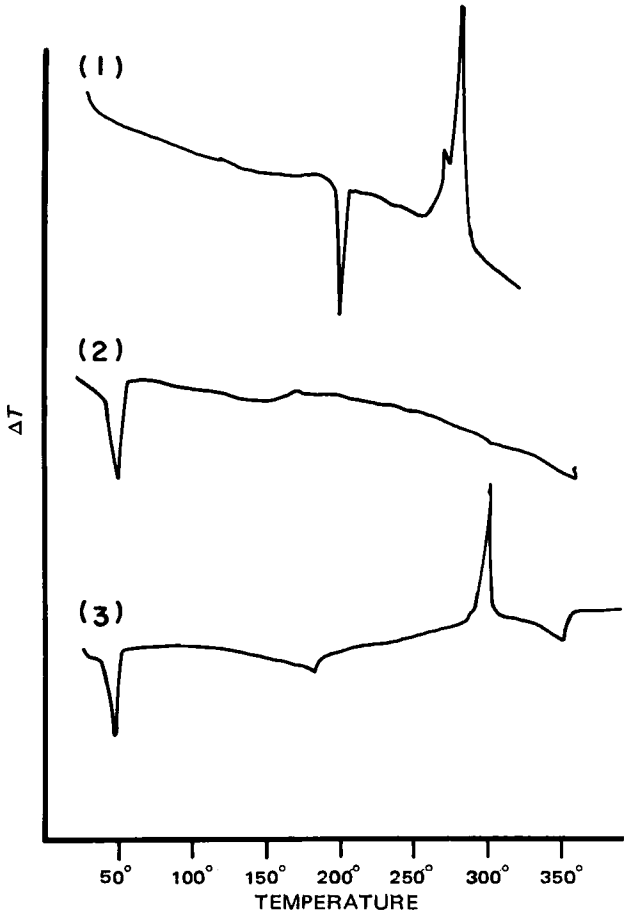

Figure 2—*Differential thermograms of I (1), lyophilized poloxamer 407 (2), and I–poloxamer 407 lyophilate (3).*

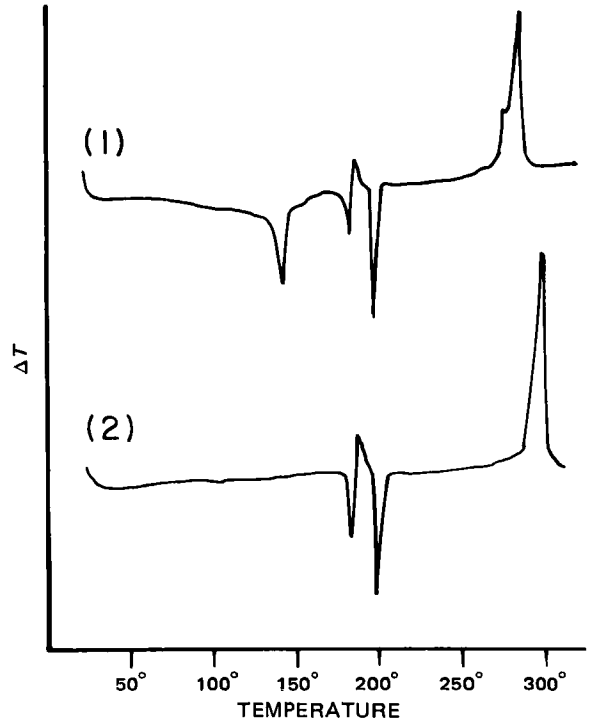

Figure 3—*Differential thermograms of undried (1) and dried (2) I lyophilized from dioxane.*

Figure 3 depicts the thermograms of I, lyophilized alone from dioxane before and after further drying as a fluid bed. The undried sample showed new endotherms at 140 and 180°, with a new exotherm at 183°. After fluid bed drying of the sample to 0% total volatiles, the endotherm at 140° disappeared; its presence can be attributed to solvate formation (dioxane), since the undried lyophilates characteristically contained more than 13% volatiles. The thermograms shown in Fig. 3 are strongly indicative of the possible existence of polymorphic forms of I.

X-Ray Diffraction—Powder X-ray diffraction patterns for lyophilized poloxamer 407, I, and the combined lyophilate product are shown in Fig. 4. Poloxamer 407 displayed two characteristic strong diffraction peaks of almost equal intensity at d values of 3.81 and 4.64 Å. Untreated I had a very rich diffraction pattern, as did the lyophilized combination product; however, there were marked differences between the patterns, *e.g.*, the triad of peaks near 5.90 Å in the case of the lyophilized combination product.

The X-ray diffraction pattern of a sample of I lyophilized alone from dioxane is shown in Fig. 5. Except for the peaks attributable to poloxamer 407, the X-ray diffraction patterns for the lyophilized combination I–poloxamer 407 and for lyophilized I alone were identical but different from that for untreated I.

IR Spectroscopy—IR spectra for untreated and lyophilized I, each prepared as mineral oil mulls and in deuterated chloroform solution, are shown in Fig. 6. The spectra for the two forms of I obtained as mulls differed, whereas the spectra for the two solutions were identical. This behavior is typical of polymorphic forms of a compound (6).

Comparative Bioavailability in Dogs—The mean plasma concentration–time curve for each of the three formulations is shown in Fig. 7; the mean area under the plasma concentration–time curve (*AUC*) for 0–4 hr is also included.

Comparative Bioavailability in Humans—Blood level–time profiles after single-dose administrations of 200 and 400 mg of I in each of the three formulations are shown in Figs. 8 and 9; the areas under the curves are also included.

DISCUSSION

The increase in solubility of I in Formulation 3 (the combined lyophilate with poloxamer 407) compared with that of I alone can be attributed mainly to the existence of a polymorphic form of the compound, as shown by differential thermal analysis, X-ray diffraction, and IR spectroscopy. The thermogram of the combined lyophilate (Fig. 2) does not indicate conclusively the existence of a polymorphic form. Poloxamer 407 melts at 48–50°, and the molten polymer dissolves I as the temperature increases. This solution accounts for the disappearance of the strong melting endotherm of I near 196°. Only the thermogram of lyophilized I alone (Fig. 3) permits attribution of the small endotherm near 180° in the combination product to undissolved polymorph Form B.

The X-ray diffraction patterns (Figs. 4 and 5) and IR spectra (Fig. 6) prove conclusively that polymorphic Form B exists in the I–poloxamer 407 lyophilate. In addition, determinations of the equilibrium solubility of isolated Form B showed the material to be approximately 50% more soluble than untreated I (Form A), *i.e.*, 0.059 mg/ml. The dissolution rate of Form B, however, was less than that of the simple admixture formulation (Formulation 1), indicating the necessity for inclusion of poloxamer 407 as a wetting agent in the preparation of Form B for use in the capsule formulation.

Microscopic examination of the combined lyophilate after the addition of water showed the presence of small crystallites of drug, approximately 1 μm in diameter. Although attempts to isolate these crystallites for further study failed, it is reasonable to conjecture that I lyophilized in combination with poloxamer 407 exists, at least in part, as extremely small crystallites of the more soluble Form B intimately enmeshed with poloxamer 407. Although this mixture is not a solid solution, as shown by the X-ray diffraction pattern (Fig. 4), the contribution of these small crystallites, in intimate admixture with the wetting agent, to the increased solubility of I cannot be completely ignored. The X-ray diffraction pattern of the combination lyophilate product (Fig. 4) shows the existence of a crystalline, rather than of an amorphous, lyophilized material. In this laboratory, freeze drying of an aqueous solution resulted in the formation of amorphous materials almost exclusively.

Figures 7–9 reveal the increase in bioavailability of I that resulted

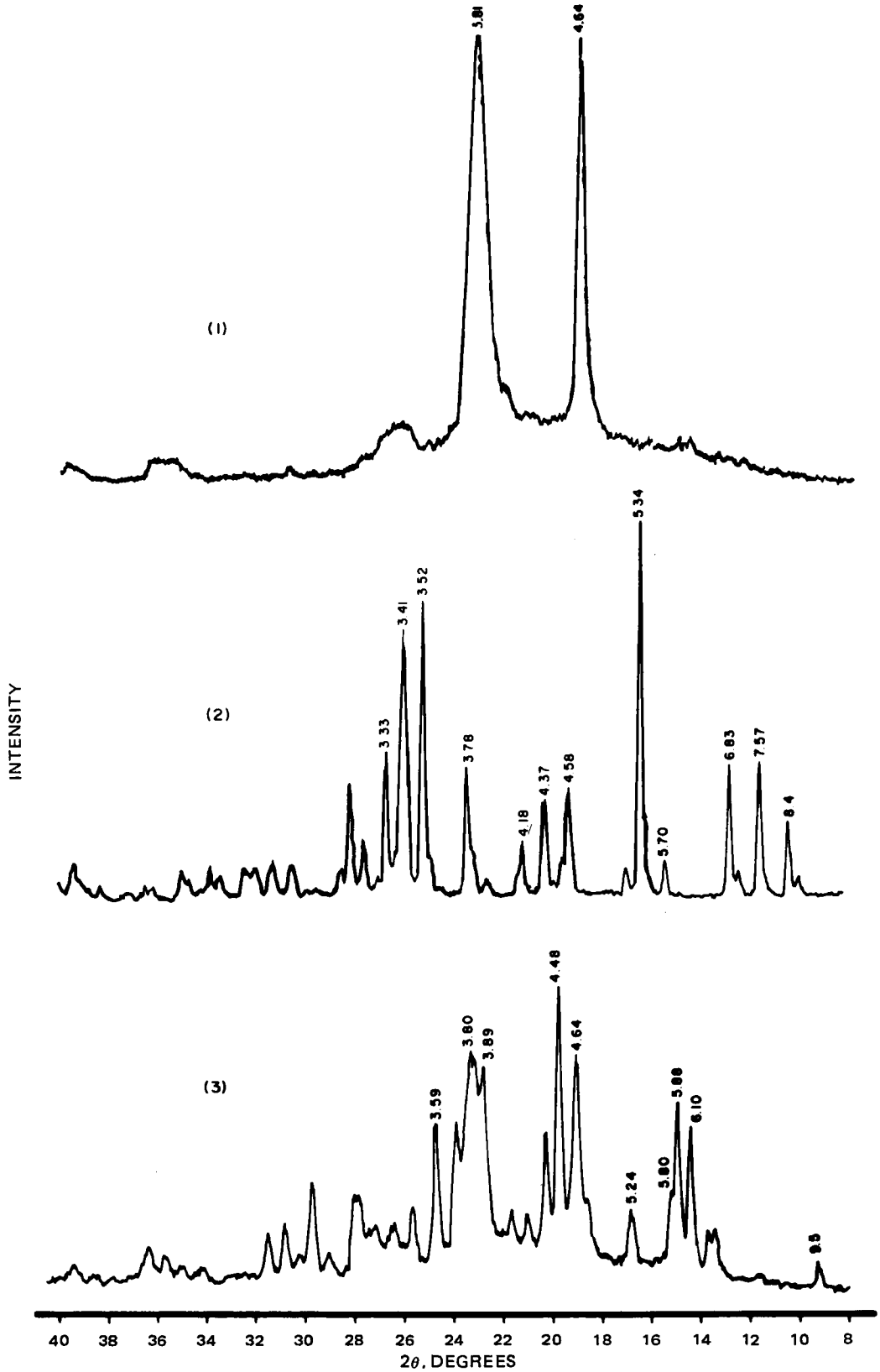

Figure 4—*Powder X-ray diffraction patterns for lyophilized poloxamer 407 (1), I (2), and I–poloxamer 407 lyophilate (3).*

from micronization of I followed by granulation with a wetting agent or from use of the combined lyophilate. In dogs given an oral dose of I, approximately 8.2 mg/kg, plasma levels were undetectable after the administration of Formulation 1, in which the untreated drug is in simple admixture with the excipients. Utilization of Formulation 2, in which micronized I exists as a granulation with sodium lauryl sulfate, led to blood levels detectable for 4 hr after dosing, with an area under the plasma level–time curve of 1.99 μg/ml × hr. Use of Formulation 3, containing the I–poloxamer 407 lyophilate in which the drug exists as polymorphic Form B, increased the bioavailability from that of Formulation 2 (peak height ratio of 1.2:0.7) and yielded an area under the plasma level–time curve of 2.78 μg/ml × hr.

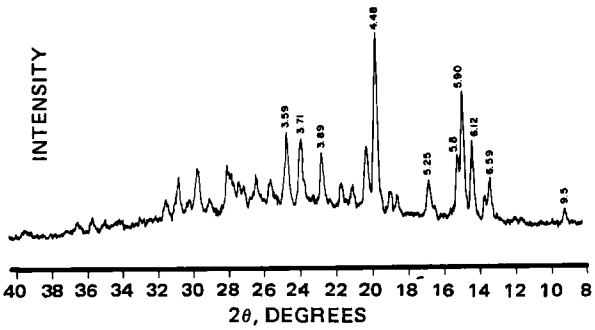

Figure 5—*Powder X-ray diffraction pattern of fluid bed dried I lyophilized from dioxane.*

In humans given oral doses of I of approximately 2.51 and 5.02 mg/kg, blood levels were detectable after the administration of each formulation. After administration of a 200-mg dose of I, the biological availability of the compound increased progressively for Formulations 1–3.

The ratio of peak heights after the administration to humans of a 200-mg dose of I as Formulations 3, 2, and 1 was 2.5:1.85:0.8; the respective areas under the serum level–time curves were 81.2, 68.2, and 43.6 μg/ml × hr. After the administration of a 400-mg dose of I, the formulations showed the same order of drug bioavailability, with peak height ratios of 3.90:2.92:1.23 and areas under the blood level–time curves of 132, 100, and 50.8 μg/ml × hr, respectively.

Within the limitations of the number of data points employed, a plot of the dissolution parameter, "amount of drug dissolved in 1 hr," *versus* blood level peak heights or areas under the plasma level–time curve yielded a linear relationship, with regression coefficients greater than 0.9 for both dose levels in the human.

In summary, the existence of a polymorphic form of I, a potential tricyclic antidepressant, has been proven. The utility of this polymorph in a solid dispersion with a polyoxypropylene–polyoxyethylene copolymer to enhance the biological availability of the drug has been demonstrated. An intermediate increase in biological availability was attained by the administration of a micronized form of the original polymorph granulated with aqueous sodium lauryl sulfate solution. Values obtained from dissolution profiles *in vitro* of the various for-

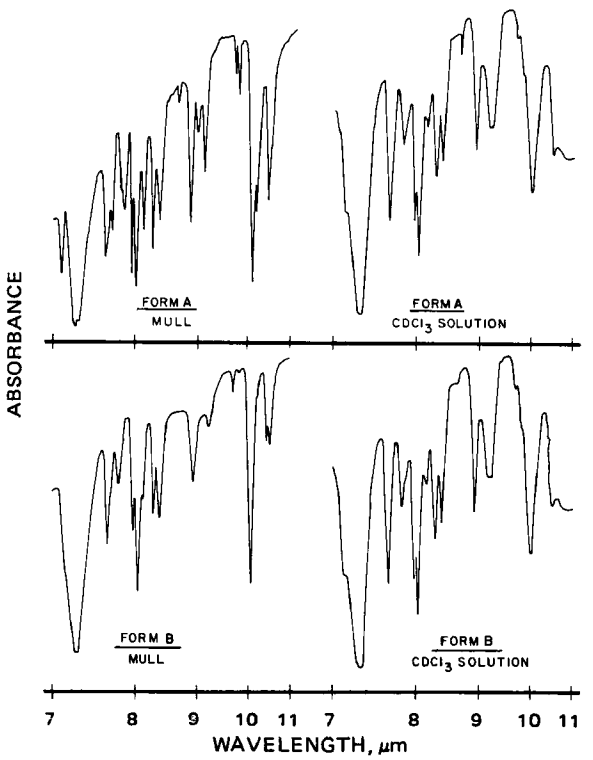

Figure 6—*IR spectra of I.*

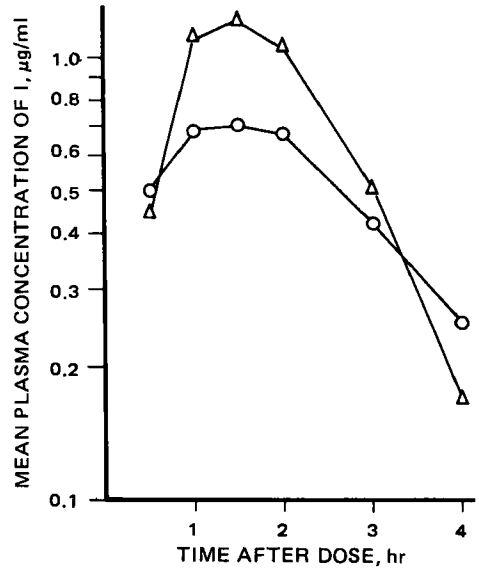

Figure 7—*Mean plasma concentrations of I after oral administration of 100-mg capsules to three male beagle dogs. Key:* ○, *Formulation 2* (AUC = *1.99 μg/ml × hr*); *and* △, *Formulation 3* (AUC = *2.78 μg/ml × hr*).

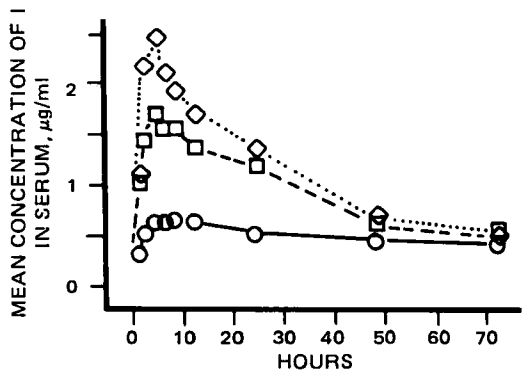

Figure 8—*Mean concentrations of unchanged drug in serum of six healthy male volunteers after oral administration of a 200-mg dose of each of three different formulations of I in a three-way crossover design study. Key:* ○, *Formulation 1* (AUC = *43.6 μg/ml × hr*); □, *Formulation 2* (AUC = *68.2 μg/ml × hr*); *and* ◇, *Formulation 3* (AUC = *81.2 μg/ml × hr*).

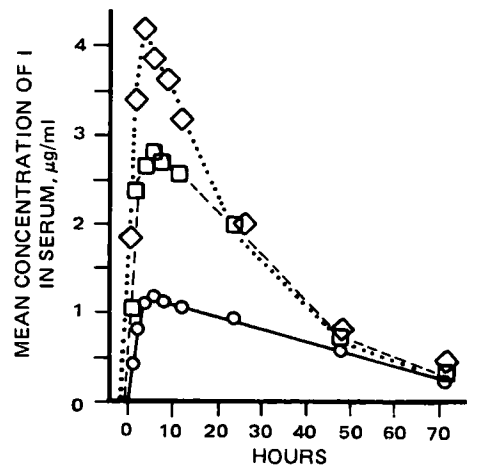

Figure 9—*Mean concentrations of unchanged drug in serum of six healthy male volunteers after oral administration of a 400-mg dose of each of three different formulations of I in a three-way crossover design study. Key:* ○, *Formulation 1* (AUC = *50.8 μg/ml × hr*); □, *Formulation 2* (AUC = *100 μg/ml × hr*); *and* ◇, *Formulation 3* (AUC = *132 μg/ml × hr*).

mulations could be correlated with the biological availability subsequently demonstrated in humans.

REFERENCES

(1) D. J. Jollow and B. B. Brodie, *Pharmacology*, **8**, 21(1972).
(2) R. M. Atkinson, C. Bedford, K. J. Child, and E. G. Tomich, *Antibiot. Chemother.*, **12**, 232(1962).
(3) J. H. Fincher, *J. Pharm. Sci.*, **57**, 1825(1968).
(4) J. D. Mullins and T. J. Macek, *J. Am. Pharm. Assoc., Sci. Ed.*, **49**, 245(1960).
(5) G. S. Mewada, D. R. Parikh, and S. Somasekhara, *Sci. Cult.*, **39**, 378(1973).
(6) J. Haleblian and W. McCrone, *J. Pharm. Sci.*, **58**, 911(1969).
(7) K. Münzel, *Pharm. Acta Helv.*, **46**, 513(1971).
(8) A. H. Goldberg, M. Gibaldi, and J. L. Kanig, *J. Pharm. Sci.*, **54**, 1145(1965).
(9) A. H. Goldberg, M. Gibaldi, J. L. Kanig, and M. Mayersohn, *ibid.*, **55**, 581(1966).
(10) W. L. Chiou and S. Riegelman, *ibid.*, **58**, 1505(1969).
(11) *Ibid.*, **60**, 1281(1971).
(12) E. I. Stupak and T. R. Bates, *J. Pharm. Sci.*, **62**, 1806(1973).
(13) H. Yale, *J. Med. Chem.*, **11**, 396(1968).
(14) "The National Formulary," 13th ed., Mack Publishing Co., Easton, Pa., 1970, p. 802.
(15) A. O. Niedermayer and R. G. Koski, *J. Pharm. Sci.*, **64**, 1531(1975).

ACKNOWLEDGMENTS AND ADDRESSES

Received July 11, 1975, from the *Squibb Institute for Medical Research, New Brunswick, NJ 08903*

Accepted for publication December 8, 1975.

The authors thank Mrs. Ethel Humphrey, Mrs. Mary Simon, Ms. Patricia Taylor, Ms. Veronica Valenti, Mr. Quentin Ochs, and Mr. Henry Roberts for technical assistance. The constructive discussions with Dr. David Frost, Dr. J. Zanos Gougoutas, Dr. James McGinity, and Mr. A. La Via are gratefully acknowledged.

[x] To whom inquiries should be directed.

Real Flow Measurements on Time-Dependent Thixotropic Fluids

ROGER L. SCHNAARE [x], RAFIQ M. SHEIKH [*], PAUL J. NIEBERGALL, and EDWIN T. SUGITA

Abstract □ An experimental procedure was developed in which shear stress *versus* time data at a constant shear rate are extrapolated to structural equilibrium conditions utilizing both the upcurve and the downcurve. This procedure allows the construction of a flow curve by plotting the equilibrium shear stress, F_e, *versus* the shear rate. Such an equilibrium flow curve is independent of all experimental conditions and of shear history and does not exhibit a hysteresis loop. The method also yields apparent rate constants for characterizing thixotropic behavior on an unequivocal basis. The extrapolation procedure was developed using a cup and bob viscometer but is generally applicable to any continuous shear viscometer.

Keyphrases □ Thixotropic systems—equilibrium flow curve constructed from shear stress and shear rate data, apparent rate constants calculated □ Viscosity—thixotropic systems, equilibrium flow curve constructed, apparent rate constants calculated □ Shear stress and rate—thixotropic systems, data used in construction of equilibrium flow curve

A thixotropic material, as defined by Bauer and Collins (1), exhibits a "time-dependent, reversible and isothermal decrease of viscosity with shear in flow." This behavior is universally accepted as being indicative of an equilibrium process between the breakdown and buildup of structure as the material is subjected to shear (2–6). It follows that quantitative measurements of the viscosity or flow of such a system must be dependent on how close the system is to equilibrium. To be completely rigorous, a flow curve should be three dimensional, including time as the third variable (4) in addition to shear stress and shear rate.

BACKGROUND

This time dependency is experimentally evident from the common observation that flow curves are highly dependent on experimental conditions, *i.e.*, the rate at which the shear rate is increased or decreased, the length of time a sample is subjected to any one rate of shear, how many times the flow curve is repeated, and the degree of agitation of the sample prior to measurement (7–9).

It is common practice to report flow data indicating as explicitly as possible the exact experimental conditions. This practice is based on the assumption that variability can be eliminated by duplicating experimental conditions, allowing results to be compared on a relative, albeit arbitrary, basis. This assumption has not been found to be true in actual experience, and experimental data will be presented to illustrate this point.

The difficulty arises from the inability to duplicate the "shear history" of the sample and the uncertainty in the degree of structural equilibrium at a given shear rate. Other investigators simply admit that certain flow curves are not reproducible (2).

It is generally agreed (10, 11) that the structural state of such a material under shear can be represented by a first-order equilibrium process (Scheme I):

$$\text{(structure)} \underset{k_2}{\overset{k_1}{\rightleftharpoons}} \text{(nonstructure)}$$

Scheme I

and that the shear stress is a function of structure such that, at equilibrium for a given shear rate:

$$\left[\frac{d(\text{structure})}{dt}\right]_S \equiv \left[\frac{dF}{dt}\right]_S = 0 \qquad \text{(Eq. 1)}$$

The correct procedure then for determining a time-dependent flow curve would be to indicate the point in time relative to the degree of structure at which shear stress measurements are made (4). The two simplest references points are at time $t = 0$, corresponding to the

mulations could be correlated with the biological availability subsequently demonstrated in humans.

REFERENCES

(1) D. J. Jollow and B. B. Brodie, *Pharmacology*, **8**, 21(1972).
(2) R. M. Atkinson, C. Bedford, K. J. Child, and E. G. Tomich, *Antibiot. Chemother.*, **12**, 232(1962).
(3) J. H. Fincher, *J. Pharm. Sci.*, **57**, 1825(1968).
(4) J. D. Mullins and T. J. Macek, *J. Am. Pharm. Assoc., Sci. Ed.*, **49**, 245(1960).
(5) G. S. Mewada, D. R. Parikh, and S. Somasekhara, *Sci. Cult.*, **39**, 378(1973).
(6) J. Haleblian and W. McCrone, *J. Pharm. Sci.*, **58**, 911(1969).
(7) K. Münzel, *Pharm. Acta Helv.*, **46**, 513(1971).
(8) A. H. Goldberg, M. Gibaldi, and J. L. Kanig, *J. Pharm. Sci.*, **54**, 1145(1965).
(9) A. H. Goldberg, M. Gibaldi, J. L. Kanig, and M. Mayersohn, *ibid.*, **55**, 581(1966).
(10) W. L. Chiou and S. Riegelman, *ibid.*, **58**, 1505(1969).
(11) *Ibid.*, **60**, 1281(1971).
(12) E. I. Stupak and T. R. Bates, *J. Pharm. Sci.*, **62**, 1806(1973).
(13) H. Yale, *J. Med. Chem.*, **11**, 396(1968).
(14) "The National Formulary," 13th ed., Mack Publishing Co., Easton, Pa., 1970, p. 802.
(15) A. O. Niedermayer and R. G. Koski, *J. Pharm. Sci.*, **64**, 1531(1975).

ACKNOWLEDGMENTS AND ADDRESSES

Received July 11, 1975, from the *Squibb Institute for Medical Research, New Brunswick, NJ 08903*

Accepted for publication December 8, 1975.

The authors thank Mrs. Ethel Humphrey, Mrs. Mary Simon, Ms. Patricia Taylor, Ms. Veronica Valenti, Mr. Quentin Ochs, and Mr. Henry Roberts for technical assistance. The constructive discussions with Dr. David Frost, Dr. J. Zanos Gougoutas, Dr. James McGinity, and Mr. A. La Via are gratefully acknowledged.

[x] To whom inquiries should be directed.

Real Flow Measurements on Time-Dependent Thixotropic Fluids

ROGER L. SCHNAARE [x], RAFIQ M. SHEIKH [*], PAUL J. NIEBERGALL, and EDWIN T. SUGITA

Abstract □ An experimental procedure was developed in which shear stress *versus* time data at a constant shear rate are extrapolated to structural equilibrium conditions utilizing both the upcurve and the downcurve. This procedure allows the construction of a flow curve by plotting the equilibrium shear stress, F_e, *versus* the shear rate. Such an equilibrium flow curve is independent of all experimental conditions and of shear history and does not exhibit a hysteresis loop. The method also yields apparent rate constants for characterizing thixotropic behavior on an unequivocal basis. The extrapolation procedure was developed using a cup and bob viscometer but is generally applicable to any continuous shear viscometer.

Keyphrases □ Thixotropic systems—equilibrium flow curve constructed from shear stress and shear rate data, apparent rate constants calculated □ Viscosity—thixotropic systems, equilibrium flow curve constructed, apparent rate constants calculated □ Shear stress and rate—thixotropic systems, data used in construction of equilibrium flow curve

A thixotropic material, as defined by Bauer and Collins (1), exhibits a "time-dependent, reversible and isothermal decrease of viscosity with shear in flow." This behavior is universally accepted as being indicative of an equilibrium process between the breakdown and buildup of structure as the material is subjected to shear (2–6). It follows that quantitative measurements of the viscosity or flow of such a system must be dependent on how close the system is to equilibrium. To be completely rigorous, a flow curve should be three dimensional, including time as the third variable (4) in addition to shear stress and shear rate.

BACKGROUND

This time dependency is experimentally evident from the common observation that flow curves are highly dependent on experimental conditions, *i.e.*, the rate at which the shear rate is increased or decreased, the length of time a sample is subjected to any one rate of shear, how many times the flow curve is repeated, and the degree of agitation of the sample prior to measurement (7–9).

It is common practice to report flow data indicating as explicitly as possible the exact experimental conditions. This practice is based on the assumption that variability can be eliminated by duplicating experimental conditions, allowing results to be compared on a relative, albeit arbitrary, basis. This assumption has not been found to be true in actual experience, and experimental data will be presented to illustrate this point.

The difficulty arises from the inability to duplicate the "shear history" of the sample and the uncertainty in the degree of structural equilibrium at a given shear rate. Other investigators simply admit that certain flow curves are not reproducible (2).

It is generally agreed (10, 11) that the structural state of such a material under shear can be represented by a first-order equilibrium process (Scheme I):

$$\text{(structure)} \underset{k_2}{\overset{k_1}{\rightleftharpoons}} \text{(nonstructure)}$$

Scheme I

and that the shear stress is a function of structure such that, at equilibrium for a given shear rate:

$$\left[\frac{d(\text{structure})}{dt}\right]_S \equiv \left[\frac{dF}{dt}\right]_S = 0 \qquad \text{(Eq. 1)}$$

The correct procedure then for determining a time-dependent flow curve would be to indicate the point in time relative to the degree of structure at which shear stress measurements are made (4). The two simplest references points are at time $t = 0$, corresponding to the

maximum structural state of the material, and at $t = \infty$ or at a time sufficiently great to ensure structural equilibrium.

Experimentally, the easiest parameter to measure is the shear stress at structural equilibrium by letting the material shear in a viscometer until no further change in stress is detected. This approach turns out to be impractical for most real time-dependent systems. Similarly, the direct determination of the shear at zero time is not possible because of instrument response and, most importantly, the effect of the sample's shear history on stress measurements.

The alternative procedure for determining F_0 or F_e is to use extrapolation methods. Oldroyd (12) indicated that shear stress should decay exponentially at a constant shear rate from an initial stress value as:

$$F = F_0 e^{-kt} \qquad \text{(Eq. 2)}$$

The constant k is equivalent to $1/t_r$, where t_r is interpreted as a relaxation time. Equation 2, corresponding to the equilibrium process in Scheme I in which $k_2 \rangle\rangle\rangle k_1$, would appear to be useful for determining F_0 from extrapolation of initial stress data. The empirical, linear relationship between F and $\log(t)$ observed by Weltman (13) appears to be valid under comparable conditions.

The equilibrium process has been considered (14), giving:

$$F = F_e + (F_0 - F_e)e^{-kt} \qquad \text{(Eq. 3)}$$

and it has been derived from thermodynamic and rheological principles by others (15–17). The predicted linear relationship between $\ln(F - F_e)$ and t is found in practice, and it appears that F_e and F_0 can be determined from shear stress data by usual numerical methods.

Unfortunately, these plotting procedures *do not* work in practice, because time, t, is not an absolute value as far as structure is concerned. In measuring a shear stress, the material at some point is transferred from a container to the viscometer, the instrument is turned on, and the time is noted as $t = 0$, the reference point denoting complete structure. However, the structure cannot be complete, since some shear must be introduced in transferring the sample.

It is possible in some cases to let the sample rest for a sufficiently long time to ensure complete structure. In that case, $t = 0$ is determined on an absolute basis. Once the material is moved or sheared, it again becomes impossible to identify $t = 0$ at any other shear rate. There is also the uncertainty as to whether, at successive shear rates, F_0 refers to the structure at rest, the equilibrium structure at the preceding shear rate, or a unique structure associated with each shear rate.

The only readily available reference point in the rheogram is the equilibrium condition, and a convenient experimental method is suggested for obtaining the shear stress at structural equilibrium independent of shear history.

EXPERIMENTAL

Preparation of Samples—The carbomer 940 dispersion was prepared by mixing the dry powder and distilled water with a mechanical stirrer for 1 hr. After standing for 30 min, potassium hydroxide solution was added to pH 7. Bentonite dispersions were prepared according to USP specifications.

Rheological Measurements—All measurements were made on a rotational cup and bob viscometer[1] at 25 ± 0.1°. The viscometer has a speed range of 5–350 rpm, with the shear stress being measured at the bob surface. The dimensions of the various cups and bobs used are listed in Table I.

Selection of Shear Rate—For Newtonian fluids, shear rates were used as derived from the Margules equation (4). At the bob surface:

$$S = 2R_c^2\Omega/(R_c^2 - R_b^2) \qquad \text{(Eq. 4)}$$

or:

$$S = 0.2094\ (\text{rpm})\ R_c^2/(R_c^2 - R_b^2) = K_s\ (\text{rpm}) \qquad \text{(Eq. 5)}$$

The shear stress is determined by:

$$F = K_f\ (\text{dial readings}) \qquad \text{(Eq. 6)}$$

where the constant K_f is obtained from calibration of the viscometer with standard Newtonian oils and the shear rates as calculated by Eq. 5 for each cup and bob combination. Values for the constants K_s and K_f are listed in Table I.

[1] Rheomat 15, Contraves Corp., Zurich, Switzerland.

Table I—Dimensions and Constants for the Viscometer

Cup and Bob Notation	R_c, cm	R_b, cm	K_s (Eq. 5)	K_f (Eq. 6)	K_1 (Eq. 7)	K_2 (Eq. 7)
A/A	2.360	2.223	1.969	1.887	0.0553	0.00100
A/B	2.360	1.556	0.3704	4.144	0.3613	0.03927
B/B	1.945	1.556	0.5817	4.136	0.2068	0.01338

If the shear rate and shear stress, as defined by Eqs. 5 and 6, are used to construct a flow curve for a time-independent non-Newtonian fluid, a separate curve results for each cup and bob combination. This experimental observation is illustrated by the upper three curves in Fig. 1. Obviously, one cannot describe the flow of a fluid with three distinct, separate curves.

Several approaches have been tried to overcome this lack of reproducibility. One approach is to use a shear rate derived on some basis thought to account for non-Newtonian behavior. Shangraw *et al.* (18) discussed several "non-Newtonian" shear rates. This approach has not eliminated the discrepancy, as depicted by the flow data for the carbomer in Fig. 1. In fact, a different flow curve will result for each shear rate using the same shear stress data obtained from a single fluid and a single cup and bob combination.

There are at least two published procedures for correcting the Newtonian shear rates as calculated by Eq. 5 for non-Newtonian behavior (19–21). The single bob procedure (19) is the most convenient and consistent.

The true non-Newtonian shear rate, S', can be obtained from the Newtonian shear rate and the experimental data with:

$$S' = S[1 + K_1(1/n - 1) + K_2(1/n - 1)^2] \qquad \text{(Eq. 7)}$$

where:

$$K_1 = (R_c^2 - R_b^2)[1 + 2/3\ \ln(R_c/R_b)]/2R_c^2 \qquad \text{(Eq. 8)}$$

$$K_2 = (R_c^2 - R_b^2)\ln(R_c/R_b)/6R_c^2 \qquad \text{(Eq. 9)}$$

and:

$$n = d(\ln F)/d(\ln S) \qquad \text{(Eq. 10)}$$

The two constants, K_1 and K_2, are functions of the instrument, *i.e.*, independent of the fluid being measured. Values of K_1 and K_2 for the viscometer are listed in Table I. The term n is a function of the instrument and the fluid and must be determined experimentally from the flow data. Fortunately, a plot of $\ln(F)$ *versus* $\ln(S)$ for many non-Newtonian fluids is linear, so n is a constant for a particular fluid measured with a particular cup and bob combination. If $d(\ln F/d(\ln S)$ is not constant, an extended form of Eq. 7 must be used (see Ref. 22).

This correction procedure was applied to the three flow curves for the carbomer in Fig. 1. The resultant corrected flow curve, obtained

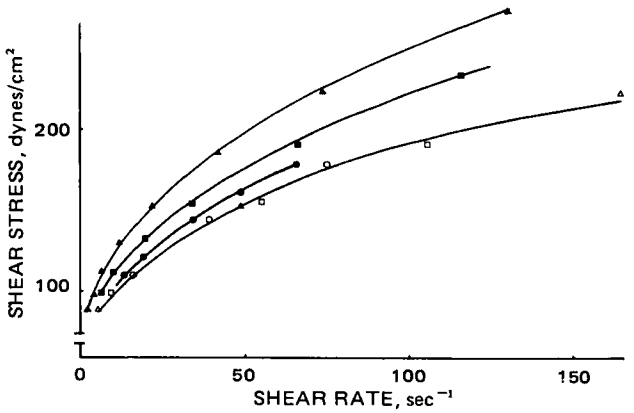

Figure 1—*Time-independent flow curves for 0.1% carbomer 940 dispersion. Key:* ▲, *measuring system A/B;* ■, *measuring system B/B;* ●, *measuring system A/A; and* △, □, ○, *data corrected according to Eq. 7.*

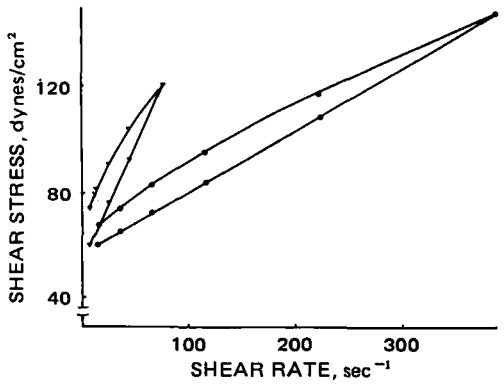

Figure 2—*Effect of the measuring system on the thixotropic flow curve of 7.0% bentonite dispersion. Key: ▼, measuring system B/B; and ●, measuring system A/A. Shear interval = 5 min.*

by plotting shear stress *versus* the corrected shear rate, is the true flow curve and is independent of the viscometer. It has been shown repeatedly (23) that viscosity data from widely differing types of viscometers, when properly corrected for non-Newtonian effects, result in a single flow curve for a given fluid. Such corrections must be applied to non-Newtonian flow data unless such corrections are shown to be insignificant.

RESULTS AND DISCUSSION

Lack of Reproducibility in Measuring Thixotropic Fluids—Figure 2 shows two flow curves for a bentonite dispersion, a typical thixotropic fluid. Two distinct hysteresis loops are observed for the same fluid measured with two different cup and bob combinations. This difference is not eliminated by applying a non-Newtonian correction to the shear rate. In addition, two loops were determined from the same fluid using the same cup and bob combination, but the time that the disperson was sheared before switching to the next shear rate was varied (Fig. 3).

It is evident that, in addition to eliminating the instrument effect, one must eliminate the time-dependent effect, *i.e.*, one must measure shear stress at the same degree of structure or at the same reference point relative to structure. Figure 4 shows some shear stress data as a function of time. All four curves were measured at the same shear rate using the same fluid and the same cup and bob combination. The two upper curves were measured on the upcurve of the hysteresis loop, and the two lower curves were measured on the downcurve.

One can see that since the values of the shear stress at $t = 0$ are not identical for the two upper curves, the degree of structure at the beginning of the measurement was not identical either. This general observation indicates that the shear history or prior treatment of a fluid makes it impossible to start a rheological measurement at the same structural reference point for a time-dependent fluid. The only other convenient structural reference point that can be used is the condition of structural equilibrium. Indeed, all four curves in Fig. 4 approach the same shear stress at equilibrium. For many time-dependent fluids, shearing until equilibrium is reached is not practical.

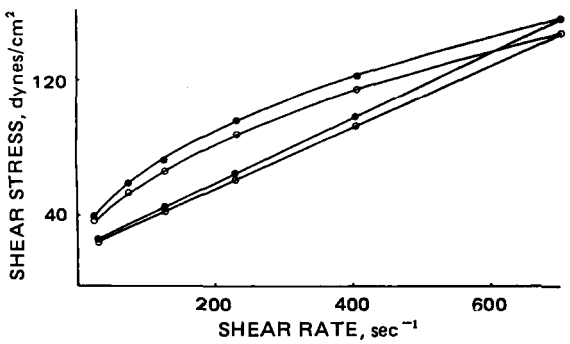

Figure 3—*Effect of shear interval on the thixotropic flow curve of 5.0% bentonite dispersion (measuring system A/A). Key: ●, shear interval of 5 min; and ○, shear interval of 10 min.*

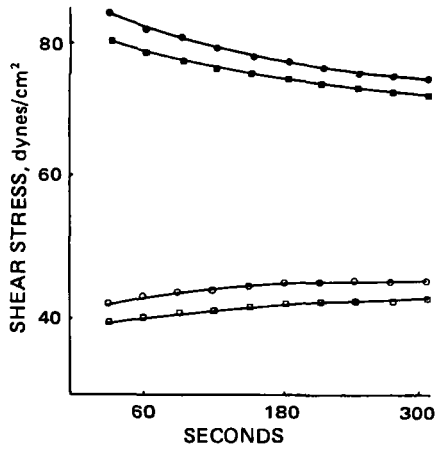

Figure 4—*Shear stress as a function of time at a constant shear rate for 5.0% bentonite dispersion (measuring system A/A). Key: ●, ■, data collected on the upcurve from two experiments; and ○, □, data collected on the downcurve from two experiments. Shear rate = 116 sec⁻¹.*

Extrapolation to Structural Equilibrium—Following Swinbourne (24, 25), Eq. 3 can be written for a time $t + \Delta$ as:

$$F_{t+\Delta} = F_e + (F_0 - F_e)e^{-(t+\Delta)k} \qquad \text{(Eq. 11)}$$

Rearrangement of Eqs. 3 and 11 gives:

$$F_t - F_e = (F_0 - F_e)e^{-kt} \qquad \text{(Eq. 12)}$$

and:

$$F_{t+\Delta} - F_e = (F_0 - F_e)e^{-kt}e^{-k\Delta} \qquad \text{(Eq. 13)}$$

Dividing Eq. 12 by Eq. 13 and rearranging give:

$$F_t = F_e(1 - e^{k\Delta}) + e^{k\Delta}F_{t+\Delta} \qquad \text{(Eq. 14)}$$

which predicts a linear relationship between the shear stress measured at time t and the shear stress measured at time $t + \Delta$. From this relationship, the equilibrium shear stress and the rate constant k can be obtained.

The predicted linear relationship is observed in Fig. 5, utilizing the data from all four curves in Fig. 4. Shear stress data from the upcurve as well as from the downcurve fall on the same line. In fact, since F_0 and t have been eliminated in Eq. 14, shear stress data at a given shear rate can be collected in any manner; the only criterion is that the time interval, Δ, be kept constant.

Determination of True Equilibrium Flow Curve—To determine such a flow curve using a cup and bob viscometer, the following steps are necessary:

1. Shear stress data are collected as a function of time at each shear rate (from both the upcurve and downcurve).

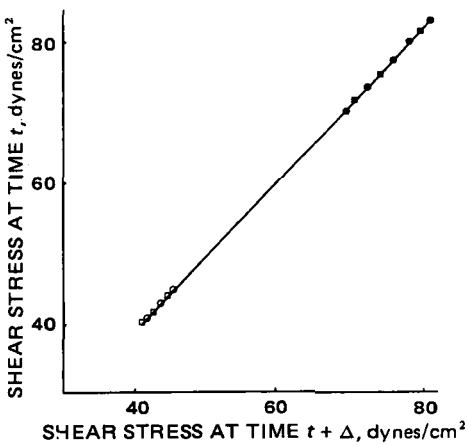

Figure 5—*Swinbourne-type plot according to Eq. 12 for the data shown in Fig. 4. Δ = 30 sec.*

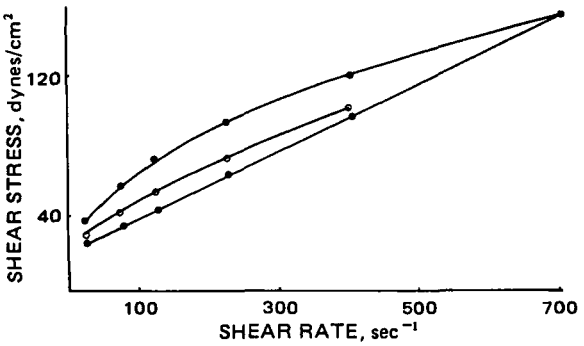

Figure 6—*Flow curve for 5.0% bentonite dispersion (measuring system A/A). Key: ●, data collected using a shear interval of 5 min; and ○, data extrapolated to equilibrium conditions.*

2. The shear stress is extrapolated to equilibrium as indicated by Eq. 14.

3. The shear rate is corrected for non-Newtonian behavior according to Eq. 7.

4. The flow curve is constructed by plotting the equilibrium shear stress *versus* the corrected shear rate.

Figure 6 shows a typical hysteresis loop for a bentonite dispersion and the corresponding equilibrium flow curve obtained by plotting the equilibrium shear stress *versus* the uncorrected or Newtonian shear rates. The equilibrium curve lies within the loop as one would expect if the upcurve corresponds to structure breakdown and the downcurve to structure buildup.

The *true* equilibrium flow curve is shown in Fig. 7, where the non-Newtonian correction was applied to two equilibrium flow curves extrapolated from data for two different cup and bob combinations.

Experimental Verification of Equilibrium—The data in Table II are offered as experimental verification of the extrapolation procedure. The predicted equilibrium shear stress values were extrapolated from shear stress *versus* time data collected over a 10-min period using a time interval of $\Delta = 30$ sec. The experimental values were obtained by shearing the dispersion at a constant rate for 10 hr, taking precautions to prevent evaporation of the solvent. The predicted and experimental values agree to within a 95% confidence limit.

SUMMARY AND CONCLUSIONS

A convenient and rapid method for obtaining the true equilibrium flow curve for non-Newtonian time-dependent fluids was developed. The method is illustrated for a cup and bob viscometer but is applicable in principle for any continuous shear viscometer. The flow curve obtained is independent of the instrument used and the shear history of the sample, enabling rheological parameters to be compared on an absolute basis.

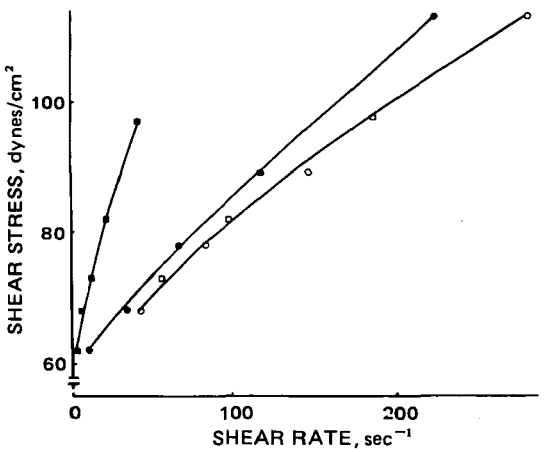

Figure 7—*Equilibrium flow curves for 7.0% bentonite dispersion. Key: ■, measuring system A/B; ●, measuring system A/A; and □, ○, data corrected according to Eq. 7.*

Table II—Experimental *versus* Predicted Equilibrium Shear Stress for Bentonite Dispersions

Predicted (10 min)	Experimental (10 hr)
Bentonite, 5.0%[a]	
30.3	31.8
34.4	35.6
41.4	40.3
52.0	49.6
69.5	66.3
98.3	95.7
Bentonite, 8.0%[b]	
116	118
129	129

[a] Cup and bob A/A. [b] B/B.

As a consequence of the method, the hysteresis loop is not encountered. The loop as a measurement of thixotropic behavior has not shown much application anyway. The rate constant k in Eq. 14 is proposed as a more meaningful measure of thixotropy; its utility is currently being investigated.

LIST OF SYMBOLS

k_1 and k_2 = first-order rate constants
t = time
F = shear stress
F_0 = shear stress at zero time, *i.e.*, the shear stress corresponding to maximum structure
F_e = shear stress at structural equilibrium
S = Newtonian shear rate
S' = non-Newtonian shear rate
R_c and R_b = radius of the viscometer cup and bob, respectively
Ω = angular velocity
K_s = constant relating shear rate with the rotational speed of the viscometer bob
K_f = constant relating shear stress to the viscometer dial reading
K_1 and K_2 = constants
n = slope of a $\ln(F)$ *versus* $\ln(S)$ plot
Δ = time interval

REFERENCES

(1) W. H. Bauer and E. A. Collins, in "Rheology," F. R. Eirich, Ed., vol. 4, Academic, New York, N.Y., 1967, chap. 8.

(2) J. H. Wood, G. Catacalos, and S. V. Lieberman, *J. Pharm. Sci.*, **52**, 354(1963).

(3) H. S. Bean, A. H. Beckett, and J. E. Carless, in "Advances in Pharmaceutical Sciences," vol. 1, Academic, New York, N.Y., 1964.

(4) J. R. Van Wazer, J. W. Lyons, K. Y. Kim, and R. E. Colwell, "Viscosity and Flow Measurements," Interscience, New York, N.Y., 1963.

(5) H. Green, "Industrial Rheology and Rheological Structure," Wiley, New York, N.Y., 1949.

(6) A. N. Martin and G. S. Banker, in "Advances in Pharmaceutical Sciences," vol. 1, Academic, New York, N.Y., 1964.

(7) A. N. Martin, J. Swarbrick, and A. Cammarata, "Physical Pharmacy," 2nd ed., Lea & Febiger, Philadelphia, Pa., 1969.

(8) I. Setnikar, G. Giuseppe, and S. Fantelli, *J. Pharm. Sci.*, **57**, 671(1968).

(9) S. Shiba, *Bull. Chem. Soc. Jpn.*, **33**, 1563(1960).

(10) T. Ree and H. Eyring, *J. Appl. Phys.*, **26**, 793(1955).

(11) D. A. Denny and R. S. Brodkey, *ibid.*, **33**, 2269(1962).

(12) J. G. Oldroyd, *Proc. Roy. Soc.*, **A218**, 122(1953).

(13) H. Weltman, *ibid.*, **14**, 343(1943).

(14) H. Umstatter, *Kolloidzeitschrift*, **70**, 174(1935).

(15) S. J. Hahn, T. Ree, and H. Eyring, *Ind. Eng. Chem.*, **51**, 856(1959).

(16) M. Seno, *Bull. Chem. Soc. Jpn.*, **39**, 1401(1966).

(17) E. K. Carver and J. R. Van Wazer, *J. Phys. Col. Chem.*, **51**, 754(1947).

(18) R. Shangraw, W. Grim, and A. M. Mattocks, *Trans. Soc. Rheol.*, **5**, 247(1961).
(19) I. M. Kreiger and S. H. Maron, *J. Appl. Phys.*, **25**, 72 (1954).
(20) C. G. Lindquist and W. C. Sierichs, *J. Colloid Sci.*, **6**, 33(1951).
(21) J. A. Lescarboura, F. J. Eichstadt, and G. W. Swift, *AIChE J.*, **13**, 169(1967).
(22) I. M. Kreiger and H. Elrod, *J. Appl. Phys.*, **24**, 134(1953).
(23) J. G. Brodnyan, F. H. Gaskins, and W. Philippoff, "Symposium on Non-Newtonian Viscometry," No. 299, American Society for Testing and Materials, Philadelphia, Pa., 1960, pp. 14–25.
(24) E. S. Swinbourne, *J. Chem. Soc.*, **1960**, 2371.
(25) P. J. Niebergall and E. T. Sugita, *J. Pharm. Sci.*, **57**, 1805(1968).

ACKNOWLEDGMENTS AND ADDRESSES

Received July 7, 1975, from the *Department of Pharmacy, Philadelphia College of Pharmacy and Science, Philadelphia, PA 19104*

Accepted for publication November 14, 1975.

* Currently a candidate for the Ph.D. degree at the Philadelphia College of Pharmacy and Science.

ˣ To whom inquiries should be directed.

NOTES

Epimeric 5-Hydroxy-5-phenyl-1-azabicyclo[5.4.0]undecanes

N. ABOUL-ENEIN and J. SAM ˣ

Abstract □ The preparation of epimeric 5-hydroxy-5-phenyl-1-azabicyclo[5.4.0]undecanes is described. One propionate ester exhibited weak analgesic activity.

Keyphrases □ Undecanes, substituted cyclic—epimers synthesized, analgesic activity evaluated □ 5-Hydroxy-5-phenyl-1-azabicyclo[5.4.0]undecanes epimers—synthesized, analgesic activity evaluated □ Analgesic agents, potential—epimers of 5-hydroxy-5-phenyl-1-azabicyclo[5.4.0]undecanes synthesized and screened

The potent analgesic activity exhibited by proheptazine (I) (1) and the esters of 2-hydroxy-2-phenylquinolizidines (II) (2) led to the investigation of epimeric 5-hydroxy-5-phenyl-1-azabicyclo[5.4.0]undecanes (III) and the corresponding propionate esters. The preparation and stereochemistry of 6-hydroxy-6-aryl-1-azabicyclo[5.4.0]undecanes and their structural relationship to biologically active phenethylamines and analgesic piperidines were reported previously (3).

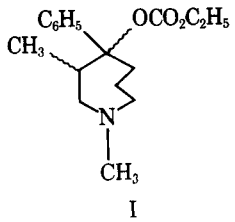

I

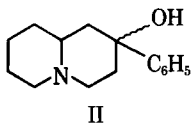

II

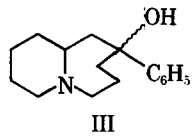

III

DISCUSSION

For the synthesis of III, 1-azabicyclo[5.4.0]undecan-5-one (V) was utilized. The procedure followed (Scheme I) for the preparation of V from ethyl 1-(3-cyanopropyl)piperidyl-2-acetate (IV) was similar to the method described (4) for the synthesis of 1-oxoquinolizidine.

Published reports (3–9) describing the stereochemical structure of bicyclo[5.4.0]undecan-2-one (VI), II, and related quinolizidines

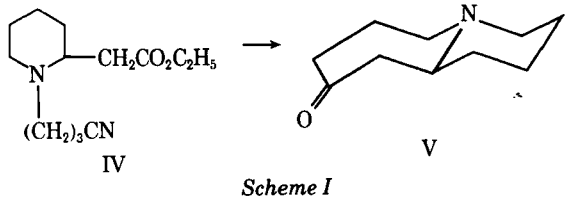

IV V

Scheme I

were utilized in determining the stereochemical nature of the ring in V. The IR spectra of V is consistent with published data (2–9) on *trans*-fused II and related *trans*-fused ring systems. Since TLC indicated the formation of only one isomer, *trans*-fused Structure V was assigned to the product.

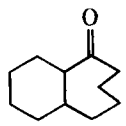

VI

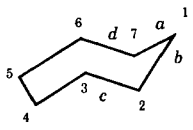

VII

The reaction of phenylmagnesium bromide with V provided an 8:1 mixture of epimeric 5-hydroxy-5-phenyl-1-azabicyclo[5.4.0]undecanes (III*a* and III*b*). Because of the lack of definitive information on the conformation of heterocyclic ring systems containing more than five carbons (10, 11) and the high flexibility of seven-membered rings (12), a conclusive delineation of the conformation of III*a* and III*b* could not be determined. Investigators noted previously (13–16) that the stable conformation of cycloheptane is in a deformed chair position (VII). Moreover, the cyclohexane chair can be fused at any one of the four bounds marked *a*, *b*, *c*, and *d* without affecting the original conformation. Structures resulting from *trans*-fusion of the cyclohexane chair at *a* or *b* are readily interconvertible by a slight manipulation of C-4 and are the most favored, while the other two structures fused at *c* or *d* are quite rigid (5, 16).

The IR spectra of both III*a* and III*b* are similar in the hydroxyl absorption region (both show absorption at 3300 cm^{-1} in carbon tetrachloride even on high dilutions) and in the aromatic region between 600 and 800 cm^{-1}. Bohlmann bands do not appear in the spectrum of III*a*; the spectrum of III*b* includes bands at 2765, 2795, and 2860 cm^{-1}, indicative of a *trans*-fused system. Sircar and Meyers

(18) R. Shangraw, W. Grim, and A. M. Mattocks, *Trans. Soc. Rheol.*, **5**, 247(1961).
(19) I. M. Kreiger and S. H. Maron, *J. Appl. Phys.*, **25**, 72 (1954).
(20) C. G. Lindquist and W. C. Sierichs, *J. Colloid Sci.*, **6**, 33(1951).
(21) J. A. Lescarboura, F. J. Eichstadt, and G. W. Swift, *AIChE J.*, **13**, 169(1967).
(22) I. M. Kreiger and H. Elrod, *J. Appl. Phys.*, **24**, 134(1953).
(23) J. G. Brodnyan, F. H. Gaskins, and W. Philippoff, "Symposium on Non-Newtonian Viscometry," No. 299, American Society for Testing and Materials, Philadelphia, Pa., 1960, pp. 14–25.
(24) E. S. Swinbourne, *J. Chem. Soc.*, **1960**, 2371.
(25) P. J. Niebergall and E. T. Sugita, *J. Pharm. Sci.*, **57**, 1805(1968).

ACKNOWLEDGMENTS AND ADDRESSES

Received July 7, 1975, from the *Department of Pharmacy, Philadelphia College of Pharmacy and Science, Philadelphia, PA 19104*

Accepted for publication November 14, 1975.

* Currently a candidate for the Ph.D. degree at the Philadelphia College of Pharmacy and Science.

ˣ To whom inquiries should be directed.

NOTES

Epimeric 5-Hydroxy-5-phenyl-1-azabicyclo[5.4.0]undecanes

N. ABOUL-ENEIN and J. SAM ˣ

Abstract □ The preparation of epimeric 5-hydroxy-5-phenyl-1-azabicyclo[5.4.0]undecanes is described. One propionate ester exhibited weak analgesic activity.

Keyphrases □ Undecanes, substituted cyclic—epimers synthesized, analgesic activity evaluated □ 5-Hydroxy-5-phenyl-1-azabicyclo[5.4.0]undecanes epimers—synthesized, analgesic activity evaluated □ Analgesic agents, potential—epimers of 5-hydroxy-5-phenyl-1-azabicyclo[5.4.0]undecanes synthesized and screened

The potent analgesic activity exhibited by proheptazine (I) (1) and the esters of 2-hydroxy-2-phenylquinolizidines (II) (2) led to the investigation of epimeric 5-hydroxy-5-phenyl-1-azabicyclo[5.4.0]undecanes (III) and the corresponding propionate esters. The preparation and stereochemistry of 6-hydroxy-6-aryl-1-azabicyclo[5.4.0]undecanes and their structural relationship to biologically active phenethylamines and analgesic piperidines were reported previously (3).

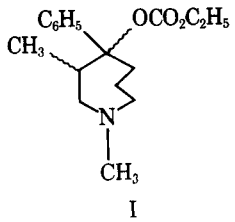

I

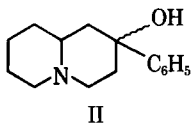

II

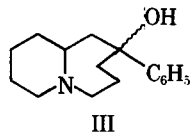

III

DISCUSSION

For the synthesis of III, 1-azabicyclo[5.4.0]undecan-5-one (V) was utilized. The procedure followed (Scheme I) for the preparation of V from ethyl 1-(3-cyanopropyl)piperidyl-2-acetate (IV) was similar to the method described (4) for the synthesis of 1-oxoquinolizidine.

Published reports (3–9) describing the stereochemical structure of bicyclo[5.4.0]undecan-2-one (VI), II, and related quinolizidines

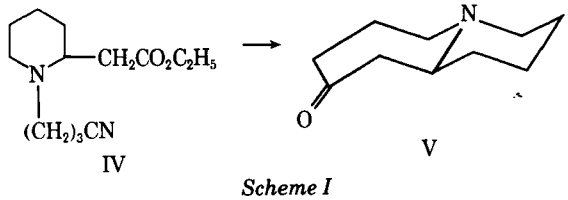

IV V

Scheme I

were utilized in determining the stereochemical nature of the ring in V. The IR spectra of V is consistent with published data (2–9) on *trans*-fused II and related *trans*-fused ring systems. Since TLC indicated the formation of only one isomer, *trans*-fused Structure V was assigned to the product.

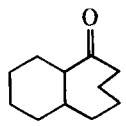

VI

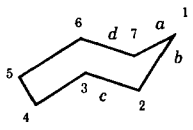

VII

The reaction of phenylmagnesium bromide with V provided an 8:1 mixture of epimeric 5-hydroxy-5-phenyl-1-azabicyclo[5.4.0]undecanes (III*a* and III*b*). Because of the lack of definitive information on the conformation of heterocyclic ring systems containing more than five carbons (10, 11) and the high flexibility of seven-membered rings (12), a conclusive delineation of the conformation of III*a* and III*b* could not be determined. Investigators noted previously (13–16) that the stable conformation of cycloheptane is in a deformed chair position (VII). Moreover, the cyclohexane chair can be fused at any one of the four bounds marked *a*, *b*, *c*, and *d* without affecting the original conformation. Structures resulting from *trans*-fusion of the cyclohexane chair at *a* or *b* are readily interconvertible by a slight manipulation of C-4 and are the most favored, while the other two structures fused at *c* or *d* are quite rigid (5, 16).

The IR spectra of both III*a* and III*b* are similar in the hydroxyl absorption region (both show absorption at 3300 cm^{-1} in carbon tetrachloride even on high dilutions) and in the aromatic region between 600 and 800 cm^{-1}. Bohlmann bands do not appear in the spectrum of III*a*; the spectrum of III*b* includes bands at 2765, 2795, and 2860 cm^{-1}, indicative of a *trans*-fused system. Sircar and Meyers

Table I—Analgesic Potency of Propionates of Phenylhydroxy-1-azabicyclo[5.4.0]undecanes

Compound	ED_{50}, mg/kg[a]	Activity, min		
		Onset	Peak	Duration
VIII	71.5 (62.5–81.8)	4.5	36.5	134.8
IX	65.9 (56.7–76.7)	2.0	39.1	160.2
Codeine	7.5 (6.8–82)	4.0	22.8	147.6

[a] Subcutaneous; numbers in parentheses are 95% confidence limits.

(17), however, reported that Bohlmann bands have not always been observed in systems known to possess *trans*-fused quinolizidine moieties. The NMR spectra of III*a* in deuterochloroform shows the hydroxyl group as a sharp peak at δ 5.33; for III*b*, it appears as a weak broad peak at δ 5.60. The aromatic nucleus appears as a multiplet centered at δ 7.48 in both III*a* and III*b*. The results are in agreement with data reported for related 1-, 2-, and 3-hydroxyquinolizidines (2, 18, 19) and 6-hydroxy-1-azabicyclo[5.4.0]undecanes (3).

On the basis of these data, Structures III*a* and III*b* are assigned to these epimers, respectively. *trans*-Fused rings are proposed for both epimers, with the hydroxyl group of III*a* in a quasiaxial position and the hydroxyl group of III*b* in a quasiequatorial position.

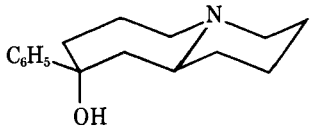

III*a*

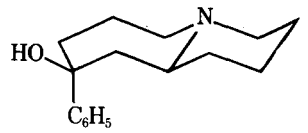

III*b*

The reaction of III*a* with propionyl chloride provided ester VIII. The IR spectrum of the ester showed the disappearance of the hydroxyl group; Bohlmann bands at 2700, 2780, 2820, and 2860 cm^{-1}, indicating *trans*-fusion of the rings; and carbonyl absorption at 1740 cm^{-1}. Because of difficulties encountered in the preparation of a sufficient quantity of III*b*, the corresponding ester was not prepared.

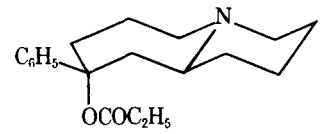

VIII

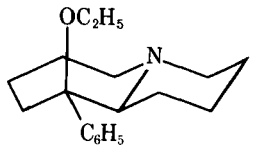

IX

The analgesic potency of VIII and the propionate ester IX of 6-hydroxy-6-phenyl-1-azabicyclo[5.4.0]undecanes, prepared in a previous study (3), was determined by the hot-plate method (20). As noted in Table I, both VIII and IX are considerably less potent than codeine. Studies are being conducted to obtain sufficient quantities of III*b* to permit biological evaluation of the corresponding propionate ester.

EXPERIMENTAL[1]

Ethyl 1-(3-Cyanopropyl)piperidyl-2-acetate (IV)—A mixture of 63.1 g (0.36 mole) of ethyl piperidyl-2-acetate (21), 43.5 g (0.29 mole) of δ-bromobutyronitrile, and 80 g of anhydrous potassium carbonate in 130 ml of dry toluene was stirred and refluxed for 24 hr. An additional 20 g of anhydrous potassium carbonate and 70 ml of dry toluene were added, and the mixture was refluxed another 24 hr. After cooling, the mixture was treated with 500 ml of benzene and with enough water to dissolve the precipitate.

The organic layer was separated and the aqueous layer was extracted with ether (2 × 300 ml). The combined organic extracts were dried over magnesium sulfate and evaporated. The oily residue was distilled at 140–142°/0.1 mm to give 60 g (69%) of IV, $n_D^{27.5}$ = 1.4686; IR (liquid film): 2240 (C≡N) and 1720 (C=O ester) cm^{-1}.

Anal.—Calc. for $C_{13}H_{22}N_2O_2$: C, 65.52; H, 9.30; N, 11.75. Found: C, 65.08; H, 9.34; N, 11.44.

1-Azabicyclo[5.4.0]undecan-5-one (V)—A solution of 54 g (0.226 mole) of the nitrile (IV) in 60 ml of dry xylene was added during 1.5 hr to a refluxing mixture of 20.5 g (0.439 mole) of a 50% dispersion of sodium hydride in mineral oil and 1000 ml of dry xylene. After the addition was completed, refluxing was continued for 5 hr. Then the mixture was cooled in ice and treated carefully with 90 ml of acetic acid. The xylene layer was extracted with concentrated hydrochloric acid (3 × 100 ml), and then the combined acidic extracts were refluxed for 24 hr.

The residue remaining after the excess acid was distilled *in vacuo* was basified with 20% sodium hydroxide solution, extracted with ether (3 × 100 ml), and dried over potassium carbonate. Distillation of the ether extract gave 14 g (36%) of V, bp 144–146°/30 mm, $n_D^{27.5}$ = 1.4959; IR (CCl_4): Bolhmann bands at 2690, 2775, 2810, and 2860 cm^{-1} and 1710 (C=O) cm^{-1}. The picrate was prepared in the usual manner and recrystallized from ethanol–acetone, mp 200–201°.

Anal.—Calc. for $C_{16}H_{20}N_4O_8$: C, 48.49; H, 5.09; N, 14.14. Found: C, 48.60; H, 5.11; N, 14.17.

5-Phenyl-5-hydroxy-1-azabicyclo[5.4.0]undecane (III*a* and III*b*)—The procedure described by England and Sam (18) was followed using 13 g (0.077 mole) of V. A viscous oil (16 g, 88%), which crystallized on standing, was obtained. The IR spectrum showed strong hydroxyl and weak carbonyl absorptions. Trituration of the mass with cold *n*-hexane and storage at 0–5° for 4 hr yielded crystalline needles, mp 116–117°. Recrystallization from *n*-hexane gave 7.8 g (44%) of III*a*, mp 117–118°. TLC, using petroleum ether (bp 30–60°)–ether (3:7) and 1-butanol–acetic acid–water (4:1:1), indicated the presence of a single component; IR (CCl_4): 3300 (—OH) cm^{-1} and no obvious Bohlmann bands; IR (KBr): 695, 730, and 765 cm^{-1} (monosubstituted aromatic absorption); NMR: δ 5.33 (s, —OH, exchangeable with D_2O) and 7.48 (m, 5H).

Anal.—Calc. for $C_{16}H_{23}NO$: C, 78.32; H, 9.45; N, 5.71. Found: C, 78.32; H, 9.64; N, 5.65.

Evaporation of the *n*-hexane from which III*a* was obtained yielded 6 g of a viscous oil, which was dissolved in a minimum amount of *n*-hexane and column chromatographed. Elution was performed with *n*-hexane at a flow rate of 7 ml/min. Fractions 4–25 yielded 1 g (6%) of crystalline III*b*, mp 65.5–67.5°. TLC showed one spot; IR (CCl_4): 3300 (—OH) cm^{-1} and Bohlmann bands at 2765, 2798, and 2860 cm^{-1}; IR (KBr): 700 and 760 (monosubstituted aromatic absorption) cm^{-1}; NMR: δ 5.60 (broad, weak, s, —OH, exchangeable with D_2O) and 7.48 (m, 5H).

Anal.—Calc. for $C_{16}H_{23}NO$: C, 78.32; H, 9.45; N, 5.71. Found: C, 78.34; H, 9.63; N, 5.70.

Further elution with *n*-hexane followed by ether yielded unreacted ketone (V).

5-Phenyl-5-propionoxy-1-azabicyclo[5.4.0]undecane (VIII)—To a solution of 7.5 g (0.031 mole) of III*a* and 15 g (0.150 mole) of triethylamine in 125 ml of dry toluene was added dropwise a solution of 7.5 g (0.081 mole) of propionyl chloride in 25 ml of dry toluene. The reaction mixture was stirred under reflux for 6–8 hr. After cooling, the mixture was filtered, and the filtrate was evaporated under reduced pressure. The residual brown oil was treated with ice-cold saturated potassium carbonate solution and extracted with ether (3 × 150 ml). The extract was dried over magnesium sulfate and evaporated.

A solution of the residue in 60 ml of 20% hydrochloric acid was extracted with ether (3 × 50 ml) and then basified under cooling with saturated potassium carbonate solution. An ether extract (3 × 150 ml) was dried over magnesium sulfate and then evaporated to give 8.5 g (94%) of brown oil. The oil was column chromatographed using *n*-hexane as the eluant, and 6.5 g (71%) of a yellow oil was obtained, $n_D^{27.5}$ = 1.5364; IR (CCl_4): no hydroxyl absorption, Bohlmann bands at 2700, 2780, 2820, and 2860 cm^{-1}, and 1740 (C=O) cm^{-1}.

Anal.—Calc. for $C_{19}H_{27}NO_2$: C, 75.71; H, 9.03; N, 4.65. Found: C, 75.91; H, 9.06; N, 4.57.

[1] Melting points were taken with a Thomas-Hoover Uni-Melt apparatus and are uncorrected. IR spectra were determined with a Perkin-Elmer 257 spectrophotometer. NMR spectra were obtained with a Jeolco C-60-HL spectrometer relative to an internal standard of tetramethylsilane. TLC and column chromatography were performed with Eastman alumina sheets and Woelm grade I neutral alumina, respectively. Elemental analyses were performed by the A. H. Robins Co., Richmond, Va.

REFERENCES

(1) R. A. Hardy, Jr., and G. Howell, in "Analgetics," vol. 5, G. DeStevens, Ed., Academic, New York, N.Y., 1965, p. 209.

(2) J. Sam, J. D. England, and D. Temple, *J. Med. Chem.*, **12**, 144(1969).
(3) M. N. Aboul-Enein and J. Sam, *J. Heterocycl. Chem.*, **8**, 7(1971).
(4) S. F. Mason, K. Schofield, and R. J. Wells, *J. Chem. Soc., C*, **1967**, 626.
(5) T. C. Joseph and S. Dev, *Tetrahedron*, **24**, 3841(1968).
(6) F. Bohlmann, *Angew. Chem.*, **69**, 641(1957); *Chem. Ber.*, **91**, 2157(1958).
(7) T. M. Moynehan, K. Schofield, R. A. Y. Jones, and A. R. Katritzky, *J. Chem. Soc.*, **1962**, 2637.
(8) H. S. Aaron and C. P. Ferguson, *Tetrahedron Lett.*, **1968**, 6191.
(9) P. J. Chivers, T. A. Crabb, and R. O. Williams, *Tetrahedron*, **24**, 4411(1968).
(10) E. L. Eliel, N. L. Allinger, S. J. Angyal, and G. A. Morrison, "Conformational Analysis," Wiley, New York, N.Y., 1965, p. 254.
(11) F. G. Riddell, *Quart. Rev.*, **21**, 364(1967).
(12) E. L. Eliel, N. L. Allinger, S. J. Angyal, and G. A. Morrison, "Conformational Analysis," Wiley, New York, N.Y., 1965, p. 207.
(13) S. Dev, *J. Indian Chem. Soc.*, **33**, 769(1956).
(14) N. L. Allinger, *J. Am. Chem. Soc.*, **81**, 5727(1959).
(15) R. Pauncz and D. Ginsburg, *Tetrahedron*, **9**, 40(1960).
(16) J. B. Hendrickson, *J. Am. Chem. Soc.*, **83**, 4537(1961).
(17) J. C. Sircar and A. I. Meyers, *J. Org. Chem.*, **32**, 1248(1967), and references cited therein.
(18) J. D. England and J. Sam, *J. Heterocycl. Chem.*, **3**, 582(1966).
(19) M. E. Rogers and J. Sam, *J. Med. Chem.*, **17**, 726(1974).
(20) A. E. Jacobson and E. L. May, *ibid.*, **8**, 563(1965); N. B. Eddy and D. Leimbach, *J. Pharmacol. Exp. Ther.*, **107**, 385(1953).
(21) H. J. Rhodes and T. O. Soine, *J. Am. Pharm. Assoc., Sci. Ed.*, **45**, 746(1956).

ACKNOWLEDGMENTS AND ADDRESSES

Received August 28, 1975, from the *Department of Medicinal Chemistry, School of Pharmacy, University of Mississippi, University, MS 38677*

Accepted for publication November 6, 1975.

The authors are grateful to Dr. E. L. May, National Institutes of Health, for the analgesic data.

[x] To whom inquiries should be directed.

Differential Thermal Analysis of Aluminum Hydroxide Gel

STEVEN L. NAIL [*], JOE L. WHITE [‡], and STANLEY L. HEM [*x]

Abstract □ The development of order during the aging of aluminum hydroxide gel prepared by the reaction of aluminum chloride and ammonium hydroxide to a final pH of 7.0 can be monitored by differential thermal analysis. The loss of acid reactivity upon aging is accompanied by an increase in the temperature and intensity of the dehydroxylation endotherm and an accompanying decrease in the intensity of the water of hydration endotherm. With continued aging, the thermogram develops the characteristics of a crystalline aluminum hydroxide.

Keyphrases □ Aluminum hydroxide gels—differential thermal analysis, development of order during aging □ Gels, aluminum hydroxide—differential thermal analysis, development of order during aging □ Aging—aluminum hydroxide gels, monitored by differential thermal analysis □ Differential thermal analysis—aging of aluminum hydroxide gels monitored

In previous investigations (1, 2), IR spectroscopy and X-ray diffraction were used to monitor the structural changes in aluminum hydroxide gel which occurred upon aging and were associated with a decreased rate of acid reactivity. The initial highly random structure changed during aging as the hydroxyls became part of an ordered structure. The degree of order increased until a crystalline form of aluminum hydroxide developed. This report demonstrates the utility of differential thermal analysis in monitoring the aging of aluminum hydroxide gel and relates the thermal behavior to a recently proposed structure of aluminum hydroxide gel (3, 4).

The physical changes detectable by differential thermal analysis when aluminum hydroxide gel is heated are the loss of water of hydration in the range of

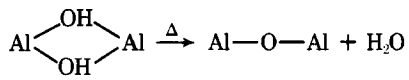

Scheme I

100–120° and the loss of structural hydroxyl as water (Scheme I). The temperature at which the dehydroxylation of the double hydroxide bridges occurs is a characteristic that allows the identification of crystalline aluminum hydroxide (5–10), although the aluminum hydroxide polymorphs cannot be distinguished from one another. Gibbsite and bayerite both have dehydroxylation endotherms at about 300°. Pseudoboehmite and boehmite undergo dehydroxylation at about 450° (9).

EXPERIMENTAL

Materials—All chemicals used were either reagent or analytical grade.

Aluminum Hydroxide Gel Preparation—A 4-liter batch of gel was prepared by the addition of 13% (v/v) strong ammonia solution to a solution of 287.2 g of aluminum chloride hexahydrate in 3340 ml of distilled water. Strong ammonia solution was added, with continuous stirring, at a rate of approximately 120 ml/min to a final pH of 7.0. After precipitation, the gel was divided into equal portions prior to washing. The first portion (I) was washed with 1 liter of distilled water by draining through a canvas bag, the second (II), was washed with 3 liters of distilled water, and the third (III) was washed with 5 liters of distilled water. The three gels were diluted to 1 liter with distilled water and were then stored in tightly closed glass containers and aged at 25°.

Differential Thermal Analysis Thermograms—The differential thermal analysis thermogram[1] was recorded from room temperature

[1] Model III, Deltatherm Instrument Co., Denver, Colo.

(2) J. Sam, J. D. England, and D. Temple, *J. Med. Chem.*, **12**, 144(1969).
(3) M. N. Aboul-Enein and J. Sam, *J. Heterocycl. Chem.*, **8**, 7(1971).
(4) S. F. Mason, K. Schofield, and R. J. Wells, *J. Chem. Soc., C*, **1967**, 626.
(5) T. C. Joseph and S. Dev, *Tetrahedron*, **24**, 3841(1968).
(6) F. Bohlmann, *Angew. Chem.*, **69**, 641(1957); *Chem. Ber.*, **91**, 2157(1958).
(7) T. M. Moynehan, K. Schofield, R. A. Y. Jones, and A. R. Katritzky, *J. Chem. Soc.*, **1962**, 2637.
(8) H. S. Aaron and C. P. Ferguson, *Tetrahedron Lett.*, **1968**, 6191.
(9) P. J. Chivers, T. A. Crabb, and R. O. Williams, *Tetrahedron*, **24**, 4411(1968).
(10) E. L. Eliel, N. L. Allinger, S. J. Angyal, and G. A. Morrison, "Conformational Analysis," Wiley, New York, N.Y., 1965, p. 254.
(11) F. G. Riddell, *Quart. Rev.*, **21**, 364(1967).
(12) E. L. Eliel, N. L. Allinger, S. J. Angyal, and G. A. Morrison, "Conformational Analysis," Wiley, New York, N.Y., 1965, p. 207.
(13) S. Dev, *J. Indian Chem. Soc.*, **33**, 769(1956).
(14) N. L. Allinger, *J. Am. Chem. Soc.*, **81**, 5727(1959).
(15) R. Pauncz and D. Ginsburg, *Tetrahedron*, **9**, 40(1960).
(16) J. B. Hendrickson, *J. Am. Chem. Soc.*, **83**, 4537(1961).
(17) J. C. Sircar and A. I. Meyers, *J. Org. Chem.*, **32**, 1248(1967), and references cited therein.
(18) J. D. England and J. Sam, *J. Heterocycl. Chem.*, **3**, 582(1966).
(19) M. E. Rogers and J. Sam, *J. Med. Chem.*, **17**, 726(1974).
(20) A. E. Jacobson and E. L. May, *ibid.*, **8**, 563(1965); N. B. Eddy and D. Leimbach, *J. Pharmacol. Exp. Ther.*, **107**, 385(1953).
(21) H. J. Rhodes and T. O. Soine, *J. Am. Pharm. Assoc., Sci. Ed.*, **45**, 746(1956).

ACKNOWLEDGMENTS AND ADDRESSES

Received August 28, 1975, from the *Department of Medicinal Chemistry, School of Pharmacy, University of Mississippi, University, MS 38677*

Accepted for publication November 6, 1975.

The authors are grateful to Dr. E. L. May, National Institutes of Health, for the analgesic data.

[x] To whom inquiries should be directed.

Differential Thermal Analysis of Aluminum Hydroxide Gel

STEVEN L. NAIL [*], JOE L. WHITE [‡], and STANLEY L. HEM [*x]

Abstract □ The development of order during the aging of aluminum hydroxide gel prepared by the reaction of aluminum chloride and ammonium hydroxide to a final pH of 7.0 can be monitored by differential thermal analysis. The loss of acid reactivity upon aging is accompanied by an increase in the temperature and intensity of the dehydroxylation endotherm and an accompanying decrease in the intensity of the water of hydration endotherm. With continued aging, the thermogram develops the characteristics of a crystalline aluminum hydroxide.

Keyphrases □ Aluminum hydroxide gels—differential thermal analysis, development of order during aging □ Gels, aluminum hydroxide—differential thermal analysis, development of order during aging □ Aging—aluminum hydroxide gels, monitored by differential thermal analysis □ Differential thermal analysis—aging of aluminum hydroxide gels monitored

In previous investigations (1, 2), IR spectroscopy and X-ray diffraction were used to monitor the structural changes in aluminum hydroxide gel which occurred upon aging and were associated with a decreased rate of acid reactivity. The initial highly random structure changed during aging as the hydroxyls became part of an ordered structure. The degree of order increased until a crystalline form of aluminum hydroxide developed. This report demonstrates the utility of differential thermal analysis in monitoring the aging of aluminum hydroxide gel and relates the thermal behavior to a recently proposed structure of aluminum hydroxide gel (3, 4).

The physical changes detectable by differential thermal analysis when aluminum hydroxide gel is heated are the loss of water of hydration in the range of

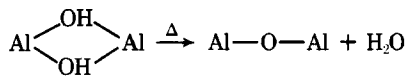

Scheme I

100–120° and the loss of structural hydroxyl as water (Scheme I). The temperature at which the dehydroxylation of the double hydroxide bridges occurs is a characteristic that allows the identification of crystalline aluminum hydroxide (5–10), although the aluminum hydroxide polymorphs cannot be distinguished from one another. Gibbsite and bayerite both have dehydroxylation endotherms at about 300°. Pseudoboehmite and boehmite undergo dehydroxylation at about 450° (9).

EXPERIMENTAL

Materials—All chemicals used were either reagent or analytical grade.

Aluminum Hydroxide Gel Preparation—A 4-liter batch of gel was prepared by the addition of 13% (v/v) strong ammonia solution to a solution of 287.2 g of aluminum chloride hexahydrate in 3340 ml of distilled water. Strong ammonia solution was added, with continuous stirring, at a rate of approximately 120 ml/min to a final pH of 7.0. After precipitation, the gel was divided into equal portions prior to washing. The first portion (I) was washed with 1 liter of distilled water by draining through a canvas bag, the second (II), was washed with 3 liters of distilled water, and the third (III) was washed with 5 liters of distilled water. The three gels were diluted to 1 liter with distilled water and were then stored in tightly closed glass containers and aged at 25°.

Differential Thermal Analysis Thermograms—The differential thermal analysis thermogram[1] was recorded from room temperature

[1] Model III, Deltatherm Instrument Co., Denver, Colo.

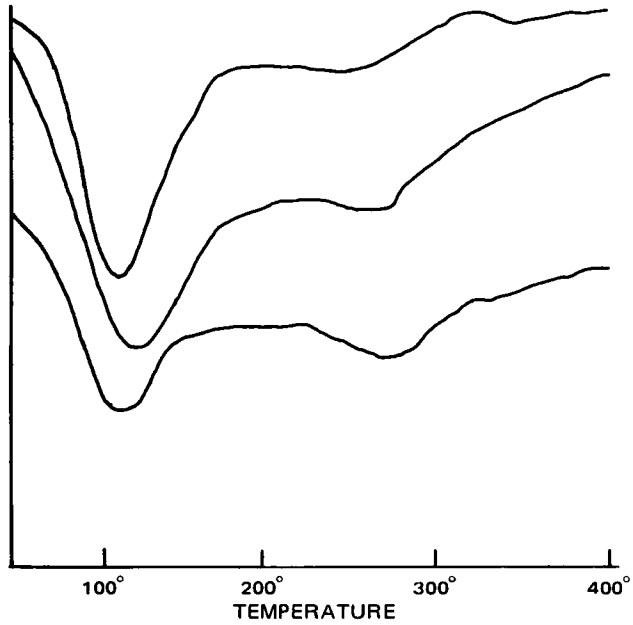

Figure 1—*Change in differential thermal analysis thermogram of Gel I during aging at 25°. Key: top, 15 days; middle, 66 days; and bottom, 161 days.*

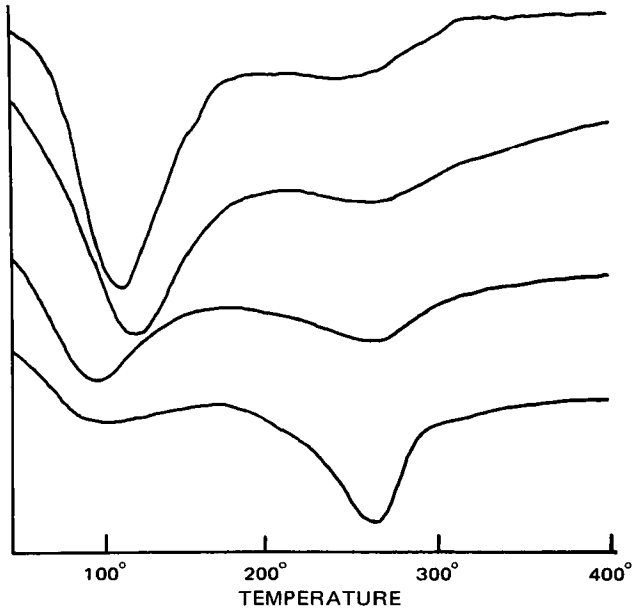

Figure 2—*Change in differential thermal analysis thermogram of Gel II during aging at 25°. Key: top, 15 days; upper middle, 64 days; lower middle, 113 days; and bottom, 161 days.*

to 500° for each gel at various times during aging. Samples were prepared by placing 5 ml of gel in a plastic centrifuge tube[2] and diluting to 12 ml with 2 *N* NaCl. Samples were then centrifuged[3] at 4000 rpm for 15 min. The supernate was discarded and replaced with 50% ethanol, and the samples were again centrifuged at 4000 rpm for 15 min.

The purpose of this washing process was to remove any residual ammonium chloride from the gel samples. It was found that 2 *N* NaCl and 50% ethanol permitted the gel to be separated by centrifugation because these vehicles prevented dispersion of the gel which occurred if the gel was washed with distilled water. Ammonium chloride sublimes at 340°, resulting in an endotherm that interferes with the detection of the dehydroxylation endotherm of the sample.

After washing, the sample was air dried at room temperature and ground to a fine powder with an agate mortar and pestle. The sample cup was filled with 40 ± 3 mg of sample and packed uniformly. The thermogram was recorded under the following conditions: heating rate, 10°/min; ΔT sensitivity, 2°/2.54 cm; and upper temperature limit, 500°. The reference was calcined alumina. The thermogram of gibbsite[4] was recorded similarly.

The temperature of the dehydration endotherm was somewhat variable due to the variable heating rate of the instrument below 100°. Daily replications indicated that the temperature of the dehydroxylation endotherm in the 200–300° range varied by less than ±1°.

The acid-consuming capacity test (11) was modified by titrating to pH 3.5 rather than using bromophenol blue TS, as given in the USP. All determinations were made in duplicate. The antacid property of each gel is given as the percentage of the theoretical acid-consuming capacity, which is based on the stoichiometric reaction of hydrochloric acid with the equivalent aluminum oxide in the sample as determined by the official chelatometric assay (11).

RESULTS AND DISCUSSION

Differential thermal analysis thermograms for the three gels studied are shown in Figs. 1–3. The earliest thermogram of each gel is characterized by an endotherm at about 100°, corresponding to loss of bound water, and by a broad, poorly defined endotherm centered at about 250°, appearing as a shoulder on the dehydration endotherm. The later endotherm is the loss of structural hydroxyl as water, resulting in an oxo linkage, Al—O—Al.

As a gel ages, the dehydroxylation endotherm becomes more defined, appears at a higher temperature, and is more intense. The fact that the endotherm is observed at a higher temperature indicates that, as the gel ages, more thermal energy is required for dehydroxylation. This is evidence that the structure is becoming more ordered with age. The differential thermal analysis thermogram of gibbsite is shown along with the thermograms of Gel III in Fig. 3. As the gels age, the features of the thermogram approach those of the highly crystalline material.

The relative rate of development of order as measured by the intensity of the dehydroxylation endotherm was greatest in Gel III (Fig. 3), which was washed with 5 liters of distilled water, and least in Gel I (Fig. 1), which was washed with 1 liter of distilled water. This rank order is the same as the loss of acid reactivity as measured by the percent of theoretical acid-consuming capacity (Table I). The crystalline aluminum hydroxide polymorphs are virtually unreactive in 0.1 *N* HCl, so the development of an ordered system leading to a

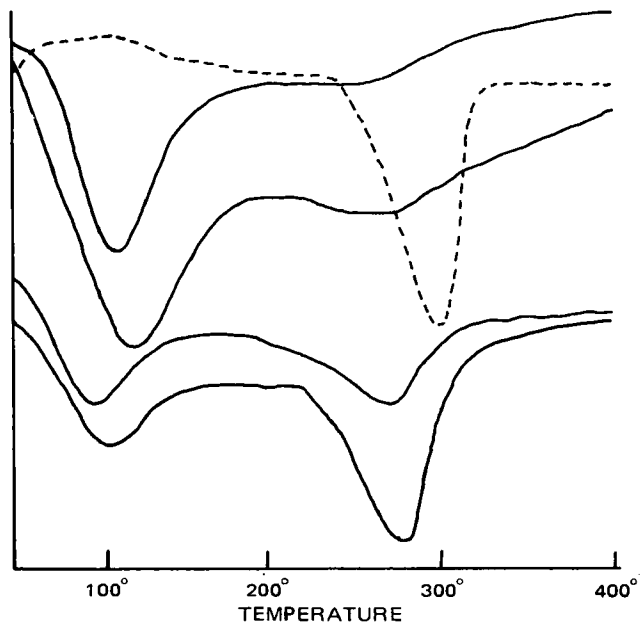

Figure 3—*Change in differential thermal analysis thermogram of Gel III during aging at 25°. Key: - - -, gibbsite; top, 13 days; upper middle, 66 days; lower middle, 113 days; and bottom, 161 days.*

[2] Polypropylene tubes, 16.0 × 102.2 mm, Ivan Sorvall, Inc., Newton, Conn.
[3] Model GLC-1, Ivan Sorvall, Inc., Newton, Conn.
[4] Reynolds Metal Co., Richmond, Va.

Table I—Change in Acid-Consuming Capacity during Aging at 25°

Days	Percent of Theoretical Acid-Consuming Capacity		
	Gel I	Gel II	Gel III
13	—	—	78
15	78	81	—
64	—	61	—
66	63	—	57
113	—	53	41
161	55	34	28

crystalline aluminum hydroxide polymorph results in a decreased acid-consuming capacity. The behavior supports the earlier hypothesis (12–14) that anions present at the time of precipitation stabilize the gel structure. The removal of these stabilizing anions by washing results in an increased rate of development of order in the gel structure, with an associated decrease in the acid reactivity.

The sequence of thermograms showing the aging process of each gel (Figs. 1–3) indicates that, as aging proceeds, the intensity of the dehydration endotherm decreases and the intensity of the dehydroxylation endotherm increases. As the gel becomes ordered, less water is bound to the gel and the structural hydroxyl content increases. The bound water is probably replaced by structural hydroxyl in the form of double hydroxide bridges.

The proposed (15) polymer model for aluminum hydroxide suggests that particle growth occurs by a deprotonation–dehydration mechanism, which results in the conversion of bound water molecules into double hydroxide bridges. This process continues until a crystalline form of aluminum hydroxide is produced. With gibbsite, a highly crystalline form of aluminum hydroxide, the thermogram (Fig. 3) indicates that virtually no bound water is present.

In summary, it appears that differential thermal analysis is a useful technique for studying aluminum hydroxide gel. It is sensitive to the structural changes that occur during aging which are responsible for the decreased acid reactivity of the aluminum hydroxide gel. Analysis of the thermograms indicates that bound water in the gels was replaced during aging by structural hydroxyl groups in the form of double hydroxide bridges. This change results in a more ordered structure which is more resistant to reaction with acid. As aging progresses, the gel assumes the characteristic thermogram of a crystalline aluminum hydroxide.

REFERENCES

(1) S. L. Nail, J. L. White, and S. L. Hem, *J. Pharm. Sci.*, **64**, 1166(1975).

(2) *Ibid.*, **65**, 231(1976).

(3) *Ibid.*, **65**, 1188(1976).

(4) *Ibid.*, **65**, 1192(1976).

(5) T. Sato, *Z. Anorg. Allg. Chem.*, **391**, 69(1972).

(6) R. C. MacKenzie, R. Meldeau, and J. A. Gard, *Min. Mag.*, **33**, 145(1962).

(7) J. M. Bracewell, A. S. Campbell, and B. D. Mitchell, *Clay Miner.*, **8**, 325(1970).

(8) H. C. Stumpf, A. S. Russell, and J. W. Newsome, *Ind. Eng. Chem.*, **42**, 1398(1950).

(9) T. Sato, *Z. Anorg. Allg. Chem.*, **391**, 167(1972).

(10) R. E. Grim, "Clay Mineralogy," 2nd ed., McGraw-Hill, New York, N.Y., 1968, pp. 285–297.

(11) "The United States Pharmacopeia," 18th rev., Mack Publishing Co., Easton, Pa., 1970, p. 26.

(12) S. L. Hem, E. J. Russo, S. M. Bahal, and R. S. Levi, *J. Pharm. Sci.*, **59**, 317(1970).

(13) G. J. Ross and R. C. Turner, *Soil Sci. Soc. Am. Proc.*, **35**, 389(1971).

(14) P. H. Hsu, *Int. Comm. Study Bauxites Aluminum Oxides-Hydroxides, 3rd*, **1973**, 613.

(15) J. D. Hem and C. E. Roberson, Geological Survey Water-Supply Paper 1827-A, U.S. Government Printing Office, Washington, D.C., 1967.

ACKNOWLEDGMENTS AND ADDRESSES

Received July 2, 1975, from the *Industrial and Physical Pharmacy Department, School of Pharmacy and Pharmacal Sciences, and the ‡Department of Agronomy, Purdue University, West Lafayette, IN 47907

Accepted for publication November 26, 1975.

Supported in part by an American Foundation for Pharmaceutical Education Fellowship (S. L. Nail).

This report is Journal Paper 5946, Purdue University Agricultural Experiment Station, West Lafayette, IN 47907

ˣ To whom inquiries should be directed.

Extraction and GLC Analysis of Pyrithyldione in Highly Putrified Human Postmortem Samples

FRANK K. MARTENS ˣ, MARK A. MARTENS, JOHAN DEMETER, and AUBIN HEYNDRICKX

Abstract □ Pyrithyldione was isolated from highly putrified human brain and small intestine samples by ether extraction followed by alumina column cleanup. The total yield was 90 ± 5%. No derivatization was necessary prior to GLC analysis.

Keyphrases □ Pyrithyldione—GLC analysis, putrified brain and intestine □ GLC—analysis, pyrithyldione in putrified brain and intestine □ Sedatives—pyrithyldione, GLC analysis in putrified brain and intestine

In forensic toxicology, many methods have been reported for extracting pyrithyldione and glutethimide from postmortem samples. Most of these methods consist of a single extraction step with chloroform, petroleum ether, or methylene chloride followed by TLC, UV spectrophotometry, or spectrofluorometry (1–4).

Impurities may be removed by gel permeation chromatography (5) or direct analysis by GLC, using various liquid phases (6, 7). If impurities interfere too much after direct extraction, ethylation with tetraethylammonium hydroxide may solve this problem (8). Three-month-old postmortem samples are difficult to analyze, and special cleanup requirements may be necessary for final unambiguous identification. To prevent interference with barbiturates and other hypnotics or sedatives, OV-275 was selected for the GLC analysis.

Table I—Change in Acid-Consuming Capacity during Aging at 25°

Days	Percent of Theoretical Acid-Consuming Capacity		
	Gel I	Gel II	Gel III
13	—	—	78
15	78	81	—
64	—	61	—
66	63	—	57
113	—	53	41
161	55	34	28

crystalline aluminum hydroxide polymorph results in a decreased acid-consuming capacity. The behavior supports the earlier hypothesis (12–14) that anions present at the time of precipitation stabilize the gel structure. The removal of these stabilizing anions by washing results in an increased rate of development of order in the gel structure, with an associated decrease in the acid reactivity.

The sequence of thermograms showing the aging process of each gel (Figs. 1–3) indicates that, as aging proceeds, the intensity of the dehydration endotherm decreases and the intensity of the dehydroxylation endotherm increases. As the gel becomes ordered, less water is bound to the gel and the structural hydroxyl content increases. The bound water is probably replaced by structural hydroxyl in the form of double hydroxide bridges.

The proposed (15) polymer model for aluminum hydroxide suggests that particle growth occurs by a deprotonation–dehydration mechanism, which results in the conversion of bound water molecules into double hydroxide bridges. This process continues until a crystalline form of aluminum hydroxide is produced. With gibbsite, a highly crystalline form of aluminum hydroxide, the thermogram (Fig. 3) indicates that virtually no bound water is present.

In summary, it appears that differential thermal analysis is a useful technique for studying aluminum hydroxide gel. It is sensitive to the structural changes that occur during aging which are responsible for the decreased acid reactivity of the aluminum hydroxide gel. Analysis of the thermograms indicates that bound water in the gels was replaced during aging by structural hydroxyl groups in the form of double hydroxide bridges. This change results in a more ordered structure which is more resistant to reaction with acid. As aging progresses, the gel assumes the characteristic thermogram of a crystalline aluminum hydroxide.

REFERENCES

(1) S. L. Nail, J. L. White, and S. L. Hem, *J. Pharm. Sci.*, **64**, 1166(1975).

(2) *Ibid.*, **65**, 231(1976).

(3) *Ibid.*, **65**, 1188(1976).

(4) *Ibid.*, **65**, 1192(1976).

(5) T. Sato, *Z. Anorg. Allg. Chem.*, **391**, 69(1972).

(6) R. C. MacKenzie, R. Meldeau, and J. A. Gard, *Min. Mag.*, **33**, 145(1962).

(7) J. M. Bracewell, A. S. Campbell, and B. D. Mitchell, *Clay Miner.*, **8**, 325(1970).

(8) H. C. Stumpf, A. S. Russell, and J. W. Newsome, *Ind. Eng. Chem.*, **42**, 1398(1950).

(9) T. Sato, *Z. Anorg. Allg. Chem.*, **391**, 167(1972).

(10) R. E. Grim, "Clay Mineralogy," 2nd ed., McGraw-Hill, New York, N.Y., 1968, pp. 285–297.

(11) "The United States Pharmacopeia," 18th rev., Mack Publishing Co., Easton, Pa., 1970, p. 26.

(12) S. L. Hem, E. J. Russo, S. M. Bahal, and R. S. Levi, *J. Pharm. Sci.*, **59**, 317(1970).

(13) G. J. Ross and R. C. Turner, *Soil Sci. Soc. Am. Proc.*, **35**, 389(1971).

(14) P. H. Hsu, *Int. Comm. Study Bauxites Aluminum Oxides-Hydroxides, 3rd*, **1973**, 613.

(15) J. D. Hem and C. E. Roberson, Geological Survey Water-Supply Paper 1827-A, U.S. Government Printing Office, Washington, D.C., 1967.

ACKNOWLEDGMENTS AND ADDRESSES

Received July 2, 1975, from the *Industrial and Physical Pharmacy Department, School of Pharmacy and Pharmacal Sciences, and the ‡Department of Agronomy, Purdue University, West Lafayette, IN 47907

Accepted for publication November 26, 1975.

Supported in part by an American Foundation for Pharmaceutical Education Fellowship (S. L. Nail).

This report is Journal Paper 5946, Purdue University Agricultural Experiment Station, West Lafayette, IN 47907

ˣ To whom inquiries should be directed.

Extraction and GLC Analysis of Pyrithyldione in Highly Putrified Human Postmortem Samples

FRANK K. MARTENS ˣ, MARK A. MARTENS, JOHAN DEMETER, and AUBIN HEYNDRICKX

Abstract □ Pyrithyldione was isolated from highly putrified human brain and small intestine samples by ether extraction followed by alumina column cleanup. The total yield was 90 ± 5%. No derivatization was necessary prior to GLC analysis.

Keyphrases □ Pyrithyldione—GLC analysis, putrified brain and intestine □ GLC—analysis, pyrithyldione in putrified brain and intestine □ Sedatives—pyrithyldione, GLC analysis in putrified brain and intestine

In forensic toxicology, many methods have been reported for extracting pyrithyldione and glutethimide from postmortem samples. Most of these methods consist of a single extraction step with chloroform, petroleum ether, or methylene chloride followed by TLC, UV spectrophotometry, or spectrofluorometry (1–4).

Impurities may be removed by gel permeation chromatography (5) or direct analysis by GLC, using various liquid phases (6, 7). If impurities interfere too much after direct extraction, ethylation with tetraethylammonium hydroxide may solve this problem (8). Three-month-old postmortem samples are difficult to analyze, and special cleanup requirements may be necessary for final unambiguous identification. To prevent interference with barbiturates and other hypnotics or sedatives, OV-275 was selected for the GLC analysis.

Table I—Concentrations of Pyrithyldione in 3-Month-Old Postmortem Samples from a Suicide Case

Samples Analyzed	Concentration Found, ppm ± *SD*
Stomach content	6.70 ± 0.15
Blood	3.50 ± 0.25
Liver	3.50 ± 0.20
Small intestine content	1.60 ± 0.17
Kidney	3.55 ± 0.20
Brain	0.75 ± 0.13
Urine	4.25 ± 0.22

EXPERIMENTAL

Reagents—Peroxide-free ether was prepared by refluxing over potassium hydroxide and distillation and was stored in bottles protected from light. The methanol-deactivated neutral alumina[1] was prepared according to the method of McClure (9) and applied in forensic toxicology according to Martens *et al.* (10).

Dry sodium sulfate and extrapure seasand[1] were used to grind the postmortem tissues. Reference standards were pyrithyldione[2] and methyprylon[3]. For routine analysis, 1- and 0.1-mg/ml pyrithyldione solutions in ethanol and a 0.1-mg/ml methyprylon solution in ethanol were prepared as internal standards.

Apparatus—A research gas chromatograph[4] equipped with a dual flame-ionization detector was used. A Pyrex glass column, not silanized (4 mm i.d., 6 mm o.d. × 1.90 m) contained 3% OV-275 on Chromosorb W-AW, not silanized[5]. About 0.07-m glass beads were placed in the injection port of the column.

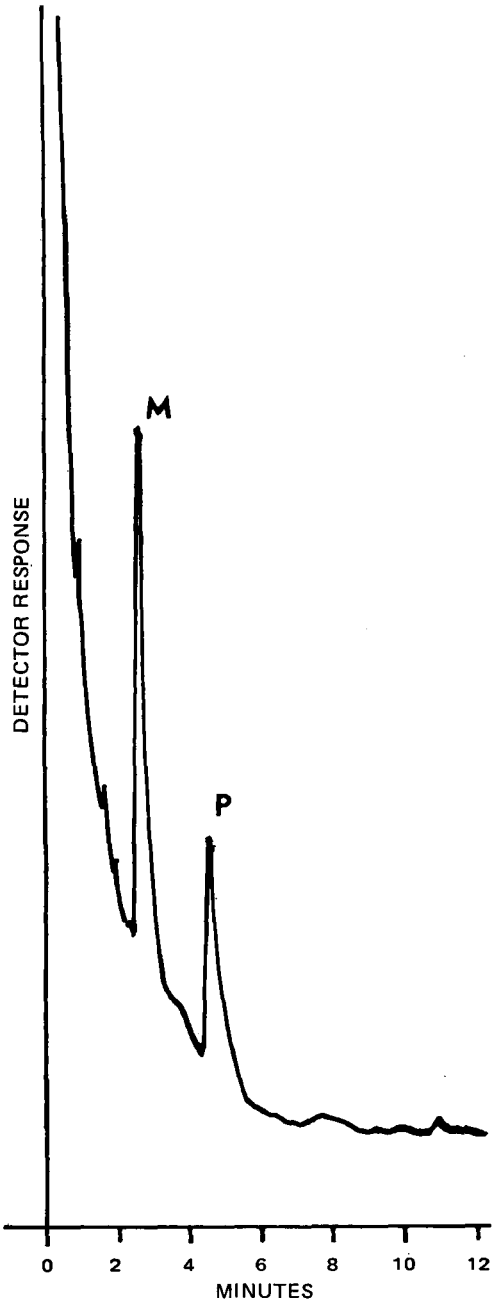

Figure 1—*GLC analysis of an extract of pyrithyldione from a 250-mg brain sample. An OV-275 column was used. Key: M, methyprylon internal standard; and P, pyrithyldione.*

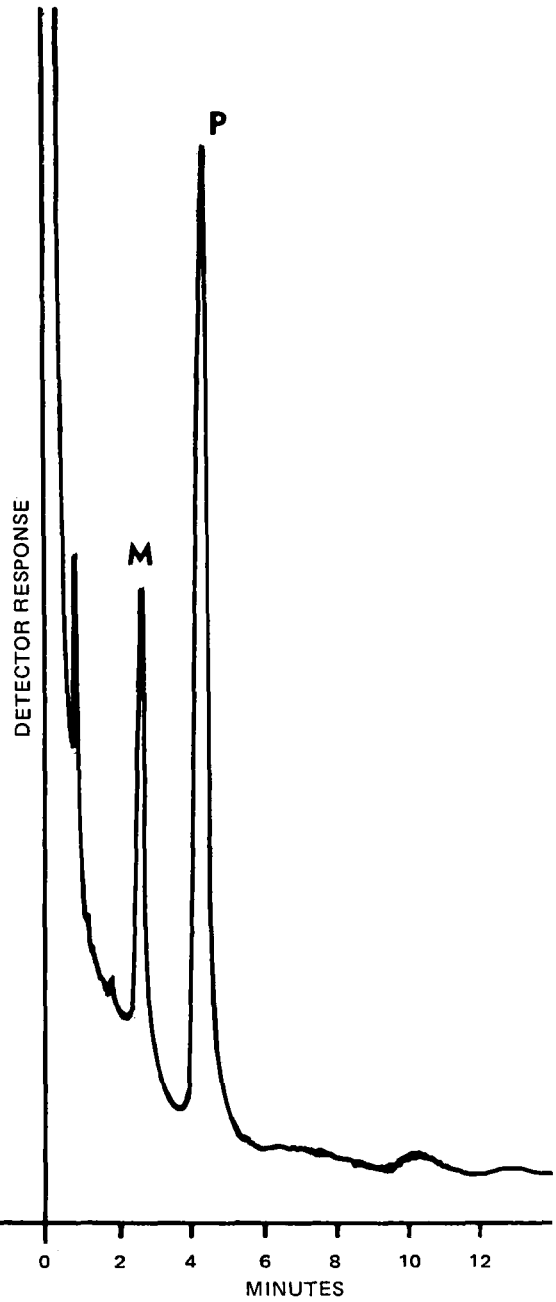

Figure 2—*GLC analysis of an extract of pyrithyldione from a 230-mg small intestine sample. An OV-275 column was used. Key: M, methyprylon internal standard; and P, pyrithyldione.*

[1] E. Merck, Darmstadt, Germany.
[2] Persedon, Roche, Basel, Switzerland.
[3] Noludar, Roche, Basel, Switzerland.
[4] Model 5750 B, Hewlett-Packard.
[5] Supelco, lot C-1249.

Table II—Relative Retention Times on OV-275

Compound	Relative R_t
Pyrithyldione	1.00
Methyprylon	0.61
Glutethimide	1.77
Methsuximide	0.58
Phensuximide	1.29
Mephenytoin	2.42

This column was conditioned as follows: 30 min, a 10-ml/min carrier gas flow at room temperature; 2.30 hr, no flow at 100°; 1.30 hr, no flow at 150°; 2.00 hr, no flow at 220°; and 24 hr, a 10-ml/min carrier gas flow at 240°. During analysis, the oven temperature was maintained at 200° isothermal, the injection port at 240° and the detector at 255°. The column showed a top performance at 37 ml/min. Injections were made with a 10-μl syringe[6]. Chromatographic cleanup columns consisted of Pyrex glass, 0.7 × 20 cm.

Procedure—In a mortar, 5–10 g of forensic sample (brain, liver, kidney, stomach content, small intestine content, blood, and urine) are thoroughly mixed and shattered with sand and sufficient sodium sulfate to obtain a free flowing dry powder. This dry mixture is transferred into a 500-ml erlenmeyer flask containing 200 ml of ether and shaken for 30 min. The extraction residue is washed twice with 20 ml of ether.

The combined ether phases, loaded with fat, impurities, and the drug, are poured into an evaporation flask together with 25 ml of distilled water. The ether phase is slowly evaporated[7] at 50°. The remaining aqueous phase contains the drug while fatty material precipitates. This aqueous phase and two 20-ml portions of water, used for rinsing, are filtered through a prewetted filter[8] into a 250-ml separator. All combined aqueous phases are washed once with 50 ml of *n*-pentane to remove the remaining fats and free fatty acids.

Ether (2 × 100 ml) is used to extract the drug out of the aqueous phase. The combined ether phases are spiked with the appropriate amount of methyprylon as the internal standard. The volume of the ethereal phase is reduced[9] to not less than 0.5 ml. After adjusting the remaining volume to 2 ml with ether, 1 ml is pipetted onto the chromatography column containing 10 cm of methanol-deactivated alumina; the drug is completely eluted with 100 ml of ether. This volume is reduced[9] and further evaporated by a gentle jet of nitrogen at room temperature until dry. This final residue is dissolved in 10–50 μl of methanol and injected in the gas chromatograph.

RESULTS

GLC data were quantified by their pyrithyldione–methyprylon peak ratios (Table I). The separation achieved is shown in Figs. 1 and 2. Methyprylon proved to be the best internal standard in all sample analyses.

[6] Hamilton Co., Reno, Nev.
[7] Buchi-Rotavapor.
[8] Whatman No. 1.
[9] Kuderna Danish evaporator.

DISCUSSION

Recovery experiments were carried out on each extraction step. Volume–volume ratios, temperature conditions, and column conditions were optimized to obtain acceptable reproducibility. Total recovery was 90 ± 5% on 25-ppm pyrithyldione-spiked samples. The aqueous phase, containing the drug, gave a 97 ± 2% yield when extracted twice with equal volumes of ether; only 2–3% losses occurred during the *n*-pentane washing. Experiments on the influence of the aqueous phase pH demonstrated a higher extraction yield of pigments and impurities at low pH. Since the keto form of pyrithyldione prevails at neutral pH, no acidification was needed.

Methyprylon was chosen as the internal standard because of its superior properties compared to other hypnotics or sedatives of analogous molecular structure. Methyprylon eluted along with pyrithyldione from the alumina column in a 100% yield, and a constant pyrithyldione–methyprylon ratio was maintained over two evaporation steps. The coefficient of variation of this ratio during the alumina column cleanup ranged from 2.2 to 5.2%. However, close attention is required for the evaporation procedure, after which the final residues may not be heated over 40°. Therefore, glutethimide and phensuximide were not suited for use as internal standards. Most common hypnotics are separated on OV-275 (Table II). Other hypnotics such as brallobarbital, secobarbital, ethosuximide, phenytoin, primidone, phenobarbital, and mephobarbital do not interfere and appear at much higher R_t values.

The developed method offers the possibility of extracting pyrithyldione with a high yield and purity. Because of its excellent performance with barbiturates and diketopiperidines, OV-275 allows a detection limit of 15 ng/g of sample with flame ionization.

REFERENCES

(1) I. Sunshine, R. Maes, and R. Faracci, *Clin. Chem.*, **14**, 595(1968).

(2) O. Pribilla, *Arzneim.-Forsch.*, **6**, 138(1956).

(3) E. Hirschberg, M. F. Greenberg, E. De Ritter, and S. H. Rubin, *J. Am. Pharm. Assoc., Sci. Ed.*, **37**, 288(1948).

(4) P. Polatin, E. Hirschberg, S. Rubin, and L. Pirk, *Am. J. Med. Sci.*, **214**, 662(1947).

(5) M. Yoshihiko, *J. Forensic Sci.*, **15**, 92(1970).

(6) E. Watson and S. Kalman, *Clin. Chim. Acta*, **38**, 33(1972).

(7) P. Grieveson and J. S. Gordon, *J. Chromatogr.*, **44**, 279(1969).

(8) J. McGee, *Clin. Chem.*, **17**, 587(1971).

(9) V. McClure, *J. Chromatogr.*, **70**, 168(1972).

(10) M. A. Martens, F. K. Martens, and A. Heyndrickx, *Meded. Fac. Landbouwwet. Gent*, **39**(2), 1279(1974).

ACKNOWLEDGMENTS AND ADDRESSES

Received August 22, 1975, from the *Department of Toxicology, State University of Ghent, Hospitaalstraat 13, B-9000 Ghent, Belgium.*

Accepted for publication October 25, 1975.

The authors are indebted to M. Creynen for technical assistance.

[x] To whom inquiries should be directed.

Pharmacokinetics of Skin Penetration

EUGENE R. COOPER

Abstract □ A model for estimating *in vivo* skin permeability coefficients is presented. Explicit expressions are derived for the permeability coefficient in terms of excretion rates and tissue absorption. The excretion rate has a linear asymptotic limit from which the permeability coefficient can be determined. The usefulness of the model is demonstrated with existing literature data.

Keyphrases □ Pharmacokinetics—model for estimating *in vivo* skin permeability coefficients in terms of excretion rates and tissue absorption □ Permeability coefficients, skin—estimated using pharmacokinetic models, in terms of excretion rates and tissue absorption □ Skin permeability coefficients—estimated using pharmacokinetic models, in terms of excretion rates and tissue absorption □ Excretion rate—data used in deriving pharmacokinetic models for estimating *in vivo* skin permeability coefficients

Quantitative studies of skin penetration have been conducted primarily with *in vitro* systems, *i.e.*, with epidermis obtained at autopsy, and Scheuplein and Blank (1) pioneered much of this important work. However, little effort has been directed toward a quantitative understanding of skin penetration *in vivo*, and it is very difficult to extract permeability coefficients from existing *in vivo* data. Thus, accurate comparisons of *in vivo* and *in vitro* skin penetration are sparse.

The *in vitro* and *in vivo* transport of alkyl methyl sulfoxides across rabbit skin was studied, and the steady-state urinary elimination rate was about one-half of the *in vitro* steady-state flux (2). Since only one-half of the sulfoxide was eliminated *via* the urinary pathway, this result is evidence for reasonable agreement between *in vivo* and *in vitro* skin penetration.

The *in vivo* skin penetration of three esters of salicylic acid was measured using urinary excretion rates in humans (3). The system (3) was somewhat more ideal than that of Sekura and Scala (2), since 90% of the intravenously injected salicylate was recovered in the urine. That is, the urinary excretion at steady state should closely reflect the diffusion rate across the skin.

The purpose of this report is to show quantitatively how permeability coefficients can be extracted from excretion data. Diffusion theory is coupled with simple elimination kinetics to derive mathematical expressions for the amount of material excreted as a function of time. The excretion rate is shown to have a linear (in time) asymptotic limit, with a lag time that is the sum of the diffusional and excretion lag times.

MATHEMATICAL MODEL

It is assumed that a drug is applied to the skin surface over an area, A, and that the diffusion across the skin into the body fluids can be represented by diffusion theory. That is, it is assumed that the concentration of material in the skin (the membrane) is governed by:

$$\frac{\partial c}{\partial t} = D\frac{\partial^2 c}{\partial x^2} \qquad \text{(Eq. 1)}$$

where c is the concentration, D is the diffusion coefficient, t is time, and x is the position inside the membrane. The flux of material into the body fluids is given by:

$$J = -D\left(\frac{\partial c}{\partial x}\right)_{x=l} = D\left[\frac{c_0}{l} + \frac{2c_0}{l}\sum_{n=1}^{\infty}(-1)^n e^{-\alpha_n t}\right] \qquad \text{(Eq. 2)}$$

where $c(x,t)$ is the solution (4) of Eq. 1 for a membrane of thickness l and boundary conditions $c(0,t) = c_0$ and $c(l,t) \ll c_0$. Here $\alpha_n = (n^2\pi^2/6)k_D$ and $k_D = 6D/l^2$, which is just the reciprocal of the diffusional lag time. The constant concentration, c_0, is related to the vehicle concentration *via* the partition coefficient, and $c(l,t)$ is related to the concentration in the body fluids.

As the drug diffuses across the stratum corneum, it is assumed to be carried away into the body fluids, where it is either in solution or bound. Furthermore, it is assumed that the drug is eliminated by parallel first-order routes of metabolism, biliary excretion, and urinary excretion and that distribution between body fluids and tissue is rapid. Thus, one can employ conservation of mass to obtain the time rate of change of drug in solution in the body fluids:

$$V_l\frac{dC_l}{dt} = AJ - V_b\frac{d\theta_b}{dt} - V_tK\frac{dC_l}{dt} - (k_M + k_B + k_U)C_lV_l \qquad \text{(Eq. 3)}$$

where C_l is the drug concentration in solution in the liquid portion of the body fluids; V_l is the volume of the liquid; $\theta_b(C_l)$ is the amount (per unit volume) of material bound to a volume, V_b, of substrate in the body fluids; and k_M, k_B, and k_U are metabolism, biliary excretion, and urinary elimination coefficients, respectively. Here, K is the distribution coefficient between the body fluids and the tissue of volume V_t. Equation 3 can now be written as:

$$\left(1 + \frac{V_b}{V_l}\frac{d\theta_b}{dC_l} + \frac{V_tK}{V_l}\right)\frac{dS}{dt} = -kS + Q\left[1 + 2\sum_{n=1}^{\infty}(-1)^n e^{-\alpha_n t}\right] \qquad \text{(Eq. 4)}$$

where $S = V_lC_l$ is the total amount of drug in solution and:

$$Q = AC_0D/l \qquad \text{(Eq. 5)}$$

$$k = k_M + k_B + k_U \qquad \text{(Eq. 6)}$$

Evaluation of Eq. 4 depends on a knowledge of θ_b. If one assumes that the body fluids contain a low concentration of drug, then one can approximate θ_b by:

$$\theta_b = \beta C_l \qquad \text{(Eq. 7)}$$

This approximation allows Eq. 4 to be written as:

$$\frac{dS}{dt} = -k_aS + Q_a\left[1 + 2\sum_{n=1}^{\infty}(-1)^n e^{-\alpha_n t}\right] \qquad \text{(Eq. 8)}$$

where $k_a = k/\delta$, $Q_a = Q/\delta$, and $\delta = 1 + \beta(V_b/V_l) + K(V_t/V_l)$.

The solution of Eq. 8 is:

$$S = \frac{Q_a}{k_a}(1 - e^{-k_at}) + 2Q_a\sum_{n=1}^{\infty}\frac{(-1)^n}{(k_a - \alpha_n)}(e^{-\alpha_n t} - e^{-k_at}) \qquad \text{(Eq. 9)}$$

from which one can obtain the urinary excretion rate, k_US, or the total excretory rate, kS. Equation 9 has a simplifying limit for $k_D \gg k$, *i.e.*, when the diffusional lag time is small with respect to the excretory time scale. In this limit:

$$\lim_{k_D \gg k} S = \frac{Q_a}{k_a}(1 - e^{-k_at}) \qquad \text{(Eq. 10)}$$

which says that the excretion rate rises exponentially.

A more useful parameter is the total amount excreted as a function of time, since it has a linear asymptotic solution from which Q_a and k_a can be estimated more easily. The total amount excreted is obtained by multiplying the appropriate excretion constant by M, where:

$$M = \int_0^t dtS = \frac{Q_a}{k_a}\left[t - \frac{1}{k_a}(1 - e^{-k_at})\right] + 2Q_a\sum_{n=1}^{\infty}\frac{(-1)^n}{k_a - \alpha_n}\left[\frac{1}{\alpha_n}(1 - e^{-\alpha_n t}) - \frac{1}{k_a}(1 - e^{-k_at})\right] \qquad \text{(Eq. 11)}$$

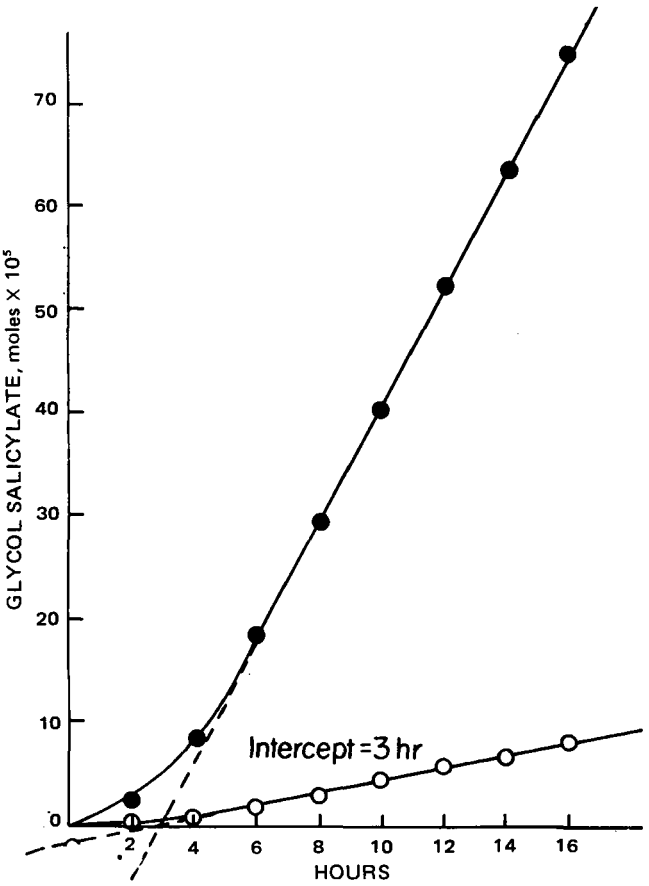

Figure 1—*Accumulative urinary salicylate data showing influence of moisture on percutaneous absorption rate of glycol salicylate. Key: ●, hydrous system rate, 11.7; and ○, anhydrous system rate, 1.3. (Reproduced, with permission, from Fig. 7 of Ref. 3.)*

which has the asymptotic limit:

$$M_A = \lim_{\substack{k_a t \gg 1 \\ k_D t \gg 1}} M = \frac{Q_a}{k_a}\left(t - \frac{1}{k_a} - \frac{1}{k_D}\right) \qquad \text{(Eq. 12)}$$

Thus, M is linear at long times and has an intercept or lag time of:

$$t_L = \frac{1}{k_a} + \frac{1}{k_D} \qquad \text{(Eq. 13)}$$

and a slope of Q_a/k_a.

For $k_a \gg k_D$, t_L is just the diffusional lag time; for $k_D \gg k_a$, the intercept is just the reciprocal of the adjusted excretion rate constant, k_a. The slope, $Q_a/k_a = Q/k$, is not affected by binding in the body fluids or by tissue absorption, whereas the lag time is increased by fluid binding and tissue absorption.

APPLICATIONS

To illustrate the usefulness of the results derived in the previous section, the model is applied to interpret the data of Wurster and Kramer (3). Figure 1 is a graph of the amount of salicylate excreted in the urine as a function of time for a topical application of glycol salicylate[1]. The amount excreted does indeed become linear after 6 hr, and the lag time is about 3 hr. The slope of the linear portion of the curve should be given by:

$$\text{slope} = k_U\left(\frac{Q}{k}\right) = \frac{Q}{1+\Delta} \qquad \text{(Eq. 14)}$$

where $\Delta = (k_M + k_B)/k_U$ (k_M refers to the rate constant for metabolism to a compound other than salicylic acid).

[1] Since the data do not distinguish between salicylic acid and glycol salicylate in the urine, it is assumed that glycol salicylate is rapidly converted to salicylic acid or that both species have the same elimination kinetics. Both of these possibilities are consistent with the lag time equal to $k_a^{-1} = 3.45$ hr.

If $\Delta \ll 1$, then the slope is a direct measure of the *in vivo* steady-state flux, and the permeability coefficient is just:

$$k_{per} \simeq \frac{\text{slope}}{AC_{GS}} \qquad \text{(Eq. 15)}$$

where C_{GS} is the concentration of glycol salicylate applied to the skin. From Eq. 14, one observes that the permeability coefficient is underestimated by the factor $1 + \Delta$. Thus, if the urinary excretion rate is not large with respect to the other elimination rates, the permeability coefficient is significantly underestimated.

The parameter Δ can be approximated from the urinary recovery after intravenous injection. The elimination is governed by:

$$\frac{dS}{dt} = -k_a S \qquad \text{(Eq. 16)}$$

which has the solution:

$$S = S_0 e^{-k_a t} \qquad \text{(Eq. 17)}$$

where S_0 is the initial amount in solution, and $S_0\delta$ is the total amount injected. Since Wurster and Kramer (3) determined the elimination rate constant from the slope of the logarithm of the urinary excretion rate, $k_U S$, *versus* time, they essentially measured k_a. The total amount excreted in the urine is:

$$\int_0^t dt k_U S = \frac{S_0\delta}{1+\Delta}(1 - e^{-k_a t}) \qquad \text{(Eq. 18)}$$

so that the 90% recovery of Wurster and Kramer estimates $\Delta = 0.11$. Thus, the *in vivo* permeability coefficient is given by:

$$k_{per} = 1.11\left(\frac{\text{slope}}{AC_{GS}}\right) \qquad \text{(Eq. 19)}$$

The diffusional lag time is small, since k_a^{-1} is almost identical with the excretion lag time of Fig. 1. Thus, a knowledge of the excretion rate constant and the urinary excretion lag time permits one to estimate the diffusional lag time.

DISCUSSION

Permeability coefficients for skin can be measured *in vivo* from excretion data, provided that the excretion rate is proportional to the drug concentration in the body fluids. The asymptotic limit for the amount of material excreted is linear in time. The slope of the asymptotic limit is dependent upon the particular excretion path, but the lag time is identical for all paths of elimination. Tissue absorption and binding to proteins in the body fluids do not alter the asymptotic slope but do increase the lag time contribution from the excretion process.

Accurate determination of the skin permeability coefficient requires a knowledge of all rates of elimination. However, the percent recovery in the urine following intravenous injection provides an estimate of the magnitude of the error involved in computing the permeability coefficient from the urinary excretion rate. Thus, one can obtain reasonable estimates of skin permeability coefficients *in vivo* by measuring urinary excretion.

If the skin metabolizes the drug to some degree before it enters the body fluids, the preceding arguments have to be modified. A term has to be added to the diffusion equation to account for the kinetics of the reaction taking place in the skin. *In vivo* permeability coefficients determined by ignoring skin metabolism would clearly be significantly smaller than those measured *in vitro* if skin metabolism is an important process.

REFERENCES

(1) R. J. Scheuplein and I. H. Blank, *Physiol. Rev.*, **51**, 702(1971).

(2) D. L. Sekura and J. Scala, in "Pharmacology and the Skin," W. Montagna, R. B. Stoughton, and E. J. Van Scott, Eds., Appleton-Century-Crofts, New York, N.Y., 1972.

(3) D. E. Wurster and S. F. Kramer, *J. Pharm. Sci.*, **50**, 288(1961).

(4) J. Crank, "The Mathematics of Diffusion," Oxford University Press, Oxford, England, 1970.

ACKNOWLEDGMENTS AND ADDRESSES

Received July 14, 1975, from the *Miami Valley Laboratories, Procter & Gamble Company, Cincinnati, OH 45247*

Accepted for publication November 21, 1975.

Antinauseant and Antiemetic Properties of Bismuth Subsalicylate in Dogs and Humans

MARVIN M. GOLDENBERG ˣ, LEROY J. HONKOMP, and CHARLES S. DAVIS

Abstract □ Laboratory and clinical investigations were carried out to determine the effectiveness of bismuth subsalicylate in allaying nausea by preventing the physical symptom of emesis. In normal conscious dogs, a bismuth subsalicylate formulation caused a dose-related reduction in the incidence of vomiting in response to an emetic dose of ipecac syrup. In normal human subjects, a bismuth subsalicylate suspension, unlike the placebo formulation, successfully subdued nausea and vomiting in 66.7 and 80% of the subjects, respectively, in response to ipecac syrup. Both findings demonstrate that bismuth subsalicylate can provide antiemetic action and that the decrease in the occurrence of emesis in humans and dogs parallels the decrease in nausea found in humans and the nausea suspected to occur prior to emesis in dogs.

Keyphrases □ Bismuth subsalicylate—antinauseant and antiemetic properties evaluated, dogs and humans □ Antinauseants—bismuth subsalicylate, effect after ipecac dosing, dogs and humans □ Antiemetics—bismuth subsalicylate, effect after ipecac dosing, dogs and humans

Nausea, retching, and vomiting comprise the typical stages relative to emesis in humans (1, 2). The symptoms of nausea and vomiting are associated with many clinical conditions, *e.g.*, acute gastritis or gastroenteritis and dyspepsia induced by alcohol, food intolerances, aspirin, steroids, pregnancy, motion, and other physical and psychological stresses. Antihistamines and phenothiazine derivatives are commonly used in the treatment of nausea and vomiting, but side effects (sedation, hypotension, and drowsiness) limit or preclude their use (3). These unwanted side effects can be avoided by the use of various salts of bismuth, which have been used in the treatment of gastritis and dyspepsia (4).

Various stimuli may induce a chain of events leading to nausea. Clinicians agree that nausea is easily and commonly described for humans (5); this symptom in intact animals, however, is virtually impossible to detect (6). Rarely does an individual vomit without first being nauseated. It follows then that, if the incidence of vomiting is decreased, so also will be the incidence of nausea.

The emetic mechanism in human gastritis parallels that of drugs that induce emesis by gastric irritation (7). The premise that a salt of bismuth, such as bismuth subsalicylate[1], would be effective in allaying nausea induced by an emetic agent (ipecac syrup) was examined in both dogs and humans. For the dog, the physiological event of emesis was used as acceptable, objective evidence of the antinauseant property of bismuth subsalicylate. In humans, both antinauseant and antiemetic activities of bismuth subsalicylate were more definitively evaluated.

EXPERIMENTAL

Dogs—Twelve adult dogs[2] of mixed breed and of either sex, 8.5–24.3 kg, were used. Preliminary screening for an emetic dose of ipecac syrup USP in the dog, representing a dose that was reliably effective but yet not overwhelmingly drastic or potentially toxic, revealed that 0.5 ml/kg orally induced such an effect in 90% of the dogs tested.

A bismuth subsalicylate formulation (an 8.75% suspension in magnesium aluminum silicate[3]–methylcellulose–water vehicle) was administered orally to each dog at doses of 0.5, 1.0, or 2.0 ml/kg 10 min prior to 0.5 ml/kg of ipecac syrup. The dog was observed for emesis for up to 3 hr after the dose of ipecac syrup. Only one dose of bismuth subsalicylate was given to each dog in any given test day, and there was always at least 1 day of rest between tests.

On one occasion, each dog was pretreated with 2 ml/kg of water (a volume equivalent to the highest dose of the bismuth subsalicylate suspension) 10 min before the standard ipecac syrup dose (0.5 ml/kg) to test a potential antiemetic effect through mere dilution of the syrup. A final experiment in which the highest dose of bismuth subsalicylate was administered (not followed by ipecac syrup) was included to rule out conditioned emesis in this group of dogs. The data obtained from these studies were statistically analyzed for significance using the Sign test (8).

Humans—Forty healthy adult men and women, between the ages of 21 and 40 with no history of GI, renal, or cardiac disease, participated in the study. All subjects refrained from food or drink 10 hr before and during the study. The subjects were matched by sex and were randomly assigned to treatment pairs without regard to weight.

One member of each pair received a dose of ipecac syrup followed immediately by 30 ml of the bismuth subsalicylate formulation (a 1.75% suspension in magnesium aluminum silicate–methylcellulose with flavor, coloring, and water); the remaining member received the same dose of ipecac syrup followed immediately by 30 ml of the placebo formulation (containing flavor, coloring, 0.1% titanium dioxide, and water). A second dose of the appropriate liquid formulation was given 30 min after the initial dose. All subjects were observed for at least 3 hr, and each subject wrote a report describing any symptoms which developed.

To minimize human discomfort, a sequential method of statistical analysis was employed. Four groups of 10 subjects were evaluated sequentially and, when a statistically significant conclusion was reached (restricted binomial plan) (9), the study was terminated. Because of the violently disagreeable nature of the response to ipecac syrup in the subjects, it was necessary to adjust the dose as the study progressed; *i.e.*, Group I received 15 ml of ipecac syrup, Group II received 7.5 ml, and Groups III and IV received 5 ml. From the study design, one of three conclusions could be reached: Treatment A (bismuth subsalicylate formulation) was more effective, Treatment B (placebo formulation) was more effective, or no difference between treatments existed.

A four-point scale was developed to evaluate the severity of symptoms described by each subject: 0, subject felt fine throughout study (possible slight gas or queasiness); 1, subject definitely nauseated with or without upset stomach, cramping, or headache; 2, subject vomited at least once (felt well within approximately 1 hr);

[1] Principal active constituent in Pepto-Bismol, Morton-Norwich Products, Inc.

[2] Raised at the Animal Research Center, Norwich Pharmacal Co., Norwich, N.Y.

[3] Veegum, R. T. Vanderbilt Co.

Table I—Effect of Bismuth Subsalicylate Formulation or Water on the Incidence of Emesis Induced by Ipecac Syrup in Dogs[a]

Dog	Weight, kg	Doses of Bismuth Subsalicylate Formulation (8.75%)[b] 0.5 ml/kg	1.0 ml/kg	2.0 ml/kg	Water[b], 2 ml/kg	Bismuth Subsalicylate Formulation (8.75%)[c], 2 ml/kg
1	23.3	+	—	+	—	—
2	20.6	—	—	—	—	—
3	21.3	—	+	—	+	—
4	17.4	+	—	—	+	—
5	23.7	—	—	—	+	—
6	20.1	+	+	—	+	—
7	11.7	—	—	—	+	—
8	12.1	—	—	—	+	—
9	8.5	+	+	—	+	—
10	9.7	+	—	—	—	—
11	10.2	—	+	—	+	—
12	11.6	+	+	+	+	—
Number of dogs vomiting		6/12	5/12	2/12[d]	9/12	0/12
Total number dosed		50	58	87[d]	25	—
Percent protected						

[a] + = emesis, and − = no emesis. [b] Ten minutes prior to 0.5 ml/kg of ipecac syrup USP. [c] Dose of ipecac syrup not administered. [d] Significantly different from water-treatment control group; $p = 0.0195$, Sign test.

Table II—Effect of Bismuth Subsalicylate Formulation and Placebo on the Relief of Symptoms Induced by Various Doses of Ipecac Syrup in Human Subjects

Group[a]	Total Dose of Ipecac Syrup, ml	Relief of Ipecac-Induced Symptoms: Treatment A[b], Average Score[d]	Treatment B[c], Average Score[d]
I	15	1.8	2.4
II	7.5	0.6	2.0
III	5.0	0.6	1.8
IV	5.0	0.8	2.0

[a] Each group consisted of five pairs of subjects. [b] Thirty milliliters of bismuth subsalicylate formulation (1.75%) followed in 0.5 hr by another 30 ml. [c] Thirty milliliters of placebo formulation followed in 0.5 hr by another 30 ml. [d] Mean of the responses obtained on the basis of the response key described under *Experimental.*

and 3, subject experienced severe nausea and vomiting with headache and malaise (symptoms lasted considerably longer than 1 hr).

The data obtained from this clinical study were analyzed statistically for significance employing the χ-square test.

RESULTS

Dogs—As summarized in Table I, the bismuth subsalicylate formulation (8.75% suspension), 0.5 ml/kg in 12 dogs, protected 50% of the animals from the vomiting dose of ipecac syrup. By increasing the doses of the bismuth subsalicylate formulation to 1 and 2 ml/kg, there was a respective dose-related increase (58 and 87%) in protection against the emetic effect of ipecac syrup.

In the control group, 2 ml/kg of water prevented vomiting in 25% of the dogs treated. However, there was still a significant difference found between this control group and the bismuth subsalicylate group (87% protection at 2 ml/kg). None of the dogs vomited with the highest dose of bismuth subsalicylate administered alone.

Humans—In 10 subjects, ipecac syrup, in 15-ml total doses, caused severe and potentially harmful GI symptoms, which were not alleviated by either Treatment A (bismuth subsalicylate formulation) or Treatment B (placebo formulation) (Table II). To avoid such symptoms, the dose of ipecac syrup was lowered to 7.5 ml. At this dose, two patients treated with placebo exhibited grade 3 responses; the average score of these placebo-treated patients was 2 (Table II), indicating relatively little protection. Less severe symptoms were noted following the bismuth subsalicylate formulation (1.75%) administration; the average score was reduced to 0.6, indicating that protection was afforded. In Groups III and IV, when the dose of ipecac syrup administered was 5 ml, treatment with bismuth subsalicylate more effectively relieved the untoward symptoms as opposed to the subjects receiving the placebo.

Table III—Effect of Bismuth Subsalicylate Formulation and Placebo on Symptoms of Nausea and Vomiting in Response to Ipecac Syrup in Human Subjects

Group[a]	Treatment A[b]: Absence of Nausea	Protection from Nausea, %	Absence of Vomiting	Protection from Vomiting, %	Treatment B[c]: Absence of Nausea	Protection from Nausea, %	Absence of Vomiting	Protection from Vomiting, %
I[d]	1/5[e]	20	1/5[f]	20	0/5[e]	0	0/5[e]	0
II	3/5	60	4/5	80	0/5	0	2/5	40
III	3/5	60	4/5	80	1/5	20	1/5	20
IV	4/5	80	4/5	80	0/5	0	0/5	0
Total number in Groups II, III, and IV	10/15		12/15		1/15		3/15	
Mean protection in Groups II, III, and IV		66.7[g]		80[g]		7		20

[a] Each group consisted of five pairs of subjects. [b] Thirty milliliters of bismuth subsalicylate formulation (1.75%) followed in 0.5 hr by another 30 ml. [c] Thirty milliliters of placebo formulation followed in 0.5 hr by another 30 ml. [d] Explanation for not pooling these data was discussed under *Results.* [e] Number without nausea/number treated. [f] Number not vomiting/number treated. [g] Significantly different from Treatment B using χ-square test; $p = 0.05$ or less.

Table III summarizes the results of the study of the two test formulations in preventing nausea and vomiting in subjects receiving ipecac syrup. Because of the small number of subjects, it was necessary to pool the results in Groups II–IV for Treatment A or B. Pooling of the data was determined to be permissible since sequential testing revealed that no differences in response existed among Groups II–IV and, according to the binomial theorem of analysis, these groups were not significantly different. However, Group I was significantly different from each of the other groups and was not pooled with the three groups. The high dose of ipecac syrup in Group I caused severe GI irritation along with other marked side effects.

When the results of Groups II–IV were combined, 66.7% of the subjects failed to experience nausea following bismuth subsalicylate while only 7% were not nauseated by the ipecac syrup after the placebo administration. The act of vomiting in response to ipecac syrup was completely prevented in 80% of the subjects (Groups II–IV) treated with the bismuth subsalicylate formulation, and the placebo formulation afforded 20% protection. χ-Square statistical evaluation for the difference between patients receiving bismuth subsalicylate and those receiving the placebo formulation indicated that bismuth subsalicylate is significantly superior in its ability to control nausea and vomiting compared to the placebo formulation.

DISCUSSION

The mechanism of action of ipecac, or its principal alkaloid emetine, with respect to the induction of vomiting is poorly understood, although standard pharmacology texts generally agree that both a local and a central component are involved. In the present study, ipecac syrup was used to induce vomiting in dogs and nausea and vomiting in humans. After establishing the dose of ipecac syrup necessary to meet the criteria of a reliably effective, but not overwhelmingly drastic, emetic, it was found that bismuth subsalicylate formulation elicited a dose-related protective effect against ipecac syrup-induced emesis in the dog.

The laboratory evidence was corroborated by clinical evidence, in which it was revealed that the bismuth subsalicylate formulation was capable of arresting both nausea and vomiting in response to doses of ipecac syrup capable of inducing mild GI upset in humans. In the clinical study, it was necessary to adjust the dose of ipecac syrup to avoid the severe and harsh symptoms induced by the emetic. When utilizing the doses (5.0 and 7.5 ml) of ipecac syrup that appeared to mimic the symptoms of nonspecific GI upset and irritation in humans, the signs and symptoms of ipecac syrup ingestion were easily reproducible. Bismuth subsalicylate, unlike the placebo suspension, successfully controlled the nausea and vomiting in 66.7 and 80% of the subjects, respectively, in response to ipecac syrup.

Thus, both laboratory and clinical findings concur that bismuth subsalicylate provides antiemetic protection against the effects of ipecac syrup and that the decrease in the incidence of emesis in humans and dogs parallels the decreased incidence of nausea noted in humans and the nausea suspected to occur prior to vomiting in the dog.

REFERENCES

(1) J. S. Fordtran, in "Vomiting in Gastrointestinal Disease," M. H. Sleisenger and J. S. Fordtran, Eds., Saunders, Philadelphia, Pa., 1973, pp. 127–143.

(2) W. H. Resnik, "Principles of Internal Medicine," 5th ed., McGraw-Hill, New York, N.Y., 1966, pp. 107–110.

(3) J. W. Bellville, in "Drugs of Choice 1972–1973," W. Modell, Ed., Mosby, St. Louis, Mo., 1972, pp. 294–305.

(4) L. Jaenicke, "Bismuth—A Survey of the Pharmacology and Medicinal Uses," Mining and Chemical Products, Ltd., London, England, 1950, pp. 1–44.

(5) F. A. Jones, J. W. P. Gummer, and J. E. Lennard-Jones, "Clinical Gastroenterology," 2nd ed., Blackwell Scientific Publications, Oxford, England, 1968, p. 15.

(6) S. Wolf, *Gastroenterology*, **12**, 212(1949).

(7) J. H. Moyer, "Effective Antiemetic Agents," Medical Clinics of North America, Saunders, Philadelphia, Pa., 1957, pp. 405–432.

(8) K. A. Brownlee, "Statistical Theory and Methodology in Science and Engineering," 2nd ed., Wiley, New York, N.Y., 1965, p. 242.

(9) P. Armitage, "Sequential Medical Trials," 1st ed., Blackwell Scientific Publications, Oxford, England, 1960, pp. 25–47.

ACKNOWLEDGMENTS AND ADDRESSES

Received September 19, 1975, from the *Norwich Pharmacal Company, Division of Morton-Norwich Products, Inc., Norwich, NY 13815*

Accepted for publication November 26, 1975.

The authors thank Mr. R. H. Burns and Mr. P. J. Schmitz for technical assistance, Dr. A. W. Castellion for advice, and Mr. Ching-Tsao Tu and Dr. R. P. Basson for assistance in the statistical analysis.

[x] To whom inquiries should be directed.

Solid-State Anomalies in IR Spectra of Compounds of Pharmaceutical Interest

S. C. MUTHA [x] and W. B. LUDEMANN

Abstract □ Solid-state anomalies in the IR spectra of lysine monohydrochloride, etoxadrol hydrochloride, thiamine hydrochloride, and L-histidine in a potassium bromide matrix were noted. With the first three compounds, the anomalies were due to metathetical exchange of the halide anion between the compound and the matrix. The anomaly seen with L-histidine was related to the crystal structure.

Keyphrases □ IR spectroscopy—solid-state anomalies, lysine monohydrochloride, etoxadrol hydrochloride, thiamine hydrochloride, and L-histidine □ Lysine monohydrochloride—IR spectra, solid-state anomalies □ Etoxadrol hydrochloride—IR spectra, solid-state anomalies □ Thiamine hydrochloride—IR spectra, solid-state anomalies □ L-Histidine—IR spectra, solid-state anomalies

It is well known that IR absorption spectra of solids depend on both structure and crystalline form. Variations between mull and pellet spectra are due either to an induced physical isomerization or to the samples having been rendered amorphous in the alkali halide pellet (1). In addition, the observed spectra from dif-

Table III summarizes the results of the study of the two test formulations in preventing nausea and vomiting in subjects receiving ipecac syrup. Because of the small number of subjects, it was necessary to pool the results in Groups II–IV for Treatment A or B. Pooling of the data was determined to be permissible since sequential testing revealed that no differences in response existed among Groups II–IV and, according to the binomial theorem of analysis, these groups were not significantly different. However, Group I was significantly different from each of the other groups and was not pooled with the three groups. The high dose of ipecac syrup in Group I caused severe GI irritation along with other marked side effects.

When the results of Groups II–IV were combined, 66.7% of the subjects failed to experience nausea following bismuth subsalicylate while only 7% were not nauseated by the ipecac syrup after the placebo administration. The act of vomiting in response to ipecac syrup was completely prevented in 80% of the subjects (Groups II–IV) treated with the bismuth subsalicylate formulation, and the placebo formulation afforded 20% protection. χ-Square statistical evaluation for the difference between patients receiving bismuth subsalicylate and those receiving the placebo formulation indicated that bismuth subsalicylate is significantly superior in its ability to control nausea and vomiting compared to the placebo formulation.

DISCUSSION

The mechanism of action of ipecac, or its principal alkaloid emetine, with respect to the induction of vomiting is poorly understood, although standard pharmacology texts generally agree that both a local and a central component are involved. In the present study, ipecac syrup was used to induce vomiting in dogs and nausea and vomiting in humans. After establishing the dose of ipecac syrup necessary to meet the criteria of a reliably effective, but not overwhelmingly drastic, emetic, it was found that bismuth subsalicylate formulation elicited a dose-related protective effect against ipecac syrup-induced emesis in the dog.

The laboratory evidence was corroborated by clinical evidence, in which it was revealed that the bismuth subsalicylate formulation was capable of arresting both nausea and vomiting in response to doses of ipecac syrup capable of inducing mild GI upset in humans. In the clinical study, it was necessary to adjust the dose of ipecac syrup to avoid the severe and harsh symptoms induced by the emetic. When utilizing the doses (5.0 and 7.5 ml) of ipecac syrup that appeared to mimic the symptoms of nonspecific GI upset and irritation in humans, the signs and symptoms of ipecac syrup ingestion were easily reproducible. Bismuth subsalicylate, unlike the placebo suspension, successfully controlled the nausea and vomiting in 66.7 and 80% of the subjects, respectively, in response to ipecac syrup.

Thus, both laboratory and clinical findings concur that bismuth subsalicylate provides antiemetic protection against the effects of ipecac syrup and that the decrease in the incidence of emesis in humans and dogs parallels the decreased incidence of nausea noted in humans and the nausea suspected to occur prior to vomiting in the dog.

REFERENCES

(1) J. S. Fordtran, in "Vomiting in Gastrointestinal Disease," M. H. Sleisenger and J. S. Fordtran, Eds., Saunders, Philadelphia, Pa., 1973, pp. 127–143.

(2) W. H. Resnik, "Principles of Internal Medicine," 5th ed., McGraw-Hill, New York, N.Y., 1966, pp. 107–110.

(3) J. W. Bellville, in "Drugs of Choice 1972–1973," W. Modell, Ed., Mosby, St. Louis, Mo., 1972, pp. 294–305.

(4) L. Jaenicke, "Bismuth—A Survey of the Pharmacology and Medicinal Uses," Mining and Chemical Products, Ltd., London, England, 1950, pp. 1–44.

(5) F. A. Jones, J. W. P. Gummer, and J. E. Lennard-Jones, "Clinical Gastroenterology," 2nd ed., Blackwell Scientific Publications, Oxford, England, 1968, p. 15.

(6) S. Wolf, *Gastroenterology*, **12**, 212(1949).

(7) J. H. Moyer, "Effective Antiemetic Agents," Medical Clinics of North America, Saunders, Philadelphia, Pa., 1957, pp. 405–432.

(8) K. A. Brownlee, "Statistical Theory and Methodology in Science and Engineering," 2nd ed., Wiley, New York, N.Y., 1965, p. 242.

(9) P. Armitage, "Sequential Medical Trials," 1st ed., Blackwell Scientific Publications, Oxford, England, 1960, pp. 25–47.

ACKNOWLEDGMENTS AND ADDRESSES

Received September 19, 1975, from the *Norwich Pharmacal Company, Division of Morton-Norwich Products, Inc., Norwich, NY 13815*

Accepted for publication November 26, 1975.

The authors thank Mr. R. H. Burns and Mr. P. J. Schmitz for technical assistance, Dr. A. W. Castellion for advice, and Mr. Ching-Tsao Tu and Dr. R. P. Basson for assistance in the statistical analysis.

[x] To whom inquiries should be directed.

Solid-State Anomalies in IR Spectra of Compounds of Pharmaceutical Interest

S. C. MUTHA [x] and W. B. LUDEMANN

Abstract □ Solid-state anomalies in the IR spectra of lysine monohydrochloride, etoxadrol hydrochloride, thiamine hydrochloride, and L-histidine in a potassium bromide matrix were noted. With the first three compounds, the anomalies were due to metathetical exchange of the halide anion between the compound and the matrix. The anomaly seen with L-histidine was related to the crystal structure.

Keyphrases □ IR spectroscopy—solid-state anomalies, lysine monohydrochloride, etoxadrol hydrochloride, thiamine hydrochloride, and L-histidine □ Lysine monohydrochloride—IR spectra, solid-state anomalies □ Etoxadrol hydrochloride—IR spectra, solid-state anomalies □ Thiamine hydrochloride—IR spectra, solid-state anomalies □ L-Histidine—IR spectra, solid-state anomalies

It is well known that IR absorption spectra of solids depend on both structure and crystalline form. Variations between mull and pellet spectra are due either to an induced physical isomerization or to the samples having been rendered amorphous in the alkali halide pellet (1). In addition, the observed spectra from dif-

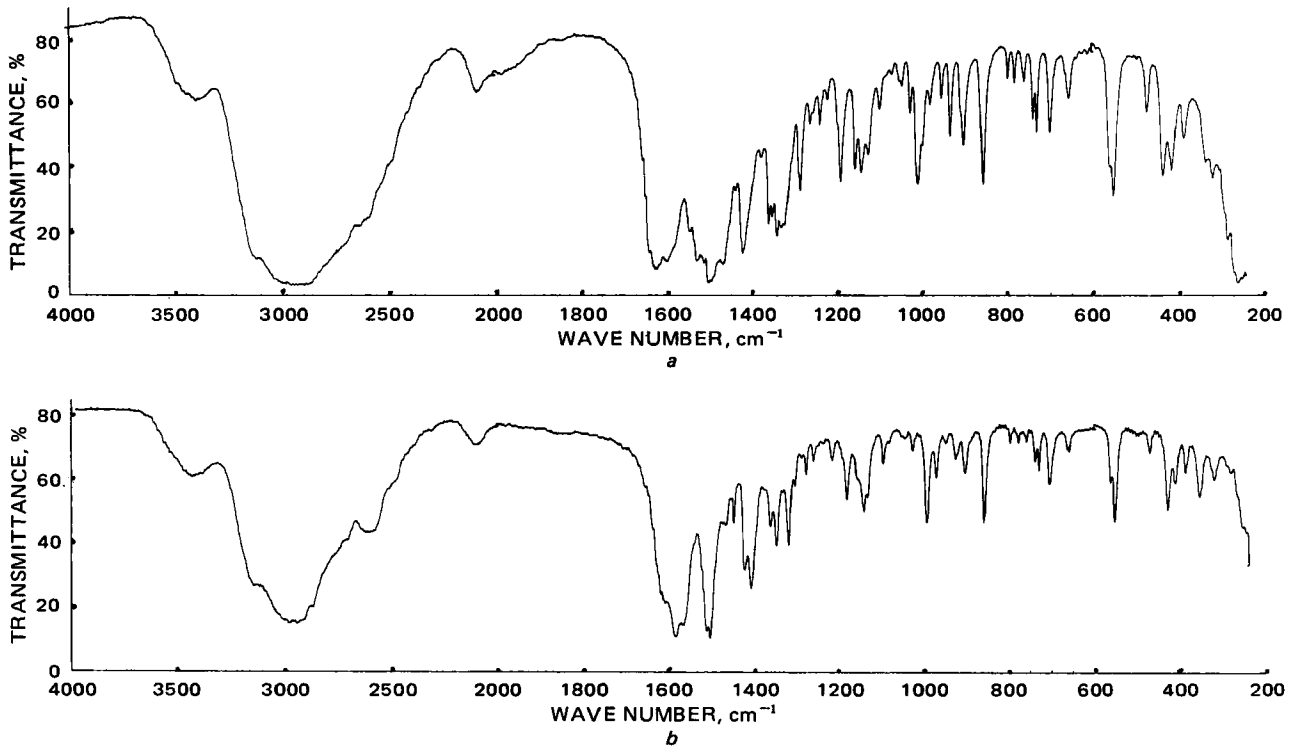

Figure 1—*IR spectra of:* (a) L-*lysine monohydrochloride in potassium chloride pellet (20,000 psi), and* (b) L-*lysine monohydrochloride in potassium bromide pellet (20,000 psi).

ferent dispersion media may not be identical because of anion exchange between the sample and the matrix. Several anomalies of these types have been noted in the IR spectra of compounds of pharmaceutical interest. This paper reports three cases demonstrating the importance of a matched matrix and one case where crystal structure is dependent on the solvent of crystallization.

EXPERIMENTAL

Materials—The following compounds were used: L-lysine monohydrochloride[1], etoxadrol hydrochloride[2] [(+)-2-(2-ethyl-2-phenyl-1,3-dioxolan-4-yl)piperidine hydrochloride] (I), etoxadrol hydrobromide[3] (II), thiamine hydrochloride[4], and L-histidine[5].

Equipment—All IR spectra were recorded on a grating spectrophotometer[6].

Procedures—Pellets of these compounds, using a potassium bromide or potassium chloride matrix, were prepared. Where necessary, spectra were obtained in mineral oil mulls between potassium bromide disks. Histidine was crystallized by the following procedures.

Water Recrystallization—One gram was dissolved in 5 ml of distilled water, heated on a steam bath until dissolved, and then cooled.

80% Ethanol Recrystallization—About 0.5 g was dissolved in 2 ml of hot distilled water, and 8 ml of absolute alcohol was added. Crystals were collected on filter paper[7] and dried overnight under vacuum at 60°

RESULTS AND DISCUSSION

L-Lysine Monohydrochloride, Etoxadrol Hydrochloride, and Thiamine Hydrochloride—Spectra of L-lysine monohydrochloride (Fig. 1*a*), I (Fig. 2*a*), and thiamine hydrochloride (Fig. 3*a*) were recorded in a potassium chloride pellet. Spectra of these compounds were also obtained in a mineral mull. No differences were noted in these two types of spectra in the window region of the mineral mull. However, when potassium bromide pellets of these compounds were prepared at 20,000 psi and spectra were recorded, significant changes were noted compared to the corresponding potassium chloride pellet spectra (Figs. 1*b*–3*b*). If the pressure used in the preparation of potassium bromide pellets was decreased to 10,000 psi, the spectra were identical to the corresponding spectra in the potassium chloride pellet.

These changes in the IR spectra were due to the exchange of halide anions between the compound and the potassium halide matrix. This result is best illustrated in the case of I. Spectra of I (Fig. 2*b*) and II (Fig. 2*c*) were obtained in the potassium bromide matrix. The pressure used in the preparation of the pellet in both cases was 20,000 psi. The spectra thus obtained were identical.

The spectrum of I obtained in the potassium chloride (Fig. 2*a*) matrix was dramatically different from the one obtained in potassium bromide (Fig. 2*b*). The potassium bromide pellets of I, prepared at 15,000 psi, contained all corresponding maxima for hydrochloride and hydrobromide salts, indicating an equilibrium situation. When the pressure was changed from 10,000 to 20,000 psi in preparing the potassium chloride pellets, no such changes were noted.

L-Histidine Base—The spectrum of L-histidine[8] was obtained in the potassium bromide pellet (Fig. 4*a*). This spectrum did not match with the in-house standard[9] spectrum (Fig. 4*b*). This lot passed all other tests, such as specific rotation, assay, nitrogen content, and TLC homogeneity, so the compound certainly was histidine. The difference seen could have been due to crystal structure.

Two common solvents used for the crystallization of amino acids are water and 80% ethanol. When L-histidine was recrystallized from 80% ethanol, it gave a spectrum identical to the in-house standard. Similarly, when the in-house reference standard was crystallized from water, it gave a spectrum identical to the L-histidine.

Conclusions—Both USP and NF recommend that the IR spectra of all hydrochlorides be obtained in potassium bromide pellets. Hayden *et al.* (2) recommended that the spectra of halide salts be obtained in the matched matrix. Three of the examples noted here

[1] Ajinomoto lot 19590 and USP reference standard.
[2] CL 1848C, Cutter Laboratories, Berkeley, Calif.
[3] Cutter Laboratories, Berkeley, Calif.
[4] Hoffmann–La Roche lot 030091 and USP reference standard.
[5] Ajinomoto lot 19060 and Calbiochem A grade lot 64418 used as the in-house standard.
[6] Perkin-Elmer model 457.
[7] Whatman No. 2.
[8] Ajinomoto lot 19060.
[9] Calbiochem A grade lot 64418.

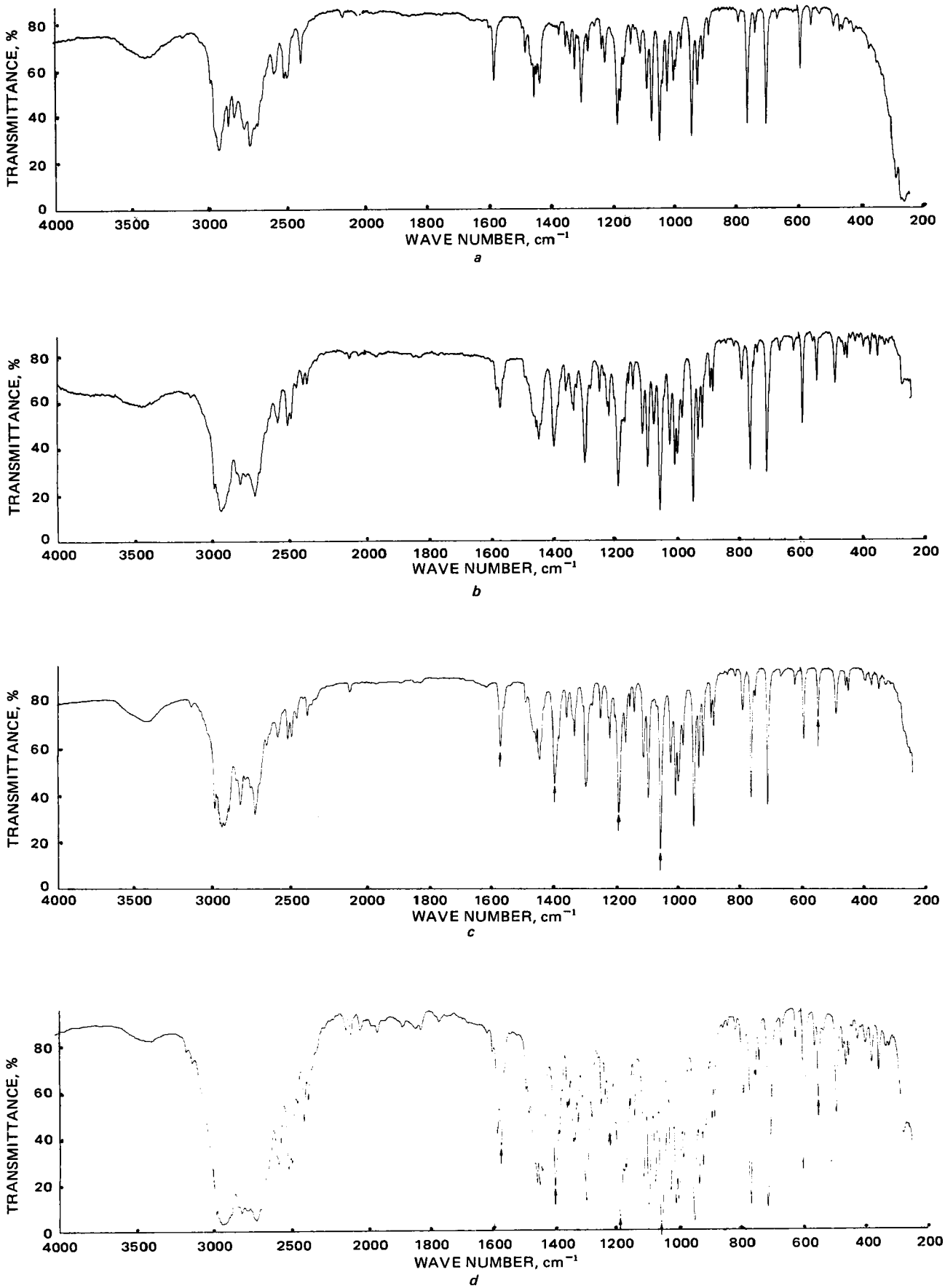

Figure 2—*IR spectra of:* (a) *I in potassium chloride pellet (20,000 psi),* (b) *I in potassium bromide pellet (20,000 psi),* (c) *II in potassium bromide pellet (20,000 psi), and* (d) *I in potassium bromide pellet (15,000 psi).*

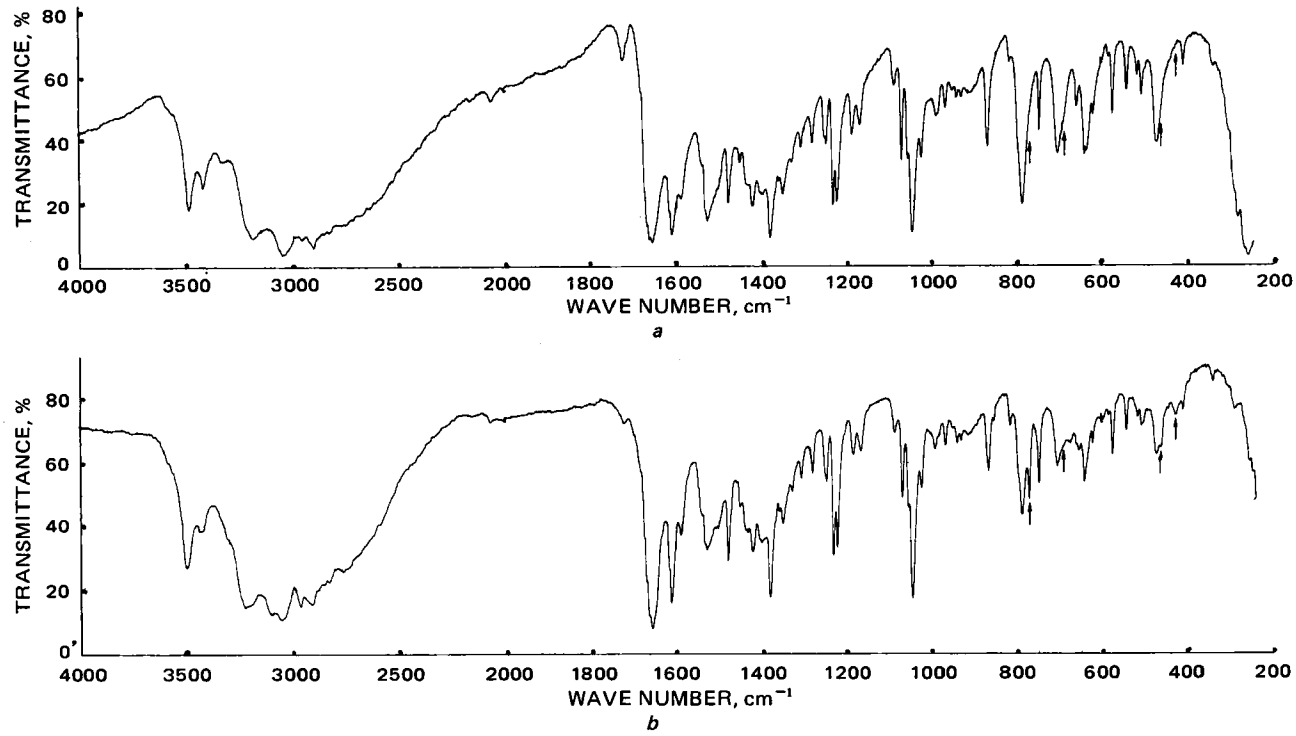

Figure 3—*IR spectra of:* (a) *thiamine hydrochloride in potassium chloride pellet (20,000 psi), and* (b) *thiamine hydrochloride in potassium bromide pellet (20,000 psi).*

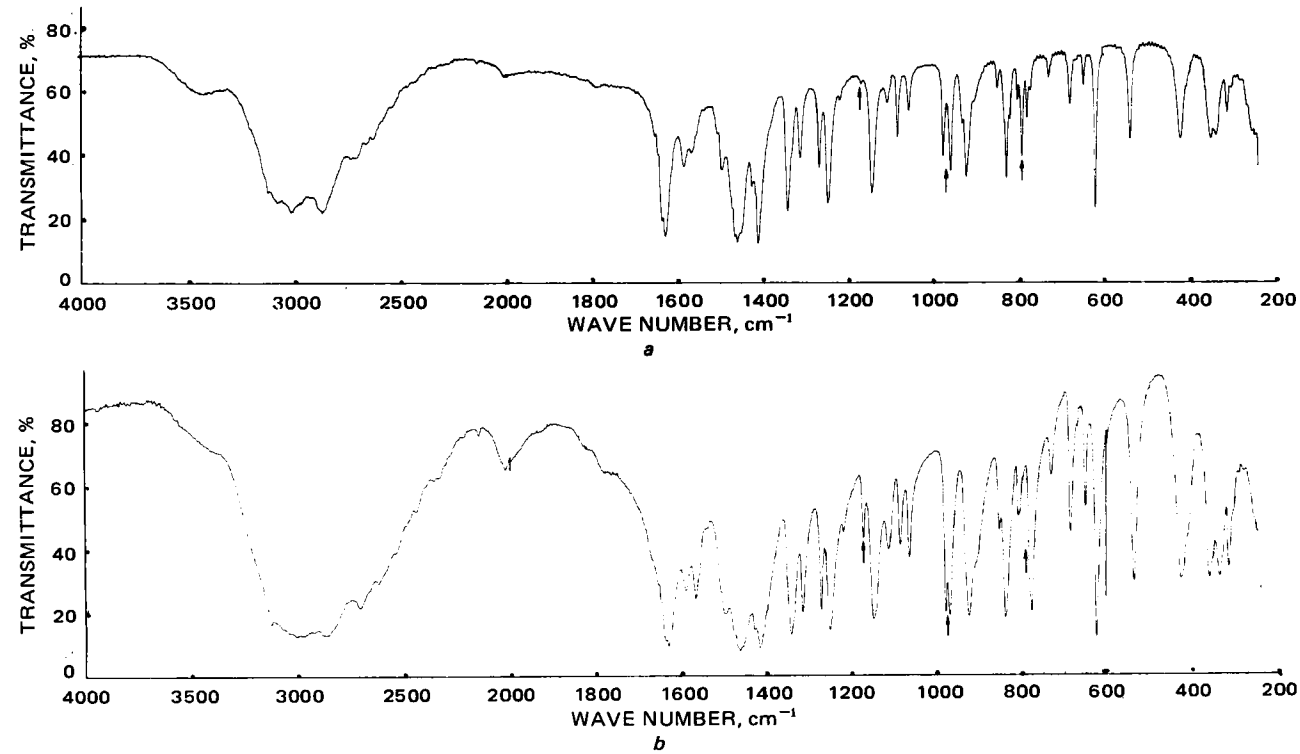

Figure 4—*IR spectra of:* (a) L-*histidine (Ajinomoto) in potassium bromide pellet (crystallized from water), and* (b) L-*histidine (Calbiochem) in potassium bromide pellet [crystallized from 80% (v/v) ethanol].*

also demonstrate that the spectra of halide salts be obtained in the corresponding potassium halide matrix.

IR spectra are dependent on the crystalline form; therefore, the solvent of recrystallization should be noted.

REFERENCES

(1) A. W. Baker, *J. Phys. Chem.*, **61**, 450(1957).

(2) A. L. Hayden, R. Sammul, G. B. Selzer, and J. Carol, *J. Assoc. Offic. Agri. Chem.*, **45**, 797(1962).

ACKNOWLEDGMENTS AND ADDRESSES

Received July 28, 1975, from the *Department of Analytical Services, Cutter Laboratories, Berkeley, CA 94710*

Accepted for publication November 7, 1975.

[x] To whom inquiries should be directed.

Topical Mosquito Repellents IX: Quinolines, Isoquinolines, and Quinoxalines

W. A. SKINNER ˣ, H. T. CRAWFORD, H. TONG, D. SKIDMORE *, and H. I. MAIBACH *

Abstract □ Various quinoxalines, quinolines, and isoquinolines were evaluated for their effectiveness as topical mosquito repellents. Several tetrahydroquinolines and isoquinolines also were included. None of the compounds tested was superior to diethyltoluamide.

Keyphrases □ Quinolines, substituted—synthesized, effectiveness as topical mosquito repellents evaluated □ Quinoxalines, substituted—synthesized, effectiveness as topical mosquito repellents evaluated □ Isoquinolines, substituted—synthesized, effectiveness as topical mosquito repellents evaluated □ Repellents, mosquito—substituted quinolines, quinoxalines, and isoquinolines synthesized and evaluated □ Structure–activity relationships—substituted quinolines, quinoxalines, and isoquinolines synthesized and evaluated for effectiveness as topical mosquito repellents

To formulate a more effective topical mosquito repellent, heterocyclic compounds in the quinoline, isoquinoline, and quinoxaline series were prepared and evaluated. The repellency of these compounds against *Aedes aegypti* was determined by topical application on human subjects as previously described (1).

In one study, 8-hydroxyquinoline was reported to be more effective against *A. aegypti* than the standard repellent, dimethyl phthalate (2). Following this report, other derivatives, chiefly in the quinoline series, were evaluated, including esters and amides of cinchoninic acid and alkyl-substituted cinchoninic acids (3, 4). Some *N*-acyl tetrahydroquinolines and isoquinolines also were reported to be effective repellents (5, 6). These reports were regarded as sufficiently promising to justify a more extensive investigation of derivatives in this series.

With few exceptions, all of the compounds tested (Tables I–IV) were either available commercially or were prepared *via* published procedures. Diethyltoluamide was used as the reference in all tests.

EXPERIMENTAL[1]

1,6-Dimethyl-8-hydroxymethyl-1,2,3,4-tetrahydroquinoline (Compound 51)—A 50-ml flask was charged with formic acid (0.1 *M*, 5.12 g of a 90% solution), aqueous formaldehyde (0.05 *M*, 4.5 g of a 37% solution), and 6-methyl-1,2,3,4-tetrahydroquinoline (0.015 *M*, 2.0 g). The reaction mixture was heated on a steam bath for 8 hr, cooled to room temperature, made basic with 10% NaOH, and then extracted with ether.

The ether layers were combined, washed with saturated sodium chloride, dried, and stripped. Distillation afforded the desired material (114°/0.20 mm) as a slightly yellow oil, 1.6 g; IR (film): 2.96, 3.41, 6.78, 8.30, and 9.62 μm; NMR ($CDCl_3$): δ 6.81 (s, 2H), 4.80 [s (sharp), 2H], 3.08 (m, 2H), 2.80 (m, 2H), 2.71 [s (sharp), 3H], 2.23 [s (sharp), 3H], and 1.86 (m, 2H).

Anal.—Calc. for $C_{12}H_{17}NO$: C, 75.35; H, 8.96; N, 7.32. Found: C, 75.63; H, 9.24; N, 7.58.

Tests on Skin—Compounds were uniformly applied in ethanol to an exposed area of the forearm of a human subject as previously described (1). Repellency was evaluated utilizing female *A. aegypti*.

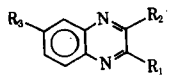

Table I—Physical Properties of Quinoxalines

Compound	R_1	R_2	R_3	Boiling Point (mm) or Melting Point	Repellency, hr[a] (0.35 mg/cm²)	Reference
1	H	H	H	31°	1.0 (1)	—[b]
2	H	H	OCH_3	57°	2.0 (1)	7
3	H	H	Cl	55°	1.0 (1)	7
4	CH_3	H	H	64° (0.5)	0.3 (1)	—[b]
5	OCH_3	H	H	33°	0.3 (1)	8
6	Cl	CH_3	H	80°	0.3 (1)	—[b]
7	$N(CH_2)_5$	H	H	62°	2.0 (1)	9
8	SCH_3	H	H	39°	2.0 (1)	9
9	$N(CH_2)_4$	H	H	89°	1.0 (1)	—[c]
10	$N(CH_2)_4$	H	H	90°	1.0 (1)	—[d]
11	2,4-$(CH_3)_2C_6H_3$	H	H	56°	1.0 (1)	10
12	OC_2H_5	OC_2H_5	H	78°	0.9 (3)	11
13	OC_4H_9	OC_4H_9	H	46°	1.1 (3)	11
14	OC_5H_{11}	OC_5H_{11}	H	154° (0.5)	2.0 (1)	11
15	CH_3	H	CH_3	100° (0.5)	1.0 (1)	12
16	$COOC_2H_5$	CH_3	H	72°	1.0 (1)	13
17	C_6H_5	CH_3	H	165° (0.5)	1.0 (1)	14
18	C_3H_7	CH_3	H	62°	0.3 (2)	15
Diethyltoluamide				100° (0.5)	6.0–7.0	

[a] Number of determinations is given in parentheses; for more than one determination, reproducibility was ±0.3 hr. [b] Commercially available compound. [c] See Ref. 9. (*Anal.*—Calc. for $C_{12}H_{13}N_3$: C, 72.33; H, 6.57; N, 21.09. Found: C, 72.08; H, 6.32; N, 21.17.) [d] See Ref. 9. (*Anal.*—Calc. for $C_{14}H_{17}N_3$: C, 73.97; H, 7.54; N, 18.49. Found: C, 73.84; H, 7.60; N, 18.21.)

[1] Melting points were determined on a Thomas-Hoover capillary melting-point apparatus and are uncorrected. Boiling points were determined using a Bantamware short path distillation apparatus and also are uncorrected. IR (Perkin-Elmer 735 B) and NMR (Varian Associates T-60) spectra were taken of all compounds and were completely consistent with the assigned structures. Elemental analyses were performed by the Microanalytical Laboratory, Department of Chemistry, Stanford University, Stanford, Calif.

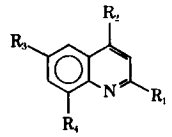

Table II—Physical Properties of Quinolines

Compound	R_1	R_2	R_3	R_4	Boiling Point (mm) or Melting Point	Repellency, hr[a] (0.35 mg/cm²)	Reference
19	Cl	H	H	H	35°	1.0	—[b]
20	CH_3	CH_3	H	H	78° (0.5)	1.0	—[b]
21	CH_3	H	CH_3	H	59°	0.3	—[b]
22	$COOC_2H_5$	H	H	H	151° (0.5)	0.4 (2)	16
23	H	H	H	$COCH_3$	111° (0.5)	3.5 (1)	16
24	$COCH_3$	H	H	H	47°	1.0 (1)	17
25	H	$COCH_3$	H	H	105° (0.5)	2.0 (1)	18
26	H	$COOC_2H_5$	H	H	113° (0.5)	2.0 (1)	18
27	H	$COOCH_3$	H	H	114° (0.5)	1.0 (1)	19
28	H	$COOC_3H_5$	H	H	156° (0.5)	Irritant	—[c]
29	H	H	COC_6H_5	H	61°	1.0 (1)	20
30	H	COC_6H_5	H	H	154° (0.5)	0.3 (2)	21
31	C_6H_5	$COOCH_3$	H	H	55°	0.5 (1)	22
32	H	$COOC_2H_5$	OCH_3	H	65°	0.3 (2)	—[d]
33	H	Cl	H	H	71° (0.5)	Irritant	—[b]
34	CH_3	H	H	H	65° (0.5)	1.3 (2)	—[b]
35	C_6H_5	$COOC_3H_5$	H	H	32°	0.5 (1)	23
36	OC_2H_5	H	H	H	82° (0.5)	0.3 (2)	24
37	H	OC_2H_5	H	H	116° (0.5)	1.5 (1)	25
38	OC_3H_7	H	H	H	110° (0.5)	0.6 (2)	26
39	$OCH(CH_3)_2$	H	H	H	100° (0.5)	0.5 (3)	—[e]
40	OC_3H_5	H	H	H	106° (0.5)	0.3 (2)	26
41	H	OC_3H_5	H	H	135° (0.5)	1.8 (2)	27
42	CH_3	CH_3	CH_3	H	36°	1.8 (4)	—[b]
43	CH_3	H	OCH_3	H	62°	2.3 (2)	—[b]
Diethyltoluamide					100° (0.5)	6.0–7.0	

[a]Number of determinations is given in parentheses; for more than one determination, reproducibility was ±0.3 hr. [b]Commercially available compound. [c]*Anal.*—Calc. for $C_{13}H_{11}NO_2$: C, 73.22; H, 5.20; N, 6.57. Found: C, 73.05; H, 5.43; N, 6.47. [d]*Anal.*—Calc. for $C_{13}H_{13}NO_3$: C, 67.51; H, 5.74; N, 6.14. Found: C, 67.58; H, 5.74; N, 6.09. [e]*Anal.*—Calc. for $C_{12}H_{12}NO$: C, 77.38; H, 6.50; N, 7.52. Found: C, 77.28; H, 6.72; N, 7.93.

RESULTS AND DISCUSSION

For topically applied repellents, an optimum volatility, which results in maximum duration of repellency, exists for each particular series of structural analogs. The variation in optimum volatility from one series of compounds to another reflects differences in intrinsic repellency for each particular series. The optimum volatility is that which results in the maintenance of the minimum effective concentration (MEC) of the repellent vapor (directly determined by the intrinsic repellency of a particular compound) for the maximum period. The optimum volatility for most compounds appears to lie within the range of 100–150°/0.5 mm.

The series of quinoxalines examined in Table I is, without exception, disappointing. The intrinsic repellency for this series of compounds appears to be far too low.

While the quinoline derivatives evaluated (Table II) are considerably more attractive than the quinoxalines in terms of the range of volatilities attainable, their apparent low level of intrinsic repellency limits their utility as repellents for *A. aegypti*.

An interesting observation concerning polarization and duration of repellency is apparent by comparing 2-(ethoxy)- and 2-(allyloxy)-quinolines (Compounds 36 and 40) with their respective 4-substituted isomers (Compounds 37 and 41). That the 4-(alkoxy)quinolines are considerably more polar than the 2-(alkoxy)quinolines is evident from the substantial increase in boiling point. This difference in polarity can affect the duration of repellency in a number of ways.

An increase in intrinsic repellency or, perhaps, simply an optimization of the boiling point as a result of the increased polarity of the 4-(alkoxy)quinolines may be responsible for the observed differences. Another possibility is that the increase in polarity results in a reduced rate of percutaneous absorption, thereby reducing the amount of repellent dissipated *via* this pathway (32). In view of the complex relationship between repellency and molecular structure, it is unlikely that any of the possibilities mentioned is solely responsible for the observed increase in the duration of repellency with increased molecular polarity. It does, however, seem reasonable that these variables are among those responsible for the observed effect.

None of the compounds included in Table III or IV is exceptional. It is interesting that the reduction of an aromatic ring (Compound 54) to the corresponding 1,4-diene (Compound 55) results in a con-

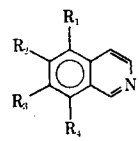

Table III—Physical Properties of Isoquinolines

Compound	R_1	R_2	R_3	R_4	Boiling Point (mm) or Melting Point	Repellency, hr[a] (0.35 mg/cm²)	Reference
43	H	Br	H	H	39°	1.5	—[b]
44	H	H	OCH_3	OCH_3	128° (0.5)	3.5 (2)	28
45	OCH_3	OCH_3	OCH_3	H	160° (0.5)	0.5 (1)	28
46	H	OCH_3	OCH_3	OCH_3	165° (0.5)	0.3 (1)	28
47	H	H	OCH_3	OCH_3	134° (0.5)	2.0 (1)	28
Diethyltoluamide					100° (0.5)	6.0–7.0	

[a]Number of determinations is given in parentheses; for more than one determination, reproducibility was ±0.3 hr. [b]Commercially available compound.

Table IV—Physical Properties of Dihydro- and Tetrahydroquinolines and Isoquinolines

Compound	Structure	Boiling Point (mm) or Melting Point	Repellency, hr[a] (0.35 mg/cm²)	Reference
48	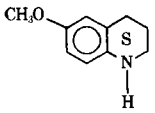	41°	1.5 (1)	—[b]
49	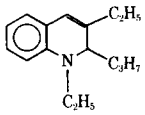	121° (0.5)	2.5 (1)	29
50	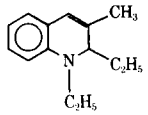	110° (0.5)	0.6 (2)	29
51	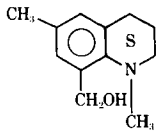	130° (0.5)	2.5 (2)	—[c]
52	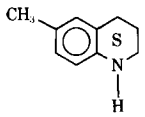	86° (0.5)	1.5 (2)	—[b]
53	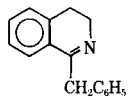	131° (0.5)	1.5 (1)	30
54	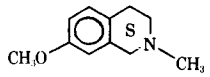	86° (0.5)	1.5 (2)	31
55	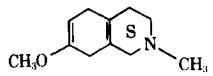	87° (0.5)	0.8 (2)	31
Diethyltoluamide		100° (0.5)	6.0–7.0	

[a] Number of determinations is given in parentheses; for more than one determination, reproducibility was ±0.3hr. [b] Commercially available compound. [c] See *Experimental.*

siderable decrease in protection time, even though the boiling points are essentially the same.

From the data summarized in Tables I–IV, it appears that none of the compounds evaluated offers a significant advantage in terms of increased protection time over topical repellents currently available.

REFERENCES

(1) H. L. Johnson, W. A. Skinner, D. Skidmore, and H. I. Maibach, *J. Med. Chem.*, **11**, 1265(1968).

(2) J. P. Linduska and F. A. Morton, *J. Econ. Entomol.*, **40**, 562(1947).

(3) U. H. Lindberg, B. Ulff, and G. Yeoman, *Acta Pharm. Suec.*, **5**, 441(1968).

(4) F. Gualtieri, P. Tsakotellis, W. A. Skinner, H. Johnson, D. Skidmore, and H. Maibach, *J. Pharm. Sci.*, **62**, 849(1973).

(5) V. P. Dremova, V. M. Tsetlin, E. B. Zhuk, E. Y. Uawkovskis, and V. V. Gorbatkova, *J. Hyg. Epidemiol. Microbiol. Immunol.*, **13**, 64(1969).

(6) P. D. Bartlett and H. J. Daaben, Jr., *Chem. Abstr.*, **47**, P3512h(1953).

(7) J. C. Cavagnol and F. Y. Wiselogle, *J. Am. Chem. Soc.*, **69**, 795(1947).

(8) G. W. H. Cheeseman, *J. Chem. Soc.*, **1955**, 1804.

(9) *Ibid.*, **1957**, 3236.

(10) R. C. Fuson, W. S. Emerson, and H. W. Gray, *J. Am. Chem. Soc.*, **61**, 480(1939).

(11) R. Patton and H. P. Schultz, *ibid.*, **73**, 5899(1951).

(12) H. Pechmann, *Ber.*, **20**, 2539(1887).

(13) R. A. Baxter and F. S. Spring, *J. Chem. Soc.*, **1945**, 229.

(14) E. C. Taylor and G. W. H. Cheeseman, *J. Am. Chem. Soc.*, **86**, 1830(1964).

(15) J. K. Landquist and G. J. Stacey, *Chem. Abstr.*, **47**, 5458i(1953).

(16) K. N. Campbell, J. F. Kerwin, and C. H. Helbing, *J. Am. Chem. Soc.*, **68**, 1840(1946).

(17) K. N. Campbell, J. F. Kerwin, R. A. LaForge, and B. K. Campbell, *ibid.*, **68**, 1844(1946).

(18) P. Rabe and R. Pasternack, *Ber.*, **46**, 1032(1913).

(19) R. C. Elderfield and M. Siegel, *J. Am. Chem. Soc.*, **73**, 5622(1951).

(20) C. E. Kaslow and E. Arnoff, *J. Org. Chem.*, **19**, 857(1954).

(21) P. Remfry and H. Decker, *Ber.*, **41**, 1007(1908).

(22) A. Claus and G. Brandt, *Justus Liebigs Ann. Chem.*, **282**, 106(1897).

(23) K. W. Rosenmund, *Ber.*, **54**, 2829(1921).

(24) P. Friedlander and H. Ostermaier, *ibid.*, **15**, 335(1882).

(25) R. Hardman and M. W. Partridge, *J. Chem. Soc.*, **1958**, 614.

(26) Y. Makisumi, *Tetrahedron Lett.*, **39**, 2833(1964).

(27) T. Itai, S. Sveyoshi, and G. Okusha, *Chem. Abstr.*, **71**, 113122a(1969).

(28) A. J. Birch, A. H. Jackson, and P. R. Shannon, *J. Chem. Soc. Perkin Trans. I*, **1974**, 2185.

(29) Y. Sato, H. Kajima, and H. Shirai, *Td.*, **30**, 2695(1974).

(30) A. Pickett and F. W. Kay, *Ber.*, **42**, 1977(1909).

(31) T. A. Crabb and J. R. Wilkinson, *J. Chem. Soc. Perkin Trans. I*, **1974**, 58.

(32) H. Johnson, J. DeGraw, J. Engstrom, W. A. Skinner, V. H.

Brown, D. Skidmore, and H. Maibach, *J. Pharm. Sci.*, **64**, 693(1975).

ACKNOWLEDGMENTS AND ADDRESSES

Received September 15, 1975, from the *Life Sciences Division, Stanford Research Institute, Menlo Park, CA 94025*

Accepted for publication December 1, 1975.

Supported by U.S. Army Medical Research and Development Command Contract DADA 17-70-C-0112 (W. A. Skinner) and DADA-70-C-0190 (H. I. Maibach).

* Present address: Division of Dermatology, School of Medicine, University of California, San Francisco Medical Center, San Francisco, CA 94143

[x] To whom inquiries should be directed.

Tumor Inhibitory Agents from *Vauquelinia corymbosa* (Rosaceae)

E. R. TRUMBULL, E. BIANCHI, D. J. ECKERT, R. M. WIEDHOPF, and J. R. COLE [x]

Abstract □ The chloroform extract of *Vauquelinia corymbosa* Correa has shown activity against the P-388 lymphocytic leukemia test system. The constituents responsible for this activity were identified as uvaol, ursolic acid, and betulinic acid. Their identity was proven by melting point; mixed melting point; elemental analysis; IR, PMR, and mass spectra; and preparation of derivatives.

Keyphrases □ *Vauquelinia corymbosa*—chloroform extract of leaves and stems, uvaol, ursolic acid, and betulinic acid isolated, screened for antitumor activity □ Antitumor agents, potential—uvaol, ursolic acid, and betulinic acid isolated from leaves and stems of *Vauquelinia corymbosa*, screened

As a result of the continuing search for plants having tumor-inhibiting constituents, the ethanol extract of the leaves and stems of *Vauquelinia corymbosa* Correa (Rosaceae)[1] was found to have inhibitory activity toward the P-388 lymphocytic leukemia test system (3PS)[2].

DISCUSSION

The chloroform extract, obtained from an ethanol extract by partition between chloroform and water, was subjected to column chromotography and yielded three pure components. These were identified as uvaol, betulinic acid, and ursolic acid by means of their melting points; mixed melting points; elemental analysis; mass, PMR, and IR spectra; and preparation of derivatives.

In the 3PS test system, uvaol demonstrated an activity of 125% test/control (T/C) at both 100 and 200 mg/kg, betulinic acid demonstrated an activity of 135% T/C at 100 mg/kg and 140% T/C at 50 mg/kg, and ursolic acid demonstrated an activity of 125% T/C at 50 mg/kg. Activity in the 3PS test system is defined as an increase in the survival of treated animals over that of controls, resulting in a test/control value greater than or equal to 125% (1).

EXPERIMENTAL[3]

The dried leaves and stems (6 kg) of *V. corymbosa* were ground and exhaustively extracted in a Lloyd-type extractor with petroleum ether. The marc was air dried and extracted similarly with ethanol. After removal of the solvent in air, the residue (750 g) was partitioned between chloroform and water (1:1), using 1 liter of each phase for each 125 g of alcohol residue.

The chloroform phases were combined and the solvent was removed in air. The residue (207 g) was chromatographed over neutral alumina (5.3 kg) (Brockmann activity grade III), eluting with solvents of increasing polarity. Three crystalline fractions were obtained: uvaol, betulinic acid, and ursolic acid (in order of elution).

Ursolic Acid—Elution with benzene–chloroform (1:1) gave 42.5 g of a semicrystalline solid. Two recrystallizations from ethanol provided pure material, mp 288–291°, $[\alpha]_D^{25}$ + 60°. An authentic specimen[4] of ursolic acid had a melting point of 285–287° and an $[\alpha]_D^{25}$ of + 62°; a mixture of the two samples had an undepressed melting point. PMR, IR, and mass spectra were identical. The methyl ester had a melting point of 168–170° [lit. (2) mp 166–168°]; the acetate had a melting point of 288–293° [lit. (3) mp 288–290°]; and the methyl ester acetate had a melting point of 247–250° [lit. (4) mp 246–247°].

Anal.—Calc. for $C_{30}H_{48}O_3$: C, 78.89; H, 10.57. Found: C, 78.57; H, 10.61.

Betulinic Acid—Elution with petroleum ether–benzene (1:1) afforded 5.8 g of semicrystalline material, 4.1 g of which was decolorized and rechromatographed over silica gel. The latter gave mostly ursolic acid along with 0.25 g of another crystalline material. Recrystallization from methanol gave needles, mp 284–286°, which was undepressed upon admixture with an authentic specimen[5] of betulinic acid. The PMR, IR, and mass spectra of the two samples were identical.

Anal.—Calc. for $C_{30}H_{48}O_3 \cdot CH_3OH$: C, 76.18; H, 10.72. Found: C, 75.86; H, 10.67.

Uvaol—The first eluate of the alumina column with petroleum ether–benzene (1:1) gave 12.5 g of a solid residue. Crystallization from acetone and recrystallization from chloroform–ethanol afforded pure material, mp 224–225°, whose PMR, IR, and mass spectra were sug-

[1] Identification was confirmed by Dr. Robert E. Perdue, Medicinal Plant Resources Laboratory, Agricultural Research Center, Beltsville, Md. A reference specimen was deposited in that herbarium. The plant was collected in Coahuila, Mexico, in July 1970.

[2] Division of Cancer Treatment, National Cancer Institute, National Institutes of Health, Bethesda, Md.

[3] Carbon and hydrogen analyses were performed by Chemalytics, Inc., Tempe, Ariz. PMR, IR, and mass spectra were determined using a Varian T-60 spectrometer, a Beckman IR-33, and a Hitachi Perkin-Elmer double-focusing spectrometer (model RMU-6E), respectively. Melting points were determined on a Kofler hot-stage apparatus and are uncorrected.

[4] From this laboratory.

[5] The authors are grateful to Dr. R. P. Rastogi, Central Drug Research Institute, Lucknow, India, for providing this sample.

Brown, D. Skidmore, and H. Maibach, *J. Pharm. Sci.*, **64**, 693(1975).

ACKNOWLEDGMENTS AND ADDRESSES

Received September 15, 1975, from the *Life Sciences Division, Stanford Research Institute, Menlo Park, CA 94025*

Accepted for publication December 1, 1975.

Supported by U.S. Army Medical Research and Development Command Contract DADA 17-70-C-0112 (W. A. Skinner) and DADA-70-C-0190 (H. I. Maibach).

* Present address: Division of Dermatology, School of Medicine, University of California, San Francisco Medical Center, San Francisco, CA 94143

[x] To whom inquiries should be directed.

Tumor Inhibitory Agents from *Vauquelinia corymbosa* (Rosaceae)

E. R. TRUMBULL, E. BIANCHI, D. J. ECKERT, R. M. WIEDHOPF, and J. R. COLE [x]

Abstract □ The chloroform extract of *Vauquelinia corymbosa* Correa has shown activity against the P-388 lymphocytic leukemia test system. The constituents responsible for this activity were identified as uvaol, ursolic acid, and betulinic acid. Their identity was proven by melting point; mixed melting point; elemental analysis; IR, PMR, and mass spectra; and preparation of derivatives.

Keyphrases □ *Vauquelinia corymbosa*—chloroform extract of leaves and stems, uvaol, ursolic acid, and betulinic acid isolated, screened for antitumor activity □ Antitumor agents, potential—uvaol, ursolic acid, and betulinic acid isolated from leaves and stems of *Vauquelinia corymbosa*, screened

As a result of the continuing search for plants having tumor-inhibiting constituents, the ethanol extract of the leaves and stems of *Vauquelinia corymbosa* Correa (Rosaceae)[1] was found to have inhibitory activity toward the P-388 lymphocytic leukemia test system (3PS)[2].

DISCUSSION

The chloroform extract, obtained from an ethanol extract by partition between chloroform and water, was subjected to column chromotography and yielded three pure components. These were identified as uvaol, betulinic acid, and ursolic acid by means of their melting points; mixed melting points; elemental analysis; mass, PMR, and IR spectra; and preparation of derivatives.

In the 3PS test system, uvaol demonstrated an activity of 125% test/control (T/C) at both 100 and 200 mg/kg, betulinic acid demonstrated an activity of 135% T/C at 100 mg/kg and 140% T/C at 50 mg/kg, and ursolic acid demonstrated an activity of 125% T/C at 50 mg/kg. Activity in the 3PS test system is defined as an increase in the survival of treated animals over that of controls, resulting in a test/control value greater than or equal to 125% (1).

EXPERIMENTAL[3]

The dried leaves and stems (6 kg) of *V. corymbosa* were ground and exhaustively extracted in a Lloyd-type extractor with petroleum ether. The marc was air dried and extracted similarly with ethanol. After removal of the solvent in air, the residue (750 g) was partitioned between chloroform and water (1:1), using 1 liter of each phase for each 125 g of alcohol residue.

The chloroform phases were combined and the solvent was removed in air. The residue (207 g) was chromatographed over neutral alumina (5.3 kg) (Brockmann activity grade III), eluting with solvents of increasing polarity. Three crystalline fractions were obtained: uvaol, betulinic acid, and ursolic acid (in order of elution).

Ursolic Acid—Elution with benzene–chloroform (1:1) gave 42.5 g of a semicrystalline solid. Two recrystallizations from ethanol provided pure material, mp 288–291°, $[\alpha]_D^{25}$ + 60°. An authentic specimen[4] of ursolic acid had a melting point of 285–287° and an $[\alpha]_D^{25}$ of + 62°; a mixture of the two samples had an undepressed melting point. PMR, IR, and mass spectra were identical. The methyl ester had a melting point of 168–170° [lit. (2) mp 166–168°]; the acetate had a melting point of 288–293° [lit. (3) mp 288–290°]; and the methyl ester acetate had a melting point of 247–250° [lit. (4) mp 246–247°].

Anal.—Calc. for $C_{30}H_{48}O_3$: C, 78.89; H, 10.57. Found: C, 78.57; H, 10.61.

Betulinic Acid—Elution with petroleum ether–benzene (1:1) afforded 5.8 g of semicrystalline material, 4.1 g of which was decolorized and rechromatographed over silica gel. The latter gave mostly ursolic acid along with 0.25 g of another crystalline material. Recrystallization from methanol gave needles, mp 284–286°, which was undepressed upon admixture with an authentic specimen[5] of betulinic acid. The PMR, IR, and mass spectra of the two samples were identical.

Anal.—Calc. for $C_{30}H_{48}O_3 \cdot CH_3OH$: C, 76.18; H, 10.72. Found: C, 75.86; H, 10.67.

Uvaol—The first eluate of the alumina column with petroleum ether–benzene (1:1) gave 12.5 g of a solid residue. Crystallization from acetone and recrystallization from chloroform–ethanol afforded pure material, mp 224–225°, whose PMR, IR, and mass spectra were sug-

[1] Identification was confirmed by Dr. Robert E. Perdue, Medicinal Plant Resources Laboratory, Agricultural Research Center, Beltsville, Md. A reference specimen was deposited in that herbarium. The plant was collected in Coahuila, Mexico, in July 1970.

[2] Division of Cancer Treatment, National Cancer Institute, National Institutes of Health, Bethesda, Md.

[3] Carbon and hydrogen analyses were performed by Chemalytics, Inc., Tempe, Ariz. PMR, IR, and mass spectra were determined using a Varian T-60 spectrometer, a Beckman IR-33, and a Hitachi Perkin-Elmer double-focusing spectrometer (model RMU-6E), respectively. Melting points were determined on a Kofler hot-stage apparatus and are uncorrected.

[4] From this laboratory.

[5] The authors are grateful to Dr. R. P. Rastogi, Central Drug Research Institute, Lucknow, India, for providing this sample.

gestive of uvaol [lit. (5) mp 222–224°]. The diacetate had a melting point of 151–152° [lit. (6) mp 150–151°]. An authentic specimen of uvaol, prepared by the lithium aluminum hydride reduction of methyl ursolate (7), had a melting point of 223–224°, which was undepressed upon admixture with the sample from *V. corymbosa*.

Anal.—Calc. for $C_{30}H_{50}O_2$: C, 81.38; H, 11.38. Found: C, 81.51; H, 11.67.

REFERENCES

(1) R. I. Geran, N. H. Greenberg, M. N. Macdonald, A. M. Schumacher, and B. J. Abbot, *Cancer Chemother. Rep.*, 3(3), 9(1972).

(2) F. B. Power and A. H. Salway, *J. Am. Chem. Soc.*, **30**, 251(1908).

(3) E. S. Ewen and F. S. Spring, *J. Chem. Soc.*, **1943**, 523.

(4) R. A. Micheli, *J. Org. Chem.*, **27**, 666(1962).

(5) M. Alanddin, T. A. Bryce, E. Clayton, M. Martin-Smith, and G. Subramanian, *J. Chem. Soc.*, **1965**, 4611.

(6) L. Ruzicka and A. Marxer, *Helv. Chim. Acta*, **23**, 144(1940).

(7) R. B. Moffett, *Org. Syn. Coll. Vol.*, **4**, 843(1964).

ACKNOWLEDGMENTS AND ADDRESSES

Received May 14, 1975, from the *Division of Pharmaceutical Chemistry, College of Pharmacy, University of Arizona, Tucson, AZ 85721*

Accepted for publication November 25, 1975.

Supported in part by Contract NO1-CM-3-3750 from the Division of Cancer Treatment, National Cancer Institute, National Institutes of Health, Bethesda, MD 20014, and the Elsa U. Pardee Foundation, Midland, Mich.

[x] To whom inquiries should be directed.

Preparation of Tri- and Tetramethyleneisoxazoles

CHARLES F. BEAM [x], KEITH D. SHEALY, CHARLES E. HARRIS, NEAL L. SHEALY, LUTHER W. DASHER, WAYNE M. HOLLINGER, RONDA M. SANDIFER, and DAVID C. REAMES

Abstract □ The syntheses of several tri- and tetramethyleneisoxazoles resulting from the condensation of C(α)O-dilithioximes with esters, followed by acid cyclization, are described.

Keyphrases □ Isoxazoles, tri- and tetramethylene—synthesized by condensation of 1,4-dianions with esters followed by acid cyclization □ Tri- and tetramethyleneisoxazoles—synthesized by condensation of 1,4-dianions with esters followed by acid cyclization

The preparation of various trimethyleneisoxazoles and tetramethyleneisoxazoles was accomplished by the condensation of the 1,4-dianions of cyclopentanone and cyclohexanone oximes with several esters.

DISCUSSION

One major use of isoxazoles and their derivatives is in the preparation of various pharmacologically important agents. These isoxazoles are prepared by synthetic routes which give more than one isomeric product, and separation of these materials can be difficult. Until the initial report on the preparation of unsymmetrical 3,5-disubstituted isoxazoles from the 1,4-dianions of aromatic oximes containing an α-hydrogen atom (1), no fundamentally new synthetic routes appeared (2).

For example, the most widely applicable method for the preparation of the isoxazole ring system is by the reaction of hydroxylamine with a 1,3-dicarbonyl compound (3); since two bonds are being formed to close the heterocyclic ring, two isomers (A and B) are formed.

A: one bond formed

B: two bonds formed

This investigation focused on the preparation of tri- and tetramethyleneisoxazoles. The literature indicates that these materials can be obtained from the 1,3-dicarbonyl compounds, benzoylcyclopentanone and benzoylcyclohexanone, which are not common reagents and are difficult to prepare (4). In addition, two products are possible; they were isolated and characterized previously.

This report deals with the preparation of these isoxazoles by the condensation of the 1,4-dianions of cyclopentanone and cyclohexanone oximes with esters such as methyl nicotinate, methyl furoate, and methyl anisate (Scheme I). The precyclization intermediate was not isolated.

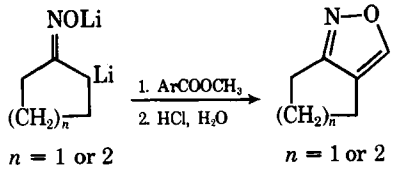

$n = 1$ or 2 $\qquad$ $n = 1$ or 2

Scheme I

All atoms of the heterocyclic ring are in position prior to cyclization, and the cyclization involves the formation of only one bond, which means only one isomer is formed and not a mixture of isomers. Table I gives the analytical and absorption spectral data for new material.

The syntheses described for the preparation of these isoxazoles have several advantages over other methods (2, 3, 5). The experimental procedure is efficient and requires the use of readily available starting materials; it is an unequivocal method for the preparation of a single isomer of unsymmetrically substituted isoxazoles.

EXPERIMENTAL

To a stirred solution of 0.025 mole of oxime in 100 ml of tetrahydrofuran, which was cooled to 0° under a nitrogen atmosphere, was added 0.05 mole of 1.6 *M* *n*-butyllithium[1] during 5 min. The mixture was stirred for 45 min and condensed with a 0.0125-mole sample of ester dissolved in 50–75 ml of tetrahydrofuran. After stirring for 15–30 min at 0°, the mixture was neutralized with 100 ml of 3 *N* hydrochloric acid.

The entire mixture was heated, with good stirring, under reflux for 1 hr and cooled; the phases separated. The aqueous layer was neutralized with sodium bicarbonate and extracted with three 75-ml portions of ether. The combined organic extracts were dried over

[1] Lithium Corporation of America, Bessemer City, N.C.

gestive of uvaol [lit. (5) mp 222–224°]. The diacetate had a melting point of 151–152° [lit. (6) mp 150–151°]. An authentic specimen of uvaol, prepared by the lithium aluminum hydride reduction of methyl ursolate (7), had a melting point of 223–224°, which was undepressed upon admixture with the sample from *V. corymbosa*.

Anal.—Calc. for $C_{30}H_{50}O_2$: C, 81.38; H, 11.38. Found: C, 81.51; H, 11.67.

REFERENCES

(1) R. I. Geran, N. H. Greenberg, M. N. Macdonald, A. M. Schumacher, and B. J. Abbot, *Cancer Chemother. Rep.*, 3(3), 9(1972).

(2) F. B. Power and A. H. Salway, *J. Am. Chem. Soc.*, **30**, 251(1908).

(3) E. S. Ewen and F. S. Spring, *J. Chem. Soc.*, **1943**, 523.

(4) R. A. Micheli, *J. Org. Chem.*, **27**, 666(1962).

(5) M. Alanddin, T. A. Bryce, E. Clayton, M. Martin-Smith, and G. Subramanian, *J. Chem. Soc.*, **1965**, 4611.

(6) L. Ruzicka and A. Marxer, *Helv. Chim. Acta*, **23**, 144(1940).

(7) R. B. Moffett, *Org. Syn. Coll. Vol.*, **4**, 843(1964).

ACKNOWLEDGMENTS AND ADDRESSES

Received May 14, 1975, from the *Division of Pharmaceutical Chemistry, College of Pharmacy, University of Arizona, Tucson, AZ 85721*

Accepted for publication November 25, 1975.

Supported in part by Contract NO1-CM-3-3750 from the Division of Cancer Treatment, National Cancer Institute, National Institutes of Health, Bethesda, MD 20014, and the Elsa U. Pardee Foundation, Midland, Mich.

[x] To whom inquiries should be directed.

Preparation of Tri- and Tetramethyleneisoxazoles

CHARLES F. BEAM [x], KEITH D. SHEALY, CHARLES E. HARRIS, NEAL L. SHEALY, LUTHER W. DASHER, WAYNE M. HOLLINGER, RONDA M. SANDIFER, and DAVID C. REAMES

Abstract □ The syntheses of several tri- and tetramethyleneisoxazoles resulting from the condensation of C(α)O-dilithioximes with esters, followed by acid cyclization, are described.

Keyphrases □ Isoxazoles, tri- and tetramethylene—synthesized by condensation of 1,4-dianions with esters followed by acid cyclization □ Tri- and tetramethyleneisoxazoles—synthesized by condensation of 1,4-dianions with esters followed by acid cyclization

The preparation of various trimethyleneisoxazoles and tetramethyleneisoxazoles was accomplished by the condensation of the 1,4-dianions of cyclopentanone and cyclohexanone oximes with several esters.

DISCUSSION

One major use of isoxazoles and their derivatives is in the preparation of various pharmacologically important agents. These isoxazoles are prepared by synthetic routes which give more than one isomeric product, and separation of these materials can be difficult. Until the initial report on the preparation of unsymmetrical 3,5-disubstituted isoxazoles from the 1,4-dianions of aromatic oximes containing an α-hydrogen atom (1), no fundamentally new synthetic routes appeared (2).

For example, the most widely applicable method for the preparation of the isoxazole ring system is by the reaction of hydroxylamine with a 1,3-dicarbonyl compound (3); since two bonds are being formed to close the heterocyclic ring, two isomers (A and B) are formed.

A: one bond formed

B: two bonds formed

This investigation focused on the preparation of tri- and tetramethyleneisoxazoles. The literature indicates that these materials can be obtained from the 1,3-dicarbonyl compounds, benzoylcyclopentanone and benzoylcyclohexanone, which are not common reagents and are difficult to prepare (4). In addition, two products are possible; they were isolated and characterized previously.

This report deals with the preparation of these isoxazoles by the condensation of the 1,4-dianions of cyclopentanone and cyclohexanone oximes with esters such as methyl nicotinate, methyl furoate, and methyl anisate (Scheme I). The precyclization intermediate was not isolated.

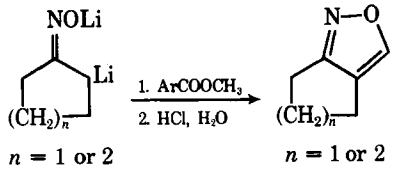

$n = 1$ or 2 $\qquad$ $n = 1$ or 2

Scheme I

All atoms of the heterocyclic ring are in position prior to cyclization, and the cyclization involves the formation of only one bond, which means only one isomer is formed and not a mixture of isomers. Table I gives the analytical and absorption spectral data for new material.

The syntheses described for the preparation of these isoxazoles have several advantages over other methods (2, 3, 5). The experimental procedure is efficient and requires the use of readily available starting materials; it is an unequivocal method for the preparation of a single isomer of unsymmetrically substituted isoxazoles.

EXPERIMENTAL

To a stirred solution of 0.025 mole of oxime in 100 ml of tetrahydrofuran, which was cooled to 0° under a nitrogen atmosphere, was added 0.05 mole of 1.6 *M* *n*-butyllithium[1] during 5 min. The mixture was stirred for 45 min and condensed with a 0.0125-mole sample of ester dissolved in 50–75 ml of tetrahydrofuran. After stirring for 15–30 min at 0°, the mixture was neutralized with 100 ml of 3 *N* hydrochloric acid.

The entire mixture was heated, with good stirring, under reflux for 1 hr and cooled; the phases separated. The aqueous layer was neutralized with sodium bicarbonate and extracted with three 75-ml portions of ether. The combined organic extracts were dried over

[1] Lithium Corporation of America, Bessemer City, N.C.

Table I—Tri- and Tetramethyleneisoxazoles[a]

Compound	Substitution	Empirical Formula	Yield, %	Melting Point[b]
I	5-(*p*-Methoxyphenyl)-3,4-tetramethylene	$C_{14}H_{15}NO_2$ [a,c,d]	30	78–79.5°
II	5-Phenyl-3,4-tetramethylene	$C_{13}H_{13}NO$	30	65–67°[e]
III	5-(*p*-Tolyl)-3,4-tetramethylene	$C_{14}H_{15}NO$	64	93–95°[f]
IV	5-(*p*-Chlorophenyl)-3,4-tetramethylene	$C_{13}H_{12}ClNO$	66	135–138°[g]
V	5-(*m*-Tolyl)-3,4-tetramethylene	$C_{14}H_{15}NO$[d,h]	29	44.5–45.5°
VI	5-(*m*-Chlorophenyl)-3,4-tetramethylene	$C_{13}H_{12}ClNO$[f]	46	53–55°[d,i]
VII	5-Phenyl-3,4-trimethylene	$C_{12}H_{11}NO$	74	104–106°[j]
VIII	5-(*p*-Chlorophenyl)-3,4-trimethylene	$C_{12}H_{10}ClNO$	29	139–140°[k]
IX	5-(*p*-Methoxyphenyl)-3,4-trimethylene	$C_{13}H_{13}NO_2$[i]	29	91–94°[d,l]
X	5-(*m*-Tolyl)-3,4-trimethylene	$C_{13}H_{13}NO$[j]	20	55–65°[d,m]
XI	5-(Nicotinyl)-3,4-tetramethylene	$C_{12}H_{12}N_2O$[k]	26	111–113°[d,n]
XII	5-(2-Furanyl)-3,4-tetramethylene	$C_{11}H_{11}NO_2$[l]	47	73–74°[d,o]

[a] The IR spectra of I–XII are consistent with the proposed structure. One or two absorption bands were noted between 6.03 and 6.29 μm (2, 6), which could be assigned to the unsaturated nitrogen stretching vibration and the aromatic moiety at position 5. [b] Melting points were taken on samples in open capillary tubes in a Thomas Hoover melting-point apparatus. [c] Calc. for: C, 73.34; H, 6.59; N, 6.11. Found: C, 73.41; H, 6.78; N, 6.05. NMR ($CDCl_3$): δ 1.58–2.00 and 2.50–4.58 [m, 8H, $(CH_2)_4$], 3.80 (s, 3H, OCH_3), and 6.87–7.72 (m, 4H, ArH). [d] Combustion analyses were performed by Robertson Laboratory, Florham Park, N.J. NMR spectra were obtained from a Varian Associates A-60 NMR spectrometer, and chemical shifts are reported in parts per million (ppm) downfield from an internal tetramethylsilane standard. IR spectra were obtained from a Perkin-Elmer 700 spectrometer using sodium chloride cells (0.1 mm). [e] Lit. (4) mp 67°. [f] Lit. (4) mp 95°. [g] Lit. (4) mp 137°. [h] Calc. for: C, 78.84; H, 7.09; N, 6.57. Found: C, 78.63; H, 7.15; N, 6.34. NMR ($CDCl_3$): δ 1.60–197 and 2.58–2.77 [m, 8H, $(CH_2)_4$], 2.38 (s, 3H, $ArCH_3$), and 7.02–7.63 (m, 4H, ArH). [i] Calc. for: C, 66.82; H, 5.18; N, 5.95. Found: C, 66.58; H, 5.28; N, 5.86. NMR ($CDCl_3$): δ 1.67–1.93 and 2.60–2.88 [m, 8H, $(CH_2)_4$] and 7.25–7.73 (m, 3H, ArH). [j] Lit. (4) mp 108–109°. [k] Lit. (4) mp 140°. [l] Calc. for: C, 72.54; H, 6.09; N, 6.51. Found: C, 72.25; H, 6.21; N, 6.25. NMR ($CDCl_3$): δ 2.58–2.79 [m, 6H, $(CH_2)_3$], 3.82 (s, 3H, OCH_3), and 6.85–7.68 (m, 4H, ArH). [m] Calc. for: C, 78.36; H, 6.58; N, 7.03. Found: C, 78.14; H, 6.77; N, 6.76. NMR ($CDCl_3$): δ 2.33 (s, 3H, $ArCH_3$), 2.42–2.95 [m, 6H, $(CH_2)_3$], and 6.93–7.35 (m, 4H, ArH). [n] Calc. for: C, 71.98; H, 6.04; N, 13.99. Found: C, 71.77; H, 6.17; N, 13.78. IR ($CHCl_3$): 6.10 (C=N) and 6.23 (C_5H_5N) μm. [o] Calc. for: C, 69.83; H, 5.86; N, 7.40. Found: C, 70.03; H, 6.16; N, 7.11. IR (CCl_4): 6.03 (C=N) μm.

anhydrous magnesium sulfate, filtered, and concentrated; the compounds were recrystallized from 95% ethanol.

REFERENCES

(1) C. F. Beam, M. C. D. Dyer, R. A. Schwarz, and C. R. Hauser, *J. Org. Chem.*, **35**, 1806(1970).

(2) N. K. Kochetkov and S. D. Sukolov, *Adv. Heterocycl. Chem.*, **2**, 367(1963).

(3) R. A. Barnes, in "Heterocyclic Compounds," vol. 5, R. C. Elderfield, Ed., Wiley, New York, N.Y., 1957, p. 454.

(4) G. Bianchi and P. Gruenanger, *Chim. Ind. (Milan)*, **46**, 425(1964).

(5) A. Quilico, in "The Chemistry of Heterocyclic Compounds," vol. 17, R. L. Wiley, Ed., Wiley, New York, N.Y., 1962, chap. 1.

(6) J. R. Dyer, "Applications of Absorption Spectroscopy of Organic Compounds," Prentice-Hall, Englewood Cliffs, N.J., p. 37.

ACKNOWLEDGMENTS AND ADDRESSES

Received August 6, 1975, from the *Department of Chemistry, Newberry College, Newberry, SC 29108*

Accepted for publication November 26, 1975.

Supported by grants from the South Carolina Heart Association, Inc.

The use of an A-60 NMR spectrometer and the cooperation of Dr. R. L. Cargill, University of South Carolina, are gratefully acknowledged.

[x] To whom inquiries should be directed.

Antitumor Agents XVII: Structure and Stereochemistry of Microhelenin-A, a New Antitumor Sesquiterpene Lactone from *Helenium microcephalum*

Keyphrases □ Antitumor agents, potential—microhelenin-A, isolated from *Helenium microcephalum*, NMR spectral identification □ Microhelenin-A—potential antitumor agent, isolated from *Helenium microcephalum*, NMR spectral identification □ *Helenium microcephalum*—microhelenin-A, potential antitumor agent, isolated and identified

To the Editor:

The search for a supply of helenalin for investigations on the relationship between the sesquiterpene lactone structure and cytotoxic antitumor activity (1) led to the isolation of a new antitumor[1] (2) sesquiterpene lactone, microhelenin-A (Structure I), from *Helenium microcephalum*[2] (3).

Microhelenin-A was isolated as colorless needles in 0.005% yield from the chloroform extract of *H. microcephalum* according to an exact literature procedure (4) followed by silica gel column chromatography. Microhelenin-A [mp 140–141°, $[\alpha]_D^{24}$ +89° (c, 1 in methanol[3], *m/e* 262 (M^+)] has the molecular formula[4] $C_{15}H_{18}O_4$ and showed the presence of a cyclopentanone ring system (1758 cm^{-1}). The presence of an α-methylene-γ-lactone moiety in Structure I was indicated by the appearance of IR bands (CCl_4) at 1772 and 1665 cm^{-1} and was substantiated by the presence in the NMR spectrum[5] of a characteristic pair of low field doublets at δ 5.77 (1H, J = 3.0 Hz, H_a − 13) and 6.34 (1H, J = 3.0 Hz, H_b − 13).

A three-proton doublet at δ 1.17 (3H, J = 7.0 Hz) was ascribed to the secondary methyl group at C-10. The one-proton signals at δ 4.77 (ddd, J = 4.0, 9.0, and 11.0 Hz) and 3.12 (m) were assigned to the hydrogens at C-8 and C-7, respectively, since irradiation at C-7 caused the signal at C-8 to collapse to a doublet of doublets at δ 4.80 (J = 4.0 and 11.0 Hz) and caused the doublet signals for H_a − 13 and H_b − 13 to collapse to two singlets at δ 5.77 and 6.34, respectively. This evidence led to the assignment of the partial Structure II to microhelenin-A.

Microhelenin-A (Structure II) and 2,3-dihydrohelenalin (III) (6) both exhibited the comparable negative Cotton effects in circular dichroism[6] (CD) studies (Structure II: $[\theta]_{253}$ −3144°; III: $[\theta]_{262}$ −3748°) and positive Cotton effects of the optical rotatory dispersion[6] (ORD) curves (Structure II: $[\Phi]_{313}$ +5633°; III: $[\Phi]_{315}$ +5016°), indicating that both possess the same C-7/C-8 *cis*-fused lactones with H-7α and H-8α as well as the *trans*-fused *A/B* rings with H-1α and alkyl-5β (7).

The NMR spectrum of I also displayed an *AB* quartet (J = 9.0 Hz)[7] at δ 3.64 (1H) and 3.85 (1H) as well as a multiplet at δ 4.53 (1H), which were assigned to the protons of —CH_2OCH—. Determination of the conformation of the B-ring as well as the position of the —CH_2OCH— linkage was achieved by an INDOR experiment (8–10). As illustrated in Fig. 1, when the quartet lines of H-6β (ax) (δ 1.67, dd, J = 13.0 and 15.0 Hz) were monitored, they gave the INDOR signals for H-6α (eq) around δ 2.30–2.50, indicating that the central seven-membered ring of Structure I (see also Structure I*a*) adopts a boat conformation:

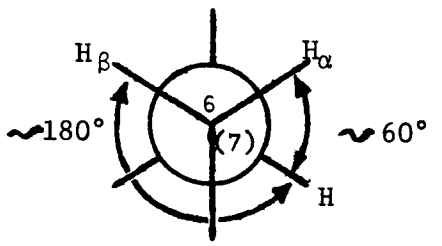

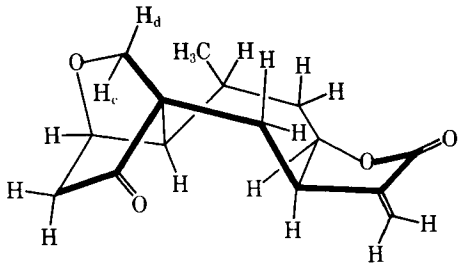

I*a*

with CH_2-5β axially disposed. The observed J values between H-6β and H-7α (J = 13.0 Hz) and between H-6α and H-7α (J = 3.0 Hz) are in accord with those derived from the Karplus rule (11), since models indicate that the dihedral angle between H-6β and H-7α is approximately 180° and that between H-6α and H-7α is approximately 60°. The downfield shift of H-6α in comparison to H-6β to δ 2.44 (dd, J = 3.0 and 15.0 Hz) is due to the coplanarity of H-6α with the carbonyl at C-4.

The position for the —CH_2OC*H*— linkage was determined as follows. The NMR data indicated the presence of a secondary methyl group at C-10 and a methylene proton at C-9. Consequently, the methine

[1] Microhelenin-A showed significant (T/C ≥125%) inhibitory activity against the Walker 256 carcinosarcoma in rats (T/C 148%) at the 2.5-mg/kg level. *In vivo* activity was assayed by Dr. I. H. Hall, Department of Medicinal Chemistry, School of Pharmacy, University of North Carolina at Chapel Hill, by a literature method (2).

[2] Specimens were gathered in June 1972 in Burleson County, Tex. We thank Professor John J. Sperry, Texas A&M University, for collecting and identifying the plant material. A voucher specimen (J. J. Sperry, No. 4020) is available for inspection at the Herbarium of the Department of Botany, University of North Carolina at Chapel Hill. The constituents of *H. microcephalum* were previously examined and reported to contain helenalin in good yield (3).

[3] Measurements were carried out on a Perkin-Elmer model 141 polarimeter. Mexicanin-H showed $[\alpha]_D$ −44.6° (see Ref. 5).

[4] Determined by high-resolution mass spectrometry.

[5] NMR spectra were measured in deuterochloroform (tetramethylsilane) with a Varian XL-100-FT instrument.

[6] CD and ORD curves were measured in methanol (c, 0.1%) on a Cary 60 recording spectropolarimeter.

[7] This quartet became a singlet at δ 3.38 when Structure I was measured in deuterated benzene–deuterochloroform (1:1).

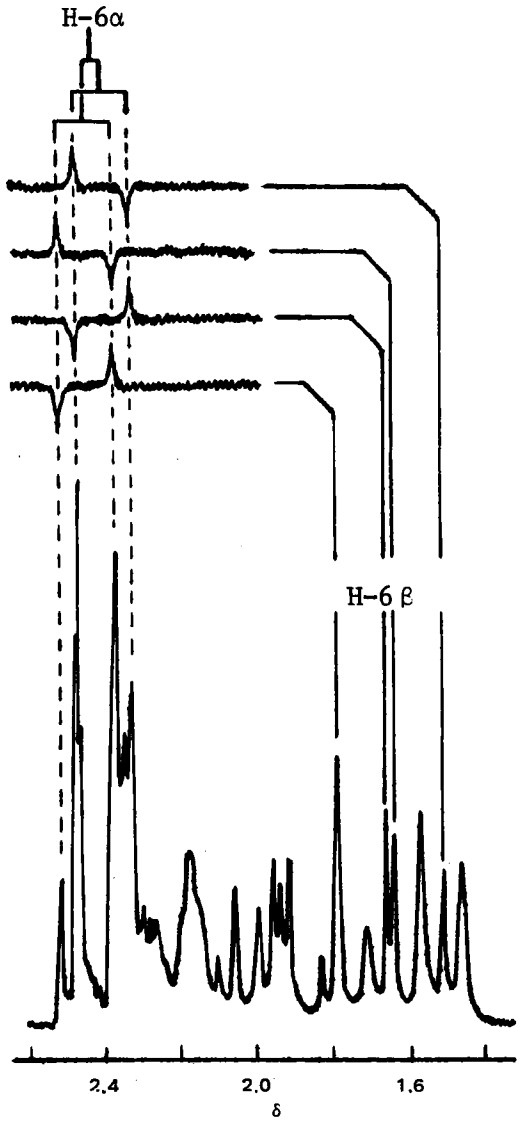

Figure 1—*The 100-MHz normal and INDOR spectra of microhelenin-A.*

proton in —CH_2OCH— can only be placed at either C-2 or C-3. Of these, the former is regarded as the most likely because monitoring the peak around δ 4.53 (H-2α) gave INDOR signals arising from H-1α and H-3 at δ 1.90–2.40. The H-1α INDOR signal would not be observed if the linkage is at C-3. Further confirmation for this assignment was obtained by sodium borohydride reduction of Structure I, which afforded a monohydroxydihydro derivative (IV).

Compound IV [$C_{15}H_{22}O_4$; ν_{max} 3590 (OH) and 1762 (γ-lactone) cm^{-1}] showed two three-proton doublets at δ 1.07 (J = 7.0 Hz, CH_3-10) and 1.18 (J = 7.5 Hz, CH_3-11) and a one-proton multiplet at δ 4.78 (H-8). The two-proton multiplet at δ 4.00 was assigned to protons at C-2 and C-4. The downfield shift of H_c, which appeared as a one-proton doublet at δ 4.18 (J = 8.0 Hz), demonstrated that H_c was adjacent to a β-OH group at C-4. The one-proton doublet of doublets (J = 2.0 and 8.0 Hz) at δ 3.50 was assigned to H_d, which was long range coupled to H-4α through an "M" arrangement of the four σ-bonds. Acetylation of IV with acetic anhydride–pyridine yielded a monoacetate [V; δ 2.14 (3H, s, $OCOCH_3$-4), 4.09 (1H, m, H-2), and 4.70–5.10 (2H, m, H-4 and H-8)].

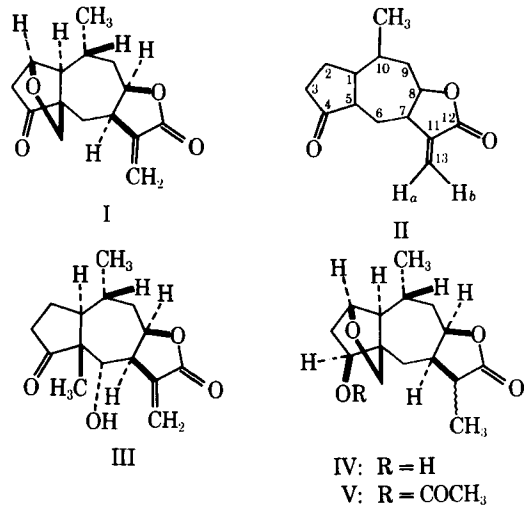

The methyl group at C-10 was assigned to an α-equatorial orientation since it appeared at δ 1.17. One would expect that, if the C-10 methyl was in the β-axial configuration, it would be shifted to a lower field due to the deshielding effect of the adjacent oxygen at C-2. This suggestion was confirmed by the fact that no NOE was observed between this C-10 methyl group and the 5 β-axial proton (H_d).

This evidence led to the assignment of Structure I for microhelenin-A[8,9] (5) beyond doubt.

(1) K. H. Lee, T. Ibuka, S. H. Kim, B. R. Vestal, I. H. Hall, and E. S. Huang, *J. Med. Chem.*, **18**, 812(1975).

(2) R. I. Geran, N. H. Greenberg, M. M. MacDonald, A. M. Schumacher, and B. J. Abbott, *Cancer Chemother. Rep. (Part 3)*, **3**, 1(1972).

(3) R. Adams and W. Herz, *J. Am. Chem. Soc.*, **71**, 2546(1949).

(4) K. H. Lee, E. S. Huang, C. Piantadosi, J. S. Pagano, and T. A. Geissman, *Cancer Res.*, **31**, 1649(1971), and references cited therein.

(5) J. Romo, A. Romo de Vivar, and P. Joseph-Nathan, *Tetrahedron Lett.*, **1966**, 1029.

(6) K. H. Lee, H. Furukawa, and E. S. Huang, *J. Med. Chem.*, **15**, 609(1972).

(7) W. Stöcklin, T. G. Waddell, and T. A. Geissman, *Tetrahedron*, **26**, 2397(1970).

(8) E. B. Baker, *J. Chem. Phys.*, **37**, 911(1962).

(9) P. N. Jenkins and L. Phillips, *J. Phys. (E)*, **4**, 530(1970).

(10) T. Kikuchi, M. Niwa, M. Takayama, T. Yokoi, and T. Shingu, *Tetrahedron Lett.*, **1973**, 1987.

(11) M. Karplus, *J. Am. Chem. Soc.*, **85**, 2870(1963).

Kuo-Hsiung Lee [x]
Yasuhiro Imakura
Donald Sims

Department of Medicinal Chemistry
School of Pharmacy
University of North Carolina
Chapel Hill, NC 27514

Received March 10, 1976.
Accepted for publication June 9, 1976.
Presented in part at the APhA Academy of Pharmaceutical Sciences, New Orleans meeting, April 1976.

[8] "Microhelenin-A" is used to differentiate "mexicanin-H" (5) since both compounds showed different melting point and $[\alpha]_D$ values as well as NMR and mass spectra, although they possess the same plane structure.

[9] This assignment was also confirmed by a single crystal X-ray analysis by Dr. A. T. McPhail and Dr. K. D. Onan of Duke University after the submission of this manuscript.

Supported by grants from the National Cancer Institute (CA-17625) and the American Cancer Society (CH-19). We thank Dr. David L. Harris, Chemistry Department, University of North Carolina at Chapel Hill, for assistance in carrying out the INDOR experiments. The XL-100 NMR spectrometer was purchased by grants from the National Science Foundation and the National Institutes of Health to the Department of Chemistry, University of North Carolina at Chapel Hill.

[x] To whom inquiries should be directed.

Method for Monitoring Hard Gelatin Capsule Disintegration Times in Humans Using External Scintigraphy

Keyphrases □ Gelatin capsules, hard—disintegration and drug release times *in vivo* monitored by external scintigraphy using technetium Tc 99m □ Disintegration time—hard gelatin capsules *in vivo*, monitored by external scintigraphy □ Drug release time—hard gelatin capsules *in vivo*, monitored by external scintigraphy □ Technetium Tc 99m—used in scintigraphic monitoring of disintegration and drug release times of gelatin capsules *in vivo* □ Scintigraphy, external—disintegration and drug release times of gelatin capsules monitored

To the Editor:

We wish to report a noninvasive and novel approach for monitoring disintegration and drug release times from a gelatin capsule in humans. The method involves the utilization of a short-lived radionuclide coupled with external scintigraphy.

Two separate formulations were used to fill identical hard gelatin capsules[1]. Formulation A consisted of 150 mg of a totally water-insoluble polystyrene resin (40–100 mesh) bearing polyamine functions which chelated the radionuclide, technetium Tc 99m, in an irreversible manner (1). Formulation B was water soluble, consisting of 145 mg of lactose and 5.9 mg of the soluble chelating agent etidronate disodium[2] labeled with technetium Tc 99m.

In a typical experiment, the subject ingested a gelatin capsule[1] filled with an appropriate material labeled with 20 mCi of technetium Tc 99m. Technetium Tc 99m is a γ-ray-emitting radionuclide (half-life = 6 hr) with an energy of 140 kev. The low energy and short half-life of this radionuclide make it suitable for external scintigraphic studies involving humans, and the radiation dose is minimal.

Following oral administration with 100 ml of water, the normal subject was placed in a supine position on a hard top stretcher for general body immobilization. The abdomen was then positioned beneath the collimated detector of a multicrystal scintillation camera[3]. Data were accumulated for up to 200 min, when necessary, at 1-min intervals. These 1-min count integrations were stored on the computer magnetic tape for future retrieval.

During data collection, scintiphotos were taken. These scintiphotos (Fig. 1) showed the release of radioactivity from the capsule region to the other portions of the stomach as a function of time. The pictures also illustrated the lack of capsule movement within the stomach, the swelling of the capsule, and, finally, the release and dispersion of the capsule contents to other stomach regions (Fig. 1).

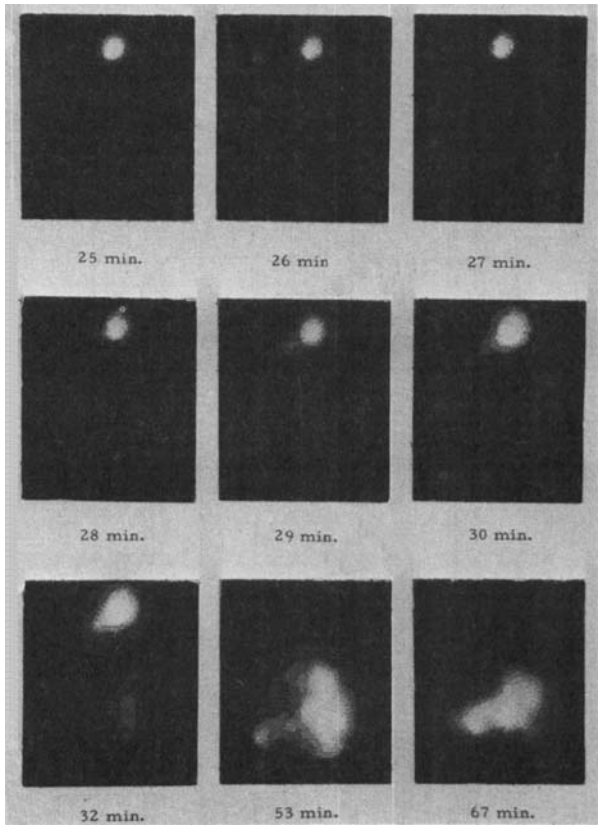

Figure 1—*Sequential scintiphotos of intermittent phases of the* in vivo *collapse of a gelatin capsule using Formulation A (empty stomach).*

Although the scintiphotos gave a qualitative picture of the release of the capsule contents, quantitative determination of the absolute capsule disintegration rate was performed with the aid of a computer. We chose an area of interest directly over the capsule and an area of

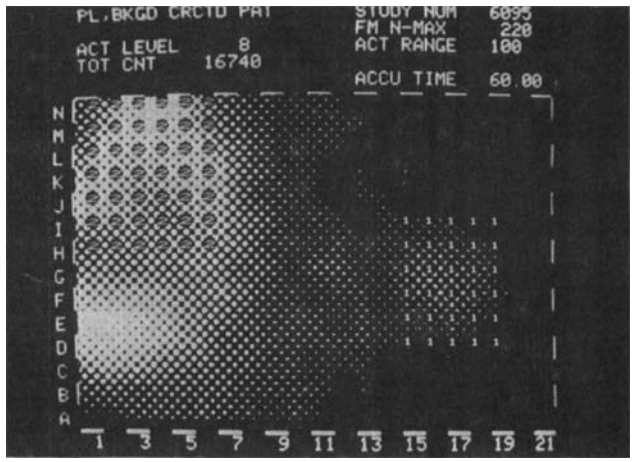

Figure 2—*Scintiphotos showing the two computer areas of interest within the stomach. Key: 1, area of interest over the capsule; and 2, area of interest over the pyloric region of the stomach.*

[1] Gelatin capsules No. 0, Eli Lilly and Co., Indianapolis, IN 46206
[2] Osteoscan, Procter and Gamble Co., Cincinnati, Ohio.
[3] Gamma-camera (Baird Atomic-System 77) equipped with a computer and magnetic tape and possessing storage and replay capability.

Supported by grants from the National Cancer Institute (CA-17625) and the American Cancer Society (CH-19). We thank Dr. David L. Harris, Chemistry Department, University of North Carolina at Chapel Hill, for assistance in carrying out the INDOR experiments. The XL-100 NMR spectrometer was purchased by grants from the National Science Foundation and the National Institutes of Health to the Department of Chemistry, University of North Carolina at Chapel Hill.

[x] To whom inquiries should be directed.

Method for Monitoring Hard Gelatin Capsule Disintegration Times in Humans Using External Scintigraphy

Keyphrases □ Gelatin capsules, hard—disintegration and drug release times *in vivo* monitored by external scintigraphy using technetium Tc 99m □ Disintegration time—hard gelatin capsules *in vivo*, monitored by external scintigraphy □ Drug release time—hard gelatin capsules *in vivo*, monitored by external scintigraphy □ Technetium Tc 99m—used in scintigraphic monitoring of disintegration and drug release times of gelatin capsules *in vivo* □ Scintigraphy, external—disintegration and drug release times of gelatin capsules monitored

To the Editor:

We wish to report a noninvasive and novel approach for monitoring disintegration and drug release times from a gelatin capsule in humans. The method involves the utilization of a short-lived radionuclide coupled with external scintigraphy.

Two separate formulations were used to fill identical hard gelatin capsules[1]. Formulation A consisted of 150 mg of a totally water-insoluble polystyrene resin (40–100 mesh) bearing polyamine functions which chelated the radionuclide, technetium Tc 99m, in an irreversible manner (1). Formulation B was water soluble, consisting of 145 mg of lactose and 5.9 mg of the soluble chelating agent etidronate disodium[2] labeled with technetium Tc 99m.

In a typical experiment, the subject ingested a gelatin capsule[1] filled with an appropriate material labeled with 20 mCi of technetium Tc 99m. Technetium Tc 99m is a γ-ray-emitting radionuclide (half-life = 6 hr) with an energy of 140 kev. The low energy and short half-life of this radionuclide make it suitable for external scintigraphic studies involving humans, and the radiation dose is minimal.

Following oral administration with 100 ml of water, the normal subject was placed in a supine position on a hard top stretcher for general body immobilization. The abdomen was then positioned beneath the collimated detector of a multicrystal scintillation camera[3]. Data were accumulated for up to 200 min, when necessary, at 1-min intervals. These 1-min count integrations were stored on the computer magnetic tape for future retrieval.

During data collection, scintiphotos were taken. These scintiphotos (Fig. 1) showed the release of radioactivity from the capsule region to the other portions of the stomach as a function of time. The pictures also illustrated the lack of capsule movement within the stomach, the swelling of the capsule, and, finally, the release and dispersion of the capsule contents to other stomach regions (Fig. 1).

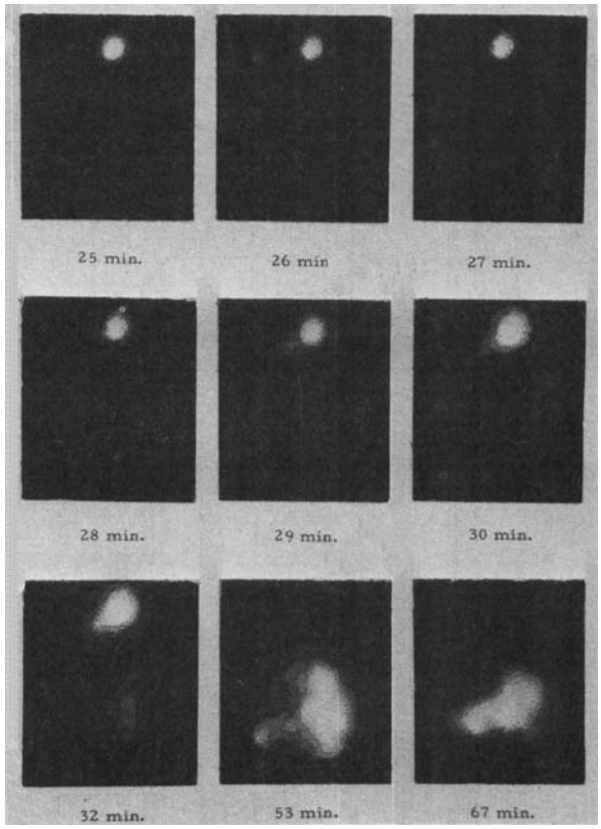

Figure 1—*Sequential scintiphotos of intermittent phases of the* in vivo *collapse of a gelatin capsule using Formulation A (empty stomach).*

Although the scintiphotos gave a qualitative picture of the release of the capsule contents, quantitative determination of the absolute capsule disintegration rate was performed with the aid of a computer. We chose an area of interest directly over the capsule and an area of

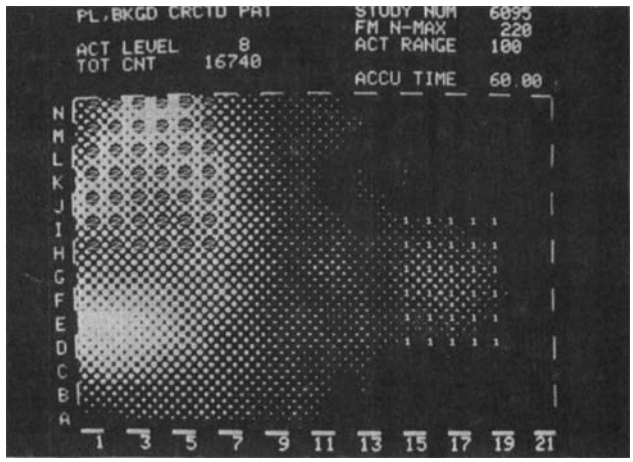

Figure 2—*Scintiphotos showing the two computer areas of interest within the stomach. Key: 1, area of interest over the capsule; and 2, area of interest over the pyloric region of the stomach.*

[1] Gelatin capsules No. 0, Eli Lilly and Co., Indianapolis, IN 46206
[2] Osteoscan, Procter and Gamble Co., Cincinnati, Ohio.
[3] Gamma-camera (Baird Atomic-System 77) equipped with a computer and magnetic tape and possessing storage and replay capability.

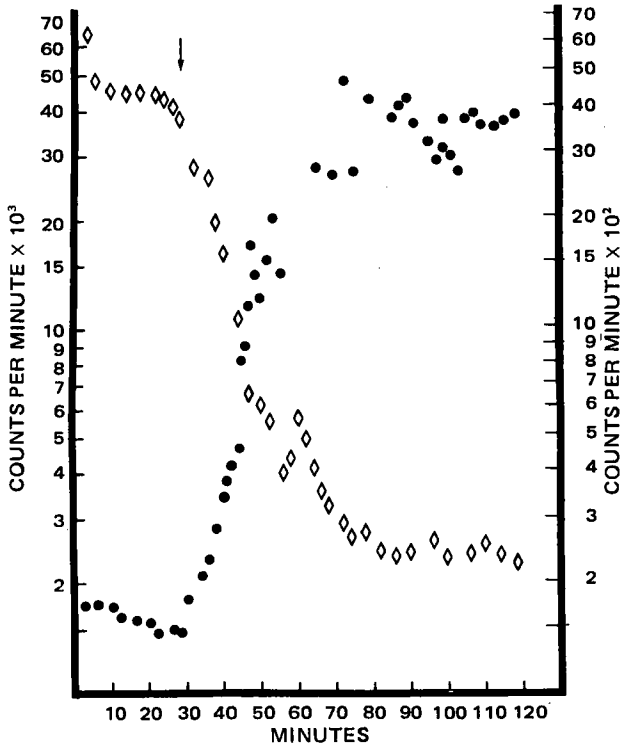

Figure 3—*Graphic display illustrating release of radioactivity from a gelatin capsule in the human stomach using Formulation A (empty stomach). Key: ◊, disappearance of radioactivity from the capsule region (Area 1, Fig. 2); and ●, concomitant appearance of radioactivity in the pyloric region of the stomach.*

interest in the lower pyloric region of the stomach (Fig. 2). Continuous monitoring of the radioactivity in the two regions, as a function of time, showed a sharp decrease in radioactivity in the capsule region, marking the time of its collapse, with a concomitant increase at the pyloric region. A typical plot is shown in Fig. 3. Further follow-up (Fig. 3) on the rate of passage of radioactivity through the lower stomach provided data for the estimation of gastric emptying times (1).

When the Formulation A capsule was administered to two subjects on an empty stomach, the scintiphotos and the integrated computer plots showed that the release of the capsule contents began 30 (Subject 1, Fig. 3) and 40 (Subject 2) min after ingestion. On a full stomach, the same two subjects exhibited much longer times for initial release of the contents, 93 and 120 min, respectively. In all cases, the capsule remained stationary and the capsule contents dispersed immediately to the other regions of the stomach after the initial release.

Upon administration of the Formulation B capsule to Subject 1 on an empty stomach, the initial release of radioactivity occurred after only 6 min. Considerable swelling of the capsule was also observed before the release. The decrease of activity from the capsule region was gradual up until 56 min after administration. At this point, there was a sharp break in the curve, indicating virtually complete disappearance of radioactivity from the capsule region.

The observed differences in the times of release of Formulations A and B from identical capsules can be explained on the basis of the differences in these formulations. The relatively large (40–100 mesh) insoluble resin particles of Formulation A can be dispersed into the stomach only after major collapse of the capsule walls, a rather lengthy process. But the water-soluble Formulation B can be released in a shorter time because the gastric juices gain access to the interior of the capsule *via* a small orifice or diffusion through the walls. These findings are consistent with the previously reported observation that increasing the water-soluble nature of a formulation will increase its rate of release from a gelatin capsule (2–4). It is also known that particle size and type of diluents or fillers used in various formulations can drastically affect the rate of their release from gelatin capsules (5).

In conclusion, this technique can provide valuable information regarding the *in vivo* behavior of capsules. The present method is noninvasive and exposes the subjects to an extremely low radiation dose. If the experiment is conducted with 20 μCi of technetium Tc 99m, the radiation dose to the whole body is 1 mrad and that to the stomach is 10 mrads (1). The present study illustrates the great potential of external scintigraphy in the assessment of drug formulations.

(1) M. C. Theodorakis, Ph.D. thesis, University of Kentucky, Lexington, Ky., 1975.

(2) L. L. Augsburger, in "Sprowls' American Pharmacy," 7th ed., L. W. Dittert, Ed., Lippincott, Philadelphia, Pa., 1974, chap. 10.

(3) J. M. Newton, G. Rowley, and J. F. V. Thornblom, *J. Pharm. Pharmacol.*, **23**, 452(1971).

(4) *Ibid.*, **23**, 156S(1971).

(5) J. G. Wagner, "Biopharmaceutics and Relevant Pharmacokinetics," 1st ed., Hamilton Press, Hamilton, Ill., 1971, p. 116.

Dennis L. Casey
Robert M. Beihn
George A. Digenis ˣ
Manvendra B. Shambhu
Divisions of Medicinal Chemistry and Nuclear Medicine
Colleges of Pharmacy and Medicine
University of Kentucky
Lexington, KY 40506

Received March 1, 1976.
Accepted for publication June 7, 1976.
We thank Ms. S. Yonts for assistance.
ˣ To whom inquiries should be directed.

High-Pressure Liquid Chromatographic Determination of Polythiazide in Pharmaceutical Dosage Forms

Keyphrases □ Polythiazide—high-pressure liquid chromatographic analysis, pharmaceutical dosage forms □ High-pressure liquid chromatography—analysis, polythiazide in pharmaceutical dosage forms □ Diuretics—polythiazide, high-pressure liquid chromatographic analysis in pharmaceutical dosage forms

To the Editor:

A recent report by Moskalyk *et al.* (1) utilized a high-pressure liquid chromatographic (HPLC) method

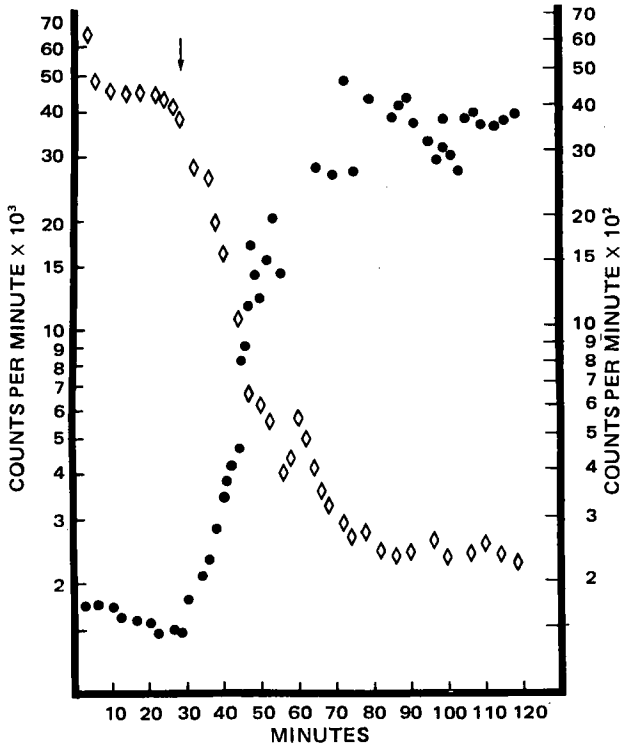

Figure 3—*Graphic display illustrating release of radioactivity from a gelatin capsule in the human stomach using Formulation A (empty stomach). Key: ◊, disappearance of radioactivity from the capsule region (Area 1, Fig. 2); and ●, concomitant appearance of radioactivity in the pyloric region of the stomach.*

interest in the lower pyloric region of the stomach (Fig. 2). Continuous monitoring of the radioactivity in the two regions, as a function of time, showed a sharp decrease in radioactivity in the capsule region, marking the time of its collapse, with a concomitant increase at the pyloric region. A typical plot is shown in Fig. 3. Further follow-up (Fig. 3) on the rate of passage of radioactivity through the lower stomach provided data for the estimation of gastric emptying times (1).

When the Formulation A capsule was administered to two subjects on an empty stomach, the scintiphotos and the integrated computer plots showed that the release of the capsule contents began 30 (Subject 1, Fig. 3) and 40 (Subject 2) min after ingestion. On a full stomach, the same two subjects exhibited much longer times for initial release of the contents, 93 and 120 min, respectively. In all cases, the capsule remained stationary and the capsule contents dispersed immediately to the other regions of the stomach after the initial release.

Upon administration of the Formulation B capsule to Subject 1 on an empty stomach, the initial release of radioactivity occurred after only 6 min. Considerable swelling of the capsule was also observed before the release. The decrease of activity from the capsule region was gradual up until 56 min after administration. At this point, there was a sharp break in the curve, indicating virtually complete disappearance of radioactivity from the capsule region.

The observed differences in the times of release of Formulations A and B from identical capsules can be explained on the basis of the differences in these formulations. The relatively large (40–100 mesh) insoluble resin particles of Formulation A can be dispersed into the stomach only after major collapse of the capsule walls, a rather lengthy process. But the water-soluble Formulation B can be released in a shorter time because the gastric juices gain access to the interior of the capsule *via* a small orifice or diffusion through the walls. These findings are consistent with the previously reported observation that increasing the water-soluble nature of a formulation will increase its rate of release from a gelatin capsule (2–4). It is also known that particle size and type of diluents or fillers used in various formulations can drastically affect the rate of their release from gelatin capsules (5).

In conclusion, this technique can provide valuable information regarding the *in vivo* behavior of capsules. The present method is noninvasive and exposes the subjects to an extremely low radiation dose. If the experiment is conducted with 20 μCi of technetium Tc 99m, the radiation dose to the whole body is 1 mrad and that to the stomach is 10 mrads (1). The present study illustrates the great potential of external scintigraphy in the assessment of drug formulations.

(1) M. C. Theodorakis, Ph.D. thesis, University of Kentucky, Lexington, Ky., 1975.

(2) L. L. Augsburger, in "Sprowls' American Pharmacy," 7th ed., L. W. Dittert, Ed., Lippincott, Philadelphia, Pa., 1974, chap. 10.

(3) J. M. Newton, G. Rowley, and J. F. V. Thornblom, *J. Pharm. Pharmacol.*, **23**, 452(1971).

(4) *Ibid.*, **23**, 156S(1971).

(5) J. G. Wagner, "Biopharmaceutics and Relevant Pharmacokinetics," 1st ed., Hamilton Press, Hamilton, Ill., 1971, p. 116.

Dennis L. Casey
Robert M. Beihn
George A. Digenis ˣ
Manvendra B. Shambhu
Divisions of Medicinal Chemistry and Nuclear Medicine
Colleges of Pharmacy and Medicine
University of Kentucky
Lexington, KY 40506

Received March 1, 1976.
Accepted for publication June 7, 1976.
We thank Ms. S. Yonts for assistance.
ˣ To whom inquiries should be directed.

High-Pressure Liquid Chromatographic Determination of Polythiazide in Pharmaceutical Dosage Forms

Keyphrases □ Polythiazide—high-pressure liquid chromatographic analysis, pharmaceutical dosage forms □ High-pressure liquid chromatography—analysis, polythiazide in pharmaceutical dosage forms □ Diuretics—polythiazide, high-pressure liquid chromatographic analysis in pharmaceutical dosage forms

To the Editor:

A recent report by Moskalyk *et al.* (1) utilized a high-pressure liquid chromatographic (HPLC) method

Table I—Comparative Analyses of Three Commercially Available Polythiazide Tablet Preparations

Product	Components	Analyses, % of Label Claim: Method of Moskalyk *et al.* (1)	Analyses, % of Label Claim: Method of Wong *et al.*[a] (3)
I[b]	Polythiazide, 1 mg	110	102
II[b]	Polythiazide, 2 mg	108	101
III[c]	Polythiazide, 1 mg, and reserpine, 0.25 mg	112	106

[a] Average of four determinations. [b] Renese, Pfizer Co. Ltd. [c] Renese-R, Pfizer Co. Ltd.

for the determination of polythiazide in pharmaceutical dosage forms. Three independent methods were used to analyze polythiazide tablets[1] (1): TLC separation followed by a UV spectrophotometric determination (2), a colorimetric method (2), and the published HPLC method (1). The results obtained by Moskalyk *et al.* (1) with their method and the compendial TLC method indicated that the polythiazide tablets were superpotent, exceeding the NF XIII limit of 110% of label claim (2). We were concerned with this implication and initiated a detailed study of the published method.

The column[2] recommended by Moskalyk *et al.* (1) was conditioned with the mobile phase, methanol–water (35:65 v/v), for at least 16 hr at 100 psig inlet pressure. The inlet pressure of the liquid chromatograph[3] then was raised to 200 psig, the reported operating pressure (1). A standard solution of polythiazide and the internal standard, quinoline, was introduced into the chromatograph using a 10-μl loop injection valve; this solution was prepared in accordance with the proposed HPLC procedure (1).

The observed polythiazide peak at a detection wavelength of 254 nm was sharp and symmetrical, having a retention time of approximately 8 min *versus* the 7 min reported previously (1). No peak was observed at the retention time reported for the internal standard. Additional column conditioning (total time of 4 days) and injections did not improve the peak characteristics or detector sensitivity for the internal standard. Increasing both the quinoline concentration from the reported 230 mg/liter to 1 g/liter and the inlet pressure to 600 psig resulted in an observed peak for quinoline at a retention time of approximately 17 min *versus* the reported 10 min at 200 psig (1). The peak was extremely broad and tailed considerably. We could not reproduce the reported observations for the internal standard.

Figure 2 in Ref. 1 does not exhibit baseline separation for polythiazide and the suggested internal standard, quinoline. In our opinion, this separation is a necessity in the establishment of a quantitative analytical procedure. Also, chromatogram III and, possibly, chromatogram II in Fig. 2 show the presence of an unknown absorption between vanillin and polythiazide. This absorption is illustrated by the shoulder on the vanillin peak and the lack of return to the minimum detector response observed in chromatogram I. Table III in Ref. 1 does not agree with our experience with the compendial method (2). The investigators (1) stated that erratic results were obtained with the NF XIII and colorimetric methods for the quantitation of polythiazide in combination with reserpine. We encountered no such interference due to reserpine in either method.

The most significant point concerns the recovery studies. The authors (1) stated that the absolute recovery of added polythiazide was 0.212 ± 0.003 mg based on four replicate determinations. They also stated that the added polythiazide was only 0.20 mg. A method in which published recoveries of 106% are presented without further explanation cannot be used with confidence. Results with such a method must be considered biased high.

At the time the article by Moskalyk *et al.* (1) appeared, research was already underway in our laboratories to develop an HPLC method for polythiazide in pharmaceutical tablet formulations. A successful assay has been developed and is described in a separate publication (3). In an effort to justify our criticism of the published method (1), we analyzed the same products. It was ascertained which batches of each product were donated to Moskalyk *et al.* (1), and our samples were taken from the same source. Results obtained by our HPLC method (3) are presented in Table I and are compared with those of Moskalyk *et al.* If the results of Moskalyk *et al.* (1) are corrected for the reported 6% high bias, their data are in excellent agreement with the results obtained by our method (3).

(1) R. E. Moskalyk, R. A. Locock, L. G. Chatten, A. M. Veltman, and M. F. Bielech, *J. Pharm. Sci.*, **64**, 1406(1975).

(2) "The National Formulary," 13th ed., Mack Publishing Co., Easton, Pa., 1970, p. 565.

(3) C. K. Wong, D. Y. J. Tsau, D. M. Cohen, and K. P. Munnelly, *J. Pharm. Sci.*, in press.

D. M. Cohen [x]
K. P. Munnelly
Quality Control
Pfizer Inc.
Brooklyn, NY 11206

Received March 19, 1976.
Accepted for publication July 1, 1976.
[x] To whom inquiries should be directed.

[1] Renese and Renese-R, Pfizer Co. Ltd.
[2] Bondapak phenyl/Corasil, Catalog No. 27283, Waters Associates.
[3] DuPont model 820.

Ciguatera I: Brine Shrimp (*Artemia salina* L.) Larval Assay for Ciguatera Toxins

Keyphrases □ Ciguatera toxins—bioassay using brine shrimp larvae □ Fish toxins—ciguatera, bioassay using brine shrimp larvae □ Toxins, ciguatera—bioassay using brine shrimp larvae □ Bioassays—screening for ciguatera toxins using brine shrimp larvae

To the Editor:

No fully satisfactory bioassay for ciguatera toxins, a major problem for tropical and subtropical reef fisheries, has been described (1). Individual fish of most reef

Table I—Comparative Analyses of Three Commercially Available Polythiazide Tablet Preparations

Product	Components	Analyses, % of Label Claim: Method of Moskalyk *et al.* (1)	Analyses, % of Label Claim: Method of Wong *et al.*[a] (3)
I[b]	Polythiazide, 1 mg	110	102
II[b]	Polythiazide, 2 mg	108	101
III[c]	Polythiazide, 1 mg, and reserpine, 0.25 mg	112	106

[a] Average of four determinations. [b] Renese, Pfizer Co. Ltd. [c] Renese-R, Pfizer Co. Ltd.

for the determination of polythiazide in pharmaceutical dosage forms. Three independent methods were used to analyze polythiazide tablets[1] (1): TLC separation followed by a UV spectrophotometric determination (2), a colorimetric method (2), and the published HPLC method (1). The results obtained by Moskalyk *et al.* (1) with their method and the compendial TLC method indicated that the polythiazide tablets were superpotent, exceeding the NF XIII limit of 110% of label claim (2). We were concerned with this implication and initiated a detailed study of the published method.

The column[2] recommended by Moskalyk *et al.* (1) was conditioned with the mobile phase, methanol–water (35:65 v/v), for at least 16 hr at 100 psig inlet pressure. The inlet pressure of the liquid chromatograph[3] then was raised to 200 psig, the reported operating pressure (1). A standard solution of polythiazide and the internal standard, quinoline, was introduced into the chromatograph using a 10-μl loop injection valve; this solution was prepared in accordance with the proposed HPLC procedure (1).

The observed polythiazide peak at a detection wavelength of 254 nm was sharp and symmetrical, having a retention time of approximately 8 min *versus* the 7 min reported previously (1). No peak was observed at the retention time reported for the internal standard. Additional column conditioning (total time of 4 days) and injections did not improve the peak characteristics or detector sensitivity for the internal standard. Increasing both the quinoline concentration from the reported 230 mg/liter to 1 g/liter and the inlet pressure to 600 psig resulted in an observed peak for quinoline at a retention time of approximately 17 min *versus* the reported 10 min at 200 psig (1). The peak was extremely broad and tailed considerably. We could not reproduce the reported observations for the internal standard.

Figure 2 in Ref. 1 does not exhibit baseline separation for polythiazide and the suggested internal standard, quinoline. In our opinion, this separation is a necessity in the establishment of a quantitative analytical procedure. Also, chromatogram III and, possibly, chromatogram II in Fig. 2 show the presence of an unknown absorption between vanillin and polythiazide. This absorption is illustrated by the shoulder on the vanillin peak and the lack of return to the minimum detector response observed in chromatogram I. Table III in Ref. 1 does not agree with our experience with the compendial method (2). The investigators (1) stated that erratic results were obtained with the NF XIII and colorimetric methods for the quantitation of polythiazide in combination with reserpine. We encountered no such interference due to reserpine in either method.

The most significant point concerns the recovery studies. The authors (1) stated that the absolute recovery of added polythiazide was 0.212 ± 0.003 mg based on four replicate determinations. They also stated that the added polythiazide was only 0.20 mg. A method in which published recoveries of 106% are presented without further explanation cannot be used with confidence. Results with such a method must be considered biased high.

At the time the article by Moskalyk *et al.* (1) appeared, research was already underway in our laboratories to develop an HPLC method for polythiazide in pharmaceutical tablet formulations. A successful assay has been developed and is described in a separate publication (3). In an effort to justify our criticism of the published method (1), we analyzed the same products. It was ascertained which batches of each product were donated to Moskalyk *et al.* (1), and our samples were taken from the same source. Results obtained by our HPLC method (3) are presented in Table I and are compared with those of Moskalyk *et al.* If the results of Moskalyk *et al.* (1) are corrected for the reported 6% high bias, their data are in excellent agreement with the results obtained by our method (3).

(1) R. E. Moskalyk, R. A. Locock, L. G. Chatten, A. M. Veltman, and M. F. Bielech, *J. Pharm. Sci.*, **64**, 1406(1975).

(2) "The National Formulary," 13th ed., Mack Publishing Co., Easton, Pa., 1970, p. 565.

(3) C. K. Wong, D. Y. J. Tsau, D. M. Cohen, and K. P. Munnelly, *J. Pharm. Sci.*, in press.

D. M. Cohen [x]
K. P. Munnelly
Quality Control
Pfizer Inc.
Brooklyn, NY 11206

Received March 19, 1976.
Accepted for publication July 1, 1976.
[x] To whom inquiries should be directed.

[1] Renese and Renese-R, Pfizer Co. Ltd.
[2] Bondapak phenyl/Corasil, Catalog No. 27283, Waters Associates.
[3] DuPont model 820.

Ciguatera I: Brine Shrimp (*Artemia salina* L.) Larval Assay for Ciguatera Toxins

Keyphrases □ Ciguatera toxins—bioassay using brine shrimp larvae □ Fish toxins—ciguatera, bioassay using brine shrimp larvae □ Toxins, ciguatera—bioassay using brine shrimp larvae □ Bioassays—screening for ciguatera toxins using brine shrimp larvae

To the Editor:

No fully satisfactory bioassay for ciguatera toxins, a major problem for tropical and subtropical reef fisheries, has been described (1). Individual fish of most reef

species sometimes contain ciguatera toxin. The only tests for its presence use living animals. The most useful bioassays involve feeding flesh or organs of a suspect fish to a mongoose (2) or cat (3) or the intraperitoneal injection of suitable extracts into mice (2); death is the primary result looked for. Research on ciguatera toxins has been hindered by the lack of a sensitive bioassay that consumes little material.

We wish to report a new and sensitive bioassay procedure, utilizing brine shrimp (*Artemia salina* L.) larvae. This procedure was developed with the aid of confirmed ciguatera fish from the Caribbean.

Brine shrimp have been used for the bioassay of fungal toxins (4, 5), dinoflagellate toxins (6), morphine-like analgesics (7), anesthetics (8), and insecticides (9–11). Brine shrimp were unaffected by finely ground ciguatera fish (2). However, we found brine shrimp to be very sensitive to certain organic extracts of toxic fish. It is postulated, therefore, that the ciguatera toxins must be released from storage sites in the flesh and that certain organic solvents can release the toxins.

Rayner (12) demonstrated that at least one ciguatera toxin caused a marked increase in the passive transport of sodium ions across certain cell membranes. We reasoned that an animal, such as *A. salina*, which has a well-developed sodium pump, might be highly sensitive to such a toxin. This prompted an investigation of this animal as a possible test organism.

Six ciguatera fish[1], confirmed to contain the toxin by the mongoose assay or recovery from cases of human poisoning, were obtained. These fish included an amberjack (*Seriola dumerili*), an almico jack (*Seriola rivoliana*), a horse eye jack (*Caranx latus*), a misty grouper (*Epinephelus mystacinus*), a snapper, and an unidentified fish. The specimens were shipped, packed in dry ice, to our laboratory. These specimens were homogenized with acetone in a blender[2], cooled to −20°, filtered, and concentrated (3). The concentrates were extracted with hexane and then ether (13). The highest concentrations of toxin were in the ether extracts; the next highest concentrations were in the *n*-hexane extracts.

Twelve extracts (six ether and six hexane) were ranked one to 12 in potency by comparing the effects of administering 1% polysorbate 60 emulsions intraperitoneally to mice (14). The dose required in the mouse assays on these crude extracts was 30 ml/mouse. Precisely the same ranking of potency was obtained with the brine shrimp. Similar extracts of several specimens of marine fish, shown by the mouse assay (14) not to contain ciguatera toxin, were nontoxic to the brine shrimp. The nontoxic marine fish thus far studied include specimens of amberjack, horse eye jack, spanish mackerel (*Scomberomorus maculatus*), and blue tang (*Acanthurus coeruleus*).

The brine shrimp assay was carried out as follows. Approximately 100 freshly hatched larvae in 1.5 ml of artificial sea water were placed in each well of a spot plate. Then 0.5 ml of a 1% polysorbate 60 suspension of an extract of known concentration was added. Brine shrimp were observed frequently for 20 min and then at 1, 2, 8, and 24 hr. Many shrimp exhibited erratic, nonproductive, swimming movements prior to death. The number of dead shrimp was noted at each reading. The percent of dead shrimp ranged from 50 to 100% in 24 hr with toxic extracts but was less than 5% with nontoxic extracts. Concentrations of crude toxin used varied from 25 to 10 μg/ml. This assay was sufficiently sensitive to assay spots from a TLC plate.

(1) B. W. Halstead, "Poisonous and Venomous Marine Animals," vol. 2, U.S. Government Printing Office, Washington, D.C., 1967, pp. 63–290.

(2) A. H. Banner, P. J. Scheuer, S. Sasaki, P. Helfrich, and C. B. Alender, *Ann. N.Y. Acad. Sci.*, **90**, 770(1960).

(3) Y. Hashimoto, T. Yasumoto, H. Kamiya, and T. Yoshida, *Bull. Jpn. Soc. Sci. Fish.*, **35**, 327(1969).

(4) J. Harwig and P. M. Scott, *Appl. Microbiol.*, **21**, 1011(1971).

(5) R. Brown, J. Wildman, and R. Eppley, *J. Assoc. Offic. Anal. Chem.*, **51**, 905(1968).

(6) N. Trieff, M. McShan, D. Grajcer, and M. Alam, *Tex. Rep. Biol. Med.*, **31**, 409(1973).

(7) J. Richtu and A. Goldstein, *Psychopharmacologia*, **17**, 327(1970).

(8) A. B. Robinson, K. F. Manly, M. P. Anthony, J. F. Catchpool, and L. Pauling, *Science*, **149**, 1255(1965).

(9) A. S. Michael, C. G. Thompson, and M. Abramovitz, *ibid.*, **123**, 464(1956).

(10) W. A. Tarpley, *J. Econ. Entomol.*, **51**, 780(1958).

(11) D. S. Grosch, *Science*, **155**, 592(1966).

(12) M. D. Rayner, *Fed. Proc.*, **31**, 1139(1972).

(13) T. Yasumoto and P. J. Scheuer, *Toxicon*, **7**, 273(1969).

(14) A. H. Banner, P. J. Scheuer, S. Sasaki, P. Helfrich, and C. B. Alender, *Nature*, **197**, 1025(1961).

H. Ray Granade
Ping C. Cheng
Norman J. Doorenbos [x]
Department of Pharmacognosy
School of Pharmacy
University of Mississippi
University, MS 38677

Received February 19, 1976.
Accepted for publication June 17, 1976.
Supported in part by the Research Institute of Pharmaceutical Sciences, School of Pharmacy, University of Mississippi.
This work is a result of research sponsored by the NOAA Office of Sea Grant, Department of Commerce, under Grant 04-3-158-53.
Appreciation is expressed to Miss Judy Buelke for assistance.
[x] To whom inquiries should be directed.

[1] Furnished by Dr. Ed Towle, Island Resources Foundation, St. Thomas.
[2] Waring.

REVIEWS

Toxicology Annual 1974. Edited by C. L. WINEK, and S. P. SHANOR. Dekker, 270 Madison Ave., New York, NY 10016, 1975. 323 pp. 16.5 × 23.5 cm. Price $29.50.

This text is, as the editor states, ". . . not an annual review of topics in toxicology, but rather an annual publication of selected topics of current concern or interest in the broad field of toxicology." Many chapters, *e.g.*, Toxicity Problems Related to Oral Ingestion of Prolonged Dosage Forms, Postmortem Drug Level Changes, Research in the Treatment of Poisoning, Testing to Predict Ocular Hazards of Household Chemicals, and The Current Status of Saccharin, fall within the above objective, and clinically useful data were found in all.

Narcotic Drug Dependence is another interesting chapter and documents various problems associated with narcotic use such as the overdose syndrome; gastrointestinal, liver, cardiac, and renal disorders; and immunological alterations. Treatment modalities are also discussed. One criticism is that in Table 2, which cites the incidence of problems in pregnant drug users (*e.g.*, breech and premature deliveries and toxemia), information is presented for only three groups: heroin addicted, methadone withdrawal, and methadone maintenance. The reader would be able to evaluate the real significance of these narcotic-induced problems if an additional column listing the usual occurrence of these problems in pregnancy was included.

In Drug and Chemical Blood Levels, one table lists many commonly used drugs (*e.g.*, acetaminophen, chlordiazepoxide, dextropropoxyphene, and methaqualone) and their therapeutic (or normal), toxic, and lethal blood levels. While only one or two of the levels are cited for some compounds, the therapeutic range is documented for most, and this in itself is a valuable offering.

Chapters that could have been deleted are This is Veterinary Toxicology (provides little significant information) and The Marihuana Dilemma: Implications of Recent Research Into the Pharmacokinetics, Psychomotor Effects, and Cardiovascular Actions of THC (more appropriate for a pharmacology text).

Overall, the *Toxicology Annual 1974* provides very worthy material in several specific areas of toxicology. Health professionals in related disciplines would also find this book informative.

Reviewed by Frederick J. Goldstein
Philadelphia College of Pharmacy and Science
Philadelphia, PA 19104

Terpenoids and Steroids, Vol. 5. Edited by K. H. OVERTON. Specialist Periodical Reports, The Chemical Society, Burlington House, London WIV OBN, England, 1975. 390 pp. 15 × 22 cm. Price $57.75. (Orders should be addressed to: Special Issues Sales, American Chemical Society, 1155 Sixteenth Street, N.W., Washington, D.C. 20036)

This is the fifth volume on terpenoids and steroids in a valuable series first published 5 years ago. The aim of the various series of Specialist Periodical Reports is to provide systematic, comprehensive, and critical review coverage of progress in the major areas of chemical research. The various series, which now total 35, are being published annually or biennially on such topics as Foreign Compound Metabolism in Mammals; Biosynthesis; Alkaloids; Carbohydrate Chemistry; Amino-acids, Peptides and Proteins; Photochemistry; and Environmental Chemistry.

This volume does not contain a subject index but is organized in a systematic manner which facilitates finding any information being sought. The six pages in the Table of Contents outline this volume in detail. The chapters are divided into many sections which are identified in boldface type in the text as well as in the Table of Contents. These sections are further divided into subsections. Chapter titles are found at the top of every second page of the text. There is an author index which includes 4000 names. It is helpful to those following the research of a given individual.

This review is illustrated with drawings of 1900 chemical structures. It is documented with 2200 references, most of which are listed at the bottom of the first page of each chapter where used.

Part I, which covers the terpenoids, is divided into chapters which include Monoterpenoids, Sesquiterpenoids, Diterpenoids, Triterpenoids, Carotenoids and Polyterpenoids, Biosynthesis of Terpenoids and Steroids, and Naturally Occurring Terpenoids whose Structures have been Determined by X-Ray Analysis. Of special interest is this last chapter which provides references covering the last decade to the determination of over 500 chemical structures by X-ray analysis.

Part II, which covers steroids, includes two large chapters and a compilation of over 100 reviews on steroid chemistry covering the period 1969–1974.

The chapter on steroid properties and reactions is divided into sections based upon more common functional groups, a section on Compounds of Nitrogen and Sulfur, and sections on such important subjects as Molecular Rearrangements, Functionalization at Non-activated Positions, Photochemical Reactions, and Structure, Stereochemistry, and Conformational Analysis.

The chapter on steroid synthesis is a 2-year review which is divided into the following sections: Total Synthesis, Halogeno-steroids, Oestranes, Androstanes, Pregnanes and Corticoids, Seco-steroids, Cholestane and Analogues, Steroidal Insect and Plant Hormones, Steroidal Alkaloids, Sapogenins, Cardenolides, and Bufadienolides.

It is a credit to the editor and 10 reporters preparing this volume that it is so well written and organized. Everyone interested in the chemistry of terpenoids and/or steroids should have access to this volume and others in the series. They would be a great time saver and a source of many new ideas. I highly recommend this series.

Reviewed by Norman J. Doorenbos
School of Pharmacy
University of Mississippi
University, MS 38677

APhA Drug Names. Edited by CHRISTINE L. BAILEY, JANET D. SHOFF, and MARGARET F. ROSE. American Pharmaceutical Association, 2215 Constitution Ave., N.W., Washington, DC 20037, 1976. 192 pp. 14 × 21.5 cm. Price $5.00 (members, $3.50).

"APhA Drug Names" is a cross-referenced alphabetical listing of approximately 7200 drug names, both proprietary (brand or trade) and nonproprietary (generic). It includes names official in USP XIX and NF XIV, as well as those names established by the United States Adopted Names Council and the Food and Drug Administration. It lists both current and discontinued trade names and names of some drugs not yet marketed. Compendial nonprescription drugs and compendial and extensively prescribed combinations also are listed.

Of special interest is the fact that the nonproprietary name entries also include the names of manufacturers that market the drugs by the nonproprietary names. There is a separate list of discontinued products based on manufacturer-supplied information, as well as a directory of manufacturers' names and addresses.

Pharmacists and other health professionals will find this book a valuable source of drug nomenclature information.

Staff Review

REVIEWS

Toxicology Annual 1974. Edited by C. L. WINEK, and S. P. SHANOR. Dekker, 270 Madison Ave., New York, NY 10016, 1975. 323 pp. 16.5 × 23.5 cm. Price $29.50.

This text is, as the editor states, ". . . not an annual review of topics in toxicology, but rather an annual publication of selected topics of current concern or interest in the broad field of toxicology." Many chapters, *e.g.*, Toxicity Problems Related to Oral Ingestion of Prolonged Dosage Forms, Postmortem Drug Level Changes, Research in the Treatment of Poisoning, Testing to Predict Ocular Hazards of Household Chemicals, and The Current Status of Saccharin, fall within the above objective, and clinically useful data were found in all.

Narcotic Drug Dependence is another interesting chapter and documents various problems associated with narcotic use such as the overdose syndrome; gastrointestinal, liver, cardiac, and renal disorders; and immunological alterations. Treatment modalities are also discussed. One criticism is that in Table 2, which cites the incidence of problems in pregnant drug users (*e.g.*, breech and premature deliveries and toxemia), information is presented for only three groups: heroin addicted, methadone withdrawal, and methadone maintenance. The reader would be able to evaluate the real significance of these narcotic-induced problems if an additional column listing the usual occurrence of these problems in pregnancy was included.

In Drug and Chemical Blood Levels, one table lists many commonly used drugs (*e.g.*, acetaminophen, chlordiazepoxide, dextropropoxyphene, and methaqualone) and their therapeutic (or normal), toxic, and lethal blood levels. While only one or two of the levels are cited for some compounds, the therapeutic range is documented for most, and this in itself is a valuable offering.

Chapters that could have been deleted are This is Veterinary Toxicology (provides little significant information) and The Marihuana Dilemma: Implications of Recent Research Into the Pharmacokinetics, Psychomotor Effects, and Cardiovascular Actions of THC (more appropriate for a pharmacology text).

Overall, the *Toxicology Annual 1974* provides very worthy material in several specific areas of toxicology. Health professionals in related disciplines would also find this book informative.

Reviewed by Frederick J. Goldstein
Philadelphia College of Pharmacy and Science
Philadelphia, PA 19104

Terpenoids and Steroids, Vol. 5. Edited by K. H. OVERTON. Specialist Periodical Reports, The Chemical Society, Burlington House, London WIV OBN, England, 1975. 390 pp. 15 × 22 cm. Price $57.75. (Orders should be addressed to: Special Issues Sales, American Chemical Society, 1155 Sixteenth Street, N.W., Washington, D.C. 20036)

This is the fifth volume on terpenoids and steroids in a valuable series first published 5 years ago. The aim of the various series of Specialist Periodical Reports is to provide systematic, comprehensive, and critical review coverage of progress in the major areas of chemical research. The various series, which now total 35, are being published annually or biennially on such topics as Foreign Compound Metabolism in Mammals; Biosynthesis; Alkaloids; Carbohydrate Chemistry; Amino-acids, Peptides and Proteins; Photochemistry; and Environmental Chemistry.

This volume does not contain a subject index but is organized in a systematic manner which facilitates finding any information being sought. The six pages in the Table of Contents outline this volume in detail. The chapters are divided into many sections which are identified in boldface type in the text as well as in the Table of Contents. These sections are further divided into subsections. Chapter titles are found at the top of every second page of the text. There is an author index which includes 4000 names. It is helpful to those following the research of a given individual.

This review is illustrated with drawings of 1900 chemical structures. It is documented with 2200 references, most of which are listed at the bottom of the first page of each chapter where used.

Part I, which covers the terpenoids, is divided into chapters which include Monoterpenoids, Sesquiterpenoids, Diterpenoids, Triterpenoids, Carotenoids and Polyterpenoids, Biosynthesis of Terpenoids and Steroids, and Naturally Occurring Terpenoids whose Structures have been Determined by X-Ray Analysis. Of special interest is this last chapter which provides references covering the last decade to the determination of over 500 chemical structures by X-ray analysis.

Part II, which covers steroids, includes two large chapters and a compilation of over 100 reviews on steroid chemistry covering the period 1969–1974.

The chapter on steroid properties and reactions is divided into sections based upon more common functional groups, a section on Compounds of Nitrogen and Sulfur, and sections on such important subjects as Molecular Rearrangements, Functionalization at Non-activated Positions, Photochemical Reactions, and Structure, Stereochemistry, and Conformational Analysis.

The chapter on steroid synthesis is a 2-year review which is divided into the following sections: Total Synthesis, Halogeno-steroids, Oestranes, Androstanes, Pregnanes and Corticoids, Seco-steroids, Cholestane and Analogues, Steroidal Insect and Plant Hormones, Steroidal Alkaloids, Sapogenins, Cardenolides, and Bufadienolides.

It is a credit to the editor and 10 reporters preparing this volume that it is so well written and organized. Everyone interested in the chemistry of terpenoids and/or steroids should have access to this volume and others in the series. They would be a great time saver and a source of many new ideas. I highly recommend this series.

Reviewed by Norman J. Doorenbos
School of Pharmacy
University of Mississippi
University, MS 38677

APhA Drug Names. Edited by CHRISTINE L. BAILEY, JANET D. SHOFF, and MARGARET F. ROSE. American Pharmaceutical Association, 2215 Constitution Ave., N.W., Washington, DC 20037, 1976. 192 pp. 14 × 21.5 cm. Price $5.00 (members, $3.50).

"APhA Drug Names" is a cross-referenced alphabetical listing of approximately 7200 drug names, both proprietary (brand or trade) and nonproprietary (generic). It includes names official in USP XIX and NF XIV, as well as those names established by the United States Adopted Names Council and the Food and Drug Administration. It lists both current and discontinued trade names and names of some drugs not yet marketed. Compendial nonprescription drugs and compendial and extensively prescribed combinations also are listed.

Of special interest is the fact that the nonproprietary name entries also include the names of manufacturers that market the drugs by the nonproprietary names. There is a separate list of discontinued products based on manufacturer-supplied information, as well as a directory of manufacturers' names and addresses.

Pharmacists and other health professionals will find this book a valuable source of drug nomenclature information.

Staff Review

REVIEWS

Toxicology Annual 1974. Edited by C. L. WINEK, and S. P. SHANOR. Dekker, 270 Madison Ave., New York, NY 10016, 1975. 323 pp. 16.5 × 23.5 cm. Price $29.50.

This text is, as the editor states, ". . . not an annual review of topics in toxicology, but rather an annual publication of selected topics of current concern or interest in the broad field of toxicology." Many chapters, *e.g.*, Toxicity Problems Related to Oral Ingestion of Prolonged Dosage Forms, Postmortem Drug Level Changes, Research in the Treatment of Poisoning, Testing to Predict Ocular Hazards of Household Chemicals, and The Current Status of Saccharin, fall within the above objective, and clinically useful data were found in all.

Narcotic Drug Dependence is another interesting chapter and documents various problems associated with narcotic use such as the overdose syndrome; gastrointestinal, liver, cardiac, and renal disorders; and immunological alterations. Treatment modalities are also discussed. One criticism is that in Table 2, which cites the incidence of problems in pregnant drug users (*e.g.*, breech and premature deliveries and toxemia), information is presented for only three groups: heroin addicted, methadone withdrawal, and methadone maintenance. The reader would be able to evaluate the real significance of these narcotic-induced problems if an additional column listing the usual occurrence of these problems in pregnancy was included.

In Drug and Chemical Blood Levels, one table lists many commonly used drugs (*e.g.*, acetaminophen, chlordiazepoxide, dextropropoxyphene, and methaqualone) and their therapeutic (or normal), toxic, and lethal blood levels. While only one or two of the levels are cited for some compounds, the therapeutic range is documented for most, and this in itself is a valuable offering.

Chapters that could have been deleted are This is Veterinary Toxicology (provides little significant information) and The Marihuana Dilemma: Implications of Recent Research Into the Pharmacokinetics, Psychomotor Effects, and Cardiovascular Actions of THC (more appropriate for a pharmacology text).

Overall, the *Toxicology Annual 1974* provides very worthy material in several specific areas of toxicology. Health professionals in related disciplines would also find this book informative.

Reviewed by Frederick J. Goldstein
Philadelphia College of Pharmacy and Science
Philadelphia, PA 19104

Terpenoids and Steroids, Vol. 5. Edited by K. H. OVERTON. Specialist Periodical Reports, The Chemical Society, Burlington House, London WIV OBN, England, 1975. 390 pp. 15 × 22 cm. Price $57.75. (Orders should be addressed to: Special Issues Sales, American Chemical Society, 1155 Sixteenth Street, N.W., Washington, D.C. 20036)

This is the fifth volume on terpenoids and steroids in a valuable series first published 5 years ago. The aim of the various series of Specialist Periodical Reports is to provide systematic, comprehensive, and critical review coverage of progress in the major areas of chemical research. The various series, which now total 35, are being published annually or biennially on such topics as Foreign Compound Metabolism in Mammals; Biosynthesis; Alkaloids; Carbohydrate Chemistry; Amino-acids, Peptides and Proteins; Photochemistry; and Environmental Chemistry.

This volume does not contain a subject index but is organized in a systematic manner which facilitates finding any information being sought. The six pages in the Table of Contents outline this volume in detail. The chapters are divided into many sections which are identified in boldface type in the text as well as in the Table of Contents. These sections are further divided into subsections. Chapter titles are found at the top of every second page of the text. There is an author index which includes 4000 names. It is helpful to those following the research of a given individual.

This review is illustrated with drawings of 1900 chemical structures. It is documented with 2200 references, most of which are listed at the bottom of the first page of each chapter where used.

Part I, which covers the terpenoids, is divided into chapters which include Monoterpenoids, Sesquiterpenoids, Diterpenoids, Triterpenoids, Carotenoids and Polyterpenoids, Biosynthesis of Terpenoids and Steroids, and Naturally Occurring Terpenoids whose Structures have been Determined by X-Ray Analysis. Of special interest is this last chapter which provides references covering the last decade to the determination of over 500 chemical structures by X-ray analysis.

Part II, which covers steroids, includes two large chapters and a compilation of over 100 reviews on steroid chemistry covering the period 1969–1974.

The chapter on steroid properties and reactions is divided into sections based upon more common functional groups, a section on Compounds of Nitrogen and Sulfur, and sections on such important subjects as Molecular Rearrangements, Functionalization at Non-activated Positions, Photochemical Reactions, and Structure, Stereochemistry, and Conformational Analysis.

The chapter on steroid synthesis is a 2-year review which is divided into the following sections: Total Synthesis, Halogeno-steroids, Oestranes, Androstanes, Pregnanes and Corticoids, Seco-steroids, Cholestane and Analogues, Steroidal Insect and Plant Hormones, Steroidal Alkaloids, Sapogenins, Cardenolides, and Bufadienolides.

It is a credit to the editor and 10 reporters preparing this volume that it is so well written and organized. Everyone interested in the chemistry of terpenoids and/or steroids should have access to this volume and others in the series. They would be a great time saver and a source of many new ideas. I highly recommend this series.

Reviewed by Norman J. Doorenbos
School of Pharmacy
University of Mississippi
University, MS 38677

APhA Drug Names. Edited by CHRISTINE L. BAILEY, JANET D. SHOFF, and MARGARET F. ROSE. American Pharmaceutical Association, 2215 Constitution Ave., N.W., Washington, DC 20037, 1976. 192 pp. 14 × 21.5 cm. Price $5.00 (members, $3.50).

"APhA Drug Names" is a cross-referenced alphabetical listing of approximately 7200 drug names, both proprietary (brand or trade) and nonproprietary (generic). It includes names official in USP XIX and NF XIV, as well as those names established by the United States Adopted Names Council and the Food and Drug Administration. It lists both current and discontinued trade names and names of some drugs not yet marketed. Compendial nonprescription drugs and compendial and extensively prescribed combinations also are listed.

Of special interest is the fact that the nonproprietary name entries also include the names of manufacturers that market the drugs by the nonproprietary names. There is a separate list of discontinued products based on manufacturer-supplied information, as well as a directory of manufacturers' names and addresses.

Pharmacists and other health professionals will find this book a valuable source of drug nomenclature information.

Staff Review

Journal of Pharmaceutical Sciences

OCTOBER 1976

VOLUME 65 NUMBER 10

MARY H. FERGUSON
Editor

L. LUAN CORRIGAN
Assistant Editor

SHELLY ELLIOTT
Production Editor

JANET D. SHOFF
Copy Editor

EDWARD G. FELDMANN
Contributing Editor

SAMUEL W. GOLDSTEIN
Contributing Editor

LELAND J. ARNEY
Publications Director

EDITORIAL ADVISORY BOARD

JOHN AUTIAN	HARRY B. KOSTENBAUDER
LYNN R. BRADY	CARL J. LINTNER, JR.
WILLIAM O. FOYE	DAVID E. MANN, JR.
WILLIAM J. JUSKO	GERALD J. PAPARIELLO

The *Journal of Pharmaceutical Sciences* is published monthly by the American Pharmaceutical Association at 2215 Constitution Ave., N.W., Washington, DC 20037. Second-class postage paid at Washington, D.C., and at additional mailing office.

All expressions of opinion and statements of supposed fact appearing in articles or editorials carried in this journal are published on the authority of the writer over whose name they appear and are not to be regarded as necessarily expressing the policies or views of the American Pharmaceutical Association.

Offices—Editorial, Advertising, and Subscription Offices: 2215 Constitution Ave., N.W., Washington, DC 20037. Printing Offices: 20th & Northampton Streets, Easton, PA 18042.

Annual Subscriptions—United States and foreign, industrial and government institutions $50, educational institutions $50, individuals *for personal use only* $30; single copies $5. All foreign subscriptions add $5 for postage. Subscription rates are subject to change without notice. Members of the American Pharmaceutical Association may elect to receive the *Journal of Pharmaceutical Sciences* as a part of their annual $60 (foreign $65) APhA membership dues.

Claims—Missing numbers will not be supplied if dues or subscriptions are in arrears for more than 60 days or if claims are received more than 60 days after the date of the issue, or if loss was due to failure to give notice of change of address. The Association cannot accept responsibility for foreign delivery when its records indicate shipment has been made.

Change of Address—Members and subscribers should notify at once both the Post Office and the American Pharmaceutical Association, 2215 Constitution Ave., N.W., Washington, DC 20037, of any change of address.

© Copyright 1976, American Pharmaceutical Association, 2215 Constitution Ave., N.W., Washington, DC 20037; all rights reserved.

RESEARCH IN THE FUTURE

A favorite, albeit harmless, pastime of those people involved in either conducting or reporting pharmaceutical research is to speculate on the future trends, directions, magnitude, and shape that such research is likely to assume. A key factor which is missing from this hypothetical equation is the thinking and viewpoint of those who "pay the tab" and who, as such, are in the ultimate position of decision making.

Recently, a high-powered conference was held in Washington to discuss various aspects of the economic impact of health-care legislation and, more specifically, to assess the probable economic effects if national health insurance were to be enacted. One of the speakers was the president of a major pharmaceutical company, with a definite reputation for being research oriented.

The speaker was John J. Pfeiffer of Winthrop Laboratories, a division of Sterling Drug, and in his remarks he included some pointed comments relative to future research in the pharmaceutical industry. He appeared to be making these predictions irrespective of national health insurance; its enactment would have no evident influence on the changes he believes will be coming in the management of drug research.

On this subject, he began by noting that progress dictated the necessity of industry continuing a major research commitment and of making sure that the necessary funds for this purpose would be available. Having stated this initial premise, he then expressed a corollary view that industry also has a "mandate that we must monitor the output of research." Recognizing and admitting that such an approach would be quite complex, he offered three specific beliefs: (*a*) that research must be subjected to some sort of business and management operating controls; (*b*) that marketing considerations must have greater input into what is done in the research arena; and (*c*) that clinical efficacy testing alone will no longer be sufficient—industry testing of drugs for comparative efficacy will become essential.

Mr. Pfeiffer went on to express the further viewpoint that:

> *"Only the projects with the greatest return on investment will be pursued. Only research that has a greater than even chance of success will be allowed to continue. Projects will be measured more frequently and a greater number of 'Go and No-Go' decision steps will be necessary. In effect, the great opportunity will be in the proper use of research as a 'tool of management'."*

He elaborated by citing the need to improve the efficiency of research efforts and to adopt new philosophies of directing and administering research. As examples, the speaker predicted that research will be more centralized as a service function, there will be greater sharing of research, and even joint ventures will be established between independent firms having a common area of interest. He concluded with the observation that management will need to develop and exercise a much more hard-nosed attitude concerning the likelihood of a payoff developing. This would be in contrast to the present relatively easy-going climate in which it is "hard to kill some projects" once they have commenced, even though it becomes apparent that the probability of achieving success is not great.

Surely, Mr. Pfeiffer's views will come as a surprise to many who are currently engaged in pharmaceutical research. Undoubtedly, many of our readers will be disturbed by these comments and disagree with them. Our purpose in stating them in this column, however, is not to debate whether these views are just or unjust, valid or invalid, necessary or unnecessary. Rather, we feel that it is important that our readers be aware of the current thinking at corporate levels, inasmuch as these policies will control the general thrust and operating budget for industry research and, thereby, will determine much of the future course and direction of pharmaceutical research activity.

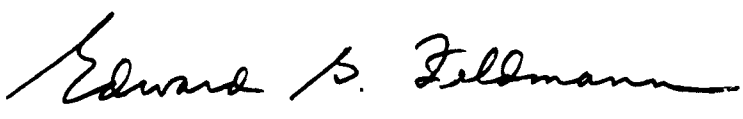

Journal of Pharmaceutical Sciences

OCTOBER 1976

VOLUME 65 NUMBER 10

MARY H. FERGUSON
Editor

L. LUAN CORRIGAN
Assistant Editor

SHELLY ELLIOTT
Production Editor

JANET D. SHOFF
Copy Editor

EDWARD G. FELDMANN
Contributing Editor

SAMUEL W. GOLDSTEIN
Contributing Editor

LELAND J. ARNEY
Publications Director

EDITORIAL ADVISORY BOARD

JOHN AUTIAN	HARRY B. KOSTENBAUDER
LYNN R. BRADY	CARL J. LINTNER, JR.
WILLIAM O. FOYE	DAVID E. MANN, JR.
WILLIAM J. JUSKO	GERALD J. PAPARIELLO

The *Journal of Pharmaceutical Sciences* is published monthly by the American Pharmaceutical Association at 2215 Constitution Ave., N.W., Washington, DC 20037. Second-class postage paid at Washington, D.C., and at additional mailing office.

All expressions of opinion and statements of supposed fact appearing in articles or editorials carried in this journal are published on the authority of the writer over whose name they appear and are not to be regarded as necessarily expressing the policies or views of the American Pharmaceutical Association.

Offices—Editorial, Advertising, and Subscription Offices: 2215 Constitution Ave., N.W., Washington, DC 20037. Printing Offices: 20th & Northampton Streets, Easton, PA 18042.

Annual Subscriptions—United States and foreign, industrial and government institutions $50, educational institutions $50, individuals *for personal use only* $30; single copies $5. All foreign subscriptions add $5 for postage. Subscription rates are subject to change without notice. Members of the American Pharmaceutical Association may elect to receive the *Journal of Pharmaceutical Sciences* as a part of their annual $60 (foreign $65) APhA membership dues.

Claims—Missing numbers will not be supplied if dues or subscriptions are in arrears for more than 60 days or if claims are received more than 60 days after the date of the issue, or if loss was due to failure to give notice of change of address. The Association cannot accept responsibility for foreign delivery when its records indicate shipment has been made.

Change of Address—Members and subscribers should notify at once both the Post Office and the American Pharmaceutical Association, 2215 Constitution Ave., N.W., Washington, DC 20037, of any change of address.

© Copyright 1976, American Pharmaceutical Association, 2215 Constitution Ave., N.W., Washington, DC 20037; all rights reserved.

RESEARCH IN THE FUTURE

A favorite, albeit harmless, pastime of those people involved in either conducting or reporting pharmaceutical research is to speculate on the future trends, directions, magnitude, and shape that such research is likely to assume. A key factor which is missing from this hypothetical equation is the thinking and viewpoint of those who "pay the tab" and who, as such, are in the ultimate position of decision making.

Recently, a high-powered conference was held in Washington to discuss various aspects of the economic impact of health-care legislation and, more specifically, to assess the probable economic effects if national health insurance were to be enacted. One of the speakers was the president of a major pharmaceutical company, with a definite reputation for being research oriented.

The speaker was John J. Pfeiffer of Winthrop Laboratories, a division of Sterling Drug, and in his remarks he included some pointed comments relative to future research in the pharmaceutical industry. He appeared to be making these predictions irrespective of national health insurance; its enactment would have no evident influence on the changes he believes will be coming in the management of drug research.

On this subject, he began by noting that progress dictated the necessity of industry continuing a major research commitment and of making sure that the necessary funds for this purpose would be available. Having stated this initial premise, he then expressed a corollary view that industry also has a "mandate that we must monitor the output of research." Recognizing and admitting that such an approach would be quite complex, he offered three specific beliefs: (*a*) that research must be subjected to some sort of business and management operating controls; (*b*) that marketing considerations must have greater input into what is done in the research arena; and (*c*) that clinical efficacy testing alone will no longer be sufficient—industry testing of drugs for comparative efficacy will become essential.

Mr. Pfeiffer went on to express the further viewpoint that:

> *"Only the projects with the greatest return on investment will be pursued. Only research that has a greater than even chance of success will be allowed to continue. Projects will be measured more frequently and a greater number of 'Go and No-Go' decision steps will be necessary. In effect, the great opportunity will be in the proper use of research as a 'tool of management'."*

He elaborated by citing the need to improve the efficiency of research efforts and to adopt new philosophies of directing and administering research. As examples, the speaker predicted that research will be more centralized as a service function, there will be greater sharing of research, and even joint ventures will be established between independent firms having a common area of interest. He concluded with the observation that management will need to develop and exercise a much more hard-nosed attitude concerning the likelihood of a payoff developing. This would be in contrast to the present relatively easy-going climate in which it is "hard to kill some projects" once they have commenced, even though it becomes apparent that the probability of achieving success is not great.

Surely, Mr. Pfeiffer's views will come as a surprise to many who are currently engaged in pharmaceutical research. Undoubtedly, many of our readers will be disturbed by these comments and disagree with them. Our purpose in stating them in this column, however, is not to debate whether these views are just or unjust, valid or invalid, necessary or unnecessary. Rather, we feel that it is important that our readers be aware of the current thinking at corporate levels, inasmuch as these policies will control the general thrust and operating budget for industry research and, thereby, will determine much of the future course and direction of pharmaceutical research activity.

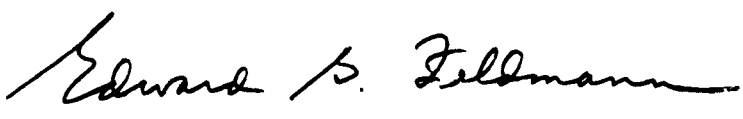

pKa for Medazepam

In the July issue of this Journal, le Petit[1] reported the pKa for medazepam in the Communications section. Since the data reported were not "new findings of outstanding importance," I assume that the impetus for publication was "corrections and reinterpretations of previously published reports."

By spectroscopic and solubility measurements, le Petit determined the pKa for medazepam to be 6.17 at 37°. He stated that "the findings disagreed with previous results." Two previous studies are cited. One[2] was a spectroscopic determination (pKa 4.4) at 20°. Thermodynamically, the pKa of a charged weak acid is expected to increase with a temperature increase. Thus, the difference between the two values is not surprising and no literature "correction" is necessary. The second study[3] reported a polarographic pK′ value of 8.7 (room temperature assumed). This value cannot be compared to the thermodynamic pKa of medazepam attributable to the azomethine functional group. Because of these erroneous comparisons, the paper is not scientifically valid, and I am surprised at the failure of our reviewing system to detect its inadequacies.

Additionally, if the comparisons had been valid and literature "corrections" necessary, I feel that the corrections should be published in the journal where the original error or misinterpretation was presented. Publication in the *Journal of Pharmaceutical Sciences* of data from other journals in need of correction is inappropriate and delays publication of original contributions.

Dale D. Maness
College of Pharmacy
University of Texas
Austin, TX 78712

Received July 30, 1976.

[1] G. F. le Petit, *J. Pharm. Sci.*, **65**, 1094(1976).
[2] J. Barrett, W. F. Smyth, and I. E. Davidson, *J. Pharm. Pharmacol.*, **25**, 387(1973).
[3] J. M. Clifford and W. F. Smyth, *Z. Anal. Chem.*, **264**, 149(1973).

Structured Water in Biology: A Revolution in the Making

The controversy over the role of structured water in cell physiology is steadily increasing in the literature[1]. The controversy is no longer about the existence of structured water in the cell but over the extent of its role in cell physiology. However, little of this controversy has appeared in the pharmaceutical literature.

Limitation of space precludes more than a resume of the contending positions. The classic position in biology holds that the cell is an aqueous medium in which various aggregates of molecules and ions are suspended, the whole of which is contained within a membrane. The membrane is a separate sac-like structure, which selectively permits reversible diffusion. Cytoplasm is considered to be in the same thermodynamic state as the extracellular aqueous medium in which the cell exists.

Therefore, when an entity such as the sodium ion is present in the extracellular fluids at a higher concentration than it is in the intracellular fluids under invariant conditions, it is necessary to postulate a mechanism, *i.e.*, a "pump," to maintain steady-state conditions. Since "pumping" is against a concentration gradient, it is also necessary to postulate the use of energy. Energy is considered to be available from metabolism.

An alternative view, referred to as "water structuring," maintains that the cytoplasm is in a different thermodynamic state, *i.e.*, lower dielectric constant, different colligative properties, *etc.*, than is the surrounding extracellular plasma. In this case, the concentration difference of intra- and extracellular sodium ions exists in equilibrium because the cytoplasm and plasma are in different thermodynamic states.

As an analogy, one may cite olive oil in contact with bulk water. If sodium chloride is introduced into this two-phase system and an equilibrium is reached, the concentration of salt in the oil will be much less than in the water. No energy-consuming pumps need be postulated to explain this equilibrium. The equilibrium is a function of chemical potential differences. The oil is thermodynamically analogous to the structured water (cytoplasm), and the bulk water is thermodynamically analogous to the bulk water of extracellular fluids.

Any critically decisive test of these concepts must involve the role of energy. Thus, how can the following fact be accounted for? The body is a perfect calorimeter, and an intake of 2000 calories in foodstuffs produces 2000 calories as heat. From the foregoing fact, the second law of thermodynamics would state that, in a reversible invariant system such as the body, there can be no energy available for work such as is required by the sodium pump[2].

A modification of the water structure concept, which has developed historically, regards the cytoplasm and all of its component molecules as being in a structured equilibrium. This structured cytoplasmic matrix is known as a coacervate phase. The membrane is an integral part of the cytoplasm and is the interface between the cytoplasm and the extracellular fluids. Since all of the components of the cytoplasm contribute to the equilibrium structure, a virtually infinite number of structural configurations are possible; these, in turn, explain the subtle solvent and other highly specific properties of the cell[3]. The growing acceptance of the concept that the membrane is a liquid structure fits more readily into the coacervate model than it does the sac-like classic model.

The basic concepts on which virtually all of the pharmaceutical sciences operate are involved in this controversy. This fact should be reflected in the pharmaceutical literature.

B. Ecanow
B. Gold
College of Pharmacy
University of Illinois
Chicago, IL 60612

R. S. Levinson
College of Pharmacy
University of Oklahoma
Norman, OK 73069

Received July 22, 1976.

[1] G. Kolata, *Science*, **192**, 1220(1976).
[2] N. Joseph, "Comparative Physical Biology," Karger, New York, N.Y., 1973.
[3] B. Ecanow and B. Gold, *J. Pharm. Sci.*, **63**(5), iv(1974); B. Ecanow and H. Klawans, in "Physical Chemical Models of Membranes in Models of Human Neurological Disease," 1st ed., H. Klawans, Ed., Excerpta Medica, Amsterdam, The Netherlands, 1974.

pKa for Medazepam

In the July issue of this Journal, le Petit[1] reported the pKa for medazepam in the Communications section. Since the data reported were not "new findings of outstanding importance," I assume that the impetus for publication was "corrections and reinterpretations of previously published reports."

By spectroscopic and solubility measurements, le Petit determined the pKa for medazepam to be 6.17 at 37°. He stated that "the findings disagreed with previous results." Two previous studies are cited. One[2] was a spectroscopic determination (pKa 4.4) at 20°. Thermodynamically, the pKa of a charged weak acid is expected to increase with a temperature increase. Thus, the difference between the two values is not surprising and no literature "correction" is necessary. The second study[3] reported a polarographic pK′ value of 8.7 (room temperature assumed). This value cannot be compared to the thermodynamic pKa of medazepam attributable to the azomethine functional group. Because of these erroneous comparisons, the paper is not scientifically valid, and I am surprised at the failure of our reviewing system to detect its inadequacies.

Additionally, if the comparisons had been valid and literature "corrections" necessary, I feel that the corrections should be published in the journal where the original error or misinterpretation was presented. Publication in the *Journal of Pharmaceutical Sciences* of data from other journals in need of correction is inappropriate and delays publication of original contributions.

Dale D. Maness
College of Pharmacy
University of Texas
Austin, TX 78712

Received July 30, 1976.

[1] G. F. le Petit, *J. Pharm. Sci.*, **65**, 1094(1976).
[2] J. Barrett, W. F. Smyth, and I. E. Davidson, *J. Pharm. Pharmacol.*, **25**, 387(1973).
[3] J. M. Clifford and W. F. Smyth, *Z. Anal. Chem.*, **264**, 149(1973).

Structured Water in Biology: A Revolution in the Making

The controversy over the role of structured water in cell physiology is steadily increasing in the literature[1]. The controversy is no longer about the existence of structured water in the cell but over the extent of its role in cell physiology. However, little of this controversy has appeared in the pharmaceutical literature.

Limitation of space precludes more than a resume of the contending positions. The classic position in biology holds that the cell is an aqueous medium in which various aggregates of molecules and ions are suspended, the whole of which is contained within a membrane. The membrane is a separate sac-like structure, which selectively permits reversible diffusion. Cytoplasm is considered to be in the same thermodynamic state as the extracellular aqueous medium in which the cell exists.

Therefore, when an entity such as the sodium ion is present in the extracellular fluids at a higher concentration than it is in the intracellular fluids under invariant conditions, it is necessary to postulate a mechanism, *i.e.*, a "pump," to maintain steady-state conditions. Since "pumping" is against a concentration gradient, it is also necessary to postulate the use of energy. Energy is considered to be available from metabolism.

An alternative view, referred to as "water structuring," maintains that the cytoplasm is in a different thermodynamic state, *i.e.*, lower dielectric constant, different colligative properties, *etc.*, than is the surrounding extracellular plasma. In this case, the concentration difference of intra- and extracellular sodium ions exists in equilibrium because the cytoplasm and plasma are in different thermodynamic states.

As an analogy, one may cite olive oil in contact with bulk water. If sodium chloride is introduced into this two-phase system and an equilibrium is reached, the concentration of salt in the oil will be much less than in the water. No energy-consuming pumps need be postulated to explain this equilibrium. The equilibrium is a function of chemical potential differences. The oil is thermodynamically analogous to the structured water (cytoplasm), and the bulk water is thermodynamically analogous to the bulk water of extracellular fluids.

Any critically decisive test of these concepts must involve the role of energy. Thus, how can the following fact be accounted for? The body is a perfect calorimeter, and an intake of 2000 calories in foodstuffs produces 2000 calories as heat. From the foregoing fact, the second law of thermodynamics would state that, in a reversible invariant system such as the body, there can be no energy available for work such as is required by the sodium pump[2].

A modification of the water structure concept, which has developed historically, regards the cytoplasm and all of its component molecules as being in a structured equilibrium. This structured cytoplasmic matrix is known as a coacervate phase. The membrane is an integral part of the cytoplasm and is the interface between the cytoplasm and the extracellular fluids. Since all of the components of the cytoplasm contribute to the equilibrium structure, a virtually infinite number of structural configurations are possible; these, in turn, explain the subtle solvent and other highly specific properties of the cell[3]. The growing acceptance of the concept that the membrane is a liquid structure fits more readily into the coacervate model than it does the sac-like classic model.

The basic concepts on which virtually all of the pharmaceutical sciences operate are involved in this controversy. This fact should be reflected in the pharmaceutical literature.

B. Ecanow
B. Gold
College of Pharmacy
University of Illinois
Chicago, IL 60612

R. S. Levinson
College of Pharmacy
University of Oklahoma
Norman, OK 73069

Received July 22, 1976.

[1] G. Kolata, *Science*, **192**, 1220(1976).
[2] N. Joseph, "Comparative Physical Biology," Karger, New York, N.Y., 1973.
[3] B. Ecanow and B. Gold, *J. Pharm. Sci.*, **63**(5), iv(1974); B. Ecanow and H. Klawans, in "Physical Chemical Models of Membranes in Models of Human Neurological Disease," 1st ed., H. Klawans, Ed., Excerpta Medica, Amsterdam, The Netherlands, 1974.

Journal of Pharmaceutical Sciences

OCTOBER 1976

VOLUME 65 NUMBER 10

REVIEW ARTICLE

Bioassays Used in Development of Topical Dosage Forms

JOHN K. HALEBLIAN

Keyphrases □ Bioassays—used in development and screening of topical dosage forms, review ■ Dosage forms, topical—development and screening, use of bioassays, review □ Topical dosage forms—development and screening, use of bioassays, review

CONTENTS

Antimicrobial Bioassays 1417
Antibacterial Formulations 1418
Antifungal Formulations 1419
Antiyeast Formulations 1420
Bioassays for Antimitotic Drugs for Topical Use 1420
Bioassays for Antiperspirant Formulations 1421
Bioassays for Sunscreen Formulations 1421
Bioassays for Antidandruff Formulations 1421
Bioassays for Anesthetic-Analgesic Formulations 1422
Bioassays for Antipruritic Formulations 1423
Bioassay for Antiwart Formulations 1423
Bioassays for Topical Formulations Used in Treatment of Rhus Dermatitis 1423
Bioassay for Topical Formulations Used in Treatment of Psoriasis 1423
Bioassays for Topical Corticosteroids 1424
Fibroblast Inhibition 1424
Thymus Involution 1424
Antigranuloma 1424
Inflammation 1424
Thinning of Epidermis 1427
Inhibition of Hair Growth 1428
Reduction of Mitotic Rate 1428
Vasoconstrictor 1428
Psoriasis Bioassay 1433
Clinical Correlation 1433
Conclusions 1434
References 1434

One main cause of the substantial decline in the introduction of new drugs in the United States in recent years is the prohibitive expense of exhaustive clinical trials required under Federal regulations (the cost of introducing a new drug entity is estimated to range from $2.25 to $15 million with an average of over $10.5 million) (1). Therefore, the pharmaceutical formulator cannot afford to submit to clinical investigation suboptimal dosage forms, which subsequently have to be reformulated and tested again.

To avoid this pitfall, model bioassays have been developed to screen various topical formulations prior to clinical trial. Many articles reviewing these bioassays have appeared in the medical and pharmaceutical literature, and a few review the entire field. Some bioassays used in developing topical corticosteroids (2–4) and for antimicrobials and corticosteroids (5) were reviewed. Similarly, a review of recent progress in the field of topical corticosteroid formulation was published (6).

The present review not only deals with the various bioassays used to test topical corticosteroid and antimicrobial formulations but also covers bioassays for antibacterials, antifungals, antiyeast formulations, antimitotics, antiperspirants, sunscreen agents, antidandruff formulations, and antipruritics. Hopefully, the reader will become informed about the use of these bioassays in the development of optimal formulations and thus avoid prematurely submitting dosage forms for expensive clinical evaluation.

ANTIMICROBIAL BIOASSAYS

Cultivating a model experimental infection that can be consistently reproduced and that persists long enough to evaluate formulations for their relative efficacy is one of the most difficult undertakings in the development of topical antimicrobial drugs. Several

antimicrobial bioassays that satisfy these requirements have been developed recently. For the purpose of this review, they are grouped under three headings: antibacterial formulations, antifungal formulations, and antiyeast formulations.

Antibacterial Formulations—A bioassay was developed which determines the penetration of bacteriostatic agents into the corium of human skin obtained from surgical specimens (7, 8). The antimicrobial agents are used either in their commercial vehicles or in special vehicles as indicated. In this procedure, plastic cylinders are attached to the epidermis with liquid adhesive, and the agent is applied to the skin circumvented by the wall of the plastic cylinder. Liquid vehicles are measured with pipets, and solid vehicles are weighed on a microbalance and then carefully transferred to the skin with a glass rod.

The specimens are incubated for 20–48 hr in a temperature- and humidity-controlled cabinet at 30° dry bulb, 27° wet bulb. After washing with soap and water, the epidermis is removed by exposure to a thermal plate (58–60°) for 2–4 min. Six-millimeter punches of the corium are taken and implanted on the culture medium, with the epidermal side of the corium in contact with the medium. Standard plastic petri dishes are used for all culture media, and bacteria are grown on a standard Mueller–Hinton medium. When inhibition of growth is seen around the implant of corium, the radius of inhibition is measured. This value refers to the distance from the edge of the corium implant to where active growth can be seen.

Penicillin and erythromycin showed definite evidence of penetration when this technique was used (7, 8). The differences in topical antibacterial effectiveness of various erythromycin esters were evaluated; ilotycin was three times as effective as its propionate, valerate, and benzoate esters. Vehicles varied in their ability to effect transport of antimicrobial agents through the epidermis. For example, 2% erythromycin in dimethylacetamide produced an average 5-mm radius of inhibition, while erythromycin in wool alcohols ointment[1] base only produced an average 1-mm radius of inhibition.

The efficacy of antibacterial formulations was studied in experimental human infections with *Staphylococcus aureus* (9–12). Infection sites were prepared by marking three 2 × 2-cm squares on the volar surface of each forearm. After delimiting the squares with adhesive tape, the horny layer was removed with cellophane tape down to the "glistening layer." These stripped sites were then left exposed for 24 hr. The inoculum was prepared by diluting 100-fold a "just hazy" saline suspension of a strain of *S. aureus* sensitive to ordinary antibiotics. Ten microliters of inoculum was applied to each square with a capillary micropipet. Then an occlusive dressing, consisting of a 2 × 2-cm square of plastic film and overlapping strips of cloth-backed adhesive tape, was applied immediately.

Six hours later, the bandages were removed and approximately 30 mg of antibacterial cream was applied in a double-blind fashion to each site (one site received no treatment). This quantity amply covered the surface when spread out under a 2 × 2-cm square of plastic film. The occlusive dressing was then reapplied for another 18 hr. The quantitative effect of the treatment on the density of *S. aureus* was measured by the detergent-scrub technique; clinical severity was assessed on a 0–4 scale, where 4 represents purulent erosion and 0 represents merely the effect of stripping (comparable to the uninoculated site) (9).

By using this technique, steroid–antibacterial formulations containing triamcinolone acetonide, neomycin, gramicidin, and nystatin were evaluated; the antibacterials were more effective in the steroid combination than when used alone.

In another set of experiments, three procedures were developed for appraising the ability of antibacterial chemicals and formulations to suppress the growth of microorganisms on human skin (13, 14). In each of the following tests, the microflora was quantified after the skin had been occluded for 1 day or more, a circumstance that normally leads to an explosive overgrowth of resident organisms.

Occlusion Test—This test is bacteriostatic and estimates the degree to which an antibacterial test agent prevents a relatively small number of microorganisms from increasing in number. In this procedure, two 5 × 5-cm squares are delimited with a marking pencil on the under surface of each forearm. The antibacterial test material is applied to one site, leaving the other site untreated as a control. Unformulated agents are applied in a volatile solvent such as water or alcohol, and rapid evaporation eliminates any antibacterial effect from the solvent. The sites are then covered with plastic film. (With creams and ointments, the materials are spread out over the test site by "massaging" the square of plastic over the site.) The plastic film is tightly sealed by encircling the arm with plastic tape. After 48 hr, the plastic is removed and the sites are immediately sampled by a detergent-scrub procedure and counted.

With this procedure, bacitracin, chloramphenicol, and neomycin were markedly inhibitory at 0.01% concentrations, while methylbenzethonium chloride and sodium pyrithione were effective at 0.1% concentrations. Hexachlorophene and povidone-iodine were effective only at 1% concentrations.

Expanded Flora Test—The expanded flora test was devised to account for circumstances in which huge numbers of organisms are already present and a bactericidal effect is also desirable. For this test, the resident organisms are allowed to reach a high population density by occluding the site for 48 hr before applying the test agent. The entire length of the forearm is wrapped snugly with several layers of plastic[2] wrap, which is sealed to the skin with plastic adhesive tape at the wrist and just below the elbow. The plastic wrapping is removed after 48 hr, and two 5 × 5-cm square test sites are marked out on each forearm. Test materials and plastic covering are then applied as in the occlusion test. After 48 hr, sampling and microbiological assays are conducted.

[1] Eucerin.

[2] Saran.

By this method, chloramphenicol and bacitracin were judged effective at 0.01%, neomycin at 0.1%, and hexachlorophene and sodium pyrithione at 1%. Methylbenzethonium chloride and povidone-iodine were ineffective.

Persistence Test—The persistence test was devised to measure the substantivity of the test antibacterial agent and to determine residual effectiveness several days after application. In this test, the 5 × 5-cm squares are marked out on the forearms as already described; test materials are applied to the sites three times per day for 3 days. The sites are left uncovered without restrictions for 3 days (washing with bland soap is permitted), followed by occlusion for 24 hr. The occluding film is then removed, and the sites are sampled and assayed as described previously. An untreated control site is not included, because there can be a transfer of activity with some very active materials, even to distant sites.

Antibiotic and chemotherapeutic compounds at 1% concentration were tested using this procedure. Of the antibiotics, chloramphenicol, neomycin, penicillin G, and gentamicin were effective.

Antifungal Formulations—Reiss *et al.* (15, 16) were among the earliest investigators to induce experimental *Microsporum lanosum* infections in dogs, cats, and rabbits for the purpose of screening antifungal compounds. The best models were newborn rabbits infected with *M. lanosum,* since they showed the least individual variation during the infection.

A controlled *in vivo* laboratory method was developed for screening antifungal ointments (17). In general, the screening procedure compares the efficacy of antifungal ointments in preventing typical *Trichophyton mentagrophytes* infections in guinea pigs.

A semi *in vivo* procedure was reported for testing antifungal agents for topical use (18). The potential activity of antifungal agents in solution is evaluated by measuring the immersion time necessary to kill *T. mentagrophytes* in infected epidermal scales obtained from guinea pigs. The fungicidal effect is dependent upon the penetrating and fungicidal activity of the test material.

Another *in vivo* model tested various vehicles for clotrimazole in experimentally induced *T. mentagrophytes* and *T. quinckeanum* infections in guinea pigs (19). A cream and a polyethylene glycol solution were identified as optimal formulations, were assessed clinically in open trials, and were highly efficacious (20).

Stoughton (7, 8) used his antibacterial technique to determine the penetration of antifungals into the corium of the human skin. Antifungal agents showed a surprising difference in their activity. For example, 1% tolnaftate[3] solution showed an average 3-mm radius of inhibition, while 1% thiabendazole showed an average 11-mm radius of inhibition.

Another experimental method, which induced inflammatory dermatophytosis on the skin of human volunteers, used purified spores of *T. mentagrophytes* (21, 22). Reproducible infections could be obtained by the application of a quantitated dose of spores to a measured skin area followed by continuous occlusion with a plastic patch for 4 days. Although not presently in use in antifungal bioassays, these infections may prove useful in the development of topical antifungals.

Knight (23–26) developed the most comprehensive human models for *in vivo* and *in vitro* assessments of topical antifungal formulations: induction of experimental human *T. mentagrophytes* infections and an *in vitro* assay using stripped human stratum corneum, respectively.

Experimental Human T. mentagrophytes *Infections*—In this bioassay, the infections are induced by applying 10,000 spores in 0.05 ml of sterile water to the upper arms. Four test sites are marked 5 cm apart on each arm. Each test site is a 4-cm square. A different antifungal compound is carefully applied to each site on one arm; the other arm serves as an untreated control. The test compound is left in place for 15 min, dabbed dry, and then washed and allowed to dry.

Inoculations are made on control and treated sites either immediately after drying or after a delay of 24 or 48 hr of normal activity. The spore solutions are covered with damp gauze, and the entire area is then covered with a square of polyethylene[4] pressed over previously sprayed adhesive to achieve a seal. The dressings are removed after 72 hr, and the sites are examined culturally and microscopically daily for 7 days. A positive infection is either culturally or microscopically positive.

In Vitro *Assay for Antifungal Compounds in Stratum Corneum*—In this bioassay, stratum corneum is stripped off by repeated application of translucent adhesive tape. The tape is then placed, with the stratum corneum surface uppermost, onto a microscope slide and fixed at each end by additional adhesive tape. The slide is placed on a bent glass rod in a petri dish and covered. The dish is sterilized in ethylene oxide gas for 4 hr at 53° at a pressure of 3.64 kg/6.45 cm^2 (8 $lb/in.^2$). The gas is allowed to disperse for 48 hr. Eight milliliters of sterile water is run into the bottom of the dish, and 0.005 ml of a spore suspension of *T. mentagrophytes* is applied to the center of the tape and spread. The lid is replaced, and the dish is stored at 30°.

After 7 days, the inoculated area is covered with a net-like mass of hyphae. If the fungus is growing under less than optimal conditions or if the stratum corneum contains an antifungal compound, the hyphae tend to be shorter. If the stratum corneum contains a high concentration of a fungistatic agent, only small, swollen, germinal tubes are produced (23). All cultures are graded from 0 to 3 on a severity scale.

The results of the evaluation of four antifungal formulations in experimental human *T. mentagrophytes* infections (23) are shown in Table I. All control sites showed positive infection when inoculated immediately after washing, while only one treated site (haloprogin) was infected. Sites treated with 1.0% dipyrithione sodium[5] cream and 5% thiabendazole in dimethylacet-

[3] Tinactin, Schering.

[4] Polythene.

[5] Omadine.

Table I—Results of Human Experimental *T. mentagrophytes* Infections after Prophylactic Use of Topical Antifungal Agents[a]

Hours	Number of Positive Infections				
		Treated Sites			
	Normal Sites	Haloprogin	Tolnaftate	Dipyrithione Sodium[b]	Thiabendazole
0	40/40	1/10	0/10	0/10	0/10
24	38/40	3/10	5/10	0/10	1/10
48	38/40	6/10	7/10	1/10	3/10

[a] Data from Ref. 23. [b] Omadine.

amide were well protected from inoculations 24 and 48 hr following application, while haloprogin and tolnaftate solutions were less effective.

Table II shows results with the same formulations using the *in vitro* stratum corneum bioassay (23). Twelve strippings were used, and all pretreatment scores approached the maximum. (On the 0–3 scale, the maximum degree of growth was 36.) At 0 hr, haloprogin, dipyrithione sodium[5], and thiabendazole completely inhibited hyphal growth, while tolnaftate proved ineffective. Haloprogin's effectiveness declined after 8 hr, and dipyrithione sodium and thiabendazole provided some protection for as long as 72 hr.

These two techniques using human models are relatively simple and produce reasonably consistent results. They indicate that topical antifungal agents are effective for prophylaxis and that one brief application may give protection lasting over 72 hr. With the exception of tolnaftate, the stratum corneum technique results indicate the same degree of prophylaxis with each agent as found in the *in vivo* human models. This finding may be helpful in future assays, because studies with the stratum corneum dermatophyte culture model are considerably easier to perform than those using *in vivo* human experimental infections.

Antiyeast Formulations—Experimental cutaneous *Candida albicans* infections have been attempted in dogs (27), mice (28), guinea pigs (29), rabbits (30), and humans (31–33). But the short duration of experimentally induced cutaneous infections has hampered the evaluation of topical antiyeast formulations. This shortcoming was overcome by using triamcinolone acetonide injections to lower the resistance of rabbits and to prolong the *Candida* infections for 1 month (30). *C. albicans* was introduced by a single scarification on the skin of albino rabbits injected subcutaneously with 10 mg of triamcinolone acetonide 1 week before infection and with 5 mg/week thereafter. The lesions were of the acute inflammatory type for about 1 week, entered a chronic stage with the formation of a thick crust (back) or desquamation of the epidermis (ear), and remained clinically evident and culturally positive for at least 35 days.

Table II—Comparison of the Effectiveness of Topical Antifungal Compounds as Shown by Inhibition of *T. mentagrophytes* Spore Growth on Stratum Corneum *In Vitro*[a]

Hours	Degree of Growth			
	Haloprogin	Tolnaftate	Dipyrithione Sodium[b]	Thiabendazole
Pretreatment	34	32	34	34
0	2	30	0	0
8	14	28	0	0
24	32	30	13	2
48	33	33	13	16
72	32	35	17	23

[a] Data from Ref. 23. [b] Omadine.

This method was used to compare the efficacy of various medications, including some currently used in the treatment of human candidiasis (30). Each rabbit was infected at 10 sites (1.5-cm diameter) on its back. One site in each rabbit was left untreated (infection control), one received a placebo, and the rest received the test medications in a random fashion. The medications were applied once a day for 5 consecutive days, and the cycle was repeated three times. Formulations containing 100,000 units of nystatin/g alone or in combination with other antibiotics and triamcinolone acetonide, 3% amphotericin B, 1% gentian violet, 1% 5-chloro-8-quinolinol, 1% 2-pyridinol 1-oxide, or 1% bis(2-pyridinyl 1-oxide) disulfide–stannous chloride complex were quite active. The latter compound was remarkably active, even at 0.25%.

Attempts to develop a human antiyeast bioassay have shown that a pustular dermatitis can be rapidly induced when a large number of *C. albicans* cells are placed on normal skin and occluded (31–33). The experimental *C. albicans* infection is produced by applying 10 μl of saline containing 10^3, 10^4, and 10^5 yeast cells on the volar surface of the forearm and immediately covering with a 2 × 2-cm square plastic film. This film is firmly sealed to the skin with 2.54-cm (1-in.) cloth-backed tape for 24 hr. Twenty-four hours after removing the dressing, the severity of dermatitis is rated + to +++++. Although this experimental human *C. albicans* infection has never been used to evaluate topical antiyeast formulations, it has a good potential for development of a useful human bioassay.

BIOASSAYS FOR ANTIMITOTIC DRUGS FOR TOPICAL USE

The effectiveness of drugs in diseases where there is an increase in cell proliferation has been generally attributed to their ability to interfere with the mitotic cycle. Since epidermal cells of skin normally have low mitotic rates, vaginal mucosa cells, which have a comparatively high rate of replication, were used (34–37). In this bioassay, test compounds were instilled intravaginally in 5–7-week-old virginal mice in 0.05-ml doses. The first dose was at time 0 and was repeated 2 hr later (concurrent with intraperitoneal injection of 2 mg of podophyllum resin). All mice were killed 6 hr later, and the vaginas were removed *en bloc* and fixed in 10% buffered formalin. Six-micrometer transverse sections were stained with hematoxylin and eosin and examined with an ocular micrometer to measure the number of mitoses per centimeter of mucosa. Only those specimens demonstrating the histological characteristics of the

estrogenic phase of the estrus cycle were included for analysis. A test drug yielding less than 100 mitoses/cm is considered antimitotic.

This bioassay was used to evaluate the efficacy of daunorubicin (daunomycin) and carmustine[6] (34), methotrexate analogs (35), and hydroxyurea and its derivatives (37). Also, it was used to compare bioassay results of 1-methylhydroxyurea and mechlorethamine to clinical efficacy in psoriasis lesions (35).

The vaginal mucosa bioassay was modified to study the effect of antimitotic agents on local DNA, RNA, and protein syntheses, and its usefulness in predicting the efficacy of topical treatments for psoriasis was recommended (38).

A bioassay using UV light was developed to stimulate epidermal hyperplasia (simulating psoriasis) in hairless mice (39–41). Antimitotic activity is measured by the mitotic index and radioactivity of extracted DNA. Among those compounds screened with the bioassay, cycloheximide has proven very effective; preliminary clinical studies with psoriasis confirmed this finding (42).

BIOASSAYS FOR ANTIPERSPIRANT FORMULATIONS

Two human bioassays were developed to determine the antiperspirant activity of topically applied anticholinergics (43, 44). In the first, the forearm antiperspirant test, 4.5-cm^2 circles are marked 1.9 cm (0.75 in.) apart on the inner aspect of the forearm. Test solutions are applied to each circle with a cotton-tipped swab and allowed to dry. This procedure is repeated three times, applying a total of 0.1–0.2 ml of solution. After about 5 hr, the forearm is washed with soap and water to remove any excess.

Sweat inhibition is measured by the starch–iodine technique (45) and is repeated without further treatment at 24 and 48 hr. Sweat inhibition is graded on a scale of 0–4: 0 = no sweat inhibition, control and treated areas are identical; 1 = poor sweat inhibition, treated area is just discernible because of fewer droplets; 2 = fair inhibition, treated area has only about half of its glands functioning; 3 = good inhibition, only a few scattered droplets are present in the treated area; and 4 = excellent inhibition, no sweat droplets are present in the treated area.

The alternative test is the axillary antiperspirant test in which 0.5–1.0 ml of the antiperspirant solution is applied to the entire axillary surface with a cotton-tipped swab or from a commercial roll-on dispenser. After a suitable time interval, the subject is placed in a room at a temperature of 37.8° (100°F) and a relative humidity of about 40–50%. Gravimetric sweat collections are made with tared pads, which are placed snugly in the axillary vault for 10 min. The pads are then placed in tared, tightly covered jars and weighed for comparison with a previously established, normal sweating pattern for each subject.

By using these techniques, various anticholinergic compounds have been found to inhibit sweating when topically applied. Among the compounds investigated, esters that contain one or more elements of atropine and scopolamine structure have the best activity of a long-lasting nature.

BIOASSAYS FOR SUNSCREEN FORMULATIONS

Since 1922, it has been known that sunburn and suntan in humans are caused by the action of only a narrow band within the UV spectrum (290–320 nm) (46). Many methods have been used to prevent actinic injury to the skin, but the most widely used is the topical application of sunscreens which absorb light and screen out harmful radiations. There are two major classifications of bioassays used to evaluate sunscreens: those using artificial light sources that mimic the UV spectrum of sunlight and those using direct sunlight.

The xenon solar simulator is one preferred artificial light source for sunscreen bioassays, because it reproduces spectral features of sunlight in the UV region (47). By means of a template, the skin of untanned adult volunteers is subdivided into small areas; fixed quantities of test sunscreens then are spread over each area. The areas are exposed for a predetermined time and examined at 24, 48, and 72 hr for severity of erythema. This technique was used to evaluate 3% concentrations of the sunscreen dipropylene glycol salicylate (dipsal) in six different vehicles, and the oil-in-water emulsions were found to be superior in promoting tanning (48). The technique also is useful in comparing the efficacy of sunscreen agents alone (47).

The procedure using direct sunlight is quite similar in that the untanned skin of adult volunteers is subdivided by a template prior to application of sunscreens and exposure to sunlight. This technique was used to evaluate selected sunscreens; 5% aminobenzoic acid in 70% ethanol and a cream containing oxybenzone and dioxybenzone were effective sunscreens (49). This procedure also can be used before and after bathing to show the water washability of various sunscreen preparations (49, 50).

Several *in vitro* methods not considered to be bioassays are also used to evaluate sunscreens. They include photographic and spectrophotometric methods (51, 52), thin-film techniques, and the solution–dilution method (53). Spectrophotometric methods also are used to evaluate the effect of vehicle components on the absorption characteristics of sunscreen compounds (54). A method was developed to evaluate the efficacy of sunscreens by analyzing stripped layers of epidermis following sunscreen application (55).

BIOASSAYS FOR ANTIDANDRUFF FORMULATIONS

Dandruff is a chronic noninflammatory scaling of the scalp in which mitosis is accelerated. Antidandruff preparations were evaluated in human volunteers with at least moderately severe dandruff (56–58). Subjects followed the shampoo regimen illustrated in Table III, and efficacy was evaluated by clinical grading or with an objective test (corneocyte count) in which the quantity of horny cells produced was measured with a hemocytometer. Clinical grading was done on a scale of 0–10: 0–1, very little scaling; 2–3, mild scaling; 4–5,

[6] BCNU.

Table III—Protocol for Complete Analysis of a Shampoo[a]

	Pretreatment Days		Treatment Days								Post-treatment Days
	−7	−4	0	3	7	10	14	17	21	24	28
Bland shampoo	x	x									
Test shampoo			x	x	x	x	x	x	x	x	
Grade			x		x		x		x		x
Corneocyte count			x				x				x

[a] Data from Ref. 56.

moderate scaling; 6–7, severe scaling; and 8–10, very strong scaling.

For the corneocyte count, a site on each side of the vertex was clipped so a glass cylinder could be snugly applied to the surface. One milliliter of buffered 0.1% octoxynol[7] was placed in a cup, and the surface was rubbed with a blunt rod[8] for 1 min. The wash fluid was then aspirated, the procedure was repeated, and the two samples were pooled. After appropriate dilution (usually 1:10 but with lesser dilutions after effective treatment), 2 drops of 2% gentian violet were added, the cell suspension was agitated mechanically, and the dispersed cells were counted in a Fuchs–Rosenthal hemocytometer (56). Table IV shows the results of a typical comparison between zinc pyrithione and its detergent base.

A more intensive version of the shampooing schedule was developed in which the test agent was applied once each weekday for 2 weeks (59). The corneocyte counts and clinical gradings were made 4, 8, and 12 days following the last exposure. This shortened version is best suited for screening and evaluating formulation changes.

Other methods measuring the severity of dandruff in humans may be useful tools for evaluating various antidandruff preparations. A method was reported in which a small vacuum cleaner is used to collect dandruff scurf from the scalp for weighing (60, 61). This technique was improved (62) by substituting a scalp brushing technique to help collect dandruff scurf for weighing. A model was described for producing a dandruff-like syndrome in guinea pigs, which requires the presence of lipid mixtures in addition to scalp organism (63). The sloughing reaction observed is probably due to the liberation of free fatty acids and the relative increase in C_{18} monoenoic acid at the irritated site. Although this method has not been used as a bioassay for the evaluation of antidandruff formulations, it could prove to be a useful model.

BIOASSAYS FOR ANESTHETIC–ANALGESIC FORMULATIONS

Both itch and pain are subserved by the same network of cutaneous nerves (64–66). Increasing the intensity of a stimulus converts the itching sensation to pricking or burning; increasing it still more induces pain.

Table IV—Comparison of 2.0% Zinc Pyrithione Shampoo with the Detergent Base Alone[a]

Treatment	Corneocyte Count			Clinical Grades		
	Day 0	Day 14	Day 28	Day 0	Day 14	Day 28
Detergent base	1,256,000	1,148,000	1,174,000	5.4	4.9	4.7
Zinc pyrithione	968,000	678,000	732,000	5.6	3.1	1.9

[a] Data from Ref. 56.

Hardy *et al.* (67) used the Hardy–Wolff–Goodell pain threshold apparatus (68) to evaluate the effect of topical anesthetics–analgesics on pain threshold measurements in human skin. In this bioassay, a 3-sec exposure to the rays from a 500-w incandescent lamp is used to produce a thermal stimulus on the volar surface of the forearm. The test areas are blackened with India ink to ensure complete absorption of the radiation and to prevent effects due to penetration of the rays below the skin surface. The stimulus is thus a purely thermal one. The subject reports on the sensation experienced at the end of the 3-sec exposure, and the stimulus intensity evoking the least perceptible pricking pain is considered to be the pain threshold. The test areas are then measured at 15-min intervals for 1.5 hr after the application of various formulations.

The effects of 3% phenol, 2% menthol, 2% tetracaine[9], and 1% dibucaine[10] in petrolatum were studied, and no significant pain threshold-rising action was found (67). When using the mucous membranes of the lips as target organs, both 5% benzocaine and 1% dibucaine in petrolatum caused marked anesthesia and analgesia.

The ointment base efficiency of local anesthetics was evaluated on the tails of albino rats using a modified Hardy–Wolff–Goodell pain threshold apparatus (69, 70). Although the technique was successful with rat tails, this success is not an indication of its usefulness in evaluating anesthetics on human skin.

Adriani *et al.* (71, 72) evaluated the effectiveness of topical anesthetics in humans. They found that local anesthetics abolished the tingling sensation caused by an electric current applied to the tip of the tongue. In this bioassay, a Burdick muscle stimulator is used to deliver a pulsatile current of 0.1–5.0 v at a frequency of 20 Hz. Although the voltage necessary to cause the tingling sensation varies from subject to subject (0.75–3.0 v), it remains constant for a given subject throughout an experiment and varies little if at all from 1 day to the next. After the application of various anesthetics, the increase in voltage necessary to elicit the tingling response serves as an index of effectiveness and makes possible a comparison of the potency of individual drugs.

The comparative potency and efficacy of more than 40 topical anesthetics were evaluated, and it was found

[7] Triton X-100, Rohm and Haas.
[8] Lined with Teflon (du Pont).
[9] Pontocaine, Winthrop.
[10] Nupercaine, Ciba.

that the latent period was shortened as the concentration was increased (71, 72). There was also a maximum effective concentration for each drug. The most effective drugs, in the order of decreasing activity, were 1% tetracaine, 0.5% dibucaine, 20% cocaine, 1% dyclonine, 4% lidocaine, 5% piperocaine, 2% pramoxine, and 5% hexylcaine.

The efficacy of local anesthetics also was evaluated using normal skin; salts of local anesthetics were ineffective in reducing itching and burning in intact normal skin (73). Only concentrated solutions of bases were efficacious. This result is not surprising since most salts are ionized and do not penetrate the intact skin. This method can be useful in developing topical anesthetic formulations, especially for anesthetics applied to mucous membranes.

BIOASSAYS FOR ANTIPRURITIC FORMULATIONS

Itching is considered a modified form of pain and is carried on afferent pain fibers with subsequent discharges of impulses in the spinothalamic tract of the sensory cortex (74). An experimental method was developed for the measurement of pruritus, and a freshly prepared histamine phosphate solution was the most satisfactory itch stimulus (74, 75). A quantitative technique was devised so that the end-point of subjective reactivity could be measured. This end-point of reactivity, called the "itch threshold," is defined as the greatest dilution of histamine that produces a recognizable pruritus. The itch threshold is then utilized as a tool to determine the effect of various topically applied drugs.

In tests with individual drugs, the itch threshold is first measured, the test drug is then administered, and the itch threshold is measured again after a suitable interval when the effect of the drug is at its peak (76). With this method, five antipruritic preparations were administered topically to 20 subjects with normal skin. The degree of threshold elevation was probably insignificant, since it was very near that of oral placebo medications. Similar results also were reported with 54 topical antipruritic preparations tested in experimental localized pruritus induced by intracutaneous injection of histamine phosphate in three normal adult male subjects (77). Not one of the 54 preparations had a consistent definite effect on histamine pruritus.

A simple method was proposed for recording the degree and duration of pruritus resulting from application of cowhage (*Mucuna pruritum*) to human skin (78). A series of antipruritics and anesthetics was studied using this method, but none of the agents significantly altered the duration of the experimental pruritus. The investigators suggested that the action of most antipruritic preparations on itching skin disease is probably a psychological one.

Although various bioassays for the evaluation of antipruritic formulations exist, none is refined enough to be useful in the development of topical antipruritics. A considerable amount of work is still needed.

BIOASSAY FOR ANTIWART FORMULATIONS

The development of topical antiwart medications is complicated, since most warts spontaneously disappear and warts are difficult to grow under experimental conditions. However, Mendelson and Kligman (79) were successful in isolating wart virus in tissue cultures and subsequently reinoculating humans. Half of 20 subjects inoculated developed banal warts.

Since such a procedure for developing experimental warts in humans has been established, it may be worthwhile to pursue the development of an animal model in which the wart virus in tissue cultures can be inoculated into the experimental animal and the subsequent warts can be treated with antiwart formulations.

BIOASSAYS FOR TOPICAL FORMULATIONS USED IN TREATMENT OF RHUS DERMATITIS

Rhus (poison oak/ivy) dermatitis is one of the most common contact dermatidides seen in the United States. A human bioassay was developed in which the oleoresin of Rhus is applied to four sites on the forearms of human volunteers (80). When dermatitis develops, three sites are treated with three different formulations; the fourth site is left as a control. Interpretation of the results is difficult.

Hypersensitivity was induced in guinea pigs, and topical anti-Rhus formulations were tested (81). This method is a modification of a previously reported method (82) for the sensitization of guinea pigs with the Rhus antigen. On Day 0, female Hartley guinea pigs, ~350 g, are sensitized with an emulsion of poison ivy/oak extract and complete Freund's adjuvant (1:1). The antigen is administered intradermally at four sites over the scapular area and also into each hindpaw, using 0.1 ml/site. On Day 10 and periodically thereafter, the guinea pigs are challenged on a shaved flank to determine sensitivity. Guinea pigs showing a reaction after 24 hr are used for testing. Guinea pigs not sensitized within 20 days are resensitized.

The test challenge consists of applying by inunction 0.01 ml of nondiluted antigen to the external basilar portion of the ear. Beginning 24 hr later, a test formulation is applied to the challenged site twice daily for 2 days. Challenged ears with or without vehicle treatment serve as controls. Nonchallenged, untreated ears are included for comparison.

The guinea pigs are sacrificed 72 hr after challenge, at which time the ears are removed and a biopsy specimen from the challenged ear is punched out with a No. 4 cork borer. The hair is clipped and the biopsy specimens are weighed. Using this bioassay, Kepel *et al.* (81) found that 0.05% fluocinonide gel markedly reduced the weight of challenged ears in comparison with those receiving vehicle alone.

This model may be useful in screening agents for the treatment of human delayed hypersensitivity reactions such as Rhus dermatitis.

BIOASSAY FOR TOPICAL FORMULATIONS USED IN TREATMENT OF PSORIASIS

A model was developed using mouse tail epidermis for the psoriatic keratinization process (83). The mouse tail scale epidermis, unlike the rest of the mouse body

skin, is histologically and biochemically similar to psoriatic skin; there is an absence of a granular layer, which is a prerequisite for orthokeratinization. Upon application of the antipsoriatic medication, formerly parakeratotic scale areas undergo granular layer induction.

Various coal tar fraction ointments were applied to male mouse tails on a daily basis (84–87). At the end of 14–21 days, the animals were sacrificed and the skin was removed and examined histologically for granular layer induction. The tar acids (phenols) with high boiling points (~400°) induced a granular layer in formerly parakeratotic skin. This mouse tail bioassay may be a useful model in the development of topical formulations used in the treatment of psoriasis.

BIOASSAYS FOR TOPICAL CORTICOSTEROIDS

Of all bioassays used in the development of topical formulations, those used for topical corticosteroids are the most sophisticated and refined. The fibroblast assay, the thymus involution bioassay, and the alcoholic vasoconstriction bioassay have been developed for the evaluation of relative potencies of the active ingredient. Other bioassays have been developed to evaluate the relative potencies of finished formulations and to measure both suppression of inflammation and formulation vasoconstriction. One main advantage of the bioassays of topical corticosteroids is their correlation with clinical trials.

Fibroblast Inhibition—It is a well-recognized phenomenon that corticosteroids act on a large number of cells, both *in vivo* and *in vitro*, where anti-inflammatory activity is one important function (88, 89). Connective tissue, which is composed mostly of fibroblasts, responds to inflammatory stimuli with a series of reactions which are inhibited by corticosteroids. At the cellular level, fibroblasts are intimately concerned with the process of inflammation, both as the manufacturer of connective tissue components and as the cells of origin or transformation for many other cell types. Therefore, it is not surprising that fibroblasts react to steroids with morphological changes, such as the disintegration of the cytoplasm and nucleus, and with inhibition of the fibroblast growth. Both of these reactions can be directly correlated with the anti-inflammatory activity of corticosteroids (89, 90).

A sensitive assay was developed based on the reaction of fibroblasts to corticosteroids (89–97). Fibroblasts of clone 929, strain L, are grown in roller tubes. Various concentrations of test corticosteroids dissolved in propylene glycol are incubated, and cells attached to the surface of the glass are counted 5 days after inoculation. Results of the experiments are expressed as dose–response curves; Fig. 1 shows a plot of fibroblast growth under the influence of hydrocortisone and fluocinolone acetonide. The dose–response lines are statistically fitted and present the relative potency of fluocinolone acetonide and hydrocortisone.

Thymus Involution—Systemic assays for assessing thymolytic anti-inflammatory activity of corticosteroids have been used to predict their possible value as a topical corticoid (98–100). The thymolytic activity is

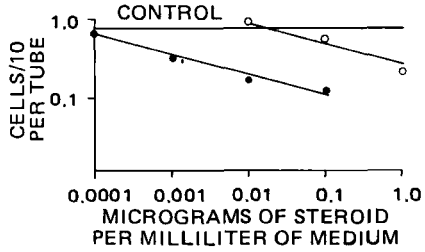

Figure 1—*Log–log plot of fibroblast growth under the influence of hydrocortisone (○) and fluocinolone acetonide (●). The lines are statistically fitted, with dose of steroid on the abscissa and millions of cells on the ordinate. (Adapted, with permission, from Ref. 90.)*

evaluated using 21–23-day-old, bilaterally adrenalectomized rats. At the time of surgery, 50-mg cotton pellets are inserted subcutaneously, one on each side of the animal. The test corticosteroid is administered subcutaneously once daily for 6 days, starting on the day of surgery. Twenty-four hours after the last injection, the thymus is removed, blotted dry, and weighed. The results are plotted as log dose–response curves, where the relative inhibition of the thymus indicates the relative potency of the corticosteroids tested.

Antigranuloma—The antigranuloma bioassay is similar to the thymus involution bioassay in that it is used to determine the relative potency of topical corticosteroids (98–102). The antigranuloma bioassay is evaluated by variants of the Hershberger and Calhoun (101) technique. Male rats, 170–200 g, are adrenalectomized and maintained on a normal diet and saline. Cotton pellets (5–8 mg) are impregnated with the test compound on the day following adrenalectomy and are implanted bilaterally into the loose subcutaneous connective tissue of the pectoral and dorsolateral neck regions. Four pellets are implanted in each animal, two impregnated with the test substance and two controls.

Six days after implantation, the pellets are removed and dried to constant weights. The results are plotted as log dose–log response curves, where the relative inhibition of granuloma formation indicates the relative potency of the corticosteroids tested.

Table V presents the relative potencies of various corticosteroids determined by the fibroblast inhibition assay, thymus involution bioassay, and antigranuloma bioassay.

Inflammation—Since topical corticosteroids are used as anti-inflammatory agents, some important bioassays involve the development of inflammation models which can then be used to evaluate the anti-inflammatory characteristics of various corticosteroid formulations.

Croton Oil—Rooks and Dorfman (98) modified the method of Tonelli *et al.* (104) and studied the relative potencies of anti-inflammatory compounds. The method employs 21-day-old male rats. A 0.05-ml mixture of 20% pyridine, 5% water, 74% ether, and 1% croton oil, with or without the test compound, is applied to the ears. One ear is treated and the other serves as an untreated control. The ears are removed 6 hr after drug administration, and uniform areas of the ear are punched out and weighed.

The anti-inflammatory effect of various corticoste-

Table V—Relative Potency of Corticosteroids Using the Fibroblast Inhibition Assay, Thymus Involution Bioassay, and Antigranuloma Bioassay

	Potency Ratios (Hydrocortisone = 1)		
	Fibroblast Inhibition Assay[a]	Anti-granuloma Bioassay[b]	Thymus Involution Bioassay[c]
Corticosterone	0.48	—	0.17
Hydrocortisone	1.0	1.0	1.0
Prednisolone	1.7	2.7	4.0
			4.1
Dexamethasone	7.5	104.0	47.0
			83.0
Paramethasone	11.3	63.6	45.1
Δ^1,9,11-Dichloro-cortisone 16,-17-acetonide	43.7	—	<1
Triamcinolone acetonide	156.0	48.5	37.7
Fluocinolone acetonide	440.0	446.0	263.0

[a] Data from Ref. 91. [b] Data from Refs. 100 and 103. [c] Data from Refs. 100, 103, and 104.

roids is determined by the relative suppression of the inflammation caused by croton oil. The results are plotted as log dose–response curves, and relative potencies are established. By using this bioassay, fluocinolone acetonide was estimated to be 150 times more potent than hydrocortisone (98).

The inflammation induced in human skin by topically applied croton oil has been suggested as a bioassay for corticosteroid potency, since it approaches the clinical inflammatory situation (105). In croton oil studies, 32 7 × 7-mm squares punched on tape[11] are applied to each forearm. Then 7 μl of 100% croton oil is applied to each square, spread evenly over the entire site, and covered with a plastic film for 3 hr. The sites are carefully marked, and the arms are washed and dried. New tapes with 12 × 12-mm punched-out squares are carefully superimposed over the croton oil-treated sites, and 3 mg of the corticosteroid preparations is applied to the sites. Each forearm is occluded with a plastic film for 18–20 hr. Reading is done at 24 hr on a 0–5 scale based on the degree of erythema, induration, and vesiculation present. The results, after decoding, are subtracted from the score of untreated croton oil sites (106, 107).

The relative potencies of several commercially available corticosteroids were evaluated using this technique. Fluocinonide 0.05% cream was found to be superior to betamethasone valerate, flumethasone pivalate, triamcinolone acetonide, and fluocortolone–fluocortolone caproate creams (107).

The anti-inflammatory activity of various corticosteroids was evaluated by measuring the suppression of croton oil-provoked pustules, and the rank order of anti-inflammatory efficacy correlated reasonably well with clinical judgments of comparative effectiveness (108).

Primary Irritants—A method was developed for evaluating the topical effectiveness of corticosteroids by inducing inflammation with the primary irritants mustard oil and nitric acid (109). Various concentrations of mustard oil were prepared by dilution with liquid petrolatum, but an 80% concentration was used primarily. Concentrations of 4, 10, and 15% nitric acid in aqueous solution were used in a small group for comparison, but the 15% concentration was employed for the main test group. Both primary irritants were kept in contact with the skin site for 24 hr by a cellophane patch and removed with a suitable solvent.

All tests are performed on the normal skin of human volunteers. The test site is a 1 × 1-cm area on the upper part of the back below the level of the dorsal spine of the scapula, and there is no pretreatment of the area. Fifty milligrams of the test ointment is applied and massaged into the skin, and the area is covered with a transparent cellophane disk. Applications are made at time intervals ranging from 24 hr before to 24 hr after the introduction of the inflammatory stimulus, and contact of the corticosteroid ointment with the skin is maintained for 0.5–8 hr. The corticosteroid ointment is removed with water, alcohol, and ether at the desired time.

In all cases, observations are made immediately after application of the inflammatory stimulus and at approximately 2-hr intervals until the maximum development of the inflammatory reaction is achieved. The time of appearance of the reaction, its rate of progress, and the final degree of response are noted. The inflammatory reaction is graded as: erythema, erythema plus obvious edema, additional formation of papules or vesicles, or necrosis.

Five major factors influenced the results obtained in the test situations (109):

1. Relationship between time of corticosteroid application and induction of inflammation. Effective inhibition of inflammation resulted from the application of the corticosteroid 2–8 hr prior to the stimulus. The maximum effect was achieved in about 6 hr. A time interval over 16 hr failed to produce any effect. If applied immediately before or after the stimulus, the corticosteroid produced no alteration in most cases, an exacerbation of inflammation in about one-third of the tests, and inhibition in only a few cases.
2. Duration of contact of corticosteroid with skin. The minimal effective contact time was 1 hr. Prolongation of the contact time over 2 hr gave no increase in effect.
3. Concentration of corticosteroid applied. Optimal and about equal effects were seen with concentrations of 1% hydrocortisone, 0.25% fluorocortisone, and 5% corticotropin.
4. Intensity of inflammatory stimulus applied. There was an inverse relationship between the intensity of the stimulus and the degree of inhibition observed in the inflammatory response.
5. Thickness of epidermis. An inverse relationship was suggested between the thickness of the epidermis in terms of cell layers and the anti-inflammatory effect.

Tetrahydrofurfuryl Alcohol—A laboratory method was developed, utilizing tetrahydrofurfuryl alcohol, which permits the rapid evaluation of topical anti-inflammatory agents (110). This method involves simultaneous application of an irritant and the test agent to human skin. Activity is judged by the ability of the

[11] Blenderm.

agent to inhibit the development of erythema. The test compounds to be evaluated are dissolved in redistilled tetrahydrofurfuryl alcohol. This agent is used because it produces a moderate irritant reaction suitable for test purposes when applied to human skin and is also an excellent solvent for a wide range of steroids and other compounds.

Flannel square patches, measuring 3.8 cm (1.5 in.) and sewn to a thin polyethylene backing, are saturated with the test solution of mixed irritant and anti-inflammatory agent. The patches are applied to the inner surface of the upper arm and held in place from late afternoon to the following morning. This time interval is sufficient to produce a moderate erythema at the control site. When the patches are removed, the sites are marked so they can be located later. Erythema at the test sites is evaluated about 1 hr after removal of the patches.

A seven-point scale is employed, ranging from 0 to +6 (severe) erythema. When the skin sites treated with the experimental agents in tetrahydrofurfuryl alcohol exhibit significantly less erythema than the irritant alone, the agent is rated as having anti-inflammatory activity. When the treated sites exhibit erythema that is equal to or greater than the control, the agent is rated as being without activity.

With this bioassay, fluorometholone was approximately 40 times as potent as hydrocortisone applied topically yet only about equal to hydrocortisone's systemic activity (111). It was suggested that fluorometholone may be a unique compound for anti-inflammatory therapy.

Tetrahydrofurfuryl alcohol was used to study the effects of flurandrenolide as an anti-inflammatory agent (112). The anti-inflammatory effect of flurandrenolide also was compared with that of hydrocortisone acetate, and 0.05% flurandrenolide was more effective than 1% hydrocortisone acetate in inhibition of erythema produced by tetrahydrofurfuryl alcohol.

Stripped Epidermis—Stripping epidermis with adhesive tape was first used by Wolf (113) in epidermal cytology studies. Since then, this method has been used to produce a standardized trauma. Möller and Rorsman (114) studied the vasodilation and exudation after the stripping of the epidermis and noticed an erythema 1–8 hr after the trauma. Wells (115), utilizing this local damage and repair stimulus, suggested that it might lend itself to a bioassay for the study of the local action of hydrocortisone and derivatives.

A flat area of normal skin with uniform surface is chosen (usually the flexor aspect of the forearm), and 1.3-cm (0.5-in.) wide cellophane tape is smoothed onto the skin for a length of about 8 cm. It is then peeled back from one end and sharply stripped off. A fresh piece of cellophane tape is applied to exactly the same area of skin and again is immediately stripped off. This process is repeated until, after about 30 pulls, glistening macules appear on the skin surface. With further stripping, they become confluent. The even, pinkish-red surface is glistening but not moist, and no more scales will peel away. Erythema persists in the strip for several days, and it is neatly confined to the rectangle that has been denuded of scales.

Immediately after stripping, the damaged area is divided into two or more parts; one part is treated with the control of unmedicated vehicle, and the other parts are treated with the hydrocortisone or other local applications. Applications are made three times in 24 hr if the experiment is prolonged. Dressings of soft plastic material are usually applied to cover the stripped area and prevent friction from clothing. Four hours after the first application of hydrocortisone at the start of the experiment, some pallor is apparent at the edges of the strip while the control is uniformly red. By 6 hr, the whole of the hydrocortisone-treated strip is more pale than the control. Twelve hours from the start of the experiment, the difference is maximal, the hydrocortisone-treated area often being as pale as normal skin.

By using the tape method (115), lotions containing 0.01, 0.025, and 0.1% triamcinolone acetonide and 1% hydrocortisone were compared (116). The results showed that 0.025 and 0.1% triamcinolone acetonide had longer and greater activity than the 1% hydrocortisone. Hydrocortisone formulations in various bases were studied using the same method (117).

UV Erythema Suppression—Since most corticosteroid responsive diseases are inflammatory in nature, the UV erythema suppression bioassay may be a useful model in evaluating the relative activity of corticosteroids.

Everall and Fisher (118) first evaluated the effect of topical corticosteroids in preventing the effects of UV rays on human skin, and they found that both cortisone acetate and hydrocortisone acetate ointment were ineffective. There were no alterations of the erythema response of the skin to UV rays if inunctions with hydrocortisone were performed after irradiation (119). When inunctions were carried out immediately prior to irradiation, the erythema response was weaker in the hydrocortisone-treated areas. A method was developed which inhibits Grenz-ray erythema by a single application of a topical corticosteroid (109, 120, 121). To be effective, formulations should be applied prior to irradiation with Grenz rays and provide an adequate concentration of corticosteroids in the tissues at the time of application of the inflammatory stimulus.

A precise UV erythema suppression bioassay was reported which could be correlated with vasoconstrictor bioassays and clinical studies (106, 122). In this bioassay, an air-cooled, hot quartz, high intensity lamp is used as the UV source. The minimum erythema dose (MED) is carefully determined on the inner upper arm of each volunteer the day before the assay is performed. On the following day, 7 × 7-mm squares punched on tape are applied, and each square is irradiated with that volunteer's minimum erythema dose before application of the preparations under study. Three milligrams of each formulation is applied to each square, and the arms are wrapped.

Six hours later, the wrapping and tapes are removed and the arms are washed with soap and water. Two readers independently assess the arms at 8 and 24 hr for both vasoconstriction and erythema. Individual sites are read as follows: 0 = no erythema, 1 = part of a square showing erythema, and 2 = a completely red square. After decoding the study, the results are calculated and

the sum of the readings for each preparation is subtracted from the sum of the readings from "blank" squares. When this bioassay was used, 0.05% fluocinonide ointment was the most active of the topical corticosteroids tested (122). The use of the UV erythema suppression bioassay was recommended along with the vasoconstrictor bioassay in evaluating various formulations before initiating expensive clinical trials.

Kerosene Inflammation Suppression—Kerosene-induced experimental inflammation in human skin has been used to evaluate various commercial corticosteroid formulations (108). In this procedure, the corticosteroids are applied directly to 1.5-cm squares of skin outlined in ink by a rubber stamp. Ointments and creams are applied in excess, spread evenly with a cotton swab, and then covered with 1.5-cm squares of nonwoven cotton. The cotton cloth mainly serves as a reservoir to keep the materials in place, and the patches are fixed to the skin by the occlusive dressing. A control patch receives hydrophilic ointment USP, an oil-in-water emulsion base.

The patches are left in place for 6 hr and then wiped dry. The irritant patches of kerosene are applied 1 hr later, at which time the degree of vasoconstriction is graded. The dressings are removed 20 hr later and the sites are immediately graded on a 5-point scale: 0 = complete absence of pustules or vesicles, 1 = pustules or vesicles not exceeding one-quarter of the area of the square, 2 = pustules or vesicles covering at most one-half of the area, 3 = pustules or vesicles occupying three-quarters of the square, and 4 = bullae. The rank order of anti-inflammatory efficacy of a series of marketed corticosteroids corresponded reasonably well with clinical judgments of comparative effectiveness (108).

By using the same technique, the relative potencies of 0.1% betamethasone valerate, 0.025% fluocinolone acetonide, and 0.1% triamcinolone acetonide creams were evaluated and found to have practically the same potency (123). These results correlated well with double-blind clinical studies. It was, therefore, suggested (108, 123) that the kerosene bioassay be used in evaluating the activity of topical corticosteroids.

6-Chloro-2,4-dinitrobenzene Inflammation Suppression—One problem of preclinical evaluation of new drugs is the simulation of human disease conditions in laboratory animals. To test the ability of topical corticosteroids to suppress eczema, a technique was developed whereby eczematous lesions are induced in guinea pigs sensitized with 6-chloro-2,4-dinitrobenzene (124). In this procedure, 0.02 ml of 50% 6-chloro-2,4-dinitrobenzene in acetone is applied to the shaved necks of young adult albino guinea pigs. Within 24 hr, an acute inflammatory reaction with ulceration develops and lasts 3–5 days before completely healing.

Ten days following this first application, a second external application of 1% 6-chloro-2,4-dinitrobenzene in acetone to any site on the animal's body provokes a local eczematous response in almost 100% of test animals. The reaction lasts 5–7 days before healing is complete, and the hypersensitive state usually lasts up to 3 months. A single application of 1% 6-chloro-2,4-dinitrobenzene fails to provoke the eczematous response in nonsensitized animals.

Scott (124) used this method to evaluate the efficacy of six commercially available corticosteroid ointments: 1% hydrocortisone, 0.25% methylprednisolone, 0.1% prednisolone, 0.1% triamcinolone acetonide, 0.05% flurandrenolide, and 0.025% fluocinolone acetonide. The shaved backs of six sensitized albino guinea pigs were marked into eight sections, and 0.02 ml of 1% 6-chloro-2,4-dinitrobenzene in acetone was applied to each section. Twenty-four hours later (when eczema had developed), one corticosteroid was applied to each of the six sites. The base alone was applied to a seventh site, while no application was made to the remaining site. The effects were observed and recorded at 2 and 4 days after treatment. Those sites treated with hydrocortisone, methylprednisolone, and prednisolone failed to show any difference compared to the control eczema site. The remainder of the compounds hastened and completed healing of the treated sites compared with the control.

This method also was used to determine the minimum concentration of fluocinolone acetonide that could suppress an established eczema (124). This bioassay was suggested for testing different dilutions and bases for a single anti-inflammatory compound in addition to tests for the comparative efficacy of any number of compounds.

Thinning of Epidermis—Two bioassays that utilize the epidermis-thinning potential of topical corticosteroids have been developed: a mouse tail epidermis bioassay and a guinea pig epidermis bioassay.

Mouse Tail Epidermis—In this bioassay, various corticosteroid preparations are applied daily to the tail skin of male mice of the "to" strain for 3 weeks (125). After the mice are killed with chloroform, the dorsal tail skin, about 3 cm from the base of the tail, is removed for histological examination. The tissue is fixed in 70% ethanol, and sagittal sections are prepared and stained with hematoxylin and eosin.

Epidermal thickness from the dermoepidermal junction to the base of the horny layer is measured with an eyepiece graticule. The mouse tail is particularly suitable for this purpose since the dermoepidermal junction is virtually flat and runs parallel to the surface. Ten different measurements are made on each tail scale, and 10 scale regions are examined from each tail.

Of the corticosteroids tested, fluocinolone acetonide and sintisone demonstrated the greatest effect. It was suggested (125) that the thinning effect of the corticosteroid preparations tested closely followed their clinical efficacy in the treatment of proliferative epidermal disorders.

Guinea Pig Epidermis—Topical application of ointment bases causes various degrees of measurable and reproducible epidermal thickening in guinea pigs (126, 127). The addition of steroids in various concentrations to the bases reduces the thickening caused by the ointment base alone. A bioassay was developed on the reduction of the epidermis thickening caused by the ointment base alone (128). Six groups of albino guinea pigs are used. The backs are clipped, and the area is divided into six equal parts. One site is used as a control, the ointment base alone is applied to a second site, and four different concentrations of steroid in the ointment

Table VI—Relative Potency of Commercial Topical Corticosteroids Using the Vasoconstrictor Bioassay[a]

Compound	Commercial Concentration, %	Potency According to Concentration	Relative Vasoconstrictor Activity (Hydrocortisone Acetate = 1)
Hydrocortisone acetate	1	1	1
Prednisolone phosphate	0.5	2	0.1
Prednisolone acetate	0.5	2	1
Prednisolone	0.5	2	0.1
Methylprednisolone acetate	0.25	4	1
9α-Fluorohydrocortisone	0.1	10	1
Dexamethasone phosphate	0.1	10	0.01
Dexamethasone	0.1	10	1
Flurandrenolide	0.05	20	10
Triamcinolone acetonide	0.1	10	100
Fluocinolone acetonide	0.025	40	100

[a] Data from Ref. 136.

base are rubbed into the four remaining sites daily for 4 or 7 days.

The animals are killed on the 5th or 8th day, the hair is removed with barium sulfide, and the treated areas and control sites are fixed in formaldehyde saline and processed for histology. Sections of 5 μm are stained with hematoxylin and eosin, and epidermal thickness is measured at 20 points on each specimen using an eyepiece graticule.

The inhibiting effect of the steroids tested was related to the type of corticosteroid, its concentration, and the base. Fluocinolone acetonide and fluocinonide in fatty alcohol–propylene glycol cream base[12] were most effective, and this bioassay was recommended to select the most suitable vehicle for topical corticosteroids (128).

Inhibition of Hair Growth—Naturally occurring corticosteroids induced inhibition of hair growth in the rat when applied directly to the skin (129, 130). Based on this observation, a bioassay was developed using the rate of hair growth in rats; it shows the comparative potency of hydrocortisone analogs (131, 132). Adult male rats of the Long-Evans strain are distributed among the experimental groups so that littermates are compared under different treatments. The analogs are dissolved in 25% ethanol, and 5.0 μg of each corticosteroid in 0.1 ml of solution is applied daily to a small area caudal to the right ear. An equal volume of 25% ethanol is applied to the same area on the control animals.

A record is made of the extent and pattern of hair growth, and hair is clipped from the dorsum of the neck prior to initiation of treatment and weekly thereafter. This procedure is continued for 7 weeks. Since the pattern of hair growth in the rat is bilaterally symmetrical, inhibition is present if hair fails to appear in the treatment area but grows in the comparable area on the untreated side.

In the scoring system, two points are given for each week in which inhibition is noted. Promptness in response is recognized by adding a figure equal to the number of weeks between the first appearance of inhibition and the end of the 7-week period of study. Two points are subtracted for each observation in which more hair is found in the treated area than in the untreated area. One point is subtracted for each week in which a small amount of hair appears in the treated area that was previously without hair. The maximum score is 21 points.

The scores for all rats treated with one analog are averaged and corrected by subtracting the average score from the alcohol-treated controls. Then, the effectiveness of each analog is compared with that of hydrocortisone in the ratio of the score for an analog/the score for hydrocortisone.

In seven hydrocortisone analogs, unsaturation at C-1 and C-2 induced moderate increases in activity according to this bioassay (131, 132). Methylation at C-2 produced a greater increase. Fluorination at C-9 produced a more highly active compound, while fluorination of 21-deoxyhydrocortisone at C-9 and C-21 produced the most potent compound (132).

Reduction of Mitotic Rate—Fisher and Maibach (133) suggested that the reduction in mitotic rate produced by corticosteroids might be used as a bioassay. A bioassay was developed using the dorsal skin of the hairless mouse which, when "stripped" with adhesive tape, provides a suitable model for the study of the antimitotic effect of corticosteroid formulations (134). Equal quantities of different formulations are applied to at least six mice. Dressings are applied and kept in place for 5–196 hr. Four hours before sacrifice, the mice are injected intraperitoneally with a solution of demecolcine[13]. After sacrifice, the dorsal skin is removed and fixed, and the mitotic index is established. When this bioassay was used, betamethasone valerate had a significant antimitotic effect at a concentration of 10^{-4}, while hydrocortisone was antimitotic at a concentration of 10^{-2} (134). This animal bioassay may be used to assay the relative potency of topical corticosteroids.

Vasoconstrictor—McKenzie and Stoughton (135, 136) noticed that, when using topical corticosteroids under plastic[2] wrap, both the lesion and the surrounding normal skin displayed a pallor. The observed vasoconstriction might be used as an index of the percutaneous absorption of steroids, and a bioassay was developed in which solutions or suspensions of various dilutions of corticosteroids are prepared in 95% alcohol and applied to areas 2.54 cm (1 in.) in diameter on the forearms. One

[12] FAPG.

[13] Colcemid.

arm is left uncovered, and the other is wrapped with plastic[2] wrap. The treated areas are left undisturbed for 16 hr, and the absence or presence of vasoconstriction is recorded.

Plastic[2] wrap caused a 100-fold increase in absorption as determined by vasoconstriction (136). The relative potency of commercially available topical corticosteroids was established (Table VI).

Alcoholic Vasoconstriction—These discoveries opened one of the most active fields of research in the development of topical corticosteroids. The alcoholic vasoconstrictor bioassay was used to evaluate the topical activity of betamethasone esters in humans, and betamethasone 17-valerate was the most active compound (137, 138). It was also utilized in the assessment of four new fluocortolone analogs (139). In these studies, diflucortolone trimethylacetate, which had 10 times the potency of triamcinolone acetonide, was the most potent analog.

The alcoholic vasoconstrictor activity and percutaneous absorption of glucocorticoids was compared (140). Contrary to previous work (137), fluocinolone acetonide was equivalent to betamethasone valerate, and fluocinolone acetonide acetate (fluocinonide) was five times more potent than both betamethasone valerate and fluocinolone acetonide (140).

In alcoholic vasoconstriction tests, flucloronide was more potent than betamethasone valerate, flurandrenolide, beclomethasone propionate, fluocortolone caproate, and flumethasone pivalate (141–143).

The vasoconstrictor bioassay was modified (144) to evaluate precisely the potency of topically applied corticosteroids. In this assay, 10-fold serial dilutions from 10^{-2} (1.0%) to 10^{-7} (0.00001%) of various corticosteroids in ethanol are first prepared. Adult white subjects are utilized, and each subject receives all serial dilutions randomly assigned to one arm. Duplicate applications randomized differently on the opposite arm provide a check on the assay. The number of sites in each study equals the number of preparations to be tested so that every test site receives every preparation.

The skin of the forearm is prepared by washing with soap and water, and the test sites are outlined by a thin film of silicone grease applied with a rubber stamp. There are three or four horizontal and six or eight vertical rows, giving 18 or 32 uniform, 7 × 7-mm squares. The square pattern reduces the problem of recognition of test sites, and the grid pattern is marked with gentian violet to assist in individual site identification. Rapid and accurate application without cross-contamination of glassware is accomplished by using a separate 10-μl pipet for each application. After evaporation of the diluent, the area is covered with plastic[2] wrap and protected by tubular gauze.

After 16–18 hr of occlusion, the dressings are removed; 1–2 hr later, the sites are viewed. Two observers independently read and record the presence or absence of vasoconstriction at each test site. Observations as well as applications are always done under double-blind conditions. For each dose of each compound, the number of responding sites is tabulated, and this value is expressed as a percentage of the number of sites to which that dose–compound combination was applied. Figure 2 shows a typical plot of results in which fluocinolone acetonide was equipotent to betamethasone valerate, while fluocinonide was five times more potent than both fluocinolone acetonide and betamethasone valerate. These results are in agreement with those of Stoughton (140).

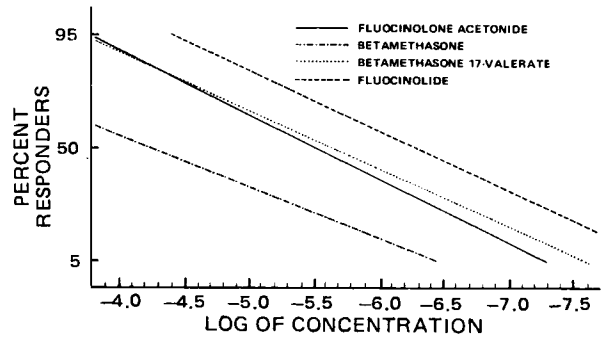

Figure 2—*Dose–response curves of various corticosteroids using the alcoholic vasoconstriction bioassay. (Reprinted, with permission, from Ref. 144.)*

Seven topical corticosteroids were evaluated with a series of vasoconstrictor tests, one of which was the alcoholic vasoconstrictor test (145).

A modified alcoholic vasoconstrictor test was reported using glassine-backed squares of absorbent paper saturated with different concentrations of alcoholic solutions and applied to the skin (146). Four new difluoroprednisolone diesters were more active than betamethasone valerate.

Barry and Brace (147), following the suggestion of Burdick *et al.* (122), adopted the "area under the curve" concept, commonly used in pharmacokinetic studies of systemic drugs, for their alcoholic vasoconstrictor studies. They evaluated vasoconstriction at 17 reading times over 26 hr and determined complete blanching curves for a series of structurally related compounds. These area under the curve determinations are indicative of the intensity and duration of action of the corticosteroids studied. Substitution or removal of the 21-hydroxy group on steroids produced compounds with a wide range of activity. Poor activity correlated with a hemisuccinate salt grouping at position 21 or with the absence of 11β-hydroxy groups.

Formulation Vasoconstriction—After selecting the compound of choice with the alcoholic vasoconstriction test, the next step in the development of topical corticosteroids is the evaluation of the active drug in various vehicles and comparisons with marketed products. The regular Stoughton–McKenzie alcoholic vasoconstriction bioassay was refined (106, 122, 148, 149) in such a way that all preparations are placed in identical tubes and coded. For each study, the forearms of 16–20 volunteers are prepared by gentle washing and drying. Strips of double adhesive-coated tape[11] with 7 × 7-mm prepunched squares are applied to both forearms so that each arm has 32 application sites. Tables of randomization are used to assign each preparation to the individual square test sites.

Three milligrams of each test formulation is applied to the skin in each square and spread evenly. On one arm, a protective cage is placed over the sites for "open"

application. On the other arm, the remaining backing is removed from the strips and the application sites are occluded with plastic[2] wrap. After 6 hr of exposure to the corticosteroid base preparations, all tapes are removed and the arms are washed. At 8, 24, and 32 hr after the original application of the formulation, the presence or absence of vasoconstriction is read independently by two experienced observers under standard lighting conditions.

The results for each application are expressed as the percentage of the total number of sites in which vasoconstriction is observed. Since variations were seen in the slopes of percent sites responding *versus* time curves for the different formulations tested, adding all readings to give a rough area under the curve evaluation was suggested (106). Commenting on the vagaries of the vasoconstriction test, Burdick (150) also suggested the following to eliminate errors inherent in the test: (*a*) preselection of subjects and use of sufficient numbers of subjects and test sites, (*b*) use of two independent readers to reduce interpretative errors, (*c*) randomization of test materials, and (*d*) use of a patterned square site and standard lighting conditions. The method was improved (151, 152) by increasing reading times to determine a complete blanching profile.

A pharmacokinetic–pharmacodynamic relationship was developed for topical corticosteroids used in the vasoconstrictor test (153, 154). Two models were obtained with good results using two-compartment open models. Model 1 makes no assumption about the progress of the blanching before the time, s, at which the source of steroid is effectively removed and thus treats times $t \geq s$ only. It assumes the concentration of steroid in stratum corneum is maximal at s. The response at s is A_s; B is the observed response at any later time. The kinetic model is $A \xrightarrow{k_1} B \xrightarrow{k_2}$, and the equation for the observed responses is solved as:

$$B_{t \geq s} = \frac{k_1 A_s}{k_2 - k_1}\left[e^{-k_1(t-s)} - e^{-k_2(t-s)}\right] + B_s e^{-k_2(t-s)} \quad \text{(Eq. 1)}$$

where k_1 and k_2 are first-order rate constants for blanching. This model gave an excellent fit to data from alcoholic steroid solution bioassays.

Model 2 extends Model 1 by assuming that the steroid enters the stratum corneum from the vehicle at a constant rate and thus permits analysis from initial application, $t = 0$. The kinetic model is source–$P \rightarrow A \xrightarrow{k_1} B \xrightarrow{k_2}$, and the equation for the observed responses is solved as forms of:

$$B_{t \geq s} = \frac{P}{k_2(k_2 - k_1)}\left[k_2 e^{-k_1 t}(e^{k_1 s} - 1) - k_1 e^{-k_2 t}(e^{k_2 s} - 1)\right] \quad \text{(Eq. 2)}$$

where P represents the constant input of pharmacological response from the source. The assumption of a constant rate of input allows A_s and B_s to be expressed in terms of P and k_1, so they do not appear in the equation. This model produced good fits to blanching data from several proprietary creams and ointments but poor fits for the alcoholic data (154).

Considerable work has been done on the evaluation of relative potencies of various topical corticosteroids using the formulation vasoconstriction bioassay. Table VII lists the corticosteroids tested along with dosage forms and the type of vasoconstrictor studies performed with each compound.

Paired Comparison Vasoconstriction—Although regular vasoconstriction studies are useful in evaluating the effect of vehicles and are used in the comparative evaluation of marketed products, they have some disadvantages. Most new corticosteroids produce maximum responses when administered at therapeutic concentrations under occlusion, thus making it difficult to demonstrate potency differences between different corticosteroids or between different concentrations of a specific drug above a certain threshold concentration. The other apparent major difficulty with the vasoconstrictor bioassay is its reliance upon subjective visual measurements. Although the human eye can perform as an effective rating device, its reliability suffers whenever comparisons are separated by distance and time.

To avoid these pitfalls, a technique was developed which involves paired comparison of vasoconstriction at adjacent sites (177). In these studies, only two formulations are tested and the direct comparison of the formulations as pairs is required. For each pair, results are reported as: one site exhibits a greater degree of vasoconstriction, both sites show equal vasoconstriction, or no vasoconstriction is observed at either site. By using this technique, statistically significant differences were found between 0.05% fluocinonide cream and 0.1% betamethasone valerate cream when applied under occlusion.

Xenon-133 Method for Evaluation of Vasoconstriction—Most methods for evaluating vasoconstriction resulting from application of topical corticosteroids are not quantitative. A method was reported which measures corticoid-induced vasoconstriction by xenon-133 clearance (178). Subjects between the ages of 18 and 50, without evidence of dermatological or vascular disease, are selected. Total resting skin blood flow in the forearm is determined by the clearance of epicutaneously applied xenon-133 in 17 control subjects. In an additional seven subjects, a comparison of differences in flow of bilateral symmetrical sites of the forearm is obtained. The experimental group consists of 14 subjects. Polyethylene tape with 4 $\mu g/cm^2$ of flurandrenolide dispersed in the adhesive layer and a similar nonmedicated tape are applied to symmetrical sites of the forearm 18–24 hr prior to the study.

Total skin blood flow is measured by a modification of the atraumatic epicutaneous labeling technique of Sejrsen (179), in which xenon-133 enters the cutaneous tissues through the intact epithelial surface. A 5 × 5-cm vinyl membrane is affixed to the skin with polyethylene tape at its margins; xenon-133 gas, with a specific activity of 5–10 mCi/ml, is introduced under the membrane from a syringe and left in contact with the skin for 2 min. The membrane is then removed, and the excess gas is blown away. This epicutaneous labeling results in diffusion into the cutaneous tissue of a minute fraction of the isotope initially brought into contact with the skin. A counting rate of 1–10 × 10^5 counts/min is obtained.

Counting is performed using a nuclear probe with a 5.1-cm (2-in.) sodium iodide crystal immediately fol-

Table VII—Review of Published Vasoconstrictor Studies with Marketed Corticosteroid Products

Compound	Formulations	Remarks	References
Beclomethasone dipropionate	Cream	Comparison with marketed products	151
	Ointment	Comparison with marketed products	152
Betamethasone benzoate	Cream, lotion, gel	Comparison with marketed products	155
	Ointment	Vehicle evaluation	156
Betamethasone dipropionate	2-Propanol–water solution	Comparison with betamethasone valerate	157
Betamethasone valerate	Cream	Comparison with marketed products	151, 155, 158, 159
		Comparison with fluocinonide	161
		Vehicle evaluation	162
		Comparison with fluclorolone acetonide	163
	Ointment	Comparison with marketed products	122, 152, 155, 159
		Comparison with fluocinonide	161
		Vehicle evaluation	162
		Comparison with flucloronide	163
		Comparison with betamethasone 17-benzoate	156
		Comparison with 21-desoxybetamethasone 17-dipropionate	160
	Lotion	Comparison with marketed products	164
	2-Propanol–water solution	Comparison with betamethasone dipropionate	157
Clobetasol propionate	Cream	Comparison with marketed products	151
	Ointment	Comparison with marketed products	152
Desonide	Cream	Comparison with marketed products	151
21-Desoxybetamethasone 17-propionate	Ointment	Comparison with betamethasone valerate	160
Flucloronide	Cream	Comparison with marketed products	151
		Comparison with betamethasone valerate	163
		Vehicle evaluation	163, 165
	Ointment	Comparison with marketed products	152
		Comparison with betamethasone valerate	163
		Vehicle evaluation	163, 165
	Gel	Vehicle evaluation and comparison with betamethasone valerate	163
Flumethasone pivalate	Cream	Comparison with marketed products	151, 155, 158, 159
	Ointment	Comparison with marketed products	152, 159
	Lotion	Comparison with marketed products	164
Fluocinolone acetonide	Cream	Comparison with marketed products	151, 155, 159
		Comparison with extemporaneous hydrocortisone creams	148
		Comparison with fluorometholone	167
		Vehicle evaluation	162, 166
	Ointment	Comparison with marketed products	152, 155, 159
		Comparison with triamcinolone acetonide	169
		Vehicle evaluation	162, 166, 168
	Gel	Comparison with marketed products	151, 159
	Lotion	Comparison with marketed products	164
		Comparison with triamcinolone acetonide	170
Fluocinonide	Fatty alcohol–propylene glycol[a]	Comparison with marketed products	151, 155, 158
		Comparison with betamethasone valerate	161
		Vehicle evaluation	106, 152, 171, 172
	Ointment	Comparison with marketed products	122
		Vehicle evaluation	152
Fluocortolone plus fluocortolone caproate	Cream, ointment	Comparison with marketed products	159
Fluocortolone pivalate plus fluocortolone hexanoate	Cream	Comparison with marketed products	151
	Ointment	Comparison with marketed products	152
Fluorometholone	Cream, ointment, solution	Vehicle evaluation	167
Fluperolone 21-acetate	Ointment	Comparison with marketed products	164
Flurandrenolide	Cream	Comparison with marketed products	151, 155, 164
	Ointment	Comparison with marketed products	122, 152, 155
Formocortol	Cream	Comparison with marketed products	151
	Ointment	Comparison with marketed products	152
Triamcinolone acetonide	Cream	Comparison with marketed products	151, 155, 158 159
		Comparison with fluocinonide	161
		Comparison with fluocinolone acetonide	148
	Ointment	Comparison with marketed products	122, 152, 155, 159
		Comparison with fluocinonide	161
		Comparison with fluocinolone acetonide	169
	Lotion	Comparison with marketed products	155, 164
		Comparison with fluocinolone acetonide	170
Miscellaneous		Placebo response to white soft paraffin–propylene glycol	173–176

[a] FAPG.

lowing removal of the vinyl membrane. The scintillation detector is coupled to a scaler registering the counting rate at 5-sec intervals and records on a strip chart for at least 30 min (178). After correction for background, the differences in blood flow are determined for symmetrical sites that received flurandrenolide and control tapes.

In one study of flurandrenolide, a mean blood flow of 5.55 ml/100 g/min was determined in the control sites compared to 3.84 ml/100 g/min in sites treated with flurandrenolide (178). Xenon-133 clearance may be better than visual observation to measure vasoconstrictor activity of topical corticosteroids.

Intradermal Injection Vasoconstriction—Studies of topical corticoid vasoconstriction involve both percutaneous penetration and inherent vasoconstrictor activity. To eliminate this penetration aspect, steroids have been studied after intradermal injection. Assays of steroids for possible local activity in human skin (180) found that 9α-fluorohydrocortisone acetate and free alcohol were superior to hydrocortisone acetate and free alcohol (181). The relative potencies of prednisone and prednisolone were studied, and prednisolone was more active (182).

A precise intradermal injection bioassay was reported in which the steroids are serially diluted and 0.1 ml of each dilution is injected intradermally into the backs and forearms of volunteers (183). In the back, five to 11 injections are made in rows, up to six rows per subject (three rows on each side). Injections are about 1.9 cm (0.75 in.) apart; rows are about 2.54 cm (1 in.) apart, always at least 3.8 cm (1.5 in.) from the midline and centered over the muscle belly. The dilutions are injected in descending order of strength from top to bottom, and no randomization is attempted. Three saline control injections are made, one at the top, middle, and bottom of the areas between rows.

In the forearm, injection sites are measured 1.9 cm (0.75 in.) apart on the flexor aspect at the edge of the hairline and not closer than 3.8 cm (1.5 in.) from the cubital fossa and wrist. Only one row of injections is made per arm with not more than seven injections in the row. One saline control is injected medial to the center of the row, about 2.54 cm (1 in.) away. The dilutions are injected in descending order of strength starting near the cubital fossa and working toward the wrist. Different subjects are used in the back and the back *versus* arm studies.

In the back *versus* arm experiment, each subject is injected with one compound on the left back and left arm and vice versa. The injection sites are read at varying intervals from 1.5 to 6 hr. The end-point, which is the most dilute concentration giving definite vasoconstriction, is noted for each subject reacting; an average end-point is figured using all subjects tested, although some fail to react. Vasoconstriction is noted as present or absent. Any questionable blanching is considered negative.

Using this technique, Sutton *et al.* (183) avoided the penetration problems and determined the relative potency of various corticosteroids as determined by skin blanching following intradermal injection. They tested a series of topically used corticosteroids and found hydrocortisone to be least effective and fluocinolone acetonide to be most effective.

Intradermal injections also were used to evaluate both vasoconstriction and atrophy produced by corticosteroids (184). Desonide and triamcinolone acetonide, which differ only by the presence of a fluorine atom, were tested. Both exhibited similar vasoconstrictor potency but only triamcinolone acetonide, the fluorinated steroid, produced atrophy (184).

Mechanism of Action—The vasoconstrictor effect of topical corticosteroids is by now well established, but its mechanism is not clear. Juhlin (185), in his work with vascular reactions in skin treated with fluocinolone acetonide, suggested that the blanching of the skin is due to a vasoconstrictor effect of the steroid *per se*. Thune (186), evaluating the vasoconstrictive effect of steroids by plethysmographic recording of skin pulses, concluded that it is due mainly to decongestion of the capillaries and small veins beneath the epidermis. Solomon *et al.* (187) demonstrated that oral guanethidine, a norepinephrine antagonist, prevents topically applied steroid vasoconstriction in normotensive subjects and suggested that corticosteroids are capable of releasing norepinephrine from cutaneous stores. Others suggested that norepinephrine is not the only factor involved.

Reis (188) showed that steroids have a local and primary effect on normal human bulbar conjunctival vessels as well as potentiating norepinephrine. Steroids suppressed the vasodilation caused by such agents as histamine, alcohol, and bradykinin as well as potentiating the effects of norepinephrine (189). In the modified hamster cheek pouch and in humans, topically applied corticosteroids potentiated catecholamine-induced vasoconstriction. Since this effect was blocked by phentolamine but not by propranolol, this action might be through the increased sensitivity of α-adrenergic receptors (190).

duVivier and Stoughton's (191) demonstration of tachyphylaxis to topically applied steroids might suggest that they act indirectly by releasing endogenous norepinephrine from nerve storage vesicles. They might also influence the metabolism of the neurotransmitter or its recapture by the vesicles after release. Alternatively, the steroid may act by attaching itself to a receptor site, causing the release of the intracellular mediator cyclic adenosine monophosphate or guanosine

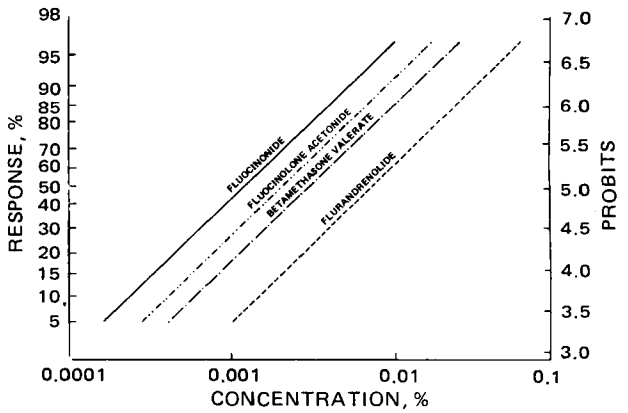

Figure 3—*Dose-response curves of various corticosteroids using the psoriasis bioassay. (Reprinted, with permission, from Ref. 193.)*

Table VIII— Vasoconstrictor and Clinical Response with Solubilized and Suspended 0.025% Fluocinolone Acetonide Ointments[a]

	Degree of Vasoconstriction[b]	Clinical Trials, % of Patients Showing Better Response		
		Eczema	Psoriasis	Total
0.025% fluocinolone acetonide in petrolatum, micronized particles	1.4	12	12	12
0.025% fluocinolone acetonide in petrolatum, solubilized in propylene glycol	1.8	56	36	46

[a] Data from Refs. 194 and 195. [b] Average of 10 subjects.

monophosphate and, thus, causing vasoconstriction (191).

Psoriasis Bioassay—Most bioassays fail to deal with spontaneously occurring skin diseases. The psoriasis bioassay was developed to deal directly with the disease state and, therefore, is the nearest approximation of the clinical trial. Chronic stabilized psoriatic patients are used as test subjects, and the test site is outlined with precut 1.1-cm^2 adhesive squares. One-half minim of medication is applied in a double-blind fashion to each site and covered with a square of plastic film. The medication is spread by light pressure on the film, and the plastic is then sealed to the underlying border. Dressings are applied daily and remain in place 24 hr.

The area is cleaned and read as either unchanged or completely normal. The final reading is made on the 5th day (106, 192, 193). The results can be presented as log dose–percentage cleared (probit) graphs. By using this technique, the relative potencies of various corticosteroids were calculated using fluocinolone acetonide as a standard (Fig. 3). Fluocinonide had 1.85 times the activity of fluocinolone acetonide; betamethasone valerate had 0.69 times the activity of fluocinolone acetonide.

CLINICAL CORRELATION

The ultimate usefulness of any bioassay is displayed when it can be correlated with clinical trials; the vasoconstrictor bioassay is one bioassay that is well correlated with clinical trials. The effect of solubilization of the corticosteroid in the vehicle has been studied (166, 194). Both the vasoconstrictor and clinical response of solubilized *versus* suspended fluocinolone acetonide in ointment form were evaluated. The results, which show the advantage of solubilization of the steroid, are given in Table VIII.

Table IX—Results of Comparison between Formulation Bioassay and Clinical Trial[a]

	Results	
	Formulation Bioassay	Double-Blind Clinical Trial
0.1% betamethasone valerate ointment *versus* 0.025% fluocinolone acetonide ointment	Betamethasone valerate superior; $p < 0.05$	Betamethasone valerate superior; $p < 0.05$
0.1% betamethasone valerate cream *versus* 0.05% fluocinonide cream	Fluocinonide superior; $p < 0.05$	Fluocinonide superior; $p < 0.05$

[a] Data from Ref. 155.

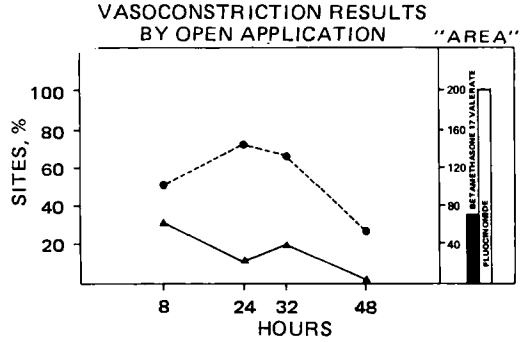

Figure 4—*Results of vasoconstrictor studies by open 16-hr application techniques and comparing 0.05% fluocinonide in fatty alcohol–propylene glycol cream (●) with 0.1% betamethasone 17-valerate cream (▲). (Adapted, with permission, from Ref. 158.)*

Stoughton (155) applied the vasoconstriction *versus* clinical correlations to comparison of marketed products and compared the vasoconstrictor response of 0.1% betamethasone valerate ointment *versus* 0.025% fluocinolone acetonide ointment and 0.05% fluocinonide cream *versus* 0.1% betamethasone valerate cream. In both vasoconstrictor studies and clinical trials, the 0.1% betamethasone valerate ointment and 0.05% fluocinonide cream were statistically superior to 0.025% fluocinolone acetonide ointment and 0.1% betamethasone valerate cream, respectively (Table IX).

The vasoconstrictor and clinical response of 0.05% fluocinonide cream and 0.1% betamethasone valerate cream also were compared (158). The 0.05% fluocinonide cream was superior to 0.1% betamethasone valerate cream as measured with the vasoconstriction bioassay (Fig. 4) and in clinical trials (Fig. 5).

These results clearly indicate that the vasoconstrictor bioassay is an excellent model in evaluating the efficacy of topical corticosteroids prior to their final testing during clinical trials.

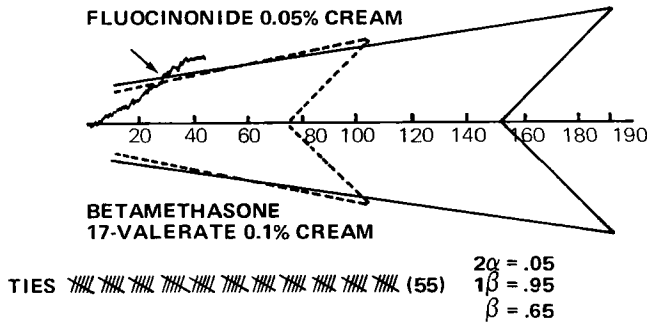

Figure 5—*Fourteen-day results in a sequential trial by paired comparisons of 0.05% fluocinonide in fatty alcohol–propylene glycol cream against 0.1% betamethasone 17-valerate cream. (Reprinted, with permission, from Ref. 158.)*

CONCLUSIONS

The ultimate systems for establishing the therapeutic efficacy of topical formulations are the qualitative and quantitative clinical trials. Since these therapeutic appraisals are full of variables and very costly to perform, they should be reserved only for careful evaluation of preselected candidates using double-blind clinical comparison between new and marketed products.

With the development of bioassays for topical antimicrobials, antimitotics, antiperspirants, sunscreens, antidandruff formulations, anesthetics, antipruritics, antiwart formulations, and corticosteroids, it is now possible to evaluate the inherent potencies of various topically active chemicals. It is also possible to evaluate the drug delivery characteristics of various vehicles.

Some bioassays discussed in this review have already been successfully used in the development of topical dosage forms. The vasoconstrictor bioassay also has been correlated with clinical trials. It is hoped that the newer bioassays which have not been used in the development of topical formulations will be regularly used along with established bioassays in the selection of optimum formulations for clinical trials, thus reducing the exorbitant cost of developing new drugs.

It is this reviewer's firm belief that intelligent use of available bioassays to evaluate test formulations of topical drugs will greatly facilitate the development of more efficacious and safer drugs. Used appropriately, these models can provide added confidence and reliability in those formulations subjected to clinical evaluation.

REFERENCES

(1) A. Burger, *Chem. Eng. News*, **53,** 37(1975).

(2) C. A. Schlagel, *J. Pharm. Sci.*, **54,** 335(1965).

(3) C. A. Schlagel, in "Pharmacology and the Skin," W. Montagna, E. J. Van Scott, and R. B. Stoughton, Eds., Appleton-Century-Crofts, New York, N.Y., 1972, p. 339.

(4) C. A. Schlagel, in "Animal Models in Dermatology," H. Maibach, Ed., Churchill Livingstone, Edinburgh, Scotland, 1975, p. 203.

(5) R. B. Stoughton, in "Pharmacology and the Skin," W. Montagna, E. J. Van Scott, and R. B. Stoughton, Eds., Appleton-Century-Crofts, New York, N.Y., 1972, p. 535.

(6) J. W. Hadgraft, *Br. J. Dermatol.*, **87,** 386(1972).

(7) R. B. Stoughton, *Arch. Dermatol.*, **101,** 160(1970).

(8) R. B. Stoughton, in "Animal Models in Dermatology," H. Maibach, Ed., Churchill Livingstone, Edinburgh, Scotland, 1975, p. 121.

(9) R. R. Marples, A. Rebora, and A. M. Kligman, *Arch. Dermatol.*, **108,** 237(1973).

(10) R. R. Marples and A. M. Kligman, in "Epidermal Wound Healing," H. Maibach and D. Rovee, Eds., Yearbook Medical Publishers, Chicago, Ill., 1972, p. 241.

(11) P. Williamson and A. M. Kligman, *J. Invest. Dermatol.*, **45,** 498(1965).

(12) G. Singh, R. R. Marples, and A. M. Kligman, *ibid.*, **57,** 149(1971).

(13) R. R. Marples and A. M. Kligman, *Antimicrob. Ag. Chemother.*, **5,** 323(1974).

(14) R. R. Marples and A. M. Kligman, *Toilet Goods Assoc. Cosmet. J.*, **1,** 26(1969).

(15) F. Reiss, L. Caroline, and L. Leonard, *J. Invest. Dermatol.*, **24,** 575(1955).

(16) F. Reiss and L. Leonard, *ibid.*, **24,** 589(1955).

(17) S. Molinas, *ibid.*, **25,** 33(1955).

(18) M. M. Dolan, J. S. Ebelhare, A. M. Kligman, and R. C. Bard, *ibid.*, **28,** 359(1957).

(19) M. Plempel and K. Bartmann, *Arzneim.-Forsch.*, **22,** 1280(1972).

(20) H. Weuta, *ibid.*, **22,** 1295(1972).

(21) J. H. Reinhardt, A. M. Allen, D. Gunnison, and W. A. Akers, *J. Invest. Dermatol.*, **63,** 419(1974).

(22) H. E. Jones, J. H. Reinhardt, and M. G. Rinaldi, *Arch. Dermatol.*, **110,** 369(1974).

(23) A. G. Knight, *Br. J. Dermatol.*, **89,** 509(1973).

(24) *Ibid.*, **91,** 49(1974).

(25) A. G. Knight, *J. Invest. Dermatol.*, **59,** 354(1972).

(26) *Ibid.*, **59,** 427(1972).

(27) R. M. Schwartzman, M. J. Deubler, and P. F. Dice, II, *J. Small Anim. Pract.*, **6,** 327(1965).

(28) I. Kubo, M. Hori, H. Niitani, I. Yokoyama, and T. Takemoto, "Studies on the Pathogenesis of Candidiasis," Studies on Candidiasis in Japan, 145, Tokyo-Research Committee of Candidiasis, Education Ministry of Japan.

(29) J. Van Cutsem and D. Thienpont, *Sabouraudia*, **9,** 17(1971).

(30) G. Maestrone and R. Semar, *Naturwissenschaften*, **55,** 87(1968).

(31) H. I. Maibach and A. M. Kligman, *Arch. Dermatol.*, **85,** 233(1962).

(32) M. C. Spencer, *ibid.*, **88,** 925(1963).

(33) A. Rebora, R. R. Marples, and A. M. Kligman, *ibid.*, **108,** 69(1973).

(34) E. J. Van Scott and R. H. Bonder, *J. Invest. Dermatol.*, **56,** 132(1971).

(35) E. J. Van Scott and R. J. Yu, in "Animal Models in Dermatology," H. Maibach, Ed., Churchill Livingstone, Edinburgh, Scotland, 1975, p. 248.

(36) E. J. Van Scott and R. J. Yu, *J. Invest. Dermatol.*, **62,** 378(1974).

(37) R. J. Yu and E. J. Van Scott, *ibid.*, **63,** 279(1974).

(38) J. L. McCullough and G. D. Weinstein, *ibid.*, **65,** 394(1975).

(39) A. duVivier and R. B. Stoughton, *Clin. Res.*, **23,** 166A(1975).

(40) A. duVivier and R. B. Stoughton, *Br. J. Dermatol., Suppl. 11,* **93,** 27(1975).

(41) A. duVivier and R. B. Stoughton, *J. Invest. Dermatol.*, **65,** 235(1975).

(42) A. duVivier, R. Bible, Jr., R. K. Mikuriya, and R. B. Stoughton, *Br. J. Dermatol.*, **94,** 1(1976).

(43) R. B. Stoughton, F. Chiu, W. Fritsch, and D. Nurse, *J. Invest. Dermatol.*, **42,** 151(1964).

(44) F. S. K. MacMillan, H. H. Reller, and F. H. Snyder, *ibid.*, **43,** 363(1964).

(45) M. Wada, *Science*, **111,** 376(1950).

(46) H. F. Blum, "Photodynamic Action and Diseases Caused by Light," American Chemical Society Monograph Series No. 85, Reinhold, New York, N.Y., 1941.

(47) I. Willis and A. M. Kligman, *J. Soc. Cosmet. Chem.*, **20,** 639(1969).

(48) E. R. Kraft, S. G. Hoch, R. A. Quisno, and E. A. Newcomb, *ibid.*, **23,** 383(1972).

(49) S. I. Katz, *Arch. Dermatol.*, **101,** 466(1970).

(50) M. A. Pathak, T. B. Fitzpatrick, and E. Frenk, *N. Engl. J. Med.*, **280,** 1459(1969).

(51) G. Kahn and G. Wilcox, *J. Soc. Cosmet. Chem.*, **20,** 807(1969).

(52) G. Kahn and G. Wilcox, *J. Invest. Dermatol.*, **53,** 200(1969).

(53) K. J. Master, R. A. Sayre, and M. A. Everett, *J. Soc. Cosmet. Chem.*, **17,** 581(1966).

(54) S. Riegelman and R. P. Penna, *ibid.*, **11,** 280(1961).

(55) O. J. Lorenzetti, J. Boltralik, E. Busby, and B. Fortenberry, *ibid.*, **26,** 593(1975).

(56) A. M. Kligman, R. R. Marples, L. R. Lantis, and K. J. McGinley, *ibid.*, **25,** 73(1974).

(57) A. B. Ackerman and A. M. Kligman, *ibid.*, **20,** 81(1969).

(58) G. Plewig and A. M. Kligman, *ibid.*, **20,** 767(1969).

(59) J. J. Leyden, K. J. McGinley, and A. M. Kligman, *ibid.*, **26,** 573(1975).

(60) R. W. Vander Wyk and F. C. Roia, Jr., *ibid.*, **15,** 761 (1964).

(61) R. W. Vander Wyk and K. E. Hechemy, *ibid.*, **18,** 629(1967).
(62) P. Finkelstein and K. Laden, *ibid.*, **19,** 669(1968).
(63) J. A. Troller, *ibid.*, **22,** 187(1971).
(64) M. von Frey, *Arch. Neerl. Physiol.*, **7,** 42(1922).
(65) W. Montagna, "The Structure and Function of Skin," 2nd ed., Academic, New York, N.Y., 1962, p. 10.
(66) E. B. Titchener, "A Textbook of Physiology," Macmillan, New York, N.Y., 1909, p. 56.
(67) J. D. Hardy, C. B. Potelunas, and M. D. Meixner, *J. Invest. Dermatol.*, **16,** 369(1951).
(68) J. D. Hardy, A. G. Wolff, and H. Goodell, *J. Clin. Invest.*, **19,** 649(1940).
(69) W. Lucas and E. P. Guth, *J. Am. Pharm. Assoc., Sci. Ed.*, **42,** 344(1953).
(70) E. W. Brockemeyer and E. P. Guth, *ibid.*, **44,** 706(1955).
(71) J. Adriani, R. Zepernick, J. Arens, and E. Authement, *Clin. Pharmacol. Ther.*, **5,** 49(1964).
(72) J. Adriani and R. Zepernick, *J. Am. Med. Assoc.*, **188,** 711(1964).
(73) H. Dalili and J. Adriani, *Clin. Pharmacol. Ther.*, **12,** 913(1971).
(74) F. E. Corima, *J. Invest. Dermatol.*, **19,** 21(1952).
(75) F. E. Corima and V. Kuykendall, *ibid.*, **20,** 429(1953).
(76) F. E. Corima and V. Kuykendall, *Arch. Dermatol.*, **69,** 206(1954).
(77) F. M. Melton and W. B. Shelley, *J. Invest. Dermatol.*, **15,** 325(1950).
(78) S. G. Macris, I. H. Blank, and H. K. Beecher, *ibid.*, **33,** 15(1959).
(79) C. G. Mendelson and A. M. Kligman, *Arch. Dermatol.*, **83,** 559(1961).
(80) L. Frank, C. Stritzler, and J. Kaufman, *ibid.*, **71,** 117(1955).
(81) E. Kepel, W. H. Rooks, II, R. W. Ferraresi, and L. D. Shott, *J. Invest. Dermatol.*, **62,** 595(1974).
(82) R. T. Bowser and H. Baer, *J. Immunol.*, **91,** 791(1963).
(83) A. Jarrett and R. I. C. Spearman, "Histochemistry of Skin-Psoriasis," English University Press, London, England, 1974.
(84) R. Wrench and A. Z. Britten, *Br. J. Dermatol.*, **92,** 569(1975).
(85) *Ibid.*, **92,** 575(1975).
(86) *Ibid.*, **93,** 67(1975).
(87) *Ibid.*, **93,** 75(1975).
(88) T. F. Dougherty and G. L. Schneebeli, *Ann. N.Y. Acad. Sci.*, **61,** 328(1955).
(89) A. G. Ruhmann and D. L. Berliner, *Endocrinology*, **76,** 916(1965).
(90) D. L. Berliner and A. G. Ruhmann, *J. Invest. Dermatol.*, **49,** 117(1967).
(91) A. G. Ruhmann and D. L. Berliner, *ibid.*, **49,** 123(1967).
(92) D. L. Berliner, *Ann. N.Y. Acad. Sci.*, **116,** 1078(1964).
(93) D. L. Berliner, A. J. Gallegos, and G. L. Schneebeli, *J. Invest. Dermatol.*, **48,** 44(1967).
(94) D. L. Berliner and A. G. Ruhmann, *Endocrinology*, **78,** 373(1966).
(95) D. L. Berliner, A. G. Ruhmann, M. L. Berliner, and T. F. Dougherty, *Excerpta Med.*, **111,** 180(1966).
(96) D. L. Berliner, M. H. Bartley, G. H. Kenner, and W. S. S. Jee, *Br. J. Dermatol., Suppl. 6,* **82,** 53(1970).
(97) D. L. Berliner and C. J. Nabors, Jr., *J. Reticuloendothel. Soc.*, **4,** 284(1967).
(98) R. I. Dorfman, *Br. J. Dermatol., Suppl. 6,* **82,** 45(1970).
(99) I. Ringler, in "Methods in Hormone Research," vol. III, R. I. Dorfman, Ed., Academic, New York, N.Y., 1964, p. 227.
(100) L. J. Lerner, A. Bianchi, A. R. Turkheimer, F. M. Singer, and A. Borman, *Ann. N. Y. Acad. Sci.*, **116,** 1071(1964).
(101) L. G. Hershberger and D. W. Calhoun, *Endocrinology*, **60,** 153(1957).
(102) G. Dipasquale, C. L. Rassaert, and E. McDougall, *J. Pharm. Sci.*, **59,** 267(1970).
(103) L. J. Lerner, A. R. Turkheimer, A. Bianchi, F. M. Singer, and A. Borman, *Proc. Soc. Exp. Biol. Med.*, **116,** 385(1964).
(104) G. Tonelli, L. Thibault, and I. Ringler, *Endocrinology*, **77,** 625(1965).
(105) J. A. Witkowski and A. M. Kligman, *J. Invest. Dermatol.*, **32,** 481(1959).
(106) K. H. Burdick, *Acta Dermatol. Venereol., Suppl. 67,* **52,** 19(1972).
(107) E. Ortega, C. Rodriguez, K. H. Burdick, V. A. Place, and L. Gonzales, *ibid.*, **52,** 95(1972).
(108) K. H. Kaidbey and A. M. Kligman, *J. Invest. Dermatol.*, **63,** 292(1974).
(109) A. Scott and F. Kalz, *ibid.*, **26,** 361(1956).
(110) M. J. Brunner and P. Finkelstein, *Arch. Dermatol.*, **81,** 453(1960).
(111) C. A. Schlagel and J. I. Northam, *Proc. Soc. Exp. Biol. Med.*, **101,** 629(1959).
(112) H. R. Gray, R. L. Wolf, and R. H. Doneff, *Arch. Dermatol.*, **84,** 18(1961).
(113) J. Wolf, *Z. Mikrosk.-Anat. Forsch.*, **46,** 170(1939).
(114) H. Möller and H. Rorsman, *Acta Dermatol. Venereol.*, **40,** 381(1960).
(115) G. C. Wells, *Br. J. Dermatol.*, **69,** 11(1957).
(116) W. W. Heseltine, J. M. McGilchrist, and R. Gartside, *Nature*, **196,** 486(1962).
(117) J. B. Shelmire, *Arch. Dermatol.*, **78,** 191(1958).
(118) J. Everall and L. Fisher, *J. Invest. Dermatol.*, **19,** 97(1952).
(119) N. B. Kanof, *ibid.*, **25,** 329(1955).
(120) A. Scott and F. Kalz, *ibid.*, **26,** 149(1956).
(121) F. Kalz and A. Scott, *ibid.*, **26,** 165(1956).
(122) K. H. Burdick, J. K. Haleblian, B. J. Poulsen, and S. E. Cobner, *Curr. Ther. Res.*, **15,** 233(1973).
(123) S. T. Zaynoun and A. K. Kurban, *Br. J. Dermatol.*, **90,** 85(1974).
(124) A. I. Scott, *ibid.*, **77,** 586(1965).
(125) R. I. C. Spearman and A. Jarrett, *ibid.*, **92,** 581(1975).
(126) I. Sarkany and P. M. Gaylarde, *Trans. St. John's Hosp. Dermatol. Soc.*, **59,** 241(1973).
(127) F. Schaaf and F. Gross, *Dermatologica*, **106,** 357(1953).
(128) H. Barnes, P. M. Gaylarde, A. P. Brock, and I. Sarkany, *Br. J. Dermatol.*, **93,** 459(1975).
(129) W. L. Whitaker and B. L. Baker, *Science*, **108,** 207(1948).
(130) B. L. Baker, *Ann. N.Y. Acad. Sci.*, **53,** 690(1951).
(131) W. L. Whitaker and B. L. Baker, *Univ. Mich. Med. Bull.*, **17,** 384(1951).
(132) K. Fukuyama and B. L. Baker, *J. Invest. Dermatol.*, **31,** 327(1958).
(133) L. B. Fisher and H. I. Maibach, *Arch. Dermatol.*, **103,** 39(1971).
(134) R. Marks, D. Pongsehirun, and T. Saylan, *Br. J. Dermatol.*, **88,** 69(1973).
(135) A. W. McKenzie and R. B. Stoughton, *Arch. Dermatol.*, **86,** 608(1962).
(136) A. W. McKenzie, *ibid.*, **86,** 611(1962).
(137) A. W. McKenzie and R. M. Atkinson, *ibid.*, **89,** 741(1964).
(138) A. W. McKenzie, in "Progress in the Biological Sciences in Relation to Dermatology," A. Rook and R. H. Champion, Eds., Cambridge University Press, Cambridge, England, 1964, pp. 283–290.
(139) H. Baker and H. A. Sattar, *Br. J. Dermatol.*, **80,** 46(1968).
(140) R. B. Stoughton, *Arch. Dermatol.*, **99,** 753(1969).
(141) M. Moore-Robinson and G. A. Christie, *Br. J. Dermatol., Suppl. 6,* **82,** 86(1970).
(142) M. Moore-Robinson, *Clin. Trials J.*, **2,** 45(1971).
(143) J. P. Garnier, *ibid.*, **2,** 55(1971).
(144) V. A. Place, J. Giner-Velazquez, and K. H. Burdick, *Arch. Dermatol.*, **101,** 531(1970).
(145) E. G. Weirich and U. Lutz, *Dermatologica*, **147,** 353 (1973).
(146) G. Falconi and G. L. Rossi, *Arch. Dermatol.*, **105,** 856(1972).
(147) B. W. Barry and A. R. Brace, *J. Invest. Dermatol.*, **64,** 418(1975).
(148) K. H. Burdick, B. Poulsen, and V. Place, *J. Am. Med. Assoc.*, **211,** 462(1970).
(149) J. Ostrenga, J. Haleblian, B. Poulsen, B. Ferrell, N. Mueller, and S. Shastri, *J. Invest. Dermatol.*, **56,** 392(1971).
(150) K. H. Burdick, *Arch. Dermatol.*, **110,** 238(1974).
(151) B. W. Barry and R. Woodford, *Br. J. Dermatol.*, **91,** 323(1974).

(152) *Ibid.*, **93,** 563(1975).
(153) B. W. Barry and A. R. Brace, *J. Pharm. Pharmacol., Suppl.*, **26,** 67P(1974).
(154) B. W. Barry, A. R. Brace, A. C. Norris, and R. Woodford, *ibid.*, **27,** 75P(1975).
(155) R. B. Stoughton, *Arch. Dermatol.*, **106,** 825(1972).
(156) A. F. Pepler, R. Woodford, and J. C. Morrison, *Br. J. Dermatol.*, **85,** 171(1971).
(157) T. Fredriksson, L. Gip, and A. Hamfelt, *Curr. Ther. Res.*, **18,** 321(1975).
(158) K. H. Burdick, *Acta Dermatol. Venereol., Suppl. 67,* **52,** 24(1972).
(159) M. F. Coldman, L. Lockerbie, and E. A. Laws, *Br. J. Dermatol.*, **85,** 381(1971).
(160) M. J. Busse, P. Hunt, K. A. Lees, P. N. D. Maggs, and T. M. McCarthy, *ibid., Suppl. 4,* **81,** 103(1969).
(161) M. F. Coldman, L. Lockerbie, and E. A. Laws, *ibid.*, **85,** 573(1971).
(162) I. Sarkany, J. W. Hadgraft, G. A. Caron, and C. W. Barrett, *ibid.*, **77,** 569(1965).
(163) G. A. Christie and M. Moore-Robinson, *ibid., Suppl. 6,* **82,** 93(1970).
(164) K. J. Child, A. F. English, H. G. Gilbert, A. Hewitt, and E. Woollett, *Arch. Dermatol.*, **97,** 407(1968).
(165) T. Malone, J. K. Haleblian, B. J. Poulsen, and K. H. Burdick, *Br. J. Dermatol.*, **90,** 187(1974).
(166) C. W. Barrett, J. W. Hadgraft, G. A. Caron, and I. Sarkany, *ibid.*, **77,** 576(1965).
(167) J. Tissot and P. E. Osmundsen, *Acta Dermatol. Venereol.*, **46,** 447(1966).
(168) M. F. Coldman and L. Lockerbie, *Br. J. Dermatol.*, **85,** 398(1971).
(169) J. Reid and D. B. Brookes, *ibid.*, **80,** 328(1968).
(170) W. W. Heseltine, J. M. McGilchrist, and R. Gartside, *ibid.*, **76,** 71(1964).
(171) M. Katz and B. J. Poulsen, *J. Soc. Cosmet. Chem.*, **23,** 565(1972).
(172) J. Reinstein, J. Ostrenga, J. Haleblian, S. Shastri, B. Poulsen, and M. Katz, *Acta Dermatol. Venereol., Suppl. 67,* **52,** 13(1972).
(173) B. W. Barry and R. Woodford, presented at British Pharmaceutical Conference, North Staffordshire, Keele, England, Paper 86, 1972.
(174) R. Woodford and B. W. Barry, *Br. J. Dermatol.*, **89,** 53(1973).
(175) *Ibid.*, **90,** 233(1974).
(176) B. W. Barry and R. Woodford, *J. Pharm. Pharmacol., Suppl.*, **24,** 174P(1972).
(177) B. J. Poulsen, K. Burdick, and S. Bessler, *Arch. Dermatol.*, **109,** 367(1974).
(178) T. P. Greeson, N. E. Levan, R. I. Freedman, and W. H. Wong, *J. Invest. Dermatol.*, **61,** 242(1973).
(179) P. Sejrsen, *Scand. J. Clin. Lab. Invest., Suppl.*, **99,** 52(1966).
(180) L. Goldman, R. Flatt, and J. Baskett, *J. Invest. Dermatol.*, **23,** 251(1954).
(181) *Ibid.*, **24,** 81(1955).
(182) *Ibid.*, **25,** 75(1955).
(183) P. M. Sutton, R. J. Feldmann, and H. I. Maibach, *J. Invest. Dermatol.*, **57,** 371(1971).
(184) D. S. Snyder and R. A. Greenberg, *ibid.*, **63,** 461(1974).
(185) L. Juhlin, *Acta Dermatol. Venereol.*, **44,** 322(1964).
(186) P. Thune, *ibid.*, **51,** 261(1971).
(187) L. M. Solomon, E. Wentzel, and M. S. Greenberg, *J. Invest. Dermatol.*, **44,** 129(1965).
(188) D. J. Reis, *J. Clin. Endocrinol.*, **20,** 446(1960).
(189) L. Frank, Y. Rapp, and L. Bird, *Arch. Dermatol.*, **89,** 55(1964).
(190) J. E. Wolf, W. R. Hubler, and N. D. Guzick, through *ibid.*, **111,** 581(1975).
(191) A. duVivier and R. B. Stoughton, *ibid.*, **111,** 581(1975).
(192) J. R. Scholtz and K. J. Dumas, "13th International Congress of Dermatology," vol. 2, Springer-Verlag, New York, N.Y., 1968, p. 179.
(193) K. J. Dumas and J. R. Scholtz, *Acta Dermatol. Venereol.*, **52,** 43(1972).
(194) B. Portnoy, *Br. J. Dermatol.*, **77,** 579(1965).

ACKNOWLEDGMENTS AND ADDRESSES

Received from the *Institute of Pharmaceutical Sciences, Syntex Research, Palo Alto, CA 94304*

The author acknowledges the following publishers for their permission to reproduce various figures used in this review article: The Society for the Publication of *Acta Dermato-Venereologica*, Stockholm, Sweden; the American Medical Association, Chicago, Ill.; and the Williams & Wilkins Co., Baltimore, Md.

Theoretical Isotropic Dissolution of Nonspherical Particles

PETER VENG PEDERSEN ˣ and K. F. BROWN

Abstract □ Equations are derived for the isotropic dissolution of single particles, considering simple forms of the six crystal systems. These can be summarized by three basic equations which are approximated well, and in some cases exactly, by the dissolution equation for a hypothetical spherical particle of specified diameter. Formulas are given to enable calculation of this diameter and to minimize the weighted errors in the approximations. Spherical approximations provide a simple basis for calculating the dissolution profile of real multiparticulate systems which are difficult to describe otherwise. Spherical approximations based on equal surface area or volume result in large errors.

Keyphrases □ Dissolution, isotropic—nonspherical particles, six crystal systems, equations derived □ Isotropic dissolution—nonspherical particles, six crystal systems, equations derived □ Particles, nonspherical—isotropic dissolution, six crystal systems, equations derived □ Crystal systems, various—nonspherical particles, isotropic dissolution, equations derived

The influence of shape factors on dissolution kinetics of drugs has been discussed for tablets and time-released tablets (1, 2), but little attention has been given to single drug particles (3, 4). Most dissolution kinetic models consider spherical particles. Application of such models to real particle systems is complicated by the fact that pure drug particles are not spherical. The usual approach has been to treat the real particles as hypothetical spherical particles having the same surface area or volume. Such approximations may introduce substantial errors.

This paper presents exact isotropic single-particle dissolution equations for several nonspherical forms and formulas, enabling calculation of the diameters of hypothetical spherical particles which closely approximate the dissolution of these forms.

THEORY

Assume that dissolution takes place isotropically, that is, that the rate of dissolution per unit surface area, J, is constant so that the following equation can be written:

$$\frac{dw}{dt} = -JA \qquad \text{(Eq. 1)}$$

where w is the amount undissolved, and A is the surface area. This equation implies that the boundary of a *plane* interface retreats with constant speed during dissolution such that:

$$\frac{ds}{dt} = -\frac{J}{\rho} \qquad \text{(Eq. 2)}$$

where ρ is the density, and s is the distance perpendicular to the interface from some fixed reference point in the dissolving solid. Equation 2 integrates to:

$$s = s_0 - \frac{J}{\rho}t \qquad \text{(Eq. 3)}$$

where s_0 is the initial ($t = 0$) distance to the reference point. When this equation is applied to the isotropic dissolution of a spherical particle, the following equation arises:

$$\frac{w}{w_0} = \left(1 - \frac{J}{r_0\rho}t\right)^3 \qquad \text{(Eq. 4)}$$

or:

$$\left(\frac{w}{w_0}\right)^{1/3} = 1 - \frac{J}{r_0\rho}t \qquad \text{(Eq. 5)}$$

where r_0 is the initial radius of the particle.

Therefore, when a spherical particle dissolves isotropically (J = constant), it obeys the Hixson and Crowell (5) cube root law; that is, a plot of $(w/w_0)^{1/3}$ *versus* time is linear.

Dissolution of Prismatic Particles—Structures I–VI are 10 simple forms of the six crystal systems and illustrate the dimensional quantities b_0, c_0, l_0, h_0, and α used in the following derivations. It is assumed that $b_0 < c_0 < l_0$.

Consider a prismatic particle of initial length l_0 and having a regular n-gonal cross section with side of initial length b_0. The distance, s, from the n sides of the polygon to the center as reference point decreases during dissolution according to Eq. 3. The area of the cross section at any time is then equal to $n[s_0 - (J/\rho)t]^2 \tan(\pi/n)$, and the length of the prism is equal to $l_0 - (2J/\rho)t$, so the particle weight at time t is:

$$w = \rho\left(l_0 - \frac{2J}{\rho}t\right) n \left(s_0 - \frac{J}{\rho}t\right)^2 \tan\frac{\pi}{n} \qquad \text{(Eq. 6)}$$

which, since $s_0 = (b_0/2)\cot(\pi/n)$, can be written as:

$$w = \rho\left(l_0 - \frac{2J}{\rho}t\right)\frac{n}{4}\left[b_0 - \left(\frac{2J}{\rho}\tan\frac{\pi}{n}\right)t\right]^2 \qquad \text{(Eq. 7)}$$

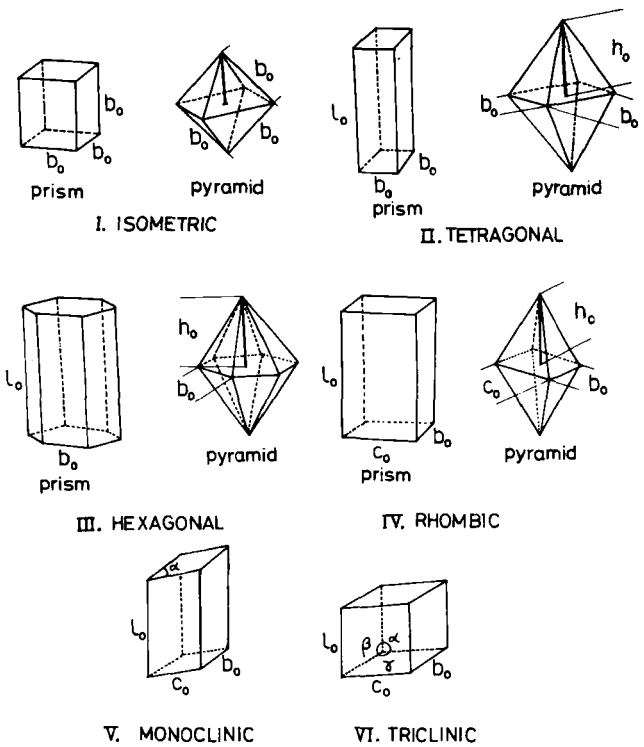

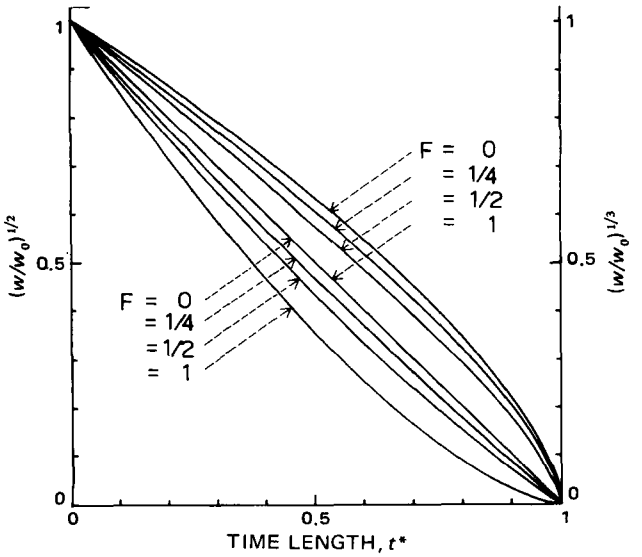

Figure 1—*Influence of the shape ratio,* F, *on the intrinsic dissolution profile of an* n*-gonal prismatic particle (tetragonal or hexagonal) or a rhombic pyramidal particle. The four curves below and including the diagonal are square root plots. The four curves above and including the diagonal are cube root plots. The dissolution deviates increasingly from the* $(w/w_0)^{1/3}$ versus t* *linear relationship (the cube root law) as the shape ratio becomes less than 1 and approaches a linear* $(w/w_0)^{1/2}$ versus t* *relationship (the square root law).*

At $t = 0$, $w_0 = \rho l_0 (n/4) b_0^2$, so Eq. 7 can be written:

$$\frac{w}{w_0} = \left(1 - \frac{2J}{l_0\rho}t\right)\left[1 - \left(\frac{2J}{b_0\rho}\tan\frac{\pi}{n}\right)t\right]^2 \qquad \text{(Eq. 8)}$$

Equation 8 comprises the exact dissolution equations for the prismatic forms of the isometric ($n = 4$, $b_0 = l_0$), tetragonal ($n = 4$, $b_0 = l_0$), and hexagonal ($n = 6$) crystal systems (I–III). The rhombic prism, having a rectangular cross section, dissolves according to:

$$w = \rho\left(b_0 - \frac{2J}{\rho}t\right)\left(c_0 - \frac{2J}{\rho}t\right)\left(l_0 - \frac{2J}{\rho}t\right) \qquad \text{(Eq. 9)}$$

because of the isotropic retreat of all surfaces. Similarly to Eq. 8, this equation can be written:

$$\frac{w}{w_0} = \left(1 - \frac{2J}{b_0\rho}t\right)\left(1 - \frac{2J}{c_0\rho}t\right)\left(1 - \frac{2J}{l_0\rho}t\right) \qquad \text{(Eq. 10)}$$

The monoclinic prismatic particle, having a parallelogram cross section with an acute angle α, has at any time a cross-sectional area equal to $bc \sin\alpha$, where $b = b_0 - [(2J/\rho)\sin\alpha]t$ and $c = c_0 - [(2J/\rho)\sin\alpha]t$, so it dissolves according to:

$$w = \rho\left(l_0 - \frac{2J}{\rho}t\right)\left[b_0 - \left(\frac{2J}{\rho}\sin\alpha\right)t\right] \times \left[c_0 - \left(\frac{2J}{\rho}\sin\alpha\right)t\right]\sin\alpha \qquad \text{(Eq. 11)}$$

or:

$$\frac{w}{w_0} = \left(1 - \frac{2J}{l_0\rho}t\right)\left[1 - \left(\frac{2J}{b_0\rho}\sin\alpha\right)t\right] \times \left[1 - \left(\frac{2J}{c_0\rho}\sin\alpha\right)t\right] \qquad \text{(Eq. 12)}$$

Dissolution of Pyramidal Particles—The regular pyramidal forms of the isometric, tetragonal, and hexagonal systems (I–III) all dissolve like a spherical particle, following the "cube root law": all plane surfaces of the pyramid retreat toward its center of symmetry with the same constant speed during isotropic dissolution. Therefore, the shape of the pyramid remains the same while its size diminishes. It can, for example, be shown geometrically that all lengths of the prism decrease by a factor of $1 - (J/r_0\rho)t$, where r_0, given by:

$$r_0 = \frac{h_0 b_0}{2\sqrt{h_0^2 + b_0^2/4}} \qquad \text{(Eq. 13)}$$

is the radius of the largest sphere that can be contained in the pyramid initially. The weight of the regular n-gonal prism at time t is equal

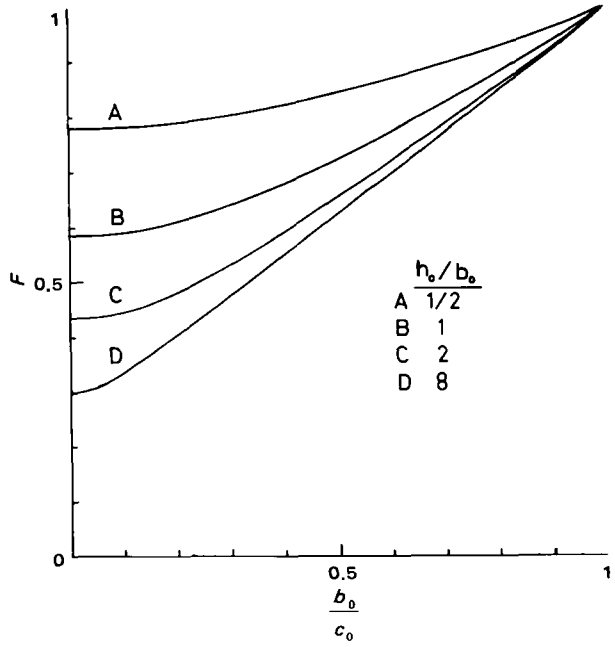

Figure 2—*Variation of the shape ratio,* F, *of a rhombic pyramidal particle having various shapes (see Structure IV for definitions of* b_0, c_0, *and* h_0).

to $\frac{1}{6}\rho n h_t b_t^2 \cot(\pi/n)$, where the height, h_t, and side, b_t, are $h_t = h_0[1 - (J/r_0\rho)t]$ and $b_t = b_0[1 - (J/r_0\rho)t]$, respectively, according to the above theory. Thus, its weight is:

$$w = \frac{1}{6}\rho n h_0 b_0^2\left(1 - \frac{J}{r_0\rho}t\right)^3 \cot\frac{\pi}{n} \qquad \text{(Eq. 14)}$$

from which it follows that:

$$\frac{w}{w_0} = \left(1 - \frac{J}{r_0\rho}t\right)^3 \qquad \text{(Eq. 15)}$$

This equation is identical to Eq. 4. Therefore, a regular pyramidal crystal form dissolves in exactly the same way as the largest (hypothetical) spherical particle that can be contained within its boundaries initially. This is also approximately true for an irregular pyramidal form such as the rhombic pyramid when the irregularity is not too extreme. It can be shown, using a double integration approach, that this crystal form dissolves according to:

$$\frac{w}{w_0} = \left(1 - \frac{J}{r_1\rho}t\right)^2\left[1 - \left(\frac{1}{4r_1} + \frac{3}{4r_2}\right)\frac{J}{\rho}t\right] \qquad \text{(Eq. 16)}$$

where:

$$r_1 = \frac{h_0 b_0}{2\sqrt{h_0^2 + b_0^2/4}} \qquad \text{(Eq. 17)}$$

$$r_2 = \frac{h_0 c_0}{2\sqrt{h_0^2 + c_0^2/4}} \qquad \text{(Eq. 18)}$$

The deviation from spherical particle dissolution (Eq. 15) arises from the fact that $b_0 < c_0$. If $b_0 = c_0$, then Eq. 16 reduces to the special case of Eq. 15 as expected.

To evaluate these single-particle dissolution equations, it is convenient to present them in a transformed simplified form which better illustrates their *intrinsic dissolution profile*[1]. For example, Eq. 8 can be transformed to:

$$\frac{w}{w_0} = (1 - Ft^*)(1 - t^*)^2 \qquad \text{(Eq. 19)}$$

or:

$$\left(\frac{w}{w_0}\right)^{1/3} = (1 - Ft^*)^{1/3}(1 - t^*)^{2/3} \qquad \text{(Eq. 20)}$$

[1] The concept of "intrinsic dissolution profile" was defined and discussed previously (6). It provides a powerful basis for the analysis of multiparticulate dissolution kinetics. In the case of single-particle dissolution, it enables the evaluation of the *shape* of the dissolution curve irrespective of the way time is scaled.

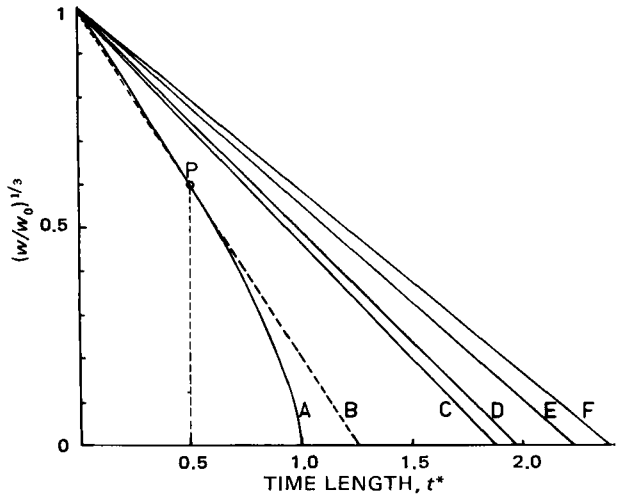

Figure 3—*Application of the use of spherical approximations to describe the dissolution of an* n*-gonal prismatic particle (curve A, Eq. 20,* F = 1/4*). Curves C and E represent the dissolution of a spherical particle with the same volume (Eq. 27,* F = 1/4, n = 4, 6*). Similarly, curves D and F represent a spherical particle having the same surface area (Eq. 26,* F = 1/4, n = 4, 6*). Curve B is the approximation (Eq. 30,* F = 1/4*) from which the equivalent spherical diameter is calculated (Eq. 31).*

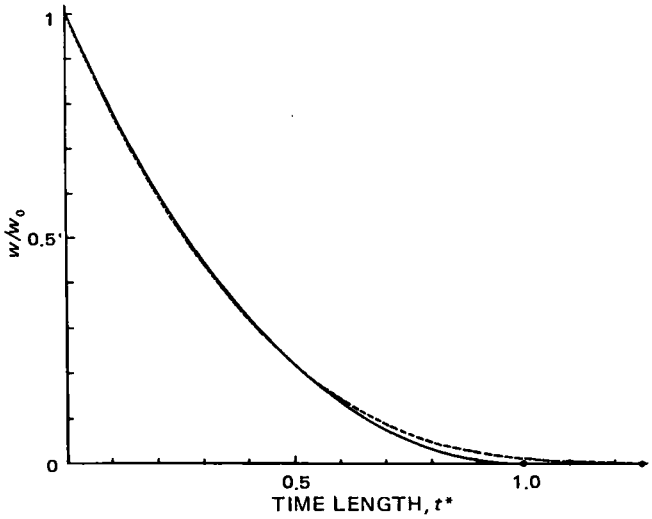

Figure 4—*Dissolution of an* n*-gonal prismatic particle (tetragonal or hexagonal) or a rhombic pyramidal particle having the shape ratio* F = 1/4 *(unbroken line, Eq. 19) and a hypothetical spherical particle (broken line) representing the approximation (Eq. 30) from which the equivalent spherical diameter is calculated (Eq. 31).*

where:

$$t^* = \left(\frac{2J}{b_0\rho}\tan\frac{\pi}{n}\right)t \qquad \text{(Eq. 21)}$$

is denoted *time length* and:

$$F = \frac{b_0}{l_0}\cot\frac{\pi}{n} \qquad \text{(Eq. 22)}$$

is denoted the *shape ratio.* This form of the equation clearly shows that the intrinsic dissolution profile depends only on the value of the dimensionless shape ratio, F, which defines the particle shape. Furthermore, the transformation makes it more convenient to evaluate the extent to which dissolution of the prismatic particle deviates from spherical particle dissolution (*i.e.*, from the cube root law). For $F = 1$, *i.e.*, when $(w/w_0)^{1/3} = 1 - t^*$, there is no such deviation; however, as F decreases, the deviation becomes more significant, *i.e.*, when the length of the particle relative to its side length or "diameter" becomes more extreme.

It is seen (Fig. 1) that as F decreases, the deviation from the cube root law becomes larger. Dissolution then approaches what can be called "the square root law," that is, a linear relationship between $(w/w_0)^{1/2}$ and time length (or time). This is in agreement with the fact that, for small F values, Eq. 19 approximates $(w/w_0)^{1/2} = 1 - t^*$. The cube root law and the square root law were each postulated previously as a model for the dissolution of a spherical particle under sink conditions (5, 7). Pure drug particles are not spherical, however, but are often prismatic in shape. Therefore, the particle shape effect should be considered in any experimental evaluation of such models.

The dissolution equation for a rhombic pyramidal particle (Eq. 16) can also be transformed to Eq. 19 where:

$$t^* = \left(\frac{2J}{\rho}\sqrt{h_0^2 + b_0^2/4}\right)t \qquad \text{(Eq. 23)}$$

and:

$$F = \frac{1}{4} + \frac{3}{4}\sqrt{\frac{h_0^2 + c_0^2/4}{h_0^2 + b_0^2/4}} \qquad \text{(Eq. 24)}$$

It is seen (Fig. 2) that the shape ratio, F, for this pyramidal particle form does not deviate much from 1 for most shapes, indicating that in most cases dissolution closely approximates that of a spherical particle.

Dissolution equations for either a rhombic (Eq. 10) or a monoclinic (Eq. 12) particle can be written similarly, in a common transformed form, as:

$$\frac{w}{w_0} = (1 - F_1t^*)(1 - F_2t^*)(1 - t^*) \qquad \text{(Eq. 25)}$$

where $F_1 = (b_0/c_0)$, $F_2 = (b_0/l_0)$, and $t^* = (2J/b_0\rho)t$ for a rhombic particle and $F_1 = (b_0/c_0)$, $F_2 = (b_0/l_0)\sin\alpha$, and $t^* = (2J/b_0\rho\sin\alpha)t$ for a monoclinic particle.

RESULTS AND DISCUSSION

The main objective of studying single-particle dissolution kinetics is to gain a better understanding and description of multiparticulate systems. In practice, the particles in such a system vary both in size and shape, thus making a rigorous mathematical description quite complex. Such a description must include a bivariate distribution function of the particle dimensions, and evaluation of this distribution function is rather difficult.

A considerable simplification can be achieved, however, if the dissolution of each particle in the multiparticulate sphere can be approximated by the dissolution of a hypothetical *spherical* particle of some specified diameter. The problem associated with the bivariate distribution function is then avoided, since the system is simplified to contain only one dimensional variable, the diameter of the spheres. The exact dissolution profile of the hypothetical particle system that approximates the real system can then be calculated using an equation presented previously (6, 8).

The usual approach to describe dissolution of nonspherical particles has been to approximate them by spherical particles having the same surface area or volume. It is of interest to evaluate the errors in such approximations. A spherical particle, having the same surface area as an n-gonal prismatic particle with shape ratio F, dissolves according to:

$$\left(\frac{w}{w_0}\right)^{1/3} = 1 - \sqrt{\frac{2\pi\cot\frac{\pi}{n}}{n(1 + 2/F)}}\,t^* \qquad \text{(Eq. 26)}$$

Or, if it has the same volume, it dissolves according to:

$$\left(\frac{w}{w_0}\right)^{1/3} = 1 - \left(\frac{2\pi F\cot\frac{\pi}{n}}{3n}\right)^{1/3} t^* \qquad \text{(Eq. 27)}$$

where t^* and F are defined by Eqs. 21 and 22. Figure 3 shows the substantial errors introduced by such approximations based on equal surface area or volume. This is not only the case for $F = 1/4$ but for all other values of the shape ratio less than 1.

The problem of finding the diameter of the spherical particle that best approximates the dissolution of an n-gonal prismatic particle is mathematically the same as finding a quantity, x, such that:

$$\frac{w}{w_0} = (1 - xt^*)^3 \qquad \text{(Eq. 28)}$$

best fits Eq. 19. Possibly the best criterion for this fit is to minimize

Table I—Summary of the Dissolution of the Particle Forms Including Expressions for Calculating the Equivalent Spherical Diameter

Dissolution of Prismatic Particles[a]

n-Gonal Prismatic Particles

Exact dissolution equation $\frac{w}{w_0} = (1 - Ft^*)(1 - t^*)^2$

Spherical approximation $\frac{w}{w_0} \doteqdot \{1 - [2 - (2 - F)^{1/3}]t^*\}^3$

Crystal System	Time Length, t^*	Shape Ratio[b], F	Equivalent Spherical Diameter $a = \frac{2Jt}{[2 - (2 - F)^{1/3}]\rho t^*}$
n-Gonal	$\left(\frac{2J}{b_0\rho} \tan\frac{\pi}{n}\right)t$	$\frac{b_0}{l_0}\cot\frac{\pi}{n}$	$\frac{b_0 \cot\frac{\pi}{n}}{2-\left(2-\frac{b_0}{l_0}\cot\frac{\pi}{n}\right)^{1/3}}$
Tetragonal ($n = 4$)	$\frac{2J}{b_0\rho}t$	$\frac{b_0}{l_0}$	$\frac{b_0}{2-\left(2-\frac{b_0}{l_0}\right)^{1/3}}$
Isometric ($n = 4$, $b_0 = l_0$)	$\frac{2J}{b_0\rho}t$	1	b_0
Hexagonal ($n = 6$)	$\frac{2\sqrt{3}J}{3b_0\rho}t$	$\sqrt{3}\frac{b_0}{l_0}$	$\frac{\sqrt{3}b_0}{2-\left(2-3\frac{b_0}{l_0}\right)^{1/3}}$

Rhombic and Monoclinic Particles

Exact dissolution equations $\frac{w}{w_0} = (1 - F_1t^*)(1 - F_2t^*)(1 - t^*)$

Spherical approximation $\frac{w}{w_0} \doteqdot \{1-[2-(2 - F_1)^{1/3}(2 - F_2)^{1/3}]t^*\}^3$

Crystal System	Time Length, t^*	Shape Ratios F_1	Shape Ratios F_2	Equivalent Spherical Diameter $a = \frac{2Jt}{[2-(2 - F_1)^{1/3}(2 - F_2)^{1/3}]\rho t^*}$
Rhombic	$\frac{2J}{b_0\rho}t$	$\frac{b_0}{c_0}$	$\frac{b_0}{l_0}$	$\frac{b_0}{2-\left(2-\frac{b_0}{c_0}\right)^{1/3}\left(2-\frac{b_0}{l_0}\right)^{1/3}}$
Monoclinic	$\frac{2J}{b_0\rho\sin\alpha}t$	$\frac{b_0}{c_0}$	$\frac{b_0}{l_0}\sin\alpha$	$\frac{b_0\sin\alpha}{2-\left(2-\frac{b_0}{c_0}\right)^{1/3}\left(2-\frac{b_0}{l_0}\sin\alpha\right)^{1/3}}$

Dissolution of Pyramidal Particles

n-Gonal Pyramidal Particles (Isometric, Tetragonal, Hexagonal)

Exact dissolution equation $\frac{w}{w_0} = (1 - t^*)^3$

Time length $t^* = \frac{2J\sqrt{h_0^2 + b_0^2/4}}{\rho}t$

Equivalent spherical diameter[c] $a = \frac{h_0 b_0}{\sqrt{h_0^2 + b_0^2/4}}$

Rhombic Pyramidal Particles

Exact dissolution equation $\frac{w}{w_0} = (1 - Ft^*)(1 - t^*)^2$

Table I—(*Continued*)

Spherical approximation	$\frac{w}{w_0} \doteq \{1-[2-(2-F)^{1/3}]t^*\}^3$
Time length	$t^* = \frac{2J\sqrt{h_0^2 + b_0^2/4}}{\rho} t$
Shape ratio	$F = \frac{1}{4} + \frac{3}{4}\sqrt{\frac{h_0^2 + c_0^2/4}{h_0^2 + b_0^2/4}}$
Equivalent spherical diameter	$a = \frac{1}{[2-(2-F)^{1/3}]\sqrt{h_0^2 + b_0^2/4}}$

[a] Structures I–VI illustrate the quantities b_0, c_0, l_0, and α used. [b] When $F = 1$, *i.e.*, $(b_0/l_0) = \tan(\pi/n)$, then the equivalent spherical diameter is equal to the biggest sphere that can be contained in the prismatic body. The spherical approximation of the dissolution then becomes exact. [c] This diameter is equal to the biggest sphere the pyramid can contain.

the sum of the squared errors where these are weighted proportionally to w/w_0, *i.e.*, to minimize the integral:

$$I = \int_0^1 [(1 - Ft^*)(1 - t^*)^2 - (1 - xt^*)^3]^2 \times (1 - Ft^*)(1 - t^*)^2\, dt^* \quad \text{(Eq. 29)}$$

by solving for x when $\partial I/\partial x = 0$. The exact expression for x is too complex to be of value. However, a very good approximation was obtained by choosing x such that Eqs. 28 and 19 intersect at $t^* = \frac{1}{2}$ (point P, Fig. 3), which corresponds to $x = 2 - (2 - F)^{1/3}$, such that the dissolution is approximated by the following equation for the hypothetical spherical particle:

$$\left(\frac{w}{w_0}\right)^{1/3} = 1 - [2 - (2 - F)^{1/3}]t^* \quad \text{(Eq. 30)}$$

The equivalent spherical diameter, a, *i.e.*, the diameter of this spherical particle, can then be obtained by equating the right-hand sides of Eqs. 30 and 5 from which it follows that:

$$a = \frac{2Jt}{[2 - (2 - F)^{1/3}]\rho t^*} \quad \text{(Eq. 31)}$$

Although the approximation given by Eq. 30 (curve B, Fig. 3) does not seem to be a particularly good fit to the exact dissolution curve calculated for the n-gonal particle (curve A), when the same two curves are plotted as w/w_0 *versus* time length (Fig. 4) instead of as $(w/w_0)^{1/3}$, it is clear that this is because of the nonlinear scaling in the cube root plot. The stippled curve (Fig. 4) representing the spherical approximation shows excellent fit to the true dissolution. The weighted errors of the spherical approximation were calculated for various values of the shape ratio F and showed (Fig. 5) that this choice for the approximation was satisfactory.

By using similar reasoning, it was found that the equation:

$$\left(\frac{w}{w_0}\right)^{1/3} = 1 - [2 - (2 - F_1)^{1/3}(2 - F_2)^{1/3}]t^* \quad \text{(Eq. 32)}$$

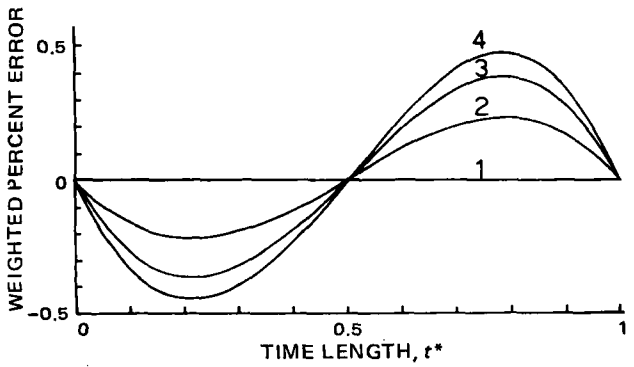

Figure 5—*Graph of errors in the spherical approximation (Eq. 30) of the dissolution (Eq. 19) of an n-gonal prismatic particle (isometric, tetragonal, or hexagonal) or a rhombic pyramidal particle of different shape ratios. The error is weighted proportionally to the fraction undissolved (w/w₀). Key: 1, F = 1; 2, F = ½; 3, F = ⅓; and 4, F = ¼.*

which is similar in form to Eq. 30, provides a good spherical approximation to Eq. 25, which describes the dissolution of rhombic and monoclinic prismatic particles. The equivalent spherical diameter in these cases is given by:

$$a = \frac{2Jt}{[2 - (2 - F_1)^{1/3}(2 - F_2)^{1/3}]\rho t^*} \quad \text{(Eq. 33)}$$

The error in this spherical approximation (Eq. 32) is substantially greater in the final stages of the dissolution process (Figs. 6 and 7) than in the previous case (Figs. 4 and 5). However, a previous study (8) showed that dissolution of a nonuniformly distributed, multiparticulate system is only slightly affected by the dissolution behavior of the smallest particles. Substantial truncation at the lower end of the particle-size distribution had very little effect on the dissolution profile calculated (8). Thus, approximation error in the later stage of the single-particle dissolution does not introduce the same degree of error when applied to a nonuniformly distributed, multiparticulate system. The approximation (Eq. 32) should, therefore, yield considerably better results when applied to a multiparticulate system than might be judged from Fig. 6. This explains the choice of the particular weighting of the errors in the approximation procedure.

Table I summarizes the dissolution of the particle forms shown in Structures I–VI and gives formulas for the calculation of the equivalent spherical diameter in each case[2]. The dissolution of these 10 forms can be described by three basic transformed equations of cubic form in time length (or time). The dissolution can thus be described exactly by a third degree polynomial in time in all cases.

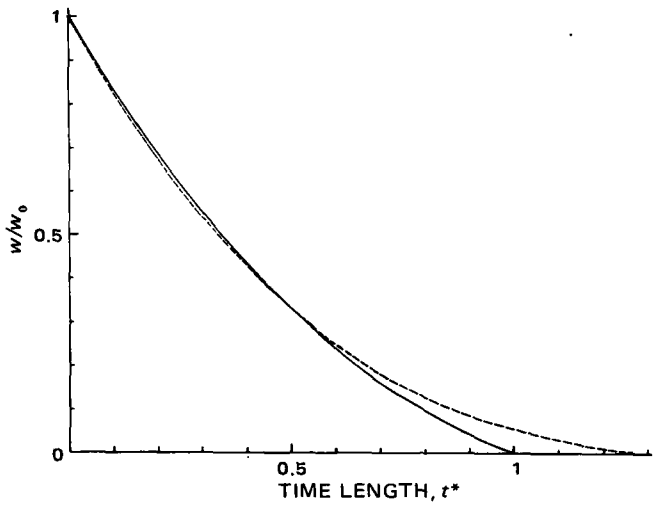

Figure 6—*Dissolution of monoclinic or rhombic prismatic particles with shape ratios $F_1 = \frac{1}{2}$ and $F_2 = \frac{1}{4}$ (unbroken line, Eq. 25) and a hypothetical spherical particle (broken line) representing the approximation (Eq. 32) from which the equivalent spherical diameter is calculated (Eq. 33).*

[2] The equation for a triclinic particle is not included because of its complexity and limited application, but it can be transformed to Eq. 25.

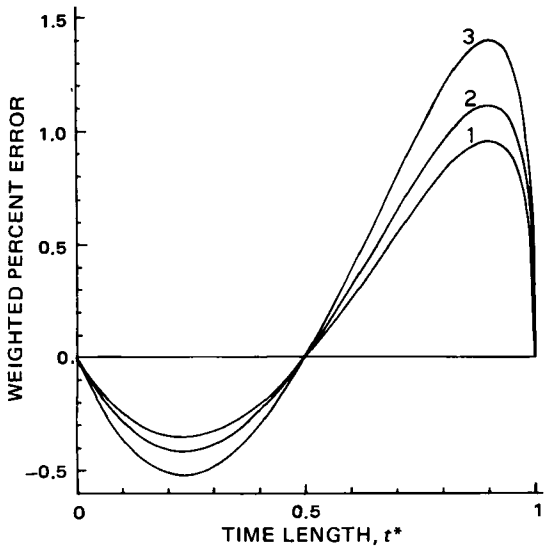

Figure 7—*Graph of errors in the spherical approximation (Eq. 32) to the dissolution (Eq. 25) of a monoclinic or rhombic prismatic particle of different shape ratios. The error is weighted proportionally to the fraction undissolved* (w/w_0). *Key: 1,* $F_2 = 1/8$; *2,* $F_2 = 1/4$; *and 3,* $F_2 = 1/3$. $F_1 = 1/2$.

The basic assumption behind these derivations is that the rate of dissolution per unit surface area, J, remains constant during dissolution and is the same everywhere at the interface of the dissolving crystal. This assumption can only be approximately true in practice under complete sink conditions. The higher activity at the crystal edges results in a larger J value in these areas and, therefore, a "rounding off" of the shape, so that dissolution in the later stages is slower than that calculated. However, this should result in an *improvement* in the fit of the spherical approximation and sometimes may result in a closer fit to the real dissolution than the exact expressions given for isotropic conditions. Thus, the approximating curve (stippled line, Figs. 4 and 6) is above the calculated dissolution curve in the later stages. The *true* dissolution curve, because of the rounding off effect, is above the calculated curve and hence closer to the approximation.

Excellent agreement between experimental and calculated results was obtained for the dissolution of a multiparticulate system of particles, approximately tetragonal prismatic in shape, when the respective spherical approximations were applied (9).

REFERENCES

(1) J. P. Cleave, *J. Pharm. Pharmacol.*, **17**, 698(1965).

(2) J. Cobby, M. Mayersohn, and G. C. Walker, *J. Pharm. Sci.*, **63**, 725(1974).

(3) I. C. Edmundson and K. A. Lees, *J. Pharm. Pharmacol.*, **17**, 193(1965).

(4) R. J. Withey, *ibid.*, **23**, 573(1971).

(5) A. W. Hixson and J. H. Crowell, *Ind. Eng. Chem.*, **23**, 923(1931).

(6) P. Veng Pedersen and K. F. Brown, *J. Pharm. Sci.*, **64**, 1981(1975).

(7) P. J. Niebergall, G. Milosovich, and J. E. Goyan, *ibid.*, **52**, 236(1963).

(8) P. Veng Pedersen and K. F. Brown, *ibid.*, **64**, 1192(1975).

(9) *Ibid.*, **65**, 1442(1976).

ACKNOWLEDGMENTS AND ADDRESSES

Received May 2, 1975, from the *Department of Pharmacy, University of Sydney, Sydney, N.S.W. 2006, Australia.*

Accepted for publication December 10, 1975.

Supported in part by Grant 72.4244 from the National Health and Medical Research Council of Australia.

[x] To whom inquiries should be directed.

Experimental Evaluation of Three Single-Particle Dissolution Models

PETER VENG PEDERSEN [x] and K. F. BROWN

Abstract □ The dissolution of the 60–85-mesh fraction of tolbutamide was investigated using a high precision, continuous recording, flow-through dissolution apparatus equipped with a dissolution cell; it was particularly suitable for kinetic analysis of multiparticulate systems. By using a time-scaling approach, experimental data are compared with theoretical calculations to evaluate, quantitatively, which of three single-particle dissolution models best describes the data and how well the multiparticulate kinetics can be explained mathematically. The nonspherical tolbutamide particles are replaced in the calculations by a hypothetical system of spherical particles that appears to be log-normally distributed. This procedure permits the calculation of the intrinsic dissolution profile, considering both size distribution and particle shape effects.

Keyphrases □ Dissolution—tolbutamide, three single-particle models evaluated and compared, mathematical analysis □ Tolbutamide—dissolution, three single-particle models evaluated and compared, mathematical analysis

There are several kinetic models for single-particle dissolution. Experimental evaluation of these models has been based on multiparticulate dissolution data, but distribution and particle shape effects have not been considered. The general theory of multiparticulate dissolution was discussed previously (1). This theory was subsequently used to develop mathematical expressions for the dissolution of log-normally distributed powders, considering three single-particle dissolution models (2).

A recent publication (3) dealt with the theory of single-particle dissolution in relation to particle shape. It gives directions for calculating the diameter of hypothetical spherical particles whose dissolution approximates nonspherical particles with minimum error. This paper demonstrates the application of

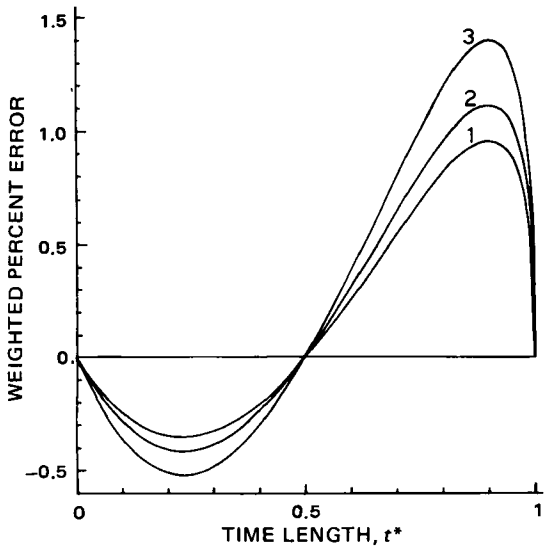

Figure 7—*Graph of errors in the spherical approximation (Eq. 32) to the dissolution (Eq. 25) of a monoclinic or rhombic prismatic particle of different shape ratios. The error is weighted proportionally to the fraction undissolved* (w/w_0). *Key: 1,* $F_2 = 1/8$; *2,* $F_2 = 1/4$; *and 3,* $F_2 = 1/3$. $F_1 = 1/2$.

The basic assumption behind these derivations is that the rate of dissolution per unit surface area, J, remains constant during dissolution and is the same everywhere at the interface of the dissolving crystal. This assumption can only be approximately true in practice under complete sink conditions. The higher activity at the crystal edges results in a larger J value in these areas and, therefore, a "rounding off" of the shape, so that dissolution in the later stages is slower than that calculated. However, this should result in an *improvement* in the fit of the spherical approximation and sometimes may result in a closer fit to the real dissolution than the exact expressions given for isotropic conditions. Thus, the approximating curve (stippled line, Figs. 4 and 6) is above the calculated dissolution curve in the later stages. The *true* dissolution curve, because of the rounding off effect, is above the calculated curve and hence closer to the approximation.

Excellent agreement between experimental and calculated results was obtained for the dissolution of a multiparticulate system of particles, approximately tetragonal prismatic in shape, when the respective spherical approximations were applied (9).

REFERENCES

(1) J. P. Cleave, *J. Pharm. Pharmacol.*, **17**, 698(1965).

(2) J. Cobby, M. Mayersohn, and G. C. Walker, *J. Pharm. Sci.*, **63**, 725(1974).

(3) I. C. Edmundson and K. A. Lees, *J. Pharm. Pharmacol.*, **17**, 193(1965).

(4) R. J. Withey, *ibid.*, **23**, 573(1971).

(5) A. W. Hixson and J. H. Crowell, *Ind. Eng. Chem.*, **23**, 923(1931).

(6) P. Veng Pedersen and K. F. Brown, *J. Pharm. Sci.*, **64**, 1981(1975).

(7) P. J. Niebergall, G. Milosovich, and J. E. Goyan, *ibid.*, **52**, 236(1963).

(8) P. Veng Pedersen and K. F. Brown, *ibid.*, **64**, 1192(1975).

(9) *Ibid.*, **65**, 1442(1976).

ACKNOWLEDGMENTS AND ADDRESSES

Received May 2, 1975, from the *Department of Pharmacy, University of Sydney, Sydney, N.S.W. 2006, Australia.*

Accepted for publication December 10, 1975.

Supported in part by Grant 72.4244 from the National Health and Medical Research Council of Australia.

[x] To whom inquiries should be directed.

Experimental Evaluation of Three Single-Particle Dissolution Models

PETER VENG PEDERSEN [x] and K. F. BROWN

Abstract □ The dissolution of the 60–85-mesh fraction of tolbutamide was investigated using a high precision, continuous recording, flow-through dissolution apparatus equipped with a dissolution cell; it was particularly suitable for kinetic analysis of multiparticulate systems. By using a time-scaling approach, experimental data are compared with theoretical calculations to evaluate, quantitatively, which of three single-particle dissolution models best describes the data and how well the multiparticulate kinetics can be explained mathematically. The nonspherical tolbutamide particles are replaced in the calculations by a hypothetical system of spherical particles that appears to be log-normally distributed. This procedure permits the calculation of the intrinsic dissolution profile, considering both size distribution and particle shape effects.

Keyphrases □ Dissolution—tolbutamide, three single-particle models evaluated and compared, mathematical analysis □ Tolbutamide—dissolution, three single-particle models evaluated and compared, mathematical analysis

There are several kinetic models for single-particle dissolution. Experimental evaluation of these models has been based on multiparticulate dissolution data, but distribution and particle shape effects have not been considered. The general theory of multiparticulate dissolution was discussed previously (1). This theory was subsequently used to develop mathematical expressions for the dissolution of log-normally distributed powders, considering three single-particle dissolution models (2).

A recent publication (3) dealt with the theory of single-particle dissolution in relation to particle shape. It gives directions for calculating the diameter of hypothetical spherical particles whose dissolution approximates nonspherical particles with minimum error. This paper demonstrates the application of

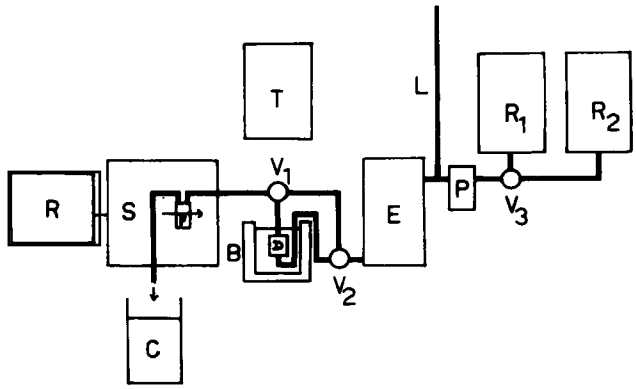

Figure 1—*Diagram of continuous-flow recording dissolution apparatus. (See text for description.)*

these theories to explain the dissolution kinetics of the 60–85-mesh fraction of tolbutamide such that both size distribution effects (2) and particle shape effects (3) are considered. By using a time-scaling approach, the three single-particle dissolution kinetic models are evaluated.

EXPERIMENTAL

A continuous-flow recording dissolution apparatus was used (Fig. 1). As shown in Fig. 1, R_1 and R_2 are 20-liter reservoirs containing the dissolution liquid, and P is a pulse-free peristaltic pump transporting liquid from R_1 or R_2 through a heat exchanger, E, which adjusts the liquid to the required temperature before it reaches the dissolution cell, D. This cell is immersed in a water-filled, jacketed beaker, B, maintained at the same temperature as the dissolution liquid leaving E. Liquid from dissolution cell D passes through a flowcell, F, in the spectrophotometer, S, fitted with a chart recorder, R, and finally accumulates in the collection vessel, C.

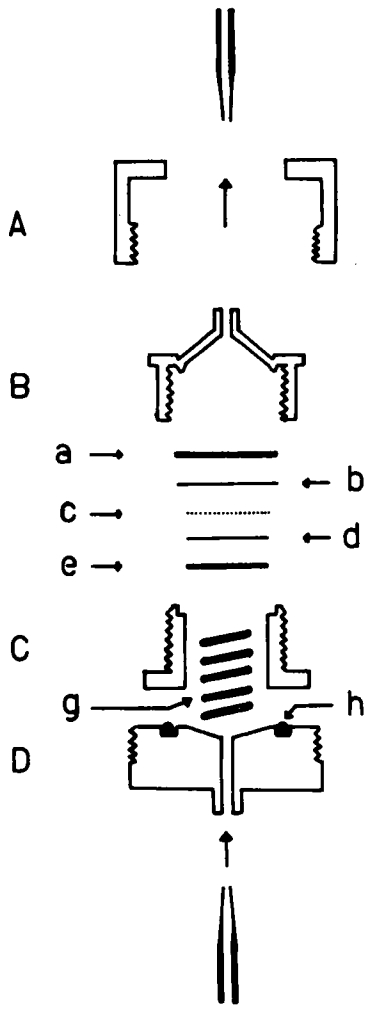

Figure 2—*Enlarged diagram of dissolution cells. (See text for description.)*

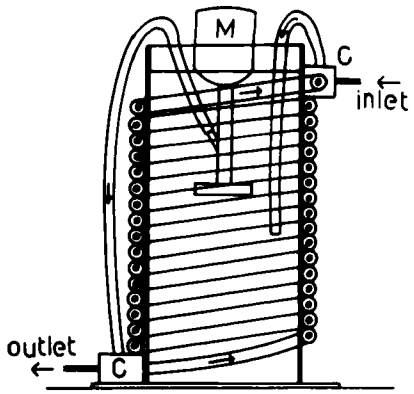

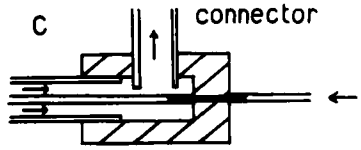

Figure 3—*Diagram of heat exchanger. (See text for description.)*

Two-way valves, V_1 and V_2, enable bypass of dissolution cell D for zero-line adjustment of the spectrophotometer with blank liquid from the reservoir; V_3 is a similar valve through which liquid can be drawn from either reservoir R_1 or R_2. Polyethylene tubing (i.d. 0.35 cm) was used throughout. The pressure governing the flow rate is monitored by the open tube-type meter L.

Figure 2 shows a detailed diagram of the dissolution cell constructed for this work. Powder to be investigated is spread in a single particle layer, c, in a sandwich line arrangement between two paper filters, b and d[1]. These filters are supported on both sides by stainless steel filter supports, a and e[2]. Filter support e and filter d have a diameter equal to the inside diameter of C (2.20 cm), whereas a and b have the same diameter as the recess in C; B and C are modified portions of a 2.54-cm (1-in.) filter holder unit[3].

Part C was modified from the commercial filter unit by increasing the depth of the recess to contain both a and b. In addition, a hole 2.20 cm in diameter was bored through the center. A watertight pressure seal is achieved by means of an O-ring, h.

The equipment for temperature regulation was also designed especially for this work to overcome the problems of maintaining large volumes of dissolution fluid at a constant temperature (Fig. 3). It consists of a cylindrical polyvinyl chloride reservoir, 40 cm in depth with internal diameter 15.5 cm, filled with distilled water. A thermostat water circulator, M, is mounted in this cylinder and connected to a polyvinyl chloride hose, which is coiled around the outer surface of the cylinder. Heated water from the cylinder is continuously recycled through the hose and returned to the reservoir. Polyethylene tubing is threaded inside the hose, carrying the dissolution fluid which requires temperature regulation.

Dissolution fluid is transported *via* the peristaltic pump and flows countercurrent to the recycled water through the inner polyethylene hose. Stainless steel connectors, C, seal the polyvinyl chloride hose at the points of entry and exit of the small bore tubing. This apparatus is very efficient in providing dissolution liquid at a constant temperature. When the water in the reservoir is

[1] Whatman quantitative filter paper.
[2] Millipore Catalog No. xx 3002503.
[3] Gelman.

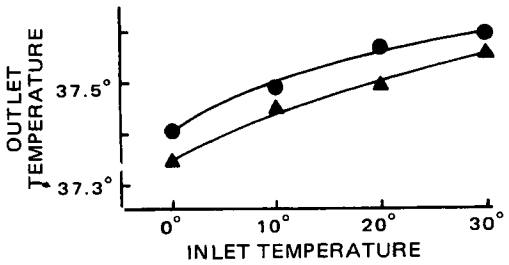

Figure 4—*Variation in temperature of water, after passage through heat exchanger, as a function of inlet water temperature. Thermostat setting was 37.7°. Key: ●, 0.24-ml/sec flow rate; and ▲, 1.90-ml/sec flow rate.*

maintained at 37.7°, the temperature of the dissolution liquid leaving the heat exchanger is 37.5 ± 0.2° for inlet temperatures ranging between 0 and 30° and flow rates of 0.24–1.90 ml/sec (Fig. 4).

Values of absorbance were read from the chart recording at 1–2.5-min intervals from the beginning of the experiment. These data, together with the volumetric flow rate, the Beer law constant, the initial amount of drug used, and the amount undissolved remaining in the dissolution cell at the end of the experiment, were processed by digital computer according to a FORTRAN program. This procedure permitted the evaluation of various dissolution kinetic models. Hydrochloric acid, 0.1 *M*, was used as liquid for all dissolution tests.

The accuracy of the apparatus in combination with the computer treatment was tested using 12.5 mg of the 60–85-mesh fraction of tolbutamide and a flow rate of 0.568 ml/sec (0.149 cm/sec linear flow rate). Dissolution liquid containing dissolved drug was collected at intervals of exactly 5 min as it left the spectrophotometer flowcell (F, Fig. 1) and was assayed for drug. Cube root plots (Fig. 5) of the dissolution data obtained from direct analysis of the samples and plots generated by the computer from the spectrophotometer recording almost coincided. The difference was similar in magnitude to the observed variation in flow rate, which was less than 1%.

THEORY

The three equations (from Refs. 4–6, respectively) for dissolution of a spherical particle under sink conditions are:

$$w^{1/3} = w_0^{1/3} - k_1 t \qquad \text{(Eq. 1)}$$

$$w^{1/2} = w_0^{1/2} - k_2 t \qquad \text{(Eq. 2)}$$

$$w^{2/3} = w_0^{2/3} - k_3 t \qquad \text{(Eq. 3)}$$

or, in general form:

$$w = (w_0^{1/m} - kt)^m \qquad \text{(Eq. 4)}$$

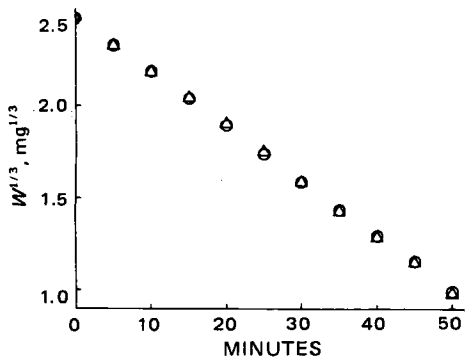

Figure 5—*Test of the accuracy of the dissolution apparatus in combination with the computer data treatment of the continuous chart recording. Dissolution is of 12.5 mg of the 60–85-mesh fraction of tolbutamide in 0.1 M HCl using dissolution cell at solvent flow rate of 0.149 cm/sec (0.568 ml/sec). Key: △, values calculated from intermittent samples collected at 5-min intervals; and ○, values generated by digital computer from continuous chart recording.*

where w and w_0 are the respective weights of the undissolved particle at times t and $t = 0$; $m = 3$, 2, and 3/2; and $k = k_1$, k_2, and k_3. The positive constants k_1, k_2, and k_3 replace the original coefficients of time. These contain quantities such as density, the diffusion coefficient, and the shape factor that are considered constant. This simplification is made because the aim is not to evaluate the theoretical basis of the three equations but solely to assess them as models for describing the dissolution kinetic data. They will be denoted as the "cube root," the "square root," and the "squared cube root" models for Eqs. 1, 2, and 3, respectively, corresponding to $m = 3$, 2, and 3/2 in Eq. 4.

These equations do not strictly describe the dissolution correctly in their present form since w does not vanish for $t \to \infty$. A more correct formulation would be:

$$w = (w_0^{1/m} - kt)^n \quad \text{for} \quad t < w_0^{1/m}/k \qquad \text{(Eq. 5a)}$$

$$w = 0 \quad \text{for} \quad t \geq w_0^{1/m}/k \qquad \text{(Eq. 5b)}$$

The general multiparticulate dissolution equation presented earlier (Eq. 13, Ref. 1), however, accepts the single-particle dissolution function in the forms of both Eqs. 4 and 5. Equation 4 will be used for simplicity.

In a previous paper (2), the following equations were presented to describe the dissolution profile of a multiparticulate system where the spherical particles dissolve according to each of the three models:

$$\frac{W}{W_0} = \sum_{n=0}^{m} \binom{m}{n} (-Kt)^{(m-n)} \times \frac{F\left(\frac{T_2 - \mu}{\sigma} - \frac{3n\sigma}{m}\right) - F\left(\frac{T_1 - \mu}{\sigma} - \frac{3n\sigma}{m}\right)}{F(j - 3\sigma) - F(-i - 3\sigma)} e^{\frac{3}{m}(n-m)\left[\mu + \frac{3}{m}(n+m)\frac{\sigma^2}{2}\right]} \qquad \text{(Eq. 6)}$$

where $m = 3$ (Eq. 6a) and $m = 2$ (Eq. 6b) and:

$$T_1 = \mu - i\sigma \quad \text{for} \quad \frac{m}{3} \ln (Kt) < \mu - i\sigma$$

$$T_1 = \frac{m}{3} \ln (Kt) \quad \text{for} \quad \frac{m}{3} \ln (Kt) \geq \mu - i\sigma$$

$$T_2 = \mu + j\sigma \quad \text{for} \quad \frac{m}{3} \ln (Kt) < \mu + j\sigma$$

$$T_2 = \frac{m}{3} \ln (Kt) \quad \text{for} \quad \frac{m}{3} \ln (Kt) \geq \mu + j\sigma$$

$$\binom{m}{n} = \frac{m!}{(m-n)!n!}$$

Furthermore ($m = 3/2$):

$$\frac{W}{W_0} = \frac{\int_{R_1}^{R_2} (w^2 - Kt)^{3/2} w^{-1} N(\ln w, \mu, \sigma) dw}{F(j - 3\sigma) - F(-i - 3\sigma)} e^{-3\mu - 9\sigma^2/2} \qquad \text{(Eq. 6c)}$$

where:

$$R_1 = e^{\mu - i\sigma} \quad \text{for} \quad (Kt)^{1/2} < e^{\mu - i\sigma}$$

$$R_1 = (Kt)^{1/2} \quad \text{for} \quad (Kt)^{1/2} \geq e^{\mu - i\sigma}$$

$$R_2 = e^{\mu + j\sigma} \quad \text{for} \quad (Kt)^{1/2} < e^{\mu + j\sigma}$$

$$R_2 = (Kt)^{1/2} \quad \text{for} \quad (Kt)^{1/2} \geq e^{\mu + j\sigma}$$

The function $F(\ )$ is the area under the standard normal curve function defined by:

$$F(x) = \int_{-\infty}^{x} (1/\sqrt{2\pi}) e^{-\frac{x^2}{2}} dx \qquad \text{(Eq. 7)}$$

The function $N(\ln w, \mu, \sigma)$ is the normal distribution function with the natural logarithm to w as the variable, defined by:

$$N(\ln w, \mu, \sigma) = \frac{1}{\sigma\sqrt{2\pi}} e^{-1/2\left(\frac{\ln w - \mu}{\sigma}\right)^2} \qquad \text{(Eq. 8)}$$

The constant K is related to k_1, k_2, and k_3 (Eqs. 1–3) by:

$$K = (6/\rho\pi)^{1/m} k_i \qquad \text{(Eq. 9)}$$

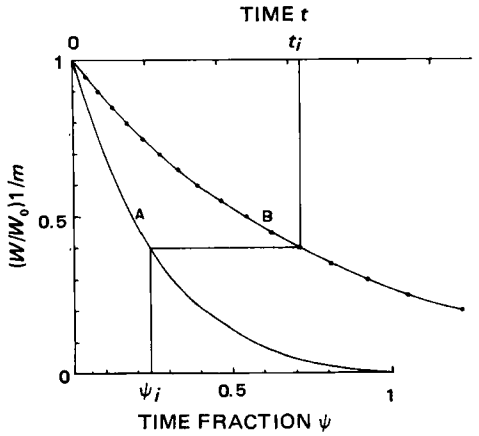

Figure 6—*Time-scaling approach (Eqs. 11–14) used in Figs. 8–10 to evaluate the agreement between the observed dissolution data (●) and the theoretical dissolution curve calculated in the form of the normalized intrinsic dissolution profile (A) on the basis of particle-size analysis.*

where ρ is the particle density, and $i = 1, 2, 3$. It is assumed that the particle diameter (a) distribution is "log normal"; that is, ln a can be approximated by a normal distribution (mean = μ, standard deviation = σ) truncated at the lower end at $\mu - i\sigma$ and at the upper end at $\mu + j\sigma$, where i and j are truncation parameters.

The multiparticulate dissolution equations (Eqs. 6*a*–6*c*) consider spherical drug particles. Such particles are only encountered when the drug exists in liquid form as an emulsion. In solid form, the particles are not spherical. The drug used for the dissolution tests was a 60–85-mesh fraction of tolbutamide consisting of particles approximately tetragonal prismatic in shape. A previous theoretical paper (3) showed that the dissolution of such particles could be approximated well by the dissolution of hypothetical spherical particles. The equivalent spherical diameter, a, is the diameter of the spherical particle that best approximates the dissolution of the nonspherical particle and is given by:

$$a = \frac{b_0}{2 - \left(2 - \frac{b_0}{l_0}\right)^{1/3}} \qquad \text{(Eq. 10)}$$

where l_0 and b_0 are the length and side, respectively, of the tetragonal particle. In this way, dissolution of the nonspherical particle system can be suitably described by the dissolution of a hypothetical spherical particle system that can be rigorously treated using Eqs. 6*a*–6*c*.

It is evident that k, μ, σ, i, j, and ρ must be known to calculate the dissolution profile. The distribution parameters μ, σ, i, and j can be obtained from micrographs, and ρ can be obtained by a standard method; however, the single-particle rate parameter k is unknown. It is possible to calculate the exact intrinsic dissolution profile with much less information[4]. According to the rules given previously (2) for multiparticulate dissolution, only the *shape* of the initial distribution (*i.e.*, of these six parameters only σ, i, and j) is required to calculate the intrinsic dissolution profile when the single-particle dissolution model is known. The concept of time scaling also was discussed previously (2). By such an approach, it is possible to evaluate quantitatively the difference between the actual dissolution data and the calculated intrinsic dissolution profile.

Figure 6 illustrates this application of time scaling. Curve B, through the experimental data points, represents the dissolution curve [$(w/w_0)^{1/m}$ *versus* t]; curve A represents the corresponding calculated normalized intrinsic dissolution profile [$(w/w_0)^{1/m}$ *versus* ψ][4].

If N is the number of data points and f is the time-scaling factor that brings curve B "into" curve A, the sum of the squared deviations between the curves given by:

$$ss = \sum_{i=1}^{N}(ft_i - \psi_i)^2 \qquad \text{(Eq. 11)}$$

[4] The intrinsic dissolution profile and normalized intrinsic dissolution profile were defined and discussed previously (2).

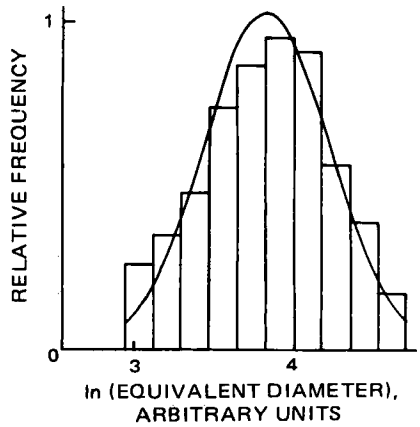

Figure 7—*Histogram of the logarithm of the equivalent spherical diameters of a sample of 500 particles from the 60–85-mesh fraction of tolbutamide powder used in the dissolution tests. The equivalent spherical diameters of the particles that are approximately tetragonal prismatic in shape were calculated according to Eq. 10 from measurements made (in arbitrary units) on electron micrographs. The parameters of the truncated log-normal distribution which best fit this diameter distribution are: σ = 0.395, μ = 3.82, i = 2.25, and j = 2.20.*

is a minimum when $\partial ss/\partial f = 0$, which gives:

$$f = \frac{\sum_{i=1}^{N}\psi_i t_i}{\sum_{i=1}^{N}t_i^2} \qquad \text{(Eq. 12)}$$

The minimum of the sum of squares is therefore:

$$ss = \sum_{i=1}^{N}\left[\left(\frac{\sum_{i=1}^{N}\psi_i t_i}{\sum_{i=1}^{N}t_i^2}\right)t_i - \psi_i\right]^2 \qquad \text{(Eq. 13)}$$

which can be simplified such that the mean squared deviation is given by:

$$\overline{ss} = \frac{1}{N}\sum_{i=1}^{N}\psi_i^2 - \frac{\left(\sum_{i=1}^{N}\psi_i t_i\right)^2}{N\sum_{i=1}^{N}t_i^2} \qquad \text{(Eq. 14)}$$

This expression is chosen as the basis for a quantitative judgment of how well the kinetic models fit the data[5].

RESULTS AND DISCUSSION

The logarithmic distribution of the equivalent spherical diameters of the 60–85-mesh fraction of tolbutamide used for the dissolution test was obtained from direct measurements of 500 particles on a series of 30 × 30-cm electron micrographs. These measurements were made in arbitrary units, disregarding the magnification power, because the calculation of the intrinsic dissolution profile does not require information about the actual sizes of the particles but only the shape of their distribution (σ, i, and j for a log-normal powder).

Each particle was approximated by the tetragonal prismatic body which fitted best, and its equivalent spherical diameter was calculated using Eq. 10. The histogram of the logarithm of these diameters (Fig. 7) shows a good fit to a normal distribution with standard deviation σ = 0.395 and mean μ = 3.82. The truncation

[5] The alternative approach to bring curve A into curve B that has the character of a curve fitting to the data points would yield the same result in a comparison of the models. The time scaling of the *data* is used for the convenience of plotting and to better illustrate the predicted time for complete dissolution.

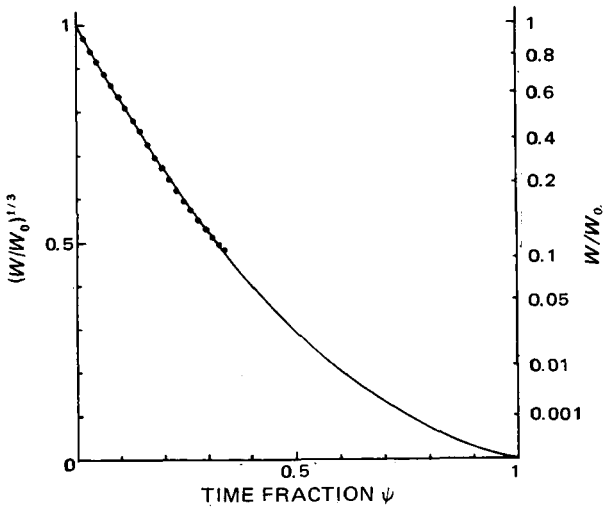

Figure 8—*Plot illustrating the agreement between data for the dissolution of 15 mg of tolbutamide (●) and the theoretical dissolution, considering the cube root model (Eq. 1) calculated (Eq. 6a) in the form of a normalized intrinsic dissolution profile using the parameters from the truncated log-normal distribution shown in Fig. 7. The data are time scaled using the scale factor given by Eq. 12. The mean squared deviation* $\overline{ss} = 1.10 \times 10^{-3}$.

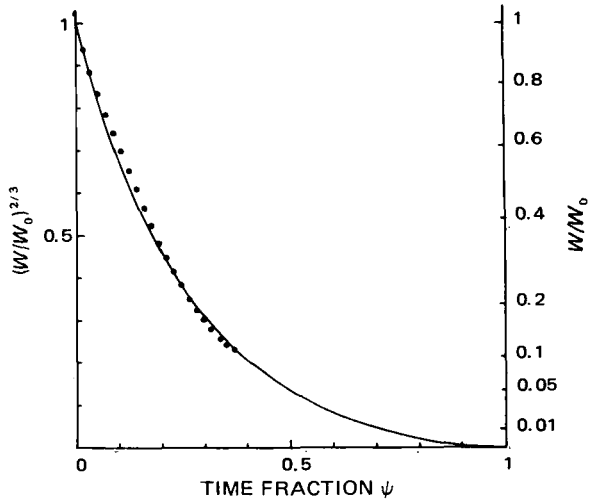

Figure 10—*Plot illustrating the agreement between data for the dissolution of 15 mg of tolbutamide (●) and the theoretical dissolution, considering the squared cube root model (Eq. 3), calculated (Eq. 6c) in the form of a normalized intrinsic dissolution profile using the parameters from the truncated log-normal distribution shown in Fig. 7. The data are time scaled using the scale factor given by Eq. 12. The mean squared deviation* $\overline{ss} = 6.70 \times 10^{-3}$.

parameters, $i = 2.25$ and $j = 2.20$, were obtained by dividing the distance from the mean to the end-points of the distribution by the standard deviation.

The normalized intrinsic dissolution profiles were calculated for each kinetic model, employing Eqs. 6a–6c and using the above values of the distribution shape parameters σ, i, and j (2). These calculated profiles are graphed as the continuous curves in Figs. 8–10, where the fraction of undissolved powder, W/W_0, is plotted according to the respective *single*-particle dissolution equation (Eqs. 1–3) to illustrate the nonlinearity caused by the distribution and particle shape effects. The same figures include a set of data for the dissolution of 15 mg of tolbutamide followed to about 90% dissolution[6]. These data are time scaled, using the optimal time-scaling factor given by Eq. 12, to illustrate the fit of the three models. The fit is very good for Eq. 6a, based on the cube root model ($\overline{ss} = 1.10 \times 10^{-3}$, Fig. 8) and for Eq. 6b, based on the square root model ($\overline{ss} = 1.92 \times 10^{-3}$, Fig. 9), but it is not so good for the squared cube root model ($\overline{ss} = 6.70 \times 10^{-3}$, Fig. 10).

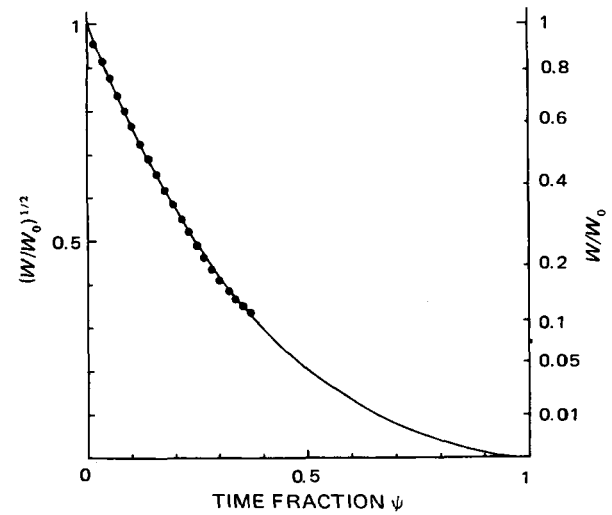

Figure 9—*Plot illustrating the agreement between data for the dissolution of 15 mg of tolbutamide (●) and the theoretical dissolution, considering the square root model (Eq. 2), calculated (Eq. 6b) in the form of a normalized intrinsic dissolution profile using the parameters from the truncated log-normal distribution shown in Fig. 7. The data are time scaled using the scale factor given by Eq. 12. The mean squared deviation* $\overline{ss} = 1.92 \times 10^{-3}$.

[6] The absorbance after 90% dissolution was so small that substantial error would have been introduced if the process had been followed much further.

The dissolution test was done several times using different amounts of tolbutamide. The $\overline{ss}$ values (Table I) indicate (F-test, $p < 0.05$) that the cube root model (Eq. 1) describes the single-particle dissolution best. The square root model (Eq. 2) is almost as good, but the squared cube root model is relatively poor.

To make the evaluations of the three models (Eqs. 1–3) by comparing dissolution data with theoretical calculations, it is necessary that the experimental conditions are consistent with the assumptions behind these calculations. A previous paper (2) discussed the three assumptions on which Eqs. 6a–6c are based:

1. The particles dissolve independently of each other. The apparatus constructed for this work is different from other published dissolution flowcell apparatus in that it guarantees this condition, which is of fundamental importance in the analysis of multiparticulate dissolution kinetics. This condition is achieved by the "absolute sink arrangement" of the drug particles in the dissolution cell. The particles are placed in a single layer such that in principle no particle receives solvent that has contacted other particles. The solvent thus contains no dissolved drug that may influence dissolution.

Table I—Mean Squared Deviation, $\overline{ss}$ (Eq. 14), as a Quantitative Comparison of the Fit of the Three Multiparticulate Dissolution Equations, Eqs. 6a–6c (Based on the Single-Particle Dissolution Models of Eqs. 1–3) to the Data from the Dissolution of Various Amounts of the 60–85-Mesh Fraction of Tolbutamide

Tolbutamide, mg	$\overline{ss} \times 10^3$		
	Eq. 6a	Eq. 6b	Eq. 6c
5	1.18	2.08	7.17
	1.22	2.20	7.40
	1.20	2.21	7.58
10	1.15	2.01	6.92
	1.21	2.18	7.41
	1.29	2.30	7.80
15	1.10	1.92	6.70
	1.19	2.10	7.12
	1.23	2.26	7.50
Mean	1.20	2.14	7.29
SE	0.050	0.119	0.337

2. The dissolution rate parameter [k_1, k_2, or k_3 (Eqs. 1–3)] is constant and the same for all particles. According to the theory on which the models are based, this condition can only be achieved experimentally if the temperature and composition of the dissolution liquid are maintained constant and the flow rate is constant or uniform in the cross section of the dissolution cell where the particles are placed.

The first two conditions are easily met. With regard to the flow rate, the dissolution cell used has a very useful feature: the process can be stopped and the cell rapidly disconnected, allowing the particles to be inspected at any stage of the dissolution process. Such inspections showed (after microscopic measurements) uniform dissolution over the whole particle layer, indicating a uniform flow rate. The fact that the particles in the dissolution cell can be inspected in this way makes it possible for dissolution data to be combined with particle-size measurements (2).

3. The initial particle-size (diameter) distribution can be approximated by a truncated log-normal distribution function. Figure 7 shows that this is the case for the 500 particles *measured*. However, it does not guarantee the correctness of the assumption that this small sample represents the particle-size distribution in the samples used for the dissolution tests, although optical investigations of the uniformity of the powder support this assumption.

This paper has shown that it is possible to describe mathematically the dissolution of a multiparticulate system with a high degree of accuracy by considering both the particle-size distribution effect and the particle shape effect discussed earlier (2, 3). It is evident from the dissolution data obtained that, of the three models investigated, the single-particle dissolution model (Eq. 1) describes the kinetics best.

More complex and flexible models for single-particle dissolution possibly could describe the dissolution more adequately. The fact that the *ss* values for the cube root and the square root model are almost the same suggests a model with properties between these two. The Danckwerts model, as discussed by Goyan (7), is given by:

$$-dw/dt = A[(Dp)^{1/2} + D/a]C_a \qquad \text{(Eq. 15)}$$

where w = weight undissolved, A = surface area, D = diffusion coefficient, p = quantity related to stirring, a = radius of the particle, and C_a = steady-state concentration.

This model is very flexible. When $(Dp)^{1/2}$ predominates, the apparent model would be the cube root model. As the quantity D/a becomes more important, the square root model becomes the apparent model. Finally, as the quantity D/a predominates, the squared cube root model becomes the apparent model. However, when applied to the log-normal case, the Danckwerts model results in a mathematical expression that is much more complex than Eqs. 6*a*–6*c*.

The fit of the dissolution data to the cube root model is excellent. Therefore, if an application of the Danckwerts model results in an even better fit, this improvement will most likely be statistically insignificant considering the magnitude of the experimental errors. The Hixon–Crowell model should be the preferred model in such a case because of its simplicity.

REFERENCES

(1) P. Veng Pedersen and K. F. Brown, *J. Pharm. Sci.*, **64,** 1192(1975).

(2) *Ibid.*, **64,** 1981(1975).

(3) *Ibid.*, **65,** 1437(1976).

(4) A. W. Hixson and J. H. Crowell, *Ind. Eng. Chem.*, **23,** 923(1931).

(5) P. J. Niebergall, G. Milosovich, and J. E. Goyan, *J. Pharm. Sci.*, **52,** 236(1963).

(6) W. I. Higuchi and E. N. Hiestand, *ibid.*, **52,** 67(1963).

(7) J. E. Goyan, *ibid.*, **54,** 645(1965).

ACKNOWLEDGMENTS AND ADDRESSES

Received May 2, 1975, from the *Department of Pharmacy, University of Sydney, Sydney, N.S.W. 2006, Australia.*

Accepted for publication July 1, 1975.

Supported in part by Grant 74/4244 from the National Health and Medical Research Council of Australia.

[x] To whom inquiries should be directed.

Antioxidant Efficiency of Polyhydric Phenols in Photooxidation of Benzaldehyde

DOUGLAS E. MOORE

Abstract □ An experimental system is described for the observation of the kinetics of photochemically initiated oxidation reactions; this system is based on the measurement of oxygen consumption with a polarographic oxygen electrode. The photooxidation of benzaldehyde in dilute aqueous solution was examined and appears to conform to a free radical chain mechanism. The antioxidant efficiency of some polyhydric phenols was determined kinetically and found to be catechol > pyrogallol > hydroquinone > resorcinol > *n*-propyl gallate for the benzaldehyde photooxidation.

Keyphrases □ Antioxidants—efficiency, various polyhydric phenols, photooxidation of benzaldehyde □ Phenols, polyhydric—antioxidant efficiency in photooxidation of benzaldehyde □ Photooxidation—benzaldehyde, antioxidant efficiency of various polyhydric phenols □ Benzaldehyde—photooxidation, antioxidant efficiency of various polyhydric phenols □ Oxidation, photochemical—benzaldehyde, antioxidant efficiency of various polyhydric phenols

The oxidative deterioration of pharmaceuticals can be initiated by UV light, both in the presence and absence of sensitizers. Two general classes of photooxidation reactions are recognized. The first is the free radical chain mechanism of autoxidation (1) initiated by sensitizers (such as benzophenone) that abstract a hydrogen atom from the oxidant. The free radical thus formed adds molecular oxygen and propagates the chain mechanism by abstracting hydrogen from a further oxidant molecule, giving rise to a hydroperoxide. The hydroperoxide is the major product but usually reacts further by a slower nonradical disproportionation mechanism. For example, it was shown (2) that the peroxy acid formed during aldehydic autoxidation undergoes an acid–base-catalyzed decomposition reaction to the carboxylic acid, which is the final reaction product.

The second class is the dye-sensitized (*e.g.*, methylene blue) photooxygenation of acceptors (3). These acceptors are either: (*a*) cyclic dienes, polycyclic aromatic compounds, or heterocyclic compounds producing cyclic

2. The dissolution rate parameter [k_1, k_2, or k_3 (Eqs. 1–3)] is constant and the same for all particles. According to the theory on which the models are based, this condition can only be achieved experimentally if the temperature and composition of the dissolution liquid are maintained constant and the flow rate is constant or uniform in the cross section of the dissolution cell where the particles are placed.

The first two conditions are easily met. With regard to the flow rate, the dissolution cell used has a very useful feature: the process can be stopped and the cell rapidly disconnected, allowing the particles to be inspected at any stage of the dissolution process. Such inspections showed (after microscopic measurements) uniform dissolution over the whole particle layer, indicating a uniform flow rate. The fact that the particles in the dissolution cell can be inspected in this way makes it possible for dissolution data to be combined with particle-size measurements (2).

3. The initial particle-size (diameter) distribution can be approximated by a truncated log-normal distribution function. Figure 7 shows that this is the case for the 500 particles *measured*. However, it does not guarantee the correctness of the assumption that this small sample represents the particle-size distribution in the samples used for the dissolution tests, although optical investigations of the uniformity of the powder support this assumption.

This paper has shown that it is possible to describe mathematically the dissolution of a multiparticulate system with a high degree of accuracy by considering both the particle-size distribution effect and the particle shape effect discussed earlier (2, 3). It is evident from the dissolution data obtained that, of the three models investigated, the single-particle dissolution model (Eq. 1) describes the kinetics best.

More complex and flexible models for single-particle dissolution possibly could describe the dissolution more adequately. The fact that the *ss* values for the cube root and the square root model are almost the same suggests a model with properties between these two. The Danckwerts model, as discussed by Goyan (7), is given by:

$$-dw/dt = A[(Dp)^{1/2} + D/a]C_a \qquad \text{(Eq. 15)}$$

where w = weight undissolved, A = surface area, D = diffusion coefficient, p = quantity related to stirring, a = radius of the particle, and C_a = steady-state concentration.

This model is very flexible. When $(Dp)^{1/2}$ predominates, the apparent model would be the cube root model. As the quantity D/a becomes more important, the square root model becomes the apparent model. Finally, as the quantity D/a predominates, the squared cube root model becomes the apparent model. However, when applied to the log-normal case, the Danckwerts model results in a mathematical expression that is much more complex than Eqs. 6*a*–6*c*.

The fit of the dissolution data to the cube root model is excellent. Therefore, if an application of the Danckwerts model results in an even better fit, this improvement will most likely be statistically insignificant considering the magnitude of the experimental errors. The Hixon–Crowell model should be the preferred model in such a case because of its simplicity.

REFERENCES

(1) P. Veng Pedersen and K. F. Brown, *J. Pharm. Sci.*, **64,** 1192(1975).

(2) *Ibid.*, **64,** 1981(1975).

(3) *Ibid.*, **65,** 1437(1976).

(4) A. W. Hixson and J. H. Crowell, *Ind. Eng. Chem.*, **23,** 923(1931).

(5) P. J. Niebergall, G. Milosovich, and J. E. Goyan, *J. Pharm. Sci.*, **52,** 236(1963).

(6) W. I. Higuchi and E. N. Hiestand, *ibid.*, **52,** 67(1963).

(7) J. E. Goyan, *ibid.*, **54,** 645(1965).

ACKNOWLEDGMENTS AND ADDRESSES

Received May 2, 1975, from the *Department of Pharmacy, University of Sydney, Sydney, N.S.W. 2006, Australia.*

Accepted for publication July 1, 1975.

Supported in part by Grant 74/4244 from the National Health and Medical Research Council of Australia.

[x] To whom inquiries should be directed.

Antioxidant Efficiency of Polyhydric Phenols in Photooxidation of Benzaldehyde

DOUGLAS E. MOORE

Abstract □ An experimental system is described for the observation of the kinetics of photochemically initiated oxidation reactions; this system is based on the measurement of oxygen consumption with a polarographic oxygen electrode. The photooxidation of benzaldehyde in dilute aqueous solution was examined and appears to conform to a free radical chain mechanism. The antioxidant efficiency of some polyhydric phenols was determined kinetically and found to be catechol > pyrogallol > hydroquinone > resorcinol > *n*-propyl gallate for the benzaldehyde photooxidation.

Keyphrases □ Antioxidants—efficiency, various polyhydric phenols, photooxidation of benzaldehyde □ Phenols, polyhydric—antioxidant efficiency in photooxidation of benzaldehyde □ Photooxidation—benzaldehyde, antioxidant efficiency of various polyhydric phenols □ Benzaldehyde—photooxidation, antioxidant efficiency of various polyhydric phenols □ Oxidation, photochemical—benzaldehyde, antioxidant efficiency of various polyhydric phenols

The oxidative deterioration of pharmaceuticals can be initiated by UV light, both in the presence and absence of sensitizers. Two general classes of photooxidation reactions are recognized. The first is the free radical chain mechanism of autoxidation (1) initiated by sensitizers (such as benzophenone) that abstract a hydrogen atom from the oxidant. The free radical thus formed adds molecular oxygen and propagates the chain mechanism by abstracting hydrogen from a further oxidant molecule, giving rise to a hydroperoxide. The hydroperoxide is the major product but usually reacts further by a slower nonradical disproportionation mechanism. For example, it was shown (2) that the peroxy acid formed during aldehydic autoxidation undergoes an acid–base-catalyzed decomposition reaction to the carboxylic acid, which is the final reaction product.

The second class is the dye-sensitized (*e.g.*, methylene blue) photooxygenation of acceptors (3). These acceptors are either: (*a*) cyclic dienes, polycyclic aromatic compounds, or heterocyclic compounds producing cyclic

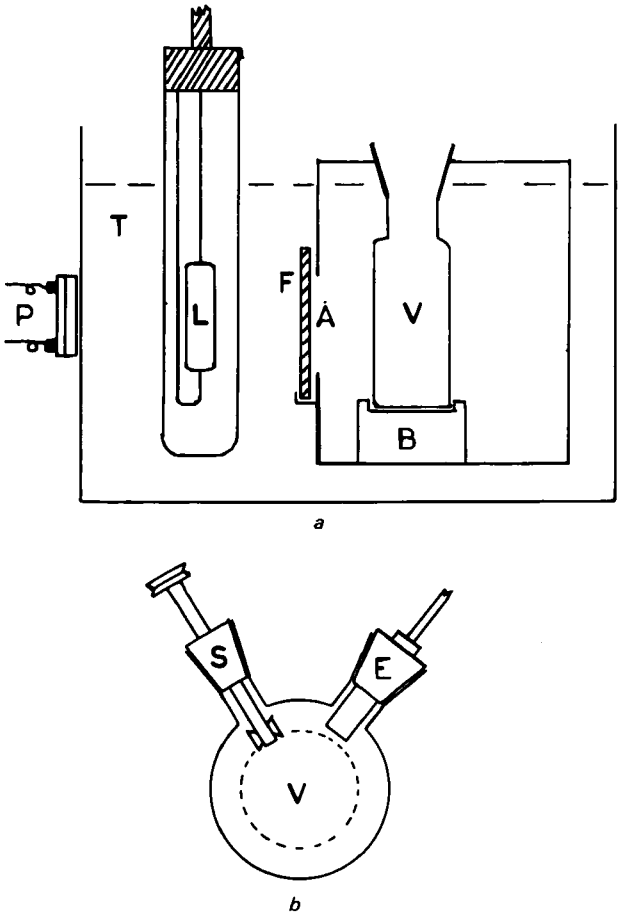

Figure 1—(a) *Schematic view of apparatus for observing the kinetics of photooxidation.* (b) *Reaction vessel, side elevation.* (*For explanation of symbols, see text.*)

peroxides, or (*b*) olefins containing allylic hydrogen atoms whereby allylic hydroperoxides are the products. As an example of the difference between the two types of oxidation, isopropyl alcohol is a very reactive acceptor for radical oxidation but is inert in the dye-sensitized photooxygenations (4). Furthermore, some acceptors can act as their own sensitizers for both classes of reaction.

An understanding of the kinetics and mechanism by which a compound is oxidized clearly enables the more judicious selection of an inhibitor or antioxidant. The traditional means of observing the kinetics of an oxidation reaction has been manometry (5), in which the rate of oxygen absorption from the gas phase into a vigorously stirred solution is measured. Only in specific cases where suitable differences in the absorption spectrum of the reactant and product exist, *e.g.*, ascorbic acid (6), can a spectrophotometric procedure be used. The major disadvantage of manometry is the requirement of a reaction slow enough that the diffusion of oxygen into the reacting solution is not rate determining. Particularly for photooxidation reactions, it is imperative that the sample be irradiated uniformly; thus the vigorous mixing of the gas phase with the solution, creating a vortex and bubbles of variable intensity, is undesirable.

One technique devised for measuring oxygen consumption in the solution directly involves following the decay of the charge transfer spectrum produced by a solution of oxygen in an organic solvent (7). More widely applicable, however, are the variants of the polarographic technique such as the oxygen electrode (8) and the galvanic cell oxygen analyzer (9). A manometric system was compared to a galvanic cell system, and the latter was more sensitive and responded faster in the measurement of oxygen-consuming enzyme systems (10).

In this paper, an experimental system is described for studying the kinetics of photooxidation reactions. The system is based on the rate of oxygen consumption measured with a polarographic oxygen electrode. As a model for the evaluation of the method, the photooxidation of benzaldehyde and its inhibition in aqueous solution were studied. Previously, benzaldehyde oxidation initiated by metal ions was used to study the role of surfactants in retarding oxidation (11–14).

The photooxidation of benzaldehyde was studied at concentrations of the order of 20% in *n*-decane solutions; a free radical mechanism was found to apply (15). The purposes of the present investigation were to determine whether the same mechanism applies in aqueous solution where the benzaldehyde solubility limit is 0.65% (16) and to determine the antioxidant efficiency of several polyhydric phenols.

EXPERIMENTAL

Materials—The oxidation of aldehydes has been stated to be very sensitive to traces of impurities (17); therefore, all chemicals were carefully purified and the reaction vessels were exceedingly clean.

Benzaldehyde[1] was distilled at a pressure of 10 mm of nitrogen, and the fraction with a boiling point of 61–63° was collected. This fraction was then twice distilled *in vacuo* using an all-glass apparatus; the middle 80% was collected each time. The final product was stored under vacuum and protected from light. Whenever a new solution of benzaldehyde was prepared, the required amount of benzaldehyde was vacuum distilled from the reservoir.

Water, first deionized and then double distilled, was used in the preparation of all solutions. Hydroquinone, resorcinol, catechol, and pyrogallol[1] were recrystallized from distilled water under an atmosphere of nitrogen. Solutions (10^{-4}–10^{-3} *M*) of these antioxidants were freshly prepared in air-saturated water when required.

Glassware was cleaned by rinsing with permanganic acid, water, and acidified hydrogen peroxide, followed by numerous rinsings with double-distilled water.

Apparatus—The reaction vessel and the arrangement of the apparatus are shown in Fig. 1. The reaction vessel (V) was constructed[2] from borosilicate glass of uniform thickness and had parallel circular faces 2.5 cm apart and 6 cm in diameter. Two standard taper sockets carried a belt-driven turbine stirrer[3] (S) and the oxygen electrode[4] (E). The UV light source (L) was a medium pressure mercury arc[5] with maximum output at 365 nm.

A glass filter[6] (F), positioned in front of the aperture (A), absorbed wavelengths below 310 nm and above 420 nm, with 28% transmission at 365 nm. The dotted circle in Fig. 1*b* indicates the approximate size of the aperture in relation to the reaction vessel. The volume of reaction mixture contained when the stirrer and oxygen electrode were in place was 135 ml.

The reaction vessel, filter, and aperture were mounted on a block (B), which could be fixed at different distances from the UV lamp to vary the light intensity incident on the reaction mixture. The whole

[1] British Drug Houses Analar grade.
[2] In the workshop at the University of Sydney.
[3] Machined from Teflon (du Pont).
[4] Radiometer (Copenhagen) E5046 oxygen electrode controlled with Radiometer PHM927 gas monitor.
[5] Engelhard Hanovia, United Kingdom.
[6] Corning filter CS 7-37.

Table I—Comparison of Rates of Photooxidation Measured by Manometry and Oxygen Electrode at 30°

Benzaldehyde, M	Reaction Rate, moles of Oxygen/liter/min × 10^6	
	Manometry[a]	Oxygen Electrode[b]
0.0540	—	15.70 ± 0.63
0.0422	—	12.52 ± 0.42
0.0309	9.07 ± 0.80	9.31 ± 0.36
0.0265	7.80 ± 0.54	8.00 ± 0.32
0.0207	6.10 ± 0.45	6.25 ± 0.20
0.0156	4.68 ± 0.47	4.75 ± 0.20
0.0112	3.36 ± 0.36	3.40 ± 0.15

[a] Means of three determinations. [b] Means of five determinations.

apparatus was immersed in a water bath thermostated to ±0.05°. Positioned on the outside face of the thermostat directly opposite the mercury arc was a photovoltaic cell[7] (P); this cell was used to monitor the lamp output.

The signals from the oxygen electrode (*via the gas monitor*) and the photocell were fed into a two-pen recorder[8].

Procedure—Benzaldehyde solutions were prepared by dissolving the required quantity of freshly vacuum-distilled benzaldehyde in air-saturated water. The benzaldehyde was weighed when cold (~0°) and transferred quickly into a volumetric flask, with copious washings of air-saturated water. Solutions were stored in the dark, with intermittent shaking, to ensure that dissolution was complete (3 hr). If this procedure was not followed, rates of photooxidation were anomolously high, corresponding to the accelerated rate of oxidation in emulsions compared to solutions observed by Carless and Nixon (11).

The reaction vessel was filled with the benzaldehyde solution, preequilibrated to the desired temperature, and the stirrer and oxygen electrode were set in place, excluding air bubbles. The oxygen electrode was calibrated each day at the appropriate temperature with air-saturated water and oxygen-free water prepared by adding sodium sulfite to a borax solution. A shutter was positioned between the lamp and the aperture, and the lamp was switched on.

In each experiment, there was no observable change in P_{O_2} (oxygen partial pressure) prior to shutter removal, indicating insignificant thermal oxidation and negligible stray light. When the lamp reached a steady intensity (7 min), the shutter was removed and the P_{O_2} was recorded. In the absence of antioxidants, there was no indication of an induction period and the change in P_{O_2} stopped immediately when the UV lamp was switched off.

A linear trace of P_{O_2} was recorded down to 50 mm Hg. For most purposes, the slope of this trace in millimeters of mercury per minute was used as a measure of the rate of oxidation. When required, the absolute rate of reaction, R, in moles of oxygen per liter per minute was obtained from[9]:

$$R = \frac{(\text{slope in mm Hg/min}) \times (\text{solubility of oxygen in water})}{P_{O_2}} \qquad \text{(Eq. 1)}$$

For the investigation of the effects of antioxidants, the desired amount of antioxidant solution (1–5 ml) was mixed with 200 ml of benzaldehyde solution immediately prior to filling the reaction vessel.

RESULTS AND DISCUSSION

Kinetic Parameters—The linearity of P_{O_2} *versus* time indicates that photooxidation of benzaldehyde is independent of oxygen concentration (for $P_{O_2} > 50$ mm). Variation of the initial benzaldehyde concentration to the near-saturated solution level showed a first-order dependence with a linear correlation coefficient of 0.9998 (Table I). As part of the preliminary testing of the technique, some photooxidation experiments were performed with a manostat similar to that described by Carlsson and Robb (18); it was connected to the reaction vessel in place of the oxygen electrode. The measured rates (Table I) compared favorably except at high initial benzaldehyde concentration (*i.e.*, high rate), emphasizing the inadequacy of manometry for following rapid oxygen absorption.

There is, of course, an upper limit to rates that can be followed by the oxygen electrode, depending as it does on the diffusion of oxygen across the 20-μm polypropylene membrane and efficient stirring of the system. Since thermal oxidation was insignificant in relation to photooxidation in the temperature range studied (15–40°), the upper limit to rate measurements was arbitrarily defined as the point at which the reading monitored from the oxygen electrode continued to decrease after the light was switched off. The upper limit for the apparatus in this study was thereby set at approximately 20 mm Hg/min or 4×10^{-5} mole/liter/min.

The catalytic interference by metal ions was declared unimportant when the presence of edetic acid (10^{-4} M) in the reaction mixture had no effect on the rate of oxidation.

Variation of light intensity gave the results in Fig. 2. The log rate *versus* log intensity plot with a slope of 0.51 ± 0.03 established that the rate of reaction depended on the square root of the incident light intensity, as determined by the ferrioxalate chemical actinometer system (19).

From the experiments in which the temperature was varied in the range of 15–40°, the overall activation energy of the reaction was 28 ± 1 kJ/mole as determined from the Arrhenius plot in Fig. 3.

Iodometric analysis of the reaction mixture immediately after irradiation was stopped for four benzaldehyde concentrations (Table I) showed a 1:1 correlation between moles of peroxide product and moles of oxygen consumed.

The unretarded rate data can be summarized by:

$$R_u = k[\text{benzaldehyde}](I^{1/2}) \qquad \text{(Eq. 2)}$$

which is the same form as found by Ingles and Melville (15) in decane solution. Thus, one can assume the same chain mechanism (Schemes I–IV).

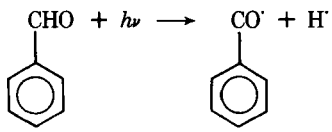

Scheme I—Initiation

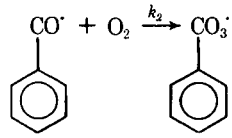

Scheme II—Propagation

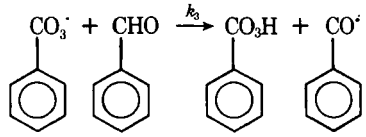

Scheme III—Propagation

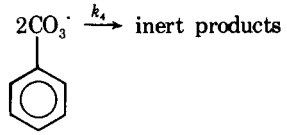

Scheme IV—Termination

Assumptions made in applying the steady-state treatment to this reaction sequence are: (*a*) the reaction chains are long, (*b*) k_3 is the rate-determining step at the oxygen pressure used, and (*c*) termination steps involving $C_6H_5CO\cdot$ radicals are unimportant. The overall rate equation is, therefore, given in Eq. 3, which is of the same form as Eq. 2:

$$R_u = k_3(R_i/k_4)^{1/2}\,[\text{benzaldehyde}] \qquad \text{(Eq. 3)}$$

[7] Evans Electroselenium Ltd., United Kingdom.
[8] Rikadenki B-241, Tokyo, Japan.
[9] The solubility of oxygen in water was obtained from Ref. 5.

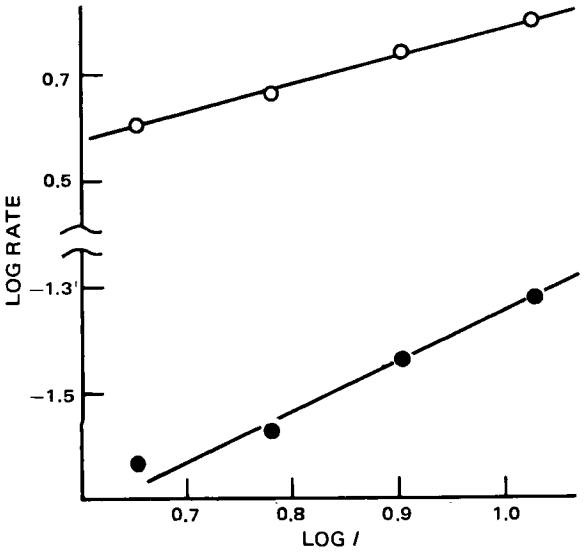

Figure 2—*Benzaldehyde photooxidation in water solution: effect of variation of light intensity on the rate (in mm Hg/min) at 30°. Each data point is the mean of four determinations. Key: ○, 0.0290 M benzaldehyde; and ●, 0.0315 M benzaldehyde + 1 × 10^{-6} M catechol.*

where R_i, the rate of the initiation step, would be expected to be directly proportional to the intensity of incident UV light, a factor considered independent of temperature.

Therefore, the overall energy of activation would be essentially that of k_3, the propagation step, since radical combination steps, such as k_4, have near zero activation energies (20).

Effects of Antioxidants—The polyhydric phenols, hydroquinone, catechol, resorcinol, pyrogallol, and *n*-propyl gallate, slowed the rate of oxidation of benzaldehyde, although none inhibited the reaction completely. These compounds were classed as retarders rather than inhibitors of this system. According to Scott (1), phenol and amine antioxidants act in radical autoxidation by terminating the chain

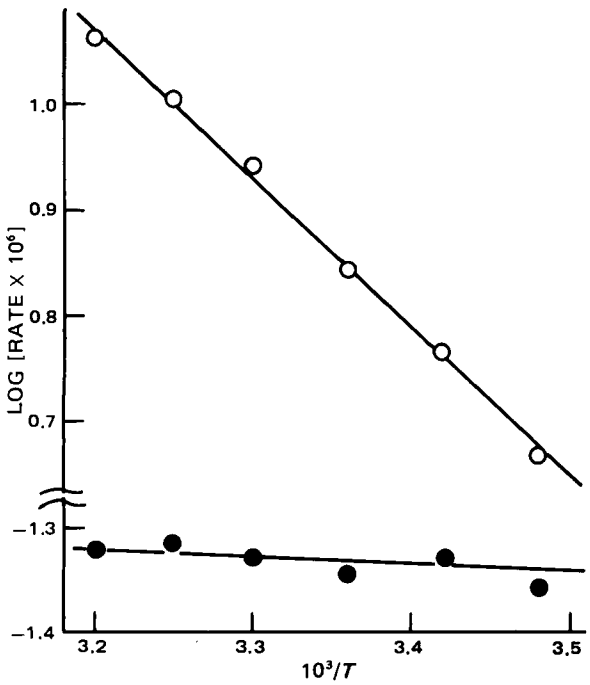

Figure 3—*Benzaldehyde photooxidation in water solution: effect of temperature variation on the rate (in moles/liter/min). Each data point is the mean of four determinations. Key: ○, 0.029 M benzaldehyde; and ●, 0.0315 M benzaldehyde + 1 × 10^{-6} M catechol.*

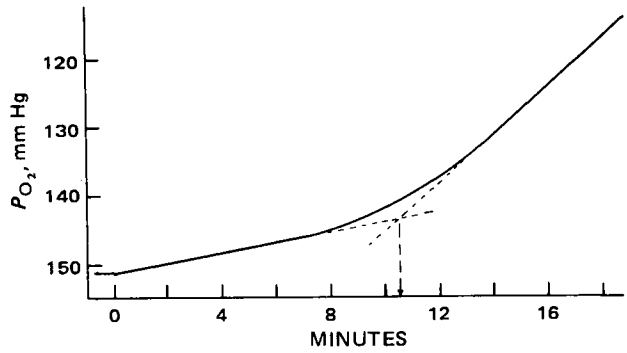

Figure 4—*Recorder trace of oxygen partial pressure during catechol-retarded photooxidation of benzaldehyde at 30° with 0.0315 M benzaldehyde + 1 × 10^{-6} M catechol. The intersection of the linear portions gives the length of the induction period as indicated by the arrow.*

carrying radical (Scheme V).

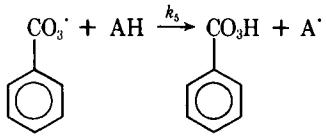

Scheme V

The antioxidant radical A· is presumed to be relatively stable and capable of reacting only with species of the same kind. In the early stages of the reaction, Scheme IV may be assumed to be negligible compared to Scheme V, so kinetic analysis gives for the rate of the retarded reaction:

$$R_a = R_i \left(1 + \frac{k_3}{k_5}\frac{[\text{benzaldehyde}]}{[\text{AH}]}\right) \qquad \text{(Eq. 4)}$$

A plot of the rate of the retarded reaction *versus* the reciprocal of retarder concentration at constant benzaldehyde concentration should be linear. As required for Eq. 4, the rates recorded here are presteady state; *i.e.*, if the reaction is allowed to proceed for a long enough time, the rate increases to the value obtained in the absence of retarder (Fig. 4). An induction period can be defined as the time at which the changeover to the unretarded rate occurs (Fig. 4). The induction period was found to be approximately proportional to retarder concentration but not sufficiently accurate to be used as a measure of antioxidant efficiency.

The presteady-state rate of the retarded reaction also was directly dependent on the incident UV light intensity but essentially independent of temperature, as shown in Figs. 2 and 3, respectively, for catechol at 1 × 10^{-6} *M*. This behavior conforms to that predicted by Eq. 4 in that R_i depends directly on the lamp intensity, and the rate constants k_3 and k_5 are both for reactions of the free radical with acceptor molecules. Thus, their activation energies are probably similar, producing an overall energy of activation near zero.

Figure 5 displays the results plotted in the form of Eq. 4. Catechol, hydroquinone, and resorcinol all appeared to act in the same way, as evidenced by the linear plots with a common intercept. The value for R_i, the rate of initiation, was 1.8 × 10^{-7} mole/liter/min.

The results for pyrogallol deviated from linearity above 2 × 10^{-6} *M*. Control experiments, at a concentration of 10^{-3} *M*, indicated that pyrogallol is itself slowly photooxidized. Whether pyrogallol oxidation contributes to the apparent oxygen uptake when benzaldehyde is present is impossible to tell without product analysis, a difficult task since the extent of reaction is less than 1%. Similar controls for hydroquinone, catechol, and resorcinol up to 5 × 10^{-3} *M* showed no oxygen uptake. Other commonly employed antioxidants, such as butylated hydroxytoluene and *n*-propyl gallate, were much less active than resorcinol. Full data over a range of concentrations for butylated hydroxytoluene could not be obtained due to its limited water solubility.

A value for the rate constant ratio k_5/k_3 can be obtained from the slopes of the lines in Fig. 5 and used as a measure of antioxidant efficiency. Bolland and tenHave (21) developed the following method for estimating antioxidant efficiencies; rate data at only one antioxidant concentration are required. At a low antioxidant concentration,

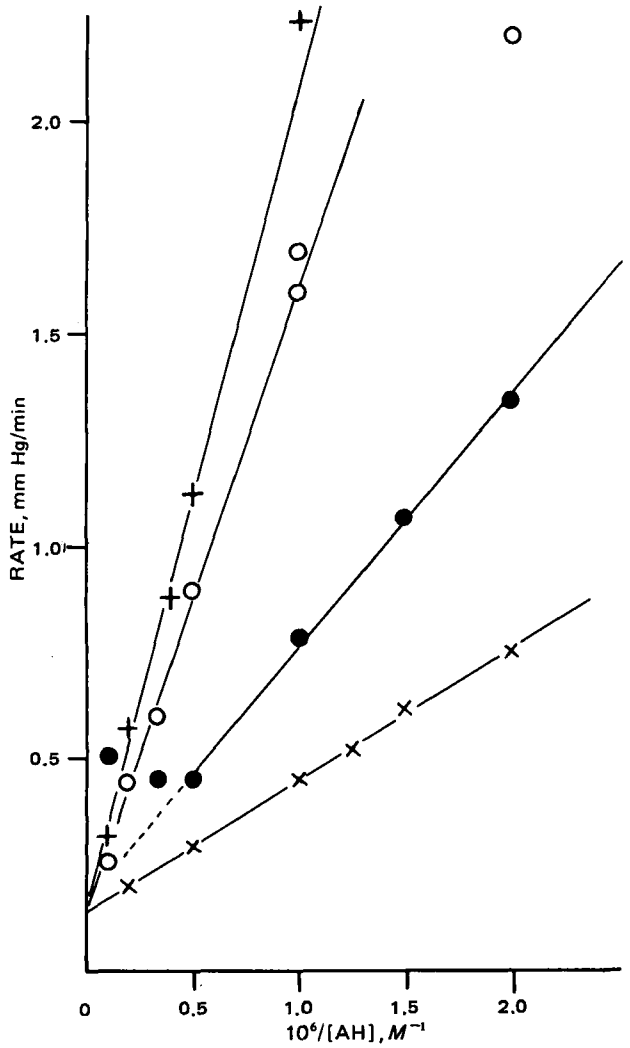

Figure 5—*Rate of the retarded reaction as a function of the reciprocal of the retarder concentration at 30°. Each data point is the mean of three determinations. Key: ×, catechol; ●, pyrogallol; ○, hydroquinone; and +, resorcinol. The benzaldehyde concentration was 0.0315* M *in all experiments.*

Eq. 4 approximates to:

$$R_a \approx R_i \frac{k_3}{k_5} \frac{[\text{benzaldehyde}]}{[\text{AH}]} \qquad \text{(Eq. 5)}$$

Combination of Eqs. 3 and 5 leads to:

$$R_a = \frac{R_u^2 k_4}{k_3 k_5 [\text{benzaldehyde}][\text{AH}]} \qquad \text{(Eq. 6a)}$$

or:

$$\frac{k_4}{k_3 k_5} = \frac{R_a}{R_u^2} [\text{benzaldehyde}][\text{AH}] = K \qquad \text{(Eq. 6b)}$$

Bolland and tenHave (21) calculated $1/K$ values for polyhydric phenol antioxidants in the benzoyl peroxide-initiated oxidation of ethyl linoleate. In Table II, their values are compared with values of $1/K$ calculated for the same antioxidants in the photooxidation of benzaldehyde. Clearly, either $1/K$ or k_5/k_3 produces the same antioxidant efficiency ranking, but the latter ratio is preferable because it is calculated over the full range of antioxidant concentrations.

Bolland and tenHave (21) also showed that a log-linear relationship existed between their measured antioxidant efficiency and the normal reduction potential of these phenolic antioxidants measured in a neutral aqueous ethanol solution (22). However, we found catechol to be a more effective antioxidant than hydroquinone and pyrogallol. Whether this result was due to a different reactivity of the semiquinone radical (A·) produced in Scheme V could not be determined at present. It is not possible from kinetic studies alone to decide the fate of the free radical A· since Schemes V and VI both give kinetics of the form of Eq. 4.

Table II—Antioxidant Efficiencies of Polyhydric Phenols in the Photooxidation of Benzaldehyde

Antioxidant	$10^2 \times k_5/k_3$	$10^2/K$, liters/mole/min[a]	$1/K$[b]
Catechol	7.5 ± 0.2	28.0 ± 1.2	0.63
Pyrogallol	4.0 ± 0.15[c]	16.0 ± 1.3	3.0
Hydroquinone	1.9 ± 0.2	7.7 ± 1.0	1.0
Resorcinol	0.85 ± 0.05	2.0 ± 0.2	0.016
n-Propyl gallate	0.48 ± 0.06	1.1 ± 0.2	—

[a] Average value from four lowest antioxidant concentrations. [b] From Ref. 21. Values referred to hydroquinone as unity. [c] From linear portion of graph, pyrogallol $< 2 \times 10^{-6}$ *M*.

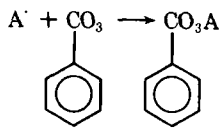

Scheme VI

REFERENCES

(1) G. Scott, "Atmospheric Oxidation and Antioxidants," Elsevier Publishing Co., Amsterdam, The Netherlands, 1965, chaps. 3, 4.

(2) W. A. Waters, *J. Chem. Soc.*, **1951**, 812.

(3) C. S. Foote, *Acc. Chem. Res.*, **1**, 104(1968).

(4) G. O. Schenck, H.-D. Becker, K.-H. Schulte-Elte, and C. H. Krauch, *Ber.*, **96**, 509(1963).

(5) W. W. Umbriet, R. H. Burris, and J. F. Stauffer, "Manometric Techniques," 4th ed., Burgess, Minneapolis, Minn., 1964.

(6) S. M. Blaug and B. Hajratwala, *J. Pharm. Sci.*, **61**, 556(1972).

(7) J. Betts and J. C. Robb, *Nature*, **215**, 274(1967).

(8) L. C. Clark, *Trans. Am. Soc. Artif. Intern. Organs*, **2**, 41(1956).

(9) K. H. Mancy, D. A. Okun, and C. N. Reilley, *J. Electroanal. Chem.*, **4**, 65(1962).

(10) H. Lipner, L. R. Witherspoon, and A. Wahlborg, *Anal. Chem.*, **37**, 347(1965).

(11) J. E. Carless and J. R. Nixon, *J. Pharm. Pharmacol.*, **9**, 963(1957).

(12) J. E. Carless and J. Swarbrick, *ibid.*, **14**, 97T(1962).

(13) J. Swarbrick and J. E. Carless, *ibid.*, **16**, 596(1964).

(14) *Ibid.*, **16**, 670(1964).

(15) T. A. Ingles and H. W. Melville, *Proc. Roy. Soc. (London)*, **A218**, 175(1953).

(16) A. G. Mitchell, L. S. C. Wan, and S. G. Bjaastad, *J. Pharm. Pharmacol.*, **16**, 632(1964).

(17) M. Niclause, J. Lemaire, and M. Letort, "Advances in Photochemistry," vol. 4, Interscience, New York, N.Y., 1966, p. 27.

(18) D. J. Carlsson and J. C. Robb, *Trans. Faraday Soc.*, **62**, 3404(1966).

(19) J. G. Calvert and J. N. Pitts, Jr., "Photochemistry," Wiley, New York, N.Y., 1966, p. 783.

(20) F. S. Dainton, "Chain Reactions," 2nd ed., Methuen, London, England, 1966, chap. 1.

(21) J. L. Bolland and P. tenHave, *Discuss. Faraday Soc.*, **2**, 252(1947).

(22) L. F. Fieser, *J. Am. Chem. Soc.*, **52**, 5204(1930).

ACKNOWLEDGMENTS AND ADDRESSES

Received August 29, 1975, from the *Department of Pharmacy, University of Sydney, Sydney, N.S.W. 2006, Australia.*

Accepted for publication December 8, 1975.

Photochromism of an Anticonvulsant, 1-Diphenylmethyl-4-(6-methyl-2-pyridylmethyleneamino)piperazine, in the Solid State

DILIP R. SANVORDEKER

Abstract □ The light-induced color change of 1-diphenylmethyl-4-(6-methyl-2-pyridylmethyleneamino)piperazine in the solid state was investigated. Light in the 420–700-nm visible region had no effect. Elevated temperature, dissolution, or prolonged storage in the dark at room temperatures restored the intrinsic color of the compound. IR, UV (solution), NMR, differential scanning calorimetry, and GC methods showed no detectable difference between the long wavelength UV light-exposed (yellow) and unexposed (colorless) samples of the pure compound. Long wavelength UV light exposure studies with several substituted piperazine analogs revealed a structure–activity requirement for the color conversion process. The data indicated that the transformation process from colorless (or faint yellow) to bright yellow is photochromism (phototropy) and is dependent on the intensity of the "action spectrum" in the 300–400-nm region. Studies in the solid state showed that heat-induced fading of the color followed apparent zero-order kinetics. The energy of activation, E_b, for the photochromic conversion process from the metastable (yellow) to the stable (colorless) state was estimated to be about 19 kcal/mole.

Keyphrases □ Photochromism—*N,N*-disubstituted piperazines in solid state, effects of temperature, dissolution, and prolonged storage □ UV—light-induced color changes, *N,N*-disubstituted piperazines in solid state, effects of temperature, dissolution, and prolonged storage □ Piperazines, *N,N*-disubstituted—photochromism in solid state, effects of temperature, dissolution, and prolonged storage □ Structure–activity relationships—photochromism of series of *N,N*-disubstituted piperazines □ Anticonvulsant agents—1-diphenylmethyl-4-(6-methyl-2-pyridylmethyleneamino)piperazine, photochromism studied

1-Diphenylmethyl -4- (6-methyl - 2-pyridylmethyleneamino)piperazine[1] (IV) is a potent anticonvulsant in animals (1). It belongs to a series of hydrazone derivatives of benzhydrylpiperazine that represents a novel chemical structure with such anticonvulsant properties.

During development of a tablet dosage form, IV in its pure state, as well as in the tablet without a color additive, exhibited a gradual change in color when exposed to daylight fluorescent light. This transformation was from colorless (or faint yellow) to bright yellow. The objectives of this investigation were to: (*a*) identify the "action spectrum" of light that induced this change in color, (*b*) study the nature of this reaction and evaluate the physicochemical aspects of the color change with reference to the chemical integrity of the drug, and (*c*) study the kinetics of the color conversion process in the solid state.

EXPERIMENTAL

Materials—Potassium bromide[2], potassium chloride[2], methanol[2], chloroform[2], and deuterated chloroform[3] were analytical reagent grade materials. 1-Diphenylmethyl-4-(6-methyl-2-pyridylmethyleneamino)piperazine[4] (IV), 1-diphenylmethyl-4-(2-pyridylmethyleneamino)piperazine[4] (III), 1-diphenylmethyl-4-(3-pyridylmethyleneamino)piperazine[4] (II), 1-diphenylmethyl-4-(4-pyridylmethyleneamino)piperazine[4] (I), 1-diphenylmethyl-4-(phenylmethyleneamino)piperazine[4] (V), 1-diphenylmethyl-4-(2-pyridyl-*N*-methylammoniummethyleneamino)piperazine bromide[4] (VI), and 1-phenyl-1- (4-chlorobenzyl)methyl-4- (6-methyl-2-pyridylmethyleneamino)piperazine[4] (VII) were supplied as pure compounds[5].

Action Spectrum of IV—Approximately 200 mg of IV[6] was spread on a 43 × 43-mm polyethylene tray[7]. A single light filter or a combination of two filters[8] was placed on the tray top to allow passage of only the desired band of wavelengths in the long wavelength UV or visible light region. The sample assembly was then placed in a light cabinet consisting of six daylight fluorescent lamps[9] mounted in a light fixture 34 cm from the samples.

The intensity of the light transmitted through the light filters was measured with a pocket-sized light meter[9]. The total fluorescent light intensity was estimated to be 900 foot-candles. Samples were checked periodically for color change and left under fluorescent light for 96 hr.

Progress of Color Change of IV—Approximately 2.5 g of IV was packed tightly in 13 × 45-mm thin glass cylindrical containers[10] with polyethylene caps. Except for the bottom surfaces, the containers were wrapped with aluminum foil to prevent light exposure. They were then placed inverted in a light cabinet, thus exposing only the unwrapped surface of the container vertically to the daylight fluorescent light for 96 hr. The reaction was monitored every 24 hr by unwrapping and rewrapping the aluminum foil around the containers and noting the color changes.

Structure–Color Activity Relationships in Light—Approximately 200-mg samples of pure crystals of IV and its six analogs were spread on polyethylene trays. These samples were then exposed vertically to a beam of 366 ± 40-nm long wavelength UV light[11]. The light intensity, as monitored by a light meter[12], was approximately 4000 $\mu w/cm^2$. The samples were exposed to light for 1 hr, after which they were compared to unexposed samples of the same lot for color change.

Physicochemical Analysis of Long Wavelength UV Light-Exposed and Unexposed Samples—*UV (Solution) Spectra*—A 10-mg % stock solution of the compound was prepared in spectral grade methanol. All UV spectra were obtained with a 1- or 3-mg % solution of the compound on a ratio recording spectrophotometer[13].

Differential Scanning Calorimetry Profiles—Approximately 4 mg of the sample was placed in the sample container of the instrument[14] under nitrogen atmosphere. The temperature program mode was set at 10°/min and the recording mode was set at 0.5°/2.54 cm for obtaining the endotherms.

IR Spectra—IR spectra on long wavelength UV-exposed and unexposed disks of IV with potassium bromide were obtained as follows. Approximately 0.8 mg of the pure compound powder was weighed on a microanalytical balance[15] and was then transferred along with 250 mg of dry potassium bromide powder into a hard plastic

[1] SC-13504.
[2] Matheson, Coleman & Bell, Norwood, Ohio.
[3] Merck & Co., Rahway, N.J.
[4] Searle Laboratories, Division of G. D. Searle & Co., Chicago, Ill.
[5] From the Chemical Research Department, Searle.
[6] Lot II-128B was used for all experiments.
[7] Sybron Corp., Rochester, N.Y.
[8] G. K. Turner Associates, Palo Alto, Calif.
[9] General Electric Co., Neela Park, Cleveland, Ohio.
[10] Corning Glass Works, Corning, N.Y.
[11] Model B-100A, Ultra-Violet Products, San Gabriel, Calif.
[12] Model J-221, Ultra-Violet Products, San Gabriel, Calif.
[13] Beckman Instruments, Fullerton, Calif.
[14] Dupont Instruments, Wilmington, Del.
[15] Metler Instruments Co., Zurich, Switzerland.

Table I—Effect of Action Spectrum of Light on the Color Change in IV (Powder) Exposed to Daylight Fluorescent Light over 0–96 hr

Light Filter Number	Light Intensity, f.c.[a]	Action Spectrum, nm	Transmitted Light	Color Change Compared with Control
58 and 2A-12	280	500–600 (λ_{max} 525)	Green	None
3 and 48	25	450–500 (λ_{max} 460)	Sky blue	None
7-60	5	300–400 (λ_{max} 360)	Violet	Bright yellow
8 and 5A	25	400–460 (λ_{max} 440)	Greenish blue	None
2A-15 and 23A	300	525–700 (λ_{max} 625)	Reddish orange	None
7-38 (silica)	900	340–700	Colorless	Bright yellow
405	15	380–430 (λ_{max} 410)	Violet blue	Pale yellow
>400 nm, UV protection Plexiglas[b]	900	>400 nm	White	None

[a] f.c. = foot-candles of light. [b] Ultra-violet Products, San Gabriel, Calif.

capsule. The mixture was shaken vigorously on a mechanical shaker[16] for 15 sec, and the powder mixture was transferred into a rectangular-shaped die mounted in a pellet press[17].

An IR spectrum on the sample disk referenced against a blank potassium bromide disk was obtained on a double-beam recording IR spectrophotometer[18]. The sample disk was then exposed to long wavelength UV light of 366 ± 40 nm for 1 hr, and another IR spectrum on the sample was obtained to note the spectral change after light exposure.

NMR Spectra—NMR spectra on samples of IV were recorded on a high-resolution NMR spectrometer[19]. The 10% solutions of IV were prepared in deuterated chloroform. The operating temperature probe was held at 37–40°, and 1% tetramethylsilane[18] solution was used as an internal standard.

GC Determination of IV—An in-house method[20] was adopted to identify the compound and its concentration before and after long wavelength UV light irradiation for 2 hr. Light-exposed and unexposed samples of IV were processed as follows.

Each sample (10 mg) was dissolved in 100 ml of spectrograde chloroform, and this stock solution was diluted to obtain a 10-μg/ml concentration of IV. Two microliters of this solution was injected into the GC column[21], which was maintained at 275°. Nitrogen, used as the carrier gas, was passed through the column at a rate of 48 ml/min; detection of the compound was achieved with a flame-ionization detector set at 250°[22].

Kinetic Studies on IV in Solid State—The objectives of these investigations were to: (*a*) identify the absorption spectrum in the visible light region attributable to the metastable (bright-yellow) state of IV, and (*b*) study the kinetics of the color conversion process as a function of temperature.

Approximately 0.5-mm thin transluscent disks from 125 mg of dry unexposed powder of IV were compressed with a 13-mm wide die and punch assembly[23]. The die cavity was filled with the powder, and the punch was placed in position. After 10 min of air evacuation from the die, an initial pressure of 25 tons was applied to the sample using a ring press[24]. The sample was then maintained under 10 tons of pressure for 5 min to obtain disks of good quality.

Two such disks were placed securely in the disk mounts[25]; one was used as a reference to obtain the visible absorption spectrum on the sample disk in the 700–370-nm range. All visible spectra were obtained on a double-beam recording spectrophotometer[26]. After initial scanning for the baseline, the sample disk was exposed on one side to long wavelength UV light of 366 ± 40 nm at 4000 μw/cm^2 intensity for 30 min and the absorption spectrum in the visible region was obtained. Care was exercised to maintain a constant geometry of both the sample and reference disks in their holders.

The sample disk was then placed in a constant-temperature oven at 50 or 70°. At predetermined time intervals, the sample assembly was withdrawn from the oven and cooled for 15 min and the absorption spectrum was recorded. Kinetic data were obtained in triplicate to derive the necessary kinetic parameters.

RESULTS AND DISCUSSION

Identification of Action Spectrum and Nature of Reaction—Experiments were designed to determine: (*a*) the band of wavelengths that induced a color change in the pure compound and (*b*) the progress of the reaction in the solid state. Table I illustrates the results of one study. It demonstrates that long wavelength UV light in the range of 300–400 nm (defined as the action spectrum) was predominantly responsible for inducing the color change. Light radiations above 400 nm were virtually ineffective.

Since transparent materials, such as Plexiglas, prevent the penetration of long wavelength UV light and protect the drug, it was suggested that their use to filter daylight fluorescent light can prevent a color change during large-scale manufacturing of any long wavelength UV light-sensitive compound. The progress of the reaction, as evidenced by color appearance in the light-exposed surface of the glass containers, was restricted to the surface area of light exposure. The possibility of nonradiative interparticulate energy transfer in the solid state was unlikely.

Physicochemical Aspects of Color Conversion—Samples of IV exposed to long wavelength UV light for 2 hr were analyzed by differential scanning calorimetry, IR (solid state), NMR, and UV (solution) spectroscopy methods. No detectable change was observed in the spectra or thermograms of either long wavelength UV-exposed or unexposed samples. Light-exposed samples that had turned yellow were subjected to elevated temperature storage at 70° for 2 hr, and the original color was restored. The UV spectrum (solution) and differential scanning calorimetry profile of this light- and heat-exposed sample were identical to those of the unexposed sample stored at room temperature.

Furthermore, repetition of the light exposure/heat (70°)/light exposure cycle for five consecutive times did not produce any observable "fatigue" in the color change phenomenon of IV. GC analysis of these exposed and unexposed controls showed the same retention time (6.0 min). The potency of the irradiated material was also retained, as evidenced by comparison of the peak heights of control and irradiated samples at equivalent concentrations in the chromatographic solvent (chloroform). Also, the TLC profiles[27] of light-exposed and unexposed samples of IV were identical and showed no impurity spots on the developed plates.

Effect of Long Wavelength UV Light on IV and Related Compounds: Possible Structure–Photochromic Activity Relationship—Photochromism refers to the ability of solid organic or inorganic compounds to undergo a transient color change on exposure to an action spectrum of light (2, 3). This color change is dependent on temperature and the duration and intensity of light exposure. However, dissolution, heat treatment, or prolonged storage in the dark

[16] Crescent Dental Manufacturing Co., Chicago, Ill.
[17] Maintenance Department, Searle Laboratories, Chicago, Ill.
[18] Model IR-12, Beckman Instruments, Fullerton, Calif.
[19] Varian Associates, Palo Alto, Calif.
[20] Mr. L. Kosobud, Bioanalytical Department, Searle Laboratories, Chicago, IL 60648, personal communication.
[21] OV-17 (1.5%) coated on Chromosorb-WH, Ohio Valley Speciality Chemical Co., Marietta, Ohio.
[22] Packard Instruments, Downers Grove, Ill.
[23] Beckman Instruments, Fullerton, Calif.
[24] Model RHC—D-01, Research & Industrial Instruments Co., London, England.
[25] Model INS-HV, Beckman Instruments, Fullerton, Calif.
[26] Acta CV double-beam recording spectrophotometer, Beckman Instruments, Fullerton, Calif.

[27] TLC analysis was performed with activated silica gel-coated glass plates. A compound sample (50 and 100 μg) dissolved in methanol was spotted and the plates were developed by the ascending technique, using benzene–ethanol–ammonium hydroxide (92.5:7:0.5) as the solvent system. Detection of the compound was done under long and short wavelength UV light.

Table II—Relationship between Some Physicochemical Parameters and the Effect of Long Wavelength UV Light Exposure on the Color of Substituted Benzhydrylpiperazines

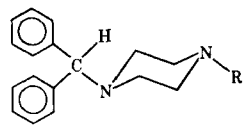

Number	R	λ_{max} (Solution), nm	Melting Point (Differential Scanning Calorimetry)	Color[a]	
				Initial	Long Wavelength UV Light Exposed
I[b]	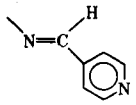	313	129°	Faint yellow	Faint yellow
II[c]	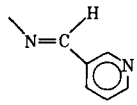	304	120°	Pale yellow	Pale yellow
III[d]	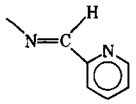	308	165°	Pale yellow	Bright yellow
IV[e]	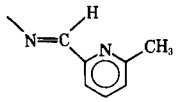	310	137°	Faint yellow	Bright yellow
V[f]	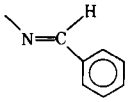	297	135°	Colorless (white)	Colorless (white)
VI[g]	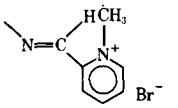	372	235°	Orange	Bright orange

[a] The color was compared to an unexposed control by visual inspection after 1 hr of irradiation of samples from the same lot. [b] SC-12757. [c] SC-13249. [d] SC-13300. [e] SC-13504. [f] SC-12123. [g] SC-21503.

at ambient temperature reverses this color change. Several organic compounds, including anils, semicarbazones, and hydrazones, exhibit photochromism in the solid state (2). Among semicarbazones, thiacetazone, an antitubercular drug, darkens in color when exposed to light (4).

To assess whether the heteroaromatic substitution (R) adjoining the hydrazone [>N—N=C(—H)R] had any effect on the light-induced color transformation process, several analogs of IV were examined for color change after exposure to long wavelength UV light for 1 hr (Table II). From these data, it is evident that *meta*- and *para*-substitution of the pyridyl moiety on the hydrazone inhibited the color change, suggesting that an electron resonance requirement was necessary for the change to occur. The time required for discoloration of III was prolonged over that necessary (about 1 min) for the discoloration of IV under similar conditions. Thus, a $+I$ (inductive) and, possibly, a hydrophobic effect of the methyl group appear to contribute to the stabilization of the light-activated intermediate.

Quaternization of the pyridyl nitrogen (VI) did not inhibit the color change significantly. However, the original color was restored in a relatively short time (about 24 hr). Except for V, which showed a shift of 7 nm toward shorter wavelengths, none of these compounds showed any significant alterations in their UV spectra after exposure to long wavelength UV light for 1 hr.

Possible Mechanisms for Photochromic Process—Longwave UV light-excited molecules of IV in the crystalline lattice are subjected to an electron delocalization process. The involvement of an *ortho*-substituted pyridyl nitrogen is likely since *meta*- and *para*-substituted analogs of IV (I and II) are relatively stable to long wavelength UV light irradiation. The melting points of the compounds studied (Table II) range from 120 to 235° and appear to show no correlation with the photochromic process. This finding suggests that crystal lattice differences between these six compounds are of minor importance.

A possible mechanism of this light-induced phenomenon is that the $n \rightarrow \pi^*$ and $\pi \rightarrow \pi^*$ electronic transitions in the excited (singlet and/or triplet) state of the molecule may lead to a stabilized resonating structure between the pyridyl and the piperazyl nitrogen atoms (Scheme I). The proposed mechanism considers the steric and resonance requirements essential for a photochromic process. A molecular model, constructed to envision the feasibility of the proposed mechanism, indicated that an *anti–syn*-transformation around the hydrazone moiety in the light-excited state may allow close proximity of the piperazine and pyridyl nitrogen. Thus, either inter- or intramolecular electrostatic forces of the molecules on the light-penetrable surface of a crystal lattice can stabilize the resonating photochromic system to produce the metastable state. Therefore, the mechanism appears to be realistically attractive and can be considered proven only if and when a compound with a carbon in place of the nitrogen atom on the piperazyl ring remains the same in color after exposure to long wavelength UV light. No such compound was available to confirm this possibility.

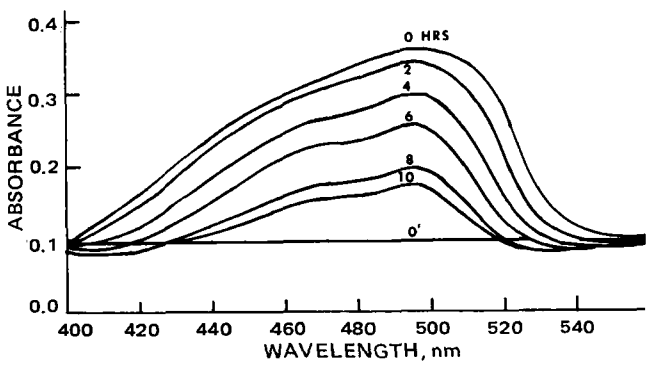

Figure 1—*Profile of visible absorption spectra obtained on a sample disk of IV prior to (0') and after (0) irradiation and successive periods of 2, 4, 6, 8, and 10 hr of heating at 50°.*

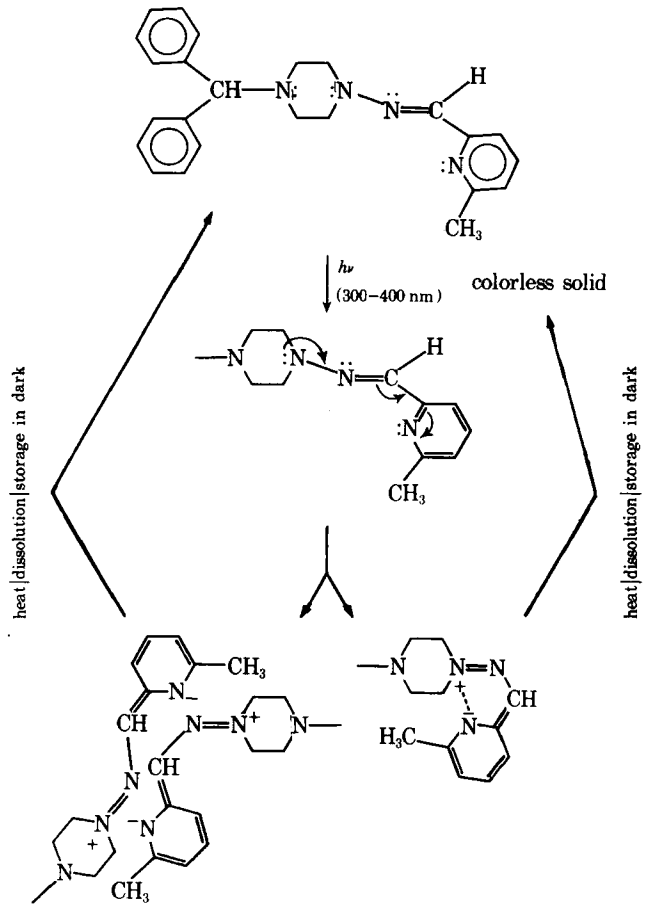

Scheme I—Mechanism for photochromism of IV

Compound VII did not produce any color change when exposed to light. The UV (solution) and IR spectra and the differential scanning calorimetry profiles of the light-exposed and unexposed samples of this compound were identical. The presence of a heavy atom, such as chlorine, in the vicinity of the resonating hydrazone moiety probably enhances the intercrossing of the excited-state electronic transitions, thus inhibiting the transformation of IV from the stable (colorless) state to a metastable (yellow) solid state. This conclusion appears consistent with the observed absence of photochromic activity of some chloro-substituted hydrazone derivatives (2).

Thus, it can be concluded that photochromism of IV in the solid state is an interesting, but known, property inherent in some hydrazone derivatives. Since the compound retains its physicochemical integrity in fluid solutions, its biological effects as a potent anticonvulsant compound in animals are most likely independent of its photochromic property in the solid state.

Kinetics of Photochromism of IV in Solid State—Figure 1 is a profile of visible absorption spectra obtained on a long wavelength UV-exposed disk of IV subjected to intermittent heat treatment at 50°. The absorption band at 500 nm (visible region) is attributed to the metastable photochromic (yellow) state. Such an assignment of the absorption spectrum is reasonable, since most yellow-colored compounds, such as riboflavin, bilirubin, and tartrazine yellow, absorb this bluish-green band of light. Furthermore, intermediates with an absorption maximum at 500 nm have been detected for a number of bioorganic reactions of pyridoxal and its derivatives with biogenic amines (5). Extension of the conjugation with the pyridyl moiety participating in such resonating structures has been proposed for the appearance of the colored intermediate (5, 6). Since the absorption maximum of the photochromic state of IV is at 494 nm (~500 nm), the possibility of an extended resonating structure lends credence to the proposed mechanism for the photochromism of IV (Scheme I).

Figure 2 is a zero-order plot of absorbance at 494 nm *versus* time of sample exposure to 50°. It illustrates the apparent zero-order kinetics of the photochromic transformation of IV from a metastable

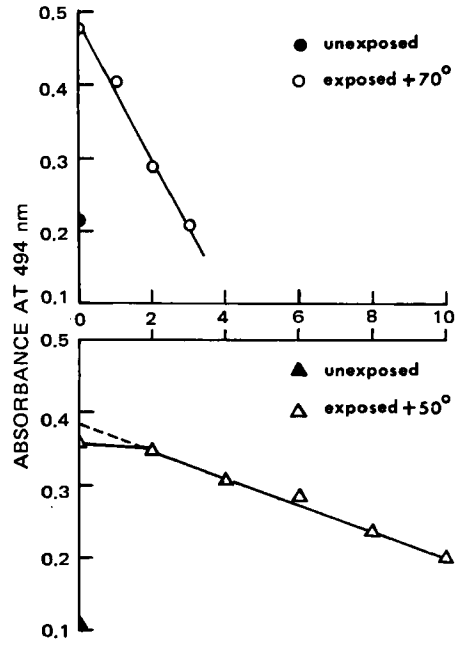

Figure 2—*Plots illustrating kinetics of photochromic conversion of IV from metastable (colored) to stable (colorless) solid state.*

(yellow) state to a stable (colorless) solid state at two defined temperatures. The rate constant for the photochromic conversion process is the slope of this plot at a given temperature. Equation 1 can be used to estimate the energy of activation, E_b, required for a reaction to proceed (7):

$$\log \frac{k_2}{k_1} = \frac{E_b}{2.303R} \frac{T_2 - T_1}{T_1 T_2} \qquad \text{(Eq. 1)}$$

where k_1 and k_2 are rate constants, T_1 and T_2 are temperatures, and R is the gas constant for the kinetic process occurring during the study of a reaction. With these parameters, the energy of activation, E_b, for the conversion of IV from a metastable (yellow) to a stable (colorless) solid state was estimated to be 19.0 kcal/mole.

Figure 3 is a proposed potential energy diagram illustrating the reversibility of the photochromic transformation of IV from a stable (colorless) state, *A*, to a metastable (yellow) state, *B*. For a reactant to go to a product *via* an intermediate requires energy and involves bond breaking processes (7). Also, in most cases, the product is at a lower energy level than the reactant. Since no bond breaking processes are involved in this case, as evidenced by the spectroscopy data, it is reasonable to expect that the metastable (yellow) state, *B*, of IV is at a higher energy level than its stable (colorless) state, *A*. Consequently, the estimated energy of activation (E_b = 19 kcal/mole) is assignable for the reversal of the metastable state, *B*, to the stable state, *A*, *via* an intermediate, X_3 (Fig. 3). This activation energy is within the range reported for photochromic systems (3). Light in the vicinity of 366 ± 40 nm provided efficient excitation energy transfer equivalent to about 80 kcal/mole (8). This was evident from the observation that

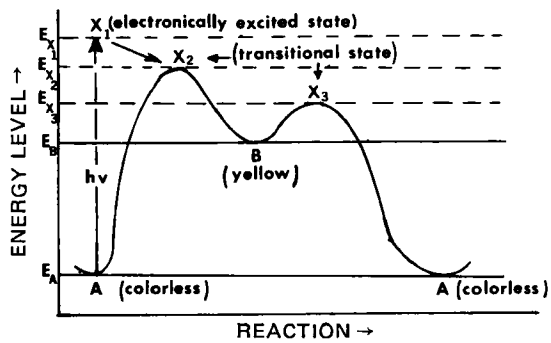

Figure 3—*Potential energy diagram illustrating the energy difference between the stable (A, colorless) and metastable (B, colored) solid state of IV; X is the transitional intermediate.*

an absorption band in the 400–550-nm region appeared within minutes after irradiation of the sample disk with long wavelength UV light of 366 ± 40 nm.

SUMMARY

Compound IV exhibited photochromism in the solid state. This light-induced color conversion process was typical of many hydrazone derivatives and did not affect the chemical nature or purity of the compound in solution. Conditions of elevated temperature, dissolution, and prolonged storage in the dark at ambient temperatures restored the original color of the compound. An action spectrum in the 300–400-nm range induced the change in color. A structure–photochromic activity relationship among several analogs of IV was observed, from which a possible mechanism for the photochromic conversion of IV from a stable to a metastable solid state was proposed.

The kinetics of photochromism of IV were apparently zero order for the return of the metastable (yellow) state to the stable (colorless) state. The energy of activation for this process was about 19 kcal/mole. The appearance and disappearance of an absorption band in the visible region, with a concomitant change in the color of the compound after exposure to long wavelength UV light, were evidence for the presence of a metastable state, which reverts back to the stable state of IV with heat treatment. These studies allowed novel and direct application of absorption spectrophotometry for determining the kinetics of photochromism in the solid state.

REFERENCES

(1) C. R. Craig, *Arch. Int. Pharmacodyn. Ther.*, **165**, 328(1967).

(2) R. Exelby and R. Grinter, *Chem. Rev.*, **65**, 247(1965).

(3) "Techniques of Chemistry," vol. III, G. H. Brown, Ed., Wiley–Interscience, New York, N.Y., 1971.

(4) "The Merck Index," 8th ed., Merck & Co., Rahway, N.J., 1968, p. 1036.

(5) J. R. Maley and T. C. Bruice, *J. Am. Chem. Soc.*, **90**, 2843(1968).

(6) P. Jencks, "Catalysis in Chemistry and Enzymology," McGraw-Hill, New York, N.Y., 1969, pp. 135–145.

(7) F. Daniels and R. A. Alberty, "Physical Chemistry," 3rd ed., Wiley, New York, N.Y., 1966, pp. 338–345.

(8) N. J. Turro, "Molecular Photochemistry," Benjamin, New York, N.Y., 1965, pp. 2–7.

ACKNOWLEDGMENTS AND ADDRESSES

Received October 14, 1975, from *Searle Laboratories, Division of G. D. Searle & Co., Chicago, IL 60680*

Accepted for publication December 8, 1975.

The author thanks Mrs. Iris A. Brener and Mr. Dale Chappelow for technical assistance. He also thanks Dr. E. LeVon, Dr. H. Dryden, Dr. G. Lenz, Dr. R. Bible, and Mr. A. Damascus for helpful discussions. The encouragement of Dr. H. J. Lambert and Dr. K. Rorig to study this phenomenon in depth is very much appreciated.

Absorption, Distribution, Metabolism, and Excretion of Furosemide in Dogs and Monkeys I: Analytical Methodology, Metabolism, and Urinary Excretion

GERALD J. YAKATAN ˣ, DALE D. MANESS, JEAN SCHOLLER, WM. J. NOVICK, Jr. *, and JAMES T. DOLUISIO

Abstract □ ^{35}S-Furosemide was administered to beagle dogs and rhesus monkeys in an oral solution on a single and a 20 repeated 5-mg/kg/day dosing regimen. Following the single dose, 25.0% (dogs) and 24.0% (monkeys) of the dose were excreted in the urine in 24 hr. TLC analysis demonstrated that both species had similar excretory patterns; *i.e.*, over 80% of the amount excreted in the urine was present as unchanged furosemide and the remainder was composed of a known metabolite, saluamine, and an as yet unidentified metabolite(s). The repetitive dosing regimen did not appear to alter significantly either the total amount recovered in the 24-hr urine or the excretion pattern. Studies in dogs showed that only 50–60% of furosemide was absorbed from oral solution. A significant biliary secretion elimination pathway for furosemide also was observed.

Keyphrases □ Furosemide and metabolite—TLC analysis, urine, dogs and monkeys □ TLC—analysis, furosemide and metabolite, urine, dogs and monkeys □ Excretion—furosemide, TLC analysis, urine, dogs and monkeys □ Pharmacokinetics—furosemide, dogs and monkeys compared □ Diuretics—furosemide, TLC analysis, urine, dogs and monkeys

Despite the widespread clinical use of diuretics in the treatment of edematous states and essential hypertension, there exist little published data on the comparative pharmacokinetics of these agents. This laboratory is involved in a major effort to elucidate the pharmacokinetic profiles of various diuretics and to compare the absorption, distribution, metabolism, and excretion patterns of these agents in several animal species including humans. The present work reports some findings with one diuretic, furosemide, in beagle dogs and rhesus monkeys.

Furosemide, 4-chloro-*N*-furfuryl-5-sulfamoylanthranilic acid (I), is a potent, orally effective diuretic. It exerts its major effect by inhibiting sodium reabsorption in the proximal convoluted tubule and the loop of Henle (1).

4-Chloro-5-sulfamoylanthranilic acid (saluamine) (II) was reported to be the major metabolite of furosemide in humans and dogs (2). Saluamine also was identified as a metabolite in a study on the distribution and urinary excretion of furosemide in the rat (3).

The purpose of the present studies was to determine

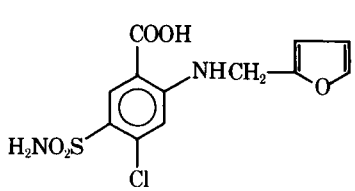

I

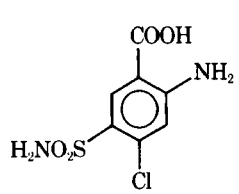

II

an absorption band in the 400–550-nm region appeared within minutes after irradiation of the sample disk with long wavelength UV light of 366 ± 40 nm.

SUMMARY

Compound IV exhibited photochromism in the solid state. This light-induced color conversion process was typical of many hydrazone derivatives and did not affect the chemical nature or purity of the compound in solution. Conditions of elevated temperature, dissolution, and prolonged storage in the dark at ambient temperatures restored the original color of the compound. An action spectrum in the 300–400-nm range induced the change in color. A structure–photochromic activity relationship among several analogs of IV was observed, from which a possible mechanism for the photochromic conversion of IV from a stable to a metastable solid state was proposed.

The kinetics of photochromism of IV were apparently zero order for the return of the metastable (yellow) state to the stable (colorless) state. The energy of activation for this process was about 19 kcal/mole. The appearance and disappearance of an absorption band in the visible region, with a concomitant change in the color of the compound after exposure to long wavelength UV light, were evidence for the presence of a metastable state, which reverts back to the stable state of IV with heat treatment. These studies allowed novel and direct application of absorption spectrophotometry for determining the kinetics of photochromism in the solid state.

REFERENCES

(1) C. R. Craig, *Arch. Int. Pharmacodyn. Ther.*, **165**, 328(1967).

(2) R. Exelby and R. Grinter, *Chem. Rev.*, **65**, 247(1965).

(3) "Techniques of Chemistry," vol. III, G. H. Brown, Ed., Wiley–Interscience, New York, N.Y., 1971.

(4) "The Merck Index," 8th ed., Merck & Co., Rahway, N.J., 1968, p. 1036.

(5) J. R. Maley and T. C. Bruice, *J. Am. Chem. Soc.*, **90**, 2843(1968).

(6) P. Jencks, "Catalysis in Chemistry and Enzymology," McGraw-Hill, New York, N.Y., 1969, pp. 135–145.

(7) F. Daniels and R. A. Alberty, "Physical Chemistry," 3rd ed., Wiley, New York, N.Y., 1966, pp. 338–345.

(8) N. J. Turro, "Molecular Photochemistry," Benjamin, New York, N.Y., 1965, pp. 2–7.

ACKNOWLEDGMENTS AND ADDRESSES

Received October 14, 1975, from *Searle Laboratories, Division of G. D. Searle & Co., Chicago, IL 60680*

Accepted for publication December 8, 1975.

The author thanks Mrs. Iris A. Brener and Mr. Dale Chappelow for technical assistance. He also thanks Dr. E. LeVon, Dr. H. Dryden, Dr. G. Lenz, Dr. R. Bible, and Mr. A. Damascus for helpful discussions. The encouragement of Dr. H. J. Lambert and Dr. K. Rorig to study this phenomenon in depth is very much appreciated.

Absorption, Distribution, Metabolism, and Excretion of Furosemide in Dogs and Monkeys I: Analytical Methodology, Metabolism, and Urinary Excretion

GERALD J. YAKATAN ˣ, DALE D. MANESS, JEAN SCHOLLER, WM. J. NOVICK, Jr. *, and JAMES T. DOLUISIO

Abstract □ ^{35}S-Furosemide was administered to beagle dogs and rhesus monkeys in an oral solution on a single and a 20 repeated 5-mg/kg/day dosing regimen. Following the single dose, 25.0% (dogs) and 24.0% (monkeys) of the dose were excreted in the urine in 24 hr. TLC analysis demonstrated that both species had similar excretory patterns; *i.e.*, over 80% of the amount excreted in the urine was present as unchanged furosemide and the remainder was composed of a known metabolite, saluamine, and an as yet unidentified metabolite(s). The repetitive dosing regimen did not appear to alter significantly either the total amount recovered in the 24-hr urine or the excretion pattern. Studies in dogs showed that only 50–60% of furosemide was absorbed from oral solution. A significant biliary secretion elimination pathway for furosemide also was observed.

Keyphrases □ Furosemide and metabolite—TLC analysis, urine, dogs and monkeys □ TLC—analysis, furosemide and metabolite, urine, dogs and monkeys □ Excretion—furosemide, TLC analysis, urine, dogs and monkeys □ Pharmacokinetics—furosemide, dogs and monkeys compared □ Diuretics—furosemide, TLC analysis, urine, dogs and monkeys

Despite the widespread clinical use of diuretics in the treatment of edematous states and essential hypertension, there exist little published data on the comparative pharmacokinetics of these agents. This laboratory is involved in a major effort to elucidate the pharmacokinetic profiles of various diuretics and to compare the absorption, distribution, metabolism, and excretion patterns of these agents in several animal species including humans. The present work reports some findings with one diuretic, furosemide, in beagle dogs and rhesus monkeys.

Furosemide, 4-chloro-*N*-furfuryl-5-sulfamoylanthranilic acid (I), is a potent, orally effective diuretic. It exerts its major effect by inhibiting sodium reabsorption in the proximal convoluted tubule and the loop of Henle (1).

4-Chloro-5-sulfamoylanthranilic acid (saluamine) (II) was reported to be the major metabolite of furosemide in humans and dogs (2). Saluamine also was identified as a metabolite in a study on the distribution and urinary excretion of furosemide in the rat (3).

The purpose of the present studies was to determine

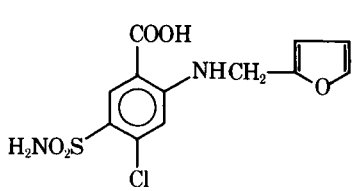

I

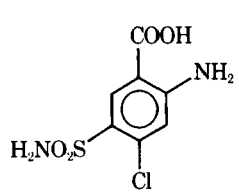

II

the absorption, distribution, metabolism, and excretion patterns of furosemide following single and repeated 5-mg/kg doses in dogs and monkeys. The generated data could then be compared to the work reported in the rat (3). This initial report describes the experimental design, analytical methodology, and application of this methodology to evaluate the metabolism and urinary excretion of furosemide.

EXPERIMENTAL

Materials—Radiochemically pure ^{35}S-furosemide (specific activity of 7.5 mCi/g initially), unlabeled furosemide, and its known metabolite, saluamine, were used as received[1]. All other chemicals used were analytical reagent or USP grade. Furosemide was administered in an aqueous sorbitol solution containing 5 mg/ml of drug, of which 1 mg/ml was labeled furosemide. The solution was stable over the period of its use.

All materials were protected from light during the preparation of the furosemide solution to prevent potential photolytic degradation. After preparation, the solution was flushed for 5 min with a stream of nitrogen and dispensed in an amber bottle with a nitrogen blanket. After each use, the furosemide solution was purged and blanketed with nitrogen.

Animal Studies—Male beagle dogs[2], 7–8 months old and weighing approximately 10 kg, were dewormed and given immunizations prior to shipment. Young, adult, male rhesus monkeys[3], 2–4 kg, were tuberculin tested prior to shipment.

The animals were individually housed in cages having stainless steel metabolism pans and were randomly assigned to experimental or control groups. Control body weights and temperatures were obtained. Water was allowed *ad libitum* throughout the experiment. Food was given daily, although no solid food was allowed for 4 hr prior to dosing. All doses of furosemide were administered by oral intubation at a level of 5.0 mg/kg. Body weights were determined weekly. Control animals received a solution identical to the one given the experimental groups except that it contained no furosemide.

Blood samples, drawn with a sterile heparinized needle and syringe, were obtained from the cephalic or saphenous veins. The samples were immediately centrifuged to obtain plasma, and the plasma was placed in a foil-wrapped tube and immediately frozen. Hematocrits were checked periodically.

Urine samples were collected in the metabolism cages at specified intervals. The volumes were measured, and an aliquot was stored frozen in a foil-wrapped tube. Urine samples were protected from light as much as possible at all times (even in metabolism cages).

All animals were sacrificed with an overdose of pentobarbital, and the liver, kidneys, and testes were removed immediately. Sections of each tissue were frozen in foil-wrapped vials, and the remainder was fixed in 10% buffered formalin for histopathological studies. The tissues were examined with hematoxylin and eosin, iron, periodic acid–Schiff, and calcium stains.

All biological specimens were stored in coded containers. The code was not broken until all samples had been assayed for radioactivity or examined by the pathologist.

Single-Dose Studies—A single 5-mg/kg dose was administered orally to four groups of dogs and monkeys. Blood, urine, and stool specimens were collected periodically from each animal. The animals were sacrificed (in groups of three) 0.25, 3, 6, and 9 days after dosing, and tissue samples were collected.

In a separate study, a single 5-mg/kg dose was administered orally to a group of three dogs. Blood, urine, and stool specimens were collected at each sampling time from each animal. These animals were not sacrificed. Two of these dogs later received single 5-mg/kg iv doses of furosemide, and blood, urine, and stool specimens were collected.

Multiple-Dose Studies—Groups of animals were given 5 mg/kg/day of furosemide for 20 days. Blood specimens from one group of three animals were obtained immediately prior to, and 2 hr following, the daily dose of drug. Urine collections from these animals were made daily. Blood specimens also were obtained from a group of six animals over 12 hr following the last dose of drug on Day 20.

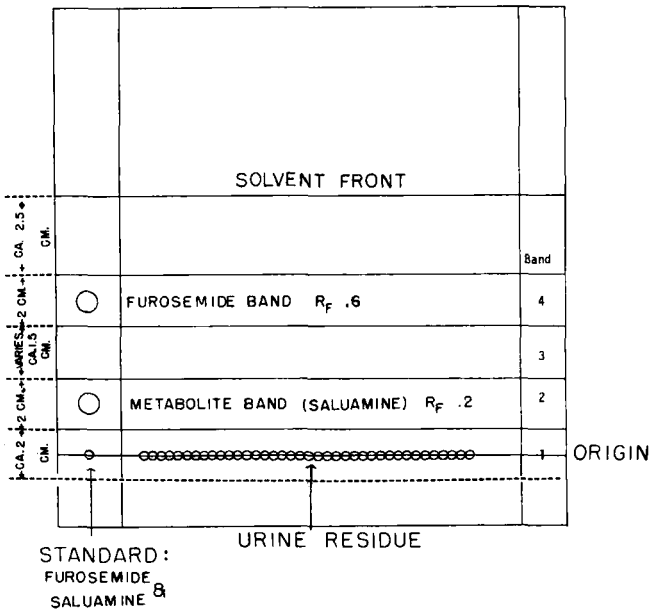

Figure 1—*TLC plate utilized for the analysis of urine samples obtained from dogs and monkeys. Each designated band was scraped and assayed for radioactivity. The band containing the* R_f *0.2 metabolite was saluamine.*

Groups of three animals were sacrificed 24 hr after doses 5, 10, 15, and 20 on a 5-mg/kg/day regimen to determine if kidney accumulation of drug and/or metabolites, or if histopathological changes, occurred. Three additional groups of animals were sacrificed and studied 3, 6, and 9 days after the 20-day dosing regimen.

TLC Analysis of Urine and Plasma Samples—The frozen urine and plasma samples were allowed to thaw, and 0.5-ml duplicate aliquots were sampled into 2-dram vials and lyophilized in the absence of light. The urine residues were extracted three times with 100-μl volumes of hot methanol. The methanolic extract from each sample was spotted on a 20 × 20-cm cellulose TLC plate[4] together with furosemide and saluamine standards, and the plates were eluted with 2-propanol–butyl acetate–water–concentrated ammonia (50:30:15:5 v/v).

Figure 1 shows a representative developed TLC plate. Excellent separation of furosemide (R_f 0.6) from saluamine (R_f 0.2) was obtained. The plates were developed in the dark after the TLC chambers had been equilibrated with the developing solvent. After development, the bands corresponding to furosemide and saluamine were visualized under UV light, marked by comparison to standards, and scraped into scintillation vials for counting of radioactivity. Three additional bands on the cellulose plate were collected to investigate and quantitate the possible existence of unknown furosemide metabolites.

The sizes of the scraped bands were chosen for assay convenience after radiochromatographic scanning and scraping of smaller bands indicated that the radioactivity on the TLC plate would be confined to the areas shown in Fig. 1. To each vial, 15 ml of a scintillation cocktail was added [80 g of naphthalene, 10 g of 2,5-diphenyloxazole, and 0.5 g of 1,4-bis[2-(5-phenyloxazolyl)]benzene dissolved in 1 liter of xylene–dioxane–2-ethoxyethanol (1:3:3 w/v)]. The vials were placed in a box and shaken for 5 min in a horizontal position on an automatic sieve shaker[5]. Then the vials were placed in a liquid scintillation spectrometer[6] and allowed to equilibrate overnight at 6° before analyzing for sulfur-35 activity.

Experiments were performed that demonstrated that: (*a*) radioactivity corresponding to furosemide was totally extracted from the cellulose by the procedures employed; (*b*) the cellulose, which settled to the bottom of the vial, did not alter the counting efficiency; (*c*) 90%

[1] Hoechst-Roussel Pharmaceuticals, Inc., Somerville, NJ 08876
[2] Marshall Research Animals.
[3] Laboratory of Aerospace Medicine, San Antonio, Tex.
[4] Celplate-22, Brinkmann Instruments, Westbury, N.Y.
[5] Model RX-21, W. X. Tyler Co., Mentor, Ohio.
[6] Tri-Carb model 3385, Packard Instrument Co., Downers Grove, Ill.

Table I—Percentages of the Administered Dose Appearing in the 24-hr Urine of Monkeys and Dogs as Unchanged Furosemide and Metabolites after Single Doses and a 20-Dose Regimen

Regimen	Band 1[a]	Band 2[a]	Band 3[a]	Band 4[a]	Total
		Monkeys			
Single dose[b]	1.50 ± 0.79 (6.1)	1.74 ± 0.85 (7.2)	0.82 ± 0.31 (3.5)	20.0 ± 7.7 (83.2)	24.0 ± 9.2
20 doses[c]	1.73 ± 1.08 (7.5)	1.75 ± 1.06 (7.6)	0.76 ± 0.50 (3.5)	17.9 ± 7.5 (81.4)	22.2 ± 9.7
		Dogs			
Single dose[c]	1.25 ± 0.41 (4.9)	1.78 ± 0.78 (6.9)	0.66 ± 0.23 (2.5)	22.4 ± 4.6 (86.0)	26.0 ± 5.1
20 doses[c]	1.27 ± 0.70 (4.7)	2.40 ± 0.82 (8.9)	0.41 ± 0.19 (1.5)	23.9 ± 9.0 (84.9)	28.0 ± 9.8

[a] The bands correspond to the areas on the TLC plates as shown in Fig. 1. The number in parentheses represents the percent of the amount excreted that appeared in that form. [b] Each value is the mean ± *SD* for nine animals for the 24-hr period following the dose (5 mg/kg). [c] Each value is the mean ± *SD* for 12 animals for the 24-hr period following the dose (5 mg/kg).

of the radioactivity was extracted from the biological sample; (*d*) reproducibility of the procedure was excellent, and processing of duplicate samples was not needed; and (*e*) total recovery of furosemide radioactivity from extraction through separation was 80%.

Thirty plasma samples, selected to represent various sampling times throughout the protocol, were assayed by essentially the same procedure used for the urine specimens. Due to the larger amount of residue after lyophilization, the extraction procedure was modified slightly by initially wetting the residue with 500 μl of hot methanol prior to three extractions with the 100-μl volumes of hot methanol. The results of these studies demonstrated that only about 1% of the total radioactivity on the plate was due to furosemide metabolites. Subsequently, all plasma samples in the study were assayed for total radioactivity only.

Preparation of Plasma Samples for Assay of Total Radioactivity—The frozen plasma samples were allowed to thaw, and 0.5-ml aliquots were added to 15 ml of a scintillation cocktail containing 15% (v/v) of a solubilizer[7], 8 g of 2-(4′-*tert*-butylphenyl)-5-(4″-biphenylyl)-1,3,4-oxadiazole, and 0.5 g of 2-(4-biphenylyl)-6-phenylbenzoxazole/liter of scintillation grade toluene and assayed for radioactivity. The samples were equilibrated at 6° overnight prior to counting.

Preparation of Tissue Samples for Assay of Total Radioactivity—A weighed sample (~100 mg) of lyophilized kidney, liver, or gonad was placed in a scintillation vial. One milliliter of 2 *N* NaOH was added, and the sample was heated in a sand bath maintained at 130°. Heating periods of up to 2–3 hr were required to digest the tissues. Careful dropwise addition of water was made as required to prevent the samples from going to dryness.

After dissolution, the sample was held at reaction temperature for 30 min, removed from the sand bath, and allowed to cool to room temperature. Where necessary, the solution was decolorized by the dropwise addition of 30% hydrogen peroxide. This addition was followed by the addition of 2.75 ml of a solubilizing agent[7], and then the samples were allowed to stand for approximately 30 min. A 10-ml volume of scintillation cocktail then was added, and the samples were mixed[8] and assayed for radioactivity.

Preparation of Feces Samples for Assay of Total Radioactivity—A weighed sample (~100 mg) of lyophilized feces was combusted by the oxygen flask method (4), using a trapping solution containing 10 ml of distilled water and 10 drops of hydrogen peroxide. A 0.1-ml aliquot of the trapping solution was counted for radioactivity in the same scintillation cocktail used for the plasma samples. Recovery experiments with "spiked" feces samples showed that 83% of the radioactivity present was recovered by this procedure.

Counting Data—All samples were assayed for total sulfur-35 activity with a counting error of 5% or less. An automatic external standardization technique was utilized to correct for sample quenching. All samples also were corrected for radioactive decay. The counting data obtained as sulfur-35 activity were converted to concentration or amount of furosemide and/or furosemide equivalents in each sample.

[7] Bio-Solv BBS-2 and BBS-3, Beckman Instruments Co., Fullerton, Calif.
[8] Vortex mixer.

RESULTS AND DISCUSSION

The TLC procedures utilized to assay the urine samples provided excellent separation of furosemide (band 4 in Fig. 1) and its major known metabolite, saluamine (band 2 in Fig. 1). Analysis of other areas on the thin-layer plate showed that significant radioactivity remained in the area of the origin (band 1 in Fig. 1). Since standards of furosemide and saluamine in spiked urine samples carried through the analytical procedures did not show significant radioactivity in band 1, this activity was assigned to the presence of a furosemide metabolite(s) of unknown structure. Preliminary data on the band 1 radioactivity utilizing alternative TLC systems and radiochromatographic scanning indicate the presence of at least two metabolites. Work is continuing to elucidate the structures.

The percentages of the administered furosemide excreted in the urine as unchanged drug and metabolite(s) in the 24-hr period following the single- and 20-dose regimens are shown in Table I. In dogs, 26% of the administered furosemide was recovered in the 24-hr urine following a single oral 5-mg/kg dose. The vast majority (86.0%) of the dose excreted in the urine was unchanged furosemide. Saluamine, the known metabolite (2), accounted for 6.9% of the amount excreted, while 4.9% was recovered as a possible metabolite(s) of unknown structure. Almost all (97%) of the radioactivity found in the urine was excreted in the first 24 hr.

The urinary excretion patterns for dogs in the 24-hr period following the last dose of the 20-dose regimen appear to be qualitatively and quantitatively similar to the single-dose data. Again, less than 30% of the total dose was recovered in 24 hr, and unchanged furosemide accounted for 85% of the drug excreted in the urine. Thus, there was no significant change in the rate or urinary elimination pattern on repetitive oral dosing in dogs.

The monkey eliminated furosemide in much the same fashion as the dog (Table I). Following an oral 5-mg/kg dose, 24.0% of the administered radioactivity was recovered in the 24-hr urine, of which 83% was unchanged furosemide. Saluamine represented 7.2% of the total radioactivity excreted, and 6.1% was recovered as a possible metabolite(s) of unknown structure.

In the 24 hr following the last dose of the 20-dose regimen, 22.2% of the administered dose was found in the urine of the monkeys (Table I). The distribution pattern for the urinary radioactivity was again similar to that observed after a single oral dose (unchanged furosemide, 81.4%; saluamine, 7.6%; unknown metabolite, 7.5%), indicating that no significant changes were occurring as a result of repetitive dosing.

In a study of the distribution and urinary excretion of ^{35}S-furosemide in rats, Seno *et al.* (3) reported recovery of 23.6% of a single oral dose in the 24-hr urine. In a metabolism study limited to the use of two rats, these investigators separated five to seven labeled compounds using TLC on urine samples collected at various time intervals. The overwhelming majority (90%) of the radioactivity resided in three major bands, which were assigned to unchanged furosemide (40–47%), saluamine (30%), and an unknown compound (20%). Schmidt (5) reported urinary recovery of 16–34% of orally administered doses of furosemide in rats and 25–45% in dogs.

Thus, the findings of these investigators regarding urinary excretion

Table II—Percentages of the Administered Dose Appearing in the 24-hr Urine of Monkeys as Unchanged Furosemide and Metabolites after Daily 5-mg/kg Doses[a]

Dose	Band 1[b]	Band 2[b]	Band 3[b]	Band 4[b]	Total
1	2.25	2.36	1.10	26.4	32.11
2	0.72	1.01	0.53	11.0	13.26
3	1.32	1.27	1.40	27.5	31.49
4	1.53	1.34	0.66	26.1	29.63
5	1.28	1.32	0.79	16.4	19.79
6	1.15	0.83	0.74	18.5	21.22
7	1.69	1.92	0.93	23.3	27.84
8	1.29	1.59	0.57	16.1	19.55
9	1.58	1.74	0.77	20.0	24.09
10	1.45	1.57	0.42	18.4	21.84
11	1.77	2.01	0.65	24.1	28.53
12	1.82	2.18	0.78	30.7	35.48
13	1.51	1.71	0.70	17.3	21.22
14	2.20	2.62	0.72	31.4	36.94
15	1.37	1.48	0.57	15.5	18.92
16	2.41	2.30	0.55	26.1	31.36
17	2.68	2.65	0.71	23.4	29.44
18	1.40	1.30	0.75	16.8	20.25
19	1.84	1.50	0.84	18.2	22.38
20	1.62	1.80	0.63	19.5	23.55
20	1.50	1.31	0.50	14.8	18.11
Mean ± *SD*	1.64 ± 0.45	1.70 ± 0.50	0.73 ± 0.22	21.0 ± 5.5	25.1 ± 6.3

[a] Each value is the mean for three animals. [b] The bands correspond to the areas on the TLC plates as shown in Fig. 1.

patterns of furosemide in various animal species are consistent with the data reported in the present study; *i.e.*, the total dose of furosemide is not recovered in the urine after oral administration, furosemide excreted in the urine is primarily in the unchanged form, and furosemide is metabolized to a minor extent to saluamine and a structurally unidentified metabolite.

Tables II and III give the percentage of the daily administered dose of furosemide excreted as unchanged drug and metabolites in the urine of monkeys and dogs for the 24-hr period after each dose. These data are qualitatively and quantitatively consistent with both the single-dose data and the data obtained following the last dose of the multiple dosing regimen (Table I). The mean recovery of the dose in the daily 24-hr urine was 25.1 ± 6.3% for the monkeys and 24.0 ± 6.7% for the dogs. The distribution of the recovered dose was 83.7% as unchanged furosemide, 6.8% as saluamine, and 6.5% as the unknown metabolite(s) for the monkeys and 85.9% as unchanged furosemide, 7.3% as saluamine, and 4.7% as the unidentified metabolite(s) for the dogs.

Although the data obtained in these studies were consistent with the few reported studies on furosemide, the reasons for the low urinary recovery of the administered dose were a cause of concern, particularly in relation to potential bioavailability problems. Two prominent possibilities to explain this problem were: (*a*) incomplete absorption of furosemide in the GI tract, and (*b*) a nonrenal elimination pathway for furosemide and/or its metabolites. The assay of feces specimens collected after oral administration showed a considerable amount of furosemide and/or metabolites present.

The answers to both possibilities dictated that furosemide be administered intravenously. A lack of sufficient ^{35}S-furosemide limited the intravenous studies to two dogs. After administration of a 5-mg/kg iv dose, the urinary excretion of radioactivity in the two dogs was 49.5 and 41.9% of the administered dose. Assay of the feces specimens demonstrated that 52.4 and 50.4% of the intravenous dose were in the feces of the same dogs. Thus, biliary secretory mechanisms appear to play a major role in the elimination of furosemide and/or metabolites in the dog.

That furosemide is not completely absorbed in dogs even from aqueous solution can be observed by comparing the total radioactivity recovered in the urine after intravenous and oral administrations in the same animals. The dog excreting 49.5% of the dose after intravenous administration excreted only 25.2% after receiving the same dose orally; the dog excreting 41.9% after intravenous administration ex-

Table III—Percentages of the Administered Dose Appearing in the 24-hr Urine of Dogs as Unchanged Furosemide and Metabolites after Daily 5-mg/kg Doses[a]

Dose	Band 1[b]	Band 2[b]	Band 3[b]	Band 4[b]	Total
1	1.30	1.54	0.63	25.0	28.5
2	1.25	1.68	0.54	23.4	26.9
3	0.97	1.31	0.82	13.5	16.6
4	1.83	1.93	0.89	32.3	37.0
5	2.07	2.31	0.82	38.8	44.0
6	1.47	1.92	0.41	28.4	32.2
7	1.76	2.55	0.56	35.7	40.6
8	1.80	2.36	1.36	23.6	29.1
9	1.45	1.78	0.58	19.0	22.8
10	1.59	2.15	0.49	27.7	31.9
11	2.13	2.20	0.68	28.2	33.2
12	1.40	2.44	0.72	25.6	30.2
13	0.91	2.38	0.57	21.1	25.0
14	0.99	2.53	0.56	21.4	25.5
15	0.96	2.06	0.41	18.3	21.7
16	0.91	1.98	0.39	22.3	25.6
17	1.18	2.53	0.71	30.5	34.9
18	0.79	1.96	0.59	20.8	24.1
19	0.62	1.40	0.41	17.1	19.5
20	2.13	2.21	0.29	25.5	30.2
20	0.99	3.24	0.41	24.4	29.0
Mean ± *SD*	1.36 ± 0.46	2.12 ± 0.45	0.61 ± 0.23	24.9 ± 6.1	29.0 ± 6.7

[a] Each value is the mean for three animals. [b] The bands correspond to the areas on the TLC plates as shown in Fig. 1.

creted 23.9% after the oral dose. Thus, based on urinary excretion of total radioactivity in dogs, it appears that only 50–60% of furosemide is absorbed from an oral solution.

The plasma and tissue levels and the pharmacokinetic parameters of furosemide in dogs and monkeys following 5-mg/kg oral and intravenous doses will be described in a subsequent paper. These data in dogs confirm the lack of complete bioavailability of furosemide from an oral solution dosage form. Less than 1% of radioactivity in the plasma of dog and monkey is attributable to metabolites.

REFERENCES

(1) P. Deetjen, *Ann. N.Y. Acad. Sci.*, **139**, 408(1966).

(2) A. Haussler and P. Hajdu, *Arzneim.-Forsch.*, **14**, 710(1964).

(3) S. Seno, S. M. Shaw, and J. E. Christian, *J. Pharm. Sci.*, **58**, 935(1969).

(4) G. J. Yakatan and M. M. Tuckerman, *ibid.*, **55**, 532(1966).

(5) H. A. E. Schmidt, "Tierversuche mit ^{35}S-markierten Lasix," International Furosemide Symposium, Bad Homburg, Germany, 1963.

ACKNOWLEDGMENTS AND ADDRESSES

Received August 18, 1975, from the *Drug Dynamics Institute, College of Pharmacy, University of Texas at Austin, Austin, TX 78712*

Accepted for publication December 8, 1975.

Presented in part at the Basic Pharmaceutics Section, APhA Academy of Pharmaceutical Sciences, San Francisco meeting, April 1975.

The authors thank Miss Winifred Ball, Mr. Guy Foster, and Miss Janet Gamble for technical assistance. They also gratefully acknowledge support of this work by grants from Hoechst-Roussel Pharmaceuticals, Inc., and the American Heart Association, Texas Affiliate, Inc.

* Hoechst-Roussel Pharmaceuticals, Inc., Somerville, NJ 08876

[x] To whom inquiries should be directed.

Interaction of Sodium Alkyl Sulfates with Everted Rat Small Intestinal Membrane

STUART FELDMAN [x] and MARK REINHARD

Abstract □ The effect of sodium alkyl sulfates (C_6–C_{14}) on the loss of protein from the everted rat small intestine was measured. At a surfactant concentration of 10 m*M*, a peak effect on protein release was noted with sodium decyl sulfate (C_{10}). Measurement of protein release as a function of sodium lauryl sulfate (C_{12}) concentration resulted in the observation that the effect appears to be due to the micellar phase of the surfactant solution. At concentrations of C_{12} above the CMC, the loss of protein from the intestinal preparation increased as the concentration of surfactant was increased. There may be a maximum amount of protein that can be released from the everted rat small intestinal sacs by surface-active agents. At equivalent micellar concentrations of C_8–C_{14} (12.5 times the CMC), there was no difference in the amount of protein released in the presence of the individual alkyl sulfates. The effect appears to be due to the micellar phase of the alkyl sulfate solutions. Other studies on salicylate transfer across the everted rat small intestine indicate that permeability changes occur with anionic and cationic surfactants but not with nonionics.

Keyphrases □ Sodium alkyl sulfates—effect on release of protein from everted rat small intestine □ Membranes, biological—everted rat small intestine, effect of sodium alkyl sulfates on release of protein □ Surfactants—sodium alkyl sulfates, effect on release of protein from everted rat small intestine □ Structure–activity relationships—sodium alkyl sulfates, effect on release of protein from everted rat small intestine

A previous report (1) indicated that sodium taurodeoxycholate, a physiological surface-active agent, accelerates the release of total phosphorus, lipid phosphorus, and protein from the everted rat small intestine. The results indicate that the interaction of the surfactant with the biological membrane accelerates the loss of structural integrity of the preparation and increases membrane permeability. The increase in membrane permeability to phenolsulfonphthalein could be correlated to the increased release of the membrane component in the presence of the physiological surface-active agent.

In view of these findings, it was of interest to examine the effect of a homologous series of anionic surfactants on the everted rat small intestinal membrane to determine the effect of the chain length of the surfactant on the biological membrane. A series of sodium alkyl sulfates from C_6 to C_{14} was chosen. The release of membrane protein was the membrane component investigated.

EXPERIMENTAL

Materials—Sodium hexyl sulfate (C_6), sodium octyl sulfate (C_8), sodium decyl sulfate (C_{10}), sodium lauryl (dodecyl) sulfate (C_{12}), and sodium tetradecyl sulfate (C_{14}) were certified as 99%+ pure by TLC analysis by the supplier[1] and were used as received. All other reagents were analytical grade and were used as received.

Modified Krebs bicarbonate buffer, pH 7.4, with no potassium dihydrogen phosphate included, was prepared as described previously (1). In all cases, the sodium-ion concentration was adjusted to 150 m*M* by the proper addition or omission of sodium chloride.

Preparation of Everted Rat Small Intestinal Sacs—Male, Sprague–Dawley-descent rats[2], 250–350 g, were fasted for 20–24 hr (water allowed *ad libitum*) and then anesthetized with ether. The sacs were prepared as described previously (1). Four consecutive 5-cm segments filled with 1 ml of buffer at pH 7.4 were incubated in a mucosal solution at 37°. The mucosal solution, consisting of 20 ml of buffer alone or buffer with various concentrations of the sodium alkyl sulfates, was oxygenated continuously with a mixture of 95% oxygen–5% carbon dioxide. One-milliliter samples were taken at 30-min intervals for 2 hr.

Protein Determinations—Protein concentrations were determined using the method of Lowry *et al.* (2). The solutions were read[3] at 750 nm against an appropriate blank. The amount of protein in the mucosal samples was calculated as bovine serum albumin equivalents.

Critical Micelle Concentrations (CMC)—The CMC's of the alkyl sulfates were determined by a method (3) based upon spectral changes of a dye in the presence of surfactant micelles. Solutions of each surfactant were prepared in modified Krebs bicarbonate buffer

[1] Schwarz/Mann, Orangeburg, N.Y.

[2] Huntingdon Farms, West Conshohocken, Pa.

[3] Spectronic 20, Bausch & Lomb.

creted 23.9% after the oral dose. Thus, based on urinary excretion of total radioactivity in dogs, it appears that only 50–60% of furosemide is absorbed from an oral solution.

The plasma and tissue levels and the pharmacokinetic parameters of furosemide in dogs and monkeys following 5-mg/kg oral and intravenous doses will be described in a subsequent paper. These data in dogs confirm the lack of complete bioavailability of furosemide from an oral solution dosage form. Less than 1% of radioactivity in the plasma of dog and monkey is attributable to metabolites.

REFERENCES

(1) P. Deetjen, *Ann. N.Y. Acad. Sci.*, **139**, 408(1966).

(2) A. Haussler and P. Hajdu, *Arzneim.-Forsch.*, **14**, 710(1964).

(3) S. Seno, S. M. Shaw, and J. E. Christian, *J. Pharm. Sci.*, **58**, 935(1969).

(4) G. J. Yakatan and M. M. Tuckerman, *ibid.*, **55**, 532(1966).

(5) H. A. E. Schmidt, "Tierversuche mit ^{35}S-markierten Lasix," International Furosemide Symposium, Bad Homburg, Germany, 1963.

ACKNOWLEDGMENTS AND ADDRESSES

Received August 18, 1975, from the *Drug Dynamics Institute, College of Pharmacy, University of Texas at Austin, Austin, TX 78712*

Accepted for publication December 8, 1975.

Presented in part at the Basic Pharmaceutics Section, APhA Academy of Pharmaceutical Sciences, San Francisco meeting, April 1975.

The authors thank Miss Winifred Ball, Mr. Guy Foster, and Miss Janet Gamble for technical assistance. They also gratefully acknowledge support of this work by grants from Hoechst-Roussel Pharmaceuticals, Inc., and the American Heart Association, Texas Affiliate, Inc.

* Hoechst-Roussel Pharmaceuticals, Inc., Somerville, NJ 08876

[x] To whom inquiries should be directed.

Interaction of Sodium Alkyl Sulfates with Everted Rat Small Intestinal Membrane

STUART FELDMAN [x] and MARK REINHARD

Abstract □ The effect of sodium alkyl sulfates (C_6–C_{14}) on the loss of protein from the everted rat small intestine was measured. At a surfactant concentration of 10 m*M*, a peak effect on protein release was noted with sodium decyl sulfate (C_{10}). Measurement of protein release as a function of sodium lauryl sulfate (C_{12}) concentration resulted in the observation that the effect appears to be due to the micellar phase of the surfactant solution. At concentrations of C_{12} above the CMC, the loss of protein from the intestinal preparation increased as the concentration of surfactant was increased. There may be a maximum amount of protein that can be released from the everted rat small intestinal sacs by surface-active agents. At equivalent micellar concentrations of C_8–C_{14} (12.5 times the CMC), there was no difference in the amount of protein released in the presence of the individual alkyl sulfates. The effect appears to be due to the micellar phase of the alkyl sulfate solutions. Other studies on salicylate transfer across the everted rat small intestine indicate that permeability changes occur with anionic and cationic surfactants but not with nonionics.

Keyphrases □ Sodium alkyl sulfates—effect on release of protein from everted rat small intestine □ Membranes, biological—everted rat small intestine, effect of sodium alkyl sulfates on release of protein □ Surfactants—sodium alkyl sulfates, effect on release of protein from everted rat small intestine □ Structure–activity relationships—sodium alkyl sulfates, effect on release of protein from everted rat small intestine

A previous report (1) indicated that sodium taurodeoxycholate, a physiological surface-active agent, accelerates the release of total phosphorus, lipid phosphorus, and protein from the everted rat small intestine. The results indicate that the interaction of the surfactant with the biological membrane accelerates the loss of structural integrity of the preparation and increases membrane permeability. The increase in membrane permeability to phenolsulfonphthalein could be correlated to the increased release of the membrane component in the presence of the physiological surface-active agent.

In view of these findings, it was of interest to examine the effect of a homologous series of anionic surfactants on the everted rat small intestinal membrane to determine the effect of the chain length of the surfactant on the biological membrane. A series of sodium alkyl sulfates from C_6 to C_{14} was chosen. The release of membrane protein was the membrane component investigated.

EXPERIMENTAL

Materials—Sodium hexyl sulfate (C_6), sodium octyl sulfate (C_8), sodium decyl sulfate (C_{10}), sodium lauryl (dodecyl) sulfate (C_{12}), and sodium tetradecyl sulfate (C_{14}) were certified as 99%+ pure by TLC analysis by the supplier[1] and were used as received. All other reagents were analytical grade and were used as received.

Modified Krebs bicarbonate buffer, pH 7.4, with no potassium dihydrogen phosphate included, was prepared as described previously (1). In all cases, the sodium-ion concentration was adjusted to 150 m*M* by the proper addition or omission of sodium chloride.

Preparation of Everted Rat Small Intestinal Sacs—Male, Sprague–Dawley-descent rats[2], 250–350 g, were fasted for 20–24 hr (water allowed *ad libitum*) and then anesthetized with ether. The sacs were prepared as described previously (1). Four consecutive 5-cm segments filled with 1 ml of buffer at pH 7.4 were incubated in a mucosal solution at 37°. The mucosal solution, consisting of 20 ml of buffer alone or buffer with various concentrations of the sodium alkyl sulfates, was oxygenated continuously with a mixture of 95% oxygen–5% carbon dioxide. One-milliliter samples were taken at 30-min intervals for 2 hr.

Protein Determinations—Protein concentrations were determined using the method of Lowry *et al.* (2). The solutions were read[3] at 750 nm against an appropriate blank. The amount of protein in the mucosal samples was calculated as bovine serum albumin equivalents.

Critical Micelle Concentrations (CMC)—The CMC's of the alkyl sulfates were determined by a method (3) based upon spectral changes of a dye in the presence of surfactant micelles. Solutions of each surfactant were prepared in modified Krebs bicarbonate buffer

[1] Schwarz/Mann, Orangeburg, N.Y.

[2] Huntingdon Farms, West Conshohocken, Pa.

[3] Spectronic 20, Bausch & Lomb.

Table I—Protein Release from Everted Rat Small Intestinal Sacs as a Function of Time and 10 m*M* Concentration of Sodium Alkyl Sulfates

Solution	Numbers of Sacs	Protein, mg[a] 30 min	60 min	90 min	120 min
Buffer	13	2.30 ± 0.69	3.04 ± 0.74	3.87 ± 0.59	4.93 ± 0.57
C_6	4	1.80 ± 0.25	2.28 ± 0.13	2.61 ± 0.13	3.40 ± 0.36
C_8	4	2.70 ± 0.24	3.61 ± 0.58	4.41 ± 0.29	5.10 ± 0.32
C_{10}	8	6.30 ± 0.61	10.1 ± 0.62	11.7 ± 0.81	12.4 ± 0.60
C_{12}	12	5.20 ± 0.63	8.46 ± 0.58	10.6 ± 0.77	11.5 ± 0.96
C_{14}	8	5.30 ± 0.91	7.60 ± 0.75	10.1 ± 0.77	11.5 ± 0.90

[a] Mean ± *SD*. Calculated as bovine serum albumin equivalents.

containing 0.0005% rhodamine 6G[4]. The solutions were maintained at 37° and were diluted at a constant dye concentration until the orange fluorescent color changed to red and the fluorescence almost disappeared. This end-point was taken as the CMC of the surfactant.

Salicylate Transfer across Everted Rat Small Intestine—Everted rat small intestinal segments, 10 cm in length, were prepared as described by Feldman and Gibaldi (4). The segments were suspended for 1 hr in 80 ml of modified Krebs bicarbonate buffer containing either sodium lauryl sulfate (10 or 50 m*M*), cetrimonium bromide (4 m*M*), polysorbate 80 (1% w/v), or poloxamer 188[5] (1%). Control segments were suspended in buffer for 1 hr.

After incubation, the segments were rinsed on both mucosal and serosal sides and then placed in 80 ml of modified Krebs buffer containing 2 mg of salicylate/ml. Modified Krebs bicarbonate buffer served as the serosal fluid. Serosal samples were withdrawn at appropriate intervals as described previously (4) and assayed for salicylic acid content according to the method of Trinder (5).

RESULTS AND DISCUSSION

The effect of 10 m*M* concentrations of sodium alkyl sulfates on the release of protein from everted rat small intestinal sacs is presented in Table I. At 30, 60, 90, and 120 min after incubation, there was an increase in the amount of protein present in the mucosal solutions. As indicated in Table I, the amount of protein at 120 min after incubation apparently reached a maximum with sodium decyl sulfate.

Figure 1 shows a plot of the ratio of the amount of protein released at 60 and 120 min after incubation in the surfactant solution to that of buffer controls *versus* the number of carbon atoms in the alkyl chain. At the 10 m*M* concentration of surfactant, the maximum ratio occurred at C_{10}. A 10 m*M* solution of sodium hexyl sulfate appeared to offer protection against the deterioration of the membrane because there was an approximate 30% reduction in the amount of protein released. The reason for this apparent stabilization of the intestinal membrane by sodium hexyl sulfate needs further evaluation.

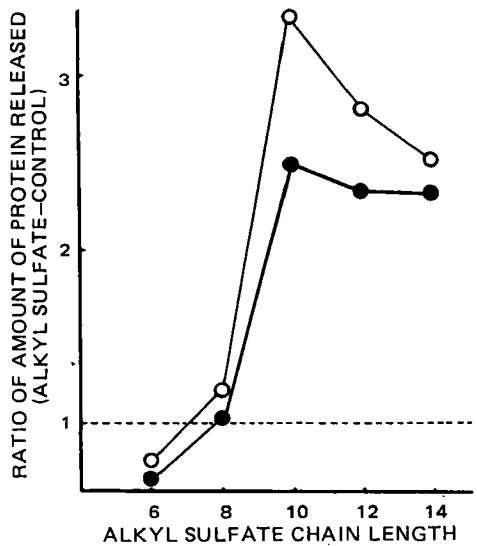

Figure 1—*Plot of the ratio of the amount of protein released in alkyl sulfate solutions to that of controls* versus *alkyl sulfate carbon atom chain length at 60 (○) and 120 (●) min after incubation.*

To investigate the effect of surfactant concentration on the efflux of membrane protein, various concentrations of sodium lauryl sulfate were incorporated into the mucosal solution. The results from this experiment, utilizing surfactant concentrations of 0, 1, 5, 7.5, 10, and 20 m*M*, are presented in Fig. 2. This figure is a plot of the amount of protein in the mucosal solution at 120 min postincubation *versus* surfactant concentration. The results indicate that a relationship exists between surfactant concentration and release of protein from the membrane. With increasing concentrations of surfactant, there was an increase in the amount of protein present in the mucosal fluid.

Inspection of Fig. 2 reveals several interesting features. For example, the largest increase in protein release for a change in surfactant concentration occurred between 0 and 1 m*M* sodium lauryl sulfate concentrations. The CMC of sodium lauryl sulfate in the present buffer system at 37° was 0.6 m*M*. Thus, the increase occurred at surfactant concentrations at or above the CMC. This finding is in agreement with previously reported data (1) on the effect of sodium taurodeoxycholate on the everted rat small intestinal membrane.

A second feature is the relationship of protein release to surfactant concentration at surfactant concentrations above the CMC. The dashed line in Fig. 2 assumes a linear relationship between protein efflux and surfactant concentration. There was an apparent linear relationship between 1 and 10 m*M* sodium lauryl sulfate concentrations, but the 20 m*M* concentration deviated from the extrapolated line. Rather than a linear relationship, the efflux of protein appeared to have asymptotically approached or reached a maximum value at 20 m*M* surfactant concentration. If one assumes that a finite amount of protein can be removed from the membrane by the surface-active agent, then the reaching of a maximum effect on protein loss from the intestinal sacs by the surface-active agent appears to be a reasonable consequence.

Inspection of the data in Table I indicates that approximately 12 mg of protein was released in 2 hr at 10 m*M* concentrations of sodium decyl sulfate, sodium lauryl sulfate, and sodium tetradecyl sulfate, which were at concentrations of 1.67, 16.7, and 83.3 times their CMC's, respectively. A 20 m*M* concentration of sodium lauryl sulfate resulted in approximately 13.5 mg of protein released in 2 hr. In a previous

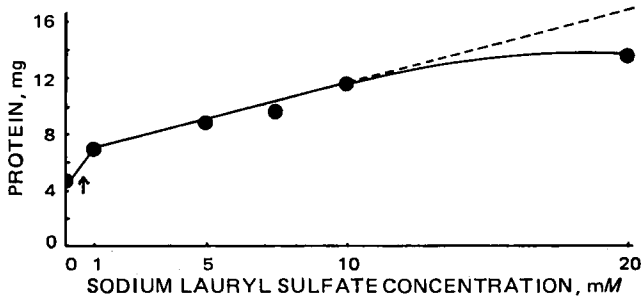

Figure 2—*Plot of the amount of protein released at 120 min after incubation* versus *concentration of sodium lauryl sulfate. See text for details.*

[4] K & K Laboratories, Plainview, N.Y.

[5] Ethylene oxide–propylene oxide polymer of average molecular weight 8350, obtained as Pluronic F-68, Wyandotte Chemicals Corp., Wyandotte, Mich.

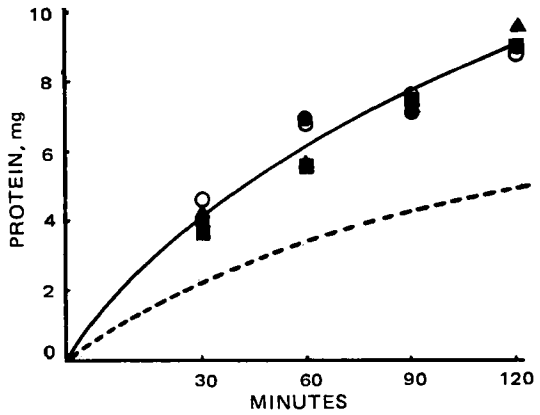

Figure 3—*Plot of the amount of protein released in various sodium alkyl sulfate solutions at a concentration 12.5 times their CMC values* versus *time. Key:* O, C_8; ●, C_{10}; ▲, C_{12}; ■, C_{14}; *and* - - -, *control experiments.*

study (1), 5 and 10 m*M* sodium taurodeoxycholate resulted in approximately 12 mg of protein released in 2 hr. Thus, a limit may exist in the maximum amount of protein that can be released from the small intestinal sacs in the presence of the surfactants.

In view of the apparent effect of concentration of sodium alkyl sulfate on the release of protein from the everted rat small intestinal sacs, the effect of equivalent micelle concentration was investigated. To measure this effect, a 12.5-fold multiple of the CMC's of the C_8–C_{14} surfactants was chosen. Sodium hexyl sulfate does not form micelles. At a constant multiple of the CMC, there should be approximately the same number of surfactant micelles present, assuming equivalent aggregation numbers.

The CMC's of the sodium alkyl sulfates at 37°, as determined in the present investigation, were 41.0, 6.0, 0.6, and 0.12 mmoles/liter for the octyl, decyl, lauryl, and tetradecyl sulfates, respectively. The results from this experiment appear in Fig. 3. Control values are included for reference. The results show that the rate of release of protein from the intestinal membrane was essentially identical for each alkyl sulfate and support the hypothesis that the micelle is responsible for the alteration in membrane structure and, thereby, its permeability.

For example, a 10 m*M* concentration of sodium octyl sulfate, which is below its CMC of 41 m*M*, produced an efflux of protein which, at 120 min, was equal in amount to the protein released in control experiments. However, at a concentration of C_8 of 12.5 times the CMC, there was a 1.83-fold increase in protein released in 120 min compared to control values. The only deviation from this observation occurred with sodium decyl sulfate, where a maximum efflux of protein occurred at a surfactant concentration of 1.7 times its CMC and less of an effect was noted at 12.5 times the CMC.

The present study utilizing anionic surfactants leads to a consideration of the effect of cationic and nonionic surfactants on membrane permeability and integrity. Reports in the literature (6) indicate that anionic and cationic surfactants alter the permeability of the GI membranes while nonionic surfactants do not. Because of cationic and nonionic surfactant interference with the protein assay, the effect of the type of surfactant on the transfer of salicylate across the everted rat small intestine was investigated.

The effect of sodium lauryl sulfate, polysorbate 80, poloxamer 188, and cetrimonium bromide on the transfer of salicylate across the everted intestinal preparation was examined (Table II). There were large increases in salicylate transfer after exposure of the intestinal segments to micellar concentrations of the anionic (sodium lauryl sulfate) and cationic (cetrimonium bromide) surfactants, but no increase was noted after the intestinal segments were exposed to micellar concentrations of two nonionic surfactants (polysorbate 80 and poloxamer 188).

Of interest is the observation (Table II) that, with both sodium lauryl sulfate and cetrimonium bromide, a maximum effect appeared to have been reached in the permeability of the everted intestinal preparation to salicylate. For example, 50 m*M* sodium lauryl sulfate resulted in an increase in salicylate transfer equivalent to the increase noted after exposure of the intestine to 4 m*M* cetrimonium bromide. Both these concentrations are far above their respective CMC's. If 13.5 mg/5 cm represents the maximum amount of protein that can be removed from the intestinal segments by a surface-active agent and if this amount results in a maximum increase in membrane permeability, then 50 m*M* sodium lauryl sulfate should yield a maximum effect while 10 m*M* surfactant should yield a permeability increase slightly below the maximum. Although not statistically significant, the data in Table II support this trend. It should be noted that 10 m*M* sodium lauryl sulfate did not produce a maximum effect on protein loss from the intestinal sacs.

Table II—Percent Change in Salicylate Transfer across the Everted Rat Small Intestine after Preexposure of Segment to Micellar Concentrations of Surfactant

Surfactant	Concentration	Change over Control[a], %
Sodium lauryl sulfate	10 m*M*	+85
	50 m*M*	+95
Polysorbate 80	1%(w/v)	−4
Poloxamer 188	1%(w/v)	+6
Cetrimonium bromide	4 m*M*	+102

[a] Mean of four determinations.

A similar effect was seen between phenolsulfonphthalein transfer and sodium taurodeoxycholate concentration in a previous study (1). In this study, 5 m*M* sodium taurodeoxycholate produced an efflux of 11.7 mg of protein and a 79% increase in phenolsulfonphthalein transfer in 2 hr, while 10 m*M* surfactant produced a protein release of 12.1 mg and a 94% increase in phenolsulfonphthalein transfer.

Based upon previous findings (1) and results of the present study, it appears that the alterations in membrane permeability in the presence of surface-active agents are due to the micellar phase of the surfactant solution as well as the charge on the surfactant molecule. It also appears that a maximum effect of the surfactant on membrane permeability may be achieved, and this maximum may be related to the amount of protein that can be removed from the intestinal segments by the micellar solutions of surface-active agents.

REFERENCES

(1) S. Feldman, M. Reinhard, and C. Willson, *J. Pharm. Sci.*, **62**, 1961(1973).

(2) O. H. Lowry, N. J. Rosenbrough, A. L. Farr, and R. J. Randall, *J. Biol. Chem.*, **193**, 265(1951).

(3) M. L. Corrin and W. D. Harkins, *J. Am. Chem. Soc.*, **69**, 679(1947).

(4) S. Feldman and M. Gibaldi, *J. Pharm. Sci.*, **58**, 425(1969).

(5) P. Trinder, *Biochem. J.*, **57**, 301(1954).

(6) M. Gibaldi and S. Feldman, *J. Pharm. Sci.*, **59**, 579(1970).

ACKNOWLEDGMENTS AND ADDRESSES

Received January 19, 1975, from the *Department of Pharmaceutics, College of Pharmacy, University of Houston, Houston, TX 77004*

Accepted for publication December 8, 1975.

Supported in part by a Grant-in-Aid of Research from Temple University.

Part of this work was conducted while S. Feldman was at Temple University School of Pharmacy. The author wishes to acknowledge the support given by that institution. The assistance given by Temple University undergraduate research project students Delores Dobler and Andrew Cuttone is gratefully acknowledged.

[x] To whom inquiries should be directed.

Automated Fluorometric Analysis of Epinephrine in Lidocaine Hydrochloride Injection

H. TARLIN ˣ, M. HUDSON, and M. SAHN *

Abstract □ A rapid automated method for determining epinephrine in lidocaine hydrochloride injection is presented. The method is an adaptation of the official USP XIX fluorometric procedure and yields equivalent results. The linearity, accuracy, precision, excipient/background effect, and carryover characteristics of the automated system are described. A recovery study indicated that intact epinephrine is measured accurately in the presence of its degradation products. Analysis of several commercial preparations is reported.

Keyphrases □ Epinephrine—automated fluorometric analysis in lidocaine hydrochloride injection □ Fluorometry—analysis, automated, epinephrine in lidocaine hydrochloride injection □ Automated analysis, fluorometric—epinephrine in lidocaine hydrochloride injection □ Lidocaine hydrochloride—injection solution, automated fluorometric analysis of epinephrine content □ Adrenergic agents—epinephrine, automated fluorometric analysis in lidocaine hydrochloride injection

The USP XIX (1) method for assaying epinephrine in lidocaine hydrochloride injection is a costly, time-consuming procedure, particularly when used to analyze large numbers of solutions. A heating step, requiring approximately 30 min, is followed by the addition of a buffer and oxidizing agent and two accurately timed operations.

In the automated system, sodium metabisulfite, which interferes with the oxidation of epinephrine (2, 3), is destroyed at 90° in a flow-through heating bath. The automated system eliminates the errors associated with accurate timing of the addition of reagents and transferring and diluting solutions and has an analysis rate of 30 samples/hr.

EXPERIMENTAL[1]

Reagents—All reagents were ACS or USP grade. Standard epinephrine solutions were prepared from USP epinephrine bitartrate reference standard. The standard solution used with the automated system consists of 10 μg of epinephrine/ml, 0.5 mg of sodium metabisulfite/ml, and 20 mg of lidocaine hydrochloride/ml.

All reagents for the manual procedure are prepared as directed in USP XIX (1). The reagents for the automated procedure are prepared as follows.

Distilled Water—Water distilled from glass was used.

Diluent Water—Add 1.0 ml of wetting agent[2] to 1 liter of distilled water and mix thoroughly.

Hydrochloric Acid, 0.5%—Add 5.0 ml of concentrated hydrochloric acid to approximately 800 ml of distilled water. Add 1.0 ml of wetting agent, dilute to 1 liter with distilled water, and mix thoroughly.

Sodium Acetate, 2%—Dissolve 20 g of sodium acetate in approximately 800 ml of distilled water. Dilute to 1 liter with distilled water and mix thoroughly.

Potassium Ferricyanide, Stock—Dissolve 6.3 g of potassium ferricyanide in approximately 800 ml of distilled water. Dilute to 1 liter with distilled water and mix thoroughly. This reagent should be made *fresh weekly*.

Potassium Ferricyanide, Working—Pipet 1.0 ml of stock potassium ferricyanide into a 100-ml volumetric flask. Dilute to volume with distilled water and mix thoroughly. This reagent should be made *fresh daily*.

Ascorbic Acid, Stock—Dissolve 1.0 g of ascorbic acid in approximately 80 ml of distilled water. Dilute to 100 ml with distilled water and mix thoroughly. This reagent should be made *fresh weekly* and kept *refrigerated*.

Ascorbic Acid, Working—Pipet 1.0 ml of stock ascorbic acid into a 100-ml volumetric flask. Dilute to volume with distilled water and mix thoroughly. This reagent should be made *fresh daily* and kept in an ice bath.

Sodium Hydroxide, 15%—Dissolve 150 g of sodium hydroxide in approximately 800 ml of distilled water. After cooling, dilute to 1 liter with distilled water and mix thoroughly.

All reagents should be in glass containers.

Manual Fluorometric Method—Follow the procedure in USP XIX (1).

Automated Fluorometric Method—A flow diagram of the automated system appears in Fig. 1. Add lidocaine hydrochloride injection, containing 2–14 μg of epinephrine/ml, to the sampling cup. Place the 10-μg/ml epinephrine standard solution in sample cups 1, 10, 20, 30, 38, 39, and 40 and optimize the fluoronephelometer using the instruction manual provided with the instrument[3]. Check for proper bubble patterns and heating bath temperature (90°).

Set the instrument baseline as soon as the reagents reach the detector. Set the recorder to a fluorescence intensity of 50 when the 10-μg/ml epinephrine standard reaches the detector. Calculate as follows:

$$\mu g \text{ of epinephrine/ml of injection solution} = \frac{\mu g \text{ of epinephrine/ml in standard}}{\text{average fluorescence intensity of standards}} \times \text{fluorescence intensity of sample} \quad \text{(Eq. 1)}$$

Standard Curve—Standards containing 2, 6, 10, 14, and 18 μg of epinephrine/ml were prepared and assayed on the automated system.

Accuracy—Standards containing variable amounts of epinephrine were prepared and analyzed over 1 year by the automated and USP XIX (1) procedures.

Precision—Thirty-nine replicate samples of a 10-μg/ml epinephrine standard were analyzed on the automated system.

Excipient/Background Effect—Solutions were prepared containing 20 mg of lidocaine hydrochloride/ml, 10 μg of epinephrine/ml, and the labeled amount of excipients found in commercial preparations of lidocaine hydrochloride injection[4]. For each solution analyzed, the concentration of one excipient was varied between zero and two or four times the labeled concentration. Solutions were also prepared in which the lidocaine hydrochloride was varied from 0 to 50 mg/ml.

Carryover—Standards containing 2, 10, and 18 μg of epinephrine/ml were prepared and analyzed in specific sample sequence to determine if there was any epinephrine carryover between samples.

Recovery of Epinephrine in Presence of Degradation Products—Varying amounts of a 50-μg/ml standard epinephrine solution were added to 20-ml aliquots of a commercial preparation of lidocaine hydrochloride in which 42% of the epinephrine was degraded. The samples were analyzed on the automated system.

[1] The automated analytical system consisted of the following Technicon (Technicon Industrial Systems, Tarrytown, N.Y.) equipment: liquid sampler IV; proportioning pump III; fluoronephelometer III fitted with an 85-w mercury lamp, a Pyrex (Corning) 2-mm i.d. flowcell, and a 420-nm primary and 520-nm secondary filter; and autoanalyzer II recorder with a chart speed of 155 cm/hr. The equipment used for the manual procedure consisted of an Aminco SPF-125 spectrophotofluorometer (American Instrument Co., Silver Spring, Md.).

[2] Brij-35, Atlas Chemical Industries, Wilmington, Del.

[3] See Technicon Publication No. TA1-0220-10, rev. July 1972.

[4] A typical formulation consists of the following excipients: 6 mg of sodium chloride/ml, 0.5 mg of sodium metabisulfite/ml, and 1.0 mg of methylparaben/ml.

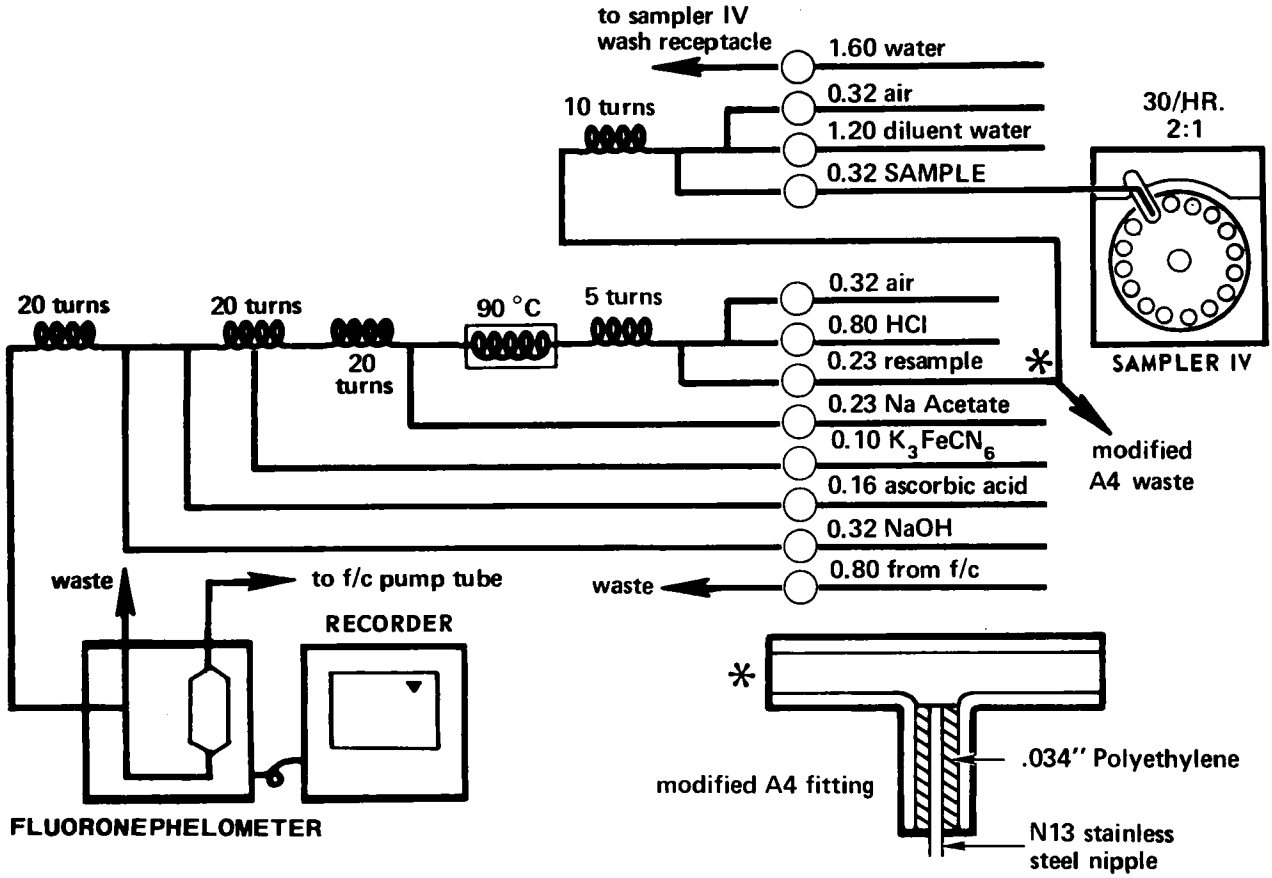

Figure 1—*Flow diagram for the automated fluorometric analysis of epinephrine. Pump tubing is given with the flow rate in milliliters per minute. All tubing is standard Tygon except on the top of the flowcell (f/c), which is 0.2-cm (0.090-in.) i.d. Acidflex.*

Analysis of Commercial Preparations—Several commercial preparations of lidocaine hydrochloride were analyzed by the automated and USP XIX (1) procedures.

RESULTS

Standard Curve—A plot of epinephrine concentration *versus* fluorescence intensity indicates that the fluorescence is linear in the concentration range of 2–18 μg of epinephrine/ml.

Table I—Recovery of Epinephrine: Comparison of Automated and Manual Procedures

Epinephrine, μg/ml		
Theoretical	Recovered by Automated Procedure[a]	Recovery by USP XIX Procedure[b]
4.0	3.9	4.0
4.5	4.4	4.6
5.0	5.0	5.0
5.4	5.5	5.4
5.5	5.3	5.5
5.6	5.5	5.7
5.8	5.6	5.7
5.8	5.6	5.9
8.0	8.1	8.0
10.0	9.9	10.0
10.0	9.9	9.9
11.0	11.2	11.1
11.0	10.9	10.9
11.0	10.9	11.0
11.0	11.2	11.1
12.0	12.1	12.2
17.0	17.0	17.2

[a] Each assay value is an average of two analyses. [b] Each value is based on one assay.

Accuracy—Table I is a summary of the recovery of epinephrine by the automated and USP XIX (1) procedures. Neither procedure yielded results that varied by more than 0.2 μg of epinephrine/ml from the theoretical concentration. The difference between the two methods never exceeded 0.3 μg/ml; the average difference was 0.12 μg/ml.

Precision—Table II shows the frequency distribution of 39 replicate samples containing 10 μg of epinephrine/ml. The average epinephrine recovery was 9.9 μg/ml ± 0.10 (*SD*), and the recovery range was 9.7–10 μg/ml.

Excipient/Background Effect—None of the excipients studied interfered with the automated epinephrine assay procedure (Table III). The fluorescence intensity was suppressed in the absence of lidocaine hydrochloride but was constant in the presence of 5–50 mg of lidocaine hydrochloride/ml.

Carryover—Table IV shows the sample sequence used to determine the effect of the samples upon one another. The fluorescence intensity of the samples indicated that the system was free from intersample carryover.

Recovery of Epinephrine in Presence of Degradation Products—Table V illustrates that intact epinephrine was recovered in the presence of epinephrine degradation products.

Analysis of Commercial Samples—Table VI is a summary of the

Table II—Automated Analysis of 39 Samples Containing 10 μg of Epinephrine/ml

	Concentration of Recovered Epinephrine, μg/ml	Frequency
	10.0	14
	9.9	9
	9.8	14
	9.7	2
Average	9.9	
Range	9.7–10.0	
SD	±0.10	

Table III—Effect of Excipients and Lidocaine Hydrochloride Concentration on Fluorescence Intensity

Compound	Concentration, mg/ml	Fluorescence Intensity[a]
Sodium metabisulfite	0.0	51, 49.5
	0.5	50.5, 50
	0.6	50.5, 50
	1.0	51, 50
	1.5	50, 49.5
	2.0	49.5, 50
Sodium chloride	0.0	51, 50
	4.0	49.5, 50
	8.0	50.5, 50
	12.0	49.5, 49
Methylparaben	0.0	50, 50.5
	1.0	49, 49.5
	2.0	50, 50
Lidocaine hydrochloride	0.0	47.5, 41
	5.0	50, 50
	10.0	51, 50.5
	20.0	51, 51
	30.0	50, 50
	40.0	50, 50
	50.0	50.5, 50.5

[a] Fluorescence intensity is for duplicate samples.

analysis of several commercial samples of lidocaine hydrochloride. The differences between the automated and USP XIX (1) methods never exceeded 0.3 μg of epinephrine/ml; the average difference was 0.18 μg of epinephrine/ml.

DISCUSSION

An accurate and precise direct method for automatically analyzing epinephrine in the presence of common excipients found in lidocaine hydrochloride injection is presented. *Both* the automated and USP XIX (1) fluorometric assay procedures yield equivalent results, since a paired t test applied to the data from Tables I and VI yielded a calculated t value of 1.430 at 28 degrees of freedom. A t value of 2.048 is required to indicate a difference between the methods at a 95% confidence level. Since fluorescence intensity is suppressed in the absence of lidocaine hydrochloride, it is essential that lidocaine hydrochloride be present in the standard.

Approximately 200 samples containing up to 14 μg of epinephrine/ml may be assayed directly in 8 hr. Samples containing more than 14 μg of epinephrine/ml may be diluted to between 2 and 14 μg of epinephrine/ml and then quantitated.

Table IV—Carryover Study: Determination of Intersample Effects

Sample[a]	Fluorescence Intensity
AAA	50, 50.5, 50.5
CCC	10, 10, 10
BBB	93.5, 94, 93.5
AAA	51, 51, 50.5
BBB	93.5, 94, 93.5
CCC	10, 10, 10
AAA	50.5, 50.5, 51
BCB	93.5, 10, 93.5
CBC	10, 93, 10
AAA	50, 50, 50
CBA	10, 93, 50
ABC	50, 92, 9.5
BBAA	92, 92.5, 49.5, 49.5

[a] Samples are shown in the order that they were assayed. Epinephrine concentrations were: A, 10 μg/ml; B, 18 μg/ml; and C, 2 μg/ml.

Table V—Recovery of Epinephrine in the Presence of Degradation Products

Total Epinephrine, μg		Total Volume of Solution Assayed, ml	Epinephrine, μg/ml	
Degraded Solution	Standard Solution		Theoretical	Recovered[a]
130	25	20.5	7.6	7.4
130	50	21	8.6	8.4
130	100	22	10.5	10.5
130	150	23	12.2	12.2

[a] Each result is an average of five determinations.

Table VI—Assay of Commercial Preparations by Automated and Manual Procedures

Dilution Range	Recovered Epinephrine, μg/ml	
	Automated[a]	Manual[b]
1:100,000	10.9	10.6
	11.0	10.8
	10.5	10.6
	10.5	10.6
	10.0	10.3
	11.0	10.7
	11.2	11.3
1:200,000	5.0	5.2
	5.0	5.2
	5.4	5.4
	5.2	5.0
	5.2	5.0

[a] Each assay value is an average of two analyses. [b] Each value is based on one analysis.

REFERENCES

(1) "The United States Pharmacopeia," 19th rev., Mack Publishing Co., Easton, Pa., 1975, p. 284.

(2) T. Canbäck and J. G. L. Harthon, *J. Pharm. Pharmacol.*, **11**, 764(1959).

(3) H. Hellberg, *Sven. Farm. Tidskr.*, **18**, 493(1960).

ACKNOWLEDGMENTS AND ADDRESSES

Received June 18, 1975, from the *Analytical Laboratory, Astra Pharmaceutical Products, Inc., Worcester, MA 01606*

Accepted for publication December 8, 1975.

The authors express their appreciation to Mr. William Webber, Dr. S. G. Davis, and Ms. Sheila Williams Tarlin for reviewing this manuscript.

* Present address: Technicon Industrial Systems, Tarrytown, NY 10591

ˣ To whom inquiries should be directed.

Stabilized Compressed Nitroglycerin Tablets

F. W. GOODHART ˣ, H. GUCLUYILDIZ, R. E. DALY, L. CHAFETZ, and F. C. NINGER

Abstract □ A stabilized compressed nitroglycerin tablet, containing microcrystalline cellulose NF and povidone NF as stabilizing agents, was formulated. Bioavailability and physical tests were conducted on the compressed tablet and two leading brands of molded tablets. There was no difference in the mean pulse rate between a molded tablet formulation and the compressed tablet in a crossover study using 10 human volunteers and three tablet strengths, 0.3, 0.4, and 0.6 mg. The compressed tablet was most uniform when tested according to the USP method for weight variation and content uniformity. Various tests for nitroglycerin loss due to volatility, *i.e.*, open dish test, thermogravimetric analysis, and a simulated in-use test, all indicated that the stabilized compressed tablet was substantially more stable than partially stabilized or unstabilized molded tablets.

Keyphrases □ Nitroglycerin—bioavailability and stability, stabilized compressed tablet compared to commercial products □ Bioavailability—nitroglycerin, stabilized compressed tablet compared to commercial products □ Stability—nitroglycerin, stabilized compressed tablet compared to commercial products □ Dosage forms—stabilized compressed nitroglycerin tablets prepared, bioavailability and stability compared to commercial products □ Tablets—stabilized compressed nitroglycerin tablets prepared, bioavailability and stability compared to commercial products □ Vasodilators, coronary—nitroglycerin, bioavailability and stability, stabilized compressed tablet compared to commercial products

Nitroglycerin, in spite of its association with a bygone era, is well recognized today as a safe and effective drug for treatment of angina pectoris. Perhaps its historical significance is that it is one of the few tablets still being manufactured as a tablet triturate. Other types of tablet triturates such as dispensing tablets and hypodermic tablets are rapidly becoming less important than they were. The drugs previously used in the hypodermic tablet form are now available as single- or multiple-dose injectable products or have been replaced by newer synthetic drugs, and the dispensing tablet form is needed less frequently because fewer prescriptions are now compounded.

However, the particular attribute of nitroglycerin tablets to disintegrate rapidly has only been obtainable thus far by manufacturing them as tablet triturates. In spite of some inherent problems in the physical stability aspects of nitroglycerin, the molded tablet method has not been satisfactorily replaced by the modern method of tablet manufacture, *i.e.*, compression.

BACKGROUND

Molded tablet manufacture has several definite disadvantages, especially for nitroglycerin, a liquid substance at room temperature whose vapor pressure is small but large enough to cause loss from conventional tablets, particularly if they are improperly stored. Molded nitroglycerin tablets are usually manufactured by mixing a lactose–nitroglycerin trituration and sucrose with a hydroalcoholic solution. After thorough wetting and mixing, the damp mass is forced into a perforated plate to form individual tablets. This process is now generally done by an automatic tablet triturate machine.

After a short time in the mold, the tablets are ejected by pegs onto a conveyor belt. The conveyor belt usually carries the tablets through a drying tunnel, which substantially removes the residual water and alcohol. The high solubility of nitroglycerin in ethanol (about 1 in 4) causes nitroglycerin to migrate to the outer tablet surface during the drying step. This concentration of nitroglycerin near the tablet surface enhances its ability to escape into the surrounding air. A study of the preparation of warfarin sodium tablets by wet granulation demonstrated unsatisfactory tablet content uniformity due to the migration of the drug during drying (1). However, the use of alginic acid in the formulation inhibited migration and gave satisfactory content uniformity.

Recent formulation improvements to inhibit nitroglycerin migration in molded tablets have increased the stability of the products of the two leading manufacturers. In Product A[1] nitroglycerin tablets, polyethylene glycol 400 is added to deter nitroglycerin migration and volatility (2). In Product B[2] nitroglycerin tablets, a small amount of stabilizer[3] (3) is added to improve stability.

The loss of nitroglycerin from tablets due to volatilization and the factors affecting such a loss were reported previously (4–8). The specific stabilizing effect of microcrystalline cellulose was first reported by Richman *et al.* (4). While older literature alluded to a loss of potency in nitroglycerin tablet formulations, the scope of the problem was not realized until a satisfactory single-tablet assay method was developed (9). In this procedure, the interference of lactose with the diazotization reaction is eliminated by using strontium hydroxide as the alkalizing agent. By this means, individual tablets were assayed accurately. A further adaptation of this procedure to the automated analyzer permitted the assay of large numbers of individual tablets, 30/hr (7), thus giving researchers the methodology for studying various factors affecting nitroglycerin stability.

Reports of nitroglycerin instability have involved several main areas concerned with packaging and storage aspects of the tablets: (*a*) the particular container employed, glass or plastic; (*b*) the type of closure used, including the cap-lining material; and (*c*) the stuffing material used in the containers.

Nitroglycerin tablets packaged in polyethylene blisters with aluminum foil backing contained only 0–10% of the labeled amount (10). However, nitroglycerin tablets were relatively stable when packaged in glass or high density polyethylene vials with screw caps but not in polystyrene, polyvinyl chloride, or polypropylene vials (5). The effect of fillers on the retention of nitroglycerin in tablets of two leading manufacturers also was reported (6). Rayon packing absorbed less nitroglycerin from commercial packages than did absorbent cotton, absorbent gauze, lamb's wool, and nonabsorbent cotton. The stabilized brand also absorbed less nitroglycerin than the nonstabilized brand.

Further studies on packaging components were carried out by Fusari (7), who noted that stuffing materials (cotton and rayon), as well as the material used in cap liners, affected the average tablet assays as well as the potency ranges. This report was the first to give data acquired by means of the automated analytic adaptation of the Bell (9) assay method. Therefore, a wide variation in the content of nitroglycerin in tablets was reported for many combinations of packaging components and storage conditions.

A typical lot of fresh 0.4-mg nitroglycerin tablets reported in this study (7) had an initial content relative standard deviation in the area of 3–6%. These tablets were aged 1–14 months at room temperature; after reassay, 12 of 32 lots fell below the minimum 75% limit of the USP XVIII. During this time the relative standard deviation of nitroglycerin content increased and ranged from 6 to 17%. It was surprising to learn of these wide variations, which occurred even in glass bottles of 100 tablets with metal screw-on caps. A later report (8) compared two nitroglycerin tablet formulations, the previous conventional formulation and a partially stabilized one, demonstrating an improvement in intertablet dose variation for the stabilized form.

[1] Parke-Davis & Co.
[2] Eli Lilly Co.
[3] Determined in these laboratories to be povidone.

Investigations in these laboratories led to the development of a compressed nitroglycerin tablet formulation that matches the traditional excellent disintegration and bioactivity of molded tablets and has significantly improved stability aspects compared to the two leading brands, particularly under stress conditions.

EXPERIMENTAL

Tablet Manufacture—Compressed tablets[4] were made by a modified direct compression process. Two stabilizers were used in the formulation, microcrystalline cellulose[5] (NF XIII) and povidone[6] (NF XIII). Microcrystalline cellulose was mixed with anhydrous lactose (USP XVIII), starch (USP XVIII), and colorant and was granulated with a solution made by dissolving povidone in nitroglycerin spirit diluted with ethanol. The granulation was dried in a forced air oven at 30–35° and milled; a small amount of tablet lubricant, calcium stearate, was blended into the granulation.

Tablets were compressed on a high-speed rotary tablet machine, producing 2000–2500 tablets/min using 3.97-mm ($\frac{5}{32}$-in.) standard concave tools. Normal quality control procedures during compression included frequent weighing of groups of tablets as well as individual tablets. Compression weight was determined by obtaining an assay of the granulation and calculating the theoretical weight required to produce the labeled potency along with a small excess. Generally, compression weight was about 29.5–30.5 mg/tablet. An in-process control of tablet disintegration was periodically made; other processing controls of the finished tablets included tablet breaking strength and friability[7].

Granulation Assay—*Reagents*—Glacial acetic acid, stronger ammonia water, and phenoldisulfonic acid TS (USP XVIII) were used.

Potassium Nitrate Standard Solution—Transfer about 65 mg of potassium nitrate standard, accurately weighed, to a 200-ml volumetric flask containing 1.0 ml of distilled water, mix to dissolve completely, dilute to volume with glacial acetic acid, and mix.

Sample Solution—Transfer an accurately weighed amount of granulation, equivalent to 1 mg of nitroglycerin, to a glass-stoppered 50-ml conical flask. Pipet 5 ml of acetic acid into the flask, stopper, and shake mechanically with a wrist-action shaker for 1 hr. Filter.

Procedure—Pipet 1 ml of sample, standard, and glacial acetic acid into separate 25-ml volumetric flasks. Add to each 2.0 ml of phenoldisulfonic acid TS, mix, and let stand 15 min. Dilute with about 8 ml of distilled water, cool to room temperature, and cautiously add 10 ml of stronger ammonia water (watch for spattering, keep solution cool); then dilute to volume with distilled water.

Concomitantly determine the absorbances of the sample and the standard at 410 nm in 1-cm cells in a suitable spectrophotometer. Calculate according to:

$$\% \text{ nitroglycerin} = \frac{A_u}{A_s} \times \frac{5C}{2SW} \times 0.749 \qquad \text{(Eq. 1)}$$

where A_u and A_s are the absorbances of the sample and the standard, respectively; 0.749 is the factor for nitrate to nitroglycerin; C is the weight, in milligrams, of potassium nitrate taken; and SW is the sample weight, in milligrams.

Semiautomatic Content Uniformity Assay—*Equipment*—The automated system[8] consisted of a sampler[9], a proportioning pump[10], a water bath[11], and a colorimeter[12]. A strip-chart recorder[13] also was utilized.

Reagents—For the 1% strontium hydroxide reagent, add about 20 g of strontium hydroxide to a 2000-ml volumetric flask and then add about 1800 ml of distilled water. Heat to hasten solution. When saturated, cool and dilute to volume. This solution should be prepared the day before use to allow the precipitate of strontium carbonate to settle out.

For the 0.3% procaine hydrochloride reagent, dissolve about 3 g of procaine hydrochloride in 1 liter of distilled water. For the 2.5 *N* HCl reagent, dilute 210 ml of hydrochloric acid cautiously to 1 liter with distilled water. For the 0.025% *N*-(1-naphthyl)ethylenediamine dihydrochloride reagent, dissolve 250 mg of *N*-(1-naphthyl)ethylenediamine dihydrochloride in 1 liter of distilled water.

Standard Preparation—Pipet 5 ml of nitroglycerin spirit (assayed by the procedure described under *Standardization of Nitroglycerin Spirit*) into a 100-ml volumetric flask. Then add 50 ml of 95% ethanol, dilute to volume with water, and mix. Pipet 10 ml of this solution into a second 100-ml volumetric flask, dilute to volume with water, and mix well. Dilute either 7.0 ml (0.6-mg tablet) or 5.0 ml (0.4-mg tablet) to exactly 100.0 ml with water or 7.0 ml (0.3-mg tablet) to exactly 200.0 ml.

Sample Preparation—Transfer one tablet to a 25-ml flask and add about 15 ml of distilled water. Swirl to mix, dilute to volume with distilled water, stopper, and shake vigorously.

Procedure—Assemble the apparatus as shown diagrammatically in Fig. 1. Turn on the recorder and the colorimeter and allow them to stabilize for at least 30 min. Charge the reagent lines. Place 2-ml sample cups in the sampler, fill with the appropriate solution, and arrange so that there are five standards initially followed by 10 samples and a standard. Each subsequent 10 samples are bracketed with a standard preparation.

Assay in the automated system, employing a 20/hr cam with a 1:4 sample to wash ratio. Set the recorder at 50 mv with a chart speed of 0.51 cm (0.2 in.)/min. Use a 550-nm filter, a No. 2 aperture, and a 15-mm flowcell.

Standardization of Nitroglycerin Spirit—Pipet 5 ml of nitroglycerin spirit, shown to be "one-spot" material by TLC, into a 100-ml volumetric flask. Then add 50 ml of 95% ethanol and dilute to volume with water. Pipet 10 ml of this dilution to a 100-ml volumetric flask and dilute to volume with acetic acid. Mix well.

Standard Preparation—Dissolve about 129 mg of potassium nitrate, accurately weighed, in 1.0 ml of water and dilute to 200.0 ml with acetic acid. Mix well.

Procedure—Pipet 1.0 ml of the standard, sample, and acetic acid to separate 100-ml volumetric flasks. Add to each 2 ml of phenoldisulfonic acid, mix well, and let stand 5 min. Dilute to about 80 ml with water, add 10 ml of ammonium hydroxide, mix, and cool to room temperature. Dilute to volume with water and mix.

Determine the absorbances at a wavelength of maximum absorbance at about 410 nm *versus* the acetic acid blank in 1-cm cells in a suitable spectrophotometer. Calculate according to:

$$\% \text{ nitroglycerin in spirit (w/v)} = 0.749 \frac{A_u}{A_s} \times C \qquad \text{(Eq. 2)}$$

where A_u and A_s are the absorbances of the sample and standard, respectively; C is the weight, in milligrams, of potassium nitrate taken; and 0.749 is a factor relating nitroglycerin to potassium nitrate.

Weight Uniformity and Content Variation—All tablets were subjected to the weight variation test given in USP XVIII (p. 951) and a content uniformity test by the automated procedure. Three lots of each of the three potencies, 0.3, 0.4, and 0.6 mg, were tested.

Disintegration, Dissolution, and *In Vitro* Availability—Three lots of each of three strengths of nitroglycerin tablets, Products A, B, and C, were tested for disintegration according to USP XVIII (p. 934) for sublingual tablets. In this test, water is the disintegration fluid and no disks are used. Six tablets of each batch were individually tested. Experiments were performed to compare the membrane permeability of nitroglycerin from solution and from all three products. The experimental apparatus was a 5-ml dialysis chamber[14]. The permeability of 5 ml of nitroglycerin solution, 0.5 mg/ml, and the same solution containing 1 mg/ml of povidone was tested. In addition, four 0.6-mg tablets of each formulation were added to 5 ml of distilled water in the dialysis chamber. The dialysis cell contained the same volume of water on the other side, and a cellulose membrane[15] was used to separate the two sides. The apparatus was mechanically agitated at room temperature, and the nitroglycerin content of both chambers was determined after 5 hr (9).

Comparative Bioactivity of Nitroglycerin Tablet Formulations—All three nitroglycerin tablet preparations were tested sub-

[4] Product C, Warner-Chilcott Division of Warner-Lambert Co. (patent pending).
[5] Avicel PH-102, American Viscose Division, FMC Corp.
[6] Plasdone K-29-32, General Aniline and Film Corp.
[7] Breaking strength was determined on a Heberlein model 2E tester with a light pendulum replacement for the heavy pendulum and a new scale with intervals of 0.1 kg. Friability was determined with a standard Roche-type friabilator made of Plexiglas.
[8] Autoanalyzer, Technicon, Inc., Tarrytown, N.Y.
[9] Sampler II.
[10] Proportioning Pump II.
[11] Adjustable heating bath, Technicon.
[12] Colorimeter I.
[13] Mosely 7100 B.
[14] Bellco No. 3221.
[15] Technicon type C.

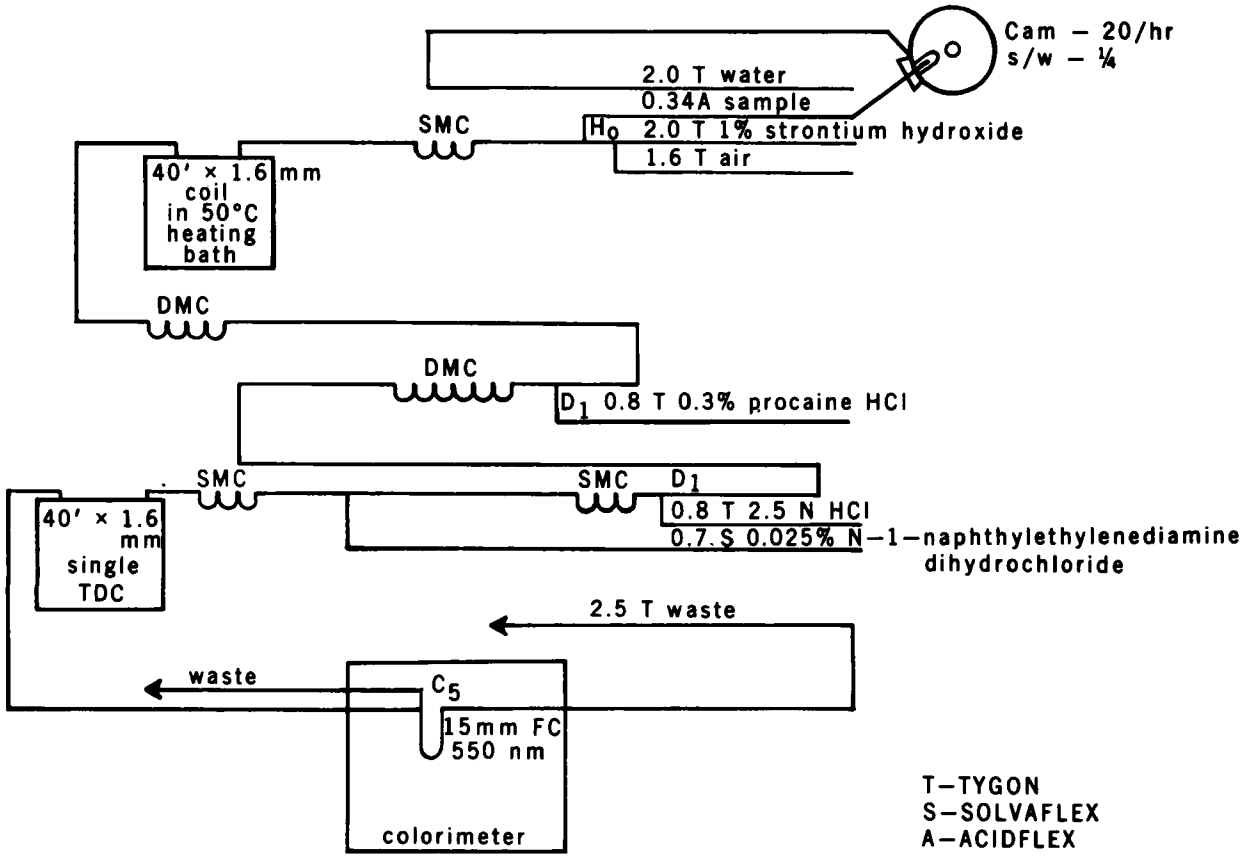

Figure 1—*Flow diagram for content uniformity assay.*

lingually in three dogs at two potency levels, 0.3 and 0.6 mg. Animals weighing 13–16 kg were anesthetized with pentobarbital sodium, 30 mg/kg iv, and aortic blood pressure and heart rate were measured. Then tablets were placed under the tongue and dissolved using a few drops of saline solution. The doses given were 22–88 μg/kg. Aortic blood pressure and pulse rate were measured again.

Products B and C and a placebo were tested in a group of 10 healthy subjects, eight males and two females, 21–47 years of age. Three tablet potencies were studied: 0.3, 0.4, and 0.6 mg. A placebo and each nitroglycerin potency of both manufacturers were studied in every subject. Prior to taking the test compound, each subject sat and rested for a minimum of 5 min and then counted his or her own pulse for 1 min every other minute for 8 min (four readings).

Beginning 1 min after taking the test drug or placebo, each subject counted his or her own pulse rate for 1 min every other minute for the next 16 min (eight readings) and then every 5 min for the next 15 min (three readings). If the pulse rate had not returned to the predrug level by this time, readings were continued every 5 min until it did.

Volatility Studies—A rapid screening method was developed to compare the effectiveness of potential stabilizing agents. Thermogravimetric analysis was found to be an excellent means of determining nitroglycerin volatility from tablets under conditions of constant temperature and controlled atmosphere. Two tablets were placed on the analyzer[16] at 80° under a nitrogen flow of 20 ml/min, and the weight loss was determined. After 90 min of treatment, a good approximation of the extent of nitroglycerin loss could be made from the curve developed (weight loss *versus* time).

Products A, B (unstabilized), and C, all 0.6 mg, were individually subjected to thermogravimetric analysis. A comparison was made among them by noting the rate of nitroglycerin loss. Furthermore, these tablets were individually assayed after exposure to verify that

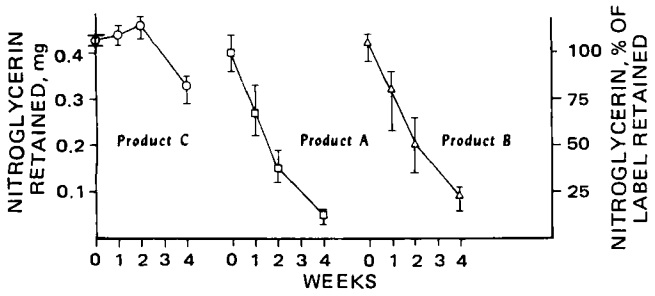

Figure 2—*Stability of nitroglycerin tablets (0.4-mg label) stored in open dishes at room temperature: average assay value and range of 10 individual tablets. Key: □, Product A; △, Product B; and ○, Product C.*

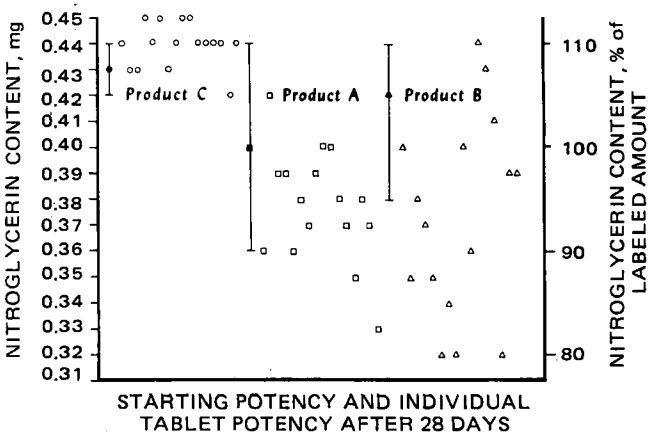

Figure 3—*Results obtained by testing the 16 individual tablets (0.4-mg label) remaining after a 28-day in-use test. Each bottle was opened three times a day for 30 sec, and one tablet was removed at each opening. Key: ●, ■, ▲, average assay and range of various tablet formulations at the start; and ○, □, △, individual tablet assays for Products C, A, and B, respectively, after 28 days of usage.*

[16] Du Pont model 950 in conjunction with model 900 console.

Table I—Comparison of Weight Uniformity of Nitroglycerin Tablets[a]

Product	Strength, mg	Lot	Tablet Weight, mg		RSD, %
			Average	Range	
Product A	0.3	PC142	34.5	32.4–36.5	3.8
	0.4	PM216	33.9	33.0–35.3	1.8
	0.6	PA165	35.5	34.2–36.5	2.7
Product B	0.3	7JSO2C	35.8	34.2–37.8	3.3
	0.4	6WF29B	35.4	34.1–38.5	4.4
	0.6	6TT84B	34.2	31.0–37.5	5.6
Product C	0.3	4900	29.5	29.2–29.8	0.7
	0.4	4902	30.8	30.4–31.4	1.2
	0.6	4906	28.9	28.2–29.7	1.8

[a] USP XVIII, p. 951.

Table II—Comparison of Content Uniformity of Nitroglycerin Tablets, Label Claim 0.4 mg

Product	Lot	Nitroglycerin Content			Number of Tablets Outside 15% Specification
		Average[a], mg	Range, mg	RSD, %	
Product A	PM216	0.40	0.36–0.44	6.72	0
	RC147	0.38	0.32–0.42	8.61	1
	PL265	0.36	0.30–0.43	10.42	2
	RB489	0.35	0.32–0.38	5.83	2
Product B	6W29B	0.42	0.38–0.44	4.71	0
	7HF65B	0.37	0.30–0.42	9.87	2
	7KJ73B	0.37	0.30–0.46	13.40	3
	7LH21B	0.43	0.34–0.55	14.05	0
Product C	4901	0.42	0.41–0.43	1.83	0
	4902	0.44	0.43–0.46	1.89	0

[a] Represents average of 10 randomly selected tablets.

the loss apparent from the weight *versus* time curve was in agreement.

Additional volatility experiments were conducted by exposing the tablets (all containing stabilizers) from the same manufacturers and of the same potencies in open dishes in the laboratory at 24–26°. Individual tablet assays were run at 1, 2, and 4 weeks.

A simulated in-use study was also carried out in which one tablet was removed from a commercial bottle three times every day for 28 days. The exposure time was 30 sec at each opening. The remaining 16 tablets were assayed individually.

RESULTS

Tables I and II give the weight variation and content uniformity of batches of tablets of various potencies. Generally, the weight variation for molded tablets was higher than for compressed tablets, and the difference was statistically significant at the 99.5% probability level when tested by Bartlett's χ-square statistic (11). Content variabilities of molded tablet formulations were also higher than with compressed tablets; this difference was also statistically significant at the 99.5% level by the Bartlett test.

Tablet disintegration of the three brands is shown in Table III. The data indicate that, although all brands disintegrated rapidly, Products B and C ranged from 3 to 7 sec while Product A ranged from 10 to 17 sec. These differences in disintegration times do not necessarily indicate a difference in rapidity of drug release or onset of pharmacological activity.

The results of the last comparative *in vitro* availability test, membrane permeability, are shown in Table IV. Nitroglycerin alone and nitroglycerin in the presence of povidone were both 31% dialyzed after 5 hr. Product A and C tablets dialyzed to the same extent as the solutions, while Product B tablets were somewhat slower.

Testing of various brands of nitroglycerin tablets in dogs indicated that the onset of activity, *i.e.*, decrease in mean aortic blood pressure and increase in heart rate, occurred within 1 min for each product at each dose level. Peak pharmacological responses occurred within 3 min after dosing regardless of the dose level. A decrease in mean aortic blood pressure, pulse pressure, and/or pulse contour and an increase in heart rate occurred with each product. There was a dose–response relationship. The higher dose had a longer lasting effect on blood pressure whereas the heart rate returned to normal in 10–20 min for all doses.

Table III—Disintegration of Nitroglycerin Tablets

Individual Tablet	Disintegration Time,[a] sec								
	0.3-mg Tablets			0.4-mg Tablets			0.6-mg Tablets		
	Product C	Product A (Lot PC142)	Product B (Lot 7BH46B)	Product C	Product A (Lot PM216)	Product B (Lot 6WF29B)	Product C	Product A (Lot MA153)	Product B (Lot 6UT66A)
1	4	15	7	6	15	5	6	10	7
2	5	17	6	7	16	5	6	17	4
3	3	15	3	7	18	5	6	12	5
4	6	16	7	7	16	5	5	13	3
5	5	12	7	7	14	4	6	10	4
6	6	14	5	7	17	6	6	14	4
Average of six	5	15[b]	6	7	16[b]	5	6	13[b]	5

[a] According to USP XVIII method for sublingual tablets, p. 934. [b] These results agree with those data reported in Product A advertising literature.

Table IV—Permeability of Nitroglycerin from Solutions and Tablet Dosage Forms[a]

Sample	Permeation, %
Nitroglycerin solution, 0.5 mg/ml	31
Nitroglycerin solution, 0.5 mg/ml, and 1.0 mg/ml of povidone	31
Product A tablets[b] (Lot PA165)	32
Product B tablets[c] (Lot 6UT66A)	20
Product C tablets	31

[a] Five-hour study; see text for details. Four tablets in 5 ml of distilled water were used. [b] Product contains a stabilizer. [c] Product contains no stabilizer.

The results obtained by testing three potencies of two drug products in human volunteers are given in Table V. Each dose of nitroglycerin caused a statistically significant increase in pulse rate whereas the placebo tablet had virtually no effect on pulse rate. The Product B nitroglycerin dose did not differ significantly from the same Product C dose with respect to the magnitude, the time of onset, the time of peak activity, or the duration of pulse rate elevation. Neither was there any significant difference in the responses between different doses. With both formulations, the onset of action was statistically significant at 3 min, the peak activity was 3–5 min after drug administration, and the duration of action was 9–11 min.

Volatility studies employing thermogravimetric analysis and chemical assay are summarized in Table VI. The loss of nitroglycerin was most pronounced with Product B tablets (unstabilized) followed by Product A. Product C tablets, on the other hand, exhibited remarkable stability under these experimental conditions.

The results obtained from open dish exposure of 0.4-mg nitroglycerin tablets are shown in Fig. 2. Tablets were spread out in a petri dish and fully exposed to air without protection. These tablets were randomly sampled at 1, 2, and 4 weeks. This type of test readily indicates the relative stability of various nitroglycerin tablet formulations. The partially stabilized brands lost substantial amounts of nitroglycerin in 1 week, *i.e.*, 32% for Product A and 24% for Product B tablets. This downward trend for these products continued until less than 13 and 23% of the drug, respectively, were retained at the end of 4 weeks. Product C tablets remain unaffected by exposure times of up to 2 weeks, after which a loss in nitroglycerin content occurred. The vertical lines in Fig. 2 indicate the range of assay values of the individually assayed tablets. These ranges were highest for Products A and B.

Results from the simulated in-use test of nitroglycerin tablets are given in Fig. 3. After 28 days of usage, again the average content of nitroglycerin in Product C tablets remained unchanged. Product A tablets and Product B averaged 0.02 and 0.05 mg, respectively, less than the initial assay values. The ranges of the content, which are also given in Fig. 3, indicate that the range of nitroglycerin content in Product C tablets after 28 days was 0.03 mg, the same as the original tablets. The ranges for the two other brands of nitroglycerin tablets increased over the initial ranges, changing from 0.08 to 0.09 mg for Product A tablets and from 0.06 to 0.12 for Product B.

Table VI—Comparison of Nitroglycerin Volatility from Various Tablet Formulations Subjected to Thermogravimetric Analysis[a]

	Nitroglycerin Remaining, %		
	Tablet 1[b]	Tablet 2[b]	Average
Product A[c] (Lot PA165)	54 54	56 59	56
Product B[d] (Lot 6MG53A)	23 21	22 21	22
Product C	97 98	93 95	96

[a] At 80° for 90 min; chemical assay values. [b] Duplicate assay results from individual tablets. [c] Product contains a stabilizer. [d] Product contains no stabilizer.

DISCUSSION

The overall quality of pharmaceutical products available from various sources has been discussed frequently in recent years by both scientific and government groups. Considerable attention has been given to the comparison of bioavailability of drug dosage forms from various sources, but the more fundamental quality aspects of drug products and their relative stabilities probably have not been compared to the same extent.

In this study, three brands of nitroglycerin tablets were compared for conformance to tests in the USP XVIII monograph; bioavailability tests were performed, and nitroglycerin instability was determined. The weight variation of the molded tablet formulations was significantly larger than that of the compressed formulation. Thus, the method of tablet manufacture is a significant factor in the dose uniformity of nitroglycerin.

The content uniformity of nitroglycerin tablets reflects both variation in weight and variation in content *per se* due to direct volatilization and tablet to tablet migration of the drug. The two molded tablet formulations had relative content variations of about 6–14%. Some of these tablets, labeled 0.4 mg, contained as little as 0.30 mg and as much as 0.55 mg. On the other hand, the compressed tablet formulation had a relative content variation of about 2% and a content range of 0.02–0.03 mg. Four of eight lots of the molded tablets contained two or three tablets out of 10 that were more than 15% below the average content, and one lot contained one tablet below the 15% average. Where more than one tablet of 10 varies by more than 15% from the average tolerance, the USP specifies that additional testing should be carried out on 20 additional individual tablets and that none should be less than 75% or more than 135% of the labeled amount. This additional test was not required for the compressed tablet formulation since it was within the 15% limit.

Comparative drug availability testing included both *in vitro* and *in vivo* tests. Similar results were obtained for all three products tested for disintegration, permeability, and bioavailability.

Volatility studies indicated that Product C was superior in retaining nitroglycerin. Thermogravimetric analysis was initially used to screen formulations in the development phase; testing at 80° for 90 min was a good screening method. In this test, the comparative losses of nitroglycerin were 4% for Product C, 56% for Product A, and 78% for Product B without stabilizer. In the open dish test, Product C was much more stable than the other two brands.

Table V—Mean Pulse Change from Baseline for Seven Treatments at 11 Time Periods[a]

Treatment	Minutes after Drug										
	1	3	5	7	9	11	13	15	20	25	30
Product B											
0.3 mg	4.8	12.0	10.8	9.4	7.6	4.0	1.7	−0.4	0.5	−1.4	−0.6
0.4 mg	4.2	12.4	11.3	10.5	8.1	6.4	5.0	3.5	−0.7	0.1	0.2
0.6 mg	4.9	12.1	10.6	10.3	6.8	6.1	2.3	1.3	0.6	−0.2	1.0
Product C											
0.3 mg	2.3	10.2	11.1	9.4	6.4	4.3	2.3	2.7	0.9	1.0	1.0
0.4 mg	3.1	10.7	11.1	9.5	6.6	4.4	2.9	2.4	−0.3	0.6	1.1
0.6 mg	3.1	13.3	12.9	10.5	9.0	6.3	4.6	3.5	0.6	−0.1	0.2
Placebo	0.0	0.1	−0.1	0.4	−0.4	−0.9	−0.9	−0.5	−0.1	−1.6	−1.6

[a] Ten human subjects; see text for details.

In the 28-day simulated use test, the remaining Product C tablets had the same original average content and content range as the starting tablets. Both Product A and B tablets experienced some potency loss as well as an increasing variability.

In conclusion, the compressed tablet formulation was as active as two other widely used nitroglycerin tablet formulations. However, the uniformity and stability significantly exceeded those of the two popularly used molded tablet formulations, particularly under the stress conditions likely to be encountered in a patient usage regimen.

REFERENCES

(1) I. A. Chaudry and R. E. King, *J. Pharm. Sci.*, **61**, 1121(1972).

(2) U.S. pat. 3,789,119 (Jan. 29, 1974).

(3) W. W. Hargrove, *Tile Till*, **59**, 65(1973).

(4) M. D. Richman, C. D. Fox, and R. F. Shangraw, *J. Pharm. Sci.*, **54**, 447(1965).

(5) B. A. Edelman, A. M. Contractor, and R. F. Shangraw, *J. Am. Pharm. Assoc.*, **NS11**, 30(1971).

(6) R. F. Shangraw and A. M. Contractor, *ibid.*, **NS12**, 633(1972).

(7) S. Fusari, *J. Pharm. Sci.*, **62**, 122(1973).

(8) *Ibid.*, **62**, 2012(1973).

(9) F. K. Bell, *J. Pharm. Sci.*, **53**, 752(1964).

(10) D. Banes, *ibid.*, **57**, 893(1968).

(11) W. J. Dixon and F. J. Massay, Jr., "Introduction to Statistical Analysis," McGraw-Hill, New York, N.Y., 1957, p. 179.

ACKNOWLEDGMENTS AND ADDRESSES

Received June 20, 1975, from the *Pharmaceutical Research and Development Laboratory, Warner-Lambert Research Institute, Morris Plains, NJ 07950*

Accepted for publication December 16, 1975.

The authors appreciate the technical assistance of Mr. Reginald Phillips in the formulation and development work. Dr. M. Winbury carried out the comparative bioactivity tests in dogs, and Dr. A. Glick and Mr. S. Jones compared the bioactivity of nitroglycerin tablets in human subjects.

[x] To whom inquiries should be directed.

Electrochemistry of Drug Action I: Electroreduction of Ferredoxins

YIE W. CHIEN

Abstract □ Ferredoxin serves as an electron carrier in the oxidation–reduction system in anaerobic microorganisms, transferring electrons from a low potential donor to electron-accepting biochemicals. The anaerobicidal activity of some drugs may be due to their interference with the electron transport function of ferredoxin. Two types of ferredoxins (isolated from *Clostridium pasteurianum* and spinach) were studied, and their electrochemical reduction and biochemical properties were analyzed using a sensitive ac polarographic technique. The reduction potential of both ferredoxins was linearly related to pH. The mechanisms of electron transport in ferredoxin molecules were found to be related to their sulfur–iron bonds. The dissociation of the sulfur–iron bonds resulted in the formation of a free sulfhydryl group and the interruption of the electroactivity of ferredoxin. This sulfur–iron dissociation process was found to be pH dependent. The electroreduction of ferredoxins was an energy-requiring, pH-dependent process.

Keyphrases □ Electrochemistry—of drug action, electrochemical reduction and biochemical properties of ferredoxins studied using ac polarography □ Ferredoxins—electrochemical reduction and biochemical properties studied using ac polarography □ Electroreduction—ferredoxins, studied using ac polarography, effect of pH □ Polarography, ac—study of electroreduction and biochemical properties of ferredoxins □ Oxidation–reduction systems—ferredoxins studied using ac polarography, effect of pH

Ferredoxin, a nonheme iron-containing protein, was first isolated from *Clostridium pasteurianum*, an anaerobe, by Mortenson *et al.* (1), and crystalline preparations were obtained later from several other anaerobic bacteria (2, 3).

Much research interest has been generated since regarding the biochemical significance of ferredoxins (4) and their relationship to the anaerobicidal activity of several drugs (5–7). These studies indicate that ferredoxin serves as an oxidation–reduction enzyme in anaerobes by transferring electrons from a low-potential donor, *e.g.*, pyruvic acid, to electron-accepting biochemicals, *e.g.*, pyridine nucleotides, or to H^+ to produce H_2, a terminal electron acceptor characteristic of anaerobes. The interruption of this vital pyruvate phosphoroclastic reaction may result in selective toxicity to the anaerobes.

Recently, dc polarography was used to measure the redox potentials of some antimicrobial agents; their antianaerobic activity was related to their redox potentials relative to the redox potential (−470 mv) of ferredoxin (5). Studies of the complexation of metronidazole, an agent effective against anaerobes, with cupric ion indicated that ac polarography has several advantages over dc polarography in terms of sensitivity and reproducibility of electrochemical measurements (8). These advantages should be beneficial to the mechanistic analysis of ferredoxin–drug interactions.

In this study, the electrochemical reduction of two types of ferredoxins was examined, using an ac polarographic technique, to gain a better understanding of the electrochemistry of their electron transport mechanisms.

EXPERIMENTAL

Materials—Clostridial and spinach ferredoxins are available as frozen solutions in neutral tromethamine buffer[1] and were used as obtained. Triple-distilled, instrument-grade mercury[2] was applied in a dropping mercury electrode. Freshly deionized, triple-distilled

[1] Trizma, Sigma Chemical Co., St. Louis, MO 63178

[2] Bethlehem Apparatus Co., Hellertown, Pa.

In the 28-day simulated use test, the remaining Product C tablets had the same original average content and content range as the starting tablets. Both Product A and B tablets experienced some potency loss as well as an increasing variability.

In conclusion, the compressed tablet formulation was as active as two other widely used nitroglycerin tablet formulations. However, the uniformity and stability significantly exceeded those of the two popularly used molded tablet formulations, particularly under the stress conditions likely to be encountered in a patient usage regimen.

REFERENCES

(1) I. A. Chaudry and R. E. King, *J. Pharm. Sci.*, **61**, 1121(1972).

(2) U.S. pat. 3,789,119 (Jan. 29, 1974).

(3) W. W. Hargrove, *Tile Till*, **59**, 65(1973).

(4) M. D. Richman, C. D. Fox, and R. F. Shangraw, *J. Pharm. Sci.*, **54**, 447(1965).

(5) B. A. Edelman, A. M. Contractor, and R. F. Shangraw, *J. Am. Pharm. Assoc.*, **NS11**, 30(1971).

(6) R. F. Shangraw and A. M. Contractor, *ibid.*, **NS12**, 633(1972).

(7) S. Fusari, *J. Pharm. Sci.*, **62**, 122(1973).

(8) *Ibid.*, **62**, 2012(1973).

(9) F. K. Bell, *J. Pharm. Sci.*, **53**, 752(1964).

(10) D. Banes, *ibid.*, **57**, 893(1968).

(11) W. J. Dixon and F. J. Massay, Jr., "Introduction to Statistical Analysis," McGraw-Hill, New York, N.Y., 1957, p. 179.

ACKNOWLEDGMENTS AND ADDRESSES

Received June 20, 1975, from the *Pharmaceutical Research and Development Laboratory, Warner-Lambert Research Institute, Morris Plains, NJ 07950*

Accepted for publication December 16, 1975.

The authors appreciate the technical assistance of Mr. Reginald Phillips in the formulation and development work. Dr. M. Winbury carried out the comparative bioactivity tests in dogs, and Dr. A. Glick and Mr. S. Jones compared the bioactivity of nitroglycerin tablets in human subjects.

[x] To whom inquiries should be directed.

Electrochemistry of Drug Action I: Electroreduction of Ferredoxins

YIE W. CHIEN

Abstract □ Ferredoxin serves as an electron carrier in the oxidation–reduction system in anaerobic microorganisms, transferring electrons from a low potential donor to electron-accepting biochemicals. The anaerobicidal activity of some drugs may be due to their interference with the electron transport function of ferredoxin. Two types of ferredoxins (isolated from *Clostridium pasteurianum* and spinach) were studied, and their electrochemical reduction and biochemical properties were analyzed using a sensitive ac polarographic technique. The reduction potential of both ferredoxins was linearly related to pH. The mechanisms of electron transport in ferredoxin molecules were found to be related to their sulfur–iron bonds. The dissociation of the sulfur–iron bonds resulted in the formation of a free sulfhydryl group and the interruption of the electroactivity of ferredoxin. This sulfur–iron dissociation process was found to be pH dependent. The electroreduction of ferredoxins was an energy-requiring, pH-dependent process.

Keyphrases □ Electrochemistry—of drug action, electrochemical reduction and biochemical properties of ferredoxins studied using ac polarography □ Ferredoxins—electrochemical reduction and biochemical properties studied using ac polarography □ Electroreduction—ferredoxins, studied using ac polarography, effect of pH □ Polarography, ac—study of electroreduction and biochemical properties of ferredoxins □ Oxidation–reduction systems—ferredoxins studied using ac polarography, effect of pH

Ferredoxin, a nonheme iron-containing protein, was first isolated from *Clostridium pasteurianum*, an anaerobe, by Mortenson *et al.* (1), and crystalline preparations were obtained later from several other anaerobic bacteria (2, 3).

Much research interest has been generated since regarding the biochemical significance of ferredoxins (4) and their relationship to the anaerobicidal activity of several drugs (5–7). These studies indicate that ferredoxin serves as an oxidation–reduction enzyme in anaerobes by transferring electrons from a low-potential donor, *e.g.*, pyruvic acid, to electron-accepting biochemicals, *e.g.*, pyridine nucleotides, or to H^+ to produce H_2, a terminal electron acceptor characteristic of anaerobes. The interruption of this vital pyruvate phosphoroclastic reaction may result in selective toxicity to the anaerobes.

Recently, dc polarography was used to measure the redox potentials of some antimicrobial agents; their antianaerobic activity was related to their redox potentials relative to the redox potential (−470 mv) of ferredoxin (5). Studies of the complexation of metronidazole, an agent effective against anaerobes, with cupric ion indicated that ac polarography has several advantages over dc polarography in terms of sensitivity and reproducibility of electrochemical measurements (8). These advantages should be beneficial to the mechanistic analysis of ferredoxin–drug interactions.

In this study, the electrochemical reduction of two types of ferredoxins was examined, using an ac polarographic technique, to gain a better understanding of the electrochemistry of their electron transport mechanisms.

EXPERIMENTAL

Materials—Clostridial and spinach ferredoxins are available as frozen solutions in neutral tromethamine buffer[1] and were used as obtained. Triple-distilled, instrument-grade mercury[2] was applied in a dropping mercury electrode. Freshly deionized, triple-distilled

[1] Trizma, Sigma Chemical Co., St. Louis, MO 63178

[2] Bethlehem Apparatus Co., Hellertown, Pa.

Table I—Characterization of the ac Polarographic Peaks for Ferredoxins

Electroactive Species[a]	ac Peak Potential, v	
	Peak 1	Peak 2
Ferric ion[b]	−0.166,	—
Cystine	—	−0.400
Ferredoxin Type I	−0.170	−0.533
Ferredoxin Type III	−0.170	−0.515

[a] pH 6.01, 37°. [b] Ferric chloride solution, 8×10^{-5} M.

water was utilized to prepare the McIlvaine buffer (5). The McIlvaine buffer at various pH's was then used as a supporting electrolyte solution for preparing all ferredoxin solutions just prior to a polarographic measurement.

Procedure—Six milliliters of McIlvaine buffer solution, alone or containing various concentrations of ferredoxins, *N*-ethylmaleimide[3], cystine[4], or ferric chlorides[4], was deaerated with pure nitrogen gas for 5 min in a thermostated (37°) three-electrode microcell system prior to measurement. A nitrogen atmosphere was maintained over the tested solution during electrochemical analysis[5] to prevent oxygen contamination.

For the ac polarogram, the controls were preset as follows: modulation amplitude, 10 mv; frequency, 100 Hz; phase, 178.6°; scan rate, 2 mv/sec; drop time, 0.5 sec; and sample duration, 10 msec. For the dc polarogram, the scan rate was 2 mv/sec, the drop time was 0.5 sec, and the time constant was 1 sec. The ac polarographic measurement of *N*-ethylmaleimide, without or with cystine or ferredoxins, was conducted under the same conditions. The current height of the *N*-ethylmaleimide peak at −0.769 v was measured to calculate the concentration of electroactive *N*-ethylmaleimide.

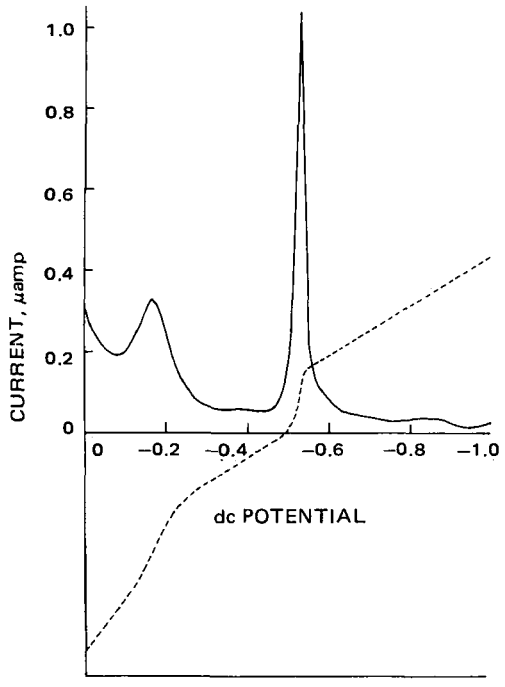

Figure 1—*The ac (solid line) and dc (dotted line) polarograms of ferredoxin (Type I, 80 μg/ml) at pH 6.01 and 37°. Two ac peaks were observed at* E_p (i_{ac}) *of −0.170 v (0.184 μamp) and −0.533 v (0.946 μamp). The second dc peak at* $E_{1/2}$ *of −0.527 v and* i_d *of 0.125 μamp is more obvious than the first dc peak.*

[3] Aldrich Chemical Co., Milwaukee, WI 53233
[4] Matheson, Coleman & Bell, Norwood, OH 45212
[5] The ac and dc polarographic analyses were performed on a PAR electrochemistry system (model 170, Princeton Applied Research Corp., Princeton, N.J.) with an automated mercury drop timer (model 172A, Princeton Applied Research Corp.).

Table II—Agreement of ac Peak Potential (E_p) with dc Half-Wave Potential ($E_{1/2}$) for Ferredoxin Type I at Various pH Values

pH Profile	E_p, v	$E_{1/2}$, v
4.51	−0.445	−0.430
6.01	−0.533	−0.527
7.52	−0.585	−0.570

RESULTS AND DISCUSSION

Electrochemical Reduction of Ferredoxins—To act as an electron transport enzyme, the ferredoxin molecule has to be active electrochemically. Using the differences in absorption spectra between the oxidized and reduced forms of ferredoxins, Tagawa and Arnon (2) estimated that the ferredoxins from *Cl. pasteurianum* and spinach have redox potentials at −0.417 and −0.432 v, respectively, at pH 7.55. However, a redox potential of −0.470 v recently was reported for clostridial ferredoxin at pH 6.0 (5).

In this investigation, both Type I (clostridial) and Type III (spinach) ferredoxins were examined by polarographic analysis, and their electrochemical activity was confirmed. One typical polarogram is illustrated in Fig. 1. In this illustration, the ac polarogram of ferredoxin Type I is compared to its dc polarogram at pH 6.01. The ac polarography gave more distinct reduction peaks for ferredoxin than did the conventional dc polarography. The distinct ac peak at a reduction potential of −0.533 v agreed well with the half-wave potential ($E_{1/2}$) of −0.527 v measured by dc polarography. In addition, the ac peak at −0.170 v was defined much more clearly than the dc polarographic curve.

This ac reduction peak (−0.170 v) was observed to superimpose on the single ac reduction peak (−0.166 v) resulting from the electrochemical reduction of ferric ion to ferrous ion under the same condition (Table I). Therefore, this reduction peak may be assigned to the electroreduction of an uncoordinated ferric ion in the ferredoxin solution tested. The uncoordinated ferric ion may have resulted from the breakdown of a small fraction of ferredoxin molecules after their isolation and purification.

The electroactivity of cystine was also examined to characterize the reduction peak at −0.533 v. The result (Table I) indicates that the electrochemical reduction of the disulfide bond in the cystine molecule is much less negative (−0.400 v) and cannot account for the functional group undergoing reduction at −0.533 v (at pH 6.01) in the ferredoxin molecule. This observation suggests that there is no disulfide linkage in the ferredoxin molecule and that the more negative reduction peak (−0.533 v) may be related to the reduction of a bond whose bond strength is stronger than that of disulfide linkage, *e.g.*, the coordinated sulfur–iron bond in the active centers of a ferredoxin molecule. The characteristics of this sulfur–iron bond will be analyzed later.

When the activities of the oxidized and reduced species of an electroactive compound at the immediate surface of an electrode are equal, an ac peak potential (E_p) should be observed in an ac polarogram and a half-wave potential ($E_{1/2}$) should be seen in a dc polaro-

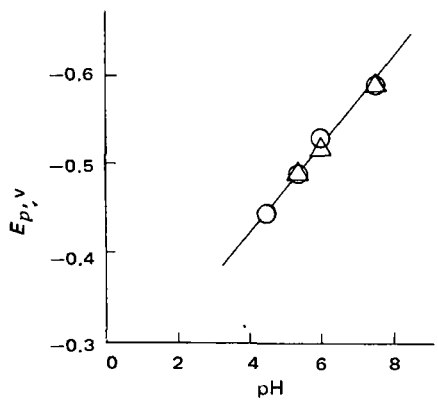

Figure 2—*Linear relationship of ac peak potential (*$-E_p$*) with pH as expected from Eq. 2. Key:* ○, *ferredoxin Type I; and* △, *ferredoxin Type III. From the slope of the linearity,* m/n *was calculated to be 0.77.*

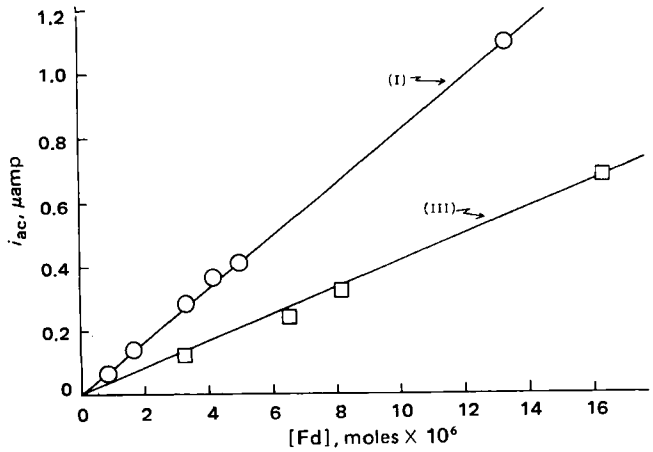

Figure 3—*Linear relationship between ac current, i_{ac}, and the molar concentration of ferredoxins, [Fd]. The slopes (i_{ac}/mole) of the linearities are 82.02 × 10^3 and 41.56 × 10^3 μamp/mole for Types I and III, respectively.*

gram. These two potentials should have the same magnitude according to electrochemical thermodynamics. As demonstrated in Table II, the values of E_p agreed with the magnitude of $E_{1/2}$ at the various pH conditions studied. This agreement permits the use of the more sensitive ac polarographic technique to study the electroreduction process of ferredoxins.

If the electrochemical reduction of ferredoxin is an electrodic reaction (Scheme I):

$$\text{ferredoxin (oxidized)} + m\text{H}^+ + ne \rightarrow \text{ferredoxin (reduced)}$$

Scheme I

then the equilibrium electrode potential, E_e, is defined by the Nernst equation (9):

$$E_e = E^\circ + \frac{2.303RT}{nF}\log\frac{[\text{oxidized}]}{[\text{reduced}]} - \frac{2.303RT}{nF}m\text{pH} \quad \text{(Eq. 1)}$$

where E° is the standard redox potential; n and m are the number of electrons transferred and the number of protons consumed, respectively; F is the Faraday constant; and R and T are the gas constant and absolute temperature, respectively.

At the peak of an ac reduction polarogram, it is reasonable to assume that [oxidized] ≃ [reduced] in view of the minor difference in the diffusivity between the oxidized and reduced species of ferredoxin molecules. So, at 37°:

$$-E_p = -E_e = -E^\circ + \frac{m}{n}0.061\ \text{pH} \quad \text{(Eq. 2)}$$

That is, a linear relationship should exist between the ac peak potential ($-E_p$) and the pH profile of the ferredoxin solution (Fig. 2). Both ferredoxins (Types I and III) followed this relationship very well. From the slope, the ratio of m/n was 0.77. This value of m/n was slightly lower than the expected value of unity for one- or two-electron reduction, indicating that the availability of proton (H^+) to ferredoxin molecules may be the rate-limiting (slower) step in the electrochemical reduction of ferredoxins.

In addition to the agreement observed between the ac peak potential and the dc half-wave potential (Table II), the data in Table III reveal that the measurement sensitivity was improved eightfold by using ac polarography. The current heights for the electrochemical reduction of ferredoxins were substantially amplified from 0.125 to 0.946 μamp for Type I ferredoxin and from 0.037 to 0.242 μamp for Type III ferredoxin.

Table III—Comparison of ac Polarography with dc Polarography for Ferredoxins[a]

	dc Polarography		ac Polarography	
Ferredoxin	$E_{1/2}$, v	i_d, μamp	E_p, v	i_{ac}, μamp
Type I	−0.527	0.125	−0.533	0.946
Type III	−0.511	0.037	−0.515	0.242

[a] Concentration of ferredoxin = 80 μg/ml, pH 6.01, 37°.

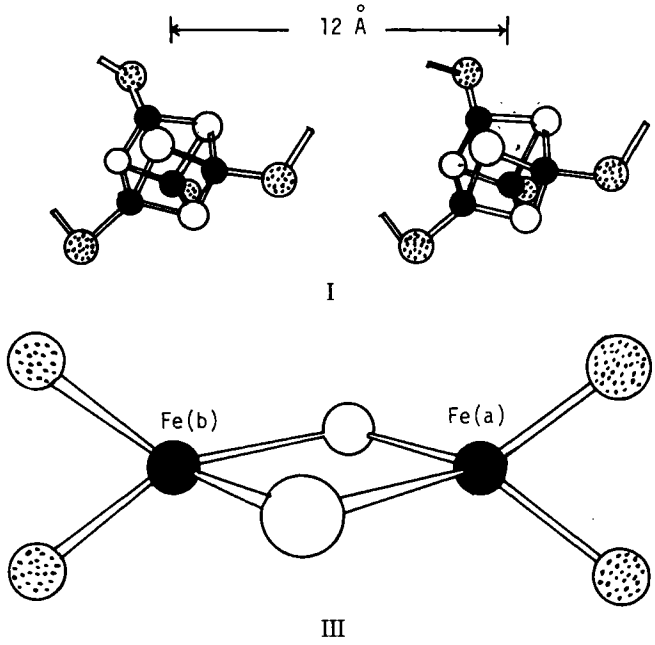

As expected from the laws of diffusion, the current height (i_{ac}) of the ac reduction peak at −0.533 v was linearly proportional to the molar concentration of ferredoxins Types I and III in solution (Fig. 3). From the slopes, the reduction current per mole, i_{ac}/mole, of ferredoxin was calculated to be 82.02 × 10^3 and 41.56 × 10^3 μamp/mole for Types I and III, respectively. The magnitude of the molar reduction current for Type I ferredoxin (82.02 × 10^3 μamp/mole) was twice that for Type III ferredoxin (41.56 × 10^3 μamp/mole). This observation supports an earlier report (10) that Type I ferredoxin functions as a two-electron carrier and that Type III ferredoxin behaves as a one-electron carrier in reduction–oxidation processes. This agreement suggests that ac polarographic measurement provides a sensitive, direct approach toward the mechanistic analysis of the electroactivity of ferredoxins.

Sulfur–Iron Coordination in Ferredoxins—A representation (11) of the current understanding of the configuration of an active site in a two(iron–sulfur) protein (ferredoxin Type III) is reproduced in Structure III. Ferric, cysteine sulfur, and inorganic sulfur atoms are represented by solid, dotted, and open circles, respectively (reproduced from Ref. 11). Each molecule of ferredoxin Type III contains one active center. The formal description of this active center is two iron atoms, two inorganic sulfur atoms, and two cysteine sulfur atoms from the peptide chain of 97 amino acid residues.

On the other hand, X-ray crystallography of an eight(iron–sulfur) ferredoxin Type I (11) revealed that there are two active centers separated by 12 Å (Structure I). The X-ray data also showed that the four iron atoms in each of the two active centers are arranged in a tetrahedron geometry, with an average iron–iron separation of 3.1 Å. The iron atoms are coordinated to the polypeptide chain of 55 amino acid residues *via* the cysteine sulfurs. The labile sulfides are located outside each face of the tetrahedron so that each iron atom is coordinated to four sulfur atoms, three inorganic and one mercaptide, which are also tetrahedrally disposed with respect to the iron atom. The mean bond lengths are 2.35 and 2.01 Å for the iron–sulfur inorganic and iron–sulfur cysteine bonds, respectively. The difference in bond length indicates that the inorganic sulfur atom binds with the iron atom less tightly than does the cysteine sulfur atom.

It was established (11) that an oxidized ferredoxin Type I molecule contained two ferrous ions and two ferric ions in each of its two active centers. Upon reduction, the ratio of ferrous to ferric ions was shifted from 2:2 to 3:1. Although the complete reduction of ferredoxin Type I required the addition of two electrons (12, 13), the oxidation–reduction behavior conformed well to the Nernst expression (Eq. 1) for n = 1, *i.e.*, with the electrons being transferred one at a time (14). It was reported that the redox potentials of these two active centers do not differ by more than a statistical factor. In the present investigation, only one electrochemical reduction peak was detected for each

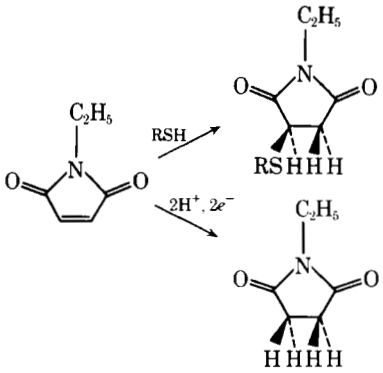

Scheme II—Electrochemical reduction and complexation of N-*ethylmaleimide with thiol group (RSH) in a protein molecule,* e.g., *ferredoxin.*

of the two types of ferredoxins examined (Table III). These observations led to the suggestion that these two redox active sites are equivalent and do not interact.

The linkage between the inorganic sulfur atom and the iron atom was reported to be labile to acid. The breakdown of this sulfur–iron inorganic bonding was related to the disappearance of the brown color and to the formation of hydrogen sulfide gas in a ferredoxin (oxidized) solution upon acidification. Experiments were designed to establish the effects of acidification on the electroactivity of ferredoxin molecules and also to characterize the relationship of the reduction peak at −0.533 v (at pH 6.01) to the sulfur–iron coordination.

It was observed that ferredoxin Type I gradually lost its electroactivity at pH 3.51; ferredoxin Type III was even more sensitive to acidity and completely lost its electroactivity after short exposure at pH 4.51. Accompanying the diminished electrochemical activity, the brown color of ferredoxin solutions faded and a white precipitate shortly formed. Upon neutralization of these acidic ferredoxin solutions to pH 6.06, the white precipitate redissolved and the reduction peak at −0.170 v was observed. However, the brown color and the reduction peak at −0.533 v could not be restored. These observations are in perfect agreement with the results reported earlier (15) and suggest that the reduction peak at −0.533 v may be related to an electroactive sulfur–iron coordination. Upon acidification, the breakdown of this electroactive sulfur–iron bond results in the loss of electroactivity of ferredoxins at the peak of −0.533 v. The following experiments with *N*-ethylmaleimide provided additional evidence concerning the correlation of the reduction peak at −0.533 v to the sulfur–iron bonding.

N-Ethylmaleimide has been used to detect thiols and thiol groups in protein molecules. The electrochemical reduction of the double bond in the *N*-ethylmaleimide molecule (Scheme II) gave a dc polarogram with an $E_{1/2}$ value of −0.775 v (16). This $E_{1/2}$ value was very close to the E_p (−0.769 v) observed in the present study. The interaction of a free sulfhydryl group with *N*-ethylmaleimide resulted in the saturation of its double bond and a quantitative reduction in the magnitude of its current height (sulfhydryl groups cannot be electrochemically reduced). This provided a sensitive procedure for detecting free sulfhydryl groups in ferredoxin molecules.

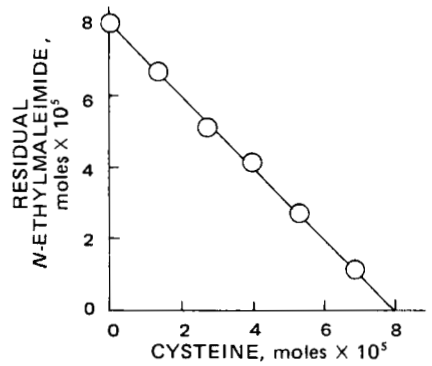

Figure 4—*Decrease in the concentration of* N-*ethylmaleimide in the presence of various concentrations of cysteine. Overall,* 8×10^{-5} *mole of cysteine is needed to complex with* 8×10^{-5} *mole of* N-*ethylmaleimide.*

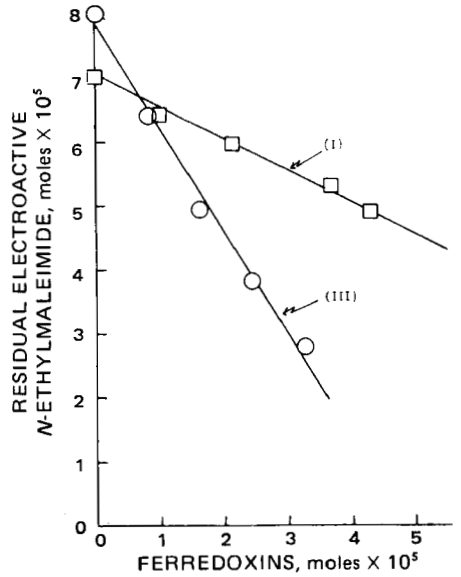

Figure 5—*Complexation of* N-*ethylmaleimide with ferredoxin Types I and III at pH 4.51 and 37°. From the slope of the linear relationships, the ratio of* N-*ethylmaleimide to ferredoxin was calculated to be 0.48 and 1.62 for Types I and III, respectively.*

As reported previously (16), the interaction of *N*-ethylmaleimide with cysteine was also measured by an ac polarographic technique to check its feasibility for detecting the quantitative interaction between *N*-ethylmaleimide and sulfhydryl groups. The result (Fig. 4) indicated that the concentration of electroactive *N*-ethylmaleimide decreased linearly as the concentration of cysteine in the mixture was increased. A quantitative 1:1 complexation between *N*-ethylmaleimide and the sulfhydryl group was observed (Fig. 4). The same results were obtained for pH values of 6.01, 4.51, and 3.51.

If the ferredoxin molecule contains any sulfhydryl groups existing in an uncoordinated state, the addition of ferredoxin to an *N*-ethylmaleimide solution also should result in a reduction in the concentration of the electroactive *N*-ethylmaleimide, as demonstrated earlier for cysteine (Fig. 4). The results shown in Fig. 5 indicated that, at pH 4.51 and 37°, ferredoxin Types I and III contain 0.48 and 1.62 uncoordinated sulfhydryl groups, respectively. The higher value of the free sulfhydryl group observed for ferredoxin Type III than for Type I suggested that Type III is less stable at pH 4.51 than Type I.

The stability of ferredoxin Type I was further studied at a lower

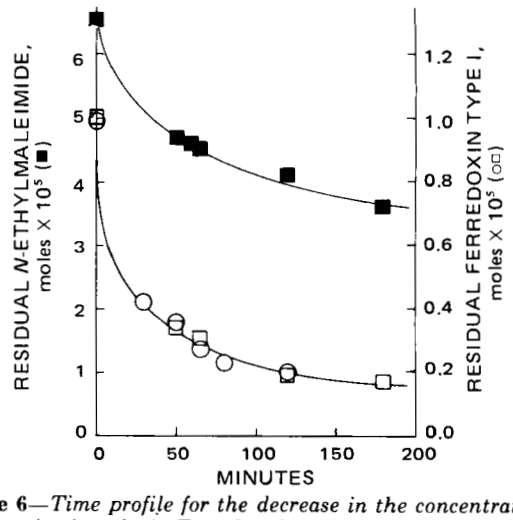

Figure 6—*Time profile for the decrease in the concentration of electroactive ferredoxin Type I and* N-*ethylmaleimide at pH 3.51 and 37°. Key:* ○, *ferredoxin alone;* □, *ferredoxin in the presence of* N-*ethylmaleimide; and* ■, N-*ethylmaleimide in the presence of ferredoxin.*

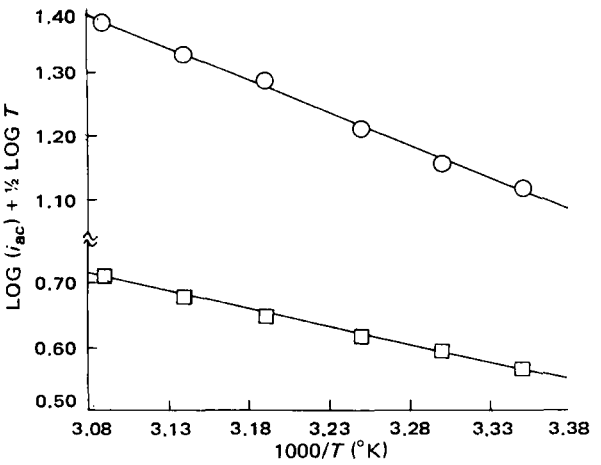

Figure 7—*Linear relationship between log (i_{ac}) + ½ log T and the reciprocal of temperature (Eq. 7) at pH 6.01. From the slope, the ΔG was calculated to be 9.64 kcal/mole for ferredoxin Type I (○) and 4.82 kcal/mole for ferredoxin Type III (□).*

pH (3.51) in the absence or presence of *N*-ethylmaleimide to characterize the relationship of its electroactivity to sulfur–iron bonds. The concentration of electroactive ferredoxin diminished with time at this pH (independent of the presence of *N*-ethylmaleimide) (Fig. 6). Meanwhile, the concentration of electroactive *N*-ethylmaleimide, which complexed with any sulfhydryl group formed, concomitantly decreased. These results (Fig. 6) indicated that more sulfhydryl groups were exposed as time went on and complexed with *N*-ethylmaleimide. The diminishing of the electroactive ferredoxin concentration followed the same pattern as the decrease in the electroactive *N*-ethylmaleimide concentration. Overall, a value of 3.6 was determined for the number of free sulfhydryl groups uncoordinated from each molecule of ferredoxin Type I after 180 min of acidic hydrolysis. Thus, the ac peak at −0.533 v (Table II and Fig. 1) is related to the electroactivity of the sulfur–iron coordination in ferredoxin.

The acidic cleavage of sulfur–iron coordination may increase the iron–iron distance and thus interrupt the antiferromagnetic interaction between iron atoms in its active center, resulting in a loss of electroactivity. The acidic conditions applied here characterize the relationship between the electroactivity of ferredoxins and their sulfur–iron coordinations. In the neutral pH range, both the electroactivity and sulfur–iron coordination were stable when some precautions, *e.g.*, the elimination of oxygen, were taken.

Temperature-Dependent Electroreduction of Ferredoxins—The effects of temperature on the electroreduction of ferredoxins were examined at pH 5.4–7.5, where the stability of ferredoxins was ascertained. In all cases, the magnitude of the ac currents, i_{ac}, for the sulfur–iron reduction peak increased as the temperature increased from 20 to 50°, while the magnitude of peak potentials (E_p) was essentially constant. On the other hand, the current height for the reduction of uncoordinated ferric ion was temperature independent.

The current height (i_{ac}) at the peak of an ac reduction wave, resulting from the application of an alternating potential (E_{ac}) at a limiting low sinusoidal frequency (W), is given by (17):

$$i_{ac} = \frac{n^2F^2AE_{ac}CW^{1/2}D_o^{1/2}}{4RT} \qquad \text{(Eq. 3)}$$

where n is the number of electrons involved, F is the Faraday constant, A is the surface area of the electrode, C is the concentration of the electroactive species, D_o is the diffusivity of the oxidized form of the electroactive species, R is the gas constant, and T is the absolute temperature.

Taking the logarithm on both sides of Eq. 3 results in:

$$\log (i_{ac}) = \log \left(\frac{n^2F^2AE_{ac}CW^{1/2}}{4R}\right) + \tfrac{1}{2}\log D_o - \log T \qquad \text{(Eq. 4)}$$

Also, it is known (18) that the diffusion is an energy-activated process, and the diffusivity of the oxidized species is thus defined by:

$$D_o = l^2\frac{RT}{Nh}e^{-\Delta G/RT} \qquad \text{(Eq. 5)}$$

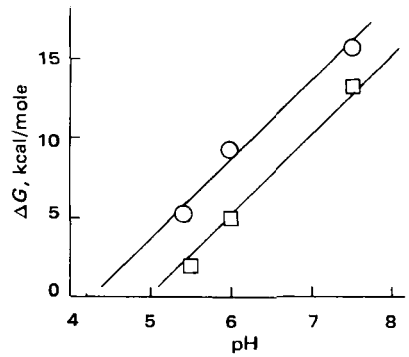

Figure 8—*Relationship between ΔG, activation free energy, and pH profile of ferredoxin solutions. Key: ○, ferredoxin Type I; and □, ferredoxin Type III.*

where l is a mean jump distance, N is Avogadro's number, h is the thickness of diffusion path, and ΔG is activation free energy. Taking the logarithm on both sides of Eq. 5 gives:

$$\log (D_o) = \log \left(l^2\frac{R}{Nh}\right) + \log T - \frac{\Delta G}{2.303R}\frac{1}{T} \qquad \text{(Eq. 6)}$$

Substituting Eq. 6 for the log D_o term in Eq. 4 results in:

$$\log (i_{ac}) + \tfrac{1}{2}\log T = \text{constant} - \frac{\Delta G}{4.606R}\frac{1}{T} \qquad \text{(Eq. 7)}$$

Equation 7 suggests that a linear relationship exists between log (i_{ac}) + ½ log T and the reciprocal of temperature (T^{-1}). A typical plot is shown in Fig. 7 for ferredoxin Types I and III at pH 6.01. The variation in the value of ½ log T was only 1.7% as the temperature was raised from 20 to 50°. From the slope of the linearity, the activation free energy (ΔG) was calculated to be 9.64 kcal/mole for ferredoxin Type I and 4.82 kcal/mole for ferredoxin Type III. The twofold higher ΔG value observed for Type I than for Type III may be related to differences in the complexity of their active centers.

The resultant ΔG values were observed to be pH dependent and increased as the pH of ferredoxin solutions increased (Fig. 8). Both ferredoxin Types I and III showed the same linear ΔG *versus* pH relationship. This observation implied that the conformation of ferredoxin molecule and, hence, its diffusivity were sensitive to the variation in proton (H^+) concentration in the solution. As the concentration of the proton decreased (as pH increased), the conformation of ferredoxin molecule was changed so that its molecular diffusion required a higher value of activation free energy (ΔG).

In summary, the results demonstrated that ac polarography is the technique of choice for studying the electroreduction of ferredoxins. The reduction peak at −0.533 v (at pH 6.01) was attributed to an electroactive sulfur–iron coordination in ferredoxin molecules. The acidic disruption of this sulfur–iron coordination led to interruption of the electroactivity of ferredoxins at low pH. The electroreduction of ferredoxins required energy and was pH dependent.

REFERENCES

(1) L. E. Mortenson, R. C. Valentine, and J. E. Carnahan, *Biochem. Biophys. Res. Commun.*, **7**, 448(1962).

(2) K. Tagawa and D. I. Arnon, *Nature*, **195**, 537(1962).

(3) W. Lovenberg, B. B. Buchanan, and J. C. Rabinowitz, *J. Biol. Chem.*, **238**, 3899(1963).

(4) R. C. Valentine, *Bacteriol. Rev.*, **28**, 497(1964).

(5) D. I. Edwards, M. Dye, and H. Carne, *J. Gen. Microbiol.*, **76**, 135(1973).

(6) D. G. Lindmark and M. Muller, *J. Protozol.*, **21**, 436(1974).

(7) R. M. J. Ings, J. A. McFadzean, and W. E. Ormerod, *Biochem. Pharmacol.*, **23**, 1421(1974).

(8) Y. W. Chien, H. J. Lambert, and D. R. Sanvordeker, *J. Pharm. Sci.*, **64**, 957(1975).

(9) J. O'M. Bockris and A. K. N. Reddy, "Modern Electrochemistry," vol. 2, Plenum, New York, N.Y., 1973, chap. 9.

(10) L. E. Mortenson and G. Nakos, in "Iron-Sulfur Proteins," vol. I, W. Lovenberg, Ed., Academic, New York, N.Y., 1973, chap. 2.

(11) G. Palmer, in "Iron-Sulfur Proteins," vol. II, W. Lovenberg,

Ed., Academic, New York, N.Y., 1973, chap. 8.
(12) S. G. Mayhew, D. Petering, G. Palmer, and G. P. Foust, *J. Biol. Chem.*, **244**, 2830(1969).
(13) M. C. W. Evans, D. O. Hall, H. Bothe, and F. R. Whatley, *Biochem. J.*, **110**, 485(1968).
(14) K. Eisenstein and J. H. Wang, *J. Biol. Chem.*, **244**, 1720(1969).
(15) R. Malkin, in "Iron–Sulfur Proteins," vol. II, W. Lovenberg, Ed., Academic, New York, N.Y., 1973, chap. 1.
(16) P. D. J. Weitzman and H. J. Tyler, *Anal. Biochem.*, **43**, 321(1971).
(17) B. Breyer and H. H. Bauer, "Alternating Current Polarography and Tensammetry," Interscience, New York, N.Y., 1963, chap. 2, p. 47.
(18) J. O'M. Bockris and A. K. N. Reddy, "Modern Electrochemistry," vol. 1, Plenum, New York, N.Y., 1973, chaps. 4, 5.

ACKNOWLEDGMENTS AND ADDRESSES

Received August 11, 1975, from the *Pharmaceutical Research Group, Development Department, Searle Laboratories, G.D. Searle & Co., Chicago, IL 60680*

Accepted for publication December 15, 1975.

The author expresses his appreciation to Dr. E. Kreider, Dr. H. Lambert, Dr. C. Mackerer, and Dr. J. Oppermann for their encouragement and constructive discussions. Thanks are also extended to Dr. D. Sanvordeker for spinach ferredoxin and to Ms. I. Wiggers and Miss S. Sering for their assistance in manuscript preparation.

Clofibrate Microcapsules: Preparation and Release Rate Studies

P. L. MADAN *¶x, DEVENDRA K. MADAN ‡, and J. C. PRICE §

Abstract □ Microencapsulation of clofibrate and dissolution characteristics of clofibrate microcapsules were investigated. Spherical droplets of clofibrate, prepared by a capillary jet method, were encapsulated in gelatin by simple coacervation, using sodium sulfate as the coacervating agent. The microcapsules, which were hardened up to 8 hr with formaldehyde, were recovered as discrete, free-flowing particles. Dissolution of clofibrate from the microcapsules was not adequately described by either square root of time or Langenbucher kinetics but followed predominantly zero-order release patterns at all hardening times. A linear correlation was found between the hardening time and the $t_{50\%}$ release time.

Keyphrases □ Clofibrate—microcapsules prepared, release rate studied □ Microcapsules—clofibrate, preparation described, release rate studied □ Dosage forms—microcapsules, clofibrate, preparation described, release rate studied □ Release rate—clofibrate from microcapsules □ Hypocholesterolemic agents—clofibrate, microcapsules, preparation described, release rate studied

Clofibrate USP, a liquid hypocholesterolemic agent with an unpleasant odor and taste, is administered at rather frequent time intervals (1). Because of these properties, microencapsulation of the drug may result in a more acceptable and effective dosage form.

Simple coacervation with gelatin has been known for many years (2) and has been studied as a means of encapsulation for various pharmaceuticals and chemicals (3). Only a few reports of the dissolution characteristics of such microcapsules are available (4–7), possibly because of the difficulty of obtaining discrete, free-flowing, and reproducible microcapsules.

This study reports the microencapsulation of clofibrate by simple coacervation with gelatin and the effect of hardening time on the dissolution of the microcapsules.

EXPERIMENTAL

Materials—All materials were of USP or reagent grade and were used without further purification. The gelatin[1] used had the following specifications as provided by the manufacturer: type, B-lime treated; bloom, 275; viscosity, 63.9 mpoises; pH (of solution of gelatin), 5.70; moisture, 10.5%; and isoionic point, 4.9.

Production of Monodisperse Spheres—The method employed for the production of monodisperse spheres of clofibrate[2] liquid was similar to that reported earlier (8). The apparatus is shown in Fig. 1. A fine capillary tube, C, was attached to an aspirator bottle, R, which served as the reservoir for the liquid to be encapsulated. The internal diameter of the capillary tube was such that air pressure had to be applied to force the liquid through the capillary. A filter, F, was fitted between the capillary and the aspirator bottle to prevent obstruction by particulate matter.

By varying the internal diameter of the capillary and/or air pressure, the diameter of the droplets produced could be changed. To attain uniformity of droplet production, all experiments were conducted under identical conditions, using the same capillary tube and forcing clofibrate from the capillary tube under identical air pressure.

The droplets leaving the capillary tube were allowed to fall into the gelatin solution. This solution was continuously stirred to prevent coalescence of clofibrate droplets.

Microencapsulation Procedure—Simple coacervation was used to achieve microencapsulation (2), and all experiments were conducted under identical conditions with the same or similar equipment. Coacervation was carried out at 40 ± 1°. The gelatin solution was prepared by soaking 10 g of gelatin in 100 ml of distilled water, allowing it to hydrate for about 12 hr, and then warming to 40° to effect solution. Then 40 ml of clofibrate in the form of monodisperse spheres was added to the gelatin solution, and the mixture was stirred continuously at 30 rpm to prevent coalescence of clofibrate droplets.

After stirring for about 5 min, a 20% (w/w) solution of sodium sulfate, also at 40°, was added to the mixture. Stirring was continued for 15 min more to ensure complete encapsulation, and the formation of coacervate-coated spheres was verified microscopically. The product was then poured into 500 ml of a 7% (w/w) sodium sulfate solution at about 4° to gel the liquid shell of the microcapsules. The mixture was maintained at less than 10° and stirred continuously for 30 min to complete the gelling process.

Recovery of Microcapsules—For this investigation, it was essential to obtain microcapsules in the form of a free-flowing powder. The method of Madan *et al.* (8) was modified slightly and, instead of 70% 2-propanol at room temperature, an equal volume of chilled 2-propanol was added to the product to dehydrate and to flocculate the coacervated droplets. The microcapsules were allowed to settle,

[1] P. Leiner and Sons, America Inc., St. Claire Shores, Mich.

[2] Ayerst Laboratories, Rouses Point, N.Y.

Ed., Academic, New York, N.Y., 1973, chap. 8.
(12) S. G. Mayhew, D. Petering, G. Palmer, and G. P. Foust, *J. Biol. Chem.*, **244**, 2830(1969).
(13) M. C. W. Evans, D. O. Hall, H. Bothe, and F. R. Whatley, *Biochem. J.*, **110**, 485(1968).
(14) K. Eisenstein and J. H. Wang, *J. Biol. Chem.*, **244**, 1720(1969).
(15) R. Malkin, in "Iron–Sulfur Proteins," vol. II, W. Lovenberg, Ed., Academic, New York, N.Y., 1973, chap. 1.
(16) P. D. J. Weitzman and H. J. Tyler, *Anal. Biochem.*, **43**, 321(1971).
(17) B. Breyer and H. H. Bauer, "Alternating Current Polarography and Tensammetry," Interscience, New York, N.Y., 1963, chap. 2, p. 47.
(18) J. O'M. Bockris and A. K. N. Reddy, "Modern Electrochemistry," vol. 1, Plenum, New York, N.Y., 1973, chaps. 4, 5.

ACKNOWLEDGMENTS AND ADDRESSES

Received August 11, 1975, from the *Pharmaceutical Research Group, Development Department, Searle Laboratories, G.D. Searle & Co., Chicago, IL 60680*

Accepted for publication December 15, 1975.

The author expresses his appreciation to Dr. E. Kreider, Dr. H. Lambert, Dr. C. Mackerer, and Dr. J. Oppermann for their encouragement and constructive discussions. Thanks are also extended to Dr. D. Sanvordeker for spinach ferredoxin and to Ms. I. Wiggers and Miss S. Sering for their assistance in manuscript preparation.

Clofibrate Microcapsules: Preparation and Release Rate Studies

P. L. MADAN *¶x, DEVENDRA K. MADAN ‡, and J. C. PRICE §

Abstract □ Microencapsulation of clofibrate and dissolution characteristics of clofibrate microcapsules were investigated. Spherical droplets of clofibrate, prepared by a capillary jet method, were encapsulated in gelatin by simple coacervation, using sodium sulfate as the coacervating agent. The microcapsules, which were hardened up to 8 hr with formaldehyde, were recovered as discrete, free-flowing particles. Dissolution of clofibrate from the microcapsules was not adequately described by either square root of time or Langenbucher kinetics but followed predominantly zero-order release patterns at all hardening times. A linear correlation was found between the hardening time and the $t_{50\%}$ release time.

Keyphrases □ Clofibrate—microcapsules prepared, release rate studied □ Microcapsules—clofibrate, preparation described, release rate studied □ Dosage forms—microcapsules, clofibrate, preparation described, release rate studied □ Release rate—clofibrate from microcapsules □ Hypocholesterolemic agents—clofibrate, microcapsules, preparation described, release rate studied

Clofibrate USP, a liquid hypocholesterolemic agent with an unpleasant odor and taste, is administered at rather frequent time intervals (1). Because of these properties, microencapsulation of the drug may result in a more acceptable and effective dosage form.

Simple coacervation with gelatin has been known for many years (2) and has been studied as a means of encapsulation for various pharmaceuticals and chemicals (3). Only a few reports of the dissolution characteristics of such microcapsules are available (4–7), possibly because of the difficulty of obtaining discrete, free-flowing, and reproducible microcapsules.

This study reports the microencapsulation of clofibrate by simple coacervation with gelatin and the effect of hardening time on the dissolution of the microcapsules.

EXPERIMENTAL

Materials—All materials were of USP or reagent grade and were used without further purification. The gelatin[1] used had the following specifications as provided by the manufacturer: type, B-lime treated; bloom, 275; viscosity, 63.9 mpoises; pH (of solution of gelatin), 5.70; moisture, 10.5%; and isoionic point, 4.9.

Production of Monodisperse Spheres—The method employed for the production of monodisperse spheres of clofibrate[2] liquid was similar to that reported earlier (8). The apparatus is shown in Fig. 1. A fine capillary tube, C, was attached to an aspirator bottle, R, which served as the reservoir for the liquid to be encapsulated. The internal diameter of the capillary tube was such that air pressure had to be applied to force the liquid through the capillary. A filter, F, was fitted between the capillary and the aspirator bottle to prevent obstruction by particulate matter.

By varying the internal diameter of the capillary and/or air pressure, the diameter of the droplets produced could be changed. To attain uniformity of droplet production, all experiments were conducted under identical conditions, using the same capillary tube and forcing clofibrate from the capillary tube under identical air pressure.

The droplets leaving the capillary tube were allowed to fall into the gelatin solution. This solution was continuously stirred to prevent coalescence of clofibrate droplets.

Microencapsulation Procedure—Simple coacervation was used to achieve microencapsulation (2), and all experiments were conducted under identical conditions with the same or similar equipment. Coacervation was carried out at 40 ± 1°. The gelatin solution was prepared by soaking 10 g of gelatin in 100 ml of distilled water, allowing it to hydrate for about 12 hr, and then warming to 40° to effect solution. Then 40 ml of clofibrate in the form of monodisperse spheres was added to the gelatin solution, and the mixture was stirred continuously at 30 rpm to prevent coalescence of clofibrate droplets.

After stirring for about 5 min, a 20% (w/w) solution of sodium sulfate, also at 40°, was added to the mixture. Stirring was continued for 15 min more to ensure complete encapsulation, and the formation of coacervate-coated spheres was verified microscopically. The product was then poured into 500 ml of a 7% (w/w) sodium sulfate solution at about 4° to gel the liquid shell of the microcapsules. The mixture was maintained at less than 10° and stirred continuously for 30 min to complete the gelling process.

Recovery of Microcapsules—For this investigation, it was essential to obtain microcapsules in the form of a free-flowing powder. The method of Madan *et al.* (8) was modified slightly and, instead of 70% 2-propanol at room temperature, an equal volume of chilled 2-propanol was added to the product to dehydrate and to flocculate the coacervated droplets. The microcapsules were allowed to settle,

[1] P. Leiner and Sons, America Inc., St. Claire Shores, Mich.

[2] Ayerst Laboratories, Rouses Point, N.Y.

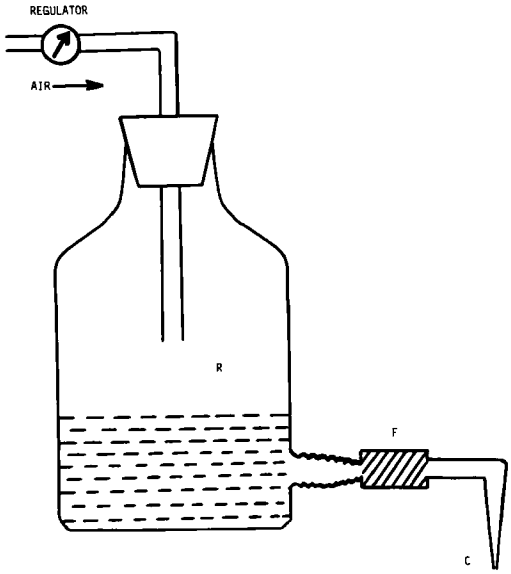

Figure 1—*Schematic diagram of the apparatus used for the production of clofibrate droplets.*

and the mother liquor was decanted. The product was washed with chilled 2-propanol (10 ml/g of microcapsules) and allowed to air dry at room temperature to yield free-flowing, discrete microcapsules.

Evaluation of Microcapsules—The microcapsules were hardened by immersing in a 10% solution of formaldehyde in 2-propanol for 0, 1, 2, 4, and 8 hr. Ten milliliters of hardening solution was used for each gram of microcapsules. The modified flask method (9) was used to evaluate the ability of dried microcapsules to resist release of the encapsulated drug. Six hundred milliliters of the dissolution medium (30% 2-propanol solution) at 37 ± 0.5° was stirred at 50 rpm using a constant-speed motor[3].

Dissolution was followed by examining triplicate samples containing approximately 30 mg of drug. In each case, microcapsules were placed on the surface of the dissolution medium and allowed to settle. At appropriate intervals, samples of the dissolution medium were withdrawn using a pipet fitted with a cotton plug. A constant volume of the dissolution medium was maintained by the addition of an equal volume of the dissolution medium after each 5-ml sample was withdrawn. The cotton plug was added to the dissolution mixture. Concentrations were determined spectrophotometrically at 226 nm.

Assay Procedure for Total Clofibrate Content of Microcapsules—Triplicate samples of approximately 30 mg of the microcapsules were accurately weighed and placed in a 150-ml homogenizing flask containing 50 ml of 30% 2-propanol. The samples were completely ruptured with a blender[4] operating at its maximum speed. In each case, two samples were blended for 10 min, and complete rupture was assured by blending a third sample for 15 min with no observed

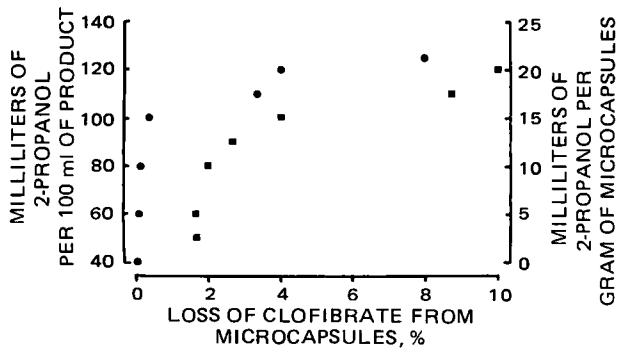

Figure 2—*Percent loss of clofibrate from the microcapsules during 2-propanol treatment. Key: ●, 2-propanol used for flocculation and dehydration; and ■, 2-propanol used for washing microcapsules.*

[3] Synchron model K12Rc 5-712.
[4] Model 45, Virtis Research Equipment, Gardner, N.Y.

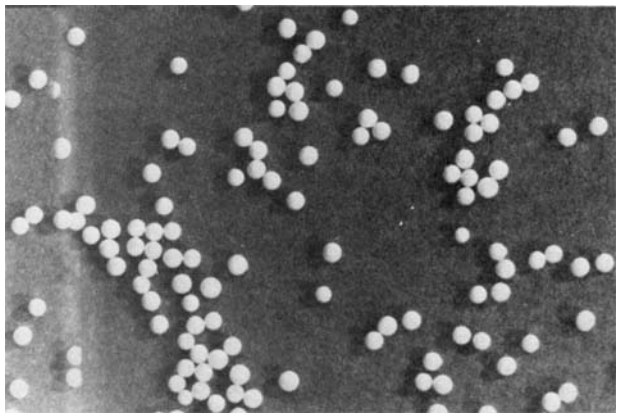

Figure 3—*Photomicrograph of clofibrate microcapsules as discrete particles.*

increase in drug content. Filtered aliquots of the mixture were then assayed spectrophotometrically.

RESULTS AND DISCUSSION

Preparation of Uniform Drug Particles—Uniform spheres of clofibrate with a mean diameter of 190 ± 10 μm were obtained when the rate of production was restricted to 100–120 particles/min. The resulting particles were essentially monodisperse and ideally suited to encapsulation and dissolution studies. Greater production rates were attempted, but they resulted in coalescence of the droplets in the gelatin dispersion.

Preparation and Recovery of Microcapsules—The usual methods of recovery by decantation and filtration or centrifugation resulted in rubbery masses which dried to hard lumps impossible to separate into individual particles. However, discrete microcapsules were successfully obtained using a chilled solution of 50% 2-propanol to dehydrate the coacervate droplets. At lower concentrations, the coacervate tended to agglomerate; at higher concentrations, an increased loss of clofibrate occurred due to leaching. The effect of the 2-propanol treatment on the loss of clofibrate from the microcapsules is summarized in Fig. 2.

Figure 3 shows a photomicrograph of clofibrate microcapsules recovered as discrete particles in the form of a free-flowing powder.

Dissolution Studies—Since clofibrate is insoluble in water (10), conventional dissolution media such as 0.1 *M* hydrochloric acid and simulated gastric fluid could not be used. The selection of a suitable dissolution medium was, therefore, based on the following criteria: (*a*) solubility of the drug, (*b*) suitability of the dissolution medium as the solvent for spectrophotometric assay, and (*c*) noninterference with the hydration of the microcapsule shell.

The USP spectrophotometric assay for clofibrate (10) uses methanol as the solvent. Neither methanol nor ethanol, in any dilution, can be employed as a dissolution medium for gelatin–acacia microcapsules because the strong dehydrating properties of these alcohols does not permit the hydration of the capsule walls. Bensusan (11) showed that soluble collagens are precipitated by aliphatic alcohols in the order methanol > ethanol > 1-propanol > 2-propanol. Thirty percent 2-propanol in water proved to have sufficient solvent property to permit dissolution without the risk of saturation and also allowed the complete hydration of the microcapsules. Microscopic examination revealed that the hydration of the microcapsules in 30% 2-propanol solution was almost identical to that in water.

The dissolution rate profiles of the microcapsules are shown in Fig. 4. Each point represents an average of at least three experiments. Most of the points had a range of less than 5%; a few points exceeded 5% but were within a 10% range.

As seen in Fig. 4, at between 10 and 85–90% release, the microcapsules yielded straight-line plots, characteristic of zero-order release irrespective of the effect of hardening. The first 5–10% clofibrate was released almost as soon as the dissolution determinations were started. This early rapid release was probably due to the clofibrate on or in the wall material of the microcapsules.

In a study dealing with the microencapsulation of sulfadiazine by a method similar to the one described here, Nixon and Walker (6)

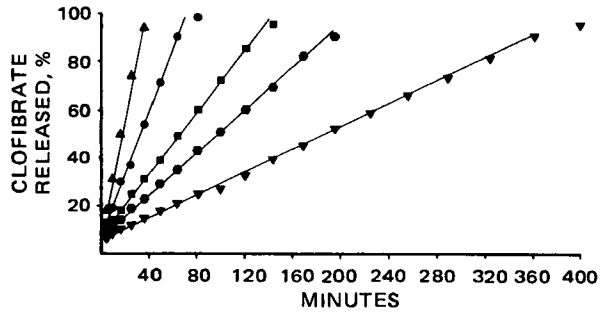

Figure 4—*Relase rate profiles of clofibrate microcapsules. Key: ●, microcapsules hardened for 1 hr; ■, microcapsules hardened for 2 hr; ●, microcapsules hardened for 4 hr; ▼, microcapsules hardened for 8 hr; and ▲, unhardened microcapsules.*

reported a similar initial rapid release. However, the results obtained in the present investigation differ in several respects. For example, Nixon and Walker (6) found that the initial rapid release approximated 25% of the core material dissolved followed by a gradual fall in the rate, with the last 20% being released very slowly. These authors found first-order release for the hardened material, but the unhardened microcapsules were better described when the percent sulfadiazine released was plotted on a probability scale as a function of the logarithm of time. They concluded that their dissolution data were not amenable to any one type of treatment.

It is possible that the nature of the core material may have been responsible for the differences observed between the present investigation and the one reported by Nixon and Walker (6). Microcapsules made from liquids usually contain only one droplet and tend to be spherical. In this investigation, the droplets were nearly monodisperse. In the case of solids, the individual microcapsules can be composed of a number of crystals, usually arranged toward the center of the microcapsule. On hardening, the wall material shrinks and the microcapsules tend to assume the shape of the solid crystals dispersed in them, thus resulting in a heterogeneous mixture.

Mechanism of Release of Clofibrate from Microcapsules—It was proposed previously (12, 13) that the release of medicaments from solid matrixes may be considered as taking place through a simple diffusional process or through leaching by dissolution into the permeating fluid. In either case, a plot of the residual fraction as a function of the square root of time should yield a straight line. Square root of time plots of the clofibrate release from microcapsules (Fig. 5) show a linear relationship only over the latter part of the dissolution. The initial portion of the graph shows that the first 5–10% clofibrate was released almost as soon as the dissolution determinations were started, while the next 25% clofibrate was released very slowly.

Here again, the results are somewhat different from those reported by Nixon and Walker (6). They found a linear relationship for the entire period with the hardened material, but the unhardened microcapsules tended to nonlinearity during the latter part of the dissolution.

Langenbucher kinetics (14) of uniform, nondisintegrating granules were also applied to the dissolution data. Figure 6 shows the cube root

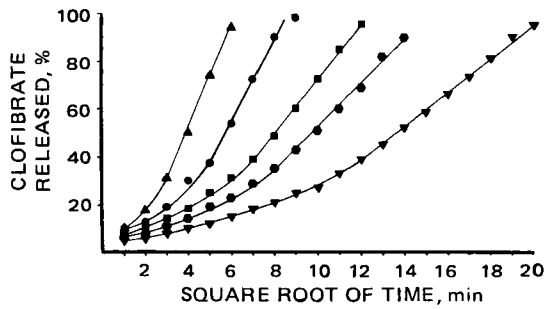

Figure 5—*Percent clofibrate released as a function of the square root of time. Key: ●, microcapsules hardened for 1 hr; ■, microcapsules hardened for 2 hr; ●, microcapsules hardened for 4 hr; ▼, microcapsules hardened for 8 hr; and ▲, unhardened microcapsules.*

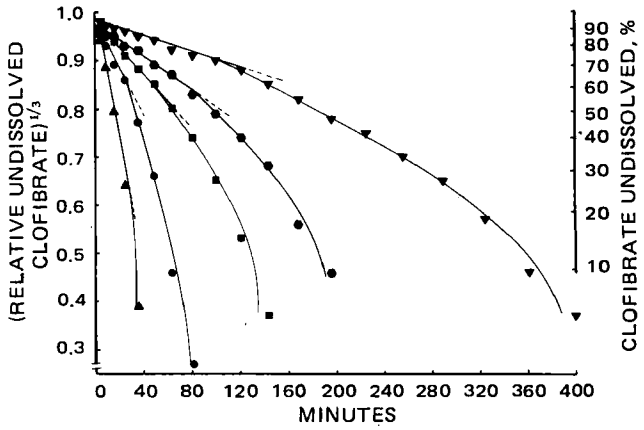

Figure 6—*Langenbucher cube root dissolution plot. Key: ●, microcapsules hardened for 1 hr; ■, microcapsules hardened for 2 hr; ●, microcapsules hardened for 4 hr; ▼, microcapsules hardened for 8 hr; and ▲, unhardened microcapsules.*

of the relative undissolved clofibrate plotted as a function of time. This treatment of the data appears to describe the dissolution of the microcapsules only in the initial portion (up to about 30–40% clofibrate released).

The predominantly zero-order release observed in the present investigation can be explained by the model shown in Fig. 7. As soon as the dissolution determinations were started, the dissolution medium (water–2-propanol) penetrated the microcapsule wall to dissolve some clofibrate. This result produced a saturated clofibrate solution within the microcapsule shell wall, thus setting up a concentration gradient between the microcapsules and the dissolution medium. As dissolution progressed, clofibrate solution diffused out slowly and therefore constituted a rate-limiting step. Since the concentration of solution inside the microcapsule shell remained constant (saturated), the diffusion rate of clofibrate out of the microcapsules would also be expected to remain constant, *i.e.*, follow zero-order dissolution, until the quantity of undissolved material was insufficient to produce a saturated solution.

Effect of Hardening Time—The effect of hardening time was studied over an 8-hr period, because hardening beyond 8 hr caused the loss of clofibrate from the microcapsules. No loss of clofibrate could be detected when the hardening time was 8 hr or less. Microscopic examination of those microcapsules hardened for more than 8 hr revealed numerous fractured and broken capsules, thus accounting for the loss of clofibrate. Prolonged hardening probably caused the walls to become brittle and subject to fracture, with subsequent loss of the liquid internal constituent.

The initial rapid release (Fig. 4) decreased with an increase in the hardening time, in contradiction to the rates reported by Nixon and Walker (6). The decrease in the initial rapid release with the corresponding increase in hardening time may be explained by the shrinkage of the wall material during the hardening process, thus leaving less room for clofibrate entrapped within the wall.

The release of clofibrate from the microcapsules was related directly to the hardening time. Figure 8 shows a linear relationship of the $t_{50\%}$ release time plotted as a function of hardening time.

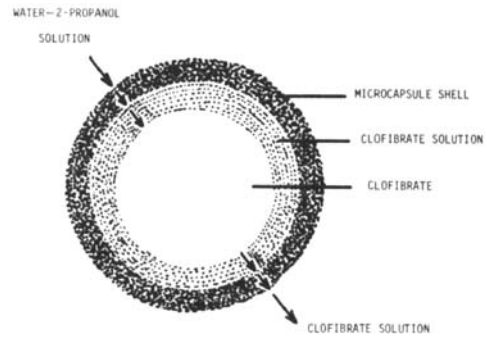

Figure 7—*Proposed model explaining the release of clofibrate from microcapsules.*

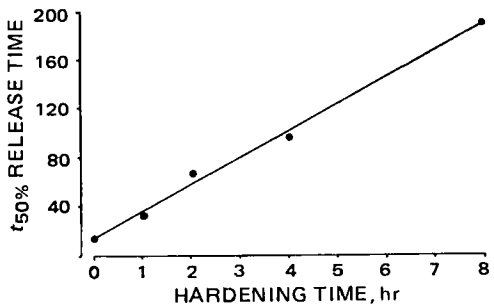

Figure 8—*The $t_{50\%}$ release time as a function of hardening time of the microcapsules.*

SUMMARY AND CONCLUSIONS

This study was undertaken to investigate the feasibility of microencapsulation of clofibrate, to collect the microcapsules in the form of a free-flowing powder, and to evaluate the dissolution characteristics of the microcapsules obtained. From the results, the following conclusions are drawn:

1. Microencapsulation of clofibrate can be successfully achieved by simple coacervation.
2. Free-flowing discrete microcapsules can be obtained by treatment with 2-propanol.
3. After an initial surge, dissolution of clofibrate from microcapsules under sink conditions followed apparent zero-order release rates until nearly 90% of the drug was released. The dissolution pattern observed can be explained by a model in which the capsule wall limits dissolution from a saturated solution of the clofibrate formed inside the microcapsule.
4. The release rates of the microcapsules were related directly to the hardening time of the microcapsules. A linear correlation was found between the hardening time and the *in vitro* $t_{50\%}$ release time of the microcapsules.
5. Hardening of microcapsules up to 8 hr did not result in a loss of clofibrate, but longer hardening times caused rupture of some of the microcapsules with subsequent loss of clofibrate.

REFERENCES

(1) "Remington's Pharmaceutical Sciences," 15th ed., Mack Publishing Co., Easton, Pa., 1975, p. 796.

(2) L. J. W. Holleman, H. G. Bungenberg de Jong, and R. S. Tjaden Modderman, *Kolloidchem. Beih.*, **39**, 334(1934).

(3) B. Green, U.S. pat. 2,800,458 (1958).

(4) R. E. Phares, Jr., and G. J. Sperandio, *J. Pharm. Sci.*, **53**, 515(1964).

(5) J. R. Nixon, S. A. H. Khalil, and J. E. Carless, *J. Pharm. Pharmacol.*, **20**, 528(1968).

(6) J. R. Nixon and S. E. Walker, *ibid.*, **23**, 147S(1971).

(7) P. L. Madan, L. A. Luzzi, and J. C. Price, *J. Pharm. Sci.*, **63**, 280(1974).

(8) *Ibid.*, **61**, 1586(1972).

(9) P. L. Madan, J. C. Price, and L. A. Luzzi, in "Microencapsulation: Processes and Applications," J. E. Vandegaer, Ed., Plenum, New York, N.Y., 1974, p. 39.

(10) "The United States Pharmacopeia," 19th rev., Mack Publishing Co., Easton, Pa., 1975, p. 96.

(11) H. B. Bensusan, *J. Am. Chem. Soc.*, **82**, 4995(1960).

(12) T. Higuchi, *J. Pharm. Sci.*, **50**, 874(1961).

(13) *Ibid.*, **52**, 1145(1963).

(14) F. Langenbucher, *J. Pharm. Sci.*, **58**, 1265(1969).

ACKNOWLEDGMENTS AND ADDRESSES

Received February 18, 1975, from the *College of Pharmacy and Allied Health Professions, St. John's University, Jamaica, NY 11439, the ‡Faculty of Pharmacy and Pharmaceutical Sciences, University of Alberta, Edmonton, Alberta, Canada, and the §School of Pharmacy, University of Georgia, Athens, GA 30602

Accepted for publication December 10, 1975.

¶ Recipient of a Lederle Pharmacy Faculty Award.

ˣ To whom inquiries should be directed.

Synthesis of Potential Mescaline Antagonists

FRANK DeSANTIS, Jr. *, and KARL A. NIEFORTH ˣ

Abstract □ 1-[2-(3,4,5-Trimethoxyphenyl)ethyl]-3-pyrroline, 2-(3,4,5-trimethoxybenzyl)-1,2,3,6-tetrahydropyridine, *N*-*n*-propylmescaline, *N*-cyclopropylmethylmescaline, and *N*-allylmescaline were synthesized as potential mescaline antagonists. The ability of these compounds to antagonize mescaline-induced disruption of swim behavior is also given.

Keyphrases □ Mescaline antagonists, potential—synthesized and screened for effect on mescaline-induced CNS stimulation □ Antagonists, mescaline, potential—synthesized and screened for effect on mescaline-induced CNS stimulation □ CNS stimulation, mescaline induced—effect of various mescaline antagonists evaluated □ Structure–activity relationships—various mescaline antagonists screened for effect on mescaline-induced CNS stimulation

The method presently used to counteract the hallucinogenic effects of mescaline (I) and other hallucinogens is administration of drugs that indirectly counteract the hallucinogenic effects, such as tranquilizers and sedatives (1). The object of this research was to synthesize compounds that would antagonize the effects of mescaline through a direct competitive mechanism. The compounds would ideally have little or no effect of their own but, when given in conjunction with mescaline, would mitigate the central nervous system (CNS) stimulation.

It has been well documented that replacement of the

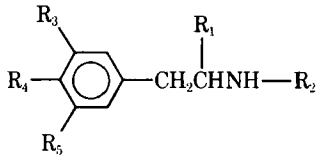

I: $R_1 = R_2 = H$, $R_3 = R_4 = R_5 = OCH_3$

II: $R_1 = CH_3$, $R_2 = R_3 = R_4 = R_5 = H$

III: $R_1 = CH_3$, $R_2 = H$, $R_3 = R_4 = R_5 = OCH_3$

IV: $R_1 = H$, $R_2 = n\text{-}C_3H_7$, $R_3 = R_4 = R_5 = OCH_3$

V: $R_1 = H$, $R_2 = CH_2$— , $R_3 = R_4 = R_5 = OCH_3$

VI: $R_1 = H$, $R_2 = CH_2$—CH=CH_2, $R_3 = R_4 = R_5 = OCH_3$

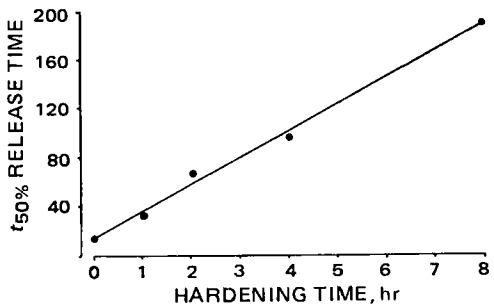

Figure 8—*The $t_{50\%}$ release time as a function of hardening time of the microcapsules.*

SUMMARY AND CONCLUSIONS

This study was undertaken to investigate the feasibility of microencapsulation of clofibrate, to collect the microcapsules in the form of a free-flowing powder, and to evaluate the dissolution characteristics of the microcapsules obtained. From the results, the following conclusions are drawn:

1. Microencapsulation of clofibrate can be successfully achieved by simple coacervation.
2. Free-flowing discrete microcapsules can be obtained by treatment with 2-propanol.
3. After an initial surge, dissolution of clofibrate from microcapsules under sink conditions followed apparent zero-order release rates until nearly 90% of the drug was released. The dissolution pattern observed can be explained by a model in which the capsule wall limits dissolution from a saturated solution of the clofibrate formed inside the microcapsule.
4. The release rates of the microcapsules were related directly to the hardening time of the microcapsules. A linear correlation was found between the hardening time and the *in vitro* $t_{50\%}$ release time of the microcapsules.
5. Hardening of microcapsules up to 8 hr did not result in a loss of clofibrate, but longer hardening times caused rupture of some of the microcapsules with subsequent loss of clofibrate.

REFERENCES

(1) "Remington's Pharmaceutical Sciences," 15th ed., Mack Publishing Co., Easton, Pa., 1975, p. 796.

(2) L. J. W. Holleman, H. G. Bungenberg de Jong, and R. S. Tjaden Modderman, *Kolloidchem. Beih.*, **39**, 334(1934).

(3) B. Green, U.S. pat. 2,800,458 (1958).

(4) R. E. Phares, Jr., and G. J. Sperandio, *J. Pharm. Sci.*, **53**, 515(1964).

(5) J. R. Nixon, S. A. H. Khalil, and J. E. Carless, *J. Pharm. Pharmacol.*, **20**, 528(1968).

(6) J. R. Nixon and S. E. Walker, *ibid.*, **23**, 147S(1971).

(7) P. L. Madan, L. A. Luzzi, and J. C. Price, *J. Pharm. Sci.*, **63**, 280(1974).

(8) *Ibid.*, **61**, 1586(1972).

(9) P. L. Madan, J. C. Price, and L. A. Luzzi, in "Microencapsulation: Processes and Applications," J. E. Vandegaer, Ed., Plenum, New York, N.Y., 1974, p. 39.

(10) "The United States Pharmacopeia," 19th rev., Mack Publishing Co., Easton, Pa., 1975, p. 96.

(11) H. B. Bensusan, *J. Am. Chem. Soc.*, **82**, 4995(1960).

(12) T. Higuchi, *J. Pharm. Sci.*, **50**, 874(1961).

(13) *Ibid.*, **52**, 1145(1963).

(14) F. Langenbucher, *J. Pharm. Sci.*, **58**, 1265(1969).

ACKNOWLEDGMENTS AND ADDRESSES

Received February 18, 1975, from the *College of Pharmacy and Allied Health Professions, St. John's University, Jamaica, NY 11439, the ‡Faculty of Pharmacy and Pharmaceutical Sciences, University of Alberta, Edmonton, Alberta, Canada, and the §School of Pharmacy, University of Georgia, Athens, GA 30602

Accepted for publication December 10, 1975.

¶ Recipient of a Lederle Pharmacy Faculty Award.

ˣ To whom inquiries should be directed.

Synthesis of Potential Mescaline Antagonists

FRANK DeSANTIS, Jr. *, and KARL A. NIEFORTH ˣ

Abstract □ 1-[2-(3,4,5-Trimethoxyphenyl)ethyl]-3-pyrroline, 2-(3,4,5-trimethoxybenzyl)-1,2,3,6-tetrahydropyridine, *N*-*n*-propylmescaline, *N*-cyclopropylmethylmescaline, and *N*-allylmescaline were synthesized as potential mescaline antagonists. The ability of these compounds to antagonize mescaline-induced disruption of swim behavior is also given.

Keyphrases □ Mescaline antagonists, potential—synthesized and screened for effect on mescaline-induced CNS stimulation □ Antagonists, mescaline, potential—synthesized and screened for effect on mescaline-induced CNS stimulation □ CNS stimulation, mescaline induced—effect of various mescaline antagonists evaluated □ Structure–activity relationships—various mescaline antagonists screened for effect on mescaline-induced CNS stimulation

The method presently used to counteract the hallucinogenic effects of mescaline (I) and other hallucinogens is administration of drugs that indirectly counteract the hallucinogenic effects, such as tranquilizers and sedatives (1). The object of this research was to synthesize compounds that would antagonize the effects of mescaline through a direct competitive mechanism. The compounds would ideally have little or no effect of their own but, when given in conjunction with mescaline, would mitigate the central nervous system (CNS) stimulation.

It has been well documented that replacement of the

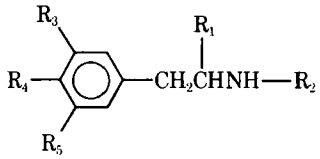

I: $R_1 = R_2 = H$, $R_3 = R_4 = R_5 = OCH_3$

II: $R_1 = CH_3$, $R_2 = R_3 = R_4 = R_5 = H$

III: $R_1 = CH_3$, $R_2 = H$, $R_3 = R_4 = R_5 = OCH_3$

IV: $R_1 = H$, $R_2 = n\text{-}C_3H_7$, $R_3 = R_4 = R_5 = OCH_3$

V: $R_1 = H$, $R_2 = CH_2$— , $R_3 = R_4 = R_5 = OCH_3$

VI: $R_1 = H$, $R_2 = CH_2$—CH=CH_2, $R_3 = R_4 = R_5 = OCH_3$

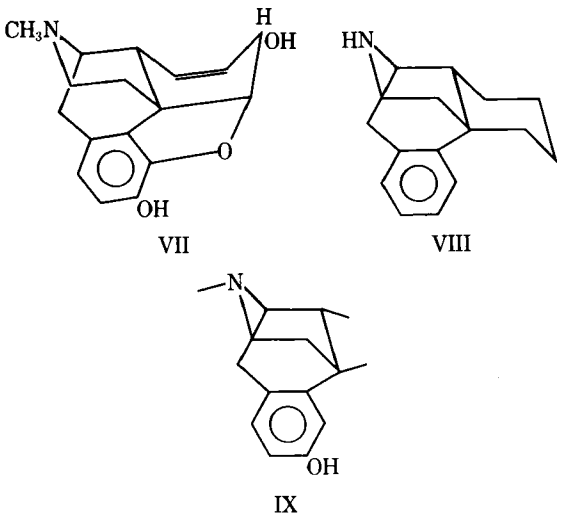

VII VIII

IX

N-methyl group of morphine (VII) with certain short chain alkyl groups produced compounds that acted as antagonists (2). Similar manipulations in the morphinan (VIII) (3–5) and benzomorphan (IX) (6, 7) series also produced narcotic antagonists.

In the amphetamine series (II), compounds more closely related to mescaline, *N*-allylation produced a compound that antagonized amphetamine-induced motor activity in mice (8). Therefore, the *N*-*n*-propyl (IV), *N*-cyclopropylmethyl (V), and *N*-allyl (VI) derivatives of mescaline were prepared as potential mescaline antagonists. These three alkyl groups were chosen because small *N*-alkyl groups generally produced the most active narcotic antagonists (9).

1-[2-(3,4,5-Trimethoxyphenyl)ethyl]-3-pyrroline (X) and 2-(3,4,5-trimethoxybenzyl)-1,2,3,6-tetrahydropyridine (XI), also synthesized, may be considered *N*-allyl derivatives of mescaline in which the relative spatial position of the double bond of the allyl group is more rigid with respect to nitrogen than in the acyclic amines. Compound XI may also be considered as an *N*-allyl derivative of 3,4,5-trimethoxyamphetamine (III) in which the double bond of the allyl group is tied back to the methyl group of the isopropyl side chain. Compound III is a hallucinogen with twice the potency of mescaline (10).

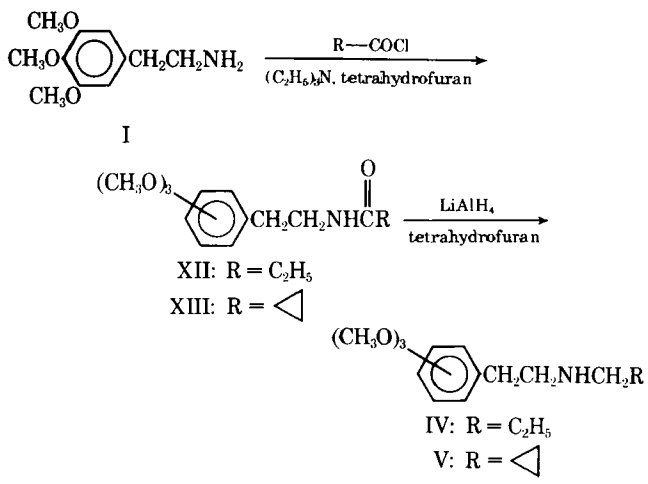

Scheme I

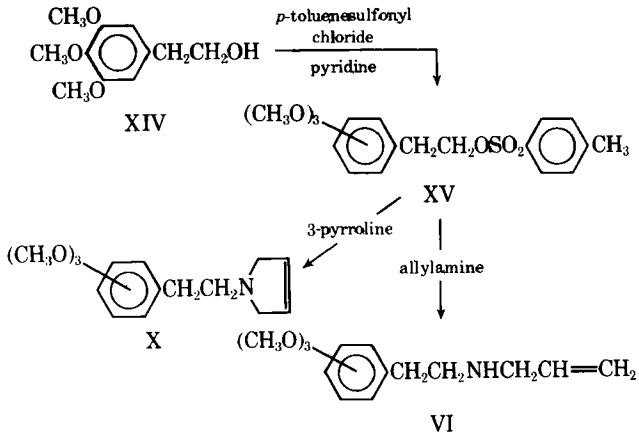

Scheme II

RESULTS AND DISCUSSION

Synthesis—Scheme I was used to prepare the *N*-*n*-propyl (IV) and *N*-cyclopropylmethyl (V) derivatives of mescaline. The procedure of Lundstrom and Agurell (11) was employed to synthesize mescaline (I). Mescaline was acylated with the suitable acid chloride to form amides XII (*N*-propionyl) and XIII (*N*-cyclopropylcarbonyl). The amides were reduced with lithium aluminum hydride to the secondary amines, IV and V, respectively.

Compounds VI and X were synthesized by utilizing Scheme II. 2-(3,4,5-Trimethoxyphenyl)ethanol (XIV), which was previously prepared (12), was converted to the *p*-toluenesulfonate ester (XV). Compounds VI and X were synthesized by displacing the *p*-toluenesulfonate of XV with allylamine and 3-pyrroline, respectively.

Scheme III was utilized for the synthesis of XI. Compound XVI (3,4,5-trimethoxybenzaldehyde) was allowed to react with 2-bromopyridine in the presence of *n*-butyllithium to form the corresponding carbinol (XVII). The carbinol was converted with thionyl chloride to the benzyl chloride (XVIII). Compound XVIII was reduced without purification with zinc and acetic acid to 2-(3,4,5-trimethoxybenzyl)-pyridine (XIX).

Compound XIX was converted to the methiodide salt (XX) and reduced with sodium borohydride to *N*-methyl-2-(3,4,5-trimethoxybenzyl)-1,2,3,6-tetrahydropyridine (XXI). Compound XXI was *N*-demethylated by initial reaction with 2,2,2-trichloroethyl chloroformate and subsequent reduction of the resultant unisolated carbamate (XXII) with zinc and acetic acid to XI.

Pharmacology—Charles River CD-1 male mice, 4–6 weeks old, were used. All drugs were given as hydrochloride salts dissolved in normal saline and were administered intraperitoneally.

The LD_{50}'s with confidence limits of the test compounds and of mescaline were determined using the procedure of Weil (13) (Table I). Also listed in Table I is the highest dose of each test compound given in this study that did not cause any overt effect (tremors, hyperactivity, or convulsions).

The ability of the test compounds to antagonize mescaline-induced disruption of swim behavior was determined by the use of the swimming maze outlined in Fig. 1 (14). The maze was constructed of Plexiglas and painted black on the outside. The walls of the maze were 25.4 cm (10 in.) high, and the maze was filled with water at 30° to a depth of 10.2 cm (4 in.). A mouse was placed in the water at the "start"

Table I—Toxicity Study of Mescaline and Synthetic Derivatives

Compound	LD_{50} with Confidence Limit (p = 0.05), mg/kg	Highest Dose without Overt Effects, mg/kg
I	346 (292–410)	—
IV	450 (418–484)	150
V	399 (366–475)	150
VI	363 (323–408)	100
X	346 (292–410)	100
XI	238 (218–261)	100

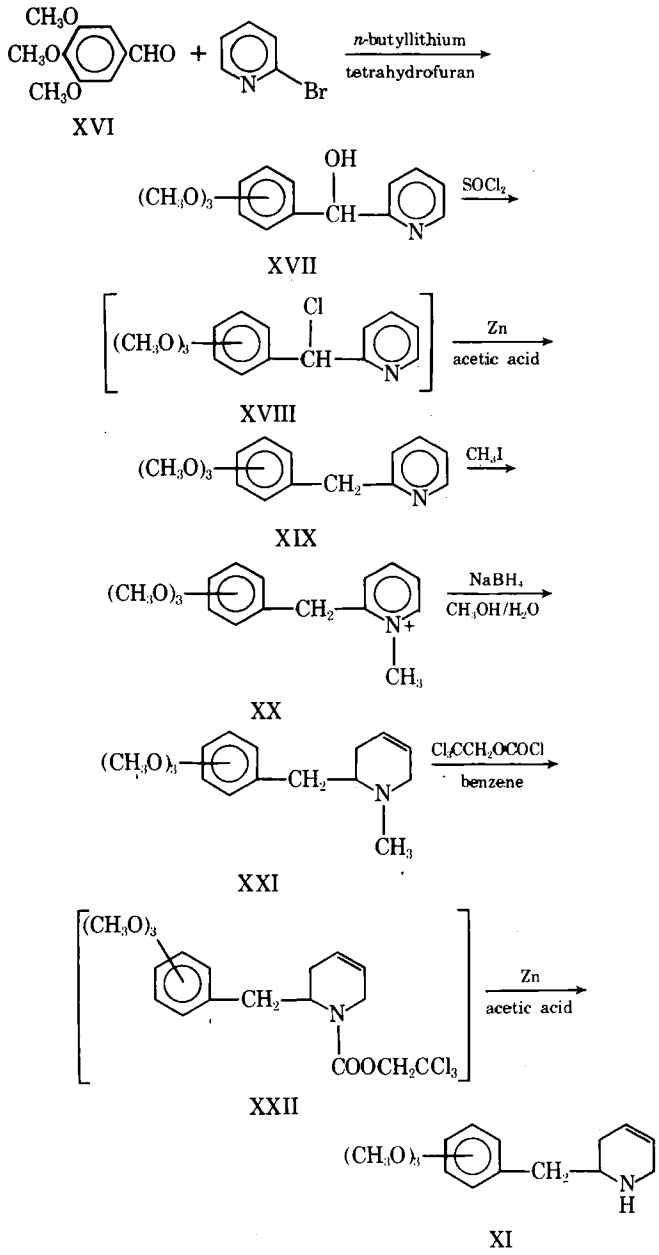

XVI XVII XVIII XIX XX XXI XXII XI

Scheme III

position and was allowed to swim to the ramp. After it climbed onto the ramp, it was lifted from the maze, placed in a sawdust-filled box, and dried by an IR heat lamp located 0.9 m (3 ft) above the box.

A group of mice was trained to swim the maze by conditioning every 2 hr for 2–3 consecutive days. Swimming times and numbers of incorrect turns were recorded. A trained mouse by definition was able to swim the maze in 4–7 sec with no more than one error. Any mouse that did not learn to swim the maze acceptably within 3 days was eliminated.

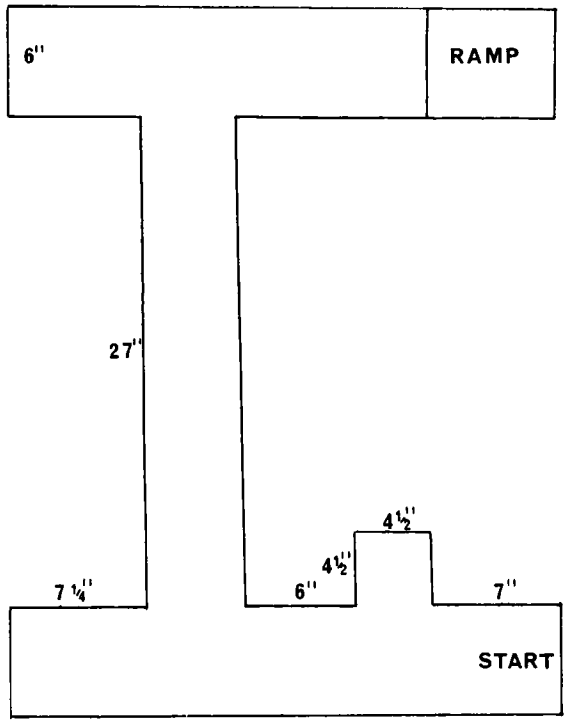

Figure 1—*Swimming maze.*

Table II contains the swim maze results of individual doses of mescaline (75 mg/kg) and the five test compounds (100 mg/kg). Disruption of swim behavior was defined as a significant ($p < 0.05$) increase in both the average number of seconds and errors generated by a group of mice 20 min after injection of drug as compared to performance 20 min after injection of saline. The data for each group (treatment *versus* saline) were analyzed using the Student t test. The group of mice given mescaline showed swim behavior disruption and hyperactivity, indicated by an increased exploring tendency. The hindleg scratching response, typical of mescaline, was also present. Compounds IV–VI did not cause disruption of swim behavior, hyperactivity, or scratching. Compounds X and XI disrupted swim behavior and produced signs of hyperactivity without scratching.

The effect of each test compound on swim behavior when given with mescaline is described in Table III. Disruption of swim behavior was defined as before. Antagonism of mescaline-induced disruption of swim behavior was measured by a significant ($p < 0.05$) decrease in both the average number of seconds and errors generated by a group of mice 20 min after injection of mescaline plus test compound as compared to performance 20 min after injection of mescaline alone (Table III). The Student t test was again used to analyze the data (mescaline plus test compound *versus* saline and *versus* mescaline).

Of the compounds that did not disrupt swim behavior, IV and VI

Table II—Effect of Mescaline and Test Compounds on Mouse Swim Behavior

Compound	n[a]	Dose of Compound, mole/kg (mg/kg)[b]	Performance 20 min after Saline[c] Time[d]	Performance 20 min after Saline[c] Errors[e]	Performance 20 min after Compound Time[d]	Performance 20 min after Compound Errors[e]	t Test[f] Time	t Test[f] Errors
I	20	3.03×10^{-4} (75)	7.10 ± 0.50	0.65 ± 0.15	22.9 ± 6.00	3.30 ± 1.01	S	S
IV	13	3.47×10^{-4} (100)	8.81 ± 0.72	0.92 ± 0.20	7.77 ± 0.61	0.69 ± 0.20	IS	IS
V	13	3.47×10^{-4} (100)	7.42 ± 0.66	0.46 ± 0.17	7.27 ± 0.60	0.54 ± 0.21	IS	IS
VI	13	3.33×10^{-4} (100)	6.96 ± 0.36	0.38 ± 0.17	7.23 ± 0.49	0.62 ± 0.21	IS	IS
X	13	3.34×10^{-4} (100)	5.88 ± 0.24	0.08 ± 0.09	11.23 ± 1.55	1.46 ± 0.38	S	S
XI	13	3.34×10^{-4} (100)	5.88 ± 0.29	0.31 ± 0.13	34.30 ± 10.1	14.5 ± 1.41	S	S

[a] Number of animals in group. [b] Weight based on hydrochloride salt. [c] Each animal was given a volume of saline equal to the volume of drug it would receive. [d] Average number of seconds ± SE for group of mice to swim maze. [e] Average number of errors ± SE made by group of mice in that period of time. [f] Student t test to compare saline *versus* drug; S ($p < 0.05$) means disruption in swim behavior, and IS ($p > 0.2$) means no disruption in swim behavior.

Table III—Effect of Test Compounds on Mescaline-Induced Disruption of Mouse Swim Behavior

Compound	n^a	Performance 20 min after Saline[b]		Performance 20 min after Mescaline plus Test Compound		*t* Test[f]		*t* Test[g]	
		Time[c]	Errors[d]	Time[c]	Errors[d]	Time	Errors	Time	Errors
IV	13	6.00 ± 0.36	0.08 ± 0.02	11.38 ± 2.30	1.08 ± 0.02	S	S	$p < 0.1$	$p < 0.1$
V	13	6.23 ± 0.33	0.15 ± 0.24	16.31 ± 4.90	1.38 ± 0.49	$p < 0.1$	S	IS	$p < 0.1$
VI	13	7.00 ± 0.58	0.69 ± 0.25	8.73 ± 1.69	0.69 ± 0.30	IS	IS	S	S
X	11	5.20 ± 0.36	0.31 ± 0.13	25.18 ± 6.15	2.55 ± 0.81	S	S	IS	IS
XI	13	6.04 ± 0.19	0.08 ± 0.07	20.04 ± 6.39	1.92 ± 0.91	S	S	IS	IS

[a] Number of animals in group. [b] Each animal was given a total volume of saline in one dose that equalled the total volume of test compound and mescaline it would receive. [c] Average number of seconds ± *SE* for group of mice to swim maze. [d] Average number of errors ± *SE* made by group of mice in that period of time. [e] Each animal was first given the test compound (100 mg/kg as hydrochloride salt) followed immediately by mescaline (75 mg/kg as hydrochloride salt). [f] Student *t* test comparing saline *versus* mescaline + test compound; S ($p < 0.05$) means disruption in swim behavior, and IS ($p > 0.2$) means no disruption in swim behavior. [g] Student *t* test comparing mescaline *versus* mescaline + test compound; S ($p < 0.05$) means antagonism of mescaline response, $p < 0.1$ means a lowering of mescaline response, and IS ($p > 0.2$) means no effect on mescaline response.

were the only ones that reduced the mescaline-induced disruption of swim behavior. Compound VI appeared more effective than IV since there was no significant difference in swim behavior of the test animals dosed with saline and the swim behavior of the same animals subsequently dosed with mescaline plus VI (Table III). On the other hand, there was a significant disruption of swim behavior when comparing mescaline plus IV to saline, but the disruption was not as great as with mescaline alone. Also, the group of mice that received mescaline plus VI showed no signs of scratching, while the group that received mescaline plus IV did exhibit the hindleg scratch response.

Compound V, when given alone, showed no disruption of swim behavior (Table II). However, when given with mescaline, V was not capable of reducing the mescaline response. The hindleg scratching response also was observed when V was given with mescaline. Compounds X and XI did not reduce the mescaline response as was anticipated since both compounds disrupted mouse swim behavior when given alone. The group of mice receiving X plus mescaline exhibited the hindleg scratch response of mescaline. However, the group of mice receiving XI plus mescaline did not exhibit this response.

Other studies will have to be completed to demonstrate that *N*-allyl- (VI) and *N*-*n*-propylmescaline (IV) antagonize the hallucinogenic as well as the swim maze effects of mescaline. Recently, Pinder *et al.* (15) reported excellent correlation between induced hyperthermia in rabbits and psychotomimetic activity in humans. Although similar correlations were described previously, there is still no test system that suitably defines hallucinogen potency in animals as related to humans.

EXPERIMENTAL[1]

***N*-Propionylmescaline (XII)**—In a three-necked flask fitted with a mechanical stirrer, dropping funnel, and reflux condenser equipped with a drying tube were placed 6.3 g (0.0284 mole) of I and 3.14 g (0.031 mole) of triethylamine dissolved in anhydrous tetrahydrofuran (Scheme I). To this solution was added dropwise 2.86 g (0.031 mole) of propionyl chloride dissolved in 20 ml of anhydrous tetrahydrofuran with stirring on an ice bath. A white precipitate began to form immediately. After addition was complete, the mixture was stirred for 1 hr at room temperature.

The white precipitate was then removed by filtration and washed with two 20-ml portions of tetrahydrofuran. The combined filtrate and washings were concentrated *in vacuo* to yield a semisolid residue which solidified upon addition of petroleum ether. The solid was collected and recrystallized from hexane to yield 6.5 g (85%) of product, mp 70–72°. The IR spectrum showed a peak at 3320 cm^{-1}, indicative of an amino group, and a peak at 1640 cm^{-1}, indicative of a carbonyl group of an amide.

Anal.—Calc. for $C_{14}H_{21}NO_4$: C, 62.89; H, 7.92; N, 5.24. Found: C, 62.76; H, 7.91; N, 5.00.

***N*-Cyclopropylcarbonylmescaline (XIII)**—The procedure used to make XII was followed for the synthesis of similar quantities of XIII (Scheme I). Compound XIII was prepared in 53% yield, mp 96–98°, after recrystallization from benzene–petroleum ether (1:1). The IR spectrum showed a peak at 3310 cm^{-1}, indicative of an amino group, and a peak at 1620 cm^{-1}, indicative of a carbonyl group of an amide.

Anal.—Calc. for $C_{15}H_{21}NO_4$: C, 64.49; H, 7.53; N, 5.02. Found: C, 64.89; H, 7.51; N, 4.83.

***N*-*n*-Propylmescaline Hydrochloride (IV)**—In a three-necked flask fitted with a mechanical stirrer, dropping funnel, and reflux condenser equipped with a drying tube were placed 3.00 g (0.1496 mole) of lithium aluminum hydride and 50 ml of anhydrous tetrahydrofuran. The mixture was stirred and heated to reflux as 5.0 g (0.0187 mole) of XII dissolved in 50 ml of anhydrous tetrahydrofuran was added dropwise (Scheme I). After addition, the reaction mixture was stirred and refluxed overnight. After cooling to room temperature, the reaction was quenched with successive dropwise additions of 1.6 ml of water, 1.3 ml of 20% NaOH, and 5.8 ml of water.

The white precipitate which formed was removed by filtration and washed with additional tetrahydrofuran. The combined filtrate and washings were concentrated *in vacuo*. The oily residue was dissolved in ether, dried over anhydrous sodium sulfate, and filtered. Hydrogen chloride gas was bubbled into the ether solution to form the hydrochloride salt. The precipitate was filtered to yield 2.1 g (39%) of IV as the hydrochloride. After recrystallization from ethyl acetate–ethanol (1:1), the melting point of the product was 174–175°. The IR spectrum showed a broad peak from 2750 to 2450 cm^{-1}, indicative of NH_2^+. The NMR spectrum (dimethyl sulfoxide-d_6) showed peaks at δ 0.8 (t, 3H, methyl), 1.6 (m, 2H, methylene α to methyl), 2.5–3.2 (b, 6H, benzylic and two methylenes α to nitrogen), 3.5 (s, 3H, *p*-methoxy), 3.7 (s, 6H, *m*-methoxy), 6.5 (s, 2H, aromatic), and 9.3 (b, 2H, NH_2^+).

Anal.—Calc. for $C_{14}H_{24}ClNO_3$: C, 58.02; H, 8.35; N, 4.83. Found: C, 57.87; H, 8.19; N, 4.84.

***N*-Cyclopropylmethylmescaline Hydrochloride (V)**—The procedure used to prepare IV was followed for the synthesis of similar quantities of V (Scheme I). Compound V was prepared in 34% yield, mp 185–187°, after recrystallization from ethyl acetate–ethanol (1:1). The IR spectrum showed a broad peak from 2750 to 2400 cm^{-1}, indicative of NH_2^+. The NMR spectrum (dimethyl sulfoxide-d_6) showed peaks at δ 0.4 (b, 4H, cyclopropyl methylenes), 1.1 (m, 1H, CH), 2.6–3.2 (b, 6H, benzylic and two methylenes α to nitrogen), 3.6 (s, 3H, *p*-methoxy), 3.8 (s, 6H, *m*-methoxy), 6.6 (s, 2H, aromatic), and 9.4 (b, 2H, NH_2^+).

Anal.—Calc. for $C_{15}H_{24}ClNO_3$: C, 59.69; H, 8.02; N, 4.64. Found: C, 59.54; H, 7.86; N, 4.50.

2-(3,4,5-Trimethoxyphenyl)ethyl *p*-Toluenesulfonate (XV)—In a three-necked flask fitted with a condenser, drying tube, and mechanical stirrer were placed 3.5 g (0.0165 mole) of 2-(3,4,5-trimethoxyphenyl)ethanol (XIV) and 5.2 g (0.066 mole) of pyridine (Scheme II). The solution was stirred and cooled on an ice–salt bath while 3.0 g (0.0182 mole) of *p*-toluenesulfonyl chloride was added in small portions. After addition, the mixture was stirred on the ice bath for 1 hr.

[1] IR spectra were determined on a Beckman Microspec model 1485 using potassium bromide pellets for solids and neat for liquids. NMR spectra were determined on the Hitachi Perkin-Elmer model R-24 spectrometer using tetramethylsilane as the internal standard when deuterochloroform was the solvent and as an external standard when deuterodimethyl sulfoxide was the solvent. The letter abbreviations used are: s, singlet; 2s, two singlets; d, doublet; 2d, two doublets; t, triplet; m, multiplet; and b, broad. Mass spectra were determined using an A.E.I. Scientific Mg-902 double-focusing spectrometer. Melting points were determined in open glass capillaries using a Thomas-Hoover Uni-Melt apparatus and are uncorrected. Microanalyses were performed by Baron Consulting Co., Orange, Conn.

The mixture was then diluted with 20 ml of cold 10% HCl and filtered, and the filter cake was washed with excess 10% HCl to yield 4.7 g (85%) of crude product, mp 88–91°. Recrystallization from ethanol gave the product, mp 92–93°. The NMR spectrum ($CDCl_3$) showed peaks at δ 2.4 (s, 3H, CH_3), 2.9 (t, 2H, benzylic), 3.8 (2s, 9H, methoxy), 4.2 (t, 2H, methylene), 6.3 (s, 2H, phenyl), and 7.5 (2d, 4H, tolyl aromatic).

Anal.—Calc. for $C_{18}H_{22}O_6S$: C, 58.99; H, 6.05. Found: C, 59.34; H, 6.05.

***N*-Allylmescaline Hydrochloride (VI)**—In a three-necked flask fitted with a reflux condenser, drying tube, and mechanical stirrer were placed 4.0 g (0.0109 mole) of XV and 75 ml of allylamine (Scheme II). The solution was stirred and refluxed for 2 hr. After cooling to room temperature, the solution was concentrated *in vacuo*. To the residue was added 50 ml of ether, and the insoluble matter was filtered. The ether layer was then dried over anhydrous sodium sulfate and filtered.

Hydrogen chloride gas was passed through the ether solution to yield the hydrochloride salt, which was collected and recrystallized from ethanol–ethyl acetate (1:1). The yield of product was 1.3 g (42%), mp 172–173°. The IR spectrum showed a broad peak from 2850 to 2350 cm^{-1}, indicative of NH_2^+. The NMR spectrum (dimethyl sulfoxide-d_6) showed peaks at δ 3.1–3.8 (b, 6H, methylenes), 3.6 (s, 3H, *p*-methoxy), 3.8 (s, 6H, *m*-methoxy), 5.3 (m, 2H, vinylic methylene), 5.8 (m, 1H, CH), 6.5 (s, 2H, aromatic), and 9.6 (b, 2H, NH_2).

Anal.—Calc. for $C_{14}H_{22}ClNO_3$: C, 60.09; H, 7.40; N, 4.83. Found: C, 59.95; H, 7.37; N, 4.58.

1-[2-(3,4,5-Trimethoxyphenyl)ethyl]-3-pyrroline Hydrochloride (X)—In a three-necked flask fitted with a mechanical stirrer, dropping funnel, and drying tube, under nitrogen atmosphere, were placed 4.0 g (0.011 mole) of XV and 50 ml of anhydrous tetrahydrofuran (Scheme II). While the solution was stirring, 3.45 g (0.05 mole) of 3-pyrroline[2] was added dropwise through the dropping funnel. After addition, the dropping funnel was replaced with a reflux condenser and the yellow solution which formed was refluxed for 3 hr. The solution was then cooled to room temperature and concentrated *in vacuo*.

To the residue was added 75 ml of ether, and the insoluble matter was filtered. The same isolation procedure used for VI was then followed. The yield of X was 1.1 g (35%), mp 176–177° (ethanol–ethyl acetate). The IR spectrum showed a broad peak centered at 2500 cm^{-1}, indicative of $>NH^+$. The NMR spectrum (dimethyl sulfoxide-d_6) showed peaks at δ 3.1 (m, 4H, ethylene), 3.6 (s, 3H, *p*-methoxy), 3.8 (s, 6H, *m*-methoxy), 4.1 (s, 4H, pyrroline methylenes), 5.9 (s, 2H, vinylic), 6.6 (s, 2H, aromatic), and 12.3 (b, 1H, NH).

Anal.—Calc. for $C_{15}H_{22}ClNO_3$: C, 60.09; H, 7.40; N, 4.83. Found: C, 59.95; H, 7.42; N, 4.57.

3,4,5-Trimethoxyphenyl-2-pyridylcarbinol (XVII)—In a 1-liter three-necked flask, placed in an acetone–dry ice bath under nitrogen atmosphere and fitted with a mechanical stirrer, dropping funnel, and thermometer, were placed 80 ml (0.16 mole) of 2 *M* *n*-butyllithium in hexane[3] and 50 ml of anhydrous tetrahydrofuran (Scheme III). The stirrer was started, and the temperature was reduced to −40°. A 50-ml solution of 17.5 g (0.11 mole) of 2-bromopyridine in anhydrous tetrahydrofuran was added dropwise while the temperature was maintained below −30°.

After addition, the dark-red mixture which formed was stirred at from −30 to −40° for 30 min. A 200-ml solution of 20.0 g (0.10 mole) of 3,4,5-trimethoxybenzaldehyde (XVI) in anhydrous tetrahydrofuran was added dropwise while the temperature of the reaction was maintained below −25°. After addition, the reaction was allowed to warm to −15° and was stirred at that temperature for 1 hr. Water (100 ml) was then added to the clear yellow solution.

The reaction mixture was made acidic with 10% HCl and washed with three 50-ml portions of ether. The acid layer was made basic (pH 8) with ammonia gas and extracted with three 75-ml portions of chloroform. The chloroform was dried over sodium sulfate, filtered, and concentrated *in vacuo* to yield 20.3 g (73%), mp 95–99°, of crude product; this product was used in the subsequent reaction without further purification. Several recrystallizations were attempted which failed to improve the melting point. An analytical sample was obtained (mp 104–106°) by passing 1 g of crude product through a silica gel column. The column was initially eluted with petroleum ether–ethyl acetate (1:1) and subsequently with ethyl acetate–methanol (1:1). The latter eluant contained the desired product. The IR spectrum showed a peak at 3100 cm^{-1}, indicative of hydroxyl. The NMR spectrum ($CDCl_3$) showed peaks at δ 3.8 (s, 9H, methoxy), 5.4 (b, 1H, OH exchanged by D_2O), 5.6 (s, 1H, CH), 6.6 (s, 2H, aromatic), 7.0–7.8 (m, 3H, 3CH, 4CH, and 5CH), and 8.5 (d, 1H, 6CH).

Anal.—Calc. for $C_{15}H_{17}NO_4$: C, 65.44; H, 6.22; N, 5.08. Found: C, 65.32; H, 6.37; N, 4.93.

2-(3,4,5-Trimethoxybenzyl)pyridine (XIX)—In a three-necked flask fitted with a condenser, drying tube, mechanical stirrer, thermometer, and dropping funnel was dissolved 26.0 g (0.095 mole) of XVII in 400 ml of anhydrous benzene (Scheme III). The solution was stirred and cooled to 0° using an ice–salt bath. A 50-ml solution of 22.0 g (0.114 mole) of thionyl chloride in anhydrous benzene was added dropwise while the temperature of the reaction was kept below 20°. After addition, the resultant reddish solution was warmed to room temperature and stirred for 1 hr.

While the solution was cooled on an ice bath, 150 ml of 25% NaOH was added slowly. The aqueous layer was washed with three 80-ml portions of chloroform. The organic layers were combined, dried over anhydrous sodium sulfate, and filtered. The solution was concentrated *in vacuo* to yield a dark-reddish oil (XVIII), which was dissolved in 125 ml of acetic acid and transferred to a three-necked flask fitted with a condenser, drying tube, and mechanical stirrer. While the solution was stirred, 17.0 g of zinc dust was added in portions and the mixture was refluxed for 4 hr.

After cooling to room temperature, the mixture was filtered of inorganic salts and the solution was concentrated *in vacuo*. To the residue was added 75 ml of 25% NaOH, and the resultant aqueous mixture was extracted with three 80-ml portions of chloroform. The organic extracts were combined, dried over anhydrous sodium sulfate, filtered, and evaporated *in vacuo*. The residue was distilled, yielding 11.5 g (47%) of XIX, bp 157–160°/0.2 mm. The NMR spectrum ($CDCl_3$) showed peaks at δ 3.8 (s, 9H, methoxy), 4.1 (s, 2H, benzylic), 6.5 (s, 2H, aromatic), 7.0–7.8 (m, 3H, 3CH, 4CH, and 5CH), and 8.5 (d, 1H, 6CH).

The methiodide salt was used for analytical purposes and also in subsequent reactions. The salt was prepared by dissolving the free amine (XIX) in methanol (approximately 15–20 times the weight of the free amine), and to this mixture was added methyl iodide (~2.5 times the weight of the free amine). The solution was then stirred at room temperature for 1 hr, followed by refluxing for 2 hr. After cooling to room temperature, the solution was concentrated *in vacuo*, yielding a solid (XX) which was recrystallized from acetone. The yield of product varied from 64 to 71%, mp 151–153°.

Anal.—Calc. for $C_{16}H_{20}INO_3$: C, 47.89; H, 5.02; N, 3.49. Found: C, 47.90; H, 5.10; N, 3.30.

***N* - Methyl-2-(3,4,5,-trimethoxybenzyl)-1,2,3,6-tetrahydropyridine (XXI)**—In a three-necked flask equipped with a condenser, dropping funnel, magnetic stirrer, and thermometer was dissolved 2.0 g (0.05 mole) of sodium borohydride in aqueous methanol (57% v/v). This solution was cooled to 0°, and 10.0 g (0.025 mole) of XX in aqueous methanol (33% v/v) at 0° was added (Scheme III). After addition, the solution was stirred for an additional 0.5 hr. A 100-ml portion of water was then added, and the mixture was extracted with three 50-ml portions of chloroform.

The combined extracts were dried over anhydrous sodium sulfate, filtered, and concentrated *in vacuo*. The residue was distilled to yield 6.0 g (87%) of product, bp 154–155°/0.27 mm. The NMR spectrum ($CDCl_3$) showed peaks at δ 2.0 (m, 2H, $3CH_2$), 2.3 (m, 1H, 2CH), 2.4 (s, 3H, methyl), 2.7 (m, 2H, benzylic), 3.0 (m, 2H, $6CH_2$), 3.8 (s, 9H, methoxy), 5.6 (m, 2H, vinylic), and 6.4 (s, 2H, aromatic); mass spectrometry: M, 277.1675. Calc. for $C_{16}H_{23}NO_3$, 277.1675. The picrate was prepared for chemical analysis and had a melting point of 168.5–170°.

Anal.—Calc. for $C_{22}H_{26}N_4O_{10}$: C, 52.17; H, 5.17; N, 11.06. Found: C, 51.90; H, 5.15; N, 10.90.

2-(3,4,5-Trimethoxybenzyl)-1,2,3,6-tetrahydropyridine Hydrochloride (XI)—In a three-necked flask fitted with a reflux condenser, drying tube, and mechanical stirrer were placed 4.0 g (0.014 mole) of XXI, 3.5 g (0.017 mole) of 2,2,2-trichloroethyl chloroformate, 1.0 g of potassium carbonate, and 50 ml of anhydrous benzene (Scheme III). The mixture was then stirred and refluxed for 24 hr. After the reaction was cooled and filtered, it was extracted twice with 20 ml of 10% hydrochloric acid. The benzene layer was then dried over anhydrous sodium sulfate, filtered, and concentrated *in vacuo* to yield

[2] Available from Aldrich Chemical Co. as a 3:1 mixture of 3-pyrroline and 1-pyrroline.

[3] Alpha Chemical Co.

6.8 g of a yellow oil (XXII). The IR spectrum showed a peak at 1700 cm^{-1}, indicative of the carbonyl of a carbamate.

The crude oil, without further purification, was reduced by dissolving it in 50 ml of acetic acid and transferred to a three-necked flask fitted with a mechanical stirrer, reflux condenser, and drying tube. After gradual addition of 3.0 g of zinc dust, the mixture was stirred at room temperature for about 60 hr. The zinc mixture was filtered, and the acetic acid was reduced in volume *in vacuo* almost to completion. The residue was made basic with 25% NaOH and extracted with three 30-ml portions of ether. The ether extracts were combined, dried over anhydrous sodium sulfate, and filtered. Hydrogen chloride gas was passed through the ether solution, forming a white precipitate. The precipitate was filtered and recrystallized from ethyl acetate–ethanol (1:1) to yield 2.2 g (51%) of product, decomposition at 230–232°. The IR spectrum showed a broad peak from 2800 to 2600 cm^{-1}, indicative of NH_2^+. The NMR spectrum (dimethyl sulfoxide-d_6) showed peaks at δ 2.3 (m, 2H, $3CH_2$), 3.0 (m, 2H, benzylic), 3.6 (m, 3H, 2CH and $6CH_2$), 3.8 (s, 3H, *p*-methoxy), 3.9 (s, 6H, *m*-methoxy), 5.9 (m, 2H, vinylic), 6.8 (s, 2H, aromatic), and 9.9 (b, 2H, NH_2).

REFERENCES

(1) A. Hoffer and H. Osmond, "The Hallucinogens," Academic, New York, N.Y., 1967, p. 42.

(2) C. A. Winter and L. Plataker, *J. Pharmacol. Exp. Ther.*, **112**, 99(1954).

(3) W. M. Benson, E. O'Gara, and S. Van Winkle, *ibid.*, **106**, 373(1952).

(4) J. Telford, C. N. Papadopoulos, and A. S. Keats, *ibid.*, **133**, 106(1961).

(5) M. Gates and T. A. Montzka, *J. Med. Chem.*, **7**, 127(1964).

(6) M. Gordon, J. J. Laffety, D. H. Tedeschi, N. B. Eddy, and E. L. May, *Nature*, **192**, 1089(1962).

(7) S. Archer, N. F. Albertson, L. S. Harris, A. K. Pierson, and J. G. Bird, *J. Med. Chem.*, **7**, 123(1964).

(8) F. Leuschner, *Arch. Exp. Pathol. Pharmakol.*, **225**, 95(1955).

(9) L. S. Harris, in "Advances in Biochemical Psychopharmacology," vol. 8, M. C. Braude, L. S. Harris, E. L. May, J. P. Smith, and J. E. Villarreal, Eds., Raven, New York, N.Y., 1973, pp. 13–20.

(10) A. T. Shulgin, *Lloydia*, **36**, 46(1973).

(11) J. Lundstrom and S. Agurell, *Acta Pharm. Suec.*, **7**, 247(1970).

(12) R. J. Mayor and K. W. Ohly, *J. Med. Pharm. Chem.*, **4**, 51(1961).

(13) C. S. Weil, *Biometrics*, **8**, 249(1952).

(14) M. E. Koosman, *Proc. Soc. Exp. Biol. Med.*, **115**, 728(1964).

(15) R. M. Pinder, F. A. B. Aldous, B. C. Barrass, K. Brewster, D. A. Buxton, D. M. Green, P. Rich, M. Skeels, and K. J. Tutt, *J. Med. Chem.*, **17**, 1100(1974).

ACKNOWLEDGMENTS AND ADDRESSES

Received June 26, 1975, from the *Medicinal Chemistry Laboratory, Section of Medicinal Chemistry and Pharmacognosy, School of Pharmacy, University of Connecticut, Storrs, CT 06268*

Accepted for publication December 17, 1975.

Abstracted in part from a thesis submitted by F. DeSantis, Jr., to the University of Connecticut in partial fulfillment of the Doctor of Philosophy degree requirements.

The authors thank Susanne Biran for technical assistance in the pharmacological evaluations and the Connecticut Drug Dependency Trust for support.

* Present address: Vick Divisions Research, Vick Chemical Co., Mt. Vernon, NY 10553

‡ To whom inquiries should be directed.

Dissolution Behavior and Bioavailability of Phenytoin from a Ground Mixture with Microcrystalline Cellulose

KEIJI YAMAMOTO *, MASAHIRO NAKANO *, TAKAICHI ARITA *‡, YOSHIKAZU TAKAYAMA *, and YOSHINOBU NAKAI ‡

Abstract □ The ground mixture of phenytoin and microcrystalline cellulose was prepared by grinding in a vibrational ball mill. The X-ray diffraction patterns indicated the amorphous nature of the ground mixture. Comparative studies were made concerning the *in vitro* dissolution and *in vivo* absorption of fine phenytoin powder, phenytoin sodium powder, and the ground mixture. The ground mixture showed a greater dissolution rate than the fine powder and attained supersaturation in the pharmacopeial disintegration media at pH 1.2 and 7.4. *In vivo* absorption studies of each preparation were carried out in five subjects, using a crossover design, by measuring the urinary excretion rate of a main metabolite, 5-(*p*-hydroxyphenyl)-5-phenylhydantoin. The blood levels of phenytoin and the corresponding urinary excretion patterns of the metabolite were determined in two subjects. The ground mixtures significantly improved the bioavailability of phenytoin. The drug was completely and rapidly absorbed after oral administration of the ground mixture. The vibrational ball milling technique for a poorly water-soluble drug with microcrystalline cellulose provides a promising way of improving the *in vivo* drug absorption.

Keyphrases □ Phenytoin—dissolution and bioavailability, ground mixture with microcrystalline cellulose compared to fine powder □ Dissolution—phenytoin, ground mixture with microcrystalline cellulose □ Bioavailability—phenytoin, ground mixture with microcrystalline cellulose □ Dosage forms—phenytoin and microcrystalline cellulose ground mixture, dissolution and bioavailability, compared to fine powder □ Cellulose, microcrystalline—ground mixture with phenytoin, effect on dissolution and bioavailability □ Anticonvulsant agents—phenytoin, dissolution and bioavailability, ground mixture with microcrystalline cellulose

When a relatively insoluble drug is administered orally, the rate of absorption and/or the extent of bioavailability are controlled by its dissolution rate in the GI fluids (1). Therefore, efforts have been made to increase the dissolution rate of poorly soluble drugs (2–5).

In an earlier study (6), a ground mixture of griseofulvin and microcrystalline cellulose significantly im-

6.8 g of a yellow oil (XXII). The IR spectrum showed a peak at 1700 cm^{-1}, indicative of the carbonyl of a carbamate.

The crude oil, without further purification, was reduced by dissolving it in 50 ml of acetic acid and transferred to a three-necked flask fitted with a mechanical stirrer, reflux condenser, and drying tube. After gradual addition of 3.0 g of zinc dust, the mixture was stirred at room temperature for about 60 hr. The zinc mixture was filtered, and the acetic acid was reduced in volume *in vacuo* almost to completion. The residue was made basic with 25% NaOH and extracted with three 30-ml portions of ether. The ether extracts were combined, dried over anhydrous sodium sulfate, and filtered. Hydrogen chloride gas was passed through the ether solution, forming a white precipitate. The precipitate was filtered and recrystallized from ethyl acetate–ethanol (1:1) to yield 2.2 g (51%) of product, decomposition at 230–232°. The IR spectrum showed a broad peak from 2800 to 2600 cm^{-1}, indicative of NH_2^+. The NMR spectrum (dimethyl sulfoxide-d_6) showed peaks at δ 2.3 (m, 2H, $3CH_2$), 3.0 (m, 2H, benzylic), 3.6 (m, 3H, 2CH and $6CH_2$), 3.8 (s, 3H, *p*-methoxy), 3.9 (s, 6H, *m*-methoxy), 5.9 (m, 2H, vinylic), 6.8 (s, 2H, aromatic), and 9.9 (b, 2H, NH_2).

REFERENCES

(1) A. Hoffer and H. Osmond, "The Hallucinogens," Academic, New York, N.Y., 1967, p. 42.

(2) C. A. Winter and L. Plataker, *J. Pharmacol. Exp. Ther.*, **112**, 99(1954).

(3) W. M. Benson, E. O'Gara, and S. Van Winkle, *ibid.*, **106**, 373(1952).

(4) J. Telford, C. N. Papadopoulos, and A. S. Keats, *ibid.*, **133**, 106(1961).

(5) M. Gates and T. A. Montzka, *J. Med. Chem.*, **7**, 127(1964).

(6) M. Gordon, J. J. Laffety, D. H. Tedeschi, N. B. Eddy, and E. L. May, *Nature*, **192**, 1089(1962).

(7) S. Archer, N. F. Albertson, L. S. Harris, A. K. Pierson, and J. G. Bird, *J. Med. Chem.*, **7**, 123(1964).

(8) F. Leuschner, *Arch. Exp. Pathol. Pharmakol.*, **225**, 95(1955).

(9) L. S. Harris, in "Advances in Biochemical Psychopharmacology," vol. 8, M. C. Braude, L. S. Harris, E. L. May, J. P. Smith, and J. E. Villarreal, Eds., Raven, New York, N.Y., 1973, pp. 13–20.

(10) A. T. Shulgin, *Lloydia*, **36**, 46(1973).

(11) J. Lundstrom and S. Agurell, *Acta Pharm. Suec.*, **7**, 247(1970).

(12) R. J. Mayor and K. W. Ohly, *J. Med. Pharm. Chem.*, **4**, 51(1961).

(13) C. S. Weil, *Biometrics*, **8**, 249(1952).

(14) M. E. Koosman, *Proc. Soc. Exp. Biol. Med.*, **115**, 728(1964).

(15) R. M. Pinder, F. A. B. Aldous, B. C. Barrass, K. Brewster, D. A. Buxton, D. M. Green, P. Rich, M. Skeels, and K. J. Tutt, *J. Med. Chem.*, **17**, 1100(1974).

ACKNOWLEDGMENTS AND ADDRESSES

Received June 26, 1975, from the *Medicinal Chemistry Laboratory, Section of Medicinal Chemistry and Pharmacognosy, School of Pharmacy, University of Connecticut, Storrs, CT 06268*

Accepted for publication December 17, 1975.

Abstracted in part from a thesis submitted by F. DeSantis, Jr., to the University of Connecticut in partial fulfillment of the Doctor of Philosophy degree requirements.

The authors thank Susanne Biran for technical assistance in the pharmacological evaluations and the Connecticut Drug Dependency Trust for support.

* Present address: Vick Divisions Research, Vick Chemical Co., Mt. Vernon, NY 10553

‡ To whom inquiries should be directed.

Dissolution Behavior and Bioavailability of Phenytoin from a Ground Mixture with Microcrystalline Cellulose

KEIJI YAMAMOTO *, MASAHIRO NAKANO *, TAKAICHI ARITA *‡, YOSHIKAZU TAKAYAMA *, and YOSHINOBU NAKAI ‡

Abstract □ The ground mixture of phenytoin and microcrystalline cellulose was prepared by grinding in a vibrational ball mill. The X-ray diffraction patterns indicated the amorphous nature of the ground mixture. Comparative studies were made concerning the *in vitro* dissolution and *in vivo* absorption of fine phenytoin powder, phenytoin sodium powder, and the ground mixture. The ground mixture showed a greater dissolution rate than the fine powder and attained supersaturation in the pharmacopeial disintegration media at pH 1.2 and 7.4. *In vivo* absorption studies of each preparation were carried out in five subjects, using a crossover design, by measuring the urinary excretion rate of a main metabolite, 5-(*p*-hydroxyphenyl)-5-phenylhydantoin. The blood levels of phenytoin and the corresponding urinary excretion patterns of the metabolite were determined in two subjects. The ground mixtures significantly improved the bioavailability of phenytoin. The drug was completely and rapidly absorbed after oral administration of the ground mixture. The vibrational ball milling technique for a poorly water-soluble drug with microcrystalline cellulose provides a promising way of improving the *in vivo* drug absorption.

Keyphrases □ Phenytoin—dissolution and bioavailability, ground mixture with microcrystalline cellulose compared to fine powder □ Dissolution—phenytoin, ground mixture with microcrystalline cellulose □ Bioavailability—phenytoin, ground mixture with microcrystalline cellulose □ Dosage forms—phenytoin and microcrystalline cellulose ground mixture, dissolution and bioavailability, compared to fine powder □ Cellulose, microcrystalline—ground mixture with phenytoin, effect on dissolution and bioavailability □ Anticonvulsant agents—phenytoin, dissolution and bioavailability, ground mixture with microcrystalline cellulose

When a relatively insoluble drug is administered orally, the rate of absorption and/or the extent of bioavailability are controlled by its dissolution rate in the GI fluids (1). Therefore, efforts have been made to increase the dissolution rate of poorly soluble drugs (2–5).

In an earlier study (6), a ground mixture of griseofulvin and microcrystalline cellulose significantly im-

proved the dissolution rate and bioavailability of griseofulvin compared with a micronized griseofulvin powder. Since microcrystalline cellulose is considered to be innocuous when taken orally, ground mixtures of poorly soluble drugs and the cellulose have been proposed to be biopharmaceutically useful formulations (6).

Phenytoin, a poorly water-soluble anticonvulsant, is incompletely and irregularly absorbed after oral administration (7). Significant variations in blood levels were reported recently when phenytoin capsules made by different manufacturers were administered (8, 9). In addition to dissolution rate-limited absorption, marked differences in biological half-lives among individuals and the closeness of the therapeutic and toxic levels (10) make phenytoin therapy very complicated and difficult. Therefore, phenytoin bioavailability recently has become a matter of great importance.

This paper describes the bioavailability of phenytoin and the physicochemical properties of the ground mixture of the drug and microcrystalline cellulose. Dissolution studies were carried out on the following preparations: the ground mixture of phenytoin and the cellulose, a fine powder, and a phenytoin sodium powder. The *in vivo* evaluation of each preparation after oral administration to healthy human volunteers also is described.

EXPERIMENTAL

Materials—Phenytoin[1] JP and phenytoin sodium[1] were used as received. The mean particle size of a phenytoin sample, as measured by nitrogen gas adsorption, was 5.3 μm. 5-(*p*-Methylphenyl)-5-phenylhydantoin[2], 5-(*p*-hydroxyphenyl)-5-phenylhydantoin[2], and microcrystalline cellulose[3] also were used. Phenyltrimethylammonium hydroxide[4] was a 20–25% solution in methanol. All other chemicals were of reagent grade, except *n*-heptane which was of spectroscopic grade.

Preparation of Ground Mixture—The ground mixture was prepared by adding 10 g of phenytoin to 90 g of microcrystalline cellulose and grinding for 2 hr with a ceramic vibrational ball mill[5]. Amorphous cellulose was similarly prepared by milling microcrystalline cellulose alone.

The X-ray powder diffraction[6] patterns of the mixture were obtained before and after the grinding process. A physical mixture (simple blend) was prepared by tumbling the fine powder with a ninefold excess of the cellulose in a bottle.

Dissolution Rate Studies—Dissolution rates of phenytoin from the different forms into 1 liter of JP VIII disintegration medium No. 1 (pH 1.2) or No. 2 (pH 7.4) were measured at 37° in a constant-temperature water bath. The amount of the drug used was 100 mg of the free acid equivalent: 100 mg of the fine powder, 109 mg of the sodium salt powder, or 1000 mg of the ground mixture.

Each preparation was transferred directly into the dissolution medium and stirred with a three-bladed stainless steel propeller at 100 rpm. A suitable aliquot was removed at the specified time using a membrane filter[7] (0.2 μm) and analyzed for drug by a UV spectrophotometric[8] method (11).

Nonequilibrium Solubility Studies—The amount of phenytoin dissolved in the disintegration medium No. 1 from the simple blend of 5 mg of the fine powder and 45 mg of amorphous cellulose and 50 or 150 mg of the ground mixture was determined at daily intervals. These preparations were weighed into 50-ml erlenmeyer flasks, which were then immersed in a constant-temperature bath. Thirty-milliliter portions of the medium, prewarmed to 37°, were added to the flasks. These flasks were immediately shaken horizontally at 70 strokes/min.

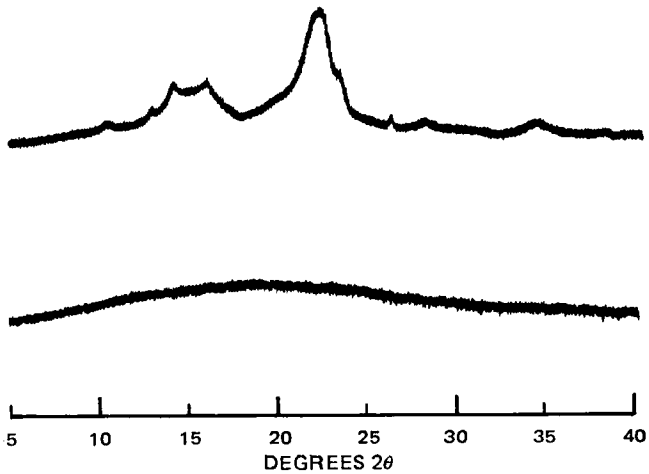

Figure 1—*X-ray powder diffraction patterns of a simple blend (upper) and the ground mixture (lower) of phenytoin and microcrystalline cellulose (1:9).*

At appropriate intervals, the samples were withdrawn through the membrane filters (0.2 μm). An aliquot was analyzed by a reported GLC method (12) with the following modifications. Phenyltrimethylammonium hydroxide (13) was employed instead of tetramethylammonium hydroxide as a methylating reagent, and 1.5% OV-101 on a solid support[9] (80–100 mesh) was used instead of DC-200 as a stationary phase.

***In Vivo* Absorption Studies**—The fine powder (250 mg), the sodium salt powder (272 mg), or the ground mixture (2500 mg) was orally administered to five normal subjects. The subjects were 21–27 years old, and the average body weight was 63 kg (range of 48–75 kg). Preparations were administered to each subject with 200 ml of water at approximately 9 am following an overnight fast using a crossover design. No food was taken for 6 hr postadministration. A minimum of 1 week was allowed between experiments.

Urine samples were collected at hourly intervals for the first 8 hr and at convenient time intervals up to 120 hr after administration. The volume and pH of each urine sample were recorded, and small portions of the urine samples were refrigerated until analyzed. In addition to the urine collection, blood samples were taken from two subjects at 0, 2, 4, 6, 8, and 24 hr. The blood samples, collected in heparinized test tubes, were centrifuged, and the plasma was stored in a refrigerator until assayed.

The amount of *p*-hydroxylated phenytoin and its conjugate, the main metabolite in humans (14), in the urine and the levels of the intact drug in the plasma were assayed by the same GLC method described for solubility measurements.

RESULTS AND DISCUSSION

Physicochemical Properties of Ground Mixture—The X-ray diffraction patterns of phenytoin–microcrystalline cellulose mixtures (1:9) before and after the grinding process are shown in Fig. 1. Before grinding (simple blend), sharp diffractional peaks derived from the drug crystals and broad diffractional peaks derived from the crystalline portions of the cellulose were observed. As the grinding progressed, however, these diffractional peaks disappeared; only the halo was observed in the X-ray diffraction pattern when complete grinding was achieved.

The changes in the X-ray diffraction patterns upon grinding indicate the decrease in the proportion of crystalline forms in the drug and the cellulose and the increase in the proportion of amorphous forms. The previous report (6) described some possible mechanisms

[1] Aleviatin, Dainippon Pharmaceutical Co., Osaka, Japan.
[2] Aldrich Chemical Co., Milwaukee, Wis.
[3] Avicel PH-101, Asahi Kasei Industrial Co., Tokyo, Japan.
[4] Tokyo Kasei Industy Co., Tokyo, Japan.
[5] Type B1, Chuokakoki Co., Toyoake, Aichi Pref, Japan.
[6] Model D-3F, Rigakudenki Co., Tokyo, Japan.
[7] Nuclepore, General Electric, Pleasanton, Calif.
[8] Spectrophotometer model 139, Hitachi Manufacturing Co., Tokyo, Japan.
[9] Shimalite W, Wako Pure Chemical Industry, Osaka, Japan.

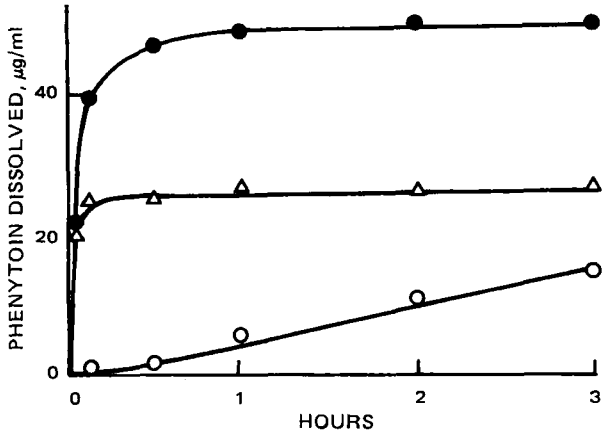

Figure 2—*Dissolution profiles of phenytoin from three preparations in 1 liter of JP VIII disintegration medium No. 1 (pH 1.2) at 37°. Each data point represents the mean of three determinations. Key: ●, 1000 mg of the ground mixture (1:9); △, 109 mg of a sodium salt powder; and ○, 100 mg of a fine powder.*

in the transition from the crystalline state to the amorphous state. IR spectra and melting-point measurements (295°) indicated no chemical change of the drug during the milling process.

Dissolution Behavior—The dissolution behavior of the fine powder, the sodium salt powder, and the ground mixture in JP VIII disintegration medium No. 1 (pH 1.2) at 37° is shown in Fig. 2. These plots show the concentration attained in solution for each preparation containing 100 mg of free acid or its equivalent. Since the drug solubility in this medium at 37° was 25.3 μg/ml, 100 mg of the drug in 1 liter of the dissolution medium corresponded to about four times its solubility. The ground mixture exhibited a faster dissolution rate than the fine powder and yielded a solution approximately 3.3 times as concentrated as a solution of the fine powder at 180 min. However, the dissolution rate of the sodium salt powder was as fast as that of the ground mixture.

Since the medium was acidic, the recrystallization of free acid took place immediately after the dissolution process and supersaturation did not occur. In the ground mixture, however, supersaturation, about twice the solubility, was observed. Although the faster dissolution rate and the phenomenon of supersaturation in the ground mixture may be due partly to deaggregation and the increased surface area, the amorphous nature of the drug may play a significant role.

Figure 3 shows the dissolution curves of three preparations in JP VIII disintegration medium No. 2 (pH 7.4) at 37°. The dissolution profile of the sodium salt powder in this medium differed significantly from that in the acidic medium Following the fast dissolution, an

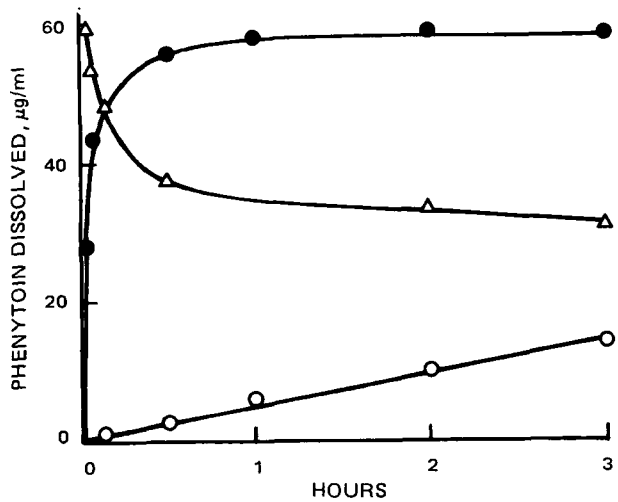

Figure 3—*Dissolution profiles of phenytoin from three preparations in 1 liter of JP VIII disintegration medium No. 2 (pH 7.4) at 37°. Each data point represents the mean of three determinations. Key: see Fig. 2.*

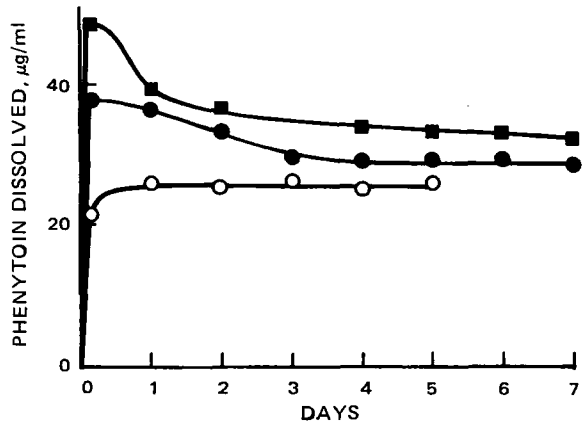

Figure 4—*Solution profiles of phenytoin in 50 ml of JP VIII disintegration medium No. 1 at 37°. Each data point represents the mean of six determinations. Key: ■, 150 mg of the ground mixture; ●, 50 mg of the ground mixture; and ○, a simple blend of 5 mg of the fine powder and 45 mg of amorphous cellulose.*

apparent decline was observed in the amount of drug dissolved. Since the pH of this medium was 7.4 and the pKa value of the drug is 8.3 (15), the slow recrystallization of free acid followed the initial rapid dissolution of the salt.

Dispersions of drugs in macromolecules such as polyethylene glycol and povidone have been employed in enhancing the dissolution and availability of drugs. Chiou and Riegelman (2) reported that the drug was molecularly and/or colloidally dispersed in the polyethylene glycol–drug solid dispersion system. Stupak *et al.* (3) suggested that reserpine in a coprecipitate with povidone had high thermodynamic activity. The exact physical nature of the ground mixture has not been determined, but drug molecules in the ground mixture probably are dispersed on the surface of cellulose and present in an amorphous state. Its energy level is expected to be higher than the original crystal.

When the solution profile of the ground mixture was followed for a longer period, the amount of drug in solution after the initial supersaturation decreased (Fig. 4). This finding may be attributed to conversion of amorphous phenytoin to a crystalline form. Moreover, with the ground mixture, the greater the amount added, the higher was the supersaturation level achieved. Even in the presence of amorphous cellulose, supersaturation was not observed when the stable fine powder was added.

***In Vivo* Absorption Studies**—The major metabolite of phenytoin in humans is the *p*-hydroxylated derivative (14). It is excreted in the urine mainly as a conjugate with glucuronic acid. Glazko *et al.* (16) reported that 76% of the dose was accounted for by a urinary metabolite over 5 days following intravenous administration of 250 mg of the sodium salt. The mean recovery of the metabolite over 96 hr was 64% when 0.5 g of the drug was orally administered to 12 subjects (17).

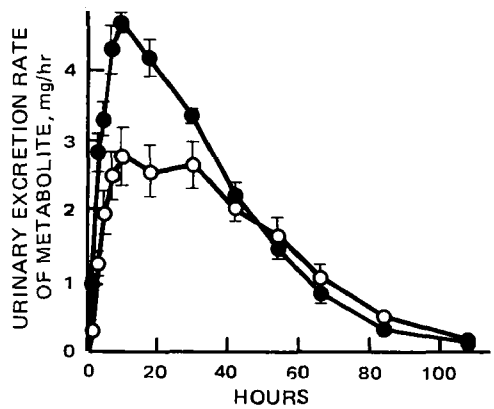

Figure 5—*Urinary excretion patterns of total 5-(p-hydroxyphenyl)-5-phenylhydantoin after oral administration of 250 mg of the fine powder (○) and 2500 mg of the ground mixture (●) to five volunteers (mean ± SEM).*

Table I—Urinary Excretion of Total *p*-Hydroxylated Phenytoin Compared by the Paired *t*-Test

Time Interval, hr	Urinary Excretion			Significance Level	
	Ground Mixture	Fine Powder	Sodium Salt Powder	Ground Mixture *versus* Fine Powder	Ground Mixture *versus* Sodium Salt Powder
	Excretion Rate[a], mg/hr				
0–2	0.98 ± 0.18	0.30 ± 0.10	1.33 ± 0.46	$p < 0.025$	N.S.[b]
2–4	2.85 ± 0.29	1.27 ± 0.17	2.08 ± 0.36	$p < 0.025$	N.S.
4–6	3.35 ± 0.24	1.98 ± 0.32	2.50 ± 0.49	$p < 0.005$	N.S.
6–8	4.32 ± 0.35	2.51 ± 0.35	2.91 ± 0.45	$p < 0.005$	N.S.
8–12	4.72 ± 0.15	2.79 ± 0.42	3.21 ± 0.66	$p < 0.005$	N.S.
12–24	4.21 ± 0.26	2.57 ± 0.38	2.71 ± 0.54	$p < 0.025$	N.S.
24–48	2.81 ± 0.16	2.37 ± 0.28	1.90 ± 0.36	N.S.	$p < 0.05$
48–72	1.19 ± 0.16	1.35 ± 0.24	0.65 ± 0.12	N.S.	$p < 0.05$
	Cumulative Amount Excreted[a], mg				
0–24	92.82 ± 4.15	53.73 ± 7.09	62.92 ± 11.07	$p < 0.005$	N.S.
0–48	160.36 ± 3.33	110.07 ± 13.51	108.19 ± 19.11	$p < 0.025$	$p < 0.05$
0–120	200.05 ± 6.68	162.76 ± 21.37	128.71 ± 22.05	N.S.	$p < 0.05$

[a] Mean ± *SEM*. [b] Not significant.

The mean urinary excretion rates of the metabolite are shown in Figs. 5 and 6. Figure 5 shows the mean urinary excretion rates after oral administration of the fine powder and the ground mixture. Excretion rates during the first 20 hr differed distinctly between the two preparations. The maximum mean excretion rate occurred in the 8–10-hr period following administration of the ground mixture. With the fine powder, however, a prolonged plateau region was observed during 10–30 hr postadministration. The intersubject variations of excretion rates were considerably smaller when the ground mixture was administered.

Figure 6 shows the mean excretion rates of the metabolite after oral administration of the sodium salt powder and the ground mixture. Their initial excretion rates did not differ significantly. However, remarkable intersubject variations in the excretion rates were observed upon the administration of the sodium salt powder. These excretion patterns were well correlated with the *in vitro* dissolution behavior of each preparation. The rapid dissolution of the ground mixture and the sodium salt powder resulted in the initially fast appearance of the metabolite in urine, and the supersaturation attained after the administration of the ground mixture resulted in the apparent high level in the maximum excretion rate.

The excretion rate of a drug is usually expected to be directly proportional to its concentration in the blood. In some cases, the excretion rate of a metabolite can reflect the blood level of its precursor (18, 19). The urinary appearance rate of hydroxylated phenytoin is expected to be controlled by its formation rate. Figure 7 shows the mean blood levels of the drug and the corresponding urinary excretion rates of the metabolite in two subjects after oral administration of the fine powder and the ground mixture. These results indicated that the drug in the ground mixture was more efficiently absorbed from the GI tract than the fine powder. Urinary excretion patterns showed that the excretion of the metabolite took many hours to reach a maximum value and was not directly proportional to the plasma levels of the drug.

Dill *et al.* (20) reported that, in a normal subject receiving a single intravenous dose of phenytoin sodium, the maximum plasma level of the metabolite occurred about 8 hr after administration and that a peak excretion rate was observed 6–8 hr after dosing, indicating a direct relationship between the plasma level of the metabolite and its urinary excretion rate. Glazko *et al.* (16) reported that the delayed appearance of the metabolite in plasma and urine could be caused by many different factors such as binding of the drug to protein, enterohepatic recirculation, and rate-limited hydroxylation or conjugation. Although the urinary excretion rate of the metabolite was not proportional to levels of the intact drug in the blood, it may be used to predict relative blood levels and relative absorption rates of the drug from different preparations if an appropriate experimental design is used.

From the *in vitro* dissolution behavior of the ground mixture and the fine powder and from the blood levels of the drug and urinary excretion rates of the metabolite following oral administration of these preparations, the following prediction may be made. After oral administration of the ground mixture, phenytoin dissolves rapidly to form a supersaturated solution in GI fluids. Subsequently, rapid absorption of the drug takes place. After oral administration of the fine powder, however, the drug dissolves slowly and the dissolution rate tends to be dependent on physiological conditions of individuals, resulting in great intersubject variations in absorption rates.

Table I summarizes the excretion data and the results of the paired *t*-test for the excretion rate and the cumulative amount excreted. Statistical analysis showed that there were significant differences,

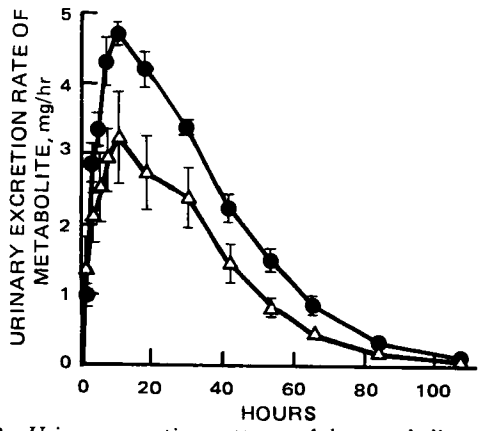

Figure 6—*Urinary excretion patterns of the metabolite after oral administration of 272 mg of the sodium salt powder (△) and 2500 mg of the ground mixture (●) to five volunteers (mean ± SEM).*

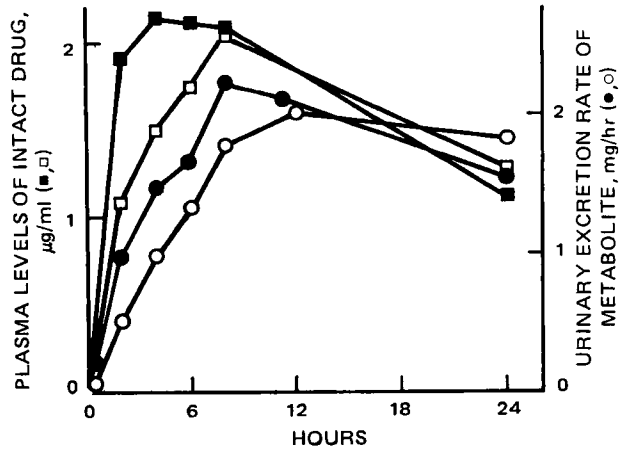

Figure 7—*Comparison of plasma levels (squares) of phenytoin with urinary excretion rates (circles) of the metabolite after oral administration of 250 mg of the fine powder (open symbols) and 2500 mg of the ground mixture (solid symbols) to two volunteers.*

at least at the 97.5% level of confidence, during the first 24 hr post-administration between the excretion rates of the metabolite following administration of the fine powder and of the ground mixture. There were significant differences among their cumulative amounts excreted during the initial time periods. The comparison of the sodium salt powder with the ground mixture, however, revealed no statistical differences in excretion rates and cumulative amounts excreted in a 0–24-hr period.

The present investigation showed that the improvement in the dissolution behavior of phenytoin due to vibrational ball milling with microcrystalline cellulose affected significantly the absorption characteristics of a drug whose absorption was dissolution rate limited. It is of interest to explore the vibrational ball milling of other poorly water-soluble drugs with microcrystalline cellulose.

REFERENCES

(1) S. A. Kaplan, in "Dosage Form Design and Bioavailability," J. Swarbrick, Ed., Lea & Febiger, Philadelphia, Pa., 1973, p. 20.

(2) W. L. Chiou and S. Riegelman, *J. Pharm. Sci.*, **58**, 1505(1969).

(3) E. I. Stupak, H. A. Rosenberg, and T. R. Bates, *J. Pharmacokinet. Biopharm.*, **2**, 511(1974).

(4) A. Ampolsuk, J. V. Mauro, A. A. Nyhuis, N. Shah, and C. I. Jarowski, *J. Pharm. Sci.*, **63**, 117(1974).

(5) S. Miyazaki, M. Nakano, and T. Arita, *Chem. Pharm. Bull.*, **23**, 552(1975).

(6) K. Yamamoto, M. Nakano, T. Arita, and Y. Nakai, *J. Pharmacokinet. Biopharm.*, **2**, 487(1974).

(7) K. Arnold, N. Gerber, and G. Levy, *Can. J. Pharm. Sci.*, **5**, 89(1970).

(8) K. S. Albert, E. Sakmar, M. R. Hallmark, D. J. Weidler, and J. G. Wagner, *Clin. Pharmacol. Ther.*, **16**, 727(1974).

(9) L. Lund, *Eur. J. Clin. Pharmacol.*, **7**, 119(1974).

(10) A. J. Glazko and T. Chang, in "Antiepileptic Drugs," D. M. Woodbury, J. K. Penry, and R. P. Schmidt, Eds., Raven, New York, N.Y., 1972, p. 127.

(11) Y. Saitoh, K. Nishihara, F. Nakagawa, and T. Suzuki, *J. Pharm. Sci.*, **62**, 206(1973).

(12) A. J. Wilensky and J. A. Lowden, *Neurology*, **23**, 318(1973).

(13) H. J. Kupferberg, *Clin. Chim. Acta*, **29**, 283(1970).

(14) T. C. Butler, *J. Pharmacol. Exp. Ther.*, **119**, 1(1957).

(15) S. P. Agarwal and M. I. Blake, *J. Pharm. Sci.*, **57**, 1434(1968).

(16) A. J. Glazko, T. Chang, J. Baukema, W. A. Dill, J. R. Goulet, and R. A. Buchanan, *Clin. Pharmacol. Ther.*, **10**, 498(1969).

(17) A. J. Glazko and T. Chang, in "Antiepileptic Drugs," D. M. Woodbury, J. K. Penry, and R. P. Schmidt, Eds., Raven, New York, N.Y., 1972, p. 130.

(18) "Guidelines for Biopharmaceutical Studies in Man," APhA Academy of Pharmaceutical Sciences, Washington, D.C., 1972.

(19) W. L. Chiou and S. Riegelman, *J. Pharm. Sci.*, **60**, 1376(1971).

(20) W. A. Dill, J. Baukema, T. Chang, and A. J. Glazko, *Proc. Soc. Exp. Biol. Med.*, **137**, 674(1971).

ACKNOWLEDGMENTS AND ADDRESSES

Received October 1, 1975, from the *Faculty of Pharmaceutical Sciences, Hokkaido University, Sapporo 060, Japan, and the ‡Faculty of Pharmaceutical Sciences, University of Chiba, Yayoicho, Chiba 280, Japan.

Accepted for publication December 16, 1975.

The authors are grateful to Dr. S. Takahashi, Department of Neurology, Hokkaido University Hospital, and to Dr. T. Minagawa and Dr. T. Sakuma, Department of Microbiology, Hokkaido University Medical School, for the help in sampling blood. Thanks are also due to Dainippon Pharmaceutical Co. and Asahi Kasei Industrial Co. for generous supplies of the materials.

ˣ To whom inquiries should be directed.

Solubility of Nonelectrolytes in Polar Solvents IV: Nonpolar Drugs in Mixed Solvents

S. H. YALKOWSKY *ˣ, S. C. VALVANI *, and G. L. AMIDON ‡

Abstract □ The molecular and group surface area approach to solubility is shown to be applicable to mixed aqueous solvent systems. An equation is derived which is consistent with the exponential increase in the aqueous solubility of nonpolar drugs that frequently accompanies the addition of a cosolvent. This equation predicts that: (*a*) the ability of a drug to be solubilized by a cosolvent is proportional to its hydrophobic surface area per molecule, and (*b*) the ability of a cosolvent to solubilize any drug is inversely proportional to its interfacial tension against a reference liquid hydrocarbon. These predictions are experimentally verified with solubility studies of several alkyl *p*-aminobenzoates in propylene glycol–water mixtures and of hexyl *p*-aminobenzoate in mixtures of water with ethanol, methanol, ethylene glycol, propylene glycol, glycerin, and formamide.

Keyphrases □ Solubility—nonelectrolytes in mixed aqueous solvent systems, molecular and group surface area approach □ Nonelectrolytes—solubility in mixed aqueous solvent systems □ Polar solvents, mixed—solubility of nonelectrolytes, molecular and group surface area approach □ Cosolvent systems, polar—solubility of nonelectrolytes, molecular and group surface area approach □ Alkyl *p*-aminobenzoates—solubility in propylene glycol–water mixtures □ Hexyl *p*-aminobenzoate—solubility in mixed polar solvent systems

Cosolvents are routinely used to increase the solubility of drugs in an aqueous medium. In general, the selection of a mixed solvent system is performed in a hit-and-miss fashion. There are few if any useful guidelines for assessing the relative solubilizing efficiency of the available liquids. Dielectric constant and solubility parameter correlations are of only limited utility, especially for drugs having very low aqueous solubilities. Yet it is precisely for these poorly soluble drugs that solubilization is most important.

A survey of the pharmaceutical literature (1–10) revealed that there is an exponential increase in aqueous solubility for many nonpolar drugs as the cosolvent is added. This increase was observed for many chemical

at least at the 97.5% level of confidence, during the first 24 hr post-administration between the excretion rates of the metabolite following administration of the fine powder and of the ground mixture. There were significant differences among their cumulative amounts excreted during the initial time periods. The comparison of the sodium salt powder with the ground mixture, however, revealed no statistical differences in excretion rates and cumulative amounts excreted in a 0–24-hr period.

The present investigation showed that the improvement in the dissolution behavior of phenytoin due to vibrational ball milling with microcrystalline cellulose affected significantly the absorption characteristics of a drug whose absorption was dissolution rate limited. It is of interest to explore the vibrational ball milling of other poorly water-soluble drugs with microcrystalline cellulose.

REFERENCES

(1) S. A. Kaplan, in "Dosage Form Design and Bioavailability," J. Swarbrick, Ed., Lea & Febiger, Philadelphia, Pa., 1973, p. 20.

(2) W. L. Chiou and S. Riegelman, *J. Pharm. Sci.*, **58**, 1505(1969).

(3) E. I. Stupak, H. A. Rosenberg, and T. R. Bates, *J. Pharmacokinet. Biopharm.*, **2**, 511(1974).

(4) A. Ampolsuk, J. V. Mauro, A. A. Nyhuis, N. Shah, and C. I. Jarowski, *J. Pharm. Sci.*, **63**, 117(1974).

(5) S. Miyazaki, M. Nakano, and T. Arita, *Chem. Pharm. Bull.*, **23**, 552(1975).

(6) K. Yamamoto, M. Nakano, T. Arita, and Y. Nakai, *J. Pharmacokinet. Biopharm.*, **2**, 487(1974).

(7) K. Arnold, N. Gerber, and G. Levy, *Can. J. Pharm. Sci.*, **5**, 89(1970).

(8) K. S. Albert, E. Sakmar, M. R. Hallmark, D. J. Weidler, and J. G. Wagner, *Clin. Pharmacol. Ther.*, **16**, 727(1974).

(9) L. Lund, *Eur. J. Clin. Pharmacol.*, **7**, 119(1974).

(10) A. J. Glazko and T. Chang, in "Antiepileptic Drugs," D. M. Woodbury, J. K. Penry, and R. P. Schmidt, Eds., Raven, New York, N.Y., 1972, p. 127.

(11) Y. Saitoh, K. Nishihara, F. Nakagawa, and T. Suzuki, *J. Pharm. Sci.*, **62**, 206(1973).

(12) A. J. Wilensky and J. A. Lowden, *Neurology*, **23**, 318(1973).

(13) H. J. Kupferberg, *Clin. Chim. Acta*, **29**, 283(1970).

(14) T. C. Butler, *J. Pharmacol. Exp. Ther.*, **119**, 1(1957).

(15) S. P. Agarwal and M. I. Blake, *J. Pharm. Sci.*, **57**, 1434(1968).

(16) A. J. Glazko, T. Chang, J. Baukema, W. A. Dill, J. R. Goulet, and R. A. Buchanan, *Clin. Pharmacol. Ther.*, **10**, 498(1969).

(17) A. J. Glazko and T. Chang, in "Antiepileptic Drugs," D. M. Woodbury, J. K. Penry, and R. P. Schmidt, Eds., Raven, New York, N.Y., 1972, p. 130.

(18) "Guidelines for Biopharmaceutical Studies in Man," APhA Academy of Pharmaceutical Sciences, Washington, D.C., 1972.

(19) W. L. Chiou and S. Riegelman, *J. Pharm. Sci.*, **60**, 1376(1971).

(20) W. A. Dill, J. Baukema, T. Chang, and A. J. Glazko, *Proc. Soc. Exp. Biol. Med.*, **137**, 674(1971).

ACKNOWLEDGMENTS AND ADDRESSES

Received October 1, 1975, from the *Faculty of Pharmaceutical Sciences, Hokkaido University, Sapporo 060, Japan, and the ‡Faculty of Pharmaceutical Sciences, University of Chiba, Yayoicho, Chiba 280, Japan.

Accepted for publication December 16, 1975.

The authors are grateful to Dr. S. Takahashi, Department of Neurology, Hokkaido University Hospital, and to Dr. T. Minagawa and Dr. T. Sakuma, Department of Microbiology, Hokkaido University Medical School, for the help in sampling blood. Thanks are also due to Dainippon Pharmaceutical Co. and Asahi Kasei Industrial Co. for generous supplies of the materials.

ˣ To whom inquiries should be directed.

Solubility of Nonelectrolytes in Polar Solvents IV: Nonpolar Drugs in Mixed Solvents

S. H. YALKOWSKY *ˣ, S. C. VALVANI *, and G. L. AMIDON ‡

Abstract □ The molecular and group surface area approach to solubility is shown to be applicable to mixed aqueous solvent systems. An equation is derived which is consistent with the exponential increase in the aqueous solubility of nonpolar drugs that frequently accompanies the addition of a cosolvent. This equation predicts that: (*a*) the ability of a drug to be solubilized by a cosolvent is proportional to its hydrophobic surface area per molecule, and (*b*) the ability of a cosolvent to solubilize any drug is inversely proportional to its interfacial tension against a reference liquid hydrocarbon. These predictions are experimentally verified with solubility studies of several alkyl *p*-aminobenzoates in propylene glycol–water mixtures and of hexyl *p*-aminobenzoate in mixtures of water with ethanol, methanol, ethylene glycol, propylene glycol, glycerin, and formamide.

Keyphrases □ Solubility—nonelectrolytes in mixed aqueous solvent systems, molecular and group surface area approach □ Nonelectrolytes—solubility in mixed aqueous solvent systems □ Polar solvents, mixed—solubility of nonelectrolytes, molecular and group surface area approach □ Cosolvent systems, polar—solubility of nonelectrolytes, molecular and group surface area approach □ Alkyl *p*-aminobenzoates—solubility in propylene glycol–water mixtures □ Hexyl *p*-aminobenzoate—solubility in mixed polar solvent systems

Cosolvents are routinely used to increase the solubility of drugs in an aqueous medium. In general, the selection of a mixed solvent system is performed in a hit-and-miss fashion. There are few if any useful guidelines for assessing the relative solubilizing efficiency of the available liquids. Dielectric constant and solubility parameter correlations are of only limited utility, especially for drugs having very low aqueous solubilities. Yet it is precisely for these poorly soluble drugs that solubilization is most important.

A survey of the pharmaceutical literature (1–10) revealed that there is an exponential increase in aqueous solubility for many nonpolar drugs as the cosolvent is added. This increase was observed for many chemical

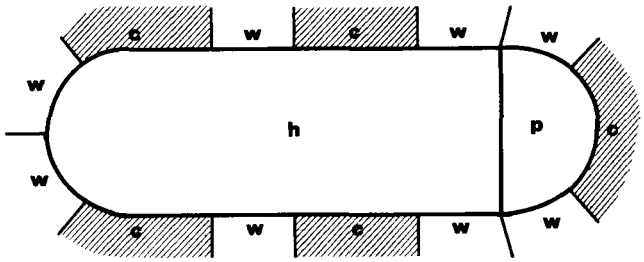

Figure 1—*Schematic diagram of a semipolar solute in a mixed solvent. Key:* h, *hydrophobic portion of solute;* p, *polar portion of solute;* c, *cosolvent; and* w, *water.*

classes of drugs in various mixed aqueous systems. The only requirement for plots of log (solubility) *versus* cosolvent composition to be linear appears to be that the solute must be less polar than the mixed solvent. Therefore, nearly all nonpolar drugs in most common mixed aqueous solvent systems are included. In spite of the ubiquitous nature of this phenomenon and its potential importance in pharmacy, there has been no systematic attempt to understand it or even to generalize about its applicability.

This work was initiated to fill this void and to elucidate the role of the cosolvent in the solution process. A simple model is developed for determining the activity coefficient and solubility of semipolar solutes in mixed solvents. The solubilities of hexyl *p*-aminobenzoate in various mixed solvent systems are used to substantiate the predictions of the model.

THEORETICAL

It is becoming increasingly popular (1–3, 11–15) to consider solute–solvent interactions in terms of solute molecular and group surface area of contact with the solvent. This concept was first proposed over 50 years ago by Langmuir (16) in his principle of independent surface action, but it received little attention until the recent development of a computer program for calculating molecular surface area (11). This program has been found useful in calculating functional group surface area as well as total molecular surface area (13).

To apply the molecular and group surface area approach to the solution of semipolar solutes in mixed solvents, all pairwise interactions between the various portions of the solute with the components of the solvent must be considered. It is assumed that the solute is sufficiently insoluble so that solute–solute contact is negligible, even in saturated solutions. This assumption restricts the applicability of the model to solutions containing low concentrations of solute. Before considering mixed solvents, the solute–solvent interactions between a drug and a pure solvent will be reviewed.

Pure Solvents—Previously (10, 13, 14), the molecular and group surface area (MGSA) approach was used to study the solubilities of hydrophobic solutes in water and other polar solvents. Based on this approach, the mole fractional solubility of a liquid solute in water, X_w^{liq}, can be related to the hydrophobic surface area, HSA, and the polar surface area, PSA, of the solute molecule by:

$$-kT \ln X_w^{liq} = (\gamma_{wh})(\text{HSA}) + (\epsilon_{wp})(\text{PSA}) \qquad \text{(Eq. 1)}$$

where γ_{wh} and ϵ_{wp} represent the microscopic surface free energy density, *i.e.*, free energy per unit area at the aqueous interface, with the hydrophobic and polar portions of the molecule, respectively, as described previously (13). [In one previous paper of this series (14), the term γ_{wp} was used instead of ϵ_{wp}.]

Equation 1 has been shown to be applicable to other polar solvents, provided that the appropriate microscopic surface free energy densities are used (14). That is:

$$-kT \ln X_c^{liq} = (\gamma_{ch})(\text{HSA}) + (\epsilon_{cp})(\text{PSA}) \qquad \text{(Eq. 2)}$$

where the subscript c denotes the solvent or cosolvent.

These equations can be extended easily to include crystalline drugs by the incorporation of the term $RT \ln X_i$, where X_i is the ideal mole fractional solubility of the drug (17, 18). Since the ideal solubility of a substance is independent of the nature of the solvent, Eqs. 1 and 2 become:

$$-kT \ln X_w = -kT \ln X_i + (\gamma_{wh})(\text{HSA}) + (\epsilon_{wp})(\text{PSA}) \qquad \text{(Eq. 3)}$$

and:

$$-kT \ln X_c = -kT \ln X_i + (\gamma_{ch})(\text{HSA}) + (\epsilon_{cp})(\text{PSA}) \qquad \text{(Eq. 4)}$$

respectively. These equations are, of course, based on the assumption that there is no specific solvation or self-association of the drug in the solvent.

The division of the solute according to its hydrophobic surface area and polar surface area is illustrated schematically in Fig. 1. There are several reasons for the choice of molecular surface area as a correlating parameter rather than molecular weight, volume, polarizability, or some other solute property. Correlation of the solubility of a large number of hydrocarbons and alcohols with surface area (13) and subsequently ethers, ketones, aldehydes, esters, acids, and olefins gives better results than with any other parameter considered. Moreover, the use of a single parameter for hydrophobic substituents eliminates the need to incorporate empirical correction factors to account for branching, ring formation, or positional isomerism. It is also possible to calculate molecular and group surface areas without performing any experimental measurements so that this parameter can be used in the design of nonexistent compounds. Finally, there is an intuitive relationship between solubility and the product of hydrophobic surface area and solvent hydrocarbon interfacial tension (10, 13, 14) which is consistent with existing theories of solubility.

Mixed Solvents—If a drug is dissolved in a mixed aqueous solvent, it will (on a microscopic level) be in contact with both water and cosolvent. According to Fig. 1 and to the proposed model, the solvent properties of a mixed solvent (*i.e.*, γ and ϵ) are a linear combination of the properties of its component species. Therefore, the mixed solvent can be described by multiplying Eq. 4 by the fraction of cosolvent, f_c, and Eq. 3 by the fraction of water, f_w, to get:

$$-kT \ln X_f = (f_c\gamma_{ch})(\text{HSA}) + (f_c\epsilon_{cp})(\text{PSA}) - f_c kT \ln X_i + (f_w\gamma_{wh})(\text{HSA}) + (f_w\epsilon_{wp})(\text{PSA}) - f_w kT \ln X_i \qquad \text{(Eq. 5)}$$

where X_f is the mole fractional solubility of the drug in the mixed solvent.

Equation 5 is based on the assumption that the microscopic interfacial tension of a mixed solvent is an additive combination of its constituent values. Langmuir (16) used fractional surface area (mole fractions times molar surface area or volume fraction times surface area per unit volume) as a weighing factor instead of volume fraction. Since the surface areas per unit volume of each cosolvent used are remarkably close[1], the two unitless fractional quantities are virtually equivalent, but the latter is easier to utilize in practice.

The assumption of additivity and constitutivity is often used in calculating solubility parameters, dielectric constants, and other properties of mixed solvents. However, in the case of surface and interfacial phenomena, it is not always valid; experimentally determined tensions are generally less than would be predicted because, at a macroscopic aqueous interface, there is a buildup of a surface excess of less polar solutes (including cosolvent molecules) that makes the surface less polar than the bulk. This effect is clearly seen from the comparison of the experimental and calculated interfacial tensions of propylene glycol–water mixtures (Table VI in Ref. 3). The following brief arguments are submitted in support of the use of Eq. 3, which does not account for a surface excess.

Development of a macroscopic surface excess is a time-dependent process (19), because the cosolvent must diffuse from the bulk to the stagnant interface. The microscopic interface, on the other hand, is not stationary; the solute has a diffusivity comparable to that of the cosolvent. Therefore, in the absence of strong attractive interactions between solute and cosolvent, the accumulation of a significant surface excess of the latter about the rapidly moving (Brownian motion) solute molecules is less likely.

Since the development of a surface excess serves to lower the interfacial tension between two phases, a low interfacial tension would not favor such accumulation. Because of its curvature, the microscopic

[1] Unpublished data.

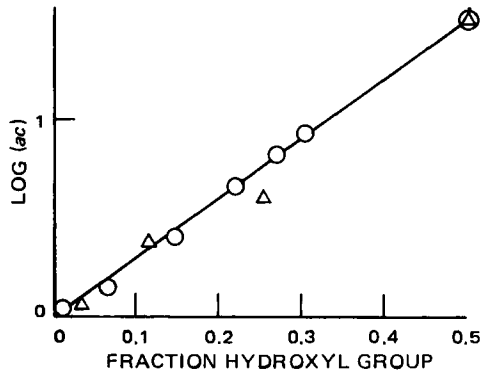

Figure 2—*Activity coefficients of heptane in pure alcohols* (△) *and ethanol–heptane mixtures* (○).

interfacial tension is much lower than a comparable macroscopic tension and thus should have a much smaller tendency to develop a surface excess.

Deal and Derr (20) showed that if the activity coefficient of *n*-heptane in various pure aliphatic alcohols and in mixtures of ethanol and heptane are plotted as a function of hydroxyl group concentration, the two sets of data fall on the same line (Fig. 2). If there is excess heptane from the mixed solvent at the microscopic interface, the triangles of Fig. 2 fall considerably above the line described by the circles; *i.e.*, the solute heptane molecules are surrounded by an excess of solvent heptane molecules.

On the basis of these arguments, it is believed that if there is a surface excess at the molecular interface, it is less than at the macroscopic interface. Since there is no way of determining its magnitude, it can, as a first approximation, be assumed to be negligible. This approximation can be made safely for aqueous glycerin and ethylene glycol, which are highly polar, but must be used cautiously for the more nonpolar cosolvents such as ethanol.

For low solute concentrations, f_w can be replaced with $1 - f_c$. Upon rearrangement of Eq. 5, the following is obtained:

$$-kT \ln X_f = (\gamma_{wh})(\text{HSA}) + (\epsilon_{wp})(\text{PSA}) - kT \ln X_i - [(\Delta\gamma)(\text{HSA}) + (\Delta\epsilon)(\text{PSA})]f_c \quad \text{(Eq. 6)}$$

where:

$$\Delta\gamma = \gamma_{wh} - \gamma_{ch} \quad \text{(Eq. 7)}$$

and:

$$\Delta\epsilon = \epsilon_{wp} - \epsilon_{cp} \quad \text{(Eq. 8)}$$

Equation 6 can be combined with Eq. 3 to give the following relationship, which serves as the basis for the rest of this paper:

$$kT \ln X_f = kT \ln X_w + [(\Delta\gamma)(\text{HSA}) + (\Delta\epsilon)(\text{PSA})]f_c \quad \text{(Eq. 9)}$$

This equation can successfully explain the exponential increase in the aqueous solubility of poorly soluble drugs that frequently accompanies the addition of cosolvent (1–10, 14). For convenience, Eq. 9 can be rewritten as:

$$\log X_f = \log X_w + \sigma f_c \quad \text{(Eq. 10)}$$

where:

$$\sigma = \frac{(\Delta\gamma)(\text{HSA}) + (\Delta\epsilon)(\text{PSA})}{2.303kT} \quad \text{(Eq. 11)}$$

(Note that Eq. 10 reduces to Eq. 1 or 2 when $f_c = 0$ or 1.)

Now the estimation of σ, the solubilizing power of a cosolvent for a drug, can be developed. In particular, the ability of various drugs to be solubilized by a particular cosolvent and the ability of various cosolvents to solubilize a particular drug will be predicted.

EXPERIMENTAL

Materials—The *p*-aminobenzoate esters studied were selected from those used in Ref. 21. All solvents were of USP grade and were used as received. The water was deionized.

Mixed Solvents—The mixed solvents were prepared by mixing 20, 40, 60, and 80 ml of cosolvent with 80, 60, 40, and 20 ml of water, respectively. The fraction of cosolvent present, f_c, is defined as the volume of cosolvent divided by the sum of the volumes of cosolvent and water.

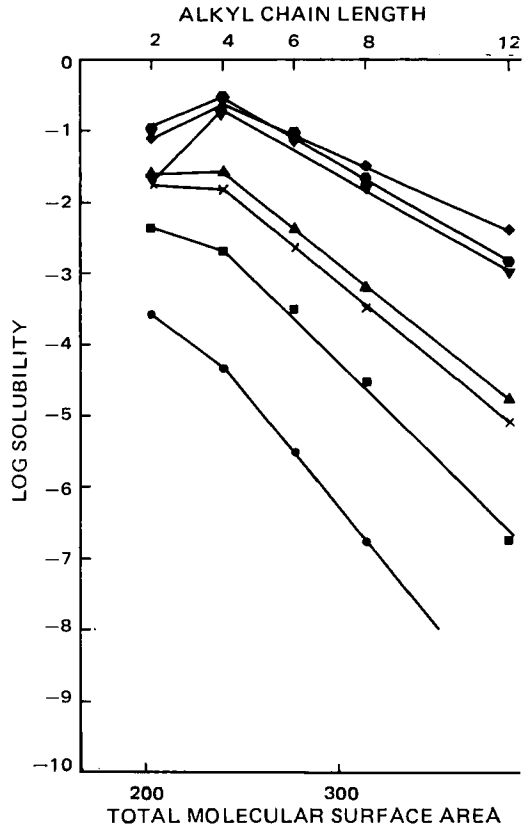

Figure 3—*Mole fractional solubilities of alkyl* p*-aminobenzoates in pure solvents. Key:* ●, *water;* ■, *glycerin;* ×, *formamide;* ▲, *ethylene glycol;* ▼, *propylene glycol;* ⬟, *methanol; and* ♦, *ethanol.*

Surface Area Calculations—The surface areas of the alkyl *p*-aminobenzoates were calculated by the preferred method described in Ref. 21. The hydrophobic surface area represents the alkyl and aryl portions of the molecules. The polar surface area is the sum of the amino and ester areas and is a constant 64 Å^2 for all esters.

Ideal Solubility Determinations—These values were calculated from the heat of fusion and the melting temperature (17, 18). The heats of fusion were determined by differential scanning calorimetry. The melting points were determined by hot-stage microscopy and differential scanning calorimetry as described previously (18).

Interfacial Tensions—The interfacial tensions were determined against tetradecane using the Wilhelmy plate method. The experimental details, along with the dependence of interfacial tension of hydrocarbon density, were described previously (22).

RESULTS

Pure Solvents—The mole fractional solubilities of the alkyl *p*-aminobenzoates studied in water, glycerin, ethylene glycol, propylene glycol, formamide, methanol, and ethanol are shown in Fig. 3. The relationship between log X and either chain length or total molecular surface area (TSA) was not linear in any of the solvents. The breaks in each curve were due to the fact that the ideal solubilities of the alkyl *p*-aminobenzoates showed a maximum at the butyl ester. This maximum was due to a change in the type of crystal formed in going from the lower to the higher homologs (18).

Since the solution interactions are of interest, it is more meaningful to look at the nonideal contribution to solubility. The nonideal solubility (often called the activity coefficient) is calculated by simply dividing the ideal solubility by the observed solubility. It is the solubility that the drug would have if it is converted to a liquid or oil by having its crystal structure destroyed. The activity coefficients (ac) of poorly soluble drugs are equivalent to the reciprocal of the liquid solubilities described by Eqs. 1 and 2.

When the observed solubilities of Fig. 3 are replaced by the nonideal

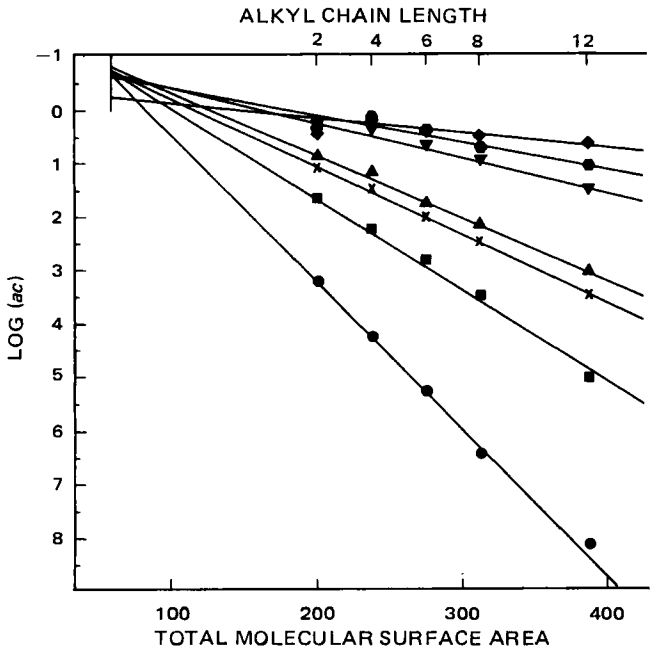

Figure 4—*Mole fractional activity coefficients of alkyl* p-*aminobenzoates in pure solvents. Key:* ●, *water;* ■, *glycerin;* ×, *formamide;* ▲, *ethylene glycol;* ▼, *propylene glycol;* ⬣, *methanol; and* ♦, *ethanol.*

solubilities, the data shown in Fig. 4 are obtained. In all solvents considered, there was good linearity between log (*ac*) and molecular surface area as predicted by Eqs. 3 and 4. The slopes of the lines appear to be related to the polarities of the solvents and the lines appear almost to converge at about 64 Å^2, the area of the polar moieties of the esters.

Mixed Solvents—The solubility data for the esters in 20, 40, 60, and 80% propylene glycol–water mixtures (Fig. 2 of Ref. 1) also show a break in the log solubility–surface area curves; when corrected for crystallinity, these data give the straight lines of Fig. 5. The data for the esters in the mixed solvents are qualitatively similar to the data

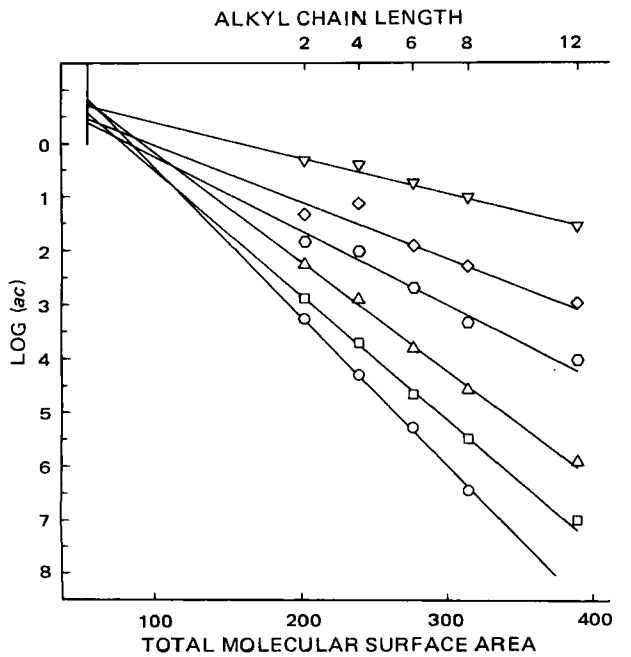

Figure 5—*Mole fractional activity coefficients of alkyl* p-*aminobenzoates in propylene glycol–water mixtures at 37°. Key:* ▽, *propylene glycol;* ◇, *80% propylene glycol in water;* ○, *60% propylene glycol in water;* △, *40% propylene glycol in water;* □, *20% propylene glycol in water; and* ○, *water.*

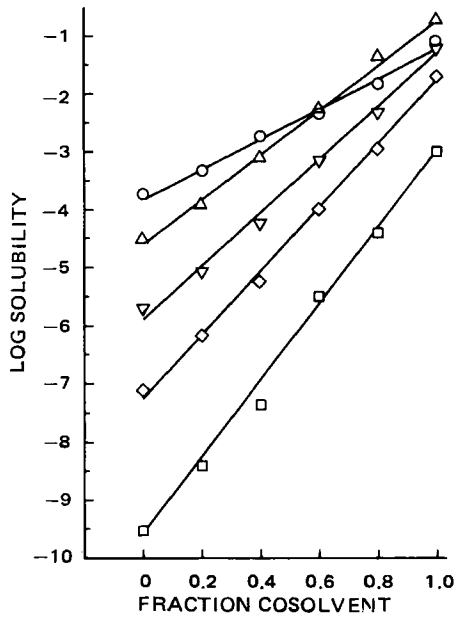

Figure 6—*Solubility of alkyl* p-*aminobenzoates in propylene glycol–water mixtures. Key:* ○, *ethyl;* △, *butyl;* ▽, *hexyl;* ◇, *octyl; and* □, *dodecyl.*

for the pure solvents. This finding indicates that a solvent blend of two liquids can indeed be treated as a pure solvent of intermediate polarity.

The data in Fig. 5 can be replotted to show the effects of altering solvent composition for each homolog. Figure 6 illustrates that increasing propylene glycol composition produces a linear increase in log X. It is apparent that the less water-soluble esters are solubilized most efficiently; *i.e.*, the solubilizing power of propylene glycol is greatest for the most nonpolar esters.

The relative solubilizing power of a variety of polar solvents for hexyl *p*-aminobenzoate can be seen from the slopes of lines of Fig. 7. The ability of the various solvents to solubilize hexyl *p*-aminobenzoate appears to be directly related to the nonpolarity of the solvent. The quantitation of these results with Eq. 11 will be discussed next.

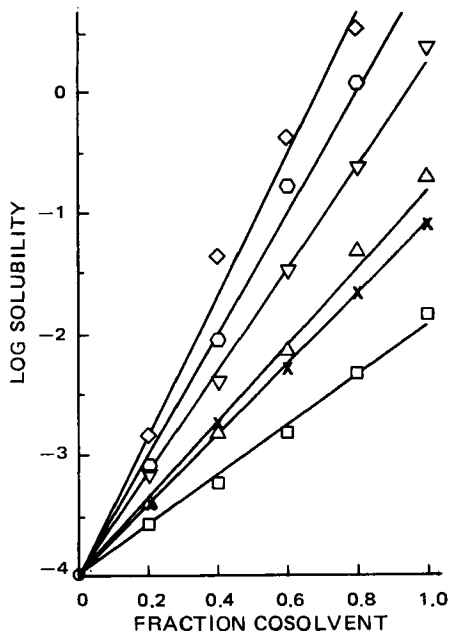

Figure 7—*Solubility of hexyl* p-*aminobenzoate in mixed solvent systems. Key:* ○, *water;* □, *glycerin–water;* ×, *formamide–water;* △, *ethylene glycol–water;* ▽, *propylene glycol–water;* ○, *methanol–water; and* ◇, *ethanol–water.*

Table I—Microscopic Interfacial Free Energy Densities for Several Solvents

Solvent, Temperature	γ, dynes/cm² (from Slope)	ϵ, dynes/cm² (from Intercept)	$\Delta\gamma$, dynes/cm² ($\gamma_w - \gamma_c$)	$\Delta\epsilon$, dynes/cm² ($\epsilon_w - \epsilon_c$)	$(\Delta\gamma)$ (HSA), dynes[a]	$(\Delta\epsilon)$ (PSA), dynes[a]
Water, 25°	28.3	10.2	0	0	0	0
Methanol, 25°	4.7	8.1	23.7	2.1	4968	143
Ethanol,[b] 25°	2.8	3.8	25.6	6.4	5367	412
Ethylene glycol, 25°	11.1	11.0	17.2	−0.8	3618	−44
Propylene glycol, 25°	6.5	8.5	21.8	1.7	4600	109
Glycerin, 25°	18.7	5.2	9.6	5.0	2026	324
Formamide, 25°	12.1	10.8	16.2	−0.6	3400	−32
Water, 37°	29.1	13.1	0	0	0	0
20% Propylene glycol, 37°	22.7	4.2	6.4	8.9	1346	569
40% Propylene glycol, 37°	20.3	9.3	8.8	3.8	1862	246
60% Propylene glycol, 37°	12.6	2.5	16.5	10.6	3456	667
80% Propylene glycol, 37°	9.9	4.3	19.2	8.8	4038	565
Propylene glycol, 37°	6.5	9.5	22.6	3.6	4739	230

[a] Hexyl *p*-aminobenzoate. [b] One data point was omitted.

DISCUSSION

Pure Solvents—*Comparison of* $(\Delta\gamma)(HSA)$ *and* $(\Delta\epsilon)(PSA)$—The relative importance of the hydrophobic and polar components of σ (Eq. 11) can be determined by the application of Eqs. 1 and 2 to the solute. The activity coefficients (or nonideal solubilities) of the esters in the various pure and mixed solvents described in Figs. 4 and 5 enable a comparison of $(\Delta\epsilon)$(PSA) and $(\Delta\gamma)$(HSA) for each ester. According to Eqs. 1 and 2, each line in these figures has a slope of $1/2.303\ kT \times \gamma$ (the microscopic interfacial free energy density at the hydrophobic portion of the solute and the pure or mixed solvent).

Since the polar surface area is the same for all esters (approximately 64 Å²), ϵ can be determined for each solvent from the extrapolated activity coefficient at TSA = PSA = 64 Å². The values of ϵ and γ in each solvent system studied are listed in Table I. The values of ϵ are not greatly different from that of water for any solvent, so $\Delta\epsilon$ is quite small in all cases. On the other hand, $\Delta\gamma$ is usually quite large. The values of $\Delta\epsilon$ and $\Delta\gamma$ are also given in Table I. It is also known that the value of HSA is significantly greater than the value of PSA for all esters studied. The last two columns of Table I show that for hexyl *p*-aminobenzoate, a typical poorly soluble solute, the value of $(\Delta\gamma)$ (HSA) is much greater than $(\Delta\epsilon)$(PSA) for all of the cosolvents considered. This finding leads to the following very useful approximation to Eq. 11:

$$\sigma \cong \frac{(\Delta\gamma)(HSA)}{2.303kT} \qquad \text{(Eq. 12)}$$

This approximation, which is applicable to solutes of low polarity, allows σ to be described in terms of a single property of each pure solvent component (γ_w and γ_c, the microscopic free energy density at the molecular hydrophobic surface) and of the pure solute (HSA, the molecular hydrophobic surface area).

Although the microscopic hydrocarbon surface areas of the solute can be calculated (21), the free energy per unit of molecular hydrocarbon surface area cannot be determined directly. However, this microscopic property can be related to the free energy per unit area at a suitable macroscopic hydrocarbon–solvent interface. This latter quantity, which is the hydrocarbon–solvent interfacial tension, is easily measurable for most polar solvents. To make this correlation, a model liquid hydrocarbon must be chosen for the macroscopic determinations and the differences between the macroscopic and microscopic interfacial tensions then must be considered.

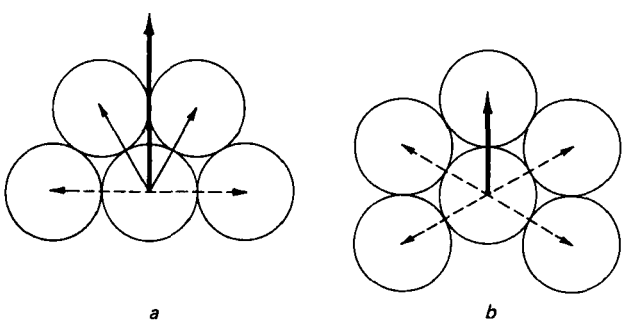

Figure 8—*Schematic diagram of the forces acting on a surface molecule of solvent at a planar interface* (a) *and at an interface having a radius of curvature equal to the solvent radius* (b).

Comparison of Macroscopic and Microscopic Interfacial Tensions—The choice of a model hydrocarbon for the macroscopic determinations is somewhat arbitrary and is governed primarily by experimental convenience. Low molecular weight hydrocarbons such as hexane are too volatile and tend to be miscible with some semipolar solvents such as ethanol. The very high molecular weight hydrocarbons are solid and cannot be used to get unambiguous interfacial tension values. Tetradecane is convenient to work with (22) and was used in all interfacial tension measurements.

The major difference between the microscopic and macroscopic interfacial tensions results from the extremely high degree of curvature of the molecular surface. The effect of high curvature can be conceptualized by consideration of the interfaces depicted in Fig. 8. Figure 8*a* shows a group of closest packed spheres at a macroscopic planar interface. (For simplicity, the region above the surface is treated as a perfect void so no transinterfacial forces have to be considered.) The balanced forces and their resultant force are indicated by solid arrows.

Figure 8*b* is a comparable diagram for the molecules surrounding a microscopic void space the size of a solvent molecule. The balanced forces are again indicated by dotted arrows. Since there is only one unbalanced interaction for each molecule surrounding the void space, this force (indicated by a solid arrow) is the resultant force. Since the

Table II—Calculation of Curvature Correction Factor from Single Solvent Data

Solvent, Temperature	γ, dynes/cm² (from Slope)	γ^0, dynes/cm² (Experimental, 25°)	c (γ/γ^0)
Water, 25°	28.3	51.9	0.55
Methanol, 25°	4.7	4.2[a]	—[a]
Ethanol, 25°	2.8	—[a]	—[a]
Ethylene glycol, 25°	11.1	19.3	0.58
Propylene glycol, 25°	6.5	12.5	0.52
Glycerin, 25°	18.7	35.2	0.53
Formamide, 25°	12.1	31.2	0.39
Water, 37°	29.1	51.9	0.56
20% Propylene glycol, 37°	22.7	44.1	0.52
40% Propylene glycol, 37°	20.3	36.2	0.56
60% Propylene glycol, 37°	12.6	28.3	0.45
80% Propylene glycol, 37°	9.9	20.4	0.49
Propylene glycol, 37°	6.5	12.5	0.52

[a] Experimental γ cannot be determined accurately because of the miscibility of the solvents with tetradecane.

Table III—Calculation of Curvature Correction Factor from Propylene Glycol–Water Data for Alkyl *p*-Aminobenzoates

Ester	HSA, A²	Slope (σ)	c
Ethyl	146	2.66	0.44
Butyl	178	3.82	0.52
Hexyl	210	4.72	0.54
Octyl	242	5.50	0.55
Dodecyl	306	6.61	0.52

imbalance of forces at the interface gives rise to the interfacial tension, the tension about a highly curved interface will be less than at a planar interface.

There is no definitive means of quantitatively predicting the effect of curvature on interfacial tension. However, several investigators proposed relationships of the same general form as the one proposed by Tolman (23):

$$\frac{\gamma^0}{\gamma} = \frac{1}{1 + \frac{2\delta}{r}} \qquad \text{(Eq. 13)}$$

where γ and γ^0 are the microscopic and macroscopic interfacial tensions, respectively; δ is a constant related to the size of the solvent (for water, $\delta \simeq 1.0$); and r is the radius of the microscopic interface in Angstroms. For cavities the size of the solvent molecule, the curvature correction factor is expected to be about 0.33; for nearly spherical solutes such as methane, neopentane, and adamantane, the factor increases to about 0.5, 0.65, and 0.77, respectively. It is not known whether nonspherical solutes can be treated as spheres of the same volume or whether some other means must be used to compute the appropriate radius of curvature.

Since there is no firm basis for choosing any particular relationship between γ and γ^0, the curvature correction must remain as an adjustable parameter, c, whose value lies somewhere between 0.33 and 1.0. Because all solvents considered are of comparable radius compared to that of the alkyl *p*-aminobenzoates, the value of c is expected to be a constant that is nearly independent of the solvent, so that:

$$\gamma = c\gamma^0 \qquad \text{(Eq. 14)}$$

applies to these systems.

The approximate constancy of c can be confirmed by another analysis of the data in Figs. 4 and 5. According to Eqs. 1 and 2, the slopes of the lines in the figure are equal to $\gamma/2.303kT$ for each solvent. The values of γ calculated from these slopes are listed in Table II along with the experimentally determined γ^0 values. It can be seen from the last column that there is very little difference in the curvature correction factors for the solvents. The values for methanol and ethanol appear to be exceptions but probably are due to the difficulties in determining interfacial tensions that result from the partial miscibility of these two pure solvents with the reference hydrocarbon, tetradecane.

Mixed Solvents—The assumed constancy of the curvature correction factor, c, allowed σ to be related directly to the measurable solvent hydrocarbon interfacial tension. Combining Eqs. 12 and 14 gives:

$$\sigma = \frac{c(\gamma_w{}^0 - \gamma_c{}^0)\text{HSA}}{2.303kT} = \frac{c\Delta\gamma^0\text{HSA}}{2.303kT} \qquad \text{(Eq. 15)}$$

which, when combined with Eq. 10, gives:

$$\log S_f = \log S_w + \frac{c}{2.303kT}\Delta\gamma^0\text{HSA}f_c \qquad \text{(Eq. 16)}$$

If c is always constant, Eq. 16 can be tested in two ways: (*a*) by relating the solubilizing power of a particular solvent system (having a constant $\Delta\gamma^0$) to the hydrophobic surface area of a series of solutes, and (*b*) by relating the solubilizing power of a series of cosolvents (having different values of $\Delta\gamma^0$) for a single solute.

According to Eq. 16, the slopes of the lines in Fig. 6 are each equal to:

$$\text{slope} = \frac{c(\gamma_w{}^0 - \gamma_{\text{PG}}{}^0)}{2.303kT} \times \text{HSA} \qquad \text{(Eq. 17)}$$

From the known values of $\gamma_w{}^0$, $\gamma_{\text{PG}}{}^0$, and HSA for each ester, the corresponding apparent values of c can be calculated. These values (Table III) are in good agreement with the values of Table II.

Table IV—Calculation of Curvature Correction Factor from Mixed Solvent Data for Hexyl *p*-Aminobenzoate

Cosolvent	σ[a]	$\Delta\gamma$, dynes/cm² (from σ)	$\Delta\gamma^0$, dynes/cm² ($\gamma_w{}^0 - \gamma_c{}^0$)	c ($\Delta\gamma/\Delta\gamma^0$)
Water	0	0	0	—
Glycerin	2.04	9.3	16.7	0.56
Formamide	2.71	12.3	20.7	0.59
Ethylene glycol	3.77	17.0	32.6	0.52
Propylene glycol	4.72	21.3	39.4	0.54
Methanol	5.45	24.6	47.7	0.52
Ethanol	6.35	28.7	51.9	0.55

[a] Calculated from $(\Delta \log X)/\Delta f_c$.

The slopes of the lines of Fig. 7 are, according to Eq. 16, equal to $(c/2.303kT)\,\Delta\gamma^0 \times \text{HSA}_{\text{hexyl }p\text{-aminobenzoate}}$. The values of c calculated for each solvent from these slopes are given in Table IV. Again, the values obtained are in agreement with all previous values. Further confirmation of the constancy of c is seen from the dependence of σ on $\Delta\gamma^0$ ($c = 0.57$ from Fig. 1 of Ref. 14) and from the slope of log (solubility) *versus* surface area for over 200 hydrocarbons and monofunctional aliphatic compounds in water [$c = 0.55$ (21)]. On the basis of the preceding observations, a constant value of 0.55 can be chosen for c and can be used in the equations.

The fact that c is constant is highly significant in that it makes Eq. 16 useful for predicting how well a particular cosolvent can solubilize a specific nonpolar drug. Table V lists the expected value of σ (both on a mole fraction scale, σ, and on a molar scale, σ_m) for each solvent considered. The last two columns of Table V list the predicted and observed increases in hexyl *p*-aminobenzoate solubility with each 10% increase in cosolvent composition. In all cases, the agreement between the two is quite good.

The constancy of c also makes it possible to predict the effect of HSA on the alkyl chain length on the solubility of a series of homologs in a given polar solvent. Table VI compares the observed decrease in the activity coefficient of the alkyl *p*-aminobenzoates in each of the pure and mixed solvents studied with the value predicted by Eq. 2 (with $c = 0.55$ and 18 Å²/methylene group). Again, the agreement between theory and experiment is quite good.

The utility of Eq. 16 extends far beyond hexyl *p*-aminobenzoate and the discussed solvents. It can be applied to nearly any nonpolar drug in a binary aqueous solvent system, even if the values of c and HSA are not explicitly known. The authors have observed[1] that the ability of propylene glycol to solubilize a number of drugs is directly related to the hydrophobicity of the drug and that the degree to which a drug is solubilized by a cosolvent is inversely proportional to its aqueous solubility. This result is expected because both aqueous solubility (corrected for crystal effects) and σ are related to hydro-

Table V—Predicted Effects of Cosolvents on Solubility of Hexyl *p*-Aminobenzoate[a]

Cosolvent	σ_X (Predicted)	σ_M (Predicted)	Factor by which Aqueous Molar Solubility Increases with Addition of 10% Cosolvent: Predicted	Observed
Water	0	0	1.0	1.0
Glycerin	2.02	1.43	1.4	1.6
Formamide	2.52	2.18	1.7	2.0
Ethylene glycol	3.97	3.48	2.2	2.2
Propylene glycol	4.79	4.19	2.6	2.6
Methanol	5.80	5.45	3.5	3.2
Ethanol	6.31	5.81	3.8	3.9

[a] All predicted values were based on a value of 0.55 for c.

Table VI—Predicted Effects of Chain Length on Activity Coefficients

Solvent	γ, dynes/cm²	Factor by which Room Temperature Activity Coefficient Decreases with Addition of Methylene Unit to Solute: Predicted	Observed
Water	51.9	3.46	3.31
Glycerin	35.2	2.19	2.13
Formamide	31.1	2.11	1.73
Ethylene glycol	19.3	1.59	1.69
Propylene glycol	12.5	1.35	1.33
Methanol	4.2	1.10	1.24
Ethanol	0	1.00	1.13

phobic surface area (Eqs. 1 and 12).

An interesting and important consequence of Eq. 16 is that the relative ability of the various cosolvents to solubilize a drug is independent of the drug (provided that it is sufficiently hydrophobic for this treatment to be applicable) and is related only to $\Delta\gamma^0$. Therefore, for any very insoluble drug, ethanol will be the most efficient solubilizer of the solvents considered, with the other solvents following in the order listed in Table IV.

SUMMARY AND CONCLUSIONS

The solubility of poorly water-soluble compounds in mixed aqueous solvents is treated as a linear combination of terms representing the pairwise interactions of each solvent component with each topographical component of the drug.

The interactions involving the hydrophobic portion of the solute are the major factors that determine how well it can be solubilized, and these interactions can be related directly to the interactions of a pure liquid hydrocarbon with the solvent components.

On this basis, an equation is derived that explains the exponential increase in the aqueous solubility of insoluble drugs with the addition of a cosolvent. This equation further predicts that the magnitude of the increase in solubility produced by the cosolvent is exponentially related to the surface (interfacial) properties of the solvent components and the hydrophobic surface area of the solute.

REFERENCES

(1) T. Higuchi, M. Gupta, and L. W. Busse, *J. Am. Pharm. Assoc., Sci. Ed.*, **42**, 157(1953).

(2) C. F. Peterson and R. E. Hopponen, *ibid.*, **42**, 540(1953).

(3) P. H. Elworthy and H. E. C. Worthington, *J. Pharm. Pharmacol.*, **20**, 830(1968).

(4) B. J. Poulson, E. Young, V. Coquilla, and M. Katz, *J. Pharm. Sci.*, **57**, 928(1968).

(5) E. R. Garrett and P. B. Chemburkar, *ibid.*, **57**, 950(1968).

(6) I. M. Korenman, *Russ. J. Phys. Chem.*, **45**, 1011(1971).

(7) Y. Kato and T. Ohuchi, *Yakugaku Zasshi*, **92**, 257(1972).

(8) A. J. Kapadia and J. Autian, *J. Am. Pharm. Assoc., Sci. Ed.*, **49**, 380(1960).

(9) G. L. Flynn and S. H. Yalkowsky, *J. Pharm. Sci.*, **61**, 852(1972).

(10) S. H. Yalkowsky, G. L. Flynn, and G. L. Amidon, *ibid.*, **61**, 893(1972).

(11) R. B. Hermann, *J. Phys. Chem.*, **76**, 2754(1972).

(12) M. J. Harris, T. Higuchi, and J. H. Rytting, *ibid.*, **77**, 2694(1973).

(13) G. L. Amidon, S. H. Yalkowsky, and S. Leung, *J. Pharm. Sci.*, **63**, 1858(1974).

(14) S. H. Yalkowsky, G. L. Amidon, G. Zografi, and G. L. Flynn, *ibid.*, **64**, 48(1975).

(15) J. A. Reynolds, D. B. Gilbert, and C. Tanford, *Proc. Nat. Acad. Sci. USA*, **71**, 2925(1974).

(16) I. M. Langmuir, *Colloid Sym. Monogr.*, **3**, 48(1925).

(17) J. H. Hildebrand and R. L. Scott, "Regular Solutions," Prentice Hall, Englewood Cliffs, N.J., 1962.

(18) S. H. Yalkowsky, G. L. Flynn, and T. G. Slunick, *J. Pharm. Sci.*, **61**, 852(1972).

(19) A. W. Adamson, "Physical Chemistry of Surfaces," Interscience, New York, N.Y., 1970.

(20) C. H. Deal and E. L. Derr, *Ind. Eng. Chem.*, **60**, 28(1968).

(21) S. C. Valvani, S. H. Yalkowsky, and G. L. Amidon, *J. Phys. Chem.*, **80**, 829(1976).

(22) G. Zografi and S. H. Yalkowsky, *J. Pharm. Sci.*, **63**, 1533(1974).

(23) R. C. Tolman, *J. Chem. Phys.*, **17**, 333(1949).

ACKNOWLEDGMENTS AND ADDRESSES

Received October 6, 1975, from **Pharmacy Research, The Upjohn Company, Kalamazoo, MI 49001*, and the *‡School of Pharmacy, University of Wisconsin, Madison, WI 53706*

Accepted for publication December 10, 1975.

ˣ To whom inquiries should be directed.

Bioavailability of 11 Sulfisoxazole Products in Humans

GERALD W. A. SLYWKA *, ARMEN P. MELIKIAN, ARTHUR B. STRAUGHN, PHILIP L. WHYATT ‡, and MARVIN C. MEYER ˣ

Abstract □ Single lots of 11 commercially available 500-mg sulfisoxazole tablets were evaluated *in vitro* and *in vivo*. All products tested met USP XVIII specifications for weight variation and product assay. However, three products failed to meet the USP XVIII dissolution requirement. The only statistically significant difference observed between the 11 products was a lower peak plasma level exhibited by one product. No useful correlation was observed between the *in vivo* and *in vitro* studies for the dosage forms tested.

Keyphrases □ Sulfisoxazole—weight variation, dissolution, and bioavailability, *in vivo* and *in vitro* evaluation, commercial dosage forms □ Weight variation product assay—USP test, sulfisoxazole, commercial dosage forms □ Dissolution—USP test, sulfisoxazole, commercial dosage forms □ Bioavailability—sulfisoxazole, *in vivo* and *in vitro* evaluation, commercial dosage forms □ Antibacterial agents—sulfisoxazole, weight variation, dissolution, and bioavailability, commercial dosage forms

Sulfisoxazole is a sulfonamide antibacterial agent employed in the treatment of urinary tract infections. Although the metabolism, distribution, and elimination of sulfisoxazole have been studied in animals and humans (1–4), few studies have been undertaken to evaluate the bioavailability of commercially available

Table VI—Predicted Effects of Chain Length on Activity Coefficients

Solvent	γ, dynes/cm²	Factor by which Room Temperature Activity Coefficient Decreases with Addition of Methylene Unit to Solute: Predicted	Observed
Water	51.9	3.46	3.31
Glycerin	35.2	2.19	2.13
Formamide	31.1	2.11	1.73
Ethylene glycol	19.3	1.59	1.69
Propylene glycol	12.5	1.35	1.33
Methanol	4.2	1.10	1.24
Ethanol	0	1.00	1.13

phobic surface area (Eqs. 1 and 12).

An interesting and important consequence of Eq. 16 is that the relative ability of the various cosolvents to solubilize a drug is independent of the drug (provided that it is sufficiently hydrophobic for this treatment to be applicable) and is related only to $\Delta\gamma^0$. Therefore, for any very insoluble drug, ethanol will be the most efficient solubilizer of the solvents considered, with the other solvents following in the order listed in Table IV.

SUMMARY AND CONCLUSIONS

The solubility of poorly water-soluble compounds in mixed aqueous solvents is treated as a linear combination of terms representing the pairwise interactions of each solvent component with each topographical component of the drug.

The interactions involving the hydrophobic portion of the solute are the major factors that determine how well it can be solubilized, and these interactions can be related directly to the interactions of a pure liquid hydrocarbon with the solvent components.

On this basis, an equation is derived that explains the exponential increase in the aqueous solubility of insoluble drugs with the addition of a cosolvent. This equation further predicts that the magnitude of the increase in solubility produced by the cosolvent is exponentially related to the surface (interfacial) properties of the solvent components and the hydrophobic surface area of the solute.

REFERENCES

(1) T. Higuchi, M. Gupta, and L. W. Busse, *J. Am. Pharm. Assoc., Sci. Ed.*, **42**, 157(1953).

(2) C. F. Peterson and R. E. Hopponen, *ibid.*, **42**, 540(1953).

(3) P. H. Elworthy and H. E. C. Worthington, *J. Pharm. Pharmacol.*, **20**, 830(1968).

(4) B. J. Poulson, E. Young, V. Coquilla, and M. Katz, *J. Pharm. Sci.*, **57**, 928(1968).

(5) E. R. Garrett and P. B. Chemburkar, *ibid.*, **57**, 950(1968).

(6) I. M. Korenman, *Russ. J. Phys. Chem.*, **45**, 1011(1971).

(7) Y. Kato and T. Ohuchi, *Yakugaku Zasshi*, **92**, 257(1972).

(8) A. J. Kapadia and J. Autian, *J. Am. Pharm. Assoc., Sci. Ed.*, **49**, 380(1960).

(9) G. L. Flynn and S. H. Yalkowsky, *J. Pharm. Sci.*, **61**, 852(1972).

(10) S. H. Yalkowsky, G. L. Flynn, and G. L. Amidon, *ibid.*, **61**, 893(1972).

(11) R. B. Hermann, *J. Phys. Chem.*, **76**, 2754(1972).

(12) M. J. Harris, T. Higuchi, and J. H. Rytting, *ibid.*, **77**, 2694(1973).

(13) G. L. Amidon, S. H. Yalkowsky, and S. Leung, *J. Pharm. Sci.*, **63**, 1858(1974).

(14) S. H. Yalkowsky, G. L. Amidon, G. Zografi, and G. L. Flynn, *ibid.*, **64**, 48(1975).

(15) J. A. Reynolds, D. B. Gilbert, and C. Tanford, *Proc. Nat. Acad. Sci. USA*, **71**, 2925(1974).

(16) I. M. Langmuir, *Colloid Sym. Monogr.*, **3**, 48(1925).

(17) J. H. Hildebrand and R. L. Scott, "Regular Solutions," Prentice Hall, Englewood Cliffs, N.J., 1962.

(18) S. H. Yalkowsky, G. L. Flynn, and T. G. Slunick, *J. Pharm. Sci.*, **61**, 852(1972).

(19) A. W. Adamson, "Physical Chemistry of Surfaces," Interscience, New York, N.Y., 1970.

(20) C. H. Deal and E. L. Derr, *Ind. Eng. Chem.*, **60**, 28(1968).

(21) S. C. Valvani, S. H. Yalkowsky, and G. L. Amidon, *J. Phys. Chem.*, **80**, 829(1976).

(22) G. Zografi and S. H. Yalkowsky, *J. Pharm. Sci.*, **63**, 1533(1974).

(23) R. C. Tolman, *J. Chem. Phys.*, **17**, 333(1949).

ACKNOWLEDGMENTS AND ADDRESSES

Received October 6, 1975, from **Pharmacy Research, The Upjohn Company, Kalamazoo, MI 49001*, and the *‡School of Pharmacy, University of Wisconsin, Madison, WI 53706*

Accepted for publication December 10, 1975.

ˣ To whom inquiries should be directed.

Bioavailability of 11 Sulfisoxazole Products in Humans

GERALD W. A. SLYWKA *, ARMEN P. MELIKIAN, ARTHUR B. STRAUGHN, PHILIP L. WHYATT ‡, and MARVIN C. MEYER ˣ

Abstract □ Single lots of 11 commercially available 500-mg sulfisoxazole tablets were evaluated *in vitro* and *in vivo*. All products tested met USP XVIII specifications for weight variation and product assay. However, three products failed to meet the USP XVIII dissolution requirement. The only statistically significant difference observed between the 11 products was a lower peak plasma level exhibited by one product. No useful correlation was observed between the *in vivo* and *in vitro* studies for the dosage forms tested.

Keyphrases □ Sulfisoxazole—weight variation, dissolution, and bioavailability, *in vivo* and *in vitro* evaluation, commercial dosage forms □ Weight variation product assay—USP test, sulfisoxazole, commercial dosage forms □ Dissolution—USP test, sulfisoxazole, commercial dosage forms □ Bioavailability—sulfisoxazole, *in vivo* and *in vitro* evaluation, commercial dosage forms □ Antibacterial agents—sulfisoxazole, weight variation, dissolution, and bioavailability, commercial dosage forms

Sulfisoxazole is a sulfonamide antibacterial agent employed in the treatment of urinary tract infections. Although the metabolism, distribution, and elimination of sulfisoxazole have been studied in animals and humans (1–4), few studies have been undertaken to evaluate the bioavailability of commercially available

products. Earlier studies (5–8) of a limited number of sulfisoxazole products failed to detect significant differences in bioavailability and reported only a moderate to poor correlation between *in vitro* dissolution rates and *in vivo* performance.

The present study of 11 sulfisoxazole products, manufactured by 10 companies, sought to determine if differences in bioavailability existed and if any differences could be related to the dissolution or disintegration properties of the dosage form.

EXPERIMENTAL

Analysis of Plasma Samples—A method similar to the Bratton–Marshall (9) procedure was employed in the determination of the free, unmetabolized sulfisoxazole present in the plasma. One-half milliliter of plasma, 4.0 ml of water, and 2.5 ml of 15% trichloroacetic acid were gently agitated and centrifuged for 30 min. Five milliliters of the supernate was transferred to a clean tube, 1.0 ml of 4 *N* HCl and then 1.0 ml of a freshly prepared 0.1% aqueous solution of sodium nitrate were added, and the mixture was vortexed. After 4 min, 1.0 ml of a 0.5% aqueous ammonium sulfamate solution was added and the tube was vigorously shaken by hand.

Upon standing for 3 additional min, 1.0 ml of a freshly prepared 0.1% aqueous solution of *N*-(1-naphthyl)ethylenediamine dihydrochloride was added and mixed. After the samples were stored in the dark for 15 min, the absorbance of each was determined at 546 nm against a distilled water blank. Blank plasma samples, collected prior to drug administration, also were analyzed. Each drug absorbance reading was corrected for the blank plasma values.

***In Vitro* Tests**—The USP XVIII (10) tablet weight variation, product assay, and dissolution tests were performed on each product[1]. Disintegration tests[2] were determined according to the USP XVII (11) procedure. More recent editions of the USP do not contain a disintegration specification for this drug.

Selection of Sulfisoxazole Products—Table I summarizes the sulfisoxazole products that were evaluated. Ten manufacturers were represented. In each case, the products tested were purchased directly from a local pharmacy or supplied by the FDA field offices.

Clinical Study Protocol—Seven healthy adult male volunteers were recruited from the staff and student body of this University. The average age of the subjects was 24 years (range 21–28), the average height was 177.4 cm (range 167.6–187.9), and the average weight was 75.6 kg (range 65.8–93.0). Each subject underwent a urine analysis as well as a hematologic and blood enzyme analysis[3] to ensure inclusion of only subjects in good health.

The bioavailability study of 11 products was divided into two separate parts, designated Groups 1 and 2. Each group consisted of six subjects who received a single 500-mg sulfisoxazole tablet in each of 6 consecutive weeks with a 7-day "washout" period between each dose. The administration of each drug to each subject every week was based on a crossover sequence designed to minimize the influence of any residual or cumulative effects of preceding doses (12).

Five subjects were common to both Groups 1 and 2. The Group 2 study was initiated following completion of the Group 1 study. Product 1 was included in both groups as a reference standard to facilitate comparison of data between groups.

Each subject was instructed to adhere to a standard protocol and abstain from taking any medication during the study. The subjects were given the tablets in the morning following an overnight fast. No food or liquid, other than water, was permitted until 4 hr following drug ingestion. Ten-milliliter blood samples were withdrawn from each subject prior to and 1, 2, 3, 4, 6, 8, 10, and 25 hr after drug ingestion. The blood samples were transferred to heparinized centrifuge tubes and the plasma was separated and frozen until assayed.

RESULTS AND DISCUSSION

Sulfisoxazole *In Vitro* Tests—Each of the 11 products tested met the USP XVIII (10) specifications for tablet weight variation. The product assays indicated that each product was within the 95–105% limits. However, three products failed to meet the USP XVIII dissolution requirement that 60% of the labeled content of the tablet must dissolve in not more than 30 min. The actual percent dissolved in 30 min ranged from approximately 12 to 97% (Table I). The three products that failed were approximately 12, 22, and 50% dissolved after 30 min.

Table I—*In Vitro* Test Data for Sulfisoxazole Bioavailability Study

Product[a] Code Number (Study Group)	Assay, % of Label	Mean Percent Dissolved in 30 min	Disintegration Time, min
1 (1, 2)	101.2	77.8	15
2 (1)	102.1	97.4	2
3 (1)	100.0	49.0	20
4 (1)	98.2	82.0	3
5 (1)	99.6	21.4	22
6 (1)	98.0	71.7	4
2 (2)	104.3	12.6	>30
3 (2)	99.7	⩾60[b]	7
4 (2)	100.0	⩾60[b]	5
5 (2)	102.6	⩾60[b]	4
6 (2)	100.2	⩾60[b]	>30

[a] Distributor (Manufacturer if different from distributor) and Lot No. are as follows: Group 1—1, Roche, 8453-02074; 2, Towne, Paulsen (Dow Chemical), 087459; 3, Arcum (Lannett), 16929; 4, Geneva Generics (Cord), 32813; 5, Ulmer Pharmaceuticals (Zenith), 2218-20; and 6, Zenith Labs, 2218-21; and Group 2—1, Roche, 8453-02074; 2, Harvey Labs, 18952; 3, Interstate Drug Exchange (Myland), 900910; 4, Upjohn, 563AT-C2; 5, West-ward, 41229; and 6, Smith Kline and French, R151163. [b] More quantitative data were not provided by the FDA.

Neither USP XVIII nor XIX contains a disintegration time specification for sulfisoxazole tablets. However, since disintegration time requirements are currently official for several tablet products and since USP XVII (11) had such a requirement for sulfisoxazole tablets, samples of each lot were tested for disintegration properties (Table I). Nine of the 11 products met the USP XVII requirement of disintegration in distilled water at 37° within 30 min. Products 2 and 6 of Group 2 failed to disintegrate in distilled water. However, when dilute hydrochloric acid (1:25) was used as the test solvent, both products disintegrated within 12 min.

Plasma Levels—Tables II and III summarize the average plasma sulfisoxazole levels for each product at each sampling time. These results are shown graphically in Figs. 1 and 2. An analysis of variance for these data indicated that there were no significant differences ($p > 0.05$) between the 11 products studied in each group in terms of mean plasma levels obtained at each sampling time.

Time of Peak Plasma Levels—In each case, the time required to reach peak plasma sulfisoxazole levels was 3 hr or less, indicating relatively rapid absorption of the drug following oral administration.

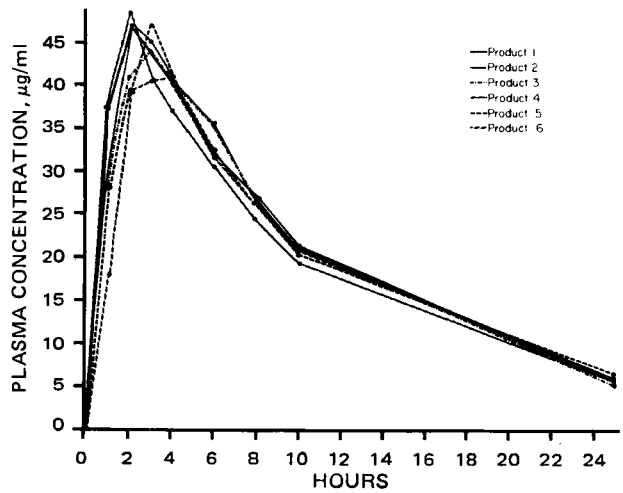

Figure 1—*Average plasma sulfisoxazole levels for Group 1. Each data point represents the mean of six subjects. (See Table I for product code numbers.)*

[1] In the laboratories of the U.S. Food and Drug Administration (FDA).
[2] In the laboratories of the University of Tennessee Center for the Health Sciences.
[3] SMA 12/60.

Table II—Average Plasma Sulfisoxazole Levels, Group 1

Product Code[a]	Average Plasma Sulfisoxazole Levels, μg/ml[b]							
	1 hr	2 hr	3 hr	4 hr	6 hr	8 hr	10 hr	25 hr
1	37.18 (9.59)	46.70 (6.70)	43.59 (3.26)	40.20 (1.91)	35.38 (2.36)	26.43 (1.18)	21.43 (1.13)	6.01 (0.54)
2	30.82 (8.21)	47.06 (9.58)	45.25 (2.63)	40.91 (2.52)	32.65 (2.07)	27.12 (1.62)	21.60 (1.02)	6.16 (0.66)
3	28.81 (7.69)	40.97 (7.79)	44.21 (2.18)	40.80 (2.17)	33.18 (1.68)	26.57 (1.36)	21.65 (1.19)	5.61 (0.72)
4	38.77 (8.33)	48.32 (2.29)	41.92 (2.43)	37.13 (2.32)	30.67 (1.99)	24.50 (1.71)	19.76 (1.37)	5.74 (0.60)
5	28.45 (10.88)	38.55 (7.13)	47.32 (4.19)	41.20 (3.17)	32.55 (3.02)	25.73 (2.49)	20.91 (2.12)	6.40 (0.95)
6	17.88 (4.90)	39.50 (8.39)	40.49 (3.50)	40.44 (2.63)	31.46 (2.31)	25.56 (1.91)	21.06 (1.83)	5.48 (0.82)

[a] See Table I. [b] Average of six subjects; standard error in parentheses.

Table III—Average Plasma Sulfisoxazole Levels, Group 2

Product Code[a]	Average Plasma Sulfisoxazole Levels, μg/ml[b]							
	1 hr	2 hr	3 hr	4 hr	6 hr	8 hr	10 hr	25 hr
1	45.21 (8.62)	48.78 (5.22)	47.81 (3.54)	43.69 (3.76)	33.77 (3.06)	26.77 (2.31)	22.17 (2.01)	7.16 (1.16)
2	7.35 (4.21)	33.14 (6.67)	43.71 (3.93)	42.50 (3.47)	35.45 (2.71)	27.89 (2.43)	24.02 (2.33)	7.22 (0.99)
3	31.82 (10.96)	36.67 (7.89)	43.12 (3.61)	43.51 (4.57)	35.44 (3.48)	29.05 (3.35)	24.43 (3.49)	7.75 (1.67)
4	29.86 (9.12)	42.13 (5.17)	44.35 (3.84)	40.86 (3.79)	32.68 (3.40)	27.25 (2.82)	22.38 (2.77)	6.64 (1.52)
5	40.49 (6.63)	44.78 (4.40)	47.18 (3.61)	40.72 (3.51)	33.79 (2.95)	27.51 (2.12)	22.99 (1.57)	7.42 (0.88)
6	32.34 (10.35)	38.28 (7.37)	40.46 (4.91)	44.02 (3.75)	36.33 (3.92)	29.80 (3.33)	25.08 (3.43)	8.74 (2.19)

[a] See Table I. [b] Average of six subjects; standard error in parentheses.

The average peak times ranged from 1.7 to 2.7 hr in Group 1 and from 2.2 to 3.0 hr in Group 2. These values are in agreement with a mean value of 2.5 hr reported previously (7, 8). There was no statistically significant ($p > 0.05$) difference in the time of peak level between any of the products in each group.

Peak Plasma Concentration—Reports in the literature (5–7) indicate that the average peak plasma levels achieved following the oral administration of sulfisoxazole may vary widely. If the previously reported peak plasma levels following 2–4-g doses are normalized to a 1-g dose, the levels range from a low of 32.2 μg/ml to a high of 84.4 μg/ml. For example, Kaplan *et al.* (7) reported a peak plasma sulfisoxazole level of 168.7 μg/ml for averaged data obtained in a study of seven subjects receiving a 2.0-g dose of the drug, with the individual peak levels ranging from 121 to 210 μg/ml.

In the present study, the average of the peak levels for each of the 11 products, obtained by averaging the individual peak levels observed for each subject, ranged from 45.5 to 57.5 μg/ml in Group 1 and from 47.6 to 56.8 μg/ml in Group 2 following administration of a single 500-mg tablet. When the average peak plasma levels observed for Products 2–6 in Groups 1 and 2 were expressed as a percentage of the average peak plasma level observed for Product 1, the values ranged from 80 to 101% in Group 1 and from 84 to 100% in Group 2. The analysis of variance indicated that Product 3 in Group 1 was significantly lower ($p < 0.05$) than the other five products in the group in terms of peak plasma level.

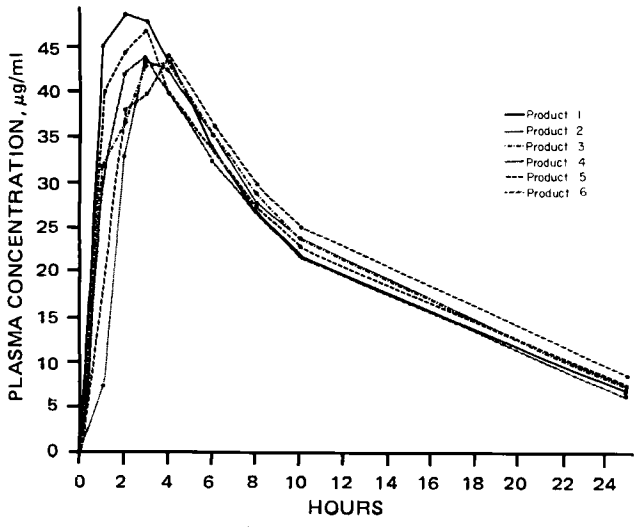

Figure 2—*Average plasma sulfisoxazole levels for Group II. Each data point represents the mean of six subjects. (See Table I for product code numbers.)*

Area under Plasma Level–Time Curve (*AUC*)—Table IV summarizes the average "uncorrected" *AUC* values computed from the individual plasma sulfisoxazole level–time curves obtained following administration of each of the 11 products. These values were estimated, using the trapezoidal rule, for the interval of 0–25 hr postadministration. For the 11 products evaluated, the average uncorrected *AUC*'s, expressed relative to Product 1, ranged from 91.0 to 100% in Group 1 and from 95 to 104% in Group 2. The analysis of variance indicated that there were no significant differences ($p > 0.05$) observed between the *AUC* values for the 11 products.

In cases where the plasma sulfisoxazole level had not reached zero at the terminal 25-hr sampling time, a "corrected" *AUC* was also calculated using:

$$(AUC)_{0-\infty} = (AUC)_{0-25\text{ hr}} + (AUC)_{25\text{ hr}-\infty} \qquad \text{(Eq. 1)}$$

and:

$$(AUC)_{25\text{ hr}-\infty} = \frac{(C_p)_{25\text{ hr}}}{K_e} \qquad \text{(Eq. 2)}$$

where $(C_p)_{25\text{ hr}}$ is the plasma level at the 25-hr sampling time, and K_e is the elimination rate constant determined from the slope of the terminal portion of a semilog plot of plasma concentration *versus* time.

Table IV—Summary of Average Areas under the Plasma Level–Time Curve (*AUC*), Uncorrected

Product Code[a]	Average *AUC*, μg/ml × hr[b]	*CV*, %[c]	Percent Relative to Product 1
	Group 1		
1	537.28 (14.8)	6.7	100.0
2	528.81 (21.7)	10.0	98.3
3	521.31 (28.3)	13.3	97.0
5	520.99 (31.8)	15.0	97.0
4	502.95 (33.5)	16.3	93.6
6	488.61 (26.8)	13.4	91.0
	Group 2		
6	583.96 (56.3)	23.6	104.6
3	575.09 (74.5)	31.7	103.1
1	558.44 (48.1)	21.1	100.0
5	555.68 (44.5)	19.6	99.5
2	533.46 (45.3)	20.8	95.5
4	532.62 (62.4)	28.7	95.4

[a] See Table I. [b] Average of six subjects per group; standard error in parentheses. [c] (Standard deviation) (100)/(mean).

Table V—Summary of Average Areas under the Plasma Level–Time Curve (*AUC*), Corrected

Product Code[a]	Average *AUC*, μg/ml × hr[b]	*CV*, %[c]	Percent Relative to Product 1
	Group 1		
1	606.98 (23.7)	9.6	100.0
5	606.94 (47.8)	19.3	99.9
2	605.60 (30.6)	12.3	99.8
3	585.90 (36.9)	15.4	96.5
4	573.45 (43.1)	18.4	94.5
6	555.89 (36.1)	15.9	91.6
	Group 2		
6	716.91 (98.1)	33.5	109.8
3	686.16 (105.6)	37.7	105.2
5	654.23 (60.4)	22.6	100.2
1	653.04 (71.2)	26.7	100.0
2	625.69 (61.0)	23.9	95.8
4	620.76 (91.1)	36.0	95.1

[a] See Table I. [b] Average of six subjects per group; standard error in parentheses. [c] (Standard deviation) (100)/(mean).

Table V summarizes the corrected average area under the plasma level–time curve. For the 11 products evaluated, the average corrected *AUC*'s, expressed relative to Product 1, ranged from 91.6 to 100% in Group 1 and from 95 to 110% in Group 2. No statistically significant differences ($p > 0.05$) were found between any of the products in terms of the corrected area under the plasma level–time curve.

Between Group Differences—Table VI summarizes the *AUC* values and peak concentrations observed following the repeat administration of Product 1 to the five subjects who were common to both Groups 1 and 2. These data indicate the reproducibility of the *in vivo* studies, since the mean uncorrected *AUC*, corrected *AUC*, and peak plasma level differed by only 4.6, 4.5, and 2.1%, respectively, between the two groups. When the data from all six subjects in each group were included in the average data for Product 1, the mean values differed by only 3.8, 7.0, and 0.04% for the uncorrected *AUC*, corrected *AUC*, and peak plasma concentration, respectively.

Differences between Subjects—Individual subjects appeared to be consistent from week to week. Subject 2, who was common to both Groups 1 and 2, exhibited the lowest *AUC* of any subject. Subject 5 exhibited the largest *AUC* of the five subjects common to both groups. The average apparent half-life for sulfisoxazole elimination, estimated from the terminal portion of a semilog plot of plasma level *versus* time for each product in each subject, was 8.5 hr. Subject 2 had an average half-life of 7.8 hr. Subject 6 of Group 2, who had the largest *AUC* values of any of the seven subjects, exhibited an average apparent half-life of 11.1 hr. In addition to possible differences in the rate and extent of GI absorption, differences in rates of elimination may have contributed to the observed differences in *AUC*'s found for the individual subjects.

Product Variability—Examination of the coefficients of variation failed to reveal any apparent deficiency in any of the 11 products. The Group 2 study yielded higher coefficients of variation readings than were observed in Group 1. This finding could be related to the fact that Subject 6 of Group 2 consistently exhibited plasma levels that were substantially greater than those observed in the other subjects.

Table VI—Comparison of Product 1 in the Group 1 and Group 2 Studies

Subject Number	Uncorrected *AUC*, μg/ml × hr		Corrected *AUC*, μg/ml × hr		Peak Plasma Level, μg/ml	
	Group 1	Group 2	Group 1	Group 2	Group 1	Group 2
1	527	494	583	551	55.94	61.40
2	485	409	538	457	58.23	51.17
3	568	545	639	635	57.77	57.02
4	563	599	655	701	49.34	45.16
5	572	542	677	607	54.06	54.71
Mean	543	518	618	590	55.07	53.89

Table VII—*In Vitro–In Vivo* Correlations

Correlation	Degrees of Freedom	Correlation Coefficient	*t* Value	*p* Level
Disintegration *versus* dissolution[a]	5	−0.90973	4.899	$p = 0.01$
Disintegration *versus* peak plasma level	10	−0.04621	0.103	NS
Disintegration *versus AUC*	10	+0.3271	0.774	NS
Dissolution *versus* peak plasma level	5	+0.1830	0.4162	NS
Dissolution *versus AUC*	5	−0.0859	0.1928	NS
Peak level *versus AUC*	10	+0.0737	0.2337	NS

[a] Disintegration time *versus* percent dissolved after 30 min.

Lot-to-lot variations were examined for Products 5 and 6 of the Group 1 study. Both lots were manufactured by the same company. The mean time of peak plasma level was 2.0 hr for Product 5 and 2.7 hr for Product 6. There was a difference of 9% in the peak plasma level between the two lots as well as differences of 6 and 8% in uncorrected *AUC* and corrected *AUC* values, respectively. The two lots of this product exhibited similar bioavailability parameters, although they had significantly different dissolution and disintegration characteristics, with Product 5 failing the USP XVIII dissolution test.

***In Vivo–In Vitro* Correlations**—Table VII summarizes the relationship observed between the various *in vitro* and *in vivo* parameters. There was a good correlation between disintegration and dissolution rate. However, no correlations were found that would be of value in predicting *in vivo* performance. A similar lack of relationship between dissolution rate and bioavailability for sulfisoxazole was noted by Solomon (6). It is significant that three lots tested in the present study failed to meet current compendial specifications for dissolution but exhibited adequate bioavailability. However, as recently discussed by Feldmann (13), this observation does not necessarily negate the validity of the USP test for the detection of products that may exhibit inadequate bioavailability.

SUMMARY AND CONCLUSIONS

Eleven lots of 500-mg sulfisoxazole tablets, manufactured by 10 companies, were evaluated in seven subjects. The study was divided into two groups, with five subjects common to both groups. All products met USP XVIII specifications except that three products did not meet the dissolution rate requirement.

The only statistically significant difference observed between the 11 products was in terms of a lower peak plasma level for Product 3 in Group 1. The peak plasma level for this product was 20% lower than that observed for the reference standard product. In view of the lack of any other statistically significant differences ($p > 0.05$) between any of the products in terms of *AUC*, time of peak plasma level, or plasma levels 1, 2, 3, 4, 6, 8, 10, and 25 hr postadministration, it was concluded that the 11 lots of sulfisoxazole could be considered as bioequivalent. It was further concluded that the current USP dissolution specifications may be of limited value in the prediction of bioavailability.

REFERENCES

(1) L. Weinstein, in "The Pharmacological Basis of Therapeutics," 5th ed., L. S. Goodman and A. Gilman, Eds., Macmillan, New York, N.Y., 1975, chap. 55.

(2) M. Cohen and R. Pocelinko, *J. Pharmacol. Exp. Ther.*, **185**, 703(1973).

(3) E. Nelson and I. O'Reilly, *ibid.*, **129**, 368(1960).

(4) R. M. O'Dell, J. P. Jarrell, and J. U. Schlegel, *Curr. Ther. Res.*, **11**, 307(1969).

(5) C. M. Martin, *Drug Info. Bull.*, **Jan./June 1969**, 72.

(6) H. Solomon, *ibid.*, **Jan/June 1969**, 75.
(7) S. A. Kaplan, R. E. Weinfeld, C. W. Abruzzo, and N. Lewis, *J. Pharm. Sci.*, **61**, 773(1972).
(8) G. R. Van Petten, G. C. Becking, and H. F. Lettau, *J. Clin. Pharmacol.*, **11**, 35(1971).
(9) A. C. Bratton and E. K. Marshall, *J. Biol. Chem.*, **128**, 537(1939).
(10) "The United States Pharmacopeia," 18th rev., Mack Publishing Co., Easton, Pa., 1970, p. 699.
(11) "The United States Pharmacopeia," 17th rev., Mack Publishing Co., Easton, Pa., 1965, p. 686.
(12) P. L. Whyatt, G. W. A. Slywka, A. P. Melikian, and M. C. Meyer, *J. Pharm. Sci.*, **65**, 652(1976).
(13) E. G. Feldmann, *ibid.*, **64**(9), iv(1975).

ACKNOWLEDGMENTS AND ADDRESSES

Received October 28, 1975, from the *Division of Drug Metabolism and Biopharmaceutics, Department of Medicinal Chemistry, College of Pharmacy, University of Tennessee Center for the Health Sciences, Memphis, TN 38163*

Accepted for publication January 8, 1976.

Supported in part by a contract from the Tennessee Department of Public Health, FDA Contract 223-74-3097, and U.S. Public Health Service Grant HL-09495.

The authors gratefully acknowledge the advice and counsel of Mr. Herbert Bates, Jr., Pharmacist Consultant, Tennessee Department of Public Health; the cooperation of the U.S. Food and Drug Administration; the technical assistance of Mrs. Irma Miller and Miss Linda Marshall; the secretarial work of Miss Marilyn McWilliams; the assistance of Mrs. Ann McEachran in the statistical and computer analysis of the data; and the medical supervision provided by Dr. Philip Lieberman.

* Present address: School of Pharmacy, Ferris State College, Big Rapids, MI 49307

‡ Present address: Division of Therapeutics, Australian Department of Health, Canberra, A.C.T. 2606, Australia.

ˣ To whom inquiries should be directed.

Effect of Certain Drugs in Perfused Human Placenta XII: Autacoid Antagonism by Phenothiazines

WAYNE W. WOLSTENHOLME and RONALD F. GAUTIERI ˣ

Abstract □ The effects of chlorpromazine, prochlorperazine, and trifluoperazine on the pressor actions of serotonin, angiotensin, and bradykinin in the perfused vessels of full-term human placentas were investigated. A significant inhibition of the effect of serotonin was observed with trifluoperazine and chlorpromazine but not with prochlorperazine. This inhibition is attributed to the ability of phenothiazines to cause adrenergic blockade. Because both bradykinin and angiotensin could not be consistently antagonized, it is concluded that they must act primarily *via* musculotropic mechanisms and only secondarily by stimulation of adrenergic receptors.

Keyphrases □ Chlorpromazine—effects on pressor actions of serotonin, angiotensin, and bradykinin in perfused human placenta □ Prochlorperazine—effects on pressor actions of serotonin, angiotensin, and bradykinin in perfused human placenta □ Trifluoperazine—effects on pressor actions of serotonin, angiotensin, and bradykinin in perfused human placenta □ Serotonin—pressor actions in perfused human placenta, effects of chlorpromazine, prochlorperazine, and trifluoperazine □ Angiotensin—pressor actions in perfused human placenta, effects of chlorpromazine, prochlorperazine, and trifluoperazine □ Bradykinin—pressor actions in perfused human placenta, effects of chlorpromazine, prochlorperazine, and trifluoperazine □ Autacoid antagonism—effects of chlorpromazine, prochlorperazine, and trifluoperazine on pressor actions of serotonin, angiotensin, and bradykinin in perfused human placenta □ Phenothiazines—chlorpromazine, prochlorperazine, and trifluoperazine, effects on pressor actions of serotonin, angiotensin, and bradykinin in perfused human placenta

It is well established that the endogenous autacoids serotonin, angiotensin, and bradykinin are present and that their levels fluctuate in human placental and/or related tissues (1–8). Several investigations linked high blood levels of angiotensin (9), renin (10), and serotonin (11) to the pathogenesis of the toxemias of pregnancy. Increased pressor response to angiotensin was observed in preeclamptic women (9); increased renin levels were reported in eclamptic and preeclamptic women (12), and decreased angiotensinase levels were found in toxemic women (13).

Serotonin, angiotensin, and bradykinin share two noticeable actions on the perfused placental vasculature: vasoconstriction with an associated increase in blood vessel pressure and increased blood vessel permeability (14–20). They also share similarities in their mechanisms of action in that they all cause α-receptor stimulation in these vessels (16, 20). Serotonin and angiotensin cause direct vascular smooth muscle stimulation, while bradykinin causes release of norepinephrine from unspecified storage sites in the placenta.

Chlorpromazine antagonizes the vasoconstrictor action of serotonin in the perfused human placental blood vessels by approximately 67.8% (21). Chlorpromazine also inhibits the ability of serotonin to cause intrauterine deaths (22). In addition, chlorpromazine and other phenothiazines block the increased vascular permeability of serotonin injections in the hindpaw of rats (23).

The phenothiazines are presently prescribed for anxiety states, tranquilization, motion sickness, night sedation, and preanesthetic medication. They are used as analgesics in labor and to prevent nausea and vomiting during labor and morning sickness (24). These compounds have strong adrenergic blocking activity and weaker cholinergic blocking activity, and they can block the actions of serotonin both *in vivo* and *in vitro* (25). The phenothiazines and the previously mentioned autacoids are capable of crossing the "placental barrier," since their molecular weight is less than 1000. Furthermore, the phenothiazines are suspected of con-

(6) H. Solomon, *ibid.*, **Jan/June 1969**, 75.
(7) S. A. Kaplan, R. E. Weinfeld, C. W. Abruzzo, and N. Lewis, *J. Pharm. Sci.*, **61**, 773(1972).
(8) G. R. Van Petten, G. C. Becking, and H. F. Lettau, *J. Clin. Pharmacol.*, **11**, 35(1971).
(9) A. C. Bratton and E. K. Marshall, *J. Biol. Chem.*, **128**, 537(1939).
(10) "The United States Pharmacopeia," 18th rev., Mack Publishing Co., Easton, Pa., 1970, p. 699.
(11) "The United States Pharmacopeia," 17th rev., Mack Publishing Co., Easton, Pa., 1965, p. 686.
(12) P. L. Whyatt, G. W. A. Slywka, A. P. Melikian, and M. C. Meyer, *J. Pharm. Sci.*, **65**, 652(1976).
(13) E. G. Feldmann, *ibid.*, **64**(9), iv(1975).

ACKNOWLEDGMENTS AND ADDRESSES

Received October 28, 1975, from the *Division of Drug Metabolism and Biopharmaceutics, Department of Medicinal Chemistry, College of Pharmacy, University of Tennessee Center for the Health Sciences, Memphis, TN 38163*

Accepted for publication January 8, 1976.

Supported in part by a contract from the Tennessee Department of Public Health, FDA Contract 223-74-3097, and U.S. Public Health Service Grant HL-09495.

The authors gratefully acknowledge the advice and counsel of Mr. Herbert Bates, Jr., Pharmacist Consultant, Tennessee Department of Public Health; the cooperation of the U.S. Food and Drug Administration; the technical assistance of Mrs. Irma Miller and Miss Linda Marshall; the secretarial work of Miss Marilyn McWilliams; the assistance of Mrs. Ann McEachran in the statistical and computer analysis of the data; and the medical supervision provided by Dr. Philip Lieberman.

* Present address: School of Pharmacy, Ferris State College, Big Rapids, MI 49307

‡ Present address: Division of Therapeutics, Australian Department of Health, Canberra, A.C.T. 2606, Australia.

ˣ To whom inquiries should be directed.

Effect of Certain Drugs in Perfused Human Placenta XII: Autacoid Antagonism by Phenothiazines

WAYNE W. WOLSTENHOLME and RONALD F. GAUTIERI ˣ

Abstract □ The effects of chlorpromazine, prochlorperazine, and trifluoperazine on the pressor actions of serotonin, angiotensin, and bradykinin in the perfused vessels of full-term human placentas were investigated. A significant inhibition of the effect of serotonin was observed with trifluoperazine and chlorpromazine but not with prochlorperazine. This inhibition is attributed to the ability of phenothiazines to cause adrenergic blockade. Because both bradykinin and angiotensin could not be consistently antagonized, it is concluded that they must act primarily *via* musculotropic mechanisms and only secondarily by stimulation of adrenergic receptors.

Keyphrases □ Chlorpromazine—effects on pressor actions of serotonin, angiotensin, and bradykinin in perfused human placenta □ Prochlorperazine—effects on pressor actions of serotonin, angiotensin, and bradykinin in perfused human placenta □ Trifluoperazine—effects on pressor actions of serotonin, angiotensin, and bradykinin in perfused human placenta □ Serotonin—pressor actions in perfused human placenta, effects of chlorpromazine, prochlorperazine, and trifluoperazine □ Angiotensin—pressor actions in perfused human placenta, effects of chlorpromazine, prochlorperazine, and trifluoperazine □ Bradykinin—pressor actions in perfused human placenta, effects of chlorpromazine, prochlorperazine, and trifluoperazine □ Autacoid antagonism—effects of chlorpromazine, prochlorperazine, and trifluoperazine on pressor actions of serotonin, angiotensin, and bradykinin in perfused human placenta □ Phenothiazines—chlorpromazine, prochlorperazine, and trifluoperazine, effects on pressor actions of serotonin, angiotensin, and bradykinin in perfused human placenta

It is well established that the endogenous autacoids serotonin, angiotensin, and bradykinin are present and that their levels fluctuate in human placental and/or related tissues (1–8). Several investigations linked high blood levels of angiotensin (9), renin (10), and serotonin (11) to the pathogenesis of the toxemias of pregnancy. Increased pressor response to angiotensin was observed in preeclamptic women (9); increased renin levels were reported in eclamptic and preeclamptic women (12), and decreased angiotensinase levels were found in toxemic women (13).

Serotonin, angiotensin, and bradykinin share two noticeable actions on the perfused placental vasculature: vasoconstriction with an associated increase in blood vessel pressure and increased blood vessel permeability (14–20). They also share similarities in their mechanisms of action in that they all cause α-receptor stimulation in these vessels (16, 20). Serotonin and angiotensin cause direct vascular smooth muscle stimulation, while bradykinin causes release of norepinephrine from unspecified storage sites in the placenta.

Chlorpromazine antagonizes the vasoconstrictor action of serotonin in the perfused human placental blood vessels by approximately 67.8% (21). Chlorpromazine also inhibits the ability of serotonin to cause intrauterine deaths (22). In addition, chlorpromazine and other phenothiazines block the increased vascular permeability of serotonin injections in the hindpaw of rats (23).

The phenothiazines are presently prescribed for anxiety states, tranquilization, motion sickness, night sedation, and preanesthetic medication. They are used as analgesics in labor and to prevent nausea and vomiting during labor and morning sickness (24). These compounds have strong adrenergic blocking activity and weaker cholinergic blocking activity, and they can block the actions of serotonin both *in vivo* and *in vitro* (25). The phenothiazines and the previously mentioned autacoids are capable of crossing the "placental barrier," since their molecular weight is less than 1000. Furthermore, the phenothiazines are suspected of con-

tributing to hyperbilirubinemia in the premature infant (26) and to respiratory depression either singly or by potentiating narcotic analgesics or the gaseous anesthetics (27, 28). They are rapidly absorbed (29), and metabolites, as well as free chlorpromazine, have been detected in the urine of patients 6–18 months after discontinuation of a therapeutic regimen (30).

Since the phenothiazines are prescribed during pregnancy and data on the antagonism of only one autacoid—serotonin—by a phenothiazine are available, the purpose of this investigation was to determine in the placental vasculature the possible antagonistic efficacy of several phenothiazines on serotonin and other autacoids that may be exerting toxic effects during some pregnancies. Possibly an assessment can then be made on the benefits of phenothiazine usage during normal as well as complicated pregnancies.

EXPERIMENTAL

Normal human placentas delivered at term were used. They were obtained no more than 20 min after parturition and were transported to the laboratory in an insulated container filled with Tyrode's solution preheated to 38°. Each placenta was then placed in a stainless steel tray filled with Tyrode's solution, and the attached membranes were dissected free. The umbilical cord was also shortened at this time to approximately 4 cm. A preheated 2.3% sodium citrate solution was perfused through the umbilical vein and one umbilical artery to remove clots and to flush the vessels free of blood.

The cannulation procedure, the methods of recording and maintaining flow and perfusion pressure, and the instrumentation were described previously (31, 32). With 40 successful placental preparations, each lasting 2–4 hr, 59 experiments were performed.

The experimental regimen was divided into four consecutive steps. After a stable baseline pressure was established, the autacoid agonist to be tested was administered as the control response. The second drug to be administered was the antagonist (a phenothiazine), usually at a 15-min interval from the first injection. The agonist was then readministered at a 5–10-min interval after the phenothiazine. Finally, another injection of agonist was made 15 min later.

The doses of the agonists, serotonin, angiotensin, and bradykinin, were all 50 μg of drug in a volume of 0.5 ml. This dose was shown previously to produce an easily observable rise in vessel pressure for all three agonists (20, 33, 34). The doses of the antagonists, chlorpromazine hydrochloride, trifluoperazine hydrochloride, and prochlorperazine edisylate, were all 1 mg. Again, this dose was based on previous work showing effective serotonin antagonism at this range (21). The mean pressure change at maximal antagonism of the pressor effect of the agonist as compared to control was the basis for comparing the antagonistic abilities of the phenothiazines. Determination of the significance of an antagonistic action to the autacoids was calculated using the paired Student *t* test, with a probability value of 0.05 being significant (35).

The following drugs were administered to the placental circulation *via* the cannula entering the arterial side of the perfused placenta: serotonin creatinine sulfate[1], 0.01%; angiotensin amide[2], 0.01%; bradykinin triacetate[3], 0.01%; chlorpromazine hydrochloride[4], 0.1%; prochlorperazine edisylate[5], 0.5%; and trifluoperazine hydrochloride[6], 0.2%.

RESULTS

The following results, summarized in Tables I–III, were obtained on the full-term human placental vessels perfused at pressures of 70–100 mm Hg. The corresponding flow rate into the vasculature ranged between 41 and 62 ml of Tyrode's solution (modified with 0.525% povidone)/min.

Table I—Comparison of the Effect of Chlorpromazine (1 mg) on Three Autacoids[a]

Autacoid[b]	Mean Change in Pressure, mm Hg	*SE*[c]	*p* Value[d]
Serotonin	−16	±7.3	<0.05
Bradykinin	−4	±7.3	<0.35
Angiotensin	−1	±2.6	<0.45

[a] Six experiments. [b] Dose of 50 μg. [c] Standard error of the difference. [d] The *p* value was calculated from a paired *t* test; a *p* value of <0.05 was significant.

Effects of Chlorpromazine on Autacoids—*Serotonin*—Serotonin in a 50-μg dose was a consistently good constrictor of placental vessels, with initial pressure increases of 6–50 mm Hg. After a 1-mg dose of chlorpromazine and a 25-min interval, the action of serotonin was markedly inhibited in five of the six experiments. The mean pressure change for the six experiments was −16 mm Hg, corresponding to a percent change of −45%.

Bradykinin—A 50-μg dose of bradykinin also gave consistent pressor responses. In the six experiments, bradykinin showed an initial range of 3–43 mm Hg. Subsequent to 1 mg of chlorpromazine at 25 min, there were percent changes of from −91 to 79%. In only two experiments was bradykinin antagonized. The mean percent pressure change was 22%.

Angiotensin—The initial responses to a 50-μg dose of angiotensin in the placental vessels ranged from 6 to 25 mm Hg. The pressure changes after 1 mg of chlorpromazine were divided equally, with three experiments showing increases and three showing decreases, with a total mean percent change of 27%.

Effects of Prochlorperazine on Autacoids—*Serotonin*—The initial pressor responses to a 50-μg dose in these six experiments ranged from 7 to 23 mm Hg. A 1-mg dose was chosen to determine the effect of prochlorperazine on the pressor actions of the autacoids. Twenty-five minutes after this dose, the percent pressure changes from a dose of serotonin ranged from −59 to 147% with a mean of 38%. Four preparations demonstrated augmented responses, while only two showed antagonism with prochlorperazine.

Bradykinin—Bradykinin at the same dose showed initial pressor responses of 6–29 mm Hg in the six preparations tested. With 1 mg of prochlorperazine and a 25-min lapse, bradykinin produced percent changes of from −31 to 59%. The resulting mean percent change was −4%.

Angiotensin—In six experiments using a 50-μg dose of agonist and a 1-mg dose of antagonist, there were responses of 4–15 mm Hg before the agonist and 5–18 mm Hg after the antagonist. The mean percent change was 7%, with three experiments showing augmentation and three showing decreased responses.

Effects of Trifluoperazine on Autacoids—*Serotonin*—The same doses of both agonist and antagonist were chosen for this series. The initial pressure increases with agonist were 4–32 mm Hg. After the 25-min interval, the pressor responses dropped to a range of 3–15 mm Hg. The mean percent change was a decrease of 6%.

Bradykinin—The initial responses to 50 μg ranged from 3 to 51 mm Hg. The mean percent change after the antagonist (1 mg) and 25 min was a 22% increase, although four of these preparations demonstrated an inhibitory action.

Table II—Comparison of the Effect of Prochlorperazine (1 mg) on Three Autacoids[a]

Autacoid[b]	Mean Change in Pressure, mm Hg	*SE*[c]	*p* Value[d]
Serotonin	1	±4.5	<0.45
Bradykinin	−2	±1.3	<0.15
Angiotensin	0	±0.6	<0.50

[a] Six experiments. [b] Dose of 50 μg. [c] Standard error of the difference. [d] The *p* value was calculated from a paired *t* test; a *p* value of <0.05 was significant.

[1] Aldrich Chemical Co., Milwaukee, Wis.
[2] Hypertensin, valyl-5-angiotensin II amide, Lot B-5578, supplied through the courtesy of Ciba Pharmaceutical Co., Summit, N.J.
[3] Nutritional Biochemicals Corp., Cleveland, Ohio.
[4] Thorazine, Smith Kline and French Laboratories, Philadelphia, Pa.
[5] Compazine, Smith Kline and French Laboratories, Philadelphia, Pa.
[6] Stelazine, Smith Kline and French Laboratories, Philadelphia, Pa.

Table III—Comparison of the Effect of Trifluoperazine (1 mg) on Three Autacoids[a]

Autacoid[b]	Mean Change in Pressure, mm Hg	SE[c]	p Value[d]
Serotonin	−6	±2.8	<0.05
Bradykinin	−9	±6.6	<0.15
Angiotensin	−1	±1.6	<0.20

[a] Six experiments. [b] Dose of 50 μg. [c] Standard error of the difference. [d] The p value was calculated from a paired t test; a p value of <0.05 was significant.

Angiotensin—A 50-μg dose of angiotensin in seven experiments demonstrated initial pressure increases of 7–20 mm Hg. Subsequent to the 1-mg dose of trifluoperazine, the change in pressure from control ranged from −10 to 2 mm Hg, with a mean percent change of −5%.

When tested alone, the phenothiazines showed slight vasodilator capabilities that were transient and the pressure rapidly returned to baseline.

DISCUSSION

Chlorpromazine had a significant inhibitory effect on the pressor action of serotonin. This result reinforces the conclusion that chlorpromazine is a potent antagonist to serotonin in the human placental blood vessels (21). At the same dose level as chlorpromazine, trifluoperazine also demonstrated powerful antagonism to the pressor action of serotonin, while prochlorperazine exhibited little ability in this direction.

Serotonin causes constriction in the perfused human blood vessels primarily *via* α-adrenergic stimulation and, secondarily, by a direct stimulation of the vascular smooth muscle (16). Since the phenothiazines have a strong adrenergic blocking action (25), it can be concluded that the major inhibition by both chlorpromazine and trifluoperazine is mediated by a blockade at the α-receptors in the placental vessels; at no time was the direct muscular action of serotonin abolished by these compounds. The lack of an inhibitory action with prochlorperazine suggests that it has less α-blocking activity than the other phenothiazines in this preparation.

Via the use of negative musculotropic agents, α-blockers, and β-blockers, it was determined that angiotensin exerts its vasopressor action primarily by direct muscular stimulation, secondarily by α-receptor stimulation, and possibly by a third component of β-receptor stimulation that offsets the other two effects (36). The effect of chlorpromazine on the pressor response to angiotensin was practically negligible, as was that with prochlorperazine. Theoretically, since the α-adrenergic component of angiotensin is blocked, one would expect a greater degree of inhibition. But since the opposing β-stimulation is also blocked by the phenothiazines, responses close to the initial values were observed. Trifluoperazine showed the greatest inhibitory potential, possibly due to a greater direct muscular depressant action.

The 1-mg dose of chlorpromazine did not yield consistent inhibitory effects on the vasopressor action of bradykinin. The responses to bradykinin after prochlorperazine and trifluoperazine were diminished slightly but not enough to be statistically significant. The mechanism of action of bradykinin on vascular beds has not, as yet, been clearly defined. Previous experiments (20) showed that its action is mechanistically unlike the actions of serotonin, acetylcholine, or histamine. It has been stated that the action of bradykinin on extravascular smooth muscle is directly mediated (37), and studies on the rat uterus (38), guinea pig intestine (38), and human umbilical arteries (19) also gave evidence of a direct positive musculotropic action with bradykinin. Therefore, it can be assumed that bradykinin's vasoconstrictor action in the perfused placental vessels is also due largely to a direct action.

One possible mode of action shared by these three autacoids is that they are all capable of releasing catecholamines. Angiotensin by itself releases catecholamines from the nerve endings in certain tissues (39), while each of the three releases catecholamines from the adrenal glands (40–42). Bucknum (43) pursued this direction by pretreatment of the placental preparation with reserpine and concluded that norepinephrine release could possibly comprise a part of the pressor activity of serotonin. This fact may be supported by the present study, in which prior administration of a phenothiazine blocked the α- and β-receptors to any norepinephrine released by serotonin. Consequently, one should expect a diminished response, which was the case for two of the three antagonists.

Bucknum (43) also found, with the same pretreatment, that angiotensin may also exert its action partially through norepinephrine release. But this hypothesis is not further solidified by the present results, since little antagonism to angiotensin by the phenothiazines was observed. Prior to that study, it had been determined that bradykinin releases norepinephrine from unspecified storage sites in the placenta (20). This finding presents the possibility of a minor α-receptor-stimulating component in bradykinin's pressor activity. The present experiments do not entirely rule out this possibility, since a diminution of the action of bradykinin, although not significant, was observed with two of the three phenothiazines.

Considerable evidence is on hand to implicate at least two of these autacoids, serotonin and angiotensin, as being partially responsible for, or contributing to, the complications arising in pregnancy. Placental infarctions are more frequent in pregnancies complicated with essential hypertension, toxemias of pregnancy, chronic nephritis, lupus erythematosus disseminata, and diabetic microangiopathy (44, 45). Marais (46) found significant correlation between clinical hypertension, especially with proteinuria, and decidual arteriolar disease, placental infarction, and premature separation of the placenta. Fetal renin also may be involved in the elevated blood pressure in the toxemias of pregnancy (47), and the ratio of the concentrations of renin in the umbilical artery over the umbilical vein was found to be highest in infants suffering respiratory distress (48).

Monoamine oxidase activity is also decreased in the placentas of toxemic patients, suggesting that serotonin may accumulate (49) and may lead to vasospasm and local placental anoxia. This finding is supported by a report of serotonin increase in placentas from toxemic patients (50). There is also a local excess of L-aromatic amino acid decarboxylase, an enzyme that synthesizes most of the important amines including serotonin (49). Bradykinin has not been found in excess amounts during complicated pregnancies, but one can easily see that, because of its vasoconstrictive effect, it may be another underlying toxic agent.

It can be suggested that if the phenothiazines are administered, they could perhaps serve the dual purpose during labor of producing sedation and diminishing the effects of autacoid toxicity in both mother and fetus. Consequently, phenothiazine usage as part of the therapeutic regimen in normal pregnancies and in those that manifest toxic symptoms should be tested clinically, although the usage should be limited to after the first trimester.

SUMMARY AND CONCLUSIONS

1. Chlorpromazine and trifluoperazine were potent antagonists to the pressor responses of serotonin in the perfused human placental vessels, while prochlorperazine was not.

2. Chlorpromazine, trifluoperazine, and prochlorperazine did not demonstrate significant antagonism to the effect of both angiotensin and bradykinin in these same vessels.

3. A possible component to the vasopressor action of serotonin is suggested to be the release of norepinephrine.

4. The primary site where the inhibition of serotonin by the phenothiazines is manifested is presumed to be at the adrenergic receptors, with only a slight possibility of direct negative musculotropic action.

5. From the degree of efficacy of antagonism in the placental vessels, it is concluded that trifluoperazine is the most potent antagonist followed by chlorpromazine. Prochlorperazine is inactive.

6. It is suggested that phenothiazine usage be tested clinically in both complicated and normal pregnancies, especially at term.

REFERENCES

(1) K. Kuriaki and T. Inoue, *C. R. Soc. Biol.*, **150**, 1835(1956).

(2) H. Pigeaud, S. Nelken, and R. Bethoux, *Presse Med.*, **68**, 170(1960).

(3) J. B. Dixon, *J. Physiol. (London)*, **147**, 144(1959).

(4) C. Delhaye, R. V. Driessche, and J. J. Reuse, *Arch. Int. Pharmacodyn. Ther.*, **197**, 203(1972).

(5) P. Periti and F. Gaspami, *Biochem. Pharmacol.*, **14**,

1396(1965).
(6) W. W. Douglas, in "The Pharmacological Basis of Therapeutics," 4th ed., L. S. Goodman and A. Gilman, Eds., Macmillan, New York, N.Y., 1970, p. 667.
(7) J. J. Brown, D. L. Davies, P. B. Doak, A. F. Lever, and J. I. S. Robertson, *Lancet*, **2**, 900(1963).
(8) J. J. Brown, D. L. Davies, P. B. Doak, A. F. Lever, J. Robertson, and M. Tree, *ibid.*, **2**, 64(1964).
(9) L. C. Chesley, *Bull. N.Y. Acad. Med.*, **41**, 811(1965).
(10) G. M. Masson, A. C. Corcoran, and I. H. Page, *J. Lab. Clin. Med.*, **38**, 213(1951).
(11) S. F. Hans and H. Kopelman, *Br. Med. J.*, **1**, 736(1964).
(12) L. Dexter and F. W. Haynes, *Proc. Soc. Exp. Biol. Med.*, **55**, 288(1944).
(13) E. W. Page, *Am. J. Med. Sci.*, **213**, 715(1947).
(14) R. Eliasson and A. Astrom, *Acta Pharmacol. Toxicol.*, **11**, 254(1955).
(15) A. Astrom and U. Samelius, *Br. J. Pharmacol.*, **12**, 410(1957).
(16) R. F. Gautieri and R. T. Mancini, *J. Pharm. Sci.*, **56**, 296(1967).
(17) E. Klinge, M. J. Mattila, O. Penttial, and E. Jukarainen, *Ann. Med. Exp. Fenn.*, **44**, 369(1966).
(18) L. G. Eltherington, J. Stoff, T. Hughes, and K. L. Melmon, *Circ. Res.*, **22**, 747(1968).
(19) J. Davignon, R. R. Lorenz, and J. T. Sheperd, *Am. J. Physiol.*, **209**, 51(1965).
(20) W. R. Sherman and R. F. Gautieri, *J. Pharm. Sci.*, **61**, 878(1972).
(21) C. O. Ward and R. F. Gautieri, *ibid.*, **55**, 474(1966).
(22) M. Marois, *C. R. Soc. Biol.*, **154**, 1200(1960).
(23) J. R. Parratt and J. B. West, *Br. J. Pharmacol.*, **13**, 65(1958).
(24) S. A. Cohen and W. A. Olson, *Pediatr. Clin. North Am.*, **17**, 835(1970).
(25) M. E. Jarvik, in "The Pharmacological Basis of Therapeutics," 4th ed., L. S. Goodman and A. Gilman, Eds., Macmillan, New York, N.Y., 1970, p. 161.
(26) J. F. Lucey, *Birth Defects*, **1**, 46(1965).
(27) S. C. James, *Anesthesiology*, **21**, 405(1960).
(28) F. Moya and V. Thorndike, *Am. J. Obstet. Gynecol.*, **84**, 1778(1962).
(29) J. Francois and J. Feher, *Exp. Eye Res.*, **14**, 65(1972).
(30) M. E. Jarvik, in "The Pharmacological Basis of Therapeutics," 4th ed., L. S. Goodman and A. Gilman, Eds., Macmillan, New York, N.Y., 1970, p. 163.
(31) H. P. Ciuchta and R. F. Gautieri, *J. Pharm. Sci.*, **53**, 184(1964).
(32) R. T. Mancini and R. F. Gautieri, *ibid.*, **53**, 1476(1964).
(33) H. P. Ciuchta and R. F. Gautieri, *ibid.*, **52**, 974(1963).
(34) C. O. Ward and R. F. Gautieri, *ibid.*, **57**, 287(1968).
(35) G. G. Simpson, A. Roe, and R. C. Lewontin, "Quantitative Zoology," Harcourt Brace, New York, N.Y., 1960, p. 180.
(36) C. O. Ward and R. F. Gautieri, *J. Pharm. Sci.*, **58**, 592(1969).
(37) W. W. Douglas, in "The Pharmacological Basis of Therapeutics," 4th ed., L. S. Goodman and A. Gilman, Eds., Macmillan, New York, N.Y., 1970, p. 671.
(38) P. H. Khairallah and I. H. Page, *Ann. N.Y. Acad. Sci.*, **104**, 212(1963).
(39) A. Distler, H. Liebau, and H. P. Wolff, *Nature (London)*, **207**, 764(1965).
(40) J. G. Reid and M. Rand, *ibid.*, **169**, 801(1952).
(41) W. Feldberg and G. P. Lewis, *J. Physiol. (London)*, **171**, 98(1964).
(42) R. S. Comline, M. Silver, and D. G. Sinclair, *ibid.*, **196**, 339(1968).
(43) T. Bucknum, Master's thesis, Temple University, Philadelphia, Pa.
(44) N. M. Falkiner, "Ciba Foundation Symposium on the Toxemias of Pregnancy," Blakinson, Philadelphia, Pa., 1950, p. 126.
(45) D. R. Shanklin, *Obstet. Gynecol.*, **13**, 325(1959).
(46) W. O. Marais, *S. Afr. Med. J.*, **37**, 117(1963).
(47) "Physiological Biochemistry of the Fetus," A. A. Hodari and F. Mariona, Eds., Proceedings of the International Symposium, Charles C Thomas, Springfield, Ill., 1972, p. 268.
(48) G. W. Geelhoed and A. J. Vander, *J. Clin. Endocrinol.*, **28**, 412(1968).
(49) K. Bernirschke and S. Driscoll, "Pathology of the Human Placenta," Springer-Verlag, New York, N.Y., 1967, p. 231.
(50) J. B. Senior, I. Fahim, F. Sullivan, and J. Robson, *Lancet*, **2**, 553(1963).

ACKNOWLEDGMENTS AND ADDRESSES

Received April 21, 1975, from the *Department of Pharmacology, School of Pharmacy, Temple University, Philadelphia, PA 19140*

Accepted for publication December 18, 1975.

Abstracted from a thesis submitted by W. W. Wolstenholme to the Graduate School, Temple University, in partial fulfillment of the Master of Science degree requirements.

The authors thank members of the obstetrical staff, Temple University Hospital, for the supply of placentas.

[x] To whom inquiries should be directed.

High-Pressure Liquid Chromatographic Analysis of Tolbutamide in Serum

DENNIS J. WEBER

Abstract □ A high-pressure liquid chromatographic (HPLC) analysis of tolbutamide in serum is described. The assay requires only 1 ml of serum and is capable of measuring as little as 2 μg of tolbutamide. The metabolites of tolbutamide do not interfere in the assay. Human serum samples, taken after a 1-g oral dose of tolbutamide, were analyzed by the HPLC and an existing GLC procedure, and the results are compared.

Keyphrases □ Tolbutamide—high-pressure liquid chromatographic analysis, compared to GLC analysis, serum □ High-pressure liquid chromatography—analysis, tolbutamide in serum □ Antidiabetic agents—tolbutamide, high-pressure liquid chromatographic analysis in serum

Tolbutamide is utilized in the control of diabetes, and simple, sensitive analytical procedures for its determination in serum or plasma are needed. An analytical procedure capable of measuring small amounts of tolbutamide in 1 ml of serum with good precision and accuracy was needed and is the subject for this report.

A literature review (1) on tolbutamide includes various UV and colorimetric assays for tolbutamide in biological fluids. All of them, however, suffer from low sensitivity when compared to modern chromatographic procedures. Several GLC procedures (2–4) for tolbutamide in plasma use dimethyl sulfate as the derivatizing reagent. It has been reported (5) that more than one peak is produced using this reagent.

A reported (6) GLC pyrolysis procedure for tolbutamide requires frequent increases in temperature to remove column contamination and needs a 3.0-ml plasma sample for analysis. An electron-capture GLC procedure was reported (7, 8) for tolbutamide in biological fluids. However, the limited linear dynamic range of electron-capture detectors requires frequent sample dilutions or repeat analyses using smaller sample aliquots to bring the measurements into the observed[1] single-decade useful concentration range. The suggested, but inconvenient, alternative (7, 8) is to reserve the sensitive GLC procedure for samples containing less than 10 μg/ml and to use the colorimetric procedure for more concentrated samples.

A high-pressure liquid chromatographic (HPLC) procedure was reported (5) for the analysis of tolbutamide in compressed tablets. The procedure uses a citrate-buffered, aqueous methanol mobile phase and a hydrocarbon polymer stationary phase to achieve separation. A reported (9) HPLC procedure for the analysis of tolbutamide in serum is capable of measuring 25 μg of tolbutamide/ml of sample. The assay uses an extraction procedure previously reported (2).

This paper reports an HPLC procedure which avoids the GLC problems of on-column decomposition and nonlinear response and is capable of measuring as little as 2 μg of tolbutamide/ml of serum. The assay uses a simple extraction procedure and requires no derivative formation. The metabolites of tolbutamide (10) elute with the solvent front and do not interfere in the assay.

[1] D. G. Kaiser, The Upjohn Co., Kalamazoo, Mich., personal communication, 1974.

EXPERIMENTAL

Reagents and Solvents—Primary standard grade tolbutamide[2] was used as received. The internal standard, *N*-(*p*-methoxybenzenesulfonyl)-*N'*-cyclohexylurea[2], had been prepared from *p*-methoxybenzenesulfonamide and cyclohexyl isocyanate and was used as received, mp 184.2–186.9°; IR: λ_{max} (mineral oil mull) 3320, 3180, 1690, 1545, 1345, 1270, and 1160 cm^{-1}; UV λ_{max} (CH_3CN): 241 nm (ϵ = 17,250).

Anal.—Calc. for $C_{14}H_{20}N_2O_4S$: C, 53.82; H, 6.45; N, 8.96; S, 10.26. Found: C, 53.83; H, 6.50; N, 8.83; S, 10.66.

TLC of the internal standard gave a single spot in two different solvent systems. All solvents were distilled in glass grade[3], and only analytical grade reagents were used. The standard solutions of the internal standard and tolbutamide were prepared by accurately weighing approximately 25 mg of material into a 25-ml volumetric flask and dissolving in 25 ml of acetonitrile. Both the tolbutamide and the internal standard solutions are stable for at least 1 month at room temperature.

Instrumentation—Samples were extracted using a two-speed reciprocating shaker[4]. Derivatization reactions were mixed using a vibromixer[5]. The GLC data were collected[6] using a 1.8-m × 3-mm i.d. glass column packed with 3% OV-17 on 60–80-mesh Gas Chrom Q. The column, injector, and ^{63}Ni-electron-capture detector temperatures were 233, 263, and 270°, respectively. Nitrogen and purge gas flow rates were 40 and 30 ml/min, respectively. Injections of 1–2 μl were made.

The mobile phase used in the liquid chromatography[7] was based on work previously reported (5) and was composed of 30% methanol and 70% water and was 0.01 *M* in monobasic sodium citrate. The flow rate at 500 psig was 0.40 ml/min. All measurements were at 26°. Detection was by UV absorption at 254 nm using sensitivity settings of 0.01–0.08 absorbance unit full scale (aufs). Quantification was by peak height ratio. Three-microliter samples were injected using a 10-μl syringe[8].

Assay Procedure—*Preparation of Standard Curve Samples*—Using microliter pipets[9] or calibrated microliter syringes[8], put 125, 100, 50, and 25 μl of a 1.0-mg/ml tolbutamide standard solution into separate 35-ml screw-capped[10] centrifuge tubes. Put 50 μl of the 0.10-mg/ml tolbutamide standard into a separate 35-ml centrifuge tube. Add 25 μl of the 1.0-mg/ml internal standard solution to each tube and also to an empty tube to be used as a blank. Blow all tubes dry with a gentle nitrogen stream. Add 1 ml of blank serum and 2 ml of pH 4.4, 0.1 *M* citrate buffer and mix well on a vibromixer. It is also possible to use 0.1 *M*, pH 4.5 phosphate buffer.

Preparation of Test Serum Samples—Put 25 μl of the 1.0-mg/ml internal standard solution into 35-ml centrifuge tubes and gently blow dry with nitrogen. Add 1 ml of test serum and 2 ml of pH 4.4 citrate buffer to each tube and mix well on a vibromixer.

[2] The Upjohn Co., Kalamazoo, Mich.
[3] Burdick & Jackson Laboratories, Muskegon, Mich. It is important to use tetrahydrofuran containing 250 ppm of butylated hydroxytoluene to avoid oxidizing the internal standard.
[4] Eberbach & Sons, Ann Arbor, Mich.
[5] Scientific Products, McGaw Park, Ill.
[6] Model MT-220, Tracor Inc., Austin, Tex.
[7] Model 820 equipped with a 1-m ETH Permaphase column, DuPont Instrument Products, Wilmington, Del.
[8] Precision Sampling Corp., Baton Rouge, La.
[9] Lang-Levy lambda pipets, Bio-Rad Labs., Richmond, Calif.
[10] Lined with Teflon (du Pont).

Table I—Extraction Efficiencies of Tolbutamide from Buffered Serum[a]

Solvent	Extraction Efficiency, %
5:95 Tetrahydrofuran–hexane	24.8
5:95 Isopentyl acetate–hexane	14.7
5:95 Butyl chloride–hexane	2.7
5:95 Methylene chloride–hexane	8.1
5:95 Isopentyl alcohol–hexane	73.1
8:92 Isopentyl alcohol–hexane	81.6

[a] Tritium-labeled tolbutamide in 4 ml of serum plus 8 ml of 0.1 *M*, pH 4.5 citrate buffer was extracted with 2 × 10 ml of organic solvent.

Treatment of Standard and Test Samples—Extract all tubes with 2 × 10 ml of 5% tetrahydrofuran in hexane for 10 min. Transfer the upper hexane layer to a 15-ml screw-capped[10] centrifuge tube and reduce the volume to about 5 ml using a warm water bath and a nitrogen stream. If emulsions form, centrifuge (3000 rpm for 10 min) and/or freeze the samples to break the emulsion. Use a pasteur pipet to transfer the hexane.

Extract the 5 ml of hexane with 10 ml of 0.1 *M* Na_2CO_3 for 10 min, centrifuge, and remove the upper hexane layer with suction.

Take an 8-ml aliquot of the sodium carbonate layer and transfer to a 35-ml screw-capped centrifuge tube. Add 2.00 ml of 1.0 *M* HCl and mix to expel gas. Extract with 10 ml of methylene chloride for 10 min, centrifuge, and remove bottom methylene chloride layer with a 5-ml gastight syringe[11] equipped with a 17.8-cm (7-in.), 20-gauge, square-cut tipped needle. Transfer the methylene chloride to 5-ml pointed, glass-stoppered centrifuge tubes and blow dry with a gentle nitrogen stream. Rinse the residue into the tip of the tube with several washes of methylene chloride and blow dry.

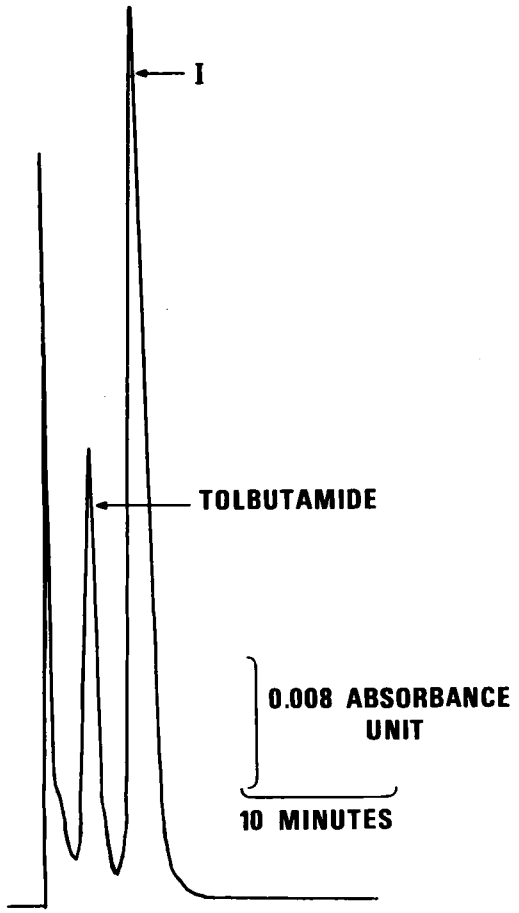

Figure 1—*Typical HPLC chromatogram of tolbutamide and the internal standard (I) from a serum sample. Sensitivity is 0.08 aufs, and the retention times of tolbutamide and the internal standard (I) are 6.0 and 9.0 min, respectively.*

Table II—Principal Peaks in the Mass Spectra of the Reaction Product of Isopentyl Alcohol with Internal Standard

m/e	Presumed Structure
301 (molecular ion)	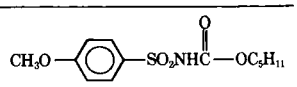
213	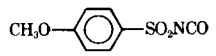
187	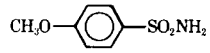
171	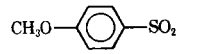
124 (base peak)	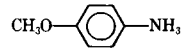
107	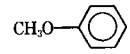
92	

Redissolve the residue in 40 μl of acetonitrile and inject 3-μl aliquots into the liquid chromatograph. Calculate the peak height ratios and plot the standard curve to be used to determine the tolbutamide content of the test samples.

Blood Level Study in Humans—Informed written consent was given by a normal human male with a fasting blood sugar not exceeding 110 mg/100 ml. The drug was given as two 0.5-g tablets of tolbutamide[12] after an 8-hr fast. Food was allowed 3 hr after drug administration. Blood samples (18 ml) were taken at the indicated time intervals and allowed to clot; the serum, harvested by centrifugation, was immediately frozen to await analysis.

GLC Assay Procedure—The procedure of Matin and Rowland (7) was used for the GLC analysis of the serum samples. The assays were run as part of a much larger study, so considerable expertise has been generated in using the procedure. Due to the nonlinearity of the calibration curve, it was necessary to use 0.1-ml serum samples instead of the 0.5-ml samples suggested by Matin and Rowland (7).

RESULTS AND DISCUSSION

Extraction Efficiency of Tolbutamide and Internal Standard from Serum Samples—Various organic solvents (tetrahydrofuran, isopentyl acetate, butyl chloride, methylene chloride, and isopentyl alcohol) in hexane were tested, and only 5% tetrahydrofuran in hexane was satisfactory. This solvent system, under the conditions of the procedure, gave an extraction efficiency of 78.7% for tolbutamide and 62% for the internal standard. Addition of 0.5 g of anhydrous sodium sulfate to the aqueous phase increased the extraction efficiency only about 3%. Tetrahydrofuran must be preserved with 250 ppm of

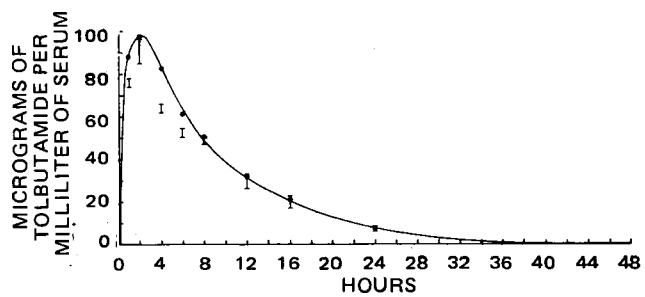

Figure 2—*Serum tolbutamide levels in a human subject after a 1-g oral dose. Key: ●, HPLC data; and* I, *GLC data. The GLC data represent the range of duplicate determinations.*

[11] Hamilton Co., Reno, Nev.

[12] Orinase, The Upjohn Co., Kalamazoo, Mich.

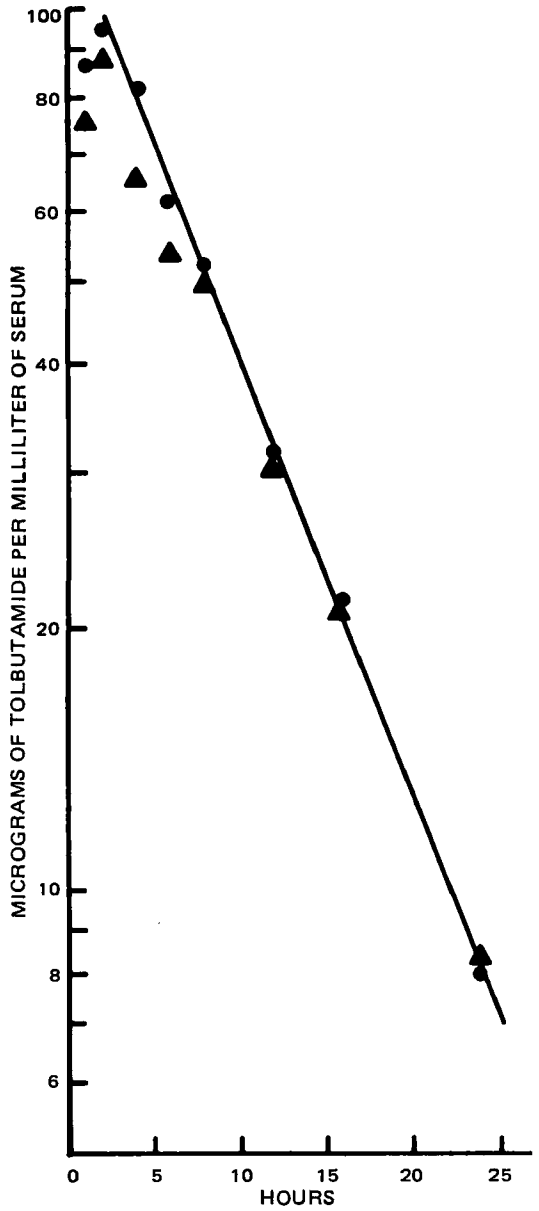

Figure 3—*First-order plot of serum tolbutamide levels after a 1-g oral dose. The* $t_{1/2}$ *is 6.03 hr. Key:* ●, *HPLC data; and* ▲, *GLC data.*

butylated hydroxytoluene to avoid oxidation of the internal standard. A comparison of extraction efficiencies of tritium-labeled tolbutamide from buffered serum using various organic solvents is shown in Table I.

Isopentyl alcohol (5%) in hexane also gave a satisfactory extraction efficiency for tolbutamide and the internal standard, but significant amounts of the isopentyl carbamate of the internal standard and tolbutamide were formed after 20 min at room temperature. The thermal dissociation of alkylsulfonylureas to give first the corresponding sulfonyl isocyanate and then, on reaction with alcohols, the alkyl carbamate is well known (11, 12). However, the reaction is usually run at 80° or higher. Therefore, the ease with which the reaction occurs, especially with the internal standard, is surprising. The reaction with the internal standard, based on peak heights, varied from 9 to 19% while tolbutamide reacted from 2 to 7%.

The identity of the reaction products was confirmed by isolating the HPLC peaks and comparing their mass spectra with those of authentic samples. The principal peaks found in the mass spectra of the reaction product of isopentyl alcohol and the internal standard are given in Table II.

Accuracy and Precision—A typical chromatogram of tolbutamide and the internal standard in a serum sample is shown in Fig. 1.

Table III—Accuracy and Precision of HPLC Assay for Tolbutamide in Human Serum

Tolbutamide Taken, μg		Amount Found, μg
128		129.9
		129.5
		133.0
		130.7
	Mean	130.7
	95% *CL*	±2.2 μg
	RSD	1.02%
64		65.5
		64.2
		65.5
		65.5
		67.7
	Mean	65.7
	95% *CL*	±1.4 μg
	RSD	1.7%
6.4		6.00
		6.31
		5.82
		5.88
	Mean	6.00
	95% *CL*	±0.30 μg
	RSD	3.1%

There was baseline separation between the drug and internal standard peaks. The calibration curve was linear from 2 to 160 μg of tolbutamide/ml of serum. The slope and associated 95% confidence interval was 0.0399 ± 0.0008, and the relative standard deviation for the slope was 1.8%. The curve passed through the origin, indicating no interference when assaying a blank serum sample.

Replicate calibration curves on different days (n = 3) gave a mean slope of 0.0381 and a mean relative standard deviation of 3.7%. The data in Table III show the accuracy and precision of the assay. The internal standard peak was measured at 0.08 aufs while the tolbutamide peak was measured at 0.01–0.08 aufs and then normalized to 0.01 aufs. It may be possible, assuming no interference, to increase the sensitivity from 2 to 0.1 μg/ml by using a variable wavelength detector at the absorption maximum (228 nm) of tolbutamide.

Comparison of GLC and HPLC Analyses—The results for the GLC and HPLC analyses of human serum samples obtained after the ingestion of 1 g of tolbutamide are given in Fig. 2. The points corresponding to the HPLC data form a smooth curve. There is a noticeable difference between the GLC and HPLC data at 4 and 6 hr, but it is not very likely that the serum tolbutamide concentration actually goes through a sharp change in slope as seen in the GLC data between 6 and 8 hr. The data from the logarithmic phase of Fig. 2 are plotted in Fig. 3 and show excellent linearity, as expected for simple first-order elimination.

REFERENCES

(1) W. F. Beyer and E. H. Jensen, in "Analytical Profiles of Drug Substances," vol. III, K. Florey, Ed., Academic, New York, N.Y., 1974, p. 530.

(2) D. L. Simmons, R. J. Ranz, and P. Picotte, *J. Chromatogr.*, **71**, 421(1972).

(3) L. F. Prescott and D. R. Redman, *J. Pharm. Pharmacol.*, **24**, 713(1972).

(4) K. Sabih and K. Sabih, *J. Pharm. Sci.*, **59**, 782(1970).

(5) W. F. Beyer, *Anal. Chem.*, **44**, 1312(1972).

(6) V. Aggarwal and I. Sunshine, *Clin. Chem.*, **20**, 200(1974).

(7) S. B. Matin and M. Rowland, *J. Pharm. Pharmacol.*, **25**, 186(1973).

(8) S. B. Matin and M. Rowland, *Anal. Lett.*, **6**, 865(1973).

(9) D. L. Simmons, A. A. Legore, P. Picotte, K. S. Lee, and N. N. Joshi, *J. Pharmacokinet. Biopharm.*, **3**, 39(1975).

(10) R. C. Thomas and G. J. Ikeda, *J. Med. Chem.*, **9**, 507(1966).

(11) F. Bottari, M. Mannelli, and M. F. Saettone, *J. Pharm. Sci.*, **59**, 1663(1970).

(12) F. Bottari, B. Giannaccini, E. Nannipieri, and M. F. Saettone, *ibid.*, **61**, 603(1972).

ACKNOWLEDGMENTS AND ADDRESSES

Received October 14, 1975, from the *Research Laboratories, The Upjohn Company, Kalamazoo, MI 49001*

Accepted for publication January 7, 1976.

The author thanks the Clinical Bioavailability Unit, The Upjohn Co., for the clinical portion of the study and Ursula M. Rykert and Janice M. Wozniak for collection of the GLC and accuracy and precision data.

Synthesis and Properties of Mesoionic Pyrimido[1,2-*b*]pyridazine-2,4-diones and Mesoionic Pyridazino[2,3-*a*]-*s*-triazine-2,4-diones: Mesoionic Analogs Structurally Related to Fervenulin

R. A. COBURN ˣ **and R. A. CARAPELLOTTI**

Abstract □ Derivatives of two new and unusual classes of heterocycles, possessing structural similarities to the broad spectrum antibiotic fervenulin, were synthesized and examined for *in vitro* antimicrobial activity. Only three of 17 mesoionic pyrimido[1,2-*b*]pyridazine-2,4-diones exhibited evidence of antimicrobial activity while seven of eight mesoionic pyridazino[2,3-*a*]-*s*-triazine-2,4-diones were active against one or more microorganisms. Susceptibility toward attack by nucleophiles of both mesoionic pyridazino[2,3-*a*]-*s*-triazine-2,4-diones and fervenulin was observed.

Keyphrases □ Pyrimido[1,2-*b*]pyridazine-2,4-diones—synthesized, *in vitro* antimicrobial activity screened □ Pyridazino[2,3-*a*]-*s*-triazine-2,4-diones—synthesized, *in vitro* antimicrobial activity screened □ Heterocycles—substituted pyrimido[1,2-*b*]pyridazines and pyridazino[2,3-*a*]-*s*-triazines synthesized, screened for antimicrobial activity □ Structure–activity relationships—substituted pyrimido[1,2-*b*]pyridazines and pyridazino[2,3-*a*]-*s*-triazines synthesized, antimicrobial activity screened □ Antimicrobial activity—substituted pyrimido[1,2-*b*]pyridazines and pyridazino[2,3-*a*]-*s*-triazines □ Mesoionic compounds—substituted pyrimido[1,2-*b*]-pyridazines and pyridazino[2,3-*a*]-*s*-triazines series synthesized, antimicrobial activity screened

The discovery of *in vitro* antibacterial activity of mesoionic thiazolo[3,2-*a*]pyrimidine-5,7-diones (I*a*, X = CH) and mesionic 1,3,4-thiadiazolo[3,2-*a*]pyrimidine-5,7-diones (I*b*, X = N) was reported recently (1). In particular, the most active I*b* compounds possess obvious structural similarities to the broad spectrum antibiotic fervenulin (II) (2, 3) (replacement of N=N by a sulfur atom). These findings prompted the examination of two other ring systems structurally similar to fervenulin, mesoionic pyrimido[1,2-*b*]pyridazine-2,4-diones[1] (III) and mesoionic pyridazino[2,3-*a*]-*s*-triazine-2,4-diones[2] (IV).

Reported here are the syntheses of a number of derivatives of mesoionic Structures III and IV and an examination of their chemical properties compared with those of fervenulin (II). These compounds were screened for *in vitro* antibacterial and antifungal activities and for *in vivo* antimalarial activity as part of an initial pharmacological investigation.

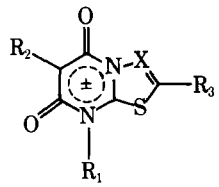

I*a*: X = CH
I*b*: X = N

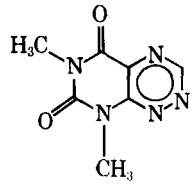

II

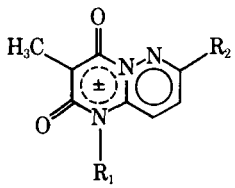

III

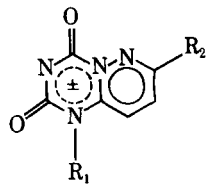

IV

CHEMISTRY

Compounds III*a*–III*q* (Table I) were prepared by the condensation of 3-aminopyridazines (secondary amines V and VI) with bis(2,4,6-trichlorophenyl) methylmalonate as previously described (1, 4), and IV*a*–IV*h* (Table II) were prepared by reaction of V and VI with phenoxycarbonyl isocyanate (Scheme I). The 3-(*N*-substituted amino)pyridazines (V) were prepared by the displacement of one chloro group of 3,6-dichloropyridazine with a primary alkyl-, aryl-, or aralkylamine. The chloro group of V could then be displaced to give VI with 6-substituents such as methoxy, morpholino, hydrogen, anilino, and *N*-methylpiperazyl (Table III).

In contrast to mesoionic thiazolopyrimidinediones (I*a*), which readily acylate benzylamine (4), mesoionic pyrimidopyridazinediones

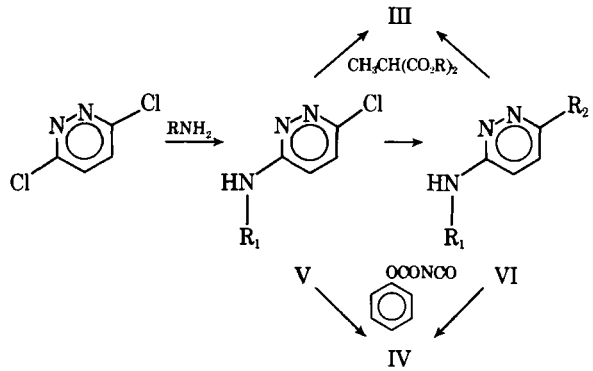

Scheme I

[1] *anhydro*-1-Substituted 2-hydroxypyrimido[1,2-*b*]pyridazinium-4-one hydroxide.

[2] *anhydro*-1-Substituted 2-hydroxypyridazino[2,3-*b*]-*s*-triazinium-4-one hydroxide.

ACKNOWLEDGMENTS AND ADDRESSES

Received October 14, 1975, from the *Research Laboratories, The Upjohn Company, Kalamazoo, MI 49001*

Accepted for publication January 7, 1976.

The author thanks the Clinical Bioavailability Unit, The Upjohn Co., for the clinical portion of the study and Ursula M. Rykert and Janice M. Wozniak for collection of the GLC and accuracy and precision data.

Synthesis and Properties of Mesoionic Pyrimido[1,2-*b*]pyridazine-2,4-diones and Mesoionic Pyridazino[2,3-*a*]-*s*-triazine-2,4-diones: Mesoionic Analogs Structurally Related to Fervenulin

R. A. COBURN ˣ **and R. A. CARAPELLOTTI**

Abstract □ Derivatives of two new and unusual classes of heterocycles, possessing structural similarities to the broad spectrum antibiotic fervenulin, were synthesized and examined for *in vitro* antimicrobial activity. Only three of 17 mesoionic pyrimido[1,2-*b*]pyridazine-2,4-diones exhibited evidence of antimicrobial activity while seven of eight mesoionic pyridazino[2,3-*a*]-*s*-triazine-2,4-diones were active against one or more microorganisms. Susceptibility toward attack by nucleophiles of both mesoionic pyridazino[2,3-*a*]-*s*-triazine-2,4-diones and fervenulin was observed.

Keyphrases □ Pyrimido[1,2-*b*]pyridazine-2,4-diones—synthesized, *in vitro* antimicrobial activity screened □ Pyridazino[2,3-*a*]-*s*-triazine-2,4-diones—synthesized, *in vitro* antimicrobial activity screened □ Heterocycles—substituted pyrimido[1,2-*b*]pyridazines and pyridazino[2,3-*a*]-*s*-triazines synthesized, screened for antimicrobial activity □ Structure–activity relationships—substituted pyrimido[1,2-*b*]pyridazines and pyridazino[2,3-*a*]-*s*-triazines synthesized, antimicrobial activity screened □ Antimicrobial activity—substituted pyrimido[1,2-*b*]pyridazines and pyridazino[2,3-*a*]-*s*-triazines □ Mesoionic compounds—substituted pyrimido[1,2-*b*]-pyridazines and pyridazino[2,3-*a*]-*s*-triazines series synthesized, antimicrobial activity screened

The discovery of *in vitro* antibacterial activity of mesoionic thiazolo[3,2-*a*]pyrimidine-5,7-diones (I*a*, X = CH) and mesionic 1,3,4-thiadiazolo[3,2-*a*]pyrimidine-5,7-diones (I*b*, X = N) was reported recently (1). In particular, the most active I*b* compounds possess obvious structural similarities to the broad spectrum antibiotic fervenulin (II) (2, 3) (replacement of N=N by a sulfur atom). These findings prompted the examination of two other ring systems structurally similar to fervenulin, mesoionic pyrimido[1,2-*b*]pyridazine-2,4-diones[1] (III) and mesoionic pyridazino[2,3-*a*]-*s*-triazine-2,4-diones[2] (IV).

Reported here are the syntheses of a number of derivatives of mesoionic Structures III and IV and an examination of their chemical properties compared with those of fervenulin (II). These compounds were screened for *in vitro* antibacterial and antifungal activities and for *in vivo* antimalarial activity as part of an initial pharmacological investigation.

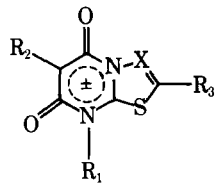

I*a*: X = CH
I*b*: X = N

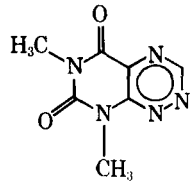

II

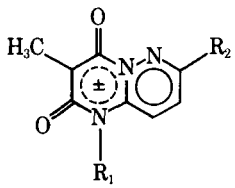

III

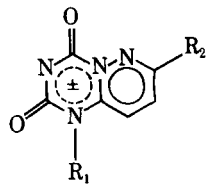

IV

CHEMISTRY

Compounds III*a*–III*q* (Table I) were prepared by the condensation of 3-aminopyridazines (secondary amines V and VI) with bis(2,4,6-trichlorophenyl) methylmalonate as previously described (1, 4), and IV*a*–IV*h* (Table II) were prepared by reaction of V and VI with phenoxycarbonyl isocyanate (Scheme I). The 3-(*N*-substituted amino)pyridazines (V) were prepared by the displacement of one chloro group of 3,6-dichloropyridazine with a primary alkyl-, aryl-, or aralkylamine. The chloro group of V could then be displaced to give VI with 6-substituents such as methoxy, morpholino, hydrogen, anilino, and *N*-methylpiperazyl (Table III).

In contrast to mesoionic thiazolopyrimidinediones (I*a*), which readily acylate benzylamine (4), mesoionic pyrimidopyridazinediones

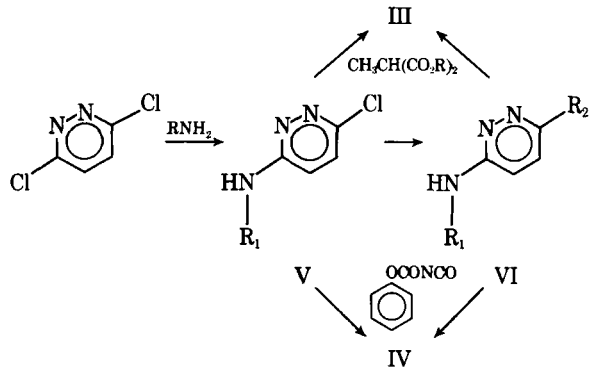

Scheme I

[1] *anhydro*-1-Substituted 2-hydroxypyrimido[1,2-*b*]pyridazinium-4-one hydroxide.

[2] *anhydro*-1-Substituted 2-hydroxypyridazino[2,3-*b*]-*s*-triazinium-4-one hydroxide.

Table I—Properties of Mesoionic Pyrimido[1,2-*b*]pyridazine-2,4-diones (III)

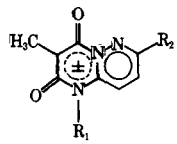

Compound	R_1	R_2	Yield, %	Melting Point	Formula	Analysis, % Calc.	Found
III*a*	CH_3	Cl	88	279–280°	$C_9H_8ClN_3O_2$	C 47.91 H 3.57 Cl 15.71 N 18.82	47.95 3.60 15.77 18.56
III*b*	$CH(CH_3)_2$	Cl	80	264–270°	$C_{11}H_{12}ClN_3O_2$	C 52.08 H 4.77 Cl 13.98 N 16.56	52.01 4.78 14.07 16.59
III*c*	$(CH_2)_3CH_3$	Cl	91	182–184°	$C_{12}H_{14}ClN_3O_2$	C 53.84 H 5.27 Cl 13.24 N 15.70	53.77 5.31 13.29 15.61
III*d*	$CH_2C_6H_4$	Cl	90	269–271°	$C_{15}H_{12}ClN_3O_2$	C 59.71 H 4.01 Cl 11.75 N 13.93	59.64 4.08 11.83 13.87
III*e*	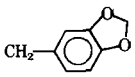	Cl	69	250–251°	$C_{16}H_{12}ClN_3O_4$	C 55.58 H 3.50 Cl 10.25 N 12.15	55.53 3.54 10.20 12.08
III*f*	C_6H_5	Cl	79	255–260°	$C_{14}H_{10}ClN_3O_2$	C 58.45 H 3.50 Cl 12.32 N 14.61	58.73 3.66 12.12 14.50
III*g*	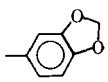	Cl	83	276–279°	$C_{15}H_{10}ClN_3O_4$	C 54.31 H 3.04 Cl 10.69 N 12.67	54.06 3.20 10.51 12.46
III*h*	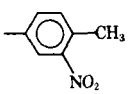	Cl	91	293–295°	$C_{15}H_{11}ClN_4O_4$	C 51.96 H 3.20 Cl 10.23 N 16.16	51.82 3.24 10.27 16.17
III*i*	CH_3	OCH_3	95	265–267°	$C_{10}H_{11}N_3O_3$	C 54.30 H 5.01 N 19.00	54.46 5.08 18.95
III*j*	$CH_2C_6H_4$	OCH_3	87	240–243°	$C_{16}H_{15}N_3O_3$	C 64.64 H 5.09 N 14.13	64.58 5.14 14.03
III*k*	C_6H_5	OCH_3	93	310–312°	$C_{15}H_{13}N_3O_3$	C 63.60 H 4.63 N 14.83	63.36 4.68 14.95
III*l*	C_6H_5	H	97	314–315°	$C_{14}H_{11}N_3O_2$	C 66.40 H 4.38 N 16.59	66.57 4.39 16.63
III*m*	C_6H_5	NHC_6H_4	87	332–334°	$C_{20}H_{16}N_4O_2$	C 69.76 H 4.68 N 16.27	69.78 4.69 16.22
III*n*	$CH(CH_3)_2$	Morpholino	92	265–266°	$C_{15}H_{20}N_4O_3$	C 59.20 H 6.62 N 18.41	58.86 6.69 18.27
III*o*	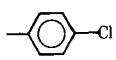	Morpholino	90	294–296°	$C_{18}H_{17}ClN_4O_3$	C 57.99 H 4.60 Cl 9.51 N 15.03	57.63 4.62 9.37 14.87
III*p*	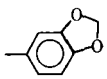	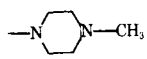	78	253–256°	$C_{20}H_{21}N_5O_4 \cdot 2H_2O$	C 55.68 H 5.84 N 16.23	55.72 5.88 16.20
III*q*	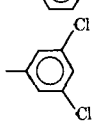	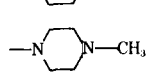	94	278–279°	$C_{19}H_{19}Cl_2N_5O_2$	C 54.30 H 4.56 Cl 16.87 N 16.66	54.23 4.60 16.91 16.66

(III) were stable to nucleophilic attack by benzylamine in refluxing chloroform, ethanol, or acetonitrile for 7 days. However, mesoionic pyridazinotriazinedione (IV*c*) reacts readily with benzylamine in acetonitrile to form VII (Scheme II). Evidence in support of the structure assignment of VII follows from the reaction of V*h* with phenyl chloroformate to yield VIII, which reacted with the sodium salt of benzylurea to give a product with identical melting point, NMR spectrum, and R_f values to VII.

Compound IV*c* in aqueous acetonitrile reacts readily with water, affording the starting material V*h* (Scheme II). Only mesoionic pyridazinotriazinediones IV*a*–IV*c*, with chloro groups at their 7-positions, appear to be sensitive to nucleophilic attack by water. From the NMR spectra of IV*a*–IV*c* in moist dimethyl sulfoxide-d_6, it was estimated that these compounds have a half-life of about 30 min; under identical conditions, the NMR spectra of IV*d*–IV*h* showed no evidence of decomposition at 37° after several days.

Little has been reported concerning the reactions of fervenulin with nucleophiles other than its susceptibility to degradation in aqueous alkali (5). Fervenulin (II) reacted with benzylamine in ethanol to afford the adduct IX (Scheme III). Evidence in support of the assign-

Table II—Properties of Mesoionic Pyridazino[2,3-*a*]-*s*-triazine-2,4-diones (IV)

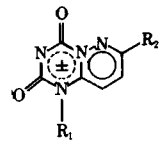

Compound	R_1	R_2	Yield, %	Melting Point	Formula	Analysis, % Calc.	Found
IV*a*	CH_3	Cl	79	215–217°	$C_7H_5ClN_4O_2$	C 39.55 H 2.37 Cl 16.68 N 26.35	39.50 2.49 16.78 26.31
IV*b*	$(CH_2)_3CH_3$	Cl	89	197–200°	$C_{10}H_{11}ClN_4O_2$	C 47.16 H 4.35 Cl 13.92 N 22.00	47.27 4.42 14.06 22.17
IV*c*	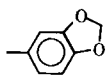	Cl	85	210–215°	$C_{13}H_7ClN_4O_4$	C 49.00 H 2.21 Cl 11.13 N 17.58	48.73 2.21 11.25 17.43
IV*d*	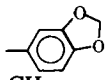	OCH_3	78	254–257°	$C_{14}H_{10}N_4O_5$	C 53.51 H 3.21 N 17.83	53.57 3.29 17.80
IV*e*	CH_3	Morpholino	94	277–280°	$C_{11}H_{13}N_5O_3$	C 50.19 H 4.98 N 26.60	50.21 5.00 26.63
IV*f*	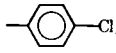	Morpholino	85	284–286°	$C_{16}H_{14}ClN_5O_3$	C 53.42 H 3.92 Cl 9.85 N 19.47	53.48 3.94 9.88 19.54
IV*g*	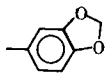	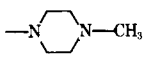	83	212–217°	$C_{18}H_{18}N_6O_4 \cdot 2H_2O$	C 50.99 H 5.23 N 21.14	51.29 4.96 21.52
IV*h*	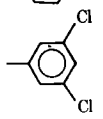	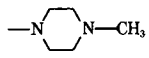	74	217–220°	$C_{17}H_{16}Cl_2N_6O_2$	C 50.14 H 3.96 Cl 17.41 N 20.64	50.17 4.00 17.37 20.68

ment of Structure IX is based upon NMR studies, IR spectrum, and elemental composition. Spin-decoupling studies carried out in dimethyl sulfoxide-d_6 showed the *N*-1 proton (δ 7.7), which undergoes rapid exchange in the presence of deuterium oxide, coupled to the C-3 proton (δ 10.8, J = 2 Hz) on the *as*-triazine nucleus. Both methyl groups appear as singlets at δ 2.7 and 2.9.

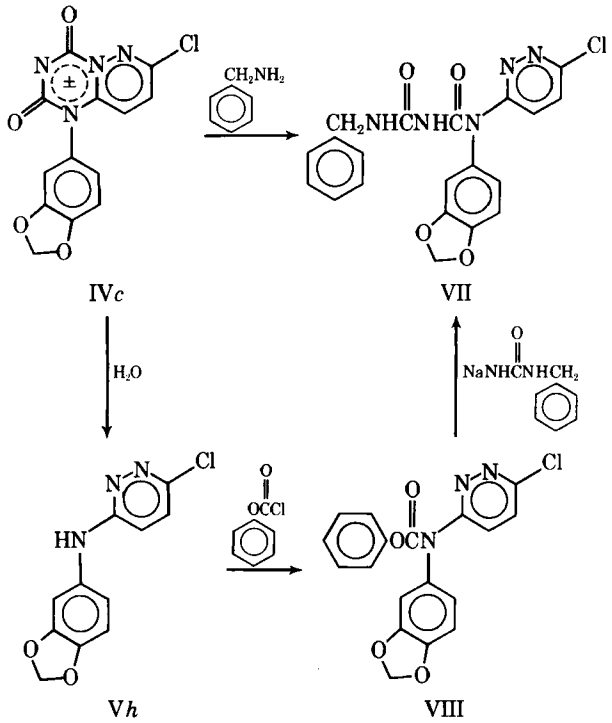

Scheme II

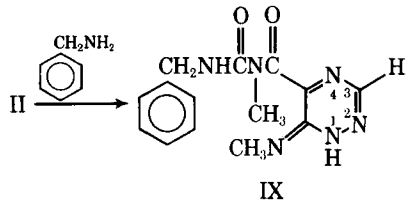

IX

Scheme III

EXPERIMENTAL[3]

3- Chloro -6- (3,4- methylenedioxybenzylamino)pyridazine (V*e*)—3,6-Dichloropyridazine (4.9 g, 33 mmoles) and 3,4-(methylenedioxy)benzylamine (10 g, 66 mmoles) in ethanol (50 ml) were stirred for 30 min at room temperature and then refluxed for 7 hr. The solvent was evaporated *in vacuo*, and the residue was stirred with water (75 ml) and ice (50 g). The resulting white crystals were filtered, washed with water (3 × 75 ml), and air dried. Recrystallization from benzene yielded 4.5 g (52%) of V*e*, mp 139–142°; NMR (dimethyl sulfoxide-d_6): δ 4.5 (d, 2), 6.1 (s, 2), 6.9 (m, 3), and 7.4 (m, 2).

3-Chloro-6-(4-methyl-3-nitroanilino)pyridazine (V*g*)—3,6-Dichloropyridazine (15.0 g, 0.1 mole) and 4-methyl-3-nitroaniline (15.2 g, 0.1 mole) in ethanol (75 ml) were refluxed with stirring for 3 hr, and the solvent was evaporated *in vacuo*. The resulting residue was neutralized with an aqueous sodium carbonate solution (1.0 *M*), and the free base was filtered, washed with water (3 × 75 ml), and air dried. Recrystallization from methanol yielded 17.6 g (86%) of V*g*, mp 188–191°; NMR (dimethyl sulfoxide-d_6): δ 7.6 (m, 4), 8.7 (d, 1), and 10.0 (s, 1).

[3] Proton magnetic resonance (PMR) spectra were obtained on a Varian T-60 spectrometer, and chemical shifts are reported relative to tetramethylsilane. IR spectra were obtained on a Perkin-Elmer 237 grating spectrophotometer. Microanalyses were performed by Atlantic Microlab, Inc., Atlanta, Ga. All melting points were determined on a Mel-Temp melting-point apparatus and are uncorrected.

Table III—Properties of 3-(*N*-Substituted Amino)pyridazines (V and VI)

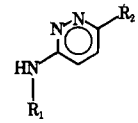

Compound	R_1	R_2	Yield, %	Melting Point[a]	Formula	Analysis, % Calc.	Found
V*a*	CH_3	Cl	65	195–196°[b]	—[b]	—	—
V*b*	$CH(CH_3)_2$	Cl	88	103–105°	—[e]	—	—
V*c*	$(CH_2)_3CH_3$	Cl	69	99–101°[c]	—[e]	—	—
V*d*	$CH_2C_6H_4$	Cl	87	150–156°	—[f]	—	—
V*e*	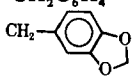	Cl	52	139–142°[c]	$C_{12}H_{10}ClN_3O_2$	C 54.66 H 3.82 Cl 13.45 N 15.94	54.79 3.90 13.39 15.91
V*f*	C_6H_5	Cl	60	185–187°	—[f]	—	—
V*g*	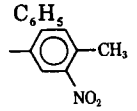	Cl	86	188–191°	$C_{11}H_9ClN_4O_2$	C 49.92 H 3.43 Cl 13.40 N 21.17	49.92 3.49 13.34 21.09
V*h*	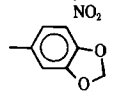	Cl	84	204–205°	$C_{11}H_8ClN_3O_2$	C 52.92 H 3.23 Cl 14.20 N 16.83	52.98 3.29 14.15 16.88
V*i*	$4\text{-}ClC_6H_4$	Cl	69	192–195°	—[f]	—	—
V*j*	$4\text{-}CH_3OC_6H_4$	Cl	62	145–147°	—[f]	—	—
VI*a*	CH_3	OCH_3	72	82–85°[c]	$C_6H_9N_3O$	C 51.79 H 6.52 N 30.20	51.75 6.44 29.98
VI*b*	$CH_2C_6H_4$	OCH_3	67	99–101°	—[f]	—	—
VI*c*	C_6H_5	OCH_3	60	112–115°	$C_{11}H_{11}N_3O$	C 65.66 H 5.51 N 20.88	65.43 5.47 20.69
VI*d*	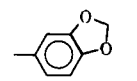	OCH_3	90	135–137°[c]	$C_{12}H_{11}N_3O_3$	C 58.77 H 4.52 N 17.14	58.92 4.62 17.18
VI*e*	CH_3	Morpholino	84	195–197°[c]	$C_9H_{14}N_4O$	C 55.65 H 7.27 N 28.85	55.63 7.30 28.93
VI*f*	$CH(CH_3)_2$	Morpholino	81	135–137°[c]	$C_{11}H_{18}N_4O$	C 59.44 H 8.16 N 25.21	59.60 8.19 25.29
VI*g*	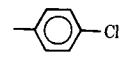	Morpholino	89	174–176°	$C_{14}H_{15}ClN_4O$	C 57.83 H 5.20 Cl 12.19 N 19.27	58.04 5.34 12.26 19.30
VI*h*	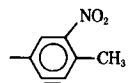	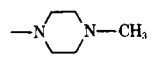	82	198–202°[c]	$C_{16}H_{20}N_6O_2$	C 58.52 H 6.14 N 25.59	58.73 6.22 25.65
VI*i*	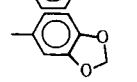	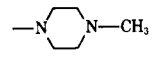	88	181–182°[c]	$C_{16}H_{19}N_5O_2$	C 61.33 H 6.11	61.20 6.17
VI*j*	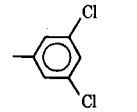	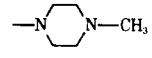	83	168–169°[c]	$C_{15}H_{17}Cl_2N_5$	C 53.27 H 5.07 Cl 20.96 N 20.71	53.01 5.15 20.84 20.57

[a] Unless otherwise indicated, the recrystallization solvent was absolute methanol. [b] Recrystallized from water. [c] Recrystallized from benzene. [d] Reference 6. [e] Reference 7. [f] Reference 8.

3-Chloro-6-(3,4-methylenedioxyanilino)pyridazine (V*h*)—This compound was prepared by the same method as V*g*, using 3,4-(methylenedioxy)aniline (13.7 g, 0.1 mole). After recrystallization from methanol, the yield was 21.0 g (84%) of V*h*, mp 204–205°; NMR (dimethyl sulfoxide-d_6): δ 6.0 (s, 2), 7.3 (m, 5), and 9.3 (s, 1).

3-(*N*-Substituted Amino)-6-methoxypyridazines (VI*a*–VI*d*)—The appropriate 3-(*N*-substituted amino)-6-chloropyridazine (100 mmoles) and sodium methoxide (0.6 g, 110 mmoles) in xylene (50 ml) were refluxed with stirring for 12 hr. The solvent was evaporated *in vacuo*, and the resulting residue was stirred in water (75 ml) for 15 min. The resulting dark-yellow crystals were filtered, washed with water (4 × 25 ml), and air dried. Recrystallization was from an appropriate solvent (Table III).

3-(*N*-Substituted Amino)-6-morpholinopyridazines (VI*e*–VI*g*)—The appropriate 3-(*N*-substituted amino)-6-chloropyridazine (10 mmoles) and morpholine (12 ml) were refluxed with stirring for 6 hr. The cooled reaction mixture was poured onto ice (30 g), producing pale-yellow crystals. Then the crystals were filtered, washed with water (3 × 25 ml), and air dried.

3-(*N*-Substituted Amino)-6-*N*-(4-methylpiperazyl)pyridazines (VI*h*–VI*j*)—The appropriate 3-(*N*-substituted amino)-6-chloropyridazine (20 mmoles) and *N*-methylpiperazine (20 ml) were refluxed with stirring for 6 hr. The excess *N*-methylpiperazine was removed *in vacuo*, and the resulting residue was stirred with water (25 ml) and ice (25 g). The resulting pale-yellow crystals were filtered, washed with water, and air dried.

Mesoionic Pyrimido[1,2-*b*]pyridazine-2,4-diones (III*a*–III*q*)—An intimate mixture of equal molar quantities of the appropriate (*N*-substituted amino)pyridazine (V or VI) and bis(2,4,6-trichlorophenyl) methylmalonate was heated on an oil bath (160°) under a slow stream of nitrogen until a clear melt was obtained (7–10 min). The cooled oil was triturated with ether, leading to the crystallization of III. Then the crystals were filtered, air dried, and recrystallized from acetonitrile.

Table IV—Zones of Inhibition[a]

Compound	*E. coli*	*Ent. cloacae*	*K. pneumoniae*	*Sal. typhimurium*	*S. marcescens*	*Staph. aureus*	*Staph. epidermidis*	*C. albicans*
IV*a*	—	—	—	—	—	—	—	11
IV*b*	—	—	11	—	12	—	—	—
IV*c*	—	—	—	—	—	—	—	—
IV*d*	—	—	—	—	—	8	—	—
IV*e*	—	—	—	—	10	—	—	—
IV*f*	—	—	—	—	12	—	—	—
IV*g*	—	—	—	—	—	8	10	—
IV*h*	—	12	8	—	12	18	13	10
Nystatin	20	22	22	18	16	18	19	15
Furazolidone	19	21	17	18	—	22	14	—

[a] Diameter (millimeters) of zones of inhibition.

Mesoionic Pyridazino[2,3-*a*]-*s*-triazine-2,4-diones (IV*a*–IV*h*)—To the appropriate (*N*-substituted amino)pyridazine (V or VI) (4.0 mmoles) in dry acetonitrile (20 ml) was added phenoxycarbonyl isocyanate (9) (1.0 g, 6.0 mmoles), and the reaction mixture was allowed to stir at room temperature for 2 hr with the exclusion of moisture. The precipitate was filtered, washed with ether, and air dried. Purification of IV was accomplished by stirring in refluxing dry acetonitrile (10–20 ml) for 20–30 min. The recrystallized mixture was filtered while still warm and dried *in vacuo*, affording only minor loss of product.

Reaction of IV*c* with Water—To IV*c* (500 mg, 1.6 mmoles) in acetonitrile (30 ml) was added water (10 ml) (Scheme II), and the reaction mixture was stirred at room temperature for 30 min and refluxed for 30 min. The reaction mixture was evaporated *in vacuo*, and the resulting residue was extracted with chloroform. The chloroform extract was dried (anhydrous sodium sulfate), filtered, and evaporated *in vacuo*, yielding a residue which was crystallized with ether–benzene (1:10). The crystalline material was chromatographed on a silica gel (Woelm) column. Elution with benzene–ethyl acetate and recrystallization from benzene yielded 135 mg (34%) of V*h*, mp 208–211° dec.

Anal.—Calc. for $C_{11}H_8ClN_3O_2$: C, 52.92; H, 3.23; Cl, 14.20; N, 16.83. Found: C, 53.19; H, 3.30; Cl, 14.32; N, 17.07.

Phenyl *N*-(3,4-Methylenedioxyphenyl)-*N*-[3-(6-chloropyridazyl)]carbamate (VIII)—Compound V*h* (500 mg, 2.0 mmoles), phenyl chloroformate (3 ml), and sodium carbonate (250 mg, 2.0 mmoles) (Scheme II) were refluxed for 30 min. The reaction mixture was filtered, and the filtrate was treated with water (5 ml) and ethyl acetate (5 ml), leading to the precipitation of white crystals. Then the crystals were filtered, washed with ether (10 ml), and air dried. Recrystallization from methanol yielded 500 mg (68%) of VIII, mp 176–182°; NMR (dimethyl sulfoxide-d_6): δ 6.2 (s, 2), 7.1 (m, 3), 7.4 (m, 5), and 8.2 (q, 2).

Anal.—Calc. for $C_{18}H_{12}ClN_3O_4$: C, 58.47; H, 3.27; Cl, 9.59; N, 11.36. Found: C, 58.35; H, 3.28; Cl, 9.51; N, 11.26.

Reaction of Fervenulin (II) with Benzylamine—Fervenulin (II) (100 mg, 0.52 mmole) and benzylamine (2 ml) in ethanol (15 ml) (Scheme III) were refluxed for 70 hr with stirring. The solvent and excess benzylamine were evaporated *in vacuo*, and the resulting residue was crystallized from ether (10 ml), filtered, and air dried. Recrystallization from chloroform–ether yielded 145 mg (94%) of IX, mp 224–226°; NMR (dimethyl sulfoxide-d_6): δ 4.3 (d, 2), 7.3 (s, 5), 7.7 (d, 1), and 10.8 (d, 1).

Anal.—Calc. for $C_{14}H_{16}N_6O_2$: C, 55.99; H, 5.37; N, 27.98. Found: C, 55.88; H, 5.39; N, 27.93.

1-(3,4- Methylenedioxyphenyl) -1- [3-(6-chloropyridazyl)]-5-benzylbiuret (VII)—*Method A: Reaction of IV*c *with Benzylamine*—To IV*c* (200 mg, 0.63 mmole) in dry acetonitrile (10 ml) was added benzylamine (0.1 ml) (Scheme II), and the mixture was allowed to stir at room temperature for 90 min. The reaction mixture was stirred with charcoal and filtered, and the filtrate was evaporated *in vacuo*. The resulting residue was crystallized from ether, producing tan crystals which were filtered and air dried. Recrystallization from benzene yielded 240 mg (90%) of VII, mp 169–170° dec.; NMR (dimethyl sulfoxide-d_6): δ 4.4 (d, 2), 6.2 (s, 2), 7.0 (m, 3), 7.4 (s, 5), and 7.7 (q, 2).

Anal.—Calc. for $C_{20}H_{16}ClN_5O_4$: C, 56.41; H, 3.79; Cl, 8.33; N, 16.45. Found: C, 56.64; H, 3.86; Cl, 8.23; N, 16.32.

Method B—To a suspension of sodium hydride (57% oil dispersion; 150 mg, 6.25 mmoles) in benzene (10 ml) was added benzylurea (150 mg, 1.0 mmole). The reaction mixture was stirred at room temperature for 1 hr, followed by the addition of VIII (250 mg, 0.7 mmole) (Scheme II). Stirring was continued at room temperature for 2.5 hr, and then the reaction mixture was washed with portions of water until neutral. The benzene layer was dried (anhydrous sodium sulfate), filtered, and evaporated *in vacuo*. The resulting yellow crystals were recrystallized from benzene, yielding 125 mg (42%) of VII, mp 167–169° (identical NMR spectra and R_f values as product prepared by reaction of IV*c* with benzylamine).

Antimicrobial Testing Procedure—The following organsms were employed: *Escherichia coli* (ATCC 25922), *Enterobacter cloacae* (ATCC 23355), *Salmonella typhimurium* (ATCC 14028), *Serratia marcescens* (ATCC 8100), *Staphylococcus epidermidis* (ATCC 12228), *Candida albicans* (ATCC 10231), *Staphylococcus aureus* (ATCC 25923), and *Klebsiella pneumoniae* (ATCC 23357). A lawn was prepared on trypticase[4] soy agar plates, using 1 ml of a 24-hr growth of the test organism in trypticase soy broth. Paper disks (6 mm), impregnated with 1 mg of the test compounds, were placed on the agar and incubated for 24 hr at 37°. Included on each plate were disks[4] impregnated with the commercially available antimicrobial agents nystatin and furazolidone[5].

RESULTS AND DISCUSSION

Only three of 17 III derivatives, III*a*, III*g*, and III*h*, showed any evidence of inhibition in this assay. They exhibited activity against *S. marcescens*, *Staph. aureus*, *Staph. epidermidis*, or *C. albicans*. This activity is in contrast to the more widespread activity (seven of eight) of the mesoionic pyridazino[2,3-*a*]-*s*-triazine-2,4-diones (IV*a*–IV*h*, Table IV) and the previously reported thiazolo- and 1,3,4-thiadiazolo[3,2-*a*]pyrimidinediones (I*a* and I*b*) (1). No significant blood schizonticidal antimalarial activity against *Plasmodium berghei*-infected mice was found[6] for III*a*, III*b*, III*d*, III*k*, III*n*, III*o*, IV*c*, and IV*f*.

While no antimicrobial mechanism of action could be established for mesoionic Structures I*a* and I*b* and series III and IV, an apparent correlation exists between the reactivity of the test compounds toward nucleophiles and their *in vitro* antibacterial activity. Thus, little activity was found among compounds in series III, which are stable to benzylamine, while a number of derivatives of IV, which readily acylate amines, display activity. This finding lends support to the hypothesis (11) that these fused-ring mesoionic compounds may act as acylating agents *in vivo*.

REFERENCES

(1) R. A. Coburn and R. A. Glennon, *J. Pharm. Sci.*, **62**, 1785(1973).

(2) C. DeBoer, A. Dietz, J. S. Evans, and R. M. Michaels, *Antibiot. Ann.*, **1959–1960**, 220.

(3) T. E. Eble, E. C. Olson, C. M. Large, and J. W. Shell, *ibid.*, **1959–1960**, 227.

(4) R. A. Coburn and R. A. Glennon, *J. Heterocycl. Chem.*, **10**, 487(1973).

(5) K. Tanabe, Y. Asahi, M. Nishikawa, T. Shima, Y. Kuwada, T. Kanzawa, and K. Ogata, *Takeda Kenkyusho Nempo*, **22**,

[4] BBL, Division Becton, Dickinson and Co., Cockeysville, Md.
[5] Furoxone, Eaton.
[6] Determined by Rane Laboratory, University of Miami (10).

133(1963); through *Chem. Abstr.*, **60**, 13242(1964).
(6) M. Fujisaka, Y. Ueno, H. Shinohara, and E. Imato, *Bull. Chem. Soc. Jpn.*, **37**, 1107(1964).
(7) D. I. Relyea, Belgian pat. 636,313 (Dec. 16, 1963); through *Chem. Abstr.*, **62**, 571(1965).
(8) F. Yoneda, T. Ohtaka, and Y. Nitta, *Chem. Pharm. Bull.*, **11**, 740(1963).
(9) A. J. Speciale, L. R. Smith, and J. E. Fedder, *J. Org. Chem.*, **30**, 4306(1965).
(10) T. S. Osdene, P. B. Russell, and L. Rane, *J. Med. Chem.*, **10**, 431(1967).
(11) R. A. Coburn and R. A. Glennon, *ibid.*, **17**, 1025(1974).

ACKNOWLEDGMENTS AND ADDRESSES

Received March 10, 1975, from the *Department of Medicinal Chemistry, School of Pharmacy, State University of New York at Buffalo, Buffalo, NY 14214*

Accepted for publication December 17, 1975.

Abstracted from a dissertation submitted by R. A. Carapellotti to the Graduate School, State University of New York at Buffalo, in partial fulfillment of the Doctor of Philosophy degree requirements.

Supported in part by the U.S. Army Medical Research and Development Command under Contract DADA-17-73-C-3054 and by Training Grant 5-T1-GM-55-08 from the Division of Medical Sciences, U.S. Public Health Service, Bethesda, MD 20014

Antimalarial test data were supplied through the Division of Medicinal Chemistry, Walter Reed Army Institute of Research.

This paper is Contribution 1395 from the Army Research Program on Malaria.

[x] To whom inquiries should be directed.

Prodrug Approaches to Enhancement of Physicochemical Properties of Drugs IV: Novel Epinephrine Prodrug

ANWAR HUSSAIN [x] and J. E. TRUELOVE

Abstract □ The synthesis and characterization of a prodrug that appears to overcome the problem of inefficient absorption of epinephrine through the lipoidal membranes of the eye are described. The enzymatic rate of regeneration of epinephrine from the prodrug was determined using a rabbit eye homogenate, rabbit plasma, and human plasma. The prodrug had no activity of its own when tested against a guinea pig smooth muscle preparation. Upon enzymatic regeneration of epinephrine from the prodrug, however, the reaction mixture exhibited α-adrenergic activity equivalent to that of epinephrine when tested in the same preparation.

Keyphrases □ Prodrugs—epinephrine prodrug synthesized, screened for adrenergic activity, rabbit eye homogenate and plasma, human plasma □ Epinephrine prodrug—synthesized, screened for adrenergic activity, rabbit eye homogenate and plasma, human plasma □ Adrenergic activity—epinephrine prodrug, screened in rabbit eye homogenate and plasma, human plasma

Previous reports in this series (1–3) presented examples of prodrug approaches that may be used to modify the physicochemical properties of drug molecules to reduce the gastric irritation of aspirin or to improve the dissolution characteristics of highly water-insoluble compounds such as allopurinol and phenytoin. This report presents an example demonstrating the utility of the prodrug approach in improving the efficiency of absorption of a highly polar molecule through lipoidal membranes.

BACKGROUND

Although epinephrine has been used for many years in eye drops for the management and treatment of glaucoma and in inhalant preparations for the treatment of bronchial asthma, problems arise with its use. One major problem is the occurrence of undesirable side effects, both ocular and systemic. McClure (4) recently listed some side effects resulting from topical applications of epinephrine.

In the treatment of glaucoma, relatively concentrated epinephrine solutions are instilled directly into the eye. However, because it is highly polar, little drug is absorbed. The remainder of the solution reaches the general circulation through the tear ducts, exerting its undesirable systemic side effects (5). Since many glaucomatous patients are over 40 years of age, some may have cardiac or circulatory disorders which could be aggravated by systemically absorbed epinephrine. Therefore, an improved form of epinephrine that would be effective at low concentrations seemed desirable.

The fundamental problem with epinephrine is its inefficient transport across lipoidal barriers due to its high polarity and low lipid solubility. It was felt that the transient blocking of the phenolic hydroxy groups would enhance the lipophilicity of epinephrine and significantly facilitate its absorption through the lipoidal membranes of the eye.

The synthesis of a novel prodrug of epinephrine (6), which has been shown to be approximately 100 times more effective clinically than epinephrine itself in the management of glaucoma (4), is reported here. Furthermore, the prodrug has been shown to be about 100–400 times weaker than epinephrine in affecting the cardiovascular systems of dogs and cats (4).

A successful epinephrine prodrug should be more lipophilic than epinephrine, possess adequate water solubility, regenerate epinephrine at a reasonable rate, and be stable enough to be formulated into conventional dosage forms. Furthermore, the blocking groups, upon cleavage, should have no toxicity of their own.

The prodrug, 3,4-dipivaloyloxy-α-(methylaminomethyl)benzyl alcohol perchlorate salt (I) (Scheme I) was a suitable candidate. Since the general pharmacology, toxicology, and clinical evaluation of the prodrug have already been reported (4), this article is concerned with the synthesis and *in vitro* enzymatic hydrolysis of the drug in a rabbit eye homogenate, rabbit plasma, and human plasma.

EXPERIMENTAL

Synthesis[1] of I—Fifty grams (0.27 mole) of α-chloro-3′,4′-dihydroxyacetophenone[2] (II) was dissolved in 200 ml of methanol. (Slight warming may be necessary to complete the solution.) Then 100 ml of

[1] The general synthetic procedure was presented in U.S. pat. 3,809,714.
[2] Obtained from a commercial source or synthesized by the reaction of pyrocatechol and chloroacetyl chloride in refluxing benzene.

133(1963); through *Chem. Abstr.*, **60**, 13242(1964).
(6) M. Fujisaka, Y. Ueno, H. Shinohara, and E. Imato, *Bull. Chem. Soc. Jpn.*, **37**, 1107(1964).
(7) D. I. Relyea, Belgian pat. 636,313 (Dec. 16, 1963); through *Chem. Abstr.*, **62**, 571(1965).
(8) F. Yoneda, T. Ohtaka, and Y. Nitta, *Chem. Pharm. Bull.*, **11**, 740(1963).
(9) A. J. Speciale, L. R. Smith, and J. E. Fedder, *J. Org. Chem.*, **30**, 4306(1965).
(10) T. S. Osdene, P. B. Russell, and L. Rane, *J. Med. Chem.*, **10**, 431(1967).
(11) R. A. Coburn and R. A. Glennon, *ibid.*, **17**, 1025(1974).

ACKNOWLEDGMENTS AND ADDRESSES

Received March 10, 1975, from the *Department of Medicinal Chemistry, School of Pharmacy, State University of New York at Buffalo, Buffalo, NY 14214*

Accepted for publication December 17, 1975.

Abstracted from a dissertation submitted by R. A. Carapellotti to the Graduate School, State University of New York at Buffalo, in partial fulfillment of the Doctor of Philosophy degree requirements.

Supported in part by the U.S. Army Medical Research and Development Command under Contract DADA-17-73-C-3054 and by Training Grant 5-T1-GM-55-08 from the Division of Medical Sciences, U.S. Public Health Service, Bethesda, MD 20014

Antimalarial test data were supplied through the Division of Medicinal Chemistry, Walter Reed Army Institute of Research.

This paper is Contribution 1395 from the Army Research Program on Malaria.

[x] To whom inquiries should be directed.

Prodrug Approaches to Enhancement of Physicochemical Properties of Drugs IV: Novel Epinephrine Prodrug

ANWAR HUSSAIN [x] and J. E. TRUELOVE

Abstract □ The synthesis and characterization of a prodrug that appears to overcome the problem of inefficient absorption of epinephrine through the lipoidal membranes of the eye are described. The enzymatic rate of regeneration of epinephrine from the prodrug was determined using a rabbit eye homogenate, rabbit plasma, and human plasma. The prodrug had no activity of its own when tested against a guinea pig smooth muscle preparation. Upon enzymatic regeneration of epinephrine from the prodrug, however, the reaction mixture exhibited α-adrenergic activity equivalent to that of epinephrine when tested in the same preparation.

Keyphrases □ Prodrugs—epinephrine prodrug synthesized, screened for adrenergic activity, rabbit eye homogenate and plasma, human plasma □ Epinephrine prodrug—synthesized, screened for adrenergic activity, rabbit eye homogenate and plasma, human plasma □ Adrenergic activity—epinephrine prodrug, screened in rabbit eye homogenate and plasma, human plasma

Previous reports in this series (1–3) presented examples of prodrug approaches that may be used to modify the physicochemical properties of drug molecules to reduce the gastric irritation of aspirin or to improve the dissolution characteristics of highly water-insoluble compounds such as allopurinol and phenytoin. This report presents an example demonstrating the utility of the prodrug approach in improving the efficiency of absorption of a highly polar molecule through lipoidal membranes.

BACKGROUND

Although epinephrine has been used for many years in eye drops for the management and treatment of glaucoma and in inhalant preparations for the treatment of bronchial asthma, problems arise with its use. One major problem is the occurrence of undesirable side effects, both ocular and systemic. McClure (4) recently listed some side effects resulting from topical applications of epinephrine.

In the treatment of glaucoma, relatively concentrated epinephrine solutions are instilled directly into the eye. However, because it is highly polar, little drug is absorbed. The remainder of the solution reaches the general circulation through the tear ducts, exerting its undesirable systemic side effects (5). Since many glaucomatous patients are over 40 years of age, some may have cardiac or circulatory disorders which could be aggravated by systemically absorbed epinephrine. Therefore, an improved form of epinephrine that would be effective at low concentrations seemed desirable.

The fundamental problem with epinephrine is its inefficient transport across lipoidal barriers due to its high polarity and low lipid solubility. It was felt that the transient blocking of the phenolic hydroxy groups would enhance the lipophilicity of epinephrine and significantly facilitate its absorption through the lipoidal membranes of the eye.

The synthesis of a novel prodrug of epinephrine (6), which has been shown to be approximately 100 times more effective clinically than epinephrine itself in the management of glaucoma (4), is reported here. Furthermore, the prodrug has been shown to be about 100–400 times weaker than epinephrine in affecting the cardiovascular systems of dogs and cats (4).

A successful epinephrine prodrug should be more lipophilic than epinephrine, possess adequate water solubility, regenerate epinephrine at a reasonable rate, and be stable enough to be formulated into conventional dosage forms. Furthermore, the blocking groups, upon cleavage, should have no toxicity of their own.

The prodrug, 3,4-dipivaloyloxy-α-(methylaminomethyl)benzyl alcohol perchlorate salt (I) (Scheme I) was a suitable candidate. Since the general pharmacology, toxicology, and clinical evaluation of the prodrug have already been reported (4), this article is concerned with the synthesis and *in vitro* enzymatic hydrolysis of the drug in a rabbit eye homogenate, rabbit plasma, and human plasma.

EXPERIMENTAL

Synthesis[1] of I—Fifty grams (0.27 mole) of α-chloro-3′,4′-dihydroxyacetophenone[2] (II) was dissolved in 200 ml of methanol. (Slight warming may be necessary to complete the solution.) Then 100 ml of

[1] The general synthetic procedure was presented in U.S. pat. 3,809,714.
[2] Obtained from a commercial source or synthesized by the reaction of pyrocatechol and chloroacetyl chloride in refluxing benzene.

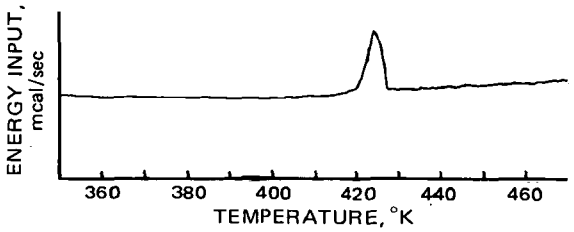

Figure 1—*Differential scanning calorimeter thermogram on heating of a sample of I.*

40% aqueous methylamine was slowly added, and the mixture was stirred at 50° for 2 hr (Scheme I). The solution was then stirred an additional 24 hr at ambient temperatures.

The crude α-methylamino-3′,4′-dihydroxyacetophenone precipitated from the reaction mixture and was recovered by filtration. After thorough washing with ether, the material was dissolved in 100 ml of 4 *N* HCl and 125 ml of methanol. After filtration through decolorizing charcoal, the product was precipitated as the hydrochloride salt (III) by the addition of seven parts of acetone. The salt, a white crystalline material, mp 242°, was used without further purification.

Compound III (25.3 g, 0.125 mole) was dissolved in 250 ml of ethyl acetate, and 0.125 mole of perchloric acid as the 70% aqueous solution was added with continuous stirring. Then 280 ml of pivaloyl chloride was added, and the mixture was slowly warmed to reflux. After 5 hr at reflux, the mixture was allowed to cool to room temperature with continuous stirring. The product, α-methylamino-3′,4′-(dipivaloyloxy)acetophenone (IV), was precipitated as the perchlorate salt by the addition of 500 ml of ether. The crude material was purified by dissolving in 75 ml of acetone and precipitating with water (150–200 ml).

Twenty grams (0.044 mole) of IV was dissolved in 300 ml of 95% ethanol in a 500-ml Parr reaction bottle. Then 1.5 g of platinic oxide was added, and the mixture was shaken under hydrogen at 50 psi for 1 hr. After filtration to remove the platinum, the solvent was removed on a rotary evaporator. The resulting oil was mixed with 200 ml of ether. The product (I) separated as a white crystalline material (mp 147–149°) when the ether solution was slowly added to an additional 1200 ml of vigorously stirred ether.

Anal.—Calc. for $C_{19}H_{30}ClNO_9$: C, 50.50; H, 6.69; Cl, 7.85; N, 3.10; O, 31.86. Found: C, 50.51; H, 6.40; Cl, 7.66; N, 3.11; O, 31.88.

The NMR, UV, TLC, and differential scanning calorimetry data were consistent with the proposed structure (I); NMR ($CDCl_3$): δ 6.6–7.4 (m, 5, aromatic and amino), 4.8–5.2 (m, 1, C*H*OH), 4.1–4.3 (d, 1, CHO*H*), 2.9–3.6 (m, 2, CHOHC*H*$_2$), 2.5–2.9 (s, 3, NCH_3), and 1.1–1.5 (s, 18, pivalyl); UV: 263 nm (ε 476); TLC [silica gel with chloroform–methanol–formic acid (30:10:1) and ninhydrin visualizer]: R_f 0.10 (epinephrine), 0.65 (I), and 0.80 (IV).

With differential scanning calorimetry, a single endotherm was observed at the melting point (421° K) of the compound, indicating

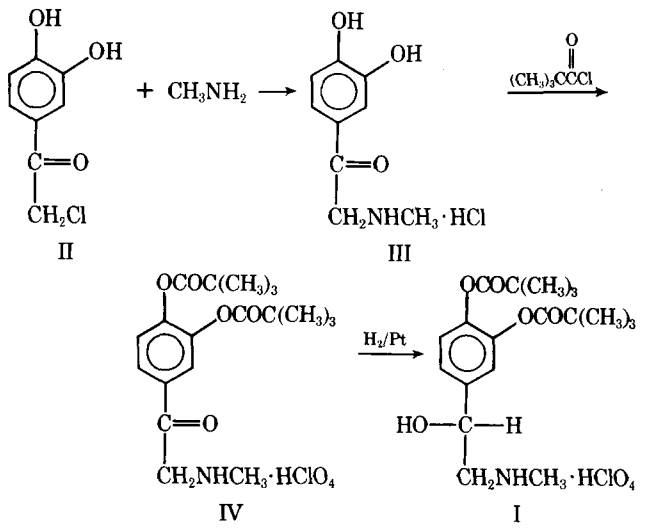

Scheme I

Table I—*In Vitro* Enzymatic Hydrolysis of the Prodrug

Minutes	Percent Hydrolysis in Rabbit Plasma	Human Plasma	Rabbit Eye Homogenate
0	0	0	0
3	12.3	—	—
8	47.7	—	—
10	—	8.0	—
13	58.0	—	—
18	—	24.1	—
20	—	—	2.3
22	96.0	—	—
28	—	47.5	—
32	100	—	—
40	—	—	5.3
45	—	85.8	—
60	—	95.1	18.2
90	—	100	34.0
105	—	—	42.5
150	—	—	68.9
190	—	—	81.8
285	—	—	100

that the material was unitary. The endotherm remained unchanged upon cooling and reheating of the sample (Fig. 1).

Compound I is a racemic mixture and was resolved employing fractional crystallization of the dibenzoyl *d*-bitartrate salt. Sodium dibenzoyl *d*-bitartrate (8.4 g) was dissolved in 200 ml of methanol. Then 20 g of I was dissolved in 200 ml of methanol, and the solution was filtered and diluted with 400 ml of water. The sodium dibenzoyl *d*-bitartrate solution was added to the solution of I, and the total volume was adjusted to 840 ml with 50% aqueous methanol. The solution was cooled slowly (about 0.8°/hr) until the final temperature was 2.6°. The product was recovered by filtration and recrystallized from 50% aqueous methanol. Crystallizations were repeated until the product had a constant specific rotation of −26° and a melting point of 142–143°.

Analytical Procedure—A high-pressure liquid chromatograph[3] with a UV monitor (254 nm) was used. A 1-m × 2.1-mm i.d. stainless steel column, packed with a strong anion-exchange resin[4], was operated at 1200 psi and ambient temperatures, resulting in a flow rate of 1 ml/min. The mobile phase employed was a 0.01 *M* phosphate buffer at pH 7.4. Ten microliters of the appropriate solution (0.4 mg of prodrug/ml of plasma or eye homogenate) was injected and analyzed for epinephrine concentration by comparing the peak area to that of a standard epinephrine solution.

***In Vitro* Enzymatic Rate of Hydrolysis in Rabbit Eye Homogenate**—Upon sacrifice, the eyes of a New Zealand white rabbit were removed and washed thoroughly with cold isotonic saline solution to eliminate any traces of blood. The eyes were then homogenized in a ground-glass homogenizer. The homogenate was subjected to centrifugation for 10 min at 5000 rpm, yielding about 3 ml of a clear supernate. The supernate was transferred to a stoppered test tube and equilibrated to 37°.

After equilibration, a 2-ml sample of the preparation was placed in another tube, mixed with 0.2 ml of a 4-mg/ml aqueous solution of the prodrug, flushed with nitrogen, and maintained at 37°. Ten-microliter aliquots were periodically injected directly onto the liquid chromatographic column, and the liberation of epinephrine was followed as a function of time.

***In Vitro* Enzymatic Rate of Hydrolysis of Prodrug in Human or Rabbit Plasma**—Blood samples (5 ml) were withdrawn and centrifuged immediately. Two milliliters of the plasma was transferred to a stoppered test tube and equilibrated to 37°. After equilibration, 0.2 ml of the 4-mg/ml solution of prodrug was added and the mixture was maintained at 37°. Liberation of epinephrine was followed as already described.

Hydrolysis of Prodrug in Aqueous Humor of Rabbit Eyes—The aqueous humor was obtained from the rabbit eye by puncturing the anterior chamber with a needle and syringe. Fifty microliters of a 4-mg/ml aqueous solution of the prodrug was added to 0.5 ml of the

[3] Du Pont 820.
[4] Zipax SAX, du Pont.

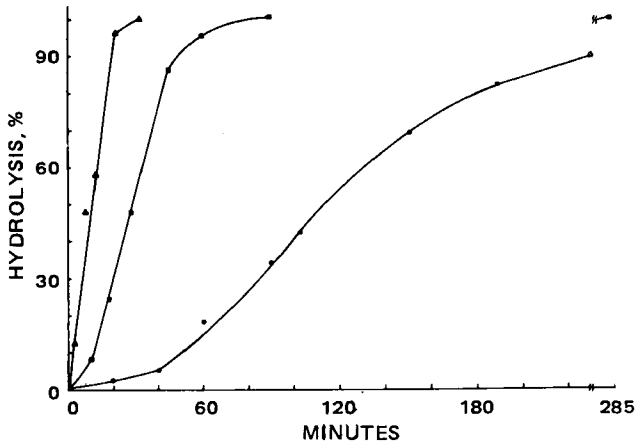

Figure 2—In vitro *enzymatic rate of hydrolysis of the prodrug at 37°. Key: ▲, rabbit plasma; ■, human plasma; and ●, rabbit eye homogenate.*

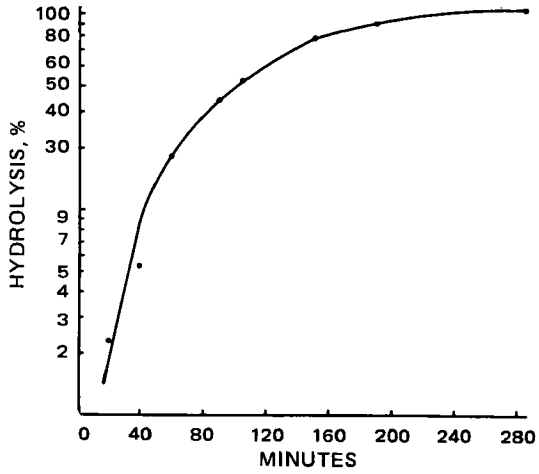

Figure 3—*Semilog plot of the rate of hydrolysis of the prodrug in the rabbit eye homogenate.*

aqueous humor, and the mixture was maintained at 37°. After 3 hr, the mixture was subjected to high-pressure liquid chromatographic analysis.

Effect of Prodrug on Guinea Pig Vas Deferens Preparation—To determine if the dipivaloyl derivative possesses pharmacological activity, its effect on the guinea pig smooth muscle was studied (7). The contraction of the guinea pig vas deferens was determined in the presence of epinephrine, the prodrug, and the product of complete hydrolysis of the prodrug in human plasma.

RESULTS AND DISCUSSION

The described synthetic procedure for the preparation of I appears satisfactory for the production of large batches of the prodrug. The same procedure was successfully applied to the preparation of the corresponding esters of isoproterenol (8) and phenylephrine (9).

Based on the reported clinical superiority of I in the management of glaucoma (4), this approach appears to be significant in improving the pharmacological activity of catecholamines. The fundamental problems with epinephrine, its high polarity and poor lipid solubility, appear to be overcome by the synthesis of the prodrug. In fact, the prodrug approach apparently is the only one capable of enhancing the pharmacological activity of epinephrine while reducing the incidence of its side effects. McClure (4) reported that the prodrug is about 100 times more effective than epinephrine in the management of glaucoma and about 100–400 times weaker than epinephrine in affecting the cardiovascular system of dogs and cats.

The lack of α-adrenergic activity of the prodrug was clearly demonstrated by its lack of activity in the guinea pig vas deferens preparation. However, the activity of epinephrine remained intact after hydrolysis of the pivaloyl groups in human plasma.

The prodrug is relatively stable toward hydrolysis in the absence of enzymes. However, in the presence of enzymes, the prodrug generates epinephrine at an acceptable rate. For example, the prodrug resists hydrolysis in the presence of aqueous humor but regenerates epinephrine in the total eye homogenate. This result may be due to the fact that enzyme levels are as much as 29 times higher in the lens tissue than in the aqueous humor (10).

The results of the hydrolytic study with the rabbit eye homogenate, rabbit plasma, and human plasma are shown in Table I and Fig. 2. These data show that the prodrug cleaves to epinephrine at a reasonable rate.

The *in vivo* cleavage rate may, in fact, be many times faster. A semilog plot of percent hydrolysis in rabbit eye homogenate *versus* time is shown in Fig. 3. It is apparent from these data that the rate of hydrolysis of the prodrug cannot be described by simple first-order kinetics.

Although other esters of epinephrine were made, the data indicate that the pivaloyl prodrug exhibits superior stability when compared to the corresponding acetate derivative (6). The pivalic acid generated upon hydrolysis of the prodrug exhibits a wide margin of safety, even when given orally in large doses (11).

Subsequent reports will investigate the effects of the pivaloyl blocking group on the activity of other catecholamines.

REFERENCES

(1) A. Hussain, M. Yamasaki, and J. E. Truelove, *J. Pharm. Sci.*, **63**, 627(1974).

(2) A. Hussain and J. H. Rytting, *ibid.*, **63**, 798(1974).

(3) V. Stella, T. Higuchi, A. Hussain, and J. Truelove, in "Prodrugs as Novel Drug Delivery Systems," T. Higuchi and V. Stella, Eds., American Chemical Society, Washington, D.C., 1975.

(4) D. A. McClure, in *ibid.*, pp. 224–235.

(5) P. P. Ellis and D. L. Smith, "Handbook of Ocular Therapeutics and Pharmacology," 4th ed., C. V. Mosby, St. Louis, Mo., 1973.

(6) A. Hussain and J. E. Truelove, U.S. pat. 3,809,714 (1974) (to INTERx Research Corp., Lawrence, Kans.).

(7) Staff of the Department of Pharmacology, University of Edinburgh, "Pharmacological Experiments on Isolated Preparations," 2nd ed., E & S Livingstone, London, England, 1970, pp. 108–111.

(8) A. Hussain and J. E. Truelove, U.S. pat. 3,868,461 (1975) (to INTERx Research Corp., Lawrence, Kans.).

(9) A. Hussain and J. E. Truelove, U.S. pat. 3,825,583 (1974) (to INTERx Research Corp., Lawrence, Kans.).

(10) R. Carlin and E. Cotlier, *Invest. Ophthalmol.*, **10**, 887(1971).

(11) D. Dziewiatkowski and H. Lewis, *J. Biol. Chem.*, **158**, 77(1945).

ACKNOWLEDGMENTS AND ADDRESSES

Received August 26, 1975, from *INTERx Research Corporation, Lawrence, KS 66044*, and the *Division of Drug Information and Technology, College of Pharmacy, University of Kentucky, Lexington, KY 40506*

Accepted for publication December 18, 1975.

[x] To whom inquiries should be directed (at the University of Kentucky).

Mass Spectral Analysis of Glucuronides from Sympathomimetic Hydroxyphenylalkylaminoethanols

KARL-HEINZ POOK ˣ, KARL-LUDWIG ROMINGER, and DIETRICH ARNDTS

Abstract □ A mass spectral method is described for the structure determination of glucuronic acid conjugates of hydroxyphenylalkylaminoethanol-type drugs. Trimethylsilylation and application of the GLC–mass spectral technique yield mass spectra with sufficient information for the identification of all structural subunits.

Keyphrases □ Hydroxyphenylalkylaminoethanols—mass spectral analysis of glucuronides □ Glucuronides—hydroxyphenylalkylaminoethanol-type drugs, mass spectral analysis □ Mass spectrometry—analysis, glucuronides from sympathomimetic hydroxyphenylalkylaminoethanols

The identification of glucuronides obviously depends on observations revealing that the role of conjugates is not exclusively one of detoxification (1). Some reports on the GLC properties of urinary steroid glucuronides presented routine separation methods (2, 3). The application of the GLC–mass spectral technique to some glucuronides derived from phenolic and steroidal aglycons showed that this method, in principle, is suitable for direct identification (4). The glucuronides derived from several barbitals (5) and aromatic acids as well as substituted phenols (6) were studied by similar techniques.

Glucuronides (I, R_1 = H, R_2 = alkyl), produced by the primary route of metabolism of the hydroxyphenylalkylaminoethanol-type drugs (II, R_1 = H, R_2 = alkyl), were investigated. The ratio of glucuronized and free drug concentrations determined in blood plasma was up to 9:1. Since a general GLC–mass spectral study (7) on catecholamine-type derivatives (II, R = trimethylsilyl or trifluoroacetyl) yielded mass spectral data for metabolite identification, the derivatizing procedure for trimethylsilyl derivatives and the inlet system conditions were modified to measure the glucuronides (I). To support the mass spectral data obtained from 10 conjugates, deuterated derivatives and one model compound were studied [Table I and Structures V–XIV, R = $Si(CH_3)_3$].

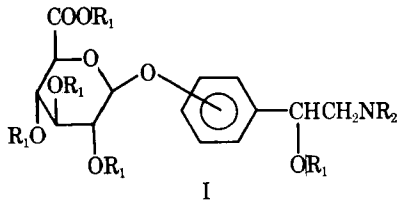

I

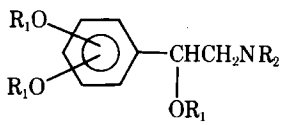

II

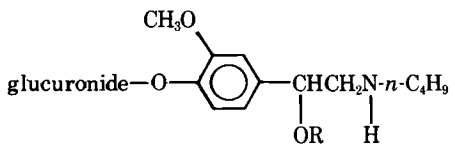

V: M^+775

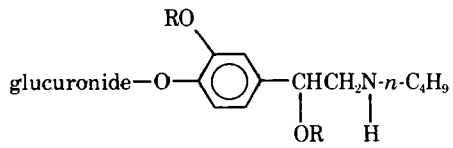

VI: M^+833

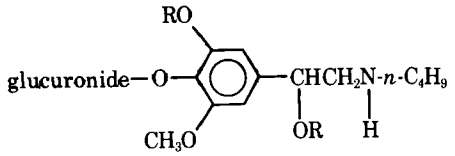

VII: M^+863

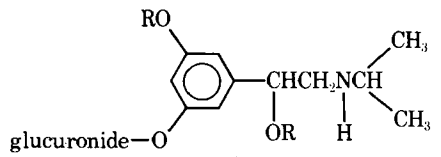

VIII: M^+819

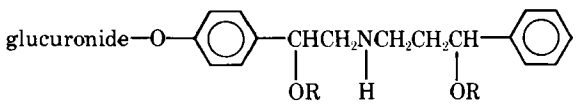

IX: M^+895

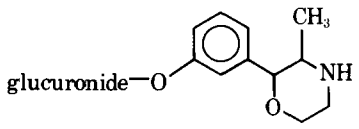

X: M^+657

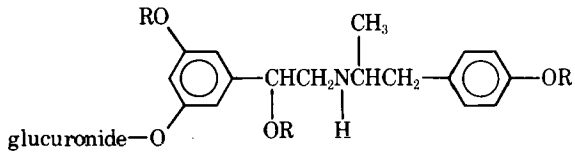

XI: M^+983

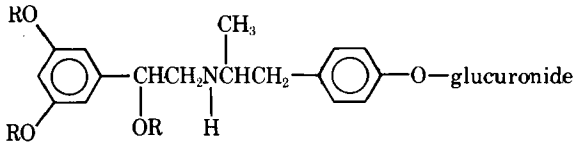

XII: M^+983

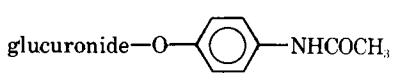

XIII: M^+615

Table I—Mass Spectra Data: *O*-Trimethylsilylglucuronides (*m/e*, Relative Intensity)

Compound	R_1	R_2	M+	M−15	M−15−90(−90)	M−α −90	M−α −465[a]	α	M−Aglycon		Metastable Transitions
III[c]	$Si(CH_3)_3$	n-C_4H_9	745 (16.6)	730 (10.0)	640 (3.8) 550 (0.5)	659 (6.6)	569 (3.6)	267 (88) 268 (22) 195 (90) 196 (37)	86 (95)	375 (100) (c)[b]	465 (2.4)	583.0 561.0 302.5	745 → 659 730 → 640 465 → 375
IIIa	$Si(CD_3)_3$	n-C_4H_9	790 (15.5)	773 (8)	673 (3)	704 (5.8)	605 (3.3)	285 (80) 286 (19) 204 (88) 205 (17)	86 (90)	402 (100) (c')[b]	501 (2)	627.5 322.8	790 → 704 501 → 402
IV[d]	$Si(CH_3)_3$	C_2H_5	717 (18)	702 (10)	612 (1.8)	659 (1.8)	569 (1.3)	267 (23) 268 (93) 195 (78) 196 (65)	58 (90)	375 (100) (c)[b]	465 (3)	606.0 302.5 196.3	717 → 659 465 ↑ 375 717 ↑ 375
IVa	$Si(CD_3)_3$	C_2H_5	762 (15)	744 (7.9)	645 (1.6)	704 (1.6)	605 (1.2)	285 (20) 286 (81) 204 (69) 205 (49)	58 (92)	402 (100) (c')[b]	501 (2.8)	651.0 322.8 212.0	762 → 704 501 ↑ 402 762 ↑ 402
								333 (30) 257 (34) 217 (93) 204 (69)	(c)[b]	360 (29) 275 (30) 235 (90) 204 (65)	(c')[b]		

[a] (M − α) − 465 + $(CH_3)_3Si/H$. [b] Indicates paths *c* and *c'* degradation of 375/402. [c] Glucuronide–O at 4-position; Vasculat (Bamethane), C. H. Boehringer Sohn, West Germany. [d] Glucuronide–O at 3-position; Effortil (Etilefrine), C. H. Boehringer Sohn, West Germany.

EXPERIMENTAL

Isolation and Preparation of Materials—The glucuronides were isolated from rat urine and purified using ion-exchange chromatography and TLC. Column materials and solvents for repeated purification steps were adapted to the various types of conjugates[1].

Additional TLC purification was necessary to isolate IX and X; 20 × 20-cm glass plates precoated with silica gel[2] and 1-butanol–acetic acid–water (50:10:40 v/v) were used. Elution time was up to 72 hr, if required. The fractions eluted were concentrated to dryness by lyophilization. The concentration ratio of radiolabeled drugs and their glucuronides in blood plasma was determined following their chromatographic separation and enzymatic hydrolysis.

Derivatizing Procedure—One milligram of glucuronide was dissolved in 40 μl of pyridine, analytical grade, and 40 μl of *N,O*-bis(trimethylsilyl)acetamide – *N,O*-bis(trimethylsilyl)trifluoroacetamide (50:50) was added. The sample was warmed slightly and kept in a closed vial at room temperature for 5 hr. Glucuronides containing larger substituents, *i.e.*, VIII, required 10–15 hr for derivatization.

GLC–Mass Spectral Conditions—One-microliter volumes were injected, using a gas chromatograph[3] equipped with a 1.50-m × 2-mm i.d. column packed with 1% OV-17 (or 3% OV-17) and operating at a helium flow rate of 25 ml/min. The temperature was programmed between 180 and 330° at 6°/min. The molecular separator[4], kept at 250°, was connected to a mass spectrometer[5] with the source at 220°, the electron energy at 70 ev, and the acceleration voltage at 3 kv. Mass spectra were obtaining by scanning 100 mass units in 2 sec and recorded on an electrostatic recorder[6].

Figure 1 shows typical elution profiles monitored by the total ion current trace, which was also used as a signal for the scan start of the mass spectrometer. In some cases (Fig. 1*a*), a peak at a shorter retention time (peak 1) was present; it was identified as the *O*-trimethylsilyl derivative of the corresponding aglycon. This peak was due to partial cleavage of the glucuronide acetal bond during derivatization. Isomeric glucuronides (Fig. 1*b*) with higher molecular weights were separated satisfactorily.

RESULTS AND DISCUSSION

In molecules such as I, the glucuronic acid moiety and the alkylaminoethanol side chain are linked together by the rather stable benzene ring. Therefore, both structural subunits give rise to a selective and characteristic fragmentation, which is easily extractable from the total pattern and may be correlated with the sugar acid and the aglycon partial structures, respectively. The data from two typical *O*-trimethylsilylglucuronides (III and IV) and their deuterated analogs (III*a* and IV*a*) are summarized in Table I.

The mass spectrum resulting from III (Fig. 2) represents the general pattern consistently observed in all spectra from homologous glucuronides IV–VIII[7]. As shown in Scheme I, three particular sequences can be deduced. The molecular ion, generally appearing with a reasonable intensity, runs through the M − 15 − 90 − 90 sequence (Path *a*), yielding *m/e* 730, 640, and 550. Loss of trimethylsilyl hydroxide from the 1,2-position in the aglycon side chain may contribute to these ions (7, 8). Numerous injections performed in this work demonstrated that there was no need to rely upon a "molecular ion set" as mentioned previously (4).

For unequivocal identification of the aglycon side chain, the *O*-aryl C-1 portion and the sugar acid moiety key fragments formed by paths *b* and *c* are used. Upon C-1–C-2 bond cleavage, the α-fragment, *m/e* 86, and the M − α ion, *m/e* 659, occur. The latter, still containing the sugar acid ring, yields (M − α) − 90, *m/e* 569, with weaker intensity. The main degradation induced by the acetal bond cleavage, as indi-

[1] For III and V–VII, the columns were Zerolit M-IP (SRA-153) and Sephadex QAE-A25 in acetate form; the elution solvent was linear gradient acetic acid–water. For IV, the columns were Amberlite CG-50-I in ammonium form and Zerolit in acetate form; the elution solvent was hydrochloric acid. For VIII (Alupent) and IX, the columns were Amberlite, Zerolit, and Sephadex; the elution solvent was the same as for III. For X, the columns were Amberlite and Sephadex; the elution solvent was the same as for III. For XI (Berotec)–XIII, the columns were Zerolit and Sephadex; the elution solvent was the same as for III.

[2] F-254, Merck 5715/0025.

[3] Varian Aerograph 700.

[4] Watson-Biemann.

[5] Varian-Mat CH-7.

[6] Varian-Statos recorder.

[7] Modifications concerning IV, IV*a*, and VIII are mentioned later.

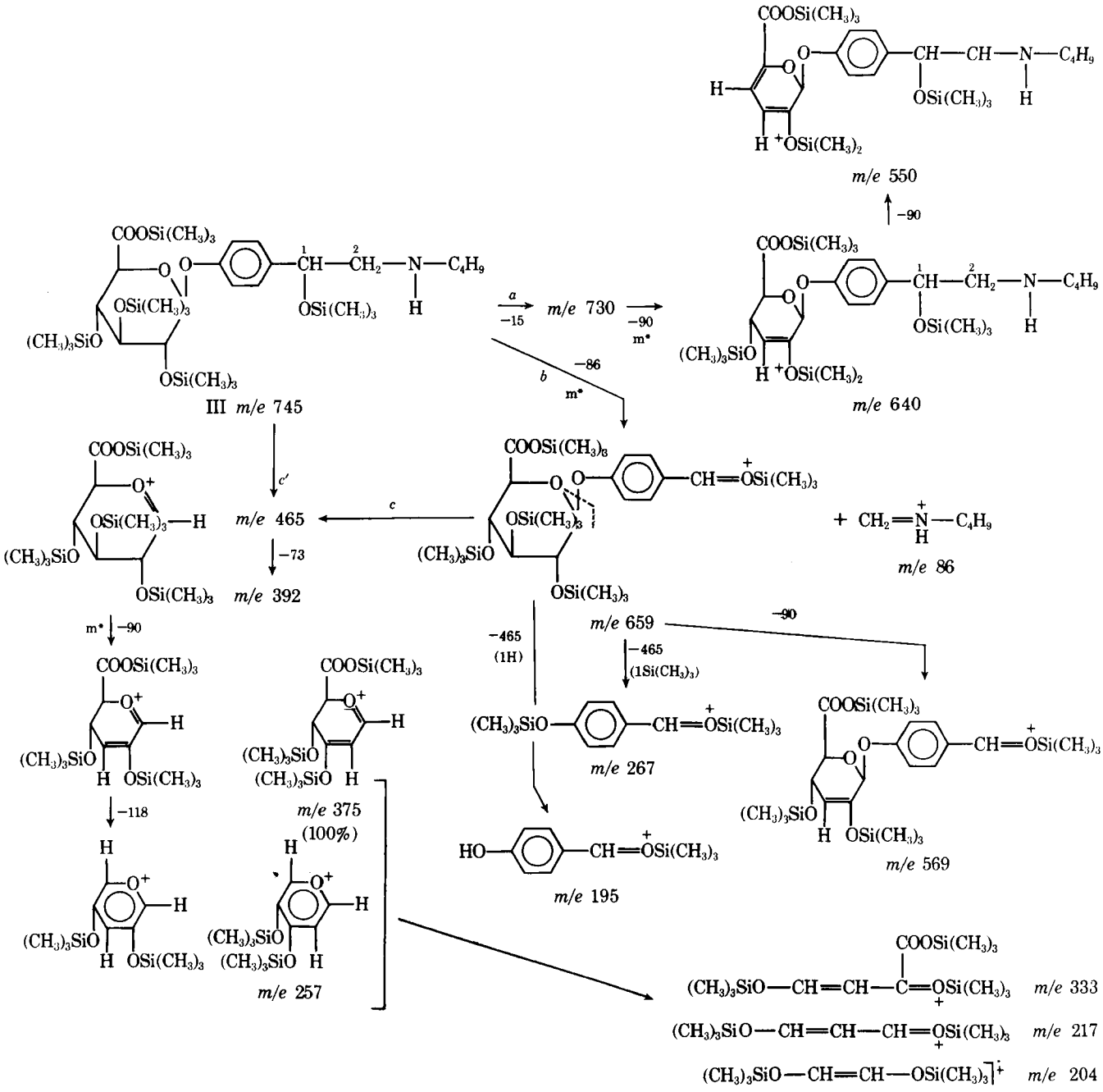

Scheme I

cated, leads to *m/e* 465 and, by stabilization of the residual fragment by trimethylsilyl or proton addition, to *m/e* 267 (7, 9) and 195.

The oxonium ion, *m/e* 465, could also be formed by path *c'* by direct acetal bond cleavage from the molecular ion; the M − 465 residue then undergoes α-cleavage and stabilization to *m/e* 267 and 195 as described. The metastable ion found for the M − α transition, however, indicates that path *b* should be predominant[8].

By multiple loss of trimethylsilyl hydroxide and ring fragmentation of *m/e* 465, the sequence of ions *m/e* 375 (normally the base peak), 333, 257, 217, and 204 is produced selectively, indicating the presence of the silylated glucuronic acid ring. Similar fragmentation was observed when carbohydrate derivatives were examined (9).

As shown in Fig. 2, the sequence resulting in paths *b* and *c* is predominant in the spectrum.

The data from V, VI, and VII clearly correspond to those of III; the appropriate ions are shifted 30, 88, and 119 mass units, respectively. The deuterium-labeled derivative (III*a*) also had the correct mass shifts at the key ions, as listed in Table I.

Glucuronides derived from aglycons with 3′- or 3′,5′-hydroxylation in the benzene ring such as IV, IV*a* (Table I), and VIII show an additional significant feature concerning the C-1–C-2 bond cleavage: the characteristic benzyl fragments (IV and IV*a*) *m/e* 267, 285 and 195, 204 are accompanied by intense peaks *m/e* 268, 286 and 196, 205, respectively (Fig. 3). For example, the ratio of intensity of *m/e* 267/268 as found for III (approximately 80:20) is completely reversed in the spectrum of IV. This result must be due to a markedly favored McLafferty rearrangement (10) for the loss of the C-2 NR portion (Scheme II) in the case of 3′- or 3′,5′-aryl substitution (the latter leading to *m/e* 356/355 due to the second trimethylsilyloxy group on the aryl ring).

Two structural variations concerning the aglycon side chain are illustrated by IX and X. Compound X obviously displays little fragmentation from the morpholine ring, except losing the methyl group and thus probably contributing to the *m/e* 642 ions (Fig. 4). Ions usually found in phenmetrazine (2-phenyl-3-methylmorpholine) mass spectra are completely absent (11). Consequently, the M − 15 frag-

[8] Several transitions are confirmed by metastable peaks, as listed in Table I.

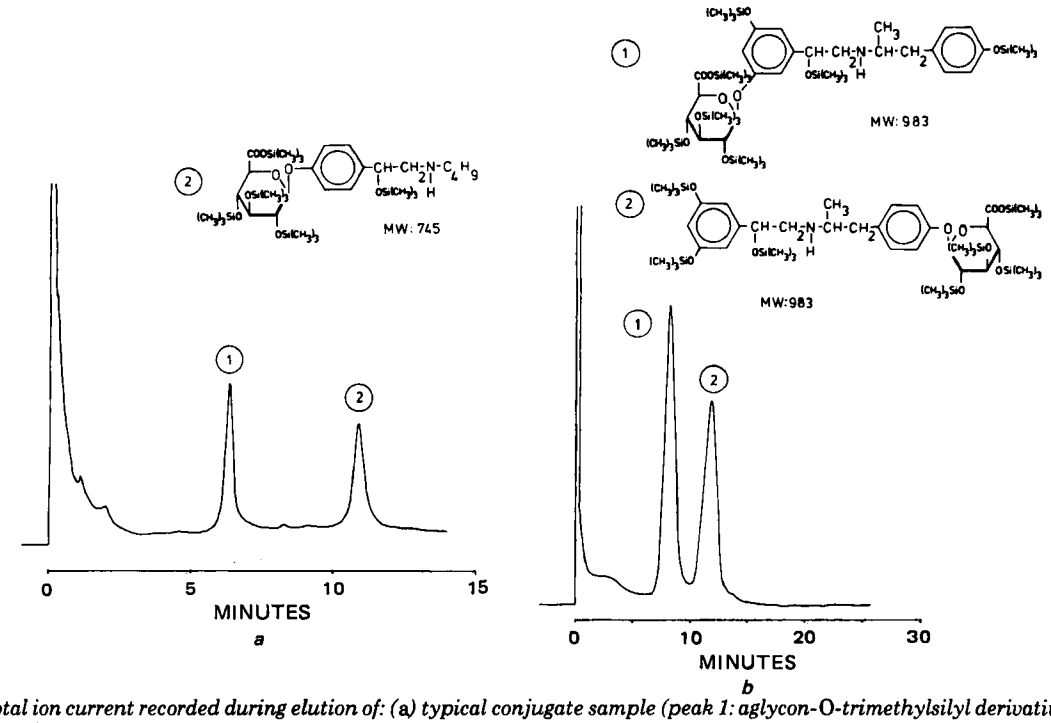

Figure 1—*Total ion current recorded during elution of: (a) typical conjugate sample (peak 1: aglycon-O-trimethylsilyl derivative, programmed at 180–310°, 10°/min); and (b) two isomeric glucuronide derivatives, XI (peak 1) and XII (peak 2).*

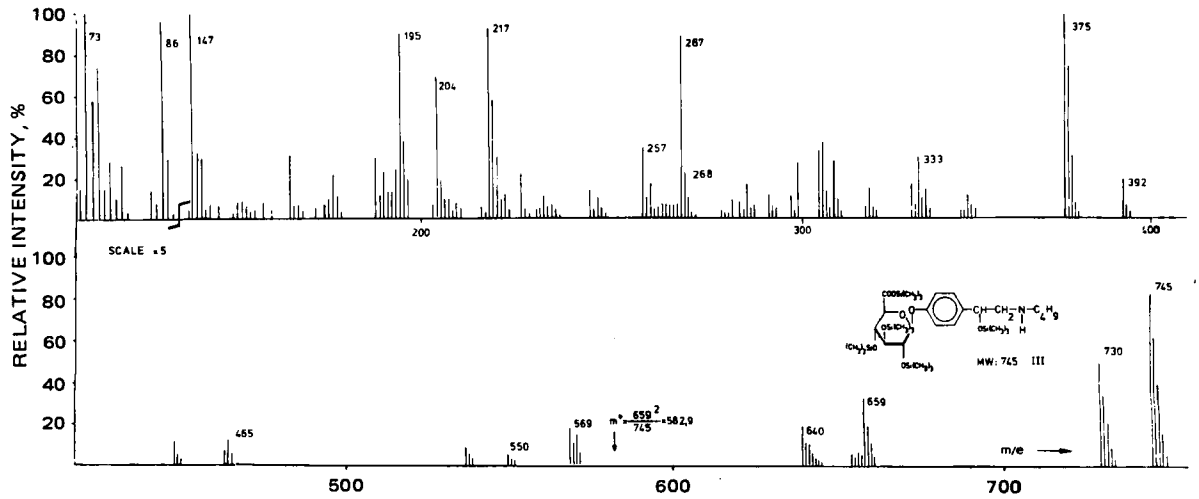

Figure 2—*Mass spectrum of glucuronide derivative III.*

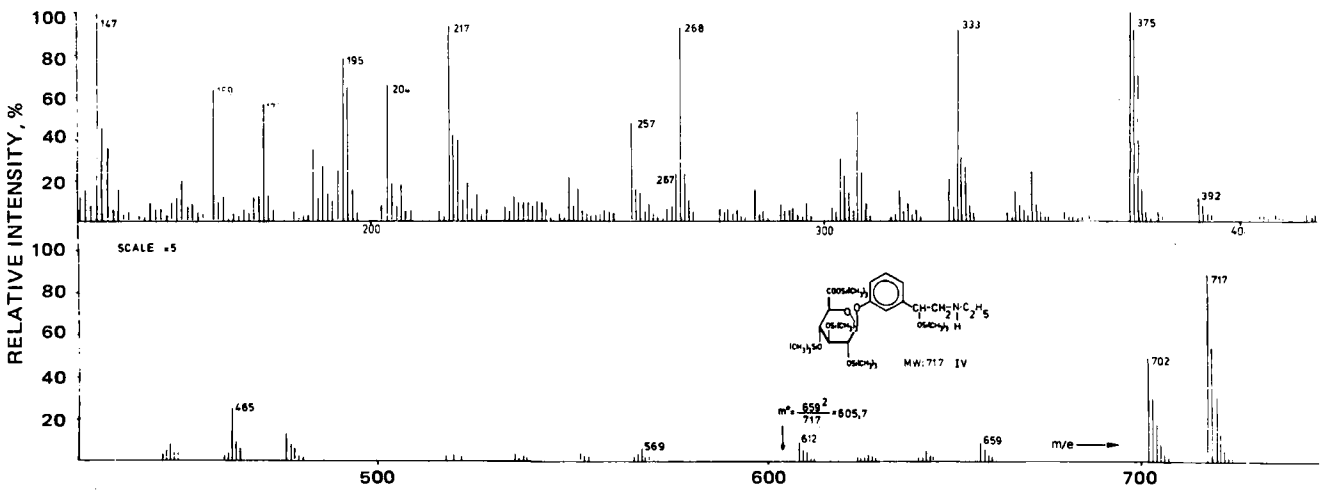

Figure 3—*Mass spectrum of glucuronide derivative IV.*

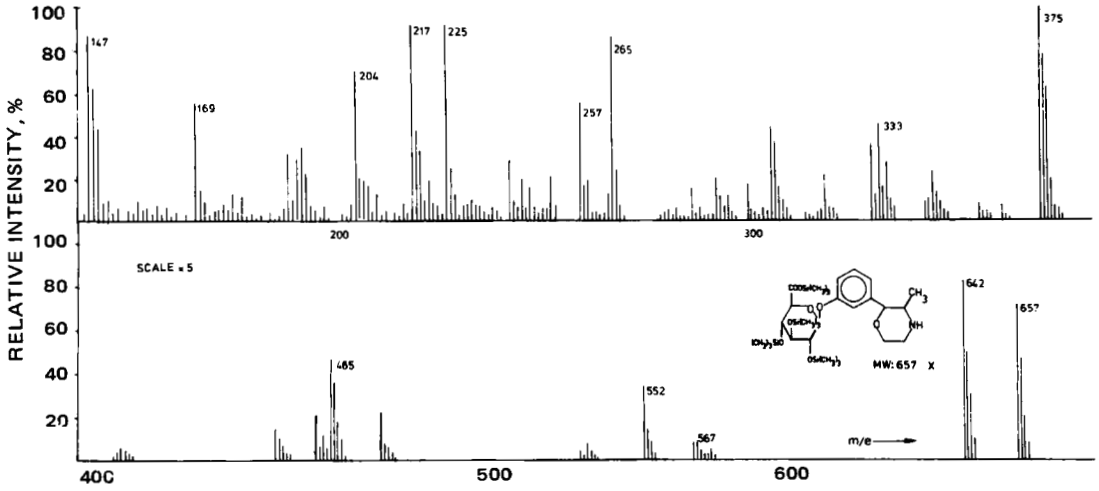

Figure 4—*Mass spectrum of glucuronide derivative X.*

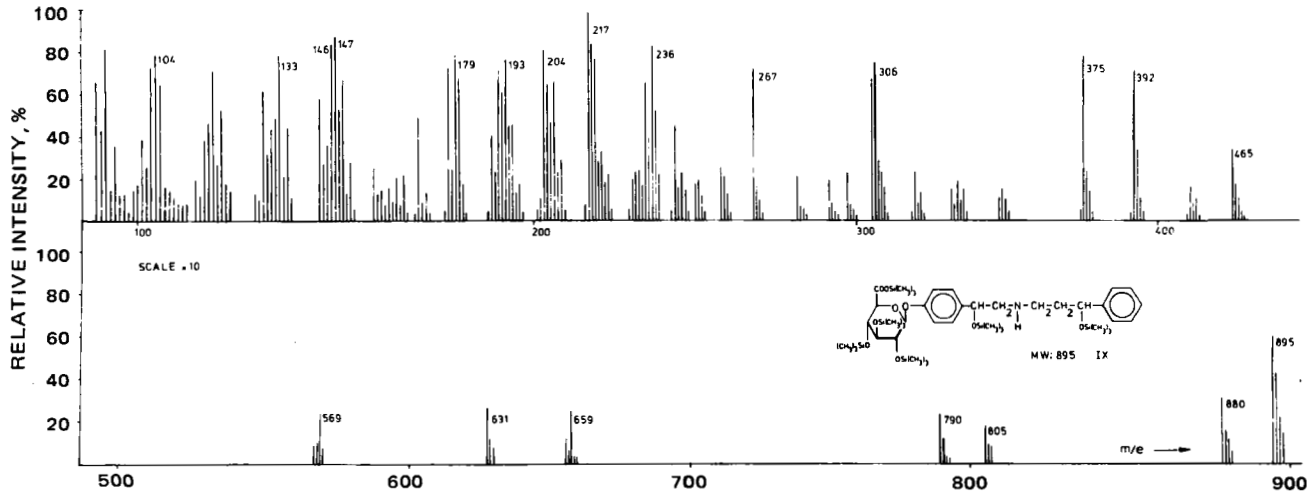

Figure 5—*Mass spectrum of glucuronide derivative IX.*

ment, *m/e* 642 (instead of the M − 15 − α analog), undergoes acetal cleavage followed by trimethylsilyl transfer, as described, to form *m/e* 265; the fragment resulting from proton stabilization, *m/e* 179, is not present in reasonable intensity. This type of spectrum also is observed if glucuronides such as XIII are measured.

Attachment of a phenylhydroxypropyl group at the nitrogen, as is present in IX (Fig. 5 and Scheme III), naturally yields an increased fragmentation within the aglycon portion due to multiple α-cleavage as the ions *m/e* 236, 193, 179, 146, and 104 reveal. The *m/e* 465 degradation sequence is not markedly suppressed in intensity but modified, *m/e* 217 forms the base peak instead of *m/e* 375, and *m/e* 392 (Scheme I and Fig. 2) appears much more intense than in normal glucuronide spectra.

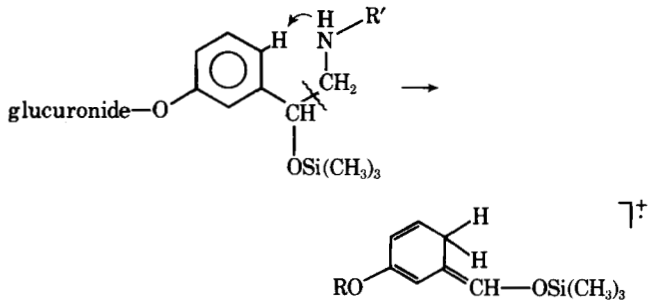

i.e. from IV: R = $Si(CH_3)_3$, *m/e* 268
R = H, *m/e* 196
from IV*a*: R = $Si(CD_3)_3$, *m/e* 286
R = H, *m/e* 205

Scheme II

In a special conjugate sample, originating from a new bronchodilator, a mixture of two glucuronides, XI and XII, could be determined after GLC separation of the trimethylsilyl derivatives (mol. wt. 983). Peak 1 (Fig. 1*b*) was identified as the 3′-conjugate species (Fig. 6). Key ions detecting the arylalkylamino side chain are generated by the first and second α-cleavage, yielding *m/e* 236 and 179, and, in addition, *m/e* 207 from *m/e* 236 by loss of 29.

The M − 179 = *m/e* 804 represents the base peak; M − 236 = *m/e* 747 incorporates the whole glucuronide–*O*-aryl–C-1 moiety. As already described, the typical stabilization steps following the acetal cleavage form *m/e* 283 and 355 (Scheme I, 195, 267). Intense ions at

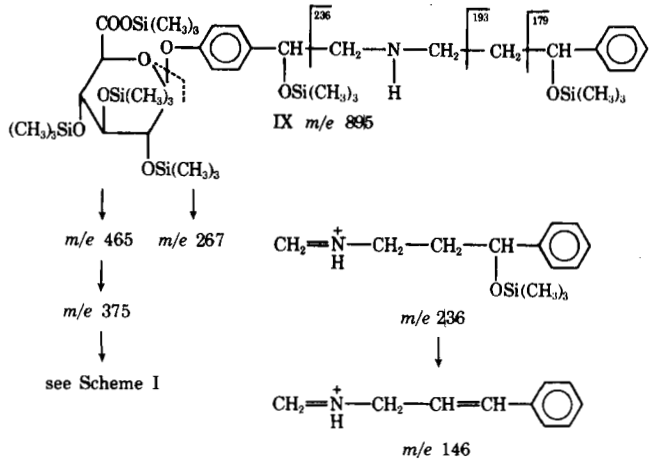

Scheme III

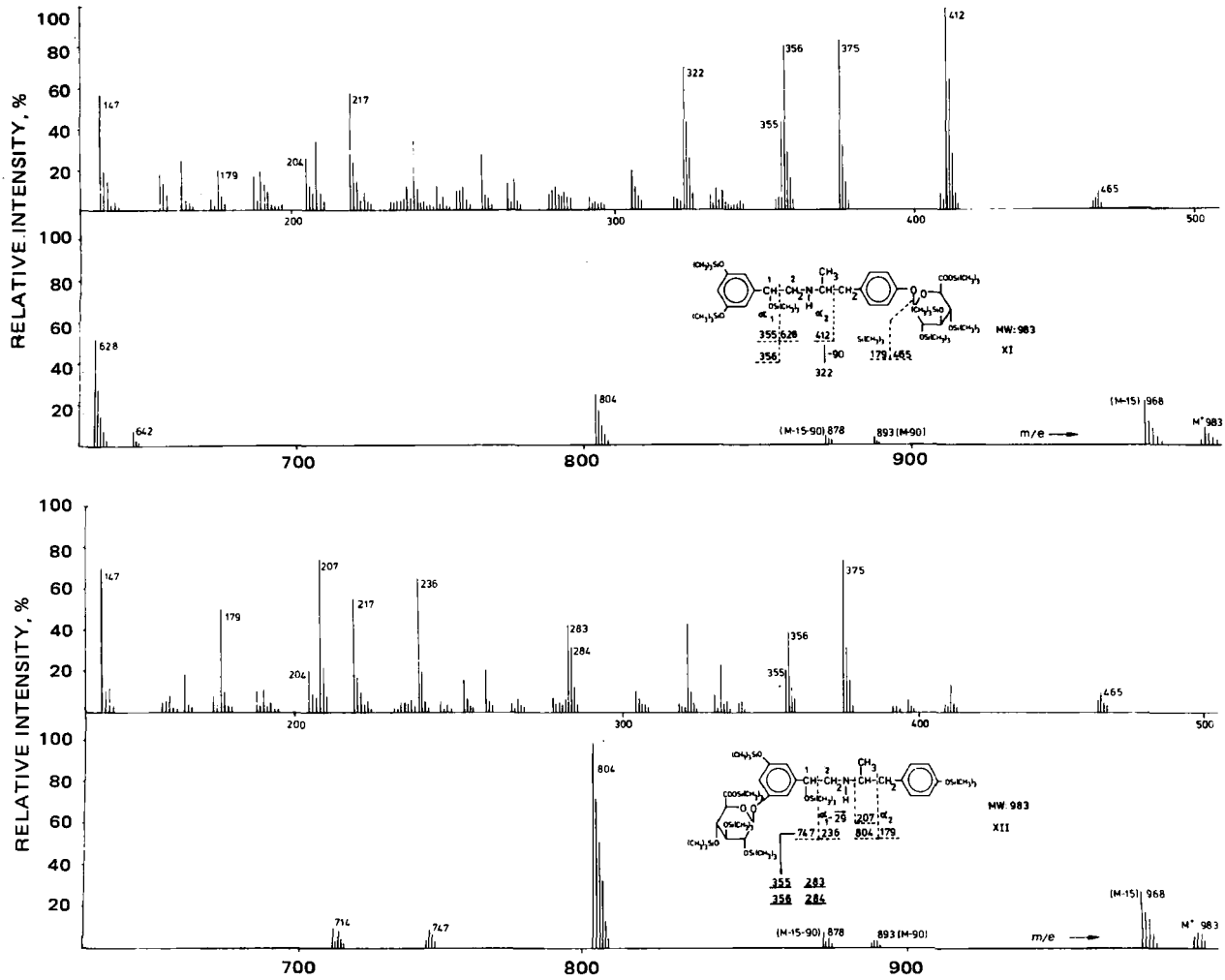

Figure 6—*Mass spectra of the isomeric glucuronide derivatives XI and XII.*

284 and 356 mass units indicate again a predominance of the McLafferty mechanism for the loss of the C-2 NR portion (Scheme II).

The mass spectrum resulting from peak 2 (Figs. 1*b* and 6) demonstrates a different pattern, since the sugar acid portion is attached at the 4′-hydroxyl function in the phenylpropyl moiety. The characteristic ions formed upon double α-cleavage are *m/e* 628 and 412; the latter loses trimethylsilyl hydroxide to give *m/e* 322. The 355/356 ions are present in approximately the same intensity ratio as is found with XI. The M − 412 (α_2) = *m/e* 517 is not detected, obviously due to rapid acetal cleavage/trimethylsilyl transfer forming *m/e* 179. Unequivocal structural differentiation of these more complicated isomeric conjugates is thus performed by interpretation of rather few typical fragments.

CONCLUSION

The method is easy to use for routine identification of 100-μg samples of glucuronides. Work is in progress to improve the mass spectrometric sensitivity and to modify the method for quantitation.

REFERENCES

(1) H. E. Hadd and R. T. Blickenstaff, "Conjugates of Steroid Hormones," Academic, New York, N.Y., 1969, p. 293.

(2) T. Imanari and Z. Tamura, *Chem. Pharm. Bull.*, **15**, 1677(1967).

(3) E. C. Horning, N. Ikekawa, E. M. Chambaz, P. J. Jaakonmaki, and C. J. W. Brooks, *J. Gas Chromatogr.*, **5**, 283(1967).

(4) S. Billets, P. S. Lietman, and C. Fenselau, *J. Med. Chem.*, **16**, 30(1973).

(5) R. M. Thompson, N. Gerber, R. A. Seibert, and D. M. Desiderio, *Drug Metab. Dispos.*, **1**, 489(1973).

(6) J. E. Mrochek and W. T. Rainey, Jr., *Anal. Biochem.*, **57**, 173(1974).

(7) K.-H. Pook, "Proceedings of the International Symposium on Gas Chromatography Spectrometry," Isle of Elba, Italy, 1972, p. 178.

(8) E. Ängård, G. Sedvall, and B. Sjöquist, *J. Chromatogr.*, **52**, 251(1970).

(9) D. C. De Jongh, T. Radford, J. D. Hribar, S. Hribar, S. Hannessian, M. Bieber, G. Dawson, and C. C. Sweeley, *J. Am. Chem. Soc.*, **91**, 1728(1969).

(10) J. D. McCollum and S. Meyerson, *ibid.*, **81**, 4116(1959).

(11) E. Ängård and A. Hankey, *Acta Chem. Scand.*, **23**, 3110(1969).

ACKNOWLEDGMENTS AND ADDRESSES

Received July 28, 1975, from the *Analytical-Research and Biochemistry Department, C. H. Boehringer Sohn, D-6507 Ingelheim/Rhein, West Germany.*

Accepted for publication December 18, 1975.

The authors thank Mr. A. Wittrock, Mr. A. Ziemann, and Mr. J. Krause for expert work in isolating and preparing the samples and in measuring and evaluating the mass spectra. They also thank Dr. W. Deckers, Professor W. Pollmann, and Professor H. Daniel for their interest.

ˣ To whom inquiries should be directed.

In Vitro Release of Therapeutically Active Ingredients from Polymer Matrixes

J. J. SCIARRA *x and S. P. PATEL ‡§

Abstract □ Several therapeutically active ingredients including benzocaine, cyclomethycaine, and methapyrilene hydrochloride were incorporated into ethylcellulose and polyamide films. The effect of cetyl alcohol and tributyl citrate upon the release of these ingredients was studied. The films containing the active ingredient and plasticizer were cast upon a mercury substrate, and the *in vitro* release of these drugs from each film into a desorbing medium of distilled water was measured. The results indicated that the film-forming agent and plasticizer affected the drug release rate and that the release followed first-order kinetics. Benzocaine was slowly released from polyamide–cetyl alcohol films and polyamide–cetyl alcohol–tributyl citrate films. Polyamide–tributyl citrate films showed enhanced release of benzocaine and cyclomethycaine. Ethylcellulose films plasticized with tributyl citrate produced a fast drug release. Based upon these results, a water-soluble, highly polar, noncomplexing additive would tend to increase the drug release from the film. When the amount of benzocaine released from ethylcellulose was plotted as a function of the square root of time, a linear plot was obtained. Since this linear plot passed through the origin, ethylcellulose should be an ideal matrix for benzocaine according to the Higuchi diffusion-controlled model. These studies demonstrated the *in vitro* release of therapeutically active agents from a polymeric film as a function of the solubility of the active agent in both the polymer matrix and the desorbing medium.

Keyphrases □ Polymer matrixes—*in vitro* drug release of benzocaine, cyclomethycaine, and methapyrilene hydrochloride, effect of plasticizers □ Drug release—*in vitro* from polymer matrixes, effect of plasticizers □ Ethylcellulose films—*in vitro* drug release, effect of plasticizers □ Polyamide films—*in vitro* drug release, effect of plasticizers □ Benzocaine—*in vitro* release from polymer matrixes, effect of plasticizers □ Cyclomethycaine—*in vitro* release from polymer matrixes, effect of plasticizers □ Methapyrilene hydrochloride—*in vitro* release from polymer matrixes, effect of plasticizers

Protective films containing therapeutic agents have been used for dermatological, surgical, and cosmetic applications. Several of these preparations have been available in pressurized containers and included the use of cellulose compounds in the management of wounds and general surgical practice (1). A spray-on bandage containing methacrylate resin and thiram dissolved in ethyl acetate has been employed as a dressing for donor sites in skin grafting (2). Ethylcellulose and carboxymethylcellulose sodium with levomycellin and nitrofurazone were employed as bactericidal film-forming liquids in treating cuts and wounds (3). Polymeric films of ethylcellulose and polyamide resins were studied for their potential use as wound dressings and, in particular, their ability to release active ingredients such as gentian violet, benzalkonium chloride, and other antiseptic agents (4, 5).

Films composed of poly(methyl vinyl ether)–maleic anhydride copolymer, cross-linked with polysorbate 20, were reported to be promising for controlling drug release (6). Inert and insoluble matrixes of plastic polymers were shown to exhibit time-dependent release profiles (7). The release rate for sodium salicylate, benzoic acid, caffeine, and benzocaine from a polyethylene matrix was significantly changed when (*a*) different plastics were used, (*b*) the amount of drug in the matrix was changed, (*c*) drug solubility was changed, and (*d*) additives were used. The release rate of gentian violet from various plastic matrixes and different desorbing media was explained by first-order kinetics based on the Whitney–Noyes equation (4–8).

In addition, the mechanism of drug release from an inert insoluble polymeric matrix was described by the Higuchi equation (9, 10). The release of benzoic acid and salicylic acid into an aqueous medium from a wax matrix using both first-order release and the Higuchi diffusion-controlled release model also was investigated (11, 12).

This study concerned the development of a suitable film–plasticizer system containing benzocaine, cyclomethycaine, and methapyrilene hydrochloride that can be applied topically as an aerosol dosage form. Additionally, the release rates of these drugs from the films were determined.

EXPERIMENTAL

Based upon data obtained previously (4), ethylcellulose[1] and a polyamide[2] film were selected for investigation. Their alkali resistance, film hardness, flexibility, water vapor transmission, and insolubility in the desorbing medium were the bases for their selection. Cetyl alcohol and tributyl citrate[3] were used as plasticizers because of their polarity and plasticizing characteristics. Benzocaine[4], cyclomethycaine[5], and methapyrilene hydrochloride[5] were used as the model drugs.

Preparation of Drug–Film Matrix—The films were prepared from a 5% (w/w) solution of the film-forming agents and plasticizers. Ethylcellulose was dissolved in absolute alcohol, and the polyamide resin was dissolved in 2-propanol. A specific amount of drug was added to the plasticized polymer solution (concentration ranging from 150 to 200 mg/5 g of resin solids) so that the resulting solutions formed a good film without any cracks or fissures and contained sufficient drug for the drug release measurements.

The films were cast using the previously developed mercury substrate technique (4), and the drug-containing films were stored in a desiccator overnight. The drug–polymer-pretreated film (4.5 cm in diameter) was mounted onto the flat surface of a glass stopper using an epoxy-bonding cement as previously described (4). The film was then immersed in the drug release apparatus (Fig. 1). The flat head of the glass stopper was suspended in a water-jacketed, 400-ml capacity beaker containing 300 ml of distilled water at 37 ± 0.5°. Two such units were used.

The compositions of the films used for the drug release profile are shown in Table I. Two plasticizers at different concentration levels were used to determine the effect of both the nature and the concentration of the plasticizer on the drug release rate profile.

At selected time intervals over 6–8 hr, samples of the desorbing medium were removed and assayed spectrophotometrically[6] for the released drug at 294, 264, and 244 nm for benzocaine, cyclomethycaine

[1] Hercules, Inc., Wilmington, Del.
[2] Emerez 1155, Emery Industries, Cincinnati, Ohio.
[3] Citroflex-4, Chas. Pfizer and Co., Brooklyn, N.Y.
[4] Mallinckrodt Chemical Works, St. Louis, Mo.
[5] Eli Lilly & Co., Indianapolis, Ind.
[6] Coleman-Hitachi model 124 double-beam spectrophotometer.

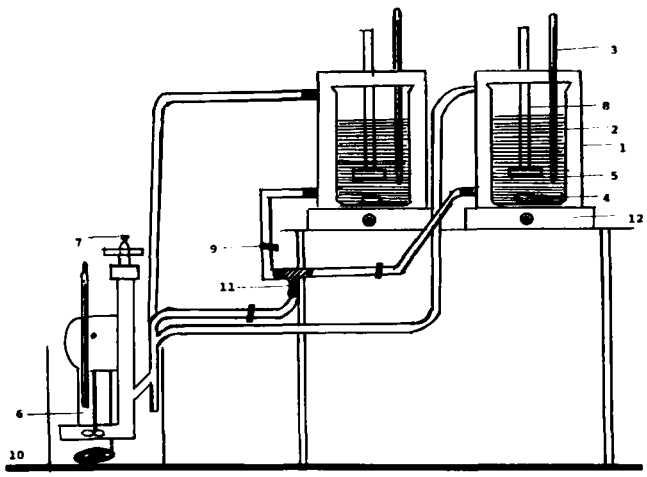

Figure 1—*Schematic diagram for* in vitro *drug release determination. Key: 1, plastic jar; 2, 400-ml beaker; 3, thermometer; 4, magnetic stirrer; 5, model drug film; 6, water circulating pump; 7, temperature variable; 8, plastic rod with a glass stopper; 9, pinch cock; 10, heating element; 11, glass T-tube; and 12, magnetic stirrer control.*

sulfate, and methapyrilene hydrochloride, respectively. The volume of desorbing medium removed (10 ml) from the release cell was replaced by an equal volume of desorbing medium, previously equilibrated at 37°. A cumulative correction was made for the previously removed samples in determining the total amount dissolved according to the following formula:

$$C_n = C_n \text{ meas} + \frac{10}{300} \times \sum_{s=1}^{n-1} C_s \text{ meas} \qquad \text{(Eq. 1)}$$

where C_n meas is the spectrophotometrically measured concentration, C_n is the concentration of the nth sampling expected in the medium if previous samples had not been removed, $n - 1$ is the total volume of all samples removed prior to the sample being measured, and C_s meas is the total of all spectrophotometrically measured concentrations at $n - 1$ samples (13).

Two to four determinations were performed on each sample. When a linear relationship was expected according to first-order kinetics, the data were treated by the least-squares method and the lines of best fit were reported using a multiaccess computer. The initial concentration of benzocaine, cyclomethycaine sulfate, or methapyrilene hydrochloride was determined spectrophotometrically by dissolving a 4.5-cm disk of the film in 1-butanol (Figs. 2–7 and Table II).

DISCUSSION

It is evident from the results that the nature of the film-forming agent affects the rate of drug release. Values of log A (drug remaining in the film) were plotted as a function of time. The linearity of these plots indicated that the drug release apparently followed first-order kinetics (Figs. 2–5). Figures 2 and 3 show the release rate profiles of benzocaine from ethylcellulose and polyamide films plasticized with varying concentrations of either tributyl citrate or cetyl alcohol. Similarly, the amounts of drug released from the polyamide film as a function of time for cyclomethycaine sulfate and methapyrilene

Table I—Film System Selected for Drug Release Studies

Film	Polymer	Plasticizer (parts per hundred)
1	Ethylcellulose	None
2	Ethylcellulose	Tributyl citrate (10)
3	Ethylcellulose	Tributyl citrate (20)
4	Ethylcellulose	Cetyl alcohol (20)
5	Ethylcellulose	Cetyl alcohol (30)
6	Ethylcellulose	Tributyl citrate–cetyl alcohol (10 and 10)
7	Polyamide	Tributyl citrate (20)
8	Polyamide	Cetyl alcohol (20)
9	Polyamide	Tributyl citrate–cetyl alcohol (10 and 10)

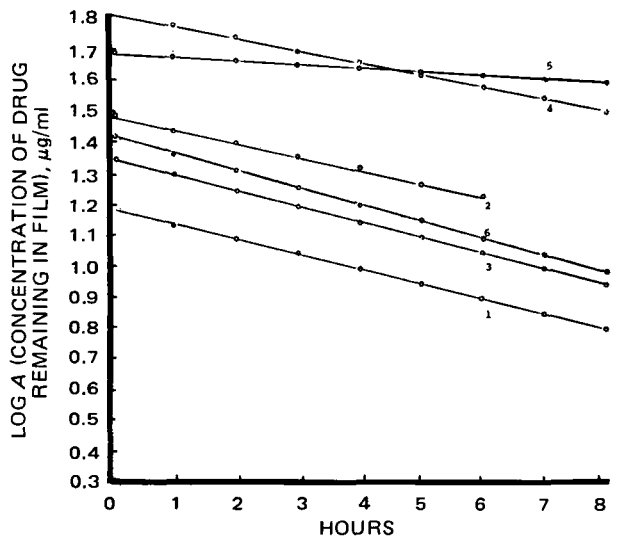

Figure 2—*Release of benzocaine from ethylcellulose films. Key: 1, unplasticized; 2, tributyl citrate (10 parts per hundred); 3, tributyl citrate (20 parts per hundred); 4, cetyl alcohol (20 parts per hundred); 5, cetyl alcohol (30 parts per hundred); and 6, tributyl citrate–cetyl alcohol (10 and 10 parts per hundred).*

hydrochloride are illustrated in Figs. 4 and 5. The incorporation of methapyrilene hydrochloride in the ethylcellulose film resulted in a film that could not be cast due to an incompatibility between ethylcellulose and the drug.

The rate constant and half-life for the release of each drug were calculated from the slope of these lines according to:

$$k = \text{slope} \times 2.303 \qquad \text{(Eq. 2)}$$

$$t_{1/2} = \frac{0.693}{k} \qquad \text{(Eq. 3)}$$

and are shown in Table II. Benzocaine was slowly released from the polyamide films plasticized with cetyl alcohol and a mixture of cetyl alcohol–tributyl citrate. Polyamide film plasticized with tributyl ci-

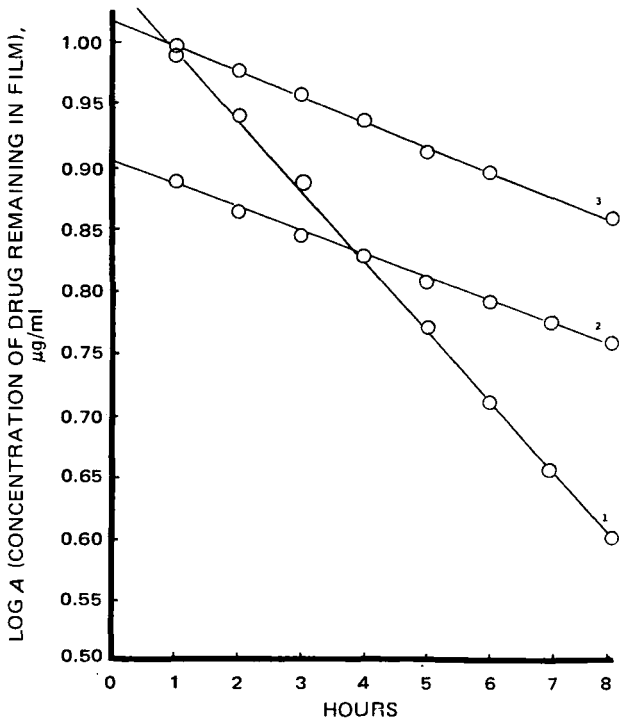

Figure 3—*Release of benzocaine from polyamide resin films. Key: 1, tributyl citrate (20 parts per hundred); 2, cetyl alcohol (20 parts per hundred); and 3, tributyl citrate–cetyl alcohol (10 and 10 parts per hundred).*

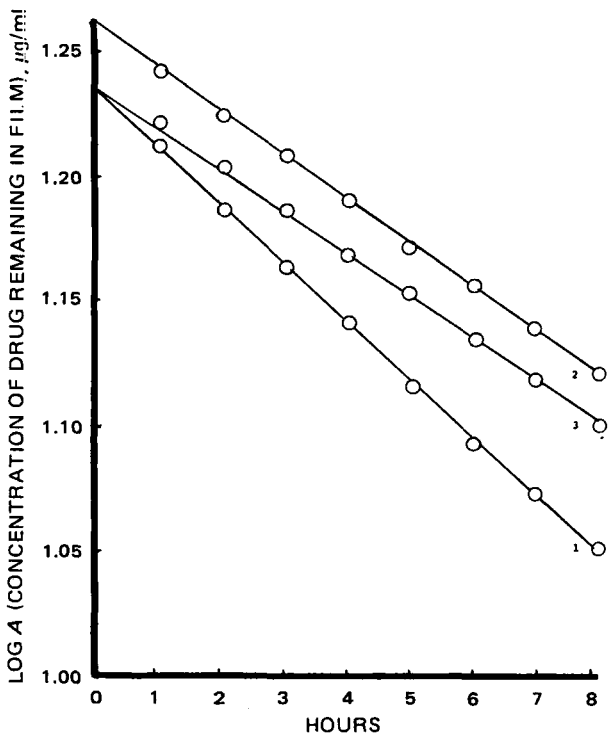

Figure 4—*Release of cyclomethycaine from polyamide resin films. Key: see Fig. 3.*

trate showed enhanced benzocaine and cyclomethycaine release. Ethylcellulose films plasticized with tributyl citrate produced a fast drug release profile. This finding indicated that water-soluble, highly polar, noncomplexing additives (plasticizers or film modifiers) would tend to increase the drug release from the film.

When the amount of drug released was plotted as a function of the square root of time, a linear plot was obtained for benzocaine from an ethylcellulose film (Fig. 6). Since this linear plot passes through the origin, ethylcellulose would be an ideal matrix for benzocaine according to the Higuchi diffusion-controlled model. The diffusion-controlled drug release data were plotted, and the value of the slope obtained from the plot of the logarithm of the amount of drug released per unit surface area *versus* the logarithm of time supports the diffusion-controlled drug release mechanism (Fig. 7).

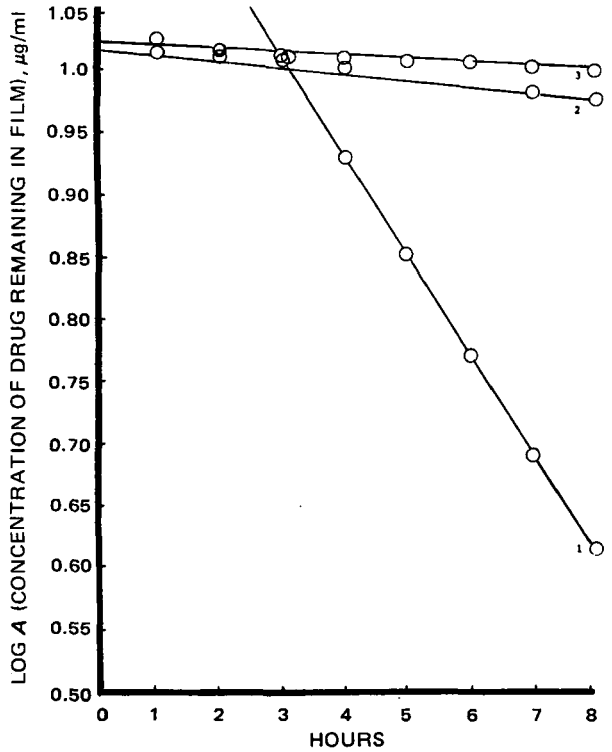

Figure 5—*Release of methapyrilene hydrochloride from polyamide resin films. Key: see Fig. 3.*

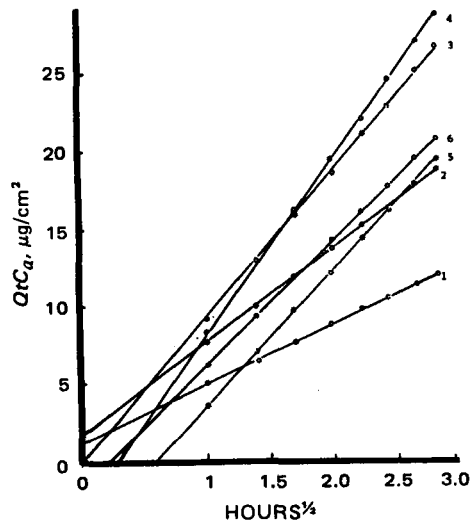

Figure 6—*Release profile of benzocaine plotted according to the diffusion model* (QtC_a = *corrected concentration of the drug released at time* t). *Key: see Fig. 2.*

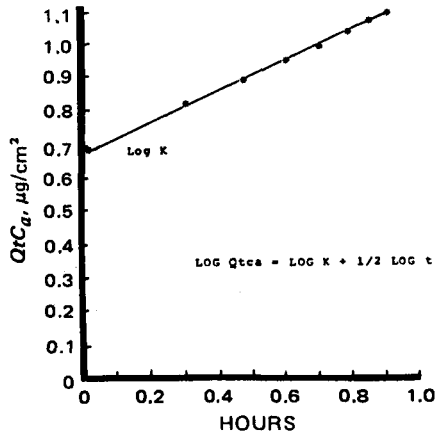

Figure 7—*Confirmation of diffusion-controlled drug release benzocaine–ethylcellulose system.*

Table II—Parameters for Release of Therapeutically Active Ingredients from Polymeric Films in Demineralized Water

Drug	Film	Slope × 10^{-2}	$K \times 10^{-2a}$, hr^{-1}	$t_{1/2}$, hr
Benzocaine	1	3.32	7.65	9.0
	2	3.00	6.90	10.0
	3	4.88	11.23	6.1
	4	2.54	5.84	11.8
	5	9.79	2.26	30.7
	6	5.18	11.94	5.8
	7	5.77	13.28	5.2
	8	1.93	4.44	15.5
	9	1.97	4.53	15.3
Cyclomethycaine sulfate	3	19.06	43.90	1.5
	6	2.40	5.52	12.5
	7	2.28	5.26	13.1
	8	1.69	3.90	17.7
	9	1.73	3.99	17.3
Methapyrilene hydrochloride	7	8.18	18.85	3.6
	8	3.43	7.90	8.7
	9	2.51	5.78	11.9

[a] First-order rate constant.

CONCLUSION

This study demonstrated a simple method that was useful for the determination of the release of certain drugs from a polymer–plasticizer combination. The drug release data indicated the usability of ethylcellulose and polyamide films. An ethylcellulose–tributyl citrate combination proved to be an excellent matrix for benzocaine. Cyclomethycaine could be incorporated into an ethylcellulose and polyamide film while methapyrilene hydrochloride was found to be incompatible with ethylcellulose.

A kinetic study of the release of benzocaine from ethylcellulose showed that the diffusion mechanism was operative according to the Higuchi diffusion-controlled model where the rate of release was inversely proportional to the concentration of drug released. The release rates were changed significantly with cetyl alcohol or tributyl citrate at different concentrations. These studies demonstrated the release of therapeutically active agents from polymeric film into the surrounding medium. The medicinal agent must be sufficiently insoluble in the film to allow for its release into the surrounding medium but not so soluble as to remain preferentially in the film.

REFERENCES

(1) J. M. Miller, M. Grinberg, and G. E. McElfatrick, *Arch. Surg.*, **82,** 326(1961).

(2) "Resifilm, Squibb Surgical Spray Dressing," *Tech. Bull. A*, **May 1964,** 6905.

(3) I. A. Istomina, S. A. Botvinik, and P. E. Rozentsveig, *Sb. Nauchn. Tr. Vitebsk. Gos. Med. Inst.*, **11,** 171(1964).

(4) J. J. Sciarra and R. Gidwani, *J. Soc. Cosmet. Chem.*, **21,** 667(1970).

(5) E. Marcus, H. K. Kim, and J. Autian, *J. Am. Pharm. Assoc., Sci. Ed.*, **48,** 457(1959).

(6) A. L. Fites, G. S. Banker, and V. F. Smolen, *J. Pharm. Sci.*, **59,** 610(1970).

(7) S. J. Desai, A. P. Simonelli, and W. I. Higuchi, *ibid.*, **54,** 1459(1965).

(8) A. A. Noyes and W. R. Whitney, *J. Amer. Chem. Soc.*, **19,** 930(1897).

(9) T. Higuchi, *J. Pharm. Sci.*, **52,** 1145(1963).

(10) *Ibid.*, **50,** 874(1961).

(11) J. B. Schwartz, A. P. Simonelli, and W. I. Higuchi, *J. Pharm. Sci.*, **57,** 274(1968).

(12) *Ibid.*, **57,** 278(1968).

(13) D. E. Wurster and P. W. Taylor, Jr., *J. Pharm. Sci.*, **54,** 670(1965).

ACKNOWLEDGMENTS AND ADDRESSES

Received April 15, 1975, from the *Brooklyn College of Pharmacy, Long Island University, Brooklyn, NY 11216, and the ‡College of Pharmacy and Allied Health Professions, St. John's University, Jamaica, NY 11439

Accepted for publication January 9, 1976.

Presented at the Industrial Pharmaceutical Technology Section, APhA Academy of Pharmaceutical Sciences, San Francisco meeting, April 24, 1975.

§ Present address: Schering Corporation, Kenilworth, NJ 07033

ˣ To whom inquiries should be directed.

NOTES

Automated Analysis of Warfarin Sodium Tablets

S. HANNA ˣ, G. DZUS, L. RASERO, and L. LACHMAN

Abstract □ An automated procedure was developed for the determination of warfarin sodium by following the steps of the manual USP procedure. The automated procedure is applicable to single tablets and composites of 20 tablets at different tablet concentrations. Sensitivity, precision, accuracy, and reproducibility are equivalent to the manual USP procedure. Sensitivity was approximately 15 μg/ml, with a coefficient of variation of 0.711%.

Keyphrases □ Warfarin sodium—automated analysis, commercial dosage forms □ Automated analyses—warfarin sodium, commercial dosage forms □ Anticoagulants—warfarin sodium, commercial dosage forms

The semiautomated method recognized officially by the Association of Official Analytical Chemists (1–3) is an adaptation of the USP compendial assay (4) for warfarin sodium tablets. This semiautomated method uses suspensions of either single tablets or portions of tablet composites equivalent to single tablets. The preparation of these suspensions requires the disintegration of individual tablets or dispersion of weighed composites in an accurately measured volume of 0.01 *N* NaOH to give a drug concentration of 0.1 mg/ml. Homogenization of the sample is achieved by using an ultrasonic generator for at least 10 min with intermittent swirling and letting the suspension stand for 1.5 hr with occasional mixing. An aliquot of the homogenized sample is then transferred to the automatic analyzer.

This report discusses an automated system that follows the manual USP procedure and saves the labor and time consumed in the semiautomated method.

EXPERIMENTAL

Apparatus—The analytical system consisted of the following modules: solid sampler II[1], programmed at 20/hr, homogenizing speed 3, and stir speed 1; proportioning pump III[1]; a continuous filter[1], speed

[1] Technicon Corp., Tarrytown, N.Y.

CONCLUSION

This study demonstrated a simple method that was useful for the determination of the release of certain drugs from a polymer–plasticizer combination. The drug release data indicated the usability of ethylcellulose and polyamide films. An ethylcellulose–tributyl citrate combination proved to be an excellent matrix for benzocaine. Cyclomethycaine could be incorporated into an ethylcellulose and polyamide film while methapyrilene hydrochloride was found to be incompatible with ethylcellulose.

A kinetic study of the release of benzocaine from ethylcellulose showed that the diffusion mechanism was operative according to the Higuchi diffusion-controlled model where the rate of release was inversely proportional to the concentration of drug released. The release rates were changed significantly with cetyl alcohol or tributyl citrate at different concentrations. These studies demonstrated the release of therapeutically active agents from polymeric film into the surrounding medium. The medicinal agent must be sufficiently insoluble in the film to allow for its release into the surrounding medium but not so soluble as to remain preferentially in the film.

REFERENCES

(1) J. M. Miller, M. Grinberg, and G. E. McElfatrick, *Arch. Surg.*, **82,** 326(1961).

(2) "Resifilm, Squibb Surgical Spray Dressing," *Tech. Bull. A*, **May 1964,** 6905.

(3) I. A. Istomina, S. A. Botvinik, and P. E. Rozentsveig, *Sb. Nauchn. Tr. Vitebsk. Gos. Med. Inst.*, **11,** 171(1964).

(4) J. J. Sciarra and R. Gidwani, *J. Soc. Cosmet. Chem.*, **21,** 667(1970).

(5) E. Marcus, H. K. Kim, and J. Autian, *J. Am. Pharm. Assoc., Sci. Ed.*, **48,** 457(1959).

(6) A. L. Fites, G. S. Banker, and V. F. Smolen, *J. Pharm. Sci.*, **59,** 610(1970).

(7) S. J. Desai, A. P. Simonelli, and W. I. Higuchi, *ibid.*, **54,** 1459(1965).

(8) A. A. Noyes and W. R. Whitney, *J. Amer. Chem. Soc.*, **19,** 930(1897).

(9) T. Higuchi, *J. Pharm. Sci.*, **52,** 1145(1963).

(10) *Ibid.*, **50,** 874(1961).

(11) J. B. Schwartz, A. P. Simonelli, and W. I. Higuchi, *J. Pharm. Sci.*, **57,** 274(1968).

(12) *Ibid.*, **57,** 278(1968).

(13) D. E. Wurster and P. W. Taylor, Jr., *J. Pharm. Sci.*, **54,** 670(1965).

ACKNOWLEDGMENTS AND ADDRESSES

Received April 15, 1975, from the *Brooklyn College of Pharmacy, Long Island University, Brooklyn, NY 11216, and the ‡College of Pharmacy and Allied Health Professions, St. John's University, Jamaica, NY 11439

Accepted for publication January 9, 1976.

Presented at the Industrial Pharmaceutical Technology Section, APhA Academy of Pharmaceutical Sciences, San Francisco meeting, April 24, 1975.

§ Present address: Schering Corporation, Kenilworth, NJ 07033

ˣ To whom inquiries should be directed.

NOTES

Automated Analysis of Warfarin Sodium Tablets

S. HANNA ˣ, G. DZUS, L. RASERO, and L. LACHMAN

Abstract □ An automated procedure was developed for the determination of warfarin sodium by following the steps of the manual USP procedure. The automated procedure is applicable to single tablets and composites of 20 tablets at different tablet concentrations. Sensitivity, precision, accuracy, and reproducibility are equivalent to the manual USP procedure. Sensitivity was approximately 15 μg/ml, with a coefficient of variation of 0.711%.

Keyphrases □ Warfarin sodium—automated analysis, commercial dosage forms □ Automated analyses—warfarin sodium, commercial dosage forms □ Anticoagulants—warfarin sodium, commercial dosage forms

The semiautomated method recognized officially by the Association of Official Analytical Chemists (1–3) is an adaptation of the USP compendial assay (4) for warfarin sodium tablets. This semiautomated method uses suspensions of either single tablets or portions of tablet composites equivalent to single tablets. The preparation of these suspensions requires the disintegration of individual tablets or dispersion of weighed composites in an accurately measured volume of 0.01 *N* NaOH to give a drug concentration of 0.1 mg/ml. Homogenization of the sample is achieved by using an ultrasonic generator for at least 10 min with intermittent swirling and letting the suspension stand for 1.5 hr with occasional mixing. An aliquot of the homogenized sample is then transferred to the automatic analyzer.

This report discusses an automated system that follows the manual USP procedure and saves the labor and time consumed in the semiautomated method.

EXPERIMENTAL

Apparatus—The analytical system consisted of the following modules: solid sampler II[1], programmed at 20/hr, homogenizing speed 3, and stir speed 1; proportioning pump III[1]; a continuous filter[1], speed

[1] Technicon Corp., Tarrytown, N.Y.

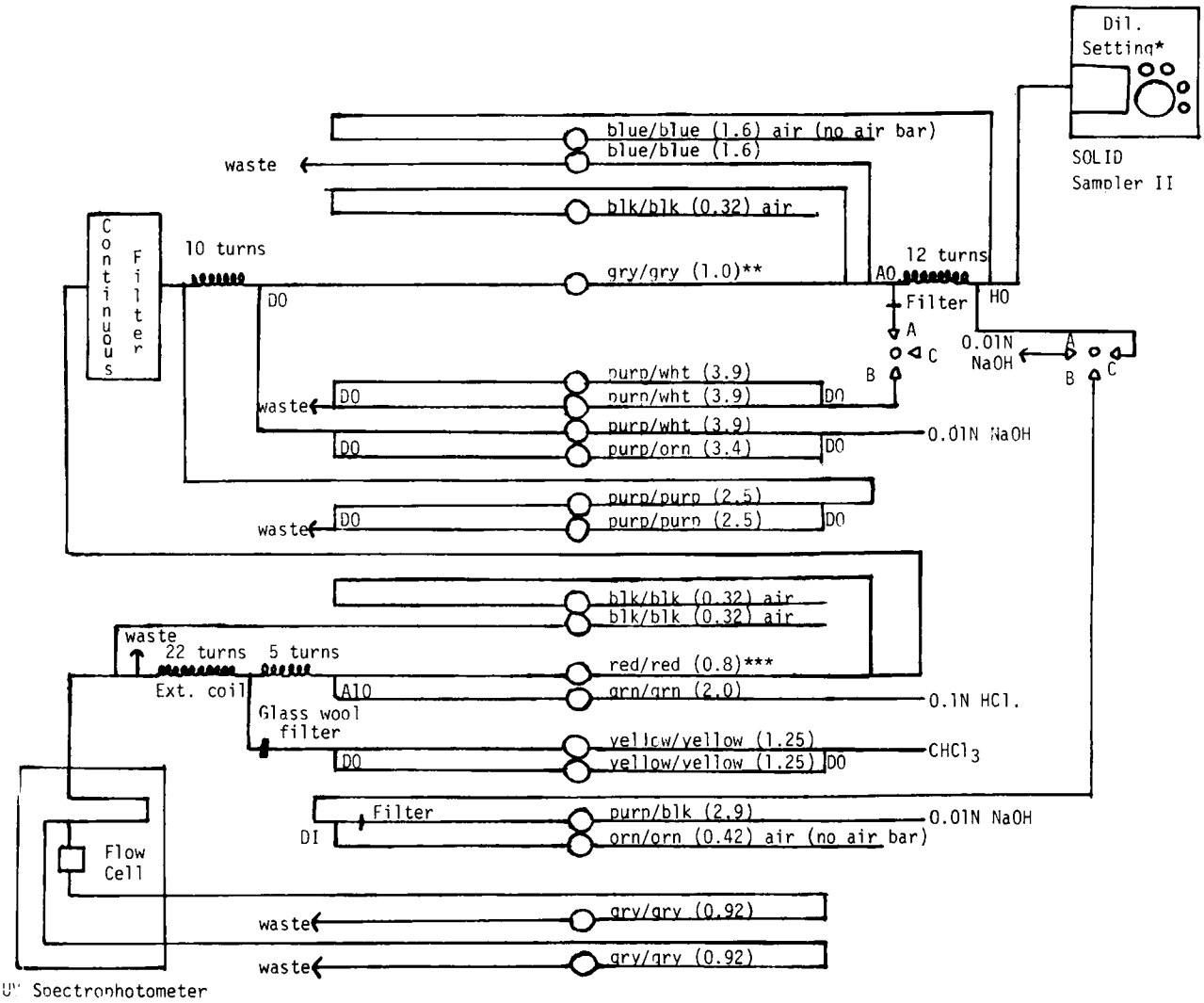

Figure 1—*Schematic diagram of the automated system for warfarin sodium analysis. * Diluent setting is adjusted to obtain absorbance between 0.4 and 0.6. ** For unit-dose analysis, remove red/red resample line and attach the gry/gry line directly to A10. *** Change to wht/wht (0.6) for warfarin sodium 10-mg tablets.*

4; a spectrophotometer[2] at a fixed wavelength of 308 nm and equipped with a 10-mm continuous flowcell[3]; and a recorder[1] with a chart speed of 45 cm/hr.

Reagents[4] and Solutions—The following were used: chloroform, spectrograde; methanol; 0.01 *N* NaOH; 0.1 *N* HCl; and USP warfarin reference standard in 0.01 *N* NaOH, 0.94 and 18.8 mg/ml.

Automated Procedure—A schematic diagram of the automated system is shown in Fig. 1. Organic solvent line tubes were pumped with methanol and chloroform, each for 5 min; then all tubes were placed in their respective solutions, and the system was allowed to equilibrate for 20–30 min. The spectrophotometer was adjusted to a baseline of 0.02 absorbance unit. Standards, baseline blanks, and samples of either individual tablets or composites of 20 tablets were placed into polystyrene cups and the system was activated.

The system was run in the sequence described in Table I. The tablets were ground to a fine powder and homogenized in the solid sampler II blender with the aliquot volume of 0.01 *N* NaOH for 1.47 min (48.9% of the complete 3-min cycle). The sampling time was 16.7% and the triple rinsing time was 14.4% of the complete cycle. A continuous filter was used to filter off the undesirable, insoluble tablet excipients from the solution before mixing with solvents.

After completing the analysis, acid, base, and sampling line tubes were placed in water while organic solvent line tubes were left in their reservoirs; pumping was continued for 5 min. Then all lines were removed from solvents, and the system was pumped until dry.

Calculations—A correction was necessary to account for the volume change resulting from the use of liquid standards. The correction

Table I—Disposition of Standards[a], Baseline Blanks[b], and Samples

Baseline
Standard solution I[c], three samples
Standard solution II[c], three samples
Baseline blank, one empty cup
Standard solution, one sample
Five samples
Standard solution, one sample
Baseline blank, one empty cup

[a] Before and after every group of five samples, average the net absorbance of the two standards to obtain the average absorbance value of standard reading. [b] Before and after every group of 10 samples and two standards, average the baseline values and subtract from the samples and standards peak values to obtain their net absorbance readings. [c] Two separate standards were accurately weighed and prepared. The percent absorbance spread for each standard should be less than 3%, and average absorbance ratios of the two standards should differ by not more than 1.5%. The standard concentrations, chosen according to sample warfarin content, of 0.375–1.88 and 7.52–37.6 mg/ml are for single-tablet and 20-tablet composite analyses, respectively.

[2] Beckman DB-G, Beckman, Fullerton, Calif.
[3] Arthur H. Thomas, Philadelphia, Pa.
[4] All chemicals were analytical grade except when specified.

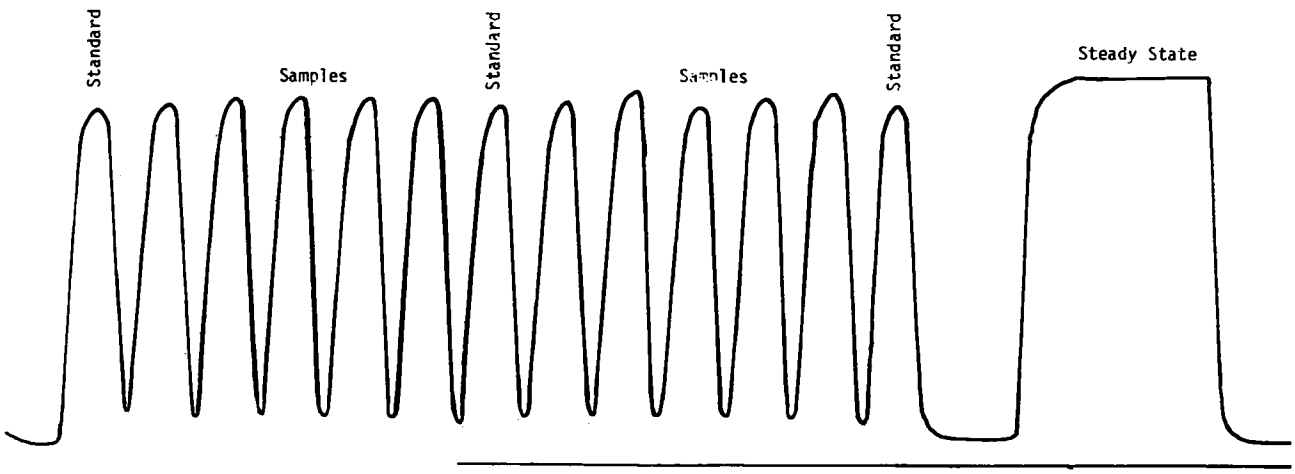

Figure 2—*Typical recordings from the automated analysis of warfarin sodium.*

Table II—Recoveries and Precision with Automated Method

Warfarin Sodium Added, mg	Warfarin Sodium Recovered[a], %
2	99.0
2.5	98.8
5	100.4
7.5	100.2
10	99.5
Average	99.58
Coefficient of variation, %	0.711

[a] Mean of 10 results.

chloroform was added and mixed in the extraction coil. Phases were separated in the phase separator fitting, and chloroform containing warfarin was debubbled. Chloroform was pumped through the continuous flowcell, where the absorbance was continuously measured and recorded on the recorder chart. A typical recording is shown in Fig. 2.

Under the experimental conditions, a linear relationship existed between the absorbance and concentration of warfarin over the ±25% range of the average standard concentration chosen according to the sample warfarin content, with a linear correlation coefficient of 0.996. The precision and recoveries obtained by the automated method were checked by running placebos of the tablet formulations with standard solutions with the same active concentrations (Table II). No significant interference from the excipients was observed.

Table III—Comparison of Results, in Milligrams of Warfarin Sodium, Obtained by Automated and USP XIX Methods

Labeled Concentration, mg	Single-Tablet Analysis[a]				20-Tablet Composite Analysis[b]			
	Automated	*CV*, %[c]	USP	*CV*, %	Automated	*CV*, %	USP	*CV*, %
2 A[d]	2.03	0.57	2.05	1.58	2.02	0.77	1.97	1.3
B[e]	1.97	1.61	2.02	1.99	1.96	0.59	1.94	1.2
2.5 A	2.47	0.50	2.49	1.42	2.48	0.57	2.47	0.73
B	2.45	1.76	2.51	1.92	2.45	0.35	2.42	0.92
5 A	5.04	0.36	5.10	0.47	5.02	0.39	4.98	0.40
B	4.91	1.37	4.95	1.25	4.97	0.50	4.92	0.85
7.5 A	7.45	0.17	7.47	0.34	7.47	0.18	7.48	0.50
B	7.42	1.27	7.46	0.95	7.50	0.32	7.48	0.67
10 A	9.95	0.18	9.8	2.29	9.96	0.19	9.88	1.17
B	9.89	0.78	9.95	1.10	10.06	0.32	9.95	0.90

[a] Mean of 10 results. [b] Mean of 30 results for Sample A and mean of 10 results for Sample B. [c] Coefficient of variation. [d] Coumadin tablets, Endo Laboratories, Garden City, N.Y. [e] Panwarfin tablets, Abbott Laboratories, Chicago, Ill.

factor, *CF*, was calculated by:

$$CF = \frac{\text{diluent pump setting + sample displacement volume}}{\text{diluent pump setting + standard volume}} \quad \text{(Eq. 1)}$$

The concentration, X, of warfarin sodium per tablet was calculated by:

$$X = \frac{A_{sample}}{A_{standard}} \times 1.071 \times CF \times C \times D \quad \text{(Eq. 2)}$$

where A = net absorbance value, 1.071 = ratio of molecular weight of warfarin sodium to warfarin, C = concentration of standard in milligrams per milliliter, and D = dilution factor.

RESULTS AND DISCUSSION

Warfarin sodium samples were withdrawn, segmented with air, and acidified with 0.1 *N* HCl. The acidified solution was mixed, and

As shown in Table III, results obtained with the automated procedure compared favorably with those of the manual USP method in the analysis of 2-, 2.5-, 5-, 7.5-, and 10-mg warfarin sodium tablets. The coefficient of variation percent with each sample, single tablets or composites of 20 tablets, was significantly smaller by the automated procedure. Results obtained by the automated method appear to demonstrate reproducibility in comparison to the official manual USP procedure.

REFERENCES

(1) R. E. Kolinski, *J. Assoc. Offic. Anal. Chem.*, **56**, 692(1973).

(2) "Official Methods of Analysis," 12th ed., Association of Official Analytical Chemists, Washington, D.C., 1975, sections 37.144–37.151.

(3) *Ibid.*, 1st supplement, 1975, Sections 37.144–37.151.

(4) "The United States Pharmacopeia," 19th rev, Mack Publishing Co., Easton, Pa., 1975, p. 539.

ACKNOWLEDGMENTS AND ADDRESSES

Received August 16, 1975, from the *Quality Control Department, Endo Laboratories, Inc., Garden City, NY 11530*

Accepted for publication December 1, 1975.

The authors thank Mr. J. Fernandez, Technicon Corp., for technical assistance.

[x] To whom inquiries should be directed.

Inhibition of *Streptococcus faecalis* by Long Chain Aliphatic Monoamines: Quantitative Structure–Activity Studies

G. E. BASS [x], LARRY J. POWERS, and E. O. DILLINGHAM

Abstract □ Primary, secondary, and tertiary long chain aliphatic amines were synthesized, and their activity against *Streptococcus faecalis* was determined. Quantitative structure–activity analyses were carried out based on the Hansch extrathermodynamic model, using partition coefficients, CMC's, quantum mechanical charges on the amine nitrogen, and the Taft steric parameter. The best correlations were obtained with the CMC. Steric properties of the ammonium head become important for tertiary amines. The structural feature of these compounds that dominates biological activity is the length of the alkyl tail. Ammonium head substituents are of only secondary importance.

Keyphrases □ *Streptococcus faecalis*—inhibition by long chain aliphatic monoamines, quantitative structure–activity relationships □ Amines, long chain aliphatic—inhibition of *Streptococcus faecalis*, structure–activity relationships □ Structure–activity relationships—long chain aliphatic monoamine inhibition of *Streptococcus faecalis*

The antibacterial activity of amines carrying long aliphatic chains has been recognized (1, 2). Although the quaternary compounds have been studied the most, simple primary, secondary, and tertiary long chain aliphatic amines, $R_1R_2N—C_nH_{2n+1}$, are also potent antibacterials. Relationships between structures and biological activities of these compounds have been investigated (3–7); but in most of these studies, structure variations were limited primarily to the length of the long aliphatic chain or "tail."

Hansch and coworkers (4–6) carried out quantitative structure–activity correlations on published activity data for primary amines using the extrathermodynamic model:

$$\log(\text{biological activity}) = a(\log P)^2 + b(\log P) + c \quad \text{(Eq. 1)}$$

where P is the octanol–water partition coefficient. Biological data included antibacterial (Gram-positive and Gram-negative species) (4, 5), antifungal (6), and hemolytic (5) activities. Very good correlations were always found.

Weiner *et al.* (3) suggested that activity variations for these compounds may be explained within the framework of the Ferguson principle (8), utilizing surface activity parameters such as the critical micelle concentration (CMC) and the surface concentration. These studies involved the inhibition of *Micrococcus pyogenes* var. *aureus*, *Escherichia coli*, and *Candida albicans* by three substituted dodecylamines.

To develop a more complete understanding of the structure–activity relationships for these compounds, the effect of alkyl substitution on the ammonium head ($R_1R_2N—$) was investigated. Physicochemical properties that might play a role in, or reflect, the bioactivities of these compounds include the partition coefficient, CMC, the Taft steric parameter (E_s) for the ammonium head, and the quantum mechanical charge (Q_N) calculated for the amine nitrogen.

Long chain aliphatic amines (primary, secondary, and tertiary) were synthesized, and their ability to inhibit the growth of *Streptococcus faecalis* was determined. The physicochemical parameters noted were evaluated, and quantitative structure–activity correlations were carried out using the generalized Hansch equation:

$$\log(\text{activity}) = a(\log P)^2 + b(\log P) + c(\log \text{CMC})^2 + d(\log \text{CMC}) + eE_s + fQ_N + g \quad \text{(Eq. 2)}$$

Not all of these parameters can be used together in a single correlation. For example, log P and log CMC reflect similar properties. In the opinion of these authors, little can be gained from these empirical correlations if more than three parameters are involved.

EXPERIMENTAL[1]

The amine salts were prepared by reacting the acyl chloride of the appropriate long chain carboxylic acid with amines to obtain the corresponding amides. After recrystallization, the amides were reduced with lithium aluminum hydride to the desired amines. The amines were isolated and converted to the hydrochloride salts. Melting points and IR spectra were in agreement with available literature data.

Partition coefficients were calculated from substituent contributions obtained from the literature (5, 9, 10). The reported value of log P = 1.85 was assumed for dodecylamine. Substituent contributions for $—NH_2$ and $—N(CH_3)_2$ were −1.85 and −0.95, respectively. The value for $—NHCH_3$ was interpolated as −1.40. Methylene groups were assumed to contribute 0.50, and branching corrections

[1] Melting points were determined on a Thomas-Hoover capillary melting-point apparatus. IR spectra were determined on a Perkin-Elmer model 257 spectrophotometer. Turbidity measurements were made using a Bausch & Lomb Spectronic 20. Surface tension was determined using a Fisher surface tensiometer. Regression analyses were performed on an IBM 1130 system.

ACKNOWLEDGMENTS AND ADDRESSES

Received August 16, 1975, from the *Quality Control Department, Endo Laboratories, Inc., Garden City, NY 11530*

Accepted for publication December 1, 1975.

The authors thank Mr. J. Fernandez, Technicon Corp., for technical assistance.

[x] To whom inquiries should be directed.

Inhibition of *Streptococcus faecalis* by Long Chain Aliphatic Monoamines: Quantitative Structure–Activity Studies

G. E. BASS [x], LARRY J. POWERS, and E. O. DILLINGHAM

Abstract □ Primary, secondary, and tertiary long chain aliphatic amines were synthesized, and their activity against *Streptococcus faecalis* was determined. Quantitative structure–activity analyses were carried out based on the Hansch extrathermodynamic model, using partition coefficients, CMC's, quantum mechanical charges on the amine nitrogen, and the Taft steric parameter. The best correlations were obtained with the CMC. Steric properties of the ammonium head become important for tertiary amines. The structural feature of these compounds that dominates biological activity is the length of the alkyl tail. Ammonium head substituents are of only secondary importance.

Keyphrases □ *Streptococcus faecalis*—inhibition by long chain aliphatic monoamines, quantitative structure–activity relationships □ Amines, long chain aliphatic—inhibition of *Streptococcus faecalis*, structure–activity relationships □ Structure–activity relationships—long chain aliphatic monoamine inhibition of *Streptococcus faecalis*

The antibacterial activity of amines carrying long aliphatic chains has been recognized (1, 2). Although the quaternary compounds have been studied the most, simple primary, secondary, and tertiary long chain aliphatic amines, $R_1R_2N—C_nH_{2n+1}$, are also potent antibacterials. Relationships between structures and biological activities of these compounds have been investigated (3–7); but in most of these studies, structure variations were limited primarily to the length of the long aliphatic chain or "tail."

Hansch and coworkers (4–6) carried out quantitative structure–activity correlations on published activity data for primary amines using the extrathermodynamic model:

$$\log(\text{biological activity}) = a(\log P)^2 + b(\log P) + c \quad \text{(Eq. 1)}$$

where P is the octanol–water partition coefficient. Biological data included antibacterial (Gram-positive and Gram-negative species) (4, 5), antifungal (6), and hemolytic (5) activities. Very good correlations were always found.

Weiner *et al.* (3) suggested that activity variations for these compounds may be explained within the framework of the Ferguson principle (8), utilizing surface activity parameters such as the critical micelle concentration (CMC) and the surface concentration. These studies involved the inhibition of *Micrococcus pyogenes* var. *aureus*, *Escherichia coli*, and *Candida albicans* by three substituted dodecylamines.

To develop a more complete understanding of the structure–activity relationships for these compounds, the effect of alkyl substitution on the ammonium head ($R_1R_2N—$) was investigated. Physicochemical properties that might play a role in, or reflect, the bioactivities of these compounds include the partition coefficient, CMC, the Taft steric parameter (E_s) for the ammonium head, and the quantum mechanical charge (Q_N) calculated for the amine nitrogen.

Long chain aliphatic amines (primary, secondary, and tertiary) were synthesized, and their ability to inhibit the growth of *Streptococcus faecalis* was determined. The physicochemical parameters noted were evaluated, and quantitative structure–activity correlations were carried out using the generalized Hansch equation:

$$\log(\text{activity}) = a(\log P)^2 + b(\log P) + c(\log \text{CMC})^2 + d(\log \text{CMC}) + eE_s + fQ_N + g \quad \text{(Eq. 2)}$$

Not all of these parameters can be used together in a single correlation. For example, log P and log CMC reflect similar properties. In the opinion of these authors, little can be gained from these empirical correlations if more than three parameters are involved.

EXPERIMENTAL[1]

The amine salts were prepared by reacting the acyl chloride of the appropriate long chain carboxylic acid with amines to obtain the corresponding amides. After recrystallization, the amides were reduced with lithium aluminum hydride to the desired amines. The amines were isolated and converted to the hydrochloride salts. Melting points and IR spectra were in agreement with available literature data.

Partition coefficients were calculated from substituent contributions obtained from the literature (5, 9, 10). The reported value of log P = 1.85 was assumed for dodecylamine. Substituent contributions for $—NH_2$ and $—N(CH_3)_2$ were −1.85 and −0.95, respectively. The value for $—NHCH_3$ was interpolated as −1.40. Methylene groups were assumed to contribute 0.50, and branching corrections

[1] Melting points were determined on a Thomas-Hoover capillary melting-point apparatus. IR spectra were determined on a Perkin-Elmer model 257 spectrophotometer. Turbidity measurements were made using a Bausch & Lomb Spectronic 20. Surface tension was determined using a Fisher surface tensiometer. Regression analyses were performed on an IBM 1130 system.

Table I—*S. faecalis* Inhibitory Activities and Physicochemical Parameters for a Series of Long Chain Aliphatic Monoamines

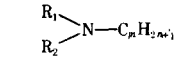

n	R_1	R_2	$ID_{50} \times 10^6$ [a]	Log P [b]	Log (CMC × 10^7) [c]	E_s [d]	Q_N [e]
8	H	H	1800	−0.150	6.26	2.48	0.131
10	H	H	230	0.850	5.54	2.48	0.131
11	H	H	84.8	1.35	4.89	2.48	0.131
12	H	H	38.0	1.85	4.15	2.48	0.131
12	H	CH_3	30.0	2.30	4.32	1.24	0.349
12	H	C_2H_5	25.0	2.80	4.02	1.17	0.347
12	H	n-C_4H_9	58.5	3.80	3.27	0.85	0.347
12	H	*tert*-C_4H_9	18.0	3.33	4.31	−0.30	0.345
12	CH_3	CH_3	60.0	2.75	4.48	0.00	0.529
12	C_2H_5	C_2H_5	31.5	3.75	4.38	−0.14	0.525
12	iso-C_3H_7	iso-C_3H_7	34.5	4.35	4.29	−0.94	0.523
12	iso-C_4H_9	iso-C_4H_9	120.0	5.35	4.19	−1.86	0.525
12	C_2H_5	n-C_4H_9	25.0	4.75	4.35	−0.46	0.525
14	H	CH_3	4.0	3.30	3.36	1.24	0.349
14	H	n-C_3H_7	3.8	4.30	2.17	0.88	0.347
14	H	$C_2H_4OCH_3$	4.2	2.82	3.35	0.47	0.348
16	H	H	2.5	3.85	2.73	2.48	0.131
16	H	C_2H_5	3.3	4.80	1.80	1.17	0.347
17	H	H	1.9	4.35	2.55	2.48	0.131
18	H	H	10.0	4.85	2.83	2.48	0.131
18	H	CH_3	3.5	5.30	2.77	1.24	0.349
18	CH_3	CH_3	3.6	5.75	2.60	0.00	0.529

[a] Amine concentration, moles per liter × 10^6, required for 50% growth inhibition. [b] P = octanol–water partition coefficient, calculated. [c] CMC in isotonic saline. [d] E_s = Taft steric factor for onium head, R_1R_2N—. [e] Q_N = quantum mechanical charge on the amine nitrogen in proton units.

Table II—Statistics for Correlation of *S. faecalis* Inhibitory Activities with Physicochemical Parameters of Long Chain Aliphatic Monoamines Using the Extrathermodynamic Model

Physicochemical Parameters	All Compounds (n = 22)		Primary Amines (n = 7)		Secondary Amines (n = 9)		Tertiary Amines (n = 6)		Dodecylamines (n = 10)	
	R^2	F	R^2	F	R^2	F	R^2	F	R^2	F
log CMC	0.81	87	0.96	117	0.46	6.0	0.71	9.8	0.06	0.5
(log CMC)², log CMC	0.84	51	0.96	51	0.47	2.6	0.80	5.8	0.08	0.3
log P	0.44	16	0.86	30	0.28	2.7	0.19	0.9	0.13	1.2
(log P)², log P	0.57	12	0.95	39	0.28	1.2	0.25	0.5	0.34	1.8
E_s	0.00	0.0	—	—	0.03	0.2	0.38	2.5	0.11	0.9
log CMC, E_s	0.81	41	—	—	0.47	2.6	0.88	11	0.24	1.1
log P, E_s	0.60	14	—	—	0.28	1.2	0.94	25	0.13	0.5
Q_N	0.01	0.1	—	—	—	—	—	—	0.07	0.6
log CMC, Q_N	0.81	41	—	—	—	—	—	—	0.20	0.9
log P, Q_N	0.54	11	—	—	—	—	—	—	0.13	0.5

of −0.20 and −0.47 were employed for iso- and *tert*-substituents, respectively.

The CMC's of the amines in isotonic saline were determined by the du Nouy ring method (11, 12). The quantum mechanical charge on the amine nitrogens was calculated using the Del Re sigma electron method (13).

Growth inhibition by the amine salts was measured turbidimetrically at 660 nm. A minimum of 12 amine concentrations (five replicates each) in NIH thioglycolate broth was assayed along with controls. Each tube (containing 5 ml of broth) was loop inoculated from an overnight growth of *S. faecalis*[2] and incubated at 37° for 8 hr. Percent growth *versus* amine concentration plots were constructed to obtain concentrations required for 50% inhibition (ID_{50}).

Quantitative structure–activity correlations using the generalized Hansch model (Eq. 2) were carried out by regression analysis, and goodness of fit was assessed statistically (14).

RESULTS AND DISCUSSION

Inhibitory activities and physicochemical parameters for 22 long chain aliphatic amines are presented in Table I. Octylamine and heptadecylamine were the least active and most active compounds tested, respectively. For the primary amines, activity increased steadily with chain length up to heptadecylamine and then began to decrease. Solubilities of $C_{20}H_{41}$—NH_2 and $C_{22}H_{45}$—NH_2 were not sufficient to allow ID_{50} determinations ($ID_{50} > 5 \times 10^{-5}$ M). No easily recognized pattern was exhibited by the secondary and tertiary amines.

Results for the quantitative structure–activity correlations are summarized in Table II. When all 22 compounds in Table I were included in the analyses, the best correlations were found with log CMC. The log P parameter was considerably less effective. The Taft steric parameters, E_s, and the quantum mechanical charge on the amine nitrogen, Q_N, taken alone, were totally incapable of explaining activity variations. These parameters did not significantly improve correlations when used together with log CMC or log P. The essence of these results is that the rather wide range of activities displayed by these compounds is best correlated with parameters sensitive to the length of the long alkyl tail. Activity correlates better with the substituent contribution for the tail, π (tail) (R^2 = 0.75, F = 58.7), than with log $P = \pi$ (head) + π (tail).

Analyses involving only the primary amines again showed log CMC to be the best parameter while appreciable correlations with log P were also obtained. No significant correlations were obtained

[2] Oral isolate was supplied by Dr. Albert T. Brown, School of Dental Medicine, University of Connecticut Health Center, Hartford, Conn.

for the secondary amines considered alone. Best correlations were found with log CMC.

Notable results were obtained for the tertiary amines. Fair correlations were found with log CMC (linear and quadratic) but not log P or E_s. However, very significant improvements were obtained when E_s was used together with either log CMC or log P. The clear implication is that for tertiary amines the bulk of the head group must be considered along with the overall hydrophobic properties of the molecule and has a deactivating effect. Somewhat similar results were found for a series of alcohols (15). Hansch and Glave (5) also noted structure–activity similarities for long chain amines and alcohols. They proposed that both classes of compounds be classified as "membrane-perturbing" agents.

The dodecylamines, like the secondary amines, yielded no significant correlations. This finding underscores the inability of the physicochemical parameters studied to represent adequately the biologically important properties of the ammonium head. However, the range of activities for this series is rather narrow.

In summary, the activity is dominated by the length of the long aliphatic tail. Best correlations are found with physicochemical properties sensitive to this feature. Substitution of small alkyl groups on the amine nitrogen has only a secondary effect on activity. For secondary amines, no rationale for the direction or magnitude of this effect was uncovered. For tertiary amines, the bulk of the ammonium head appears to be important when considered with hydrophobic properties. CMC was superior to the partition coefficient for quantitative structure–activity correlations.

REFERENCES

(1) G. Domagk, *Deut. Med. Wochenschr.*, **61**, 829(1935); through *Chem. Abstr.*, **29**, 7018(1935).

(2) A. T. Fuller, *Biochem. J.*, **36**, 548(1942).

(3) N. D. Weiner, F. Hart, and G. Zografi, *J. Pharm. Pharmacol.*, **17**, 350(1965).

(4) E. J. Lien, C. Hansch, and S. M. Anderson, *J. Med. Chem.*, **11**, 430(1968).

(5) C. Hansch and W. R. Glave, *Mol. Pharmacol.*, **7**, 337(1971).

(6) C. Hansch and E. J. Lein, *J. Med. Chem.*, **14**, 653(1971).

(7) J. J. Kabara, A. J. Conley, and J. P. Truant, *Antimicrob. Ag. Chemother.*, **2**, 492(1972).

(8) J. Ferguson, *Proc. Roy. Soc., Ser. B*, **127**, 387(1939).

(9) J. Iwasa, T. Fujita, and C. Hansch, *J. Med. Chem.*, **8**, 150(1965).

(10) C. Hansch, J. E. Quinlan, and G. L. Lawrence, *J. Org. Chem.*, **33**, 347(1968).

(11) A. W. Adamson, "Physical Chemistry of Surfaces," 2nd ed., Interscience, New York, N.Y., 1967, pp. 24–491.

(12) L. J. Powers, E. O. Dillingham, and G. E. Bass, *J. Pharm. Sci.*, **64**, 883(1975).

(13) G. Del Re, in "Electronic Aspects of Biochemistry," B. Pullman, Ed., Academic, New York, N.Y., 1964, p. 221. G. Del Re, *J. Chem. Soc.*, **1958**, 4031.

(14) W. P. Purcell, G. E. Bass, and J. M. Clayton, "Strategy of Drug Design," Wiley, New York, N.Y., 1973, pp. 69–71.

(15) E. O. Dillingham, R. W. Mast, G. E. Bass, and J. Autian, *J. Pharm. Sci.*, **62**, 22(1973).

ACKNOWLEDGMENTS AND ADDRESSES

Received September 9, 1974, from the *Department of Molecular Biology, College of Pharmacy, University of Tennessee Center for the Health Sciences, Memphis, TN 38163*

Accepted for publication February 11, 1975.

Supported in part by U.S. Public Health Service Grants DE-03429 and HL-09495.

The authors gratefully acknowledge the technical assistance of J. N. Warren and I. Bilsky.

[x] To whom inquiries should be directed.

5-Aryloxy-6-methoxy-8-aminoquinolines as Potential Prophylactic Antimalarials

KALIDAS PAUL and C. DeWITT BLANTON, Jr. [x]

Abstract □ 5-(*p*-Anisyloxy)-6-methoxy-8-(5-isopropylaminopentylamino)quinoline was resynthesized for evaluation in the *Plasmodium berghei* and monkey prophylactic (*Plasmodium cynomolgi*) tests. A new primary amine, three secondary amines, and one structurally modified side-chain analog of the 5-aryloxy series were also prepared. None of these compounds showed significant antimalarial or prophylactic activity.

Keyphrases □ 8-Aminoquinolines, 5- and 6-substituted—series synthesized, screened for antimalarial activity □ Antimalarial agents, potential—5- and 6-substituted 8-aminoquinolines synthesized and screened □ Structure–activity relationships—5- and 6-substituted 8-aminoquinolines synthesized and screened for antimalarial activity

During studies (1, 2) on the synthesis and evaluation of various derivatives of the 8-aminoquinoline nucleus as potential prophylactic antimalarials, a known compound, 5-(*p*-anisyloxy)-6-methoxy-8-(5-isopropylaminopentylamino)quinoline (I) (3, 4), was proposed for resynthesis and evaluation in the *Plasmodium berghei* and monkey prophylactic (*Plasmodium cynomolgi*) tests. In *Plasmodium gallinaceum* studies (4), I was relatively nontoxic and highly active, displaying the highest therapeutic index (177) of any 8-aminoquinoline tested. It was suggested that I and related compounds may be more conveniently converted to the *o*-quinoid structure *in vivo*, a structural feature proposed for the active metabolite (5, 6). Primaquine and pentaquine exhibited therapeutic indexes of 30 and 57, respectively, in this test (4).

Although the 8-aminoquinolines are quite toxic, primaquine has had a prominent place in malaria prophylaxis. The possibility that 5-aryloxy-substituted 8-aminoquinolines may offer a lead in the search for more effective and less toxic agents led to a reexamination of I as well as a few selective, structurally modified analogs (II–VI). For example, the 5-aryloxy analog (II) of primaquine was considered since primaquine has been recognized as the least toxic and most effective 8-aminoquinoline tested in humans (5, 7). It was reported (7, 8) that occasional aromatic interruption in

for the secondary amines considered alone. Best correlations were found with log CMC.

Notable results were obtained for the tertiary amines. Fair correlations were found with log CMC (linear and quadratic) but not log P or E_s. However, very significant improvements were obtained when E_s was used together with either log CMC or log P. The clear implication is that for tertiary amines the bulk of the head group must be considered along with the overall hydrophobic properties of the molecule and has a deactivating effect. Somewhat similar results were found for a series of alcohols (15). Hansch and Glave (5) also noted structure–activity similarities for long chain amines and alcohols. They proposed that both classes of compounds be classified as "membrane-perturbing" agents.

The dodecylamines, like the secondary amines, yielded no significant correlations. This finding underscores the inability of the physicochemical parameters studied to represent adequately the biologically important properties of the ammonium head. However, the range of activities for this series is rather narrow.

In summary, the activity is dominated by the length of the long aliphatic tail. Best correlations are found with physicochemical properties sensitive to this feature. Substitution of small alkyl groups on the amine nitrogen has only a secondary effect on activity. For secondary amines, no rationale for the direction or magnitude of this effect was uncovered. For tertiary amines, the bulk of the ammonium head appears to be important when considered with hydrophobic properties. CMC was superior to the partition coefficient for quantitative structure–activity correlations.

REFERENCES

(1) G. Domagk, *Deut. Med. Wochenschr.*, **61**, 829(1935); through *Chem. Abstr.*, **29**, 7018(1935).

(2) A. T. Fuller, *Biochem. J.*, **36**, 548(1942).

(3) N. D. Weiner, F. Hart, and G. Zografi, *J. Pharm. Pharmacol.*, **17**, 350(1965).

(4) E. J. Lien, C. Hansch, and S. M. Anderson, *J. Med. Chem.*, **11**, 430(1968).

(5) C. Hansch and W. R. Glave, *Mol. Pharmacol.*, **7**, 337(1971).

(6) C. Hansch and E. J. Lein, *J. Med. Chem.*, **14**, 653(1971).

(7) J. J. Kabara, A. J. Conley, and J. P. Truant, *Antimicrob. Ag. Chemother.*, **2**, 492(1972).

(8) J. Ferguson, *Proc. Roy. Soc., Ser. B*, **127**, 387(1939).

(9) J. Iwasa, T. Fujita, and C. Hansch, *J. Med. Chem.*, **8**, 150(1965).

(10) C. Hansch, J. E. Quinlan, and G. L. Lawrence, *J. Org. Chem.*, **33**, 347(1968).

(11) A. W. Adamson, "Physical Chemistry of Surfaces," 2nd ed., Interscience, New York, N.Y., 1967, pp. 24–491.

(12) L. J. Powers, E. O. Dillingham, and G. E. Bass, *J. Pharm. Sci.*, **64**, 883(1975).

(13) G. Del Re, in "Electronic Aspects of Biochemistry," B. Pullman, Ed., Academic, New York, N.Y., 1964, p. 221. G. Del Re, *J. Chem. Soc.*, **1958**, 4031.

(14) W. P. Purcell, G. E. Bass, and J. M. Clayton, "Strategy of Drug Design," Wiley, New York, N.Y., 1973, pp. 69–71.

(15) E. O. Dillingham, R. W. Mast, G. E. Bass, and J. Autian, *J. Pharm. Sci.*, **62**, 22(1973).

ACKNOWLEDGMENTS AND ADDRESSES

Received September 9, 1974, from the *Department of Molecular Biology, College of Pharmacy, University of Tennessee Center for the Health Sciences, Memphis, TN 38163*

Accepted for publication February 11, 1975.

Supported in part by U.S. Public Health Service Grants DE-03429 and HL-09495.

The authors gratefully acknowledge the technical assistance of J. N. Warren and I. Bilsky.

[x] To whom inquiries should be directed.

5-Aryloxy-6-methoxy-8-aminoquinolines as Potential Prophylactic Antimalarials

KALIDAS PAUL and C. DeWITT BLANTON, Jr. [x]

Abstract □ 5-(*p*-Anisyloxy)-6-methoxy-8-(5-isopropylaminopentylamino)quinoline was resynthesized for evaluation in the *Plasmodium berghei* and monkey prophylactic (*Plasmodium cynomolgi*) tests. A new primary amine, three secondary amines, and one structurally modified side-chain analog of the 5-aryloxy series were also prepared. None of these compounds showed significant antimalarial or prophylactic activity.

Keyphrases □ 8-Aminoquinolines, 5- and 6-substituted—series synthesized, screened for antimalarial activity □ Antimalarial agents, potential—5- and 6-substituted 8-aminoquinolines synthesized and screened □ Structure–activity relationships—5- and 6-substituted 8-aminoquinolines synthesized and screened for antimalarial activity

During studies (1, 2) on the synthesis and evaluation of various derivatives of the 8-aminoquinoline nucleus as potential prophylactic antimalarials, a known compound, 5-(*p*-anisyloxy)-6-methoxy-8-(5-isopropylaminopentylamino)quinoline (I) (3, 4), was proposed for resynthesis and evaluation in the *Plasmodium berghei* and monkey prophylactic (*Plasmodium cynomolgi*) tests. In *Plasmodium gallinaceum* studies (4), I was relatively nontoxic and highly active, displaying the highest therapeutic index (177) of any 8-aminoquinoline tested. It was suggested that I and related compounds may be more conveniently converted to the *o*-quinoid structure *in vivo*, a structural feature proposed for the active metabolite (5, 6). Primaquine and pentaquine exhibited therapeutic indexes of 30 and 57, respectively, in this test (4).

Although the 8-aminoquinolines are quite toxic, primaquine has had a prominent place in malaria prophylaxis. The possibility that 5-aryloxy-substituted 8-aminoquinolines may offer a lead in the search for more effective and less toxic agents led to a reexamination of I as well as a few selective, structurally modified analogs (II–VI). For example, the 5-aryloxy analog (II) of primaquine was considered since primaquine has been recognized as the least toxic and most effective 8-aminoquinoline tested in humans (5, 7). It was reported (7, 8) that occasional aromatic interruption in

the aminoalkylamino side chain provides relatively nontoxic compounds with a high therapeutic index. Compound VI has incorporated this structural feature.

DISCUSSION

The approach for the synthesis of I is a modification of the original literature procedure (3). In this modification (Scheme I), the new primary amine (II) (Table I) was obtained as an intermediate during the preparation of the known agent, I. Compound II served as the key intermediate for the preparation of additional analogs (III–V). The original procedure (3) called for nucleophilic displacement of the 5-bromo atom of VIII by potassium *p*-methoxyphenoxide, which was generated *in situ*. This method gave inconsistent results (10–30% yields). However, if the potassium *p*-methoxyphenoxide is prepared and isolated, the dried salt reacts with VIII, in dimethylformamide, to give yields consistently greater than 70%. A second modification employed 5-bromo-1-phthalimidopentane instead of the 1-halo-5-(isopropylamino)pentane of the original method (3).

Although elemental analyses for the key intermediate (XI) employed to synthesize I and II gave a consistently low value for carbon when it was not considered as a hemihydrate, the product obtained by Methods A and B gave identical IR and NMR spectra. TLC results were homogeneous and identical. Preparation of VI employed a similar process, utilizing 1,4-bis(chloromethyl)benzene for the synthesis of the intermediate, 4-phthalimidomethylbenzyl chloride (XII), required for reaction with X.

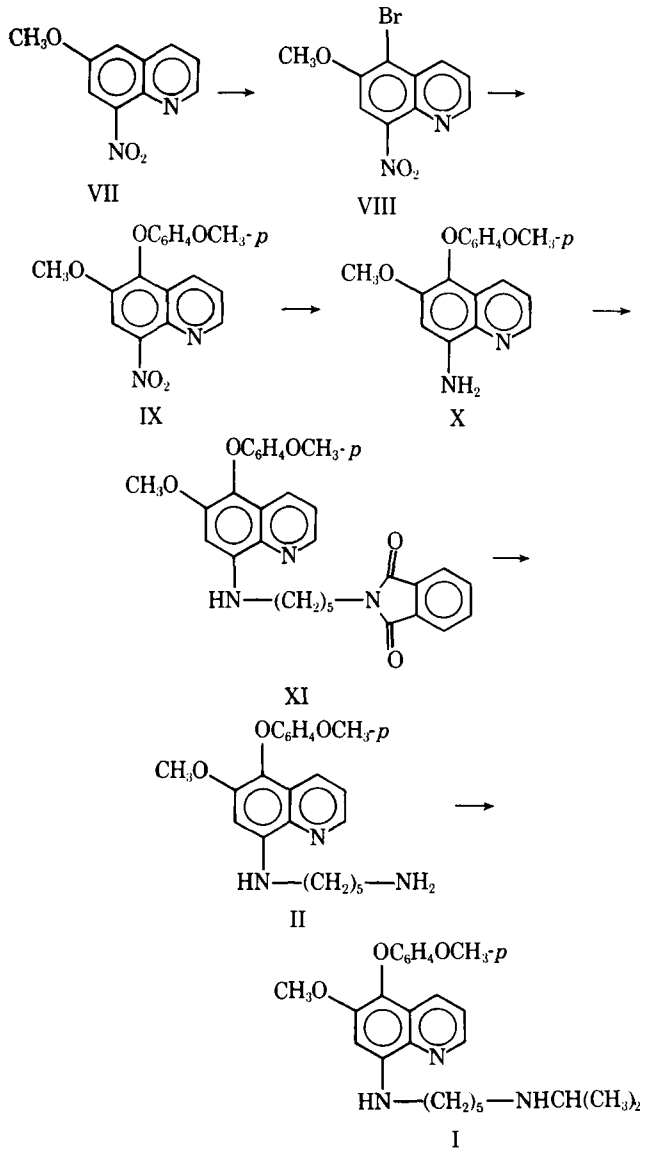

Scheme I

BIOLOGICAL ACTIVITY

The antimalarial activity[1] was assessed against *P. berghei* in mice by the method of Osdene *et al.* (9) (Table II). With this test, only IIa met the criteria to be considered "active." Furthermore, I, which was such a promising candidate in the *P. gallinaceum* test (4), was a failure in terms of activity and toxicity when compared to primaquine in the *P. berghei* test.

Compounds I, II, and VI also were evaluated in monkeys for prophylactic and radical curative activity by the Schmidt technique (10, 11). This method involves sporozoite-induced *P. cynomolgi* infections of rhesus monkeys. All compounds were inactive at 10 mg/kg. Primaquine was active at 1 mg/kg. The activity patterns did not justify expanded testing or further extension of the present group.

EXPERIMENTAL[2]

5-Bromo-6-methoxy-8-nitroquinoline (VIII)—Compound VIII was prepared in 86% yield according to the procedure of Elderfield *et al.* (12), mp 207–209° [lit. (12) mp 203–205.5°].

5-(*p*-Anisyloxy)-6-methoxy-8-nitroquinoline (IX)—Preparation of this compound by the existing procedure (3) gave irreproducible yields, varying from 10 to 30%. The literature procedure for reaction of VIII and potassium *p*-methoxyphenoxide was modified to give yields as high as 70%. The modifications included a change in the reaction solvent from butyl cellulose to dimethylformamide and isolation of the potassium *p*-methoxyphenoxide, instead of generating *in situ*, and drying.

5-(*p*-Anisyloxy)-6-methoxy-8-aminoquinoline (X)—Compound X was prepared in 55–90% yield according to the procedure of Lauer *et al.* (13), mp 112–115° [lit. (13) mp 115–116°].

5 - (*p*-Anisyloxy)-6-methoxy-8-(5-phthalimidopentylamino)quinoline (XI)—*Method A*—An intimate mixture of 11.84 g (40 mmoles) of X and 5.94 g (20 mmoles) of 5-bromophthalimidopentane was heated at 155–160° for 3 hr (under nitrogen). The resulting black mass was extracted with 1600 ml of benzene (200-ml portions). The extract was treated with charcoal, filtered, and concentrated to give 3 g of canary yellow solid, mp 150–152° (after recrystallization from ethanol–chloroform, mp 152–153°).

Anal.—Calc. for $C_{30}H_{29}N_3O_5$: C, 70.43; H, 5.71; N, 8.21. Calc. for $C_{30}H_{29}N_3O_5 \cdot 0.5H_2O$: C, 69.22; H, 5.80; N, 8.07. Found: C, 69.14, 69.06; H, 5.91, 5.86; N, 8.06.

Method B—5-Bromophthalimidopentane (6 g) and 6 g of X in 100 ml of 66% ethanol and 136 g of sodium acetate were refluxed for 72 hr. After 24 hr, 6 g of 5-bromophthalimidopentane and 13.6 g of sodium acetate were added; after 48 hr, 27.2 g of sodium acetate was added to keep the pH at 7–8. The reaction mixture was cooled, saturated with potassium carbonate, and extracted with ether (some canary yellow precipitate appeared at the interphase). This solid was taken with the ether layer and filtered to give 5 g (50% yield). Evaporation of the dried ether layer gave a dark oil, which was mainly unreacted amine (X) and 5-bromophthalimidopentane. The analytical material obtained from ethanol–chloroform melted at 152–153°.

Anal.—Calc. for $C_{30}H_{29}N_3O_5$: N, 8.21. Found: N, 8.08.

5-(*p*-Anisyloxy)-6-methoxy-8-(5-aminopentylamino)quinoline Dimaleate (IIa)—Compound XI (39 g, 0.0763 mole) was suspended in 400 ml of 95% ethanol and 35 ml of 85% hydrazine hydrate. The suspension was heated in an oil bath (90–100°) for 1 hr to give a clear solution, followed by the appearance of a voluminous white precipitate. After heating for an additional 1 hr, a portion of the ethanol was removed *in vacuo*. The solid residue was cooled to room temperature and dissolved in 45 ml of water containing 45 g of sodium

[1] Antimalarial test results were provided by the Walter Reed Army Institute of Research.

[2] Melting points were determined on a Thomas-Hoover apparatus (capillary method) and are uncorrected. NMR spectra were determined on a Hitachi Perkin-Elmer R 20A high-resolution NMR spectrometer using tetramethylsilane as the internal reference. IR spectra were determined on a Perkin-Elmer 237B grating spectrophotometer using the potassium bromide technique. Elemental analyses were determined by Atlantic Microlab, Inc., Atlanta, Ga. TLC was performed on Eastman Chromatogram sheets, type 6060 (silica gel).

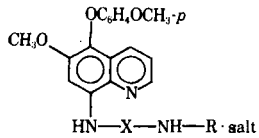

Table I—5-Aryloxy-6-methoxy-8-aminoquinolines

Compound	X	R	Salt	Yield, %	Melting Point	Formula	Analysis, % Calc.	Analysis, % Found
I	$(CH_2)_5$	$CH(CH_3)_2$	Maleate	84.0	120–122°	$C_{29}H_{37}N_3O_7$	C 64.54 H 6.91 N 7.78	64.66 6.94 7.72
IIa	$(CH_2)_5$	H	Dimaleate	68.4	118–120°	$C_{30}H_{35}N_3O_{11}$	C 58.72 H 5.74 N 6.84	58.54 6.05 6.83
IIb	$(CH_2)_5$	H	Maleate	—	127–128°	$C_{26}H_{31}N_3O_7$	C 62.76 H 6.28 N 8.45	62.92 6.38 8.36
IIc	$(CH_2)_5$	H	—	—	61–65[a]	$C_{22}H_{27}N_3O_3$	—	—
III	$(CH_2)_5$	2-Adamantyl	Maleate	87.0	153–155°	$C_{36}H_{45}N_3O_7$	C 68.44 H 7.17 N 6.65	68.21 7.28 6.62
IV	$(CH_2)_5$	3,4,5-Trimethoxybenzyl	Tartrate	51.5	119–121°	$C_{37}H_{45}N_3O_{12}\cdot H_2O$	C 59.90 H 6.34 N 5.66	59.83 6.53 5.68
V	$(CH_2)_5$	2-Hydroxybenzyl	Tartrate	96.0	90–95°	$C_{33}H_{39}N_3O_{10}$	C 62.16 H 6.16 N 6.58	61.93 6.20 6.54
VI	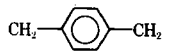	H	Maleate	77.5	158–160°	$C_{29}H_{29}N_3O_7$	C 65.53 H 5.50 N 7.90	65.23 5.59 7.86

hydroxide. This solution was treated with 300 ml of ether, stirred at room temperature for 1 hr, and allowed to stand overnight at room temperature.

The ether layer was separated, washed with water and a saturated salt solution, and dried over anhydrous sodium sulfate. Concentration of the ether gave an oil (32 g). This oil was redissolved in 300 ml of ether and treated with 500 ml of a saturated solution of maleic acid in ether (20 g of maleic acid/500 ml of ether). A red precipitate (32 g, 68.4%) was obtained, mp 120–122°. The analytical sample was prepared by recrystallizing from chloroform, mp 118–120° (see Table I for physical constants).

By continuous recrystallization, it was possible to obtain the monomaleate (IIb), mp 127–128°. Suspension of IIa or IIb in 1 *N* sodium hydroxide gave a yellow solid, mp 61–65°. The free base (IIc) was not analyzed but was used directly for the synthesis of III–V. These compounds gave expected NMR and IR spectra.

5-(*p*-Anisyloxy)-6-methoxy-8-(5-isopropylaminopentylamino)quinoline Maleate (I)—Compound IIc (5.7 g, 15 mmoles), 3 ml of acetone, 0.5 g of prereduced platinum oxide, and 75 ml of absolute ethanol were shaken at room temperature on a Parr hydrogenation apparatus (initial pressure of 50 psi). After 5 hr, 0.6 kg (1.3 lb) of pressure had been lost. The catalyst was removed, and the ethanol solution was concentrated *in vacuo*.

The resulting oil was dissolved in ether and dried over anhydrous sodium sulfate. The ether was removed *in vacuo*, and the oil was redissolved in anhydrous ether. This solution was treated with a saturated ether solution of maleic acid to give a red precipitate (6.8 g, 84%), mp 110–112°. The maleate salt was dissolved in chloroform, treated with charcoal, and precipitated by addition of ether as a yellow solid (5.5 g), mp 120–122°.

5 - (*p*-Anisyloxy)-6-methoxy-8-[5-(3,4,5-trimethoxybenzyl)-aminopentylamino]quinoline *d*-Tartrate (IV)—Compound IIc (1.2 g, 315 mmoles), 0.8 g of 3,4,5-trimethoxybenzaldehyde, 50 ml of benzene, and 2–3 drops of piperidine were refluxed, with azeotropic removal of water, for 18 hr. On removal of the benzene, an oil was obtained; this oil gave a yellow solid (mp 65–70°) on trituration with methanol (1.9 g). Without further purification, this yellow solid (Schiff base) was dissolved in 50 ml of absolute ethanol, warmed to 50°, and treated with 2 g of sodium borohydride.

After the addition was completed, the solution was heated at 60° for 0.5 hr, cooled to room temperature, and diluted with water. The aqueous solution was extracted with ether, the ether layer was dried over sodium sulfate, and the product was isolated as a *d*-tartrate salt. The analytical sample was obtained by dissolving in chloroform and reprecipitating (1.2 g, 51.5%) with ether, mp 119–121°.

5 - (*p*-Anisyloxy)-6-methoxy-8-[5-(2-adamantyl)aminopentylamino]quinoline Maleate (III)—This compound was prepared from 2-adamanone and the free base (IIc) in 87% yield by the procedure already outlined, mp 153–155°.

5-(*p*-Anisyloxy)-6- methoxy-8-[5- (2-hydroxybenzyl)amino-

Table II—Antimalarial Activity against *P. berghei*[a]

Compound	ΔMST (days) after a Single Dose 20 mg/kg sc	40 mg/kg sc	80 mg/kg sc	160 mg/kg sc	320 mg/kg sc	640 mg/kg sc
I	—	0.3	—	0.9 (2T)	—	(5T)
IIa	1.1	1.7	3.1	4.7	5.7	7.3
IIb	0.7	0.9	2.1	4.3	4.7	5.7
IIc	0.5	1.3	3.1	3.5	4.5	5.9
III	0.3	0.5	1.5	2.5	3.3	5.7
IV	—	0.1	—	0.1	—	0.1
V	—	0.3	—	0.5	—	0.5
VI	—	0.3	—	0.5	—	0.5
Primaquine phosphate	4.0	5.0	9.4	10.8 (2T)	(5T)	(5T)

[a] Increase in mean survival time (MST), in days, of the test group (five mice) is reported. The mean survival time of untreated mice is 6.1 days. A compound is "active" if ΔMST exceeds 6.1 days. Animals that survive to 60 days postinfection are considered "cured" (C). Deaths from Days 2–5 after drug administration are attributed to drug toxicity (T).

pentylamino]quinoline *d*-Tartrate (V)—This compound was prepared from salicylaldehyde by the procedure previously described. A yield of 96% was obtained, mp 90–95° (with bubbling at 80°).

4-Phthalimidomethylbenzyl Chloride (XII)—1,4-Bis(chloromethyl)benzene (43.7 g, 0.25 mole) was added to 300 ml of dimethylformamide. Potassium phthalimide (46 g, 0.25 mole) was added in two portions. The second portion was added after 3 hr together with another 300 ml of dimethylformamide. The mixture was heated for 3 hr at 85°, and 500 ml of dimethylformamide distilled off under aspirator vacuum (about 18–19 hr). The residue was poured into water, and a white material was collected. This material was extracted with 1 liter of acetone, leaving 18.5 g of the insoluble diphthalimido product. Extraction of the acetone solution with hot petroleum ether (bp 30–60°) removed 12 g of unreacted 1,4-bis(chloromethyl)benzene. From the acetone solution was obtained 33.5 g of desired product, mp 143–146°.

5 - (*p*-Anisyloxy)-6-methoxy-8-(4-phthalimidomethylbenzylamino)quinoline (XIII)—Compound XII (2.8 g), 1.6 g of potassium iodide, and 20 ml of acetone were boiled for 1 hr and concentrated. The aminoquinoline (X) (3 g) was added together with 1.3 g of anhydrous potassium carbonate and 20 ml of 2-propanol. This mixture was heated in an open flask on a steam bath for 1.5 hr, allowing the 2-propanol to evaporate. The residue was poured into water, made basic with potassium carbonate, extracted with chloroform, and dried (sodium sulfate).

The chloroform was removed *in vacuo*, and the residue was heated with absolute ethanol to give an orange solid. This solid was dissolved in benzene, treated with charcoal, filtered, and concentrated to an oily residue. Addition of warm absolute ethanol gave an orange solid, which was collected and washed with absolute ethanol, mp 164–165°. The yield was 3 g (55%). In a second experiment, the yield was increased to 76%.

Anal.—Calc. for $C_{33}H_{27}N_3O_5$: C, 72.65; H, 4.99; N, 7.70. Found: C, 72.82; H, 5.04; N, 7.58.

5-(*p*-Anisyloxy)-6-methoxy-8-(4-aminomethylbenzylamino)-quinoline Maleate (VI)—The phthalimido compound (XIII) (11 g, 0.02 mole) in 200 ml of 95% ethanol and 10 ml of 85% hydrazine hydrate was refluxed for 1.5 hr at 90–100°. Ethanol was removed, 20 g of potassium hydroxide in 20 ml of water was added, and the mixture was stirred for 0.5 hr. The solution was extracted with ether (500 ml), dried over sodium sulfate, concentrated, and redissolved in ether. A saturated ether solution of maleic acid (11 g/500 ml of ether) was added. The yellowish orange precipitate (hygroscopic) was filtered, dissolved in chloroform, and reprecipitated with ether, mp 136–139°. It analyzed as the dimaleate salt.

Anal.—Calc. for $C_{25}H_{25}N_3O_3 \cdot (C_4H_4O_4)_2$: C, 61.20; H, 5.16; N, 6.49. Found: C, 60.91; H, 5.24; N, 6.72.

Two additional reprecipitations from chloroform by ether gave the product as the monomaleate salt (77.5%), mp 158–160° (Table I).

REFERENCES

(1) K. Paul and C. D. Blanton, Jr., *J. Med. Chem.*, **16**, 1391(1973).

(2) W. P. Wetter and C. D. Blanton, Jr., *ibid.*, **17**, 620(1974).

(3) N. L. Drake, R. A. Hayes, J. A. Garman, R. B. Johnston, G. W. Kelley, S. Melamed, and R. M. Peck, *J. Am. Chem. Soc.*, **71**, 455(1949).

(4) G. R. Coatney, W. C. Cooper, N. B. Eddy, and J. Greenberg, "Survey of Antimalarial Agents," Public Health Monograph No. 9, U.S. Government Printing Office, Washington, D.C., 1953, p. 47.

(5) P. B. Russell, in "Medicinal Chemistry," 2nd ed., A. Burger, Ed., Interscience, New York, N.Y., 1960, p. 814.

(6) F. Schonhofer, *Z. Physiol. Chem.*, **274**, 1(1942).

(7) P. E. Thompson and L. M. Werbel, "Antimalarial Agents," Academic, New York, N.Y., 1972, p. 100.

(8) A. Funke, D. Bovet, and G. Montezin, *Ann. Inst. Pasteur, Paris*, **72**, 264(1946).

(9) T. S. Osdene, P. B. Russell, and L. Rane, *J. Med. Chem.*, **10**, 431(1967).

(10) "Chemotherapy of Malaria and Resistance to Antimalarials," *WHO Tech. Rep. Ser.*, No. 529 (1973).

(11) "WHO Report of Procedures for Screening Potential Antimalarial Compounds," in World Health Organization (1972b); WHO/MAL/72.763 (cyclostyled report), WHO, Geneva.

(12) R. C. Elderfield, W. R. Vaughan, B. R. Millward, and J. H. Ross, *J. Org. Chem.*, **23**, 1378(1958).

(13) W. M. Lauer, C. Rondestvedt, R. T. Arnold, N. L. Drake, J. VanHook, and J. Tinker, *J. Am. Chem. Soc.*, **68**, 1546(1946).

ACKNOWLEDGMENTS AND ADDRESSES

Received September 8, 1975, from the *Department of Medicinal Chemistry, School of Pharmacy, University of Georgia, Athens, GA 30602*

Accepted for publication December 1, 1975.

Supported by the U.S. Army Medical and Development Command under Contract DADA 17-71-C1068.

This paper is Contribution No. 1375 from the Army Research Program on Malaria.

The authors thank Dr. R. E. Strube, Dr. E. A. Steck, and Dr. T. R. Sweeney of the Walter Reed Army Institute of Research for interest and encouragement.

[x] To whom inquiries should be directed.

Determination of Salicylates by GLC

JOHN P. TISCHIO

Abstract □ Silylation of salicylic acid by hexamethyldisilazane, *N,O*-bis(trimethylsilyl)acetamide, and *N,N*-bis(trimethylsilyl)trifluoroacetamide was compared using GLC. The completeness of the reaction, the stability of products, and the reproducibility of results with time were investigated. Different reaction vessels were examined for their reliability and application for a routine assay procedure.

Keyphrases □ GLC—analysis, salicylic acid, different silylating reagents and different reaction vessels compared □ Salicylic acid—GLC analysis, different silylating reagents and different reaction vessels compared □ Silylating reagents, various—compared in GLC analysis of salicylic acid □ Keratolytic agents—salicylic acid, GLC analysis

Several methods for the determination of salicylates in physiological fluids were reviewed previously (1). One of these, GLC, is attractive because it affords a sensitive quantitative method for the simultaneous determination of aspirin and salicylic acid. Several papers have reported different GLC procedures (1–5), but the most promising incorporate a silylation process after extraction of the salicylates from the physiological fluid. The silylating reagents that have been utilized include hexamethyldisilazane (2), *N,O*-bis(trimethylsilyl)-acetamide (3), and *N,N*-bis(trimethylsilyl)trifluoroacetamide (4).

pentylamino]quinoline *d*-Tartrate (V)—This compound was prepared from salicylaldehyde by the procedure previously described. A yield of 96% was obtained, mp 90–95° (with bubbling at 80°).

4-Phthalimidomethylbenzyl Chloride (XII)—1,4-Bis(chloromethyl)benzene (43.7 g, 0.25 mole) was added to 300 ml of dimethylformamide. Potassium phthalimide (46 g, 0.25 mole) was added in two portions. The second portion was added after 3 hr together with another 300 ml of dimethylformamide. The mixture was heated for 3 hr at 85°, and 500 ml of dimethylformamide distilled off under aspirator vacuum (about 18–19 hr). The residue was poured into water, and a white material was collected. This material was extracted with 1 liter of acetone, leaving 18.5 g of the insoluble diphthalimido product. Extraction of the acetone solution with hot petroleum ether (bp 30–60°) removed 12 g of unreacted 1,4-bis(chloromethyl)benzene. From the acetone solution was obtained 33.5 g of desired product, mp 143–146°.

5 - (*p*-Anisyloxy)-6-methoxy-8-(4-phthalimidomethylbenzylamino)quinoline (XIII)—Compound XII (2.8 g), 1.6 g of potassium iodide, and 20 ml of acetone were boiled for 1 hr and concentrated. The aminoquinoline (X) (3 g) was added together with 1.3 g of anhydrous potassium carbonate and 20 ml of 2-propanol. This mixture was heated in an open flask on a steam bath for 1.5 hr, allowing the 2-propanol to evaporate. The residue was poured into water, made basic with potassium carbonate, extracted with chloroform, and dried (sodium sulfate).

The chloroform was removed *in vacuo*, and the residue was heated with absolute ethanol to give an orange solid. This solid was dissolved in benzene, treated with charcoal, filtered, and concentrated to an oily residue. Addition of warm absolute ethanol gave an orange solid, which was collected and washed with absolute ethanol, mp 164–165°. The yield was 3 g (55%). In a second experiment, the yield was increased to 76%.

Anal.—Calc. for $C_{33}H_{27}N_3O_5$: C, 72.65; H, 4.99; N, 7.70. Found: C, 72.82; H, 5.04; N, 7.58.

5-(*p*-Anisyloxy)-6-methoxy-8-(4-aminomethylbenzylamino)-quinoline Maleate (VI)—The phthalimido compound (XIII) (11 g, 0.02 mole) in 200 ml of 95% ethanol and 10 ml of 85% hydrazine hydrate was refluxed for 1.5 hr at 90–100°. Ethanol was removed, 20 g of potassium hydroxide in 20 ml of water was added, and the mixture was stirred for 0.5 hr. The solution was extracted with ether (500 ml), dried over sodium sulfate, concentrated, and redissolved in ether. A saturated ether solution of maleic acid (11 g/500 ml of ether) was added. The yellowish orange precipitate (hygroscopic) was filtered, dissolved in chloroform, and reprecipitated with ether, mp 136–139°. It analyzed as the dimaleate salt.

Anal.—Calc. for $C_{25}H_{25}N_3O_3 \cdot (C_4H_4O_4)_2$: C, 61.20; H, 5.16; N, 6.49. Found: C, 60.91; H, 5.24; N, 6.72.

Two additional reprecipitations from chloroform by ether gave the product as the monomaleate salt (77.5%), mp 158–160° (Table I).

REFERENCES

(1) K. Paul and C. D. Blanton, Jr., *J. Med. Chem.*, **16**, 1391(1973).

(2) W. P. Wetter and C. D. Blanton, Jr., *ibid.*, **17**, 620(1974).

(3) N. L. Drake, R. A. Hayes, J. A. Garman, R. B. Johnston, G. W. Kelley, S. Melamed, and R. M. Peck, *J. Am. Chem. Soc.*, **71**, 455(1949).

(4) G. R. Coatney, W. C. Cooper, N. B. Eddy, and J. Greenberg, "Survey of Antimalarial Agents," Public Health Monograph No. 9, U.S. Government Printing Office, Washington, D.C., 1953, p. 47.

(5) P. B. Russell, in "Medicinal Chemistry," 2nd ed., A. Burger, Ed., Interscience, New York, N.Y., 1960, p. 814.

(6) F. Schonhofer, *Z. Physiol. Chem.*, **274**, 1(1942).

(7) P. E. Thompson and L. M. Werbel, "Antimalarial Agents," Academic, New York, N.Y., 1972, p. 100.

(8) A. Funke, D. Bovet, and G. Montezin, *Ann. Inst. Pasteur, Paris*, **72**, 264(1946).

(9) T. S. Osdene, P. B. Russell, and L. Rane, *J. Med. Chem.*, **10**, 431(1967).

(10) "Chemotherapy of Malaria and Resistance to Antimalarials," *WHO Tech. Rep. Ser.*, No. 529 (1973).

(11) "WHO Report of Procedures for Screening Potential Antimalarial Compounds," in World Health Organization (1972b); WHO/MAL/72.763 (cyclostyled report), WHO, Geneva.

(12) R. C. Elderfield, W. R. Vaughan, B. R. Millward, and J. H. Ross, *J. Org. Chem.*, **23**, 1378(1958).

(13) W. M. Lauer, C. Rondestvedt, R. T. Arnold, N. L. Drake, J. VanHook, and J. Tinker, *J. Am. Chem. Soc.*, **68**, 1546(1946).

ACKNOWLEDGMENTS AND ADDRESSES

Received September 8, 1975, from the *Department of Medicinal Chemistry, School of Pharmacy, University of Georgia, Athens, GA 30602*

Accepted for publication December 1, 1975.

Supported by the U.S. Army Medical and Development Command under Contract DADA 17-71-C1068.

This paper is Contribution No. 1375 from the Army Research Program on Malaria.

The authors thank Dr. R. E. Strube, Dr. E. A. Steck, and Dr. T. R. Sweeney of the Walter Reed Army Institute of Research for interest and encouragement.

[x] To whom inquiries should be directed.

Determination of Salicylates by GLC

JOHN P. TISCHIO

Abstract □ Silylation of salicylic acid by hexamethyldisilazane, *N,O*-bis(trimethylsilyl)acetamide, and *N,N*-bis(trimethylsilyl)trifluoroacetamide was compared using GLC. The completeness of the reaction, the stability of products, and the reproducibility of results with time were investigated. Different reaction vessels were examined for their reliability and application for a routine assay procedure.

Keyphrases □ GLC—analysis, salicylic acid, different silylating reagents and different reaction vessels compared □ Salicylic acid—GLC analysis, different silylating reagents and different reaction vessels compared □ Silylating reagents, various—compared in GLC analysis of salicylic acid □ Keratolytic agents—salicylic acid, GLC analysis

Several methods for the determination of salicylates in physiological fluids were reviewed previously (1). One of these, GLC, is attractive because it affords a sensitive quantitative method for the simultaneous determination of aspirin and salicylic acid. Several papers have reported different GLC procedures (1–5), but the most promising incorporate a silylation process after extraction of the salicylates from the physiological fluid. The silylating reagents that have been utilized include hexamethyldisilazane (2), *N,O*-bis(trimethylsilyl)-acetamide (3), and *N,N*-bis(trimethylsilyl)trifluoroacetamide (4).

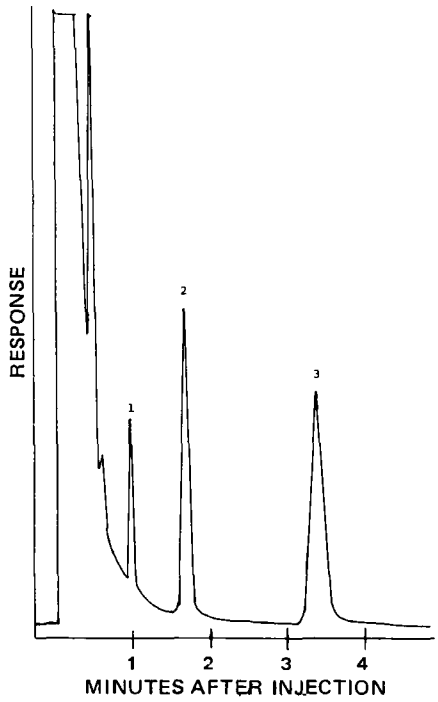

Figure 1—*Typical chromatogram. Key: 1, naphthalene; 2, trimethylsilyl-p-toluic acid; and 3, trimethylsilylsalicylic acid.*

However, when analyzing blood samples for salicylates, different results are obtained depending upon which silylating reagent is used, which reaction vessel is employed, and when the samples are analyzed after derivatization. In this report, a comparison is made of these silylating agents for their completeness of reaction, the stability of trimethylsilylated derivatives in the silylating mixture, and the reproducibility of results. In addition, three different vessels (a polyseal screw-capped centrifuge tube, a ground-glass-stoppered centrifuge tube, and a cork-stoppered centrifuge tube) were examined for their applicability for a routine assay procedure.

EXPERIMENTAL

Materials—The following chemicals were of analytical reagent quality unless otherwise noted: salicylic acid[1] USP, *p*-toluic acid[2], naphthalene[3], acetone[3], anhydrous ether[3], and the silylating reagents hexamethyldisilazane[4], *N,O*-bis(trimethylsilyl)acetamide[4], and *N,N*-bis(trimethylsilyl)trifluoroacetamide[4]. Other materials included screw-capped 15-ml conical centrifuge tubes fitted with polyseal screw caps[5], ground-glass 15-ml conical centrifuge tubes fitted with ground-glass stoppers[5], and plain 15-ml centrifuge tubes fitted with corks[5].

Apparatus—A flame-ionization gas chromatograph[6] was employed with a 1.2-m (4-ft) × 4-mm silanized glass column packed with 3% OV-17 on Gas Chrom Q (100–120 mesh), acid washed and silanized[4].

Analytical Procedure—*GLC Conditions*—The injector and detector temperatures were 200°, the column temperature was 130°, and the helium carrier gas flow rate was 18 ml/min.

Silylation Procedure—A standard stock solution of *p*-toluic acid and salicylic acid was made in anhydrous ether and had a final concentration of 50 μg of each acid/ml. A 0.5-ml aliquot of this solution was pipetted into each of nine silylating vessels (three screw-capped tubes, three ground-glass tubes, and three plain tubes), and each was evaporated on a heating block maintained at 60°. After evaporation, 50 μl of each silylating reagent was added to each type of reaction vessel.

All tubes were flushed with a stream of nitrogen, capped with their respective stoppers immediately, and then incubated in an oven maintained at 60°. After 1 hr, the tubes were removed and allowed to return to room temperature (~5 min). Then 50 μl of an acetone solution containing 100 μg of naphthalene/ml was added to each tube. A 5-μl sample of this last mixture was then subjected to GLC analysis.

[1] Merck and Co.
[2] Matheson, Coleman and Bell Co.
[3] Baker Chemical Co.
[4] Supelco Inc.
[5] Arthur H. Thomas Co.
[6] Gow Mac model 750.

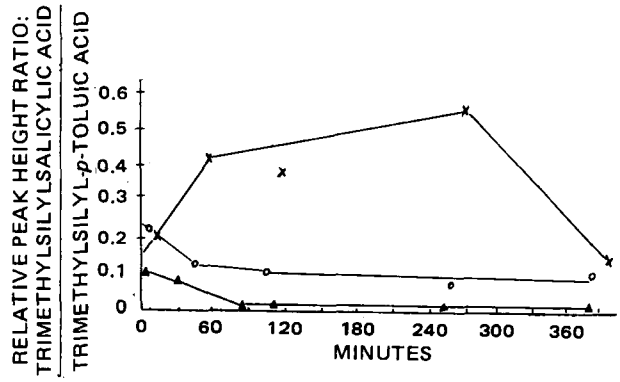

Figure 2—*Comparison of the hexamethyldisilazane reagent in screw-capped tubes (×), ground-glass-stoppered tubes (○), and cork-stoppered tubes (△).*

RESULTS AND DISCUSSION

Hexamethyldisilazane, *N,O*-bis(trimethylsilyl)acetamide, and *N,N*-bis(trimethylsilyl)trifluoroacetamide have been reported as reagents for derivatizing salicylates for their subsequent GLC analysis. This study was conducted over a 6-hr period to determine the relative completeness of the silylation reaction, the stability of trimethylsilyl derivatives in the silylating reagent, and the relative qualitative and quantitative GLC response with respect to time. In addition, several different reaction tubes were investigated as to their suitability for routine analysis.

Figure 1 illustrates a typical *N,N*-bis(trimethylsilyl)trifluoroacetamide chromatogram tracing, showing the separation of naphthalene, trimethylsilyl-*p*-toluic acid, and trimethylsilylsalicylic acid. Their relative retention times under the experimental conditions were 1, 1.8, and 3.5 min, respectively, in close agreement with retention times found by others (4).

Naphthalene, which is not silylatable, is used as an internal standard to ensure consistency in sampling size, with the intensity of its peak not varying more than 3% between samples. The trimethylsilyl-*p*-toluic acid peak is employed as an internal silylatable standard,

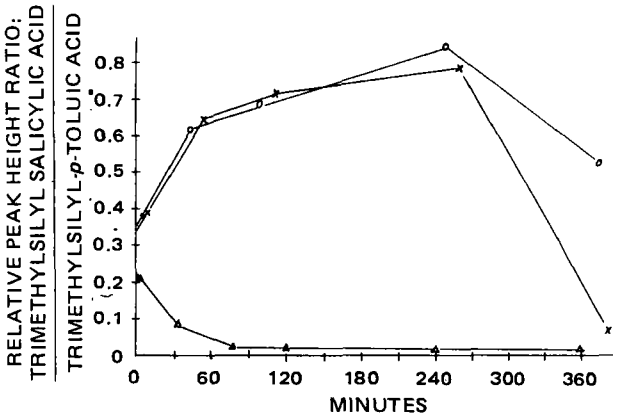

Figure 3—*Comparison of the N,O-bis(trimethylsilyl)acetamide reagent in screw-capped tubes (×), ground-glass-stoppered tubes (○), and cork-stoppered tubes (△).*

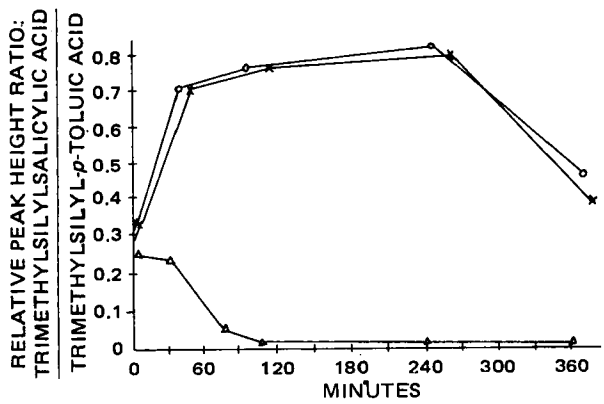

Figure 4—*Comparison of the* N,N-*bis(trimethylsilyl)trifluoroacetamide reagent in screw-capped tubes* (×), *ground-glass-stoppered tubes* (○), *and cork-stoppered tubes* (△).

and the ratio of trimethylsilylsalicylic acid to trimethylsilyl-*p*-toluic acid peaks is a relative measurement of the trimethylsilylsalicylic acid concentration from sample to sample.

The data obtained for each silylating reagent in the three different reaction vessels are compared in Figs. 2–4. In each figure, the ratio of relative peak heights of trimethylsilylsalicylic acid to trimethylsilyl-*p*-toluic acid is plotted *versus* time. All time intervals indicated on the graph for each sample are the times elapsed after removal from incubation.

The hexamethyldisilazane reagent did not silylate the salicylic acid to the same extent as the other reagents under the conditions described. In addition, as time elapsed, the hexamethyldisilazane chromatograms became complex due to the appearance of many interfering peaks (Figs. 5 and 6). Qualitatively as well as quantitatively, this reagent proved to be unsatisfactory.

The *N,O*-bis(trimethylsilyl)acetamide reagent appeared to give the same completeness of derivatization of salicylic acid as *N,N*-bis-(trimethylsilyl)trifluoroacetamide. However, the former showed a deterioration with time as was evident by the peaks tailing and becoming unsymmetrical (Fig. 7).

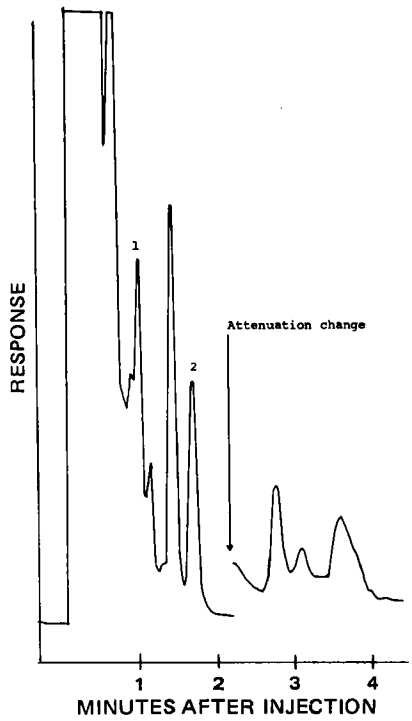

Figure 6—*Typical hexamethyldisilazane gas chromatogram 260 min after derivatization. Key: 1, naphthalene; and 2, trimethylsilyl-*p*-toluic acid.*

The *N,N*-bis(trimethylsilyl)trifluoroacetamide proved to be the best silylating reagent with respect to completeness of derivatization, stability, and reproducibility of the peaks with time under these conditions. Therefore, *N,N*-bis(trimethylsilyl)trifluoroacetamide is the reagent of choice for the silylation of salicylates.

In addition to the differences obtained due to the silylation reagents, the reaction vessel can be a diminishing factor in the amount of measurable derivatives remaining in the tube. Samples silylated in cork-stoppered vessels, whether hexamethyldisilazane, *N,O*-bis-

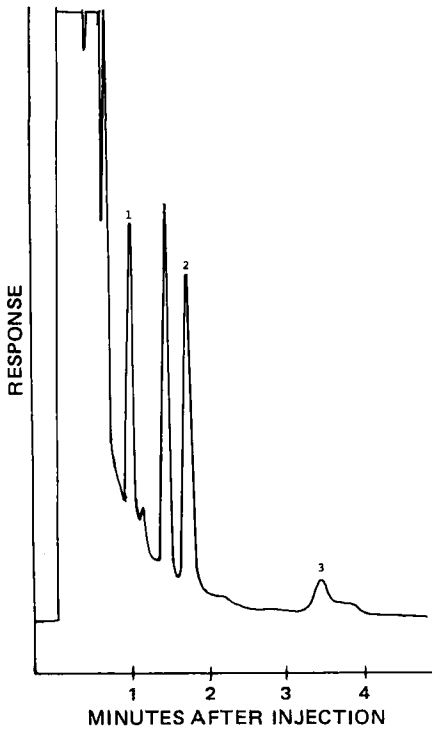

Figure 5—*Typical hexamethyldisilazane gas chromatogram 70 min after derivatization. Key: 1, naphthalene; 2, trimethylsilyl-*p*-toluic acid; and 3, trimethylsilylsalicylic acid.*

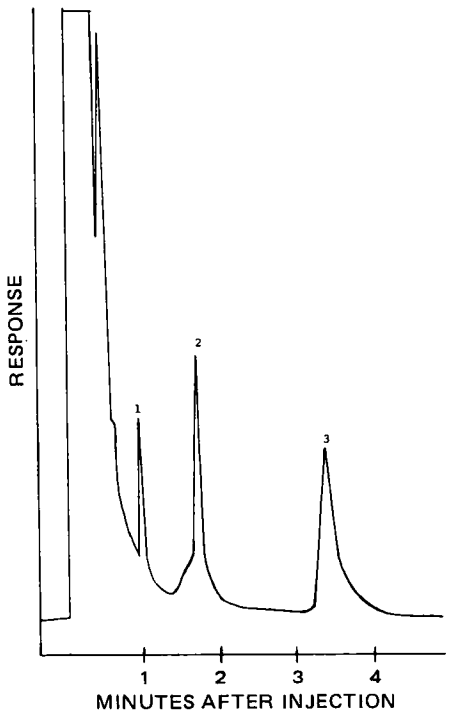

Figure 7—*Typical* N,O-*bis(trimethylsilyl)acetamide gas chromatogram 65 min after derivatization. Key: 1, naphthalene; 2, trimethylsilyl-*p*-toluic acid; and 3, trimethylsilylsalicylic acid.*

(trimethylsilyl)acetamide, or *N,N*-bis(trimethylsilyl)trifluoroacetamide, were totally unsatisfactory. The disappearance of trimethylsilylsalicylic acid with respect to trimethylsilyl-*p*-toluic acid over time was most demonstrable under the cork-stoppered vessel conditions. Polyseal screw-capped and ground-glass-stoppered vessels were satisfactory.

To determine the difficulty with the cork-stoppered tubes, pieces of cork were suspended in three screw-capped tubes, each containing a sample to be silylated along with one silylating reagent. A polyseal cap was used to seal off the tube, and incubation and analysis were performed as described. The chromatograms showed the same pattern as was found for the cork-stoppered vessels for each reagent. The cork probably absorbed the trimethylsilyl derivatives and thereby reduced the amount of measurable derivative.

Regarding the optimal time for injection of samples, the most reliable time for consistent results for salicylic acid was between 1 and 4 hr after incubation. On the other hand, aspirin was reported to be silylated almost instantaneously (4), and its trimethylsilyl derivative probably should be analyzed as soon as possible to reduce the extent of hydrolysis by the presence of moisture. If both salicylates are being analyzed simultaneously, a prescribed time for injection of the sample should be followed closely, recognizing the variables involved for optimizing each determination.

In conclusion, certain recommendations can be made pertaining to the routine assaying of salicylates by GLC. For the qualitative and quantitative analysis of the silylated derivative of salicylic acid, *N,N*-bis(trimethylsilyl)trifluoroacetamide is the silylating reagent of choice. Polyseal screw-capped stoppered tubes are also recommended as the reaction vessel due to their ease and reliability of use. In addition, injection should be performed between 1 and 4 hr after incubation for optimal and reliable results for salicylic acid.

REFERENCES

(1) L. J. Walter, D. F. Biggs, and R. T. Coutt, *J. Pharm. Sci.*, **63**, 1754(1974).

(2) M. Rowland and S. Riegelman, *ibid.*, **56**, 717(1967).

(3) S. Patel, J. H. Perrin, and J. J. Windheuser, *ibid.*, **61**, 1794(1972).

(4) B. H. Thomas, G. Solomonraj, and B. B. Coldwell, *J. Pharm. Pharmacol.*, **25**, 201(1973).

(5) R. C. Crippen and H. C. Freimuth, *Anal. Chem.*, **36**, 273(1964).

ACKNOWLEDGMENTS AND ADDRESSES

Received September 22, 1975, from the *Department of Chemistry, Philadelphia College of Pharmacy and Science, Philadelphia, PA 19104*

Accepted for publication December 10, 1975.

Supported by the Henry Leffmann Research Grant of the Wagner Free Institute of Science, Philadelphia.

The author expresses his appreciation for the criticism and help of Dr. Alfonso Gennaro.

High-Performance Liquid Chromatographic Separation of C-15-Epimers of 15-Methylprostaglandin E_2 Methyl Ester and 15-Methylprostaglandin E_2

R. K. LUSTGARTEN

Abstract □ A high-performance liquid chromatographic system that permits quantitation of 15-methylprostaglandin E_2 and its methyl ester is described. Separation from the corresponding C-15 epimers is effected by adsorption chromatography on microparticulate silica with refractive index detection.

Keyphrases □ 15-Methylprostaglandin E_2 and methyl ester—high-performance liquid chromatographic analysis and separation from C-15-epimers □ High-performance liquid chromatography—analysis, 15-methylprostaglandin E_2 and methyl ester, separation from C-15-epimers □ Prostaglandins—15-methylprostaglandin E_2 and methyl ester, high-performance liquid chromatographic analysis and separation from C-15-epimers

The methyl ester of 15-(*R*)-methylprostaglandin E_2 (I*a*) and its corresponding acid (I*b*) are potentially pharmacologically active in the treatment of gastric hyperacidity (1, 2). Procedures are known that would separate them from possible degradation products, *e.g.*, the prostaglandin A_2 and prostaglandin B_2 analogs (3–5), but there has been no efficient way of quantitating them in the presence of their 15-epimers (II*a* and II*b*). This paper presents a precise, rapid, and efficient method for doing so. The technique and data are discussed for the I*a*–II*a* system. Except for the composition of the mobile phase, the procedure and results for the I*b*–II*b* system directly parallel those for the esters, so this system will not be discussed in detail.

EXPERIMENTAL

Materials—Prostaglandin[1] samples, methyl acetate[2], and all other materials were obtained from commercial sources and used directly.

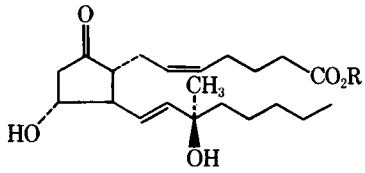

I*a*: R = CH_3
I*b*: R = H

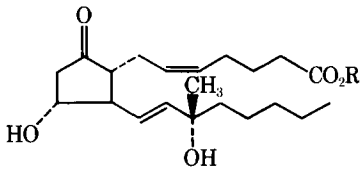

II*a*: R = CH_3
II*b*: R = H

[1] The Upjohn Co.
[2] Fisher Certified grade.

(trimethylsilyl)acetamide, or *N,N*-bis(trimethylsilyl)trifluoroacetamide, were totally unsatisfactory. The disappearance of trimethylsilylsalicylic acid with respect to trimethylsilyl-*p*-toluic acid over time was most demonstrable under the cork-stoppered vessel conditions. Polyseal screw-capped and ground-glass-stoppered vessels were satisfactory.

To determine the difficulty with the cork-stoppered tubes, pieces of cork were suspended in three screw-capped tubes, each containing a sample to be silylated along with one silylating reagent. A polyseal cap was used to seal off the tube, and incubation and analysis were performed as described. The chromatograms showed the same pattern as was found for the cork-stoppered vessels for each reagent. The cork probably absorbed the trimethylsilyl derivatives and thereby reduced the amount of measurable derivative.

Regarding the optimal time for injection of samples, the most reliable time for consistent results for salicylic acid was between 1 and 4 hr after incubation. On the other hand, aspirin was reported to be silylated almost instantaneously (4), and its trimethylsilyl derivative probably should be analyzed as soon as possible to reduce the extent of hydrolysis by the presence of moisture. If both salicylates are being analyzed simultaneously, a prescribed time for injection of the sample should be followed closely, recognizing the variables involved for optimizing each determination.

In conclusion, certain recommendations can be made pertaining to the routine assaying of salicylates by GLC. For the qualitative and quantitative analysis of the silylated derivative of salicylic acid, *N,N*-bis(trimethylsilyl)trifluoroacetamide is the silylating reagent of choice. Polyseal screw-capped stoppered tubes are also recommended as the reaction vessel due to their ease and reliability of use. In addition, injection should be performed between 1 and 4 hr after incubation for optimal and reliable results for salicylic acid.

REFERENCES

(1) L. J. Walter, D. F. Biggs, and R. T. Coutt, *J. Pharm. Sci.*, **63**, 1754(1974).

(2) M. Rowland and S. Riegelman, *ibid.*, **56**, 717(1967).

(3) S. Patel, J. H. Perrin, and J. J. Windheuser, *ibid.*, **61**, 1794(1972).

(4) B. H. Thomas, G. Solomonraj, and B. B. Coldwell, *J. Pharm. Pharmacol.*, **25**, 201(1973).

(5) R. C. Crippen and H. C. Freimuth, *Anal. Chem.*, **36**, 273(1964).

ACKNOWLEDGMENTS AND ADDRESSES

Received September 22, 1975, from the *Department of Chemistry, Philadelphia College of Pharmacy and Science, Philadelphia, PA 19104*

Accepted for publication December 10, 1975.

Supported by the Henry Leffmann Research Grant of the Wagner Free Institute of Science, Philadelphia.

The author expresses his appreciation for the criticism and help of Dr. Alfonso Gennaro.

High-Performance Liquid Chromatographic Separation of C-15-Epimers of 15-Methylprostaglandin E_2 Methyl Ester and 15-Methylprostaglandin E_2

R. K. LUSTGARTEN

Abstract □ A high-performance liquid chromatographic system that permits quantitation of 15-methylprostaglandin E_2 and its methyl ester is described. Separation from the corresponding C-15 epimers is effected by adsorption chromatography on microparticulate silica with refractive index detection.

Keyphrases □ 15-Methylprostaglandin E_2 and methyl ester—high-performance liquid chromatographic analysis and separation from C-15-epimers □ High-performance liquid chromatography—analysis, 15-methylprostaglandin E_2 and methyl ester, separation from C-15-epimers □ Prostaglandins—15-methylprostaglandin E_2 and methyl ester, high-performance liquid chromatographic analysis and separation from C-15-epimers

The methyl ester of 15-(*R*)-methylprostaglandin E_2 (I*a*) and its corresponding acid (I*b*) are potentially pharmacologically active in the treatment of gastric hyperacidity (1, 2). Procedures are known that would separate them from possible degradation products, *e.g.*, the prostaglandin A_2 and prostaglandin B_2 analogs (3–5), but there has been no efficient way of quantitating them in the presence of their 15-epimers (II*a* and II*b*). This paper presents a precise, rapid, and efficient method for doing so. The technique and data are discussed for the I*a*–II*a* system. Except for the composition of the mobile phase, the procedure and results for the I*b*–II*b* system directly parallel those for the esters, so this system will not be discussed in detail.

EXPERIMENTAL

Materials—Prostaglandin[1] samples, methyl acetate[2], and all other materials were obtained from commercial sources and used directly.

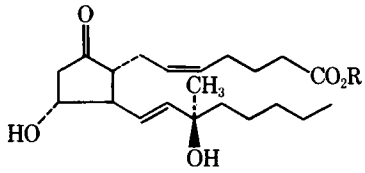

I*a*: R = CH_3
I*b*: R = H

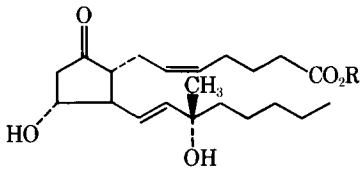

II*a*: R = CH_3
II*b*: R = H

[1] The Upjohn Co.
[2] Fisher Certified grade.

High-Performance Liquid Chromatographic (HPLC) Procedure—The instrumentation was a modular setup consisting of a solvent delivery system[3], a loop injector[4], a 30-cm microparticulate silica gel column[5], and a differential refractometer for detection (attenuation = 8)[6] linked to a strip-chart recorder[7]. The mobile phases were 100% methyl acetate for I*a*–II*a* and 99.5% methyl acetate–0.5% acetic acid for I*b*–II*b*. The flow rate was 1.25 ml/min (~450 psi), and the injection volume was 8–10 μl.

Internal Standard Solution—This solution was prepared by dissolving sufficient 1,3-butanediol in the mobile phase to obtain a concentration of about 25 mg/ml. 1,6-Hexanediol, at 30 mg/ml, is a satisfactory alternative internal standard.

Reference Standard Solution—This solution was prepared by accurately weighing about 6.6 mg of the reference material and dissolving it in 1.0 ml of the internal standard solution.

Sample Solution—This solution was prepared in the same way as the reference standard solution.

Computation—Peak heights were measured and expressed in three significant figures. The following equation for the percent purity of the sample was then applied:

$$\text{percent purity} = \left(\frac{H_{is}W_r}{H_r}\right)\left(\frac{H_s}{H_{is}W_s}\right)(P) \qquad \text{(Eq. 1)}$$

where:

W_r = weight of reference material (milligrams)
W_s = weight of sample (milligrams)
H_r = peak height of reference material
H_s = peak height of sample
H_{is} = peak height of internal standard
P = percent purity of reference material

RESULTS AND DISCUSSION

Figure 1 shows a chromatogram of a simulated mixture of I*a*, II*a*, and the internal standard. Chloroform was added to mark the solvent front. Essentially baseline resolution of the epimers was achieved. The time from injection to complete elution of internal standard was about 7 min. Since dehydration products of I (*e.g.*, prostaglandin B and A analogs) are considerably less polar, they would appear on the solvent front and would not interfere with quantitation (3–5). Furthermore, products due to deesterification, *e.g.*, I*b* and II*b*, would remain on the column. Thus, the chromatography is highly selective for the compounds of interest. Moreover, the prostaglandin $F_{2\alpha}$ analogs of I*a* and II*a* have significantly longer retention times than II*a* under the conditions of Fig. 1.

The refractive index detector is inherently less sensitive than other popular forms of detection. This creates no problem in the present case, since there is virtually no limitation on sample size. The amount of sample injected corresponds to about 70 μg of material. Up to several hundred micrograms may be injected without loss of efficiency. The absolute limit of detection is about 1 μg. The sensitivity with respect to trace contamination by II*a* was studied separately (*vide infra*); about 1% could be detected. This limit could presumably be reduced if larger quantities of sample are injected.

The experimental response curve was measured over a range corresponding to about 40–85 μg of I*a*. (The concentration range was ~3–9 mg of drug/ml of internal standard solution.) Linear regression analysis revealed excellent linearity over this range. The correlation coefficient was 0.9998. Within experimental error, the response curve passed through the origin. Indeed, no interfering peaks were detected in a sample blank. Therefore, the procedure contains no systematic bias on accuracy.

Table I demonstrates the precision for the assay of an impure sample *versus* the reference standard. Satisfactory results were obtained: *RSD* = 0.87%.

Table II demonstrates the precision in measuring less than 1% of II*a* in I*a*. The sample was a synthetic mixture of the two epimers. The peak height for II*a* was measured by decreasing the detector attenuation by a factor of four relative to the attenuation of I*a*.

In quantitating II*a* relative to I*a*, a relative response factor was needed. This factor was determined by using the well-known base-catalyzed conversion of prostaglandin E_2 systems to the corresponding prostaglandin B_2 chromophore (6–8). The procedure was as follows. First, a peak height ratio was carefully determined for several synthetic mixtures of I*a* and II*a*. The mobile phase was then changed to ethyl acetate. This less polar mobile phase gives even better resolution of the two epimers and allows the quantitative collection of each peak.

The samples were reinjected, and each peak was collected in a small vial. The mobile phase was evaporated, and the residue was dissolved in 10.0 ml of a solution of 0.2 *N* KOH in 90% methanol. The solutions were allowed to stand for 0.5 hr, and the UV absorbance was determined at the maximum (278 nm) (6). The ratio of the absorbances was taken to be the true ratio of the two epimers. (It was shown independently that the absorptivities of the corresponding prostaglandin B_2 epimers are equal within experimental error.)

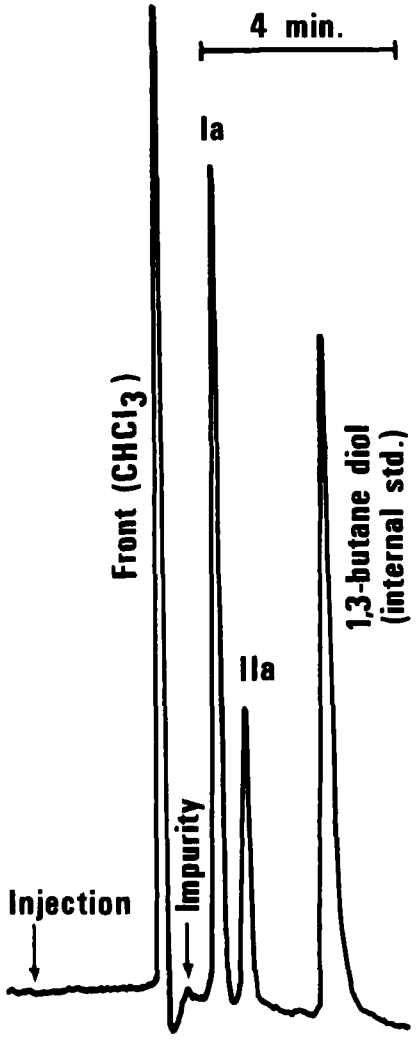

Figure 1—*HPLC chromatogram of synthetic mixture. Chromatographic conditions are given in the text.*

Table I—Precision of Assay

Sample Weight, mg	Assay Result, mg		Purity, %
3.855	3.687		95.6
5.994	5.600		93.4
7.088	6.704		94.6
5.233	4.930		94.2
7.892	7.388		93.6
4.351	4.127		94.9
		Average	94.4
		RSD	0.87

[3] LDC Corp.
[4] Waters model U6K.
[5] μ-Porasil, Waters.
[6] Waters model 401.
[7] Hewlett-Packard model 7127A.

Table II—Precision of Assay for Trace Quantity of IIa in a Simulated Mixture

Measurement	IIa Found, %[a]
1	0.86
2	0.78
3	0.82
4	0.82
5	0.72
6	0.83
7	0.84
Average	0.81
RSD	5.7

[a] Relative to Ia + IIa = 100% and computed with a correction for detector response as described in the text.

The original chromatographic peak height ratio could then be adjusted accordingly. The net result was that the Ia peak height had to be divided by 1.25; *i.e.*, Ia showed an apparent enhancement relative to IIa by a factor of 1.25 under the assay conditions. Equivalent experiments with the acids were performed, and IIa was enhanced relative to IIb by a factor of 1.23. The reason for the difference in detector response between the epimers is not known.

Sample and reference preparations are equivalent, quick, and routine. Consecutive chromatographic injections may be repeated every 7 min, or the injections may be staggered between the drug and internal standard to effect even shorter intervals.

The silica gel column appears to be quite stable. After several weeks of constant use, it gave chromatograms insignificantly different from the one shown in Fig. 1. This finding was also true for Ib, indicating that a small amount of acetic acid in the mobile phase does not cause significant deterioration of column performance. Some variability was noted, however, between different columns. For best results, the use of a column with 4000 or more plates/0.305 m, as measured and reported by the manufacturer, is recommended. Alternatively, ethyl acetate may be substituted for methyl acetate in the mobile phase. Because the former solvent is less polar than the latter, it gives better resolution of the epimers, albeit with a longer analysis time.

Preliminary experiments showed that the chromatographic system described here has good potential for separating various prostaglandin pairs, each characterized by being epimeric at C-15. Interestingly, the 15-(*R*)-epimer always was eluted before the 15-(*S*)-epimer. This trend was noted previously for some naturally occurring prostaglandins and their C-15-epimers (4).

REFERENCES

(1) S. M. M. Karim, D. C. Carter, D. Bhana, and P. A. Ganesan, *Adv. Biosci.*, **9**, 255(1973).

(2) A. Robert and E. W. Yankee, *Proc. Soc. Exp. Biol. Med.*, **148**, 1155(1975).

(3) E. W. Dunham and M. W. Anders, *Prostaglandins*, **4**, 85(1973).

(4) N. H. Anderson and E. M. K. Leovey, *ibid.*, **6**, 361(1974).

(5) E. G. Daniels, in "Lipid Chromatographic Analysis," G. V. Marinetti, Ed., Dekker, New York, N.Y., 1976, pp. 611–662.

(6) N. H. Andersen, *J. Lipid Res.*, **10**, 320(1969).

(7) R. M. Zusman, *Prostaglandins*, **1**, 167(1972).

(8) D. C. Monkhouse, L. Van Campen, and A. J. Aguiar, *J. Pharm. Sci.*, **62**, 576(1973).

ACKNOWLEDGMENTS AND ADDRESSES

Received September 17, 1975, from *Control Research and Development, The Upjohn Company, Kalamazoo, MI 49001*

Accepted for publication December 2, 1975.

Comparison of Observed and Predicted First-Pass Metabolism of Nortriptyline in Humans

SARFARAZ NIAZI

Abstract □ The extent of first-pass metabolism of nortriptyline, calculated by comparing the areas under the plasma concentration–time curves following intravenous and oral dosing in six individuals, varied from 41 to 54%. Theoretically predicted values ranged from 41 to 61% based on a plasma flow model, indicating that the clearance takes place mainly from the plasma, which does not represent the whole blood concentration.

Keyphrases □ Nortriptyline—first-pass metabolism predicted using plasma flow rates, compared to observed rates □ Metabolism, first pass—nortriptyline, predicted using plasma flow rates, compared to observed rates □ Pharmacokinetics—nortriptyline, first-pass metabolism predicted using plasma flow rates, compared to observed rates □ Antidepressant agents—nortriptyline, first-pass metabolism predicted, compared to observed rates

The systemic availability of nortriptyline in humans was recently reported to vary from 46 to 59% (1). This low bioavailability compared to intravenous dosing was attributed to the first-pass metabolism of nortriptyline, assuming complete absorption from the GI tract and no extrahepatic metabolism (1). It was also postulated (1) that the plasma concentration represents the whole blood concentration.

The purpose of this report is to show that the last assumption may not be correct, since a theoretical prediction of first-pass metabolism can be made if plasma flow rates are considered instead of total blood flow, indicating restriction of nortriptyline to plasma or slow partitioning between plasma and blood cells (2).

DISCUSSION

Theoretical prediction of the first-pass metabolism of imipramine based on the equation of Gibaldi *et al.* (2) was reported (3):

$$\% FP = \frac{(\text{dose}/AUC)(100)}{\text{flow rate} + (\text{dose}/AUC)} \qquad \text{(Eq. 1)}$$

where % *FP* is the percent of drug metabolized during each pass through the liver, *AUC* is the area under the plasma concentration–time curve following oral administration, and flow rate is the blood or plasma flow rate through the liver.

It was shown (3) that good correlations can be obtained for im-

Table II—Precision of Assay for Trace Quantity of IIa in a Simulated Mixture

Measurement	IIa Found, %[a]
1	0.86
2	0.78
3	0.82
4	0.82
5	0.72
6	0.83
7	0.84
Average	0.81
RSD	5.7

[a] Relative to Ia + IIa = 100% and computed with a correction for detector response as described in the text.

The original chromatographic peak height ratio could then be adjusted accordingly. The net result was that the Ia peak height had to be divided by 1.25; *i.e.*, Ia showed an apparent enhancement relative to IIa by a factor of 1.25 under the assay conditions. Equivalent experiments with the acids were performed, and IIa was enhanced relative to IIb by a factor of 1.23. The reason for the difference in detector response between the epimers is not known.

Sample and reference preparations are equivalent, quick, and routine. Consecutive chromatographic injections may be repeated every 7 min, or the injections may be staggered between the drug and internal standard to effect even shorter intervals.

The silica gel column appears to be quite stable. After several weeks of constant use, it gave chromatograms insignificantly different from the one shown in Fig. 1. This finding was also true for Ib, indicating that a small amount of acetic acid in the mobile phase does not cause significant deterioration of column performance. Some variability was noted, however, between different columns. For best results, the use of a column with 4000 or more plates/0.305 m, as measured and reported by the manufacturer, is recommended. Alternatively, ethyl acetate may be substituted for methyl acetate in the mobile phase. Because the former solvent is less polar than the latter, it gives better resolution of the epimers, albeit with a longer analysis time.

Preliminary experiments showed that the chromatographic system described here has good potential for separating various prostaglandin pairs, each characterized by being epimeric at C-15. Interestingly, the 15-(*R*)-epimer always was eluted before the 15-(*S*)-epimer. This trend was noted previously for some naturally occurring prostaglandins and their C-15-epimers (4).

REFERENCES

(1) S. M. M. Karim, D. C. Carter, D. Bhana, and P. A. Ganesan, *Adv. Biosci.*, **9**, 255(1973).

(2) A. Robert and E. W. Yankee, *Proc. Soc. Exp. Biol. Med.*, **148**, 1155(1975).

(3) E. W. Dunham and M. W. Anders, *Prostaglandins*, **4**, 85(1973).

(4) N. H. Anderson and E. M. K. Leovey, *ibid.*, **6**, 361(1974).

(5) E. G. Daniels, in "Lipid Chromatographic Analysis," G. V. Marinetti, Ed., Dekker, New York, N.Y., 1976, pp. 611–662.

(6) N. H. Andersen, *J. Lipid Res.*, **10**, 320(1969).

(7) R. M. Zusman, *Prostaglandins*, **1**, 167(1972).

(8) D. C. Monkhouse, L. Van Campen, and A. J. Aguiar, *J. Pharm. Sci.*, **62**, 576(1973).

ACKNOWLEDGMENTS AND ADDRESSES

Received September 17, 1975, from *Control Research and Development, The Upjohn Company, Kalamazoo, MI 49001*

Accepted for publication December 2, 1975.

Comparison of Observed and Predicted First-Pass Metabolism of Nortriptyline in Humans

SARFARAZ NIAZI

Abstract □ The extent of first-pass metabolism of nortriptyline, calculated by comparing the areas under the plasma concentration–time curves following intravenous and oral dosing in six individuals, varied from 41 to 54%. Theoretically predicted values ranged from 41 to 61% based on a plasma flow model, indicating that the clearance takes place mainly from the plasma, which does not represent the whole blood concentration.

Keyphrases □ Nortriptyline—first-pass metabolism predicted using plasma flow rates, compared to observed rates □ Metabolism, first pass—nortriptyline, predicted using plasma flow rates, compared to observed rates □ Pharmacokinetics—nortriptyline, first-pass metabolism predicted using plasma flow rates, compared to observed rates □ Antidepressant agents—nortriptyline, first-pass metabolism predicted, compared to observed rates

The systemic availability of nortriptyline in humans was recently reported to vary from 46 to 59% (1). This low bioavailability compared to intravenous dosing was attributed to the first-pass metabolism of nortriptyline, assuming complete absorption from the GI tract and no extrahepatic metabolism (1). It was also postulated (1) that the plasma concentration represents the whole blood concentration.

The purpose of this report is to show that the last assumption may not be correct, since a theoretical prediction of first-pass metabolism can be made if plasma flow rates are considered instead of total blood flow, indicating restriction of nortriptyline to plasma or slow partitioning between plasma and blood cells (2).

DISCUSSION

Theoretical prediction of the first-pass metabolism of imipramine based on the equation of Gibaldi *et al.* (2) was reported (3):

$$\% FP = \frac{(\text{dose}/AUC)(100)}{\text{flow rate} + (\text{dose}/AUC)} \qquad \text{(Eq. 1)}$$

where % *FP* is the percent of drug metabolized during each pass through the liver, *AUC* is the area under the plasma concentration–time curve following oral administration, and flow rate is the blood or plasma flow rate through the liver.

It was shown (3) that good correlations can be obtained for im-

Table I—Predicted and Observed First-Pass Metabolism of Nortriptyline in Six Subjects

Subject	AUC, μg/liter × hr	% FP (Observed)	% FP (Predicted) Blood Flow Model	% FP (Predicted) Plasma Flow Model
5	895	54	38	53
6	860	50	39	54
7	925	41	37	53
8	670	53	45	61
9	885	49	38	54
10	1500	50	27	41
Mean ± SEM	—	49.50 ± 1.88	37.33 ± 2.38	52.67 ± 2.64
T, predicted:observed		—	4.02 $p<0.0025$	0.98 (n.s.)

ipramine using a blood flow model, indicating that the plasma indeed represents the total blood concentration. A similar approach is made here using both blood and plasma flow models for nortriptyline.

EXPERIMENTAL

The extent of the first-pass effect was calculated, using Eq. 1, from the *AUC* values reported following oral administration of 50 mg of nortriptyline to six subjects (1). A mean blood flow of 91.8 liters/hr (4) and a plasma flow of 48.65 liters/hr were used for these calculations (hematocrit = 0.47).

RESULTS

Table I lists the predicted and experimentally observed values of the first-pass metabolism of nortriptyline in humans. The blood flow model, with the assumption that the plasma concentration represents the whole blood concentration, fails to predict the first-pass metabolism, whereas the plasma flow model accurately describes the first-pass metabolism. If it is assumed that the absorption of nortriptyline is complete and that there is no extrahepatic metabolism of nortriptyline, it can be concluded that the clearance takes place mainly from the plasma, which does not represent the whole blood concentration.

REFERENCES

(1) L. F. Gram and K. F. Overø, *Clin. Pharmacol. Ther.*, **18**, 305(1975).

(2) M. Gibaldi, R. N. Boyes, and S. Feldman, *J. Pharm. Sci.*, **60**, 1338(1971).

(3) S. Niazi, *ibid.*, **65**, 1063(1976).

(4) M. Gibaldi, *ibid.*, **64**, 1036(1975).

ACKNOWLEDGMENTS AND ADDRESSES

Received September 29, 1975, from the *Department of Pharmacy, College of Pharmacy, University of Illinois at the Medical Center, Chicago, IL 60612*

Accepted for publication December 8, 1975.

Liquid Chromatography in Pharmaceutical Analysis V: Determination of an Isoniazid–Pyridoxine Hydrochloride Mixture

J. T. STEWART, I. L. HONIGBERG ˣ, J. P. BRANT, W. A. MURRAY, J. L. WEBB, and J. B. SMITH

Abstract □ Operating parameters are described for the qualitative and quantitative analysis of an isoniazid–pyridoxine hydrochloride mixture by high-pressure liquid chromatography. Each compound was chromatographed on an octadecyl column, using absolute methanol–water (60:40) (pH 2.5) containing 0.01 *M* dioctyl sodium sulfosuccinate. The flow rate was 2.0 ml/min (2500 psig), and the peaks were detected at 293 nm. The analysis was accomplished using ion-pair formation for effecting chromatographic separation. The time required for separation of the drug mixture is approximately 12 min with an accuracy of 0.17–0.30%.

Keyphrases □ High-pressure liquid chromatography—analysis, isoniazid and pyridoxine hydrochloride in mixtures □ Isoniazid—high-pressure liquid chromatographic analysis in mixtures with pyridoxine hydrochloride □ Pyridoxine hydrochloride—high-pressure liquid chromatographic analysis in mixtures with isoniazid □ Antitubercular agents—isoniazid, high-pressure liquid chromatographic analysis in mixtures with pyridoxine hydrochloride □ Vitamins—pyridoxine hydrochloride, high-pressure liquid chromatographic analysis in mixtures with isoniazid

The separation and quantification of the antitubercular mixture, isoniazid–pyridoxine hydrochloride, are reported as a continuation of investigations into the use of high-pressure liquid chromatography (HPLC) in the analysis of multicomponent dosage forms. Previous studies dealt with the separation, detection, and quantification of cough–cold, diuretic–antihypertensive, and antispasmodic mixtures (1–4) by HPLC. Some analytical problems associated with the isoniazid–pyridoxine hydrochloride mixture include a 10-fold difference in concentration of the ingredients and a much greater molar absorptivity for isoniazid than pyridoxine at 254 nm, the fixed wavelength presently used in most HPLC UV detectors.

Isoniazid and pyridoxine hydrochloride have been analyzed by various methods. Techniques used for isoniazid include colorimetry (5–9), UV spectrophotometry (6), fluorescence (10), polarography (6), and titrimetry (11). Procedures for pyridoxine hydrochloride involve nonaqueous titrimetry (12), UV spectrophotometry (12), colorimetry (13–15), and fluorescence (16).

The determination of the isoniazid–pyridoxine hydrochloride mixture by HPLC overcomes or circumvents many shortcomings in the reported methods. This paper describes an analysis of the drugs using ion-pair

Table I—Predicted and Observed First-Pass Metabolism of Nortriptyline in Six Subjects

Subject	AUC, μg/liter × hr	% FP (Observed)	% FP (Predicted) Blood Flow Model	% FP (Predicted) Plasma Flow Model
5	895	54	38	53
6	860	50	39	54
7	925	41	37	53
8	670	53	45	61
9	885	49	38	54
10	1500	50	27	41
Mean ± SEM	—	49.50 ± 1.88	37.33 ± 2.38	52.67 ± 2.64
T, predicted:observed		—	4.02 $p<0.0025$	0.98 (n.s.)

ipramine using a blood flow model, indicating that the plasma indeed represents the total blood concentration. A similar approach is made here using both blood and plasma flow models for nortriptyline.

EXPERIMENTAL

The extent of the first-pass effect was calculated, using Eq. 1, from the *AUC* values reported following oral administration of 50 mg of nortriptyline to six subjects (1). A mean blood flow of 91.8 liters/hr (4) and a plasma flow of 48.65 liters/hr were used for these calculations (hematocrit = 0.47).

RESULTS

Table I lists the predicted and experimentally observed values of the first-pass metabolism of nortriptyline in humans. The blood flow model, with the assumption that the plasma concentration represents the whole blood concentration, fails to predict the first-pass metabolism, whereas the plasma flow model accurately describes the first-pass metabolism. If it is assumed that the absorption of nortriptyline is complete and that there is no extrahepatic metabolism of nortriptyline, it can be concluded that the clearance takes place mainly from the plasma, which does not represent the whole blood concentration.

REFERENCES

(1) L. F. Gram and K. F. Overø, *Clin. Pharmacol. Ther.*, **18**, 305(1975).

(2) M. Gibaldi, R. N. Boyes, and S. Feldman, *J. Pharm. Sci.*, **60**, 1338(1971).

(3) S. Niazi, *ibid.*, **65**, 1063(1976).

(4) M. Gibaldi, *ibid.*, **64**, 1036(1975).

ACKNOWLEDGMENTS AND ADDRESSES

Received September 29, 1975, from the *Department of Pharmacy, College of Pharmacy, University of Illinois at the Medical Center, Chicago, IL 60612*

Accepted for publication December 8, 1975.

Liquid Chromatography in Pharmaceutical Analysis V: Determination of an Isoniazid–Pyridoxine Hydrochloride Mixture

J. T. STEWART, I. L. HONIGBERG ˣ, J. P. BRANT, W. A. MURRAY, J. L. WEBB, and J. B. SMITH

Abstract □ Operating parameters are described for the qualitative and quantitative analysis of an isoniazid–pyridoxine hydrochloride mixture by high-pressure liquid chromatography. Each compound was chromatographed on an octadecyl column, using absolute methanol–water (60:40) (pH 2.5) containing 0.01 *M* dioctyl sodium sulfosuccinate. The flow rate was 2.0 ml/min (2500 psig), and the peaks were detected at 293 nm. The analysis was accomplished using ion-pair formation for effecting chromatographic separation. The time required for separation of the drug mixture is approximately 12 min with an accuracy of 0.17–0.30%.

Keyphrases □ High-pressure liquid chromatography—analysis, isoniazid and pyridoxine hydrochloride in mixtures □ Isoniazid—high-pressure liquid chromatographic analysis in mixtures with pyridoxine hydrochloride □ Pyridoxine hydrochloride—high-pressure liquid chromatographic analysis in mixtures with isoniazid □ Antitubercular agents—isoniazid, high-pressure liquid chromatographic analysis in mixtures with pyridoxine hydrochloride □ Vitamins—pyridoxine hydrochloride, high-pressure liquid chromatographic analysis in mixtures with isoniazid

The separation and quantification of the antitubercular mixture, isoniazid–pyridoxine hydrochloride, are reported as a continuation of investigations into the use of high-pressure liquid chromatography (HPLC) in the analysis of multicomponent dosage forms. Previous studies dealt with the separation, detection, and quantification of cough–cold, diuretic–antihypertensive, and antispasmodic mixtures (1–4) by HPLC. Some analytical problems associated with the isoniazid–pyridoxine hydrochloride mixture include a 10-fold difference in concentration of the ingredients and a much greater molar absorptivity for isoniazid than pyridoxine at 254 nm, the fixed wavelength presently used in most HPLC UV detectors.

Isoniazid and pyridoxine hydrochloride have been analyzed by various methods. Techniques used for isoniazid include colorimetry (5–9), UV spectrophotometry (6), fluorescence (10), polarography (6), and titrimetry (11). Procedures for pyridoxine hydrochloride involve nonaqueous titrimetry (12), UV spectrophotometry (12), colorimetry (13–15), and fluorescence (16).

The determination of the isoniazid–pyridoxine hydrochloride mixture by HPLC overcomes or circumvents many shortcomings in the reported methods. This paper describes an analysis of the drugs using ion-pair

Table I—Calibration Data for Standard Drug Solutions

Compound	Final Concentration, mg[a]	D/IS Ratio[b]	Slope	Intercept	$r \pm s$[c]
Isoniazid	5.0	2.237 ± 0.031[d]	0.479	−0.180	0.9999
	10.0	4.580 ± 0.007			±0.0226
	20.0	9.413 ± 0.049			
Pyridoxine hydrochloride	0.5	1.386 ± 0.030	2.631	0.062	0.9999
	1.0	2.680 ± 0.010			±0.0091
	2.0	5.328 ± 0.020			

[a] Total milligrams per 10-ml sample. [b] Data represent four replicate injections of standard solutions; D/IS is the ratio of the integrated area of the drug at some concentration divided by the integrated area of isonicotinic acid at 5 mg/10 ml. [c] Correlation coefficient ± standard deviation. [d] Confidence limits at $p = 0.05$.

formation for effecting chromatographic separation. The use of ion-pairs in the separation of tartrazine and its intermediates by HPLC was reported recently (17). A quantitative study is described for a simulated dosage form. The time required for chromatographic separation of the drug mixture is approximately 12 min.

EXPERIMENTAL[1]

Reagents and Chemicals—Powdered samples of isoniazid[2] and pyridoxine hydrochloride[3] were used in the analytical procedure. In addition, dioctyl sodium sulfosuccinate[4] was a component of the mobile phase. All other chemicals and solvents were the highest commercially available materials.

Mobile Phases—The mobile phases were various concentrations of absolute methanol mixed with distilled water. Dioctyl sodium sulfosuccinate was added to make a 0.01 *M* solution, and the pH was adjusted to 2.5 with sulfuric acid. The solutions were prepared fresh daily.

Internal Standard Solution—The stock internal standard solution (50 mg/10 ml) was prepared by dissolving isonicotinic acid[5] in distilled water.

Standard Solutions for Calibration Curves—Stock solutions of isoniazid (50 mg/10 ml) and pyridoxine hydrochloride (5 mg/10 ml) were prepared in distilled water. Accurately pipetted volumes of 1.0, 2.0, and 4.0 ml of each stock solution were placed in 10-ml volumetric flasks. One milliliter of the internal standard stock solution was added to each flask, followed by the addition of distilled water to volume.

The three concentrations of each drug were subjected to a linear regression analysis, and the slope and intercept were calculated (Table I).

Conditions for Chromatographic Separation and Quantification—The degassed mobile phase was pumped through a column containing a monomolecular layer of octadecyltrichlorosilane (C_{18}), chemically bonded to a high efficiency porous silica surface[6], at a flow rate of 2.0 ml/min (2500 psig) at room temperature until a stable baseline was obtained. Replicate 40-μl injections of sample and standard solutions were made using a 100-μl syringe[7]. The chart recorder provided a record of drug elution from the column as peaks on a chromatogram. In all cases, the solute was measured by digital integration of the peak area[1].

RESULTS AND DISCUSSION

The analysis of the dosage form, isoniazid–pyridoxine hydrochloride, involved two separate analytical problems: (*a*) the development of operating parameters of HPLC that would separate the two components without peak overlap, and (*b*) the detection and quantification of each component at the level in the dosage form.

Initial attempts to separate isoniazid and pyridoxine hydrochloride were made using cation-exchange chromatography. Table II shows the effect of mobile phase pH on the separation of the two drugs as expressed in R_s values. The R_s value (18), a theoretical parameter, is a reasonable measurement of the separation of two species on a column[8]. Satisfactory quantification of a multicomponent dosage form is dependent on adequate resolution of the components. The use of cation-exchange chromatography in the separation and quantification of isoniazid–pyridoxine hydrochloride was not satisfactory because:

1. There was a marked variation in the resolution of the drugs using two batches of resin from the same supplier.
2. The sensitivity of the R_s value of the two components to changing pH, with a maximum near pH 4.5, made it difficult to develop an analytical method with reproducible resolution values on a repetitive basis.

The separation of isoniazid and pyridoxine hydrochloride on conventional reversed-phase chromatography was also unsuccessful. The affinity of the components for the stationary phase was too low. However, addition of a small quantity of dioctyl sodium sulfosuccinate to the mobile phase gave sufficient selectivity to effect the separation. Solvent composition was varied to include absolute methanol with

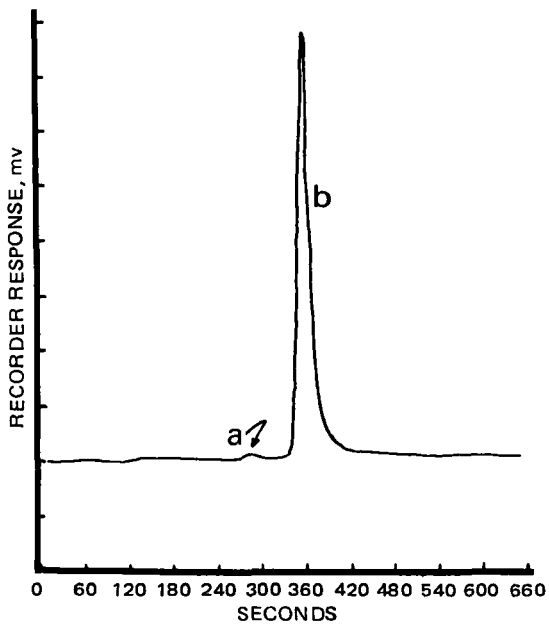

Figure 1—*Liquid chromatogram of isoniazid–pyridoxine hydrochloride (10:1) mixture at 254 nm on octadecyl column with absolute methanol–water (60:40, pH 2.5) containing 0.01* M *dioctyl sodium sulfosuccinate. Key: a, pyridoxine hydrochloride; and b, isoniazid.*

[1] A Waters Associates liquid chromatograph (model ALC/GPC 201), equipped with an M-6000 pump, a Perkin-Elmer model LC-55 variable wavelength UV–visible detector, and an Infotronics integrator (model CRS-204) with digital printout, and a Waters packed column, 4 mm i.d. × 30 cm, were used.
[2] Matheson, Coleman and Bell, East Rutherford, N.J.
[3] Nutritional Biochemicals Corp., Cleveland, Ohio.
[4] Sigma Chemical Co., St. Louis, Mo.
[5] Eastman Organic Chemicals, Rochester, N.Y.
[6] Micro-Bondapak/C_{18}, <10 μm, Waters Associates, Milford, Mass.
[7] Model B-110, Precision Sampling Corp., Baton Rouge, La.

[8] It is possible to calculate the approximate resolution (R_s) of two components by the equation $R_s = 2(t_2 - t_1)/(w_1 + w_2)$, where t_1 and t_2 are retention times, and w_1 and w_2 are base peak widths of Compounds 1 and 2, respectively. In past experience, two components with an R_s value >1.5 showed satisfactory resolution for quantification by this analytical technique if the peak areas were approximately equal. A significant difference in peak area for two components may require R_s values of 2 or greater.

Table II—Effect of Mobile Phase pH on Approximate Resolution (R_s) Values for Isoniazid–Pyridoxine Hydrochloride on Cation-Exchange Column

Cation-Exchange Resin[b]	pH of Mobile Phase[a]			
	3.5	4.5	5.5	6.5
Batch 1	<0.24[c]	3.08	2.15	0.36
Batch 2	0.62	4.95	2.40	1.18

[a] Mobile phase was aqueous 0.01 *M* ammonium acetate containing 0.01% sodium azide. The pH was adjusted to the desired level with acetic acid. The flow rate was 2.0 ml/min (1000 psig), and the peaks were measured using UV detection at 254 nm. [b] A sulfonated alkyl phenyl chemically bonded to solid glass cores with a porous silica surface (CX-Corasil, Waters Associates, Milford, Mass.). [c] See Footnote 8. Resolution values were measured under experimental conditions that produced equivalent peak areas for both components.

changing concentrations of distilled water. The pH of the mobile phase (pH 2.5) and of the octadecyl (lipophilic) stationary phase remained constant during the investigation.

Apparently, the separation depends on the reversible formation of ion-pairs within the chromatographic system and separation of the drugs on the basis of differences in the lipophilicity of the ion-pairs formed. The effect of changing solvent composition on retention times

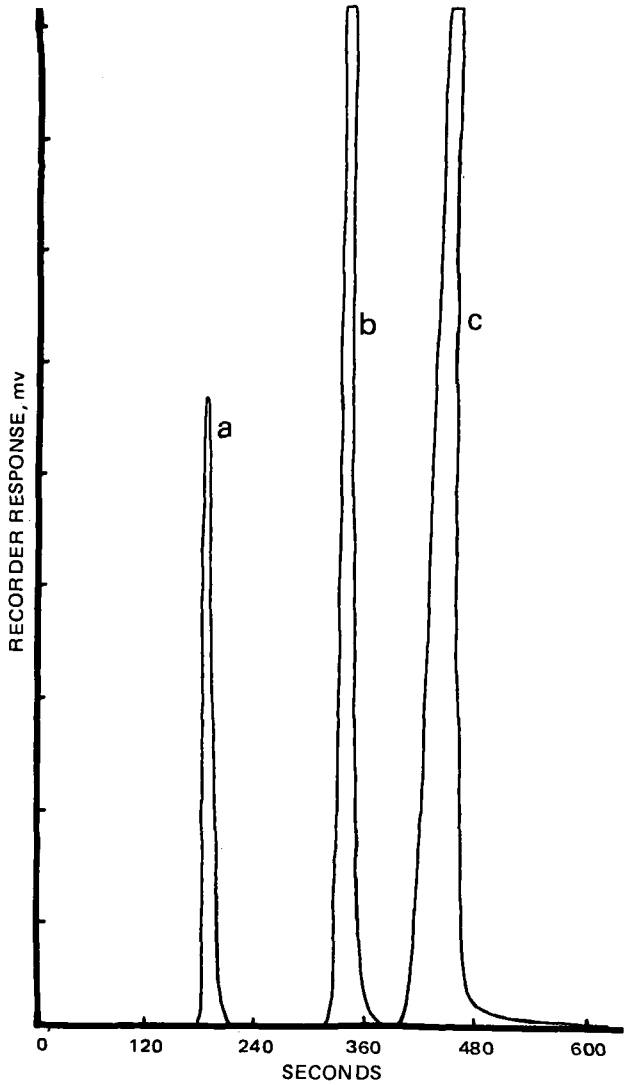

Figure 2—*Liquid chromatogram of isoniazid–pyridoxine hydrochloride mixture at 293 nm on octadecyl column with absolute methanol–water (60:40, pH 2.5) containing 0.01* M *dioctyl sodium sulfosuccinate. Key: a, isonicotinic acid; b, pyridoxine hydrochloride; and c, isoniazid.*

Table III—Effect of Mobile Phase Composition on Retention Times[a]

Compound	Mobile Phase Composition, Methanol–Water[b]			
	70:30	60:40	50:50	40:60
Isoniazid	261[a] (14)[d]	578 (60)	1332 (116)	—[c]
Pyridoxine hydrochloride	239 (37)	388 (39)	656 (60)	1228 (96)
R_s[e] =	0.86	3.84	7.68	>16.7[f]

[a] Retention time is expressed as seconds measured as elapsed time between injection and attainment of the chromatographic peak maximum. Eluted peaks were monitored using UV detection at 293 nm. [b] Solvents contained 0.01 *M* dioctyl sodium sulfosuccinate and were buffered to pH 2.5 with sulfuric acid. [c] Retention time greater than 3000 sec. [d] Base peak width expressed as seconds. [e] See Footnote 8. [f] Calculated on the basis of a retention time of 3000 sec and a base peak width of 116 sec for isoniazid.

Table IV—Analysis of Isoniazid–Pyridoxine Hydrochloride in Known Mixture

Mixture	Added, mg	Amount Found[a], mg	Accuracy, %
Isoniazid	10.0	10.017 ± 0.073[b]	0.17
Pyridoxine hydrochloride	1.0	0.997 ± 0.004	0.30

[a] Based on four replicate determinations of known mixture. [b] Confidence limits at $p = 0.05$.

and base peak widths is shown in Table III. The table also shows calculated R_s values for both drugs in various solvent systems on the octadecyl column. A mobile phase containing methanol–water (60:40) was chosen for the quantification since adequate resolution could be achieved in the shortest time.

Initially, the separation was monitored at 254 nm. However, at this wavelength, the molar absorptivity of isoniazid is much greater than that of pyridoxine hydrochloride (Fig. 1). When the wavelength of the detector was changed to 293 nm (the λ_{max} of pyridoxine hydrochloride in acid media), the detector response was approximately equivalent for the different molarities of the drugs. Therefore, 293 nm was used to facilitate the simultaneous determination of the two drugs.

Figure 2 illustrates a chromatogram of the drugs being assayed. Various concentrations of standard solutions of each drug dissolved in the absolute methanol–water (60:40) mixture containing 0.01 *M* dioctyl sodium sulfosuccinate were chromatographed using the octadecyl column. Isonicotinic acid was added to each solution as the internal standard[9]. The area under the curve for each peak on the chromatograms was evaluated with a digital integrator[1]. The ratio of each peak area to the area of the internal standard was calculated for each chromatogram. A linear regression line of these data at three concentrations of each drug gave the slope, intercept, and correlation coefficient for each calibration curve (Table I).

A known mixture containing a quantity of each drug was chromatographed, and the ratios of drug peak areas to internal standard peak areas (D/IS) were calculated for each drug. The constants (slope and intercept) for the linear regression equation (Table I) were used to solve for drug concentration [D/IS = (slope × concentration) + intercept]. The calculations were performed on a programmable calculator[10].

The data in Table IV demonstrate the quantitative results obtained for a simulated isoniazid–pyridoxine hydrochloride (10:1) dosage form. The method is also capable of detecting and subsequently quantifying a 20:1 mix of the two drugs (Table I). The utility of HPLC

[9] It has been suggested that, in certain circumstances, isoniazid might degrade to yield isonicotinic acid as a major contaminant. If this is suspected, an alternative choice for the internal standard is either nicotinic acid (retention time and base peak width of 159 and 21 sec, respectively) or nicotinamide (retention time and base peak width of 198 and 30 sec, respectively). The stock solution concentration given under *Experimental* for isonicotinic acid can be used for either compound.

[10] Olivetti-Underwood programma 101.

in the analysis of the isoniazid–pyridoxine hydrochloride (10:1) mixture is clearly demonstrated, with an accuracy of 0.17–0.30%.

REFERENCES

(1) I. L. Honigberg, J. T. Stewart, and A. P. Smith, *J. Pharm. Sci.*, **63**, 766(1974).

(2) I. L. Honigberg, J. T. Stewart, A. P. Smith, R. D. Plunkett, and D. W. Hester, *ibid.*, **63**, 1762(1974).

(3) *Ibid.*, **64**, 1201(1975).

(4) I. L. Honigberg, J. T. Stewart, A. P. Smith, R. D. Plunkett, and E. L. Justice, *J. Pharm. Sci.*, **64**, 1389(1975).

(5) P. G. W. Scott, *J. Pharm. Pharmacol.*, **4**, 681(1952).

(6) N. F. Poole and A. E. Meyer, *Proc. Soc. Exp. Biol. Med.*, **98**, 375(1958).

(7) H. S. I. Tan, *J. Pharm. Sci.*, **62**, 993(1973).

(8) H. G. Boxenbaum and S. Riegelman, *ibid.*, **63**, 1191(1974).

(9) J. T. Stewart and D. A. Settle, *ibid.*, **64**, 1403(1975).

(10) E. M. Scott and R. C. J. Wright, *J. Lab. Clin. Invest.*, **70**, 355(1967).

(11) "The United States Pharmacopeia," 18th rev., Mack Publishing Co., Easton, Pa., 1970, p. 349.

(12) "The United States Pharmacopeia," 19th rev., Mack Publishing Co., Easton, Pa., 1975, p. 429.

(13) *Ibid.*, p. 120.

(14) R. Adamski and J. Skibicki, *Farm. Pol.*, **28**, 1073(1972); through *Anal. Abstr.*, **24**, 3010(1973).

(15) P. Moszczynski and C. Kubicka, *Zesz. Nauk. Politech. Lodz., Chem. Spozyw.*, **20**, 159(1972); through *Chem. Abstr.*, **79**, 139668(1973).

(16) D. Mikac-Deric and C. Tomanic, *Clin. Chim. Acta*, **38**, 235(1972).

(17) D. P. Wittmer, N. O. Nuessle, and W. G. Haney, *Anal. Chem.*, **47**, 1422(1975).

(18) B. L. Karger, L. R. Synder, and C. Horvath, "An Introduction to Separation Science," Wiley, New York, N.Y., 1973, pp. 146–150.

ACKNOWLEDGMENTS AND ADDRESSES

Received August 22, 1975, from the *Department of Medicinal Chemistry, School of Pharmacy, University of Georgia, Athens, GA 30602*

Accepted for publication December 10, 1975

[x] To whom inquiries should be directed.

Selectivity of 4-Methoxyphenethylamine Derivatives as Inhibitors of Monoamine Oxidase

WILLIAM J. KELLER [x] and GARY G. FERGUSON

Abstract □ It has been established that the oxidative deamination of tyramine by monoamine oxidase is inhibited by (±)-4-methoxy-β-hydroxyphenethylamine and its *N*-methylated derivatives. This particular series of compounds does not inhibit the action of monoamine oxidase when tryptamine is used as the substrate. In contrast, 4-methoxyphenethylamine and its *N*-methylated homologs inhibit the monoamine oxidase-catalyzed deamination of both tyramine and tryptamine.

Keyphrases □ 4-Methoxyphenethylamine and *N*-methylated homologs—effect on monoamine oxidase-catalyzed deamination of tyramine and tryptamine □ Monoamine oxidase—deamination of tyramine and tryptamine, effect of 4-methoxyphenethylamine and *N*-methylated homologs □ Tyramine—monoamine oxidase-catalyzed oxidative deamination, effect of 4-methoxyphenethylamine and *N*-methylated homologs □ Tryptamine—monoamine oxidase-catalyzed oxidative deamination, effect of 4-methoxyphenethylamine and *N*-methylated homologs □ Enzymes—monoamine oxidase, deamination of tyramine and tryptamine, effect of 4-methoxyphenethylamine and *N*-methylated homologs □ Structure–activity relationships—4-methoxyphenethylamine and *N*-methylated homologs, effect on monoamine oxidase-catalyzed deamination of tyramine and tryptamine

4-Methoxy-β-hydroxyphenethylamine [1-(4-methoxyphenyl)-2-aminoethanol] has been detected in extracts of *Coryphantha cornifera* (DC.) Br. and R. var. *echinus* (Engelm.) L. Benson (1), while *Dolichothele longimamma* (DC.) Br. and R. was recently shown to contain *N*-methyl-4-methoxy-β-hydroxyphenethylamine [1-(4-methoxyphenyl)-2-(methylamino)ethanol] (2). These naturally occurring compounds, together with *N,N*-dimethyl-4-methoxy-β-hydroxyphenethylamine [1-(4-methoxyphenyl)-2-(dimethylamino)ethanol], have been found to inhibit the oxidative deamination of tyramine by monoamine oxidase (3). These data resulted from a screen used to correlate the pharmacological activity of cactus alkaloids and related compounds with the folkloric uses of various cacti.

Recently, it was noted that certain compounds inhibit the reaction of monoamine oxidase with tryptamine or serotonin but not with tyramine (4–7). The possibility of finding selective monoamine oxidase inhibitory activity prompted a reexamination of 4-methoxy-β-hydroxyphenethylamine and its *N*-methylated derivatives using tryptamine as the substrate.

N-Methyl-4-methoxyphenethylamine [1-(4-methoxyphenyl)-2-(methylamino)ethane] has been isolated from a number of cacti with potential psychoactivity (1, 8–12). This compound, as well as its *N*-methyl and *N*-demethyl derivatives, was tested for monoamine oxidase inhibitory activity using both tyramine and tryptamine as substrates. These studies revealed the significance of the β-hydroxy group in a series of phenethylamines with known monoamine oxidase inhibitory activity. In addition, the effects of the naturally occurring *N*-methyl-4-methoxyphenethylamine and its *N*-methyl homologs on monoamine oxidase were established.

EXPERIMENTAL

Synthesis—The synthesis of racemic 4-methoxy-β-hydroxyphenethylamine hydrochloride (I), *N*-methyl-4-methoxy-β-hy-

in the analysis of the isoniazid–pyridoxine hydrochloride (10:1) mixture is clearly demonstrated, with an accuracy of 0.17–0.30%.

REFERENCES

(1) I. L. Honigberg, J. T. Stewart, and A. P. Smith, *J. Pharm. Sci.*, **63**, 766(1974).

(2) I. L. Honigberg, J. T. Stewart, A. P. Smith, R. D. Plunkett, and D. W. Hester, *ibid.*, **63**, 1762(1974).

(3) *Ibid.*, **64**, 1201(1975).

(4) I. L. Honigberg, J. T. Stewart, A. P. Smith, R. D. Plunkett, and E. L. Justice, *J. Pharm. Sci.*, **64**, 1389(1975).

(5) P. G. W. Scott, *J. Pharm. Pharmacol.*, **4**, 681(1952).

(6) N. F. Poole and A. E. Meyer, *Proc. Soc. Exp. Biol. Med.*, **98**, 375(1958).

(7) H. S. I. Tan, *J. Pharm. Sci.*, **62**, 993(1973).

(8) H. G. Boxenbaum and S. Riegelman, *ibid.*, **63**, 1191(1974).

(9) J. T. Stewart and D. A. Settle, *ibid.*, **64**, 1403(1975).

(10) E. M. Scott and R. C. J. Wright, *J. Lab. Clin. Invest.*, **70**, 355(1967).

(11) "The United States Pharmacopeia," 18th rev., Mack Publishing Co., Easton, Pa., 1970, p. 349.

(12) "The United States Pharmacopeia," 19th rev., Mack Publishing Co., Easton, Pa., 1975, p. 429.

(13) *Ibid.*, p. 120.

(14) R. Adamski and J. Skibicki, *Farm. Pol.*, **28**, 1073(1972); through *Anal. Abstr.*, **24**, 3010(1973).

(15) P. Moszczynski and C. Kubicka, *Zesz. Nauk. Politech. Lodz., Chem. Spozyw.*, **20**, 159(1972); through *Chem. Abstr.*, **79**, 139668(1973).

(16) D. Mikac-Deric and C. Tomanic, *Clin. Chim. Acta*, **38**, 235(1972).

(17) D. P. Wittmer, N. O. Nuessle, and W. G. Haney, *Anal. Chem.*, **47**, 1422(1975).

(18) B. L. Karger, L. R. Synder, and C. Horvath, "An Introduction to Separation Science," Wiley, New York, N.Y., 1973, pp. 146–150.

ACKNOWLEDGMENTS AND ADDRESSES

Received August 22, 1975, from the *Department of Medicinal Chemistry, School of Pharmacy, University of Georgia, Athens, GA 30602*

Accepted for publication December 10, 1975

[x] To whom inquiries should be directed.

Selectivity of 4-Methoxyphenethylamine Derivatives as Inhibitors of Monoamine Oxidase

WILLIAM J. KELLER [x] and GARY G. FERGUSON

Abstract □ It has been established that the oxidative deamination of tyramine by monoamine oxidase is inhibited by (±)-4-methoxy-β-hydroxyphenethylamine and its *N*-methylated derivatives. This particular series of compounds does not inhibit the action of monoamine oxidase when tryptamine is used as the substrate. In contrast, 4-methoxyphenethylamine and its *N*-methylated homologs inhibit the monoamine oxidase-catalyzed deamination of both tyramine and tryptamine.

Keyphrases □ 4-Methoxyphenethylamine and *N*-methylated homologs—effect on monoamine oxidase-catalyzed deamination of tyramine and tryptamine □ Monoamine oxidase—deamination of tyramine and tryptamine, effect of 4-methoxyphenethylamine and *N*-methylated homologs □ Tyramine—monoamine oxidase-catalyzed oxidative deamination, effect of 4-methoxyphenethylamine and *N*-methylated homologs □ Tryptamine—monoamine oxidase-catalyzed oxidative deamination, effect of 4-methoxyphenethylamine and *N*-methylated homologs □ Enzymes—monoamine oxidase, deamination of tyramine and tryptamine, effect of 4-methoxyphenethylamine and *N*-methylated homologs □ Structure–activity relationships—4-methoxyphenethylamine and *N*-methylated homologs, effect on monoamine oxidase-catalyzed deamination of tyramine and tryptamine

4-Methoxy-β-hydroxyphenethylamine [1-(4-methoxyphenyl)-2-aminoethanol] has been detected in extracts of *Coryphantha cornifera* (DC.) Br. and R. var. *echinus* (Engelm.) L. Benson (1), while *Dolichothele longimamma* (DC.) Br. and R. was recently shown to contain *N*-methyl-4-methoxy-β-hydroxyphenethylamine [1-(4-methoxyphenyl)-2-(methylamino)ethanol] (2). These naturally occurring compounds, together with *N,N*-dimethyl-4-methoxy-β-hydroxyphenethylamine [1-(4-methoxyphenyl)-2-(dimethylamino)ethanol], have been found to inhibit the oxidative deamination of tyramine by monoamine oxidase (3). These data resulted from a screen used to correlate the pharmacological activity of cactus alkaloids and related compounds with the folkloric uses of various cacti.

Recently, it was noted that certain compounds inhibit the reaction of monoamine oxidase with tryptamine or serotonin but not with tyramine (4–7). The possibility of finding selective monoamine oxidase inhibitory activity prompted a reexamination of 4-methoxy-β-hydroxyphenethylamine and its *N*-methylated derivatives using tryptamine as the substrate.

N-Methyl-4-methoxyphenethylamine [1-(4-methoxyphenyl)-2-(methylamino)ethane] has been isolated from a number of cacti with potential psychoactivity (1, 8–12). This compound, as well as its *N*-methyl and *N*-demethyl derivatives, was tested for monoamine oxidase inhibitory activity using both tyramine and tryptamine as substrates. These studies revealed the significance of the β-hydroxy group in a series of phenethylamines with known monoamine oxidase inhibitory activity. In addition, the effects of the naturally occurring *N*-methyl-4-methoxyphenethylamine and its *N*-methyl homologs on monoamine oxidase were established.

EXPERIMENTAL

Synthesis—The synthesis of racemic 4-methoxy-β-hydroxyphenethylamine hydrochloride (I), *N*-methyl-4-methoxy-β-hy-

Table I—Inhibiting Effects of Compounds on Oxidation of Tyramine Hydrochloride and Tryptamine Hydrochloride by Rat Brain Mitochondria[a]

Compound	Tyramine Hydrochloride			Tryptamine Hydrochloride		
	Percent Inhibition	Significance	SD	Percent Inhibition	Significance	SD
I	59	+	1.6	7	—	3.4
II	70	+	1.5	17	—	3.8
III	61	+	1.4	16	—	4.3
IV	59	+	0.7	55	+	1.5
V	44	+	1.5	42	+	1.1
VI	47	+	1.2	64	+	0.9
Isocarboxazid[b]	100	+	1.5	67	+	1.0

[a] Each value represents the results obtained using three or more flasks per compound for each substrate. Percent inhibition was calculated by comparing control and experimental values for each compound with each substrate. [b] Reference.

droxyphenethylamine hydrochloride (II), and *N,N*-dimethyl-4-methoxy-β-hydroxyphenethylamine hydrochloride (III) was described previously (3).

4-Methoxyphenethylamine [1-(4-methoxyphenyl)-2-aminoethane] hydrochloride (IV) was available commercially[1] and served as the starting point for the synthetic production of the other two members of this series. *N*-Methyl-4-methoxyphenethylamine hydrochloride (V) was synthesized by refluxing equimolar quantities of 4-methoxyphenethylamine and ethyl formate[2] to give an *N*-formyl intermediate, which was subsequently reduced with lithium aluminum hydride. The free base resulting from this reaction was converted to a fluffy white hydrochloride, mp 181–182° [lit. (10) mp 182–184°].

N,N-Dimethyl-4-methoxyphenethylamine [1-(4-methoxyphenyl)-2-(dimethylamino)ethane] hydrochloride (VI) was produced by reacting V with 36% formaldehyde[3] followed by a sodium borohydride reduction of the Schiff-base intermediate. Conversion of the resulting colorless oil to the hydrochloride salt gave short white needles, mp 173–174° [lit. (13) mp 175–176°].

In each case, the identity of the final product was verified by IR and NMR spectra in addition to the melting-point data.

Warburg Studies—As an evaluation of possible monoamine oxidase inhibition, the effects of the compounds on the oxidation of tyramine and tryptamine hydrochlorides by rat brain mitochondria were investigated. Brain mitochondria (containing monoamine oxidase) were prepared from albino Wistar female rats, 150–200 g, according to the method of Brody and Bain (14). Monoamine oxidase activity was determined in the presence and absence of the respective compounds by conventional manometric techniques[4] (15).

In the manometric determinations, the main compartment of the Warburg flasks contained 0.8 ml of a 0.1 *M* buffered solution of the compound studied (or buffer), 1 ml of mitochondrial suspension (representing 500 mg wet weight of original brain tissue), and sufficient 0.01 *M* phosphate buffer (pH 7.4) to make a total volume of 2.7 ml. All aliquots for a given run were taken from the same mitochondrial preparation. The side arm of each flask contained 0.3 ml of 0.1 *M* tyramine or tryptamine hydrochloride. After the flasks were allowed to equilibrate for 15 min at 37°, the manometer valves were closed and the side arm contents of each were tipped in.

Manometers were set at 150 mm, and readings were taken at 15-min intervals for 90 min. Values for the 90-min reaction period were obtained for each flask and were multiplied by the respective flask constants after adjusting for changes in the thermobarometer. The total microliters of oxygen uptake for each flask was thus obtained.

Reference flasks, using 0.05 *M* isocarboxazid (0.8 ml) as the monoamine oxidase inhibitor, were employed as already described and were used for comparison.

Statistical Analysis—The mean and standard error were determined for each control or treated group. Values thus obtained were compared, using the difference between the means and the standard error of the difference between the means for the respective control-treated pairs of groups. The Student *t* test was applied to the results, and the probability was determined; *p* values of less than 0.05 were considered significant.

[1] Calbiochem.
[2] Eastman Kodak Co.
[3] Fisher Scientific Co.
[4] Precision Warburg apparatus, Precision Scientific Co.

RESULTS AND DISCUSSION

Direct measurements of monoamine oxidase inhibition using Warburg studies revealed a certain degree of selectivity among a series of 4-methoxyphenethylamine derivatives (Table I). Significant ($p < 0.05$) inhibition was observed for all compounds tested when tyramine was the substrate. However, with tryptamine as the substrate, only 4-methoxyphenethylamine and its *N*-methyl homologs (IV–VI) revealed significant inhibitory effects. These positive results were validated by the activity exhibited by reference isocarboxazid.

Substrate selectivity was observed with the 4-methoxy-β-hydroxyphenethylamine series (I–III) when these substances failed to inhibit the enzymatic oxidative deamination of tryptamine. These data suggest that rat brain monoamine oxidase possesses one active site for the oxidation of tyramine and another for tryptamine. An alternative explanation would involve the presence of an isozyme specific for each of the two substrates examined. Apparently, the presence of a β-hydroxy group in the 4-methoxyphenethylamine moiety interferes with the binding of these derivatives with the active site and/or isozyme responsible for the oxidation of tryptamine.

Mescaline is a well-known hallucinogenic substance and is responsible for the effects produced upon ingesting *Lophophora williamsii* (Lem.) Coult., the famed peyote cactus. However, many reputedly psychoactive cacti do not contain mescaline. It has always been difficult to substantiate the purported actions of these cacti with the known pharmacological properties of the isolated alkaloids. Based upon evidence presented in this paper, the monoamine oxidase inhibitory effects of some phenethylamines found in alleged mind-altering cacti may provide a partial explanation. The potency and selectivity of the monoamine oxidase-inhibiting phenethylamines, together with the cooccurrence of indirectly acting amines, might help to explain the long-term and short-term pharmacological effects of the cactus in question.

REFERENCES

(1) K. M. Kelley Hornemann, J. M. Neal, and J. L. McLaughlin, *J. Pharm. Sci.*, **61**, 41(1972).

(2) R. L. Ranieri and J. L. McLaughlin, *J. Org. Chem.*, **41**, 319(1976).

(3) G. G. Ferguson and W. J. Keller, *J. Pharm. Sci.*, **64**, 1431(1975).

(4) M. Winn, B. W. Harrom, R. R. Rasmussen, E. B. Chappell, and N. P. Plotnikoff, *J. Med. Chem.*, **18**, 437(1975).

(5) C. Goridis and N. H. Neff, *Neuropharmacology*, **10**, 557(1971).

(6) R. W. Fuller, B. J. Warren, and B. B. Malloy, *Biochem. Pharmacol.*, **19**, 2934(1970).

(7) B. T. Ho, *J. Pharm. Sci.*, **61**, 821(1972).

(8) W. J. Keller, J. L. McLaughlin, and L. R. Brady, *ibid.*, **62**, 408(1973).

(9) J. G. Bruhn, S. Agurell, and J. E. Lindgren, *Acta Pharm. Suec.*, **12**, 199(1975).

(10) J. M. Neal and J. L. McLaughlin, *Lloydia*, **33**, 395(1970).

(11) P. T. Sato, J. M. Neal, L. R. Brady, and J. L. McLaughlin, *J. Pharm. Sci.*, **62**, 411(1973).

(12) S. Agurell, *Experientia*, **25**, 1132(1969).

(13) G. D. Cherayil, *J. Pharm. Sci.*, **62**, 2054(1973).

(14) T. M. Brody and J. A. Bain, *J. Biol. Chem.*, **195**, 685(1952).

(15) W. W. Umbreit, R. H. Burris, and J. F. Stauffer, "Manometric Techniques," 4th ed., Burgess, Minneapolis, Minn., 1964, pp. 61, 76.

ACKNOWLEDGMENTS AND ADDRESSES

Received October 21, 1975, from the *School of Pharmacy, Northeast Louisiana University, Monroe, LA 71201*

Accepted for publication December 18, 1975.

[x] To whom inquiries should be directed.

Volume of Distribution and Tissue Level Errors in Instantaneous Intravenous Input Assumptions

SARFARAZ NIAZI

Abstract □ A comparison was made between instantaneous input assumption and short-term zero-order infusion for 1 and 2 min for several drugs showing fast distribution to the tissue compartments. The errors ranged from 9 to 40% for the volume of the central compartment, from 0.7 to 11% for the volume of distribution following pseudo-distribution equilibrium, and from 11 to 34% for the volume of distribution change at the end of the 2-min infusion period. Significant errors in the tissue levels also were observed. It was suggested that all intravenous administrations be considered as short-term zero-order inputs.

Keyphrases □ Distribution, volume—comparison of instantaneous input assumption and short-term zero-order infusion, tissue compartments, various drugs □ Tissue levels—various drugs, comparison of instantaneous input assumption and short-term zero-order infusion, various drugs □ Intravenous input assumption, instantaneous—compared to short-term zero-order infusion, volume of distribution calculations, various drugs □ Volume of distribution—comparison of instantaneous input assumption and short-term zero-order infusion, tissue compartments, various drugs

The concept of possible errors in assuming that a drug can be instantaneously placed in the central compartment of a mammillary model was recently introduced (1). The simplifying assumption of instantaneous input invariably results in erroneous volume of distribution and tissue level calculations, the extent of which depends on the distribution half-lives in a mammillary model system. The purposes of this report are to cite several examples where such errors may have occurred and to review the pharmacokinetic and pharmacological aspects of these observations.

THEORY

In the conventional treatment of the data following a quick intravenous dose, the blood concentration, C_1, is expressed as:

$$C_1 = \sum_{i=1}^{n} A_i e^{-a_i t} \qquad \text{(Eq. 1)}$$

where A_i = intercepts on the feathered plot, and a_i = hybrid rate constants. If, however, the intravenous administration is considered as short-term zero-order infusion (1), the blood concentration can be expressed as (1):

$$C_1 = \sum_{i=1}^{n} \frac{A_i(1 - e^{-a_i\theta})e^{-a_i t'}}{a_i\theta} \qquad \text{(Eq. 2)}$$

where θ = dosing duration, and t' = time following the infusion period $(t - \theta)$.

The volume of the central compartment, V_{d_0}, is expressed as:

$$V_{d_0} = \frac{\text{dose}}{\sum_{i=1}^{n} A_i} \qquad \text{(Eq. 3)}$$

Therefore, the corrected definition would read (1):

$$V_{d_0} = \frac{\text{dose}}{\sum_{i=1}^{n} \frac{\theta a_i A_i}{(1 - e^{-a_i\theta})}} \qquad \text{(Eq. 4)}$$

The volume of distribution following pseudo-distribution equilibrium is expressed as (2, 3):

$$V_{d_{eq}} = \frac{\text{dose}}{a_n x \sum_{i=1}^{n} \frac{A_i}{a_i}} \qquad \text{(Eq. 5)}$$

which can be corrected for short-term zero-order infusion to give:

$$V_{d_{eq}} = \frac{\text{dose}}{a_n x \sum_{i=1}^{n} \frac{\theta A_i}{(1 - e^{-a_i\theta})}} \qquad \text{(Eq. 6)}$$

A single definition of the volume of distribution, treating this term as a function of time, was proposed (3):

$$V_d = \frac{\text{dose} \sum_{i=1}^{n} \frac{A_i}{a_i} e^{-a_i t}}{\sum_{i=1}^{n} \frac{A_i}{a_i} \sum_{i=1}^{n} A_i e^{-a_i t}} \qquad \text{(Eq. 7)}$$

It can be modified for short-term zero-order infusion to give:

$$V_d = \frac{\text{dose} \sum_{i=1}^{n} \frac{\theta A_i e^{-a_i t'}}{(1 - e^{-a_i\theta})}}{\sum_{i=1}^{n} \frac{\theta A_i}{(1 - e^{-a_i\theta})} \sum_{i=1}^{n} \frac{\theta a_i A_i}{(1 - e^{-a_i\theta})} e^{-a_i t'}} \qquad \text{(Eq. 8)}$$

This equation has the same limits at $t = \theta$ and t = pseudo-distribution equilibrium time as expressed in Eqs. 4 and 6, respectively.

The concept of the volume of distribution as a function of time was applied to evaluate the thermodynamic activity of the drug in the central compartment (3). The rate of the volume of distribution change with time reflects the distribution to the tissues from the central compartment; at time $t = \theta$, the volume of distribution derivative, RV_{d_0}, will be maximum. Applied to the short-term zero-order infusion, this concept can be expressed as:

$$RV_{d_0} = \text{dose}\left[\frac{\sum_{i=1}^{n} \frac{\theta a_i^2 A_i}{(1 - e^{-a_i\theta})}}{\left\{\sum_{i=1}^{n} \frac{\theta a_i A_i}{(1 - e^{-a_i\theta})}\right\}^2} - \frac{1}{\sum_{i=1}^{n} \frac{\theta A_i}{(1 - e^{-a_i\theta})}}\right] \qquad \text{(Eq. 9)}$$

The fraction of the available dose remaining in the body, f_B, is expressed as (3, 4):

$$f_B = \frac{\sum_{i=1}^{n} \frac{A_i}{a_i} e^{-a_i t}}{\sum_{i=1}^{n} \frac{A_i}{a_i}} \qquad \text{(Eq. 10)}$$

and the fraction remaining in the central compartment, f_C, is expressed as:

$$f_C = \frac{\sum_{i=1}^{n} A_i e^{-a_i t}}{\sum_{i=1}^{n} A_i} \qquad \text{(Eq. 11)}$$

The fraction of the available dose in the tissues, f_T, can be expressed as the difference between Eqs. 10 and 11. By incorporating the correction due to short-term zero-order infusion, this fraction can be expressed as:

$$f_T = \frac{\sum_{i=1}^{n} \frac{\theta A_i e^{-a_i t'}}{(1 - e^{-a_i\theta})}}{\sum_{i=1}^{n} \frac{\theta A_i}{(1 - e^{-a_i\theta})}} - \frac{\sum_{i=1}^{n} \frac{\theta a_i A_i e^{-a_i t'}}{(1 - e^{-a_i\theta})}}{\sum_{i=1}^{n} \frac{\theta a_i A_i}{(1 - e^{-a_i\theta})}} \qquad \text{(Eq. 12)}$$

Therefore, it is possible to calculate the tissue levels without calculating the transfer rate constants and comparisons made at different values of θ.

DISCUSSION

For drugs exhibiting multicompartment pharmacokinetics, the nature of distribution can be expressed in terms of the volume of the central compartment, the volume of distribution following pseudo-

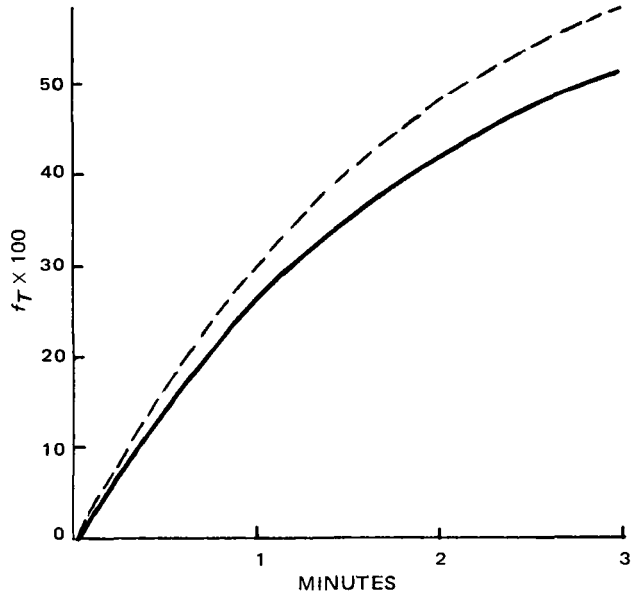

Figure 1—*Fraction of clonazepam remaining in the tissue compartment as a function of time according to the instantaneous input assumption (—) and short-term zero-order infusion for 2 min (----).*

distribution equilibrium, and, recently (3), the volume of distribution as a function of time and the change in the volume of distribution at time $t = \theta$. The assumption of instantaneous input will not affect these parameters significantly in most cases. However, where the distribution half-lives are short, an overestimation of these parameters will invariably result, as shown in Table I for several drugs where the volume terms were calculated for dosing intervals of 1 and 2 min and compared with the reported values. The selection of 1- and 2-min dosing intervals was based on the range of generally observed time intervals for intravenous injection. Of course, time periods greater than 2 min sometimes are necessary for administering an appropriate amount of the drug.

As shown in Table I, a 40% overestimation of volume of the central compartment was observed for clonazepam if the dose was administered over a 2-min period. The volume of distribution following pseudo-distribution equilibrium was little changed, but the RV_{d_0} showed a 23% overestimation. The largest overestimation of RV_{d_0} was observed for methohexital at 34% at the 2-min dosing interval. The overestimations of $V_{d_{eq}}$ were generally small, the highest being about 11% for aspirin.

Several interesting observations can be made from these analyses. First, the volume of the central compartment is much more sensitive to erroneous calculation if an instantaneous input assumption is made than is the volume of distribution following pseudo-distribution equilibrium. This observation was applicable to all but one situation for aspirin, where $V_{d_{eq}}$ values varied more (18%) than V_{d_0} values (11%). This discrepancy can be explained on the basis of the ratio of $V_{d_{eq}}$ and V_{d_0}. This ratio, 2.11, was the lowest for aspirin (compared to 36 for methohexital). Obviously, for aspirin the central compartment provides for a significant fraction of the total body distribution, increasing the error involved in $V_{d_{eq}}$. However, as shown in other examples, the volume of the so-called tissue compartments ($V_{d_{eq}} - V_{d_0}$) accounts for the major contribution to $V_{d_{eq}}$.

The rate of the volume of distribution change at time $t = \theta$ indicates the chemical potential of the drug in the central compartment (3). As shown in Table I, this parameter was overestimated in instantaneous input assumptions by 11–34% at the 2-min dosing interval. Such significant variations decrease its utility in various thermodynamic and pharmacological correlations.

The concept of the volume of distribution as a function of time makes it possible to compare tissue levels as a function of time in an instantaneous input assumption and the corresponding short-term zero-order infusion without any calculation of transfer rate constants between compartments. Figure 1 shows the tissue levels of clonazepam as determined from the reported pharmacokinetic parameters (5) assuming an instantaneous input and the tissue levels if the drug is

Table I—Reported and Corrected Pharmacokinetic Parameters for Several Drugs

Drug (Reference)	Dose, mg	A_1, mg/liter	A_2, mg/liter	A_3, mg/liter	a_1, hr^{-1}	a_2, hr^{-1}	a_3, hr^{-1}	V_{d_0}, liters	V_{d_0}', liters, θ = 1 min	V_{d_0}', liters, θ = 2 min	$V_{d_{eq}}'$ liters	$V_{d_{eq}}'$, liters, θ = 1 min	$V_{d_{eq}}'$, liters, θ = 2 min	RV_{d_0}', liters/hr	RV_{d_0}', liters/hr, θ = 1 min	RV_{d_0}', liters/hr, θ = 2 min
Aspirin (6)	650	67	33	—	13.880	2.976	—	6.50	5.97	5.49	13.72	13.02	12.35	26.00	23.88	21.92
Penicillin G (7)	100	8.4	2.3	—	6.250	1.351	—	9.34	8.95	8.58	24.29	23.59	22.91	15.74	14.93	14.17
Methohexital (8)	190	21.15	1.85	0.280	16.666	1.077	0.1234	8.16	7.20	6.39	292.95	282.09	271.24	88.13	76.04	65.73
Pralidoxime chloride (9)	411	14.94	3.73	—	7.060	0.531	—	22.01	20.98	20.01	84.68	83.24	81.80	81.74	77.76	73.94
Lysergide (10)	0.12	0.01464	0.002016	0.006531	26.230	2.480	0.2170	5.17	4.49	3.92	17.57	17.46	17.34	83.33	77.26	70.83
Pentazocine (11)	2.4	0.15412	0.04852	0.02112	25.000	1.100	0.2200	10.72	9.28	8.06	74.58	73.59	72.55	171.06	155.02	139.35
Clonazepam (5)	30	1.205	0.601	—	30.620	0.129	—	16.61	14.02	11.88	49.49	49.33	49.14	333.70	302.70	271.04

administered over 2 min. Such differences can result in correlation variations between pharmacological activity and blood concentration if the site of action resides in the tissue compartments. It would be reasonable to assume that the site of action probably will be, at least in part, in one or more of the tissue compartments, since the compartments simply represent time-dependent equilibration processes. Even if the organ on which the drug is acting can be clearly classified as part of the central compartment, such as the heart, the actual site of action may reside in tissue compartments because of the essential nature of time-dependent processes involved in the tissue equilibration.

From these data, it is clear that some degree of error will invariably result if an instantaneous input assumption is made. Therefore, all intravenous administrations should be considered as short-term zero-order inputs.

REFERENCES

(1) S. Niazi, *J. Pharm. Sci.*, **65**, 750(1976).

(2) M. Gibaldi, R. Nagashima, and G. Levy, *ibid.*, **58**, 193(1969).

(3) S. Niazi, *ibid.*, **65**, 452(1976).

(4) S. Niazi, *Math. Biosci.*, **27**, 169(1975).

(5) S. A. Kaplan, K. Alexander, M. L. Jack, C. V. Puglisi, J. A. F. de Silva, T. L. Lee, and R. E. Weinfeld, *J. Pharm. Sci.*, **63**, 527(1974).

(6) S. Riegelman, J. C. K. Loo, and M. Rowland, *ibid.*, **57**, 128(1968).

(7) N. G. Heatley, *Antibiot. Med. Clin. Ther.*, **11**, 33(1956).

(8) D. B. Breimer, Ph.D. dissertation, University of Nijmegen, The Netherlands, 1974.

(9) F. R. Sidell, W. A. Groff, and A. Kaminskis, *J. Pharm. Sci.*, **61**, 1765(1972).

(10) G. Levy, M. Gibaldi, and W. Jusko, *ibid.*, **58**, 422(1969).

(11) K. A. Pefman and G. A. Portman, *ibid.*, **63**, 84(1974).

ACKNOWLEDGMENTS AND ADDRESSES

Received July 16, 1975, from the *Department of Pharmacy, College of Pharmacy, University of Illinois at the Medical Center, Chicago, IL 60612*

Accepted for publication December 16, 1975.

Simple and Rapid Determination of a New Pharmaceutically Active Amine Hydrochloride

ZUI L. CHANG ˣ and VICTOR E. PAPENDICK

Abstract □ The quantitative analysis of a new pharmaceutically active amine hydrochloride is described. Samples are extracted with chloroform. A yellow amine–dye complex is formed by buffering a sample–bromthymol blue solution at pH 8.5 ± 0.1 and subsequently extracted with chloroform. The complex is treated with 0.01 *N* NaOH to convert it back to the sodium salt of bromthymol blue, which is then measured at 615 nm in the aqueous layer. The amount of complex extracted is linearly related to the amount of amine present, from 0.020 to 0.20 mg/ml. Under the selected conditions, the compound can be determined in the presence of degradation products and there is no interference from common pharmaceutical excipients. The method is suitable for stability studies.

Keyphrases □ Amine hydrochlorides—pharmaceutically active substituted benzopyranopyridine, complexation with bromthymol blue, colorimetric analysis □ Benzopyranopyridine, substituted—pharmaceutically active compound, colorimetric analysis □ Colorimetry—analysis, pharmaceutically active substituted benzopyranopyridine □ Bromthymol blue—use in colorimetric analysis of pharmaceutically active substituted benzopyranopyridine

A new biologically active compound with a benzopyran nucleus (I) was synthesized. Chemically, I is 5,5-dimethyl-10-[4-(1-piperidine)butyryloxy]-8-(3-methyl-2-octyl)-2-(2-propynyl)-1,2,3,4-tetrahydro-5*H*-[1]benzopyrano[3,4-*d*]pyridine hydrochloride. It is readily soluble in water, chloroform, and ethanol, and its melting point[1] is 103–106°.

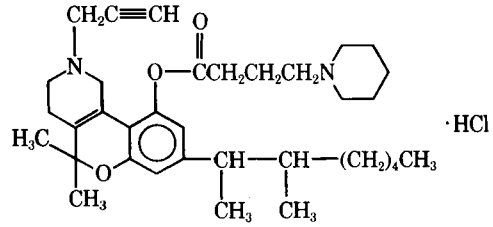

I

The method for the determination of amine salts, involving the formation of an ion-pair with indicator, is based on Prudhomme's (1) discovery that alkaloids form chloroform-soluble complexes with acid dyes such as eosin, the reaction being quantitative (2). The methods available for the determination of quaternary ammonium salts were reviewed previously (3). The extraction of the amine–bromthymol blue complexes of numerous compounds into methylene chloride was studied, and the optimum pH value was 7.4 (4). Thiamine was analyzed using bromthymol blue with a pH 6.6 buffer solution (5).

The indicator extraction method has the advantages of high sensitivity, rapidity, and partial selectivity and appeared to be of potential value for pharmaceutical preparations. The purpose of this investigation was to develop a stability method for the assay of a new pharmaceutically active amine hydrochloride (I) in various dosage forms.

EXPERIMENTAL

Instruments—The following were used: a UV–visible spectrophotometer[2] with 1-cm cells[3], a pH meter[4], a centrifuge[5], and an analytical balance[6].

[1] Thomas-Hoover, USP Class I.
[2] Beckman DU (or equivalent), Beckman Instruments, Fullerton, Calif.
[3] Bausch and Lomb.
[4] Beckman expandomatic instrument (or equivalent).
[5] International clinical centrifuge.
[6] Type H-51, Mettler Instrument Corp., Princeton, N.J.

administered over 2 min. Such differences can result in correlation variations between pharmacological activity and blood concentration if the site of action resides in the tissue compartments. It would be reasonable to assume that the site of action probably will be, at least in part, in one or more of the tissue compartments, since the compartments simply represent time-dependent equilibration processes. Even if the organ on which the drug is acting can be clearly classified as part of the central compartment, such as the heart, the actual site of action may reside in tissue compartments because of the essential nature of time-dependent processes involved in the tissue equilibration.

From these data, it is clear that some degree of error will invariably result if an instantaneous input assumption is made. Therefore, all intravenous administrations should be considered as short-term zero-order inputs.

REFERENCES

(1) S. Niazi, *J. Pharm. Sci.*, **65**, 750(1976).

(2) M. Gibaldi, R. Nagashima, and G. Levy, *ibid.*, **58**, 193(1969).

(3) S. Niazi, *ibid.*, **65**, 452(1976).

(4) S. Niazi, *Math. Biosci.*, **27**, 169(1975).

(5) S. A. Kaplan, K. Alexander, M. L. Jack, C. V. Puglisi, J. A. F. de Silva, T. L. Lee, and R. E. Weinfeld, *J. Pharm. Sci.*, **63**, 527(1974).

(6) S. Riegelman, J. C. K. Loo, and M. Rowland, *ibid.*, **57**, 128(1968).

(7) N. G. Heatley, *Antibiot. Med. Clin. Ther.*, **11**, 33(1956).

(8) D. B. Breimer, Ph.D. dissertation, University of Nijmegen, The Netherlands, 1974.

(9) F. R. Sidell, W. A. Groff, and A. Kaminskis, *J. Pharm. Sci.*, **61**, 1765(1972).

(10) G. Levy, M. Gibaldi, and W. Jusko, *ibid.*, **58**, 422(1969).

(11) K. A. Pefman and G. A. Portman, *ibid.*, **63**, 84(1974).

ACKNOWLEDGMENTS AND ADDRESSES

Received July 16, 1975, from the *Department of Pharmacy, College of Pharmacy, University of Illinois at the Medical Center, Chicago, IL 60612*

Accepted for publication December 16, 1975.

Simple and Rapid Determination of a New Pharmaceutically Active Amine Hydrochloride

ZUI L. CHANG ˣ and VICTOR E. PAPENDICK

Abstract □ The quantitative analysis of a new pharmaceutically active amine hydrochloride is described. Samples are extracted with chloroform. A yellow amine–dye complex is formed by buffering a sample–bromthymol blue solution at pH 8.5 ± 0.1 and subsequently extracted with chloroform. The complex is treated with 0.01 *N* NaOH to convert it back to the sodium salt of bromthymol blue, which is then measured at 615 nm in the aqueous layer. The amount of complex extracted is linearly related to the amount of amine present, from 0.020 to 0.20 mg/ml. Under the selected conditions, the compound can be determined in the presence of degradation products and there is no interference from common pharmaceutical excipients. The method is suitable for stability studies.

Keyphrases □ Amine hydrochlorides—pharmaceutically active substituted benzopyranopyridine, complexation with bromthymol blue, colorimetric analysis □ Benzopyranopyridine, substituted—pharmaceutically active compound, colorimetric analysis □ Colorimetry—analysis, pharmaceutically active substituted benzopyranopyridine □ Bromthymol blue—use in colorimetric analysis of pharmaceutically active substituted benzopyranopyridine

A new biologically active compound with a benzopyran nucleus (I) was synthesized. Chemically, I is 5,5-dimethyl-10-[4-(1-piperidine)butyryloxy]-8-(3-methyl-2-octyl)-2-(2-propynyl)-1,2,3,4-tetrahydro-5*H*-[1]benzopyrano[3,4-*d*]pyridine hydrochloride. It is readily soluble in water, chloroform, and ethanol, and its melting point[1] is 103–106°.

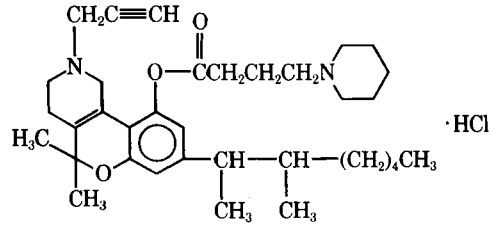

I

The method for the determination of amine salts, involving the formation of an ion-pair with indicator, is based on Prudhomme's (1) discovery that alkaloids form chloroform-soluble complexes with acid dyes such as eosin, the reaction being quantitative (2). The methods available for the determination of quaternary ammonium salts were reviewed previously (3). The extraction of the amine–bromthymol blue complexes of numerous compounds into methylene chloride was studied, and the optimum pH value was 7.4 (4). Thiamine was analyzed using bromthymol blue with a pH 6.6 buffer solution (5).

The indicator extraction method has the advantages of high sensitivity, rapidity, and partial selectivity and appeared to be of potential value for pharmaceutical preparations. The purpose of this investigation was to develop a stability method for the assay of a new pharmaceutically active amine hydrochloride (I) in various dosage forms.

EXPERIMENTAL

Instruments—The following were used: a UV–visible spectrophotometer[2] with 1-cm cells[3], a pH meter[4], a centrifuge[5], and an analytical balance[6].

[1] Thomas-Hoover, USP Class I.
[2] Beckman DU (or equivalent), Beckman Instruments, Fullerton, Calif.
[3] Bausch and Lomb.
[4] Beckman expandomatic instrument (or equivalent).
[5] International clinical centrifuge.
[6] Type H-51, Mettler Instrument Corp., Princeton, N.J.

Table I—Effect of the Aqueous Phase pH on the Reagent Blank

pH of Aqueous Phase	Absorbance at 615 nm[a]
6.4	0.500
6.6	0.350
7.0	0.162
7.4	0.065
7.6	0.042
8.3	0.015
8.6	0.013
9.1	0.006
9.6	0.002
10.1	0.000

[a] The absorbance was obtained by comparing the reagent blank solution at each pH against distilled water as a blank.

Reagents and Solutions—All reagents were ACS grade.

Borate Buffer, pH 8.4—Dissolve 12.5 g of boric acid and 14.9 g of potassium chloride in water to make 1 liter (Solution A). Make a 0.8% sodium hydroxide solution (Solution B). Mix 500 ml of Solution A with 85.5 ml of Solution B and adjust to pH 8.4 ± 0.1, if necessary, with either Solution A or B.

Bromthymol Blue Solution—Use a 0.1% bromthymol blue sodium in 0.08% sodium hydroxide solution.

Buffer–Dye Mixture—On the day of use, mix 100 ml of borate buffer, pH 8.4, with 20 ml of bromthymol blue solution. The pH of the final solution is 8.5 ± 0.1. The pH of the solution decreases when allowed to stand overnight.

Standard Preparation—Weight accurately about 20 mg of reference standard, transfer to a 200-ml volumetric flask, dilute to volume with chloroform, and mix. This standard preparation should have a concentration of about 0.1 mg/ml.

Assay Preparation—Transfer an accurately weighed portion of the pharmaceutical preparation, equivalent to about 2 mg of I, to a 30-ml centrifuge tube. Add 20.0 ml of chloroform, shake the tube mechanically for 30 min, and then centrifuge for about 10 min. Filter the solution into a 30-ml centrifuge tube through a 0.45-μm silver membrane filter[7], using a 20-ml syringe attached to a suitable filter holder[8], and stopper immediately. The filtrate is the assay preparation.

Assay Procedure—Pipet 4.0 ml of the assay preparation and 4.0 ml of the standard preparation into separate 50-ml centrifuge tubes. Pipet 4.0 ml of chloroform into a similar 50-ml centrifuge tube to provide a blank. Add 20.0 ml of chloroform to each tube and mix. Taking one tube at a time, add 10.0 ml of buffer–dye mixture, shake the tube horizontally for 2 min, centrifuge for about 3 min, and then remove the upper aqueous layer by aspiration.

Pipet 10.0 ml of each chloroform layer into separate 30-ml centrifuge tubes. To each tube, add 10.0 ml of 0.04% sodium hydroxide; shake the tube horizontally for 2 min and then centrifuge for about 5 min. Concomitantly determine the absorbance of the upper layers obtained from the assay preparation (A_u) and the standard preparation (A_s) in 1-cm cells at 615 nm, with a suitable spectrophotometer, against the blank.

Calculate the milligrams of I as follows:

$$\text{mg of I per dose} = \frac{A_u}{A_s} CD \frac{F}{W} \qquad \text{(Eq. 1)}$$

where A_u = absorbance of the unknown, A_s = absorbance of the standard, C = concentration of the standard preparation (milligrams per milliliter), D = dilution factor, F = average dosage weight (grams per dose), and W = sample weight (grams).

RESULTS AND DISCUSSION

Compound I degrades in water, acid, and base by hydrolysis to 5,5-dimethyl-10-hydroxy-8-(3-methyl-2-octyl)-2-(2-propynyl)-1,-2,3,4-tetrahydro-5*H*-[1]benzopyrano[3,4-*d*]pyridine (II) and γ-piperidinobutyric acid hydrochloride (III). The degradation products were identified by TLC and compared with authentic samples of II and III. The type of plate used was silica gel GF_{254}, and the developing solvent was chloroform–methanol (80:20). Arsenomolybdate spray reagent was used for detection.

GLC cannot be used since the compound cannot be silylated without degradation. Also, direct UV spectrophotometry cannot be used as a stability method because I has a characteristic band at 300 nm (maximum) that is partially overlapped by II.

The described dye transfer method is a stability method. It has been used to assay I when formulated with various materials and compounded with approved excipients for pharmaceutical formulations.

A single chloroform extraction of the yellow amine–dye complex is made possible by buffering the dye solution to pH 8.5 ± 0.1. An amount of the dye proportional to the concentration of the drug was carried into the chloroform phase as a yellow complex compound. The complex appeared to form rapidly in the aqueous phase. The absorbance at 410 nm was obtained from the standard solution (0.10 mg/ml in chloroform) of I through the procedure using the buffer–dye mixture at pH 8.5 and compared against the reagent blank. The absorbances after 1, 2, 3, and 4 min of shaking were 0.261, 0.265, 0.264, and 0.265, respectively, indicating that the phase equilibrium was complete after 2 min of shaking.

Aqueous alkali produced dissociation of the ion-pair, resulting in the stable soluble sodium salt of bromthymol blue which was determined colorimetrically. The absorbance at 615 nm was obtained from the standard solution (0.10 mg/ml in chloroform) of I through the procedure using the buffer–dye mixture at pH 8.5 and compared against the reagent blank. The absorbances determined initially and after 1, 2, 3, and 4 hr at ambient temperature (25 ± 2°) were 0.520, 0.521, 0.520, 0.520, and 0.521, respectively. The conversion of the yellow ion-pair (ϵ_m = 9300 at 410 nm) to the blue color of the sodium salt of bromthymol blue (ϵ_m = 18,300 at 615 nm) makes it possible to assay lower concentrations of sample accurately because of the higher molar extinction and prevents interference caused by any yellow color imparted by the sample.

The effect of pH variation in the aqueous phase on the extraction of the complex into chloroform was studied (Tables I–III). The absorbance was measured after the complex was converted to the sodium salt of bromthymol blue and extracted.

Experimental results indicate that the optimum pH range of the aqueous phase is 8.4–8.6. Samples containing as little as 0.25 mg of active amine salt/dose were analyzed by this method. Beer's law is obeyed from 0.02 to 0.20 mg of I/ml of solution.

The validity of the single-extraction procedure was demonstrated

Table II—Effect of the Aqueous Phase pH on Compounds I and II

pH of Aqueous Phase	*A* at 615 nm[a], Compound I	*A* at 615 nm[a], Compound II
8.1	0.910	0.035
8.3	0.735	0.010
8.5	0.525	0.000
8.7	0.260	0.000
8.9	0.068	0.000

[a] The absorbance was obtained from the standard solution (0.10 mg/ml in chloroform) of I or II through the procedure and compared against the reagent blank at each pH.

Table III—Effect of the Aqueous Phase pH on Compound III

pH of Aqueous Phase	Absorbance at 615 nm[a]
8.1	0.035
8.3	0.013
8.5	0.003
8.7	0.000
8.9	0.000

[a] The absorbance was obtained from the saturated solution of III through the procedure and compared against the reagent blank at each pH. The saturated solution of III used for dye transfer was obtained by shaking 10 mg of III in 200 ml of chloroform for 30 min and then filtering the solution through a 0.45-μm silver membrane filter, using a 20-ml syringe attached to a suitable filter holder. The solubility of III in chloroform at room temperature is about 0.02 mg/ml.

[7] FM-25, Selas Flotronics, Spring House, Pa.
[8] Swinnex-25, Millipore Corp., Bedford, Mass.

on nine assays conducted on 3 days. Mean and standard deviation values were 9.66 mg/g ± 0.12 mg for the powder. The relative standard deviation was ±1.3%.

On the basis of this investigation, it is concluded that the proposed method is a superior stability assay of this new pharmaceutically active amine hydrochloride.

REFERENCES

(1) M. R. O. Prudhomme, *Bull. Soc. Pathol. Exot.*, **31**, 929(1938).

(2) M. R. O. Prudhomme, *J. Pharm. Chim.*, **9**, 8(1940).

(3) O. B. Hager, E. M. Young, T. L. Flanagan, and H. B. Walker, *Anal. Chem.*, **19**, 885(1947).

(4) G. Schill, *Acta Pharm. Suec.*, **2**, 13(1965).

(5) V. D. Gupta and D. E. Cadwallader, *J. Pharm. Sci.*, **57**, 112(1968).

ACKNOWLEDGMENTS AND ADDRESSES

Received July 5, 1974, from the *Analytical Research Department, Abbott Laboratories, North Chicago, IL 60064*

Accepted for publication December 15, 1975.

[x] To whom inquiries should be directed.

Stereochemistries of Geometric Isomers of 4-(2-Bromo-1,2-diphenylvinyl)phenol, 4-(2-Bromo-1,2-diphenylvinyl)anisole, and 2-[*p*-(2-Bromo-1,2-diphenylvinyl)phenoxy]triethylamine: Corrections of the Literature

A. RICHARDSON, Jr. [*], H. D. BENSON [*], and G. HITE [‡x]

Abstract □ The stereochemistries of geometric isomers of 4-(2-bromo-1,2-diphenylvinyl)phenol, 4-(2-bromo-1,2-diphenylvinyl)anisole, and 2-[*p*-(2-bromo-1,2-diphenylvinyl)phenoxy]triethylamine were determined by conversion of the phenolic analog to the ethers and subsequent comparison of physical properties with those of 2-[*p*-(2-chloro-1,2-diphenylvinyl)phenoxy]triethylamine of known stereochemistry.

Keyphrases □ Stereochemistry—geometric isomers of various substituted 1,2-diphenylvinyl compounds determined, literature correction □ Geometric isomers—various substituted 1,2-diphenylvinyl compounds, stereochemistry determined, literature correction □ Isomers, geometric—various substituted 1,2-diphenylvinyl compounds, stereochemistry determined, literature correction □ 1,2-Diphenylvinyl compounds, substituted—various, stereochemistry of geometric isomers determined, literature correction

The more estrogenic geometric isomers of 2-[*p*-(2-chloro-1,2-diphenylvinyl)phenoxy]triethylamine, clomiphene[1] (I) (1), and of 2-[*p*-(1,2-diphenyl-1-butenyl)phenoxy]-*N,N*-dimethylethylamine (II) (2) were designated *trans-(E)* (3) and *cis-(Z)* (4), respectively. Single-crystal X-ray diffraction studies on isomers of I and II (5) established the *cis*-stereochemistry for the more estrogenic isomers, permitted a consistent correlation of the biological data with structure and stereochemistry, and provided insight into the molecular mechanisms of action (6). Numerous conflicting aspects of the structural determinations of I and II prompted this report, which will review the chemical and physical lines of evidence, place them in perspective, and record the correct stereochemistries and physical properties of 4-(2-bromo-1,2-diphenylvinyl)anisole (III), 2-[*p*-(2-bromo- 1,2- diphenylvinyl)phenoxy]triethylamine (IV), and 4-(2-bromo-1,2-diphenylvinyl)phenol (V), which played the dominant role in the earlier incorrect assignments of stereochemistry to geometric isomers of I (5, 7).

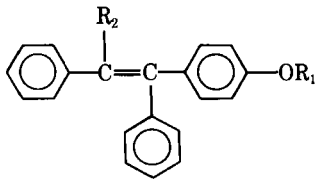

cis-configuration

I: $R_1 = CH_2CH_2N(CH_2CH_3)_2$, $R_2 = Cl$

II: $R_1 = CH_2CH_2N(CH_3)_2$, $R_2 = CH_3CH_2$

III: $R_1 = CH_3$, $R_2 = Br$

IV: $R_1 = CH_2CH_2N(CH_2CH_3)_2$, $R_2 = Br$

V: $R_1 = H$, $R_2 = Br$

EXPERIMENTAL

(*Z*)-4-(2-Bromo-1,2-diphenylvinyl)phenol (V*a*)—This compound was prepared as described by Longfellow and Jackson (8), mp 145–147° [lit. (8) mp 147–149°].

(*Z*)- and (*E*)-4-(2-Bromo-1,2-diphenylvinyl)anisoles (III*a* and III*b*)—These isomers, previously identified incorrectly as *E* and *Z*, respectively, were prepared by the method described by Koelsch (9): (*Z*), mp 117.5–119° [lit. (9) mp 118–120°, lit. (10) mp 118.5–119.5°], and by Curtin *et al.* (10): (*E*), mp 93–94.5° [lit. (10) mp 97–98°]. In addition, III*a* was obtained by treatment of a solution of V*a* with methyl iodide and base.

(*Z*)- and (*E*)-2-[*p*-(2-Bromo-1,2-diphenylvinyl)phenoxy]triethylamines (IV*a* and IV*b*)—These compounds were prepared as described by Palopoli *et al.* (3). Their physical properties are summarized in Table I.

[1] Clomid, Merrell-National Laboratories, Division of Richardson-Merrell Inc., Cincinnati, Ohio.

on nine assays conducted on 3 days. Mean and standard deviation values were 9.66 mg/g ± 0.12 mg for the powder. The relative standard deviation was ±1.3%.

On the basis of this investigation, it is concluded that the proposed method is a superior stability assay of this new pharmaceutically active amine hydrochloride.

REFERENCES

(1) M. R. O. Prudhomme, *Bull. Soc. Pathol. Exot.*, **31**, 929(1938).

(2) M. R. O. Prudhomme, *J. Pharm. Chim.*, **9**, 8(1940).

(3) O. B. Hager, E. M. Young, T. L. Flanagan, and H. B. Walker, *Anal. Chem.*, **19**, 885(1947).

(4) G. Schill, *Acta Pharm. Suec.*, **2**, 13(1965).

(5) V. D. Gupta and D. E. Cadwallader, *J. Pharm. Sci.*, **57**, 112(1968).

ACKNOWLEDGMENTS AND ADDRESSES

Received July 5, 1974, from the *Analytical Research Department, Abbott Laboratories, North Chicago, IL 60064*

Accepted for publication December 15, 1975.

[x] To whom inquiries should be directed.

Stereochemistries of Geometric Isomers of 4-(2-Bromo-1,2-diphenylvinyl)phenol, 4-(2-Bromo-1,2-diphenylvinyl)anisole, and 2-[*p*-(2-Bromo-1,2-diphenylvinyl)phenoxy]triethylamine: Corrections of the Literature

A. RICHARDSON, Jr. [*], H. D. BENSON [*], and G. HITE [‡x]

Abstract □ The stereochemistries of geometric isomers of 4-(2-bromo-1,2-diphenylvinyl)phenol, 4-(2-bromo-1,2-diphenylvinyl)anisole, and 2-[*p*-(2-bromo-1,2-diphenylvinyl)phenoxy]triethylamine were determined by conversion of the phenolic analog to the ethers and subsequent comparison of physical properties with those of 2-[*p*-(2-chloro-1,2-diphenylvinyl)phenoxy]triethylamine of known stereochemistry.

Keyphrases □ Stereochemistry—geometric isomers of various substituted 1,2-diphenylvinyl compounds determined, literature correction □ Geometric isomers—various substituted 1,2-diphenylvinyl compounds, stereochemistry determined, literature correction □ Isomers, geometric—various substituted 1,2-diphenylvinyl compounds, stereochemistry determined, literature correction □ 1,2-Diphenylvinyl compounds, substituted—various, stereochemistry of geometric isomers determined, literature correction

The more estrogenic geometric isomers of 2-[*p*-(2-chloro-1,2-diphenylvinyl)phenoxy]triethylamine, clomiphene[1] (I) (1), and of 2-[*p*-(1,2-diphenyl-1-butenyl)phenoxy]-*N,N*-dimethylethylamine (II) (2) were designated *trans-(E)* (3) and *cis-(Z)* (4), respectively. Single-crystal X-ray diffraction studies on isomers of I and II (5) established the *cis*-stereochemistry for the more estrogenic isomers, permitted a consistent correlation of the biological data with structure and stereochemistry, and provided insight into the molecular mechanisms of action (6). Numerous conflicting aspects of the structural determinations of I and II prompted this report, which will review the chemical and physical lines of evidence, place them in perspective, and record the correct stereochemistries and physical properties of 4-(2-bromo-1,2-diphenylvinyl)anisole (III), 2-[*p*-(2-bromo- 1,2- diphenylvinyl)phenoxy]triethylamine (IV), and 4-(2-bromo-1,2-diphenylvinyl)phenol (V), which played the dominant role in the earlier incorrect assignments of stereochemistry to geometric isomers of I (5, 7).

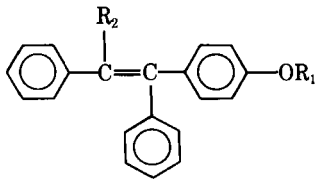

cis-configuration

I: $R_1 = CH_2CH_2N(CH_2CH_3)_2$, $R_2 = Cl$

II: $R_1 = CH_2CH_2N(CH_3)_2$, $R_2 = CH_3CH_2$

III: $R_1 = CH_3$, $R_2 = Br$

IV: $R_1 = CH_2CH_2N(CH_2CH_3)_2$, $R_2 = Br$

V: $R_1 = H$, $R_2 = Br$

EXPERIMENTAL

(*Z*)-4-(2-Bromo-1,2-diphenylvinyl)phenol (V*a*)—This compound was prepared as described by Longfellow and Jackson (8), mp 145–147° [lit. (8) mp 147–149°].

(*Z*)- and (*E*)-4-(2-Bromo-1,2-diphenylvinyl)anisoles (III*a* and III*b*)—These isomers, previously identified incorrectly as *E* and *Z*, respectively, were prepared by the method described by Koelsch (9): (*Z*), mp 117.5–119° [lit. (9) mp 118–120°, lit. (10) mp 118.5–119.5°], and by Curtin *et al.* (10): (*E*), mp 93–94.5° [lit. (10) mp 97–98°]. In addition, III*a* was obtained by treatment of a solution of V*a* with methyl iodide and base.

(*Z*)- and (*E*)-2-[*p*-(2-Bromo-1,2-diphenylvinyl)phenoxy]triethylamines (IV*a* and IV*b*)—These compounds were prepared as described by Palopoli *et al.* (3). Their physical properties are summarized in Table I.

[1] Clomid, Merrell-National Laboratories, Division of Richardson-Merrell Inc., Cincinnati, Ohio.

Table I—Physical Properties of Geometric Isomers of I and III–V[a]

Property	Ia, *cis*-(*Z*)	Ib, *trans*-(*E*)	IIIa, *cis*-(*Z*)	IIIb, *trans*-(*E*)	IVa, *cis*-(*Z*)	IVb, *trans*-(*E*)
Melting point[b]	50–51.5°	73.5–75°	117.5–119°	93–94.5°	51.5–53°	65–66°
λ_{max}[c], nm (CH_3OH)	231 (ε 20,200)	242 (ε 22,100)	233 (ε 23,500)	241 (ε 22,000)	232 (ε 25,400)	240 (ε 23,200)
	246 (ε 15,800) sh	300 (ε 11,400)	257 (ε 11,000) sh	302 (ε 9190)	258 (ε 12,200) sh	302 (ε 9570)
	292 (ε 12,600)		292 (ε 8940)		291 (ε 9860)	
μ[d], D (C_6H_6, 25°)	1.98	2.86	1.92	2.53	1.95	2.85
ν[e], cm^{-1} (KBr)	693, 696 sh	693, 696	690	687, 699	691, 696 sh	690, 696
δf[f], ppm (tetramethylsilane in $CDCl_3$, A_2B_2)	6.82, 7.26	6.52, 6.82	6.87, 7.34	6.53, 6.86	6.82, 7.25	6.53, 6.85

[a] The melting point for Va, which has the *cis*-(*Z*) geometry, is 145–147°. [b] Melting points were determined in a Thomas-Hoover Unimelt apparatus and are uncorrected. [c] UV spectra were determined in 1-cm corex cells with a Cary 118 recording spectrophotometer. Band assignments are believed accurate to within ±1 nm. [d] Dipole moments were measured with a Kahl DM 01 dipolmeter. [e] IR spectra were determined with a Perkin-Elmer model 421 recording spectrophotometer. Band assignments are believed accurate to within ±3 cm^{-1}. [f] PMR spectra were determined on 10% solutions with a Varian model A60-A spectrometer. Band assignments are believed accurate to within ±0.05 ppm. The two entries in each set refer to the *ortho*- and *meta*-protons, respectively, of the disubstituted aromatic ring.

DISCUSSION

The longest wavelength UV maximum appears at a shorter wavelength for Ia (mp 50–51.5°), the more potent estrogenic isomer. Thus, Ia was designated *trans*, since this structure contains the less easily excited *trans*-stilbene chromophore while the more easily excited *trans*-*p*-alkoxystilbene chromophore is a feature of the *cis*-isomer (3). The A_2B_2 PMR pattern occurs at a lower field (0.4 ppm) for the lower melting, more potent estrogenic isomer of II (mp 72–74° and 96–98°). This isomer was designated *cis*. The assignment is consistent with the proposed sandwiching of the disubstituted ring between the monosubstituted rings, a feature unique to the *trans*-structure in which double shielding of the protons of the disubstituted ring by the ring currents of the monosubstituted rings is expected to lead to a higher field A_2B_2 PMR pattern (4).

It was assumed that the three rings exhibit a time-averaged orientation nearly perpendicular to the plane of the vinyl group. Interpreted in the same way, the PMR data for isomers of I contradicted the geometric assignment made on the basis of the UV evidence (*cf.*, Table I) (7). A similar inconsistency exists in the PMR and UV interpretations for II (5). In view of the previously demonstrated inconsistencies in the correlation of UV spectra with geometries of stilbenes (11) and the structural and electronic differences between I and II, the advent of a chemical line of evidence in support of the *trans* assignment for Ia demanded a completely different interpretation of the PMR data for isomers of I (7).

This rationale assumed a time-averaged coplanar stilbene with a nearly perpendicular geminal alkoxyphenyl substituent (*trans*-structure) and a time-averaged coplanar alkoxystilbene with a nearly perpendicular geminal phenyl substituent (*cis*-isomer). The A_2B_2 protons in the *cis*-structure were expected to be shielded by the ring currents of the geminal phenyl moiety. Thus, the *trans* assignment to Ia was made on the basis of the less shielded A_2B_2 PMR absorption exhibited by this isomer. The validity of the chemical evidence (and the PMR interpretation for isomers of I) rested on an earlier designation of the *trans*-geometry for IIIa (mp 117.5–119°) (9, 10). This isomer and IVa (mp 51.5–53°) were prepared by conventional methods (phenol, base, RX) (7) from Va (mp 145–147°) (8). Comparisons of dipole moments and UV, IR, and PMR spectra (Table I) (7) established that Ia has the same geometry as IIIa–Va.

The X-ray diffraction analysis (5) of the hydrobromide salt of the *cis*-isomer of II confirmed not only the geometric assignment but also the conformational assumptions made on the basis of the PMR studies (4). The latter point in particular called into question the geometric assignments made for isomers of I on the basis of the chemical evidence and the stereochemistry originally assigned to IIIa and of the PMR spectra and led to the X-ray diffraction studies of both Ib hydrochloride (mp 149–150.5°) and Ia hydroiodide (mp 170–171°). Full accounts of these studies will appear elsewhere. These studies revealed that Ia is *cis*-(*Z*) and not *trans*-(*E*). The disposition of the aromatic rings in I is much the same as that found in the solid state for II. Accordingly, while the UV data for isomers of both I and II are misleading, the PMR data, properly interpreted (4), are not. This proves that the geometries for isomers of III (9, 10), IV, and V (7) were also incorrectly assigned. The correct stereochemistries and the physical properties of geometric isomers of III–V are recorded in Table I.

REFERENCES

(1) L. W. Self, D. E. Holtkamp, and W. L. Kuhn, *Fed. Proc.*, **26**, 534(1967).

(2) M. J. K. Harper and A. L. Walpole, *Nature*, **212**, 87(1966).

(3) F. P. Palopoli, V. L. Feil, R. E. Allen, D. E. Holtkamp, and A. Richardson, Jr., *J. Med. Chem.*, **10**, 84(1967).

(4) G. R. Bedford and D. N. Richardson, *Nature*, **212**, 733(1966).

(5) B. T. Kilbourn and P. G. Owston, *J. Chem. Soc. B*, **1970**, 1.

(6) S. Ernst, G. Hite, J. S. Cantrell, A. Richardson, Jr., and H. D. Benson, *J. Pharm. Sci.*, **65**, 148(1976).

(7) A. Richardson, Jr., and H. D. Benson, "Abstracts of the 153rd Meeting of the American Chemical Society," American Chemical Society, Washington, D.C., 1967, p. M4.

(8) C. F. Longfellow and A. O. Jackson, U.S. pat. 2,429,556 (1947); through *Chem. Abstr.*, **42**, 1029(1948).

(9) C. F. Koelsch, *J. Am. Chem. Soc.*, **54**, 2487(1932).

(10) D. Y. Curtin, E. E. Harris, and E. K. Meislich, *ibid.*, **74**, 2901(1952).

(11) M. Katayama, S. Fujiwara, H. Suzuki, Y. Nagai, and O. Simamura, *J. Mol. Spectrosc.*, **5**, 85(1960).

ACKNOWLEDGMENTS AND ADDRESSES

Received October 20, 1975, from *Merrell-National Laboratories, Division of Richardson-Merrell Inc., Cincinnati, OH 45215, and the ‡Section of Medicinal Chemistry and Pharmacognosy, School of Pharmacy, University of Connecticut, Storrs, CT 06268

Accepted for publication December 17, 1975.

Supported in part by the Department of Health, Education, and Welfare, U.S. Public Health Service, under special Postdoctoral Fellowship GM 49037.

x To whom inquiries should be directed.

Chemical Constituents of Gentianaceae XIX: CNS-Depressant Effects of Swertiamarin

S. K. BHATTACHARYA *, P. K. S. P. REDDY *, S. GHOSAL‡x, A. K. SINGH ‡, and P. V. SHARMA ‡

Abstract □ CNS activity of swertiamarin, a secoiridoid glucoside from *Swertia chirata*, was evaluated. An apparent anomaly, associated with the unanticipated finding that the alcoholic extracts (excluding mangiferin) of *S. chirata* significantly reversed the mangiferin-induced CNS-stimulating effects in albino mice and rats, was resolved. The results indicate that swertiamarin and mangiferin antagonize each other *in vivo* and thereby reverse their CNS effects.

Keyphrases □ Gentianaceae—*Swertia chirata*, CNS activity of swertiamarin evaluated □ Swertiamarin—CNS activity evaluated, interaction with mangiferin □ CNS activity—swertiamarin evaluated □ Mangiferin—CNS activity, effect of swertiamarin

One result of a prior study, dealing with the active principles of *Swertia chirata* (Gentianaceae) (1), was the unanticipated finding that the alcoholic extracts, containing xanthones (excluding mangiferin) and secoiridoid glucosides, in doses of 50–100 mg/kg ip, significantly reversed the mangiferin-induced hyperactivity in albino mice and rats and also the potentiating effect of mangiferin on amphetamine toxicity in aggregated mice. Mangiferin (I), isolated in appreciable quantities from *S. chirata* (1.2 g/kg of whole plant) (1) and from *Canscora decussata* (30 g/kg of whole plant) (2), was earlier shown to produce significant pharmacological actions on the central nervous system (CNS) of laboratory animals (3, 4). In doses of 50–100 mg/kg ip, it produced definite signs of CNS stimulation in albino mice and rats as evidenced by hyperactivity, fine tremors, piloerection, increased spontaneous motility, reversal of reserpine-induced ptosis and sedation, potentiation of the analgesic effect of subanalgesic doses of morphine, and potentiation of amphetamine toxicity in aggregated mice.

The actions of mangiferin were subsequently found to be mediated *via* monoamine oxidase inhibition (5). Also, it was shown recently (6) that mangiferin-induced potentiation of the antinociceptive effect of morphine, like that of nialamide, was 5-hydroxytryptamine mediated. This paper describes findings that indicate that the reversal of mangiferin-induced pharmacological effects by the alcoholic extracts of *S. chirata* is due to the presence of an appreciable quantity (about 4 g/kg of whole plant) (5) of a CNS depressant swertiamarin (II).

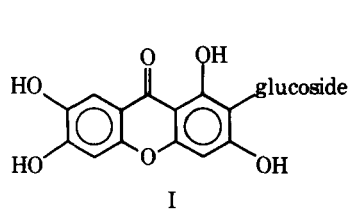

I

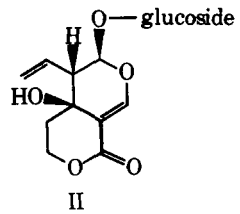

II

EXPERIMENTAL

The isolation and purification of swertiamarin from *S. chirata* were reported previously (5). Pharmacological studies were conducted on albino mice (18–25 g) and albino rats[1] (80–120 g). The animals were fed a standard pellet diet[2]. All experiments were conducted at ambient temperature of 24 ± 2°.

The drug was tested in doses of 25–100 mg/kg ip. Unless stated otherwise, the data given indicate the effect of swertiamarin in doses of 50 mg/kg ip and a pretreatment time of 1 hr. In experiments where combined effects of mangiferin and swertiamarin were investigated, mangiferin was administered at 100 mg/kg ip and the pretreatment time was 2 hr.

In all experiments, 10 animals were used for the drug-treated and control groups; controls received only the vehicle, distilled water. Statistical analyses were done by the Student t test and χ-square test at appropriate places.

RESULTS AND DISCUSSION

In primary observational tests (7), swertiamarin produced a transient stimulation followed by signs of marked central depression in albino mice. The initial stimulation was absent in albino rats. The depressant activity was characterized by considerably diminished spontaneous motility, grouping of animals on one side of the cage, and ptosis. However, reflexes were intact, and the animals responded to external stimuli.

With higher doses (75–100 mg/kg ip), normal activities of the mice such as grooming were further reduced, the gait became abnormal, and the animals lost their ability to remain on an inclined plane. They responded to painful stimuli, although the righting reflex was sluggish. In these doses, swertiamarin produced significant hypothermia in albino rats as recorded by a rectal thermister probe (Table I). Since these observations were indicative of CNS depressant activity, swertiamarin was subjected to further pharmacological screening as follows.

The effects of swertiamarin on hexobarbital hypnosis (8) and amphetamine toxicity in aggregated and isolated mice (9) were evaluated

[1] The animals were supplied by Messrs B. N. Ghosh & Co., Calcutta, India.

[2] Hindusthan Levers, Calcutta, India.

(11) M. Katayama, S. Fujiwara, H. Suzuki, Y. Nagai, and O. Simamura, *J. Mol. Spectrosc.*, **5**, 85(1960).

ACKNOWLEDGMENTS AND ADDRESSES

Received October 20, 1975, from *Merrell-National Laboratories, Division of Richardson-Merrell Inc., Cincinnati, OH 45215, and the ‡Section of Medicinal Chemistry and Pharmacognosy, School of Pharmacy, University of Connecticut, Storrs, CT 06268

Accepted for publication December 17, 1975.

Supported in part by the Department of Health, Education, and Welfare, U.S. Public Health Service, under special Postdoctoral Fellowship GM 49037.

x To whom inquiries should be directed.

Chemical Constituents of Gentianaceae XIX: CNS-Depressant Effects of Swertiamarin

S. K. BHATTACHARYA *, P. K. S. P. REDDY *, S. GHOSAL‡x, A. K. SINGH ‡, and P. V. SHARMA ‡

Abstract □ CNS activity of swertiamarin, a secoiridoid glucoside from *Swertia chirata*, was evaluated. An apparent anomaly, associated with the unanticipated finding that the alcoholic extracts (excluding mangiferin) of *S. chirata* significantly reversed the mangiferin-induced CNS-stimulating effects in albino mice and rats, was resolved. The results indicate that swertiamarin and mangiferin antagonize each other *in vivo* and thereby reverse their CNS effects.

Keyphrases □ Gentianaceae—*Swertia chirata*, CNS activity of swertiamarin evaluated □ Swertiamarin—CNS activity evaluated, interaction with mangiferin □ CNS activity—swertiamarin evaluated □ Mangiferin—CNS activity, effect of swertiamarin

One result of a prior study, dealing with the active principles of *Swertia chirata* (Gentianaceae) (1), was the unanticipated finding that the alcoholic extracts, containing xanthones (excluding mangiferin) and secoiridoid glucosides, in doses of 50–100 mg/kg ip, significantly reversed the mangiferin-induced hyperactivity in albino mice and rats and also the potentiating effect of mangiferin on amphetamine toxicity in aggregated mice. Mangiferin (I), isolated in appreciable quantities from *S. chirata* (1.2 g/kg of whole plant) (1) and from *Canscora decussata* (30 g/kg of whole plant) (2), was earlier shown to produce significant pharmacological actions on the central nervous system (CNS) of laboratory animals (3, 4). In doses of 50–100 mg/kg ip, it produced definite signs of CNS stimulation in albino mice and rats as evidenced by hyperactivity, fine tremors, piloerection, increased spontaneous motility, reversal of reserpine-induced ptosis and sedation, potentiation of the analgesic effect of subanalgesic doses of morphine, and potentiation of amphetamine toxicity in aggregated mice.

The actions of mangiferin were subsequently found to be mediated *via* monoamine oxidase inhibition (5). Also, it was shown recently (6) that mangiferin-induced potentiation of the antinociceptive effect of morphine, like that of nialamide, was 5-hydroxytryptamine mediated. This paper describes findings that indicate that the reversal of mangiferin-induced pharmacological effects by the alcoholic extracts of *S. chirata* is due to the presence of an appreciable quantity (about 4 g/kg of whole plant) (5) of a CNS depressant swertiamarin (II).

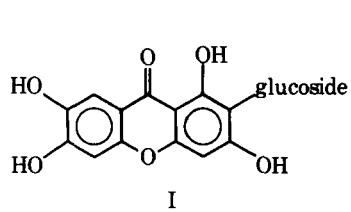

I

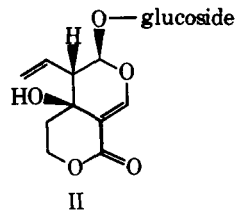

II

EXPERIMENTAL

The isolation and purification of swertiamarin from *S. chirata* were reported previously (5). Pharmacological studies were conducted on albino mice (18–25 g) and albino rats[1] (80–120 g). The animals were fed a standard pellet diet[2]. All experiments were conducted at ambient temperature of 24 ± 2°.

The drug was tested in doses of 25–100 mg/kg ip. Unless stated otherwise, the data given indicate the effect of swertiamarin in doses of 50 mg/kg ip and a pretreatment time of 1 hr. In experiments where combined effects of mangiferin and swertiamarin were investigated, mangiferin was administered at 100 mg/kg ip and the pretreatment time was 2 hr.

In all experiments, 10 animals were used for the drug-treated and control groups; controls received only the vehicle, distilled water. Statistical analyses were done by the Student t test and χ-square test at appropriate places.

RESULTS AND DISCUSSION

In primary observational tests (7), swertiamarin produced a transient stimulation followed by signs of marked central depression in albino mice. The initial stimulation was absent in albino rats. The depressant activity was characterized by considerably diminished spontaneous motility, grouping of animals on one side of the cage, and ptosis. However, reflexes were intact, and the animals responded to external stimuli.

With higher doses (75–100 mg/kg ip), normal activities of the mice such as grooming were further reduced, the gait became abnormal, and the animals lost their ability to remain on an inclined plane. They responded to painful stimuli, although the righting reflex was sluggish. In these doses, swertiamarin produced significant hypothermia in albino rats as recorded by a rectal thermister probe (Table I). Since these observations were indicative of CNS depressant activity, swertiamarin was subjected to further pharmacological screening as follows.

The effects of swertiamarin on hexobarbital hypnosis (8) and amphetamine toxicity in aggregated and isolated mice (9) were evaluated

[1] The animals were supplied by Messrs B. N. Ghosh & Co., Calcutta, India.

[2] Hindusthan Levers, Calcutta, India.

Table I—Effect of Swertiamarin on Rectal Temperature (RT), Spontaneous Motor Activity (SMA), Forced Locomotor Activity (FLA) (Rotarod Test), and Pentylenetetrazol-Induced Convulsions (PIC)[a]

Group	Dose, mg/kg ip	RT, Mean ± *SEM*	SMA, Mean ± *SEM*	FLA, % Fall within 180 sec	PIC, % Incidence of Convulsions
Control	—	36.5 ± 0.96°	298 ± 42	0	100
Swertiamarin	50	35.2 ± 0.21°, $p > 0.05$[b]	74 ± 14, $p < 0.01$	70, $p < 0.01$	50, $p > 0.05$
Swertiamarin	100	34.3 ± 0.34°, $p < 0.05$	33 ± 9, $p < 0.001$	90, $p < 0.001$	70, $p < 0.01$

[a] Number of animals was 10 in each case. [b] The p value shows significance in relation to respective control groups.

(Tables II and III). Swertiamarin significantly potentiated (110% over the control) hexobarbital- (100 mg/kg ip) induced sleeping time in albino mice. It diminished amphetamine- (20 mg/kg ip) induced toxicity in both aggregated and isolated mice in similar doses. The ED_{50}'s of swertiamarin (in milligrams per kilogram ± *SEM*) against the lethal effect of amphetamine in aggregated and isolated mice were 6.25 ± 5.9 and 58.6 ± 6.3, respectively.

The effects of swertiamarin on rats and mice on the rotarod test (10) and on their conditioned avoidance response (11) were examined. It markedly inhibited the ability of trained mice to remain on a rotating rod for a maximum trial of 180 sec. With higher doses, the incidence of fall increased (Table I). Swertiamarin had no effect on the avoidance response to the conditioned stimulus (buzzer) in trained rats. However, in higher doses (75–100 mg/kg ip), it significantly blocked the escape response to both conditioned and unconditioned (electric shock) stimuli in 65% of the animals ($p < 0.05$) and there was a marked loss of motor tone.

Table II—Effect of Swertiamarin on Hexobarbital Hypnosis in Absence and Presence of Mangiferin[a]

Group	Drugs (Dose, mg/kg ip)	Hexobarbital Sleeping Time, min, Mean ± *SEM*	p
1	Hexobarbital (100)	21.4 ± 1.4	
2	Swertiamarin (50) plus hexobarbital (100)	43.8 ± 4.3	<0.001[b]
3	Mangiferin (100) plus hexobarbital (100)	31.8 ± 3.2	<0.01[b]
4	Mangiferin (100) plus swertiamarin (50) plus hexobarbital (100)	56.3 ± 3.1	<0.01[c]

[a] Number of animals was 10 in each case. [b] Significance in relation to Group 1. [c] Significance in relation to Group 2.

Table III—Effect of Swertiamarin on Amphetamine Toxicity in Aggregated Mice in Absence and Presence of Mangiferin[a]

Group	Drugs (Dose, mg/kg ip)	Mortality (18 hr), %	p
1	Amphetamine (20)	100	—
2	Swertiamarin (50) plus amphetamine (20)	60	>0.05[b]
3	Swertiamarin (100) plus amphetamine (20)	20	<0.001[b]
4	Mangiferin (100) plus amphetamine (20)	100	—
5	Mangiferin (100) plus swertiamarin (100) plus amphetamine (20)	80	<0.05[c]
6	Amphetamine (10)	20	—
7	Mangiferin (100) plus amphetamine (10)	80	<0.05[d]
8	Mangiferin (100) plus swertiamarin (100) plus amphetamine (10)	40	>0.05[e]

[a] Number of animals was 10 in each case. [b] Significance in relation to Group 1. [c] Significance in relation to Group 3. [d] Significance in relation to Group 6. [e] Significance in relation to Group 7.

The effects of swertiamarin on morphine analgesia (12), anticonvulsant action of phenytoin (13), electroshock seizure (13), and pentylenetetrazol convulsion (14) were also determined (Tables I, IV, and V). Swertiamarin significantly potentiated the analgesic activity of a subanalgesic dose (2 mg/kg ip) of morphine (15) but had no analgesic activity *per se*. It also significantly potentiated the anticonvulsant activity of a subanticonvulsant dose (2.5 mg/kg ip) of phenytoin but had no anticonvulsant activity *per se*. In higher doses (75–100 mg/kg ip), swertiamarin offered significant protection against pentylenetetrazol- (70 mg/kg sc) induced convulsion. However, as mentioned earlier, there was marked loss of motor tone in the animals with these doses.

In view of the initial observation and the cooccurrence of mangiferin and swertiamarin as the two major chemical constituents of *S. chirata*, their interactions on selected pharmacological parameters were examined. Mangiferin significantly inhibited swertiamarin-induced sedation, ptosis, and hypothermia. It further potentiated (160%) swertiamarin-induced potentiation (110%) of hexobarbital-induced sleeping time in mice (Table II). Since mangiferin itself potentiated (50%) hexobarbital hypnosis in mice, the combined effect appears to be additive.

In mangiferin-pretreated animals, swertiamarin produced significant anticonvulsant effect (against electroshock seizure). Likewise,

Table IV—Effect of Swertiamarin on Morphine Analgesia and Its Analgesic Effect *per se* in Absence and Presence of Mangiferin[a]

Group	Drugs (Dose, mg/kg ip)	Latent Period of Tail-Flick Response, sec, Mean ± *SEM*	p
1	Morphine (2)	3.9 ± 0.7	—
2	Swertiamarin (50)	2.4 ± 0.96	—
3	Swertiamarin (50) plus morphine (2)	10.7 ± 1.1	<0.001[b]
4	Mangiferin (100)	3.2 ± 0.7	—
5	Mangiferin (100) plus swertiamarin (50)	9.3 ± 1.06	<0.001[c]

[a] Number of animals was 10 in each case. [b] Significance in relation to Group 1. [c] Significance in relation to Group 2.

Table V—Effect of Swertiamarin on Anticonvulsant Effect of Phenytoin and Its Anticonvulsant Effect *per se* against Electroshock Seizure in Absence and Presence of Mangiferin[a]

Group	Drugs (Dose, mg/kg ip)	Anticonvulsant Effect, %	p
1	Phenytoin (2.5)	0	—
2	Swertiamarin (50)	0	—
3	Swertiamarin (100)	40	>0.05[b]
4	Swertiamarin (50) plus phenytoin (2.5)	60	<0.05[b]
5	Mangiferin (100)	0	—
6	Mangiferin (100) plus swertiamarin (50)	60	<0.05[c]

[a] Number of animals was 10 in each case. [b] Significance in relation to Group 1. [c] Significance in relation to Group 2.

in mangiferin-pretreated animals, swertiamarin produced significant analgesic effect (Tables IV and V). Mangiferin significantly reduced the protective effect of swertiamarin against amphetamine (20 mg/kg ip) toxicity in aggregated mice (Table III).

The toxicity (16) and the LD_{50} of swertiamarin after single intraperitoneal administration in albino rats were studied; the LD_{50} (in milligrams per kilogram ± *SEM*) was 368 ± 45.

Earlier reports (17) indicated that iridoids are the active ingredients of some folk medicines and have been used for centuries, but the properties of specific iridoids have been evaluated only in a few cases. To the knowledge of the authors, this is the first report of a pharmacological evaluation of a pure secoiridoid, swertiamarin, occurring widely in members of the family Gentianaceae.

REFERENCES

(1) S. Ghosal, P. V. Sharma, R. K. Chaudhuri, and S. K. Bhattacharya, *J. Pharm. Sci.*, **62**, 926(1973).

(2) R. K. Chaudhuri and S. Ghosal, *Phytochemistry*, **10**, 2425(1971).

(3) S. K. Bhattacharya, S. Ghosal, R. K. Chaudhuri, and A. K. Sanyal, *J. Pharm. Sci.*, **61**, 1838(1972).

(4) S. K. Bhattacharya, A. K. Sanyal, and S. Ghosal, *Naturwissenschaften*, **59**, 650(1972).

(5) P. V. Sharma, Ph.D. thesis, Banaras Hindu University, Varanasi, India, 1974, p. 118.

(6) S. K. Bhattacharya, A. K. Sanyal, and S. Ghosal, in "Drugs and Central Synaptic Transmission," P. B. Bradley and B. N. Dhawan, Eds., Macmillan, London, England, 1975, p. 94.

(7) R. A. Turner, in "Screening Methods in Pharmacology," vol. 1, Academic, New York, N.Y., 1965, p. 26.

(8) W. L. Kuhn and E. F. Van Maanen, *J. Pharmacol. Exp. Ther.*, **134**, 60(1961).

(9) J.H. Mennear and A. D. Rudzik, *Life Sci.*, **5**, 349(1966).

(10) W. J. Kinnard and C. J. Carr, *J. Pharmacol. Exp. Ther.*, **121**, 354(1957).

(11) L. Cook and E. Weidley, *Ann. N.Y. Acad. Sci.*, **66**, 740(1957).

(12) O. L. Davies, J. Faventos, and W. J. Walpole, *Br. J. Pharmacol.*, **1**, 255(1946).

(13) E. A. Swinyard, W. C. Brown, and W. K. Young, *J. Pharmacol. Exp. Ther.*, **106**, 319(1952).

(14) L. S. Goodman, M. S. Grewal, W. C. Brown, and E. A. Swinyard, *ibid.*, **108**, 168(1953).

(15) S. K. Bhattacharya, M. K. Raina, D. Banerjee, and N. C. Neogi, *Indian J. Exp. Biol.*, **9**, 257(1971).

(16) L. C. Miller and M. L. Tainter, *Proc. Soc. Exp. Biol. Med.*, **57**, 261(1944).

(17) J. M. Bobbit and K.-P. Segebarth, in "Cyclopentanoid Terpene Derivatives," W. I. Taylor and A. R. Battersby, Eds., Dekker, New York, N.Y., 1969, p. 135.

ACKNOWLEDGMENTS AND ADDRESSES

Received April 7, 1975, from the *Departments of *Pharmacology and ‡Pharmaceutics, Banaras Hindu University, Varanasi-5, India.*

Accepted for publication January 6, 1976.

The authors thank the Council of Scientific and Industrial Research, New Delhi, India, for financial assistance.

ˣ To whom inquiries should be directed.

Chemical Constituents of Gentianaceae XX: Natural Occurrence of (−)-Loliolide in *Canscora decussata*

S. GHOSAL ˣ, A. K. SINGH, and R. K. CHAUDHURI *

Abstract □ (−)-Loliolide was isolated as a native compound from *Canscora decussata* Schult (Gentianaceae). Physical and spectral (UV, IR, PMR, CMR, and mass spectra) properties of the compound and its acetate derivative established its identity. The significance of the cooccurrence of loliolide with a number of carotenoids in *C. decussata* and the facile transformation of violaxanthin into loliolide and violoxin are discussed in the light of the biogenesis of the degraded carotenoid.

Keyphrases □ Loliolide—isolated from *Canscora decussata* aerial parts, transformation from violaxanthin, UV, IR, NMR, and mass spectral data □ *Canscora decussata*—loliolide isolated from extract of aerial parts, UV, IR, NMR, and mass spectral data □ Violaxanthin—transformation into loliolide and violoxin □ Carotenoids—violaxanthin, transformation into loliolide and violoxin

The isolation of nearly two dozen polyoxygenated xanthones and two tetracyclic triterpenes from different parts of *Canscora decussata* Schult (Gentianaceae) was reported previously (1, 2). This paper describes the isolation and identification of (−)-loliolide (I), as a native compound, from this species. Additionally, the significance of the cooccurrence of loliolide and a number of carotenoids (acyclic, cyclic, and xanthophylls) in *C. decussata* and the facile transformation of violaxanthin (II) into loliolide and violoxin (III) are appraised in the light of the biogenesis of the degraded carotenoid (I).

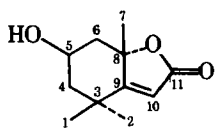

I

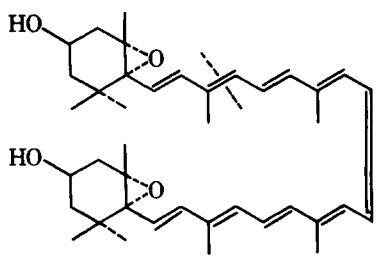

II

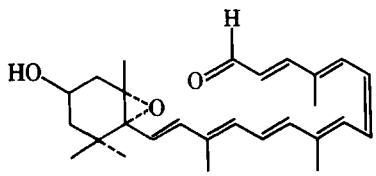

III

in mangiferin-pretreated animals, swertiamarin produced significant analgesic effect (Tables IV and V). Mangiferin significantly reduced the protective effect of swertiamarin against amphetamine (20 mg/kg ip) toxicity in aggregated mice (Table III).

The toxicity (16) and the LD_{50} of swertiamarin after single intraperitoneal administration in albino rats were studied; the LD_{50} (in milligrams per kilogram ± *SEM*) was 368 ± 45.

Earlier reports (17) indicated that iridoids are the active ingredients of some folk medicines and have been used for centuries, but the properties of specific iridoids have been evaluated only in a few cases. To the knowledge of the authors, this is the first report of a pharmacological evaluation of a pure secoiridoid, swertiamarin, occurring widely in members of the family Gentianaceae.

REFERENCES

(1) S. Ghosal, P. V. Sharma, R. K. Chaudhuri, and S. K. Bhattacharya, *J. Pharm. Sci.*, **62**, 926(1973).

(2) R. K. Chaudhuri and S. Ghosal, *Phytochemistry*, **10**, 2425(1971).

(3) S. K. Bhattacharya, S. Ghosal, R. K. Chaudhuri, and A. K. Sanyal, *J. Pharm. Sci.*, **61**, 1838(1972).

(4) S. K. Bhattacharya, A. K. Sanyal, and S. Ghosal, *Naturwissenschaften*, **59**, 650(1972).

(5) P. V. Sharma, Ph.D. thesis, Banaras Hindu University, Varanasi, India, 1974, p. 118.

(6) S. K. Bhattacharya, A. K. Sanyal, and S. Ghosal, in "Drugs and Central Synaptic Transmission," P. B. Bradley and B. N. Dhawan, Eds., Macmillan, London, England, 1975, p. 94.

(7) R. A. Turner, in "Screening Methods in Pharmacology," vol. 1, Academic, New York, N.Y., 1965, p. 26.

(8) W. L. Kuhn and E. F. Van Maanen, *J. Pharmacol. Exp. Ther.*, **134**, 60(1961).

(9) J.H. Mennear and A. D. Rudzik, *Life Sci.*, **5**, 349(1966).

(10) W. J. Kinnard and C. J. Carr, *J. Pharmacol. Exp. Ther.*, **121**, 354(1957).

(11) L. Cook and E. Weidley, *Ann. N.Y. Acad. Sci.*, **66**, 740(1957).

(12) O. L. Davies, J. Faventos, and W. J. Walpole, *Br. J. Pharmacol.*, **1**, 255(1946).

(13) E. A. Swinyard, W. C. Brown, and W. K. Young, *J. Pharmacol. Exp. Ther.*, **106**, 319(1952).

(14) L. S. Goodman, M. S. Grewal, W. C. Brown, and E. A. Swinyard, *ibid.*, **108**, 168(1953).

(15) S. K. Bhattacharya, M. K. Raina, D. Banerjee, and N. C. Neogi, *Indian J. Exp. Biol.*, **9**, 257(1971).

(16) L. C. Miller and M. L. Tainter, *Proc. Soc. Exp. Biol. Med.*, **57**, 261(1944).

(17) J. M. Bobbit and K.-P. Segebarth, in "Cyclopentanoid Terpene Derivatives," W. I. Taylor and A. R. Battersby, Eds., Dekker, New York, N.Y., 1969, p. 135.

ACKNOWLEDGMENTS AND ADDRESSES

Received April 7, 1975, from the *Departments of *Pharmacology and ‡Pharmaceutics, Banaras Hindu University, Varanasi-5, India.*

Accepted for publication January 6, 1976.

The authors thank the Council of Scientific and Industrial Research, New Delhi, India, for financial assistance.

ˣ To whom inquiries should be directed.

Chemical Constituents of Gentianaceae XX: Natural Occurrence of (−)-Loliolide in *Canscora decussata*

S. GHOSAL ˣ, A. K. SINGH, and R. K. CHAUDHURI *

Abstract □ (−)-Loliolide was isolated as a native compound from *Canscora decussata* Schult (Gentianaceae). Physical and spectral (UV, IR, PMR, CMR, and mass spectra) properties of the compound and its acetate derivative established its identity. The significance of the cooccurrence of loliolide with a number of carotenoids in *C. decussata* and the facile transformation of violaxanthin into loliolide and violoxin are discussed in the light of the biogenesis of the degraded carotenoid.

Keyphrases □ Loliolide—isolated from *Canscora decussata* aerial parts, transformation from violaxanthin, UV, IR, NMR, and mass spectral data □ *Canscora decussata*—loliolide isolated from extract of aerial parts, UV, IR, NMR, and mass spectral data □ Violaxanthin—transformation into loliolide and violoxin □ Carotenoids—violaxanthin, transformation into loliolide and violoxin

The isolation of nearly two dozen polyoxygenated xanthones and two tetracyclic triterpenes from different parts of *Canscora decussata* Schult (Gentianaceae) was reported previously (1, 2). This paper describes the isolation and identification of (−)-loliolide (I), as a native compound, from this species. Additionally, the significance of the cooccurrence of loliolide and a number of carotenoids (acyclic, cyclic, and xanthophylls) in *C. decussata* and the facile transformation of violaxanthin (II) into loliolide and violoxin (III) are appraised in the light of the biogenesis of the degraded carotenoid (I).

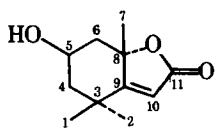

I

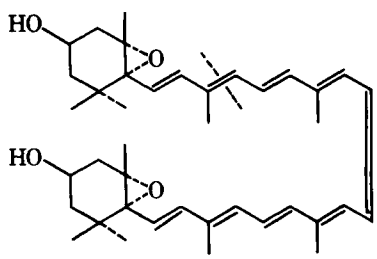

II

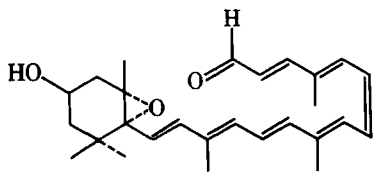

III

RESULTS AND DISCUSSION

(−)-Loliolide (I) was isolated previously (3, 4) in low yields (10^{-6}–10^{-4}%) from three plant species—*viz.*, *Lolium perenne* (Gramineae), *Digitalis purpurea*, and *D. lanata* (Scrophulariaceae). However, the process of isolation and the plant parts used did not eliminate the possibility of its formation from the carotenoids present in these plants in appreciable quantities. Thus, the question of whether loliolide is an artifact or a native compound in these plants remained unsettled. It has now been obtained in an appreciable yield (7×10^{-3}%) from aerial parts and in a lower yield (1×10^{-4}%) from roots of *C. decussata*.

The compound, mp 149–150°, $C_{11}H_{16}O_3$ (M^+, 196), showed optical rotation, UV, IR, and ^{1}H-NMR spectra identical with those reported for (−)-loliolide (3, 4). Additional spectral data (mass and ^{13}C-NMR spectra) have now been obtained for the compound and its acetate derivative. The mass spectral data can be conveniently used for the identification of loliolide even when it is obtained in a very low yield.

The mass spectrum of loliolide shows, aside from the molecular ion peak, significant fragment ion peaks at *m/e* 181 ($M - CH_3$), 178 ($M - H_2O$), 163 ($M - H_2O - CH_3$), 153 ($M - C_2H_3O$), and 111 (base peak). In the acetate derivative, only the molecular ion peak is shifted (M^+, 238), by 42 amu; the position and intensity of the fragment ion peaks remain essentially unaltered. The formation of the fragment ion species has been substantiated by metastable ions (m*).

The 100-MHz ^{1}H-NMR spectrum of loliolide (in $CDCl_3$) is very informative. Apart from the three methyl singlets appearing at 1.3, 1.5, and 1.8 ppm and a one-proton sharp singlet due to >C═CH— at 5.7 ppm, a complex pattern ranging from 1.4 to about 2.6 ppm, corresponding to five protons, is discernible. The broad resonance at 2.25 ppm is assigned to hydroxyl. The remaining signals could be analyzed by using double resonance techniques.

Irradiation of the quintuplet at 4.35 ppm ($J \sim 3.5$ Hz) showed the presence of two *AB* systems originating from magnetically nonequivalent methylene protons ($J \sim 14$ Hz). This result indicates that the molecular framework of loliolide is conformationally rigid. The small coupling ($J = 2$ Hz) is due to a four-bond long-range coupling (W-coupling). In the absence of the decoupling field, a further coupling appears (to the proton resonating at 4.35 ppm). The magnitude (3–4 Hz) for this coupling is not equal for all protons. Since the proton at 4.35 ppm is ascribable to a >CH—O function, the partial structure IV can be deduced from these data.

The absence of any further coupling suggests that the carbons alpha to the methylene protons are fully substituted, thus permitting extension of the partial structure IV to V. The methyl chemical shifts further imply that one quaternary carbon bears a *gem*-dimethyl group while the other one carries one methyl group and one >C—O— function.

The 25.2-MHz ^{13}C-NMR spectrum (Fourier transform) of loliolide exhibits chemical shifts and relative intensities from which straightforward assignments can be made (Table I).

The strong deshielding of the quaternary olefinic carbon (C-9) is due to its β-position relative to the lactonic carbonyl. The low intensity of the line indicates a particularly long T_1. Thus, the two other carbons (C-3 and C-8) attached to the quaternary olefinic carbon (C-9) are also quaternary. The two lines around 26 ppm indicate that one of these two quaternary carbons bears a *gem*-dimethyl group; the line around 30 ppm indicates that the other one bears a methyl and an oxygen function.

The line at 183 ppm is due to an α,β-unsaturated carbonyl. The high intensity of the line at 112 ppm must be due to a proton-bearing olefinic carbon (C-10). The remaining lines at 45, 47, and 66 ppm are due to methylene (C-4 and C-6) and hydroxymethine (C-5) carbons, respectively. The spectral data thus fit in excellently with Structure I for the C_{11} compound isolated from *C. decussata*.

Several naturally occurring compounds of terpene origin are known to arise through oxidative degradation in terpene biosynthesis. The

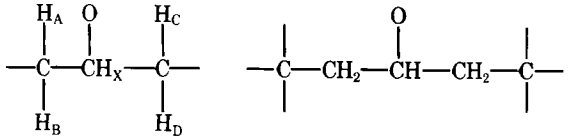

IV V

Table I—^{13}C-NMR Spectral Data of Loliolide

Carbon	δ_C, ppm (Relative to Internal Tetramethylsilane)
1	26.45
2	26.95
3	35.98
4	45.29
5	66.42
6	47.22
7	30.62
8	87.08
9	172.10
10	112.54
11	183.03

compounds have such degraded structures that it becomes difficult to postulate their precise biosynthetic precursors. Thus, the ionones (C_{13} terpenes) may be built up of monoterpenes (C_{10} unit), degraded sesquiterpenes (C_{15} unit), or degraded carotenoids (C_{40} unit), while the carotenoid origin is currently favored (5, 6). Isoe *et al.* showed that photooxygenation of β-carotene yields dihydroactinidiolide, β-ionone, and 2-hydroxy-2,6,6-trimethylcyclohexanone (5) and that exhaustive photooxygenation of zeaxanthin yields (−)-loliolide and (+)-isololiolide plus other products (6). Taylor and Burden (7) reported that violaxanthin (II), on photochemical oxidation, yields loliolide, 3-hydroxy-5,6-epoxy-β-ionone, and xanthoxin. Lutein *trans*-epoxide was shown recently (8) to produce loliolide on cautious oxidation with nickel peroxide.

The weight of evidence thus favors that loliolide is a degraded carotenoid, and evidence from the present study supports this conclusion. From a benzene solution of II, loliolide and a C_{27} aldehyde (named violoxin) were isolated as products of autoxidation. Violoxin, an oil, $C_{27}H_{36}O_3$ (M^+, 408), shows an orange spot by TLC when sprayed with 2,4-dinitrophenylhydrazine. Benzene solution of violoxin on prolonged sitting also furnishes loliolide. These results and the spectral properties are consistent with Structure III for violoxin. During autoxidation, II seems to be cleaved at the dotted line, yielding 3-hydroxy-5,6-epoxy-β-ionone (or equivalent) and violoxin (III). The formation of loliolide from 3-hydroxy-5,6-epoxy-β-ionone is a well-documented phenomenon (6).

Definite evidence has now been obtained that loliolide is a native compound in *C. decussata*. A qualitative survey of the distribution of carotenoids in flowers and fruits of some members of the genera *Canscora*, *Gentiana*, and *Swertia*, belonging to the family Gentianaceae, was made recently by chromatographic and spectroscopic methods (9, 10). From aerial parts of *C. decussata*, five carotenoids—*viz.*, phytoene, phytofluene, β-carotene, lutein epoxide, and violaxanthin, were isolated and identified. The roots of the plant, however, were found to be free from carotenoids.

The isolation of loliolide from the roots, therefore, suggests that it is a native compound in *C. decussata* and is not formed by the autoxidation of any one of the oxycarotenoids during the extraction of these compounds. A portion of loliolide probably is formed as a metabolite of one of the oxycarotenoids (or equivalent) *in vivo* moves to the roots from the flowers and fruits of *C. decussata* during the growth of the plant. The possible role of this and related carotenoid metabolites in the ontogeny of plants is currently being investigated.

EXPERIMENTAL[1]

Extraction of *C. decussata*[2]—In a typical experiment, air-dried and milled aerial parts (2.1 kg) of the plant, collected from the local area and properly identified[3], were extracted (30 hr) under reflux in a 3-liter soxhlet apparatus with petroleum ether (bp 60–80°). The petroleum ether extract was concentrated (to about 400 ml), and the concentrate was extracted with aqueous citric acid (12.5%, 200 ml) using a mechanical stirrer (8 hr).

[1] The general directions are the same as were reported recently (1).

[2] The plant material was supplied by Mr. B. Singh. A voucher specimen has been preserved in the Pharmaceutical Chemistry Research Laboratory, Department of Pharmaceutics, Banaras Hindu University.

[3] Through the courtesy of Dr. C. S. P. Rao, Department of Botany, Banaras Hindu University.

Isolation of (−)-Loliolide (I)—The clarified aqueous citric acid solution was cooled and made basic with ammonia (pH 8.5–9.0), and this solution was extracted with chloroform (five 50-ml portions). The chloroform extract was washed and dried, and the solvent was removed; a straw-colored amorphous solid (0.51 g) was obtained. It was again dissolved in chloroform (10 ml) and chromatographed over alumina (30 g). The elution was carried out with benzene. Fractions (50 ml) were collected and monitored by analytical TLC. *n*-Butyl alcohol–acetic acid–water (4:1:2) was used as the solvent system, and iodine vapor was used for staining.

Fractions 9–11 were combined and evaporated. The residue crystallized from acetone–petroleum ether (1:2) as colorless fine needles (143 mg), mp 149–150° [lit. (3, 4) mp 149°, 149–151°]; R_f 0.82; $[\alpha]_D^{25}$ −116.3° (c 0.98, $CHCl_3$); UV: λ_{max} (ethanol) 216 nm (log ϵ, 4.17); IR: ν_{max} (mineral oil) 3425, 1720, and 1622 cm^{-1}; mass spectrometry: *m/e* 196 (M^+, 36%), 181 (7), 179 (5), 178 (50, m* 162, $178^2/196 = 161.6$), 163 (15, m* 149.5, $163^2/178 = 149.2$), 153 (16), 140 (50), 135 (15), 112 (18), and 111 (100).

Anal.—Calc. for $C_{11}H_{16}O_3$: C, 67.34; H, 8.16. Found: C, 67.32; H, 8.16.

The acetyl derivative, prepared with pyridine and acetic anhydride (in equal proportions) at ordinary temperature for 40 hr, was purified by column chromatography over alumina[4]. Benzene–ether (1:1) was used as the eluent. The middle eluates furnished loliolide acetate, which crystallized from hexane–methylene chloride as colorless prisms, mp 86–87° [lit. (3, 4) mp 86–87°, 86.5°]; $[\alpha]_D^{25}$ −74.7° (c 0.77, $CHCl_3$); UV: λ_{max} (ethanol) 214 nm (log ϵ, 4.28); mass spectrometry: *m/e* 238 (M^+, 21%), 223 (4), 195 (12), 178 (54), 163 (11), 135 (8), and 111 (100).

Autoxidation of Violaxanthin (II)—Violaxanthin (52 mg), obtained from *C. decussata* (10), was dissolved in benzene (50 ml) containing traces of methanol and was kept at room temperature for about 3 weeks. The yellow color of the solution faded gradually, and the solution was practically colorless at the end of the reaction. After evaporation of the solvent, the residue was partitioned between aqueous methanol and petroleum ether (bp 60–80°). The residue from the methanol layer was dissolved in benzene and chromatographed over a silicic acid (100-mesh) column, using benzene–ethyl acetate (2:1) as the eluent.

Fractions (50 ml) were collected, and fractions 10–15 showed the presence of loliolide and an aldehyde (2,4-dinitrophenylhydrazine reagent positive) component. The latter had a slightly lower R_f, 0.62, in acetone–petroleum ether (1:3). These compounds were separated by preparative TLC (plate thickness, 2 mm) with the same solvent system. The component having the lower R_f value was identified as violoxin.

Violoxin (III)—This compound was obtained as an oil (11 mg); UV: λ_{max} (ethanol) 230 (0.56), 262 sh (0.38), and 300 (0.08) nm; IR: ν_{max} (liquid) 3450, 1658, 1628, and 972 cm^{-1}; mass spectrometry: *m/e* 408 (51%), 393 (26), 390 (5), and 375 (12).

[4] Brockman alumina, grade IV.

REFERENCES

(1) S. Ghosal, R. K. Chaudhuri, and K. R. Markham, *J. Chem. Soc. Perkin Trans. 1*, **1974**, 2538.

(2) S. Ghosal, R. K. Chaudhuri, and A. Nath, *Phytochemistry*, **12**, 1763(1973).

(3) R. Hodges and A. L. Porte, *Tetrahedron*, **20**, 1463(1964).

(4) T. Wada, *Chem. Pharm. Bull.*, **13**, 43(1965).

(5) S. Isoe, S. B. Hyeon, and T. Sakan, *Tetrahedron Lett.*, **1969**, 279.

(6) S. Isoe, S. B. Hyeon, S. Katsumura, and T. Sakan, *ibid.*, **1972**, 2517.

(7) H. F. Taylor and R. S. Burden, *Phytochemistry*, **9**, 2217(1970).

(8) H. Cadosch and C. H. Eugster, *Helv. Chim. Acta*, **57**, 1466(1974).

(9) S. Ghosal and A. K. Singh, "Abstract Book," 35th International Congress of Pharmaceutical Sciences (FIP), Dublin, Ireland, 1975.

(10) A. K. Singh, Ph.D. thesis, Banaras Hindu University, Varanasi, India, 1976.

ACKNOWLEDGMENTS AND ADDRESSES

Received September 10, 1975, from the *Pharmaceutical Chemistry Research Laboratory, Department of Pharmaceutics, Banaras Hindu University, Varanasi-5, India.*

Accepted for publication November 14, 1975.

The authors are grateful to Dr. F. W. Wehrli, Varian AG, Zug, Switzerland, Dr. Nitya Nand, Central Drug Research Institute, Lucknow, India, and Dr. B. C. Das, CNRS, Gif-Sur-Yvette, France, for the NMR and mass spectral data. Financial assistance from the Council of Scientific and Industrial Research, New Delhi, India, is also gratefully acknowledged.

* Present address: Pharmazeutisches Institut der Universität, Bonn, West Germany.

[x] To whom inquiries should be directed.

Antimicrobial Activity of Newly Synthesized Isothiocyanate Derivatives against Pathogenic Plant Microorganisms

MISAO KOJIMA [x] and M. KADO *

Abstract □ Fifteen reaction products of isothiocyanates with cysteine, seven reaction products of isothiocyanates with 2,3-dimercapto-1-propanol, and four reaction products of isothiocyanates with sulfanilamide were synthesized. Their antimicrobial activity against pathogenic plant microorganisms was investigated.

Keyphrases □ Isothiocyanate derivatives—synthesized and screened for antimicrobial activity □ 1-Propanols, 2,3-bis(alkylthiocarbamoylthio)—synthesized and screened for antimicrobial activity □ Cysteines, *N*-(*N*-substituted thiocarbamoyl)—synthesized and screened for antimicrobial activity □ Thioureas, *N*-substituted *N'*-*p*-sulfonamidophenyl—synthesized and screened for antimicrobial activity □ Antimicrobial activity—isothiocyanate derivatives screened □ Structure–activity relationships—isothiocyanate derivatives synthesized, screened for antimicrobial activity

It was reported previously (1) that some reaction products of isothiocyanates with cysteine and 2,3-dimercapto-1-propanol (dimercaprol) exhibited antimicrobial activity against some bacteria and fungi. This paper reports the antimicrobial activity against pathogenic plant microorganisms of these compounds and

Isolation of (−)-Loliolide (I)—The clarified aqueous citric acid solution was cooled and made basic with ammonia (pH 8.5–9.0), and this solution was extracted with chloroform (five 50-ml portions). The chloroform extract was washed and dried, and the solvent was removed; a straw-colored amorphous solid (0.51 g) was obtained. It was again dissolved in chloroform (10 ml) and chromatographed over alumina (30 g). The elution was carried out with benzene. Fractions (50 ml) were collected and monitored by analytical TLC. *n*-Butyl alcohol–acetic acid–water (4:1:2) was used as the solvent system, and iodine vapor was used for staining.

Fractions 9–11 were combined and evaporated. The residue crystallized from acetone–petroleum ether (1:2) as colorless fine needles (143 mg), mp 149–150° [lit. (3, 4) mp 149°, 149–151°]; R_f 0.82; $[\alpha]_D^{25}$ −116.3° (c 0.98, $CHCl_3$); UV: λ_{max} (ethanol) 216 nm (log ϵ, 4.17); IR: ν_{max} (mineral oil) 3425, 1720, and 1622 cm^{-1}; mass spectrometry: *m/e* 196 (M^+, 36%), 181 (7), 179 (5), 178 (50, m* 162, $178^2/196 = 161.6$), 163 (15, m* 149.5, $163^2/178 = 149.2$), 153 (16), 140 (50), 135 (15), 112 (18), and 111 (100).

Anal.—Calc. for $C_{11}H_{16}O_3$: C, 67.34; H, 8.16. Found: C, 67.32; H, 8.16.

The acetyl derivative, prepared with pyridine and acetic anhydride (in equal proportions) at ordinary temperature for 40 hr, was purified by column chromatography over alumina[4]. Benzene–ether (1:1) was used as the eluent. The middle eluates furnished loliolide acetate, which crystallized from hexane–methylene chloride as colorless prisms, mp 86–87° [lit. (3, 4) mp 86–87°, 86.5°]; $[\alpha]_D^{25}$ −74.7° (c 0.77, $CHCl_3$); UV: λ_{max} (ethanol) 214 nm (log ϵ, 4.28); mass spectrometry: *m/e* 238 (M^+, 21%), 223 (4), 195 (12), 178 (54), 163 (11), 135 (8), and 111 (100).

Autoxidation of Violaxanthin (II)—Violaxanthin (52 mg), obtained from *C. decussata* (10), was dissolved in benzene (50 ml) containing traces of methanol and was kept at room temperature for about 3 weeks. The yellow color of the solution faded gradually, and the solution was practically colorless at the end of the reaction. After evaporation of the solvent, the residue was partitioned between aqueous methanol and petroleum ether (bp 60–80°). The residue from the methanol layer was dissolved in benzene and chromatographed over a silicic acid (100-mesh) column, using benzene–ethyl acetate (2:1) as the eluent.

Fractions (50 ml) were collected, and fractions 10–15 showed the presence of loliolide and an aldehyde (2,4-dinitrophenylhydrazine reagent positive) component. The latter had a slightly lower R_f, 0.62, in acetone–petroleum ether (1:3). These compounds were separated by preparative TLC (plate thickness, 2 mm) with the same solvent system. The component having the lower R_f value was identified as violoxin.

Violoxin (III)—This compound was obtained as an oil (11 mg); UV: λ_{max} (ethanol) 230 (0.56), 262 sh (0.38), and 300 (0.08) nm; IR: ν_{max} (liquid) 3450, 1658, 1628, and 972 cm^{-1}; mass spectrometry: *m/e* 408 (51%), 393 (26), 390 (5), and 375 (12).

[4] Brockman alumina, grade IV.

REFERENCES

(1) S. Ghosal, R. K. Chaudhuri, and K. R. Markham, *J. Chem. Soc. Perkin Trans. 1*, **1974**, 2538.

(2) S. Ghosal, R. K. Chaudhuri, and A. Nath, *Phytochemistry*, **12**, 1763(1973).

(3) R. Hodges and A. L. Porte, *Tetrahedron*, **20**, 1463(1964).

(4) T. Wada, *Chem. Pharm. Bull.*, **13**, 43(1965).

(5) S. Isoe, S. B. Hyeon, and T. Sakan, *Tetrahedron Lett.*, **1969**, 279.

(6) S. Isoe, S. B. Hyeon, S. Katsumura, and T. Sakan, *ibid.*, **1972**, 2517.

(7) H. F. Taylor and R. S. Burden, *Phytochemistry*, **9**, 2217(1970).

(8) H. Cadosch and C. H. Eugster, *Helv. Chim. Acta*, **57**, 1466(1974).

(9) S. Ghosal and A. K. Singh, "Abstract Book," 35th International Congress of Pharmaceutical Sciences (FIP), Dublin, Ireland, 1975.

(10) A. K. Singh, Ph.D. thesis, Banaras Hindu University, Varanasi, India, 1976.

ACKNOWLEDGMENTS AND ADDRESSES

Received September 10, 1975, from the *Pharmaceutical Chemistry Research Laboratory, Department of Pharmaceutics, Banaras Hindu University, Varanasi-5, India.*

Accepted for publication November 14, 1975.

The authors are grateful to Dr. F. W. Wehrli, Varian AG, Zug, Switzerland, Dr. Nitya Nand, Central Drug Research Institute, Lucknow, India, and Dr. B. C. Das, CNRS, Gif-Sur-Yvette, France, for the NMR and mass spectral data. Financial assistance from the Council of Scientific and Industrial Research, New Delhi, India, is also gratefully acknowledged.

* Present address: Pharmazeutisches Institut der Universität, Bonn, West Germany.

[x] To whom inquiries should be directed.

Antimicrobial Activity of Newly Synthesized Isothiocyanate Derivatives against Pathogenic Plant Microorganisms

MISAO KOJIMA [x] and M. KADO *

Abstract □ Fifteen reaction products of isothiocyanates with cysteine, seven reaction products of isothiocyanates with 2,3-dimercapto-1-propanol, and four reaction products of isothiocyanates with sulfanilamide were synthesized. Their antimicrobial activity against pathogenic plant microorganisms was investigated.

Keyphrases □ Isothiocyanate derivatives—synthesized and screened for antimicrobial activity □ 1-Propanols, 2,3-bis(alkylthiocarbamoylthio)—synthesized and screened for antimicrobial activity □ Cysteines, *N*-(*N*-substituted thiocarbamoyl)—synthesized and screened for antimicrobial activity □ Thioureas, *N*-substituted *N'*-*p*-sulfonamidophenyl—synthesized and screened for antimicrobial activity □ Antimicrobial activity—isothiocyanate derivatives screened □ Structure–activity relationships—isothiocyanate derivatives synthesized, screened for antimicrobial activity

It was reported previously (1) that some reaction products of isothiocyanates with cysteine and 2,3-dimercapto-1-propanol (dimercaprol) exhibited antimicrobial activity against some bacteria and fungi. This paper reports the antimicrobial activity against pathogenic plant microorganisms of these compounds and

Table I—Characteristics of *N*-(*N*-Substituted Thiocarbamoyl)cysteines

Compound[b]	R	Melting Point[c]	Formula	Analysis, %[d] Calc.	Found
VI	$CH_3CH_2(CH_3)CH$	206° dec.	$C_6H_{16}N_2O_2S_2$	C 40.67	40.57
				H 6.83	6.81
				N 11.86	11.77
				S 27.10	27.36
VII	$(CH_3)_3C$	243° dec.	$C_6H_{16}N_2O_2S_2$	C 40.67	40.39
				H 6.83	6.91
				N 11.86	12.05
				S 27.10	27.00
VIII	$CH_3(CH_2)_4$	193° dec.	$C_9H_{18}N_2O_2S_2$	C 43.19	43.19
				H 7.25	7.33
				N 11.20	11.10
				S 25.07	25.55
IX	$(CH_3)_2CH(CH_2)_2$	210° dec.	$C_9H_{18}N_2O_2S_2$	C 43.19	42.81
				H 7.25	7.27
				N 11.20	11.30
				S 25.07	25.40
X	$CH_3CH_2(CH_3)CH(CH_2)_4$	226° dec.	$C_{12}H_{24}N_2O_2S_2$	C 49.30	49.00
				H 8.28	8.51
				N 9.58	10.05
				S 21.89	21.30
XI	$(CH_3)_2CHCH_2C(CH_3)_2CH_2$	235° dec.	$C_{12}H_{24}N_2O_2S_2$	C 49.30	49.51
				H 8.28	8.20
				N 9.58	9.50
				S 21.89	21.50
XII	$CH_2{=}CHCH_2$[e]	185° dec.	$C_7H_{12}N_2O_2S_2$	—	—

[a] Obtained commercially or synthesized from corresponding primary amines by the method of Mumm and Richter (3). [b] Characteristics of I (R = CH_3CH_2), II [R = $CH_3(CH_2)_2$], III [R = $(CH_3)_2CH$], IV [R = $CH_3(CH_2)_3$], V [R = $(CH_3)_2CHCH_2$], XIII (R = C_6H_5), XIV (R = $C_6H_5CH_2$), and XV [R = $C_6H_5(CH_2)_2$] were detailed previously (1). [c] Uncorrected. [d] Carbon and hydrogen were analyzed by the reduction method (5), nitrogen was analyzed by use of a Coleman type-29 nitrogen analyzer, and sulfur was analyzed by the silver absorption method (6). [e] This compound was originally synthesized by Todrick and Walker (4).

Table II—Characteristics of 2,3-Bis(alkylthiocarbamoylthio)-1-propanols[a]

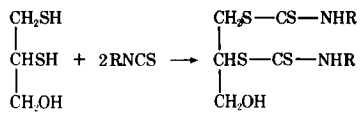

Compound	R	Melting Point	Formula	Analysis, % Calc.	Found
XVI	CH_3	—	—	—	—
XVII	CH_3CH_2	132–133°	$C_9H_{18}N_2OS_4$	C 36.21	36.09
				H 6.08	6.16
				N 9.39	9.09
				S 42.96	43.38
XVIII	$CH_3(CH_2)_2$	—	—	C 40.45	40.55
				H 6.79	6.77
				N 8.58	8.67
				S 39.27	38.96
XIX	$(CH_3)_2CH$	111–112°	$C_{11}H_{22}N_2OS_4$	C 47.08	46.92
				H 7.91	7.95
				N 7.33	7.42
				S 33.51	33.06
XX	$(CH_3)_2CHCH_2$	—	—		
XXI	$(CH_3)_2CHCH_2$	131–132°	$C_{15}H_{30}N_2OS_4$		
XXII	$CH_2{=}CHCH_2$	—	—		

[a] Characteristics of XVI, XVIII, XX, and XXII were detailed previously (1). Other notations are the same as in Table I.

Table III—Characteristics of *N*-Substituted *N'*-*p*-Sulfonamidophenylthioureas[a]

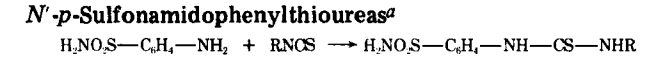

Compound	R	Melting Point	Formula
XXIII[b]	$CH_3(CH_2)_2$	182–183°	$C_{10}H_{15}N_3O_2S_2$
XXIV[b]	$CH_2{=}CHCH_2$	188–189°	$C_{10}H_{13}N_3O_2S_2$
XXV[b]	C_6H_5	190–191°	$C_{13}H_{13}N_3O_2S_2$
XXVI[c]	$C_6H_5CH_2$	176–177°	$C_{14}H_{15}N_3O_2S_2$

[a] Notations are the same as in Table I. [b] Reported by Roth and Degering (2). [c] Reported by Budeanu *et al.* (7).

some additional compounds of the same series.

EXPERIMENTAL

***N*-(*N*-Substituted Thiocarbamoyl)cysteines and 2,3-Bis(alkylthiocarbamoylthio)-1-propanols**—These compounds were prepared by the method described previously (1).

***N*-Substituted *N'*-*p*-Sulfonamidophenylthioureas**—These compounds were obtained by the method of Roth and Degering (2).

Antimicrobial Activity—The antimicrobial activity was determined by obtaining the minimum inhibitory concentration (MIC) macroscopically using the agar dilution method. The tested compound

Table IV—Effects of Isothiocyanate Derivatives on Growth of Pathogenic Plant Microorganisms

Compound	MIC										
	Ascomycetes		Basidiomycetes	Fungi imperfecti					Bacteria		
	Cochliobolus miyabeanus[a]	*Diaporthe citri*[b]	*Corticium rolfsii*[c]	*Gloeosporium laeticolor*[b]	*Pyricularia oryzae*[d]	*Cladosporium carpophilum*[b]	*Alternaria kikuchiana*[b]	*Fusarium oxysporum f. niveum*[e]	*Xanthomonus oryzae*[f]	*Xanthomonus citri*[b]	*Corynebacterium sepedonlicum*[f]
I	10	10	100	10	10	10	100	10	100	100	1000
II	1000	1000	1000	1000	1000	1000	1000	1000	1000	1000	1000
III	1000	100	1000	1000	1000	1000	1000	1000	1000	1000	1000
IV	1000	100	1000	1000	1000	1000	1000	1000	1000	1000	1000
V	100	10	1000	100	10	100	100	10	1000	10	1000
VI	10	10	100	100	10	10	100	100	1000	1000	1000
VII	10	10	1000	100	10	10	1000	100	1000	1000	1000
VIII	10	10	100	10	10	10	100	10	100	100	1000
IX	10	10	100	10	10	10	100	10	100	100	1000
X	1000	1000	1000	1000	1000	1000	1000	1000	1000	1000	1000
XI	1000	1000	1000	1000	1000	1000	1000	1000	1000	1000	1000
XII	10	10	100	10	10	10	10	10	100	10	1000
XIII	1000	1000	1000	1000	1000	1000	1000	1000	1000	1000	1000
XIV	10	10	10	100	10	10	100	10	10	10	100
XV	10	10	100	100	10	10	100	100	10	10	100
XVI	10	10	1000	10	10	10	10	10	100	1000	1000
XVII	100	10	100	100	100	100	1000	1000	100	1000	1000
XVIII	10	10	1000	10	10	10	1000	10	100	1000	1000
XIX	100	10	1000	100	10	10	100	10	1000	1000	1000
XX	10	10	1000	10	10	10	1000	10	100	100	1000
XXI	10	10	1000	1000	10	10	100	10	1000	1000	1000
XXII	100	10	100	100	100	100	100	100	100	100	100
XXIII	1000	1000	1000	1000	1000	1000	1000	1000	1000	1000	1000
XXIV	1000	1000	1000	1000	1000	1000	1000	1000	1000	1000	1000
XXV	1000	1000	1000	1000	1000	1000	1000	1000	1000	1000	1000
XXVI	1000	1000	1000	1000	1000	1000	1000	1000	1000	1000	1000
A[g]	1	1	10	1	1	1	1	1	1	1	10
B[g]	—	—	—	—	—	—	—	—	—	10	—

[a] Supplied by Department of Agriculture, Kyoto University. [b] Supplied by Fruit-tree Institute, Ministry of the Agriculture and Forestry. [c] Isolated from sugar beet. [d] Supported by the Physical and Chemical Research Institute. [e] Isolated from watermelon. [f] Supported by Department of Agriculture, Shizuoka University. [g] Compound A is phenylmercuric acetate, and B is streptomycin sulfate. Both A and B were used as the standard samples.

was added in the agar medium[1] containing 1% soluble starch, 0.2% yeast extract, and 1.5% agar. This medium was solidified in petri dishes (diameter 9 cm), pathogenic microorganisms were seeded on the plates, and the plates were cultured for 3 days at 28°.

DISCUSSION

All experimental compounds were synthesized in this laboratory. Tables I–III show the characteristics of newly synthesized compounds.

Compounds I–XV were used as their hydrochlorides because of their water solubility. Compounds XVI–XXVI were used as dilute ethanol solutions.

The antimicrobial activity of a solution of these compounds is shown as the MIC (micrograms per milliliter) in Table IV.

Compounds V, XII, XIV, and XV exhibited the same potencies as streptomycin sulfate, which was used as the standard sample on *Xanthomonas citri*. Compound XIV also exhibited the same potency as phenylmercuric acetate on *Corticium rolfsii*.

[1] Misato.

REFERENCES

(1) M. Kojima, *J. Pharm. Sci.*, **63**, 1801(1974).

(2) J. S. Roth and E. F. Degering, *J. Am. Chem. Soc.*, **67**, 126(1945).

(3) O. Mumm and H. Richter, *Chem. Ber.*, **73**, 843(1940).

(4) A. Todrick and E. Walker, *Biochem. J.*, **31**, 297(1937).

(5) K. Narita, *Anal. Instrum.*, **6**, 35(1968).

(6) T. Mitsui and H. Sato, *Mikrochim. Acta*, **1956**, 103.

(7) C. H. Budeanu, E. Budeanu, I. Sechter, and D. Cahan, *Mat. Fiz. Chem.*, **1**, 336(1955); through *Chem. Abstr.*, **51**, 10409g(1957).

ACKNOWLEDGMENTS AND ADDRESSES

Received May 12, 1975, from the *Faculty of Pharmaceutical Sciences, Fukuoka University, Nanakuma, Nishi-ku, Fukuoka 814, Japan.*

Accepted for publication January 5, 1976.

The authors thank Mr. K. Narita, Analytical Center, Shizuoka College of Pharmacy, for the elemental analyses.

* Present address: Research Laboratory, Kumiai Chemical Industries Ltd., Shibukawa, Shimizu 424, Japan.

x To whom inquiries should be directed.

Sulfur Analogs of Psychotomimetic Amines

DAVID E. NICHOLS ˣ and ALEXANDER T. SHULGIN *

Abstract □ The syntheses and physical properties are described for 2,5-dimethoxy-4-methylthiophenylethylamine and 2,5-dimethoxy-4-methylthiophenylisopropylamine. The latter compound is the sulfur analog of the psychotomimetic phenylisopropylamines 2,4,5-trimethoxyphenylisopropylamine and 2,5-dimethoxy-4-methylphenylisopropylamine wherein the methylthio group replaces a methoxy group or a methyl group, respectively. This compound is predicted to be about 30 times as active as mescaline.

Keyphrases □ Amines, phenylalkyl, substituted—sulfur analogs of psychotomimetic agents synthesized □ Sulfur analogs—psychotomimetic substituted phenylalkylamines synthesized □ Psychotomimetic agents, potential—sulfur analogs of substituted phenylalkylamines synthesized

The 2,4,5-substituent orientation provides maximum potency in the trisubstituted psychotomimetic phenylisopropylamines (1), and recent studies focused attention upon the pharmacological importance of the chemical nature of specific 4-substituents (2, 3). 2,5-Dimethoxy-4-methylphenylisopropylamine[1] (I) is a potent compound which produces severe sensory disturbances and hallucinations. Increasing the length of the alkyl chain at the 4-position results in an increase in activity. Optimum activity is realized when the alkyl chain is three carbons (2, 3), and this result may be related to lipid partitioning (4).

The qualitative nature of intoxication induced also varies with the 4-substituent. For example, 2,5-dimethoxy-4-ethylphenylisopropylamine (II) and 2,5-dimethoxy-4-bromophenylisopropylamine (III) are about two and 10 times more potent, respectively, than I (5–7) in producing threshold central nervous system effects. In contrast, neither elicits the severe visual disturbances characteristic of I. Both the quantitative and the qualitative nature of the drug's action apparently are determined by the 4-substituent, although these relationships have not been defined clearly.

DISCUSSION

One route for the metabolism of I is through oxidation of the 4-methyl group (8, 9). It might be anticipated that such oxidation would be less favored in the higher alkyl homologs and that it could not occur with the 4-bromo compound. It was shown recently that II is metabolized in rats at the 4-ethyl position, but more slowly than with I (10), and that III generates no detectable inorganic bromide in humans (11).

The ability of a compound to produce hallucinatory disturbances may be lost when the 4-substituent is resistant to oxidation. The concept that facile oxidation of the 4-function might be involved in the production of hallucinations by psychotomimetic amphetamine derivatives may receive support through study of an amphetamine derivative with a 4-substituent that is unusually susceptible to oxidative metabolism.

The sulfur atom would appear to be an excellent choice for such a substituent. Metabolically, it should retain the chemical properties of oxygen in reactions such as *S*-demethylation but should allow the formation of sulfoxides and sulfones as products of oxidative metabolism (12). The lipophilicity, electronic character, and size of sulfur also seem ideal. A comparison of the σ_p and π values for methoxy, methyl, methylthio, and bromo shows that the methylthio group lies intermediate between methyl and bromo (13–15). Barfknecht *et al.* (4) correlated human activity with octanol–water partition coefficients; by using the principles of additivity (16), one can predict that the methylthio analog should be some 30 times as potent as mescaline.

This paper describes the syntheses and properties of 2,5-dimethoxy-4-methylthiophenylisopropylamine (IV) and 2,5-dimethoxy-4-methylthiophenylethylamine (V). Compounds IV and V, as well as the intermediates IX, X*a*, and X*b*, have not been reported previously.

EXPERIMENTAL[2]

2,5-Dihydroxyphenylthiosulfuric Acid, Sodium Salt (VI)—The method of Alcalay (17) was modified as follows (Scheme I). A solution of 43.2 g of benzoquinone (0.4 mole) in 200 ml of acetic acid was added over 10 min to a solution of 149 g of sodium thiosulfate in 300 ml of water. The mixture was stirred for 1 hr and then reduced under vacuum to a thick syrup. The residue crystallized on standing and was slurried in a saturated salt solution and filtered. The solids were washed with small portions of a saturated salt solution, sucked dry, and finally dissolved in methanol and filtered through diatomaceous earth[3]. The methanol filtrate was concentrated *in vacuo*, yielding 67 g (68%) of VI as a yellow powder. This powder was used directly in the next step.

2,5-Dihydroxythiophenol (VII)—Fifty grams of VI (0.205 mole) was dissolved in a mixture of 200 ml of water and 400 ml of concentrated hydrochloric acid. Zinc dust (250 g) was added slowly over 1.5 hr, with external ice bath cooling applied as needed to keep the temperature at 50–60°. Adequate ventilation was needed because a large quantity of hydrogen sulfide was generated. Near the end of the reduction, the reaction mixture changed to a semisolid gray mass.

An additional 50 ml of concentrated hydrochloric acid was added to the mixture, and the solution was decanted from unreacted zinc metal. The aqueous acid solution was extracted with ether (6 × 100 ml), and the pooled extracts were washed with saturated sodium chloride solution (3 × 75 ml), dried (sodium sulfate), and concentrated *in vacuo*. The resulting yellow solid was recrystallized from ether to yield 24.7 g (85%) of pale-yellow needles, mp 118–119° [lit. (17) mp 118°].

2,5-Dimethoxymethylthiophenol (VIII)—The method of Butenandt *et al.* (18) was modified as follows. To 200 ml of 9 *N* KOH (1.8 *M*) stirred under nitrogen was added 24 g (0.169 mole) of VII. Methyl sulfate (160 g, 1.27 mole) was added, with vigorous stirring, over 2 hr. The temperature (50–60°) was maintained by the rate of addition. The mixture was then heated to reflux for 3 hr, stirred overnight at room temperature, and filtered. The filtrate was extracted with 6 × 100 ml of ether, and the combined ether extracts were washed with 2 × 50 ml of saturated sodium chloride solution, dried (sodium sulfate), and concentrated *in vacuo*. The residue was vacuum distilled to give 25.9 g (83%) of product, bp 86–88°/0.04 mm [lit. (18) bp 96–97°/0.07 mm] and mp 33–34° [lit. (18) mp 35°].

2,5-Dimethoxy-4-methylthiobenzaldehyde (IX)—The aldehyde was prepared using the method of Rieche *et al.* (19). A solution of 6.07 g (0.033 mole) of VIII in 40 ml of dry dichloromethane under nitrogen was cooled in an ice bath. To the solution was added 13.02 g (0.05 mole) of stannic chloride over 2 min. Dichloromethyl methyl ether, 3.45 g (0.03 mole), was then added dropwise over 5 min, and stirring was continued with ice bath cooling for 15 min. The reaction was allowed to warm to room temperature over 30 min and was stirred for

[1] Also referred to as DOM and STP.

[2] NMR spectra were obtained on a Varian A-60 or EM-360 spectrometer. IR spectra were obtained using a Beckman IR-18. Melting points were determined in open glass capillaries and are uncorrected.

[3] Celite.

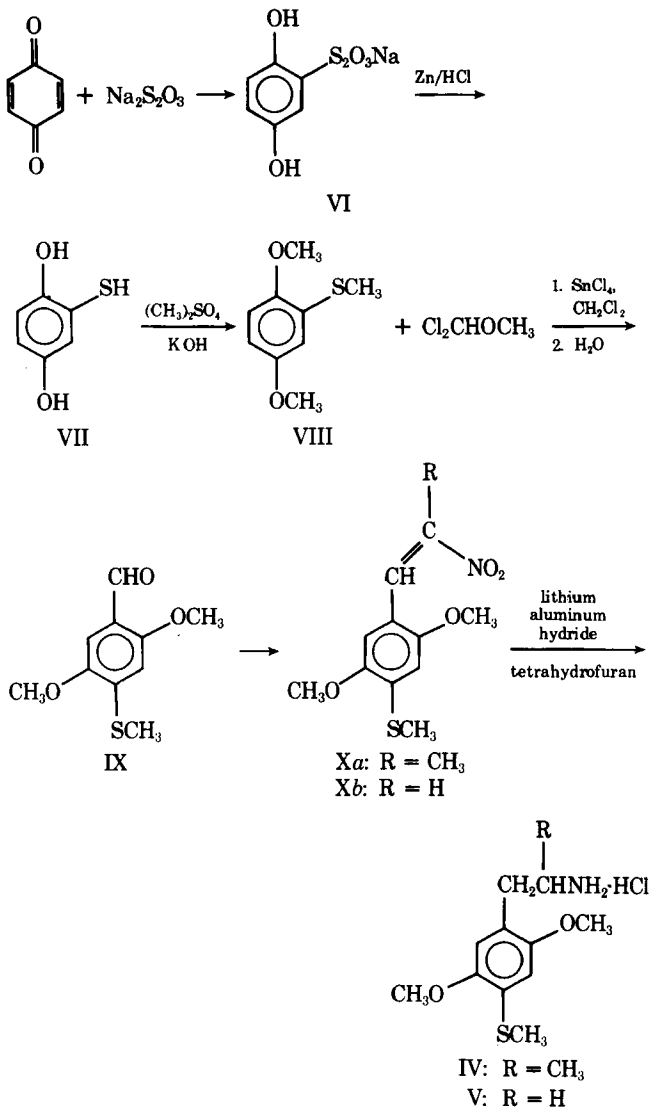

Scheme I

an additional 1 hr, at which time hydrogen chloride evolution had ceased.

Then the mixture was slowly poured onto 15 g of ice in a separator, and the aqueous layer was separated and discarded. The organic phase was washed with 3 × 25 ml of 3 *N* HCl and 3 × 25 ml of saturated sodium chloride solution and dried (sodium sulfate), and the solvent was removed *in vacuo*. The solid residue was dissolved in methanol, filtered, and recrystallized from methanol–water to give 5.86 g (92%) of yellow needles. TLC (silica gel, chloroform) showed only one product. An analytical sample was further purified *via* the sodium bisulfite adduct and recrystallized from methanol–water, mp 99–100°; NMR ($CDCl_3$): δ 2.48 (s, 3H, SCH_3), 3.92, 3.97 (2s, 6H, OCH_3), 6.74, 7.29 (2s, 2H, ArH), and 10.45 (s, 1H, CHO).

Anal.—Calc. for $C_{10}H_{12}O_3S$: C, 56.58; H, 5.70; S, 15.11. Found: C, 56.85; H, 5.51; S, 14.72.

The ylidinemalononitrile derivative of IX was prepared from equal weights of the benzaldehyde and malononitrile in ethanol with triethylamine catalysis, mp 185–186° after recrystallization from ethanol.

Anal.—Calc. for $C_{13}H_{12}N_2O_2S$: C, 59.98; H, 4.62; N, 10.76; S, 12.32. Found: C, 59.78; H, 4.83; N, 10.80; S, 11.96.

1-(2,5-Dimethoxy-4-methylthiophenyl)-2-nitropropene (X*a*)—A solution of 2.3 g (0.011 mole) of IX in 7.5 ml of nitroethane containing 0.45 g of ammonium acetate was heated on the steam bath for 6 hr. Removal of most of the nitroethane *in vacuo*, followed by the addition of 10 ml of methanol, gave crystals. After filtering and washing with cold methanol, the product was recrystallized from 140 ml of boiling ethanol, yielding 1.8 g (62%) of bright-orange crystals, mp 137–138°; NMR ($CDCl_3$): δ 2.42 (s, 3H, CH_3), 2.50 (s, 3H, SCH_3), 3.88 (s, 6H, OCH_3), 8.29 (broad s, 1H, =CH), 6.79, and 6.83 (2s, 2H, ArH).

Anal.—Calc. for $C_{12}H_{15}NO_4S$: C, 53.51; H, 5.61; N, 5.20; S, 11.91. Found: C, 53.47; H, 5.71; N, 5.27; S, 11.99.

1- (2,5-Dimethoxy -4- methylthiophenyl) -2- nitroethylene (X*b*)—Essentially the same procedure as for X*a* was used, but use of nitromethane instead of nitroethane gave the homologous nitrostyrene. Recrystallization from ethanol gave rust-orange crystals (yield 68%), mp 165.5–166°.

Anal.—Calc. for $C_{11}H_{13}NO_4S$: C, 51.75; H, 5.13; N, 5.49; S, 12.56. Found: C, 50.81; H, 5.12; N, 5.57; S, 11.96.

2,5-Dimethoxy-4-methylthiophenylisopropylamine (IV)—To a gently refluxing suspension of 1.4 g of lithium aluminum hydride in 40 ml of tetrahydrofuran was added dropwise a saturated solution of 1.7 g (0.006 mole) of X*a* in tetrahydrofuran. Reflux with stirring was continued for 7 hr. The reaction mixture was then cooled externally with ice water; 1.6 ml of water, 1.6 ml of 15% NaOH, and finally 4.8 ml of water were added dropwise. Stirring was continued until no gray-colored solids remained. The mixture was filtered, the filter cake was washed with tetrahydrofuran, and the mother liquor and washings were combined and evaporated to dryness *in vacuo*.

The free base was a white solid; an analytical sample, after recrystallization from hexane, had a melting point of 91–93°. The product was dissolved in 25 ml of 2-propanol, titrated with concentrated hydrochloric acid to a persistent pink color (0.57 ml), and diluted with 100 ml of anhydrous ether. After a few moments, there was spontaneous formation of white crystals, 1.2 g (68% yield), mp 204–205°.

Anal.—Calc. for $C_{12}H_{20}NO_2S$: C, 51.87; H, 7.25; N, 5.04. Found: C, 51.40; H, 7.07; N, 5.52.

2,5-Dimethoxy-4-methylthiophenylethylamine (V)—The same procedure as was used for IV but with X*b* instead of X*a* gave the corresponding phenethylamine hydrochloride (V) as white crystals from 2-propanol–ether (57% yield). Recrystallization from ethanol gave melting point of 240–241° with prior darkening.

Anal.—Calc. for $C_{11}H_{18}ClNO_2S$: C, 50.08; H, 6.87; N, 5.31; S, 12.15. Found: C, 50.03; H, 6.83; N, 5.54; S, 12.10.

REFERENCES

(1) A. T. Shulgin, T. Sargent, and C. Naranjo, *Nature*, **221**, 537(1969).

(2) A. T. Shulgin and D. C. Dyer, *J. Med. Chem.*, **18**, 1201(1975).

(3) R. D. Morin, F. Benington, S. R. Mitchell, J. M. Beaton, R. J. Bradley, and J. R. Smythies, *Experientia*, **31**, 93(1975).

(4) C. F. Barfknecht, D. E. Nichols, and W. J. Dunn, III, *J. Med. Chem.*, **18**, 208(1975).

(5) S. H. Snyder, L. Faillace, and H. Weingartner, *Am. J. Psychiat.*, **125**, 113(1967).

(6) S. H. Snyder, S. Unger, B. Blatchley, and C. F. Barfknecht, *Arch. Gen. Psychiat.*, **31**, 103(1974).

(7) A. T. Shulgin, T. Sargent, and C. Naranjo, *Pharmacology*, **5**, 103(1971).

(8) B. T. Ho and L. W. Tansey, *J. Med. Chem.*, **14**, 156(1971).

(9) S. B. Matin, P. S. Callery, J. S. Zweig, A. O'Brien, R. Rapoport, and N. Castagnoli, Jr., *ibid.*, **17**, 877(1974).

(10) L. W. Tansey, V. S. Estevez, and B. T. Ho, *Proc. West. Pharmacol. Soc.*, **18**, 362(1975).

(11) T. Sargent, D. A. Kalbhen, A. T. Shulgin, G. Braun, H. Stauffer, and N. Kusubov, *Neuropharmacology*, **14**, 165(1975).

(12) H. G. Mandel, in "Fundamentals of Drug Metabolism and Drug Disposition," B. N. La Du, H. G. Mandel, and E. L. Way, Eds., Williams & Wilkins, Baltimore, Md., 1971, p. 149.

(13) R. W. Taft, Jr., in "Steric Effects in Organic Chemistry," M. S. Newman, Ed., Wiley, New York, N.Y., 1956, p. 556.

(14) T. Fujita, J. Iwasa, and C. Hansch, *J. Am. Chem. Soc.*, **86**, 5175(1964).

(15) C. Hansch, E. Kutter, and A. Leo, *J. Med. Chem.*, **12**, 746(1969).

(16) A. Leo, C. Hansch, and D. Elkins, *Chem. Rev.*, **71**, 525(1971).

(17) W. Alcalay, *Helv. Chim. Acta*, **30**, 578(1947).

(18) A. Butenandt, E. Biekert, and E. Haerle, *Chem. Ber.*, **97**, 285(1964).

(19) A. Rieche, H. Gross, and E. Höft, *Org. Syn.*, **47**, 1(1967).

ACKNOWLEDGMENTS AND ADDRESSES
Received October 28, 1975, from the *Department of Medicinal Chemistry and Pharmacognosy, School of Pharmacy and Pharmacal Sciences, Purdue University, West Lafayette, IN 47907*

Accepted for publication December 24, 1975.
Supported in part by General Research Support funds.
* Present address: 1483 Shulgin Road, Lafayette, CA 94549
x To whom inquiries should be directed.

Rapid Procedure for Assessment of Compounds that Modify Uptake and Release of Tritiated Norepinephrine

MORTON LEVITT x, WAYNE R. CUMISKEY, MICHAEL B. McGRATH, and LEON SHARGEL *

Abstract □ A rapid procedure to estimate tritiated norepinephrine (levarterenol) in a single mouse heart is described. The method is based upon oxidation of the tritium in the tissue to tritiated water, which is then determined by liquid scintillation spectroscopy. Large numbers of samples can be assayed with great facility. The effects of standard compounds that modify the uptake and release of ^{3}H-norepinephrine in heart tissue were determined with this system, and a procedure for studying their interactions is described.

Keyphrases □ Norepinephrine, tritiated—liquid scintillation spectroscopic analysis, effects of various compounds on uptake and release, mouse heart □ Spectroscopy, liquid scintillation—analysis, tritiated norepinephrine, mouse heart □ Radiolabeled compounds—tritiated norepinephrine, liquid scintillation spectroscopic analysis, mouse heart □ Adrenergic agents—norepinephrine, liquid scintillation spectroscopic analysis, mouse heart

Compounds that modify norepinephrine (levarterenol) uptake, release, storage, or turnover are frequently used in clinical medicine and in many procedures for the investigation, development, and characterization of new therapeutic agents (1–4). Norepinephrine metabolism has been studied by measuring changes in tritiated norepinephrine concentrations in the hearts of several species (5–7). Since some of these procedures are tedious and time consuming, only small numbers of individual or pooled samples can be conveniently assayed in a single experiment.

Introduction of instrumentation for the oxidation of small tissue samples allowed the development of a rapid and sensitive assay of ^{3}H-norepinephrine. This report describes a rapid screening procedure for studying compounds that affect the uptake and release of ^{3}H-norepinephrine in individual mouse hearts. The interactions of several test compounds with tyramine, reserpine, metaraminol, amphetamine, and tetrabenazine determined with this procedure are presented.

EXPERIMENTAL

Materials—The radiochemical purity (>95%) of 7-^{3}H-*l*-norepinephrine[1], specific activity of 4.1 Ci/mmole, was verified by ascending paper chromatography in 1-butanol–acetic acid–water (4:1:1). The following compounds were used: *l*-norepinephrine bitartrate[2], *l*-metaraminol bitartrate[2], tyramine hydrochloride[3], reserpine hydrochloride[4], dextroamphetamine sulfate[5], tetrabenazine methanesulfonate[6], chlorpromazine hydrochloride[7], guanethidine sulfate[8], bretylium *p*-toluenesulfonate[9], desipramine hydrochloride[10], and cocaine hydrochloride[10].

Animals and Dosage—Swiss Webster mice, 20 ± 2 g, were used. All compounds were administered as a solution in 0.2 ml of distilled water. ^{3}H-Norepinephrine (1 μCi) was administered intravenously in the tail vein. Test compounds were administered subcutaneously.

^{3}H-Norepinephrine Assay—Mice were killed by cervical dislocation. Hearts were removed, blotted, and weighed on tared low ash filter paper disks[11] and dried overnight in a refrigerator (4°). The tissue sample was compressed in a tablet press and oxidized in a sample oxidizer[12]. The resulting tritiated water was collected in counting vials, and 15 ml of scintillation fluid[13] was added. Radioactivity was measured in a liquid scintillation spectrometer[12]. The counting efficiency was determined by the channels ratio method.

Heart tritium concentrations were proportional to dose over the range studied, 0.25–5.0 μCi of tritiated norepinephrine. The dose used in these studies, 1 μCi, yielded about 10,000 cpm/mouse heart (220 nCi/g) after 2 hr.

Uptake and Release Study—Effects on the uptake of ^{3}H-norepinephrine by the heart were determined by administering the test compounds subcutaneously 15 min before the intravenous administration of 1 μCi of ^{3}H-norepinephrine. The animals were sacrificed 2 hr after the administration of the radiotracer. Release of ^{3}H-norepinephrine was determined by administering the test compound subcutaneously 15 min after the administration of ^{3}H-norepinephrine. After 2 hr, the animals were sacrificed, hearts were removed, and radioactivity was determined.

Interaction Study—The interactions of desipramine, chlorpromazine, and cocaine with tyramine, reserpine, metaraminol, amphetamine, and tetrabenazine were estimated by their effects in combination on the release of ^{3}H-norepinephrine from the heart. ^{3}H-Norepinephrine (1 μCi) was administered intravenously to 11 groups of mice, and the test compound was administered to five groups after 15 min. Then 15 min later, the releasing agents were administered to the pretreated animals and to additional control groups. One group served as unmedicated controls. The animals were sacrificed 2 hr after administration of ^{3}H-norepinephrine.

[1] Amersham/Searle.
[2] Sterling-Winthrop Research Institute.
[3] Eastman Organic Chemicals.
[4] Knoll Pharmaceutical.
[5] Mann Research Labs.
[6] Hoffmann-La Roche.
[7] Smith Kline and French Labs.
[8] Ciba-Geigy Pharmaceuticals.
[9] Burroughs Wellcome Co.
[10] Merck & Co.
[11] Carl Schleicher and Scheull.
[12] Packard Tri-Carb.
[13] Consisting of 5 g of 2,5-diphenyloxazole, 0.75 g of 1,4-bis[2-(5-phenyloxazolyl)]benzene, 100 g of naphthalene, 150 ml of toluene, 40 ml of ethyl alcohol, and dioxane to make 1 liter.

ACKNOWLEDGMENTS AND ADDRESSES
Received October 28, 1975, from the *Department of Medicinal Chemistry and Pharmacognosy, School of Pharmacy and Pharmacal Sciences, Purdue University, West Lafayette, IN 47907*

Accepted for publication December 24, 1975.
Supported in part by General Research Support funds.
* Present address: 1483 Shulgin Road, Lafayette, CA 94549
x To whom inquiries should be directed.

Rapid Procedure for Assessment of Compounds that Modify Uptake and Release of Tritiated Norepinephrine

MORTON LEVITT x, WAYNE R. CUMISKEY, MICHAEL B. McGRATH, and LEON SHARGEL *

Abstract □ A rapid procedure to estimate tritiated norepinephrine (levarterenol) in a single mouse heart is described. The method is based upon oxidation of the tritium in the tissue to tritiated water, which is then determined by liquid scintillation spectroscopy. Large numbers of samples can be assayed with great facility. The effects of standard compounds that modify the uptake and release of ^{3}H-norepinephrine in heart tissue were determined with this system, and a procedure for studying their interactions is described.

Keyphrases □ Norepinephrine, tritiated—liquid scintillation spectroscopic analysis, effects of various compounds on uptake and release, mouse heart □ Spectroscopy, liquid scintillation—analysis, tritiated norepinephrine, mouse heart □ Radiolabeled compounds—tritiated norepinephrine, liquid scintillation spectroscopic analysis, mouse heart □ Adrenergic agents—norepinephrine, liquid scintillation spectroscopic analysis, mouse heart

Compounds that modify norepinephrine (levarterenol) uptake, release, storage, or turnover are frequently used in clinical medicine and in many procedures for the investigation, development, and characterization of new therapeutic agents (1–4). Norepinephrine metabolism has been studied by measuring changes in tritiated norepinephrine concentrations in the hearts of several species (5–7). Since some of these procedures are tedious and time consuming, only small numbers of individual or pooled samples can be conveniently assayed in a single experiment.

Introduction of instrumentation for the oxidation of small tissue samples allowed the development of a rapid and sensitive assay of ^{3}H-norepinephrine. This report describes a rapid screening procedure for studying compounds that affect the uptake and release of ^{3}H-norepinephrine in individual mouse hearts. The interactions of several test compounds with tyramine, reserpine, metaraminol, amphetamine, and tetrabenazine determined with this procedure are presented.

EXPERIMENTAL

Materials—The radiochemical purity (>95%) of 7-^{3}H-*l*-norepinephrine[1], specific activity of 4.1 Ci/mmole, was verified by ascending paper chromatography in 1-butanol–acetic acid–water (4:1:1). The following compounds were used: *l*-norepinephrine bitartrate[2], *l*-metaraminol bitartrate[2], tyramine hydrochloride[3], reserpine hydrochloride[4], dextroamphetamine sulfate[5], tetrabenazine methanesulfonate[6], chlorpromazine hydrochloride[7], guanethidine sulfate[8], bretylium *p*-toluenesulfonate[9], desipramine hydrochloride[10], and cocaine hydrochloride[10].

Animals and Dosage—Swiss Webster mice, 20 ± 2 g, were used. All compounds were administered as a solution in 0.2 ml of distilled water. ^{3}H-Norepinephrine (1 μCi) was administered intravenously in the tail vein. Test compounds were administered subcutaneously.

^{3}H-Norepinephrine Assay—Mice were killed by cervical dislocation. Hearts were removed, blotted, and weighed on tared low ash filter paper disks[11] and dried overnight in a refrigerator (4°). The tissue sample was compressed in a tablet press and oxidized in a sample oxidizer[12]. The resulting tritiated water was collected in counting vials, and 15 ml of scintillation fluid[13] was added. Radioactivity was measured in a liquid scintillation spectrometer[12]. The counting efficiency was determined by the channels ratio method.

Heart tritium concentrations were proportional to dose over the range studied, 0.25–5.0 μCi of tritiated norepinephrine. The dose used in these studies, 1 μCi, yielded about 10,000 cpm/mouse heart (220 nCi/g) after 2 hr.

Uptake and Release Study—Effects on the uptake of ^{3}H-norepinephrine by the heart were determined by administering the test compounds subcutaneously 15 min before the intravenous administration of 1 μCi of ^{3}H-norepinephrine. The animals were sacrificed 2 hr after the administration of the radiotracer. Release of ^{3}H-norepinephrine was determined by administering the test compound subcutaneously 15 min after the administration of ^{3}H-norepinephrine. After 2 hr, the animals were sacrificed, hearts were removed, and radioactivity was determined.

Interaction Study—The interactions of desipramine, chlorpromazine, and cocaine with tyramine, reserpine, metaraminol, amphetamine, and tetrabenazine were estimated by their effects in combination on the release of ^{3}H-norepinephrine from the heart. ^{3}H-Norepinephrine (1 μCi) was administered intravenously to 11 groups of mice, and the test compound was administered to five groups after 15 min. Then 15 min later, the releasing agents were administered to the pretreated animals and to additional control groups. One group served as unmedicated controls. The animals were sacrificed 2 hr after administration of ^{3}H-norepinephrine.

[1] Amersham/Searle.
[2] Sterling-Winthrop Research Institute.
[3] Eastman Organic Chemicals.
[4] Knoll Pharmaceutical.
[5] Mann Research Labs.
[6] Hoffmann-La Roche.
[7] Smith Kline and French Labs.
[8] Ciba-Geigy Pharmaceuticals.
[9] Burroughs Wellcome Co.
[10] Merck & Co.
[11] Carl Schleicher and Scheull.
[12] Packard Tri-Carb.
[13] Consisting of 5 g of 2,5-diphenyloxazole, 0.75 g of 1,4-bis[2-(5-phenyloxazolyl)]benzene, 100 g of naphthalene, 150 ml of toluene, 40 ml of ethyl alcohol, and dioxane to make 1 liter.

Table I—Effect of Several Compounds on the Uptake and Release of ^{3}H-Norepinephrine[a]

Compound and Dose, mg/kg	Norepinephrine Released, nCi/g[b]	Compound and Dose, mg/kg	Norepinephrine Released, nCi/g[c]
Tyramine, 15	62.8[d]	Desipramine, 1.0	21.6[d]
Reserpine, 1.0	12.6[d]	Cocaine, 10	31.3[d]
Guanethidine, 1.0	64.6[d]	Chlorpromazine, 10	48.5[d]
Metaraminol, 5	19.1[d]	Bretylium, 20	76.9[d]
Control	131	Control	185
Pooled *SE*	±7.0%		±8.5%

[a] Each value (nanocuries per gram) is the geometric mean for six hearts. [b] Compounds were injected 15 min after injection of ^{3}H-norepinephrine. [c] Compounds were injected 15 min before injection of ^{3}H-norepinephrine. [d] Significantly different from corresponding control, $p \leq 0.01$.

Table II—Interaction of Desipramine, Chlorpromazine, and Cocaine with Compounds that Release ^{3}H-Norepinephrine[a]

Compound and Dose, mg/kg	Desipramine		Chlorpromazine		Cocaine	
	None	5 mg/kg	None	5 mg/kg	None	10 mg/kg
Tyramine, 15	94	146	78	114	68	92
Reserpine, 1	42	56	32	133[b]	39	36
Metaraminol, 5	37	58	38	82[b]	34	33
Amphetamine, 10	163	174	111	170	112	122
Tetrabenazine, 10	83	156[c]	80	147	89	112
Control	190	217	195	248	214	215
Pooled *SE*[d]	±11%		±11%		±10%	

[a] Each value (nanocuries per gram) is the geometric mean for six mouse hearts. [b] Significant nonadditivity (interaction), $p \leq 0.01$. [c] $p = 0.05$. [d] Based on residual error estimate from corresponding analysis of variance.

Experimental Design and Statistical Analysis—In all experiments, animals were randomly assigned to treatment groups. The values from the radioactivity determinations were routinely transformed to logarithms prior to analysis to minimize the correlation between means and standard deviations (8) and to facilitate the study of multiplicative interactions.

The primary method for testing hypotheses and determining statistical significance of associated linear contrasts was through analysis of variance techniques applied to the classic fixed-effects model for the resulting data (9).

RESULTS

Uptake and Release of ^{3}H-Norepinephrine—The effects of compounds known to release or block the uptake of ^{3}H-norepinephrine in mouse heart were determined (Table I). Tyramine, reserpine, guanethidine, and metaraminol released ^{3}H-norepinephrine from heart, as demonstrated by the significantly ($p \leq 0.01$) decreased tritium concentrations. Desipramine, cocaine, chlorpromazine, and bretylium significantly ($p \leq 0.01$) blocked uptake of ^{3}H-norepinephrine into cardiac tissue.

Interaction Studies—The interaction of desipramine, chlorpromazine, and cocaine with several compounds that release norepinephrine is illustrated in Table II. Although the interactions were variable, the three compounds slightly decreased the effect of tyramine and tetrabenazine. Chlorpromazine significantly ($p \leq 0.01$) decreased the effect of reserpine and metaraminol. Since these compounds have similar inhibitory effects on norepinephrine uptake but different pharmacological and clinical effects, interaction studies may be of value in elucidating the mechanisms of action (1, 2).

DISCUSSION

Norepinephrine stores in sympathetically innervated tissues such as heart can be labeled by administering ^{3}H-norepinephrine (10). Tritium concentrations in the heart after administration of ^{3}H-norepinephrine are almost entirely due to the parent compound (6, 10, 11). Thus, changes in the concentration of tritium in the heart have been used to determine norepinephrine uptake, release, and turnover (6, 7, 12).

The reported effects of standard compounds that block the uptake or release norepinephrine are consistent with the results obtained with the oxidation procedure (1, 6, 7) where the assay was simplified by isolation of the tritium as tritiated water. This method is rapid, simple, sensitive, and reproducible. The quantity of tissue sample that can be assayed is limited by the tritium concentration of the tissue. Ten to 100 mg are convenient sample sizes, while larger samples (0.5–2 g) may be combusted in several parts.

The test compounds and doses used here were selected after preliminary experiments primarily as examples of the method. Other compounds may be substituted, and different time periods, species, tissues, and numbers of animals can be used within the framework of this procedure.

Studies on the interactions of two or more compounds in animals and humans have provided basic information on the mechanisms of drug action (13, 14). The oxidation procedure provides a convenient means of determining both the actions and interactions of compounds affecting adrenergic neurons.

REFERENCES

(1) I. J. Kopin, *Pharmacol. Rev.*, **18**, 513(1966).

(2) P. A. Shore, *Ann. Rev. Pharmacol.*, **12**, 209(1972).

(3) J. J. Schildkraut, *Am. J. Psychiat.*, **122**, 509(1965).

(4) L. L. Iversen, "The Uptake and Storage of Noradrenaline in Sympathetic Nerves," Cambridge University Press, London, England, 1967, pp. 147–174.

(5) R. Montanari, E. Costa, M. A. Beaven, and B. B. Brodie, *Life Sci.*, **4**, 232(1963).

(6) J. W. Daly, C. R. Creveling, and B. Witkop, *J. Med. Chem.*, **9**, 273(1966a).

(7) *Ibid.*, **9**, 280(1966b).

(8) G. W. Snedecor, "Statistical Methods," 4th ed., Iowa State College Press, Ames, Iowa, 1946.

(9) B. J. Winer, "Statistical Principles in Experimental Design," McGraw-Hill, New York, N.Y., 1971.

(10) J. Axelrod, L. G. Whitby, and G. Hertting, *Science*, **133**, 388(1961).

(11) L. G. Whitby, J. Axelrod, and H. Weil-Malherbe, *J. Pharmacol. Exp. Ther.*, **132**, 193(1961).

(12) A. Oliverio and L. Stjarne, *Life Sci.*, **4**, 2339(1965).

(13) J. A. Oates, J. R. Mitchell, O. T. Feagin, J. S. Kaufmann, and D. G. Shand, *Ann. N.Y. Acad. Sci.*, **179**, 302(1971).

(14) J. R. Mitchell, L. Arias, and J. A. Oates, *J. Am. Med. Assoc.*, **202**, 973(1967).

ACKNOWLEDGMENTS AND ADDRESSES

Received August 18, 1975, from the Sterling-Winthrop Research

Institute, Rensselaer, NY 12144
Accepted for publication December 24, 1975.
* Present address: Department of Pharmacy and Pharmacology, College of Pharmacy and Allied Health Professions, Northeastern University, Boston, MA 02115
x To whom inquiries should be directed. Present address: Division of Neuroscience, New York State Psychiatric Institute, New York, NY 10032

COMMUNICATIONS

Antineoplastic Agents XLV: Sea Cucumber Cytotoxic Saponins

Keyphrases □ Antineoplastic agents, potential—three saponins isolated from sea cucumbers, structures partially determined, activity evaluated □ Cytotoxic activity—evaluated in three saponins isolated from sea cucumbers □ Sea cucumbers—three saponins isolated and identified, screened for antineoplastic and cytotoxic activity □ Saponins—isolated from sea cucumbers, structures partially determined, antineoplastic and cytotoxic activity evaluated

To the Editor:

In Asia, various sea cucumbers (Echinodermata phylum, Holothurioidea class) are readily available under the name Trepang. One of these, *Stichopus japonicus* Selenka, is used for various medicinal purposes[1] (1) and human food. In 1929, Yamanouchi began to explore sea cucumber toxins; in 1942, he reported the isolation of a crystalline saponin mixture from *Holothuria vagabunda* Selenka (2). Subsequently, such saponin mixtures from sea cucumbers have been shown to possess various physiological activities, *e.g.*, neurotoxic (3), hemolytic (4), and the ability to inhibit growth of Crocker mouse sarcoma 180 and Krebs-2 ascites tumors in Swiss mice (5).

The actual composition of these saponin mixtures continues to be a challenging area for chemical study. So far, evidence has been presented only for the structure of the antifungal agent holotoxin A (I) from *S. japonicus* Selenka (6). However, the lanostane derivatives obtained by acid hydrolysis of the saponin mixtures received detailed investigation (7), particularly by Tan *et al.* (8) who recently provided definitive structural evidence for holotoxinogenin (II*a*) (6) and its 25-methyl ether derivative (II*b*).

About 10 years ago, in collaboration with the National Cancer Institute, we began the first systematic and worldwide survey of marine animals as potential sources of new antineoplastic agents (9). Many marine animal species have been located which yield extracts with a confirmed level of activity in the National Cancer Institute's P-388 murine lymphocytic leukemia, 9KB cell culture, and/or the P-388 and L-1210 cell culture evaluation systems (10). Of these potentially important marine animal species, six were Holothurioidea. Three were selected for detailed study: two from the family Stichopodidae, namely, *Stichopus chloronotus* Brandt (from Australia) and *Thelenota ananas* Jaeger (from Taiwan and the Marshall Islands), and one from the family Holothuriidae, *Actinopyga mauritiana* (from Hawaii).

We now wish to report that separation of the cytotoxic and antineoplastic constituents, guided by bioassay, led in each case to a complex mixture of lanostane-type saponins characteristic of sea cucumber Cuvierian organ toxins. The major cytotoxic component of each saponin mixture was isolated and designated stichostatin 1, thelenostatin 1, and actinostatin 1, respectively. A description of the isolation, purification, and partial characterization of stichostatin 1 (P-388, ED_{50} = 2.9) provides a summary of the techniques found most useful in this first detailed study of sea cucumber cytotoxic constituents.

A 2-propanol extract (59 g) obtained from *S. chloronotus* Brandt was partitioned between benzene and water. The water phase was separated and extracted with 1-butanol, and the extracted material was partitioned between ether and water. Freeze drying of the water phase afforded 1 g of the saponins, which were carefully separated on a specially prepared (11) prepacked silica gel column [elution with chloroform–methanol–water (20:5:0.5)].

Fractions 71–106 (6-ml volumes) contained stichostatin 1 (0.19 g). Recrystallization from methanol–chloroform gave needles (0.13 g) melting at 279–280°. Elemental analyses and molecular weight determinations by osmometry methods suggested a molecular weight of 1200 and an empirical formula of $C_{54-56}H_{93-98}O_{27-28}$. A series of mass (molecular ions were not observed), PMR, IR, and UV spectral studies, combined with preliminary chemical evidence, suggests that stichostatin 1 contains a lanostane nucleus related to that of Structure II*c* (8) and a glycoside system related to that of holotoxin A (I).

The structurally related cytotoxic saponins thelenostatin 1 (needles, mp 213–217°, from chloroform–methanol–water) and actinostatin 1 (needles, mp 218–220°, from chloroform–methanol–water) were obtained and partially characterized by similar methods from *T. ananas* Jaeger and *A. mauritiana*, respectively. In addition, both thelenostatin 1 (P-388, ED_{50} = 1.5) and actinostatin 1 (KB, ED_{50} = 2.6 and L-1210, ED_{50} = 2.1) were found to be half-esters of sulfuric acid similar to holothurin A, which is believed to contain the lanostane system illustrated by Structure III (12).

A definitive structural elucidation of these three new cytotoxic saponins, combined with further cytotoxic and antineoplastic evaluations, will be undertaken. Pres-

[1] Trepang is prepared by boiling the sea cucumber to cause evisceration and partial deactivation of the toxins.

Institute, Rensselaer, NY 12144
Accepted for publication December 24, 1975.
* Present address: Department of Pharmacy and Pharmacology, College of Pharmacy and Allied Health Professions, Northeastern University, Boston, MA 02115
x To whom inquiries should be directed. Present address: Division of Neuroscience, New York State Psychiatric Institute, New York, NY 10032

COMMUNICATIONS

Antineoplastic Agents XLV: Sea Cucumber Cytotoxic Saponins

Keyphrases □ Antineoplastic agents, potential—three saponins isolated from sea cucumbers, structures partially determined, activity evaluated □ Cytotoxic activity—evaluated in three saponins isolated from sea cucumbers □ Sea cucumbers—three saponins isolated and identified, screened for antineoplastic and cytotoxic activity □ Saponins—isolated from sea cucumbers, structures partially determined, antineoplastic and cytotoxic activity evaluated

To the Editor:

In Asia, various sea cucumbers (Echinodermata phylum, Holothurioidea class) are readily available under the name Trepang. One of these, *Stichopus japonicus* Selenka, is used for various medicinal purposes[1] (1) and human food. In 1929, Yamanouchi began to explore sea cucumber toxins; in 1942, he reported the isolation of a crystalline saponin mixture from *Holothuria vagabunda* Selenka (2). Subsequently, such saponin mixtures from sea cucumbers have been shown to possess various physiological activities, *e.g.*, neurotoxic (3), hemolytic (4), and the ability to inhibit growth of Crocker mouse sarcoma 180 and Krebs-2 ascites tumors in Swiss mice (5).

The actual composition of these saponin mixtures continues to be a challenging area for chemical study. So far, evidence has been presented only for the structure of the antifungal agent holotoxin A (I) from *S. japonicus* Selenka (6). However, the lanostane derivatives obtained by acid hydrolysis of the saponin mixtures received detailed investigation (7), particularly by Tan *et al.* (8) who recently provided definitive structural evidence for holotoxinogenin (II*a*) (6) and its 25-methyl ether derivative (II*b*).

About 10 years ago, in collaboration with the National Cancer Institute, we began the first systematic and worldwide survey of marine animals as potential sources of new antineoplastic agents (9). Many marine animal species have been located which yield extracts with a confirmed level of activity in the National Cancer Institute's P-388 murine lymphocytic leukemia, 9KB cell culture, and/or the P-388 and L-1210 cell culture evaluation systems (10). Of these potentially important marine animal species, six were Holothurioidea. Three were selected for detailed study: two from the family Stichopodidae, namely, *Stichopus chloronotus* Brandt (from Australia) and *Thelenota ananas* Jaeger (from Taiwan and the Marshall Islands), and one from the family Holothuriidae, *Actinopyga mauritiana* (from Hawaii).

We now wish to report that separation of the cytotoxic and antineoplastic constituents, guided by bioassay, led in each case to a complex mixture of lanostane-type saponins characteristic of sea cucumber Cuvierian organ toxins. The major cytotoxic component of each saponin mixture was isolated and designated stichostatin 1, thelenostatin 1, and actinostatin 1, respectively. A description of the isolation, purification, and partial characterization of stichostatin 1 (P-388, ED_{50} = 2.9) provides a summary of the techniques found most useful in this first detailed study of sea cucumber cytotoxic constituents.

A 2-propanol extract (59 g) obtained from *S. chloronotus* Brandt was partitioned between benzene and water. The water phase was separated and extracted with 1-butanol, and the extracted material was partitioned between ether and water. Freeze drying of the water phase afforded 1 g of the saponins, which were carefully separated on a specially prepared (11) prepacked silica gel column [elution with chloroform–methanol–water (20:5:0.5)].

Fractions 71–106 (6-ml volumes) contained stichostatin 1 (0.19 g). Recrystallization from methanol–chloroform gave needles (0.13 g) melting at 279–280°. Elemental analyses and molecular weight determinations by osmometry methods suggested a molecular weight of 1200 and an empirical formula of $C_{54-56}H_{93-98}O_{27-28}$. A series of mass (molecular ions were not observed), PMR, IR, and UV spectral studies, combined with preliminary chemical evidence, suggests that stichostatin 1 contains a lanostane nucleus related to that of Structure II*c* (8) and a glycoside system related to that of holotoxin A (I).

The structurally related cytotoxic saponins thelenostatin 1 (needles, mp 213–217°, from chloroform–methanol–water) and actinostatin 1 (needles, mp 218–220°, from chloroform–methanol–water) were obtained and partially characterized by similar methods from *T. ananas* Jaeger and *A. mauritiana*, respectively. In addition, both thelenostatin 1 (P-388, ED_{50} = 1.5) and actinostatin 1 (KB, ED_{50} = 2.6 and L-1210, ED_{50} = 2.1) were found to be half-esters of sulfuric acid similar to holothurin A, which is believed to contain the lanostane system illustrated by Structure III (12).

A definitive structural elucidation of these three new cytotoxic saponins, combined with further cytotoxic and antineoplastic evaluations, will be undertaken. Pres-

[1] Trepang is prepared by boiling the sea cucumber to cause evisceration and partial deactivation of the toxins.

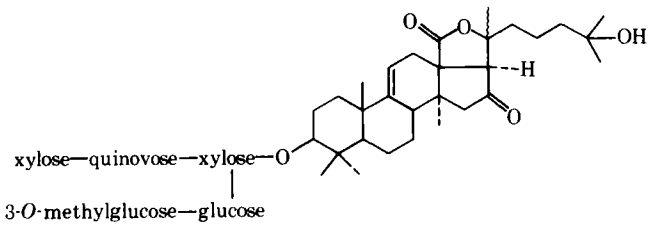

I

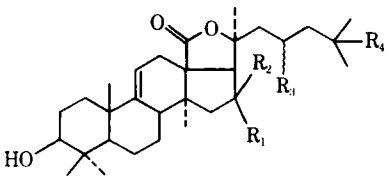

IIa: $R_1 = R_2 = O, R_3 = H, R_4 = OH$
IIb: $R_1 = R_2 = O, R_3 = H, R_4 = OCH_3$
IIc: $R_1 = OH, R_2 = H, R_3 = OCOCH_3, R_4 = H$

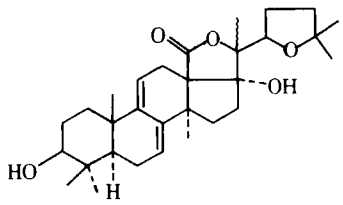

III

ently available evidence strongly indicates that such sea cucumber saponins have potentially useful and interesting biological properties. The inhibition of cell growth by the three tetracyclic triterpene saponins described in this report may be due to the ability of certain sea cucumber saponins to inhibit protein synthesis (rat bone marrow tissue culture) and RNA synthesis (yeast cell culture) (13).

(1) G. B. Elyakov, T. A. Kuznetsova, and V. E. Vaskovsky, *Khim. Prir. Soedin*, **4**, 253(1968); through *Chem. Abstr.*, **70**, 45173(1969).

(2) T. Yasumoto, K. Nakamura, and Y. Hashimoto, *Agr. Biol. Chem.*, **31**, 7(1967). B. W. Halstead, "Poisonous and Venomous Marine Animals of the World," vol. 1, U.S. Government Printing Office, Washington, D.C., 1965, p. 574.

(3) S. L. Friess, F. G. Standaert, E. R. Whitcom, R. F. Nigrelli, J. D. Chanley, and H. Sobotka, *J. Pharmacol. Exp. Ther.*, **126**, 323(1959).

(4) J. Lasley and R. F. Nigrelli, *Zoologica*, **56**, 1(1971).

(5) R. F. Nigrelli, *ibid.*, **37**, 89(1952). T. D. Sullivan, K. T. Ladue, and R. F. Nigrelli, *ibid.*, **40**, 49(1955).

(6) I. Kitagawa, T. Sugawara, and I. Yosioka, *Tetrahedron Lett.*, **1975**, 963; I. Kitagawa, T. Sugawara, and I. Yosioka, *Chem. Pharm. Bull.*, **24**, 275(1976).

(7) J. D. Chanley and C. Rossi, *Tetrahedron*, **25**, 1897(1969). B. Tursch, R. Cloetens, and C. Djerassi, *Tetrahedron Lett.*, **1970**, 467. P. Roller, C. Djerassi, R. Cloetens, and B. Tursch, *J. Am. Chem. Soc.*, **91**, 4918(1969). G. Habermehl and G. Volkwein, *Justus Liebigs Ann. Chem.*, **731**, 53(1970). P. Roller, B. Tursch, and C. Djerassi, *J. Org. Chem.*, **35**, 2585(1970). I. Rothberg, B. M. Tursch, and C. Djerassi, *ibid.*, **38**, 209(1973). J. D. Chanley, R. Ledeen, J. Wax, R. F. Nigrelli, and H. Sobotka, *J. Am. Chem. Soc.*, **81**, 5180(1959).

(8) W. L. Tan, C. Djerassi, J. Fayos, and J. Clardy, *J. Org. Chem.*, **40**, 466(1975). G. B. Elyakov, V. A. Stonik, E. V. Levina, V. P. Slanke, T. A. Kuznetsova, and V. S. Levin, *Comp. Biochem. Physiol.*, **44B**, 325(1973).

(9) G. R. Pettit, J. F. Day, J. L. Hartwell, and H. B. Wood, *Nature*, **227**, 962(1970) and Abstracts (No. 190) of the 30th Annual Northwest Regional Meeting of the American Chemical Society, University of Hawaii, Honolulu, Hawaii, June 12–13, 1975.

(10) R. I. Gueran, N. H. Greenberg, M. M. Macdonald, A. M. Schumacher, and B. J. Abbott, *Cancer Chemother. Rep., Part 3*, **3**, No. 2 (Sept. 1972).

(11) D. L. Herald, R. H. Ode, and G. R. Pettit, *J. Chromatogr. Sci.*, **14**, 356(1976).

(12) S. L. Friess, R. C. Durant, W. L. Fink, and J. D. Chanley, *Toxicol. Appl. Pharmacol.*, **22**, 115(1972).

(13) M. M. Anisimov, N. G. Prokof'eva, T. A. Juznetsova, and N. V. Peretolchin, *Izv. Akad. Nauk SSSR, Ser. Biol.*, **1**, 137(1971); through *Chem. Abstr.*, **74**, 73825(1971). S. I. Baranova, A. L. Kul'ga, M. M. Anisimov, V. A. Stonik, E. V. Levina, V. S. Levin, and G. B. Elyakov, *ibid.*, **2**, 284(1973); through *Chem. Abstr.*, **78**, 143997(1973).

George R. Pettit [x]
Cherry L. Herald
Delbert L. Herald

Cancer Research Institute and Department of Chemistry
Arizona State University
Tempe, AZ 85281

Received February 23, 1976.

Accepted for publication June 24, 1976.

Supported by the National Cancer Institute (performed pursuant to Contract NO1-CM-12308 with the Division of Cancer Treatment, National Cancer Institute, National Institutes of Health, Department of Health, Education, and Welfare), Public Health Research Grant CA-16049-02 from the National Cancer Institute, the Fannie E. Rippel Foundation, the J. W. Kieckhefer Foundation, Talley Industries, and the Phoenix Coca-Cola Bottling Co.

Grateful acknowledgment is extended to Dr. R. H. Ode, Mr. L. D. Vanell, and Mr. G. C. Bryan for assistance with preliminary and analytical experiments and to members of the Smithsonian Institution for their valuable contributions. We also wish to thank Dr. C. Djerassi, Dr. I. Kitagawa, and Dr. J. D. Chanley for various specimens of sea cucumber constituents.

For Part XLIV of this series, see G. R. Pettit, *China Q.*, in press.

[x] To whom inquiries should be directed.

Starch Paste Granulations: Factors Causing Binder Dilution Effects on Granulations and Tablets

Keyphrases □ Starch paste granulations—effect of mixing time, speed, and binder dilution on physical properties of tablets □ Granulations, starch paste—effect of mixing time, speed, and binder dilution on physical properties of tablets □ Dosage forms—tablets, effect of mixing time, speed, and binder dilution on physical properties of tablets

To the Editor:

In a recent communication (1), the dilution factor of starch paste binder and its effects on granulations and tablets were reported. The conventional wet granulation process was used to prepare granulations in a small

Table I—Starch Paste Dilutions

	Formulation A	Formulation B	Formulation C
Lactose, g	860	860	860
Starch (in dry mix), g	47	47	47
Starch (in paste), g	26	26	26
Water (for paste), ml	100	130	160
Water (used to *qs*), ml	100	70	40

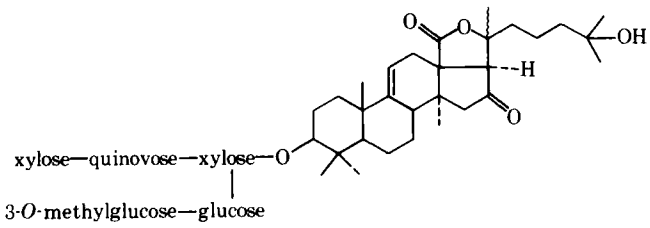

I

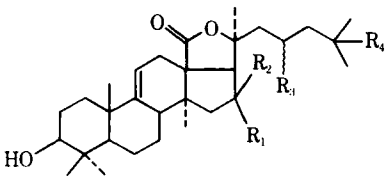

IIa: $R_1 = R_2 = O, R_3 = H, R_4 = OH$
IIb: $R_1 = R_2 = O, R_3 = H, R_4 = OCH_3$
IIc: $R_1 = OH, R_2 = H, R_3 = OCOCH_3, R_4 = H$

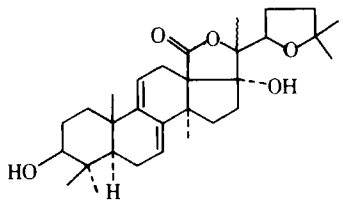

III

ently available evidence strongly indicates that such sea cucumber saponins have potentially useful and interesting biological properties. The inhibition of cell growth by the three tetracyclic triterpene saponins described in this report may be due to the ability of certain sea cucumber saponins to inhibit protein synthesis (rat bone marrow tissue culture) and RNA synthesis (yeast cell culture) (13).

(1) G. B. Elyakov, T. A. Kuznetsova, and V. E. Vaskovsky, *Khim. Prir. Soedin*, **4**, 253(1968); through *Chem. Abstr.*, **70**, 45173(1969).

(2) T. Yasumoto, K. Nakamura, and Y. Hashimoto, *Agr. Biol. Chem.*, **31**, 7(1967). B. W. Halstead, "Poisonous and Venomous Marine Animals of the World," vol. 1, U.S. Government Printing Office, Washington, D.C., 1965, p. 574.

(3) S. L. Friess, F. G. Standaert, E. R. Whitcom, R. F. Nigrelli, J. D. Chanley, and H. Sobotka, *J. Pharmacol. Exp. Ther.*, **126**, 323(1959).

(4) J. Lasley and R. F. Nigrelli, *Zoologica*, **56**, 1(1971).

(5) R. F. Nigrelli, *ibid.*, **37**, 89(1952). T. D. Sullivan, K. T. Ladue, and R. F. Nigrelli, *ibid.*, **40**, 49(1955).

(6) I. Kitagawa, T. Sugawara, and I. Yosioka, *Tetrahedron Lett.*, **1975**, 963; I. Kitagawa, T. Sugawara, and I. Yosioka, *Chem. Pharm. Bull.*, **24**, 275(1976).

(7) J. D. Chanley and C. Rossi, *Tetrahedron*, **25**, 1897(1969). B. Tursch, R. Cloetens, and C. Djerassi, *Tetrahedron Lett.*, **1970**, 467. P. Roller, C. Djerassi, R. Cloetens, and B. Tursch, *J. Am. Chem. Soc.*, **91**, 4918(1969). G. Habermehl and G. Volkwein, *Justus Liebigs Ann. Chem.*, **731**, 53(1970). P. Roller, B. Tursch, and C. Djerassi, *J. Org. Chem.*, **35**, 2585(1970). I. Rothberg, B. M. Tursch, and C. Djerassi, *ibid.*, **38**, 209(1973). J. D. Chanley, R. Ledeen, J. Wax, R. F. Nigrelli, and H. Sobotka, *J. Am. Chem. Soc.*, **81**, 5180(1959).

(8) W. L. Tan, C. Djerassi, J. Fayos, and J. Clardy, *J. Org. Chem.*, **40**, 466(1975). G. B. Elyakov, V. A. Stonik, E. V. Levina, V. P. Slanke, T. A. Kuznetsova, and V. S. Levin, *Comp. Biochem. Physiol.*, **44B**, 325(1973).

(9) G. R. Pettit, J. F. Day, J. L. Hartwell, and H. B. Wood, *Nature*, **227**, 962(1970) and Abstracts (No. 190) of the 30th Annual Northwest Regional Meeting of the American Chemical Society, University of Hawaii, Honolulu, Hawaii, June 12–13, 1975.

(10) R. I. Gueran, N. H. Greenberg, M. M. Macdonald, A. M. Schumacher, and B. J. Abbott, *Cancer Chemother. Rep., Part 3*, **3**, No. 2 (Sept. 1972).

(11) D. L. Herald, R. H. Ode, and G. R. Pettit, *J. Chromatogr. Sci.*, **14**, 356(1976).

(12) S. L. Friess, R. C. Durant, W. L. Fink, and J. D. Chanley, *Toxicol. Appl. Pharmacol.*, **22**, 115(1972).

(13) M. M. Anisimov, N. G. Prokof'eva, T. A. Juznetsova, and N. V. Peretolchin, *Izv. Akad. Nauk SSSR, Ser. Biol.*, **1**, 137(1971); through *Chem. Abstr.*, **74**, 73825(1971). S. I. Baranova, A. L. Kul'ga, M. M. Anisimov, V. A. Stonik, E. V. Levina, V. S. Levin, and G. B. Elyakov, *ibid.*, **2**, 284(1973); through *Chem. Abstr.*, **78**, 143997(1973).

George R. Pettit [x]
Cherry L. Herald
Delbert L. Herald

Cancer Research Institute and Department of Chemistry
Arizona State University
Tempe, AZ 85281

Received February 23, 1976.

Accepted for publication June 24, 1976.

Supported by the National Cancer Institute (performed pursuant to Contract NO1-CM-12308 with the Division of Cancer Treatment, National Cancer Institute, National Institutes of Health, Department of Health, Education, and Welfare), Public Health Research Grant CA-16049-02 from the National Cancer Institute, the Fannie E. Rippel Foundation, the J. W. Kieckhefer Foundation, Talley Industries, and the Phoenix Coca-Cola Bottling Co.

Grateful acknowledgment is extended to Dr. R. H. Ode, Mr. L. D. Vanell, and Mr. G. C. Bryan for assistance with preliminary and analytical experiments and to members of the Smithsonian Institution for their valuable contributions. We also wish to thank Dr. C. Djerassi, Dr. I. Kitagawa, and Dr. J. D. Chanley for various specimens of sea cucumber constituents.

For Part XLIV of this series, see G. R. Pettit, *China Q.*, in press.

[x] To whom inquiries should be directed.

Starch Paste Granulations: Factors Causing Binder Dilution Effects on Granulations and Tablets

Keyphrases □ Starch paste granulations—effect of mixing time, speed, and binder dilution on physical properties of tablets □ Granulations, starch paste—effect of mixing time, speed, and binder dilution on physical properties of tablets □ Dosage forms—tablets, effect of mixing time, speed, and binder dilution on physical properties of tablets

To the Editor:

In a recent communication (1), the dilution factor of starch paste binder and its effects on granulations and tablets were reported. The conventional wet granulation process was used to prepare granulations in a small

Table I—Starch Paste Dilutions

	Formulation A	Formulation B	Formulation C
Lactose, g	860	860	860
Starch (in dry mix), g	47	47	47
Starch (in paste), g	26	26	26
Water (for paste), ml	100	130	160
Water (used to *qs*), ml	100	70	40

Table II—Sieve Analysis of the Three Formulations

Formulation	Percent Remaining on Corresponding Screens after Dry Granulation Step							Percent Remaining on Corresponding Screens following Attrition at 500 Revolutions						
	20 Mesh	40 Mesh	60 Mesh	80 Mesh	120 Mesh	140 Mesh	Pan	20 Mesh	40 Mesh	60 Mesh	80 Mesh	120 Mesh	140 Mesh	Pan
A	9.0	56.6	16.6	6.9	6.5	2.4	2.0	7.0	39.4	16.9	6.7	7.8	3.3	18.9
B	13.3	53.9	18.6	6.4	4.7	1.8	1.3	12.8	46.4	16.9	5.4	5.0	2.0	11.5
C	10.3	56.7	16.8	6.9	5.8	2.3	1.2	5.9	40.7	15.1	7.1	6.5	3.3	21.4

planetary-type mixer. The three formulations tested are given in Table I. The lactose and starch were dry mixed in the mixer bowl for 5 min. The amount of water used to make the starch paste was varied from a 4:1 to a 6:1 water to starch ratio. The total amount of water used in each experiment was kept constant by varying the amount of water added to the mass after the starch paste had been mixed with the lactose–starch mixture for 1 min.

The total mixing time was kept constant at 5 min. The wet mass was passed through a 6-mesh screen, dried at 50° to a moisture content of 1%, and then passed through a 16-mesh screen. These granules were evaluated for friability and compressibility. It was reported that the friability and compressibility of the granules improved with increasing starch paste dilution. Disintegration time increased slightly with each dilution of the starch paste.

Important parameters in the conventional wet granulation process are mixing time and speed of mixing. Mixing time is generally determined by the type and speed of mixing equipment. It is important to reach an appropriate degree of wetting in the powder particles during the wet granulation procedure. The properties of the dried granules with regard to hardness, friability, and compressibility vary with the varying degree of wetting in the wet granulation.

It should be obvious to the formulator that gross changes in the viscosity or thickness of the starch paste binder require changes in the mixing time for reaching a similar degree of wetting during the wet granulation process. Thick starch paste requires a longer time for mixing compared to a thin starch paste. Unless a thick starch paste is mixed for a longer period compared to a thin starch paste, one should expect differences in the degree of wetting of the powder particles. These differences would be reflected in the hardness, friability, and compressibility of the dried granulation. Obviously, Hill (1) optimized the degree of wetting of the lactose–starch mixture in favor of the thin starch paste to show the binder dilution effects.

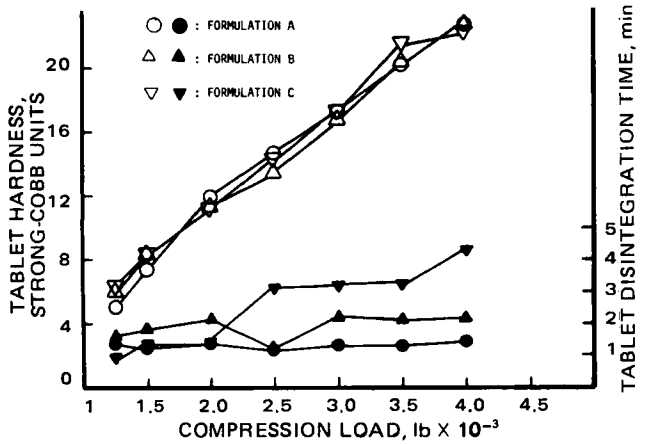

Figure 1—*Tablet hardness–compression load profiles and corresponding disintegration times of the three formulations. Mixing time and mixing speed were 10 min and 60 rpm, respectively. Key:* ○, △, *and* ▽, *tablet hardness; and* ●, ▲, *and* ▼, *tablet disintegration time.*

Careful evaluations should be carried out for any changes in the process, such as dilution of the binder solution, or in the size or type of mixing equipment during the tableting scale-up operations. Mixing time should be adjusted to ensure similar wetness of the powders. In view of these considerations, we consider it important to present data that clearly show that the binder dilution effects on the dry granulation friability and compressibility reported recently (1) are a consequence of improper mixing and are readily eliminated by increasing the mixing time from 5 to 10 min, ensuring a similar degree of wetting of the powders using the thick and thin starch pastes.

Similar procedures (1) were used in the preparation of granules and tablets. The lactose and starch were dry mixed in the mixer bowl for 5 min. The amount of water used to make the paste was varied from a 4:1 to a 6:1 water to starch ratio. The total amount of water used in each experiment was kept constant by varying the amount of water added to the mass after the starch paste had been mixed with the lactose–starch mixture for 1 min. The total amount of mixing time was increased from 5 to 10 min. The mixing speed was constant at 60 rpm. The wet mass was put through a 6-mesh screen by hand, dried at 50° to a moisture content of 1%, and then passed through an oscillator using a 16-mesh screen.

Granulation friability was measured by tumbling 25 g of granulation larger than 150 mesh end to end in a Plexiglas cylinder, 3.81 cm in diameter and 30.49 cm long. Sieve analysis[1] of the granulations before and after attrition was made. The sieve assembly was vibrated and sifted for 5 min at a pulse and sift setting of 7. The granulations were mixed with 0.5% magnesium stearate and 0.5% talc and compressed by an instrumented single-punch machine[2]. The punches and dies were 1.11 cm flat-faced beveled edge. The tablet hardness was determined[3]. The disintegration was carried out by the USP procedure.

The sieve analysis of the three granulations before

[1] Model L3P, Allen Bradley Co., Milwaukee, Wis.
[2] Stokes model E.
[3] Strong Cobb Arner Inc., Cleveland, Ohio.

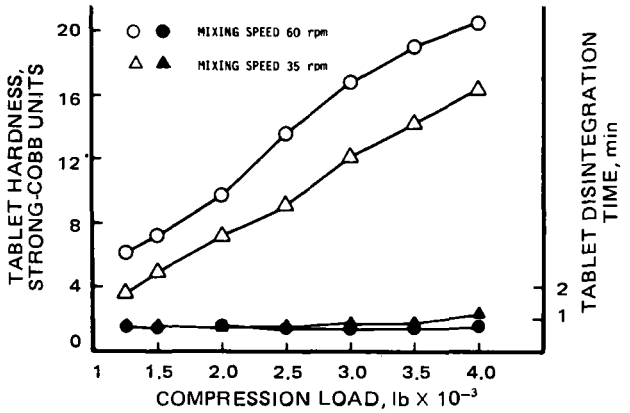

Figure 2—*Tablet hardness–compression load profiles and corresponding disintegration times. Mixing time was 5 min. Key: ○ and △, tablet hardness; and ● and ▲, tablet disintegration time.*

and after attrition is given in Table II. These results indicate no significant differences in the granulation size before and after attrition. Figure 1 gives the results of the tablet hardness–compression load profiles. The compressibility of the three granulations was essentially the same. These data indicate that when the three formulations were mixed for 10 min instead of for 5 min (1), the dilution factor effects on granule hardness and compressibility disappeared. A similar degree of wetting in the powders was reached by adequate mixing, which resulted in no differences in hardness, friability, and compressibility of the dried granules prepared from thick and thin starch pastes. Thus, we have shown clearly that the dilution factor effects on hardness, friability, and compressibility of granules are a consequence of improper mixing during the wet granulation procedure.

Figure 2 also gives the average disintegration times as a function of the compression load for the three formulations given in Table I. At lower compression forces, the differences in the disintegration times of the three formulations are slight and do not appear to follow any definite trend relating to the viscosity of the starch paste. However, at higher compression loads, the differences in the disintegration time might be significant and thus relate to a slightly longer disintegration time for tablets made with thin starch paste compared to thick starch paste.

In the conventional wet granulation procedure, the speed of mixing generally determines the mixing time. The results in Fig. 2 show the effect of mixing speed at a constant mixing time on the tablet hardness–compression load profiles from tablets prepared using Formulation C. The harder tablets at the 60-rpm mixing speed are in agreement with the smaller percentage of fines formed after attrition. The tablet disintegration time was not affected by the change in mixing speed at a constant mixing time.

(1) P. M. Hill, *J. Pharm. Sci.*, **65**, 313(1976).

Z. T. Chowhan [x]
L. Palagyi
Syntex Research
Institute of Pharmaceutical Sciences
Palo Alto, CA 94304

Received April 13, 1976.
Accepted for publication July 7, 1976.
[x] To whom inquiries should be directed.

Starch Paste Granulations: Factors Causing Binder Dilution Effects on Granulations and Tablets — A Response

Keyphrases□ Starch paste granulations—effect of starch paste viscosity on granule hardness and physical properties of tablets □ Granulations, starch paste—effect of starch paste viscosity on granule hardness and physical properties of tablets □ Dosage forms—tablets, effect of starch paste viscosity on granule hardness and physical properties of tablets

To the Editor:

Granulation mixing time is an important variable, of course. That fact is recognized by often specifying maximum mixing times for the manufacture of granulations. However, the purpose of my communication was to show the unexpected effect of starch paste viscosity on the hardness of the resulting granules. This effect is of interest because the same total amount of water was used in each experiment and it would not be immediately apparent that the paste viscosity would affect the rate of wetting under this circumstance.

A 5-min mixing time was used because the mass appeared to be maximally wet in that time. This is usually the case in the production setting for products made today. The granulating operator has the flexibility to mix until the mass appears granular. It would not be feasible to place a finite limit on mixing time because the actual time required often varies with some physical aspect of the powders such as moisture content, particle size, or shape. The paste dilution study lends support, in fact, to Chowhan and Palagyi's statement that: "Careful evaluations should be carried out for any changes in the process, such as dilution of the binder solution, ..."

The authors also stated that the dilution factor effects disappeared when the three formulations were mixed for 10 min instead of 5 min. This is not entirely true. Even though they showed that the effect on compressibility disappears as shown by similar hardness–pressure profiles, some effect is still reflected in increasing tablet disintegration times. Admittedly, the changes are small and would not be expected to affect tablet acceptability unless a product had a very short disintegration time limit.

Philip M. Hill
Tablet Products Research and Development
Abbott Laboratories
North Chicago, IL 60064

Received May 17, 1976.
Accepted for publication June 16, 1976.

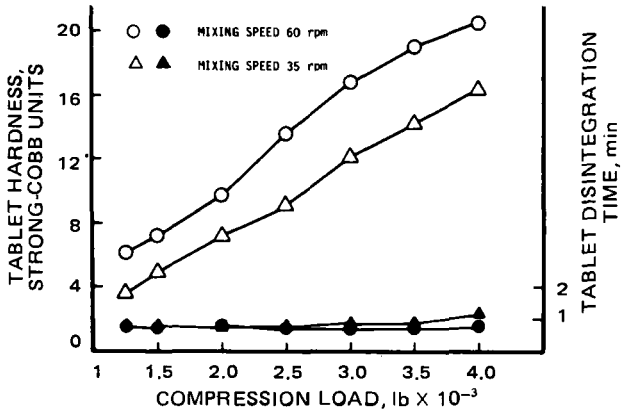

Figure 2—*Tablet hardness–compression load profiles and corresponding disintegration times. Mixing time was 5 min. Key: ○ and △, tablet hardness; and ● and ▲, tablet disintegration time.*

and after attrition is given in Table II. These results indicate no significant differences in the granulation size before and after attrition. Figure 1 gives the results of the tablet hardness–compression load profiles. The compressibility of the three granulations was essentially the same. These data indicate that when the three formulations were mixed for 10 min instead of for 5 min (1), the dilution factor effects on granule hardness and compressibility disappeared. A similar degree of wetting in the powders was reached by adequate mixing, which resulted in no differences in hardness, friability, and compressibility of the dried granules prepared from thick and thin starch pastes. Thus, we have shown clearly that the dilution factor effects on hardness, friability, and compressibility of granules are a consequence of improper mixing during the wet granulation procedure.

Figure 2 also gives the average disintegration times as a function of the compression load for the three formulations given in Table I. At lower compression forces, the differences in the disintegration times of the three formulations are slight and do not appear to follow any definite trend relating to the viscosity of the starch paste. However, at higher compression loads, the differences in the disintegration time might be significant and thus relate to a slightly longer disintegration time for tablets made with thin starch paste compared to thick starch paste.

In the conventional wet granulation procedure, the speed of mixing generally determines the mixing time. The results in Fig. 2 show the effect of mixing speed at a constant mixing time on the tablet hardness–compression load profiles from tablets prepared using Formulation C. The harder tablets at the 60-rpm mixing speed are in agreement with the smaller percentage of fines formed after attrition. The tablet disintegration time was not affected by the change in mixing speed at a constant mixing time.

(1) P. M. Hill, *J. Pharm. Sci.*, **65**, 313(1976).

Z. T. Chowhan [x]
L. Palagyi
Syntex Research
Institute of Pharmaceutical Sciences
Palo Alto, CA 94304

Received April 13, 1976.
Accepted for publication July 7, 1976.
[x] To whom inquiries should be directed.

Starch Paste Granulations: Factors Causing Binder Dilution Effects on Granulations and Tablets — A Response

Keyphrases□ Starch paste granulations—effect of starch paste viscosity on granule hardness and physical properties of tablets □ Granulations, starch paste—effect of starch paste viscosity on granule hardness and physical properties of tablets □ Dosage forms—tablets, effect of starch paste viscosity on granule hardness and physical properties of tablets

To the Editor:

Granulation mixing time is an important variable, of course. That fact is recognized by often specifying maximum mixing times for the manufacture of granulations. However, the purpose of my communication was to show the unexpected effect of starch paste viscosity on the hardness of the resulting granules. This effect is of interest because the same total amount of water was used in each experiment and it would not be immediately apparent that the paste viscosity would affect the rate of wetting under this circumstance.

A 5-min mixing time was used because the mass appeared to be maximally wet in that time. This is usually the case in the production setting for products made today. The granulating operator has the flexibility to mix until the mass appears granular. It would not be feasible to place a finite limit on mixing time because the actual time required often varies with some physical aspect of the powders such as moisture content, particle size, or shape. The paste dilution study lends support, in fact, to Chowhan and Palagyi's statement that: "Careful evaluations should be carried out for any changes in the process, such as dilution of the binder solution, ..."

The authors also stated that the dilution factor effects disappeared when the three formulations were mixed for 10 min instead of 5 min. This is not entirely true. Even though they showed that the effect on compressibility disappears as shown by similar hardness–pressure profiles, some effect is still reflected in increasing tablet disintegration times. Admittedly, the changes are small and would not be expected to affect tablet acceptability unless a product had a very short disintegration time limit.

Philip M. Hill
Tablet Products Research and Development
Abbott Laboratories
North Chicago, IL 60064

Received May 17, 1976.
Accepted for publication June 16, 1976.

Orthogonal Least Squares

Keyphrases □ Linear regression methods—both variables measured subject to error, equations derived □ Orthogonal least squares—linear regression methods, both variables measured subject to error, equations derived

To the Editor:

The usual least-squares linear regression of y on x assumes that y is measured subject to error and that x is fixed or measured without error. The line of best fit:

$$\frac{y-\bar{y}}{s_y} = r\frac{x-\bar{x}}{s_x} \qquad \text{(Eq. 1)}$$

therefore minimizes the sums of squares of vertical deviations (along y) from the set of n observed points $(x_1, y_1), \ldots, (x_n, y_n)$ to this line, where the sample means are $\bar{x} = \Sigma x_i/n$ and $\bar{y} = \Sigma y_i/n$, the sample variances are $s_x^2 = \Sigma(x_i - \bar{x})^2/n$ and $s_y^2 = \Sigma(y_i - \bar{y})/n$, the sample covariance is $s_{xy} = \Sigma(x_i - \bar{x})(y_i - \bar{y})/n$, and the sample correlation coefficient is $r = s_{xy}/s_x s_y$.

The purpose of this communication is to outline the known methods of linear regression when *both* x and y are measured subject to error. Reference is made to statistical textbooks on multivariate analysis.

Morrison (1) considered the problem of the minimization of the sums of squares of *perpendicular* deviations from the points to the line and indicated that it is equivalent to a rotation of axes such that the perpendicular projection of these points onto the new axis has a maximum variance. This approach gives as the line of best fit:

$$\frac{y-\bar{y}}{s_y} = [\text{sign } (r)]\frac{x-\bar{x}}{s_x} \qquad \text{(Eq. 2)}$$

Kendall and Stuart (2) gave a more general model when both x and y are subject to the errors δ and ϵ, respectively. Their development leads to the line of best fit:

$$y - \bar{y} = (x-\bar{x})\frac{(s_y^2 - \lambda s_x^2) + \sqrt{(s_y^2 - \lambda s_x^2)^2 + 4\lambda s_{xy}^2}}{2s_{xy}} \qquad \text{(Eq. 3)}$$

where $\lambda = \sigma_\epsilon^2/\sigma_\delta^2$ is assumed known, σ_ϵ^2 is the population error variance of y, and σ_δ^2 is the population error variance of x.

When $\lambda = 1$, Eq. 3 reduces to Eq. 2; when $\sigma_\delta^2 = 0$, it reduces to Eq. 1. Thus, if both variables are subject to errors of the same magnitude, then Eq. 2 can be used. If the errors differ markedly, Eq. 3 should be used.

(1) D. F. Morrison, "Multivariate Statistical Methods," McGraw-Hill, New York, N.Y., 1967, pp. 84, 85, 230–234.

(2) M. G. Kendall and A. Stuart, "The Advanced Theory of Statistics, vol. 2, Inference and Relationship," 3rd ed., Charles Griffin, London, England, 1973, Sect. 29.9–29.12.

J. R. Howell

Department of Pharmacy and Pharmaceutics
School of Pharmacy
Medical College of Virginia
Virginia Commonwealth University
Richmond, VA 23298

Received March 4, 1976.
Accepted for publication July 27, 1976.

BOOKS

REVIEWS

Progress in Medicinal Chemistry, Vol. 12. Edited by G. P. ELLIS and G. B. WEST. American Elsevier, 52 Vanderbilt Avenue, New York, NY 10017, 1975. 484 pp. 15.5 x 21.5 cm. Price $58.50.

In keeping with the tradition of the series, the editors have assembled excellent reviews of timely topics. The first five of the eight chapters emphasize the utility of specific instrumentation to the study of biological samples.

In Chapter 1, A. M. Lawson and G. H. Draffon briefly describe basic principles of mass spectrometry and GC–mass spectrometry and give attention to developments concerned with the role of computers in data analysis, selected ion monitoring methods, the use of stable isotopes, and alternative ionization processes. Numerous examples of specific applications are presented to demonstrate the present scope of the methods in the areas of biochemistry, pharmacology, and toxicology.

The basic principles, applications, and the more recent technological advances in affinity chromatography, gel chromatography, and high-pressure liquid chromatography are reviewed by K. W. Williams and R. C. Smith in Chapter 2.

P. J. Sadler, in Chapter 3, has chosen examples from recent literature to highlight progress in the NMR study of biological materials. The examples include the use of isotopic labels, paramagnetic probes, and other techniques.

In Chapter 4, D. L. Williams-Smith and S. J. Wyard briefly explain electron spin resonance spectroscopy and review its application to the study of metalloproteins, biological free radicals, and complex multicomponent enzyme systems. Also the use of spin labeling in enzymology, membrane studies, and immunochemistry is discussed.

The application of polarography to analytical and mechanistic problems in biochemistry, pharmacology, and toxicology is reviewed in Chapter 5 by M. Brezina and J. Volke.

The rapidly growing literature on cyclic nucleotides is reviewed by B. G. Benfey in Chapter 6. The discussion includes a review of the methods of determining the cyclic nucleotides as well as assays of certain other enzyme activities.

The increasing importance of *Pseudomonas aeruginosa* as a human pathogen makes Chapter 7 by R. B. Sykes and A. Morris a timely review. The sensitivity of the organism, as well as possible mechanisms by which the organism becomes resistant to various classes of antibacterial agents, is discussed.

The final chapter by J. C. Jaszberenyi and T. E. Gunda is the first of a two-part series (Part II is scheduled to appear in Volume 13 of this series) on the synthetic analogs of the β-lactam antibiotics. This chapter reviews changes in the thiazolidine and thiazine rings as well as substituents on rings. In one section, the literature on the mode of action of these antibotics is discussed from the view of a "structural analog" model *versus* a "conformational response" model.

In the preface, the editors state that "Biochemists, pharmacologists and toxicologists are finding increasing use for methods which have hitherto been used mainly by chemists, and the aim of the first six reviews is to allow biologists to assess the potential value of the techniques in their own work." Therefore, the book should find an interested audience among biochemists, pharmacologists, toxicologists, medicinal, and natural products chemists.

Reviewed by Charles M. Darling
Auburn University
School of Pharmacy
Auburn, AL 36830

Orthogonal Least Squares

Keyphrases □ Linear regression methods—both variables measured subject to error, equations derived □ Orthogonal least squares—linear regression methods, both variables measured subject to error, equations derived

To the Editor:

The usual least-squares linear regression of y on x assumes that y is measured subject to error and that x is fixed or measured without error. The line of best fit:

$$\frac{y-\bar{y}}{s_y} = r\frac{x-\bar{x}}{s_x} \qquad \text{(Eq. 1)}$$

therefore minimizes the sums of squares of vertical deviations (along y) from the set of n observed points $(x_1, y_1), \ldots, (x_n, y_n)$ to this line, where the sample means are $\bar{x} = \Sigma x_i/n$ and $\bar{y} = \Sigma y_i/n$, the sample variances are $s_x^2 = \Sigma(x_i - \bar{x})^2/n$ and $s_y^2 = \Sigma(y_i - \bar{y})/n$, the sample covariance is $s_{xy} = \Sigma(x_i - \bar{x})(y_i - \bar{y})/n$, and the sample correlation coefficient is $r = s_{xy}/s_x s_y$.

The purpose of this communication is to outline the known methods of linear regression when *both* x and y are measured subject to error. Reference is made to statistical textbooks on multivariate analysis.

Morrison (1) considered the problem of the minimization of the sums of squares of *perpendicular* deviations from the points to the line and indicated that it is equivalent to a rotation of axes such that the perpendicular projection of these points onto the new axis has a maximum variance. This approach gives as the line of best fit:

$$\frac{y-\bar{y}}{s_y} = [\text{sign } (r)]\frac{x-\bar{x}}{s_x} \qquad \text{(Eq. 2)}$$

Kendall and Stuart (2) gave a more general model when both x and y are subject to the errors δ and ϵ, respectively. Their development leads to the line of best fit:

$$y - \bar{y} = (x-\bar{x})\frac{(s_y^2 - \lambda s_x^2) + \sqrt{(s_y^2 - \lambda s_x^2)^2 + 4\lambda s_{xy}^2}}{2s_{xy}} \qquad \text{(Eq. 3)}$$

where $\lambda = \sigma_\epsilon^2/\sigma_\delta^2$ is assumed known, σ_ϵ^2 is the population error variance of y, and σ_δ^2 is the population error variance of x.

When $\lambda = 1$, Eq. 3 reduces to Eq. 2; when $\sigma_\delta^2 = 0$, it reduces to Eq. 1. Thus, if both variables are subject to errors of the same magnitude, then Eq. 2 can be used. If the errors differ markedly, Eq. 3 should be used.

(1) D. F. Morrison, "Multivariate Statistical Methods," McGraw-Hill, New York, N.Y., 1967, pp. 84, 85, 230–234.

(2) M. G. Kendall and A. Stuart, "The Advanced Theory of Statistics, vol. 2, Inference and Relationship," 3rd ed., Charles Griffin, London, England, 1973, Sect. 29.9–29.12.

J. R. Howell

Department of Pharmacy and Pharmaceutics
School of Pharmacy
Medical College of Virginia
Virginia Commonwealth University
Richmond, VA 23298

Received March 4, 1976.
Accepted for publication July 27, 1976.

BOOKS

REVIEWS

Progress in Medicinal Chemistry, Vol. 12. Edited by G. P. ELLIS and G. B. WEST. American Elsevier, 52 Vanderbilt Avenue, New York, NY 10017, 1975. 484 pp. 15.5 x 21.5 cm. Price $58.50.

In keeping with the tradition of the series, the editors have assembled excellent reviews of timely topics. The first five of the eight chapters emphasize the utility of specific instrumentation to the study of biological samples.

In Chapter 1, A. M. Lawson and G. H. Draffon briefly describe basic principles of mass spectrometry and GC–mass spectrometry and give attention to developments concerned with the role of computers in data analysis, selected ion monitoring methods, the use of stable isotopes, and alternative ionization processes. Numerous examples of specific applications are presented to demonstrate the present scope of the methods in the areas of biochemistry, pharmacology, and toxicology.

The basic principles, applications, and the more recent technological advances in affinity chromatography, gel chromatography, and high-pressure liquid chromatography are reviewed by K. W. Williams and R. C. Smith in Chapter 2.

P. J. Sadler, in Chapter 3, has chosen examples from recent literature to highlight progress in the NMR study of biological materials. The examples include the use of isotopic labels, paramagnetic probes, and other techniques.

In Chapter 4, D. L. Williams-Smith and S. J. Wyard briefly explain electron spin resonance spectroscopy and review its application to the study of metalloproteins, biological free radicals, and complex multicomponent enzyme systems. Also the use of spin labeling in enzymology, membrane studies, and immunochemistry is discussed.

The application of polarography to analytical and mechanistic problems in biochemistry, pharmacology, and toxicology is reviewed in Chapter 5 by M. Brezina and J. Volke.

The rapidly growing literature on cyclic nucleotides is reviewed by B. G. Benfey in Chapter 6. The discussion includes a review of the methods of determining the cyclic nucleotides as well as assays of certain other enzyme activities.

The increasing importance of *Pseudomonas aeruginosa* as a human pathogen makes Chapter 7 by R. B. Sykes and A. Morris a timely review. The sensitivity of the organism, as well as possible mechanisms by which the organism becomes resistant to various classes of antibacterial agents, is discussed.

The final chapter by J. C. Jaszberenyi and T. E. Gunda is the first of a two-part series (Part II is scheduled to appear in Volume 13 of this series) on the synthetic analogs of the β-lactam antibiotics. This chapter reviews changes in the thiazolidine and thiazine rings as well as substituents on rings. In one section, the literature on the mode of action of these antibotics is discussed from the view of a "structural analog" model *versus* a "conformational response" model.

In the preface, the editors state that "Biochemists, pharmacologists and toxicologists are finding increasing use for methods which have hitherto been used mainly by chemists, and the aim of the first six reviews is to allow biologists to assess the potential value of the techniques in their own work." Therefore, the book should find an interested audience among biochemists, pharmacologists, toxicologists, medicinal, and natural products chemists.

Reviewed by Charles M. Darling
Auburn University
School of Pharmacy
Auburn, AL 36830

Journal of Pharmaceutical Sciences

NOVEMBER 1976

VOLUME 65 NUMBER 11

MARY H. FERGUSON
Editor

L. LUAN CORRIGAN
Assistant Editor

SHELLY ELLIOTT
Production Editor

JANET D. SHOFF
Copy Editor

EDWARD G. FELDMANN
Contributing Editor

SAMUEL W. GOLDSTEIN
Contributing Editor

LELAND J. ARNEY
Publications Director

EDITORIAL ADVISORY BOARD

JOHN AUTIAN	HARRY B. KOSTENBAUDER
LYNN R. BRADY	CARL J. LINTNER, JR.
WILLIAM O. FOYE	DAVID E. MANN, JR.
WILLIAM J. JUSKO	GERALD J. PAPARIELLO

The *Journal of Pharmaceutical Sciences* is published monthly by the American Pharmaceutical Association at 2215 Constitution Ave., N.W., Washington, DC 20037. Second-class postage paid at Washington, D.C., and at additional mailing office.

All expressions of opinion and statements of supposed fact appearing in articles or editorials carried in this journal are published on the authority of the writer over whose name they appear and are not to be regarded as necessarily expressing the policies or views of the American Pharmaceutical Association.

Offices—Editorial, Advertising, and Subscription Offices: 2215 Constitution Ave., N.W., Washington, DC 20037. Printing Offices: 20th & Northampton Streets, Easton, PA 18042.

Annual Subscriptions—United States and foreign, industrial and government institutions $50, educational institutions $50, individuals *for personal use only* $30; single copies $5. All foreign subscriptions add $5 for postage. Subscription rates are subject to change without notice. Members of the American Pharmaceutical Association may elect to receive the *Journal of Pharmaceutical Sciences* as a part of their annual $60 (foreign $65) APhA membership dues.

Claims—Missing numbers will not be supplied if dues or subscriptions are in arrears for more than 60 days or if claims are received more than 60 days after the date of the issue, or if loss was due to failure to give notice of change of address. The Association cannot accept responsibility for foreign delivery when its records indicate shipment has been made.

Change of Address—Members and subscribers should notify at once both the Post Office and the American Pharmaceutical Association, 2215 Constitution Ave., N.W., Washington, DC 20037, of any change of address.

© Copyright 1976, American Pharmaceutical Association, 2215 Constitution Ave., N.W., Washington, DC 20037; all rights reserved.

PASSING THE BATON AT FDA

This editorial is being written prior to the U.S. presidential election, although it will not be published and read until after the results are in. Consequently, at this writing, there are much discussion and conjecture about what changes will soon take place on the Washington scene—and particularly within the top echelons of executive branch agencies—depending upon the outcome of the national elections.

Some cynics have asserted that it really doesn't matter who wins the Presidency and who the President appoints to Cabinet positions because the various bureaucratic machines will relentlessly continue to ramble along irrespective of personnel changes that may occur in the offices of the pertinent Secretary. Indeed, a number of presidential appointees have resigned in anguish during recent administrations, expressing frustration at their inability to have any dramatic impact on the course of operation of the very agencies which they were assigned to run.

Although speculation may be currently rife with respect to many top government posts, even at this writing it is known that one post will become vacant at the end of this year regardless of whom the voters may choose. We refer to the annoucement by FDA Commissioner Alexander M. Schmidt that he is resigning from FDA to return to the academic life at the University of Illinois.

Dr. Schmidt's resignation makes this an appropriate time to review the modern-day history of FDA and to do so particularly from the standpoint of what impact recent Commissioners have had on the agency.

From its establishment on through the World War II period, the FDA was principally oriented toward enforcement *via* on-site inspection procedures; moreover, it appeared to concentrate its efforts primarily in the food area. The entire line of FDA Commissioners had traditionally come up through the ranks, with a heavy orientation in the inspection field. The agency appeared, therefore, to be ill prepared for the dramatic post-World War II pharmaceutical boom which culminated at the legislative level with the enactment of the 1962 Drug Amendments. Despite a dedicated and well-intentioned group of administrators, FDA leadership of the early 1960's was simply unprepared for this rapid turn of events in the drug field. To draw an analogy from the military world, they were old line cavalry generals suddenly facing an enemy equipped with tanks, armored vehicles, and aircraft. FDA went into a state of virtual paralysis, and it was evident that some major change was necessary.

Early in 1966, change did occur—and quickly and dramatically—with President Johnson's appointment of James L. Goddard to the Commissionership. As a starter, for the first time in the agency's history, its leader was drawn from outside the career staff. "Dr. God," as many of his critics referred to him in private, was accused of being unduly impulsive, shooting from the hip, and operating in a disorganized, helter-skelter fashion. There may have been some truth to these criticisms but, nonetheless, there is no disputing the fact that this vigorous Commissioner breathed new life into the agency, gave it a sense of purpose, and effectively divorced it from the regulated industries. For better or for worse, FDA would never again be the same.

Dr. Goddard's successor, Herbert L. Ley, during his relatively brief tenure as Commissioner, primarily attempted to digest and integrate the radical changes initiated by his predecessor—changes that had had a traumatic effect upon the agency staff.

Despite Dr. Ley's efforts, however, the need for a major reorganization of the FDA operating structure was clearly evident. In early 1970, Charles C. Edwards was appointed to succeed Dr. Ley and brought in a background of managerial and administrative skills which he translated into an effective system of operations. For the first time, FDA operation began to show at least some organizational resemblance to the modern and efficient business operations in the industries that it regulated and dealt with on a daily basis.

In 1973, when Dr. Edwards' managerial skills were further tapped by promoting him to the position of HEW Assistant Secretary of Health, he was succeeded by Dr. Schmidt. In turn, it appears that Dr. Schmidt's major contributions during his tenure of office were (*a*) to reestablish meaningful communications with the health professions, the industry, and the public through pragmatic diplomacy, and (*b*) to imbue the agency with an aura of honesty, fair-dealing, and integrity, which he himself personally exemplified.

Hence, each of these modern-era FDA Commissioners has left his own mark on the agnecy and has, in fact, had some sort of meaningful influence on its course and direction. Despite this, however, the FDA remains part of that peculiar institution known as "the Washington bureaucracy." Consequently, just as in the case of Cabinet officials, there has been only so much that these respective FDA Commissioners were able to achieve in a quantitative sense.

Hopefully, Dr. Schmidt's successor will have the capacity, ability, and persistence to move the agency forward in each of those areas in which his recent predecessors have made notable starts. As the slang expression goes in the field of sports and in the entertainment world, FDA now needs someone at the helm "who can get it all together!"

—EGF

Journal of Pharmaceutical Sciences

NOVEMBER 1976

VOLUME 65 NUMBER 11

MARY H. FERGUSON
Editor

L. LUAN CORRIGAN
Assistant Editor

SHELLY ELLIOTT
Production Editor

JANET D. SHOFF
Copy Editor

EDWARD G. FELDMANN
Contributing Editor

SAMUEL W. GOLDSTEIN
Contributing Editor

LELAND J. ARNEY
Publications Director

EDITORIAL ADVISORY BOARD

JOHN AUTIAN	HARRY B. KOSTENBAUDER
LYNN R. BRADY	CARL J. LINTNER, JR.
WILLIAM O. FOYE	DAVID E. MANN, JR.
WILLIAM J. JUSKO	GERALD J. PAPARIELLO

The *Journal of Pharmaceutical Sciences* is published monthly by the American Pharmaceutical Association at 2215 Constitution Ave., N.W., Washington, DC 20037. Second-class postage paid at Washington, D.C., and at additional mailing office.

All expressions of opinion and statements of supposed fact appearing in articles or editorials carried in this journal are published on the authority of the writer over whose name they appear and are not to be regarded as necessarily expressing the policies or views of the American Pharmaceutical Association.

Offices—Editorial, Advertising, and Subscription Offices: 2215 Constitution Ave., N.W., Washington, DC 20037. Printing Offices: 20th & Northampton Streets, Easton, PA 18042.

Annual Subscriptions—United States and foreign, industrial and government institutions $50, educational institutions $50, individuals *for personal use only* $30; single copies $5. All foreign subscriptions add $5 for postage. Subscription rates are subject to change without notice. Members of the American Pharmaceutical Association may elect to receive the *Journal of Pharmaceutical Sciences* as a part of their annual $60 (foreign $65) APhA membership dues.

Claims—Missing numbers will not be supplied if dues or subscriptions are in arrears for more than 60 days or if claims are received more than 60 days after the date of the issue, or if loss was due to failure to give notice of change of address. The Association cannot accept responsibility for foreign delivery when its records indicate shipment has been made.

Change of Address—Members and subscribers should notify at once both the Post Office and the American Pharmaceutical Association, 2215 Constitution Ave., N.W., Washington, DC 20037, of any change of address.

© Copyright 1976, American Pharmaceutical Association, 2215 Constitution Ave., N.W., Washington, DC 20037; all rights reserved.

PASSING THE BATON AT FDA

This editorial is being written prior to the U.S. presidential election, although it will not be published and read until after the results are in. Consequently, at this writing, there are much discussion and conjecture about what changes will soon take place on the Washington scene—and particularly within the top echelons of executive branch agencies—depending upon the outcome of the national elections.

Some cynics have asserted that it really doesn't matter who wins the Presidency and who the President appoints to Cabinet positions because the various bureaucratic machines will relentlessly continue to ramble along irrespective of personnel changes that may occur in the offices of the pertinent Secretary. Indeed, a number of presidential appointees have resigned in anguish during recent administrations, expressing frustration at their inability to have any dramatic impact on the course of operation of the very agencies which they were assigned to run.

Although speculation may be currently rife with respect to many top government posts, even at this writing it is known that one post will become vacant at the end of this year regardless of whom the voters may choose. We refer to the annoucement by FDA Commissioner Alexander M. Schmidt that he is resigning from FDA to return to the academic life at the University of Illinois.

Dr. Schmidt's resignation makes this an appropriate time to review the modern-day history of FDA and to do so particularly from the standpoint of what impact recent Commissioners have had on the agency.

From its establishment on through the World War II period, the FDA was principally oriented toward enforcement *via* on-site inspection procedures; moreover, it appeared to concentrate its efforts primarily in the food area. The entire line of FDA Commissioners had traditionally come up through the ranks, with a heavy orientation in the inspection field. The agency appeared, therefore, to be ill prepared for the dramatic post-World War II pharmaceutical boom which culminated at the legislative level with the enactment of the 1962 Drug Amendments. Despite a dedicated and well-intentioned group of administrators, FDA leadership of the early 1960's was simply unprepared for this rapid turn of events in the drug field. To draw an analogy from the military world, they were old line cavalry generals suddenly facing an enemy equipped with tanks, armored vehicles, and aircraft. FDA went into a state of virtual paralysis, and it was evident that some major change was necessary.

Early in 1966, change did occur—and quickly and dramatically—with President Johnson's appointment of James L. Goddard to the Commissionership. As a starter, for the first time in the agency's history, its leader was drawn from outside the career staff. "Dr. God," as many of his critics referred to him in private, was accused of being unduly impulsive, shooting from the hip, and operating in a disorganized, helter-skelter fashion. There may have been some truth to these criticisms but, nonetheless, there is no disputing the fact that this vigorous Commissioner breathed new life into the agency, gave it a sense of purpose, and effectively divorced it from the regulated industries. For better or for worse, FDA would never again be the same.

Dr. Goddard's successor, Herbert L. Ley, during his relatively brief tenure as Commissioner, primarily attempted to digest and integrate the radical changes initiated by his predecessor—changes that had had a traumatic effect upon the agency staff.

Despite Dr. Ley's efforts, however, the need for a major reorganization of the FDA operating structure was clearly evident. In early 1970, Charles C. Edwards was appointed to succeed Dr. Ley and brought in a background of managerial and administrative skills which he translated into an effective system of operations. For the first time, FDA operation began to show at least some organizational resemblance to the modern and efficient business operations in the industries that it regulated and dealt with on a daily basis.

In 1973, when Dr. Edwards' managerial skills were further tapped by promoting him to the position of HEW Assistant Secretary of Health, he was succeeded by Dr. Schmidt. In turn, it appears that Dr. Schmidt's major contributions during his tenure of office were (*a*) to reestablish meaningful communications with the health professions, the industry, and the public through pragmatic diplomacy, and (*b*) to imbue the agency with an aura of honesty, fair-dealing, and integrity, which he himself personally exemplified.

Hence, each of these modern-era FDA Commissioners has left his own mark on the agnecy and has, in fact, had some sort of meaningful influence on its course and direction. Despite this, however, the FDA remains part of that peculiar institution known as "the Washington bureaucracy." Consequently, just as in the case of Cabinet officials, there has been only so much that these respective FDA Commissioners were able to achieve in a quantitative sense.

Hopefully, Dr. Schmidt's successor will have the capacity, ability, and persistence to move the agency forward in each of those areas in which his recent predecessors have made notable starts. As the slang expression goes in the field of sports and in the entertainment world, FDA now needs someone at the helm "who can get it all together!"

—EGF

1976

December 1–3
Symposium on New Biochemical Aspects of Prostaglandins and Thromboxanes, Los Angeles, Calif. (Contact Marilyn Cheung, Intra-Science Research Foundation, P.O. Box 18589, Los Angeles, CA 90018)

December 2
Pharmaceutical Processing Symposium, American Institute of Chemical Engineers, Palmer House, Chicago, Ill. (Contact N. L. Henderson, Hoechst-Roussel Pharmaceuticals Inc., Route 202–206 North, Somerville, NJ 08876)

December 4–8
American Medical Association, Clinical Meeting, Philadelphia, Pa.

December 5–10
American Society of Hospital Pharmacists, Midyear Meeting, Anaheim, Calif.

December 6–10
International Symposium on Biological Applications of Stable Isotopes, Leipzig, West Germany (Contact John H. Kane, Energy Research and Development Administration, Washington, DC 20545)

December 9–10
Toxic Substances Seminar, Washington, D.C. (Contact Nancy McNerney, Government Institutes, 4733 Bethesda Ave., Washington, DC 20014)

December 13–15
International Congress on Advances in Automated Analysis and Information Systems, New York, N.Y. (Contact Michele Barth, Technicon Corp., Tarrytown, NY 10591)

December 14–15
Food and Drug Law Institute, Annual Meeting, Washington Hilton, Washington, D.C.

1977

January 9–12
Symposium on Quantum Biology and Quantum Pharmacology, Sanibel Island, Fla. (Contact John R. Sabin, Williamson Hall, University of Florida, Gainesville, FL 32611)

February 11–13
Clinical Pharmacy Symposium, Tallahassee, Fla. (Contact Charles A. Walker, Florida Agricultural and Mechanical University, School of Pharmacy, Tallahassee, FL 32307)

February 15–19
The American Academy of Forensic Sciences, San Diego, Calif. (Contact Dr. Naresh C. Jain, Rancho Los Amigos Hospital, 7601 E. Imperial Highway, Downey, CA 90242)

February 20–26
American Association for the Advancement of Science, Annual Meeting, Denver, Colo.

February 28–March 4
Pittsburgh Conference on Analytical Chemistry and Applied Spectroscopy, Cleveland, Ohio (Contact John E. Graham, Koppers Co., 440 College Park Dr., Monroeville, PA 15146)

March 7–11
Symposium on Biologically Active Polypeptides, Le Chateau Montebello, Montebello, Quebec, Canada (Contact Chemical Institute of Canada, 151 Slater St., Suite 906, Ottawa, Ontario K1P 5H3, Canada)

March 20–25
American Chemical Society National Meeting, New Orleans, La. (Contact A. T. Winstead, American Chemical Society, 1155 16th St., N.W., Washington, DC 20036)

March 30–April 2
First International Congress on Toxicology, Toronto, Canada (Contact Dr. R. G. Burford, G. D. Searle Co. of Canada, 400 Iroquois Shore Rd., Oakville, Ontario L6H 1M5, Canada)

April 16–19
Annual Meeting of Society for Biomaterials and International Biomaterials Symposium, Hyatt Regency Hotel, New Orleans, La. (Contact Dr. Allan M. Weinstein, Biomaterials Lab, Tulane University, New Orleans, LA 70118)

April 26–28
Pharmaceutical Manufacturers Association, Annual Convention, Boca Raton Hotel, Boca Raton, Fla.

April 30–May 5
Pahlavi Medical Congress, School of Medicine, Pahlavi University, Shiraz, Iran (Contact Dr. T. Fakouhi, Director, 8th Pahlavi Medical Congress, School of Medicine, Pahlavi University, Shiraz, Iran)

May 14–19
APhA Annual Meeting, New York, N.Y.

May 15–18
Proprietary Association, Annual Meeting, The Greenbrier, White Sulphur Springs, W.Va.

May 31–June 1
International Conference on Pharmaceutical Technology, Paris, France (Contact Professor D. Duchêne, Association De Pharmacie Galenique Industrielle, Rue J. B. Clement, 92290 Chatenay-Malabry, France)

June 13–15
American Chemical Society Annual Summer Symposium, American Chemical Society Division of Analytical Chemistry, University of Massachusetts, Amherst, Mass. (Contact S. Siggia, GRC Tower I, University of Massachusetts, Amherst, MA 01002)

June 18–23
American Medical Association, Annual Meeting, San Francisco, Calif.

June 20–24
International Conference on Fourier Transform Infrared Spectroscopy, University of South Carolina, Columbia, S.C. (Contact Dr. R. O. Kagel, Environmental Services, 628 Bldg., Dow Chemical, Midland, MI 48640)

August 29–September 1
Symposium on Drugs Affecting Lipid Metabolism, Philadelphia, Pa. (Contact William L. Holmes, Scientific Secretary, Symposium on Drugs Affecting Lipid Metabolism, Lankenau Hospital, Philadelphia, PA 19151)

August 30–September 2
IUPAC–IUPHAR Symposium, Noordwijkerhout, The Netherlands (Contact the Secr. Dept., c/o Merck Sharpe & Dohme B.V., Waarderweg 39, P.O. Box 581, Haarlem, The Netherlands)

November 13–17
APhA Academy of Pharmaceutical Sciences, Annual Meeting, The Adams, Phoenix, Ariz.

Journal of Pharmaceutical Sciences

NOVEMBER 1976

VOLUME 65 NUMBER 11

RESEARCH ARTICLES

Comparative Stability of Cephalosporins in Aqueous Solution: Kinetics and Mechanisms of Degradation

TSUKINAKA YAMANA [x] **and AKIRA TSUJI**

Abstract □ The acidic, neutral, and alkaline degradations of six therapeutically useful cephalosporins (cephalothin, cephaloridine, cephaloglycin, cephalexin, cephradine, and cefazolin), 7-aminocephalosporanic acid, 7-aminodeacetoxycephalosporanic acid, and some 7-substituted derivatives were followed by high-pressure liquid chromatographic, UV spectrometric, iodometric, and hydroxamic acid assays. The pH–rate profiles were determined at 35° and $\mu = 0.5$. The acidic degradation pathway for the 3-acetoxymethyl and 3-pyridinylmethyl derivatives was the specific hydrogen-ion-catalyzed hydrolysis of the β-lactam bonds. The β-lactam hydrolyses of these antibiotics exhibited half-lives of about 25 hr at pH 1.0 and 35°. The acetyl functions of 3-acetoxymethylcephalosporins were hydrolyzed eight times faster than their β-lactam moieties to yield the corresponding deacetyl intermediates, which were rapidly converted to the lactones. Deacetoxycephalosporins were fairly acid stable; *e.g.*, cephalexin and cephradine were about 25 times more stable than cephalothin, cephaloridine, and cephaloglycin and about 180 times more stable than ampicillin at pH 1.0. In the neutral degradation of 3-acetoxymethyl compounds, the competitive reactions of the direct water attack and intramolecular catalysis by the side-chain amido upon the β-lactams were proposed. The pH–rate profiles near pH 8 for cephaloglycin, cephalexin, and cephradine could be explained by the intramolecular–nucleophilic attack of the side-chain α-amino group upon the β-lactam carbonyls to produce diketopiperazine-type compounds. The reactivity of the cephalosporins in the hydroxide-ion-catalyzed degradation was influenced significantly by the C-3 methylene substituents.

Keyphrases □ Cephalosporins—stability in aqueous solutions, kinetics and mechanisms of degradation, effect of pH □ Stability—cephalosporins in aqueous solutions, kinetics and mechanisms of degradation, effect of pH □ Degradation—cephalosporins in aqueous solutions, kinetics and mechanisms, effect of pH □ Antibiotics—cephalosporins, stability in aqueous solutions, kinetics and mechanisms of degradation, effect of pH □ Structure–activity relationships—various cephalosporins, stability in aqueous solutions, kinetics and mechanisms of degradation, effect of pH

Penicillins and cephalosporins have been known to undergo remarkably facile cleavage of their β-lactam bonds in aqueous solution. Interest in the kinetics of cephalosporin degradation arose from previous studies (1–5) on penicillins which showed that their instability may affect possible chemical reactions involved in penicillin allergy (6) as well as the formulation of pharmaceutical dosage forms (7).

The kinetic approaches to the degradation of cephalosporins have been utilized in a few instances. These studies include the degradation of cephalosporin C in a wide pH range at 25° (8) and of several cephalosporins at pH 10 and 35° (9). However, many questions regarding the acidic, neutral, and alkaline degradations of cephalosporins have not been completely answered. The present studies on therapeutically useful cephalosporins and other semisynthetic compounds (Table I) were begun with the expectation that a systematic and quantitative approach to the degradation would help answer some questions. Some preliminary aspects were reported earlier (10).

EXPERIMENTAL

Materials—Cephalothin sodium, cephaloridine, cephaloglycin, deacetylcephalothin sodium[1], and cephradine[2] were used as supplied. Cefazolin sodium was purchased commercially[3]. The substituted phenylcephalosporins (I*a*–I*e*), substituted phenyldeacetoxycephalosporins (II*a*–II*d*), and 7-benzenesulfonamidocephalosporanic acid (III) were prepared as sodium salts by the acylation of 7-aminocephalosporanic acid and 7-aminodeacetoxycephalosporanic acid, in the manner described by Flynn (11). The UV and IR spectra of these synthesized cephalosporins confirmed the presence of an intact β-lactam ring. Deacetylcephalothin lactone was obtained by the method of Neidleman *et al.* (12).

All other chemicals used were the highest commercial grade available.

Kinetic Procedures—An accurately weighed cephalosporin was

[1] Shionogi & Co., Osaka, Japan.
[2] Sankyo Co., Ltd., Tokyo, Japan.
[3] Fujisawa Pharmaceutical Co., Osaka, Japan.

Table I—Properties of Investigated Cephalosporins

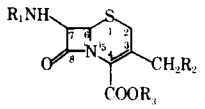

Cephalosporin	Substituents R_1	R_2	R_3	Analytical Method	pKa[a]
Cephalothin	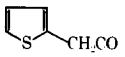	$OCOCH_3$	Na	HPLC, UV, iodometry	pKa_1 = 2.22
Deacetylcephalothin	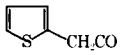	OH	Na	HPLC	—
Cephaloridine	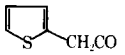		—	HPLC, UV, iodometry	pKa_1 = 1.67
Cephaloglycin	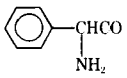	$OCOCH_3$	H	HPLC, UV, iodometry	pKa_1 = 1.91, pKa_2 = 6.90
Cephalexin	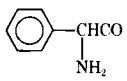	H	H	HPLC, UV, iodometry, hydroxamic acid assay	pKa_1 = 2.56, pKa_2 = 6.88
Cephradine	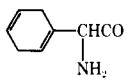	H	H	HPLC, UV, iodometry, hydroxamic acid assay	pKa_1 = 2.53, pKa_2 = 7.30
Cefazolin	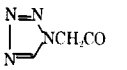	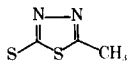	Na	HPLC, UV, iodometry	pKa_1 = 2.54, pKa_3 = 1.70[b]
Substituted phenylcephalosporin (I) [*a*, 4-CH_3; *b*, H; *c*, 4-Cl; *d*, 4-NO_2; *e*, 3,5-$(NO_2)_2$]	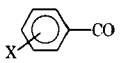	$OCOCH_3$	Na	UV, iodometry	—
Substituted phenyldeacetoxycephalosporin (II) (*a*, 4-CH_3; *b*, H; *c*, 4-Cl; *d*, 4-NO_2)	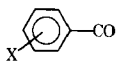	H	Na	UV, iodometry, hydroxamic acid assay	—
7-Benzenesulfonamidocephalosporin (III)	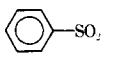	$OCOCH_3$	Na	UV, iodometry	—
7-Aminocephalosporanic acid	H	$OCOCH_3$	H	UV, iodometry	pKa_1 = 2.02, pKa_2 = 4.42
7-Aminodeacetoxycephalosporanic acid	H	H	H	UV, iodometry, hydroxamic acid assay	pKa_1 = 2.95, pKa_2 = 4.87

[a] Values determined potentiometrically at 35° and μ = 0.5. These values were computed from the equations of Glasstone and Hammel (20) for the data corresponding to 25–75% of neutralization and were the averages from at least three experiments, never deviating more than ±0.05 pK unit. pKa_1, pKa_2, and pKa_3 refer to 4-carboxylic acid, 7-ammonium or α-ammonium of the 7-side chain, and other dissociable groups, respectively. [b] Kinetically determined.

dissolved in (in experiments at low pH, aliquots from stock solution were diluted with) acid, alkaline, or an appropriate buffer solution preheated at a desired temperature to produce a final cephalosporin concentration of about 5×10^{-5}–5×10^{-3} *M* according to an employed analytical method or the solubility. The fast reacting solutions in acid and alkaline media were studied in 100-ml volumetric flasks. Where the half-life was more than 1 day, the reaction solution was sealed in 5-ml ampuls. The reactions were conducted in a constant-temperature water bath at 35 ± 0.1°. Samples were withdrawn at suitable time intervals, diluted with distilled water, if necessary, and analyzed.

All reactions were run under pseudo-first-order conditions with catalysts in excess and followed first-order kinetics. The kinetic parameters describing degradation of cephalosporins were determined by a combination of appropriate analytical methods. The pseudo-first-order rate constants were obtained by least-squares analysis.

The reaction solution pH was maintained at the desired value by the use of a pH-stat[4] or appropriate buffer systems. The buffer solutions used were hydrochloric acid–potassium chloride, phosphoric acid–monobasic sodium phosphate, acetic acid–sodium acetate, monobasic–dibasic sodium phosphates, sodium bicarbonate–sodium carbonate, boric acid–sodium borate, and dibasic–tribasic sodium phosphates. The ionic strength of each solution was adjusted to 0.5 by addition of potassium chloride. The pH values of the reaction solutions were measured at the experimental temperature initially and at the end of the experiment on a pH meter[5] standardized with standard buffer solutions of pH 4, 7, and 9 at the same temperature. No significant changes in pH were observed.

Deuterium Oxide Solvent Isotope Effects—Solvent isotope effects on the degradation rates of cephalothin were determined at 35° in 98% deuterium oxide by the use of an autotitrator[4] to maintain a constant pD. The pD values were taken as the pH meter[5] reading plus the proper correction at 35° (13).

Analytical Procedures—*Liquid Chromatography*—High-pressure liquid chromatography (HPLC) was used to follow the kinetics of the degradation of several cephalosporins. The liquid chromatograph[6] was equipped with a UV detector[7] set at 254 nm and a stainless steel column, 2 mm i.d. For cephalothin, cephalexin, and cephradine, a strong anion-exchange resin[8] was used as the stationary phase. The mobile phase was aqueous 0.02 *M* NaH_2PO_4 adjusted to pH 8.5 with sodium hydroxide. For cephaloridine, cephaloglycin, and cefazolin, reversed-phase chromatography[9] was used with a mobile phase of 30% methanol–70% 0.05 *M* ammonium carbonate.

Samples were eluted at 100 kg/cm^2 at room temperature for ion-exchange chromatography and at 150 kg/cm^2 at 50° for reversed-phase chromatography, resulting in flow rates of about 1 and 0.3 ml/min, respectively.

Five microliters of degradation solution (5×10^{-4}–5×10^{-3} *M* total antibiotic) at suitable intervals was injected with the flow stopped. Peak heights were measured, and the concentrations were calculated from the calibration curves (obtained daily). The calibration curves

[4] Radiometer pH stat–titrimeter assembly consisting of TTT2 titrator, SBR2 titrigraph, and SBU12b autoburet or TTT1 titrator, PHM 26 pH meter, SBR2 titrigraph, and SBU12b autoburet.
[5] Radiometer PHM 26 pH meter or TTT2 titrator.
[6] Shimadzu-Dupont model 830.
[7] Shimadzu UV 202 recording spectrophotometer.
[8] SAX on Zipax, 1 m, Dupont.
[9] ODS on Sorbax, 0.25 m, Dupont.

of the peak height against the concentration of the antibiotics were satisfactorily linear.

Spectrophotometric Method—Since all intact cephalosporins gave the UV absorption band near 260 nm due to O=CNC=C linkage, the disappearance of this band absorption is characteristic of β-lactam opening, either chemically or enzymatically (14). The UV spectra[10] of the reaction solutions were monitored periodically.

Iodometric Method—It has been known that iodometric analysis is also applicable for the determination of intact cephalosporins as well as penicillins (15, 16). The procedure employed was essentially the same reported for the determination of penicillin G (17).

From the degradation solution (5×10^{-3} *M* total cephalosporin), two samples of 2 ml were pipetted into separate conical flasks. To the first sample, 5 ml of 1 *N* NaOH was added. After standing for 20 min at room temperature, 5 ml of 0.2 *M* phthalate buffer solution (pH 4.5), 5 ml of 1 *N* HCl, and 10 ml of 0.01 *N* iodine were added. The flask was kept for 20 min in darkness at room temperature. Back-titration with 0.01 *N* thiosulfate gave *a* ml of 0.01 *N* iodine consumed by this sample. The second sample was treated with 5 ml of pH 4.5 phthalate buffer solution and 10 ml of 0.01 *N* iodine for 20 min in darkness at room temperature and then back-titrated with 0.01 *N* thiosulfate. The iodine uptake corresponded to *b* ml. The difference, $(a - b)$ ml, represents the amount of intact cephalosporin present in the degradation solution.

Solutions containing known amounts of cephalosporin and its alkaline degradation products were prepared so that the total concentration became 5×10^{-3} *M*. These solutions were analyzed according to the analytical method. The excellent linear relationship between the extent of iodine consumption, $(a - b)$ ml, and the concentration of intact cephalosporin in solutions containing degradation products was obtained, although the iodine consumption depended upon the time treated with 1 *N* NaOH and the pH of the test solution.

Hydroxamic Acid Method—The method for the assay of remaining β-lactam of deactoxycephalosporins was adapted from a literature procedure (18). To 2 ml of reaction solution (about 5×10^{-3} *M* cephalosporin) in a 20-ml volumetric flask were added 2 ml of an aqueous 3 *M* solution of hydroxylamine hydrochloride and 2 ml of aqueous 3.5 *N* NaOH. After the mixture was allowed to stand for 3 min at room temperature, 2 ml of aqueous 3.5 *N* HCl and then 1 ml of an aqueous 35% ferric ammonium sulfate–0.1 *N* H_2SO_4 solution were pipetted into the flask. The solution was diluted to 20 ml with distilled water, and the resultant color was read at 510 nm[11] after exactly 3 min.

pKa Determination—The apparent pKa values of the tested cephalosporins were determined potentiometrically (19) at an ionic strength of 0.5 at 35°. The initial concentrations of cephalosporins were in the range of approximately 2×10^{-3}–2×10^{-2} *M* according to their solubility. For cephaloglycin, cephalexin, cephradine, 7-aminocephalosporanic acid, and 7-aminodeacetoxycephalosporanic acid, the titration with acid was a process of proton association (proton gain) from zwitterion to cation; the titration with base was a process of proton dissociation (proton loss) from zwitterion to anion (Scheme I).

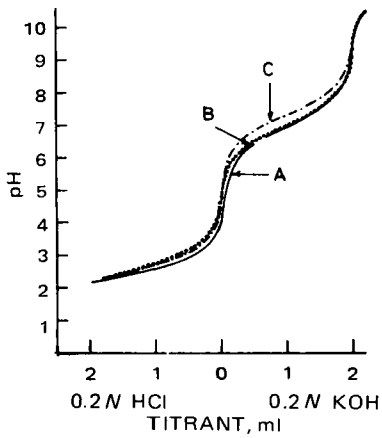

Figure 1—*Titration curves of 1.0 × 10⁻² M amphoteric cephalosporins at 35° and μ = 0.5. Key: A, cephaloglycin; B, cephalexin; and C, cephradine.*

[10] Shimadzu multipurpose recording spectrophotometer model MPS-5000 or Hitachi recording spectrophotometer model 323.

[11] Hitachi spectrophotometer model 101.

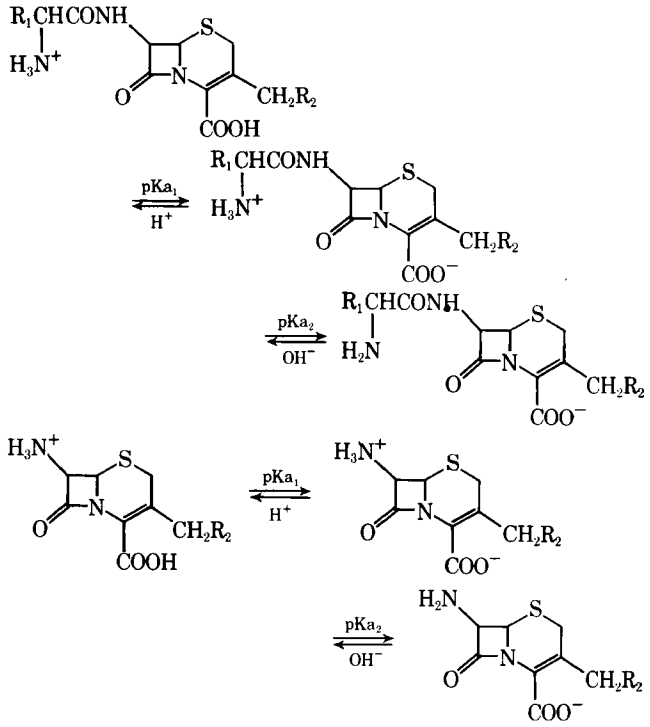

Scheme I

Figure 1 shows the typical titration curves obtained from the titration of these amphoteric cephalosporins, cephaloglycin, cephalexin, and cephradine, with hydrochloric acid and potassium hydroxide solutions. The apparent pKa values, computed by the equations of Glasstone and Hammel (20), are listed in Table I, where pKa_1, pKa_2, and pKa_3 refer to the dissociation of the 4-carboxylic acid, the conjugated acid of the 7-amino or 7-(α-amino) group, and another dissociation group, respectively. Each pKa value is an average of the data obtained in most cases to 25–75% of neutralization.

RESULTS

HPLC Studies and Rate Constants—*Degradation Kinetics of 3-Acetoxymethylcephalosporins*—3- Acetoxymethylcephalosporins such as cephalothin and cephaloglycin have another possible site, in addition to the β-lactam moiety, susceptible to degradation. This site is the ester group of the acetoxy side chain. In fact, acidic and alkaline degradations of cephalosporin C (8, 21), cephalothin (12, 22), and cephaloglycin (23) lead to the formation of the corresponding deacetyl derivatives and their lactones as the hydrolytic intermediates. However, except for cephalosporin C (8), no quantification of these hydrolytic reactions has appeared.

The kinetics for cephalothin degradation were followed at various pH values by HPLC. Typical chromatograms of basic (pH 10.00), neutral (pH 5.00), and acidic (pH 2.00) reaction mixtures, sampled at about 50–60% degradation of cephalothin, are shown in Fig. 2. The peaks designated 1, 2, and 3 are the parent compound, deacetylcephalothin, and its lactone, respectively. The peaks designated U were not identified.

Figure 3 shows the typical time course, expressed as mole percent of the initial concentration (C_0) of the substrate, for the disappearance of cephalothin and simultaneously for the formation and disappearance of deacetylcephalothin in the degradation of cephalothin at pH 10.00 and 35°. At relatively low pH, no accumulation of deacetylcephalothin was observed during the reaction due to the rapid lactonization to deacetylcephalothin lactone (Fig. 2).

Scheme II, expressed as a general formula, is valid in the entire pH range, where k_1, k_3, and k_5 correspond to the rates of β-lactam cleavage in the nucleus. In neutral and basic pH regions, the k_4 reaction process is negligible, and the following equations can be ob-

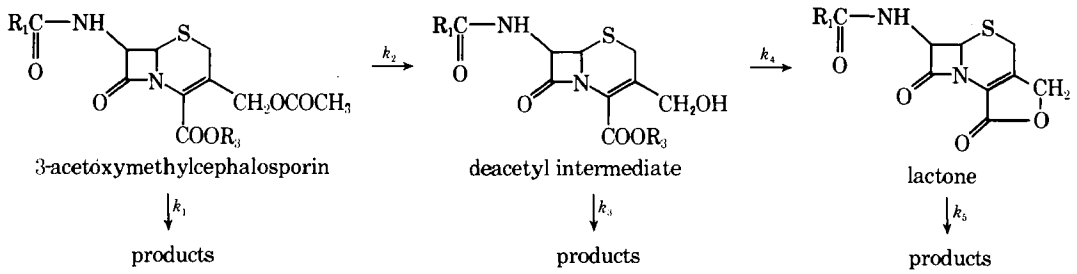

Scheme II

tained for the degradation of cephalothin:

$$[CET]/C_0 = e^{-(k_1+k_2)t} \quad \text{(Eq. 1)}$$

$$[DAT]/C_0 = \frac{k_2}{(k_1 + k_2) - k_3}[e^{-k_3 t} - e^{-(k_1+k_2)t}] \quad \text{(Eq. 2)}$$

where [CET] and [DAT] represent the concentrations at time t of cephalothin and deacetylcephalothin, respectively. The values $k_{app} = k_1 + k_2$ were obtained from the slopes of the apparent first-order plots of the disappearance of cephalothin (Fig. 3). The rate constants k_2 and k_3 were determined from the analog computer fitting of the $[DAT]/C_0$ data.

Analysis of the data at pH 10.00 gave $k_1 = 0.217\ hr^{-1}$, $k_2 = 0.346\ hr^{-1}$, and $k_3 = 0.210\ hr^{-1}$. Treatment of data at any other pH verified the general relationships $k_1/k_2 = 1.1$ and $k_2/k_1 = 1.6$, which are similar to those reported for cephalosporin C ($k_1 = k_3$ and $k_2/k_1 = 4$) (8). The lactonization of deacetylcephalothin became significant below pH 4. For example, at pH 2.00 and 35°, the value of k_4 was $0.708\ hr^{-1}$. Because of this rapid lactonization rate, the extremely low concentration of deacetylcephalothin and the appreciable production of deacetylcephalothin lactone were observed during the degradation of cephalothin (Fig. 2).

The degradation pathway for cephaloglycin was confirmed by HPLC analysis to be as shown in Scheme II.

Degradation Kinetics of Deacetoxycephalosporins—It is expected that the degradation of deacetoxycephalosporins such as cephalexin and cephradine occurs only at the β-lactam moiety.

The chromatographic changes of the degraded solutions of cephalexin and cephradine exhibited the same pattern for all solutions. Figure 4 illustrates the data in 0.3 *M* borate buffer at pH 8.02 and 35°. The semilogarithmic plots of the data obtained at various pH values were reasonably linear (Fig. 5), indicating that the degradation of cephalexin and cephradine follows simple first-order kinetics. The pseudo-first-order rate constants, k_{obs}, were obtained from the slopes.

Determination of Rate Constants by UV Spectroscopy, Iodometry, and Hydroxamic Acid Assay—During the kinetic runs, all cephalosporins studied lost their characteristic UV absorbance at about 260–270 nm. Typical spectral changes as a function of time are illustrated for the degradation of cephalothin (at pH 10.00, maintained by the use of a pH-stat), cephaloglycin (at pH 8.00, maintained by the use of a pH-stat), and cefazolin (in 0.24 *M* acetate buffer of pH 3.53) at 35° and $\mu = 0.5$ in Figs. 6, 7, and 8, respectively.

Plots of $(A_t - A_\infty)$ at λ_{max} *versus* time t were reasonably linear according to the first-order expression:

$$\ln (A_t - A_\infty) = \ln (A_0 - A_\infty) - k_{obs}t \quad \text{(Eq. 3)}$$

where A_t, A_0, and A_∞ are the absorbances at time t, zero, and infinity, respectively. All reactions were followed for at least one or two half-lives, and the values of the pseudo-first-order rate constant, k_{obs}, were obtained by plots of Eq. 3 or by the method of Guggenheim (24). Several typical first-order plots for the degradation of cephalothin, cephaloglycin, and cefazolin according to Eq. 3 are shown in Fig. 9.

For 3-acetoxymethylcephalosporins, the obtained k_{obs} values were approximately equal to the k_1 values (Scheme II) determined by HPLC. Since the absorptivity of the corresponding deacetyl intermediates with an intact nucleus did not differ appreciably from the parent compounds (12, 23, 25, 26), this agreement suggests that the rates for β-lactam cleavage of these deacetyl intermediates are almost the same as those for the parent acetoxy derivatives. This speculation was shown to be reasonable for cephalothin and for cephalosporin C (8).

The pseudo-first-order rate constants, k_{obs}, were also determined by the iodometric titration method and/or hydroxamic acid assay. Typical first-order plots determined iodometrically for the degra-

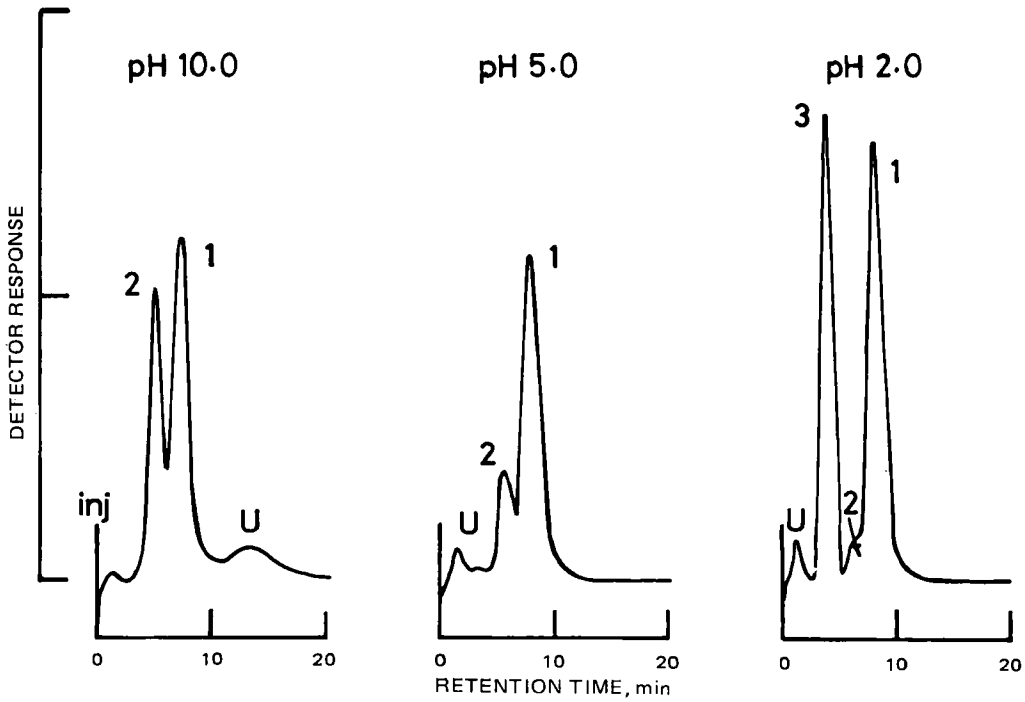

Figure 2—*High-pressure liquid chromatograms of 50–60% degraded cephalothin at 35° and several pH values. Key: 1, cephalothin; 2, deacetylcephalothin; 3, deacetylcephalothin lactone; and U, unknown peak.*

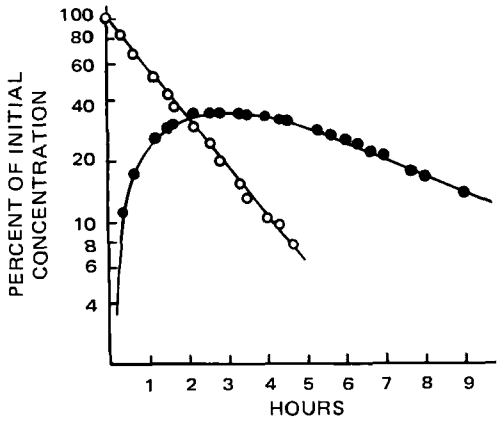

Figure 3—*Time courses for cephalothin (○) and deacetylcephalothin (●) during the degradation of cephalothin at pH 10.00 (pH was maintained by the use of a pH-stat), 35°, and μ = 0.5. The lines were generated using an analog computer programmed according to Scheme II (k_1 = 0.217/hr, k_2 = 0.346/hr, and k_3 = 0.210/hr); the points are experimental values measured by HPLC.*

dation of cephalothin at pH 10.00 and 5.00 and at several temperatures are shown in Fig. 10.

The rate constants determined by the different analytical methods at the same pH and 35° are listed in Table II. The values evaluated from UV spectrophotometric analysis are in relatively good agreement with those determined by Indelicato *et al.* (9) under the same conditions. Although agreement among the rate constants determined by the different analytical methods was not always obtained, the differences did not prevent the determinations of the specific rate constants for the interpretation of their pH–rate dependencies (Figs. 11–15) and for a discussion of the relative stabilities. From the present results and previous discussions (8, 9, 16) of analytical methods for the cephalosporin stability tests, it appears that UV spectrophotometric and chemical methods such as iodometry and colorimetry are acceptable for good estimations of the β-lactam opening rate of the starting cephalosporins. However, HPLC seems to be the most desirable analytical method.

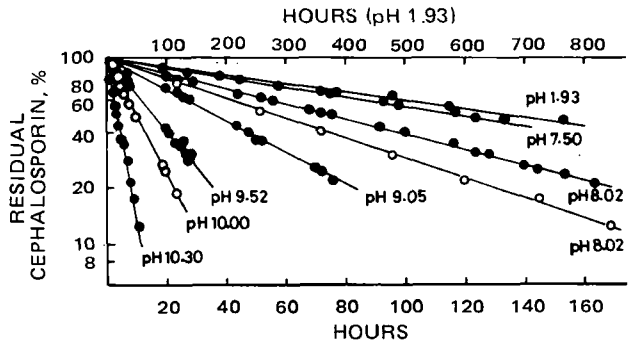

Figure 5—*Apparent first-order plots followed by HPLC for the degradation of cephalexin (○) and cephradine (●) at various pH values, 35°, and μ = 0.5. Key: pH 1.93, 0.06 M phosphate buffer; pH 7.50, pH-stat; pH 8.02, 0.3 M borate buffer; pH 9.05, 0.18 M borate buffer; pH 9.52, 0.08 M carbonate buffer; pH 10.00, pH-stat; and pH 10.30, pH-stat.*

Dependence of Rate on Temperature—Arrhenius plots of the observed first-order rate constants, k_{obs}, for the degradation of cephalothin at two different pH values are given in Fig. 16. The energy of activation, E_a, calculated from the slope of the line was 22.6 kcal/mole at pH 5.00. The calculated apparent energy of activation at pH 10.00 was 28.5 kcal/mole. However, the heat of ionization of water was included in this value. By employing the value of 13.1 kcal/mole as the heat of water (27), the net energy of activation of the degradation of cephalothin in the basic solution, 15.4 kcal/mole, was obtained.

Log k_{pH}–pH Profile—At constant pH and in the presence of excess buffer, the degradation of all types of cephalosporins at low concentration (below 5×10^{-3} *M*) followed pseudo-first-order kinetics and gave rate constants k_{obs} and k_1 for their β-lactam cleavage. General acids and bases served as effective catalysts for the degradation of cephalosporins, although these catalytic effects were not always observed. Typical plots for borate buffer catalytic effects on the rates of cephradine are shown in Fig. 11, giving a reasonable straight line at constant pH. Extrapolation of such plots to zero buffer concentration provides, as intercepts, the values of the pseudo-first-order rate constants, k_{pH}, corresponding to the nonbuffer-cat-

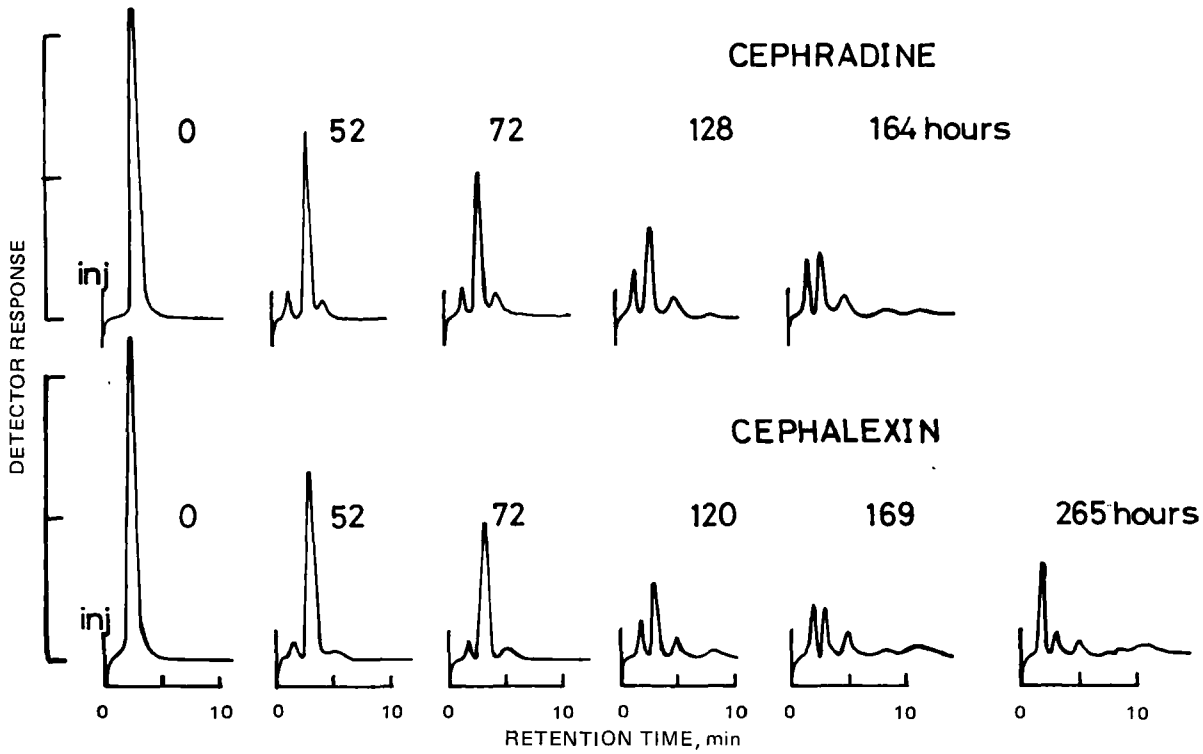

Figure 4—*HPLC changes for the degradations of cephalexin and cephradine in 0.3 M borate buffer (pH 8.02) at 35° and μ = 0.5 with time in hours (listed on graph).*

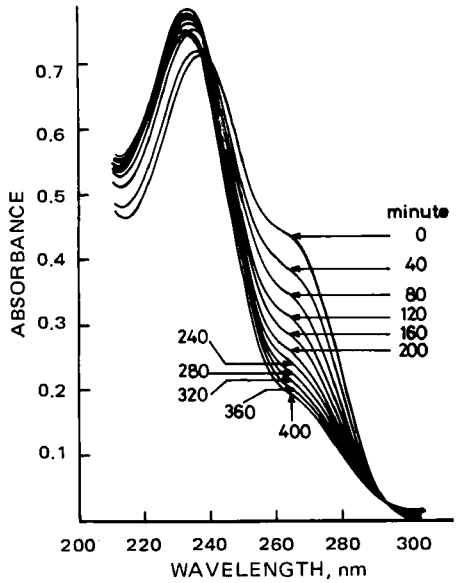

Figure 6—*Spectral changes for the degradation of 5.0 × 10^{-5} M cephalothin at pH 10.00, 35°, and μ = 0.5 with time in minutes (listed on graph). The reaction pH was maintained by the use of a pH-stat.*

alyzed degradation of the cephalosporin nucleus. The k_{pH} values were also determined by the use of a pH-stat.

Figure 12 shows log k_{pH} *versus* pH for the degradation of cephalothin and cephaloridine at 35° and μ = 0.5. Figure 13 shows the log k_{pH}–pH profiles for I, II, and III. There were three important pH regions: one where a hydrogen-ion-catalyzed reaction took place, a pH-independent region, and a region where the reaction was hydroxide ion catalyzed. The degradation rates of these cephalosporins were not influenced by the dissociation of 4-carboxylic acid groups (pKa = ~2–3; Table I), whereas all types of penicillins are apparently influenced by the dissociation of the 3-carboxylic acid group (pKa = ~2.7), as illustrated for penicillin G (28) in Fig. 12. These observations imply that the degradation rates of both undissociated and dissociated cephalosporins are of almost the same magnitude. Therefore, the

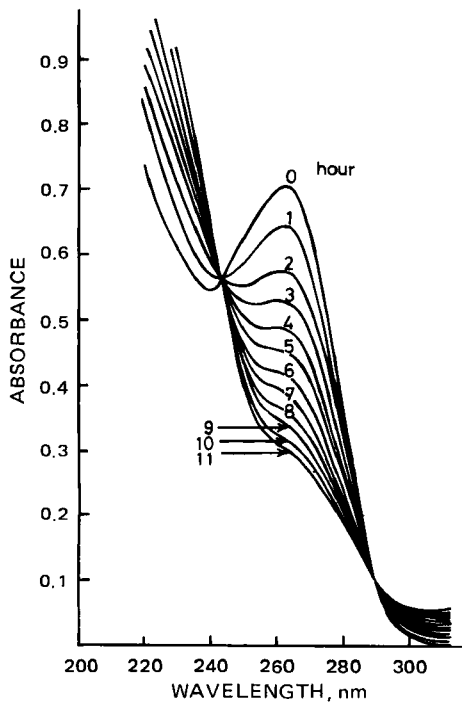

Figure 7—*Spectral changes for the degradation of 1.0 × 10^{-4} M cephaloglycin at pH 8.00, 35°, and μ = 0.5 with time in hours (listed on graph). The reaction pH was maintained by a pH-stat.*

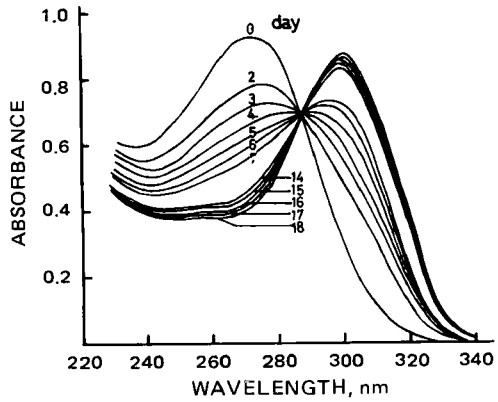

Figure 8—*Spectral changes for the degradation of 5.0 × 10^{-5} M cefazolin in 0.24 M acetate buffer of pH 3.53 at 35° and μ = 0.5 with time in days (listed on graph).*

apparent first-order rate constant at a given pH can be expressed as the following rate law:

$$k_{pH} = k_H a_H + k_0 + k_{OH}(K_w/a_H) \qquad \text{(Eq. 4)}$$

where k_H and k_{OH} are the second-order rate constants for the hydrogen-ion-catalyzed degradation and hydroxide-ion-catalyzed degradation, respectively; k_0 is the first-order rate constant for spontaneous or water-catalyzed degradation; and a_H is the activity of hydrogen ion as measured by the glass electrode. The value for the autoprotolysis constant of water, K_w, at 35° is 2.09 × 10^{-14} (27). These rate constants that produced the best fits of the observed rate–pH profiles are given in Table III. Figure 12 shows the plateau rate of cephalothin at 35° in deuterium oxide; this rate ($k_0^{D_2O}$ = 1.17 × 10^{-2} hr^{-1}) was almost the same as that in water ($k_0^{H_2O}$ = 1.09 × 10^{-2} hr^{-1}). For comparison, the corresponding rate constants recalculated from the literature (references are cited in Ref. 1) and determined (1) in this laboratory for several penicillins are recorded in Table III.

Figure 12 also includes the log k_{pH}–pH profile for the degradation of cefazolin. The profile bent over at pH values lower than 2 and indicated that a dissociation constant, K_{a_3}, affected the degradation rate, most probably in the thiadiazole moiety. The log k_{pH}–pH profile for cefazolin was fitted by:

$$k_{pH} = k_a\left(\frac{a_H}{K_{a_3} + a_H}\right) + k_0 + k_{OH}(K_w/a_H) \qquad \text{(Eq. 5)}$$

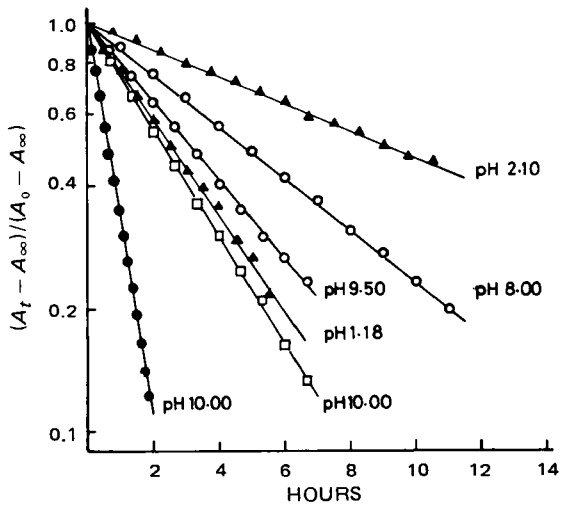

Figure 9—*Apparent first-order plots followed spectrophotometrically for the degradation of cephalothin (□), cephaloridine (●), cephaloglycin (○), and cefazolin (▲) at various pH values, 35°, and μ = 0.5. The reaction pH was maintained by a pH-stat. The absorbance values, A_t, were measured at 265 nm for cephalothin, 260 nm for cephaloridine, 263 nm for cephaloglycin, and 273 nm for cefazolin; A_0 and A_∞ are the absorbances at zero time and at infinite time, respectively.*

Table II—Comparison of the Rate Constants[a] Determined by the Different Analytical Methods at the Same pH Values and 35°

Cephalosporin	pH[b]	10^2k, hr^{-1} HPLC	UV[c]	Iodometry	Hydroxamic Acid[d]	Reported Value[e]
Cephalothin	5.00	1.20[f]	—	1.14	—	—
	9.84	20.2[f]	21.8	—	—	—
	10.00	21.7[f]	30.0	13.9	—	34.9
	10.25	49.1[f]	40.7	21.2	—	—
Cephaloridine	10.00	106	108	103	—	67.7
Cephaloglycin	8.00	15.4	12.0	14.6	—	—
	9.50	—	21.5	18.4	—	—
	10.00	71.8	69.0	—	—	60.1
Cephalexin	8.00	—	0.80	0.92	—	—
	10.00	7.14	14.5	8.39	11.0	3.78[g]
Cephradine	10.00	—	6.70	7.00	7.08	—
	11.00	100	116	76.2	73.7	—
Cefazolin	1.18	16.4	26.8	—	—	—
	6.00	—	0.20	0.24	—	—
	9.70	—	13.7	13.5	—	—
	10.00	24.9	21.7	21.2	—	—

[a] All rate constants were obtained by least-squares analysis. [b] Reaction pH was maintained by the use of a pH-stat. [c] Rate constants were obtained from Eq. 3 or the Guggenheim method (24). [d] Rate constants were obtained from the Guggenheim method (24). [e] Rate constants were determined UV spectrophotometrically by Indelicato *et al.* (9). [f] k_1 values in Scheme II. [g] Rate constants were determined by the pH-stat alkalimetric titration method.

The values of the various rate constants and the kinetically determined pKa_3 value for cefazolin are given in Tables III and I, respectively. As compared with cephalothin and cephaloridine, cefazolin was two to five times more stable in neutral pH solutions and about 10 times more unstable at pH 1.0. The instability of cefazolin itself in acidic media may result in the β-lactam cleavage and/or the thiadiazole elimination, since the acidic degradation rates of this antibiotic followed the apparent rates of the loss of the starting material by UV spectroscopy and HPLC.

The rate–pH profiles for cephaloglycin, cephalexin, and cephradine, which contain α-amino groups in their side chains, have interesting shapes (Fig. 14). A linear increase of the log k_{pH} for cephaloglycin with decreasing pH below 2, to give a negative unity slope, indicated specific hydrogen-ion catalysis, and the k_{pH} became pH independent between pH 2 and 5. On the other hand, rate constants for cephalexin and cephradine were independent of pH below 5, indicating that the hydrogen-ion-catalyzed degradation was negligible compared with spontaneous degradation. The k_{pH} values for these cephalosporins increased with pH values above 5. The fact that there were inflections in the log k_{pH}–pH plots near pH 7 indicates that the dissociation equilibria of the α-amino groups (pKa_2 = 6.90, 6.88, and 7.30 for cephaloglycin, cephalexin, and cephradine, respectively) (Table I) influenced the degradation rates. Above pH 10, the positive unity slopes of their log k_{pH}–pH profiles reflects the specific hydroxide-ion-catalyzed degradation. Accordingly, the apparent first-order rate constants for the degradation of cephaloglycin, cephalexin, and cephradine can be formulated as:

$$k_{pH} = k_H a_H + k_0 + k_b \left(\frac{K_{a_2}}{K_{a_2} + a_H}\right) + k_{OH}(K_w/a_H) \quad \text{(Eq. 6)}$$

where k_b represents the spontaneous degradation of the anionic species of cephaloglycin, cephalexin, and cephradine. The lines of Fig. 14 were generated from Eq. 6 by the use of their rate constants listed in Table III and the dissociation constants, pKa_2, in Table I. Figure 14 also shows the log k_{pH}–pH profile at 35° and μ = 0.5 for ampicillin (29), which contains the α-amino group in the penicillin side chain; there was no facilitation of the degradation rate near the pKa of the α-ammonium group (pKa_2 = 7.05) (29).

The pH–rate profiles obtained for 7-aminocephalosporanic acid and 7-aminodeacetoxycephalosporanic acid are shown in Fig. 15, indicating that specific hydrogen-ion-catalyzed, spontaneous, and specific hydroxide-ion-catalyzed degradations were proceeding, but the spontaneous reaction rates could be influenced by the dissociation of 7-ammonium groups. The rate enhancement of water attack on the β-lactam moiety may be attributed to the inductive effect of the protonated amino group at the α-position, as was observed (1) in the degradation of 6-aminopenicillanic acid (Fig. 15). The rate constants for 7-aminodeacetoxycephalosporanic acid were independent of pH below 3, where the compound was completely protonated, implying that the hydrogen-ion-catalyzed reaction of its protonated form is

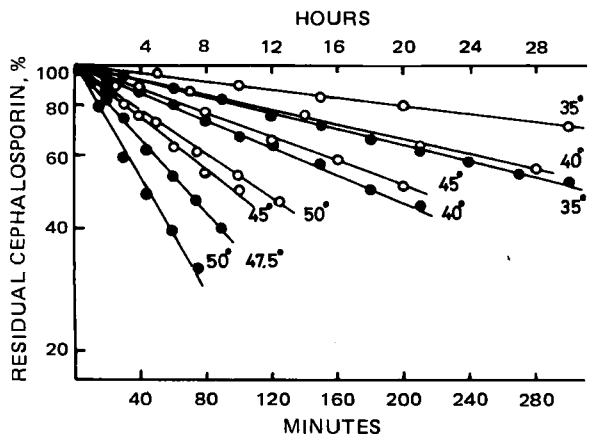

Figure 10—*Apparent first-order plots followed iodometrically for the degradation of cephalothin at various temperatures, pH 5.00 (○, upper scale), pH 10.00 (●, lower scale), and μ = 0.5. The reaction pH was maintained by a pH-stat.*

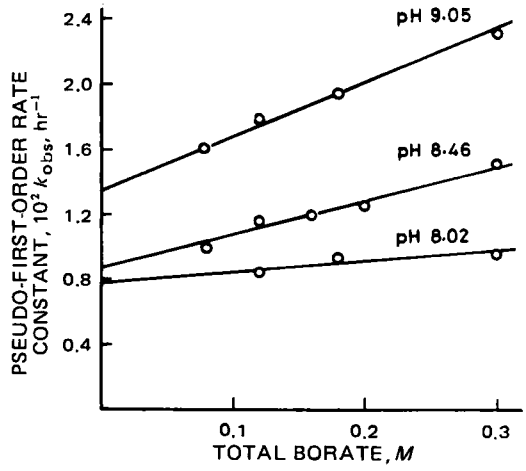

Figure 11—*Plots of the pseudo-first-order rate constants,* k_{obs}, *versus the total buffer concentration for the degradation of cephradine in borate buffer at 35° and μ = 0.5. The rate constants were determined from the HPLC analysis.*

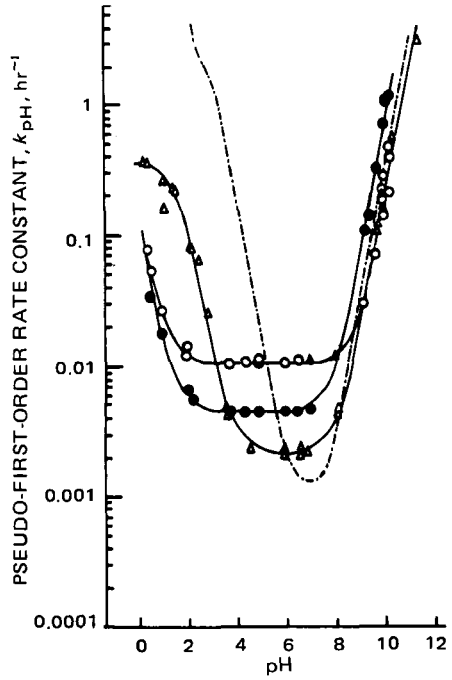

Figure 12—*Log* k_{pH}*–pH profiles for the degradation of cephalothin (○, in* H_2O*; ▲, in* D_2O*), cephaloridine (●), and cefazolin (△) at 35° and* $\mu = 0.5$*. The lines represent the curves calculated from Eq. 4 or 5 and the constants in Tables I and III; the points are the experimental values. The dashed-dotted line refers to the pH–rate profile for penicillin G at 35° and* $\mu = 0.5$ *(28).*

negligible. The reactions are kinetically described by:

$$k_{pH} = k_H a_H + k_c\left(\frac{a_H}{K_{a_2} + a_H}\right) + k_d\left(\frac{K_{a_2}}{K_{a_2} + a_H}\right) + k_{OH}(K_w/a_H) \quad \text{(Eq. 7)}$$

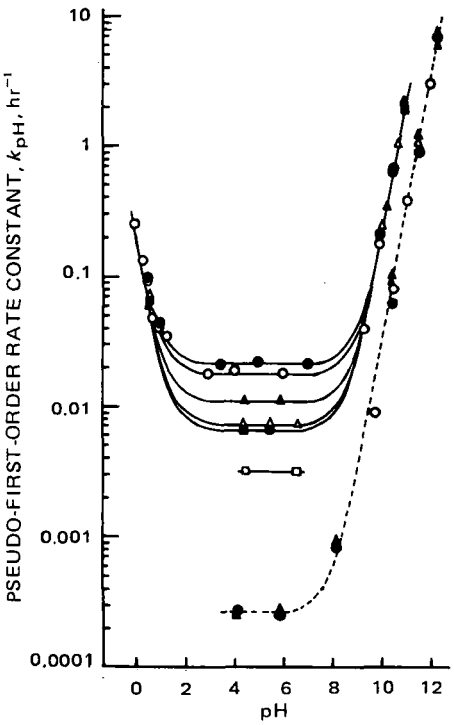

Figure 13—*Log* k_{pH}*–pH profiles for the degradation of I, II, and III at 35° and* $\mu = 0.5$*. The lines represent the curves calculated from Eq. 4 and the constants in Table III; the points are the experimental values. Key: —●—, Ia; —○—, Ib; —▲—, Ic; —△—, Id; —■—, Ie; - - -●- - -, IIa; - - -○- - -, IIb; - - -▲- - -, IIc; - - -△- - -, IId; and —□—, III.*

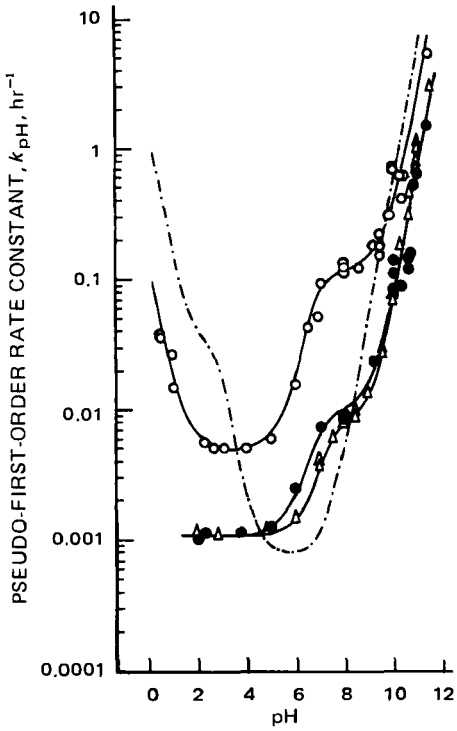

Figure 14—*Log* k_{pH}*–pH profiles for the degradation of cephaloglycin (○), cephalexin (●), and cephradine (△) at 35° and* $\mu = 0.5$*. The lines represent the curves calculated from Eq. 6 and the constants in Tables I and III; the points are the experimental values. The dashed-dotted line refers to the pH–rate profile for ampicillin at 35° and* $\mu = 0.5$ *(29).*

The various rate constants are given in Table III, including those for 6-aminopenicillanic acid (1).

DISCUSSION

Acidic Degradation Mechanism and Relative Stability of Cephalosporins and Penicillins—The acidic degradation rates of penicillins are known to depend on the side-chain structure (7, 30). Penicillin G is extremely acid unstable with a half-life of only 0.7 min at pH 1 and 35° (28); ampicillin is the most acid stable (29), with the difference in acid stability between the two penicillins being about 300-fold. The side-chain reactivity of the penicillin molecule is attributed to the rearrangement initiated by the attack of the side-chain amido carbonyl upon the β-lactam to produce the corresponding penicillenic and penillic acids (6).

In contrast to the penicillin reactivity, 3-acetoxymethylcephalosporins (R_2 = $OCOCH_3$; cephalothin and cephaloglycin) undergo degradation of their β-lactams at almost the same rate regardless of the side-chain structure, R_1. The fact that there was no significant contribution of the side chain to the acidic degradation rates indicates that the reactions exclusively proceed *via* a simple and specific hydrogen-ion-catalyzed hydrolysis of the β-lactam bond rather than the acid-catalyzed intramolecular attack of the side-chain amido on the β-lactam moiety.

β-Lactams of these cephalosporins exhibit half-lives of about 25 hr at pH 1.0 and 35° and are about seven times more stable than ampicillin under the same conditions. However, their acetyl functions are hydrolyzed eight times faster than the β-lactam moiety to yield the corresponding deacetyl compounds, which are easily converted to the lactones (Scheme II). Calculated half-lives for the loss of the original 3-acetoxymethylcephalosporins are about 7 hr at pH 1.0 and 35°.

The acidic degradations of cephalexin, cephradine, II, and 7-aminodeacetoxycephalosporanic acid were pH independent even in strong acid solution. These deacetoxycephalosporins were fairly acid stable; *e.g.*, cephalexin and cephradine were about 25 times more stable than the other cephalosporins and approximately 180 times more stable than ampicillin at pH 1.0.

Competitive Degradations of Direct Water Attack and Intramolecular Catalysis by Side-Chain Amido Group—A com-

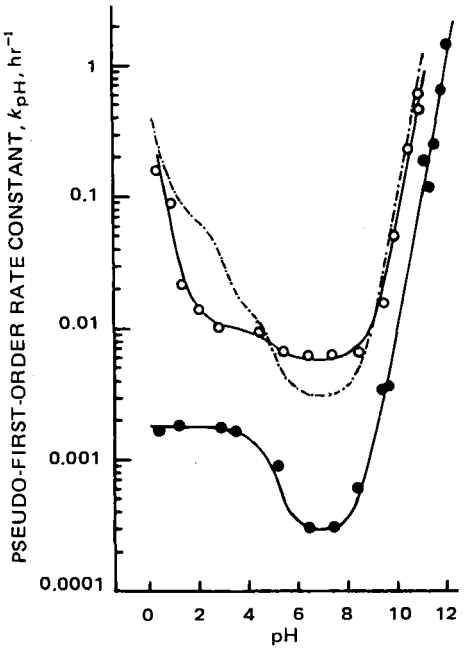

Figure 15—*Log* k_{pH}*–pH profiles for the degradation of 7-aminocephalosporanic acid (○) and 7-aminodeacetoxycephalosporanic acid (●) at 35° and* $\mu = 0.5$*. The lines represent the curves calculated from Eq. 7 and the constants in Tables I and III; the points are the experimental values. The dashed-dotted line refers to the pH–rate profile for 6-aminopenicillanic acid at 35° and* $\mu = 0.5$ *(1).*

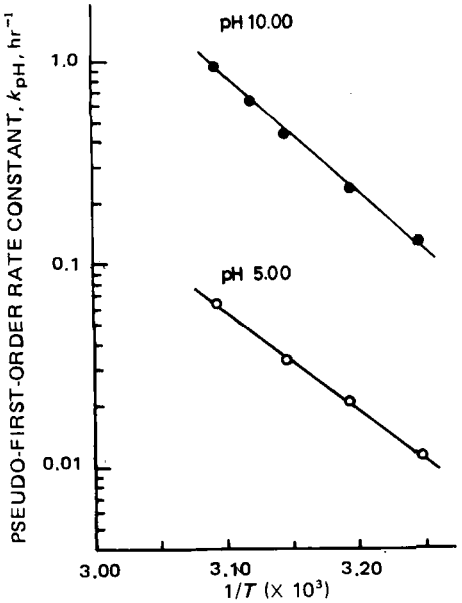

Figure 16—*Arrhenius plots for the apparent first-order rate constants,* k_{pH}*, for cephalothin at pH 5.00 and 10.00 and* $\mu = 0.5$*.*

parison of the degradation rates of several cephalosporins in neutral and basic regions illustrates an apparent dependence on the nature of both substituents, R_1 and R_2.

The most striking feature of the pH–rate profiles shown in Figs. 12 and 13 is the large plateau, extending from approximately pH 3 to 8, with the rates of the degradations being pH independent in this range. The chromatography of the neutral degradation solution of cephalothin, although resulting in a somewhat different elution pattern from that obtained in the alkaline degradation, showed the absence of products with appreciable absorptivity at 254 nm except for small amounts of deacetylcephalothin (Fig. 2). These chromatographic observations, together with agreement of the degradation rates measured by HPLC, UV spectroscopy, and the iodometric method, imply that the principal degradation in the flat region for cephalothin and probably for other 3-acetoxymethylcephalosporins should be the β-lactam cleavage of their nucleus.

The β-lactam opening rate of cephalothin ($k_0 = 1.09 \times 10^{-2}$ hr^{-1}) was about 10 times faster than the spontaneous water-catalyzed degradation rates of penicillins (k_0 = about $1–2 \times 10^{-3}$/hr, regardless of their side-chain structure) (Table III). The enhanced plateau rate is interpretable in terms of the competitive reaction of the hydrolytic cleavage of the β-lactam bond by the direct attack of water (Scheme III) and the degradation caused by intramolecular participation of the neighboring side-chain amido group (Scheme IV) as suggested previously (10).

If the neutral degradation of cephalosporins involves such an intramolecular reaction (Scheme IV), the introduction of an electron-donating substituent into the 7-acylamino moiety should increase the susceptibility of the β-lactam bond to nucleophilic attack of the side-chain amido while an electron-withdrawing substituent should decrease it. The result obtained with a series of substituted phenylcephalosporins (Ia–Ie) showed that the order of decreasing k_0 was the same as the predicted order, the variation of k_0 being about fourfold. The benzenesulfonyl compound (III) prevented the plateau rate as expected and exhibited the minimum k_0 value of 3.3×10^{-3}/hr, which corresponds to a k_{H_2O} value of the direct water reaction (Scheme III) for 3-acetoxymethylcephalosporins.

The ρ value of −0.7 was obtained from the Hammett plot of k_{intra} ($= k_0 - k_{H_2O}$) for I. The negative value is consistent with the intramolecular participation of the side-chain amido group in spontaneous rearrangement of the substituted phenylcephalosporins (k_0 value in Table III). The deuterium solvent isotope effect for cephalothin ($k_0^{H_2O}/k_0^{D_2O} = 0.93$) strongly indicates no significant participation of water in the transition state, which would rule out the large contribution of the direct water reaction to the total plateau rate.

The plateau rate of cephalosporin C ($k_0 = 5.0 \times 10^{-3}$/hr at 25°) (8) was slightly faster than that of cephalothin ($k_0 = 4.0 \times 10^{-3}$/hr at 25°), suggesting that the intramolecular degradation was also proceeding. Cephaloridine, in spite of the same 7-acylamido side chain as cephalothin, showed lower reactivity than cephalothin, probably due to the block of the nucleophilic attack to β-lactam by the 3-bulkyl substituent as suggested by the molecular model.

This report is the first to suggest the occurrence of the side-chain amido group participation in the spontaneous degradation of cephalosporin β-lactam. The spontaneous degradation by the side-chain amido attack on the β-lactam of undissociated penicillins (1, 17) was confirmed to produce the corresponding penicillenic acid (6). While such a penicillenate analog was not confirmed for cephalosporins, considerable kinetic evidence has been presented in support of Scheme IV producing, most probably, the penicillenate analog intermediate or an unstable compound with the oxazolone structure as one spontaneous degradation product.

However, Abraham (31) stated that stable compounds analogous to penicillenate do not appear to be formed in the cephalosporin

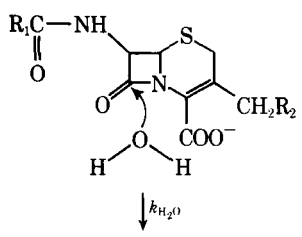

Scheme III

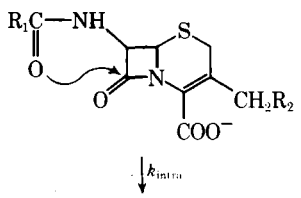

Scheme IV

Table III—Various Rate Constants for the Degradation of Cephalosporins and Penicillins at 35° and μ = 0.5

β-Lactam Antibiotic	k_H, M^{-1} hr^{-1}	10^3k_0, hr^{-1}	$10^{-2}k_{OH}$, M^{-1}hr^{-1}	10^2k_a[a], hr^{-1}	10^2k_b[b], hr^{-1}	10^3k_c[c], hr^{-1}	10^3k_d[c], hr^{-1}
Cephalosporins							
Cephalothin	0.172	10.9	10.6	—	—	—	—
Cephaloridine	0.134	4.40	38.8	—	—	—	—
Cephaloglycin	0.148	5.00	13.1	—	13.5	—	—
Cephalexin	—[d]	1.15	2.64	—	1.01	—	—
Cephradine	—[d]	1.10	3.98	—	0.740	—	—
Cefazolin	—[d]	2.15	11.4	37.0	—	—	—
Ia	0.238	21.0	9.08	—	—	—	—
Ib	0.206	18.7	8.56	—	—	—	—
Ic	0.186	11.4	8.45	—	—	—	—
Id	0.265	7.06	9.55	—	—	—	—
Ie	0.176	6.56	8.85	—	—	—	—
IIa	—[e]	0.270	1.43	—	—	—	—
IIb	—[e]	—[e]	1.33	—	—	—	—
IIc	—[e]	0.270	1.56	—	—	—	—
IId	—[e]	—[e]	1.52	—	—	—	—
III	—[e]	3.30	—[e]	—	—	—	—
7-Aminocephalosporanic acid	0.579	—	2.32	—	—	10.4	6.00
7-Aminodeacetoxycephalosporanic acid	—[d]	—	0.36	—	—	1.84	0.28
Penicillins[f]							
Penicillin G	601	0.90	11.9	341	—	—	—
Carbenicillin	52.2	2.04	12.1	183	—	—	—
Cloxacillin	35.6	0.94	13.4	21.0	—	—	—
Propicillin	30.7	0.89	17.3	13.3	—	—	—
Cyclacillin	4.61	2.49	11.0	4.33	—	—	—
Ampicillin	1.82	0.75	25.7	5.56	—	—	—
Substituted phenylpenicillins							
4-CH_3	—[e]	—[e]	17.0	2188	—	—	—
H	—[e]	—[e]	—[e]	977	—	—	—
4-Cl	—[e]	—[e]	18.3	399	—	—	—
3,4-$(Cl)_2$	301	1.45	16.2	104	—	—	—
4-NO_2	127	1.45	17.9	49.8	—	—	—
3,5-$(NO_2)_2$	15.0	1.55	17.4	5.98	—	—	—
6-Aminopenicillanic acid	0.608	—	3.15	—	—	11.4	3.03

[a] Rate constant is defined in Eq. 5. For penicillins, k_a represents the rate constants for the uncatalyzed intramolecular rearrangement of the undissociated penicillins. [b] Rate constant is defined in Eq. 6. [c] Rate constant is defined in Eq. 7. [d] Not determined because of the large contribution of other kinetic terms. [e] Not determined. [f] Value was recalculated according to this work from the data summarized by Yamana *et al.* (1).

degradations. Instead, Jeffery *et al.* (32) isolated small amounts of thiazole from the neutral degradation solution of cephalosporin C at 37°. They (32) argued that this compound was formed by β-lactam opening and nucleophilic attack of sulfur on carbon of the acyl side chain. Although their arguments (31, 32) are inconsistent with our assumption based on the kinetic evidence, the possibility cannot be excluded that the thiazole may be produced by the nucleophilic attack of sulfur on the oxazolone moiety of the reactive intermediate resulting from Scheme IV. Since rapid fragmentation of β-lactam opening products of cephalosporins can occur in neutral aqueous solutions (31), confirmation of Scheme IV appears to be difficult from product analysis rather than from kinetic analysis.

If such a highly reactive intermediate can be produced from cephalosporins under physiological pH and temperature conditions, it may play a possible role in cephalosporin allergy, analogous to penicillenic acid in penicillin allergy (6). This possibility is now being investigated.

Intramolecular Nucleophilic Attack of Side-Chain α-Amino Group on β-Lactam—The pH–rate profiles for cephaloglycin, cephalexin, and cephradine degradations represent a unique shape in comparison with the profile of ampicillin, which has the same side-chain structure (Fig. 14). The results are consistent with a mechanism involving intramolecularly catalyzed degradation of the anionic species of these cephalosporin molecules at neutral pH, superseded in importance at high pH by hydroxide-ion attack on the anionic cephalosporins and in the lower pH region from 3 to 5 by direct water-catalyzed degradation of the β-lactams. At pH 8, about 10–20 times higher degradation rates of cephaloglycin, cephalexin, and cephradine were observed as compared with those of the corresponding cephalosporins not involving the side-chain α-amino function.

The mechanisms plausible to the neighboring α-amino group participation for the facilitation of β-lactam cleavage of cephaloglycin, cephalexin, and cephradine include intramolecular nucleophilic reaction (Mechanism A), intramolecular general-base catalysis (Mechanism B), and intramolecular general-acid and specific-base catalysis (Mechanism C).

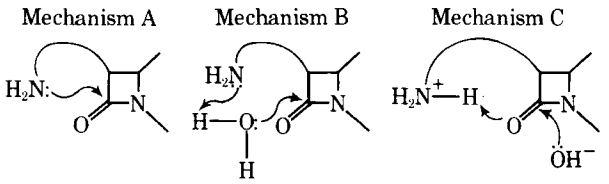

These mechanisms are kinetically indistinguishable. However, if Mechanism A is participating in the degradations, the corresponding stable δ-lactams, diketopiperazines, may be produced. From an aqueous sodium carbonate solution of cephradine, Cohen *et al.* (33) recently isolated the diketopiperazine-type compound, IV, as the major alkaline degradation product. The authors (33) demonstrated the $\Delta^{4,5}$-double bond migration in the degradation of cephradine from NMR observation.

In this laboratory, the degradation of cephalexin was also followed by NMR spectroscopy according to Cohen *et al.* (33) and by HPLC. In deuterium oxide–sodium deuteroxide solution at pD 8.0 and 60°, the 3-methyl group in cephalexin showed a singlet at δ 1.84, which gradually decreased as the degradation proceeded, and a new singlet

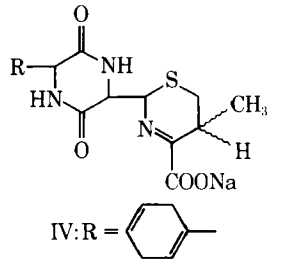

IV: R =

Table IV—Effect of Solvent on the Degradation Rate of Cephaloglycin in 0.05 *M* Borate Buffer (pH 8.00) at 35° and $\mu = 0.5$

Solvent Composition	k_{obs}[a], hr^{-1}
Water	0.166
10% Dioxane–water	0.234
25% Dioxane–water	0.261
50% Dioxane–water	0.262

[a] Rate constants were determined spectrophotometrically.

for the secondary methyl group was observed at δ 1.22. When the degradation was performed in water at pH 8.0, the methyl proton signal appeared as a doublet (J = 8 Hz). The NMR spectral changes for cephalexin indicated the double bond migration probably to the 4,5-position during the degradation and exhibited the same behavior as found for cephradine (33). The HPLC studies also showed the same elution pattern between cephalexin and cephradine (Fig. 4).

With regard to cephaloglycin, no decrease in the degradation rates in aqueous dioxane at pH 8.00 was observed (Table IV), indicating no significant participation of water in this reaction.

Additionally, Indelicato *et al.* (9, 34) isolated similar $\Delta^{3,4}$-diketopiperazines, which were produced without migration of the double bond from the refluxed benzene solution of esters of cephaloglycin and cephalexin. Although these reactions were conducted in a nonaqueous solvent, the results (9, 34) serve to support that intramolecular nucleophilic attack of the α-amino group toward β-lactam is possible conformationally in cephalosporin molecules and may also proceed in aqueous media. The evidence obtained in the present study and previous findings (9, 33, 34) are consistent with Mechanism A rather than the kinetically equivalent alternatives.

In contrast, ampicillin did not exhibit such a rate enhancement of the β-lactam opening by the direct intramolecular attack of the side-chain α-amino group (Fig. 14). In spite of the structural similarity between cephalosporin and penicillin, this difference in reactivity is attributed to the steric hindrance of the *gem*-dimethyl group and the 3-proton to the attack of the α-amino group at the β-face as suggested by Indelicato *et al.* (9, 34).

According to the present study, under biological conditions at pH 7.4 and 37°, the β-lactam of cephalogylcin may be degraded nonenzymatically with a half-life of only about 5 hr. This intramolecular degradation process may proceed competitively with enzymatic deacetylation (35), yielding deacetylcephaloglycin.

Alkaline Degradation Mechanism and Relative Stability of Cephalosporins and Penicillins—The k_{OH} values (Table III) for cephalosporins and penicillins are approximately 10^2–10^3 times greater than those for simple and unfused β-lactams (k_{OH} = about 10^{-1} M^{-1} hr^{-1} at 35°) (36). Some investigators stated that the enhanced sensitivity to alkaline degradation of these antibiotics may be attributed mainly to a suppression of the usual amido resonance resulting from the nonplanarity in the β-lactam nitrogen atom (37, 38) and to the intramolecular participation of the neighboring acylamino groups (39, 40). The latter contribution to penicillin reactivity was ruled out by other researchers (1, 41, 42), because changing the substituent of the acylamino group in penicillin only influenced the reaction rates slightly with amines, oxyanion compounds, and hydroxide ion (1, 4, 5, 41, 42).

A similar possibility for intramolecular participation of acylamino groups can also be excluded in the alkaline degradation of cephalosporins, because no significant variations of k_{OH} for the series of Compounds I and II with various acylamino substituents were observed (Table III and Fig. 13). The relatively low reactivities observed for 6-aminopenicillanic acid, 7-aminocephalosporanic acid, and 7-aminodeacetoxycephalosporanic acid (Table III and Fig. 15) as compared with *N*-acylated compounds of the corresponding nucleus may result from the inductive effect of the 6- or 7-amino (electron-donating) group.

The sensitivity of cephalosporins to degrade varied greatly with different 3-methylene substituents. In the series of 7-acylated cephalosporins, cephaloridine was the most reactive; cephalothin, cephaloglycin, and cefazolin exhibited the intermediate reactivity; and cephalexin and cephradine were the most resistant to the hydroxide-ion-catalyzed degradation. The reactivity variation among these cephalosporins was about 20-fold. The significant influence of the substituents at the 3-methylene position upon the chemical reactivity of the β-lactam may be attributed to the long-range inductive effect on the electrophilicity of the β-lactam carbonyl carbon atom toward hydroxide-ion attack (43) and/or the leavability of the 3-methylene moiety, R_2, which may lower the energy of the transition state (44).

The order (cephaloridine > cephalothin = cefazolin = cephaloglycin > cephradine = cephalexin) of the alkaline degradation rates of therapeutically useful cephalosporins parallels their antibacterial activities against Gram-negative bacteria. The present kinetic data support the suggestions of several investigators (38, 43, 45) that the biological activity of penicillins and cephalosporins is related to the chemical reactivity of the β-lactam carbon–nitrogen bond as well as to the physicochemical properties such as lipophilic character of the antibiotic molecules.

REFERENCES

(1) T. Yamana, A. Tsuji, and Y. Mizukami, *Chem. Pharm. Bull.*, **22**, 1186(1974).

(2) A. Tsuji and T. Yamana, *ibid.*, **22**, 2434(1974).

(3) T. Yamana, T. Tsuji, and Y. Itatani, *J. Antibiot.*, **28**, 242(1975).

(4) T. Yamana, A. Tsuji, E. Miyamoto, and E. Kiya, *J. Pharm. Pharmacol.*, **27**, 283(1975).

(5) A. Tsuji, T. Yamana, E. Miyamoto, and E. Kiya, *ibid.*, **27**, 580(1975).

(6) M. A. Schwartz, *J. Pharm. Sci.*, **58**, 643(1969).

(7) M. A. Schwartz and F. H. Buckwalter, *ibid.*, **51**, 1119(1962).

(8) J. Konecny, E. Felber, and J. Gruner, *J. Antibiot.*, **26**, 135(1973).

(9) J. M. Indelicato, T. T. Norvilas, R. R. Pfeiffer, W. J. Wheeler, and W. L. Wilham, *J. Med. Chem.*, **17**, 523(1974).

(10) T. Yamana, A. Tsuji, K. Kanayama, and O. Nakano, *J. Antibiot.*, **27**, 1000(1974).

(11) E. H. Flynn, in "Cephalosporins and Penicillins, Chemistry and Biology," E. H. Flynn, Ed., Academic, New York, N.Y., 1972, chap. 16.

(12) S. L. Neidleman, S. C. Pan, J. A. Last, and J. E. Dolfini, *J. Med. Chem.*, **13**, 386(1970).

(13) T. H. Fife and T. C. Bruice, *J. Phys. Chem.*, **65**, 1079(1961).

(14) L. D. Sabath, M. Jago, and E. P. Abraham, *Biochem. J.*, **96**, 739(1965).

(15) J. F. Alicino, *Anal. Chem.*, **33**, 648(1961).

(16) L. P. Marrelli, in "Cephalosporins and Penicillins, Chemistry and Biology," E. H. Flynn, Ed., Academic, New York, N.Y., 1972, chap. 14.

(17) P. Finholt, G. Jurgensen, and H. Kristiansen, *J. Pharm. Sci.*, **54**, 387(1965).

(18) J. H. Ford, *Anal. Chem.*, **19**, 1004(1947).

(19) A. Albert and E. P. Serjeant, "The Determination of Ionization Constants," Chapman and Hall, London, England, 1971, chap. 2.

(20) S. Glasstone and E. F. Hammel, Jr., *J. Am. Chem. Soc.*, **63**, 243(1941).

(21) J. D. A. Jeffery, E. P. Abraham, and G. G. F. Newton, *Biochem. J.*, **81**, 591(1961).

(22) R. J. Simmons, in "Analytical Profiles of Drug Substances," vol. 1, K. Florey, Ed., Academic, New York, N.Y., 1972, pp. 319–341.

(23) S. Kukolja, *J. Med. Chem.*, **11**, 1067(1968).

(24) E. A. Guggenheim, *Phil. Mag.*, **2**, 538(1926).

(25) E. V. Heyningen, *J. Med. Chem.*, **8**, 22(1965).

(26) J. W. Chamberlin and J. B. Campbell, *ibid.*, **10**, 966(1967).

(27) H. S. Harned and W. J. Hamer, *J. Am. Chem. Soc.*, **55**, 2194(1933).

(28) R. Broderson, *Acta Pharmacol.*, **3**, 345(1947).

(29) J. P. Hou and J. W. Poole, *J. Pharm. Sci.*, **58**, 447(1969).

(30) *Ibid.*, **60**, 503(1971).

(31) E. P. Abraham, in "Topics in Pharmaceutical Sciences," D. Perlman, Ed., Interscience, New York, N.Y., 1968, pp. 1–31.

(32) J. D. A. Jeffery, E. P. Abraham, and G. G. F. Newton, *Biochem. J.*, **75**, 216(1960).

(33) A. I. Cohen, P. T. Funke, and M. S. Puar, *J. Pharm. Sci.*, **62**, 1558(1973).

(34) J. M. Indelicato, T. T. Norvilas, and W. J. Wheeler, *Chem. Commun.*, **1972**, 1162.

(35) J. S. Welles, in "Cephalosporins and Penicillins, Chemistry

and Biology," E. H. Flynn, Ed., Academic, New York, N.Y., 1972, chap. 13.
(36) R. J. Washkuhn and J. R. Robinson, *J. Pharm. Sci.*, **60**, 1169(1971).
(37) J. R. Johnson, R. B. Woodward, and R. Robinson, in "The Chemistry of Penicillin," H. T. Clarke, J. R. Johnson, and R. Robinson, Eds., Princeton University Press, Princeton, N.J., 1949, p. 440.
(38) R. M. Sweet and L. F. Dahl, *J. Am. Chem. Soc.*, **92**, 5489(1970).
(39) E. P. Doyle and J. H. C. Nayler, in "Advances in Drug Research," vol. 1, N. J. Harper and A. B. Simmonds, Ed., Academic, New York, N.Y., 1964, pp. 1–69.
(40) F. Moll, *Arch. Pharm.*, **301**, 272(1968).
(41) M. A. Schwartz and G.-M. Wu, *J. Pharm. Sci.*, **55**, 550(1966).
(42) H. Bundgaard, *Dansk. Tidsskr. Farm.*, **46**, 85(1972).
(43) R. B. Hermann, *J. Antibiot.*, **26**, 223(1973).
(44) D. B. Boyd, R. B. Hermann, D. E. Presti, and M. M. Marsh, *J. Med. Chem.*, **18**, 408(1975).
(45) R. B. Morin, B. G. Jackson, R. A. Mueller, E. R. Lavagnino, W. B. Scanlor, and S. L. Andrews, *J. Am. Chem. Soc.*, **91**, 1401(1969).

ACKNOWLEDGMENTS AND ADDRESSES

Received May 5, 1975, from the *Faculty of Pharmaceutical Sciences, Kanazawa University, Takara-machi, Kanazawa 920, Japan.*

Accepted for publication January 12, 1976.

Presented in part at the 94th annual meeting of the Pharmaceutical Society of Japan, Sendai, Japan, April 1974.

The authors acknowledge the gifts of cephalosporins from Shionogi & Co., Ltd. and Sankyo, Co., Ltd. They also thank Mr. O. Nakano, Mr. K. Kanayama, Mr. E. Takahashi, Ms. S. Kikuchi, Ms. R. Mishima, Ms. A. Ito, and Ms. T. Takamura for technical assistance. They thank Mr. Y. Itatani for the NMR studies and Professor T. Fujii of this University for discussions.

[x] To whom inquiries should be directed.

Systems Approach to Vaginal Delivery of Drugs II: *In Situ* Vaginal Absorption of Unbranched Aliphatic Alcohols

S. HWANG, E. OWADA, T. YOTSUYANAGI, L. SUHARDJA, N. F. H. HO, G. L. FLYNN, and W. I. HIGUCHI [x]

Abstract □ The absorption of unbranched aliphatic alcohols in the rabbit vagina was studied using a perfusion method, and the absorption rates were found to be first order with respect to the drug concentration in the vagina from methanol to octanol. A physical model involving an aqueous diffusion layer in series with a membrane consisting of aqueous pores and lipoidal pathways was used for analyzing the data. The physically based parameters in the model were determined. An effective diffusion layer thickness ("unstirred layer") of around 0.035 cm was found. The increase in the permeability coefficient for the lipoidal pathway per methylene group was around 2.5 for this homologous series.

Keyphrases □ Drug delivery, vaginal—*in situ* absorption of unbranched aliphatic alcohols, rabbits □ Absorption, vaginal—unbranched aliphatic alcohols, rabbits □ Alcohols, unbranched aliphatic—vaginal absorption, rabbits □ Permeability—unbranched aliphatic alcohols, vaginal absorption, rabbits

The objectives of this investigation were: (*a*) to develop suitable methodology in an appropriate animal system and to obtain firm, baseline data on vaginal absorption; (*b*) to delineate the general barrier properties of the vaginal mucosa; and (*c*) to develop quantitative, integrated models describing both the release of drugs from vaginal devices and subsequent drug absorption.

A method was described previously (1) for evaluating drug absorption in the vagina, using the rabbit doe as a prototype animal. A rib-cage-type cell, which provides a closed absorptive compartment in the vaginal tract, was designed and surgically implanted in the rabbit. Drug absorption was determined by perfusing the drug solution through this system and following the time changes in drug concentration in the system. The study showed that the method generally affords good precision and should provide a sound basis for meeting the objectives of this research.

The present study employed this general perfusion technique and was concerned with the permeability behavior of a homologous series of unbranched aliphatic alcohols in the rabbit vaginal membrane. These compounds were expected to exhibit a systematic increase in the permeability coefficient with increasing carbon number, and a systems analysis of the resulting data was expected to define the operational barrier characteristics of the rabbit vaginal mucosa.

The method of data analysis essentially follows that delineated in previous studies on the human buccal membrane (2, 3), the rat intestinal membrane (4–7), and the silicone rubber membrane (8, 9).

An improved technique employing two simultaneously permeating species with different radiolabels (tritium and carbon-14) is introduced. By using one species as a control, the precision of the method is substantially improved. In addition, a GLC procedure was developed to investigate solutes that are not conveniently available with a radiolabel. Finally, a new cell with a magnetic stirrer was developed to manipulate the hydrodynamics within the absorption cell compartment independently of the hydrodynamics induced by the perfusate flow itself.

and Biology," E. H. Flynn, Ed., Academic, New York, N.Y., 1972, chap. 13.
(36) R. J. Washkuhn and J. R. Robinson, *J. Pharm. Sci.*, **60**, 1169(1971).
(37) J. R. Johnson, R. B. Woodward, and R. Robinson, in "The Chemistry of Penicillin," H. T. Clarke, J. R. Johnson, and R. Robinson, Eds., Princeton University Press, Princeton, N.J., 1949, p. 440.
(38) R. M. Sweet and L. F. Dahl, *J. Am. Chem. Soc.*, **92**, 5489(1970).
(39) E. P. Doyle and J. H. C. Nayler, in "Advances in Drug Research," vol. 1, N. J. Harper and A. B. Simmonds, Ed., Academic, New York, N.Y., 1964, pp. 1–69.
(40) F. Moll, *Arch. Pharm.*, **301**, 272(1968).
(41) M. A. Schwartz and G.-M. Wu, *J. Pharm. Sci.*, **55**, 550(1966).
(42) H. Bundgaard, *Dansk. Tidsskr. Farm.*, **46**, 85(1972).
(43) R. B. Hermann, *J. Antibiot.*, **26**, 223(1973).
(44) D. B. Boyd, R. B. Hermann, D. E. Presti, and M. M. Marsh, *J. Med. Chem.*, **18**, 408(1975).
(45) R. B. Morin, B. G. Jackson, R. A. Mueller, E. R. Lavagnino, W. B. Scanlor, and S. L. Andrews, *J. Am. Chem. Soc.*, **91**, 1401(1969).

ACKNOWLEDGMENTS AND ADDRESSES

Received May 5, 1975, from the *Faculty of Pharmaceutical Sciences, Kanazawa University, Takara-machi, Kanazawa 920, Japan.*

Accepted for publication January 12, 1976.

Presented in part at the 94th annual meeting of the Pharmaceutical Society of Japan, Sendai, Japan, April 1974.

The authors acknowledge the gifts of cephalosporins from Shionogi & Co., Ltd. and Sankyo, Co., Ltd. They also thank Mr. O. Nakano, Mr. K. Kanayama, Mr. E. Takahashi, Ms. S. Kikuchi, Ms. R. Mishima, Ms. A. Ito, and Ms. T. Takamura for technical assistance. They thank Mr. Y. Itatani for the NMR studies and Professor T. Fujii of this University for discussions.

[x] To whom inquiries should be directed.

Systems Approach to Vaginal Delivery of Drugs II: *In Situ* Vaginal Absorption of Unbranched Aliphatic Alcohols

S. HWANG, E. OWADA, T. YOTSUYANAGI, L. SUHARDJA, N. F. H. HO, G. L. FLYNN, and W. I. HIGUCHI [x]

Abstract □ The absorption of unbranched aliphatic alcohols in the rabbit vagina was studied using a perfusion method, and the absorption rates were found to be first order with respect to the drug concentration in the vagina from methanol to octanol. A physical model involving an aqueous diffusion layer in series with a membrane consisting of aqueous pores and lipoidal pathways was used for analyzing the data. The physically based parameters in the model were determined. An effective diffusion layer thickness ("unstirred layer") of around 0.035 cm was found. The increase in the permeability coefficient for the lipoidal pathway per methylene group was around 2.5 for this homologous series.

Keyphrases □ Drug delivery, vaginal—*in situ* absorption of unbranched aliphatic alcohols, rabbits □ Absorption, vaginal—unbranched aliphatic alcohols, rabbits □ Alcohols, unbranched aliphatic—vaginal absorption, rabbits □ Permeability—unbranched aliphatic alcohols, vaginal absorption, rabbits

The objectives of this investigation were: (*a*) to develop suitable methodology in an appropriate animal system and to obtain firm, baseline data on vaginal absorption; (*b*) to delineate the general barrier properties of the vaginal mucosa; and (*c*) to develop quantitative, integrated models describing both the release of drugs from vaginal devices and subsequent drug absorption.

A method was described previously (1) for evaluating drug absorption in the vagina, using the rabbit doe as a prototype animal. A rib-cage-type cell, which provides a closed absorptive compartment in the vaginal tract, was designed and surgically implanted in the rabbit. Drug absorption was determined by perfusing the drug solution through this system and following the time changes in drug concentration in the system. The study showed that the method generally affords good precision and should provide a sound basis for meeting the objectives of this research.

The present study employed this general perfusion technique and was concerned with the permeability behavior of a homologous series of unbranched aliphatic alcohols in the rabbit vaginal membrane. These compounds were expected to exhibit a systematic increase in the permeability coefficient with increasing carbon number, and a systems analysis of the resulting data was expected to define the operational barrier characteristics of the rabbit vaginal mucosa.

The method of data analysis essentially follows that delineated in previous studies on the human buccal membrane (2, 3), the rat intestinal membrane (4–7), and the silicone rubber membrane (8, 9).

An improved technique employing two simultaneously permeating species with different radiolabels (tritium and carbon-14) is introduced. By using one species as a control, the precision of the method is substantially improved. In addition, a GLC procedure was developed to investigate solutes that are not conveniently available with a radiolabel. Finally, a new cell with a magnetic stirrer was developed to manipulate the hydrodynamics within the absorption cell compartment independently of the hydrodynamics induced by the perfusate flow itself.

EXPERIMENTAL

Animals—Mature female rabbits (7–9 months old, New Zealand White) were used. Their body weights normally ranged from 3.5 to 5.0 kg. They were maintained in a temperature-controlled animal room (25°) with free access to water and a regular diet.

Materials—The homologous series of alcohols included methanol (^{3}H-methyl)[1], 1-^{14}C-1-propanol[1], 1-^{14}C-1-butanol[1], 1-pentanol[2], 1-^{14}C-1-hexanol, 1-heptanol[2], and 1-^{14}C-1-octanol[3]. They were used without further purification. Approximately 1.5 μCi of ^{14}C-labeled compound and 5 μCi of ^{3}H-labeled compound were used for each experiment. Pentanol and heptanol were studied at a concentration of 2–3 m*M*.

Perfusion System—The perfusion system basically consisted of an outside solution reservoir and the rib-cage cell surgically implanted in the vaginal tract. The entire perfusion path was made of glass tubing and stainless steel material except the short portion [about 2.54 cm (1 in.) polyethylene tube] between the rib-cage cell and the fenestra rotunda. The vaginal membrane was in direct contact with the drug solution in the rib-cage cell.

Because preliminary studies showed that solute losses to the perfusion system could become serious, especially for the higher alcohols, special measures were taken to eliminate this problem. All surfaces including the reservoir were coated with a silicone solution[4] to prevent solute binding onto the parts of the system. The carbon-lined cylinder on the pump[5] was replaced by a stainless steel cylinder.

As previously described, the rib-cage provided an interior volume of 8.1 cm^3 and a geometrical surface area of 22.5 cm^2. It was inserted through the wall of the upper part of the vaginal tract after an appropriate incision.

Also, to minimize solute losses, all exposed Teflon surfaces in the rib-cage cell were covered with stainless steel sheeting. With all of the described measures, solute losses were reduced to a negligible level for all tested steroids and for all alcohols up to octanol.

Rib-Cage with Magnetic Stirring Bar—To assess the importance of the diffusion layer, a cell with a magnetic stirring bar (about 1 cm long) was designed to manipulate the hydrodynamics within the absorption cell compartment. The stirring bar was coated with gold by vacuum deposition. A hole was drilled perpendicular to the axis of the stirring bar, and the bar was mounted to rotate about the inlet center tube as the axis when a magnetic stirrer (300 rpm) was positioned appropriately (1–2 cm) above the rabbit abdomen.

Because of the unreliable performance of the stirring bar when the experiments were conducted more than 1 day after the rib-cage cell implantation, all stirring experiments were carried out on the same day of the surgery.

Absorption Studies—The absorption experiments were carried out in a manner described previously (1), except for a dual-solute transport modification. Experiments were scheduled on 5 successive days beginning 2 days after the surgical implantation of the rib-cage cell. On each day, two successive experiments were conducted with each rabbit. The rabbit was first anesthetized with pentobarbital sodium, 25 mg/kg, and the perfusion system was connected through the fenestra rotunda. The vaginal tract was then washed with normal saline solution for about 5 min at 35 ml/min and then for an additional 2 min with the buffer solution to be used in the experiment.

The buffer used was pH 6.0, 0.1 *M* phosphate buffer with isotonic sodium chloride. All absorption experiments were conducted with a perfusion flow rate of 35 ml/min at 37°.

To improve the precision of the results, a reference compound, usually methanol (^{3}H-methyl), was employed in all runs with ^{14}C-labeled compounds. An aliquot of the tritiated methanol was introduced simultaneously with the ^{14}C-labeled alcohol into the reservoir at time zero. Samples were removed periodically and analyzed for both activities with a liquid scintillation counter[6] employing a dioxane cocktail[7].

GLC Analysis of Pentanol and Heptanol—GLC measurements were made with a gas chromatograph[8] equipped with a hydrogen flame-ionization detector and an electronic integrator. A coiled stainless steel column (0.9 m × 2 mm i.d.) of 80–100-mesh Porapak Q[9] was used.

During analysis, the column, the injection port, and the detector block were maintained isothermally at 230, 260, and 300°, respectively. Nitrogen was used as the carrier gas at 25 ml/min. Under these conditions, butanol, pentanol, and heptanol had retention times of 0.9, 1.7, and 5.3 min, respectively. Butanol was used as an internal standard for the analysis of pentanol and heptanol.

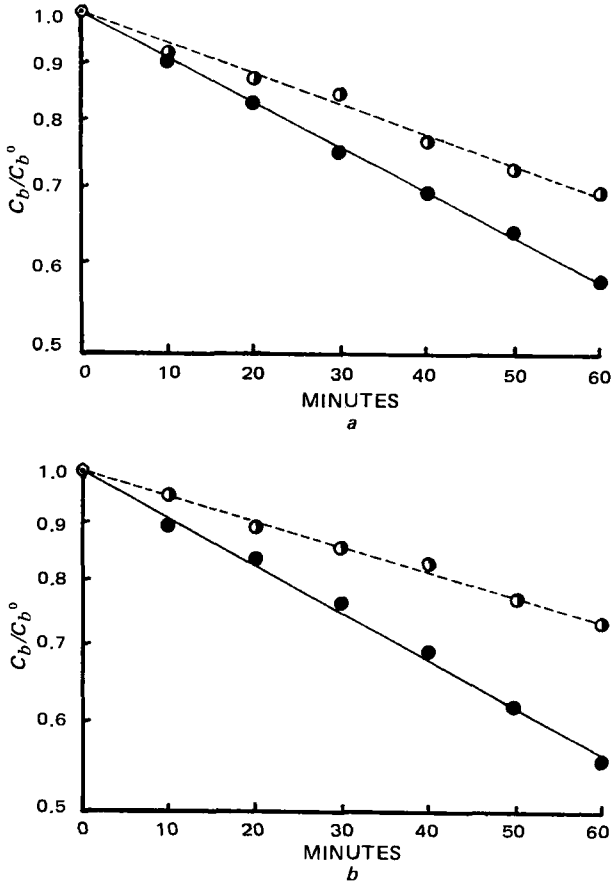

Figure 1—*Typical results for the vaginal absorption of the alcohols using the dual permeant technique. Key (for* a*):* ◑, *methanol; and* ●, *hexanol. Key (for* b*):* ◑, *methanol; and* ●, *octanol.*

RESULTS AND DISCUSSION

Absorption Experiments with Alcohols—The absorption data were treated as previously described (1) using:

$$\frac{dC_b}{dt} = -K_u C_b \qquad \text{(Eq. 1)}$$

$$K_u = P_{app}\left(\frac{A}{V}\right) \qquad \text{(Eq. 2)}$$

where C_b is the concentration of the drug in the bulk solution, K_u is the first-order rate constant, A is the geometrical surface area of the vaginal tract, V is the volume of the perfusion solution, and P_{app} is the apparent permeability coefficient of the membrane.

Without exception, the log (C_b/C_b^0) (where C_b^0 is the zero-time concentration) *versus* time plots of the data were linear with all of the alcohols as was found previously with butanol (Fig. 1). The P_{app} values were computed from the K_u values taken from the slopes of the plots using A = 22.5 cm^2 and V = 34 ml.

Tables I–IV summarize the results of all experiments with the ^{14}C-labeled alcohols. The data also show the value of having the reference solute, methanol, run simultaneously with the alcohol. Although the standard deviation of the absolute P_{app} varied from 14 to 28%, the standard deviation of the ratio, $R = P_{app}/P_{app}$ (methanol), was much less (5–8%).

[1] New England Nuclear Corp., Boston, Mass.
[2] Analytical standard, provided by PolyScience Corp., Niles, Ill.
[3] International Chemical and Nuclear Corp., Irvine, Calif.
[4] Siliclad, Clay Adams, Parsippany, N.J.
[5] FMI lab pump, model RRP 2G 150, Fluid Metering Inc., Oyster Bay, N.Y.
[6] Beckman LS 200.
[7] 2,5-Diphenyloxazole, 6 g; naphthalene, 100 g; and dioxane *qs*, 1000 ml.
[8] Model 5830A, Hewlett-Packard, Avondale, Pa.
[9] Alltech Associates, Inc., Arlington Heights, Ill.

Table I—Apparent Permeability Coefficients for 1-Propanol and Methanol in the Rabbit Vagina at pH 6 (37°)[a]

	$P_{app} \times 10^4$, cm/sec		Propanol/ Methanol
	Methanol	Propanol	
	1.32	1.52	1.15
	1.48	1.42	0.962
	1.74	2.05	1.17
	1.40	1.44	1.03
	1.06	1.18	1.12
	1.03	1.23	1.19
	1.21	1.36	1.13
Mean	1.32	1.46	1.11
SD	0.249	0.287	0.082

[a] Three rabbits were used.

Pentanol and heptanol were studied using GLC after all ^{14}C-labeled alcohol experiments were completed. Methanol was included in the schedule of every rabbit. However, simultaneous methanol–pentanol or methanol–heptanol two-solute runs were not carried out with the GLC procedure. The mean P_{app} values for each rabbit were used for the ratio calculation (Table V). Octanol was also run in these three rabbits so that there would be a common solute between the two groups. The good agreement between the octanol–methanol ratio in Table IV and that in Table V indicates that the results in Table V may be compared to the previous results (Tables I–IV).

Figure 2 is a plot of the mean ratio (R) as a function of the carbon number for the alcohols up to octanol. The data in Fig. 2 possess a strong resemblance to the alcohol absorption data obtained with the rat intestine (jejunum) previously reported (7). Both in the present experiments and in the rat intestine studies, the P_{app} showed little or no chain length effect at the low carbon numbers (≤3). Then, from butanol, the P_{app} began to increase rapidly up to octanol. At octanol, the ratio in the rat intestine studies ranged between 2.0 and 2.8, depending upon the hydrodynamics.

In the present study with the rabbit vagina, P_{app} (octanol)/P_{app} (methanol) approximately equaled 2.0. Beyond octanol, the P_{app} values plateaued in the rat intestine studies. The alcohol data beyond octanol for the present study with the rabbit vagina are not reported because of significant solute loss to the perfusion system. Experiments with decanol in the rabbit vagina indicated, however, that P_{app} may plateau around decanol. Therefore, the parallel behavior appears to be total for these two biological systems.

A physical model was reported (6) for the rat intestine data based upon a composite barrier comprised of an aqueous diffusion layer in series with a membrane having two parallel pathways for solute transport, a lipoidal pathway and an aqueous pore pathway. This model has been remarkably successful in treating the rat jejunum data. It is proposed that this same physical model may apply to alcohol absorption in the rabbit vagina.

Demonstration of Existence of Diffusion Layer by Additional Stirring in Rib-Cage Cell—Uptake experiments of ^{14}C-octanol–^{3}H-methanol with magnetic stirring (with 35-ml/min flow) were carried out on the same day after surgical implantation of the cell. Four runs—with or without stirring—were carried out with each of four rabbits (Table VI). The variation in the results was much greater than when the experiments were conducted 2 or more days after surgery (Tables I–IV). The effect of stirring was to increase the R(octanol) ratio by about 10%. A statistical analysis of the data showed this difference to be significant.

Table II—Apparent Permeability Coefficients for 1-Butanol and Methanol in the Rabbit Vagina at pH 6 (37°)[a]

	$P_{app} \times 10^4$, cm/sec		Butanol/ Methanol
	Methanol	Butanol	
	2.02	2.16	1.07
	2.03	2.13	1.05
	1.52	1.73	1.13
	1.34	1.62	1.21
	1.74	2.08	1.20
	1.44	1.65	1.14
	1.51	1.65	1.09
Mean	1.66	1.86	1.13
SD	0.279	0.250	0.062

[a] Four rabbits were used.

Table III—Apparent Permeability Coefficients for 1-Hexanol and Methanol in the Rabbit Vagina at pH 6 (37°)[a]

	$P_{app} \times 10^4$, cm/sec		Hexanol/ Methanol
	Methanol	Hexanol	
	2.64	3.71	1.41
	1.89	2.88	1.52
	1.83	2.65	1.45
	1.25	1.61	1.29
	1.53	2.55	1.67
	1.53	2.55	1.67
	1.33	2.08	1.56
Mean	1.71	2.53	1.48
SD	0.471	0.666	0.120

[a] Three rabbits were used.

Proposed Physical Model and Analysis of Alcohol Data—Figure 3 illustrates the proposed model in which there is an aqueous diffusion layer[10] on the lumen side in series with the membrane, consisting of parallel lipoidal and aqueous pore pathways for passive diffusion of the solutes. Immediately beyond the membrane, there is a perfect sink (serosal). The appropriate equation expressing P_{app} for this situation is (7):

$$P_{app} = \frac{1}{\frac{1}{P_{aq}} + \frac{1}{P_p + P_l}} \qquad \text{(Eq. 3)}$$

where P_{aq} is the permeability coefficient of the diffusion layer, P_p is the permeability coefficient of the pore pathway, and P_l is the permeability coefficient of the lipoidal pathway.

Following the concept of the incremental partition coefficient (2, 3):

$$P_l = P_l^0 \times 10^{\pi n} \qquad \text{(Eq. 4)}$$

where P_l^0 is the permeability coefficient of the lipoidal pathway for the hypothetical solute of zero carbon number, n is the carbon number, and π is the logarithm of the incremental constant.

Although the permeability coefficient for the aqueous pore, P_p, might be expected to be a function of the molecular size and/or aqueous diffusivity (7) for a given homologous series, it will be as-

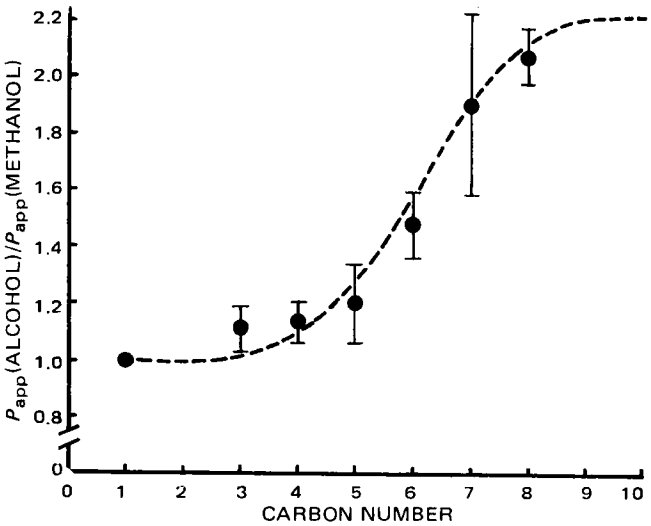

Figure 2—*Effect of carbon number on the normalized permeability coefficient,* $P_{app}(alcohol)/P_{app}(methanol)$, *at pH 6 (37°). Bar indicates mean ± SD.*

[10] The diffusion layer is an effective diffusion layer. In fact, both convective and molecular diffusive components should contribute to the transport (10).

Table IV—Apparent Permeability Coefficients for 1-Octanol and Methanol in the Rabbit Vagina at pH 6 (37°)[a]

	$P_{app} \times 10^4$, cm/sec		
	Methanol	Octanol	Octanol/ Methanol
	1.59	3.33	2.09
	1.64	3.48	2.12
	1.65	3.52	2.13
	1.38	2.92	2.12
	1.36	2.68	1.97
	1.23	2.39	1.94
	1.16	2.56	2.21
Mean	1.43	2.98	2.08
SD	0.199	0.462	0.095

[a] Three rabbits were used.

sumed to be a constant for the alcohols. The consequence of assuming P_p proportional to the aqueous diffusivity will be examined later.

The permeability coefficient of the aqueous diffusion layer, P_{aq}, will be assumed to be described by:

$$P_{aq}(n) = \frac{D_{aq}(n)}{h} \qquad \text{(Eq. 5)}$$

where $D_{aq}(n)$ is the aqueous diffusion coefficient for the alcohol of carbon number n, and h is diffusion layer thickness. The consequence of assuming P_{aq} to be proportional to the two-thirds power[11] instead of the first power of D_{aq} will be examined later. The Stokes–Einstein relationship, $D_{aq} \propto 1/(\text{molar volume})^{1/3}$ will be used to account for the n-dependence of D_{aq}.

With these considerations, Eq. 3 may be written:

$$P_{app} = \frac{1}{\left(\frac{MV}{91.5}\right)^{1/3} \frac{h}{D_{aq}(\text{butanol})} + \frac{1}{P_p + P_l^0 \times 10^{\pi n}}} \qquad \text{(Eq. 6)}$$

where MV is the molar volume of the alcohol in question (molecular weight divided by density), and 91.5 is the molar volume of butanol. The diffusivity for butanol, D_{aq}(butanol), was taken to be 1.42×10^{-5} cm²/sec as reported previously (11).

A best fit theoretical curve of $R[P_{app}/P_{app}(\text{methanol})]$ *versus* n was deduced using Eq. 6 and varying the parameters P_p, P_l^0, π, and h. A P_{app} value for methanol of $1.41 \pm 0.26 \times 10^{-4}$ cm/sec was used, based on experiments involving 13 rabbits. The best fit curve is shown in Fig. 2 and the following "best" parameter values were used: $P_p = 1.9 \times 10^{-4}$ cm/sec, $P_l^0 = 1.5 \times 10^{-6}$ cm/sec, $\pi = 0.40$, and $h = 0.035$ cm.

An analysis of the results given in Fig. 2 showed that the goodness of fit of the theoretical curve with the experimental data was rather

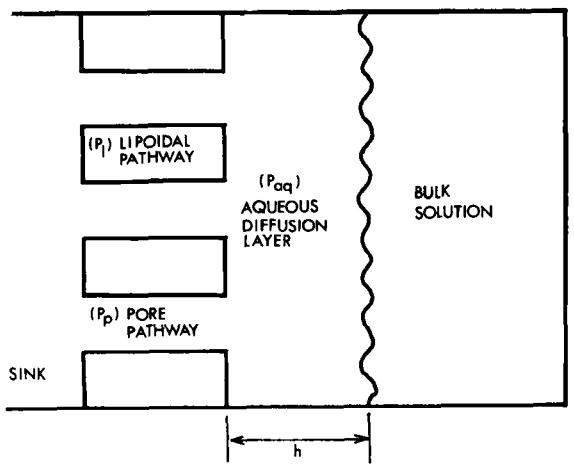

Figure 3—*Schematic model of the vaginal membrane as a transport barrier. Aqueous diffusion layer is in series with the membrane consisting of parallel lipoidal and aqueous pore pathways.*

[11] A D_{aq} two-thirds power dependence may be more appropriate if convection as well as molecular diffusion is taken into account.

Table V—Normalized Permeability Coefficients, P_{app} (Compound)/P_{app} (Methanol), for Pentanol, Heptanol, Octanol, and Hexanoic Acid

Compound	pH	P_{app}(Compound)/ P_{app}(Methanol)[a]
Hexanoic acid	3	2.29 ± 0.71
Octanol	6	2.15 ± 0.61
Heptanol	6	1.91 ± 0.32
Pentanol	6	1.20 ± 0.14

[a] Mean ± *SD* from three rabbits.

Table VI—Effect of Stirring on Octanol Absorption in the Rabbit Vagina

Rabbit	Experimental Order[a]	Ratio of P_{app} (Octanol/Methanol) NS	S
98	S–NS	1.98	2.43
	NS–S	1.90	1.92
99	NS–S	1.83	1.98
	S–NS	1.69	2.00
103	S–NS	2.33	2.74
	NS–S	2.73	2.90
104	NS–S	2.76	2.90
	S–NS	2.50	2.83
	Mean ± *SE*	2.22 ± 0.149	2.46 ± 0.155[b]

[a] NS = nonstirring condition; S = stirring condition. [b] Significantly different from NS, $p < 0.01$ (paired t-test).

sensitive to the P_p, P_l^0, and π values and somewhat insensitive to the choice of h. Interestingly, each of the four parameters dominated in different regions of the curve. Therefore, other combinations of P_p, π, and P_l^0 that are significantly different from this set do not yield good fitting curves.

That the h value of 0.035 cm is reasonably good was confirmed by the hexanoic acid data. Another experiment[12] showed that hexanoic acid absorption at pH 3 was nearly completely aqueous diffusion controlled, *i.e.*, nearly completely determined by the P_{aq} (or D_{aq}/h) term. This finding would correspond to an expected R value of around 2.6. The R value actually found for hexanoic acid in the present experiments (Table V) was 2.29 ± 0.71, in good agreement with $h = 0.035$ cm.

Further Examination of Proposed Model—Two variations in the method of data treatment were considered. First, to assess the possible influence of convective transport, a two-thirds power dependence of D_{aq} for P_{aq} (instead of Eq. 5) was investigated. In this case, the best curve based on Eq. 6 gave a somewhat smaller dip at the lower end of the curve in Fig. 2, but the best fitting value of π deduced for this situation was not significantly different from the one obtained from the original model.

The second modification assumed P_p to be proportional to D_{aq}. This modification made the dip at ethanol deeper and wider. However, the best π value was not significantly altered.

Both this latter analysis and that based upon Eq. 6 (Fig. 2) indicate that the behavior of the alcohols at the lower carbon numbers, *i.e.*, methanol, propanol, and butanol, is not in complete quantitative accord with the simple model (Fig. 3). Such a deviation from the model predications would suggest at least two possibilities. First, the effective aqueous pores may not be truly "aqueous" but somewhat semipolar in character and may have an associated modest π value. Second, an effective third parallel pathway with a modest π value for alcohol transport may exist.

Both of these modifications would tend to influence somewhat the interpretation of the transport data for the lower alcohols but would have relatively little influence upon that for the higher alcohols that are dominated by the principal lipoidal pathway and the aqueous diffusion layer.

In conclusion, the simple two-phase model works well in describing

[12] S. Hwang, E. Owada, L. Suhardja, N. F. H. Ho, G. L. Flynn, and W. I. Higuchi, to be published.

the alcohol absorption in the rabbit vagina. However, the possibility of more sophisticated models is not precluded.

REFERENCES

(1) T. Yotsuyanagi, A. Molokhia, S. Hwang, N. F. H. Ho, G. L. Flynn, and W. I. Higuchi, *J. Pharm. Sci.*, **64**, 71(1975).

(2) N. F. H. Ho and W. I. Higuchi, *ibid.*, **60**, 537(1971).

(3) K. Vora, W. I. Higuchi, and N. F. H. Ho, *ibid.*, **61**, 1785(1972).

(4) A. Suzuki, N. F. H. Ho, and W. I. Higuchi, *ibid.*, **59**, 644(1970).

(5) *Ibid.*, **59**, 651(1970).

(6) N. F. H. Ho, J. S. Turi, and W. I. Higuchi, *J. Pharm. Sci.*, **61**, 192(1972).

(7) K. Desai, Ph.D. thesis, University of Michigan, Ann Arbor, Mich., 1975.

(8) G. L. Flynn, O. S. Carpenter, and S. H. Yalkowsky, *J. Pharm. Sci.*, **61**, 312(1972).

(9) G. L. Flynn and S. H. Yalkowsky, *ibid.*, **61**, 838(1972).

(10) P. Singh, S. J. Desai, D. R. Flanagan, A. P. Simonelli, and W. I. Higuchi, *ibid.*, **57**, 959(1968).

(11) C. M. Gary-Bobo and H. W. Weber, *J. Phys. Chem.*, **73**, 1155(1969).

ACKNOWLEDGMENTS AND ADDRESSES

Received May 21, 1975, from the *College of Pharmacy, University of Michigan, Ann Arbor, MI 48104*

Accepted for publication December 22, 1975.

Supported by Contract NO1-HD-3-2740, National Institute of Child Health and Human Development, Bethesda, Md.

[x] To whom inquiries should be directed.

Systems Approach to Vaginal Delivery of Drugs III: Simulation Studies Interfacing Steroid Release from Silicone Matrix and Vaginal Absorption in Rabbits

N. F. H. HO [x], L. SUHARDJA, S. HWANG, E. OWADA, A. MOLOKHIA, G. L. FLYNN, W. I. HIGUCHI, and J. Y. PARK

Abstract □ A composite physical model involving the simultaneous receding boundary release of drug from a drug suspension–silicone polymer matrix system, diffusion across the aqueous layer, and passive transport across the vaginal membrane consisting of parallel lipoidal and aqueous pore pathways is described. Simulation studies with progesterone and hydrocortisone illustrate matrix release-limiting, membrane absorption, and aqueous diffusion layer-limiting cases when the cylindrical silicone delivery device is interfaced with the vaginal membrane of the rabbit.

Keyphrases □ Drug delivery, vaginal—progesterone and hydrocortisone release from silicone matrix, vaginal absorption, rabbits □ Absorption, vaginal—progesterone and hydrocortisone from silicone matrix, rabbits □ Silicone matrix system—release of progesterone and hydrocortisone, vaginal absorption, rabbits □ Progesterone—release from silicone matrix, vaginal absorption, rabbits □ Hydrocortisone—release from silicone matrix, vaginal absorption, rabbits □ Steroids—progesterone and hydrocortisone, release from silicone matrix, vaginal absorption, rabbits

As part of continuing research on the systems approach to an understanding of the vaginal delivery of drugs from a quantitative mechanistic standpoint, results of studies on membrane permeability of the rabbit vagina (1, 2) and *in vitro* release from the silicone polymer[1] matrix (3–5) and the composite physical model and equations are interfaced and integrated in this report. A rigorous description is presented for the drug release–drug absorption process. Several combination mechanisms are predicted from the analyses of these model simulation studies with progesterone and hydrocortisone. The simulations serve as the basis for the experimental design and subsequent interpretation of ongoing *in situ* studies in which the steroid–silicone polymer matrix is interfaced with the rabbit vagina.

[1] Silastic, Dow Corning, Midland, Mich.

THEORY

Physical Model—The model for the simultaneous release of a nonelectrolyte drug from a water-insoluble polymer matrix and transport across an aqueous diffusion layer and vaginal membrane is shown in Fig. 1. Following Roseman and Higuchi (3), it is assumed that: (*a*) the finely divided drug particles are uniformly dispersed in the matrix shaped as a cylinder, (*b*) the drug has a finite solubility in the matrix, (*c*) it diffuses through the matrix rather than the pores, and (*d*) there is no penetration of water into the matrix and no release of drug from the ends of the cylindrical matrix.

An aqueous diffusion layer surrounding the matrix is in series with the vaginal membrane, consisting of parallel lipoidal and aqueous pore pathways. Sink conditions on the serosal side prevail. Quasi-steady-state kinetics are assumed everywhere.

Total Flux Expressions—The fluxes of the drug in the matrix, aqueous diffusion layer, and vaginal membrane are:

$$J_{ma} = -\frac{2\pi h D_e (C_s - C_s')}{\ln a/a_0} \qquad \text{(Eq. 1)}$$

$$J_{aq} = 2\pi h a_0 \frac{D_{aq}}{h_{aq}} (C_a - C_b) \qquad \text{(Eq. 2)}$$

$$J_{me} = 2\pi h a_m \left[\frac{\alpha D_0 C_0}{h_m} + \frac{(1-\alpha) D_p C_p}{h_m} \right] \qquad \text{(Eq. 3)}$$

where h is the length of the cylinder; D_e is the effective diffusion coefficient in the matrix; a, a_0, and a_m are the radial dimensions of the receding boundary in the matrix, cylinder, and vaginal membrane

the alcohol absorption in the rabbit vagina. However, the possibility of more sophisticated models is not precluded.

REFERENCES

(1) T. Yotsuyanagi, A. Molokhia, S. Hwang, N. F. H. Ho, G. L. Flynn, and W. I. Higuchi, *J. Pharm. Sci.*, **64**, 71(1975).

(2) N. F. H. Ho and W. I. Higuchi, *ibid.*, **60**, 537(1971).

(3) K. Vora, W. I. Higuchi, and N. F. H. Ho, *ibid.*, **61**, 1785(1972).

(4) A. Suzuki, N. F. H. Ho, and W. I. Higuchi, *ibid.*, **59**, 644(1970).

(5) *Ibid.*, **59**, 651(1970).

(6) N. F. H. Ho, J. S. Turi, and W. I. Higuchi, *J. Pharm. Sci.*, **61**, 192(1972).

(7) K. Desai, Ph.D. thesis, University of Michigan, Ann Arbor, Mich., 1975.

(8) G. L. Flynn, O. S. Carpenter, and S. H. Yalkowsky, *J. Pharm. Sci.*, **61**, 312(1972).

(9) G. L. Flynn and S. H. Yalkowsky, *ibid.*, **61**, 838(1972).

(10) P. Singh, S. J. Desai, D. R. Flanagan, A. P. Simonelli, and W. I. Higuchi, *ibid.*, **57**, 959(1968).

(11) C. M. Gary-Bobo and H. W. Weber, *J. Phys. Chem.*, **73**, 1155(1969).

ACKNOWLEDGMENTS AND ADDRESSES

Received May 21, 1975, from the *College of Pharmacy, University of Michigan, Ann Arbor, MI 48104*

Accepted for publication December 22, 1975.

Supported by Contract NO1-HD-3-2740, National Institute of Child Health and Human Development, Bethesda, Md.

[x] To whom inquiries should be directed.

Systems Approach to Vaginal Delivery of Drugs III: Simulation Studies Interfacing Steroid Release from Silicone Matrix and Vaginal Absorption in Rabbits

N. F. H. HO [x], L. SUHARDJA, S. HWANG, E. OWADA, A. MOLOKHIA, G. L. FLYNN, W. I. HIGUCHI, and J. Y. PARK

Abstract □ A composite physical model involving the simultaneous receding boundary release of drug from a drug suspension–silicone polymer matrix system, diffusion across the aqueous layer, and passive transport across the vaginal membrane consisting of parallel lipoidal and aqueous pore pathways is described. Simulation studies with progesterone and hydrocortisone illustrate matrix release-limiting, membrane absorption, and aqueous diffusion layer-limiting cases when the cylindrical silicone delivery device is interfaced with the vaginal membrane of the rabbit.

Keyphrases □ Drug delivery, vaginal—progesterone and hydrocortisone release from silicone matrix, vaginal absorption, rabbits □ Absorption, vaginal—progesterone and hydrocortisone from silicone matrix, rabbits □ Silicone matrix system—release of progesterone and hydrocortisone, vaginal absorption, rabbits □ Progesterone—release from silicone matrix, vaginal absorption, rabbits □ Hydrocortisone—release from silicone matrix, vaginal absorption, rabbits □ Steroids—progesterone and hydrocortisone, release from silicone matrix, vaginal absorption, rabbits

As part of continuing research on the systems approach to an understanding of the vaginal delivery of drugs from a quantitative mechanistic standpoint, results of studies on membrane permeability of the rabbit vagina (1, 2) and *in vitro* release from the silicone polymer[1] matrix (3–5) and the composite physical model and equations are interfaced and integrated in this report. A rigorous description is presented for the drug release–drug absorption process. Several combination mechanisms are predicted from the analyses of these model simulation studies with progesterone and hydrocortisone. The simulations serve as the basis for the experimental design and subsequent interpretation of ongoing *in situ* studies in which the steroid–silicone polymer matrix is interfaced with the rabbit vagina.

[1] Silastic, Dow Corning, Midland, Mich.

THEORY

Physical Model—The model for the simultaneous release of a nonelectrolyte drug from a water-insoluble polymer matrix and transport across an aqueous diffusion layer and vaginal membrane is shown in Fig. 1. Following Roseman and Higuchi (3), it is assumed that: (*a*) the finely divided drug particles are uniformly dispersed in the matrix shaped as a cylinder, (*b*) the drug has a finite solubility in the matrix, (*c*) it diffuses through the matrix rather than the pores, and (*d*) there is no penetration of water into the matrix and no release of drug from the ends of the cylindrical matrix.

An aqueous diffusion layer surrounding the matrix is in series with the vaginal membrane, consisting of parallel lipoidal and aqueous pore pathways. Sink conditions on the serosal side prevail. Quasi-steady-state kinetics are assumed everywhere.

Total Flux Expressions—The fluxes of the drug in the matrix, aqueous diffusion layer, and vaginal membrane are:

$$J_{ma} = -\frac{2\pi h D_e (C_s - C_s')}{\ln a/a_0} \qquad \text{(Eq. 1)}$$

$$J_{aq} = 2\pi h a_0 \frac{D_{aq}}{h_{aq}} (C_a - C_b) \qquad \text{(Eq. 2)}$$

$$J_{me} = 2\pi h a_m \left[\frac{\alpha D_0 C_0}{h_m} + \frac{(1-\alpha) D_p C_p}{h_m} \right] \qquad \text{(Eq. 3)}$$

where h is the length of the cylinder; D_e is the effective diffusion coefficient in the matrix; a, a_0, and a_m are the radial dimensions of the receding boundary in the matrix, cylinder, and vaginal membrane

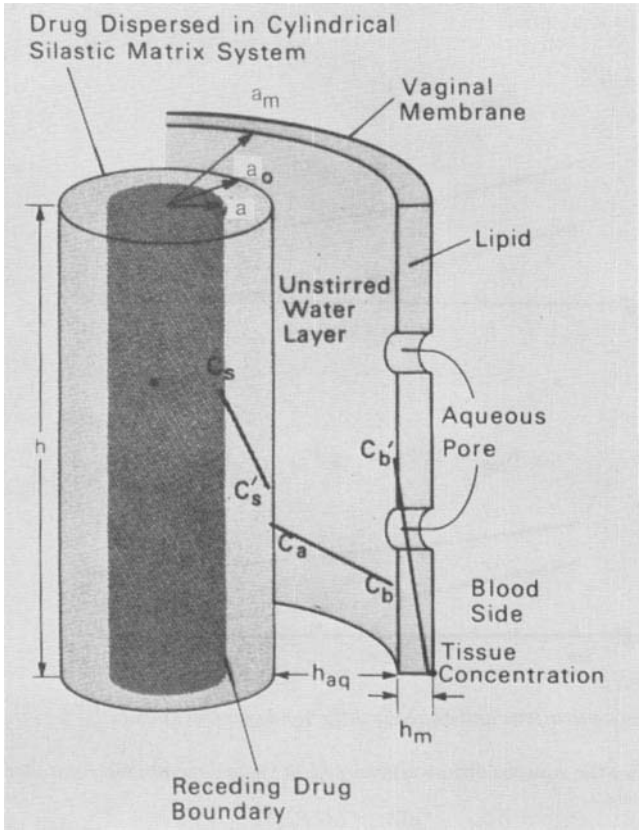

Figure 1—*Physical model of the simultaneous release of a contraceptive drug, which is uniformly dispersed in a water-insoluble silicone polymer matrix in cylindrical form, and the transport of the drug across the unstirred water layer and then the parallel lipoidal and aqueous pore pathways of the vaginal membrane. The shaded interior indicates the cylindrical region of drug in the polymer matrix, which diminishes uniformly as drug is released. (See text for details.)*

surface, respectively; h_{aq} and h_m are the thicknesses of the aqueous diffusion layer and the vaginal membrane, respectively; D_{aq}, D_0, and D_p are the diffusion coefficients in the aqueous layer, lipoidal membrane, and aqueous pores, respectively; α is the volume fraction of lipid biophase in the membrane; C_s and C_s' are the solubility of the drug in the matrix and the concentration at the surface on the matrix side, respectively; C_a and C_b are the concentrations in the aqueous layer at the matrix surface and membrane surface, respectively; and C_0 and C_p are the concentrations in the membrane at the interface of the lipid, pores, and aqueous layer.

The radial receding boundary, a, is a function of the amount of drug released and time. The effective diffusion coefficient in the matrix is also described by:

$$D_e = \frac{\epsilon D}{\tau} \qquad \text{(Eq. 4)}$$

where D is the intrinsic diffusion coefficient, ϵ is the porosity, and τ is the tortuosity.

The partition coefficients of the drug for the polymer matrix–water, K_s, and lipoidal biophase–water, K, are defined as follows:

$$K_s = \frac{C_s'}{C_a} \qquad \text{(Eq. 5)}$$

$$K = \frac{C_0}{C_b} = \frac{C_0}{C_p} \qquad \text{(Eq. 6)}$$

The continuity of flow across the various barriers is given by:

$$J_{ma} = J_{aq} = J_{me} \qquad \text{(Eq. 7)}$$

With Eqs. 1–3 and 5–7:

$$J_{ma} = \frac{2\pi h D_e C_s}{\frac{D_e K_s}{a_0}\left(\frac{1}{P_{aq}} + \frac{1}{P_m}\right) - \ln a/a_0} \qquad \text{(Eq. 8)}$$

The permeability coefficient of the aqueous diffusion layer is:

$$P_{aq} = \frac{D_{aq}}{h_{aq}} \qquad \text{(Eq. 9)}$$

A linear approximation of the aqueous diffusion layer thickness, h_{aq}, has been shown to be sufficient when the radial distance from the center of the cylinder to the vaginal membrane, a_m, is not too different from the radius of the cylinder, a_0; *i.e.*, $a_m/a_0 \leq 1.10$ (6). The permeability coefficient[2] of the membrane is the sum of the permeability coefficients of the lipoidal and aqueous pore pathways, *i.e.*:

$$P_m = \frac{\alpha D_0 K}{h_m} + \frac{(1-\alpha)D_p}{h_m} \qquad \text{(Eq. 10}a\text{)}$$

$$P_m = P_0 + P_p \qquad \text{(Eq. 10}b\text{)}$$

Change in Receding Boundary in Matrix and Amount of Drug Released with Time—The flux in the matrix is related to the rate of drug release from the matrix and to the rate of change in the receding boundary in the matrix. Accordingly:

$$J_{ma} = \frac{dQ}{dt} = -2\pi h A a \frac{da}{dt} \qquad A \gg C_s \qquad \text{(Eq. 11)}$$

where Q is the amount of drug released, h is the length of the cylinder, a is the radial coordinate of the receding boundary, and t is time. An important assumption made here is that A, the initial amount of drug per volume of cylinder, is much greater than C_s, the solubility of the drug in the matrix.

By combining Eqs. 8 and 11 and integrating between $a(0) = a_0$ and $a(t)$, the change in the receding boundary with time is:

$$\left[\frac{D_e K_s}{2a_0}\left(\frac{1}{P_{aq}} + \frac{1}{P_m}\right) + \frac{1}{4}\right](a_0^2 - a^2) + \frac{a^2}{2}\ln a/a_0 = \frac{D_e C_s}{A}t \qquad \text{(Eq. 12)}$$

Because of Eq. 11, the amount and fraction of drug released are:

$$Q = \pi h A(a_0^2 - a^2) \qquad \text{(Eq. 13}a\text{)}$$

$$\frac{Q}{\pi a_0^2 h A} = \left[1 - \left(\frac{a}{a_0}\right)^2\right] \qquad \text{(Eq. 13}b\text{)}$$

It follows that:

$$\frac{1}{2\pi h A}\left[\frac{D_e K_s}{a_0}\left(\frac{1}{P_{aq}} + \frac{1}{P_m}\right) + \frac{1}{2}\right]Q + \frac{1}{2}\left(a_0^2 - \frac{Q}{\pi h A}\right)\ln\sqrt{1 - \frac{Q}{\pi h a_0^2 A}} = \frac{D_e C_s}{A}t \qquad \text{(Eq. 14)}$$

or:

$$\left[\frac{D_e K_s}{a_0}\left(\frac{1}{P_{aq}} + \frac{1}{P_m}\right) + \frac{1}{2}\right]Q + (\pi h a_0^2 A - Q)\ln\left(1 - \frac{Q}{\pi h a_0^2 A}\right)^{1/2} = (2\pi h D_e C_s)t \qquad \text{(Eq. 15)}$$

Simplified Expressions of Receding Boundary and Amount Released with Time—It is useful to obtain more simplified forms of Eqs. 12 and 15 for the changes of the receding boundary in the matrix and the amount released with time, particularly at relatively early time periods.

Recognizing that $a/a_0 \leq 1.0$, one gets $\ln a/a_0 \approx (a/a_0) - 1$. Thus, Eq. 12 becomes:

$$\left[\frac{D_e K_s}{2a_0}\left(\frac{1}{P_{aq}} + \frac{1}{P_m}\right) + \frac{1}{4}\right](a_0^2 - a^2) - \frac{a^2}{2a_0}(a_0 - a) = \frac{D_e C_s}{A}t \qquad \text{(Eq. 16)}$$

It is recognized that when $(Q/\pi h a_0^2 A) \ll 1.0$, it follows that $1/2 \ln [1 - (Q/\pi h a_0^2 A)] \approx -(Q/2\pi h a_0^2 A)$.

With some rearrangement in the algebra, Eq. 15 reduces to a quadratic expression:

$$\frac{Q^2}{2\pi h a_0^2 A} + \frac{D_e K_s}{a_0}\left(\frac{1}{P_{aq}} + \frac{1}{P_m}\right)Q = (2\pi h D_e C_s)t \qquad \text{(Eq. 17)}$$

[2] The permeability coefficient of the pore can also be defined in a more descriptive manner, *i.e.*, $P_p = [(1-\alpha)D_{aq}F]/h_m$, where D_{aq} is the bulk aqueous diffusion coefficient, and F is the filtration factor (7).

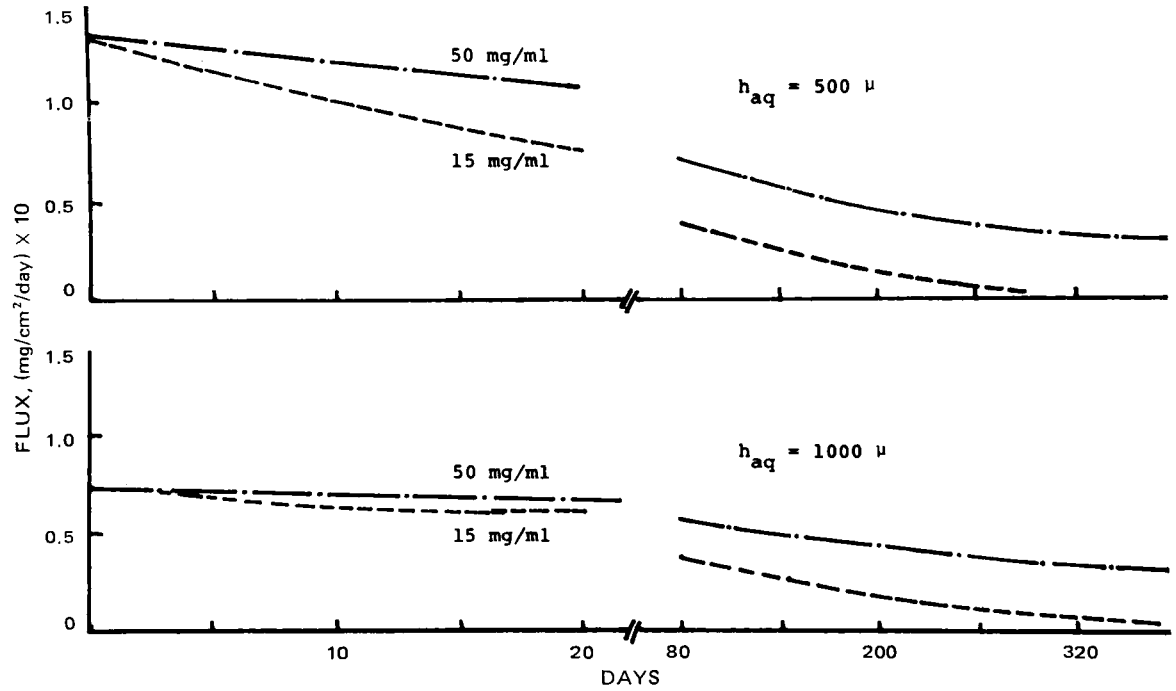

Figure 2—*Predicted flux of progesterone with time at various loading concentrations and aqueous diffusion layer thicknesses.*

After differentiating with respect to time, the rate of the amount of drug released from the matrix per unit area is:

$$\frac{1}{2\pi h a_0}\frac{dQ}{dt} = \frac{dQ'}{dt} = \frac{D_e C_s A}{\sqrt{\left[D_e K_s\left(\frac{1}{P_{aq}} + \frac{1}{P_m}\right)\right]^2 + 4D_e C_s A t}} \quad \text{(Eq. 18)}$$

For the aqueous diffusion layer and/or vaginal membrane-controlled case:

$$\frac{dQ'}{dt} = \frac{C_s P_{aq} P_m}{K_s(P_{aq} + P_m)} \quad \text{(Eq. 19)}$$

and for the matrix-controlled case:

$$\frac{dQ'}{dt} = \frac{1}{2}\sqrt{\frac{D_e C_s A}{t}} \quad \text{(Eq. 20)}$$

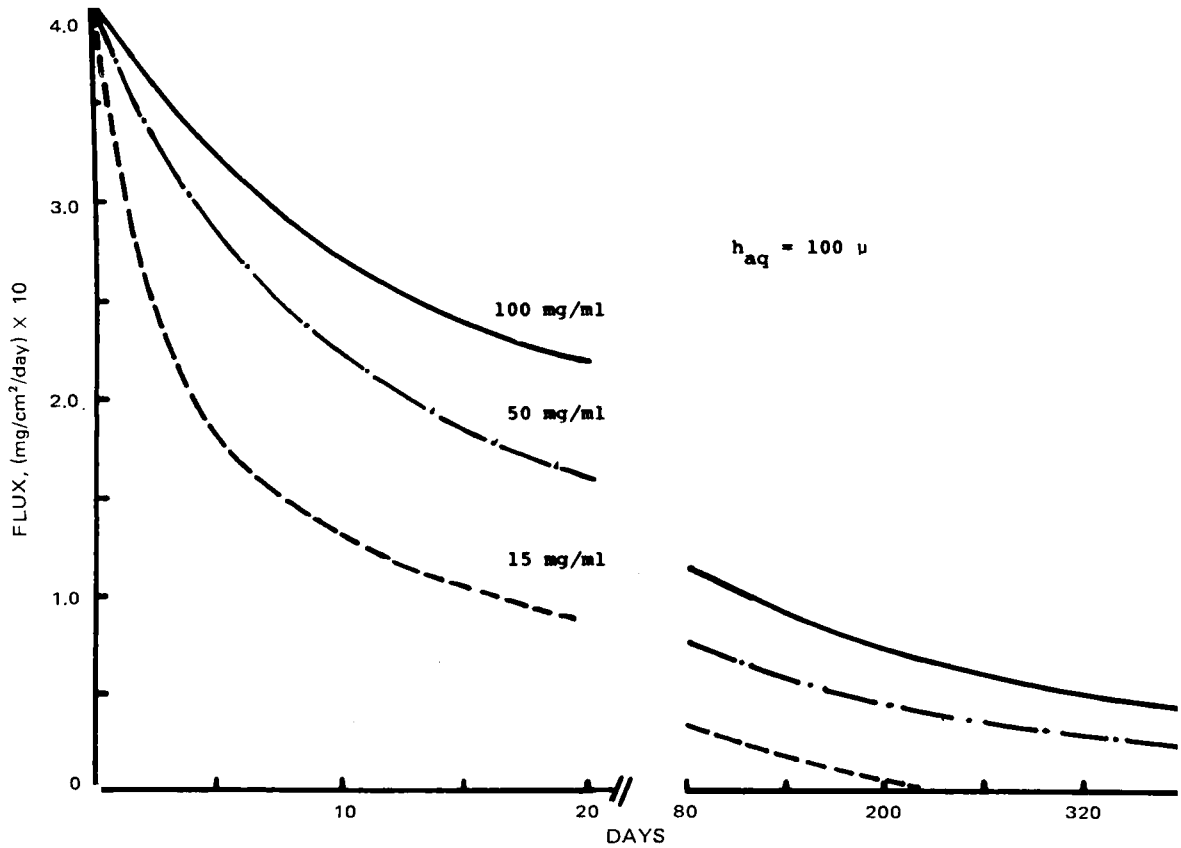

Figure 3—*Predicted flux of progesterone with time at various loading concentrations and 100-μm diffusion layer thickness.*

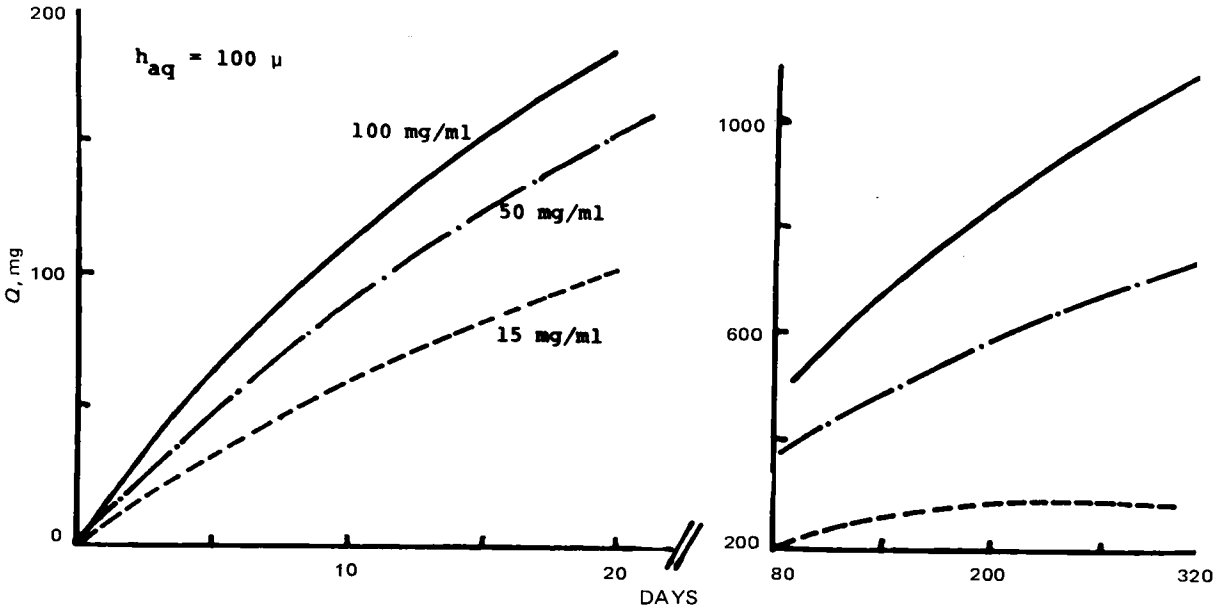

Figure 4—*Predicted total amount of progesterone released with time at various concentrations and 100-μm aqueous diffusion layer thickness.*

Taking Eqs. 18–20 together, one readily observes that the rate (or flux) changes from the non-matrix-controlled case to the matrix-controlled case with time as the resistance in the receding boundary increases.

SIMULATION STUDIES

By using the preliminary results of the *in situ* vaginal absorption of the various steroids in the rabbit, the *in vitro* physicochemical characterization of the steroids with the silicone membrane, the *in vitro* release kinetic studies of steroids from the silicone matrix (3), and the theoretical physical model, the findings of these studies will now be integrated. Simulations of the simultaneous release of progesterone from a cylindrical poly(dimethyl siloxane) matrix and vaginal absorption will serve as the prototype in assessing the concurrent physicochemical roles of the membrane, aqueous diffusion, and receding boundary layers. Another steroid in these simulation studies is hydrocortisone. Table I gives the values of the physical parameters of progesterone and hydrocortisone and the silicone cylinder. The size of the cylinder is the same as the rib-cage cell used previously (1).

The predictions obtained here are being used in ongoing studies where the steroid release from a silicone matrix is interfaced with vaginal membrane absorption in the rabbit.

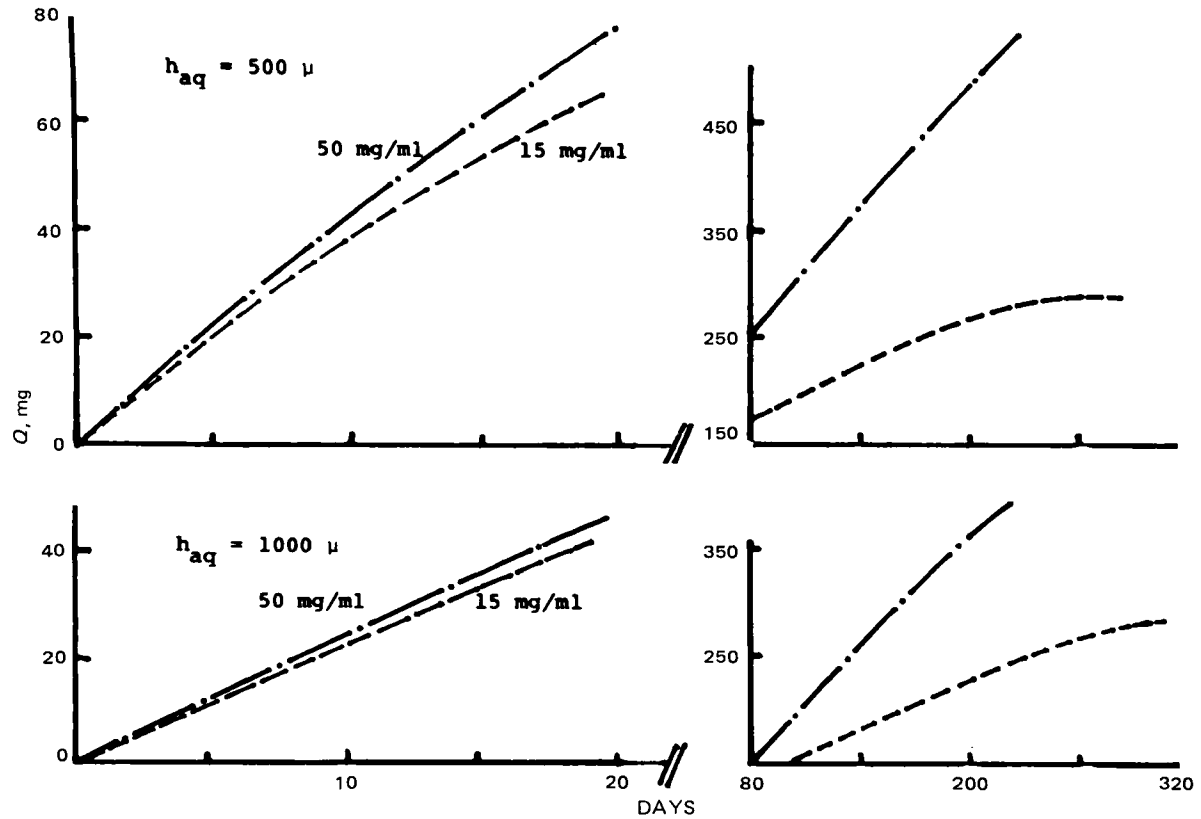

Figure 5—*Predicted total amount of progesterone released with time at various concentrations and aqueous diffusion layer thicknesses.*

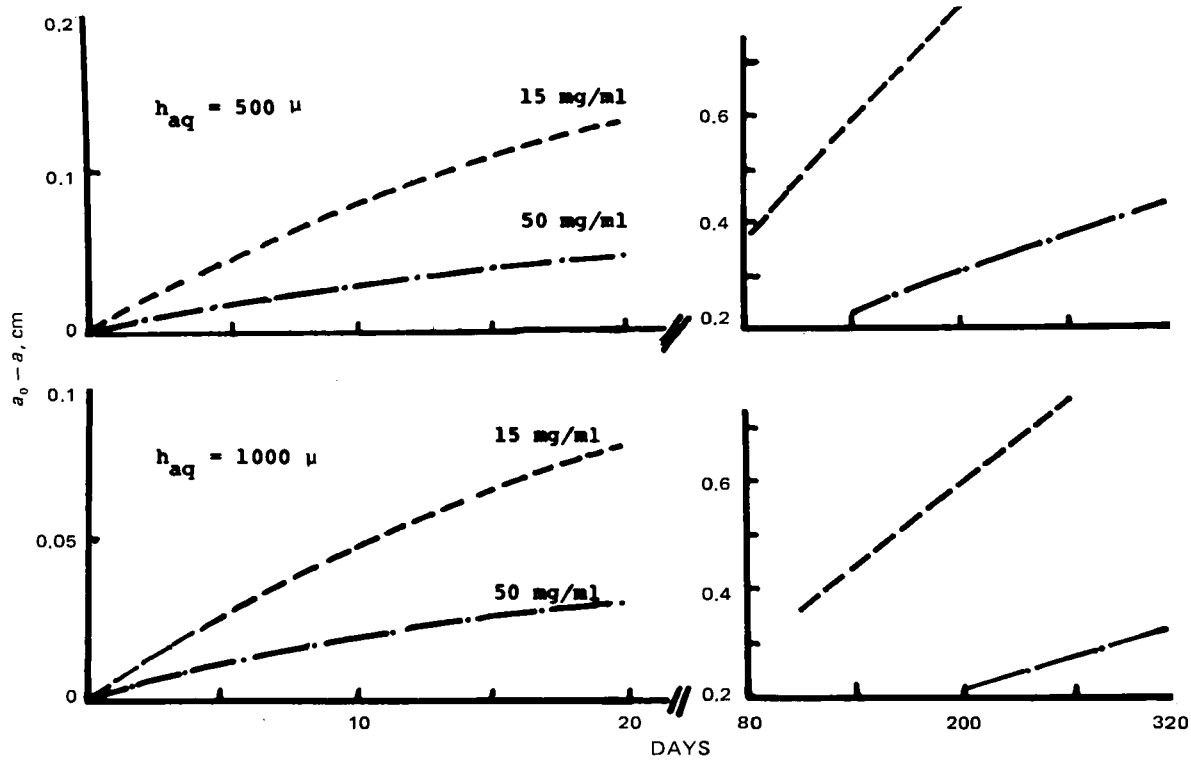

Figure 6—*Predicted change in receding boundary zone thickness with time at various concentrations of progesterone and diffusion layer thicknesses.*

Simulation Studies with Progesterone—The flux per unit area of the cylinder *versus* time profiles are shown in Figs. 2 and 3 for different aqueous diffusion layer thicknesses and initial concentrations of progesterone in the matrix. When the aqueous diffusion layer is 500–1000 μm thick (Fig. 2), the fluxes tend to be invariant with time for relatively long periods and then to decrease gradually with time. This time-independent characteristic is maintained longer when the aqueous layer between the cylinder and vaginal membrane is quite thick (1000 *versus* 500 μm) and the initial loading steroid concentration is also high (50 *versus* 15 mg/ml).

The mechanistic interpretation is that the rate in the first time period is determined by the aqueous diffusion layer barrier. The membrane resistance is a factor of 10 less than the diffusion layer resistance when the aqueous layer is 1000 μm thick and, similarly, a factor of 5 less when it is 500 μm thick. Also, the high loading concentrations tend to counterbalance the increasing resistance due to the receding boundary of drug in the cylindrical matrix with time by providing a sufficiently high effective concentration gradient in the matrix. At later times, the rate changes to the more matrix-controlled mechanism. It is significant that the rate in Fig. 2 remains fairly constant for about 6 months. Thus, one can expect the metering out of reasonably constant increments of drug in that period.

The early time profiles of Fig. 3 are in sharp contrast to those in Fig. 2. Here the aqueous diffusion layer thickness is 100 μm, which would be the likely situation when the progesterone–silicone cylinder is in snug fit with the membrane of the vaginal tract. The rate is essentially matrix controlled. Again, the effect of the loading concentration on the rate is observed. With the 100-mg/ml concentration, the early time periods are more influenced by the diffusion layer than they are at the lower concentrations. At low concentrations, the release of the

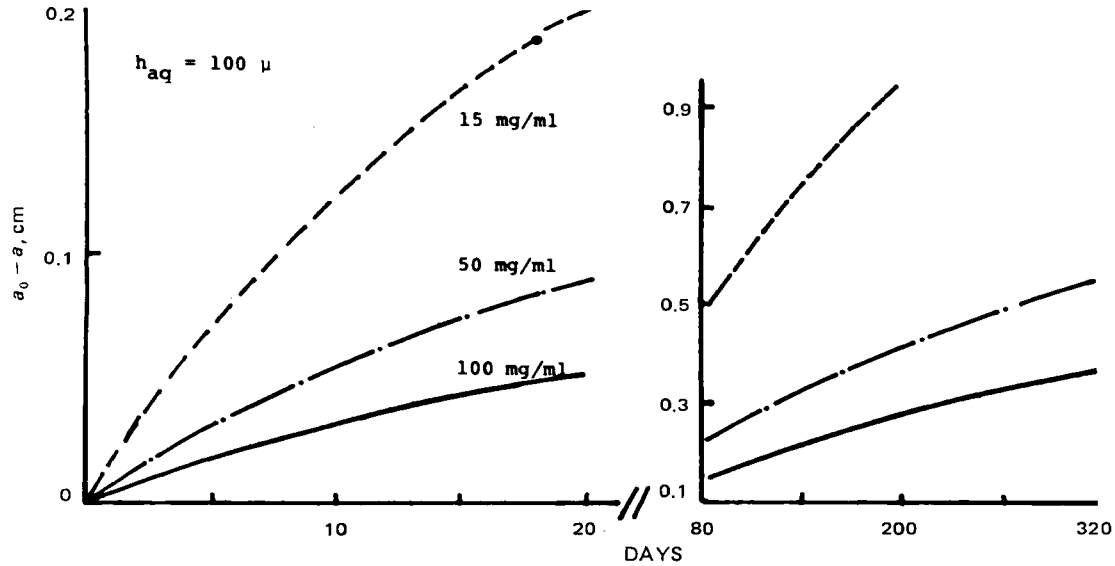

Figure 7—*Predicted change in receding boundary zone thickness with time at various loading concentrations of progesterone and 100-μm aqueous diffusion layer thickness.*

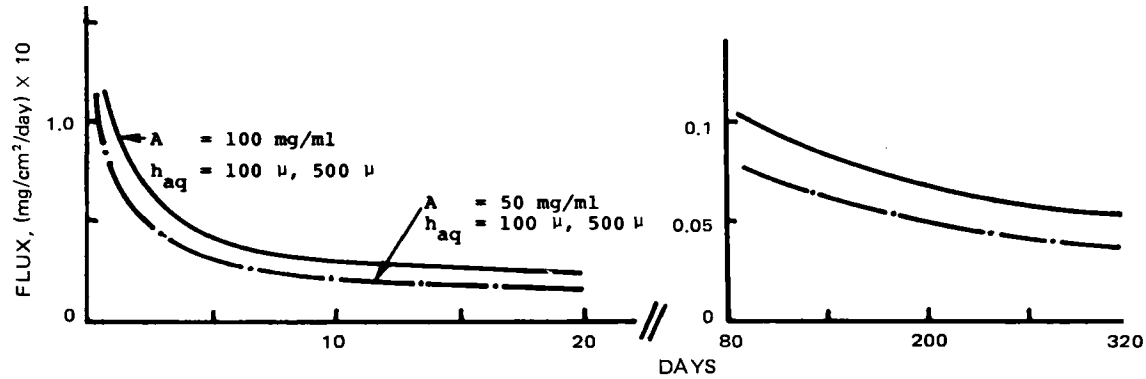

Figure 8—*Predicted fluxes of hydrocortisone with time at various loading concentrations and aqueous diffusion layer thicknesses.*

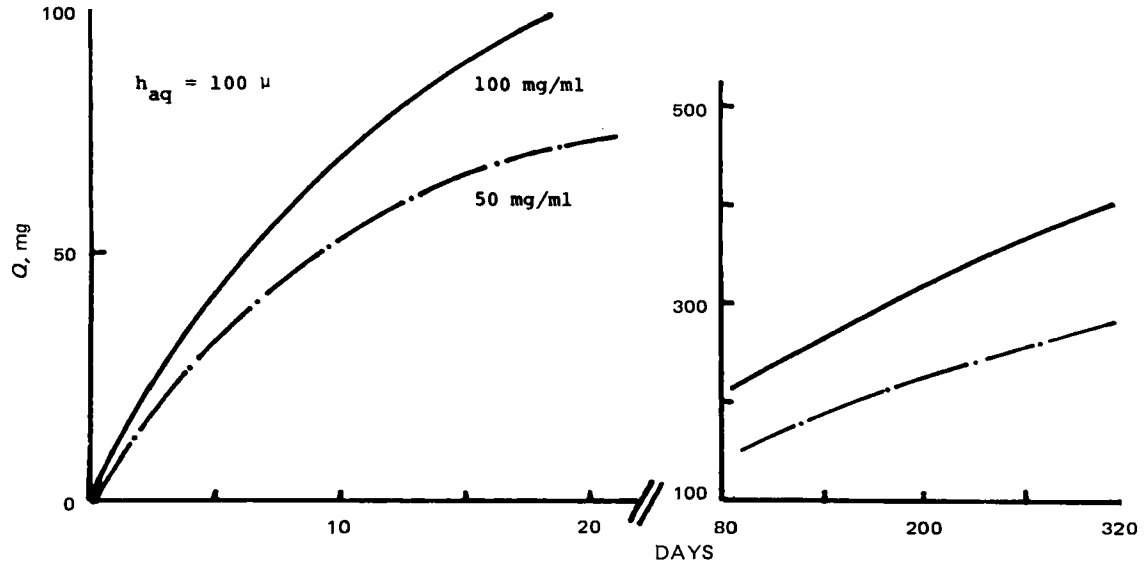

Figure 9—*Predicted total amount of hydrocortisone released with time at various loading concentrations and 100-μm aqueous diffusion layer thickness.*

steroid from the matrix is the predominantly rate-controlling factor once the cylinder is inserted into the vagina.

Figures 4 and 5 show the predicted total amounts of progesterone released from the cylinder (6 cm long and 2 cm diameter) as a function of time for various loading concentrations (15, 50, and 100 mg/ml) and aqueous diffusion layer thicknesses (100, 500, and 1000 μm). In the 500- and 1000-μm diffusion layer situations (Fig. 5), the initial slopes are unaffected by the loading concentrations since the transport kinetics are diffusion controlled. The initial rates are zero order as predicted in Eq. 19. Because the 15-mg/ml concentration cannot sustain the duration of the diffusion-controlled period as long as the 50-mg/ml concentration case, the slope monotonically decreases with

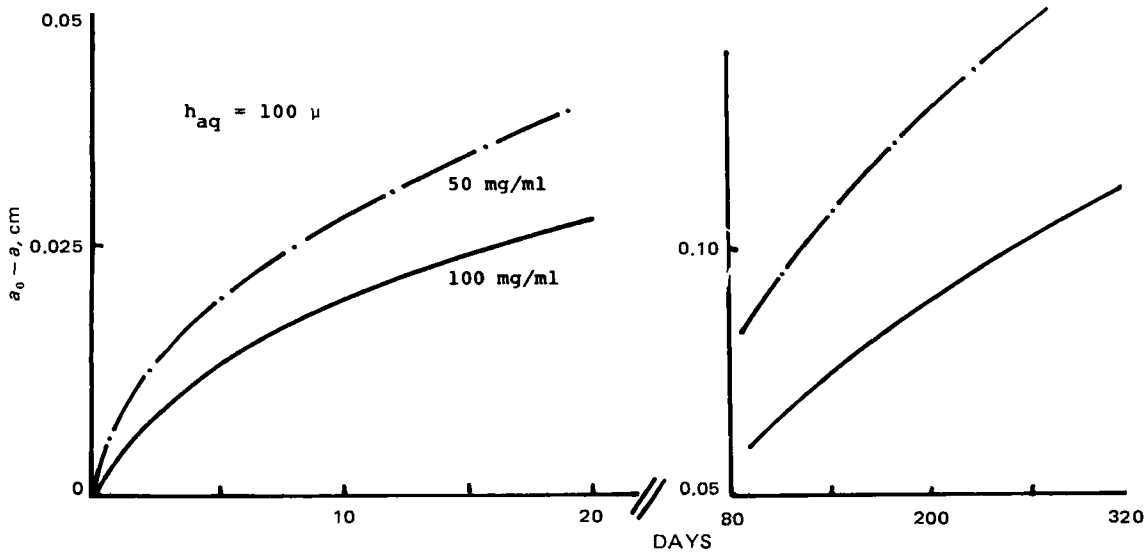

Figure 10—*Predicted change in the receding boundary zone thickness with time at various concentrations of hydrocortisone and 100-μm aqueous diffusion layer thickness.*

Table I—Values of Physical Parameters Used in the Simulation Studies Interfacing Steroid Release from Silicone Matrix with Vaginal Absorption in the Rabbit[a]

Parameter	Progesterone[b]	Hydrocortisone
Structure	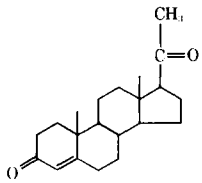	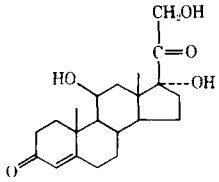
Solubility in matrix, C_s, mg/ml	0.572	0.014
Solubility in water, C_{aq}, mg/ml	0.0114	0.28
Diffusion coefficient in matrix, D_e, cm²/sec	4.5×10^{-7}	4.5×10^{-7}
Diffusion coefficient in water, D_{aq}, cm²/sec	7×10^{-6}	7×10^{-6}
Silicone–water partition coefficient, K_s	50.2	0.05[c]
Permeability coefficient[d] of rabbit vaginal membrane, P_m, cm/sec	7×10^{-4}	5.8×10^{-5}
P_{aq} (when h_{aq} = 100 μm)	7×10^{-4}	7×10^{-4}
P_{aq} (when h_{aq} = 1000 μm)	0.7×10^{-4}	0.7×10^{-4}

[a] Other pertinent specifications were: silicone cylinder, 1.0-cm radius, 6.0-cm height; steroid concentrations, 15, 50, and 100 mg/ml; and aqueous diffusion layer, 10^{-2}, 5×10^{-2}, and 10^{-1} cm. [b] Physical constants of progesterone in Silastic 382 such as C_s, C_{aq}, D_e, and K_s were determined previously (3). [c] The K_s value of hydrocortisone was determined with Silastic 382. [d] The P_m values of progesterone and hydrocortisone were obtained from vaginal absorption studies (to be reported).

time until the total drug delivery capacity is depleted. The initial steroid concentration and size of the cylinder determine the drug capacity. The curves in Fig. 4 with the 100-μm diffusion layer are indicative of the situation where the transport mechanism is essentially matrix controlled at the onset. Other factors being constant, the total delivery capacity depends upon the loading concentration as expected; however, the total time taken to release the total amount of drug depends on both the concentration and transport mechanism.

The predicted changes in the receding boundary zone thickness with time at various progesterone concentrations and aqueous diffusion layer thicknesses are shown in Figs. 6 and 7. This zone of depleted drug would be translucent as compared to the opaque core of the drug–matrix suspension. According to Roseman and Higuchi (3), the measurement of this zone with time gives a rapid estimation of the amount of drug released with time. For a fixed diffusion layer thickness, the radial thickness of the zone increases more rapidly with time with the lower concentration. In general, the rate of change in zone thickness is rapid when the progesterone concentration is low and the diffusion layer is small.

Simulation Studies with Hydrocortisone—As can be seen in Fig. 8 by the rapid fall in the fluxes with time, the overall transport kinetics are mechanistically controlled by the release of hydrocortisone from the silicone cylinder at concentrations of 50 and 100 mg/ml and aqueous boundary layers of 100- and 500-μm thickness. From the 8th

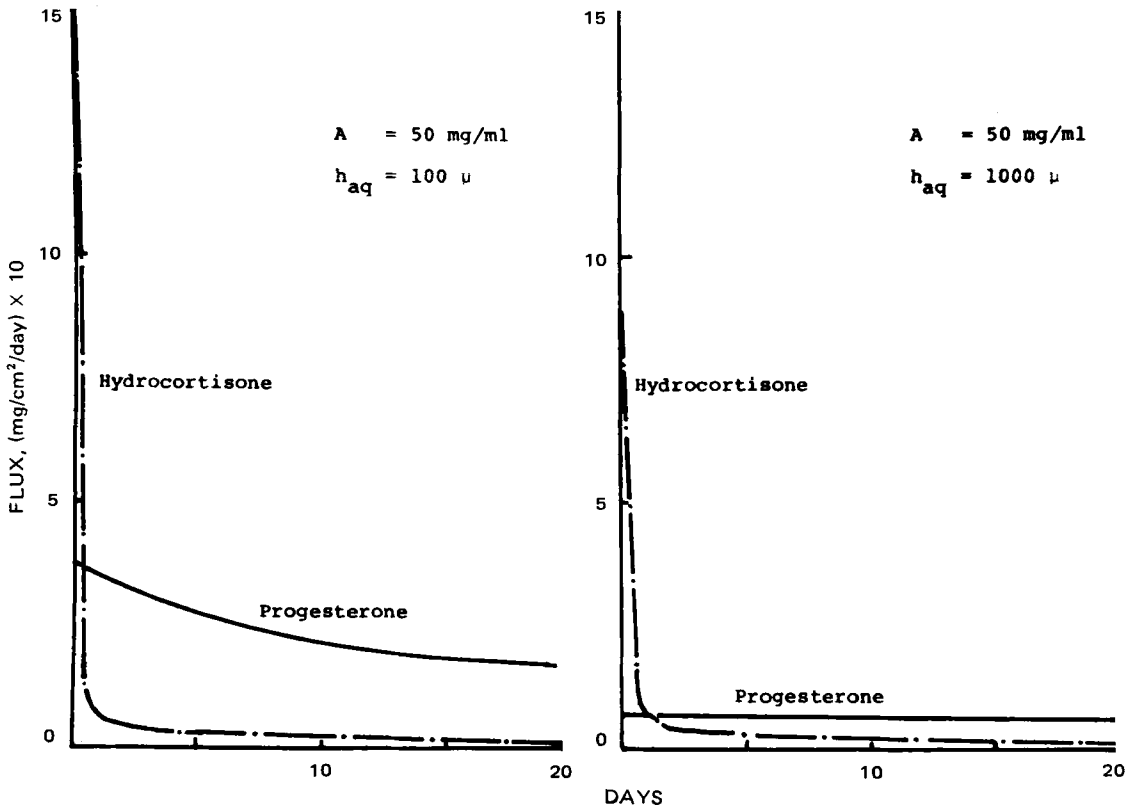

Figure 11—*Comparison of fluxes of progesterone and hydrocortisone with time.*

day, the fluxes decrease very slowly and, perhaps from a practical viewpoint, may be considered to be fairly constant between the 10th and 80th day.

For a given concentration of 50 or 100 mg/ml, the initial flux per unit area of the cylinder is 1.5×10^{-1} for the 100-μm diffusion layer case and 1.15×10^{-1} for the 500-μm layer case; however, the fluxes converge in 6 hr. The corresponding time changes in the total amount of drug released from the matrix and the receding boundary zone thickness are found in Figs. 9 and 1, respectively.

Physical Significance between Progesterone and Hydrocortisone Simulation Studies—A comparison between the progesterone and hydrocortisone simulation studies gives an interesting mechanistic insight into the transport processes involved. It is believed that these model simulations, which encompass the interactions among the drug delivery device, the vaginal membrane, and the aqueous diffusion layer between the device and membrane, are the first of their kind.

The flux per unit area of the cylinder *versus* time profiles in Fig. 11 typify the differences in the transport mechanisms of progesterone and hydrocortisone. The concentration is fixed at 50 mg/ml, but the diffusion layer thickness is varied from 100 to 1000 μm. The pertinent physically meaningful parameters of these steroids (C_s, K_s, P_m, and P_{aq}) are given in Table I.

Considering only the aqueous diffusion layer and the vaginal membrane, one finds that for progesterone the resistance[3] of the diffusion layer is equal to that of the membrane when the diffusion layer thickness (h_{aq}) is 100 μm and is 10-fold greater when h_{aq} is 100 μm. Correspondingly, for the more polar hydrocortisone, the resistance of the diffusion layer is 12-fold less than that of the membrane when h_{aq} is 100 μm and the resistances are about equal when h_{aq} is 1000 μm. Thus, in general, the transport of progesterone across the aqueous and membrane layers tends to be more on the aqueous diffusion-controlled side and the transport of hydrocortisone is more membrane controlled.

When one now brings in the steroid–silicone device, the additional resistance in the matrix, which increases with the recession of the boundary with time and is in series with the aqueous layer and membrane resistances, must be considered. With the large matrix–aqueous partition coefficient, K_s, for progesterone, the change in the net flux with time is largely influenced by the aqueous diffusion layer in the first 20 days. In comparison with the small K_s of 0.05 for hydrocortisone, the net flux changes quite rapidly with time from membrane control to matrix control.

In conclusion, the *in vivo* studies of progesterone-containing silicone vaginal devices in Rhesus monkeys (8) support the physical model simulations in this present paper. In particular, it was noted (8) that the amount of steroid released was independent of progesterone concentration in the silicone device at the high 10 and 30% dose levels (in other words, pseudo-zero-order release rates); these observations were compatible with the rate-controlling process being the diffusion of the steroid across the aqueous boundary layer and the vaginal membrane until the depleted layer in the matrix is large. In another *in vivo* situation involving the matrix release of medroxyprogesterone in the human female, Roseman and Higuchi (3) estimated the aqueous layer between the device and the vaginal membrane to be about 500 μm.

Studies are continuing in which the steroid–silicone matrix is interfaced *in situ* in the rabbit vagina to demonstrate the concept of the systems model approach to drug delivery in the vagina.

[3] The resistance is defined as the reciprocal of the permeability coefficient; hence, the resistances of the diffusion layer and membrane are $1/P_{aq}$ and $1/P_m$, respectively.

REFERENCES

(1) T. Yotsuyanagi, A. Molokhia, S. Hwang, N. F. H. Ho, G. L. Flynn, and W. I. Higuchi, *J. Pharm. Sci.*, **64**, 71(1975).

(2) S. Hwang, E. Owada, T. Yotsuyanagi, L. Suhardja, N. F. H. Ho, G. L. Flynn, and W. I. Higuchi, *ibid.*, **65**, 1574(1976).

(3) T. J. Roseman and W. I. Higuchi, *ibid.*, **59**, 353(1970).

(4) T. J. Roseman, *ibid.*, **61**, 46(1972).

(5) T. J. Roseman and S. H. Yalkowsky, *ibid.*, **63**, 1639(1974).

(6) G. L. Flynn, N. F. H. Ho, W. I. Higuchi, and J. Kent, *ibid.*, **65**, 157(1976).

(7) K. Desai, Ph.D thesis, University of Michigan, Ann Arbor, Mich., 1976.

(8) K. T. Kirton, T. J. Roseman, and A. D. Forbes, *Contraception*, **8**, 561(1973).

ACKNOWLEDGMENTS AND ADDRESSES

Received October 6, 1975, from the *College of Pharmacy, University of Michigan, Ann Arbor, MI 48104*

Accepted for publication December 22, 1975.

Supported by Contract NO1-HD-3-2740, National Institute of Child Health and Human Development, Bethesda, Md.

The authors thank Dr. Theodore Roseman, The Upjohn Co., Kalamazoo, Mich., for the generous supply of Silastic 382 membranes.

[x] To whom inquiries should be directed.

Systematic Identification of Drugs of Abuse II: TLC

ASAAD N. MASOUD

Abstract □ A limited number of spray reagents and solvent systems were selected or developed to separate and identify over 40 of the most commonly encountered drugs of abuse. A new reagent is reported, and new uses were developed for well-known reagents. A flowsheet for the systematic utilization of the spray reagents is given, and use of this sequence made it possible to identify systematically an unknown drug using only two to four TLC plates, providing that the drug was one of the compounds investigated. This TLC system also can be used to complement and confirm results obtained from spot tests.

Keyphrases □ Drugs of abuse—TLC identification, spray reagents and solvent systems selected and developed □ Abuse drugs—TLC identification, spray reagents and solvent systems selected and developed □ TLC—identification, drugs of abuse, spray reagents and solvent systems selected and developed

TLC is presently considered one of the most suited techniques for drug analysis. It is fast, requires minimal equipment, can be carried out using a minimal amount of sample, and provides highly reliable results (1).

TLC analysis with different solvent systems and different modes of detection presents a reinforced selectivity. The corroborative findings show that this technique, when properly performed, achieves effectual specificity. Thus, the multiple TLC identity test is considered equivalent in its relevancy, analytical power,

day, the fluxes decrease very slowly and, perhaps from a practical viewpoint, may be considered to be fairly constant between the 10th and 80th day.

For a given concentration of 50 or 100 mg/ml, the initial flux per unit area of the cylinder is 1.5×10^{-1} for the 100-μm diffusion layer case and 1.15×10^{-1} for the 500-μm layer case; however, the fluxes converge in 6 hr. The corresponding time changes in the total amount of drug released from the matrix and the receding boundary zone thickness are found in Figs. 9 and 1, respectively.

Physical Significance between Progesterone and Hydrocortisone Simulation Studies—A comparison between the progesterone and hydrocortisone simulation studies gives an interesting mechanistic insight into the transport processes involved. It is believed that these model simulations, which encompass the interactions among the drug delivery device, the vaginal membrane, and the aqueous diffusion layer between the device and membrane, are the first of their kind.

The flux per unit area of the cylinder *versus* time profiles in Fig. 11 typify the differences in the transport mechanisms of progesterone and hydrocortisone. The concentration is fixed at 50 mg/ml, but the diffusion layer thickness is varied from 100 to 1000 μm. The pertinent physically meaningful parameters of these steroids (C_s, K_s, P_m, and P_{aq}) are given in Table I.

Considering only the aqueous diffusion layer and the vaginal membrane, one finds that for progesterone the resistance[3] of the diffusion layer is equal to that of the membrane when the diffusion layer thickness (h_{aq}) is 100 μm and is 10-fold greater when h_{aq} is 100 μm. Correspondingly, for the more polar hydrocortisone, the resistance of the diffusion layer is 12-fold less than that of the membrane when h_{aq} is 100 μm and the resistances are about equal when h_{aq} is 1000 μm. Thus, in general, the transport of progesterone across the aqueous and membrane layers tends to be more on the aqueous diffusion-controlled side and the transport of hydrocortisone is more membrane controlled.

When one now brings in the steroid–silicone device, the additional resistance in the matrix, which increases with the recession of the boundary with time and is in series with the aqueous layer and membrane resistances, must be considered. With the large matrix–aqueous partition coefficient, K_s, for progesterone, the change in the net flux with time is largely influenced by the aqueous diffusion layer in the first 20 days. In comparison with the small K_s of 0.05 for hydrocortisone, the net flux changes quite rapidly with time from membrane control to matrix control.

In conclusion, the *in vivo* studies of progesterone-containing silicone vaginal devices in Rhesus monkeys (8) support the physical model simulations in this present paper. In particular, it was noted (8) that the amount of steroid released was independent of progesterone concentration in the silicone device at the high 10 and 30% dose levels (in other words, pseudo-zero-order release rates); these observations were compatible with the rate-controlling process being the diffusion of the steroid across the aqueous boundary layer and the vaginal membrane until the depleted layer in the matrix is large. In another *in vivo* situation involving the matrix release of medroxyprogesterone in the human female, Roseman and Higuchi (3) estimated the aqueous layer between the device and the vaginal membrane to be about 500 μm.

Studies are continuing in which the steroid–silicone matrix is interfaced *in situ* in the rabbit vagina to demonstrate the concept of the systems model approach to drug delivery in the vagina.

[3] The resistance is defined as the reciprocal of the permeability coefficient; hence, the resistances of the diffusion layer and membrane are $1/P_{aq}$ and $1/P_m$, respectively.

REFERENCES

(1) T. Yotsuyanagi, A. Molokhia, S. Hwang, N. F. H. Ho, G. L. Flynn, and W. I. Higuchi, *J. Pharm. Sci.*, **64**, 71(1975).

(2) S. Hwang, E. Owada, T. Yotsuyanagi, L. Suhardja, N. F. H. Ho, G. L. Flynn, and W. I. Higuchi, *ibid.*, **65**, 1574(1976).

(3) T. J. Roseman and W. I. Higuchi, *ibid.*, **59**, 353(1970).

(4) T. J. Roseman, *ibid.*, **61**, 46(1972).

(5) T. J. Roseman and S. H. Yalkowsky, *ibid.*, **63**, 1639(1974).

(6) G. L. Flynn, N. F. H. Ho, W. I. Higuchi, and J. Kent, *ibid.*, **65**, 157(1976).

(7) K. Desai, Ph.D thesis, University of Michigan, Ann Arbor, Mich., 1976.

(8) K. T. Kirton, T. J. Roseman, and A. D. Forbes, *Contraception*, **8**, 561(1973).

ACKNOWLEDGMENTS AND ADDRESSES

Received October 6, 1975, from the *College of Pharmacy, University of Michigan, Ann Arbor, MI 48104*

Accepted for publication December 22, 1975.

Supported by Contract NO1-HD-3-2740, National Institute of Child Health and Human Development, Bethesda, Md.

The authors thank Dr. Theodore Roseman, The Upjohn Co., Kalamazoo, Mich., for the generous supply of Silastic 382 membranes.

[x] To whom inquiries should be directed.

Systematic Identification of Drugs of Abuse II: TLC

ASAAD N. MASOUD

Abstract □ A limited number of spray reagents and solvent systems were selected or developed to separate and identify over 40 of the most commonly encountered drugs of abuse. A new reagent is reported, and new uses were developed for well-known reagents. A flowsheet for the systematic utilization of the spray reagents is given, and use of this sequence made it possible to identify systematically an unknown drug using only two to four TLC plates, providing that the drug was one of the compounds investigated. This TLC system also can be used to complement and confirm results obtained from spot tests.

Keyphrases □ Drugs of abuse—TLC identification, spray reagents and solvent systems selected and developed □ Abuse drugs—TLC identification, spray reagents and solvent systems selected and developed □ TLC—identification, drugs of abuse, spray reagents and solvent systems selected and developed

TLC is presently considered one of the most suited techniques for drug analysis. It is fast, requires minimal equipment, can be carried out using a minimal amount of sample, and provides highly reliable results (1).

TLC analysis with different solvent systems and different modes of detection presents a reinforced selectivity. The corroborative findings show that this technique, when properly performed, achieves effectual specificity. Thus, the multiple TLC identity test is considered equivalent in its relevancy, analytical power,

Table I—Summary of R_f Values and Detection Modes

Compound	Solvent System[a] 1	2	3	4	5	Visibility[b] Visible	Longwave UV	Shortwave UV	Spray Reagents[b] Ninhydrin–Phenylacetaldehyde	Iodoplatinate	Ninhydrin–Phenylacetaldehyde Iodoplatinate	Ehrlich's	Ehrlich's–Iodoplatinate	Mercuric Chloride–Diphenylcarbazone	Diazotized Benzidine
Alkaloids															
Atropine	0	11	18	47	0					+	+				
Caffeine	45	46	72	68	0			+					+		
Cocaine hydrochloride	81	81	65	47	0			+		+	+				
Codeine phosphate	27	25	38	47	0			+		+	+				
Ephedrine sulfate	2	14	32	63	0			+					+		
Heroin	48	40	46	52	0			+		+	+				
Lysergide	42	56	73	69	0		+	+				+			
Mescaline hydrochloride	22	17	26	69	0			+	+	+	+		+		
Morphine sulfate	5	15	36	53	0			+		+	+				
Nicotine salicylate	68	47	64	34	0			+		+	+				
Opium	6	16	36	53	0			+		+	+				
Papaverine	86	72	72	65	0		+	+		+	+				
Physostigmine salicylate	64	52	62	55	0			+		+	+				
Psilocin	22	33	36	60	0	+		+	+	+	+	+	+		
Psilocybin	0	41	5	31	0			+					+		
Quinine sulfate	19	52	53	63	0		+	+		+	+				
Scopolamine hydrobromide	21	27	67	52	0					+	+				
Strychnine	28	77	16	51	0			+		+	+				
Yohimbine hydrochloride	43	79	83	71	0		+	+		+	+				
Nonalkaloids that give positive alkaloidal reactions															
Lidocaine hydrochloride	80	82	84	60	0			+		+	+				
Meperidine[c]	65	65	53	60	0			+		+	+				
Methadone hydrochloride	64	77	38	72	0			+		+	+				
Methapyrilene hydrochloride[d]	28	46	62	48	0			+		+	+[e]	+			
Methaqualone	85	80	81	91	0			+					+		
Methylphenidate hydrochloride	68	73	65	74	0			+		+	+				
Pentazocine hydrochloride[f]	50	83	60	82	0			+		+	+				
Phencyclidine hydrochloride	83	82	48	70	0			+		+	+				
Procaine hydrochloride	31	60	71	54	0			+				+	+		
Propoxyphene napsylate[g]	77	81	80	73	0			±		+	+				
Barbiturates															
Amobarbital	65	82	86	95	0			+						+	
Phenobarbital sodium	49	77	85	95	0			+						+	
Secobarbital	70	84	84	94	0			+					+	+	
Amphetamines															
Dextroamphetamine sulfate	15	30	41	69	0			+	+						
Methamphetamine hydrochloride	26	34	26	70	0			+		+	+			+	
Miscellaneous															
Aspirin	0	25	71	92	10		±	+						+	
Benzocaine	79	78	84	92	14			+				+	+		
Cannabidiol	84	86	82	98	50			+							+
Cannabinol	82	86	81	98	45			+							+
Glutethimide[h]	77	86	85	95	0			±						+	
Meprobamate	30	76	72	86	0							+			
Phenytoin sodium[i]	48	83	86	95	0			±						+	
Δ^9-Tetrahydrocannabinol	83	85	83	98	42										+
Thiopental	82	82	90	94	10			+	+[j]	+		+	+	+	

[a] The composition of the solvent systems is given under *Experimental*. The R_f values are averages of three determinations. [b] + = easily detected spot, and ± = very faint spot. The empty spaces indicate negative reactions with the exception of the last three columns. These reagents were not attempted on the alkaloids, the compounds that give positive alkaloidal reactions, and the cannabinoids. [c] Demerol. [d] Histadyl, Dormin. [e] The intensity of the color produced by methapyrilene hydrochloride was less than that produced with iodoplatinate spray on a fresh plate. [f] Talwin. [g] Darvon-N. [h] Doriden. [i] Dilantin. [j] Thiopental produced a faint white spot 15-20 min after the application of iodoplatinate.

and utility to the IR identity test for regulatory drug analysis (2).

The purpose of this study was to develop systems, reagents, and specific techniques suited for the identification of the most commonly encountered street drugs. Forty-three drugs were considered along with these goals: (*a*) to limit the number of spray reagents needed, (*b*) to reduce the number of TLC plates run per sample, and (*c*) to limit the number of solvent systems to a minimum.

EXPERIMENTAL

Materials—The 43 drugs investigated in this work had been subjected to spot tests previously (3). Based on the results obtained from the alkaloidal precipitating agents (3), drugs that give a positive test to Mayer's, Dragendorff's, or Wagner's reagents are grouped to-

Table II—Results Produced by Ninhydrin–Phenylacetaldehyde Spray

Compound	Color	Remarks
Mescaline hydrochloride	Fluorescent yellow	Visible with other reagents
Psilocin	White spot with dark center	Visible upon standing and with other reagents
Dextroamphetamine sulfate	Fluorescent yellow	Becomes pink with Ehrlich's reagent; not visible with any other reagent investigated

gether and referred to as nonalkaloids that give a positive alkaloidal reaction. Otherwise, the drugs[1] listed in Table I are grouped according to their chemical nature.

Preparation of Reference Standards—Examination of the solubility of the compounds investigated showed that most were soluble in alcohol USP except for the following (4). Lysergide was obtained as an aqueous solution and was diluted using distilled water. Yohimbine hydrochloride and dextroamphetamine sulfate were dissolved in 50% ethanol. A solution of 2 mg/ml was prepared in the appropriate solvent, with the exception of lysergide where a concentration of 0.1 mg/ml was used.

These solutions were kept in tightly closed vials in the refrigerator. They were stable for several months under these conditions, with the exception of the alkaloid psilocin. Psilocin, once in solution, had to be used within a few days. It decomposed completely, even in the refrigerator, to a dark-brown solution which did not contain any of the original reference alkaloid. However, it is recommended that fresh reference standards be prepared every 3–4 months.

Preparation of Unknown Samples—If a sample is suspected to contain a certain compound or compounds, it is dissolved in the same solvent as the standards. But if it is completely unknown, the sample is divided into three parts and three solutions are prepared using alcohol USP, 50% ethanol, and water as solvents.

To assure dissolution of the drug, the test tube is shaken thoroughly using a vortex apparatus and is also heated for a few minutes over a steam bath. Then the sample is either filtered or allowed to sit so that the suspended material can settle prior to spotting.

Chromatography Equipment—Silica gel GF-254 TLC plates[2], 0.25 mm, were activated by warming at 110° for 1 hr.

Standard size development tanks were lined[3] and allowed to equilibrate. The paper lining should be wetted with solvent before the chromatography is started (5). Solvent systems were changed frequently for reproducible results.

Application of Drugs—Approximately 5 μl of the standard solution was applied on the TLC plates. When the concentration of the sample is unknown, it is advisable to apply larger quantities to assure detection of compounds present in low concentrations.

Solvent Systems—Five solvent systems were satisfactory for the screening and identification of all drugs studied. These solvents were: 1, chloroform–ether–methanol–concentrated ammonium hydroxide (75:25:5:1) (6); 2, ethyl acetate–1-propanol–concentrated ammonium hydroxide (40:30:3) (7); 3, methanol–concentrated ammonium hydroxide (100:1.5) (8); 4, alcohol USP–acetic acid–water (60:30:10) (8); and 5, benzene (9).

Systematic Utilization of Solvent Systems—If the substance is completely unknown, two plates are prepared and developed in Solvent Systems 1 and 2. After detection and tentative identification, one or two more plates may be prepared and developed in one or more of the other solvent systems.

If the substance is suspected to be a specific compound, it is sufficient to select two appropriate systems based on the information in Table I.

Solvent System 5 was used previously for the identification of marijuana constituents (9) and was incorporated in this study specifically to separate cannabinoids.

[1] These drugs were obtained from the United States Pharmacopeial Convention, Inc., the National Institute of Mental Health, and miscellaneous pharmaceutical and chemical companies.

[2] Prepared in-house using Desage equipment.

[3] Using Whatman No. 1 chromatography paper.

Table III—Compounds Reacting with Ehrlich's Reagent and Ehrlich's–Iodoplatinate Combination Reagent

Compound	Color Produced with Ehrlich's Reagent	Color Produced with Combination Reagent
Lysergide	Purple	Color disappears
Psilocin	Blue	Violet purple
Procaine hydrochloride	Yellow	Dark brown
Thiopental	Chalky white	Orange
Benzocaine	Yellow	Dark brown
Meprobamate	White; becomes yellow with heating	Color disappears

Detection—Developed plates were placed in a fume hood and allowed to dry for 10 min or until the odor of ammonium hydroxide disappeared. The plates were examined for visible spots and then viewed under both longwave and shortwave UV light and marked.

If the compound is completely unknown, the systematic utilization scheme of the spray reagents (Scheme I) should be followed. If the substance is suspected to be a certain compound, the appropriate spray reagent or combination of reagents can be selected from Table I. The composition and application of the spray reagents used are discussed here.

Ninhydrin–Phenylacetaldehyde Spray—Solution A is 0.4% ninhydrin in pH 9 phosphate buffer. Solution B is 0.5% phenylacetaldehyde in alcohol USP.

Spray lightly with Solution A and then apply a heavier spray with Solution B. Let the plate sit for about 10 min. Heating the plate in an oven at 100° for a few minutes speeds the reaction.

This reagent has not been reported in the literature. However, the use of the condensation products of ninhydrin with aldehydes for the detection of amines was reported (10). Fluorescamine, which forms the same fluorophores with amines, was reported (11) for the assay of minute quantities of amines and later was used for the detection of amphetamines in urine (11, 12).

Iodoplatinate Spray (13)—Solution A is 10% hexachloroplatinic(IV) acid solution. Solution B is 6% aqueous potassium iodide solution.

Mix 3 ml of Solution A with 100 ml of Solution B and add 97 ml of distilled water.

Ehrlich's Spray (14)—Prepare 0.2% solution of *p*-dimethylaminobenzaldehyde in 10% hydrochloric acid. To each 100 ml, add 0.2 ml of 5% ferric chloride solution. The reagent decomposes with time and is light sensitive. Therefore, it should be prepared weekly and protected from light.

Mercuric Chloride–Diphenylcarbazone Spray (15)—Solution A is 0.2% (w/v) diphenylcarbazone in 95% ethanol. Solution B is 2.0% (w/v) mercuric chloride in 95% ethanol.

Mix equal volumes of the two solutions prior to use.

Diazotized Benzidine Spray (9, 16)—Solution A is 5 mg of benzidine dihydrochloride in 14 ml of concentrated hydrochloric acid diluted to 1 liter with distilled water. Solution B is 10% sodium nitrite solution.

Mix equal volumes of the two solutions immediately prior to use. The mixed spray deteriorates in a few hours.

RESULTS AND DISCUSSION

The two main parameters involved in the identification of unknown substances by TLC are related to detection and R_f values. Detection involves the visibility of the substance or substances with visible light, under long- or shortwave UV light, or by the chromogenic reaction produced by a certain spray reagent or a combination of spray reagents. The R_f values are only approximate values and are affected by many variables. Therefore, it is absolutely necessary to use different solvent systems and different modes of detection to identify unknown substances.

Detection—The visibility characteristics of substances and the color reactions that they produce with certain spray reagents are an important part of the identification process by TLC. The results pertaining to each detection mode are discussed in the sequence of actual utilization during identification procedures. Utilization of these detection modes in this particular sequence is particularly useful if

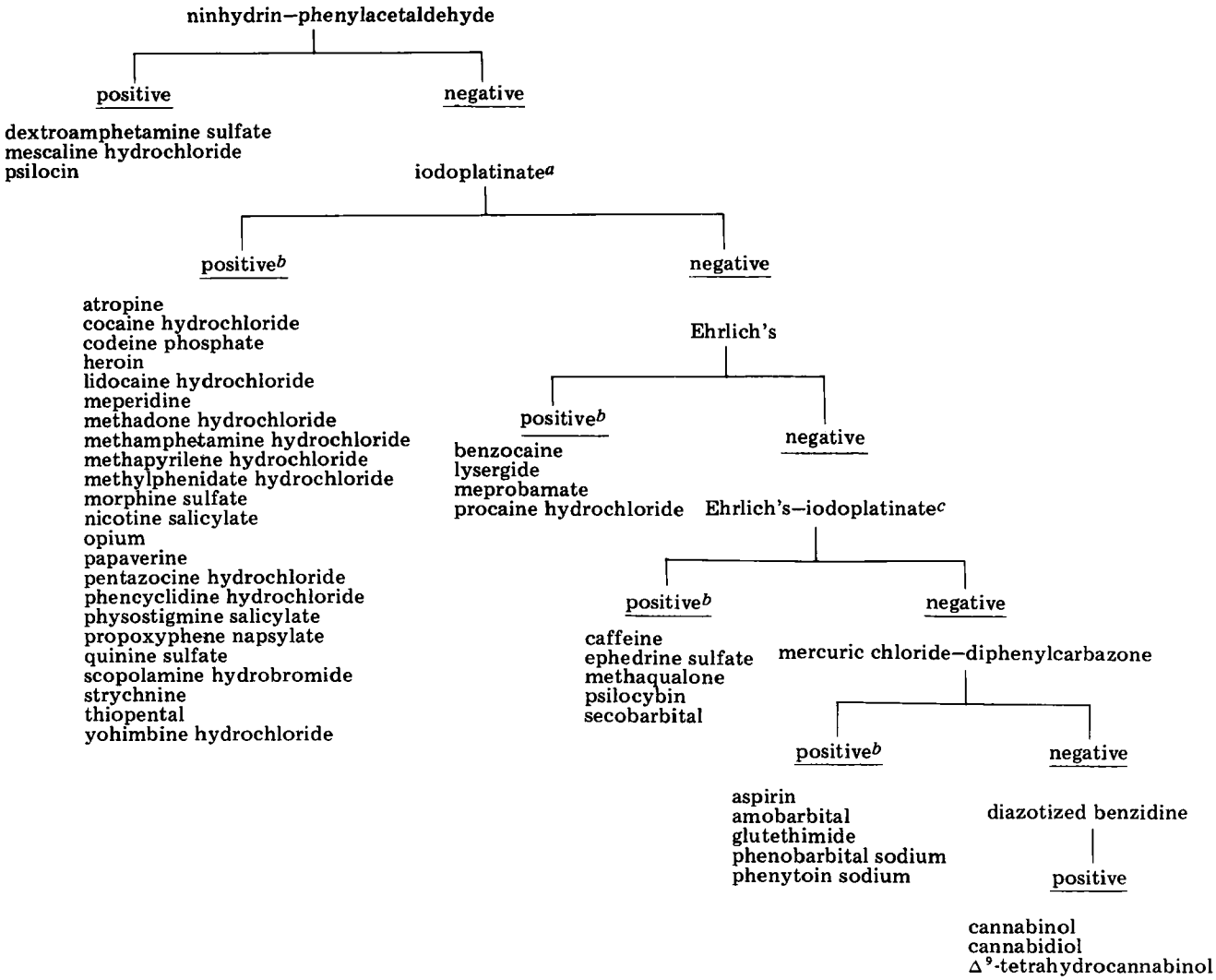

Scheme I—Systematic utilization of spray reagents. [a] Iodoplatinate may be sprayed on the same plate on which ninhydrin–phenylacetaldehyde has been sprayed. However, the color reactions produced by thiopental and methapyrilene hydrochloride may become difficult to detect. [b] Compounds producing color reactions with earlier reagents not included. See Table I for more complete information. [c] Iodoplatinate should be sprayed on the same plate previously sprayed with Ehrlich's reagent.

the substance is of a completely unknown nature. Furthermore, this sequence provides maximum information from each TLC plate, thus reducing the number of plates necessary for the identification of the unknown.

Scheme I provides the sequence in which the spray reagents are utilized, and Table I includes data pertaining to color reactions and R_f values.

Visible Compounds—Psilocin was the only compound visible under visible light. The alkaloid developed a gray color which darkened with time. The color developed in a few minutes in a 100° oven or in 15–20 min at room temperature. This color was produced by the decomposition product(s) of the compound.

Visibility under UV Light—All compounds investigated were visible under shortwave UV light except atropine, scopolamine hydrobromide, Δ^9-tetrahydrocannabinol, and meprobamate. However, only lysergide, papaverine, quinine, yohimbine hydrochloride, and aspirin were visible under longwave UV light. The visibility of these compounds was due to their fluorescent nature or to their quenching of the fluorescent background of the adsorbent material used in this work.

Ninhydrin–Phenylacetaldehyde Spray—Dextroamphetamine sulfate has been a very difficult compound to detect by TLC. Several techniques including potassium permanganate spray (8), fast blue B followed by sodium hydroxide and again by fast blue B (13), acid–base extraction of the dextroamphetamine salt to produce the base prior to the application of the iodoplatinate (7), and iodine solution in methanol (6) were attempted but did not produce satisfactory results.

It was possible to detect amphetamines using 0.5% ninhydrin in butanol as described by Kaistha and Jaffe (17). However, many of the drugs used in this work produced similar chromogenic reactions to those of amphetamines, thus rendering the reagent less specific than ninhydrin–phenylacetaldehyde.

The ninhydrin–phenylacetaldehyde described in this work is highly sensitive, easy to use, and can be stored for months without deterioration. The yellow fluorescent color produced by the application of this reagent to dextroamphetamine sulfate was converted to a very characteristic pink color upon the application of Ehrlich's reagent. This new color adds to the value of the reagent in the identification process.

Mescaline hydrochloride produced a similar chromogenic reaction with the reagent, but the color was not converted to pink upon the application of Ehrlich's reagent. Psilocin produced a white spot with a dark center with this reagent. The results pertaining to the application of this reagent are summarized in Table II.

In conclusion, ninhydrin–phenylacetaldehyde is used only if dextroamphetamine or any of its salts are suspected. However, methamphetamine hydrochloride did not produce any color reaction with this reagent. After obtaining the information sought from the plates sprayed with this reagent, the plates can be sprayed with iodoplatinate spray without interference with the results, with the exception of methapyrilene hydrochloride and thiopental which may

Table IV—Compounds Reacting Only upon the Use of the Combination of Ehrlich's Reagent followed by Iodoplatinate Spray

Compound	Color Produced
Caffeine	Purple
Ephedrine sulfate	Brown
Mescaline hydrochloride	Orange
Psilocybin	Brown
Methaqualone	Brown
Methapyrilene hydrochloride	Deep blue
Secobarbital	Pink

become difficult to detect (Table I).

Iodoplatinate Spray—This reagent, as expected, reacted with all alkaloids investigated (Table I) except caffeine, ephedrine sulfate, and lysergide. It also reacted with all nonalkaloids that give a positive alkaloidal reaction except methaqualone and procaine hydrochloride (3). Of the drugs listed in other groups, thiopental and methamphetamine hydrochloride produced a color reaction.

Ehrlich's Spray—This reagent is known to produce blue or purple colors with ergot alkaloids and other indole compounds (8, 14). In this study, a number of other compounds produced various chromogenic reactions with this reagent. Those colors underwent certain changes upon the application of iodoplatinate spray following Ehrlich's spray. The color change is considered a valuable additional characteristic for the identification of these compounds (Table III). The compounds listed in Table III, except psilocin and thiopental, were not detected by ninhydrin–phenylacetaldehyde or iodoplatinate sprays.

Furthermore, a number of compounds that did not produce a color reaction with Ehrlich's reagent produced characteristic colors upon the application of iodoplatinate spray on a plate previously sprayed with Ehrlich's reagent (Table IV). Thus, Ehrlich's–iodoplatinate combination reagent made it possible to detect and identify some new compounds not visible by either spray separately. All of the compounds listed in Table IV, except mescaline hydrochloride, methapyrilene hydrochloride, and secobarbital, were not detected by any other reagent.

Mercuric Chloride–Diphenylcarbazone Spray—This reagent is used for the detection of barbiturates (15). It produced a characteristic purple color with these compounds, with the exception of secobarbital which developed a white spot with a purple margin. Other compounds that reacted with this reagent are listed in Table V.

Diazotized Benzidine Spray—This reagent is used to detect cannabinoids and marijuana (9, 16). It produced a characteristic orange color with the three cannabinoids studied.

R_f Values—The data pertaining to the R_f values of all compounds investigated in Solvent Systems 1–5 are summarized in Table I. These solvent systems were satisfactory in most cases.

If the unknown is suspected to be a certain chemical, two appropriate solvent systems may be chosen. However, if the sample is completely unknown, Solvent Systems 1 and 2 are recommended first; then one or more of the other solvents may be used if confirmatory tests are necessary.

Solvent System 5 is suggested only when cannabinoids or marijuana extracts are suspected.

Table V—Results of Mercuric Chloride–Diphenylcarbazone Spray

Compound	Color Produced
Aspirin[a]	White
Amobarbital[a]	Purple
Phenobarbital sodium[a]	Purple
Phenytoin sodium[a]	Purple
Glutethimide[a]	Purple
Methamphetamine hydrochloride	Blue
Secobarbital	White center and purple margin
Thiopental	Purple

[a] These compounds did not produce colors with any other reagent.

REFERENCES

(1) E. Stahl, "Drug Analysis by Chromatography and Microscopy," 1st ed., Ann Arbor Science Publishers, Ann Arbor, Mich., 1973, p. 3.

(2) D. Banes, "A Chemists Guide to Regulatory Drug Analysis," The Association of Official Analytical Chemists, Benjamin Franklin Station, Washington, D.C., 1974, p. 63.

(3) A. N. Masoud, *J. Pharm. Sci.*, **64**, 841(1975).

(4) "Handbook of Analytical Toxicology," I. Sunshine, Ed., The Chemical Rubber Co., Cleveland, Ohio, 1969, pp. 2–123.

(5) J. Bobbitt, A. Schwarting, and R. Gritter, "Introduction to Chromatography," Reinhold, New York, N.Y., 1968, pp. 54, 58.

(6) R. A. Van Welsum, *J. Chromatogr.*, **78**, 237(1973).

(7) J. K. Brown, L. Shapazian, and G. D. Griffin, *ibid.*, **64**, 129(1972).

(8) E. G. C. Clarke, "Isolation and Identification of Drugs," Pharmaceutical Press, London, England, 1969, pp. 46, 51, 192.

(9) A. N. Masoud and N. J. Doorenbos, *J. Pharm. Sci.*, **62**, 313(1973).

(10) K. Samejima, W. Dairman, J. Stone, and S. Udenfriend, *Anal. Biochem.*, **42**, 237(1971).

(11) S. Udenfriend, S. Stein, P. Bohlen, and W. Dairman, *Science*, **178**, 871(1972).

(12) B. Klein, J. Sheehan; and E. Grunberg, *Clin. Chem.*, **20**, 272(1974).

(13) E. Stahl, "Thin-Layer Chromatography, A Laboratory Handbook," 2nd ed., Springer-Verlag, New York, N.Y., 1969, pp. 883, 893, 520, 869.

(14) S. K. Sim, "Medicinal Plant Alkaloids," 2nd ed., University of Toronto Press, Toronto, Canada, 1965, p. 97.

(15) D. J. Berry and J. Grove, *J. Chromatogr.*, **80**, 205(1973).

(16) H. Aramaki, N. Tomiyasu, H. Yoshimura, and H. Tsukamoto, *Chem. Pharm. Bull.*, **16**, 822(1968).

(17) K. K. Kaistha and J. H. Jaffe, *J. Pharm. Sci.*, **61**, 679(1972).

ACKNOWLEDGMENTS AND ADDRESSES

Received August 23, 1974, from the *School of Pharmacy, Creighton University, Omaha, NE 68178*

Accepted for publication January 12, 1976.

Presented at the joint meeting of the American Society of Pharmacognosy and the Pharmacognosy and Natural Products Section, APhA Academy of Pharmaceutical Sciences, Chicago meeting, August 1974. The presentation of this paper at the meeting was made possible by the award granted to the author by Lederle Co.

The author expresses his appreciation to Dr. Irving Sunshine, Chief Toxicologist, Cuyahoga County Coroner's Office, Cleveland, Ohio, for suggesting the use of the reagent ninhydrin–phenylacetaldehyde and for his encouragement to publish the method described in this paper.

Present address: Department of Anesthesiology, University of Nebraska Medical Center, Omaha, NE 68105

Simultaneous Semiautomated Assay of Pyrrobutamine Phosphate, Cyclopentamine Hydrochloride, and Methapyrilene Hydrochloride in Pharmaceutical Mixtures

J. L. HALE

Abstract □ Antihistamine preparations containing methapyrilene hydrochloride, pyrrobutamine phosphate, and cyclopentamine hydrochloride were assayed by introducing an aqueous sample solution into the appropriate automated system. Methapyrilene hydrochloride was determined by UV spectrophotometry. Pyrrobutamine phosphate was extracted as an ion-pair and quantitated colorimetrically by forming the bromcresol purple acid–dye complex. Cyclopentamine hydrochloride was determined colorimetrically by using the copper dithiocarbamate reaction for secondary amines.

Keyphrases □ Pyrrobutamine phosphate—semiautomated colorimetric analysis, pharmaceutical mixtures □ Cyclopentamine hydrochloride—semiautomated colorimetric analysis, pharmaceutical mixtures □ Methapyrilene hydrochloride—semiautomated UV spectrophotometric analysis, pharmaceutical mixtures □ Colorimetry—semiautomated analyses, pyrrobutamine phosphate and cyclopentamine hydrochloride, pharmaceutical mixtures □ UV spectrophotometry—semiautomated analysis, methapyrilene hydrochloride, pharmaceutical mixtures □ Automated analyses—pyrrobutamine phosphate, cyclopentamine hydrochloride, and methapyrilene hydrochloride, pharmaceutical mixtures □ Antihistamine preparations—pyrrobutamine phosphate, cyclopentamine hydrochloride, and methapyrilene hydrochloride, semiautomated analyses

Pharmaceutical mixtures of pyrrobutamine phosphate (I), cyclopentamine hydrochloride (II), and methapyrilene hydrochloride (III) are assayed by manual spectrophotometric methods and by temperature-programmed GLC[1]. These methods are time consuming and do not lend themselves to control work where numerous samples are involved. An automated method was developed to determine the content uniformity of capsules[2] containing these antihistamines.

A modification of the bromcresol purple acid–dye method for tertiary amines (1) was used to assay pyrrobutamine phosphate. A manual method for secondary amines (2) was modified and adapted to the automated system for the colorimetric determination of cyclopentamine hydrochloride. Methapyrilene hydrochloride was determined using UV spectrophotometry by basically the same method as reported by Fernandez *et al.* (3).

EXPERIMENTAL

Equipment—The analytical train consisted of a liquid sampler[3], a proportioning pump[4], spectrophotometers[5] equipped with 10-mm flowcells, and suitable recorders.

Reagents—*Pyrrobutamine Phosphate*—The wash solution was 0.02 *N* hydrochloric acid and was the same for the three systems. The bromcresol purple reagent was prepared by dissolving 350 mg of bromcresol purple (5′,5″-dibromo-*o*-cresolsulfonphthalein sodium salt[6]) in about 200 ml of purified water contained in a 1-liter flask, adding 250 ml of 0.2 *M* potassium biphthalate and 22.6 ml of 1 *N* sodium hydroxide, and diluting to volume with purified water (pH should be 5.0 ± 0.1). The hydrochloric acid solution was 1% (v/v). Chloroform (analytical reagent) was used as the displaced organic solvent.

Cyclopentamine Hydrochloride—The displaced organic solvent was prepared by mixing 50 ml of carbon disulfide with 950 ml of chloroform.

Copper reagent was prepared by dissolving 800 mg of copper sulfate pentahydrate and 10 g of ammonium acetate in about 500 ml of purified water, adding 100 ml of 28% ammonia solution, and diluting to 1 liter with purified water.

Table I—Precision Determined by Assaying Common Solutions and Powders

Formulation	Cyclopentamine Hydrochloride, %	Pyrrobutamine Phosphate, %	Methapyrilene Hydrochloride, %
1	1.11	0.68	0.50 (solution)
	0.76	0.99	— (powder)
2	0.70	0.83	0.58 (solution)
	0.90	0.66	— (powder)

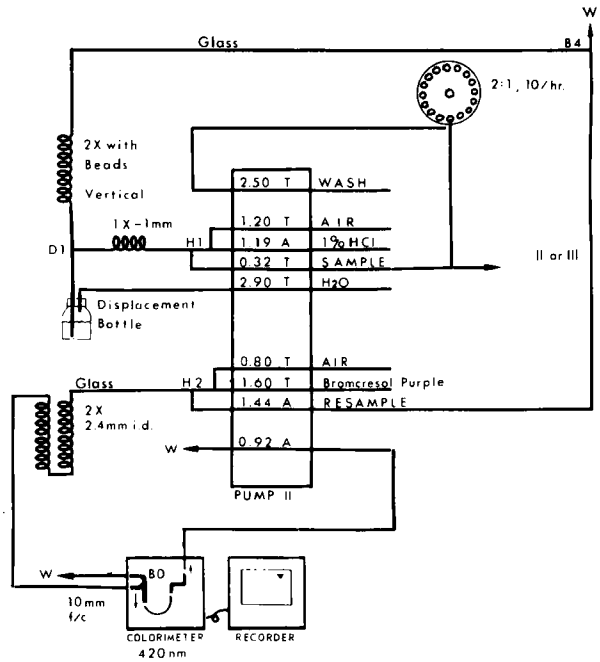

Figure 1—*Components for semiautomated analysis of pyrrobutamine phosphate.*

[1] Unpublished methods, Eli Lilly and Co.
[2] Co-Pyronil, Eli Lilly and Co., Indianapolis, IN 46206
[3] Technicon Liquid Sampler II.
[4] Technicon Proportioning Pump II.
[5] Perkin-Elmer model 55 or 124D.
[6] Eastman No. 6266.

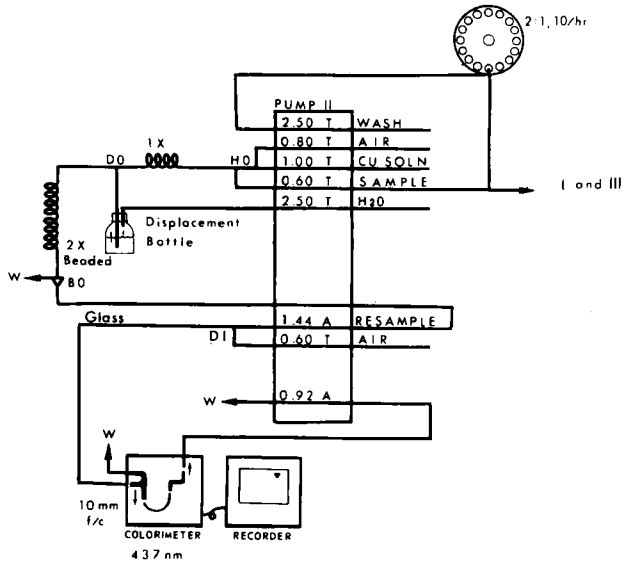

Figure 2—*Components for semiautomated analysis of cyclopentamine hydrochloride.*

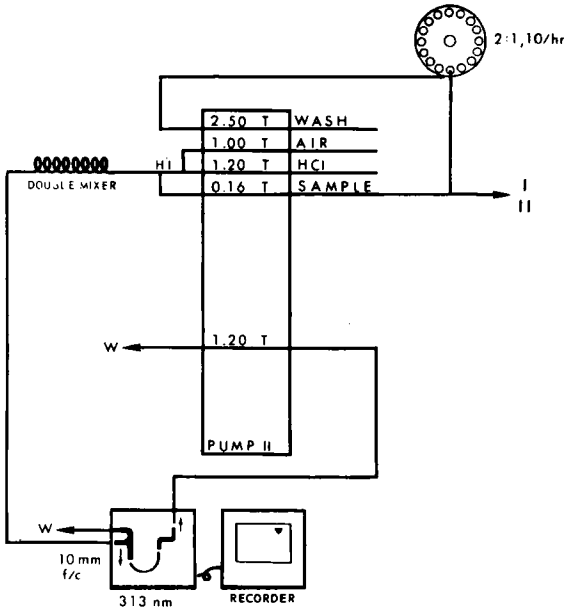

Figure 3—*Components for semiautomated analysis of methapyrilene hydrochloride.*

Methapyrilene Hydrochloride—One percent hydrochloric acid (v/v) was used.

Standards—For the standards, 25.0 mg of methapyrilene hydrochloride, 15.0 mg of pyrrobutamine phosphate, and 12.5 mg of cyclopentamine hydrochloride were dissolved in about 100 ml of purified water. Then the solution was diluted to 200.0 ml with purified water. The standard solution is stable for at least 2 weeks.

Procedure—Dissolve the contents of each capsule in sufficient purified water to achieve a concentration of about 125 μg/ml for methapyrilene hydrochloride, 75 μg/ml for pyrrobutamine phosphate, and 62.5 μg/ml for cyclopentamine hydrochloride. If the formulation contains magnesium carbonate, silicone fluid, or mineral oil, use 0.02 *M* hydrochloric acid as the sample diluent and heat the solution gently on a steam bath for 15 min with intermittent swirling. Allow the solution to stand until the insolubles settle or, alternatively, centrifuge and use the supernate as the assay solution.

Place the sample solution in 8.5-ml sample cups and place on the liquid sampler. The automated modules should be arranged as shown in Figs. 1–3. A common sampler may be used with a stream splitter. The usual practice in this laboratory is to place two components on one pump and use another pump for the third component, if present. The usual sampling pattern is three standards, five samples, one standard, five samples, and one standard.

RESULTS AND DISCUSSION

The manual assay involves a chloroform extraction of the acidified sample solution wherein the extractable ion-pair formed by pyrrobutamine is quantitatively separated from the other two components. The chloroform extract is evaporated to dryness, the residue is taken up in methanol, and the UV absorbance at 226 nm is determined. Methapyrilene hydrochloride is determined by UV spectrophotometry using an acidified, aqueous solution of the sample. Cyclopentamine hydrochloride is determined colorimetrically by forming the extractable copper dithiocarbamate complex and determining the absorbance in methanol–chloroform solution at 437 nm.

The manual procedure for methapyrilene hydrochloride was easily adapted to automation. The pyrrobutamine phosphate assay was more difficult because of the chloroform evaporation step. This portion of the assay was avoided by employing the bromcresol purple reaction for tertiary amines. The acid–dye complex is ordinarily formed by placing the analyte and the bromcresol purple in an acidic aqueous solution and then extracting into an immiscible organic solvent. It was found that the extracted ion-pair reacted quantitatively with an aqueous bromcresol purple solution buffered at pH 5.0. The reaction was linear throughout the concentration range of interest (0–100 μg/ml). A 100-μg/ml pyrrobutamine phosphate solution gave an absorbance of about 0.450.

Cyclopentamine hydrochloride was adapted to automation by making several changes in the reported manual methods (2, 4, 5). Attempts to incorporate chloroform-miscible solvents such as methanol, propanol, and pyridine were made, but little or no advantage was gained so they were eliminated from the system. A sludge buildup in the beaded extraction coil was largely eliminated by using a large excess of ammonium hydroxide. Use of the displacement bottle helped prevent particles of acid-flex tubing from entering the system. The reaction obeys Beers law from 0 to 75 μg/ml with an absorbance of about 0.490 for a 75-μg/ml solution.

The precision of the assay was determined by performing 10 replicate assays from a common solution and from a common powder. Table I shows the relative standard deviation values obtained. Accuracy was determined by preparing authentic mixtures of the various formulations encountered (Table II). The excipient materials encountered were silica gel, starch, talc, magnesium stearate, silicone fluid, and mineral oil. Magnesium carbonate, when present, reduced pyrrobutamine phosphate recovery by as much as 50%. Silicone fluid and mineral oil reduced pyrrobutamine phosphate recovery by 5–8%. Dissolution of the sample with 0.02 *M* hydrochloric acid followed by mild heating eliminated these interferences. Satisfactory recoveries

Table II—Accuracy Determined by Assaying Authentic Mixtures

Cyclopentamine Hydrochloride			Pyrrobutamine Phosphate			Methapyrilene Hydrochloride		
Milligrams Added	Milligrams Found	Recovery, %	Milligrams Added	Milligrams Found	Recovery, %	Milligrams Added	Milligrams Found	Recovery, %
10.73	10.80	100.6	12.81	12.64	98.6	21.7	21.3	98.2
12.52	12.62	100.6	15.09	14.82	98.2	25.2	24.8	98.4
14.31	14.32	100.1	17.19	16.87	98.1	29.2	28.7	98.1
5.39	5.44	100.9	6.43	6.47	100.6	10.69	10.64	99.5
6.32	6.35	100.4	7.52	7.44	98.9	12.68	12.49	98.4
7.17	7.21	100.5	8.68	8.62	93.3	14.54	12.28	98.2

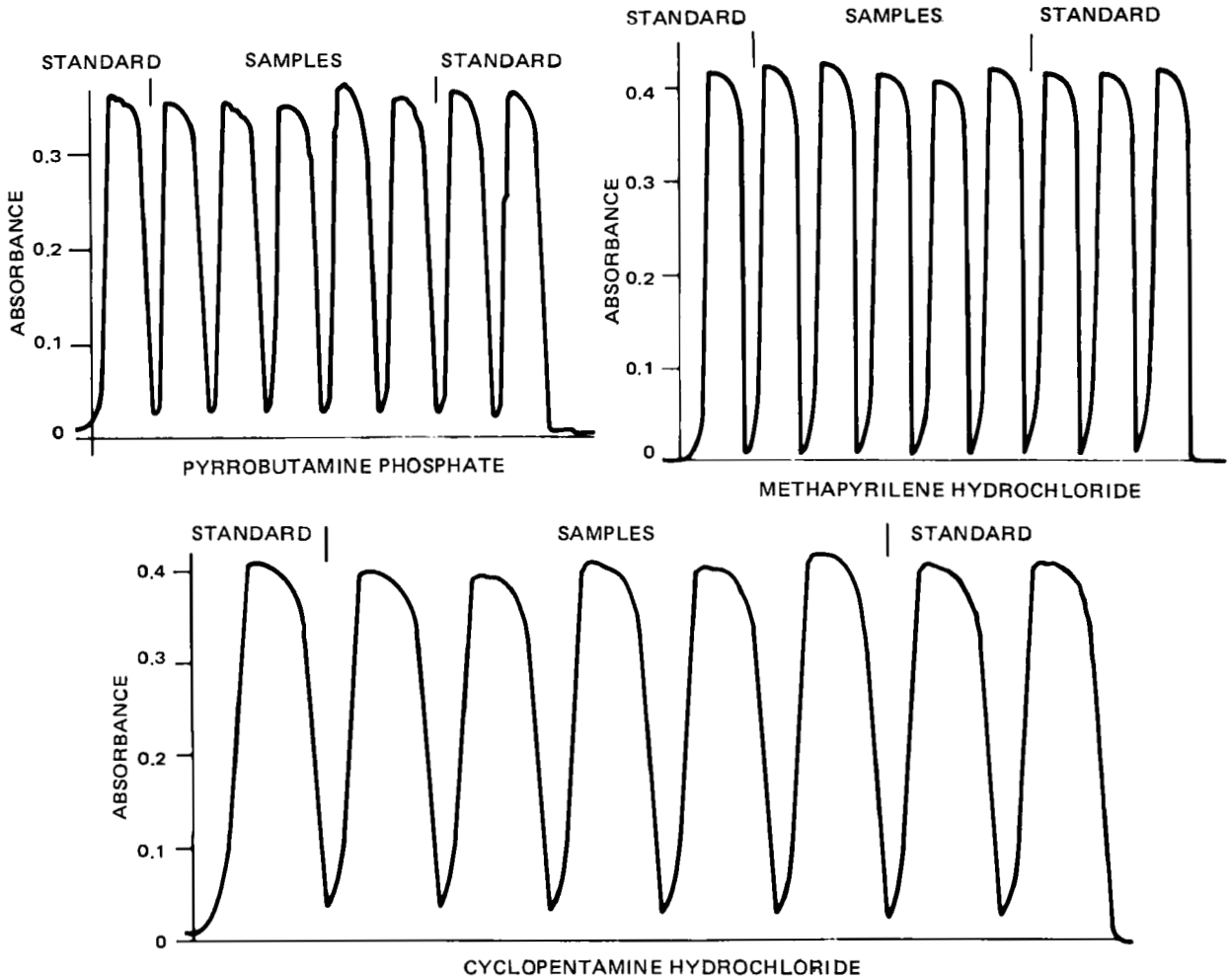

Figure 4—*Recorder traces for semiautomated assay of methapyrilene hydrochloride, pyrrobutamine phosphate, and cyclopentamine hydrochloride.*

were exhibited for the three components at 85, 100, and 115% of theoretical amounts. Typical curves are shown in Fig. 4.

The system has been in use for more than a year in this laboratory for content uniformity assays on capsules, bulk powder analyses, new formulation development, and homogeneity studies. The method is accurate and precise and offers a substantial time saving over manual spectrophotometric and GLC assays.

REFERENCES

(1) N. R. Kuzel, "Automation in Analytical Chemistry, Technicon Symposia 1966," vol. 1, Mediad, White Plains, N.Y., 1967, pp. 218–221.

(2) G. R. Umbreit, *Anal. Chem.*, **33**, 1572(1961).

(3) J. Fernandez, E. Laszlo, and L. C. Leeper, "Automation in Analytical Chemistry, Technicon Symposia 1967," vol. 1, Mediad, White Plains, N.Y., 1968, pp. 471–482.

(4) F. E. Critchfield and J. B. Johnson, *Anal. Chem.*, **28**, 430 (1956).

(5) S. Siggia, "Quantitative Organic Analysis via Functional Groups," 3rd ed., Wiley, New York, N.Y., 1963, p. 497.

ACKNOWLEDGMENTS AND ADDRESSES

Received September 22, 1975, from *Eli Lilly and Company, Indianapolis, IN 46206*

Accepted for publication January 8, 1976.

The author thanks W. G. Richardson, A. D. Garner, and R. W. Roller for their guidance and assistance in preparing the paper.

Pharmacokinetics of Chlorpromazine-Induced Miotic Response in Rabbits

PAUL B. KUEHN *, ASHOK K. JHAWAR ‡, WILLIAM A. WEIGAND §, and VICTOR F. SMOLEN ˣ

Abstract □ The time variation of changes in the chlorpromazine-induced pupil diameter decrease was studied following varying bolus and slowly infused intravenous doses administered to rabbits. The observed pharmacological response data were converted, *via* the use of a dose–effect curve, to values theoretically corresponding to relative biophasic drug levels. These values were, in turn, used to construct a linear pharmacokinetic model of the drug bioavailability input ⇆ pharmacological response output dynamics of the system. The use of a time domain, MULTIFIT, computerized method of fitting the data to obtain a pharmacokinetic model was compared to the use of a frequency response, PLTEST, approach. The fidelity of the model in quantitatively relating the time course of systemic drug bioavailability to observed pupil response was verified by the satisfactory agreement obtained by directly comparing experimentally known amounts of drug intravenously infused with corresponding values computed from observed changes in pupil size. The applicability of using pharmacological data for quantitative bioavailability and pharmacokinetic analysis of chlorpromazine is demonstrated. This finding is particularly significant because no suitable chemical or radiological direct assay technique exists for determining levels of chlorpromazine, except for high doses, in body fluids.

Keyphrases □ Chlorpromazine—pharmacokinetic model relating induced miotic response to systemic bioavailability, rabbits □ Pharmacokinetic models—chlorpromazine-induced miotic response related to systemic bioavailability, rabbits □ Bioavailability, systemic—related to chlorpromazine-induced miotic response, pharmacokinetic model, rabbits □ Miotic response—chlorpromazine induced, related to systemic bioavailability, pharmacokinetic model, rabbits □ Tranquilizers—chlorpromazine, pharmacokinetic model relating induced miotic response to systemic bioavailability, rabbits

One principal objective of pharmacokinetic research involves the development of mathematical models to characterize the dynamics of drug transfer and drug effects in pharmacologically responding systems. For such models to be of maximum value for the elucidation of the pharmacokinetic system behavior, they must allow the prediction of the time course of drug-induced responses as a function of the manner in which the drug is made available to the biological system.

To elucidate the operative mechanisms involved in pharmacodynamic systems in terms of mathematical models, one must develop a means by which the transfer of a drug from its site of administration to its site(s) of action can be quantitated. This may be done by methods first made familiar by Wagner and Nelson (1) and further developed by Loo and Riegelman (2) if the drug level at the site of administration or in some body compartment can be periodically determined. Such direct methods are seldom practical for the detection of small quantities of drug, and an adequate direct assay may not exist for certain drugs such as chlorpromazine.

Methods of analysis that rely on the detection of the drug in the body fluids are generally applicable only to systemic routes of administration. However, the appropriate use of graded pharmacological response intensity data, when applicable, permits the bioavailability characteristics of a drug to be determined following its administration by any route and obviates detection by direct assay methods.

A theoretical basis has been developed for the quantitative determination of relative biophasic drug levels at any time following dosing by any route of administration using data obtained from the observation of the time course of pharmacological response intensity (3). Engineering analysis techniques for dynamic systems can be directly applied to describe the pharmacokinetic processes that determine the quantitative nature of drug effects (4).

The concept of a direct and rapidly reversible pharmacological effect implies that a given intensity of response is associated with a particular drug concentration at the site(s) of action (5). Smolen and coworkers, *e.g.*, (6), developed a theoretical basis for a pharmacokinetic analysis of data obtained by observing the time course of pharmacological response intensity following single, multiple, or continuous dosing of a drug by any route of administration. Through the suitable use of experimentally determined dose–effect curves, the observed intensities of pharmacological response could be transferred into relative biophasic drug levels at all times following dosing (7), thereby obviating the postulation of hypothetical models for drug–receptor site interaction. This method is general and does not require the assumptions of earlier methods, other than requiring the dynamics of drug disposition to be linear or at least to be linear in an operational range of interest.

The drug chlorpromazine[1] was chosen because of its known effects on the intraocular pressure and pupil diameter in both animals and humans. The extreme lowering of intraocular pressure was demonstrated in cataractous eyes after preoperative administration of chlorpromazine (8). A brief ocular hypotensive effect was noted with chlorpromazine in experimental animals given 25–100 mg im (9), and the drug also caused miosis in rabbits and mydriasis in cats (9, 10). The adrenolytic and ganglionic blocking actions of chlorpromazine might explain the mechanisms for this response.

THEORETICAL

Pharmacokinetic Models—The biokinetic behavior of a drug can be characterized most concisely in terms of mathematical models, and the input for the construction of such models is provided by data reflecting the time course of variation of drug levels in the biophase. By treating the biophase as a compartment, its level of drug at any time

[1] Thorazine, Smith Kline and French, Philadelphia, Pa.

following dosing is by definition uniform throughout its volume and is responsible for the observed intensity of response to the drug.

Since the biophase is a hypothetical concept and often cannot be assayed directly for its drug content, the use of the time course of change of pharmacological response intensities can be an advantageous alternative to the use of data derived from direct chemical or radiological assay of drugs in plasma or other body fluids. However, a functional relationship must be established between the level of drug in the biophase at any time and the observable pharmacological response to that drug. Once this relationship has been established, the mathematical methods employed for the pharmacokinetic analysis of drug action using pharmacological response data are usually identical to the methods used to treat drug assay data.

The conversion of pharmacological response intensity data into biophasic drug levels (or relative biophasic drug levels) is accomplished using an experimentally determined dose–effect curve or the drug's resolution in the manner of a calibration curve. The theoretical basis for the use of dose–effect curves to transform pharmacological data into relative biophasic drug levels prior to further analysis was described previously (5–7).

Model Determination—The principal objective of pharmacokinetic research is the quantitative characterization of the biokinetic behavior of a drug in terms of mathematical models. Engineering analysis techniques for dynamic systems can be applied directly to describe the pharmacokinetic processes determining the quantitative nature of drug effects (4). These powerful techniques involve the areas of engineering control theory and signal processing. Interest in the pharmacokinetic analysis of pharmacological data has been spurred by the need to understand the rates of transfer of a drug to sites of action; such knowledge can facilitate the assessment of factors that account for individual variations in effects elicited by a drug (11, 12).

Except for the transduction between biophasic drug levels and drug response, most drug transfer systems can be described in terms of linear mathematical models or models that are linear piecewise over an operational range of interest. To characterize a pharmacologically responding system in mathematical terms, it is necessary to establish the relationship between drug input and response output (in terms of biophasic drug levels) for bolus intravenous administration of the drug. Such an injection represents an impulse of drug input. If the time course of pharmacological response is then observed following this impulse input and transformed into the corresponding time course of biophasic drug levels *via* the dose–effect curve, the unit impulse response or transfer function for the system is obtained. By assuming the initial conditions to be zero, the transfer function may be mathematically described as:

$$\frac{Y(s)}{X(s)} = G(s) = \text{transfer function} \qquad \text{(Eq. 1)}$$

where s is the independent variable in the Laplace Transform Domain. When the input function is a unit impulse [*i.e.*, $X(s) = 1$], the response output of the system, $Y(s)$, is equal to the transfer function, $G(s)$.

Several techniques can be used to determine a transfer function model for a system. Traditionally, methods are used to best "fit" the data by the technique of nonlinear least squares, *i.e.*, estimation of model parameters such that they minimize the sum of squares of differences between observed and predicted values.

Other methods of fitting sums of exponentials to data are available but are usually for restricted cases (13). A powerful technique, widely used in engineering analysis (14–17) but which has not been applied to pharmacological data, is the frequency response method. General frequency response methods require the excitation of the system for several sinusoidal functions until a new steady state is achieved. In practice, this is impractical because it requires the system to be disturbed several times for prolonged periods. A more practical approach to obtain frequency response information is a "pulse testing" method. The use of frequency response *via* the pulse testing approach was discussed in detail (18). A digital computer program PLTEST was developed by the authors to perform the computations efficiently. A detailed presentation of this method will be reported separately.

Frequency response methods have certain inherent advantages over nonlinear least-squares-type fitting procedures. The prinicpal advantage of pulse testing is that no *a priori* knowledge of the order of the system is required. For least-squares fitting, a form of the model and the number of terms in it must be assumed. In frequency response techniques, the number of asymptotes required to approximate the Bode diagram give rise to the number of poles and zeros of the transfer function.

Table I—Intensity of Pupillary Diameter Decrease (Miosis) in Rabbits Measured as $(P_0 - P)/P_0 \times 10^4$ as a Function of Five Bolus Intravenous Doses of Chlorpromazine

	Dose, mg/kg iv				
Minutes	4.0	3.0	2.0	1.0	0.5
10	1668	1540	923	967	345
20	2321	2020	1399	1307	937
30	2333	2236	1814	1380	1266
40	2561	2280	1928	1520	1375
50	2533	2280	2047	1500	1424
60	2454	2460	2028	1630	1448
70	2495	2360	2082	1703	1498
80	2442	2110	1987	1703	1438
90	2361	2200	1946	1563	1408
100	2352	2180	1973	1550	1337
110	2360	2150	1927	1497	1320
120	2317	2140	1820	1417	1323
130	2240	2200	1813	1407	1270
140	2176	2180	1830	1410	1197
150	2104	2103	1817	1413	1123
160	2048	2113	1733	1360	1033
170	1986	2007	1677	1320	950
180	1907	1837	1636	1300	867
190	1894	1820	1630	1237	830
200	1886	1790	1620	1180	802
210	1875	1757	1617	1157	777
220	1860	1767	1580	1183	683
230	1846	1720	1553	1147	603
240	1820	1630	1527	1060	529
250	1768	1580	1482	1003	443
260	1706	1553	1435	957	377
270	1640	1530	1377	880	317
280	1610	1457	1282	827	250
290	1580	1367	1180	773	180
300	1556	1280	1090	727	107
310	1532	1283	1050	653	93
320	1522	1283	997	583	80
330	1486	1260	937	527	65
340	1450	1240	847	537	49
350	1410	1123	763	527	37
360	1378	963	680	483	25

Another advantage of this method is that it can handle any general input pulse, whereas fitting procedures usually require data from a specific type of pulse. Furthermore, PLTEST takes only a fraction of the time that MULTIFIT takes for the same order system. This advantage becomes particularly important with higher order systems.

Model Confirmation—The inverse transformation to the time domain of the product of two Laplace transformed functions results in the convolution integral. As an example, the output of a system would be computed using the convolution integral if the system transfer function and the input to the system are known:

$$Y(S) = G(S)^*X(S) \qquad \text{(Eq. 2)}$$

or:

$$Y(t) = \int_0^t g(\tau)X(t-\tau)\,d\tau \qquad \text{(Eq. 3)}$$

In the case of model confirmation, it is assumed that the input function is unknown. With an observed output response and a previously obtained transfer function, the task is now to determine the input that caused the given response. This problem is often termed "deconvolution."

There are several possible methods of performing a deconvolution: (*a*) numerical deconvolution, (*b*) analog deconvolution, and (*c*) digital deconvolution. Each method has its advantages and disadvantages (19). A digital deconvolution scheme has been implemented for this purpose. The method essentially involves converting the deconvolution problem into a system of linear differential equations in vector–matrix notation. The details will be presented in a future report.

For all real systems, the numerator of the transfer function is of a lower order than the denominator. This condition causes problems in deconvolution by the above procedure because it gives rise to in-

Table II—Pupillary Diameter Response Intensities from Table I Transduced to $f(I)$ Values (Relative Biophasic Drug Levels) Using the Dose–Effect Curve as a Calibration Curve and Normalized by Dividing by the Corresponding Dose

	$f(I)$/Dose						
	Dose, mg/kg iv						
Minutes	4.0	3.0	2.0	1.0	0.5	Average	*SEM*
10	0.236	0.258	0.155	0.325	0.166	0.228	0.07
20	0.631	0.555	0.313	0.545	0.630	0.535	0.13
30	0.644	0.758	0.600	0.603	1.026	0.726	0.18
40	1.000	0.800	0.727	0.750	1.206	0.897	0.20
50	0.956	0.800	0.869	0.728	1.296	0.930	0.22
60	0.782	1.053	0.844	0.888	1.350	0.984	0.23
70	0.872	0.894	0.910	1.000	1.456	1.026	0.25
80	0.773	0.629	0.797	1.000	1.320	0.904	0.27
90	0.671	0.713	0.747	0.8000	1.266	0.839	0.24
100	0.663	0.698	0.775	0.788	1.150	0.815	0.19
110	0.671	0.667	0.727	0.728	1.100	0.779	0.18
120	0.631	0.662	0.613	0.640	1.100	0.729	0.21
130	0.569	0.713	0.600	0.633	1.026	0.708	0.19
140	0.524	0.698	0.625	0.638	0.936	0.684	0.15
150	0.469	0.625	0.613	0.638	0.830	0.635	0.13
160	0.434	0.629	0.525	0.588	0.730	0.581	0.11
170	0.399	0.542	0.481	0.550	0.640	0.522	0.09
180	0.350	0.420	0.450	0.538	0.550	0.462	0.08
190	0.344	0.408	0.444	0.493	0.526	0.443	0.07
200	0.342	0.389	0.438	0.455	0.500	0.425	0.06
210	0.335	0.367	0.438	0.440	0.486	0.413	0.06
220	0.325	0.373	0.412	0.455	0.410	0.395	0.05
230	0.319	0.342	0.394	0.428	0.340	0.365	0.04
240	0.306	0.296	0.379	0.380	0.290	0.330	0.05
250	0.280	0.275	0.352	0.348	0.226	0.296	0.05
260	0.250	0.263	0.330	0.323	0.190	0.271	0.06
270	0.225	0.253	0.302	0.285	0.150	0.243	0.06
280	0.215	0.229	0.262	0.263	0.116	0.217	0.06
290	0.206	0.197	0.228	0.238	0.090	0.192	0.06
300	0.197	0.175	0.197	0.218	0.050	0.167	0.07
310	0.189	0.175	0.188	0.188	0.046	0.157	0.06
320	0.188	0.175	0.173	0.160	0.040	0.147	0.06
330	0.176	0.169	0.157	0.145	0.030	0.135	0.06
340	0.169	0.164	0.134	0.150	0.026	0.129	0.06
350	0.160	0.138	0.118	0.145	0.020	0.116	0.06
360	0.151	0.108	0.100	0.128	0.010	0.099	0.05

tegral equations rather than differential equations which are easier to solve digitally. To overcome this problem, the procedure involves the addition of as many zeros as required to make the order of the numerator equal to that of the denominator. Quite obviously, the transfer function of the system is changed. However, this change is minimized by the addition of zeros at frequencies 10 times higher than any other frequency present in the system transfer function. This provision ensures that distortions are minimal; it also permits the representation of the problem by means of a system of differential equations. For example, the system:

$$\frac{Y(S)}{X(S)} = \frac{A}{(S+m_1)(S+m_2)(S+m_3)} \qquad m_1 > m_2 > m_3 \qquad \text{(Eq. 4)}$$

can then be written as:

$$X(S) = \frac{(s+m_1)(s+m_2)(s+m_3)}{A(s+10m_1)(s+10m_1)(s+10m_1)}\,Y(S) \qquad \text{(Eq. 5)}$$

Now, this problem is rewritten in the form:

$$\mathbf{x}(t) = \underline{A}\mathbf{x}(t) + \underline{B}y(t) \qquad \text{(Eq. 6)}$$

where bold face denotes a vector and a single underline denotes a matrix.

This vector equation is integrated using the modified Euler numerical integration scheme. Practically speaking, it is difficult to obtain accurate results digitally if the input function was an impulse function or a pulse of very short duration. Hence, an extra s is introduced in the denominator of Eq. 5 so that the result of the numerical integration gives the cumulative or integrated input. Symbolically:

$$X'(S) = \frac{1}{s}\,\frac{(s+m_1)(s+m_2)(s+m_3)}{A(s+10m_1)(s+10m_1)(s+10m_4)}\,Y(S) \qquad \text{(Eq. 7)}$$

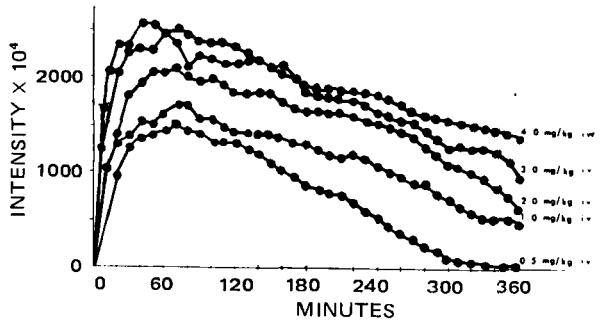

Figure 1—*Intensity of pupillary diameter decrease (miosis) in rabbits measured as* $(P_0 - P)/P_0$, *using a TV pupillometer, as a function of five bolus intravenous doses of chlorpromazine. Each curve represents averaged data from three or four rabbits.*

and:

$$\mathbf{X}'(t) = \underline{A}'x'(t) + \underline{B}y(t) \qquad \text{(Eq. 8)}$$

where:

$$\mathbf{X}'(t) = \int_0^t \mathbf{x}(t)\,dt \qquad \text{(Eq. 9)}$$

A future report will discuss the numerical deconvolution procedure in detail; a simplified overview appeared elsewhere (20, 21).

Experimental and Computational Procedure for Performing a Pharmacokinetic Analysis Using Pharmacological Data—The most commonly applicable procedure for performing a pharmacokinetic analysis of drug action using pharmacological data involves the following steps (20, 21):

1. Administration of several bolus intravenous doses of the drug and monitoring of the time course of pharmacological response intensities. The drug should induce a graded response intensity, and the maximum response resulting from each dose should occur at approximately the same time. If it does not, the assumption of linearity does not hold and an alternative approach must be implemented.

2. Construction of a dose–effect curve by plotting the maximum observed response intensities as a function of dose. The intensity of pharmacological response should be a single-valued, nonhysteretic function of biophasic drug levels (6).

3. Conversion of each I *versus* time–response profile resulting from each dose into a corresponding $f(I)$ *versus* time profile.

4. Dose normalization of the $f(I)$ values for each dose and plotting of all $f(I)/D$ values on the same set of coordinates. All points should scatter around the same curve to confirm the assumption of linearity.

5. Fitting of a sum of exponential equation to the $f(I)/D$ *versus* time curve using various weighted least-squares, regression, computer techniques or other techniques derived from engineering systems analysis such as the pulse testing technique to yield values of equation parameters.

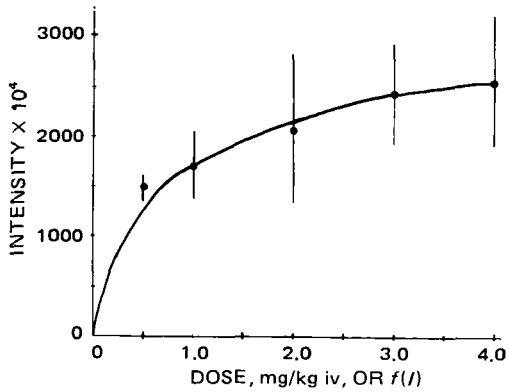

Figure 2—*Intravenous dose–effect curve for chlorpromazine-induced pupillary diameter decrease in rabbits constructed from the maximum response intensities from Fig. 1, with the standard error of the mean indicated for each value. The abscissa is relabeled* f(I), *which corresponds to a relative biophasic drug level.*

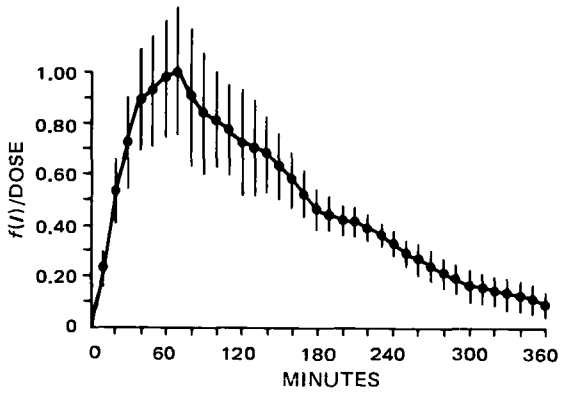

Figure 3—*Pupillary diameter response intensities from Fig. 1 transduced to* f(I) *values (relative biophasic drug levels) using the dose–effect curve as a calibration curve and normalized by dividing by the corresponding dose. The average* f(I)*/dose values are indicated along with the standard error of the mean for each value.*

6. Development of a model transfer function describing the relationship between drug input and response output. The transfer function, $G(s)$, may be defined as the Laplace Transform of the $f(I)/D$ *versus* time function obtained in Step 5. The form of $G(s)$ is given by:

$$G(s) = Lg(t) = L\sum_{i=1}^{N} A_i e^{-m_i t} = \sum_{i=1}^{N} \frac{A_i}{m_i + s} \qquad \text{(Eq. 10)}$$

where $g(t)$ is the "weighting function," and L signifies the Laplace operator.

7. Verification of the transfer function model for use in pharmacokinetic computations by a direct comparison of experimentally known drug inputs obtained by programmed intravenous infusion with results computed from monitoring the pharmacological response intensities during the intravenous administration of the drug. These observed time variations of drug response intensities are converted into their corresponding relative biophasic drug level *versus* time profile using the dose–effect curve. The cumulative amount of drug absorbed (or infused), A_t, is then obtained by deconvolving the biophasic drug levels, Q_B, with the transfer function, $G(s)$, which in the time domain is $g(t)$, in the following manner:

$$A_t = \int_0^t \int_0^t [g(t-\tau)^{-1} Q_B(\tau) d\tau]\, dt \qquad \text{(Eq. 11)}$$

where τ is a dummy variable used to perform the necessary integrations. Good agreement between known and experimentally determined A_t values verifies the mathematical model.

EXPERIMENTAL

Materials—Chlorpromazine hydrochloride[1] was supplied in powder form and used as received without further purification. This drug was freshly solubilized before each experiment using normal saline for injection USP[2]. All syringes used were disposable plastic[3], and the plastic cannulas with needles attached were 23-gauge butterfly infusion sets[2]. Male New Zealand white rabbits[4], 3–4 months old and 2.5–3.5 kg, were used as long as they remained physically healthy. They were not screened in any way prior to experimentation and were utilized as received.

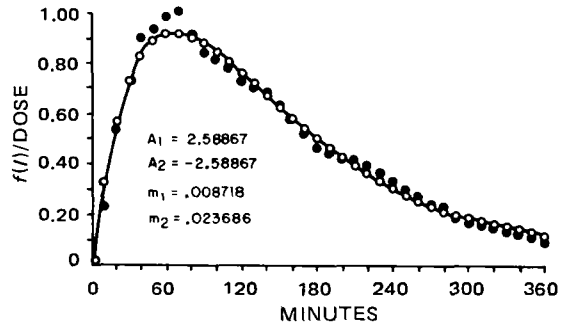

Figure 4—*The* f(I)*/dose values experimentally determined from pupillary diameter decreases* (●) *and computer-predicted values* (○) *based upon a biexponential model obtained by fitting the data via a least-squares procedure. The model has the general form:*

$$y = \sum_{i=1}^{n} A_i e^{-m_i t}$$

where the A_i*'s and* m_i*'s are constants.*

Table III—Intensity of Pupillary Diameter Decrease in a Single Rabbit (No. 17) Measured as $(P_0 - P)/P_0 \times 10^4$ in Response to a Slow Intravenous Infusion of Chlorpromazine, the Infusion Rate Being 0.50 mg/kg/hr

Minutes	I^a	$f(I)$
10	508	0.133
20	740	0.225
30	915	0.300
40	1070	0.383
50	1205	0.470
60	1325	0.555
70	1415	0.635
80	1480	0.705
90	1535	0.768
100	1580	0.825
110	1625	0.885
120	1650	0.923
130	1675	0.962
140	1690	0.993
150	1705	1.000
160	1710	1.013
170	1720	1.025
180	1725	1.037
190	1730	1.050
200	1735	1.067
210	1740	1.075
220	1745	1.081
230	1750	1.088
240	1755	1.096
250	1760	1.105
260	1770	1.121
270	1775	1.138
280	1780	1.150
290	1785	1.159
300	1790	1.168

[a] The intensity values were transduced to $f(I)$ values (relative biophasic drug levels) using the dose–effect curve as a calibration curve.

Methods—The animals were fasted for 24 hr prior to the experiment and were then restrained in an appropriate holder and weighed. A butterfly infusion cannula was inserted in the marginal ear vein, secured with a paper clip, and flushed with normal saline. The restrained animal was placed in a darkened room where the small amount of constant illumination necessary for the experiment was provided by two microscope lamps[5]. The animal was allowed 60 min to acclimate to the darkened room, during which time measurements of pupil diameter were taken for determining baseline values.

Pupil diameters were determined using a television pupillometer[6] equipped with a video camera and a low intensity, red illumination light. The signal from the video camera was relayed to a 63.5-cm (25-in.) professional size television monitor where the pupil size could be measured easily on the screen using compass dividers and a meter stick. Normal baseline pupil diameters measured from 29.0 to 32.0 cm using this method.

Once the animal's pupil diameter reached constant values, normal saline or a dose of chlorpromazine was administered *via* the cannula in the marginal ear vein in approximately 40–60 sec. The chlorpromazine dosage range employed was 0.5–4.0 mg/kg. Following dosing, pupillometry readings were taken for 5–6 hr depending on the animal's rate of recovery. The degree of pupil diameter decrease due to chlorpromazine doses was calculated in the following manner: the initial value at zero time minus the value at time t divided by the initial value.

[2] Abbott Laboratories, Chicago, Ill.
[3] Becton-Dickinson.
[4] Nicely Farms, Greenfield, Ind.
[5] Bausch & Lomb.
[6] Model 800, Whittaker Industries, Space Sciences Division, Waltham, Mass.

Table IV—Intensity of Pupillary Diameter Decrease in a Single Rabbit (No. 20) Measured as $(P_0 - P)/P_0 \times 10^4$ in Response to a Slow Intravenous Infusion of Chlorpromazine, the Infusion Rate Being 0.50 mg/kg/hr

Minutes	I^a	$f(I)$
10	241	0.053
20	655	0.188
30	975	0.333
40	1225	0.485
50	1375	0.603
60	1500	0.728
70	1598	0.850
80	1695	0.993
90	1725	1.035
100	1775	1.138
110	1820	1.223
120	1850	1.275
130	1875	1.338
140	1890	1.373
150	1900	1.388
160	1918	1.418
170	1925	1.448
180	1935	1.463
190	1950	1.495
200	1965	1.525
210	1975	1.550
220	1980	1.563
230	1995	1.605
240	2005	1.625
250	2015	1.650
260	2025	1.675
270	2035	1.705
280	2050	1.738
290	2065	1.765
300	2075	1.800

[a] The intensity values were transduced to $f(I)$ values (relative biophasic drug levels) using the dose–effect curve as a calibration curve.

Table V—Intensity of Pupillary Diameter Decrease in a Single Rabbit (No. 20) Measured as $(P_0 - P)/P_0 \times 10^4$ in Response to a Slow Intravenous Infusion of Chlorpromazine, the Infusion Rate Being 0.75 mg/kg/hr

Minutes	I^a	$f(I)$
10	625	0.175
20	1025	0.363
30	1315	0.550
40	1515	0.740
50	1640	0.900
60	1725	1.037
70	1765	1.120
80	1775	1.138
90	1780	1.150
100	1785	1.159
110	1790	1.168
120	1795	1.175
130	1800	1.183
140	1855	1.198
150	1810	1.205
160	1810	1.205
170	1815	1.213
180	1820	1.223
190	1825	1.238
200	1825	1.238
210	1825	1.238
220	1830	1.250
230	1830	1.250
240	1835	1.255
250	1840	1.263
260	1845	1.268
270	1850	1.275
280	1855	1.288
290	1860	1.300
300	1865	1.305

[a] The intensity values were transduced to $f(I)$ values (relative biophasic drug levels) using the dose–effect curve as a calibration curve.

RESULTS AND DISCUSSION

Time Course of Drug Response—The intensities of pupillary diameter decrease (miosis) in rabbits as a function of five bolus intravenous doses of chlorpromazine are shown in Fig. 1. The average miotic values for each dose of drug are also indicated in Table I. These averages were determined from data from two to four rabbits for each dose; the dosing schedule was randomized according to a Youden square design. A clearly discernible graded response profile is evidenced by Fig. 1. The times of absolute response intensity maximums were not identical here but the times all were within a narrow time band between 40 and 70 min, with no trend observable with increasing dose.

It can be seen from Fig. 1 that the times of maximum response intensity were removed from zero time. Strictly speaking, the times of maximum response must be identical for the system to be considered linear and modeled using linear mathematical techniques. However, one may still choose to model a system that is nonlinear with a linear mathematical model, depending, of course, on the degree of nonlinearity. Thus, one may obtain an accurate representation of the biokinetic behavior of the drug in that system over the range of doses and intensities of response studied. The intensity maximums did not occur at time zero, indicating that the biophase is a compartment kinetically distinct from the systemic circulation where the drug was administered.

Construction of Dose–Effect Curve—The intravenous dose–effect curve for chlorpromazine-induced pupillary diameter decrease in rabbits was constructed from the maximum response intensities shown in Fig. 1 and can be seen as Fig. 2. The shape of the curve appears as expected because chlorpromazine is known to have a very high therapeutic index and the curve plateaus over a wide dose range. The dose–effect curve represents a single-valued functional relationship between dose or relative biophasic drug levels and miotic response intensity (21).

Transduction of I Values to $f(I)$—Pupillary diameter response intensities were transformed to $f(I)$ values (relative biophasic drug levels) using the dose–effect curve as a calibration curve. The individual dose-normalized $f(I)$ values can be seen in Table II, which also lists the average $f(I)$/dose values and the standard deviations of the means. These average values were plotted as a function of time (Fig. 3), and these data represent the unit impulse response output of the system. The MULTIFIT and PLTEST curve-fitting procedures were then employed to fit these data with a mathematical function in the form of a sum of exponentials.

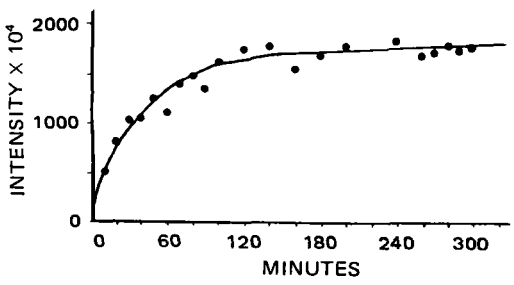

Figure 5—*Intensity of pupillary diameter decrease in a single rabbit (No. 17) in response to a slow intravenous infusion of chlorpromazine, the infusion rate being 0.50 mg/kg/hr.*

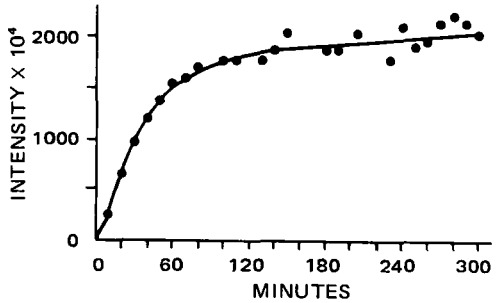

Figure 6—*Intensity of pupillary diameter decrease in a single rabbit (No. 20) in response to a slow intravenous infusion of chlorpromazine, the infusion rate being 0.50 mg/kg/hr.*

Table VI—Amount of Chlorpromazine Infused Determined Experimentally from Pupillary Diameter Decreases in Rabbit 17 *versus* Actual Amount of Chlorpromazine Theoretically Infused at 0.50 mg/kg/hr

$A(t)_{theor}$	$A(t)_{exp}$
0.0833	0.3650
0.1667	0.4030
0.2500	0.4500
0.3333	0.5400
0.4167	0.6450
0.5000	0.7300
0.5833	0.8200
0.6667	0.8900
0.7500	0.9700
0.8333	1.0400
0.9167	1.1380
1.0000	1.1800
1.0333	1.2560
1.1667	1.3125
1.2500	1.3300
1.3333	1.4000
1.4167	1.4628
1.5000	1.5290
1.5833	1.5970
1.6667	1.6725
1.7500	1.7204
1.8333	1.7790
1.9167	1.8433
2.0000	1.9100
2.0833	1.9800
2.1667	2.0650
2.2500	2.1400
2.3333	2.2000
2.4167	2.2600
2.5000	

Model Determination—Figure 4 represents the $f(I)$/dose values experimentally determined from chlorpromazine-induced pupillary diameter decreases plotted with values predicted from computerized MULTIFIT mathematical model parameters. The model so obtained appears to be a reasonable approximation of the true solution as evidenced by the closeness of the fit to the experimental data points.

As noted previously, the PLTEST procedure can be utilized to obtain frequency response information about the system that can lead to the determination of the mathematical model parameters for the system transfer function by an alternative route to be compared with those obtained by the MULTIFIT process. The parameters so obtained were compared with those obtained by the MULTIFIT procedure, and there was no significant difference between the two sets of parameters (22).

Model Verification—The intensities of pupillary diameter decrease in single rabbits in response to various slow intravenous infusions of chlorpromazine can be seen in Tables III–V. The infusion rates employed here *were* 0.50 and 0.75 mg/kg/hr. The purpose of the slow intravenous infusions was to introduce a type of input into the system other than that for which the transfer function had been determined; by using the output from these infusions and this transfer function model, the fidelity of the model was determined by calculating the known input function from pharmacological data alone and comparing experimentally determined values with theoretical values.

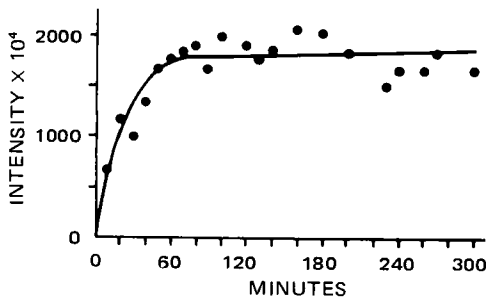

Figure 7—*Intensity of pupillary diameter decrease in a single rabbit (No. 20) in response to a slow intravenous infusion of chlorpromazine, the infusion rate being 0.75 mg/kg/hr.*

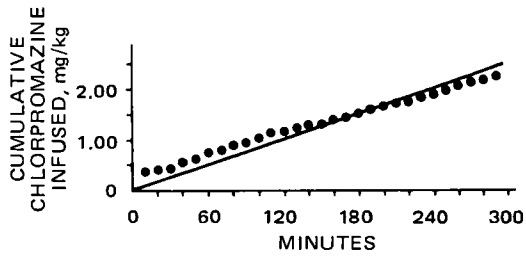

Figure 8—*Experimentally determined amounts of chlorpromazine slowly infused to a single rabbit (No. 17) as a function of time using intensities of pupillary diameter decrease and the transfer function model in a deconvolution procedure. The response intensity values were transduced to* f(I) *values (relative biophasic drug levels) using the dose–effect curve and deconvolved to yield cumulative amounts of chlorpromazine infused. The solid line represents the actual amount of chlorpromazine infused during the experiment, 0.50 mg/kg/hr.*

Figures 5–7 represent graphically the slow intravenous responses from Tables III–V; the curves were smoothed to facilitate their use in the deconvolution procedure.

The response intensity values from Tables III–V were transduced to $f(I)$ values (relative biophasic drug levels) using the dose–effect curve. These $f(I)$ values from the slow intravenous infusions then served as inputs to the deconvolution computer program that calculates cumulative drug input values once the transfer function and the response output from the system are known. Figure 8 indicates the computationally determined amounts of chlorpromazine slowly infused in a single rabbit at 0.50 mg/kg/hr, using intensities of pupillary diameter decrease and the transfer function model in a deconvolution procedure; cumulative amounts of chlorpromazine infused were plotted as a function of time.

Table VI lists the known amounts of chlorpromazine infused for comparison to the amount infused calculated wholly from pharmacological response intensities. The values are plotted in Fig. 9, where the slope of the best straight line forced through the origin is indicated along with the Pearson R correlation coefficient. Table VII summarizes the results from the deconvolution of response intensities from all slow intravenous infusions. It indicates good agreement when the experimentally known amounts of drug slowly infused are compared to the amounts calculated from pharmacological data.

The results indicate excellent agreement, as judged by the linear correlation coefficient and slope of plots of theoretically predicted *versus* experimentally observed values of drug bioavailability inputs of chlorpromazine. The validity of the mathematical model describing drug transfer in this system for the dosage range employed is confirmed.

SUMMARY AND CONCLUSIONS

The principal purpose of the present study was to investigate and confirm a method of performing a pharmacokinetic analysis of drug-responding biological systems using pharmacological response data. The results demonstrate that, through the suitable use of intravenous dose–effect curves to transform observed intensities of pharmacological response into values of relative biophasic drug levels, the postulation of hypothetical models for the drug–receptor interaction is obviated. The following conclusions were also evident:

1. As exemplified for the drug chlorpromazine, the method was confirmed and illustrated using results derived from the drug-induced

Table VII—Summary of the Deconvolution Results of Pupillary Diameter Response Intensities from Slow Intravenous Infusions of Chlorpromazine Where the Amount Theoretically Infused Was Compared with the Amount Calculated Using Pharmacological Data Alone

Rabbit	Infusion Rate, mg/kg/hr	$A(t)$ Slope	Pearson R
17	0.50	1.00405	0.99373
20	0.50	1.42894	0.99650
20	0.75	0.84010	0.98148

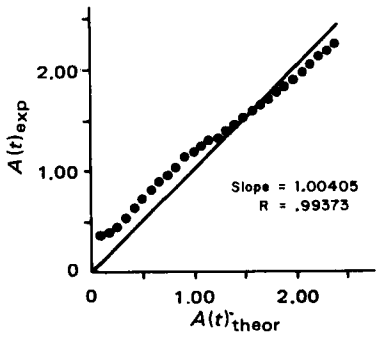

Figure 9—*Amount of chlorpromazine infused determined experimentally from pupillary diameter decreases of a single rabbit (No. 17)* versus *actual amount of chlorpromazine theoretically infused at 0.50 mg/kg/hr. The slope of the best line through the data points was determined using a linear regression technique.*

decrease in pupil diameter in rabbits. Agreement was observed between the quantities of drug known to be infused at any time and the amounts calculated wholly from pharmacological response data.

2. Through the proper selection of linear mathematical equation parameters, a system that is not strictly linear can be modeled in a linear fashion over an appreciable dose range. For chlorpromazine, this dose range was 0.5–4.0 mg/kg iv. The appropriate mathematical model to describe drug-induced changes in pupillary diameter in rabbits was a biexponential equation.

Subsequent reports will demonstrate results for other pharmacological responses to chlorpromazine (*e.g.*, intraocular pressure change and body temperature lowering) similar to those obtained for pupillometry. The use of pharmacological data for bioavailability testing of chlorpromazine in humans was reported elsewhere (22, 23).

REFERENCES

(1) J. G. Wagner and E. Nelson, *J. Pharm. Sci.*, **53**, 1392 (1964).

(2) J. C. K. Loo and S. Riegelman, *ibid.*, **57**, 918(1968).

(3) V. F. Smolen, *Can. J. Pharm. Sci.*, **7**, 1(1972).

(4) V. F. Smolen, B. D. Turrie, and W. A. Weigand, *J. Pharm. Sci.*, **61**, 1941(1972).

(5) G. Levy and M. Gibaldi, *Ann. Rev. Pharmacol.*, **12**, 85(1972).

(6) V. F. Smolen and R. D. Schoenwald, *J. Pharm. Sci.*, **60**, 96(1971).

(7) V. F. Smolen, R. G. Barile, and T. G. Theophanous, *ibid.*, **61**, 467(1972).

(8) A. B. Nutt and H. L. Wilson, *Br. Med. J.*, **1**, 1457(1955).

(9) S. D. Paul and I. H. Leopold, *Am. J. Ophthalmol.*, **42**, 107(1956).

(10) S. Oono, *Jpn. J. Pharmacol.*, **15**, 81(1965).

(11) G. Levy, *Clin. Pharmacol. Ther.*, **7**, 362(1966).

(12) R. E. Notari, *J. Pharm. Sci.*, **62**, 865(1973).

(13) W. J. Westlake, *ibid.*, **62**, 1579(1973).

(14) D. S. Riggs, "The Mathematical Approach to Physiological Problems," Williams & Wilkins, Baltimore, Md., 1963, pp. 193–217.

(15) J. G. Truxal, "Automatic Feedback Control System Synthesis," McGraw-Hill, New York, N.Y., 1955.

(16) D. R. Coughanower and L. B. Koppel, "Process Systems Analysis and Control," McGraw-Hill, New York, N.Y., 1965.

(17) P. Harriott, "Process Control," 1st ed., McGraw-Hill, New York, N.Y., 1964.

(18) W. L. Luyben, "Process Modeling, Simulation, and Control for Chemical Engineers," McGraw-Hill, New York, N.Y., 1973.

(19) R. Rodeman and J. T. P. Yao, "Structural Identification—Literature Review," School of Civil Engineering, Purdue University, Lafayette, Ind., Dec. 1973.

(20) V. F. Smolen, *J. Pharmacokinet. Biopharm.*, **4**, 337(1976).

(21) *Ibid.*, **4**, 353(1976).

(22) V. F. Smolen, E. J. Williams, and P. B. Kuehn, *Can. J. Pharm. Sci.*, **10**, 95(1975).

(23) V. F. Smolen, H. R. Murdock, Jr., W. P. Stoltman, J. W. Clevenger, L. W. Combs, and E. J. Williams, *J. Clin. Pharmacol.*, **15**, 734(1975).

ACKNOWLEDGMENTS AND ADDRESSES

Received November 25, 1974, from the *Interdisciplinary Drug Engineering and Assessment Laboratory, School of Pharmacy and Pharmacal Sciences, Purdue University, West Lafayette, IN 47907*

Accepted for publication January 8, 1976.

Presented at the Pharmacology and Toxicology Section, APhA Academy of Pharmaceutical Sciences, Chicago meeting, 1974.

Abstracted in part from theses submitted by P. B. Kuehn and A. K. Jhawar to Purdue University in partial fulfillment of the Doctor of Philosophy degree requirements.

Supported by the National Institutes of Health, Predoctoral Fellowship 5 F01 G543208-03, and Food and Drug Administration Contract 73-23.

* Present address: School of Pharmacy, University of Washington, Seattle, WA 98195

‡ Present address: AMACO Oil Co., Naperville, Ill.

§ Department of Chemical Engineering, School of Engineering, Purdue University, West Lafayette, IN 47907

ˣ To whom inquiries should be directed (Department of Industrial and Physical Pharmacy, School of Pharmacy and Pharmacal Sciences, Purdue University, West Lafayette, IN 47907).

Bioavailability and Pharmacokinetic Analysis of Chlorpromazine-Induced Rectal Temperature Depression in Rabbits

VICTOR F. SMOLEN [x], ASHOK K. JHAWAR *, WILLIAM A. WEIGAND [‡], RONALD M. PAOLINO [§], and PAUL B. KUEHN [¶]

Abstract □ Chlorpromazine-induced depression of rectal temperatures in rabbits kept at 20° was used to determine relative biophasic drug levels corresponding to observed hypothermic response intensities, which then served to establish a triexponential linear mathematical model describing drug transference and drug action in this system. Comparisons of various experimentally known, slow intravenous infusion drug inputs of chlorpromazine with drug inputs computed by deconvolution, using the derived model and observed temperature depressions, served to verify the accuracy of the model for the 0.50–4.0-mg/kg dosage range.

Keyphrases □ Chlorpromazine—bioavailability and pharmacokinetics, evaluated by measurement of rectal temperature depression, rabbits □ Bioavailability—chlorpromazine, evaluated by measurement of rectal temperature depression, rabbits □ Pharmacokinetics—chlorpromazine, evaluated by measurement of rectal temperature depression, rabbits □ Tranquilizers—chlorpromazine, bioavailability and pharmacokinetics, evaluated by measurement of rectal temperature depression, rabbits

The use of pharmacological response *versus* time data can often represent an advantageous alternative to the use of data derived from the direct assay of drugs in the plasma or other body fluids. A routinized procedure for the use of pharmacological data to perform pharmacokinetic and bioavailability analyses by observing drug effects in a given system was described previously (1–3). The present report further illustrates the application of pharmacological response data to pharmacokinetic modeling for the drug chlorpromazine. Chlorpromazine-induced changes in the rectal temperature recorded in rabbits were transformed to relative biophasic drug levels, using a dose–effect curve, and subsequently utilized to establish a biomathematical model relating the drug transference and drug response behavior of the system to drug bioavailability inputs as defined by the dynamics of how the drug enters the systemic circulation.

Chlorpromazine produces a fall in body temperature in most species exposed to neutral environmental temperatures (4, 5). However, the mechanism by which the drug produces its effect on temperature is unclear. Chlorpromazine has a strong antiadrenergic effect but little or no anticholinergic activity (6), and it also exhibits a peripheral ganglionic action (7). The drug is a remarkably potent antagonist of epinephrine and norepinephrine (8). The drug could act within the central nervous system by reducing the sensitivity of the thermoregulatory process at the level of the hypothalamus or peripherally by interfering with thermoregulatory vasomotor control due to vasodilation (9, 10). Total body heat loss could be explained on the basis of an increased heat loss through vasodilation and a decrease in heat production through muscle relaxation or prevention of shivering (10–13).

Some investigations speculated that chlorpromazine might have an effect on lowering body metabolism (10), while others discount this possibility (11). In any event, the effect of chlorpromazine on body temperature is said to be poikilothermic (14) in that the body temperature tends to assume the ambient temperature of the surrounding environment. Previous animal studies also showed that the drug's effect on body temperature is dose dependent (15), with the maximum intensity of effect occurring between 1 and 3 hr after administration, depending on the species studied (11, 16). The time for maximum intensity of response to occur is relatively long, because the mechanism of drug action involves both heat production and heat loss processes which are relatively slow and continuous phenomena.

Despite the complications and the lack of definitive knowledge concerning the precise mechanism by which chlorpromazine induces its hypothermic activity, pharmacokinetic relationships between drug input and the resulting time variation of its effects can still be established provided the temporal pharmacological data are observed to behave in conformity with the assumption that the transference behavior of the drug in the body can be described by linear dynamics. Whether this is the case or not can be judged from the observed behavior of pharmacological data alone without utilizing any direct assay methods to detect the presence of the drug in the body.

When certain criteria justifying the assumption of linear system behavior are even approximately met, the relationship between the rates and extents to which a drug enters the body, *i.e.*, the drug bioavailability input, and the pharmacological effects it induces can be reliably established, even for natural product drugs whose exact chemical composition is not known or for drugs such as chlorpromazine whose rapid and complex metabolism and distribution into tissues renders it extremely difficult to detect in body fluids. As illustrated by the results of the present study, such drug input → output response relationships can be established without any specific knowledge of the site(s) and mechanism of the drug's action(s) and observed effect.

EXPERIMENTAL

Materials—Chlorpromazine hydrochloride[1] was supplied in powder form and used as received. The drug was freshly solubilized

[1] Thorazine, Smith Kline and French, Philadelphia, Pa.

Table I—Average Intensity of Rectal Temperature Depression in Rabbits Measured at 20°, Recorded as $(T_0 - T)/T_0 \times 10^4$, as a Function of Five Bolus Doses of Chlorpromazine

Minutes	Dose, mg/kg iv				
	4.0	3.0	2.0	1.0	0.5
10	49	66	42	32	26
20	96	109	87	63	49
30	149	155	132	99	81
40	197	202	174	132	112
50	242	251	213	169	140
60	285	299	250	198	162
70	327	340	282	223	180
80	365	377	309	242	191
90	396	408	339	255	204
100	426	436	369	266	213
110	452	459	392	271	221
120	474	474	406	278	219
130	493	484	412	278	217
140	513	493	416	279	209
150	525	496	422	280	212
160	533	401	421	279	212
170	537	499	414	275	209
180	543	493	418	264	203
190	544	487	412	256	204
200	540	488	403	259	196
210	531	483	396	253	189
220	527	473	385	244	180
230	519	464	375	240	173
240	514	454	364	229	171
250	505	446	354	228	169
260	491	442	343	220	163
270	480	430	331	212	158
280	475	424	326	208	—
290	464	412	319	196	—
300	452	406	312	190	—
310	441	401	298	181	—
320	434	394	291	173	—

before each experiment using normal saline for injection USP[2]. Disposable plastic syringes[3] were used, and the plastic cannulas with needles attached were 23-gauge butterfly infusion sets[3].

New Zealand white rabbits[4], 3–4-month-old males, were caged individually and received a regular diet with no restrictions on the amount of food and water consumed. All rabbits weighed between 2.5 and 3.5 kg and were used as long as they remained physically healthy.

Methods—The animals were fasted for 24 hr prior to the experiment. They were then restrained in an appropriate holder and weighed. A rectal thermistor probe[5] was inserted 8 cm into the animal's rectum and secured to the tail using several rubberbands. The rabbits were then placed into a constant-temperature incubator[6] with the ambient temperature set at 20°.

The animals were allowed 60 min to equilibrate, in which time their rectal temperatures reached a constant value of 38.5–38.8°. Rectal temperatures were observed using a temperature monitor[7] with automatic channel scanning capability and recorded on a strip-chart recorder[8] that had been previously calibrated using the rectal probes and monitor.

Once the animal's rectal temperature reached a constant value, normal saline (the control dose) or a dose of chlorpromazine was administered *via* the marginal ear vein in approximately 20 sec. The chlorpromazine dosage range was 0.5–4.0 mg/kg. The dosing schedule was randomized according to an Youden square design. Following dosing, the rectal temperature was continuously monitored for 6 hr.

The saline dose produced no change in rectal temperature. The intensity of rectal temperature depression elicited by chlorpromazine was calculated as the initial temperature at time zero minus the temperature at time t; dividing this number by the initial temperature

[2] Abbott Laboratories, Chicago, Ill.
[3] Becton-Dickinson.
[4] Nicely Farms, Greenfield, Ind.
[5] Model 402.
[6] New Brunswick Psychotherm.
[7] Model 47 Telethermonitor, Yellow Springs Instrument Co.
[8] E. H. Sargent model SR6G.

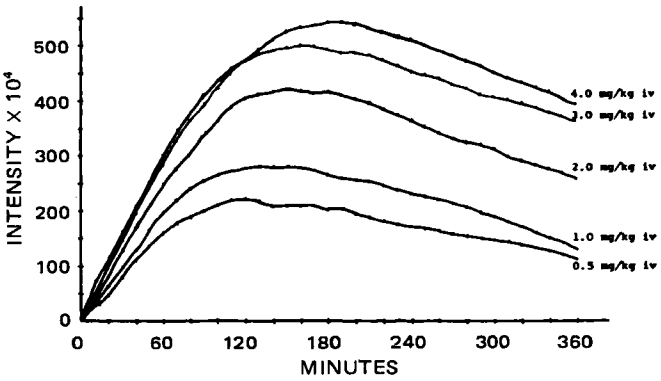

Figure 1—*Intensity of rectal temperature depression in rabbits kept at 20°, reported as* $(T_0 - T)/T \times 10^9$, *as a function of five bolus intravenous doses of chlorpromazine. Each curve represents averaged data from seven to nine rabbits.*

gave the hypothermic response intensity. These experiments were used to construct the dose–effect curve.

The validity of the models developed was checked by using the response to slow intravenous infusion of chlorpromazine. The infusion rates employed were 0.50 and 0.75 mg/kg/hr.

RESULTS AND DISCUSSION

Time Course of Drug Response—The observed time variations of the intensity of chlorpromazine-induced rectal temperature depression in rabbits kept at 20° as a function of five bolus intravenous doses of the drug are shown in Fig. 1; the average values are listed in Table I. Each curve in Fig. 1 represents averaged data from seven to nine rabbits. The observed maximum response intensities for each dose and the times of their occurrence are summarized in Table II.

It is apparent that the drug-induced rectal temperature depression is a graded response, but the times of absolute maximum response are not exactly identical. Despite this apparent nonlinear characteristic of the data, it was felt that a linear model might still adequately describe this system because virtually 90% of the response intensity maximums fell within a rather narrow time band.

Figure 1 shows that the times of maximum response occur far beyond zero time. This behavior can be taken to indicate that the biophase is removed and can be described as a "deep" compartment separate from the systemic circulation or plasma space into which the drug was administered. However, the sites of action may not necessarily be as far removed as the intensity maximums indicate since the temperature regulation mechanisms involve both direct and indirect effects on the hypothalamus and vasoconstriction. Moreover, there is the influence of the body's large heat capacity acting in a manner analogous to a low pass filter in an electrical system with regard to transmitting the results of the drug's action at receptor sites to

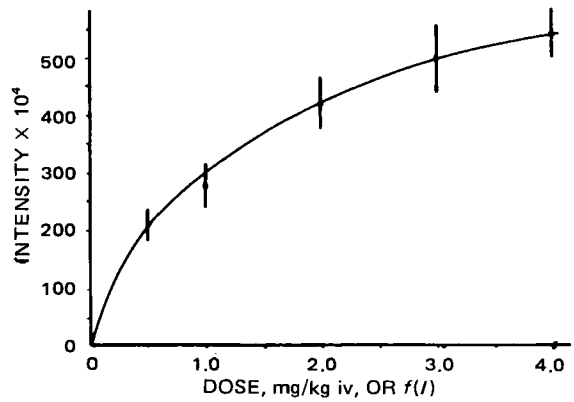

Figure 2—*Intravenous dose–effect curve for chlorpromazine-induced rectal temperature depression in rabbits constructed from the maximum intensities of temperature depression in Fig. 1, with the standard error of the mean indicated for each value. The abscissa is relabeled* f(I), *which corresponds to a relative biophasic drug level.*

Table II—Range of Maximum Intensities of Rectal Temperature Depression and Times of Maximum Response in Individual Rabbits as a Function of Five Bolus Intravenous Doses of Chlorpromazine

	Dose, mg/kg iv									
	4.0		3.0		2.0		1.0		0.5	
Rabbit	I_{max}	t_{max}	I_{max}	t_{max}	I_{max}	t_{max}	I_{max}	t_{max}	I_{max}	t_{max}
1	493	170	—	—	353	130	219	130	235	170
4	512 473	180 180	389	170	539	190	—	—	255	190
5	637	160	609	140	404	130	252	100	—	—
A	594	200	582	200	578	160	331	140	397	170
B	447	150	370	120	332	120	315	120	81	140
C	519	190	697	190	409	170	382	150	—	—
D	443	140	434	120	335	150	185	170	225	110
E	656	210	578	160	434	160	397	170	—	—
F	564	180	582	160	425	140	252	130	170	180
H	671	190	506	120	568	170	337	150	322	110
$\bar{X}$	546	177	527	153	438	152	297	140	241	153
SEM	25.06	6.34	33.20	9.17	28.06	6.64	22.10	6.91	30.65	9.96

manifest as an observed hypothermic effect. Conceivably, the slow loss and gain of heat by the system itself could be responsible for the peak response intensities being observed at times later than zero following the administration of the bolus intravenous doses, even though the actual drug levels at the site(s) of action are at all times in equilibrium with drug levels in the blood. In any case, the actual biophysical mechanisms involved are irrelevant to the purely phenomenological description of the developed system.

Construction of Dose–Effect Curve—Table II indicates the intensities of maximum rectal temperature depression and their times of occurrence for each dose of chlorpromazine administered to each rabbit. The average values are also indicated along with their standard deviations of the means. These average values were plotted as a function of the dose, and the resulting intravenous dose–effect curve is shown in Fig. 2. The shape of the curve appears as expected based upon the fact that chlorpromazine is known to have a high therapeutic index and the curve plateaus over a wide dose range.

When the dose–effect curve is represented by a single-valued functional relationship between dose and response intensity, as exemplified by Fig. 2, it can be used as a calibration curve to convert intensities of drug effect, observed at any time following dosing by any route, into actual or relative biophasic drug levels. The basis and purpose of the conversion were discussed previously (1–3, 17).

Transduction of I Values to $f(I)$— The observed rectal temperature response intensities were transduced to $f(I)$ values (relative biophasic drug levels) using the dose–effect curve as a calibration curve, as described in detail elsewhere (2, 17, 18). The individual dose-normalized $f(I)$ values are listed in Table III, which also contains the average $f(I)$/dose values and the standard deviations of the means. These average values, plotted as a function of time, are shown in Fig.

Table III—Rectal Temperature Response Intensities from Table I Transduced to $f(I)$ Values (Relative Biophasic Drug Levels) Using the Dose–Effect Curve as a Calibration Curve and Normalized by Dividing by the Corresponding Dose

	$f(I)$ Dose						
	Dose, mg/kg iv						
Minutes	4.0	3.0	2.0	1.0	0.5	Average	*SEM*
10	0.019	0.037	0.032	0.050	0.0	0.028	0.009
20	0.040	0.062	0.072	0.100	0.150	0.085	0.023
30	0.069	0.100	0.123	0.170	0.260	0.144	0.031
40	0.109	0.153	0.78	0.245	0.400	0.337	0.120
50	0.162	0.233	0.252	0.335	0.520	0.301	0.063
60	0.256	0.345	0.345	0.440	0.650	0.407	0.067
70	0.306	0.442	0.505	0.550	0.750	0.511	0.072
80	0.375	0.533	0.555	0.650	0.820	0.587	0.072
90	0.438	0.617	0.655	0.725	0.940	0.675	0.081
100	0.500	0.700	0.762	0.810	1.010	0.756	0.081
110	0.569	0.787	0.855	0.860	1.060	0.826	0.072
120	0.637	0.850	0.920	0.975	1.050	0.886	0.058
130	0.706	0.903	0.945	0.975	1.040	0.914	0.036
140	0.800	0.942	0.962	0.990	0.980	0.935	0.027
150	0.869	0.963	0.992	1.000	1.000	0.965	0.013
160	0.940	1.000	0.988	0.990	1.000	0.983	0.013
170	0.944	0.983	0.950	0.900	0.980	0.951	0.036
180	0.994	0.942	0.970	0.785	0.930	0.924	0.036
190	1.000	0.917	0.945	0.730	0.940	0.906	0.040
200	0.969	0.920	0.902	0.750	0.860	0.880	0.036
210	0.900	0.895	0.875	0.710	0.840	0.844	0.040
220	0.881	0.850	0.830	0.655	0.750	0.793	0.036
230	0.831	0.775	0.788	0.635	0.710	0.748	0.036
240	0.806	0.767	0.750	0.575	0.700	0.720	0.031
250	0.762	0.737	0.712	0.570	0.670	0.690	0.036
260	0.700	0.723	0.672	0.530	0.650	0.655	0.036
270	0.659	0.683	0.630	0.500	0.620	0.618	0.045
280	0.644	0.662	0.613	0.480	0.550	0.590	0.045
290	0.581	0.630	0.593	0.430	0.500	0.547	0.054
300	0.571	0.613	0.580	0.410	0.420	0.519	0.035
310	0.540	0.595	0.530	0.385	0.370	0.484	0.037
320	0.521	0.575	0.517	0.355	0.310	0.456	0.042
330	0.506	0.563	0.500	0.315	0.260	0.429	0.058

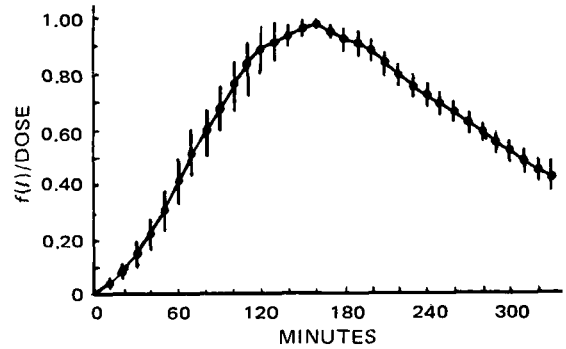

Figure 3—*Rectal temperature depression intensities from Fig. 1 transduced to* f(I) *values (relative biophasic drug levels) using the dose–effect curve as a calibration curve and normalized by dividing by the corresponding dose. The average* f(I)*/dose values are indicated along with the standard error of the mean for each value.*

3. The resulting curve represents the unit impulse response output of the system (19–21).

Curve-fitting procedures such as MULTIFIT, which operates in the time domain, and PLTEST, which performs in the frequency domain (19, 22), were then used to fit this curve with a mathematical function having the form of a sum of exponential terms.

Model Determination—Figure 4 depicts the $f(I)$/dose values experimentally determined from chlorpromazine-induced rectal temperature depression plotted for comparison with values predicted from computerized MULTIFIT mathematical model parameters. Based on this comparison, the mathematical model obtained by the use of the MULTIFIT computer program appears to be a reasonable approximation of the observed data, as evidenced by the closeness of the computed points to the experimental data points.

The parameters of the mathematical model also were determined using the PLTEST procedure (19, 22), which has the advantage of requiring less computer time than the MULTIFIT program and serves as an alternative method of obtaining the desired model parameters. A Bode diagram was constructed from the output of the PLTEST program, and the model parameters were determined from the corner frequencies (23). The details of this analysis will appear in a future report. The parameters obtained from PLTEST were compared with those obtained by the MULTIFIT procedure as listed in Table IV. The two procedures yielded essentially the same result. The MULTIFIT model was used for the remainder of the calculations.

Model Verification—The time variations of intensities of rectal temperature depression observed in single rabbits kept at 20° in response to various slow intravenous infusions of chlorpromazine are depicted by the curves in Figs. 5 and 6. These curves were smoothed to facilitate deconvolution, which is sensitive to noisy data. The smoothed data for the curves are listed in Tables V and VI. The

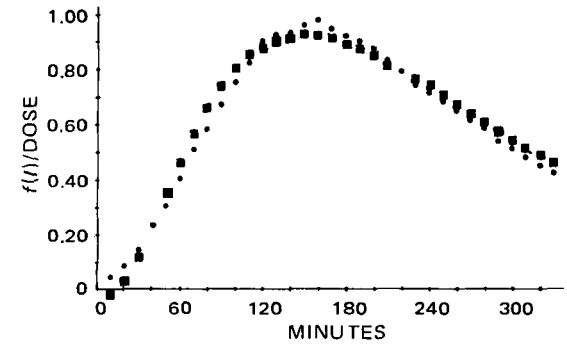

Figure 4—*The* f(I)*/dose values experimentally determined from rectal temperature depression (●) and computer-predicted values (■) based upon a triexponential model obtained by fitting the data via a least-squares procedure. The model has the general form:*

$$y = \sum_{i=1}^{n} A_i e^{-m_i t}$$

where the A_i*'s and* m_i*'s are constants* ($A_1 = 4.86563$, $A_2 = -9.26821$, $A_3 = 4.40259$, $m_1 = 0.006803$, $m_2 = 0.015532$, *and* $m_3 = 0.026769$).

Table IV—Comparison of the Mathematical Model Parameters Describing Chlorpromazine-Induced Rectal Temperature Depression in Rabbits Calculated from MULTIFIT and PLTEST Procedures

MULTIFIT	PLTEST
$A_1 = 4.86563$	$A_1 = 3.83573$
$A_2 = -9.26821$	$A_2 = -7.66823$
$A_3 = 4.40259$	$A_3 = 3.83300$
$m_1 = 0.006803$	$m_1 = 0.0063708$
$m_2 = 0.015532$	$m_2 = 0.020332$
$m_3 = 0.026769$	$m_3 = 0.020337$

Table V—Intensity of Rectal Temperature Depression in a Single Rabbit at 20°, Expressed as $(T_0 - T)/T_0 \times 10^4$, in Response to a Slow Intravenous Infusion of Chlorpromazine, the Infusion Rate Being 0.50 mg/kg/hr

Minutes	I^a	$f(I)$
10	5	0.013
20	31	0.050
30	46	0.073
40	75	0.123
50	100	0.173
60	121	0.218
70	147	0.275
80	170	0.350
90	185	0.398
100	208	0.483
110	237	0.620
120	257	0.738
130	283	0.913
140	296	1.005
150	311	1.125
160	325	1.220
170	332	1.263
180	335	1.275
190	335	1.275
200	335	1.275
210	335	1.275
220	335	1.275
230	335	1.275
240	335	1.275
250	335	1.275
260	335	1.275
270	335	1.275
280	335	1.275
290	335	1.275
300	335	1.275

[a] The intensity values were transduced to $f(I)$ values (relative biophasic drug levels) using the dose–effect curve as a calibration curve.

infusion rates employed were 0.50 and 0.75 mg/kg/hr. These slow intravenous infusions served as test inputs into the system and are obviously different from the bolus drug inputs that provided the data from which the transfer function model had been determined.

By using the response output elicited by these infusions and the transfer function model, the fidelity of the linear model may be evaluated. This is done by calculating the input function responsible for the observed pharmacological response output and comparing the experimentally known inputs with the values computed from the

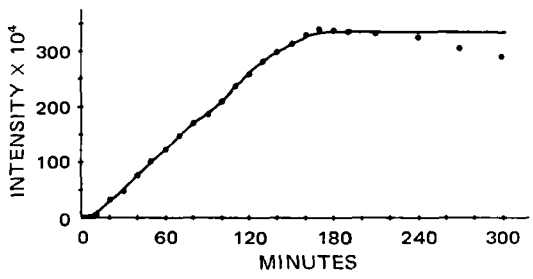

Figure 5—*Intensity of rectal temperature depression in a single rabbit at 20° in response to a slow intravenous infusion of chlorpromazine, the infusion rate being 0.50 mg/kg/hr.*

Table VI—Intensity of Rectal Temperature Depression in a Single Rabbit at 20°, Expressed as $(T_0 - T)/T_0 \times 10^4$, in Response to a Slow Intravenous Infusion of Chlorpromazine, the Infusion Rate Being 0.75 mg/kg/hr

Minutes	I^a	$f(I)$
10	5	0.013
20	15	0.025
30	52	0.080
40	98	0.163
50	131	0.243
60	170	0.350
70	209	0.488
80	245	0.663
90	282	0.913
100	315	1.150
110	350	1.400
120	375	1.575
130	395	1.750
140	410	1.875
150	420	1.962
160	423	1.987
170	424	1.995
180	425	2.000
190	425	2.000
200	425	2.000
210	425	2.000
220	425	2.000
230	425	2.000
240	425	2.000
250	425	2.000
260	425	2.000
270	425	2.000
280	425	2.000
290	425	2.000
300	425	2.000

[a] The intensity values were transduced to $f(I)$ values (relative biophasic drug levels) using the dose–effect curve as a calibration curve.

pharmacological response data observed following administration of the drug input used to test the fidelity of the model.

This comparison of known and computed drug inputs was performed using the response intensity values listed in Tables V and VI, which were transduced to $f(I)$ values (relative biophasic drug levels) using the dose–effect curve in the manner described in detail elsewhere (1, 2, 17, 18–22). These $f(I)$ values observed for the slow intravenous infusions then served as inputs to a deconvolution digital computer program (22), which calculated the cumulative drug input from the transfer function and the relative biophasic drug level response output of the system. These calculated inputs were compared with the known inputs to verify the transfer function model for chlorpromazine-induced rectal temperature depression in rabbits (Figs. 7 and 8).

Table VII indicates the amounts of chlorpromazine known to have been infused at 0.50 mg/kg/hr *versus* the amounts calculated wholly from observed pharmacological response intensities. Table VIII presents a similar comparison of results for a 0.75-mg/kg/hr infusion rate.

All data indicate good agreement between experimentally known chlorpromazine drug inputs and corresponding values calculated from the drug-induced rectal temperature depression. Based on these results, the mathematical model describing the dynamics of the drug's input–output response behavior for the dosage range employed may be considered as satisfactory, even though a linear model does not rigorously describe the dynamics of the system's response behavior.

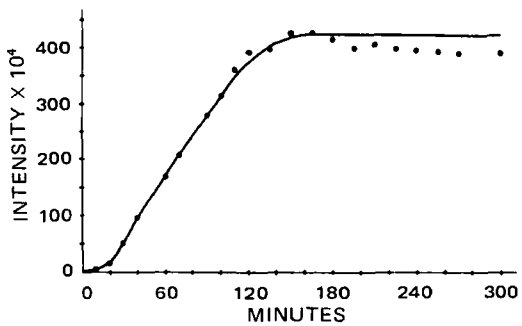

Figure 6—*Intensity of rectal temperature depression in a single rabbit at 20° in response to a slow intravenous infusion of chlorpromazine, the infusion rate being 0.75 mg/kg/hr.*

Table VII—Comparison of Experimentally Known Amounts of Chlorpromazine Infused at a Rate of 0.50 mg/kg/hr with Theoretical Amounts Computed from Rectal Temperature Depression Measured in a Single Rabbit

$A(t)_{theor}$	$A(t)_{exp}$
0.0833	0.3100
0.1667	0.2600
0.2500	0.2923
0.3333	0.5028
0.4167	0.4100
0.5000	0.4950
0.5833	0.7353
0.6667	0.6400
0.7500	0.7500
0.8333	1.3907
0.9167	1.4753
1.000	1.7200
1.0833	1.6000
1.1667	1.3705
1.2500	1.7760
1.3333	1.4000
1.4167	1.1797
1.5000	1.2458
1.5833	1.3900
1.6667	1.5078
1.7500	1.5639
1.8333	1.6100
1.9167	1.6550
2.0000	1.7000
2.0833	1.7459
2.1667	1.7900
2.2500	1.8343
2.3333	1.8806
2.4167	1.9300
2.5000	

SUMMARY AND CONCLUSIONS

A method of performing a pharmacokinetic analysis of drug-responding systems was further confirmed using the results of observed intensities of chlorpromazine-induced rectal temperature depression to establish a pharmacokinetic model to relate drug bioavailability inputs to the time variation of hypothermic response intensity induced by the drug in rabbits. A simplified explication and details of the method were described elsewhere (24, 25). The dosage range of chlorpromazine employed was 0.5–4.0 mg/kg; a third-order (triexponential) transfer function model describing the drug's dynamic response behavior in this system was determined from the results of bolus intravenous dosing in this range and confirmed the use of slow intravenous infusions of the drug as test inputs.

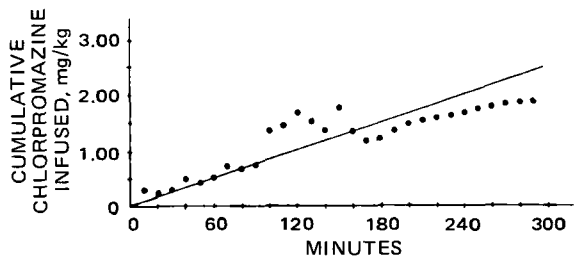

Figure 7—*Experimentally determined amounts of chlorpromazine slowly infused in a single rabbit as a function of time using intensities of rectal temperature depression from Fig. 5 and the transfer function model from Fig. 4 in a deconvolution procedure. The response intensity values were transduced to* f(I) *values (relative biophasic drug levels) using the dose–effect curve and deconvolved with the transfer function to yield cumulative amounts of chlorpromazine infused. The solid line represents the actual amount of chlorpromazine infused during the experiment, 0.50 mg/kg/hr.*

Table VIII—Comparison of Experimentally Known Amounts of Chlorpromazine Infused at a Rate of 0.75 mg/kg/hr with Theoretical Amounts Computed from Rectal Temperature Depression Measured in a Single Rabbit

$A(t)_{theor}$	$A(t)_{exp}$
0.125	0.1136
0.250	0.3500
0.375	0.7286
0.500	0.7276
0.625	0.8200
0.750	1.2030
0.875	1.5820
1.000	2.2500
1.125	2.5000
1.250	2.4698
1.375	2.3100
1.500	2.2000
1.625	2.4089
1.750	2.1834
1.875	1.9800
2.000	1.9000
2.125	2.1573
2.250	2.2950
2.375	2.3700
2.500	2.4651
2.625	2.5411
2.750	2.6100
2.875	2.6830
3.000	2.7528
3.125	2.8250
3.250	2.8940
3.375	2.9640
3.500	3.0366
3.625	3.1050
3.750	

Although the linear mathematical model described here was considered to be relatively adequate in describing the biokinetic behavior of the drug in this system, the systematic differences of computed values from the experimentally known amounts of drug infused (Figs. 7 and 8) indicate a need for further model tuning. It was considered that the application of further linear mathematical modeling techniques would be of little value in improving the fidelity of the drug's input–output response relationship describing the dynamics of chlorpromazine-induced temperature depression. Therefore, future studies will explore an approach involving a systematic variation of the transfer function parameters which is dependent at any time upon the level of response intensity observed at that time. It is anticipated that this type of linear approximation transfer function model will yield improved results as compared with those using the linear transference model presently employed.

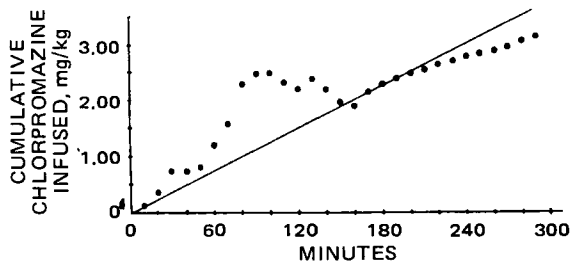

Figure 8—*Experimentally determined amounts of chlorpromazine slowly infused in a single rabbit as a function of time using intensities of rectal temperature depression from Fig. 6 and the transfer function model from Fig. 4 in a deconvolution procedure. The response intensity values were transduced to* f(I) *values (relative biophasic drug levels) using the dose–effect curve and deconvolved with the transfer function to yield cumulative amounts of chlorpromazine infused. The solid line represents the actual amount of chlorpromazine infused during the experiment, 0.75 mg/kg/hr.*

REFERENCES

(1) V. F. Smolen, *J. Pharm. Sci.*, **60**, 354(1971).

(2) V. F. Smolen and R. D. Schoenwald, *ibid.*, **60**, 96(1971).

(3) V. F. Smolen, *Can. J. Pharm. Sci.*, **7**, 1(1972).

(4) W. E. Kirkpatrick and P. Lomax, *Neuropharmacology*, **10**, 61(1971).

(5) H. Bachtold and A. Pletscher, *Experientia*, **13**, 163(1957).

(6) O. Benesova and I. Trinerova, *Int. J. Neuropharmacol.*, **3**, 473(1964).

(7) V. G. Longo, G. P. Von Berger, and D. Vovet, *J. Pharmacol. Exp. Ther.*, **111**, 349(1954).

(8) S. D. Gokhale, O. D. Gulati, and H. M. Parikh, *Br. J. Pharmacol.*, **23**, 508(1964).

(9) W. I. Cranston, T. H. Folwy, R. H. Luff, and M. D. Rawlins, *ibid.*, **46**, 555p(1972).

(10) J. Kollias and R. W. Bullard, *J. Pharmacol. Exp. Ther.*, **145**, 373(1964).

(11) J. Kopera and A. K. Armitage, *Br. J. Pharmacol.*, **9**, 392(1954).

(12) H. F. Lettan, E. A. Sellers, and E. Schonbaum, *Can. J. Physiol. Pharmacol.*, **42**, 745(1964).

(13) S. Courvoisier, J. Fournel, R. Ducrot, M. Kolsky, and P. Koetschnet, *Arch. Int. Pharmacodyn. Ther.*, **92**, 305(1953).

(14) "The Pharmacological Basis of Therapeutics," 4th ed., L. S. Goodman and A. Gilman, Eds., Macmillan, New York, N.Y. 1970, p. 159.

(15) T. G. Reigle and H. H. Wolf, *Life Sci. (I)*, **10**, 121(1971).

(16) F. Ratcliffe, *Arch. Int. Pharmacodyn. Ther.*, **197**, 305(1972).

(17) V. F. Smolen, R. G. Barile, and T. G. Theophanous, *J. Pharm. Sci.*, **61**, 467(1972).

(18) V. F. Smolen, P. B. Kuehn, and E. J. Williams, *Drug Dev. Commun.*, **1**, 143(1975).

(19) V. F. Smolen, E. J. Williams, and P. B. Kuehn, *Can. J. Pharm. Sci.*, **10**, 95(1975).

(20) V. F. Smolen, *Am. J. Pharm. Ed.*, **37**, 107(1973).

(21) V. F. Smolen and W. A. Weigand, *J. Pharm. Sci.*, **61**, 1941(1972).

(22) A. K. Jhawar, Ph.D. thesis, Purdue University, Lafayette, Ind., 1974.

(23) D. R. Coughanower and L. B. Koppel, "Process Systems Analysis and Control," McGraw-Hill, New York, N.Y., 1966, chaps. 18 and 19.

(24) V. F. Smolen, *J. Pharmacokinet. Biopharm.*, **4**, 337(1976).

(25) *Ibid.*, **4**, 355(1976).

ACKNOWLEDGMENTS AND ADDRESSES

Received December 18, 1974, from the *Interdisciplinary Drug Engineering and Assessment Laboratory, School of Pharmacy and Pharmacal Sciences, Purdue University, West Lafayette, IN 47907*

Accepted for publication January 16, 1976.

Presented at the Pharmacology and Toxicology Section, APhA Academy of Pharmaceutical Sciences, Chicago meeting, 1974.

Abstracted in part from theses submitted by P. B. Kuehn and A. K. Jhawar to Purdue University in partial fulfillment of the Doctor of Philosophy degree requirements.

Supported in part by the National Institutes of Health, General Medical Division, through Predoctoral Fellowship 1 F-1 GM43208 and Food and Drug Administration Contract 73-23.

* Present address: AMACO Oil Co., Naperville, Ill.

‡ Department of Chemical Engineering, School of Engineering, Purdue University, West Lafayette, IN 47907

§ Present address: Department of Psychiatry, Brown University, Providence, R.I.

¶ Present address: School of Pharmacy, University of Washington, Seattle, WA 98195

x To whom inquiries should be directed (Department of Industrial and Physical Pharmacy, School of Pharmacy and Pharmacal Sciences, Purdue University, West Lafayette, IN 47907).

High-Pressure Liquid Chromatographic Separation, Identification, and Determination of Sulfa Drugs and Their Metabolites in Urine

J. P. SHARMA *, E. G. PERKINS *, and R. F. BEVILL ‡ ×

Abstract □ A high-pressure liquid chromatographic method for the separation and quantitative determination of sulfamethazine, sulfamerazine, sulfathiazole, and their N^4-acetylated metabolites on an amino-bonded reversed-phase column was developed. The method is suitable for the analysis of these compounds in pure solutions as well as in cattle urine. Retention times were reproducible. Injection volumes containing 0.2 μg of individual sulfonamides or their acetyl derivatives were successfully quantitated; coefficients of variation ranged from 0 to 0.073 for individual sulfonamides.

Keyphrases □ Sulfamethazine—and metabolites, high-pressure liquid chromatographic analysis, pure solutions and cattle urine □ Sulfamerazine—and metabolites, high-pressure liquid chromatographic analysis, pure solutions and cattle urine □ Sulfathiazole—and metabolites, high-pressure liquid chromatographic analysis, pure solutions and cattle urine □ High-pressure liquid chromatography—analysis, sulfamethazine, sulfamerazine, sulfathiazole, and acetyl derivatives, pure solutions and cattle urine □ Antibacterial agents—sulfamethazine, sulfamerazine, and sulfathiazole, high-pressure liquid chromatographic analysis, pure solutions and cattle urine

Solutions containing a mixture of three sulfonamides are commonly administered to food-producing animals for the treatment of bacterial diseases. In some instances, treated animals may be slaughtered before the concentrations of sulfonamides have declined to predetermined tolerance limits (≤0.1 ppm) in edible tissues. Animal carcasses containing sulfonamide concentrations in excess of 0.1 ppm are destroyed (1).

The disappearance of a drug from edible animal tissues is a function of time (2). Carcass destruction can be avoided if animals containing excessive tissue concentrations of sulfonamides can be identified and withheld from slaughter. Preslaughter sampling and analysis of animal plasma and urine could be used to identify these animals if a meaningful correlation exists between the concentrations of drug in plasma, urine, and tissues.

A rapid, accurate method for the separation and quantitation of sulfonamides and their metabolites in animal urine was requisite to a projected urine–plasma–tissue study. Previous work (3–5) indicated that the parent sulfonamides and the N^4-acetylated derivatives were major urinary excretion products of sulfonamides.

Previously reported quantitative methods based on TLC or colorimetry (6–12) did not distinguish between parent drugs and/or metabolites. These methods were intended for the analysis of the parent drug in pure solutions and extracts of pharmaceutical preparations and animal feeds. No provisions were included to eliminate possible interference due to biological components in urine.

GLC methods (13–15) were unsuited for this purpose because the derivatization, extraction, and isolation procedures were too exhaustive for routine sample analysis.

High-pressure liquid chromatography (HPLC) can be used to separate nonpolar, polar, and ionized materials. Kram (16) surveyed the conditions required for the separation of pure sulfonamide samples on an anion-exchange column. Poet and Pu (17) described the separation and determination of trisulfapyrimidines in pharmaceutical dosage forms by HPLC. No reports concerning the separation and determination of sulfonamides and their metabolites in pure solutions or biological fluids have appeared.

This paper describes an HPLC method for the separation and quantitative determination of sulfamethazine, sulfamerazine, sulfathiazole (a common triple sulfa preparation), and their N^4-acetylated metabolites in pure solutions and urine.

EXPERIMENTAL

Apparatus—A liquid chromatograph[1] equipped with a digitally controlled dual pumping system, having a 3000-psi pressure limit, was used. Prepacked columns (2.6 mm i.d. and 0.5 m in length) containing amino-bonded phase material[2] were used to effect separations.

A single-beam spectrophotometer[3] equipped with an 8-μl flowcell and digital readout was used for the UV detection (254 nm) of separated components. The detector output was recorded on a variable-span potentiometric recorder[4].

All separations were effected at ambient temperature.

Reagents and Materials—The mobile phase was methanol, spectroscopic grade[5]. A 0.1 *N* sodium hydroxide solution in distilled water was prepared. USP sulfamethazine, sulfamerazine[6], and sulfathiazole[7] were used as received.

Acetyl derivatives of sulfonamides were prepared by acetylation with acetic anhydride, precipitation with water, and recrystallization in dioxane–water (1:1 v/v). Purity of dried samples was checked by TLC and HPLC.

Sulfonamide Stock Solutions—From 200 to 250 mg of each of the three sulfonamides and their acetylated products was weighed and transferred to a clean 100-ml volumetric flask, and distilled water (5 ml) was added. The sulfonamides were solubilized by dropwise addition of 0.1 *N* sodium hydroxide and constant shaking, followed by dilution to volume with distilled water.

Working Standards—Aliquots (1–7 ml) of the stock solution were transferred to 25-ml volumetric flasks and diluted to volume with distilled water. Five microliters of each solution was injected onto the column.

Urine Standards—Six aliquots (2–12 ml) of the stock solution were transferred to 25-ml volumetric flasks and diluted to volume with cattle urine. Aliquots (2 ml) of each dilution were pipetted into 20-ml screw-capped glass tubes containing 8 ml of methanol. Each tube was centrifuged for 5 min at 2000 rpm to remove the gelatinous precipitate

[1] Model 1220, Perkin-Elmer Corp., Norwalk, Conn.
[2] Amino-Sil-X-I, Perkin-Elmer Corp., Norwalk, Conn.
[3] Model LC-55, Perkin-Elmer Corp., Norwalk, Conn.
[4] Linear Instruments Corp., Irvine, Calif.
[5] Burdick and Jackson Laboratories, Muskegan, Mich.
[6] American Cyanamid Co., Pearl River, N.Y.
[7] Merck and Co., Rahway, N.J.

Table I—Retention Times and Standard Curve Parameters for Sulfa Drugs and Their Metabolites in Pure Sample and Urine

Compound	Solution Injected	Retention Time, min	Slope (Response Factor), Absorbance/ μg	Intercept, Absorbance Unit	Correlation Coefficient of Standard Curves	*SE* of Estimate	Range of Sample Sizes Used, μg
Sulfamethazine	Sample	2.3	0.0462	−0.0001	0.999	0.0004	0.20–1.65
	Urine	2.6	0.0537	−0.0015	0.998	0.0008	0.14–0.86
Sulfamerazine	Sample	3.6	0.0319	+0.0005	0.999	0.0006	0.2–2.13
	Urine	3.8	0.0310	+0.00002	0.999	0.0002	0.14–0.88
Sulfamethazine	Sample	5.7	0.0311	−0.0001	0.999	0.0006	0.33–1.67
acetyl derivative	Urine	5.8	0.0280	−0.00005	0.999	0.0003	0.18–1.09
Sulfathiazole	Sample	8.1	0.0188	+0.0007	0.999	0.0003	0.40–2.02
	Urine	9.0	0.0163	−0.0001	0.999	0.0002	0.19–1.16
Sulfamerazine	Sample	11.0	0.0166	+0.0015	0.998	0.0007	0.53–2.14
acetyl derivative	Urine	11.0	0.0216	−0.0007	0.999	0.0003	0.16–0.99
Sulfathiazole	Sample	13.8	0.0153	+0.0002	0.999	0.0004	0.39–1.94
acetyl derivative	Urine	15.6	0.0108	+0.0006	0.993	0.0004	0.14–1.15

which formed. The clear supernate (5 μl) was injected onto the column. Unspiked control urine was treated in an identical manner, except that no stock sulfonamide solution was added.

Chromatographic Procedures—Columns[2] were preconditioned with methanol until a stable recorder output was obtained. A flow rate of 1.5 ml of methanol/min was established at a pressure of about 700 psi. Sample aliquots were injected onto the column under stop-flow conditions. Column eluants were monitored at 254 nm. As the peak maxima emerged, the peak absorbance of each component was recorded from the digital spectrophotometer readout as well as on a potentiometric recorder.

RESULTS AND DISCUSSION

Solutions of pure sulfonamides were completely separated with a reversed-phase column packing[2] (Fig. 1).

Raw urine containing sulfonamides and their acetyl derivatives could not be injected directly onto the column packing, since operating pressures increased with each successive injection. This result may be explained by precipitation of urine components onto the column packing in the presence of methanol and other organic solvents. The problem was circumvented by pretreating urine samples with methanol. Following the addition of methanol to urine samples, a gelatinous precipitate was formed; it was subsequently removed by centrifugation. Separation of all sulfonamides in the supernate was then obtained without the attendant problems resulting from the injection of samples containing raw urine.

The separations obtained after the injection of methanol-pretreated urine containing sulfonamides and metabolites as well as a pretreated urine blank are included in Fig. 2. The effect of various flow rates between 1.0 and 1.5 ml/min was investigated to improve the resolution. Although slight improvements in peak resolution were noted at lower flow rates, a rate of 1.5 ml/min was selected to obtain maximum resolution in the shortest possible time.

The separation patterns of sulfonamides following their injection in distilled water or urine were similar but not identical. Although the relative order of elution was maintained, the retention times of certain

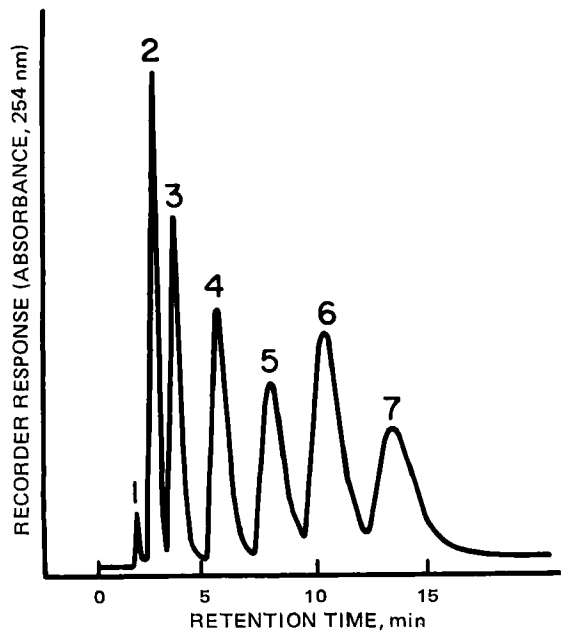

Figure 1—*Separation of sulfa drugs and their acetylated derivatives. Key: 1, solvent front; 2, sulfamethazine; 3, sulfamerazine; 4, sulfamethazine acetyl derivative; 5, sulfathiazole; 6, sulfamerazine acetyl derivative; and 7, sulfathiazole acetyl derivative (7.5 μg total sample).*

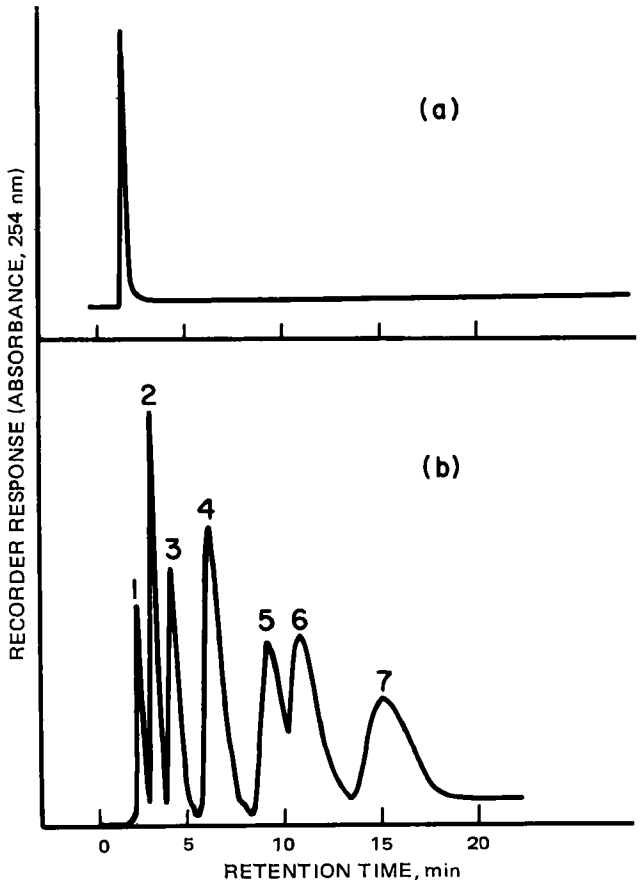

Figure 2—*Separation of sulfa drugs and their metabolites in urine. (a) Blank, urine treated with methanol showing solvent front. (b) Key: 1, solvent front; 2, sulfamethazine; 3, sulfamerazine; 4, sulfamethazine acetyl derivative; 5, sulfathiazole; 6, sulfamerazine acetyl derivative; and 7, sulfathiazone acetyl derivative (3.6 μg total sample).*

Table II—Determination of Sulfa Drugs and Their Metabolites in Pure Samples and Urine

Compound	Amount in Pure Samples, μg			Amount in Urine, μg		
	Added[a]	Recovered[a,b]	SD	Added[a]	Recovered[a,b]	SD
Sulfamethazine	0.83	0.86	±0.012	0.29	0.29	±0.011
	1.65	1.65	±0.012	0.58	0.55	±0.000
Sulfamerazine	0.85	0.87	±0.018	0.30	0.32	±0.000
	1.71	1.72	±0.018	0.59	0.63	±0.019
Sulfamethazine acetyl derivative	0.67	0.67	±0.019	0.37	0.38	±0.021
	1.34	1.31	±0.018	0.75	0.81	±0.021
Sulfathiazole	0.81	0.80	±0.031	0.39	0.41	±0.035
	1.62	1.63	±0.031	0.78	0.82	±0.035
Sulfamerazine acetyl derivative	1.07	1.13	±0.035	0.33	0.37	±0.000
	2.14	2.10	±0.035	0.67	0.71	±0.027
Sulfathiazole acetyl derivative	0.78	0.79	±0.038	0.38	0.43	±0.054
	1.55	1.53	±0.038	0.77	0.75	±0.055

[a] Values reported are correct up to second decimal place. [b] Recovered amounts are averages of triplicate injections of the same amount.

peaks were altered. When urine supernates were injected, the sulfathiazole and acetyl derivative of sulfamerazine peaks merged to some degree and the overall elution time increased slightly (2 min) when compared with that obtained after the injection of sulfonamides in distilled water. Differences in the separation patterns of the sulfonamides in water and urine may have been due to the presence of nonabsorbing inorganic ions in urine and their influence on column characteristics. However, the peak maxima of all components remained well separated.

Mean retention times (T_R) obtained following the injection of identical volumes (5 μl) of sulfonamide mixtures in water and urine are presented in Table I. The retention times were highly reproducible under the experimental conditions previously described.

Slight changes in retention times (and hence peak heights) were observed when the sample volume injected was gradually increased. These changes may be due to the gradual accumulation of inorganic ions on the columns. This problem was minimized by the injection of small sample volumes.

Column regeneration was required after 15–30 urine samples were injected and was effected by flushing the column for 1 hr with methanol–water (98:2 v/v) at a flow of 1.5 ml/min. However, water itself produced changes in column characteristics, as denoted by a complete merging of some peaks when samples were injected immediately after the flushing step. To reduce the water content of the column and provide complete column regeneration, pure methanol was pumped through the column for 2 hr at a rate of 1.5 ml/min.

Peak heights were proportional to the concentration of individual components and were used for their quantitative determination. Peak heights were measured in terms of the absorbance value obtained at the peak maxima of each component. A recent report (18) indicated that the use of peak heights for quantitative determinations gives the same degree of precision and accuracy as may be obtained with electronically measured peak areas.

Standard curves were calculated by linear regression analysis of the peak heights obtained for each component following the injection of sulfonamide mixtures in water and urine. The parameters for these curves are presented in Table I. Ideally, the straight lines should have a zero intercept; in most cases, the intercept values listed in Table I approached zero.

The high correlation of individual results to the line of best fit and the small standard deviation among data points were indicative of the accuracy and precision of the method.

The recovery of individual components following their injection in water and urine is reported in Table II. Recoveries were calculated from the equation for a straight line using slopes (response factors) and intercepts presented in Table I.

CONCLUSION

The present work demonstrates the capability of an amino-bonded reversed-phase packing to separate sulfonamides and their metabolites. The present procedure is suitable for routine analysis of cattle urine for the compounds mentioned and also may serve as a method for screening urine samples for sulfonamides and their metabolites.

REFERENCES

(1) *Fed. Regist.*, **40** (60), part II, 13957(1974).

(2) B. N. La Du, H. G. Mandel, and E. L. Way, "Fundamentals of Drug Metabolism and Drug Disposition," Williams & Wilkins, Baltimore, Md., 1971, p. 22.

(3) P. Nielsen, *Biochem. J.*, **136,** 1039(1973).

(4) E. G. C. Clarke, "Isolation and Identification of Drugs," Pharmaceutical Press, London, England, 1969, p. 557.

(5) R. M. Sharma, Ph.D. thesis, University of Illinois, Urbana, Ill., 1975.

(6) "The United States Pharmacopeia," 18th rev., Mack Publishing Co., Easton, Pa., 1970, pp. 760, 761.

(7) F. M. Kunze, *J. Assoc. Offic. Agr. Chem.*, **47,** 474(1964).

(8) M. Maienthal, J. Carol, and F. M. Kunze, *ibid.*, **44,** 313(1961).

(9) H. M. Miller, *J. Assoc. Offic. Anal. Chem.*, **53,** 1100(1970).

(10) R. A. Dezeeuw, *J. Chromatogr.*, **48,** 27(1970).

(11) U. G. Cieri, *J. Assoc. Offic. Anal. Chem.*, **56,** 1475(1973).

(12) B. R. Rader, *J. Pharm. Sci.*, **62,** 1148(1973).

(13) R. J. Daun, *J. Assoc. Offic. Anal. Chem.*, **54,** 1277(1971).

(14) E. Roder and W. Stuthe, *Justus Liebigs Anal. Chem.*, **266,** 358(1973).

(15) O. Gyllenhaal and H. Ehrsson, *J. Chromatogr.*, **107,** 327(1975).

(16) T. C. Kram, *J. Pharm. Sci.*, **61,** 254(1972).

(17) R. B. Poet and H. H. Pu, *ibid.*, **62,** 809(1973).

(18) A. Janik, *J. Chromatogr. Sci.*, **13,** 93(1975).

ACKNOWLEDGMENTS AND ADDRESSES

Received October 3, 1975, from the *Department of Food Science and the ‡Department of Veterinary Physiology and Pharmacology, University of Illinois at Urbana–Champaign, Urbana, IL 61801

Accepted for publication January 15, 1976.

Supported in part by Food and Drug Administration Contract 223-74-7178.

ˣ To whom inquiries should be directed.

High-Performance Liquid Chromatographic Analysis of Prostaglandins Formed during *In Vitro* Incubations with Prostaglandin 15-Dehydrogenase

F. A. FITZPATRICK

Abstract □ Dinoprost, dinoprostone, and prostaglandin E_1 were each separated from their major 15-keto metabolites by high-performance liquid chromatography on a microparticulate, bonded, reversed-phase column after conversion to their *p*-bromophenacyl esters. Detection and simultaneous quantitation of prostaglandins in 1.0 ml of a 5-μM solution is possible. The method was applied to monitor prostaglandins formed during *in vitro* incubations with prostaglandin 15-dehydrogenase from monkey lungs. The advantages of this technique for assessing enzyme purity and activity are discussed.

Keyphrases □ Prostaglandins—formed during *in vitro* incubation with prostaglandin 15-dehydrogenase, high-performance liquid chromatographic analysis □ Dinoprost and dinoprostone—derivatives formed during *in vitro* incubation with prostaglandin 15-dehydrogenase, high-performance liquid chromatograpic analysis □ High-performance liquid chromatography—analysis, prostaglandins formed during *in vitro* incubation with prostaglandin 15-dehydrogenase □ Oxytocic agents—dinoprost and dinoprostone derivatives formed during *in vitro* incubation with prostaglandin 15-dehydrogenase, high-performance liquid chromatographic analysis

A significant strategy for prolonging pharmacological effects of prostaglandins focuses on inhibiting their metabolic inactivation. The first stage in the metabolism of most prostaglandins is dehydrogenation of the secondary hydroxyl group at the C-15 position along with concomitant formation of a 15-keto derivative. Several investigators recently isolated and characterized prostaglandin 15-dehydrogenase enzyme in different tissues from various species including pig, beef, and monkey lungs (1–3); dog heart (4); pig and monkey kidneys, and human placenta (5–8). With the availability of highly active, purified prostaglandin 15-dehydrogenase preparations, further advances should occur in the development of prostaglandin analogs resistant to metabolic inactivation and also in the development of drugs capable of direct *in vivo* inhibition of the enzyme (9).

A prominent obstacle remaining is the lack of analytical methodology capable of accurately quantitating substrate and metabolic conversion products from prostaglandin 15-dehydrogenase incubations *in vitro*. Enzyme activity is usually measured indirectly by fluorometric or spectrophotometric determination of the rate of formation of NADH, the product of the NAD-linked reaction. Another widely used spectrophotometric method, based on the alkaline-catalyzed formation of a transient chromophore (λ_{max} 500 nm) from the enzymatic oxidation products of prostaglandin E_1, has the drawback of limited utility, except with prostaglandin E-type substrates, and poor reproducibility relative to NADH measurements. The validity of the analytical results for both approaches depends greatly on the purity of the enzyme preparation, which is often judged by electrophoretic homogeneity.

Characterizations of enzymes by indirect methods must always be regarded with some skepticism. Except for the limited use of radiometric TLC (10) and a radioimmunoassay procedure for the 15-keto derivative of dinoprost (8), virtually no specific analytical methods have been employed to determine 15-keto derivatives from *in vitro* prostaglandin 15-dehydrogenase incubations. This report describes the development of a reversed-phase, high-performance liquid chromatographic (HPLC) system for the separation of several prostaglandins from their principal 15-keto metabolites after conversion to *p*-bromophenacyl esters. Quantitative analysis is easily performed on the basis of peak height measurements for 1 ml of solution containing prostaglandins in concentrations greater than 5 μM.

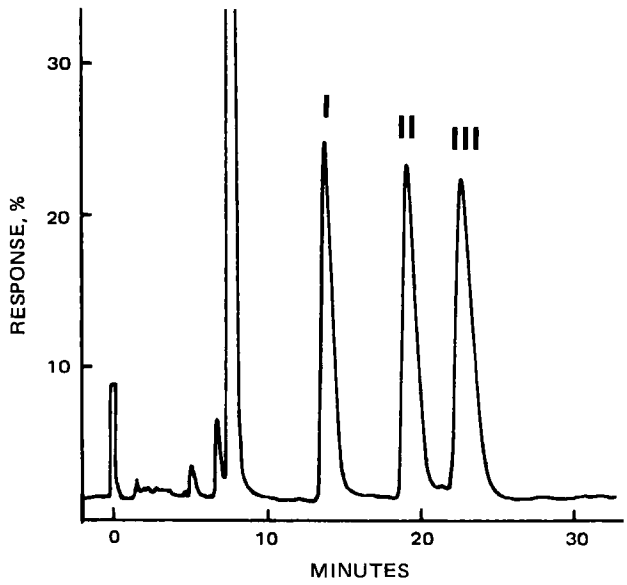

Figure 1—*Separation of* p-*bromophenacyl esters of dinoprostone (I), 15-keto derivative (II), and 13,14-dihydro-15-keto derivative (III).*

EXPERIMENTAL

Apparatus—A high-performance liquid chromatograph[1] with a pneumatic drive, positive displacement pump, and a single-wavelength (254 nm) UV detector was used. The chromatographic column was operated at ambient temperature (25 ± 3°), and injections were made into a stopped-flow injection port with a 10-μl syringe[2]. Chromatograms were recorded on a single-pen recorder[3], 0–1 mv full-scale.

Chromatographic Column—A prepacked, pretested, microparticulate, reversed-phase column[4] was used as received. Low dead volume fittings were easily constructed to adapt this column to the stopped-flow injection port of the chromatograph. A mobile phase

[1] Chromatec model 5100, Tracor Instruments, Austin, Tex.
[2] Hamilton model 701.
[3] Varian A-25.
[4] μBondapak C18, Waters Associates, Milford, Mass.

Table I—Prostaglandin Recovery Experiments

Dinoprostone		Dinoprostone 15-Keto Derivative		Dinoprost		Dinoprost 15-Keto Derivative	
μg/0.5 ml	% Recovery	μg/0.5 ml	% Recovery	μg/0.5 ml	% Recovery	μg/0.5 ml	% Recovery
112.2	97.9 ± 4.5	105.0	97.8 ± 5.6	122.2	102.7 ± 4.0	80.4	101.5 ± 8.9
56.1	93.7 ± 2.2[a]	52.5	94.9 ± 5.4[a]	61.2	88.9 ± 3.7	40.2	93.2 ± 4.3
22.4	92.6 ± 2.8	21.0	96.6 ± 5.7	24.4	83.5 ± 4.5	16.1	93.8 ± 4.9
				12.2	88.3 ± 6.9	8.04	99.2 ± 8.7

[a] $n = 3$; in all other cases, $n = 6$ determinations.

composition of acetonitrile–water (50:50) at a flow rate of 1.2 ml/min (1000 psig) eluted the prostaglandins in less than 30 min.

Reagents[5]—Distilled-in-glass acetonitrile[6], methanol[6], methylene chloride[6], and α,p-dibromoacetophenone[7] were used as received. Diisopropylethylamine[8] was redistilled (bp 127°) before use.

Procedure—*Derivatization*—Prostaglandin p-bromophenacyl esters were prepared by a modification of the procedure of Morozowich and Douglas (11). Briefly, the prostaglandin (500 μg or greater) was dissolved in 1.0 ml of anhydrous acetonitrile containing a threefold molar excess of α,p-dibromoacetophenone. Two microliters of diisopropylethylamine was added to catalyze the reaction, which was >95% complete in 1 hr at 25°. For 1–100 μg of prostaglandin, the volume of acetonitrile should be reduced to 0.1–0.2 ml and the amount of diisopropylethylamine should be reduced to 0.5 μl.

A threefold molar excess of reagent gave complete conversion without an unduly large reagent peak. For extracts from enzymatic incubations, an amount of derivatizing reagent corresponding to a threefold molar excess of initial prostaglandin substrate should be added.

Enzyme Incubation—Purified prostaglandin 15-dehydrogenase[9]

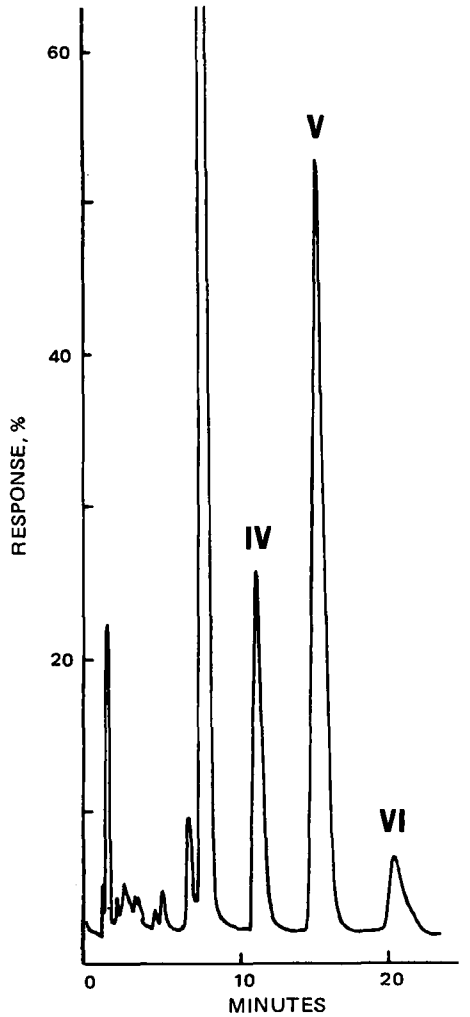

Figure 2—*Separation of* p-*bromophenacyl esters of dinoprost (IV), 15-keto derivative (V), and 13,14-dihydro-15-keto derivative (VI).*

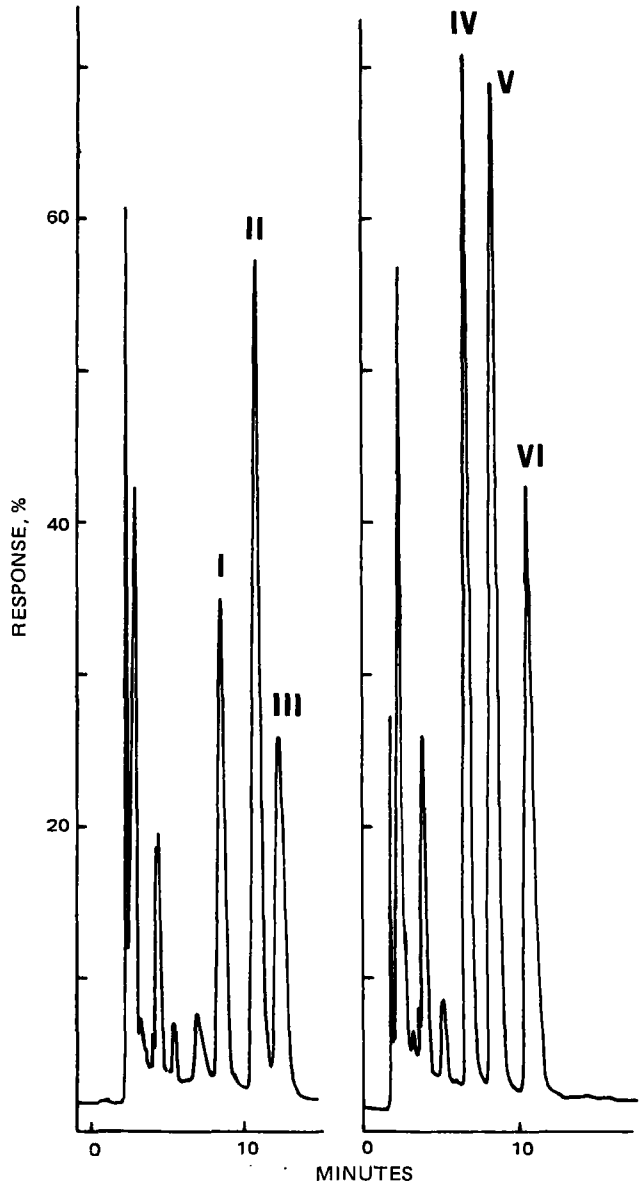

Figure 3—*Separation of* p-*nitrophenacyl esters of I–III and IV–VI.*

[5] All prostaglandins were supplied by the Experimental Chemistry Laboratories, The Upjohn Co.

[6] Burdick & Jackson, Muskegon, Mich.

[7] Eastman Kodak, Rochester, N.Y.

[8] Aldrich Chemical Co., Milwaukee, Wis.

[9] Supplied by J. Mc Guire, Experimental Biology Unit, The Upjohn Co.

Table II—Incubation and Analysis Reproducibility

50 μl of Enzyme					25 μl of Enzyme				
	Dinoprostone		Dinoprostone 15-Keto Derivative			Dinoprostone		Dinoprostone 15-Keto Derivative	
Minutes	A[a]	B[a]	A	B	Minutes	A	B	A	B
0	209[b]	216	0	0	0	196	196	0	0
2	199	201	12	16	5	186	180	16	20
5	184	198	26	37	10	181	183	31	34
7.5	183	191	38	52	30	127	120	62	65
10	170	173	53	54	45	101	97	73	79
15	148	149	62	66	60	87	87	85	96
20	121	129	64	83	90	69	64	94	84
30	97	106	76	105	120	50	43	91	77
60	56	56	102	119	180	41	41	84	69
180	39	33	149	131					

[a] A and B represent completely separate incubations and assays. [b] Values given are micrograms per 0.5 ml, the assay volume.

enzyme was isolated from monkey lungs. The soluble enzyme present in the high speed supernate of a tissue homogenate was obtained by standard procedures (12).

A volume of enzyme preparation from 10 to 50 μl, depending upon the activity desired, was added to 5.0 ml of 0.1 *M* phosphate buffer (pH 7.4), 180 mg of NAD, and 2.5 μl of mercaptoethanol in a 75 × 130-mm disposable tube. The mixture was preincubated to a temperature of 37°, and the enzymatic reaction was initiated by adding 200 μl of prostaglandin (100–2000 μg) dissolved in 0.1 *M* phosphate buffer (pH 7.4) at 37° and then vortexing.

Samples (0.5 ml) were withdrawn for analysis at appropriate time intervals and immediately quenched in a 12 × 75-mm tube containing 1.0 ml of methanol. Usually, 0-, 2-, 5-, 7.5-, 10-, and 15-min samples provided sufficient data points to characterize the initial reaction rate adequately. The contents of the tube were quantitatively transferred to a 60-ml separator containing 4 ml of 0.1 *M* citric acid and 500 mg of anhydrous sodium sulfate.

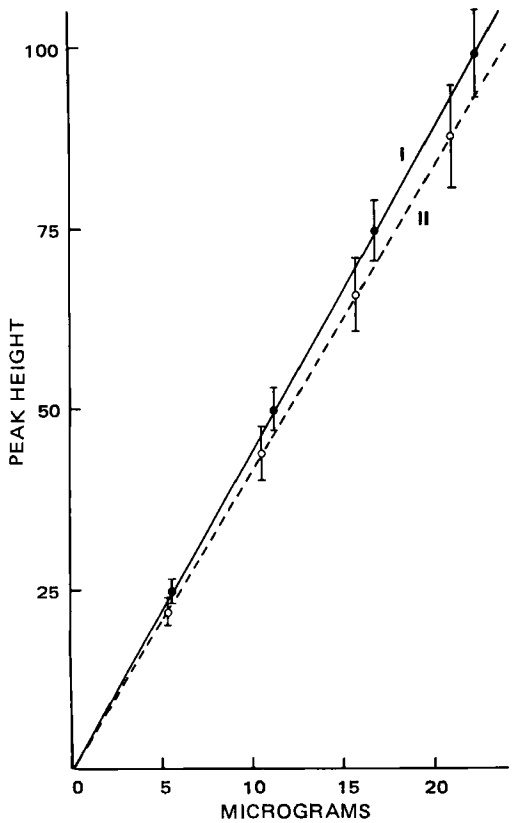

Figure 4—*Calibration curve based on peak height* versus *micrograms derivatized. Key: I, dinoprostone; and II, 15-keto derivative.*

For prostaglandin E_1 and dinoprostone[10], the aqueous phase was extracted twice with 5 ml of methylene chloride; for dinoprost[11], it was extracted three times with 5 ml. The pooled organic phases were desiccated by passage through a funnel containing about 1 g of anhydrous sodium sulfate and then evaporated to dryness under nitrogen. The residue concentrated in the bottom of the tube was derivatized, evaporated to dryness, and reconstituted in 200 μl of methanol for analysis. Ten-microliter aliquots were chromatographed.

RESULTS AND DISCUSSION

Chromatography—The principle of forming *para*-substituted phenacyl esters of prostaglandins to improve the detection limit with a 254-nm UV detector was described previously, and separations were reported by adsorption chromatography on microparticulate silica gel (11). The rationale for using reversed-phase, liquid chromatography as the basis for a quantitative assay on the *in vitro* enzyme system is due to the fact that the 15-keto metabolites are less polar than their parent compounds and elute close to the chromatographic void volume with only partial resolution on a microparticulate silica gel adsorption column, thereby presenting difficulties for quantitative analysis. On a reversed-phase column, the metabolites are retained more strongly than the parent prostaglandins but still elute in a reasonable time with good chromatographic resolution.

Figures 1 and 2 show the separation of dinoprostone and dinoprost from their respective 15-keto metabolites. Resolution of the Δ^{13},15-keto derivative from the 13,14-dihydro-15-keto derivative is

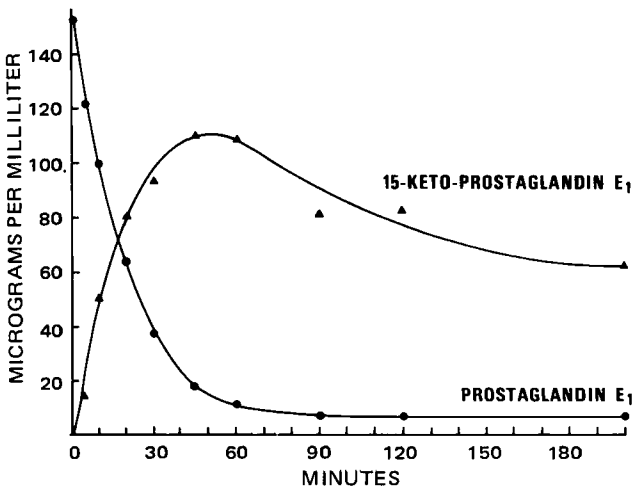

Figure 5—*Concentration* versus *time for the prostaglandin* E_1 *substrate. Enzyme = 25 μl. Total incubation volume = 5.2 ml; samples assayed = 0.5 ml.*

[10] Prostaglandin E_2.
[11] Prostaglandin $F_{2\alpha}$.

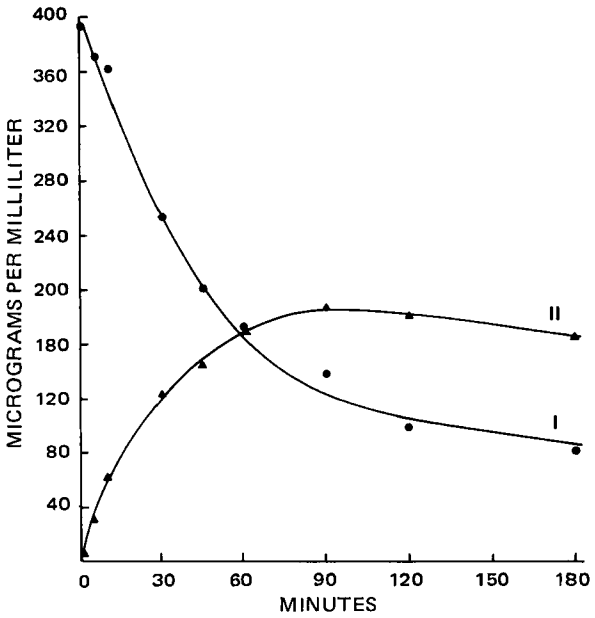

Figure 6—*Concentration* versus *time. I = dinoprostone substrate. II = 15-keto derivative. Enzyme = 25 μl. Total incubation volume = 5.2 ml; samples assayed = 0.5 ml.*

essential to determine the purity of the enzyme preparation, since crude preparations generally contain Δ^{13}-reductase activity. The *p*-nitrophenacyl esters of these prostaglandins (Fig. 3) are also easily separated; however, for routine quantitation of less than 50 μg, the *p*-bromophenacyl esters were preferred because of a lower reagent blank.

Calibration—Typical calibration curves based on peak height response for dinoprostone and its 15-keto derivative are shown in Fig. 4, with the 95% confidence limits predicted by linear regression analysis. Similar results were obtained for dinoprost and its 15-keto metabolite. An internal standard could have been selected from a variety of prostaglandin analogs; however, the prostaglandin 15-dehydrogenase enzyme is water soluble, so quantitative transfers in steps prior to chromatography are simple. With the use of external standard calibration curves, 15–20 samples/day can be assayed.

Sample Analysis—Accuracy and precision were verified by several recovery experiments. Phosphate buffer (pH 7.4), spiked with varying amounts of prostaglandin substrate and the corresponding 15-keto derivatives, was incubated under conditions identical to an active enzyme preparation for 15 min before extraction and chromatographic analysis (Table I). Recovery was nearly quantitative for all prostaglandins except dinoprost. This disadvantage can be compensated for by running the calibration curve for dinoprost after extraction from buffer or by applying a correction factor based on a single recovery experiment.

Application of Method—Figures 5–7 show the time course for the prostaglandin 15-dehydrogenase reaction under identical conditions for three substrates, prostaglandin E_1, dinoprostone, and dinoprost. The corresponding 13,14-dihydro-15-keto derivative, prostaglandin A, and prostaglandin B can also be determined if present. Replicate incubations with dinoprostone (Table II) at two different enzyme concentrations showed reasonable reproducibility, and a comparative radioimmunoassay analysis for the dinoprost 15-keto derivative provided additional authentication of the chromatographic method (Table III). High values at the last two time intervals may reflect

Table III—Comparative Analysis for Dinoprost 15-Keto Derivative by Radioimmunoassay (RIA) and HPLC

Method	Minutes						
	0	2	5	10	15	20	60
HPLC, μg/0.5 ml	3.7	16.2	34.0	49.2	80.9	82.6	76.0
RIA, μg/0.5 ml	<8	36	38	48	82	112	116

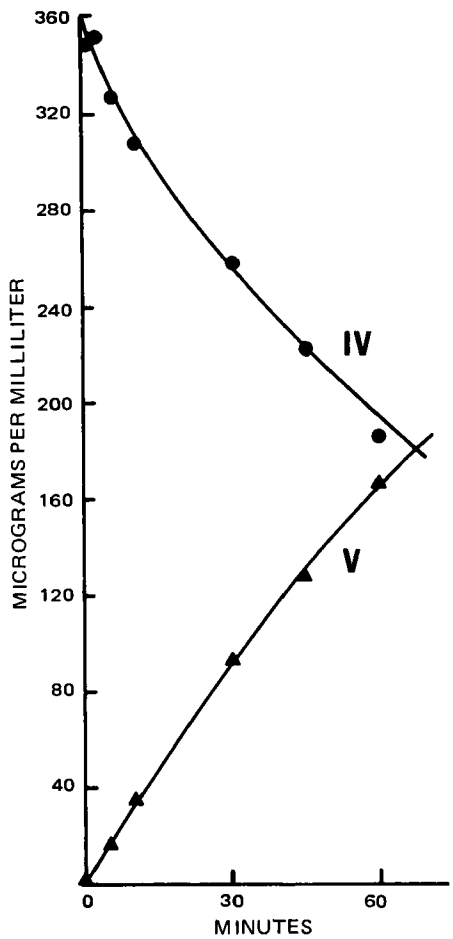

Figure 7—*Concentration* versus *time. IV = dinoprost substrate. V = 15-keto derivative. Enzyme = 25 μl. Total incubation volume = 5.2 ml; samples assayed = 0.5 ml.*

cross-reactivity with small amounts of unidentified material formed during the incubation.

Figures 8 and 9 show the application of the method to kinetic studies. Rate constants for substrate decline can be compared with product appearance to verify enzymatic purity.

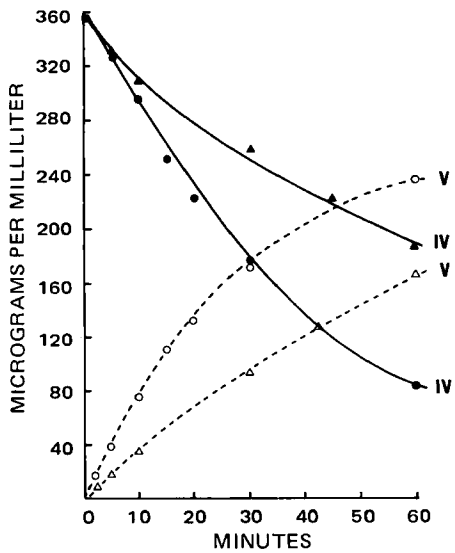

Figure 8—*Concentration* versus *time for two concentrations of prostaglandin 15-dehydrogenase. Key: Δ, ▲, 25 μl; ○, ●, 50 μl; —, dinoprost (IV); and - - -, 15-keto derivative (V). Total incubation volume = 5.2 ml; samples assayed = 0.5 ml.*

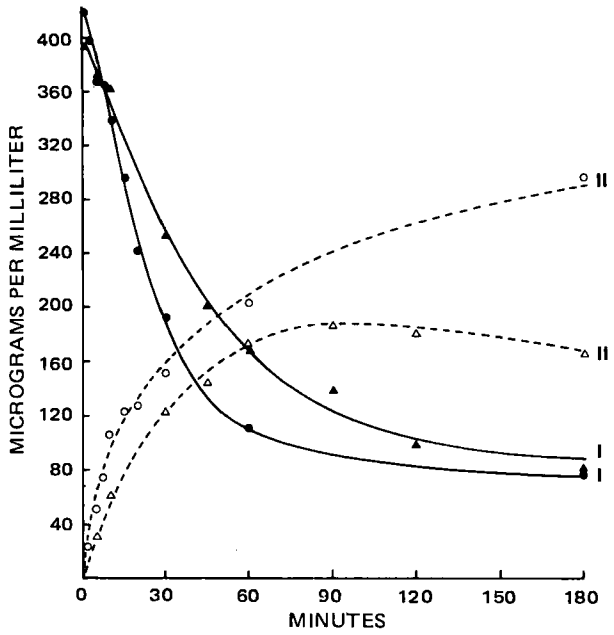

Figure 9—*Concentration* versus *time for two concentrations of prostaglandin 15-dehydrogenase enzyme. Key:* Δ, ▲, *25 μl;* ○, ●, *50 μl;* —, *dinoprostone (I); and* - - -, *15-keto derivative (II). Total incubation volume = 5.2 ml; samples assayed = 0.5 ml.*

CONCLUSIONS

An HPLC method was developed, allowing the simultaneous determination of substrate and metabolic conversion products from *in vitro* incubations with prostaglandin 15-dehydrogenase. The specific nature of the assay provides vital information for a complete characterization of enzyme quality and activity. Preliminary results pointed toward differences in *in vitro* enzyme kinetics for different substrates. Dinoprost, while showing the lowest initial reaction rate (*cf.*, Figs. 5–7), is completely consumed while prostaglandin E_1 and dinoprostone reach an asymptote with time.

The method may be useful as a: (*a*) screen for prostaglandin 15-dehydrogenase inhibitors, (*b*) reference method for questionable results from other screening assays, and (*c*) control method to ensure that the inhibitor screening assay is employing a satisfactorily specific and active enzyme.

If reasonably high activities can be obtained, then HPLC probably may be used to characterize other prostaglandin-metabolizing enzymes. With the availability of superfused organ techniques, it also may be possible to compare, by an accurate physical–chemical technique, the effect of inhibitors on the enzyme in this system and *in vitro* enzymes to distinguish differences.

REFERENCES

(1) H. Vonkeman, D. H. Nugteren, and D. A. van Dorp, *Biochim. Biophys. Acta*, **187**, 581(1969).

(2) S. A. Saeed and A. C. Roy, *Biochem. Biophys. Res. Commun.*, **47**, 96(1972).

(3) H. S. Hansen, *Prostaglandins*, **8**, 95(1974).

(4) C. J. Limas and J. N. Cohn, *Proc. Soc. Exp. Biol. Med.*, **142**, 1230(1973).

(5) H. H. Tai, C. L. Tai, and C. S. Hollander, *Biochem. Biophys. Res. Commun.*, **57**, 457(1974).

(6) J. Jarabak, *Proc. Nat. Acad. Sci. USA*, **69**, 533(1972).

(7) W. Schlegel, L. M. Demers, H. E. Hildebrandt-Stark, H. R. Behrman, and R. O. Greep, *Prostaglandins*, **5**, 417(1974).

(8) S. C. Lee and L. Levine, *J. Biol. Chem.*, **250**, 548(1975).

(9) L. J. Lerner, P. Carminali, F. Luzzani, and A. Soffientini, presented at the International Conference on Prostaglandins, Florence, Italy, 1975, Session 13.

(10) C. Pace-Asciak, *J. Biol. Chem.*, **250**, 2789(1975).

(11) W. Morozowich and S. Douglas, *Prostaglandins*, **10**, 19(1975).

(12) F. F. Sun, S. B. Armour, and V. R. Bockstanz, presented at the International Conference on Prostaglandins, Florence, Italy, 1975, Session 10.

ACKNOWLEDGMENTS AND ADDRESSES

Received September 29, 1975, from the *Research Laboratories, The Upjohn Company, Kalamazoo, MI 49001*

Accepted for publication January 16, 1976.

The author acknowledges valuable discussions with Dr. E. G. Daniels, The Upjohn Co. Special thanks are due to J. C. Mc Guire for supplying purified prostaglandin 15-dehydrogenase enzyme.

Preparation and Properties of Solid Dispersion System Containing Citric Acid and Primidone

M. P. SUMMERS and R. P. ENEVER ˣ

Abstract □ Solid dispersions containing 1–32% (w/w) primidone were prepared by fusing the drug with citric acid and rapidly cooling the melt. The solidified dispersions were clear glasses which devitrified on aging or when stored at 60° for up to 3 days. The phase diagram of the devitrified system indicated that the drug may exist as a solid solution at 1–3% (w/w) concentrations but that a eutectic mixture is formed at higher concentrations. The solubility of primidone increased in the presence of citric acid. Preliminary dissolution studies showed that the dissolution rate from the solid dispersion was greater than that of the pure drug or the physical mixture.

Keyphrases □ Solid dispersion systems—primidone with citric acid, effect of concentration, aging, and temperature □ Primidone—solid dispersion with citric acid, effect of concentration, aging, and temperature □ Citric acid—solid dispersion with primidone, effect of concentration, aging, and temperature □ Anticonvulsant agents—primidone, solid dispersion with citric acid, effect of concentration, aging, and temperature

Sekiguchi and Obi (1) first demonstrated the use of a eutectic mixture of a sparingly soluble drug and a water-soluble compound in increasing the rates of dissolution and absorption of the drug. This type of formulation, a "solid dispersion system," has undergone much investigation and has been extended to include

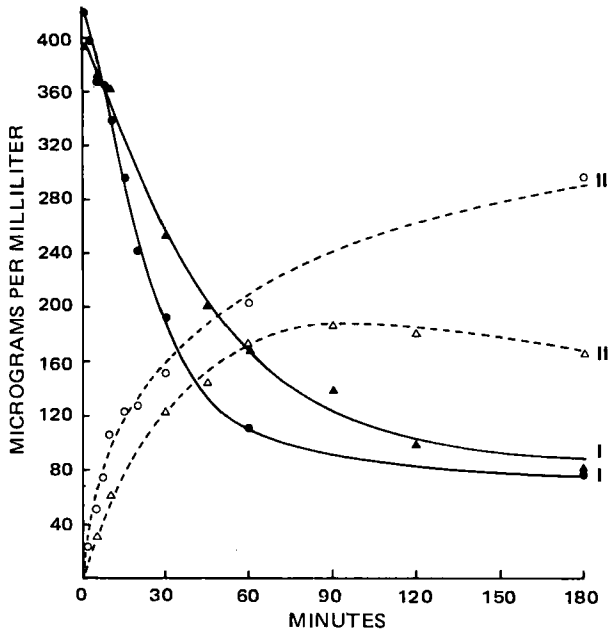

Figure 9—*Concentration* versus *time for two concentrations of prostaglandin 15-dehydrogenase enzyme. Key:* Δ, ▲, *25 μl;* ○, ●, *50 μl;* —, *dinoprostone (I); and* - - -, *15-keto derivative (II). Total incubation volume = 5.2 ml; samples assayed = 0.5 ml.*

CONCLUSIONS

An HPLC method was developed, allowing the simultaneous determination of substrate and metabolic conversion products from *in vitro* incubations with prostaglandin 15-dehydrogenase. The specific nature of the assay provides vital information for a complete characterization of enzyme quality and activity. Preliminary results pointed toward differences in *in vitro* enzyme kinetics for different substrates. Dinoprost, while showing the lowest initial reaction rate (*cf.*, Figs. 5–7), is completely consumed while prostaglandin E_1 and dinoprostone reach an asymptote with time.

The method may be useful as a: (*a*) screen for prostaglandin 15-dehydrogenase inhibitors, (*b*) reference method for questionable results from other screening assays, and (*c*) control method to ensure that the inhibitor screening assay is employing a satisfactorily specific and active enzyme.

If reasonably high activities can be obtained, then HPLC probably may be used to characterize other prostaglandin-metabolizing enzymes. With the availability of superfused organ techniques, it also may be possible to compare, by an accurate physical–chemical technique, the effect of inhibitors on the enzyme in this system and *in vitro* enzymes to distinguish differences.

REFERENCES

(1) H. Vonkeman, D. H. Nugteren, and D. A. van Dorp, *Biochim. Biophys. Acta*, **187**, 581(1969).

(2) S. A. Saeed and A. C. Roy, *Biochem. Biophys. Res. Commun.*, **47**, 96(1972).

(3) H. S. Hansen, *Prostaglandins*, **8**, 95(1974).

(4) C. J. Limas and J. N. Cohn, *Proc. Soc. Exp. Biol. Med.*, **142**, 1230(1973).

(5) H. H. Tai, C. L. Tai, and C. S. Hollander, *Biochem. Biophys. Res. Commun.*, **57**, 457(1974).

(6) J. Jarabak, *Proc. Nat. Acad. Sci. USA*, **69**, 533(1972).

(7) W. Schlegel, L. M. Demers, H. E. Hildebrandt-Stark, H. R. Behrman, and R. O. Greep, *Prostaglandins*, **5**, 417(1974).

(8) S. C. Lee and L. Levine, *J. Biol. Chem.*, **250**, 548(1975).

(9) L. J. Lerner, P. Carminali, F. Luzzani, and A. Soffientini, presented at the International Conference on Prostaglandins, Florence, Italy, 1975, Session 13.

(10) C. Pace-Asciak, *J. Biol. Chem.*, **250**, 2789(1975).

(11) W. Morozowich and S. Douglas, *Prostaglandins*, **10**, 19(1975).

(12) F. F. Sun, S. B. Armour, and V. R. Bockstanz, presented at the International Conference on Prostaglandins, Florence, Italy, 1975, Session 10.

ACKNOWLEDGMENTS AND ADDRESSES

Received September 29, 1975, from the *Research Laboratories, The Upjohn Company, Kalamazoo, MI 49001*

Accepted for publication January 16, 1976.

The author acknowledges valuable discussions with Dr. E. G. Daniels, The Upjohn Co. Special thanks are due to J. C. Mc Guire for supplying purified prostaglandin 15-dehydrogenase enzyme.

Preparation and Properties of Solid Dispersion System Containing Citric Acid and Primidone

M. P. SUMMERS and R. P. ENEVER ˣ

Abstract □ Solid dispersions containing 1–32% (w/w) primidone were prepared by fusing the drug with citric acid and rapidly cooling the melt. The solidified dispersions were clear glasses which devitrified on aging or when stored at 60° for up to 3 days. The phase diagram of the devitrified system indicated that the drug may exist as a solid solution at 1–3% (w/w) concentrations but that a eutectic mixture is formed at higher concentrations. The solubility of primidone increased in the presence of citric acid. Preliminary dissolution studies showed that the dissolution rate from the solid dispersion was greater than that of the pure drug or the physical mixture.

Keyphrases □ Solid dispersion systems—primidone with citric acid, effect of concentration, aging, and temperature □ Primidone—solid dispersion with citric acid, effect of concentration, aging, and temperature □ Citric acid—solid dispersion with primidone, effect of concentration, aging, and temperature □ Anticonvulsant agents—primidone, solid dispersion with citric acid, effect of concentration, aging, and temperature

Sekiguchi and Obi (1) first demonstrated the use of a eutectic mixture of a sparingly soluble drug and a water-soluble compound in increasing the rates of dissolution and absorption of the drug. This type of formulation, a "solid dispersion system," has undergone much investigation and has been extended to include

solid solutions, such as those believed to be formed at low drug concentrations with the high molecular weight polyethylene glycols (2–5), and the amorphous or glassy dispersions formed with povidone (3, 6–8). The theories and pharmaceutical applications of such solid dispersions were reviewed extensively (3).

Chiou and Riegelman (2) proposed the use of organic glass-forming compounds to form binary glass systems with water-insoluble drugs and demonstrated the increased dissolution rate of griseofulvin in a glass of citric acid. The glass system gave faster drug release than other solid dispersion systems studied.

In the present investigation, the applicability of the glass system for the formulation of primidone was investigated. This drug is relatively water insoluble (1 in 2000 at 20°) and melts (with decomposition) at the relatively high temperature of 295°. It appears to be a suitable candidate for such formulation since binary systems can be prepared containing low drug concentrations at temperatures below which the drug decomposes. Furthermore, primidone exists in two polymorphic forms (9), and one (Form II) can be prepared from a melt.

It was, therefore, of interest to determine whether this method of formulation could cause a change in the polymorphic form of a drug. Chiou and Niazi (10) showed that different polymorphic forms of a drug can give different phase diagrams and that crystalline changes may occur in such solid dispersion systems on aging.

EXPERIMENTAL

Preparation of Solid Dispersions—Primidone[1] was intimately mixed in a pestle and mortar with citric acid monohydrate[2]. Mixtures containing 1–32% (w/w) primidone were prepared. The mixtures were transferred to Pyrex tubes and gently heated over a flame until complete melting occurred. Heating was continued to remove any water of crystallization condensed on the tube walls.

Gentle heating had to be used to prevent decomposition of citric acid. Mixtures containing more than 32% (w/w) primidone could not be prepared because primidone decomposition occurred on melting. Subsequently, the melt was poured into a glass petri dish and immediately placed in a desiccator to prevent moisture absorption.

Chiou and Riegelman (3) found that the griseofulvin–anhydrous citric acid glass became brittle and transparent after storage at 37° for a few days. In this system, however, devitrification of the glasses occurred. Since high temperatures aided devitrification, the glasses were stored at 60° until complete devitrification occurred, usually in less than 3 days.

Construction of Phase Diagram—The phase diagram of the devitrified system was constructed by determining the onset and completion of melting of a 125–180-μm size fraction of each dispersion. Hot-stage microscopy[3] and differential scanning calorimetry[4] were used to determine the melting points. A heating rate of 2°/min was used.

Hot-stage microscopy was performed using scattered particles on a glass slide, with a field of view containing at least eight particles.

At least two determinations were performed on each dispersion, and at least two batches were prepared and tested at each primidone concentration.

X-Ray Diffraction—X-ray diffraction[5] was used to assess the nature of the solid dispersion system before and after devitrification and to characterize the two polymorphic forms of primidone. Powdered samples of a mixed size range were mounted on adhesive tape, and the X-ray diffraction pattern was determined using CuKα radiation.

Powdered samples of devitrified glasses were compared with physical mixtures of the same concentration. Physical mixtures were prepared using citric acid monohydrate and anhydrous citric acid to establish the nature of the citric acid in the devitrified system. Furthermore, physical mixtures were prepared using both polymorphic forms of primidone to determine the polymorphic form in the devitrified system.

Solubility Determinations—Solution concentration–time profiles ("dynamic solubility" determinations) of the two polymorphic forms of primidone (prepared using the method in Ref. 9) were determined by shaking suspensions of the polymorphs in distilled water (pH 5.5) in a water bath at 37°. At 5-min intervals, 5-ml samples were removed with a pipet fitted with a grade 3 sintered-glass filter stick. The solutions were assayed at 257 nm using a UV spectrophotometer[6]. Saturation concentration was usually achieved within 1 hr, but samples were withdrawn for periods up to 12 hr to check this fact.

Equilibrium solubility values of the two polymorphs and the commercial sample of primidone were determined by equilibrating aqueous suspensions at 37° in the same apparatus for 12 hr. The commercial sample was also equilibrated with citric acid solutions of various concentrations for the same period. At the end of this time, 5-ml samples were removed and assayed in the manner already described.

Aqueous suspensions of the two polymorphic forms were also equilibrated at 37° for 21 days. Subsequently, the crystals were removed and analyzed by IR spectroscopy[7].

Dissolution Studies of Powdered Materials—The experiments were conducted in a 1-liter, flat-bottom, glass reaction vessel held in a water bath maintained at 37°. The dissolution medium was stirred by a T-shaped glass stirrer inserted through a gland in the lid of the vessel and connected to a constant-speed motor *via* a belt drive. The stirrer was positioned 1.2 cm from the base of the vessel, and a stirring speed of 110 rpm was used.

Stainless steel stirrers could not be used because a reaction took place between steel and citric acid. Pitting and discoloration were observed, and the soluble products of the reaction interfered with the UV assay.

All dissolution studies were performed using a 150–250-μm size fraction of powdered material. When physical mixtures of primidone and citric acid were tested, a 150–250-μm size fraction of both powders was used.

The powder was placed on the vessel base at the beginning of the dissolution experiment. The vessel top and stirrer were replaced and, after the stirrer motor was started, 400 ml of distilled water (pH 5.5), previously equilibrated at 37°, was added. Then 5-ml samples were withdrawn at frequent intervals using a pipet fitted with a grade 3 sintered-glass filter stick. Sampling was continued for 20 min. The volume withdrawn was not replaced with fresh dissolution medium. Samples were assayed at 257 nm[6].

The studies were performed with the following systems: (*a*) 200-mg quantities of both powdered devitrified glasses and physical mixtures containing either 16 or 32% (w/w) primidone (equivalent to 32 or 64 mg of primidone, respectively), and (*b*) amounts of powdered devitrified glasses equivalent to a primidone content of 32 mg [200 mg of 16% (w/w) or 100 mg of 32% (w/w) concentrations].

Rotating-Disk Dissolution Studies—Disks of each polymorphic form of primidone were prepared by compressing powdered samples at 5000 kg in a 1.2-cm diameter die using a hydraulic press[8]. Preliminary experiments established that a minimum force of 4500 kg was necessary to obtain constant dissolution rate data.

The experiments were carried out using the apparatus described under *Dissolution Studies of Powdered Materials*, except that the glass stirrer was replaced by a stainless steel shaft bearing a disk support. The disks were attached to the support with microcrystalline wax[9], and their edges were sealed with the wax to ensure that only one surface was exposed to the dissolution medium.

The dissolution medium was distilled water (pH 5.5), which had previously been boiled to remove air and subsequently equilibrated at 37° before use. At 30-min intervals, 5-ml samples were withdrawn

[1] Batch No. ADM 16619/73, I.C.I. Pharmaceuticals Ltd., Macclesfield, England.
[2] Analar Grade, B.D.H. Chemicals Ltd., Poole, England.
[3] Mettler FP2, Mettler Instrument Corp, Switzerland.
[4] D.S.C. 1B, Perkin-Elmer, Beaconsfield, United Kingdom.
[5] Nonius Mk. 2 self-focusing Guinier diffractometer.
[6] SP 1800, Pye-Unicam, Cambridge, United Kingdom.
[7] 175 G spectrophotometer, Perkin-Elmer, Norwalk, Conn.
[8] Apex hydraulic press, Apex Construction Ltd., United Kingdom.
[9] B.D.H. Chemicals Ltd., Poole, England.

and assayed as described previously. Sections from the disk were subjected, before and after dissolution, to IR spectroscopy to determine the effect of compression and dissolution on the polymorphic form of the drug.

RESULTS AND DISCUSSION

Preparation and Devitrification of Glass System—Chiou and Riegelman (3) suggested the use of citric acid monohydrate for preparing solid dispersions of this type, because the lower melting point of the monohydrate would be advantageous in preventing decomposition of citric acid and the drug. Hot-stage microscopy showed that the monohydrate lost water of crystallization at approximately 70° before finally melting at the melting point of the anhydrous material (153°).

It was confirmed, however, that the monohydrate was the better form to use, became decomposition of primidone occurred at lower concentrations of primidone in anhydrous citric acid. It is possible that the released water of crystallization in the restricted environment of the test tube caused the formation of a citric acid solution which then acted to dissolve the primidone.

The glasses were unstable and devitrified after preparation. This devitrification was concentration dependent; glasses containing low concentrations of primidone devitrified faster than those of higher concentration. A 1% glass started to devitrify within 15 min, whereas a glass containing 30% primidone remained clear for longer than 6 months.

Although no quantitative data are available, the glasses containing low concentrations of primidone were less viscous than those of greater concentrations. The glass containing 30% (w/w) primidone was hard, brittle, and very hygroscopic. Glasses of concentrations lower than about 28% (w/w) were softer and did not harden until devitrified. When vitreous, these glasses were also hygroscopic.

The time taken for the onset of devitrification reflects this increase in viscosity with an increased concentration of primidone. It is thought that the decreased viscosity of the lower concentrations permits the ordering of the molecules necessary for crystallization (11).

Moreover, the increasing viscosity of the glass with an increasing primidone concentration is probably due to the extent of hydrogen bond formation between the citric acid and primidone molecules and the strength of these bonds. If the bonds formed between citric acid and primidone are stronger than those between citric acid molecules, the cooling melt is composed of a network of noncrystallizing molecules. These molecules are responsible for the increased viscosity of the melt and the glass that subsequently forms.

Phase Diagram of Devitrified System—A portion of the phase diagram of the devitrified solid dispersion system is shown in Fig. 1. The upper line shows the liquidus line obtained from hot-stage microscopy. The lower portion is the phase diagram found by differential scanning calorimetry. The two methods gave similar results, but the diagrams were displaced by approximately 2°. The calibration of both instruments had been checked before use, and the discrepancy is probably due to the errors inherent in the hot-stage technique when observing a binary system without a sharp melting point. The liquidus line obtained from hot-stage microscopy ceases at the boiling point of the melt.

The primidone concentration is expressed as a percent (w/w) in anhydrous citric acid, because X-ray diffraction indicated that the citric acid in the devitrified system was anhydrous.

The phase diagram of the system indicates that a solid solution of primidone in citric acid exists at very low concentrations of primidone (up to 3%) and that a eutectic mixture is formed at higher primidone concentrations. Because the phase diagram in Fig. 1 is not complete, it is not possible to define the nature of the eutectic mixture. It may consist of a mixture of the solid solution of primidone in citric acid with primidone. Alternatively, if a solid solution of citric acid in primidone is formed at high primidone concentrations, the eutectic consists of a mixture of the solid solutions of primidone in citric acid and citric acid in primidone. The eutectic contains 20% (w/w) primidone, and the melting point of this eutectic is 141° by differential scanning calorimetry.

X-ray diffraction patterns (Fig. 2) show that a physical mixture containing 15% (w/w) primidone in anhydrous citric acid resembles the diffraction pattern of the devitrified glass containing 15% (w/w) primidone. This result is typical of devitrified glasses containing 5–30% (w/w) primidone. There was no change in citric acid lattice

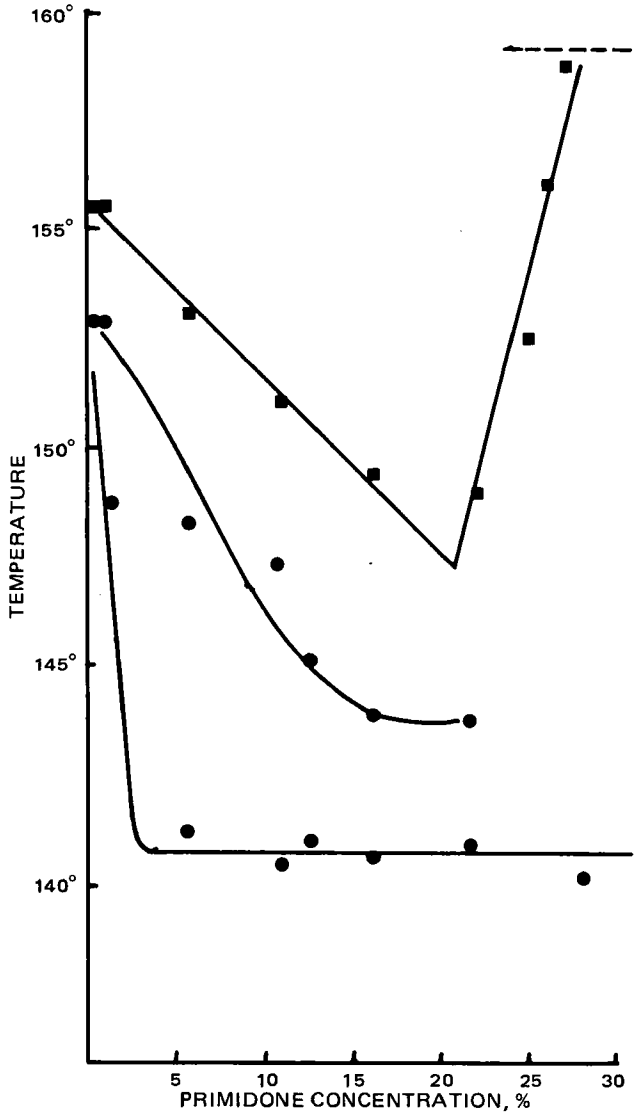

Figure 1—*Phase diagram of the primidone–citric acid system. Key: ■, hot-stage microscope; ●, differential scanning calorimetry; and - - -, boiling point of citric acid–primidone melt.*

parameters with increasing concentration of primidone. Such changes would indicate solid solution formation. The presence of typical primidone lines at all concentrations in which it could be detected suggests that a simple eutectic mixture is formed and that the solid solubility of primidone in citric acid is very small.

The apparent discrepancy in the X-ray diffraction data and the differential scanning calorimetry–hot-stage phase diagram may be attributed to the fact that the latter data relate to the solubility of primidone in citric acid at the temperature of the solid–liquid equilibrium. If this solubility is greater than the room temperature solubility of primidone in citric acid, precipitation of primidone from the solid solution under ambient conditions would account for the simple eutectic mixture observed with X-ray diffraction studies.

The results of dispersions containing up to 3% (w/w) primidone were inconclusive; at these low concentrations, X-ray diffraction failed to detect primidone in the physical mixtures.

The results also show that primidone existed in the devitrified system as the Form II polymorph, whereas the starting material (*i.e.*, the commercial sample) was the Form I polymorph.

The diffraction pattern of the 30% (w/w) vitreous glass exhibits only very broad lines typical of the backing tape, suggesting that primidone is molecularly dispersed in the glassy state throughout the citric acid glass or exists in the amorphous form. This behavior is likely to be observed with all glasses prepared.

Solubility Studies—The polymorphic forms of primidone have

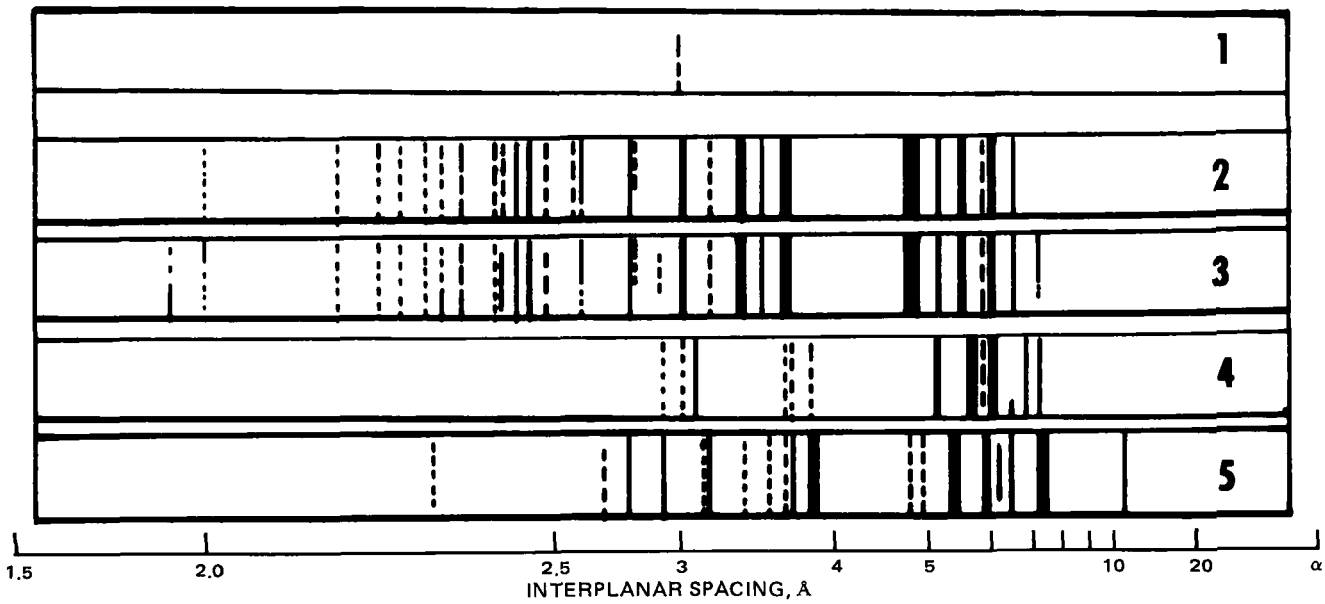

Figure 2—*X-ray powder diffraction pattern of (1) 30% vitreous glass, (2) 15% devitrified glass, (3) 15% physical mixture of anhydrous citric acid and primidone Form II polymorph, (4) primidone Form II polymorph, and (5) primidone Form I polymorph. Dotted lines indicate bands of weaker intensity.*

solubilities of 56.4 mg/100 ml (Form I) and 56.5 mg/100 ml (Form II) at 37°. There was no evidence of a phase change during the dynamic solubility determinations, and IR spectroscopy confirmed that there was no change in aqueous suspensions equilibrated for 21 days.

Figure 3 shows that citric acid increased the solubility of primidone. A solution containing 500 mg/ml of citric acid increased the solubility of primidone from 56.4 to 172.2 mg/100 ml. The effect of citric acid on the solubility of primidone would be expected to influence the dissolution rate of the drug from the solid dispersion system.

Dissolution Studies—Figure 4 shows the results of the rotating-disk dissolution study of the two primidone polymorphs. There was no difference in the dissolution rates of the polymorphs at 37°. Neither compression of powder into disks nor the process of dissolution caused any change in polymorphic form. Thus, the results of both the dissolution and solubility studies suggest that the dissolution rate of primidone will not be altered by precipitation of the Form II polymorph in the devitrified system.

Dissolution studies of the devitrified glasses were initially carried out using the rotating-disk method, but this attempt failed. During dissolution from the disk of the solid dispersion, primidone precipitated on the disk surface and subsequently flaked off into the dissolution medium. Within 5 min, complete breakdown of the disk occurred because of this phenomenon.

Dissolution studies were finally performed using the powder method described. Vitreous glasses could not be tested, because they became very cohesive during comminution due to moisture absorption. A suitable size fraction could not be prepared.

Large particles of the glass were placed in the dissolution medium, however, and it was found that primidone was precipitated on the surface of the glass during dissolution. When devitrified glasses dissolve, a similar process may occur if a solution of primidone in citric acid is formed in the diffusion layer around the particle. Therefore, dissolving devitrified glasses may be covered with a layer of primidone crystals precipitated during devitrification and dissolution.

The results of the powder dissolution experiments are shown in Fig. 5. All results were corrected to a 400-ml volume of dissolution medium

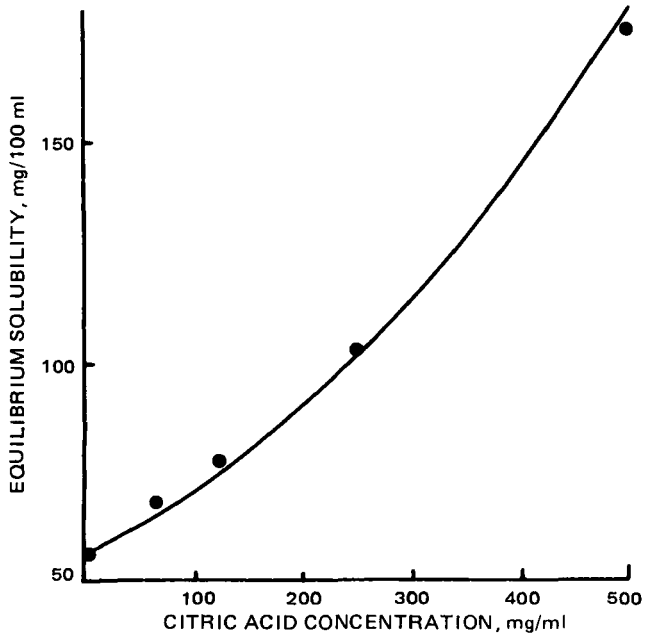

Figure 3—*Effect of citric acid on primidone solubility.*

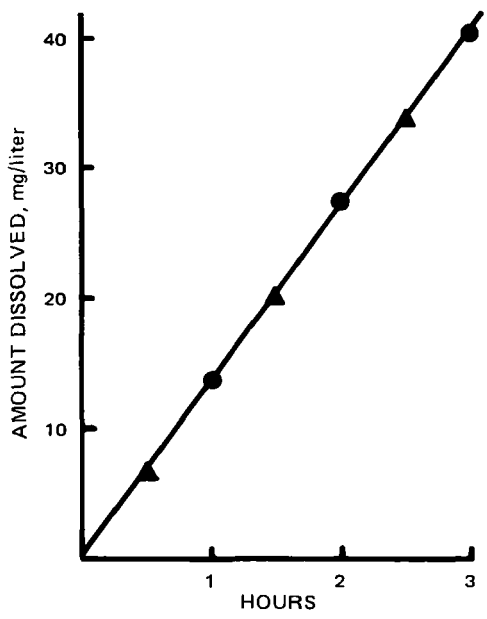

Figure 4—*Dissolution rate of two primidone polymorphs. Key: ▲, Form II; and ●, Form I.*

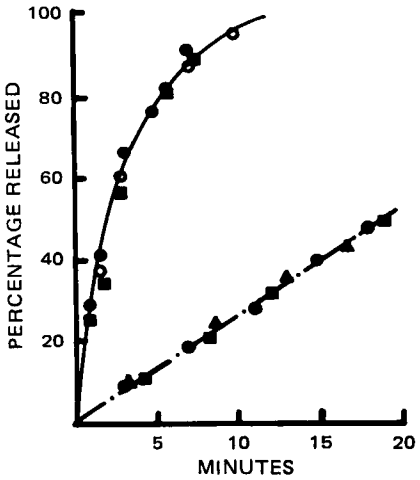

Figure 5—*Dissolution of primidone expressed as a percentage of the total drug content. Key: —, devitrified glass; —·—, physical mixtures; ●, 16% primidone (200 mg); ○, 32% primidone (100 mg); ■, 32% primidone (200 mg); and ▲, primidone Form II powder.*

at each sample time. The dissolution rates of the devitrified glasses were faster than those of the physical mixtures. This could be due to the solubility increase associated with the presence of citric acid or the small particle size of the primidone precipitated during devitrification and dissolution. The dissolution rates of the physical mixtures would not be expected to show any significant increase due to the presence of citric acid, because the acid concentration in the bulk of the dissolution medium is relatively low. This assumption is supported by the data in Fig. 5, which show that primidone Form II powder dissolves at the same rate as the physical mixtures.

When the glasses and devitrified glasses dissolve, however, citric acid forms a saturated solution in the diffusion layer around the particle, and this would be expected to aid dissolution because of the solubility increase. When this concentrated acidic solution is diluted during diffusion away from the particle, the primidone is present in a supersaturated solution, accounting for its precipitation from the glass during dissolution.

Because citric acid is very soluble (592 g in 1 liter at 20°), rapid depletion of the citric acid probably occurs and, in the later stage of dissolution, the rate depends upon the size of the precipitated primidone crystals. These crystals are smaller than the particles in the physical mixtures and, therefore, dissolution from the devitrified glasses would be expected to be greater than that from the physical mixtures even in the later stages.

The results in Fig. 5 are plotted as a percentage of the drug content and show that the dissolution rates of the two devitrified glasses are the same irrespective of sample size. This finding tends to indicate that the dissolution rates are dependent upon the concentration of drug in the devitrified glasses and that the particle-size distribution of primidone is similar in both during drug dissolution. One explanation of this phenomenon would be that rapid depletion of the citric acid causes the formation of a suspension of primidone particles that were precipitated during devitrification. These particles would control the rate of dissolution and would account for the dependence of the dissolution rate on primidone concentration.

CONCLUSIONS

Solid dispersions of primidone can be prepared by fusing the drug with citric acid to form a glass. The glass is unstable and devitrifies, and X-ray diffraction indicates that this devitrified state is a eutectic mixture of primidone and citric acid.

The devitrified glass has a faster dissolution rate than the pure drug and a physical mixture of the drug with citric acid. This increased dissolution rate is probably due to three factors:

1. Citric acid has been shown to increase the solubility of primidone and this may affect the solubility of primidone in the diffusion layer around the dissolving devitrified glass.
2. Primidone is precipitated as fine crystals during devitrification, and this will increase the effective surface area of the drug in the devitrified state.
3. The glass and the devitrified glass have superior wetting characteristics compared with the pure drug, and this will also affect the surface area available for dissolution. This aspect was discussed by Chiou and Riegelman (2).

REFERENCES

(1) K. Sekiguchi and N. Obi, *Chem. Pharm. Bull.*, **9**, 866 (1961).

(2) W. L. Chiou and S. Riegelman, *J. Pharm. Sci.*, **58**, 1505(1969).

(3) *Ibid.*, **60**, 1281(1971).

(4) W. L. Chiou and L. D. Smith, *J. Pharm. Sci.*, **60**, 125(1971).

(5) W. L. Chiou and S. Riegelman, *ibid.*, **60**, 1569(1971).

(6) M. Mayersohn and M. Gibaldi, *ibid.*, **55**, 1323(1966).

(7) A. P. Simonelli, S. C. Mehta, and W. I. Higuchi, *ibid.*, **58**, 538(1969).

(8) T. R. Bates, *J. Pharm. Pharmacol.*, **21**, 710(1969).

(9) R. D. Daley, in "Analytical Profiles of Drug Substances," vol. 2, K. Florey, Ed., Academic, New York, N.Y., 1973, p. 417.

(10) W. L. Chiou and S. Niazi, *J. Pharm. Sci.*, **60**, 1333(1971).

(11) G. O. Jones, "Glass," Wiley, New York, N.Y., 1958.

ACKNOWLEDGMENTS AND ADDRESSES

Received April 28, 1975, from the *Department of Pharmaceutics, School of Pharmacy, University of London, Brunswick Square, London, WC1N 1AX, England.*

Accepted for publication January 9, 1976.

[x] To whom inquiries should be directed.

Effect of Polymers on Dissolution from Drug Suspensions

NUTAN B. SHAH * and BHOGI B. SHETH ˣ

Abstract □ The effect of three viscosity grades of methylcellulose on the dissolution–dialysis rate of nitrofurantoin suspensions was investigated using a cell designed to provide a large surface area for dialysis. Apparent dialytic rate constants of drug dispersions and solutions were measured in 0.1 *N* HCl and in pH 7.4 buffer. Samples containing methylcellulose had lower rates of dialysis, with the lowest rate being observed for samples in which the polymer was used as the suspending agent. The reduced rate of dialysis of the drug suspension containing methylcellulose is thought to be due to complexation of the drug in solution with the polymer as well as formation of microscopic regions of high viscosity surrounding the undissolved drug particles leading to a reduction in the dissolution rate of the drug. An empirical relationship was obtained to enable the estimation of the effective drug concentration in the dissolution chamber for drug dispersions. The method is based on utilizing dialysis rate data of drug solutions. This relationship could be used for comparing suspension formulations in terms of the amount of drug available for dialysis.

Keyphrases □ Nitrofurantoin—suspensions, dissolution–dialysis rate, effect of three viscosity grades of methylcellulose □ Dissolution–dialysis rates—nitrofurantoin suspensions, effect of three viscosity grades of methylcellulose □ Methylcellulose—three viscosity grades, effect on dissolution–dialysis rates of nitrofurantoin suspensions □ Suspensions, drug—nitrofurantoin, dissolution–dialysis rates, effect of three viscosity grades of methylcellulose □ Viscosity—three grades, methylcellulose, effect on dissolution–dialysis rates of nitrofurantoin suspensions □ Antibacterial agents, urinary—nitrofurantoin suspensions, dissolution–dialysis rates

The dissolution rate of a drug from a suspension is generally assumed to be similar to that of its dispersion in water. However, lower cumulative excretion of nitrofurantoin was reported from a dispersion in 5% methylcellulose solution as compared to that of the drug dispersion in water (1). Other reports also indicated unsatisfactory bioavailability of drugs from suspensions (2–8). These findings suggest the possibility of drug–adjuvant interactions in suspension formulations that could affect drug dissolution and absorption. Therefore, there was a need for a systematic investigation of factors affecting the drug dissolution from suspension formulations.

This investigation was concerned with the effect of polymeric suspending agents on the dissolution rate of nitrofurantoin. Its dissolution rate was investigated by a dissolution–dialysis technique, because conventional dissolution rate measurement methods were not suitable for precise determination of dissolution behavior. A specially designed dissolution–dialysis technique was used.

EXPERIMENTAL

The model drug selected was nitrofurantoin[1]. Three viscosity grades of methylcellulose[2], 50, 400, and 4000 cps, were used as suspending agents. Dissolution–dialysis experiments were carried out at 37° using 0.1 *N* HCl and 0.1 *M* phosphate buffer (pH 7.4) as the dissolution and dialysis media. Rates of dialysis of the drug from dispersions of nitrofurantoin in deionized water and in polymer solutions were determined. In addition, dialysis rates were measured using solutions of the drug in deionized water and in the polymer solutions.

Dissolution–Dialysis Cell—A diagram of the dissolution–dialysis cell is shown in Fig. 1. The dissolution chamber consisted of a cylindrical Plexiglas frame made up of two Plexiglas disks (C and D) connected with three Plexiglas supports (F) onto which a cellulose dialysis tubing[3] was mounted. The dissolution chamber was placed in a 2-liter resin reaction kettle[4] which served as the recipient chamber.

The cell had provision for a sample introduction port (I) for the addition of the test sample to the dissolution chamber (B) and a port (J) for removing samples of the desorbing solution from the dialysis chamber (A). In a typical experiment, 50 ml of the dissolution medium was placed in the dissolution chamber and agitated at 70 rpm using a constant-speed mixer[5] and a three-blade stainless steel propeller. Eleven hundred milliliters of the desorbing solution (identical to the dissolution medium) was placed in the dialysis chamber and stirred at approximately 500 rpm with a controlled magnetic stirrer[6].

The cellulose dialysis tubing was obtained as a 150-mm flat width tubing, having an average pore diameter of 50 Å and a thickness of 3.25×10^{-2} mm when fully hydrated. A piece of tubing approximately 30 cm long was thoroughly washed several times in deionized water and soaked in deionized water for 24 hr in a refrigerator to achieve hydration. The hydrated dialysis tubing was then mounted on the Plexiglas frame (Fig. 1). The dissolution chamber was filled with 500 ml of deionized water and observed for at least 3 hr for possible leakage. The diameter of this chamber was about 90 mm and, when filled with 500 ml of the dissolution medium, the level of the medium rose to about 95 mm from the bottom of the dissolution chamber.

Procedure—Appropriate volumes of the dissolution medium and desorbing solution were placed in the dissolution–dialysis cell and allowed to equilibrate for 1 hr at 37°. The test sample was quantitatively transferred to the dissolution chamber. Five-milliliter samples of the desorbing solution were withdrawn at 2, 5, 10, 20, 30, 40, 50, 60, 75, 90, 120, 150, and 180 min, and the sample volume was immediately replaced with fresh desorbing solution.

The concentrations of nitrofurantoin in the samples were determined after appropriate dilutions by spectrophotometric analysis at 369 nm for 0.1 *N* HCl and at 380 nm for the pH 7.4 buffer. A cumulative correction for the amount of drug dialyzed was made for the previously removed sample using an equation described in the literature (9).

Test Systems—To analyze the specific effects of the polymer on the dissolution behavior of the drug from suspensions, five test systems were investigated. They were dispersions and solutions of the model drug in water and in methylcellulose solutions.

System A, for measuring the dialysis rate of drug dispersions with suspending agent, consisted of a dispersion of 40 mg of drug in 20 g of methylcellulose solution added to 480 ml of the dissolution medium.

System B, for measuring the dialysis rate of aqueous drug dispersions, consisted of a dispersion of 40 mg of drug in 20 g of deionized water added to 480 ml of the dissolution medium.

System C, for measuring the effect of methylcellulose present in the dissolution medium, consisted of an aqueous dispersion of 40 mg of drug in 20 g of deionized water added to the dissolution medium

[1] Nitrofurantoin, Lot 100C-1300, Sigma Chemical Co., St. Louis, Mo.
[2] Methocel, Dow Chemical Co., Midland, Mich.
[3] Cellulose dialysis tubing (150 mm flat width), Union Carbide Corp., Chicago, Ill.
[4] Pyrex, Fisher Catalog No. 110847C (1974), Fisher Scientific Co., Pittsburgh, Pa.
[5] Servodyn constant-speed and torque control unit, model 600-013, Cole-Parmer Instrument Co., Chicago, Ill.
[6] Micro-submersible magnetic stirrer, Tri-R Instrument, Inc., Rockville Center, N.Y.

Table I—Composition of Samples of Test System A Prepared for Dissolution–Dialysis Experiments

Polymer	Concentration of Stock Solution of Polymer, % w/w	Amount of Polymer Stock Solution in Test Sample, g	Amount of Deionized Water in Test Sample, g	Final Concentration of Polymer in Test Sample, % w/w
Methylcellulose, 50 cps	6.45	15.50	4.50	5.00
Methylcellulose, 400 cps	3.26	17.63	2.37	2.87
Methylcellulose, 4000 cps	1.96	18.13	1.87	1.77

containing the same amount of methylcellulose as would be present if a methylcellulose suspension of the drug were being tested.

System D, for measuring the dialysis rate of drug solutions containing methylcellulose, consisted of a solution of 40 mg of drug plus the same amount of methylcellulose as in a drug suspension in 500 g of total solution.

System E, for measuring the dialysis rate of aqueous drug solutions, consisted of drug solutions ranging from 8 to 53 mg of drug in 500 g of the dissolution medium.

Preparation of Test Samples—*Test System A*—Dispersions of Test System A were made using predetermined amounts of the drug, the polymer stock solution, and deionized water. The specific amounts used for the preparation of each sample of Test System A are shown in Table I. The predetermined amount of the drug was weighed into a 40-ml screw-capped vial, and then the predetermined amount of water and 5 g of the appropriate polymer stock solution were added.

The sample was mixed[7] and then dispersed by sonification for 6 min, using the microtip horn of the sonifier[8] at a power output of 40 w. The vial was immersed in an ice and water bath to keep it cool during sonification. The sample vial was closed with the screw cap, using an additional polyethylene liner to obtain a leakproof seal. The sample was equilibrated at 37° for 24 hr in a rotating-bottle apparatus.

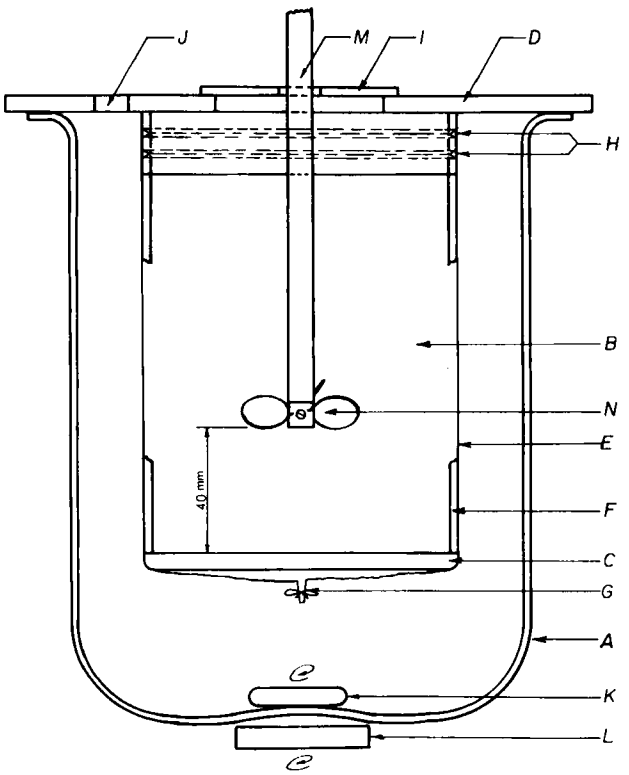

Figure 1—*Dissolution–dialysis cell. Key: A, 2-liter reaction kettle (dialysis chamber); B, dissolution chamber; C, Plexiglas disk (98 mm diameter, 5 mm thick); D, Plexiglas top (184 mm diameter, 5 mm thick); E, cellulose dialysis tubing (150 mm flat width); F, Plexiglas support (115 mm long, 10 mm wide, and 5 mm thick); G, lower end of dialysis membrane; H, heavy duty rubber bands; I, Plexiglas lid for sample introduction port (63 mm diameter); J, sample withdrawing port (10 mm diameter); K, magnetic spinning bar; L, microsubmersible magnetic stirrer; M, stirring shaft attached to a constant-speed motor; and N, stainless steel propeller.*

[7] S/P delux mixer, Scientific Products, Division of American Hospital Supply Corp., McGaw Park, Ill.

Test Systems B and C—The procedure outlined for preparing samples of Test System A was used for preparing samples of Test Systems B and C with some necessary changes. For Test System B, the drug was dispersed in 10 g of water initially and the dispersion was made up to 20 g with deionized water. Test System C was the same as Test System B, but the dissolution measurements were made using the dissolution medium as described earlier.

Test System D—The predetermined amount of the drug was weighed and transferred to a 500-ml volumetric flask. About 200 ml of dissolution medium was added to the flask, and the drug was dissolved with heat and mixing. The solution was allowed to cool to room temperature, and then the amount of the appropriate polymer stock solution was added to the contents of the flask necessary to obtain a polymer concentration in solution corresponding to that in System A. The solution was made up to 500 g with the dissolution medium. The test sample was then equilibrated at 37° for 24 hr in a water bath.

Test System E—The required amount of the drug as shown in Table II was dissolved in the appropriate test medium with the aid of heating and stirring. The samples were made up to 500 g with the appropriate test medium and were equilibrated at 37° for 24 hr prior to measurement.

The amount of nitrofurantoin to be used in the various test systems was such that, when all of the added drug had been dissolved, the final concentration was less than 20% of the equilibrium solubility of the drug in the dissolution–dialysis medium. The equilibrium solubility of nitrofurantoin at 37° was 143.8 μg/ml in 0.1 *N* HCl and 304.18 μg/ml in the pH 7.4 buffer solution.

The selection of each methylcellulose concentration was based on obtaining suspension vehicles with viscosity values in the range representative of commercial suspension products. The viscosity[9] values of four commercial suspensions at 60 rpm were 950–1250 cps. A solution of 50-cps methylcellulose, 5.0% (w/w), had a viscosity value of 1300 ± 100 cps. Therefore, this concentration was selected for 50-cps methylcellulose. Concentrations of the higher viscosity grades of methylcellulose were selected to give suspension vehicles of viscosities similar to the 5.0% (w/w) 50-cps methylcellulose solution. These concentrations were 2.78% (w/w) for 400-cps methylcellulose and 1.77% (w/w) for 4000-cps methylcellulose.

RESULTS AND DISCUSSION

Dissolution–Dialysis Cell—The rationale for the specific design of the dissolution–dialysis cell was to maintain dialysis conditions such that the dialysis rate measurements would reflect the dissolution behavior of the drug under sink conditions. The dialysis technique was employed in the past to maintain sink conditions in dissolution rate measurements of solid dosage forms (10, 11). However, reported dissolution–dialysis cells were unsuitable for the present investigation for two main reasons. First, the suspension formulations dissolved at a much faster rate than solid dosage forms. Second, the surface area for dialysis was quite small.

The net effect would be a rapid buildup of drug concentration in

[8] Sonifier cell disrupter model W185 with microtip, Heat Systems-Ultrasonics, Inc., Plainview, Long Island, N.Y.

[9] Brookfield Synchro-Lectric viscometer model LVT and No. 3 spindle, Brookfield, Stoughton, Mass.

Table II—Typical Amounts of Nitrofurantoin Used for Preparing Solutions of Various Concentrations for Test System E for Dialysis Experiments

Nitrofurantoin, mg	
0.1 *N* HCl	pH 7.4 Buffer
7.80	7.35
12.97	12.22
26.59	25.27
41.84	39.60
52.48	49.77

the dissolution medium, resulting in the loss of adequate sink conditions for drug dissolution. Therefore, the dialysis rate obtained by using small cells would not be an index of dissolution behavior because the rate-limiting factor would be the dialysis rate and not the dissolution rate. A cell was constructed to provide a large surface area for dialysis and thus prevent the concentration buildup in the dissolution chamber. The dialysis rate measurements under these conditions should reflect the dissolution behavior of drugs in suspensions.

Data Treatment—For calculation of the apparent dialytic rate constant, the following equation, developed by Davis *et al.* (12), was used:

$$\log [V_0A_T - (V_0 + V_i)A_0] = -\left[\frac{V_0 + V_i}{2.3V_iV_0}\right]Kt + \log (V_0A_T) \quad \text{(Eq. 1)}$$

where V_0 = volume of the test medium in the dialysis chamber, V_i = volume of the test medium in the dissolution chamber, A_0 = amount of drug dialyzed into the dialysis chamber, A_T = total amount of drug in the test sample, t = time in minutes, and K = apparent dialytic rate constant.

The term $\log [V_0A_T - (V_0 + V_i)A_0]$ represents the amount of drug remaining in the dissolution chamber at time t. When $\log [V_0A_T - (V_0 + V_i)A_0]$ is plotted *versus* time, t, a straight line is obtained. The slope of the line is:

$$\text{slope} = -\left[\frac{V_0 + V_i}{2.3V_iV_0}\right]K \quad \text{(Eq. 2)}$$

Therefore, the apparent dialytic rate constant, K, can be evaluated as follows:

$$K \text{ min}^{-1} = \frac{-(\text{slope})(2.303)(V_iV_0)}{V_i + V_0} \quad \text{(Eq. 3)}$$

A representative plot of the log amount of drug remaining in the dissolution chamber as a function of time is shown in Fig. 2 for Test System C. The value of the apparent dialytic rate constant, K, for this system was evaluated using the slope of this plot, calculated by the method of least squares.

In the case of drug dispersions, Test Systems A, B, and C, the amount of drug in solution at zero time is not known. Therefore, the amount of drug added to the system was used as the value of A_T for the data treatment. Hence, the values of K for these samples represent apparent dialytic rate constants. Similarly, the extent, if any, of complexation between the drug and the polymer was not determined for Test System D. Hence, the values of the dialytic rate constant for this test system should also be considered as the apparent dialytic rate constant. With Test System E, however, K should be considered as representing the dialytic rate constant of the drug solution.

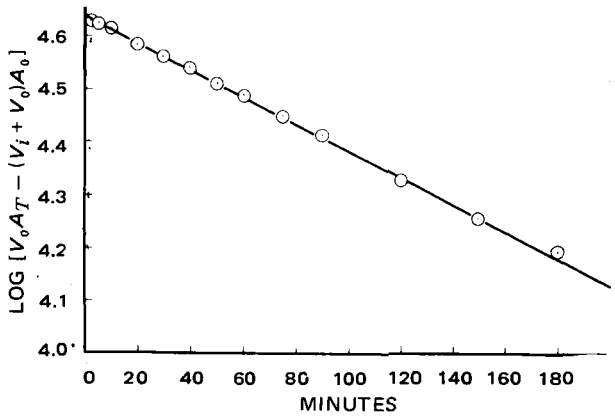

Figure 2—*Plot of logarithm of amount of drug remaining in the dissolution chamber* versus *time for Test System C of nitrofurantoin with 4000-cps methylcellulose as the suspending agent in 0.1* N *HCl.*

The rate of dialysis of dissolved drug is a function of the concentration of the dissolved drug, the diffusion coefficient of the drug, and the surface area of the dialyzing membrane. Therefore, with a suitable design of the dialysis cell, the rate of dialysis should serve as a more reliable index of the dissolution behavior of drug from the dosage formulation. Other investigators (13, 14) also indicated that the dissolution rate was an inadequate parameter for assessing the amount of drug available for absorption from a dosage form in the GI tract. They proposed that the rate of dialysis or the rate of permeation would be more appropriate.

Furthermore, conventional dissolution rate measurement methods involve filtration of the dissolution medium samples through a filter, usually a glass wool, a sintered-glass disk, or a membrane filter with an average pore diameter of 0.22 μm or larger. The finer particles of drugs could pass through the filter medium and continue to dissolve in the filtrate. A soluble drug–excipient complex could also be present in the filtrate and be measured as free drug if a nonspecific assay procedure is used for the analysis of the filtrate. Therefore, the dissolution–dialysis technique was used for the investigation of the dissolution of drugs from suspensions.

Dissolution–Dialysis of Nitrofurantoin in 0.1 *N* HCl—The apparent dialytic rate constants for the various samples of Test Systems A, B, C, and D in 0.1 *N* HCl are shown in Table III. Values for Test System E in this test medium are shown in Table IV.

As might be expected, the highest value of K was obtained for Test System E, the aqueous solution of the drug. The lowest value of K was obtained for Test System A, the suspension of the drug in methylcellulose solution. Essentially the same value of K was obtained for Test Systems B, C, and D; these values were intermediate between those for Test Systems A and E.

The values of K for drug suspensions would be expected to be lower than those for drug solutions since the drug concentration in the dissolution chamber should be dissolution controlled for these systems. The apparent dialytic rate constant values of Test System A were significantly lower than those of Test System B at the 90% confidence level using the F test.

The value obtained for Test System A indicated the effect of

Table III—Values of Apparent Dialytic Rate Constant, K, in 0.1 *N* HCl Test Medium for Systems Containing Nitrofurantoin

Test System	Methylcellulose[a]			
	None	50 cps	400 cps	4000 cps
A	—	1.67 (1.58–1.78)	1.64 (1.52–1.71)	1.66 (1.60–1.72)
B	1.98 (1.84–2.05)	—	—	—
C	—	2.02 (1.87–2.21)	1.83 (1.81–1.84)	1.95 (1.92–1.98)
D	—	1.97 (2.07–1.87)	1.93 (1.86–1.98)	2.05 (2.00–2.10)

[a] Average value (K, min^{-1}) of three experiments; range given in parentheses.

Table IV—Values of Dialytic Rate Constant, K, and Coefficient of Variation of K for Test System E Containing Nitrofurantoin

Test Medium	K[a], min^{-1}	Coefficient of Variation of K
0.1 N HCl	2.36	6.25
pH 7.4 buffer	2.21	3.82

[a] Average of five values obtained for each of five test samples of Test System E.

methylcellulose in retarding drug dissolution. This effect could be due to entrapment of the drug in the polymer chain or adsorption of polymer on the drug particles, forming a weak drug–polymer adsorbate. One example of such an interaction, the adsorption of a hydrophilic polymer on barium sulfate particles in barium meal preparations, was reported previously (15). The formation of a drug–polymer adsorbate or the entrapment of the drug in the polymer chain would prevent easy access of the solvent to the drug particles. Such a possibility was proposed (1) for nitrofurantoin suspensions with methylcellulose as the suspending agent.

Also possible is the formation in the dissolution medium of regions of high viscosity due to the hydrated polymer surrounding drug particles in the sample. The dissolved drug molecules in these regions would encounter a high resistance in the diffusion process. This resistance would be reflected as a slow concentration buildup of dissolved drug in the dissolution medium, which would then be reflected as a slower dialysis rate when compared to aqueous dispersions of the drug (Test System B) under similar conditions.

The combined effect of these phenomena is named "dissolution-controlled dialysis" in this investigation. The dialysis of dissolved drug from drug suspensions in polymer solutions could also be affected by possible complex formation of drug in solution with polymer and the effect of increased bulk viscosity of the dissolution medium due to the polymer.

The apparent dialytic rate constant of Test System C, containing the same total amount of polymer in the dissolution chamber as Test System A, was similar to that of Test System B. This finding indicates that the presence of methylcellulose in the dissolution medium did not appreciably affect drug dissolution behavior as was noted for Test System A, where the same amount of polymer was present but as a suspending agent in the drug suspension. This finding is consistent with the observations of Braun and Parrott (16). They found that when methylcellulose was present in the dissolution medium, a substantial increase in the relative viscosity was necessary to decrease the dissolution rate of benzoic acid. At the polymer concentrations used in this study, a high relative viscosity might occur in a microscopic region surrounding drug particles in Test System A but not in Test System C.

The values of K for Test System D were significantly lower ($p < 0.1$) than those for Test System E, both of which were solutions. The lower value of K might be due to formation of drug–polymer complex or to the effect of bulk viscosity of the dissolution medium due to the presence of polymer. The amount of polymer in each test system was 0.2% for the 50-cps, 0.115% for the 400-cps, and 0.071% for the 4000-cps methylcellulose, which increased the bulk viscosity of the dissolution medium approximately 1.6 times.

Table VI—Values of the Dialytic Rate Constant, K, and the Apparent Dialytic Rate Constant, K_f, for Test System E: Nitrofurantoin in 0.1 N HCl and pH 7.4

Test Medium	Amount of Nitrofurantoin in Test System, A_T, mg[a]	K, min^{-1}	K_f, min^{-1}
0.1 N HCl	7.80	2.18	0.35
	12.97	2.32	0.62
	26.59	2.28	1.32
	41.48	2.53	2.86
	52.48	2.50	3.71
pH 7.4 buffer	7.35	2.25	0.33
	12.22	2.14	0.55
	25.27	2.34	1.55
	39.60	2.15	2.11
	49.77	2.17	3.10

[a] Data from Table II.

Reduced dialysis rates as a result of an increase in the relative viscosity were reported previously (17–19), with the effect being evident at relative viscosities of approximately 4.0 or higher. Hence, a relative viscosity value of 1.6 would not be expected to affect substantially the dialysis rate of dissolved drug from the dissolution chamber. Moreover, the same apparent rate constant was observed for Test Systems B and C. Therefore, the reduced dialysis rate observed for Test System D probably was due to complex formation between the drug and the polymer, as suggested by Seager (1).

Samples of Test System D were equilibrated for 24 hr at 37° prior to measurement, thus allowing enough time for the formation of possible complexes. Since Test Systems B and C have essentially similar K values, the possible effect of complex formation is not evident in the samples of Test System C. This result might be due to the relatively rapid dialysis rate of the drug from the dissolution chamber not permitting sufficient time for a complexation equilibrium to be achieved in the dissolution chamber.

Dissolution–Dialysis of Nitrofurantoin in pH 7.4 Buffer—The apparent dialytic rate constants for Test Systems A, B, C, and D are shown in Table V, and those for Test System E are shown in Table VI.

Forty milligrams of nitrofurantoin was used for preparing samples of the various test systems with 50-cps methylcellulose as the suspending agent; twice that amount, 80 mg, was used for test samples with 400- and 4000-cps methylcellulose as suspending agents.

The results indicate that the effect of the polymer on the dissolution behavior of the drug in pH 7.4 buffer was essentially the same as its effect on drug dissolution in 0.1 N HCl for samples of the test systems with 400- and 4000-cps methylcellulose as suspending agents. The apparent dialytic rate constants for all samples with 50-cps methylcellulose were similar. A measurable difference between samples of Test System A and Test Systems B, C, and D was not detected in this case. This result was probably due to the lower amount of drug used and to the higher dissolution rate of the drug in the pH 7.4 buffer system because of its higher solubility in this medium.

Table V—Values of Apparent Dialytic Rate Constant, K, in pH 7.4 Buffer for Systems Containing Nitrofurantoin

Test System	Methylcellulose[a] None	50 cps[b]	400 cps[c]	4000 cps[c]
A	—	1.99[a] (1.96–2.03)	1.57[d] (1.54–1.61)	1.62[d] (1.61–1.63)
B	2.10[a] (2.04–2.17) 1.97[a,c] (1.87–2.07)	—	—	—
C	—	2.01[a] (1.91–2.11)	2.00[d] (1.95–2.05)	1.82[d] (1.79–1.85)
D	—	1.98[a] (1.85–2.11)	1.93[d] (1.92–1.95)	2.00[d] (1.94–2.05)

[a] Average value (K, min^{-1}) of three experiments; range given in parentheses. [b] Amount of nitrofurantoin used was approximately 40 mg. [c] Amount of nitrofurantoin used was approximately 80 mg. [d] Average value of two experiments; range given in parentheses.

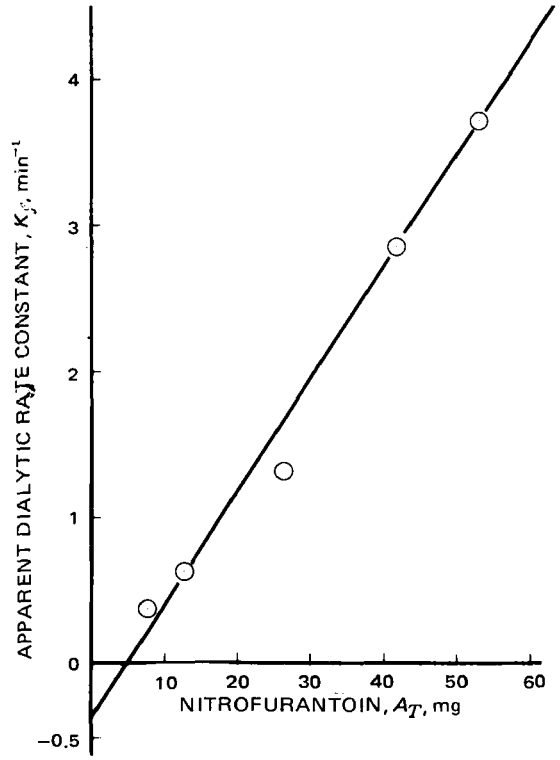

Figure 3—*Plot of the apparent dialytic rate constant,* K_f, *versus the amount of nitrofurantoin,* A_T, *in the dissolution chamber for 0.1 N HCl.*

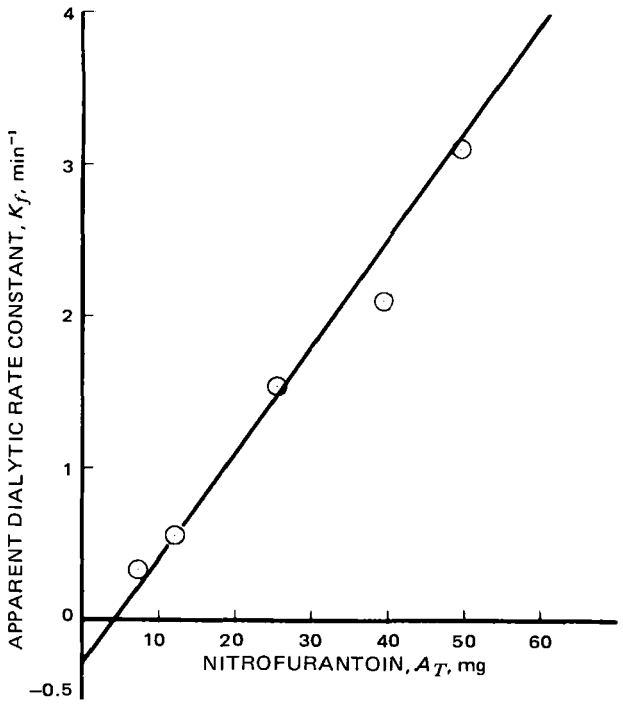

Figure 4—*Plot of the apparent dialytic rate constant,* K_f, *versus the amount of nitrofurantoin,* A_T, *in the dissolution chamber for pH 7.4 buffer.*

Prediction of Effective Drug Concentration—The rate of dialysis of drug in dissolution–dialysis measurements depends upon its effective concentration in the dissolution chamber at any given time. The effective concentration is the drug concentration in solution available for dialysis that would be the concentration of free drug in solution (3). This concentration was not known for the drug dispersion samples of this study. Therefore, the total quantity of drug in the dispersion was used for the term A_T in Eq. 1 in calculating apparent dialytic rate constants for these samples.

However, an estimate of the effective drug concentration, A_e, for these samples can be obtained by applying a modification of Eq. 1 to the dialysis rate data of drug solutions (Test System E). For the term A_T in Eq. 1, the total amount of drug in the dispersion sample of interest is used in place of the known initial concentration of the drug in solution:

$$\log [V_0A_f - (V_0 + V_i)A_0] = -\left[\frac{V_0 + V_i}{2.3V_iV_0}\right] K_f t + \log (V_0A_f) \quad \text{(Eq. 4)}$$

where A_f replaces the term A_T in Eq. 1 and represents the total amount of drug in the dispersion sample of interest being evaluated. The term K_f is the apparent dialytic rate constant corresponding to the value of A_f used in applying Eq. 4. The rest of the terms are the same as in Eq. 1.

The solution dialysis studies (Test System E) utilized drug solutions at five concentrations (Table II). Values of K_f were calculated from dialysis rate data of these samples by means of Eq. 4, using 40 mg for the value of A_f for dispersion samples tested in 0.1 *N* HCl and 80 mg for samples tested in pH 7.4 buffer. The values of K_f, the apparent dialytic rate constant per Eq. 4 thus calculated, are shown in Table VI along with the values of K, the dialytic rate constant calculated per Eq. 1, for the same samples. A linear relationship was obtained when K_f was plotted as a function of A_T, the initial concentration of the drug solutions of Test System E, as shown in Figs. 3 and 4. This relationship can be expressed as:

$$K_f = \alpha A_T + \beta \quad \text{(Eq. 5)}$$

where α and β are constants characteristic of the specific value of A_f used for the calculation of K_f values. The values of α and β obtained and their correlation coefficients are shown in Table VII.

For evaluating the effective concentration in the dissolution–dialysis measurement of drug dispersions, the term A_T in Eq. 5 is replaced by the term A_e, the effective drug concentration in the dissolution chamber, and the term K_f is replaced by K, the apparent dialytic rate constant of the dispersion obtained using Eq. 1 to obtain:

$$K = \alpha A_e + \beta \quad \text{(Eq. 6)}$$

where α and β are the same as in Eq. 5, and K is the apparent dialytic rate constant of test samples as shown in Tables III and V. The effective drug concentration in the dissolution chamber for a given drug dispersion sample corresponding to its measured apparent dialytic rate constant can be obtained as follows:

$$A_e = \frac{K - \beta}{\alpha} \quad \text{(Eq. 7)}$$

Tables VIII and IX show A_e values calculated for the dispersion test systems of nitrofurantoin in 0.1 *N* HCl and pH 7.4 buffer.

It is thought that this procedure provides a useful method of opti-

Table VII—Regression Analysis Data for Nitrofurantoin

Test Medium	α^a	β^a	r^b
0.1 *N* HCl	0.0768	−0.4004	0.9915
pH 7.4 buffer	0.0636	−0.2556	0.9892

[a] The α and β are coefficients of Eq. 6. [b] Coefficient of correlation.

Table VIII—A_e Values[a] for Systems Containing Nitrofurantoin in 0.1 *N* HCl

Test System	Methylcellulose			
	None	50 cps	400 cps	4000 cps
A	—	26.93	26.54	26.80
B	30.96	—	—	—
C	—	31.48	29.00	30.57
D	—	28.94	30.31	30.56

[a] Average value (milligrams) of three experiments. Values were obtained using Eq. 7 and the K values from Table III.

Table IX—A_e Values[a] for Systems Containing Nitrofurantoin in pH 7.4 Buffer

Test System	Methylcellulose			
	None	50 cps[b]	400 cps[c]	4000 cps[c]
A	—	35.30[d]	57.80[e]	59.39[e]
B	37.03[d] 40.47[d,b]	—	—	—
C	—	35.62[d]	71.42[e,c]	65.72[e,c]
D	—	35.39[d]	69.20[e]	71.42[e]

[a] Values (milligrams) were obtained using Eq. 7 and the K values from Table V. [b] Amount of nitrofurantoin used was 40.0 mg. [c] Amount of nitrofurantoin used was 80.0 mg. [d] Average value of three experiments. [e] Average value of two experiments.

mum design of suspension formulations by enabling comparisons of the formulations in terms of equivalent drug solutions.

SUMMARY

The effect of selected suspending agents on the dissolution behavior of nitrofurantoin from suspension formulations was investigated utilizing the dissolution–dialysis technique. A dissolution–dialysis cell of special design was developed to provide a large surface area for dialysis to minimize concentration buildup in the dissolution chamber. Three viscosity grades of methylcellulose, 50, 400, and 4000 cps, were used as suspending agents.

The measurement procedure used was to determine the dialysis rate of the dissolved drug after addition of the test sample, drug dispersion or drug solution, to the dissolution chamber of the cell. The dissolution–dialysis measurements were carried out using 0.1 N HCl and pH 7.4 buffer. The dissolution behavior of the drug was evaluated in terms of the apparent dialytic rate constants of the test samples.

Methylcellulose caused a reduction in the dialysis rate of nitrofurantoin from both the drug solution and drug suspension. However, the maximum retardation effect was observed when methylcellulose was used as a suspending agent in preparing drug dispersions. The dialysis rate of the drug suspension in the methylcellulose solution was significantly less than that of the drug dispersion in water. The dialysis rates of (*a*) the drug dispersion in water, (*b*) the drug dispersion in water with an equivalent amount of polymer added to the test medium, and (*c*) the drug solution in the test medium containing the equivalent amount of polymer were similar but significantly less than the dialytic rate of the drug solution.

The reduction in the dialysis rate of the drug solution containing the polymer is thought to be due to the possible formation of a drug–polymer complex. The greater effect observed with the drug suspension in polymer solution is thought to be due to complex formation as well as to the formation of microscopic regions of high viscosity surrounding the drug particles, leading to the possible formation of a diffusion layer of high viscosity.

An empirical relationship was developed from solution dialysis rate data to estimate the amount of free drug available for dialysis when a fixed amount of drug was added to the dissolution chamber. This relationship permits consideration of suspensions in terms of equivalent drug solutions. Therefore, it could find application in the *in vitro* evaluation of test products in the development of suspension formulations.

REFERENCES

(1) H. Seager, *J. Pharm. Pharmacol.*, **20**, 968(1968).

(2) K. H. Harper and A. N. Wordan, *Toxicol. Appl. Pharmacol.*, **8**, 325(1966).

(3) C. Davison, J. L. Guy, M. Levitt, and P. R. Smith, *J. Pharmacol. Exp. Ther.*, **134**, 176(1961).

(4) M. H. Malone, R. D. Gibson, and T. S. Miya, *J. Am. Pharm. Assoc., Sci. Ed.*, **49**, 529(1960).

(5) G. Levy and W. J. Jusko, *J. Pharm. Sci.*, **54**, 219(1965).

(6) R. R. Hewitt and G. Levy, *ibid.*, **60**, 784(1971).

(7) J. J. Ashley and G. Levy, *ibid.*, **62**, 688(1973).

(8) A. Berlin, B. Siwers, S. Agurell, A. Hiort, F. Sjoqvist, and S. Strom, *Clin. Pharmacol. Ther.*, **13**, 733(1972).

(9) D. E. Wurster and P. W. Taylor, Jr., *J. Pharm. Sci.*, **54**, 670(1965).

(10) E. Marlowe and R. F. Shangraw, *ibid.*, **56**, 498(1967).

(11) P. C. Sheen, Ph.D. thesis, University of Iowa, Iowa City, Iowa, 1971.

(12) R. E. Davis, C. W. Hartman, and J. H. Fincher, *J. Pharm. Sci.*, **60**, 429(1971).

(13) R. E. Northern, J. L. Lach, and J. H. Fincher, *Am. J. Hosp. Pharm.*, **30**, 622(1973).

(14) E. G. Lovering and K. B. McRae, *J. Pharm. Sci.*, **62**, 971(1973).

(15) A. M. James and G. H. Goddard, *Pharm. Acta Helv.*, **47**, 244(1972).

(16) R. J. Braun and E. L. Parrott, *J. Pharm. Sci.*, **61**, 175(1972).

(17) G. D. Redman, J. E. Christian, and G. J. Sperandio, *J. Am. Pharm. Assoc., Sci. Ed.*, **49**, 98(1960).

(18) L. H. Block and P. P. Lamy, *Pharm. Acta Helv.*, **44**, 44(1969).

(19) P. P. Lamy, *ibid.*, **44**, 79(1969).

ACKNOWLEDGMENTS AND ADDRESSES

Received April 10, 1975, from the *Division of Drug Product Technology, College of Pharmacy, University of Tennessee Center for the Health Sciences, Memphis, TN 38163*

Accepted for publication January 15, 1976.

Presented at the Industrial Pharmaceutical Technology Section, APhA Academy of Pharmaceutical Sciences, New Orleans meeting, November 1974.

Abstracted in part from a dissertation submitted by N. B. Shah to the University of Tennessee Center for the Health Sciences in partial fulfillment of the Doctor of Philosophy degree requirements.

* Present address: Vick Division Research, Mount Vernon, NY 10553

[x] To whom inquiries should be directed.

In Vitro Studies of Poly(methyl Methacrylate) Adjuvants

JÖRG KREUTER and PETER P. SPEISER[x]

Abstract □ Poly(methyl methacrylate) adjuvants, prepared by polymerizing monomeric methyl methacrylate in the presence of influenza virions or by addition of the virions to previously polymerized poly(methyl methacrylate) particles, were studied by means of the hemagglutination test, antibody binding, and electron microscopy. The results indicated that the virions were coated partly when the polymerization was carried out in the presence of the virus, whereas the virions were probably adsorbed when added to polymerized particles.

Keyphrases □ Poly(methyl methacrylate) adjuvants—for influenza vaccine, preparation, evaluation by hemagglutination, antibody binding, and electron microscopy □ Adjuvants, poly(methyl methacrylate)—for influenza vaccine, preparation, evaluation by hemagglutination, antibody binding, and electron microscopy □ Influenza vaccines—preparation of poly(methyl methacrylate) adjuvants, evaluation by hemagglutination, antibody binding, and electron microscopy □ Vaccines, influenza—preparation of poly(methyl methacrylate) adjuvants, evaluation by hemagglutination, antibody binding, and electron microscopy □ Virus vaccines, influenza—preparation of poly(methyl methacrylate) adjuvants, evaluation by hemagglutination, antibody binding, and electron microscopy

A previous publication (1) reported the preparation of potent new adjuvants for influenza vaccines. The new adjuvants were produced by γ-ray-induced polymerization of monomeric methyl methacrylate in the presence or absence of influenza virus. In the case of polymer preparation in the absence of the antigen, the virus was later added to the polymer particles. These two methods resulted in adjuvants characterized by different antibody-inducing properties.

The present investigation obtained additional information on the two different adjuvants.

EXPERIMENTAL

Virus—Whole formalin-inactivated, zonal centrifugation-purified influenza virions of the A2/Aichi and the A2/Hongkong X-31 strains were used.

Production of Clear Virion Suspension—The following simplified version of a purification method (2) was used. Allantoic fluid, containing 4800 hemagglutinating units/ml of A2/Hongkong X-31, was taken from embryonated chicken eggs that had been infected with live virus. Then 600 ml of a 1.5% chicken erythrocyte suspension was centrifuged at 1500 rpm for 15 min. The deposit was resuspended in 75 ml of the allantoic fluid by gentle agitation. This suspension was placed in an ice bath for 1–2 hr, the cells being kept in suspension by gentle agitation, and then the suspension was centrifuged again for 15 min at 1500 rpm.

The deposit (erthrocytes plus adsorbed virions) was washed two times by resuspending in 75 ml of phosphate-buffered saline at pH 7.2 and centrifuging under the described conditions. After washing, the deposit was resuspended in 40 ml of phosphate-buffered saline at pH 7.2; the virus was eluted by placing the suspension in a water bath at 37 ± 1° for 2 hr. The cells were then removed by centrifugation, and the supernatant fluid served as the clear virion suspension (content = 3200 hemagglutinating units/ml).

Production of Antibody Solution—Two guinea pigs were given 2 ml of an influenza vaccine (A2 / Hongkong X-31, 3200 hemagglutinating units/ml) containing 50% of complete Freund adjuvant. After 7 and 14 days, the animals were boosted with the same vaccine. Twenty-four days after the primary vaccination, blood was taken from the animals. The serum was inactivated by heating at 56° for 30 min and was then diluted with phosphate-buffered saline at pH 7.2 to obtain an antibody solution with a hemagglutination inhibition titer of 1600.

Table I—Hemagglutination Titers of Poly(methyl Methacrylate) Adjuvant Influenza Vaccines and Intermediate Products

Treatment	Hemagglutination Titer
Fluid virus suspension, untreated	3200
Fluid virus suspension, γ-radiated	3200
Fluid virus suspension + 0.8% monomeric methyl methacrylate, not radiated	3200
0.8% Poly(methyl methacrylate) particles without virions	160
Virus suspension + 0.8% poly(methyl methacrylate), polymerized in presence of virions	160
Virus suspension + 0.8% poly(methyl methacrylate), polymerized in absence of virions	1200

Monomer—Methyl methacrylate[1] was purified from polymerization inhibitors by the method described by Riddle (3) or Tessmar (4).

Preparation of Poly(methyl Methacrylate) Adjuvants—The poly(methyl methacrylate) adjuvants were produced by polymerization in the presence or absence of the virions (1).

Polymerization in Presence of Virions—An amount of methyl methacrylate, 0–2% (Tables I and II and Figs. 1 and 2), was dissolved

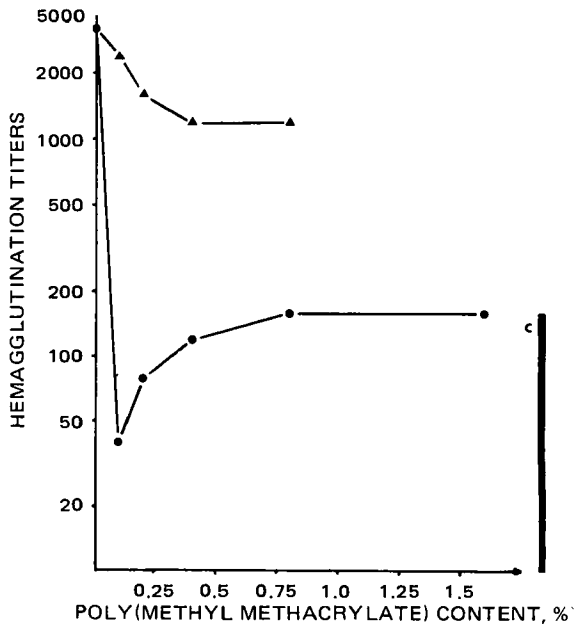

Figure 1—*Dependency of the hemagglutination titers on the poly(methyl methacrylate) content of influenza vaccines. Key: ●, polymerization in the presence of the virus; ▲, polymerization in the absence of the virus; and C, 0.8% poly(methyl methacrylate) particles without virus.*

[1] Fluka, Fluka AG, Buchs, Switzerland.

Table II—Hemagglutination Titers of Poly(methyl Methacrylate) Adjuvant Influenza Vaccines with Increasing Poly(methyl Methacrylate) Contents

Poly(methyl Methacrylate) Content, %	Mean ($\bar{x}$) and Standard Deviation (s)	Polymerization in Presence of Virus		Polymerization in Absence of Virus	
		Complete Vaccine	Supernatant Fluid	Complete Vaccine	Supernatant Fluid
0.0	$\bar{x}$	960	960	960	960
	s	109	109	109	109
0.025	$\bar{x}$	120	64	—	—
	s	13	0		
0.05	$\bar{x}$	48	1	320	12
	s	25	0	65.5	1.65
0.1	$\bar{x}$	20	0	240	2
	s	7		135.5	0
0.2	$\bar{x}$	60	0	160	1
	s	13		0	0
0.4	$\bar{x}$	120	0	160	0
	s	4.5		65.5	
0.6	$\bar{x}$	160	0	—	—
	s	26			
0.8	$\bar{x}$	160	0	320	0
	s	0		0	
1.0	$\bar{x}$	160	0	—	—
	s	26			
2.0	$\bar{x}$	240	0	—	—
	s	65.5			
1.0 Control[a]	$\bar{x}$	160	0	160	0
	s	0		0	
2.0 Control[a]	$\bar{x}$	240	0	240	0
	s	65.5		65.5	

[a] Poly(methyl methacrylate) particles without virus.

in the virus suspension. The oxygen content was reduced by bubbling nitrogen for 3–5 min through the suspension by means of an injection needle. The polymerization was carried out by γ-radiation with a dosage of 0.46 Mrad with a cobalt-60 source.

Polymerization in Absence of Virions—The monomer was polymerized as already described, using phosphate-buffered saline at pH 7.2 instead of the virus suspension. The resulting particles were centrifuged (1000 rpm for 10 min) and resuspended in the virus suspension after being washed three times in phosphate-buffered saline at pH 7.2.

Monomer Solubility—Erlenmeyer flasks (150 ml) were filled with 100.0 ml each of one of the following fluids: double-distilled water, phosphate-buffered saline at pH 7.2, or clear virion suspension. The fluids were placed in a water bath at 20.0 ± 0.1° and stirred with a magnetic stirrer. Methyl methacrylate was added with a 0.05-ml repeating pipet[2] and, in a repetition of the experiment drop by drop, with a 0.01-ml graded microburet. The clearly soluble amount of methyl methacrylate was measured (Table III).

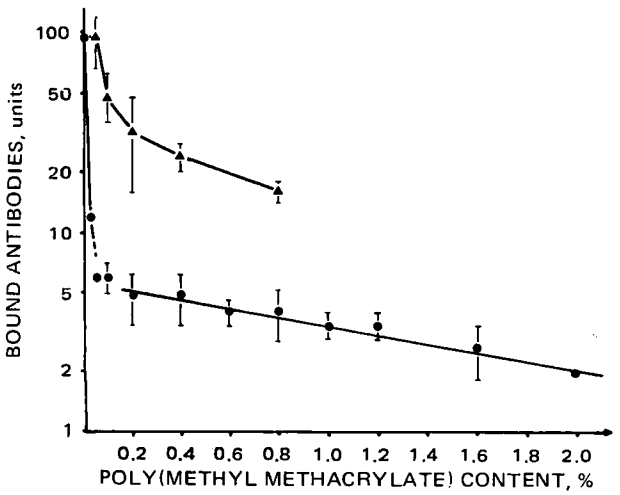

Figure 2—*Dependency of the amount of bound antibodies on the poly(methyl methacrylate) content of influenza vaccines. Key: ●, polymerization in the presence of the virus; and ▲, polymerization in the absence of the virus.*

[2] Oxford sampler.

Hemagglutination Titers—The hemagglutination titers of the following preparations were determined, using the methods of Hirst (5) and Bonin (6): (*a*) initial fluid virus suspension; (*b*) γ-ray-radiated fluid virus suspension; (*c*) fluid virus suspension containing 0.8% monomeric methyl methacrylate (this mixture was stored at 4° without radiation for 3 weeks); (*d*) poly(methyl methacrylate) particles without virus (plastic control); (*e*) virus suspensions containing various amounts of poly(methyl methacrylate) (Tables I and II and Fig. 1), polymerized in the presence of the virions; and (*f*) virus suspensions containing various amounts of poly(methyl methacrylate) (Tables I and II and Fig. 1), polymerized in the absence of the virions.

In addition to the hemagglutination test of the complete suspensions, the determination of the supernatant fluids of these preparations was carried out after centrifugation at 2000 rpm for 10 min.

Antibody Binding Properties—A 1% albumin solution (0.5 ml) in phosphate-buffered saline was added to 2.0 ml of different poly(methyl methacrylate) adjuvant preparations and to 2.0 ml of the initial virus suspension. The mixtures were shaken vigorously and stored overnight at 4°. Then 0.50 ml of the antibody solution was added, and the mixture was vigorously shaken again. After 1 hr, the polymer particles were removed by centrifugation at 2000 rpm for 10 min. The remaining antibodies in the supernatant fluid were determined by the hemagglutination inhibition test as described by Bonin (7). Polymer particle suspensions without virus served as controls.

The amount of antibodies bound by the polymer–virus preparations was calculated using:

$$\log BU = \log PP - \log AP \qquad \text{(Eq. 1)}$$

Table III—Solubility of Monomeric Methyl Methacrylate

Solvent (100 ml)	Maximum Solubility (20°) of Methyl Methacrylate, ml
Double-distilled water	1.55 ± 0.03
Phosphate-buffered saline, pH 7.2	1.50 ± 0.03
Clear influenza virion suspension	2.00 ± 0.03

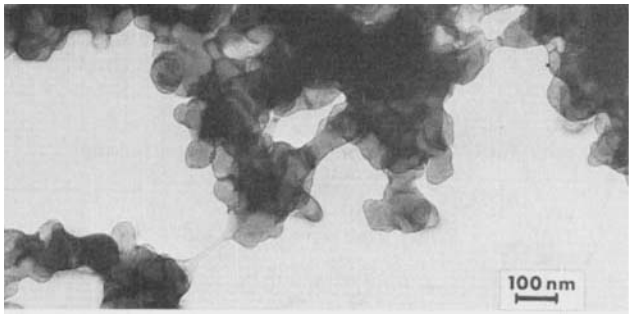

Figure 3—*Influenza vaccine with 0.5% poly(methyl methacrylate) adjuvant polymerized in the presence of the virus. No virions or virion surface structures such as spikes are visible.*

Equation 1 can be transformed into:

$$\log BU = \log \frac{PP}{AP} \qquad \text{(Eq. 2)}$$

where BU = bound antibodies in units, PP = hemagglutination inhibition titer of polymer particles without virus, and AP = hemagglutination inhibition titer of adjuvant preparation.

Transmission Electron Microscopy—The samples were produced by polymerization of 0.5% methyl methacrylate in the presence (Fig. 3) and absence (Fig. 4) of the virions (A2/Aichi, content = 32,000 hemagglutinating units/ml). The virion suspension without adjuvant was examined as a control (Fig. 5). Formvar-coated copper grids were floated on the samples for 3 min. Without removing excess fluid, the grids were brought in contact with 2% phosphotungstic acid for a few seconds. Excess fluid was then removed, and the grids were examined immediately in an electron microscope[3].

RESULTS AND DISCUSSION

Monomer Solubility—Table III shows that about 30% more methyl methacrylate was soluble in the clear virion suspension than in phosphate-buffered saline at pH 7.2. This finding supports the assumption (1) that a certain amount of monomeric methyl methacrylate is adsorbed by the virions.

Hemagglutination Titers—The results of the hemagglutination test are shown in Tables I and II and Fig. 1. Neither addition of the methyl methacrylate monomer and storage for 3 weeks without radiation nor γ-radiation alone decreased the hemagglutination titers of the virus suspension (Table I). These treatments had no changing or damaging effects on the hemagglutinating properties of the virions.

Polymerization in the presence of the virions decreased the hemagglutination titers to a minimum at a poly(methyl methacrylate) concentration of 0.1% and increased the hemagglutination titers at higher poly(methyl methacrylate) contents to the level of the plastic control without virus (Fig. 1 and Table II). This increase above 0.1% poly(methyl methacrylate) was due to prevention of free sedimentation of the erythrocytes by the polymeric particles and thus to simulated hemagglutination.

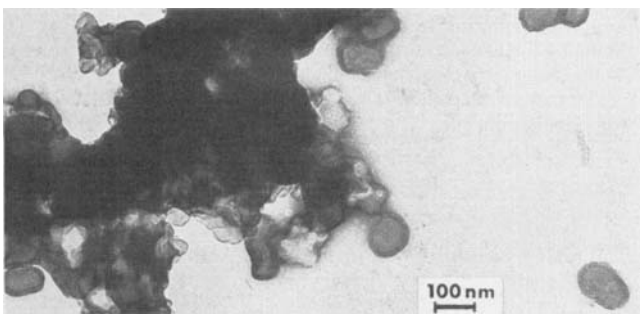

Figure 4—*Influenza vaccine with 0.5% poly(methyl methacrylate) adjuvant polymerized in the absence of the virus. Virions are visible at the surface of the polymer particles as well as independent from the polymer.*

[3] Philips E. M. 301.

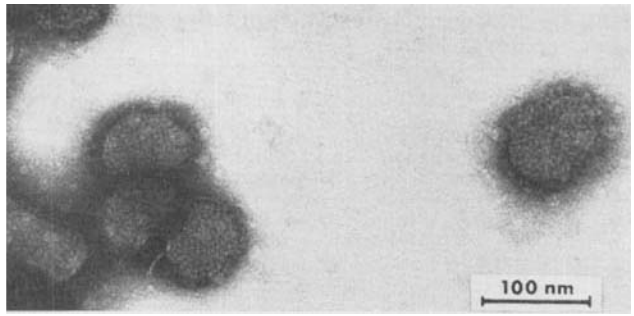

Figure 5—*Initial fluid influenza vaccine without adjuvant (A2/Aichi, content = 32,000 hemagglutinating units/ml).*

If the virions were added to previously polymerized particles, a decrease of the hemagglutination titers was also obtained, although it was much less pronounced (Fig. 1). However, this decrease indicated certain interactions of virions with the plastic particles.

The hemagglutination test of the supernatant fluid after centrifugation of the polymer particles only gave information about the virus that was not associated with the polymer material. A rapid decrease of the hemagglutination activity was obtained with increasing poly(methyl methacrylate) contents (Table II). This decrease again was more pronounced if the polymerization was carried out in the presence of the virions.

Antibody Binding Properties—The antibody binding properties of the poly(methyl methacrylate) adjuvant influenza vaccines gave information about the amount of virus surface not covered by or interacting with polymer. Unbound antibodies could be determined in the supernatant fluid by the hemagglutination inhibition test after removal of the polymer by centrifugation. Therefore, the complication that the polymer particles simulated hemagglutination by preventing the free sedimentation of erythrocytes was avoided. Nonspecific adsorption of antibodies was prevented by addition of 1% albumin.

Figure 2 demonstrates that the amount of antibodies bound by the polymer–virus preparations decreased with an increasing content of poly(methyl methacrylate) in both preparations. However, a much lower amount was bound by preparations polymerized in the presence of the virions than by preparations polymerized in their absence.

Interpretation of Results—These results clearly demonstrate that the products obtained after polymerization in the presence of virus and those obtained after addition of virus to previously polymerized particles were not identical. Moreover, the previous hypothesis (1) that the monomeric methyl methacrylate was adsorbed by the virions and that the virions were coated to a certain extent by the developing polymer during radiation is supported. The electron microscopic picture (Fig. 3) further confirmed this hypothesis: no virions or virion surface structures, such as spikes, can be identified if the polymerization is carried out in the presence of the virions. The extent of coating is dependent on the initial monomer content. Accordingly, increasing contents of the resulting polymer lead to a decrease of virions in the supernatant fluid (Table II) and to a decrease in antibody binding surface (Fig. 2).

As mentioned previously, the virions also interacted with poly(methyl methacrylate) particles prepared by previous polymerization in the absence of virions. These products also decreased the hemagglutination titers and the amount of bound antibodies and yielded a good, but less pronounced, adjuvant effect (1). It can be assumed that adsorption of virions onto the plastic particles took place. Correspondingly, virions were found on the surface of the polymer by electron microscopy (Fig. 4).

The products described here are very similar in size (1) to the "nanoparticles" prepared by Birrenbach and Speiser (8). They produced adjuvants by secondary solubilization of monomeric acrylamide in the presence of tetanus toxoid or γ-globulin in n-hexane and following polymerization. However, the preparation of the products described here is considerably less complicated, thus offering certain advantages over the other procedure.

SUMMARY

1. Monomeric methyl methacrylate was adsorbed by influenza virions in a virus suspension.

2. After polymerization of methyl methacrylate in the presence

of influenza virions, the virions were coated to a certain extent by the polymer.

3. The extent of coating was dependent on the monomer concentration before polymerization.

4. Influenza virions were adsorbed by previously polymerized poly(methyl methacrylate) particles.

REFERENCES

(1) J. Kreuter and P. P. Speiser, *Infect. Immun.*, **13**, 204(1976).

(2) F. W. Sheffield, W. Smith, and G. Belyavin, *Br. J. Exp. Pathol.*, **35**, 214(1954).

(3) E. H. Riddle, "Monomeric Acrylic Esters," Reinhold, New York, N.Y., 1954, p. 15.

(4) K. Tessmar, in "Methoden der Organischen Chemie," (Houben-Weyl), vol. XIV/1, E. Müller, Ed., Makromolekulare Stoffe, G. Thieme-Verlag, Stuttgart, Germany, 1961, p. 1037.

(5) G. K. Hirst, *J. Exp. Med.*, **75**, 47(1942).

(6) O. Bonin, "Quantitativ-Virologische Methodik," G. Thieme-Verlag, Stuttgart, Germany, 1973, p. 203.

(7) O. Bonin, *ibid.*, p. 227.

(8) G. Birrenbach and P. P. Speiser, *J. Pharm. Sci.*, in press.

ACKNOWLEDGMENTS AND ADDRESSES

Received October 16, 1975, from the *School of Pharmacy, Federal Institute of Technology, CH-8006 Zürich, Clausiusstr. 25, Switzerland.*

Accepted for publication January 15, 1976.

Abstracted in part from a thesis submitted by J. Kreuter to the Federal Institute of Technology, Zürich, Switzerland, in partial fulfillment of the Doctor of Science degree requirements.

Supported by a grant from Deutscher Akademischer Austauschdienst, Bonn-Bad Godesberg, West Germany, and by Behringwerke AG, Marburg, West Germany.

The authors thank Mr. M. Müller, Laboratory for Electron Microscopy, Federal Institute of Technology, Zürich, Switzerland, for the preparation of the electron micrographs and Mr. H. J. Zehnder, Eidgenössiche Forschungsanstalt Wädenswil, for the γ-radiation of the samples, and recognize Prof. E. Ullmann for her contributions.

[x] To whom inquiries should be directed.

Rapid Spectrophotometric Determination of Salicylamide in Analgesic Tablets

SOBHI A. SOLIMAN [x] and ALI SALAHELDIN *

Abstract □ An independent, simple, and rapid procedure is suggested for the routine analysis of salicylamide in analgesic tablets containing acetaminophen, phenobarbital, caffeine, codeine phosphate, prednisone, ascorbic acid, and chloroquine phosphate. The method does not require the preliminary separation of salicylamide from other constituents by the time-consuming solvent extraction technique or by chromatography prior to determination. The absorbance was linear for investigated concentrations of salicylamide from 0 to 4.0 mg/100 ml of solution at 308 nm.

Keyphrases □ Salicylamide—spectrophotometric analysis in tablets containing other drugs □ Spectrophotometry—analysis, salicylamide in tablets containing other drugs □ Dosage forms—multicomponent analgesic tablets, spectrophotometric analysis of salicylamide □ Analgesics—salicylamide, spectrophotometric analysis in tablets containing other drugs

Salicylamide, an analgesic, antipyretic, and antirheumatic drug, can be determined by visual titration in dimethylformamide against standard sodium methoxide solution with thymol blue indicator (1). Although this method is perfectly suitable for the determination of the drug in pure form, it is totally unsuitable for selective determination in the presence of such acidic substances as acetaminophen, phenobarbital, and codeine phosphate.

Salicylamide can be determined colorimetrically by several methods. The color produced when salicylamide reacts with ferric nitrate in the presence of nitric acid (2) has been the basis for colorimetric determination of the drug after its separation from sodium salicylate and sodium gentisate by extraction with ether. The same reaction was employed for colorimetric determination of salicylamide in serum and urine (3), but after hydrolysis with hydrochloric acid and extraction in ethylene dichloride. Measurements of absorbance were performed at 450 nm. Use of the color resulting from the condensation reaction of salicylamide with *p*-amino-*N*,*N*-dimethylaniline sulfate in the presence of potassium ferricyanide (4) was suggested.

A spectrophotometric procedure was described (5) for the simultaneous determination of five analgesic compounds including salicylamide. Absorbance was measured at three different wavelengths and under three different conditions of acid and base content. Salicylamide also was determined by differential spectrophotometry (6) in the presence of aspirin, acetaminophen, and caffeine. A spectrophotofluorometric method (7) was reported for the simultaneous determination of salicylamide and salicylic acid in blood serum and urine after acid hydrolysis of the salicylamide metabolites.

Salicylamide was determined bromometrically (8) in anhydrous acetic acid by adding aceteous bromine solution and determining unreacted bromine by adding potassium iodide and titrating against thiosulfate.

The objective of this study was to develop a rapid routine analytical method for salicylamide in analgesic tablets containing acetaminophen, phenobarbital, caffeine, codeine phosphate, prednisone, ascorbic acid, and chloroquine phosphate which would be useful for pharmaceutical control purposes.

EXPERIMENTAL

Chemicals—The following were used: salicylamide[1], acetamino-

[1] El-Nasr Pharmaceutical Chemicals Co., A.R.E.

of influenza virions, the virions were coated to a certain extent by the polymer.

3. The extent of coating was dependent on the monomer concentration before polymerization.

4. Influenza virions were adsorbed by previously polymerized poly(methyl methacrylate) particles.

REFERENCES

(1) J. Kreuter and P. P. Speiser, *Infect. Immun.*, **13**, 204(1976).

(2) F. W. Sheffield, W. Smith, and G. Belyavin, *Br. J. Exp. Pathol.*, **35**, 214(1954).

(3) E. H. Riddle, "Monomeric Acrylic Esters," Reinhold, New York, N.Y., 1954, p. 15.

(4) K. Tessmar, in "Methoden der Organischen Chemie," (Houben-Weyl), vol. XIV/1, E. Müller, Ed., Makromolekulare Stoffe, G. Thieme-Verlag, Stuttgart, Germany, 1961, p. 1037.

(5) G. K. Hirst, *J. Exp. Med.*, **75**, 47(1942).

(6) O. Bonin, "Quantitativ-Virologische Methodik," G. Thieme-Verlag, Stuttgart, Germany, 1973, p. 203.

(7) O. Bonin, *ibid.*, p. 227.

(8) G. Birrenbach and P. P. Speiser, *J. Pharm. Sci.*, in press.

ACKNOWLEDGMENTS AND ADDRESSES

Received October 16, 1975, from the *School of Pharmacy, Federal Institute of Technology, CH-8006 Zürich, Clausiusstr. 25, Switzerland.*

Accepted for publication January 15, 1976.

Abstracted in part from a thesis submitted by J. Kreuter to the Federal Institute of Technology, Zürich, Switzerland, in partial fulfillment of the Doctor of Science degree requirements.

Supported by a grant from Deutscher Akademischer Austauschdienst, Bonn-Bad Godesberg, West Germany, and by Behringwerke AG, Marburg, West Germany.

The authors thank Mr. M. Müller, Laboratory for Electron Microscopy, Federal Institute of Technology, Zürich, Switzerland, for the preparation of the electron micrographs and Mr. H. J. Zehnder, Eidgenössiche Forschungsanstalt Wädenswil, for the γ-radiation of the samples, and recognize Prof. E. Ullmann for her contributions.

[x] To whom inquiries should be directed.

Rapid Spectrophotometric Determination of Salicylamide in Analgesic Tablets

SOBHI A. SOLIMAN [x] and ALI SALAHELDIN *

Abstract □ An independent, simple, and rapid procedure is suggested for the routine analysis of salicylamide in analgesic tablets containing acetaminophen, phenobarbital, caffeine, codeine phosphate, prednisone, ascorbic acid, and chloroquine phosphate. The method does not require the preliminary separation of salicylamide from other constituents by the time-consuming solvent extraction technique or by chromatography prior to determination. The absorbance was linear for investigated concentrations of salicylamide from 0 to 4.0 mg/100 ml of solution at 308 nm.

Keyphrases □ Salicylamide—spectrophotometric analysis in tablets containing other drugs □ Spectrophotometry—analysis, salicylamide in tablets containing other drugs □ Dosage forms—multicomponent analgesic tablets, spectrophotometric analysis of salicylamide □ Analgesics—salicylamide, spectrophotometric analysis in tablets containing other drugs

Salicylamide, an analgesic, antipyretic, and antirheumatic drug, can be determined by visual titration in dimethylformamide against standard sodium methoxide solution with thymol blue indicator (1). Although this method is perfectly suitable for the determination of the drug in pure form, it is totally unsuitable for selective determination in the presence of such acidic substances as acetaminophen, phenobarbital, and codeine phosphate.

Salicylamide can be determined colorimetrically by several methods. The color produced when salicylamide reacts with ferric nitrate in the presence of nitric acid (2) has been the basis for colorimetric determination of the drug after its separation from sodium salicylate and sodium gentisate by extraction with ether. The same reaction was employed for colorimetric determination of salicylamide in serum and urine (3), but after hydrolysis with hydrochloric acid and extraction in ethylene dichloride. Measurements of absorbance were performed at 450 nm. Use of the color resulting from the condensation reaction of salicylamide with *p*-amino-*N*,*N*-dimethylaniline sulfate in the presence of potassium ferricyanide (4) was suggested.

A spectrophotometric procedure was described (5) for the simultaneous determination of five analgesic compounds including salicylamide. Absorbance was measured at three different wavelengths and under three different conditions of acid and base content. Salicylamide also was determined by differential spectrophotometry (6) in the presence of aspirin, acetaminophen, and caffeine. A spectrophotofluorometric method (7) was reported for the simultaneous determination of salicylamide and salicylic acid in blood serum and urine after acid hydrolysis of the salicylamide metabolites.

Salicylamide was determined bromometrically (8) in anhydrous acetic acid by adding aceteous bromine solution and determining unreacted bromine by adding potassium iodide and titrating against thiosulfate.

The objective of this study was to develop a rapid routine analytical method for salicylamide in analgesic tablets containing acetaminophen, phenobarbital, caffeine, codeine phosphate, prednisone, ascorbic acid, and chloroquine phosphate which would be useful for pharmaceutical control purposes.

EXPERIMENTAL

Chemicals—The following were used: salicylamide[1], acetamino-

[1] El-Nasr Pharmaceutical Chemicals Co., A.R.E.

Table I—Absorbance of Salicylamide in Chloroform at 308 nm

Concentration, mg/100 ml	Average Absorbance[a]
0.5	0.158
1.0	0.318
1.5	0.473
2.0	0.628
2.5	0.776
3.0	0.932
3.5	1.060
4.0	1.236

[a] Average of three readings.

phen[2], phenobarbital[3], codeine phosphate[4], caffeine[5], prednisone[6], ascorbic acid[6], chloroquine phosphate[6], and chloroform[1].

Calibration Curve—Prepare a stock solution of salicylamide in chloroform containing 50.0 mg/100.0 ml. Transfer by pipets 1.0, 2.0, 3.0, 4.0, 5.0, 6.0, 7.0, and 8.0 ml of the stock solution to eight 100-ml volumetric flasks, dilute to volume with chloroform, and mix well. These working solutions contain 0.5, 1.0, 1.5, 2.0, 2.5, 3.0, 3.5, and 4.0 mg of salicylamide/100.0 ml of solution, respectively.

Measure the absorbance[7] of each solution in 1-cm cells against a proper blank at 308 nm (Table I). These values give a straight line whose equation was determined by the method of least squares.

Sample Preparation and Assay—Weigh and powder 20 tablets. Weigh an aliquot of the powder corresponding to 50.0 mg of salicylamide and transfer quantitatively to a 100-ml volumetric flask. Add about 70 ml of chloroform, shake for about 30 min, and dilute to volume with the same solvent. Filter through paper, to remove excipients and chloroform-insoluble materials, into a suitable dry receiver, discarding the first portion of the filtrate.

Accurately measure 5.0–6.0 ml of the filtrate, transfer into a 100-ml volumetric flask, dilute to volume with chloroform, and mix. Measure the absorbance as described previously. Calculate milligrams of salicylamide in the aliquot of powder taken from the straight-line equation using the measured absorbance.

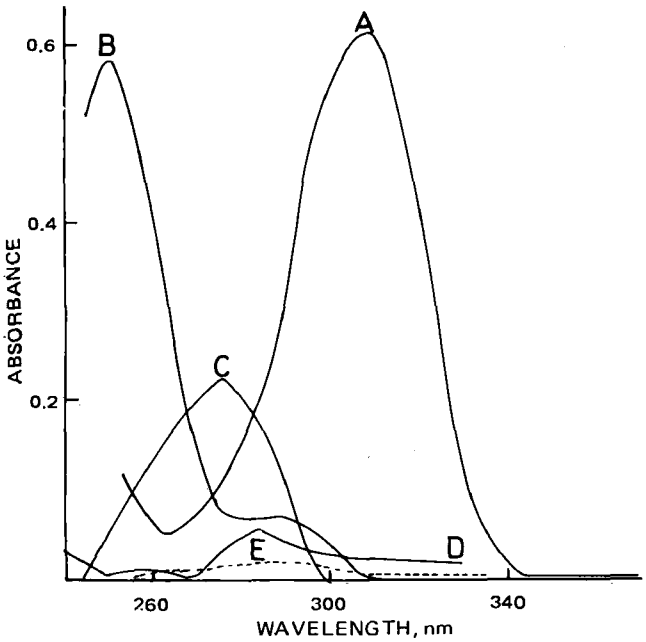

Figure 1—*Absorbance spectra. Key: A, salicylamide (2.0 mg %); B, acetaminophen (4.0 mg %); C, caffeine (0.5 mg %); D, phenobarbital (2 mg %); and E, codeine phosphate (0.125 mg %).*

[2] Rhone Poulenc, France.
[3] Alkaloid, Hungary.
[4] Macfarlan Smith, Germany.
[5] China.
[6] BP grade.
[7] Prolabo Jean et Constant UV spectrophotometer.

Table II—Recoveries of Salicylamide by the Proposed Procedure

Added, mg	Found, mg	Recovery, %
20.1	19.7	98.0
30.2	30.2	100.0
39.8	41.0	103.3
50.3	50.8	100.9
60.0	60.4	100.7
70.1	71.0	101.1
Mean percent recovery ± *SD*		100.7 ± 1.72

Bromometric Determination—Accurately weigh about 100.0 mg of salicylamide and place in a stoppered 250-ml erlenmeyer flask. Add 50.0 ml, accurately measured, of 0.1 *N* bromine solution and warm to dissolve. Cool, add 15 ml of concentrated hydrochloric acid, and stopper the flask immediately. Leave for 30 min, add 3 g of potassium iodide, and titrate against 0.1 *N* sodium thiosulfate. Carry out a blank experiment.

RESULTS AND DISCUSSION

Salicylamide is often compounded in a multicomponent system with several analgesic compounds such as acetaminophen, phenobarbital, caffeine, and codeine phosphate. The separation for analysis of salicylamide from such a system is difficult and time consuming. The complicated spectrophotometric methods, requiring the solution of several algebraic equations, may make the determination tedious because of computational problems. Therefore, an independent and simple spectrophotometric method is suggested for the determination of salicylamide in the presence of the previously mentioned drugs. Separation of the drug by solvent extraction or chromatography prior to analysis is avoided.

Data obtained for the construction of a calibration curve for salicylamide are listed in Table I. The calibration curve, obtained by plotting eight average values of the absorbance at 308 nm as a function of concentration, indicated that the Beer–Lambert law was obeyed. No trials, however, were made to extend the investigations to concentrations higher or lower than those listed, since the absorbance values obtained with the concentrations studied are most suitable for minimum experimental errors.

The straight-line equation for the calibration curve, as determined by the method of least squares, is $A = 0.0130 + 0.3043C$, where A is the absorbance and C is the concentration (milligrams per 100 ml). The concentration of salicylamide in an unknown sample may be calculated readily. According to the experimental results, the average molar absorptivity of salicylamide at 308 nm is $\epsilon = 4.28 \times 10^3$ liters/mole/cm. Data obtained from the determination of salicylamide in simple chloroform solutions of varying concentrations are listed in Table II.

Time–absorbance studies on standard solutions of salicylamide and on test solutions containing in addition acetaminophen, phenobarbital, caffeine, and codeine phosphate indicated that the solutions can be kept for 12 hr without appreciable change in absorbance.

The spectra of the compounds commonly encountered with sali-

Table III—Compounds Studied for Interference with the Determination of Salicylamide

Compound	Relative Concentration in Working Solution, mg %	Tested Concentration, mg %	Absorbance of Tested Concentration at 308 nm	Molar Absorptivity
Caffeine	0.625	5.0	None	—
Phenobarbital	0.313	1.25	0.010	186
Codeine phosphate	0.125	2.0	0.004	81
Acetaminophen	2.5	2.5	None	—
	3.75	3.75	0.010	40
Ascorbic acid	Insoluble	Insoluble	None	—
Chloroquine phosphate	Insoluble	Insoluble	None	—
Prednisone	0.01	0.75	0.002	95

Table IV—Recoveries of Salicylamide from Synthetic Tablets

Labeled Content in Assay Aliquot, mg	Found, mg	Recovery, %
	Formula A	
40.1	40.1	100.00
50.2	50.5	100.59
53.3	53.2	99.81
60.2	61.4	101.99
62.0	61.5	99.19
Mean percent recovery ± *SD*		100.32 ± 1.06
	Formula B	
41.1	42.7	103.89
51.4	52.2	101.56
61.6	61.1	99.19
Mean percent recovery ± *SD*		100.55 ± 2.35
	Product C	
50.6	50.4	99.60
50.8	50.8	100.00
61.0	61.4	100.65
61.2	60.9	99.51
Mean percent recovery ± *SD*		99.94 ± 0.52
	Product D	
50.3	50.0	99.40
50.7	50.6	99.80
59.7	60.4	101.17
60.9	62.0	101.80
Mean percent recovery ± *SD*		100.54 ± 1.13

cylamide in tablets were determined in chloroform (Fig. 1). However, the concentrations employed for determining the spectra of acetaminophen and phenobarbital were higher than their relative concentrations in analgesic tablets. As may be seen from Fig. 1, the absorbance of salicylamide at the working wavelength is high enough to make errors due to absorbance by other compounds, if any, minimal. The spectra of the other compounds tested for interference with the proposed procedure (ascorbic acid, chloroquine phosphate, and prednisone) also were determined in chloroform.

Table V—Results of Recoveries of Salicylamide from Commercial Tablets

Product[a]	Labeled Content in Assay Aliquot, mg	Found, mg	Recovery, %
A	40.0	41.1	102.75
	40.0	41.4	103.50
	50.0	49.6	99.20
	60.0	61.4	102.33
Mean percent recovery ± *SD*			101.94 ± 1.89
B	51.07	50.93	99.73
	61.29	61.78	100.80
	61.40	61.58	100.29
Mean percent recovery ± *SD*			100.27 ± 0.54
C	50.93	51.59	101.29
	61.11	61.45	100.55
	61.57	58.82	95.53
Mean percent recovery ± *SD*			99.12 ± 3.13
D	43.54	42.72	98.12
	54.42	53.17	97.70
	65.30	63.08	96.60
Mean percent recovery ± *SD*			97.47 ± 0.78

[a] Trade names, suppliers, and weights of components per tablet are: A, Dolviran, The Alexandria Co. for Pharmaceuticals under licence of Bayer, salicylamide (200 mg), acetaminophen (200 mg), caffeine (50 mg), phenobarbital (25 mg), and codeine phosphate (10 mg); B, Cidal Forte, CID, salicylamide (500 mg); C, Salestol, CID, salicylamide (200 mg), chloroquine phosphate (40 mg), and prednisone (0.75 mg); and D, Vicemide, Kahira, salicylamide (500 mg) and ascorbic acid (100 mg).

Table VI—Recoveries of Added Salicylamide to Commercial Tablets[a]

Labeled Salicylamide, mg	Added Salicylamide, mg	Recovery of Added Salicylamide, mg	Recovery, %
42.16	21.08	20.90	99.14
40.69	15.81	15.18	96.02
39.97	15.75	15.64	99.30
39.97	26.25	27.92	106.36
Mean percent recovery ± *SD*			100.20 ± 4.37

[a] Product A.

Table III lists all tested compounds and their relative concentrations in the working chloroform solution corresponding to their relative amounts in tablets. The table also includes the highest concentrations used to test the interference with the proposed procedure. The data indicate that the contributions to the absorbance of the working solution corresponding to the relative amounts of these drugs in tablets are negligibly small compared to the absorbance of salicylamide. Such a property may lend itself to the independent routine spectrophotometric analysis of salicylamide without serious interference from the tested drugs. Ascorbic acid and chloroquine phosphate were insoluble in chloroform. Codeine phosphate, however, dissolved with difficulty on heating, and the solution had to be filtered from the few undissolved particles before the absorbance was measured.

The suggested procedure was applied to the analysis of salicylamide in two types of synthetic tablets containing the same amounts of salicylamide (200.0 mg), caffeine (50.0 mg), phenobarbital (25.0 mg), and codeine phosphate (10.0 mg) and different amounts of acetaminophen (200.4 and 299.7 mg in Formulas A and B, respectively). The mean percent recoveries (Table IV) were 100.32 ± 1.06 and 101.55 ± 2.35. Further investigations indicated that, at a higher content of acetaminophen (400.0 mg/tablet) a positive error was introduced in the recovery of salicylamide. Recoveries of salicylamide from synthetic tablets containing the same amounts of active ingredients as Products C and D also are listed in Table IV. Common tablet excipients such as starch, talc, and magnesium stearate do not interfere.

The suggested method also was applied to the determination of salicylamide in a number of commercial tablets containing different components such as acetaminophen, phenobarbital, caffeine, codeine phosphate, ascorbic acid, chloroquine phosphate, and prednisone. The results obtained agree with the labeled amounts of salicylamide (Table V).

To differentiate between experimental errors and errors due to bulk production, recoveries of known amounts of added salicylamide to one of the commercial tablets were determined (Table VI).

For purity determination and comparative purposes, salicylamide was determined by two different methods: the nonaqueous titration method of NF XIII (1) and a bromometric titration procedure. The results (Table VII) show that the mean percent purities of salicylamide used in this study were 98.63 ± 0.73 and 99.41 ± 0.25, respectively.

The suggested procedure is simple and rapid and may be quite useful for routine analysis of salicylamide in analgesic tablets.

Table VII—Determination of Purity of Salicylamide by the NF XIII Nonaqueous Titration Method and Bromometric Titration

NF Assay			Bromometric Assay		
Weight Taken, mg	Weight Found, mg	Recovery, %	Weight Taken, mg	Weight Found, mg	Recovery, %
205.4	204.6	99.62	101.3	100.8	99.51
209.5	207.9	99.23	103.1	102.5	99.42
211.7	207.3	97.92	104.3	103.2	98.94
223.4	219.1	98.07	100.2	99.6	99.45
249.7	245.6	98.33	100.7	99.9	99.26
			100.8	100.4	99.64
			100.6	100.3	99.66
Mean percent recovery ± *SD*		98.63 ± 0.75	Mean percent recovery ± *SD*		99.41 ± 0.25

REFERENCES

(1) "The National Formulary," 13th ed., Mack Publishing Co., Easton, Pa., 1970, p. 627.

(2) R. Rutkowski, *Arzneim.-Forsch.*, **4**, 209(1954); through *Anal. Abstr.*, **2**, 1313(1955).

(3) J. M. Crampton and E. Voss, *J. Am. Pharm. Assoc., Sci. Ed.*, **43**, 470(1954); through *Anal. Abstr.*, **2**, 139(1955).

(4) O. Hardy and J. Cerny, *Cesk. Farm.*, **8**, 73(1959); through *Anal. Abstr.*, **6**, 4947(1959).

(5) A. W. Clayton and R. E. Thiers, *J. Pharm. Sci.*, **55**, 404(1966).

(6) N. Shane and M. Kowblansky, *ibid.*, **57**, 1218(1968).

(7) S. A. Veresh, F. S. Hom, and J. J. Miskel, *ibid.*, **60**, 1092(1971).

(8) B. Miszczuk-Lucka and H. Taborska, *Przem. Chem.*, **11**, 706(1955); through *Anal. Abstr.*, **4**, 1016(1957).

ACKNOWLEDGMENTS AND ADDRESSES

Received February 7, 1975, from the *Pharmaceutical Analytical Chemistry Department, College of Pharmacy, University of Alexandria, Alexandria, Egypt.*

Accepted for publication December 8, 1975.

The authors are grateful to Dr. Ibrahim H. Abdallah, Alexandria Co. for Pharmaceuticals, for encouraging this study and generously supplying chemicals.

* Present address: The Alexandria Co. for Pharmaceuticals, Alexandria, Egypt.

[x] To whom inquiries should be directed.

In Vitro and *In Vivo* Availability of Spironolactone from Oral Dosage Forms

ALLEN Y. CHAO, DILIP R. SANVORDEKER [x], JUDY ZAGARELLA, KIRK MATTES, BILIANA NICHOLOVA, and AZIZ KARIM

Abstract □ Tablet formulations of spironolactone with hydrochlorothiazide were studied *in vitro* and *in vivo* to evaluate the effect of formulation parameters on the bioavailability of spironolactone. The time required for 50% tablet dissolution (T_{50}) in simulated gastric fluid was linearly correlated with the disintegration times of four experimental formulations and one commercial tablet of spironolactone and hydrochlorothiazide. Bioavailability studies were conducted in four healthy, female beagle dogs. The mean time to peak concentration of canrenone, the major metabolite of spironolactone, was proportional to the T_{50} dissolution parameter. A study of spironolactone administered orally with and without hydrochlorothiazide showed that the bioavailability of spironolactone is not affected by hydrochlorothiazide. No significant differences in the bioavailability of spironolactone from one 100-mg and four 25-mg tablets were observed. Estimates of some pharmacokinetic parameters for canrenone closely agreed with those previously reported.

Keyphrases □ Spironolactone—dissolution and bioavailability, tablet formulations with and without hydrochlorothiazide, effect of formulation parameters □ Dissolution—spironolactone tablet formulations with and without hydrochlorothiazide, effect of formulation parameters □ Bioavailability—spironolactone, tablet formulations with and without hydrochlorothiazide, effect of formulation parameters □ Hydrochlorothiazide—effect on dissolution and bioavailability of spironolactone in tablet formulations □ Dosage forms—tablets, spironolactone with and without hydrochlorothiazide, dissolution and bioavailability, effect of formulation parameters □ Diuretic agents—spironolactone, dissolution and bioavailability, tablet formulations with and without hydrochlorothiazide

Bioavailability of a drug from a dosage form is of public health interest (1–4). Several investigations have documented the importance of formulation factors affecting drug bioavailability (4–7). Consequently, it has become increasingly important to recognize and evaluate the *in vitro* availability of existing drug products and to determine the influence of formulation on *in vivo* availability from oral dosage formulations. With this approach, effective *in vitro–in vivo* correlations can be established so that improvements in the drug bioavailability from a given drug combination can be achieved (6–10).

Spironolactone (I), a potent aldosterone antagonist, in combination with hydrochlorothiazide (II) is an effective antihypertensive agent. It is also used for the treatment of edema and ascites of congestive heart failure (11–13).

The objectives of this study were: (*a*) to test whether differences exist in the bioavailability of tablet formulations of I given orally with and without II, (*b*) to assess the *in vitro–in vivo* relationship for four experimental and one commercial tablet preparations of I and II, and (*c*) to determine the pharmacokinetics of canrenone (III), a major metabolite of I, with and without II.

EXPERIMENTAL

Materials—Starch USP[1], microcrystalline cellulose[2], povidone NF[3], calcium sulfate dihydrate NF[4], spironolactone USP[5] (I), hydrochlorothiazide USP[6] (II), magnesium stearate USP[4], polyethylene glycol 400[7], and methanol, analytical reagent grade, were used.

Methods—*Tablet Preparation*—Batches (2 kg) of each formulation, except the commercial tablets[8] containing 25 mg each of I and II, were processed. The drugs and excipients, except magnesium stearate, were mixed and wet granulated with distilled water.

The granulations were oven dried, comminuted, and then lubricated with 0.5% magnesium stearate. Each batch was compressed on a rotary tablet press[9] equipped with 16 sets of 0.95-cm (0.375-in.) standard concave tablet punches. Each batch was analyzed for the content of I per tablet (discussed later).

[1] Anheuser-Busch Inc., St. Louis, Mo.
[2] FMC Corp., Newark, N.J.
[3] Plasdone, GAF Corp., New York, N.Y.
[4] Mallinckrodt Chemical Works, St. Louis, Mo.
[5] Searle & Co., San Juan, Puerto Rico.
[6] Ciba-Geigy Corp., Summit, N.J.
[7] Matheson, Coleman & Bell, Norwood, Ohio.
[8] Aldactone, 25-mg tablets (Lot 273-438), and Aldactazide, 25-mg tablets (Lot 21).
[9] Stokes B-2, Pennwalt Corp., Philadelphia, Pa.

REFERENCES

(1) "The National Formulary," 13th ed., Mack Publishing Co., Easton, Pa., 1970, p. 627.

(2) R. Rutkowski, *Arzneim.-Forsch.*, **4**, 209(1954); through *Anal. Abstr.*, **2**, 1313(1955).

(3) J. M. Crampton and E. Voss, *J. Am. Pharm. Assoc., Sci. Ed.*, **43**, 470(1954); through *Anal. Abstr.*, **2**, 139(1955).

(4) O. Hardy and J. Cerny, *Cesk. Farm.*, **8**, 73(1959); through *Anal. Abstr.*, **6**, 4947(1959).

(5) A. W. Clayton and R. E. Thiers, *J. Pharm. Sci.*, **55**, 404(1966).

(6) N. Shane and M. Kowblansky, *ibid.*, **57**, 1218(1968).

(7) S. A. Veresh, F. S. Hom, and J. J. Miskel, *ibid.*, **60**, 1092(1971).

(8) B. Miszczuk-Lucka and H. Taborska, *Przem. Chem.*, **11**, 706(1955); through *Anal. Abstr.*, **4**, 1016(1957).

ACKNOWLEDGMENTS AND ADDRESSES

Received February 7, 1975, from the *Pharmaceutical Analytical Chemistry Department, College of Pharmacy, University of Alexandria, Alexandria, Egypt.*

Accepted for publication December 8, 1975.

The authors are grateful to Dr. Ibrahim H. Abdallah, Alexandria Co. for Pharmaceuticals, for encouraging this study and generously supplying chemicals.

* Present address: The Alexandria Co. for Pharmaceuticals, Alexandria, Egypt.

[x] To whom inquiries should be directed.

In Vitro and *In Vivo* Availability of Spironolactone from Oral Dosage Forms

ALLEN Y. CHAO, DILIP R. SANVORDEKER [x], JUDY ZAGARELLA, KIRK MATTES, BILIANA NICHOLOVA, and AZIZ KARIM

Abstract □ Tablet formulations of spironolactone with hydrochlorothiazide were studied *in vitro* and *in vivo* to evaluate the effect of formulation parameters on the bioavailability of spironolactone. The time required for 50% tablet dissolution (T_{50}) in simulated gastric fluid was linearly correlated with the disintegration times of four experimental formulations and one commercial tablet of spironolactone and hydrochlorothiazide. Bioavailability studies were conducted in four healthy, female beagle dogs. The mean time to peak concentration of canrenone, the major metabolite of spironolactone, was proportional to the T_{50} dissolution parameter. A study of spironolactone administered orally with and without hydrochlorothiazide showed that the bioavailability of spironolactone is not affected by hydrochlorothiazide. No significant differences in the bioavailability of spironolactone from one 100-mg and four 25-mg tablets were observed. Estimates of some pharmacokinetic parameters for canrenone closely agreed with those previously reported.

Keyphrases □ Spironolactone—dissolution and bioavailability, tablet formulations with and without hydrochlorothiazide, effect of formulation parameters □ Dissolution—spironolactone tablet formulations with and without hydrochlorothiazide, effect of formulation parameters □ Bioavailability—spironolactone, tablet formulations with and without hydrochlorothiazide, effect of formulation parameters □ Hydrochlorothiazide—effect on dissolution and bioavailability of spironolactone in tablet formulations □ Dosage forms—tablets, spironolactone with and without hydrochlorothiazide, dissolution and bioavailability, effect of formulation parameters □ Diuretic agents—spironolactone, dissolution and bioavailability, tablet formulations with and without hydrochlorothiazide

Bioavailability of a drug from a dosage form is of public health interest (1–4). Several investigations have documented the importance of formulation factors affecting drug bioavailability (4–7). Consequently, it has become increasingly important to recognize and evaluate the *in vitro* availability of existing drug products and to determine the influence of formulation on *in vivo* availability from oral dosage formulations. With this approach, effective *in vitro–in vivo* correlations can be established so that improvements in the drug bioavailability from a given drug combination can be achieved (6–10).

Spironolactone (I), a potent aldosterone antagonist, in combination with hydrochlorothiazide (II) is an effective antihypertensive agent. It is also used for the treatment of edema and ascites of congestive heart failure (11–13).

The objectives of this study were: (*a*) to test whether differences exist in the bioavailability of tablet formulations of I given orally with and without II, (*b*) to assess the *in vitro–in vivo* relationship for four experimental and one commercial tablet preparations of I and II, and (*c*) to determine the pharmacokinetics of canrenone (III), a major metabolite of I, with and without II.

EXPERIMENTAL

Materials—Starch USP[1], microcrystalline cellulose[2], povidone NF[3], calcium sulfate dihydrate NF[4], spironolactone USP[5] (I), hydrochlorothiazide USP[6] (II), magnesium stearate USP[4], polyethylene glycol 400[7], and methanol, analytical reagent grade, were used.

Methods—*Tablet Preparation*—Batches (2 kg) of each formulation, except the commercial tablets[8] containing 25 mg each of I and II, were processed. The drugs and excipients, except magnesium stearate, were mixed and wet granulated with distilled water.

The granulations were oven dried, comminuted, and then lubricated with 0.5% magnesium stearate. Each batch was compressed on a rotary tablet press[9] equipped with 16 sets of 0.95-cm (0.375-in.) standard concave tablet punches. Each batch was analyzed for the content of I per tablet (discussed later).

[1] Anheuser-Busch Inc., St. Louis, Mo.
[2] FMC Corp., Newark, N.J.
[3] Plasdone, GAF Corp., New York, N.Y.
[4] Mallinckrodt Chemical Works, St. Louis, Mo.
[5] Searle & Co., San Juan, Puerto Rico.
[6] Ciba-Geigy Corp., Summit, N.J.
[7] Matheson, Coleman & Bell, Norwood, Ohio.
[8] Aldactone, 25-mg tablets (Lot 273-438), and Aldactazide, 25-mg tablets (Lot 21).
[9] Stokes B-2, Pennwalt Corp., Philadelphia, Pa.

Table I—Formulation Parameters of Tablet Preparations of Spironolactone (I) and Hydrochlorothiazide (II)

Formulation	Excipient[a], %			*In Vitro* Parameter		
	Starch USP	Microcrystalline Cellulose	Calcium Sulfate Dihydrate	Potency, %	Hardness, kg	Disintegration Time, min
1	20	2	60.5	100.8	4.8	3.0
2	5	2	75.5	100.4	5.5	13.5
3	5	10	67.5	99.6	8.3	15.4
4	20	10	52.5	103.5	7.6	5.8
5	—	—	—	100.3	4.0	2.5

[a] Povidone and magnesium stearate made up the rest of the excipients.

Disintegration Test—The disintegration times for six randomly sampled tablets of each formulation were measured in simulated gastric fluid without pepsin using the USP test apparatus. Disintegration tests were run without disks, and the mean disintegration time was recorded.

Hardness Test—Tablet hardness[10] was measured using 20 randomly sampled tablets from each formulation, and the mean was recorded.

Dissolution Test—The dissolution of four randomly selected tablets from each formulation was determined on an individual basis in the following manner.

Due to solubility limitations of I, one tablet was dropped in 1500 ml of simulated gastric fluid (without pepsin) maintained at 37 ± 0.5° in a constant-temperature bath and stirred at 100 rpm. A 20-ml aliquot of the dissolution fluid was withdrawn at 5, 10, 20, 40, 60, 90, and 120 min. The sample was filtered through a glass wool filter[11] fitted in a filtration unit[12]. Upon appropriate dilution, the filtrate was assayed spectrophotometrically at 241 nm on a dual-beam spectrophotometer[13].

Analysis of Spironolactone in Tablets—Twenty tablets were ground to a fine powder in a mortar and pestle. A weighed amount of this powder, equivalent to one tablet, was dissolved in 100 ml of methanol. After filtering and appropriate dilution, the sample was assayed spectrophotometrically as already described.

Bioavailability Studies in Dogs—Bioavailability studies were conducted in four healthy, female beagle dogs. A 2-week washout period was allowed prior to administration of each preparation. The animals were dosed orally with either one 100-mg[14] or four 25-mg tablets of each formulation of I with or without II. A 100-mg dose of I with and without II in 15 ml of polyethylene glycol 400 solution was administered intragastrically to each dog. An additional 15 ml of the vehicle was then administered to ensure total delivery of the dose.

Approximately 3 ml of blood was collected in heparinized tubes *via* a butterfly catheter[15] implanted securely into the saphenous vein of the right leg. Blood samples were collected at 0.25, 0.75, 1.0, 1.5, 2.0, 2.5, 3.0, 4.0, 5.0, 6.0, 7.0, 8.0, and 24 hr after dosing of each preparation. Sterile normal saline solution[16] was infused in the animals at approximately 20 ml/hr prior to and after blood sampling. The blood samples were centrifuged immediately, and the plasma was stored frozen until analysis.

Assay of Canrenone in Dog Plasma—The fluorometric[17] method of Gochman and Gantt (14) was used to quantify the concentration of canrenone (III) in the dog plasma. Due to limitations on the sample size, levels of III below 50 ng/ml were not considered reliable.

RESULTS AND DISCUSSION

Formulation Characteristics *In Vitro*—The composition and characteristics of four experimental tablet formulations are shown in Table I. In these formulations, magnesium stearate and povidone were kept constant at 0.5 and 3%, respectively, to eliminate their influence as variables in drug release and dissolution. Comparison of Formulation 1 with 2 and of Formulation 3 with 4 (Table I) shows that increasing the amount of corn starch with a constant level of microcrystalline cellulose in the formulations resulted in a shorter disintegration time while maintaining the hardness in a relatively close range. This finding agrees with the reported results on improved disintegration properties due to starch (15, 16). Comparison of Formulation 1 with 4 and of Formulation 2 with 3 shows that increasing the amount of microcrystalline cellulose from 2 to 10%, while maintaining a constant starch level, resulted in improved tablet hardness. However, the disintegration time was not affected significantly.

The dissolution profiles of I from four experimental formulations and one commercial tablet are illustrated in Fig. 1. Each point on the graph is a mean of four separate determinations. The T_{50} value, defined as the time required for 50% of I to dissolve in the dissolution medium, was estimated for each formulation from these data.

When the T_{50} value for each formulation was plotted against the corresponding disintegration time, a linear relationship (Fig. 2) was

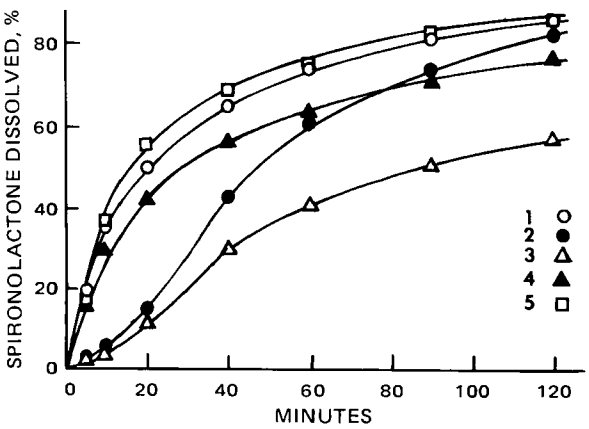

Figure 1—*Dissolution profile of I from four experimental (1–4) and one commercial (5) tablet formulations of I and II.*

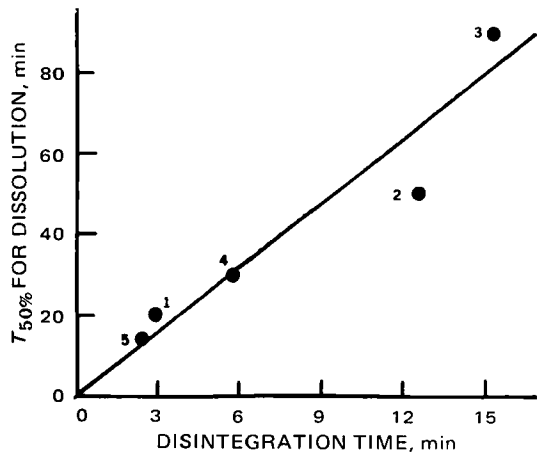

Figure 2—*Linear relationship between tablet disintegration time and $T_{50\%}$ for dissolution of I from four experimental (1–4) and one commercial (5) tablet formulations of I and II.*

[10] Heberlein, Vector Corp., Hiawatha, Iowa.
[11] Reeve-Angel Co., Clifton, N.J.
[12] Millipore Corp., Bedford, Mass.
[13] Model 124-D, Coleman, Perkin-Elmer Corp., Maywood, Ill.
[14] Aldactone, 100-mg tablets (Lot 912-1068), prepared for clinical trials, Searle Laboratories, Chicago, Ill.
[15] Butterfly-19 infusion catheter, Abbott Laboratories, North Chicago, Ill.
[16] Baxter Laboratories, Morton Grove, Ill.
[17] All fluorometric measurements were performed on an Aminco-Bowman spectrophotofluorometer, American Instrument Co., Silver Spring, Md.

Table II—*In Vivo* and *In Vitro* Parameters for Five Tablet Formulations of Spironolactone (I) and Hydrochlorothiazide (II)

Formulation	Dog	Observed Maximum		Smoothed Maximum		Disintegration Time, min	T_{50}, min
		Time, hr	Concentration, ng/ml	Time, hr	Concentration, ng/ml		
1	1	2.0	190	2.36	175		
	2	1.5	190	1.86	182		
	3	1.25	150	1.34	150		
	4	1.5	390	1.75	422		
	Mean:	1.56	230	1.83	232	3.0	21.0
2	1	2.0	100	—	—		
	2	2.5	210	2.77	204		
	3	2.5	120	2.34	111		
	4	3.0	150	2.78	152		
	Mean:	2.5	145	2.63	156	13.5	46.8
3	1	2.5	250	2.07	222		
	2	3.0	240	3.41	233		
	3	1.5	170	1.75	162		
	4	7.0	520	10.75	599		
	Mean:	3.5	295	4.50	304	15.4	89.2
4	1	1.5	300	1.92	286		
	2	2.25	160	2.07	158		
	3	2.0	170	1.86	138		
	4	5.0	410	4.72	276		
	Mean:	2.69	260	2.64	215	5.8	30.8
5	1	2.0	330	2.17	319		
	2	2.0	210	2.22	194		
	3	2.0	190	2.27	181		
	4	1.0	500	1.37	590		
	Mean:	1.75	308	2.01	321	2.5	15.0

observed. Since the dissolution process of a drug from a tablet is dependent on its disintegration into dispersed aggregates, it is reasonable to expect that a longer disintegration time for a given tablet formulation would give a longer T_{50} value.

Bioavailability Studies in Dogs—Previous studies (17–21) demonstrated that the bioavailability of I can be measured by the appearance of III, a major fluorogenic metabolite in the plasma. In a series of investigations, Sadée *et al.* (20–22) showed that I was rapidly metabolized to III and nonfluorogenic metabolites in dog plasma.

In Vitro–In Vivo *Correlation for Tablet Formulations of I and II*—Figure 3 is a semilogarithmic plot of the plasma concentration of III *persus* time and illustrates the comparative bioavailability of I from the five tablet formulations of I and II. It is apparent that the bioavailability of the commercial preparation (Formulation 5), as reflected by the plasma levels of III, was optimal compared to the other four experimental formulations. The plasma levels of III achieved from Formulations 1 and 4 during the absorption phase (0–1 hr) were higher, while those achieved from 2 and 3 were below the detectable level of 50 ng/ml. Whereas Formulations 2 and 3 exhibited a lag phase in the dissolution profile (Fig. 2), Formulations 1, 4, and 5 did not. These differences in the dissolution profiles were reflected in the plasma levels of III monitored during the absorption phase. It was deemed important to evaluate whether there was a correlation between the T_{50} parameter and mean time to peak concentration of III in the plasma.

Table II illustrates the individual dog data and the observed *in vitro* parameters for the five tablet preparations of I and II. The mean time

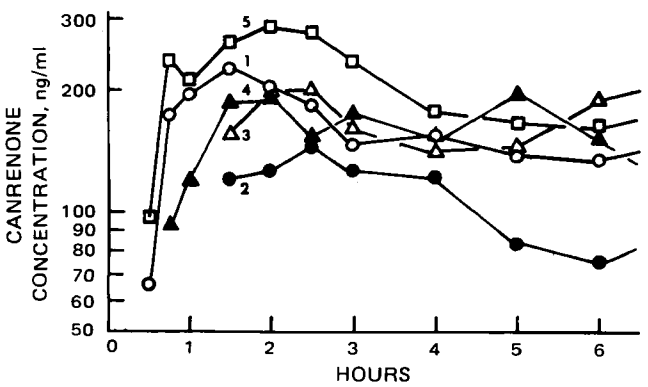

Figure 3—*Semilogarithmic plots of mean plasma levels of III monitored as a function of time after oral dosing of four experimental (1–4) and one commercial (5) tablet formulations of I and II to four dogs.*

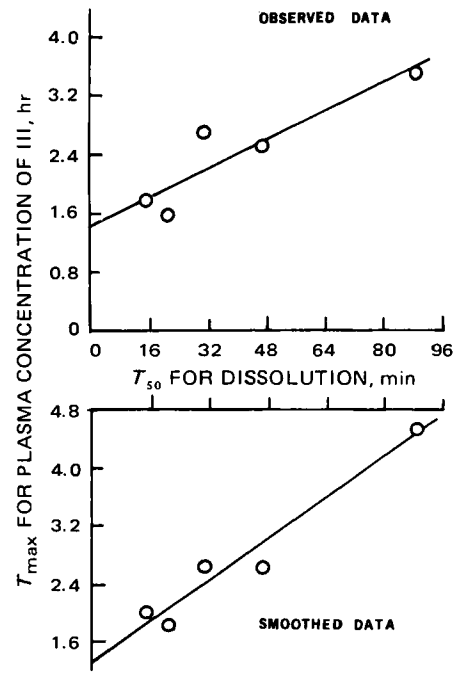

Figure 4—*Linear relationship between time for maximum concentration of III in dog plasma (T_{max}) and T_{50} value for dissolution of I from four experimental and one commercial tablet formulations of I and II.*

Table III—Pharmacokinetic Parameters of Canrenone (III) in Dog Plasma after Oral Dosing of Spironolactone

Mode of Oral Administration of I	Apparent Pharmacokinetic Parameter: Half-Life for Appearance in Plasma, hr	Half-Life for Distribution from Plasma, hr	Half-Life for Elimination from Plasma, hr (Mean ± *SE*)	*AUC* (0.25–8 hr), ng/ml × hr (Mean ± *SE*)
100 mg in polyethylene glycol 400	0.40[a]	0.82[a]	13.5 ± 2.9[b]	5042 ± 599[c]
Four 25-mg tablets	—	—	15.5 ± 1.3[b]	1582 ± 612[d]
One 100-mg tablet	—	—	20.4 ± 4.8[b]	958 ± 70

[a] Determined on the basis of the mean plasma concentration–time profile of III in four dogs. [b] Determined on the basis of the slope of the terminal portion (4–24 hr) of the plasma concentration–time profile of III in each dog. Difference was not statistically significant at $p < 0.05$ level. [c] The difference between polyethylene glycol and both tablet formulations was statistically significant at the $p < 0.05$ level. [d] The difference between the two tablet formulations was not statistically significant at the $p < 0.05$ level.

to peak and the peak plasma concentration of III were estimated by a quadratic spline "smoothening" technique (23) (Table II). The Pearson product moment correlation coefficients (r) were calculated to correlate both the observed and "smoothed" *in vivo* data with the *in vitro* dissolution times, *i.e.*, T_{50} value (Table II).

The correlation of mean time to peak with T_{50} value for the five formulations was statistically significant ($p < 0.05$) based on the observed *in vivo* data ($r = 0.91$) and confirmed by the smoothed *in vivo* data ($r = 0.97$). This correlation indicated that there was a significant linear relationship between the *in vitro* and *in vivo* parameters established for the five tablet preparations of I and II (Fig. 4).

Bioavailability of 100- and 25-mg Tablets of I—Figure 5 is a semilogarithmic plot of the mean plasma concentration of III achieved after oral administration of one 100[14]- or four 25-mg tablets[8] of I and four 25-mg tablets[8] of I and II to the four dogs used in the previous studies. The mean time to peak plasma concentration of III fell in the 1.5–2-hr range after dosing, regardless of the dose distribution of I in the three different tablet types. This finding suggests that the drug release from these tablet preparations of I and/or I and II (4 × 25 mg) during the absorptive phase was virtually equivalent. The plasma elimination profile of III observed for these tablet preparations indicates that the presence of II did not affect the pharmacokinetic disposition of III.

Bioavailability of I with and without II in Polyethylene Glycol 400 Solution—Figure 6 is a semilogarithmic plot of the mean plasma concentration of III *versus* time following oral administration of a 100-mg dose of I and II in 15 ml of polyethylene glycol 400 solution. The peak plasma concentration of III occurred at about 1.5 hr after drug administration. The half-life for the biological disposition of III, $(t/2)_\beta$, as estimated from the terminal portion of the plasma concentration–time profile, was about 8 hr. These observations are consistent with reported results (20–22).

To test whether coadministration of II in solution had any significant effect on the bioavailability of I, an additional study with a 100-mg dose of only I in 15 ml of polyethylene glycol 400 solution was conducted in the same dogs. Statistical analysis of the area under the plasma concentration–time curve (*AUC*) of III for the four dogs revealed no significant difference ($p < 0.05$) in the bioavailability of I with and without coadministration of II.

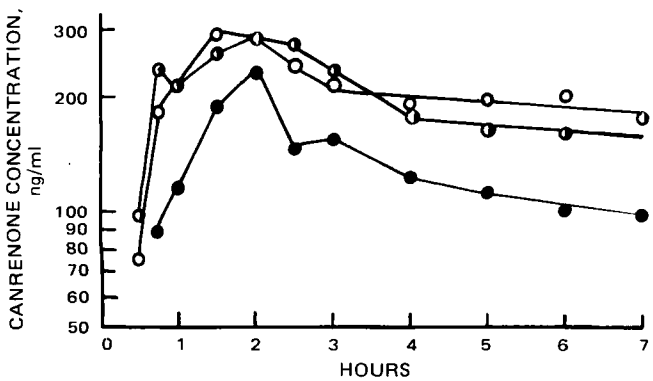

Figure 5—*Semilogarithmic plots of mean plasma levels of III. Key: ◑, tablets of I and II; ○, four 25-mg tablets of I; and ●, one 100-mg tablet of I.*

Pharmacokinetic Analysis—Since I is rapidly metabolized to III in the dog (21), it is reasonable to assume that biotransformation of I by a first-order process during the absorptive phase results in a first-order appearance or input of III and other metabolities in the plasma. An equation that describes the first-order input (or appearance) of III and its subsequent distribution and elimination from the plasma (central) compartment of a two-compartment open model is:

$$C_{p(t)} = -C'e^{-k_{III}(t)} + A'e^{-\alpha(t)} + B'e^{-\beta(t)} \qquad \text{(Eq. 1)}$$

where A', B', and C' are the zero-time plasma concentration intercepts, in nanograms per milliliter, derived from a graphical analysis of the plasma concentration–time profile by the method of residuals (24). As illustrated in Fig. 6, such an analysis was performed; the apparent rate constants k_{III} (input rate constant for III) and the hybrid rate constants α and β (for distribution and elimination of III) were obtained.

Table III illustrates some biopharmaceutical parameters estimated for III following oral dosing of I in polyethylene glycol solution and tablet dosage forms to four beagle dogs. The biological half-life, $(t/2)_\beta$, for the elimination of III for the plasma did not show any statistical difference ($p < 0.05$) regardless of the mode of administration of I. Moreover, no difference ($p < 0.05$) was observed for the *AUC* parameter of four 25-mg and one 100-mg tablets of I.

The apparent differences observed in the plasma concentration–time profile (Fig. 5) of III after oral dosing of one 100-mg and four 25-mg tablets of I may be attributed to the surface area of tablets and their aggregates exposed for dissolution and then absorption of I from the GI tract. The *AUC* parameter indicates that administration of polyethylene glycol 400 solutions of I resulted in significantly ($p <$

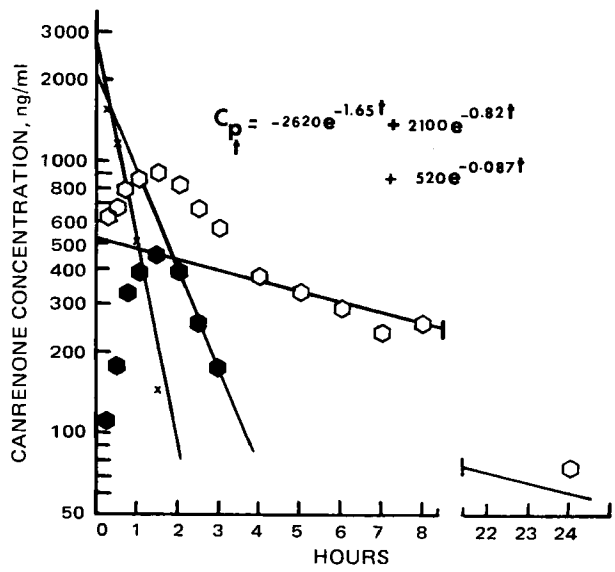

Figure 6—*Graphical analysis of mean plasma levels of III achieved in four dogs after oral dosing of I and II in polyethylene glycol 400 solution. Key: ○, mean plasma levels of III; ●, first residual plot; and ×, second residual plot.*

0.05) higher levels of III in the plasma than those achieved from tablet dosage forms.

Although such differences have not been observed in humans (25), it is possible that the presence of a cosolvent, such as polyethylene glycol, in the dog gut provided an effective dissolution medium for I, thus allowing increased amounts of the drug to be absorbed over a given period of the drug transit in the GI tract. This could explain the observed differences in the relative bioavailability of I in the plasma from a solution and tablet dosage forms.

REFERENCES

(1) W. H. Barr, *Drug Inform. Bull.*, **3**, 27(1969).

(2) J. G. Wagner, "The Physiological Equivalence of Drug Dosage Forms," Department of National Health and Welfare, Canada, 1969, pp. 40–43.

(3) "Bioavailability of Drugs," B. B. Brodie and W. M. Heller, Eds., S. Karger, Basel, Switzerland, 1972.

(4) "Current Concepts in Pharmaceutical Sciences," J. Swarbrick, Ed., Lea & Febiger, Philadelphia, Pa., 1973, pp. 77–96.

(5) WHO Scientific Group, "Bioavailability of Drugs: Principles and Problems", Tech. Rep. Ser. No. 536, WHO, Geneva, Switzerland, 1974.

(6) J. G. Wagner, *Drug Intell. Clin. Pharm.*, **5**, 115(1971).

(7) W. H. Barr, *Pharmacology*, **8**, 55(1972).

(8) L. F. Prescott and J. Nimmo, *Acta Pharmacol. Toxicol., Suppl.*, **3**, 288(1971).

(9) J. G. Wagner, *Drug Intell. Clin. Pharm.*, **4**, 190(1970).

(10) J. Koch-Weser, *N. Engl. J. Med.*, **291**, 233(1974); *ibid.*, **291**, 503(1974).

(11) S. Shaldon, J. R. McLaren, and S. Sherlock, *Lancet*, **1**, 609(1960).

(12) E. J. Ross, *Br. Med. J.*, **1**, 1508(1961).

(13) C. M. Kagawa and V. A. Drill, *Arch. Int. Pharmacodyn. Ther.*, **136**, 283(1962).

(14) N. Gochman and C. L. Gantt, *J. Pharmacol. Exp. Ther.*, **135**, 312(1962).

(15) W. Lowenthal, *Pharm. Acta Helv.*, **48**, 589(1972).

(16) A. M. Sakr, A. A. Kassem, and A. Farrag, *Chem. Aerosol News*, **44**, 37(1973).

(17) C. M. Kagawa, D. J. Bouska, and M. L. Anderson, *J. Pharm. Sci.*, **53**, 450(1964).

(18) C. M. Kagawa, D. J. Bouska, and M. L. Anderson, *Proc. Soc. Exp. Biol. Med.*, **115**, 837(1964).

(19) A. Karim, R. E. Ranney, and H. I. Maibach, *J. Pharm. Sci.*, **60**, 708(1971).

(20) W. Sadée, M. Dagcioglu, and S. Riegelman, *ibid.*, **61**, 1126(1972).

(21) W. Sadée, S. Riegelman, and S. C. Jones, *ibid.*, **61**, 1129(1972).

(22) *Ibid.*, **61**, 1132(1972).

(23) S. Wold, *Technometrics*, **16**, 1(1974).

(24) A. Rescigno and G. Segré, "Drug and Tracer Kinetics," Blaisdell, Waltham, Mass., 1966.

(25) A. Karim, J. Zagarella, T, C. Hutsell, and A. Chao, *Clin. Pharmacol. Ther.*, **19**, 170(1976).

ACKNOWLEDGMENTS AND ADDRESSES

Received August 4, 1975, from the *Departments of Pharmaceutical Research and Development and Drug Metabolism, Searle Laboratories, Chicago, IL 60680*

Accepted for publication January 26, 1976.

The authors thank Mrs. Beatrice Gerstel and Miss Charlotte Craig for technical assistance and Miss Suzanne Sering for manuscript preparation. Appreciation is also expressed to Dr. H. J. Lambert and Dr. E. Lau for suggestions and encouragement.

[x] To whom inquiries should be directed.

Dissolution Rate Equations in Column-Confined Dissolution

J. T. CARSTENSEN [x] and KAILASH DHUPAR

Abstract □ Equations are derived for the dissolution of a soluble solid in a column into a liquid stream. The equations are substantiated by experiments using oxalic acid dihydrate as a test substance. The dissolution rate constant, k, of oxalic acid dihydrate depends on linear velocity, $\bar{v}$ (centimeters per second), by the following equation: $k = (2.54 \pm 0.76) \times 10^{-4}\ \bar{v}$, where k is measured in centimeters per second.

Keyphrases □ Dissolution—soluble solid in a column into a liquid stream, equations derived □ Column-confined dissolution—soluble solid into a liquid stream, equations derived □ Solids, soluble—dissolution in a column into a liquid stream, equations derived

Numerous recent publications have discussed dissolution testing[1]. Pernarowski (1) cited 100 different published methods. LeHir (2) also described the technology in depth.

Some reported work relates to the use (or potential use) of column apparatuses for dissolution of dosage forms (3–13). The scope of this article is the experimental probing of an actual monodisperse system dissolving in a column at low liquid velocities[2]. Oxalic acid was used because it was tested previously under other conditions (14) and found to be easy to reproduce by controlled recrystallization from water.

EXPERIMENTAL

Oxalic acid[3] was recrystallized as the dihydrate and classified by sieving as described previously (14). The dissolution experiments were performed in a column such as the one shown in Fig. 1. A female ground joint (A_1) was fused[4] onto the top of a 50-ml buret. A male ground joint (A_2) was fused onto a sintered-glass filter in a 1-cm i.d. Pyrex tube. A stopcock (C), Pyrex tubing, and a female joint were fused onto the other end of the sintered-glass filter tube, and the tube was bent beyond C at the angle shown. The female joint fit the outlet

[1] There was no attempt here to make a complete bibliography; only articles directly relevant to the particular arguments in this study are cited. For a bibliography of methodology, the reader is referred to Ref. 1.

[2] Reynolds numbers between 10 and 100.

[3] Mallinckrodt analytical reagent oxalic acid dihydrate, Mallinckrodt Chemical Works, Saint Louis, Mo.

[4] All fusing was done by glass blowing using Pyrex glass and a gas–oxygen flame.

0.05) higher levels of III in the plasma than those achieved from tablet dosage forms.

Although such differences have not been observed in humans (25), it is possible that the presence of a cosolvent, such as polyethylene glycol, in the dog gut provided an effective dissolution medium for I, thus allowing increased amounts of the drug to be absorbed over a given period of the drug transit in the GI tract. This could explain the observed differences in the relative bioavailability of I in the plasma from a solution and tablet dosage forms.

REFERENCES

(1) W. H. Barr, *Drug Inform. Bull.*, **3**, 27(1969).

(2) J. G. Wagner, "The Physiological Equivalence of Drug Dosage Forms," Department of National Health and Welfare, Canada, 1969, pp. 40–43.

(3) "Bioavailability of Drugs," B. B. Brodie and W. M. Heller, Eds., S. Karger, Basel, Switzerland, 1972.

(4) "Current Concepts in Pharmaceutical Sciences," J. Swarbrick, Ed., Lea & Febiger, Philadelphia, Pa., 1973, pp. 77–96.

(5) WHO Scientific Group, "Bioavailability of Drugs: Principles and Problems", Tech. Rep. Ser. No. 536, WHO, Geneva, Switzerland, 1974.

(6) J. G. Wagner, *Drug Intell. Clin. Pharm.*, **5**, 115(1971).

(7) W. H. Barr, *Pharmacology*, **8**, 55(1972).

(8) L. F. Prescott and J. Nimmo, *Acta Pharmacol. Toxicol., Suppl.*, **3**, 288(1971).

(9) J. G. Wagner, *Drug Intell. Clin. Pharm.*, **4**, 190(1970).

(10) J. Koch-Weser, *N. Engl. J. Med.*, **291**, 233(1974); *ibid.*, **291**, 503(1974).

(11) S. Shaldon, J. R. McLaren, and S. Sherlock, *Lancet*, **1**, 609(1960).

(12) E. J. Ross, *Br. Med. J.*, **1**, 1508(1961).

(13) C. M. Kagawa and V. A. Drill, *Arch. Int. Pharmacodyn. Ther.*, **136**, 283(1962).

(14) N. Gochman and C. L. Gantt, *J. Pharmacol. Exp. Ther.*, **135**, 312(1962).

(15) W. Lowenthal, *Pharm. Acta Helv.*, **48**, 589(1972).

(16) A. M. Sakr, A. A. Kassem, and A. Farrag, *Chem. Aerosol News*, **44**, 37(1973).

(17) C. M. Kagawa, D. J. Bouska, and M. L. Anderson, *J. Pharm. Sci.*, **53**, 450(1964).

(18) C. M. Kagawa, D. J. Bouska, and M. L. Anderson, *Proc. Soc. Exp. Biol. Med.*, **115**, 837(1964).

(19) A. Karim, R. E. Ranney, and H. I. Maibach, *J. Pharm. Sci.*, **60**, 708(1971).

(20) W. Sadée, M. Dagcioglu, and S. Riegelman, *ibid.*, **61**, 1126(1972).

(21) W. Sadée, S. Riegelman, and S. C. Jones, *ibid.*, **61**, 1129(1972).

(22) *Ibid.*, **61**, 1132(1972).

(23) S. Wold, *Technometrics*, **16**, 1(1974).

(24) A. Rescigno and G. Segré, "Drug and Tracer Kinetics," Blaisdell, Waltham, Mass., 1966.

(25) A. Karim, J. Zagarella, T, C. Hutsell, and A. Chao, *Clin. Pharmacol. Ther.*, **19**, 170(1976).

ACKNOWLEDGMENTS AND ADDRESSES

Received August 4, 1975, from the *Departments of Pharmaceutical Research and Development and Drug Metabolism, Searle Laboratories, Chicago, IL 60680*

Accepted for publication January 26, 1976.

The authors thank Mrs. Beatrice Gerstel and Miss Charlotte Craig for technical assistance and Miss Suzanne Sering for manuscript preparation. Appreciation is also expressed to Dr. H. J. Lambert and Dr. E. Lau for suggestions and encouragement.

[x] To whom inquiries should be directed.

Dissolution Rate Equations in Column-Confined Dissolution

J. T. CARSTENSEN [x] and KAILASH DHUPAR

Abstract □ Equations are derived for the dissolution of a soluble solid in a column into a liquid stream. The equations are substantiated by experiments using oxalic acid dihydrate as a test substance. The dissolution rate constant, k, of oxalic acid dihydrate depends on linear velocity, $\bar{v}$ (centimeters per second), by the following equation: $k = (2.54 \pm 0.76) \times 10^{-4}\ \bar{v}$, where k is measured in centimeters per second.

Keyphrases □ Dissolution—soluble solid in a column into a liquid stream, equations derived □ Column-confined dissolution—soluble solid into a liquid stream, equations derived □ Solids, soluble—dissolution in a column into a liquid stream, equations derived

Numerous recent publications have discussed dissolution testing[1]. Pernarowski (1) cited 100 different published methods. LeHir (2) also described the technology in depth.

Some reported work relates to the use (or potential use) of column apparatuses for dissolution of dosage forms (3–13). The scope of this article is the experimental probing of an actual monodisperse system dissolving in a column at low liquid velocities[2]. Oxalic acid was used because it was tested previously under other conditions (14) and found to be easy to reproduce by controlled recrystallization from water.

EXPERIMENTAL

Oxalic acid[3] was recrystallized as the dihydrate and classified by sieving as described previously (14). The dissolution experiments were performed in a column such as the one shown in Fig. 1. A female ground joint (A_1) was fused[4] onto the top of a 50-ml buret. A male ground joint (A_2) was fused onto a sintered-glass filter in a 1-cm i.d. Pyrex tube. A stopcock (C), Pyrex tubing, and a female joint were fused onto the other end of the sintered-glass filter tube, and the tube was bent beyond C at the angle shown. The female joint fit the outlet

[1] There was no attempt here to make a complete bibliography; only articles directly relevant to the particular arguments in this study are cited. For a bibliography of methodology, the reader is referred to Ref. 1.

[2] Reynolds numbers between 10 and 100.

[3] Mallinckrodt analytical reagent oxalic acid dihydrate, Mallinckrodt Chemical Works, Saint Louis, Mo.

[4] All fusing was done by glass blowing using Pyrex glass and a gas–oxygen flame.

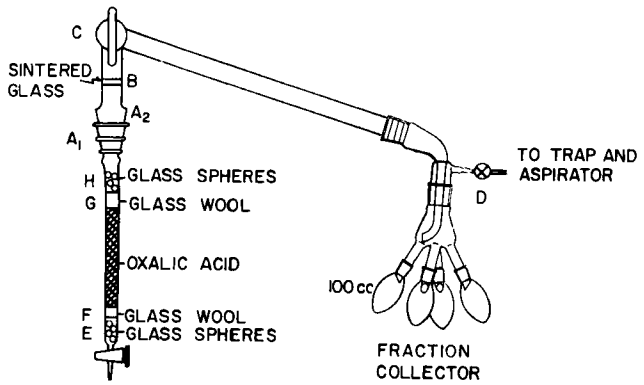

Figure 1—*Apparatus used for dissolution rate studies.*

joint of a commercial glass fraction collector[5] with four 100-ml collecting bulbs.

The vacuum outlet of the fraction collector was connected to an erlenmeyer vacuum flask, serving as a trap; this flask, in turn, was connected to a water aspirator *via* a stopcock (D). The tip of the buret stopcock was attached *via* a piece of Tygon tubing to a micrometric flow valve[6]. The rate of liquid flow could be governed by both this valve and the position of D.

The column was loaded with glass spheres at E to a depth of 1 cm, then with 1 cm of glass wool (at F), and then with 40 cm (~ 33 g) of oxalic acid dihydrate crystals of a given mesh sieve fraction. Glass wool (1 cm) and glass beads (8 cm) were then added at points G and H. The purpose of the glass beads at E is to rectify the turbulence that occurs at the pipe widening beyond the stopcock (5). The purpose of the glass beads at H is to weight down the column so that it does not move upward during experiments performed at high liquid velocity. The purpose of the sintered-glass filter is to prevent passage of entrained small particles into the efflux beyond C.

After the column had been packed, the buret stopcock was closed, C and D were opened, and the aspirator was started. Just prior to the start of the experiment, C was closed, a 500-ml beaker with 0.1 *N* HCl was lifted over the tip of the flow valve, and the buret stopcock and C then were opened. Timers were started, and the time required to fill each of the four collecting bulbs (t_i) was recorded. The collector was turned by hand at the point when collection was changed from one bulb to the next.

The length of the column[7] as a function of time was recorded by noting the time at which the column reached prefixed marks at the buret and then noting the position of the top of the column; the latter

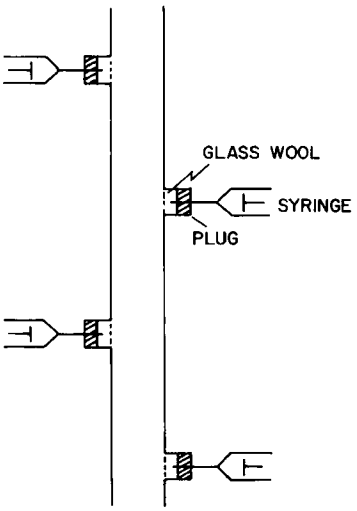

Figure 2—*Apparatus for studying the dependence of* C *on* x.

[5] Catalog No. 10525 and No. 10515, Eck and Krebs Scientific Laboratory Glass Apparatus Inc., Long Island City, NY 11101

[6] Catalog No. M7110, Roger Gilmon Instruments Inc., Great Neck, NY 11021

[7] Two persons are needed to collect results from one experiment.

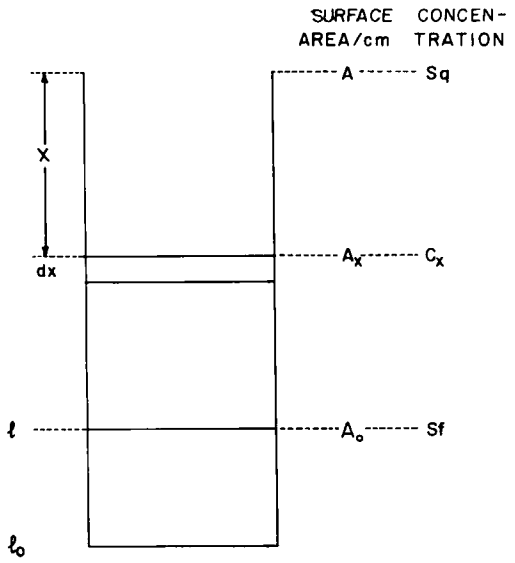

Figure 3—*Nomenclature used.* A_x = *surface area per centimeter of column length,* x = *distance from top of column,* l = *length of column at time* t, S = *saturation concentration,* f = *degree of saturation of feed,* q = *degree of saturation of efflux and* C_x = *concentration at point* x *in the column.*

moved very slightly downward (3 mm during an experiment). The volume flow rate, V (milliliters per second), could then be calculated by weighing the collected fraction (w_i) and dividing by the density (ρ_i) and the time elapsed for the collection (t_i). The densities, ρ_i, were obtained by pycnometry; the amount of oxalic acid present in a fraction (x_i) was determined titrimetrically.

The feeds used in the experiments were (*a*) 0.1 *N* HCl and (*b*) 0.1 *N* HCl containing varying concentrations of oxalic acid—*viz.*, degrees of saturation of 0.2, 0.4, 0.6, and 0.8

The specific surface area of a coarse solid as used here is small and cannot be determined by gas adsorption or by permeametry. The geometric surface areas can be obtained by microscopy, since the crystals can be approximated by parallelepipeds (15) of side L, breadth $\alpha\overline{B}$, and height $\overline{B}$. Then $N = 50$ crystals of a 10–20-mesh cut were weighed, and their dimensions (L and $\alpha\overline{B}$) were determined microscopically. The volume was then (since the sample is fairly monodisperse) $\alpha\overline{L}(\overline{B})^2$. Comparing the theoretical weight, $N\alpha\overline{L}(\overline{B})^2(\rho)$ (where $\rho = 1.66$ g/ml) to the actual weight allows calculation of α; hence, the specific geometric surface area can be found to be $(2\alpha\overline{L})(\overline{B}) + 2[\overline{L}(\overline{B})] + 2[\alpha(\overline{B})^2]$. The same procedure was carried out for all mesh fractions.

The surface area term of interest, as will be discussed later, is A, the surface area present in a 1-cm length of column. It is of interest to see if or how A changes as a function of position and time. For this purpose, a column was packed alternately with glass wool and oxalic acid (10–20 mesh); the column, in this fashion, consisted of seven subcolumns. A dissolution experiment was then carried out for 67 sec and the lengths of the various sections were measured. The geometric surface area was then determined microscopically and divided by the length to give the value of A.

At one point, it was desired to check the concentration profile along the column. For this purpose, a duplicate column was prepared, with four side arms (Fig. 2). The sidearms were short (8 mm) and could accommodate a rubber plug, into which a hypodermic syringe was inserted. Prior to insertion of the plug, the space in front of it was filled with glass wool (Fig. 2). At a particular point in an experiment, the flow was stopped and samples were removed from the four positions and assayed for oxalic acid.

RESULTS AND DISCUSSION

Consider a column of solid powder of length l cm and cross section σ cm^2 (Fig. 3). The surface area (square centimeters) of the amount of powder (b g) in 1-cm length of column is denoted A (square centimeters per centimeter). The liquid enters from the bottom of the column at a flow rate of V_i cm^3/sec. It dissolves solid from the column and exits with a rate of V' cm^3/sec, where V' includes the volume in-

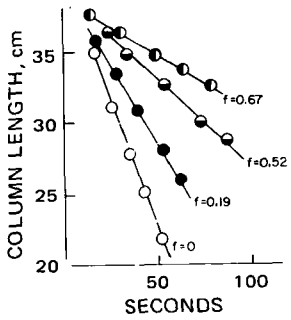

Figure 4—*Column length as a function of time. Key:* ○, f = *0 and* V = *3.42 ml/sec;* ●, f = *0.19 and* V = *2.56 ml/sec;* ⊖, f = *0.52 and* V = *2.53 ml/sec; and* ◐, f = *0.67 and* V = *2.35 ml/sec. Particles are −20/+40 mesh.*

crease due to the dissolved solid. If V denotes the average of V_i and V', then, if ϵ is the porosity of the powder, the magnitude of the average linear velocity (simply denoted the linear velocity, $\bar{v}$) is given by (15):

$$\bar{v} = V/(\sigma\epsilon) \qquad \text{(Eq. 1)}$$

Since σ cm^3 contains b g of density ρ g/ml, the porosity is given by:

$$\epsilon = 1 - (b/\sigma\rho) \qquad \text{(Eq. 2)}$$

It was observed that, under the conditions imposed, the liquid was always fairly close to saturation, S (grams per milliliter), upon exit. If one denotes the exit concentration qS, where q, the degree of saturation, is close to unity, then the following holds: in t sec, Vt ml will have passed through the column and will have saturated to a degree of Sq, *i.e.*, will have dissolved $VtS(q - f)$ g, if the incoming liquid is of a degree of saturation of f. Since there is b g of solid powder per linear column centimeter, $VtS(q - f)/b$ cm will have disappeared, *i.e.*:

$$l = l_0 - \frac{VS(q-f)}{b}t = l_0 - \alpha t \qquad \text{(Eq. 3)}$$

so that the column length should decrease linearly in time. That this is so is seen directly from Fig. 4. The slopes should be proportional to the liquid velocity. That this is so is seen in Fig. 5, where slopes of plots of the type shown in Fig. 4 are plotted against the flow rates, V. The plot is linear and goes through the origin as dictated by:

$$\alpha = [S(q-f)/b]V = \beta V \qquad \text{(Eq. 4)}$$

where:

$$\beta = (S/b)(q-f) = -\frac{S}{b}f + \frac{S}{b}q \qquad \text{(Eq. 5)}$$

Hence, if the slopes, β, from Fig. 5 are plotted *versus* the degree of saturation, f, of the incoming liquid, a linear plot should result; this plot is shown in Fig. 6[8].

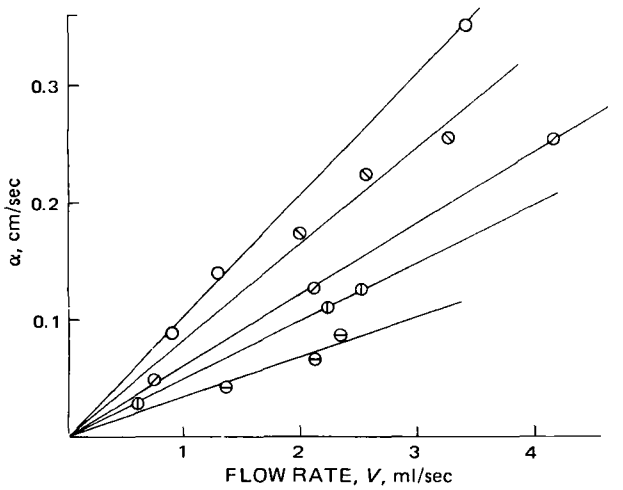

Figure 5—*Column decrease rate, α, as a function of flow rate,* V, *of −20/+40-mesh particles. Key:* ○, f = *0.0;* ⊘, f = *0.19;* ⊘, f = *0.35;* ⊖, f = *0.52; and* ⊖, f = *0.67.*

[8] Here $q \sim 1$ and is considered constant in these plots.

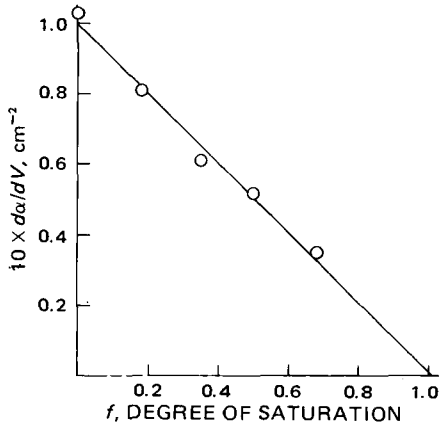

Figure 6—Plot of dα/dV *as a function of* f *for −20/+40-mesh particles.*

It is noted from Fig. 6 that the plot is fairly linear and cuts the f-axis close to $f = q = 1$ in accordance with Eq. 5. The slope in Fig. 6 is − 0.1; *i.e.*, from Eq. 5, S/b should equal 0.1. For the 10–20-mesh cut depicted, there is 36 g of solid/39 cm of column so that b = 36/39. Furthermore, S = 0.13 g/ml so the slope, by these values, should be −0.13/(36/39) = −0.13, *i.e.*, of the same order of magnitude, albeit higher, than the value obtained from the slope in Fig. 6.

When referring to Fig. 3 and using the terminology of this figure, it is noted that a volume element $\sigma\,dx$, which is x cm from the top of the column, contains solid with a surface area of $A_x\,dx$, so that the dissolution rate in this volume element would be:

$$\text{dissolution rate} = kA_x\,dx(S - C_x) \qquad \text{(Eq. 6)}$$

where k (centimeters per second) is the intrinsic dissolution rate constant. Hence, the dissolution rate over the entire column at time t, when the length is l cm, is:

$$dm/dt = \int_0^l kA_x(S - C_x)\,dx \qquad \text{(Eq. 7)}$$

The results from the experimental determination of A_x *versus* x are shown in Fig. 7. It appears[9] (as expected) that A_x is high at the bottom of the solid column and then rapidly drops to a constant value. This drop occurs over a length of less than 3 cm (*i.e.*, less than 10% of the length of the column); therefore, A_x is given by:

$$A_x = A_0 \qquad x < l' \qquad \text{(Eq. 8}a\text{)}$$

$$A_x = A_0 + \zeta(x - l') \qquad l' < x \leq l \qquad \text{(Eq. 8}b\text{)}$$

where ζ is the slope of the nonlinear portion of Fig. 7, and where l' denotes the point where A_x starts increasing (and is close to l, the total

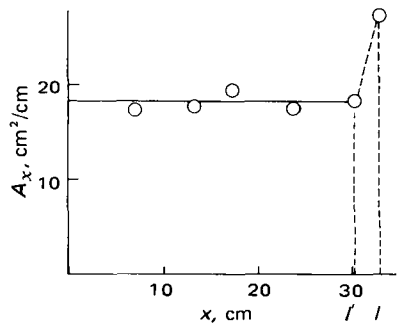

Figure 7—*Surface area per centimeter column length after a dissolution experiment.* A_x *is plotted as a function of* x *for a −10/+20-mesh particle sample.*

[9] For example, the number of particles of diameter d_1 in a single layer (d_1 cm thick) is O/d_1^2, assuming a "square" packing. The solid surface area is then $[O/(d_1^2)]\pi d_1^2 = \pi O$, so that the area per column length is $A_1 = O\pi/(d_1)$. If, after some dissolution, the diameter decreases to d_2, then by a similar argument $A_2 = O\pi/(d_2) > A_1$ (because $d_2 < d_1$).

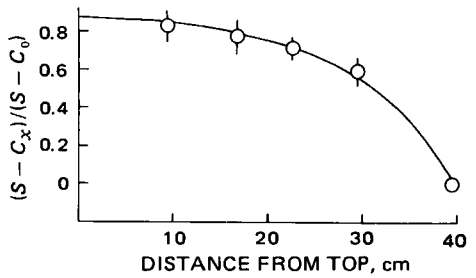

Figure 8—*Concentration,* C_x, *as a function of* x. *Particles are −20/+40 mesh.*

length of the column). Entering this into Eq. 7 then gives:

$$-\frac{dm}{dt} = kA_0 \int_0^l (S - C_x)\,dx + k \int_{l'}^l \zeta(x - l')(S - C_x)\,dx \quad \text{(Eq. 9)}$$

The concentration profile was determined (Fig. 8). The shape of the curve suggests that (with real particles in real packings as opposed to hypothetical spheres with theoretical porosities) the concentration C_x is a function of x by:

$$\ln [(S - C_x)/(S - C_l)] = gx + j \quad \text{(Eq. 10}a\text{)}$$

That this is so is seen in Fig. 9. Since $x = l$ implies that the left-hand side of Eq. 10a is zero, it follows that $0 = gl + j$, *i.e.*, $j = -gl$, so:

$$\ln [(S - C_x)/(S - C_l)] = g(x - l) \quad \text{(Eq. 10}b\text{)}$$

or:

$$S - C_x = (S - C_l)e^{g(x-l)} \quad \text{(Eq. 11)}$$

At $x = 0$, $C_x = Sq$; and since $C_l = Sf$, it follows that:

$$S(1 - q) = S(1 - f)e^{-gl} \quad \text{(Eq. 12}a\text{)}$$

or:

$$e^{gl} = (1 - f)/(1 - q) \quad \text{(Eq. 12}b\text{)}$$

Introducing Eq. 11 into Eq. 9 gives:

$$-\frac{dm}{dt} = kA_0 \int_0^l S(1 - f)e^{g(x-l)}dx + k \int_{l'}^l \zeta(x - l')S(1 - f)e^{g(x-l)}dx \quad \text{(Eq. 13)}$$

It is shown in the *Appendix* that, under the assumption that $l \sim l'$, this equation can be simplified to:

$$-\frac{dm}{dt} = \frac{kA_0Sl(q - f)}{\ln[(1 - f)/(1 - q)]} \quad \text{(Eq. 14)}$$

The rate constants were calculated according to Eq. 14 for all conditions used, and an example of such a calculation is shown in Table I. The experimental values of k obtained in this fashion were then plotted as a function of flow rate (Fig. 10). It is obvious from Table I and from the lengths of the bars in Fig. 10 that the values of k are time independent, *i.e.*, that k indeed is a constant; this finding is experimental support for the views put forth so far.

As mentioned, the time independence of k is implied by the small magnitude of the length of the bars in Fig. 10; these bars are the 95% confidence intervals calculated conventionally (as shown in Table I)

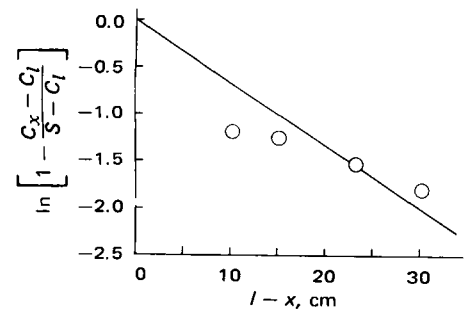

Figure 9—*Data in Fig. 8 plotted as a* σ^- *plot.*

Table I—k Values According to Eq. 14 from a 10–20-Mesh Sample

	V, ml/sec	10^4k, cm/sec
	2.20	43.7
	2.29	41.9
	2.33	42.2
	2.28	45.8
Average	2.27	43.4
$t_{3,0.05}$	3.18	—
σ =	0.054	—
$t\sigma/\sqrt{n} = \gamma$ =	0.086	—

according to $\gamma = t_{0.05}\,\sigma/\sqrt{n}$, where $\sigma\sqrt{n}$ is the standard error and $t_{0.05,n-1}$ is the Student t value for $n - 1$ degrees of freedom.

The least-squares fit line for the data in Fig. 11, weighted by factors of $(1/\gamma)$, is:

$$k = 4.76 \times 10^{-4}\,V - 0.31 \times 10^{-4} \quad \text{(Eq. 15)}$$

where k is in centimeters per second, and V is in milliliters per second.

As discussed later, the liquid velocity is of a magnitude dictating laminar (or slightly turbulent) flow. This flow is presumably the type around a particle in most dissolution methods. Extrapolating to zero velocity is possible *via* Eq. 15, but the confidence limits around this extrapolated value include zero. Carstensen and Patel (14) showed that static dissolution rate constants are at least an order of magnitude smaller than those found from "usual" beaker-type dissolution rate methods.

The flow rates used here (Figs. 5 and 10) are of the order of 2 ml/sec. With a cross section of 0.8 cm^2 and a porosity of 0.4, this rate would give a linear velocity of $2/(0.4 \times 0.8) = 6.25$ cm/sec. For a 20-mesh particle, the diameter is $d = 0.082$ cm, so that the Reynolds number (calculated according to Refs. 16 and 17) is $Re = (vd\rho)/\eta$, where ρ (grams per milliliter) is the density of the liquid and η is the viscosity in poises. Assuming these values to be $\rho = 1.00$ g/ml and $\eta = 0.01$ poise gives $Re = 6.25 \times 0.082 \times 1.0 \div 0.01 \sim 50$. Groves *et al.* (18), in column work with tablets, found backflow at $Re < 10$ and instability at $Re > 100$. Therefore, the flow rates found in the present study correspond to what they found to be a stable range.

The work reported here does *not* intend to describe another dissolution method with application to dosage forms. The apparatus was constructed because it appears to be the best way of creating well-defined linear liquid velocities; the sole intent of its construction was to study the dissolution of an easily reproducible crystal. In the pro-

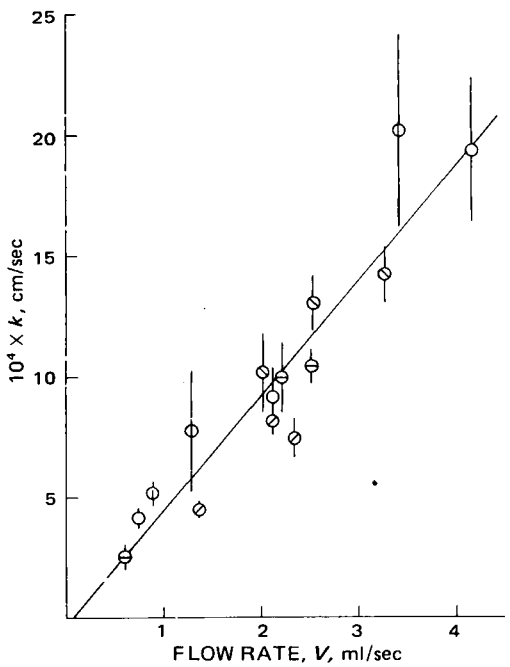

Figure 10—*Dissolution rate constants,* k, *as a function of liquid flow rate,* V.

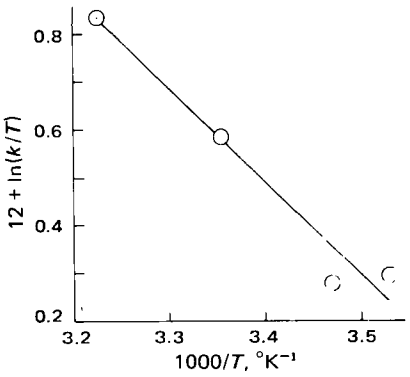

Figure 11—*Plot of* (k/T) *as a function of reciprocal absolute temperature.* E_a = *3900 kcal/mole.*

cess, the equations for dissolution of a dissolving powder in a column-type operation were derived. Mass transport equations for column apparatuses have appeared (19), but they relate primarily to solid supports (which adsorb and desorb solutes from and into the feed but themselves remain of constant weight) and nondisintegrating entities (9). Actual dissolution in columns has been reported (20) but at high Reynolds numbers (100–1000).

Oxalic acid was used because it is easily reproducible in fairly coarse particle size and remains isometric during dissolution (14). The experiments were carried out at a series of temperatures. The k values obtained were plotted as ln (k/T) *versus* $(1/T)$ and, according to Puisieux and Carstensen (21), should be linear with slopes between E_η/R and $2E_\eta/R$, where E_η is the energy of activation of the viscosity of the dissolving liquid. That this is the case is seen in Fig. 11. According to this figure, oxalic acid dihydrate has a dissolution rate constant that can be presented by:

$$\ln (k/T) = -(1880/T) + 6.87 \qquad \text{(Eq. 16)}$$

This gives an activation energy of −3770 cal/mole, which is close to the activation energy of water (−4000 cal/mole).

The least-squares fit shown in Eq. 15 was made with flow rate, V (milliliters per second), as the independent variable. This rate is, in the following, converted to liquid velocity, $\bar{v}$ (centimeters per second), *via* Eq. 1. The intercept value (0.31) is shown not to differ significantly from zero, and the least-squares fits are confined to the zero intercept, *i.e.*, slope = $\Sigma xy/(\Sigma x^2)$. The slopes and 95% confidence limits of the slopes calculated in this fashion are shown in Table II.

It is expected that k values should be a function of $\bar{v}$ and, indeed, at smaller particle sizes they are (21). The studies here failed to show significant differences at the coarse particle sizes tested (Table II). The last line gives the composite value of all mesh fractions tested; *i.e.*, oxalic acid dihydrate has a dissolution rate constant that can be represented by:

$$k = (2.54 \pm 0.76) \times 10^{-4}\,\bar{v} \qquad \text{(Eq. 17)}$$

where k and $\bar{v}$ are in centimeters per second.

SUMMARY

1. Equations for dissolution of a solid in a column into a flowing liquid stream were developed.

2. The results obtained by dissolving oxalic acid dihydrate by such a method are consistent with the equations as far as: (*a*) the column length is a function of time; (*b*) the rate of decrease of the column length is a function of liquid velocity; (*c*) the slope–intercept relations of plots are of type (*b*); (*d*) k, the intrinsic dissolution rate constant, is time independent at a particular velocity; and (*e*) k has the predicted activation energy.

Table II—Slopes of k *versus* $\bar{v}$ Plot

Mesh Fraction	Slope × 10^{-4}	95% Confidence Limits on Slope	Degrees of Freedom
10–20	3.7	1.1	8
20–40	1.8	0.7	14
40–60	1.2	0.6	8
60–80	1.2	0.8	8
Composite	2.54	0.76	41

APPENDIX

Equation 13 may be written:

$$-\frac{e^{gl}}{kS(1-f)}\frac{dm}{dt} = A_0\int_0^l e^{gx}\,dx + \zeta\int_{l'}^{l} xe^{gx}\,dx - \zeta l'\int_{l'}^{l} e^{gx}\,dx \qquad \text{(Eq. A1)}$$

The substitution $u = gx$ (*i.e.*, $dx = (1/g)du$) is then made with the appropriate change in the limits: for $x = 0$, $u = 0$; for $x = l$, $u = gl$. Equation A1 then becomes:

$$-\frac{e^{gl}}{kS(1-f)}\frac{dm}{dt} = \frac{A_0}{g}\int_0^{gl} e^u\,du + \frac{\zeta}{g^2}\int_{gl'}^{gl} ue^u\,du - \frac{\zeta l'}{g}\int_{gl'}^{gl} e^u\,du \qquad \text{(Eq. A2)}$$

Noting that $\int ue^u\,du = ue^u - u$ plus an integration constant allows integration of Eq. A2; multiplying through by g then gives:

$$-\frac{ge^{gl}}{kS(1-f)}\frac{dm}{dt} = A_0(e^{gl}-1) + \frac{\zeta}{g}(gle^{gl} - e^{gl} - gl'e^{gl'} + e^{gl'}) - \zeta l'(e^{gl} - e^{gl'}) \qquad \text{(Eq. A3)}$$

With the assumption that $l \sim l'$ so that also $e^{gl} \sim e^{gl'}$, the last two parentheses vanish and the equation becomes:

$$-\frac{ge^{gl}}{kS(1-f)}\frac{dm}{dt} = A_0(e^{gl}-1) \qquad \text{(Eq. A4)}$$

Introducing Eq. 12 for e^{gl} and the logarithmic form of Eq. 12 for g:

$$g = (1/l)\ln[(1-f)/(1-q)] \qquad \text{(Eq. A5)}$$

into Eq. A4 then gives:

$$-\frac{(1/l)\{\ln[(1-f)/(1-q)]\}[(1-f)/(1-q)]}{kS(1-f)}\frac{dm}{dt} = A_0\left[\frac{(1-f)}{(1-q)} - 1\right] \qquad \text{(Eq. A6)}$$

which is synonymous with Eq. 14.

REFERENCES

(1) M. Pernarowski, in "Dissolution Technology," L. Leeson and J. T. Carstensen, Eds., IPT of APhA Academy of Pharmaceutical Sciences, Washington, D.C., 1974, p. 58.

(2) A. LeHir, "Abrégé de Pharmacie Galénique," Masson et Cie, Paris, France, 1974, p. 109.

(3) J. T. Carstensen, in "Dissolution Technology," L. Leeson and J. T. Carstensen, Eds., IPT of APhA Academy of Pharmaceutical Sciences, Washington, D.C., 1974, p. 19.

(4) R. J. Whithey and A. J. Bowker, *J. Pharm. Pharmacol.*, **24,** 346(1972).

(5) J. Tingstad, J. Dudzinski, L. Lachman, and E. Shami, *J. Pharm. Sci.*, **62,** 1527(1973).

(6) J. E. Tingstad and S. Riegelman, *ibid.*, **59,** 692(1970).

(7) J. E. Tingstad, E. Gropper, L. Lachman, and E. Shami, *ibid.*, **61,** 1985(1972).

(8) *Ibid.*, **62,** 293(1973).

(9) F. Langenbucher, *J. Pharm. Sci.*, **58,** 1265(1969).

(10) K. Marshall and D. B. Drook, *J. Pharm. Pharmacol.*, **21,** 790(1969).

(11) D. C. Baun and G. C. Walker, *J. Pharm. Sci.*, **58,** 611(1969).

(12) C. F. Lerk and K. Zuurman, *J. Pharm. Pharmacol.*, **22,** 319(1970).

(13) A. Richter, R. Myhre, and S. C. Khama, *ibid.*, **21,** 409(1969).

(14) J. T. Carstensen and M. Patel, *J. Pharm. Sci.*, **64,** 1770(1975).

(15) W. A. Gray, "The Packing of Solid Particles," Chapman and Hall, Ltd., London, England, 1968, p. 129.

(16) V. G. Levich, "Physicochemical Hydrodynamics," Prentice-Hall, Englewood Cliffs, N.J., 1962, p. 7.
(17) F. Langenbucher, *Pharm. Acta Helv.*, **49**, 187(1974).
(18) M. J. Groves, M. H. Alkan, and M. A. Deer, *J. Pharm. Pharmacol.*, **27**, 400(1975).
(19) S. Ergun, *Chem. Eng. Progr.*, **48**, 227(1952).
(20) J. W. Mullen and T. P. Cook, *J. Appl. Chem.*, **15**, 145(1965).
(21) F. Puisieux and J. T. Carstensen, *Ann. Pharm. Fr.*, in press.

ACKNOWLEDGMENTS AND ADDRESSES

Received August 4, 1975, from the *School of Pharmacy, University of Wisconsin, Madison, WI 53706*
Accepted for publication January 21, 1976.
[x] To whom inquiries should be directed.

Microenvironmental Kinetic Effects within a Lyotropic Smectic Biophase Model: Conformational Restrictions in Fischer Indole Cyclization

HUSSEIN G. IBRAHIM [*] and EDWARD G. RIPPIE [x]

Abstract □ The microenvironmental orientation effects, arising from an ordered solvent structure, were studied in a model liquid crystalline biophase for the cyclization of a series of 2-substituted cyclohexanone phenylhydrazones. The magnitude of such solvent-induced intramolecular conformational constraints was determined from a comparison of the kinetics of the Fischer indole rearrangement in a lyotropic smectic liquid crystal *versus* those in an isotropic liquid of similar chemical composition but lacking the structured nature of the mesophase. Solutions consisting of 50% (w/w) polyoxyethylene 6 tridecyl ether or 44% (w/v) polyethylene glycol in aqueous buffers comprised the smectic or isotropic media, respectively. The apparent dissociation constants of the conjugate acids of the phenylhydrazones were determined kinetically, as were their partition coefficients between lipid and polar isotropic phases approximating the compositions of the smectic lamellae. Intrinsic first-order rate constants, corrected for partitioning within the lamellar mesophase, were used to compute the enthalpies and entropies of activation. The somewhat slower intrinsic rates of cyclization and the accompanying less negative entropies of activation generally observed in the liquid crystalline medium, as opposed to the isotropic system, are attributed to the orienting effects of the lamellar lyotropic mesophase.

Keyphrases □ Cyclohexanone phenylhydrazones, 2-substituted—cyclization reaction kinetics, effect of ordered solvent structure on microenvironmental orientation and intramolecular conformational constraints □ Phenylhydrazones, 2-substituted cyclohexanone—cyclization reaction kinetics, effect of ordered solvent structure on microenvironmental orientation and intramolecular conformational constraints □ Cyclization reaction kinetics—2-substituted cyclohexanone phenylhydrazones, effect of ordered solvent structure □ Solvent structure, ordered—effect on cyclization reaction kinetics of 2-substituted cyclohexanone phenylhydrazones □ Conformational constraints, intramolecular—2-substituted cyclohexanone phenylhydrazones, effect of ordered solvent structure □ Orientation, microenvironmental—2-substituted cyclohexanone phenylhydrazones, effect of ordered solvent structure

Mobile liquid crystalline phases composed of nonrandomly oriented molecules constitute the media for many, if not most, catalytic processes at the cellular level (1–3). In such cases, it is likely that they modify the rates and extent of biochemical reactions and receptor site interactions as well as the processes of active and passive transport. Investigation of the influences of such structured environments on the kinetics and thermodynamics of chemical reactions may explain the nature of their control of the biological processes occurring within them.

BACKGROUND

It is extremely difficult to assess the functions and effects of ordered fluids in a biological system by direct experimentation on living matter. Results from kinetic and thermodynamic solution studies in structured lyotropic solvents, such as the liquid crystals used in this work, can reveal significant information concerning both intra- and intermolecular orientation effects arising solely from the medium structure. Effects of solvent-hindered molecular mobility and the influence of various liquid crystalline structural features on reaction rates also indicate the relative importance of molecular grouping and interaction factors in mesophasic solvent systems and provide a basis for an understanding of the effects of the structured environment on the behavior of drugs in living organisms.

The principal structural feature characteristic of the liquid crystalline state is the parallel arrangement of the component molecules, with rotation primarily being permitted only about the long axis. Because of increasing interest in the mesomorphic states, the characteristic features and properties associated with these systems have been extensively reviewed (4, 5). However, studies of reaction kinetics in such novel solvents are relatively few (6–10).

Since solute species (reactants) dissolved in liquid crystalline media lose freedom of molecular motion to varying degrees due to microenvironmental effects arising from solvent structure, orientation-dependent rearrangement or cyclization reactions can be expected to undergo substantial entropic changes. Also, because of the specific orientations that reactant molecules experience in such ordered fluids, solvent-induced changes in conformation populations can influence significantly any stereospecificity characteristic of the reaction.

Preliminary studies of certain polymerization processes indicated that the molecular order of a nematic solvent often directs the reaction, generally forming isotactic polymers in preference to atactic ones (6). It is also known that molecular diffusion fluxes are functions of molecular orientation as well as the usual driving forces of diffusion. Thus, a reactant molecule dissolved in an ordered fluid experiences anisotropic or directed diffusion, which can significantly affect the kinetics of certain diffusion-controlled reactions.

Fendler and Fendler (11) stressed the importance of studies of chemical reactions in micellar systems because of the recognized analogies between micellar and solvated protein structures and between micellar and enzymatic catalysis. Most of these studies have been conducted in dilute micellar solutions. However, since lyotropic liquid crystals can be regarded as bulk micellar media, they probably would be more representative and better suited for such an analogy.

(16) V. G. Levich, "Physicochemical Hydrodynamics," Prentice-Hall, Englewood Cliffs, N.J., 1962, p. 7.
(17) F. Langenbucher, *Pharm. Acta Helv.*, **49**, 187(1974).
(18) M. J. Groves, M. H. Alkan, and M. A. Deer, *J. Pharm. Pharmacol.*, **27**, 400(1975).
(19) S. Ergun, *Chem. Eng. Progr.*, **48**, 227(1952).
(20) J. W. Mullen and T. P. Cook, *J. Appl. Chem.*, **15**, 145(1965).
(21) F. Puisieux and J. T. Carstensen, *Ann. Pharm. Fr.*, in press.

ACKNOWLEDGMENTS AND ADDRESSES

Received August 4, 1975, from the *School of Pharmacy, University of Wisconsin, Madison, WI 53706*
Accepted for publication January 21, 1976.
[x] To whom inquiries should be directed.

Microenvironmental Kinetic Effects within a Lyotropic Smectic Biophase Model: Conformational Restrictions in Fischer Indole Cyclization

HUSSEIN G. IBRAHIM [*] and EDWARD G. RIPPIE [x]

Abstract □ The microenvironmental orientation effects, arising from an ordered solvent structure, were studied in a model liquid crystalline biophase for the cyclization of a series of 2-substituted cyclohexanone phenylhydrazones. The magnitude of such solvent-induced intramolecular conformational constraints was determined from a comparison of the kinetics of the Fischer indole rearrangement in a lyotropic smectic liquid crystal *versus* those in an isotropic liquid of similar chemical composition but lacking the structured nature of the mesophase. Solutions consisting of 50% (w/w) polyoxyethylene 6 tridecyl ether or 44% (w/v) polyethylene glycol in aqueous buffers comprised the smectic or isotropic media, respectively. The apparent dissociation constants of the conjugate acids of the phenylhydrazones were determined kinetically, as were their partition coefficients between lipid and polar isotropic phases approximating the compositions of the smectic lamellae. Intrinsic first-order rate constants, corrected for partitioning within the lamellar mesophase, were used to compute the enthalpies and entropies of activation. The somewhat slower intrinsic rates of cyclization and the accompanying less negative entropies of activation generally observed in the liquid crystalline medium, as opposed to the isotropic system, are attributed to the orienting effects of the lamellar lyotropic mesophase.

Keyphrases □ Cyclohexanone phenylhydrazones, 2-substituted—cyclization reaction kinetics, effect of ordered solvent structure on microenvironmental orientation and intramolecular conformational constraints □ Phenylhydrazones, 2-substituted cyclohexanone—cyclization reaction kinetics, effect of ordered solvent structure on microenvironmental orientation and intramolecular conformational constraints □ Cyclization reaction kinetics—2-substituted cyclohexanone phenylhydrazones, effect of ordered solvent structure □ Solvent structure, ordered—effect on cyclization reaction kinetics of 2-substituted cyclohexanone phenylhydrazones □ Conformational constraints, intramolecular—2-substituted cyclohexanone phenylhydrazones, effect of ordered solvent structure □ Orientation, microenvironmental—2-substituted cyclohexanone phenylhydrazones, effect of ordered solvent structure

Mobile liquid crystalline phases composed of nonrandomly oriented molecules constitute the media for many, if not most, catalytic processes at the cellular level (1–3). In such cases, it is likely that they modify the rates and extent of biochemical reactions and receptor site interactions as well as the processes of active and passive transport. Investigation of the influences of such structured environments on the kinetics and thermodynamics of chemical reactions may explain the nature of their control of the biological processes occurring within them.

BACKGROUND

It is extremely difficult to assess the functions and effects of ordered fluids in a biological system by direct experimentation on living matter. Results from kinetic and thermodynamic solution studies in structured lyotropic solvents, such as the liquid crystals used in this work, can reveal significant information concerning both intra- and intermolecular orientation effects arising solely from the medium structure. Effects of solvent-hindered molecular mobility and the influence of various liquid crystalline structural features on reaction rates also indicate the relative importance of molecular grouping and interaction factors in mesophasic solvent systems and provide a basis for an understanding of the effects of the structured environment on the behavior of drugs in living organisms.

The principal structural feature characteristic of the liquid crystalline state is the parallel arrangement of the component molecules, with rotation primarily being permitted only about the long axis. Because of increasing interest in the mesomorphic states, the characteristic features and properties associated with these systems have been extensively reviewed (4, 5). However, studies of reaction kinetics in such novel solvents are relatively few (6–10).

Since solute species (reactants) dissolved in liquid crystalline media lose freedom of molecular motion to varying degrees due to microenvironmental effects arising from solvent structure, orientation-dependent rearrangement or cyclization reactions can be expected to undergo substantial entropic changes. Also, because of the specific orientations that reactant molecules experience in such ordered fluids, solvent-induced changes in conformation populations can influence significantly any stereospecificity characteristic of the reaction.

Preliminary studies of certain polymerization processes indicated that the molecular order of a nematic solvent often directs the reaction, generally forming isotactic polymers in preference to atactic ones (6). It is also known that molecular diffusion fluxes are functions of molecular orientation as well as the usual driving forces of diffusion. Thus, a reactant molecule dissolved in an ordered fluid experiences anisotropic or directed diffusion, which can significantly affect the kinetics of certain diffusion-controlled reactions.

Fendler and Fendler (11) stressed the importance of studies of chemical reactions in micellar systems because of the recognized analogies between micellar and solvated protein structures and between micellar and enzymatic catalysis. Most of these studies have been conducted in dilute micellar solutions. However, since lyotropic liquid crystals can be regarded as bulk micellar media, they probably would be more representative and better suited for such an analogy.

The effect of solvent anisotropicity on ester hydrolysis in lyotropic smectic mesophases was studied (7). Also, the hydrolysis of *p*-nitrophenyl laurate was studied in a similar system (8), and a catalytic effect comparable to that of micelles was found. These results gave evidence of changes in the catalytic effect with changes in medium structure. The present investigation is concerned with the effects of such solvent-modified intramolecular mobility on the kinetics of an orientation-sensitive reaction.

The cyclization of a series of 2-substituted cyclohexanone phenylhydrazones was conducted in a lamellar lyotropic liquid crystal composed of 50% (w/w) polyoxyethylene 6 tridecyl ether in aqueous buffer. The neat phase of this system exists over a broad range of surfactant concentration, as shown by the composition–temperature phase diagram (12, 13), and maintains its ordered structure in the presence of relatively high concentrations of added solutes (7). Reaction rates were determined in such a medium and in a medium simulating the chemical environment of the substrate in the liquid crystal but lacking the structured nature of the mesophase. The isotropic medium fulfilling these requirements was provided by a solution of 44% (w/v) polyethylene glycol 400 in aqueous buffer.

EXPERIMENTAL[1]

Materials—Triple-distilled water and reagent grade potassium chloride and hydrochloric acid were used in preparing the buffer solutions. Polyoxyethylene 6 tridecyl ether[2], polyethylene glycol 400[3], phenylhydrazine[4], cyclohexanone[5], 2-methylcyclohexanone[4], 2-*n*-propylcyclohexanone[6], and *n*-heptane[5] were used as received without further purification.

The cyclohexanone phenylhydrazones were prepared by condensing the hydrazine with the corresponding cyclohexanone and were purified by crystallization or separation from aqueous ethanol immediately before use (14). Identity and purity of the compounds were checked by melting or boiling points and UV and IR spectra: cyclohexanone phenylhydrazone (I), $C_{12}H_{16}N_2$, mol. wt. 194, mp 77°; 2-methylcyclohexanone phenylhydrazone (II), $C_{13}H_{18}N_2$, mol. wt. 208, bp 220°/35–40 mm; and 2-*n*-propylcyclohexanone phenylhydrazone (III), $C_{15}H_{22}N_2$, mol. wt. 236.

Medium Preparation—Initial hydrazone concentrations of 2×10^{-3} *M* were used in the various isotropic and anisotropic systems; they were adequate for UV assay and did not disrupt the liquid crystalline phases. Anisotropic reaction mixtures for the kinetic experiments were prepared by adding aqueous solutions, containing the calculated amounts of the hydrazones and buffer ingredients, to previously weighed quantities of surfactant in small, wide-mouth, erlenmeyer flasks.

To ensure the homogeneity of the media, the mixtures were stirred with a glass rod, rapidly heated in a water bath to 70°, and then rapidly cooled with stirring to the desired reaction temperature. Thus, the resultant very viscous liquid crystalline gels contained the required concentration of surfactant and were at the proper pH and ionic strength.

When examined under a polarizing microscope with crossed polars at a magnification of 100×, they showed the characteristics typical of a smectic-type structure. The 50% (w/w) polyoxyethylene 6 tridecyl ether aqueous systems had a smectic–isotropic transition temperature of 69°, in agreement with the previously reported value (7). In the presence of buffer ingredients and the reactant compounds, a lowering of 1° of the transition temperature was noted.

For the preparation of the isotropic reaction media, accurately weighed quantities of polyethylene glycol 400 in volumetric flasks were diluted to volume with aqueous solutions containing the calculated amounts of the hydrazones and buffer ingredients. Clark and Lub's potassium chloride–hydrochloric acid buffers were used to maintain a constant pH (±0.05) in the media. Whenever necessary, the ionic strength was adjusted to 0.08 using potassium chloride.

Analytical and Kinetic Procedures—Reactions in the liquid crystalline gels were followed by means of samples withdrawn at appropriate time intervals and quickly cooled. Approximately 1 g of each sample was accurately weighed in a 10-ml volumetric flask, dissolved and diluted to volume with 95% ethanol, and assayed. For reactions carried out in the isotropic media, 2-ml samples were withdrawn and cooled and a 1-ml aliquot was pipetted into a 10-ml volumetric flask and diluted to volume with 95% ethanol.

Absorbance measurements were taken immediately at 275 nm, using an appropriately treated blank in all instances. All measurements were made in alcoholic solutions because of the cloudiness characteristic of dilute aqueous solutions of the surfactant. In all cases, the flasks containing the reaction mixtures were maintained at constant temperature ±0.05° in thermostated water baths. The temperature dependence of the reaction was determined from the rates of cyclization at three temperatures under conditions of constant pH and ionic strength. Duplicate runs were made for each kinetic experiment.

Partition Studies—Partitioning of the hydrazones between the polar and hydrocarbon regions of the lamellar liquid crystals was simulated by studying the distribution of the reactants between 44% (w/v) polyethylene glycol in an aqueous buffer and *n*-heptane. The immiscible solvents were first equilibrated by shaking together for 3 hr at the desired temperature. The mixture was allowed to stand for 24 hr to permit complete separation. Equal volumes of the equilibrated solvents containing the calculated amount of the reactants were placed in an erlenmeyer flask and shaken in a constant-temperature water bath.

The reaction in the two-phase system was followed kinetically by withdrawing an aliquot of the aqueous phase and simultaneously removing and discarding an equal volume of the *n*-heptane, so that the ratio between the volumes of the phases remained constant. Duplicate runs were made for each experiment, and the samples were assayed in the normal manner.

NMR and UV Studies—Comparisons of the NMR shifts, as well as the band shapes and peak positions in the UV spectrum, of a solubilizate in a micellar system to those in polar and nonpolar solvents have been used to furnish information on the nature of the environment of the solubilizate (15–20). In the current investigation, the recorded spectra of the reactant compounds in the liquid crystalline solvent were compared with those in *n*-heptane, aqueous buffer, and a series of aqueous polyethylene glycol 400 solutions of various concentration to obtain information concerning the location of the reactant species within the lamellar mesophase.

The NMR spectra were recorded at room temperature, with tetramethylsilane as the external standard. In preparing the liquid crystalline system for the study, a syringe was used to introduce the viscous gel into the NMR tube or the Beckman cell (7). Except for *n*-heptane, all media were buffered to pH 1.0 and adjusted to an ionic strength of 0.08. For the UV study, spectra were recorded between wavelengths of 210 and 350 nm at room temperature, using appropriate blanks in all instances.

RESULTS AND DISCUSSION

Fischer Indole Reaction Kinetics—Aside from its general importance and wide scope of application, the Fischer indole synthesis, involving the intramolecular cyclization of the arylhydrazones of aldehydes or ketones, is known to involve a substantial entropy change during ring closure and can be expected to be sensitive to an ordered microenvironment. The reaction mechanism (Scheme I), as originally proposed by Robinson and Robinson in 1918, has been subsequently well supported by experimental observations (21).

While it has been reported that the phenylhydrazones of 2-substituted cylohexanones may yield both a tetrahydrocarbazolenine and the expected indole, the latter product is strongly favored in the presence of mineral acids such as were used in the present study. The concentration of the reactive protonated form of the enehydrazine depends upon the pH of the medium, so the rate of cyclization is a function of the hydrogen-ion concentration. Cyclohexanone phenylhydrazone and its 2-methyl and 2-*n*-propyl derivatives, I, II, and III, respectively, were selected for this study.

The determination of liquid crystal medium effects necessitates the adjustment of the kinetic rate constants to account for both the degree of protonation and the extent of partitioning of the reactant within the smectic phase itself. These calculated intrinsic first-order

[1] UV absorption readings were taken with a Hitachi Perkin-Elmer 139 visible-UV spectrophotometer and a Cary 14 recording spectrophotometer. NMR measurements were made with Varian A-60D and XL-100 NMR spectrometers. A Bausch and Lomb polarizing microscope fitted with a Kofler hot stage was used to determine phase transition temperatures.

[2] Renex 36, Atlas Chemical Industries, Wilmington, Del.

[3] Ruger Chemical Co., Irvington, N.Y.

[4] Aldrich Chemical Co., Milwaukee, Wis.

[5] Mallinckrodt Chemical Works, St. Louis, Mo.

[6] Pfaltz and Bauer, Flushing, N.Y.

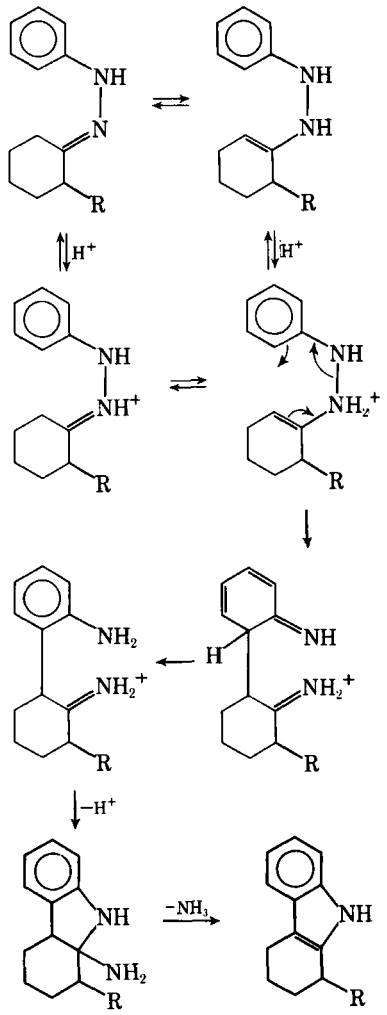

Scheme I

rate constants thus correspond to the reaction of the protonated enehydrazine within the polar polyoxyethylene aqueous lamellae. The data required for making these necessary rate constant adjustments were obtained in isotropic systems, and the procedures and calculations involved are discussed subsequently.

The measured pseudo-first-order rate constants of cyclization, both in the isotropic and anisotropic media, were determined by monitoring the disappearance of the reactants spectrophotometrically at 275 nm with subsequent treatment of data by the Guggenheim (22) method. For simplicity, they will be referred to subsequently as observed, k_{obs}, and apparent, k_{app}, rate constants. Equation 1 was used for these calculations:

$$\ln(A_t - A_{t+\tau}) = -kt + C \qquad \text{(Eq. 1)}$$

where A_t and $A_{t+\tau}$ represent the absorbance at time t and $t + \tau$, respectively, where τ is an appropriate constant time interval. This method of data handling was chosen to avoid the necessity of knowing with accuracy the initial and final concentrations of the reactants. Also, interference from other species in the various media could be avoided by this technique.

The slopes of plots corresponding to Eq. 1 were calculated by the method of least squares and are reported, together with their estimated standard deviations, in Table I.

Apparent Acid Dissociation Constants and Intrinsic First-Order Rate Constants in Isotropic Media—The apparent dissociation constants of the conjugate acids of I–III were determined kinetically from the pH dependency of the measured pseudo-first-order rate constants of cyclization. The study was conducted in the isotropic solvent at various hydrogen-ion concentrations and under conditions of constant temperature and ionic strength. The functional relationship between the hydrogen-ion concentration and the observed rate constants, k_{obs}, as derived in *Appendix I*, can be represented by:

$$\frac{1}{k_{obs}} = \frac{1}{k^*} + \frac{K_a}{k^*[H^+]} \qquad \text{(Eq. 2)}$$

Graphs of $1/k_{obs}$ *versus* $1/[H^+]$ yield linear plots such as that shown in Fig. 1, with slopes equal to K_a/k^* and intercepts of $1/k^*$, where K_a and k^* are the apparent acid dissociation constants and intrinsic first-order rate constants, respectively. Data from these measurements and calculations are presented in Tables I and II, together with the estimated standard deviations of the dissociation constants and their corresponding correlation coefficients. For reasons discussed later, no attempt was made to account for the temperature dependency of K_a in computing intrinsic first-order rate constants.

Kinetic Determination of Intrinsic Partition Coefficients—As previously indicated, the lyotropic smectic solvent used has a structure characterized by lamellae of alternating hydrocarbon and polyoxyethylene–water composition. Since, in the reaction under investigation, only the protonated form of the reactant can cyclize at a measurable rate and its concentration in the hydrocarbon lamellae is expected to be negligible, it is reasonable to assume that the cyclization reaction occurs solely in the polyoxyethylene–water regions of the liquid crystal.

Table I—Pseudo and Intrinsic First-Order Rate Constants[a] of Cyclization of 2-Substituted Cyclohexanone Phenylhydrazones

Medium	pH	Temperature	k_{obs} or k_{app} × 10^3, min^{-1}	k^* × 10^3, min^{-1}
Cyclohexanone Phenylhydrazone				
Aqueous polyethylene glycol	1.0	35.0°	5.38 ± 0.21	7.2
	1.0	40.0°	7.26 ± 0.42	9.7
	1.0	49.5°	14.54 ± 0.48	20.5
	1.4	49.5°	12.31 ± 0.39	20.5
	1.8	49.5°	6.77 ± 0.14	20.5
	2.0	49.5°	4.63 ± 0.11	20.5
	2.2	49.5°	3.43 ± 0.11	20.5
Liquid crystal	1.0	40.0°	1.57 ± 0.11	2.2
	1.0	49.5°	3.57 ± 0.10	5.1
	1.0	60.0°	8.80 ± 0.24	12.5
Biphase	1.0	49.5°	12.68 ± 0.53	
2-Methylcyclohexanone Phenylhydrazone				
Aqueous polyethylene glycol	1.0	35.0°	7.67 ± 0.45	10.4
	1.0	40.0°	9.38 ± 0.97	12.7
	1.0	49.5°	15.36 ± 0.91	22.3
	1.8	49.5°	7.56 ± 0.14	22.3
	2.2	49.5°	3.55 ± 0.08	22.3
Liquid crystal	1.0	40.0°	3.06 ± 0.11	5.1
	1.0	49.5°	5.48 ± 0.21	9.2
	1.0	60.0°	11.20 ± 0.90	18.8
Biphase	1.0	49.5°	8.98 ± 0.77	
2-*n*-Propylcyclohexanone Phenylhydrazone				
Aqueous polyethylene glycol	1.0	35.0°	5.84 ± 0.45	8.4
	1.0	40.0°	8.08 ± 0.24	11.5
	1.0	49.5°	16.67 ± 0.65	29.3
	1.8	49.5°	9.55 ± 0.11	29.3
	2.2	49.5°	3.86 ± 0.06	29.3
Liquid crystal	1.0	40.0°	2.18 ± 0.09	6.1
	1.0	49.5°	5.71 ± 0.07	15.9
	1.0	60.0°	14.23 ± 0.92	39.6
Biphase	1.0	49.5°	4.74 ± 0.76	

[a] The ± indicates 1 estimated standard deviation.

Table II—Apparent Conjugate Acid Dissociation Constants[a]

Compound	K_a × 10^2, M	r
I	3.40 ± 0.13	0.997
II	3.51 ± 0.17	0.999
III	4.30 ± 0.65	0.990

[a] The ± indicates 1 estimated standard deviation. All measurements were made at 49.5°.

Table III—Intrinsic Partition Coefficients[a] in Biphase Systems

Compound	K_p*[b]
I	0.81 ± 0.03
II	3.23 ± 0.22
III	11.05 ± 1.72

[a] The ± indicates 1 estimated standard deviation. [b] Determined in systems of *n*-heptane–44% (w/v) polyethylene glycol–aqueous buffer at 49.5°, pH 1.0, and ionic strength of 0.08.

Because of the reactivity of the phenylhydrazones under the conditions of interest, partition coefficients cannot be determined directly but were calculated from kinetic data gathered in two-phase systems. Data were obtained from *n*-heptane–aqueous polyethylene glycol systems under the same conditions of temperature, pH, and ionic strength as those used in determining the rates of reaction in the liquid crystals. All determinations were made in duplicate on systems containing initial overall hydrazone concentrations of $2 \times 10^{-3} M$.

Semilog plots of residual hydrazone concentration *versus* time exhibited linear correlation coefficients in excess of 0.99. The relationship between the intrinsic partition coefficients, K_p*, and the observed first-order rate constants, k_{obs}, as determined in these biphase systems is derived in *Appendix II* and represented by:

$$K_p^* = \frac{1}{r}\left(\frac{k^*[H^+]}{k_{obs}K_a} - 1 - \frac{[H^+]}{K_a}\right) \qquad \text{(Eq. 3)}$$

The intrinsic partition coefficients reported in Table III were calculated by substituting the experimentally measured values of k_{obs}, together with the previously determined values of K_a and k*, into Eq. 3. The ratio, r, of the hexane volume to that of aqueous polyethylene glycol was held at unity by withdrawing equal volumes of both phases when obtaining samples for assay.

NMR and UV Spectral Evidence of Solute Environment—Fendler and Fendler (11) and Winsor (15) observed that comparisons of the NMR shifts of solubilizates in micellar systems with those in polar and nonpolar solvents can be used to provide information on the nature of the environment of the solubilizate. In the current investigation, the recorded spectra of the phenylhydrazones in the media employed for the kinetic studies were used to furnish evidence concerning the location of the reactant species in the mesophase. Line positions of the aromatic protons of I–III in *n*-heptane, liquid crystals, aqueous polyethylene glycol, and aqueous buffer are listed in Table IV. If small allowances are made for differences in bulk susceptibility, comparisons are readily made between phases.

Spectra in the liquid crystal solvent resembled those in the isotropic solvents, except for an expected line broadening (23) due to decreased thermal mobility. In the present study, both the high microviscosity and the hindered rotational mobility experienced by solubilizates in the lamellar structure contributed to the observed line broadening. The strong shifts accompanying the change of solvent from *n*-heptane to the polar media can be attributed to field effects resulting from these media.

The correspondence of the line positions of I and II in the liquid crystal to those in aqueous polyethylene glycol indicates that the microenvironment of these compounds lies within the palisade-like polyoxyethylene layers of the mesophase. In contrast, III showed a line position intermediate to those in *n*-heptane and aqueous polyethylene glycol. Thus, its immediate environment is not purely hydrocarbon nor typically polar but is within the transition regions of lamellae and predominantly in the polar layers.

Table IV—NMR Line Positions[a] of Aromatic Protons of the Phenylhydrazones in Several Media, Isotropic and Anisotropic

Compound	*n*-Heptane	Liquid Crystal	Aqueous Polyethylene Glycol	Aqueous Buffer
I	366	309	309	310
II	398	345	345	348
III	400	333	310	310

[a] Line positions are in hertz relative to tetramethylsilane as the external standard. All measurements in the aqueous systems were made at pH 1.0.

Table V—UV Absorption Wavelength Maxima of the Phenylhydrazones in Several Media, Isotropic and Anisotropic

Medium[a]	Compound I, λ_{max}, nm	Compound II, λ_{max}, nm	Compound III, λ_{max}, nm
Liquid crystal[b]	276	270	260
n-Heptane	268	269	268
Buffer[b]	280	273	285
Polyethylene[b] glycol:			
30% (w/v)	277	274	278
44% (w/v)	276	274	276
50% (w/v)	278	276	276

[a] The temperature was held at 23° for all measurements. [b] Spectra were recorded at pH 1.0.

No NMR spectral differences were found between spectra of the pure liquid crystal and of the liquid crystal containing dissolved reactants. This finding can be attributed to the low concentrations of reactants used and to the marked stability and tolerance of the lyotropic lamellar neat phase both to water content and to added third components (24).

UV spectra are sensitive to solute characteristics (19, 20, 25, 26). Table V shows UV absorption spectra maxima of the three hydrazones in several media. The effects observed in the present studies are consistent with the expected behavior based on dielectric and hydrogen bonding properties of the media (27, 28).

Compound I exhibited the same λ_{max} in both 44% (w/v) aqueous polyethylene glycol and the liquid crystal. This fact, together with the NMR data, indicates the existence of the compound within the palisade layer of the lamellar structure.

Compound III exhibited a λ_{max} in the liquid crystal below that in *n*-heptane. A similar effect due to steric crowding was reported to cause comparable line shifts of stilbene and azobenzene (29). An increased energy for the $n \rightarrow \pi$ transition, with a resultant shorter absorption wavelength, is consistent with the existence of the compound in a strained configuration close to the plane of separation of the hydrocarbon and polar layers. This interpretation is in agreement with that reached from NMR results.

The spectrum of II can be readily explained on the basis of the behavior of the other hydrazones. The lesser steric crowding effect for the methyl derivative accounts for the similarity of λ_{max} in the liquid crystal and *n*-heptane. Since the hydrophobic character of II is between those of I and III, it is reasonable to expect it to locate within the polyoxyethylene layers in a region intermediate to those proposed for the other compounds.

Intrinsic First-Order Rate Constants in Anisotropic Media—The apparent first-order rate constants of cyclization in the liquid crystal system were adjusted for partitioning between polar and hydrocarbon layers and for dissociation of the conjugate acids. The resultant intrinsic rate constants, k*, were calculated from a rearranged form of Eq. 3:

$$k^* = \frac{k_{app}K_a}{[H^+]}\left(1 + \frac{[H^+]}{K_a} + rK_p^*\right) \qquad \text{(Eq. 4)}$$

The experimental values of K_a and K_p*, as determined previously, and k_{app} were substituted into Eq. 4 to give the corresponding values of k* presented in Table I.

Kinetic Activation Parameters—The enthalpies, $\Delta H^{\pm}$, and entropies, $\Delta S^{\pm}$, of activation (Table VI) were calculated from the Eyring equation using the calculated intrinsic first-order rate constants of cyclization. The primary significance of these data resides in the differences that can be observed between the kinetic activation parameters in the liquid crystalline media and the corresponding isotropic media. For this reason, no attempt was made to account for the relatively small contributions to $\Delta H^{\pm}$ and $\Delta S^{\pm}$ arising from the temperature dependence of the intrinsic partition coefficients and the apparent conjugate acid dissociation constants.

Plots of pKa for the dissociation of most weak electrolytes pass

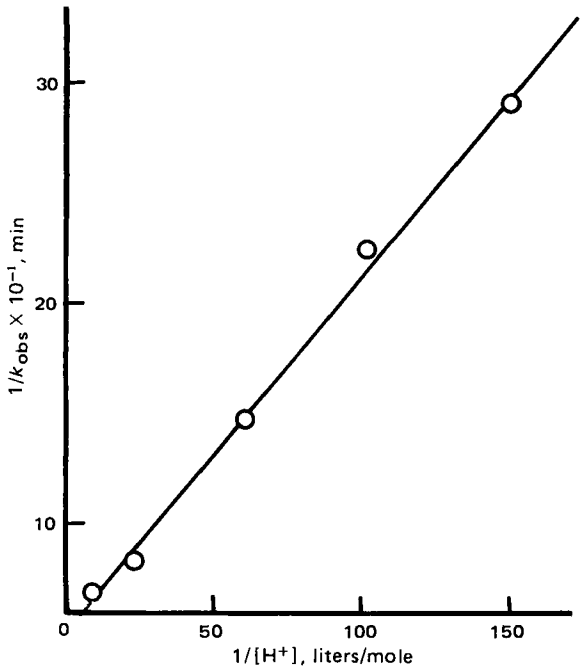

Figure 1—*Double reciprocal plot of* $[H^+]$ versus k_{obs} *for I at 49.5°.*

through a minimum in the 0–60° range (30). Consequently, the absolute value of the observed change is expected to be small; in the present study, it was zero within experimental error. Furthermore, no statistically significant change in K_p* with temperature could be found.

Similar trends in $\Delta H^{\ddagger}$ were evident in both isotropic and anisotropic media, although values of $\Delta H^{\ddagger}$ were generally higher in the latter solvent. Cyclization involves simultaneous nitrogen–nitrogen bond cleavage and carbon–carbon bond formation at the rate-determining step. In accordance with the accepted mechanism, carbon–carbon bond formation results from partial charges on the α-carbon atoms in the cyclohexane and benzene rings. The activation enthalpy would thus be expected to increase with an increase in the average distance separating the two partially charged centers. The experimentally observed increase in $\Delta H^{\ddagger}$ in the liquid crystal systems can likely be related, therefore, to solvent-restricted molecular bending.

Relatively large negative entropies of activation were found in both solvent systems. However, less negative values were observed in the anisotropic solvent, suggesting that the reactants in this system are less randomly disposed since their corresponding activated complexes are not likely to change significantly with solvent.

The combined effects of $\Delta H^{\ddagger}$ and $\Delta S^{\ddagger}$ were manifested in the reaction in such a manner that the reaction rates were only moderately lower in the ordered system as opposed to the structureless isotropic liquid. The existence of a linear relationship between $\Delta H^{\ddagger}$ and $\Delta S^{\ddagger}$ was seen in both solvent systems. This latter behavior is well known as the thermodynamic compensation law or more commonly as the

Table VI—Kinetic Activation Parameters of Cyclization[a]

Compound	$\Delta H^{\ddagger}$, kcal/mole	$\Delta S^{\ddagger}$, cal/deg mole
	44% (w/v) Aqueous Polyethylene Glycol	
I	13.8 ± 1.1	−31.9 ± 3.5
II	10.0 ± 1.1	−43.5 ± 3.5
III	16.8 ± 1.9	−21.9 ± 6.0
	Lyotropic Liquid Crystal	
I	17.3 ± 0.3	−23.6 ± 1.0
II	12.9 ± 0.7	−36.2 ± 2.1
III	18.9 ± 0.5	−16.6 ± 1.5

[a] The ± indicates 1 estimated standard deviation. The pH was held at 1.0 and the ionic strength at 0.08 in all measurements.

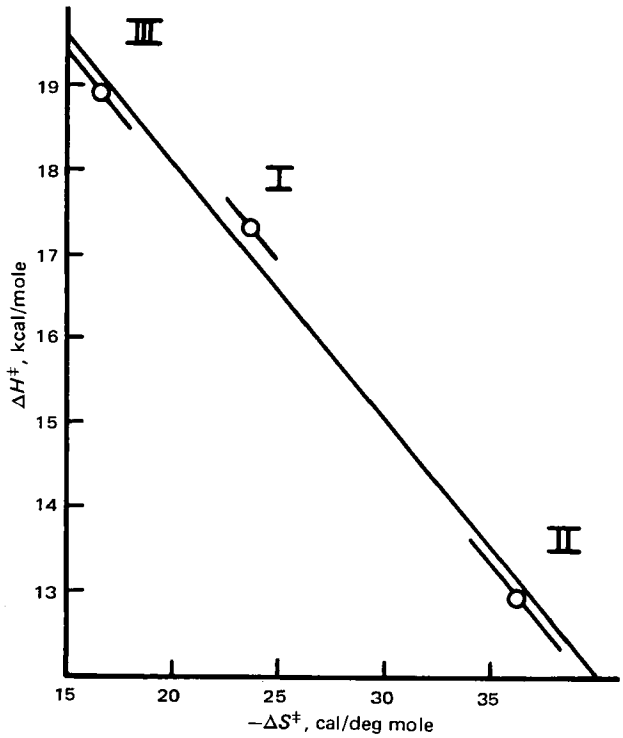

Figure 2—*Entropy–enthalpy correlation for cyclization of 2-substituted cyclohexanone phenylhydrazones in the lyotropic liquid crystalline phase. Points correspond to Compounds I, II, and III.*

isokinetic relationship (31). It takes the form:

$$\Delta H^{\ddagger} = \alpha + \beta \Delta S^{\ddagger} \qquad \text{(Eq. 5)}$$

where α is a constant, and β corresponds to the isokinetic temperature of the reaction. At this temperature, the measured rate constants for a series of structurally related compounds undergoing a well-defined chemical reaction will be the same irrespective of the effects arising from the structural changes. Since such an apparent relationship can result from experimental error in measuring the temperature coefficient of reaction, care must be exercised in its interpretation.

Leffler (32) outlined the criteria that must be satisfied before a valid isokinetic relationship can be claimed to exist. Only those data obtained in the liquid crystal meet these requirements and are illustrated in Fig. 2 as a plot of $\Delta H^{\ddagger}$ *versus* $\Delta S^{\ddagger}$. Slopes equal to 312 and 315 in the anisotropic and isotropic media, respectively, with correlation coefficients greater than 0.99 were found; however, the precision of measurement was insufficient to support strongly isokinetic behavior in the latter case.

SUMMARY AND CONCLUSIONS

The lyotropic smectic liquid crystalline medium provided by an aqueous solution of polyoxyethylene 6 tridecyl ether was found to possess sufficient thermal, chemical, and compositional stability to serve as a useful structured biophase model. While this medium is not chemically similar to a proteinaceous liquid crystal, its ability to orient and hinder the rotation and bending of solutes within it may be presumed to be comparable. The Fischer indole synthesis is sensitive to such a medium, and similar kinetic manifestations of liquid crystalline structure can be expected of biochemical processes. The fact that an increasing number and variety of tissues, including muscles, tendons, nerve fibers, erythrocytes, ovaries, and bone, have been shown to contain a wide variety of liquid crystalline media serves to underline their importance in living matter.

APPENDIX I

For a first-order reaction in which only the conjugate acid, BH^+, of a weak base, B, is able to react, the rate is given by:

$$d[B]_T/dt = -k^*[BH^+] \qquad \text{(Eq. A1)}$$

where $[B]_T$ is the stoichiometric concentration of the base, and k^* is the intrinsic first-order rate constant. The concentration of conjugate acid is given by:

$$[BH^+] = \left(\frac{[H^+]}{K_a + [H^+]}\right)[B]_T \qquad \text{(Eq. A2)}$$

where K_a is the apparent dissociation constant of the conjugate acid. By combining Eqs. A1 and A2, the rate equation takes the form:

$$\frac{d[B]_T}{dt} = -k^* \left(\frac{[H^+]}{K_a + [H^+]}\right)[B]_T \qquad \text{(Eq. A3)}$$

However, the expression $k^*[H^+]/(K_a + [H^+])$ is defined as the observed pseudo-first-order rate constant, k_{obs}, and can be rearranged to give the linear form in Eq. 2.

APPENDIX II

In a biphase system, the hydrazone compounds used in this study distribute between the hydrocarbon phase and the aqueous polyethylene glycol phase in a manner such that the total quantity of the compound, Q, will be given by:

$$Q = [B]_w V_w + [B]_o V_o + [BH^+]_w V_w \qquad \text{(Eq. A4)}$$

where the subscripts w and o denote aqueous and hydrocarbon phases, respectively; and V denotes volume. Equation A4 can be expressed in terms of K_a and $[H^+]$ in the form:

$$Q = [BH^+]_w V_w \left(1 + \frac{K_a}{[H^+]} + \frac{K_a[B]_o V_o}{[H^+][B]_w V_w}\right) \qquad \text{(Eq. A5)}$$

By setting $r = V_o/V_w$ and $K_p^* = [B]_o/[B]_w$, Eq. A5 can be written as:

$$Q = \frac{[BH^+]_w K_a V_w}{[H^+]} \left(1 + \frac{[H^+]}{K_a} + rK_p^*\right) \qquad \text{(Eq. A6)}$$

where r is the phase volume ratio and K_p^* is the intrinsic partition coefficient. The overall mass rate equation:

$$dQ/dt = -k_{obs}Q = -k^*[BH^+]_w V_w \qquad \text{(Eq. A7)}$$

can be combined with Eq. A6, rearranged in the form of Eq. 3, and used to calculate K_p^*.

REFERENCES

(1) J. D. Bernal, *Trans. Faraday Soc.*, **29,** 1082(1933).

(2) D. B. DuPré, E. T. Samulski, and A. V. Tobolsky, "Polymer Sciences and Materials," Wiley, New York, N.Y., 1971.

(3) C. L. Khetrapal, "Lyotropic Liquid Crystals," Springer-Verlag, New York, N.Y., 1975.

(4) G. Gray, "Molecular Structure and the Properties of Liquid Crystals," Academic, New York, N.Y., 1962.

(5) G. H. Brown, J. W. Doan, and V. D. Neff, "A Review of the Structure and Physical Properties of Liquid Crystals," CRC Press, Cleveland, Ohio, 1971.

(6) G. H. Brown, *Am. Sci.*, **60,** 64(1972).

(7) E. G. Rippie and K. S. Murthy, *J. Pharm. Sci.*, **59,** 459(1970).

(8) S. I. Ahmad and S. Friberg, *J. Am. Chem. Soc.*, **94,** 5196(1972).

(9) W. E. Bacon and G. H. Brown, *Mol. Cryst. Liq. Cryst.*, **6,** 155 (1969).

(10) *Ibid.*, **12,** 229(1971).

(11) E. J. Fendler and J. H. Fendler, *Adv. Phys. Org. Chem.*, **8,** 271(1970).

(12) K. S. Murthy, Ph.D. thesis, University of Minnesota, Minneapolis, Minn., 1968.

(13) A. R. Morad, Ph.D. thesis, University of Minnesota, Minneapolis, Minn., 1973.

(14) K. H. Pausacker and C. I. Schubert, *J. Chem. Soc.*, **1950,** 1814.

(15) P. A. Winsor, *Chem. Rev.*, **68,** 1(1968).

(16) J. C. Eriksson and G. Gilberg, *Surf. Chem.*, **1965,** 148.

(17) J. C. Eriksson and G. Gilberg, *Acta Chem. Scand.*, **20,** 2019(1966).

(18) J. C. Eriksson, *ibid.*, **17,** 1478(1963).

(19) S. Riegelman, N. A. Allawalla, M. K. Hrenoff, and L. A. Strait, *J. Colloid Sci.*, **13,** 208(1958).

(20) S. J. Rehfeld, *J. Phys. Chem.*, **74,** 117(1970).

(21) B. Rolinson, *Chem. Rev.*, **63,** 373(1963).

(22) E. A. Guggenheim, *Phil. Mag.*, **2,** 538(1926).

(23) L. M. Jackman, "Application of Nuclear Magnetic Resonance Spectroscopy in Organic Chemistry," Pergamon Press, London, England, 1959.

(24) P. Ekwall, L. Mandell, and K. Fontell, *Acta Chem. Scand.*, **22,** 1543(1968).

(25) C. F. Hisky and T. A. Downey, *J. Phys. Chem.*, **58,** 853(1954).

(26) B. A. Mully and A. D. Metcalf, *J. Pharm. Pharmacol.*, **8,** 774(1956).

(27) L. G. S. Brooker and R. H. Sprague, *J. Chem. Soc.*, **63,** 3214(1941).

(28) S. Nagakura, *J. Am. Chem. Soc.*, **76,** 3070(1954).

(29) H. H. Jaffé and M. Orchin, *J. Chem. Soc.*, **1960,** 1078.

(30) R. G. Bates, "Determination of pH; Theory and Practice," Wiley, New York, N.Y., 1964, p. 114.

(31) L. P. Hammett, "Physical Organic Chemistry," 2nd ed., McGraw-Hill, New York, N.Y., 1970, pp. 397–401.

(32) J. E. Leffler, *J. Org. Chem.*, **20,** 1202(1955).

ACKNOWLEDGMENTS AND ADDRESSES

Received November 12, 1975, from the *Department of Pharmaceutics, College of Pharmacy, University of Minnesota, Minneapolis, MN 55455*

Accepted for publication February 4, 1976.

* Present address: Pharmacy Research and Development, Pharmaceuticals Division, Ciba-Geigy Corp., Suffern, NY 10901

x To whom inquiries should be directed.

Correlation of Dielectric Constant and Solubilizing Properties of Tetramethyldicarboxamides

T. REBAGAY and P. DeLUCA ˣ

Abstract □ The dielectric constants of aqueous solutions of four tetramethyldicarboxamides (tetramethylpimelamide, tetramethylsuberamide, tetramethylazelamide, and tetramethylsebacamide) were measured at 25°. The values obtained were utilized in assessing the solubility behavior patterns of glutethimide, a semipolar, water-insoluble drug in these amide–water systems. At equimolar concentrations of water-rich amide solutions, the solubilizing power paralleled the chain length of the amides. The higher homologs appeared to favor more extensive solvation, as shown by the lower dielectric constants of their resulting solutions. Deviation in solubilizing action between the odd-carbon amides and the even-carbon amides, however, was exhibited at higher amide concentrations. The two odd-carbon amides, tetramethylpimelamide and tetramethylazelamide, showed consistently greater solubilizing action. This phenomenon was attributed to the greater association tendencies of the odd-carbon amides with water, which effectively reduced self-associations of glutethimide.

Keyphrases □ Dielectric constants—aqueous solutions of various tetramethyldicarboxamides, correlated with solubilizing properties □ Solubilizing properties—aqueous solutions of various tetramethyldicarboxamides, correlated with dielectric constants □ Tetramethyldicarboxamides—aqueous solutions, dielectric constants correlated with solubilizing properties □ Glutethimide—solubility assessed using dielectric constants of aqueous solutions of various tetramethyldicarboxamides

Substituted carboxamides exhibit potential as solubilizing agents for hydrophobic molecules (1). The solvent properties of amides are attributed in part to the strong dipole of the amide function and to the good electron-donating properties of the carbonyl group. Recent studies on a series of tetramethyl-substituted dicarboxamides possessing Structure I (n = 5–8) revealed that these amides show strong association tendencies in very dilute solutions and suggested that further aggregation of associated amide molecules leads to micellization (2).

A stronger amide–water interaction has been suggested for the odd-carbon amides of the homologous series, tetramethylpimelamide and tetramethylazelamide, using partial molal volume and viscosity behavior patterns (3). A minimum in the partial molal volume and a maximum in viscosity were observed at definite integral mole fractions for the odd-carbon homologs. Such behavior was not observed for the even-carbon amides, tetramethylsuberamide and tetramethylsebacamide. The stronger amide–water association for the odd-carbon amides could lead to greater disruption of the structure of the surrounding water molecules.

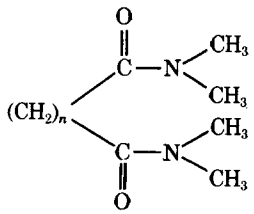

I

The extent of water structure disruption can be reflected in the dielectric constant of the resulting solution. The change in dielectric constant may then be used as a measure of the degree of interaction of a particular amide with water. In general, such interactions could lead to the formation of ordered molecular aggregates of varying sizes that are made up of statistically preferred arrangements of different molecular species, either as hydrates or complexes (4).

The enhanced solubility of various substances as a function of dielectric constants has been reported (5–8). It is believed that solubility can be correlated with the dielectric constant when the solvent or solvent mixture exhibits similar bonding characteristics as the substance of interest. Correlation also can be obtained by using compounds belonging to the same homologous series, either alone or in combination as solvent blends (9).

To gain further knowledge of the tetramethyldicarboxamides as solubilizing agents for poorly soluble drugs, the dielectric constants of aqueous solutions of these amides were measured. The values obtained were then utilized in assessing the solubility behavior patterns of glutethimide, a semipolar, water-insoluble drug. Since the amides differ only in the number of methylene units in the hydrocarbon chain, the effect of chain length on the dielectric solubility profile of glutethimide was assessed.

EXPERIMENTAL

Materials—The tetramethyl-substituted dicarboxamides were prepared according to a previously reported procedure (2). The purity of the amides was determined by vapor phase chromatography, and the conductivity of aqueous amide solutions was checked by the method described previously (10).

Apparatus for Capacitance Measurements—An impedance bridge assembly[1] was used in conjunction with two-terminal parallel plate cells for capacitance measurements at 1 MHz. Similar cells with platinum electrodes are structurally satisfactory[2] and convenient for measuring low conducting liquids (11, 12). The ends of the external leads to the cell electrodes were fitted with special adapters so that the cell, which was suspended in an oil bath during measurements, could be easily attached to the bridge by a shielded coaxial cable having a dual banana plug connection at each end.

The principal aspects for determining the cell constants and for calculating dielectric constants were described previously (13, 14). The standard media used in the determination of cell constants were air and water, which have dielectric constants of 1.0005 and 78.304 (15), respectively, at 25°.

The temperature for the dielectric constant determinations was controlled to within ±0.05° using a constant-temperature bath[3] filled with light paraffin oil. Readings from the bath thermometer, with 0.1° subdivisions, were compared with those from an NBS-calibrated thermometer; appropriate corrections were applied.

[1] Twin-T, General Radio Co., Cambridge, Mass.

[2] Measurements of the dielectric constant of water were made at 5° intervals in the 25–55° range to check the calibrations of the cells and the experimental procedure in general. No variations in the cell constants were observed, indicating that the cell configuration remained constant.

[3] Model H-1, Cannon Instrument Co., State College, Pa.

Table I—Dielectric Constants of Tetramethyldicarboxamides–Water Systems in Relation to Solubility of Glutethimide

Substituted Amide				Glutethimide	
Molarity	Weight Percent	Mole Fraction × 100	Dielectric Constant	Solubility, $M \times 10^3$	Relative Solubility, S/S_0
		Tetramethylpimelamide			
0.0			78.3	4.60	1.00
0.04	1.71	0.146	78.0	5.20	1.13
0.10	2.95	0.255	77.8	6.06	1.32
0.25	6.04	0.537	77.2	8.23	1.79
0.4	9.14	0.838	76.6	11.3	2.46
1.0	21.51	2.25	73.6	29.1	6.33
2.0	42.13	5.76	66.9	103.4	22.5
2.8	58.63	10.64	60.1	318.	69.1
3.0	62.75	12.40	58.2	399.	86.7
3.9	81.31	26.76	48.5[a]	1343.	292.0
4.76	100.00	100.	37.6		
		Tetramethylsuberamide			
0.0	0.0	0	78.3	4.6	1.00
0.04	1.04	0.083	78.0	4.6	1.00
0.10	2.38	0.192	77.6	4.6	1.00
0.25	5.73	0.477	76.4	4.7	1.02
0.40	9.08	0.781	75.1	11.9	2.59
0.50	11.31	0.995	74.3	16.6	3.61
1.00	22.48	2.24	69.8[a]	34.5	7.5
2.00	44.80	6.01	59.7[a]	138.0	30.0
2.40	53.73	8.39	55.2[a]	330.0	71.7
		Tetramethylazelamide			
0.0	0.0	0	78.3	4.60	1.00
0.04	0.99	0.074	78.1	4.85	1.05
0.10	2.43	0.185	77.6	5.70	1.24
0.25	6.03	0.474	76.4	7.5	1.63
0.5	12.04	1.006	74.4	18.0	3.91
1.00	24.05	2.30	70.1	39.5	8.59
2.00	48.08	6.44	60.3	230	50.0
3.00	72.10	16.10	49.2	700	152
3.90	93.72	52.57	38.0[a]	1472	320
		Tetramethylsebacamide			
0.0	0.0	0	78.3	4.60	1.00
0.04	1.03	0.073	77.9	4.60	1.00
0.10	2.57	0.185	77.5	4.60	1.00
0.25	6.42	0.486	76.1	8.56	1.86
0.40	10.16	0.788	74.7	17.6	3.83
0.50	12.82	1.022	73.8[a]	22.2	4.83

[a] Value calculated from Eq. 1.

Dielectric Constant Determination—All amide–water solutions were prepared on a weight basis, with the necessary weight in vacuum corrections applied[4]. The cells were cleaned with distilled conductivity water and rinsed with acetone. They were then blown dry with air before they were filled with the test solutions. The cells were placed in the constant-temperature bath and allowed to equilibrate for at least 15 min.

RESULTS AND DISCUSSION

The dielectric constant data for the amide–water systems are given in Table I. Plotting the solution dielectric constant *versus* concentration for the amides resulted in a linear relationship only at dilute concentrations (Fig. 1). At concentrations greater than 20% amide, a curvature was produced. The curvature may be assumed arbitrarily as due to molecular associations resulting in the formation of molecular aggregates. Molecular association with water is likely to occur with the two unshared pairs of electrons on the carbonyl oxygen or on the sterically more obstructed lone pair of electrons on the dimethyl-substituted nitrogen on each end of the amide molecule. This assumption is supported by light-scattering studies on these amides, which showed a rapid increase in the number of aggregates with increasing concentration, resembling the behavior of high polymer solutions (2).

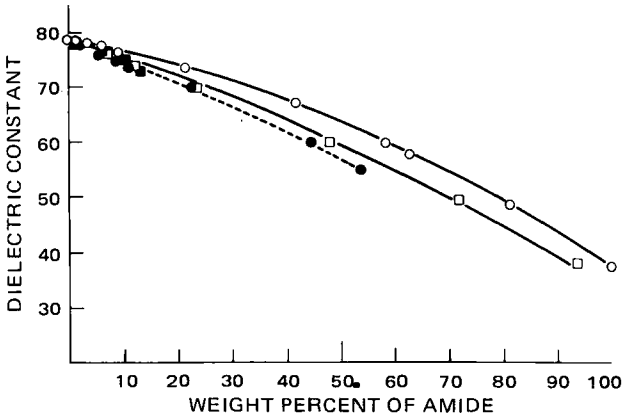

Figure 1—*Dielectric constant* versus *composition of tetramethyldicarboxamides. Key:* ○, *tetramethylpimelamide;* ●, *tetramethylsuberamide;* □, *tetramethylazelamide; and* ■, *tetramethylsebacamide.*

An equation[5] of the type:

$$\epsilon = a + bx + cx^2 \qquad \text{(Eq. 1)}$$

where ϵ is the solution dielectric constant, x is the concentration, and a, b, and c are constants, describes the behavior of the solution dielectric constant. The constants for each amide are obtained through fitting the mean experimental ϵ values to Eq. 1, using a nonlinear least-squares program of the type described by Wentworth (16). Some ϵ values of the even-carbon amides listed in Table I are calculated with Eq. 1.

The solubility data of glutethimide in the different amide–water systems are listed in Table I, and solubility profiles are depicted in Fig. 2. The solubility patterns showed an almost exponential rise with a decreasing solution dielectric constant. This finding may imply more effective hydration of the glutethimide molecules as the concentration increases and the formation of various hydrates having their own solubility characteristics.

A clearer illustration of the phenomenon occurring at the water-rich region (high ϵ) is depicted in Fig. 3*a*. The solubility ratios, S/S_0 (S refers to the solubility of glutethimide in the amide–water mixture, and S_0 is its solubility in water), are plotted as a function of the dielectric constant. Below a certain amide concentration, the solubility ratios remained almost constant, indicating that addition of small amounts of amides did not significantly change the solubility pattern.

Previous studies on these amides (2) suggested the formation of micelles at very dilute concentrations of the amides. Critical micelle concentrations (CMC) were reported to be at 0.41, 0.20, 0.031, and 0.11 M for the pimelamide, suberamide, azelamide, and sebacamide, respectively. A sudden change in the solubility pattern was also observed, which may correspond to the CMC of the amide micelle or any mixed micelles arising from the addition of glutethimide. At the micellar region, it is believed that micellization removes the alkyl or nonpolar groups of the amides from the aqueous to nonaqueous environment, producing a high density of hydrophilic groups at the micellar surface and resulting in the hydrophobic solvation of nonpolar moieties (3).

The micellar interior behaves in the same way as an organic phase in a two-immiscible phase system in which water is one phase. It is

[4] Weight in vacuum corrections applied using:

$$M_{vac} = M_{air} + \frac{K(M_{air})}{1000}$$

where M_{vac} is the weight of the object in vacuum, M_{air} is the observed weight in air, and K is a correction factor related to the density of the object ("Handbook of Chemistry and Physics," 47th ed., R. C. Weast and S. M. Selby, Eds., Chemical Rubber Co., Cleveland, Ohio, 1966, p. D-75).

[5] An equally applicable alternative expression is:

$$\epsilon_{12} = \epsilon_1 + KW_2 + K_1W_1W_2$$

where ϵ_{12} and ϵ_1 are the dielectric constants of the mixture and water, respectively; K and K_1 are constants; and W_1 and W_2 refer to the weight fractions of the water and amide, respectively.

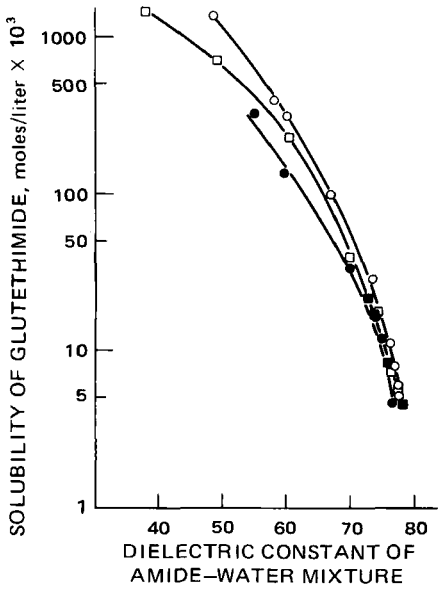

Figure 2—*Solubility of glutethimide in relation to the solution dielectric constant of amide–water mixtures. Key:* O, *tetramethylpimelamide;* ●, *tetramethylsuberamide;* □, *tetramethylazelamide; and* ■, *tetramethylsebacamide.*

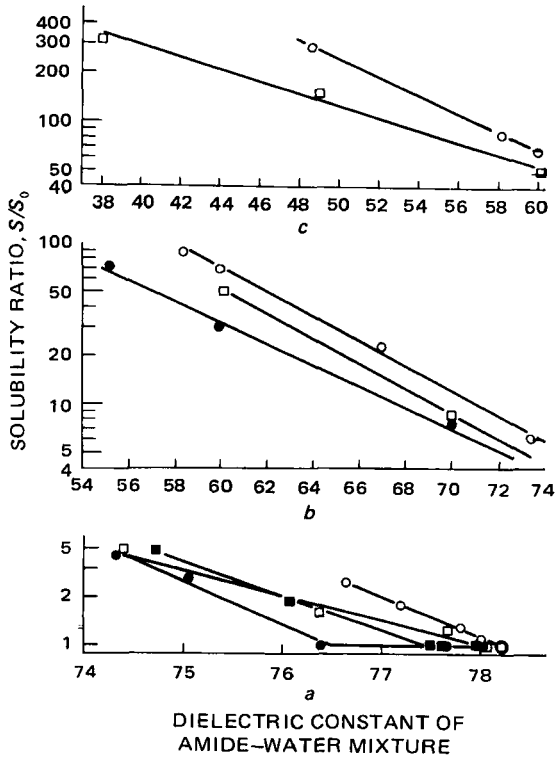

Figure 3—*Solubility ratios of glutethimide* versus *dielectric constants of amide–water mixtures. Key:* a, *water-rich mixtures;* b, *moderate amide concentrations;* c, *amide-rich mixtures;* O, *tetramethylpimelamide;* ●, *tetramethylsuberamide;* □, *tetramethylazelamide; and* ■, *tetramethylsebacamide.*

felt that the glutethimide molecule is of a favorable size to penetrate or incorporate itself into the micelle, causing an increase in solubility. A globular type of micelle for the odd-carbon amides, while an open micelle shape that is configurationally constrained to accommodate more glutethimide molecules, may account for their higher solubility.

As depicted by Fig. 3*b*, with a moderate increase in amide concentrations beyond the micellar region, it is apparent that an environment favorable for the solubilization of glutethimide is created. The odd-carbon amides exhibited a minimum in partial molal volume in this region, and this phenomenon was attributed to maximum cooperation of water clusters in the amide environment with the amides to form "clathrate-like" structures (3). The amides aid in the solubilization of glutethimide by breaking up water clusters surrounding the glutethimide molecules and effectively reducing self-association of glutethimide.

As the environment of the glutethimide molecules becomes progressively reduced in dielectric constant (amide-rich region, Fig. 3*c*) a strong interaction between glutethimide molecules and water clusters persists. Viscosity data of the odd-carbon amide systems reveal a maximum in viscosity in this region (3). It was postulated that an amide-hydrate with an approximate 2:1 solvent–amide ratio was formed at the maximum in the viscosity curve. Formation of this hydrate involved further breakdown of more clusters of hydrogen-bonded water in the vicinity of the glutethimide molecules. The possibility of glutethimide–water associations through hydrophobic bonding is apparent.

SUMMARY AND CONCLUSIONS

Examination of the structures of the tetramethyldicarboxamides indicates that their solubilizing properties can be correlated with the length of the carbon chain to which the amide groups are terminally attached. When taking equimolar concentrations of the amides and noting their corresponding solution dielectric constants (Table I), the following trends are evident:

1. At the water-rich regions of the amide–water systems, just beyond the CMC, the solubilizing action of the amides varies slightly. The solubilizing power parallels the chain length of the amides. This result is to be expected, since the dielectric constants corresponding to equimolar concentrations decrease with the length of the chain. It appears that the higher homologs favor more extensive solvation by water, resulting in the lowering of the solution dielectric constant. Also, since the magnitude and direction of the resultant electrostatic field depend on the orientation of the amide molecules and/or molecular aggregates of varying sizes, it seems that the smaller the amide molecule or its aggregates, the more it can adjust its position to accommodate a variety of orientations favoring higher polarizations.

2. While there is a definite correlation between the dielectric constant and solubilizing properties, deviations occur at higher amide concentrations, indicating a more complex nature of their interactions with water. The two odd-carbon amides, tetramethylpimelamide and tetramethylazelamide, showed consistently greater solubilizing power relative to their even-carbon amide analog, tetramethylsuberamide, within the solubility range of the suberamide. The better solubilizing action of the odd-carbon amides may be attributed to their greater association tendencies with water clusters in the vicinity of the glutethimide molecules; self-associations of glutethimide molecules are effectively reduced, thus promoting solubility. However, the dielectric properties of these amides alone as the parameter for determining solubilizing action could not give a firm interpretation of the molecular events occurring because of the complexity of their association tendencies in aqueous solutions.

REFERENCES

(1) E. H. Gans and T. Higuchi, *J. Am. Pharm. Assoc., Sci. Ed.*, **46**, 587(1957).

(2) P. P. DeLuca, L. Lachman, and H. Schroeder, *J. Pharm. Sci.*, **62**, 1320(1973).

(3) P. P. DeLuca and T. V. Rebagay, *J. Phys. Chem.*, **79**, 2493(1975).

(4) J. E. Anderson, *J. Chem. Phys.*, **51**, 3578(1969).

(5) A. N. Paruta, B. J. Sciarrone, and N. G. Lordi, *J. Pharm. Sci.*, **51**, 704(1962).

(6) *Ibid.*, **53**, 1349(1964).

(7) *Ibid.*, **54**, 1325(1965).

(8) W. G. Gorman and G. D. Hall, *J. Pharm. Sci.*, **53**, 1017(1964).

(9) A. N. Martin, "Physical Pharmacy," Lea & Febiger, Philadelphia, Pa., 1960.

(10) T. V. Rebagay, J. F. Casteel, and P. G. Sears, *J. Electrochem. Soc.*, **121**, 977(1974).

(11) G. Akerlof, *J. Am. Chem. Soc.*, **54**, 4125(1932).

(12) R. Kempa and W. H. Lee, *J. Chem. Soc.*, **1958**, 1936.

(13) G. R. Leader, *J. Am. Chem. Soc.*, **73**, 856(1951).
(14) J. W. Vaughn and P. G. Sears, *J. Phys. Chem.*, **62**, 183(1958).
(15) C. G. Malmberg and A. A. Maryott, *J. Res. Nat. Bur. Stand.*, **56**, 1(1956).
(16) W. E. Wentworth, *J. Chem. Educ.*, **42**, 96, 162(1965).

ACKNOWLEDGMENTS AND ADDRESSES

Received October 3, 1975, from the *College of Pharmacy, University of Kentucky, Lexington, KY 40506*
Accepted for publication January 26, 1976.
[x] To whom inquiries should be directed.

Effects of Bis(2-ethylhexyl) Phthalate on Chromosomes of Human Leukocytes and Human Fetal Lung Cells

MORTON A. STENCHEVER [*x], MARJORIE A. ALLEN [*], LESLIE JEROMINSKI [*], and ROBERT V. PETERSEN [‡]

Abstract □ Blood from two male and two female donors was exposed at 37° for 4 hr to concentrations of 60.0, 6.0, 0.6, and 0.06 μg of a widely used plasticizer, bis(2-ethylhexyl) phthalate, per milliliter of blood. The bis(2-ethylhexyl) phthalate was solubilized with polysorbate 80. Appropriate polysorbate and nonpolysorbate controls also were established. Following the 4 hr of incubation, phytohemagglutinin was added and tissue cultures were established. In addition, human fetal lung cells were exposed in tissue culture to a medium containing 6.0 μg/ml of bis(2-ethylhexyl) phthalate in polysorbate 80 for 5 days. Similar controls also were established for these experiments. Analysis of chromosome preparations from all cultures obtained failed to show any increased evidence of isochromatid and chromatid breaks or gaps or abnormal forms at any studied concentration when compared to the control cultures. In addition, analysis of fetal lung cell preparations for aneuploidy failed to reveal any differences between cells from study and control cultures. This study involved a short-term exposure to bis(2-ethylhexyl) phthalate in various concentrations which did not cause damage in leukocytes or fetal lung cells.

Keyphrases □ Bis(2-ethylhexyl) phthalate—effect on chromosomes of human leukocytes and fetal lung cells □ Phthalate esters—bis(2-ethylhexyl) phthalate, effect on chromosomes of human leukocytes and fetal lung cells □ Chromosomes, human leukocyte and fetal lung cell—effect of incubation with bis(2-ethylhexyl) phthalate □ Toxicity, potential—bis(2-ethylhexyl) phthalate, effect on chromosomes of human leukocytes and fetal lung cells □ Plasticizers—bis(2-ethylhexyl) phthalate, effect on chromosomes of human leukocytes and fetal lung cells

Bis(2-ethylhexyl) phthalate (I) is a plasticizer used in the fabrication of polyvinyl chloride medical devices such as blood storage bags, blood administration assemblies, hemodialysis units, and cardiopulmonary bypass units, and it is one of the most widely used of the phthalate esters. In many instances, it represents 40% or more of the total weight of the finished plastic (1). Roll *et al.* (2) demonstrated by GLC techniques that

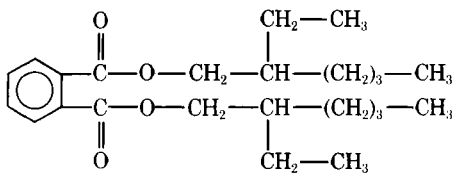

I

phthalate esters are found almost universally as contaminants on or in items such as laboratory glassware, laboratory chemicals, metal foils, rubber stoppers, and distilled water.

Trimble *et al.* (3) and Guess *et al.* (4, 5) were among the first to note that I leaches out of polyvinyl chloride in the presence of blood or certain other solvents. Since that time, several investigators quantitated the rate of leaching of I from various polyvinyl chloride devices under various conditions (6–10).

Jaeger and Rubin (11) first demonstrated the presence of I in various human tissues following transfusion of blood stored in polyvinyl chloride blood bags. Much research has since been performed to quantify the toxicogenic implications of phthlates in various organs and tissues. Petersen *et al.* (12) showed that I can be detected in liver, lung, and spleen of calves following exposure to cardiopulmonary procedures and in the same organs of humans exposed to prolonged renal hemodialysis.

Recent publications and reviews confirmed that I probably has a low order of acute toxicity (13–15). However, the long-range, subtle toxicogenic potential of this agent is becoming of paramount concern. Guess and coworkers (5, 16) were among the first to suggest potential hazards from long-term exposure of this agent. Observations of cells in tissue culture (19, 20), teratogenic effects (16, 17, 21–24), and effects on reproduction (12, 25) and related studies appear to substantiate this suggestion. While the data are not conclusive and there is incomplete agreement between laboratories, evidence suggests that I and/or its metabolites are toxic at the cellular level, that I interferes with normal reproductive patterns, and that lower molecular weight phthalate esters are teratogenic.

To evaluate possible mechanisms of toxicity and add a dimension to previous studies, human leukocytes and human fetal lung cells were exposed to I at various concentrations and their chromosomes were analyzed for possible changes.

(13) G. R. Leader, *J. Am. Chem. Soc.*, **73**, 856(1951).
(14) J. W. Vaughn and P. G. Sears, *J. Phys. Chem.*, **62**, 183(1958).
(15) C. G. Malmberg and A. A. Maryott, *J. Res. Nat. Bur. Stand.*, **56**, 1(1956).
(16) W. E. Wentworth, *J. Chem. Educ.*, **42**, 96, 162(1965).

ACKNOWLEDGMENTS AND ADDRESSES

Received October 3, 1975, from the *College of Pharmacy, University of Kentucky, Lexington, KY 40506*
Accepted for publication January 26, 1976.
[x] To whom inquiries should be directed.

Effects of Bis(2-ethylhexyl) Phthalate on Chromosomes of Human Leukocytes and Human Fetal Lung Cells

MORTON A. STENCHEVER [*x], MARJORIE A. ALLEN [*], LESLIE JEROMINSKI [*], and ROBERT V. PETERSEN [‡]

Abstract □ Blood from two male and two female donors was exposed at 37° for 4 hr to concentrations of 60.0, 6.0, 0.6, and 0.06 μg of a widely used plasticizer, bis(2-ethylhexyl) phthalate, per milliliter of blood. The bis(2-ethylhexyl) phthalate was solubilized with polysorbate 80. Appropriate polysorbate and nonpolysorbate controls also were established. Following the 4 hr of incubation, phytohemagglutinin was added and tissue cultures were established. In addition, human fetal lung cells were exposed in tissue culture to a medium containing 6.0 μg/ml of bis(2-ethylhexyl) phthalate in polysorbate 80 for 5 days. Similar controls also were established for these experiments. Analysis of chromosome preparations from all cultures obtained failed to show any increased evidence of isochromatid and chromatid breaks or gaps or abnormal forms at any studied concentration when compared to the control cultures. In addition, analysis of fetal lung cell preparations for aneuploidy failed to reveal any differences between cells from study and control cultures. This study involved a short-term exposure to bis(2-ethylhexyl) phthalate in various concentrations which did not cause damage in leukocytes or fetal lung cells.

Keyphrases □ Bis(2-ethylhexyl) phthalate—effect on chromosomes of human leukocytes and fetal lung cells □ Phthalate esters—bis(2-ethylhexyl) phthalate, effect on chromosomes of human leukocytes and fetal lung cells □ Chromosomes, human leukocyte and fetal lung cell—effect of incubation with bis(2-ethylhexyl) phthalate □ Toxicity, potential—bis(2-ethylhexyl) phthalate, effect on chromosomes of human leukocytes and fetal lung cells □ Plasticizers—bis(2-ethylhexyl) phthalate, effect on chromosomes of human leukocytes and fetal lung cells

Bis(2-ethylhexyl) phthalate (I) is a plasticizer used in the fabrication of polyvinyl chloride medical devices such as blood storage bags, blood administration assemblies, hemodialysis units, and cardiopulmonary bypass units, and it is one of the most widely used of the phthalate esters. In many instances, it represents 40% or more of the total weight of the finished plastic (1). Roll *et al.* (2) demonstrated by GLC techniques that

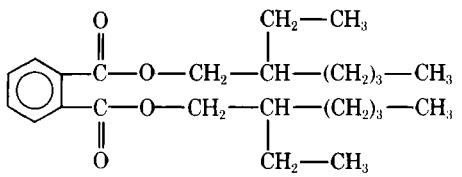

I

phthalate esters are found almost universally as contaminants on or in items such as laboratory glassware, laboratory chemicals, metal foils, rubber stoppers, and distilled water.

Trimble *et al.* (3) and Guess *et al.* (4, 5) were among the first to note that I leaches out of polyvinyl chloride in the presence of blood or certain other solvents. Since that time, several investigators quantitated the rate of leaching of I from various polyvinyl chloride devices under various conditions (6–10).

Jaeger and Rubin (11) first demonstrated the presence of I in various human tissues following transfusion of blood stored in polyvinyl chloride blood bags. Much research has since been performed to quantify the toxicogenic implications of phthlates in various organs and tissues. Petersen *et al.* (12) showed that I can be detected in liver, lung, and spleen of calves following exposure to cardiopulmonary procedures and in the same organs of humans exposed to prolonged renal hemodialysis.

Recent publications and reviews confirmed that I probably has a low order of acute toxicity (13–15). However, the long-range, subtle toxicogenic potential of this agent is becoming of paramount concern. Guess and coworkers (5, 16) were among the first to suggest potential hazards from long-term exposure of this agent. Observations of cells in tissue culture (19, 20), teratogenic effects (16, 17, 21–24), and effects on reproduction (12, 25) and related studies appear to substantiate this suggestion. While the data are not conclusive and there is incomplete agreement between laboratories, evidence suggests that I and/or its metabolites are toxic at the cellular level, that I interferes with normal reproductive patterns, and that lower molecular weight phthalate esters are teratogenic.

To evaluate possible mechanisms of toxicity and add a dimension to previous studies, human leukocytes and human fetal lung cells were exposed to I at various concentrations and their chromosomes were analyzed for possible changes.

Table I—Chromosome Breaks, Gaps, and Abnormal Forms Seen in Leukocytes from Various Cultures for Each Subject[a]

Subject	Concentration of I, μg/ml	Number of Breaks	Percent	Number of Gaps	Percent	Number of Abnormal Forms	Percent
1 (Male)	60.0	2	2.0	5	5.00	0	0
	6.0	1	1.0	7	7.00	0	0
	0.6	2	2.0	4	4.00	0	0
	0.06	1	1.0	0	0	0	0
	Polysorbate control	0	0	0	0	0	0
	Pure control	1	1.0	3	3.00	0	0
2 (Male)	60.0	3	3.0	1	1.0	0	0
	6.0	0	0	2	2.0	0	0
	0.6	2	2.0	1	1.0	0	0
	0.06	0	1.0	2	2.0	0	0
	Polysorbate control	0	0	4	4.0	0	0
	Pure control	0	0	3	3.0	0	0
3 (Female)	60.0	4	4.0	3	3.0	1	1.0[b]
	6.0	3	3.0	6	6.0	0	0
	0.6	0	0	0	0	0	0
	0.06	1	1.0	1	1.0	0	0
	Polysorbate control	1	1.0	1	1.0	0	0
	Pure control	0	1.0	1	1.0	0	0
4 (Female)	60.0	3	3.0	1	1.0	1	1.0[c]
	6.0	1	1.0	2	2.0	0	0
	0.6	2	2.0	3	3.0	0	0
	0.06	2	2.0	3	3.0	0	0
	Polysorbate control	4	4.0	5	5.0	0	0
	Pure control	1	1.0	2	2.0	0	0

[a] Number of cells scored was 100 in each case. [b] Triradial. [c] Ring.

EXPERIMENTAL

For all experiments, I[1] was solubilized in polysorbate 80[2] (1:3) prior to dispersing in fetal calf serum by sonication. Following addition of I to fetal calf serum, the dispersion was filtered through a 0.22-μm filter[3] and diluted such that the concentrations of I desired for a particular experiment would be produced when it was added in 0.1-ml aliquots to 9.9 ml of blood or in 0.2-ml aliquots to 19.8 ml of cells in a tissue culture medium.

Leukocyte Cultures—Sixty milliliters of heparinized blood was obtained from each of two male and two female donors. The donors had been exposed to no medications or known chromosome-damaging agents for at least 1 year and had been exposed to no ionizing radiation for at least 6 months. At the time of obtaining the blood, these individuals were in their early twenties, were in good health, and showed no evidence or stigmata of viral infections.

Each 60-ml sample was divided into six 9.9-ml aliquots. The appropriate I–polysorbate solution was added in 0.1-ml quantities to the first four samples to give final concentrations of 60.0, 6.0, 0.6, and 0.06 μg of I/ml of blood. To the fifth tube, 0.1 ml of polysorbate 80 solution was added to serve as a polysorbate control. Nothing was added to the sixth tube of blood, which served as a pure control tube.

All tubes were incubated at 37° for 4 hr. Phytohemagglutinin then was added, and each tube was placed in cracked ice for 30 min and then centrifuged at 500 rpm for 5 min. The serum containing the leukocytes from each tube was divided equally into three tissue culture flasks, to which Minimal Eagle's medium was added to make a final total volume of 10 ml. All flasks were then incubated at 37° for 72 hr. Two hours prior to harvesting, 0.3 ml of demecolcine[4] was added to each flask. Following this step, harvesting and production of air-dried preparations were carried out.

Slides prepared from each culture were then coded for blind scoring to eliminate the possibility of scorer bias. Each slide was stained with Giemsa stain and permanently coverslipped. Fifty consecutive, intact-appearing metaphase spreads were scored by two observers for total chromosome count, evidence of chromatid and isochromatid breaks and gaps, and the presence of abnormal forms such as tetraploid chromosome count, ring chromosome, and tri- and quadriradials. Each observer dealt with cells from at least two different slides for scoring purposes; thus, 100 metaphase spreads were evaluated for each concentration of I and each control tube.

[1] Eastman Organic Chemicals, Rochester, N.Y.
[2] Tween 80, ICI America, Wilmington, Del.
[3] Millipore Corp., San Mateo, Calif.
[4] Colcemid, Grand Island Biological Co., Grand Island, N.Y.

Fetal Lung Cell Cultures—A stock culture of fetal lung cells was established from a normal appearing 16-week fetus delivered by hysterotomy. For this experiment, an early subculture of cells was used. T-60 flasks were inoculated with 5×10^5 cells, each in Minimal Eagle's medium plus 20% fetal calf serum (heat inactivated). Twenty-four hours after inoculation, all cultures were renewed with medium as follows: two flasks with 19.8 ml of Minimal Eagle's medium with 20% fetal calf serum and 0.2 ml of I–polysorbate 80 solution, and two flasks with 20 ml of Minimal Eagle's medium and 20% fetal calf serum. All flasks were cultured in a 5% CO_2 in air environment at 37°.

Five days after the first renewal, all flasks were renewed with 10 ml of Minimal Eagle's medium with 20% fetal calf serum and 0.8 ml of demecolcine[4]. Eight hours later, harvesting was carried out by removing the monolayer from the glass using 0.25% trypsin in Hank's salt solution. Slides were then prepared by an air-dried method, coded for blind scoring, and scored in the fashion already described.

RESULTS

Table I summarizes the chromosome breaks, gaps, and abnormal forms seen in cells from various leukocyte cultures of the four donor subjects. Since isochromatid and chromatid breaks and gaps were at a minimum, they were combined for statistical purposes. No statistically significant differences were seen between the various concentrations in the two control flasks for each subject. One female subject did show a 4% breakage rate in the 60.0-μg/ml concentration, a 3% breakage rate in at the 6.0-μg/ml concentration, and one triradial in her 60.0-μg/ml concentration culture. The second female subject showed a 3% breakage rate at 60.0 μg/ml but also a 4% breakage rate in the polysorbate control. This subject had a ring chromosome present in the 60.0-μg/ml concentration. However, when all data from each of the four subjects were combined (Table II), no statistically significant differences were noted at the various concentrations when compared to the control cultures.

Table III summarizes the chromosome breaks, gaps, and abnormal forms, as well as percentages of cells with aneuploid counts, seen in the fetal lung cell cultures. Again, isochromatid and chromatid breaks were combined because of the small numbers in each group. No statistically significant differences were noted in any of these categories. Abnormal cells present in each case were tetraploid cells.

DISCUSSION

Since it has been noted that I migrates into blood stored in plastic bags (6, 7) and that it tends to concentrate in certain tissues such as

Table II—Combined Data from All Four Subjects[a] (Leukocyte Experiments)

Concentration of I, μg/ml	Number of Breaks	Percent	Number of Gaps	Percent	Number of Abnormal Forms	Percent
60.0	12	3.00	10	2.50	2	0.5
6.0	5	1.25	17	4.25	0	0
0.6	6	1.50	8	2.25	0	0
0.06	5	1.25	6	1.50	0	0
Polysorbate control	5	1.25	10	2.50	0	0
Pure control	3	0.75	9	2.25	0	0

[a]Number of cells scored was 400 in each case.

Table III—Cells with Breaks, Gaps, and Abnormal Forms Seen in Fetal Lung Cell Experiments[a]

Sample	Number of Breaks	Percent	Number of Gaps	Percent	Number of Tetraploid Cells	Percent	Number of Aneuploid Cells	Percent
I (6.0 μg/ml)	7	3.5	5	2.5	6	3.0	17	8.5
Polysorbate control	9	4.5	5	2.5	3	1.5	11	5.5
Pure control	11	5.5	1	0.5	5	2.5	20	10.0

[a]Number of cells scored was 200 in each case.

the lung (12), it was decided to study the potential chromosome-damaging effect of this agent on both blood leukocytes and fetal lung cells. The 60.0-μg/ml concentration was chosen because it represented the highest concentration used in other experiments wherein I was dispersed in serum by sonication and, following the steps of the experimental protocol, represented a 10-fold dilution of this concentration. Recent data by Turner *et al.* (26) demonstrated that these levels are within the range of those seen in blood stored in plastic bags. These investigators recently studied the effects of I on chromosomes of leukocytes found in blood-bank blood stored in plastic bags and failed to find any significant chromosome damage.

The 6.0-μg/ml concentration was chosen for the fetal lung experiment because a good mitotic index was desired, but a relatively high concentration seemed appropriate for the 5-day exposure. The leukocyte experiments demonstrated a good mitotic rate at this concentration, whereas the mitotic rate was poor at 60.0 μg/ml.

Polysorbate 80 was chosen as a solvent for I since it is one of the few relatively innocuous agents that could serve this purpose for this agent. Although not known to be cytotoxic, polysorbate 80 was added to a control culture as an added precaution.

Four-hour incubations were used for the blood leukocyte experiments because longer periods had resulted in significant red cell hemolysis in pilot studies designed to expose leukocytes prior to phytohemagglutinin addition to mimic *in vivo* exposure. Once phytohemagglutinin is added, the mitotic process is initiated and, by the procedure followed, the concentration of I is reduced. However, by this point, the cells have been exposed and some intracellular binding can be anticipated. While exposure to I would vary *in vivo* depending on the type of medical procedure, the design of the experiment allowed for a variety of concentrations of I, which do occur in many of these circumstances for a specific period.

The fetal lung experiment allowed for a more chronic exposure to I during all stages of the cell cycle.

Chromosome damage and induction of abnormal chromosome forms and aneuploidy are signs of cytotoxicity. It is comforting to note that cells exposed for short periods to I do not show such signs. However, data suggesting toxic effects on cells in tissue culture, teratogenicity, and adverse effects on the outcome of reproductivity, as previously cited, seem to imply that these agents have potentially harmful effects. The results of these studies and those of Turner *et al.* (26) indicate that these effects are not mediated through a mechanism that damages chromosomes.

Although chromosome damage is often interpreted as evidence for potential mutagenicity, either may occur separately. This report in no way rules out a mutagenic potential of this agent; studies using bacterial and animal systems will be necessary to establish such a possibility. Likewise, this report cannot be interpreted as ruling out a teratogenic effect of the agent since that was outside the scope of the experimental design and specific relationships between chromosome damage and teratogenicity have not been defined. Further animal studies will be necessary to investigate such a potential problem.

Nonetheless, the results of the cited studies imply that exposure to I during pregnancy should be kept to a minimum. Perhaps other substances should be used in the production of blood bags, intravenous tubings, and dialysis equipment when pregnant or potentially pregnant women are to be treated until a clearer understanding of the mechanism of action of I is obtained. It also seems prudent to seek data that describe the specific effects on various tissues after prolonged exposure to these agents.

REFERENCES

(1) A. Hall, *Mod. Plast.*, **48**(9), 58(1971).

(2) D. B. Roll, J. D. Douglas, and R. V. Petersen, *J. Pharm. Sci.*, **63**, 1629(1974).

(3) A. S. Trimble, B. S. Goldman, J. K. Yao, L. K. Kovats, and W. G. Bigelow, *Surgery*, **59**, 857(1966).

(4) W. L. Guess, J. Jacob, and J. Autian, *Drug Intell.*, **1**, 120(1967).

(5) W. L. Guess and S. Haberman, *J. Biomed. Mater. Res.*, **2**, 313(1968).

(6) R. J. Jaeger, Ph.D. dissertation, Johns Hopkins University, Baltimore, Md., 1971.

(7) R. J. Jaeger and R. J. Rubin, *Environ. Health Perspect., Exp. Issue*, **3**, 53(1973).

(8) M. S. Jacobson, R. Parkman, L. N. Button, R. J. Jaeger, and S. V. Kevy, *Chem. Pathol. Pharmacol.*, **9**, 315(1974).

(9) R. E. Esterling, E. Johnson, and E. A. Napier, Jr., *Proc. Soc. Exp. Biol. Med.*, **147**, 573(1974).

(10) J. Neergaard, B. Nielsen, V. Faurby, D. H. Christensen, and O. F. Nielsen, *Nephron*, **14**, 263(1974).

(11) R. J. Jaeger and R. J. Rubin, *Science*, **170**, 460(1970).

(12) R. V. Petersen, D. B. Roll, E. A. Swinyard, D. J. Lyman, M. A. Stenchever, R. W. Rhees, P. S. Nicholes, S. W. Kim, and J. R. Cardinal, "Toxicology of Plastic Devices Having Contact with Blood," Final Report to NHLI, Contract NIH-NHLI-73-2908-B, 1975.

(13) *Environ. Health Perspect., Exp. Issue*, **3** (Jan. 1973).

(14) "Flexible Vinyls and Human Safety: An Objective Analysis," Society of Plastic Engineers Inc., Greenwich, Conn., Mar. 1973.

(15) J. Autian, *Environ. Health Perspect., Exp. Issue*, **4**, 3(1973).

(16) W. L. Guess, S. Haberman, D. F. Rowan, R. K. Bower, and J. Autian, *Am. J. Hosp. Pharm.*, **24**, 495(1967).

(17) E. O. Dillingham and J. Autian, *Environ. Health Perspect., Exp. Issue*, **3**, 81(1973).

(18) D. Calley, J. Autian, and W. L. Guess, *J. Pharm. Sci.*, **55**, 158(1966).

(19) H. Lee and G. W. Kalmus, *Experientia*, **30**, 800(1974).
(20) A. E. Jones, R. H. Kahn, J. T. Groves, and E. A. Napier, Jr., *Toxicol. Appl. Pharmacol.*, **31**, 283(1975).
(21) M. J. Verrett, M. K. Mutchler, W. F. Scott, E. F. Reynaldo, and J. McLaughlin, *Ann. N.Y. Acad. Sci.*, **160**, 334(1969).
(22) R. K. Bower, S. Haberman, and P. D. Minton, *J. Pharmacol. Exp. Ther.*, **171**, 314(1970).
(23) A. R. Singh, W. H. Lawrence, and J. Autian, *J. Pharm. Sci.*, **61**, 51(1972).
(24) *Ibid.*, **62**, 1596(1973).
(25) A. R. Singh, W. H. Lawrence, and J. Autian, *Toxicol. Appl. Pharmacol.*, **29**, 35(1974).
(26) J. H. Turner, J. C. Petricciani, M. L. Crouch, and S. Wenger, *Transfusion*, **14**, 560(1974).

ACKNOWLEDGMENTS AND ADDRESSES

Received October 7, 1975, from the *Department of Obstetrics and Gynecology, College of Medicine, and the ‡Department of Applied Pharmaceutical Sciences, College of Pharmacy, University of Utah, Salt Lake City, UT 84112

Accepted for publication January 26, 1976.

Supported by Contract NIH-NHLI-73-2908-B, National Institutes of Health, and the Brush Foundation of Cleveland.

ˣ To whom inquiries should be directed.

Biotransformation of Drugs: Quantitative Structure–Activity Relationships for Barbiturates, Tertiary Amines, and Substituted Imidazoles

GEORGE L. TONG ˣ and ERIC J. LIEN

Abstract □ When using free energy-related physicochemical parameters, stimulation of NADPH oxidation by barbiturates and the *N*-oxidation of tertiary amines was found to be primarily dependent upon the lipophilic character of the substrates as measured by log *P*, where *P* is the partition coefficient from either 1-octanol–water or corn oil–water solvent systems. In contrast, the inhibition of epoxidation of aldrin by a series of substituted imidazoles appears to be much more dependent on electronic (σ) and steric (E_s) effects of the inhibitors.

Keyphrases □ Biotransformation, drug—quantitative structure–activity relationships for barbiturates, tertiary amines, and substituted imidazoles, physicochemical properties □ Structure–activity relationships—barbiturates, tertiary amines, and substituted imidazoles, biotransformation, physicochemical properties □ Barbiturates—effect on NADPH oxidation, quantitative structure–activity relationships, physicochemical properties □ Amines, tertiary—*N*-oxidation, quantitative structure–activity relationships, physicochemical properties □ Imidazoles, substituted—effect on epoxidation of aldrin, quantitative structure–activity relationships, physicochemical properties □ Metabolism, drug—quantitative structure–activity relationships for barbiturates, tertiary amines, and substituted imidazoles

Since early work (1, 2), the importance of lipophilic character in drug metabolism has been well established and documented (3–6). While there have been many elegant and well-designed *in vivo* and *in vitro* metabolism studies on single drugs, there have been relatively few good investigations of series of compounds to account for their differences in biotransformation in terms of their physicochemical properties. From the tremendous amount of published work on drug metabolism, there are relatively few good sets of data suitable for multiple regression analysis using free energy-related substituent constants. This paper reports the quantitative correlations obtained for the stimulation of NADPH oxidation by barbiturates, the *N*-oxidation of tertiary amines including chlorpromazine and morphine, and the inhibition of epoxidation of aldrin by substituted imidazoles.

EXPERIMENTAL

The microsomal oxidation data in Table I were obtained from the literature (7–9). The biological data were converted to log *C* or log 1/*C*, where *C* is the molar concentration required to elicit a standard biological response, *i.e.*, log (oxidation rate) in moles per minute per milligram or log $1/I_{50}$. The physicochemical constants used in the regression analysis (Table I) were obtained from the literature or calculated taking advantage of their additive and constitutive nature. All equations assembled in Table II were derived *via* the method of nonweighted least-squares fit using a computer program executed through a computer communicating terminal[1].

RESULTS AND DISCUSSION

Jannson *et al.* (7) studied the effects of a series of substituted barbituric acids on the rat hepatic microsomal monooxygenase system. They reported that there were no significant correlations of the microsomal oxidation with various measured physicochemical properties of the barbiturates such as the oil–water partition coefficient ($P_{o/w}$), pKa, cytochrome P_{450} dissociation constant (K_s), and maximal type I spectral change (ΔE). In contrast, they reported the importance of the partition coefficient in the inhibition of membrane-bound mitochondrial NADH oxidase. They suggested that although the lipid solubility was required for a substance to reach the microsomal cytochrome P_{450}, other properties of the barbiturates were important for determining the affinity of their interaction with the cytochrome system whereas the inhibition of the mitochondrial respiratory chain by uncoupling oxidative phosphorylation could be explained simply in terms of lipoid solubility.

In reanalyzing their results by using the free energy-related log *P* term instead of the partition coefficient itself, there was an excellent linear correlation (Eq. 2) with the 50% inhibition of NADH oxidation by the barbiturates. The coefficient or the slope associated with the log *P* term (0.88) is comparable to a similar dependence obtained for identical inhibition by barbiturates (10). The addition of either the pKa or the $(\log P)^2$ term did not result in a statistically significant improvement in correlation.

From the same work, only slightly improved correlations were found of the stimulation of microsomal NADPH oxidation by barbiturates with their free energy-related parameters (Eqs. 3–6). Closer inspection of the results of the regression analysis revealed that all allyl-substi-

[1] IBM 2741.

(19) H. Lee and G. W. Kalmus, *Experientia*, **30**, 800(1974).
(20) A. E. Jones, R. H. Kahn, J. T. Groves, and E. A. Napier, Jr., *Toxicol. Appl. Pharmacol.*, **31**, 283(1975).
(21) M. J. Verrett, M. K. Mutchler, W. F. Scott, E. F. Reynaldo, and J. McLaughlin, *Ann. N.Y. Acad. Sci.*, **160**, 334(1969).
(22) R. K. Bower, S. Haberman, and P. D. Minton, *J. Pharmacol. Exp. Ther.*, **171**, 314(1970).
(23) A. R. Singh, W. H. Lawrence, and J. Autian, *J. Pharm. Sci.*, **61**, 51(1972).
(24) *Ibid.*, **62**, 1596(1973).
(25) A. R. Singh, W. H. Lawrence, and J. Autian, *Toxicol. Appl. Pharmacol.*, **29**, 35(1974).
(26) J. H. Turner, J. C. Petricciani, M. L. Crouch, and S. Wenger, *Transfusion*, **14**, 560(1974).

ACKNOWLEDGMENTS AND ADDRESSES

Received October 7, 1975, from the *Department of Obstetrics and Gynecology, College of Medicine, and the ‡Department of Applied Pharmaceutical Sciences, College of Pharmacy, University of Utah, Salt Lake City, UT 84112

Accepted for publication January 26, 1976.

Supported by Contract NIH-NHLI-73-2908-B, National Institutes of Health, and the Brush Foundation of Cleveland.

ˣ To whom inquiries should be directed.

Biotransformation of Drugs: Quantitative Structure–Activity Relationships for Barbiturates, Tertiary Amines, and Substituted Imidazoles

GEORGE L. TONG ˣ and ERIC J. LIEN

Abstract □ When using free energy-related physicochemical parameters, stimulation of NADPH oxidation by barbiturates and the *N*-oxidation of tertiary amines was found to be primarily dependent upon the lipophilic character of the substrates as measured by log *P*, where *P* is the partition coefficient from either 1-octanol–water or corn oil–water solvent systems. In contrast, the inhibition of epoxidation of aldrin by a series of substituted imidazoles appears to be much more dependent on electronic (σ) and steric (E_s) effects of the inhibitors.

Keyphrases □ Biotransformation, drug—quantitative structure–activity relationships for barbiturates, tertiary amines, and substituted imidazoles, physicochemical properties □ Structure–activity relationships—barbiturates, tertiary amines, and substituted imidazoles, biotransformation, physicochemical properties □ Barbiturates—effect on NADPH oxidation, quantitative structure–activity relationships, physicochemical properties □ Amines, tertiary—*N*-oxidation, quantitative structure–activity relationships, physicochemical properties □ Imidazoles, substituted—effect on epoxidation of aldrin, quantitative structure–activity relationships, physicochemical properties □ Metabolism, drug—quantitative structure–activity relationships for barbiturates, tertiary amines, and substituted imidazoles

Since early work (1, 2), the importance of lipophilic character in drug metabolism has been well established and documented (3–6). While there have been many elegant and well-designed *in vivo* and *in vitro* metabolism studies on single drugs, there have been relatively few good investigations of series of compounds to account for their differences in biotransformation in terms of their physicochemical properties. From the tremendous amount of published work on drug metabolism, there are relatively few good sets of data suitable for multiple regression analysis using free energy-related substituent constants. This paper reports the quantitative correlations obtained for the stimulation of NADPH oxidation by barbiturates, the *N*-oxidation of tertiary amines including chlorpromazine and morphine, and the inhibition of epoxidation of aldrin by substituted imidazoles.

EXPERIMENTAL

The microsomal oxidation data in Table I were obtained from the literature (7–9). The biological data were converted to log *C* or log 1/*C*, where *C* is the molar concentration required to elicit a standard biological response, *i.e.*, log (oxidation rate) in moles per minute per milligram or log $1/I_{50}$. The physicochemical constants used in the regression analysis (Table I) were obtained from the literature or calculated taking advantage of their additive and constitutive nature. All equations assembled in Table II were derived *via* the method of nonweighted least-squares fit using a computer program executed through a computer communicating terminal[1].

RESULTS AND DISCUSSION

Jannson *et al.* (7) studied the effects of a series of substituted barbituric acids on the rat hepatic microsomal monooxygenase system. They reported that there were no significant correlations of the microsomal oxidation with various measured physicochemical properties of the barbiturates such as the oil–water partition coefficient ($P_{o/w}$), pKa, cytochrome P_{450} dissociation constant (K_s), and maximal type I spectral change (ΔE). In contrast, they reported the importance of the partition coefficient in the inhibition of membrane-bound mitochondrial NADH oxidase. They suggested that although the lipid solubility was required for a substance to reach the microsomal cytochrome P_{450}, other properties of the barbiturates were important for determining the affinity of their interaction with the cytochrome system whereas the inhibition of the mitochondrial respiratory chain by uncoupling oxidative phosphorylation could be explained simply in terms of lipoid solubility.

In reanalyzing their results by using the free energy-related log *P* term instead of the partition coefficient itself, there was an excellent linear correlation (Eq. 2) with the 50% inhibition of NADH oxidation by the barbiturates. The coefficient or the slope associated with the log *P* term (0.88) is comparable to a similar dependence obtained for identical inhibition by barbiturates (10). The addition of either the pKa or the $(\log P)^2$ term did not result in a statistically significant improvement in correlation.

From the same work, only slightly improved correlations were found of the stimulation of microsomal NADPH oxidation by barbiturates with their free energy-related parameters (Eqs. 3–6). Closer inspection of the results of the regression analysis revealed that all allyl-substi-

[1] IBM 2741.

Table I—Microsomal Oxidation Data and Physicochemical Constants Used in Deriving the Equations in Table II

Inhibition of Mitochondrial NADH Oxidation: Log $1/I_{50}$		Stimulation of Microsomal NADPH Oxidation: Log (Oxidation Rate)			ΣE_s				
Obs.[a]	Calc.[b]	Obs.[c]	Calc.[d]	Calc.[e]	$(R_1 + R_2)$	Log $P_{o/w}$	ΔE	pKa	Compound
3.34	3.55	1.37	1.30	1.32	−0.79	0.88	0.045	8.35	Hexobarbital
3.28	3.25	1.13	1.10	1.16	−1.17	0.54	0.031	7.75	Heptabarbital
3.52	3.46	1.08	1.24	1.15	−1.20	0.78	0.030	8.05	Pentobarbital
3.74	3.67	—	—	—	−1.49	1.02	0.021	8.00	Secobarbital[f]
2.92	2.92	0.86	0.88	0.96	−0.86	0.16	0.013	7.65	Cyclobarbital
3.54	3.38	1.12	1.19	1.07	−0.42	0.69	0.023	7.95	Amobarbital
2.66	2.79	—	—	—	−0.83	0.02	0.0035	7.95	Aprobarbital[f]
3.11	3.00	0.97	0.94	0.92	−0.46	0.26	0.0095	7.95	Butabarbital
2.96	2.73	0.94	0.76	0.92	−1.20	−0.05	0.010	7.55	Vinbarbital
3.14	3.32	—	—	—	−2.10	0.62	0.006	7.80	Allylneopentylbarbituric acid[f]
3.30	3.25	—	—	—	−0.75	0.54	0.0085	7.85	Allylbutylbarbituric acid[f]
2.51	2.56	—	—	—	−0.72	−0.24	—	7.70	Diallylbarbituric acid[f]
2.66	2.78	0.87	0.79	0.85	−0.45	0.01	0.003	7.35	Phenobarbital
2.05	2.05	0.18	0.31	—	−0.14	−0.82	—	7.90	Barbital

Log (Oxidation Rate)					
Obs.[g]	Calc.[h]	Log P	pKa	Compound	
−6.84	−6.96	0.27	9.27	Trimethylamine	
−6.47	−6.50	1.77	10.02[i]	*N,N*-Dimethyl-*n*-butylamine	
−6.11	−6.12	3.77	10.02[i]	*N,N*-Dimethyl-*n*-octylamine	
−6.08	−6.07	4.27	10.02[i]	*N,N*-Dimethyl-*n*-nonylamine	
−6.09	−6.00	5.77	10.02[i]	*N,N*-Dimethyl-*n*-dodecylamine	
−6.31	−6.31	8.77	10.02[i]	*N,N*-Dimethyl-*n*-hexadecylamine	
−6.30	−6.37	2.31	5.06	*N,N*-Dimethylaniline	
−6.33	−6.27	2.81	5.23	*N,N*-Dimethyl-*p*-toluidine	
−5.90	−6.01	5.35	10.02[i]	Chlorpromazine	
−6.96	−6.80	0.76	9.85	Morphine	

Inhibition of Microsomal Epoxidation of Aldrin by Imidazole Derivative: Log $1/I_{50}$										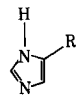
Obs.[j]	Calc.[k]	Calc.[l]	E_s (p)		Log P	$\sigma_{(p)}$	$\Sigma\sigma_{(m+p)}$	$F_{(p)}$	$R_{(p)}$	R
6.06	5.82	5.88	H	1.24	2.03	0.00	0.00	0.00	0.00	$C_6H_5OCH_2$—
5.94	6.07	6.07	H	1.24	2.62	0.00	0.00	0.00	0.00	2-$ClC_6H_4OCH_2$—
5.62	5.70	5.59	Cl	0.18	2.73	0.23	0.23	0.41	−0.15	4-$ClC_6H_4OCH_2$—
6.19	6.13	6.13	H	1.24	2.78	0.00	0.00	0.00	0.00	2-$BrC_6H_4OCH_2$—
5.68	5.67	5.67	Br	0.00	3.05	0.23	0.23	0.44	−0.17	4-$BrC_6H_4OCH_2$—
5.66	5.85	5.89	H	1.24	2.04	0.00	0.00	0.00	0.00	2-$FC_6H_4OCH_2$—
6.28	6.20	6.18	H	1.24	2.95	0.00	0.00	0.00	0.00	2-$IC_6H_4OCH_2$—
5.84	5.92	6.02	Cl	0.18	4.09	0.23	0.09	0.41	−0.15	3,5-$(CH_3)_2$,4-$ClC_6H_2OCH_2$—
6.10	6.09	6.09	H	1.24	2.67	0.00	0.00	0.00	0.00	$C_6H_5SCH_2$—
6.07	5.94	6.07	I	−0.20	3.93	0.28	0.28	0.40	−0.19	4-$IC_6H_4SCH_2$—
5.30	5.28	5.30	CH_3O	0.99	2.63	−0.27	−0.27	0.26	−0.51	4-$CH_3OC_6H_4SCH_2$—
6.13	6.17	5.98	Cl	0.18	3.96	0.23	0.23	0.41	−0.15	2,4-$Cl_2C_6H_3SCH_2$—
6.26	6.28	6.25	H	1.24	3.17	0.00	0.00	0.00	0.00	$C_6H_5CH_2SCH_2$—

[a] I_{50} is the molar concentration required to inhibit 50% NADH oxidation (7). [b] Calculated from Eq. 2. [c] The oxidation rate is the increase in substrate-induced NADPH in moles per minute per milligram of protein (7). [d] Calculated from Eq. 9. [e] Calculated from Eq. 10. [f] Allyl-containing barbiturate. [g] The oxidation rate of substrate-dependent NADPH in moles per minute per milligram of protein (8). [h] Calculated from Eq. 12. [i] Estimated from the pKa of *N,N*-dimethyl-*n*-butylamine. [j] I_{50} is the molar concentration required to inhibit 50% epoxidation of aldrin (9). [k] Calculated from Eq. 21. [l] Calculated from Eq. 22.

tuted barbiturates were poorly predicted, and they stimulated the rate of metabolism to a lesser extent than the nonallyl barbiturates.

In a well-designed controlled study, allyl-containing barbiturates administered to rats treated with a microsomal enzyme inducer caused a rapid destruction of the hemeprotein cytochrome P_{450}, while corresponding nonallyl barbiturates did not have this effect (11). The results suggested that the allyl group in the biotransformation process is probably converted to a highly reactive epoxide intermediate, which leads to the reduction of the terminal oxidase involved in drug metabolism (11).

Upon deletion of the allyl barbiturates from the regression analysis, two highly significant equations (Eqs. 9 and 10) were obtained correlating the log of the oxidation rate with either the log $P_{o/w}$ or the maximal type I spectral change (ΔE). The coefficient of 0.58 in Eq. 9 associated with log $P_{o/w}$ is within the range (0.60 ± 0.1) of the log $P_{\text{octanol-water}}$ reported for various types of drug metabolism (6), as well as for the nonspecific binding of organic compounds to a wide variety of proteins and proteinaceous materials (12–14). The relationship between log P values measured in these two solvent systems was reported previously (15) to be $\log P_{\text{oil-water}} = 1.099 \log P_{\text{octanol-water}} - 1.310$ with $n = 65$, $r = 0.98$, and $s = 0.27$.

Table II—Equations Correlating Various Microsomal Oxidations with Physicochemical Constants

Equation	n^a	s^b	r^c	Equation Number
Inhibition of beef heart submitochondrial NADH oxidation by barbiturates				
$\log 1/I_{50} = 0.68$ pKa $- 2.25$	14	0.446	0.372	1
$= 0.88 \log P_{(\text{corn oil-water})} + 2.78$	14	0.133	0.961	2
Stimulation of rat liver microsomal NADPH oxidation by barbiturates				
log (oxidation rate) $= 0.05\ \Sigma E_{s(R_1+R_2)} + 0.91$	14	0.317	0.082	3
$= 0.27$ pKa $- 1.25$	14	0.310	0.223	4
$= 0.36 \log P_{(\text{corn oil-water})} + 0.75$	14	0.256	0.593	5
$= 13.16\ \Delta E_{(\text{max type I})} + 0.72$	12	0.175	0.718	6
Exclusion of allyl-containing barbiturates				
log (oxidation rate) $= 0.29$ pKa $- 1.31$	9	0.338	0.273	7
$= 0.46\ \Sigma E_{s(R_1+R_2)} + 0.61$	9	0.294	0.547	8
$= 0.58 \log P_{(\text{corn oil-water})} + 0.79$	9	0.116	0.944	9
$= 11.25\ \Delta E_{(\text{max type I})} + 0.81$	8	0.063	0.939	10
Pork liver microsomal NADPH dependent *N*-oxidation of tertiary amines				
log (oxidation rate) $= 0.09 \log P - 6.61$	10	0.269	0.672	11
$= -0.03 (\log P)^2 + 0.37 (\log P) - 7.06$				
$\log P_o = 5.69\ (5.12 - 6.64)^d$	10	0.106	0.962	12
Inhibition of rat liver microsomal epoxidation of aldrin by imidazole derivatives				
$\log 1/I_{50} = 0.11 \log P + 5.61$	13	0.298	0.247	13
$= 0.12\ E_{s(p)} + 5.84$	13	0.299	0.239	14
$= 0.35\ \sigma_{(p)} + 5.91$	13	0.302	0.186	15
$= 0.43\ \Sigma\sigma_{(m+p)} + 5.91$	13	0.300	0.219	16
$= 0.42\ E_{s(p)} + 0.37 \log P + 4.52$	13	0.249	0.637	17
$= 2.22\ \sigma_{(p)} + 0.61\ E_{s(p)} + 5.31$	13	0.227	0.713	18
$= 2.07\ \Sigma\sigma_{(m+p)} + 0.53\ E_{s(p)} + 5.40$	13	0.232	0.696	19
$= 1.96\ \sigma_{(p)} + 0.81\ E_{s(p)} + 0.32 \log P + 4.22$	13	0.166	0.872	20
$= 2.15\ \Sigma\sigma_{(m+p)} + 0.86\ E_{s(p)} + 0.39 \log P + 4.00$	13	0.125	0.930	21
$= -1.75\ F_{(p)} + 0.78\ R_{(p)} - 0.29\ E_{s(p)} + 0.32 \log P + 5.58$	13	0.147	0.914	22

[a] The number of data points or compounds used in the regression analysis. [b] The standard deviation from the regression. [c] The correlation coefficient. [d] The 95% confidence interval on $\log P_o$.

The *N*-oxidation rates of various amines were studied using a purified microsomal mixed function amine oxidase system (8). A relationship was found between the oxidation rate and the chain length up to nine carbons for the tertiary amines studied (8).

Analysis of only the substituted *N,N*-dimethyl tertiary amines, forming detectable corresponding *N*-oxide metabolites, showed a highly statistically significant (99.95 percentile level) parabolic equation (Eq. 12) using the *F* test. Included in the regression analysis were chlorpromazine and morphine, which are also tertiary amines. When these compounds were tested under the same conditions, they gave the corresponding *N*-oxide and fit reasonably well into the regression curve (Fig. 1). By setting the $d \log(\text{oxidation rate})/(d \log P) = 0$, the optimal $\log P_o$ of 5.69 for maximal *N*-oxidation with a 95% confidence interval of 5.12–6.64 was obtained. Chlorpromazine, with a log *P* of 5.35, is close to the $\log P_o$, and it was metabolized at the fastest rate among all of the compounds examined. The log *P* values are for the unprotonated forms, so under physiological conditions at pH 7.4, most aliphatic tertiary amines would be protonated and the log *P* of the charged species would be approximately 3 log units lower (16). The addition of the pKa term to account for differences in the basicity of aromatic *versus* aliphatic tertiary amines did not significantly improve the correlation.

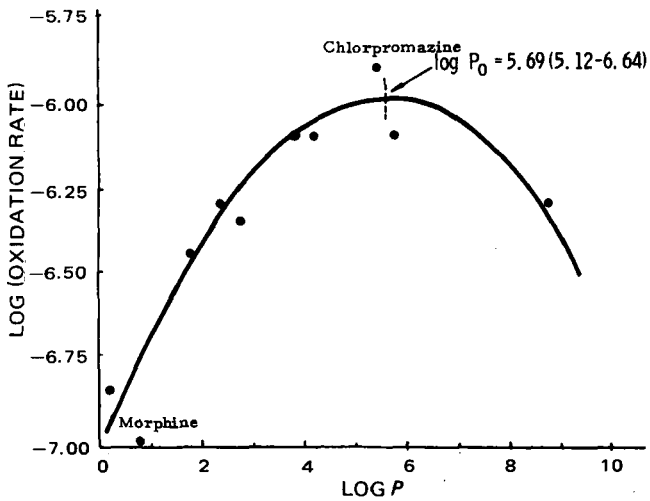

Figure 1—*Parabolic dependence of the* N*-oxidation rate of tertiary amines on log* P *(Eq. 12).*

In contrast to the relatively nonspecific microsomal oxidations where the lipophilicity of the substrate is of primary importance, the inhibition of the rat liver microsomal epoxidation of aldrin by substituted imidazoles (9) appears to be much more specific on both electronic and steric parameters.

The best equations obtained from all possible combinations of linear and quadratic equations are Eqs. 20–22. In Eq. 21, the positive coefficient on the summation of Hammett's (σ) constant for both the *meta*- and *para*-positions on the benzene ring suggests that an electron-withdrawing group enhances the inhibitory activity. The positive dependence on Taft's (E_s) steric constant suggests the importance of a small substituent in the *para*-position. The addition of log *P* of the whole molecule is statistically significant but is only of secondary importance. This equation reflects the importance of electronic and steric effects in the inhibition of drug metabolism, probably due to greater specificity at the active site.

Similar dependence on σ and E_s also was noted previously for several types of enzyme inhibition such as carbonic anhydrase, D-amino acid oxidase, and monoamine oxidase by various inhibitors (17). Swain's and Lupton's *F* and *R* aromatic substituent constants (18) for field and resonance effects, respectively, gave comparable but not better correlations (Eq. 22).

CONCLUSION

In summary, it is gratifying to see that the fairly complicated biotransformations of various drugs by different microsomal systems can be well correlated with a few physicochemical constants. The results obtained from the available data suggest that the modification of organic compounds by microsomal enzymes can be understood in terms of their physicochemical properties in a quantitative way. This type of approach in the future may be useful in the understanding of drug metabolism and possibly aid the medicinal chemist in drug design *via* molecular modification to affect biotransformation.

REFERENCES

(1) B. B. Brodie, J. R. Gillette, and B. N. LaDu, *Ann. Rev. Biochem.*, **27**, 427(1958).

(2) L. E. Gaudette and B. B. Brodie, *Biochem. Pharmacol.*, **2**, 89(1959).

(3) E. J. Lien and C. Hansch, *J. Pharm. Sci.*, **57**, 1027(1968).

(4) C. Hansch, E. J. Lien, and F. Helmer, *Arch. Biochem. Biophys.*, **128**, 139(1968).

(5) Y. C. Martin and C. Hansch, *J. Med. Chem.*, **14**, 777(1971).

(6) C. Hansch, *Drug Metab. Rev.*, **1**, 1(1972).

(7) I. Jannson, S. Orrenius, L. Ernster, and J. B. Schenkman, *Arch. Biochem. Biophys.*, **151**, 391(1972).

(8) D. M. Ziegler, C. H. Mitchell, and D. Jollow, "Microsomes and Drug Oxidation," Academic, New York, N.Y., 1969, pp. 173–188.

(9) C. F. Wilkinson, K. Hetnarski, and T. O. Yellin, *Biochem. Pharmacol.*, **21**, 3187(1972).

(10) C. Hansch and S. M. Anderson, *J. Med. Chem.*, **10**, 745(1967).

(11) W. Levin, E. Sernatinger, M. Jacobson, and R. Kuntzman, *Science*, **176**, 1341(1972).

(12) C. Hansch, *Proc. Int. Congr. Pharmacol.*, **4**, 128(1969).

(13) C. Hansch, in "Drug Design," vol. 1, E. J. Ariens, Ed., Academic, New York, N.Y., 1971, p. 271.

(14) C. Hansch, "Biological Correlations—The Hansch Approach," American Chemical Society, Washington, D.C., 1972, pp. 20–40.

(15) A. Leo, C. Hansch, and D. Elkins, *Chem. Rev.*, **71**, 525(1972).

(16) E. J. Lien and G. L. Tong, *Cancer Chemother. Rep.*, **57**, 251(1973).

(17) E. J. Lien, M. Hussain, and G. L. Tong, *J. Pharm. Sci.*, **59**, 865(1970).

(18) C. Hansch, A. Leo, S. H. Unger, K. H. Kim, D. Nikaitani, and E. J. Lien, *J. Med. Chem.*, **16**, 1207(1973).

ACKNOWLEDGMENTS AND ADDRESSES

Received November 3, 1975, from the *Section of Biomedicinal Chemistry, School of Pharmacy, University of Southern California, Los Angeles, CA 90033*

Accepted for publication January 26, 1976.

Presented in part at the Medicinal Chemistry Section, 167th American Chemical Society National Meeting, Los Angeles, Calif., April 5, 1974.

The authors thank the staff of the Computer Science Laboratory of this University for data processing service. G. L. Tong is especially grateful to Dr. Wolfgang Sadee for kind and helpful discussions.

[x] To whom inquiries should be directed.

Effect of Topically Applied Pilocarpine on Tear Film pH

A. LONGWELL [x], S. BIRSS, N. KELLER, and D. MOORE

Abstract □ Changes in tear film pH were observed during the 1st hr after instillation of pilocarpine in various dosage forms to the rabbit eye. In anesthetized rabbits, with periodic blinking induced electrically, commercial formulations of pilocarpine salts applied as drops or a spray acutely lowered tear film pH by 1.1–1.6 pH units. The pH remained below pretreatment levels for 45–>60 min after instillation. Pilocarpine base, administered continuously at the rates of 20 or 80 μg/hr from ocular therapeutic systems, had little or no effect on tear film pH in this same animal preparation. The reduction in tear film pH produced by pilocarpine eyedrops or spray solution is attributable to the acid pH and buffer capacity of these solutions. Delivery of pilocarpine base without pH change was achieved with ocular therapeutic systems, because the drug (pKa = 7.07) was delivered free, or virtually so, of excipients. These observed differences in tear film pH after application may partially explain the four- to eightfold reduction in total effective pilocarpine dose with ocular therapeutic systems compared to eyedrops or spray, since the cornea is less permeable to ionized than to unionized molecules.

Keyphrases □ Pilocarpine—topically applied base and salts, effect on tear film pH, rabbits □ Tear film pH—effect of topically applied pilocarpine, base and salts compared, rabbits □ pH—tear film, effect of topically applied pilocarpine, base and salts compared, rabbits □ Ophthalmic cholinergic agents—pilocarpine base and salts, topically applied, effect on tear film pH, rabbits

The pH of the tear film is of interest to ophthalmic pharmacologists for two reasons. Tear pH is an important factor in the penetration of any topically applied ophthalmic drug that is a weak base, since the cornea is less permeable to ionized than to unionized molecules. In addition, well-buffered acid solutions are known to cause more sensation of stinging or burning to the eye than do weakly buffered acid solutions, because the concentrated acid buffer overwhelms the *in vivo* buffer capacity of tear film.

The major buffering system in extracellular fluids, including tears, is the bicarbonate system. Tear film concentration of bicarbonate is the same as that of plasma. However, the total buffering capacity of tear film is obviously very small, since its volume is only about 7 μl. Thus, the addition of eyedrop solutions such as 1–4% pilocarpine at pH 4–5, in volumes five to 10 times that of the tear film, might be expected to overwhelm, for a time, the buffering capacity of the tears.

Pilocarpine is dispensed as a nitrate or hydrochloride in solutions ranging from 0.5 to 10% (0.025–0.5 *M*); even at the commonly prescribed concentration of 2% (0.1 *M*), a solution of pilocarpine nitrate alone, which has an equilibrium pH of 3.9, is a fairly concentrated buffer. The pH of most pilocarpine ophthalmic solutions, however, is adjusted to 4.5–5.5, but no higher, for reasons of drug stability in solution. The topical application of these low pH solutions of pilocarpine, either in eyedrops or in sprays, should reduce tear film pH for some time after administration.

CONCLUSION

In summary, it is gratifying to see that the fairly complicated biotransformations of various drugs by different microsomal systems can be well correlated with a few physicochemical constants. The results obtained from the available data suggest that the modification of organic compounds by microsomal enzymes can be understood in terms of their physicochemical properties in a quantitative way. This type of approach in the future may be useful in the understanding of drug metabolism and possibly aid the medicinal chemist in drug design *via* molecular modification to affect biotransformation.

REFERENCES

(1) B. B. Brodie, J. R. Gillette, and B. N. LaDu, *Ann. Rev. Biochem.*, **27**, 427(1958).

(2) L. E. Gaudette and B. B. Brodie, *Biochem. Pharmacol.*, **2**, 89(1959).

(3) E. J. Lien and C. Hansch, *J. Pharm. Sci.*, **57**, 1027(1968).

(4) C. Hansch, E. J. Lien, and F. Helmer, *Arch. Biochem. Biophys.*, **128**, 139(1968).

(5) Y. C. Martin and C. Hansch, *J. Med. Chem.*, **14**, 777(1971).

(6) C. Hansch, *Drug Metab. Rev.*, **1**, 1(1972).

(7) I. Jannson, S. Orrenius, L. Ernster, and J. B. Schenkman, *Arch. Biochem. Biophys.*, **151**, 391(1972).

(8) D. M. Ziegler, C. H. Mitchell, and D. Jollow, "Microsomes and Drug Oxidation," Academic, New York, N.Y., 1969, pp. 173–188.

(9) C. F. Wilkinson, K. Hetnarski, and T. O. Yellin, *Biochem. Pharmacol.*, **21**, 3187(1972).

(10) C. Hansch and S. M. Anderson, *J. Med. Chem.*, **10**, 745(1967).

(11) W. Levin, E. Sernatinger, M. Jacobson, and R. Kuntzman, *Science*, **176**, 1341(1972).

(12) C. Hansch, *Proc. Int. Congr. Pharmacol.*, **4**, 128(1969).

(13) C. Hansch, in "Drug Design," vol. 1, E. J. Ariens, Ed., Academic, New York, N.Y., 1971, p. 271.

(14) C. Hansch, "Biological Correlations—The Hansch Approach," American Chemical Society, Washington, D.C., 1972, pp. 20–40.

(15) A. Leo, C. Hansch, and D. Elkins, *Chem. Rev.*, **71**, 525(1972).

(16) E. J. Lien and G. L. Tong, *Cancer Chemother. Rep.*, **57**, 251(1973).

(17) E. J. Lien, M. Hussain, and G. L. Tong, *J. Pharm. Sci.*, **59**, 865(1970).

(18) C. Hansch, A. Leo, S. H. Unger, K. H. Kim, D. Nikaitani, and E. J. Lien, *J. Med. Chem.*, **16**, 1207(1973).

ACKNOWLEDGMENTS AND ADDRESSES

Received November 3, 1975, from the *Section of Biomedicinal Chemistry, School of Pharmacy, University of Southern California, Los Angeles, CA 90033*

Accepted for publication January 26, 1976.

Presented in part at the Medicinal Chemistry Section, 167th American Chemical Society National Meeting, Los Angeles, Calif., April 5, 1974.

The authors thank the staff of the Computer Science Laboratory of this University for data processing service. G. L. Tong is especially grateful to Dr. Wolfgang Sadee for kind and helpful discussions.

[x] To whom inquiries should be directed.

Effect of Topically Applied Pilocarpine on Tear Film pH

A. LONGWELL [x], S. BIRSS, N. KELLER, and D. MOORE

Abstract □ Changes in tear film pH were observed during the 1st hr after instillation of pilocarpine in various dosage forms to the rabbit eye. In anesthetized rabbits, with periodic blinking induced electrically, commercial formulations of pilocarpine salts applied as drops or a spray acutely lowered tear film pH by 1.1–1.6 pH units. The pH remained below pretreatment levels for 45–>60 min after instillation. Pilocarpine base, administered continuously at the rates of 20 or 80 μg/hr from ocular therapeutic systems, had little or no effect on tear film pH in this same animal preparation. The reduction in tear film pH produced by pilocarpine eyedrops or spray solution is attributable to the acid pH and buffer capacity of these solutions. Delivery of pilocarpine base without pH change was achieved with ocular therapeutic systems, because the drug (pKa = 7.07) was delivered free, or virtually so, of excipients. These observed differences in tear film pH after application may partially explain the four- to eightfold reduction in total effective pilocarpine dose with ocular therapeutic systems compared to eyedrops or spray, since the cornea is less permeable to ionized than to unionized molecules.

Keyphrases □ Pilocarpine—topically applied base and salts, effect on tear film pH, rabbits □ Tear film pH—effect of topically applied pilocarpine, base and salts compared, rabbits □ pH—tear film, effect of topically applied pilocarpine, base and salts compared, rabbits □ Ophthalmic cholinergic agents—pilocarpine base and salts, topically applied, effect on tear film pH, rabbits

The pH of the tear film is of interest to ophthalmic pharmacologists for two reasons. Tear pH is an important factor in the penetration of any topically applied ophthalmic drug that is a weak base, since the cornea is less permeable to ionized than to unionized molecules. In addition, well-buffered acid solutions are known to cause more sensation of stinging or burning to the eye than do weakly buffered acid solutions, because the concentrated acid buffer overwhelms the *in vivo* buffer capacity of tear film.

The major buffering system in extracellular fluids, including tears, is the bicarbonate system. Tear film concentration of bicarbonate is the same as that of plasma. However, the total buffering capacity of tear film is obviously very small, since its volume is only about 7 μl. Thus, the addition of eyedrop solutions such as 1–4% pilocarpine at pH 4–5, in volumes five to 10 times that of the tear film, might be expected to overwhelm, for a time, the buffering capacity of the tears.

Pilocarpine is dispensed as a nitrate or hydrochloride in solutions ranging from 0.5 to 10% (0.025–0.5 *M*); even at the commonly prescribed concentration of 2% (0.1 *M*), a solution of pilocarpine nitrate alone, which has an equilibrium pH of 3.9, is a fairly concentrated buffer. The pH of most pilocarpine ophthalmic solutions, however, is adjusted to 4.5–5.5, but no higher, for reasons of drug stability in solution. The topical application of these low pH solutions of pilocarpine, either in eyedrops or in sprays, should reduce tear film pH for some time after administration.

The purpose of these studies was to compare the magnitude and duration of pH changes in tear film of anesthetized rabbits produced by: (*a*) a spray or various pilocarpine eyedrop solutions; (*b*) solutions of a strong acid (hydrochloric), and (*c*) pilocarpine free base delivered continuously without excipients or exogenous fluid from ocular therapeutic systems at rates that span the range used clinically.

EXPERIMENTAL

Animals—New Zealand White rabbits of either sex, 2.0–3.5 kg, were caged individually and fed and watered *ad libitum*.

pH Measurements—A combination electrode pH probe[1] with a sensing bulb diameter of 1.2 mm is easily accommodated in the nasal corner of the lower cul-de-sac. Recordings of pH were made with a digital pH meter[2]. Before and after each experiment, the electrode was calibrated with a pH 7 buffer and checked for linearity with pH 5 and 8 buffers.

Prior to pH measurements in the tear film, rabbits were anesthetized with 0.016 g of thiopental sodium[3]/kg iv. Additional thiopental sodium, injected as needed, maintained anesthesia throughout the experiment as gauged by absence of the blink reflex. After a tracheotomy was performed, the tracheal tube was connected to a respirator with the tidal volume set at less than 20 cm^3/stroke and the frequency set at 30–40 strokes/min. The animal's head was immobilized in the upright position, and the pH electrode was set in place. Care was taken to avoid covering the lacrimal punctum with the electrode.

Because lacrimation is at a minimum in the unstimulated anesthetized animal (1), tear production was maintained by electrically induced blinking. A stimulating electrode, inserted through the skin into the palpebral portion of the orbicularis muscle of the upper eyelid, was connected to a stimulator[4]. Every 5 sec, the stimulator induced a blink by applying a pulse of 5–7 v and 20-msec duration. This interval between blinks is considerably shorter than the interval in a conscious rabbit but is characteristic of the blink rate in humans. Tear production in anesthetized rabbits with electrically induced blinking every 5 sec was measured previously (2).

The nasolacrimal duct was cannulated, and fluid collected over 30-min intervals was weighed. The average rate of tear production over 90 min was 0.78 ± 0.18 (*SE*) μl/min. The rate of tear production did not decline during this 90-min period. When pH measurements were made, blinking was stimulated for several minutes before the first pH measurement was taken. Subsequent pH measurements were taken every 5 min. One minute before a pH reading was made, the blink stimulator was turned off, the measurement was made, and blinking was reestablished.

Before any test solution was instilled or any ocular therapeutic system was placed in the eye, baseline pH measurements were taken every 5 min for 20–30 min. When four successive pH readings varied no more than ± 0.05 pH unit, the preparation was considered stable. To date, in 10 out of 82 of these eye preparations, a "constant" level of ±0.05 pH unit was not observed during nine successive 5-min measurements. Such preparations were rejected as "unstable." Once stable tear film pH levels were observed, test solutions or systems were applied; tear film pH was recorded every 5 min for 60 min following application.

Experimental Design—Eyes of each experimental animal were treated sequentially, but no rabbit received the same treatment in both eyes. Eight eyes in a control group received no eyedrops or pilocarpine in any form. Two groups of six eyes each received a 50-μl drop of 10^{-2} or 10^{-4} *M* HCl.

Four groups of six eyes each received solutions of pilocarpine salts and excipients. Four different commercially available pilocarpine solutions were used: Solution A[5], 2% pilocarpine hydrochloride at pH 4.5; Solution B[6], 2% pilocarpine nitrate at pH 4.8; Solution C[7], 2% pilocarpine hydrochloride at pH 5.3, supplied in a spray bottle; and Solution D[8], 2% pilocarpine hydrochloride at pH 5.0. The eyedrops were applied as 50-μl drops, and the spray was applied in a quantity estimated to be about 85 μl. Two groups of six eyes each received ocular therapeutic systems designed to deliver unbuffered pilocarpine base to the tear film at the rate of 20 or 80 μg/hr[9].

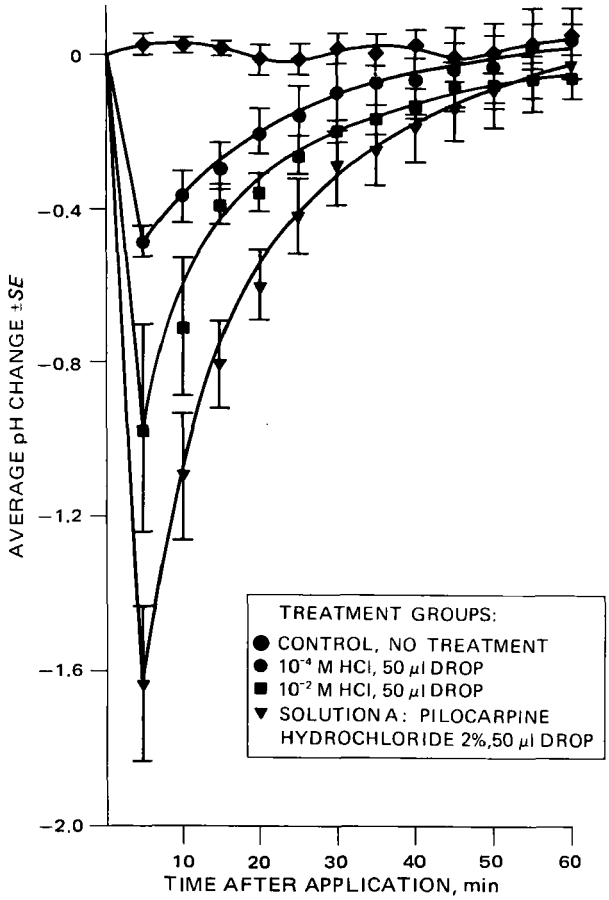

Figure 1—*Comparison of effect of instillation of hydrochloric acid on rabbit tear film pH with that of instillation of pilocarpine ophthalmic solution.*

The initial, pretreatment pH values were averaged. For untreated controls, values taken in the first 30 min after insertion of the probe were averaged. Changes from this average baseline pH after each type of treatment, including *no* treatment, were recorded for each rabbit eye. The response to any of the treatment regimens (including no treatment) is expressed as the average, over all animals in the treatment group, of the changes in tear film pH from each animal's baseline period average.

RESULTS

The undisturbed tear film pH of 56 rabbit eyes measured every 5 min over the 20-min pretreatment period averaged 7.47 (n = 56, SE ± 0.03). This value is very like the average normal human tear film pH of 7.4 (range of 7.3–7.7) (3). The change in pH over a 60-min period in untreated eyes was determined by measuring tear film pH in eight untreated eyes every 5 min for 80 min, averaging the first four values, and comparing the last 12 values with this initial average. The largest range of pH change for individual eyes was +0.18, −0.27 pH unit, observed during the experimental period. Thus, the pH of the normal, undisturbed tear film was quite stable.

The average variation of pH in untreated eyes is shown in Fig. 1. No evidence of drift, either to acid or basic pH, was apparent in tears of untreated eyes.

[1] Microelectrodes, Inc.
[2] Beckman.
[3] Pentothal sodium, Abbott.
[4] Grass S-6.
[5] Isopto Carpine ophthalmic solution, 2%, Alcon Laboratories.
[6] P. V. Carpine Liquifilm ophthalmic solution, 2%, Allergan Pharmaceuticals.
[7] Mistura P, ophthalmic solution sterile, 2%, Lederle Laboratories.
[8] Adsorbocarpine ophthalmic solution USP, 2%, Burton, Parsons and Co.
[9] OCUSERT Pilo-20 ocular therapeutic system, 20 μg/hr, for 1 week, Alza Pharmaceuticals. The 80-μg/hr system is an Investigational New Drug, Alza Research Division of Alza Corp.

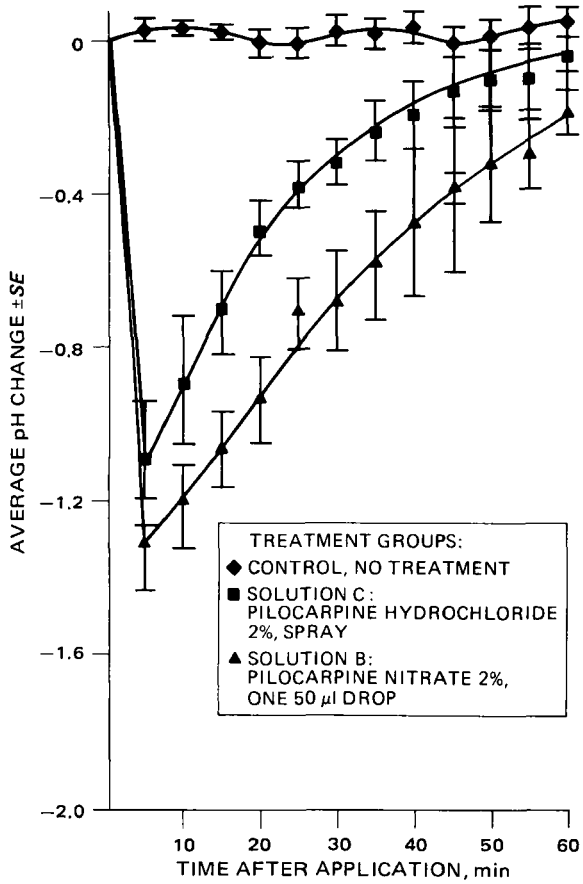

Figure 2—*Effect of administration of pilocarpine solutions in drop forms or spray on rabbit tear film pH.*

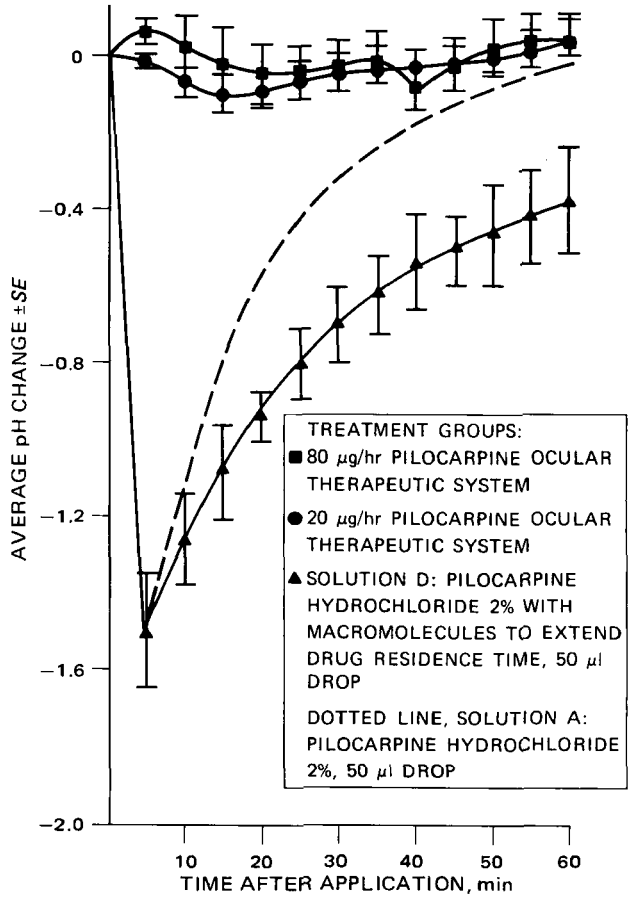

Figure 3—*Comparison of effect on rabbit tear film pH of a pilocarpine hydrochloride ophthalmic solution formulated to extend drop residence time with continuous delivery of pilocarpine* via *ocular therapeutic systems. The dashed line indicates the pH change observed in tears when a pilocarpine hydrochloride ophthalmic solution from another manufacturer was applied.*

Figure 1 also compares the perturbations of tear film pH in rabbit eyes produced by a single drop of pilocarpine ophthalmic solution with those produced by the addition of a single drop of either 10^{-2} or 10^{-4} *M* HCl. The pilocarpine solution produced a change of greater magnitude and longer duration than did the strong acids. For the strong acid, the magnitude and duration of the response were concentration dependent. Within 5 min after addition of a 10^{-4} *M* HCl drop, an average decrease of 0.5 pH unit occurred in tear film pH, which returned to the control level at 30 min. Instillation of a drop of 10^{-2} *M* HCl solution caused an average pH reduction of 1 pH unit within 5 min; the recovery time was 45 min. The instillation of pilocarpine preparations at pH 4.4–5.3, however, caused a greater and more persistent reduction in tear film pH than did hydrochloric acid alone at pH 4 or even at pH 2 (Figs. 1 and 2).

Following administration of these eyedrop solutions or the spray, the mean maximum pH decrease measured at the 5-min observation time could be correlated with the pH of the bulk solution. Solution C, pH 5.3, caused an average maximum decrease in tear pH of 1.10 pH units; Solution A, pH 4.5, caused a maximum tear pH decrease of 1.63 pH units. Solution B, with an intermediate pH, produced a maximum decrease in tear pH that was intermediate between those produced by Solutions A and C.

In all cases, recovery times were prolonged compared to those observed for the pH 4 hydrochloric acid solution. In contrast to the 30 min required for recovery of tear film pH after 10^{-4} *M* HCl, recovery time after a pilocarpine eyedrop ranged from 45 to >60 min. At 60 min after application of Solution B, the tear film pH values were still significantly below pretreatment levels ($p < 0.05$).

Figure 3 compares the effects on tear film pH of two different rates of pilocarpine release, 20 and 80 µg/hr, from ocular therapeutic systems and the effect of Solution D. The latter is a pilocarpine solution made with water-soluble polymers to increase the residence time of the drug in the eye. For comparison, the average curve of Solution A is repeated from Fig. 1. Solution D lowered pH below control levels for more than 60 min ($p < 0.05$), and the average pH change at 60 min was the greatest of all observed changes for that time. In contrast, the fluctuations in pH during 1 hr of continuous delivery of pilocarpine from ocular therapeutic systems were ±0.1 pH unit.

DISCUSSION

This study compared the magnitude and duration of pH changes in tear film induced by various forms of topical pilocarpine. Solutions were applied at the same volumes or, in the case of the spray, at higher volumes, and under the same conditions as was hydrochloric acid at two different concentrations. These pilocarpine solutions lowered tear pH more than did hydrochloric acid of the same pH. In addition, the duration of the pH change was longer than that produced by a strong acid.

Since this study was carried out in anesthetized animals with artifically stimulated, relatively constant tear flow, some effects of applying drops, sprays, or ocular therapeutic systems to the eye of a conscious animal may be absent. Extensive reflex tearing in response to a burning sensation, common in conscious humans, will probably not be observed, and differences in the rate of tear drainage between conscious and anesthetized animals (1) will affect the absolute rate at which tear film returns to normal pH after instillation of a drop. However, the observed relationships between various forms of ophthalmic medication and acid drops should remain valid under other conditions, *i.e.*, in the conscious animal.

The rate of change of pilocarpine concentration in the tear film is a function of the tear drainage rate. For a given tear production, the concentration of pilocarpine in tear film changes slowly when drainage is slow and vice versa. For drops, when tear film pilocarpine concentration is maximum, presumably at the instant of drop instillation, tear pH is at a minimum, at or below that measured at 5 min after application. Then, concomitant with the subsequent decline in tear pilocarpine concentration, tear pH returns to normal.

Changes in tear film pH alter the rate of ocular penetration of topically applied drugs that are weak acids or bases, because the ratio of their ionized to unionized form is a function of pH and because ionized molecules do not easily penetrate the cornea. Pilocarpine, a case in point, is a weak base, pKa 7.07, but is formulated as a salt in eyedrop preparations. Pilocarpine nitrate at 0.1 *M* in water at 20° has an equilibrium pH of 3.9, but the pH of pilocarpine nitrate ophthalmic formulations is adjusted to 4–5. Altering the pH of tears toward the acid side increases the proportion of protonated pilocarpine to the unionized pilocarpine base in the tears, and the rate of penetration of the drug to the internal eye is expected to decrease.

Anderson and Cowles (4) showed that pilocarpine is a more effective ocular hypotensive agent when administered at pH 6.5 (22% unionized) than at pH 5 (1% unionized). They suggested that this enhanced efficacy at pH 6.5 is a result of increased penetration of pilocarpine due to a greater concentration of the unionized form of the drug. These results suggest that, for a given pilocarpine concentration, more drug will enter the eye if the physiological pH of the tear film can be maintained coincident with drug administration. Unfortunately, the pH of eyedrop solutions must be kept low at present to stabilize the pilocarpine, necessitating larger doses for therapeutic effect than would otherwise be required with more nearly physiological pH.

Fairbairn *et al.* (5) indicated that a more concentrated acid buffer causes a stronger sensation of stinging or burning than does a less concentrated buffer of the same acid pH. Presumably, this sensory effect occurs because the tear film remains at a lower pH for a longer time with the more concentrated buffer. Fairbairn *et al.* (5) recommended minimum buffering of acidic ophthalmic solutions to permit the tear film to return to the physiological pH range rapidly. This conclusion, that the stronger the acid buffer the more subjectively irritating the eyedrop, appears valid for pilocarpine solutions.

Pilocarpine exerts no known topical anesthetic effect, so it should not suppress any stinging sensation caused by a lowering of eye surface pH. The combination of drug and excipients causes at least as great a sensation of burning and stinging as a solution of pharmacologically inactive salt with identical buffer capacity. Whether or not pilocarpine solutions are subjectively more irritating at lower pH values depends not only on the extent and duration of the induced pH change but also on the relative potential for irritation of the protonated *versus* the base form of drug. This question awaits further investigation.

Hydrochloric acid alone in pH 4 solutions produced smaller decreases in tear film pH, and the recovery time to pretreatment tear film pH was shorter by 15 min than with any 2% pilocarpine solution tested. Attempts to prolong residence time of pilocarpine in the eye by adding macromolecules to the formulation (Solution D) appeared to prolong the duration of pH change as well.

The results of this study indicate that reduction of tear film pH by pilocarpine eyedrop formulations is not a simple function of solution pH. On the contrary, both the contact time and the acidic buffer capacity of these solutions contribute to the magnitude and duration of lowered tear film pH after an eyedrop of an ophthalmic pilocarpine formulation is instilled.

The continuous delivery of pilocarpine base in the absence of concomitant delivery of acid buffers favors the prevalence of the neutral base form of pilocarpine. The neutral form of pilocarpine should readily penetrate the lipophilic corneal epithelial barrier, in contrast to the protonated form which predominates at pH < 7. This reasoning may partially explain why continuous delivery of pilocarpine is clinically effective at daily doses of one-fourth to one-eighth (6, 7), and occasionally as little as one-fourteenth (8), those usually administered by eyedrops.

REFERENCES

(1) S. S. Chrai, T. Patton, A. Mehta, and J. Robinson, *J. Pharm. Sci.*, **62**, 1112(1973).

(2) N. Keller, D. M. Moore, and J. Urquhart, "Pilocarpine Kinetics in Rabbit Eye Tear Film during Continuous Administration," presented at ARVO meeting, Sarasota, Fla., Apr. 28, 1976.

(3) R. A. Moses, "Adler's Physiology of the Eye," 5th ed., Mosby, St. Louis, Mo., 1970, p. 21.

(4) R. A. Anderson and J. B. Cowles, *Br. J. Ophthalmol.*, **52**, 607(1968).

(5) W. Fairbairn, W. Shepherd, and S. Eriksen, in preparation, cited by Allergan Pharmaceuticals, *J. Am. Optom. Assoc.*, **40**, 720(1969).

(6) P. Lee, Y. Shen, and M. Eberle, *Invest. Ophthalmol.*, **14**, 43(1975).

(7) M. S. Armaly and K. R. Rao, in "Symposium on Ocular Therapy," I. H. Leopold, Ed., Mosby, St. Louis, Mo., 1973, pp. 80–94.

(8) K. L. Macoul and D. Pavan-Langston, *Arch. Ophthalmol.*, **93**, 587(1975).

ACKNOWLEDGMENTS AND ADDRESSES

Received October 15, 1975, from *Alza Research, a Division of Alza Corporation, Palo Alto, CA 94304*

Accepted for publication February 9, 1976.

[x] To whom inquiries should be directed.

Bioavailability Assessment under Quasi- and Nonsteady-State Conditions III: Application

J. V. BONDI, H. B. HUCKER, K. C. YEH, and K. C. KWAN [x]

Abstract □ The applicability of bioavailability assessment at quasi- and nonsteady state is illustrated with data from a study comparing two formulations of amitriptyline hydrochloride in humans. Relative bioavailability as a function of the observed mean plasma concentrations may be expressed in closed form, provided the affected intervals begin and end in the log–linear region. Alternatively, numerical, graphical, and/or electronic computational techniques may be used to simulate the appropriate $[\overline{C}p^{(i)}]_{sim}$, the proximity of which to $[\overline{C}p^{(i)}]_{obs}$ is a function of relative bioavailability and of ω. If a model can be found to fit the data adequately, it would be sufficient that only one sampled interval end in the log–linear phase.

Keyphrases □ Bioavailability—amitriptyline hydrochloride, assessment at quasi- and nonsteady state, equations derived □ Amitriptyline hydrochloride—bioavailability assessment at quasi- and nonsteady state, equations derived □ Antidepressants—amitriptyline hydrochloride, bioavailability assessment at quasi- and nonsteady state, equations derived

Previous reports (1, 2) in this series dealt with the theoretical basis for bioavailability assessment at quasi- and nonsteady state and its versatility in accommodating variations in experimental design. The purpose of this report is to apply the proposed technique to data from a study comparing two different formulations of

Changes in tear film pH alter the rate of ocular penetration of topically applied drugs that are weak acids or bases, because the ratio of their ionized to unionized form is a function of pH and because ionized molecules do not easily penetrate the cornea. Pilocarpine, a case in point, is a weak base, pKa 7.07, but is formulated as a salt in eyedrop preparations. Pilocarpine nitrate at 0.1 *M* in water at 20° has an equilibrium pH of 3.9, but the pH of pilocarpine nitrate ophthalmic formulations is adjusted to 4–5. Altering the pH of tears toward the acid side increases the proportion of protonated pilocarpine to the unionized pilocarpine base in the tears, and the rate of penetration of the drug to the internal eye is expected to decrease.

Anderson and Cowles (4) showed that pilocarpine is a more effective ocular hypotensive agent when administered at pH 6.5 (22% unionized) than at pH 5 (1% unionized). They suggested that this enhanced efficacy at pH 6.5 is a result of increased penetration of pilocarpine due to a greater concentration of the unionized form of the drug. These results suggest that, for a given pilocarpine concentration, more drug will enter the eye if the physiological pH of the tear film can be maintained coincident with drug administration. Unfortunately, the pH of eyedrop solutions must be kept low at present to stabilize the pilocarpine, necessitating larger doses for therapeutic effect than would otherwise be required with more nearly physiological pH.

Fairbairn *et al.* (5) indicated that a more concentrated acid buffer causes a stronger sensation of stinging or burning than does a less concentrated buffer of the same acid pH. Presumably, this sensory effect occurs because the tear film remains at a lower pH for a longer time with the more concentrated buffer. Fairbairn *et al.* (5) recommended minimum buffering of acidic ophthalmic solutions to permit the tear film to return to the physiological pH range rapidly. This conclusion, that the stronger the acid buffer the more subjectively irritating the eyedrop, appears valid for pilocarpine solutions.

Pilocarpine exerts no known topical anesthetic effect, so it should not suppress any stinging sensation caused by a lowering of eye surface pH. The combination of drug and excipients causes at least as great a sensation of burning and stinging as a solution of pharmacologically inactive salt with identical buffer capacity. Whether or not pilocarpine solutions are subjectively more irritating at lower pH values depends not only on the extent and duration of the induced pH change but also on the relative potential for irritation of the protonated *versus* the base form of drug. This question awaits further investigation.

Hydrochloric acid alone in pH 4 solutions produced smaller decreases in tear film pH, and the recovery time to pretreatment tear film pH was shorter by 15 min than with any 2% pilocarpine solution tested. Attempts to prolong residence time of pilocarpine in the eye by adding macromolecules to the formulation (Solution D) appeared to prolong the duration of pH change as well.

The results of this study indicate that reduction of tear film pH by pilocarpine eyedrop formulations is not a simple function of solution pH. On the contrary, both the contact time and the acidic buffer capacity of these solutions contribute to the magnitude and duration of lowered tear film pH after an eyedrop of an ophthalmic pilocarpine formulation is instilled.

The continuous delivery of pilocarpine base in the absence of concomitant delivery of acid buffers favors the prevalence of the neutral base form of pilocarpine. The neutral form of pilocarpine should readily penetrate the lipophilic corneal epithelial barrier, in contrast to the protonated form which predominates at pH < 7. This reasoning may partially explain why continuous delivery of pilocarpine is clinically effective at daily doses of one-fourth to one-eighth (6, 7), and occasionally as little as one-fourteenth (8), those usually administered by eyedrops.

REFERENCES

(1) S. S. Chrai, T. Patton, A. Mehta, and J. Robinson, *J. Pharm. Sci.*, **62**, 1112(1973).

(2) N. Keller, D. M. Moore, and J. Urquhart, "Pilocarpine Kinetics in Rabbit Eye Tear Film during Continuous Administration," presented at ARVO meeting, Sarasota, Fla., Apr. 28, 1976.

(3) R. A. Moses, "Adler's Physiology of the Eye," 5th ed., Mosby, St. Louis, Mo., 1970, p. 21.

(4) R. A. Anderson and J. B. Cowles, *Br. J. Ophthalmol.*, **52**, 607(1968).

(5) W. Fairbairn, W. Shepherd, and S. Eriksen, in preparation, cited by Allergan Pharmaceuticals, *J. Am. Optom. Assoc.*, **40**, 720(1969).

(6) P. Lee, Y. Shen, and M. Eberle, *Invest. Ophthalmol.*, **14**, 43(1975).

(7) M. S. Armaly and K. R. Rao, in "Symposium on Ocular Therapy," I. H. Leopold, Ed., Mosby, St. Louis, Mo., 1973, pp. 80–94.

(8) K. L. Macoul and D. Pavan-Langston, *Arch. Ophthalmol.*, **93**, 587(1975).

ACKNOWLEDGMENTS AND ADDRESSES

Received October 15, 1975, from *Alza Research, a Division of Alza Corporation, Palo Alto, CA 94304*

Accepted for publication February 9, 1976.

[x] To whom inquiries should be directed.

Bioavailability Assessment under Quasi- and Nonsteady-State Conditions III: Application

J. V. BONDI, H. B. HUCKER, K. C. YEH, and K. C. KWAN [x]

Abstract □ The applicability of bioavailability assessment at quasi- and nonsteady state is illustrated with data from a study comparing two formulations of amitriptyline hydrochloride in humans. Relative bioavailability as a function of the observed mean plasma concentrations may be expressed in closed form, provided the affected intervals begin and end in the log–linear region. Alternatively, numerical, graphical, and/or electronic computational techniques may be used to simulate the appropriate $[\overline{C}p^{(i)}]_{sim}$, the proximity of which to $[\overline{C}p^{(i)}]_{obs}$ is a function of relative bioavailability and of ω. If a model can be found to fit the data adequately, it would be sufficient that only one sampled interval end in the log–linear phase.

Keyphrases □ Bioavailability—amitriptyline hydrochloride, assessment at quasi- and nonsteady state, equations derived □ Amitriptyline hydrochloride—bioavailability assessment at quasi- and nonsteady state, equations derived □ Antidepressants—amitriptyline hydrochloride, bioavailability assessment at quasi- and nonsteady state, equations derived

Previous reports (1, 2) in this series dealt with the theoretical basis for bioavailability assessment at quasi- and nonsteady state and its versatility in accommodating variations in experimental design. The purpose of this report is to apply the proposed technique to data from a study comparing two different formulations of

amitriptyline hydrochloride in humans. Details of the study design and of the results were given elsewhere (3); only elements pertinent to the present discussion are repeated here. This example was chosen because several aspects in its design permit considerations of alternative means of estimating relative bioavailability from a given set of results.

The possible analytical options considered include those that attempt to make projections concerning the steady state, those that attempt the opposite of extrapolating to time zero, and some combinations of the two. It is shown that the various approaches are equivalent and that similar conclusions result from these divergent lines of reasoning. Since the various ramifications of the method cannot be exhaustively treated with a single example, other approaches that may have been possible are also discussed.

EXPERIMENTAL

The study was conducted with 12 healthy volunteers over 2 weeks. In Period I (Days 1–7), each subject ingested one 25-mg amitriptyline hydrochloride tablet at 8 am, 2 pm, and 8 pm daily. During Period II (Days 8–14), the same subjects ingested one 75-mg amitriptyline hydrochloride capsule at 8 am daily. On Days 7 and 14, plasma samples were drawn at 8, 9, 10, and 11 am, 12 noon, 2, 5, and 8 pm, and 8 am of the following day. Plasma amitriptyline concentrations were determined by the method of Hucker and Stauffer (4).

DRUG ACCUMULATION

Closed-Form Solutions (Method A)—Since the daily dosage is the same between treatments, the simplest approach would have been to compare individual mean steady-state plasma concentrations, $\overline{C}p^{(ss)}$, projected from the observed mean plasma levels on Day 7, $\overline{C}p^{(7)}$, and on Day 14, $\overline{C}p^{(7+7)}$. The mean plasma concentration on Day 7 is the weighted sum of the mean plasma levels $\overline{C}p^{(7,\tau_1)}$, $\overline{C}p^{(7,\tau_2)}$, and $\overline{C}p^{(7,\tau_3)}$ over each of the three dosing intervals τ_1, τ_2, and τ_3; *i.e.*:

$$\overline{C}p^{(7)} = \frac{\tau_1\overline{C}p^{(7,\tau_1)} + \tau_2\overline{C}p^{(7,\tau_2)} + \tau_3\overline{C}p^{(7,\tau_3)}}{\tau_1 + \tau_2 + \tau_3} \qquad \text{(Eq. 1)}$$

since $\tau_1 + \tau_2 + \tau_3 = 24$ hr, the mean daily plasma concentration at steady state for the prescribed tablet dosage regimen is:

$$[\overline{C}p^{(ss)}]_T = \frac{\overline{C}p^{(7)}}{1 - e^{-7\omega(\tau_1+\tau_2+\tau_3)}} \qquad \text{(Eq. 2)}$$

where ω is the observed terminal slope. Similarly, the mean plasma level over a 24-hr interval at steady state following daily administrations of the capsule formulation is given by:

$$[\overline{C}p^{(ss)}]_C = \frac{\overline{C}p^{(7+7)} - \overline{C}p^{(7)}e^{-7\omega\phi}}{1 - e^{-7\omega\phi}} \qquad \text{(Eq. 3)}$$

where ϕ is the dosing interval for capsules, and the subscripts T and C refer to tablets and capsules, respectively. The numerator of Eq. 3 is the expected mean plasma level after seven daily doses of the capsule formulation represented as the difference between the observed mean on Day 14 and the residual contributions resulting from the prior administration of tablets for 7 days.

The relative bioavailability between the tablet and capsule formulations, F_C/F_T, can be estimated by the ratio of their mean plasma levels at steady state. Combining Eqs. 2 and 3 and rearranging give:

$$\frac{F_C}{F_T} = \frac{\overline{C}p^{(7+7)}}{\overline{C}p^{(7)}} - e^{-7\omega\phi} \qquad \text{(Eq. 4)}$$

Unfortunately, the sampling schedule does not permit satisfactory estimates of $\overline{C}p^{(7,\tau_2)}$ and $\overline{C}p^{(7,\tau_3)}$. Thus, prudence dictates that the analysis should be based on $\overline{C}p^{(7,\tau_1)}$ and $\overline{C}p^{(14,\phi)}$, mean plasma levels during τ_1 on Day 7 and during ϕ on Day 14, respectively. This type of study design is similar to previously described types (2). However, an extension of the general solutions (2) is necessary to account for the intervention of two additional tablet doses between the sampled interval of Period I and the beginning of Period II. In the prevailing situation of r daily doses of tablets for L days in Period I followed by u daily doses of capsules for M days in Period II, it can be shown that the appropriate solution is:

$$\left(\frac{F_{II}}{F_I}\right)_{T/C} = \frac{D_I}{D_{II}}\left\{\frac{[R_I]}{[R_{II}]}\frac{\overline{C}p^{(II,\phi)}}{\overline{C}p^{(I,\tau_1)}}\frac{\phi(1 - e^{-\omega\tau_1})}{\tau_1(1 - e^{-\omega\phi})} - \frac{[R_I']}{[R_{II}]}W\right\} \qquad \text{(Eq. 5)}$$

where D is the dose, $[R_i]$'s are the regimen factors, W is the residue factor, I is identified with tablets in Period I, and II is identified with capsules in Period II. In particular, when $r = 3$, $u = 1$, $l = 3$, $\tau_1 = \tau_2 = 6$ hr, $\tau_3 = 12$ hr, and $\overline{C}p^{(I,\tau_1)}$ is estimated on the Kth ($K \leq L$) day of Period I:

$$[R_I] = (e^{-24\omega})\sum_{j=1}^{r}\left(\prod_{i=1}^{j} e^{\omega\tau_i}\right) - (e^{-24K\omega})\left[1 + \sum_{j=1}^{r-1}\left(\prod_{i=1}^{j} e^{\omega\tau_i}\right)\right] \qquad \text{(Eq. 6a)}$$

$$[R_I] = 1 + e^{-12\omega} + e^{-18\omega} - e^{-24K\omega}(1 + e^{6\omega} + e^{12\omega}) \qquad \text{(Eq. 6b)}$$

$$[R_I'] = (e^{\omega\tau_l})\sum_{j=1}^{l}\left(\prod_{i=j}^{l} e^{-\omega\tau_i}\right) + (e^{-24\omega})\sum_{j=l}^{r-1}\left(\prod_{i=l}^{j} e^{\omega\tau_i}\right) - (e^{-24L\omega})\left(\prod_{i=1}^{l-1} e^{-\omega\tau_i}\right)\left[1 + \sum_{j=1}^{r-1}\left(\prod_{i=1}^{j} e^{\omega\tau_i}\right)\right] \qquad \text{(Eq. 7a)}$$

$$[R_I'] = (1 - e^{-24L\omega})(1 + e^{-6\omega} + e^{-12\omega}) \qquad \text{(Eq. 7b)}$$

$$[R_{II}] = (e^{-24\omega})\sum_{j=1}^{u}\left(\prod_{i=1}^{j} e^{\omega\phi_i}\right) - (e^{-24M\omega})\left[1 + \sum_{j=1}^{u-1}\left(\prod_{i=1}^{j} e^{\omega\phi_i}\right)\right] \qquad \text{(Eq. 8a)}$$

$$[R_{II}] = 1 - e^{-24M\omega} \qquad \text{(Eq. 8b)}$$

and:

$$W = \left(\prod_{i=l}^{r} e^{-\omega\tau_i}\right) e^{-24(M-1)\omega} = (e^{-12\omega})e^{-24(M-1)\omega} \qquad \text{(Eq. 9)}$$

For the present study, $K = L = M = 7$ days such that $\overline{C}p^{(I,\tau_1)}$ is synonymous with $\overline{C}p^{(7,\tau_1)}$ and $\overline{C}p^{(II,\phi)}$ is synonymous with $\overline{C}p^{(14,\phi)}$. However, for the time being, the general notation is retained to facilitate discussion. Whereas the regimen factors, $[R_i]$, serve the same functions previously ascribed (2), their specific combinations in this case should be noted. The inequality between $[R_I]$ and $[R_I']$ is caused by the two additional tablet dosages on Day 7. The ratio $[R_I]/[R_{II}]$ tracks the dosage intervals over which mean plasma levels are determined; the ratio $[R_I']/[R_{II}]$ accounts for the fact that the washout period begins two doses after the one for which estimates of mean plasma concentrations are made in Period I. In other words, the mean plasma concentration ratio and the residue factor share a common regimen factor only when the sampled interval and the washout period begin at the same time.

Simulations (Methods B and C)—Even though relative bioavailability ratios for any tractable dosing sequence would be amenable to solution in closed form, their complexity multiplies rapidly with each additional variant in dosage and dosage regimen and may become a deterrent in general usage. For this reason and for completeness, a somewhat more circuitous approach is suggested that may be of practical utility in some instances.

The strategy evolves with some initial assumptions concerning the ratio of F_C to F_T, which results in the observed plasma concentrations on Day 14. From the observed terminal slope ω and the mean plasma level $\overline{C}p^{(14,\phi)}$, the entire time course of change in plasma concentrations from time zero can be reconstructed through simulation. The validity of the initial assumptions will be reflected in the agreement, or the lack thereof, between simulated and observed plasma levels on Day 7. It will be shown that the ratio of simulated to observed mean plasma levels is a function of the relative bioavailability between treatments I and II. Alternatively, the bioavailability ratio can be varied iteratively until there is agreement between simulated and observed values.

For the prescribed dosing sequence, the mean plasma concentration during any capsule dosage interval in Period II can be represented by:

$$\overline{C}p^{(II,\phi)} = \frac{(1 - e^{-\omega\phi})}{\omega\phi V_0(1 - e^{-24\omega})}\{F_T D_T[R_I']W + F_C D_C[R_{II}]\} \qquad \text{(Eq. 10)}$$

where V_0 is as defined previously (1).

If Period II is prolonged indefinitely (*i.e.*, $M \to \infty$), a steady state for the capsule dosage regimen is attained. When $L = 7$ days and ϕ

= 24 hr:

$$[\overline{C}p^{(II,\phi)}] \lim_{M \to \infty} = [\overline{C}p^{(ss)}]_C = \frac{F_C D_C}{\omega \phi V_0} \quad \text{(Eq. 11)}$$

By substituting Eq. 11 into Eq. 10 and specifying $M = 7$:

$$\overline{C}p^{(14,\phi)} = [\overline{C}p^{(ss)}]_C \left\{ \frac{F_T D_T}{F_C D_C} [R_I'] W + [R_{II}] \right\} \quad \text{(Eq. 12)}$$

Initially, it is assumed that $F_C = F_T$. Under this assumption, $[\overline{C}p^{(ss)}]_C$ can be calculated from $[\overline{C}p^{(14,\phi)}]_{obs}$, the observed mean plasma level on Day 14; *i.e.*:

$$[\overline{C}p^{(ss)}]_C = \frac{D_C [\overline{C}p^{(14,\phi)}]_{obs}}{D_T [R_I'] W + D_C [R_{II}]} = \frac{F_C D_C}{\omega \phi V_0} \quad \text{(Eq. 13)}$$

and:

$$\frac{F_C}{V_0} = \frac{\omega \phi [\overline{C}p^{(14,\phi)}]_{obs}}{D_T [R_I'] W + D_C [R_{II}]} \quad \text{(Eq. 14)}$$

Next, it is assumed also that drug disposition kinetics obey a one-compartment open model with first-order absorption, for which the time course of change of Cp following a single dose of the tablet is given by the familiar:

$$Cp(t) = \frac{k_a F_T D_T}{(k_a - \omega) V_0} (e^{-\omega t} - e^{-k_a t}) \quad \text{(Eq. 15)}$$

In a one-compartment open model, $V_0 = V_d$, the apparent volume of distribution. The entire time course of drug accumulation during Period I according to the actual dosage schedule can now be simulated by appropriate summations of Eq. 15 over all dosing intervals, preferably with the aid of analog (5) or digital (6) computational techniques. Given the assumption of $F_C = F_T$, the only indeterminate quantity on the right-hand side of Eq. 15 is k_a, which can be chosen to reflect best the shape of the data on Day 7, with particular emphasis given to the morning dose.

From the simulated data, the mean plasma levels over τ_1 on Day 7, $[\overline{C}p^{(7,\tau_1)}]_{sim}$, can be calculated and compared with those observed, $[\overline{C}p^{(7,\tau_1)}]_{obs}$. Perfect agreement between observed and simulated data affirms the initial assumption of $F_C = F_T$. In any event, the ratio of simulated to observed data is a measure of F_C/F_T. For the prescribed tablet regimen, the general relationship between F_C/F_T and $[\overline{C}p^{(K,\tau_1)}]_{sim}/[\overline{C}p^{(K,\tau_1)}]_{obs}$ can be represented by:

$$\frac{F_C}{F_T} = \left\{ 1 + \frac{D_T}{D_C} \frac{[R_I']}{[R_{II}]} W \right\} \frac{[\overline{C}p^{(K,\tau_1)}]_{sim}}{[\overline{C}p^{(K,\tau_1)}]_{obs}} - \frac{D_T}{D_C} \frac{[R_I']}{[R_{II}]} W \quad \text{(Eq. 16)}$$

which is the equation of a straight line whose slope and intercept are functions of D, L, M, and ω. A diagrammatic representation of this relationship as a function of ω for the prevailing conditions of $D_T/D_C = 1/3$ and $L = M = 7$ is shown in Fig. 1. It is apparent that plots of F_C/F_T *versus* $[\overline{C}p^{(K,\tau_1)}]_{sim}/[\overline{C}p^{(K,\tau_1)}]_{obs}$ result in a family of straight lines, each passing through the point (1,1) with a different slope. The slopes vary inversely with ω. The lines converge to a limiting slope of unity (and, therefore, an intercept of zero) as ω becomes large.

In other words, with a given dosage regimen, steady state can be achieved sooner with drugs having shorter half-lives; at steady state, there is a one-to-one correspondence between the ratio $[\overline{C}p^{(K,\tau_1)}]_{sim}/[\overline{C}p^{(K,\tau_1)}]_{obs}$ and relative bioavailability. The regimen factor $[R_I]$ does not appear in Eq. 16, because the relationship between F_C/F_T and $[\overline{C}p^{(K,\tau_1)}]_{sim}/[\overline{C}p^{(K,\tau_1)}]_{obs}$ is independent of the location of the sampled interval in Period I.

In the present example, the specific comparison is between $[\overline{C}p^{(7,\tau_1)}]_{sim}$ and $[\overline{C}p^{(7,\tau_1)}]_{obs}$. Estimates of relative bioavailability can be obtained by setting $L = M = 7$ in Eq. 16 or by interpolating directly from Fig. 1 (Method B). Alternatively, F_C/F_T can be varied iteratively through repeated simulations such that equality between $[\overline{C}p^{(7,\tau_1)}]_{sim}$ and $[\overline{C}p^{(7,\tau_1)}]_{obs}$ and between $[\overline{C}p^{(14,\phi)}]_{sim}$ and $[\overline{C}p^{(14,\phi)}]_{obs}$ is achieved simultaneously after k_a has been fixed by the shape of the observed plasma concentration profile on Day 7 (Method C).

RESULTS

The mean plasma amitriptyline concentrations following the first tablet dosage on Day 7, $\overline{C}p^{(7,\tau_1)}$, and following the capsule dosage on Day 14, $\overline{C}p^{(14,\phi)}$ were estimated by:

$$\overline{C}p^{(7,\tau_1)} = \frac{\int_0^{\tau_1} Cp(t')dt'}{\tau_1} \quad \text{(Eq. 17)}$$

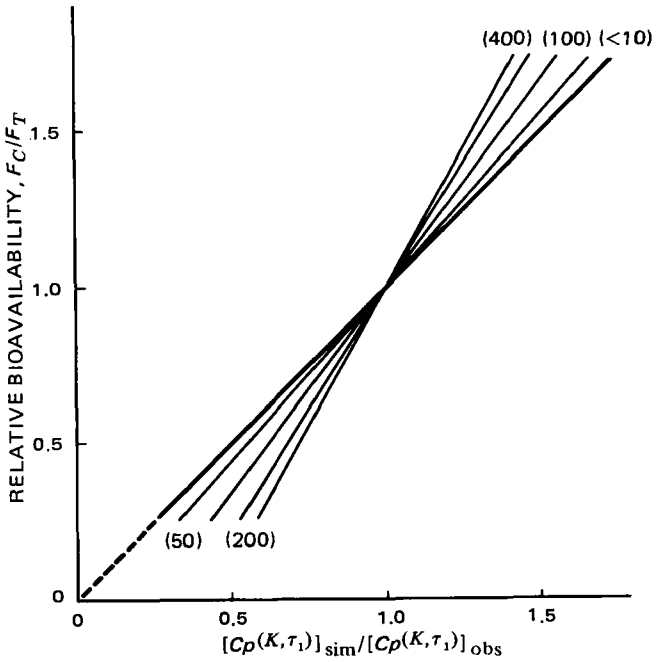

Figure 1—*Graphical representation of Eq. 16 for the prescribed dosing regimen. Values in parentheses correspond to plasma half-lives in hours.*

and:

$$\overline{C}p^{(14,\phi)} = \frac{\int_0^{\phi} Cp(t')dt'}{\phi} \quad \text{(Eq. 18)}$$

where τ_1 and ϕ equal 6 and 24 hr, respectively; t' is time from the last dose; and the areas under the plasma–time curve are trapezoidal approximations. Terminal slopes, ω, were estimated from the last data points on Day 14. Apparent lag times, t_0', and peak times, t'_{max}, for the sampled interval τ_1 on Day 7 were estimated visually from graphs of plasma concentration *versus* time. Individual values for $\overline{C}p^{(7,\tau_1)}$, $\overline{C}p^{(14,\phi)}$, t_0', t'_{max}, ω, and plasma half-life ($0.693/\omega$) are shown in Table I.

Method A—Estimates of relative bioavailability between the tablet and capsule formulations calculated by Eq. 5 are shown in Table II, which also includes the corresponding dosage, regimen, correction, and residue factors. Since the residue factor W is zero at steady state, its relatively minor contributions signify the fact that steady state is being approached in nearly every case. That is, given the observed terminal slopes, the plasma levels attained after 7 days of either treatment are very nearly those expected at steady state. On the other hand, the proximity between $\overline{C}p^{(14,\phi)}/\overline{C}p^{(7,\tau_1)}$ and F_C/F_T is purely coincidental since, in general, $[\overline{C}p^{(II,\phi)}]/[\overline{C}p^{(I,\tau_1)}]$ does not equal F_{II}/F_I at steady state.

Method B—Alternatively, estimates of relative bioavailability can be made from data presented in Table I under the initial assumption

Table I—Summary of Experimentally Observed Variables

Subject	Day 7 $\overline{C}p^{(7,\tau_1)}$, ng/ml	Day 7 t_0', hr	Day 7 t'_{max}, hr	Day 14 $\overline{C}p^{(14,\phi)}$, ng/ml	Day 14 ω, hr^{-1}	Day 14 $0.693/\omega$, hr
1	38.5	2	3	43.5	0.0133	52
2	65.4	0	1	74.5	0.0182	38
3	82.6	0	2	75.5	0.0204	34
4	71.3	1	4	72.3	0.0330	21
5	52.0	1	2	52.8	0.0433	16
6	22.8	2	6	39.5	0.0144	48
7	66.8	2	4	56.2	0.0347	20
8	52.9	2	6	68.4	0.0178	39
9	30.8	1	4	22.5	0.0231	30
10	60.2	1	3	79.2	0.0173	31
11	38.3	1	4	55.1	0.0217	32
12	64.3	0	1	52.1	0.0267	26

Table II—Estimates of Bioavailability by Projections to Steady State[a] (Eq. 5)

Subject	Mean Plasma Ratio, $\bar{C}p^{(II,\phi)}/\bar{C}p^{(I,\tau_1)}$	Regimen Factors $[R_I]/[R_{II}]$	Regimen Factors $[R_I']/[R_{II}]$	Correction Factor, $\phi(1-e^{-\omega\tau_1})/\tau_1(1-e^{-\omega\phi})$	Residue Factor, W	Bioavailability Ratio, F_C/F_T
1	1.130	2.566	2.776	1.123	0.126	0.97
2	1.139	2.483	2.700	1.169	0.058	1.05
3	0.914	2.444	2.668	1.190	0.041	0.85
4	1.014	2.219	2.490	1.313	0.006	0.98
5	1.015	2.052	2.366	1.416	0.001	0.98
6	1.732	2.548	2.759	1.133	0.106	1.57
7	0.845	2.190	2.471	1.330	0.004	0.82
8	1.293	2.490	2.706	1.165	0.062	1.19
9	0.750	2.396	2.628	1.216	0.027	0.70
10	1.316	2.499	2.714	1.161	0.067	1.21
11	1.439	2.421	2.649	1.203	0.034	1.37
12	0.810	2.331	2.578	1.251	0.016	0.77

[a] The dose ratio, D_I/D_{II}, used was 1:3.

that $F_C = F_T$. By Eqs. 13 and 14, $[\bar{C}p^{(ss)}]_C$ and F_C/V_0 are projected from $\bar{C}p^{(14,\phi)}$. The time courses of change of plasma levels in accordance with the prescribed dosing sequence are then simulated digitally by the appropriate accumulation of Eq. 15 with due consideration for t_0' and appropriate choices of k_a such that simulated plasma peak times approximate the observed t'_{max}. Finally, the bioavailability ratio of capsule to tablet formulations is calculated from the ratio of $[\bar{C}p^{(7,\tau_1)}]_{sim}$ to $[\bar{C}p^{(7,\tau_1)}]_{obs}$ with the aid of Eq. 16. Individual values of $[\bar{C}p^{(ss)}]_C$, F_C/V_0, k_a, $[\bar{C}p^{(7,\tau_1)}]_{sim}$, and F_C/F_T are summarized in Table III. When comparing corresponding entries in the last column of Table III with those of Table II, it is evident that the two methods of calculation result in similar conclusions.

A comparison of simulated and observed plasma concentrations for a typical subject is shown in Fig. 2. Whereas the perfect agreement between simulated and observed mean plasma levels on Day 14 is predestined as a consequence of Eqs. 13 and 14, their juxtaposition on Day 7 is a function of their relative bioavailabilities. By the same token, the poor agreement point by point is not unexpected, because the method is dependent mainly on area estimates and because the assumptions of a one-compartment open model and of first-order absorption are merely expedients to facilitate the simulation. Nevertheless, the effect of these assumptions on the validity of the conclusion deserves further consideration.

Method C—No attempt is made in the present example to obtain iterative solutions of F_C/F_T by repeated simulations. Instead, a theoretically equivalent calculation is made to illustrate what would have been achieved if such attempts were implemented.

For linear systems, general solutions in closed form descriptive of drug accumulation as a function of time for any tractable dosing sequence were presented previously (7). In the case of a one-compartment open model with first-order absorption, when equal doses are administered at recurring intervals of τ_1, τ_2, and τ_3, the temporal change in plasma concentrations during the ith dosage interval is given by:

$$Cp^{(i)} = \frac{k_a FD}{V_0(k_a-\omega)}\left\{e^{-\omega t}\sum_{\pi,\rho,\sigma}^{i-1} e^{\omega(\pi\tau_1+\rho\tau_2+\sigma\tau_3)} - e^{-k_a t}\sum_{\pi,\rho,\sigma}^{i-1} e^{k_a(\pi\tau_1+\rho\tau_2+\sigma\tau_3)}\right\} \quad \text{(Eq. 19)}$$

where t is real time; and π, ρ, and σ are positive integers such that $(\pi+\rho+\sigma) = 0, 1, 2, \ldots, i-1$, $\pi \geq \rho \geq \sigma$, and $\pi - \sigma \geq 1$.

By applying Eq. 19 specifically to the present example, the mean plasma level following the 19th dose of the tablet formulation can be calculated by specifying $i = 19$ and integrating over the appropriate time intervals:

$$[\bar{C}p^{(7,\tau_1)}]_{sim} = [\bar{C}p^{(i)}]_{sim} \quad \text{(Eq. 20a)}$$

$$[\bar{C}p^{(7,\tau_1)}]_{sim} = \frac{k_a F_T D_T}{\tau_1 V_0(k_a-\omega)}\left\{\frac{[R_a][1-e^{-\omega\tau_1}]e^{-144\omega}}{\omega} - \frac{[R_b](1-e^{-k_a\tau_1})e^{-144k_a}}{k_a}\right\} \quad \text{(Eq. 20b)}$$

where:

$$[R_a] = \sum_{\pi,\rho,\sigma}^{i-1} e^{\omega(\pi\tau_1+\rho\tau_2+\sigma\tau_3)} \quad \text{(Eq. 21)}$$

$$[R_b] = \sum_{\pi,\rho,\sigma}^{i-1} e^{k_a(\pi\tau_1+\rho\tau_2+\sigma\tau_3)} \quad \text{(Eq. 22)}$$

Similarly, the mean plasma level after the seventh dose of the capsule formulation on Day 14 can be calculated by appropriate extensions of Eqs. 19 and 20b:

$$[\bar{C}p^{(14,\phi)}]_{sim} = \frac{k_a F_T D_T}{\phi V_0(k_a-\omega)}\left\{\frac{[R_a'](1-e^{-\omega\phi})e^{-312\omega}}{\omega} - \frac{[R_b'](1-e^{-k_a\phi})e^{-312k_a}}{k_a}\right\} + \frac{k_a F_C D_C}{\phi V_0(k_a-\omega)}\left\{\frac{[R_c](1-e^{-\omega\phi})e^{-312\omega}}{\omega} - \frac{[R_d](1-e^{-k_a\phi})e^{-312k_a}}{k_a}\right\} \quad \text{(Eq. 23)}$$

where:

$$[R_a'] = \sum_{\pi,\rho,\sigma}^{j} e^{\omega(\pi\tau_1+\rho\tau_2+\sigma\tau_3)} \quad \text{(Eq. 24)}$$

$$[R_b'] = \sum_{\pi,\rho,\sigma}^{j} e^{k_a(\pi\tau_1+\rho\tau_2+\sigma\tau_3)} \quad \text{(Eq. 25)}$$

$$[R_c] = (e^{24L\omega})\left(1+\sum_{n=1}^{M-1} e^{n\omega\phi}\right) \quad \text{(Eq. 26)}$$

$$[R_d] = (e^{24Lk_a})\left(1+\sum_{n=1}^{M-1} e^{nk_a\phi}\right) \quad \text{(Eq. 27)}$$

with $j = 21$ and $L = M = 7$.

Table III—Estimates of Bioavailability by Simulations Based on a One-Compartment Open Model

Subject	$[\bar{C}p^{(ss)}]_C$, ng/ml	F_C/V_0, $10^4 \times$ liters^{-1}	k_a, hr^{-1}	$[\bar{C}p^{(7,\tau_1)}]_{sim}$, ng/ml	Bioavailability Ratio, F_C/F_T
1	43.6	1.877	2.40	39.2	1.02
2	74.3	4.333	2.40	68.8	1.05
3	75.3	4.955	0.96	70.9	0.85
4	72.2	7.582	0.36	67.9	0.95
5	52.8	7.316	2.00	53.3	1.03
6	39.5	1.820	0.12	34.7	1.57
7	56.2	6.229	0.84	57.3	0.86
8	68.2	3.896	0.16	63.7	1.22
9	22.4	1.648	0.10	21.4	0.71
10	78.9	4.379	1.00	73.3	1.23
11	54.9	3.819	0.32	52.3	1.38
12	52.0	4.451	2.00	49.0	0.76

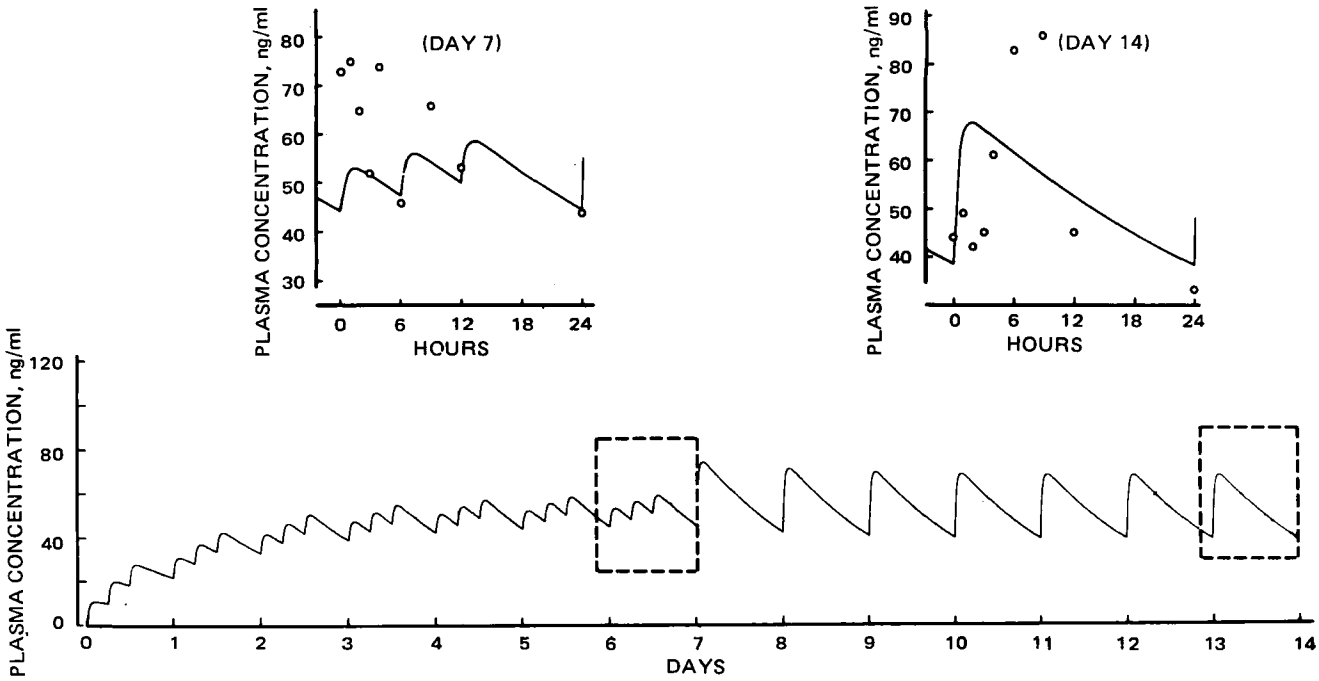

Figure 2—*Typical simulated plasma concentration–time course using a one-compartment open model approximation under the initial assumption of* $F_C = F_T$. *Insets represent enlargements comparing observed (O) and simulated (—) events on Days 7 and 14 (Subject 12).*

The theoretical equivalent of an iterative solution is obtained by replacing the left-hand side of Eqs. 20*b* and 23 by $[\overline{C}p^{(7,\tau_1)}]_{obs}$ and $[\overline{C}p^{(14,\phi)}]_{obs}$, respectively, and solving for F_C/F_T:

$$\frac{F_C}{F_T} = \frac{D_T}{D_C}\frac{[Q_I]}{[Q_{II}]}\left\{\frac{\phi[\overline{C}p^{(14,\phi)}]_{obs}}{\tau_1[\overline{C}p^{(7,\tau_1)}]_{obs}} - \frac{[Q_I']}{[Q_I]}\right\} \quad \text{(Eq. 28)}$$

where:

$$[Q_I] = k_a[R_a]\,(1 - e^{-\omega\tau_1})\,e^{-144\omega} - \omega[R_b]\,(1 - e^{-k_a\tau_1})\,e^{-144k_a} \quad \text{(Eq. 29)}$$

$$[Q_I'] = k_a[R_a']\,(1 - e^{-\omega\phi})\,e^{-312\omega} - \omega[R_b']\,(1 - e^{-k_a\phi})\,e^{-312k_a} \quad \text{(Eq. 30)}$$

$$[Q_{II}] = k_a[R_c]\,(1 - e^{-\omega\phi})\,e^{-312\omega} - \omega[R_d](1 - e^{-k_a\phi})\,e^{-312k_a} \quad \text{(Eq. 31)}$$

There is evidently a close resemblance in form between Eqs. 5 and 28. This finding is not surprising, because the only difference resides in the fact that Eq. 5 is model independent while Eq. 28 is predicated on a one-compartment open model approximation with first-order absorption for the plasma–time course. The application of Eq. 5 requires that the sampled intervals on both Days 7 (τ_1) and 14 (ϕ) begin and end in the log–linear phase. On the other hand, the application of Eq. 28 requires such conformance only on Day 14, so that $[\overline{C}p^{(ss)}]_C$ can be competently estimated from $\overline{C}p^{(14,\phi)}$. In general, only one sampled interval needs to begin and end during the log–linear region, provided an adequate model fits the data adequately in all other sampled intervals. Conversely, when all sampled intervals begin and terminate in ω, Eqs. 5 and 28, and extensions thereof, may be used interchangeably.

The factors $[Q_i]$ in Eq. 28 are composites of terms previously defined (2) as regimen, correction, and residue factors; their identities are readily discernible in Eqs. 29–31. Individual estimates of F_C/F_T by Eq. 28 are shown in Table IV, which also includes values for the factors $[Q_i]$. The values of k_a employed in these calculations were those chosen (Table III) to approximate best the shape of the plasma concentration profiles during τ_1 on Day 7. The agreement between corresponding estimates of F_C/F_T shown in Tables III and IV verifies the previous assertion of equivalence between the two methods of calculation. Figure 3 compares the observed plasma levels and those simulated with the aid of F_C/F_T from Table IV. In contrast to Fig. 2, there is now also equality between simulated and observed mean concentrations during the interval τ_1 on Day 7.

Role of k_a—Estimates of relative bioavailability (Tables III and IV) depend in part on choices of k_a to approximate best the data during τ_1 on Day 7. It is evident from Figs. 2 and 3 that agreement point by point is poor. Thus, an attempt is made to determine the effect of k_a on the estimates of F_C/F_T. It is convenient, and perhaps informative, to classify the results according to the relative magnitudes of k_a to ω (*e.g.*, $\gg 1$, $\simeq 1$, or <1) and to consider each category in relation to previously cited (1) conditions under which the rate of drug accumulation approaches model independence. Table V summarizes the results on selected subjects whose plasma half-lives appear to be representative of the observed range.

When k_a is to be selected from a family, each member of which is much larger than ω, the conditions for model independence are most likely to be satisfied. That is to say, when ω is much smaller than the next larger eigenvalue and when the terminal slope is not k_a, succeeding doses are most probably administered during the log–linear phase. Under these circumstances, the rate of drug accumulation should be predictable from a knowledge of ω. In other words, given an estimate of ω, the observed mean plasma concentration represents a known position in the time course of drug accumulation. Consequently, estimates of F_C/F_T should be relatively insensitive to the choice of a model or parameters therein.

The choice of k_a, even though $>\omega$, becomes progressively more important as the ratio of k_a/ω approaches unity. This result is a manifestation of ω being no longer much smaller than the next larger eigenvalue. The rate of drug accumulation is not entirely predictable from ω alone but is subject also to the residual influence of other eigenvalues. However, a reasonable estimate of F_C/F_T should result, provided the model fits the data adequately during τ_1 on Day 7.

Table IV—Estimates of Bioavailability by Iterations Based on a One-Compartment Open Model (Eq. 28)

Subject	$[Q_I]$	$[Q_I']$	$[Q_{II}]$	$[Q_I]/[Q_{II}]$	$[Q_I']/[Q_{II}]$	F_C/F_T
1	1.530	0.844	2.130	0.718	0.396	0.95
2	1.642	0.423	2.269	0.724	0.186	1.04
3	0.655	0.122	0.908	0.721	0.135	0.83
4	0.232	0.007	0.326	0.712	0.021	0.96
5	1.409	0.008	1.955	0.720	0.004	0.97
6	0.068	0.036	0.095	0.720	0.382	1.53
7	0.576	0.012	0.803	0.717	0.015	0.80
8	0.097	0.030	0.134	0.721	0.223	1.17
9	0.054	0.008	0.075	0.729	0.114	0.69
10	0.668	0.201	0.928	0.720	0.216	1.19
11	0.208	0.034	0.290	0.717	0.116	1.34
12	1.415	0.099	1.951	0.725	0.051	0.77

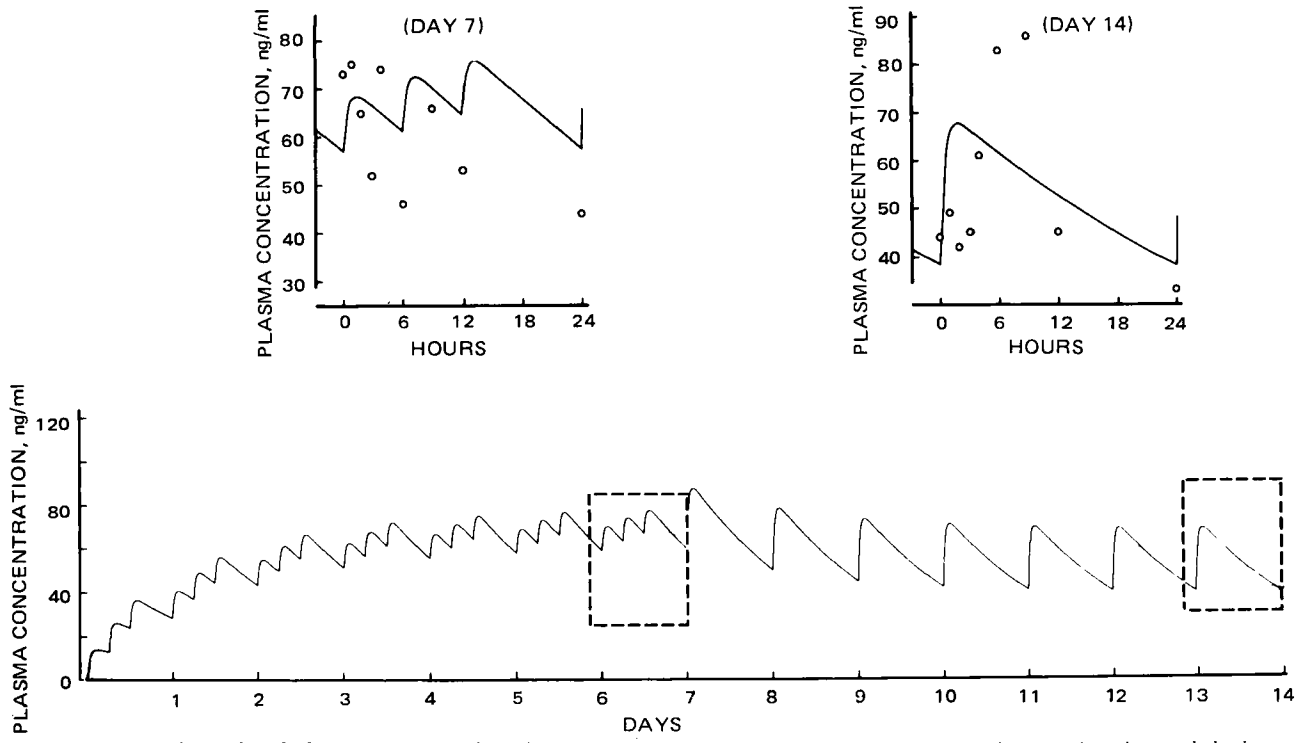

Figure 3—*Typical simulated plasma concentration–time course using a one-compartment open model approximation and the iterative solution of* F_C/F_T. *Insets represent enlargements comparing observed (O) and simulated (—) events on Days 7 and 14 (Subject 12).*

Finally, Table V includes entries for cases where $(k_a/\omega) < 1$, even though the terminology is imprecise. By definition (1), ω is the terminal slope; thus, if k_a is the smallest eigenvalue, it should be properly designated as ω. Nevertheless, this category reflects the magnitude of potential errors resulting from changing half-lives between treatments. If the terminal slope had been experimentally determined for each of the two treatments, one would be designated ω_I and the other ω_{II}, on the basis of which F_C/F_T could be calculated by projections to steady state (2). In the present example, only ω_{II} can be estimated experimentally such that k_a should be viewed simply as the other eigenvalue chosen in an attempt to fit the data on Day 7 by a one-compartment open model. Thus, simulation and iterative techniques may be useful when changes in terminal slope between treatments are suspected but cannot be experimentally verified. They can be attempted if the study design includes at least one sampled interval that begins and ends in the log-linear region.

Table V—Influence of k_a on Estimates of Bioavailability by Eq. 28 for Selected Subjects

	Relative Bioavailability, F_C/F_T				
k_a/ω	Subject 1	Subject 2	Subject 12	Subject 7	Subject 5
0.5	0.18	0.50	0.50	0.67	0.91
0.6	0.28	0.59	0.56	0.72	0.95
0.7	0.36	0.66	0.61	0.75	0.97
0.8	0.43	0.72	0.65	0.77	0.98
0.9	0.49	0.77	0.68	0.79	0.98
1.0	0.54	0.81	0.70	0.80	0.99
2.0	0.80	0.97	0.76	0.82	0.98
3.0	0.87	1.00	0.77	0.81	0.97
4.0	0.90	1.02	0.77	0.81	0.96
5.0	0.91	1.02	0.76	0.80	0.96
6.0	0.92	1.02	0.76	0.80	0.95
8.0	0.93	1.02	0.76	0.80	0.95
10.0	0.93	1.02	0.76	0.79	0.95
12.0	0.93	1.02	0.76	0.80	0.95
14.0	0.93	1.02	0.76	0.80	0.96
16.0	0.93	1.02	0.76	0.80	0.96
18.0	0.94	1.02	0.76	0.80	0.96
20.0	0.94	1.02	0.76	0.80	0.96
Observed (ω, hr^{-1})	0.0133	0.0182	0.0267	0.0347	0.0433

The effect of k_a is negligible for large values of ω but assumes progressively greater significance as ω diminishes, indicating that the model and goodness of fit become less important as steady state is approached.

Model Dependency—An attempt can be made to achieve better agreement point by point on Day 14. The shapes of the plasma concentration profiles suggest that they may be approximated by a two-compartment open model with zero-order absorption.

Slopes, α and β, and apparent intercepts, A' and B', are obtained graphically from the "postabsorptive" phase. The actual intercepts, A and B, at time zero following a single dose can be calculated by correcting for the kinetics during the time of absorption, t_a', and for the influence of all preceding dosages:

$$A = \frac{\alpha t_a' A'(1 - e^{-\alpha\phi})}{(1 - e^{-\alpha t_a'})\{(D_T[R_I']_\alpha W_\alpha/D_C) - [R_{II}]_\alpha\}} \quad \text{(Eq. 32)}$$

$$B = \frac{\beta t_a' B'(1 - e^{-\beta\phi})}{(1 - e^{-\beta t_a'})\{(D_T[R_I']_\beta W_\beta/D_C) - [R_{II}]_\beta\}} \quad \text{(Eq. 33)}$$

from which:

$$\frac{V_1}{F_C} = \frac{D_C}{A + B} \quad \text{(Eq. 34)}$$

The other model parameters, k_{12}, k_{21}, and k_{10}, are calculated in the usual manner. The subscripts α and β on $[R_I']$, $[R_{II}]$, and W signify that ω in Eqs. 7–9 is to be replaced by α or β, as the case may be.

Implicit in Eqs. 32–34 is the assumption that $F_C = F_T$. By analogy, therefore, $[\overline{C}p^{(\tau,\tau_1)}]_{sim}$ can be calculated by appropriate superpositions of Eq. 35, again with due regard for t_0' and t'_{max}:

$$Cp(t) = \frac{k_a' F_T D_T}{V_1}\left\{\frac{(k_a' - k_{21})\, e^{-k_a'(t-t_0')}}{(\alpha - k_a')\,(\beta - k_a')} + \frac{(\alpha - k_{21})\, e^{-\alpha(t-t_0')}}{(k_a' - \alpha)(\beta - \alpha)} + \frac{(\beta - k_{21})\, e^{-\beta(t-t_0')}}{(k_a' - \beta)(\alpha - \beta)}\right\} \quad \text{(Eq. 35)}$$

where k_a' is the fitting constant for apparent absorption which, in general, is different from k_a in Eq. 15 (8). Relative bioavailability between capsule and tablet formulations then can be estimated with the aid of Eq. 16.

Model parameters, including t_a', and estimates of F_C/F_T are shown in Table VI. When comparing the last columns in Tables III, IV, and VI, it is evident that the conclusions are little affected, despite the fact that considerable improvement in point by point agreement has been achieved with the two-compartment open model (Fig. 4). Iterative

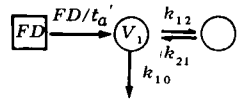

Table VI—Estimates of Bioavailability by Simulations Based on a Two-Compartment Open Model

Subject	Model Parameters[a] from Day 14						$[\bar{C}p^{(\tau,\tau_1)}]_{sim}$, ng/ml	Bioavailability Ratio[a], F_C/F_T
	k_{12}, hr^{-1}	k_{21}, hr^{-1}	k_{10}, hr^{-1}	V_1/F_C, liters	t_a', hr	k_a', hr^{-1}		
1	0.457	0.045	0.204	340	5.0	1.0	41.3	1.08
2	0.620	0.092	0.173	245	4.0	0.6	71.6	1.10
3	0.861	0.124	0.190	217	8.0	0.4	72.6	0.87
4	0.796	0.210	0.182	230	7.0	0.4	72.2	1.01
5	0.505	0.260	0.144	407	6.0	1.0	51.8	1.00
6	0.308	0.106	0.063	1224	5.0	0.2	34.3	1.55
7	0.406	0.118	0.203	279	4.0	0.5	51.1	0.77
8	0.411	0.089	0.121	370	6.0	0.1	62.4	1.19
9	0.619	0.071	0.323	408	7.5	0.1	22.1	0.73
10	1.020	0.079	0.305	125	5.0	0.1	74.0	1.24
11	0.620	0.049	0.507	110	5.0	0.1	51.4	1.35
12	0.264	0.096	0.129	464	6.0	1.0	52.6	0.82

[a] By Eq. 16.

solutions based on simulations of the two-compartment open model are shown in Fig. 5, which is the counterpart of Fig. 3.

There is one important conceptual difference between the one-compartment and the two-compartment simulations attempted in the present example. In the first instance, F_C/V_0 is estimated from $[Cp^{(ss)}]_C$, thus requiring at least one sampled interval to begin and end in the log-linear phase. In the second instance, F_C/V_1 is calculated by modeling the data from a suitable interval and extrapolating to time zero, whereby it is sufficient for the affected interval to terminate in the log-linear phase to provide a starting point to model.

Finally, it is evident that the rate of accumulation varies depending on whether drug disposition is approximated by a one-compartment (Figs. 2 and 3) or two-compartment (Figs. 4 and 5) model. This model dependency is a manifestation of ω being not sufficiently smaller than either E_j or the next larger eigenvalue or both (1). In the present example, since k_a' is always much larger than β (the observed terminal slope), the dependency is attributable to the fact that the term containing $e^{-\alpha\tau_1}$ is not sufficiently close to zero to be ignored or that k_{21} is not always a good approximation of $(k_{21} - \beta)$ or both. Thus, if the two-compartment model is thought to be a more appropriate representation of amitriptyline disposition, the one-compartment model approximation will always underestimate the time course of drug accumulation, particularly during the early stages.

Part of the problem may be overcome by lengthening the sampled interval τ such that $e^{-\alpha\tau} \simeq 0$. However, a better solution, as evidenced by the present example, is to sample at quasisteady state, where model-related differences become negligible.

DISCUSSION

The study comparing amitriptyline formulations was not designed specifically to demonstrate the applicability of the proposed method. Nevertheless, it appears to have been useful in exemplifying the principle of bioavailability assessment at quasi- and nonsteady state and in illustrating some alternative techniques of data analysis. Obviously, there are numerous ways to obtain estimates of bioavailability from a given set of data. Some are theoretical equivalents so that they can be used interchangeably, while others are sufficiently different so that they may be used as checks for each other.

Even though data analysis can be greatly facilitated by keeping

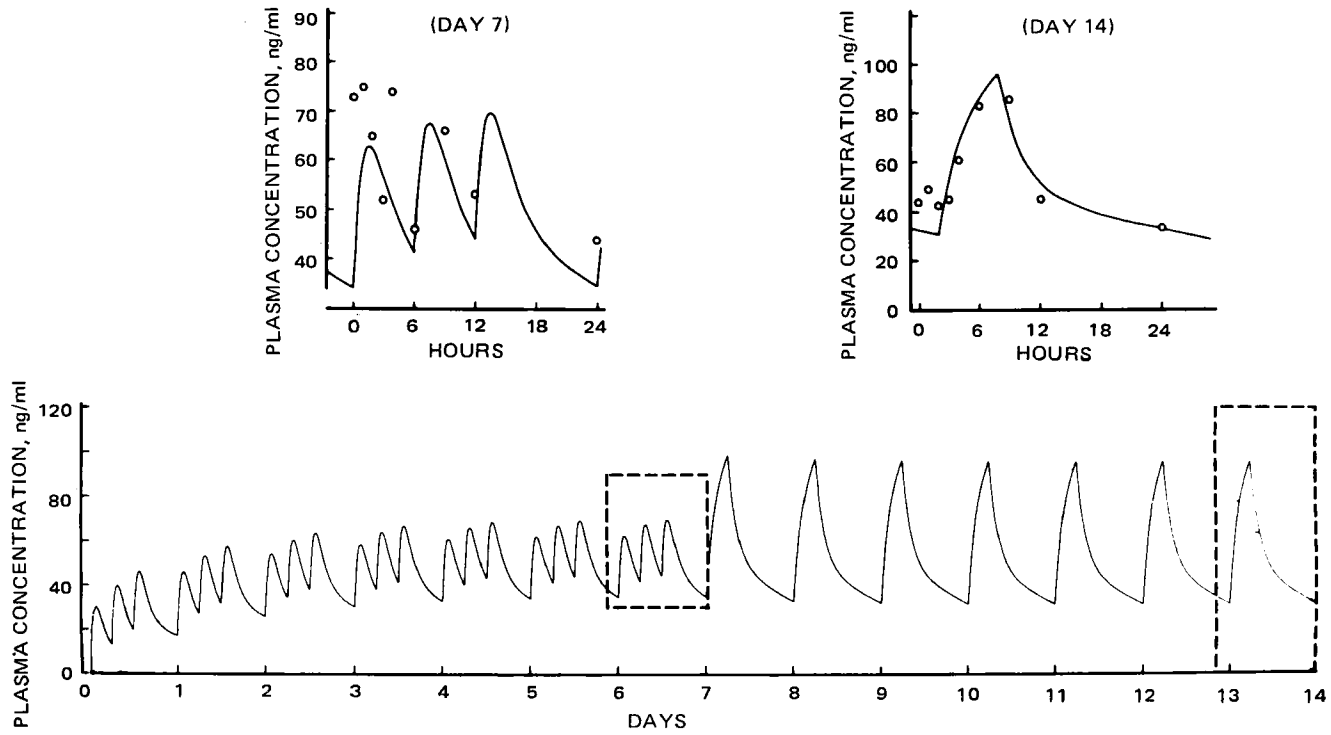

Figure 4—*Typical simulated plasma concentration–time course using a two-compartment open model approximation under the initial assumption of* F_C/F_T. *Insets represent enlargements comparing observed (O) and simulated (—) events on Days 7 and 14 (Subject 12).*

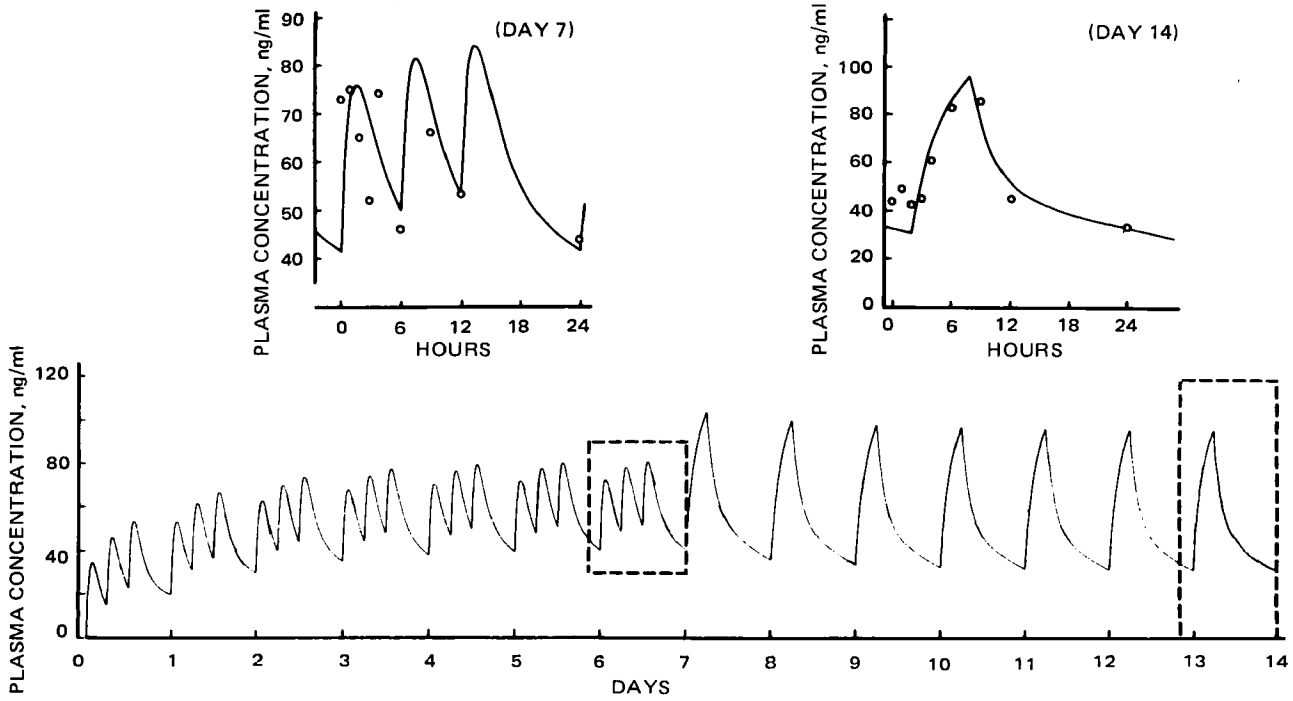

Figure 5—*Typical simulated plasma concentration–time course using a two-compartment open model approximation and the iterative solution of* F_C/F_T. *Insets represent enlargements comparing observed (O) and simulated (—) events on Days 7 and 14 (Subject 12).*

dosages, dosing intervals, and sampling intervals uniform throughout, planned deviations should be considered to accommodate the ease of execution and subject convenience, both of which are particularly important in multiple-dose studies. Analytical options based on extrapolations to steady state require that the sampled intervals begin and end in the log–linear region (2). However, alternatives based on comparative mean plasma levels between simulated and observed values require only that the sample interval over which F/V_0 is estimated begins and ends in the log–linear phase. Finally, if the simulations are predicated on model parameters derived from a suitable dosage interval, it is sufficient that the affected interval terminates in the log–linear region. Thus, the close agreement between corresponding estimates of F_C/F_T in Table II and, for example, Table IV provides verification for one of the underlying assumptions. Namely, the sampled intervals on Days 7 and 14 probably began and terminated in the log–linear phase for most subjects.

In the present example, F/V_0 estimates are derived from data on Day 14, and the temporal changes in plasma concentrations on Day 7 are interpolated through simulation. In general, the sequence may be reversed without compromise with rigor. In other words, it is equally valid to simulate the events on Day 14 through estimates of F/V_0 obtained on Day 7. When all mean plasma levels are determined over intervals beginning and ending in the log–linear region, precise point by point agreement between simulated and observed values is not necessary because an estimate of relative bioavailability would always be possible by projecting the observed means to steady state. This would be true even when ω is identified with k_a, provided that ω is experimentally determined for all affected treatments.

On the other hand, if some sampled intervals begin and terminate under the influence of continued (non-first-order) absorption or before the attainment of pseudosteady state in drug distribution, the validity of the estimated bioavailability ratios would depend on the goodness of fit, the importance of which diminishes as steady state is approached. Therefore, bioavailability assessment at quasi- and nonsteady state may be more or less model independent, depending on drug disposition and experimental design. The relative insensitivity of the present example to alternative methods of calculation is probably the result of having satisfied most of the criteria for model independence; it cannot be generally anticipated.

The techniques employed to effect estimates of bioavailability at quasi- and nonsteady state are simply variations of those used in single-dose and steady-state comparisons. To the extent that a one-to-one correspondence between estimates following single doses and those at steady state can be assured under the principle of superposition, the proposed method is conceptually equivalent to both in that it is a necessary intermediate. Under certain circumstances, there are unique experimental advantages at quasi- and nonsteady state.

In planning single-dose comparisons, sample points must be judiciously placed to ensure a competent estimate of the total area under the plasma–time curve, and sufficient time must elapse between treatments to prevent undesirable residual effects. Whether or not the planned effects are achieved in any given test subject depend largely on the observed terminal slope, which is ascertainable only after the fact. Difficulties may arise when ω is small or when ω cannot be conveniently sampled because it is manifested near or below assay sensitivity or during the subject's normal sleeping hours.

In planning comparisons at steady state, a sufficiently large number of dosing cycles must be included to guarantee experimental attainment of steady state in every treatment; where the dosage and sampled intervals are not uniform throughout, care must be exercised to ensure that all sampled intervals begin and end in the log–linear region. Whether or not the desired effects have been achieved in any given test subject is again dependent on the observed terminal slope and also on subject compliance. Difficulties may arise when so many doses must be given that perfect adherence to the prescribed sequence and timing becomes unrealistic or when the observed ω for some subjects is smaller than anticipated. It is evident that most, possibly all, of these problems can be circumvented at quasi- and nonsteady state. Thus, the proposed techniques appear to be particularly useful when plasma half-lives are long and variable, such as is the case with amitriptyline.

SUMMARY

In summary, some possible techniques for effecting estimates of bioavailability at quasi- and nonsteady state have been illustrated with data from a study comparing two formulations of amitriptyline hydrochloride in humans. It is learned that some previously established (1, 2) experimental constraints may be further relaxed. Minimally, only one sampled interval needs to end in the log–linear region, provided a model can be found to fit the data adequately in all other sampled intervals. There is a demonstrable parallelism in the concepts and in the techniques used to estimate bioavailability, whether the comparisons are made after single doses, at steady state, or somewhere in between.

In a sense, steady-state comparisons can be construed to be a special case of the proposed method in which the residual effect of preceding treatments is zero; and single-dose studies can be considered to be a

special case in which all doses after the first dose of each treatment are skipped to permit more extensive sampling of ω. Conversely, the proposed method may be thought of as a salvage operation for planned steady-state comparisons that fall short of target and for planned single-dose studies where the washout period is too short.

APPENDIX

The validity of Eq. 5 (and, therefore, Eqs. 16 and 28) can be demonstrated with a set of simulated data generated with the aid of a one-compartment open model, in which $F_I = 0.8$, $F_{II} = 0.6$, $k_a = 1.0$ hr^{-1}, $\omega = 0.015$ hr^{-1}, and $V_0 = 10$ liters in accordance with the prescribed regimen. Under these circumstances, the correction factor $\phi(1 - e^{-\omega\tau_1})/\tau_1(1 - e^{-\omega\phi})$ is 1.139; the residue factor W is 0.096; and the regimen factors $R_I = 2.334$, $R_I' = 2.528$, and $R_{II} = 0.920$. Given $D_I = 25$ mg, $D_{II} = 75$ mg, $\bar{C}p^{(I,\tau_1)} = 0.15$ μg/ml, and $\bar{C}p^{(II,\phi)} = 0.13$ μg/ml, $F_{II}/F_I = 0.75$.

REFERENCES

(1) K. C. Kwan, J. V. Bondi, and K. C. Yeh, *J. Pharm. Sci.*, **64**, 1639(1975).

(2) K. C. Yeh and K. C. Kwan, *ibid.*, **65**, 512(1976).

(3) H. B. Hucker, S. C. Stauffer, F. G. Clayton, B. R. S. Nakra, and R. Gaind, *J. Clin. Pharmacol.*, **15**, 168(1975).

(4) H. B. Hucker and S. C. Stauffer, *J. Pharm. Sci.*, **63**, 296(1974).

(5) L. Kirschner, T. H. Simon, and C. E. Rasmussen, *ibid.*, **62**, 117(1973).

(6) P. J. Niebergall, E. T. Sugita, and R. L. Schnaare, *ibid.*, **63**, 100(1974).

(7) K. C. Kwan, M. P. Zirrith, R. A. Castello, and A. D. Marcus, "A Mathematical Treatment of Repetitive Dose Kinetics," presented at the Basic Pharmaceutics Section, APhA Academy of Pharmaceutical Sciences, Dallas meeting, Apr. 1965.

(8) J. C. K. Loo and S. Riegelman, *J. Pharm. Sci.*, **57**, 918 (1968).

ACKNOWLEDGMENTS AND ADDRESSES

Received May 1, 1975, from the *Merck Sharp & Dohme Research Laboratories, West Point, PA 19486*

Accepted for publication January 30, 1976.

[x] To whom inquiries should be directed.

Effect of Formulation of Intramuscular Injections of Phenothiazines on Duration of Activity

A. T. FLORENCE [x], A. W. JENKINS [*], and A. H. LOVELESS

Abstract □ Trifluoperazine and pericyazine were formulated using both the hydrochloride and embonate salts, and some comparisons were made with the activity of fluphenazine salt and ester formulations. Simple solutions in polyethylene glycol, gelled aqueous solutions, nonaqueous suspensions, multiple emulsions, and microencapsulated preparations were formulated, and their duration of activity was tested in dogs. While the multiple emulsion system showed some promise, a nylon microcapsule system produced significant prolonged activity of the drug after deep intramuscular injection.

Keyphrases □ Phenothiazines—effect of various pharmaceutical formulations on duration of biological activity, dogs □ Trifluoperazine hydrochloride and embonate—effect of various pharmaceutical formulations on duration of biological activity, dogs □ Pericyazine embonate—effect of various pharmaceutical formulations on duration of biological activity, dogs □ Pharmaceutical formulations, various—phenothiazines, effect on duration of biological activity, dogs □ Tranquilizers—trifluoperazine hydrochloride and embonate and pericyazine embonate, effect of various pharmaceutical formulations on duration of biological activity, dogs

Long-acting injectable phenothiazines are valuable in extended aftercare therapy in certain psychiatric states (1, 2). Currently available long-acting neuroleptics include solutions in oils such as sesame oil of poorly water-soluble esters of fluphenazine[1] and flupentixol[2], the duration of activity being up to 40 days. However, not all phenothiazines can be esterified to form lipid-soluble derivatives. Therefore, this work was directed toward alternative methods of prolonging the activity of two such drugs, trifluoperazine and pericyazine, using physicochemical rather than chemical or pharmacological methods.

Various formulation techniques, similar to those reviewed by Ritschel (3), were utilized. Resulting preparations were tested in dogs by an apomorphine challenge test utilizing the antiemetic as opposed to the tranquilizing properties of the phenothiazine, since levels of phenothiazine attained cannot be measured readily by available chemical assay techniques. Some experiments were carried out for comparative purposes using fluphenazine embonate. In all cases, fluphenazine enanthate in sesame oil was used as a reference formulation.

EXPERIMENTAL

Materials—Trifluoperazine hydrochloride and embonate salts[3] and pericyazine embonate[3] were used as received. Fluphenazine embonate was recovered after mixing equimolar solutions of sodium embonate[4] and fluphenazine hydrochloride[5]. Fluphenazine enanthate in sesame oil[6] (25 mg/ml) was obtained commercially.

Drug Solubilities—The solubilities of the bases were determined by a turbidity method (4). The solubilized embonate salts were determined by a modification of this method. Various solutions of drug hydrochloride were mixed with buffered sodium embonate (pamoate) to give equimolar mixtures. The turbidity of the solutions at 560 nm was plotted against the final concentration of drug embonate in the

[1] Moditen and Moditen Enanthate, Modecate; Squibb, United Kingdom; Prolixin Enanthate, Squibb, Princeton, N.J.

[2] Depixol, Lundbeck.

[3] May and Baker, Dagenham, Essex, United Kingdom.

[4] Eastman Kodak.

[5] Donated by Squibb, United Kingdom.

[6] Moditen, Squibb.

special case in which all doses after the first dose of each treatment are skipped to permit more extensive sampling of ω. Conversely, the proposed method may be thought of as a salvage operation for planned steady-state comparisons that fall short of target and for planned single-dose studies where the washout period is too short.

APPENDIX

The validity of Eq. 5 (and, therefore, Eqs. 16 and 28) can be demonstrated with a set of simulated data generated with the aid of a one-compartment open model, in which $F_I = 0.8$, $F_{II} = 0.6$, $k_a = 1.0$ hr^{-1}, $\omega = 0.015$ hr^{-1}, and $V_0 = 10$ liters in accordance with the prescribed regimen. Under these circumstances, the correction factor $\phi(1 - e^{-\omega\tau_1})/\tau_1(1 - e^{-\omega\phi})$ is 1.139; the residue factor W is 0.096; and the regimen factors $R_I = 2.334$, $R_I' = 2.528$, and $R_{II} = 0.920$. Given $D_I = 25$ mg, $D_{II} = 75$ mg, $\bar{C}p^{(I,\tau_1)} = 0.15$ μg/ml, and $\bar{C}p^{(II,\phi)} = 0.13$ μg/ml, $F_{II}/F_I = 0.75$.

REFERENCES

(1) K. C. Kwan, J. V. Bondi, and K. C. Yeh, *J. Pharm. Sci.*, **64**, 1639(1975).

(2) K. C. Yeh and K. C. Kwan, *ibid.*, **65**, 512(1976).

(3) H. B. Hucker, S. C. Stauffer, F. G. Clayton, B. R. S. Nakra, and R. Gaind, *J. Clin. Pharmacol.*, **15**, 168(1975).

(4) H. B. Hucker and S. C. Stauffer, *J. Pharm. Sci.*, **63**, 296(1974).

(5) L. Kirschner, T. H. Simon, and C. E. Rasmussen, *ibid.*, **62**, 117(1973).

(6) P. J. Niebergall, E. T. Sugita, and R. L. Schnaare, *ibid.*, **63**, 100(1974).

(7) K. C. Kwan, M. P. Zirrith, R. A. Castello, and A. D. Marcus, "A Mathematical Treatment of Repetitive Dose Kinetics," presented at the Basic Pharmaceutics Section, APhA Academy of Pharmaceutical Sciences, Dallas meeting, Apr. 1965.

(8) J. C. K. Loo and S. Riegelman, *J. Pharm. Sci.*, **57**, 918 (1968).

ACKNOWLEDGMENTS AND ADDRESSES

Received May 1, 1975, from the *Merck Sharp & Dohme Research Laboratories, West Point, PA 19486*

Accepted for publication January 30, 1976.

[x] To whom inquiries should be directed.

Effect of Formulation of Intramuscular Injections of Phenothiazines on Duration of Activity

A. T. FLORENCE [x], A. W. JENKINS [*], and A. H. LOVELESS

Abstract □ Trifluoperazine and pericyazine were formulated using both the hydrochloride and embonate salts, and some comparisons were made with the activity of fluphenazine salt and ester formulations. Simple solutions in polyethylene glycol, gelled aqueous solutions, nonaqueous suspensions, multiple emulsions, and microencapsulated preparations were formulated, and their duration of activity was tested in dogs. While the multiple emulsion system showed some promise, a nylon microcapsule system produced significant prolonged activity of the drug after deep intramuscular injection.

Keyphrases □ Phenothiazines—effect of various pharmaceutical formulations on duration of biological activity, dogs □ Trifluoperazine hydrochloride and embonate—effect of various pharmaceutical formulations on duration of biological activity, dogs □ Pericyazine embonate—effect of various pharmaceutical formulations on duration of biological activity, dogs □ Pharmaceutical formulations, various—phenothiazines, effect on duration of biological activity, dogs □ Tranquilizers—trifluoperazine hydrochloride and embonate and pericyazine embonate, effect of various pharmaceutical formulations on duration of biological activity, dogs

Long-acting injectable phenothiazines are valuable in extended aftercare therapy in certain psychiatric states (1, 2). Currently available long-acting neuroleptics include solutions in oils such as sesame oil of poorly water-soluble esters of fluphenazine[1] and flupentixol[2], the duration of activity being up to 40 days. However, not all phenothiazines can be esterified to form lipid-soluble derivatives. Therefore, this work was directed toward alternative methods of prolonging the activity of two such drugs, trifluoperazine and pericyazine, using physicochemical rather than chemical or pharmacological methods.

Various formulation techniques, similar to those reviewed by Ritschel (3), were utilized. Resulting preparations were tested in dogs by an apomorphine challenge test utilizing the antiemetic as opposed to the tranquilizing properties of the phenothiazine, since levels of phenothiazine attained cannot be measured readily by available chemical assay techniques. Some experiments were carried out for comparative purposes using fluphenazine embonate. In all cases, fluphenazine enanthate in sesame oil was used as a reference formulation.

EXPERIMENTAL

Materials—Trifluoperazine hydrochloride and embonate salts[3] and pericyazine embonate[3] were used as received. Fluphenazine embonate was recovered after mixing equimolar solutions of sodium embonate[4] and fluphenazine hydrochloride[5]. Fluphenazine enanthate in sesame oil[6] (25 mg/ml) was obtained commercially.

Drug Solubilities—The solubilities of the bases were determined by a turbidity method (4). The solubilized embonate salts were determined by a modification of this method. Various solutions of drug hydrochloride were mixed with buffered sodium embonate (pamoate) to give equimolar mixtures. The turbidity of the solutions at 560 nm was plotted against the final concentration of drug embonate in the

[1] Moditen and Moditen Enanthate, Modecate; Squibb, United Kingdom; Prolixin Enanthate, Squibb, Princeton, N.J.

[2] Depixol, Lundbeck.

[3] May and Baker, Dagenham, Essex, United Kingdom.

[4] Eastman Kodak.

[5] Donated by Squibb, United Kingdom.

[6] Moditen, Squibb.

Table I—Formulation Compositions and Summary of Biological Results

Drug	Formulation	Drug Concentration in Formulation, mg/ml	Administered Dose[a], mg/kg	Duration of Total Inhibition of Retching, days	Time for Return to 25% Control Response, days
Trifluoperazine hydrochloride	5% Bentonite aqueous gel	100	2.5	1	8.5
	35% Polysorbate 80 aqueous gel	100	2.5	1	6
	Multiple emulsion	20	2.5	1	10
			5	3	21
Trifluoperazine embonate	Suspension in 1% aluminum stearate–gelled sesame oil	100	5	1	6.5
	Solution in polyethylene glycol 400	100	5	1	9
	Solution in polyethylene glycol 600	100	5	—	14.5
			5	3	17.5
	Sesame oil suspension of microencapsulated polyethylene glycol 400 drug solution	30	10	3	21
Pericyazine embonate	Suspension in 1% aluminum stearate–gelled sesame oil	100	5	1	6.5
	Solution in polyethylene glycol 400	100	5	1	5.5
	Solution in polyethylene glycol 600	100	5	1	5
	Aqueous suspension of microencapsulated polyethylene glycol 400–aqueous (50:50) mixture drug solution	30	5	Total inhibition	19
			5	not achieved	19
	Sesame oil suspension of microencapsulated polyethylene glycol 400–aqueous (50:50) mixture drug solution	30	10	Total inhibition not achieved	23
Fluphenazine embonate	Solution in polyethylene glycol 400	100	2	1	11
Fluphenazine enanthate	Solution in sesame oil	25	2	7	28
			0.8	3	21
			0.2	3	11.5

[a] Approximate dose equivalents as regards antiemetic activity: 2.5 mg of trifluoperazine hydrochloride/kg ≡ 5 mg of trifluoperazine embonate/kg ≡ 5 mg of pericyazine embonate/kg ≡ 2 mg of fluphenazine embonate/kg ≡ 1.5 mg of fluphenazine enanthate/kg.

buffered solution, and extrapolation to zero turbidity gave the solubility value.

Sample Preparation—All samples contained from 20 to 100 mg of drug/ml. Due to its relative instability, the multiple emulsion containing trifluoperazine hydrochloride was prepared immediately prior to use; the other preparations were inherently stable (Table I).

Aqueous Gels—Aqueous solutions of trifluoperazine hydrochloride were gelled by incorporation into solutions of 5% bentonite, 35% polysorbate 80, or up to 5% povidone (molecular weight 44,000) to give gels containing 100 mg of drug/ml.

Solutions—Solutions of drug embonates were prepared in liquid polyethylene glycols 400 and 600.

Suspensions—Powdered drugs, either as the hydrochloride (trifluoperazine) or embonate (pericyazine and trifluoperazine), were dispersed in sesame oil by grinding in a mortar.

Multiple Emulsions—Multiple emulsions were prepared as follows. An aqueous solution of trifluoperazine hydrochloride (2.75 g) in 15 ml of water containing polysorbate 85[7] (0.6 g) in sesame oil (40 ml containing 2.4 g of sorbitan trioleate[8]) was redispersed in an aqueous 5% polysorbate 40[9] solution to give a water-in-oil in water multiple emulsion containing 20 mg/ml of trifluoperazine hydrochloride.

Microcapsule Formulations—These formulations were prepared using an interfacial polymerization process in which the drug embonates were dissolved in polyethylene glycol 400. This process was described in detail elsewhere (5), and the properties of the microcapsules were discussed previously (6).

Formulation Evaluation *In Vivo*—Four beagle dogs of either sex, 10–17 kg, were injected with apomorphine, 0.1 mg/kg sc, on three occasions during the week before the test compound was administered. The number of retches occurring in the 30 min after dosing was counted. Two days after the final control session, the test formulation was administered by deep intramuscular injection into the thigh at a dose of 2.5, 5, or 10 mg/kg. After 24 hr, 3 days, 7 days, and weekly intervals, the apomorphine challenge was repeated.

The number of retches of all four dogs receiving a particular phenothiazine preparation was averaged and compared to the prephenothiazine response. Results are expressed as the percentage of prephenothiazine response that the apomorphine challenge stimulated and were plotted against the number of days after the phenothiazine was administered. Standard errors of the results from four dogs receiving the same dose of phenothiazine were from ±12 to ±15%.

[7] Tween 85, Atlas, supplied by Honeywill-Atlas, Surrey, England.
[8] Span 85, Atlas, supplied by Honeywill-Atlas, Surrey, England.
[9] Tween 40, Atlas, supplied by Honeywill-Atlas, Surrey, England.

RESULTS

The results in Fig. 1 can be considered as a baseline with which to gauge the success of other formulations. It could be anticipated that solutions of trifluoperazine and pericyazine embonates might be relatively short acting. However, the nature of the glycol vehicle might be expected to influence the duration of activity. The use of a suspension of the drug embonate in sesame oil (in which the drug is virtually insoluble) also might have influenced the result.

Figure 1 shows that there was no appreciable advantage in using a solution of poorly water-soluble salts such as the embonates to prolong activity beyond a few days, since the duration of activity shown was of the same order as that from an aqueous injection of trifluoperazine hydrochloride. Trifluoperazine embonate apparently was longer acting than pericyazine embonate, but this result may simply have been a reflection of the greater potency of the former drug. Because the two drugs have similar physicochemical characteristics, the reversal of the order of results for the two polyethylene glycol solutions and the dispersion (Fig. 1) was seen as a reflection of the experimental error in the assay.

The results obtained with sesame oil solutions of fluphenazine enanthate at various doses and with fluphenazine embonate in polyethylene glycol solution are shown in Fig. 2. These results show that: (*a*) the duration of activity of fluphenazine enanthate at 2 mg/kg, *i.e.*, 28 days, was comparable with the normal maximum clinical response; and (*b*) fluphenazine itself had no inherent prolonged activity, because fluphenazine embonate in glycol solution showed no significant difference in duration of activity from the embonate solutions of trifluoperazine and pericyazine (Fig. 1). This finding is in agreement with that of Laffan *et al.* (7).

Formulation of trifluoperazine hydrochloride as a multiple emulsion, thereby creating an interfacial barrier to drug diffusion, yielded more promising results (Fig. 3). At both 2.5 and 5 mg/kg, activity was prolonged, although complete inhibition of retching was of limited

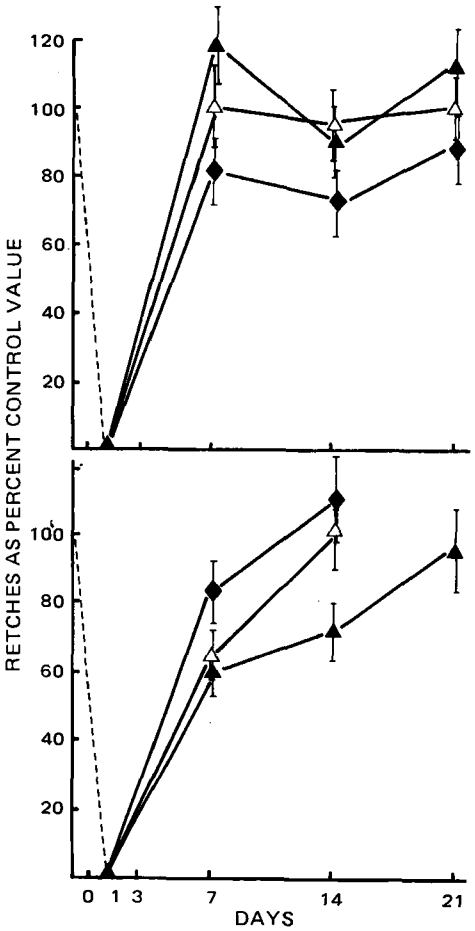

Figure 1—*(Top) Duration of activity of intramuscular injections of pericyazine embonate (5 mg/kg) as a solution in polyethylene glycol 400 (△), a solution in polyethylene glycol 600 (▲), and a dispersion of drug in sesame oil (♦). (Bottom) Duration of activity of intramuscular injection of trifluoperazine embonate (5 mg/kg) as a solution in polyethylene glycol 400 (△), a solution in polyethylene glycol 600 (▲), and a dispersion of drug and sesame oil (♦).*

duration. At 5 mg/kg, complete inhibition of the retching response was extended to 3 days and was followed by a more gradual return to the predrug response (Fig. 3). The polysorbate 80 gel formulation (Fig. 3) had no advantage over a solution of the embonate in polyethylene glycol; it was too rapidly dispersed from the injection site. The bentonite gel formulation, which had a slow release pattern *in vitro*, displayed a slightly longer activity than the polyethylene glycol solutions, but this finding was not sufficient to encourage further work on the formulation. This result led to the realization that a more efficient and more stable barrier to drug diffusion was required, so microencapsulation of the drug solution was attempted.

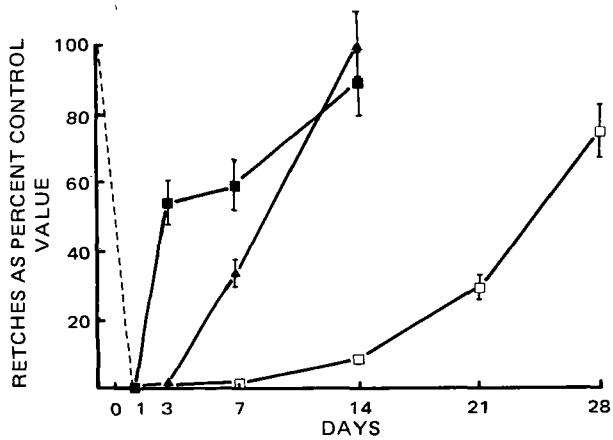

Figure 2—*Duration of activity of fluphenazine preparations. Key: ■, fluphenazine embonate solution in polyethylene glycol 400 (2 mg/kg); ▲, fluphenazine enanthate solution in sesame oil (0.2 mg/kg); and □, fluphenazine enanthate solution in sesame oil (2 mg/kg).*

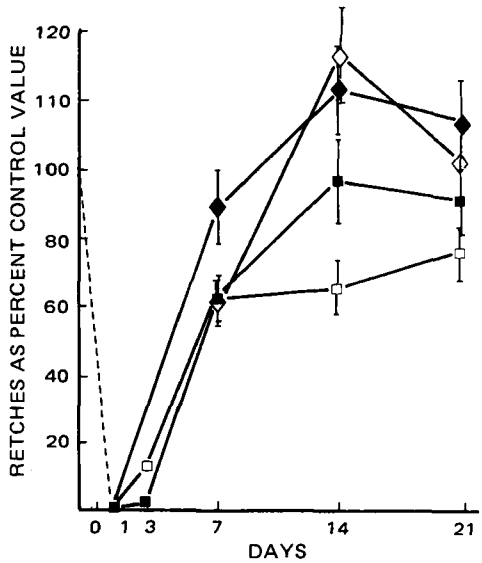

Figure 3—*Results for various formulations of trifluoperazine hydrochloride. Key: ◊, 2.5 mg/kg of drug in bentonite gel; ♦, 2.5 mg/kg of drug in polysorbate 80 gel; □, 2.5 mg/kg of drug in multiple emulsion; and ■, 5.0 mg/kg of drug in multiple emulsion.*

Results with a microencapsulated pericyazine embonate in 50% polyethylene glycol 400 aqueous solution are presented in Fig. 4. Insufficient drug was released initially to give complete inhibition of drug response on Day 1, as was obtained with all previous formulations. Doubling the injected dose increased the response up to 2 weeks. This result was more pronounced when an additional barrier in the form of the sesame oil suspending vehicle was present. However, after 2 weeks, by which time the sesame oil was removed from the injection site, no significant difference between the two preparations was observed. Microencapsulation of a polyethylene glycol 400 solution of trifluoperazine embonate resulted in a more satisfactory response–time profile (Fig. 4), where the time for return to predrug response was about 28 days.

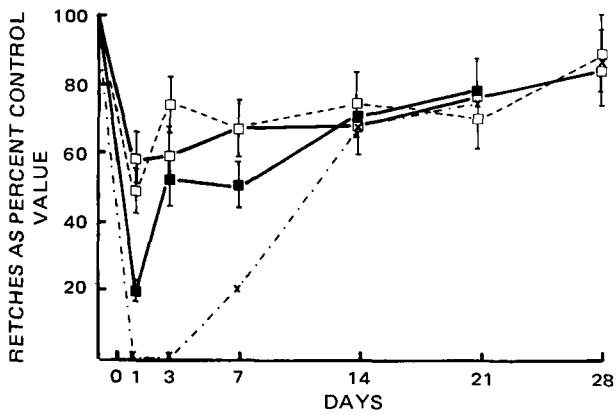

Figure 4—*Results for microencapsulated preparations of pericyazine embonate and trifluoperazine embonate. Key: □—□, pericyazine microencapsulated in nylon 610 (dose 5 mg/kg), with the microcapsule suspension being injected intramuscularly as a suspension in sesame oil; □- -□, pericyazine microencapsulated in nylon 610 (dose 10 mg/kg), with the microcapsule suspension being injected intramuscularly as a suspension in sesame oil; ■—■, pericyazine microencapsulated in nylon 610 (dose 5 mg/kg), with the preparation being injected as an aqueous suspension; and ×- -×-, trifluoperazine microencapsulated (dose 10 mg/kg) and dispersed in sesame oil for injection.*

Table II—Drug Solubilities at 37° in pH 7.4 Buffer

Drug	Solubility, 10^6 M
Trifluoperazine	36
Trifluoperazine embonate	30
Pericyazine	104
Pericyazine embonate	63
Fluphenazine	71
Fluphenazine embonate	25
Fluphenazine enanthate[a]	0.2

[a] The solubility of fluphenazine enanthate was determined in various aqueous ethanol solutions, and the logarithm of solubility was plotted against percent ethanol (six points). Extrapolation to zero ethanol gave the value quoted in the table.

These results are summarized in Table I.

DISCUSSION

The approach made here to prolong drug activity is typical of previous attempts in this field (3). Wai *et al.* (8), formulating a long-acting pentagastrin preparation, increased vehicle viscosity, formed a suspension, and finally coated the suspended particles to give the desired extension of drug activity. Formation of drug–embonate complexes was used successfully to prolong the release of intramuscular dihydrostreptomycin (9) and cycloguanil (10) but had little value in usefully extending the duration of activity of the three studied phenothiazines.

The lack of difference in activity between the trifluoperazine hydrochloride in aqueous solution and the embonate in suspension and solution may be due to the similarity in solubilities of these salts in pH 7.4 buffer, which has a pH close to that of the tissue fluids. Trifluoperazine hydrochloride has a solubility of 36×10^{-6} M at 37°, while the embonate has a solubility of 30×10^{-6} M at 37° (Table II). Thus, trifluoperazine precipitates from either hydrochloride or embonate solutions on encountering a pH of 7.4 at the injection site. Pericyazine is more soluble and appears to have a shorter duration of activity in all forms. The fluphenazine enanthate has a very low solubility (2×10^{-7} M), which undoubtedly contributes to its prolonged action.

Multiple emulsions of antitoxins extended antibody response time after injection (11), and this technique was used to give slow release of chemotherapeutic agents (12, 13). Our multiple emulsion formulation showed promise but had insufficient stability to prolong complete activity beyond 3 days. Undoubtedly, a stable emulsion system would be of interest. The logical extension of these approaches was to use microencapsulated drug derivatives; in this instance, the formulation performance approached the desired objective.

The microencapsulating agent used (nylon 610) was chosen to determine the feasibility and suitability of the microencapsulation technique for long-acting parenterals. Nylon is not likely to be acceptable in human medicine. Control of drug release by increasing the amount of nylon-forming materials, or alternative polymers (piperazine–phthalamide) or gelatin produced by coacervation, has been attempted. No significant improvement over the best results shown in this paper has been achieved.

REFERENCES

(1) S. R. Hirsch, R. Gaind, P. D. Rohde, B. S. Stevens, and J. K. Wing, *Br. Med. J.*, **1**, 633(1973).

(2) H. E. Lehman, *Dis. Nerv. Syst., Suppl.*, **31**, 7(1970).

(3) W. A. Ritschel, in "Drug Design," vol. IV, E. J. Ariens, Ed., Academic, London, England, 1973, p. 175.

(4) A. L. Green, *J. Pharm. Pharmacol.*, **19**, 10(1967).

(5) A. T. Florence and A. W. Jenkins, in "Microencapsulation," J. R. Nixon, Ed., Dekker, New York, N.Y., 1975, pp. 39–55.

(6) A. W. Jenkins and A. T. Florence, *J. Pharm. Pharmacol.*, **25**, 57P(1973).

(7) R. J. Laffan, J. P. High, and J. C. Burke, *Int. Neuropsychiat.*, **1**, 300(1965).

(8) K. N. Wai, E. E. L. Gerring, and R. D. Broad, *ibid.*, **22**, 923(1970).

(9) H. C. Caldwell, A. B. Rednick, G. C. Scott, G. J. Yakatan, and D. Ziv, *J. Pharm. Sci.*, **59**, 1689(1970).

(10) R. E. Thomson, B. J. Olszenski, E. F. Elslager, and D. F. Worth, *Am. J. Trop. Med. Hyg.*, **12**, 481(1963).

(11) W. J. Herbert, *Lancet*, **2**, 771(1965).

(12) A. J. Collings and R. Schneider, *Br. J. Pharmacol.*, **38**, 468P(1970).

(13) C. J. Benoy, L. A. Elson, and R. Schneider, *ibid.*, **45**, 135P(1972).

ACKNOWLEDGMENTS AND ADDRESSES

Received March 29, 1975, from the *Department of Pharmaceutical Chemistry, University of Strathclyde, Glasgow G1 1XW, United Kingdom,* and the *Research and Development Laboratories, May & Baker Ltd., Dagenham, Essex, United Kingdom.*

Accepted for publication January 29, 1976.

The authors thank Dr. D. R. Maxwell for his interest in this work. A. W. Jenkins was financed by May & Baker Ltd. and the University of Strathclyde.

* Present address: Fisons Ltd., Pharmaceutical Division, Loughborough, England.

[x] To whom inquiries should be directed (at the Department of Pharmaceutical Technology, University of Strathclyde).

Pulmonary Absorption Studies Utilizing *In Situ* Rat Lung Model: Designing Dosage Regimen for Bronchial Delivery of New Drug Entities

Z. T. CHOWHAN [x] and A. A. AMARO

Abstract □ The absorption of 7-methylsulfinylxanthone-2-carboxylic acid, 7-(methylthio)xanthone-2-carboxylic acid, and their sodium salts from the respiratory tract of anesthetized rats was studied after intratracheal administration of 0.1 ml of a solution or suspension containing the drug. At various times after administration, the lungs and trachea were removed and assayed radiochemically for unabsorbed drug. Sodium 7-(methylthio)xanthone-2-carboxylate from solution was absorbed approximately 20 times faster than sodium 7-methylsulfinylxanthone-2-carboxylate from a solution. The absorption from solutions was three to four times faster than the absorption from suspensions. For inhalation aerosol dosage forms intended for prophylactic use, the drug entity with slower systemic absorption probably would be more desirable than the drug entity with rapid absorption. Rapid systemic absorption following inhalation of powder or liquid aerosols would lead to more frequent dosing if the biological activity is related to the drug concentration in the tracheobronchial tissues. Therefore, the powder or liquid inhalation aerosols of organic acids rather than the corresponding sodium salts may be preferable for designing a dosage regimen. However, if the dosage form is intended for utilizing the bronchodilator activity of the compound, the drug entity with rapid absorption is more desirable. Therefore, in the treatment of asthmatic attacks, liquid or powder inhalation aerosols of the sodium salt of the rapidly absorbing drug entity are preferable. The absorption rates were directly proportional to concentration when the initial concentration of sodium 7-methylsulfinylxanthone-2-carboxylate was varied over a 333-fold range. The effect of the pH of the drug solution administered intratracheally to the rat lung indicated a sharp increase in the pulmonary absorption at a pH near the pKa. The results suggested that structurally related xanthones are absorbed possibly by passive diffusion across the lipoidal region of the pulmonary membranes and that the absorption of organic acids and organic electrolytes is mainly controlled by the lipid solubility of the unionized species.

Keyphrases □ Xanthone-2-carboxylic acids, substituted—pulmonary absorption after intratracheal administration, solution and suspension compared, rat lungs □ Absorption, pulmonary—substituted xanthone-2-carboxylic acids and sodium salts, intratracheal administration, solution and suspension compared, rat lungs □ Bronchial delivery—substituted xanthone-2-carboxylic acids and sodium salts, intratracheal administration, solution and suspension compared, rat lungs □ Dosage forms—solutions and suspensions of substituted xanthone-2-carboxylic acids and sodium salts, pulmonary absorption, rat lungs

The delivery of drugs to the tracheobronchial tree has been used for centuries. The use of inhalation aerosols, however, has not gained as much popularity as many conventional dosage forms. The drugs are generally subjected to systemic absorption through the mouth, nose, trachea, lungs, and GI tract after aerosol inhalation. The determination of the site and extent of drug delivery becomes difficult because of the complications resulting from the various mechanisms of deposition, clearance, and retention of aerosol particles. In spite of these disadvantages, the bronchial route of drug administration is the most direct route to the tracheobronchial tree. In some situations, bronchial administration is the only practical way of delivering a drug to the respiratory tract because of the loss of important biological activity by acid or enzymatic hydrolysis in the stomach, first-pass metabolism in the liver, or poor absorption in the GI tract.

Although the major objectives of inhalation therapy are to provide the drug directly to the site of action and to treat the conditions within the tracheobronchial tree, the potential absorption of the drug across alveolar capillary membranes must be considered. The knowledge of the absorption rates of new drug entities becomes extremely important if the biological activity is directly related to drug concentration at the site of action. From a dosage regimen viewpoint, the slow systemic absorption of a drug may be more desirable than rapid systemic absorption from the lungs. Therefore, the pulmonary absorption of potential drug entities should be compared quantitatively before the most suitable drug species is selected.

A quantitative method of measuring the absorption of various nonvolatile organic solutes from the anesthetized rat lung was introduced recently (1–11). The results of these studies indicated that the respiratory tract epithelium conforms to the classical lipid pore model of biological membranes. Lipid-soluble compounds were absorbed more rapidly than lipid-insoluble compounds, and the latter substances crossed the membranes at rates inversely related to their molecular size. With most compounds, absorption appeared to occur by passive diffusion. Notable exceptions were the absorption of phenolsulfonphthalein (8) and cromolyn sodium (9), which were absorbed in part by a saturable carrier-type transport process and in part by diffusion.

This investigation utilized the *in situ* rat lung model for quantitative determination of the absorption rates of two structurally related xanthone-2-carboxylic acids and their sodium salts. It was hoped that the comparisons would provide useful information in the selection of the most suitable drug entity for an appropriate dosage regimen for bronchial delivery. Furthermore, this study was expected to elucidate the processes involved in the absorption of these compounds from the lungs.

EXPERIMENTAL

Chemicals—Monobasic and dibasic sodium phosphate[1] (anhydrous), citric acid[1], sodium citrate[1], calcium chloride[1], sodium chloride[2], potassium chloride[2], dextrose[2] (anhydrous), and acetic acid[3] were analytical reagent grade.

The two xanthones, 7-methylsulfinylxanthone-2-carboxylic acid[4]

[1] J. T. Baker Chemical Co., Phillipsburg, NJ 08865
[2] Mallinckrodt Chemical Works, St. Louis, MO 63147
[3] E. I. du Pont de Nemours and Co., Wilmington, Del.
[4] Institute of Organic Chemistry, Syntex Research, Palo Alto, Calif.

Table I—Apparent First-Order Rate Constants and Half-Times of Absorption of the Sodium Salts and Free Acids of Two Xanthones

Compound	Primary Absorption Rate Constant, min^{-1}	Primary Half-Time of Absorption, min	Secondary Rate Constant, min^{-1}	Secondary Half-Time of Absorption, min
7-Methylsulfinylxanthone-2-carboxylic acid	0.0304	23	0.0112	61.7
Sodium 7-methylsulfinylxanthone-2-carboxylate	0.0534	13	—	—
7-(Methylthio)xanthone-2-carboxylic acid	—	—	0.231	3.0
Sodium 7-(methylthio)xanthone-2-carboxylate	—	—	0.232	3.0

and 7-(methylthio)xanthone-2-carboxylic acid[4], were used as received. The radiochemical purity of 7-methylsulfinylxanthone-2-carboxylic acid and its sodium salt was greater than 95%. The chemical purity as determined by quantitative TLC, using chlorform–methanol–acetic acid (95:5:1), was greater than 99.5%. The radiochemical purity of 7-(methylthio)xanthone-2-carboxylic acid was greater than 98%, and its chemical purity was 99.7%.

Naphthalene[1], 1,4-bis[2-(4-methyl-5-phenyloxazolyl)]benzene[5], 2,5-diphenyloxazole[5], methanol[2], dioxane[6] (spectrograde), and toluene[2] (scintillation grade) were used in making the scintillation cocktail.

Doses—Doses for the sodium 7-(methylthio)xanthone-2-carboxylate were prepared by dissolving radioactive and nonlabeled compounds in pH 7.4 phosphate buffer. Sodium 7-methylsulfinylxanthone-2-carboxylate doses were prepared by dissolving the radioactive and nonlabeled materials together in appropriate buffer solutions. The doses of the free acids were prepared by coprecipitating the free acid from a solution of radioactive and nonlabeled materials by adding an equimolar quantity of hydrochloric acid and then adding the buffer species to obtain the appropriate buffer concentration and pH. The particle-size distribution of suspensions resulting from the two compounds were similar.

The buffers contained 0.134 *M* sodium chloride, 0.011 *M* potassium chloride, 0.0001 *M* calcium chloride, 0.02 *M* glucose, and 0.008 *M* buffer salts. Sodium 7-methylsulfinylxanthone-2-carboxylate was used for studying the effects of concentration and pH on pulmonary absorption. For pH 3, 3.5, and 4 experiments, acetate buffer was used. For pH 5 and 7.4 experiments, citrate–phosphate and phosphate buffers, respectively, were used. All buffers were of the same molarity (0.008 *M*). Except as indicated under the concentration effect, the dose per rat for the solutions was 10 μg; for the suspensions, it was 1 mg.

Procedure in Animals—Young male Sprague–Dawley-derived rats[7], 160–190 g, were used. Animals were anesthetized with pentobarbital and placed on their backs on a small animal operating board[8]; the limbs were secured. After exposing the trachea through a longitudinal incision along the ventral aspect of the neck, the trachea was cut traversely, halfway through between the fourth and fifth tracheal rings caudal to the thyroid cartilage.

Medical grade tubing[9] [0.07 cm (0.027 in.) i.d., 0.09 cm (0.039 in.) o.d., and 6.3 cm (2.5 in.) in length] was inserted around the needle of a 100-μl syringe[10] so that 1.2 cm remained exposed from the needle. The tubing was inserted through the tracheal incision to a depth of 2.5 cm below the tracheal incision, so the tip of the tubing was slightly above the bifurcation of the trachea. With the tubing in this position, the solution or suspension was injected over 1–2 sec. The tubing was then withdrawn completely, and the animal was maintained under light anesthesia for the remainder of the experiment. The body temperature of the animal was maintained at 36 ± 1° throughout the experiment by heat from a 100-w incandescent lamp in a reflector suspended over the animal at about 20 cm.

Absorption of the xanthones was allowed to occur for various times. One minute before the end of the absorption period, removal of the lungs was begun. The trachea just below the incision was tied by means of a nylon thread, and the lungs were quickly removed along with the trachea up to just above the tied end. Any surrounding tissue was then trimmed, and the lungs were cut into two parts so as not to exceed the sample weight of the combustor. Each part was placed on a 7-cm diameter filter paper[11] and dried overnight in a petri dish using a vacuum oven at 50°.

Measurement of Radioactivity—Both parts of the dried lungs from each animal, along with the filter paper, were pelletized and then combusted[12]. The pelletized samples were ignited on a platinum filament in the combustion chamber and burned completely. The vapors from each sample passed through a refrigerated condenser and then into a scintillation vial. After complete combustion, the flask and condenser were flushed with five injections of distilled water to cleanse the system of radioactivity. The wash was also passed into the scintillation vial. The condenser was again flushed with water and added along with the scintillation fluid to the scintillation vial. The composition of the scintillation fluid was: naphthalene, 100 g; 2,5-diphenyloxazole, 5 g; 1,4-bis[2-(4-methyl-5-phenyloxazolyl)]benzene, 0.3 g; dioxane, 720 ml; toluene, 135 ml; and methanol, 45 ml.

To minimize radioactivity overlap, a blank pellet was combusted in a similar fashion between each pair of samples. Radioactivity was determined by a scintillation counter[13]. Background counts were determined from combustion of blank filter paper and subtracted from the sample counts. Quench corrections were made by comparing the counts gained from spiking both the blanks and the samples with a known amount of radioactivity. The ratio of the average spike from blanks to the average spike from samples determined the quench correction applied to the samples.

To determine the combustion efficiency of the oxidizer, two sets of standards were prepared from the same solution used for dosing the animals. Each standard of the first set was prepared by placing a known volume of solution on a filter paper, and then pelletizing and combusting it. The second set of standards were noncombustion standards. The combustion efficiency equaled the counts per minute of the combustion standard divided by the counts per minute of the noncombustion standard. This value then represented the percent of radioactivity retained in the combustion procedure. The counts per minute value of the sample was multiplied by the reciprocal of the combustion efficiency.

The percent radioactivity remaining in the lungs for any given time point was determined from the counts per minute obtained from the noncombustion standards. The counts per minute values obtained from the two lung samples for each rat were combined to give the radioactivity remaining at that time point. The percent radioactivity remaining was determined from the counts per minute of the lung sample divided by the counts per minute of the dose given intratracheally.

Octanol–Water Partition Coefficient—The octanol[1]–water partition coefficients were determined by equilibrating at 23° 100 ml of 0.008 *M* HCl in which the compound was dissolved with 0.5 ml of 1-octanol. The initial concentration of 7-(methylthio)xanthone-2-carboxylic acid (tritiated) was 0.009 μg/ml, and the initial concentration of 7-methylsulfinylxanthone-2-carboxylic acid (tritiated) was 0.004 μg/ml. The samples were shaken on a wrist-action shaker[14] until equilibrium was reached. Samples from both phases were taken, and concentrations were determined by the radiochemical method.

RESULTS AND DISCUSSION

The results of pulmonary absorption studies with sodium 7-

[5] Arapahoe Chemicals, Boulder, Colo.
[6] Matheson, Coleman & Bell, Norwood, OH 45212
[7] Simonsen Laboratories Inc., Gilroy, CA 94020
[8] Americal Hospital Supply Corp., McGaw Park, IL 60085
[9] Lined with Teflon (du Pont), Becton, Dickinson and Co., Rutherford, N.J.
[10] Hamilton Co., Whittier, Calif.
[11] Whatman No. 1.
[12] Tri-Carb sampler oxidizer model 305, Packard Instruments.
[13] Nuclear Chicago, Des Plaines, IL 60018
[14] Burrell Corp., Pittsburgh, Pa.

Table II—Effect of Concentration on Absorption of Sodium 7-Methylsulfinylxanthone-2-carboxylate from Rat Lungs

Initial Concentration	Number of Animals	Time for Absorption, min	Mean Percent Unabsorbed	Range	*SE*
3 μg/ml	6	5	75.91	64.9–84.7	2.72
100 μg/ml	10	5	72.31	66.7–82.5	1.74
0.5 mg/ml	5	5	81.18	76.5–88.3	2.46
1 mg/ml	9	5	83.25	76.2–88.7	1.27

methylsulfinylxanthone-2-carboxylate solution and 7-methylsulfinylxanthone-2-carboxylic acid suspension are given in Fig. 1. The drug from the solution appeared to be absorbed by a first-order process. The semilogarithmic plots of pulmonary absorption from the suspension did not follow a linear relationship with time. This finding indicated that the dissolution of the drug from a suspension was superimposed on the absorption process. The slower rate of absorption in the secondary phase might indicate that the rate of dissolution rather than the rate of absorption may be the rate-limiting step.

Estimates of the absorption rate constant and half-time for absorption are given in Table I. The half-time of absorption from solutions was 13 min. However, the half-time of absorption from suspensions after the initial rapid phase was 61.7 min. According to these results, it would be possible to obtain different rates of drug clearance from the lungs by proper selection of the drug species.

Drugs intended for bronchial delivery from powders or inhalation aerosols are generally developed for topical treatment within the respiratory tract. For a suitable dosage regimen of these dosage forms, rapid systemic absorption from the lungs may not be desirable if the compound has only prophylactic activity. For a powder inhalation aerosol dosage form or propelled[15] aerosol dosage form, absorption data from solutions and suspensions suggest that the free acid of the drug would be absorbed at a slower rate compared to the sodium salt because the absorption from the lungs would be limited by the slower dissolution from the solid particles of the free acid. The slower systemic absorption from the lungs would provide drug concentrations for longer periods for the mast cell protective activity. Based on these considerations, the free acid rather than the sodium salt may be more desirable.

The results of pulmonary absorption studies with sodium 7-(methylthio)xanthone-2-carboxylate solution and 7-(methylthio)-xanthone-2-carboxylic acid suspension are given in Fig. 2. The semilogarithmic plots of the absorption data from solutions as well as suspensions suggest that the absorption process is biphasic. Because of the extremely rapid rate of absorption of the drug in the primary phase, this model did not permit the determination of primary rates of absorption. At the end of 90 sec, only about 20% drug was remaining in the lungs after intratracheal administration of a solution.

The secondary half-time of absorption of this compound both from solutions and suspensions was 3 min. Although the absorption from suspensions was somewhat slower in the primary phase, probably because of the dissolution step from the suspended drug in the free acid form, the amount remaining in the lungs at the end of 10 min was less than 10%. Rapid absorption of this compound in combination with bronchodilator activity provides a useful dosage regimen for the treatment of asthmatic attacks.

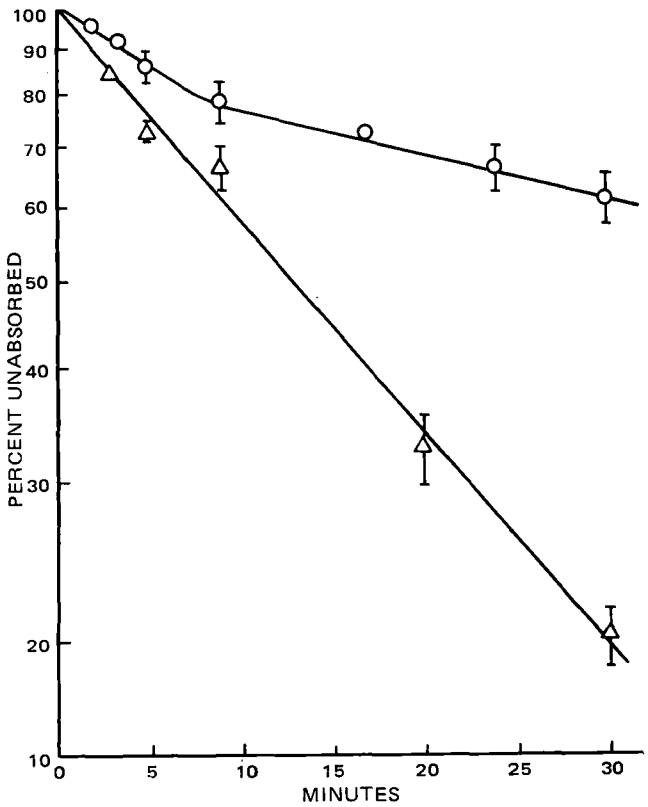

Figure 1—*Absorption of 7-methylsulfinylxanthone-2-carboxylic acid after intratracheal administration of a sodium salt solution (Δ) and an acid suspension (O) to the lungs of anesthetized rats. Data points are averages of at least three rats. Vertical bars represent standard error; the absence of vertical bars indicates that the standard error was too small to be shown.*

[15] Freon.

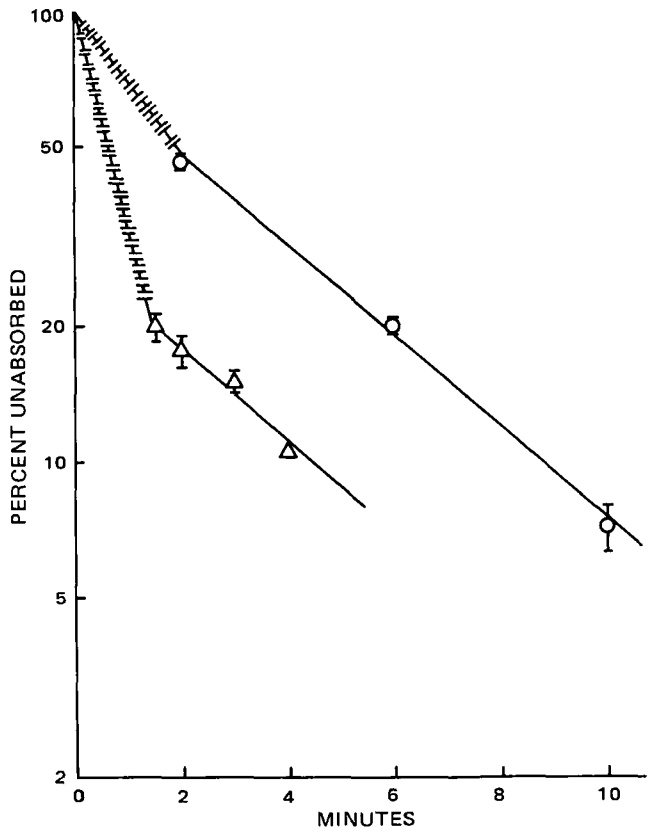

Figure 2—*Absorption of 7-(methylthio)xanthone-2-carboxylic acid and its sodium salt after intratracheal administration of a sodium salt solution (Δ) and an acid suspension (O) to the lungs of anesthetized rats. Data points are averages of at least three rats. Vertical bars represent standard error; the absence of vertical bars indicates that the standard error was too small to be shown.*

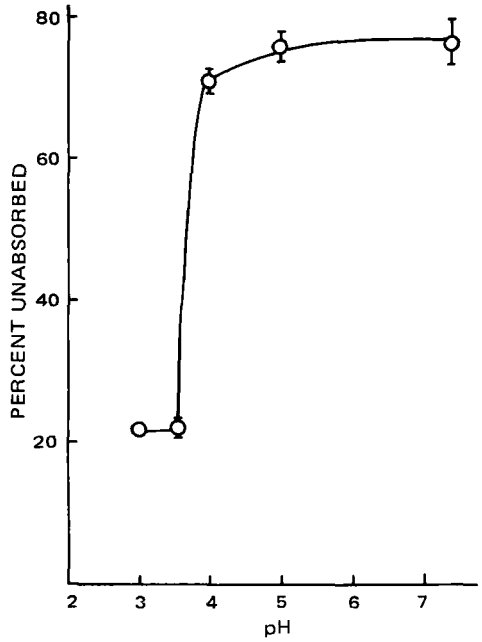

Figure 3—*Effect of pH of the solution administered intratracheally to rat lungs on absorption of sodium 7-methylsulfinylxanthone-2-carboxylate. Data points are averages of at least three rats. Vertical bars represent standard error; the absence of vertical bars indicates that the standard error was too small to be shown.*

The apparent first-order absorption of sodium 7-methylsulfinylxanthone-2-carboxylate and the biphasic absorption of sodium 7-(methylthio)xanthone-2-carboxylate from solution are similar to the absorption of cardiac glycosides from the rat lungs (7). The pulmonary absorption of digoxin and digitoxin was apparent first order, while ouabain and dihydroouabain appeared to fit a biexponential function. These differences in the mode of absorption of structurally related xanthones can probably be explained in terms of the large differences in the partition coefficients between the aqueous and the lipoidal phases. These data appear to agree with the octanol–water partition coefficient data. The octanol–water partition coefficient of 7-methylsulfinylxanthone-2-carboxylic acid was 58 compared to 2493 obtained for 7-(methylthio)xanthone-2-carboxylic acid. These differences in octanol–water partition coefficients and in the pulmonary absorption are in agreement with earlier (4, 5) observations that compounds with higher lipid solubility are absorbed faster than the compounds with lower lipid solubility.

In Table II, the effect of concentration on absorption of sodium 7-methylsulfinylxanthone-2-carboxylate from the rat lung administered in the form of a solution is given. Over a 3-μg/ml–1-mg/ml range, the absorption did not vary significantly. Since the percent unabsorbed remained essentially constant over a wide concentration range, the amount absorbed being proportional to the concentration, the results suggested that the absorption occurred mainly by a nonsaturable process such as passive diffusion.

The results of the percent sodium 7-methylsulfinylxanthone-2-carboxylate unabsorbed at 5 min as a function of pH of the drug solution administered intratracheally to rat lungs are given in Fig. 3. These results indicate a relatively small change in absorption in the pH 4–8 range. There was a sharp increase in the pulmonary absorption when the pH of the administered solution was changed to 3.5. The pKa of this compound, as determined by the solubility method, was 3.8. A considerable increase in the unionized species at the absorption site was reflected by a rapid increase in absorption. These results further support the hypothesis that pulmonary absorption of these organic electrolytes and organic acids is mainly controlled by the lipid solubility of the unionized species.

REFERENCES

(1) G. F. Moss and J. T. Richie, *Toxicol. Appl. Pharmacol.*, **17**, 699(1970).

(2) S. J. Enna and L. S. Schanker, *Am. J. Physiol.*, **223**, 409(1972).

(3) *Ibid.*, **223**, 1227(1972).

(4) J. A. Burton and L. S. Schanker, *Proc. Soc. Exp. Biol. Med.*, **145**, 752(1974).

(5) J. A. Burton and L. S. Schanker, *Steroids*, **23**, 617(1974).

(6) J. A. Burton and L. S. Schanker, *Xenobiotica*, **4**, 291 (1974).

(7) R. C. Lanman, R. M. Grillilan, and L. S. Schanker, *J. Pharmacol. Exp. Ther.*, **187**, 105(1973).

(8) S. J. Enna and L. S. Schanker, *Life Sci.*, **12**, 231(1973).

(9) T. S. Gardiner and L. S. Schanker, *Xenobiotica*, **4**, 725(1974).

(10) E. W. Mitchell and L. S. Schanker, *Fed. Proc., Fed. Am. Soc. Exp. Biol.*, **32**, 258(1973).

(11) *Ibid.*, **33**, 422(1974).

ACKNOWLEDGMENTS AND ADDRESSES

Received November 21, 1975, from the *Institute of Pharmaceutical Sciences, Syntex Research, Division of Syntex Corporation, Palo Alto, CA 94304*

Accepted for publication February 9, 1976.

[x] To whom inquiries should be directed.

Effect of Temperature on Binding of Warfarin by Human Serum Albumin

Y. T. OESTER, STEVEN KERESZTES-NAGY, ROLAND F. MAIS ˣ, JACK BECKTEL, and JOHN F. ZAROSLINSKI

Abstract □ The *in vitro* binding of warfarin by human serum albumin was studied at various temperatures and at pH 7.4 by a frontal gel filtration technique. The results can be best described in terms of a two class-of-binding site model, in which the numbers of primary and secondary sites are constrained to the average values for all experiments (n_1 = 1.38 and n_2 = 3.73). Analysis of the temperature dependence of the binding yielded the following thermodynamic parameters: $\Delta H_1 = -2.55$ kcal/mole, $\Delta S_1 = 16.1$ eu, and $\Delta F_1 = -7.34$ kcal/mole for the primary binding and $\Delta H_2 = -5.08$ kcal/mole, $\Delta S_2 = -1.10$ eu, and $\Delta F_2 = 4.72$ kcal/mole for the secondary binding. Calculations based on these results showed that, for the therapeutic concentration range, warfarin was over 99% bound to albumin present in physiological concentration. These findings are compared and contrasted to binding data in the literature for warfarin and salicylate.

Keyphrases □ Warfarin—binding to human serum albumin, effect of temperature □ Albumin, human serum—binding of warfarin, effect of temperature □ Binding, drug–protein—warfarin to human serum albumin, effect of temperature □ Anticoagulants—warfarin, binding to human serum albumin, effect of temperature

Drug binding studies carried out *in vivo* provide practical information about the fraction bound and free drug concentrations. The unbound drug in circulation affects the degree of pharmacological response *via* tissue distribution and clearance, while the bound fraction influences drug absorption and transport. Unfortunately, the interpretation of *in vivo* studies is complicated by many factors, such as the existence of specific transport proteins, binding by red cells, and competition for binding sites by endogenous and exogenous substances.

An example of displacement of drug bound to albumin by other drugs is the potentiation of the anticoagulant effect of warfarin by phenylbutazone (1); chloral hydrate (2); mefenamic, ethacrynic, and nalidixic acids (3); and salicylate (4). However, the exact mechanism of displacement of warfarin by these drugs has not been settled. To clarify the nature of binding and the type of inhibition involved, a detailed study of the interaction of warfarin and salicylate with human serum albumin was begun.

As the first step, new binding methodology was developed, combining the sensitivity and precision of radioisotope dilution with the rapidity and reproducibility of the frontal gel filtration technique. Subsequently, this methodology was employed in the study of salicylate binding to human serum albumin at various temperatures (5). Analyses of the data were carried out by computer programs corresponding to the various binding models considered.

As a further development, this paper describes a study of the binding of warfarin to human serum albumin. It compares the results with similar data already available. The mathematical basis for analysis and comparison of binding data presented in various forms was published recently (6). The detailed description of salicylate and warfarin binding to human serum albumin in terms of the two class-of-site model paves the way for the quantitative analysis of the mutual displacement of these two drugs from albumin. Some aspects of these interactions were discussed previously (7).

EXPERIMENTAL

Materials and Methods—Gel filtration frontal analysis chromatography, which was successfully employed in previous drug binding studies (5–8), was used for the determination of bound warfarin. Various concentrations of drug were prepared in 0.067 *M* phosphate buffer, pH 7.4, containing 0.3 g/100 ml of crystalline human serum albumin[1]. Labeled ^{14}C-warfarin[2], of 99% radiochemical purity and a specific activity of 23 mCi/mmole, was added to the drug solutions at a constant level to provide about 20,000 cpm/ml. Initial studies were conducted with ^{14}C-warfarin[3], 0.2 mCi/mmole, which was found to be identical to the higher activity labeled material.

The gel filtration technique used was that described by Cooper and Wood (9). A cross-linked dextran gel[4] was allowed to swell in 0.067 *M* phosphate buffer, pH 7.4, at the temperature prescribed (6–37°). Precision bore columns[5] were modified for more rapid flow by replacing the fritted polyethylene disk with nylon mesh[6]. The gel was packed into the column to a depth of 25 cm, providing a bed volume of about 20 ml. The columns and system were equilibrated for 1 hr prior to making the runs. The system was maintained at the desired temperature with a constant-temperature regulator[7].

The samples were maintained for several hours at the prescribed temperature in the water bath that comprised part of the thermoregulator system. Because of a slight retention of the warfarin by the gel, the sample volume had to be increased to 60 ml from the usual 45 ml reported previously for salicylate (8). The absorption was inconsequential in the frontal analysis system, as reported previously (9). Preliminary studies indicated that satisfactory plateaus in the total and free drug regions were obtainable for this volume of sample. Three 1-ml aliquots were taken in the β-plateau region and four in the γ-region. The results were averaged from the duplicate samples.

Warfarin Determinations—The test solutions, containing warfarin in varying concentrations, were prepared accurately by weight from standardized stock solutions, which were verified for exact concentration by UV absorption spectrophotometry. One-milliliter aliquots of the fractions obtained on a fraction collector[8] from the gel column were added to 10 ml of scintillation solution[9] in a conventional low K-I glass counting vial[10].

The carbon-14 activity was measured in a three-channel beta liquid scintillation spectrometer[11]. Each sample was counted to less than

[1] Miles Laboratories, Kankakee, Ill.
[2] CFA. 499, Amersham/Searle, Arlington Heights, Ill.
[3] Wisconsin Alumni Research Foundation Institute, Madison, Wis.
[4] Sephadex G-25, coarse grade, Pharmacia Fine Chemicals, Piscataway, N.J.
[5] Adjusto-Chrom 5919, 1 × 60-cm set for 25-cm column, Ace Glass Inc., Vineland, N.J.
[6] Kontes Glass Co., Vineland, N.J.
[7] Haake Series FE constant-temperature circulator with KR refrigerated chiller, Polyscience Corp., Evanston, Ill.
[8] Brinkmann-Serva Linear II, Brinkmann Instruments, Westbury, N.Y.
[9] Insta-Gel, Packard Instrument Co., Downers Grove, Ill.
[10] Packard Instrument Co., Downers Grove, Ill.
[11] Model 3380, Packard Instrument Co., Downers Grove, Ill.

Table I—Calculated Fraction Bound (*FB*) of Warfarin to 4 g/100 ml of Human Serum Albumin at 37°[a]

Plasma Warfarin Concentration, mg/liter	*FB*, %	FB_1, %
2	99	96
5	99	96
55	99	96
500	88	55

[a] Data obtained by iterative calculation with the PDP-8e computer.

1% *SD*. Instrument efficiency was monitored by including matched standards for the counting. Quenching, which was evaluated by the channels ratio method of Baillie (10), was insignificant for the protein level encountered in these solutions.

Warfarin content of the samples was determined by comparison of sample counts against the counts of the standard for the total drug level, and recovery was greater than 98%. Protein was determined by the microbiuret method of Goa (11), and recoveries exceeded 98%. Sodium, as a measure of the Donnan effect, was determined by flame photometry[12], using lithium as an internal standard.

Calculations—The extent of binding was calculated as follows:

$$\text{warfarin bound} = \text{warfarin total} - \text{warfarin free} \quad \text{(Eq. 1)}$$

The concentrations of total and free warfarin were determined by radioassay of aliquots from the β- and γ-plateaus. The molecular weight of albumin was taken as 69,000 for these calculations. The concentrations were corrected for solute space, and the free warfarin concentration was adjusted for the Donnan equilibrium using the sodium distribution according to the procedure of Keen (12).

The molar ratio of the bound warfarin (r) and the free warfarin concentrations (c) was used to obtain a two class-of-site solution by means of an iterative least-squares program[13]. The data were also tested for aptness of fit to a three class-of-site model using a much faster computer[14] for the program execution; this approach represents an improvement over the procedure previously described (8)[15].

The resulting values for n_1 and n_2, the primary and secondary binding sites, were averaged for the entire set of duplicate runs encompassing the full range of temperatures studied. These values were then used, in a modification of the two-site computer program, to evaluate the original data. This method resulted in new primary and secondary association constants constrained to average values for the number of primary and secondary sites. These values of the association constants were then used in the least-squares linear regression for the van't Hoff plot. The thermodynamic parameters were derived from the van't Hoff regressions.

The partial and total fractions bound, FB_1 and *FB*, were calculated from the total warfarin concentration by means of an iterative procedure employing a digital computer[16] (13). The data of Table I were derived in this way. Garten and Wosilait (14) described a solution to this problem, employing a computer[17], when there are two classes of sites. The advantage of our solution is that it can be done with a programmable calculator and is applicable to more than two classes of sites.

RESULTS AND DISCUSSION

Figure 1 compares typical elution patterns for warfarin and salicylate for a level of albumin of 0.3 g/100 ml. The β- and γ-plateaus correspond to the total and free drug concentrations, respectively. The column size and sample volume necessary to achieve the proper plateaus are determined experimentally, the main factor being absorption to the gel with some drugs. Presumably, because of interaction of warfarin with the gel, a larger sample volume is required with this drug than with salicylate to establish a satisfactory elution pattern. However, as long as flat β- and γ-plateaus are present, the binding equilibrium between warfarin and albumin is not altered by the retardation of the drug in the column. In contrast to large volume frontal analysis, small volume zonal chromatography would provide erroneous data as to the degree of binding of warfarin to albumin.

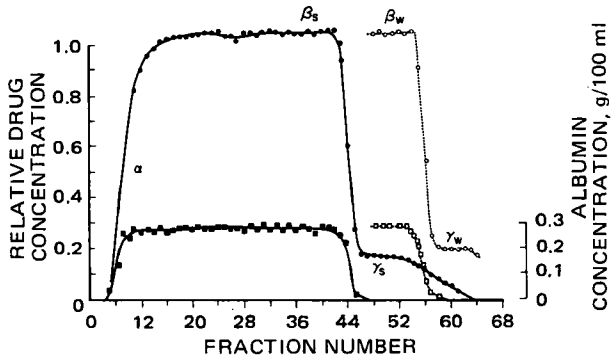

Figure 1—*Comparison of elution profiles for 45 ml of salicylate–human serum albumin (●) and human serum albumin (■) and 60 ml of warfarin–human serum albumin (○) and human serum albumin (□). Frontal gel chromatographic separation was on 1 × 25-cm columns of Sephadex G-25 coarse. The fractions were 1.3 ml.*

Figure 2 is a Scatchard display of the binding data for duplicate runs of eight points each. The sample concentrations are selected to provide optimal spacing of the points along the curve. The plot is curvilinear, an invariable finding with warfarin–albumin binding

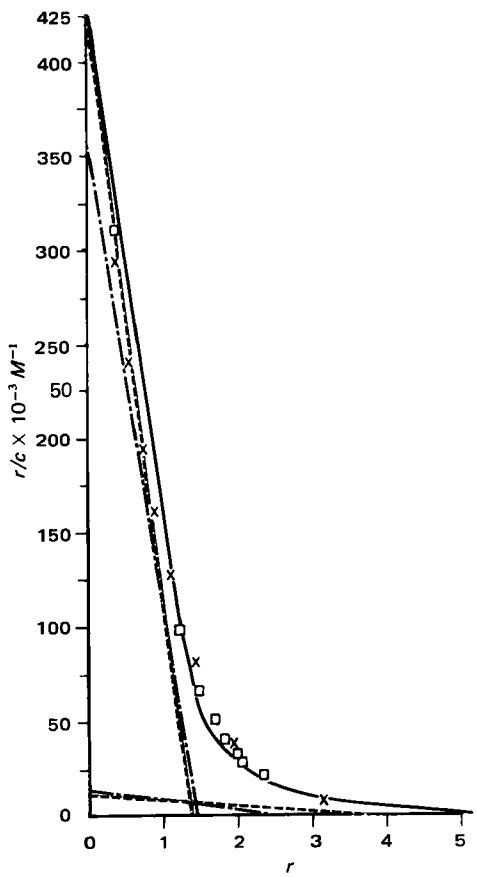

Figure 2—*Binding of warfarin to albumin in 0.067 M phosphate buffer, pH 7.4, at 25°. Two sets of data are displayed, each representing separate eight-point trials (×,□). Each point is a duplicate determination. The smooth curve is the best fit to these data resulting from the computer solution based on predetermined values for the number of sites ($n_1 = 1.38$, and $n_2 = 3.73$). Key: – · –, unconstrained solution; and - - - -, constrained solution.*

[12] Flame photometer 343, Instrumentation Laboratories, Lexington, Mass.
[13] IBM 1620, IBM Data Processing Division, White Plains, N.Y.
[14] IBM 360.
[15] Specific details of the computer programs employed are available upon request from the authors.
[16] PDP-8e, Digital Equipment Corp., Maynard, Mass.
[17] IBM 360/65.

Table II—Comparison of the Number of Primary and Secondary Binding Sites on Human Serum Albumin Reported for Warfarin and Salicylate

n_1	n_2	Drug	Reference
1.38	3.73	Warfarin	This paper
1.46	4.10	Salicylate	5
2	4	Warfarin	14
1 (1.3)[a]	6 (5.7)[a]	Warfarin	13
2 (2.38)[b]	(9.03)[b]	Warfarin	22
(2.13)[c]	(21.75)[c]		
3.5[d]	—	Warfarin	2
1.4[e]	—	Warfarin	2

[a]Our computer evaluation of the published data. [b]Our computer evaluation of the published data at 3°. [c]Our computer evaluation of the published data at 27°. [d]Reported value at 3°. [e]Reported value at 37°.

studies. A possible explanation for this result is that electrostatic interactions of the bound and incoming charged drug molecules significantly influence the binding process. However, appropriate electrostatic corrections for this effect, when applied to the present data, failed to produce a linear plot as was mentioned.

Similarly, electrostatic considerations were inadequate to explain the curvilinear Scatchard plots reported with an azo dye (15), various fatty acid anions (16), penicillin (12), and salicylate (5) binding to albumin. In these studies, the data were interpreted in terms of multiple binding sites and the electrostatic corrections were not employed. Generally, analysis based on two independent classes of sites adequately fits the binding data. Such a model is characterized for four parameters, n_1, K_1, n_2, and K_2; these are the number of sites and their respective association constants. The computer program derived values for these constants corresponding to the best fit to the experimental r and c values.

The unconstrained solution of the experimental data is illustrated in Fig. 2, where $n_1 = 1.46$ and $n_2 = 2.42$. These best-fit n values from all experiments were averaged, and the means were used in a computer program accepting fixed numbers of binding sites. The resulting constrained solution is also portrayed in the graph. There is no appreciable difference between the constrained and unconstrained evaluation, as reflected by the single smooth curve through the experimental points. This curve represents the vectorial summation of the linear components. The residual sum of squares, an additional indicator of the goodness of fit, is not significantly different in the two cases. This constrained model is in accord with the concept that the number of binding sites is invariate under the same experimental conditions for a particular system. Indeed, no trend was noted in the variation of n values relative to temperature and to warfarin or albumin concentration that would upset this idea.

A three class-of-site resolution of the experimental data was also attempted. This model resulted in low fractional primary sites and extraordinarily high tertiary sites. Additionally, an F test comparison of the residual sum of squares for the two and three class-of-site models revealed that the latter fits the data no better than the former. Similar findings for the binding of salicylate led to the adoption of the two class-of-site interpretation as the most appropriate.

Table II lists the various reported n values for the primary and secondary sites. The 95% confidence limits for n_1 are 1.08 and 1.59; for n_2, they are 0.22 and 7.14. For comparison, the number of binding sites for salicylate is also shown. Clearly, the number of primary and secondary binding sites for warfarin and salicylate are nearly identical. This finding suggests that these two drugs may displace one another from albumin by competing for identical sites on the albumin molecule.

As is evident from Table II, many investigators prefer to report integral number of binding sites. These numbers are most likely adjusted values, based on the reasonable assumption that, with homogeneous albumin, the number of sites should be integers. To estimate the degree of adjustment, published data from several studies (17–19) were analyzed by our computer program. The results are shown in Table II in parentheses. On the basis of the information collected, it is not possible to determine conclusively whether n_1 is 1 or 2; the degree of uncertainty is even larger with n_2. Thus, in all calculations, the fractional number of sites was employed, ensuring the best agreement of calculated and experimental information.

A summary of the binding data obtained at various temperatures

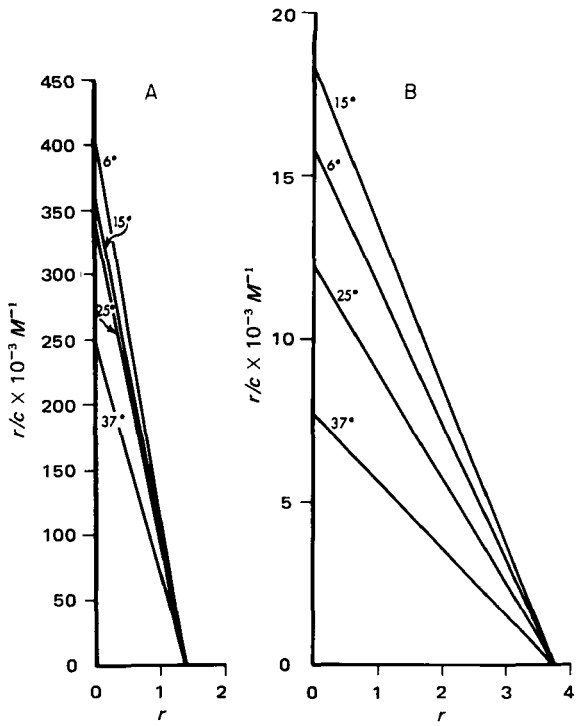

Figure 3—*Temperature dependence of the binding of warfarin to human serum albumin, as shown by the constrained two-site resolution of the binding data. The variation of binding with temperature at the primary and secondary binding sites is represented in sections A and B, respectively. In all experiments, the pH (7.4) and protein concentrations (0.3 g/100 ml) were maintained constant.*

is shown in Fig. 3 in the form of a Scatchard display of the constrained two class-of-site resolutions. The slopes of the lines correspond to the experimental primary and secondary association constants. Decreasing temperature results in an increase of the binding constants for both classes of sites. The van't Hoff plot, log K *versus* the reciprocal of the absolute temperature, is shown in Fig. 4. The straight lines were derived by regression analysis and serve to calculate corrected binding constants as well as standard enthalpies for the primary and secondary binding.

A summary of the association constants for the binding of warfarin to albumin is assembled in Table III. In general, the agreement among the reported K_1 and K_2 values can be considered good, especially since the experimental techniques used were different and the interpretation of the data, as reflected in the calculation of binding parameters, was not uniform. An apparent exception is the unusually large K_1 value reported by Meyer and Guttman (19). In an attempt to analyze the reasons for this discrepancy, the data from their curvilinear Scatchard plot were resolved in our computer program. Corresponding

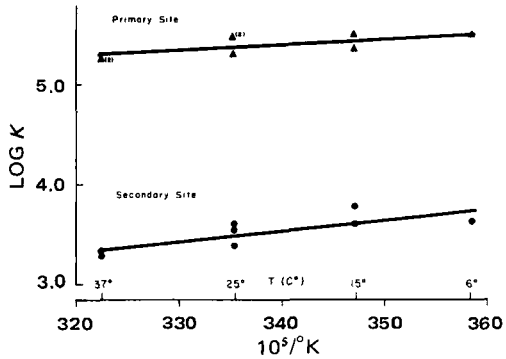

Figure 4—*Van't Hoff plot of the data for primary (▲) and secondary (●) sites. The regressions are: log* $K_1 = 0.00557\ (10^5/T) + 3.51201$, *and log* $K_2 = 0.01110\ (10^5/T) - 0.23081$. *The correlation coefficients are 0.67 and 0.81, respectively.*

Table III—Comparison of Primary and Secondary Binding Constants Reported for Warfarin and Human Serum Albumin

Temperature	$K_1 \times 10^3, M^{-1}$					$K_2 \times 10^3, M^{-1}$				
	This Study	Ref. 23	Ref. 19	Ref. 20	Ref. 2	This Study	Ref. 23	Ref. 19	Ref. 20	Ref. 2
3°	—	385 (114)[a]	—	—	160	—	— (0.6)[a]	—	—	—
6°	321	—	—	—	—	5.6	—	—	—	—
15°	278	350	—	—	—	4.2	—	—	—	—
25°	240	—	6240 (174)[a]	—	—	3.1	—	2.6 (2.2)[a]	—	—
27°	—	231 (97)[a]	—	89	—	—	— (0.3)[a]	—	6.7	—
37°	203	217	—	—	180	2.2	—	—	—	—
42°	190	—	—	—	—	2.0	—	—	—	—

[a] Our computer evaluation of the published data.

r and r/c values from the Scatchard plot least-squares fit of Meyer and Guttman were read by means of a microcomparator. The best fit to these readings was obtained with a K_1 value of 174×10^3 ($n_1 = 1.3$) and a K_2 value of 2.2×10^3 ($n_2 = 5.7$). This solution differs substantially from that of Meyer and Guttman only in the value for K_1.

Clearly, very minor variations or errors in r/c at low r values have a large influence on the derived value for K_1, especially when steep curves are extrapolated to zero r/c values. The spectrophotometric method used by these authors (19) for the determination of warfarin did not allow measurement of experimental r values much below 1.2. This limitation is contrasted with the ability of the radioisotope technique, which allowed routine determinations at r values as low as 0.2. Thus, while the generally much lower K_1 values shown in Table III are consistent with the experimental data of Meyer and Guttman, their reported K_1 value is out of line with the experimental binding data observed at r values below 1.

O'Reilly's extensive binding studies with warfarin largely parallels the present work. This author, while recognizing multiple binding sites, did not attempt to resolve his data in these terms. His K_1 association constant, shown in Table III, represents the limiting slope of the curvilinear Scatchard plot. For a better comparison of the reported binding data as well as the binding parameters, the data of O'Reilly and Kowitz (17) were subjected to our computer analysis. The results at two temperatures are also included in Table III. The derived K_1 values are two- to threefold lower than the association constants reported previously (17). This difference is an example of another interpretation of binding data. The value reported previously (17) is the association constant for the first anion bound, while the present value is the association constant for the binding by the primary class of sites. The four parameters derived from the data of O'Reilly and Kowitz are in good agreement with their data over the entire range of experimental measurements.

The binding constant reported by Garten and Wosilait (20) (Table III) is somewhat lower than would be expected from interpolation of our K values to 27°. These workers employed Hart's procedure (21), which produces a least-squares fit to a linearized form of the mass action expression for binding. This procedure considers r the "independent" and r/c the "dependent" variables and minimizes the sum of squared deviations in r/c. Such a comparison is not entirely valid, however, since the n_1, n_2, and K_2 values are different and the evaluation of K is interdependent with them.

A better comparison of the binding data is on the basis of fraction bound and free drug concentrations at identical drug and protein levels. This type of comparison shows the present data to be essentially the same as those of Garten and Wosilait (20). The binding constants at 37° given by Sellers and Koch-Weser (2) are in excellent agreement with the present data. Notably, their n_1 value at this temperature is identical with the average n_1 value obtained in this study. The agreement no longer exists for the comparison of association constants at 3°, mainly for the reason that they reported an increase in the number of binding sites with a decrease in temperature. This increase was not evident in the present work.

Comparison of binding studies on the basis of fraction of bound drug of identical drug and albumin concentrations is highly desirable. A computer program for this purpose was developed (6). Calculations show that at therapeutic plasma warfarin levels, warfarin is more than 99% bound to albumin at a concentration of 4 g/100 ml, regardless of which published set of binding parameters is used. The secondary sites contribute less than 4% of the binding at a warfarin concentration of 55 mg/liter. A 10-fold increase in the total plasma warfarin level would reduce the fraction bound to 88% and increase the contribution of the secondary binding to 45% of the total. A summary of these calculations is given in Table I.

These findings may be compared to those for the binding of salicylate published previously (5). In general, salicylate is somewhat less strongly bound than warfarin. Under identical conditions, 96% would be bound at the 20-mg/liter level; at 300 mg/liter, the therapeutic limit for salicylate, 83% would be in the bound form. The major importance of such considerations is to point out that drugs capable of displacing warfarin from its albumin binding sites may raise the effective free drug level manyfold, thereby leading to hemorrhagic complications (22).

The data presented here on the temperature dependence of warfarin binding agree well with those reported by O'Reilly (23). From the variation of the association constant with temperature, he derived a standard enthalpy change of −3.48 kcal/mole and a standard entropy change of +11 eu. Microcalorimetric measurements yielded a ΔH of −3.14 kcal/mole. These values, together with the other selected thermodynamic data for the binding of the various ligands by albumin, are shown in Table IV. Comparison of primary and secondary thermodynamic parameters reveals that the binding to primary sites is associated with significant positive entropy, while the secondary binding is exclusively enthalpy driven.

Furthermore, the temperature dependence of the secondary binding sites is about twice as large as that for the primary sites. Thus, at lower temperatures, the contribution of the secondary binding would increase. Such a shift toward binding to the more numerous secondary sites may explain the increased numbers of binding sites

Table IV—Standard Thermodynamic Parameters for Various Ligands Binding to Human Serum Albumin

Ligand	ΔF_1[a], kcal/mole	ΔH_1, kcal/mole	ΔS_1, eu	ΔF_2, kcal/mole	ΔH_2, kcal/mole	ΔS_2, eu
Warfarin[b]	−7.34	−2.55	+16.1	−4.76	−5.08	−1.10
Warfarin (Ref. 23)	−7.37	−3.50	+11.0	—	—	—
Azo dyes (Ref. 15)	−6.54	−3.93	+8.8	—	—	—
d-Tryptophan (Ref. 25)	−5.40	−11.3	−20.0	—	—	—
Salicylate (Ref. 5)	−6.45	−9.8	−11.2	−4.72	−4.70	+0.10
Thiocyanate (Ref. 26)	−6.20	−8.8	−8.8	—	—	—

[a] In Ref. 5, the thermodynamic parameters were expressed in units promoted by the Systeme International. However, these units have found little usage so far and the comparison with literature values is facilitated by employing the more familiar calorie unit. Conversion from one system to the other is based on the equivalence of 1 cal with 4.1868 J. [b] This paper.

reported by Sellers and Koch-Weser (2, 3) at the lower temperature.

According to Klotz (24), thermodynamic parameters in themselves do not provide a diagnostic criterion for distinguishing the types of forces involved in ligand binding by proteins. Indeed, as shown in Table IV, these parameters are nearly identical for the small thiocyanate ion and the larger organic molecule of salicylate containing the aromatic ring. Despite this anomaly, it is possible to draw relevant conclusions from the strikingly different thermodynamic parameters recorded for warfarin and azo dyes (15) as contrasted with those for *d*-tryptophan (25), salicylate (5), and thiocyanate (26). The binding of the first group is characterized by a low negative enthalpy and a considerable positive entropy; the binding by the second group is characteristically enthalpy driven opposed by the negative entropy.

From these considerations, it seems that hydrophobic forces predominate in the binding of warfarin since electrostatic forces were shown not to contribute to the positive entropy term (18). With salicylate, it appears that van der Waals forces are the most significant in the binding of this drug in albumin. This striking contrast between the binding parameters for warfarin and salicylate raises some serious doubts as to the coincidence of their binding sites on the albumin molecule, despite their nearly identical number of binding sites and their proven displacement interactions with albumin.

In line with this observation is the earlier finding that the inhibitor constants characterizing the displacement abilities of these two drugs are severalfold smaller than the primary association constants (4). Thus, purely competitive inhibition of binding between warfarin and salicylate can be ruled out. In contrast to the primary site parameters, binding to the secondary sites results in similar ΔH and ΔS values for these two drugs (Table IV). In both cases, the entropy term is nearly zero and the negative enthalpy drives the reaction. Therefore, competition at these sites might be expected to conform to a more strictly competitive inhibition model.

REFERENCES

(1) P. M. Aggeler, R. A. O'Reilly, L. Leong, and P. E. Kowitz, *N. Engl. J. Med.*, **276**, 496(1967).

(2) E. M. Sellers and J. Koch-Weser, *ibid.*, **283**, 827(1970).

(3) E. M. Sellers and J. Koch-Weser, *Clin. Pharmacol. Ther.*, **11**, 524(1970).

(4) J. F. Zaroslinski, Y. T. Oester, R. F. Mais, and S. Keresztes-Nagy, Fifth International Congress of Pharmacology, July 23–28, 1972.

(5) J. F. Zaroslinski, S. Keresztes-Nagy, R. F. Mais, and Y. T. Oester, *Biochem. Pharmacol.*, **32**, 1767(1974).

(6) R. F. Mais, S. Keresztes-Nagy, J. F. Zaroslinski, and Y. T. Oester, *J. Pharm. Sci.*, **63**, 1423(1974).

(7) Y. T. Oester, R. F. Mais, S. Keresztes-Nagy, and J. F. Zaroslinski, *Pharmacologist*, **13**, 309(1971).

(8) S. Keresztes-Nagy, R. F. Mais, Y. T. Oester, and J. F. Zaroslinski, *Anal. Biochem.*, **48**, 80(1972).

(9) P. F. Cooper and G. C. Wood, *J. Pharm. Pharmacol., Suppl.*, **20**, 150S(1968).

(10) L. A. Baillie, *Int. J. Appl. Radiat. Isotopes*, **8**, 1(1960).

(11) J. Goa, *Scand. J. Clin. Lab. Invest., Suppl. 22*, **7**, 15(1955).

(12) P. M. Keen, *Biochem. Pharmacol.*, **15**, 447(1966).

(13) R. F. Mais, R. D. McCook, and Y. T. Oester, "Fraction Bound and Total Drug," DECUS No. Focal 8-262 Digital Equipment Computer Users Society Library, Maynard, Mass., Dec. 1972.

(14) S. Garten and W. D. Wosilait, *Comput. Programs Biomed.*, **2**, 61(1971).

(15) F. Karush, *J. Am. Chem. Soc.*, **72**, 2705(1950).

(16) J. D. Teresi and J. M. Luck, *J. Biol. Chem.*, **194**, 823(1952).

(17) R. A. O'Reilly and P. E. Kowitz, *J. Clin. Invest.*, **46**, 829(1967).

(18) R. A. O'Reilly, *ibid.*, **48**, 193(1969).

(19) M. C. Meyer and D. E. Guttman, *J. Pharm. Sci.*, **59**, 39(1970).

(20) S. Garten and W. D. Wosilait, *Comp. Gen. Pharmacol.*, **3**, 83(1972).

(21) H. E. Hart, *Bull. Math. Biophys.*, **27**, 87(1965).

(22) R. A. O'Reilly and G. Levy, *J. Pharm. Sci.*, **59**, 1258(1970).

(23) R. A. O'Reilly, *Ann. N.Y. Acad. Sci.*, **226**, 293(1973).

(24) I. M. Klotz, *ibid.*, **226**, 18(1973).

(25) G. F. Fairclough and J. S. Fruton, *Biochemistry*, **5**, 673(1966).

(26) G. Scatchard and W. T. Yap, *J. Am. Chem. Soc.*, **86**, 3434(1964).

ACKNOWLEDGMENTS AND ADDRESSES

Received December 8, 1975, from the *Research Service, Veterans Administration Hospital, Hines, IL 60141*, and the *Department of Pharmacology and Biochemistry, Loyola University Stritch School of Medicine, Maywood, IL 60153*

Accepted for publication January 26, 1976.

Supported in part by Veterans Administration Research Project No. 6320-02.

[x] To whom inquiries should be directed (at the Neuropharmacology Research Section, Veterans Administration Hospital, Hines, IL 60141).

Synthesis of Substituted Anilino-(3-methoxy-4-substituted Acetoxy)benzylidenes and Their Monoamine Oxidase Inhibitory and Anticonvulsant Properties

SHIVA P. SINGH *§, ANSHUMALI CHAUDHARI §, VIRGIL I. STENBERG *, and SURENDRA S. PARMAR ‡§x

Abstract □ Several substituted anilino-(3-methoxy-4-substituted acetoxy)benzylidenes were synthesized and characterized by their sharp melting points and elemental analyses. All substituted benzylidenes competitively inhibited the *in vitro* monoamine oxidase activity of rat brain homogenates and possessed anticonvulsant activity against pentylenetetrazol-induced convulsions in mice.

Keyphrases □ Benzylidenes, substituted—synthesized, screened for effect on monoamine oxidase activity and anticonvulsant properties □ Monoamine oxidase activity—effect of various substituted anilinobenzylidenes, rat brain homogenate □ Anticonvulsant activity—various substituted anilinobenzylidenes screened, mice □ Structure–activity relationships—various substituted anilinobenzylidenes synthesized and screened for effect on monoamine oxidase activity and anticonvulsant properties

Mixed excitatory and depressant actions on the central nervous system activity have been shown to be associated with numerous tertiary alkylamines containing one or more aromatic groups. Of the several azacycloalkylbenzaldehyde hydrazones examined, 3-[2-(4- methyl-1-piperazinyl)-5- nitrobenzylidene]amino-2-oxazolidinone produced the most marked inhibition of rat brain monoamine oxidase (1). Monoamine oxidase inhibitors also possess pronounced anticonvulsant properties (2). Earlier studies indicated that substituted benzylidenes have anticonvulsant and monoamine oxidase inhibitory activity (3). These observations prompted the synthesis of substituted anilino- (3-methoxy-4- morpholino/pyrrolidino/piperidinoacetoxy)benzylidenes. These substituted benzylidenes were evaluated for their ability to inhibit rat brain monoamine oxidase and anticonvulsant activity against pentylenetetrazol-induced convulsions in mice.

The various substituted anilino-(3-methoxy-4-substituted acetoxy)benzylidenes were synthesized by following the route outlined in Scheme I.

EXPERIMENTAL

Substituted Anilino-(3-methoxy-4-hydroxy)benzylidenes—These benzylidenes were prepared by the condensation of substituted anilines with vanillin as reported previously (3).

Substituted Anilino-(3-methoxy-4-chloroacetoxy)benzylidenes (I–III)—To a substituted anilino-(3-methoxy-4-hydroxy)-benzylidene (0.05 mole) in 25 ml of dry benzene was added chloroacetyl chloride (0.055 mole), gradually and with shaking, and the mixture was refluxed on a steam bath for 4 hr. Excess benzene was removed by distillation; the solid mass which separated was collected by filtration, washed with water to remove the traces of chloroacetyl chloride, dried, and recrystallized from ethanol. All compounds were characterized by their sharp melting points and elemental analyses (Table I).

Substituted Anilino-(3-methoxy-4-substituted Acetoxy)benzylidenes (IV–XXI)—These compounds were synthesized by refluxing a mixture of a substituted anilino-(3-methoxy-4-chloroacetoxy)benzylidene (0.005 mole) and an appropriate secondary amine (0.01 mole) in 25 ml of dry benzene on a steam bath for 6 hr. Excess benzene was removed by distillation; the solid mass which separated was collected by filtration, dried, and recrystallized from ethanol. All substituted benzylidenes were characterized by their sharp melting points and elemental analyses (Table II).

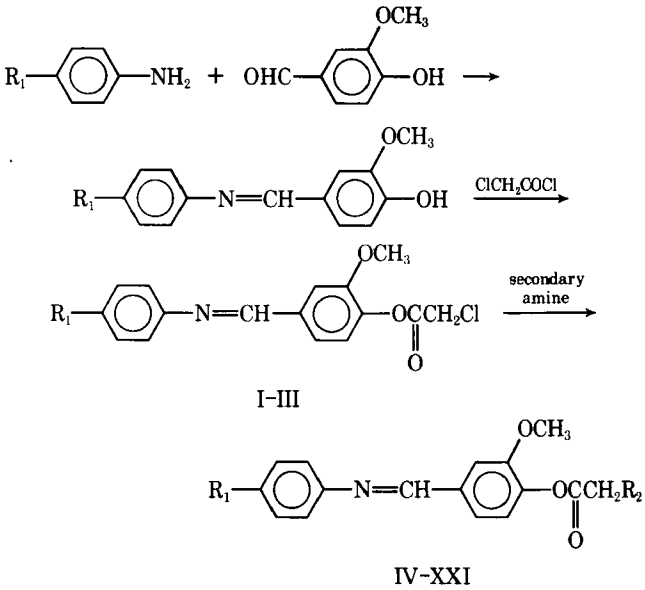

Scheme I

Monoamine Oxidase Activity—Monoamine oxidase activity of rat brain homogenate was determined by a spectrophotofluorometric method, using kynuramine as the substrate (4). Male albino rats, 100–150 g, were allowed food and water *ad libitum*. They were sacrificed by decapitation, and the brains were removed immediately and homogenized[1] in ice-cold 0.25 *M* sucrose (1:9 w/v). The monoamine oxidase activity of rat brain homogenate was determined by incubation at 37° in air for 30 min. The reaction mixture in a total volume of 3 ml consisted of 0.5 ml of phosphate buffer (0.5 *M*, pH 7.5), 0.1 m*M* kynuramine, and 0.5 ml of brain homogenate (equivalent to 10 mg wet weight of the tissue).

The various substituted benzylidenes were dissolved in propylene glycol (100%) and used at a final concentration of 0.166 m*M*. An equivalent amount of propylene glycol was added to the control tubes. All benzylidenes were incubated with rat brain homogenates for 10 min before the addition of kynuramine. The mixture, after the addition of kynuramine, was further incubated for 30 min. The enzymatic reaction was stopped by the addition of 1 ml of 10% trichloroacetic acid (w/v), and the precipitated proteins were removed by centrifugation.

Suitable 1-ml aliquots of the supernatant solution were taken in 2 ml of 1 *N* NaOH solution and assayed for 4-hydroxyquinoline, formed during deamination of kynuramine. They then were measured fluorometrically[2], using activating light of 315 nm and measuring fluorescence at 380 nm. An increase in absorbance provided a direct

[1] Potter-Elvehjem.
[2] Aminco-Bowman spectrophotofluorometer.

Table I—Physical Constants of Substituted Anilino-(3-methoxy-4-chloroacetoxy)benzylidenes

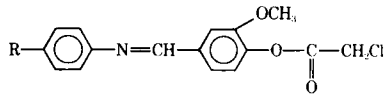

Compound	R	Melting Point[a]	Yield, %	Molecular Formula[b]	Analysis, % Calc.	Found
I	Cl	105°	80	$C_{16}H_{13}Cl_2NO_3$	C 56.80	56.32
					H 3.85	3.76
					N 4.14	4.12
II	CH_3	115°	82	$C_{17}H_{16}ClNO_3$	C 64.25	63.85
					H 5.04	4.92
					N 4.40	4.22
III	OCH_3	130°	85	$C_{17}H_{16}ClNO_4$	C 61.17	61.00
					H 4.79	4.57
					N 4.19	3.88

[a] Melting points were taken in open capillary tubes and are corrected. [b] All compounds were recrystallized from ethanol.

Table II—Physical Constants of Substituted Anilino-(3-methoxy-4-substituted Acetoxy)benzylidenes

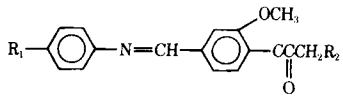

Compound	R_1	R_2	Melting Point[a]	Yield, %	Molecular Formula[b]	Analysis, % Calc.	Found
IV	Cl	Morpholino	115°	78	$C_{20}H_{21}ClN_2O_4 \cdot HCl$	C 56.47	56.23
						H 5.18	4.98
						N 6.59	6.44
V	Cl	Pyrrolidino	112°	80	$C_{20}H_{21}ClN_2O_3 \cdot HCl$	C 58.68	58.28
						H 5.38	5.12
						N 6.85	6.52
VI	Cl	Piperidino	68°	74	$C_{21}H_{23}ClN_2O_3 \cdot HCl$	C 59.57	59.34
						H 5.67	5.41
						N 6.62	6.21
VII	Cl	2-Methylpiperidino	98°	58	$C_{22}H_{25}ClN_2O_3 \cdot HCl$	C 60.41	60.20
						H 5.95	5.75
						N 6.41	6.30
VIII	Cl	3-Methylpiperidino	103°	60	$C_{22}H_{25}ClN_2O_3 \cdot HCl$	C 60.41	59.98
						H 5.95	5.58
						N 6.41	6.13
IX	Cl	4-Methylpiperidino	118°	60	$C_{22}H_{25}ClN_2O_3 \cdot HCl$	C 60.41	60.38
						H 5.95	5.84
						N 6.41	6.40
X	CH_3	Morpholino	167°	76	$C_{21}H_{24}N_2O_4 \cdot HCl$	C 62.29	62.12
						H 6.18	5.83
						N 6.92	6.48
XI	CH_3	Pyrrolidino	222°	73	$C_{21}H_{24}N_2O_3 \cdot HCl$	C 64.86	64.54
						H 6.43	6.27
						N 7.21	7.15
XII	CH_3	Piperidino	226°	72	$C_{22}H_{26}N_2O_3 \cdot HCl$	C 65.59	65.37
						H 6.71	6.29
						N 6.96	6.38
XIII	CH_3	2-Methylpiperidino	215°	56	$C_{23}H_{28}N_2O_3 \cdot HCl$	C 66.27	66.00
						H 6.96	6.88
						N 6.72	6.55
XIV	CH_3	3-Methylpiperidino	235°	61	$C_{23}H_{28}N_2O_3 \cdot HCl$	C 66.27	66.22
						H 6.96	6.76
						N 6.72	6.42
XV	CH_3	4-Methylpiperidino	237°	68	$C_{23}H_{28}N_2O_3 \cdot HCl$	C 66.27	66.14
						H 6.96	6.58
						N 6.72	6.46
XVI	OCH_3	Morpholino	134°	85	$C_{21}H_{24}N_2O_5$	C 65.62	65.46
						H 6.25	6.08
						N 7.29	7.21
XVII	OCH_3	Pyrrolidino	128°	83	$C_{21}H_{24}N_2O_4$	C 68.48	68.28
						H 6.52	6.37
						N 7.61	7.48
XVIII	OCH_3	Piperidino	125°	80	$C_{22}H_{26}N_2O_5$	C 69.11	69.02
						H 6.81	6.72
						N 7.33	7.12
XIX	OCH_3	2-Methylpiperidino	122°	60	$C_{23}H_{28}N_2O_4$	C 69.69	69.35
						H 7.07	6.86
						N 7.07	6.65
XX	OCH_3	3-Methylpiperidino	124°	64	$C_{23}H_{28}N_2O_4$	C 69.69	69.29
						H 7.07	7.02
						N 7.07	6.59
XXI	OCH_3	4-Methylpiperidino	127°	72	$C_{23}H_{28}N_2O_4$	C 69.69	69.46
						H 7.07	6.88
						N 7.07	6.78

[a] Melting points were taken in open capillary tubes and are corrected. [b] All compounds were recrystallized from ethanol.

Table III—Monoamine Oxidase Inhibitory and Anticonvulsant Properties of Substituted Anilino-(3-methoxy-4-substituted Acetoxy)benzylidenes

Compound	Monoamine Oxidase Inhibition[a]		Anticonvulsant Activity[b], % Protection	Pentylenetetrazol Mortality[c], %
	% Inhibition	I_{50} Values[d] ($\times 10^{-4}$ M)		
IV	65.0 ± 0.5	1.16	40	50
V	67.5 ± 0.8	1.14	20	40
VI	51.8 ± 0.6	1.60	30	70
VII	70.1 ± 0.6	1.10	20	50
VIII	62.2 ± 1.1	1.22	20	60
IX	45.3 ± 1.0	1.76	20	80
X	57.3 ± 0.5	1.40	50	30
XI	72.7 ± 0.6	1.06	70	90
XII	65.0 ± 0.7	1.16	20	90
XIII	75.2 ± 0.8	1.00	20	80
XIV	70.1 ± 0.6	1.10	30	60
XV	66.1 ± 0.5	1.15	30	50
XVI	64.8 ± 0.9	1.15	70	20
XVII	64.8 ± 0.5	1.15	10	90
XVIII	63.5 ± 0.7	1.20	30	70
XIX	68.7 ± 0.5	1.20	50	50
XX	71.2 ± 0.6	1.11	30	80
XXI	64.5 ± 0.8	1.20	20	70
Methaqualone	—	—	60	20
Meprobamate	—	—	80	10

[a]Contents of the reaction mixture and assay procedures are as described in the text. Each experiment was done in triplicate, and the values are the mean values of three separate experiments with ±*SEM*. Kynuramine and substituted benzylidenes were used at a final concentration of 0.1 and 0.166 m*M*, respectively. [b]Screening procedures for the determination of anticonvulsant activity of substituted benzylidenes and methaqualone and meprobamate, the two reference drugs, at a dose of 100 mg/kg ip are described in the text. [c]Mortality in pentylenetetrazol-treated animals was observed during 24 hr. [d]Various substituted benzylidenes were used at final concentrations ranging between 0.05 and 0.2 m*M* for the determination of their I_{50} values.

measurement of 4-hydroxyquinoline formation, which was taken as an index of the monoamine oxidase activity. The percentage inhibition was calculated from the decrease observed in absorbance, and this value provided an index of the inhibitory property of these substituted benzylidenes.

In the preincubation studies, the rat brain homogenates in the incubation mixture were incubated with or without substituted benzylidenes at 37° for 10, 20, and 30 min prior to the addition of kynuramine. In zero-time experiments, the substituted benzylidenes and kynuramine were added simultaneously to the reaction mixture containing the brain homogenate. The I_{50} values (concentrations producing 50% inhibition) were determined graphically from the values obtained for the inhibition of rat brain monoamine oxidase by using these benzylidenes in concentrations ranging between 0.05 and 0.2 m*M*. In addition, the nature of the enzyme inhibition caused by XI, XIII, and XX was evaluated by the graphic method of Lineweaver and Burk (5) as modified by Dixon (6).

Determination of Anticonvulsant Activity—The anticonvulsant activity of substituted benzylidenes was determined against pentylenetetrazol-induced seizures. Albino mice of either sex, 25–30 g, were divided into groups of 10, keeping the group weights as near the same as possible. All substituted benzylidenes were suspended in 5% aqueous gum acacia, which was devoid of anticonvulsant activity, to give a concentration of 1% (w/v). An arbitrary dose of 100 mg/kg of benzylidene was administered intraperitoneally to one group of 10 mice.

The mice were injected with pentylenetetrazol (90 mg/kg sc) 4 hr after the administration of the test compounds (7). This dose of pentylenetetrazol has been shown to produce convulsions in almost all untreated mice and to exhibit 100% mortality during 24 hr. No mortality was observed during 24 hr for animals treated with 100 mg/kg of the benzylidenes alone. The mice were observed for 60 min for the occurrence of seizures. An episode of clonic spasm persisting for a minimum of 6 sec was considered a threshold convulsion. Transient intermittent jerks and tremulousness were not counted.

Mice devoid of threshold convulsions during 60 min were considered protected. The number of mice protected in each group was recorded, and the anticonvulsant activity of these benzylidenes was represented as the percent protection. The animals were then ob-

Table IV—Preincubation Studies on the *In Vitro* Inhibition of Monoamine Oxidase by Substituted Benzylidenes

Compound	Preincubation Time, min			
	0	10	20	30
	Percent Inhibition[a]			
XI	68.2 ± 0.4	72.0 ± 0.8	71.8 ± 0.5	72.6 ± 0.7
XIII	73.5 ± 0.5	75.6 ± 0.6	74.3 ± 0.6	75.0 ± 0.9
XX	70.2 ± 0.8	71.4 ± 0.5	70.9 ± 0.8	71.7 ± 0.5

[a]Contents of the reaction mixture and the assay procedures are as indicated in Table III. The enzyme preparations were incubated with substituted benzylidenes for varying times before the addition of kynuramine. Zero-time experiments indicated that both kynuramine and benzylidenes were added to the reaction mixture containing rat brain homogenates simultaneously. Each experiment was done in triplicate, and the values are the mean values of three separate experiments with ±*SEM*. Compounds XI, XIII, and XX were used in the final concentration of 0.166 m*M*.

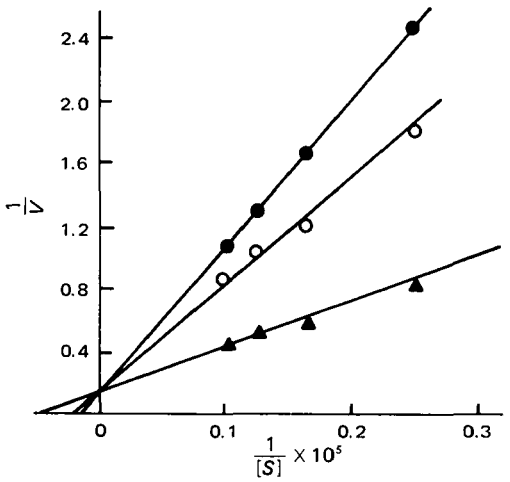

Figure 1—*Competitive inhibition of rat brain monoamine oxidase by XV. Assay procedures and the contents of the reaction mixture are as described in the text.* [S] *denotes molar concentration of kynuramine, and 1/V represents the reciprocal of the change in percent absorbance/10 mg fresh tissue wet weight/30 min. Key:* ▲, *control;* ○, *0.1 m*M *of the benzylidene (XI);* and ●, *0.15 m*M *of the benzylidene (XI). The* K_m *value for kynuramine was 0.19 m*M.

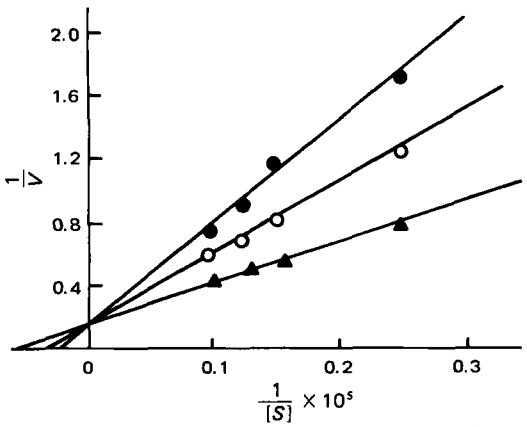

Figure 2—*Competitive inhibition of rat brain monoamine oxidase by XIII. Details of the assay procedure are as described in Fig. 1.*

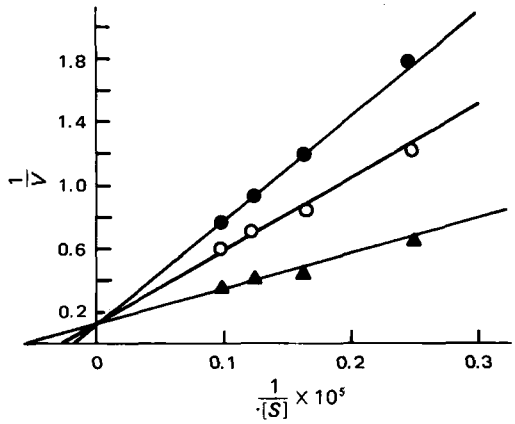

Figure 3—*Competitive inhibition of rat brain monoamine oxidase by XX. Details of the assay procedures are as described in Fig. 1.*

served for 24 hr, and the mortality of mice in each group was recorded. In the present study, methaqualone[3].(8) and meprobamate[4] (9) were used intraperitoneally at a dose of 100 mg/kg as reference anticonvulsant drugs for comparative evaluation.

RESULTS AND DISCUSSION

The monoamine oxidase inhibitory activity possessed by substituted anilino-(3-methoxy-4-morpholino/pyrrolidino/piperidinoacetoxy)benzylidenes is recorded in Table III. All benzylidenes inhibited *in vitro* monoamine oxidase activity of rat brain homogenates at a final concentration of 0.166 m*M*, and the degree of inhibition ranged from 45.3 to 75.2%. Maximum inhibition was observed with XIII, while IX was the least effective inhibitor. The effectiveness of these benzylidenes in inhibiting rat brain monoamine oxidase correlated well with their I_{50} values. The I_{50} values were 0.1 and 0.176 m*M* for XIII and IX, respectively.

Preincubation of XI, XIII, and XX at a final concentration of 0.166 m*M* for varying times prior to the addition of the substrate in *in vitro* studies in no way altered the degree of monoamine oxidase inhibition. These studies thus indicated a rapidly reversible and possibly competitive nature of the inhibition of monoamine oxidase by substituted benzylidenes (Table IV). These findings were further supported by kinetic studies with XI (Fig. 1), XIII (Fig. 2), and XX (Fig. 3), which revealed the competitive nature of inhibition of rat brain monoamine oxidase by these three substituted benzylidenes. The intercept at the $1/S$ axis was taken at $-1/K_m$; the value of 0.19 m*M* was obtained as the apparent Michaelis constant (K_m) in these experiments, using kynuramine as the substrate.

The results of anticonvulsant activity studies (Table III) demonstrated that most of these substituted benzylidenes possess significantly low anticonvulsant activity; the degree of protection against pentylenetetrazol-induced convulsions afforded by these compounds at a dose of 100 mg/kg ranged from 10 to 70%. Maximum anticonvulsant activity was observed with XI and XVI, while the rest of benzylidenes possessed low anticonvulsant activity. In the present study, intraperitoneal administration of methaqualone and meprobamate at 100 mg/kg provided protection of 60 and 80%, respectively, against pentylenetetrazol-induced convulsions in mice under similar experimental conditions. These studies also indicated that there appears to be some connection, but no uniform trend, between the percent protection afforded by substituted benzylidenes and the reference drugs against pentylenetetrazol-induced convulsions and their ability to protect against pentylenetetrazol-induced mortality during a 24-hr period.

[3] Arnar-Stone Laboratories, Mount Prospect, Ill.
[4] Wyeth Laboratories, Philadelphia, Pa.

REFERENCES

(1) T. George, C. L. Mehta, R. S. Grewal, and D. V. Mehta, *J. Med. Chem.*, **14**, 909(1971).

(2) D. J. Prokop, P. A. Shore, and B. B. Brodie, *Ann. N.Y. Acad. Sci.*, **80**, 643(1959).

(3) C. Dwivedi, R. D. Harbison, B. Ali, and S. S. Parmar, *J. Pharm. Sci.*, **63**, 1124(1974).

(4) M. Krajl, *Biochem. Pharmacol.*, **14**, 1684(1965).

(5) H. Lineweaver and D. Burk, *J. Am. Chem. Soc.*, **56**, 658(1934).

(6) M. Dixon, *Biochem. J.*, **55**, 170(1953).

(7) S. S. Parmar, A. K. Gupta, T. K. Gupta, and V. I. Stenberg, *J. Pharm. Sci.*, **64**, 154(1975).

(8) M. L. Gujral, P. N. Saxena, and R. P. Kohli, *Indian J. Med. Res.*, **45**, 207(1957).

(9) M. A. Perlstein, *J. Am. Med. Assoc.*, **161**, 1040(1956).

ACKNOWLEDGMENTS AND ADDRESSES

Received March 17, 1975, from the **Department of Chemistry and the [1]Department of Physiology and Pharmacology, University of North Dakota, Grand Forks, ND 58202,* and the *[8]Department of Pharmacology and Therapeutics, King George's Medical College, Lucknow University, Lucknow 226003, India.*

Accepted for publication February 4, 1976.

Supported in part by U.S. Public Health Service Grants GM-21590, 1 T01 HL-05939-02, and 1 R01 DA-00996-01 and U.S. Public Health Service Career Development Award 1-K4-GM-09888 to V. I. Stenberg.

The authors thank Professor Roland G. Stevenson and Professor Stanley J. Brumleve for their advice and encouragement. Grateful acknowledgment is made to the Atomic Energy Commission, Bombay, India, and the Indian National Science Academy, New Delhi, India, for providing research fellowships to S. P. Singh and A. Chaudhari, respectively.

[x] To whom inquiries should be directed (at the University of North Dakota).

Derivatives of Apomorphine and of Other *N*-Substituted Norapomorphines

EDWARD R. ATKINSON *x, S. P. BATTISTA *, ISTVAN E. ARY *, DONALD G. RICHARDSON *, LOUIS S. HARRIS ‡, and WILLIAM L. DEWEY ‡

Abstract □ Derivatives of apomorphine and of *N*-*n*-propylnorapomorphine were prepared to obtain modified pharmacological activity and enhanced chemical stability. Mouse profile and dog emesis screens were performed, and the activity of various *N*-substituted derivatives and their esters was evaluated and compared to the parent compounds. The *N*-*n*-propyl diacetate derivative and *N*-methyl and *N*-*n*-propyl ascorbate salts were remarkably stable to air; apomorphine etherate was no more stable than the free base. The dimers, the major products formed during the acid-catalyzed rearrangement of morphines to apomorphines, were all potent emetics. Additionally, two showed a significant antagonism to morphine in mice and dogs.

Keyphrases □ Apomorphine—*N*-substituted derivatives synthesized, screened for emetic activity, stabiliy □ Structure–activity relationships—*N*-substituted derivatives of apomorphine screened for emetic activity □ Emetic activity—*N*-substituted derivatives of apomorphine screened

Following the conclusion that *N*-*n*-propylnorapomorphine was the most potent member of the apomorphine series (1–3), derivatives were prepared (I–IX, Table I) that might possess appropriately modified pharmacological activity or greater stability. In this work, apomorphine was used as a model; the *n*-propyl compound was used only for the synthesis of the more promising derivatives. The work was restricted to compounds preparable from morphine and belonging to the (6aR) (−) series. Some parallel work with apomorphines prepared by total synthesis was reported previously (4).

The pharmacological activity of four "dimers" (X–XIII), the major products formed during the acid-catalyzed rearrangement of normorphine and its *N*-substituted derivatives to the corresponding apomorphines, is also reported.

DISCUSSION

Chemistry—Conventional procedures for the synthesis of I–IX and workup procedures for X–XIII are described under *Experimental*. Little is known about the structure and chemistry of the dimers (X–XIII). Their behavior in gel chromatography indicates that they have molecular weights considerably higher than the 535 required for a true dimer[1], and a parent peak in their mass spectra has not been identified. They are readily soluble in dilute acid but insoluble in all other solvents. Although it was possible to free them from the corresponding apomorphine, homogeneous samples were not obtained; the analytical values given in Table I are for the specific sample used for pharmacological evaluation. They are formed during the rearrangement reaction (even at room temperature) and are not formed from the apomorphine itself under the conditions of rearrangement (3).

Compound III was prepared by the reaction of apomorphine with ethyl chloroformate in pyridine. When aqueous Schotten–Bauman conditions were used, ring opening occurred to give the phenanthrene

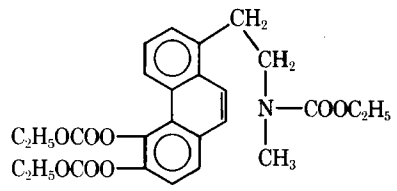

XIV

(XIV). Analogous reactions were reported for the conditions of the Hoffmann and Emde degradation reactions (5).

Compound XIV was evaluated because of the possibility that hydrolysis *in vivo* might give an aminoalkylphenanthrenediol known (5) to have apomorphine-like activity.

Pharmacology[2]—The mouse profile and dog emesis screens were those used previously (3). Quaternary derivatives of apomorphine and of morphine are known to differ markedly from the parent compounds because of their inability to enter the central nervous system (CNS) (6); the unusally low activity of VII in comparison to its parent tertiary amine is a striking example of this effect. The quaternary compound was also much more toxic.

Alkyl ethers derived from apomorphine compounds do not cause the apomorphine response or syndrome (4, 7, 8). Compound V was prepared in the hope that, as a formal, it might undergo cleavage to apomorphine *in vivo*. Its low activity suggests that this cleavage does not occur readily.

The quantitative pharmacological equivalence of apomorphine and its ester derivatives was reported previously (9, 10). In the treatment of parkinsonism, the esters have a prolonged effect and a lower toxicity than apomorphine itself (10). The esters of catecholamines enter the CNS more rapidly and provide for a sustained release of the catecholamine within the CNS (11).

The equivalence of diacetates to the parent phenols (3) is confirmed by the activity of I and II. TLC showed that the hydrolysis of II *in vitro* was slow. The onset of emesis in dogs following intravenous administration of the carbonate ester (III) was slightly delayed. At a dose of 0.05 mg/kg, 2 min was required. At 0.1 mg/kg, emesis occurred at 90 sec and again at 2 hr. At 0.2 mg/kg, emesis occurred at 90 sec and again at 30 min. These observations are in accord with the hypothesis that hydrolysis of III to apomorphine is slower than with the acetates (I and II).

The carbamate (IV) and the methoxyacetate (VI) were relatively inactive in mice, suggesting that hydrolysis *in vivo* is slow. The LD_{50} and MED values in mice for XIV were both greater than 20 mg/kg; had hydrolysis occurred, greater activity would have been expected for the resulting aminoalkylphenanthrenediol (5).

The dimers (X–XIII) were all quite active in the mouse screen, although less potent than the related apomorphines (3). Their emetic potency in dogs was only slightly less than that of the apomorphines. During a routine study of other pharmacological properties, it was observed that all four dimers showed insignificant analgesia in a modified mouse tail-flick test (12) at doses up to 100 mg/kg iv but that only XII and XIII showed marked antagonism to morphine in that test. For example, when 18 mice were treated with 10 mg/kg of morphine (which produced 79% analgesia), XII had a morphine antagonist value (AD_{50}) of 9.0 mg/kg; the values ranged between 82% analgesia at 3 mg/kg of XII and 8% analgesia at 30 mg/kg. The AD_{50} for XIII was 21 mg/kg.

[1] J. G. Cannon, University of Iowa, Iowa City, Iowa, personal communication.

[2] In conducting the described research, the investigators adhered to the "Guide for the Care and Use of Laboratory Animals," as promulgated by the Committee on Revision of the "Guide for Laboratory Animals, Facilities and Care" of the Institute of Laboratory Animal Resources, National Research Council.

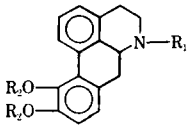

Table I—Derivatives of Apomorphine and of Other *N*-Substituted Norapomorphines

Compound	R_1	R_2	Melting Point	Yield, %	Formula	Analysis, % Calc.	Analysis, % Found	MED[a], mg/kg iv, Mouse (Fiducial Limits)	LD_{50}, mg/kg iv, Mouse (Fiducial Limits)	Dog Emesis, Minimum Effective Dose, mg/kg iv
I	CH_3	CH_3CO	125–128°[b]	50	$C_{21}H_{21}NO_4$	—	—	0.042 (0.024–0.075)	40.0 (18.0–89.0)	0.006
II	n-C_3H_7	CH_3CO	138.5–139.5°	50	$C_{23}H_{25}NO_4$	C 72.73 H 6.64 N 3.68	72.18 6.71 3.60	0.0042 (0.0024–0.0075)	50.0 (39.0–63.0)	—
III	CH_3	C_2H_5OCO	111–113°	55	$C_{23}H_{24}NO_6$	C 67.14 H 6.12 N 3.40	67.09 6.04 3.31	0.056 (0.034–0.094)	36.0 (28.0–45.0)	<0.05
IV	CH_3	$(CH_3)_2NCO$	75–125°	50	$C_{23}H_{27}N_3O_4$	C 67.46 H 6.65 N 10.26	67.48 6.47 10.27	1.8 (0.56–5.6)	18.0 (5.6–56.0)	>0.1
V[c]	CH_3	CH_3OCH_2	164–166° dec.	58	$C_{21}H_{25}NO_4 \cdot C_4H_6O_6$	C 59.39 H 6.18 N 2.77	58.86 6.12 2.64	1.8 (0.56–5.6)	>100	>0.1
VI[c]	CH_3	CH_3OCH_2CO	162–163°	67	$C_{23}H_{25}NO_6 \cdot C_4H_6O_6$	C 57.75 H 5.56 N 2.49	57.56 5.63 2.45	0.13 (0.075–0.24)	63 (50.0–79.0)	
VII[d]	n-C_3H_7, CH_3	H	—[e]	40	$C_{20}H_{24}INO_2$	C 54.92 H 5.53 I 29.02 N 3.30	54.26 5.30 29.58 3.30	1.8 (0.56–5.6)	5.6 (1.8–18.0)	>0.1
VIII[f]	CH_3	H	100° dec.	95	$C_{17}H_{17}NO_2 \cdot C_6H_8O_6 \cdot H_2O$	C 59.86 H 5.90 N 3.04	59.48 5.74 2.69	—	—	—
IX[f]	n-C_3H_7	H	85° dec.	80	$C_{19}H_{21}NO_2 \cdot C_6H_8O_6 \cdot 2H_2O$	C 59.16 H 6.55 N 2.76	58.90 6.07 2.37	—	—	—
X[g]	CH_3	H	290–300° dec.	60	—	C H Cl N Ash	61.6 6.04 11.21 4.22 1.44	0.13 (0.075–0.24)	32.0 (25.0–40.0)	0.01
XI[g]	C_2H_5	H	285° dec.	70	—	C H Cl N Ash	62.8 5.99 10.60 4.14 1.83	0.042 (0.024–0.075)	32.0 (20.0–50.0)	0.005
XII[g]	n-C_3H_7	H	270–280° dec.	70	—	C H Cl N Ash	65.4 6.59 8.46 4.48 0.9	0.01 (0.005–0.019)	36.0 (28.0–45.0)	0.002
XIII[g]	CH_2=$CHCH_2$	H	270–290° dec.	40	—	C H Cl N Ash	66.9 6.51 10.1 3.75 1.93	0.56 (0.18–1.8)	56.0 (18.0–180.0)	0.1

[a] Minimum dose at which reactive signs were observed in half of mice tested (3). [b] Recrystallized from ethyl acetate–petroleum ether; lit. (21) mp 128–129°. [c] Tartrate salt. [d] Quaternary methiodide. [e] Shrinks at 220°, decomposes at much higher temperature. [f] L-Ascorbate salt hydrate. [g] Dimer hydrochloride.

The morphine antagonism of XII and XIII was also observed in dogs, where these compounds reversed morphine-induced respiratory depression as measured by both respiration rate and pulmonary ventilation rate. Thus, 5 mg/kg of morphine was administered intravenously to anesthetized beagle dogs of either sex, and the well-known respiratory depression was observed. After 5 min, 0.1 mg/kg of XII was administered intravenously and caused an immediate reversal of depression. The antagonism persisted for at least 1 hr, because two subsequent 5-mg/kg doses of morphine given at 15 and 65 min caused no further respiratory depression. A dose of 0.01 mg/kg of XII did not prevent respiratory depression caused by 5 mg/kg of morphine, but it did prevent additional depression by a second 5-mg/kg dose of morphine. Similar results were observed with doses of 0.03 and 0.1 mg/kg of XIII. An alternative explanation of the apparent morphine antagonism of XII and XIII is that the dogs rapidly developed a tolerance to morphine.

Stability Studies—All apomorphines are easily oxidized by air to form a green oxidation product, which has been identified (13) and used as the basis of an analytical method for apomorphine (14, 15). Dilute solutions of apomorphine hydrochloride at pH 3 develop no color when protected by sulfite and an inert gas. When the solutions contain sulfite and the sodium salt of ethylenediaminetetraacetic acid, they can still be exposed intermittently to air and yet suffer only a 7% deterioration during 7 months (16). The standard procedure for liberating apomorphine bases from their hydrochloride salts by the use of aqueous sulfite solutions was undoubtedly developed to take advantage of the protective effect of sulfite. Thiourea also protects apomorphine (17).

Ascorbic acid protects apomorphine hydrochloride solutions from oxidation by air (18). The ascorbate salts (VIII and IX) were characterized and found to be nonhygroscopic and to develop no color after prolonged exposure to air. The protective effect of the ascorbate ion is so great that these salts do not react in the standard iodine oxidation color test for apomorphines (19). No attempt was made to establish the pharmacological potency of VIII and IX; it is likely that these salts are equivalent to the hydrochloride salts *in vivo*.

It was expected that the diacetate ester (II) would also resist oxidation. It did not become discolored in air and was very stable even in the molten state. Samples were repeatedly melted (pronounced supercooling was observed) on a microscope stage, and the melting point fell only to 131–136°. Solutions of II in dimethyl sulfoxide remained colorless for 1 week; when allowed to evaporate in air, long colorless needles of II separated.

A 24% solution of II in dimethylacetamide at 22° had a very pale-green color. During 8 weeks of storage in contact with air, the absorption coefficient at 266 nm did not change within experimental error; the color darkened somewhat. It has been the authors' experience [as with others (16)] that marked discoloration of apomorphine compounds in contact with air can occur before significant decreases in actual apomorphine content. A 1% aqueous stock solution of *N*-*n*-propylnorapomorphine (pH 4–5) became dark green, but the MED value in the mouse screen was unchanged after 24 hr.

When apomorphine base is liberated from its hydrochloride salt by aqueous sulfite and then extracted into ether, concentration by boiling of the ether solution gives a remarkably stable etherate [$C_{17}H_{17}NO_2 \cdot (C_2H_5)_2O$], whose stability was noted previously (20). The compound loses ether at 145° to form the apomorphine base, mp 208°. Evaporation of an acetone solution of the etherate does not decompose it, but evaporation of a chloroform solution causes complete loss of ether. An analogous etherate could not be prepared from *N*-*n*-propylnorapomorphine. Apomorphine etherate developed a faint green color after contact with air in the dark during 3 months; but in parallel experiments, the discoloration of the apomorphine base and of the free base of *N*-*n*-propylnorapomorphine (mp 195–197°) was about the same. Thus, etherates do not possess greatly enhanced stability to air.

While the stability studies are qualitative in nature, the results confirm the observations of other investigators who found that significant stabilization of apomorphine can be achieved by use of appropriate salts. They also show that the diacetate esters (I and II) are very stable derivatives with high pharmacological potency.

EXPERIMENTAL[3]

***N*-*n*-Propylnorapomorphine Diacetate (II)**—The procedure was similar to that used for the preparation of apomorphine diacetate (21). Following acetylation by acetic anhydride in pyridine, the crude product hydrochloride was dissolved in water and the base was liberated by addition of potassium bicarbonate. The base was extracted into chloroform, recovered by evaporation, and recrystallized from ethyl acetate–hexane.

Apomorphine Bis(ethyl Carbonate) (III)—Ethyl chloroformate (1.6 g, 0.0148 mole) was added rapidly to a stirred, cold (0°) solution of 1.5 g (0.00454 mole) of apomorphine hydrochloride[4] NF in 60 ml of pyridine. The mixture was stirred in the dark for 36 hr, during which time a transient pale-yellow precipitate was observed. Pyridine was removed by vacuum evaporation to 20 ml, 20 ml of toluene was added, and the solution was evaporated to dryness. The gelatinous residue was taken up in 100 ml of water, and the base was liberated by addition of excess sodium sulfite solution. It was extracted into ether, recovered by evaporation, and recrystallized from acetone–heptane.

Ethyl *N*-[2-[1-[5,6-Bis(ethoxycarbonyloxy)]phenanthryl]-ethyl]-*N*-methylcarbamate (XIV)—To a stirred mixture of 5 g (0.0158 mole) of apomorphine hydrochloride, 50 ml of water, and 30 g (0.28 mole) of ethyl chloroformate under nitrogen at 0–3° was added 10% aqueous sodium hydroxide (containing a little sodium dithionite) until the mixture became permanently basic to litmus. The mixture was stirred in the dark at room temperature for 3 days. The solid that separated was washed with water, dried in air, and recrystallized from ether–hexane to give almost colorless XIV in 60% yield, mp 84–87°.

Anal.—Calc. for $C_{26}H_{29}NO_8$: C, 64.61; H, 6.05; N, 2.88. Found: C, 65.19; H, 6.06; N, 2.91.

Because of its insolubility in standard solvents for intravenous administration, XIV was administered as a solution in 85% lactic acid.

Apomorphine Bis(dimethylcarbamate) (IV)—To a solution of apomorphine etherate (21) (1.7 g, 0.005 mole) in 15 ml of dry pyridine was added 1.08 g (0.01 mole) of freshly distilled dimethylcarbamyl chloride[5]. The yellow solution was warmed under nitrogen on the steam bath until TLC (silica, methyl alcohol–chloroform) of an aliquot (free base liberated by sodium sulfite and extracted into ether) showed little remaining apomorphine. Pyridine was removed under vacuum and by evaporation of its azeotrope with toluene.

The residual hydrochloride salt was treated with sodium sulfite solution, and the free base was recovered after extraction into ether. TLC showed a trace of residual apomorphine, which was removed by passing a chloroform solution of the product through a column of neutral alumina. The product recovered by evaporation of chloroform was a pale-yellow glass, homogeneous by TLC. It developed a pronounced yellow color when exposed to light and air. It was examined in the animal screens without delay.

10,11-Di(methoxymethoxy)aporphine Tartrate (V)—Apomorphine etherate (20) was prepared from 1.5 g (0.00492 mole) of apomorphine hydrochloride. A solution of naphthalene sodium was prepared by stirring a mixture of 2 g of naphthalene, 226 mg (0.00984 mole) of sodium, and 60 ml of dry 1,2-dimethoxyethane for 3.5 hr. A solution of the etherate in 30 ml of the same solvent was added dropwise under nitrogen to the stirred naphthalene sodium solution, and a clear pale-green solution formed.

A solution of 800 mg (0.00994 mole) of chloromethyl methyl ether in 10 ml of the solvent was added, and the mixture was refluxed for 2 hr, during which time sodium chloride precipitated and an orange color developed. When the product could not be characterized as the free base, it was converted to a tartrate salt in boiling isopropyl alcohol solution and then recrystallized from ethyl alcohol–ether.

Apomorphine Bis(methoxyacetate) Tartrate (VI)—Acylation in pyridine, as for III, was used with methoxyacetyl chloride (22). The product was characterized as the tartrate salt from boiling isopropyl alcohol.

***N*-*n*-Propylnorapomorphine Methiodide (VII)**—Excess methyl iodide was added to a dry (magnesium sulfate) ether solution of *N*-*n*-propylnorapomorphine under nitrogen, and a heavy colorless

[3] Melting points were obtained in capillaries in a bath heated from room temperature at 5°/min and are uncorrected. Elemental analyses were performed by Galbraith Laboratories, Knoxville, Tenn., and by the late Dr. S. M. Nagy (Belmont, Mass.). Satisfactory IR, UV, and NMR spectra were recorded for all synthesized compounds. All workup procedures were designed to eliminate unreacted starting material that might have significantly affected the pharmacological evaluation.

[4] Penick.

[5] Aldrich.

crystalline solid separated during 24 hr. The quaternary salt was recrystallized twice from methyl alcohol–acetone and additionally leached with ether until free (TLC) from unreacted base. The salt formed a 1.8% solution in water at room temperature; both the salt and its solution discolored rapidly in air.

Ascorbate Salts (VIII and IX)—Apomorphine hydrochloride (2 g, 0.0066 mole) was dissolved in 150 ml of water, and the colorless base was precipitated by addition of excess sodium sulfite solution. The base was extracted into ether, and a solution of 1.16 g (0.0066 mole) of ascorbic acid[6] USP in 10 ml of methyl alcohol was added to the dry (magnesium sulfate) ether solution. The colorless ascorbate salt (VIII) that precipitated was washed with ether and dried in air at 65°.

Ascorbate salt IX was prepared similarly from *N*-*n*-propylnorapomorphine. The hydrate character was assigned on the basis of analytical data and melting-point behavior.

Dimers (X–XIII)—The starting materials for these preparations were the tan-colored pastes formed as the major product during the rearrangement of morphine and its *N*-alkyl derivatives to the corresponding apomorphines, from which the apomorphines had been extracted by ether (3). No distinction between the dimers formed in the hot phosphoric acid process and those formed in methanesulfonic acid at room temperature was made, except that the latter were less discolored. The yields given in Table I are based on quantities used in specific earlier preparations (3); no allowance was made for manipulative losses experienced during the following procedure.

Crude dimer pastes were obtained as free bases. The bases became green on standing in air, particularly when exposed to light. Dried samples often contained up to 10% ash on analysis. The ash is believed to be derived from occluded or adsorbed sodium sulfite because sulfur dioxide evolved when the bases were dissolved in dilute hydrochloric acid.

The pastes were boiled with acetone to remove any remaining apomorphine and then were suspended in water at 60°. Then, 6 *N* HCl was added to the stirred suspension until the solid dissolved. The brown solution was stirred at 60° until no odor of the sulfur dioxide remained and then was filtered by gravity unless clear. The solution was then stirred at 40°, and an equal volume of concentrated hydrochloric acid was added slowly to precipitate the dimer hydrochloride. The precipitate was washed by stirring with 6 *N* HCl and then was allowed to dry in air at 40° until no odor of hydrogen chloride remained; forced drying at 65° caused severe discoloration. Final drying was at 65°/1 mm to give an olive-colored powder.

Typical analyses are given in Table I. It was apparent that these polymeric materials held metal ions tenaciously; ash-free samples were never obtained. In a standard color test for apomorphine (20), the dimer hydrochloride salts gave very weak colors. Their UV spectra in ethyl alcohol all showed λ_{max} 275 nm and a shoulder at 310 nm. Their IR spectra were not well resolved but showed absorption at 1700 cm^{-1} and a double band at 1600 cm^{-1}.

[6] Pfizer.

REFERENCES

(1) M. V. Koch, J. G. Cannon, and A. M. Burkman, *J. Med. Chem.*, **11**, 977(1968).

(2) S. Archer (to Sterling Drug, Inc.), U.S. pat. 3,717,643 (1973).

(3) E. R. Atkinson, F. J. Bullock, F. E. Granchelli, S. Archer, F. J. Rosenberg, D. G. Teiger, and F. C. Nachod, *J. Med. Chem.*, **18**, 1000(1975).

(4) J. L. Neumeyer, B. R. Neustadt, K. H. Oh, K. K. Weinhardt, and C. B. Boyce, *ibid.*, **16**, 1223(1973).

(5) J. G. Cannon, R. J. Borgman, M. A. Aleem, and J. P. Long, *ibid.*, **16**, 219(1973).

(6) R. S. Foster, D. J. Jenden, and P. Lomax, *J. Pharmacol. Exp. Ther.*, **157**, 185(1967).

(7) J. G. Cannon, R. V. Smith, A. Modiri, S. P. Sood, R. J. Borgman, M. A. Aleem, and J. P. Long, *J. Med. Chem.*, **15**, 273(1972).

(8) W. S. Saari, S. W. King, and V. J. Lotti, *ibid.*, **16**, 171 (1973).

(9) J. G. Cannon, J. F. Hensiak, and A. M. Burkman, *J. Pharm. Sci.*, **52**, 1112(1963).

(10) D. Seidelmann, R. Schmiechen, R. Horowski, W. Kehr, D. Palenschat, and G. Paschelke, German Offen. 2,154,162 (1973).

(11) C. R. Creveling, J. W. Daly, T. Tokuyama, and B. Witkop, *Experientia*, **25**, 26(1969).

(12) L. S. Harris and A. K. Pierson, *J. Pharmacol. Exp. Ther.*, **143**, 141(1964).

(13) H. H. A. Linde and M. S. Ragab, *Helv. Chim. Acta*, **51**, 683(1968).

(14) K. Rehse, *Arch. Pharm. (Weinheim, Ger.)*, **302**, 487(1969).

(15) K. Rehse and G. Dreke, *Fresenius' Z. Anal. Chem.*, **248**, 179(1969).

(16) P. Lundgren and L. Landersjo, *Acta Pharm. Suec.*, **7**, 133(1970).

(17) M. Struhar and M. Heliova, *Pharmazie*, **22**, 38(1967).

(18) R. J. Englehardt, F. M. Schell, and J. L. Lichtin, *J. Am. Pharm. Assoc.*, **NS8**, 198(1968).

(19) "The National Formulary," 13th ed., Mack Publishing Co., Easton, Pa., 1970, p. 61 (Identification Test A).

(20) R. Pschorr, B. Jaeckel, and H. Fecht, *Chem. Ber.*, **35**, 4383(1902).

(21) L. Small, B. F. Faris, and J. E. Mallonee, *J. Org. Chem.*, **5**, 347(1940).

(22) F. Benington and R. D. Morin, *ibid.*, **26**, 194(1961).

ACKNOWLEDGMENTS AND ADDRESSES

Received September 4, 1975, from **Arthur D. Little, Inc., Cambridge, MA 02140,* and the *‡Department of Pharmacology, School of Medicine, University of North Carolina, Chapel Hill, NC 27514*

Accepted for publication February 2, 1976.

[x] To whom inquiries should be directed.

GLC Assay for Fenclorac

ANTHONY J. VISALLI ˣ, DAHYABHAI M. PATEL, and NELSON H. REAVEY-CANTWELL

Abstract □ A rapid stability-indicating GLC method is described for the determination of fenclorac as the diethylamine salt in dosage formulations. The procedure is also applied in detecting and quantitating the weight percent of 3-chloro-4-cyclohexylphenylglycolic acid and α-chloro-4-cyclohexylphenylacetic acid impurities associated with the synthesis of the fenclorac drug substance. The former compound, in addition to being an impurity, is also the degradation product of fenclorac. The procedure involves preparation of the silyl derivatives, addition of an internal standard (triphenylethylene), and use of a hydrogen flame-ionization detector. The column, with a phenyl methyl silicone liquid phase and operated at about 195°, is well suited for the separation. The silyl derivatives were characterized by GLC–mass spectrometry.

Keyphrases □ Fenclorac—GLC analysis, pharmaceutical dosage formulations □ GLC—analysis, fenclorac in pharmaceutical dosage formulations □ Anti-inflammatory agents—fenclorac, GLC analysis in pharmaceutical dosage formulations

Anti-inflammatory properties have been attributed (1) to aryl- and alkyl-substituted phenoxyacetic acids. Recently, a U.S. patent (2) was issued for a series of substituted phenylacetic acid compounds having high anti-inflammatory, analgesic, and antipyretic activities and low toxicity. Preferred compounds of this series are fenclorac (α,3-dichloro-4-cyclohexylphenylacetic acid) and its esters and salts. The pharmacological activity of fenclorac diethylamine (I) has been investigated[1].

This publication is one of a series designed to provide information concerning the chemical kinetics[2] and analytical chemistry of I. A procedure is described for the determination of I in pharmaceutical dosage forms. The procedure is also applied in detecting and quantitating the impurities associated with the synthesis of I. These impurities are 3-chloro-4-cyclohexylphenylglycolic acid (II) and the diethylamine salt of α-chloro-4-cyclohexylphenylacetic acid (III). Compound II, in addition to being an impurity, is also the degradation product of I.

The developed GLC method requires little sample manipulations. Sample preparation is restricted solely to a simple solution of the drug and a silylation reaction with *N,O*-bis(trimethylsilyl)acetamide[3], necessitating approximately 15 min for completion.

This procedure offers several advantages over derivatizing reagents such as diazomethane or boron trifluoride. Diazomethane is toxic, potentially explosive, and rather difficult to prepare and use. Boron trifluoride in methanol can promote side reactions through hydrolysis of labile compounds and complicate quantitation.

EXPERIMENTAL

Instrumentation—A gas chromatograph[4] and electronic integrator[5], equipped with a flame-ionization detector and glass column [1.2 m (4 ft) × 2 mm i.d., packed with 5% phenyl methyl silicone[6] on 80–100-mesh silanized diatomaceous earth[7]], were used. The operating temperatures were: column, 195 or 185°; detector, 235°; and injection port, 235°. Nitrogen, with a flow rate of 30 ml/min, was the carrier gas.

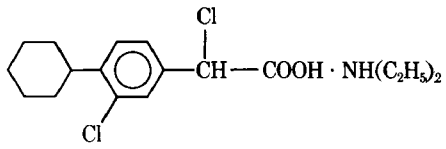

I

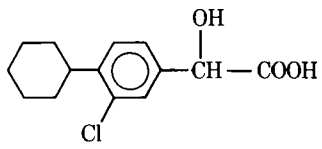

II

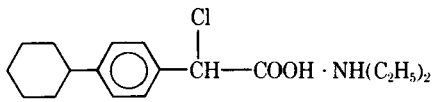

III

Materials—Methylene chloride[8] and triphenylethylene[9] were used without further purification. *N,O*-Bis(trimethylsilyl)acetamide was used as the silylating reagent.

Assay of I in Dosage Formulations—*Internal Standard Preparation*—Triphenylethylene (125 mg) was transferred to a 50-ml volumetric flask and dissolved in and diluted to volume with methylene chloride.

Reference Standard Preparation— Reference I (125 mg) was accurately weighed into a 50-ml volumetric flask and dissolved in and diluted to volume with methylene chloride. This solution was prepared fresh daily.

Sample Preparation—A suitable quantity of tablets or the contents of capsules, after determining the average weight, was transferred to a mortar and pestle and ground to a fine powder. The equivalent of 125 mg of I was accurately weighed into a 50-ml volumetric flask, and about 30 ml of methylene chloride was added. The flask was stoppered and shaken vigorously for about 5 min, and the solution was diluted to volume with methylene chloride. A portion of the solution was centrifuged in a screw-capped[10] test tube to clear it of insoluble formulation excipients.

Two-milliliter aliquots of the sample and reference standard preparations, equivalent to 5.0 mg of I, were transferred to respective glass vials. To each vial were added 1.0 ml of the internal standard preparation and 0.20 ml of *N,O*-bis(trimethylsilyl)acetamide. The vials were securely closed with polyethylene stoppers, shaken vigorously, and allowed to stand at room temperature for not less than 15 min.

Procedure—The chromatographic column was preconditioned with several injections of the derivatized standard solution prior to analysis. Two microliters of this solution was injected until a constant peak area ratio of I to the internal standard was obtained; then 2 μl of the derivatized sample solution was injected in duplicate.

[1] Nuss *et al.*, to be published.
[2] C. M. Won *et al.*, to be published.
[3] Pierce Chemical Co., Rockford, Ill.
[4] Hewlett-Packard 7620A.
[5] Hewlett-Packard 3370A.
[6] OV-25, Analabs, Inc., Northhaven, Conn.
[7] Chromosorb W-H. P., Celite Division, Johns-Manville Products Corp.
[8] GC spectrophotometric grade, J. T. Baker Co.
[9] Eastman Kodak Co.
[10] Lined with Teflon (du Pont).

Table I—Response Factors and Relative Retention Time

Compound	Response Factor	Relative Retention
I	1.00	1.00
II	1.42	0.76
III	1.02	0.67

Calculations—The I content in pharmaceutical dosage forms was calculated as follows:

$$\text{mg of I/dosage unit} = \frac{(R_u)(C_s)(A.W.)}{(R_s)(W)} \quad \text{(Eq. 1)}$$

where R_u and R_s are the peak area ratios of I to the internal standard for sample and standard solutions, respectively; C_s is the milligrams of I in the reference standard preparation; $A.W.$ is the average dosage weight; and W is the weight of sample taken in the sample preparation.

Assay of Related Impurities in I Drug Substance—*Instrumentation*—The instrumentation was the same as previously described, except that the column operating temperature was lowered to 185°.

Determination of Response Factors—Two milligrams each of I, II, and III were accurately weighed and combined in a glass vial. To the vial were added 1.0 ml of methylene chloride and 0.20 ml of *N,O*-bis(trimethylsilyl)acetamide. The vial was securely closed with a polyethylene stopper, shaken vigorously, and allowed to stand at room temperature for not less than 15 min.

The chromatographic column was preconditioned with several injections of the standard mixture prior to analysis; then 2 μl of this mixture was injected in duplicate. The response factors of II and III relative to I were determined using the following sample calculations:

$$\text{specific response for II} = \frac{\text{peak area of II}}{\text{mg of II in mixture}} \quad \text{(Eq. 2)}$$

and:

$$\text{response factor for II} = \frac{\text{specific response for II}}{\text{specific response for I}} \quad \text{(Eq. 3)}$$

Typical response factors and retention times relative to I are shown in Table I. A chromatogram is given in Fig. 1 for a typical mixture.

Sample Preparation—Ten milligrams of I drug substance was transferred to a glass vial, and 1.0 ml of methylene chloride and 0.20 ml of *N,O*-bis(trimethylsilyl)acetamide were added. The vial was securely closed with a polyethylene stopper, shaken vigorously, and allowed to stand at room temperature for not less than 15 min. Two microliters of the sample preparation was injected, and the peak areas of each impurity, if any, and I were recorded. The peak area of each impurity was normalized by dividing by its respective response factor calculated previously.

Calculations—The weight percent of an impurity was calculated as follows:

$$\%\ \text{impurity} = \frac{\text{normalized peak area of impurity} \times 100}{\text{sum of all normalized peak areas in chromatogram}} \quad \text{(Eq. 4)}$$

RESULTS AND DISCUSSION

Derivatization Reagent—The use of *N,O*-bis(trimethylsilyl)-acetamide as the derivatizing reagent was prompted by the failure of boron trifluoride in methanol to form a stable derivative. Under the conditions of esterification, which required the application of heat to catalyze the reaction, partial decomposition of I to II occurred, resulting in a mixture of the methyl esters. With *N,O*-bis(trimethylsilyl)acetamide, derivatization was complete at room temperature within 2 min and the derivatives were stable up to 8 hr.

Table II—Fragmentation Pattern in Mass Spectral Examination of the Trimethylsilyl Derivative of I

Mass *m/e*	Fragment Ion
358	Molecular ion (M)
343	$M - CH_3$
314	$M - CO_2$
260	$M - [CH_3 + C_6H_{11}]$

Table III—Fragmentation Pattern in Mass Spectral Examination of the Trimethylsilyl Derivative of II

Mass *m/e*	Fragment Ion
412	Molecular ion (M), not observed
397	$M - CH_3$
369	$M - [CH_3 + CO]$
295	$M - [CH_3 + CO + OSi^+(CH_3)_2]$

Peak Characterization—GLC–mass spectrometry data[11] indicated the molecular ion of the derivative of I to be at *m/e* 358, corresponding to the monotrimethylsilyl derivative. The molecular ion of the derivative of II was not observed at *m/e* 412; however, an ion fragment found at *m/e* 397 was considered to be the disubstituted trimethylsilyl derivative minus one methyl group. This finding confirmed the formation of the ditrimethylsilyl derivative.

GLC–mass spectrometry was not performed on III due to its structural similarity to I, having only one active hydrogen capable of being silylated. The fragmentation pattern of the mass spectral examination of the trimethylsilyl derivatives of I and II are listed in Tables II and III, respectively.

Column Conditioning—Earlier work indicated that preconditioning of the GLC column was necessary to prevent excessive adsorption and peak loss of the trimethylsilyl derivatives of I and III. These phenomena did not occur with II. Apparently, the α-chlorine of I and III, which is of a labile nature, combined with active sites on the column support or glass column wall. Various solid supports were tried without success. Removal of the silanized glass wool plug at the head of the column did not rectify the problem.

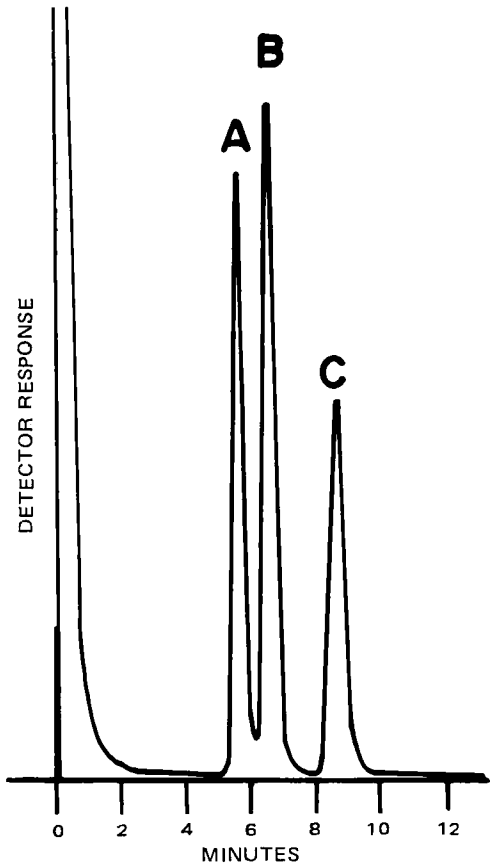

Figure 1—*Gas chromatogram of the trimethylsilyl derivatives of a mixture (prepared in the determination of response factors) containing III (A), II (B), and I (C).*

[11] Analysis performed by Analytical Development Corp., Monument, CO 80132

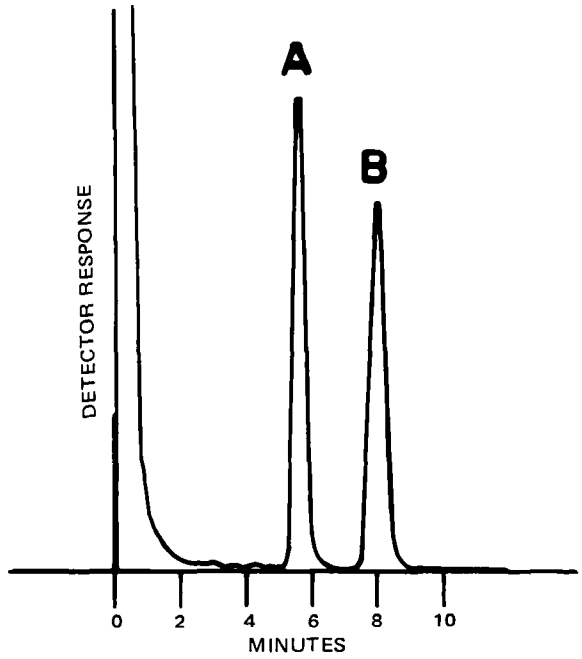

Figure 2—*Gas chromatogram of a sample preparation containing I as the trimethylsilyl derivative (A) and triphenylethylene, the internal standard (B).*

Preconditioning was a necessity when columns were initially packed; it was then only necessary to condition the column at normal operating conditions overnight before analyses were performed. The following preconditioning procedure was employed: 150° for 1 hr with a 30-ml/min carrier gas flow, 250° for 2 hr with no carrier gas flow followed by rapid cooling to room temperature, and 195° for 50–60 hr with a 30-ml/min carrier gas flow.

Table IV—Recovery Data

Mixture	I Added, mg	I Recovered, mg	Recovery, %
A	80.1	75.8	94.6
B	101.3	102.0	100.7
C	125.2	126.4	101.0
D	149.0	153.8	103.2
E	176.0	184.6	104.9

Table V—Statistical Evaluation

Determinations	I, mg
1	128.2
2	130.0
3	127.8
4	129.3
5	129.6
6	128.9
Mean	129.0
SD	±0.84
Precision, %	±0.65

Linearity—The detector response for I was linear in the 0.31–3.13-mg/ml range at a constant internal standard concentration. Column adsorption of I was indicated by the linear plot intersecting the concentration axis. By saturating the column with multiple sample injections until a constant peak area ratio of I to the internal standard was obtained, the adsorption phenomenon was kept relatively constant.

A minimum detectable quantity of II and III in the I drug substance was 0.01%.

Recovery—A study was undertaken to estimate the recovery of I from a synthetic mixture containing some common pharmaceutical excipients. Various amounts of I were added to a placebo mixture containing starch, lactose, microcrystalline cellulose, magnesium stearate, dibasic calcium phosphate, colloidal silicon dioxide, and hydroxypropyl cellulose. The mixtures were contained in 50-ml volumetric flasks, and the I content was assayed according to the procedure for dosage formulations. Results indicated essentially complete recovery (Fig. 2 and Table IV).

Precision—A statistical evaluation of the precision of the method was performed by making replicate injections of a placebo mixture containing I (Table V).

REFERENCES

(1) B. J. Northover, *J. Pathol. Bacteriol.*, **85**, 361(1963).

(2) J. Diamond and N. J. Santora, U.S. pat. 3,864,384 (Feb. 4, 1975).

ACKNOWLEDGMENTS AND ADDRESSES

Received September 11, 1975, from the *Analytical and Physical Chemistry Department, Rorer Research Laboratories, William H. Rorer, Inc., Fort Washington, PA 19034*

Accepted for publication February 9, 1976.

The authors thank Dr. George H. Douglas for his contribution in identifying III and also Mrs. Mary Pellak for secretarial assistance.

[x] To whom inquiries ahould be directed.

Colorimetric Assay for Guaiacol O-Methyltransferase

JOHN O. MacFARLANE ˣ, JOHN W. LEE, and C. C. CHENG

Abstract □ A relatively simple colorimetric assay was developed for guaiacol O-methyltransferase. Monomethylated phenolic acid substrates are enzymatically methylated to their corresponding dimethoxyl compounds; S-adenosylmethionine serves as the methyl donor. Enzymatic activity is measured by colorimetric assay of the monomethylated (nonreacted) substrate by coupling of the phenolic acid with a diazotized sulfanilic acid. The methoxyl and hydroxyl groups may be in the 3,4- or 4,3-positions on the substrate molecules; however, a side chain (COOH) or a substituted side chain is necessary for enzyme action. The radioactive demonstration of guaiacol O-methyltransferase as a separate entity from catechol O-methyltransferase was confirmed.

Keyphrases □ Guaiacol O-methyltransferase—colorimetric analysis of enzymatic activity □ Colorimetry—analysis, guaiacol O-methyltransferase, enzymatic activity □ Enzymatic activity—guaiacol O-methyltransferase, colorimetric analysis □ Methylation, enzymatic—guaiacol O-methyltransferase, colorimetric analysis

Enzymatic changes essential for the metabolism of the catecholamines have been the subject of numerous investigations. Catechol O-methyltransferase (EC 2.1.1.6), the enzyme capable of methylating a number of catechol derivatives, generally methylates at the 3-position, thus converting the hydroxyl to a methoxyl function. However, only one of the two hydroxyl groups is methylated. Recently, Friedhoff *et al.* (1, 2) reported the probable existence of a separate enzyme capable of methylating guaiacol derivatives giving rise to dimethoxy compounds. This guaiacol O-methyltransferase is derived from rat livers and capable of *in vitro* methylation. Schemes I and II illustrate the basic reactions for catechol O-methyltransferase and guaiacol O-methyltransferase, respectively.

As part of an ongoing program for the synthesis of new anticancer compounds, methods were developed to evaluate the inhibition of the new materials on methyltransferase enzymes. Nonradioactive methods were elected for these assays. Since the early investigations on guaiacol O-methyltransferase used radioactive substrates or radioactive methyl donors (1, 2), a new, simple, colorimetric assay for guaiacol O-methyltransferase has been developed.

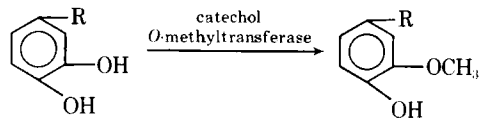

Scheme I

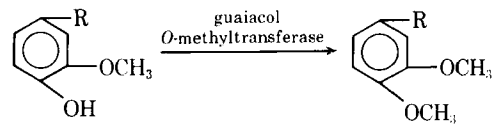

Scheme II

EXPERIMENTAL

The assay involves two major steps: (*a*) the enzyme reaction and (*b*) conjugation of the nonreacted guaiacol compound used as the substrate with diazotized sulfanilic acid and colorimetric determination of the conjugate.

Since the enzyme is most reactive at pH 9.0, 1.5 ml of 0.1 *M* trometh amine buffer at pH 9.0 is used. As with catechol O-methyltransferase, Mg^{+2} ions are required; therefore, 0.2 ml of 1 *M* $MgCl_2$ is added. The enzyme is a partially purified rat liver extract prepared according to the procedure of Friedhoff (3) using ultracentrifugation, ammonium sulfate precipitation, and dialysis.

The 0.3 ml used per assay contains approximately 15 mg of protein nitrogen, as determined by the method of Oyama and Eagle (4), which is a modification of the protein assay of Lowry *et al.* (5). As the methyl donor, 0.5 ml of 5×10^{-3} *M* S-adenosylmethionine is added. As the substrate, 0.1 ml of the guaiacol derivative (1×10^{-2} *M*) is added. For consistent and reproducible results, the substrate is added last. All reagents are added at 0–5°. Ninety minutes at 37° is allowed for the complete enzyme reaction.

Following this enzyme reaction, the mixture is tested for unreacted (nonmethylated) substrate. Low speed centrifugation (800×*g*) for 10 min at 5° removes the agglomerated protein, and 2.3 ml of the supernate is treated with 0.2 ml of the 0.2% diazotized sulfanilic acid, a reagent commonly used in chromatographic studies of the phenolic acids (6–9). The diazotized sulfanilic acid is prepared fresh daily by dissolving in distilled water the commercially available powder[1] (dry stable Pauley's reagent: diazotized sulfanilate trifluoroborate salt).

The conjugation reaction is performed at room temperature; however, temperature does not appear to be critical for this step. The diazotized sulfanilic acid reagent combines with the monomethylated phenol derivatives but not with the dimethylated compounds. The absorbance (*A*) of the conjugate is measured[2] at 520 nm within 1–15 min after the addition of the diazotized sulfanilic acid. The enzyme activity is the ΔA difference between a reaction without enzyme and with enzyme. The reaction without enzyme serves as a control of the reagents in the absence of protein as well as the basis for enzyme calculations.

RESULTS AND DISCUSSION

Several guaiacol compounds were tested as substrates for guaiacol O-methyltransferase and for their ability to convert the monohydroxyl–monomethoxyl groups to the corresponding dimethoxyl functions.

Scheme III illustrates the enzymatic action of guaiacol O-methyltransferase on homovanillic acid (I, 4-hydroxy-3-methoxyphenylacetic acid). It is methylated by transfer of the methyl group from the S-adenosylmethionine to position 4 on the ring. Homovanillic acid can be linked to the diazotized reagent, but 3,4-dimethoxyphenylacetic acid (II) cannot.

The enzyme converted 38.3, 30.5, 30.2, and 23.4% of ferulic acid, homovanillyl alcohol, vanillylmandelic acid, and homovanillic acid, respectively, from the monohydroxylated guaiacol derivatives to the dimethoxyl compounds. Guaiacol, the parent compound, was not significantly methylated (1.1%) since it has no side chain. On the other hand, ferulic acid has a double bond in the side chain, homovanillyl alcohol has a primary alcohol side chain, vanillylmandelic acid has a secondary alcohol side chain, and homovanillic acid has a short aliphatic acid side chain.

[1] Calbiochem 28656.
[2] Beckman DU spectrometer.

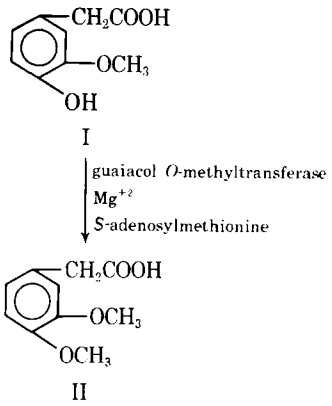

Scheme III

Vanillic acid and isovanillic acid have the hydroxyl and methoxyl groups reversed, but both were methylated (15.0 and 16.7%, respectively) by guaiacol *O*-methyltransferase. 4-Hydroxy-3-methoxyphenethylamine was also methylated (14.9%). These three compounds are superior substrates to normetanephrine, a phenethanolamine derivative (2.5% methylated). Vanillin (4-hydroxy-3-methoxybenzaldehyde) did not react with the diazo reagent but did yield some color upon standing in the presence of air and enzyme. This vanillin reaction needs additional study.

Based upon the reactions with the various substrates, it appears that the side chain may be an important determinant in the enzyme's specificity and influence the enzyme reaction.

The amount of enzyme used in the guaiacol *O*-methyltransferase reaction determines the amount of methylated product; however, for routine assays, the enzyme activity is standardized to yield the most optimal optical readout. The substrate concentration also is adjusted to give optimal optical readings. No problems of substrate inhibition were encountered in studies using multiple levels of substrate.

The colorimetric assay of guaiacol *O*-methyltransferase was used for several types of studies. A study of the influence of pH on the methylation of homovanillic acid showed the absence of methylation at pH 7.0, the maximum activity at pH 9.0, and somewhat less (47.4%) methylation at pH 9.5. These findings confirm previous data (1, 2) and indicate that catechol *O*-methyltransferase and guaiacol *O*-methyltransferase are two separate enzymes.

Studies by this colorimetric assay on the need for Mg^{+2} and the inhibitory effect of edetic acid, which ties up the Mg^{+2}, also confirmed data from the radioactive guaiacol *O*-methyltransferase assays (2).

Routine assays are currently being run for guaiacol *O*-methyltransferase inhibitors by this colorimetric assay. The enzyme (0.3 ml) and inhibitor (0.5 ml) are mixed and held for 5 min at 0–5°. Then the mixture is incubated to bring about enzyme activity using homovanillic acid as a substrate. The inhibitory effects are determined by comparing the absorbance changes of the combined substrate in the presence and absence of inhibitor according to:

$$\text{percent inhibition} = \frac{\Delta A \text{ enzyme (no inhibitor)} - \Delta A \text{ enzyme and inhibitor}}{\Delta A \text{ enzyme (no inhibitor)}} \times 100 \quad \text{(Eq. 1)}$$

The ED_{50}'s for the inhibitors may be calculated from assays at three inhibitor levels.

A second colorimetric reagent may be used as a modification of the conjugation reaction and its use provides additional information about the influence of substrate structure on the enzyme reaction. Studies conducted with the dichloroquinone chlorimide reagent, which reacts with phenolic acids having a hydroxyl function in position 3 (λ_{max} = 600 nm), demonstrated guaiacol *O*-methyltransferase methylation of isovanillic acid (43.9%) and isovanillin (27.0%) but not of vanillin. No blue color was expected with vanillin.

REFERENCES

(1) A. J. Friedhoff, J. W. Schweitzer, and J. Miller, *Res. Commun. Chem. Pathol. Pharmacol.*, **3**, 293(1972).

(2) A. J. Friedhoff, J. W. Schweitzer, J. Miller, and E. VanWinkle, *Experientia*, **28**, 517(1972).

(3) A. J. Friedhoff, *Biol. Psychiat.*, **6**, 187(1973).

(4) V. I. Oyama and H. Eagle, *Proc. Soc. Exp. Biol. Med.*, **91**, 305(1955).

(5) O. H. Lowry, N. J. Rosebrough, A. L. Farr, and R. J. Randall, *J. Biol. Chem.*, **193**, 265(1951).

(6) M. D. Armstrong, K. N. F. Shaw, and P. E. Wall, *ibid.*, **218**, 293(1956).

(7) S. Senoh, J. Daly, J. Axelrod, and B. Witkop, *J. Am. Chem. Soc.*, **81**, 6240(1959).

(8) H. G. Bray, W. V. Thorpe, and K. White, *Biochem. J.*, **46**, 271(1950).

(9) I. Smith, "Chromatographic and Electrophoretic Techniques. Vol. I. Chromatography," Interscience, New York, N.Y., 1969, p. 280.

ACKNOWLEDGMENTS AND ADDRESSES

Received August 11, 1975, from the *Biological Sciences Division, Midwest Research Institute, Kansas City, MO 64110*

Accepted for publication December 10, 1975.

Supported by Contract N01-CM-33743, Drug Research and Development Division of Cancer Treatment, National Cancer Institute, National Institutes of Health, Department of Health, Education, and Welfare.

[x] To whom inquiries should be directed.

Dissolution Testing of Nitroglycerin Tablets

CHARLES A. GAGLIA, Jr., JOSEPH J. LOMNER, BERDINE L. LEONARD, and LESTER CHAFETZ ˣ

Abstract □ The available types of dissolution testing apparatus for tablets and capsules are inapplicable to sublingual tablets, since these tablets are formulated to release their drug content within minutes in a small volume of fluid. A simple dissolution test method was developed for nitroglycerin tablets based on the reduction of nitroglycerin at a rotating platinum electrode, which provides reproducible stirring. The system provides instantaneous and continuous measurement of dissolved nitroglycerin in a small constant volume of buffered isotonic sodium chloride solution over a period of seconds to several minutes, when reduction is complete as shown by the current–time curve. Since the height of the curve is directly proportional to the amount of nitroglycerin in solution, the method also can be used to determine the drug content of individual tablets.

Keyphrases □ Nitroglycerin—sublingual tablets, polarographic dissolution test □ Polarography—determination of dissolution of nitroglycerin sublingual tablets □ Dissolution—nitroglycerin sublingual tablets, polarographic determination □ Vasodilators, coronary—nitroglycerin, polarographic determination of dissolution of sublingual tablets

Absorption of drug from a buccal or sublingual tablet requires dissolution in a small volume of fluid in the mouth, affording prompt pharmacodynamic effect. Although the dissolution of drugs from such a dosage form is thus an important parameter, methods for studying it have been limited. Apparatus such as those described by USP (1), NF (2), and Goodhart *et al.* (3) use relatively large volumes of fluid and are not suitable for sublingual tablets.

Dorsch and Shangraw (4) recently described a discontinuous technique for nitroglycerin tablets. The tablet is placed on top of a microporous membrane filter[1] (0.45-μm pore size) in the upper chamber of a plastic syringe-type filter holder[2], and five 1-ml portions of water at 30° are flushed through the chamber at 0, 30, 60, 90, and 120 sec. The method is tedious and affords only discrete data points. Karlsen[3] suggested that a polarographic method could be worked out to provide a continuous record of the dissolution rate profile of a nitroglycerin tablet. This report describes an amperometric procedure for measurement of the dissolution rate of individual nitroglycerin tablets.

Nitroglycerin is electrochemically reducible. Flann (5) described the polarographic determination of nitroglycerin tablets, reporting a single, irreversible, diffusion-controlled wave consuming two electrons for each nitrate group, independent of pH in the range of 3–13. In the work reported here, amperometry at a polarized rotating platinum electrode in conjunction with a time-based recorder affords a graphical representation of nitroglycerin concentration against time. Constant stirring is provided by the rotating electrode, and the reduction current is unaffected by suspended solids.

EXPERIMENTAL

Electrolyte (Dissolution Medium)—Dissolve 8.5 g of sodium chloride, 245 mg of monobasic sodium phosphate, and 700 mg of anhydrous dibasic sodium phosphate in water and dilute to 1 liter. Adjust the pH, if necessary, to 7.1 ± 0.1 by adding more of either phosphate salt.

Apparatus—The rotating platinum electrode comprised a platinum electrode[4] and a 600-rpm motor[5]. The potentiostat[6] was fitted with a recorder[7]. Silver wire was used as the reference and counter electrode. The cell was a flat-bottom glass cylinder, about 5 cm long by 2.1 cm i.d., held in place under the rotating platinum electrode with a round-jaw buret clamp and charged with 5.0 ml of the electrolyte. The nitrogen gas used to flush the oxygen from the cell was bubbled through 100 ml of the electrolyte in a gas-washing bottle.

The cell was positioned below the rotating platinum electrode so that the rotating platinum electrode wire was 1 mm below the surface of the solution, the silver wire extended to the bottom of the cell, and the nitrogen inlet tube was inserted at one side of the cell, away from the rotating platinum electrode, with its tip extended under the solution surface. The cell bottom was flush with the bottom of the clamp, allowing easy repositioning of the cell after removal for cleaning between samples by using a flat surface to line up the bottoms of the clamp and the cell.

The following settings were used for the polarographic analyzer: drop timer, two electrodes; modulation amplitude, 50 mv; operating mode, pulse; initial voltage, −0.99 v; display direction, +; drop time, 2 sec; potential scan direction, −; range, 1.5 v; current range, 0.5 mamp full scale; and low pass filter, 3.

Standard Preparation—Standardize nitroglycerin spirit against potassium nitrate by the phenoldisulfonic acid method. Transfer 1.0 ml to a 100-ml volumetric flask, add 25 ml of alcohol USP, and dilute to volume with the electrolyte. Further dilute the solution with the electrolyte to obtain concentrations of about 40 and about 80 μg/ml.

Standardization Procedure—Transfer 5.0 ml of the less concentrated standard preparation to the cell. Place the electrodes so that the platinum wire of the rotating platinum electrode is about 1 mm below the surface of the solution and the silver reference electrode extends to the bottom of the cell and arrange the nitrogen inlet tube at one side of the cell under the solution surface so that it does not contact the rotating platinum electrode. Start the rotating platinum electrode motor and deaerate with nitrogen for about 5 min. After 5 min, lift the nitrogen inlet tube about 2 mm above the solution surface.

Start the chart and turn the selector switch to EXT CELL, marking "zero time" on the recorder chart at this point. Run the chart about 3 min at 5.1 cm (2 in.)/min. Reset the chart and perform a blank determination with the electrolyte in the cell. Measure the difference between the standard and the blank at 2 min to obtain the standard reading.

Repeat the procedure for the more concentrated standard preparation.

Dissolution Procedure—Pipet 5.0 ml of the electrolyte into the cell, arranged as already described; then start the rotating platinum electrode motor and deaerate with nitrogen. After 5 min, lift the nitrogen inlet tube about 2 mm above the solution surface. Turn the electrode selector switch to EXT CELL, zero the chart, and start the recorder. Within 30 sec of the time the nitrogen inlet tube is lifted, drop in the tablet to be tested and mark the recorder chart "zero time." Allow the system to operate until no further increase in reduction current is observed.

[1] Millipore.
[2] Millipore Swinnex 25.
[3] J. Karlsen, University of Oslo, Oslo, Norway, personal communication *via* R. F. Shangraw, School of Pharmacy, University of Maryland, Baltimore, MD 21201, 1974.
[4] Sargent-Welch S30421.
[5] Sargent-Welch S76485.
[6] Princeton Applied Research polarographic analyzer, model 174.
[7] Heath-Schlumberger model EU-205-11 recorder with model EU-200-01 potentiometric amplifier.

Table I—Nitroglycerin Dissolution from Three 0.4-mg Sublingual Tablet Lots

Lot	Average Percent Dissolved at 0.25 min	0.5 min	0.75 min	1.0 min	t_{90} Average	t_{100} Average	Average Micrograms per Tablet
1	31 (16–37)[a]	78 (66–84)	93 (88–95)	97 (95–98)	0.70	1.6 (1.2–2.4)[b]	433 (418–452)[b]
2	24 (19–30)	72 (69–76)	89 (86–94)	96 (94–98)	0.78	1.5 (1.2–1.8)	443 (424–459)
3	33 (28–39)	82 (71–90)	94 (92–97)	98 (95–100)	0.57	1.2 (1.0–1.5)	394 (360–415)

[a] Range for 10-tablet sample. [b] Range.

Perform a blank determination with the electrolyte to compensate for the small amount of oxygen that diffuses into the cell and take the difference in recorder chart reading between the sample and the blank at each time interval as the sample reading. With no change in experimental conditions, the blank remains constant during the day and only one blank determination need be obtained each day.

Calculate the quantity of nitroglycerin, in milligrams per tablet, from the formula $5C(U/S)$, where C is the concentration, in milligrams per milliliter, of the standard preparation used, whichever is closer to the sample reading; and U and S are the chart readings for the tablet and the standard preparation, respectively.

Note as t_{100} the time required for 100% of the drug to dissolve; this value is determined from the chart as that point where no further rise in reduction current occurs. Calculate the percent of drug released at any time, t, in seconds from the formula (milligrams measured at time t/total milligrams released) × 100.

RESULTS AND DISCUSSION

The proposed dissolution test was performed using 10-tablet samples of each of three lots of a commercial 0.4-mg sublingual tablet formulation[8]. Table I shows the average percentage of drug dissolved from the tablets at 15-sec intervals during the 1st min and the average time required for 90 and 100% of the drug content of the tablets to dissolve. Use of percentage affords direct comparison among individual tablets of differing drug content, thus normalizing the data. Since prompt onset of action is an important criterion for a sublingual nitroglycerin tablet, these data may have clinical significance.

Another advantage of the method is that it provides a measure of the nitroglycerin in each tablet. The data shown in Table I (last column) are consistent with those obtained for these tablets by Dorsch and Shangraw (4), who used an automated assay method. Their method is less time consuming than the dissolution procedure and probably would be preferable if content uniformity information is the only consideration.

[8] NITROPRN Tablets, Warner-Chilcott Laboratories, Morris Plains, NJ. Lot 1 was control number 490254B, Lot 2 was control number 4917124B, and Lot 3 was control number 5964124A.

REFERENCES

(1) "The United States Pharmacopeia," 19th rev., Mack Publishing Co., Easton, Pa., 1975, p. 651.

(2) "The National Formulary," 14th ed., Mack Publishing Co., Easton, Pa., 1975, p. 893.

(3) F. W. Goodhart, R. H. McCoy, and F. C. Ninger, *J. Pharm. Sci.*, **62**, 304(1973).

(4) B. Dorsch and R. Shangraw, *Am. J. Hosp. Pharm.*, **32**, 795(1975).

(5) B. C. Flann, *J. Pharm. Sci.*, **58**, 122(1969).

ACKNOWLEDGMENTS AND ADDRESSES

Received October 3, 1975, from the *Pharmaceutical Research and Development Laboratories, Warner-Lambert Research Institute, Morris Plains, NJ 07950*

Accepted for publication January 8, 1976.

[x] To whom inquiries should be directed.

Synthesis and Preliminary Antimicrobial Screening of Two Thiosulfonates

LaVERNE D. SMALL

Abstract □ Tetramethylene bis(methanethiosulfonate), the *S*-ester analog of busulfan, was prepared by reacting 1,4-dibromobutane with potassium methanethiosulfonate. 2,4-Dichlorophenyl methanethiosulfonate was prepared by reacting sodium methanesulfinate with 2,4-dichlorobenzenesulfenyl chloride. Neither compound showed antifungal activity against *Microsporum audouini* or *Trichophyton mentagrophytes*. Although tetramethylene bis(methanethiosulfonate) was more active against *Staphylococcus aureus* than was 2,4-dichlorophenyl methanethiosulfonate, neither compound was as active as the streptomycin control.

Keyphrases □ Thiosulfonates—synthesis of tetramethylene bis(methanethiosulfonate) and 2,4-dichlorophenyl methanethiosulfonate, antimicrobial screening □ Sulfur analog of busulfan—synthesized, antimicrobial screening □ Structure–activity relationships—thiosulfonates synthesized, antimicrobial screening □ Antimicrobial activity—thiosulfonates synthesized and screened

Although thiosulfonates have been known for more than 100 years, the demonstration of antimicrobial activity of some members of this chemical class has been relatively recent (1–3). Two different types of thiosulfonates were made for antimicrobial screening. Busulfan, a bis(sulfonate) ester, is used for treatment of chronic myelocytic leukemia (4). The bis(*S*-ester) analog of this compound was prepared for testing of its antibacterial and antifungal activities and for future screening for antileukemic activity. In addition, the *S*-ester analog of 2,4-dichlorophenyl methanesulfonate, a long acting soil nematocide (5), was prepared. These new thiosulfonates were tested for antibacterial activity against *Staphylococcus aureus* and for antifungal ac-

Table I—Nitroglycerin Dissolution from Three 0.4-mg Sublingual Tablet Lots

Lot	Average Percent Dissolved at 0.25 min	0.5 min	0.75 min	1.0 min	t_{90} Average	t_{100} Average	Average Micrograms per Tablet
1	31 (16–37)[a]	78 (66–84)	93 (88–95)	97 (95–98)	0.70	1.6 (1.2–2.4)[b]	433 (418–452)[b]
2	24 (19–30)	72 (69–76)	89 (86–94)	96 (94–98)	0.78	1.5 (1.2–1.8)	443 (424–459)
3	33 (28–39)	82 (71–90)	94 (92–97)	98 (95–100)	0.57	1.2 (1.0–1.5)	394 (360–415)

[a] Range for 10-tablet sample. [b] Range.

Perform a blank determination with the electrolyte to compensate for the small amount of oxygen that diffuses into the cell and take the difference in recorder chart reading between the sample and the blank at each time interval as the sample reading. With no change in experimental conditions, the blank remains constant during the day and only one blank determination need be obtained each day.

Calculate the quantity of nitroglycerin, in milligrams per tablet, from the formula $5C(U/S)$, where C is the concentration, in milligrams per milliliter, of the standard preparation used, whichever is closer to the sample reading; and U and S are the chart readings for the tablet and the standard preparation, respectively.

Note as t_{100} the time required for 100% of the drug to dissolve; this value is determined from the chart as that point where no further rise in reduction current occurs. Calculate the percent of drug released at any time, t, in seconds from the formula (milligrams measured at time t/total milligrams released) × 100.

RESULTS AND DISCUSSION

The proposed dissolution test was performed using 10-tablet samples of each of three lots of a commercial 0.4-mg sublingual tablet formulation[8]. Table I shows the average percentage of drug dissolved from the tablets at 15-sec intervals during the 1st min and the average time required for 90 and 100% of the drug content of the tablets to dissolve. Use of percentage affords direct comparison among individual tablets of differing drug content, thus normalizing the data. Since prompt onset of action is an important criterion for a sublingual nitroglycerin tablet, these data may have clinical significance.

Another advantage of the method is that it provides a measure of the nitroglycerin in each tablet. The data shown in Table I (last column) are consistent with those obtained for these tablets by Dorsch and Shangraw (4), who used an automated assay method. Their method is less time consuming than the dissolution procedure and probably would be preferable if content uniformity information is the only consideration.

[8] NITROPRN Tablets, Warner-Chilcott Laboratories, Morris Plains, NJ. Lot 1 was control number 490254B, Lot 2 was control number 4917124B, and Lot 3 was control number 5964124A.

REFERENCES

(1) "The United States Pharmacopeia," 19th rev., Mack Publishing Co., Easton, Pa., 1975, p. 651.

(2) "The National Formulary," 14th ed., Mack Publishing Co., Easton, Pa., 1975, p. 893.

(3) F. W. Goodhart, R. H. McCoy, and F. C. Ninger, *J. Pharm. Sci.*, **62**, 304(1973).

(4) B. Dorsch and R. Shangraw, *Am. J. Hosp. Pharm.*, **32**, 795(1975).

(5) B. C. Flann, *J. Pharm. Sci.*, **58**, 122(1969).

ACKNOWLEDGMENTS AND ADDRESSES

Received October 3, 1975, from the *Pharmaceutical Research and Development Laboratories, Warner-Lambert Research Institute, Morris Plains, NJ 07950*

Accepted for publication January 8, 1976.

[x] To whom inquiries should be directed.

Synthesis and Preliminary Antimicrobial Screening of Two Thiosulfonates

LaVERNE D. SMALL

Abstract □ Tetramethylene bis(methanethiosulfonate), the *S*-ester analog of busulfan, was prepared by reacting 1,4-dibromobutane with potassium methanethiosulfonate. 2,4-Dichlorophenyl methanethiosulfonate was prepared by reacting sodium methanesulfinate with 2,4-dichlorobenzenesulfenyl chloride. Neither compound showed antifungal activity against *Microsporum audouini* or *Trichophyton mentagrophytes*. Although tetramethylene bis(methanethiosulfonate) was more active against *Staphylococcus aureus* than was 2,4-dichlorophenyl methanethiosulfonate, neither compound was as active as the streptomycin control.

Keyphrases □ Thiosulfonates—synthesis of tetramethylene bis(methanethiosulfonate) and 2,4-dichlorophenyl methanethiosulfonate, antimicrobial screening □ Sulfur analog of busulfan—synthesized, antimicrobial screening □ Structure–activity relationships—thiosulfonates synthesized, antimicrobial screening □ Antimicrobial activity—thiosulfonates synthesized and screened

Although thiosulfonates have been known for more than 100 years, the demonstration of antimicrobial activity of some members of this chemical class has been relatively recent (1–3). Two different types of thiosulfonates were made for antimicrobial screening. Busulfan, a bis(sulfonate) ester, is used for treatment of chronic myelocytic leukemia (4). The bis(*S*-ester) analog of this compound was prepared for testing of its antibacterial and antifungal activities and for future screening for antileukemic activity. In addition, the *S*-ester analog of 2,4-dichlorophenyl methanesulfonate, a long acting soil nematocide (5), was prepared. These new thiosulfonates were tested for antibacterial activity against *Staphylococcus aureus* and for antifungal ac-

tivity against *Microsporum audouini* and *Trichophyton mentagrophytes*.

Tetramethylene bis(methanethiosulfonate) (I), the analog of busulfan, was prepared by reacting 1,4-dibromobutane with 2 equivalents of potassium methanethiosulfonate, using a modification of the procedure of Spring (6). The 2,4-dichlorophenyl methanethiosulfonate (II) was prepared by reacting sodium methanesulfinate with 2,4-dichlorobenzenesulfenyl chloride.

Both I and II were purified with the aid of TLC, using aluminum sheets coated with silica gel F-254. The sulfur-containing compound, as well as compounds containing aromatic groups, was visualized as fluorescent quenching spots under short wavelength UV light. This technique was used to determine the best solvents for separating various components from the final reaction mixture and to check the purity of the final product.

EXPERIMENTAL[1]

TLC sheets, precoated with 0.25-mm silica gel F-254[2] on an aluminum backing, were used for the TLC separations. The NMR spectra[3] of I and II were obtained using deuterated chloroform and deuterated dimethyl sulfoxide as the solvents, respectively. Tetramethylsilane was used as the internal standard for all NMR measurements. The IR spectra[4] were obtained using chloroform as the solvent for I and carbon tetrachloride for II.

Potassium Methanethiosulfonate—An alcoholic solution of potassium sulfide was prepared by dissolving 12 g (0.3 mole) of bright metallic potassium in 600 ml of anhydrous ethanol under an atmosphere of dry nitrogen. One-half of this solution was saturated with hydrogen sulfide according to the procedure described by Brauer (7) for the preparation of potassium trisulfide. Water, 60 ml, was added to this alcohol solution containing 0.15 mole of potassium sulfide, and the solution was cooled in an ice–water bath to less than 10°.

Methanesulfonyl chloride, 11.6 g (0.15 mole), was slowly dropped into the cold sulfide solution while the mixture was stirred rapidly. Stirring was continued for 3 hr while the mixture was allowed to warm to room temperature. The potassium methanethiosulfonate was not isolated from the reaction mixture.

Tetramethylene Bis(methanethiosulfonate) (I)—To the alcoholic suspension of potassium methanethiosulfonate was added 1,4-dibromobutane, 8.1 ml (0.068 mole). The mixture was heated under gentle reflux for 36 hr. The reaction mixture was allowed to cool to room temperature and then was stirred for an additional 12 hr. The white precipitate was removed by filtration, and the alcoholic filtrate of the reaction mixture was placed in a freezer for 24 hr to obtain additional material.

The precipitated material was washed with cold water, dried under reduced pressure at 40°, and crystallized by dissolving in boiling acetone and allowing the solution to cool. The substance was recrystallized by dissolving in boiling benzene. After the addition of hexane to the warm benzene solution and cooling, I, 12.4 g (66% yield), mp 90.0–90.5°, was obtained. The NMR spectrum and the melting point were the same as those of the product previously obtained from commercial potassium sulfide by TLC.

The NMR spectrum showed a strong, sharp absorption peak at δ 3.40, a smaller peak at δ 3.30, and a third broad peak centered at δ 1.93. If the integration of the peak at δ 1.93 represents four protons, the integration of the two peaks at δ 3.30 and 3.40 represents 10 protons. The NMR spectrum of 1,4-dibromobutane showed two broad band peaks at δ 2.03 and 3.50.

The IR spectrum for I showed absorption at 1130 (1) (strongest absorption), 1321 (2), 949 (3), and 1182 (4) cm^{-1}. Literature values (8) for ethyl methanethiosulfonate indicate absorption at 1136 (SO_2), 1321, 962, and 751 cm^{-1}. The mass spectrum for I indicated 278 (M^+, $C_6H_{14}O_4S_4$).

Anal.—Calc. for $C_6H_{14}O_4S_4$: C, 25.88; H, 5.07; S, 46.06. Found: C, 26.00; H, 4.96; S, 46.22.

Bis(2,4-dichlorophenyl) Disulfide—Sodium 2,4-dichlorothiophenol was prepared by a slight modification of the method of Baddeley and Bennett (9), starting with 20 g (0.123 mole) of 2,4-dichloroaniline. About 200 ml of 50% (w/w) sulfuric acid was necessary to dissolve and maintain the dichloroaniline in solution. This amount was more than twice the concentration of acid used by Baddeley and Bennett (9).

After preparing the diazonium sulfate, about 85% of the acid was neutralized by the addition of sodium hydroxide solution while the temperature of the mixture was maintained below 10°. Sodium borate solution was then used to adjust the reaction mixture to about pH 4. The dichlorophenyl xanthogenate was prepared and then hydrolyzed as described by Baddeley and Bennett (9). The resulting sodium 2,4-dichlorothiophenol was oxidized in the aqueous alcoholic solution by addition of excess iodine and sodium iodide solution.

After the mixture was stirred for 20 min, sodium thiosulfate solution was added until the color of the iodine was discharged. The disulfide was extracted from the mixture by the addition of chloroform. The chloroform extract was dried, using anhydrous sodium sulfate, and the chloroform was evaporated. The residue, crystallized from a mixture of acetone and methanol, provided 7.6 g (17% yield) of bis(2,4-dichlorophenyl) disulfide, mp 82–84° [lit. (10) mp 82–83°].

2,4-Dichlorobenzenesulfenyl Chloride—A solution containing 7.6 g (0.02 mole) of bis(2,4-dichlorophenyl) disulfide in 100 ml of dry carbon tetrachloride was treated with chlorine according to the method of Hubacher (11) for the preparation of *o*-nitrophenylsulfur chloride, except for the reaction time. The flow of chlorine through the warm reaction mixture was maintained for 20 hr. The solvent was then evaporated, and the residual dark oil was distilled at about 5 mm of pressure. The fractions distilling at 100–102° and showing a constant refractive index, n_D^{25} 1.6330 ± 0.0002, were combined. A fuming red oil, 4.5 g (98% yield), was obtained [lit. (10) bp 94–96°/4 mm].

2,4-Dichlorophenyl Methanethiosulfonate (II)—Methanesulfinyl chloride, 1.4 g (0.014 mole), was prepared by the reaction of chlorine on methyl disulfide in acetic anhydride (12) and was then added dropwise, with stirring, to 25 ml of a cold (5°) aqueous solution containing 1.13 g (0.028 mole) of sodium hydroxide to form sodium methanesulfinate. A solution containing 3.0 g (0.014 mole) of 2,4-dichlorobenzenesulfenyl chloride in 5 ml of dichloromethane was slowly added, with stirring, to the cold aqueous solution of the sodium methanesulfinate. The cold mixture was stirred for 1 hr and then allowed to warm to room temperature.

The reaction mixture was extracted with carbon tetrachloride, and the extract was washed with 5% sodium bicarbonate solution and dried with anhydrous sodium sulfate. A thin-layer chromatogram of a small portion of the carbon tetrachloride extract was developed as indicated below. The carbon tetrachloride was removed in a flash evaporator, and the remaining white solid was washed with hexane until a thin-layer chromatogram showed a single spot. The remaining compound, II, 2.1 g (58% yield), was crystallized from benzene–hexane, mp 88–88.5°.

The NMR spectrum, using deuterated dimethyl sulfoxide as the solvent, showed a sharp absorption peak at δ 3.6 that integrated for three protons. A multiplet, integrating for three protons, occurred between δ 7.6 and 8.1.

The IR spectrum for II showed strong absorption at 1347 (1), 1146 (2), and 956 (3) cm^{-1} and a broad band of absorption between 710 and 840 cm^{-1}. The mass spectrum showed M^+ 256, M + 2 at 258, and a lower peak M + 4 at 260.

Anal.—Calc. for $C_7H_6Cl_2O_2S_2$: C, 32.69; H, 2.35; S, 24.94. Found: C, 32.59; H, 2.26; S, 24.83.

Isolation of Products I and II—The desired compound was initially separated from the reaction mixture by TLC. Solvents and other volatile substances were removed from the reaction mixture by means of a flash vacuum evaporator and heating at 50°. Several drops or a few milligrams of the reaction residue was dissolved in about 0.3 ml of acetone or carbon tetrachloride. About 5 μl of this solution was applied to a 5 × 20-cm sheet coated with silica gel F-254. A diluted solution of methyl disulfide or 2,4-dichlorophenyl disulfide was applied to the chromatographic sheet as a control. The chromatogram of the reaction product of I was developed with benzene–hexane–ether (8:8:1), and the chromatogram of II was developed with benzene–0.5% acetic acid.

Four or five spots were visible on the developed chromatograms when viewed under short wavelength UV light. The solubility of each

[1] Element analyses were performed by Galbraith Laboratories, Inc., Knoxville, Tenn.
[2] Brinkmann Instruments, Des Plaines, Ill.
[3] Varian model EM-360 spectrometer.
[4] Beckman IR-18A spectrophotometer.

spot on the developed chromatogram was determined by the dropwise addition of hexane to each spot and reexamination of the chromatogram under UV light. The areas apparently not influenced by the hexane were then treated with benzene. The areas containing the more polar substances had either little or no apparent solubility in benzene. Most impurities in the reaction products of both I and II were removed by washing the reaction residues with hexane. The washed residues, representing nearly pure I and II, were recrystallized from mixtures of benzene and hexane until a chromatogram indicated a pure substance.

Antibacterial and Antifungal Testing—Both I and II were tested for antifungal activity against *M. audouini*[5] and *T. mentagrophytes*[5] in Sabouraud liquid medium by the serial dilution method (13). Griseofulvin, used as the control agent, prevented growth of the microsporum at 1.25 μg/ml, as indicated by the absence of turbidity in the culture. Griseofulvin prevented growth of the trichophyton at 2.5 μg/ml. Neither thiosulfonate showed antifungal activity at the highest concentration tested, 125 μg/ml.

The antibacterial activity was tested by the serial dilution method using a culture of *S. aureus* (subcultured from FDA 209) in nutrient broth[6] (14). Streptomycin, used as the control agent, prevented growth of the *S. aureus* at 5 μg/ml but not at 2.5 μg/ml.

Compound I prevented growth of the *S. aureus* at 16 μg/ml but not at 8 μg/ml, while II prevented growth at 62.5 μg/ml but not at 31.3 μg/ml.

DISCUSSION

Compound I was first prepared by reacting methanesulfonyl chloride with a solution of commercial potassium sulfide to form potassium methanethiosulfonate. After combining the product of this reaction with 1,4-dibromobutane and purifying the products as described, 150 mg (representing a 2% yield) of a white crystalline compound was obtained. IR, NMR, and mass spectra were obtained for this material, Compound I.

The small yield of I obtained by this procedure was probably due to the fact that much of the commercial potassium sulfide is actually sulfurated potash, a mixture of potassium sulfides. Knowledge of the properties of I obtained from this initial preparation facilitated the separation of I in a much better yield from the reaction mixture as described. Previous attempts to synthesize I using commercial sodium sulfide had proven unsuccessful.

[5] University of Nebraska Hospital isolate No. 1.
[6] Bacto.

REFERENCES

(1) L. D. Small, J. H. Bailey, and C. J. Cavallito, *J. Am. Chem. Soc.*, **71**, 3565(1949).

(2) J. P. Weidner and S. S. Block, *J. Med. Chem.*, **7**, 671(1964).

(3) *Ibid.*, **10**, 1167(1967).

(4) "AMA Drug Evaluations," 2nd ed., Publishing Science Group, Acton, Mass., 1973, p. 838.

(5) C. W. McBeth, L. V. White, and S. T. Ichikawa, *Plant Dis. Rep.*, **48**, 634(1964).

(6) W. Spring, *Ber.*, **7**, 1157(1874).

(7) G. Brauer, "Handbook of Preparative Inorganic Chemistry," vol. I, 2nd ed., Academic, New York, N.Y., 1963, p. 364.

(8) E. Block and J. O'Connor, *J. Am. Chem. Soc.*, **96**, 3921(1974), including supplemental material 3929M-3.

(9) G. Baddeley and G. M. Bennett, *J. Chem. Soc.*, **1933**, 46.

(10) M. B. Sparke, J. L. Cameron, and N. Kharasch, *J. Am. Chem. Soc.*, **75**, 4907(1953).

(11) M. H. Hubacher, in "Organic Syntheses," col. vol. II, A. H. Blatt, Ed., Wiley, New York, N.Y., 1943, p. 455.

(12) I. B. Douglass and R. V. Norton, in "Organic Syntheses," col. vol. V, H. E. Baumgarten, Ed., Wiley, New York, N.Y., 1973, p. 709.

(13) M. C. Bryant, "Antibiotics and Their Laboratory Control," Appleton-Century-Crofts, New York, N.Y., 1968, pp. 45, 46.

(14) *Ibid.*, pp 36, 37.

ACKNOWLEDGMENTS AND ADDRESSES

Received August 8, 1975, from the *Department of Medicinal Chemistry and Pharmacognosy, College of Pharmacy, University of Nebraska, Lincoln, NE 68588*

Accepted for publication January 16, 1976.

Presented at the Medicinal Chemistry Section, APhA Academy of Pharmaceutical Sciences, April 23, 1975.

Supported by a grant from the University of Nebraska Medical Center.

The author wishes to thank Dr. M. J. Weinstein, Director of Microbiological Sciences, Schering Corp., Bloomfield, N.J., for the griseofulvin used in the antifungal screening; Ms. Doris Malone, University of Nebraska Medical Center, for the cultures of *M. audouini* and *T. mentagrophytes;* Dr. T. L. Thompson, Department of Microbiology, University of Nebraska, for the culture of *S. aureus;* Dr. M. L. Gross, Department of Chemistry, University of Nebraska, for the mass spectral analysis; and Mr. Rick Larrabee for technical assistance.

Effect of Compression Force and Corn Starch on Tablet Disintegration Time

PHILIP M. HILL

Abstract □ An unusual occurrence of decreasing tablet disintegration time with increasing tablet hardness was explored. Tablets were made with varying ratios of starch disintegrant to starch paste and compressed with eight different forces. This unusual disintegration pattern is modified by changes in the starch ratios. The reason for this phenomenon is ascribed to grain swelling as the mechanism by which starch acts as a disintegrant.

Keyphrases □ Tablets—disintegration time, hardness, effect of various ratios of starch disintegrant to starch paste and various compression forces □ Disintegration time, tablet—effect of various ratios of starch disintegrant to starch paste and various compression forces □ Hardness, tablet—effect of various ratios of starch disintegrant to starch paste and various compression forces □ Dosage forms—tablets, disintegration time, hardness, effect of various ratios of starch disintegrant to starch paste and various compression forces □ Starch—effect of various ratios of disintegrant to paste on tablet disintegration time and hardness

Most articles dealing with tablet compressing report that increased compression forces result in tablets with longer disintegration times. Lowenthal (1) cited 31 references supporting this conclusion in a review of tablet disintegration. This cause–effect relationship is logical and not surprising. Higher compression forces

spot on the developed chromatogram was determined by the dropwise addition of hexane to each spot and reexamination of the chromatogram under UV light. The areas apparently not influenced by the hexane were then treated with benzene. The areas containing the more polar substances had either little or no apparent solubility in benzene. Most impurities in the reaction products of both I and II were removed by washing the reaction residues with hexane. The washed residues, representing nearly pure I and II, were recrystallized from mixtures of benzene and hexane until a chromatogram indicated a pure substance.

Antibacterial and Antifungal Testing—Both I and II were tested for antifungal activity against *M. audouini*[5] and *T. mentagrophytes*[5] in Sabouraud liquid medium by the serial dilution method (13). Griseofulvin, used as the control agent, prevented growth of the microsporum at 1.25 μg/ml, as indicated by the absence of turbidity in the culture. Griseofulvin prevented growth of the trichophyton at 2.5 μg/ml. Neither thiosulfonate showed antifungal activity at the highest concentration tested, 125 μg/ml.

The antibacterial activity was tested by the serial dilution method using a culture of *S. aureus* (subcultured from FDA 209) in nutrient broth[6] (14). Streptomycin, used as the control agent, prevented growth of the *S. aureus* at 5 μg/ml but not at 2.5 μg/ml.

Compound I prevented growth of the *S. aureus* at 16 μg/ml but not at 8 μg/ml, while II prevented growth at 62.5 μg/ml but not at 31.3 μg/ml.

DISCUSSION

Compound I was first prepared by reacting methanesulfonyl chloride with a solution of commercial potassium sulfide to form potassium methanethiosulfonate. After combining the product of this reaction with 1,4-dibromobutane and purifying the products as described, 150 mg (representing a 2% yield) of a white crystalline compound was obtained. IR, NMR, and mass spectra were obtained for this material, Compound I.

The small yield of I obtained by this procedure was probably due to the fact that much of the commercial potassium sulfide is actually sulfurated potash, a mixture of potassium sulfides. Knowledge of the properties of I obtained from this initial preparation facilitated the separation of I in a much better yield from the reaction mixture as described. Previous attempts to synthesize I using commercial sodium sulfide had proven unsuccessful.

[5] University of Nebraska Hospital isolate No. 1.
[6] Bacto.

REFERENCES

(1) L. D. Small, J. H. Bailey, and C. J. Cavallito, *J. Am. Chem. Soc.*, **71**, 3565(1949).

(2) J. P. Weidner and S. S. Block, *J. Med. Chem.*, **7**, 671(1964).

(3) *Ibid.*, **10**, 1167(1967).

(4) "AMA Drug Evaluations," 2nd ed., Publishing Science Group, Acton, Mass., 1973, p. 838.

(5) C. W. McBeth, L. V. White, and S. T. Ichikawa, *Plant Dis. Rep.*, **48**, 634(1964).

(6) W. Spring, *Ber.*, **7**, 1157(1874).

(7) G. Brauer, "Handbook of Preparative Inorganic Chemistry," vol. I, 2nd ed., Academic, New York, N.Y., 1963, p. 364.

(8) E. Block and J. O'Connor, *J. Am. Chem. Soc.*, **96**, 3921(1974), including supplemental material 3929M-3.

(9) G. Baddeley and G. M. Bennett, *J. Chem. Soc.*, **1933**, 46.

(10) M. B. Sparke, J. L. Cameron, and N. Kharasch, *J. Am. Chem. Soc.*, **75**, 4907(1953).

(11) M. H. Hubacher, in "Organic Syntheses," col. vol. II, A. H. Blatt, Ed., Wiley, New York, N.Y., 1943, p. 455.

(12) I. B. Douglass and R. V. Norton, in "Organic Syntheses," col. vol. V, H. E. Baumgarten, Ed., Wiley, New York, N.Y., 1973, p. 709.

(13) M. C. Bryant, "Antibiotics and Their Laboratory Control," Appleton-Century-Crofts, New York, N.Y., 1968, pp. 45, 46.

(14) *Ibid.*, pp 36, 37.

ACKNOWLEDGMENTS AND ADDRESSES

Received August 8, 1975, from the *Department of Medicinal Chemistry and Pharmacognosy, College of Pharmacy, University of Nebraska, Lincoln, NE 68588*

Accepted for publication January 16, 1976.

Presented at the Medicinal Chemistry Section, APhA Academy of Pharmaceutical Sciences, April 23, 1975.

Supported by a grant from the University of Nebraska Medical Center.

The author wishes to thank Dr. M. J. Weinstein, Director of Microbiological Sciences, Schering Corp., Bloomfield, N.J., for the griseofulvin used in the antifungal screening; Ms. Doris Malone, University of Nebraska Medical Center, for the cultures of *M. audouini* and *T. mentagrophytes;* Dr. T. L. Thompson, Department of Microbiology, University of Nebraska, for the culture of *S. aureus;* Dr. M. L. Gross, Department of Chemistry, University of Nebraska, for the mass spectral analysis; and Mr. Rick Larrabee for technical assistance.

Effect of Compression Force and Corn Starch on Tablet Disintegration Time

PHILIP M. HILL

Abstract □ An unusual occurrence of decreasing tablet disintegration time with increasing tablet hardness was explored. Tablets were made with varying ratios of starch disintegrant to starch paste and compressed with eight different forces. This unusual disintegration pattern is modified by changes in the starch ratios. The reason for this phenomenon is ascribed to grain swelling as the mechanism by which starch acts as a disintegrant.

Keyphrases □ Tablets—disintegration time, hardness, effect of various ratios of starch disintegrant to starch paste and various compression forces □ Disintegration time, tablet—effect of various ratios of starch disintegrant to starch paste and various compression forces □ Hardness, tablet—effect of various ratios of starch disintegrant to starch paste and various compression forces □ Dosage forms—tablets, disintegration time, hardness, effect of various ratios of starch disintegrant to starch paste and various compression forces □ Starch—effect of various ratios of disintegrant to paste on tablet disintegration time and hardness

Most articles dealing with tablet compressing report that increased compression forces result in tablets with longer disintegration times. Lowenthal (1) cited 31 references supporting this conclusion in a review of tablet disintegration. This cause–effect relationship is logical and not surprising. Higher compression forces

Table I—Formula Variations

Component, mg/Tablet	Formula A	B	C	D	E	F
Lactose	172	177	181	172	172	172
Corn starch (disintegrant)	9.4	4.7	0	9.4	4.7	0
Corn starch (paste)	5.2	5.2	5.2	5.2	9.9	14.6
Talcum powder	6.8	6.8	6.8	6.8	6.8	6.8
Magnesium stearate	1.95	1.95	1.95	1.95	1.95	1.95

Table II—Water Penetration Rate (Time in Seconds for Penetration of 10 μl) of Tablets Compressed at Various Forces

Formula	Compression Force, tons 1.0	1.3	1.7	2.0	2.3	2.7	3.0	3.3
A	9.4	10.3	13.5	15.5	18.1	20.9	26.1	31.1
B	16.9	19.0	20.5	21.1	23.5	30.7	34.0	45.7
C	34.6	63.1	266.0	—	—	—	—	>15 min
D	14.1	16.3	16.5	18.4	24.1	25.0	29.3	33.5
E	14.0	15.8	16.2	18.4	22.5	29.1	40.7	45.9
F	18.4	24.9	25.5	35.2	30.5	46.1	75.1	93.7

result in less porous tablets with the particles more strongly bonded together, as reflected by increasing tablet hardness values. Comparatively few investigators (2, 3) reported the opposite effect of faster tablet disintegration times with increasing compression forces.

The study of starch as a tablet disintegrant has not been neglected by pharmaceutical scientists (4–9). Two major theories as to how starch performs as a tablet disintegrant were proposed. One is that the starch grains form channels or pores that act to draw water into the tablet by capillarity or wicking (10). Disintegration or erosion occurs when the water dissolves the soluble components in the tablet. The other theory is that the starch grains swell upon contact with water and cause the tablet to disintegrate by physically rupturing the particle-to-particle bonds (2).

As compression force increases, a tablet becomes more dense and consequently less porous. Particle-to-particle bonds also usually become stronger. The reduced porosity, *i.e.*, smaller pore diameter, results in a longer penetrating time for water into the tablet (3, 11, 12). If wicking is the primary mode of action, disintegration time should increase with increased compression force. If grain swelling is the mechanism by which starch acts as a disintegrant, a decreasing tablet porosity should result in faster disintegration times because the starch grains can exert a force on the surrounding particles more effectively. A lightly compressed tablet has larger intergranular spaces, and the starch grains can swell considerably before they begin to exert a disruptive pressure (2).

The purpose of this paper is to present data on studies of tablet disintegration times *versus* compression force, showing that tablet disintegration times can become faster when compression force is increased. It is proposed that this occurrence indicates that the starch grain swelling mechanism of tablet disintegration is in force.

EXPERIMENTAL

A lactose–starch paste formula (Table I) was used to make the granulations. The portion of starch added to the granulations as a dry powder is referred to as disintegrant starch. The lactose and dry starch were mixed in a planetary action mixer. The starch for paste was cooked in five parts of water by weight and added to the lactose–starch blend. This was mixed to form granules and then passed through a 6-mesh screen and dried at 50°. The dried granules were sized to 16 mesh and then blended with the talcum powder and magnesium stearate. To control process variables, the starch paste was cooked to the same temperature (72 ± 1°) in each experiment.

The granulations were compressed with special semistandard, concave, 0.714-cm square punches on an instrumented rotary tablet machine[1] at eight different forces, starting at 900 kg and increasing in approximately 300-kg increments. Mean tablet thickness varied between 3.29 mm at the lowest compression force and 2.99 mm at the highest force. In Formulas A, B, and C (Table I), the total amount of starch (dry mix plus paste) per tablet decreased as the disintegrant starch was decreased. In Formulas D, E, and F, the total amount of starch in the tablet was kept constant by increasing the amount in the paste as the disintegrant starch was decreased.

Tablet disintegration times were measured in the USP tablet disintegration apparatus in 37 ± 1° water. Disintegration testing was performed without disks to avoid obscuring the differences in times between tablets compressed at the various forces. When disks are used, the disintegration time always shows an increasing trend starting from the lowest compressing force in all experiments. The mechanical action exerted by the disks apparently aids the disintegrating tablet to break up into smaller pieces which are even more susceptible to breakage by mechanical force. Use of disks thus seems to result in disintegration times that reflect the mechanical strength of the tablets, as do hardness values.

Tablet hardness values were obtained on an air-operated hardness tester[2]. The water penetration rate was measured by observing the disappearance of a 10-μl drop of water into the tablet under a low power microscope. The end-point was determined by extinction of reflected light. The values shown in Table II are the averages of three determinations.

RESULTS

Disintegration times are shown by a bar chart (Fig. 1) and are the averages of six tablets. The corresponding tablet hardness values at each compression force are shown by the curves on the same chart and are the averages of 10 tablets. Tablets compressed at the lower forces had longer disintegration times (A, B, and D, Fig. 1), except for those formulations containing no disintegrant starch (C and F, Fig. 1).

Formula E contained an increased quantity of starch paste and did not clearly show the longer disintegration times at lower pressures. In the A, B, and C series, disintegrant starch was reduced in B and absent in C. The disintegration profile in C differed completely from

[1] Stokes model B-2.
[2] Modified Strong-Cobb.

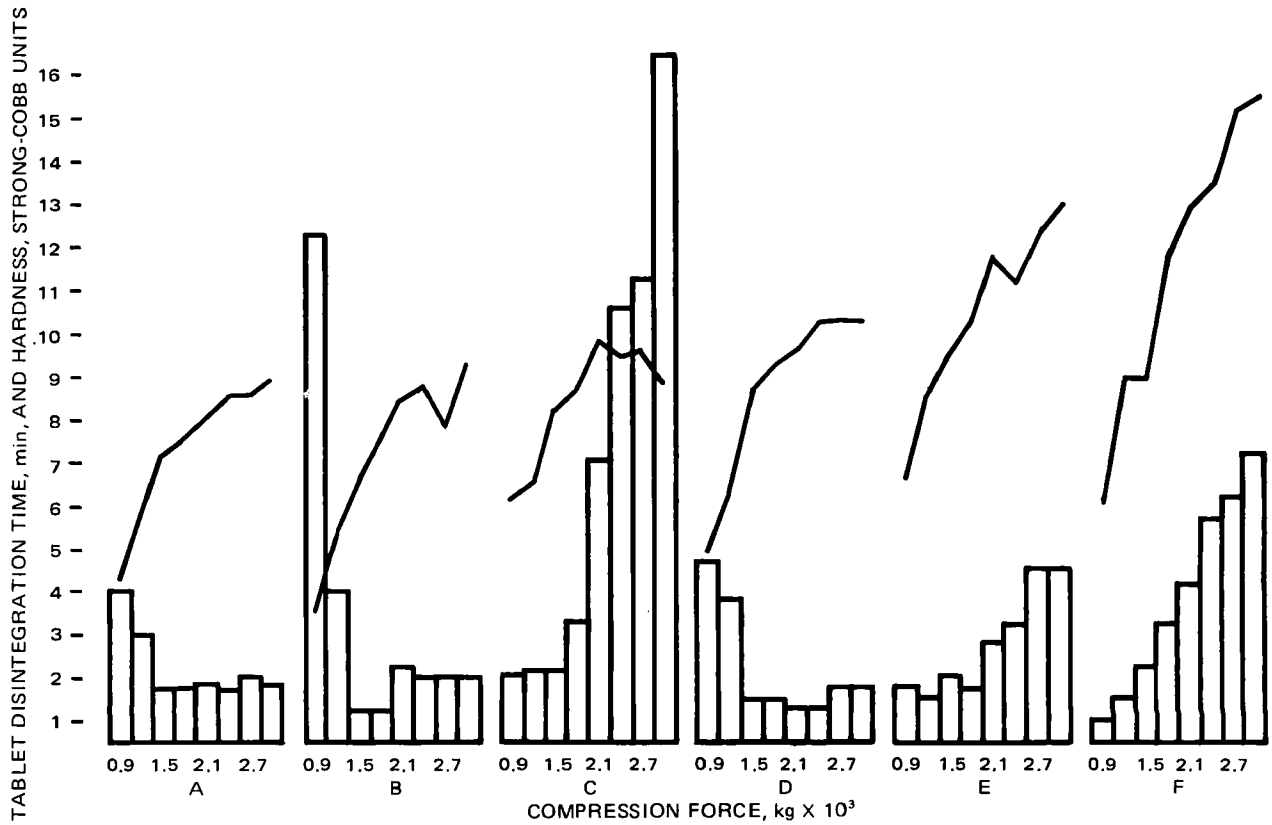

Figure 1—*Tablet disintegration times at various compression forces. Bars show disintegration time; lines show tablet hardness.*

that of A and B, illustrating the effect exerted by starch. With no disintegrant starch in C, the disintegration times at the higher compression forces were much longer than in A or B. The disintegrant starch in A and B was shown to be more effective at the higher compression forces, despite increased tablet hardness.

In D, E, and F, where the total amount of starch per tablet was kept constant, the disintegration profiles differed from those of A, B, and C. In this case, the tablet with reduced disintegrant starch (E) had a disintegration profile similar to that of tablets without disintegrant starch (C and F). The extra binder activity of the increased paste starch in E, as reflected in higher tablet hardness values, may counter the grain swelling of the disintegrant starch.

DISCUSSION

The water penetration rate values in Table II show that paste starch by itself is not as effective as disintegrant starch (uncooked starch) in providing water absorbency to a tablet (compare Formula C with A or B in Table II). However, of the two formulas containing paste starch only, the one with the greater quantity had better water absorbency (compare Formula F with C, Table II). This improved absorbency of F probably accounts for its generally faster disintegration time as compared to C (Fig. 1).

The varying disintegration times of tablets compressed at the same compression forces is related to the presence or absence of disintegrant starch in the tablet as well as to the ratio of disintegrant starch to paste starch. When disintegrant starch was present in a quantity approximately equal to or greater than the quantity of paste starch, disintegration time was shorter at the higher compression forces. When disintegrant starch was absent or was greatly exceeded in quantity by paste starch, tablet disintegration times at the higher compression forces were longer. This effect was very striking in the A, B, and C series, where the paste starch quantity was kept constant.

If it is accepted that the longer disintegration times at the low compression forces are typical of the starch grain swelling mechanism of disintegration, then it might be expected that tablets without disintegrant starch will disintegrate by a different mechanism and show a different disintegration time–compression force profile. With Formulas C and F, tablet disintegration time followed the more generally expected pattern of increasing time with increasing compression force. Here the mechanism might be postulated to be water penetration by capillary movement and disintegration by dissolution of particle bonds. The disintegration time–compression force profile shows a positive correlation with the water penetration time *versus* compression force data for these trials and suggests that tablet porosity is controlling disintegration time.

This finding is in contrast to that for Formulas A, B, and D, where the disintegration time–compression force profile does not correlate positively with water penetration times. The water penetration data show that water readily entered the tablets compressed at the lowest forces. The fact that the tablets did not disintegrate as quickly as those compressed at higher forces supports the starch grain swelling theory, and this theory would explain why the water penetration rates do not correlate with disintegration times in A, B, and D.

Tablets without a disintegrant have a shorter disintegration time at the lowest compression forces than do the tablets containing a disintegrant. The starch seems to inhibit disintegration at low compression forces. This result could be explained by theorizing that the expanded starch granules occlude some of the relatively larger channels of the softer tablets, resulting in nonuniform water penetration and breakup of the tablet.

REFERENCES

(1) W. Lowenthal, *J. Pharm. Sci.*, **61**, 1695(1972).

(2) H. Berry and C. Ridout, *J. Pharm. Pharmacol.*, **2**, 619(1950).

(3) D. Ganderton and D. R. Fraser, *ibid.*, **22**, 95S(1970).

(4) J. T. Ingram and W. Lowenthal, *J. Pharm. Sci.*, **55**, 614(1966).

(5) *Ibid.*, **57**, 187(1968).

(6) *Ibid.*, **57**, 393(1968).

(7) W. Lowenthal and R. A. Burruss, *J. Pharm. Sci.*, **60**, 1325(1971).

(8) W. Lowenthal, *ibid.*, **61**, 455(1972).
(9) W. Lowenthal and J. H. Wood, *ibid.*, **62**, 287(1973).
(10) L. C. Curlin, *J. Am. Pharm. Assoc., Sci. Ed.*, **44**, 16(1955).
(11) H. Nogami, J. Hasegawa, and M. Miyamoto, *Chem. Pharm. Bull.*, **15**, 279(1967).
(12) D. Ganderton, *J. Pharm. Pharmacol.*, **21**, 9S(1969).

ACKNOWLEDGMENTS AND ADDRESSES

Received July 28, 1975, from *Tablet Products Research and Development, Pharmaceutical Products Division, Abbott Laboratories, North Chicago, IL 60064*

Accepted for publication January 23, 1976.

Quantitative Determination of Morphine in Paregoric USP by High-Pressure Liquid Chromatography

V. DAS GUPTA

Abstract □ The quantitative determination of morphine in paregoric by reversed-phase high-pressure liquid chromatography is described. The method is simple, accurate, and fast compared to the USP method. Benzoic acid in paregoric also can be determined quantitatively with the same column. The method was applied to two commercial samples with excellent results.

Keyphrases □ Morphine—high-pressure liquid chromatographic analysis in commercial samples of paregoric □ High-pressure liquid chromatography—analysis, morphine in commercial samples of paregoric □ Paregoric—high-pressure liquid chromatographic analysis of morphine and benzoic acid, commercial samples □ Analgesic agents—morphine, high-pressure liquid chromatographic analysis in commercial samples of paregoric

The USP method (1) for the quantitative determination of morphine in paregoric is tedious and time consuming. No other easy method is available for determining morphine in paregoric USP. The purpose of these investigations was to develop a simple, accurate, and fast method for the analysis of morphine using high-pressure liquid chromatography (HPLC). A method for the quantitative determination of benzoic acid in paregoric using the same column also is described.

EXPERIMENTAL

Apparatus—A high-pressure liquid chromatograph[1] capable of operating at an inlet pressure up to 6000 psig was used.

Column—The column[2] (30 cm long and 4 mm i.d.) was purchased and used as received. It consisted of a monomolecular layer of octadecyltrichlorosilane permanently bonded to silica *via* silicon–carbon bonds.

Recorder—The recorder[3] was equipped with an integrator.

Chromatographic Conditions—The chromatographic solvents were: (*a*) 0.1 *M* KH_2PO_4 buffer solution in 7% (v/v) methanol in water for morphine and (*b*) 0.1 *M* KH_2PO_4 buffer solution in 10% (v/v) methanol in water for benzoic acid. The temperature was ambient. The flow rate was 1.8 ml/min (inlet pressure approximately 1000 psig) for morphine or 3 ml/min (inlet pressure approximately 2100 psig) for benzoic acid. The absorbance unit full scale was 0.16, and the chart speed was 30.5 cm (12 in.)/hr.

Chemicals and Reagents—All chemicals and reagents were USP, NF, or ACS grade. Morphine sulfate[4] USP and all other reagents were used without further purification.

Solutions—*Benzoic Acid Standard Solution*—Weigh 100.32 mg of benzoic acid, dissolve in 15.0 ml of approximately 0.1 *N* NaOH solution, and dilute to volume (100.0 ml) with water.

Morphine Standard Solution—Weigh 53.3 mg of morphine sulfate (equivalent to 40.0 mg of anhydrous morphine) and dissolve in enough water, containing 8.0 ml of approximately 0.1 *N* H_2SO_4, to bring to 250.0 ml.

Standard Mixture Similar to Paregoric—Dissolve 53.3 mg of morphine sulfate in 4–5 ml of water; dissolve 0.38 ml of anise oil, 0.38 g of benzoic acid, 0.38 g of camphor, and 3.8 ml of glycerin in 48 ml of alcohol. Mix the aqueous and alcoholic solutions and dilute to volume (100.0 ml) with water.

Assay Procedure for Morphine in Standard Mixture and Paregoric—Transfer 10.0 ml of the standard mixture or paregoric to a 150-ml beaker and add 2.0 ml of ~0.1 *N* H_2SO_4 and 20 ml of water. Boil on a hot plate until the volume is approximately 8 ml, cool, and dilute to volume (25.0 ml) with water. Filter if necessary and inject 40.0 μl, using the described chromatographic conditions.

The detector response to the standard mixture and one commercial sample is presented in Fig. 1. Since preliminary investigations indicated that concentration (4–8 μg) was directly related to the peak area,

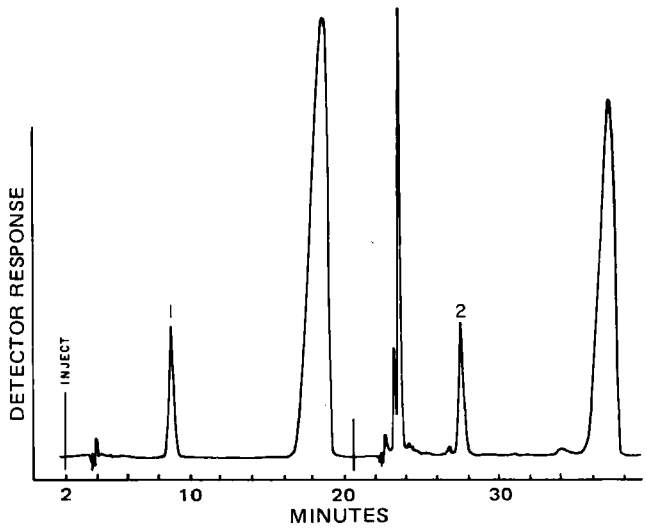

Figure 1—*HPLC analysis of morphine in paregoric USP (for chromatographic conditions, see text). Key: 1, standard mixture; and 2, paregoric sample.*

[1] Waters ALC 202 equipped with U6K Universal liquid chromatograph injector and UV detector (254 nm), Waters Associates, Milford, Mass.
[2] μBondapak/C_{18}, Waters Associates, Milford, Mass.
[3] Omniscribe model 5213-12, Houston Instruments, Austin, Tex.
[4] Merck & Co.

(8) W. Lowenthal, *ibid.*, **61**, 455(1972).
(9) W. Lowenthal and J. H. Wood, *ibid.*, **62**, 287(1973).
(10) L. C. Curlin, *J. Am. Pharm. Assoc., Sci. Ed.*, **44**, 16(1955).
(11) H. Nogami, J. Hasegawa, and M. Miyamoto, *Chem. Pharm. Bull.*, **15**, 279(1967).
(12) D. Ganderton, *J. Pharm. Pharmacol.*, **21**, 9S(1969).

ACKNOWLEDGMENTS AND ADDRESSES

Received July 28, 1975, from *Tablet Products Research and Development, Pharmaceutical Products Division, Abbott Laboratories, North Chicago, IL 60064*

Accepted for publication January 23, 1976.

Quantitative Determination of Morphine in Paregoric USP by High-Pressure Liquid Chromatography

V. DAS GUPTA

Abstract □ The quantitative determination of morphine in paregoric by reversed-phase high-pressure liquid chromatography is described. The method is simple, accurate, and fast compared to the USP method. Benzoic acid in paregoric also can be determined quantitatively with the same column. The method was applied to two commercial samples with excellent results.

Keyphrases □ Morphine—high-pressure liquid chromatographic analysis in commercial samples of paregoric □ High-pressure liquid chromatography—analysis, morphine in commercial samples of paregoric □ Paregoric—high-pressure liquid chromatographic analysis of morphine and benzoic acid, commercial samples □ Analgesic agents—morphine, high-pressure liquid chromatographic analysis in commercial samples of paregoric

The USP method (1) for the quantitative determination of morphine in paregoric is tedious and time consuming. No other easy method is available for determining morphine in paregoric USP. The purpose of these investigations was to develop a simple, accurate, and fast method for the analysis of morphine using high-pressure liquid chromatography (HPLC). A method for the quantitative determination of benzoic acid in paregoric using the same column also is described.

EXPERIMENTAL

Apparatus—A high-pressure liquid chromatograph[1] capable of operating at an inlet pressure up to 6000 psig was used.

Column—The column[2] (30 cm long and 4 mm i.d.) was purchased and used as received. It consisted of a monomolecular layer of octadecyltrichlorosilane permanently bonded to silica *via* silicon–carbon bonds.

Recorder—The recorder[3] was equipped with an integrator.

Chromatographic Conditions—The chromatographic solvents were: (*a*) 0.1 *M* KH_2PO_4 buffer solution in 7% (v/v) methanol in water for morphine and (*b*) 0.1 *M* KH_2PO_4 buffer solution in 10% (v/v) methanol in water for benzoic acid. The temperature was ambient. The flow rate was 1.8 ml/min (inlet pressure approximately 1000 psig) for morphine or 3 ml/min (inlet pressure approximately 2100 psig) for benzoic acid. The absorbance unit full scale was 0.16, and the chart speed was 30.5 cm (12 in.)/hr.

Chemicals and Reagents—All chemicals and reagents were USP, NF, or ACS grade. Morphine sulfate[4] USP and all other reagents were used without further purification.

Solutions—*Benzoic Acid Standard Solution*—Weigh 100.32 mg of benzoic acid, dissolve in 15.0 ml of approximately 0.1 *N* NaOH solution, and dilute to volume (100.0 ml) with water.

Morphine Standard Solution—Weigh 53.3 mg of morphine sulfate (equivalent to 40.0 mg of anhydrous morphine) and dissolve in enough water, containing 8.0 ml of approximately 0.1 *N* H_2SO_4, to bring to 250.0 ml.

Standard Mixture Similar to Paregoric—Dissolve 53.3 mg of morphine sulfate in 4–5 ml of water; dissolve 0.38 ml of anise oil, 0.38 g of benzoic acid, 0.38 g of camphor, and 3.8 ml of glycerin in 48 ml of alcohol. Mix the aqueous and alcoholic solutions and dilute to volume (100.0 ml) with water.

Assay Procedure for Morphine in Standard Mixture and Paregoric—Transfer 10.0 ml of the standard mixture or paregoric to a 150-ml beaker and add 2.0 ml of ~0.1 *N* H_2SO_4 and 20 ml of water. Boil on a hot plate until the volume is approximately 8 ml, cool, and dilute to volume (25.0 ml) with water. Filter if necessary and inject 40.0 μl, using the described chromatographic conditions.

The detector response to the standard mixture and one commercial sample is presented in Fig. 1. Since preliminary investigations indicated that concentration (4–8 μg) was directly related to the peak area,

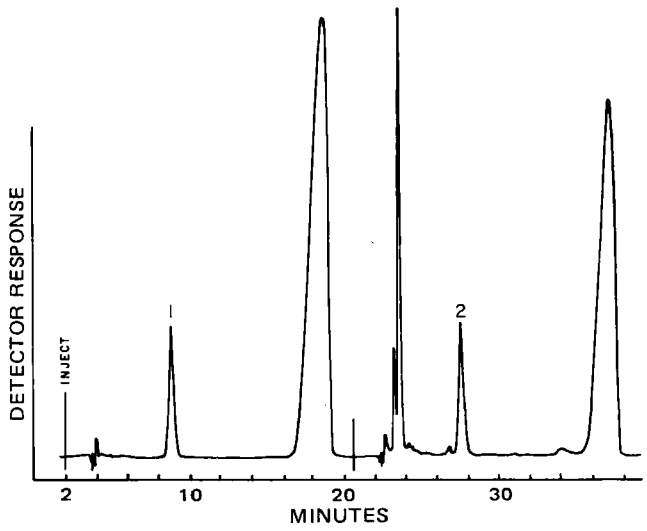

Figure 1—*HPLC analysis of morphine in paregoric USP (for chromatographic conditions, see text). Key: 1, standard mixture; and 2, paregoric sample.*

[1] Waters ALC 202 equipped with U6K Universal liquid chromatograph injector and UV detector (254 nm), Waters Associates, Milford, Mass.
[2] μBondapak/C_{18}, Waters Associates, Milford, Mass.
[3] Omniscribe model 5213-12, Houston Instruments, Austin, Tex.
[4] Merck & Co.

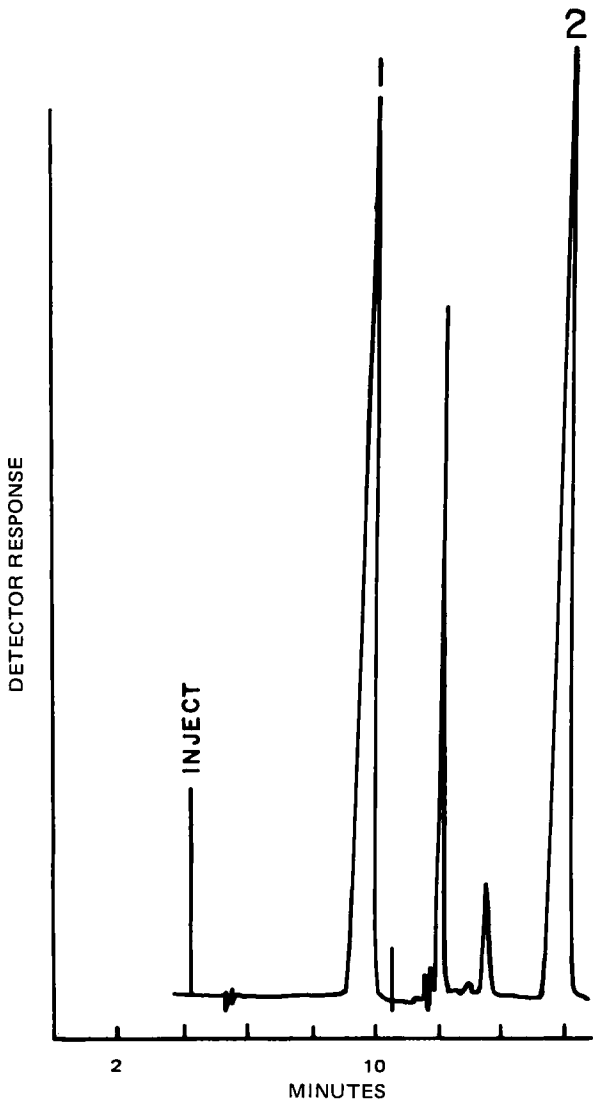

Figure 2—*HPLC analysis of benzoic acid in paregoric USP (for chromatographic conditions, see text). Key: 1, standard solution; and 2, commercial paregoric sample.*

the results on commercial samples were calculated by comparing the peak areas of morphine using:

$$\frac{A_a}{A_s} \times 100 = \text{percent of claim} \qquad \text{(Eq. 1)}$$

where A_a is the peak area of the assay, and A_s is the peak area of the standard. The time of retention and the peak for morphine from the morphine standard solution were identical to those from the standard mixture.

Table I—Assay Results on Two Commercial Samples of Paregoric

Sample	Morphine[a], %	Benzoic Acid[a], %
Standard mixture	100.4	99.7
I	104.3[b]	101.4
II[c]	105.5[d]	101.8
Average deviation	±2.6	±1.9
SD	3.22	2.35

[a] Average of three. [b] The manufacturer reported assay results of 105.3% using the USP (2) method. [c] From a different manufacturer. [d] The manufacturer reported assay results of 107.0% using the modified USP method.

Assay Procedure for Benzoic Acid—Transfer 6.6 ml of paregoric to a 150-ml beaker and add 20 ml of water and 3.1 ml of ~0.1 *N* NaOH. Boil on a hot plate until the volume is approximately 8 ml, cool, dilute to volume (25 ml) with water, and inject 20.0 μl.

The detector response to a commercial sample is presented in Fig. 2. Since preliminary investigations indicated that concentration (12–25 μg) of benzoic acid was directly related to peak area, the results were calculated by comparing the peak area of the unknown sample with that of the standard (Table I).

DISCUSSION

The assay results (Table I) on morphine and benzoic acid indicate that HPLC can be used for the quantitative analysis of these ingredients in commercial samples of paregoric. At least in a twofold range, the areas of peaks were related to the concentrations of both morphine and benzoic acid. This result was considered satisfactory for analysis. In the case of morphine, the time required was about 20 min *versus* about 4–6 hr by the USP method (1). The ratio of methanol and the flow rate (1.8 ml/min) were adjusted to separate the small peak immediately on the left side of the morphine peak (Fig. 1). This peak must be separated from the morphine peak or the results may be high. This was a major problem, especially with Sample II.

As far as benzoic acid is concerned, the conditions (*e.g.*, lesser flow rate or higher percent of methanol) may be changed without difficulties in separation.

REFERENCES

(1) "The United States Pharmacopeia," 19th rev., Mack Publishing Co., Easton, Pa., 1975, p. 360.

(2) *Ibid.*, 17th rev., 1965, p. 441.

ACKNOWLEDGMENTS AND ADDRESSES

Received October 14, 1975, from the *College of Pharmacy, University of Houston, Houston, TX 77004*

Accepted for publication January 26, 1976.

Potential CNS Antitumor Agents—Phenothiazines I: Nitrogen Mustard Derivatives

TADASHI HIRATA * **and JOHN S. DRISCOLL** ˣ

Abstract □ Four phenothiazine derivatives containing the bis(β-chloroethyl)aminopropyl side chain were prepared and evaluated in the murine L-1210, P-388, and B-16 melanoma intraperitoneal tumor systems. Moderate P-388 activity was observed. An aminoethyl phenothiazine mustard was compared with the aminopropyl analogs and was superior in all test systems. None of the compounds tested against the murine ependymoblastoma brain tumor system was active.

Keyphrases □ Phenothiazines—derivatives containing bis(β-chloroethyl)aminopropyl side chain synthesized, CNS antitumor activity screened □ CNS antitumor activity—substituted phenothiazines synthesized, screened □ Antitumor activity, CNS—substituted phenothiazines synthesized, screened □ Structure–activity relationships—substituted phenothiazines synthesized, screened for CNS antitumor activity

Phenothiazine derivatives are well known for their central nervous system (CNS) activity (1–3). Several studies also showed that some common psychotropic agents within this family (*e.g.*, chlorpromazine) produce antitumor effects (4–7). Phenothiazines containing reactive alkylating groups also have been evaluated. Haloacyl derivatives (8, 9) were active in the sarcoma 180 system. Jackson and Shirley (10) prepared several phenothiazine derivatives containing the nitrogen mustard function. These compounds were reported to show no significant antitumor activity, but they were 10-aminoethyl derivatives rather than the more common 10-aminopropyl analogs.

Three methylene groups between N-10 and the amino group in the side chain are known to be optimum for phenothiazine antipsychotic potency (1). Four aminopropyl nitrogen mustard analogs (X*a*–X*d*) were prepared and evaluated to determine whether the extra methylene group might enhance the antitumor activity and provide a potentially useful CNS antitumor agent. These compounds were compared with the aminoethyl analog (I) that had been reported and evaluated earlier (11, 12). This compound was among a group of similar materials that had activity in the Yoshida ascites system (11, 12).

Compound I was also prepared by Shirley *et al.* (13) for testing at the National Cancer Institute, but the results of the initial limited testing were not published. Therefore, I was used as a model 10-aminoethyl analog for comparison testing with the synthesized 10-aminopropyl compounds.

CHEMISTRY

The necessary intermediate compound, 2-ethylphenothiazine (VI), was prepared through the sequence (II–VI) described previously (12).

The bis(β-chloroethyl)aminopropyl derivatives of phenothiazine were synthesized as described in Scheme I (Table I). Intermediates VIII*a*–VIII*d* and IX*a*–IX*d* were oils which could be used in the next step without further purification.

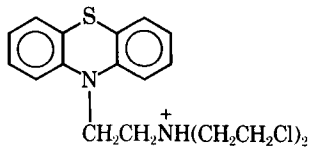

I

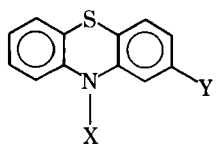

II: X = Y = H
III: X = CH_3CO, Y = H
IV: X = Y = CH_3CO
V: X = H, Y = CH_3CO
VI: X = H, Y = C_2H_5

RESULTS AND DISCUSSION

Standard National Cancer Institute protocols (15) were followed. The results of *in vivo* studies in the intraperitoneal lymphoid leukemia L-1210, lymphocytic leukemia P-388, and B-16 melanocarcinoma models as well as in the intracerebral ependymoblastoma system are shown in Table II. Also included are *in vitro* KB cell culture assays. Compounds were considered active *in vivo* if they gave activity (T/C) values (15) equal to or greater than the following: L-1210 leukemia, 125%; P-388 leukemia, 125%; B-16 melanoma, 140%; and ependymoblastoma, 140%. Compounds were considered cytotoxic in the KB cell culture system if they possessed an LD_{50} of 4 μg/ml or less.

All compounds reported here, including intermediates, were evaluated in the L-1210 leukemia system. No intermediate was active. Only I and X*a* were marginally active against the L-1210 tumor. Significant activity was observed in the more sensitive P-388 system with I, X*a*, and X*d*. Marginal activity was observed with the trifluoromethyl (X*b*) and chloro (X*c*) analogs.

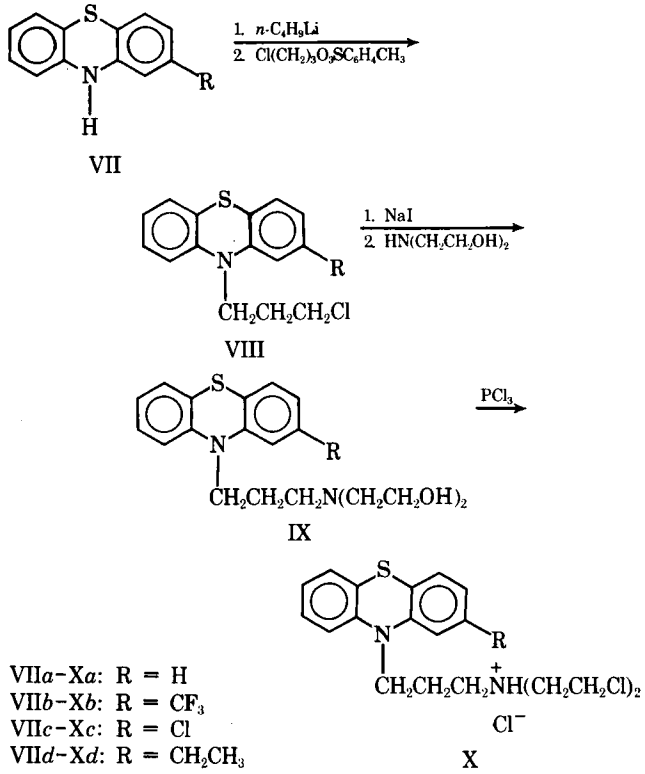

VII

VIII

IX

X

VII*a*–X*a*: R = H
VII*b*–X*b*: R = CF_3
VII*c*–X*c*: R = Cl
VII*d*–X*d*: R = CH_2CH_3

Scheme I

Table I—Physical and Chemical Data

Compound	Melting Point	Yield, %	Formula	Analysis, % Calc.	Found
X*a*	156–159°	42	$C_{19}H_{23}Cl_3N_2S \cdot \frac{1}{2}H_2O$	C 53.48 H 5.43 Cl 24.92 N 6.56 S 7.50	53.75 5.31 24.47 6.37 7.44
X*b*	181°	53	$C_{20}H_{22}Cl_3F_3N_2S$	C 49.44 H 4.56 Cl 21.89 N 5.77 S 6.60	49.01 4.72 21.77 5.73 6.59
X*c*	136–139°[a]	54	$C_{19}H_{22}Cl_4N_2S \cdot \frac{1}{2}H_2O$	C 49.47 H 5.03 Cl 30.75 N 6.07 S 6.95	49.85 4.90 30.93 5.78 6.94
X*d*	144°	70	$C_{21}H_{27}Cl_3N_2S$	C 56.56 H 6.10 Cl 23.86 N 6.28 S 7.19	56.25 6.09 23.56 5.95 7.50

[a] Lit. (14) mp 145°.

Earlier studies (5) indicated that chlorpromazine had a marked affinity for melanin-containing tissues and affected tumor growth in the B-16 melanoma system. It was suspected that this property might be a characteristic of the phenothiazine structure. However, of the four compounds tested, only I was active in that system.

The initial objective of this investigation was the preparation of potential CNS antitumor agents. Since intracerebral antitumor activity is normally significantly less than intraperitoneal activity in any given tumor system (16), the compounds in this study were considered to have insufficient L-1210, P-388, or B-16 activity intraperitoneally to be tested in the corresponding intracerebral tumor system. Three compounds were tested in the intracerebral ependymoblastoma murine brain tumor model (16, 17), but no activity was observed. This finding is in contrast to the high activity observed when hydantoins rather than phenothiazine were used as the carrier for the bis(β-chloroethyl)amino group (18). The poor activity might be related to the very high ($\log P > 7$) partition coefficients (19) calculated for the free base of the phenothiazine alkylating agents.

Compounds X*a* and X*c* were reported to affect cell respiration and to increase murine survival time when injected with Ehrlich sarcoma cells (20). Borderline KB activity was observed only with the 2-ethyl derivative, X*d*, in our *in vitro* test. *In vitro* activity did not correlate with activity in any *in vivo* test system.

The antitumor results show the aminoethyl compound (I) to be clearly superior to the aminopropyl derivatives (X*a*–X*d*). This relationship between the number of methylene groups and antitumor activity is more similar to that observed for phenothiazine antihistaminergic activity (21) than that for antipsychotic activity. The antihistaminergic parallel is also consistent with the general trend among X*a*–X*d*, which indicates a reduction of antitumor activity with electronegative substitution in the 2-position of the phenothiazine ring.

Based on available data, further synthetic studies with phenothiazines as carriers for nitrogen mustard groups are not planned.

EXPERIMENTAL[1]

10-Bis(2-chloroethyl)aminoethylphenothiazine (I)—This compound was prepared and supplied by Shirley *et al.* (13).

10-Acetylphenothiazine (III)—Phenothiazine (50.0 g, 0.25 mole) was refluxed in a mixture of acetic anhydride (50 ml) and xylene (90 ml) for 6 hr. Upon cooling, the resulting crystals were filtered and washed with petroleum ether to give 55 g (92%) of a light-gray-green powder, mp 197° [lit. (22) mp 197–198°].

2,10-Diacetylphenothiazine (IV)—This compound was prepared on a 40-g scale in 74% yield by the method of Takada and Nishimura (23). The crude solid was used without purification for the next step in the sequence.

2-Acetylphenothiazine (V)—Crude IV was hydolyzed with 10% HCl in acetic acid at reflux for 15 min. The resulting product was recrystallized from benzene to give yellow crystals, mp 188–190° [lit. (23) mp 189–195°].

2-Ethylphenothiazine (VI)—This compound was prepared on a 6-g scale. Recrystallization from hexane and benzene gave crystals, mp 132–133° [lit. (23) mp 135°].

2-(Trifluoromethyl)-10-[3-[bis(2-hydroxyethyl)amino]propyl]phenothiazine (IX*b*) (General Procedure for IX*a*–IX*d*)—To a solution of 5.21 g (19.5 mmoles) of 2-trifluoromethylphenothiazine in 120 ml of dry ether was added 15 ml of 1.6 *M* butyllithium (24 mmoles) in hexane under dry, deoxygenated, nitrogen gas (passed through alkaline pyrogallol solution, calcium chloride, and potassium hydroxide tubes in that order). The solution was stirred under reflux for 30 min and cooled in an ice bath. A solution of 5.25 g (21 mmoles) of γ-chloropropyl *p*-toluenesulfonate in 30 ml of dry ether was added. The mixture was stirred (ice bath) for 1 hr and then at room temperature for 18 hr. A brown precipitate was formed.

Benzene and water were added to the reaction mixture; the benzene layer was then separated, washed with saturated sodium chloride, and dried over anhydrous sodium sulfate. Evaporation of benzene *in vacuo* gave a dark oil, which was mixed with 3.05 g (20 mmoles) of sodium iodide and 50 ml (520 mmoles) of diethanolamine. The stirred mixture was heated at 150–165° for 18 hr. After cooling, 100 ml of water was added to the reaction mixture and the resulting emulsion was extracted with ether. The ether extracts were washed with water and extracted with cold 5 *N* HCl. 2-(Trifluoromethyl)phenothiazine (850 mg) was recovered from the ether layer. Dark oil drops were present in the aqueous layer. The aqueous layer was made alkaline with concentrated potassium hydroxide and extracted with ether.

The ether solution was dried (sodium sulfate) and evaporated to give 4.0 g of an oil, which was then chromatographed on silica gel (60–200 mesh, 100 g). Unreacted 2-(trifluoromethyl)phenothiazine was first eluted with benzene, and then a homogeneous oily product (3.5 g, 44%) was eluted with benzene–acetone (1:1); NMR ($CDCl_3$): δ 1.90 (2H, t, $CH_2CH_2CH_2$), 2.53 (6H, distorted triplet, CH_2 adjacent to ammonium nitrogen), 2.71 (2H, s, OH), 3.50 (4H, t, CH_2OH), 3.95 (2H, t, CH_2 adjacent to N-10), and 6.8–~ 7.2 (7H, m, aromatic).

All derivatives in this series were oils. The following yields were obtained: IX*a*, 40%; IX*b*, 44%; IX*c*, 55%; and IX*d*, 52%. Compounds obtained in this manner were used without further purification to obtain the final products.

General Procedure for 2-Substituted 10-[3-[Bis(2-chlo-

[1] Melting points were recorded on a Thomas-Hoover melting-point apparatus and are uncorrected. Elemental analyses were performed by the National Institute of Arthritis, Metabolism, and Digestive Diseases, National Institutes of Health, Bethesda, Md. Phenothiazine and its 2-chloro and 2-trifluoromethyl analogs were obtained commercially. NMR spectra were obtained on a Varian HA-100D spectrometer, with tetramethylsilane as an internal standard.

Table II—Biological Activity[a]

Compound	Antitumor Activity								KB Cell Culture Activity, μg/ml[e]
	L-1210 Lymphoid Leukemia[b]		P-388 Lymphocytic Leukemia[b]		B-16 Melanocarcinoma[c]		Ependymoblastoma[d]		
	OD[f]	T/C[g]	OD	T/C	OD	T/C	OD	T/C	
I	300[h]	141	35	210	12.5	147	30	126	100
Xa	25	125	12.5	169	12.5	128	25	110	100
Xb	25	113	12.5	128					59
Xc	50	122	6.25	125	6.25	138			19
Xd	12.5	111	12.5	163	12.5	115	25	108	5

[a] Protocols and test systems were described in Ref. 15. [b] Day 1, 5, and 9 treatment schedule, unless noted otherwise. [c] Day 1–9 treatment schedule of intraperitoneally implanted tumor. [d] Day 1–5 treatment schedule: intraperitoneal treatment of intracerebrally implanted tumor. [e] Concentration required to inhibit cell growth to 50% that of the control. Cells were derived from a human epidermoid carcinoma of the mouth. [f] Optimum dose (milligrams per kilogram per injection). [g] T/C = (treated survival ÷ control survival) × 100%. [h] Day 1 only treatment schedule.

roethyl)amino]propyl]phenothiazine Hydrochlorides (Xa–Xd)—A solution of 4 mmoles of phosphorus trichloride in 10 ml of dry benzene was added dropwise to a solution of 2 mmoles of 2-substituted 10-[3-[bis(2-hydroxyethyl)amino]propyl]phenothiazine in 20 ml of dry benzene. The solution was heated gently during the 30-min addition period. The reaction solution was then refluxed for 3.5–5 hr, cooled, and treated with 20 ml of water.

Sodium carbonate was added to the cold mixture with vigorous shaking until the aqueous layer turned to a thick paste. The mixture was extracted repeatedly with benzene. The benzene extracts were dried (sodium carbonate) and evaporated to give an oil, which was dissolved in 30 ml of dry ether and treated with hydrogen chloride gas. The resulting crude hydrochloride was recrystallized from chloroform–ether; NMR ($CDCl_3$) for Xc: δ 2.35 (2H, broad, $CH_2CH_2CH_2$), 3.33 (6H, t, CH_2 adjacent to ammonium nitrogen), 3.85 (4H, t, CH_2Cl), 4.06 (2H, t, CH_2 adjacent to N-10), and 6.8 –~ 7.2 (7H, m, aromatic).

REFERENCES

(1) "Psychopharmacological Agents," vol. III, M. Gordon, Ed., Academic, New York, N.Y., 1974.

(2) "Psychopharmacological Agents," vol. II, M. Gordon, Ed., Academic, New York, N.Y., 1967.

(3) "Progress in Drug Research," vol. 5, E. Jucker, Ed., Birkhauser Verlag, Basel, Switzerland, 1965.

(4) F. Kanazawa, A. Hoshi, and K. Kuretani, *Gann*, **61**, 529(1970).

(5) M. H. Van Woert and S. H. Palmer, *Cancer Res.*, **29**, 1952(1969).

(6) R. Hilf, C. Bell, H. Goldenberg, and I. Michel, *ibid.*, **31**, 1111(1971).

(7) A. Polliack and I. S. Levij, *ibid.*, **32**, 1912(1972).

(8) F. Kanazawa, A. Hoshi, and K. Kuretani, *Gann*, **63**, 225(1972).

(9) *Ibid.*, **63**, 375(1972).

(10) T. G. Jackson and D. A. Shirley, *J. Med. Chem.*, **11**, 622(1968).

(11) I. Aiko, Japanese pat. 2377 (Mar. 17, 1960).

(12) M. Ishidate, Y. Sakurai, and I. Aiko, *Chem. Pharm. Bull.*, **8**, 99(1960).

(13) D. A. Shirley, K. Sen, and J. C. Gilmer, *J. Org. Chem.*, **26**, 3587(1961).

(14) R. J. Horclois, British pat. 762,711 (Dec. 5, 1956); Rhone-Poulenc, French pat. 1,167,514 (Nov. 26, 1958).

(15) R. I. Geran, N. H. Greenberg, M. M. Macdonald, A. M. Schumacher, and B. J. Abbott, *Cancer Chemother. Rep., Part 3*, **3** (2), 1(1972).

(16) P. C. Merker, I. Wodinsky, and R. I. Geran, *Cancer Chemother. Rep.*, **59**, 729(1975).

(17) R. I. Geran, G. F. Congleton, L. E. Dudeck, B. J. Abbott, and J. L. Gargus, *Cancer Chemother. Rep., Part 2*, **4**, 53(1974).

(18) G. W. Peng, V. E. Marquez, and J. S. Driscoll, *J. Med. Chem.*, **18**, 846(1975).

(19) A. Leo, C. Hansch, and D. Elkins, *Chem. Rev.*, **71**, 525(1971).

(20) G. Carraz, A. Boucherle, H. Beriel, and L. H. Duc, *Therapie*, **17**, 8(1962).

(21) "Drugs Affecting the Central Nervous System," vol. 2, A. Burger, Ed., Dekker, New York, N.Y., 1968, p. 382.

(22) H. Gilman and R. D. Nelson, *J. Am. Chem. Soc.*, **75**, 5422(1953).

(23) A. Takada and H. Nishimura, *Chem. Pharm. Bull.*, **10**, 1(1962).

ACKNOWLEDGMENTS AND ADDRESSES

Received November 24, 1975, from the *Drug Design and Chemistry Section, Laboratory of Medicinal Chemistry and Biology, Drug Research and Development Program, Division of Cancer Treatment, National Cancer Institute, National Institutes of Health, Bethesda, MD 20014*

Accepted for publication January 16, 1976.

The authors thank Mr. Leo Dudeck and Mr. George Congelton, Hazleton Laboratories, for the *in vivo* antitumor results, and Dr. David A. Shirley, University of Tennessee, for permission to use the biological data obtained on the sample of Compound I which he supplied to the National Cancer Institute.

* National Institutes of Health Visiting Fellow 1971–1973. Present address: Kyowa Hakko Kogyo Co. Ltd., Tokyo, Japan.

x To whom inquiries should be directed.

Enhancement of Dissolution Rates of Poorly Water-Soluble Drugs by Crystallization in Aqueous Surfactant Solutions I: Sulfathiazole, Prednisone, and Chloramphenicol

WIN L. CHIOU ˣ, SHAW-JEN CHEN, and NARAYAN ATHANIKAR

Abstract □ Effects of crystallization of poorly water-soluble drugs in aqueous surfactant solutions on *in vitro* dissolution rates were investigated. Marked enhancement was observed for chloramphenicol, sulfathiazole, and prednisone. Differential thermal analysis studies indicated the presence of small amounts of surfactant in surfactant-treated crystals. Possible mechanisms of dissolution enhancement are discussed.

Keyphrases □ Dissolution rates—chloramphenicol, sulfathiazole, prednisone, effect of crystallization in aqueous surfactant solutions □ Chloramphenicol—dissolution rate, effect of crystallization in aqueous surfactant solutions □ Sulfathiazole—dissolution rate, effect of crystallization in aqueous surfactant solutions □ Prednisone—dissolution rate, effect of crystallization in aqueous surfactant solutions □ Surfactants, aqueous—crystallization of chloramphenicol, sulfathiazole, and prednisone in polysorbate 80, effect on dissolution rates

Many methods have been used to enhance dissolution rates of poorly water-soluble or insoluble drugs. The methods include, for example, salt and polymorphic formation (1); micronization, microcrystallization, solid dispersion, and coprecipitation using inert, water-soluble compounds as carriers (2–6); and grinding with (7), and adsorption onto (8), an inert water-insoluble compound.

The purpose of this article is to report the preliminary findings of another unique method to enhance the dissolution rate of poorly water-soluble or insoluble drugs. The basic method simply involves the recrystallization of the drug in an aqueous surfactant solution. Three drugs will be used for illustration.

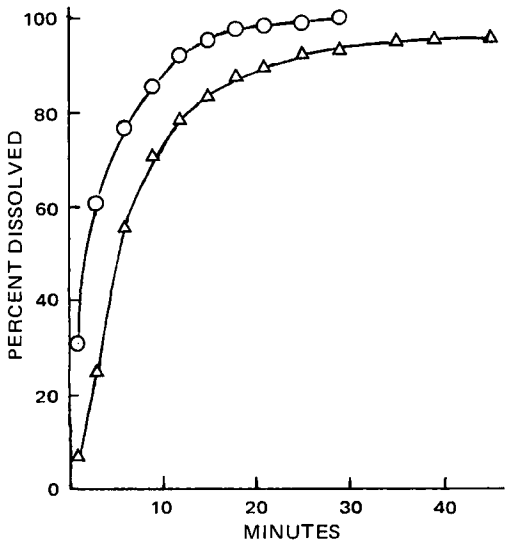

Figure 1—*Average percent of sulfathiazole dissolved as a function of time. Key: △, control; and ○, surfactant treated.*

Table I—Average Time (Minutes) for 50% of Drug to Dissolve during the Dissolution Study

Drug	Crystallization in Absence of Surfactant	Crystallization in Presence of Surfactant
Prednisone	9	2
Sulfathiazole	6	2
Chloramphenicol	2	<1

EXPERIMENTAL

Materials—Chloramphenicol[1], sulfathiazole[2], and prednisone[3] were obtained from commercial sources and used without further purification.

Method of Crystallization—A certain amount of drug powder was initially dissolved in a small volume of a water-miscible organic solvent at ambient temperature. The drug precipitated after this solution was diluted with an equal volume of water or 2.5% aqueous solution of polysorbate 80[4] kept at about 0° in a water bath. The precipitated crystals were immediately collected by filtration and dried in a desiccator. They were pulverized with a mortar and pestle, and the 80–100-mesh portion after sieving was collected for the dissolution study.

The volumes of the water-miscible solvents or solvent system used to dissolve the drugs were 14 ml of ethanol for 2 g of chloramphenicol, 9 ml of dimethylformamide[5] for 8 g of sulfathiazole, and a mixture of 30 ml of ethanol and 50 ml of methanol for 1 g of prednisone.

Dissolution Studies—The dissolution studies were conducted in water at 37° by the beaker method (9). A three-blade, 4.4-cm (1.75-in.)

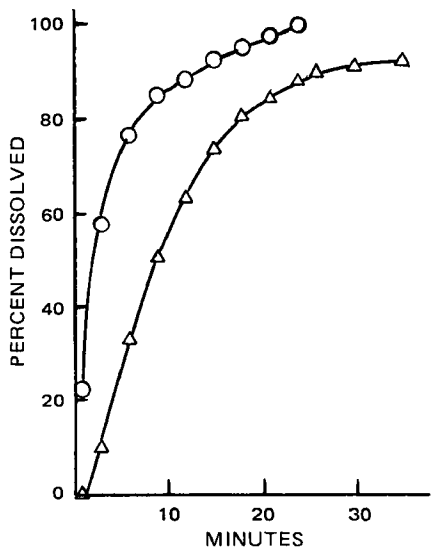

Figure 2—*Average percent of prednisone dissolved as a function of time. Key: △ control; and ○, surfactant treated.*

[1] Parke, Davis & Co., Detroit, Mich.
[2] Merck Sharp & Dohme Research Laboratories, West Point, Pa.
[3] Schering Corp., Bloomfield, N.J.
[4] Tween 80, Atlas Powder Co., Chicago, Ill.
[5] J. T. Baker Chemical Co., Phillipsburg, N.J.

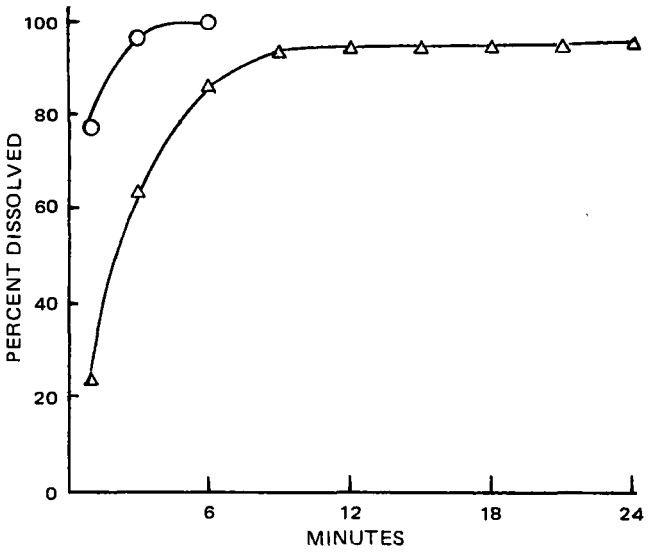

Figure 3—*Average percent of chloramphenicol dissolved as a function of time. Key: Δ, control; and O, surfactant treated.*

stirrer[6] with a stirring rate of 50 rpm was employed. The drug powder was spread onto the surface of the dissolution medium, and the amount of drug dissolved was analyzed directly after filtration by a spectrophotometric method. The wavelengths used were 278, 320, and 238 nm for chloramphenicol, sulfathiazole, and prednisone, respectively. The amounts of drug used were 25, 50, and 5 mg, respectively.

For sulfathiazole, 1 liter of the dissolution medium was used; for the other two drugs, only 500 ml was used. Four dissolution studies were performed on each type of crystal preparation. The Student *t* test was employed for the statistical analysis.

Differential Thermal Analysis—Powders of each drug, prepared in the absence or presence of the surfactant, were studied with a differential thermal analyzer[7] (3–5). A heating rate of 20°/min was used.

RESULTS AND DISCUSSION

The results of the dissolution studies, expressed in terms of percent dissolved as a function of time for the three drugs, are shown in Figs. 1–3. Due to the high reproducibility of the dissolution study, the data on standard errors are not shown in the figures. During the first few minutes of study, the dissolution rates of crystals prepared in the presence of the surfactant were all significantly higher (*e.g.*, $p < 0.005$ for prednisone up to 9 min, $p < 0.01$ for sulfathiazole up to 6 min, and $p < 0.001$ for chloramphenicol up to 6 min). Times estimated for the 50% dissolution for the three drugs are summarized in Table I.

The mechanisms of dissolution rate enhancement by this unique crystallization method are not discussed fully in this preliminary report. The results of the differential thermal analysis studies (Figs. 4 and 5) indicate that the presence of the surfactant during the crystallization process did not result in a different polymorphic form. The depression of final melting points by approximately 0.5–1.0° for all three surfactant-treated drugs strongly suggests the presence of a small amount of surfactant in these crystals.

Some surfactant molecules, due to their surface activity, might be adsorbed onto the hydrophobic surface of the crystals. This adsorption would undoubtedly increase the wettability of the powder or crystals and thereby increase their dissolution rate (2). The presence of the surfactant during the crystallization process might also cause a defect in the crystal structure and the crystal would become thermodynamically unstable and, hence, dissolve faster. The possibility of the formation of a solid solution of the water-soluble surfactant in the drug crystal might also enhance the dissolution (2).

Although it has been shown that surfactants can increase the solubility of poorly soluble compounds (10), the amount of the surfactant present in the crystals studied in the present investigation was probably too negligible to affect the solubility of the drug in bulk solution. However, the surfactant, present inside and/or outside of the crystals, might enhance the solubility of a drug in the diffusion layer during the dissolution process.

The effects of concentration and types of surfactants on the extent of dissolution rate enhancement, together with the nature of the surfactant present in the crystal, are currently being investigated in this laboratory.

Although only three drugs were studied, it is believed that such an approach can be applied to many poorly water-soluble or insoluble drugs.

[6] Nalgene stirrer, Fisher Scientific Co., Skokie, Ill.
[7] Model 990, E. I. du Pont de Nemours & Co., Wilmington, Del.

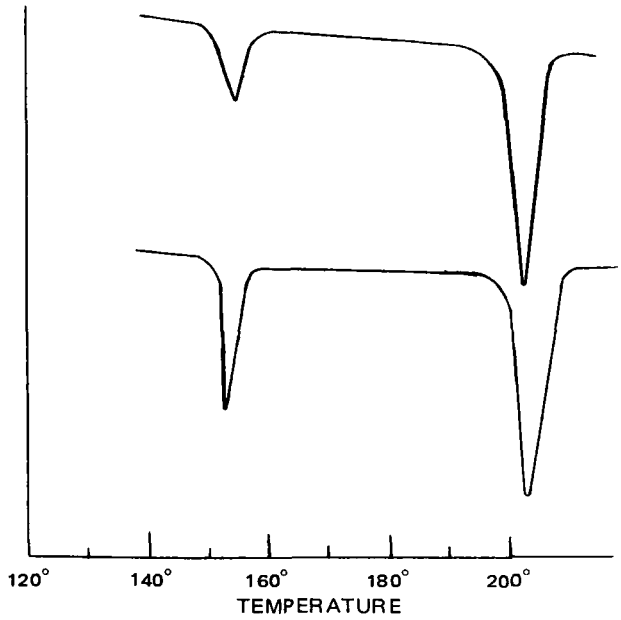

Figure 4—*Differential thermal analysis thermograms of sulfathiazole. Key: top, surfactant treated; and bottom, control.*

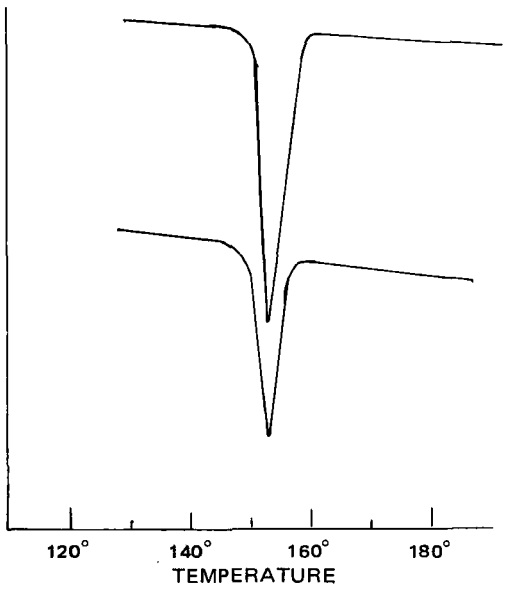

Figure 5—*Differential thermal analysis thermograms of chloramphenicol. Key: top, control; and bottom, surfactant treated.*

REFERENCES

(1) J. Haleblian and W. McCrone, *J. Pharm. Sci.*, **58**, 911(1969).

(2) W. L. Chiou and S. Riegelman, *ibid.*, **60**, 1281(1971).

(3) W. L. Chiou, *ibid.*, **60**, 1406(1971).

(4) W. L. Chiou and S. Niazi, *ibid.*, **60**, 1333(1971).
(5) *Ibid.*, **62**, 498(1973).
(6) E. I. Stupak, H. A. Rosenberg, and T. R. Bates, *J. Pharmacokinet. Biopharm.*, **2**, 511(1974).
(7) K. Yamamoto, M. Nakano, T. Arita, and Y. Nakai, *ibid.*, **2**, 487(1974).
(8) D. C. Monkhouse and J. L. Lach, *J. Pharm. Sci.*, **61**, 1430(1972).
(9) W. L. Chiou and I. Onyemelukae, *J. Clin. Pharmacol.*, **14**, 497(1974).
(10) A. N. Martin, J. Swarbrick, and A. Cammarata, "Physical Pharmacy," 2nd ed., Lea & Febiger, Philadelphia, Pa., 1969, p. 463.

ACKNOWLEDGMENTS AND ADDRESSES

Received July 7, 1975, from the *Department of Pharmacy and the Clinical Pharmacokinetics Laboratory, College of Pharmacy, University of Illinois at the Medical Center, Chicago, IL 60612*

Accepted for publication February 5, 1976.

[x] To whom inquiries should be directed.

Molecular Orbital Studies of Antischistosomal Agents

HAVEN S. ALDRICH [*x] and DONALD C. CLAGETT [‡§]

Abstract □ Molecular orbital calculations were used to investigate the antischistosomal agent, niridazole, and an inactive derivative, 1-(5-nitro-2-thiazolyl)-2-ethylurea. The CNDO/2 calculations revealed that the inactive derivative had a preferred conformation stabilized by an intramolecular hydrogen bond. The molecular profile, the relative three-dimensional arrangement of constituent atoms, of the inactive derivative was different than that of the niridazole compound. The likelihood of similar intramolecular interactions rendering niridazole derivatives inactive is discussed. The results of the calculations suggest select structural modifications that might increase the efficacy of niridazole derivatives.

Keyphrases □ Niridazole and derivative—preferred molecular conformations, effect on biological activity □ Molecular orbital calculations—preferred conformations of niridazole and derivative □ Structure–activity relationships—niridazole and derivative, preferred molecular conformations, effect on biological activity □ Antischistosomal agents—niridazole, preferred molecular conformation, effect on biological activity

Recent studies concerning the structure–activity relationships of antischistosomal agents revealed certain essential molecular features necessary for activity insofar as nitroheterocyclic compounds of the niridazole (I) type are concerned. One study (1) showed that the activity of niridazole was dependent upon the presence of the nitro and sulfuryl moieties and that the presence of a nonpolar side chain was necessary. This work was definitive and covered many structural variants.

However, one feature that remains unaccounted for is the inactivity of niridazole derivatives in which the imidazolidinone ring is ruptured at the N-1′–C-5′-position. Thus, 1-(5-nitro-2-thiazolyl)-2-ethylurea (II) possesses no antischistosomal activity. The potential importance of a biologically preferred conformation was noted previously (1) and, because of the increased lability of ureido side chain over the imidazolidinone ring, the conformational differences were studied using the molecular orbital approach.

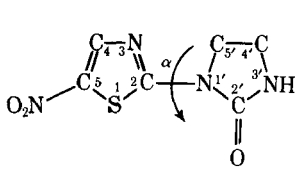

I

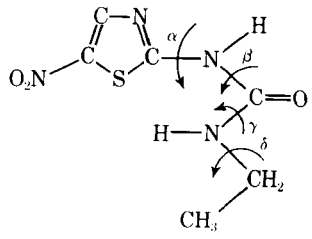

IIa

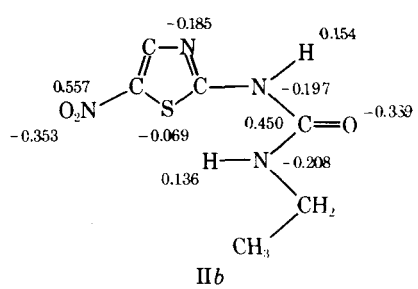

IIb

EXPERIMENTAL

A series of semiempirical molecular orbital calculations was performed to determine the preferred conformations of the active niridazole compound and its inactive derivative. The Complete Neglect of Differential Overlap (CNDO/2) molecular orbital technique was used for this purpose. The CNDO/2 method assumes that two center overlap integrals are zero, greatly simplifying the Hamiltonian matrix. The success of the method, providing that proper parameterization is used, has been well documented (2–4).

The CNDO/2 method has been used to compute stabilization energies for hydrogen-bonded systems as well as barriers to internal rotation (5, 6). Because of certain limitations concerning the CNDO/2 method, an *ab initio* approach may be preferable. Hydrogen bond energies are usually overestimated while internal barriers to rotation are underestimated. However, with a clear understanding of the method's limitations, one should, in principle, be able to compute potential surfaces in which intramolecular hydrogen bonding plays

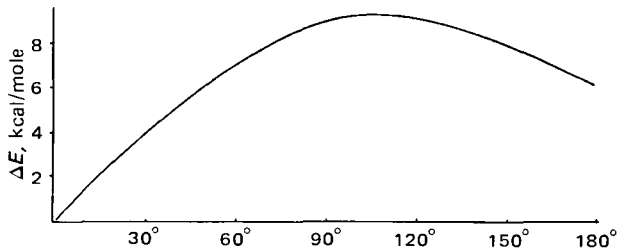

Figure 1—*Potential energy contour for the α-rotomer in niridazole. Energies are plotted relative to the lowest energy conformation, α = 0°.*

(4) W. L. Chiou and S. Niazi, *ibid.*, **60**, 1333(1971).
(5) *Ibid.*, **62**, 498(1973).
(6) E. I. Stupak, H. A. Rosenberg, and T. R. Bates, *J. Pharmacokinet. Biopharm.*, **2**, 511(1974).
(7) K. Yamamoto, M. Nakano, T. Arita, and Y. Nakai, *ibid.*, **2**, 487(1974).
(8) D. C. Monkhouse and J. L. Lach, *J. Pharm. Sci.*, **61**, 1430(1972).
(9) W. L. Chiou and I. Onyemelukae, *J. Clin. Pharmacol.*, **14**, 497(1974).
(10) A. N. Martin, J. Swarbrick, and A. Cammarata, "Physical Pharmacy," 2nd ed., Lea & Febiger, Philadelphia, Pa., 1969, p. 463.

ACKNOWLEDGMENTS AND ADDRESSES

Received July 7, 1975, from the *Department of Pharmacy and the Clinical Pharmacokinetics Laboratory, College of Pharmacy, University of Illinois at the Medical Center, Chicago, IL 60612*

Accepted for publication February 5, 1976.

[x] To whom inquiries should be directed.

Molecular Orbital Studies of Antischistosomal Agents

HAVEN S. ALDRICH [*x] and DONALD C. CLAGETT [‡§]

Abstract □ Molecular orbital calculations were used to investigate the antischistosomal agent, niridazole, and an inactive derivative, 1-(5-nitro-2-thiazolyl)-2-ethylurea. The CNDO/2 calculations revealed that the inactive derivative had a preferred conformation stabilized by an intramolecular hydrogen bond. The molecular profile, the relative three-dimensional arrangement of constituent atoms, of the inactive derivative was different than that of the niridazole compound. The likelihood of similar intramolecular interactions rendering niridazole derivatives inactive is discussed. The results of the calculations suggest select structural modifications that might increase the efficacy of niridazole derivatives.

Keyphrases □ Niridazole and derivative—preferred molecular conformations, effect on biological activity □ Molecular orbital calculations—preferred conformations of niridazole and derivative □ Structure–activity relationships—niridazole and derivative, preferred molecular conformations, effect on biological activity □ Antischistosomal agents—niridazole, preferred molecular conformation, effect on biological activity

Recent studies concerning the structure–activity relationships of antischistosomal agents revealed certain essential molecular features necessary for activity insofar as nitroheterocyclic compounds of the niridazole (I) type are concerned. One study (1) showed that the activity of niridazole was dependent upon the presence of the nitro and sulfuryl moieties and that the presence of a nonpolar side chain was necessary. This work was definitive and covered many structural variants.

However, one feature that remains unaccounted for is the inactivity of niridazole derivatives in which the imidazolidinone ring is ruptured at the N-1′–C-5′-position. Thus, 1-(5-nitro-2-thiazolyl)-2-ethylurea (II) possesses no antischistosomal activity. The potential importance of a biologically preferred conformation was noted previously (1) and, because of the increased lability of ureido side chain over the imidazolidinone ring, the conformational differences were studied using the molecular orbital approach.

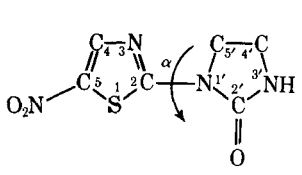

I

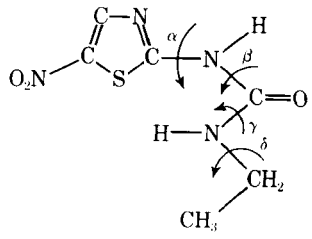

IIa

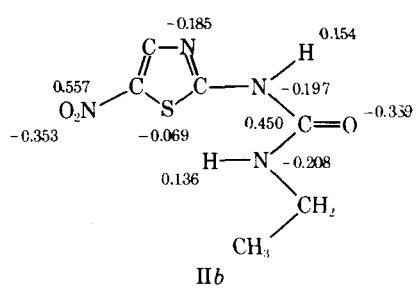

IIb

EXPERIMENTAL

A series of semiempirical molecular orbital calculations was performed to determine the preferred conformations of the active niridazole compound and its inactive derivative. The Complete Neglect of Differential Overlap (CNDO/2) molecular orbital technique was used for this purpose. The CNDO/2 method assumes that two center overlap integrals are zero, greatly simplifying the Hamiltonian matrix. The success of the method, providing that proper parameterization is used, has been well documented (2–4).

The CNDO/2 method has been used to compute stabilization energies for hydrogen-bonded systems as well as barriers to internal rotation (5, 6). Because of certain limitations concerning the CNDO/2 method, an *ab initio* approach may be preferable. Hydrogen bond energies are usually overestimated while internal barriers to rotation are underestimated. However, with a clear understanding of the method's limitations, one should, in principle, be able to compute potential surfaces in which intramolecular hydrogen bonding plays

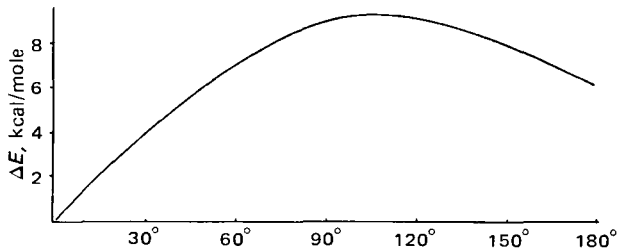

Figure 1—*Potential energy contour for the α-rotomer in niridazole. Energies are plotted relative to the lowest energy conformation, α = 0°.*

Table I—Interatomic Distances in Angstroms

	Niridazole	Niridazole Derivative
O_2N—O	7.27	5.82
O_2N—N	5.50	7.61
S—N	2.63	4.77
S—H	1.70	—

a dominant role. In this study, the pattern of net atom charges is considered concurrently with the preferred conformation because this approach is consistent with the remote recognition hypothesis postulated by Kier (7).

For the calculations, 30° increments were used for generating the potential surfaces for both niridazole and the inactive derivative. The niridazole compound has only one degree of freedom for internal rotation. The inactive derivative has been treated as a three-rotomer problem. The δ-rotomer has been held fixed at 180°. The terminal methyl group assumes a staggered conformation with respect to the C-4′-methylene hydrogens.

DISCUSSION

The potential surface for the niridazole compound is shown in Fig. 1. The preferred conformation of the imidazolidinone ring is *cis* (α = 0°). This conformation is somewhat unexpected but understandable. The dipole–dipole interaction of the carbonyl moiety with the sulfur of the thiazolyl ring is probably stabilizing or at least less destabilizing than the similar interaction with the N-3 atom of the thiazolyl ring.

Critical interatomic separations are shown in Table I for the preferred conformation. Figure 2 illustrates the potential surface for the inactive derivative. The preferred conformation (II*b*) must be stabilized by an intramolecular hydrogen bond between the amide proton and the sulfur. This conformation is, of course, impossible for most antischistosomal compounds of the niridazole family to assume.

The calculated barrier to rotation for niridazole is 8.90 kcal/mole. The barrier to rotation is substantial and implies that a large percentage of the compound should exist in the planar *cis*-conformation. The difference in energy between the preferred conformation of the inactive derivative and the closest secondary minima energetically is 12.6 kcal/mole. The corresponding conformation for the inactive derivative that is comparable to the preferred conformation of the niridazole compound is 7.00 kcal/mole higher in energy. There is a low probability that the open ring inactive derivative could assume the related conformation of the niridazole compound.

These results are consistent with previous findings for other open ring compounds. The calculations imply that the N-3′-methyl derivative should be more active than the derivative shown, since the favorable hydrogen bonding interaction with the thiazolyl ring would be replaced with a repulsive interaction. To date, activity for the N-3′-methyl derivative has not been reported.

SUMMARY

Semiempirical molecular orbital calculations have shown that there are significant conformational differences between the active antischistosomal agent niridazole and the inactive derivative, 1-(5-nitro-2-thiazolyl)-2-ethylurea. The derivative has a folded preferred conformation that causes the critical interatomic distances to differ greatly from those of niridazole. The preferred conformations of these two molecules have been obtained for vacuum free space; consequently, definitive correlations for the molecules in the biological milieu must be drawn carefully. However, the conformational differences are interesting and represent a possible basis for difference in efficacy.

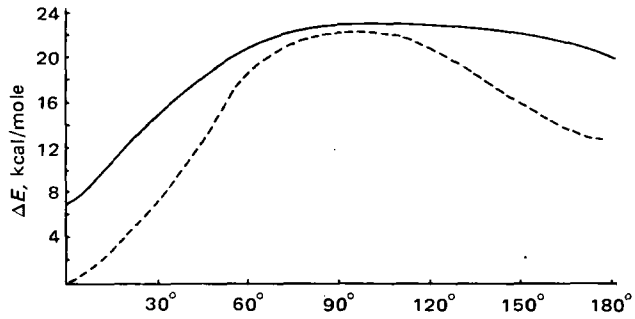

Figure 2—*Potential energy contour for the open ring derivative of niridazole. Dashed line corresponds to the α-rotomer with β = 0° and γ and δ = 180°.*

REFERENCES

(1) C. H. Robinson, E. Bueding, and J. Fisher, *Mol. Pharmacol.*, **6**, 604(1972).

(2) J. R. Hoyland, in "Molecular Orbital Studies in Chemical Pharmacology," L. B. Kier, Ed., Springer, New York, N.Y., 1970, p. 31.

(3) J. A. Pople and G. A. Segal, *J. Chem. Phys.*, **43**, S136(1965).

(4) J. A. Pople, D. L. Beveridge, and N. S. Ostlund, *Int. J. Quant. Chem.*, **IS**, 293(1967).

(5) P. A. Kollman and L. C. Allen, *Chem. Rev.*, **72**, 285(1972).

(6) J. A. Pople and D. L. Beveridge, "Approximate Molecular Orbital Theory," Academic, New York, N.Y., 1972.

(7) L. B. Kier, "Molecular Orbital Theory in Drug Research," Academic, New York, N.Y., 1971.

ACKNOWLEDGMENTS AND ADDRESSES

Received September 2, 1975, from the *Department of Chemistry, St. Mary's Dominican College, New Orleans, LA 70118, and the ‡Department of Chemistry, Northeastern University, Boston, MA 02115

Accepted for publication February 4, 1976.

§ Present address: Dewey and Almy Chemical Division, W. R. Grace & Co, Lexington, MA 02173

x To whom inquiries should be directed.

Quantitative Determinations of Phenol and Resorcinol in Pharmaceutical Dosage Forms by High-Pressure Liquid Chromatography

V. DAS GUPTA

Abstract □ The quantitative determinations of phenol in phenolated calamine lotion USP and of phenol and resorcinol in phenol–resorcinol–boric acid solution by high-pressure liquid chromatography are reported. The procedures are simple, rapid (no special preliminary treatment is required), and accurate. There is no interference from other ingredients of the lotion (bentonite magma, calamine, and zinc oxide) or solution (acetone and boric acid).

Keyphrases □ Phenol—high-pressure liquid chromatographic analysis, pharmaceutical dosage forms □ Resorcinol—high-pressure liquid chromatographic analysis, pharmaceutical dosage forms □ High-pressure liquid chromatography—analysis, phenol and resorcinol, pharmaceutical dosage forms □ Preservatives—phenol, high-pressure liquid chromatographic analysis, pharmaceutical dosage forms □ Keratolytic agents—resorcinol, high-pressure liquid chromatographic analysis, pharmaceutical dosage forms

No method is available for the direct quantitative determination of phenol and resorcinol in each other's presence. A reported method (1) required a combined assay on both compounds by a bromometric technique and then division of the data based on the molar ratio obtained from the NMR spectroscopic analysis.

The purpose of this investigation was to develop a simple, rapid, and accurate method for the direct quantitative determination of both phenol and resorcinol in a pharmaceutical dosage form. The developed high-pressure liquid chromatographic (HPLC) method was successfully applied to the quantitative determination of phenol in phenolated calamine lotion USP.

EXPERIMENTAL

Chemicals and Reagents—All chemicals and reagents were ACS, USP, or NF quality and were used without further purification.

Apparatus—A high-pressure liquid chromatograph[1] equipped with a UV detector (254 nm) and a recorder[2] was used.

Column—A column (30 cm × 4 mm i.d.) of a very nonpolar packing material[3] consisting of a monomolecular layer of octadecyltrichlorosilane permanently bonded by silicon–carbon bonds was used.

Chromatographic Conditions—The chromatographic solvent was 0.02 *M* NH_4HCO_3 in 10% by volume of methanol in water[4] (pH 7.67). The temperature was ambient, and the solvent flow rate was 3.0 ml/min (at an inlet pressure of approximately 2200 psig). The detector was set at a sensitivity of 0.16 absorbance unit full scale, and the chart speed was 30.5 cm (12 in.)/hr.

Preparation of Solutions—An aqueous standard solution of phenol (45.0 mg/100 ml), resorcinol (100.0 mg/100 ml) or a combination of phenol and resorcinol was prepared using the simple solution method. Phenol–resorcinol–boric acid solution was prepared according to a procedure reported earlier (1). The phenolated calamine lotion was prepared according to directions in the USP (2).

Assay Procedure for Phenol and Resorcinol in Phenol–Resorcinol–Boric Acid Solutions—Dilute 10.0 ml of the solution to 1000.0 ml with water, mix, and inject 10–20 μl.

[1] Waters ALC 202 equipped with U6K universal chromatograph injector.
[2] Omniscribe 5213-12 equipped with an integrator.
[3] Waters μBondapack-C18, Catalog No. 27324.
[4] Must be used within 3 days since pH changes on standing.

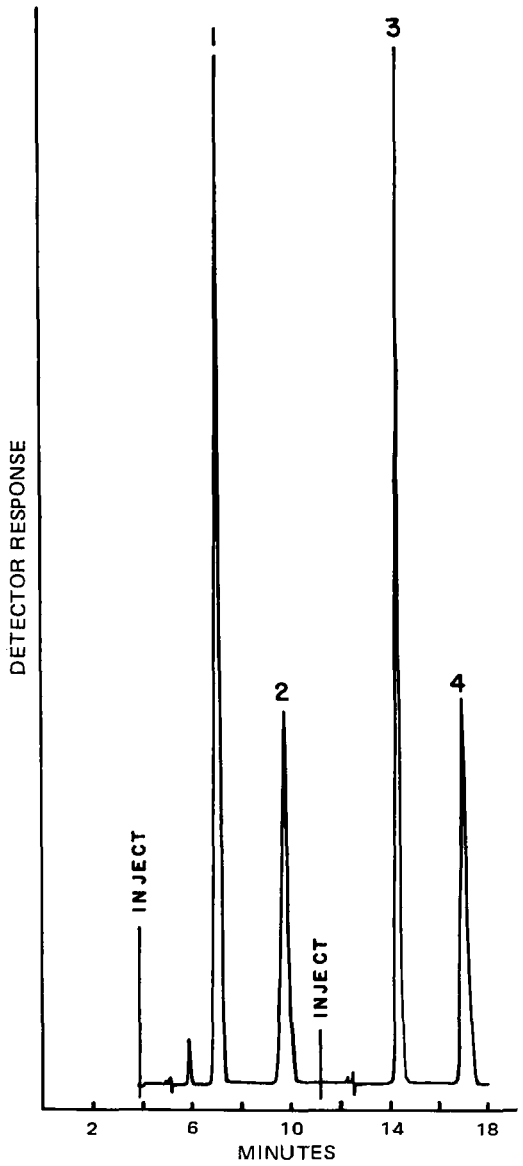

Figure 1—*HPLC analysis of phenol and resorcinol in combination (for chromatographic conditions, see text). Peaks 1 and 2 are resorcinol and phenol, respectively, from an assay sample; peaks 3 and 4 are resorcinol and phenol, respectively, from a standard sample.*

Assay Procedure for Phenol in Phenolated Calamine Lotion USP—Shake the lotion thoroughly and dilute 5.0 ml to 100 ml with water. Mix, filter, reject the first 8–10 ml of the filtrate, collect the clear filtrate, and inject 10–20 μl.

For the purpose of comparison, inject an identical volume of the appropriate standard solution after the assay solution is eluted.

Calculations—Since preliminary investigations indicated that the peak areas of phenol and resorcinol were directly related to the concentrations, the results were calculated using:

$$\frac{A_a}{A_s} \times 100 = \text{percent of label claim} \qquad \text{(Eq. 1)}$$

Table I—Assay Results on Phenol and Resorcinol

Sample	Percent Results[a] on Phenol	Resorcinol
1[b]	99.6	100.2
2[b]	98.7	99.4
3[c]	100.5	0.0
Average deviation	±2.4	±1.8

[a] Average of three. [b] Phenol–resorcinol–boric acid solution. [c] Phenolated calamine lotion.

where A_a = peak area of the assay sample, and A_s = peak of the standard sample.

The results are presented in Table I, and the chromatogram is presented in Fig. 1.

DISCUSSION

The assay results (Table I) indicate that phenol and resorcinol in combination can be separated (Fig. 1) and assayed accurately. The procedure developed for the quantitative determinations of phenol and resorcinol by HPLC is very simple and rapid (no special preliminary treatment is required). No interference from other ingredients of the phenol–resorcinol–boric acid solution (acetone and boric acid) or phenolated calamine lotion USP (bentonite magma, calamine, and zinc oxide) was noted. The method provides direct results on phenol and resorcinol rather than determining one or the other by difference.

REFERENCES

(1) V. D. Gupta and L. A. Cates, *J. Pharm. Sci.*, **63**, 93(1974).

(2) "The United States Pharmacopeia," 19th rev., Mack Publishing Co., Easton, Pa., 1975, p. 60.

ACKNOWLEDGMENTS AND ADDRESSES

Received November 11, 1975, from the *College of Pharmacy, University of Houston, Houston, TX 77004*

Accepted for publication February 2, 1976.

Electron-Capture GC Determination of Subnanogram Amounts of Emepronium Bromide in Serum

PER HARTVIG *×, BARBRO NÄSLUND *, and JÖRGEN VESSMAN ‡

Abstract □ Barium peroxide in an acidic medium was utilized to increase the sensitivity in the benzophenone method for the determination of the quaternary ammonium compound emepronium bromide. The method is comprised of ion-pair extraction, oxidation, and quantitative determination of benzophenone by electron-capture GC. By employing small extraction and reaction volumes, the method was used in the 0.2–8-ng/ml range with a relative standard deviation of 2.5% at the 1-ng/ml level. The application of the method to human serum samples after a single oral dose demonstrated that the elimination phase for emepronium in serum had a half-life of 7–11 hr.

Keyphrases □ Emepronium bromide—electron-capture GC analysis in human serum, elimination profile described □ GC, electron capture—analysis, emepronium bromide in human serum □ Elimination profile—emepronium bromide, electron-capture GC analysis in human serum □ Anticholinergic agents—emepronium bromide, electron-capture GC analysis in human serum, elimination profile described

Emepronium bromide[1] [(3,3-diphenyl-1-methylpropyl)dimethylethylammonium bromide], a quaternary ammonium compound with anticholinergic properties, was determined by electron-capture GC in biological samples after oxidation with chromic acid to benzophenone (1). The oxidation conditions as well as the extraction of emepronium were studied in detail. Special attention was paid to the interference from metabolites. The lower limit of detection of that method was about 1 ng/ml, and down to 3 ng/ml could be determined with acceptable precision. The fate of emepronium bromide in dogs (2) and humans (3) was studied with this sensitive method.

From a pharmacokinetic point of view, there was a need for a method with a higher sensitivity to follow the fate of emepronium over a longer time. Subnanogram analysis of emepronium bromide could be realized when a study of barium peroxide oxidation in sulfuric acid revealed very low reagent blanks (4). The sensitivity was also increased by the use of small extraction and reaction volumes and by the employment of a purer internal standard (5). This paper describes the development of a barium peroxide oxidation procedure for emepronium and its application to the analysis of human serum samples for the drug after single oral doses.

[1] Cetiprin.

EXPERIMENTAL

Apparatus and Glass Equipment—*GC*—A gas chromatograph[2] equipped with a tritium electron-capture detector operating in the dc mode was used. The glass column (1.5 m × 1.8 mm) was filled with 3% DC 560 and 0.3% polyethylene glycol[3]–terephthalic acid on 100–120-mesh Gas Chrom P, acid washed and silanized. The column temperature was 139°; the flow rate of the carrier gas, nitrogen, was 30 ml/min. The detector temperature was 155°, corresponding to 138° at the detector foil.

Heating Bath—The reaction was performed in a dry bath[4] at 114°. The reaction tubes were emersed in sand so that only the water phase was covered.

Glass Equipment—The extraction was performed in 15-ml centrifuge tubes with a tapered base of 0.3 ml. The oxidation was performed in glass tubes with a height of 10 cm and an inner diameter of 0.6 cm. The tubes had a restriction at the half-height, and no condenser was necessary with this arrangement.

Reagents and Chemicals—Barium peroxide[5], anhydrous powder,

[2] Varian 1400.
[3] Carbowax, Union Carbide.
[4] Thermolyne.
[5] Matheson, Coleman and Bell.

Table I—Assay Results on Phenol and Resorcinol

Sample	Percent Results[a] on Phenol	Resorcinol
1[b]	99.6	100.2
2[b]	98.7	99.4
3[c]	100.5	0.0
Average deviation	±2.4	±1.8

[a] Average of three. [b] Phenol–resorcinol–boric acid solution. [c] Phenolated calamine lotion.

where A_a = peak area of the assay sample, and A_s = peak of the standard sample.

The results are presented in Table I, and the chromatogram is presented in Fig. 1.

DISCUSSION

The assay results (Table I) indicate that phenol and resorcinol in combination can be separated (Fig. 1) and assayed accurately. The procedure developed for the quantitative determinations of phenol and resorcinol by HPLC is very simple and rapid (no special preliminary treatment is required). No interference from other ingredients of the phenol–resorcinol–boric acid solution (acetone and boric acid) or phenolated calamine lotion USP (bentonite magma, calamine, and zinc oxide) was noted. The method provides direct results on phenol and resorcinol rather than determining one or the other by difference.

REFERENCES

(1) V. D. Gupta and L. A. Cates, *J. Pharm. Sci.*, **63**, 93(1974).

(2) "The United States Pharmacopeia," 19th rev., Mack Publishing Co., Easton, Pa., 1975, p. 60.

ACKNOWLEDGMENTS AND ADDRESSES

Received November 11, 1975, from the *College of Pharmacy, University of Houston, Houston, TX 77004*

Accepted for publication February 2, 1976.

Electron-Capture GC Determination of Subnanogram Amounts of Emepronium Bromide in Serum

PER HARTVIG *×, BARBRO NÄSLUND *, and JÖRGEN VESSMAN ‡

Abstract □ Barium peroxide in an acidic medium was utilized to increase the sensitivity in the benzophenone method for the determination of the quaternary ammonium compound emepronium bromide. The method is comprised of ion-pair extraction, oxidation, and quantitative determination of benzophenone by electron-capture GC. By employing small extraction and reaction volumes, the method was used in the 0.2–8-ng/ml range with a relative standard deviation of 2.5% at the 1-ng/ml level. The application of the method to human serum samples after a single oral dose demonstrated that the elimination phase for emepronium in serum had a half-life of 7–11 hr.

Keyphrases □ Emepronium bromide—electron-capture GC analysis in human serum, elimination profile described □ GC, electron capture—analysis, emepronium bromide in human serum □ Elimination profile—emepronium bromide, electron-capture GC analysis in human serum □ Anticholinergic agents—emepronium bromide, electron-capture GC analysis in human serum, elimination profile described

Emepronium bromide[1] [(3,3-diphenyl-1-methylpropyl)dimethylethylammonium bromide], a quaternary ammonium compound with anticholinergic properties, was determined by electron-capture GC in biological samples after oxidation with chromic acid to benzophenone (1). The oxidation conditions as well as the extraction of emepronium were studied in detail. Special attention was paid to the interference from metabolites. The lower limit of detection of that method was about 1 ng/ml, and down to 3 ng/ml could be determined with acceptable precision. The fate of emepronium bromide in dogs (2) and humans (3) was studied with this sensitive method.

From a pharmacokinetic point of view, there was a need for a method with a higher sensitivity to follow the fate of emepronium over a longer time. Subnanogram analysis of emepronium bromide could be realized when a study of barium peroxide oxidation in sulfuric acid revealed very low reagent blanks (4). The sensitivity was also increased by the use of small extraction and reaction volumes and by the employment of a purer internal standard (5). This paper describes the development of a barium peroxide oxidation procedure for emepronium and its application to the analysis of human serum samples for the drug after single oral doses.

[1] Cetiprin.

EXPERIMENTAL

Apparatus and Glass Equipment—*GC*—A gas chromatograph[2] equipped with a tritium electron-capture detector operating in the dc mode was used. The glass column (1.5 m × 1.8 mm) was filled with 3% DC 560 and 0.3% polyethylene glycol[3]–terephthalic acid on 100–120-mesh Gas Chrom P, acid washed and silanized. The column temperature was 139°; the flow rate of the carrier gas, nitrogen, was 30 ml/min. The detector temperature was 155°, corresponding to 138° at the detector foil.

Heating Bath—The reaction was performed in a dry bath[4] at 114°. The reaction tubes were emersed in sand so that only the water phase was covered.

Glass Equipment—The extraction was performed in 15-ml centrifuge tubes with a tapered base of 0.3 ml. The oxidation was performed in glass tubes with a height of 10 cm and an inner diameter of 0.6 cm. The tubes had a restriction at the half-height, and no condenser was necessary with this arrangement.

Reagents and Chemicals—Barium peroxide[5], anhydrous powder,

[2] Varian 1400.
[3] Carbowax, Union Carbide.
[4] Thermolyne.
[5] Matheson, Coleman and Bell.

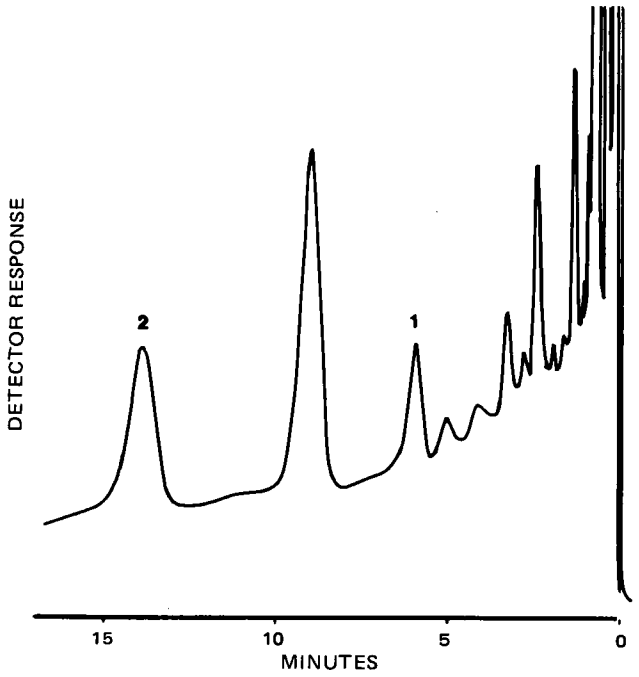

Figure 1—*Gas chromatogram of the oxidation extract from a human serum sample of emepronium. Key: 1, benzophenone from emepronium, 2.5 ng/ml; and 2,* p*-chlorobenzophenone from the internal standard, 5 ng/ml.*

was used as received. Methylene chloride[6], analytical grade, was extracted with 0.5 *M* sodium carbonate, 0.5 *M* sodium bisulfite, and water. After drying with sodium sulfate, it was distilled. Sodium perchlorate[6] solution, 0.5 *M*, was shaken with double-distilled heptane before use. Sulfuric acid solution, 3.6 *M*, was prepared from high purity sulfuric acid[7]. The sodium hydroxide[6] solution used was 1 *M*.

Internal Standard Solution—Ethyl-(3-*p*-chlorophenyl-3-phenyl-1-methylpropyl)dimethylammonium bromide was purified by a reversed-phase, ion-pair chromatographic procedure (5). It was dissolved in water and diluted to a final concentration of 9 ng/ml.

Standard Solution of Emepronium Bromide—Emepronium bromide was dissolved in water and diluted to 2 ng/ml.

Determination of Emepronium in Serum—To a serum volume containing 0.2–4 ng of emepronium in a centrifuge tube were added 1 ml of the internal standard solution, 1 ml of 0.5 *M* sodium perchlorate, water to 5 ml, and 1 ml of methylene chloride. The tube was shaken for 30 min and centrifuged. The methylene chloride phase was then transferred to an oxidation tube and evaporated to dryness in a gentle stream of nitrogen.

To the residue, 0.25 ml of 3.6 *M* sulfuric acid and about 20 mg of barium peroxide were added. Then 50 μl of heptane was added, and the tube was heated for 30 min in the heating bath. After cooling, the organic phase was shaken with 3 drops of 1 *M* sodium hydroxide. A 10–20-μl aliquot of the heptane phase was then injected into the gas chromatograph.

A standard curve was prepared by treating five samples containing 0, 0.5, 1, 2, and 4 ng of emepronium bromide from the standard solution and 1 ml of blank serum according to the described procedure.

RESULTS AND DISCUSSION

Extraction Conditions—The extraction of emepronium and the internal standard (the *p*-chloro analog) from the serum sample was as described in the chromic acid oxidation procedure (1). To increase the sensitivity of the method, the phase volumes were diminished four times compared to the previous method.

Reaction Conditions—Emepronium bromide can be converted to benzophenone by several oxidizing reagents (6–8). The oxidation yield was about 70% in all cases. However, the reagent blank was much less in the oxidation with acidic barium peroxide (4), and this reagent was chosen for a more sensitive method.

The conditions for the barium peroxide oxidation of emepronium bromide and the internal standard in a two-phase system were studied previously (6). The sulfuric acid concentration in the oxidation solution was important, and 3.6 *M* was necessary for optimum yield in both cases. The oxidation time for emepronium bromide and the internal standard was 30 and 60 min, respectively. In this study, a somewhat higher reaction temperature, 114°, was used; the reaction was complete in 30 min for both compounds. Prolonged reaction time increased the interferences on the gas chromatograms.

Purification of Reagents—An advantage of oxidation procedures in electron-capture GC is that clean extracts are obtained because interfering materials often are completely decomposed during oxidation. However, in this low concentration range, special attention had to be paid to the reagent purity. All reagents were of the highest analytical quality but, in many cases, were not sufficiently pure for a successful analysis. For example, use of other qualities of sulfuric acid increased the control background so much that subnanogram analysis was impossible. Good results were achieved by shaking organic solvents with water followed by distillation. In some cases, the aqueous reagents were shaken with heptane before use.

Although these precautions were taken, some unidentified peaks remained in the chromatogram (Fig. 1). These peaks mainly originated from sodium perchlorate and methylene chloride. Methylene chloride has a high electron-capture response, and some impurities in that solvent remained after the evaporation procedure. The interference from serum components was low.

Reagent Blank—Due to a reagent blank in the chromic acid oxidation of emepronium, the lowest level that could be determined with acceptable precision was 3 ng/ml (1). About half of the reagent blank was due to a batch of internal standard being contaminated with emepronium bromide. By use of the reversed-phase, ion-pair liquid chromatographic procedure, this contaminant was eliminated (5). The reagent blank that originates from the oxidation procedure was much lower in acidic barium peroxide oxidation, and determinations were possible down to 0.2 ng/ml of emepronium. The blank from an aqueous sample in this procedure corresponded to approximately 100 pg of emepronium. The blank from serum varied with the individuals and added 0–200 pg to the blank from the aqueous sample.

Selectivity—The interferences from metabolites in the chromic acid oxidation procedure were discussed earlier (1–3). Barium peroxide oxidation also gives interferences from metabolites and other compounds containing the diphenylmethane moiety. Most diphenylmethane-substituted compounds gave a benzophenone yield of about 70% when oxidized in acidic barium peroxide (6). The only emepronium metabolite of importance in humans is the 4-hydroxylated one (3), and this metabolite will not interfere (1). Studies in the dog indicated that the interference from other metabolites is small (2).

Precision and Recovery—In the chromic acid oxidation procedure, the relative recovery of emepronium from serum was 100 ± 3% at the 6-ng/ml level (1). The absolute drug recoveries were studied previously with ^{14}C-labeled material in a series of experiments where quantitative recoveries were obtained. The relative recovery of the drug using the present method was 100%.

The precision of this microprocedure was good. At the 1-ng/ml level, six samples were determined with a relative standard deviation of 2.5%.

Although the interferences from peaks in the vicinity of benzophenone and 4-chlorobenzophenone peaks in the chromatograms were small (Fig. 1), an injection of a sample in the gas chromatograph could be done only at 40-min intervals. Very large peaks were eluted after the 4-chlorobenzophenone peak, and some of them could be recognized as phthalate derivatives. This problem reduced the capacity of the present method; six samples and the standard curve were processed each day.

Analysis of Emepronium Bromide in Human Serum after Oral Administration—Due to the sensitivity increase of the present method for emepronium, 10–20 times lower serum levels of the drug could be determined. The high sensitivity is of value in the determination of emepronium long after its administration and in the determination of emepronium in small sample volumes from small experimental animals.

The method was used in the establishment of serum levels of

[6] Pro analysi quality, Merck, Darmstadt, West Germany.
[7] Merck, Suprapur.

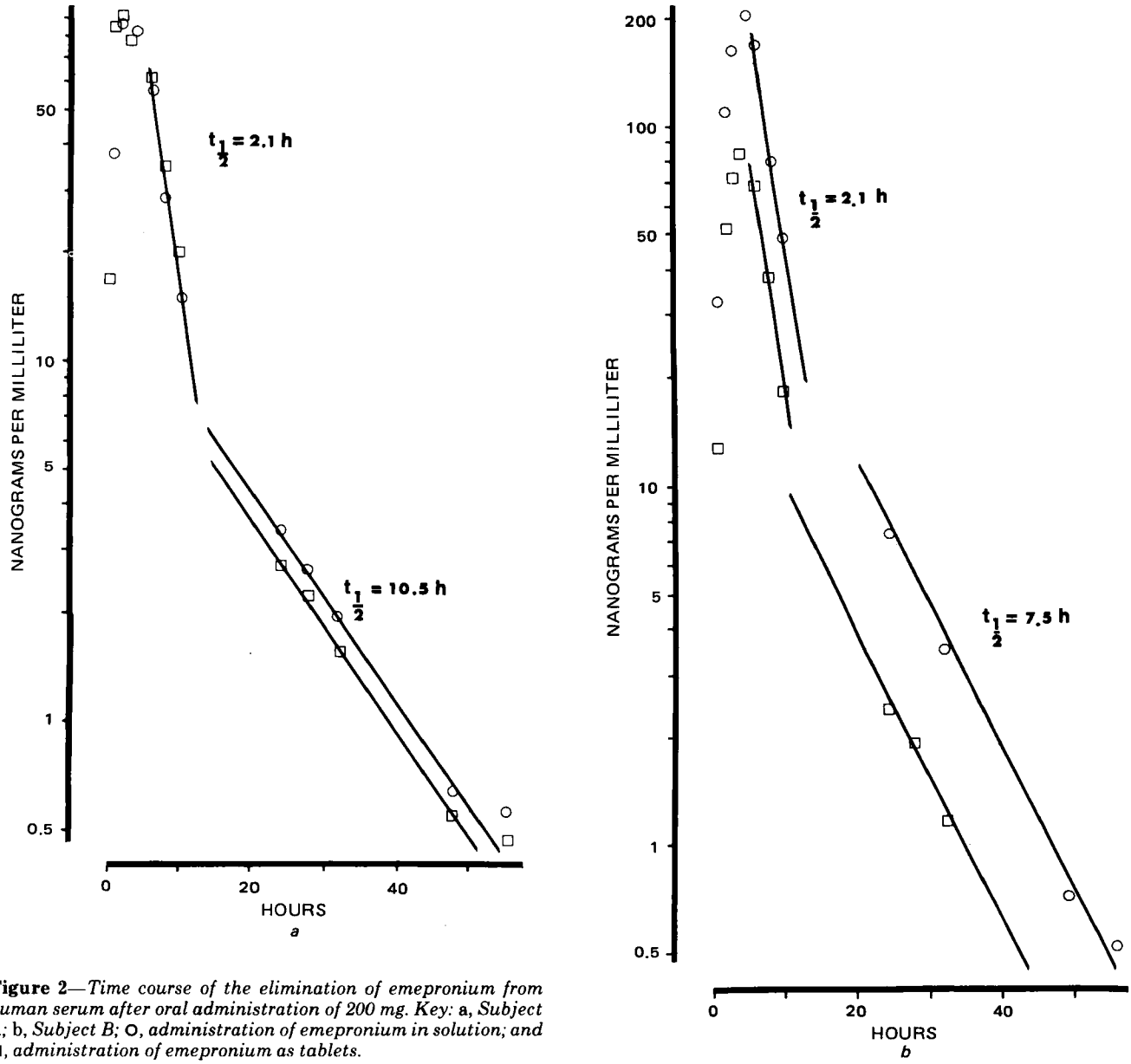

Figure 2—*Time course of the elimination of emepronium from human serum after oral administration of 200 mg. Key:* a, *Subject A;* b, *Subject B;* O, *administration of emepronium in solution; and* □, *administration of emepronium as tablets.*

emepronium in samples taken 24–56 hr after drug administration. The samples taken up to 24 hr were analyzed by the less sensitive chromic acid oxidation procedure. A few samples were analyzed with both procedures, and the results were as expected within the same order of magnitude. The time course for the concentration of emepronium in serum from two volunteers after oral administration of 200 mg in solution and as tablets is shown in Figs. 1 and 2. With this sensitivity of detection, it can be demonstrated clearly that emepronium in serum exhibits an elimination phase, the so-called β-phase, after about 24 hr. The drug half-life in serum was calculated from the slope of the curves and varied from 7.5 to 10.5 hr for these two subjects. With the earlier procedure, only the distribution phase, with a half-life of 1.5–2.5 hr, could be evaluated (1).

REFERENCES

(1) J. Vessman, S. Strömberg, and G. Rietz, *Acta Pharm. Suec.*, **7**, 363(1970).

(2) A. Sundwall, K. Uthne, and J. Vessman, *Acta Pharmacol. Toxicol.*, **29**, 385(1970).

(3) A. Sundwall, J. Vessman, and B. Strindberg, *Eur. J. Clin. Pharmacol.*, **6**, 191(1973).

(4) P. Hartvig and B. Näslund, *J. Chromatogr.*, **111**, 347(1975).

(5) K. Gröningsson, P. Hartvig, and L. Molin, *Acta Pharm. Suec.*, **10**, 53(1973).

(6) P. Hartvig and W. Handl, *ibid.*, **12**, 349(1975).

(7) J. Vessman, P. Hartvig, and S. Strömberg, *ibid.*, **7**, 363(1970).

(8) P. Hartvig, H. Sundin, and J. Vessman, *ibid.*, **9**, 269(1972).

ACKNOWLEDGMENTS AND ADDRESSES

Received August 25, 1975, from the *Department of Analytical Pharmaceutical Chemistry, University of Uppsala, Box 574, S-751 23 Uppsala, Sweden, and †Analytical Chemistry, Research Department, AB KABI, Fack, S-104 25 Stockholm, Sweden.

Accepted for publication February 9, 1976.

[x] To whom inquiries should be directed.

Potential Problem in GLC Determination of Ibuprofen Caused by Solid Support

Keyphrases □ Ibuprofen—GLC analysis in plasma, effect of varying solid support materials □ GLC—analysis, ibuprofen in plasma, effect of varying solid support materials □ Solid supports, GLC—effect on ibuprofen analysis □ Anti-inflammatory agents—ibuprofen, GLC analysis in plasma, effect of varying solid support materials

To the Editor:

A sensitive and specific GLC method for the determination of ibuprofen [(±)-2-(*p*-isobutylphenyl)propionic acid] in plasma was reported previously (1). The assay involves a single extraction followed by methylation of the carboxyl moiety of ibuprofen to form ibuprofen methyl ester. Chromatography is carried out on a column packed with 6% diethylene glycol succinate on 80–100-mesh silanized diatomaceous earth. The purpose of this communication is to report a problem encountered due to differences between apparently equivalent solid support materials obtained from different manufacturers.

Using Diatoport-S[1] as the solid support, Kaiser and VanGiessen (1) obtained chromatograms that showed a return to a consistently clean baseline 10 min after sample injection. Essentially identical results were obtained when Gas Chrom Q[2] was used as the solid support. In a slightly different chromatographic system (using nitrogen rather than helium as the carrier at a flow rate of 50 ml/min and a 1.82-m × 2-mm i.d. coiled glass column), Anakrom-SD[3] (90–100 mesh) coated with 6% diethylene glycol succinate was used as received from the manufacturer. With this support material, a contaminant was eluted with a retention time of 23 min; return to baseline was achieved only 70–90 min after sample injection (Fig. 1). Similar results were obtained when Anakrom-SD was used under the exact chromatographic conditions described by Kaiser and VanGiessen (1).

Sequential elimination of reagents from the methylation scheme revealed that the contaminant was associated with the use of triethylamine, which functions to increase the rate of methylation. Essentially identical results were obtained with triethylamine (reagent grade) from three different sources[4]. Mass spectral analysis of the eluate comprising the contaminant peak indicated that it was triethylamine or a closely related compound.

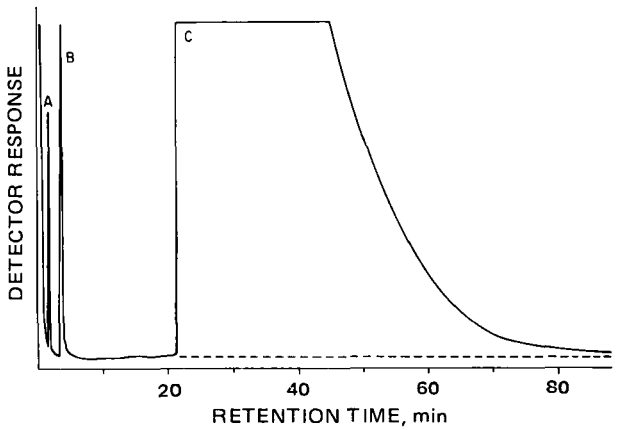

Figure 1—*Gas–liquid chromatogram of ibuprofen recovered from chloroform and methylated (1), using Anakrom-SD as the solid support. Key: A, naphthalene internal standard; B, ibuprofen methyl ester; C, peak obtained when triethylamine is included in the methylation procedure; and - - - -, normal baseline when triethylamine is omitted.*

Triethylamine can be eliminated from the procedure by allowing methanol to react with the imidazole intermediate for 20 min. This step has no effect on the specificity or sensitivity of the assay. However, it may be preferred to retain triethylamine (which reduces the reaction time to less than 5 min) and to use a solid support material that does not produce the chromatographic peak associated with triethylamine.

(1) D. G. Kaiser and G. J. VanGiessen, *J. Pharm. Sci.*, **63**, 219(1974).

John T. Slattery
Avraham Yacobi
Gerhard Levy ˣ
Department of Pharmaceutics
School of Pharmacy
State University of New York
at Buffalo
Buffalo, NY 14214

David G. Kaiser
Research Laboratories
The Upjohn Company
Kalamazoo, MI 49001

Received July 12, 1976.
Accepted for publication August 18, 1976.
Supported in part by Grant GM 20852 from the National Institute of General Medical Sciences, National Institutes of Health.
ˣ To whom inquiries should be directed.

[1] Hewlett-Packard Co., Avondale, Pa.
[2] Supelco, Inc., Bellefonte, Pa.
[3] Analabs, Inc., North Haven, Conn.
[4] Matheson, Coleman and Bell, Norwood, Ohio; Eastman Kodak Co., Rochester, N.Y.; J.T. Baker Chemical Co., Phillipsburg, N.J.

REVIEWS

Pharmacology: An Introduction to Drugs. By MICHAEL C. GERALD. Prentice-Hall, Englewood Cliffs, NJ 07632, 1974. 524 pp. 15.5 × 23.5 cm. Price $11.95.

The writing of a general pharmacology textbook intended primarily (though not exclusively) for individuals possessing little or no scientific background is an ambitious undertaking. Author Michael Gerald has taken on this onerous task and, in the opinion of this reviewer, has succeeded splendidly.

"Pharmacology: An Introduction to Drugs" is unlike other recently published introductory pharmacology texts (*e.g.*, Levine, "Pharmacology: Drug Actions and Reactions" and Ray, "Drugs, Society and Human Behavior") in that it does not confine itself to the basic principles governing chemical–biologic interactions or to a discussion of only those drugs possessing abuse potential; rather, it encompasses the entire scope of the science of pharmacology. It is a textbook well suited to the needs of both nonprofessional students and lay persons who seek an understanding of what drugs are, how they act, and what they can and cannot do.

Dr. Gerald has a delightfully disarming style of writing and has organized his book in a logical, easy-to-follow sequence. The book contains very few ambiguities and is relatively free of minutiae and detailed information which might prove confusing to the novice. Where knowledge is lacking or when scientific opinion is conflicting on some drug-related subject, this is so stated. Many erroneous beliefs and popular misconceptions about drugs are dispelled outright.

The book is divided into seven sections covering the following topics (the number of pages devoted to each topic is given in parentheses): I, General Concepts of Pharmacology (79); II, Drugs Affecting the Peripheral Nervous System (91); III, Drugs Affecting the Central Nervous System (185); IV, Drugs Affecting the Cardiovascular System (32); V, Drugs Affecting the Endocrine System (35); VI, Chemotherapeutic Agents (42); and VII, Toxicology (11). Each chapter is concluded with a summary and a list of supplementary readings. The first chapters of Sections II–V are devoted to an overview of basic anatomy and physiology. The overviews covering the autonomic and central nervous systems are particularly good and include a number of instructive diagrams.

What I enjoyed most about the book was Dr. Gerald's liberal use of quotations, epigrams, and historical anecdotes, each of which he has been careful to document. Since much of the material will be new even to the antediluvian pharmacologist, it should prove invaluable to instructors in other fields who might make use of it in speeches, lectures, and other pedagogic endeavors. Here is a sampling.

Recounting his second voyage around the world, Captain James Cook describes his experience after eating the liver and roe of the puffer fish (now known to contain tetrodotoxin):

> *"About three to four o'clock in the morning, we were seized with most extraordinary weakness in all our limbs attended with numbness of sensation like to that caused by exposing one's hands and feet to a fire after having been pinched much by frost. I had almost lost the sense of feeling nor could I distinguish between light and heavy objects, a quart potfull of water and a feather was the same in my hand. We each took a vomit and after that a sweat which gave great relief. In the morning, one of the pigs which had eaten the entrails was found dead."*

The following quote attributed to F. Scott Fitzgerald precedes the chapter on sedative–hypnotic agents:

> *"It appears that every man's insomnia is as different from his neighbor's as are their daytime hopes and aspirations."*

This review would be incomplete without mention of the few misgivings I had about the book. For one thing, it seemed to me as though the author had reneged on a prefatory promise to "sprinkle but a modest number of chemical structures among the pages of his book" when he incorporated nine complex chemical structures of narcotic analgesics and antagonists in Figure 13-1 and 14 chemical structures of aminergic psychotomimetic agents in Figure 17-1. Second, the overview of the cardiovascular system suffered somewhat from overdistillation. It probably will leave the casual reader with little comprehension of cardiac function or what "blood pressure" is really all about. Third, considering the fact that many would-be readers will have had no formal courses in biology or physiology, I think it unfortunate that Dr. Gerald did not spend time early in his book developing the concept of homeostasis, *i.e.*, the maintenance of a stable internal environment. This fundamental concept supplies the basis for understanding the common denominator of the functions carried out by all organ systems. I believe it would have paid off handsomely had the author driven this point home right from the outset.

The above criticisms are in no way intended to discourage adoption of the book for appropriate undergraduate courses. It is a well-written, informative, and entertaining text. Dr. Gerald is to be complimented on a truly fine contribution.

Reviewed by Louis Diamond
College of Pharmacy
University of Kentucky
Lexington, KY 40506

Advances in Pharmaceutical Sciences. Volume 4. Edited by H. S. BEAN, A. H. BECKETT, and J. E. CARLESS. Academic, 111 5th Avenue, New York, NY 10003, 1974. 444 pp. 15 × 22.5 cm. Price $35.00.

This volume is composed of four unrelated chapters, each supported by numerous references. The subjects considered are different from those in previous volumes except for the chapter on rheology. In Volume 1, this chapter included discussions of Newtonian flow, plastic flow, pseudoplastic flow, dilatancy, and thixotropy; a description of various instruments designed for measuring rheologic properties; and a consideration of the application of rheology to various pharmaceutical systems.

In Volume 4, rheology is considered in its application to pharmaceutical and cosmetic semisolids using two drug delivery systems: (*a*) soft paraffins and their formulations, and (*b*) ternary systems and oil-in-water emulsions containing mixed emulsifiers of surfactant–long-chain alcohol types. The author describes continuous shear rheometry of semisolids. Most of the chapter is devoted to the nature of viscoelastic behavior and viscoelastic analysis of semisolids.

The author states that a considerable amount of mathematics is necessary for a complete understanding of the viscoelastic theory. However, in this chapter he uses only elementary mathematics in his consideration of the simpler shear case in order to make the information usable by someone not so well versed in mathematics. The researcher will need to be very knowledgeable in mathematics to conduct research at the academic level, whereas the formulation pharmacist who has a deadline to meet on the production line can still use the viscoelastic approach if he or she uses strain techniques and control tools. A protocol is presented for the examination of raw materials and products using the viscoelastic theory. The author used over 100 references, including about 30 of his own publications.

The second chapter, "Determination of Thermodynamics of Functional Groups in Solutions of Drug Molecules," is supported by about 540 references in a variety of publications. The authors also describe some of their own research on this subject. First, the authors review some relevant areas of equilibrium thermodynamics and the meanings of some terms. Then they discuss the group contribution concept by activity coefficients, solubility, heat capacity, molar volume, and partition coefficients. They present experimental determinations of thermodynamic quantities and group contribution values. The functional groups considered are methylene, methyl, branched alkyl chains, double bonds, ring compounds, halogens, and various polar groupings. Finally, they discuss the application of the group contribution concept in pharmaceutical sciences.

REVIEWS

Pharmacology: An Introduction to Drugs. By MICHAEL C. GERALD. Prentice-Hall, Englewood Cliffs, NJ 07632, 1974. 524 pp. 15.5 × 23.5 cm. Price $11.95.

The writing of a general pharmacology textbook intended primarily (though not exclusively) for individuals possessing little or no scientific background is an ambitious undertaking. Author Michael Gerald has taken on this onerous task and, in the opinion of this reviewer, has succeeded splendidly.

"Pharmacology: An Introduction to Drugs" is unlike other recently published introductory pharmacology texts (*e.g.*, Levine, "Pharmacology: Drug Actions and Reactions" and Ray, "Drugs, Society and Human Behavior") in that it does not confine itself to the basic principles governing chemical–biologic interactions or to a discussion of only those drugs possessing abuse potential; rather, it encompasses the entire scope of the science of pharmacology. It is a textbook well suited to the needs of both nonprofessional students and lay persons who seek an understanding of what drugs are, how they act, and what they can and cannot do.

Dr. Gerald has a delightfully disarming style of writing and has organized his book in a logical, easy-to-follow sequence. The book contains very few ambiguities and is relatively free of minutiae and detailed information which might prove confusing to the novice. Where knowledge is lacking or when scientific opinion is conflicting on some drug-related subject, this is so stated. Many erroneous beliefs and popular misconceptions about drugs are dispelled outright.

The book is divided into seven sections covering the following topics (the number of pages devoted to each topic is given in parentheses): I, General Concepts of Pharmacology (79); II, Drugs Affecting the Peripheral Nervous System (91); III, Drugs Affecting the Central Nervous System (185); IV, Drugs Affecting the Cardiovascular System (32); V, Drugs Affecting the Endocrine System (35); VI, Chemotherapeutic Agents (42); and VII, Toxicology (11). Each chapter is concluded with a summary and a list of supplementary readings. The first chapters of Sections II–V are devoted to an overview of basic anatomy and physiology. The overviews covering the autonomic and central nervous systems are particularly good and include a number of instructive diagrams.

What I enjoyed most about the book was Dr. Gerald's liberal use of quotations, epigrams, and historical anecdotes, each of which he has been careful to document. Since much of the material will be new even to the antediluvian pharmacologist, it should prove invaluable to instructors in other fields who might make use of it in speeches, lectures, and other pedagogic endeavors. Here is a sampling.

Recounting his second voyage around the world, Captain James Cook describes his experience after eating the liver and roe of the puffer fish (now known to contain tetrodotoxin):

> *"About three to four o'clock in the morning, we were seized with most extraordinary weakness in all our limbs attended with numbness of sensation like to that caused by exposing one's hands and feet to a fire after having been pinched much by frost. I had almost lost the sense of feeling nor could I distinguish between light and heavy objects, a quart potfull of water and a feather was the same in my hand. We each took a vomit and after that a sweat which gave great relief. In the morning, one of the pigs which had eaten the entrails was found dead."*

The following quote attributed to F. Scott Fitzgerald precedes the chapter on sedative–hypnotic agents:

> *"It appears that every man's insomnia is as different from his neighbor's as are their daytime hopes and aspirations."*

This review would be incomplete without mention of the few misgivings I had about the book. For one thing, it seemed to me as though the author had reneged on a prefatory promise to "sprinkle but a modest number of chemical structures among the pages of his book" when he incorporated nine complex chemical structures of narcotic analgesics and antagonists in Figure 13-1 and 14 chemical structures of aminergic psychotomimetic agents in Figure 17-1. Second, the overview of the cardiovascular system suffered somewhat from overdistillation. It probably will leave the casual reader with little comprehension of cardiac function or what "blood pressure" is really all about. Third, considering the fact that many would-be readers will have had no formal courses in biology or physiology, I think it unfortunate that Dr. Gerald did not spend time early in his book developing the concept of homeostasis, *i.e.*, the maintenance of a stable internal environment. This fundamental concept supplies the basis for understanding the common denominator of the functions carried out by all organ systems. I believe it would have paid off handsomely had the author driven this point home right from the outset.

The above criticisms are in no way intended to discourage adoption of the book for appropriate undergraduate courses. It is a well-written, informative, and entertaining text. Dr. Gerald is to be complimented on a truly fine contribution.

Reviewed by Louis Diamond
College of Pharmacy
University of Kentucky
Lexington, KY 40506

Advances in Pharmaceutical Sciences. Volume 4. Edited by H. S. BEAN, A. H. BECKETT, and J. E. CARLESS. Academic, 111 5th Avenue, New York, NY 10003, 1974. 444 pp. 15 × 22.5 cm. Price $35.00.

This volume is composed of four unrelated chapters, each supported by numerous references. The subjects considered are different from those in previous volumes except for the chapter on rheology. In Volume 1, this chapter included discussions of Newtonian flow, plastic flow, pseudoplastic flow, dilatancy, and thixotropy; a description of various instruments designed for measuring rheologic properties; and a consideration of the application of rheology to various pharmaceutical systems.

In Volume 4, rheology is considered in its application to pharmaceutical and cosmetic semisolids using two drug delivery systems: (*a*) soft paraffins and their formulations, and (*b*) ternary systems and oil-in-water emulsions containing mixed emulsifiers of surfactant–long-chain alcohol types. The author describes continuous shear rheometry of semisolids. Most of the chapter is devoted to the nature of viscoelastic behavior and viscoelastic analysis of semisolids.

The author states that a considerable amount of mathematics is necessary for a complete understanding of the viscoelastic theory. However, in this chapter he uses only elementary mathematics in his consideration of the simpler shear case in order to make the information usable by someone not so well versed in mathematics. The researcher will need to be very knowledgeable in mathematics to conduct research at the academic level, whereas the formulation pharmacist who has a deadline to meet on the production line can still use the viscoelastic approach if he or she uses strain techniques and control tools. A protocol is presented for the examination of raw materials and products using the viscoelastic theory. The author used over 100 references, including about 30 of his own publications.

The second chapter, "Determination of Thermodynamics of Functional Groups in Solutions of Drug Molecules," is supported by about 540 references in a variety of publications. The authors also describe some of their own research on this subject. First, the authors review some relevant areas of equilibrium thermodynamics and the meanings of some terms. Then they discuss the group contribution concept by activity coefficients, solubility, heat capacity, molar volume, and partition coefficients. They present experimental determinations of thermodynamic quantities and group contribution values. The functional groups considered are methylene, methyl, branched alkyl chains, double bonds, ring compounds, halogens, and various polar groupings. Finally, they discuss the application of the group contribution concept in pharmaceutical sciences.

The chapter on "Radiopharmaceuticals" is introduced with an outline of radioactivity and definitions, choice of radionuclide, principles of radiation hygiene, historical aspects of radioactive materials, and the radioactive products official in the *British Pharmacopoeia*. The diagnostic applications of radiopharmaceuticals are presented, and descriptions of radionuclide generators are given. Hospital preparation of radiopharmaceuticals, including the use of ampuls and multidose vials, the use of bactericides, and quality control, is described. A section on toxic ingredients and adverse reactions includes control by drug regulatory authorities. A final section discusses radioisotopes in clinical chemistry, professional collaboration, and future developments.

The chapter on "Rectal Administration of Drugs" is introduced with a discussion of lipid materials and water-soluble compositions as bases for suppositories. Sections on formulation development and quality control include drug release, problems with suspended solids, viscosity adjustments, melting ranges, solidification ranges, and physical breakdown in water. The manufacture and packaging of suppositories are included. Finally, a section on the rectal absorption of drugs (several different examples are given) in animals and humans is presented.

An index makes it possible to find most topics covered in the book.

The authors of this volume have cited over 800 references, including many of their own research papers, in their chapters. This broad coverage not only makes the volume valuable in itself but also is an advantage to the reader who may want to follow up on specific subjects.

Reviewed by Elmer M. Plein
University of Washington
School of Pharmacy
Seattle, Washington 98195

Beta-blockers—Present Status and Future Prospects. Edited by W. SCHWEIZER. University Park Press, Chamber of Commerce Building, Baltimore, MD 21202, 1974. 325 pp. 17.5 × 24.5 cm. Price $19.50.

This publication contains the proceedings of an International Symposium held May 27–29, 1974. The book starts out with introductory remarks by Dr. C. Bartorelli describing the various points to be considered when evaluating beta-adrenergic blocking agents as potential antihypertensive drugs. The following chapter describes in great detail the relative beta-adrenergic blocking activity of various beta-blockers and their advantages and disadvantages when used as antihypertensive agents. Various possible mechanisms of action for the antihypertensive property of beta-blockers are also discussed.

The remaining chapters deal with various aspects of beta-blockers when prescribed as antihypertensive agents. All of these chapters are concise and well written, and certain aspects such as the renin–angiotensin–aldosterone interaction and the effect of beta-blockers on this system are covered rather thoroughly. In addition, there are chapters dealing with the importance of plasma volume in the treatment of hypertension and clinical experience with beta-blockers in the treatment of hypertension in the United Kindgom. Most of the chapters are followed by discussion sections which are very stimulating. Finally, the use of beta-blockers as antihypertensives is covered in a general discussion session, which is interesting, thought-provoking, and invaluable to the practicing physician as well as various research investigators.

Another aspect of beta-blockers covered in this book deals with their use in ischemic heart diseases, angina pectoris, cardiac arrhythmias, and hypertrophic cardiomyopathy. All of these chapters are written very thoroughly. The book also contains separate chapters that cover such topics as cardiological aspects of beta-blockade in stress situations and oxygen dissociation from hemoglobin. Finally, the last portion of the book is devoted to describing the metabolic effects of beta-blockers as well as their pharmacokinetic properties, followed by a general discussion session on guidelines for the use of beta-blockers in general practice.

This book can serve as an excellent reference source for clinicians, research investigators, graduate students, and clinical pharmacists. Considering the wealth of information contained in this volume, the price is very reasonable.

Reviewed by Mustafa F. Lokhandwala
Department of Pharmacology
College of Pharmacy
University of Houston
Houston, TX 77004

The Alkaloids. Vol. 5. Edited by J. E. SAXTON. The Chemical Society, Burlington House, London, England, W1V OBN, 1975. 303 pp. 14 × 22 cm. Price $48.25.

This book, the fifth of a series on alkaloids, is divided into 16 chapters and covers the literature from July 1973 to June 1974. As is the custom with previous books in this series, the first chapter is concerned with the biosynthesis of various classes of alkaloids and constitutes approximately 20% of the total book volume. This chapter begins with a quick, light introductory review of alkaloid biosynthesis, followed by detailed discussions on newer findings.

Chapters 2–16 are concerned with the phytochemistry of the alkaloids of pyrrolidine, piperidine, and pyridine; tropane; pyrrolizidine; indolizidine; quinolizidine; quinoline, quinazoline, acridone, and related compounds; β-phenylethylamines and isoquinoline; Amaryllidaceae and related plants; *Erythrina* and related plants; indole; diterpenoid; and steroidal and miscellaneous alkaloids. As is the case in past books of this series, the chapters on indole and isoquinoline alkaloids are more extensive than the discussions of other groups of compounds simply because of the abundance of literature on the chemistry of these two groups of alkaloids.

Of particular interest to students of indole alkaloids is J. A. Joule's compilation of ^{13}C-NMR data in a table of 36 typical indole and two biogenetically related quinoline alkaloid structures. These data should be of invaluable aid in the identification and structure elucidation of similar indole alkaloids.

Other than the relatively high price, one can recommend this book unequivocably to students of natural products chemistry.

Reviewed by Harry H. S. Fong
Department of Pharmacognosy
College of Pharmacy
University of Illinois at the Medical Center
Chicago, IL 60612

Symposium on Clinical Pharmacology. Sponsored by the National Cancer Institute. Pergamon Press, Maxwell House, Fairview Park, Elmsford, NY 10523. 236 pp. 16 × 23 cm. Price $20.00.

This book is a collection of the papers presented at the Symposium on Clinical Pharmacology sponsored by the National Cancer Institute in the spring of 1973. Its purpose was to present and collate the most recent advances in the field of cancer chemotherapy. The papers are divided into five broad areas: Pharmacological Factors in Drug Action, Factors Influencing Drug Selectivity, Mechanisms of Clinical Drug Resistance, Combination Chemotherapy, and New Information on Mechanisms of Drug Action. This book should be of value to those involved in development of potential therapies for cancer.

Staff Review

The chapter on "Radiopharmaceuticals" is introduced with an outline of radioactivity and definitions, choice of radionuclide, principles of radiation hygiene, historical aspects of radioactive materials, and the radioactive products official in the *British Pharmacopoeia*. The diagnostic applications of radiopharmaceuticals are presented, and descriptions of radionuclide generators are given. Hospital preparation of radiopharmaceuticals, including the use of ampuls and multidose vials, the use of bactericides, and quality control, is described. A section on toxic ingredients and adverse reactions includes control by drug regulatory authorities. A final section discusses radioisotopes in clinical chemistry, professional collaboration, and future developments.

The chapter on "Rectal Administration of Drugs" is introduced with a discussion of lipid materials and water-soluble compositions as bases for suppositories. Sections on formulation development and quality control include drug release, problems with suspended solids, viscosity adjustments, melting ranges, solidification ranges, and physical breakdown in water. The manufacture and packaging of suppositories are included. Finally, a section on the rectal absorption of drugs (several different examples are given) in animals and humans is presented.

An index makes it possible to find most topics covered in the book.

The authors of this volume have cited over 800 references, including many of their own research papers, in their chapters. This broad coverage not only makes the volume valuable in itself but also is an advantage to the reader who may want to follow up on specific subjects.

Reviewed by Elmer M. Plein
University of Washington
School of Pharmacy
Seattle, Washington 98195

Beta-blockers—Present Status and Future Prospects. Edited by W. SCHWEIZER. University Park Press, Chamber of Commerce Building, Baltimore, MD 21202, 1974. 325 pp. 17.5 × 24.5 cm. Price $19.50.

This publication contains the proceedings of an International Symposium held May 27–29, 1974. The book starts out with introductory remarks by Dr. C. Bartorelli describing the various points to be considered when evaluating beta-adrenergic blocking agents as potential antihypertensive drugs. The following chapter describes in great detail the relative beta-adrenergic blocking activity of various beta-blockers and their advantages and disadvantages when used as antihypertensive agents. Various possible mechanisms of action for the antihypertensive property of beta-blockers are also discussed.

The remaining chapters deal with various aspects of beta-blockers when prescribed as antihypertensive agents. All of these chapters are concise and well written, and certain aspects such as the renin–angiotensin–aldosterone interaction and the effect of beta-blockers on this system are covered rather thoroughly. In addition, there are chapters dealing with the importance of plasma volume in the treatment of hypertension and clinical experience with beta-blockers in the treatment of hypertension in the United Kindgom. Most of the chapters are followed by discussion sections which are very stimulating. Finally, the use of beta-blockers as antihypertensives is covered in a general discussion session, which is interesting, thought-provoking, and invaluable to the practicing physician as well as various research investigators.

Another aspect of beta-blockers covered in this book deals with their use in ischemic heart diseases, angina pectoris, cardiac arrhythmias, and hypertrophic cardiomyopathy. All of these chapters are written very thoroughly. The book also contains separate chapters that cover such topics as cardiological aspects of beta-blockade in stress situations and oxygen dissociation from hemoglobin. Finally, the last portion of the book is devoted to describing the metabolic effects of beta-blockers as well as their pharmacokinetic properties, followed by a general discussion session on guidelines for the use of beta-blockers in general practice.

This book can serve as an excellent reference source for clinicians, research investigators, graduate students, and clinical pharmacists. Considering the wealth of information contained in this volume, the price is very reasonable.

Reviewed by Mustafa F. Lokhandwala
Department of Pharmacology
College of Pharmacy
University of Houston
Houston, TX 77004

The Alkaloids. Vol. 5. Edited by J. E. SAXTON. The Chemical Society, Burlington House, London, England, W1V OBN, 1975. 303 pp. 14 × 22 cm. Price $48.25.

This book, the fifth of a series on alkaloids, is divided into 16 chapters and covers the literature from July 1973 to June 1974. As is the custom with previous books in this series, the first chapter is concerned with the biosynthesis of various classes of alkaloids and constitutes approximately 20% of the total book volume. This chapter begins with a quick, light introductory review of alkaloid biosynthesis, followed by detailed discussions on newer findings.

Chapters 2–16 are concerned with the phytochemistry of the alkaloids of pyrrolidine, piperidine, and pyridine; tropane; pyrrolizidine; indolizidine; quinolizidine; quinoline, quinazoline, acridone, and related compounds; β-phenylethylamines and isoquinoline; Amaryllidaceae and related plants; *Erythrina* and related plants; indole; diterpenoid; and steroidal and miscellaneous alkaloids. As is the case in past books of this series, the chapters on indole and isoquinoline alkaloids are more extensive than the discussions of other groups of compounds simply because of the abundance of literature on the chemistry of these two groups of alkaloids.

Of particular interest to students of indole alkaloids is J. A. Joule's compilation of ^{13}C-NMR data in a table of 36 typical indole and two biogenetically related quinoline alkaloid structures. These data should be of invaluable aid in the identification and structure elucidation of similar indole alkaloids.

Other than the relatively high price, one can recommend this book unequivocably to students of natural products chemistry.

Reviewed by Harry H. S. Fong
Department of Pharmacognosy
College of Pharmacy
University of Illinois at the Medical Center
Chicago, IL 60612

Symposium on Clinical Pharmacology. Sponsored by the National Cancer Institute. Pergamon Press, Maxwell House, Fairview Park, Elmsford, NY 10523. 236 pp. 16 × 23 cm. Price $20.00.

This book is a collection of the papers presented at the Symposium on Clinical Pharmacology sponsored by the National Cancer Institute in the spring of 1973. Its purpose was to present and collate the most recent advances in the field of cancer chemotherapy. The papers are divided into five broad areas: Pharmacological Factors in Drug Action, Factors Influencing Drug Selectivity, Mechanisms of Clinical Drug Resistance, Combination Chemotherapy, and New Information on Mechanisms of Drug Action. This book should be of value to those involved in development of potential therapies for cancer.

Staff Review

The chapter on "Radiopharmaceuticals" is introduced with an outline of radioactivity and definitions, choice of radionuclide, principles of radiation hygiene, historical aspects of radioactive materials, and the radioactive products official in the *British Pharmacopoeia*. The diagnostic applications of radiopharmaceuticals are presented, and descriptions of radionuclide generators are given. Hospital preparation of radiopharmaceuticals, including the use of ampuls and multidose vials, the use of bactericides, and quality control, is described. A section on toxic ingredients and adverse reactions includes control by drug regulatory authorities. A final section discusses radioisotopes in clinical chemistry, professional collaboration, and future developments.

The chapter on "Rectal Administration of Drugs" is introduced with a discussion of lipid materials and water-soluble compositions as bases for suppositories. Sections on formulation development and quality control include drug release, problems with suspended solids, viscosity adjustments, melting ranges, solidification ranges, and physical breakdown in water. The manufacture and packaging of suppositories are included. Finally, a section on the rectal absorption of drugs (several different examples are given) in animals and humans is presented.

An index makes it possible to find most topics covered in the book.

The authors of this volume have cited over 800 references, including many of their own research papers, in their chapters. This broad coverage not only makes the volume valuable in itself but also is an advantage to the reader who may want to follow up on specific subjects.

Reviewed by Elmer M. Plein
University of Washington
School of Pharmacy
Seattle, Washington 98195

Beta-blockers—Present Status and Future Prospects. Edited by W. SCHWEIZER. University Park Press, Chamber of Commerce Building, Baltimore, MD 21202, 1974. 325 pp. 17.5 × 24.5 cm. Price $19.50.

This publication contains the proceedings of an International Symposium held May 27–29, 1974. The book starts out with introductory remarks by Dr. C. Bartorelli describing the various points to be considered when evaluating beta-adrenergic blocking agents as potential antihypertensive drugs. The following chapter describes in great detail the relative beta-adrenergic blocking activity of various beta-blockers and their advantages and disadvantages when used as antihypertensive agents. Various possible mechanisms of action for the antihypertensive property of beta-blockers are also discussed.

The remaining chapters deal with various aspects of beta-blockers when prescribed as antihypertensive agents. All of these chapters are concise and well written, and certain aspects such as the renin–angiotensin–aldosterone interaction and the effect of beta-blockers on this system are covered rather thoroughly. In addition, there are chapters dealing with the importance of plasma volume in the treatment of hypertension and clinical experience with beta-blockers in the treatment of hypertension in the United Kindgom. Most of the chapters are followed by discussion sections which are very stimulating. Finally, the use of beta-blockers as antihypertensives is covered in a general discussion session, which is interesting, thought-provoking, and invaluable to the practicing physician as well as various research investigators.

Another aspect of beta-blockers covered in this book deals with their use in ischemic heart diseases, angina pectoris, cardiac arrhythmias, and hypertrophic cardiomyopathy. All of these chapters are written very thoroughly. The book also contains separate chapters that cover such topics as cardiological aspects of beta-blockade in stress situations and oxygen dissociation from hemoglobin. Finally, the last portion of the book is devoted to describing the metabolic effects of beta-blockers as well as their pharmacokinetic properties, followed by a general discussion session on guidelines for the use of beta-blockers in general practice.

This book can serve as an excellent reference source for clinicians, research investigators, graduate students, and clinical pharmacists. Considering the wealth of information contained in this volume, the price is very reasonable.

Reviewed by Mustafa F. Lokhandwala
Department of Pharmacology
College of Pharmacy
University of Houston
Houston, TX 77004

The Alkaloids. Vol. 5. Edited by J. E. SAXTON. The Chemical Society, Burlington House, London, England, W1V OBN, 1975. 303 pp. 14 × 22 cm. Price $48.25.

This book, the fifth of a series on alkaloids, is divided into 16 chapters and covers the literature from July 1973 to June 1974. As is the custom with previous books in this series, the first chapter is concerned with the biosynthesis of various classes of alkaloids and constitutes approximately 20% of the total book volume. This chapter begins with a quick, light introductory review of alkaloid biosynthesis, followed by detailed discussions on newer findings.

Chapters 2–16 are concerned with the phytochemistry of the alkaloids of pyrrolidine, piperidine, and pyridine; tropane; pyrrolizidine; indolizidine; quinolizidine; quinoline, quinazoline, acridone, and related compounds; β-phenylethylamines and isoquinoline; Amaryllidaceae and related plants; *Erythrina* and related plants; indole; diterpenoid; and steroidal and miscellaneous alkaloids. As is the case in past books of this series, the chapters on indole and isoquinoline alkaloids are more extensive than the discussions of other groups of compounds simply because of the abundance of literature on the chemistry of these two groups of alkaloids.

Of particular interest to students of indole alkaloids is J. A. Joule's compilation of ^{13}C-NMR data in a table of 36 typical indole and two biogenetically related quinoline alkaloid structures. These data should be of invaluable aid in the identification and structure elucidation of similar indole alkaloids.

Other than the relatively high price, one can recommend this book unequivocably to students of natural products chemistry.

Reviewed by Harry H. S. Fong
Department of Pharmacognosy
College of Pharmacy
University of Illinois at the Medical Center
Chicago, IL 60612

Symposium on Clinical Pharmacology. Sponsored by the National Cancer Institute. Pergamon Press, Maxwell House, Fairview Park, Elmsford, NY 10523. 236 pp. 16 × 23 cm. Price $20.00.

This book is a collection of the papers presented at the Symposium on Clinical Pharmacology sponsored by the National Cancer Institute in the spring of 1973. Its purpose was to present and collate the most recent advances in the field of cancer chemotherapy. The papers are divided into five broad areas: Pharmacological Factors in Drug Action, Factors Influencing Drug Selectivity, Mechanisms of Clinical Drug Resistance, Combination Chemotherapy, and New Information on Mechanisms of Drug Action. This book should be of value to those involved in development of potential therapies for cancer.

Staff Review

The chapter on "Radiopharmaceuticals" is introduced with an outline of radioactivity and definitions, choice of radionuclide, principles of radiation hygiene, historical aspects of radioactive materials, and the radioactive products official in the *British Pharmacopoeia*. The diagnostic applications of radiopharmaceuticals are presented, and descriptions of radionuclide generators are given. Hospital preparation of radiopharmaceuticals, including the use of ampuls and multidose vials, the use of bactericides, and quality control, is described. A section on toxic ingredients and adverse reactions includes control by drug regulatory authorities. A final section discusses radioisotopes in clinical chemistry, professional collaboration, and future developments.

The chapter on "Rectal Administration of Drugs" is introduced with a discussion of lipid materials and water-soluble compositions as bases for suppositories. Sections on formulation development and quality control include drug release, problems with suspended solids, viscosity adjustments, melting ranges, solidification ranges, and physical breakdown in water. The manufacture and packaging of suppositories are included. Finally, a section on the rectal absorption of drugs (several different examples are given) in animals and humans is presented.

An index makes it possible to find most topics covered in the book.

The authors of this volume have cited over 800 references, including many of their own research papers, in their chapters. This broad coverage not only makes the volume valuable in itself but also is an advantage to the reader who may want to follow up on specific subjects.

Reviewed by Elmer M. Plein
University of Washington
School of Pharmacy
Seattle, Washington 98195

Beta-blockers—Present Status and Future Prospects. Edited by W. SCHWEIZER. University Park Press, Chamber of Commerce Building, Baltimore, MD 21202, 1974. 325 pp. 17.5 × 24.5 cm. Price $19.50.

This publication contains the proceedings of an International Symposium held May 27–29, 1974. The book starts out with introductory remarks by Dr. C. Bartorelli describing the various points to be considered when evaluating beta-adrenergic blocking agents as potential antihypertensive drugs. The following chapter describes in great detail the relative beta-adrenergic blocking activity of various beta-blockers and their advantages and disadvantages when used as antihypertensive agents. Various possible mechanisms of action for the antihypertensive property of beta-blockers are also discussed.

The remaining chapters deal with various aspects of beta-blockers when prescribed as antihypertensive agents. All of these chapters are concise and well written, and certain aspects such as the renin–angiotensin–aldosterone interaction and the effect of beta-blockers on this system are covered rather thoroughly. In addition, there are chapters dealing with the importance of plasma volume in the treatment of hypertension and clinical experience with beta-blockers in the treatment of hypertension in the United Kindgom. Most of the chapters are followed by discussion sections which are very stimulating. Finally, the use of beta-blockers as antihypertensives is covered in a general discussion session, which is interesting, thought-provoking, and invaluable to the practicing physician as well as various research investigators.

Another aspect of beta-blockers covered in this book deals with their use in ischemic heart diseases, angina pectoris, cardiac arrhythmias, and hypertrophic cardiomyopathy. All of these chapters are written very thoroughly. The book also contains separate chapters that cover such topics as cardiological aspects of beta-blockade in stress situations and oxygen dissociation from hemoglobin. Finally, the last portion of the book is devoted to describing the metabolic effects of beta-blockers as well as their pharmacokinetic properties, followed by a general discussion session on guidelines for the use of beta-blockers in general practice.

This book can serve as an excellent reference source for clinicians, research investigators, graduate students, and clinical pharmacists. Considering the wealth of information contained in this volume, the price is very reasonable.

Reviewed by Mustafa F. Lokhandwala
Department of Pharmacology
College of Pharmacy
University of Houston
Houston, TX 77004

The Alkaloids. Vol. 5. Edited by J. E. SAXTON. The Chemical Society, Burlington House, London, England, W1V OBN, 1975. 303 pp. 14 × 22 cm. Price $48.25.

This book, the fifth of a series on alkaloids, is divided into 16 chapters and covers the literature from July 1973 to June 1974. As is the custom with previous books in this series, the first chapter is concerned with the biosynthesis of various classes of alkaloids and constitutes approximately 20% of the total book volume. This chapter begins with a quick, light introductory review of alkaloid biosynthesis, followed by detailed discussions on newer findings.

Chapters 2–16 are concerned with the phytochemistry of the alkaloids of pyrrolidine, piperidine, and pyridine; tropane; pyrrolizidine; indolizidine; quinolizidine; quinoline, quinazoline, acridone, and related compounds; β-phenylethylamines and isoquinoline; Amaryllidaceae and related plants; *Erythrina* and related plants; indole; diterpenoid; and steroidal and miscellaneous alkaloids. As is the case in past books of this series, the chapters on indole and isoquinoline alkaloids are more extensive than the discussions of other groups of compounds simply because of the abundance of literature on the chemistry of these two groups of alkaloids.

Of particular interest to students of indole alkaloids is J. A. Joule's compilation of ^{13}C-NMR data in a table of 36 typical indole and two biogenetically related quinoline alkaloid structures. These data should be of invaluable aid in the identification and structure elucidation of similar indole alkaloids.

Other than the relatively high price, one can recommend this book unequivocably to students of natural products chemistry.

Reviewed by Harry H. S. Fong
Department of Pharmacognosy
College of Pharmacy
University of Illinois at the Medical Center
Chicago, IL 60612

Symposium on Clinical Pharmacology. Sponsored by the National Cancer Institute. Pergamon Press, Maxwell House, Fairview Park, Elmsford, NY 10523. 236 pp. 16 × 23 cm. Price $20.00.

This book is a collection of the papers presented at the Symposium on Clinical Pharmacology sponsored by the National Cancer Institute in the spring of 1973. Its purpose was to present and collate the most recent advances in the field of cancer chemotherapy. The papers are divided into five broad areas: Pharmacological Factors in Drug Action, Factors Influencing Drug Selectivity, Mechanisms of Clinical Drug Resistance, Combination Chemotherapy, and New Information on Mechanisms of Drug Action. This book should be of value to those involved in development of potential therapies for cancer.

Staff Review

Journal of Pharmaceutical Sciences

DECEMBER 1976

VOLUME 65 NUMBER 12

MARY H. FERGUSON
Editor

L. LUAN CORRIGAN
Assistant Editor

SHELLY ELLIOTT
Production Editor

JANET D. SHOFF
Copy Editor

EDWARD G. FELDMANN
Contributing Editor

SAMUEL W. GOLDSTEIN
Contributing Editor

LELAND J. ARNEY
Director of Publications

EDITORIAL ADVISORY BOARD

JOHN AUTIAN	HARRY B. KOSTENBAUDER
LYNN R. BRADY	CARL J. LINTNER, JR.
WILLIAM O. FOYE	DAVID E. MANN, JR.
WILLIAM J. JUSKO	GERALD J. PAPARIELLO

The *Journal of Pharmaceutical Sciences* is published monthly by the American Pharmaceutical Association at 2215 Constitution Ave., N.W., Washington, DC 20037. Second-class postage paid at Washington, D.C., and at additional mailing office.

All expressions of opinion and statements of supposed fact appearing in articles or editorials carried in this journal are published on the authority of the writer over whose name they appear and are not to be regarded as necessarily expressing the policies or views of the American Pharmaceutical Association.

Offices—Editorial, Advertising, and Subscription Offices: 2215 Constitution Ave., N.W., Washington, DC 20037. Printing Offices: 20th & Northampton Streets, Easton, PA 18042.

Annual Subscriptions—United States and foreign, industrial and government institutions $50, educational institutions $50, individuals *for personal use only* $30; single copies $5. All foreign subscriptions add $5 for postage. Subscription rates are subject to change without notice. Members of the American Pharmaceutical Association may elect to receive the *Journal of Pharmaceutical Sciences* as a part of their annual $60 (foreign $65) APhA membership dues.

Claims—Missing numbers will not be supplied if dues or subscriptions are in arrears for more than 60 days or if claims are received more than 60 days after the date of the issue, or if loss was due to failure to give notice of change of address. The Association cannot accept responsibility for foreign delivery when its records indicate shipment has been made.

Change of Address—Members and subscribers should notify at once both the Post Office and the American Pharmaceutical Association, 2215 Constitution Ave., N.W., Washington, DC 20037, of any change of address.

© Copyright 1976, American Pharmaceutical Association, 2215 Constitution Ave., N.W., Washington, DC 20037; all rights reserved.

SCIENTIFIC RESEARCH FREEDOM

In November 1969, the APhA House of Delegates held a special meeting during which George E. Schreiner, M.D., Professor of Medicine at Georgetown University School of Medicine, delivered the luncheon address on the subject of "Scientific Freedom."

In his opening remarks, Dr. Schreiner observed that *"Research scientists have been recognized by society as being creative persons, very analogous to the artist and poet, and they, therefore, have been accorded considerable latitude in expressions of freedom in an open society which recognizes innovation and imagination."* He then went on to list seven specific scientific freedoms, ranging from choosing the research area, through conducting the project and communicating the results, to drawing conclusions from the data developed.

Having made these points, the speaker devoted the balance of his presentation to emphasizing that *"such extreme degrees of freedom carry with them quite definite responsibilities"*—namely, that the researcher must develop a personal code of professional conduct. He spoke of general codes, such as those of Nuremberg and Helsinki, as well as the traditional obligation of the scientist to strive for accuracy, integrity, and honesty in the work conducted and reported.

He then went on to point out that the scientific and moral criteria used by society as a benchmark for arriving at an attitude of general "approval" were becoming more and more specific—largely as a cause and effect result of omissions or errors in judgment by scientific investigators. For example, he attributed the series of New York State trials involving the injection of cancer cells into elderly patients at the Jewish Chronic Disease Hospital as the prime stimulus leading to adoption of the requirement for written informed consent.

In the ensuing seven years, we have heard of a number of other disturbing incidents—such as the careless use of prisoners in a poorly planned and inadequately supervised syphilis study. In turn, this revelation has led to severe restrictions being applied to the use of prisoners for any kind of medically related research, irrespective of how well controlled, conducted, and supervised.

Currently, the National Institutes of Health is attempting to anticipate the potential risk and hazard which might ensue from any slip or careless step in the conduct of recombinant DNA research. These are the so-called "creation of life" experiments which involve combining gene-containing fragments of DNA (deoxyribonucleic acid), the molecule that transmits heredity, with chromosomes of another sort of organism to produce an entirely new or different type of organism.

The NIH has set forth proposed guidelines and published these for public comment. In part, the preamble cryptically states: *"The promise of recombinant DNA research for better understanding and improved treatment of human disease is great. There is also a possible risk that microorganisms with foreign genes might cause disease or alter the environment should they escape from the laboratory and infect human beings, animals, or plants."*

World history is replete with examples of such "escapes from the laboratory" and elsewhere of microorganisms, insects, rodents, and other animal pests which previously were unknown to a certain part of the world and which then rapidly proliferated to produce a wave of destruction. Current laws restricting the import of agricultural products are one means now used to control such problems.

During the past fifteen years, space science turned into reality the Buck Rogers-type fantasies of the 1930's. Recombinant DNA research has the potential of turning the present day horror films depicting seven-foot long rats and man-eating spiders into tomorrow's realities. Consequently, we believe that NIH is acting prudently, wisely, and timely in its effort to establish guidelines designed to ensure proper safeguard and controls in conducting this research.

Moreover, the seriousness of this subject would lead us to expect that all other responsible parties would share this view. And it appears that most do.

For a while it appeared that there would be one sour note. It seems that one special interest group was reluctant to support or embrace these guidelines out of fear that the guidelines for voluntary compliance would eventually become obligatory and thereby be enforced. Frankly, we were stunned by this attitude.

Since there is ample precedent to believe that a real danger does exist if this kind of research is not properly monitored, it strikes us that—rather than be concerned that the guidelines *might* become mandatory—we should ask why they were not proposed in a fashion that would definitely provide for them to become mandatory after appropriate review, comment, and possible revision.

Dr. Schreiner put this proposition very well in his scientific freedom speech of seven years ago when he quoted Teddy Roosevelt: *"Your right to swing ends where my chin begins!"*

Edward G. Feldmann

Journal of Pharmaceutical Sciences

DECEMBER 1976

VOLUME 65 NUMBER 12

MARY H. FERGUSON
Editor

L. LUAN CORRIGAN
Assistant Editor

SHELLY ELLIOTT
Production Editor

JANET D. SHOFF
Copy Editor

EDWARD G. FELDMANN
Contributing Editor

SAMUEL W. GOLDSTEIN
Contributing Editor

LELAND J. ARNEY
Director of Publications

EDITORIAL ADVISORY BOARD

JOHN AUTIAN	HARRY B. KOSTENBAUDER
LYNN R. BRADY	CARL J. LINTNER, JR.
WILLIAM O. FOYE	DAVID E. MANN, JR.
WILLIAM J. JUSKO	GERALD J. PAPARIELLO

The *Journal of Pharmaceutical Sciences* is published monthly by the American Pharmaceutical Association at 2215 Constitution Ave., N.W., Washington, DC 20037. Second-class postage paid at Washington, D.C., and at additional mailing office.

All expressions of opinion and statements of supposed fact appearing in articles or editorials carried in this journal are published on the authority of the writer over whose name they appear and are not to be regarded as necessarily expressing the policies or views of the American Pharmaceutical Association.

Offices—Editorial, Advertising, and Subscription Offices: 2215 Constitution Ave., N.W., Washington, DC 20037. Printing Offices: 20th & Northampton Streets, Easton, PA 18042.

Annual Subscriptions—United States and foreign, industrial and government institutions $50, educational institutions $50, individuals *for personal use only* $30; single copies $5. All foreign subscriptions add $5 for postage. Subscription rates are subject to change without notice. Members of the American Pharmaceutical Association may elect to receive the *Journal of Pharmaceutical Sciences* as a part of their annual $60 (foreign $65) APhA membership dues.

Claims—Missing numbers will not be supplied if dues or subscriptions are in arrears for more than 60 days or if claims are received more than 60 days after the date of the issue, or if loss was due to failure to give notice of change of address. The Association cannot accept responsibility for foreign delivery when its records indicate shipment has been made.

Change of Address—Members and subscribers should notify at once both the Post Office and the American Pharmaceutical Association, 2215 Constitution Ave., N.W., Washington, DC 20037, of any change of address.

© Copyright 1976, American Pharmaceutical Association, 2215 Constitution Ave., N.W., Washington, DC 20037; all rights reserved.

SCIENTIFIC RESEARCH FREEDOM

In November 1969, the APhA House of Delegates held a special meeting during which George E. Schreiner, M.D., Professor of Medicine at Georgetown University School of Medicine, delivered the luncheon address on the subject of "Scientific Freedom."

In his opening remarks, Dr. Schreiner observed that *"Research scientists have been recognized by society as being creative persons, very analogous to the artist and poet, and they, therefore, have been accorded considerable latitude in expressions of freedom in an open society which recognizes innovation and imagination."* He then went on to list seven specific scientific freedoms, ranging from choosing the research area, through conducting the project and communicating the results, to drawing conclusions from the data developed.

Having made these points, the speaker devoted the balance of his presentation to emphasizing that *"such extreme degrees of freedom carry with them quite definite responsibilities"*—namely, that the researcher must develop a personal code of professional conduct. He spoke of general codes, such as those of Nuremberg and Helsinki, as well as the traditional obligation of the scientist to strive for accuracy, integrity, and honesty in the work conducted and reported.

He then went on to point out that the scientific and moral criteria used by society as a benchmark for arriving at an attitude of general "approval" were becoming more and more specific—largely as a cause and effect result of omissions or errors in judgment by scientific investigators. For example, he attributed the series of New York State trials involving the injection of cancer cells into elderly patients at the Jewish Chronic Disease Hospital as the prime stimulus leading to adoption of the requirement for written informed consent.

In the ensuing seven years, we have heard of a number of other disturbing incidents—such as the careless use of prisoners in a poorly planned and inadequately supervised syphilis study. In turn, this revelation has led to severe restrictions being applied to the use of prisoners for any kind of medically related research, irrespective of how well controlled, conducted, and supervised.

Currently, the National Institutes of Health is attempting to anticipate the potential risk and hazard which might ensue from any slip or careless step in the conduct of recombinant DNA research. These are the so-called "creation of life" experiments which involve combining gene-containing fragments of DNA (deoxyribonucleic acid), the molecule that transmits heredity, with chromosomes of another sort of organism to produce an entirely new or different type of organism.

The NIH has set forth proposed guidelines and published these for public comment. In part, the preamble cryptically states: *"The promise of recombinant DNA research for better understanding and improved treatment of human disease is great. There is also a possible risk that microorganisms with foreign genes might cause disease or alter the environment should they escape from the laboratory and infect human beings, animals, or plants."*

World history is replete with examples of such "escapes from the laboratory" and elsewhere of microorganisms, insects, rodents, and other animal pests which previously were unknown to a certain part of the world and which then rapidly proliferated to produce a wave of destruction. Current laws restricting the import of agricultural products are one means now used to control such problems.

During the past fifteen years, space science turned into reality the Buck Rogers-type fantasies of the 1930's. Recombinant DNA research has the potential of turning the present day horror films depicting seven-foot long rats and man-eating spiders into tomorrow's realities. Consequently, we believe that NIH is acting prudently, wisely, and timely in its effort to establish guidelines designed to ensure proper safeguard and controls in conducting this research.

Moreover, the seriousness of this subject would lead us to expect that all other responsible parties would share this view. And it appears that most do.

For a while it appeared that there would be one sour note. It seems that one special interest group was reluctant to support or embrace these guidelines out of fear that the guidelines for voluntary compliance would eventually become obligatory and thereby be enforced. Frankly, we were stunned by this attitude.

Since there is ample precedent to believe that a real danger does exist if this kind of research is not properly monitored, it strikes us that—rather than be concerned that the guidelines *might* become mandatory—we should ask why they were not proposed in a fashion that would definitely provide for them to become mandatory after appropriate review, comment, and possible revision.

Dr. Schreiner put this proposition very well in his scientific freedom speech of seven years ago when he quoted Teddy Roosevelt: *"Your right to swing ends where my chin begins!"*

Edward G. Feldmann

GC Determination of Pilocarpine and Isopilocarpine

Although Urbányi *et al.*[1] recently reported an interesting method for the determination of pilocarpine and its *trans*-isomer, isopilocarpine, in pharmaceutical preparations using liquid chromatography, I would like to draw attention to a report by Aboul-Enein[2] which described the separation of pilocarpine and isopilocarpine by GC.

A Beckman 45G instrument was used, and the separation was effective using a 1.8-m (6-ft) long column packed with 5% OV-17 on Gas Chrom P (80–100 mesh). The injector, column, and detector temperatures were 235, 225, and 235°, respectively. The gas flow rates were: hydrogen, 40 ml/min; air, 250 ml/min; and helium as a carrier gas, 100 ml/min. This method is applicable for the analysis of commercial pilocarpine ophthalmic preparations and for the detection and determination of isopilocarpine in these solutions.

This method is suitable and sensitive, and it offers an alternative method to the liquid chromatographic technique.

Hassan Y. Aboul-Enein
Department of Pharmaceutical and Medicinal Chemistry
Faculty of Pharmacy
Riyadh University
Riyadh, Saudi Arabia

Received June 14, 1976.

[1] T. Urbányi, A. Piedmont, E. Willis, and G. Manning, *J. Pharm. Sci.*, **65**, 257(1976).
[2] H. Y. Aboul-Enein, *Acta Pharm. Suec.*, 11, 387(1974).

Bolus Intravenous Injections: Round 2

Dr. Wagner[1] recently criticized my paper[2], stating that the limiting assumption:

$$\frac{1 - e^{-b_i\theta}}{b_i\theta} = 1 \qquad \text{(Eq. 1)}$$

is "incorrect" and cautioned readers "*not* to make such corrections" as suggested. I believe this criticism resulted due to the different terminology Dr. Wagner uses in his calculations. The plasma concentration following infusion is given by[1]:

$$C_p = \sum_{i=1}^{n} C_i \frac{(e^{+b_i\theta} - 1)}{b_i\theta} e^{-b_i t} \qquad \text{(Eq. 2)}$$

where t is time from the start of infusion, and θ is the infusion time. I used the terminology t', which is:

$$t' = t - \theta \qquad \text{(Eq. 3)}$$

Substitution of Eq. 3 into Eq. 2 gives:

$$C_p = \sum_{i=1}^{n} C_i \frac{(1 - e^{-b_i\theta})}{b_i\theta} e^{-b_i t'} \qquad \text{(Eq. 4)}$$

This equation is identical to one described in the published report[2]. This terminology was used to allow direct comparisons between equations used for infusion and bolus administration since the term Y_i used by Dr. Wagner is:

$$Y_i = \text{(observed intercept, postinfusion) } e^{+b_i\theta} \qquad \text{(Eq. 5)}$$

If postinfusion data are used to calculate the pharmacokinetic parameters assuming an instantaneous input, an invalid assumption is made (Eq. 1), which should be corrected as described in the published report.

Sarfaraz Niazi
Department of Pharmacy
College of Pharmacy
University of Illinois at the Medical Center
Chicago, IL 60612

Received August 25, 1976.

[1] J. G. Wagner, *J. Pharm. Sci.*, **65**(8), viii(1976).
[2] S. Niazi, *ibid.*, **65**, 750(1976).

Bolus Intravenous Injections: Round 3

The paper of Niazi[1] prompted me to make a comment in the Open Forum[2]. Now Niazi[3] has written a comment in the Open Forum, which implies that the only problem was his use of t' rather than my t. But this is not so.

If postinfusion data are fitted to a polyexponential equation, one uses the equations of Loo and Riegelman[4]; then no "corrections," as proposed by Niazi[1], are needed. Such corrections are only needed when one applies equations derived from the bolus intravenous equation. Niazi is actually talking to scientists who give infusions and then disregard that they gave an infusion and *treat the data as if they had administered a bolus intravenous injection.* It is unfortunate that there is such misunderstanding of pharmacokinetics, but I wished to eliminate further misunderstanding. I do not believe that Dr. Niazi made it clear what he was discussing.

My comment[2] about the "incorrectness" of the equation shown as Eq. 1 in both my Open Forum comment[2] and his[3] refers to his approach. The equation is inconsistent for $\theta = 0$ (case for bolus intravenous injection), since the left-hand side is equal to zero and the right-hand side is equal to unity. It is preferable to discuss the change of a coefficient obtained by fitting "during infusion" or "postinfusion" data to a coefficient that would have been obtained if the same dose had been administered as a bolus intravenous injection to the same subject; this is what I did in my Open Forum comment[2] in Eqs. 5 and 6.

I hope that this letter clarifies my comment[2].

John G. Wagner
College of Pharmacy and Upjohn Center for Clinical Pharmacology
University of Michigan
Ann Arbor, MI 48109

Received September 1, 1976.

[1] S. Niazi, *J. Pharm. Sci.*, **65**, 750(1976).
[2] J. G. Wagner, *ibid.*, **65**(8), viii(1976).
[3] S. Niazi, *ibid.*, **65**(12), iv(1976).
[4] J. C. K. Loo and S. Riegelman, *ibid.*, **59**, 53(1970).

GC Determination of Pilocarpine and Isopilocarpine

Although Urbányi *et al.*[1] recently reported an interesting method for the determination of pilocarpine and its *trans*-isomer, isopilocarpine, in pharmaceutical preparations using liquid chromatography, I would like to draw attention to a report by Aboul-Enein[2] which described the separation of pilocarpine and isopilocarpine by GC.

A Beckman 45G instrument was used, and the separation was effective using a 1.8-m (6-ft) long column packed with 5% OV-17 on Gas Chrom P (80–100 mesh). The injector, column, and detector temperatures were 235, 225, and 235°, respectively. The gas flow rates were: hydrogen, 40 ml/min; air, 250 ml/min; and helium as a carrier gas, 100 ml/min. This method is applicable for the analysis of commercial pilocarpine ophthalmic preparations and for the detection and determination of isopilocarpine in these solutions.

This method is suitable and sensitive, and it offers an alternative method to the liquid chromatographic technique.

Hassan Y. Aboul-Enein
Department of Pharmaceutical and Medicinal Chemistry
Faculty of Pharmacy
Riyadh University
Riyadh, Saudi Arabia

Received June 14, 1976.

[1] T. Urbányi, A. Piedmont, E. Willis, and G. Manning, *J. Pharm. Sci.*, **65**, 257(1976).
[2] H. Y. Aboul-Enein, *Acta Pharm. Suec.*, 11, 387(1974).

Bolus Intravenous Injections: Round 2

Dr. Wagner[1] recently criticized my paper[2], stating that the limiting assumption:

$$\frac{1 - e^{-b_i\theta}}{b_i\theta} = 1 \qquad \text{(Eq. 1)}$$

is "incorrect" and cautioned readers "*not* to make such corrections" as suggested. I believe this criticism resulted due to the different terminology Dr. Wagner uses in his calculations. The plasma concentration following infusion is given by[1]:

$$C_p = \sum_{i=1}^{n} C_i \frac{(e^{+b_i\theta} - 1)}{b_i\theta} e^{-b_i t} \qquad \text{(Eq. 2)}$$

where t is time from the start of infusion, and θ is the infusion time. I used the terminology t', which is:

$$t' = t - \theta \qquad \text{(Eq. 3)}$$

Substitution of Eq. 3 into Eq. 2 gives:

$$C_p = \sum_{i=1}^{n} C_i \frac{(1 - e^{-b_i\theta})}{b_i\theta} e^{-b_i t'} \qquad \text{(Eq. 4)}$$

This equation is identical to one described in the published report[2]. This terminology was used to allow direct comparisons between equations used for infusion and bolus administration since the term Y_i used by Dr. Wagner is:

$$Y_i = \text{(observed intercept, postinfusion) } e^{+b_i\theta} \qquad \text{(Eq. 5)}$$

If postinfusion data are used to calculate the pharmacokinetic parameters assuming an instantaneous input, an invalid assumption is made (Eq. 1), which should be corrected as described in the published report.

Sarfaraz Niazi
Department of Pharmacy
College of Pharmacy
University of Illinois at the Medical Center
Chicago, IL 60612

Received August 25, 1976.

[1] J. G. Wagner, *J. Pharm. Sci.*, **65**(8), viii(1976).
[2] S. Niazi, *ibid.*, **65**, 750(1976).

Bolus Intravenous Injections: Round 3

The paper of Niazi[1] prompted me to make a comment in the Open Forum[2]. Now Niazi[3] has written a comment in the Open Forum, which implies that the only problem was his use of t' rather than my t. But this is not so.

If postinfusion data are fitted to a polyexponential equation, one uses the equations of Loo and Riegelman[4]; then no "corrections," as proposed by Niazi[1], are needed. Such corrections are only needed when one applies equations derived from the bolus intravenous equation. Niazi is actually talking to scientists who give infusions and then disregard that they gave an infusion and *treat the data as if they had administered a bolus intravenous injection.* It is unfortunate that there is such misunderstanding of pharmacokinetics, but I wished to eliminate further misunderstanding. I do not believe that Dr. Niazi made it clear what he was discussing.

My comment[2] about the "incorrectness" of the equation shown as Eq. 1 in both my Open Forum comment[2] and his[3] refers to his approach. The equation is inconsistent for $\theta = 0$ (case for bolus intravenous injection), since the left-hand side is equal to zero and the right-hand side is equal to unity. It is preferable to discuss the change of a coefficient obtained by fitting "during infusion" or "postinfusion" data to a coefficient that would have been obtained if the same dose had been administered as a bolus intravenous injection to the same subject; this is what I did in my Open Forum comment[2] in Eqs. 5 and 6.

I hope that this letter clarifies my comment[2].

John G. Wagner
College of Pharmacy and Upjohn Center for Clinical Pharmacology
University of Michigan
Ann Arbor, MI 48109

Received September 1, 1976.

[1] S. Niazi, *J. Pharm. Sci.*, **65**, 750(1976).
[2] J. G. Wagner, *ibid.*, **65**(8), viii(1976).
[3] S. Niazi, *ibid.*, **65**(12), iv(1976).
[4] J. C. K. Loo and S. Riegelman, *ibid.*, **59**, 53(1970).

GC Determination of Pilocarpine and Isopilocarpine

Although Urbányi *et al.*[1] recently reported an interesting method for the determination of pilocarpine and its *trans*-isomer, isopilocarpine, in pharmaceutical preparations using liquid chromatography, I would like to draw attention to a report by Aboul-Enein[2] which described the separation of pilocarpine and isopilocarpine by GC.

A Beckman 45G instrument was used, and the separation was effective using a 1.8-m (6-ft) long column packed with 5% OV-17 on Gas Chrom P (80–100 mesh). The injector, column, and detector temperatures were 235, 225, and 235°, respectively. The gas flow rates were: hydrogen, 40 ml/min; air, 250 ml/min; and helium as a carrier gas, 100 ml/min. This method is applicable for the analysis of commercial pilocarpine ophthalmic preparations and for the detection and determination of isopilocarpine in these solutions.

This method is suitable and sensitive, and it offers an alternative method to the liquid chromatographic technique.

Hassan Y. Aboul-Enein
Department of Pharmaceutical and Medicinal Chemistry
Faculty of Pharmacy
Riyadh University
Riyadh, Saudi Arabia

Received June 14, 1976.

[1] T. Urbányi, A. Piedmont, E. Willis, and G. Manning, *J. Pharm. Sci.*, **65**, 257(1976).
[2] H. Y. Aboul-Enein, *Acta Pharm. Suec.*, 11, 387(1974).

Bolus Intravenous Injections: Round 2

Dr. Wagner[1] recently criticized my paper[2], stating that the limiting assumption:

$$\frac{1 - e^{-b_i\theta}}{b_i\theta} = 1 \qquad \text{(Eq. 1)}$$

is "incorrect" and cautioned readers "*not* to make such corrections" as suggested. I believe this criticism resulted due to the different terminology Dr. Wagner uses in his calculations. The plasma concentration following infusion is given by[1]:

$$C_p = \sum_{i=1}^{n} C_i \frac{(e^{+b_i\theta} - 1)}{b_i\theta} e^{-b_i t} \qquad \text{(Eq. 2)}$$

where t is time from the start of infusion, and θ is the infusion time. I used the terminology t', which is:

$$t' = t - \theta \qquad \text{(Eq. 3)}$$

Substitution of Eq. 3 into Eq. 2 gives:

$$C_p = \sum_{i=1}^{n} C_i \frac{(1 - e^{-b_i\theta})}{b_i\theta} e^{-b_i t'} \qquad \text{(Eq. 4)}$$

This equation is identical to one described in the published report[2]. This terminology was used to allow direct comparisons between equations used for infusion and bolus administration since the term Y_i used by Dr. Wagner is:

$$Y_i = \text{(observed intercept, postinfusion) } e^{+b_i\theta} \qquad \text{(Eq. 5)}$$

If postinfusion data are used to calculate the pharmacokinetic parameters assuming an instantaneous input, an invalid assumption is made (Eq. 1), which should be corrected as described in the published report.

Sarfaraz Niazi
Department of Pharmacy
College of Pharmacy
University of Illinois at the Medical Center
Chicago, IL 60612

Received August 25, 1976.

[1] J. G. Wagner, *J. Pharm. Sci.*, **65**(8), viii(1976).
[2] S. Niazi, *ibid.*, **65**, 750(1976).

Bolus Intravenous Injections: Round 3

The paper of Niazi[1] prompted me to make a comment in the Open Forum[2]. Now Niazi[3] has written a comment in the Open Forum, which implies that the only problem was his use of t' rather than my t. But this is not so.

If postinfusion data are fitted to a polyexponential equation, one uses the equations of Loo and Riegelman[4]; then no "corrections," as proposed by Niazi[1], are needed. Such corrections are only needed when one applies equations derived from the bolus intravenous equation. Niazi is actually talking to scientists who give infusions and then disregard that they gave an infusion and *treat the data as if they had administered a bolus intravenous injection.* It is unfortunate that there is such misunderstanding of pharmacokinetics, but I wished to eliminate further misunderstanding. I do not believe that Dr. Niazi made it clear what he was discussing.

My comment[2] about the "incorrectness" of the equation shown as Eq. 1 in both my Open Forum comment[2] and his[3] refers to his approach. The equation is inconsistent for $\theta = 0$ (case for bolus intravenous injection), since the left-hand side is equal to zero and the right-hand side is equal to unity. It is preferable to discuss the change of a coefficient obtained by fitting "during infusion" or "postinfusion" data to a coefficient that would have been obtained if the same dose had been administered as a bolus intravenous injection to the same subject; this is what I did in my Open Forum comment[2] in Eqs. 5 and 6.

I hope that this letter clarifies my comment[2].

John G. Wagner
College of Pharmacy and Upjohn Center for Clinical Pharmacology
University of Michigan
Ann Arbor, MI 48109

Received September 1, 1976.

[1] S. Niazi, *J. Pharm. Sci.*, **65**, 750(1976).
[2] J. G. Wagner, *ibid.*, **65**(8), viii(1976).
[3] S. Niazi, *ibid.*, **65**(12), iv(1976).
[4] J. C. K. Loo and S. Riegelman, *ibid.*, **59**, 53(1970).

Journal of Pharmaceutical Sciences

DECEMBER 1976
VOLUME 65 NUMBER 12

RESEARCH ARTICLES

Effect of Micellization on Rate of Cupric-Ion-Promoted Hydrolysis of Dicarboxylic Acid Hemiesters

JOHN T. H. ONG * and H. B. KOSTENBAUDER ˣ

Abstract □ The effect of micellar sodium lauryl sulfate on the rate of cupric-ion-promoted hydrolysis of some dicarboxylic acid hemiesters was investigated at pH 5, ionic strength 0.1 *M*, and 40, 45, and 50°. The rate of cupric-ion-promoted hydrolysis of sodium *n*-decyl oxalate in the micellar phase is about 50 times as fast as that in the bulk solution. The formation constant of the intermediate chelate complex, cupric decyl oxalate, was decreased in the micellar phase, while the rate of attack of hydroxide ion upon the chelate complex was increased. The overall rate increase is attributed to the increase in the entropy of activation for the reaction in the micellar phase. The rates of hydrolysis of sodium hydrocortisone 21-hemisuccinate and sodium hydrocortisone 21-hemi-(3,3-dimethylglutarate) were unaffected by copper ion.

Keyphrases □ Micellization—sodium lauryl sulfate, effect on rate of cupric-ion-promoted hydrolysis of dicarboxylic acid hemiesters □ Sodium lauryl sulfate—micellization, effect on rate of cupric-ion-promoted hydrolysis of dicarboxylic acid hemiesters □ Cupric-ion-promoted hydrolysis—dicarboxylic acid hemiesters, effect of micellar sodium lauryl sulfate on rate □ Hydrolysis, cupric ion promoted—dicarboxylic acid hemiesters, effect of micellar sodium lauryl sulfate on rate □ Dicarboxylic acid hemiesters—cupric-ion-promoted hydrolysis, effect of micellar sodium lauryl sulfate on rate

Monoesters of some dicarboxylic acids are subject to metal-ion catalysis, as indicated by the unusually large kinetic salt effects exerted by Tl^{+}, Ba^{+2}, Ca^{+2}, and $Co(NH_3)_6^{+3}$ ions on the rate of hydrolysis of ethyl esters of oxalic, malonic, and adipic acids (1). The catalytic effect of a series of divalent metal ions on the hydrolysis of potassium ethyl oxalate has been interpreted in terms of a mechanism in which the ester, which is coordinated to the metal ion to form an intermediate chelate complex (I) in a prior rapid equilibrium, is attacked by OH^{-} in the rate-determining step (2).

The present study was undertaken to assess the possible influence of micellization on the metal-ion-promoted hydrolysis of a dicarboxylic acid hemiester. Succinate or glutarate hemiesters of 21-hydroxy steroids have been commonly employed as water-soluble derivatives of several important corticosteroid drugs. There is evidence that corticosteroid 21-phosphate esters are capable of association colloid formation (3), and it is conceivable that corticosteroid 21-hemiesters of dicarboxylic acids might also exhibit either self-aggregation or association with micellar surface-active agents. It was of interest to evaluate the potential of such association colloids for increasing product lability to metal-ion-promoted hydrolysis.

Furthermore, although metal ions are sometimes required as a cofactor for reactions occurring in the organized structure characteristic of an enzyme system, the mechanisms of such reactions are commonly studied in nonenzymatic model systems (4, 5). The present work involves a detailed study of a model system that incorporates the effects of both metal ion and micellization on the rate of ester hydrolysis.

For this study, it was necessary to use an ester that would: (*a*) be sufficiently soluble so that the reactions could be carried out in aqueous solution, (*b*) exhibit metal-ion-catalyzed hydrolysis, and (*c*) have sufficient hydrophobic properties to either undergo self-aggre-

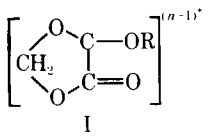

I

gation or be strongly bound to added surfactant micelles. Sodium *n*-decyl oxalate was selected as the model compound for extensive study. Since Cu^{+2} would form a sparingly soluble salt with the long chain oxalate, it was necessary to run the nonmicellar reactions in relatively dilute solutions.

EXPERIMENTAL

Materials—Sodium *n*-decyl oxalate, $C_{10}H_{21}OCOCOONa$, was prepared by means of half-saponification of bis(*n*-decyl) oxalate according to a modified procedure of Backer and Hóman (6) for the preparation of potassium *tert*-butyl oxalate, using dioxane as solvent and for recrystallization of the product, mp 202–205° dec. (uncor.). The IR and NMR spectra were consistent with the structure, and elemental analysis[1] gave the expected content of carbon (calc. 57.13; found 57.20) and hydrogen (calc. 8.39; found 8.42).

Bis(*n*-decyl) oxalate was prepared by esterification of oxalic acid with *n*-decyl alcohol, following the method of Bondar *et al.* (7).

Sodium lauryl sulfate was prepared from dodecyl alcohol and chlorosulfonic acid by the method of Dreger *et al.* (8). To remove trace quantities of dodecyl alcohol, the product was extracted with petroleum ether (bp 30–80°) in a soxhlet apparatus for 36 hr, recrystallized twice from absolute ethanol, and dried under vacuum. A plot of apparent surface tension–concentration did not show any minimum (9).

Sodium hydrocortisone 21-hemisuccinate[2] and sodium hydrocortisone 21-hemi-(3,3-dimethylglutarate)[3] were used as received.

Standard cupric nitrate solution[4] and analytical grade sodium nitrate were used in all experiments. The water was distilled water redistilled from glass.

Kinetics—Rates of hydrolysis were determined by a pH-stat technique[5]. The reaction flask was immersed in a constant-temperature water bath (±0.1°). Inserted into the reaction vessel was a glass electrode, a saturated calomel reference electrode, a stirrer, and a delivery tube for the sodium hydroxide titrant. The proportional band was set at 0.1.

The amount of sodium hydroxide solution delivered, which corresponded to the amount of ester hydrolyzed, was recorded as a percentage of the total capacity of the syringe buret. Pseudo-first-order rate constants, k_{obs}, were calculated from the slopes of the logarithm of the rate of sodium hydroxide consumed, $\Delta\%/\Delta t$, against time at the midpoint of the time interval. The plots were linear to about two half-lives. Reactions were run at constant pH 5.00, ionic strength 0.1 *M* with sodium nitrate, and 40, 45, and 50°.

For reactions in micellar systems, the concentrations of the components were 0.0200 *M* NaOH, 5×10^{-4} *M* sodium *n*-decyl oxalate, $4–30 \times 10^{-3}$ *M* sodium lauryl sulfate, and $2–5 \times 10^{-3}$ *M* $Cu(NO_3)_2$.

For reactions in nonmicellar systems, concentrations were 0.000475 *M* NaOH, $3–6 \times 10^{-5}$ *M* sodium *n*-decyl oxalate, and $0.4–1.25 \times 10^{-3}$ *M* $Cu(NO_3)_2$.

For hydrolysis of sodium hydrocortisone 21-hemisuccinate and sodium hydrocortisone 21-hemi-(3,3-dimethylglutarate), the procedure was the same as for sodium *n*-decyl oxalate hydrolysis.

Cu^{+2}-Ion Activity—The activity of Cu^{+2} ion in the bulk of the solution was measured using a specific cupric-ion electrode[6] in conjunction with a single-junction reference electrode[7]. The potentials were read on a digital, expanded scale, pH meter[8]. Calibration plots of the logarithm of activity *versus* potential were made at 40, 45, and 50° using cupric nitrate standard solution within the range of the activity of Cu^{+2} used in the reactions.

Critical Micelle Concentration (CMC)—The CMC of sodium *n*-decyl oxalate was determined at 40° and ionic strength 0.1 *M* using the surface tension method[9] and was 2.4×10^{-3} *M*.

[1] Performed by Micro-Analysis, Inc., Wilmington, Del.
[2] U-4905, batch MR 676, The Upjohn Co., Kalamazoo, Mich.
[3] U-5242, batch 3059-ESG-84, The Upjohn Co., Kalamazoo, Mich.
[4] Orion 0.1 *M* standard, Orion Research Inc., Cambridge, Mass.
[5] Radiometer A/S (Copenhagen, Denmark) comprised of TTT2 automatic titrator, TTA3 titration assembly, SBR2c titrigraph, and ABU 11 autoburet (2.5 ml).
[6] Orion 94-29, Orion Research Inc., Cambridge, Mass.
[7] Orion 90-01, Orion Research Inc., Cambridge, Mass.
[8] Model 110, Corning Scientific Instruments, Medfield, Mass.
[9] Fisher surface tensiometer, model 20, Fisher Scientific Co., Pittsburgh, Pa.

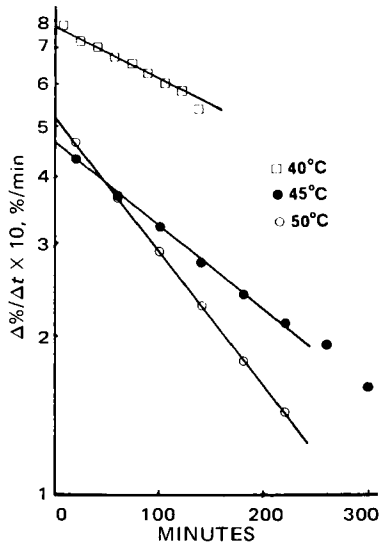

Figure 1—*Finite increments of sodium hydroxide solution and time as a function of time for representative studies of sodium* n*-decyl oxalate hydrolysis in the absence of sodium lauryl sulfate micelles at pH 5.00 and ionic strength 0.1* M.

RESULTS AND DISCUSSION

Kinetics in Absence of Sodium Lauryl Sulfate Micelles—The mechanism of sodium *n*-decyl oxalate hydrolysis should follow that proposed (2) for potassium ethyl oxalate shown in Scheme I.

$$DOx^- + Cu^{+2} \underset{}{\overset{K_f}{\rightleftharpoons}} CuDOx^+$$

$$CuDOx^+ + OH^- \xrightarrow[\text{slow}]{k_o} CuOx + DOH$$

Scheme I

The rate law can be written as:

$$\text{rate} = k_o[OH^-][CuDOx^+] \qquad \text{(Eq. 1)}$$

$$\text{rate} = \frac{k_o K_f a_{Cu^{+2}}[OH^-]}{1 + K_f a_{Cu^{+2}}}[DOx^-]_{total} \qquad \text{(Eq. 2)}$$

where $a_{Cu^{+2}}$ is the activity of Cu^{+2} ion in the bulk of the solution; K_f is the formation constant of the $CuDOx^+$ chelate complex; and subscript *o* denotes a nonmicellar system.

The pseudo-first-order rate constant, k_{obs}, is:

$$(k_{obs})_o = \frac{k_o K_f a_{Cu^{+2}}[OH^-]}{1 + K_f a_{Cu^{+2}}} \qquad \text{(Eq. 3)}$$

Figure 1 illustrates a typical plot of the logarithm of the rate of hydroxide consumption *versus* time, from which $(k_{obs})_o$ is calculated. Rearranging Eq. 3 gives:

$$\frac{[OH^-]}{(k_{obs})_o} = \frac{1}{k_o K_f a_{Cu^{+2}}} + \frac{1}{k_o} \qquad \text{(Eq. 4)}$$

Therefore, a plot of $[OH^-]/(k_{obs})_o$ *versus* $1/a_{Cu^{+2}}$ should give a straight line with the slope of $1/k_o K_f$ and the intercept of $1/k_o$. From the extrapolated intercept and slope, the values of k_o and K_f can be determined.

The value of $[OH^-]$ was calculated at pH 5.00 from the data given by Harned and Hamer (10). In solution of ionic strength 0.1 *M*, $[OH^-]$ is 3.06×10^{-9}, 4.23×10^{-9}, and 5.69×10^{-9} *M* at 40, 45, and 50°, respectively.

Figure 2 shows plots according to Eq. 4 at 40, 45, and 50°. Linear regression lines were drawn to obtain the best fit. The values of k_o and K_f are recorded in Table I.

Kinetics in Presence of Sodium Lauryl Sulfate Micelles—Both substrate and micelle have a similar long hydrocarbon hydrophobic group. The interaction would be very strong, and thus the solubilization would be such that the hydrocarbon hydrophobic group would be in the core of the micelle while the polar oxalate group would be exposed on the micelle surface to coordinate with Cu^{+2} and subsequently react with OH^-. The reactions involved in the micellar sodium

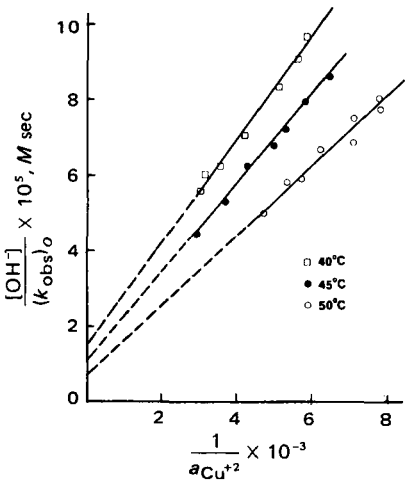

Figure 2—*Plots according to Eq. 4 for studies of sodium* n*-decyl oxalate hydrolysis in the absence of sodium lauryl sulfate micelles at pH 5.00 and ionic strength 0.1* M. *The lines were determined by linear regression analysis of the individual studies.*

lauryl sulfate system can then be written as shown in Scheme II, where M is the sodium lauryl sulfate micelles; K_b and K are the substrate–micelle and Cu^{+2}–micelle binding constants, respectively; K_f and K_f' are the formation constants of the chelate complex $CuDOx^+$ in nonmicellar and micellar phases, respectively; subscript o denotes the nonmicellar phase; and m denotes the micellar phase.

$$(DOx^-)_o + M \overset{K_b}{\rightleftharpoons} (DOx^-)_m$$

$$Cu^{+2} + M \overset{K}{\rightleftharpoons} (Cu^{+2})_m$$

$$(DOx^-)_o + Cu^{+2} \overset{K_f}{\rightleftharpoons} (CuDOx^+)_o$$

$$(CuDOx^+)_o + OH^- \overset{k_o}{\underset{\text{slow}}{\rightleftharpoons}} \text{products}$$

$$(DOx^-)_m + Cu^{+2} \overset{K_f'}{\rightleftharpoons} (CuDOx^+)_m$$

$$(CuDOx^+)_m + OH^- \overset{k_m}{\underset{\text{slow}}{\longrightarrow}} \text{products}$$

Scheme II

The rate law is given by:

$$\text{rate} = k_o[OH^-][CuDOx^+]_o + k_m[OH^-][CuDOx^+]_m \quad \text{(Eq. 5)}$$

$$\text{rate} = \frac{k_o K_f a_{Cu^{+2}}[OH^-]}{1 + K_f a_{Cu^{+2}}}[DOx^-]_o^{\text{total}} + \frac{k_m K_f' a_{Cu^{+2}}[OH^-]}{1 + K_f' a_{Cu^{+2}}}[DOx^-]_m^{\text{total}} \quad \text{(Eq. 6)}$$

$$\text{rate} = \left[\frac{k_o K_f a_{Cu^{+2}}[OH^-]}{(1 + K_f a_{Cu^{+2}})(1 + K_b[M])} + \frac{k_o K_f' a_{Cu^{+2}}[OH^-]K_b[M]}{(1 + K_f' a_{Cu^{+2}})(1 + K_b[M])}\right][DOx^-]_{\text{total}} \quad \text{(Eq. 7)}$$

The pseudo-first-order rate constant is given by:

$$k_{obs} = \frac{k_o K_f a_{Cu^{+2}}[OH^-]}{(1 + K_f a_{Cu^{+2}})(1 + K_b[M])} + \frac{k_m K_f' a_{Cu^{+2}}[OH^-]K_b[M]}{(1 + K_f' a_{Cu^{+2}})(1 + K_b[M])} \quad \text{(Eq. 8)}$$

Figure 3 illustrates a typical plot of the logarithm of the rate of hydroxide consumption *versus* time, from the slope of which the pseudo-first-order rate constant, k_{obs}, can be determined.

According to Eq. 8, at constant $a_{Cu^{+2}}$ in the bulk of the solution, k_{obs} will increase with increasing micelle concentration [M] until an asymptotic value is reached with [M] → ∞. This asymptotic value is given by:

$$k_{obs}^{max} = \frac{k_m K_f' a_{Cu^{+2}}[OH^-]}{1 + K_f' a_{Cu^{+2}}} = (k_{obs})_m \quad \text{(Eq. 9)}$$

which is the observed rate constant in the micellar phase. The asymptotic value is approached when $K_b[M] \gg 1$. Thus, at sufficiently

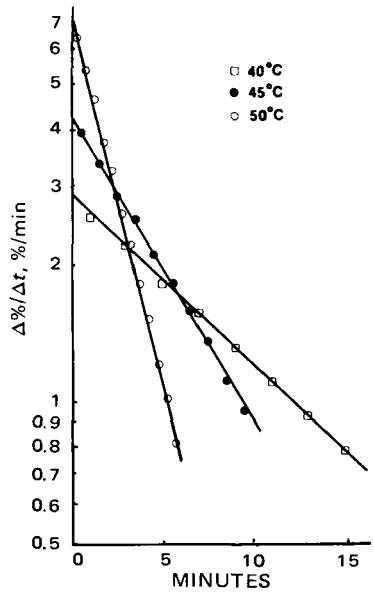

Figure 3—*Finite increments of sodium hydroxide solution and time as a function of time for representative studies of sodium* n*-decyl oxalate hydrolysis in the presence of sodium lauryl sulfate micelles at pH 5.00 and ionic strength 0.1* M.

high [M], there is no contribution of $(k_{obs})_o$, all of the n-decyl oxalate substrate being solubilized in the micelles.

Equation 9 predicts that, if $a_{Cu^{+2}}$ is held constant, further increases in [M] should give no observable change in the asymptotic value. In the experiments, a constant concentration of Cu^{+2} was added to the solution, so that $a_{Cu^{+2}}$ decreased with increasing [M] because more Cu^{+2} bound as counterions of the anionic micelles (11). However, a plot of $k_{obs}/a_{Cu^{+2}}$ reaches an asymptotic value and remains constant with a further increase of micelle concentration [M] or surfactant concentration. Such plots are shown in Fig. 4 at three different temperatures. At the asymptotic level:

$$\frac{(k_{obs})_m}{a_{Cu^{+2}}} = \frac{k_m K_f'[OH^-]}{1 + K_f' a_{Cu^{+2}}} \quad \text{(Eq. 10)}$$

This value is essentially constant since $a_{Cu^{+2}}$ is small and the denominator on the right-hand side is ≈1. An inhibitory salt effect with a higher concentration of surfactant was not observed in the present study because of the relatively high ionic strength maintained and the range of the surfactant concentration used.

It was observed from Fig. 4 that all of the substrate is in the micellar phase at surfactant concentrations above 20×10^{-3} *M*. Therefore, to simplify the system, all kinetic runs in the micellar system were carried out at a surfactant concentration of 24×10^{-3} *M*. Under this condition, rearrangement of Eq. 9 gives:

$$\frac{[OH^-]}{(k_{obs})_m} = \frac{1}{k_m K_f' a_{Cu^{+2}}} + \frac{1}{k_m} \quad \text{(Eq. 11)}$$

Equation 11 is analogous to Eq. 4 for nonmicellar systems.

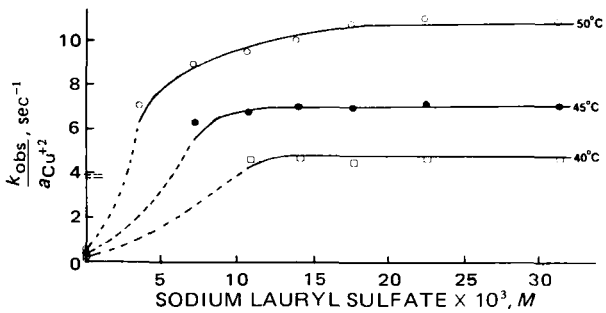

Figure 4—*Observed pseudo-first-order rate constant per unit activity of cupric ion as a function of sodium lauryl sulfate concentration for studies of sodium* n*-decyl oxalate hydrolysis in a micellar system at a constant cupric-ion concentration added of 22.1* × 10^{-4} M, *pH 5.00, and ionic strength 0.1* M.

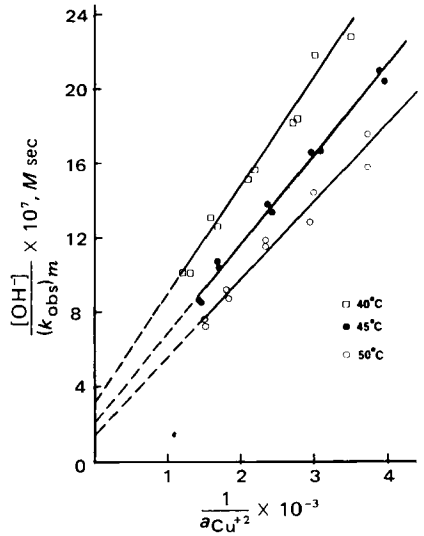

Figure 5—*Plots according to Eq. 11 for studies of sodium* n-*decyl oxalate hydrolysis in the presence of sodium lauryl sulfate micelles at pH 5.00 and ionic strength 0.1* M. *The lines were determined by linear regression analysis of the individual studies.*

Figure 5 shows plots according to Eq. 11 at 40, 45, and 50°. By using linear regression analysis, the extrapolated intercepts and slopes were determined, from which k_m and K_f' were calculated (Table I).

The extent of the rate enhancement can be taken as the ratio of k_m/k_o; at 40, 45, and 50°, this ratio was 47.8, 50.5, and 46.9, respectively.

Under the conditions of the present study, no observable reaction occurred in the absence of Cu^{+2}. Also, micellar sodium lauryl sulfate, which is known to undergo an enhanced rate of H^+-catalyzed hydrolysis compared to the monomer (12, 13), did not hydrolyze appreciably in this weakly acidic solution.

Estimate of Substrate–Sodium Lauryl Sulfate Binding Constant—The constant K_b for binding of the substrate sodium *n*-decyl oxalate to micelles of sodium lauryl sulfate can be estimated from Eq. 8, using data obtained at 50° and a surfactant concentration of 3.47×10^{-3} *M*, at which the substrate was not completely solubilized in the micelles (Fig. 4). The measured $a_{Cu^{+2}}$ was 7.75×10^{-4} *M*, and the k_{obs} was 56.6×10^{-4} sec^{-1}. If it is assumed that the CMC of sodium lauryl sulfate does not change appreciably with temperature in the range of 5–90° (14), the CMC might be taken as 1.46×10^{-3} *M* at 25° and ionic strength 0.1 *M* (15). Although this CMC value is for sodium lauryl sulfate in the absence of Cu^{+2}, it is quite reasonable because the CMC of pure cupric lauryl sulfate micelles is 1.2×10^{-3} *M* in a salt solution (16). If the aggregation number *N* is taken as 62 (17) in the presence of 25×10^{-4} *M* added Cu^{+2} and ionic strength 0.1 *M*, compared to 52 in the presence of 4.83×10^{-4} *M* Cu^{+2} (11), then the concentration of micelles [M] is:

$$[M] = \frac{[\text{sodium lauryl sulfate}] - CMC}{N} = 3.24 \times 10^{-5} M \qquad \text{(Eq. 12)}$$

Substituting all known parameters into Eq. 8 gives $K_b = 7.83 \times 10^4$ M^{-1} at 50°. This high value indicates a strong interaction between the substrate and micelle. It is comparable to that obtained for the binding constant of mono-*p*-nitrophenyl dodecanedioate to sodium laurate, which was 4.5×10^3 M^{-1} (18).

Table I—Second-Order Rate Constants for Hydroxyl Attack on the Chelate Complex (k_o and k_m) and Formation Constants (K_f and K_f') of the Complex in the Absence and Presence of Sodium Lauryl Sulfate Micelles at pH 5.00 and Ionic Strength 0.1 *M*

	Nonmicellar		Micellar	
Temperature	$10^{-5}\ k_o$, M^{-1} sec^{-1}	$10^{-3}\ K_f$, M^{-1}	$10^{-7}\ k_m$, M^{-1} sec^{-1}	$10^{-3} K_f'$, M^{-1}
40°	0.67 ± 0.09	1.09 ± 0.25	0.32 ± 0.06	0.54 ± 0.13
45°	0.93 ± 0.09	0.94 ± 0.13	0.47 ± 0.07	0.43 ± 0.07
50°	1.45 ± 0.39	0.74 ± 0.29	0.68 ± 0.22	0.32 ± 0.05

Table II—Activation Parameters Associated with the Second-Order Rate Constants, k_o and k_m, at pH 5.00 and Temperature 318°K

	E_a, kcal/mole	ΔH^*, kcal/mole	ΔS^*, eu
Micellar solution	15.1 ± 0.1[a]	13.5 ± 0.1[a]	14.3 ± 0.4[a]
Nonmicellar solution	15.5 ± 0.1	13.9 ± 0.1	7.8 ± 0.4

[a] Standard deviation.

Formation Constant for Chelate Complex—Surprisingly, the formation constant K_f of the chelate complex $CuDOx^+$ was not increased in the anionic micellar phase. This finding could be explained by considering the nature of counterion binding to the micelle. Generally, the binding is nonspecific and the counterions or oppositely charged reactants form a "mobile monolayer" in the Stern layer (19–22). The micelles concentrate the reactants on the surface and, in the case of an equilibrium, the apparent formation constant is increased (23).

In the particular case of interaction between the transition metal Cu^{+2} and the negatively charged micelles of sodium lauryl sulfate, it is possible that a coordinate covalent bond is formed, as is the case with polycarboxylic acid anion (20). It was suggested that micelles of divalent metal lauryl sulfate be treated as weak electrolytes (16). The Cu^{+2} bound covalently to sodium lauryl sulfate micelles would not be available to chelate with the substrate, or at least there would be a competitive binding between the micelle and solubilized substrate for the Cu^{+2}. Thus, sodium lauryl sulfate micelles do not appreciably serve to increase the concentration of reactants as generally is the case.

Steric factors could also have some influence. In the micellar phase, the formation of the copper chelate complex could be somewhat more difficult. After one coordination with the anion oxygen, the Cu^{+2} should coordinate with the carbonyl oxygen, which might be located farther inside the micelle. This second coordination might be hindered by the crowded neighboring lauryl sulfate ions. These could be the reasons that the formation constant K_f was not increased but rather decreased by twofold in the micellar phase. The rate enhancement must then be attributed to some other factors, which will be discussed further.

Effect of Temperature—Arrhenius-type plots (Fig. 6) for the hydrolysis of sodium *n*-decyl oxalate in nonmicellar and micellar systems are parallel, indicating similar temperature dependencies for the hydrolysis reactions in both systems. Experimental energy of activation was calculated from the slope of each plot. The enthalpy of activation was calculated from $\Delta H^* = E_a - RT$ for reactions in solution (24) and corrected for the enthalpy associated with the coordination of a carboxylate donor ligand to Cu^{+2}. The entropy of activation, ΔS^*, was calculated from the Eyring method (25):

$$k = \frac{RT}{Nh} e^{-\Delta H^*/RT} e^{\Delta S^*/R} \qquad \text{(Eq. 13)}$$

The values of E_a, ΔH^*, and ΔS^* are given in Table II.

It appears that the enhanced rate for the reaction in the micellar system is associated with an increase in ΔS^* rather than a decrease in ΔH^*. The larger entropy change can be attributed to the larger hydration and electrostatic entropy changes in the micellar phase. In terms of hydration of ions, the explanation of the entropy factor is that the two ions coming together to form a neutral molecule become partially dehydrated in the transition state so that some "frozen" water molecules are released, resulting in an increase of the entropy. The large charge density of the sodium lauryl sulfate micelle causes the formation of a more ordered structure, consisting of water molecules and counterions about its outer, polar surface. There is evidence from hydrodynamic data that, in dilute solution, sodium lauryl sulfate micelles are spherical and highly hydrated, with 10–12 water molecules bound by each surfactant molecule in the micelle (26). On the other hand, sodium lauryl sulfate is hydrated by only two or three water molecules when present in solution below the CMC (27). The sodium *n*-decyl oxylate in the present study contains about the same hydrocarbon chain length and would be expected to follow the same pattern of hydration. Thus, there would be a greater overall change

Table III—Studies of Cupric-Ion-Promoted Hydrolysis[a] of Sodium Hydrocortisone 21-Hemisuccinate and Sodium Hydrocortisone 21-Hemi-(3,3-dimethylglutarate) in the Absence and Presence of Sodium Lauryl Sulfate Micelles

Hydrocortisone 21-Hemi-(3,3-dimethylglutarate), m*M*	Hydrocortisone 21-Hemisuccinate, m*M*	$Cu(NO_3)_2$, m*M*	Sodium Lauryl Sulfate, m*M*	pH	Temperature
—	0.5	—	—	6.0	40°
—	0.5	0.5	—	6.0	40°
—	0.5	1.0	—	5.0	40°
—	0.05	0.5	—	5.0	50°
0.05	—	0.5	—	5.0	50°
0.5	—	2.0	24.3	5.0	50°

[a] No reactions occurred after 3–4 hr.

in randomness in the micellar phase, since the quantity of electrostatically bound water molecules released in the formation of the neutral transition state would be considerably greater than the amount released in the single ion state.

In terms of electrostatic interaction between the two reacting ions, the free energy change resulting solely from bringing two ions from infinite separation to the equilibrium distance in the activated complex is given by (28):

$$\Delta F^*_{el} = \frac{Z_A Z_B e^2}{Dr_*} \qquad \text{(Eq. 14)}$$

where Z_A and Z_B are the charges on the ions forming the activated complex; D is the dielectric constant of the medium; and r_* is the equilibrium separation of the charges in the transition state. The change in entropy can be written as:

$$\Delta S^*_{el} = \frac{Z_A Z_B e^2}{Dr_*}\left(\frac{\partial \ln D}{\partial T}\right)_p \qquad \text{(Eq. 15)}$$

The quantity $(\partial \ln D/\partial T)$ is always negative, because thermal motion overcomes the orientation of dipoles in an electric field (29). Therefore, for a reaction of two opposite charges, ΔS^*_{el} has a positive value and is inversely proportional to the dielectric constant of the medium. The surface of micelles appears to be less polar than water itself (30). For instance, Mukerjee and Ray (31) assigned an approximate value of 36 for the dielectric constant of the surface of micelles derived from *N*-dodecylpyridinium iodide. In the present system, the oxalate charged group might be regarded as being attached to a region of lower dielectric constant than water in the bulk of the solution; therefore, ΔS^*_{el} is larger and more positive than in nonmicellar solution.

It is apparent that the micellar rate enhancement was completely controlled by the entropy factor. The increase in entropy of activation was sufficient to overwhelm the unfavorable electrostatic repulsion of OH^- by the sodium lauryl sulfate micelles. The observed micellar rate enhancement for attack of hydroxide ion upon the positively charged intermediate chelate complex is in contrast to the inhibition by micellar sodium lauryl sulfate of attack of hydroxide ion upon a neutral solubilizate such as benzocaine (32) and upon lauryl sulfate anion (13).

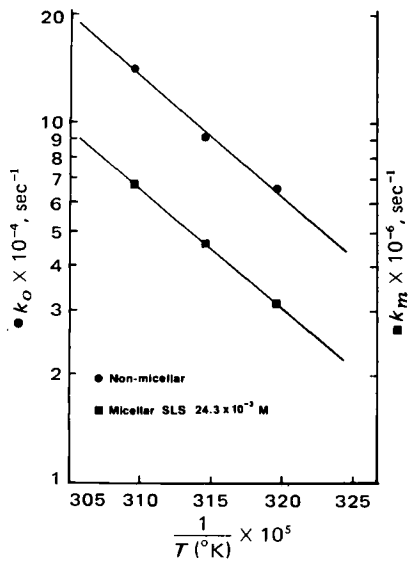

Figure 6—*Temperature dependence of the second-order rate constant for the cupric-ion-promoted hydrolysis of sodium* n*-decyl oxalate in the absence and presence of sodium lauryl sulfate (SLS) micelles at pH 5.00 and ionic strength 0.1* M.

The results in Table III clearly indicate that no copper-ion catalysis was observed in the hydrolysis of hydrocortisone hemisuccinate and hemi-(3,3-dimethylglutarate). The formation of a chelate complex is necessary for a metal ion to exert a catalytic effect on ester hydrolysis (4), and generally the extent of catalysis parallels the stability of the corresponding chelate complex. For example, Hoppe and Prue (1) reported that divalent cations such as barium and calcium show a lesser catalytic effect with malonate than with oxalate. The formation constants of barium and calcium oxalate are 213 and 1000 M^{-1} (33), compared to 51 and 313 M^{-1} for the respective malonate complexes (34). Going from oxalate to glutarate, the metal ion forms five- through eight-membered ring complexes with a decreasing order of stability. For the succinate complexes, the chelate effect may be almost entirely lost (35).

REFERENCES

(1) J. I. Hoppe and J. E. Prue, *J. Chem. Soc.*, **1957**, 1775.

(2) G. L. Johnson and R. J. Angelici, *J. Am. Chem. Soc.*, **93**, 1106(1971).

(3) G. L. Flynn and D. J. Lamb, *J. Pharm. Sci.*, **59**, 1433(1970).

(4) M. L. Bender and B. W. Turnquest, *J. Am. Chem. Soc.*, **79**, 1889(1957).

(5) R. Breslow and C. McAllister, *ibid.*, **93**, 7096(1971).

(6) H. J. Backer and J. D. H. Homan, *Rec. Trav. Chim.*, **58**, 1048(1939).

(7) L. S. Bondar, P. P. Rodionov, and R. A. Okunev, *Izv. Akad. Nauk, SSSR, Ser. Khim.*, **5**, 1102(1968); through *Chem. Abstr.*, **69**, 43365g(1968).

(8) E. E. Dreger, G. I. Keim, G. D. Miles, L. Shedlovsky, and J. Ross, *Ind. Eng. Chem.*, **36**, 610(1944).

(9) G. D. Miles and L. Shedlovsky, *J. Phys. Chem.*, **48**, 57(1944).

(10) H. S. Harned and W. J. Hamer, *J. Am. Chem. Soc.*, **55**, 2194(1933).

(11) M. U. Oko and R. L. Venable, *J. Colloid Interface Sci.*, **35**, 53(1971).

(12) V. A. Motsavage and H. B. Kostenbauder, *J. Colloid Sci.*, **18**, 603(1963).

(13) J. L. Kurz, *J. Phys. Chem.*, **66**, 2239(1962).

(14) Z. N. Markina, N. Z. Kostova, and P. A. Rebinder, *Dokl. Akad. Nauk, SSSR*, **177**, 640(1967); through *Chem. Abstr.*, **68**, 63010c(1968).

(15) R. J. Williams, J. N. Phillips, and K. J. Mysels, *Trans. Faraday Soc.*, **51**, 728(1955).

(16) I. Satake, I. Iwamatus, S. Hosokawa, and R. Matsuura, *Bull. Chem. Soc. Jpn.*, **36**, 204(1963).

(17) E. J. Fendler and J. H. Fendler, *Adv. Phys. Org. Chem.*, **8**, 271(1970).

(18) F. M. Menger and C. E. Portnoy, *J. Am. Chem. Soc.*, **89**, 4698(1967).

(19) S. Lapanje and S. A. Rice, *ibid.*, **83**, 496(1961).

(20) L. Kotin and M. Nagasawa, *ibid.*, **83**, 1026(1961).

(21) P. Mukerjee, *J. Phys. Chem.*, **66**, 943(1962).

(22) D. Stigter, *ibid.*, **68**, 3603(1964).

(23) K. Martinek, A. K. Yatsimirski, A. P. Osipov, and I. V. Berezin, *Tetrahedron*, **29**, 963(1973).

(24) A. A. Frost and R. G. Pearson, "Kinetics and Mechanism,"

Wiley, New York, N.Y., 1965, p. 100.
(25) A. Glasstone, K. J. Laidler, and H. Eyring, "The Theory of Rate Processes," McGraw-Hill, New York, N.Y., 1941, pp. 22, 196, 454.
(26) W. L. Courchene, *J. Phys. Chem.*, **68**, 1870(1964).
(27) A. N. Potanin and N. A. Dubovich, *Dokl. Akad. Nauk SSSR*, **188**, 849(1969); through *Chem. Abstr.*, **72**, 33536u(1970).
(28) A. A. Frost and R. G. Pearson, "Kinetics and Mechanism," Wiley, New York, N.Y., 1965, pp. 143, 144.
(29) L. L. Schaleger and F. A. Long, *Adv. Phys. Org. Chem.*, **1**, 1(1963).
(30) R. B. Dunlap and E. H. Cordes, *J. Am. Chem. Soc.*, **90**, 4395(1968).
(31) P. Mukerjee and A. Ray, *J. Phys. Chem.*, **70**, 2144(1966).
(32) S. Riegelman, *J. Am. Pharm. Assoc., Sci. Ed.*, **49**, 339(1960).
(33) R. W. Money and C. W. Davies, *Trans. Faraday Soc.*, **28**, 609(1932).
(34) D. I. Stock and C. W. Davies, *J. Chem. Soc.*, **1949**, 1371.
(35) G. H. Nancollas, "Interactions in Electrolyte Solutions," Elsevier, New York, N.Y., 1966, p. 151.

ACKNOWLEDGMENTS AND ADDRESSES

Received July 28, 1975, from the *Division of Pharmaceutics and Pharmaceutical Analysis, College of Pharmacy, University of Kentucky, Lexington, KY 40506*

Accepted for publication February 13, 1976.

Abstracted in part from a thesis submitted by J. T. H. Ong to the Graduate School, University of Kentucky, in partial fulfillment of the Doctor of Philosophy degree requirements.

* Present address: Eli Lilly and Co., Indianapolis, IN 46206

ˣ To whom inquiries should be directed.

Optimally Predictive *In Vitro* Drug Dissolution Testing for *In Vivo* Bioavailability

VICTOR F. SMOLEN ˣ and WILLIAM A. WEIGAND *

Abstract □ A systematic method for optimally adjusting the conditions for *in vitro* drug dissolution testing is presented. Although the basic approach also can be applied to other types of dissolution apparatus, a scheme is described using a flow-through dissolution apparatus for the design and implementation of *in vitro* drug release tests. The tests have an optimized capability to simulate and, under predetermined conditions, predict *in vivo* drug bioavailability, blood levels, or pharmacological response *versus* time profiles of appropriate drug products. The apparatus is operated in two (simulative and predictive) stages. First, different dosage forms are used to calibrate the apparatus by operating it in a feedback-controlled mode to find a program for varying the composition, recycle flow, and flow rate of the dissolution medium that provides *in vitro* results that best simulate the different *in vivo* drug release properties of the dosage forms. The variables governing the operation of the apparatus are systematically modified until the differences between the *in vitro* and *in vivo* behavior of the dosage forms become: (*a*) minimized, (*b*) the same for every dosage form, and (*c*) independent of time. Second, predictive tests of the *in vivo* behavior of other drug formulations are performed. The apparatus is now operated without feedback control, using the program determined to be optimal in Stage 1. If necessary, an analog computer is used to vary continuously the composition and recycle flow of the dissolution medium. Mathematical expressions for the performance criteria on which the optimization of the apparatus is based are derived. The optimization procedures are described, and limitations of the method are discussed.

Keyphrases □ Dissolution, drug—flow-through-type apparatus described, used to predict *in vivo* bioavailability □ Drug release tests—flow-through-type dissolution apparatus described, used to predict *in vivo* bioavailability □ Bioavailability—predicted using flow-through-type dissolution apparatus

The advent of potent drugs emphasizes the need to develop pharmaceutical dosage forms that possess optimal effectiveness, safety, and reliability. Although approaches to rationally designing the dynamic bioavailability properties of dosage forms have been described (1–3), it is seldom practical to perform the exhaustive *in vivo* testing required to develop new oral drug products possessing the desired behavior. An inexpensive and rapid *in vitro* method of evaluation is needed.

It has become apparent in recent years that the formulation and manufacturing specifications of different manufacturers, while conforming to USP and NF requirements, can vary and alter the bioavailability characteristics of a drug. Such variations in bioavailability of drug products have often only been detectable by extensive human testing. Consequently, in some cases, products with inadequate *in vivo* drug bioavailability have been marketed and sold for long periods prior to the discovery of their inadequacy. Commonly prescribed drugs continue to be released from patent. Not only does this situation serve as a stimulus for increased generic usage, it also makes it necessary for medical researchers to have a ready means for evaluating the bioavailability of chemical equivalents of these drugs as they enter the market. The compendia should have precise laboratory tests for gauging their bioavailability, but only *in vivo* testing in humans is fully reliable at present.

In the extensive literature on *in vitro* drug release testing (3–17), it is often stated that the problem is quite complicated because a correlation of *in vivo* to *in vitro* release found with a particular test for a particular drug in a particular dosage form may not exist if another drug is substituted or the dosage form is altered. Few attempts have been reported to determine the full extent to which this is the case. The *in vitro* to *in vivo* drug availability correlations found have always been after the fact, as were the single-point correlations of 50% *in vitro–in vivo* release times (7) and the multiple-point correlations (8–11) that linearly related the cumulative amounts of drug released from the dosage form *in vitro* to similar amounts absorbed *in vivo*.

Previous reports from this laboratory (3, 4, 12) sug-

Wiley, New York, N.Y., 1965, p. 100.
(25) A. Glasstone, K. J. Laidler, and H. Eyring, "The Theory of Rate Processes," McGraw-Hill, New York, N.Y., 1941, pp. 22, 196, 454.
(26) W. L. Courchene, *J. Phys. Chem.*, **68**, 1870(1964).
(27) A. N. Potanin and N. A. Dubovich, *Dokl. Akad. Nauk SSSR*, **188**, 849(1969); through *Chem. Abstr.*, **72**, 33536u(1970).
(28) A. A. Frost and R. G. Pearson, "Kinetics and Mechanism," Wiley, New York, N.Y., 1965, pp. 143, 144.
(29) L. L. Schaleger and F. A. Long, *Adv. Phys. Org. Chem.*, **1**, 1(1963).
(30) R. B. Dunlap and E. H. Cordes, *J. Am. Chem. Soc.*, **90**, 4395(1968).
(31) P. Mukerjee and A. Ray, *J. Phys. Chem.*, **70**, 2144(1966).
(32) S. Riegelman, *J. Am. Pharm. Assoc., Sci. Ed.*, **49**, 339(1960).
(33) R. W. Money and C. W. Davies, *Trans. Faraday Soc.*, **28**, 609(1932).
(34) D. I. Stock and C. W. Davies, *J. Chem. Soc.*, **1949**, 1371.
(35) G. H. Nancollas, "Interactions in Electrolyte Solutions," Elsevier, New York, N.Y., 1966, p. 151.

ACKNOWLEDGMENTS AND ADDRESSES

Received July 28, 1975, from the *Division of Pharmaceutics and Pharmaceutical Analysis, College of Pharmacy, University of Kentucky, Lexington, KY 40506*

Accepted for publication February 13, 1976.

Abstracted in part from a thesis submitted by J. T. H. Ong to the Graduate School, University of Kentucky, in partial fulfillment of the Doctor of Philosophy degree requirements.

* Present address: Eli Lilly and Co., Indianapolis, IN 46206

ˣ To whom inquiries should be directed.

Optimally Predictive *In Vitro* Drug Dissolution Testing for *In Vivo* Bioavailability

VICTOR F. SMOLEN ˣ and WILLIAM A. WEIGAND *

Abstract □ A systematic method for optimally adjusting the conditions for *in vitro* drug dissolution testing is presented. Although the basic approach also can be applied to other types of dissolution apparatus, a scheme is described using a flow-through dissolution apparatus for the design and implementation of *in vitro* drug release tests. The tests have an optimized capability to simulate and, under predetermined conditions, predict *in vivo* drug bioavailability, blood levels, or pharmacological response *versus* time profiles of appropriate drug products. The apparatus is operated in two (simulative and predictive) stages. First, different dosage forms are used to calibrate the apparatus by operating it in a feedback-controlled mode to find a program for varying the composition, recycle flow, and flow rate of the dissolution medium that provides *in vitro* results that best simulate the different *in vivo* drug release properties of the dosage forms. The variables governing the operation of the apparatus are systematically modified until the differences between the *in vitro* and *in vivo* behavior of the dosage forms become: (*a*) minimized, (*b*) the same for every dosage form, and (*c*) independent of time. Second, predictive tests of the *in vivo* behavior of other drug formulations are performed. The apparatus is now operated without feedback control, using the program determined to be optimal in Stage 1. If necessary, an analog computer is used to vary continuously the composition and recycle flow of the dissolution medium. Mathematical expressions for the performance criteria on which the optimization of the apparatus is based are derived. The optimization procedures are described, and limitations of the method are discussed.

Keyphrases □ Dissolution, drug—flow-through-type apparatus described, used to predict *in vivo* bioavailability □ Drug release tests—flow-through-type dissolution apparatus described, used to predict *in vivo* bioavailability □ Bioavailability—predicted using flow-through-type dissolution apparatus

The advent of potent drugs emphasizes the need to develop pharmaceutical dosage forms that possess optimal effectiveness, safety, and reliability. Although approaches to rationally designing the dynamic bioavailability properties of dosage forms have been described (1–3), it is seldom practical to perform the exhaustive *in vivo* testing required to develop new oral drug products possessing the desired behavior. An inexpensive and rapid *in vitro* method of evaluation is needed.

It has become apparent in recent years that the formulation and manufacturing specifications of different manufacturers, while conforming to USP and NF requirements, can vary and alter the bioavailability characteristics of a drug. Such variations in bioavailability of drug products have often only been detectable by extensive human testing. Consequently, in some cases, products with inadequate *in vivo* drug bioavailability have been marketed and sold for long periods prior to the discovery of their inadequacy. Commonly prescribed drugs continue to be released from patent. Not only does this situation serve as a stimulus for increased generic usage, it also makes it necessary for medical researchers to have a ready means for evaluating the bioavailability of chemical equivalents of these drugs as they enter the market. The compendia should have precise laboratory tests for gauging their bioavailability, but only *in vivo* testing in humans is fully reliable at present.

In the extensive literature on *in vitro* drug release testing (3–17), it is often stated that the problem is quite complicated because a correlation of *in vivo* to *in vitro* release found with a particular test for a particular drug in a particular dosage form may not exist if another drug is substituted or the dosage form is altered. Few attempts have been reported to determine the full extent to which this is the case. The *in vitro* to *in vivo* drug availability correlations found have always been after the fact, as were the single-point correlations of 50% *in vitro–in vivo* release times (7) and the multiple-point correlations (8–11) that linearly related the cumulative amounts of drug released from the dosage form *in vitro* to similar amounts absorbed *in vivo*.

Previous reports from this laboratory (3, 4, 12) sug-

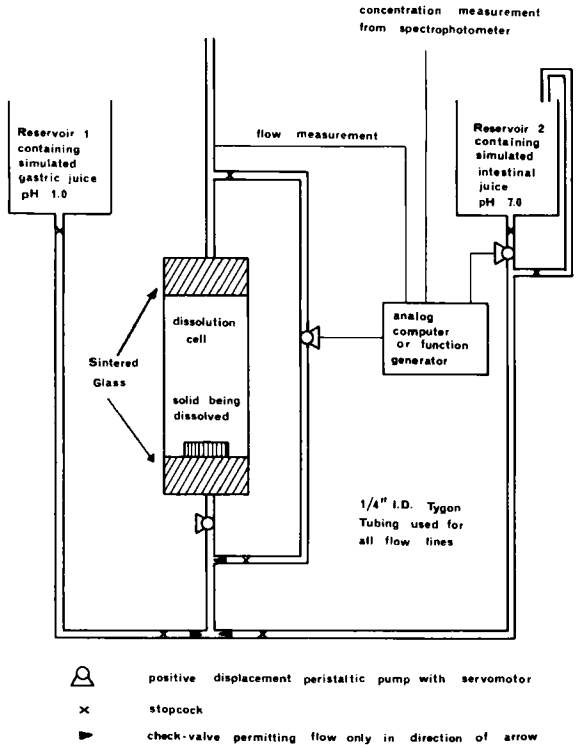

Figure 1—*Schematic diagram of a simple flow-through apparatus with modifications appropriate for use in optimized drug release testing. See text for details.*

gested that *in vitro* to *in vivo* correlations can be improved through a systematic adjustment of test conditions such as agitation or flow rates, composition of the release medium, geometry of the apparatus, solubility volume of a sink, and permeability of membranous barriers. The use of optimization methods was suggested to determine test conditions that would provide uniformly simulative results for drug dosage formulations with different *in vivo* drug release properties. Such a test could be expected to predict the *in vivo* drug release behavior of other formulations with release properties similar to those of the dosage forms for which the test conditions were optimized (4, 17).

The present report describes a methodology employing a flow-through dissolution apparatus similar to that described previously (13, 14). The apparatus is initially operated with closed loop analog computer feedback control of the recycling of the dissolution medium; this phase is followed by an optimized open loop automated operation to predict *in vivo* dosage form bioavailability behavior. It is postulated that this procedure, or a manually operated variation thereof, can provide a relatively simple, economical, and versatile approach to improving the predictive capability of *in vitro* drug bioavailability testing and, therefore, reduce, but not eliminate, the need for *in vivo* bioavailability studies.

EXPERIMENTAL

Apparatus—The use of a single apparatus to test most drug products is theoretically feasible, provided its mode of operation is sufficiently flexible (17). Compared to other types of apparatus, a flow-through dissolution cell, such as that described previously (13, 14), possesses good flexibility and involves no arbitrary and material-dependent parameters (14, 15). Its operating conditions can be well defined and readily standardized.

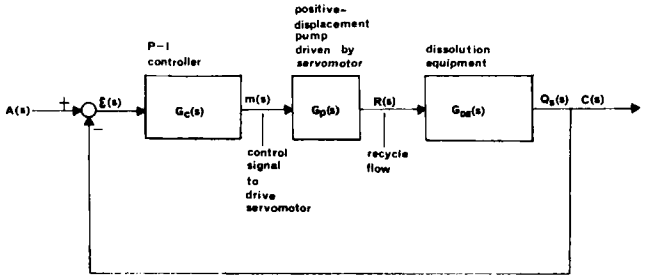

Figure 2—*Block diagram for closed loop feedback control of recycle flow,* R(t), *in the operation of the* in vitro *drug release testing apparatus.*

Figure 1 shows a flow-through apparatus with provisions to change the composition of the dissolution medium and recycle flow through the cell. A change in solvent pH can be used to simulate the *in vivo* change from the stomach to the duodenum. The recycling of solvent through the dissolution chamber allows variable sink conditions to be achieved to simulate existing *in vivo* conditions due to differing barrier properties of drug-absorbing biological membranes. Resistance to biological absorption is simulated by mixing the fresh solvent with the solution leaving the cell. The recycling of solution through the dissolution chamber in this manner decreases the driving force for dissolution.

As shown in Fig. 1, the time-varying recycle flow, $R(t)$, can be controlled to reproduce *in vivo* dissolution rates by using a preprogrammed analog computer. A time-varying mixing of the two reservoirs of dissolution media also can be controlled by an analog computer or a variable diode function generator. The pumps indicated in Fig. 1 are positive-displacement peristaltic pumps with a servomotor. The pumps on the recycle line and second reservoir require a speed modulator to allow the pump to be driven by a signal generated by an analog computer, diode function generator, or analog tape recorder.

Once the pumping rate is set at the outlet of the dissolution cell, the pumping arrangement and use of positive-displacement pumps ensure a constant flow through the apparatus. This is the case despite a time-varying recycle flow and a changing flow from the simulated gastric and intestinal juice reservoirs. The apparatus includes a spectrophotometer or other instrument to measure the concentration of drug in the liquid leaving the cell.

The analog computer is used for either the open loop control of the recycle flow (during a predictive *in vitro* run) or for the closed loop feedback control of the recycle flow (during the calibration or simulation stage of operating the apparatus). During the feedback-controlled mode of operation, the analog computer converts the signal from the spectrophotometer to a voltage representing the drug concentration and then multiplies this voltage with the voltage representing the flow of medium leaving the apparatus. This signal is compared with a signal produced by a diode function generator, programmed to reproduce the *in vivo* bioavailability rate, blood level, or pharmacological response *versus* time profile being simulated. The error signal is formed from the comparison. The error signal then goes to the PID (proportional integral differential) controller, which produces the control signal (usually PI modes are adequate) and drives the recycle flow at the desired rate.

The block diagram for the feedback-controlled mode is given in Fig. 2. When the apparatus is operated to obtain a predictive result, the analog computer produces an open loop control signal which varies the recycle flow without a concentration measurement from the spectrophotometer. The open loop block diagram for this operation is given in Fig. 3.

The dissolution cell (Fig. 1) has a length of 5.0 cm and a diameter

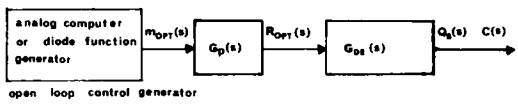

Figure 3—*Block diagram for open loop programmed control of recycle flow,* $\bar{R}_{opt}(t)$, *during operation of the* in vitro *drug release apparatus.*

of 2.5 cm. The volume of fluid held by the chamber can be changed by altering its length or filling the chamber with glass beads. The solid to be dissolved rests on a flow distributor; flow usually is in the laminar range.

The dissolution apparatus in Fig. 1 is in its simplest form and is probably adequate for most drugs and dosage forms. However, the flow-through apparatus can be modified to overcome such possible problems as clogging of the upper sintered-glass filter with undissolved particles or formation of soluble, but *in vivo* nonabsorbable, complexes between the drug and excipients contained in the dosage form. Possible filter clogging might easily be eliminated by filling the chamber with glass beads or replacing the stationary sintered-glass filter with a cone-shaped, rotating filter; such use of spin filters in a dissolution apparatus has been described (18).

A membrane system to simulate biological absorption could be incorporated using a scheme similar to that employed in a commercially available apparatus (19). However, since lipoid membranes are not entirely satisfactory for simulating the transport properties of biological structures (20, 21), membranes having the properties described by Smolen and Hagman (22) or Ling (23) could be applied more successfully. When considered advantageous, other dissolution media including nonaqueous solvents could be used in place of simulated gastric and intestinal juices.

Another possible problem is interferences of dissolved excipients with a spectrophotometric assay for the drug. In this case, discrete sampling techniques may need to be employed. Although this can be done within the context of the described scheme, it would require complicating both the equipment and the computer control of the dissolution process. Obviously, the problems described as possibly necessitating complications in the flow-through apparatus are also common to all other types of continuous sampling drug dissolution apparatus.

General Operation—The operation of the flow-through apparatus consists of two parts. First, the apparatus is calibrated (or adjusted) by operating it in the feedback-controlled mode to find the required recycle flow for two or more dosage forms chosen for having different drug release properties. The operating parameters are adjusted until an optimum combination is found. The optimum set of parameters consists of an optimum flow rate, a program for varying the composition of the dissolution medium, and a single recycle flow function. The relationship between the operating parameters (the process variables) and the dissolution parameters is discussed later. These results are then applied to set the conditions of operation of the apparatus in the optimally predictive open loop mode. In this second stage, the analog computer controls the recycle flow in accordance with the previously found optimal recycle flow function. Predictive tests are then performed on other drug dosage formulations, and the time courses of absorption rates, blood levels, drug effects, or urinary drug recovery rates of the test dosage form are produced. Various performance criteria can be used to optimize the operation of the apparatus by minimizing the differences between *in vivo* bioavailability results and values generated by the apparatus. The performance criteria developed in the *Appendix* also distribute the differences uniformly over time and the different dosage forms used to calibrate the apparatus.

THEORY AND DISCUSSION

Relation between Process Variables (Extrinsic to Drug Product) and Dissolution Rate—The dissolution process often may be described by a simple diffusion layer model (6):

$$\frac{dw}{dt} = \frac{DS}{T}(C_s - C) \qquad \text{(Eq. 1)}$$

where:

$\frac{dw}{dt}$ = dissolution rate (milligrams per minute)

D = diffusion coefficient for the solvent and solute under consideration (square centimeters per minute)

S = surface area for dissolution (square centimeters)

C_s = concentration of solute required to saturate the solvent (milligrams per milliliter)

C = actual solute concentration in solution (milligrams per milliliter)

T = effective thickness of the film or diffusion layer (centimeters)

The process variables are:

Q = volumetric flow rate (milliliters per minute)

$Q_A = Q/A_C$ = velocity through the cell (centimeters per minute)

A_C = cross-sectional area of the cell (square centimeters)

R or $R(t)$ = volumetric flow of recycle (milliliters per minute); *i.e.*, it can be a constant or time-varying quantity

τ_1 = time during which all solvent is drawn from the reservoir containing the simulated gastric juice (minutes)

τ_2 = time after which all solvent is drawn from the reservoir containing the simulated intestinal juice (minutes)

Once A_C is chosen, the process variables become Q, R, τ_1, and $(\tau_2 - \tau_1)$. The variables τ_1 and τ_2 can be assumed to be related to gastric and intestinal emptying time, which can vary significantly. However, average values in the neighborhood of 1–2 hr for τ_1 may be initially chosen. In most instances, the experiments would not exceed 2–4 hr, although runs with dosage forms with prolonged-release characteristics could last 12 hr. However, through appropriate time scaling, the actual experimental time can be contracted approximately 10–30-fold.

The solvent solutions can resemble gastric juice (0.1 *N* HCl) and intestinal juice (a phosphate-buffered solution of pH 7.0). An appropriate surfactant can be added to lower the surface tensions of the solutions into the range for human gastric juice, *i.e.*, from 34 to 50 dynes/cm (24). The rationale for adjusting the surface tension into the *in vivo* range, especially for a hydrophobic drug or dosage form, was demonstrated by Finholt and Solvang (25). They showed that the dissolution of phenacetin was progressively accelerated as the surface tension of the dissolution medium was reduced by the addition of a surfactant, primarily due to the increased wetting of the solid particles. They presented data showing that the dissolution rates obtained using a sample of gastric juice and a solution of hydrochloric acid (0.1 *N*) adjusted to the same surface tension were similar. A surfactant of the cholate type could also be added to the simulated intestinal fluid.

The relationship between variables in the diffusion layer equation and the process variables are easily seen as given for a fixed value of A_C:

T = a function of Q

C = a function of the volume of the dissolution chamber, V, and the volumetric flow rate, Q, *i.e.*, the residence time, V/Q, and the flow of recycle, R or $R(t)$
To avoid changing the volume of the dissolution chamber by changing its length to change C, this could also be effected by changing the recycle flow.

C_s = a function of the properties of the solvent
Using the simulated gastric and intestinal juices mentioned previously, the process variables to be manipulated here are τ_1 and τ_2, as graphically depicted in Fig. 4. The variables D and C_s are obviously affected by the solvents used; but once the solvents have been specified, D and C_s are reflective of the solid being dissolved.

S = in addition to being a function of Q, a function of the initial amount of drug, m_0, and the physical properties of the solid
Once these variables are fixed, *i.e.*, once a drug and a dosage form are decided upon, the time course of S as the experiment proceeds is reflective of the properties of the drug product.

Automatic Feedback Control to Produce a Time-Varying Recycle Flow and Simulate $\dot{A}(t)$—The objective is to devise an apparatus that will predictively simulate *in vivo* drug availability data. The dissolution data produced by the flow-through apparatus are in a differential form. Using the symbol $A(t)$ (milligrams) for the cumulative *in vivo* availability, the output of the apparatus should reproduce $\dot{A}(t)$ (milligrams per minute), *i.e.*, the rate of bioavailability, blood level, urinary excretion rate, or pharmacological response *versus* time profiles. If $Q_s(t)$ is the volumetric flow rate out of the apparatus to the sink, it is given by $Q_s(t) = Q - R(t)$ (milliliters per minute). The rate of flow of dissolved drug to the sink is then given by $Q_s(t)C(t)$, where $C(t)$(milligrams per milliliter) is the concentration of the stream leaving the dissolution cell. It is then desired to have:

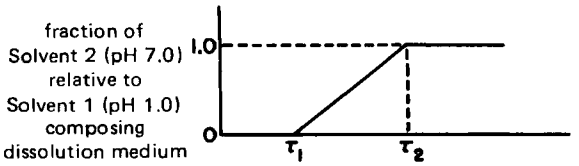

Figure 4—*Relationship between solvent compositions and dissolution rates; τ_1 and τ_2 are described in the text.*

$$\dot{A}(t) = Q_s(t)C(t) \qquad \text{(Eq. 2)}$$

or:

$$\dot{A}(t) - Q_s(t)C(t) = \epsilon(t) \qquad \text{(Eq. 3)}$$

where, in the ideal case, the error $\epsilon(t) = 0$. It may not be possible to obtain $\epsilon(t) = 0$, but it is possible to produce a small $\epsilon(t)$ with the feedback control scheme indicated in Fig. 1 and described in terms of the block diagram in Fig. 2. Although Q can be held constant with time, $Q_s(t)$ can be changed by changing $R(t)$ by PI control action generated by an analog computer. In fact, all variables needed for the feedback control of $R(t)$, *i.e.*, the calculation of $R(t)$ and $Q_s(t)$, the multiplication of $Q_s(t)$ by $C(t)$ (measured by a spectrophotometer or other appropriate device and fed back to the computer), the comparison of $\dot{A}(t)$ (*e.g.*, produced by a diode function generator) with $Q_s(t)C(t)$ to produce the error signal, and the desired control action to drive the servomotor of the pump on the recycle stream, are all easily accomplished with an analog computer. In addition, the servomotor on the second reservoir can be driven according to the desired τ_1 and $\tau_2 - \tau_1$ quite easily by a function generator or a signal prerecorded on magnetic tape.

The effect of increasing the recycle flow is to lower the amount of drug entering the sink. This effect is produced by a lowering of the volumetric flow to the reservoir as well as by an increase in the inlet concentration of drug in the liquid entering the dissolution apparatus, which lowers the driving force for mass transfer. Furthermore, if the recycle flow is a controlled function of time, $R(t)$, which is prescribed by an experimentally determined differential *in vivo* drug availability rate, $\dot{A}(t)$, it is not considered as an ordinary process variable as is the constant recycle flow, R. It is now reflective of the experimentally obtained *in vivo* data and is, therefore, not an arbitrary process variable extrinsic of the drug product. Instead, it is an intrinsic variable of the drug product and the *in vivo* system from which $A(t)$ was obtained.

Closed Loop Operation for Optimization of $R(t)$ and Subsequent Open Loop Operation of Apparatus with a Programmed Optimal Recycle Flow—The objective of the operation of the *in vitro* drug release apparatus is to obtain results that uniformly reflect the *in vivo* drug availability with optimal fidelity over time and varying drug release behavior of the dosage forms. For any given set of process variables, *i.e.*, Q_A, τ_1, and $\tau_2 - \tau_1$, the closed loop operation of the *in vitro* testing apparatus will produce a function $Q_{s,i}(t)C_i(t)$ for each ith dosage form so that the expression $\dot{A}_i(t) - [Q - R_i(t)]C(t)$ closely approximates zero. A function $R_i(t)$ will be obtained for each dosage form of the drug tested that was chosen to possess different drug release dynamics. The $R_i(t)$ functions can be readout by the computer on magnetic tape or a potentiometric recorder during the closed loop operation of the apparatus.

At this stage, the apparatus merely simulates the $A(t)$ functions determined from *in vivo* experimentation. Analog $R_i(t)$ function signals recorded on magnetic tape for each dosage form can be conveniently processed on an analog computer, or digitized, and their values can be averaged, over dosage forms, at each time to obtain an average, $\bar{R}(t)$, function representing the mean behavior of all dosage forms included in the closed loop operations. A second set of *open loop* runs must then be performed for each dosage form with the $\bar{R}(t)$ function programmed to control recycle flow. The second set of runs is needed because different $C_i(t)$ functions will result, since it may be expected that $R_i(t) \neq \bar{R}(t)$ for any dosage form. The second set of $C_i(t)$ functions are again obtained from the readout of a spectrophotometer or other analytical devices used to monitor continuously the concentration of drug in the dissolution medium recycle stream or the stream flowing out of the apparatus.

An objective function, F_0, defined in the *Appendix*, can be formed from the $\bar{R}(t)$, $C_i(t)$, and $\dot{A}(t)$ functions. A minimal value of the objective function is achieved by systematically adjusting the process variables. A minimal value of the objective function corresponds to optimal open loop operation of the apparatus under determined conditions of Q_{opt}, $\tau_{1\,opt}$, $(\tau_2 - \tau_1)_{opt}$, and $\bar{R}(t)_{opt}$. As mentioned, various means can be implemented to control the recycle flow dynamics to conform to $\bar{R}(t)_{opt}$. The open loop operation of the apparatus with $R(t)_{opt}$ is block diagrammed in Fig. 3.

Procedural Steps—The *in vitro* test apparatus should be operated in the simplest manner that provides acceptable *in vitro* results with regard to *in vivo* drug availability behavior. To determine the magnitude of sensitivity of the fidelity of the test to different operating conditions, the test can be initially performed in four successive phases of increasing complexity and equipment requirements.

Phase I can be performed without automatic control, using fixed, time invariant, values of the process variables, Q and R; R is then a constant recycle flow. An optimal composition and pH of the dissolution medium may be found and thereafter maintained constant; *i.e.*, τ_1 and $\tau_2 - \tau_1$ are not included as process variables.

Phase II can be performed similarly to Phase I but with the inclusion of τ_1 and $\tau_2 - \tau_1$ as process variables.

Phase III can employ an analog computer control of a time-varying recycle flow, $R_i(t)$, and involve the optimization of one process variable, Q. In this case, it will be recalled that $R_i(t)$ is not an arbitrary process variable but is prescribed by the feedback control implemented with the analog computer; *i.e.*, this is a servo problem where $R_i(t)$ is manipulated so that the output from the *in vitro* apparatus is made to follow (or match) closely the experimental *in vivo* dissolution rate data in differential form.

Phase IV is the most complicated case of optimizing three process variables, Q, τ_1, and $\tau_2 - \tau_1$, with feedback control-driven $R_i(t)$.

These four modes of operation can be repeated for different dosage forms of the same drug to obtain the optimal conditions over all dosage forms. One would then have the optimal process conditions, ranging from the simplest arrangement, that would yield Q_{opt}, $\tau_{1\,opt}$, $(\tau_2 - \tau_1)_{opt}$, and $\bar{R}(t)_{opt}$. The simplest mode of operation possessing an acceptable fidelity would then be chosen for future studies with the drug.

Statistical Design—At any stage of the experiment, an objective function may be minimized with minimal experimental effort. The optimization of the process variables and $\bar{R}(t)$ can be accomplished using a fractional two-level factorial experimental design in the process variables (26). A quarter or half, duplicated, replicate experiment can be performed and an objective function, F_0, can be evaluated. To minimize F_0 and, therefore, uniformly minimize the discrepancy between *in vitro* and *in vivo* results, a "path of steepest descent" in the objective function should be followed. This path represents changes in the independent (process) variables so that the most gain (least discrepancy) is made by proceeding in this direction rather than any other.

Optimization is continued by planning another experiment around the best values found along the path of steepest descent. Ultimately, a more extensive experiment such as a three-level factorial or a central composite can be designed to develop a mathematical model of the effects of the process variables on the discrepancies represented by the objective function. The optimum set of conditions can then be determined by differentiating this model and locating the minimum (26).

Possible Limitations and Properties of the Test—The *in vitro* testing apparatus can be calibrated to predict bioavailability rates, $\dot{A}(t)$. These rates can be integrated to provide cumulative amount of drug absorbed profiles, $A(t)$. Alternatively, blood level–time profiles $[C_b(t)]$, urinary excretion rates $[\dot{A}_u(t)]$, or pharmacological response intensities $[I(t)]$, can be predicted. When quantities other than $\dot{A}(t)$ are used as *in vivo* bioavailability criteria, the $C_b(t)$, $\dot{A}_u(t)$, or $I(t)$ values are merely substituted for $\dot{A}(t)$ in all equations in which it appears.

When using pharmacological data (1–3, 27–30), the observed response intensity *versus* time profiles $[I(t)]$ should first be converted to their corresponding biophasic drug level *versus* time profiles $[Q_B(t)]$; the details of the basis and procedures for the interconversion were reported previously (2, 27, 28). Of the various *in vivo* bioavailability criteria, only $\dot{A}(t)$ has a directly corresponding *in vitro* counterpart in $[Q - R(t)]C(t)$ to which it is compared. For this reason, it would theoretically be preferred. However, $\dot{A}(t)$ is computed from blood, urine, or pharmacological data using a pharmacokinetic model (1–3, 28–32). As such, it may be a large step removed from the actual observed $C_b(t)$, $\dot{A}_u(t)$, or $I(t)$ data used for its computation. Since these latter quantities are usually of primary interest, they could be used directly without first converting them to $\dot{A}(t)$.

The direct comparison of $C_b(t)$, $\dot{A}_u(t)$, or $I(t)$ to *in vitro* drug release rates cannot be justified as easily as $\dot{A}(t)$ on mechanistic grounds. However, considering that the pharmacokinetic behavior of most systems can be described by linear compartment models (1), the relationship between $\dot{A}(t)$ and $C_b(t)$, $\dot{A}_u(t)$, or $I(t)$ [converted to $Q_B(t)$] will usually be given by a first- or higher order transfer function (1–3, 6). Therefore, $C_b(t)$, $\dot{A}_u(t)$, or $Q_B(t)$ profiles will resemble and possess the essential features of $\dot{A}(t)$, except for differing from them by the first or higher lag time always imposed in the same way by the transfer functions. The operation of the apparatus should be sufficiently versatile to compensate for this effect.

In vitro drug release results are obviously only of interest in bioequivalency testing when they reflect *in vivo* bioavailability behavior of drug formulations. *In vitro* drug release testing can never obviate performing *in vivo* studies in human subjects. However, the described approach to optimized *in vitro* drug bioavailability testing minimizes *in vivo* experimentation by confining it to what is needed to optimize and verify the predictive operation of the apparatus. Thereafter, the apparatus will optimally simulate and predict the bioavailability behavior of the panel of human subjects who contributed the *in vivo* data used in its calibration. Within the discussed limitations, the calibrated apparatus can then be considered to serve as a substitute for this same panel of subjects who, in theory, are no longer needed to test additional dosage forms.

The results obtained from *in vitro* testing can, of course, be no better than the *in vivo* bioavailability data used to calibrate the apparatus. However, once properly calibrated, the *in vitro* apparatus can provide predictive results rapidly (the *in vitro* dissolution can be accelerated up to approximately 10–30 times the *in vivo* rates), conveniently, and inexpensively. Therefore, it can be used routinely to screen large numbers of generic drug products or preliminary formulations prepared in developing a new drug product. Such large-scale routine screening is not practical with human testing. However, when a particular drug product is brought into question on the basis of *in vitro* testing results, it would generally be prudent also to evaluate it *in vivo*.

The optimized *in vitro* drug release test apparatus is conceived as a drug bioavailability simulator. In principle, the apparatus can be adjusted to predict optimally the bioavailability behavior of any drug-absorbing biological system when it is operated with drug dosage forms possessing drug release dynamics similar to, and within the range for which, the process variables have been optimized. In other words, the dynamics of drug release in the apparatus are optimized to simulate the drug absorption dynamics of the specific *in vivo* system from which the $\dot{A}(t)$ or other bioavailability results are obtained.

If the dynamic behavior of both the *in vitro* and *in vivo* drug transference systems could be assumed to be linear, then, in principle, it would only be necessary to optimize the operation of the *in vitro* drug release apparatus for a single dosage form having any arbitrary drug release properties. However, this situation will not be the general case; two or more different dosage forms will minimally be required to optimize the test. The apparatus will then possess fidelity in directly reflecting *in vivo* drug availability for a range of drug release behavior in the vicinity of that characteristic of the dosage forms for which the apparatus was specifically calibrated.

In *in vivo* bioavailability testing of generic drug products, the objective of the test may be merely to establish whether a given generic formulation is bioequivalent to an innovating drug company's product which is chosen as a standard (33). Similarly, in an *in vitro* test, if only a relatively qualitative determination of bioequivalence is sought, as opposed to a quantitative prediction of the *in vivo* performance of the test formulation, it may not be necessary to calibrate the apparatus optimally. In this case, it may only be required to choose values arbitrarily for the process variables, τ_1, $\tau_2 - \tau_1$, and Q, that permit the apparatus, when operated in the closed loop mode, to simulate an *in vivo* response *versus* time profile for the standard formulation.

In the process of performing this simulation, a recycle flow function, $R(t)$, will be obtained; $R(t)$ can subsequently be used to control open loop dissolution tests performed with the generic products under evaluation. The resulting *in vitro* release profiles for the tested formulations can then be statistically compared (33) with results obtained from the standard to determine whether their profiles fall within the range observed for different, acceptable lots of the standard dosage form. Although this shortcut procedure can provide a rapid and simple means of detecting *in vitro* differences in drug formulations relating to their *in vivo* bioavailability behavior, the direct relationship between *in vitro* and *in vivo* performance obtained when the apparatus is optimally calibrated cannot be assumed.

No *in vitro* dissolution apparatus, however complex and how well it simulates known *in vivo* data, can be fully relied upon to predict *in vivo* performance. Human testing must always be performed, not only to obtain the data required to calibrate the apparatus but also to ensure that the unpredictable biological and/or chemical factors specific for a particular dosage form are not operating to vitiate the predictive capability of the apparatus. The probability of this occurrence may be diminished if the chemical composition of the dosage forms used in its calibration differs only quantitatively from the composition subsequently tested. The determination of the full extent of applicability of a test for any particular drug must always be performed by experimentation.

Conceivably, an extension of the presently described scheme for *in vitro* drug bioavailability testing could provide an approach to the ideal of an ultimately "universal" drug release test. The limits to which optimized *in vitro* drug release testing could be generalized to drugs for which the tests have not been specifically developed may be explored through the determination and subsequent testing of any observed dependencies of optimized fixed process variables on the physical properties of the drugs (*e.g.*, water solubility, diffusion coefficient, pK, and oil–water partition coefficient). Such correlations would obviously require studies with various dosage forms of several drugs possessing physical properties sufficient to permit extrapolations and interpolations.

The accuracy of such estimations of optimal test conditions for a previously unstudied drug may, of course, be expected to increase with the number of drugs for which the *in vitro* test conditions have previously been optimized. The possible occurrence of unpredictable or nonlinear biological influences that could vitiate the predictive capability of tests performed under extrapolatively on interpolatively estimated conditions would obviously always require an *in vivo* verification of *in vitro* test results. The periodic pooling of results reported by different laboratories could serve to accelerate the accumulation of information required to determine the "universality" and reliability of optimized *in vitro* drug bioavailability testing.

APPENDIX: OBJECTIVE FUNCTION

A performance criterion for the *in vitro* test should reflect both the magnitude of deviations from the ideal, as represented by *in vivo* bioavailability results, and the uniformity of deviations. Consider an *in vitro* apparatus operating with a fixed set of process variables and an average recycle flow $\bar{R}(t)$. Nonzero deviations will generally occur between comparisons of *in vivo* bioavailability rates, *i.e.*, $\dot{A}(t)$, and their *in vitro* counterparts, *i.e.*, $Q_s(t)C(t)$. Such differences may be referred to as apparatus errors. For any dosage form, the apparatus produces errors that vary as a function of time over the *in vitro* drug release test process.

It is desired to both minimize the magnitude of the average error for the entire drug dissolution process and to distribute the error uniformly over time. The error tends to be uniformly distributed when the variance of the error at each instant of time from the average error is minimized. An apparatus performance criterion meeting these objectives may be developed as follows. For the ith dosage form, the squared deviation, d_{i,t_j}, of the *in vitro* from the *in vivo* data at each discrete *in vivo* sampling time, t_j, is defined by:

$$d_{i,t_j} = [\dot{A}_{i,t_j}(t) - P_{i,t_j}(t)]^2 \qquad \text{(Eq. A1)}$$

The quantity:

$$\bar{A}_{i,t_j} = \frac{\sum_{k=1}^{N_i} A_{i,t_j,k}}{N_i} \qquad \text{(Eq. A2)}$$

defines the average *in vivo* value at sampling time t_j, N_i is the number of *in vivo* replicate experiments performed with the ith dosage form, and P_{i,t_j} represents the value of the *in vitro* counterpart of $\dot{A}_{i,t_j}$. The average value of the squared error, d_i, for the ith dosage form over the entire *in vitro* testing time can be calculated by:

$$d_i = \frac{\sum_{j=1}^{n_i} w_{i,t_j} d_{i,t_j}}{n_i} \qquad \text{(Eq. A3)}$$

where n_i is the number of discrete *in vivo* sampling times; and w_{i,t_j} represents a weighting factor, defined by Eq. A4, which attenuates each sampling time contribution to d_i. As seen here, the degree of

attenuation depends upon the magnitude of the error at each time that is determined from the replicated *in vivo* data:

$$w_{i,t_j} = \frac{q_i}{q_i + q_{i,t_j}} \qquad \text{(Eq. A4)}$$

where q_{i,t_j} represents the variance of each *in vivo* result about the average value, *i.e.*, $\bar{A}_{i,t_j}$ at sampling time t_j, as defined by:

$$q_{i,t_j} = \frac{\sum_{k=1}^{N_i} (\dot{A}_{i,t_j,k} - \bar{A}_{i,t_j})^2}{N_i - 1} \qquad \text{(Eq. A5)}$$

The variance of the *in vivo* data averaged over the entire experimental time is symbolized by q_i and defined by:

$$q_i = \frac{\sum_{j=1}^{n_i} q_{i,t_j}}{n_i} \qquad \text{(Eq. A6)}$$

For each ith dosage form, a measure of the uniformity of the distribution of the error over the experimental run can be expressed as the variance, v_i, of the squared error at the jth discrete sampling time about the average squared error for the entire time of the *in vitro* experiment:

$$v_i = \frac{\sum_{j=1}^{n_i} (d_i - w_{i,t_j} d_{i,t_j})^2}{n_i - 1} \qquad \text{(Eq. A7)}$$

Combining Eqs. A3 and A7 results in an objective function, F_i, for each dosage form. This function expresses both the magnitude of the total error and the uniformity of its distribution over time as expressed by:

$$F_i = g_{m,i} d_i + g_{u,i} v_i \qquad \text{(Eq. A8)}$$

and:

$$F_i = F_{m,i} + F_{u,i} \qquad \text{(Eq. A9)}$$

where $g_{m,i}$ and $g_{u,i}$ represent a magnitude (*i.e.*, average value) weighting factor for the ith dosage form and a uniformity (*i.e.*, variance) weighting factor, respectively; $F_{m,i}$ is the weighted average magnitude of the deviation over time for the ith dosage form; and $F_{u,i}$ is the weighted uniformity in the deviations over time for the ith dosage form.

In addition to the average error and distribution of error over experimental time for a single dosage form, an *in vitro* drug release apparatus operating with fixed process variables may be expected to produce different average errors and error distributions for different dosage forms. Therefore, the optimum set of process variables is one that:

1. Produces the smallest *overall* average error for all dosage forms; *i.e.*, the smallest value of $\bar{F}_M$ as defined by Eq. A10, where p is the number of dosage forms:

$$\bar{F}_M = \frac{\sum_{i=1}^{p} F_{m,i}}{p} \qquad \text{(Eq. A10)}$$

2. Produces a uniform distribution of average error between dosage forms. A measure of this is represented as the variance of the average error of the individual dosage forms, $F_{m,i}$, about the overall average error for all dosage forms as expressed by:

$$F_{u,D} = \frac{\sum_{i=1}^{p} (\bar{F}_M - F_{m,i})^2}{p - 1} \qquad \text{(Eq. A11)}$$

3. Produces the greatest degree of *overall* uniformity of error over time for all dosage forms. This will be reflected by the value of the *overall average* weighted time variance for all dosage forms as expressed by:

$$F_{M,u,D,T} = \frac{\sum_{i=1}^{p} F_{u,i}}{p} \qquad \text{(Eq. A12)}$$

4. Produces a uniform distribution of uniformity of error over experimental time among all dosage forms. A measure of this criterion is provided by the variance of the weighted time variance of the individual dosage forms, $F_{u,i}$, above the overall average weighted time variance, $F_{u,u,D,T}$, as expressed by:

$$F_{u,u,D,T} = \frac{\sum_{i=1}^{h} (F_{M,u,D,T} - F_{u,i})^2}{p - 1} \qquad \text{(Eq. A13)}$$

The quantities defined by Eqs. A10–A13 are the average values and variances, over the dosage forms, of the terms in Eq. A9. The overall objective function, F_0, as expressed by Eq. A14, represents both the magnitude and uniformity performance criteria enumerated above:

$$F_0 = G_M \bar{F}_M + G_{u,D} F_{u,D} + G_{M,u,D,T} F_{M,u,D,T} + G_{u,u,D,T} F_{u,u,D,T} \qquad \text{(Eq. A14)}$$

The weighting factors, G's and g's in Eqs. A14 and A8, may be chosen with respect to the relative importance of each consideration and the relative magnitudes of each term constituting F_0. Each value of G and g can be defined to constitute a product factor a and G' and a and g', *i.e.*, $G = aG'$ and $g = ag'$. The values of a will compensate for innate differences in the magnitudes of the terms in the objective function; *i.e.*, the ratio of any two terms multiplied by their values of a may be chosen to be unity at the optimum, *e.g.*, $a_M F_M / a_{u,D} F_{u,D} = 1$.

The values of G may be selected on the basis of the relative importance of the reduction of magnitudes of errors and uniform simultaneous convergence to the optimum. If desirable, the complexity of the objective function, as defined by Eq. A14, can readily be reduced by setting weighting factors equal to zero. Obviously, in each case the simplest form of an objective function found to be appropriate should be implemented.

As noted previously, when operating with feedback control of recycle flow, it is necessary first to obtain $R_i(t)$ for each dosage form to determine a $\bar{R}(t)$. A second set of open loop runs using the programmed $\bar{R}(t)$ on each dosage is required to obtain corresponding $C_i(t)$'s that will be different since, in general, $R_i(t) \neq \bar{R}(t)$. The $C_i(t)$ values obtained in the second run of experiments are required for the evaluation of the performance index, as defined by Eq. A14, whose minimization indicates that an optimal set of fixed process variables, *i.e.*, Q, τ_1, and $\tau_2 - \tau_1$, has been determined. The operation of the apparatus with this set of variables and their corresponding $\bar{R}(t)$ values provides an *in vitro* drug release test that is optimally reflective of *in vivo* bioavailability.

An alternative, although somewhat less rigorous, procedure may serve to diminish the amount of open loop duplication of the experimentation for optimization. With closed loop feedback control of recycle flow, the differences between the *in vitro* and *in vivo* dissolution process can be made very small for each individual dosage form. However, since $R(t) \neq \bar{R}(t)$, the error increases when open loop operation with $\bar{R}(t)$ is performed. Therefore, if a set of fixed process variables can be found such that the average deviation between the individual $[R_i(t)]$ and average $[\bar{R}(t)]$ recycle time functions is a minimum, then the average error produced when the individual dosage forms are tested with the apparatus operated with $\bar{R}(t)$ will tend to be a minimum. This set of fixed variables would minimize the quantity M expressed by Eq. A15, where T_i is the length of the experimental run on the ith dosage form:

$$M = \frac{\sum_{i=1}^{p} \frac{I}{T_i} \int_0^{T_i} [R_i(t) - \bar{R}(t)]^2 \, dt}{p} \qquad \text{(Eq. A15)}$$

For a finite set of discrete sampling times, M can be approximated by Eq. A16, where n_i is the number of equally spaced discrete sampling times:

$$M_A = \frac{\sum_{i=1}^{p} \frac{1}{n_i} \sum_{j=1}^{n_i} [R_{ij}(t) - \bar{R}_j(t)]^2}{p} \qquad \text{(Eq. A16)}$$

The rationale for Eq. A16 may be seen to develop from the consideration that the test conditions producing uniformly accurate results for every dosage form would tend to minimize the quantity $S(t)$ given by:

$$S(t) = \sum_{i=1}^{p} S_i(t) = \sum_{i=1}^{p} \{[Q - R_i(t)] C_{ii}(t) - [Q - \bar{R}(t)] C_{iA}(t)\} \qquad \text{(Eq. A17)}$$

where $C_{ii}(t)$ is the concentration of drug entering the sink with the dissolution apparatus operated with the recycle time function, $R_i(t)$, for the ith dosage form, and $C_{iA}(t)$ is similarly defined for a recycle time function, $\bar{R}(t)$. With all process variables fixed in value, the concentration in the effluent stream is a function of only the recycle time function, *i.e.*, $C_{ii} = f[R_i(t)]$ and $C_{iA} = f[\bar{R}(t)]$. Therefore, as $R_i(t)$ approaches $\bar{R}(t)$ for each ith dosage form, then $C_{ii}(t)$ approaches $C_{iA}(t)$ and $S_i(t)$ tends to zero.

It is not considered likely that a set of process variables exists such that $R_i(t)$ will precisely equal $\bar{R}(t)$ for $i = 1, 2, \ldots, p$. However, one set will minimize the sum of the deviations for all dosage forms. One approach to determining an approximation to this set of process variables is to find the minimum value of Eqs. A15 and A16.

This alternative approach is seen to obviate open loop operation runs which would otherwise be required to be performed with $\bar{R}(t)$. It should be noted that with the alternative performance criterion for optimization, as expressed by Eqs. A15 and A16, the influence of the *in vivo* bioavailability data for each dosage form is implicit in $R_i(t)$ by virtue of its use in providing a reference for the closed operation of the apparatus. In any event, this alternative procedure is an indirect approach to the problem of minimizing the deviation of *in vitro* data from *in vivo* data. It may best be considered as a method for more rapidly attaining a set of process variables in the neighborhood of the optimum set. The fidelity of an *in vitro* test may best be gauged from a statistical comparison between drug release results obtained with the apparatus operated with optimal $R(t)$ and fixed process variables with *in vivo* bioavailability data using dosage forms previously unstudied *in vitro* and not included in the optimization procedure.

REFERENCES

(1) V. F. Smolen, B. D. Turrie, and W. A. Weigand, *J. Pharm. Sci.*, **61**, 1941(1972).

(2) V. F. Smolen, P. B. Kuehn, and E. J. Williams, *Drug Dev. Commun.*, **1**, 143(1975).

(3) *Ibid.*, **1**, 231(1975).

(4) V. F. Smolen, *J. Pharm. Sci.*, **60**, 878(1971).

(5) J. G. Wagner, "Biopharmaceutics and Relevant Pharmacokinetics," Drug Intelligence Publications, Hamilton, Ill., 1971, pp. 64–147.

(6) "Current Concepts in the Pharmaceutical Sciences: Biopharmaceutics," J. Swarbrick, Ed., Lea & Febiger, Philadelphia, Pa., 1970, pp. 265–294.

(7) W. A. Cressman, C. A. Janicki, P. C. Johnson, J. T. Dolusio, and G. A. Braun, *J. Pharm. Sci.*, **58**, 1516(1969).

(8) G. Levy, *ibid.*, **52**, 1039(1963).

(9) G. Levy and L. E. Hollister, *ibid.*, **53**, 1446(1964).

(10) H. Weintraub and M. Gibaldi, *ibid.*, **58**, 1368(1969).

(11) *Ibid.*, **59**, 1792(1970).

(12) V. F. Smolen, *Hosp. Pharm.*, **4**, 14(1969).

(13) J. E. Tingstad and S. Riegelman, *J. Pharm. Sci.*, **59**, 692(1970).

(14) F. Langenbucher, *ibid.*, **58**, 1265(1969).

(15) G. H. Elliot, *Pharm. J.*, **131**, 514(1933).

(16) E. Nelson, *J. Am. Pharm. Assoc., Sci. Ed.*, **47**, 297(1958).

(17) W. Brownell, S. Riegelman, and W. J. Mader, "Committee Report on Drug Dissolution Methodology," APhA Academy of Pharmaceutical Sciences, Pharmaceutical Analysis Control Section, 1968.

(18) A. C. Shah and J. F. Ochs, *J. Pharm. Sci.*, **63**, 110(1974).

(19) "Sartorius Membrane Filter: Absorption and Solubility Simulation," Tech. Bull. SM 2300, Beckman Instruments, Inc., Anaheim, Calif.

(20) G. Levy and E. J. Mroczak, *J. Pharm. Sci.*, **57**, 235(1968).

(21) T. Khalil and A. N. Martin, *ibid.*, **56**, 1225(1967).

(22) V. F. Smolen and D. E. Hagman, *J. Colloid Interface Sci.*, **42**, 70(1973).

(23) G. N. Ling, *Int. J. Neurosci.*, **1**, 129(1970).

(24) M. Gibaldi and S. Feldman, *J. Pharm. Sci.*, **56**, 1238(1967).

(25) P. Finholt and S. Solvang, *ibid.*, **57**, 1322(1968).

(26) C. R. Hicks, "Fundamental Concepts in the Design of Experiments," Holt, Reinhart, and Winston, New York, N.Y., 1964, pp. 224–245.

(27) V. F. Smolen and W. A. Weigand, *J. Pharmacokinet. Biopharm.*, 1, 329(1973).

(28) V. F. Smolen, E. J. Williams, and P. B. Kuehn, *Can. J. Pharm. Sci.*, **10**, 95(1975).

(29) V. F. Smolen, R. G. Barile, and T. G. Theophanous, *J. Pharm. Sci.*, **61**, 467(1972).

(30) V. F. Smolen and R. D. Schoenwald, *ibid.*, **60**, 96(1971).

(31) J. G. Wagner and E. Nelson, *ibid.*, **53**, 1392(1964).

(32) J. C. K. Loo and S. Riegelman, *ibid.*, **57**, 918(1968).

(33) W. J. Westlake, in "Current Concepts in the Pharmaceutical Sciences: Dosage Form Design and Bioavailability," J. Swarbrick, Ed., Lea & Febiger, Philadelphia, Pa., 1973, pp. 149–179.

ACKNOWLEDGMENTS AND ADDRESSES

Received September 25, 1972, from the *Interdisciplinary Drug Engineering and Assessment Laboratory, School of Pharmacy and Pharmacal Sciences, Purdue University, West Lafayette, IN 47907*

Accepted for publication February 12, 1976.

* Department of Chemical Engineering.

ˣ To whom inquiries should be directed (at the Department of Industrial and Physical Pharmacy).

Subnanogram Assay for Pilocarpine in Biological Fluids

W. F. BAYNE ˣ, L.-C. CHU, and F. T. TAO

Abstract □ A method for the determination of pilocarpine was developed in which the imidazole ring of pilocarpine was acylated with heptafluorobutyric anhydride, using triethylamine as a catalyst. After cleanup, the pilocarpine derivative was analyzed using GLC with electron-capture detection. The limit of sensitivity was 25–50 pg of pilocarpine, which had been subjected to the derivatization and cleanup procedures. The method was specific for pilocarpine, with the isopilocarpine derivative eluting prior to the pilocarpine derivative.

Keyphrases □ Pilocarpine—GLC analysis, biological fluids □ GLC—analysis, pilocarpine, biological fluids □ Ophthalmic cholinergic agents—pilocarpine, GLC analysis in biological fluids

Pilocarpine is used extensively in clinical ophthamology as a topical agent for lowering intraocular pressure of patients suffering from open- and closed-angle primary glaucoma. Much interest and analytical development (1) have recently been focused on this drug because of its incorporation into a new dosage form called an ocular therapeutic system (2, 3). This system is placed beneath the eyelid and provides continuous delivery of pilocarpine at a controlled low rate into the tear film, as opposed to intermittent pulses of drug into the tear film by conventional eyedrops.

Colorimetric methods based on the oxidation of the tertiary amino group or on opening the lactone ring with hydroxylamine have been reported (4). Pilocarpine has

It is not considered likely that a set of process variables exists such that $R_i(t)$ will precisely equal $\bar{R}(t)$ for $i = 1, 2, \ldots, p$. However, one set will minimize the sum of the deviations for all dosage forms. One approach to determining an approximation to this set of process variables is to find the minimum value of Eqs. A15 and A16.

This alternative approach is seen to obviate open loop operation runs which would otherwise be required to be performed with $\bar{R}(t)$. It should be noted that with the alternative performance criterion for optimization, as expressed by Eqs. A15 and A16, the influence of the *in vivo* bioavailability data for each dosage form is implicit in $R_i(t)$ by virtue of its use in providing a reference for the closed operation of the apparatus. In any event, this alternative procedure is an indirect approach to the problem of minimizing the deviation of *in vitro* data from *in vivo* data. It may best be considered as a method for more rapidly attaining a set of process variables in the neighborhood of the optimum set. The fidelity of an *in vitro* test may best be gauged from a statistical comparison between drug release results obtained with the apparatus operated with optimal $R(t)$ and fixed process variables with *in vivo* bioavailability data using dosage forms previously unstudied *in vitro* and not included in the optimization procedure.

REFERENCES

(1) V. F. Smolen, B. D. Turrie, and W. A. Weigand, *J. Pharm. Sci.*, **61**, 1941(1972).

(2) V. F. Smolen, P. B. Kuehn, and E. J. Williams, *Drug Dev. Commun.*, **1**, 143(1975).

(3) *Ibid.*, **1**, 231(1975).

(4) V. F. Smolen, *J. Pharm. Sci.*, **60**, 878(1971).

(5) J. G. Wagner, "Biopharmaceutics and Relevant Pharmacokinetics," Drug Intelligence Publications, Hamilton, Ill., 1971, pp. 64–147.

(6) "Current Concepts in the Pharmaceutical Sciences: Biopharmaceutics," J. Swarbrick, Ed., Lea & Febiger, Philadelphia, Pa., 1970, pp. 265–294.

(7) W. A. Cressman, C. A. Janicki, P. C. Johnson, J. T. Dolusio, and G. A. Braun, *J. Pharm. Sci.*, **58**, 1516(1969).

(8) G. Levy, *ibid.*, **52**, 1039(1963).

(9) G. Levy and L. E. Hollister, *ibid.*, **53**, 1446(1964).

(10) H. Weintraub and M. Gibaldi, *ibid.*, **58**, 1368(1969).

(11) *Ibid.*, **59**, 1792(1970).

(12) V. F. Smolen, *Hosp. Pharm.*, **4**, 14(1969).

(13) J. E. Tingstad and S. Riegelman, *J. Pharm. Sci.*, **59**, 692(1970).

(14) F. Langenbucher, *ibid.*, **58**, 1265(1969).

(15) G. H. Elliot, *Pharm. J.*, **131**, 514(1933).

(16) E. Nelson, *J. Am. Pharm. Assoc., Sci. Ed.*, **47**, 297(1958).

(17) W. Brownell, S. Riegelman, and W. J. Mader, "Committee Report on Drug Dissolution Methodology," APhA Academy of Pharmaceutical Sciences, Pharmaceutical Analysis Control Section, 1968.

(18) A. C. Shah and J. F. Ochs, *J. Pharm. Sci.*, **63**, 110(1974).

(19) "Sartorius Membrane Filter: Absorption and Solubility Simulation," Tech. Bull. SM 2300, Beckman Instruments, Inc., Anaheim, Calif.

(20) G. Levy and E. J. Mroczak, *J. Pharm. Sci.*, **57**, 235(1968).

(21) T. Khalil and A. N. Martin, *ibid.*, **56**, 1225(1967).

(22) V. F. Smolen and D. E. Hagman, *J. Colloid Interface Sci.*, **42**, 70(1973).

(23) G. N. Ling, *Int. J. Neurosci.*, **1**, 129(1970).

(24) M. Gibaldi and S. Feldman, *J. Pharm. Sci.*, **56**, 1238(1967).

(25) P. Finholt and S. Solvang, *ibid.*, **57**, 1322(1968).

(26) C. R. Hicks, "Fundamental Concepts in the Design of Experiments," Holt, Reinhart, and Winston, New York, N.Y., 1964, pp. 224–245.

(27) V. F. Smolen and W. A. Weigand, *J. Pharmacokinet. Biopharm.*, 1, 329(1973).

(28) V. F. Smolen, E. J. Williams, and P. B. Kuehn, *Can. J. Pharm. Sci.*, **10**, 95(1975).

(29) V. F. Smolen, R. G. Barile, and T. G. Theophanous, *J. Pharm. Sci.*, **61**, 467(1972).

(30) V. F. Smolen and R. D. Schoenwald, *ibid.*, **60**, 96(1971).

(31) J. G. Wagner and E. Nelson, *ibid.*, **53**, 1392(1964).

(32) J. C. K. Loo and S. Riegelman, *ibid.*, **57**, 918(1968).

(33) W. J. Westlake, in "Current Concepts in the Pharmaceutical Sciences: Dosage Form Design and Bioavailability," J. Swarbrick, Ed., Lea & Febiger, Philadelphia, Pa., 1973, pp. 149–179.

ACKNOWLEDGMENTS AND ADDRESSES

Received September 25, 1972, from the *Interdisciplinary Drug Engineering and Assessment Laboratory, School of Pharmacy and Pharmacal Sciences, Purdue University, West Lafayette, IN 47907*

Accepted for publication February 12, 1976.

* Department of Chemical Engineering.

ˣ To whom inquiries should be directed (at the Department of Industrial and Physical Pharmacy).

Subnanogram Assay for Pilocarpine in Biological Fluids

W. F. BAYNE ˣ, L.-C. CHU, and F. T. TAO

Abstract □ A method for the determination of pilocarpine was developed in which the imidazole ring of pilocarpine was acylated with heptafluorobutyric anhydride, using triethylamine as a catalyst. After cleanup, the pilocarpine derivative was analyzed using GLC with electron-capture detection. The limit of sensitivity was 25–50 pg of pilocarpine, which had been subjected to the derivatization and cleanup procedures. The method was specific for pilocarpine, with the isopilocarpine derivative eluting prior to the pilocarpine derivative.

Keyphrases □ Pilocarpine—GLC analysis, biological fluids □ GLC—analysis, pilocarpine, biological fluids □ Ophthalmic cholinergic agents—pilocarpine, GLC analysis in biological fluids

Pilocarpine is used extensively in clinical ophthamology as a topical agent for lowering intraocular pressure of patients suffering from open- and closed-angle primary glaucoma. Much interest and analytical development (1) have recently been focused on this drug because of its incorporation into a new dosage form called an ocular therapeutic system (2, 3). This system is placed beneath the eyelid and provides continuous delivery of pilocarpine at a controlled low rate into the tear film, as opposed to intermittent pulses of drug into the tear film by conventional eyedrops.

Colorimetric methods based on the oxidation of the tertiary amino group or on opening the lactone ring with hydroxylamine have been reported (4). Pilocarpine has

successfully been chromatographed by GLC using several stationary liquid phases (5–7); one article (7) reported the separation of pilocarpine and isopilocarpine. This laboratory observed significant tailing and loss of resolution when pilocarpine and isopilocarpine were chromatographed and a tendency for pilocarpine to epimerize thermally to isopilocarpine, even with rigid control of the injector and column temperatures.

Repta and Higuchi (8) developed an analytical method for pilocarpine based on the catalytic action of its imidazole ring on the hydrolysis of 2,4-dinitrophenyl acetate. The product of hydrolysis, the 2,4-dinitrophenoxide ion, was determined spectrophotometrically. They suggested that the assay was capable of measuring 100 ng of pilocarpine with suitable modifications. Since the ability to measure absolute quantities of pilocarpine as low as 0.05 ng was desired, development of such an assay was undertaken with the intent to measure pilocarpine in biological fluids.

EXPERIMENTAL

Reagents—Methylene chloride, hexane, benzene, and ethyl acetate[1], used in the derivatization and cleanup procedures, were highly purified, commercially available solvents. Methylene chloride was distilled from phosphorus pentoxide prior to use; the other solvents were used as received. All other chemicals were reagent grade unless otherwise specified. Triethylamine[2] (I) and heptafluorobutyric anhydride[2] (II) were used for the acylation of pilocarpine.

Pilocarpine base, when used as the standard, was prepared by extracting pilocarpine with methylene chloride from an aqueous solution of pilocarpine nitrate adjusted to pH 9, followed by evaporation of the organic solvent, which had been dried with sodium sulfate. This pilocarpine base contained less than 1% isopilocarpine as determined using a liquid chromatographic procedure (1). A methanol[1] solution of the extracted pilocarpine was diluted down to a working standard and was stable at 0° for at least 1 month.

Borate buffer was made from 0.0625 *M* sodium tetraborate and 0.25 *M* H_3BO_3 adjusted to pH 8.5. Similarly, carbonate buffer was made from 1 *M* $KHCO_3$ adjusted to pH 9.25 with fresh concentrated potassium hydroxide. Hydrochloric acid, 0.5 *N*, was prepared by diluting the concentrated acid.

The dimethylated derivative of methazolamide, verified by mass spectrometry, was synthesized by an extractive alkylation technique using iodomethane in methylene chloride and tetrahexylammonium hydrogen sulfate[3] and used as an internal standard. This technique has been used to form a peralkylated derivative of chlorthalidone, which also contains a primary sulfonamide group (9). The suggestion (10) that silver sulfate be used to remove any tetrahexylammonium iodide formed during the alkylation from the organic phase was also followed.

Glassware—All glassware was silanized by soaking for several hours in 5% dimethyldichlorosilane in toluene and rinsing with toluene, methanol, and methylene chloride.

Apparatus—A gas chromatograph equipped with a scandium tritide detector[4] was used. A 2-mm i.d., 1.8-m (6-ft) silanized glass column was packed with 3% OV-17[5] on Chromosorb W[5] (100–120 mesh). This support was inactivated and coated with the liquid phase according to a published procedure (11). Nitrogen was used as the carrier gas.

Retention times were 5 min for dimethylmethazolamide (III) and 6 min for the pilocarpine derivative (IV) at a column temperature of 190° and a gas flow of 25 ml/min. The detector temperature was 250°. To prevent on-column formation of the isopilocarpine derivative, the injector temperature was kept below 210°.

Mass spectra of the pilocarpine derivative and the internal standard were obtained with a quadrupole mass spectrometer[6] interfaced with a gas chromatograph. The electron energy was 70 ev, and the emission current was 1 mamp. The column conditions and flow rate were identical with those employed in the GLC analysis, using either a flame-ionization detector or an electron-capture detector.

The PMR spectra were obtained on a spectrometer[7] in the pulse mode. The solutions analyzed were 20% (w/v), using chloroform-d_1 as a solvent with tetramethylsilane as an internal reference.

Derivatization and Purification for Electron-Capture Detection—An aliquot of a dilution of a pilocarpine nitrate aqueous solution (1 μg/ml) was added with a microsyringe to a stoppered[8] 15-ml centrifuge tube. Then 0.5 ml of borate buffer was added to the aliquot, and the aqueous solution was extracted twice with 1 ml of methylene chloride. The combined organic extract was evaporated at 40° under a stream of nitrogen. Then 0.5 ml of benzene was added to the residue, and the organic solvent was evaporated at 40° with nitrogen.

When an aliquot of pilocarpine base in methanol was used, the methanol was evaporated before the addition and evaporation of benzene since any residual methanol will consume II. In either case, 200 μl of methylene chloride, 2 μl of I, and 4 μl of II were added to the residue with careful mixing. After 15 min at 50°, 1 ml of borate buffer was added, and the solution was vortexed for 1 min and centrifuged. Excess II was thus removed from the organic phase by hydrolysis to the acid, with the pH chosen to minimize the breakdown of IV.

After the addition of 0.5 ml of 0.5 *N* HCl and vigorous vortexing, first nine volumes and then 2.5 volumes of hexane were used to wash the derivative to eliminate any organic soluble impurities. Complete removal of hexane was followed by the addition of 0.5 ml of benzene and approximately 0.8 ng of III. (Observation in this laboratory indicated that III had an appropriate retention time under similar chromatographic conditions for use as an internal standard.)

Adjusting the pH of the solution to 9 by addition of 1 ml of carbonate buffer permitted the partitioning of IV into the benzene layer. This benzene was transferred to a clean vessel, evaporated to dryness under a nitrogen flow, and then reconstituted in 50 μl of 20% ethyl acetate in hexane. Aliquots of this solution were injected into the gas chromatograph.

Preparation of Microgram Quantities of Derivative—Microgram samples were prepared in the same manner outlined for the submicrogram procedure, except that 4 μl of I and 8 μl of II in 200 μl of methylene chloride were used to derivatize pilocarpine. A few microliters of the final ethyl acetate–hexane solution was either injected onto a gas chromatograph equipped with a flame-ionization detector and chromatographed or onto a GLC–mass spectrometry system, which was employed to obtain the mass spectrum of IV.

Preparation of Milligram Quantities of Derivative—Milligram quantities of IV were prepared by reacting 100 mg of pilocarpine base with 2 ml of I and 4 ml of II in 90 ml of methylene chloride overnight at 40°. The solution was then transferred to a 250-ml separator and washed with 100 ml of carbonate buffer. After removal of the aqueous phase and addition of 90 ml of hexane to the methylene chloride, the organic layer was extracted three times with 50 ml of 1 *N* HCl.

The pooled acid extract was adjusted to pH 9 with sodium carbonate followed by two extractions of IV with 75 ml of carbon tetrachloride. The organic solvent was then removed with a rotary evaporator. The resulting 93 mg of yellow, oily residue was reconstituted with chloroform-d_1 to make a 20% (w/v) solution for PMR analysis.

Derivatization of Base-Catalyzed, Hydrolyzed Pilocarpine—A methanol solution (1 μg/μl) of a pilocarpine sample that had been subjected to base-catalyzed hydrolysis in butanol was prepared. Aliquots of this working solution, representing approximately 100 μg of hydrolyzed pilocarpine, were either derivatized directly after removal of methanol or extracted twice with 1 ml of methylene chloride from 0.5 ml of borate buffer after removal of the methanol. The conditions employed were those described in the microderivatization procedure.

Standard Curve and Calibration—The standard curve was constructed by transferring microliter quantities of pilocarpine nitrate aqueous solution, ranging from 0.05 to 10 ng of pilocarpine base, to the centrifuge tubes. The derivatization was then conducted as al-

[1] Nanograde solvents, Mallinckrodt, St. Louis, Mo.
[2] Sequanal grade, Pierce Chemical Co., Rockford, Ill.
[3] Synthesized by a method supplied by Labkemi AB, Sweden.
[4] Varian model 2100, Walnut Creek, Calif.
[5] Applied Science Labs, State College, Pa.
[6] Finnigan 1015 SL, Sunnyvale, Calif.
[7] Varian XL-100 FT, Palo Alto, Calif.
[8] Lined with Teflon (du Pont).

Table I—Proton Chemical Shifts (Parts per Million) Relative to Tetramethylsilane for Pilocarpine and Derivative in Chloroform-d_1 [a]

	CH_3CH_2—	CH_3CH_2—	—CH_2 (Bridge) 3H, 4H	$5H_a$	$5H_b$	Imidazole Protons 4'H	Imidazole Protons 2'H	N—CH_3
Pilocarpine	1.12 (t)	1.71 (m)	2.64 (m)	4.05 (dd)	4.19 (dd)	6.76 (s)	7.42 (s)	3.63 (s)
Derivative	1.14 (t)	1.72 (m)	2.70 (m)	4.04 (dd)	4.26 (dd)	7.22 (s)	(2'H or 4'H)	4.00 (s)

[a] s = singlet, t = triplet, m = multiplet, and dd = doublet of doublet.

ready described; a constant amount of III, approximately 0.8 ng, was added after the addition of benzene in the cleanup procedure. The standard curve was constructed by measuring the area, peak height times width at half-height, for IV and III. The ratio of the area of IV to III was then plotted against the amount of pilocarpine and yielded a linear plot (slope, 0.37; intercept, 0.008; and r^2, 0.997).

Sampling of Aqueous Humor in Rabbits—Samples of aqueous humor, 24 hr after instillation of 50 μl of a 2% pilocarpine nitrate[9] solution or insertion of a membrane-controlled delivery system[10], were obtained using a 1-ml syringe with a 27-gauge needle. The cornea of anesthetized rabbits was punctured near the limbus, and 50–100 μl of fluid was withdrawn. A few microliters of aqueous humor was added to 0.5 ml of borate buffer, and the assay was conducted as already described.

RESULTS

Samples containing subnanogram quantities of pilocarpine were derivatized and analyzed with good detection (Fig. 1). The minimum detectable quantity was between 25 and 50 pg/25 μl of 20% ethyl acetate–hexane when 9 μl of solution was injected. This limit is practical since 25–50 pg of pilocarpine can be derivatized and carried through the cleanup procedure.

The mass spectrum of IV (Fig. 2) exhibited a molecular ion peak, *m/e* 404, which was consistent with a monoacylated heptafluorobutyryl derivative of pilocarpine. The *m/e* 291 fragment resulted from the loss of the lactone ring from the molecular ion. Further cleavage with the loss of the heptafluorobutyryl group resulted in the *m/e* 94 fragment, which was the base peak. The *m/e* 235 fragment arose from the loss of the C_3F_7 radical from the molecular ion and underwent further loss of the lactone ring to give the *m/e* 122 fragment. Thus, the mass spectrum indicated the loss of one imidazole proton during the acylation.

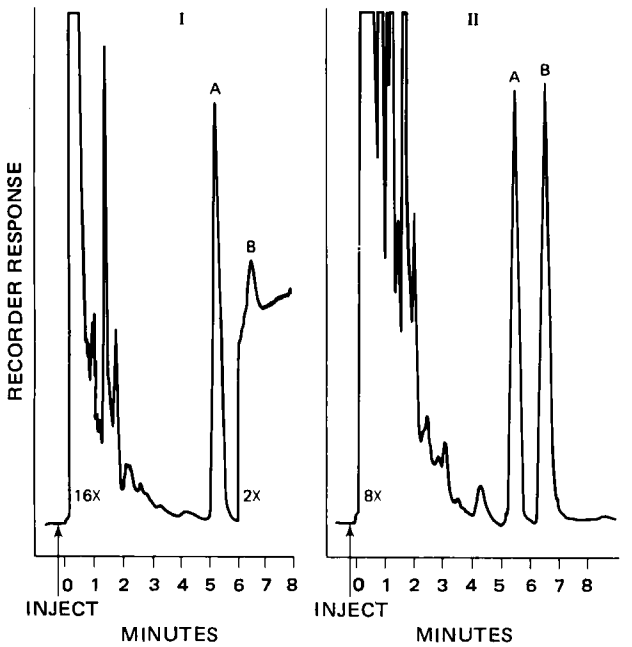

Figure 1—*Representative chromatograms of pilocarpine derivative prepared from aqueous pilocarpine nitrate solutions carried through extraction, derivatization, and cleanup steps. Key: A, internal standard, methazolamide derivative; B, pilocarpine derivative; I, pilocarpine base equivalent to 50 pg; and II, pilocarpine base equivalent to 1 ng.*

The PMR spectrum of the derivative contained only one imidazole proton, whereas pilocarpine had two distinct resonances for the two imidazole protons (Table I). The PMR spectrum also showed a large downfield shift of the *N*-methyl protons in the derivative relative to pilocarpine. This shift can readily be explained by the withdrawal of electron density from the nitrogen by the fluorinated acyl group. It has been reported that a direct correlation between the electron density on the nitrogen and the chemical shift of the attached methyl group exists for a large number of azoles (12). No coupling of the 4'-imidazole proton to the methylene bridge protons was observed in pilocarpine; such coupling has been shown to occur in some 1,5-disubstituted imidazoles (13). Therefore, it is not possible to assign unequivocally the acyl group to either the 2'- or 4'-position of the imidazole ring.

When 100 μg of pilocarpine, which had been subjected to base-catalyzed hydrolysis, was derivatized, only isopilocarpine was obtained. When an extraction from borate buffer (pH 8.5) was performed prior to derivatization, no derivative was obtained. When a sample of pilocarpine was either derivatized directly or extracted and derivatized, the same response was obtained. This response was the same as that obtained for the derivatized sample of pilocarpine subjected to hydrolysis. Thus, it may be concluded that:

1. The sample subjected to hydrolysis was isopilocarpic acid or isopilocarpate.
2. Isopilocarpic acid was not extracted with methylene chloride from a pH 8.5 aqueous solution.
3. Isopilocarpic acid underwent quantitative ring closure to isopilocarpine under the reaction conditions of the derivatization procedure.
4. Pilocarpine can be extracted quantitatively.

The derivatives of pilocarpine and isopilocarpine elicited the same responses from the flame-ionization detector used in this study. Therefore, an extraction from a borate buffer should be performed for biological samples to separate the acids from the lactones if pilocarpine and isopilocarpine are to be specifically determined.

When the described procedure was used to measure pilocarpine concentrations in the aqueous humor of rabbits 24 hr after administration of 50 μl of a 2% solution of pilocarpine nitrate, no pilocarpine was detected (<3 ng/g). However, 24 hr after insertion of the membrane-controlled delivery system, the average concentration in the aqueous humor was 520 ± 16 (*SE*) ng/g (n = 5). This value compares favorably with results obtained using N-$^{14}CH_3$-pilocarpine (14) incorporated into the membrane-controlled delivery system; after appropriate corrections for metabolism (15), an average concentration of 450 ± 16 (*SE*) ng/g (n = 5) was obtained during steady-state delivery.

DISCUSSION

Grimison and Ridd (16) studied the kinetics and deuterium isotope effects of the reaction of imidazole with the electrophiles formed from iodine and iodide and diazotized sulfanilic acid. The 4- or 5-position was the initial site of attack by the iodonium electrophile, while the 2-position was attacked by the diazonium electrophile. The difference in site of attack was rationalized in terms of the position of the transition states along the reaction coordinate, attack by the diazonium species being governed by charge density of imidazole and attack by the iodonium species being controlled by the localization energy of

[9] P. V. Carpine Liquifilm, Allergan, Irvine, Calif.
[10] Ocusert P-20, Alza Corp., Palo Alto, CA 94304

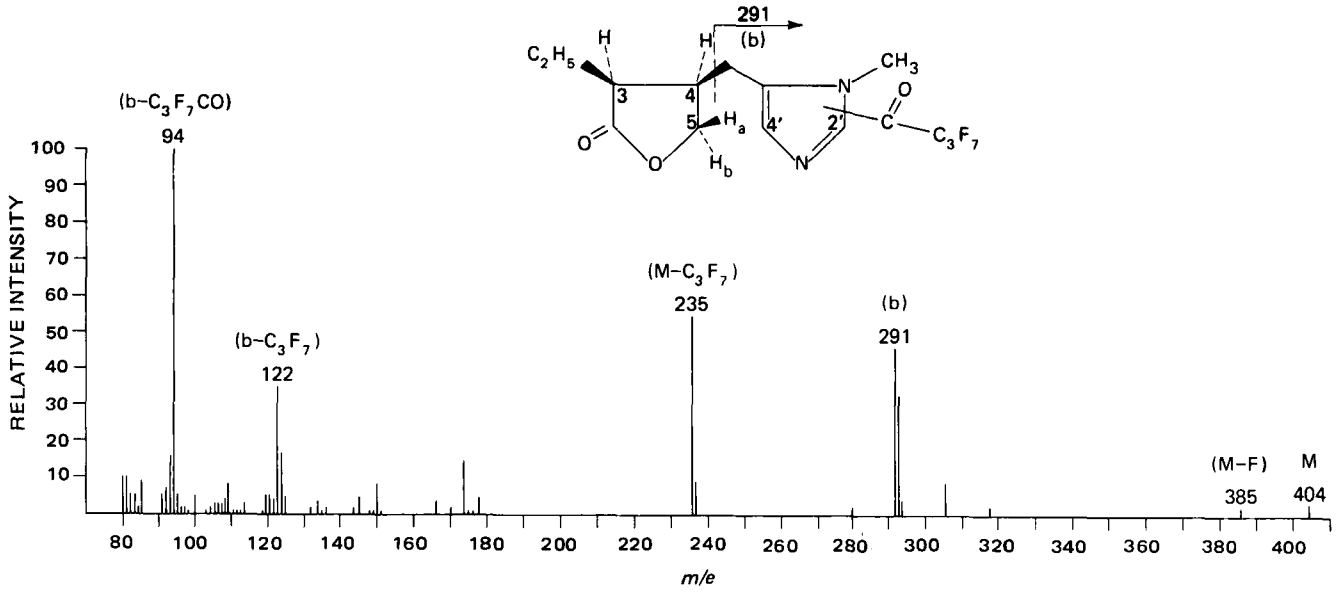

Figure 2—*Mass spectrum of pilocarpine derivative obtained with electron energy of 70 ev and emission current of 1 μamp.*

a high energy intermediate (17). The investigators postulated that the conjugate base of imidazole was the species that reacted with the electrophiles. No reaction occurred when 1-methylimidazole was used.

However, in this laboratory, the acylium electrophile generated from I and II acylated, in methylene chloride or benzene, the imidazole ring of pilocarpine, which has a tertiary amino group. Sulfonation and nitration of imidazole have been reported to occur in the 4- or 5-position, the conjugate base not existing in the acidic medium (18). Blake *et al.* (19) indicated that aromatic compounds can be acylated with fluorinated anhydrides in ethyl acetate, using aluminum chloride as a catalyst. This approach was not successful with pilocarpine in this laboratory.

The derivative (IV) could be made with no apparent epimerization of pilocarpine to isopilocarpine. When microgram samples of pilocarpine were derivatized and chromatographed, separation between the isopilocarpine and pilocarpine derivatives was achieved. The small peak proceeding IV in Fig. 3 had the same retention time as a derivatized sample of isopilocarpine. Figure 3 is a chromatogram of derivatized pilocarpine base, reported to contain less than 1% isopilocarpine. The GLC analysis indicated that the sample contained 0.65% isopilocarpine. Therefore, the derivatization can be conducted without significant epimerization to the more thermodynamically stable *trans*-configuration of the 3- and 4-protons of the lactone ring (isopilocarpine).

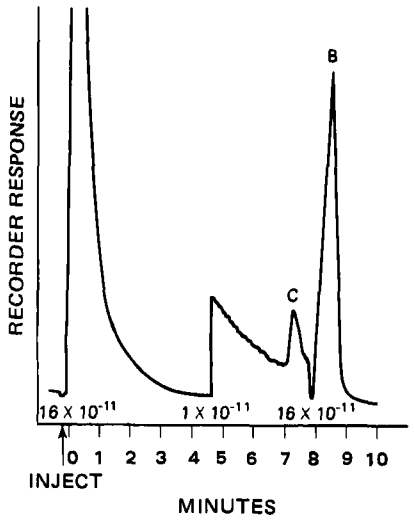

Figure 3—*Chromatogram of derivatized pilocarpine base, showing presence of isopilocarpine. Key: B, pilocarpine derivative; and C, isopilocarpine derivative. The column temperature was lowered to 170° to ensure complete resolution of the two peaks.*

The base-catalyzed epimerization of pilocarpine to isopilocarpine and the base-catalyzed ring opening to pilocarpate, reported previously (20), were minimized due to the high lipophilicity of IV. The derivative (IV) cannot be reextracted to any measurable extent from benzene or methylene chloride with pH 4.5 acetate buffer. Thus, when the benzene and internal standard are added to the aqueous acid and the aqueous phase is made alkaline, IV overwhelmingly favors the organic phase, minimizing residence time in the basic medium. Thus, the extraction procedure could be conducted with little or no epimerization. Furthermore, a linear standard curve resulted.

The cleanup procedure was checked by derivatizating microgram samples of pilocarpine, injecting a microliter of the solution, and comparing the response after the cleanup. The procedure was nearly 100% efficient.

The internal standard was a matter of convenience. Any compound that has favorable partitioning toward benzene relative to an aqueous basic phase, a favorable retention time relative to the pilocarpine derivative, good chromatographic properties in the subnanogram range, and reasonably good sensitivity toward electron-capture detection can be used.

REFERENCES

(1) T. Urbányi, A. Piedmont, E. Willis, and G. Manning, *J. Pharm. Sci.*, **65**, 257(1976).

(2) D. M. Worthen, T. J. Zimmerman, and C. A. Wind, *Invest. Ophthalmol.*, **13**, 296(1974).

(3) M. G. Holland, *Ann. Ophthalmol.*, **6**, 447(1974).

(4) M. S. Karawya and M. G. Ghourab, *J. Assoc. Offic. Anal. Chem.*, **55**, 1180(1972), and references cited therein.

(5) E. Brochmann-Hanssen and A. B. Svendson, *J. Pharm. Sci.*, **51**, 1095(1962).

(6) E. Brochmann-Hanssen and C. R. Fontan, *J. Chromatogr.*, **19**, 296(1965).

(7) J. L. Massingill, Jr., and J. E. Hodgkins, *Anal. Chem.*, **37**, 952(1965).

(8) A. Repta and T. Higuchi, *J. Pharm. Sci.*, **60**, 1468(1971).

(9) M. Ervik and K. Gustavii, *Anal. Chem.*, **46**, 39(1974).

(10) H. Ehrsson, *ibid.*, **46**, 922(1974).

(11) R. J. Leibrand and L. L. Dunham, *Res. Dev.*, **Sept. 1973**, 32.

(12) R. N. Butler, *Can. J. Chem.*, **51**, 2315(1973).

(13) H. R. Matthews nd H. Rapoport, *J. Am. Chem. Soc.*, **95**, 2297(1973).

(14) J. I. DeGraw, J. S. Ingstrom, and E. Willis, *J. Pharm. Sci.*, **64**, 1700(1975).
(15) L. Sendelbeck, D. Moore, and J. Urquhart, *Am. J. Ophthalmol.*, **80**, 274(1975).
(16) G. Grimison and J. H. Ridd, *J. Chem. Soc.*, **1959**, 3019.
(17) G. Grimison and J. H. Ridd, *Proc. Chem. Soc.*, **1958**, 256.
(18) R. J. Gillespie, A. Grimison, J. H. Ridd, and R. F. M. White, *J. Chem. Soc.*, **1958**, 3228.
(19) J. W. Blake, R. Huffman, J. Noonan, and R. Ray, *Am. Lab.*, **May 1973**, 63.
(20) M. A. Nunes and E. Brochmann-Hanssen, *J. Pharm. Sci.*, **63**, 716(1974).

ACKNOWLEDGMENTS AND ADDRESSES

Received November 24, 1975, from *Alza Research, Palo Alto, CA 94304*

Accepted for publication February 2, 1976.

The authors acknowledge N. Keller, L. Sendelbeck, and D. Moore of the Biological Sciences Department, Alza, for obtaining the biological samples.

Note added in proof: The authors of a recent Communication in *J. Pharm. Sci.* [**65**, 1262(1976)], accepted after this research article, reported the formation of a heptafluorobutyramide derivative of pilocarpine. The chemical structure of pilocarpine would seem to preclude formation of an amide. The evidence presented in this research article indicates that either the 2′- or 4′-position of the imidazole ring is acylated with heptafluorobutyric anhydride when the reaction is catalyzed with triethylamine. Since the authors of the Communication employed reaction conditions similar to those presented in this article, it is likely that they formed the same acylated derivative of pilocarpine.

[x] To whom inquiries should be directed.

Circular Dichroism Spectra of Tetracycline Complexes with Mg^{+2} and Ca^{+2}

E. C. NEWMAN [*] and C. W. FRANK [x]

Abstract □ The study of Ca^{+2} and Mg^{+2} complexes of tetracycline in buffered solution was undertaken to determine their stoichiometry and the chelation sites. Circular dichroism was used to follow complex formation. Modified tetracyclines, in which potential complexation sites were blocked, were used to determine the participation of particular sites in complexation. Calcium formed a 2:1 metal-ion to ligand complex, while the magnesium complex formed at a 1:1 ratio. Formation of the calcium complex involved addition of one metal ion to the C-10, C-11 site with subsequent addition of a second metal ion at the C-12, C-1 site. The magnesium chelate occurred at the C-11, C-12 β-diketone site.

Keyphrases □ Tetracycline—complexes with Ca^{+2} and Mg^{+2}, circular dichroism spectral investigation of binding properties □ Metal-ion complexes—Ca^{+2} and Mg^{+2} with tetracycline, circular dichroism spectral investigation of binding properties □ Complexes, metal ion—Ca^{+2} and Mg^{+2} with tetracycline, circular dichroism spectral investigation of binding properties □ Spectrometry, circular dichroism—investigation of binding properties of tetracycline complexes with Ca^{+2} and Mg^{+2} □ Antibiotics—tetracycline, complexes with Ca^{+2} and Mg^{+2}, circular dichroism spectral investigation of binding properties

The mode of action of the tetracycline (I) antibiotics is dependent upon the presence of certain metal ions, and the metal-ion complexation of these drugs has been the subject of numerous investigations. The complex chemistry of the tetracyclines and the large number of potential binding sites have led to much confusion as to the location of these sites. A major contributing factor in this problem has been the failure of the commonly used spectroscopic techniques to pinpoint the complexation centers. Circular dichroism, however, seems to be capable of filling this void, as indicated by recent work (1–4).

From an antimicrobial standpoint, the tetracycline complexes with Mg^{+2} and Ca^{+2} are probably the most important, because the concentrations of these cations

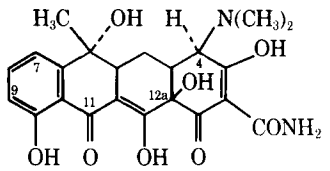

I

and the large formation constants of their complexes with tetracycline dictate that *in vivo* tetracycline would exist as one of these two complexes.

The tetracycline complexes of Mg^{+2} and Ca^{+2} were studied in pH 7.4 buffered 90% methanol, and differences found in the circular dichroism (as well as fluorescence and UV–visible) spectra were attributed to different conformations and thus different binding sites for the two complexes (1). A four-coordinate binding involving positions C-11, C-12, C-2, and C-3 was proposed for the Ca^{+2} complex; the Mg^{+2} complex was thought to be at a different, unspecified site.

Mitscher *et al.* (2) concluded that, in aqueous solutions of pH 7.4 or below, Ca^{+2} and Mg^{+2} both bind somewhere at the B, C, or D complexation site (C-10, C-11; C-11, C-12; or C-12, C-1) of tetracycline. Above pH 7.5, Ca^{+2} binds between the C-4 dimethylamine group and the C-12a hydroxyl group, but Mg^{+2} cannot.

EXPERIMENTAL

Circular Dichroism Spectra—All circular dichroism spectra were recorded on an optical rotatory dispersion–circular dichroism instrument[1]. Concentrations of tetracyclines were always 1×10^{-4} *M*.

[1] Cary 60.

(14) J. I. DeGraw, J. S. Ingstrom, and E. Willis, *J. Pharm. Sci.*, **64**, 1700(1975).
(15) L. Sendelbeck, D. Moore, and J. Urquhart, *Am. J. Ophthalmol.*, **80**, 274(1975).
(16) G. Grimison and J. H. Ridd, *J. Chem. Soc.*, **1959**, 3019.
(17) G. Grimison and J. H. Ridd, *Proc. Chem. Soc.*, **1958**, 256.
(18) R. J. Gillespie, A. Grimison, J. H. Ridd, and R. F. M. White, *J. Chem. Soc.*, **1958**, 3228.
(19) J. W. Blake, R. Huffman, J. Noonan, and R. Ray, *Am. Lab.*, **May 1973**, 63.
(20) M. A. Nunes and E. Brochmann-Hanssen, *J. Pharm. Sci.*, **63**, 716(1974).

ACKNOWLEDGMENTS AND ADDRESSES

Received November 24, 1975, from *Alza Research, Palo Alto, CA 94304*

Accepted for publication February 2, 1976.

The authors acknowledge N. Keller, L. Sendelbeck, and D. Moore of the Biological Sciences Department, Alza, for obtaining the biological samples.

Note added in proof: The authors of a recent Communication in *J. Pharm. Sci.* [**65**, 1262(1976)], accepted after this research article, reported the formation of a heptafluorobutyramide derivative of pilocarpine. The chemical structure of pilocarpine would seem to preclude formation of an amide. The evidence presented in this research article indicates that either the 2′- or 4′-position of the imidazole ring is acylated with heptafluorobutyric anhydride when the reaction is catalyzed with triethylamine. Since the authors of the Communication employed reaction conditions similar to those presented in this article, it is likely that they formed the same acylated derivative of pilocarpine.

[x] To whom inquiries should be directed.

Circular Dichroism Spectra of Tetracycline Complexes with Mg^{+2} and Ca^{+2}

E. C. NEWMAN [*] and C. W. FRANK [x]

Abstract □ The study of Ca^{+2} and Mg^{+2} complexes of tetracycline in buffered solution was undertaken to determine their stoichiometry and the chelation sites. Circular dichroism was used to follow complex formation. Modified tetracyclines, in which potential complexation sites were blocked, were used to determine the participation of particular sites in complexation. Calcium formed a 2:1 metal-ion to ligand complex, while the magnesium complex formed at a 1:1 ratio. Formation of the calcium complex involved addition of one metal ion to the C-10, C-11 site with subsequent addition of a second metal ion at the C-12, C-1 site. The magnesium chelate occurred at the C-11, C-12 β-diketone site.

Keyphrases □ Tetracycline—complexes with Ca^{+2} and Mg^{+2}, circular dichroism spectral investigation of binding properties □ Metal-ion complexes—Ca^{+2} and Mg^{+2} with tetracycline, circular dichroism spectral investigation of binding properties □ Complexes, metal ion—Ca^{+2} and Mg^{+2} with tetracycline, circular dichroism spectral investigation of binding properties □ Spectrometry, circular dichroism—investigation of binding properties of tetracycline complexes with Ca^{+2} and Mg^{+2} □ Antibiotics—tetracycline, complexes with Ca^{+2} and Mg^{+2}, circular dichroism spectral investigation of binding properties

The mode of action of the tetracycline (I) antibiotics is dependent upon the presence of certain metal ions, and the metal-ion complexation of these drugs has been the subject of numerous investigations. The complex chemistry of the tetracyclines and the large number of potential binding sites have led to much confusion as to the location of these sites. A major contributing factor in this problem has been the failure of the commonly used spectroscopic techniques to pinpoint the complexation centers. Circular dichroism, however, seems to be capable of filling this void, as indicated by recent work (1–4).

From an antimicrobial standpoint, the tetracycline complexes with Mg^{+2} and Ca^{+2} are probably the most important, because the concentrations of these cations

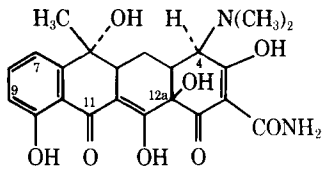

I

and the large formation constants of their complexes with tetracycline dictate that *in vivo* tetracycline would exist as one of these two complexes.

The tetracycline complexes of Mg^{+2} and Ca^{+2} were studied in pH 7.4 buffered 90% methanol, and differences found in the circular dichroism (as well as fluorescence and UV–visible) spectra were attributed to different conformations and thus different binding sites for the two complexes (1). A four-coordinate binding involving positions C-11, C-12, C-2, and C-3 was proposed for the Ca^{+2} complex; the Mg^{+2} complex was thought to be at a different, unspecified site.

Mitscher *et al.* (2) concluded that, in aqueous solutions of pH 7.4 or below, Ca^{+2} and Mg^{+2} both bind somewhere at the B, C, or D complexation site (C-10, C-11; C-11, C-12; or C-12, C-1) of tetracycline. Above pH 7.5, Ca^{+2} binds between the C-4 dimethylamine group and the C-12a hydroxyl group, but Mg^{+2} cannot.

EXPERIMENTAL

Circular Dichroism Spectra—All circular dichroism spectra were recorded on an optical rotatory dispersion–circular dichroism instrument[1]. Concentrations of tetracyclines were always 1×10^{-4} *M*.

[1] Cary 60.

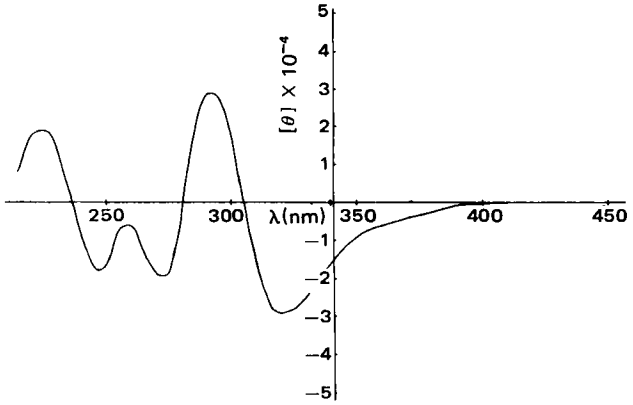

Figure 1—*Circular dichroism spectrum of tetracycline in methanol–water (90:10).*

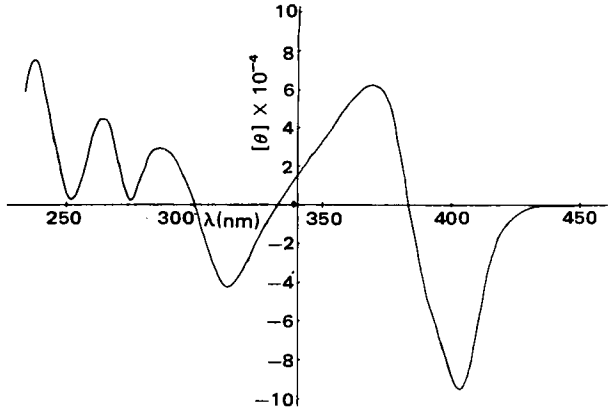

Figure 2—*Circular dichroism spectrum of the calcium complex of tetracycline in methanol–water (50:50).*

The buffer was 0.1 *M* tromethamine, adjusted to pH 7.4 with concentrated hydrochloric acid. The circular dichroism spectra of solutions in this buffer were identical to those of solutions in 0.1 *M* KCl adjusted to pH 7.4, indicating no buffer interference. Solutions were prepared by adding 1 ml of 2.5×10^{-3} *M* tetracycline and an aliquot of 1.25×10^{-2} *M* metal ion to give the desired metal-ion to ligand ratio, and these solutions were diluted to 25 ml with the buffer.

Modified Tetracyclines—Dedimethylaminotetracycline was prepared according to the method of Boother *et al.* (5). The 2-cyanotetracycline was prepared according to the method of Soder and Siedel (6).

RESULTS AND DISCUSSION

The circular dichroism spectrum of tetracycline in 90% methanol contained up to seven clearly defined Cotton effect peaks (as compared to two UV–visible peaks). Since there were also seven potential binding sites, it is theoretically possible to assign each peak to a binding site. Unfortunately, most Cotton effects are not as yet assigned. Some Cotton effects, however, can be assigned to particular portions of the tetracycline molecule on the basis of model compounds. Those Cotton effects that are not assigned are at least useful for fingerprint comparisons.

The circular dichroism spectrum of tetracycline (Fig. 1) in pH 7.4 buffer in 90% methanol contained positive Cotton effects at 225 and 291 nm and negative peaks at 247, 273, and 321 nm with a weak shoulder in the 360-nm region. The two negative peaks at 247 and 273 nm were assigned to the combination of two Cotton effects centered at about 260 nm, one positive and the other negative. One of these two peaks resulted from the β-diketone system of the A-ring, while the other resulted from the phenolic β-diketone system of the B-, C-, and D-rings.

A comparison of the circular dichroism spectra of the complexes of tetracycline and dedimethylaminotetracycline serves to establish the possible involvement of the C-4 dimethylamino group in complexation. Similarly, the use of 2-cyanotetracycline can be used to determine the involvement of the C-2 amide group.

Ca^{+2} Complex of Tetracycline—As Ca^{+2} was added to a buffered solution of tetracycline, some striking spectral changes were noted (Fig. 2). The positive Cotton effect at 225 nm underwent a bathochromic shift to 236 nm and was greatly increased in intensity. These effects were complete once the Ca^{+2} concentration gave a 1:1 metal-ion to ligand ratio. The positive peak at 260 nm was shifted to 264 nm and the intensity was enhanced; the 247- and 273-nm peaks were slightly shifted to 251 and 274 nm, respectively, and decreased in intensity. These effects were complete when a metal-ion to ligand ratio of 1:1 was achieved.

The intensity of the positive Cotton effect at 291 nm was not affected by complexation; however, the peak was shifted to 286 nm. This shift did not begin until the metal-ion to ligand ratio was 1:1 and was complete at a 2:1 ratio. The negative Cotton effect at 321 nm was slightly enhanced and shifted to 313 nm at a metal-ion to ligand ratio of 1:1, after which there was no change. Two new Cotton effects, a positive absorption at 370 nm and a negative absorption at 403 nm, developed from the shoulder near 360 nm and became very intense. These Cotton effects remained unchanged after the metal-ion to ligand ratio reached 2:1 (Fig. 3).

These changes are consistent with the stepwise formation of a 2:1 Ca^{+2}–tetracycline complex. The first Ca^{+2} is added to a site that affects the positive peak at 225 nm, the positive peak at 260 nm, and, to a lesser extent, the positive peak at 291 nm.

The circular dichroism spectrum of dedimethylaminotetracycline is presented in Fig. 4. Its similarity to that of tetracycline indicates that the removal of the dedimethylamino group does not produce major conformational changes in the molecule. There were positive Cotton effects at 225, 256, and 284 nm and negative peaks at 246, 264, and 319 nm.

The addition of Ca^{+2} to a solution of dedimethylaminotetracycline buffered to pH 7.4 produced effects in its circular dichroism spectrum similar to those observed with tetracycline (Fig. 5). The positive Cotton effect at 225 nm was shifted to 236 nm, and its intensity was enhanced up to a metal-ion to ligand ratio of 1:1. This behavior was identical to that observed with tetracycline. The positive peak at 256 nm was also enhanced and shifted to 261 nm, while the intensity of the negative peaks at 246 and 264 nm decreased and shifted to 250 and 273 nm, respectively. These changes were essentially complete at a metal-ion to ligand ratio of 1:1. As with tetracycline, the positive Cotton effect at 284 nm was unchanged in intensity while the negative Cotton effect at 319 nm was slightly enhanced and shifted to 307 nm. These changes were complete up to a metal-ion to ligand ratio of 1:1. Two new Cotton effects, a positive absorption at 366 nm and a nega-

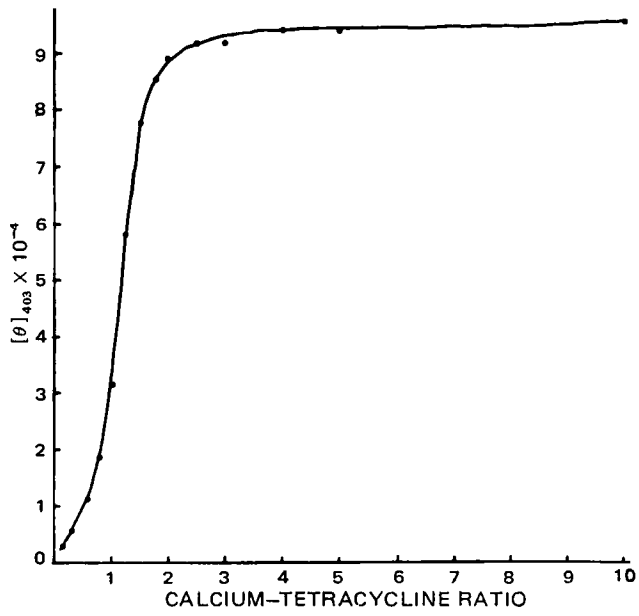

Figure 3—*Mole ratio plot for the calcium–tetracycline complex at 403 nm in methanol–water (50:50).*

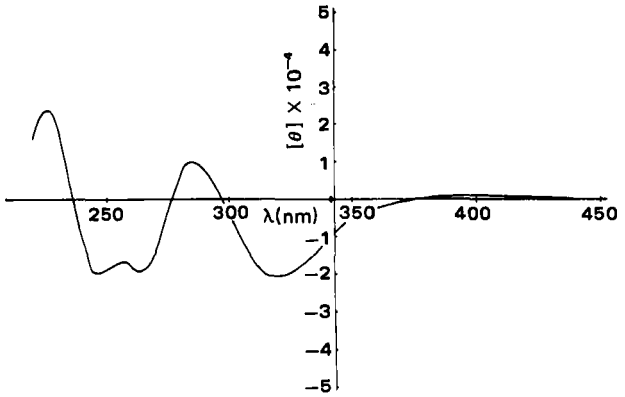

Figure 4—*Circular dichroism spectrum of dedimethylaminotetracycline in methanol–water (50:50).*

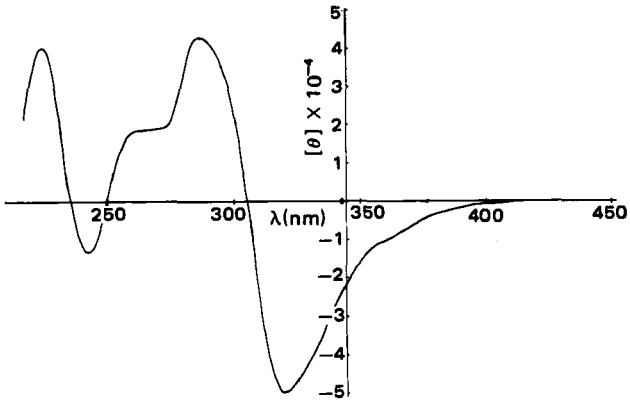

Figure 6—*Circular dichroism spectrum of 2-cyanotetracycline in methanol–water (50:50).*

tive absorption at 403 nm, were produced and became very intense at a metal-ion to ligand ratio of 2:1.

The spectra of the calcium complexes of tetracycline and dedimethylaminotetracycline were strikingly similar at the various stages of the development of the complexes. Both ligands formed 2:1 metal-ion to ligand complexes with Ca^{+2}. It is concluded that tetracycline and dedimethylaminotetracycline complex with Ca^{+2} at the same sites. Furthermore, neither of these sites involves the C-4 dimethylamino group, since this group is absent in dedimethylaminotetracycline.

The circular dichroism spectrum of 2-cyanotetracycline (Fig. 6) was slightly different from the spectra of tetracycline and dedimethylaminotetracycline in that the negative peak at 273 nm was absent. Thus, the positive 260-nm peak appeared as a shoulder on the larger, positive peak at 289 nm. The conversion of the amide group to a nitrile would be expected to change the contribution of the A-ring chromophores to the circular dichroism spectrum in the 260-nm region. The other Cotton effects, the positive peaks at 225, 260, and 289 nm, and the negative peaks at 244 and 320 nm were all present. These peaks were similar in shape and intensity to the corresponding peaks in the tetracycline spectrum. The circular dichroism spectrum was similar to that of tetracycline, indicating that no major conformational changes took place in the conversion of the amide to a nitrile.

The addition of Ca^{+2} to a pH 7.4 buffered solution of 2-cyanotetracycline changed the circular dichroism spectrum (Fig. 7) to one similar to spectra of tetracycline and dedimethylaminotetracycline. The positive Cotton effect at 225 nm was shifted to 236 nm and increased in intensity. This effect was complete when the metal-ion to ligand ratio reached 1:1. In addition, the positive peak at 260 nm was enhanced, the negative peak at 273 nm observed in tetracycline reappeared, and the negative peak at 244 nm was decreased in intensity and shifted to 249 nm. These three changes were complete at a metal-ion to ligand ratio of 1:1 and resulted in a spectrum that was similar to that of tetracycline in the 260-nm region. The 289-nm positive chromophore was only slightly enhanced, as was the 320-nm negative peak. Changes of these two Cotton effects were complete at a metal-ion to ligand ratio of 1:1. As with tetracycline and dedimethylaminotetracycline, two new peaks, a positive absorption at 356 nm and a negative absorption at 393 nm, were produced. These peaks were approximately 10 nm lower than the corresponding peaks in tetracycline and changed only slightly after the metal-ion to ligand ratio reached 1:1.

The circular dichroism spectrum of the calcium chelate of 2-cyanotetracycline was similar to spectra of tetracycline and dedimethylaminotetracycline in the region below 340 nm but differed significantly at longer wavelengths. This finding indicates that the first Ca^{+2} chelates at the same site as the first Ca^{+2} in tetracycline or dedimethylaminotetracycline but that complexation at the other site is incomplete.

The failure of 2-cyanotetracycline to bind the second calcium ion is explained by identifying one A-ring site, or an adjacent site, as the region of interaction for this second cation. The absorptions affected by chelation of the second Ca^{+2} to tetracycline are at 370 and 403 nm, which are assigned to the B-, C-, and D-rings of the tetracycline molecule. Neither of the A-ring sites gives rise to these spectral changes; therefore, assignment of the binding of Ca^{+2} to the C-12, C-1 site accounts for both the long wavelength absorptions and the failure of the 2-cyano derivatives to add the second calcium ion.

The first Ca^{+2} to complex with tetracycline and dedimethylaminotetracycline also complexes with 2-cyanotetracycline. Because the derivative without the C-4 dimethylamino group forms this chelate, sites involving this position (C-4, C-12 and C-3, C-4) are removed as possibilities for the first binding site. Sites involving the C-2 amide (C-1, C-2 and C-2, C-3) are removed as sites because this same complex is formed by 2-cyanotetracycline.

Thus, only three sites (C-10, C-11; C-11, C-12; and C-12, C-1) remain as viable possibilities. Since the second Ca^{+2} chelates at the C-12 position and the calcium ions are chelated by tetracycline at two of three sites, the first Ca^{+2} must bind in the C-10, C-11 site. The C-12, C-1 site must be assigned to the second Ca^{+2} to account for the only partial complexation of this second cation with 2-cyanotetracycline.

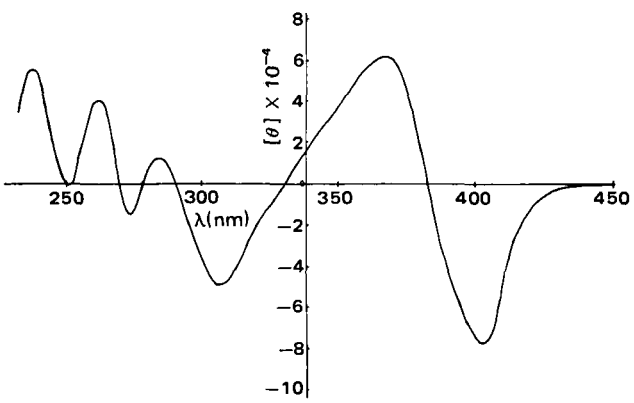

Figure 5—*Circular dichroism spectrum of the calcium complex of dedimethylaminotetracycline in methanol–water (50:50).*

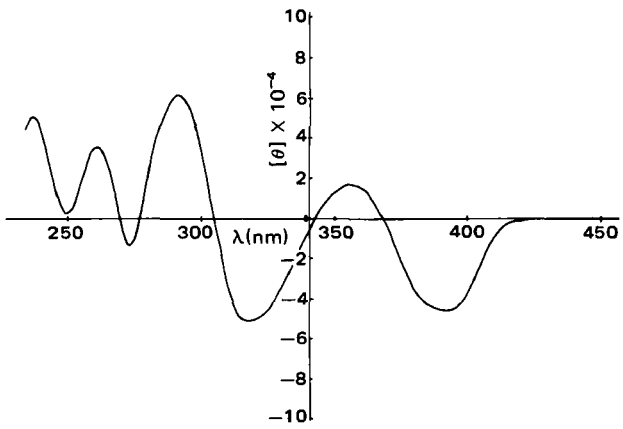

Figure 7—*Circular dichroism spectrum of the calcium complex of 2-cyanotetracycline in methanol–water (50:50).*

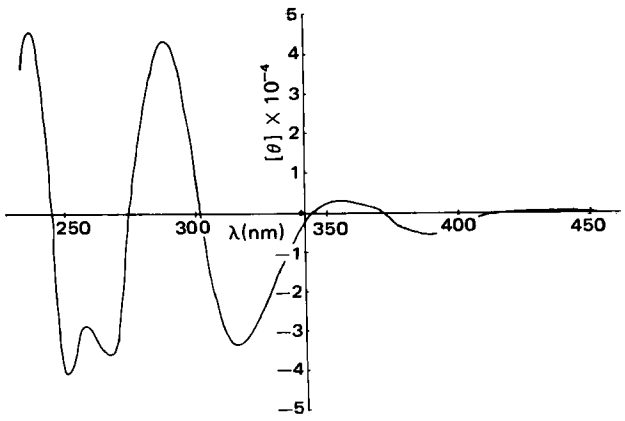

Figure 8—*Circular dichroism spectrum of the magnesium complex of tetracycline in methanol–water (90:10).*

This order of complexation also explains the effect on the longer wavelength region of the circular dichroism spectrum of this molecule.

Mg^{+2} Complex of Tetracycline—The addition of Mg^{+2} to a solution of tetracycline buffered to pH 7.4 produced changes in its circular dichroism spectrum (Fig. 8) that differed from those observed for the Ca^{+2} complex of tetracycline. The 225-nm positive Cotton effect was shifted to 237 nm and was enhanced in intensity, an effect similar to that with Ca^{+2}. The two negative peaks at 247 and 273 nm were also increased in intensity at the expense of the positive 260-nm peak. The opposite effect was noted for the calcium chelate as the positive 260-nm Cotton effect was increased. The positive Cotton effect at 291 nm, which was essentially unchanged by the addition of Ca^{+2}, was greatly increased in magnitude by the addition of Mg^{+2}. The negative peak at 320 nm was only slightly affected by the addition of Mg^{+2}. Two new peaks, a positive absorption at 355 nm and a negative absorption at 390 nm (similar to those produced in the circular dichroism spectrum of the Ca^{+2} complex of tetracycline), formed only to a minor extent.

All changes in the circular dichroism spectrum of the tetracycline complex with Mg^{+2} were complete once the metal-ion to ligand ratio was 1:1 (Fig. 9). Because the spectral changes accompanying the formation of this complex were different from those observed with

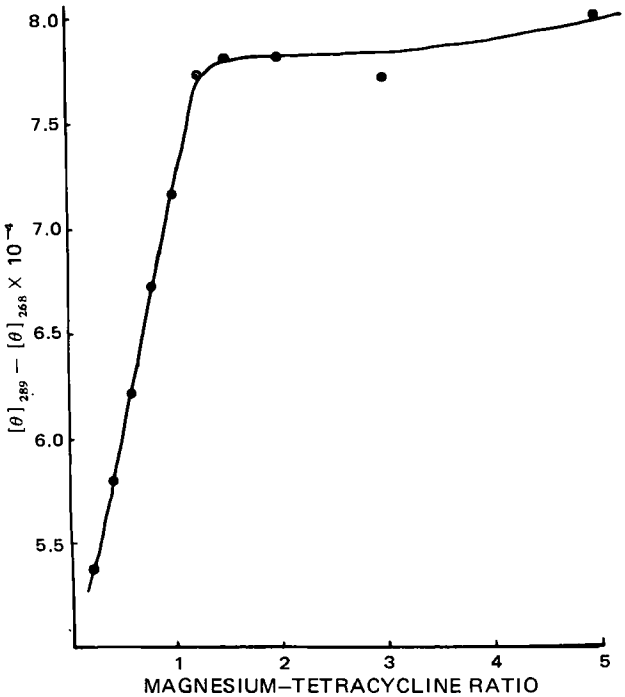

Figure 9—*Mole ratio plot for the magnesium complex of tetracycline in methanol–water (90:10).*

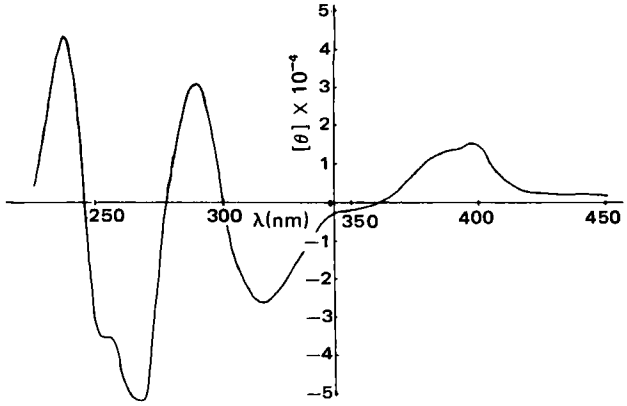

Figure 10—*Circular dichroism spectrum of the magnesium complex of dedimethylaminotetracycline in methanol–water (90:10).*

the addition of metal ion to either site proposed for the tetracycline complex with calcium, a third complexation site is indicated.

When Mg^{+2} was added to a solution of dedimethylaminotetracycline in 90% methanol buffered to an effective pH of 7.4, its circular dichroism spectrum (Fig. 10) was affected in a manner similar to the spectrum of the Mg^{+2} complex with tetracycline. The positive peaks at 246 and 264 nm were enhanced and shifted to 252 and 265 nm, respectively, while the positive Cotton effect at 283 nm was greatly increased in intensity and shifted to 289 nm. The negative peak at 318 nm was slightly increased in intensity and shifted to 316 nm. All these changes were complete at a metal-ion to ligand ratio of 1:1.

A comparison of the circular dichroism spectra of the magnesium chelates of tetracycline and dedimethylaminotetracycline indicates that they are identical; thus, the same complexation site is used in both cases. This precludes binding at any site utilizing the dimethylamino group of C-4.

The changes in the circular dichroism spectrum of 2-cyanotetracycline (Fig. 11) with addition of Mg^{+2} were similar to those of the Mg^{+2} complexes with tetracycline and dedimethylaminotetracycline. The positive Cotton effect at 225 nm was increased in size and shifted to 235 nm. The 260-nm region gave rise to the two negative peaks at 251 and 271 nm, which were increased in intensity, masking the positive peak at 259 nm. The positive peak at 286 nm was shifted to 284 nm and slightly decreased in intensity along with the negative Cotton effect at 320 nm.

Most of these changes took place when the metal-ion to ligand ratio reached 1:1, but minor changes occurred as more Mg^{+2} was added. These data indicate that the 1:1 complex between Mg^{+2} and 2-cyanotetracycline is not as favorably formed as 1:1 complexes of Mg^{+2} with tetracycline and dedimethylaminotetracycline. A comparison of the circular dichroism spectrum of the Mg^{+2} complex with 2-cyanotetracycline to that of tetracycline shows that they are essentially the same and thus indicates the same complexation site. The fact that 2-cyanotetracycline forms this complex indicates that neither of the A-ring sites (C-1, C-2 or C-2, C-3) is used.

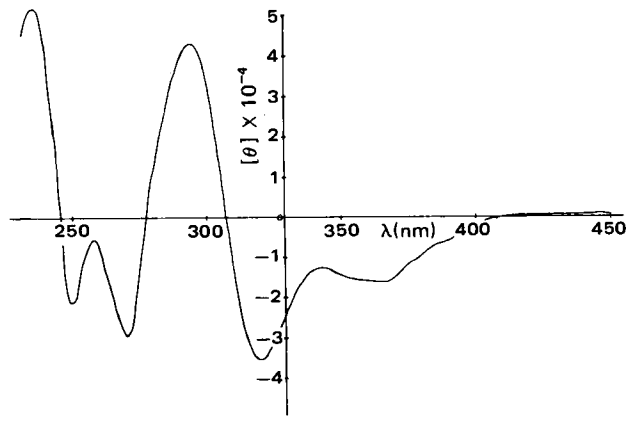

Figure 11—*Circular dichroism spectrum of the magnesium complex of 2-cyanotetracycline in methanol–water (90:10).*

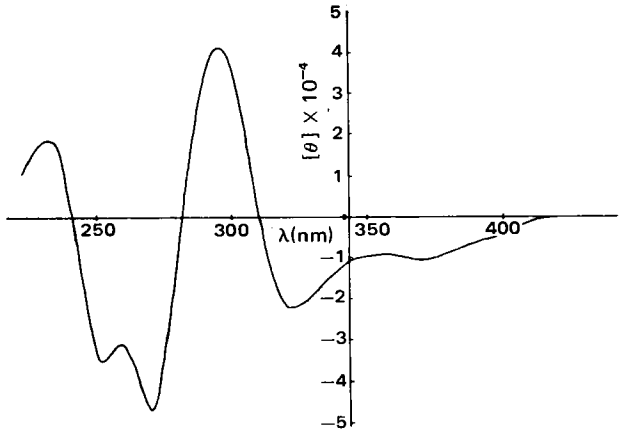

Figure 12—*Circular dichroism spectrum of the magnesium complex of tetracycline in aqueous solution.*

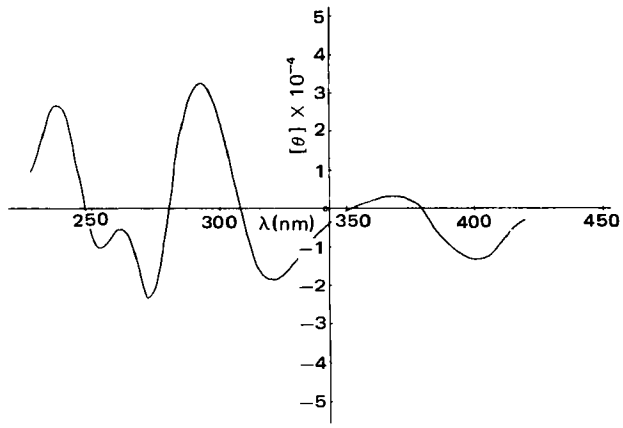

Figure 13—*Circular dichroism spectrum of the calcium complex of tetracycline in aqueous solution.*

Since tetracycline, dedimethylaminotetracycline, and 2-cyanotetracycline all form the same 1:1 complex with Mg^{+2}, there are only three possible sites of complexation: C-10, C-11; C-11, C-12; and C-12, C-1. As stated previously, the calcium ions bind at the C-10, C-11 and C-12, C-1 sites and the Mg^{+2} complex binds at a different position, as indicated by the circular dichroism spectra. Thus, the Mg^{+2} complex of tetracycline binds at the C-11, C-12 β-diketone site.

Comparison of Solvent Systems—The circular dichroism spectrum of the Mg^{+2} complex of tetracycline in aqueous solution (Fig. 12) buffered to pH 7.4 was similar to the corresponding spectrum in 90% methanol. However, the formation of the complex was not favorable in the aqueous solution, since a fourfold excess of Mg^{+2} was necessary to force the complexation. The 225-nm positive Cotton effect was shifted to 232 nm and increased in intensity, the negative peaks at 251 and 272 nm were significantly increased in intensity, and the negative peaks at 293 and 323 nm were slightly affected by complexation. It is apparent from these data that the Mg^{+2} complex of tetracycline is the same in both aqueous and methanolic solutions.

In pH 7.4 buffered solution, the circular dichroism spectrum of the Ca^{+2} complex of tetracycline (Fig. 13) was similar to that of tetracycline in 90% methanol in the wavelength region below 340 nm. But the two Cotton effects at 370 and 403 nm were only slightly developed with a metal-ion to ligand ratio of 4:1. Thus, it appears that the second Ca^{+2} is not complexed significantly in aqueous solution. The positive peak at 225 nm was shifted to 234 nm and increased in intensity, and there was an increase in intensity of the positive 260-nm peak, as attested by the change of the 251- and 270-nm peaks. The positive peak at 292 nm was slightly decreased, while the 322-nm peak was unchanged. As with the Mg^{+2} complex in aqueous solution, the complexation of even the first Ca^{+2} was not as favorable a process in aqueous solution as in methanolic solution.

In pH 7.4 methanolic buffers, tetracycline and several related compounds formed different complexes with Mg^{+2} and Ca^{+2}. Magnesium complexed in a 1:1 ratio at the C-11, C-12 β-diketone site. The complex in 90% methanol was much stronger than the same complex in water, requiring only stoichiometric quantities of metal ion and ligand to achieve essentially 100% complexation. In aqueous solution at pH 7.4, higher concentrations of Mg^{+2} were necessary to complete the complexation.

The calcium chelate of tetracycline in 90% methanol was a 2:1 metal-ion to ligand complex. The two metal ions added stepwise, the first at the C-10, C-11 site and the second at the C-12, C-1 site. Formation of this 2:1 complex was very favorable, requiring only stoichiometric quantities of metal ion and tetracycline to achieve essentially 100% complexation. However, formation of the calcium chelate in pH 7.4 aqueous solution was not as favorable as in 90% methanol. An excess of Ca^{+2} was necessary to force the addition of the first cation onto the C-10, C-11 site, and the second cation did not add to any significant extent. Apparently, in aqueous solution, the removal of water molecules from the hydration sphere of the metal ion is much more difficult; therefore, both steps in the formation of the complex are more difficult. Since the first metal ion must add to the C-10, C-11 site before the C-12, C-1 site is capable of accommodating a cation, incomplete addition of this first cation inhibits addition of the second cation.

REFERENCES

(1) A. H. Caswell and J. D. Hutchison, *Biochem. Biophys. Res. Commun.*, **43**, 625(1971).

(2) L. A. Mitscher, A. C. Bonacci, and T. D. Sokoloski, *Tetrahedron Lett.*, **51**, 5361(1968).

(3) L. A. Mitscher, A. C. Bonacci, and T. D. Sokoloski, *Antimicrob. Ag. Chemother.*, **1968**, 78.

(4) L. A. Mitscher, A. C. Bonacci, B. Slater-Eng, and T. D. Sokoloski, *ibid.*, **1972**, 66.

(5) J. H. Boother, G. E. Bonvincino, C. W. Waller, J. P. Petisi, R. W. Wilkinson, and R. B. Broschard, *J. Am. Chem. Soc.*, **80**, 1654(1958).

(6) A. Soder and W. Siedel, German pat. 1,091,564 (Oct. 27, 1969); through *Chem. Abstr.*, **55**, 198825(1961).

ACKNOWLEDGMENTS AND ADDRESSES

Received December 4, 1975, from the *Department of Chemistry, University of Iowa, Iowa City, IA 52242*

Accepted for publication February 13, 1976.

Supported in part by Pfizer, Inc.

* Present address: 3M Center, 3M Co., St. Paul, Minn.

ˣ To whom inquiries should be directed.

N-Halo Derivatives IV: Synthesis of Low Chlorine Potential Soft *N*-Chloramine Systems

JAMES J. KAMINSKI, NICOLAE BODOR ˣ, and TAKERU HIGUCHI

Abstract □ A number of low chlorine potential, soft *N*-chloramines containing nitrogen–chlorine bonds of different polarity were prepared. These novel *N*-chloramine systems were based on derivatization of 2-amino-2-methyl-1-propanol.

Keyphrases □ *N*-Halo derivatives—series of low chlorine potential, soft *N*-chloramines synthesized from 2-amino-2-methyl-1-propanol □ *N*-Chloramine systems, soft—series with low chlorine potential synthesized from 2-amino-2-methyl-1-propanol □ Antimicrobial agents, potential—*N*-chloramine series synthesized

Recently, the chlorination of α-amino acids and their related derivatives was examined (1) to investigate the relationship between the antimicrobial activity of the *N*-chloramine and the degree of polarization of the nitrogen–chlorine bond (2). As a result of the kinetic studies conducted on these *N*-chlorinated products, factors significantly influencing the stability and reactivity of the nitrogen–chlorine bond in these *N*-chloramines were elucidated.

More importantly, these investigations led to the development of a class of stable, low-chlorine potential (3, 4), soft *N*-chloramines based on α-aminoisobutyric acid and related derivatives. The low chlorine potential of these *N*-chloramines was a result of the reduced polarity of the nitrogen–chlorine bond. By decreasing the polarity of the nitrogen–chlorine bond, the chemical reactivity of the *N*-chloramine was minimized. Therefore, these low chlorine potential *N*-chloramines were less readily deactivated by extraneous reaction with denaturing agents and exhibited a high degree of antimicrobial activity.

The soft nature of the *N*-chloramines rested primarily upon the mechanism of their antimicrobial action and upon the transient character of the *N*-chloramine precursor to generate nontoxic degradation products. It was hypothesized that the bactericidal action of *N*-chloramines was a manifestation of a chemical reaction involving the direct transfer of a positive chlorine from the *N*-chloramine to an appropriate receptor in the cell. This chemical reaction can effectively destroy or inhibit an enzymatic or metabolic cell process, resulting in the expiration of the organism. If it is assumed that the transfer of positive chlorine to an appropriate receptor in the cell is responsible for eliciting the antimicrobial effect of the *N*-chloramine, detoxification of the microorganism ultimately regenerates the parent molecule from which the *N*-chloramine is derived. By judiciously selecting the *N*-chloramine precursor from nontoxic entities and selectively incorporating into the molecular structure specific functional groups susceptible to hydrolysis, the inherent toxicity of the soft *N*-chloramine antimicrobial agents can be effectively controlled.

In continuing the investigation of the relationship between the antimicrobial activity of the *N*-chloramine and the degree of polarization of the nitrogen–chlorine bond, the present study describes the preparation of several novel classes of soft *N*-chloramines. Based on previous investigations (1) of the stability and reactivity of the nitrogen–chlorine bond in soft *N*-chloramines, derivatives of 2-amino-2-methyl-1-propanol were investigated as precursors to these soft *N*-chloramines.

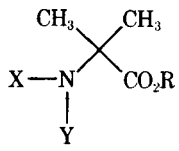

Ia: X = Cl, Y = Cl, R = CH_3
Ib: X = H, Y = Cl, R = $(CH_2)_5CH_3$
Ic: X = H, Y = Cl, R = $(CH_2)_7CH_3$
Id: X = H, Y = Cl, R = $(CH_2)_{11}CH_3$
Ie: X = H, Y = Cl, R = $(CH_2)_{13}CH_3$
If: X = H, Y = Cl, R = $(CH_2)_{17}CH_3$
Ig: X = H, Y = Cl, R = $(CH_2)_2O(CH_2)_2O(CH_2)_3CH_3$
Ih: X = Cl, Y = Cl, R = $(CH_2)_5CH_3$
Ii: X = Cl, Y = Cl, R = $(CH_2)_7CH_3$
Ij: X = Cl, Y = Cl, R = $(CH_2)_{11}CH_3$
Ik: X = Cl, Y = Cl, R = $(CH_2)_{13}CH_3$
Il: X = Cl, Y = Cl, R = $(CH_2)_{17}CH_3$
Im: X = Cl, Y = Cl, R = $(CH_2)_2O(CH_2)_2O(CH_2)_3CH_3$

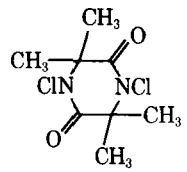

II

RESULTS AND DISCUSSION

Investigation of the chlorination of α-aminoisobutyrate esters and related derivatives led to the preparation of a number of low chlorine potential, soft *N*-chloramines, Ia–Im and II (1). To conduct a comprehensive and systematic investigation of the relationship between the antimicrobial activity of the *N*-chloramine and the degree of polarization of the nitrogen–chlorine bond, the preparation of additional low chlorine potential, soft *N*-chloramines containing nitrogen–chlorine bonds of different polarity was necessary.

Based on the low polarity of the nitrogen–chlorine bond and the soft nature of the *N*-chloramines desired, derivatization of 2-amino-2-methyl-1-propanol was particularly attractive because of its inherent low toxicity (5). In addition, 2-amino-2-methyl-1-propanol contains the specific structural requirement essential for optimizing the stability and reactivity of the nitrogen–chlorine bond of the *N*-chloramine; that is, the *gem*-dimethyl substitution at the carbon atom adjacent to the nitrogen–chlorine bond in the *N*-chloramine (1). With these considerations in mind, 2-amino-2-methyl-1-propyl carboxylate hydrochlorides (IIIa–IIIf) were examined initially as precursors to an alternative class of low chlorine potential, soft *N*-chloramines.

CHEMISTRY

Compounds IIIa–IIIf were prepared by: (a) *N*- to *O*-acyl transfer

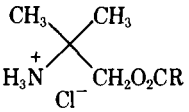

IIIa: R = CH_3
IIIb: R = $(CH_2)_2CH_3$
IIIc: R = $C(CH_3)_3$
IIId: R = $(CH_2)_4CH_3$
IIIe: R = $(CH_2)_6CH_3$

IIIf: R = 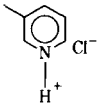

in the corresponding *N*-acylated amino alcohol *via* ethanolic hydrogen chloride (Scheme I) (6), (*b*) hydrolysis of the corresponding Δ^2-1,3-oxazoline (Scheme II), or (*c*) *O*-acylation of the *N*-protected amino alcohol with subsequent removal of the *N*-protective group (Scheme III).

The synthetic approaches utilized to obtain IIIa–IIIf merit discussion. Classically, several analogous derivatives have been prepared by *N*- to *O*-acyl transfer from the kinetically formed *N*-acylated amino alcohol by ethanolic hydrogen chloride (6). However, this method is ineffective for the preparation of *n*-aliphatic carboxylate derivatives of ethanolamines. More recently, Δ^2-1,3-oxazolines, based on 2-amino-2-methyl-1-propanol, received attention as a reversible protecting group for the carboxyl function in carboxylic acids (7). In certain instances, hydrolysis of the Δ^2-1,3-oxazoline afforded the 2-amino-2-methyl-1-propyl carboxylate hydrochloride as an intermediate in the regeneration of the initially protected carboxylic acid.

Utilization of either of these procedures to obtain the *N*-chloramine precursors IIIa–IIIe resulted in complete hydrolysis to the corresponding carboxylic acid and 2-amino-2-methyl-1-propanol. However, using a modification of the procedure described by Meyers and Temple (7), IIIb and IIIc could be conveniently obtained in satisfactory yields. Unfortunately, this approach was ineffective for the preparation of IIIa; IIIa was prepared by *O*-acetylation of the *N*-protected amino alcohol, with subsequent removal of the *N*-protective group by catalytic hydrogenation.

The *N*-chloramine precursors (IIIa–IIIf) were particularly interesting, since their *N*-chlorinated products (IVa–IVl) should contain a nitrogen–chlorine bond of lower polarity relative to the *N*-chloramines (Ia–Im and II). The lower polarity of the nitrogen–chlorine bond is a result of the decreased inductive effect of the carboxyl group on the nitrogen–chlorine bond in these *N*-chloramines. More importantly, IVd, IVh and IVe, IVi are isomeric with the *N*-chloramines Ib, Ih and Ic, Ii, respectively. The isomeric relationship between these *N*-chloramines provides an opportunity for comparing the antimicrobial activity of structurally related *N*-chloramines of different chlorine potentials.

In addition, chlorination of the longer chain homologs (IIIb–IIIe) resulted in the preparation of both the *N*-chloroamino and *N,N*-dichloroamino derivatives. Therefore, the effect of the degree of chlorination of the nitrogen atom, as well as the effect of a branched

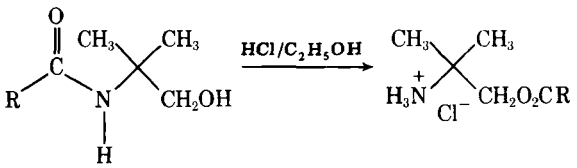

Scheme I

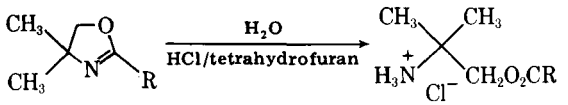

Scheme II

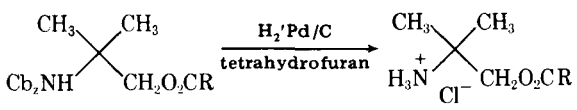

Scheme III

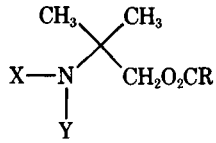

IVa: X = Cl, Y = Cl, R = CH_3
IVb: X = H, Y = Cl, R = $(CH_2)_2CH_3$
IVc: X = H, Y = Cl, R = $C(CH_3)_3$
IVd: X = H, Y = Cl, R = $(CH_2)_4CH_3$
IVe: X = H, Y = Cl, R = $(CH_2)_6CH_3$
IVf: X = Cl, Y = Cl, R = $(CH_2)_2CH_3$
IVg: X = Cl, Y = Cl, R = $C(CH_3)_3$
IVh: X = Cl, Y = Cl, R = $(CH_2)_4CH_3$
IVi: X = Cl, Y = Cl, R = $(CH_2)_6CH_3$

IVj: X = Cl, Y = Cl, R =

IVk: X = Cl, Y = Cl, R = 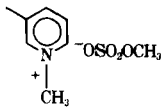

IVl: X = Cl, Y = Cl, R = 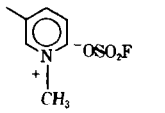

alkyl carboxyl chain on the antimicrobial activity of the *N*-chloramine, could be investigated. Furthermore, the effect of a delocalized positive charge in the *N*-chloramine and of different *gegen*-ions on the antimicrobial activity of the *N*-chloramine could be examined by comparison among IVj, IVk, and IVl. The identification of a number of low chlorine potential, soft *N*-chloramines based on the *N*-chlorinated products of 2-amino-2-methyl-1-propyl carboxylate hydrochlorides led to an investigation of alternative 2-amino-2-methyl-1-propanol derivatives as precursors to additional low chlorine potential, soft *N*-chloramine systems containing nitrogen–chlorine bonds of different polarity.

The ideal proximity between the amino and hydroxyl groups in 2-amino-2-methyl-1-propanol suggested investigation of the 2-oxazolidinone and the 1,3-oxazolidine systems as precursors to low chlorine potential, soft *N*-chloramines. 4,4-Dimethyl-2-oxazolidinone (V) was prepared by the reaction between 2-amino-2-methyl-1-propanol and diethyl carbonate in the presence of a catalytic amount of sodium methoxide (Scheme IV) (8). On the other hand, azeotropic removal of water from benzene or toluene solutions containing 2-amino-2-methyl-1-propanol and acetone, cyclohexanone, or 1-methyl-4-piperidone gave the corresponding *N*-chloramine precursors, VIa, VIb, and VIc, respectively (Scheme V) (9).

Chlorination of V gave 3-chloro-4,4-dimethyl-2-oxazolidinone (VII) (10). Relative to 1,4-dichloro-2,2,5,5-tetramethyl-3,6-piperazinedione (II), the degree of polarization of the nitrogen–chlorine bond in VII should be decreased as a result of the inductive and resonance effects of the oxygen atom adjacent to the carbonyl group in the 2-oxazolidinone structure. Compounds VIa–VIc are particularly interesting, since their *N*-chlorinated products (VIIIa–VIIIf) should contain the least polar nitrogen–chlorine bond of all the low chlorine potential, soft *N*-chloramine systems examined. The low polarity of the nitrogen–chlorine bond in these systems is a result of the electron-donating inductive effect of the tetraalkyl substitution adjacent to the nitrogen–chlorine bond. More importantly, VIIIc–VIIIf provide an opportunity for comparing the effect of a localized positive charge in the *N*-chloramine on its antimicrobial activity. With the preparation of a number of low chlorine potential, soft *N*-chloramine systems containing nitrogen–chlorine bonds of different polarity accomplished, comparative antimicrobial activity studies for these systems were initiated (11).

EXPERIMENTAL

2-Amino-2-methyl-1-propyl Acetate Hydrochloride (IIIa) —To a dichloromethane solution containing 17.1 g (0.1 mole) of carbobenzoxy chloride at 0° was added dropwise, with stirring, 18.4 g (0.2 mole) of 2-amino-2-methyl-1-propanol. The reaction mixture was stirred at room temperature overnight, and the 2-amino-2-methyl-

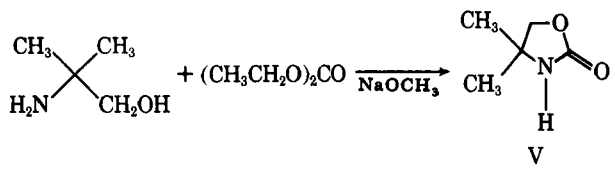

V

Scheme IV

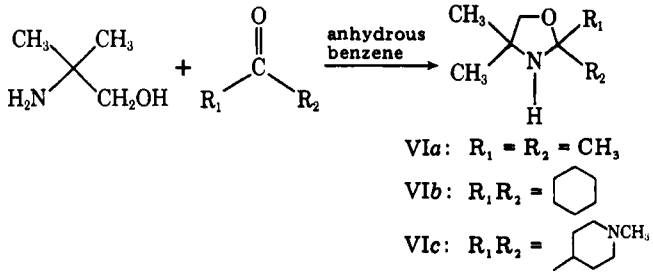

VI*a*: $R_1 = R_2 = CH_3$

VI*b*: R_1R_2 =

VI*c*: R_1R_2 =

Scheme V

1-propanol hydrochloride which formed was removed by filtration. Removal of the dichloromethane under reduced pressure afforded a colorless, viscous liquid. Distillation gave 14.9 g (0.07 mole), 70%, of 2-carbobenzoxyamino-2-methyl-1-propanol, bp 144–148°/0.3 mm; IR (neat): 3400, 3020, 2980, 1710, 1510, 1455, 1270, 1070, 730, and 680 cm^{-1}; PMR ($CDCl_3$): δ 7.2 (s, 5H), 5.4 (broad s, 1H), 4.9 (s, 2H), 4.2 (broad s, 1H), 3.4 (s, 2H), and 1.2 (s, 6H) ppm.

To a dichloromethane solution containing 2.52 g (0.011 mole) of 2-carbobenzoxyamino-2-methyl-1-propanol and 1.17 g (0.015 mole) of acetyl chloride was added dropwise, with stirring, 1.11 g (0.011 mole) of triethylamine. The reaction was stirred at ambient temperature overnight, and the dichloromethane was removed under reduced pressure. The triethylamine hydrochloride residue was triturated in anhydrous ether. Following filtration, the ether was removed under reduced pressure to afford 2.38 g (0.009 mole), 82%, of crude 2-carbobenzoxyamino-2-methyl-1-propyl acetate as a pale-yellow liquid; PMR ($CDCl_3$): δ 7.2 (s, 5H), 5.4 (broad s, 1H), 5.0 (s, 2H), 4.2 (s, 2H), 2.0 (s, 3H), and 1.2 (s, 6H) ppm.

2-Carbobenzoxyamino-2-methyl-1-propyl acetate, 2.38 g (0.009 mole), was dissolved in 100 ml of anhydrous hydrogen chloride in tetrahydrofuran (2 *M*). Then 1.0 g of 10% palladium on carbon was added to the solution, and the resulting mixture was hydrogenated at 50 psi for 2 hr. The catalyst was removed by filtration and thoroughly washed with tetrahydrofuran. Removal of the tetrahydrofuran under reduced pressure gave an off-white solid. Recrystallization from acetone–hexane afforded 1.0 g (0.006 mole) of III*a* as a hygroscopic white solid, mp 146–149°; PMR (D_2O): δ 4.0 (s, 2H), 2.0 (s, 3H), and 1.2 (s, 6H) ppm.

Anal.—Calc. for $C_6H_{14}ClNO_2 \cdot \frac{1}{2}H_2O$: C, 40.79; H, 8.56; N, 7.93. Found: C, 40.31; H, 8.36; N, 8.28.

2-Amino-2-methyl-1-propyl Butanoate Hydrochloride (III*b*)—To 65 ml of a solution of anhydrous hydrogen chloride in tetrahydrofuran (1 *M*) containing 1 ml of water was added 7.3 g (0.052 mole) of 2-*n*-propyl-4,4-dimethyl-Δ^2-1,3-oxazoline, which was prepared using the method of Allen and Ginos (12). The solution was heated under reflux with stirring for 1 hr. The tetrahydrofuran was removed under reduced pressure to afford a semisolid residue, which crystallized at 0° upon the addition of anhydrous ether. The solid was triturated in anhydrous ether overnight and isolated by filtration under a nitrogen atmosphere. After drying *in vacuo* over calcium sulfate, 7.0 g (0.036 mole), 70%, of III*b*, was obtained, mp 104–107°; IR (KBr): 2900, 1740, and 1160 cm^{-1}; PMR [$(CD_3)_2CO$–D_2O]: δ 4.2 (s, 2H), 3.8 (broad s, 3H), 2.5 (t, 2H), 1.6 (m, 2H), 1.5 (s, 6H), and 1.0 (t, 3H) ppm.

Anal.—Calc. for $C_8H_{18}ClNO_2$: C, 49.10; H, 9.27; N, 7.16. Found: C, 50.01; H, 9.62; N, 7.54.

By using the procedure described for the preparation of III*b*, the following 2-amino-2-methyl-1-propyl carboxylate hydrochlorides were prepared:

2-Amino-2-methyl-1-propyl 2,2-Dimethylpropanoate Hydrochloride (III*c*)—mp 113–118°; IR (KBr): 3430, 2980, 1735, 1520, 1470, 1270, and 1150 cm^{-1}; PMR (D_2O): δ 4.10 (s, 2H), 1.40 (s, 6H), and 1.23 (s, 9H) ppm.

Anal.—Calc. for $C_9H_{20}ClNO_2 \cdot H_2O$: C, 47.46; H, 9.74; N, 6.15. Found: C, 47.86; H, 9.34; N, 6.06.

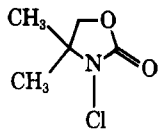

VII

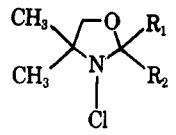

VIII*a*: $R_1 = R_2 = CH_3$

VIII*b*: R_1R_2 =

VIII*c*: R_1R_2 =

VIII*d*: R_1R_2 =

VIII*e*: R_1R_2 =

VIII*f*: R_1R_2 =

2-Amino-2-methyl-1-propyl Hexanoate Hydrochloride (III*d*)—mp 100–101°; IR (KBr): 2900, 1745, and 1165 cm^{-1}; PMR [$(CD_3)_2CO$–D_2O]: δ 4.3 (s, 2H), 3.7 (broad s, 3H), 2.5 (t, 2H), 1.2–1.8 (m, 6H), 1.5 (s, 6H), and 0.9 (t, 3H) ppm.

Anal.—Calc. for $C_{10}H_{22}ClNO_2$: C, 53.68; H, 9.91; N, 6.26. Found: C, 53.02; H, 10.21; N, 6.71.

2-Amino-2-methyl-1-propyl Octanoate Hydrochloride (III*e*)—mp 106–108°; IR (KBr): 2900, 1750, and 1175 cm^{-1}; PMR (D_2O): δ 4.2 (s, 2H), 2.5 (t, 2H), 1.5 (s, 6H), 1.2–1.8 (m, 10H), and 0.9 (t, 3H) ppm.

Anal.—Calc. for $C_{12}H_{26}ClNO_2$: C, 57.24; H, 10.41; N, 5.56. Found: C, 57.29; H, 10.52; N, 5.28.

2-Amino-2-methyl-1-propyl Nicotinate Dihydrochloride (III*f*)—Ethyl nicotinate, 100 g (0.66 mole), and 88 g (0.99 mole) of 2-amino-2-methyl-1-propanol were mixed and heated together under reflux for 2 hr. The excess amino alcohol was removed by distillation, bp 50–60°/1 mm. The yellow residue was recrystallized from ether–acetone to give 87.3 g (0.45 mole), 68%, of *N*-(1-hydroxy-2-methyl-2-propyl)nicotinamide, mp 91–93°; IR (KBr): 3385, 3200, 1665, and 1590 cm^{-1}; PMR ($CDCl_3$): δ 7.3–8.8 (m, 4H), 6.7 (broad s, 1H), 5.0 (s, 1H), 3.7 (s, 2H), and 1.4 (s, 6H) ppm.

Anal.—Calc. for $C_{10}H_{14}N_2O_4$: C, 61.90; H, 7.23; N, 14.50. Found: C, 61.87; H, 7.26; N, 14.55.

A suspension of 73.3 g (0.38 mole) of *N*-(1-hydroxy-2-methyl-2-propyl)nicotinamide in 300 ml of anhydrous hydrogen chloride in absolute ethanol (4 *M*) was heated under reflux for 2 hr. The ethanol was removed under reduced pressure to afford a semisolid residue, which crystallized from acetone on standing. The solid was isolated by filtration under a nitrogen atmosphere and was thoroughly washed with acetone. After drying *in vacuo* over calcium sulfate, 74 g (0.28 mole), 74%, of III*f* was obtained, mp 215–216° dec.; IR (KBr): 3200–2500, 1735, 1630, and 1600 cm^{-1}; PMR (D_2O): δ 9.5 (broad s, 1H), 9.1–9.4 (m, 2H), 8.3 (q, 1H), 4.6 (s, 2H), and 1.6 (s, 6H) ppm.

Anal.—Calc. for $C_{10}H_{16}Cl_2N_2O_2$: C, 44.98; H, 5.99; N, 10.49. Found: C, 45.29; H, 6.15; N, 10.06.

2-*N,N*-Dichloroamino-2-methyl-1-propyl Acetate (IV*a*)—To 50 ml of 0.75 *M* sodium hypochlorite at 0° was added, in portions over 5 min, 3.19 g (0.019 mole) of III*a*. The reaction mixture was adjusted to pH 4–6 by the addition of 1 *M* HCl, and the suspension was vigorously stirred at 0° for 1 hr. The *N*-chloramine was extracted into dichloromethane, and the extracts were combined and dried over anhydrous sodium sulfate. Following filtration, the dichloromethane was removed under reduced pressure to afford a dark-yellow liquid. Distillation gave 2.0 g (0.010 mole), 55%, of IV*a*, bp 55–60°/0.4 mm; IR (neat): 1750, 1230, and 1040 cm^{-1}; PMR ($CDCl_3$): δ 4.2 (s, 2H), 2.1 (s, 3H), and 1.4 (s, 6H) ppm.

Anal.—Calc. for $C_6H_{11}Cl_2NO_2$: C, 36.02; H, 5.54; N, 7.00. Found: C, 36.40; H, 5.63; N, 6.90.

By using the procedure described for the preparation of IV*a*, the following 2-*N,N*-dichloroamino-2-methyl-1-propyl carboxylates were prepared:

2-N,N-*Dichloroamino-2-methyl-1-propyl Butanoate* (IV*f*)—bp 70–75°/0.4 mm; IR (neat): 2940, 1740, and 1160 cm^{-1}; PMR ($CDCl_3$): δ 4.3 (s, 2H), 2.4 (t, 2H), 1.7 (m, 2H), 1.4 (s, 6H), and 1.0 (t, 3H) ppm.

Anal.—Calc. for $C_8H_{15}Cl_2NO_2$: C, 42.14; H, 6.63; N, 6.14. Found: C, 42.30; H, 6.60; N, 6.04.

2-N,N-*Dichloroamino-2-methyl-1-propyl 2,2-Dimethylpropanoate* (*IV*g)—bp 67.5–68.5°/0.45 mm; IR (neat): 2990, 1740, 1475, 1360, 1270, and 1140 cm^{-1}; PMR ($CDCl_3$): δ 4.3 (s, 2H), 1.4 (s, 6H), and 1.2 (s, 9H) ppm.

Anal.—Calc. for $C_9H_{17}Cl_2NO_2$: C, 44.64; H, 7.08; N, 5.70. Found: C, 44.51; H, 7.11; N, 5.58.

2-N,N-*Dichloroamino-2-methyl-1-propyl Hexanoate* (*IV*h)—IR (neat): 2930, 2910, 2840, 1745, and 1155 cm^{-1}; PMR ($CDCl_3$): δ 4.2 (s, 2H), 2.3 (t, 2H), 1.2–1.8 (m, 6H), 1.4 (s, 6H), and 0.9 (t, 3H) ppm.

Anal.—Calc. for $C_{10}H_{19}Cl_2NO_2$: C, 46.88, H, 7.48; N, 5.47. Found: C, 46.90; H, 7.49; N, 5.22.

2-N,N-*Dichloroamino-2-methyl-1-propyl Octanoate* (*IV*i)—IR (neat): 2940, 2860, 1750, and 1150 cm^{-1}; PMR ($CDCl_3$): δ 4.2 (s, 2H), 2.3 (t, 2H), 1.1–2.0 (m, 8H), 1.4 (s, 6H), and 0.9 (t, 3H) ppm.

Anal.—Calc. for $C_{12}H_{23}Cl_2NO_2$: C, 50.71; H, 8.16; N, 4.93. Found: C, 50.38; H, 8.00; N, 4.70.

2-*N*-Chloroamino-2-methyl-1-propyl Butanoate (IV*b*)—To 50 ml of 0.75 *M* sodium hypochlorite at 0° was added, in portions over 5 min, 7.41 g (0.038 mole) of III*b*. The suspension was vigorously stirred at 0° for 1 hr. The *N*-chloramine was extracted into dichloromethane, and the extracts were combined and dried over anhydrous sodium sulfate. Following filtration, the dichloromethane was removed under reduced pressure to afford a pale-yellow liquid. Distillation gave 5.2 g (0.027 mole) of IV*b*, bp 60–65°/0.4 mm; IR (neat): 3230, 2930, 1740, and 1160 cm^{-1}; PMR ($CDCl_3$): δ 4.2 (s, 2H), 2.4 (t, 2H), 1.7 (m, 2H), 1.4 (s, 6H), and 1.0 (t, 3H) ppm.

Anal.—Calc. for $C_8H_{16}ClNO_2$: C, 49.61; H, 8.33; N, 7.23. Found: C, 49.00; H, 8.47; N, 6.94.

By using the procedure described for the preparation of IV*b*, the following *N*-chloroamino-2-methyl-1-propyl carboxylates were prepared:

2-N-*Chloroamino - 2-methyl - 1-propyl 2,2-Dimethylpropanoate* (*IV*c)—bp 61.5–63°/0.45 mm; IR (neat): 3280, 2990, 1730, 1475, 1275, and 1140 cm^{-1}; PMR ($CDCl_3$): δ 4.6 (broad s, 1H), 4.0 (s, 2H), 1.3 (s, 9H), and 1.2 (s, 6H) ppm.

Anal.—Calc. for $C_9H_{18}ClNO_2$: C, 52.04; H, 8.73; N, 6.75. Found: C, 52.04; H, 8.70; N, 6.37.

2-N-*Chloroamino-2-methyl-1-propyl Hexanoate* (*IV*d)—IR (neat): 3240, 1745, and 1160 cm^{-1}; PMR ($CDCl_3$): δ 4.5 (broad s, 1H), 4.1 (s, 2H), 2.2 (t, 2H), 1.1–2.0 (m, 6H), 1.3 (s, 6H), and 1.0 (t, 3H) ppm.

Anal.—Calc. for $C_{10}H_{20}ClNO_2$: C, 54.16; H, 9.09; N, 6.32. Found: C, 55.04; H, 9.82; N, 6.70.

2-N-*Chloroamino-2-methyl-1-propyl Octanoate* (*IV*e)—IR (neat): 3260, 2920, 1740, and 1150 cm^{-1}; PMR ($CDCl_3$): δ 4.5 (broad s, 1H), 4.1 (s, 2H), 2.4 (t, 2H), 1.1–2.0 (m, 8H), 1.3 (s, 6H), and 0.9 (t, 3H) ppm.

Anal.—Calc. for $C_{12}H_{24}ClNO_2$: C, 57.70; H, 9.68; N, 5.61. Found: C, 57.14; H, 9.72; N, 5.39.

2-*N,N*-Dichloroamino-2-methyl-1-propyl Nicotinate (IV*j*)—To 58 ml of 0.7 *M* sodium hypochlorite at 0° was added, in portions over 10 min, 5.32 g (0.02 mole) of III*f*. After 0.5 hr at 0°, the pale-yellow solid was isolated by filtration and thoroughly washed with cold water. The solid was dried *in vacuo* over calcium sulfate to give 3.7 g (0.014 mole), 70%, of IV*j*, mp 53–55° with sublimation at 50°/0.25 mm; IR (KBr): 3020, 3000, 1720, 1580, 1280, 1110, 720, and 670 cm^{-1}; PMR ($CDCl_3$): δ 9.3 (s, 1H), 8.9 (d, 1H), 7.6–8.2 (m, 2H), 4.6 (s, 2H), and 1.5 (s, 6H) ppm.

Anal.—Calc. for $C_{10}H_{12}Cl_2N_2O_2$: C, 45.64; H, 4.60; N, 10.65. Found: C, 45.69; H, 4.71; N, 10.46.

2-*N,N*-Dichloroamino-2-methyl-1-propyl *N*-Methylnicotinate Methylsulfate (IV*k*)—To 1.3 g (0.005 mole) of IV*j* was added 0.63 g (0.005 mole) of dimethyl sulfate. The mixture was heated at 60° under a nitrogen atmosphere for 2.5 hr and the solid mass was triturated with anhydrous ether. The solid was isolated by filtration under a nitrogen atmosphere and thoroughly washed with anhydrous ether. After drying *in vacuo* over calcium sulfate, 1.87 g (0.0048 mole), 93%, of IV*k* was obtained, mp 95–100° dec.; IR (KBr): 3020, 2980, 1730, 1240, 1200, 1000, and 730 cm^{-1}; PMR (D_2O): δ 9.5 (s, 1H), 9.2 (d, 2H), 8.3 (t, 1H), 4.6 (s, 2H), 3.8 (s, 3H), and 1.6 (s, 6H) ppm; UV (H_2O): λ_{max} 303 nm ($\epsilon = 263\ M^{-1}\ cm^{-1}$).

Anal.—Calc. for $C_{12}H_{18}Cl_2N_2O_6S$: C, 37.02; H, 4.66; N, 7.20. Found: C, 36.84; H, 4.75; N, 6.92.

2-*N,N*-Dichloroamino-2-methyl-1-propyl *N*-Methylnicotinate Fluorosulfonate (IV*l*)—To an ethereal solution containing 1.3 g (0.005 mole) of IV*j* at 0° was added dropwise, with stirring, 0.57 g (0.005 mole) of methyl fluorosulfonate in 25 ml of anhydrous ether. After stirring at room temperature for 4 days, the yellow gummy mass was crystallized by repeated scratching at ambient temperature to a white solid. The solid was triturated with anhydrous ether and isolated by filtration under a nitrogen atmosphere. Then 1.32 g (0.0035 mole), 70%, of IV*l* was obtained as an extremely hygroscopic white solid, mp (sealed) 112–118° dec.; PMR (D_2O): δ 9.4 (s, 1H), 9.0 (d, 2H), 8.2 (t, 1H), 4.6 (s, 2H), 4.5 (s, 3H), and 1.6 (s, 6H) ppm.

Anal.—Calc. for $C_{11}H_{15}Cl_2FN_2O_5S{\cdot}H_2O$: C, 33.42; H, 4.34; N, 7.09. Found: C, 33.37; H, 4.42; N, 6.58.

2,2,4,4-Tetramethyl-1,3-oxazolidine (VI*a*)—To 237 g (3.0 moles) of 2-amino-2-methyl-1-propanol was added 750 ml of anhydrous benzene containing 174 g (3.0 moles) of acetone. A few crystals of *p*-toluenesulfonic acid were added to the reaction mixture, and the solution was heated at reflux temperature. When the theoretical amount of water was collected, the reaction mixture was distilled. Compound VI*a* was collected, 220 g (1.7 mole), 57%, as a clear, colorless liquid, bp 128–130°; IR (neat): 3300, 2950, 1450, 1380, 1230, 1050, and 790 cm^{-1}; PMR ($CDCl_3$): δ 3.6 (s, 2H), 1.85 (broad s, 1H), 1.4 (s, 6H), and 1.3 (s, 6H) ppm.

Anal.—Calc. for $C_7H_{15}NO$: C, 65.07; H, 11.70; N, 10.84. Found: C, 65.34; H, 11.80; N, 11.00.

By using the procedure described for the preparation of VI*a*, the following 1,3-oxazolidine derivatives were prepared:

3,3-Dimethyl-1-oxa-4-azaspiro[4,5]decane (*VI*b) (*13*)—bp 99–103°/21 mm; IR (neat): 3300, 2910, 1440, 1350, 1110, 1040, 910, and 780 cm^{-1}; PMR ($CDCl_3$): δ 3.4 (s, 2H), 1.8 (broad s, 11H), and 1.2 (s, 6H) ppm.

Anal.—Calc. for $C_{10}H_{19}NO$: C, 70.96; H, 11.31; N, 8.28. Found: C, 71.03; H, 11.60; N, 8.08.

3,3,8-Trimethyl-1-oxa-4,8-diazaspiro[4,5]decane (*VI*c)—bp 63–65°/1.2 mm; IR (neat): 3300, 2920, 1460, 1350, 1260, 1100, 1040, 890, and 800 cm^{-1}; PMR ($CDCl_3$): δ 3.5 (s, 2H), 2.4 (t, 4H), 2.2 (s, 3H), 1.7 (t, 4H), and 1.2 (s, 6H) ppm.

Anal.—Calc. for $C_{10}H_{20}N_2O$: C, 65.17; H, 10.94; N, 15.21. Found: C, 64.88; H, 11.19; N, 15.33.

3-Chloro-2,2,4,4-tetramethyl-1,3-oxazolidine (VIII*a*)—To 175 ml of 0.65 *M* sodium hypochlorite at 0° was added dropwise, with vigorous stirring, 14.2 g (0.11 mole) of VI*a*. The reaction mixture was adjusted to pH 4–6 by the addition of 1 *M* HCl. After 0.5 hr at 0°, the reaction mixture was extracted with dichloromethane. The extracts were combined and dried over anhydrous sodium sulfate. Following filtration, the dichloromethane was removed under reduced pressure to afford a pale-yellow liquid. Distillation gave 9.78 g (0.06 mole), 56%, of VIII*a*, bp 51–53°/12 mm; IR (neat): 2990, 1460, 1370, 1230, 1140, 1040, 900, 820, and 790 cm^{-1}; PMR ($CDCl_3$): δ 3.6 (s, 2H), 1.3 (s, 6H), and 1.2 (s, 6H) ppm; UV (H_2O): λ_{max} 265 nm ($\epsilon = 228\ M^{-1}\ cm^{-1}$).

Anal.—Calc. for $C_7H_{14}ClNO$: C, 51.37; H, 8.62; N, 8.56. Found: C, 51.36; H, 8.77; N, 8.77.

By using the procedure described for the preparation of VIII*a*, the following *N*-chloro-1,3-oxazolidine derivatives were prepared:

3,3-Dimethyl-4-chloro-1-oxa-4-azaspiro[4,5]decane (*VIII*b)—bp 45–47°/0.3 mm; IR (neat): 2920, 1440, 1360, 1090, 1050, 900, 830, and 780 cm^{-1}; PMR ($CDCl_3$): δ 3.8 (s, 2H), 1.7 (broad s, 10H), and 1.2 (s, 6H) ppm; UV (H_2O): λ_{max} 265 nm ($\epsilon = 160\ M^{-1}\ cm^{-1}$).

Anal.—Calc. for $C_{10}H_{18}ClNO$: C, 58.96; H, 8.90; N, 6.88. Found: C, 58.84; H, 8.76; N, 6.28.

3,3,8 - Trimethyl - 4-chloro - 1-oxa-4,8 - diazaspiro[4,5]decane (*VIII*c)—mp 46–48° with sublimation at 35°/0.5 mm; IR (neat/melt): 2930, 1460, 1300, 1090, 840, and 790 cm^{-1}; PMR ($CDCl_3$): δ 3.8 (s, 2H), 1.4–3.0 (m, 8H), 2.4 (s, 3H), and 1.4 (s, 6H) ppm; UV (H_2O): λ_{max} 265 nm ($\epsilon = 270\ M^{-1}\ cm^{-1}$).

Anal.—Calc. for $C_{10}H_{19}ClN_2O$: C, 54.91; H, 8.76; N, 12.81. Found: C, 54.77; H, 8.90; N, 12.85.

3,3,8,8-Tetramethyl-4-chloro-1-oxa-4,8-diazaspiro[4,5]decane Fluorosulfonate (*VIII*d)—mp 123–125°; PMR (D_2O): δ 3.8 (s, 2H), 3.4 (m, 4H), 3.1 (s, 6H), 1.5–3.0 (m, 4H), and 1.2 (s, 6H) ppm; UV (H_2O): λ_{max} 265 nm ($\epsilon = 261\ M^{-1}\ cm^{-1}$).

Anal.—Calc. for $C_{11}H_{22}ClFNO_4S$: C, 39.68; H, 6.66; N, 8.42. Found: C, 39.07; H, 6.67; N, 7.91.

3,3,8,8-Tetramethyl-4-chloro-1-oxa-4,8-diazaspiro[4,5]decane Methylsulfate (*VIII*e)—mp 131–133°; PMR (D_2O): δ 3.8 (s, 2H), 3.6 (s, 3H), 3.4 (m, 4H), 3.1 (s, 6H), 1.5–3.0 (m, 4H), and 1.2 (s, 6H) ppm; UV (H_2O): λ_{max} 268 nm ($\epsilon = 263\ M^{-1}\ cm^{-1}$).

Anal.—Calc. for $C_{12}H_{25}ClN_2O_5S$: C, 41.79; H, 7.31; N, 8.12. Found: C, 41.71; H, 7.29; N, 7.84.

3,3,8,8-Tetramethyl-4-chloro-1-oxa-4,8-diazaspiro[4,5]decane p-Toluenesulfonate (*VIII*f)—mp 94–97°; PMR (D_2O): δ 7.8–7.0 (s,

4H), 3.8 (s, 2H), 3.2–3.7 (m, 4H), 3.0 (s, 6H), 1.4–2.9 (m, 4H), 2.3 (s, 3H), and 1.2 (s, 6H) ppm.

Anal.—Calc. for $C_{18}H_{29}ClN_2O_4S \cdot H_2O$: C, 51.11; H, 7.39; N, 6.62. Found: C, 50.70; H, 7.37; N, 6.59.

REFERENCES

(1) J. J. Kaminski, N. Bodor, and T. Higuchi, *J. Pharm. Sci.*, **65**, 553(1976).

(2) N. Bodor, J. J. Kaminski, S. D. Worley, R. J. Colton, T. H. Lee, and J. W. Rabalais, *ibid.*, **63**, 1387(1974).

(3) T. Higuchi, A. Hussain, and I. Pitman, *J. Chem. Soc., B*, **1969**, 626.

(4) I. Pitman, H. Dawn, T. Higuchi, and A. Hussain, *ibid.*, **1969**, 1230.

(5) "The Toxic Substances List, 1974 Edition," U.S. Department of Health, Education, and Welfare, National Institute for Occupational Safety and Health, Rockville, Md., 1974, p. 650.

(6) A. P. Phillips and R. Baltzly, *J. Am. Chem. Soc.*, **69**, 200(1947).

(7) A. I. Meyers and D. L. Temple, Jr., *ibid.*, **92**, 6646(1970).

(8) A. H. Homeyer, U.S. pat. 2,399,118 (1946); through *Chem. Abstr.*, **40**, 4081[6](1946).

(9) J. J. Carnes, U.S. pat. 2,629,740 (1953); through *Chem. Abstr.*, **48**, 9407[b](1954).

(10) M. Kosugi, J. J. Kaminski, S. H. Selk, I. H. Pitman, N. Bodor, and T. Higuchi, *J. Pharm. Sci.*, **65**, 1743(1976).

(11) J. J. Kaminski, M. M. Huycke, S. H. Selk, N. Bodor, and T. Higuchi, *ibid.*, **65**, 1737(1976).

(12) P. Allen and J. Ginos, *J. Org. Chem.*, **28**, 2759(1963).

(13) F. M. Hancock and A. C. Cope, *J. Am. Chem. Soc.*, **66**, 1738(1944).

ACKNOWLEDGMENTS AND ADDRESSES

Received July 14, 1975, from *INTERx Research Corporation, Lawrence, KS 66044*

Accepted for publication February 5, 1976.

[x] To whom inquiries should be directed.

N-Halo Derivatives V: Comparative Antimicrobial Activity of Soft *N*-Chloramine Systems

JAMES J. KAMINSKI, M. MAUREEN HUYCKE, SALLY H. SELK, NICOLAE BODOR [x], and TAKERU HIGUCHI

Abstract □ Comparative antimicrobial activity studies for certain new classes of soft *N*-chloramines derived from α-aminoisobutyric acid and 2-amino-2-methyl-1-propanol were examined using the minimum inhibitory concentration (MIC) and/or the contact germicidal efficiency (CGE) procedures. Several factors significantly influence the antimicrobial activity of the soft *N*-chloramines: (*a*) the aliphatic chain length in a homologous series, (*b*) the degree of chlorination of the nitrogen atom, (*c*) the solution pH, (*d*) the presence of a denaturant, and (*e*) the nature of a positive charge.

Keyphrases □ *N*-Halo derivatives—low chlorine potential, soft *N*-chloramines, antimicrobial activity evaluated and compared □ *N*-Chloramines, soft—series with low chlorine potential, antimicrobial activity evaluated and compared □ Antimicrobial activity—*N*-chloramine derivatives of α-aminoisobutyric acid and 2-amino-2-methyl-1-propanol evaluated □ Structure–activity relationships—*N*-chloramine derivatives of α-aminoisobutyric acid and 2-amino-2-methyl-1-propanol evaluated for antimicrobial activity

Recently, the *N*-chlorinated derivatives of α-amino acids and their related derivatives were synthesized and their various reactions were studied (1). Based on the stability and reactivity of the nitrogen–chlorine bond in these *N*-chloramines, new types of soft *N*-chloramines were developed which are derivatives of 2-amino-2-methyl-1-propanol (2).

RESULTS AND DISCUSSION

A comprehensive and systematic investigation of the relationship between the antimicrobial activity of the *N*-chloramines and the various factors influencing the polarity, reactivity, and stability of the nitrogen–chlorine bond was examined using the following compounds. Class I represents the esters of the monochloro and dichloro derivatives of α-aminoisobutyric acid; Class II represents the corresponding diketopiperazines. Compounds in Class III have an even lower chlorine potential than those in Class I, while a number of the compounds are structural isomers, such as the III*h*–I*e*, III*i*–I*d*, III*k*–I*f*, and III*l*–I*g* isomeric pairs, which permit a direct comparison of the structure–activity relationship. Compound IV is a stable derivative of 2-amino-2-methyl-1-propanol, representing a whole series of *N*-chloro-2-oxazolidinones. Class V represents the corresponding 1,3-oxazolidine derivatives characterized by a lower chlorine potential and an enhanced soft character.

Minimum Inhibitory Concentration (MIC)—The antimicrobial activity of the various soft *N*-chloramine systems was examined first

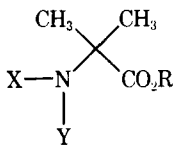

I*a*: X = Cl, Y = Cl, R = CH_3
I*b*: X = H, Y = H, R = $C_6H_{13} \cdot HCl$
I*c*: X = H, Y = Cl, R = C_6H_{13}
I*d*: X = Cl, Y = Cl, R = C_6H_{13}
I*e*: X = H, Y = H, R = $C_8H_{17} \cdot HCl$
I*f*: X = H, Y = Cl, R = C_8H_{17}
I*g*: X = Cl, Y = Cl, R = C_8H_{17}
I*h*: X = H, Y = H, R = $C_{12}H_{25} \cdot HCl$
I*i*: X = H, Y = Cl, R = $C_{12}H_{25}$
I*j*: X = Cl, Y = Cl, R = $C_{12}H_{25}$
I*k*: X = H, Y = H, R = $C_{14}H_{29} \cdot HCl$
I*l*: X = H, Y = Cl, R = $C_{14}H_{29}$
I*m*: X = Cl, Y = Cl, R = $C_{14}H_{29}$
I*n*: X = H, Y = H, R = $C_{18}H_{37} \cdot HCl$
I*o*: X = H, Y = Cl, R = $C_{18}H_{37}$
I*p*: X = Cl, Y = Cl, R = $C_{18}H_{37}$
I*q*: X = H, Y = H, R = $(CH_2)_2O(CH_2)_2O(CH_2)_3CH_3 \cdot HCl$
I*r*: X = H, Y = Cl, R = $(CH_2)_2O(CH_2)_2O(CH_2)_3CH_3$
I*s*: X = Cl, Y = Cl, R = $(CH_2)_2O(CH_2)_2O(CH_2)_3CH_3$

4H), 3.8 (s, 2H), 3.2–3.7 (m, 4H), 3.0 (s, 6H), 1.4–2.9 (m, 4H), 2.3 (s, 3H), and 1.2 (s, 6H) ppm.

Anal.—Calc. for $C_{18}H_{29}ClN_2O_4S \cdot H_2O$: C, 51.11; H, 7.39; N, 6.62. Found: C, 50.70; H, 7.37; N, 6.59.

REFERENCES

(1) J. J. Kaminski, N. Bodor, and T. Higuchi, *J. Pharm. Sci.*, **65**, 553(1976).

(2) N. Bodor, J. J. Kaminski, S. D. Worley, R. J. Colton, T. H. Lee, and J. W. Rabalais, *ibid.*, **63**, 1387(1974).

(3) T. Higuchi, A. Hussain, and I. Pitman, *J. Chem. Soc., B*, **1969**, 626.

(4) I. Pitman, H. Dawn, T. Higuchi, and A. Hussain, *ibid.*, **1969**, 1230.

(5) "The Toxic Substances List, 1974 Edition," U.S. Department of Health, Education, and Welfare, National Institute for Occupational Safety and Health, Rockville, Md., 1974, p. 650.

(6) A. P. Phillips and R. Baltzly, *J. Am. Chem. Soc.*, **69**, 200(1947).

(7) A. I. Meyers and D. L. Temple, Jr., *ibid.*, **92**, 6646(1970).

(8) A. H. Homeyer, U.S. pat. 2,399,118 (1946); through *Chem. Abstr.*, **40**, 4081[6](1946).

(9) J. J. Carnes, U.S. pat. 2,629,740 (1953); through *Chem. Abstr.*, **48**, 9407[b](1954).

(10) M. Kosugi, J. J. Kaminski, S. H. Selk, I. H. Pitman, N. Bodor, and T. Higuchi, *J. Pharm. Sci.*, **65**, 1743(1976).

(11) J. J. Kaminski, M. M. Huycke, S. H. Selk, N. Bodor, and T. Higuchi, *ibid.*, **65**, 1737(1976).

(12) P. Allen and J. Ginos, *J. Org. Chem.*, **28**, 2759(1963).

(13) F. M. Hancock and A. C. Cope, *J. Am. Chem. Soc.*, **66**, 1738(1944).

ACKNOWLEDGMENTS AND ADDRESSES

Received July 14, 1975, from *INTERx Research Corporation, Lawrence, KS 66044*

Accepted for publication February 5, 1976.

[x] To whom inquiries should be directed.

N-Halo Derivatives V: Comparative Antimicrobial Activity of Soft *N*-Chloramine Systems

JAMES J. KAMINSKI, M. MAUREEN HUYCKE, SALLY H. SELK, NICOLAE BODOR [x], and TAKERU HIGUCHI

Abstract □ Comparative antimicrobial activity studies for certain new classes of soft *N*-chloramines derived from α-aminoisobutyric acid and 2-amino-2-methyl-1-propanol were examined using the minimum inhibitory concentration (MIC) and/or the contact germicidal efficiency (CGE) procedures. Several factors significantly influence the antimicrobial activity of the soft *N*-chloramines: (*a*) the aliphatic chain length in a homologous series, (*b*) the degree of chlorination of the nitrogen atom, (*c*) the solution pH, (*d*) the presence of a denaturant, and (*e*) the nature of a positive charge.

Keyphrases □ *N*-Halo derivatives—low chlorine potential, soft *N*-chloramines, antimicrobial activity evaluated and compared □ *N*-Chloramines, soft—series with low chlorine potential, antimicrobial activity evaluated and compared □ Antimicrobial activity—*N*-chloramine derivatives of α-aminoisobutyric acid and 2-amino-2-methyl-1-propanol evaluated □ Structure–activity relationships—*N*-chloramine derivatives of α-aminoisobutyric acid and 2-amino-2-methyl-1-propanol evaluated for antimicrobial activity

Recently, the *N*-chlorinated derivatives of α-amino acids and their related derivatives were synthesized and their various reactions were studied (1). Based on the stability and reactivity of the nitrogen–chlorine bond in these *N*-chloramines, new types of soft *N*-chloramines were developed which are derivatives of 2-amino-2-methyl-1-propanol (2).

RESULTS AND DISCUSSION

A comprehensive and systematic investigation of the relationship between the antimicrobial activity of the *N*-chloramines and the various factors influencing the polarity, reactivity, and stability of the nitrogen–chlorine bond was examined using the following compounds. Class I represents the esters of the monochloro and dichloro derivatives of α-aminoisobutyric acid; Class II represents the corresponding diketopiperazines. Compounds in Class III have an even lower chlorine potential than those in Class I, while a number of the compounds are structural isomers, such as the III*h*–I*e*, III*i*–I*d*, III*k*–I*f*, and III*l*–I*g* isomeric pairs, which permit a direct comparison of the structure–activity relationship. Compound IV is a stable derivative of 2-amino-2-methyl-1-propanol, representing a whole series of *N*-chloro-2-oxazolidinones. Class V represents the corresponding 1,3-oxazolidine derivatives characterized by a lower chlorine potential and an enhanced soft character.

Minimum Inhibitory Concentration (MIC)—The antimicrobial activity of the various soft *N*-chloramine systems was examined first

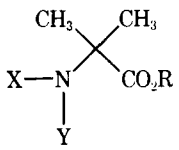

I*a*: X = Cl, Y = Cl, R = CH_3
I*b*: X = H, Y = H, R = $C_6H_{13} \cdot HCl$
I*c*: X = H, Y = Cl, R = C_6H_{13}
I*d*: X = Cl, Y = Cl, R = C_6H_{13}
I*e*: X = H, Y = H, R = $C_8H_{17} \cdot HCl$
I*f*: X = H, Y = Cl, R = C_8H_{17}
I*g*: X = Cl, Y = Cl, R = C_8H_{17}
I*h*: X = H, Y = H, R = $C_{12}H_{25} \cdot HCl$
I*i*: X = H, Y = Cl, R = $C_{12}H_{25}$
I*j*: X = Cl, Y = Cl, R = $C_{12}H_{25}$
I*k*: X = H, Y = H, R = $C_{14}H_{29} \cdot HCl$
I*l*: X = H, Y = Cl, R = $C_{14}H_{29}$
I*m*: X = Cl, Y = Cl, R = $C_{14}H_{29}$
I*n*: X = H, Y = H, R = $C_{18}H_{37} \cdot HCl$
I*o*: X = H, Y = Cl, R = $C_{18}H_{37}$
I*p*: X = Cl, Y = Cl, R = $C_{18}H_{37}$
I*q*: X = H, Y = H, R = $(CH_2)_2O(CH_2)_2O(CH_2)_3CH_3 \cdot HCl$
I*r*: X = H, Y = Cl, R = $(CH_2)_2O(CH_2)_2O(CH_2)_3CH_3$
I*s*: X = Cl, Y = Cl, R = $(CH_2)_2O(CH_2)_2O(CH_2)_3CH_3$

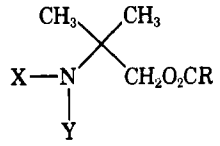

IIIa: X = Cl, Y = Cl, R = CH_3
IIIb: X = H, Y = H, R = $(CH_2)_2CH_3 \cdot HCl$
IIIc: X = H, Y = Cl, R = $(CH_2)_2CH_3$
IIId: X = Cl, Y = Cl, R = $(CH_2)_2CH_3$
IIIe: X = H, Y = Cl, R = $C(CH_3)_3$
IIIf: X = Cl, Y = Cl, R = $C(CH_3)_3$
IIIg: X = H, Y = H, R = $(CH_2)_4CH_3 \cdot HCl$
IIIh: X = H, Y = Cl, R = $(CH_2)_4CH_3$
IIIi: X = Cl, Y = Cl, R = $(CH_2)_4CH_3$
IIIj: X = H, Y = H, R = $(CH_2)_6CH_3 \cdot HCl$
IIIk: X = H, Y = Cl, R = $(CH_2)_6CH_3$
IIIl: X = Cl, Y = Cl, R = $(CH_2)_6CH_3$

IIIm: X = Cl, Y = Cl, R =

IIIn: X = Cl, Y = Cl, R =

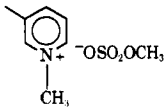

IIIo: X = Cl, Y = Cl, R =

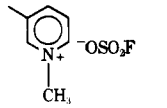

using the MIC procedure. This method is based on incubation of the microorganism tested with solutions containing different concentrations of the soft *N*-chloramine. The MIC of the soft *N*-chloramine is the lowest concentration of the *N*-chloramine for which growth of the microorganism tested is not observed. The MIC is indicative of the *N*-chloramine's bacteriostatic activity but may also represent the *N*-chloramine's bactericidal activity.

Differentiation between the bacteriostatic or bactericidal activity of the *N*-chloramine can be deduced by subculturing the test organism from the MIC and observing the growth or expiration of the organism. However, regardless of the inhibitory mode of bacterial growth, it is important to consider that the activity of the *N*-chloramine observed using this procedure is determined essentially under equilibrium conditions. The microorganism tested and the different concentrations of the *N*-chloramine can attain an equilibrium state. The antimicrobial activity of the soft *N*-chloramine observed under these conditions can be considered its equilibrium thermodynamic activity.

The MIC's of three representative soft *N*-chloramines containing nitrogen–chlorine bonds of different polarity were determined (Table I). Comparison between the MIC's determined for these agents (II, IV, and V*a*) suggests that as the polarity of the nitrogen–chlorine bond is decreased, the MIC against both Gram-positive and Gram-negative microorganisms is increased. The MIC's for the soft *N*-chloramines of α-aminoisobutyrate esters and of 2-amino-2-methyl-1-propyl carboxylates also were determined (Tables II and III).

Comparison between the MIC's determined for the α-*N*-chloroamino and α-*N,N*-dichloroaminoisobutyrate homologous esters (Table II) suggests that the dodecyl homologs (I*i* and I*j*) exhibit the optimum antimicrobial activity against a broad spectrum of Gram-positive, Gram-negative, and fungal organisms. However, compared

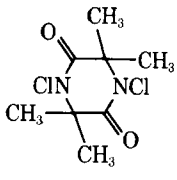

II

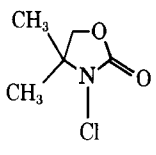

IV

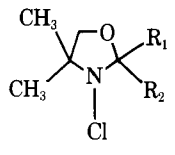

V*a*: $R_1 = R_2 = CH_3$

V*b*: R_1R_2 =

V*c*: R_1R_2 =

Table I—MIC[a] of *N*-Chloramines Containing Nitrogen–Chlorine Bonds of Different Polarity

Compound	*Staph. aureus*	*Strep. pyogenes*	*E. coli*	*S. typhimurium*	*B. subtilis*
II	237	>473[b]	118	237	118
IV	1052	>1052	1052	1052	1052
V*a*	3260	3260	3260	3260	3260

[a] Expressed in parts per million of compound. [b] Greater than indicates that the MIC for the test organism is greater than the highest concentration of the compound that could be tested.

to the MIC determined for dodecyl α-aminoisobutyrate hydrochloride (I*h*), it appears that the activity observed for I*i* and I*j* is primarily an effect of the inherent activity of the parent molecular structure. Unlike the MIC's of the *N*-chlorinated α-aminoisobutyrates, comparison between the MIC's determined for the 2-*N*-chloroamino- and the 2-*N,N*-dichloroamino-2-methyl-1-propyl carboxylates (Table III) suggests that these *N*-chlorinated products are no more efficacious antimicrobial agents than their unchlorinated parent precursors.

Contact Germicidal Efficiency (CGE)—Since the proposed mechanism of bactericidal action for the *N*-chloramines is a result of the direct transfer of positive chlorine from the *N*-chloramine to an appropriate receptor in the cell, the determination of the MIC, which is based on an equilibrium condition, may be an inappropriate means to observe the kinetic effect of the *N*-chloro function in determining the bactericidal activity of the *N*-chloramine. To investigate the kinetic effect of different positive chlorine transfer rates from *N*-chloramines containing nitrogen–chlorine bonds of different polarity on the bactericidal activity, the various soft *N*-chloramine systems were examined using the CGE procedure.

The CGE method is based on treating the microorganism tested with a solution of a given concentration of the soft *N*-chloramine. At various times, aliquots of this solution are subcultured into sterile nutrient broth; the dilution of the aliquot subculture must be sufficient to ensure no further bacteriostatic action of the *N*-chloramine. The subcultured time interval samples are incubated, and the growth behavior of the microorganism tested is observed. The shortest time interval for which growth of the microorganism is not observed is the sterilization time for the soft *N*-chloramine against the particular microorganism tested.

Effect of Homologous Chain Length and Degree of N-*Chlorination*—The sterilization times for the soft *N*-chloramines of α-aminoisobutyrate esters and of the 2-amino-2-methyl-1-propyl carboxylates were determined (Tables IV and V). Comparison between the sterilization times determined for the homologous *N*-chlorinated α-aminoisobutyrates (Table IV) suggests that III*a* is the most active soft *N*-chloramine of the series from a kinetic standpoint. However, an accurate comparison between the sterilization times for the homologs in the series is difficult because of the marked differences in the equilibrium solubilities of the *N*-chloramines.

Nevertheless, the inherent activity of the parent molecular structure for dodecyl α-aminoisobutyrate hydrochloride (I*h*), which is observed in the MIC procedure, is also observed in the CGE procedure. The inherent activity of the parent molecule effectively masks the bactericidal effect of the *N*-chloro function at the relatively low concentrations of the *N*-chloramines. Comparison between the sterilization times determined for 2-(2-*n*-butoxyethoxy)ethyl α-aminoisobutyrate hydrochloride (I*q*) and its *N*-chlorinated products (I*r* and I*s*) supports this hypothesis. The parent molecular structure, I*q*, does not exhibit any antimicrobial activity against any of the microorganisms examined using the CGE procedure. However, comparison of the sterilization times determined for I*r* and I*s* relative to the parent precursor demonstrates the substantial kinetic bactericidal effect of the *N*-chloro function.

Furthermore, comparison between the sterilization times determined for I*r* and I*s* at essentially the same concentration of positive chlorine suggests that the *N,N*-dichloroamino derivative (I*s*) is a more effective antimicrobial agent relative to the *N*-chloroamino derivative (I*r*). Unlike the behavior observed in the determination of the MIC of the *N*-chlorinated products of 2-amino-2-methyl-1-propyl carboxylates, comparison between the sterilization times determined for these derivatives demonstrates that the parent molecular structures are essentially inactive against the microorganisms tested and the kinetic bactericidal effect of the *N*-chloro function is observable for these *N*-chloramines.

Table II—MIC[a] of α-Aminoisobutyrates

Compound	*Staph. aureus*	*Strep. pyogenes*	*E. coli*	*K. pneumoniae*	*P. aeruginosa*	*A. niger*	*C. albicans*	*T. mentagrophytes*
I*a*	125	>250[b]	125	>250	250	>250	>250	>250
I*b*	>500	>500	>500	>500	>500	>500	>500	>500
I*c*	>121	>61	>121	>121	>61	>121	>121	>121
I*d*	>131	>66	>131	>131	>66	>131	>131	66
I*e*	125	125	250	250	500	250	250	250
I*f*	150	75	150	150	>75	>150	150	140
I*g*	142	71	142	>142	>71	>142	142	142
I*h*	3.9	7.8	15.6	15.6	>500	31.3	15.6	15.6
I*i*	9	9	>131	>131	>66	33	33	17
I*j*	80	10	>159	>159	>80	>159	159	20
I*k*	3.9	7.8	500	>500	>500	62.5	15.6	7.8
I*l*	1.6	6.3	>250	>250	250	250	250	125
I*m*	62.5	31.3	500	500	125	>62.5	125	7.8
I*n*	3.9	7.8	>500	>500	>500	>125	125	62.5
I*o*	139	18	>139	>139	>70	>151	>151	76
I*p*	>118	>59	>118	>118	>59	>118	>118	>118
I*q*	>500	>500	>500	>500	>500	>500	>500	>500
I*r*	>125	>62.5	>125	>125	>125	>125	>250	>125
I*s*	>125	>62.5	>125	>125	>62.5	>125	250	>125

[a] Expressed in parts per million of compound. [b] Greater than indicates that the solvent in the dilution sequence inhibited the test organism at the higher concentrations.

Table III—MIC[a] of 2-Amino-2-methyl-1-propyl Carboxylates

Compound	*Staph. aureus*	*Strep. pyogenes*	*E. coli*	*K. pneumoniae*	*P. aeruginosa*	*A. niger*	*C. albicans*	*T. mentagrophytes*
III*a*	>62.5[b]	62.5	>62.5	>62.5	62.5	>62.5	>62.5	62.5
III*b*	>62.5	>62.5	>62.5	>62.5	>62.5	>62.5	>62.5	>62.5
III*c*	>62.5	62.5	>62.5	>62.5	>62.5	>62.5	>62.5	>62.5
III*d*	>62.5	62.5	>62.5	>62.5	>62.5	>62.5	>62.5	>62.5
III*e*	>250	>125	>250	>250	>250	>250	>250	>250
III*f*	250	250	>125	>125	250	>125	>125	>125
III*g*	>62.5	62.5	>62.5	>62.5	62.5	>62.5	>62.5	>62.5
III*h*	>62.5	>62.5	>62.5	>62.5	>62.5	>62.5	>62.5	>62.5
III*i*	>62.5	62.5	>62.5	>62.5	>62.5	>62.5	>62.5	62.5
III*j*	>62.5	>62.5	>62.5	>62.5	>62.5	>62.5	>62.5	>62.5
III*k*	>62.5	>62.5	>62.5	>62.5	>62.5	>62.5	>62.5	>62.5
III*l*	62.5	62.5	>62.5	>62.5	>62.5	>62.5	>62.5	62.5
III*n*	>250	>250	>250	>250	>250	125	>250	125

[a] Expressed in parts per million of compound. [b] Greater than indicates that the solvent in the dilution sequence inhibited the test organism at the higher concentrations.

Table IV—CGE of α-Aminoisobutyrates

Compound	Concentration[a]		Sterilization Time[b], min				
	ppm	ppm, Cl^+	*Staph. aureus*	*Strep. pyogenes*	*E. coli*	*S. typhimurium*	*B. subtilis*
I*a*	887	334	0.5	2.5	0.5	2.5	2.5
I*b*	806	—	>60	10	30	45	30
I*c*	664	106	2.5	0.5	0.5	2.5	0.5
I*d*	79	22	5	2.5	2.5	15	5
I*e*	327		60	10	0.5	15	15
I*f*	275	39	30	0.5	0.5	2.5	2.5
I*g*	71	18	10	2.5	>60	45	15
I*h*	241		0.5	0.5	45	5	2.5
I*i*	159	18	30	0.5	2.5	60	15
I*j*	71	15	30	30	>60	>60	60
I*k*	114		60	2.5	45	15	45
I*l*	83	9	30	0.5	45	>60	30
I*m*	66	13	45	30	>60	>60	45
I*n*	113		10	10	5	30	15
I*o*	59	5	>60	30	>60	>60	45
I*p*	68	11	60	30	30	>60	45
I*q*	2506		>60	>60	>60	>60	>60
I*r*	2263	285	15	2.5	2.5	15	5
I*s*	1142	256	2.5	0.5	2.5	10	2.5

[a] Solubility in 30% methanol—0.1 *M* sodium dihydrogen phosphate, pH 7.0. [b] Time intervals screened were 0.5, 2.5, 5, 10, 15, 30, 45, and 60 min.

Although differences in the equilibrium solubilities of the *N*-chloramines investigated do exist, comparison of the sterilization times determined for the *N*-chloramines (Table V) suggests that III*f* is the most active in the series. Compound III*f* contains a branched (tertiary) aliphatic carboxyl chain and, analogous to the antimicrobial activity observed for the *N*-chlorinated α-aminoisobutyrates, the most

Table V—CGE of 2-Amino-2-methyl-1-propyl Carboxylates

Compound	Concentration[a] ppm	Concentration[a] ppm, Cl+	Sterilization Time[b], min *Staph. aureus*	*Strep. pyogenes*	*E. coli*	*S. typhimurium*	*B. subtilis*
III*a*	1292	458	5	2.5	0.5	2.5	2.5
III*b*	1070	—	>60	>60	>60	>60	>60
III*c*	2078	389	2.5	0.5	0.5	2.5	2.5
III*d*	979	304	2.5	0.5	0.5	2.5	0.5
III*e*	1886	323	5	0.5	0.5	2.5	2.5
III*f*	409	120	5	2.5	2.5	5	2.5
III*g*	1037	—	>60	>60	>60	>60	>60
III*h*	1319	211	2.5	0.5	2.5	5	2.5
III*i*	95	26	10	2.5	10	10	2.5
III*j*	1040	—	>60	30	15	30	5
III*k*	300	43	10	2.5	5	10	0.5
III*l*	85	21	15	5	10	10	2.5

[a] Solubility in 30% methanol—0.1 *M* sodium dihydrogen phosphate, pH 7.0. [b] Time intervals screened were 0.5, 2.5, 5, 10, 15, 30, 45, and 60 min.

active *N*-chlorinated 2-amino-2-methyl-1-propyl carboxylate, III*f*, also is an *N,N*-dichloroamino derivative. With the kinetic bactericidal effect of the *N*-chloro function in the *N*-chloramines established using the CGE procedure, the effects of (*a*) the solution pH, (*b*) the presence of a denaturant, and (*c*) the nature of a positive charge in the *N*-chloramine on the antimicrobial activity of *N*-chloramines containing nitrogen–chlorine bonds of different polarity were examined.

Effect of Solution pH—The sterilization time for the soft *N*-chloramine system as a function of the solution pH was investigated (Table VI). Comparison between the sterilization times determined for these *N*-chloramines suggests that all of the *N*-chloramines investigated appear to be equally effective antimicrobial agents against the less resistant Gram-positive and Gram-negative microorganisms. However, this conclusion is based on an inherent limitation in the time scale of the CGE procedure. Since the shortest time interval that could be examined was 0.5 min, expiration of the organism tested during this interval is not a true indication of the actual contact time required to detoxify the organism.

Despite the inherent limitation in the method, the antimicrobial activity determined for each *N*-chloramine against the less resistant organisms under essentially the same conditions appears to be pH independent. On the other hand, for the more resistant Gram-positive organisms, *Staphylococcus epidermidis* and *Staph. aureus*, only II and IV, which contain the most polar nitrogen–chlorine bonds, exhibit a pH-independent antimicrobial activity. The antimicrobial activity of I*a*, III*e*, III*f*, and V*a*, which contain less polar nitrogen–chlorine bonds, appears to be decreased marginally as the solution pH is increased.

Effect of Denaturant—The sterilization times for the same soft *N*-chloramines under identical conditions but in the presence of a denaturant such as horse serum were determined (Table VII). Comparison between these sterilization times relative to those described in Table VI demonstrates that II, which contains the most polar nitrogen–chlorine bond and should most readily transfer its positive chlorine atom, is also the *N*-chloramine most readily deactivated by the denaturant.

The antimicrobial activity of IV is also decreased by the presence of a denaturant under neutral (pH 7.0) or basic (pH 9.3) conditions. Furthermore, the extent of deactivation appears to increase as the solution pH is increased. The antimicrobial activities of V*a* and III*e*, which contain even less polar nitrogen–chlorine bonds relative to II and IV, are also decreased by the presence of the denaturant. The antimicrobial activity of the *N*-chloroamino derivative (III*e*) is completely removed by the denaturant. On the other hand, the sterilization times determined for the *N,N*-dichloroamino derivative (I*a*) in the presence and the absence of the denaturant are essentially unchanged. The lack of deactivation of I*a* by the denaturant further supports the previous conclusion from the CGE studies (Table IV) that the *N,N*-dichloroamino derivatives are more efficacious antimicrobial agents relative to the *N*-chloroamino derivatives.

Effect of Nature of a Positive Charge—The effect on the antimicrobial activity of the presence and nature of a positive charge in *N*-chloramines containing nitrogen–chlorine bonds of different polarity was examined (Table VIII). Comparison between the sterilization times determined for the *N,N*-dichloroamino derivative (III*m*) and the *N*-chloroamino derivative (V*b*) suggests that both *N*-chloramines are equally effective antimicrobial agents at the concentrations examined.

Comparison between the sterilization times determined for V*b* relative to V*c* demonstrates that, even at the same positive chlorine

Table VI—CGE of *N*-Chloramines as a Function of the Solution pH in the Absence of Horse Serum

Compound	Concentration ppm	Concentration ppm, Cl+	pH	Sterilization Time[a], min *Staph. epidermidis*	*Staph. aureus*	*E. coli*	*K. pneumoniae*	*P. aeruginosa*	*B. bronchiseptica*
	1071	403	4.6	0.5	1	0.5	0.5	0.5	0.5
I*a*	1071	403	7.0	3	3	0.5	1	0.5	0.5
	1071	403	9.3	4	4	0.5	1	0.5	0.5
	404	69	4.6	0.5	1	0.5	0.5	0.5	0.5
III*e*	1886	323	7.0	3	4	0.5	2	1	1
	1704	292	9.3	4	3	1	2	1	1
	489	143	4.6	0.5	2	0.5	0.5	0.5	1
III*f*	409	120	7.0	2	4	1	3	0.5	2
	319	94	9.3	2	2	1	2	0.5	2
	139	41	4.6	2	3	1	2	3	1
II	126	36	7.0	2	4	1	4	5	4
	146	43	9.3	2	4	1	4	4	4
	1332	311	4.6	2	2	0.5	1	0.5	0.5
IV	1146	267	7.0	1	2	0.5	1	0.5	0.5
	1061	247	9.3	2	2	1	1	0.5	1
	1355	289	4.6	0.5	0.5	0.5	0.5	0.5	0.5
V*a*	1463	312	7.0	1	3	0.5	0.5	1	1
	1333	285	9.3	5	5	2	4	2	3

[a] Time intervals screened were 0.5, 1, 2, 3, 4, and 5 min.

Table VII—CGE of *N*-Chloramines as a Function of the Solution pH in the Presence of Horse Serum

Compound	Concentration			Sterilization Time[a], min					
	ppm	ppm, Cl^+	pH	*Staph. epidermidis*	*Staph. aureus*	*E. coli*	*K. pneumoniae*	*P. aeruginosa*	*B. bronchiseptica*
	1071	403	4.6	1	2	0.5	0.5	1	0.5
Ia	1071	403	7.0	3	4	1	1	3	1
	1071	403	9.3	4	7	1	3	2	3
IIIe	468	80	4.6	>10	>10	>10	>10	>10	>10
	139	41	4.6[b]	>15	>15	>10	>10	>10	>10
II	126	36	7.0[b]	>15	>15	>15	>15	>15	>15
	146	43	9.3[b]	>15	>15	>15	>15	>15	>15
	1332	311	4.6	3	3	0.5	1	0.5	0.5
IV	1146	267	7.0	6	10	5	4	3	4
	1061	247	9.3	>10	>10	>10	>10	>10	>10
	1355	289	4.6	>10	>10	3	>10	4	6
Va	1463	312	7.0	6	>10	3	5	7	>10
	1333	285	9.3	>10	>10	4	9	4	4

[a]Time intervals screened were 0.5, 1, 2, 3, 4, 5, 6, 7, 8, 9, and 10 min unless otherwise noted. [b]Time intervals screened were 0.5, 1, 2, 3, 4, 5, 6, 7, 8, 9, 10, and 15 min.

Table VIII—CGE of *N*-Chloramines Containing a Positive Charge

Compound	Concentration			Sterilization Time[a], min					
	ppm	ppm, Cl^+	pH	*Staph. epidermidis*	*Staph. aureus*	*E. coli*	*K. pneumoniae*	*P. aeruginosa*	*B. bronchiseptica*
IIIm	79	21	4.6	3	5	2	1	2	4
IIIn	3100	565	4.6	4	5	1	2	2	1
IIIo	1112	209	4.6	3	5	1	5	3	5
Vb	1428	231	4.6	1	5	0.5	0.5	0.5	0.5
Vc	2594	267	4.6	>5	>5	>5	>5	>5	>5

[a]Time intervals screened were 0.5, 1, 2, 3, 4, and 5 min.

concentration, the presence of a localized positive charge completely removes the antimicrobial activity of Vc. This observation suggests several points regarding the detoxification mechanism of *N*-chloramines that requires further amplification. The only major difference between Vb and Vc is the presence of a remote, localized, positive charge from the *N*-chloro function. If hydrolytic degradation of each *N*-chloramine to another positive chlorine-containing species, *e.g.*, HOCl, were important, essentially the same antimicrobial activity would be expected for Vb and Vc. The difference observed in their antimicrobial activity suggests that the *N*-chloramine as an entity exerts the bactericidal effect upon the microorganism.

Furthermore, the loss of antimicrobial activity only for the *N*-chloramine containing the localized positive charge suggests that the *N*-chloramine must penetrate the cell wall of the microorganism to exert its bactericidal effect. Since the presence of a remote, localized, positive charge would not be expected to perturb the *N*-chloramine bond polarity significantly and, therefore, the rate at which positive chlorine is transferred, the localized positive charge must inhibit the antimicrobial activity of the *N*-chloramine by preventing effective penetration through the cell wall.

The *N*-chloramines IIIn and IIIo also contain a positive charge. However, in this case, the positive charge of the *N*-chloramine can be effectively delocalized by resonance. Comparison between the sterilization times determined for IIIn and IIIo suggests that the *gegen*-ion does not significantly influence the antimicrobial activity of the *N*-chloramine. Most importantly, the antimicrobial activity of the *N*-chloramine is not altered by the presence of a delocalized positive charge. Although differences in the *N*-chloramine concentrations examined do exist, the sterilization times determined for IIIm relative to IIIn or IIIo demonstrate that the delocalized positive charge in the *N*-chloramine does not significantly affect antimicrobial activity.

Furthermore, the antimicrobial activity of IIIn determined in the presence of a denaturant such as horse serum is identical to that observed in the absence of the denaturant under identical concentration conditions. This observation supports the proposal that delocalization of the positive charge permits sufficient penetration of the *N*-chloramine into or through the cell wall of the microorganism to exert a bactericidal effect. In addition, delocalization of the positive charge apparently prevents a significant protein binding of the *N*-chloramine, which would affect the antimicrobial activity of the *N*-chloramine. The identical antimicrobial activity observed for IIIn in the absence and presence of a denaturant once again demonstrates the superior bactericidal effect of an *N,N*-dichloroamino derivative.

With the comparative antimicrobial activity studies for the various low chlorine potential, soft *N*-chloramine systems accomplished using the MIC and/or CGE procedures, the utility of these agents as effective, soft antimicrobial agents necessitated an evaluation of their hydrolytic stabilities. The hydrolytic stability of three representative soft *N*-chloramines (II, IV, and Va) containing nitrogen–chlorine bonds of different polarity was examined in solutions of pH values corresponding to those in which their antimicrobial activities were determined (Table IX); the rate of change in the concentration of positive chlorine was followed iodometrically. The kinetic data obtained could be interpreted as first-order kinetic processes. The stability of the *N*-chloramines under the experimental conditions was characterized using the observed rate constant and reaction half-life.

Comparison between the hydrolytic stability determined for II and IV as a function of the solution pH is consistent with the degree of polarization of the nitrogen–chlorine bond in the *N*-chloramines. That is, II, which contains the nitrogen–chlorine bond most susceptible to hydrolytic cleavage, is also the *N*-chloramine that contains the most polar nitrogen–chlorine bond. The apparent discrepancy observed between the hydrolytic stability of Va and the degree of polarization of the nitrogen–chlorine bond in the *N*-chloramine is a result of the inherent instability of the 1,3-oxazolidine system. The 1,3-oxazolidine is the mono-*N*-analog of the 1,3-dioxolane system. These systems are susceptible to cleavage under acidic and basic conditions.

Comparison between the hydrolytic stability determined for Va as a function of the solution pH indicates an optimum stability for the *N*-chloramine under neutral conditions and relatively rapid degradation under acidic and basic conditions. This observation supports the hypothesis of cleavage of the 1,3-oxazolidine system and suggests that the loss of positive chlorine from Va is not solely due to hydrolytic cleavage of the nitrogen–chlorine bond.

The degree of polarization of the nitrogen–chlorine bond in II and IV confirmed by the hydrolytic stability studies is also consistent with the explanation of the antimicrobial activity of these *N*-chloramines based on different positive chlorine transfer rates determined by the degree of polarization of the nitrogen–chlorine bond.

Further chemical and microbiological investigations of IV to cor-

Table IX—Hydrolytic Stability of *N*-Chloramines Containing Nitrogen–Chlorine Bonds of Different Polarity

Compound	Solution pH	Rate Constant[a] $\times 10^{-2}$, hr^{-1}	Half-Life, hr
II	4.6	0.06	1260
	7.0	0.21	330
	9.3	1.95	35.5
IV	4.6	0.007	9600
	7.0	0.018	3792
	9.3	0.495	140
Va	4.6	27.7	2.5
	7.0	1.39	50
	9.3	13.9	5.0

[a] Rate constants were determined at 40°.

relate the degree of polarization of the nitrogen–chlorine bond and the rate of positive chlorine transfer to the antimicrobial activity of the *N*-chloramine are forthcoming (3).

EXPERIMENTAL

MIC—Prior to determination of the MIC, all bacteria were cultured for 18–20 hr (37°) in tryptose phosphate broth, except *Streptococcus pyogenes* (ATCC 19615) which was cultured in brain heart infusion broth plus 10% normal horse serum. Immediately prior to testing, each culture was adjusted to an optical density of 0.10 (650 nm) and diluted subsequently into double strength medium to approximately 2×10^5 viable organisms/ml.

Spore suspensions of the fungi, *Aspergillus niger* (ATCC 16404) and *Trichophyton mentagrophytes* (ATCC 9129), were diluted into maltose peptone broth to approximately 2×10^5 spores/ml. *Candida albicans* (ATCC 10231) was adjusted to an optical density of 0.10 and diluted into double strength maltose peptone to approximately 2×10^5 organisms/ml. The other organisms used were: *Staphylococcus aureus* (ATCC 6538), *Escherichia coli* (ATCC 10536), *Klebsiella pneumoniae* (ATCC 10031), *Pseudomonas aeruginosa* (ATCC 9027), *Salmonella typhimurium* (ATCC 14028), and *Bacillus subtilis* (ATCC 6051).

The diluted cultures were aseptically distributed in 1-ml amounts to five sterile culture tubes for each organism. The test solution of the compound to be investigated was prepared using 0.1 *M* sodium dihydrogen phosphate buffered to pH 7.0 and subjected to twofold dilutions into sterile water. Then 1 ml of each dilution was dispensed to separate tubes containing the organisms. The inoculated tubes were incubated at 37° for 18–20 hr, and the MIC of the compound was determined. Yeast and fungi were tested in the same manner, except that the incubation period was 5 days at 25°.

Controls were run to ensure viability of the organisms, sterility, and lack of bactericidal effect from the buffer.

CGE—A modified serial dilution analysis was used to determine the time taken for various concentrations of the compounds to sterilize suspensions of the microorganisms. The organisms used and their concentrations (organisms per milliliter) in overnight broth culture were: *Staphylococcus epidermidis* (ATCC 12228), 5×10^6; *Escherichia coli* (ATCC 10536), 10×10^6; *Klebsiella pneumoniae* (ATCC 10031), 12×10^6–13×10^6; *Pseudomonas aeruginosa* (ATCC 9027), 12×10^6–13×10^6; *Staphylococcus aureus* (ATCC 6538), 6×10^6–8×10^6; and *Bordetella bronchiseptica* (ATCC 4617), 3×10^6.

Nutrient Broth—The broth contained 5 g of gelysate peptone and 3 g of beef extract/1000 ml of distilled water, pH 6.9.

Nutrient Agar—The nutrient contained 5 g of gelysate peptone, 3 g of beef extract, and 15 g of agar/1000 ml of distilled water.

Horse Serum T.C.—A 10% horse serum solution in distilled water was freshly prepared and adjusted to pH 7, using carbon dioxide.

Method—A stock solution containing a known concentration of the *N*-chloro compound in an appropriate buffer was prepared. Aliquots of this stock solution were then diluted with equal volumes of distilled water or 10% horse serum to give the solutions to be tested. In some cases, the pH of the test solution was adjusted with 1 *M* HCl. Test solutions were left at room temperature for 30 min prior to their use in the screen.

In the screen, 0.2 ml of an overnight broth culture of an organism was added to 5 ml of the test solution. At time intervals of 0.5, 1, 2, 3, 4, 5, *etc.*, min, a loop of the suspension was subcultured into 5 ml of sterile nutrient broth. The subcultures were incubated at 37° for 7 days and observed daily for evidence of bacterial growth. The time reported for sterilization of a suspension of an organism corresponds to the smallest time interval in which a subculture that gave no growth during 7 days was prepared.

The following controls were conducted:

1. A 0.2-ml aliquot of an overnight culture was added to 5 ml of sterile 0.9% NaCl, and a loop of the suspension was subcultured into 5 ml of sterile nutrient broth. Bacterial growth in the subculture, when it was incubated at 37°, indicated that the overnight culture was viable.
2. A loop of a test solution of an *N*-chloro compound and a loop of a 25-fold dilution of an overnight culture with sterile 0.9% NaCl were added to 5 ml of nutrient broth, and the subculture was incubated at 37°. Bacterial growth indicated that the concentration of chlorinating agent in the subcultures did not inhibit bacterial growth.
3. At the same time intervals that subcultures were made of suspensions of microorganisms in test solutions, a loop of the suspension was subcultured on sterile nutrient agar plates. Following incubation of the plates at 37°, the morphology of the colonies was examined for contamination by foreign organisms.
4. Solutions that were identical to the test solutions but that did not contain the *N*-chloro compounds were subjected to the same screen as the test solutions. The purpose of this control was to ensure that the buffers in the test solutions were not bactericidal.

Replicate experiments demonstrated that there were no significant differences in the results within and between experiments.

The hydrolytic stability of the *N*-chloramines investigated was conducted using the procedure described previously (4).

SUMMARY

The preparation of a number of low chlorine potential, soft *N*-chloramines containing nitrogen–chlorine bonds of different polarity was investigated. These novel *N*-chloramine systems were based on derivatization of 2-amino-2-methyl-1-propanol. Comparative antimicrobial studies for these new classes of soft *N*-chloramines, as well as the soft *N*-chloramines of α-aminoisobutyrate esters and related derivatives (1), were examined using the MIC and/or CGE procedures.

The results of the comparative microbiological investigations demonstrate that the antimicrobial activity of the *N*-chloramine is significantly influenced by a number of factors. Comparison between the MIC's of the *N*-chloramines (Table I) suggests that the bacteriostatic activity is decreased as the nitrogen–chlorine bond polarity is decreased. The kinetic bactericidal effect of the *N*-chloro function in the *N*-chloramines is observable using the CGE procedure. Comparison between the sterilization times determined for the *N*-chloramines (Table VI) suggests that only the *N*-chloramines containing the more polar nitrogen–chlorine bonds give a pH-independent antimicrobial activity against the Gram-positive and Gram-negative microorganisms.

Comparison between the sterilization times determined for the same soft *N*-chloramines, but in the presence of a denaturant (Table VII), suggests that the *N,N*-dichloroamino derivative is the most resistant to deactivation by a denaturant. Furthermore, antimicrobial activity is completely removed by the presence of a localized positive charge in the *N*-chloramine but not significantly influenced by the presence of a delocalized positive charge (Table VIII).

REFERENCES

(1) J. J Kaminski, N. Bodor, and T. Higuchi, *J. Pharm. Sci.*, **65**, 553(1976).

(2) *Ibid.*, **65**, 1733(1976).

(3) M. Kosugi, J. J. Kaminski, S. H. Selk, I. H. Pitman, N. Bodor, and T. Higuchi, *ibid.*, **65**, 1743(1976).

(4) N. Bodor, J. J. Kaminski, S. D. Worley, R. J. Colton, T. H. Lee, and J. W. Rabalais, *ibid.*, **63**, 1387(1974).

ACKNOWLEDGMENTS AND ADDRESSES

Received November 17, 1975, from *INTERx Research Corporation, Lawrence, KS 66044*

Accepted for publication February 5, 1976.

Acknowledgment is made to Dr. Joseph Collins and Dr. William Goss for helpful discussions.

[x] To whom inquiries should be directed.

N-Halo Derivatives VI: Microbiological and Chemical Evaluations of 3-Chloro-2-oxazolidinones

MASANORI KOSUGI *, JAMES J. KAMINSKI, SALLY H. SELK, IAN H. PITMAN ‡, NICOLAE BODOR ˣ, and TAKERU HIGUCHI ‡

Abstract □ Comparative antimicrobial activity of 3-chloro-2-oxazolidinone (I), 3-chloro-4-methyl-2-oxazolidinone (II), 3-chloro-4,4-dimethyl-2-oxazolidinone (III), and *N*-chlorosuccinimide (IV) was evaluated in aqueous buffers in the absence and presence of 5% horse serum. All four compounds had similar bactericidal activity in the absence of horse serum, but I and III had superior activity relative to IV when serum was present. Compound III was considerably more stable with respect to loss of positive chlorine and bactericidal activity than I and II when stored in 0.1 *M* sodium dihydrogen phosphate buffered to pH 7.0 at 40°. Thus, III is potentially the most useful bactericidal agent of those evaluated. The chlorine potentials of I, II, and III, the rate constants for transfer of positive chlorine from I and III to morpholine in aqueous solutions, and the hydrolytic stabilities of I and III with respect to loss of positive chlorine were evaluated. These data, together with previously calculated data for IV, are used to rationalize the observed bactericidal activities.

Keyphrases □ Nitrogen–halogen compounds—3-chloro-2-oxazolidinones, antimicrobial activity screened, chlorine potentials evaluated □ 3-Chloro-2-oxazolidinones—antimicrobial activity screened, chlorine potentials evaluated □ Antimicrobial agents, potential—3-chloro-2-oxazolidinones screened □ Chlorine potentials—3-chloro-2-oxazolidinones evaluated □ Structure–activity relationships—3-chloro-2-oxazolidinones and antimicrobial activity

Recent studies on the chemical (1–4) and antimicrobial properties (4, 5) of *N*-chloro compounds led to the conclusion that 3-chloro-4,4-dimethyl-2-oxazolidinone (III) should be an extremely useful bactericidal agent (6). The minimum inhibitory concentration (MIC) of III against bacteria such as *Staphylococcus aureus, Escherichia coli, Salmonella typhimurium,* and *Bacillus subtilis* was approximately 1000 ppm, and III was an effective bactericidal agent in the presence of 5% horse serum, a potential denaturing agent (5). In addition, the absence from the molecule of hydrogen atoms adjacent to the nitrogen–chlorine bond (3) is expected to stabilize its solutions against loss of positive chlorine [*cf.*, the stability of its 3-bromo analog (2)], and the product of hydrolytic decomposition of its nonchlorinated analog would be the relatively nontoxic 2-amino-2-methyl-1-propanol (7).

The objectives of these studies were twofold: (*a*) to compare the antimicrobial activity of III with that of related compounds, 3-chloro-2-oxazolidinone (I), 3-chloro-4-methyl-2-oxazolidinone (II), and *N*-chlorosuccinimide (IV); and (*b*) to compare some chemical properties of these compounds such as the chlorine potential, rate of positive chlorine transfer to a nitrogen-containing acceptor, and stability of aqueous solutions with respect to loss of positive chlorine with their antimicrobial properties.

This comparative study was made to provide useful information for the design of new *N*-chloro antimicrobial agents.

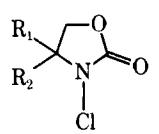

I: $R_1 = R_2 = H$
II: $R_1 = CH_3$, $R_2 = H$
III: $R_1 = R_2 = CH_3$

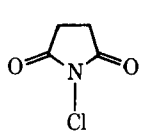

IV

EXPERIMENTAL

Equipment—Spectrophotometric measurements were made on instruments[1] with thermostated cell compartments. All thermostated water baths were maintained at 25.0 ± 0.1°.

Materials—All reagents were of analytical grade unless otherwise stated. *N*-Chlorosuccinimide[2] was used without further purification. All water was double distilled using a Pyrex still. 2-Oxazolidinone and 4,4-dimethyl-2-oxazolidinone were prepared as described previously (8).

3-Chloro-2-oxazolidinone (I)—Chlorine was bubbled through 30 ml of an aqueous solution of 2-oxazolidinone (8.7 g, 0.1 mole) for 0.5 hr at 0°. A white solid, which precipitated, was extracted with dichloromethane. The dichloromethane extract was dried over anhydrous sodium sulfate, filtered, and evaporated to dryness. The white solid that was obtained was sublimed (40°/0.2 mm Hg) and yielded 8.57 g (0.071 mole, 71%) of I, mp 59–61°; UV (H_2O): λ_{max} 248 nm (ϵ = 296 M^{-1} cm^{-1}); PMR ($CDCl_3$): δ 3.6–5.0 (*AA'BB'*, 4H) ppm.

Anal.—Calc. for $C_3H_4ClNO_2$: C, 29.65; H, 3.32; Cl, 29.2; N, 11.53. Found: C, 29.95; H, 3.65; Cl, 28.7; N, 11.77.

3-Chloro-4-methyl-2-oxazolidinone (II)—This compound was prepared from 4-methyl-2-oxazolidinone in essentially the same way as I was prepared from 2-oxazolidinone, resulting in a liquid, bp 85–90°/1 mm Hg; IR (neat): 3000, 1780, 1390, 1195, and 1040 cm^{-1};

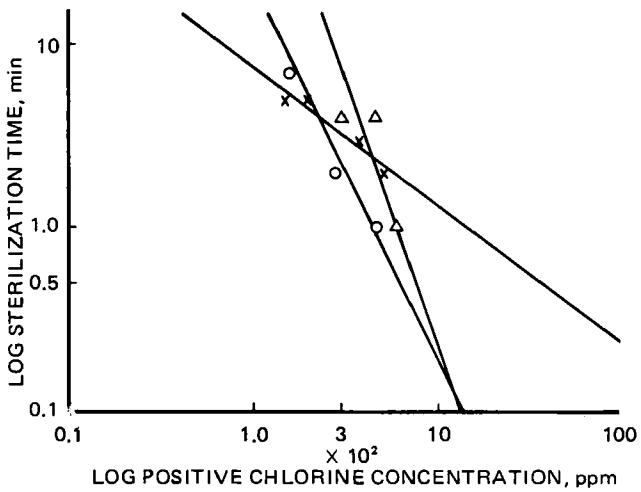

Figure 1—*Plot of the sterilization time for a suspension of* Staph. aureus *against the concentration of I* (○), *II* (△), *and III* (×) *expressed as parts per million of positive chlorine. Solutions were buffered to pH 7.0 with sodium dihydrogen phosphate.*

[1] Cary 14, 15, and 16 spectrophotometers, Varian Instruments, Inc.; and Durrum-Gibson stopped-flow spectrophotometer, Durrum Instrument Corp.

[2] Aldrich Chemical Co.

Table I—Effect of Horse Serum on the Contact Bactericidal Efficiency of I, III, and IV[a]

Compound	Positive Chlorine, ppm	Horse Serum, %	Sterilization Time[b], min					
			Staph. epidermidis	*E. coli*	*K. pneumoniae*	*P. aeruginosa*	*Staph. aureus*	*B. bronchiseptica*
I	298	0	0.5[c]	0.5	0.5	0.5	1	0.5
	298	5	1	0.5	0.5	0.5	3	0.5
III	311	0	2	0.5	1	0.5	2	0.5
IV	311	5	3	0.5	1	0.5	3	0.5
	301	0	0.5	0.5	0.5	0.5	0.5	0.5
	301	5	7	3	8	9	>10	5

[a] pH 4.6 in 0.1 *M* sodium acetate. [b] Time intervals screened were 0.5, 1, 2, 3, 4, 5, 6, 7, 8, 9, and 10 min. [c] Due to limitations in the time scale of the antimicrobial experiment, sterilization time intervals of 0.5 min may not be a true indication of the actual contact time required to sterilize the microorganisms tested. Sterilization of the organisms during this time interval should be more correctly interpreted as less than or equal to 0.5 min.

PMR ($CDCl_3$): δ 4.5 (m, 1H), 4.0 (m, 2H), and 1.4 (d, 3H, J = 6 Hz) ppm.

Anal.—Calc. for $C_4H_6ClNO_2$: C, 35.44; H, 4.46; Cl, 26.2; N, 10.33. Found: C, 35.64; H, 4.59; Cl, 26.5; N, 10.14.

3-Chloro-4,4-dimethyl-2-oxazolidinone (III)—This compound was prepared from 4,4-dimethyl-2-oxazolidinone, using the method described for I and II. Sublimation of the reaction product at 60°/0.25 mm Hg yielded a white solid, mp 71–72.5°; UV (H_2O): λ_{max} 248 nm (ϵ = 274 M^{-1} cm^{-1}); PMR ($CDCl_3$): δ 4.23 (s, 2H) and 1.40 (s, 6H) ppm.

Anal.—Calc. for $C_5H_8ClNO_2$: C, 40.15; H, 5.39; Cl, 23.7; N, 9.37. Found: C, 40.36; H, 5.36; Cl, 23.4; N, 9.35.

Chlorine Potentials—Chlorine potentials were calculated from the measured equilibrium constants for the reactions of I, II, or III with succinimide to yield the appropriate 2-oxazolidinone and IV or from those for the reverse reactions. The calculation method was described previously (9). In a typical experiment, a volume of a freshly prepared solution of the *N*-chloro compound in water was mixed with an equal volume of a solution of the appropriate nonchlorinated compound in 0.1 *M* phosphate buffer. The ionic strength of the reaction solution was 1.0 *M*. The reaction solution was equilibrated at 25°, and then its UV absorbance was measured. The method of calculating equilibrium constants from absorbance measurements was essentially the same as that described previously (10).

Rates of Chlorine Transfer—A volume of a freshly prepared solution of I or III (10^{-3}–10^{-4} *M*) in water was mixed with an equal volume of an aqueous solution of morpholine (10^{-1}–10^{-2} *M*). The pH value of the latter solution was adjusted with perchloric acid, and the ionic strength was maintained at 2.0 *M* with sodium perchlorate. Pseudo-first-order rate constants for the chlorine transfer were calculated from UV absorbance changes accompanying the reaction.

Table II—Stability of Aqueous Solutions[a] of I–III at 40° with Respect to Loss of Positive Chlorine and Bactericidal Activity

Compound	Positive Chlorine[b], Initial, ppm	Sterilization[c] Time, min	Positive Chlorine[d], Final, ppm	Sterilization[c] Time, min
I	465	1	30	>30
II	610	1	4	>30
III	534	2	527	2

[a] The solutions were buffered to pH 7.0 using 0.1 *M* sodium dihydrogen phosphate. [b] Concentration expressed as parts per million of positive chlorine at the time of preparation of the sterilizing solutions. [c] Time for sterilization of a suspension of *Staph. aureus*. Time intervals screened were 0.5, 1, 2, 3, 4, 5, 6, 7, 8, 9, 10, 15, and 30 min. [d] Concentration of positive chlorine remaining in the sterilizing solution after storage for 14 days at 40°.

Table III—Chlorine Potentials, pK_{cp} Values, of I–IV at 25°

Compound	pK_{cp}
I	7.01[a]
II	7.41[a]
III	8.01[a]
IV	7.71[b]

[a] The ionic strength of 1.0 *M* was adjusted using sodium perchlorate. [b] From Ref. 9.

Stability of I and III in Aqueous Solutions—Solutions of I and III in 0.1 *M* sodium acetate solutions buffered at pH 4.6, in 0.1 *M* sodium dihydrogen phosphate solutions buffered at pH 7.0, and in sodium borate solutions buffered at pH 9.3 were stored at 40°. The stability of the solutions with respect to loss of positive chlorine was determined from results of iodometric assays for positive chlorine.

Antimicrobial Activity of I–IV—The organisms and methods were the same as those described previously (5).

RESULTS AND DISCUSSION

A bactericidal efficiency test was conducted to determine the contact time required to sterilize a bacterial suspension by particular concentrations of the test substances. *Staphylococcus aureus* (ATCC 6538) was the bacterium used, and the test solutions were buffered to pH 7.0 with 0.1 *M* sodium dihydrogen phosphate. The concentration of positive chlorine and, hence, the concentration of *N*-chloro compound in the solutions were determined by iodometric assay. Each compound had similar bactericidal activities as judged by this test[3] (Fig. 1).

The second type of test involved comparison of the time required to sterilize suspensions of various organisms in aqueous buffers and in the same buffers containing 5% horse serum (Table I). The data demonstrate that IV was much less active in the solution containing the serum (*i.e.*, in the presence of extraneous organic material including proteins) than in the pure buffer, whereas I and III were active bactericidal agents in the absence and presence of the horse serum denaturant.

The third test was designed to evaluate the length of time that aqueous solutions of I–III remain bactericidal. Such solutions were prepared in 0.1 *M* sodium dihydrogen phosphate buffered to pH 7.0 and divided into two portions. One portion was assayed for positive chlorine content and then subjected to the bactericidal efficiency test using *Staph. aureus*. The other portion was stored at 40° for 14 days when it was assayed for positive chlorine content and subjected to the bactericidal efficiency test. The solutions of I and II lost most of their

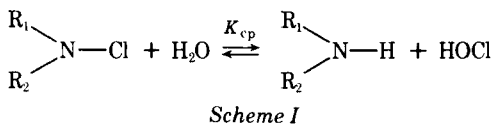

Scheme I

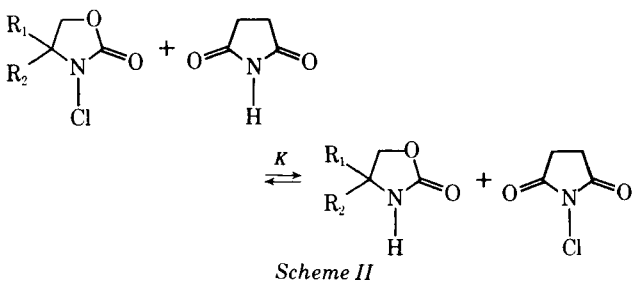

Scheme II

[3] The nonchlorinated oxazolidinone analogs of I (1823 ppm), II (1554 ppm), and III (1404 ppm) did not sterilize the bacterial suspension in 30 min. Therefore, the bactericidal activity of the 3-chloro derivatives is much greater than that of the parent compounds.

Table IV—Equilibrium Constants[a] for Exchange of Positive Chlorine between an *N*-Chloro Compound and a Nitrogen-Containing Receptor

Reaction	pH	*K*
IV + 2-oxazolidinone	6.59	0.2
I + succinimide	6.76	5.0
IV + 4-methyl-2-oxazolidinone	6.85	0.5
IV + 4,4-dimethyl-2-oxazolidinone	6.83	2.0
III + succinimide	6.68	0.5

[a] The ionic strength of 1.0 *M* was adjusted using sodium perchlorate. The analytical wavelength was 270 nm.

Table V—Second-Order Rate Constants for Transfer of Positive Chlorine from I, III, and IV to Morpholine at 25° and Ionic Strength 1.0 *M*

Compound	pH	k_{obs}, M^{-1} sec^{-1}	k, M^{-1} sec^{-1}[a]
I	6.78	1.0	
	7.19	3.2	112 ± 13
	7.72	9.2	
III	6.76	0.24	
	7.25	0.82	
	7.33	0.78	24 ± 3
	7.70	2.2	
	7.73	1.7	
IV			6667[b]

[a] Values of k are independent of pH and refer to the reaction between the morpholine neutral molecule and the neutral *N*-chloro compound:

$$k_{obs}\left[1 + \frac{[H^+]}{K_{a,\text{morpholine}}}\right] = k$$

The pKa of morpholine was taken to be 8.77 (15). [b] From Ref. 9.

positive chlorine content during 14 days; consequently, the bactericidal activity of the solutions was reduced (Table II). The solution of III retained both its original positive chlorine content and its bactericidal activity during 14 days at 40°.

The second phase of this study was concerned with comparing the bactericidal properties of I–IV with some of their chemical properties. The chlorine potential, pK_{cp} value of an *N*-chloro compound has been defined (9) as $-\log K_{cp}$, where K_{cp} is the equilibrium constant for the reaction shown in Scheme I.

The chlorine potential values (Table III) were calculated from the equilibrium constants described in Table IV, which are for positive chlorine exchange between I, II, or III and succinimide or for the reverse reactions (Scheme II).

The methods used for converting the latter equilibrium constants into chlorine potential, pK_{cp}, values were described previously (9). The chlorine potential is thus a measure of the thermodynamic stability of an *N*-chloro compound relative to its nonchlorinated analog. An *N*-chloro compound spontaneously transfers its chlorine to another nitrogen-containing molecule if the chlorine potential of the product is larger than that of the reactant. Hence, the fact that I–IV have similar chlorine potentials (within the range of 7.51 ± 0.50) indicates that they would have similar "thermodynamic tendencies" to transfer their positive chlorine to receptor molecules.

These receptor molecules may be constituents of the solvent (*i.e.*, to yield hypochlorous acid in water), of extraneous organic material (*e.g.*, proteins and other denaturing agents), or of bacteria. The reaction of the *N*-chloro molecule or of hypochlorous acid with molecules that are constituents of bacteria has been suggested (5, 11) to be involved in the bactericidal action of *N*-chloro compounds. The similarity of the chlorine potentials of these molecules thus seems to be consistent with the observation that they have similar bactericidal activity in aqueous suspensions of bacteria that are not contaminated with a denaturing agent such as horse serum.

Earlier (12), it was suggested that pK_{cp} values of *N*-chlorinated imides and amides were related to the acid dissociation constants of the imides or amides by a rather complex relationship. The use of this relationship leads to the prediction that the pK_{cp} values of I, II, and III would be 8.0, 8.5, and 8.4, respectively. The fact that the actual values were slightly smaller than the predicted values is probably due to the different electronic character of the nitrogen atom in the oxazolidinones as compared to that in the amides and imides discussed previously (12). However, it is apparent that the linear free energy relationship described previously (12) does provide a useful means of obtaining an estimate of the pK_{cp} value of an *N*-chloro compound.

The mechanism of chlorine transfer from *N*-chloro compounds to other organic molecules (*e.g.*, proteins or bacterial constituents) may involve hydrolysis of the molecules to hypochlorous acid, their chlorination by hypochlorous acid, and direct transfer of the chlorine to the receptor (13). It was argued previously (14) that the second mechanism was likely to be relatively important because the rate of chlorine exchange between molecules such as IV and nitrogen-containing receptors was much faster than the rate of hydrolysis of the *N*-chloro compound.

The second-order rate constants for transfer of chlorine from I, III, and IV to morpholine to yield *N*-chloromorpholine are described in Table V. The value for IV was reported earlier; those for I and III were calculated from the pseudo-first-order rate constants for formation of *N*-chloromorpholine in solutions containing I or III (10^{-4} *M*) and morpholine (5×10^{2}–2×10^{-1} *M*). Measurements of UV absorbance at the conclusion of the reactions indicated that stoichiometric amounts of *N*-chloromorpholine were formed. Values of a pH-dependent second-order rate constant, k_{obs}, were calculated from the slope of linear plots of pseudo-first-order rate constants against the concentration of morpholine plus morpholine cation in the solution. A pH-independent rate constant, k, was obtained when k_{obs} values were multiplied by the factor $(1 + [H^+]/K_{a,\text{morpholine}})$. Hence, k values are believed to be the second-order rate constants for a reaction between the *N*-chloro compound and morpholine neutral molecules. Values of both k_{obs} and k are described in Table V.

It can be seen that while I, III, and IV have similar chlorine potentials, the rates at which they transferred positive chlorine to morpholine differed considerably. Compound IV was nearly 300 times more reactive than III and 60 times more reactive than I. This difference in reactivity may explain why IV was less bactericidal than I and III in solutions containing horse serum. These solutions were kept for 30 min before being inoculated with bacteria, and a higher fraction of molecules of IV may have transferred their positive chlorine to protein molecules or other receptors than was the case with I and III.

The results in Table II clearly indicate that III is much more stable with respect to loss of positive chlorine than I or II in aqueous solution. Further confirmation of this fact comes from a comparison of the half-lives, $t_{1/2}$, for the positive chlorine content of solutions of I and III (Table VI). The positive chlorine content was determined by iodometric titration. Hence, III was considerably more stable than I at pH values of 4.6, 7.0, and 9.3. The products of these reactions were not determined, but the relative stabilities of the reactants are consistent with an earlier observation (3) that *N*-chloro compounds that do not contain hydrogen atoms adjacent to the nitrogen–chlorine bond are more stable with respect to loss of positive halogen than are compounds that do contain these α-hydrogen atoms.

The results of this study led to the following three conclusions that should be generally applicable in the design of *N*-chloro compounds:

1. Compounds with chlorine potentials between 7 and 8.5 are ef-

Table VI—Hydrolytic Stabilities of I and III at 40°

Compound	Solvent	Half-Life, hr
I	0.1 *M* Sodium acetate, pH 4.6	1872
	0.1 *M* Sodium dihydrogen phosphate, pH 7.0	42.3
	0.1 *M* Sodium borate, pH 9.3	1.3
III	0.1 *M* Sodium acetate, pH 4.6	9600
	0.1 *M* Sodium dihydrogen phosphate, pH 7.0	3792
	0.1 *M* Sodium borate, pH 9.3	140

fective bactericidal agents against various bacteria.

2. The rate at which chlorine is transferred from an *N*-chloro compound to a nitrogen-containing receptor should be considered along with the chlorine potential of the molecules in estimating the likely bactericidal activity of the compound in solutions containing proteins and other organic material.

3. *N*-Chloro compounds that do not contain hydrogen atoms adjacent to the nitrogen–chlorine bond are likely to be more stable than those that do with respect to loss of bactericidal activity in aqueous solution.

REFERENCES

(1) J. J. Kaminski, S. D. Worley, and N. Bodor, *Org. Mass Spectrum.*, in press.

(2) J. J. Kaminski and N. Bodor, *Tetrahedron*, **32**, 1097(1976).

(3) J. J. Kaminski, N. Bodor, and T. Higuchi, *J. Pharm. Sci.*, **65**, 553(1976).

(4) N. Bodor, J. J. Kaminski, S. D. Worley, R. J. Colton, T. H. Lee, and J. W. Rabalais, *ibid.*, **63**, 1387(1974).

(5) J. J. Kaminski, M. M. Huycke, S. H. Selk, N. Bodor, and T. Higuchi, *ibid.*, **65**, 1737(1976).

(6) J. J. Kaminski and N. Bodor, U.S. pat. 3,931,213 (Jan. 6, 1976).

(7) "The Toxic Substances List, 1974 Edition," U.S. Department of Health, Education, and Welfare, National Institutes of Occupational Safety and Health, Rockville, Md., 1974, p. 650.

(8) A. H. Homeyer, U.S. pat. 2,399,118 (1946); through *Chem. Abstr.*, **40**, 4081^6(1946).

(9) T. Higuchi, A. Hussain, and I. H. Pitman, *J. Chem. Soc.*, **1969**, 626.

(10) T. Higuchi and J. Hasegawa, *J. Phys. Chem.*, **69**, 796(1965).

(11) G. R. Dychdala, in "Disinfection, Sterilization, and Preservation," C. Lawrence and S. Block, Eds., Lea & Febiger, Philadelphia, Pa., 1971.

(12) I. H. Pitman, H. Dawn, T. Higuchi, and A. Hussain, *J. Chem. Soc.*, **1969**, 1230.

(13) H. C. Marks, O. Wyss, and F. B. Strandskov, *J. Bacteriol.*, **49**, 299(1945).

(14) A. Hussain, T. Higuchi, A. Hurwitz, and I. H. Pitman, *J. Pharm. Sci.*, **61**, 371(1972).

(15) G. S. Rork and I. H. Pitman, *J. Am. Chem. Soc.*, **96**, 4654(1974).

ACKNOWLEDGMENTS AND ADDRESSES

Received July 24, 1975, from *INTERx Research Corporation, Lawrence, KS 66044*

Accepted for publication September 10, 1975.

* Present address: Department of Chemistry, Gunma University, Kiryu, Gunma, Japan.

‡ Department of Pharmaceutical Chemistry, University of Kansas, Lawrence, KS 66045

ˣ To whom inquiries should be directed.

Effect of Storage at Specified Temperature and Humidity on Properties of Three Directly Compressible Tablet Formulations

S. T. HORHOTA *, J. BURGIO *, L. LONSKI *, and C. T. RHODES ˣ

Abstract □ Direct compression tablets containing sodium starch glycolate, an alginate derivative, or povidone as a disintegrant, magnesium stearate as a lubricant, amaranth as a tracer, and dibasic calcium phosphate dihydrate as the matrix were stored for 30 days at 23° and 75% relative humidity (R.H.), 45° and 75% R.H., and 65° and 40% R.H. Samples were evaluated after 0, 10, 20, and 30 days for size, hardness, and dissolution characteristics. Although no significant changes in the dimensions or hardness of the three tablet formulations, prepared at three different compaction pressures, were observed, the dissolution efficiency of the systems showed significant changes, some systems dissolving more rapidly and some more slowly after storage. In some cases, the changes were so substantial as to indicate the possibility of significant changes of the bioavailability of drugs formulated in such systems. The relevance of this work to the problem of evaluating aging effects on the physical properties of tablets is discussed.

Keyphrases □ Tablets, direct compression—size, hardness, and dissolution, effect of storage at various temperatures and humidity □ Size, tablet—effect of storage at various temperatures and humidity □ Hardness, tablet—effect of storage at various temperatures and humidity □ Dissolution, tablet—effect of storage at various temperatures and humidity □ Dosage forms—direct compression tablets, size, hardness, and dissolution, effect of storage at various temperatures and humidity

Methods for evaluating the chemical stability of drug substances and pharmaceutical products are well established, and the industry now makes considerable use of storage under temperature stress conditions to predict chemical shelflife. Recently, the problem of biological availability has received considerable attention, both scientific and political, and there is particular concern about factors that may modify the dissolution of drugs from compressed tablets (1, 2).

The problem of tablet aging with accompanying changes in dissolution time has received little attention, although it has been the cause of some recalls, and there now is increasing concern within the industry regarding this problem. Some formulators are using accelerated storage samples to screen for possible aging effects. Furthermore, some workers are placing considerable reliance on tablet hardness as a general indicator of tablet aging, the implicit assumption being that invariance in hardness contraindicates changes in dissolution. Unlike simple chemical decomposition, no well-established theory relates the effects of storage under stress conditions to shelflife.

The present paper reports a study of the effect of storage of compressed tablets, under three sets of stress conditions, on tablet hardness, size, and dissolution properties. The purpose of this investigation was to determine if any simple relationship exists between changes in dissolution properties and storage under

fective bactericidal agents against various bacteria.

2. The rate at which chlorine is transferred from an *N*-chloro compound to a nitrogen-containing receptor should be considered along with the chlorine potential of the molecules in estimating the likely bactericidal activity of the compound in solutions containing proteins and other organic material.

3. *N*-Chloro compounds that do not contain hydrogen atoms adjacent to the nitrogen–chlorine bond are likely to be more stable than those that do with respect to loss of bactericidal activity in aqueous solution.

REFERENCES

(1) J. J. Kaminski, S. D. Worley, and N. Bodor, *Org. Mass Spectrum.*, in press.

(2) J. J. Kaminski and N. Bodor, *Tetrahedron*, **32**, 1097(1976).

(3) J. J. Kaminski, N. Bodor, and T. Higuchi, *J. Pharm. Sci.*, **65**, 553(1976).

(4) N. Bodor, J. J. Kaminski, S. D. Worley, R. J. Colton, T. H. Lee, and J. W. Rabalais, *ibid.*, **63**, 1387(1974).

(5) J. J. Kaminski, M. M. Huycke, S. H. Selk, N. Bodor, and T. Higuchi, *ibid.*, **65**, 1737(1976).

(6) J. J. Kaminski and N. Bodor, U.S. pat. 3,931,213 (Jan. 6, 1976).

(7) "The Toxic Substances List, 1974 Edition," U.S. Department of Health, Education, and Welfare, National Institutes of Occupational Safety and Health, Rockville, Md., 1974, p. 650.

(8) A. H. Homeyer, U.S. pat. 2,399,118 (1946); through *Chem. Abstr.*, **40**, 4081^6(1946).

(9) T. Higuchi, A. Hussain, and I. H. Pitman, *J. Chem. Soc.*, **1969**, 626.

(10) T. Higuchi and J. Hasegawa, *J. Phys. Chem.*, **69**, 796(1965).

(11) G. R. Dychdala, in "Disinfection, Sterilization, and Preservation," C. Lawrence and S. Block, Eds., Lea & Febiger, Philadelphia, Pa., 1971.

(12) I. H. Pitman, H. Dawn, T. Higuchi, and A. Hussain, *J. Chem. Soc.*, **1969**, 1230.

(13) H. C. Marks, O. Wyss, and F. B. Strandskov, *J. Bacteriol.*, **49**, 299(1945).

(14) A. Hussain, T. Higuchi, A. Hurwitz, and I. H. Pitman, *J. Pharm. Sci.*, **61**, 371(1972).

(15) G. S. Rork and I. H. Pitman, *J. Am. Chem. Soc.*, **96**, 4654(1974).

ACKNOWLEDGMENTS AND ADDRESSES

Received July 24, 1975, from *INTERx Research Corporation, Lawrence, KS 66044*

Accepted for publication September 10, 1975.

* Present address: Department of Chemistry, Gunma University, Kiryu, Gunma, Japan.

‡ Department of Pharmaceutical Chemistry, University of Kansas, Lawrence, KS 66045

ˣ To whom inquiries should be directed.

Effect of Storage at Specified Temperature and Humidity on Properties of Three Directly Compressible Tablet Formulations

S. T. HORHOTA *, J. BURGIO *, L. LONSKI *, and C. T. RHODES ˣ

Abstract □ Direct compression tablets containing sodium starch glycolate, an alginate derivative, or povidone as a disintegrant, magnesium stearate as a lubricant, amaranth as a tracer, and dibasic calcium phosphate dihydrate as the matrix were stored for 30 days at 23° and 75% relative humidity (R.H.), 45° and 75% R.H., and 65° and 40% R.H. Samples were evaluated after 0, 10, 20, and 30 days for size, hardness, and dissolution characteristics. Although no significant changes in the dimensions or hardness of the three tablet formulations, prepared at three different compaction pressures, were observed, the dissolution efficiency of the systems showed significant changes, some systems dissolving more rapidly and some more slowly after storage. In some cases, the changes were so substantial as to indicate the possibility of significant changes of the bioavailability of drugs formulated in such systems. The relevance of this work to the problem of evaluating aging effects on the physical properties of tablets is discussed.

Keyphrases □ Tablets, direct compression—size, hardness, and dissolution, effect of storage at various temperatures and humidity □ Size, tablet—effect of storage at various temperatures and humidity □ Hardness, tablet—effect of storage at various temperatures and humidity □ Dissolution, tablet—effect of storage at various temperatures and humidity □ Dosage forms—direct compression tablets, size, hardness, and dissolution, effect of storage at various temperatures and humidity

Methods for evaluating the chemical stability of drug substances and pharmaceutical products are well established, and the industry now makes considerable use of storage under temperature stress conditions to predict chemical shelflife. Recently, the problem of biological availability has received considerable attention, both scientific and political, and there is particular concern about factors that may modify the dissolution of drugs from compressed tablets (1, 2).

The problem of tablet aging with accompanying changes in dissolution time has received little attention, although it has been the cause of some recalls, and there now is increasing concern within the industry regarding this problem. Some formulators are using accelerated storage samples to screen for possible aging effects. Furthermore, some workers are placing considerable reliance on tablet hardness as a general indicator of tablet aging, the implicit assumption being that invariance in hardness contraindicates changes in dissolution. Unlike simple chemical decomposition, no well-established theory relates the effects of storage under stress conditions to shelflife.

The present paper reports a study of the effect of storage of compressed tablets, under three sets of stress conditions, on tablet hardness, size, and dissolution properties. The purpose of this investigation was to determine if any simple relationship exists between changes in dissolution properties and storage under

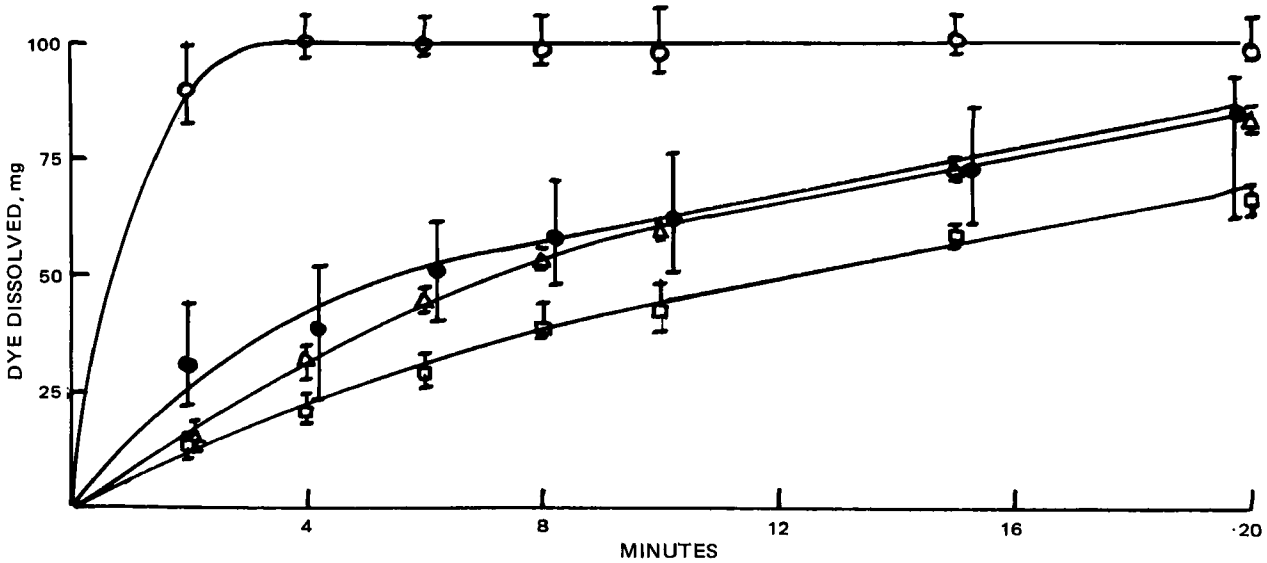

Figure 1—*Typical dissolution profile (III-C, 23°, and 75% R.H.). Key: ○, zero time; □, 10 days; △, 20 days; and ●, 30 days.*

conditions of varying stress. It also seemed useful to check whether changes in dissolution properties of tablets were reflected by changes in hardness.

EXPERIMENTAL

Materials—Dibasic calcium phosphate dihydrate[1], sodium starch glycolate[2], an alginate derivative[3], povidone[4], amaranth[5], and magnesium stearate[6] were used as received.

Three formulations (I, II, and III) were each prepared at three compaction pressures: A (low), B (medium), and C (high). All formulations contained 0.5% magnesium stearate, 2.5% disintegrant (sodium starch glycolate in I, alginate in II, and povidone in III), 7.5% amaranth, and dibasic calcium phosphate dihydrate to 100%; the theoretical tablet weight was 200 mg.

Methods—Amaranth was blended with an equal weight of dibasic calcium phosphate dihydrate, and the mixture was passed twice through a 100-mesh screen. The disintegrant and the remaining dibasic calcium phosphate dihydrate were blended with the color mixture, and the product was passed once through a 60-mesh screen. Magnesium stearate was added, and the product was bag blended for 5 min. Compression was effected using a single-punch tablet[7] press with 8-mm dies and flat punches.

Hardness values, five replicate readings for each sample, were determined using an electric tablet hardness tester[8].

Thickness and diameter values, 10 tablets for each sample, were evaluated in millimeters by use of a micrometer screw gauge.

Dissolution properties of the tablets, three tablets for each sample, were determined using a USP dissolution apparatus. Samples were withdrawn (appropriate volumes of solvent being added to compensate for those removed) at 0, 2, 4, 6, 8, 10, 15, and 20 min and passed through a paper filter[9]. Samples were assayed, without dilution, on a single-beam spectrophotometer[10] at 525 nm.

The Beer–Lambert law was obeyed over the concentration range used in this work. Dissolution efficiency values at 20 min were calculated as described by Khan and Rhodes (3), using the trapezoidal rule to integrate areas under the dissolution curves.

Tablets were stored on petri dishes in ovens at 23 ± 2, 45 ± 2, or 65 ± 2°. Humidity control was effected by storing large beakers containing saturated sodium chloride solution in the ovens. If care was taken to minimize opening of the oven doors, the humidity remained quite constant. Checks, conducted during storage, indicated that the relative humidity (R.H.) values were 75 ± 3% at both 23 and 45° and 40 ± 4% at 65°.

[1] Encompress Special, Edward Mendell Co., Carmel, N.Y.
[2] Primogel, Edward Mendell Co., Carmel, N.Y.
[3] Langoline, Edward Mendell Co., Carmel, N.Y.
[4] Plasdone XL, GAF Corp.
[5] Amend Drug and Chemical Co., New York, N.Y.
[6] Ruger, New Brunswick, N.J.
[7] Erweka.
[8] Strong-Cobb.
[9] Whatman No. 40.
[10] Hitatchi model 139.

RESULTS AND DISCUSSION

Figure 1 exemplifies the type of dissolution profile determined in this study. In all cases, the general form of the curve was the same; lag times (as are often seen in capsule dissolution) were never observed. Therefore, measurement of dissolution efficiency provides a convenient and precise way of characterizing *in vitro* dissolution.

Tables I–III list the hardness values, and Table IV and Fig. 2 show the dissolution efficiency data. The thickness and diameter measurements showed no significant change in any system and are not

Table I—Strong-Cobb Hardness (±*SD*) of Tablets Stored at 23° and 75% R.H.

	Days of Storage			
Batch	0	10	20	30
I-A	5.98 (1.24)	2.84 (0.50)	3.54 (0.40)	2.88 (0.62)
I-B	5.82 (1.47)	2.74 (0.73)	2.72 (0.50)	2.26 (0.85)
I-C	9.06 (2.07)	4.70 (0.73)	4.22 (0.94)	4.22 (0.98)
II-A	5.84 (1.03)	2.94 (0.21)	2.88 (0.39)	2.50 (0.71)
II-B	5.26 (1.03)	2.70 (0.26)	2.84 (0.52)	1.82 (0.49)
II-C	5.74 (0.06)	3.30 (0.56)	3.14 (0.15)	2.30 (0.97)
III-A	4.02 (1.00)	1.32 (0.28)	1.48 (0.23)	1.30 (0.14)
III-B	4.70 (0.92)	1.52 (0.11)	1.84 (0.64)	1.34 (0.22)
III-C	6.92 (1.98)	2.52 (0.28)	2.40 (0.40)	2.60 (0.29)

Table II—Strong-Cobb Hardness (±*SD*) of Tablets Stored at 45° and 75% R.H.

	Days of Storage			
Batch	0	10	20	30
I-A	5.98 (1.24)	2.50 (0.60)	4.04 (1.03)	3.92 (1.00)
I-B	5.82 (1.47)	3.10 (0.27)	3.02 (0.52)	3.61 (0.97)
I-C	9.06 (2.07)	4.80 (0.82)	4.82 (1.13)	5.00 (0.73)
II-A	5.84 (1.03)	6.24 (2.35)	5.16 (1.56)	5.76 (0.95)
II-B	5.26 (1.03)	3.96 (0.88)	4.04 (0.53)	4.32 (0.80)
II-C	5.74 (0.06)	5.38 (0.22)	5.66 (1.62)	5.18 (0.84)
III-A	4.02 (1.00)	2.04 (0.67)	1.70 (0.20)	—[a]
III-B	4.70 (0.92)	3.22 (1.14)	2.64 (0.78)	3.06 (0.42)
III-C	6.92 (1.98)	4.76 (0.46)	4.42 (1.03)	4.34 (0.87)

[a] Hardness too low to measure.

Table III—Strong-Cobb Hardness (±*SD*) of Tablets Stored at 65° and 40% R.H.

Batch	Days of Storage 0	10	20	30
I-A	5.98 (1.24)	3.86 (1.05)	3.94 (0.77)	2.92 (0.58)
I-B	5.82 (1.47)	2.72 (0.80)	2.48 (0.56)	2.86 (0.74)
I-C	9.06 (2.07)	5.06 (1.35)	4.40 (0.98)	4.56 (0.79)
II-A	5.84 (1.03)	1.62 (0.16)	2.50 (0.54)	2.60 (0.52)
II-B	5.26 (1.03)	1.90 (0.52)	1.96 (0.33)	1.85 ($n = 2$)
II-C	5.74 (0.06)	2.54 (0.13)	2.08 (0.40)	2.05 ($n = 2$)
III-A	4.02 (1.00)	1.32 (0.27)	1.38 (0.25)	—[a]
III-B	4.70 (0.92)	1.48 (0.13)	1.26 (0.22)	1.53 ($n = 2$)
III-C	6.92 (1.98)	1.86 (0.50)	1.80 (0.41)	2.02 (0.65)

[a] Hardness too low to measure.

reported in detail; a representative set of data, given in Table V, exemplifies the general findings.

Tables I–III show that, with few exceptions, the same general pattern emerged. Storage at all three stress conditions caused a substantial reduction in hardness in the first 10 days, after which there was little change. Moreover, hardness values did not have a direct relationship with changes in dissolution. The reduction in hardness after 30 days was, somewhat surprisingly, greatest in the systems stored at 23° and least in those stored at 45°.

For the sodium starch glycolate at time zero, the best dissolution efficiency was obtained at the higher compression values (B and C). On storage, the systems prepared at all three compaction pressures showed a similar pattern. The systems stored at 23 and 45° showed no significant change in dissolution efficiency over the storage period. Those stored at 65° showed little change in the first 10 days (the period when hardness values changed most significantly) but then showed a substantial decrease, with a possible leveling out or increase in the last 10 days.

Table V—Change in Thickness and Diameter (±*SD*) of Tablet Batch I-A Stored at 45° and 75% R.H.

	Days of Storage 0	10	20	30
Thickness, mm	2.346 (0.30)	2.32 (0.08)	2.227 (0.10)	2.278 (0.13)
Diameter, mm	—	8.119 (0.16)	7.972 (0.05)	7.986 (0.04)

Type II systems (alginate) had more complex dissolution efficiency changes. The initial dissolution efficiency, which showed little evidence of dependence on compaction pressure, was significantly lower than for the sodium starch glycolate formulations. For the system prepared at all three compaction pressures and stored at 23°, the dissolution efficiency decreased to less than 30% of the original value after 10 days and then returned to approximately the original value. The systems stored at 63° showed an initial increase after 10 days and little change thereafter. Systems stored at 45° showed a slight increase in dissolution efficiency after 10 days and then little further change.

The systems containing povidone as a disintegrant showed an initial high dissolution efficiency. On storage at 65°, little change occurred. However, after 10 days of storage at 23°, dissolution efficiency in III-A and III-B dropped to less than 30% of the initial value; the decrease in III-C was somewhat less. After 10 days of storage, all systems stored at 23° showed no further decrease in dissolution efficiency. Systems stored at 45° showed a decrease and then an increase.

Consideration *in toto* of the reported results leads to several general conclusions for the systems studied. First, neither hardness nor measurement of thickness and diameter bears any relationship to changes in dissolution efficiency. Indeed, substantial changes in dissolution efficiency occur without any changes in either hardness or tablet size. The appearance of the tablets at the start in no way

Table IV—Dissolution Efficiency (Percent) of Various Tablet Batches Stored under Different Stress Conditions[a]

Batch	Storage Time, days	23° and 75% R.H.	45° and 75% R.H.	65° and 40% R.H.
I-A	0	83.3 (82.6–84.1)	—	—
	10	86.3 (84.5–88.6)	85.0 (80.7–91.5)	78.8 (67.0–85.2)
	20	84.4 (79.1–88.5)	85.5 (83.3–89.7)	28.4 (25.8–30.5)
	30	88.4 (86.4–90.0)	79.6 (77.0–82.1)	30.4 (28.7–33.2)
I-B	0	75.7 (75.2–76.2)	—	—
	10	83.9 (81.9–86.4)	83.8 (82.1–85.9)	82.2 (81.3–83.7)
	20	75.7 (75.3–75.9)	74.7 (74.4–75.3)	49.9 (43.8–53.4)
	30	82.4 (81.3–83.7)	79.8 (77.6–80.9)	31.8 (26.9–35.0)
I-C	0	79.8 (74.3–83.2)	—	—
	10	87.3 (86.1–88.9)	86.2 (84.5–88.2)	86.3 (83.7–89.9)
	20	77.5 (69.1–84.1)	78.6 (71.7–83.4)	28.9 (26.9–30.7)
	30	84.6 (84.1–85.5)	73.9 (71.2–77.2)	32.2 (28.1–39.2)
II-A	0	67.2 (62.0–75.0)	—	—
	10	26.7 (20.9–36.5)	81.8 (72.9–94.3)	110.2 (102.2–124.5)
	20	36.4 (27.6–50.0)	81.1 (78.5–84.7)	91.6 (80.4–101.1)
	30	75.4 (73.7–78.3)	78.1 (75.9–81.3)	97.3 (95.2–100.5)
II-B	0	63.0 (61.9–64.1)	—	—
	10	32.7 (31.4–33.4)	52.9 (50.0–62.1)	94.4 (90.8–101.1)
	20	44.8 (41.3–48.1)	88.1 (81.4–92.3)	95.9 (93.1–98.9)
	30	66.7[b]	70.1 (67.2–71.8)	93.9[b]
II-C	0	69.8 (63.6–77.9)	—	—
	10	28.2 (26.8–29.1)	52.0 (50.9–52.9)	96.1 (95.2–97.6)
	20	33.5 (17.0–53.2)	91.6 (88.4–93.9)	97.0 (94.1–98.9)
	30	47.6[b]	75.2 (74.0–77.6)	89.9[b]
III-A	0	94.8 (86.6–102.8)	—	—
	10	25.3 (23.2–27.4)	31.8 (28.6–36.5)	92.5 (90.6–95.3)
	20	31.9 (30.7–32.8)	39.2 (36.5–42.1)	94.9 (93.6–96.4)
	30	29.8[b]	68.9 (67.7–70.1)	—
III-B	0	92.9 (92.5–93.4)	—	—
	10	27.9 (23.3–36.3)	87.9 (79.5–94.2)	91.9 (87.5–96.2)
	20	32.4 (22.1–38.6)	60.6 (38.3–75.1)	89.4 (74.0–74.9)
	30	35.2 (34.1–36.2)	97.2 (96.7–97.8)	95.4 (94.7–96.1)
III-C	0	96.9 (94.2–101.0)	—	—
	10	42.0 (40.9–42.9)	57.1 (55.5–59.9)	96.4 (94.2–98.9)
	20	55.4 (54.9–55.6)	67.5 (64.4–69.6)	95.6 (95.0–96.5)
	30	58.7 (39.1–71.0)	97.7 (96.1–99.4)	97.0 (94.0–99.5)

[a] Values are the means (range) for three trials unless otherwise noted. [b] Single determination.

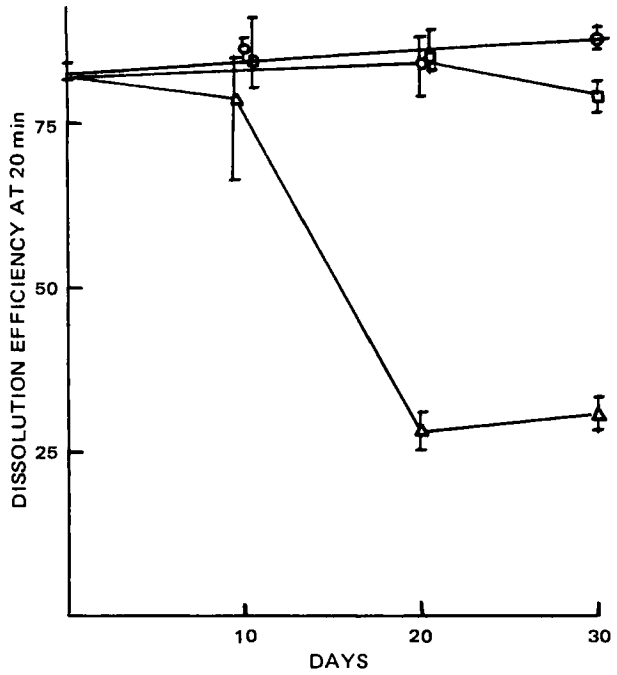

Figure 2—*Effect of storage time on the dissolution efficiency of I-A tablets. Key: ○, 23° and 75% R.H.; □, 45° and 75% R.H.; and △, 65° and 40% R.H.*

differed from that at the end of the storage stress period. Thus, those who rely upon hardness values as an indication of changes in dissolution may be following an unreliable practice.

Second, the reported data cast considerable doubt on the use of accelerated stability-type tests to predict changes at room temperature. Predictions of behavior at room temperature from data obtained at 45 and 65° would lead to unreliable results for the investigated systems.

It is interesting to speculate on the reasons for these results. The direct effect of water vapor on the disintegrant, as described by Khan and Rhodes (4), is probably involved. Also, in the case of povidone, it is reasonable to postulate a direct interaction between the dye and disintegrant. Fung *et al.* (5) made use of the stabilizing effect of the interaction between povidone and nitroglycerin for the formulation of that drug. More than one mechanism probably underlies the reported data, and further work in various tablet matrixes would be valuable to elucidate the principles operating in such systems.

REFERENCES

(1) "Dissolution Technology," L. J. Leeson and J. T. Carstensen, Eds., Industrial Pharmaceutical Technology Section, APhA Academy of Pharmaceutical Sciences, Washington, D.C., 1974.

(2) D. E. Cadwallader, "Biopharmaceutics and Drug Interactions," 2nd ed., Rocom, Montclair, N.J., 1974.

(3) K. A. Khan and C. T. Rhodes, *Pharm. Acta Helv.*, **47**, 594(1972).

(4) K. A. Khan and C. T. Rhodes, *J. Pharm. Sci.*, **64**, 444(1975).

(5) H.-L. Fung, S. K. Yap, and C. T. Rhodes, *ibid.*, **65**, 558(1976).

ACKNOWLEDGMENTS AND ADDRESSES

Received October 6, 1975, from the *Department of Pharmacy, University of Rhode Island, Kingston, RI 02881*

Accepted for publication January 30, 1976.

Financial assistance from Merck Sharp and Dohme is gratefully acknowledged.

* Present address: Department of Pharmaceutics, State University of New York at Buffalo, Buffalo, NY 14214

ˣ To whom inquiries should be directed.

Disaggregation of Compressed Tablets

MICHAEL H. RUBINSTEIN ˣ and DOROTHY M. BODEY

Abstract □ Tablets of dibasic calcium phosphate containing varying proportions of intra- to extragranular maize starch were prepared at three compaction pressures. The surface area generated per tablet after 10 and 30 min of disintegration was measured with an automated counter by a new technique. The optimum starch combination that produced the maximum surface area in a tablet formulation was either 2.5% intra–12.5% extragranular or 15% intragranular starch alone. The distribution of starch did not affect the resultant strength of the tablets, and maximum generation of surface area was achieved by compacting the tablets at as low a pressure as practical.

Keyphrases □ Disaggregation—compressed tablets of dibasic calcium phosphate, with varying proportions of intra- to extragranular starch, effect of compaction pressure □ Dosage forms—compressed tablets, dibasic calcium phosphate with varying proportions of intra- to extragranular starch, disaggregation, effect of compaction pressure □ Tablets, compressed—dibasic calcium phosphate with varying proportions of intra- to extragranular starch, disaggregation, effect of compaction pressure □ Calcium phosphate, dibasic—compressed tablets with varying proportions of intra- to extragranular starch, disaggregation, effect of compaction pressure □ Starch, intra- and extragranular—varying proportions in dibasic calcium phosphate compressed tablets, disaggregation, effect of compaction pressure

Disintegration of a compressed tablet is the process by which a whole tablet breaks up into small pieces when in contact with fluid. If the process is considered to be a zero- or first-order reaction, the specific rate constant is inversely proportional to the disintegration time, as measured by the USP disintegration test. This official test is concerned solely with the breakdown of tablets to particles that pass the 10-mesh screen. No indication is given as to whether the undermesh material consists of coarse aggregates or fine particles, even though, as long ago as 1945, Kelly and Green (1) reported that it was clinically important that tablets disintegrated beyond the size of the original granules.

BACKGROUND

The official disintegration tests assume that two tablets with the same disintegration times disintegrate in the same manner to produce fragments that, for all intents and purposes, have similar size distri-

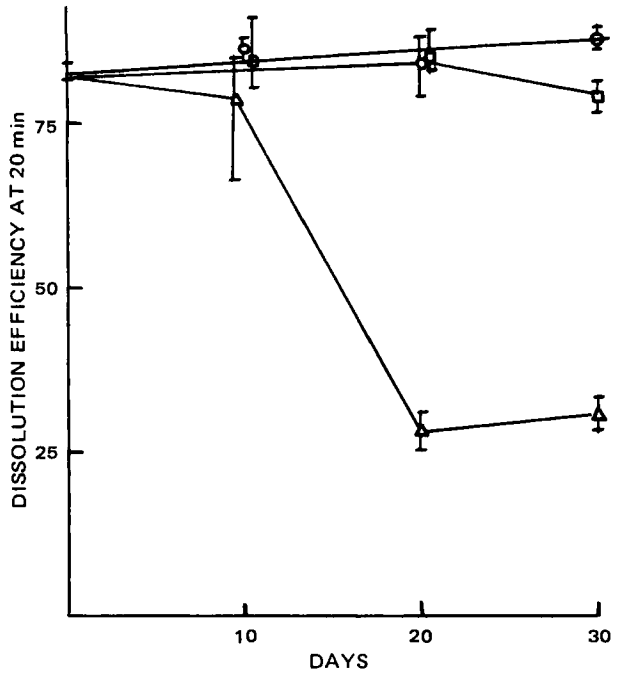

Figure 2—*Effect of storage time on the dissolution efficiency of I-A tablets. Key: ○, 23° and 75% R.H.; □, 45° and 75% R.H.; and △, 65° and 40% R.H.*

differed from that at the end of the storage stress period. Thus, those who rely upon hardness values as an indication of changes in dissolution may be following an unreliable practice.

Second, the reported data cast considerable doubt on the use of accelerated stability-type tests to predict changes at room temperature. Predictions of behavior at room temperature from data obtained at 45 and 65° would lead to unreliable results for the investigated systems.

It is interesting to speculate on the reasons for these results. The direct effect of water vapor on the disintegrant, as described by Khan and Rhodes (4), is probably involved. Also, in the case of povidone, it is reasonable to postulate a direct interaction between the dye and disintegrant. Fung *et al.* (5) made use of the stabilizing effect of the interaction between povidone and nitroglycerin for the formulation of that drug. More than one mechanism probably underlies the reported data, and further work in various tablet matrixes would be valuable to elucidate the principles operating in such systems.

REFERENCES

(1) "Dissolution Technology," L. J. Leeson and J. T. Carstensen, Eds., Industrial Pharmaceutical Technology Section, APhA Academy of Pharmaceutical Sciences, Washington, D.C., 1974.

(2) D. E. Cadwallader, "Biopharmaceutics and Drug Interactions," 2nd ed., Rocom, Montclair, N.J., 1974.

(3) K. A. Khan and C. T. Rhodes, *Pharm. Acta Helv.*, **47**, 594(1972).

(4) K. A. Khan and C. T. Rhodes, *J. Pharm. Sci.*, **64**, 444(1975).

(5) H.-L. Fung, S. K. Yap, and C. T. Rhodes, *ibid.*, **65**, 558(1976).

ACKNOWLEDGMENTS AND ADDRESSES

Received October 6, 1975, from the *Department of Pharmacy, University of Rhode Island, Kingston, RI 02881*

Accepted for publication January 30, 1976.

Financial assistance from Merck Sharp and Dohme is gratefully acknowledged.

* Present address: Department of Pharmaceutics, State University of New York at Buffalo, Buffalo, NY 14214

ˣ To whom inquiries should be directed.

Disaggregation of Compressed Tablets

MICHAEL H. RUBINSTEIN ˣ and DOROTHY M. BODEY

Abstract □ Tablets of dibasic calcium phosphate containing varying proportions of intra- to extragranular maize starch were prepared at three compaction pressures. The surface area generated per tablet after 10 and 30 min of disintegration was measured with an automated counter by a new technique. The optimum starch combination that produced the maximum surface area in a tablet formulation was either 2.5% intra–12.5% extragranular or 15% intragranular starch alone. The distribution of starch did not affect the resultant strength of the tablets, and maximum generation of surface area was achieved by compacting the tablets at as low a pressure as practical.

Keyphrases □ Disaggregation—compressed tablets of dibasic calcium phosphate, with varying proportions of intra- to extragranular starch, effect of compaction pressure □ Dosage forms—compressed tablets, dibasic calcium phosphate with varying proportions of intra- to extragranular starch, disaggregation, effect of compaction pressure □ Tablets, compressed—dibasic calcium phosphate with varying proportions of intra- to extragranular starch, disaggregation, effect of compaction pressure □ Calcium phosphate, dibasic—compressed tablets with varying proportions of intra- to extragranular starch, disaggregation, effect of compaction pressure □ Starch, intra- and extragranular—varying proportions in dibasic calcium phosphate compressed tablets, disaggregation, effect of compaction pressure

Disintegration of a compressed tablet is the process by which a whole tablet breaks up into small pieces when in contact with fluid. If the process is considered to be a zero- or first-order reaction, the specific rate constant is inversely proportional to the disintegration time, as measured by the USP disintegration test. This official test is concerned solely with the breakdown of tablets to particles that pass the 10-mesh screen. No indication is given as to whether the undermesh material consists of coarse aggregates or fine particles, even though, as long ago as 1945, Kelly and Green (1) reported that it was clinically important that tablets disintegrated beyond the size of the original granules.

BACKGROUND

The official disintegration tests assume that two tablets with the same disintegration times disintegrate in the same manner to produce fragments that, for all intents and purposes, have similar size distri-

Table I—Tablet Formulation Composition

	Dry Weight Percentage in Formulation						
	I	II	III	IV	V	VI	VII
Dibasic calcium phosphate	83	83	83	83	83	83	83
Maize starch:							
Intragranular	0	2.5	5.0	7.5	10.0	12.5	15.0
Extragranular	15	12.5	10.0	7.5	5.0	2.0	0
Starch mucilage	2	2	2	2	2	2	2

butions and surface areas. The equivalency of particle distribution and surface area is important, since these parameters directly determine the dissolution rate as defined by the Noyes–Whitney (2) equation. However, two formulated tablets can have the same disintegration times but different generated surface areas.

Figure 1 shows the disintegration of two tablet formulations, A and B, both having identical disintegration times. With Formulation A, large fragments break into two to produce smaller fragments; these fragments, in turn, break down into finer fragments until, at the disintegration time, the largest aggregates just pass through the 10-mesh sieve. With this type of breakdown, there is a relatively large number of large fragments.

With Formulation B, however, the fragments erode away so that their size gradually diminishes. The time taken for the largest particles to erode and pass through the screen is the disintegration time. This type of disintegration yields a lot of fine material with few large fragments. The fragments from Formulation A have a relatively small surface area while those from B have a relatively large surface area, even though both formulations have the same disintegration times.

A better method, therefore, of characterizing the disintegration process is to measure directly the surface area generated with respect to time. The first attempt to do this was described by Nogami *et al.* (3), who modified a thermal analysis method used by Suito and Hirai (4). Several applications of the thermal analysis method have been described subsequently (5–7). Sanders (8) and Sandell (9), recognizing that the extent of disaggregation was important, used a crude wet-sieving method to measure the particle size produced by tablets after disintegration. This technique was refined by Shotton and Leonard (10), who used a wet-sieving process to measure coarse fragments and an automated counter[1] to measure very fine particles. These tests, however, were crude and were not sensitive enough to measure the change of particle size at different time intervals.

The purpose of the present investigation was to evaluate a disintegration test based upon measurements of generated surface area at fixed disaggregation times. The method utilized an automated counter[1] and was used to compare tablets of calcium orthophosphate containing varying proportions of intra- to extragranular maize starch.

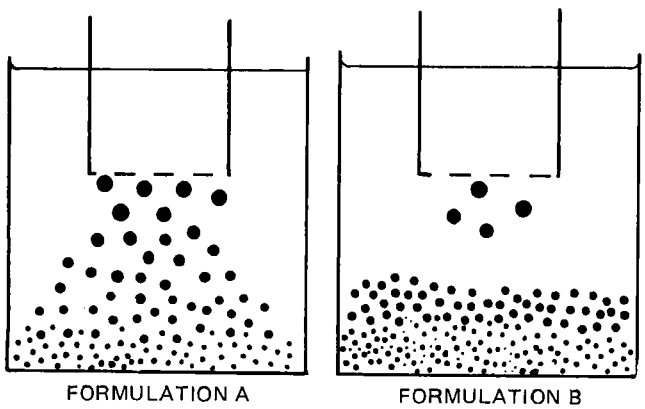

Figure 1—*Comparison of the mechanism of disintegration of two formulated tablets, A (small surface area of tablet fragments) and B (large surface area of tablet fragments).*

[1] Coulter.

EXPERIMENTAL

Materials—The dibasic calcium phosphate was reagent grade, and the maize starch and magnesium stearate used were of BP quality. The moisture content of the maize starch, dibasic calcium phosphate, and magnesium stearate was 0.5, 0.5, and 3% (w/w), respectively. The dibasic calcium phosphate was milled so that the mean particle size was 48 μm with 100% by weight less than 90 μm (automated counter).

Methods—*Granulation*—Granules were prepared by wet massing and screening. Formulations were produced according to the data in Table I. Each formulation (I–VII) contained the same amount of maize starch [15% (w/w)], but it was distributed in varying proportions as intra- or extragranular starch. In all batches, a consistent amount of binder, 10% (w/w) starch mucilage, was used [equivalent to 2% (w/w) dry binder in the final tablet]. If an intragranular disintegrant was required in the formulation, it was dry mixed with the dibasic calcium phosphate before the addition of the granulating agent.

The wet granules were passed through a 44-mesh screen and dried in a hot air oven at 55° for 2 hr. The 44–60-mesh sieve fraction was collected, extragranular starch was added (if required), and the granules were dried in a hot oven at 55° for 12 hr. In all cases, the granules contained less than 0.5% of moisture.

Compression—The tablets were prepared individually between 9.5-mm diameter flat-faced punches. Each formulation was compressed at three compaction pressures: 58.5, 87.6, and 116.4 MNm^{-2}. The die wall was dusted lightly with magnesium stearate as a lubricant, and the lower and upper faces of the punches were cleaned after the production of each tablet. Individual tablets were blown free of fine powder before storage in sealed jars.

Hardness Testing—Tablet hardness[2] was determined using each formulation. Each stroke was timed to take 1 sec in an effort to apply a uniform force at a uniform rate. Ten determinations were carried out for each formulation and at each compaction pressure.

Disintegration Testing—The BP disintegration test was carried out on each group of tablets. In addition, the test was performed at room temperature (20°) and in the electrolyte (discussed later) at 20°.

Disaggregation Apparatus—The apparatus (Fig. 2) consisted of a USP dissolution test basket[3] submerged 3 cm below the surface of 200 ml of electrolyte contained in a 250-ml measuring cylinder (internal diameter of 3.5 cm and height of 31.5 cm). The basket containing the tablet was rotated at a constant speed of 100 rpm (±1%). The narrow diameter of the measuring cylinder produced a lot of turbulence in the area around and within the basket but little turbulence 3 cm below the basket base. This arrangement ensured that there was adequate agitation while the tablet disintegrated in the basket. However, once the tablet fragments passed through the mesh, they were not subjected to any further mixing action.

Disintegration measurements with the apparatus were carried out by timing how long it took individual tablets to pass completely through the basket mesh.

Counter and Surface Area Determinations—An automated counter[4] with a 560-μm diameter orifice sampling tube was used. Sampling times were kept constant at 4 sec, and this time was consistently equivalent to a sample volume of 4.40 ml. When using a 560-μm tube and calibrating at the high end, particles in the 321–25-μm range could be measured.

Preliminary experimentation showed that the most suitable electrolyte for this work was a filtered mixture of 60% (v/v) glycerin BP and 40% (v/v) modified Eagle's solution[5]. This mixture possessed a reasonable rate of flow through the 560-μm orifice tube, had the right electrical resistivity, and was viscous enough to prevent quick settlement of any large tablet fragments. In addition, the viscosity of the mixture (measured with a U-tube viscometer) was close to that of gastric juice. The electrolyte was filtered through a 0.22-μm membrane.

A tablet was placed in the basket of the disaggregation apparatus

[2] Strong-Cobb tester, Strong Cobb Arner Inc.
[3] See USP XIX, p. 651.
[4] Coulter, model B, with model M volume converter.
[5] Isoton, Coulter Electronics Ltd.

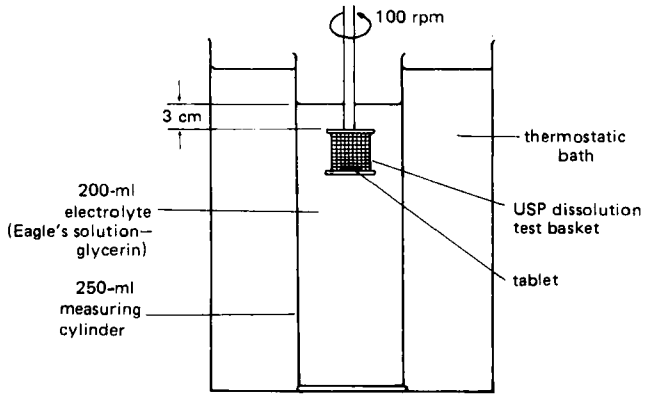

Figure 2—*Disaggregation test apparatus.*

and allowed to revolve for 10 min. The basket assembly was then removed from the electrolyte, and the contents of the measuring cylinder were immediately transferred to a 250-ml beaker containing a magnetic stirrer. The suspension was carefully poured down the inside of the beaker to avoid the production of air bubbles. The beaker contents were allowed to mix for 15 sec, and then a 12-point automated analysis was performed. With a 4-sec count, a complete analysis could be accomplished in about 1 min. All counts were within the recommended 5% coincidence level. From each tablet batch, five replicate determinations were performed.

The whole procedure was repeated with fresh tablets from each batch at a disaggregation time of 30 min. However, the 5% coincidence level was exceeded with these counts, and a 1:5 electrolyte dilution had to be performed before a count could be taken.

In addition to the size analysis, the data from the counter directly produced values for the volume occupied by the tablet fragments within each specific size interval. By using these data and assuming that the fragments were solid spheres, the total surface area of the tablet fragments in 200 ml of suspension could be calculated.

The volume converter produced values of ΔnV_i, the total volume (in arbitrary units) occupied by the tablet fragments within the size interval i. Conversion to real units was accomplished by calibration with spheres of known size, number, and volume. The calibration factor was 2.1×10^{-6} ml; thus, $2.1 \times 10^{-6}\ \Delta nV_i$ cm^3 represents the total volume in cubic centimeters occupied by the tablet fragments in the size interval i. If $\overline{di}$ is the mean particle diameter (in micrometers) within size interval i, then the total surface area (S) of fragments within this size interval is:

$$S = \frac{2.1 \times 10^{-6}\ \Delta nV_i 6}{\overline{di}\ 10^{-4}}\ \text{cm}^2 \qquad \text{(Eq. 1}a\text{)}$$

$$S = \frac{12.6 \times 10^{-2}\ \Delta nV_i}{\overline{di}}\ \text{cm}^2 \qquad \text{(Eq. 1}b\text{)}$$

The total surface area, S_T, in 200 ml of suspension is then:

$$S_T = \frac{12.6 \times 10^{-2}\ V_1 f}{V_2} \sum_{i=12}^{i=1} \frac{\Delta nV_i}{\overline{di}}\ \text{cm}^2 \qquad \text{(Eq. 2)}$$

where V_1 = total volume of suspension (200 ml), V_2 = sample volume passing through orifice tube (4.40 ml), and f = dilution factor.

Values for S_T were plotted for each formulation at each of the two disaggregation times.

RESULTS AND DISCUSSION

Figure 3 shows the graphs obtained when the BP disintegration time was plotted for each tablet formulation. Similarly shaped graphs were obtained when using electrolyte as the disintegration medium and when disintegration was carried out in the disaggregation apparatus. As expected, an increase in compaction pressure increased the disintegration time. Increasing the ratio of extragranular starch above 5% (w/w) produced a decrease in disintegration time, although the reduction was not very great.

The data from these graphs were found statistically to fit a first-order polynomial ($p = 0.05$) relating disintegration time with starch content and compaction pressure. If D_e is the disintegration time in electrolyte (minutes), P is the compaction pressure (MNm^{-2}), and s equals (percent extragranular starch–percent intragranular starch), then by using the method of least squares to fit the response surface,

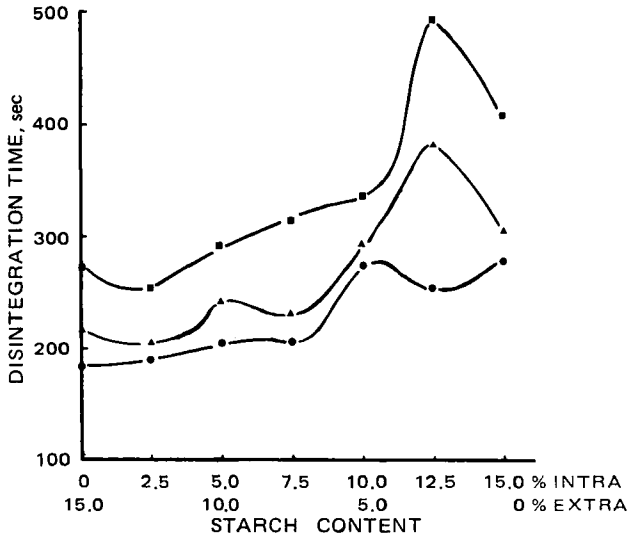

Figure 3—*Effect of starch distribution on tablet disintegration time. Key: ●, 58.5 MNm^{-2}; ▲, 87.6 MNm^{-2}; and ■, 116.4 MNm^{-2}.*

it was found that:

$$D_e = 1.85 - 0.08s + 0.032P \qquad \text{(Eq. 3)}$$

A minimum value for D_e occurs when s is high and P is low, *i.e.*, with tablets produced at as low a compaction pressure as possible and with a formulation containing 15% extra-0% intragranular starch. All other things being equal, this set of formulation and production conditions would be applied to produce the best disintegrating tablets as far as the BP disintegration test is concerned.

Figure 4 depicts tablet hardness values for the various formulations at the three compaction pressures. Again, as expected, increasing the compaction pressure increased the hardness. Variation in the proportion of extragranular starch did not appear to produce a significant variation in hardness, and this finding was confirmed by calculating the respective correlation coefficients (r). At 58.5 MNm^{-2}, r was −0.388; at 87.6 MNm^{-2}, r equaled 0.029; at 116.4 MNm^{-2}, r was 0.474 ($p = 0.05$, $\phi = 5$). Again, these data were found statistically to fit a first-order polynomial ($p = 0.05$):

$$H = 0.005s - 1.76 + 0.07P \qquad \text{(Eq. 4)}$$

where H = hardness in Strong-Cobb units.

From Eq. 4, it can be seen that the siting of the starch does not greatly affect the hardness of the resultant tablets. The compaction pressure appears to be the dominant factor.

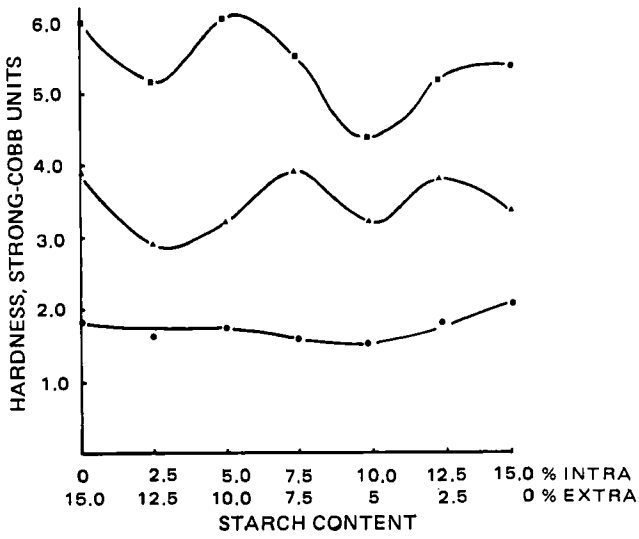

Figure 4—*Variation of tablet hardness with starch distribution. Key: ●, 58.5 MNm^{-2}; ▲, 87.6 MNm^{-2}; and ■, 116.4 MNm^{-2}.*

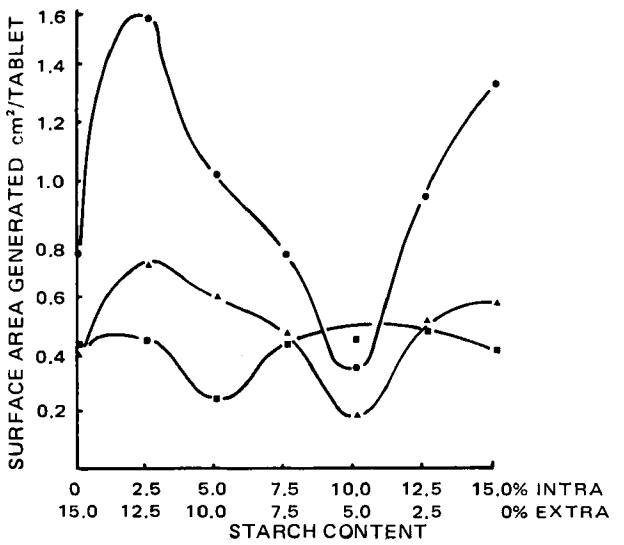

Figure 5—*Effect of starch distribution on the surface area generated per tablet after 10 min of disintegration. Key: ●, 58.5 MNm^{-2}; ▲, 87.6 MNm^{-2}; and ■, 116.4 MNm^{-2}.*

Correlation coefficients for the hardness and disintegration measurements at similar compaction pressures showed that there was no correlation between tablet hardness and disintegration time at all compaction pressures [disintegration in water: r = 0.191 (58.5 MNm^{-2}), −0.311 (87.6 MNm^{-2}), and −0.648 (116.4 MNm^{-2}); disintegration in electrolyte: r = 0.303 (58.5 MNm^{-2}), 0.213 (87.6 MNm^{-2}), and −0.334 (116.4 MNm^{-2})].

The particle-size distributions of the suspensions recovered from the disaggregation test were log normally distributed and, in all cases, were bimodal or occasionally trimodal. Increasing the time of disaggregation did not greatly affect the particle-size distributions, and no meaningful conclusions could be elucidated from comparisons of the median particle diameters obtained from each group of tablets. At 58.5 MNm^{-2}, the number of small particles increased as the proportion of extragranular starch increased from 0%. However, this

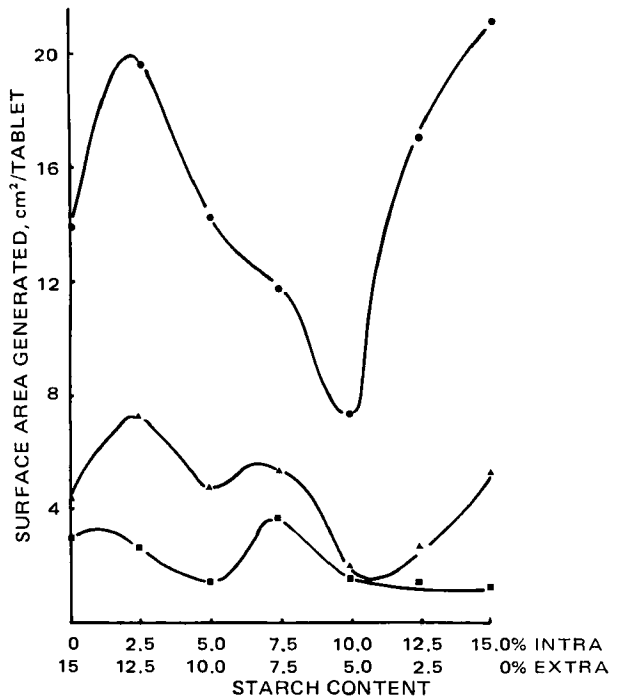

Figure 6—*Effect of starch distribution on the surface area generated per tablet after 30 min of disintegration. Key: ●, 58.5 MNm^{-2}; ▲, 87.6 MNm^{-2}; and ■, 116.4 MNm^{-2}.*

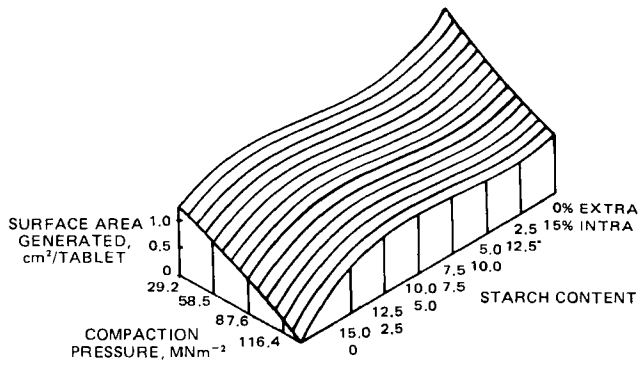

Figure 7—*Computer-produced three-dimensional contour model. The contour system shows how variation in starch content and compaction pressure affects the generated surface area per tablet after 10 min of disintegration.*

pattern was not exhibited at higher pressures.

One very prominent feature that was observed was the large number of particles between 63.7 and 80.3 μm for all formulations containing 2.5% extra–12.5% intragranular starch. A satisfactory explanation for this phenomenon has not been found. These results do not bear out the findings of Shotton and Leonard (10), who found that the use of intragranular starch resulted in the recovery of much finer particles than did the use of extragranular starch. However, Shotton and Leonard did not report the compaction pressure at which comparisons were made, and it seems from the present investigation that compacting pressure plays a large part in determining the extent of disaggregation. Shotton and Leonard assumed that the size values obtained from sieving and by automated counter measurement were directly compatible. This assumption has been shown not to be the case (11) and could give rise to misleading results. In addition, these workers took no account of the possibility that disintegration probably took place by dissolution of the water-soluble binder povidone (included in their tablets) as well as by the breakdown resulting from starch disintegration.

For the various formulations, the surface area generated per tablet after 10 and 30 min are shown in Figs. 5 and 6, respectively. Each point on these graphs was calculated from the individual measurements of some 35,000 fragments; therefore, a very high degree of precision could be expected.

Roughly 12 times the surface area is generated after 30 min than after 10 min. After 30 min, decreasing the compaction pressure increased the generated surface area of the tablet fragments. However, after 10 min there appeared to be an interaction between compaction pressure and starch content.

The surface area data were found statistically to fit a third-order polynomial (p = 0.05), confirming that an interaction did exist. After 10 min:

$$S_T = 1.2000 + 0.0156s - 0.0107P + 0.0030s^2 + 0.004sP - 0.002s^3 \quad \text{(Eq. 5)}$$

and after 30 min:

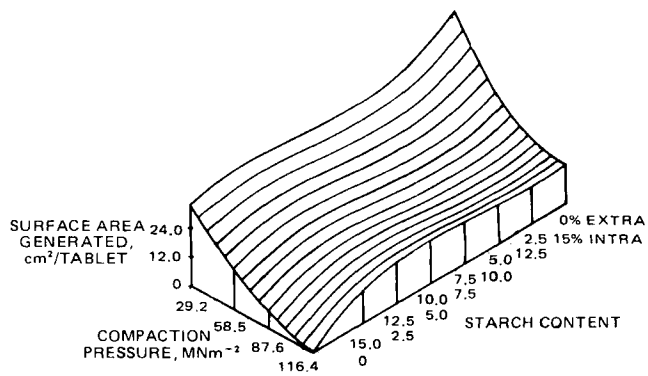

Figure 8—*Effect of compaction pressure and starch distribution on the surface area generated per tablet after 30 min of disintegration.*

$$S_T = 52.048 - 0.324s - 0.955P - 0.232s^2 + 0.016sP - 0.053s^2 - 0.003s^2P \quad \text{(Eq. 6)}$$

By computer simulation, the three-dimensional contour systems were produced from these equations. The mathematical models are shown in Figs. 7 and 8, respectively. As was found from disintegration time measurements, decreasing the compaction pressure increased the generated surface area of the tablet fragment with all formulations. However, with this test, the highest values of surface area occurred with formulations containing 2.5% intra–12.5% extragranular starch and 15% intragranular starch. On the basis of this test, these formulations should be selected, not the one containing 15% extragranular starch, as found from BP disintegration test determinations. This test also shows that there are large differences in surface area values for starch combinations less than 10% intra–5% extragranular, a fact not shown by simple disintegration time measurements. In addition, the common practice of incorporating 5% extragranular starch into a formulation actually produced the lowest values of surface area, again a fact not shown by simple disintegration time measurements.

This new type of disaggregation test appears to be particularly sensitive. It is capable of monitoring small formulation differences with a high degree of precision and of producing an index that is more directly relatable to tablet dissolution. The official disintegration test, however, may produce misleading results, because the insensitivity of the test can mask real and significant differences between tablets. The new disaggregation test reported here thus appears to provide a more sensitive tool for evaluating the disintegrating properties of tablets.

CONCLUSIONS

The authors consider that the official disintegration test is only sufficiently sensitive to detect gross differences between tablets. An alternative and more sensitive technique is proposed; it utilizes an automated counter and measures the surface area generated per tablet during disintegration. This new disaggregation method was used to show that the optimum starch combination in a tablet formulation is either 2.5% intra–12.5% extragranular or 15% intragranular starch alone. Furthermore, the distribution of starch will not affect the resultant hardness of the tablets and, to achieve maximum generation of surface area, tablets should be compacted at as low a pressure as possible.

REFERENCES

(1) K. L. Kelly and M. W. Green, *Bull. Nat. Formul. Comm.*, **13**, 48(1945).

(2) A. A. Noyes and W. R. Whitney, *J. Am. Chem. Soc.*, **19**, 930(1897).

(3) H. Nogami, J. Hasegawa, and Y. Nakai, *Chem. Pharm. Bull.*, **7**, 331(1959).

(4) E. Suito and N. Hirai, *J. Chem. Soc. Jpn.*, **72**, 713(1951).

(5) Y. Nakai and Y. Kubo, *Chem. Pharm. Bull.*, **8**, 634(1960).

(6) Y. Nakai, *ibid.*, **8**, 641(1960).

(7) H. Nogami, J. Hasegawa, and M. Mujamoto, *ibid.*, **15**, 297(1967).

(8) J. C. Sanders, *Pharm. Weekbl.*, **104**, 485(1969).

(9) E. Sandell, *Acta Pharm. Suec.*, **7**, 55(1970).

(10) E. Shotton and G. S. Leonard, *J. Pharm. Pharmacol.*, **24**, 798(1972).

(11) T. Allen, "A Critical Evaluation of the Coulter Counter," Particle-Size Analysis Conference, Bradford, United Kingdom, 1966.

ACKNOWLEDGMENTS AND ADDRESSES

Received March 18, 1975, from the *Department of Pharmaceutics, School of Pharmacy, Liverpool Polytechnic, Byrom Street, Liverpool L3 3AF, United Kingdom.*

Accepted for publication January 12, 1976.

The authors thank Mr. J. Higgins, Mathematics Department, Liverpool Polytechnic, for assistance with the computer programs.

[x] To whom inquiries should be directed.

Dissolution Characteristics and Oral Absorption of Digitoxin and Digoxin Coprecipitates

RANJIT K. REDDY, SAID A. KHALIL [*], and M. WAFIK GOUDA [x]

Abstract □ A marked increase in the dissolution rates of digitoxin and digoxin was attained by dispersing the drugs in two inert solid carriers, poloxamer 188 and deoxycholic acid. The 1 and 10% (w/w) drug–carrier solid dispersions were prepared by the solvent method. The former dissolved significantly faster than the latter. The oral administration of 10% (w/w) digitoxin–carrier coprecipitates to mice significantly increased toxicity. This observed increase is attributed to an increase in the rate and, possibly, the extent of oral absorption of the drug. Although a 10% coprecipitate of digoxin in both carriers showed an increase in the dissolution rate, no increase in oral toxicity was observed. X-ray diffraction patterns indicated that both digitoxin and deoxycholic acid undergo crystalline modifications due to treatment by the solvent, but the exact nature of the drug–carrier solid dispersions was not revealed.

Keyphrases □ Digitoxin—coprecipitates with inert solid carriers, dissolution and oral absorption, mice □ Digoxin—coprecipitates with inert solid carriers, dissolution and oral absorption, mice □ Dissolution—digitoxin and digoxin, coprecipitates with inert solid carriers, mice □ Absorption, oral—digitoxin and digoxin, coprecipitates with inert solid carriers, mice □ Coprecipitates—digitoxin and digoxin with inert solid carriers, dissolution and oral absorption, mice □ Dosage forms—digitoxin and digoxin coprecipitates with inert solid carriers, dissolution and oral absorption, mice

It is well documented that the bioavailability of digoxin from commercial tablet dosage forms is not uniform (1–7). Furthermore, the absorption efficiency from tablets is considerably less than from an oral solution (6, 8). Solid dosage forms of digitoxin are also suspected of exhibiting bioavailability differences (9).

Mortar grinding increased the dissolution rate of three digoxin samples studied (10). Tablets and capsules of digoxin made after crushing material that passed the BP requirements gave higher area under the concentration–time curves than did formulations made of the same material before crushing (11). It was concluded

$$S_T = 52.048 - 0.324s - 0.955P - 0.232s^2 + 0.016sP - 0.053s^2 - 0.003s^2P \quad \text{(Eq. 6)}$$

By computer simulation, the three-dimensional contour systems were produced from these equations. The mathematical models are shown in Figs. 7 and 8, respectively. As was found from disintegration time measurements, decreasing the compaction pressure increased the generated surface area of the tablet fragment with all formulations. However, with this test, the highest values of surface area occurred with formulations containing 2.5% intra–12.5% extragranular starch and 15% intragranular starch. On the basis of this test, these formulations should be selected, not the one containing 15% extragranular starch, as found from BP disintegration test determinations. This test also shows that there are large differences in surface area values for starch combinations less than 10% intra–5% extragranular, a fact not shown by simple disintegration time measurements. In addition, the common practice of incorporating 5% extragranular starch into a formulation actually produced the lowest values of surface area, again a fact not shown by simple disintegration time measurements.

This new type of disaggregation test appears to be particularly sensitive. It is capable of monitoring small formulation differences with a high degree of precision and of producing an index that is more directly relatable to tablet dissolution. The official disintegration test, however, may produce misleading results, because the insensitivity of the test can mask real and significant differences between tablets. The new disaggregation test reported here thus appears to provide a more sensitive tool for evaluating the disintegrating properties of tablets.

CONCLUSIONS

The authors consider that the official disintegration test is only sufficiently sensitive to detect gross differences between tablets. An alternative and more sensitive technique is proposed; it utilizes an automated counter and measures the surface area generated per tablet during disintegration. This new disaggregation method was used to show that the optimum starch combination in a tablet formulation is either 2.5% intra–12.5% extragranular or 15% intragranular starch alone. Furthermore, the distribution of starch will not affect the resultant hardness of the tablets and, to achieve maximum generation of surface area, tablets should be compacted at as low a pressure as possible.

REFERENCES

(1) K. L. Kelly and M. W. Green, *Bull. Nat. Formul. Comm.*, **13**, 48(1945).

(2) A. A. Noyes and W. R. Whitney, *J. Am. Chem. Soc.*, **19**, 930(1897).

(3) H. Nogami, J. Hasegawa, and Y. Nakai, *Chem. Pharm. Bull.*, **7**, 331(1959).

(4) E. Suito and N. Hirai, *J. Chem. Soc. Jpn.*, **72**, 713(1951).

(5) Y. Nakai and Y. Kubo, *Chem. Pharm. Bull.*, **8**, 634(1960).

(6) Y. Nakai, *ibid.*, **8**, 641(1960).

(7) H. Nogami, J. Hasegawa, and M. Mujamoto, *ibid.*, **15**, 297(1967).

(8) J. C. Sanders, *Pharm. Weekbl.*, **104**, 485(1969).

(9) E. Sandell, *Acta Pharm. Suec.*, **7**, 55(1970).

(10) E. Shotton and G. S. Leonard, *J. Pharm. Pharmacol.*, **24**, 798(1972).

(11) T. Allen, "A Critical Evaluation of the Coulter Counter," Particle-Size Analysis Conference, Bradford, United Kingdom, 1966.

ACKNOWLEDGMENTS AND ADDRESSES

Received March 18, 1975, from the *Department of Pharmaceutics, School of Pharmacy, Liverpool Polytechnic, Byrom Street, Liverpool L3 3AF, United Kingdom.*

Accepted for publication January 12, 1976.

The authors thank Mr. J. Higgins, Mathematics Department, Liverpool Polytechnic, for assistance with the computer programs.

[x] To whom inquiries should be directed.

Dissolution Characteristics and Oral Absorption of Digitoxin and Digoxin Coprecipitates

RANJIT K. REDDY, SAID A. KHALIL [*], and M. WAFIK GOUDA [x]

Abstract □ A marked increase in the dissolution rates of digitoxin and digoxin was attained by dispersing the drugs in two inert solid carriers, poloxamer 188 and deoxycholic acid. The 1 and 10% (w/w) drug–carrier solid dispersions were prepared by the solvent method. The former dissolved significantly faster than the latter. The oral administration of 10% (w/w) digitoxin–carrier coprecipitates to mice significantly increased toxicity. This observed increase is attributed to an increase in the rate and, possibly, the extent of oral absorption of the drug. Although a 10% coprecipitate of digoxin in both carriers showed an increase in the dissolution rate, no increase in oral toxicity was observed. X-ray diffraction patterns indicated that both digitoxin and deoxycholic acid undergo crystalline modifications due to treatment by the solvent, but the exact nature of the drug–carrier solid dispersions was not revealed.

Keyphrases □ Digitoxin—coprecipitates with inert solid carriers, dissolution and oral absorption, mice □ Digoxin—coprecipitates with inert solid carriers, dissolution and oral absorption, mice □ Dissolution—digitoxin and digoxin, coprecipitates with inert solid carriers, mice □ Absorption, oral—digitoxin and digoxin, coprecipitates with inert solid carriers, mice □ Coprecipitates—digitoxin and digoxin with inert solid carriers, dissolution and oral absorption, mice □ Dosage forms—digitoxin and digoxin coprecipitates with inert solid carriers, dissolution and oral absorption, mice

It is well documented that the bioavailability of digoxin from commercial tablet dosage forms is not uniform (1–7). Furthermore, the absorption efficiency from tablets is considerably less than from an oral solution (6, 8). Solid dosage forms of digitoxin are also suspected of exhibiting bioavailability differences (9).

Mortar grinding increased the dissolution rate of three digoxin samples studied (10). Tablets and capsules of digoxin made after crushing material that passed the BP requirements gave higher area under the concentration–time curves than did formulations made of the same material before crushing (11). It was concluded

that particle size may be an important determinant of digoxin bioavailability. A comparison of human plasma digoxin levels after administration of tablets made from particles of 3.7-, 12-, and 22-μm diameter showed that the smaller the particle size, the higher was the plasma level (12). A number of reports (6, 7, 13) correlated digoxin tablet dissolution rate *in vitro* to biological availability, showing that the absorption of this drug is dissolution rate limited.

As noted previously (14), if a drug is more rapidly and/or more completely absorbed from solution than from a solid form, its absorption is quite likely to be dissolution rate limited. Slow dissolution results in incomplete, erratic, and unpredictable absorption, and the potential for variability in absorption increases greatly with incompletely absorbed drugs. The purpose of this study was to improve the dissolution of digitoxin and digoxin to reduce the variability in their absorption. The usefulness of solid dispersions of poorly soluble drugs in inert carriers for increasing their dissolution rate has been widely reported (15–28). Soluble carriers such as povidone, polyethylene glycol, urea, citric acid, and succinic acid and poorly soluble ones such as deoxycholic acid, lithocholic acid, and cholic acid have been used.

In this report, the effects of coprecipitating digitoxin and digoxin with two carriers, poloxamer 188 and deoxycholic acid, on the *in vitro* dissolution rate and oral absorption in mice are presented. Deoxycholic acid increased the dissolution and absorption of reserpine (23, 26) and nitrofurantoin (27). To the authors' knowledge, poloxamer 188 has not been used previously to prepare solid dispersions of drugs. It is a block polymer of ethylene oxide and propylene oxide, with an average molecular weight of 8350. It is highly water soluble (>10 g/100 ml at 25°) and is currently used medicinally as a fecal softener. It is a nonionic surfactant which was shown to have no membrane effects (29). High molecular weight polymers are expected to form interstitial solid solutions with many drugs (22). Because it possesses these properties, poloxamer 188 was investigated for its possible use as a matrix for solid-dispersing insoluble drugs.

EXPERIMENTAL

Materials—Digoxin[1], digitoxin[2], poloxamer 188[3], and deoxycholic acid[4] were used as received. All other chemicals were either USP or analytical grade.

Preparation of Coprecipitates—The 1 and 10% (w/w) drug–carrier coprecipitates were prepared by dissolving the two components in 95% alcohol. The solvent was removed under vacuum in a rotary evaporator[5] at room temperature; the vacuum was maintained overnight. The material was then scraped and screened, and the fraction that passed through an 80-mesh sieve and was retained on a 100-mesh sieve was used. Precipitated digitoxin and digoxin were prepared by treating them in a similar manner in the absence of any carrier. Physical mixtures composed of 1 and 10% (w/w) of the drugs and carriers were prepared by mixing the components on paper with a spatula.

Analysis of Drug in Coprecipitates—Two to four accurately weighed fractions of the coprecipitate were dissolved in alcohol and, after suitable dilution with water, were subjected to the described assay procedure. The drug content was between 98.8 and 102.2%.

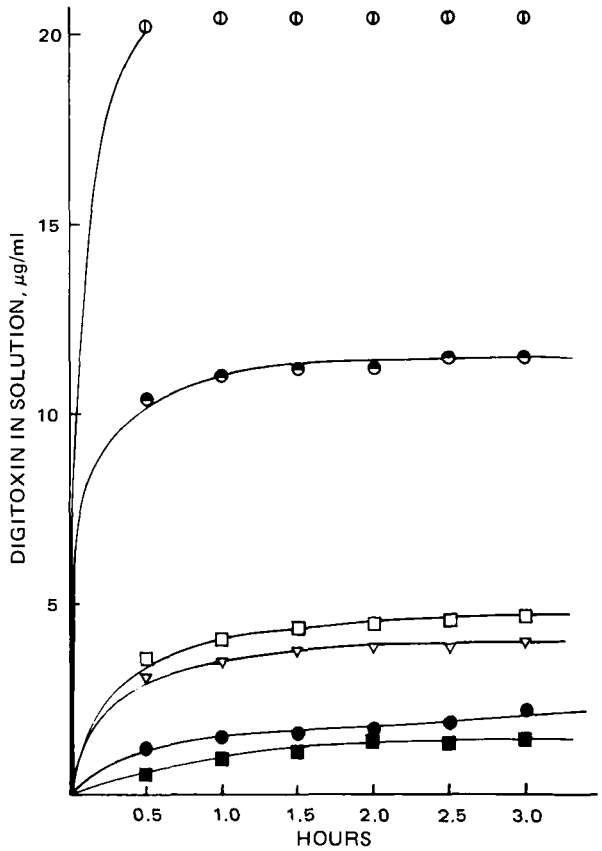

Figure 1—*Dissolution of digitoxin from poloxamer 188 test preparations. Key:* ■, *untreated drug;* ●, *treated drug;* ▽, *10% physical mixture;* □, *1% physical mixture;* ⊖, *10% coprecipitate; and* ⊙, *1% coprecipitate.*

Dissolution Rates—The dissolution characteristics (under nonsink conditions) of (*a*) pure digitoxin and digoxin, (*b*) precipitated digitoxin and digoxin, (*c*) digitoxin and digoxin in 1 and 10% (w/w) coprecipitates, and (*d*) physical mixtures of the drugs with the carriers were determined. In all cases, 80–100-mesh powders (particle size 149–177 μm) containing 15 mg of drug were used. All dissolution experiments were carried out with samples not more than 2 days old.

The beaker method of Levy and Hayes (30), with slight modification, was employed. The dissolution medium consisted of 500 ml of water maintained at 37° in a 1-liter beaker immersed in a constant-temperature water bath. Stirring was provided by a three-blade, 4.45-cm diameter polyethylene stirrer[6] rotating at 60 rpm and dipped in the water to 3.5 cm. The test system was added to the dissolution medium, and 5-ml samples were removed as a function of time and analyzed for drug content. Five milliliters of the dissolution medium was added back to the beaker after each sampling. Each experiment was done in duplicate. A cumulative correction was made for the previously removed samples (31).

Solubility Determinations—The equilibrium solubility of digitoxin and digoxin in water at 37° was determined, and the effect of the carriers on the solubility of the drugs was studied. Excess drug was placed in erlenmeyer flasks along with 20 ml of water or 20 ml of water and carriers. The flasks were tightly stoppered and equilibrated in a water bath shaker[7]. Equilibrium solubility was determined by repetitive sampling.

Assay Procedure—The colorimetric method of Mesnard and Devaux (32) was employed, with slight modification, to assay for the amount of digitoxin and digoxin in solution. The presence of the carriers did not interfere with the assay. To 3 ml of drug solution was

[1] Lanoxin, lot 57177, Burroughs Wellcome Co.
[2] Lot W11097, supplied by Eli Lilly and Co.
[3] Pluronic F-68, supplied by Wyandotte Chemical Co.
[4] Nutritional Biochemicals Corp.
[5] Rotavapor-R, Brinkmann Instruments.
[6] Nalge, No. 6160.
[7] Metabolyte, New Brunswick Scientific.

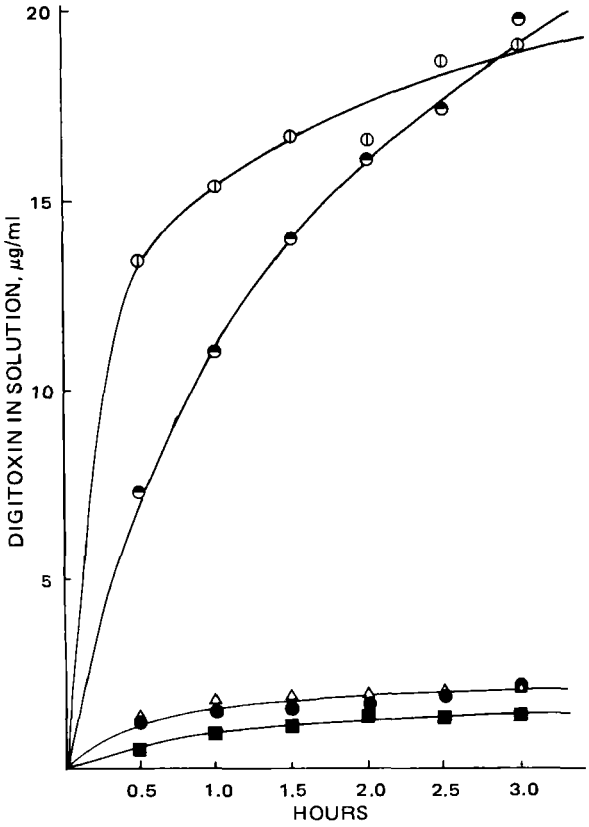

Figure 2—*Dissolution of digitoxin from deoxycholic acid test preparations. Key: ■, untreated drug; ●, treated drug; △, 10 and 1% physical mixtures; ⊖, 10% coprecipitate; and ⊙, 1% coprecipitate.*

added 0.5 ml of 0.01 *N* periodic acid in 0.1 *N* H_2SO_4. After allowing a 10-min oxidation period, 1 ml of 2% sodium arsenite solution in 0.5 *N* HCl was added to stop the oxidation. Four milliliters of the mixture was added to 4 ml of a 0.6% aqueous solution of thiobarbituric acid, adjusted to pH 2, in a 10-ml volumetric flask. The flask was heated in a boiling water bath for 20 min, after which it was cooled to room temperature and the volume was made up with distilled water. The absorbance was determined at 530 nm[8] against a blank treated similarly. The slopes obtained from Beer's law plots were used to determine drug concentrations in the dissolution and solubility studies and in analyzing the coprecipitate systems for drug content.

The direct spectrophotometric assay for digitoxin was tried first. Filtration of the sample through the membrane filters[9] used drastically increased the absorbance of the solution at 220 nm.

Protocol for *In Vivo* Studies—The GI absorption characteristics of digitoxin and digoxin were assessed by comparing the relative oral toxicity of pure drugs, 10% (w/w) physical mixtures with the carriers, and 10% (w/w) coprecipitates. Male albino mice[10], 16–30 g, were deprived of feed 16–18 hr prior to drug administration. Water was freely allowed. The drugs were administered by gastric intubation as a suspension in 0.5% (w/v) methylcellulose (100 cps) aqueous vehicle.

The concentration of the suspension was adjusted such that the dose to be administered would be contained in a volume of 0.2 ml (digitoxin) and 0.4 ml (digoxin)/10 g of body weight. The animals were returned to cages after drug administration, and food and water were allowed *ad libitum*. The number of deaths in the next 168 hr was noted. The 1% coprecipitates were not investigated because the dose to be administered would have been prohibitive.

X-Ray Diffraction Studies—Powdered samples were packed firmly on an aluminum slide having a cavity with a glass window. All diffraction spectra[11] were obtained by scanning at 2°/min in terms of a 2θ angle.

RESULTS AND DISCUSSION

Digitoxin Coprecipitates—The dissolution characteristics of digitoxin–poloxamer 188 test preparations are illustrated in Fig. 1. Digitoxin in both 1 and 10% coprecipitates dissolved at a significantly faster rate than the pure drug. The 1% coprecipitate released the drug much faster than the 10% coprecipitate. The former contained 11 times as much poloxamer 188 as the latter. Complete dissolution of the carrier in the 1% coprecipitates yielded a 0.297% solution, about three times the critical micelle concentration (CMC) value of this surfactant (33).

Surfactants increase the dissolution rate of drugs because of lowering of interfacial tension, which results in an increase in the effective surface area of the drug, or due to micellar solubilization. Therefore, the effect of two poloxamer 188 concentrations, 0.027 and 0.297% (corresponding to the 10 and 1% coprecipitates, respectively), on the dissolution of digitoxin was studied. Digitoxin dissolved at a faster rate in the presence of both concentrations of the surfactant. Equilibrium solubility in these surfactant solutions at 37° was determined. No difference between the solubility of digitoxin in water (0.62 mg/100 ml) and in the surfactant solutions was observed. This result indicates the lack of drug–carrier interaction in the concentrations employed. The slightly faster dissolution of the drug in the more concentrated poloxamer 188 solution (Fig. 1) might be due to better wetting of the drug.

Figure 2 shows the dissolution of digitoxin from the deoxycholic acid test systems. Both coprecipitates dissolved much faster than the pure drug, and the 1% coprecipitate dissolved faster than the 10% coprecipitate, at least in the initial stages. The dissolution of digitoxin from both the 1 and 10% physical mixtures proceeded at equal rates. The studies with physical mixtures indicated that the mere presence of the carrier in an amount equivalent to that present in the coprecipitates was not responsible for the enhanced dissolution of digitoxin from the coprecipitates. Equilibrium solubility studies indicated that there was no interaction between digitoxin and deoxycholic acid.

Digitoxin is known to form solvates with alcohol which are stable *in vacuo* (34). Since drug solvates may have markedly different rates

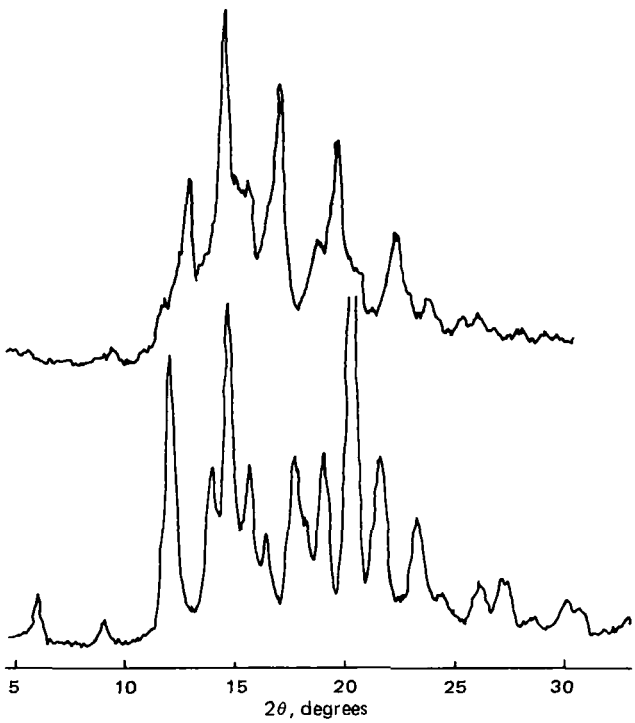

Figure 3—*X-ray diffraction spectra of treated (top) and untreated (bottom) digitoxin.*

[8] Beckman ACTA CIII.
[9] Millipore, 0.45-µm filters.
[10] Horton Laboratories, Oakland, Calif.
[11] Norelco, Philips Electronic.

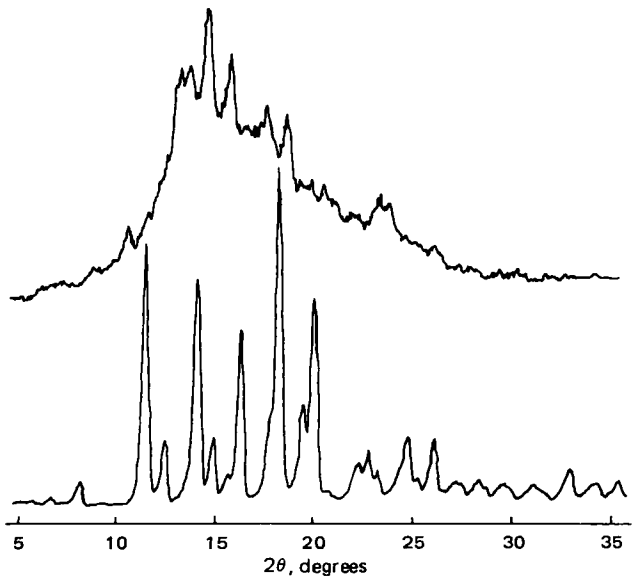

Figure 4—*X-ray diffraction spectra of untreated (top) and treated (bottom) deoxycholic acid.*

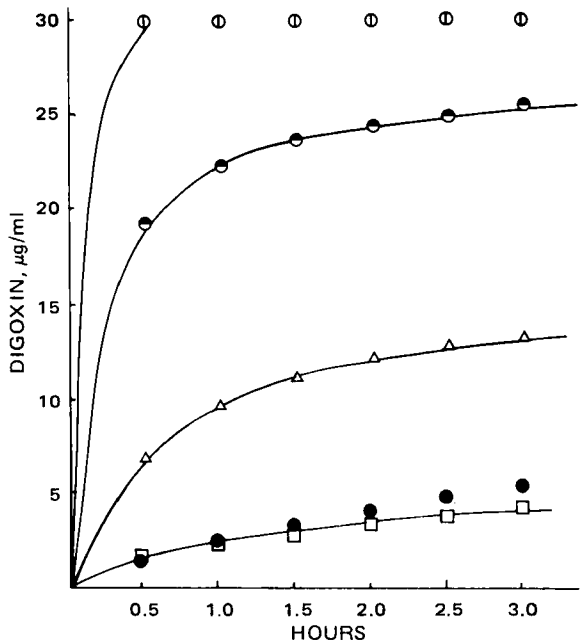

Figure 5—*Dissolution of digoxin from poloxamer 188 test preparations. Key: ●, treated drug; □, untreated drug; △, 10 and 1% physical mixtures; ⊖, 10% coprecipitate; and ⊙, 1% coprecipitate.*

of dissolution compared to the pure drugs (35), the effect of treating (dissolving in alcohol and removing the solvent *in vacuo*) digitoxin on its dissolution was studied. As shown in Fig. 1, treated digitoxin dissolved at a slightly faster rate than did the untreated sample. To determine if digitoxin had undergone any crystalline modifications due to solvent treatment, X-ray diffraction spectra were obtained. Treated digitoxin (Fig. 3) had a diffraction spectrum different from the untreated digitoxin, indicating the possibility of polymorphic modification or solvate formation. The X-ray diffraction pattern ruled out the possibility that solvent treatment changes digitoxin to an amorphous form. The small difference in the dissolution rates of the pure and precipitated digitoxin does not account for the considerably faster dissolution of the drug from the coprecipitates.

Since these facts indicate that the enhanced dissolution of digitoxin from the coprecipitates cannot be fully accounted for as due to surface tension lowering by the carriers, drug–carrier complexation, or solvate formation, other factors must be considered. The enhanced dissolution of the coprecipitated digitoxin could be due to its presence in an amorphous state, as a high energy polymorph, in a microcrystalline state, or as a solid solution. The X-ray diffraction technique has been used to study solid dispersions (36–38). In the present study, the digitoxin coprecipitates as well as the physical mixtures showed the diffraction patterns of the carriers only. Simple dilution with the carriers masked the diffraction peaks of digitoxin. Hence, the X-ray studies neither confirmed nor ruled out any of the mentioned possibilities as the specific cause of enhanced drug dissolution from the coprecipitates. The X-ray diffraction pattern of deoxycholic acid after solvent treatment (Fig. 4) indicated a change in its crystalline nature. There was no change in the X-ray spectrum of poloxamer 188 due to solvent treatment.

Both the poloxamer 188 and deoxycholic acid coprecipitates achieved supersaturation, but there was no indication of drug precipitation and decline toward the equilibrium value, as was the case with a digitoxin–povidone coprecipitate (28). A distinct difference existed in the pattern of dissolution of the poloxamer 188 (Fig. 1) and deoxycholic acid (Fig. 2) coprecipitates. The drug from the former went into solution rapidly during the first 30 min, but there was almost no change in the amount of the drug in solution after this period. In contrast, the deoxycholic acid coprecipitates released digitoxin over a greater time. This difference in the release pattern of the drug could be due to the differences in the solubilities of the two carriers in water. Since poloxamer 188 is highly soluble, it dissolves rapidly and all drug dispersed in it comes in contact with the dissolution medium. Deoxycholic acid, because of its low solubility, does not let all of the dispersed drug come in contact with the dissolution medium immediately. The shapes of the dissolution curves of the deoxycholic acid coprecipitates (Fig. 2) suggest that the initial steeply rising portion may represent the dissolution of the drug present on the surface of the carrier or the dissolution of a high energy or amorphous form of the drug. Once this surface-dispersed or high energy form dissolves, the dissolution is rate limited by the leaching out of the drug in the interior of the carrier or by the erosion of the drug crystals.

Preliminary *in vivo* absorption studies were undertaken to find if the *in vitro* dissolution enhancement of digitoxin from its coprecipitates increases in the GI absorption of the drug. Drug absorption from the test preparations was assessed indirectly by determining their oral toxicity. Oral drug absorption was assessed by determining the number of deaths in mice given the same dose of digitoxin as pure drug, as a 10% drug–carrier physical mixture, and as a 10% coprecipitate (Table I).

The administration of digitoxin as the poloxamer 188 coprecipitate caused a significant ($p < 0.001$) increase in its oral toxicity, but the administration of the physical mixture did not result in any significant change. Administration of up to 2.7 g of poloxamer 188 alone/kg did not result in any toxicity to the mice, in agreement with the reported toxicity of poloxamer 188 (39). The mice that received the poloxamer 188 coprecipitate died at a much earlier time than those receiving the other two preparations. While 62% of the deaths resulting from the coprecipitate occurred between 12 and 36 hr after administration, only 33% of the deaths due to the pure drug occurred in 72 hr.

Table I also summarizes the results of the toxicity studies with

Table I—Oral Toxicity of Various Digitoxin Preparations in Mice[a]

Test System	Number of Animals Dead[b]	Mortality, %
Digitoxin	6	20
Digitoxin–poloxamer 188[c] coprecipitate	29	97
Digitoxin–deoxycholic acid[c] coprecipitate	30	100
Digitoxin–poloxamer 188[c] physical mixture	11	37
Digitoxin–deoxycholic acid[c] physical mixture	9	30
Poloxamer 188[d]	0	0
Deoxycholic acid[e]	0	0

[a] A dose of 70 mg of digitoxin/kg was administered as a suspension in 0.5% methylcellulose. Thirty animals were used for each test system. [b] Animals were observed for 7 days postadministration. [c] A 700-mg/kg dose was administered containing 10% (w/w) digitoxin. [d] A 2.7-g/kg dose was used. [e] A 630-mg/kg dose was used.

Table II—Effect of Poloxamer 188 and Deoxycholic Acid on the Solubility of Digoxin in Water at 37°

Test System	Solubility, mg/100 ml
Water	3.47
Poloxamer 188 in concentration equivalent to 10% coprecipitate	4.77
Poloxamer 188 in concentration equivalent to 1% coprecipitate	5.38
Deoxycholic acid in concentration equivalent to 10% coprecipitate	4.62
Deoxycholic acid in concentration equivalent to 1% coprecipitate	4.25

deoxycholic acid test preparations. Like the poloxamer 188 coprecipitate, the deoxycholic acid coprecipitate caused a significant ($p < 0.001$) increase in oral toxicity. Once again, the mice receiving the coprecipitate died much earlier than those receiving the other two test forms. Of 30 mice that received only deoxycholic acid in amounts present in the coprecipitate, none died. Therefore, the inherent toxicity of deoxycholic acid is not a contributing factor to the enhanced toxicity of the coprecipitated drug.

Although these toxicity studies suffer from the limitation of being a single-dose method, they do indicate a highly significant increase in the rate and, possibly, the extent of oral absorption of digitoxin from the coprecipitates.

Digoxin Coprecipitates—The dissolution characteristics of digoxin from poloxamer 188 test systems are illustrated in Fig. 5. The coprecipitates dissolved significantly faster than the pure drug, and the 1% coprecipitate dissolved faster than the 10% coprecipitate. Precipitating digoxin from ethanol did not significantly alter the dissolution of the drug. The X-ray diffraction patterns of the treated and untreated digoxin were similar. Although the physical mixtures showed a significant enhancement of drug dissolution, there was no difference between the 1 and 10% mixtures.

Equilibrium solubility studies (Table II) showed that poloxamer 188 increased drug solubility, indicating the possibility of micellar complexation. It is evident, however, that although the surface tension-lowering and solubilizing effects of poloxamer 188 do contribute to the enhanced dissolution of the coprecipitated drug, these effects do not fully account for the differences in dissolution of the pure and coprecipitated drug.

The dissolution of digoxin from deoxycholic acid coprecipitates (Fig. 6) proceeded at a faster rate compared to the dissolution of the drug alone. The 1:9 and 1:99 physical mixtures also dissolved faster than the drug. The dissolution of the drug from both physical mixtures proceeded at a rate that was higher than its dissolution from the 10% coprecipitate. Equilibrium solubility studies (Table II) indicated that there was an interaction between digoxin and deoxycholic acid. Deoxycholic acid is known to form inclusion compounds with many drugs (40), including those with a steroidal nucleus (41). It seems possible that the presence of an extra hydroxyl group in the digoxin molecule (compared to digitoxin) is favoring an interaction between the drug and the carrier in the coprecipitate. In the 10% coprecipitate,

Table III—Oral Toxicity of Various Digoxin Preparations in Mice[a]

Test System	Number of Animals Dead[b]	Mortality, %
Digoxin	1	3
Digoxin–poloxamer 188[c] coprecipitate	0	0
Digoxin–deoxycholic acid[c] coprecipitate	30	100
Digoxin–poloxamer 188[c] physical mixture	0	0
Digoxin–deoxycholic acid[c] physical mixture	26	87
Deoxycholic acid[d]	27	90

[a] A dose of 300 mg of digoxin/kg was administered as a suspension in 0.5% methylcellulose. Thirty animals were used for each test system. [b] Animals were observed for 7 days postadministration. [c] A 3-g/kg dose was administered containing 10% (w/w) digoxin. [d] A 2.7-g/kg dose was used.

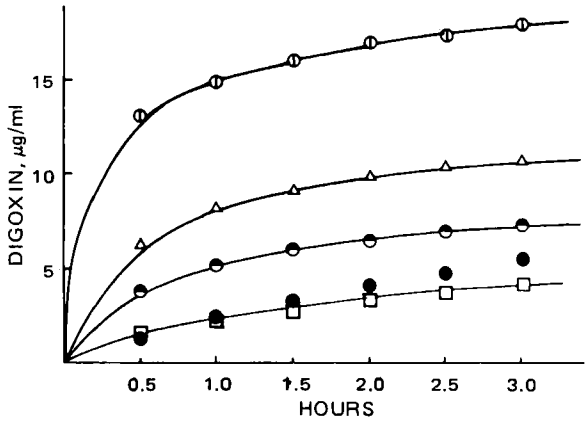

Figure 6—*Dissolution of digoxin from deoxycholic acid test preparations. Key: ●, treated drug; □, untreated drug; △, 10 and 1% physical mixtures; ◓, 10% coprecipitate; and ◔, 1% coprecipitate.*

such an interaction seems to have a negative effect on the increase in the dissolution rate obtained through coprecipitation.

As discussed under digitoxin coprecipitates, dilution of digoxin with the carriers caused loss of diffraction peaks of the drug. Therefore, the X-rays did not aid in elucidating the exact nature of the coprecipitated drug. It is reasonable to assume, however, that coprecipitation changes the nature of digoxin in the same way as mentioned under digitoxin coprecipitates.

The data in Table III indicate that for this particular dose of digoxin (300 mg/kg), the digoxin–poloxamer 188 coprecipitate was no more toxic to mice than was the drug alone. The drug suspension administered to mice contained 6.75% poloxamer 188, which is above its CMC. Surfactants hinder drug absorption due to micellar complexation (42), and poloxamer 188 retarded the absorption of phenolsulfonphthalein from the rat intestine (29). It is, therefore, possible that entrapment of the digoxin in the surfactant micelles was the reason for the lack of enhancement of toxicity of the digoxin–poloxamer 188 coprecipitate. The oral toxicity of the administered dose of digoxin as a 10% digoxin–deoxycholic acid coprecipitate (Table III) did not increase significantly beyond that of deoxycholic acid alone (in the amount present in the coprecipitate). It is probable that the toxicity of the carrier is masking any increase in toxicity of the coprecipitate. More sensitive tests of bioavailability, such as plasma level curves, might differentiate the potencies of the various test systems.

The 1% coprecipitates of both digitoxin and digoxin dissolved faster than the 10% coprecipitates. Because the ratio of drug to carrier was smaller in the 1% systems, precipitation of the drug could have been hindered more than in the 10% systems, resulting in a finer particle size of the drugs. The difference in the dissolution rates also could be due to the presence of the drugs as solid solutions in the 1% coprecipitates.

In summary, coprecipitation of digitoxin and digoxin with two inert carriers, poloxamer 188 and deoxycholic acid, resulted in a dramatic increase in the dissolution rate of the two cardiac glycosides. The increased dissolution of the coprecipitated digitoxin caused an increase in its oral toxicity in mice, but the increased dissolution of the coprecipitated digoxin did not cause such an increase.

REFERENCES

(1) J. Lindenbaum, M. D. Mellow, M. O. Blackstone, and V. P. Butler, Jr., *N. Engl. J. Med.*, **285**, 1344(1971).

(2) T. G. Vitti, D. Banes, and T. E. Byers, *ibid.*, **285**, 1433(1971).

(3) V. Manninen, J. Melin, and G. Hartel, *Lancet*, **2**, 434 (1971).

(4) T. R. D. Shaw, M. R. Howard, and J. Hammer, *ibid.*, **2**, 303(1972).

(5) P. F. Binnion and M. McDermott, *ibid.*, **2**, 592(1972).

(6) J. G. Wagner, M. Christensen, E. Sakmar, D. Blair, J. D. Yates, P. K. Willis, III, A. J. Sedman, and R. G. Stoll, *J. Am. Med. Assoc.*, **224**, 199(1973).

(7) J. Lindenbaum, M. P. Butler, Jr., J. E. Murphy, and R. M.

Creswell, *Lancet*, **1**, 1215(1973).
(8) D. H. Huffmann and D. L. Azarnoff, *J. Am. Med. Assoc.*, **222**, 957(1972).
(9) F.D.C. Reports, "The Pink Sheet," **36** (28)(1974).
(10) A. T. Florence, E. G. Salole, and J. B. Stenlake, *J. Pharm. Pharmacol.*, **26**, 480(1974).
(11) A. J. Jounela and A. Sothman, *Lancet*, **1**, 202(1973).
(12) T. D. R. Shaw, J. E. Carless, M. R. Howard, and K. Raymond, *ibid.*, **2**, 209(1973).
(13) B. F. Johnson, H. Greer, T. McCrerie, C. Bye, and A. Fowle, *ibid.*, **1**, 1473(1973).
(14) M. Gibaldi, "Introduction to Biopharmaceutics," Lea & Febiger, Philadelphia, Pa., 1971, p. 21.
(15) K. Sekiguchi and N. Obi, *Chem. Pharm. Bull.*, **9**, 866 (1961).
(16) T. Tachibana and A. Nakamura, *Kolloid-Z. Polym.*, **203**, 130(1965).
(17) A. H. Goldberg, M. Gibaldi, and J. L. Kanig, *J. Pharm. Sci.*, **54**, 1145(1965).
(18) *Ibid.*, **55**, 482(1966).
(19) *Ibid.*, **55**, 487(1966).
(20) A. H. Goldberg, M. Gibaldi, J. L. Kanig, and M. Mayersohn, *J. Pharm. Sci.*, **55**, 581(1966).
(21) M. Mayersohn and M. Gibaldi, *ibid.*, **55**, 1323(1966).
(22) W. L. Chiou and S. Riegelman, *ibid.*, **58**, 1505(1969).
(23) M. Gibaldi, S. Feldman, and T. R. Bates, *ibid.*, **57**, 708(1968).
(24) *Ibid.*, **60**, 1569(1971).
(25) E. I. Stupak and T. R. Bates, *J. Pharm. Sci.*, **61**, 400(1972).
(26) M. H. Malone, H. I. Hochman, and K. A. Nieforth, *ibid.*, **55**, 972(1966).
(27) R. B. Stoll, T. R. Bates, and J. Swarbrick, *ibid.*, **62**, 65(1973).
(28) E. I. Stupak and T. R. Bates, *ibid.*, **62**, 1806(1973).
(29) S. N. Malik, D. H. Canham, and M. W. Gouda, *ibid.*, **64**, 987(1975).
(30) G. Levy and B. A. Hayes, *N. Engl. J. Med.*, **262**, 1053 (1960).
(31) D. E. Wurster and P. W. Taylor, *J. Pharm. Sci.*, **54**, 670(1965).
(32) P. Mesnard and G. Devaux, *C. R.*, **253**, 497(1961).
(33) W. Saski and S. G. Shah, *J. Pharm. Sci.*, **54**, 71(1965).
(34) "The Merck Index," 8th ed., Merck and Co., Rahway, N.J., 1968, p. 364.
(35) E. Shefter and W. I. Higuchi, *J. Pharm. Sci.*, **52**, 781(1963).
(36) W. L. Chiou and S. Niazi, *ibid.*, **60**, 1333(1971).
(37) *Ibid.*, **62**, 498(1973).
(38) W. L. Chiou, *J. Pharm. Sci.*, **60**, 1406(1971).
(39) "Pluronic® Polyols Toxicity and Irritation Data," 3rd ed., BASF Wyandotte Corp., Wyandotte, Mich.
(40) S. G. Frank, *J. Pharm. Sci.*, **64**, 1585(1975).
(41) J. L. Lach and W. A. Pauli, *ibid.*, **55**, 32(1966).
(42) A. T. Florence, *J. Pharm. Pharmacol.*, **22**, 265(1970).

ACKNOWLEDGMENTS AND ADDRESSES

Received August 25, 1975, from the *School of Pharmacy, University of Montana, Missoula, MT 59801*

Accepted for publication February 12, 1976.

Supported by the National Science Foundation under SFC Program Grants GF 38851 and GF 39207 and by the Montana Heart Association.

* Present address: Faculty of Pharmacy, University of Alexandria, Alexandria, Egypt.

[x] To whom inquiries should be directed.

Electrochemical Evidence for Interaction between Chlorpromazine Hydrochloride and Trifluoperazine Hydrochloride and the Flavin Coenzymes

LENA A. DeLISSER-MATTHEWS [x] and ALI KHALAJ

Abstract □ Polarographic and chronopotentiometric methods were applied to study the effects of the phenothiazine tranquilizers chlorpromazine hydrochloride and trifluoperazine hydrochloride on the electrochemical behavior of the flavin coenzymes flavin mononucleotide and flavin adenine dinucleotide. The effects of the drugs were measured mainly by decreases in the diffusion currents, i_d, developed in the polarographic experiments and by a similar decrease in the chronopotentiometric constant, $i_0\tau^{1/2}$, in the chronopotentiometric experiments when the coenzymes were reduced in the presence of the added drugs. The observed interference with the redox properties of the coenzymes could conceivably be related to the reported ability of the drugs to inhibit respiration and produce their tranquilizing effect.

Keyphrases □ Chlorpromazine hydrochloride—effect on electrochemical behavior of flavin coenzymes, polarographic and chronopotentiometric investigation □ Trifluoperazine hydrochloride—effect on electrochemical behavior of flavin coenzymes, polarographic and chronopotentiometric investigation □ Flavin coenzymes—electrochemical behavior, effect of chlorpromazine and trifluoperazine hydrochlorides □ Electrochemical behavior—flavin coenzymes, effect of chlorpromazine and trifluoperazine hydrochlorides □ Polarography—investigation of effect of chlorpromazine and trifluoperazine hydrochlorides on electrochemical behavior of flavin coenzymes □ Chronopotentiometry—investigation of effect of chlorpromazine and trifluoperazine hydrochlorides on electrochemical behavior of flavin coenzymes □ Tranquilizers—chlorpromazine and trifluoperazine hydrochlorides, effect on electrochemical behavior of flavin coenzymes □ Coenzymes, flavin—electrochemical behavior, effect of chlorpromazine and trifluoperazine hydrochlorides

One mechanism proposed to account for the tranquilizing action of the phenothiazine drugs involves the possible interaction between the drugs and certain electron-transferring coenzymes of the respiratory chain. The inhibitory effects of chlorpromazine on respiration were suggested to result from complex formation between chlorpromazine and flavin adenine dinucleotide (1). The studies involved observation of changes in the fluorescent and spectrophotometric properties of the coenzymes upon the addition of the drug.

Similar inhibitory effects were reported in studies of the effects of chlorpromazine upon the mitochondrial systems of both the brain and heart of rats (2, 3). It was

Creswell, *Lancet*, **1**, 1215(1973).
(8) D. H. Huffmann and D. L. Azarnoff, *J. Am. Med. Assoc.*, **222**, 957(1972).
(9) F.D.C. Reports, "The Pink Sheet," **36** (28)(1974).
(10) A. T. Florence, E. G. Salole, and J. B. Stenlake, *J. Pharm. Pharmacol.*, **26**, 480(1974).
(11) A. J. Jounela and A. Sothman, *Lancet*, **1**, 202(1973).
(12) T. D. R. Shaw, J. E. Carless, M. R. Howard, and K. Raymond, *ibid.*, **2**, 209(1973).
(13) B. F. Johnson, H. Greer, T. McCrerie, C. Bye, and A. Fowle, *ibid.*, **1**, 1473(1973).
(14) M. Gibaldi, "Introduction to Biopharmaceutics," Lea & Febiger, Philadelphia, Pa., 1971, p. 21.
(15) K. Sekiguchi and N. Obi, *Chem. Pharm. Bull.*, **9**, 866 (1961).
(16) T. Tachibana and A. Nakamura, *Kolloid-Z. Polym.*, **203**, 130(1965).
(17) A. H. Goldberg, M. Gibaldi, and J. L. Kanig, *J. Pharm. Sci.*, **54**, 1145(1965).
(18) *Ibid.*, **55**, 482(1966).
(19) *Ibid.*, **55**, 487(1966).
(20) A. H. Goldberg, M. Gibaldi, J. L. Kanig, and M. Mayersohn, *J. Pharm. Sci.*, **55**, 581(1966).
(21) M. Mayersohn and M. Gibaldi, *ibid.*, **55**, 1323(1966).
(22) W. L. Chiou and S. Riegelman, *ibid.*, **58**, 1505(1969).
(23) M. Gibaldi, S. Feldman, and T. R. Bates, *ibid.*, **57**, 708(1968).
(24) *Ibid.*, **60**, 1569(1971).
(25) E. I. Stupak and T. R. Bates, *J. Pharm. Sci.*, **61**, 400(1972).
(26) M. H. Malone, H. I. Hochman, and K. A. Nieforth, *ibid.*, **55**, 972(1966).
(27) R. B. Stoll, T. R. Bates, and J. Swarbrick, *ibid.*, **62**, 65(1973).
(28) E. I. Stupak and T. R. Bates, *ibid.*, **62**, 1806(1973).
(29) S. N. Malik, D. H. Canham, and M. W. Gouda, *ibid.*, **64**, 987(1975).
(30) G. Levy and B. A. Hayes, *N. Engl. J. Med.*, **262**, 1053 (1960).
(31) D. E. Wurster and P. W. Taylor, *J. Pharm. Sci.*, **54**, 670(1965).
(32) P. Mesnard and G. Devaux, *C. R.*, **253**, 497(1961).
(33) W. Saski and S. G. Shah, *J. Pharm. Sci.*, **54**, 71(1965).
(34) "The Merck Index," 8th ed., Merck and Co., Rahway, N.J., 1968, p. 364.
(35) E. Shefter and W. I. Higuchi, *J. Pharm. Sci.*, **52**, 781(1963).
(36) W. L. Chiou and S. Niazi, *ibid.*, **60**, 1333(1971).
(37) *Ibid.*, **62**, 498(1973).
(38) W. L. Chiou, *J. Pharm. Sci.*, **60**, 1406(1971).
(39) "Pluronic® Polyols Toxicity and Irritation Data," 3rd ed., BASF Wyandotte Corp., Wyandotte, Mich.
(40) S. G. Frank, *J. Pharm. Sci.*, **64**, 1585(1975).
(41) J. L. Lach and W. A. Pauli, *ibid.*, **55**, 32(1966).
(42) A. T. Florence, *J. Pharm. Pharmacol.*, **22**, 265(1970).

ACKNOWLEDGMENTS AND ADDRESSES

Received August 25, 1975, from the *School of Pharmacy, University of Montana, Missoula, MT 59801*

Accepted for publication February 12, 1976.

Supported by the National Science Foundation under SFC Program Grants GF 38851 and GF 39207 and by the Montana Heart Association.

* Present address: Faculty of Pharmacy, University of Alexandria, Alexandria, Egypt.

[x] To whom inquiries should be directed.

Electrochemical Evidence for Interaction between Chlorpromazine Hydrochloride and Trifluoperazine Hydrochloride and the Flavin Coenzymes

LENA A. DeLISSER-MATTHEWS [x] and ALI KHALAJ

Abstract □ Polarographic and chronopotentiometric methods were applied to study the effects of the phenothiazine tranquilizers chlorpromazine hydrochloride and trifluoperazine hydrochloride on the electrochemical behavior of the flavin coenzymes flavin mononucleotide and flavin adenine dinucleotide. The effects of the drugs were measured mainly by decreases in the diffusion currents, i_d, developed in the polarographic experiments and by a similar decrease in the chronopotentiometric constant, $i_0\tau^{1/2}$, in the chronopotentiometric experiments when the coenzymes were reduced in the presence of the added drugs. The observed interference with the redox properties of the coenzymes could conceivably be related to the reported ability of the drugs to inhibit respiration and produce their tranquilizing effect.

Keyphrases □ Chlorpromazine hydrochloride—effect on electrochemical behavior of flavin coenzymes, polarographic and chronopotentiometric investigation □ Trifluoperazine hydrochloride—effect on electrochemical behavior of flavin coenzymes, polarographic and chronopotentiometric investigation □ Flavin coenzymes—electrochemical behavior, effect of chlorpromazine and trifluoperazine hydrochlorides □ Electrochemical behavior—flavin coenzymes, effect of chlorpromazine and trifluoperazine hydrochlorides □ Polarography—investigation of effect of chlorpromazine and trifluoperazine hydrochlorides on electrochemical behavior of flavin coenzymes □ Chronopotentiometry—investigation of effect of chlorpromazine and trifluoperazine hydrochlorides on electrochemical behavior of flavin coenzymes □ Tranquilizers—chlorpromazine and trifluoperazine hydrochlorides, effect on electrochemical behavior of flavin coenzymes □ Coenzymes, flavin—electrochemical behavior, effect of chlorpromazine and trifluoperazine hydrochlorides

One mechanism proposed to account for the tranquilizing action of the phenothiazine drugs involves the possible interaction between the drugs and certain electron-transferring coenzymes of the respiratory chain. The inhibitory effects of chlorpromazine on respiration were suggested to result from complex formation between chlorpromazine and flavin adenine dinucleotide (1). The studies involved observation of changes in the fluorescent and spectrophotometric properties of the coenzymes upon the addition of the drug.

Similar inhibitory effects were reported in studies of the effects of chlorpromazine upon the mitochondrial systems of both the brain and heart of rats (2, 3). It was

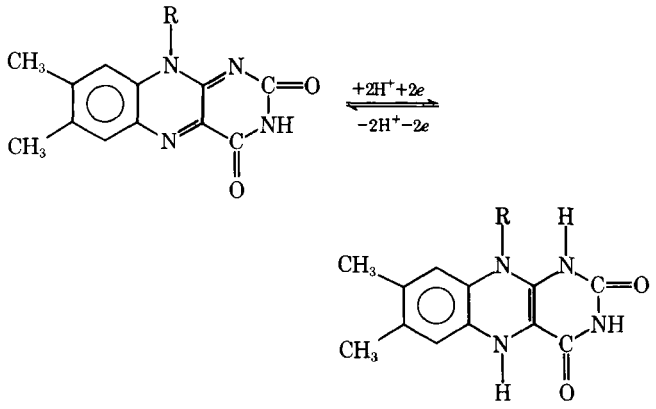

Scheme I

proposed that the drug inhibited electron transport between reduced nicotinamide adenine dinucleotide (NADH) and cytochrome c and must, therefore, exert its effect between NADH and the flavo-proteins, including riboflavin phosphate (flavin mononucleotide) (I) and flavin adenine dinucleotide (II).

In other studies, the electron-donor properties of chlorpromazine were investigated, and the drug was found to be an "extraordinary electron donor" (4). Therefore, the assumption was made that charge-complex formation between the coenzyme, I, and the drug could form the basis for the pharmacological action. When a solution of riboflavin, the parent moiety of the flavins, was frozen in the presence of chlorpromazine, the solution turned greenish brown and lost all fluorescence, an indication of complex formation. In subsequent studies, the phenothiazines did not possess the exceptional electron-donating ability formerly attributed to them. It was proposed that the tranquilizing action of the drugs might be due to the "ability of the S atom to form complexes with the localized electrons" (5).

The isoalloxazine moiety of the flavin coenzymes constitutes a reversible redox system (Scheme I). The redox activity of I and II has been extensively studied by several techniques, and their electrochemical behavior has been well established (6–8). The effect of pH on the reduction potentials and the tendency of the compounds to be adsorbed on electrode surfaces have also been well documented (9). Complex formation between I and iron(III) was studied by polarography and chronopotentiometry (10).

Any correlation between the processes involved in intact biological redox systems and those occurring in electrolytic cells must, of necessity, be made with due caution. Nevertheless, it is reasonable to believe that useful information might be gained from the electrochemical behavior of some of these compounds of biological significance. As pointed out previously (11), several points of similarity between the two processes seem to permit an evaluation of the biological processes on the basis of the electrochemical reactions.

The purpose of this study was to utilize electrochemistry to determine whether any interaction between the phenothiazine drugs and the flavin coenzymes would be reflected in changes in the electrochemical behavior of the latter. Such a study would help elucidate the mechanism by which the drugs produce their pronounced tranquilizing effect. Since electron-transfer processes are involved, electrochemical methods could be a direct approach. Furthermore, since the phenothiazines undergo electrochemical oxidation in solutions ranging from pH 1.5 to 9.5 (12, 13), interference due to their electroactivity was not anticipated during electrolytic reductions.

EXPERIMENTAL

Apparatus and Equipment—*Polarographic experiments* were performed with a polarograph[1] and a suitable recorder. The polarographic H-cell had a conventional dropping mercury electrode as the working electrode and a mercury–mercurous chloride reference electrode. The dropping mercury electrode had an open circuit drop time of about 3.65 sec in 0.1 *M* potassium chloride at a column height of 60 cm and a mercury flow rate of 1.25 mg/sec.

Chronopotentiometric measurements were made with an instrument[2] equipped with a high speed recorder, with chart speeds ranging from 100 to 1 sec/2.54 cm (1 in.). The controlled current was checked by measuring with a potentiometer[3] the voltage drop across a precision resistor in series with the electrolysis cell.

The electrolysis cell consisted of a glass cylinder fitted with a stopcock at the bottom to permit easy drainage. An outer glass jacket connected to a constant-temperature bath provided for the circulation of water to maintain the temperature at 25°. The cover[4] had openings for introducing the electrodes and provided an inlet for the nitrogen used to deaerate the solutions.

A conventional three-electrode assembly was used for the chronopotentiometric measurements. A mercury pool electrode, consisting of about 1 ml of mercury contained in a cup[4] and calculated to have an area of 2.75 cm^2, was the working electrode. A saturated calomel electrode and a platinum electrode (supplied with the chronopotentiometer) were used as the reference and counter electrodes, respectively. The counter electrode was placed in a separate compartment and connected to the main cell by a sintered-glass disk. The solutions to be analyzed were placed in both compartments.

Chemicals and Reagents—All chemicals used as supporting electrolytes and for the preparation of buffer solutions were of reagent grade. The mercury used in preparing the pool electrode and the dropping mercury electrode was triple distilled and of high purity. Prepurified nitrogen was used for degassing the solutions.

Compounds I and II[5] were reportedly of high purity and were used without further purification. Chlorpromazine hydrochloride and trifluoperazine hydrochloride[6] were also of high purity.

Procedure—Solutions to be analyzed were prepared with double-distilled water. In all experiments, solutions of I and II were made 10^{-4} *M* in phosphate or phosphate–citrate buffers to which the appropriate supporting electrolytes were added. In experiments involving the phenothiazines, the analytical amounts of chlorpromazine hydrochloride and trifluoperazine hydrochloride were added to the coenzyme solutions. These solutions were prepared in pH 6.5 phosphate buffer, since the drugs exhibited maximum solubility at this pH and this value was close to the physiological pH range.

Solutions of potassium chloride, potassium nitrate, ammonium chloride, tetrabutylammonium chloride, tetraethylammonium chloride, and tetrabutylammonium bromide were used as supporting electrolytes in the different experiments. To maintain the alkylammonium salt concentrations at 0.1 *M* throughout a series of experiments, potassium chloride was added to adjust the ionic strength where necessary.

All solutions were freshly prepared daily, deoxygenated with prepurified nitrogen, and prewashed by passage through a gas washing bottle containing distilled water. Due to the reported tendency of the phenothiazines to form complexes with elemental oxygen, the degassing periods were extended to between 20 and 30 min for each run for both the polarographic and chronopotentiometric experiments.

[1] Sargent model XV.
[2] Electroscan 30 electroanalytical system, Beckman Instruments, Inc.
[3] Leeds & Northrup 7553-5 type K-3 Universal potentiometer.
[4] Lined with Teflon (du Pont).
[5] Nutritional Biochemicals Corp., Cleveland, Ohio.
[6] Courtesy of SmithKline Corp., Philadelphia, Pa.

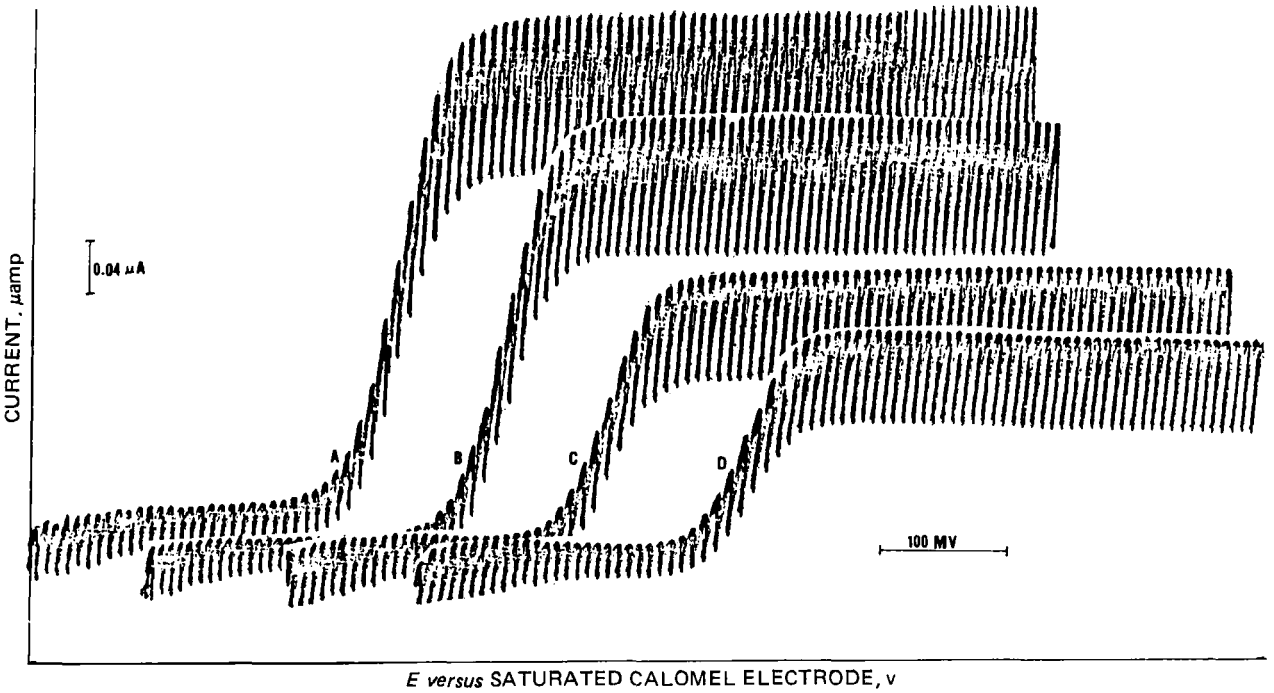

Figure 1—*Effect of chlorpromazine hydrochloride on polarography of 10^{-4} M II. Key: A, no chlorpromazine; B, with 10^{-2} M chlorpromazine; C, with 10^{-1} M chlorpromazine; and D, with 2×10^{-1} M chlorpromazine. All waves start at −0.15 v.*

As an added precaution, the coenzyme solutions were degassed prior to drug addition and then the additional degassing process was continued. Furthermore, because of the possibility of adsorption of the coenzymes onto the mercury electrode, the solutions were constantly agitated between runs and sufficient time was allowed for the mercury pool potential to return to its initial value after each run. To avoid photolytic decomposition of the coenzymes, all preparations and experiments were carried out with minimum light.

RESULTS AND DISCUSSION

Polarographic Behavior of Coenzymes—Polarographic reduction of I and II at the dropping mercury electrode gave results similar to those reported previously (6–13). Both compounds showed single well-defined polarographic waves in solutions buffered to pH 6–8 with all supporting electrolytes at 25°. The half-wave potentials, $E_{1/2}$, for both compounds at pH 6.5 were observed between −0.42 and −0.45 v *versus* the saturated calomel electrode. The pH dependence of the reductions was evidenced by an increase in the $E_{1/2}$ values as the pH increased from 6.0 to 8.0, ranging from about −0.42 to −0.50 v for I and from −0.40 to −0.52 v for II. At pH 2.2, the polarograms exhibited two reduction waves, thus supporting the evidence for an adsorption-controlled prewave and a diffusion-controlled main wave in acidic solutions. The prewave appeared between −0.05 and −0.10 v, while the primary wave was observed between −0.15 and −0.20 v for both compounds.

The diffusion currents for the I systems were significantly higher than those for the II systems of the same composition. When the tetraalkylammonium salts were used as supporting electrolytes, the diffusion currents for both compounds were somewhat lower than those observed with the other electrolytes such as potassium chloride, potassium nitrate, and ammonium chloride.

Chronopotentiometric Behavior of Coenzymes—Chronopotentiograms obtained upon reduction of the coenzymes at the mercury electrode showed single well-defined waves in solutions buffered to pH 6–8 at 25°. The apparent conformity of the systems to the diffusion control model was reflected in the constancy of the $i_0\tau^{1/2}$ values at the applied current densities, with transition times ranging from above 20 to below 0.5 sec. Good reproducibility was obtained when the solutions were degassed for 20–30 min and sufficient time was allowed for the system to return to its equilibrium potential after each run. As with the polarographic experiments, the observed $i_0\tau^{1/2}$ values decreased with the tetraalkylammonium salts as compared with those obtained with potassium chloride and other ionic electrolytes.

The pH dependence of the reductions also was apparent from the chronopotentiometric results. The $Er/4$ values (corresponding roughly to the $E_{1/2}$ values) for I ranged from about −0.40 to −0.48 v *versus* the saturated calomel electrode for solutions buffered between pH 6.0 and 8.0. The values for similar II systems ranged from −0.39 to −0.47 v. At pH 2.2, the potential for both reductions was about −0.19 v.

Reversible chronopotentiometric waves were observed for both compounds. At pH 6.5, the ratio of the forward cathodic to the reverse anodic transition time, τ_f/τ_r, was about 3, in accordance with the value expected for a completely reversible system. This relationship between the forward and reverse transition times supported the absence of any kinetic complications resulting from coenzyme adsorption onto the electrode surface. By careful control of experimental conditions, it was possible to get good reproducibility and no interference due to adsorption.

Effect of Chlorpromazine Hydrochloride and Trifluoperazine Hydrochloride on Polarography of I and II—The pronounced

Table I—Polarographic Data Showing Effects of Drugs on I Reduction

System[a]	i_d, μamp	$E_{1/2}$, v
10^{-4} *M* I	0.422	0.44
10^{-4} *M* I plus 10^{-3} *M* chlorpromazine[b]	0.412	0.44
10^{-4} *M* I plus 5×10^{-3} *M* chlorpromazine	0.400	0.44
10^{-4} *M* I plus 10^{-2} *M* chlorpromazine	0.345	0.44
10^{-4} *M* I plus 5×10^{-2} *M* chlorpromazine	0.241	0.42
10^{-4} *M* I plus 10^{-1} *M* chlorpromazine	0.205	0.40
10^{-4} *M* I plus 10^{-3} *M* trifluoperazine[c]	0.412	0.44
10^{-4} *M* I plus 5×10^{-3} *M* trifluoperazine	0.375	0.42
10^{-4} *M* I plus 10^{-2} *M* trifluoperazine	0.341	0.41
10^{-4} *M* I plus 5×10^{-2} *M* trifluoperazine	0.235	0.25
10^{-4} *M* I plus 10^{-1} *M* trifluoperazine	0.203	0.23

[a] Tetraethylammonium chloride was the supporting electrolyte. [b] Hydrochloride salt. [c] Dihydrochloride salt.

Table II—Polarographic Data Showing Effects of Drugs on II Reduction

System[a]	i_d, μamp	$E_{1/2}$, v
10^{-4} *M* II	0.304	0.43
10^{-4} *M* II plus 10^{-3} *M* chlorpromazine	0.310	0.43
10^{-4} *M* II plus 5×10^{-3} *M* chlorpromazine	0.299	0.43
10^{-4} *M* II plus 10^{-2} *M* chlorpromazine	0.268	0.43
10^{-4} *M* II plus 5×10^{-2} *M* chlorpromazine	0.196	0.41
10^{-4} *M* II plus 10^{-1} *M* chlorpromazine	0.165	0.40
10^{-4} *M* II plus 10^{-3} *M* trifluoperazine	0.296	0.44
10^{-4} *M* II plus 5×10^{-3} *M* trifluoperazine	0.294	0.43
10^{-4} *M* II plus 10^{-2} *M* trifluoperazine	0.271	0.42
10^{-4} *M* II plus 5×10^{-2} *M* trifluoperazine	0.188	0.25
10^{-4} *M* II plus 10^{-1} *M* trifluoperazine	0.156	0.22

[a] Tetraethylammonium chloride was the supporting electrolyte.

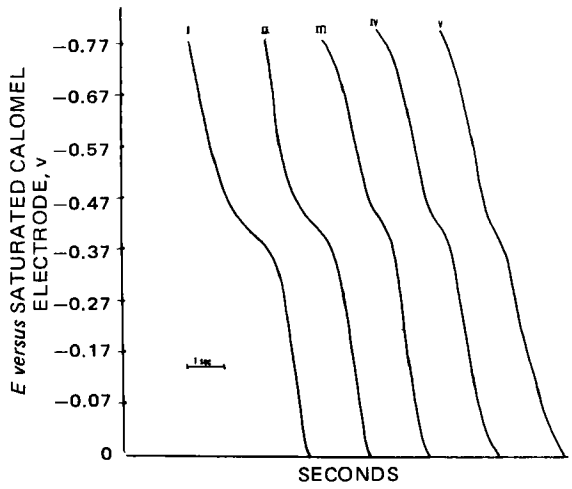

Figure 2—*Effect of chlorpromazine hydrochloride on chronopotentiometry of 10^{-4} M II. Key: I, with 10^{-4} M chlorpromazine; II, with 10^{-3} M chlorpromazine; III, with 10^{-2} M chlorpromazine; IV, with 5×10^{-2} M chlorpromazine; and V, with 10^{-1} M chlorpromazine.*

surface activity of the phenothiazines made it impossible to carry out the experiments using ordinary ionic electrolytes. Excessive foaming during the degassing period resulted in loss of solution from the electrolysis cell. For this reason, the tetraalkylammonium salts were used; they were reported (14) to cause marked reduction in the surface activity of the phenothiazines. Several of these cationic agents were used as supporting electrolytes, and the tetraethyl- and the tetrabutylammonium chloride salts were equally effective in reducing surface activity. Figure 1 shows that with various amounts of chlorpromazine hydrochloride added, well-defined polarograms with no apparent distortions due to adsorption were obtained, and it was possible to get adequate reproducibility.

The results shown in Tables I and II indicate that, even at high concentrations of drug, chlorpromazine hydrochloride had little or no effect on the reduction potential for either I or II. On the other hand, with concentrations of trifluoperazine hydrochloride in excess of 10^{-2} *M*, a reduction in the $E_{1/2}$ for both coenzymes was observed. This result was probably due to the high acidity of the drug, resulting in a decrease in the pH of the system from approximately pH 6.5 to 3.0. The effect of pH on the reduction potential of the coenzymes has already been established. However, even at this lower pH, there was no evidence of the adsorption prewave observed earlier when the coenzymes were run in more acidic solutions.

That the diffusion currents for both coenzymes showed a progressive decrease as the concentration of the added drugs increased is clearly indicated in Tables I and II and Fig. 1. With the addition of either drug at 0.10 *M*, the diffusion currents decreased to approximately one-half of the original values obtained in the absence of the drugs. Since the direct proportionality between concentration and i_d had clearly been established in preceding experiments, these results could only be interpreted to mean that the amount of the coenzymes available for electroreduction at the dropping mercury electrode was greatly reduced in the presence of large amounts of the drugs.

Effect of Chlorpromazine Hydrochloride and Trifluoperazine Hydrochloride on Chronopotentiometry of I and II—It was more difficult to obtain reproducible results in the chronopotentiometric experiments than in the polarographic studies. Some distortion of the chronopotentiometric waves was observed unless the systems were degassed for prolonged periods and sufficient time was allowed for equilibration. The tetrabutylammonium salts were most effective in controlling the surface activity of the drugs and in obtaining reproducible results. The chronopotentiometric data of Table III and the potential–time curves of Figs. 2 and 3 clearly show the effect of the added drugs.

From the data, it was once again apparent that chlorpromazine exerted little or no influence on the reduction potential for II even at high drug concentrations. There was, however, clear evidence of a progressive decrease in the calculated $i_0\tau^{1/2}$ values in the presence of increased amounts of the drug (Fig. 2). At the same applied current density, the transition time for the reduction of II showed a decrease as the concentration of added chlorpromazine increased. This finding indicates once again that the amount of II available for reduction at the electrode surface becomes progressively less as the added amount of the drug increases. Although the apparent decrease in the concentration of II observed in the chronopotentiometric experiments was not as pronounced as observed with the polarographic determinations, there was indeed some effect.

Close scrutiny of the chronopotentiograms of Fig. 2 also reveals slight evidence of what would appear to be a prewave at very high concentrations of chlorpromazine. This prewave could possibly be considered as evidence of some drug adsorption onto the mercury

Table III—Chronopotentiometric Data Showing Effects of Chlorpromazine on II Reduction

System Composition[a]	τ Range, sec	Average $i_0\tau^{1/2}$, amp $sec^{1/2}$ $cm^{-2} \times 10^4$[b]	$Er/4$, v
10^{-4} *M* II	13.98–0.63	0.530 ± 0.018	0.42
10^{-4} *M* II plus 10^{-4} *M* chlorpromazine	12.60–0.35	0.505 ± 0.038	0.41
10^{-4} *M* II plus 10^{-3} *M* chlorpromazine	10.24–0.35	0.512 ± 0.029	0.43
10^{-4} *M* II plus 10^{-2} *M* chlorpromazine	7.09–0.26	0.403 ± 0.037	0.42
10^{-4} *M* II plus 10^{-1} *M* chlorpromazine	11.42–0.25	0.303 ± 0.009	0.40
System Composition[c]			
10^{-4} *M* II	16.53–0.79	0.449 ± 0.023	0.44
10^{-4} *M* II plus 10^{-3} *M* chlorpromazine	12.60–0.39	0.434 ± 0.021	0.40
10^{-4} *M* II plus 10^{-2} *M* chlorpromazine	14.17–0.35	0.382 ± 0.029	0.41
10^{-4} *M* II plus 10^{-1} *M* chlorpromazine	10.24–0.98	0.293 ± 0.010	0.41

[a] Tetrabutylammonium chloride was the supporting electrolyte. [b] Uncertainties are based on 95% confidence intervals. [c] Tetrabutylammonium bromide was the supporting electrolyte.

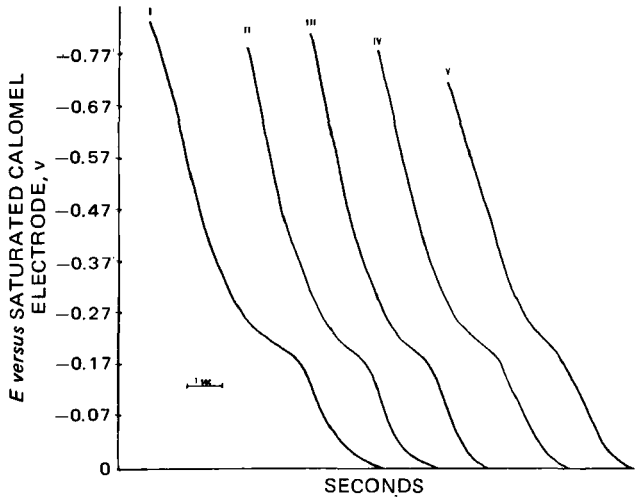

Figure 3—*Effect of 10^{-1} M trifluoperazine hydrochloride on chronopotentiometry of II. Current density was increased from I to V.*

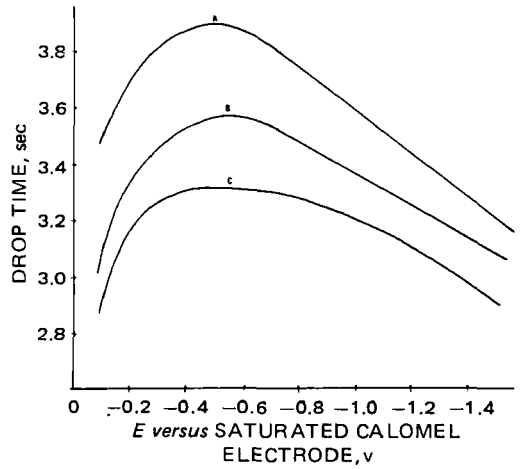

Figure 5—*Effect of trifluoperazine hydrochloride on the electrocapillary curve for II in 0.1 M tetrabutylammonium bromide and pH 6.5 phosphate buffer. Key: A, 10^{-4} M II; B, with 10^{-2} M trifluoperazine; and C, with 10^{-1} M trifluoperazine.*

electrode surface, thus causing interference with the normal single-wave reduction for II at this pH. However, if adsorption is primarily responsible for the observed decreases both in the transition times in chronopotentiometry and the diffusion currents in polarography, then the evidence for such adsorption should be significantly more pronounced.

Investigation of possible adsorption of the phenothiazines onto the mercury electrode was carried out by preparing electrocapillary curves for the systems in the presence of the drugs at several different concentrations. For clarity, only a few of the electrocapillary curves are shown in Figs. 4 and 5. The curves of Fig. 4 show that neither II nor II with added chlorpromazine appreciably altered the electrocapillary curve, A, for 0.1 *M* tetraethylammonium chloride in pH 6.5 phosphate buffer. There was no obvious shift in the electrocapillary maximum; and although there was slight lowering of the surface tension of the mercury drop with increasing amounts of added chlorpromazine, as reflected in the decrease in drop time, the decrease was so small that the amount of adsorption indicated could not conceivably account for the changes observed in the polarographic and chronopotentiometric experiments. Moreover, the curve for II alone gives no indication of the reportedly strong adsorption of the coenzymes observed in highly acidic solutions.

That adsorption becomes an important factor when trifluoperazine is added to the coenzymes is evident from the electrocapillary curves of Fig. 5. Not only was there an observed decrease in the surface tension of the mercury drop, but the electrocapillary maximum disappeared and the curve flattened out over a span of potentials at 10^{-1} *M* trifluoperazine. This surface activity was observed in earlier chronopotentiometric experiments, and it was considered advisable to increase the tetrabutylammonium salt concentration used as the supporting electrolyte to 0.15 *M* to minimize this effect. Even with this increase, however, it was difficult to obtain reproducible results in the presence of high drug concentrations.

Figure 3 shows some chronopotentiograms obtained for II upon the addition of 10^{-1} *M* trifluoperazine. As with the polarographic experiments, the reduction potential for II was lowered considerably when large amounts of the drug were added. Lowering of the pH was again believed to be the cause of this decrease in the $Er/4$ value.

The shape of the chronopotentiograms (Fig. 3) made it virtually impossible to make any meaningful transition time measurements at this high drug concentration. Even at concentrations of trifluoperazine below 10^{-2} *M*, the curves showed some distortions. Had there been a clear indication of more than one chronopotentiometric wave, then perhaps measurements could have been made and some interpretations proposed. The curves were, however, similar to those observed at the higher concentrations, only somewhat less distorted.

Due to the similarity in the electrochemical behavior of I and II as observed in the polarographic experiments, even with the added drugs, it was considered unnecessary to repeat all of the chronopotentiometric experiments on the I systems. It seemed advantageous, however, to verify some results at the highest concentrations of both chlorpromazine and trifluoperazine. Upon the addition of 0.10 *M* chlorpromazine, the $i_0\tau^{1/2}$ value for 10^{-4} *M* I in tetrabutylammonium chloride decreased from 0.564×10^{-4} to 0.294×10^{-4} amp $sec^{1/2}$ cm^{-2}. In the presence of trifluoperazine, a decrease in the reduction potential for I was observed, as were the distortions of the chronopotentiometric waves obtained with II.

Current reversal chronopotentiometry carried out on solutions of the coenzymes containing the drugs resulted in well-defined reversible waves similar to those previously obtained for the coenzymes alone. However, the ratio of the forward to the reverse transition times was in all cases greater than that obtained with the former systems. Instead of being of the order of 3, as was found for the coenzymes alone, the ratio increased to values between 5 and 6, indicating that all reduced material was not being reoxidized at the electrode surface.

Since the defined purpose of this study was to determine whether electrochemical methods could provide evidence of the effect of the phenothiazine drugs on the electrochemical behavior of the coenzymes, the results obtained indicate that this purpose has to some extent been achieved. The role of adsorption as a conflicting factor in the case of the highly surface-active trifluoperazine must be recognized, but the evidence for adsorption in the case of chlorpromazine is virtually nonexistent. Therefore, changes in the measured quantities

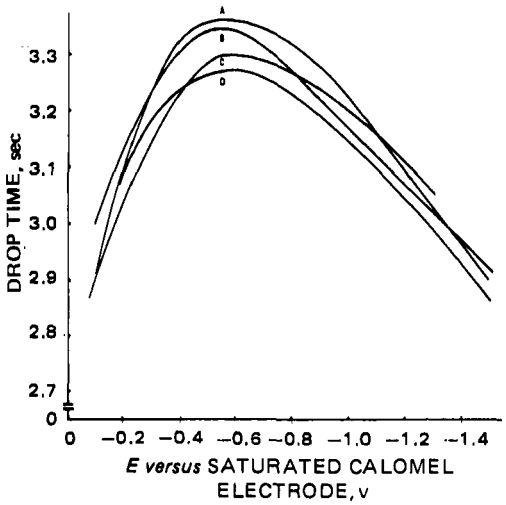

Figure 4—*Effect of II and chlorpromazine hydrochloride on the electrocapillary curve for 0.1 M tetraethylammonium chloride in pH 6.5 phosphate buffer. Key: A, normal curve; B, with 10^{-4} M II; C, with 10^{-4} M II and 10^{-2} M chlorpromazine; and D, with 10^{-4} M II and 10^{-1} M chlorpromazine.*

observed upon the addition of the latter drug to the coenzymes must be attributed to an interaction between the two species.

Whether this interaction provides a basis for the pharmacological activity of the drug is, of course, mere speculation at this stage. Obviously, further and more detailed studies are needed, utilizing other phenothiazines and employing other techniques. The main thrust of the investigation at this point is that electrochemical methods can and do provide a direct and feasible approach to the study of the possible interactions between the drugs and the coenzymes; further studies should lead to the acquisition of some definite knowledge in this area.

REFERENCES

(1) K. Yagi, T. Ozawa, and T. Nagatsu, *Biochim. Biophys. Acta*, **43**, 310(1960).

(2) M. J. R. Dawkins, J. D. Judah, and K. R. Rees, *Biochem. J.*, **72**, 204(1959).

(3) *Ibid.*, **76**, 200(1960).

(4) G. Karreman, I. Isenberg, and A. Szent-Gyorgi, *Science*, **130**, 1191(1959).

(5) J. E. Bloor, B. R. Gilson, R. J. Haas, and C. L. Zirkle, *J. Med. Chem.*, **13**, 922(1970).

(6) Y. Asahi, *J. Pharm. Soc. Jpn.*, **76**, 378(1956).

(7) B. Ke, *Arch. Biochem. Biophys.*, **68**, 330(1957).

(8) M. Senda, M. Senda, and I. Tachi, *Rev. Polarogr.*, **10**, 142(1962).

(9) A. M. Hartley and G. S. Wilson, *Anal. Chem.*, **38**, 681 (1966).

(10) Y. Takemori, *Rev. Polarogr.*, **11**, 225(1964).

(11) P. J. Elving, J. E. O'Reilly, and C. O. Schmakel, "Methods of Biochemical Analysis," vol. 21, Wiley, New York, N.Y., 1973, pp. 293–295.

(12) P. Kabasakalian and J. McGlotten, *Anal. Chem.*, **31**, 431(1959).

(13) F. H. Merkle and C. A. Discher, *J. Pharm. Sci.*, **53**, 620(1964).

(14) R. M. Patel and G. Zografi, *ibid.*, **55**, 1345(1966).

ACKNOWLEDGMENTS AND ADDRESSES

Received November 18, 1974, from the *Philadelphia College of Pharmacy and Science, Philadelphia, PA 19104*

Accepted for publication February 13, 1976.

The authors thank the SmithKline Corp. for supplying the phenothiazine drugs and Dr. John P. Tischio for interest and advice.

[x] To whom inquiries should be directed.

Polymerized Micelles and Their Use as Adjuvants in Immunology

G. BIRRENBACH and P. P. SPEISER [x]

Abstract □ A polymerization process is described for the preparation of hydrophilic micelles containing solubilized drug molecules in a colloidal aqueous system of dissolved monomers. A hydrocarbon medium constitutes the outer phase. After secondary solubilization with the aid of selected surfactants, polymerization of micelles under different conditions takes place. The formulation of drugs including labile proteins in the ultrafine polymer components ("nanoparts") and their isolation are possible without noticeable destruction of the encapsulated molecules. Entrapped tagged material (human ^{125}I-immunoglobulin G) shows a stable fixation in such nanoparts during long-term *in vitro* liberation trials. Nanoparts are visible with the aid of an electron microscope. They are mostly spherical in shape and smaller than 80 nm in diameter. They form real colloidal aqueous solutions. Nanoparts are suitable to embed antigenic material (tetanus toxoid and human immunoglobulin G) for parenteral use. These preparations show intact biological activity and high antibody production in animals.

Keyphrases □ Polymerization—hydrophilic micelles containing drug molecules (nanoparts), use as immunological adjuvants □ Micelles, hydrophilic—containing drug molecules, polymerization, use as immunological adjuvants □ Nanoparts—hydrophilic micelles containing drug molecules, polymerization, use as immunological adjuvants □ Adjuvants, immunological—hydrophilic micelles containing drug molecules, polymerization □ Immunological adjuvants—hydrophilic micelles containing drug molecules, polymerization

"Nanoparts" are solidified micelles containing drugs; they are spherical particles of nontoxic polymeric material with entrapped bioactive materials. The extremely small diameter of nanoparts, smaller than 80 nm, is measured by electron scanning microscopy. The lower limit for the particle diameter ranges between 20 and 35 nm, as shown by ultrafiltration with special diaphragms of an average pore size between 20 and 50 nm.

These ultrafine capsules or polymer pellets represent a narrow distribution in particle size. The electron scanning photographs show an aggregation of homogeneous, spherical particles of nearly the same shape and size, being small enough to give colloidal aqueous solutions.

According to polarity, dielectric constant, and steric effect of the reactants, a more or less shell-like polymer construction ("nanocapsule") or a compact polymer particle ("nanopellet") can be proposed (Scheme I). The minuteness of the nanoparts and the homogeneity of the final product also enable the formulation of parenteral drug delivery systems.

EXPERIMENTAL

Synthesis—Water-soluble polymerizable monomers and the enclosure material, *e.g.*, the biologically or pharmacologically active agent, are dissolved in water to form a true, or at least a colloidal, solution. This solution is distributed with the aid of surfactants by stirring in a hydrophobic phase (*n*-hexane) in which the precursors and the drugs are practically insoluble. Minute aqueous micelles, containing the polymerizable monomers, drugs, and possibly other auxiliary agents, are thus solubilized in a relatively large volume of the lipophilic outer phase and form extremely small reaction regions for the ensuing polymerization. The polymerization is induced by known methods (1–7).

The mechanism of micelle polymerization is definitely different from emulsion polymerization. In most cases, mainly in micellar reaction regions, water-insoluble monomers polymerize in water during emulsion polymerization. Here, the radical-containing polymerizing regions may swell to many times their original size. This swelling is due to diffusion of monomers from a stock of monomer droplets in the emulsion into growing latex polymer particles (8, 9). In this process, polymerization is strictly restricted to the micellar regions, since

observed upon the addition of the latter drug to the coenzymes must be attributed to an interaction between the two species.

Whether this interaction provides a basis for the pharmacological activity of the drug is, of course, mere speculation at this stage. Obviously, further and more detailed studies are needed, utilizing other phenothiazines and employing other techniques. The main thrust of the investigation at this point is that electrochemical methods can and do provide a direct and feasible approach to the study of the possible interactions between the drugs and the coenzymes; further studies should lead to the acquisition of some definite knowledge in this area.

REFERENCES

(1) K. Yagi, T. Ozawa, and T. Nagatsu, *Biochim. Biophys. Acta*, **43**, 310(1960).

(2) M. J. R. Dawkins, J. D. Judah, and K. R. Rees, *Biochem. J.*, **72**, 204(1959).

(3) *Ibid.*, **76**, 200(1960).

(4) G. Karreman, I. Isenberg, and A. Szent-Gyorgi, *Science*, **130**, 1191(1959).

(5) J. E. Bloor, B. R. Gilson, R. J. Haas, and C. L. Zirkle, *J. Med. Chem.*, **13**, 922(1970).

(6) Y. Asahi, *J. Pharm. Soc. Jpn.*, **76**, 378(1956).

(7) B. Ke, *Arch. Biochem. Biophys.*, **68**, 330(1957).

(8) M. Senda, M. Senda, and I. Tachi, *Rev. Polarogr.*, **10**, 142(1962).

(9) A. M. Hartley and G. S. Wilson, *Anal. Chem.*, **38**, 681 (1966).

(10) Y. Takemori, *Rev. Polarogr.*, **11**, 225(1964).

(11) P. J. Elving, J. E. O'Reilly, and C. O. Schmakel, "Methods of Biochemical Analysis," vol. 21, Wiley, New York, N.Y., 1973, pp. 293–295.

(12) P. Kabasakalian and J. McGlotten, *Anal. Chem.*, **31**, 431(1959).

(13) F. H. Merkle and C. A. Discher, *J. Pharm. Sci.*, **53**, 620(1964).

(14) R. M. Patel and G. Zografi, *ibid.*, **55**, 1345(1966).

ACKNOWLEDGMENTS AND ADDRESSES

Received November 18, 1974, from the *Philadelphia College of Pharmacy and Science, Philadelphia, PA 19104*

Accepted for publication February 13, 1976.

The authors thank the SmithKline Corp. for supplying the phenothiazine drugs and Dr. John P. Tischio for interest and advice.

[x] To whom inquiries should be directed.

Polymerized Micelles and Their Use as Adjuvants in Immunology

G. BIRRENBACH and P. P. SPEISER [x]

Abstract □ A polymerization process is described for the preparation of hydrophilic micelles containing solubilized drug molecules in a colloidal aqueous system of dissolved monomers. A hydrocarbon medium constitutes the outer phase. After secondary solubilization with the aid of selected surfactants, polymerization of micelles under different conditions takes place. The formulation of drugs including labile proteins in the ultrafine polymer components ("nanoparts") and their isolation are possible without noticeable destruction of the encapsulated molecules. Entrapped tagged material (human ^{125}I-immunoglobulin G) shows a stable fixation in such nanoparts during long-term *in vitro* liberation trials. Nanoparts are visible with the aid of an electron microscope. They are mostly spherical in shape and smaller than 80 nm in diameter. They form real colloidal aqueous solutions. Nanoparts are suitable to embed antigenic material (tetanus toxoid and human immunoglobulin G) for parenteral use. These preparations show intact biological activity and high antibody production in animals.

Keyphrases □ Polymerization—hydrophilic micelles containing drug molecules (nanoparts), use as immunological adjuvants □ Micelles, hydrophilic—containing drug molecules, polymerization, use as immunological adjuvants □ Nanoparts—hydrophilic micelles containing drug molecules, polymerization, use as immunological adjuvants □ Adjuvants, immunological—hydrophilic micelles containing drug molecules, polymerization □ Immunological adjuvants—hydrophilic micelles containing drug molecules, polymerization

"Nanoparts" are solidified micelles containing drugs; they are spherical particles of nontoxic polymeric material with entrapped bioactive materials. The extremely small diameter of nanoparts, smaller than 80 nm, is measured by electron scanning microscopy. The lower limit for the particle diameter ranges between 20 and 35 nm, as shown by ultrafiltration with special diaphragms of an average pore size between 20 and 50 nm.

These ultrafine capsules or polymer pellets represent a narrow distribution in particle size. The electron scanning photographs show an aggregation of homogeneous, spherical particles of nearly the same shape and size, being small enough to give colloidal aqueous solutions.

According to polarity, dielectric constant, and steric effect of the reactants, a more or less shell-like polymer construction ("nanocapsule") or a compact polymer particle ("nanopellet") can be proposed (Scheme I). The minuteness of the nanoparts and the homogeneity of the final product also enable the formulation of parenteral drug delivery systems.

EXPERIMENTAL

Synthesis—Water-soluble polymerizable monomers and the enclosure material, *e.g.*, the biologically or pharmacologically active agent, are dissolved in water to form a true, or at least a colloidal, solution. This solution is distributed with the aid of surfactants by stirring in a hydrophobic phase (*n*-hexane) in which the precursors and the drugs are practically insoluble. Minute aqueous micelles, containing the polymerizable monomers, drugs, and possibly other auxiliary agents, are thus solubilized in a relatively large volume of the lipophilic outer phase and form extremely small reaction regions for the ensuing polymerization. The polymerization is induced by known methods (1–7).

The mechanism of micelle polymerization is definitely different from emulsion polymerization. In most cases, mainly in micellar reaction regions, water-insoluble monomers polymerize in water during emulsion polymerization. Here, the radical-containing polymerizing regions may swell to many times their original size. This swelling is due to diffusion of monomers from a stock of monomer droplets in the emulsion into growing latex polymer particles (8, 9). In this process, polymerization is strictly restricted to the micellar regions, since

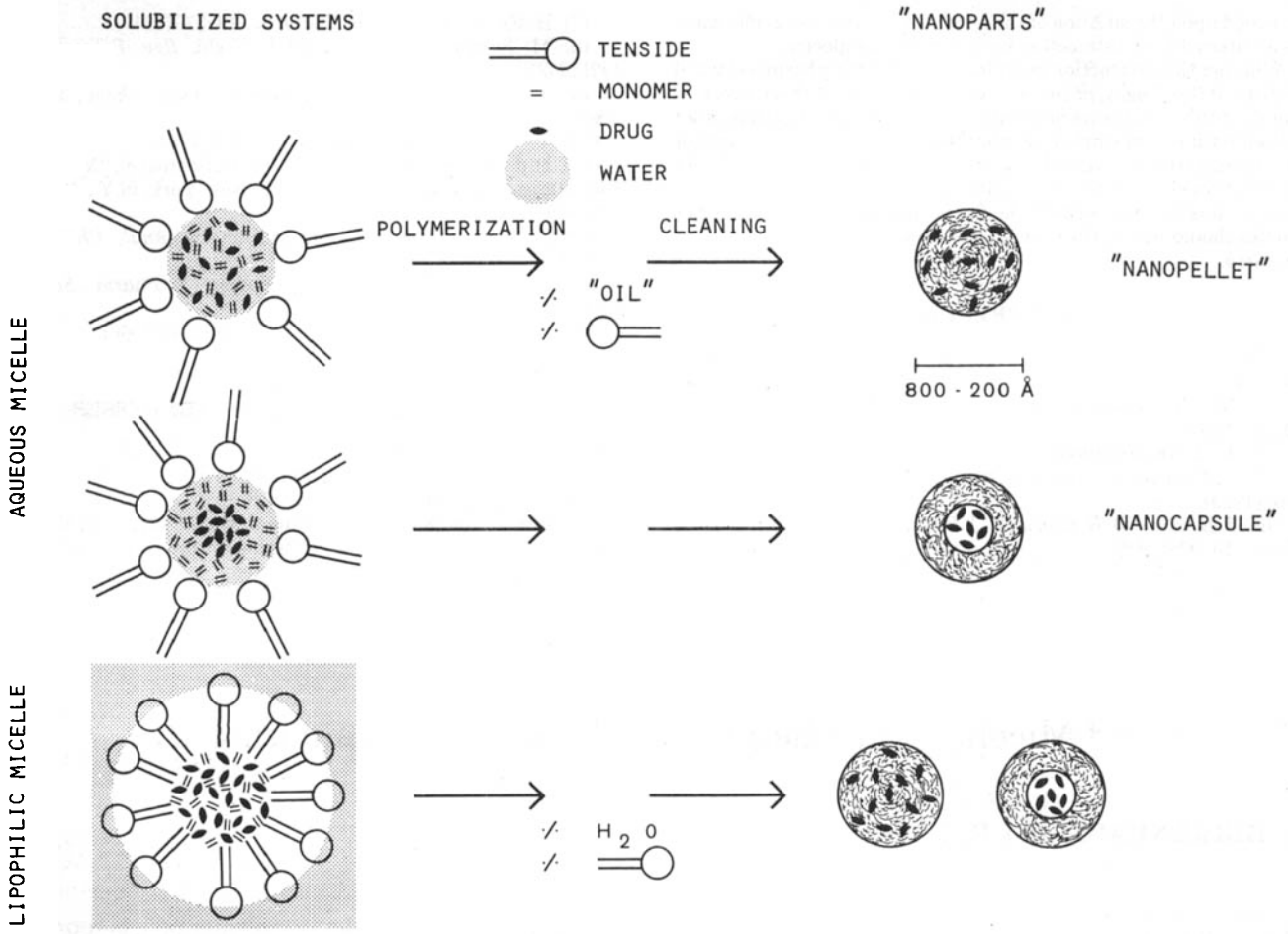

Scheme I—Schematic presentation of nanoparts

the hydrophobic outer phase contains no polymerizable material. A diffusion of monomers into this phase is largely prevented because of the low partition coefficient.

To encapsulate water-insoluble materials, the system can be modified so that a lipophilic phase with the dissolved weak polar drug can be solubilized in a hydrophilic outer medium, usually water. In this case, the precursors must have a high partition coefficient and the diffusion of monomers into the hydrophilic outer phase has to be prevented (Scheme I). The polymer micelle formed can usually be cleaned and isolated by precipitation or by ultrafiltration, dialysis, or centrifugation.

The procedure for preparing nanoparts, however, requires the following three steps: (*a*) solubilization of enclosure material (drug) and polymerizable molecules to form micelles, (*b*) polymerization of the monomers, and (*c*) purification and isolation of the solidified micelle.

Solubilization—All materials used were analytical grade.

Procedure A—A mixture of 12.0 g of bis(2-ethylhexyl) sodium sulfosuccinate[1] (I) and 6.0 g of polyoxyethylene 4 lauryl ether[2] (II), with an average of four ethylene oxide units in the chain, was dissolved in 80 ml of *n*-hexane by stirring at room temperature until the solution was clear. By adding 5.0 ml of distilled water dropwise into the solution and by continuous stirring, the crystalline monomers, 0.25 g of *N,N'*-methylenebisacrylamide[3] (III) and 2.00 g of acrylamide[3] (IV), were dissolved.

The soluble portion was filtered through membrane filters[4] to produce a sterile solution. Under aseptic conditions, 5.0 g of tetanus toxoid solution containing 3100 limit flocculation (Lf) units/ml[5] were added dropwise, with stirring, until a clear solution resulted.

Procedure B—A mixture of 12.0 g of bis(2-ethylhexyl) sodium sulfosuccinate and 6.0 g of polyoxyethylene 4 lauryl ether was dissolved in 80.0 ml of *n*-hexane at room temperature. Then 35 ml of distilled water was slowly added while the solution was stirred. Then the crystalline monomers, 0.50 g of III and 4.00 g of IV, were dissolved in this solution. The solution was sterile filtered[4], and 0.30 g of freeze-dried urease[6] was added to form a micellar solution with a weak Tyndall effect.

Procedure C—A mixture of 45.0 g of I and 25.0 g of II was dissolved in 215 ml of *n*-hexane at room temperature. Then 2.5 ml of ethanol, 2.5 ml of methanol, 40.0 ml of distilled water, 1.00 g of III, and 8.00 g of IV were added and dissolved successively.

The solubilized mixture was sterile filtered, and *n*-hexane was added to form 340 ml of solution. While stirring under aseptic conditions, 10.0 ml of a ^{125}I-labeled human immunoglobulin G (IgG) solution[5] (aggregate free in tromethamine buffer with 0.100 g of sodium chloride corresponding to ~1.4% human IgG) was added dropwise at room temperature.

Human IgG was alcohol fractioned, with approximately 10–15% of aggregated material, and was purified by molecular sieving with dextran gel[7]. Labeling with iodine-125 was performed by the method of Helmkamp *et al.* (10).

Polymerization with γ-Radiation (1)—Solutions prepared according to Procedures A and C were placed under nitrogen, sealed tightly, and exposed continuously to the radiation of a cobalt-60 source at about 20–30°. A dosage of 0.3 Mrad ensured complete polymerization. The end-point of polymerization, *i.e.*, the disappearance of the monomers, could be determined with the aid of an acidimetric color titration method to determine unsaturated compounds by reaction with morpholine (11).

[1] Fluka, Ltd., Buchs, Switzerland.
[2] Brij 30, Atlas Powder Co.
[3] Ciba-Geigy Ltd., Basle, Switzerland.
[4] Millipore HA 45 nm and GS 22 nm, Millipore, Bedford, Mass.
[5] Serum- & Impfinstitut, Bern, Switzerland.
[6] Merck Ltd., Darmstadt, Germany.
[7] Sephadex G 200.

Polymerization with Visible Light (3–7)—A solution prepared according to Procedure B was placed in a cylindrical, temperature-stable, double-walled reaction vessel of Pyrex glass with an internal diameter of 6 cm[8]. Then 0.2 mg of riboflavin 5′-sodium phosphate[1] and 0.2 mg of potassium peroxodisulfate[6], as an initiator, were added and dissolved. While stirring at 35 ± 1°, the solution was continuously perfused with a weak stream of nitrogen gas. The opalescent solution was then radiated from outside the column at a distance of 15 cm with an electric bulb of 300 w for 7 hr until the monomers disappeared completely.

Polymerization with UV Light (2)—One solution was prepared according to Procedure B and placed in a cylindrical reaction vessel as already described. It then was continuously stirred at 35 ± 1° and perfused by a weak stream of nitrogen gas while being radiated from inside by a UV dipping lamp (quartz burner of 70 w) for 45 min until the monomers completely disappeared.

Isolation and Purification According to Procedure C—After complete polymerization, the *n*-hexane hydrophobic phase was removed by azeotropic distillation at room temperature under vacuum. From the remaining aqueous residue containing the nanoparts and the surfactants, the surfactants were removed completely by ultrafiltration and repeated washing with distilled water under nitrogen pressure (~2–4 atm). Ultrafiltration[9] assays of the polymerized nanoparts were performed in special cells of 65, 200, or 400 ml and with a special diaphragm.

Finally an opalescent aqueous solution of the polymer product was obtained. Freeze drying of this solution gave a white free-flowing powder, which was redispersable in aqueous solution.

Isolation and Purification According to Procedures A and C—The polymeric product containing the antigen could be precipitated at −5° with an excess of a mixture containing 60% water and 40% (v/v) methanol. The isolation and purification of the nanoparts were done by centrifugation or ultrafiltration[9] at −5° to remove all surfactants. Freeze drying, preferably with a methanol content of 5% (v/v), removed the solvent and yielded products that formed a white free-flowing powder.

Immunological Assays—The antibody levels of human IgG in guinea pig serum were measured by a passive hemagglutination test (12, 13). For this purpose, sheep erythrocytes, which had been sensitized with the antigen by means of benzidine, were used. Antitoxin titer levels are average values for surviving animals of a group of five to 10 guinea pigs from a serum dilution series with factor 2 (Fig. 1). The antibody levels (antitoxin titers in International Units per milliliter) against tetanus toxoid in guinea pig serum were determined as the LD+ dose of the toxoid (14, 15). The serum of four to 10 animals of one group was analyzed in pools.

***In Vitro* Release Studies**—According to Procedure C, nanoparts containing ^{125}I-labeled human IgG were synthesized by polymerization with γ-radiation. The resulting product was isolated and purified by following ultrafiltration and freeze drying as described for Procedures A and C.

The release of the globulin from the polymer material was studied by a modified beaker method (16). Therefore, 38.44 mg of nanocapsules, corresponding to 1 mg of labeled human IgG, was redissolved in a 300-ml well-closed beaker with 250 ml of aqueous phosphate-buffered medium of pH 7.2 (0.645 g of monobasic potassium phosphate and 2.125 g of dibasic sodium phosphate dihydrate). The solution was magnetically stirred at 60 rpm, and the whole medium was thermostated in a water bath of 37 ± 0.2°.

The liberation of the free globulin from the polymer material was followed by membrane filtration[10]. Therefore, every 24 hr, 0.050 ml of the solution was diluted with 1000 ml of the phosphate buffer and filtered under a nitrogen pressure of 5 atm in a special cell[11] and washed five times with 1000 ml of the buffer. ^{125}I-Activity measurements were performed in a liquid scintillation counter[12], and probes were diluted with Bray solution (4.0 g of 2,5-diphenyloxazole, 0.2 g of 1,4-bis[2-(5-phenyloxazolyl)]benzene, 60 g of naphthalene, 20 ml of ethylene glycol, 100 ml of methanol, and 815 ml of dioxane).

[8] W. Möller, Glass-Blower Ltd., Zurich, Switzerland.
[9] Diaphragm: Diaflo PK 30, Amicon Ltd., Oosterhout, The Netherlands.
[10] Diaphragm SM 115.30, 35–20-nm pore size, Sartorius GmbH, Göttingen, Germany.
[11] Ultrafiltration cell SM 162 25 with an effective filtration area of 16 cm^2, Sartorius GmbH, Göttingen, Germany.
[12] Packard Tri-Carb liquid scintillation spectrometer 3320, Packard Instrument Corp., Frankfurt, Germany.

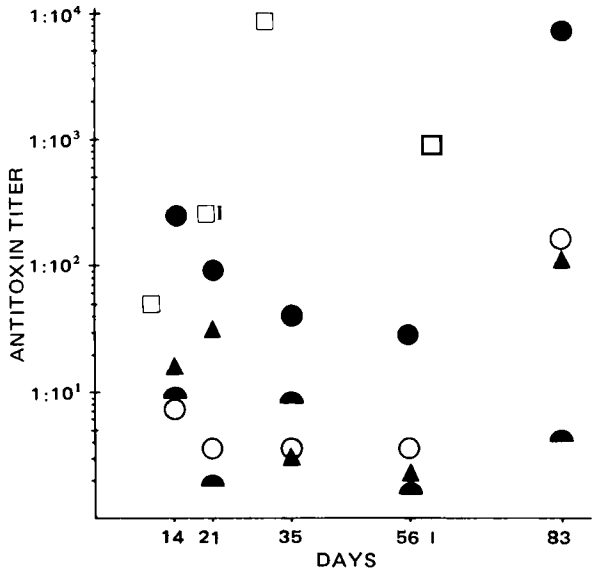

Figure 1—*Immunization of guinea pigs with human IgG preparations (antibody levels as a function of time). Key: ◓, immunization with IgG basic material (aqueous buffered solution, pH 7.2, 0.3 mg of IgG/kg sc); ▲, IgG basic material plus aluminum oxide (4 mg/ml) (0.3 mg/kg sc); ○, IgG in nanoparts (0.3 mg of IgG/kg sc); ●, IgG in nanoparts (1 mg of IgG/kg sc); □, IgG basic material plus complete Freund adjuvant (1:1) (1 mg of IgG/kg im); and I, booster injection after 21 days and booster injections with basic material after 60 days.*

Each day, the activity of 0.050 ml of the test medium was set at 100%. The activity of collected filtrates corresponded to percent free globulin (as could be proven by test filtrations with free globulin in the presence of "empty" nanocapsules in solution).

RESULTS AND DISCUSSION

Activity and Stability of Biological Material in Nanoparts—Even labile proteins can be embedded in nanoparts. After a "simulated" micelle polymerization, *i.e.*, in the absence of monomers, urease, tetanus toxoid, and human IgG, no noticeable loss of enzymatic reactivity or immunological response was shown. The urea-decomposing activity of urease and the immunoelectrophoretic behavior of the toxoid and the globulin remained unchanged after the "simulated" synthesis (17).

Embedded active substance, *e.g.*, human IgG, forms a deposit in the nanoparts. With labeled human IgG as a model, a maximum of only 25% of the incorporated substance could be released unaltered from nanocapsules over 48 days. It is reasonable to assume that only radioactive fragments of the globulin molecule were recorded, suggesting that the fixed portion of IgG may be greater than 75%.

Adjuvant Effect—In theory, stable antigen fixation and the physical properties of nanoparts offer rich prospects for immunological applications. Favorable characteristics of nanoparts for use as adjuvants include their compatibility with only slight local reactions at the place of application, their stability in solution, their easy method of application in a water-based solution, their protective effect with only slowly expected metabolism or corrosion and with only minimal release of antigenic material, and their possible affinity to lipoid cell membranes. Furthermore, a highly dispersed amount of antigenic material can be incorporated in the nanoparts.

Another advantage is the possible disseminating effect of colloid particles with a tendency to spread over the whole lymphoid system. The antigen appears in the polymerized state as a considerably larger complex. As a result, phagocytosis is strongly stimulated. The antigen–adjuvant complex penetrates into the immunosystem; it is transferred into the lymphatic ganglions and into the spleen, where it is degraded slowly and can be distributed.

Expected good adjuvant effects have been confirmed experimentally. Animal experiments also showed that nanoparts are well tolerated parenterally.

Human IgG—Studies of the adjuvant effect of nanoparts with

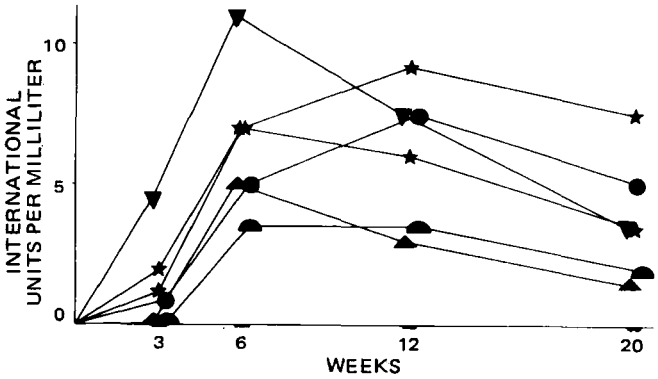

Figure 2—*Immunization of guinea pigs with tetanus toxoid preparations (antitoxin titers as a function of time) using intramuscular vaccination with no booster injection. Key: ▲, tetanus toxoid embedded in nanoparts (5 Lf); ▼, tetanus toxoid embedded in nanoparts (50 Lf); ◓, tetanus toxoid embedded (5 Lf) plus basic material (aqueous buffered solution, 5 Lf); ●, tetanus toxoid embedded (50 Lf) plus basic material (aqueous buffered solution, 50 Lf); ★, tetanus toxoid adsorbed on aluminum phosphate (5 Lf); and ☆, tetanus toxoid adsorbed on aluminum phosphate (50 Lf).*

enclosed human IgG in immunization trials on guinea pigs showed that higher antibody titers are obtained as compared with aluminum oxide as the adjuvant. Furthermore, a level comparable to Freund's adjuvant, the most effective jet toxic adjuvant, is approached (Fig. 1).

Tetanus Toxoid—Nanoparts with tetanus toxoid as antigen produce in guinea pigs slightly less immunization (antibody production) than the standard aluminum phosphate adjuvant (see Fig. 2).

CONCLUSION

The embedding of biologically active materials in ultrafine components (nanoparts) offers considerable technological possibilities and flexibility, as shown with the example of human IgG, tetanus toxoid, and urease. Accordingly, the partition of drugs in such nanoparts seems to be promising as a new parenteral drug delivery system for long-term therapy. Other biological drug models and the mechanism of drug incorporation and release will be studied.

REFERENCES

(1) E. Collinson, F. S. Dainton, and G. S. McNaughton, *J. Chim. Phys. Phys.-Chim. Biol.*, **52**, 556(1955).

(2) G. D. Jones, U.S. pat. 2,533,166 (1945).

(3) G. Oster, *Nature*, **173**, 300(1954).

(4) G. K. Oster, G. Oster, and G. Prati, *J. Am. Chem. Soc.*, **79**, 595(1957).

(5) G. K. Oster, U.S. pat. 2,850,495 (1955).

(6) G. Oster, U.S. pat. 2,875,047 (1955).

(7) A. A. Hiltz and E. G. Lendrat, U.S. pat. 2,880,152/153 (1957).

(8) H. Fikentscher, H. Gerrens, and H. Schuller, *Angew. Chem.*, **72**, 856(1960).

(9) W. D. Harkins, *J. Polym. Sci.*, **5**, 217(1950).

(10) R. W. Helmkamp, R. L. Godland, W. F. Bale, J. L. Spar, and L. E. Mutschler, *Cancer Res.*, **20**, 1495(1960).

(11) F. E. Critchfield, G. L. Funk, and J. B. Johnson, *Anal. Chem.*, **28**, 76(1956).

(12) E. A. Kabat and M. M. Mayer, "Experimental Immunochemistry," Charles C Thomas, Springfield, Ill., 1967, p. 119.

(13) J. H. Humphrey and R. G. White, "Kurzes Lehrbuch der Immunologie," E. Macker, G. Thieme Verlag, Stuttgart, Germany, 1971, p. 235.

(14) G. Ramon and R. Richou, *Rev. Immunol. (Paris)*, **14**, 161(1950).

(15) H. Schmidt, "Praxis der Auswertung von Toxinen und Antitoxinen," Jena, E. Germany, 1931, p. 21.

(16) G. Levy and B. A. Hayes, *N. Engl. J. Med.*, **262**, 1053(1960).

(17) G. Birrenbach, thesis 5071 ETH-Zurich, 1973, pp. 82, 88, 89.

ACKNOWLEDGMENTS AND ADDRESSES

Received June 30, 1975, from the *School of Pharmacy, Federal Institut of Technology, Clausiusstrasse 25, CH-8006 Zurich, Switzerland.*

Accepted for publication January 28, 1976.

Abstracted in part from a dissertation submitted by G. Birrenbach to the Swiss Federal Institut of Technology in partial fulfillment of the Doctor of Natural Sciences degree requirements.

Supported in part by a grant of the Swiss Serum- & Impfinstitut, Bern, Switzerland.

The authors thank the Swiss Serum- & Impfinstitut, Bern, Switzerland, for the antigenic material, the labeled IgG, and the performance of animal trials.

[x] To whom inquiries should be directed.

Fluorometric Determination of Trifluoromethyl-Substituted 2,3-Bis(4-methoxyphenyl)indoles in Biological Materials

DAVID G. KAISER ˣ, WALTER F. LIGGETT, and ARLINGTON A. FORIST

Abstract □ Interest in the 5-, 6-, and 7-trifluoromethyl-substituted 2,3-bis(4-methoxyphenyl)indoles as potent, orally active anti-inflammatory agents required a method for their determination in serum, urine, and feces to permit studies of their absorption, metabolism, and excretion. A simple, rapid, sensitive, and specific procedure was developed based on an ethyl acetate extraction of alkaline specimens and subsequent fluorometric analysis of ethanolic solutions of the extract residues. The method is sensitive to 0.1 μg/ml, 0.5 μg/ml, and 0.7 μg/100 mg of these compounds in serum, urine, and feces, respectively. Overall mean recoveries and standard deviations of the 5-, 6-, and 7-trifluoromethyl-substituted compounds from biological samples were 102.2 ± 3.0, 102.2 ± 5.4, and 100.5 ± 5.7%, respectively. The procedure was applied successfully to absorption studies with 2,3-bis(4-methoxyphenyl)-7-(trifluoromethyl)indole in the dog.

Keyphrases □ 2,3-Bis(4-methoxyphenyl)indoles, trifluoromethyl substituted—fluorometric analysis, serum, urine, and feces □ Fluorometry—analysis, trifluoromethyl-substituted 2,3-bis(4-methoxyphenyl)indoles in serum, urine, and feces □ Anti-inflammatory agents—trifluoromethyl-substituted 2,3-bis(4-methoxyphenyl)-indoles, fluorometric analysis in serum, urine, and feces

In a continuing search for nonsteroidal anti-inflammatory drugs, the trifluoromethyl-substituted 2,3-bis(4-methoxyphenyl)indoles were found to be potent orally active agents (1). Studies of their absorption, metabolism, and excretion required a method for their determination in serum, urine, and feces.

Previous reports described fluorometric procedures for the determination of indoxole [2,3-bis(4-methoxyphenyl)indole, I] (2), 4,5-bis(4-methoxyphenyl)-2-phenylpyrrole-3-acetonitrile (3), and 2,3-bis(4-methoxyphenyl)imidazo[1,2-*a*]pyrimidine (4) in biological materials. These methods were successfully used in investigations in animals and humans (3–7).

Exploratory studies showed that the 5-, 6-, and 7-trifluoromethyl-substituted 2,3-bis(4-methoxyphenyl)indoles (II, III, and IV, respectively) possessed useful fluorescence characteristics. Therefore, a simple, rapid, sensitive, and specific fluorometric procedure was developed for their determination in biological materials.

EXPERIMENTAL

Reagents and Materials—Aqueous sodium hydroxide (1 *N*) was stored in glass containers. Ethyl acetate was equilibrated with an equal volume of water prior to use in the extraction step. A solution

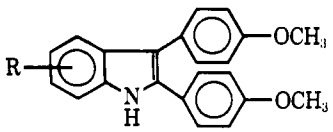

I: R = H
II: R = 5-CF_3
III: R = 6-CF_3
IV: R = 7-CF_3

Table I—Excitation and Fluorescence Maxima for 2,3-Bis(4-methoxyphenyl)indoles in 95% Ethanol

Compound	Excitation Maximum, nm	Emission Maximum, nm
I[a]	320	420
II	330	415
III	325	415
IV	325	415

[a] Reference 2.

Table II—Effect of Extraction Time on Recovery of II[a] from Rat Serum

Extraction Time, min	II Found, μg/ml	Recovery, %
5	1.85	74.3
10	2.03	81.5
15	2.26	90.7
20	2.48	99.6
25	2.50	100.5
30	2.50	100.5

[a] The amount of II added was 2.49 μg/ml in all cases.

of quinine sulfate[1] (2.25 μg/ml in 0.1 *N* aqueous sulfuric acid) was utilized as a spectrophotofluorometric standard. All pipets and centrifuge tubes were thoroughly rinsed with alcohol or acetone and air dried prior to use.

Instrumentation—A blender[2] and/or a homogenizer[3] were used in the preparation of fecal specimens for extraction. A two-speed reciprocating shaker[4] was utilized for sample extractions in the horizontal position. Fluorometric measurements[5] were made with a spectrophotofluorometer[6] equipped with a xenon lamp dc power supply[7], a compact xenon arc lamp[8] (150 w), a potted photomultiplier tube[9], and a two-axis recorder[10].

Standards—Stock solutions of II–IV were prepared by dissolving 5–10 mg in 100 ml of 95% ethanol with shaking. Working standards were prepared by dilution of the stock solutions with 95% ethanol to give final concentrations of approximately 0.05, 0.1, 0.2, 0.4, 0.6, and 0.8 μg/ml. Standard solutions were stored in the dark since II, III, and IV solutions are susceptible to photochemical decomposition.

Collection and Storage of Specimens—Blood samples were allowed to clot at room temperature (27°) for 1 hr and then were centrifuged at 2000 rpm for 10 min, and the serum was harvested. Urine specimens were collected, and 1 ml of 37% formaldehyde was added for each 50 ml. All serum, urine, and fecal specimens were stored at −18° until analyzed.

Extractions—In a 15-ml glass-stoppered centrifuge tube were placed 1 ml of serum or urine, 0.05 ml of 1 *N* aqueous sodium hydroxide, and 3 ml of ethyl acetate. The mixture was shaken in a horizontal position for 20 min, avoiding exposure to direct sunlight, and then centrifuged at 2000 rpm for 10 min. A 1-ml aliquot of the ethyl acetate layer was transferred to a glass-stoppered centrifuge tube and

[1] Matheson, Coleman, and Bell, Milwaukee, Wis.
[2] Model PB-5A, Waring Products Corp., Winsted, Conn.
[3] Virtis 45, Virtis Co., Gardiner, N.Y.
[4] Eberbach & Sons, Ann Arbor, Mich.
[5] Identical results were obtained with a Hitachi Perkin-Elmer (model MPF-2A) spectrophotofluorometer, Perkin-Elmer Corp., Norwalk, Conn.
[6] Aminco-Bowman, American Instrument Co., Silver Spring, Md.
[7] Sola Electric Co., Elk Grove, Ill.
[8] Engelhard Hanovia, Inc., Newark, N.J.
[9] 1P28, Aminco-Bowman, American Instrument Co., Silver Spring, Md.
[10] Autograf, F. L. Moseley Co., Pasadena, Calif.

Table III—Lower Limits of Detection[a] for II–IV in Rat and Dog Serum, Urine, and Feces

Sample	II	III	IV
Rat serum, μg/ml	0.06	0.04	0.08
Dog serum, μg/ml	0.04	0.04	0.12
Rat urine, μg/ml	0.20	0.28	0.14
Dog urine, μg/ml	0.30	0.48	0.22
Rat feces, μg/100 mg	0.46	0.42	0.28
Dog feces, μg/100 mg	0.62	0.74	0.64

[a] Based on sample response two times that of the appropriate blank.

evaporated to dryness in a stream of nitrogen. The residue was reconstituted in 5 ml of 95% ethanol and stored in the dark until analyzed.

For rat feces, the frozen specimen was weighed and placed in the homogenizer[3]. A volume of water equivalent to twice the sample weight was added, and the mixture was homogenized at high speed for 1 min. A 100-mg aliquot of the slurry was weighed into a 15-ml glass-stoppered centrifuge tube; then 1 ml of water, 0.05 ml of 1 *N* aqueous sodium hydroxide, and 3 ml of ethyl acetate were added. The extraction was completed as described for serum and urine.

For dog feces, the total specimen was weighed and placed in the blender[2]. A volume of water equivalent to twice the sample weight was added, and the mixture was homogenized at high speed for 1 min. An aliquot (about 20 ml) was removed and homogenized[3] at high speed until a fine slurry was produced. A 100-mg aliquot was weighed into a 15-ml glass-stoppered centrifuge tube; then 1 ml of water, 0.05 ml of 1 *N* aqueous sodium hydroxide, and 3 ml of ethyl acetate were added. The extraction was completed as described for serum and urine.

Fluorometric Analysis—The spectrophotofluorometer was standardized with the quinine sulfate solution (60% transmission at 0.3 multiplier setting[9]), using the excitation and emission maxima for the specific compound to be determined (Table I). Fluorescence intensities of the samples were measured at these wavelength settings.

Table IV—Recovery of II from Aqueous Solution and Biological Materials

Sample	II Added[a]	II Found[b]	Recovery, %
Water	0.50	0.50	100.0
	1.00	0.99	99.0
	2.00	1.99	99.5
		Mean ± *SD*	99.5 ± 0.5
Rat serum	0.50	0.49	98.0
	1.00	1.01	101.0
	2.00	2.00	100.0
		Mean ± *SD*	99.7 ± 1.5
Dog serum	0.50	0.50	100.0
	1.00	1.05	105.0
	2.00	2.05	102.5
		Mean ± *SD*	102.5 ± 2.5
Rat urine	0.50	0.55	110.0
	1.00	1.04	104.0
	2.00	2.04	102.0
		Mean ± *SD*	105.3 ± 4.2
Dog urine	0.50	0.53	106.0
	1.00	1.01	101.0
	2.00	1.98	99.0
		Mean ± *SD*	102.0 ± 3.6
Rat feces	4.99	5.01	100.4
	9.98	10.14	101.6
	19.96	20.74	103.9
		Mean ± *SD*	101.9 ± 1.8
Dog feces	4.99	4.89	98.0
	9.98	10.43	104.5
	19.96	20.51	102.7
		Mean ± *SD*	101.7 ± 3.4

[a] Values for water, serum, and urine are expressed as micrograms per milliliter. Values for feces are expressed as micrograms per 100 mg. [b] Corrected for appropriate specimen blank.

Table V—Recovery of III from Aqueous Solution and Biological Materials

Sample	III Added[a]	III Found[b]	Recovery, %
Water	0.49	0.50	102.0
	0.98	0.98	100.0
	1.97	1.96	99.4
		Mean ± *SD*	100.5 ± 1.4
Rat serum	0.49	0.48	97.9
	0.98	0.99	101.0
	1.97	1.96	99.4
		Mean ± *SD*	99.4 ± 1.6
Dog serum	0.49	0.47	95.9
	0.98	0.97	98.9
	1.97	1.98	100.5
		Mean ± *SD*	98.4 ± 2.3
Rat urine	0.49	0.53	108.1
	0.98	1.02	104.1
	1.97	1.99	101.0
		Mean ± *SD*	104.4 ± 3.6
Dog urine	0.49	0.53	110.2
	0.98	1.05	107.1
	1.97	1.98	100.5
		Mean ± *SD*	105.9 ± 5.0
Rat feces	5.03	5.03	100.0
	10.05	9.90	98.5
	20.10	22.21	110.5
		Mean ± *SD*	103.0 ± 6.5
Dog feces	5.03	4.95	98.4
	10.05	9.55	95.0
	20.10	22.81	113.4
		Mean ± *SD*	102.3 ± 9.8

[a] Values for water, serum, and urine are expressed as micrograms per milliliter. Values for feces are expressed as micrograms per 100 mg. [b] Corrected for appropriate specimen blank.

Drug concentrations were calculated from a standard curve (working standards) with appropriate corrections for serum, urine, or feces blanks.

Animal Preparation—In studies designed to determine the utility of the method, three male beagle dogs, 12.5 ± 1.2 kg, were fasted for 16 hr prior to single-dose oral drug administration. Two dogs received approximately 20 mg of IV/kg in polysorbate 80, and the remaining animal served as a vehicle-treated control. All animals were fasted for an additional 4 hr after drug administration and were then allowed free access to food and water.

Blood specimens were withdrawn from the jugular veins at 0, 1, 2, 3, 4, 6, 8, 12, and 24 hr postadministration. Urine specimens were collected at predetermined time intervals during the first 24 hr after drug administration. All specimens were stored at −18°.

TLC—All chromatography was conducted on thin layers (250 μm) of silica gel F_{254}[11], ascendingly developed in 20% (v/v) ethyl acetate in cyclohexane. The separated materials were visualized by: (*a*) irradiation of the plates with short wavelength (254 nm) and long wavelength (366 nm) UV lamps, or (*b*) spraying with 50% (v/v) aqueous sulfuric acid and heating at 110° for 20 min. Under these conditions, intact II, III, and IV had R_f values of 0.22, 0.30, and 0.44, respectively.

RESULTS AND DISCUSSION

Earlier studies with indoxole (2) and 4,5-bis(4-methoxyphenyl)-2-phenylpyrrole-3-acetonitrile (3) showed those compounds to be susceptible to photochemical degradation. Similar behavior was found for II–IV. Therefore, as a precaution, all specimen extracts were stored in the dark until analyzed.

Fluorescence responses for II–IV were compared with those for indoxole (I), using the excitation and emission maxima of the latter (Table I). On a molar basis relative to a value of unity for I, responses for II, III, and IV were 1.89, 2.69, and 1.67, respectively. A preferential

[11] Brinkmann Instruments, Westbury, N.Y.

Table VI—Recovery of IV from Aqueous Solution and Biological Materials

Sample	IV Added[a]	IV Found[b]	Recovery, %
Water	0.51	0.49	96.0
	1.01	1.04	102.9
	2.02	2.04	100.9
		Mean ± *SD*	99.9 ± 3.6
Rat serum	0.51	0.46	90.2
	1.01	1.00	99.0
	2.02	2.11	104.4
		Mean ± *SD*	97.8 ± 7.8
Dog serum	0.51	0.50	98.0
	1.01	1.07	105.9
	2.02	2.11	104.4
		Mean ± *SD*	102.7 ± 4.2
Rat urine	0.51	0.40	96.0
	1.01	1.00	99.0
	2.02	2.14	105.9
		Mean ± *SD*	100.3 ± 5.1
Dog urine	0.51	0.46	90.2
	1.01	1.04	102.9
	2.02	2.26	111.8
		Mean ± *SD*	101.6 ± 10.9
Rat feces	5.1	5.4	105.8
	10.1	10.3	101.9
	20.2	20.2	100.0
		Mean ± *SD*	102.5 ± 3.0
Dog feces	5.1	5.1	100.0
	10.1	9.4	93.0
	20.2	20.3	100.4
		Mean ± *SD*	97.8 ± 4.2

[a] Values for water, serum, and urine are expressed as micrograms per milliliter. Values for feces are expressed as micrograms per 100 mg. [b] Corrected for appropriate specimen blank.

electronic distribution in the resonance states of the trifluoromethyl-substituted compounds is suggested.

Low recoveries (80–90%) of II and III from rat serum were obtained utilizing the 10-min extraction previously described for indoxole (2). A determination of the recovery of II from rat serum as a function of extraction time (Table II) established the need for a 20-min extraction and suggested that the trifluoromethyl-substituted analogs are more tightly bound to serum proteins than is the parent compound, indoxole.

The maximum fluorometric sensitivity for II–IV in 95% ethanol was 0.005 μg/ml (meter multiplier[9] setting of 0.003). However, the practical lower limits of detection in biological matrixes are controlled by the magnitude of the specimen blanks in addition to the inherent fluorescence emissions of the specific compounds. Calculated lower detection limits for II–IV, based on sample responses twice those of the appropriate blanks, are shown in Table III. Taken collectively, II–IV may be detected in serum, urine, and feces at levels of ≥0.1 μg/ml, ≥0.5 μg/ml, and ≥0.7 μg/100 mg, respectively.

Under the described conditions, a linear relationship between fluorescence response and concentration of II–IV was obtained over the 0–0.8-μg/ml range in 95% ethanol. Direct quantification from a standard curve was adequate.

To determine recoveries from biological samples, known amounts of II–IV in 95% ethanol were evaporated to dryness in centrifuge tubes, and water or specimens of rat or dog serum, urine, or feces were added. The samples were thoroughly mixed and analyzed by the standard procedure. Overall mean recoveries and standard deviations for II, III, and IV from biological samples were 102.2 ± 3.0% (Table IV), 102.2 ± 5.4% (Table V), and 100.5 ± 5.7% (Table VI). These results validate the use of simple standard curves in routine analyses as described previously.

The utility of the method was established by a limited study with IV in dogs. Following oral administration of approximately 30 mg of IV/kg, peak serum IV levels of 1.85–2.19 μg/ml were observed between

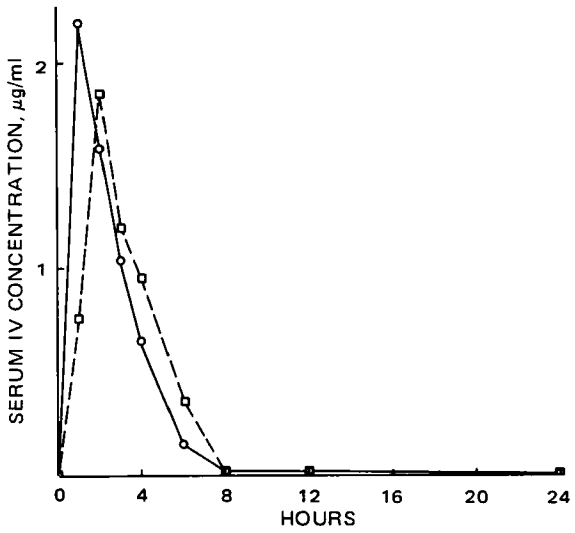

Figure 1—*Serum concentrations of IV in dogs after single-dose oral drug administration in polysorbate 80. Key:* ○, *Dog 478 (male), 20.9 mg/kg; and* □, *Dog 479 (male), 20.3 mg/kg.*

1 and 2 hr (Fig. 1). Measurable concentrations were present during the first 12 hr after drug administration. These results are similar to those reported for indoxole (2, 6), 4,5-bis(4-methoxyphenyl)-2-phenylpyrrole-3-acetonitrile (3), and 2,3-bis(4-methoxyphenyl)imidazo[1,2-*a*]pyrimidine (4) in dogs.

The present method detects materials that are extractable from an alkaline solution with ethyl acetate and that possess excitation and fluorescence characteristics in 95% ethanol similar to the administered drug. Interference by endogenous materials in most specimens is very low, as indicated by the lower limits of detection (Table III). However, metabolic transformations could give rise to compounds responding in the assay. Accordingly, excitation spectra were routinely obtained on serum extracts as a check on specificity; metabolic changes would be expected to result in altered UV spectra and, therefore, fluorescence excitation spectra. No such changes were observed in the dog. Moreover, TLC of serum extracts showed that the major component (>85%) was similar to IV, confirming the measurement of intact drug. Thus, the method possesses adequate sensitivity and specificity for drug absorption studies in animals.

Based on fluorometric and TLC analyses, less than 1% of the dose was excreted in urine as intact IV by the dog during the 24-hr collection interval. Extensive metabolism and/or biliary secretion are indicated.

REFERENCES

(1) J. Szmuszkovicz, U.S. pat. 3,551,451 (1970); through *Chem. Abstr.*, **74**, 141523n(1971).

(2) D. G. Kaiser, B. J. Bowman, and A. A. Forist, *Anal. Chem.*, **38**, 977(1966).

(3) D. G. Kaiser and E. M. Glenn, *J. Pharm. Sci.*, **61**, 1908(1972).

(4) D. G. Kaiser and A. A. Forist, *ibid.*, **64**, 2011(1975).

(5) J. G. Wagner, E. S. Gerard, and D. G. Kaiser, *Clin. Pharmacol. Ther.*, **7**, 610(1966).

(6) D. G. Kaiser, E. M. Glenn, R. H. Johnson, and R. L. Johnston, *J. Pharmacol. Exp. Ther.*, **155**, 174(1967).

(7) D. G. Kaiser and A. A. Forist, *J. Pharm. Pharmacol.*, **26**, 563(1974).

ACKNOWLEDGMENTS AND ADDRESSES

Received December 8, 1975, from the *Research Laboratories, The Upjohn Company, Kalamazoo, MI 49001*

Accepted for publication February 9, 1976.

The authors thank Mr. S. R. Shaw for technical assistance.

[x] To whom inquiries should be directed.

GLC Determination of a Novel Polyvalent Saluretic Agent, (6,7-Dichloro-2-methyl-1-oxo-2-phenyl-5-indanyloxy)acetic Acid, in Biological Fluids

ANTHONY G. ZACCHEI ˣ and THEODORE WISHOUSKY

Abstract □ Highly specific and sensitive GLC methods were developed for the determination of (6,7-dichloro-2-methyl-1-oxo-2-phenyl-5-indanyloxy)acetic acid, a novel saluretic–uricosuric agent, in biological fluids. The procedures involve the addition of an internal standard, (6,7-dichloro-2-cyclopentyl-2-methyl-1-oxo-5-indanyloxy)acetic acid, to the biological specimens followed by extraction of the acids into benzene at pH 1. The indanones are back-extracted into sodium hydroxide and reextracted into methylene chloride under acidic conditions. The acids are subsequently converted to the methyl esters for GLC analysis by reaction with diazomethane. The sensitivity of the method is such that 1.0 μg of material/ml of plasma can be analyzed using a flame-ionization detector. When the derivatized samples are analyzed using a ^{63}Ni-electron-capture detector, the sensitivity is such that 2.5 ng of compound can be detected. These levels are suitable for the analysis of samples obtained following a therapeutic dose. A recovery of 98.8 ± 11.9% was obtained using the electron-capture method for plasma (n = 322). Recoveries using flame ionization were 99.1 ± 4.4% (plasma, n = 207) and 99.8 ± 4.9% (urine, n = 163). Quantitation of the major ring-hydroxylated metabolite (in chimpanzee and human) was accomplished following silylation of the methyl esters.

Keyphrases □ Indanyloxyacetic acid, substituted—GLC analysis, biological fluids □ GLC—analysis, (6,7-dichloro-2-methyl-1-oxo-2-phenyl-5-indanyloxy)acetic acid in biological fluids □ Saluretic agents—(6,7-dichloro-2-methyl-1-oxo-2-phenyl-5-indanyloxy)acetic acid, GLC analysis in biological fluids

(6,7-Dichloro-2-methyl-1-oxo-2-phenyl-5-indanyloxy)acetic acid (I) is a new nonsulfonamide saluretic agent with polyvalent action, *i.e.*, with uricosuric and antihypertensive activities as additional attributes. The synthesis of this material and other similar analogs was described recently (1–3). The compound has pronounced saluretic activity in rats, dogs, and chimpanzees (4, 5). In the latter species, pronounced saluretic and uricosuric effects were found over a wide range of oral doses (5). The compound has significant antihypertensive effects in the renal hypertensive monkey and in the spontaneously hypertensive rat, the duration of this effect exceeding 24 hr in the latter species (4). Preliminary studies on the physiological disposition of this compound were described previously (6, 7).

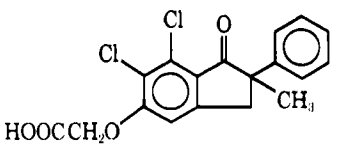

I

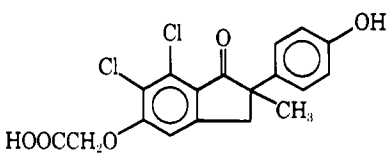

III

This report describes highly specific and sensitive GLC methods for the determination of I using an internal standard, (6,7-dichloro-2-cyclopentyl-2-methyl-1-oxo-5-indanyloxy)acetic acid (II), derivatization with diazomethane, and a flame-ionization or ^{63}Ni-electron-capture detector. Biological specimens from dogs, monkeys, chimpanzees, and humans were utilized to demonstrate the applicability of the assay procedures following pharmacological doses of I. Studies on the physiological disposition of the drug (6–8) indicated that the major metabolite in chimpanzees and humans is [6,7-dichloro-2-(4-hydroxyphenyl)-2-methyl-1-oxo-5-indanyloxy]acetic acid (III). During these studies, quantitative determinations were made on this metabolite following derivatization with diazomethane and *N,O*-bis(trimethylsilyl)acetamide.

EXPERIMENTAL

Reagents and Chemicals—The reagents and chemicals used were: (6,7-dichloro-2-methyl-1-oxo-2-phenyl-5-indanyloxy)acetic acid (I), the internal standard (6,7-dichloro-2-cyclopentyl-2-methyl-1-oxo-5-indanyloxy)acetic acid (II), pesticide grade benzene, methylene chloride, freshly prepared 0.5 *M* diazomethane, and *N,O*-bis(trimethylsilyl)acetamide[1] in pyridine (2:1).

Instrumentation—*GLC*—Analyses during the past 2 years were carried out on three different gas chromatographs. A gas chromatograph[2] equipped with a flame-ionization detector and a 122-cm × 4-mm (i.d.) glass column packed with 3% OV-210[3] was employed. Helium was used as the carrier gas at a flow rate of 48 ml/min. A gas chromatograph[4] equipped with a ^{63}Ni-electron-capture detector and a 122-cm × 4-mm (i.d.) glass column containing 3% OV-210 was used in the isothermal (264°) electron-capture analysis of I and III. Nitrogen was used as the carrier gas at a flow rate of 80 ml/min. A gas chromatograph[5] equipped with a flame-ionization detector and a ^{63}Ni-electron-capture detector was also utilized. The injection port and detector temperatures were 10–30° higher than the column temperatures.

GLC–Mass Spectrometry—All mass spectra were obtained on a mass spectrometer[6] using a GLC inlet. A 122-cm × 3-mm (i.d.) glass column packed with 3% OV-210 was used. The gas chromatograph was operated isothermally at 250° with a helium flow rate of 30 ml/min. The mass spectrometer ionizing and accelerating potentials were 70 ev and 3.5 kv, respectively. The source, separator, and injection port temperatures were 270, 265, and 260°, respectively.

Measurement of I in Biological Samples—The concentration of I was determined in biological specimens as follows. To 1.0 ml of plasma (or an appropriate aliquot of urine) in a 50-ml glass-stoppered centrifuge tube were added 10.0 μg of II in 1 ml of pH 7 phosphate buffer, 1 ml of 2 *N* HCl, and 25 ml of reagent grade benzene. The tube was shaken for 10 min and centrifuged, and at least 20 ml of the organic phase was transferred to a similar tube containing 2 ml of 0.1 *N* NaOH. After the tube was shaken for 5 min, it was centrifuged and the organic phase was removed by aspiration.

[1] Aldrich Chemical Co.
[2] Hewlett-Packard model 5750.
[3] Applied Science Laboratories; 100–120-mesh Gas Chrom Q.
[4] Packard model 7400.
[5] Hewlett-Packard model 5830A.
[6] LKB-9000S.

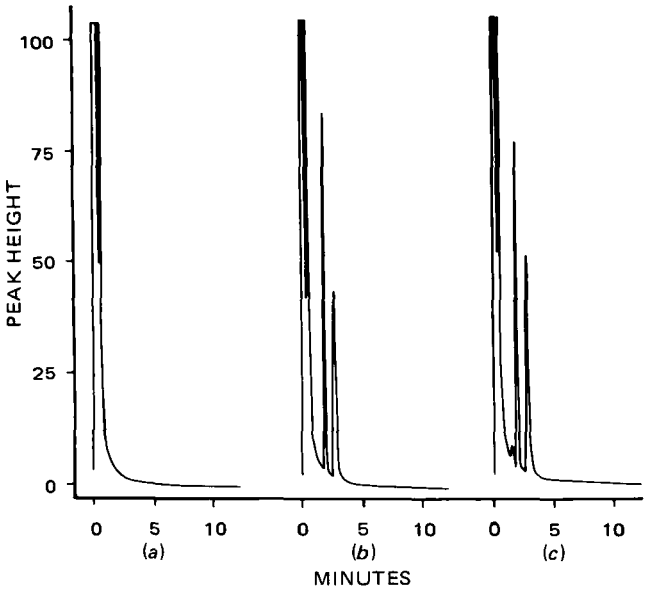

Figure 1—*Gas chromatograms of:* (a) *control chimpanzee plasma,* (b) *chimpanzee plasma obtained 40 min after dosing, and* (c) *I (10 μg) and II (10 μg) added to control chimpanzee plasma. All samples were carried through the flame-ionization detection method. Five microliters was injected out of a 100-μl final volume.*

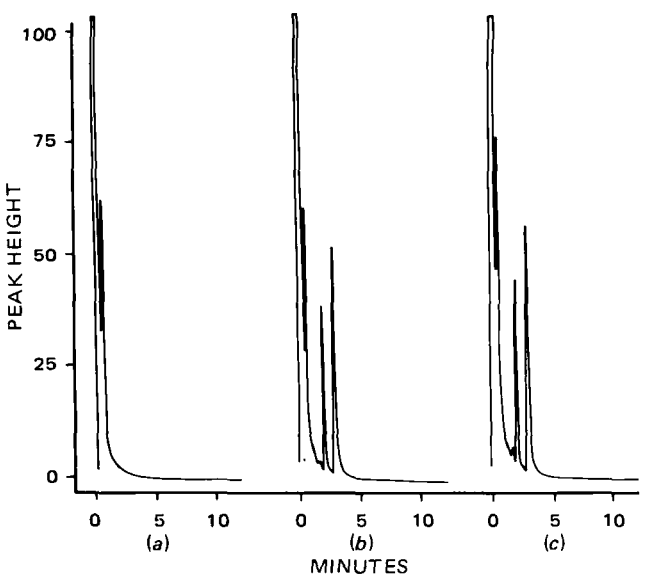

Figure 2—*Gas chromatograms of:* (a) *control chimpanzee urine,* (b) *chimpanzee urine obtained 30 min postadministration, and* (c) *I (20 μg) and II (10 μg) added to control urine. Samples were carried through the flame-ionization detection method. Five microliters was injected out of 50–100 μl of final volume.*

The pH of the aqueous phase was adjusted to 1 by the addition of 0.2 ml of 2 *N* HCl, and the free acids were extracted into 5 ml of methylene chloride (vortex, 1 min). After centrifugation, the methylene chloride phase was transferred to a 13-ml centrifuge tube and reacted with 100 μl of ethereal diazomethane. The contents of the tube were evaporated to dryness under nitrogen in a warm water bath (~50°), the residue was then dissolved in 50 μl of ethyl acetate, and appropriate aliquots (2–5 μl) were injected into the gas chromatograph. At a column temperature of 250°, I and II exhibited retention times of 2.8 and 2.0 min as the methyl esters, respectively. Over 6 months, the retention times of the compounds decreased slightly due to slight losses of the liquid phase at the high temperatures.

Standard plasma and urine curves were constructed by plotting the peak height ratios (I/II) *versus* weight ratios (I/II). A linear relationship was obtained in the 1–60-μg range. The peak height ratio of an unknown sample was then used to determine the amount of I present. The standard samples were run concurrently with the unknown samples as previously described.

The electron-capture method of analysis was employed when increased sensitivity was required. The procedure was similar to that described for flame-ionization detection. The minor changes were: (*a*) 25 ng of internal standard was added rather than 10 μg of II, and

Table I—Recovery of I from Plasma and Urine Using Flame-Ionization Detection Method

I Added, μg		Amount Recovered[a] Plasma *n*	Plasma Mean ± *SD*	Urine *n*	Urine Mean ± *SD*
60.0	A	12	60.2 ± 0.75	8	59.1 ± 2.32
	B		100.3 ± 1.3		98.5 ± 3.8
50.0	A	19	50.1 ± 1.13	15	50.2 ± 0.84
	B		100.1 ± 2.2		100.5 ± 1.7
40.0	A	24	40.6 ± 1.07	16	40.5 ± 0.89
	B		101.5 ± 2.7		101.5 ± 2.2
30.0	A	25	30.0 ± 0.70	18	30.2 ± 1.00
	B		100.0 ± 2.3		100.6 ± 3.3
20.0	A	27	19.9 ± 0.77	18	20.0 ± 0.39
	B		99.9 ± 3.8		99.9 ± 1.9
10.0	A	29	9.8 ± 0.38	27	10.0 ± 0.42
	B		98.3 ± 3.8		100.2 ± 4.2
5.0	A	31	4.9 ± 0.22	26	5.0 ± 0.25
	B		98.1 ± 4.4		100.3 ± 4.9
2.5	A	26	2.4 ± 0.13	21	2.5 ± 0.14
	B		97.6 ± 5.3		98.5 ± 5.6
1.0	A	14	1.0 ± 0.09	14	1.0 ± 0.10
	B		96.6 ± 9.1		96.6 ± 11.0
1–60	B	207	99.1 ± 4.4	163	99.8 ± 4.9

[a] Values in A rows represent micrograms recovered; values in B rows represent percent recovery.

(*b*) 10 ng of internal standard was added rather than 25 ng of III.

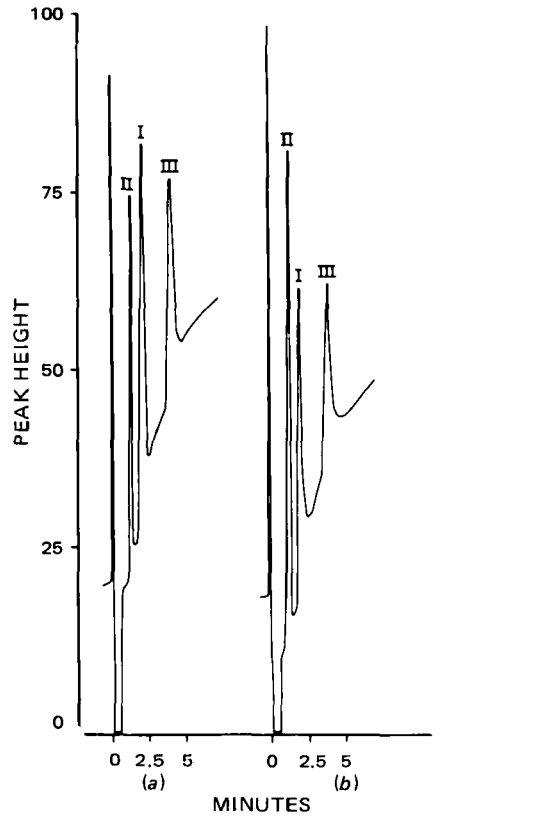

Figure 3—*Gas chromatograms of:* (a) *I, III, and II added to control urine in a 2:2:1 ratio and carried through the electron-capture method; and* (b) *chimpanzee urine (1–2 hr). Five microliters out of 100 μl was injected and analyzed with the* ^{63}*Ni-detector.*

Table II—Plasma Levels of I following Administration of I to Monkeys at a Dose of 2.5 mg/kg

Hours	I, μg/ml				
	Monkey 1	Monkey 2	Monkey 3	Monkey 4	Mean ± *SD*
			Oral		
0.5	7.3	7.8	4.1	6.6	6.4 ± 1.6
1	13.4	12.9	6.4	11.5	11.0 ± 3.2
2	15.1	21.8	7.0	16.4	15.1 ± 6.1
4	13.3	19.2	8.2	16.0	14.2 ± 4.7
6	11.4	16.9	8.2	14.6	12.8 ± 3.8
24	3.1	4.2	7.2	7.8	5.6 ± 2.3
48	1.7	1.5	5.4	5.1	3.4 ± 2.1
72[a]	0.51	0.38	2.78	3.60	1.8 ± 1.6
96	0.078	0.066	1.35	2.35	0.96 ± 1.10
120	0.028	0.029	0.68	1.85	0.64 ± 0.85
144	0.021	0.045	0.58	1.37	0.50 ± 0.63
168	0.015	0.050	0.081	1.50	0.41 ± 0.72
336	0.002	0.007	0.016	0.005	0.008 ± 0.006
			Intravenous		
0.08	39.6	34.7	41.6	36.4	38.1 ± 3.1
0.27	33.7	28.5	34.3	30.5	31.8 ± 2.7
0.5	28.8	22.4	31.5	25.5	27.0 ± 3.9
1	21.6	16.6	23.9	20.5	20.7 ± 3.0
2	16.0	13.0	18.5	15.7	15.8 ± 2.2
4	11.9	10.1	17.3	12.1	12.9 ± 3.1
6	9.6	8.7	14.2	10.5	10.8 ± 2.4
24	3.2	2.5	5.6	5.8	4.3 ± 1.7
48	1.4	1.0	2.8	3.8	2.3 ± 1.3
72	0.43	0.22	1.53	2.54	1.18 ± 1.07
96	0.069	0.073	0.44	1.55	0.53 ± 0.70

[a] Samples (72–336 hr) were analyzed by electron-capture GLC method.

(*b*) pesticide grade benzene was used to dissolve the esters prior to injection. Standard plasma and urine recovery curves were obtained by plotting peak height ratios (I/II) *versus* weight ratios (I/II) in the range of 2.5–100 ng of I.

Measurement of III in Biological Samples—Compound III was determined in the biological samples by a method similar to the ones described for flame-ionization detector or electron-capture detector analysis. The minor changes were: (*a*) initial extraction was performed with benzene–ethyl acetate (8:2), and (*b*) following derivatization with diazomethane, the solution was taken to dryness under nitrogen and subsequently treated with 100 μl of the *N,O*-bis(trimethylsilyl)-acetamide reagent for 30 min at 60°. Samples were then injected directly into the gas chromatograph. Depending on the concentration of III, either the flame-ionization detector or electron-capture detector method was utilized. Appropriate standard curves were obtained in a manner similar to that described previously.

Biological Studies—Four beagle dogs, 6.6–10.0 kg, received I orally in a water solution at a dose of 2.5 mg/kg. Four Rhesus monkeys, 3.0–3.4 kg, received a 2.5-mg/kg oral dose of I by gavage. One month later, the same four monkeys received 2.5 mg/kg iv. Anesthetized chimpanzees (*Pam troglodytes*) were given I at a dose of 1 mg/kg iv. Four healthy male volunteers each received 10.1 mg of ^{14}C-I orally in solution.

Table III—Recovery of I from Plasma Using Electron-Capture Detection

I Added, ng	*n*	Amount Recovered, ng, Mean ± *SD*	Percent Recovery, Mean ± *SD*
100.0	22	98.9 ± 4.3	98.9 ± 4.3
80.0	20	79.0 ± 8.9	98.7 ± 11.1
65.0	21	65.7 ± 5.4	101.1 ± 8.3
50.0	37	48.7 ± 3.4	97.4 ± 6.8
40.0	27	39.4 ± 3.1	98.4 ± 7.7
25.0	42	25.0 ± 2.1	100.1 ± 8.4
20.0	30	19.8 ± 2.3	99.1 ± 11.3
12.5	31	12.9 ± 1.6	103.5 ± 13.0
10.0	26	9.9 ± 1.0	99.1 ± 10.6
6.25	27	5.9 ± 1.1	93.9 ± 17.8
5.0	23	4.9 ± 0.65	97.6 ± 13.0
2.5	16	2.4 ± 0.64	96.2 ± 26.3
2.5–100	322	—	98.8 ± 11.9

The animals and human volunteers were fasted overnight prior to compound administration. Blood specimens were collected in heparinized tubes, plasma was separated by centrifugation, and aliquots were removed for analysis. Urine specimens were immediately frozen upon collection and kept frozen until analyzed. The samples were analyzed for I and III using the described procedures.

RESULTS AND DISCUSSION

During the development of I for potential use as a polyvalent saluretic agent with uricosuric and hypotensive properties, a method was needed to determine blood and urinary levels of the compound for absorption and excretion studies. GLC analysis of the indanyloxyacetic acids as the methyl esters provided a means for the determination of I. Figure 1 presents gas chromatograms of the following

Table IV—Mean Human Plasma Levels of Radioactivity, I, and III following Oral Administration of ^{14}C-I (10 mg)

Hours	Nanograms per Milliliter[a]			
	A	B	C	D
0.17	156	145 (93.2)[b]	1 (0.8)[b]	94.0
0.33	429	369 (86.0)	7 (1.7)	87.7
0.67	508	431 (84.9)	19 (3.7)	88.6
1.0	474	426 (90.0)	41 (8.7)	98.7
1.33	447	360 (80.4)	52 (11.7)	92.1
1.67	437	325 (74.3)	66 (15.3)	89.6
2	411	341 (82.9)	68 (16.7)	99.6
3	376	293 (77.9)	85 (22.6)	100.5
4	364	242 (66.4)	100 (27.7)	94.1
6	298	209 (70.0)	101 (33.9)	103.9
8	242	145 (60.2)	89 (40.0)	100.2
12	181	99 (54.8)	63 (35.1)	89.9
24	85	26 (30.8)	27 (32.1)	62.9
36	62	10 (16.5)	22 (35.6)	52.1

[a] Values in A column represent nanogram equivalents of I from ^{14}C-data; B values represent nanograms of I per milliliter of plasma; C values represent nanograms of III per milliliter of plasma; D values represent the sum of percent of radioactivity equivalents (A) as I and III. Values represent the mean from three subjects. [b] Values in parentheses represent the percent of plasma radioactivity attributed to unchanged drug or metabolite.

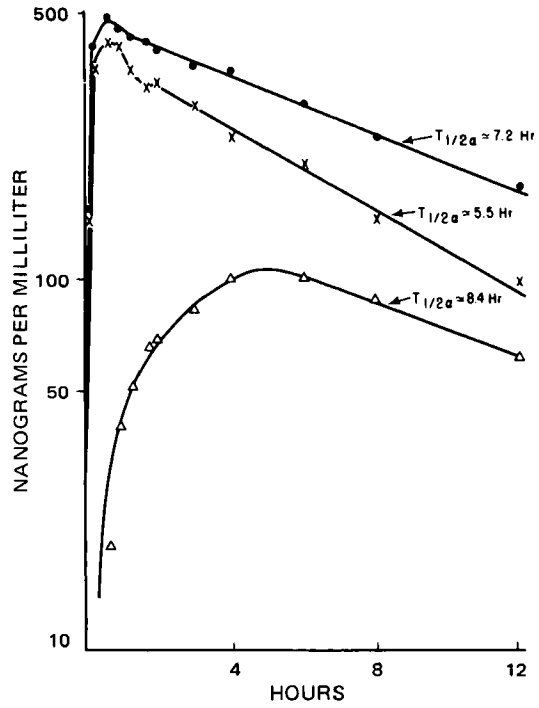

Figure 4—*Human plasma levels of I, III, and total radioactivity (calculated as I equivalents). Key: ●, radioactivity; ×, I; and △, III.*

samples using flame-ionization detection: (*a*) control chimpanzee plasma, (*b*) chimpanzee plasma obtained 40 min after dosing, and (*c*) I and II added to control chimpanzee plasma. Figure 2 presents gas chromatograms (flame-ionization detection) of: (*a*) control chimpanzee urine, (*b*) chimpanzee urine obtained 30 min postadministration, and (*c*) I and II added to control urine.

All samples were carried through the described procedure. As indicated in Figs. 1*a* and 2*a*, no interfering peaks were obtained from the control plasma or urine specimens. The methyl ester of I exhibited a retention time of 2.8 min, and the corresponding internal standard had a retention time of 2.0 min. A linear relationship was observed when peak height (or peak area) was plotted *versus* amount of I injected. A typical standard ratio curve was obtained after various amounts of I (1.0–50.0 μg) and II (10 μg) were carried through the entire procedure.

A summary of the results obtained following analysis of various amounts of I in control plasma or urine from rat, dog, chimpanzee, monkey, or human studies is presented in Table I. All analyses were performed using the flame-ionization detector over 1 year. In the 1–60-μg range, the mean recovery of I from control plasma was 99.1 ± 4.4% (n = 207); the recovery from urine was 99.8 ± 4.9% (n = 163). As is evident, the GLC method for I in biological fluids is sensitive and exhibits a high degree of accuracy and precision. Typical levels of I in monkey plasma following oral or intravenous administration of I at a dose of 2.5 mg/kg are seen in Table II.

The electron-capture method of detection was required for samples that were too low for detection with the flame-ionization detector (Table II). Table III summarizes the results obtained following electron-capture analysis of various amounts of I (2.5–100 ng) added to plasma. The mean recovery (n = 322) of I from control plasma (dog, monkey, human, and rat) in the 2.5–100-ng range was 98.8 ± 11.9%. The electron-capture GLC method is extremely sensitive and exhibits a high degree of accuracy and precision over the entire range. Typical values obtained in monkeys and humans are seen in Tables II and IV, respectively.

The analysis of III by the electron-capture procedure gave a recovery of 98.3 ± 6.5% (n = 62) in the 5–5000-ng range. A typical gas chromatogram is shown in Fig. 3. Recovery of I and III from the same tube at a 2:1 ratio is seen in Fig. 3*a*. Figure 3*b* shows the response obtained following analysis of chimpanzee urine (1–2 hr).

Table V—Comparison of the Mass Spectra of Isolated I and III with the Spectra of Authentic I and III[a]

	Relative Abundance, %			
m/e	I[b]	I[c]	III[b]	III[c]
378	100	100	—	—
363	68	70	—	—
301	11	11	—	—
466	—	—	100	100
451	—	—	22	23
393	—	—	7	12

[a] I was analyzed as the methyl ester; III was analyzed as the methyl ester–silyl ether. In both cases, the molecular ion was the base peak. [b] Spectra were obtained from the material present in biological specimens at retention times corresponding to authentic I and III. [c] Spectra were obtained from authentic I and III carried through the procedure.

Human plasma levels of I and III are presented in Fig. 4. As indicated, the plasma half-life of total radioactivity (calculated as nanogram equivalents of I per milliliter) was about 7 hr. The initial phase of the I elimination curve indicated an apparent $t_{1/2\alpha}$ of 5.5 hr; the III value gave an apparent plasma half-life of 8.4 hr. Peak levels of drug and radioactivity occurred about 1 hr after oral administration of drug. Essentially, all plasma radioactivity was accounted for as I and III.

Confirmation of the specificity of analysis was obtained when representative unknown biological specimens were analyzed by combined GLC–mass spectrometry, using the technique described previously. The spectra obtained from analysis of the GLC peaks corresponding to I and III (from an unknown biological sample) were identical to those obtained when authentic I and III were carried through the entire procedure. Details of the fragmentation pattern for these compounds were reported previously (8). A comparison of the relative abundance of the major ions (≥10%) for I and III with authentic I and III is presented in Table V.

REFERENCES

(1) E. J. Cragoe, Jr., E. M. Schultz, J. D. Schneeberg, G. E. Stokker, O. W. Woltersdorf, Jr., G. M. Fanelli, Jr., and L. S. Watson, *J. Med. Chem.*, **18**, 225(1975).

(2) O. W. Woltersdorf, Jr., E. J. Cragoe, Jr., and L. S. Watson, 169th National American Chemical Society Meeting, Philadelphia, Pa., Apr. 1975, Medicinal Chemistry Division Paper 48.

(3) O. W. Woltersdorf, Jr., J. D. Schneeberg, E.M. Schultz, G. E. Stokker, E. J. Cragoe, Jr., L. S. Watson, and G. M. Fanelli, Jr., 169th National American Chemical Society Meeting, Philadelphia, Pa., Apr. 1975, Medicinal Chemistry Division Paper 49.

(4) L. S. Watson and G. M. Fanelli, *Fed. Proc.*, **34**, 802(1975).

(5) G. M. Fanelli, D. L. Bohn, C. A. Horbaty, K. H. Beyer, and A. Scriabine, International Congress of Nephrology, Florence, Italy, June 8–12, 1975.

(6) A. G. Zacchei and T. Wishousky, *Fed. Proc.*, **34**, 802(1975).

(7) A. G. Zacchei and T. I. Wishousky, *Drug Metab. Dispos.*, **4**, 490(1976).

(8) A. G. Zacchei, T. I. Wishousky, B. H. Arison, and G. M. Fanelli, Jr., *ibid.*, **4**, 479(1976).

ACKNOWLEDGMENTS AND ADDRESSES

Received June 8, 1975, from the *Merck Institute for Therapeutic Research, West Point, PA 19486*

Accepted for publication February 13, 1976.

The authors thank Mr. O. Woltersdorf, Ms. J. Schneeberg, and Dr. E. J. Cragoe for supplies of I and related compounds. They are also indebted to Dr. G. M. Fanelli who gave I to chimpanzees and to Dr. S. Dziewanowska for supervision of the human study.

[x] To whom inquiries should be directed.

Reinvestigation of Disulfiram-Like Biological Activity of *Coprinus atramentarius* (Bull. *ex* Fr.) Fr. Extracts

M. VANHAELEN ˣ, R. VANHAELEN-FASTRÉ, J. HOYOIS, and Y. MARDENS

Abstract □ A ninhydrin-positive aqueous fraction isolated from *Coprinus atramentarius* (Bull. *ex* Fr.) Fr. showed significant disulfiram-like activity in mice. The isolation of this fraction from the mushroom crude extract and a convenient pharmacological test for following the physiological activity in each fraction are described.

Keyphrases □ *Coprinus atramentarius*—mushroom crude extract, aqueous fraction isolated, biological activity evaluated □ Mushrooms—*Coprinus atramentarius* crude extract, methanolic fraction isolated, biological activity evaluated □ Alcohol-potentiating activity—evaluated in methanolic fraction of extract of *Coprinus atramentarius* mushroom

Among several species of *Coprinus*, *Coprinus atramentarius* (Bull. *ex* Fr.) Fr. has given rise to the greatest interest because of its ability to sensitize humans to ethanol (1–4). However, controversial conclusions about this potentiation have been reported (5–8). Isolation of disulfiram from *C. atramentarius* (9) was not confirmed (10, 11). Although no disulfiram was detected, recent investigations unequivocally confirmed that polar extracts of *C. atramentarius* significantly potentiate the action of ethanol in mice (12, 13). Recently, an active constituent isolated from *C. atramentarius* increased blood acetaldehyde levels in mice (14).

To investigate the chemical structure of the active compound(s), a ninhydrin-positive fraction was isolated from a crude extract of *C. atramentarius*[1]. Its disulfiram-like activity in mice was determined using a convenient pharmacological test.

EXPERIMENTAL

Collection of Mushrooms—*Coprinus atramentarius* (Bull. *ex* Fr.) Fr. was collected[2] on lawns around Brussels during the autumn of 1972. The mushrooms were stored in ethanol at −18° for 1.5–3 months before extraction.

Apparatus—GLC was performed on an instrument[3] equipped with a dual flame-ionization detector and using 2-m × 4-mm (i.d.) glass columns packed with 80–100-mesh Chromosorb W coated with 10% SE 30.

The following conditions were used. For fatty acid methyl esters, the column temperature was 150–200° programmed at 5°/min and the carrier gas was 30 ml of nitrogen/min. For silyl derivatives of amino acids, the column temperature was 50–200° programmed at 7.5°/min and the carrier gas was 20 ml of nitrogen/min. In both cases, the injector and detector temperature was 250°.

Mass spectra were recorded after direct inlet in the source of the mass spectrometer[4].

PMR spectra[5] were obtained in deuterochloroform, with tetramethylsilane as the internal standard.

Ion-exchange chromatography was carried out on a two-column automatic amino acid analyzer[6], as described by the manufacturer. A cation-exchange resin[7] (sulfonated polystyrene) was used.

Evaporations were performed in a rotary evaporator at temperatures lower than 40°.

Reagents—For preparative TLC (thickness of 2 mm), 70 g of silica gel[8] or 60 g of cellulose[9] on 20 × 40-cm glass plates was used. Prepared chromatoplates were prewashed by developing with methanol–water (1:1 v/v) and then were activated by heating for 2 hr at 120° (silica gel) or 60° (cellulose).

Analytical TLC was carried out on the same adsorbents (thickness of 0.25 mm; 5 g on 20 × 20-cm glass plates).

Cellulose powder[10] was used for percolation of the ethanol–water extract (Scheme I).

All solvents and reagents were analytical grade[11].

Methods—*Extraction Procedures*—The general treatment of the crude extract in Procedure I is described in Scheme I.

In addition, two separate analyses were performed on crushed fresh mushrooms. In Procedure II, mushrooms (500 g) were treated by steam distillation under nitrogen to obtain a distillate volume of 200 ml. In Procedure III, mushrooms (500 g) were extracted by shaking with 1 liter of benzene. The benzene extract was dried on anhydrous sodium sulfate and evaporated to 10 ml.

Chromatographic Studies—The 10-ml final benzene extract of Procedure III was screened for disulfiram by partition paper chromatography as described by Simandl and Franc (9) and by TLC performed on silica gel, with benzene as solvent and 0.5% $PdCl_2$ aqueous solution as the reagent spray. It was not possible to identify disulfiram under these conditions, but an unknown compound was detected at the previously reported (9) R_f value corresponding to disulfiram. Therefore, the total benzene extract was subjected to preparative TLC on silica gel with benzene as solvent. The pertinent band at R_f 0.6 was eluted with chloroform to afford, after evaporation, 200 mg of a compound, mp 68–72°.

The mass spectrum of the isolated compound showed a molecular ion at *m/e* 882.

Glycerol was detected directly by dehydration to acrolein (15). After methanolysis, the methyl esters of the constitutive fatty acids were identified by GLC as methyl stearate and methyl linoleate in a ratio of 1:2. These two esters were purified by preparative TLC, using the same conditions as described for the initial compound. Further evidence of the chemical structure of these purified fatty acids methyl esters was obtained by direct comparison of their PMR and mass spectra with those of authentic samples.

These results suggested that the compound under investigation was a triglyceride containing one molecule of stearic acid for two of linoleic acid. Because of the biological inactivity of this triglyceride, the relative position of the fatty acids was not studied.

Five hundred milligrams of the ninhydrin-positive fraction (Fraction C_3, Scheme I) was isolated from 10 g of Fraction C_2 by means of preparative TLC, first on silica gel (100 plates) and then on cellulose

[1] *Note added in proof:* Since this paper was accepted, the disulfiram-like constituent of *C. atramentarius* was identified as N^5-(1-hydroxycyclopropyl)-glutamine by two groups: G. M. Hatfield and I. P. Schaumberg, *Lloydia*, **38**, 489(1975), and P. Lindberg, R. Bergman, and B. Wickberg, *J. Chem. Soc. Chem. Commun.*, **1975**, 946. These works confirmed our preliminary results, which located the active compound in a fraction containing amino acids.

[2] Identified at the Botanical Institute of the Free University of Brussels. Specimens, preserved at −18°, are available for inspection in this laboratory.

[3] Packard-Becker model 421.

[4] AEI model MS 902.

[5] Jeol 100 MHz.

[6] Technicon sequential multisample amino acid analyzer (TSM).

[7] Chromobeads C_3 Technicon resin.

[8] Silica gel H, Merck type 60.

[9] Cellulose Macherey-Nagel MN 300.

[10] Cellulose Macherey-Nagel MN 2100 ff.

[11] Merck.

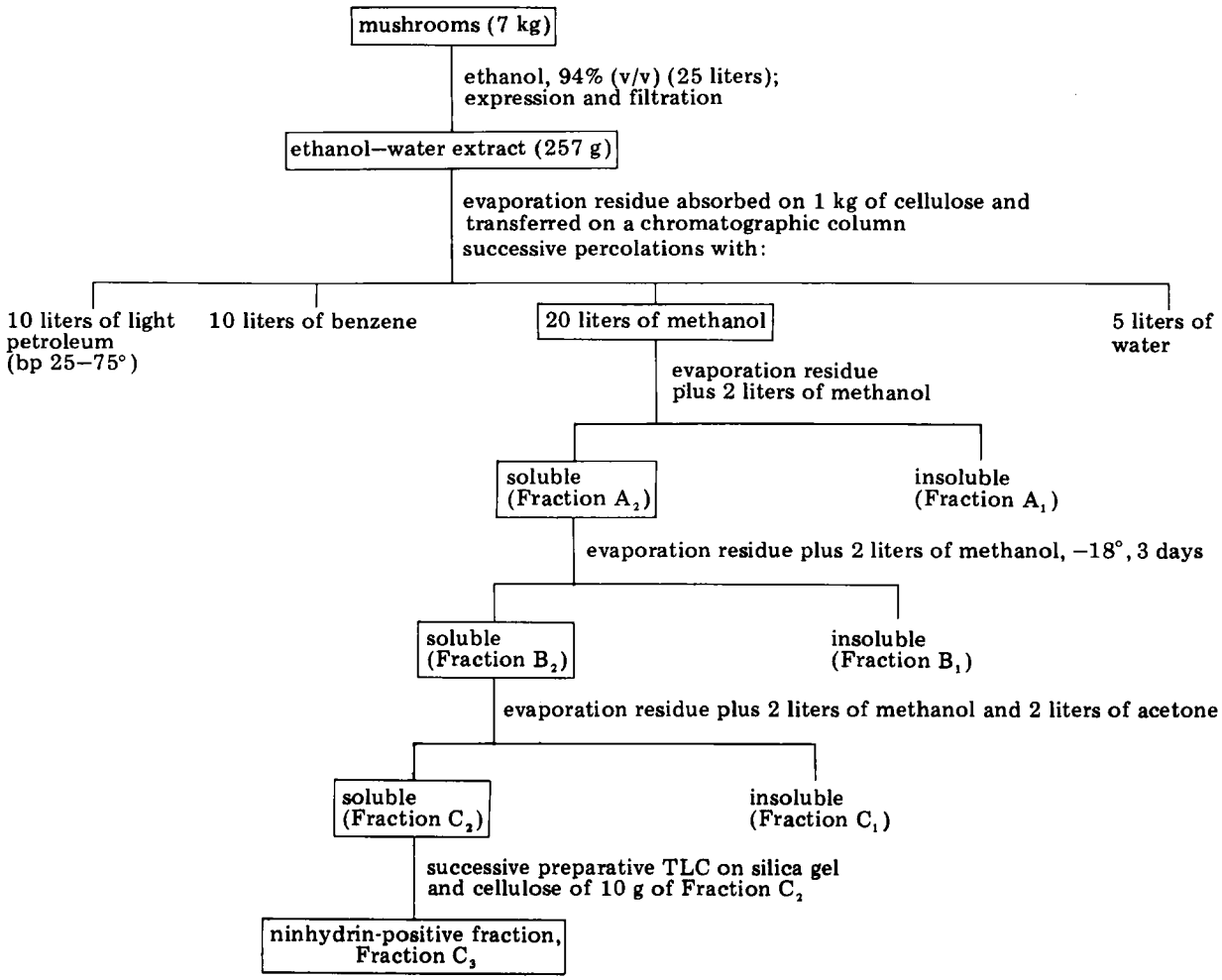

Scheme I—Extraction Procedure I for the crude extract from C. atramentarius

(20 plates). The silica gel plates were developed with ethyl acetate–2-propanol–methanol–water (5:2:1.5:1.5 v/v). The cellulose plates were developed with the same solvent system in 1:1:1:1 (v/v) proportions. The physiologically active band (R_f 0.25 on silica gel and R_f 0.45 on cellulose) was eluted from the adsorbent by methanol–water (1:1 v/v).

Identification of the main amino acids present in Fraction C_3 was carried out by TLC on cellulose under the conditions described for a commercial device[12]. Visualization of amino acids after TLC was performed by separate spraying of ninhydrin, isatin, Ehrlich, anisidin, iodoplatinate, and nitroprussiate reagents (16). For betaines, Bregoff-Delwiche's modification of Dragendorff's reagent was used (17).

Further identification of the amino acids of Fraction C_3 was obtained by ion-exchange chromatography and by GLC of silyl derivatives.

Experimental Conditions—*Methanolysis of Fatty Acids*—A 100-mg sample, dissolved in 10 ml of dry 0.5 *M* methanolic hydrochloric acid, was placed into a glass-stoppered vial at 75–80° overnight. The methyl esters were extracted twice with 10 ml of *n*-hexane.

Silylation of Amino Acids—Twenty milligrams of sample was dispersed in 1 ml of *N,O*-bis(trimethylsilyl)acetamide and 3 ml of carbon tetrachloride in a stoppered vial and heated at 50° until a clear solution was obtained.

Pharmacological Test—The investigated fraction was dissolved or dispersed in 0.4% tragacanth or 1% polysorbate 80 aqueous dispersions. Following the method of Coldwell *et al.* (13), the dose levels used for any fraction were calculated from: (*a*) the active amount of the precedent fraction and (*b*) the weight of the fraction under investigation, which was assumed to contain at least 80% of the activity shown by the precedent fraction.

Female albino mice (Swiss species), 23 ± 1.5 g, were allowed free access to water but no food 15 hr before the test. They were divided into two groups of seven animals each. Mice of Group I were given 32 ml of solution/kg by stomach tube administration. Group II (controls) received an equal volume of the corresponding vehicle without the mushroom fraction.

Four hours after this treatment, both groups received orally a solution of 9.5% (w/w) absolute ethanol in water (2 g of ethanol/kg). Oral administration of diluted ethanol–water solutions causes a lack of balance in mice. After an induction period of 2–3 min, a sufficient loss of the grasping reflex on a narrow rod is seen (18). Under these experimental conditions, this loss of reflex was observed at 110 ± 20 min (n = 40) for control mice. This period was significantly increased in mice receiving disulfiram before ethanol administration (Table I).

In Procedure I (Scheme I), any investigated fraction giving a significant increase of this period was considered as active (Table I). Further purification of a fraction was achieved if: (*a*) p was lower than 0.01 (Student t test between the results of Groups I and II), and (*b*) this statistical test gave a similar conclusion when applied to the results of a second experiment with the same fraction.

RESULTS AND DISCUSSION

Extraction Procedure III—Contrary to the work of Simandl and Franc (9), the crude benzene extract from *C. atramentarius* failed to show the presence of disulfiram. A compound characterized as a triglyceride, with one molecule of stearic acid for two of linoleic acid, was isolated from the benzene extract. This compound was physiologically inactive when tested in mice at a dose of 200 mg/kg po (Table

[12] Merckotest, CCM Merck 3345 for plasmatic amino acids.

Table I—Pharmacological Activity of Fractions Related to Extraction Procedures I, II, and III, Ergothionein, and Disulfiram

Tested Material	Weight of Fraction, g	Dose Used, mg/kg	Pharmacological Activity, Time (Minutes) of Loss of Reflex	
			Group I	Group II (Control)
Procedure I:				
Ethanol–water extract	257	2400	210	91
Light petroleum extract	38	445	126	113
Benzene extract	1	12	107	113
Methanol extract	44	515	238	130
Fraction A_1	2.5	37	112	93
Fraction A_2	41	515	253	97
Fraction B_1	3	40	131	127
Fraction B_2	38	515	233	95
Fraction C_1	14.5	200	98	114
Fraction C_2	23	310	276	104
Fraction C_3	0.5	150	335	129
Water extract	160	1870	111	121
Procedure II	200 ml of distillate from 500 g of mushrooms	32 ml/kg	99	123
Procedure III:				
Triglyceride	0.2	200	110	105
Ergothionein		200	123	128
Disulfiram		40	292	105

I). This result is supported by the inactivity of the light petroleum extract obtained by Procedure I (Scheme I and Table I).

Extraction Procedure II—To detect physiologically active volatile compound(s) that might have been overlooked using Procedures I and III, the aqueous distillate from extraction Procedure II was administered to mice (32 ml/kg po). This distillate was inactive (Table I).

Extraction Procedure I—The initial ethanol–water extract, prepared from the mushroom material, was subjected to a systematic fractionation (Scheme I), with all steps guided by pharmacological assays. Fraction C_2 was found to exhibit the biological activity present in the starting mushroom material. Further separation of Fraction C_2 (10 g), using preparative TLC, afforded the physiologically active ninhydrin-positive Fraction C_3 (500 mg).

Fraction C_3 exhibited physiological activity at doses (Table I) that were nontoxic when administered with or without ethanol (*i.e.*, no deaths were observed up to 2 months following these experiments). TLC and GLC of Fraction C_3 showed the presence of amino acids and of two unidentified compounds which could be connected to betaines [positive reaction with Bregoff-Delwiche's modification of Dragendorff's reagent (17) after TLC].

Ion-exchange chromatography allowed the identification of the following 20 amino acids (listed in order of decreasing concentrations): glutamine, alanine, threonine, serine, valine, proline, glutamic acid, tyrosine, glycine, aspartic acid, isoleucine, taurine, asparagine, leucine, tryptophan, citrulline, lysine, histidine, arginine, and 3-methylhistidine. Amino acids related to some central nervous system activity were actively sought. Ibotenic acid, muscazon, and muscimol, which were identified in many species of *Amanita* (19), could not be detected in Fraction C_3 by TLC or ion-exchange chromatography (comparison with authentic samples).

In this connection, ergothionein, found together with hercynin in *C. atramentarius* (20), *C. comatus* (21, 22), and *C. micaceus* (23) was tested on mice. Although this amino acid appeared only in trace amounts on thin-layer chromatograms of Fraction C_3, doses of 200 mg/kg of authentic compound were tested on mice and were inactive (Table I).

These results suggest that the structure of the disulfiram-like compound(s) of *C. atramentarius* could be connected to some particular oligopeptides, amino acids, and amines such as tryptamine derivatives. Further work is underway to isolate and characterize the compound(s) responsible for the disulfiram-like activity exhibited by Fraction C_3.

REFERENCES

(1) R. W. Buck, *N. Engl. J. Med.*, **265**, 681(1961).

(2) J. W. Groves, "Edible and Poisonous Mushrooms of Canada," Department of Agriculture, Ottawa, Canada, 1962, p. 210.

(3) V. E. Tyler, Jr., in "Progress in Toxicology," A. Stolman, Ed., Academic, New York, N.Y., 1963, p. 368.

(4) W. A. Reynolds and F. H. Lowe, *N. Engl. J. Med.*, **272**, 630(1965).

(5) L. C. C. Krieger, *Mycologia*, **3**, 200(1911).

(6) L. Zeitlmayr, "Knaurs Pilzbuch," Droemer, Munich, Germany, 1955, pp. 65, 145.

(7) G. P. Child, *Mycologia*, **44**, 200(1952).

(8) J. W. Groves, *ibid.*, **54**, 779(1964).

(9) J. Simandl and J. Franc, *Chem. Listy*, **50**, 1862(1956).

(10) P. H. List and H. Reith, *Arzneim.-Forsch.*, **10**, 34(1960).

(11) J. K. Wier and V. E. Tyler, *J. Am. Pharm. Assoc., Sci. Ed.*, **49**, 426(1960).

(12) K. Genest, B. B. Coldwell, and D. W. Hughes, *J. Pharm. Pharmacol.*, **20**, 102(1968).

(13) B. B. Coldwell, K. Genest, and D. W. Hughes, *ibid.*, **21**, 176(1969).

(14) G. M. Hatfield, J. P. Schaumberg, and R. G. Brummel, "Abstracts," 121st Annual Meeting of the American Pharmaceutical Association, Chicago, Ill., Aug. 3–8, 1974, Vol. 4, No. 1.

(15) F. Feigl, "Spot-Tests in Organic Analysis," Elsevier, Amsterdam, The Netherlands, 1971, p. 705.

(16) I. Smith, "Chromatographic and Electrophoretic Techniques, Vol. I, Chromatography," 3rd ed., William Heineman, Ed., Medical Books, 1969, pp. 119–122.

(17) E. Stahl, "Thin-Layer Chromatography," Academic, New York, N.Y., 1965, p. 491.

(18) J. R. Boissier, L'apport de la pharmacologie expérimentale à l'étude des neuroleptiques et des tranquillisants, *Actualités pharmacologiques*, XIIe série, Masson, Paris, France, 1959, pp. 1–69.

(19) C. H. Eugster, in "Progress in the Chemistry of Organic Natural Products," vol. 27, L. Zechmeister, Ed., Springer-Verlag, Wien, Austria, 1969, pp. 261–321.

(20) P. H. List and H. Hetzel, *Planta Med.*, **8**, 105(1960).

(21) P. H. List, *Arch. Pharm.*, **290/62**, 517(1957).

(22) *Ibid.*, **291/63**, 502(1958).

(23) P. H. List and H. Reith, *Z. Physiol. Chem.*, **319**, 17(1960).

ACKNOWLEDGMENTS AND ADDRESSES

Received October 21, 1974, from the *Laboratories of Pharmacognosy, Pharmaceutical Organic Chemistry, and Medical Biochemistry, Pharmaceutical Institute, Free University of Brussels, Campus Plaine B205/4, Boulevard du Triomphe, B-1050 Brussels, Belgium.*

Accepted for publication February 19, 1976.

The authors thank Professor A. Lowenthal and Mr. F. Lavinha for the column chromatography of amino acids, Dr. C. H. Eugster for ibotenic acid, and Dr. A. R. Gagneux for assistance.

[x] To whom inquiries should be directed.

Stability of Aqueous Solutions of Mibolerone

M. I. AMIN ˣ, K. T. KOSHY, and J. T. BRYAN

Abstract □ The kinetics and mechanism of degradation of mibolerone were studied in aqueous buffered solutions in the pH range of 1–8 at 67.5°. Mibolerone showed maximum stability between pH 5.5 and 6.4. At pH 1–2, the major degradative pathway was dehydration followed by migration of the 18-methyl group to form 7α,17,17-trimethylgona-4,13-dien-3-one. While there was only one degradation product at pH 1–2, the degradation at pH 7–8 was complex. As many as 12 degradation products were detected by GLC. Mass spectral data indicated that the majority of these products were either oxidation products or isomers. At pH 7.6, the apparent first-order rate constants exhibited marked dependency on buffer concentration. Incorporation of a sequestering agent into the solutions eliminated this dependency, suggesting that trace metal impurities from the buffer reagents were catalyzing the degradation. This was confirmed by degradation studies of solutions in water for injection containing 5 ppm of trace metal ions. Sn^{+2}, Cu^{+2}, and Fe^{+2} accelerated the degradation, with Fe^{+2} having the most catalytic effect. The temperature dependence of the rate of degradation was studied in 0.05 *M* phosphate buffer at pH 6.4. The activation energy was 19.6 ± 1.63 kcal/mole.

Keyphrases □ Mibolerone—aqueous solutions, kinetics and mechanism of degradation, GLC evaluation □ Stability—mibolerone aqueous solutions, kinetics and mechanism of degradation, GLC evaluation □ GLC—evaluation, kinetics and mechanism of degradation of mibolerone aqueous solutions □ Anabolic–androgenic agents—mibolerone, aqueous solutions, kinetics and mechanism of degradation, GLC evaluation

Mibolerone[1] (7α,17α-dimethyl-19-nortestosterone) (I) is an androgenic–anabolic nonprogestational steroid. Given orally on a continuous basis, it effectively inhibits estrus in a high percentage of bitches and queens (1).

The purpose of this study was to investigate the factors affecting its degradation in aqueous solutions and the nature of its degradation products so that liquid and semisolid dosage forms could be formulated.

EXPERIMENTAL

Kinetic Studies—*pH–Rate Studies*—Solutions of 0.2 *M* KH_2PO_4 were adjusted to pH 1–8 using either hydrochloric acid or 0.2 *M* sodium hydroxide and were diluted with water for injection to 0.05 *M* phosphate concentration. To 99 ml of the buffer solution at each pH, 1 ml of a 0.2% mibolerone solution in alcohol was added and the contents were mixed. About 11 ml of the solutions was poured into ampuls, sealed, and placed in a 67.5° constant-temperature oven. At appropriate times, two samples were withdrawn; the pH of one was measured, and the other was stored at 4° until GLC analysis. During the study, the pH did not vary by more than 0.15 pH unit.

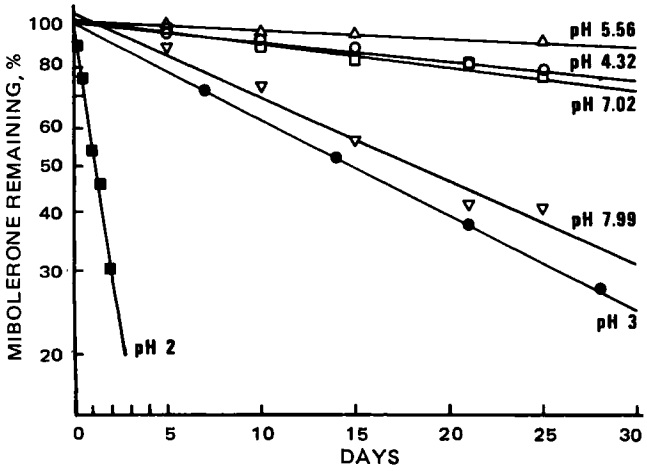

Figure 1—*Apparent first-order disappearance of mibolerone in 0.05 M phosphate buffers at 67.5°.*

Table I—Apparent First-Order Rate Constants of Degradation of Mibolerone in 0.05 *M* Phosphate Buffer at 67.5°

pH	k, days^{-1} × 10^3
1.00	10,219
2.00	6,302
3.00	46.46
4.32	9.22
5.56	3.73
6.40	4.28
7.02	10.40
7.99	39.97

Table II—GLC–Mass Spectral Data for Mibolerone, pH 7.95, 67.5°, 28 Days

Peak	*m/e*	Remarks
1	249	Not likely to be the molecular ion
2		Very weak spectrum
3	279	Not likely to be the molecular ion
4	304	Two more mass units than mibolerone; reduction product?
5	302, 304	An isomer and a reduction product?
6	302	Another isomer of mibolerone?
7		Did not scan
8	302	Mibolerone
9	316	An epoxide?
10	316, 318	Oxidation products
11	314, 318	Oxidation products
12	316, 318	Oxidation products
13		Did not scan

Temperature–Rate Studies—The effect of temperature on the rate of mibolerone degradation was studied in 0.05 *M* KH_2PO_4 buffer, pH 6.4, at 40, 47, 56, 80, and 95°. At appropriate intervals, samples were withdrawn and stored at 4° until GLC analysis.

Assay Procedure: GLC—The samples stored at 4° were brought to room temperature. Ten milliliters of the sample was pipetted into a 50-ml glass-stoppered centrifuge tube. Exactly 10 ml of a chloroform solution containing 15.0 μg/ml of stanolone (17β-hydroxy-5α-androstan-3-one) was added as the internal standard. The tube was shaken, the layers were allowed to separate, and the aqueous layer was removed by aspiration.

The chloroform was removed by a stream of nitrogen, and the residue was redissolved in 0.5 ml of chloroform and transferred to a 1-ml tube. Then 1.0 μl of solution was injected into a gas chromatograph[2]

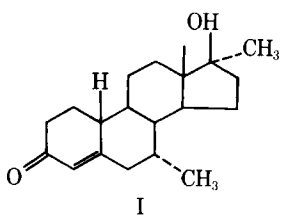

I

[1] The Upjohn Co.

[2] Mikrotek MT-220, Tracor Inc., Austin, Tex.

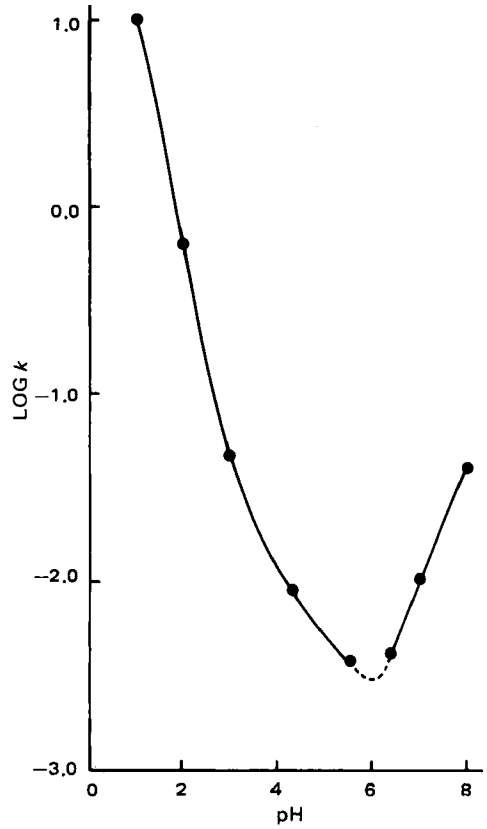

Figure 2—*The pH–rate profile of mibolerone degradation at 67.5°.*

under the following conditions. The column used was 1% QF-1 on Gas Chrom Q (100–120 mesh) in a 3-mm i.d. glass tube, 0.46 m (18 in.). The temperatures were: column, 190°; inlet, 230°; and flame-ionization detector, 260°. The gas flow rates were: helium, 70 ml/min; hydrogen, 40 ml/min; and air, 400 ml/min.

The retention times for stanolone and mibolerone were 2.5 and 4 min, respectively. The concentration of mibolerone in each sample was calculated by comparing mibolerone–internal standard peak height ratios to the peak height ratios of a standard solution of mibolerone treated in the same manner as the sample.

RESULTS AND DISCUSSION

Kinetic Studies—*pH–Rate Studies*—At constant pH and temperature, the degradation of mibolerone followed an apparent first-order process (Fig. 1). The apparent first-order rate constants were calculated from the slopes of log percent residual concentration–time data by means of a computer-programmed least-squares regression analysis (Table I).

The pH–rate relationship for mibolerone is shown in Fig. 2, and the maximum stability was observed between pH 5.5 and 6.4 (the dotted line).

Temperature–Rate Studies—The temperature dependence of the rate of degradation was studied in 0.05 *M* phosphate buffer at pH 6.4. This pH was selected because the semisolid dosage form had a pH of 6.4. The Arrhenius plot is shown in Fig. 3. From the slope of this line, the activation energy was calculated as 19.6 ± 1.63 kcal/mole, from

Table III—Apparent First-Order Rate Constants of Degradation of Mibolerone in Phosphate Buffers in the Presence and Absence of Edetate Disodium at 80°, pH 7.6, and Ionic Strength 0.4

Buffer Concentration	k, Days^{-1} × 10^3 With Edetate Disodium	k, Days^{-1} × 10^3 Without Edetate Disodium
0.1 *M*	3.52	56.19
0.2 *M*	5.88	67.69

Table IV—Apparent First-Order Rate Constants of Degradation of Mibolerone in Water for Injection at 95° and with Different Trace Metal Ions at 5-ppm Concentration

Trace Metal Ions Salt	k, days^{-1} × 10^3
None	15.65
Stannous sulfate	21.49
Cupric sulfate pentahydrate	31.64
Ferrous sulfate heptahydrate	122.88

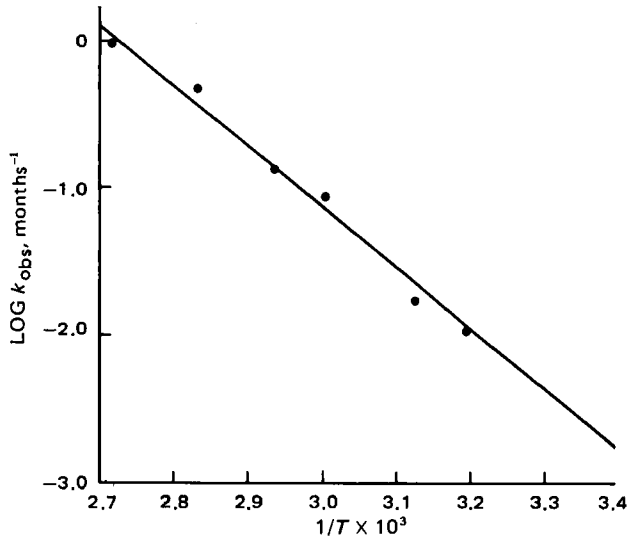

Figure 3—*Arrhenius plot for degradation of mibolerone at pH 6.4.*

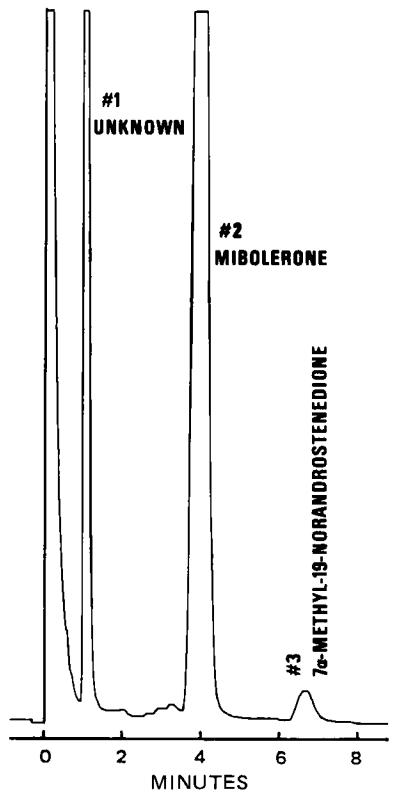

Figure 4—*Gas–liquid chromatogram of a chloroform extract of a buffered aqueous solution of mibolerone, pH 2, heated for 72 hr at 67.5°.*

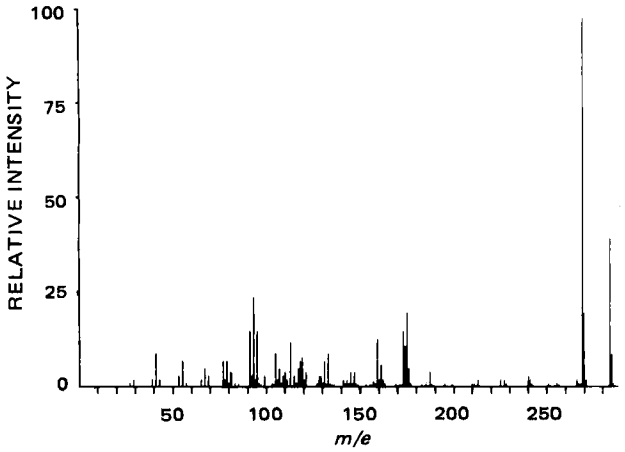

Figure 5—*Mass spectrum of degradation compounds isolated from a buffered aqueous solution of mibolerone, pH 2, heated for 72 hr at 67.5°.*

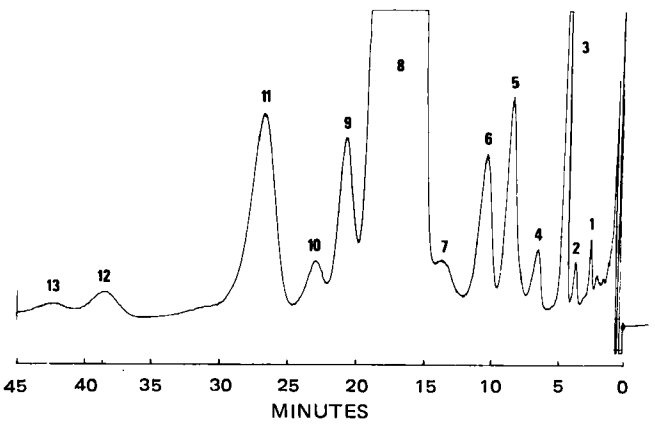

Figure 6—*Gas–liquid chromatogram of a chloroform extract (total ion current detector) of a buffered aqueous solution of mibolerone, pH 7.95, heated for 28 days at 67.5°.*

which the prediction was made that at pH 6.4 mibolerone will not degrade by more than 10% after 3 years at 25°.

Mechanism of Degradation and Identification of Degradation Products—A gas–liquid chromatogram of a chloroform extract of a degraded solution of mibolerone at pH 2 is shown in Fig. 4. A similar chromatogram was also obtained from a chloroform extract of a degraded solution of mibolerone at pH 1.

To determine the mechanism of degradation, the degradation product (peak 1) was isolated and identified. The extract of a degraded solution at pH 2 was subjected to TLC on silica gel plates (GF_{254}, 250 μm), using benzene–acetone (4:1) as the developing solvent. The unknown degradation product was nicely separated from mibolerone; the R_f values were 0.57 and 0.31, respectively. The band representing the unknown was scraped and eluted with ethanol, the ethanol was removed, and the residue was redissolved in chloroform. This extract was subjected to GLC–mass spectrometry[3] using 1% QF-1 on a Gas Chrom Q column [0.61 m (2 ft), 3 mm i.d.], and the response was monitored using a total ion current detector.

The mass spectrum is shown in Fig. 5. The molecular ion was *m/e* 284, 18 less than mibolerone. It was suspected that mibolerone had undergone Wagner–Meerwein rearrangement (2), which involves dehydration and migration of the 18-methyl group to form 7α,17,17-trimethylgona-4,13-dien-3-one (II). Authentic Compound II was synthesized by refluxing mibolerone with 3 *N* HCl for 5 hr in a nitrogen atmosphere. Crystals that separated on cooling were recrystallized from methanol (mp 97–99°). The structure was identified by elemental analysis and IR, NMR, and mass spectra. The unknown had TLC and GLC characteristics and a mass spectrum identical to those of the authentic compound.

At pH 7.95, mibolerone degraded more slowly than at pH 2, but the mechanism of degradation was more complex. A degraded buffered solution of mibolerone at pH 7.95 was extracted with chloroform, and the extract was directly subjected to GLC–mass spectrometry as already described [except that the column length was 0.9 m (3 ft)] (Fig. 6 and Table II). As many as 12 degradation products were found. Even though none of the degradation products was identified, it is evident that they were mostly oxidation products.

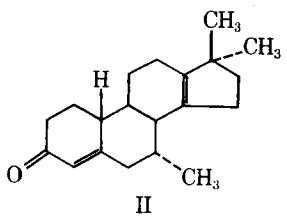

II

[3] LKB 9000 gas chromatograph–mass spectrometer.

Effect of Buffer Concentration—It was reported (3) that degradation of prednisolone in solutions is autoxidative and is catalyzed by trace metal impurities present in buffer reagents. Thus, the degradation of mibolerone was studied at pH 7.6 at two different buffer concentrations, but at a constant ionic strength, and in the presence and absence of a sequestering agent. In the absence of a sequestering agent, the apparent first-order rate constants showed a dependency on the buffer concentration, suggesting that trace metal impurities in the buffer reagents were catalyzing the degradation (Table III).

Effect of Specific Trace Metal Ions—The effect of specific trace metal ions on the degradation of mibolerone was confirmed by addition of known amounts of metal ions to a solution of mibolerone in water for injection. The amounts of salts used corresponded to 5 ppm of the specific metal ions. The data (Table IV) indicated that Sn^{+2}, Cu^{+2}, and Fe^{+2} accelerated the degradation, with Fe^{+2} having the most catalytic effect. Furthermore, when no metal ions were added, the apparent first-order rate constant was about 2000 times slower than the apparent first-order rate constant obtained from 0.05 *M*, pH 6.4 phosphate buffer at 95° (Fig. 3).

REFERENCES

(1) J. H. Sokolowski, "Proceedings 41st Annual Meeting, American Animal Hospital Association," Apr. 1974.

(2) C. R. Noller, "Chemistry of Organic Compounds," 2nd ed., Saunders, Philadelphia, Pa., 1958, p. 857.

(3) T. O. Oesterling and D. E. Guttman, *J. Pharm. Sci.*, **53**, 1189(1964).

ACKNOWLEDGMENTS AND ADDRESSES

Received May 7, 1975, from the *Agricultural Division, The Upjohn Company, Kalamazoo, MI 49001*

Accepted for publication February 9, 1976.

Presented at the Basic Pharmaceutics Section, APhA Academy of Pharmaceutical Sciences, New Orleans meeting, November 1974.

The authors thank J. A. Campbell for suggestions in the identification of degradation products.

[x] To whom inquiries should be directed.

Effect of Nonionic Surfactants on Percutaneous Absorption of Salicylic Acid and Sodium Salicylate in the Presence of Dimethyl Sulfoxide

WU-WEI SHEN *, AUGUST G. DANTI ˣ, and FRANK N. BRUSCATO

Abstract □ Fifteen nonionic surfactants, 10% (w/w), were each incorporated into white petrolatum USP ointment base containing 10% (w/w) salicylic acid or 11.6% (w/w) sodium salicylate with 10% (w/w) dimethyl sulfoxide. Percutaneous absorption was determined from blood salicylate levels in New Zealand white rabbits at regular intervals for 8 hr following application of the ointment. Percutaneous absorption of salicylic acid was increased significantly when sorbitan monopalmitate, sorbitan trioleate, poloxamer 231, poloxamer 182, polyoxyethylene 4 lauryl ether, polyoxyethylene 2 oleyl ether, or polyoxyl 8 stearate was added to the ointment containing dimethyl sulfoxide, salicylic acid, and white petrolatum. Percutaneous absorption of sodium salicylate was increased significantly when sorbitan monolaurate, sorbitan monopalmitate, or poloxamer 182 was added to the ointment containing dimethyl sulfoxide, sodium salicylate, and white petrolatum.

Keyphrases □ Surfactants, nonionic—effect on percutaneous absorption of salicylic acid and sodium salicylate from ointment bases containing dimethyl sulfoxide, rabbits □ Absorption, percutaneous—salicylic acid and sodium salicylate from ointment bases containing dimethyl sulfoxide, effect of nonionic surfactants, rabbits □ Salicylic acid—percutaneous absorption from ointment bases containing dimethyl sulfoxide, effect of nonionic surfactants, rabbits □ Sodium salicylate—percutaneous absorption from ointment bases containing dimethyl sulfoxide, effect of nonionic surfactants, rabbits □ Petrolatum, white—ointment base, percutaneous absorption of salicylic acid and sodium salicylate, effect of nonionic surfactants □ Ointment bases—white petrolatum, percutaneous absorption of salicylic acid and sodium salicylate, effect of nonionic surfactants

Dimethyl sulfoxide has demonstrated a broad spectrum of activities, including the enhancement of penetration through plant and animal membranes (1). It has been suggested for possible use as an analgesic agent, anti-inflammatory adjunct, bacteriostatic agent, diuretic, tranquilizer, potentiator of other compounds, and penetrant carrier (2). Dimethyl sulfoxide facilitates the transport of sodium salicylate, sulfadiazine sodium, aminophylline, Evans blue dye, and heparin sodium across the mucous membrane of a dog's bladder (3). Kligman (1) concluded from his experimentation that, if dimethyl sulfoxide is to be clinically useful, quite concentrated solutions, perhaps 80–90%, would be required to accelerate the rate of topical medicaments such as corticosteroids through the skin. Dimethyl sulfoxide enhanced the percutaneous absorption of salicylic acid from hydrophilic ointment USP and hydrophilic petrolatum USP (4).

In November 1965, dimethyl sulfoxide was removed from the market by the Food and Drug Administration because it was reported to have a possible harmful effect on human eyes. The lens of eyes of dimethyl sulfoxide-treated animals were characterized by division into two zones, a central area stimulating a lens nucleus and a peripheral area (5).

The mechanism of increased membrane permeability effected by dimethyl sulfoxide is essentially unknown. It was pointed out that the carrier mechanism produced by dimethyl sulfoxide might be related to the fact that it forms complexes with various substances (2). The attraction of dimethyl sulfoxide for water should be considered as a possible factor in altered membrane permeability.

Since enhanced percutaneous absorption of drugs can be achieved *via* dimethyl sulfoxide (4), substances possessing a particular affinity for the membranous structure may contribute to the overall enhancement. Such substances are classified as surface-active agents. Of the three major surface-active agents, a nonionic surfactant can possibly emulsify the sebum, enhance the thermodynamic activity of drugs, or change the diffusion constant and activity coefficient of drugs (6), consequently permitting drugs to penetrate into the cells easily.

This study determined the effects of selected nonionic surfactants on the percutaneous absorption of salicylic acid and sodium salicylate in white petrolatum USP with dimethyl sulfoxide.

EXPERIMENTAL

The following ointments were used: 10% (w/w) salicylic acid[1] in white petrolatum[2], 11.6% (w/w) sodium salicylate[3] in white petrolatum, 10% (w/w) dimethyl sulfoxide[4] plus 10% (w/w) salicylic acid in white petrolatum, 10% (w/w) dimethyl sulfoxide plus 11.6% (w/w) sodium salicylate in white petrolatum, 10% (w/w) surfactant plus 10% (w/w) salicylic acid plus 10% (w/w) dimethyl sulfoxide in white petrolatum, and 10% (w/w) surfactant plus 11.6% (w/w) sodium salicylate plus 10% (w/w) dimethyl sulfoxide in white petrolatum.

The property of absorption was compared between an ointment consisting of 10% (w/w) dimethyl sulfoxide plus 10% (w/w) salicylic acid in white petrolatum and one containing 10% (w/w) surfactant plus 10% (w/w) salicylic acid plus 10% (w/w) dimethyl sulfoxide in white petrolatum. This comparison was repeated with sodium salicylate replacing the salicylic acid.

Surfactants—The nonionic surfactants selected [and hydrophilic–lipophilic balance (HLB) values] were poloxamer 231[5] (2), poloxamer 182[6] (7), poloxamer 184[7] (15), polyoxyethylene 20 oleyl ether[8] (15.3), polyoxyethylene 4 lauryl ether[9] (9.5), polyoxyethylene 2 oleyl ether[10] (4.9), sorbitan monolaurate[11] (8.6), sorbitan monopalmitate[12] (6.7), sorbitan trioleate[13] (1.8), polysorbate 20[14] (16.7), polysorbate 40[15] (15.6), polysorbate 60[16] (14.9), polyoxyl 8 stearate[17]

[1] USP grade, lot 61416, Merck & Co.
[2] USP grade, lot 731214, Fisher Scientific.
[3] USP grade, lot 71610, Merck & Co.
[4] Experimental drug grade, lot 50509, Crown Zellerbach.
[5] Pluronic L81, Wyandotte Chemical Corp., Wyandotte, Mich.
[6] Pluronic L62, Wyandotte Chemical Corp., Wyandotte, Mich.
[7] Pluronic L64, Wyandotte Chemical Corp., Wyandotte, Mich.
[8] Brij 99, Atlas Chemical Industries, Wilmington, Del.
[9] Brij 30, Atlas Chemical Industries, Wilmington, Del.
[10] Brij 93, Atlas Chemical Industries, Wilmington, Del.
[11] Span 20, Atlas Chemical Industries, Wilmington, Del.
[12] Span 40, Atlas Chemical Industries, Wilmington, Del.
[13] Span 85, Atlas Chemical Industries, Wilmington, Del.
[14] Tween 20, Atlas Chemical Industries, Wilmington, Del.
[15] Tween 40, Atlas Chemical Industries, Wilmington, Del.
[16] Tween 60, Atlas Chemical Industries, Wilmington, Del.
[17] Myrj 45, Atlas Chemical Industries, Wilmington, Del.

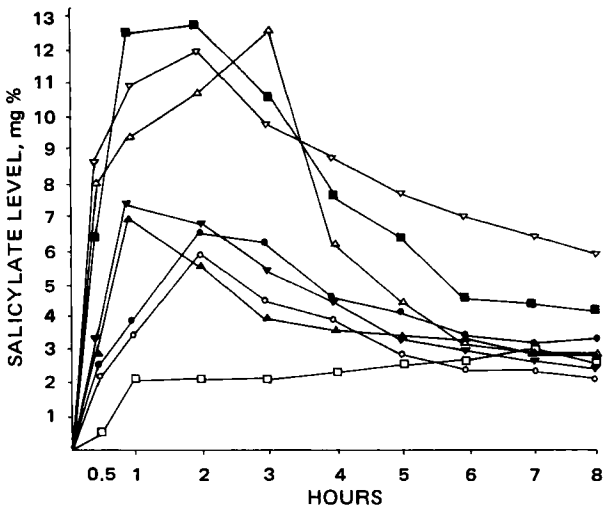

Figure 1—*Effect of sorbitan and polysorbate surfactants on percutaneous absorption of salicylic acid in the presence of dimethyl sulfoxide. Key: △, 10% sorbitan monolaurate plus 10% dimethyl sulfoxide plus 10% salicylic acid; ▽, 10% sorbitan monopalmitate plus 10% dimethyl sulfoxide plus 10% salicylic acid; ■, 10% sorbitan trioleate plus 10% dimethyl sulfoxide plus 10% salicylic acid; ●, 10% polysorbate 20 plus 10% dimethyl sulfoxide plus 10% salicylic acid; ▲, 10% polysorbate 40 plus 10% dimethyl sulfoxide plus 10% salicylic acid; ▼, 10% polysorbate 60 plus 10% dimethyl sulfoxide plus 10% salicylic acid; ○, 10% dimethyl sulfoxide plus 10% salicylic acid; and □, 10% salicylic acid.*

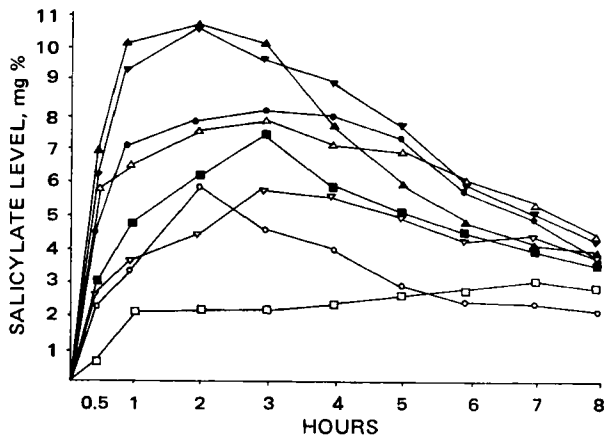

Figure 3—*Effect of polyoxyethylene esters and mixed surfactants on percutaneous absorption of salicylic acid in the presence of dimethyl sulfoxide. Key: △, 10% polyoxyl 8 stearate plus 10% dimethyl sulfoxide plus 10% salicylic acid; ▽, 10% polyoxyethylene 30 monostearate plus 10% dimethyl sulfoxide plus 10% salicylic acid; ■, 10% polyoxyethylene 40 monostearate plus 10% dimethyl sulfoxide plus 10% salicylic acid; ●, 5% sorbitan trioleate plus 5% polysorbate 40 plus 10% dimethyl sulfoxide plus 10% salicylic acid; ▲, 5% polyoxyethylene 2 oleyl ether plus 5% polyoxyethylene 20 oleyl ether plus 10% dimethyl sulfoxide plus 10% salicylic acid; ▼, 5% polyoxyl 8 stearate plus 5% polyoxyethylene 40 monostearate plus 10% dimethyl sulfoxide plus 10% salicylic acid; ○, 10% dimethyl sulfoxide plus 10% salicylic acid; and □, 10% salicylic acid.*

(11.1), polyoxyethylene 30 monostearate[18] (16), and polyoxyethylene 40 monostearate[19] (16.9).

To investigate the effect of the HLB value on percutaneous absorption of salicylic acid and sodium salicylate, the following matched surfactants were used: 5% (w/w) sorbitan trioleate plus 5% (w/w) polysorbate 40 with an HLB of 8.7, 5% (w/w) polyoxyethylene 20 oleyl ether plus 5% (w/w) polyoxyethylene 2 oleyl ether with an HLB of 10.1, and 5% (w/w) polyoxyl 8 stearate plus 5% (w/w) polyoxyethylene 40 monostearate with an HLB of 14.0.

Ointment Preparation—Salicylic acid and sodium salicylate, previously reduced to fine powders in a ball mill, were each passed through an 80-mesh sieve and dried at 50° in a heated vacuum desiccator for at least 48 hr before use. The ointments prepared contained 10% (w/w) milled salicylic acid or 11.6% (w/w) milled sodium salicylate, 10% (w/w) surfactant, and 10% (w/w) dimethyl sulfoxide. Each ingredient was accurately weighed[20] and incorporated into the white petrolatum.

Test Animals—Each ointment was applied to a New Zealand white rabbit, 3.0–4.0 kg, randomly selected without regard to sex. Each rabbit was used only three times and received the same surfactant in each test. Only one pair of rabbits was utilized during any one ex-

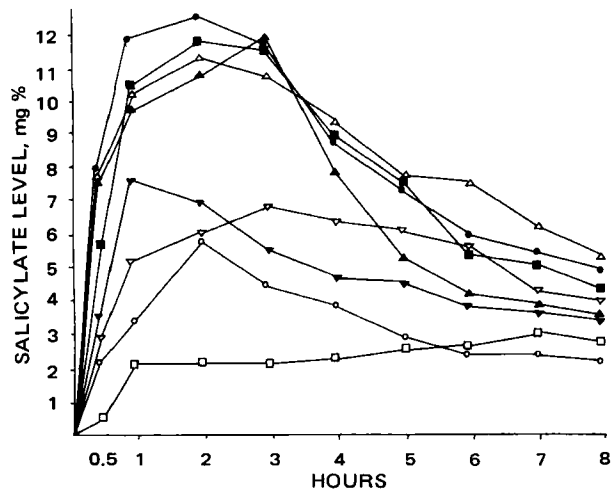

Figure 2—*Effect of poloxamer and polyoxyethylene surfactants on percutaneous absorption of salicylic acid in the presence of dimethyl sulfoxide. Key: △, 10% poloxamer 182 plus 10% dimethyl sulfoxide plus 10% salicylic acid; ▽, 10% poloxamer 184 plus 10% dimethyl sulfoxide plus 10% salicylic acid; ■, 10% poloxamer 231 plus 10% dimethyl sulfoxide plus 10% salicylic acid; ●, 10% polyoxyethylene 2 oleyl ether plus 10% dimethyl sulfoxide plus 10% salicylic acid; ▲, 10% polyoxyethylene 4 lauryl ether plus 10% dimethyl sulfoxide plus 10% salicylic acid; ▼, 10% polyoxyethylene 20 oleyl ether plus 10% dimethyl sulfoxide plus 10% salicylic acid; ○, 10% dimethyl sulfoxide plus 10% salicylic acid; and □, 10% salicylic acid.*

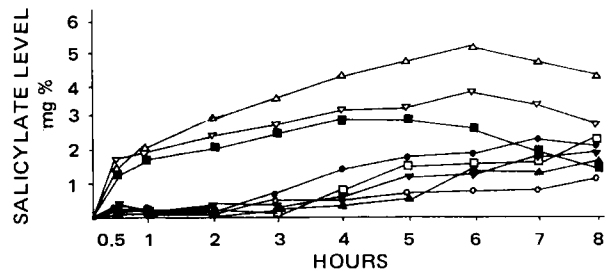

Figure 4—*Effect of sorbitan and polysorbate surfactants on percutaneous absorption of sodium salicylate in the presence of dimethyl sulfoxide. Key: △, 10% sorbitan monolaurate plus 10% dimethyl sulfoxide plus 11.6% sodium salicylate; ▽, 10% sorbitan monopalmitate plus 10% dimethyl sulfoxide plus 11.6% sodium salicylate; ■, 10% sorbitan trioleate plus 10% dimethyl sulfoxide plus 11.6% sodium salicylate; ●, 10% polysorbate 20 plus 10% dimethyl sulfoxide plus 11.6% sodium salicylate; ▲, 10% polysorbate 40 plus 10% dimethyl sulfoxide plus 11.6% sodium salicylate; ▼, 10% polysorbate 60 plus 10% dimethyl sulfoxide plus 11.6% sodium salicylate; ○, 10% dimethyl sulfoxide plus 11.6% sodium salicylate; and □, 11.6% sodium salicylate.*

[18] Myrj 51, Atlas Chemical Industries, Wilmington, Del.
[19] Myrj 52, Atlas Chemical Industries, Wilmington, Del.
[20] Harvard Trip Balance, Ohaus, N.J.

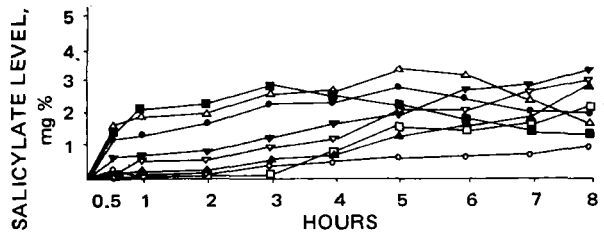

Figure 5—*Effect of polyoxyethylene and poloxamer surfactants on percutaneous absorption of sodium salicylate in the presence of dimethyl sulfoxide. Key: △, 10% poloxamer 182 plus 10% dimethyl sulfoxide plus 11.6% sodium salicylate; ▽, 10% poloxamer 184 plus 10% dimethyl sulfoxide plus 11.6% sodium salicylate; ■, 10% poloxamer 231 plus 10% dimethyl sulfoxide plus 11.6% sodium salicylate; ●, 10% polyoxyethylene 2 oleyl ether plus 10% dimethyl sulfoxide plus 11.6% sodium salicylate; ▲, 10% polyoxyethylene 4 lauryl ether plus 10% dimethyl sulfoxide plus 11.6% sodium salicylate; ▼, 10% polyoxyethylene 20 oleyl ether plus 10% dimethyl sulfoxide plus 11.6% sodium salicylate; ○, 10% dimethyl sulfoxide plus 11.6% sodium salicylate; and □, 11.6% sodium salicylate.*

perimental period due to space and time limitations. A 7-day rest period was allowed before reapplication of the ointment.

The animals were maintained on rabbit chow[21] and water and housed individually in an animal room maintained at 25°. Twenty-four hours prior to the application of the ointment to the rabbit, hair was removed from the ears and the dorsal area between the forelegs and hindlegs on both sides of the spine (4) with an animal clipper and a depilatory cream[22].

Application of Ointment—A specially prepared bandage restricted and controlled the area of contact between the rabbit and the ointment. The edges of an 8.4 × 14.7-cm^2 piece of aluminum foil were doubled over and flattened 1 cm on each side to produce a rectangular plate measuring 6.4 × 12.7 cm^2 with 1-cm reinforced margin. A 5.0-g sample of the selected ointment was uniformly spread over one surface of the plate, whose opposite side was centered on an 8.9 × 20-cm^2 strip of adhesive tape. The entire assembly was then applied to the shaved dorsal skin of the rabbit and adjusted to conform to contours of the area.

The assembly was covered with a bandage to ensure adequate contact between the ointment and the skin to minimize the possibility of contamination. The bandage arrangement was adapted from Stolar *et al.* (7). The ointment remained in contact with the skin for 8 hr, during which time the rabbit did not receive food or water.

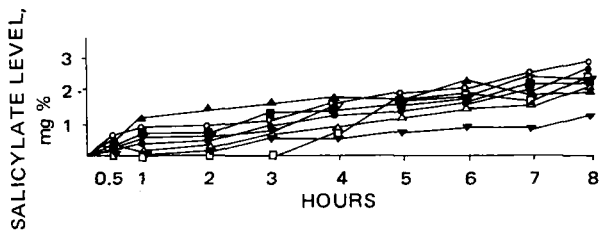

Figure 6—*Effect of polyoxyethylene esters and mixed surfactants on percutaneous absorption of sodium salicylate in the presence of dimethyl sulfoxide. Key: △, 10% polyoxyl 8 stearate plus 10% dimethyl sulfoxide plus 11.6% sodium salicylate; ▽, 10% polyoxyethylene 30 monostearate plus 10% dimethyl sulfoxide plus 11.6% sodium salicylate; ■, 10% polyoxyethylene 40 monostearate plus 10% dimethyl sulfoxide plus 11.6% sodium salicylate; ●, 5% sorbitan trioleate plus 5% polysorbate 40 plus 10% dimethyl sulfoxide plus 11.6% sodium salicylate; ▲, 5% polyoxyethylene 2 oleyl ether plus 5% polyoxyethylene 20 oleyl ether plus 10% dimethyl sulfoxide plus 11.6% sodium salicylate; ▼, 5% polyoxyl 8 stearate plus 5% polyoxyethylene 40 monostearate plus 10% dimethyl sulfoxide plus 11.6% sodium salicylate; ○, 10% dimethyl sulfoxide plus 11.6% sodium salicylate; and □, 11.6% sodium salicylate.*

[21] Purina.
[22] Surgex, Ciba, Summit, N.J.

Table I—*t* Test Value from the Comparison of the Overall Average of Percutaneous Salicylate Absorption from the Rabbit between Surfactant (S) plus Salicylic Acid (I) plus White Petrolatum USP (II) and Salicylic Acid plus White Petrolatum USP Ointments and also between Dimethyl Sulfoxide (III) plus Salicylic Acid plus White Petrolatum USP and Dimethyl Sulfoxide plus Surfactant plus Salicylic Acid plus White Petrolatum USP Ointments

Surfactant	*t* Value between I + II and S + I + II	*t* Value between III + S + I + II and III + I + II
Poloxamer 231	4.905[a]	3.886[a]
Poloxamer 182	4.050[a]	5.737[a]
Poloxamer 184	2.992[a]	2.960[a]
Polyoxyethylene 20 oleyl ether	2.461[a]	2.112[a]
Polyoxyethylene 4 lauryl ether	3.154[a]	2.944[a]
Polyoxyethylene 2 oleyl ether	5.918[a]	3.245[a]
Sorbitan monolaurate	3.038[a]	4.537[a]
Sorbitan monopalmitate	11.308[a]	9.877[a]
Sorbitan trioleate	5.435[a]	9.014[a]
Polysorbate 20	2.104[a]	1.165[b]
Polysorbate 40	2.385[a]	0.745[b]
Polysorbate 60	2.886[a]	0.937[b]
Polyoxyl 8 stearate	2.815[a]	3.972[a]
Polyoxyethylene 30 monostearate	1.901[a]	2.164[a]
Polyoxyethylene 40 monostearate	1.851[a]	3.669[a]
Sorbitan trioleate plus polysorbate 40	3.784[a]	3.804[a]
Polyoxyethylene 20 oleyl ether plus polyoxyethylene 2 oleyl ether	4.846[a]	4.226[a]
Polyoxyl 8 stearate plus polyoxyethylene 40 monostearate	3.380[a]	3.879[a]

[a] Significant difference at 95% level. [b] No significant difference.

Sample Collection Procedure—Blood samples were withdrawn, and the plasma salicylate concentration was determined. One-half milliliter of blood was withdrawn from the marginal ear vein of the rabbit at the following time periods: prior to application of ointment, 0.5 hr after ointment application, and at hourly intervals for 8 hr after application of the ointment. Blood samples were collected in 1-ml sterile disposable 26-gauge tuberculin syringes[23], 1.27 cm containing 0.1 ml of heparin sodium[24]. This blood and heparin mixture was added to 5.0 ml of the combined protein color reagent in a centrifuge tube and analyzed for salicylate content according to the method described by Trinder (8).

After centrifugation and filtration, the colorimetric analysis for salicylate was performed at a wavelength of 540 nm using a spectrophotometer[25]. The absorbance reading obtained from the blood sample withdrawn prior to application was considered the zero reading and subtracted from the other reading to account for the absorbance contributed by other blood constituents. The salicylate content was obtained from a curve previously drawn by using 0.1 ml of heparin sodium and 0.5 ml of sodium salicylate solutions containing the equivalent of 1, 5, 10, 15, and 20 mg % of salicylic acid with 5.0 ml of coloring reagent.

Statistical Analysis of Data—Three replications were run in each individual test. A *t* test with two degrees of freedom at the 95% significance level was used to test the null hypothesis.

[23] Plastipak, Becton, Dickinson & Co., Rutherford, N.J.
[24] USP grade, lot 3AK90A, 10,000 units/ml, Eli Lilly.
[25] Beckman DT-DB model 95.

Table II—t Test Value from the Comparison of the Overall Average of Percutaneous Salicylate Absorption from the Rabbit between Surfactant (S) plus Sodium Salicylate (IV) plus White Petrolatum USP (II) and Sodium Salicylate plus White Petrolatum USP Ointments and also between Dimethyl Sulfoxide (III) plus Sodium Salicylate plus White Petrolatum USP and Dimethyl Sulfoxide plus Surfactant plus Sodium Salicylate plus White Petrolatum USP Ointments

Surfactant	t Value from IV + II and S + IV + II	t Value from III + IV + II and III + S + IV + II
Poloxamer 231	2.011[a]	1.996[a]
Poloxamer 182	3.189[a]	1.645[b]
Poloxamer 184	4.258[a]	1.687[b]
Polyoxyethylene 20 oleyl ether	4.084[a]	2.246[a]
Polyoxyethylene 4 lauryl ether	2.556[a]	2.961[a]
Polyoxyethylene 2 oleyl ether	1.582[b]	3.011[a]
Sorbitan monolaurate	3.858[a]	4.365[a]
Sorbitan monopalmitate	1.878[a]	3.614[a]
Sorbitan trioleate	2.237[a]	3.564[a]
Polysorbate 20	6.209[a]	3.548[a]
Polysorbate 40	4.923[a]	3.854[a]
Polysorbate 60	4.289[a]	3.123[a]
Polyoxyl 8 stearate	3.458[a]	2.843[a]
Polyoxyethylene 30 monostearate	5.464[a]	2.853[a]
Polyoxyethylene 40 monostearate	5.614[a]	2.964[a]
Sorbitan trioleate plus polysorbate 40	3.460[a]	3.224[a]
Polyoxyethylene 20 oleyl ether plus polyoxyethylene 2 oleyl ether	4.162[a]	2.765[a]
Polyoxyl 8 stearate plus polyoxyethylene 40 monostearate	6.040[a]	2.367[a]

[a]Significant difference at 95% level. [b]No significant difference.

RESULTS

The altered percutaneous absorption patterns of salicylic acid and sodium salicylate obtained upon addition of selected surfactants to 10% (w/w) salicylic acid plus 10% (w/w) dimethyl sulfoxide in white petrolatum USP or to 11.6% (w/w) sodium salicylate plus 10% (w/w) dimethyl sulfoxide in white petrolatum USP ointments are shown in Figs. 1–6.

The results of the statistical t test (Tables I and II) indicate that percutaneous absorption of salicylic acid was increased significantly when sorbitan monopalmitate, sorbitan trioleate, poloxamer 231, poloxamer 182, polyoxyethylene 4 lauryl ether, polyoxyethylene 2 oleyl ether, and polyoxyl 8 stearate were each added to the ointment containing dimethyl sulfoxide and salicylic acid in white petrolatum USP. The percutaneous absorption of sodium salicylate was increased significantly when sorbitan monolaurate, sorbitan monopalmitate, and poloxamer 182 were each added to the ointment containing dimethyl sulfoxide and sodium salicylate in white petrolatum USP.

DISCUSSION

A statistical analysis of the results seems to indicate that some surfactants functioned as penetrant carriers, enhancing the percutaneous absorption of salicylic acid and sodium salicylate. When these surfactants were added to an ointment containing salicylic acid and dimethyl sulfoxide, percutaneous absorption of salicylic acid rapidly increased during the first 2 hr following ointment application.

Salicylic acid, which is lipid soluble, penetrates more readily through the skin than the nonlipid-soluble sodium salicylate (9). Substances that are lipid soluble penetrate the cell membrane because of their fat-soluble nature; on the other hand, the uptake of the water by the cell membrane protein provides entry for water-soluble substances (10).

The 10% (w/w) salicylic acid in the ointment was completely solubilized by the quantity of dimethyl sulfoxide and surfactant added to the ointment. Approximately one-third of the 11.6% (w/w) sodium salicylate, equivalent to 10% (w/w) salicylic acid, was solubilized in the amount of dimethyl sulfoxide and surfactant. Adding surfactants and dimethyl sulfoxide to the ointment containing 10% (w/w) salicylic acid in white petrolatum resulted in a significantly rapid increased absorption of the salicylic acid. This increase could possibly be attributed to the ability of dimethyl sulfoxide to solubilize salicylic acid and serve as a penetrant carrier for salicylic acid.

Mixed surfactants of varying HLB values resulted in a prolonged percutaneous absorption effect of both salicylic acid and sodium salicylate.

The mechanism by which percutaneous absorption of salicylic acid and sodium salicylate is increased by nonionic surfactants in the presence of dimethyl sulfoxide is unknown. However, Higuchi (6) suggested that the activity coefficient of the acid and salt plays a major role in percutaneous absorption. Salicylic acid and sodium salicylate, held firmly by the white petrolatum, form a drug–vehicle complex exhibiting a low activity coefficient. The rate of release from such drug–vehicle combinations is slow. When dimethyl sulfoxide and surfactants are added to the ointment containing 11.6% (w/w) sodium salicylate in white petrolatum or 10% (w/w) salicylic acid in white petrolatum, the rate of release of salicylic acid and sodium salicylate may be increased by forming high activity coefficient complexes such as surfactant–drug, dimethyl sulfoxide–drug, and dimethyl sulfoxide–surfactant–drug. Therefore, the percutaneous absorption of salicylic acid and sodium salicylate may be enhanced by these complexes.

REFERENCES

(1) A. M. Kligman, *J. Am. Med. Assoc.*, **193**, 746(1965).

(2) S. W. Jacob, M. Bischel, and R. J. Herschler, *Curr. Ther. Res.*, **6**, 134(1964).

(3) *Ibid.*, **9**, 193(1964).

(4) J. M. Stelzer, J. L. Colaizzi, and P. J. Wurdack, *J. Pharm. Sci.*, **57**, 1732(1968).

(5) L. B. Rubin and K. C. Barnett, *Ann. N.Y. Acad. Sci.*, **141**, 355(1967).

(6) T. Higuchi, "Physical Chemical Analysis of Percutaneous Absorption Process from Creams and Ointments," presented to the Society of Cosmetic Chemists Seminar, New York, N.Y., Sept. 23, 1959.

(7) M. E. Stolar, G. V. Rossi, and M. Barr, *J. Am. Pharm. Assoc., Sci. Ed.*, **49**, 144(1960).

(8) P. Trinder, *Biochem. J.*, **57**, 301(1954).

(9) S. Rothman, "Physiology and Biochemistry of the Skin," University of Chicago Press, Chicago, Ill., 1954, pp. 40, 48.

(10) W. Montagna and W. C. Lobitz, "The Epidermis," Academic, New York, N.Y., 1964, p. 440.

ACKNOWLEDGMENTS AND ADDRESSES

Received May 20, 1975, from the *School of Pharmacy, College of Pharmacy and Health Sciences, Northeast Louisiana University, Monroe, LA 71201*

Accepted for publication February 23, 1976.

Abstracted in part from a thesis submitted by Wu-wei Shen to the Graduate School, Northeast Louisiana University, in partial fulfillment of the Master of Science degree requirements.

* Present address: 200 East Chestnut St., Bordertown, NJ 08505

x To whom inquiries should be directed.

Dissolution of Two-Component Solids

SHIRISH A. SHAH * and EUGENE L. PARROTT ˣ

Abstract □ The dissolution rates of compressed two-component mixtures were investigated. A good correlation between the composition of the solid and its observed dissolution rate was demonstrated by regression analysis. A model for dissolution was applied to compressed mixtures of aspirin–salicylic acid, aspirin–phenacetin, phenacetin–caffeine, and aspirin and caffeine (the last mixture complexes in solution).

Keyphrases □ Dissolution—compressed two-component mixtures, rate correlated with composition □ Solids, two component—dissolution rate correlated with composition □ Aspirin—compressed mixtures with salicylic acid, phenacetin, or caffeine, dissolution rates compared □ Salicylic acid—compressed mixture with aspirin, dissolution rate compared to other mixtures □ Phenacetin—compressed mixtures with aspirin or caffeine, dissolution rates compared □ Caffeine—compressed mixtures with phenacetin or aspirin, dissolution rates compared

The models and kinetics of dissolution for pure materials have received considerable attention in the past 2 decades, but much less attention has been given to models of dissolution from multicomponent systems. An early pharmaceutical study of the dissolution of a two-component system was reported in which the dissolution rates of several poorly soluble weak acids and trisodium phosphate in various mole fractions were studied (1). As the mole fraction of the acid was increased, the dissolution rate increased to a maximum rate; then a further increase in the mole fraction of the acid decreased the dissolution rate.

The dissolution rates of salicylic acid and povidone from compressed disks also were reported (2). Diffusion models were proposed (3) for the dissolution of nondisintegrating polyphasic mixtures, which contained noninteracting components and complexing components. This approach also has been applied to mixtures of polymorphs (4).

Because the relationship of the dissolution rate of a tableted material to compressional force has not been clearly defined, it was desirable to determine this relationship for the materials used in this study of the dissolution kinetics of two-component systems. Increasing precompressional force caused an increase in the dissolution rate of salicylic acid (5). The $t_{50\%}$ decreased for two conventional sulfamethazine tablet formulations and increased for another formulation with increased compressional force. The effect of formulation was also suggested by Khan and Rhodes (7), who reported that an increase in compressional force enhanced the dissolution rate for dicalcium phosphate dihydrate systems but decreased it for microcrystalline cellulose systems. Similarly, Knoechel *et al.* (8) found that, although force influenced the dissolution rate, the formulation and particular medicinal compound had a greater effect on it.

A steady increase in the dissolution rate was found with increasing compressional force until a maximal value, coinciding with the maximum apparent density, was reached (9, 10). An increase in the dissolution rate with an increased compressional force to a maximum and then a decrease with a further increase in compressional force were reported (11). Other studies (12, 13) reported one or two maxima. In contrast, a decrease in the dissolution rate with increasing compressional force to a minimum and then an increase in the dissolution rate with a further increase in compressional force were observed (14, 15).

Kanke and Sekiguchi (16) confirmed earlier reports (17, 18) that for benzoic acid the force exerted no influence on the dissolution rate and that the size of sulfathiazole particles being compressed had no effect on the dissolution rate.

The purpose of this investigation was to apply a diffusion layer model to the dissolution of compressed two-component solids containing interacting and noninteracting components.

EXPERIMENTAL

Preparation of Compressed Spheres and Measurement of Densities—Material that passed through an 80-mesh sieve but was retained on a 100-mesh sieve was compacted by means of a hydraulic press[1] into compressed spheres having a diameter of 1.270 ± 0.005 cm. Depending on the compressibility of the material, compressional forces ranged from 270 to 10,900 kg. The apparent density of the compressed spheres was determined by the displacement method. The sphere was suspended by a short, thin wire from an analytical balance, and its weight was measured when the sphere was immersed in a saturated solution of the material comprising the sphere. The apparent density, ρ_a, was calculated from:

$$\rho_a = \frac{w_{air}}{w_{air} - w_{sol}} \rho_{sol} \qquad \text{(Eq. 1)}$$

where ρ_{sol} is the density of the saturated solution, and w_{air} and w_{sol} are the weights of the sphere in air and the saturated solution, respectively. The true density of the material was determined by means of a pycnometer using *n*-heptane. The percent porosity was calculated by:

$$\text{percent porosity} = 100\,(1 - \rho_a/\rho) \qquad \text{(Eq. 2)}$$

Dissolution Rate—The dissolution rate was determined in distilled water at 25 ± 0.1°, as previously described (17, 19), under conditions where the concentration of the solute did not exceed 5% of its solubility. The dissolution apparatus consisted of a 2-liter beaker in which a 3.0 × 1.5-cm stainless steel paddle was positioned 6.0 cm from the bottom of the beaker. A speed of 324 rpm and a volume of 2 liters of distilled water were used. Each sphere was weighed initially and upon withdrawal from the dissolution medium at appropriate times.

The dissolution medium was analyzed for the component(s) of the sphere by a UV spectrophotometric method. The amount of each component was determined, and the total solid dissolved was calculated. In all analyses, a material balance was demonstrated between the loss of weight of the solid and the components in solution. For each time interval, the difference between the cube root of the initial weight of the sphere and the cube root of the weight at each interval of time was plotted against time. By knowing the shape–volume factor (4.85 for a sphere) and the density of the material, the dissolution rate was calculated (17).

Analytical Procedures—For single-component spheres of benzoic acid, aspirin, and salicylic acid, standard concentration–absorbance

[1] Carver press, model C.

curves were prepared at 273, 275, and 297 nm, respectively. All standard curves exhibited a Beer's law relationship in the concentration range employed. At each time interval during dissolution, an aliquot was withdrawn by a pipet fitted with a filter. If required, the aliquot was diluted with distilled water, and the absorbance was measured spectrophotometrically at the appropriate wavelength.

For multicomponent spheres, a simultaneous analysis was made by use of simultaneous equations (20, 21). For aspirin and salicylic acid, a series of aqueous solutions of known concentrations of aspirin and salicylic acid was prepared, and the absorbance was measured at 275 and 297 nm. From the data, coefficients of the simultaneous equations were determined. Since absorbance is directly proportional to absorptivity and concentration, if the length of the absorbing solution is constant:

$$C_{ASA} = \frac{a_{2\lambda_2}A_1 - a_{2\lambda_1}A_2}{a_{1\lambda_1}a_{2\lambda_2} - a_{2\lambda_1}a_{1\lambda_2}} \quad \text{(Eq. 3)}$$

and:

$$C_{SAL} = \frac{a_{1\lambda_1}A_2 - a_{1\lambda_2}A_1}{a_{1\lambda_1}a_{2\lambda_2} - a_{2\lambda_1}a_{1\lambda_2}} \quad \text{(Eq. 4)}$$

where C_{ASA} and C_{SAL} are the concentrations of aspirin and salicylic acid, respectively; A_1 and A_2 are the absorbances at 275 and 297 nm, respectively; $a_{1\lambda_1}$ and $a_{1\lambda_2}$ are the molar absorptivities for aspirin at 275 and 297 nm, respectively; and $a_{2\lambda_1}$ and $a_{2\lambda_2}$ are the molar absorptivities for salicylic acid at 275 and 297 nm, respectively. Substitution of experimental values into Eqs. 3 and 4 yielded:

$$C_{ASA} = (1.3228A_1 - 0.4499A_2)\ mM \quad \text{(Eq. 5)}$$

and:

$$C_{SAL} = (0.2961A_2 - 0.0352A_1)\ mM \quad \text{(Eq. 6)}$$

For convenience, Eqs. 5 and 6 were expressed in milligrams per milliliter:

$$C_{ASA} = (0.2383A_1 - 0.0811A_2)\ mg/ml \quad \text{(Eq. 7)}$$

and:

$$C_{SAL} = (0.0409A_2 - 0.00486A_1)\ mg/ml \quad \text{(Eq. 8)}$$

At each time interval during dissolution, an aliquot was withdrawn and, after dilution with distilled water if required, the absorbance was measured[2] at 275 and 297 nm. The concentrations of aspirin and salicylic acid in solution were determined using Eqs. 7 and 8.

By using the method described previously (22), the amount of salicylic acid in the batch of aspirin used was 0.07%. Since aspirin hydrolyzes, the extent of hydrolysis during the dissolution interval was considered. At 30-, 60-, and 90-min intervals, colorimetric analysis (22) and UV spectroscopy detected no salicylic acid. Since both methods detected no salicylic acid and the usual interval was 15 min, aspirin hydrolysis during the dissolution interval apparently did not occur to a significant extent to affect dissolution values.

The concentrations of caffeine, phenacetin, and aspirin in solution were determined spectrophotometrically by the method of Clayton and Thiers (23). In the manner previously described, coefficients for simultaneous equations were determined. The simultaneous equations used in studying the dissolution of aspirin–caffeine spheres are:

$$C_{ASA} = (0.05046A_1 - 0.00158A_2)\ mg/ml \quad \text{(Eq. 9)}$$

and:

$$C_{CAF} = (0.019904A_2 - 0.006078A_1)\ mg/ml \quad \text{(Eq. 10)}$$

where A_1 is the absorbance of hydrolyzed solution at 301 nm, and A_2 is the absorbance of the acidic solution at 273 nm.

Simultaneous equations for the analysis of aspirin and phenacetin dissolved from an aspirin–phenacetin sphere are:

$$C_{ASA} = (0.05035A_1 - 0.00166A_2)\ mg/ml \quad \text{(Eq. 11)}$$

and:

$$C_{PH} = (0.01632A_2 - 0.00521A_1)\ mg/ml \quad \text{(Eq. 12)}$$

where A_1 is the absorbance of the hydrolyzed solution at 301 nm, and A_2 is the absorbance of the acidic solution at 250 nm.

[2] Beckman DU.

Table I—Relationship of Compressional Force to Dissolution Rate, Apparent Density, and Percent Porosity

Force, kg	Dissolution Rate[a], g/hr/cm²	Apparent Density, g/ml	Porosity, %
	Benzoic Acid		
900	0.0429	1.29	5.1
2,270	0.0405	1.31	3.7
4,540	0.0408	1.31	3.7
6,800	0.0429	1.31	3.7
9,080	0.0450	1.31	3.7
10,900	0.0429	1.31	3.7
	Salicylic Acid		
270	0.0275	1.19	20.1
454	0.0283	1.24	16.8
910	0.0276	1.31	12.1
1,360	0.0274	1.34	10.1
1,800	0.0278	1.36	8.7
2,270	0.0288	1.38	7.4
4,450	0.0273	1.39	6.7
6,800	0.0270	1.40	6.0
9,080	0.0276	1.40	6.0
10,900	0.0281	1.39	6.7
	Aspirin		
270	0.0428	1.30	9.1
454	0.0440	1.32	7.7
910	0.0438	1.35	5.6
1,360	0.0435	1.36	4.9
1,800	0.0432	1.36	4.9
2,270	0.0446	1.37	4.2
4,450	0.0430	1.38	3.5
6,800	0.0429	1.38	3.5
9,080	0.0429	1.38	3.5
10,900	0.0432	1.37	4.2

[a] Average of two determinations.

Simultaneous equations for the analysis of phenacetin and caffeine dissolved from a phenacetin–caffeine sphere are:

$$C_{PH} = (0.01762A_1 - 0.00587A_2)\ mg/ml \quad \text{(Eq. 13)}$$

and:

$$C_{CAF} = (0.02145A_2 - 0.00522A_1)\ mg/ml \quad \text{(Eq. 14)}$$

where A_1 and A_2 are the absorbances of the acidic solution at 250 and 273 nm, respectively.

RESULTS AND DISCUSSION

Influence of Compressional Force on Apparent Density, Porosity, and Dissolution Rate—Numerous reports (8, 9, 24, 25) showed the relationship of porosity and apparent density to the force of compression of tablets. The data in Tables I and II for the com-

Table II—Relationship of Compressional Force to Dissolution Rate, Apparent Density, and Percent Porosity of Equimolar Binary Mixtures

Force, kg	Dissolution Rate[a], g/hr/cm²	Apparent Density, g/ml	Porosity, %
	Aspirin and Salicylic Acid		
270	—	1.24	15.1
454	—	1.32	9.6
910	0.0484	1.35	7.5
4,540	0.0498	1.39	4.8
10,900	0.0480	1.40	4.1
	Aspirin and Caffeine		
910	0.2171	1.33	8.3
2,270	—	1.34	7.6
4,540	0.2207	1.38	4.8
9,080	—	1.40	3.4

[a] Average of two determinations.

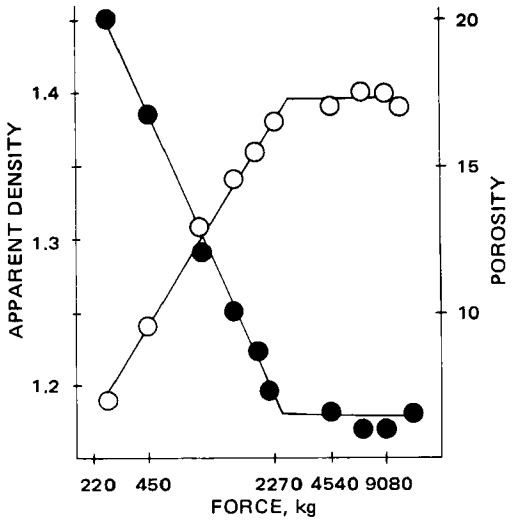

Figure 1—*Influence of compressional force on the apparent density and porosity of salicylic acid. Key: ○, apparent density; and ●, porosity.*

pressed spheres of benzoic acid, salicylic acid, aspirin, an equimolar mixture of aspirin and caffeine, and an equimolar mixture of aspirin and salicylic acid are in agreement with these reports that the apparent density is increased to an asymptotic value as the compressional force is increased. The apparent density is linearly related to the logarithm of the compressional force to a maximal value, as illustrated for salicylic acid in Fig. 1. The porosity of the sphere is decreased as the compressional force is increased. The porosity is linearly related to the logarithm of the compressional force to a minimum porosity (Fig. 1).

Examination of Tables I and II shows that, under essentially sink conditions, the dissolution rate is independent of compressional force for nondisintegrating spheres of benzoic acid, salicylic acid, aspirin, an equimolar mixture of aspirin and salicylic acid, and an equimolar mixture of aspirin and caffeine. Thus, it appears that, in this dissolution study of nondisintegrating solids, the compressional force and the apparent density are insignificant factors and need not be rigidly controlled.

Regression Analysis of Dissolution—Aspirin and salicylic acid mixtures of various mole fractions were compressed at 4540 kg into spheres. During dissolution of the compressed sphere, disintegration did not occur; each retained its spherical shape as dissolution occurred. The compositions and dissolution rates of aspirin–salicylic acid spheres are given in Table III. Since the experimentally determined ratio of the components in solution was the same as the ratio of the components in the solid, the dissolution rate may be calculated by multiplying the dissolution rate of the sphere by the mass fraction of the component in the solid.

Table III—Composition and Observed Dissolution Rate of Aspirin and Salicylic Acid Mixtures Compressed at 4540 kg

Mole Fraction		Mass Fraction		Dissolution Rate, g/hr/cm²		
N_{ASA}	N_{SAL}	F_{ASA}	F_{SAL}	ASA	SAL	Sphere
1.0	0	1.000	0	0.0430	—	0.0430
0.9	0.1	0.922	0.078	0.0423	0.0036	0.0459
0.8	0.2	0.839	0.161	0.0415	0.0080	0.0495
0.7	0.3	0.753	0.247	0.0382	0.0125	0.0507
0.6	0.4	0.662	0.338	0.0336	0.0171	0.0507
0.5	0.5	0.566	0.434	0.0282	0.0216	0.0498
0.4	0.6	0.465	0.535	0.0215	0.0248	0.0463
0.3	0.7	0.359	0.641	0.0148	0.0264	0.0412
0.2	0.8	0.246	0.754	0.0088	0.0271	0.0359
0.1	0.9	0.127	0.873	0.0039	0.0272	0.0311
0	1.0	0	1.000	—	0.0272	0.0272

A stepwise regression analysis was performed using the STEPREGN program. The regression equation for the dissolution rate, R, of aspirin–salicylic acid spheres is:

$$R = (0.02438 + 0.07048F_{ASA}) - 0.05008F_{ASA}^2 \text{ g/hr/cm}^2 \quad \text{(Eq. 15)}$$

where F_{ASA} is the mass fraction of aspirin in the aspirin–salicylic acid mixture. The coefficient of determination, r^2, is 0.9466, a value that indicates a good correlation of the experimental data with the regression equation. The experimental dissolution rate and the dissolution rate calculated by the regression equation are shown in Fig. 2.

In a similar manner, the dissolution rates of aspirin–phenacetin spheres of various mole fractions compressed at 4540 kg were determined (Table IV). The regression equation for the dissolution rate of aspirin–phenacetin spheres is:

$$R = (0.00541 + 0.04483F_{ASA}) - 0.00492F_{ASA}^2 \text{ g/hr/cm}^2 \quad \text{(Eq. 16)}$$

The r^2 value is 0.9733, a value that indicates an excellent correlation

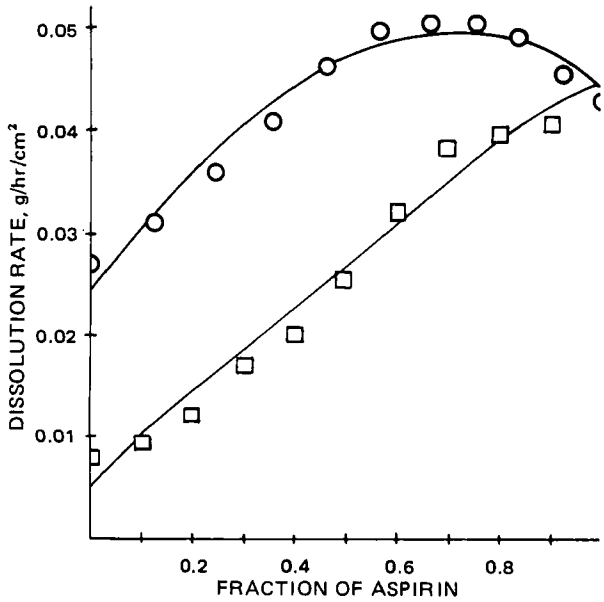

Figure 2—*Comparison of experimental dissolution rates of compressed mixtures and regression equation represented by the smooth curves. Key: ○, aspirin and salicylic acid; and □, aspirin and phenacetin.*

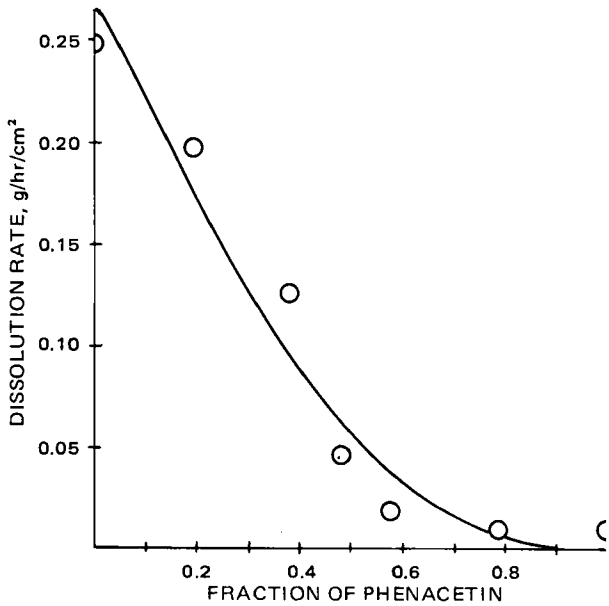

Figure 3—*Comparison of experimental dissolution rates of compressed phenacetin and caffeine mixtures and regression equation represented by the smooth curve.*

Table IV—Composition and Observed Dissolution Rate of Aspirin and Phenacetin Mixtures Compressed at 4540 kg

Mole Fraction		Mass Fraction		Dissolution Rate, g/hr/cm²		
N_{ASA}	N_{PH}	F_{ASA}	F_{PH}	ASA	PH	Sphere
1.0	0	1.000	0	0.0430	—	0.0430
0.9	0.1	0.900	0.100	0.0370	0.0041	0.0411
0.8	0.2	0.801	0.199	0.0320	0.0079	0.0399
0.7	0.3	0.701	0.299	0.0269	0.0115	0.0384
0.6	0.4	0.601	0.399	0.0195	0.0129	0.0324
0.5	0.5	0.501	0.499	0.0130	0.0125	0.0255
0.4	0.6	0.401	0.599	0.0081	0.0120	0.0201
0.3	0.7	0.301	0.699	0.0051	0.0120	0.0171
0.2[a]	0.8	0.201	0.799	0.0025	0.0098	0.0123
0.1[b]	0.9	0.100	0.900	0.0010	0.0086	0.0096
0	1.0[b]	0	1.000	—	0.0080	0.0080

[a] Compressed at 680 kg. [b] Melt method.

of the experimental data with the regression equation. The experimental dissolution rate and the dissolution rate calculated by the regression equation are shown in Fig. 2.

Attempts to compress phenacetin and caffeine mixtures were unsuccessful, and a melt process was used. Mixtures of phenacetin and caffeine were compressed at 4540 kg for 5 min within a hot stage at 265°. The compositions and dissolution rates are given in Table V. The regression equation for the dissolution rate of phenacetin–caffeine spheres is:

$$R = (0.26689 - 0.54995F_{PH}) + 0.28451F_{PH}^2 \text{ g/hr/cm}^2 \quad \text{(Eq. 17)}$$

where F_{PH} is the mass fraction of the phenacetin in the phenacetin–caffeine mixture. The r^2 value is 0.9562, a value that indicates good correlation of the experimental data with the regression equation. The experimental dissolution rate and the dissolution rate calculated by the regression equation are shown in Fig. 3.

Aspirin and caffeine mixtures of various mole fractions were compressed at 4540 kg into spheres. The compositions and dissolution rates are given in Table VI. The regression equation for the dissolution rate of aspirin–caffeine spheres is:

$$R = (0.27378 + 0.0924F_{ASA}) - 0.3809F_{ASA}^2 \text{ g/hr/cm}^2 \quad \text{(Eq. 18)}$$

The r^2 value for the aspirin–caffeine system is 0.8199. The experimental dissolution rates and the dissolution rates calculated by the regression equation are shown in Fig. 4.

Dissolution of Noninteracting Solids—Higuchi *et al.* (3) presented a theory for the dissolution of polyphasic mixtures using a diffusion layer model. For a mixture in which F_A and F_B are the amounts of components A and B, both components tend to dissolve at rates proportional to their respective solubilities, C_A and C_B, and diffusion coefficients, D_A and D_B. At some composition (critical mixture), the two components always coexist at the solid–liquid interface, and the dissolution rates are proportional to their relative amounts in the mixture. Thus:

$$\frac{F_A}{F_B} = \frac{D_A C_A}{D_B C_B} \quad \text{(Eq. 19)}$$

At other compositions after some time, one component is dissolved from the solid–liquid interface fast enough to leave a layer of the other component. If:

$$\frac{F_A}{F_B} > \frac{D_A C_A}{D_B C_B} \quad \text{(Eq. 20)}$$

component B dissolves fast enough to leave a layer of A at the solid–liquid interface. The dissolution rates are:

$$R_A = \frac{D_A C_A}{h} \quad \text{(Eq. 21)}$$

where h is the thickness of the effective diffusion layer, and:

$$R_B = \frac{F_B}{F_A} R_A \quad \text{(Eq. 22)}$$

If:

$$\frac{F_A}{F_B} < \frac{D_A C_A}{D_B C_B} \quad \text{(Eq. 23)}$$

component A dissolves fast enough to leave a layer of B at the solid–liquid interface. The dissolution rates are:

Table V—Composition and Observed Dissolution Rate of Phenacetin and Caffeine Mixtures Prepared by the Melt Method

Mole Fraction		Mass Fraction		Dissolution Rate, g/hr/cm²		
N_{PH}	N_{CAF}	F_{PH}	F_{CAF}	PH	CAF	Sphere
1.0	0	1.000	0	0.0080	—	0.0080
0.8	0.2	0.787	0.213	0.0091	0.0024	0.0115
0.6	0.4	0.581	0.491	0.0126	0.0090	0.0216
0.5	0.5	0.480	0.520	0.0227	0.0245	0.0472
0.4	0.6	0.381	0.619	0.0482	0.0782	0.1264
0.2	0.8	0.188	0.812	0.0372	0.1612	0.1984
0	1.0	0	1.000	—	0.2493	0.2493

Table VI—Composition and Observed Dissolution Rate of Aspirin and Caffeine Mixtures Compressed at 4540 kg

Mole Fraction		Mass Fraction		Dissolution Rate, g/hr/cm²		
N_{ASA}	N_{CAF}	F_{ASA}	F_{CAF}	ASA	CAF	Sphere
1.0	0	1.000	0	0.0430	—	0.0430
0.9	0.1	0.893	0.107	0.0450	0.0050	0.0500
0.8	0.2	0.788	0.212	0.0510	0.0140	0.0650
0.7	0.3	0.684	0.316	0.0680	0.0310	0.0990
0.6	0.4	0.582	0.418	0.0940	0.0680	0.1620
0.5	0.5	0.481	0.519	0.1045	0.1125	0.2170
0.4	0.6	0.382	0.618	0.1250	0.2010	0.3260
0.3	0.7	0.284	0.716	0.0900	0.2250	0.3150
0.2	0.8	0.188	0.812	0.0590	0.2560	0.3150
0.1[a]	0.9	0.094	0.906	0.0260	0.2530	0.2790
0	1.0	0	1.000	—	0.2152	0.2152

[a] Compressed at 3600 kg.

$$R_B = \frac{D_B C_B}{h} \quad \text{(Eq. 24)}$$

and:

$$R_A = \frac{F_A}{F_B} R_B \quad \text{(Eq. 25)}$$

Application of the theory can be demonstrated for the compressed aspirin–salicylic acid spheres. Edwards (26) reported that the solubility of aspirin, C_{ASA}, in water at 25° was 4.44×10^{-3} g/ml and that the diffusion coefficient of aspirin, D_{ASA}, in water at 25° was 8.01×10^{-6} cm²/sec. Hall (27) reported that the solubility of salicylic acid,

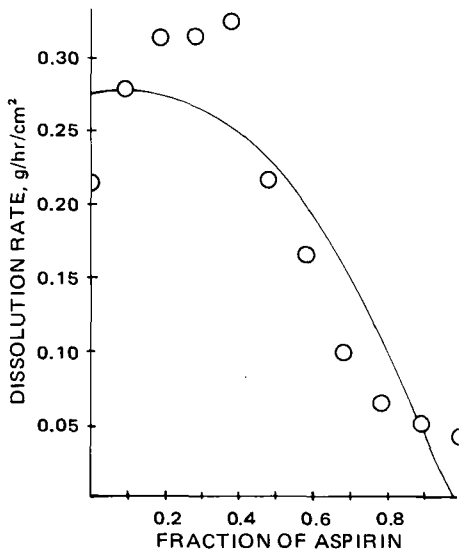

Figure 4—*Comparison of experimental dissolution rates of compressed aspirin and caffeine mixtures and regression equation represented by the smooth curve.*

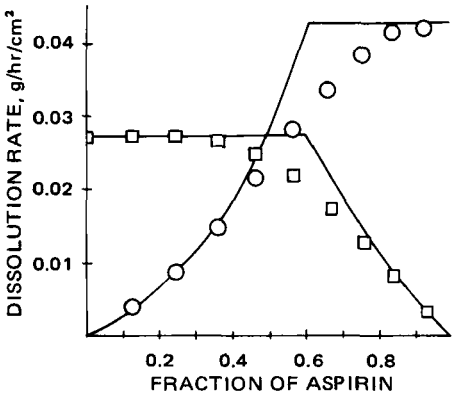

Figure 5—*Comparison of observed dissolution rates of the components of compressed aspirin and salicylic acid mixtures and smooth curve representing the theoretical rates. Key:* ○, *aspirin; and* □, *salicylic acid.*

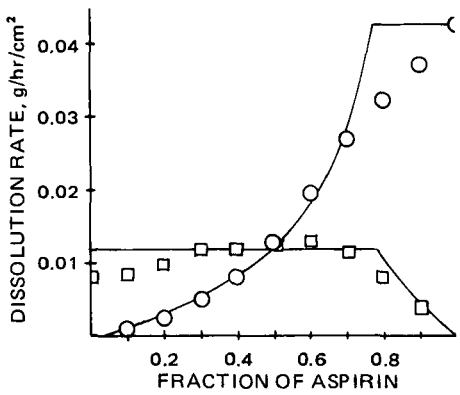

Figure 6—*Comparison of observed dissolution rates of the components of compressed aspirin and phenacetin mixtures and smooth curve representing the theoretical rates. Key:* ○, *aspirin; and* □, *phenacetin.*

C_{SAL}, in water at 25° was 2.24×10^{-3} g/ml. Mullin and Cook (28) reported that the diffusion coefficient of salicylic acid, D_{SAL}, in water at 25° was 10.12×10^{-6} cm²/sec. The thickness of the effective diffusion layer was chosen as 30 μm (29).

For the aspirin and salicylic acid mixture, the critical ratio is:

$$\frac{F_{ASA}}{F_{SAL}} = \frac{D_{ASA}C_{ASA}}{D_{SAL}C_{SAL}} \quad \text{(Eq. 26a)}$$

$$\frac{F_{ASA}}{F_{SAL}} = \frac{(8.01 \times 10^{-6})(4.44 \times 10^{-3})}{(10.12 \times 10^{-6})(2.24 \times 10^{-3})} \quad \text{(Eq. 26b)}$$

$$\frac{F_{ASA}}{F_{SAL}} = \frac{0.611}{0.389} \quad \text{(Eq. 26c)}$$

At the critical ratio, the dissolution rates are:

$$R_{ASA} = \frac{D_{ASA}C_{ASA}}{h} \quad \text{(Eq. 27a)}$$

$$R_{ASA} = \frac{(8.01 \times 10^{-6})(4.44 \times 10^{-3})}{3 \times 10^{-3}} \quad \text{(Eq. 27b)}$$

$$R_{ASA} = 1.18548 \times 10^{-5} \text{ g/sec/cm}^2 \text{ (0.0427 g/hr/cm}^2\text{)} \quad \text{(Eq. 27c)}$$

and:

$$R_{SAL} = \frac{D_{SAL}C_{SAL}}{h} \quad \text{(Eq. 28a)}$$

$$R_{SAL} = \frac{(10.12 \times 10^{-6})(2.24 \times 10^{-3})}{3 \times 10^{-3}} \quad \text{(Eq. 28b)}$$

$$R_{SAL} = 7.556 \times 10^{-6} \text{ g/sec/cm}^2 \text{ (0.0272 g/hr/cm}^2\text{)} \quad \text{(Eq. 28c)}$$

For compositions of $F_{ASA} > 0.611$, the condition described by Eq. 20 exists so that aspirin is present to a greater extent on the solid–liquid interface. For example, at $F_{ASA} = 0.753$ and $F_{SAL} = 0.247$, the dissolution rate as expressed by Eq. 21 for aspirin is:

$$R_{ASA} = \frac{D_{ASA}C_{ASA}}{h} \quad \text{(Eq. 29a)}$$

$$R_{ASA} = \frac{(8.01 \times 10^{-6})(4.44 \times 10^{-3})}{3 \times 10^{-3}} \quad \text{(Eq. 29b)}$$

$$R_{ASA} = 11.8548 \times 10^{-6} \text{ g/sec/cm}^2 \text{ (0.0427 g/hr/cm}^2\text{)} \quad \text{(Eq. 29c)}$$

and the dissolution rate as expressed by Eq. 22 for salicylic acid is:

$$R_{SAL} = \frac{F_{SAL}}{F_{ASA}} R_{ASA} \quad \text{(Eq. 30a)}$$

$$R_{SAL} = \frac{0.247}{0.753} (0.0427) \quad \text{(Eq. 30b)}$$

$$R_{SAL} = 0.0082 \text{ g/hr/cm}^2 \quad \text{(Eq. 30c)}$$

For compositions of $F_{ASA} < 0.611$, the condition described by Eq. 23 exists so that salicylic acid exists to a greater extent on the solid–liquid interface. For example, at $F_{ASA} = 0.465$ and $F_{SAL} = 0.535$, the dissolution rate as expressed by Eq. 24 for salicylic acid is:

$$R_{SAL} = \frac{D_{SAL}C_{SAL}}{h} \quad \text{(Eq. 31a)}$$

$$R_{SAL} = \frac{(10.12 \times 10^{-6})(2.24 \times 10^{-3})}{3 \times 10^{-3}} \quad \text{(Eq. 31b)}$$

$$R_{SAL} = 7.5563 \times 10^{-6} \text{ g/sec/cm}^2 \text{ (0.0272 g/hr/cm}^2\text{)} \quad \text{(Eq. 31c)}$$

and the dissolution rate as expressed by Eq. 25 for aspirin is:

$$R_{ASA} = \frac{F_{ASA}}{F_{SAL}} R_{SAL} \quad \text{(Eq. 32a)}$$

$$R_{ASA} = \frac{0.465}{0.641} (0.0272) \quad \text{(Eq. 32b)}$$

$$R_{ASA} = 0.0236 \text{ g/hr/cm}^2 \quad \text{(Eq. 32c)}$$

The dissolution rates calculated for various compositions are compared to the experimental dissolution rates of Table III in Fig. 5.

In a similar manner, the theoretical dissolution rates were calculated for aspirin and phenacetin mixtures. Seidell (30) reported that the solubility of phenacetin, C_{PH}, in water at 25° was 1.1×10^{-3} g/ml. Shively and Kildsig (31) reported that the diffusion coefficient of phenacetin, D_{PH}, in water at 30° was 9×10^{-6} cm²/sec. The dissolution rates calculated for various compositions of aspirin and phenacetin are compared to the experimental dissolution rates of Table IV in Fig. 6.

In Figs. 5 and 6, the observed dissolution rates approximate the smooth curves representing the theoretical dissolution rates, thereby substantiating the model. At the critical ratio, deviation probably is caused by small local variations in compositions. It was reported (3) that solid mixtures prepared by a melt method deviate less because they are more homogeneous.

The theoretical dissolution rates were calculated for phenacetin and caffeine mixtures. Paruta *et al.* (32) reported that the solubility of caffeine, C_{CAF}, in water at 25° was 23.2×10^{-3} g/ml. McCabe (33) reported that the diffusion coefficient of caffeine, D_{CAF}, in water at 25° was 6.79×10^{-6} cm²/sec. The dissolution rates calculated for various compositions of caffeine and phenacetin are compared to the experimental dissolution rates of Table V in Fig. 7.

As shown in Fig. 7, the theoretical and observed dissolution rates of caffeine and phenacetin are similar for mixtures containing more than half phenacetin. For compositions containing a large fraction of caffeine, there is deviation. Caffeine is 21 times more soluble than phenacetin, and it readily dissolves to produce a rough surface with minute flaking. As a result, the effective surface area is increased, and the observed dissolution of both components is faster than predicted by the model.

The dissolution rate of caffeine from solids prepared using a melt

method was reported as 20% faster than from a compressed disk, and the assumption was that the solubility of the melt was greater (3). Experimentally, the dissolution rate of spheres made by the melt method was 16% faster than by compression only. This result could also contribute to the faster observed dissolution rate of the phenacetin spheres, which contain a large fraction of caffeine.

Dissolution of Interacting Solids—Aspirin and caffeine in solution undergo the interaction: aspirin + caffeine → (aspirin–caffeine). The equilibrium constant:

$$K = \frac{\text{(aspirin–caffeine)}}{\text{(aspirin)(caffeine)}} \qquad \text{(Eq. 33)}$$

was reported as 17.4 liters/mole (34).

The model of Higuchi was extended to two-component systems in which the components interacted to form a complex and was supported by experimental data obtained from benzocaine and caffeine mixtures (3). When assuming that the interaction is represented by $B + C = BC$, the equilibrium constant is:

$$K = \frac{C_{BC}}{C_B C_C} \qquad \text{(Eq. 34)}$$

where C_B, C_C, and C_{BC} are the concentrations of components B, C, and BC, respectively.

The composition of the critical ratio is:

$$\frac{N_B}{N_C} = \frac{D_B C_B + D_{BC} K C_B C_C}{D_C D_C + D_{BC} K C_B C_C} \qquad \text{(Eq. 35)}$$

at which the dissolution rates are:

$$R_C = \frac{D_C C_C + D_{BC} K C_B C_C}{h} \qquad \text{(Eq. 36)}$$

and:

$$R_B = \frac{D_B C_B + D_{BC} K C_B C_C}{h} \qquad \text{(Eq. 37)}$$

When the ratio of the components is such that pure C is the surface phase, the dissolution rates may be determined by:

$$R_B h = \frac{D_B C_B}{1 - \dfrac{N_C D_{BC} K C_B}{N_B (D_B + D_{BC} K C_B)}} \qquad \text{(Eq. 38)}$$

and:

$$R_C h = \frac{D_B C_B}{\dfrac{N_B}{N_C} - \dfrac{D_{BC} K C_B}{D_C + D_{BC} K C_B}} \qquad \text{(Eq. 39)}$$

When the ratio of the components is such that pure C is the surface phase, the dissolution rates may be determined by:

$$R_B h = \frac{D_C C_C}{\dfrac{N_C}{N_B} - \dfrac{D_{BC} K C_C}{D_B + D_{BC} K C_C}} \qquad \text{(Eq. 40)}$$

and:

$$R_C h = \frac{D_C C_C}{1 - \dfrac{N_B D_{BC} K C_C}{N_C (D_B + D_{BC} K C_C)}} \qquad \text{(Eq. 41)}$$

For the aspirin and caffeine mixture investigated, the critical ratio calculated by Eq. 35 is $N_{ASA}/N_{CAF} = 0.32/0.68$. The diffusion coefficient of the aspirin–caffeine complex ($D_{ASA\text{–}CAF}$) was assumed to be the same as the diffusion coefficient of caffeine because there is a tendency for caffeine to associate as a dimer (35).

At the critical ratio, the dissolution rate of aspirin calculated by Eq. 36 is:

$$R_{ASA}(0.003) = (2.8836 \times 10^{-2})(2.46 \times 10^{-5}) + (2.4444 \times 10^{-2})(17{,}400)(2.46 \times 10^{-5})(11.95 \times 10^{-5}) \qquad \text{(Eq. 42a)}$$

$$R_{ASA} = 6.53232 \times 10^{-4} \text{ mole/hr/cm}^2 \ (0.1177 \text{ g/hr/cm}^2) \qquad \text{(Eq. 42b)}$$

and the dissolution rate of caffeine calculated by Eq. 37 is:

$$R_{CAF}(0.003) = (2.4444 \times 10^{-2})(11.95 \times 10^{-5}) + (2.4444 \times 10^{-2})(17{,}400)(2.46 \times 10^{-5})(11.95 \times 10^{-5}) \qquad \text{(Eq. 43a)}$$

$$R_{CAF} = 1.39 \times 10^{-3} \text{ mole/hr/cm}^2 \ (0.2700 \text{ g/hr/cm}^2) \qquad \text{(Eq. 43b)}$$

For compositions of $N_{ASA} > 0.32$, aspirin is the surface phase, and the dissolution rate of aspirin is calculated by Eq. 38. For example, at $N_{ASA} = 0.6$, the dissolution rate of aspirin is:

$$R_{ASA}(0.003) = \frac{(2.46 \times 10^{-5})(2.8836 \times 10^{-2})}{1 - \dfrac{0.4(2.4444 \times 10^{-2})(17{,}400)(2.46 \times 10^{-5})}{0.6(2.8836 \times 10^{-2}) + (2.4444 \times 10^{-2})(17{,}400)(2.46 \times 10^{-5})}} \qquad \text{(Eq. 44a)}$$

$$R_{ASA} = 2.874667 \times 10^{-4} \text{ mole/hr/cm}^2 \ (0.0518 \text{ g/hr/cm}^2) \qquad \text{(Eq. 44b)}$$

In a similar manner, the dissolution rate of caffeine calculated by Eq. 39 is 0.0383 g/hr/cm^2.

For compositions of $N_{ASA} < 0.32$, caffeine is the surface phase, and the dissolution rate is calculated by Eq. 41. For example, at $N_{ASA} = 0.2$, the dissolution rate of aspirin is 0.0522 g/hr/cm^2. From Eq. 40, the dissolution rate of caffeine is 0.2250 g/hr/cm^2.

The dissolution rates calculated for various compositions are compared to the experimental dissolution rates of Table VI in Fig. 8.

As the fraction of aspirin in the mixture is increased, the dissolution rate of aspirin and caffeine is increased to a maximum dissolution rate

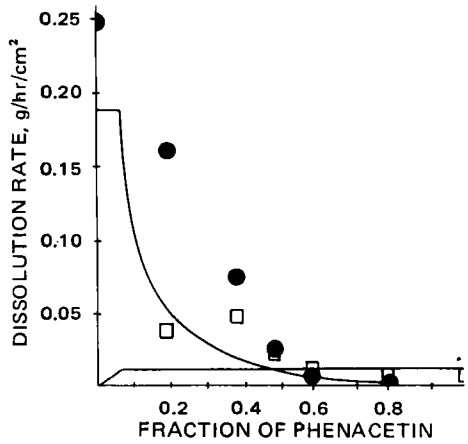

Figure 7—*Comparison of observed dissolution rates of the components of compressed caffeine and phenacetin mixtures and smooth curve representing the theoretical rates. Key: ●, caffeine; and □, phenacetin.*

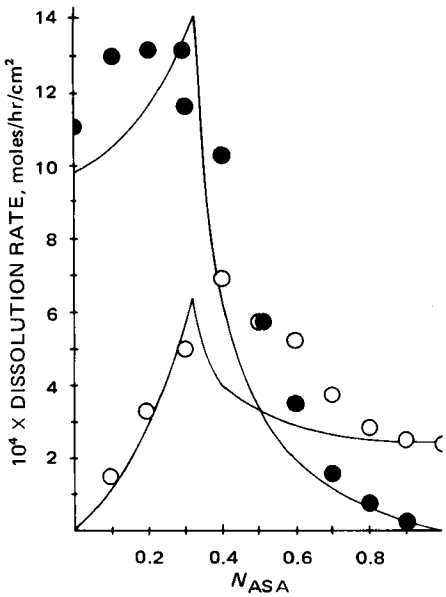

Figure 8—*Comparison of observed dissolution rates of the components of compressed aspirin and caffeine mixtures and smooth curve representing the theoretical rates. Key: ○, aspirin; and ●, caffeine.*

at the critical ratio, and then a further increase in the fraction of aspirin causes a decrease in the dissolution rates of aspirin and caffeine. The model predicts the observed dissolution rates of aspirin for compositions less than 0.3 and more than 0.8 mass fraction of aspirin. At other compositions, the dissolution rate of aspirin is faster than the theoretical rates. Caffeine has five times as great a solubility as aspirin; since it dissolves faster than the aspirin, minute flaking would occur because the aspirin matrix remaining would be porous and mechanically weak. It is likely that minute particles of aspirin flake from the solid–liquid surface with an increase in the effective surface area of the aspirin and, consequently, a faster observed dissolution rate of aspirin than predicted.

The dissolution rate of caffeine conforms to the model at compositions greater than 0.7 mass fraction of aspirin, but at other compositions the dissolution rate of caffeine is faster than predicted by the model. The increased dissolution rate of caffeine at other compositions may be due to several assumptions. In developing the model, it was assumed that only a 1:1 aspirin–caffeine complex was formed and increased the solubility of the caffeine; however, other complexes may exist (34) and at small fractions of caffeine increase the dissolution rate. The faster dissolution may also occur if the caffeine associates as a dimer or tetramer (35). From 0.4 to 0.6 mass fraction of aspirin, the rough surface caused by minute flaking may also increase the observed dissolution rate of caffeine.

REFERENCES

(1) E. Nelson, *J. Am. Pharm. Assoc., Sci. Ed.*, **46,** 607(1957).

(2) M. Gibaldi and H. Weintraub, *J. Pharm. Sci.*, **57,** 832(1968).

(3) W. I. Higuchi, N. A. Mir, and S. J. Desai, *ibid.*, **54,** 1405(1965).

(4) W. I. Higuchi, P. D. Bernardo, and S. C. Mehta, *ibid.*, **56,** 200(1967).

(5) G. L. Levy, J. M. Antkowiak, J. A. Procknal, and D. C. White, *ibid.*, **52,** 1047(1963).

(6) M. C. B. van Oudtshoorn, F. J. Potgieter, G. J. de Blaey, and J. Polderman, *J. Pharm. Pharmacol.*, **23,** 583(1971).

(7) K. A. Khan and C. T. Rhodes, *Pharm. Acta Helv.*, **47,** 116(1967).

(8) E. L. Knoechel, C. C. Sperry, and C. J. Lintner, *J. Pharm. Sci.*, **56,** 116(1967).

(9) J. Polderman and D. R. Braakman, *J. Pharm. Pharmacol.*, **20,** *323(1968).*

(10) C. J. de Blaey, M. C. B. van Oudtshoorn, and J. Polderman, *Pharm. Weekbl.*, **106,** 589(1971).

(11) E. Cid and F. Jaminet, *Pharm. Acta Helv.*, **46,** 167(1971).

(12) H. L. Smith, C. A. Baker, and J. H. Wood, *J. Pharm. Pharmacol.*, **23,** 536(1971).

(13) D. Ganderton, J. W. Hadgraft, W. T. Respin, and A. G. Thompson, *Pharm. Acta Helv.*, **42,** 152(1963).

(14) E. R. Kristoffersson, *Farm. Aikak.*, **78,** 185(1969).

(15) C. J. de Blaey, A. B. Weekers-Andersen, and J. Polderman, *Pharm. Weekbl.*, **106,** 893(1971).

(16) M. Kanke and K. Sekiguchi, *Chem. Pharm. Bull.*, **21,** 871(1973).

(17) E. L. Parrott, D. E. Wurster, and T. Higuchi, *J. Am. Pharm. Assoc., Sci. Ed.*, **44,** 269(1955).

(18) G. Milosovich, *J. Pharm. Sci.*, **53,** 484(1964).

(19) R. J. Braun and E. L. Parrott, *ibid.*, **61,** 175(1972).

(20) H. H. Willard, L. L. Merritt, and J. A. Dean, "Instrumental Methods of Analysis," Van Nostrand, Princeton, N.J., 1958, p. 120.

(21) R. B. Tinker and A. J. McBay, *J. Am. Pharm. Assoc., Sci. Ed.*, **43,** 315(1954).

(22) R. E. Pankratz and F. J. Bandelin, *ibid.*, **41,** 267(1952).

(23) A. W. Clayton and R. E. Thiers, *J. Pharm. Sci.*, **55,** 404(1966).

(24) T. Higuchi, A. N. Rao, L. W. Busse, and J. V. Swintosky, *J. Am. Pharm. Assoc., Sci. Ed.*, **42,** 194(1953).

(25) C. J. Lewis and D. Train, *J. Pharm. Pharmacol.*, **17,** 1(1965).

(26) L. J. Edwards, *Trans. Faraday Soc.*, **47,** 1191(1951).

(27) N. A. Hall, *Amer. J. Pharm.*, **132,** 406(1960).

(28) J. W. Mullin and T. P. Cook, *J. Appl. Chem.*, **15,** 145(1965).

(29) R. J. Braun and E. L. Parrott, *J. Pharm. Sci.*, **61,** 592(1972).

(30) A. Seidell, *J. Am. Chem. Soc.*, **92,** 1088(1970).

(31) C. D. Shively and D. O. Kildsig, *J. Pharm. Sci.*, **61,** 1589(1972).

(32) A. N. Paruta, B. J. Sciarrone, and N. G. Lordi, *ibid.*, **54,** 838(1965).

(33) M. McCabe, *Biochem. J.*, **127,** 249(1972).

(34) T. Higuchi and D. A. Zuck, *J. Am. Pharm. Assoc., Sci. Ed.*, **42,** 138(1953).

(35) D. Guttman and T. Higuchi, *ibid.*, **46,** 4(1957).

ACKNOWLEDGMENTS AND ADDRESSES

Received October 14, 1975, from the *College of Pharmacy, University of Iowa, Iowa City, IA 52242*

Accepted for publication February 13, 1976.

Abstracted in part from a dissertation submitted by S. A. Shah to the Graduate College, University of Iowa, in partial fulfillment of the Doctor of Philosophy degree requirements.

* Present address: Johnson & Johnson, Raritan, NJ 08869

x To whom inquiries should be directed.

Pharmacology of *Quercus infectoria*

MOHAMMAD S. DAR ˣ, M. IKRAM, and T. FAKOUHI

Abstract □ The galls of *Quercus infectoria* (Fagaceae), a commonly available plant in Iran, were studied pharmacologically. Two fractions were employed, a dried acetone-treated methanol extract dissolved in water (Fraction A) and a subfraction prepared by chloroform–methanol extraction (Fraction B). Fraction A was active as an analgesic in rats and significantly reduced blood sugar levels in rabbits. Fraction B had CNS depressant activity. Data obtained with a treadmill indicated a decreased activity ratio by Fraction B, suggesting a possible interference in motor coordination. It potentiated the barbiturate sleeping time significantly without changing the onset time or the loss of the righting reflex. In addition, Fraction B exhibited a moderate antitremorine activity by causing a delay in the onset and a decrease in the severity of tremorine-induced tremors. The local anesthetic action of Fraction B was evident due to the complete blockade of the isolated frog sciatic nerve conduction.

Keyphrases □ *Quercus infectoria*—extracts of galls, analgesic, antidiabetic, and CNS depressant activity screened, mice, rats, and rabbits □ Analgesic activity—*Quercus infectoria* extracts of galls screened, mice, rats, and rabbits □ Antidiabetic activity—*Quercus infectoria* extracts of galls screened, mice, rats, and rabbits □ CNS depressant activity—*Quercus infectoria* extracts of galls screened, mice, rats, and rabbits

Quercus infectoria (Fagaceae) is a commonly available plant in Iran. Its bark is used for treating eczema and impetigo (1). Its galls are reported to contain ellagic acid (1), gallotannins (2), sitosterol (3), methyl betulate (3), and methyl oleanolate (3). Other species of *Quercus* have hypoglycemic, antiviral, and anticholinergic activities (4). Leaves of certain species of *Quercus*, such as *Q. sessiliflora*, *Q. cerris*, and *Q. pedunculate*, have been reported to cause nephrosonephritis and glomerulonephritis in calves (5). Poisoning by *Q. havardi* also was reported (6). Therefore, it was considered of interest to study *Q. infectoria* pharmacologically, and work was undertaken on the galls of this species.

EXPERIMENTAL

Isolation and Fractionation—The dry, powdered galls of the plant were cold percolated four times with methanol, and the combined extracts were freed of the solvent under reduced pressure at a temperature not exceeding 50°. The semisolid residue thus obtained was dissolved in acetone and filtered to remove a small quantity of insoluble material.

The clear filtrate was distilled in a vacuum rotary evaporator at 50° to remove the solvent. The pale-yellow material thus obtained was again dissolved in acetone and filtered, and the filtrate was freed of the solvent under reduced pressure and temperature. The resulting pale-yellow amorphous powder, which is a partially purified material, is called Fraction A.

Fraction A was subjected to further fractionation by dissolving it in water and extracting four times with chloroform–methanol (2:1). The organic extracts were combined, dried over anhydrous sodium sulfate, treated with charcoal, and filtered. The clear filtrate was freed of the solvent under reduced pressure and temperature, and a pale-yellow amorphous solid (Fraction B) was obtained. The aqueous phase was further fractionated into 1-butanol (Fraction C) and ethyl acetate (Fraction D).

During this study, the isolation of Fraction B was carried out on three different occasions. Each time, Fraction B was subjected to TLC. The R_f values were identical in all cases, confirming the chemical identity and the stability of Fraction B.

During isolation and fractionation, the temperature was never allowed to increase beyond 50° to avoid any decomposition. TLC [chloroform–methanol–petroleum ether (8:1:1)] of the three fractions (B, C, and D) gave three spots with R_f values of 0.09, 0.214, and 0.6, but the intensity of the spot at R_f 0.6 was much higher in Fraction B than in Fractions C and D. Fractions C and D and the aqueous phase were also tested, but the pharmacological activity was negligible.

Fraction B was crystallized from hot water, mp 130–190°, but it was impure and the TLC pattern was the same as before crystallization. Aromatic carboxylic acids like gallic, ellagic, and syringic acids have been obtained from other species of *Quercus* (7) and may be present in this fraction. Fraction B gives a deep-blue color with ferric chloride solution, indicating that it may also contain aromatic carboxylic acids.

The IR spectrum of Fraction B showed peaks for hydroxyl, carbonyl, and aromatic groups, showing the aromatic carboxylic acid nature of the compounds. The IR spectrum of Fraction B was compared with the known constituents of *Quercus* species, but it was not identical to any one of them.

The concentration of Fraction B with respect to the dry plant was 1%; with respect to Fraction A, it was 8%.

Pharmacological Methods—In most of these experiments, mice (white Swiss, Charles River strain) of both sexes were used once; they were previously untreated with any drug and permitted to feed *ad libitum*. However, female rabbits (albino strain) were used in testing the hypoglycemic activity of Fraction A. Adult Sprague–Dawley rats of either sex, 200–225 g, were used for analgesic experiments.

Analgesic Activity of Fraction A in Rats—Fraction A was tested for its possible analgesic activity using the rat tail-flick test. This test was carried out using a modification of the procedure of Dewey *et al.* (8). A 6-sec cutoff time was established for experimental conditions. Reaction time was measured to the nearest 0.10 sec by an electric stopwatch synchronized with the lamp.

Ten rats were used at each dose level and were selected at random. The average of two control readings taken 30 min apart constituted the control reaction time. Any animal for which the average of two controls was greater than 3 sec was discarded. Twenty minutes after the second control reading, Fraction A (30, 100, and 200 mg/kg) was administered intraperitoneally. The concentration of Fraction A was adjusted so that 0.75 ml/100 g was always injected.

Any increase in reaction time was noted at 30, 60, 90, and 120 min after the administration of Fraction A. Results were evaluated by the Wilcoxon Signed Rank Test (9) at each time, using 10% likelihood as the cutoff point.

Hypoglycemic Activity of Fraction A in Rabbits—Female rabbits, 1.5–2.5 kg, were used. The blood sugar determinations were carried out according to the Folin Wu method (10). Fraction A (500 mg/kg) was administered orally by means of a rubber catheter to two groups of four rabbits each. The results were compared with a control group that received normal saline orally and a group that received tolbutamide orally, the standard oral hypoglycemic agent (250 mg/kg).

Blood samples were drawn from the marginal ear vein of animals just before and at 30, 60, 120, 180, 240, and 300 min after Fraction A administration. Blood sugar levels in the control and test animals were then subjected to statistical treatment (Student t test) to determine any significant hypoglycemic activity of Fraction A.

Sedative—Hypnotic Activity of Fraction B in Mice—The central nervous system (CNS) depressant activity of Fraction B was determined by observation of its effect on the spontaneous motor activity and the righting reflex of 20–30-g mice. Fraction B was given intraperitoneally as a suspension in normal saline. The degree of CNS depression, as evidenced by reduction in spontaneous motor activity, was subjectively graded and compared with that of the control animals, who were given normal saline only.

The effect of Fraction B was described in the following terms. When 100% of the normal animals equalled the control animals in spontaneous motor activity, the effect was considered nil. When 50% or more of the test population showed a slight or intermediate decrease in

activity, the effect was considered slight or intermediate. When 50% or more of the test animals showed a loss of the righting reflex, the loss of spontaneous motor activity was considered marked. For each dose (250, 500, and 1000 mg/kg), 10 control and 10 test mice were used.

Experiments Using Treadmill[1] *for Mice*—Mice, 20–25 g, were used. Fraction B, 100 mg/kg ip, was administered to the test group; the vehicle was administered to the control. Control and test experiments were based on two groups of five mice each. All animals were acclimated to the treadmill by placing them on the mill two or three times just before the start of the experiment. Only five mice (the maximum number that could be placed on the treadmill) were used at one time, and a cutoff time of 180 sec was established for both the control and test groups.

The animals were placed on the mill 5 min before and 15, 30, 45, 60, 90, and 120 min after the administration of the drug or vehicle. At the end of the 120-min experimental period, the data were computed to obtain the activity ratio. The computation involved division of time in seconds that the test animals stayed on the mill by the control time. A ratio of one or nearly one was obtained in control experiments. A ratio of less than one indicated possibly a certain degree of precise motor incoordination. The degree of motor incoordination, therefore, was reflected by the extent to which the activity ratio fell below one.

Barbiturate Potentiation in Mice—Mice, 20–30 g, were employed, and Fraction B was administered intraperitoneally as already described. Pentobarbital sodium (50 mg/kg ip) was administered 30 min after Fraction B. For each test and control experiment, 10 mice were used. Animals that went to sleep were placed on their backs until spontaneous righting occurred. They were again placed on their backs until righting was effected within 5 sec, at which time the animals were considered to have regained their righting reflex. The measure of potentiation used was the ratio of (drug plus barbiturate sleep time) divided by (barbiturate sleep time plus drug sleep time).

Antitremorine Activity in Mice—Mice, 20–30 g, were used. Fraction B was administered at a dose of 500 mg/kg ip. Tremorine (20 mg/kg ip) in a 0.25% methylcellulose sterile vehicle was given 30 min after Fraction B. In control mice, the dose produced centrally mediated tremors along with signs of increased cholinergic activity such as salivation, lacrimation, diarrhea, and urination.

Subjective grading was used to establish the degree of protection against tremorine. To evaluate the degree of protection, animals were suspended by the tail. When the tremors were the same as for the controls, protection was rated as nil. For a slight reduction in tremor intensity, the degree of protection was considered as slight; for a slight tremor, protection was moderate. No tremor was rated as complete protection. For each control and test experiment, 10 mice were used.

Local Anesthetic Activity—The procedure employed to test the local anesthetic activity of Fraction B was the one applied by Rud (11) and Jefferson (12). The isolated sciatic nerve of the frog, 44–52 mm in length, was the test object. It was mounted in a wax chamber (153 × 17 × 10 mm internal dimensions) in such a manner that the nerve, while hanging on the two wire electrodes, was fully bathed in Fraction B solution or frog Ringer solution. However, the internal dimensions of the portion of the wax chamber that held Fraction B or frog Ringer solution were 13 × 17 × 14 mm. Fraction B was prepared in two different concentrations, 2 and 4% in frog Ringer solution, and the pH was maintained between 6.5 and 7.0.

Recording of the action potentials was by means of a dual-beam oscilloscope[2], and the nerve was excited by the stimulator[3]. All stimulations were for 0.1 msec, and the voltage was 0.4 mv above that required for the maximal control action potential. The induced action potentials were recorded simultaneously from electrodes placed on each side of that portion of the nerve exposed to the Fraction B solution.

The percent reduction of the action potential at different time intervals after bathing the isolated nerve in Fraction B solution was determined. In addition, the time after which the action potential was completely abolished, indicating a complete nerve blockade, was recorded. At each drug concentration, six isolated frog nerves were employed. Control experiments in which isolated nerves were bathed in frog Ringer solution only were carried out in a similar manner.

[1] Rota Rod treadmill type 7600, Ugo Basile, Milan, Italy.
[2] Type 565, Tektronix, Inc., Portland, Ore.
[3] Type S8, Grass Medical Instruments, Quincy, Mass.

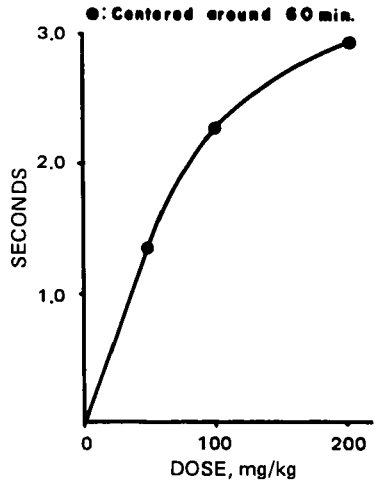

Figure 1—*Analgesic action of Fraction A. Each point represents an average increment in cutoff time in 10 rats after intraperitoneal administration.*

RESULTS AND DISCUSSION

When using Fraction A, data obtained from the analgesic and hypoglycemic experiments were statistically significant.

Analgesic Activity—The time increment in seconds observed due to the administration of Fraction A was plotted against the dose of Fraction A (Fig. 1). It is evident that the test drug is active as an analgesic (administered intraperitoneally) in a subsedative dose range that does not show any effect on the gross behavior of the animal. The onset of the analgesic activity occurred within 30 min and lasted for over 120 min. The peak analgesic action was around 60 min after drug administration. The action started declining after this period but could still be measured up to 120 min after Fraction A administration. The analgesic component of Fraction A has not been isolated.

Hypoglycemic Activity—From the experimental data, it appears that Fraction A possesses hypoglycemic activity. The effect of Fraction A on lowering the blood sugar was significantly greater than that of the control. However, the blood sugar did not fall much below the normal range of 80–120 mg %. The percent reduction in the blood sugar by Fraction A was 25.44, as compared with 47.43 produced by tolbutamide and 3.40 as seen in control animals.

The hypoglycemic action of Fraction A could be seen from the 3rd hr after its administration. The peak hypoglycemic activity was observed between 4 and 5 hr, after which it started returning toward the preadministration level. The reduction in blood sugar produced by Fraction A and tolbutamide was statistically significant ($p < 0.05$ and $p < 0.01$, respectively) (Table I), while the difference between the pre- and posttreatment blood sugar levels was not significant for control

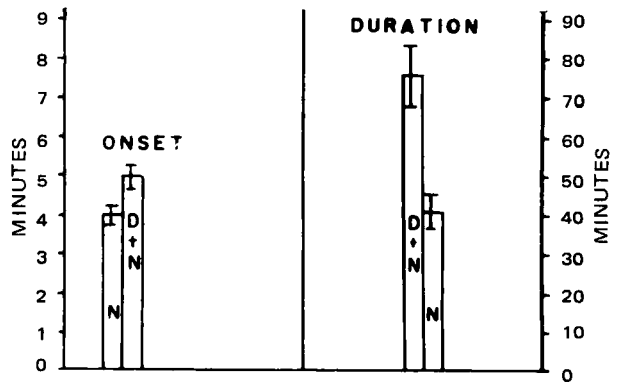

Figure 2—*Effect of Fraction B pretreatment on the hypnosis produced by pentobarbital in mice. Vertical bars represent the standard error of the mean. Key: N, saline (injection volume same as that of Fraction B) followed 30 min later by pentobarbital (50 mg/kg); and N + D, Fraction B (500 mg/kg) followed 30 min later by pentobarbital (50 mg/kg).*

Table I—Effect of Fraction A on the Blood Sugar Levels in Rabbits

Drug	Mean of Initial Blood Sugar, mg %	Mean of Lowest Blood Sugar Levels after Drug Administration, mg %	Percent Reduction	*t* Value
Tolbutamide, 250 mg/kg po	124.50 ± 3.23[a]	65.45 ± 2.11	47.43	$p < 0.01$
Control	111.50 ± 2.39	107.70 ± 3.86	3.40	NS[b]
Q. infectoria, 500 mg/kg po	119.70 ± 4.34	89.25 ± 3.04	25.44	$p < 0.05$

[a] *SEM*. [b] Not significant.

animals. Peak hypoglycemic action was attained between the 3rd and 4th hr after tolbutamide administration, after which the blood sugar gradually returned to the normal level. However, unless additional studies are carried out, it will be difficult to state the antidiabetic status of Fraction A as well as to explain the mechanism of its hypoglycemic action.

Sedative–Hypnotic Activity—At a dose level of 1000 mg/kg, Fraction B significantly reduced the spontaneous motor activity of animals. The animals lost their righting reflex within the average period of 5 min after Fraction B administration. However, at a dose of 500 mg/kg, Fraction B caused an intermediate loss of spontaneous motor activity; the animals did not lose their righting reflex but exhibited some sedation with a significant reduction in spontaneous activity. Fraction B produced only a slight reduction in spontaneous motor activity at a dose of 250 mg/kg. The data suggest a dose-dependent depressive action of Fraction B on the CNS, perhaps through the inhibition of sensory inputs into the brain.

Further insight into the action of Fraction B on the motor functions of the animals was obtained by experiments using the treadmill for mice. The data obtained indicate that Fraction B at a dose level of 100 mg/kg significantly reduced the cutoff time of animals after about 60 min until 120 min postadministration. The decrease in cutoff time, as compared to the control group, possibly suggests that Fraction B causes motor incoordination. A dose of 200 mg/kg or above caused so much motor incoordination that the animals could hardly stay on the treadmill.

Thus, a dose much smaller than the sedative–hypnotic dose significantly disturbed the motor functions of the animals, as measured by the treadmill, without any visible sedative–hypnotic action. The motor incoordination produced by Fraction B probably is due to its action on the higher areas of the brain and seems to suggest that, at a lower concentration, Fraction B is more specific to higher CNS areas only.

Barbiturate Potentiation—The locus for barbiturate potentiation appears to be functionally different from the sites involved in the directly measured depressant effect (13). Fraction B was tested for possible pentobarbital potentiation activity at a dose of 500 mg/kg; a sleep prolongation factor, *R*, was used as the criterion for effect (14). The significance of these data was determined by the use of Duncan's multiple range test (15).

As is evident from Fig. 2, Fraction B at the employed dose level acted both as a significant potentiator ($p < 0.005$) of pentobarbital as well as a CNS depressant. The value of *R* was 3.4. Nevertheless, the possibility that Fraction B causes potentiation of barbiturate sleeping time *via* the inhibition of the liver microsomal enzyme system cannot be excluded. Consequently, a definite conclusion regarding the mechanism of barbiturate potentiation cannot be made.

Local Anesthetic Activity—The data obtained (Fig. 3) indicate that Fraction B is potent as a local anesthetic. The action potential was completely abolished within an average of 7 min when the isolated nerve was placed in a 4% solution of Fraction B. However, in a 2% concentration, there was a significant reduction of the action potential but not complete nerve blockade. With the available data, it is difficult to explain the mechanism of complete nerve blockade, except that Fraction B perhaps interferes with nerve membrane permeability.

Antitremorine Activity—Fraction B also was tested for its ability to antagonize tremorine-induced peripheral parasympathetic stimulation and parkinsonian-like tremors of central origin (16, 17). At a dose of 500 mg/kg, Fraction B exhibited moderate antitremorine activity, shown by 60% of the animals, but none of the animals was completely protected. There was a slight degree of protection in 40% of the animals. Fraction B, therefore, could be classified as moderately active, since a highly active compound should be able to protect 100% of the test animals completely at a dose much lower than used to test this compound. Standard agents such as atropine, scopolamine, and trihexyphenidyl block tremorine effects in doses of 5–10 mg/kg in mice. Fraction B showed very little protection against tremorine-induced peripheral parasympathetic stimulation.

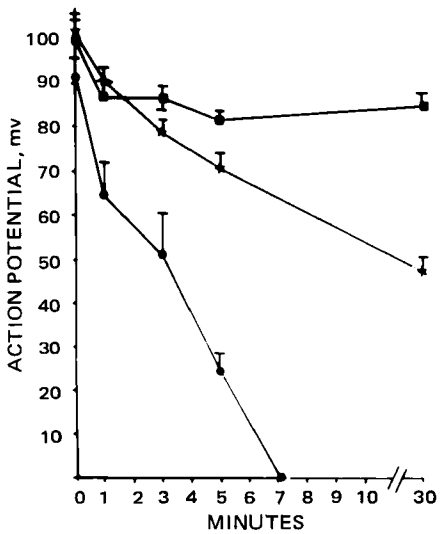

Figure 3—*Local anesthetic activity of Fraction B. Each point represents an average of six frog nerves. Vertical bars represent the standard error of the mean. Key:* ■, *control (frog Ringer);* ★, *drug (2% solution); and* ●, *drug (4% solution).*

REFERENCES

(1) R. N. Chopra, S. L. Nayar, and I. C. Chopra, "Glossary of Indian Medicinal Plants," Council of Scientific and Industrial Research, India, 1956, p. 208.

(2) E. Haslam, "Chemistry of Vegetable Tannins," Academic, London, England, 1962, p. 92.

(3) A. K. Batta and S. Rangaswami, *Phytochemistry*, **12**, 214(1973).

(4) A. K. Dhar, M. L. Dhar, B. N. Dhawan, B. N. Mehrotra, and C. Ray, *Indian J. Exp. Biol.*, **6**, 232(1968).

(5) A. Tomov *et al.*, *Izv. Vet. Nauchnoizsled. Inst. Nezarazni Boles. Zookhig. Akad. Selskostop., Nauki Bulg.*, **3**, 103(1963); through *Chem. Abstr.*, **62**, 990b(1965).

(6) G. T. Householder and J. W. Dollahite, *Southwest. Vet.*, **16**, 107(1963); through *Chem. Abstr.*, **64**, 18291d(1966).

(7) G. Alibert, G. Marigo, and A. Boudet, *Physiol. Veg.*, **7**, 57(1969).

(8) W. L. Dewey, J. F. Harris, and J. A. Nuite, *J. Pharmacol. Exp. Ther.*, **125**, 237(1959).

(9) R. Sokol and F. Rohlf, "Biometry," Freeman, San Francisco, Calif., 1969.

(10) "Hawk's Physiological Chemistry," 14th ed., B. L. Oser, Ed., McGraw-Hill, New York, N.Y., 1965, p. 1052.

(11) J. Rud, *Acta Physiol. Scand., Suppl.*, **51**, 178(1961).

(12) G. C. Jefferson, *J. Pharm. Pharmacol.*, **15**, 92(1963).

(13) K. A. Zirvi and C. H. Jarboe, *J. Med. Chem.*, **12**, 923(1969).

(14) K. A. Zirvi, M. S. Dar, and T. Fakouhi, *J. Pharm. Sci.*, **64**, 649(1975).

(15) D. Duncan, *Biometries*, **11**, 1(1955).

(16) G. M. Everett, L. E. Blockus, and I. M. Sheppered, *Science*, **124**, 79(1965).

(17) D. L. Trepanier, P. E. Krieger, and J. N. Eble, *J. Med. Chem.*, **8**, 802(1965).

ACKNOWLEDGMENTS AND ADDRESSES

Received May 16, 1975, from the *Department of Pharmacology, School of Medicine, Pahlavi University, Shiraz, Iran.*

Accepted for publication February 9, 1976.

The authors thank Dr. M. H. Bokhari of the Department of Biology, Pahlavi University, for plant identification.

[x] To whom inquiries should be directed.

Potentiometric and Spectral Investigations of Anhydrotetracycline and Its Metal-Ion Complexes

L. J. STOEL [*], E. C. NEWMAN [‡], G. L. ASLESON [§], and C. W. FRANK [x]

Abstract □ The interaction of various metal ions with anhydrotetracycline was investigated. A comparison of the UV–visible and fluorescence spectral characteristics of anhydrotetracycline and its metal-ion complexes with a number of modified anhydrotetracyclines in the presence of metal ions suggested that the C-11 oxygen was involved in metal-ion binding. Secondary binding was observed in the A-ring by circular dichroism when the primary site was blocked.

Keyphrases □ Anhydrotetracycline—and various metal-ion complexes, potentiometric and spectral investigation of binding properties □ Metal-ion complexes, various—with anhydrotetracycline, potentiometric and spectral investigation of binding properties □ Complexes, metal ion, various—with anhydrotetracycline, potentiometric and spectral investigation of binding properties □ Spectrometry, UV–visible, fluorescence, and circular dichroism—investigation of binding properties of anhydrotetracycline with various metal ions □ Potentiometry—investigation of complexation of anhydrotetracycline with various metal ions □ Antibiotics—anhydrotetracycline, complexation with various metal ions, potentiometric and spectral investigation

As a result of the extensive use of tetracyclines, several adverse side effects have been reported (1). Many of these side effects have been traced to impurities in the tetracycline preparation, as in the case of the "reversible Fanconi-type syndrome," which is thought to be induced by anhydrotetracycline (I) and 4-epianhydrotetracycline (1, 2). Tetracycline degradation in an acidic medium was investigated previously, and the principal degradation products were 5a,6-anhydrotetracycline and 4-epitetracycline (3).

Treatment of tetracycline with warm mineral acid results in the loss of a molecule of water from the C-5a and C-6 positions, forming anhydrotetracycline (4). X-ray diffraction studies revealed that the bond lengths of anhydrotetracycline agree with those of tetracycline, except for the C-ring and adjacent bonds. The anhydrotetracycline molecule was more planar in the C–D-ring region than its tetracycline parent (5). A slightly different conformation of the A-ring of anhydrotetracycline also was revealed. The nitrogen of the C-4 position was reported to be closer to the C-12a oxygen than to the C-3 oxygen in anhydrotetracycline (5). All active tetracyclines were reported to have the same conformation of the A-ring, with the C-4 nitrogen closer to the C-3 oxygen than to the C-12a oxygen (6, 7).

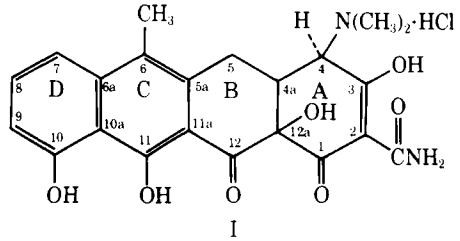

I

This investigation concerned the complexing properties of anhydrotetracycline, with particular emphasis on the determination of the complexation sites in this molecule. The functional groups proposed as binding sites in tetracycline remain in anhydrotetracycline and are considered possible binding sites of this compound. On the A-ring, these sites include a carbonyl and hydroxyl group at the C-1 or C-3 position, the amide group at the C-2 position, and the dimethylamine group at the C-4 position. The C-10–C-12 position carbonyl and hydroxyl groups of the B-, C-, and D-rings are also considered possible complexation sites.

While the UV region of both tetracycline and anhydrotetracycline contains multiple chromophore absorptions, the visible region of anhydrotetracycline exhibits a single absorption at 430 nm. This absorption is assigned to the $\pi \rightarrow \pi^*$ transition of the B–C–D-ring chromophore of anhydrotetracycline. In the presence of certain metal ions, this absorption band undergoes a bathochromic shift, strongly suggesting participation of this region of the molecule in complexation. However, the degree of intramolecular transfer of complexation effects is not known.

To establish the primary binding site(s) of metal ions to anhydrotetracycline, some modified anhydrotetracyclines were prepared. The effects of complexation within the A-ring were observed by comparison of the spectral properties of anhydrotetracycline with those of 4-dedimethylaminoanhydrotetracycline and 2-cyanoanhydrotetracycline. Possible complexation involving the C-10 hydroxyl was removed when 10-benzenesulfonyl-2-cyanoanhydrotetracycline was used; finally, any complexation through the C-11 hydroxyl was blocked using 4-dedimethylamino-11-methoxyanhydrotetracycline.

(14) K. A. Zirvi, M. S. Dar, and T. Fakouhi, *J. Pharm. Sci.*, **64**, 649(1975).

(15) D. Duncan, *Biometries*, **11**, 1(1955).

(16) G. M. Everett, L. E. Blockus, and I. M. Sheppered, *Science*, **124**, 79(1965).

(17) D. L. Trepanier, P. E. Krieger, and J. N. Eble, *J. Med. Chem.*, **8**, 802(1965).

ACKNOWLEDGMENTS AND ADDRESSES

Received May 16, 1975, from the *Department of Pharmacology, School of Medicine, Pahlavi University, Shiraz, Iran.*

Accepted for publication February 9, 1976.

The authors thank Dr. M. H. Bokhari of the Department of Biology, Pahlavi University, for plant identification.

[x] To whom inquiries should be directed.

Potentiometric and Spectral Investigations of Anhydrotetracycline and Its Metal-Ion Complexes

L. J. STOEL [*], E. C. NEWMAN [‡], G. L. ASLESON [§], and C. W. FRANK [x]

Abstract □ The interaction of various metal ions with anhydrotetracycline was investigated. A comparison of the UV–visible and fluorescence spectral characteristics of anhydrotetracycline and its metal-ion complexes with a number of modified anhydrotetracyclines in the presence of metal ions suggested that the C-11 oxygen was involved in metal-ion binding. Secondary binding was observed in the A-ring by circular dichroism when the primary site was blocked.

Keyphrases □ Anhydrotetracycline—and various metal-ion complexes, potentiometric and spectral investigation of binding properties □ Metal-ion complexes, various—with anhydrotetracycline, potentiometric and spectral investigation of binding properties □ Complexes, metal ion, various—with anhydrotetracycline, potentiometric and spectral investigation of binding properties □ Spectrometry, UV–visible, fluorescence, and circular dichroism—investigation of binding properties of anhydrotetracycline with various metal ions □ Potentiometry—investigation of complexation of anhydrotetracycline with various metal ions □ Antibiotics—anhydrotetracycline, complexation with various metal ions, potentiometric and spectral investigation

As a result of the extensive use of tetracyclines, several adverse side effects have been reported (1). Many of these side effects have been traced to impurities in the tetracycline preparation, as in the case of the "reversible Fanconi-type syndrome," which is thought to be induced by anhydrotetracycline (I) and 4-epianhydrotetracycline (1, 2). Tetracycline degradation in an acidic medium was investigated previously, and the principal degradation products were 5a,6-anhydrotetracycline and 4-epitetracycline (3).

Treatment of tetracycline with warm mineral acid results in the loss of a molecule of water from the C-5a and C-6 positions, forming anhydrotetracycline (4). X-ray diffraction studies revealed that the bond lengths of anhydrotetracycline agree with those of tetracycline, except for the C-ring and adjacent bonds. The anhydrotetracycline molecule was more planar in the C–D-ring region than its tetracycline parent (5). A slightly different conformation of the A-ring of anhydrotetracycline also was revealed. The nitrogen of the C-4 position was reported to be closer to the C-12a oxygen than to the C-3 oxygen in anhydrotetracycline (5). All active tetracyclines were reported to have the same conformation of the A-ring, with the C-4 nitrogen closer to the C-3 oxygen than to the C-12a oxygen (6, 7).

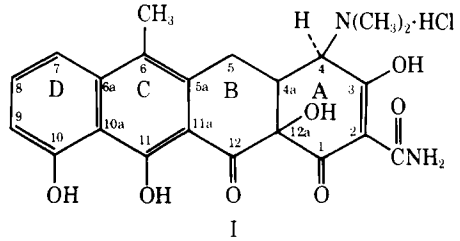

I

This investigation concerned the complexing properties of anhydrotetracycline, with particular emphasis on the determination of the complexation sites in this molecule. The functional groups proposed as binding sites in tetracycline remain in anhydrotetracycline and are considered possible binding sites of this compound. On the A-ring, these sites include a carbonyl and hydroxyl group at the C-1 or C-3 position, the amide group at the C-2 position, and the dimethylamine group at the C-4 position. The C-10–C-12 position carbonyl and hydroxyl groups of the B-, C-, and D-rings are also considered possible complexation sites.

While the UV region of both tetracycline and anhydrotetracycline contains multiple chromophore absorptions, the visible region of anhydrotetracycline exhibits a single absorption at 430 nm. This absorption is assigned to the $\pi \rightarrow \pi^*$ transition of the B–C–D-ring chromophore of anhydrotetracycline. In the presence of certain metal ions, this absorption band undergoes a bathochromic shift, strongly suggesting participation of this region of the molecule in complexation. However, the degree of intramolecular transfer of complexation effects is not known.

To establish the primary binding site(s) of metal ions to anhydrotetracycline, some modified anhydrotetracyclines were prepared. The effects of complexation within the A-ring were observed by comparison of the spectral properties of anhydrotetracycline with those of 4-dedimethylaminoanhydrotetracycline and 2-cyanoanhydrotetracycline. Possible complexation involving the C-10 hydroxyl was removed when 10-benzenesulfonyl-2-cyanoanhydrotetracycline was used; finally, any complexation through the C-11 hydroxyl was blocked using 4-dedimethylamino-11-methoxyanhydrotetracycline.

EXPERIMENTAL

Methods—The UV and visible spectra were obtained on a recording spectrophotometer[1] utilizing 1.0-cm quartz cells. Complete spectra of the compounds investigated were initially obtained in acetonitrile at concentrations of approximately 1.5×10^{-5} *M*. Samples for the visible studies were prepared at approximately 1×10^{-4} *M* in 50% chloroform in absolute ethanol. All studies of complexation with modified anhydrotetracyclines were carried out in the presence of equimolar amounts of triethylamine. The stock solutions of the various metal ions used were prepared from their chloride or nitrate salts in absolute ethanol.

Circular dichroism spectra were recorded on an optical rotatory dispersion–circular dichroism spectrometer[2]. Solutions of tetracycline and of anhydrotetracyclines were 1×10^{-4} *M* and 2.5×10^{-5} *M* in 90% methanol in water, respectively. The pH of all solutions was maintained at 7.4 with 0.1 *M* trimethylamine. A range of 0.1–0.2° full scale was used with a time constant of 3 sec.

The fluorescence spectra of the sample solutions were obtained using a spectrophotofluorometer[3]. Solutions were prepared in 50% chloroform in absolute ethanol at an approximate concentration of 1×10^{-4} *M*. Spectra were calibrated to the 450-nm fluorescence maximum of quinine sulfate.

Aqueous pKa values for the tetracycline hydrochloride salts were determined from potentiometric data by incorporation into a modified computer program (8); this program calculates pKa values from pH *versus* volume of titrant data utilizing the Noyes (9) method. Less soluble tetracyclines were titrated in 50% dimethylformamide in water, and apparent pH values were used to calculate the pKa values in these instances. Samples approximately 1.4×10^{-3} *M* were titrated with 0.5 ml of standardized 1.0 *M* sodium hydroxide in 0.01-ml increments using a micrometer syringe[4]. A constant ionic strength of 1.0 was maintained by the addition of potassium chloride. All pH values were taken on a servo-digital pH/volt meter[5] equipped with a glass electrode[6] and a calomel reference electrode.

Nonaqueous titrations in dimethylformamide of approximately 1.5×10^{-4} *M* samples were carried out using 20% tetra-*n*-butylammonium bromide as the supporting electrolyte. The dimethylformamide solvent was purified by vacuum distillation after standing for several days over barium oxide and stored over a type 4A (4–8-mesh) molecular sieve. A micrometer syringe[4] was used to deliver 0.01-ml aliquots of titrant accurately. A semimicro silver–silver chloride combination electrode[7] containing 2-propanol saturated with potassium chloride was used for all potential measurements made on a servo-digital pH/volt meter[5].

The analytical TLC method for tetracycline and related hydrochloride salts was described previously (2). Because the dedimethylaminotetracyclines remained on the solvent front in the previously described TLC system, these compounds were separated using silica gel H as the solid support and acetone–ethyl acetate–water (20:10:3) as the eluting solution.

Compounds—*Anhydrotetracycline Hydrochloride*—Tetracycline hydrochloride[8] (5.0 g) was added to a boiling solution of 2-propanol (42 ml), methanol (3 ml), and concentrated hydrochloric acid (15 ml). After refluxing for 20 min, the resulting precipitate was filtered, washed with 2-propanol, and dried under vacuum for 2 hr. The crude product was then boiled in 500 ml of benzene, removing excess water, methanol, and 2-propanol as azeotropes. The remaining precipitate was filtered and dried under vacuum for 18 hr to yield 3.9 g of product.

TLC yielded only one spot on a 5% edetate sodium[9]-treated Kieselguhr plate with R_f 0.88. An NMR peak was observed at 2.40 ppm for the C-6 methyl protons. The mass spectrum contained a parent ion at *m/e* 426. Titration in 50% dimethylformamide and water resulted in an equivalent weight of 446 ± 24 compared to a calculated value for the hydrochloride salt of 463. The calculated apparent pKa values were 4.6, 6.6, and 9.0.

2-Cyanotetracycline—The synthesis of 2-cyanotetracycline as outlined by Mani and Foltran (10) was followed. TLC using silica gel revealed a single spot at R_f 0.33. The decomposition temperature of the isolated yellow crystals was in excess of 280°. A mass spectrum of this compound could not be obtained because of its low volatility. Nonaqueous titration of the sample in dimethylformamide resulted in an equivalent weight of 427 ± 4 (calculated 426). The IR spectrum contained the nitrile absorption at 4.55 μm.

Anal.—Calc. for $C_{22}H_{22}N_2O_7$: C, 61.97; H, 5.20; N, 6.57. Found: C, 61.74; H, 5.12; N, 6.56.

2-Cyanoanhydrotetracycline—A sample of 2-cyanotetracycline was dissolved in a minimum volume of 50% anhydrous dimethylformamide in anhydrous acetone at 5°. Anhydrous hydrogen chloride was bubbled through the solution for 5 min. The resulting reaction mixture was maintained at 5° for 18 hr. The product was precipitated from the reaction mixture by treatment with anhydrous ether, purified by recrystallization from ethanol and water, and dried in a vacuum oven at 60° for 24 hr.

TLC of the sample on silica gel revealed one spot at R_f 0.25. Nonaqueous titration of the sample produced an equivalent weight of 406 ± 5 (calculated 408).

Anal.—Calc. for $C_{22}H_{20}N_2O_6$: C, 64.71; H, 4.90; N, 6.86. Found: C, 63.43; H, 5.01; N, 6.47.

10-Benzenesulfonyl-2-cyanotetracycline—The 10-benzenesulfonyl ester of tetracycline was prepared as outlined previously (4, 11). Nonaqueous titration of the dried product resulted in an equivalent weight of 546 ± 15 (calculated 566).

Anal.—Calc. for $C_{22}H_{26}N_2O_9S \cdot H_2O$: C, 57.53; H, 4.83; N, 4.79. Found: C, 57.37; H, 4.57; N, 4.81.

10-Benzenesulfonyl-2-cyanoanhydrotetracycline—A solution of 10-benzenesulfonyl-2-cyanotetracycline dissolved in anhydrous acetone was cooled to 5°. After the solution was treated for 5–10 min with anhydrous hydrogen chloride, the reaction mixture was allowed to stand for 18 hr. A 10-fold excess of distilled water was added, and the resulting precipitate was isolated and recrystallized from ethanol and water.

After drying in a vacuum oven at 60° for 24 hr, the sample revealed a single spot by TLC (silica gel) at R_f 0.57. Nonaqueous titration resulted in an equivalent weight of 265 ± 5 (calculated 274). The NMR spectrum in dimethyl sulfoxide-d_6 contained the typical anhydro C-6 methyl peak at 2.45 ppm.

4-Dedimethylaminotetracycline—The synthesis described by McCormick *et al.* (11) was used. The analytical data appeared previously (12).

4-Dedimethylaminoanhydrotetracycline and 4-Dedimethylamino-11-methoxyanhydrotetracycline—These compounds were prepared and identified as described previously (12).

DISCUSSION

Potentiometric Investigations—The titration of anhydrotetracycline hydrochloride in 50% dimethylformamide in water resulted in three pKa values: 4.6, 6.6, and 9.0. Tetracycline hydrochloride under similar conditions yielded pKa values of 4.3, 7.7, and 9.7. Comparison of these values indicates that the acidity of anhydrotetracycline is approximately the same as tetracycline, with the second and third pKa values being slightly more acidic. Doluisio and Martin (13) reported only two aqueous pKa values for anhydrochlortetracycline hydrochloride, 3.28 and 5.37, compared to 3.66, 7.40, and 9.27 for chlortetracycline hydrochloride, indicating a definite increase in the acidity of the anhydro analog.

The observed titration curves and calculated pKa values are the result of complex, multiple deprotonations of more than one acidic site within the molecule (14). The formation of anhydrotetracycline significantly changes the character of the C and D rings of tetracycline and is expected to alter significantly the acidity of any site(s) associated with this region of the molecule. The second and third dissociation values are strongly dependent on the microdissociation values (k_n) associated with the individual deprotonation sites. The theory and equations that apply to aqueous systems were developed previously (15). The equations that apply in this case are:

$$K_{a_1}K_{a_2}K_{a_3} = k_1k_{12}k_{123} = k_1k_{13}k_{132} \quad \text{(Eq. 1)}$$

$$1/K_{a_3} = 1/k_{123} + 1/k_{132} \quad \text{(Eq. 2)}$$

$$k_{12}k_{123} = k_{13}k_{132} \quad \text{(Eq. 3)}$$

[1] Cary model 14.
[2] Cary model 60.
[3] Aminco-Bowman.
[4] Agla, Burroughs Wellcome & Co.
[5] Heath model EU-302A.
[6] Sargent No. 5-30050-15C.
[7] Corning No. 476050.
[8] Pfizer, Inc., New York, N.Y.
[9] Versene.

Table I—Half-Neutralization Potentials (—Millivolts) of Various Tetracyclines and Model Compounds in Dimethylformamide

Compound	C-1 or C-3 Hydroxyl	C-4 Dimethylamine	C-10, C-11, or C-12 Hydroxyl
Tetracycline hydrochloride	474	788	976
Anhydrotetracycline hydrochloride	457	634	819 974
Tetracycline base	Zwitterionic	794	990
Tetracycline methiodide	622	Blocked	855 1240[a]
4-Dedimethylaminotetracycline	798	Not present	993
4-Dedimethylaminoanhydrotetracycline	635	Not present	893
4-Dedimethylamino-11-methoxyanhydrotetracycline	815	Not present	917[b]
2-Cyanotetracycline	Zwitterionic	649	914
2-Cyanoanhydrotetracycline	Zwitterionic	619	776
10-Benzenesulfonyl-2-cyanotetracycline	Zwitterionic	624	1038[c]
10-Benzenesulfonyl-2-cyanoanhydrotetracycline	Zwitterionic	564	652
2-Carbamoylcyclohexane-1,3-dione	932	—	—
1-Hydroxyanthraquinone	—	—	971
8,9,10-Trihydroxy-1-keto-1,2,3,4-tetrahydroanthracene	—	—	731
1,8-Dihydroxynaphthalene	—	—	735
1-Hydroxy-8-methoxynaphthalene	—	—	—

[a] Very small break in the titration curve. [b] C-11 blocked. [c] C-10 blocked.

$$K_{a_2} = k_{12} + k_{13} \quad \text{(Eq. 4)}$$

where K_{a_n}'s are the observed macroscopic dissociation constants, and k_n's are the dissociation constants of each individual site along a particular dissociation scheme. An increase in the acidity of the site assigned as the third deprotonation site (β-diketone system of C-10–C-12) results in an increase in k_{13} and k_{123} and is observed as an increase in the macroscopic dissociation values, K_{a_2} and K_{a_3}.

Because of the favorable solubility characteristics of the various modified tetracyclines and anhydrotetracyclines in dimethylformamide, all nonaqueous titrations were carried out in this solvent. The half-neutralization potential values for a number of tetracyclines and their anhydro analogs, as well as a number of tetracycline model compounds, are presented in Table I. Although the previously discussed equations do not apply directly to nonaqueous systems, the same trends were observed for the half-neutralization potentials of the tetracyclines and their anhydro analogs. The increase in the acidity of this region was also noted by the appearance of a fourth titratable proton from anhydrotetracycline, which was not observed with tetracycline under the same conditions.

As was the case with anhydro formation, the alteration of functional groups changed the acidity of the resulting compounds. The removal of the C-4 position dimethylamine group, for example, decreased the value of the first dissociation constant for both the tetracycline and the anhydrotetracycline derivatives (Table I). It is generally accepted that this dissociation should be assigned to the acidic proton of the A-ring tricarbonyl system, and a decrease in the acidity of this proton is expected as a result of removal of the electron-withdrawing dimethylamine group. A decrease in acidity was also observed for the proton dissociating from the B–C–D-ring system of these derivatives. Although the effect was not as great as that observed for the tricarbonyl proton, it does imply some intramolecular interaction between the A-ring and the remaining portion of the anhydrotetracycline molecule.

Conversion of the C-2 position amide to a nitrile would be expected to increase the acidity of the A-ring tricarbonyl proton; however, titration of the 2-cyano derivatives of anhydrotetracycline produced only two titratable protons, both weaker than predicted for this proton in these compounds (Table I). The 2-cyano derivatives may exist in zwitterionic form in solution with a weaker acidic site, probably the dimethylamine group of the C-4 position, acting as the proton receptor. The low vapor pressure and high melting points observed for these derivatives also were indicative of this ionic character. As observed for the 4-dedimethylamino derivatives, modification of the A-ring of both tetracycline and anhydrotetracycline to the 2-cyano derivative affected the acidity of the B–C–D-ring proton as well.

Conversion of the C-11 hydroxyl to the methyl ether decreased the hydrogen bonding of the C-10 hydroxyl proton, allowing this proton to be titrated. However, titration of the monomethyl ether of 1,8-dihydroxynaphthalene did not produce an observable break in the titration curve, indicating that the effect of hydrogen bonding alone was not sufficient to explain the observed increase in the acidity of this proton. The presence of the C-12 carbonyl was assumed to provide additional stabilization for the anion formed from 4-dedimethylamino-11-methoxyanhydrotetracycline. The increased carbonyl character of the C-12 position also resulted in an increase in the hydrogen bonding by the A-ring tricarbonyl proton on the C-1 oxygen. An accompanying decrease in acidity of this proton was observed, as indicated by the drop of the half-neutralization potential from −635 to −835 mv.

Spectral Characteristics—The UV–visible spectrum of anhydrotetracycline contained peaks of maximum absorption at 223 nm (ϵ = 36,900), 269 nm (ϵ = 58,370), and 430 nm (ϵ = 9820). The absorption maxima for model compounds of the B–C–D-chromophoric region and the A-ring of anhydrotetracycline are given in Table II. The bands at 430 and 269 nm were assigned to the $\pi \rightarrow \pi^*$ transitions of the B–C–D-chromophoric region. The absorption at 269 nm also contained a contribution from the A-ring chromophore. The 223-nm band was assigned to a $\pi \rightarrow \pi^*$ transition of the aromatic system of this compound, with accompanying benzenoid absorption bands observed in the 300-nm region of the spectrum.

The λ_{max} (ϵ) in the UV–visible spectra of the modified anhydrotetracyclines is presented in Table III. Comparison of the λ_{max} values of 4-dedimethylaminoanhydrotetracycline with anhydrotetracycline

Table II—UV-Visible Absorption Maxima of Model Compounds of Tetracycline and Anhydrotetracycline Chromophores

Compound	λ_{max}, nm (ϵ)	Reference
2-Carbamoylcyclohexane-1,3-dione	258 (17,800)	16
2-Methylcarbamoylcyclohexane-1,3-dione	260 (17,800)	16
2-Carbamoyl-4-dedimethylaminocyclohexane-1,3-dione	261 (15,500)	16
8-Hydroxytetralone	260 (9300), 335 (3600)	4
2-Acetyltetralone	235 (6800), 257 (5000), 300 (6400), 341 (13,000)	17
2-Acetyl-8-hydroxytetralone	236 (12,000), 267 (5500), 348 (12,000)	4
2-Acetyl-8-benzyloxytetralone	260 (4600), 343 (13,200)	17
2-Hydroxyacetophenone	252 (9300), 327 (3200)	18
2-Methoxyacetophenone	246 (11,500), 305 (3800)	18
2-Hydroxybenzaldehyde	255 (10,000), 325 (3000)	18
2-Methoxybenzaldehyde	253 (11,800), 319 (4300)	18
8,9,10-Trihydroxy-1-keto-1,2,3,4-tetrahydroanthracene	267 (35,500), 425 (6800)	4

Table III—UV-Visible Absorption Maxima, λ (ε), of Anhydrotetracyclines in Acetonitrile

Compound	λ_{max}, nm (ε)
Anhydrotetracycline hydrochloride	269 (58,400), 430 (9800)
2-Cyanoanhydrotetracycline	267 (45,000), 426 (6900)
4-Dedimethylaminoanhydrotetracycline	268 (51,400), 426 (9300)
10-Benzenesulfonyl-2-cyanoanhydrotetracycline	267 (26,500), 404 (41,00)
4-Dedimethylamino-11-methoxyanhydrotetracycline	266 (57,100), 392 (5900)

indicates that removal of the C-4 dimethylamine group only slightly affected the spectral characteristics of anhydrotetracycline. The λ_{max} values for 2-cyanoanhydrotetracycline were shifted slightly to shorter wavelengths, with a decrease in the intensity relative to anhydrotetracycline. The decrease in intensity (ε) was attributed to the change in the ionic character of the A-ring. The sulfonyl ester at the C-10 position produced a still further decrease in the intensity of the UV–visible absorptions of 10-benzenesulfonyl-2-cyanoanhydrotetracycline. The dramatic hypsochromic shift of the long wavelength maximum of 10-benzenesulfonyl-2-cyanoanhydrotetracycline and 4-dedimethylamino-11-methoxyanhydrotetracycline was the result of decreased intramolecular hydrogen bonding in these compounds. Conover (17) reported similar behavior in the spectra of *o*-hydroxy and *o*-alkoxy aldehydes and ketones.

Conversion to the anhydrotetracycline resulted in an enhancement of the fluorescent properties of the tetracycline. A single fluorescent maximum was observed for anhydrotetracycline at 520 nm, with an activation wavelength of 430 nm. Similar maxima were observed for the other modified anhydrotetracyclines (Table IV). The fluorescence intensity was observed to be pH dependent, decreasing with increasing pH. Fluorescence enhancement, as well as maxima shifts, was observed from solutions of anhydrotetracycline with some metal ions. Solutions containing the transition metal ions usually resulted in fluorescence quenching.

The results of visible and fluorescence investigations of metal-ion complexation with the modified anhydrotetracyclines are presented in Table IV. The metal ions chosen for this study all exhibited complexation with anhydrotetracycline, as indicated by either a bathochromic shift of the long wavelength $\pi \rightarrow \pi^*$ transition in the visible spectrum of metal ion–ligand solutions or a change in the fluorescence properties of these solutions. Metal-ion-containing solutions of both 4-dedimethylaminoanhydrotetracycline and 2-cyanoanhydrotetracycline produced the same spectral alterations observed for complexation with anhydrotetracycline. Any contribution to the visible absorption spectrum by complexation within the A-ring was apparently minimal. However, the bathochromic shift indicative of metal-ion complexation with anhydrotetracycline was not observed for metal-ion solutions of 4-dedimethylamino-11-methoxyanhydrotetracycline. It can be concluded that the C-11 hydroxyl is most likely involved as a binding site of these metal ions to anhydrotetracycline. A slight shoulder in the 460-nm region of the visible spectrum of the 11-methoxy derivative with Al^{+3} and Zr^{+4} suggests that possibly another site may become involved in the complexation of these metals. This contention is supported by an accompanying shift in the fluorescence maxima of these solutions.

The 10-benzenesulfonyl derivative also was not observed to form complexes with most of the metal ions investigated. Only the strong oxygen binding metals, antimony, aluminum, and zirconium, produced the spectral changes indicative of complexation with this derivative. Possible explanations for the inability of this derivative to form metal-ion complexes are direct participation of the C-10 oxygen in metal-ion chelation, steric interference of the bulky benzenesulfonyl ester, and complex formation too weak to be observed by the methods employed.

The formation of a metal-ion complex of anhydrotetracycline at the C-10 and C-11 hydroxyls would involve the loss of both protons of these functional groups or the rearrangement of the β-diketone system displacing a hydrogen to the C-12 oxygen. Potentiometric studies indicated that the displacement of a second proton from this region of the molecule is difficult. Although it was reported that strong oxygen binding metals such as zirconium and titanium do form such

Table IV—Visible Absorption Maxima and Fluorescence Emission Maxima of Metal-Ion Solutions of Anhydrotetracycline

Metal	Absorption λ_{max}, nm	Absorption ε	Fluorescence, λ_{max}, nm	Relative Intensity	Activation, λ_{max}, nm
Anhydrotetracycline					
None	433	7,300	520	1.0[a]	430
Antimony	442	7,800	545	1.0	440
Manganese	472	10,000	—	—[b]	—
Calcium	459	10,400	530	1.3	460
Magnesium	450	9,400	520	29.8	450
Tin	439	7,200	570	1.2	450
Zinc	441	9,600	530	11.0	450
Aluminum	480	8,500	550	25.0	475
Zirconium	475	8,000	557	13.5	470
4-Dedimethylaminoanhydrotetracycline					
None	432	8,200	523	1.0[a]	430
Antimony	430	8,300	536	1.0	435
Manganese	440	8,900	—	—[b]	445
Calcium	455	9,700	547	1.3	462
Magnesium	440	10,400	519	24.8	452
Tin	430	8,200	541	1.1	453
Zinc	448	10,200	532	10.5	451
Aluminum	478	11,000	556	24.4	475
Zirconium	490	8,507	577	10.5	488
2-Cyanoanhydrotetracycline					
None	430	8,300	538	1.0[a]	432
Antimony	437	9,000	560	1.8	456
Manganese	445	10,600	529	—[b]	430
Calcium	455	12,100	544	2.2	450
Magnesium	443	11,800	531	27.2	454
Tin	435	7,600	565	4.4	480
Zinc	450	10,500	531	16.1	454
Aluminum	475	10,100	559	18.3	475
Zirconium	497	9,300	578	14.5	485
10-Benzenesulfonyl-2-cyanoanhydrotetracycline					
None	405	5,100	500	1.0[a]	412
Antimony	412	5,100	505	0.8	415
Manganese	405	5,200	500	1.0	415
Calcium	406	5,000	505	1.1	412
Magnesium	405	4,900	500	1.0	415
Tin	405	5,300	505	1.0	415
Zinc	404	5,300	500	1.0	415
Aluminum	435	4,200	523	1.6	452
Zirconium	470	4,200	547	0.9	478
4-Dedimethylamino-11-methoxyanhydrotetracycline					
None	401	5,400	495	1.0[a]	400
Antimony	400	5,200	497	0.6	400
Manganese	398	5,200	500	0.5	400
Calcium	396	5,100	508	0.7	400
Magnesium	395	5,200	504	0.8	400
Tin	398	5,300	505	0.6	400
Zinc	397	5,300	503	0.8	400
Aluminum	396	5,100	521	0.7	400
Zirconium	400	5,200	534	0.8	425

[a] Intensity of anhydrotetracycline assigned as 1.0. [b] Fluorescence quenched.

double-proton displaced complexes with 1,8-dihydroxynaphthalene (19, 20), none of the other metals used in this investigation was reported to form complexes with this model compound of the C-10–C-11 chelating site. The data indicate that the C-11 oxygen participates as a chelating site in the interaction of metal ions with anhydrotetracycline. Much of the literature suggests that this is also the site of chelation in tetracycline along with the C-12 oxygen (17, 21). In the case of anhydrotetracycline, participation of the C-10 oxygen has not been eliminated by the evidence presented; however, it is highly unlikely that it would be involved in most cases. The similarities of the spectral changes induced by complexation of anhydrotetracycline with the various metal ions studied suggest that the same site is involved in all cases, namely the C-11–C-12 oxygens.

Positive evidence for additional involvement by other sites on the

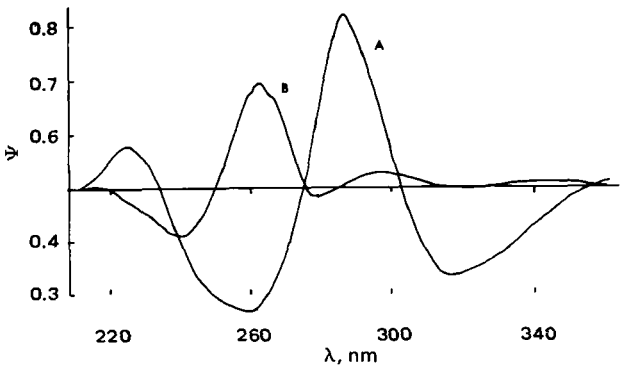

Figure 1—*Circular dichroism spectra of tetracycline hydrochloride and anhydrotetracycline hydrochloride.*

anhydrotetracycline molecules was observed only when the principal site investigated was blocked. This result is illustrated by the changes in the fluorescent properties of 4-dedimethylamino-11-methoxyanhydrotetracycline in the presence of Al^{+3} or Zr^{+4} (Table IV).

Circular Dichroism Investigations—The circular dichroism spectra of a number of tetracyclines were reported previously (6, 22). The stereochemistry at the ring junctures, C-12a, C-4a, and C-5a, are the principal factors contributing to the chirality of the B–C–D-ring chromophore of tetracycline. Therefore, the formation of anhydrotetracycline dramatically affects the circular dichroism spectra by removing the C-5a asymmetry. The circular dichroism spectra of tetracycline hydrochloride and anhydrotetracycline in methanol are shown in Fig. 1. While not all the absorptions observed have been assigned to specific chromophores, investigations of model compounds of the A-ring chromophore showed that a single absorption for this chromophore occurred in the 255–270-nm region (16).

The circular dichroism spectrum of 4-dedimethylamino-11-methoxyanhydrotetracycline in 90% methanol–water is presented in Fig. 2. At low pH, identical spectra were obtained for this compound in the presence of Ca^{+2} and Mg^{+2}, indicating no complex formation. At pH 7 and above, however, a 10-fold increase in the intensities of the principal absorptions for both Mg^{+2} and Ca^{+2} was observed.

The circular dichroism spectrum of the 11-methoxy derivative in the presence of Zr^{+4} is also presented in Fig. 2. A different type of complex is suggested by this spectrum. The definite shift observed in the 272-nm region is interpreted as participation of the A-ring chromophore in the complexation of this strong oxygen binding metal. Participation by the tricarbonyl system of the A ring has been generally disregarded because of the high acidity of this region. However, potentiometric studies indicated that the acidity of this region is greatly reduced in this derivative.

Table V presents the results of a study of the effect of complexation on the UV spectrum of a model A-ring compound, 2-carbamoylcyclohexane-1,3-dione (16). Complexation by Zr^{+4} with this compound resulted in a significant bathochromic shift, while no evidence of complexation was observed for Ca^{+2} until after the solution was treated with a base.

Because of the large shift observed for the Zr^{+4} complex of the model compound, it is postulated that similar complexation is observed in the circular dichroism spectrum of the 4-dedimethylamino-11-methoxyanhydrotetracycline–Zr^{+4} complex. No shifts were observed in the 270-nm region of the circular dichroism spectra for the Ca^{+2} and Mg^{+2} complexes; therefore, another site must be involved, possibly the C-1 and C-12 oxygens.

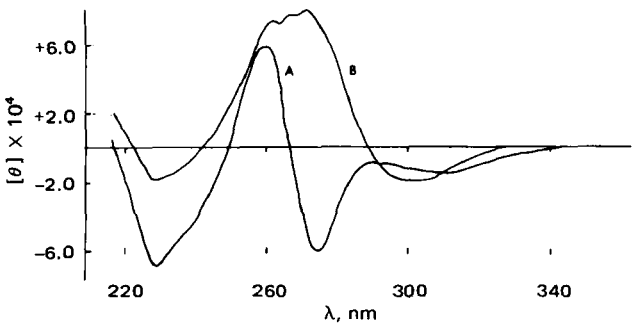

Figure 2—*Circular dichroism spectra of 4-dedimethylamino-11-methoxyanhydrotetracycline and its Zr^{+4} complex.*

Table V—Effect of Metal-Ion Complexation on the Absorption Maximum of an A-Ring Model Compound

	λ_{max}, nm (ϵ)
2-Carbamoylcyclohexane-1,3-dione[a]	257 (17,850)
Plus 1×10^{-3} *M* base	257 (18,300)
Plus 2×10^{-3} *M* Ca^{+2}	257 (17,500)
Plus 1×10^{3} *M* base and 2×10^{-3} *M* Ca^{+2}	264 (20,600)[b]
Plus 2×10^{-3} *M* Zr^{+4}	272 (18,100)
Plus 1×10^{3} *M* base and 2×10^{-3} *M* Zr^{+4}	272 (18,000)

[a] All solutions were 3×10^{5} *M* in absolute ethanol. [b] Additional shoulder at 245 nm.

It has been shown that secondary A-ring complexation can be observed in the circular dichroism spectra of modified anhydrotetracyclines. Mitscher *et al.* (22) observed such A-ring complexation of tetracycline; however, model compounds of the B–C–D-ring chromophore also yielded absorptions in the 260–270-nm region. Until the B–C–D-ring complexation site is blocked, it will remain extremely difficult to determine the effects of A-ring complexation from B–C–D-ring complexation in tetracycline.

SUMMARY

In conclusion, these studies indicate that anhydrotetracycline binds metals at more than one site. The visible spectra of anhydrotetracycline and A-ring-modified anhydrotetracycline exhibited a bathochromic shift of the 430-nm band in the presence of metal ions. The spectral properties, however, of the C-10 or C-11 blocked derivatives remained unchanged when metal ions were present. The fluorescent properties of the modified anhydrotetracyclines reflected the changes observed in the visible spectra in the presence of metal ions. Fluorescence evidence for A-ring complexation was noted when B–C–D-ring complexation was prevented. Circular dichroism investigations with the blocked C-11 position derivative confirmed metal-ion complexation within the A-ring. Variations in the circular dichroism spectra with metal ions indicated multiple binding possibilities within the A-ring.

REFERENCES

(1) M. M. Mull, *Am. J. Dis. Child.*, **112**, 483(1966).

(2) A. A. Fernandez, V. T. Noceda, and E. S. Carrera, *J. Pharm. Sci.*, **58**, 443(1969).

(3) V. N. Dobrynin, A. I. Gurevitch, M. G. Karapetyan, M. N. Kolosov, and M. M. Shemyakin, *Tetrahedron Lett.*, **1962**, 901.

(4) F. A. Hochstein, C. R. Stephens, L. H. Conover, P. P. Regna, R. Pasternack, P. N. Gordon, F. J. Pilgrim, K. J. Brunings, and R. B. Woodward, *J. Am. Chem. Soc.*, **75**, 5455(1953).

(5) R. Restivo and G. J. Palenik, *Biochem. Biophys. Res. Commun.*, **36**, 621(1969).

(6) L. A. Mitscher, A. C. Bonacci, and T. D. Sokoloski, *Antimicrob. Ag. Chemother., 1968*, **1969**, 70.

(7) H. Cid-Dresdner, *Z. Kristallogr., Kristallogeom., Kristallphys., Kristallchem.*, **121**, 170(1965).

(8) R. E. Jensen, R. G. Grvey, and B. A. Paulson, *J. Chem. Educ.*, **47**, 149(1970).

(9) A. A. Noyes, *Z. Phys. Chem.*, **11**, 495(1893).

(10) J. C. Mani and G. Foltran, *Bull. Soc. Chim. Fr.*, **11**, 4141(1971).

(11) R. D. McCormick, S. M. Fox, L. L. Smith, B. A. Bitler, J. Reichenthal, V. E. Origoni, W. H. Miller, R. Winterbottom, and A. P. Doerschuk, *J. Am. Chem. Soc.*, **79**, 2849(1957).

(12) L. Stoel, E. Newman, G. Asleson, and C. W. Frank, *J. Pharm. Sci.*, **64**, 1635(1975).

(13) J. T. Doluisio and A. N. Martin, *J. Med. Chem.*, **6**, 16(1963).

(14) L. J. Leeson, J. E. Krueger, and R. A. Nash, *Tetrahedron Lett.*, **1963**, 1155.

(15) J. T. Edsall and J. Wyman, "Biophysical Chemistry," vol. 1, Academic, New York, N.Y., 1958, p. 495.
(16) K. Tomino, *Chem. Pharm. Bull.*, **6**, 648(1958).
(17) L. H. Conover, Chem. Soc. Special Publication No. 5, 1956, p. 48.
(18) R. A. Morton and A. L. Stubbs, *J. Chem. Soc.*, **1940**, 1347.
(19) K. Andrae, *Chem. Ber.*, **101**, 1013(1968).
(20) K. Andrae, *Z. Anorg. Allg. Chem.*, **1968**, 254; through *Chem. Abstr.*, **69**, 102663k.
(21) D. J. Clive, *Quart. Rev.*, **22**, 439(1968).
(22) L. A. Mitscher, A. C. Bonacci, B. Slater-Eng, A. K. Hacker, and T. D. Sokoloski, *Antimicrob. Ag. Chemother., 1969*, **1970**, 111.

ACKNOWLEDGMENTS AND ADDRESSES

Received August 1, 1975, from the *Department of Chemistry, University of Iowa, Iowa City, IA 52242*

Accepted for publication February 13, 1976.

The partial support of Pfizer, Inc. is gratefully acknowledged.

* Present address: Department of Chemistry, Augustana College, Rock Island, IL 61201

‡ Present address: 3M Center, 3M Co., St. Paul, MN 55075

§ Present address: Department of Chemistry, College of Charleston, Charleston, SC 29401

ˣ To whom inquiries should be directed.

Lipid–Protein Interactions: Enhancement of Enzyme Activity of L-Glutamic Acid Dehydrogenase by Nonionic Detergents

DAVID H. KEMPNER and BRIAN J. JOHNSON ˣ

Abstract □ Five nonionic detergents enhanced the activity of L-glutamic acid dehydrogenase [L-glutamate:nicotinamide adenine dinucleotide phosphate oxidoreductase (deaminating) (EC 1.4.1.3)]. These detergents activated the enzyme toward α-ketoglutaric acid reduction, causing a decrease in the sensitivity of the enzyme to allosteric regulation by guanosine 5-triphosphate. There was also a diminution of the enhancing effect of the modifier adenosine 5-diphosphate on the enzyme's L-glutamic acid dehydrogenase activity. These detergents may cause a conformational change in the enzyme, and this change could lead to an increase in the binding of the substrates for the α-ketoglutaric acid reduction. Accompanied with this conformational change would be a decrease in the binding of the modifier guanosine 5′-triphosphate, with no concomitant change in the binding of the adenosine 5′-diphosphate modifier.

Keyphrases □ Lipid–protein interactions—L-glutamic acid dehydrogenase activity, effect of various nonionic detergents □ L-Glutamic acid dehydrogenase—effect of various nonionic detergents on activity □ Detergents, nonionic—effect on activity of L-glutamic acid dehydrogenase □ Enzyme activity—L-glutamic acid dehydrogenase, effect of various nonionic detergents

Nonionic detergents have been used for the isolation of membrane proteins (1, 2). However, the use of detergents can sometimes produce materials that possess altered activity. Thus, the cell surface antigen Thy-1.2 found on mouse thymocytes loses all activity when isolated with a polyoxyethylene ether nonionic detergent (3) whereas its activity is retained when it is solubilized by papain digestion (4, 5).

These changes in the biological activity of a protein in the presence of nonionic detergents prompted the investigation of the effects of such materials on a defined protein possessing an easily assayable biological activity. The enzyme L-glutamic acid dehydrogenase [L-glutamate:nicotinamide adenine dinucleotide phosphate oxidoreductase (deaminating) (EC 1.4.1.3)] was chosen as a model because it shows activity toward various substrates (6) and its activity is altered by allosteric modifiers (7).

EXPERIMENTAL

The concentration of L-glutamic acid dehydrogenase solutions was determined using an $E^{1\%}_{280}$ of 10.0 (8). Quantitation of the enzyme in detergent solutions and of ovalbumin was determined by fluorescamine (9).

L-Glutamic Acid Dehydrogenase Activity—This reaction was assayed in the direction of α-ketoglutaric acid reduction. A 6-μl aliquot of the enzyme, 0.4 mg/ml, was added to 3 ml of phosphate buffer (10^{-4} *M* ethylenediaminetetraacetic acid and 0.04 *M* sodium phosphate, pH 7.6) containing 3×10^{-4} mole of nicotinamide adenine dinucleotide phosphate reduced form, 1.5×10^{-3} mmole of α-ketoglutaric acid, and 3×10^{-1} mmole of ammonium chloride. The assays were monitored by recording the disappearance of the chromophore at 340 nm. An ϵ_{340} of $6.22 \times 10^3\ M^{-1}\ cm^{-1}$ was used. All initial rates were calculated between 15 and 30 sec after the start of the assay, during which time the reaction rate was linear.

L-Glutamic Acid Dehydrogenase Activity in Presence of Detergent[1]—This reaction was also assayed in the direction of α-ketoglutaric acid reduction. The L-glutamic acid dehydrogenase solutions in 25% (v/v) detergent were prepared by adding 0.5 ml of detergent to a 1.5-ml aliquot of a 0.53-mg/ml solution of the enzyme in phosphate buffer (1×10^{-4} *M* ethylenediaminetetraacetic acid and 0.04 *M* sodium phosphate, pH 7.4). A control was prepared by adding 0.5 ml of deionized water to a 1.5-ml aliquot of the same enzyme solution.

All samples were incubated at 37° for 15 min and then at 4° for 24 hr. Then 6-μl aliquots of this enzyme preparation were added to 3-ml aliquots of the phosphate buffer such that the detergent concentration in the assay mixture was 0.05%, and the assays were monitored as already described. The assays were performed immediately upon addition of the detergent solution of enzyme and at various time intervals over 42 hr.

A further control consisting of L-glutamic acid dehydrogenase solutions in 0.05% (v/v) detergent was prepared by adding 0.75 μl of detergent to a 1.5-ml aliquot of a 0.53-mg/ml solution of the enzyme in phosphate buffer (1×10^{-4} *M* ethylenediaminetetraacetic acid and 0.04 *M* sodium phosphate, pH 7.4). Then 6-μl aliquots of this enzyme mixture were added to 3-ml aliquots of the phosphate buffer con-

[1] The following nonionic detergents were purchased from Sigma Chemical Co.: Triton X-100, Triton X-102, Triton X-35, Triton X-45, Triton X-65, Triton CF-54, Triton CF-32, Triton N-101, Triton DF-12, Triton QS-15, Triton B-1956, Tween 20, Tween 40, Tween 60, Tween 80, Brij 96, and NP-40.

(15) J. T. Edsall and J. Wyman, "Biophysical Chemistry," vol. 1, Academic, New York, N.Y., 1958, p. 495.
(16) K. Tomino, *Chem. Pharm. Bull.*, **6**, 648(1958).
(17) L. H. Conover, Chem. Soc. Special Publication No. 5, 1956, p. 48.
(18) R. A. Morton and A. L. Stubbs, *J. Chem. Soc.*, **1940**, 1347.
(19) K. Andrae, *Chem. Ber.*, **101**, 1013(1968).
(20) K. Andrae, *Z. Anorg. Allg. Chem.*, **1968**, 254; through *Chem. Abstr.*, **69**, 102663k.
(21) D. J. Clive, *Quart. Rev.*, **22**, 439(1968).
(22) L. A. Mitscher, A. C. Bonacci, B. Slater-Eng, A. K. Hacker, and T. D. Sokoloski, *Antimicrob. Ag. Chemother., 1969*, **1970**, 111.

ACKNOWLEDGMENTS AND ADDRESSES

Received August 1, 1975, from the *Department of Chemistry, University of Iowa, Iowa City, IA 52242*

Accepted for publication February 13, 1976.

The partial support of Pfizer, Inc. is gratefully acknowledged.

* Present address: Department of Chemistry, Augustana College, Rock Island, IL 61201

‡ Present address: 3M Center, 3M Co., St. Paul, MN 55075

§ Present address: Department of Chemistry, College of Charleston, Charleston, SC 29401

ˣ To whom inquiries should be directed.

Lipid–Protein Interactions: Enhancement of Enzyme Activity of L-Glutamic Acid Dehydrogenase by Nonionic Detergents

DAVID H. KEMPNER and BRIAN J. JOHNSON ˣ

Abstract □ Five nonionic detergents enhanced the activity of L-glutamic acid dehydrogenase [L-glutamate:nicotinamide adenine dinucleotide phosphate oxidoreductase (deaminating) (EC 1.4.1.3)]. These detergents activated the enzyme toward α-ketoglutaric acid reduction, causing a decrease in the sensitivity of the enzyme to allosteric regulation by guanosine 5-triphosphate. There was also a diminution of the enhancing effect of the modifier adenosine 5-diphosphate on the enzyme's L-glutamic acid dehydrogenase activity. These detergents may cause a conformational change in the enzyme, and this change could lead to an increase in the binding of the substrates for the α-ketoglutaric acid reduction. Accompanied with this conformational change would be a decrease in the binding of the modifier guanosine 5′-triphosphate, with no concomitant change in the binding of the adenosine 5′-diphosphate modifier.

Keyphrases □ Lipid–protein interactions—L-glutamic acid dehydrogenase activity, effect of various nonionic detergents □ L-Glutamic acid dehydrogenase—effect of various nonionic detergents on activity □ Detergents, nonionic—effect on activity of L-glutamic acid dehydrogenase □ Enzyme activity—L-glutamic acid dehydrogenase, effect of various nonionic detergents

Nonionic detergents have been used for the isolation of membrane proteins (1, 2). However, the use of detergents can sometimes produce materials that possess altered activity. Thus, the cell surface antigen Thy-1.2 found on mouse thymocytes loses all activity when isolated with a polyoxyethylene ether nonionic detergent (3) whereas its activity is retained when it is solubilized by papain digestion (4, 5).

These changes in the biological activity of a protein in the presence of nonionic detergents prompted the investigation of the effects of such materials on a defined protein possessing an easily assayable biological activity. The enzyme L-glutamic acid dehydrogenase [L-glutamate:nicotinamide adenine dinucleotide phosphate oxidoreductase (deaminating) (EC 1.4.1.3)] was chosen as a model because it shows activity toward various substrates (6) and its activity is altered by allosteric modifiers (7).

EXPERIMENTAL

The concentration of L-glutamic acid dehydrogenase solutions was determined using an $E^{1\%}_{280}$ of 10.0 (8). Quantitation of the enzyme in detergent solutions and of ovalbumin was determined by fluorescamine (9).

L-Glutamic Acid Dehydrogenase Activity—This reaction was assayed in the direction of α-ketoglutaric acid reduction. A 6-μl aliquot of the enzyme, 0.4 mg/ml, was added to 3 ml of phosphate buffer (10^{-4} *M* ethylenediaminetetraacetic acid and 0.04 *M* sodium phosphate, pH 7.6) containing 3×10^{-4} mole of nicotinamide adenine dinucleotide phosphate reduced form, 1.5×10^{-3} mmole of α-ketoglutaric acid, and 3×10^{-1} mmole of ammonium chloride. The assays were monitored by recording the disappearance of the chromophore at 340 nm. An ϵ_{340} of $6.22 \times 10^3\ M^{-1}\ cm^{-1}$ was used. All initial rates were calculated between 15 and 30 sec after the start of the assay, during which time the reaction rate was linear.

L-Glutamic Acid Dehydrogenase Activity in Presence of Detergent[1]—This reaction was also assayed in the direction of α-ketoglutaric acid reduction. The L-glutamic acid dehydrogenase solutions in 25% (v/v) detergent were prepared by adding 0.5 ml of detergent to a 1.5-ml aliquot of a 0.53-mg/ml solution of the enzyme in phosphate buffer (1×10^{-4} *M* ethylenediaminetetraacetic acid and 0.04 *M* sodium phosphate, pH 7.4). A control was prepared by adding 0.5 ml of deionized water to a 1.5-ml aliquot of the same enzyme solution.

All samples were incubated at 37° for 15 min and then at 4° for 24 hr. Then 6-μl aliquots of this enzyme preparation were added to 3-ml aliquots of the phosphate buffer such that the detergent concentration in the assay mixture was 0.05%, and the assays were monitored as already described. The assays were performed immediately upon addition of the detergent solution of enzyme and at various time intervals over 42 hr.

A further control consisting of L-glutamic acid dehydrogenase solutions in 0.05% (v/v) detergent was prepared by adding 0.75 μl of detergent to a 1.5-ml aliquot of a 0.53-mg/ml solution of the enzyme in phosphate buffer (1×10^{-4} *M* ethylenediaminetetraacetic acid and 0.04 *M* sodium phosphate, pH 7.4). Then 6-μl aliquots of this enzyme mixture were added to 3-ml aliquots of the phosphate buffer con-

[1] The following nonionic detergents were purchased from Sigma Chemical Co.: Triton X-100, Triton X-102, Triton X-35, Triton X-45, Triton X-65, Triton CF-54, Triton CF-32, Triton N-101, Triton DF-12, Triton QS-15, Triton B-1956, Tween 20, Tween 40, Tween 60, Tween 80, Brij 96, and NP-40.

Table I—Chemical Composition of the Nonionic Detergents[a]

Detergent	Hydrophile Polyoxyethylene n[b]	Other	Lipophile
1[c]	20	Sorbitan	Monolaurate
2[c]	20	Sorbitan	Monopalmitate
3[c]	20	Sorbitan	Monostearate
4[c]	20	Sorbitan	Monooleate
5[c]	10	—	Oleyl alcohol
6[d]	3	Sorbitan	Octylphenyl
7[d]	5	Sorbitan	Octylphenyl
8[d]	—	—	Alkyl polyether alcohol
9[d]	9.5	—	Octylphenyl
10[d]	12.5	—	Octylphenyl
11[d]	9.5	—	Nonylphenyl
12[d]	—	—	Arylaryl polyether
13[d]	—	—	Modified polyether adduct
14[d]	—	—	Modified polyethoxylated alcohol
15[d]	—	—	Amine polyglycol condensate
16[d]	—	—	Sodium salt of amphoteric surfactant
17[d]	—	—	—
18[e]	9	—	Octylphenyl

[a] The nonionic detergents had the general formula of hydrophile–lipophile. The hydrophilic portion was a polyoxyethylene moiety and/or sorbitan. The lipophilic portion consisted of monolaurate, *etc.* The difficulty encountered in arriving at a comprehensible chemical name for each detergent led to the assigning of numbers as given in the left-hand column. Their respective trade names are Tween 20, Tween 40, Tween 60, Tween 80, Brij 96, Triton X-35, Triton X-45, Triton X-65, Triton X-100, Triton X-102, Triton N-101, Triton CF-10, Triton CF-54, Triton DF-12, Triton CF-32, Triton QS-15, Triton B-1956, and NP-40. [b] Number of ethylene oxide units. [c] From the General Characteristics of Atlas Surfactants, Atlas Chemical Industries, Wilmington, Del. [d] From Rohm and Haas Surfactants Technical Bulletin, Rohm and Haas Co., Philadelphia, Pa. [e] From Shell Oil Co. Data Sheet 2A003.

taining 0.05% (v/v) detergent. The assays were monitored as already described.

Determination of V_m and K_m of L-Glutamic Acid Dehydrogenase—Aliquots of 6 μl of the enzyme in a 25% (v/v) detergent solution were added to 3-ml aliquots of the following assay mixtures. Incremental amounts of a solution of nicotinamide adenine dinucleotide phosphate reduced form at a concentration of 2×10^{-4} *M* in a buffer solution (1×10^{-4} *M* ethylenediaminetetraacetic acid and 0.04 *M* sodium phosphate, pH 7.6) were added to a similar buffer solution containing 5×10^{-4} *M* α-ketoglutaric acid and 1×10^{-1} *M* NH_4Cl such that the concentration of the nicotinamide adenine dinucleotide phosphate reduced form was varied from 1×10^{-4} to 5×10^{-5} *M*. The assays were monitored as already described.

Inhibition of L-Glutamic Acid Dehydrogenase Activity Using Guanosine 5′-Triphosphate in Presence of Detergent—Incremental amounts of a guanosine 5′-triphosphate solution at a concentration of 4×10^{-3} *M* were added to a phosphate buffer solution (1×10^{-4} *M* ethylenediaminetetraacetic acid and 0.04 *M* sodium phosphate, pH 7.6) such that the concentrations of nicotinamide adenine dinucleotide phosphate reduced form, α-ketoglutaric acid, and ammonium chloride were 1×10^{-4}, 5×10^{-4}, and 1×10^{-1} *M*, respectively.

The final concentrations of guanosine 5′-triphosphate in the assay mixture were 0, 1, 2, 5, and 8×10^{-6} *M*. Three-milliliter aliquots of this solution were taken, and 6 μl of a 25% (v/v) detergent solution of the enzyme was added. The assays were monitored as already described.

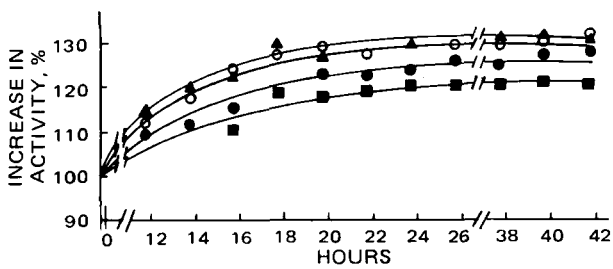

Figure 1—*Activity of L-glutamic acid dehydrogenase in detergent solutions with time. The assay conditions are given in the text. Key:* ▲, *enzyme in Detergent 10;* ●, *enzyme in Detergent 13;* ○, *enzyme in Detergent 18; and* ■, *enzyme in Detergent 2.*

Table II—Enzyme Activities of L-Glutamic Acid Dehydrogenase in Detergents[a]

Detergent	Activity[b], %	K_{GTP}, $M \times 10^{-6}$	Activity[c], %
—	100	1.55 ± 10%	100
12	0	—	—
14	0	—	—
16	8	—	—
1	120	4.3 ± 4.5%	120
2	118	3.4 ± 9.9%	97
3	10	—	—
18	130	2.65 ± 12%	43
9	94	—	—
10	130	9.25 ± 3%	103
15	74	—	—
13	125	4.9 ± 5%	110

[a] Assay conditions as stated in the text. [b] Measured in the direction of α-ketoglutaric acid reduction. [c] Measured as a monocarboxylic acid dehydrogenase.

Activation of L-Glutamic Acid Dehydrogenase Activity Using Adenosine 5′-Diphosphate in Presence of Detergent—Incremental amounts of an adenosine 5′-diphosphate solution at a concentration of 2×10^{-1} *M* were added to a phosphate buffer solution (1×10^{-4} *M* ethylenediaminetetraacetic acid and 0.04 *M* sodium phosphate, pH 7.4) such that the concentrations of nicotinamide adenine dinucleotide phosphate reduced form, α-ketoglutaric acid, and ammonium chloride were 1×10^{-4}, 5×10^{-4}, and 1×10^{-1} *M*, respectively.

The final concentrations of adenosine 5′-diphosphate in the assay mixture were 0, 0.5, 1.0, 3, and 6×10^{-4} *M*. Three-milliliter aliquots of this solution were taken, and 6 μl of a 25% (v/v) detergent solution of the enzyme was added. The assays were monitored as already described.

Monocarboxylic Acid Dehydrogenase of L-Glutamic Acid Dehydrogenase Activity in Presence of Detergent—This reaction was assayed in the direction of pyruvate reduction. Aliquots of 250 μl of a 25% (v/v) detergent solution of the enzyme were added to 2.75 ml of phosphate buffer (10^{-4} *M* ethylenediaminetetraacetic acid and 0.04 *M* sodium phosphate, pH 9.0) containing 1.28×10^{-4} mmole of nicotinamide adenine dinucleotide phosphate reduced form, 3×10^{-1} mmole of ammonium chloride, and 1.2×10^{-1} mmole of sodium pyruvate. The assays were monitored as already described.

RESULTS AND DISCUSSION

In preliminary screening experiments, 18 detergents (Table I) were investigated for their effects on L-glutamic acid dehydrogenase. Of those in which the enzyme was soluble, many destroyed much or all enzyme activity. These detergents were 3, 12, 14, and 16 (Table I). This loss could have been due to denaturation or disruption of the enzyme into its nonactive subunits, possessing molecular weights of 55,000 (10). Detergents 4, 5, 6, 7, 8, 11, and 17 did not solubilize the enzyme under the described conditions. Detergents 9 and 15 solubilized the enzyme, but these solutions showed some loss in enzyme activity.

Five detergents, 1, 2, 10, 13, and 18, gave an enhanced activity of the enzyme when α-ketoglutaric acid was used as the substrate. This change in enzyme activity was observed when the enzyme was initially incubated in a 25% (v/v) detergent solution and then diluted to the assay concentration of 0.05% detergent (Table II). When the assays were repeated such that the enzyme and substrates were only in an environment of a 0.05% detergent solution, there were no changes in enzyme activity. Thus, it appears that when the enzyme is incubated in 25% detergent solution, some change is produced that enhances the enzyme's activity toward the α-ketoglutaric acid reduction.

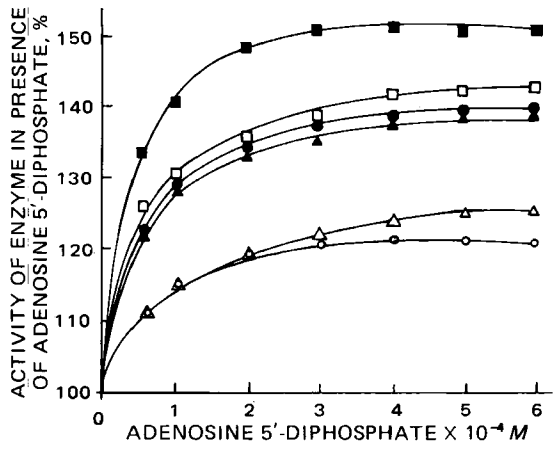

Figure 2—*Effect of detergent on the activation of* L-*glutamic acid dehydrogenase by adenosine 5′-diphosphate. The assay conditions are given in the text. Key:* ■, *enzyme in buffer;* □, *enzyme in Detergent 18;* ●, *enzyme in Detergent 13;* △, *enzyme in Detergent 10;* ▲, *enzyme in Detergent 1; and* ○, *enzyme in Detergent 2.*

The stability of the enhanced activity in detergent solution over time was investigated (Fig. 1). A similar enhancement was obtained with the nonionic detergent, 1, which showed a maximum activity of 120%. Possibly, the effects shown by the detergents on the catalytic activity of the enzyme were caused by a change in the Michaelis–Menton constant, K_m, or in the maximum number of moles of substrate that 1 mole of enzyme can convert per minute, the V_m of the enzyme. An investigation of these parameters was undertaken. The initial enzyme velocities obtained from the various enzyme assays were obtained graphically (11). The K_m and V_m of the enzyme control were 6.8×10^{-5} *M* and 17,000, respectively. Detergents 2, 10, 1, and 13 had K_m values of 8.0×10^{-5}, 8.3×10^{-5}, 4.8×10^{-5}, and 7.6×10^{-5} *M* and V_m values of 19,825, 21,525, 14,000, and 21,000, respectively. All of these detergents showed parallel changes in their V_m and K_m values.

The influence of the detergents on the regulatory properties of L-glutamic acid dehydrogenase was investigated. In general, any modifier of the enzyme that produced an increase in its activity toward the α-ketoglutaric acid conversion caused a decrease in the monocarboxylic acid dehydrogenase activity of the enzyme and vice versa. It is known that adenosine 5′-diphosphate causes an increase in the activity of the enzyme toward the α-ketoglutaric acid conversion and a decrease in its monocarboxylic acid dehydrogenase activity. The allosteric modifier guanosine 5′-triphosphate stimulates the monocarboxylic acid dehydrogenase activity of the enzyme and inhibits its activity toward the α-ketoglutaric acid conversion. Both of these materials probably mediate the equilibrium between the two modifications of the enzyme (7, 12).

In these studies with detergent solutions of the enzyme and the modifier adenosine 5′-diphosphate and guanosine 5′-triphosphate, all detergents lowered the activating effect of adenosine 5′-diphosphate (Fig. 2). The guanosine 5′-triphosphate inhibition of the α-ketoglutaric acid conversion activity of detergent solutions of the enzyme was quantitated by calculation of the reciprocal of the affinity of guanosine 5′-triphosphate (GTP) for the enzyme, the K_{GTP} in each detergent (13). The presence of detergent decreased the sensitivity of the enzyme to inhibition of the α-ketoglutaric acid conversion activity by guanosine 5′-triphosphate. In the absence of guanosine 5′-triphosphate, the monocarboxylic dehydrogenase activity of the enzyme (6, 14) was not altered greatly by detergents, with the exception of Detergent 18 which produced a decrease in activity (Table II). This decrease could have been due to this detergent influencing the equilibrium between the α-ketoglutaric acid conversion and the monocarboxylic acid dehydrogenase modifications.

A possible explanation for this enhanced enzyme activity in detergent solutions, when α-ketoglutaric acid was used as the substrate, could be related to the relative rates of the α-ketoglutaric acid reduction and the glutamate oxidation. It was shown previously that the former reaction is an order of magnitude faster than the latter reaction (15). This information indicates that the substrates for the glutamate oxidation are not bound as well as the substrates for the α-ketoglutaric acid reduction. The binding of detergents may cause a slight conformational change in the enzyme, thereby causing an increase in the binding of the substrates for the α-ketoglutaric acid reduction and accounting for the enhanced activity of the enzyme. It could be construed that this change in conformation is sufficient to lower the binding of guanosine 5′-triphosphate and, thereby, reduce this modifier's inhibitory ability of the α-ketoglutaric acid conversion activity of the enzyme. This conformational change in the enzyme could reduce the ability of the adenosine 5′-diphosphate to enhance the α-ketoglutaric acid conversion activity but not reduce the binding of this modifier with the enzyme.

REFERENCES

(1) A. Helenius and K. Simons, *Biochim. Biophys. Acta*, **415**, 29(1975).

(2) J. N. Umbreit and J. L. Strominger, *Proc. Nat. Acad. Sci. USA*, **70**, 2997(1973).

(3) E. S. Vitetta, E. A. Boyse, and J. W. Uhr, *Eur. J. Immunol.*, **3**, 446(1973).

(4) B. J. Johnson, U. N. Kucich, and J. C. Bennett, *Fed. Proc.*, **34**, 553(1975).

(5) U. N. Kucich, J. C. Bennett, and B. J. Johnson, *J. Immunol.*, **115**, 626(1975).

(6) J. Struck and I. W. Sizer, *Arch. Biochem. Biophys.*, **86**, 260(1960).

(7) G. M. Tomkins, K. L. Yielding, J. Curran, M. R. Summers, and M. W. Bitensky, *J. Biol. Chem.*, **240**, 3793(1965).

(8) M. W. Bitensky, K. L. Yielding, and G. M. Tomkins, *ibid.*, **240**, 668(1965).

(9) S. Udenfriend, S. Stein, P. Bohlen, W. Dairman, W. Leimgruber, and W. Weigele, *Science*, **178**, 871(1972).

(10) N. Talal, G. M. Tomkins, J. F. Mushinski, and K. L. Yielding, *J. Mol. Biol.*, **8**, 46(1964).

(11) H. Lineweaver and D. Burk, *J. Am. Chem. Soc.*, **56**, 658(1934).

(12) J. Monod, J. Wyman, and C. J. Changeux, *J. Mol. Biol.*, **12**, 88(1965).

(13) M. Dixon, *Biochem. J.*, **55**, 70(1953).

(14) G. M. Tomkins, K. L. Yielding, and J. Curran, *Proc. Nat. Acad. Sci. USA*, **47**, 270(1961).

(15) D. A. Olson and C. B. Anfinsen, *J. Biol. Chem.*, **197**, 67(1952).

ACKNOWLEDGMENTS AND ADDRESSES

Received September 24, 1975, from the *Department of Microbiology, University of Alabama Medical School, Birmingham, AL 35294*

Accepted for publication February 19, 1976.

Supported in part by Grant AI 11970 from the National Institutes of Health.

The encouragement of Dr. K. Lemone Yielding is gratefully acknowledged.

[x] To whom inquiries should be directed.

High-Pressure Liquid Chromatographic Determination of Chlorphenesin Carbamate and the β-Isomeric Carbamate

WILLIAM F. BEYER

Abstract □ A high-pressure liquid chromatographic assay was developed for the determination of chlorphenesin carbamate and its β-isomeric carbamate. A single 4-mm i.d. × 30-cm column, prepacked with 10-μm fully porous silica gel particles, is used with 3% methanol in 50% water-saturated butyl chloride as the mobile phase. The procedure separates chlorphenesin carbamate from several possible impurities in addition to the β-isomeric carbamate. The assay was applied to bulk drug and compressed tablets. The relative standard deviations for the assays of chlorphenesin carbamate and the β-isomer are approximately 1 and 2%, respectively.

Keyphrases □ Chlorphenesin carbamate and β-isomer—high-pressure liquid chromatographic analysis, pharmaceutical formulations □ High-pressure liquid chromatography—analysis, chlorphenesin carbamate and β-isomer in pharmaceutical formulations □ Relaxants, skeletal muscle—chlorphenesin carbamate and β-isomer, high-pressure liquid chromatographic analysis in pharmaceutical formulations

Chlorphenesin carbamate, 3-(*p*-chlorophenoxy)-1,2-propanediol 1-carbamate (III), is commercially available in tablet form as an adjunct in short-term therapy as a skeletal muscle relaxant. The drug is produced from chlorphenesin (I) through the intermediate cyclic carbonate (II). In addition to III, the reaction can also yield the isomeric chlorphenesin 2-carbamate (IV) *in limited* quantity. Therefore, process impurities may be present in bulk chlorphenesin carbamate. Chlorphenesin also has been identified as a minor potential degradation product in the tablet formulation.

Compound III may be quantitated by spectrophotofluorometric (1), GLC (2), colorimetric (3), and IR (4) methods. Spectrophotometric (5) and GLC (6) methods are available for I. The cyclic carbonate of chlorphenesin may be quantitatively assayed using IR based on the absorption of the carbonyl at 1800 cm^{-1}. NMR spectroscopy (7) has been used in the quantitative determination of IV.

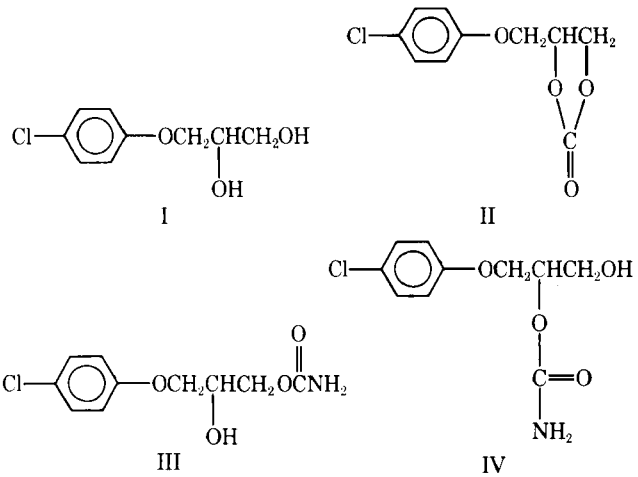

This report describes a high-pressure liquid chromatographic (HPLC) procedure for the quantitative determination of III and IV. Although I and II can be chromatographically resolved, HPLC assays for their determination were not performed due to the assay requirements.

EXPERIMENTAL

Apparatus—A commercial liquid chromatograph[1] was used at ambient temperature with UV detection at 254 nm. The column was 316 stainless steel, 4 mm i.d. × 30 cm long, prepacked with 10-μm microparticulate silica gel[2]. Chromatographic recordings were made with a standard 1-mv commercially available recorder with an integrator[3].

Reagents and Solutions—Approximately 1 part of double-distilled water is added to 3 parts of butyl chloride[4]. The mixture is shaken mechanically for approximately 3 hr and allowed to stand overnight. The upper water-saturated butyl chloride layer is removed and added to an equal volume of butyl chloride to give a 50% water-saturated butyl chloride solution. The mobile phase is 3% methanol[4] in 50% water-saturated butyl chloride.

The internal standard solution is a 0.80-mg/ml solution of 9α-fluoroprednisolone acetate[5] (V) prepared in ethanol[4]–butyl chloride (1:3). With the internal standard solution as a solvent, a 40-mg/ml reference standard[5] solution of chlorphenesin carbamate is prepared.

Sample Preparation—*Bulk Drug*—A 40-mg/ml solution of the chlorphenesin carbamate bulk drug is prepared in the internal standard solution.

Tablets—The average weight of at least 10 tablets[6] is determined, and the tablets are reduced to a fine powder. Approximately 700 mg of accurately weighed powder (equivalent to about 400 mg of chlorphenesin carbamate) is added to 10.0 ml of internal standard solution along with 10–12 6-mm glass beads. After shaking for approximately 15 min, the container is centrifuged to obtain a clear sample for injection.

Chromatography—*Bulk Drug*—Approximately 10 μl is injected; the volume should be kept constant throughout the assay. The chromatograph is operated at 1 ml/min (about 400 psig), with the UV detector sensitivity at 0.32 aufs for III and at 0.04 aufs for IV. Peak height ratios are used in the determination of III; peak heights are used in the determination of IV.

Tablets—Approximately 5 μl is injected. The chromatograph is operated at 1.8 ml/min (about 700 psig), with the UV detector sensitivity at 0.16 aufs.

Calculations—*Bulk Drug*—The amount of III is calculated by the internal standard–reference standard method, using peak height ratios. The percent of IV in the bulk drug is calculated by dividing the peak height of the isomeric carbamate (corrected for deattenuation and response factor) by the sum of the peak height of III and the corrected peak height of IV and multiplying by 100.

Tablets—The chlorphenesin carbamate content of tablets is calculated using peak height ratios and the internal standard–reference standard method. Corrections are made for the amount of powdered sample used and the average tablet weight.

[1] Model 820, du Pont, Wilmington, Del.
[2] μPorasil, Waters Associates, Milford, Mass.
[3] Electronic 19K Honeywell recorder with a Disc integrator.
[4] Burdick and Jackson, Muskegon, Mich.
[5] Control reference standards, The Upjohn Co., Kalamazoo, Mich.
[6] Maolate tablets, 400 mg of chlorphenesin carbamate, The Upjohn Co., Kalamazoo, Mich.

Table I—HPLC Linearity Data for III and IV Using 10-μm Porous Silica Gel Prepacked in a 4.0-mm i.d. × 30-cm Stainless Steel Tube[a]

Injection Number	III mg/ml	III Peak Height Ratio	III Response[b] Factor	IV mg/ml	IV Peak Height Ratio[c]	IV Response[a] Factor	Response Ratio (IV ÷ III)
			Peak Heights Used as Response Parameters				
1	2.51	0.0646	0.0257	0.1060	0.0200	0.0236	0.9183
2	4.85	0.1294	0.0267	0.3095	0.0556	0.0225	0.8427
3	9.90	0.2696	0.0272	0.6900	0.1281	0.0232	0.8529
4	20.23	0.5599	0.0277	1.2050	0.2242	0.0233	0.8412
5	39.93	1.1239	0.0281	2.5000	0.4798	0.0240	0.8541
		Average	0.0271		Average	0.0233	0.8618
		RSD	3.45%		*RSD*	2.37%	3.72%
			Peak Areas Used as Response Parameters				
1	2.51	0.1028	0.0410	0.1060	0.0335	0.0395	0.96
2	4.85	0.2072	0.0427	0.3095	0.1036	0.0418	0.98
3	9.90	0.4133	0.0417	0.6900	0.2362	0.0428	1.03
4	20.23	0.8799	0.0435	1.2050	0.4174	0.0433	1.00
5	39.93	1.7664	0.0442	2.5000	0.8890	0.0445	1.01
		Average	0.0426		Average	0.0424	1.00
		RSD	2.97%		*RSD*	4.44%	2.71%

[a]The mobile phase consisted of 3% methanol in 50% water-saturated butyl chloride. [b]Response arameters divided by milligrams per milliliter. [c]Corrected for detector sensitivity of 0.04 aufs for IV *versus* 0.32 for the internal standard.

RESULTS

A representative chromatogram of III, V (internal standard), and possible process impurities (I, II, and IV) is shown in Fig. 1. The compounds had the following relative retentions: II, 0.26; V, 0.59, I, 0.67; III, 1.0; and IV, 1.15. The number of theoretical plates for III was 4100.

Detector linearity studies for III and IV were made at five concentration levels of the compounds dissolved in the internal standard solution. Information relative to the study and calculation results based on both peak heights and peak height ratios appear in Table I. The peak area response ratio for IV:III was 0.9942, near 1.0, as would be expected for the positional isomer. When using peak heights, the ratio was 0.8618, a reflection of the later elution of IV. Correlation coefficients not significantly different from 1.0 and y-intercepts not significantly different from zero were calculated for the two compounds.

Figure 2 gives a typical chromatogram of III and IV reference standards in the internal standard solution. The peak for III was quite symmetrical for a column loading of 394 μg. The purity of III and IV reference standards was established at near 100% by differential scanning calorimetry, phase solubility, and other purity-indicating tests. A chromatogram of an impure lot of III bulk drug is shown in Fig. 3, from which 1.77% of IV was found. The relative standard deviation (*RSD*) for III obtained by replicate injections of a sample preparation of bulk drug was 0.86% when peak heights were used in calculations *versus* 2.10% for peak area ratios (Table II). Values for III were similar except for injections 1 and 6, where high and low values contributed to the high *RSD* values for peak area ratios. The content of III for this lot by replicate injection was 95.71% by peak height and 95.75% by peak area ratios. Because of better precision, ease of collecting data, and satisfactory peak symmetry, subsequent calculations were made using peak heights.

The *RSD* of the assay for IV based on repeat injections was 0.69% (Table II). The assayed value for IV was 4.43% in the bulk drug, selected for this particular study because of its unusually high IV content. The table also gives data for replicate assays for III and IV in the same bulk drug. The *RSD* for III was 1% with a purity value of 95.29%.

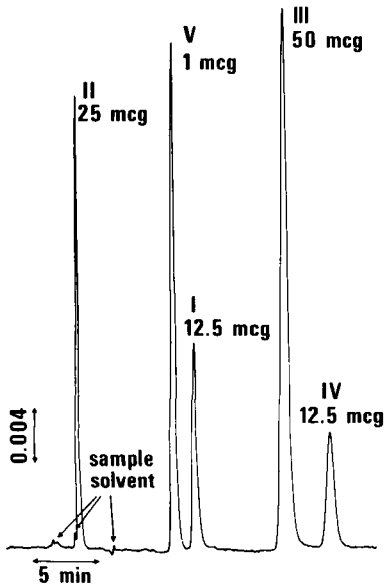

Figure 1—*Chromatogram of the cyclic carbonate of chlorphenesin (II), 9α-fluoroprednisolone acetate internal standard (V), chlorphenesin (I), chlorphenesin carbamate (III), and the β-isomeric carbamate (IV).*

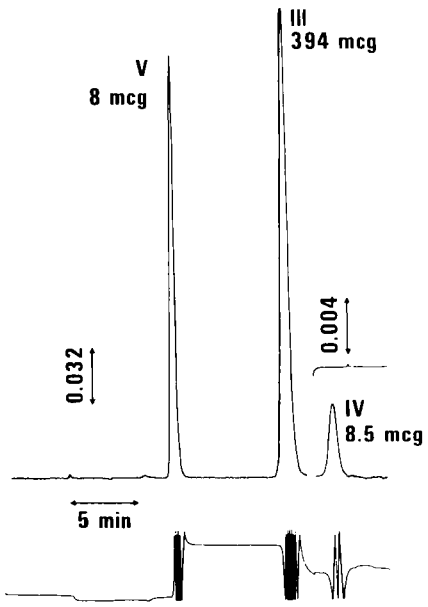

Figure 2—*Chromatogram of III, IV (2.11%), and V.*

Table II—Precision of HPLC Procedure for the Assay of III and IV in Chlorphenesin Carbamate Bulk Drug

Replicate Injections of a Single Sample Preparation for III Bulk Drug (Lot J)			
Injection	Peak Height Ratios, III, %	Peak Area Ratios, III, %	Peak Heights, IV, %
1	95.06	99.32	4.44
2	95.06	95.43	4.46
3	95.00	95.85	4.48
4	95.02	95.59	4.44
5	96.99	95.57	4.40
6	95.66	91.91	4.42
7	96.13	96.61	4.41
8	96.78	95.77	4.39
Average	95.71	95.75	4.43
RSD	0.86	2.10	0.69

Replicate Assays of Chlorphenesin Carbamate Bulk Drug (Lot J)			
Sample Weight, mg		III, %	IV, %
400.0		95.71	4.43
399.3		95.54	4.40
399.6		95.59	4.42
393.5		95.52	4.46
395.0		95.66	4.48
398.3		92.80	4.50
402.3		95.10	4.20
402.1		95.97	4.42
402.2		95.95	4.42
	Average	95.29	4.42
	RSD	1.01	1.97

For IV, the *RSD* was 1.97% and the average IV content was 4.42%. The mass balance for this lot of bulk drug was near 100% based on HPLC assays for III and IV.

Additional HPLC assays of bulk drug were conducted to verify the conditions of the assay and to ensure its manageability in a routine quality control laboratory environment. Thirty lots of the drug, manufactured over 3 years, were assayed (Table III).

HPLC conditions for the determination of III in tablets containing 400 mg of III were changed slightly from those used for the bulk drug. The injection volume was reduced from 10 to 5 μl, corresponding with a detection sensitivity setting of 0.16 aufs, and the flow rate was increased to 1.8 ml/min. These conditions increased the efficiency of the chromatographic procedure when only the assay of III was required. Representative chromatograms of sample preparations for tablet excipients and tablets are shown in Fig. 4. The excipients had no effect on the chromatogram and I and IV, if present, were below detectable limits.

The recovery of III from tablet excipients was determined by adding varying weighed amounts of III and approximately 320 mg of tablet excipients to internal standard solutions. Chromatography was then carried out on the clear extract, with an average recovery of 99.5% for the seven concentration levels of III (Table IV). The *RSD* for the determination was 0.81%, quite low considering that III was spiked at about 50–150% of the standard. Seventeen lots of tablets, varying

Table III—HPLC Assay for III and IV in Chlorphenesin Carbamate Bulk Drug

Lot	Age, months	III, %	IV, %
A	36	99.42	0.18
B	34	101.8	0.16
C	34	99.47	0.20
D	23	100.7	<0.10
E	23	99.28	<0.10
F	23	98.25	0.11
G	10	98.41	0.10
H	10	98.74	0.23
I	9	100.8	0.26
J	5	95.29	4.42[a]
K	5	100.7	0.68
L	5	99.63	0.27
M	5	102.5	0.54
N	5	100.3	0.20
O	5	102.2	<0.10
P	5	101.0	<0.10
Q	Current	98.59	1.68[a]
R	Current	100.0	0.18
S	Current	97.00	1.77[a]
T	Current	99.72	0.23
U	Current	100.7	0.20
V	Current	100.4	1.18
W	Current	99.67	0.15
X	Current	100.8	0.19
Y	Current	99.40	0.56
Z	Current	99.38	0.52
2A	Current	99.0	0.29
2B	Current	100.4	0.17
2C	Current	99.81	0.22
2D	Current	98.99	0.20

[a] Assay values confirmed by NMR.

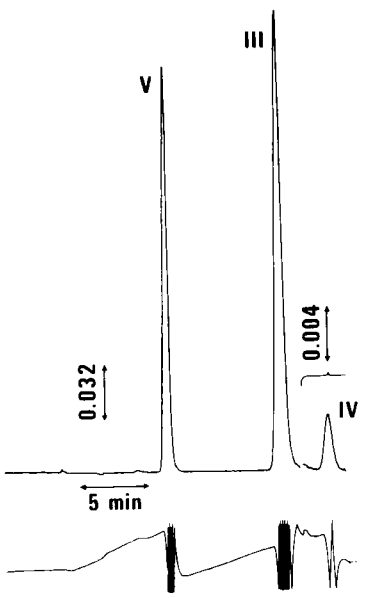

Figure 3—*Chromatogram of chlorphenesin carbamate bulk drug (Lot 5) in the internal standard solution. Compound IV assayed at 1.77%.*

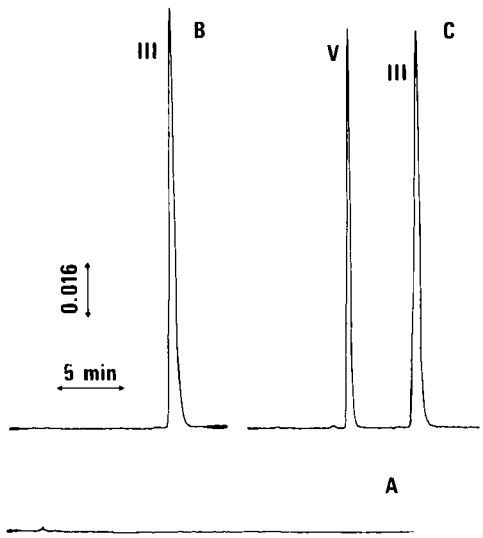

Figure 4—*Chromatograms of tablet excipients in the sample solvent (A), a sample preparation for tablets (50 months) without the internal standard (B), and a sample preparation for the same lot of tablets in the internal standard solution (C).*

Table IV—Recovery of III from Chlorphenesin Carbamate Tablet Excipients

Weight of Excipients, mg	III Added, mg	Percent of Assay Level	III Assayed, mg	Recovery, %
317.7	202.2	50.6	198.0	97.9
315.2	300.9	75.2	298.2	99.1
322.1	330.2	82.6	330.4	100.1
319.1	398.8	99.7	396.9	99.5
326.2	450.1	112.5	449.4	99.8
316.5	502.6	125.7	502.7	100.0
320.4	600.8	150.2	601.8	100.2
			Average	99.5
			RSD	0.81

in age from 7 to 62 months, were assayed by this HPLC method (Table V). Only the 62-month-old lot (Ta) gave chromatographic evidence of I, but it assayed at 99.2%.

DISCUSSION

Preliminary experiments made with HPLC to chromatograph III and possible process impurities or degradation products (I, II, and IV) using packings of 30–50-μm diameter were not considered satisfactory. Nonpolar[7] and polar[8] packings of this diameter gave less than the desired resolution for the four compounds, coupled with tailing of peaks. The properties of 10-μm fully porous silica gel[2], prepacked in a column of 4-mm i.d. dimension and modified by special drilling, were especially suited for the HPLC assay of III and IV. The application of a large amount of III to the column was required because of the relatively low degree of absorbance of the compound at 254 nm and because the determination of low levels of IV was desired.

Relatively rapid analysis was possible at low pressure requirements of the column. Reverse-flow flushing of the filter frits in the column end fittings was carried out as increased pressure was required to maintain the required flow rate. The hard surface filter paper at both ends of the column, maintained with plastic[9] washers, was replaced as needed. On occasion, small voids occurred at column ends when the end fittings were removed. Careful "troweling" with an excess of 10 μm of silica gel, wetted with a small amount of ethanol, filled the void and minimized the effect of the washer.

Water added to the mobile phase as 50% water-saturated butyl chloride provided a uniform degree of activation of the column packing for durable and uniform column performance. The addition of water also eliminated much of the peak tailing prevalent with a water-free mobile phase.

The relative insolubility of III and its possible impurities in butyl chloride required the addition of a solvent such as ethanol to the sample preparation [ethanol–butyl chloride (1:3)]. To determine IV as a minor impurity in III, a concentrated solution of III was required, *e.g.*, 40 mg/ml for a detector sensitivity of 0.32 aufs and an injection volume of 10 μl. Reasonable care was taken to keep the injection volume constant so that the ethanol added to the column from this source would contribute uniformly to the composition of the mobile phase, thereby influencing chromatography to the same degree (if at all). Controlling the injection volume was no problem with the use of a good syringe and the relatively low pressure requirements of the assay for IV (400 psig).

[7] HCP and ODS, du Pont; and C-18 reversed phase, Waters.
[8] ETH and BOP, du Pont; and Corasil, Waters.
[9] Teflon, du Pont.

Table V—HPLC Assays for III in Chlorphenesin Carbamate Tablets

Lot	Age, months	III, mg/tablet	Percent of Label
Ta	62	396.6	99.2
Tb	61	389.7	97.4
Tc	60	391.1	97.8
Td	56	395.5	98.9
Te	50	395.5	98.9
Tf	48	400.5	100.1
Tg	42	393.5	98.4
Th	42	400.2	100.0
Ti	39	398.1	99.5
Tj	39	396.5	99.1
Tk	38	388.9	97.2
Tl	27	400.8	100.2
Tm	26	392.0	98.0
Tn	26	395.3	98.8
To	9	397.4	99.4
Tp	9	394.9	98.7
Tq	7	398.7	99.7

These data for chlorphenesin carbamate bulk drug and tablets indicate that this HPLC assay is simple and rapid, with a high degree of specificity. Previous to this report, the only published procedure for the quantitation of the isomeric chlorphenesin 2-carbamate used NMR (7). The advantages of the HPLC method from standpoints of ease of operation, availability and economy of instruments, and rapidity of test results are apparent.

REFERENCES

(1) A. M. Gillespie and S. W. Walters, *Anal. Lett.*, **6**, 61(1973).
(2) D. G. Kaiser and S. R. Shaw, *J. Pharm. Sci.*, **63**, 1094(1974).
(3) A. A. Forist and R. W. Judy, *ibid.*, **60**, 1686(1971).
(4) E. F. Salim and R. E. Booth, *ibid.*, **56**, 623(1967).
(5) A. A. Forist and R. W. Judy, *ibid.*, **53**, 1244(1964).
(6) J. F. Douglas, J. A. Stockage, and N. B. Smith, *ibid.*, **59**, 107(1970).
(7) G. Slomp, R. H. Baker, and F. A. MacKellar, *Anal. Chem.*, **36**, 375(1964).

ACKNOWLEDGMENTS AND ADDRESSES

Received November 25, 1975, from *The Upjohn Company, Kalamazoo, MI 49001*

Accepted for publication February 23, 1976.

Molecular Connectivity VII: Specific Treatment of Heteroatoms

LEMONT B. KIER * and LOWELL H. HALL ‡x

Abstract □ The molecular connectivity index, χ, initially designed for hydrocarbons, has been formally extended to molecules containing heteroatoms. The δ value of the heteroatom is modified to take account of its number of attached hydrogen atoms, $\delta_i^v = Z^v - h_i$. These values were successfully tested on boiling points and molar refractions. A table of δ^v values is presented for nitrogen, oxygen, fluorine, chlorine, bromine, and iodine in various bonding situations.

Keyphrases □ Molecular connectivity—heteroatomic molecules, correlated with boiling points and molar refractions □ Heteroatomic molecules—molecular connectivity indexes calculated, correlated with boiling points and molar refractions □ Boiling points—heteroatomic molecules, correlated with molecular connectivity indexes □ Molar refractions—heteroatomic molecules, correlated with molecular connectivity indexes

In earlier studies using the molecular connectivity index, χ, to describe structural features, the heteroatoms oxygen and nitrogen were considered to contribute equally with carbon (1–7). This designation inevitably led to redundant values of χ for isomers such as 2-methyl-1-propanol and 2-methyl-2-propanol. An initial approach to the resolution of these redundancies was used in an alcohol solubility study (2). A second regression variable was introduced simply as the contribution to total χ from the C—OH bond. This bond value varies in primary, secondary, and tertiary alcohols. Redundancies are destroyed, and there is a 16% decrease in the standard error for the log of the solubility. A 33% decrease in the boiling-point standard error is also observed for this empirical approach.

In a second empirical approach, the total degree of branching, $\Delta\chi$, in the heteroatom-containing molecule is partitioned. The branching attributed to functional group position, $\Delta\chi^F$, is separated from that due to carbon skeleton branching, $\Delta\chi^S$. In a study of the heat of atomization of 20 saturated noncyclic alcohols, the standard error was reduced 40% when these quantities were introduced into the regression (3).

These approaches are now considered to be an interim or first-order solution to a more basic problem of calculating the molecular connectivity contribution of any atom other than carbon.

METHOD

An alternative approach to heteroatom calculation has a basis in earlier considerations of unsaturated molecules (4). That study used the valence connectedness of the atom as a δ value for carbon atoms in a double bond. Thus, the central carbon of propene has a δ of 3, the central carbon of 2-methylpropene has a δ of 4, and both carbons of ethene have a δ of 2. Use of these values gives rise to a χ for the molecule designated as a valence χ or χ^v. Benzene would thus have a χ^v of 2.000 [not modifying for the cyclic nature of the molecule (1)].

There are several ways that this δ value can be understood within the framework of the connectivity theory already developed (1–7). It can be derived from the total number of bonds emanating from the atom, counting the π electron bonds as well as the σ bonds.

Another derivation for the δ value is its equivalence to the number of valence electrons, Z^v, minus the number of hydrogen atoms, h, bonded to the atom under consideration, $Z^v - h$.

Table I—Valence Delta (δ^v) Values for Heteroatoms

Group	δ^v	Group	δ^v
NH_2	3	OH	5
NH	4	O	6
N	5	C=O	6
C≡N	5	Furan O	6
C=NH	4	O=NO	6
Pyridine N	5	H_2O	4
Nitro N	6	H_3O^+	3
NH_3	2	F	(−)20
NH_4^+	1	Cl	0.690
$>N<^+$	6	Br	0.254
$=NH_2^+$	3	I	0.085

Both derivations give identical values for simple unsaturated systems, but the second derivation has more wide ranging applications, especially as an approach to parameterizing the connectivity of heteroatoms.

Using the expression $\delta^v = Z^v - h$, the valence δ^v values for oxygen and nitrogen in several variations of bonding can be calculated (Table I). Ammonia and water are unique limiting cases of the $Z^v - h$ expression. The nitro group nitrogen has a $\delta^v = 6$, since it can be considered to be derived from a nitroso group ($\delta_N^v = 5$) by appending another connection, namely an oxygen atom bonded to the nitrogen atom. The nitrogen atom of a tetraalkylammonium ion can, by the same argument, be assigned a δ^v of 6.

Boiling Point and Solubility—The validity of these values can be tested by determining their ability to destroy redundant χ values in a series of molecules and to improve a correlation with a physical property. The first test of the influence of the χ^v term is with a series of aliphatic alcohols (Table II). When using the standard connectivity χ, the regression equation and statistics for the boiling points are:

$$\text{boiling point} = 38.79\ (\pm 1.61)\chi + 11.26\ (\pm 5.85)$$
$$r = 0.963 \quad s = 8.39° \quad n = 48 \qquad \text{(Eq. 1)}$$

If the χ^v value is introduced, the relationship improves to:

$$\text{boiling point} = 196.58\ (\pm 11.34)\chi - 157.6\ (\pm 11.31)\chi^v - 41.24\ (\pm 4.56)$$
$$r = 0.993 \quad s = 3.68° \quad n = 48 \qquad \text{(Eq. 2)}$$

The use of the second term, χ^v, leads to over a twofold improvement in the standard deviation of the mean. This equation leads to a prediction of the boiling point to within 2.5%.

For this same list of alcohols, the log molar solubility is related to χ by:

$$\log S = -2.61\ (\pm 0.086)\chi + 6.52\ (\pm 0.31)$$
$$r = 0.976 \quad s = 0.447 \quad n = 48 \qquad \text{(Eq. 3)}$$

When using the χ^v term, the multiple regression equation is:

$$\log S = 9.27\ (\pm 0.98)\chi + 6.64\ (\pm 0.97)\chi^v + 8.73\ (\pm 0.39)$$
$$r = 0.988 \quad s = 0.317 \quad n = 48 \qquad \text{(Eq. 4)}$$

The predicted values are shown in Table II.

Again, the improvement in the relationship is noteworthy upon the introduction of the χ^v term. The major effect is the influence of χ^v in destroying the seven pairs of redundant χ values in the list. Furthermore, the χ^v term reorders these redundancies in the correct order relative to the boiling point and log solubility.

The value of the χ^v term is dramatically illustrated in the case of the boiling points of several glycols (Table III):

$$\text{boiling point} = 20.71\ (\pm 24.28)\chi + 159.38\ (\pm 67.23)$$
$$r = 0.307 \quad s = 34.0° \quad n = 9 \qquad \text{(Eq. 5)}$$

and:

Table II—Boiling Points and Solubilities of Saturated Alcohols

Compound	Boiling Point		Log Solubility	
	Obs.[a]	Calc.	Obs.[b]	Calc.
1-Butanol	117.7°	114.56°	0.005	−0.191
2-Methylpropanol	107.9°	108.74°	0.022	0.195
2-Butanol	99.5°	97.40°	0.065	0.673
1-Pentanol	137.8°	134.27°	−1.347	−1.511
3-Methylbutanol	131.2°	128.25°	−1.167	−1.115
2-Methylbutanol	128.7°	129.74°	−1.058	−1.214
2-Pentanol	119.0°	116.91°	−0.634	−0.636
3-Pentanol	115.3°	118.39°	−0.486	−0.736
3-Methyl-2-butanol	111.5°	111.76°	−0.404	−0.294
2-Methyl-2-butanol	102.0°	102.33°	0.338	0.180
1-Hexanol	157.0°	153.58°	−2.790	−2.812
2-Hexanol	139.9°	136.42°	−1.995	−1.947
3-Hexanol	135.4°	137.90°	−1.832	−2.046
3-Methyl-3-pentanol	122.4°	124.23°	−0.830	−1.289
2-Methyl-2-pentanol	121.4°	121.85°	−1.117	−1.129
2-Methyl-3-pentanol	126.5°	132.75°	−1.609	−1.704
3-Methyl-2-pentanol	134.2°	132.75°	−1.639	−1.704
2,3-Dimethyl-2-butanol	118.6°	117.08°	−0.850	−0.813
3,3-Dimethyl-1-butanol	143.0°	139.81°	−2.590	−1.887
3,3-Dimethyl-2-butanol	120.0°	123.86°	−1.410	−1.099
4-Methyl-1-pentanol	151.8°	147.77°	−2.282	−2.425
4-Methyl-2-pentanol	131.7°	130.61°	−1.814	−1.560
2-Ethylbutanol	146.5°	150.73°	−2.787	−2.624
1-Heptanol	176.3°	173.09°	−4.166	−4.122
2-Methyl-2-hexanol	142.5°	141.36°	−2.473	−2.440
3-Methyl-3-hexanol	142.4°	143.74°	−2.263	−2.600
3-Ethyl-3-pentanol	142.5°	146.12°	−1.917	−2.759
2,3-Dimethyl-2-pentanol	139.7°	130.99°	−2.002	−1.924
2,3-Dimethyl-3-pentanol	139.0°	138.97°	−1.937	−2.284
2,4-Dimethyl-2-pentanol	133.0°	135.54°	−2.145	−2.053
2,4-Dimethyl-3-pentanol	138.8°	147.47°	−2.800	−2.689
2,2-Dimethyl-3-pentanol	136.0°	144.85°	−2.643	−2.509
3-Heptanol	156.8°	157.42°	−3.194	−3.357
4-Heptanol	155.0°	157.42°	−3.196	−3.357
1-Octanol	195.2°	192.61°	−5.401	−5.433
2,2,3-Trimethyl-3-pentanol	152.5°	151.11°	−2.931	−3.095
2-Octanol	179.8°	175.45°	−4.755	−4.568
2-Ethylhexanol	184.6°	189.76°	−5.005	−5.245
1-Nonanol	213.1°	212.12°	−6.907	−6.743
2-Nonanol	198.5°	194.96°	−6.319	−5.878
3-Nonanol	194.7°	196.44°	−6.119	−5.978
4-Nonanol	193.0°	196.44°	−5.952	−5.978
5-Nonanol	195.1°	196.44°	−5.744	−5.978
2,6-Dimethyl-3-heptanol	178.0°	174.40°	−5.776	−4.785
3,5-Dimethyl-4-heptanol	187.0°	189.45°	−5.298	−5.509
1,1-Diethylpentanol	192.0°	185.14°	−5.572	−5.381
7-Methyloctanol	206.0°	206.30°	−5.744	−6.357
3,5,5-Trimethylhexanol	193.0°	194.1°	−5.769	−5.531

[a] Boiling points are in degrees centigrade, and the logarithms of the solubility (expressed as molality) were taken from the following sources and references cited therein: G. L. Amidon, S. H. Yalkowski, and S. J. Leung, *J. Pharm. Sci.*, **63**, 1858(1974), and "Handbook of Chemistry and Physics," 51st ed., Chemical Rubber Co., Cleveland, Ohio, 1971.

$$\text{boiling point} = 249.64\ (\pm 10.04)\chi - 222.1\ (\pm 9.38)\chi^{v} - 29.11\ (\pm 10.92)$$
$$r = 0.995 \quad s = 3.78° \quad n = 9 \qquad \text{(Eq. 6)}$$

The use of χ^{v} with the χ term lowers the s value almost 10-fold.

The use of the χ^{v} terms in the case of primary and secondary amines (Table IV) also significantly improves the correlation of connectivity indexes with the boiling points. For a series of primary amines, the equations and statistics are:

$$\text{boiling point} = 50.93\ (\pm 1.00)\chi - 49.17\ (\pm 3.30)$$
$$r = 0.996 \quad s = 4.59° \quad n = 21 \qquad \text{(Eq. 7)}$$

and:

$$\text{boiling point} = 154.09\ (\pm 17.20)\chi - 103.5\ (\pm 17.84)\chi^{v} - 75.92\ (\pm 5.03)$$
$$r = 0.999 \quad s = 2.79° \quad n = 21 \qquad \text{(Eq. 8)}$$

For secondary amines, the relationships are:

Table III—Boiling Points of Polyols

	Boiling Point		Connectivity Index	
	Obs.[a]	Calc.	χ	χ^{v}
2-Methyl-2,4-pentanediol	196.0°	197.3°	3.417	2.821
Ethanediol	197.8°	197.3°	1.914	1.132
1,3-Butanediol	207.5°	204.8°	2.770	2.060
1,3-Propanediol	214.7°	211.0°	2.414	1.632
1,2-Propanediol	187.4°	191.1°	2.270	1.560
2,3-Butanediol	181.7°	185.6°	2.643	2.004
1,4-Butanediol	230.0°	224.8°	2.914	2.132
1,5-Pentanediol	238°	238.5°	3.414	2.632
Glycerol	290°	292.7°	2.808	1.707

[a] Boiling points were taken from the "Handbook of Tables for Organic Compound Identification," 3rd ed., CRC Press, Cleveland, Ohio, 1967.

$$\text{boiling point} = 48.50\ (\pm 1.15)\chi - 58.55\ (\pm 4.07)$$
$$r = 0.997 \quad s = 4.28° \quad n = 13 \qquad \text{(Eq. 9)}$$

and:

$$\text{boiling point} = 171.40\ (\pm 21.84)\chi - 120.07\ (\pm 21.45)\chi^{v} - 102.4\ (\pm 8.07)$$
$$r = 0.999 \quad s = 2.20° \quad n = 13 \qquad \text{(Eq. 10)}$$

The primary and secondary amines must apparently be considered separately with the framework of the present development of connectivity indexes. The intermolecular forces between primary amines differ enough from intermolecular forces between secondary amines,

Table IV—Boiling Points of Primary and Secondary Aliphatic Amines

Compound	Boiling Point		Residual
	Obs.[a]	Calc.	
Primary Amines			
n-Propylamine	49.0°	51.91°	−2.91
2-Aminopropane	33.0°	37.00°	−4.00
2-Amino-2-methylpropane	46.0°	47.15°	−1.15
2-Aminobutane	63.0°	64.23°	−1.23
2-Methylpropylamine	69.0°	69.93°	−0.93
n-Butylamine	77.0°	77.21°	−0.21
2-Amino-2-methylbutane	78.0°	75.66°	2.35
2-Aminopentane	92.0°	89.54°	2.45
3-Methylbutylamine	96.0°	95.23°	0.77
2-Methylbutylamine	96.0°	97.16°	−1.16
n-Pentylamine	104.0°	102.52°	1.47
4-Methylpentylamine	125.0°	120.54°	4.45
n-Hexylamine	130.0°	127.83°	2.17
3-Methylpentylamine	114.0°	114.85°	−0.85
4-Aminoheptane	139.0°	142.08°	−2.58
2-Aminoheptane	142.0°	136.44°	5.56
n-Heptylamine	155.0°	153.14°	1.86
n-Octylamine	180.0°	178.45°	1.55
n-Nonylamine	201.0°	203.76°	−2.76
2-Aminoundecane	237.0°	241.40°	−4.40
3-Aminopentane	91.0°	91.47°	−0.47
Secondary Amines			
N-(Methyl)ethylamine	36.0°	37.19°	−1.19
N-Methyl-1-methylethylamine	50.0°	52.09°	−2.09
Diethylamine	56.0°	55.28°	0.72
N-Methyl-1-methylpropylamine	78.5°	79.35°	−0.85
N-(Ethyl)propylamine	80.5°	80.62°	−0.12
Bis(1-methylethyl)amine	84.0°	84.84°	−0.84
N-(Methyl)butylamine	90.5°	87.86°	2.64
N-Methyl-1-methylbutylamine	105.0°	104.69°	0.31
Dipropylamine	109.5°	105.95°	3.55
Bis(2-methylpropyl)amine	139.0°	142.03°	−3.03
Dibutylamine	159.0°	156.62°	2.38
Bis(3-methylbutyl)amine	187.5°	186.66°	0.84
Dipentylamine	205.0°	207.29°	−2.29

[a] Boiling points were taken from the "Handbook of Tables for Organic Compound Identification," 3rd ed., CRC Press, Cleveland, Ohio, 1967.

Table V—Substituent Parameters for Molar Refraction (R_m)

Substituent	Molar Refraction		Connectivity Index[b]	
	Obs.[a]	Calc.	χ^c	χ^v
Methyl	4.7	4.14	0.577	0.500
Ethyl	9.4	9.58	1.115	1.06
Propyl	14.0	14.48	1.615	1.561
1-Methylethyl	14.0	13.30	1.488	1.443
Butyl	18.7	19.37	2.115	2.061
1,1-Dimethylethyl	18.5	16.29	1.789	1.750
Phenyl	24.3	22.84	3.150	2.161
Hydroxyl	1.5	2.17	0.577	0.224
Methoxyl	6.5	6.37	1.115	0.612
Ethoxyl	11.3	11.90	1.615	1.200
Propoxyl	15.9	16.80	2.115	1.700
1-Methylethoxyl	16.0	15.66	1.971	1.595
Butoxyl	20.7	21.69	2.615	2.200
Pentoxyl	25.3	26.59	3.115	2.700
Phenoxyl	26.6	25.25	3.633	2.319
Acetate	11.6	12.22	1.971	1.112
Amino	4.2	2.95	0.577	0.333
Acetamido	14.6	12.87	1.971	1.204
Nitro	6.0	6.83	1.488	0.537
Aldehydo	5.3	5.74	1.115	0.524
Acyl	9.9	9.81	1.488	0.954
Methylcarboxylate	11.4	12.03	2.026	1.066
Ethylcarboxylate	16.2	17.56	5.526	1.654
Amido	8.8	8.30	1.488	0.743
Cyano	5.2	5.85	1.115	0.539
Fluoro[c]	−0.4	—	0.577	−0.124
Chloro[c]	4.8	—	0.577	0.602
Bromo[c]	7.6	—	0.577	0.992
Iodo[c]	12.8	—	0.577	1.719

[a] Data were taken from Ref. 8. [b] Connectivity index was calculated only for the substituent as if attached to the phenyl ring. [c] No R_m values are shown as calculated for the halogens because the observed R_m values were used to calculate the δ^v value for the halogens.

in the bulk phase, to give rise to a different boiling point for comparable connectivity indexes. Thus, diethylamine and butylamine have similar χ^v values (2.121 and 2.115), but the boiling points differ by 21°. The difference is probably due to differing electron densities in the lone-pair electron orbitals and the different number of amino hydrogen atoms capable of hydrogen bonding. These effects are not encoded in the connectivity indexes at the present level of development. Therefore, it is necessary to consider classes of amines when relating boiling point with molecular connectivity indexes. This question will be discussed in a subsequent paper.

Molar Refraction—If these or similar intermolecular effects are minimal in influencing a physical property, it may be possible to relate the connectivity of various molecules, containing different heteroatoms, with that property. This approach appears to be possible with molar refraction (Table V). A comparison of χ and χ^v values with molar refraction provides a severe test of the χ^v values because they must recreate connectivity properties of carbon, nitrogen, and oxygen in a self-consistent manner.

Twenty-five phenyl substituent group molar refractions, listed by Norrington *et al.* (8), were used. This list includes alkyls, ethers, amines, esters, amides, ketones, an aldehyde, alcohol, and a nitro group. The relationship is:

$$R_m = 2.656\ (\pm 0.593)\chi + 7.140\ (\pm 0.688)\chi^v - 0.958\ (\pm 0.518)$$
$$r = 0.990 \quad s = 1.03 \quad n = 25 \qquad \text{(Eq. 11)}$$

This successful relationship illustrates the consistency of the oxygen and nitrogen connectivity parameters with the parameters established for the carbon atom. All χ and χ^v parameters are derived nonempirically from basic considerations of connectivity defined in terms of simple branching and the number of valence electrons not bonding to a hydrogen atom.

With these parameters, we have increased the ability of connectivity indexes to correlate with certain properties such as the boiling point within classes of molecular types. Furthermore, with other properties like molar refraction, these heteroatom parameters permit the correlation of connectivity indexes among mixed molecular types.

Table V includes a number of halogen-containing molecules. It would be highly desirable if these atoms could be considered within the framework of molecular connectivity. A derivation of δ^v values based upon the $\delta^v = Z^v - h$ relationship is not satisfactory. The values would obviously be 7 for each halogen. At this time, it is necessary to develop empirical parameters for the halogens, fitting them to molar refraction data such as those in Table V. These empirical δ^v values for halogens are listed in Table I.

A test of the δ^v values for the halogens to determine their internal consistency can be made by considering the ability of χ and χ^v to predict the boiling points of a mixed list of alkyl halides (Table VI). This objective is accomplished quite satisfactorily from the equation:

$$\text{boiling point} = -69.55\ (\pm 5.17) + 19.91\ (\pm 2.41)\chi + 38.07\ (\pm 1.27)\chi^v$$
$$r = 0.992 \quad s = 4.79° \quad n = 24 \qquad \text{(Eq. 12)}$$

Thus, δ^v values empirically derived from molar refraction are useful in correlating the boiling points in a mixed list of alkyl halides.

To test the consistency of the halogen parameters in a larger list with molecules containing oxygen and nitrogen, calculations of molar

Table VI—Boiling Points of Alkyl Halides

Compound	Boiling Point		Residual	Connectivity Index	
	Obs.	Calc.		χ^c	χ^v
Ethyl chloride	13.0°	17.9°	−4.9	1.414	1.558
Ethyl bromide	38.0°	38.9°	−0.9	1.414	2.110
Ethyl iodide	72.0°	77.8°	−5.8	1.414	3.132
Propyl chloride	46.5°	46.9°	−0.4	1.914	2.058
Propyl bromide	71.0°	67.9°	3.1	1.914	2.610
Propyl iodide	102.5°	106.8°	−4.3	1.914	3.632
1-Methylethyl chloride	36.5°	35.4°	1.1	1.732	1.850
1-Methylethyl bromide	60.0°	54.5°	7.5	1.732	2.300
1-Methylethyl iodide	90.0°	84.3°	5.7	1.732	3.135
1-Methylpropyl chloride	69.0°	67.5°	1.5	2.270	2.414
1-Methylpropyl bromide	91.0°	88.6°	2.4	2.270	2.966
1-Methylpropyl iodide	120.0°	127.5°	−7.5	2.270	3.988
1,1-Dimethylethyl chloride	51.0°	50.3°	0.7	2.000	2.102
1,1-Dimethylethyl bromide	72.5°	65.1°	7.4	2.000	2.492
1,1-Dimethylethyl iodide	98.0°	92.7°	5.3	2.000	3.215
Butyl chloride	78.0°	75.9°	2.1	2.414	2.558
Butyl bromide	101.0°	96.9°	4.1	2.414	3.110
Butyl iodide	130.0°	135.8°	−5.8	2.414	4.132
1-Methylbutyl chloride	97.0°	95.5°	1.5	2.770	2.888
1-Methylbutyl bromide	117.0°	112.7°	4.3	2.770	3.338
1-Methylbutyl iodide	142.0°	144.5°	−2.5	2.770	4.173
Propyl fluoride	2.5°	8.5°	−6.0	1.914	1.049
Butyl fluoride	32.5°	37.5°	−5.0	2.414	1.549
Pentyl fluoride	62.8°	66.5°	−3.7	2.914	2.049

Table VII—Molar Refraction of Mixed Classes of Compounds

Compound	Molar Refraction		Connectivity Index		Compound	Molar Refraction		Connectivity Index	
	Obs.	Calc.	χ^c	χ^v		Obs.	Calc.	χ^c	χ^v
Butyl methyl ether	27.020	28.519	2.914	2.560	2-Ethyl-1-butanol	31.180	32.163	3.346	2.955
Dibutyl ether	40.987	42.173	4.414	4.121	2-Methyl-2-pentanol	31.210	30.225	3.060	2.784
Dipropyl ether	32.226	33.282	3.414	3.121	2-Methyl-3-pentanol	31.138	31.068	3.180	2.861
Ethyl 1-methylethyl ether	27.678	27.695	2.770	2.504	4-Methyl-2-pentanol	31.351	30.581	3.125	2.806
Ethyl pentyl ether	36.363	37.727	3.914	3.621	2,2-Dimethyl-1-butanol	31.268	30.165	3.121	2.730
1-Methylpropyl ethyl ether	31.560	32.478	3.308	3.042	3-Methyl-3-pentanol	31.182	30.764	3.121	2.844
Butyl 1-methylethyl ether	36.027	36.586	3.770	3.504	2-Methyl-1-hexanol	35.930	36.271	3.808	3.417
1-Methylpropyl methyl ether	31.337	30.585	3.121	2.810	3-Ethyl-3-pentanol	35.821	35.748	3.681	3.405
Butyldimethylamine	33.816	31.689	3.270	2.917	2-Ethyl-1-hexanol	40.625	41.054	4.346	3.955
Methyl-2-methylpropylamine	33.852	34.520	4.201	2.806	2-Methyl-1-propanol	22.103	22.597	2.270	1.879
Dimethylpentylamine	38.281	36.135	3.770	3.417	4-Ethyl-4-heptanol	44.919	44.639	4.681	4.405
Triethylamine	33.793	32.764	3.346	3.070	6-Methyl-1-heptanol	40.736	40.378	4.270	3.879
Trimethylamine	19.594	17.816	1.732	1.341	3-Methyl-3-heptanol	40.446	39.655	4.121	3.844
Tripropylamine	47.783	46.100	4.846	4.570	4-Methyl-4-heptanol	40.439	39.655	4.121	3.844
1-Aminopropane	19.400	19.915	1.914	1.615	1-Octanol	40.637	41.660	4.414	4.023
1-Aminobutane	24.079	24.360	2.414	2.115	1-Chloropropane	20.847	22.231	1.914	2.058
1-Amino-3-methylbutane	28.672	27.523	2.770	2.471	2-Chlorobutane	25.506	25.257	2.270	2.387
1-Aminopentane	28.727	28.805	2.914	2.615	1-Chloro-2-methylpropane	25.359	25.395	2.270	2.414
3-Aminopentane	28.617	28.148	2.808	2.564	2-Chlorobutane	25.440	26.677	2.414	2.558
1-Aminohexane	33.290	33.251	3.414	3.115	3-Chloropentane	30.160	30.040	2.808	2.925
1-Aminoheptane	38.003	37.696	3.914	3.615	2-Bromopropane	23.935	22.877	1.732	2.309
2-Aminoheptane	38.037	36.701	3.770	3.526	1-Bromopropane	23.679	25.176	1.914	2.621
1-Aminononane	47.277	46.586	4.914	4.615	1-Bromo-2-methylpropane	28.537	28.339	2.270	2.977
2-Propanol	17.705	18.189	1.732	1.412	2-Bromobutane	28.651	27.661	2.270	2.847
2-Pentanol	26.680	27.418	2.770	2.450	1-Bromobutane	28.347	29.621	2.414	3.121
3-Pentanol	26.639	28.048	2.914	2.470	3-Bromopentane	33.067	32.444	2.808	3.385
1-Hexanol	31.428	32.769	3.414	3.023	2-Iodobutane	33.939	32.297	2.270	3.733
1-Heptanol	36.093	37.215	3.914	3.523	2-Iodopentane	38.314	36.742	2.770	4.233
3-Methyl-1-butanol	26.904	27.042	2.770	2.379	3-Iodopentane	38.354	37.080	2.808	4.271
2-Methyl-1-butanol	26.697	27.380	2.808	2.417	1-Iodopentane	38.263	39.745	2.914	4.707
2-Methyl-2-butanol	26.721	25.779	2.560	2.284	1-Iodohexane	42.891	44.190	3.414	5.207
4-Methyl-1-pentanol	31.489	31.487	3.270	2.879	1-Iodoheptane	47.610	48.635	3.914	5.707
2-Methyl-1-pentanol	31.164	31.825	3.308	2.917					

refraction were compared with experimentally derived values (Table VII). The consistency of all δ^v values appears to be quite good as seen from:

$$R_m = 4.460 + 5.230\ (\pm 0.211)\chi^v + 3.661\ (\pm 0.227)\chi$$
$$r = 0.990 \quad s = 1.022 \quad n = 65 \qquad \text{(Eq. 13)}$$

CONCLUSIONS

A set of valence δ values were developed for use in calculating the connectivity index, χ, for heteroatom-containing molecules. The improvement in the correlations with the boiling point and molar refraction for a wide range of molecules suggests the general applicability of these values.

The use of the number of valence electrons together with the number of attached hydrogen atoms provides a firm relationship between the structural characteristics expressed in the hydrogen-suppressed graph and the properties of molecules (3).

An important advance is made by this development in that drug molecules containing heteroatoms may now be considered with a more sophisticated molecular connectivity treatment. These δ^v values are currently being used in biological studies in this laboratory (3, 9).

REFERENCES

(1) L. B. Kier, L. H. Hall, W. J. Murray, and M. Randić, *J. Pharm. Sci.*, **64**, 1971(1975).

(2) L. H. Hall, L. B. Kier, and W. J. Murray, *ibid.*, **64**, 1974(1975).

(3) L. B. Kier and L. H. Hall, "Molecular Connectivity in Chemistry and Drug Research," Academic, New York, N.Y., 1976.

(4) W. J. Murray, L. B. Kier, and L. H. Hall, *J. Pharm. Sci.*, **64**, 1978(1975).

(5) L. B. Kier, W. J. Murray, and L. H. Hall, *J. Med. Chem.*, **18**, 1272(1975).

(6) W. J. Murray, L. B. Kier, and L. H. Hall, *ibid.*, **19**, 573(1976).

(7) L. B. Kier, W. J. Murray, M. Randic, and L. H. Hall, *J. Pharm. Sci.*, **65**, 1226(1976).

(8) F. E. Norrington, R. M. Hyde, S. G. Williams, and R. Wooten, *J. Med. Chem.*, **18**, 604(1975).

(9) L. H. Hall and L. B. Kier, *J. Pharm. Sci.*, in press.

ACKNOWLEDGMENTS AND ADDRESSES

Received October 9, 1975, from the *Massachusetts College of Pharmacy, Boston, MA 02115, and the ‡Eastern Nazarene College, Quincy, MA 02170

Accepted for publication February 23, 1976.

Supported in part by a grant from the Research Corp. and by Grant DA01353 from the National Institutes of Health.

The authors thank Mr. Phillip Coy for assistance with computerized calculations and the computer centers at Eastern Nazarene College and Massachusetts College of Pharmacy for use of their facilities.

ˣ To whom inquiries should be directed.

Trace Analysis of 2,4,5-Trichlorophenoxyacetic Acid, Its Glycineamide, and Their Alkaline Hydrolyzable Conjugates in Mouse Blood, Urine, and Feces

CHARLES R. NONY, MALCOLM C. BOWMAN ˣ, CLAUDE L. HOLDER, JOHN F. YOUNG, and WILLIAM L. OLLER

Abstract □ Chemical methods were developed for the trace analysis of the herbicide 2,4,5-trichlorophenoxyacetic acid, its glycineamide, and their alkaline hydrolyzable conjugates in mouse blood, urine, and feces. The salient elements of the methods are extraction of the free acids with benzene, methylation, cleanup on a silica gel column, and quantification *via* electron-capture GLC. Any unextracted conjugates remaining in the substrates are then subjected to alkaline hydrolysis, and the liberated 2,4,5-trichlorophenoxyacetic acid is assayed. Data are presented concerning recoveries of the compounds from the three spiked substrates. The utility of the procedures is illustrated by a preliminary pharmacokinetic study employing parallel electron-capture GLC and radioassays of the three substrates from mice injected with a single intravenous dose of ^{14}C-2,4,5-trichlorophenoxyacetic acid. GLC characteristics and partition values of the compounds and hydrolysis of the glycineamide under various conditions also are discussed.

Keyphrases □ 2,4,5-Trichlorophenoxyacetic acid—electron-capture GLC and radiochemical analyses, mouse blood, urine, and feces, pharmacokinetics □ GLC, electron capture—analysis, 2,4,5-trichlorophenoxyacetic acid, mouse blood, urine, and feces □ Radiochemistry—analysis, 2,4,5-trichlorophenoxyacetic acid, mouse blood, urine, and feces □ Pharmacokinetics—2,4,5-trichlorophenoxyacetic acid, mice □ Herbicides—2,4,5-trichlorophenoxyacetic acid, electron-capture GLC and radiochemical analyses, mouse blood, urine, and feces

In 1971, the Panel on Herbicides of the President's Science Advisory Committee (1) indicated that additional information was needed to understand the effects of 2,4,5-trichlorophenoxyacetic acid (2,4,5-T, I) in humans and animals; therefore, further research on this compound was initiated. The major objective of studies with I in this laboratory was to ascertain any potential relationships between embryonic and/or fetal exposure to the chemical and the abnormalities. To obtain a pharmacokinetic profile of the chemical in relation to its teratogenic effects, pharmacokinetic data must be available on the unbred female and at various intervals during the gestation period. Therefore, chemical methodology was required for the trace analysis of I, its glycineamide (II, a known conjugate produced under certain conditions in the liver of most mammalian systems), and other possible conjugates in mouse blood, urine, and feces.

Recently, pharmacokinetic studies were conducted using rats, dogs, and humans and single doses of (^{14}C-carboxy)-I (2) and analytical grade I (3). Also, the absorption, elimination, and metabolism of I were studied in rats, pigs, calves, and chickens (4, 5). A method was reported for determining I, 2,4-dichlorophenoxyacetic acid, and related compounds in rat urine based on ethylation, cleanup on silica gel, and analysis of the derivative by electron-capture GLC (6). The liquid–liquid extraction properties of phenoxy acid herbicides from water were investigated (7). However, no methods meeting high sensitivity requirements (low nanogram level) were applicable to the present study.

This paper describes procedures to determine traces of I, II, and their alkaline hydrolyzable conjugates *via* electron-capture GLC under the restrictions imposed by pharmacokinetic studies in mice. The procedures were tested in a preliminary pharmacokinetic study with mice injected with ^{14}C-I by parallel analyses of these substrates *via* liquid scintillation radioassays and electron-capture GLC. Data from these tests, partition values of the compounds, and ancillary information on the effectiveness of acids and bases in hydrolyzing the glycineamide are presented.

EXPERIMENTAL

GLC—A gas chromatograph[1] equipped with a ^{63}Ni-electron-capture detector[2] and a 100-cm glass column (4 mm i.d.) containing 10% OV-101 on Gas Chrom Q (80–100 mesh), conditioned overnight at 275° prior to use, was operated isothermally at 200° in the dc mode. The nitrogen carrier gas flow rate was 160 ml/min. Temperatures of the injection port and detector were 240 and 280°, respectively. Under these conditions, retention times, t_R, of the methyl esters of I and II were 1.40 and 8.00 min, respectively.

Samples of unknown residue content were quantified by relating their peak heights to dilutions of standards of the two esters prepared by methylating 1-mg amounts of the free acids. Samples for injection contained up to 25 and 160 pg of the methyl esters of I and II, respectively, in 5 μl of benzene or hexane–20% benzene.

Where a more rapid and sensitive analysis of only the methyl ester of II was sought, the instrument was operated isothermally at 240°. Under this condition, the t_R was 2.25 min and the response was linear up to about 70 pg/injection.

Radioassays—Radiolabeled samples were counted with a liquid scintillation instrument[3] equipped with a data reduction system. A one-tenth aliquot (0.5–1.0 ml) from each sample assayed by electron-capture GLC was added to a vial containing 12 ml of solubilizer[4] and counted for 20 min. Residual samples (*e.g.*, after hydrolysis and extraction) and the adsorbent from the cleanup column were combusted[5], and any ^{14}C-labeled carbon dioxide was assayed by liquid scintillation.

Materials—Benzene and hexane, pesticide grade, were redistilled in glass and screened for interfering electron-capture GLC peaks by analyzing 5 μl of a 25-fold concentrate. Solvent concentrates having responses less than 1- and 5-pg equivalents of the methyl esters of I and II (per 5-μl injection), respectively, were considered satisfactory.

Diazomethane reagent was prepared from *N*-methyl-*N*-nitroso-*p*-toluenesulfonamide[6] by using the reagent, kit, and instructions provided by the manufacturer. The ethereal diazomethane was then

[1] Model 5750, Hewlett-Packard Corp., Palo Alto, Calif.
[2] Tracor, Inc., Austin, Tex.
[3] Mark II instrument with model PDS/3 data reduction system, Nuclear-Chicago Corp., Houston, Tex.
[4] PCS solubilizer, Amersham/Searle Corp., Arlington Heights, Ill.
[5] Model JA 101 Oxymat, Teledyne, Inc., Westwood, N.J.
[6] Diazald, Catalog No. D 2800-0, Aldrich Chemical Co., Milwaukee, Wis.

Table I—GLC Data for the Quantification of 2,4,5-Trichlorophenoxyacetic Acid (I) and Its Glycineamide (II) as Their Methyl and Ethyl Esters

Compound	Retention Time, min[a] 200°	240°	Upper Limit of Linearity, pg[b] 200°	240°
I methyl ester	1.40	—[c]	25	—[c]
I ethyl ester	1.90	—[c]	44	—[c]
II methyl ester	8.00	2.25	160	70
II ethyl ester	8.80	2.52	250	125

[a] Column oven operated isothermally at stated temperatures. [b] Response was for 5-μl injection at about 5×10^{-10} amp. [c] Solvent interference precluded determination.

dried by percolation through a plug of anhydrous sodium sulfate, redistilled, and stored at −10° until used. A hexane solution of diazoethane also was prepared from *N*-ethyl-*N*,*N*′-dinitroguanidine[7] for ethylating I and II.

Silica gel[8] (oven dried at 110°) was deactivated with 2% buffer[9] (0.05 *M* monobasic potassium phosphate–sodium hydroxide, pH 7). The appropriate amount of buffer was dispersed on the inner surface of a dry, glass-stoppered bottle, and dry silica gel was added. The contents were then mixed by mechanically rolling the bottle for 1 hr. The adsorbent was prepared fresh daily.

The ^{14}C-2,4,5-trichlorophenoxyacetic acid[10], uniformly ring labeled (1.92 μCi/mg), was assayed as the methyl ester by electron-capture GLC and was essentially identical to the unlabeled standard and free of extraneous GLC peaks.

Animal Chamber—A special sampling chamber for an individual mouse was fabricated from a 2-liter beaker by reshaping the bottom to form a cone (~50 mm deep) and attaching a glass drain tube (~6 mm i.d. × 10 mm long). A disk of stainless steel screen (~2 × 2-mm square openings), approximately the same diameter of the beaker, rested on the bottom of the vessel; a 30-ml culture tube with a screw cap[11] was placed under the drain tip. This arrangement allowed urine to be collected in the tube while feces were retained on the screen. The animal was supported by a heavier disk of larger mesh (8 × 25-mm diamond-shaped openings, measured from opposite corners) equipped with metal legs, which suspended the animal about 25 mm above the bottom screen.

Several animal chambers of this type were used to collect urine and feces from untreated mice for use in developing the analytical methodology *via* electron-capture GLC; they were also used in preliminary pharmacokinetic and other studies with the ^{14}C-I. Composites of samples collected for use in developing the analytical methodology were stored at −10° prior to use; all others were extracted immediately after collection.

Hydrolysis Studies—Samples, 100 ng, of the methyl and ethyl esters of II were subjected to alkaline hydrolysis (1 *N* NaOH) for 2 hr at 85° to determine the completeness of cleaving the compound and of recovering the I reaction product. The hydrolysates were acidified, extracted with benzene, methylated, and assayed by electron-capture GLC. One hundred nanograms of II was also subjected to aqueous acid and alkali treatments at three different temperatures for various periods to determine its stability during extraction and analysis.

Animal Experiments—Unbred female CD-1 mice, 32–33 g, were

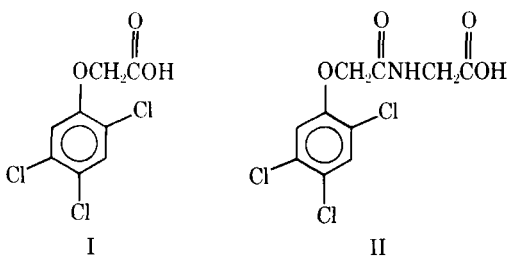

I II

[7] Catalog No. E 4160-5, Aldrich Chemical Co., Milwaukee, Wis.
[8] Catalog No. 3405, J. T. Baker Chemical Co., Glen Ellyn, Ill.
[9] Catalog No. S0-B-108, Fisher Scientific Co., St. Louis, Mo.
[10] Mallinckrodt Chemical Works, St. Louis, Mo.
[11] Lined with Teflon (du Pont).

Table II—Extraction Partition Values of the Methyl and Ethyl Esters of 2,4,5-Trichlorophenoxyacetic Acid (I) and Its Glycineamide (II)

Solvent System	I Methyl Ester	I Ethyl Ester	II Methyl Ester	II Ethyl Ester
Chloroform–water	1.00	1.00	1.00	1.00
Chloroform–60% methanol	1.00	1.00	1.00	1.00
Hexane–water	1.00	1.00	0.95	1.00
Hexane–acetonitrile	0.078	0.12	0.011	0.018
Isooctane–80% acetone	0.73	0.81	0.27	0.40
Isooctane–dimethylformamide	0.035	0.048	—[a]	—[a]
Isooctane–85% dimethylformamide	0.12	0.21	0.00	0.01
Heptane–90% ethanol	0.39	0.50	0.050	0.076
Benzene–water[b]	1.00	0.96	1.00	0.98

[a] Detection was by electron-capture GLC. All others were by flame-ionization detection GLC. [b] Solvent interference precluded determination.

individually confined in the special sampling chambers. The mice were allowed free access to food and water throughout the experiment, and control samples of urine and feces were collected for 24 hr preceding the injection of radiolabeled I. The control sample of blood was withdrawn from each mouse just prior to an intravenous injection of 1.86 mg of ^{14}C-I (contained in 100 μl of water–60% ethanol) into the tail vein of the animal; this dosage was equivalent to about 57 mg of I/kg. In the pharmacokinetic studies, samples of blood (5 or 20 μl), urine, and feces were collected at various intervals and assayed.

In experiments prior to the pharmacokinetic studies, mice injected with the ^{14}C-I were confined overnight. Various solvents in different combinations were used to determine the most efficient means of recovering the radioactive urine deposits from the inner surface of the chamber.

Analysis of Blood—An accurately measured sample of mouse blood was withdrawn from the tip of the animal's tail and immediately delivered into an 8-ml culture tube, containing 0.5 ml of distilled water, by using either a 5- or 20-μl micropipet[12]. Serial samples were taken from the same three animals throughout the experiment. The tube was sealed with a screw cap[11], subjected to vortex mixing for a few seconds until the blood was uniformly dispersed, acidified by adding 0.5 ml of 2 *N* HCl, and again subjected to vortex mixing. Then 5 ml of benzene was added, and the tube was vigorously shaken for 1 min and centrifuged at 2000 rpm for 5 min.

The benzene layer was carefully transferred to a 50-ml glass-stoppered flask with a syringe and cannula, and the aqueous layer in the tube was extracted with an additional 5-ml portion of benzene in an identical manner. [*Note:* Care was taken to withdraw as much of the benzene layer as possible (~4.75 ml) with each extraction; however, none of the aqueous phase should ever be withdrawn into the cannula or syringe. Anhydrous sodium sulfate was shown to absorb nanogram amounts of I from benzene solutions. Therefore, it cannot be used to remove water from the benzene extracts in these procedures.]

The aqueous phase was reserved for subsequent alkaline hydrolysis of possible conjugates. One milliliter of "keeper" solution (100 μg of paraffin oil[13]/ml of benzene) and a boiling bead were added to the flask containing the combined benzene extracts (I and II), and the contents were evaporated just to dryness by using water pump vacuum and a 60° water bath. Residues of the free acids were then converted to their methyl esters by the addition of 2 ml of an ethereal solution of diazomethane. After 15-min, the diazomethane solution was evaporated under water pump vacuum at ambient temperature, and the residue was dissolved in 5 ml of hexane–20% benzene for the subsequent column cleanup or in an appropriate volume of benzene (1 ml or more) for direct injection into the gas chromatograph.

The aqueous phase was subjected to alkaline hydrolysis by adding 0.5 ml of 4 *N* NaOH and heating the sealed tube at 85° for 2 hr with occasional shaking. After the tube had cooled, 1 ml of 4 *N* HCl was added; any I or II freed from the conjugates by the digestion was extracted as I, methylated, and analyzed as previously described. (Any

[12] Drummond Wiretrol, Bolab, Inc., Derry, N.H.
[13] Catalog No. 8501-2850, Hewlett-Packard Corp., Palo Alto, Calif.

Table III—Electron-Capture GLC Analysis of 2,4,5-Trichlorophenoxyacetic Acid (I) and Its Glycineamide (II) from Mouse Blood before and after Silica Gel Cleanup of Free Acid and Hydrolyzed Fractions

Added		Recovered[a]			
		Before Cleanup		After Cleanup	
Compound	ng	ng	%[b]	ng	%[b]
I[c]	0	1.2 ± 0.07	—	1.0 ± 0.44	—
	10	9.2 ± 0.70	80 ± 7	9.2 ± 1.05	82 ± 10
	100	96 ± 2.1	95 ± 2	66 ± 2.1	65 ± 2
	1000	987 ± 11.6	99 ± 1	718 ± 20.2	72 ± 2
I[d]	0	—[e]	—	0.9 ± 0.25	—
	10	—[e]	—	6.5 ± 0.91	54 ± 9
	100	99 ± 3.1	99 ± 3	75 ± 3.1	74 ± 3
	1000	1063 ± 63.5	106 ± 6	863 ± 35.9	86 ± 4
II[f]	0	1.7 ± 0.25	—	1.4 ± 0.00	—
	10	7.6 ± 0.75[g]	59 ± 7[g]	9.9 ± 0.75	85 ± 8
	100	91 ± 3.8	89 ± 4	85 ± 7.9	84 ± 8
II[h] (10 ng = 8.2 ng of I)	0	—[e]	—	0.7 ± 0.16	—
	10	—[e]	—	5.4 ± 3.1	66 ± 4
	100	79 ± 1.2	96 ± 1	68 ± 3.2	83 ± 4

[a] Mean and standard error from triplicate assays. [b] Corrected for background interference in the unspiked sample. [c] Analyzed as the methyl ester of I. [d] Respiked after extraction of I and then hydrolyzed. [e] High background interference precluded assay without column cleanup. [f] Analyzed as the methyl ester of II. [g] High background interference; quantitation is an estimate. [h] Respiked after extraction of II and then hydrolyzed.

conjugate of II freed by the hydrolysis would also be further hydrolyzed to I). GLC analysis of the methylated extracts without column chromatographic cleanup was performed whenever possible, because the recovery was higher and the time per analysis was shorter than analysis with column cleanup. However, total residues of 10 ng or less of the compounds, particularly after alkaline hydrolysis, must be subjected to the cleanup because the high electron-capturing background precludes accurate quantitation at these low levels.

The chromatographic cleanup column[14] consisted of 0.5 g of the silica gel supported by a small plug of glass wool; it was prewashed with 10 ml of hexane. The methylated extract from the free acid fraction or from the alkaline hydrolysis dissolved in 5 ml of hexane–20% benzene was added to the column and allowed to percolate into the adsorbent; then the flask and column were washed with two additional 1.5-ml portions of the solvent. The effluent was discarded, and the original 50-ml boiling flask was placed under the column to receive the subsequent eluate. The column was then eluted with 20 ml of hexane–40% benzene. This eluate, containing the methyl ester of I, was evaporated just to dryness, and the residue was dissolved in an appropriate amount of benzene (1 ml or more) for injection.

When residues of the methyl ester of II were also sought from the column, the adsorbent was deactivated by the addition of 1 ml of absolute methanol and eluted with 10 ml of benzene. The eluate was evaporated and reconstituted in benzene for GLC analysis as described for the methyl ester of I. (*Note:* If a column cleanup of the ethyl ester of I is sought, the extract is added to the column with 15 ml of hexane–20% benzene and the eluate is discarded. The ethyl ester is then eluted from the column with 25 ml of hexane–40% benzene.)

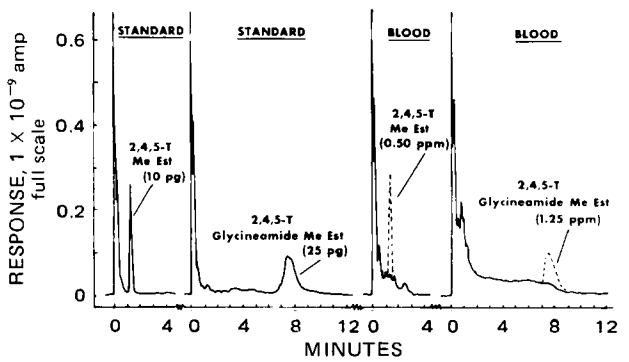

Figure 1—*Gas chromatograms of methyl ester (MeEst) standards of 2,4,5-trichlorophenoxyacetic acid (2,4,5-T), its glycineamide, and cleaned-up blood extracts in benzene spiked with the standards (injection = 5 μl).*

[14] Catalog No. 420,000, Kontes Glass Co., Vineland, N.J.

Analysis of Urine—The urine samples were collected in the 30-ml tube of the animal chamber. The animal and its metal support were removed, and any feces collected on the screen were reserved for separate analysis. The screen and walls of the chamber were then washed three times with 5-ml portions of 1 *N* HCl and twice with 5-ml portions of benzene. The 30-ml culture tube containing the urine and washings was removed, sealed, vigorously shaken for 1 min, and centrifuged at 2000 rpm for 5 min. The benzene layer was transferred to a 50-ml glass-stoppered flask, and the aqueous layer was extracted with two additional 10-ml portions of benzene; the combined extracts were evaporated, methylated, and analyzed as described for the blood.

The aqueous phase was subjected to alkaline hydrolysis by adding

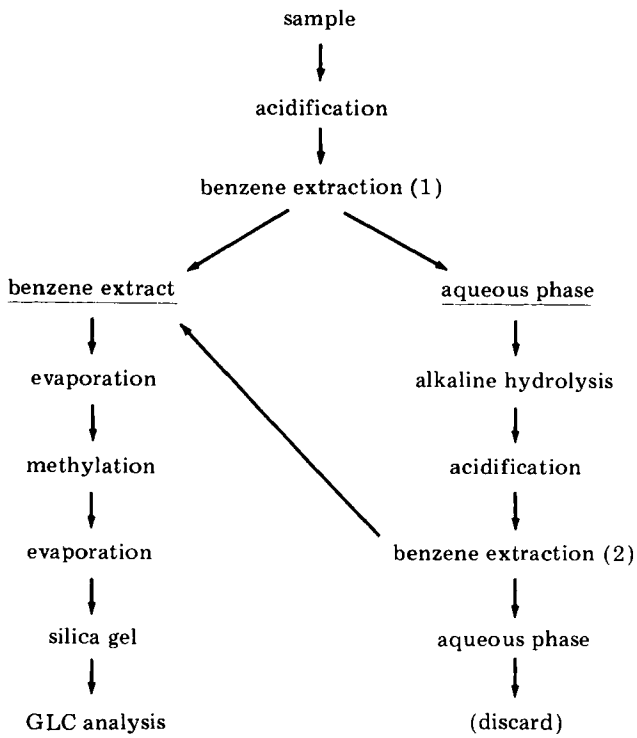

Scheme I

Table IV—Electron-Capture GLC Analysis of 2,4,5-Trichlorophenoxyacetic Acid (I) and Its Glycineamide (II) from Mouse Urine before and after Silica Gel Cleanup of Free Acid and Hydrolyzed Fractions

Added		Recovered[a]			
		Before Cleanup		After Cleanup	
Compound	ng	ng	%[b]	ng	%[b]
I[c]	0	35.3 ± 1.16	—	5.1 ± 0.00	—
	10	43.6 ± 0.00	83 ± 0	15.3 ± 1.01	102 ± 10
	100	147 ± 0.0	112 ± 0	113 ± 3.8	108 ± 4
	1000	1200 ± 10	116 ± 1	987 ± 130	98 ± 13
I[d]	0	15.0 ± 2.25	—	0.68 ± 0.13	—
	10	18.5 ± 0.17	35 ± 2	5.6 ± 0.14	49 ± 1
	100	97 ± 2.2	82 ± 2	110 ± 1.7	109 ± 2
	1000	1053 ± 13	104 ± 1	1043 ± 46	104 ± 5
II[e]	0	12.3 ± 2.24	—	5.8 ± 0.70	—
	25	27.0 ± 1.07	59 ± 4	29.4 ± 1.34	94 ± 5
	250	246 ± 7.5	94 ± 3	259 ± 8.3	101 ± 3
II[c,f] (25 ng = 20.4 ng of I)	0	15.0 ± 2.25	—	0.7 ± 0.13	—
	25	26.3 ± 1.52	55 ± 7	20.3 ± 0.91	96 ± 4
	250	218 ± 7	100 ± 3	205 ± 18	100 ± 9

[a] Mean and standard error from triplicate assays. [b] Corrected for background interference in the unspiked sample. [c] Analyzed as the methyl ester of I. [d] Respiked after extraction of I and then hydrolyzed. [e] Analyzed as the methyl ester of II. [f] Respiked after extraction of II and then hydrolyzed.

2.5 ml of 10 *N* NaOH and heating the sealed tube at 85° for 2 hr with occasional shaking. After the tube had cooled, 2.5 ml of 12 *N* HCl was added, and the aqueous phase was extracted with three 10-ml portions of benzene. The combined extracts were then prepared and analyzed as described for blood. Column chromatographic cleanup of the samples was performed as described for blood. The cleanup was usually required for all samples containing residues of 10 ng or less.

Analysis of Feces—The excrement obtained from the screen of the animal chamber was transferred to a 12-ml culture tube, and three glass beads (5 mm diameter) and 3 ml of 1 *N* HCl were added. The sealed tube was subjected to vigorous vortex mixing for 1 min. After the addition of 5 ml of benzene, the acidified sample was gently shaken for 1 min and centrifuged at 2000 rpm for 5 min; the benzene layer was transferred to a 50-ml glass-stoppered flask as described for blood. The extraction was repeated with two additional 5-ml portions of benzene, and the combined extracts were prepared and analyzed as described for blood.

The aqueous phase was subjected to alkaline hydrolysis as described for blood, except that 1 ml of 6 *N* NaOH was used. After hydrolysis, 1 ml of 8 *N* HCl was added; then the sample was extracted, prepared, and analyzed as described for blood. The column cleanup of fecal extracts on silica gel also was performed as described for blood; this cleanup was required for extracts containing residues of 100 ng or less.

Recovery Experiments—Forty-four 24-hr collections of urine and feces from untreated mice in the sampling chambers yielded a mean volume of 0.48 ± 0.26 ml of urine and 0.19 ± 0.05 g of feces/animal/day. The urine was composited and diluted with distilled water to produce 0.48 ml of undiluted mouse urine/3 ml of solution. The feces were composited and mixed by grinding with a mortar and pestle to ensure uniformity. Portions of these samples and fresh mouse blood (20 μl) were used as substrates in the development of analytical methodology based on electron-capture GLC analysis.

Amounts, 0.5 ml, of distilled water, each containing the equivalent of 20 μl of whole mouse blood, were added to triplicate 8-ml culture tubes containing 0-, 10-, 100-, or 1000-ng amounts of I or 0-, 10-, or 100-ng amounts of II as dry residues. After vortex mixing, the samples were analyzed for free acids as described. After extraction, the aqueous samples were again spiked at the same levels by adding 50 μl of acetone containing the appropriate amount of acid or glycineamide. These samples then were subjected to alkaline hydrolysis and analyzed as described.

Triplicate 0.19-g portions of the composited feces in 12-ml culture tubes or 3-ml portions of the diluted urine composite in 30-ml culture tubes were spiked with 0, 10, 100, or 1000 ng of I or 0, 25, or 250 ng of II in 50 μl of acetone. After vortex mixing, the samples were analyzed as described. The aqueous phases were then spiked again in an identical manner, hydrolyzed, and analyzed as described.

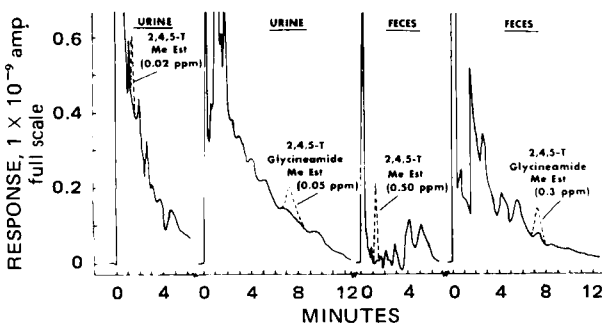

Figure 2—*Gas chromatograms of cleaned-up urine and feces extracts spiked with the methyl esters (MeEst) of 2,4,5-trichlorophenoxyacetic acid (2,4,5-T) and its glycineamide. (Extracts containing 10 and 25 pg of the methyl esters of 2,4,5-trichlorophenoxyacetic acid and its glycineamide, respectively, were injected in 5 μl of benzene.)*

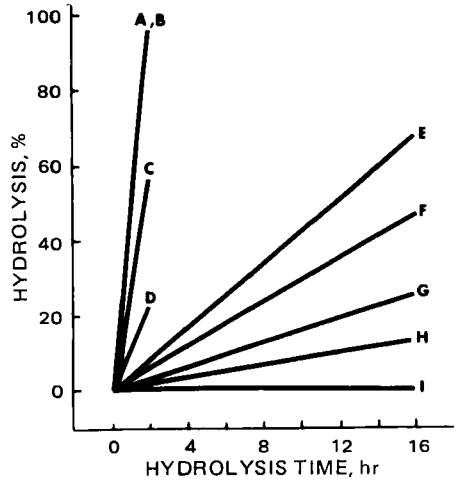

Figure 3—*Percent hydrolysis of the glycineamide of 2,4,5-trichlorophenoxyacetic acid under various conditions. Key: A, 1 N NaOH at 85°; B, 5 N HCl at 85°; C, 1 N HCl at 85°; D, 0.5 N NaOH at 25°; E, 5 N NaOH at 5°; F, 1 N NaOH at 5°; G, 0.5 N NaOH at 5°; H, 0.1 N NaOH at 25°; and I, 0.1 N NaOH at 5° or 0.1, 1, or 5 N HCl at 5 and 25°.*

Table V—Electron-Capture GLC Analysis of 2,4,5-Trichlorophenoxyacetic Acid (I) and Its Glycineamide (II) from Mouse Feces before and after Silica Gel Cleanup of Free Acid and Hydrolyzed Fractions

Added		Recovered[a]			
		Before Cleanup		After Cleanup	
Compound	ng	ng	%[b]	ng	%[b]
I[c]	0	18[d]	—	1.0 ± 0.67	—
	10	26[d]	80	8.4 ± 0.79	74 ± 8
	100	128[d]	110	91 ± 3.8	90 ± 4
	1000	983 ± 10	96 ± 1	950 ± 23	95 ± 2
I[c,e]	0	34.3 ± 13.9	—	0.7 ± 0.29	—
	10	45.1 ± 1.00	108 ± 10	7.8 ± 0.10	71 ± 1
	100	116 ± 13	82 ± 13	104 ± 6	103 ± 6
	1000	1006 ± 1	97 ± 0	1013 ± 6	101 ± 1
II[f]	0	71.4 ± 0.0	—	23.8 ± 4.0	—
	25	138 ± 6	266 ± 24	75.3 ± 2.9	105 ± 12
	250	297 ± 6	90 ± 2	274 ± 2	100 ± 1
II[c,g] (25 ng = 20.4 ng of I)	0	—[h]	—	0.7 ± 0.29	—
	25	—[h]	—	18.5 ± 3.21	87 ± 16
	250	194 ± 26	95 ± 13	208 ± 3	102 ± 2

[a] Mean and standard error from triplicate assays. [b] Corrected for background interference in the unspiked sample. [c] Analyzed as the methyl ester of I. [d] High background interference; quantitation is an estimate. [e] Respiked after extraction of I and then hydrolyzed. [f] Analyzed as the methyl ester of II. [g] Respiked after extraction of II and then hydrolyzed. [h] High background interference precluded assay without column cleanup.

Table VI—Electron-Capture GLC and Radiochemical Analysis of 2,4,5-Trichlorophenoxyacetic Acid (I), Its Glycineamide (II), and Alkaline Hydrolyzable Conjugates in Blood from Mice Injected with ^{14}C-2,4,5-Trichlorophenoxyacetic Acid (Nanograms per Microliter of Blood)[a]

Sampling Time	Assay	I	II	Alkaline Hydrolyzable Conjugates	Total as I
Pretreatment	Electron-capture GLC	0.31 ± 0.06	0.20 ± 0.03	0.26 ± 0.40	0.73
	Radiochemical	3.73 ± 1.61[b]	—	12.0 ± 1.6	15.7
5 min	Electron-capture GLC	950 ± 431	0.36 ± 0.12	0.41 ± 0.64	951
	Radiochemical	904 ± 410[b]	—	23.0 ± 15.1	927
30 min	Electron-capture GLC	672 ± 101	0.41 ± 0.17	0.19 ± 0.32	673
	Radiochemical	690 ± 109[b]	—	3.53 ± 1.88	694
1 hr	Electron-capture GLC	450 ± 126	0.36 ± 0.08	<0.26 ± 0.40[c]	450
	Radiochemical	423 ± 125[b]	—	8.72 ± 2.60	432
2 hr	Electron-capture GLC	381 ± 111	0.73 ± 0.31	5.37 ± 3.12	387
	Radiochemical	355 ± 104[b]	—	6.18 ± 5.41	361
4 hr	Electron-capture GLC	489 ± 157	1.01 ± 0.14	11.8 ± 3.9	502
	Radiochemical	472 ± 157[b]	—	6.03 ± 4.41	478
8 hr	Electron-capture GLC	279 ± 65	1.05 ± 0.15	5.80 ± 3.63	286
	Radiochemical	266 ± 71[b]	—	26.6 ± 8.62	293
24 hr[d]	Electron-capture GLC	68.9	0.05	2.24	71.2
	Radiochemical	57.8[b]	—	<12.0[c]	69.8
48 hr[d]	Electron-capture GLC	60.1	0.13	1.46	61.7
	Radiochemical	50.4[b]	—	0.23	50.6
72 hr	Electron-capture GLC	47.5 ± 34.0	0.43 ± 0.55	2.95 ± 3.19	50.8
	Radiochemical	41.3 ± 30.8[b]	—	11.5 ± 1.5	52.8

[a] Mean and standard error from three mice. Results are corrected for pretreatment sample background. [b] The ^{14}C-assay did not resolve the individual free acids; therefore, this result represents both. [c] None detected above background. [d] Data from a single and different mouse treated in the same manner. Physical condition of the other three animals precluded sampling at this interval.

RESULTS AND DISCUSSION

The analytical methods previously described were developed specifically for the mouse substrates to be assayed in pharmacokinetic studies with I (Scheme I). The binding of the free acids to proteins, especially in the whole blood, is considered to be relatively weak, since acidification with hydrochloric acid and extraction with benzene yielded good recoveries from samples spiked with both I and II. Nevertheless, the acidification and extraction of free acids should be expedited and the residues should be methylated and stored as the esters to prevent losses due to the tendency of nanogram amounts of the free acids to become associated with various surfaces. The aqueous phase remaining after extraction of the free acids may be stored in a refrigerator until alkaline hydrolysis.

Data concerning the electron-capture GLC characteristics of the methyl and ethyl esters of I and II are presented in Table I. Although ethylation of the compounds was not required in this study, information pertaining to the ethyl esters may be useful for assaying other substrates having background interferences at the t_R's of the methyl esters.

Typical chromatograms of standards of the methyl esters of I and II and extracts of untreated mouse blood before and after being spiked with the esters of the two compounds are presented in Fig. 1. Similar chromatograms of mouse urine and feces are presented in Fig. 2.

Partition values (the fraction of solute partitioning into the nonpolar phase of an equivolume immiscible binary solvent system) for the methyl and ethyl esters of the two compounds were determined as described by Beroza and Bowman (8, 9). The partition values of the methyl and ethyl esters of I and II, which are extremely useful in developing extraction and cleanup methods and confirming identity at trace levels, are presented in Table II. The partition values for I and II in chloroform–water or benzene–water (pH 0–2) were in line with those reported (7) for I (*i.e.*, 0.96–1.0). The identity of trace levels of I and II extracted from the blood and excreta of animals dosed with I in the present studies was confirmed by using partition values.

In tests pertaining to the efficiency of hydrolyzing the methyl and ethyl esters of II with aqueous sodium hydroxide at 85° for 2 hr, recoveries of I accounted for 98 and 97% of the compounds, respectively. Since no trace of intact II could be detected, these hydrolysis conditions were adopted for the analytical procedure.

Table VII—Electron-Capture GLC and Radiochemical Analysis of 2,4,5-Trichlorophenoxyacetic Acid (I), Its Glycineamide (II), and Alkaline Hydrolyzable Conjugates in Urine from Mice Injected with ^{14}C-2,4,5-Trichlorophenoxyacetic Acid (Micrograms per Sampling Interval)[a]

Sampling Interval, hr	Assay	I	II	Alkaline Hydrolyzable Conjugates	Total as I
Pretreatment	Electron-capture GLC	0.01 ± 0.00	0.06 ± 0.05	<0.01 ± 0.00[b]	0.07
	Radiochemical	0.02 ± 0.01[c]	—	0.03 ± 0.02	0.05
0–6	Electron-capture GLC	1.86 ± 1.45	<0.06 ± 0.05[b]	<0.01 ± 0.00[b]	1.92
	Radiochemical	1.83 ± 1.41[c]	—	0.05 ± 0.02	1.88
6–24	Electron-capture GLC	13.7 ± 5.0	11.7 ± 6.25	<0.01 ± 0.00[b]	23.3
	Radiochemical	29.8 ± 11.5[c]	—	2.16 ± 0.98	32.0
24–30	Electron-capture GLC	7.10 ± 4.86	3.61 ± 4.18	<0.01 ± 0.00	10.1
	Radiochemical	9.16 ± 5.70[c]	—	1.03 ± 1.05	10.2
30–48	Electron-capture GLC	61.7 ± 76.6	28.3 ± 25.7	38.1 ± 39.9	123
	Radiochemical	83.8 ± 92.2[c]	—	39.8 ± 41.5	124
48–52	Electron-capture GLC	35.8 ± 54.6	7.28 ± 8.94	13.6 ± 2.9	55.4
	Radiochemical	39.5 ± 56.7[c]	—	14.2 ± 2.4	53.7
52–72	Electron-capture GLC	40.0 ± 32.4	22.0 ± 17.2	36.5 ± 12.8	94.5
	Radiochemical	59.4 ± 46.7[c]	—	37.1 ± 13.9	96.5

[a] Mean and standard error from three mice. Results are corrected for pretreatment sample background. [b] None detected above background. [c] The ^{14}C-assay did not resolve the individual free acids; therefore, this result represents both.

Table VIII—Electron-Capture GLC and Radiochemical Analysis of 2,4,5-Trichlorophenoxyacetic Acid (I), Its Glycineamide (II), and Alkaline Hydrolyzable Conjugates in Feces from Mice Injected with ^{14}C-2,4,5-Trichlorophenoxyacetic Acid (Micrograms per Sampling Interval)[a]

Sampling Interval, hr	Mean Sample Weight, mg + *SE*	Assay	I	II	Alkaline Hydrolyzable Conjugates	Total as I
Pretreatment	538 ± 108	Electron-capture GLC	0.01 ± 0.00	0.04 ± 0.03	0.01 ± 0.00	0.05 ± 0.02
		Radiochemical	0.02 ± 0.01[b]	—	0.02 ± 0.01	0.04 ± 0.01
0–6	43.6 ± 42.1	Electron-capture GLC	1.44 ± 1.07	<0.06 ± 0.01[c]	0.10 ± 0.07	1.54 ± 1.14
		Radiochemical	1.52 ± 1.05[b]	—	0.10 ± 0.06	1.62 ± 1.11
6–24	89.0 ± 7.4	Electron-capture GLC	4.62 ± 0.78	<0.04 ± 0.02[c]	0.89 ± 0.61	5.51 ± 0.71
		Radiochemical	5.56 ± 0.82[b]	—	1.01 ± 0.60	6.57 ± 0.48
24–30	57.7 ± 29.1	Electron-capture GLC	2.07 ± 1.14	<0.04 ± 0.03[c]	0.73 ± 0.42	2.80 ± 1.56
		Radiochemical	2.75 ± 1.55[b]	—	0.85 ± 0.53	3.60 ± 2.08
30–48	262 ± 203	Electron-capture GLC	16.9 ± 11.8	1.47 ± 1.96	7.10 ± 9.23	25.2 ± 21.7
		Radiochemical	19.4 ± 13.8[b]	—	7.30 ± 9.32	26.7 ± 22.4
48–52	25.8 ± 14.8	Electron-capture GLC	0.99 ± 0.44	<0.05 ± 0.01[c]	0.11 ± 0.06	1.12 ± 0.45
		Radiochemical	1.09 ± 0.52[b]	—	0.10 ± 0.06	1.19 ± 0.54
52–72	363 ± 265	Electron-capture GLC	7.30 ± 6.70	0.12 ± 0.10	2.56 ± 2.40	9.95 ± 9.07
		Radiochemical	7.96 ± 7.86[b]	—	2.50 ± 2.39	10.5 ± 10.2

[a] Mean and standard error from three mice. Results are corrected for pretreatment sample background. [b] The ^{14}C-assay did not resolve the individual free acids; therefore, this result represents both. [c] None detected above background.

The extent of hydrolysis of II under various conditions is illustrated in Fig. 3. Aqueous sulfuric acid (0.01, 0.05, 0.10, 0.50, and 1.0 *N*) failed to yield any detectable hydrolysis at 25° for 2 hr. Also, aqueous hydrochloric acid (0.1, 1.0, and 5.0 *N*) failed to hydrolyze the glycineamide at 5 or 25° over 16 hr. However, significant hydrolysis occurred with aqueous sodium hydroxide (0.1–0.5 *N*) at 25°. These data indicated that residues of II should not be mixed with sodium hydroxide unless hydrolysis is intended. Therefore, samples containing II or conjugates were immediately acidified and extracted to ensure the integrity of the analytical results.

Results from blood, urine, and feces of untreated mice, spiked and analyzed *via* electron-capture GLC, are presented in Tables III, IV, and V, respectively. Excellent recoveries were obtained from all three substrates spiked with 100- and 1000-ng amounts of I analyzed both before and after the silica gel cleanup. Results from the aqueous sample residues respiked prior to hydrolysis indicated that the previous extractions had efficiently removed I and that the additional I was recovered from the hydrolysis procedure. Samples of blood or urine containing 100 ng or more of I should be analyzed without utilizing the silica gel cleanup to obtain higher recoveries and to speed the analysis. The background interference in urine was reduced from about 35.3- to 5.1-ng equivalents of I by utilizing a silica gel column; therefore, the cleanup is required where low levels of residues are sought. Feces should be cleaned up at all residue levels below 1000 ng.

Good recoveries were obtained for II from the three substrates spiked at all levels and especially after the extracts were cleaned up on silica gel. Results from the analysis of the residual aqueous substrates respiked with II prior to hydrolysis and assayed as I demonstrated that the previous extraction of II was complete and that hydrolysis of II and recovery of the I moiety were accomplished.

Rinses of the animal chambers with various amounts, combinations, and sequences of aqueous sodium hydroxide (1 *N*), hydrochloric acid (1 *N*), benzene, methanol, acetone, ether, and aqueous (ethylenedinitrilo)tetraacetate (1 mg/ml) were performed to determine the most efficient means of conveniently recovering the radioactivity deposited by the urine from mice injected with ^{14}C-I. The use of aqueous sodium hydroxide followed by benzene yielded a slightly better recovery (99.4%) of the total radioactivity than did aqueous hydrochloric acid followed by benzene (97.3%). Nevertheless, the use of hydrochloric acid was adopted to prevent any possible hydrolysis of II or conjugates by the alkali during the rinsing process.

Results of the preliminary pharmacokinetic studies with mice injected with ^{14}C-I, as determined by parallel electron-capture GLC and radiochemical assays, are presented for blood, urine, and feces in Tables VI, VII, and VIII, respectively. No results are reported for II *via* radioassay; since the radioassay did not resolve I and II, the value reported for I includes both compounds. The concentration of I and its products found in the blood was highest (>900 ng/μl) at the first sampling period (5 min after injection) and declined to about 50 ng/μl during the 72-hr test period, as expected after intravenous injection. Residues of II and the alkaline hydrolyzable conjugates accounted for only a small percentage of radioactivity of the material present, which existed primarily as I.

Results from the urine assays indicated that only trace amounts of I and its products were excreted during the 6-hr period immediately after injection. However, during the 6–24-hr interval and thereafter, appreciable amounts of I, II, and conjugates were excreted. Low levels

of I and lesser amounts of conjugates were found in the mouse feces at all intervals of sampling. No significant amount of II was obtained from the feces.

Radioassay results from the blood, urine, and feces generally correlated well with those from the electron-capture GLC procedure. Radioassays of the residual substrates (after hydrolysis and extraction), column adsorbents, and discarded solvents indicated that essentially all radioactivity had been extracted from the samples and that losses during the analytical procedure were negligible.

REFERENCES

(1) Report on 2,4,5-T: A Report of the Panel on Herbicides of the President's Science Advisory Committee, Executive Office of the President, Office of Science and Technology, U.S. Government Printing Office, Washington, DC 20402, Mar. 1971.

(2) W. N. Piper, J. Q. Rose, M. L. Leng, and P. J. Gehring, *Toxicol. Appl. Pharmacol.*, **26**, 339(1973).

(3) P. J. Gehring, C. G. Kramer, B. A. Schwetz, J. Q. Rose, and V. K. Rowe, *ibid.*, **26**, 352(1973).

(4) K. Erne, *Acta Vet. Scand.*, **7**, 240(1966).

(5) *Ibid.*, **7**, 264(1966).

(6) M. T. Shafik, H. C. Sullivan, and H. F. Enos, *Int. J. Environ. Anal. Chem.*, **1**, 23(1971).

(7) I. H. Suffet, *J. Agr. Food Chem.*, **21**, 591(1973).

(8) M. Beroza and M. C. Bowman, *Anal. Chem.*, **37**, 291(1965).

(9) M. C. Bowman and M. Beroza, *ibid.*, **38**, 1544(1966).

ACKNOWLEDGMENTS AND ADDRESSES

Received December 8, 1975, from the *Department of Health, Education, and Welfare, Food and Drug Administration, National Center for Toxicological Research, Jefferson, AR 72079*

Accepted for publication February 17, 1976.

The authors acknowledge the assistance of Judith E. McAninch, Percy M. Draper, Kenneth L. Rowland, Daniel M. Nestorick, James B. LaBorde, and Johnny J. Bazare, Jr., in conducting ancillary studies related to the development of analytical methods and animal sampling techniques.

[x] To whom inquiries should be directed.

Mechanistic Studies on Transcorneal Permeation of Pilocarpine

JAMES W. SIEG and JOSEPH R. ROBINSON [x]

Abstract □ The mechanism of corneal pilocarpine penetration was studied in the albino rabbit using radiochemical techniques. The apparent rate and extent of pilocarpine accumulation in the aqueous humor and the various cell layers of the cornea were determined for both intact and abraded eyes. For the first time, drug levels were monitored in the epithelium and stroma-endothelium of the intact cornea using a tissue-scraping technique. In addition, a new postinstillation rinsing method was devised to evaluate the rate of corneal uptake. The results demonstrate a dual role for the corneal epithelium, both as a barrier to drug penetration and as a reservoir for drug in the intact cornea. The transcorneal pilocarpine flux is slower than the data appear to indicate, and previous overestimates of the apparent absorption rate constant are due to parallel elimination processes occurring at the absorption site. Pharmacokinetic parameters were determined for each tissue to generate an overall mechanism for corneal permeation.

Keyphrases □ Pilocarpine—mechanism of corneal penetration, rate and extent of accumulation in aqueous humor and various cell layers, rabbits □ Corneal penetration mechanism—pilocarpine, rate and extent of accumulation in aqueous humor and various cell layers, rabbits □ Ophthalmic cholinergic agents—pilocarpine, mechanism of corneal penetration, rabbits

The cornea is an easily accessible tissue of the body. However, because of its small size and great degree of specialization, studies on corneal drug transport have been limited, with the net result that the understanding of transcorneal permeation is sketchy. Studies of inorganic ion movement have been fairly extensive (1) due to their great physiological importance to the cornea, and these ions are transported primarily through specialized transport systems associated with the epithelial potential. A relatively large number of studies also have been performed using organic molecules, both drug and nondrug, as recently described (2). However, these studies have been generally restricted to simple quantitation of drug penetration to a specific target tissue, often the aqueous humor, without elucidating the mechanism of corneal permeation. The experimental design in most of these studies does not permit anything but qualitative speculation regarding corneal penetration. The present study examines the corneal kinetics of pilocarpine in an effort to ascertain its transcorneal mechanism.

BACKGROUND

The prevailing theories on corneal penetration of pilocarpine often include, all or in part, a number of principal speculations: (*a*) the existence of a barrier to penetration in the lipophilic corneal epithelium, (*b*) rapid uptake and transport of pilocarpine by the cornea, (*c*) controlled release of pilocarpine to the anterior chamber by the endothelium, and (*d*) the presence of a depot, or reservoir, of pilocarpine somewhere in the cornea.

For most drugs, the existence of a barrier in the corneal epithelium is well documented (2, 3). This barrier is often considered to vary in magnitude according to the solubility character of the drug. A very water-soluble drug is unable to penetrate this barrier, and a very lipid-soluble drug penetrates it easily but is unable to leave; therefore, some degree of solubility in both aqueous and lipid media is deemed desirable for optimum transcorneal permeation (4, 5). Recently, the location of this barrier function was specifically attributed to the outermost cell layer of the epithelium (6, 7), and the sensitivity of this barrier to surfactants has been carefully studied (8–10).

The premise that pilocarpine has a rapid corneal penetration rate has been professed by a number of investigators whose conclusions were derived from both *in vitro* (11, 12) and *in vivo* (13) data. The basis for this assumption is usually the observation that pilocarpine exhibits early peak times in the target tissues. In addition, the flux of pilocarpine from the cornea to the anterior chamber has been attributed to some property, as yet undisclosed, of the corneal endothelium (12).

The speculation that pilocarpine accumulates somewhere in the corneal tissues arises from analogy to early studies with fluorescein (14, 15) and accurate determinations of aqueous humor drug dynamics after dosing with pilocarpine (16). In the latter case, the elimination rate constant for pilocarpine from the anterior chamber was significantly smaller than the normal aqueous humor turnover rate, and the presence of a depot in the cornea was offered as an explanation.

of I and lesser amounts of conjugates were found in the mouse feces at all intervals of sampling. No significant amount of II was obtained from the feces.

Radioassay results from the blood, urine, and feces generally correlated well with those from the electron-capture GLC procedure. Radioassays of the residual substrates (after hydrolysis and extraction), column adsorbents, and discarded solvents indicated that essentially all radioactivity had been extracted from the samples and that losses during the analytical procedure were negligible.

REFERENCES

(1) Report on 2,4,5-T: A Report of the Panel on Herbicides of the President's Science Advisory Committee, Executive Office of the President, Office of Science and Technology, U.S. Government Printing Office, Washington, DC 20402, Mar. 1971.

(2) W. N. Piper, J. Q. Rose, M. L. Leng, and P. J. Gehring, *Toxicol. Appl. Pharmacol.*, **26**, 339(1973).

(3) P. J. Gehring, C. G. Kramer, B. A. Schwetz, J. Q. Rose, and V. K. Rowe, *ibid.*, **26**, 352(1973).

(4) K. Erne, *Acta Vet. Scand.*, **7**, 240(1966).

(5) *Ibid.*, **7**, 264(1966).

(6) M. T. Shafik, H. C. Sullivan, and H. F. Enos, *Int. J. Environ. Anal. Chem.*, **1**, 23(1971).

(7) I. H. Suffet, *J. Agr. Food Chem.*, **21**, 591(1973).

(8) M. Beroza and M. C. Bowman, *Anal. Chem.*, **37**, 291(1965).

(9) M. C. Bowman and M. Beroza, *ibid.*, **38**, 1544(1966).

ACKNOWLEDGMENTS AND ADDRESSES

Received December 8, 1975, from the *Department of Health, Education, and Welfare, Food and Drug Administration, National Center for Toxicological Research, Jefferson, AR 72079*

Accepted for publication February 17, 1976.

The authors acknowledge the assistance of Judith E. McAninch, Percy M. Draper, Kenneth L. Rowland, Daniel M. Nestorick, James B. LaBorde, and Johnny J. Bazare, Jr., in conducting ancillary studies related to the development of analytical methods and animal sampling techniques.

[x] To whom inquiries should be directed.

Mechanistic Studies on Transcorneal Permeation of Pilocarpine

JAMES W. SIEG and JOSEPH R. ROBINSON [x]

Abstract □ The mechanism of corneal pilocarpine penetration was studied in the albino rabbit using radiochemical techniques. The apparent rate and extent of pilocarpine accumulation in the aqueous humor and the various cell layers of the cornea were determined for both intact and abraded eyes. For the first time, drug levels were monitored in the epithelium and stroma-endothelium of the intact cornea using a tissue-scraping technique. In addition, a new postinstillation rinsing method was devised to evaluate the rate of corneal uptake. The results demonstrate a dual role for the corneal epithelium, both as a barrier to drug penetration and as a reservoir for drug in the intact cornea. The transcorneal pilocarpine flux is slower than the data appear to indicate, and previous overestimates of the apparent absorption rate constant are due to parallel elimination processes occurring at the absorption site. Pharmacokinetic parameters were determined for each tissue to generate an overall mechanism for corneal permeation.

Keyphrases □ Pilocarpine—mechanism of corneal penetration, rate and extent of accumulation in aqueous humor and various cell layers, rabbits □ Corneal penetration mechanism—pilocarpine, rate and extent of accumulation in aqueous humor and various cell layers, rabbits □ Ophthalmic cholinergic agents—pilocarpine, mechanism of corneal penetration, rabbits

The cornea is an easily accessible tissue of the body. However, because of its small size and great degree of specialization, studies on corneal drug transport have been limited, with the net result that the understanding of transcorneal permeation is sketchy. Studies of inorganic ion movement have been fairly extensive (1) due to their great physiological importance to the cornea, and these ions are transported primarily through specialized transport systems associated with the epithelial potential. A relatively large number of studies also have been performed using organic molecules, both drug and nondrug, as recently described (2). However, these studies have been generally restricted to simple quantitation of drug penetration to a specific target tissue, often the aqueous humor, without elucidating the mechanism of corneal permeation. The experimental design in most of these studies does not permit anything but qualitative speculation regarding corneal penetration. The present study examines the corneal kinetics of pilocarpine in an effort to ascertain its transcorneal mechanism.

BACKGROUND

The prevailing theories on corneal penetration of pilocarpine often include, all or in part, a number of principal speculations: (*a*) the existence of a barrier to penetration in the lipophilic corneal epithelium, (*b*) rapid uptake and transport of pilocarpine by the cornea, (*c*) controlled release of pilocarpine to the anterior chamber by the endothelium, and (*d*) the presence of a depot, or reservoir, of pilocarpine somewhere in the cornea.

For most drugs, the existence of a barrier in the corneal epithelium is well documented (2, 3). This barrier is often considered to vary in magnitude according to the solubility character of the drug. A very water-soluble drug is unable to penetrate this barrier, and a very lipid-soluble drug penetrates it easily but is unable to leave; therefore, some degree of solubility in both aqueous and lipid media is deemed desirable for optimum transcorneal permeation (4, 5). Recently, the location of this barrier function was specifically attributed to the outermost cell layer of the epithelium (6, 7), and the sensitivity of this barrier to surfactants has been carefully studied (8–10).

The premise that pilocarpine has a rapid corneal penetration rate has been professed by a number of investigators whose conclusions were derived from both *in vitro* (11, 12) and *in vivo* (13) data. The basis for this assumption is usually the observation that pilocarpine exhibits early peak times in the target tissues. In addition, the flux of pilocarpine from the cornea to the anterior chamber has been attributed to some property, as yet undisclosed, of the corneal endothelium (12).

The speculation that pilocarpine accumulates somewhere in the corneal tissues arises from analogy to early studies with fluorescein (14, 15) and accurate determinations of aqueous humor drug dynamics after dosing with pilocarpine (16). In the latter case, the elimination rate constant for pilocarpine from the anterior chamber was significantly smaller than the normal aqueous humor turnover rate, and the presence of a depot in the cornea was offered as an explanation.

EXPERIMENTAL

Materials—Tritiated pilocarpine alkaloid, specific activity of 4.1 Ci/mmole, was obtained commercially[1] and purified by vacuum distillation (17). Purification of the pilocarpine was carried out immediately prior to each experimental run to minimize tritium exchange. All other chemicals were either reagent or analytical grade and were used as received.

Male albino rabbits[2], 1.8–2.4 kg, were used. Lighting was maintained on a 24-hr basis in the caging facilities. The animals were fed a regular diet, with no restrictions on the amount of food or water consumed.

Preparation of Pilocarpine Solutions—Drug solutions were prepared by addition of a solution of 10^{-2} *M* pilocarpine to the purified labeled material. The standard buffer solution was isotonic Sorensen's buffer, pH 6.24. It was determined that 0.25 mCi of tritiated pilocarpine/ml of final solution was sufficient to ensure good counting efficiency throughout the studies, *i.e.*, 150,000–175,000 cpm/μl. The small amount of labeled material did not alter significantly the molarity of the final solutions.

Removal of Corneal Epithelium—To facilitate removal of the corneal epithelium, 2 drops of a 0.5% tetracaine hydrochloride solution[3] were instilled into the eyes of test animals. Five minutes later the eye was proptosed, and the epithelial layer was removed *in toto* by scraping with a scalpel. The eye was then blotted with moist tissue to remove any loose fragments of epithelium from the precorneal area.

Aqueous Humor Drug Concentration–Time Profiles—*Pilocarpine Solutions*—The basic experimental techniques used were presented previously (18, 19). Unanesthetized animals were used, and a standard 25-μl dose was instilled.

Rinsing Studies—At various specified times following dosing, the eyes were thoroughly flushed with isotonic saline injection containing no preservatives. A polyethylene wash bottle with a fine-drawn tip was used so that a stream of saline could be directed into all precorneal parts of the eye to ensure complete removal of the instilled dose. The eyes were then left untouched, and no changes in the basic routine were made beyond the time of rinsing with saline.

Corneal Drug Concentration–Time Profiles—Corneal samples were taken immediately after the aqueous humor was aspirated from the anterior chamber. The eyes were proptosed and secured with a hemostat behind the globe. The tip of a scalpel was then inserted at the corneal margin, and the entire cornea was excised. Each corneal sample was carefully rinsed in saline and blotted on tissue. The corneas were then placed into tared combustion cones[4], and the wet weight was determined using an analytical balance. A tissue oxidizer[5] was used to burn each cornea, and samples were counted in plastic vials[6] using a commercial liquid scintillation solution[7] and scintillation spectrometer[8]. The final count for each sample then was converted to micrograms of pilocarpine per gram of cornea.

The only changes in this basic corneal sampling technique occurred in runs in which the corneal epithelium was removed just prior to taking the corneal samples. In these instances, the animals were sacrificed in the usual manner and the eyes were proptosed. A scalpel was used to scrape away the epithelium carefully. The aqueous humor was then withdrawn, and the corneal samples were removed and analyzed using the described techniques.

Throughout the studies, the surgical procedures were carried out as quickly as possible to minimize redistribution of drug during the time required to obtain samples. This precaution was especially important for very early sample times, and the eye was routinely rinsed with saline immediately at the end of the sampling interval as an added precaution against further influx of drug from the precorneal area. While some error may have been introduced due to the time required for sampling (usually less than 1 min), every effort was made to keep this source of error to a minimum.

Crossover Study to Determine Systemic Contribution to Aqueous Humor Pilocarpine—Drainage of the instilled solution into the nasolacrimal duct presents the possibility for systemic absorption of pilocarpine. A crossover study was performed to verify that all pilocarpine detected in the aqueous humor came from transcorneal penetration and was not due in part to systemic circulation. Rabbits were dosed only in the left eyes with pilocarpine solution. Aqueous humor samples were then taken from the anterior chamber of both eyes at 20, 60, and 120 min after instillation. No detectable pilocarpine was found in samples from the right eyes. On this basis, entry of pilocarpine into the anterior chamber *via* systemic circulation was discounted.

Analysis for Tritium Exchange in the Samples—A portion of the tritium label on the isotopic species was labile to exchange with water. Although careful solution purification procedures were used, there was concern that exchange could occur in the ocular tissues after dosing. This exchange could lead to misinterpretation of results due to rapid passage of tritiated water through the cornea (17). To discount this factor, corneal and aqueous humor samples were taken after dosing with purified tritiated pilocarpine solution. Corneal samples were cut into two pieces, weighed, and labeled A and B. Likewise, aqueous humor samples were divided into two 50-μl portions.

In each case, the A portion was immediately burned as a wet sample using the tissue oxidizer. The B samples were first desiccated and similarly treated. Any tritiated water present in the tissues would be expected to volatilize from the dried samples. The results showed no differences in activity between the A and B portions of each sample, indicating that the tritium label remained as a nonvolatile entity during passage through the cornea.

Table I—Concentration of Pilocarpine in Aqueous Humor following Topical Application of a 10^{-2} *M* Solution in Intact and Abraded Eyes

Minutes	Number of Eyes	Micrograms per Milliliter of Aqueous Humor
	Intact Eyes	
0.5	12	0.025 (0.001)[a]
5	18	0.60 (0.02)
10	36	0.85 (0.04)
20	36	1.06 (0.05)
30	28	0.95 (0.05)
60	32	0.52 (0.04)
90	36	0.33 (0.03)
120	32	0.20 (0.02)
	Abraded Eyes	
0.5	6	2.57 (0.17)
1	6	4.32 (0.49)
5	10	8.44 (0.61)
10	12	7.06 (0.53)
20	10	7.36 (0.53)
30	12	4.24 (0.46)
60	14	3.21 (0.60)
90	8	1.20 (0.13)
120	14	0.78 (0.07)

[a] Numbers in parentheses represent standard error of the mean.

RESULTS

Aqueous Humor Drug Levels following Dosing with Pilocarpine Solution—Aqueous humor drug levels were determined at various times following topical application of pilocarpine nitrate solution (Table I). The data indicate that pilocarpine penetrated the intact cornea and reached an apparent peak concentration in the aqueous humor within 20 min, in agreement with earlier work (17, 19). Immediately following this peak concentration, the level of pilocarpine in the aqueous humor began to decline. One-compartment pharmacokinetic computer analysis of the data gave an apparent transcorneal flux rate constant of 0.08 min^{-1} and an apparent elimination rate constant of 0.017 min^{-1}.

When the corneal epithelium was removed prior to dosing, both the rate and extent to which pilocarpine penetrated to the anterior chamber increased. A comparison of the aqueous humor concentration–time profiles for intact and abraded corneas can be made (Fig. 1). Removal of the epithelium produced a seven- to eightfold increase

[1] New England Nuclear, Boston, Mass.
[2] Klubertanz, Edgerton, Wis.
[3] Pontocaine, Winthrop Laboratories, Division of Sterling Drug Inc., New York, NY 10016
[4] Combusto-Cone, Packard Instrument Co., Downers Grove, Ill.
[5] Model 306, Packard Instrument Co., Downers Grove, Ill.
[6] The Vial, Research Products International Corp., Elk Grove Village, Ill.
[7] Monophase-40, Packard Instrument Co., Downers Grove, Ill.
[8] Model 2002, Packard Instrument Co., Downers Grove, Ill.

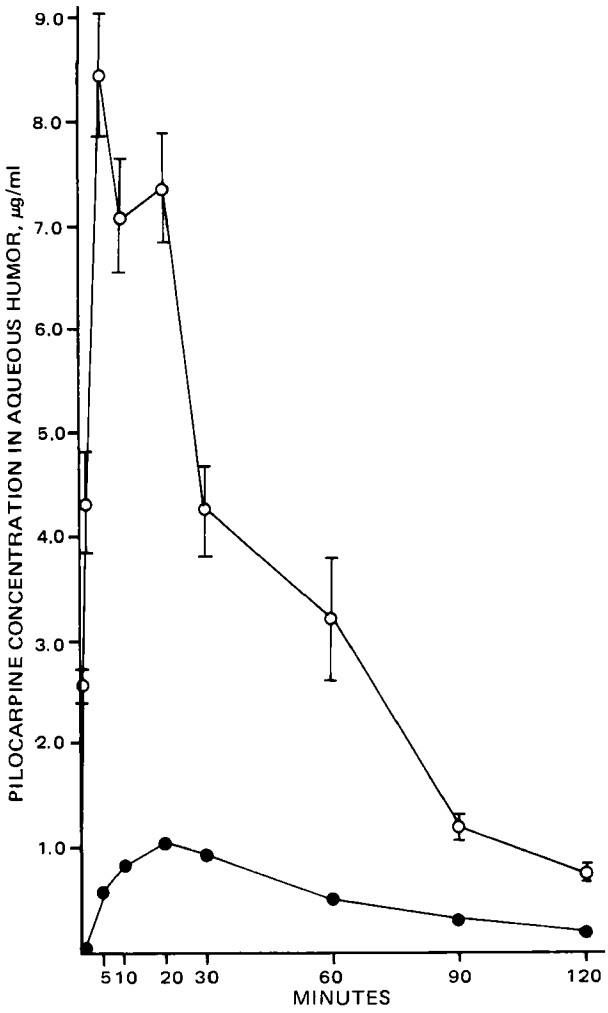

Figure 1—*Aqueous humor drug concentration after topical dosing with pilocarpine solution. Key: ●, intact eyes; and ○, abraded eyes. Error bars represent the standard error of the mean. Where no error bar is indicated, the standard error of the mean is smaller than the size of the symbol used.*

in aqueous humor levels. In addition, the drug reached a maximum level by at least 5 min. This decrease in the time required to reach a peak aqueous humor concentration suggests a change in the rate constant for transcorneal flux when the epithelium is removed. The rate constant for elimination of pilocarpine from the aqueous humor was the same as that observed for intact eyes.

Corneal Concentration of Pilocarpine following Dosing with 10^{-2} *M* Solution—The corneal pilocarpine levels for intact and abraded eyes are presented in Table II. In the intact eye, drug reached an apparent peak concentration within 5 min. If the epithelium was removed prior to dosing, the amount of pilocarpine entering the cornea markedly increased and the peak time decreased to 1 min (Fig. 2).

Analysis of whole cornea samples can only give a measure of the total amount of drug, without any indication of its distribution in the various cellular layers. To use such information, homogeneity of the cornea and uniform drug distribution must be assumed. This shortcoming is severe if an accurate mechanistic interpretation is to be attempted. The corneal epithelium has long been considered a major barrier to the penetration of drugs into and through the cornea. If this structure is to be implicated in the transcorneal mechanism for pilocarpine, the disposition of drug in the intact cornea must be determined. The current studies provide an accurate simple procedure for determining stromal and epithelial drug levels as a function of time.

The distribution of pilocarpine in the cornea at any specified time can be determined by scraping away the epithelium immediately before the corneal sample is excised. Analysis of the samples gives the

Table II—Concentration of Pilocarpine in the Cornea following Topical Application of a 10^{-2} *M* Solution

Minutes	Number of Eyes	Micrograms per Gram of Cornea
Corneas with Intact Epithelium[a]		
0.5	12	1.91 (0.20)[b]
2	12	4.31 (0.24)
5	12	5.50 (0.63)
10	10	4.77 (0.41)
20	12	3.07 (0.39)
30	10	2.72 (0.22)
60	10	0.83 (0.09)
90	12	0.50 (0.05)
120	12	0.29 (0.03)
Corneas with Epithelium Removed prior to Dosing[c]		
0.5	6	19.70 (0.98)
1	6	31.82 (1.48)
5	6	13.99 (0.69)
10	6	7.66 (1.32)
20	6	7.49 (1.37)
30	6	4.16 (0.79)
60	6	3.58 (0.57)
120	6	0.83 (0.22)
Corneas with Epithelium Removed just prior to Taking Sample[c] (Stroma-Endothelium)		
2	6	0.23 (0.03)
5	6	0.53 (0.05)
10	6	0.81 (0.08)
20	6	1.14 (0.15)
30	6	0.89 (0.11)
60	6	0.32 (0.04)
90	6	0.19 (0.08)
120	6	0.09 (0.01)
Calculated Concentration in Epithelium		
2	6	29.4
5	6	35.8
10	6	28.5
20	6	13.9
30	6	13.2
60	6	3.7
90	6	2.2
120	6	1.4

[a] Average wet weight of intact corneas was 46.1 ± 0.64 mg. [b] Numbers in parentheses represent standard error of the mean. [c] Average wet weight of corneas with epithelium removed was 39.7 ± 0.53 mg.

stroma-endothelium drug concentration of the intact cornea, since the epithelium is removed after dosing. The epithelial concentration can be determined simply by comparing the stroma-endothelium data to the data obtained for the whole intact cornea. This amount is calculated by determining the difference between the two quantities at each time point and then applying appropriate corrections for the weights of the individual tissues. The results are presented in Table II, and a graphical representation of the relative disposition of pilocarpine in the intact cornea is shown in Fig. 3.

It is clear from the data that pilocarpine concentrates in the epithelium. At very early times in the profile, up to 80% of the total pilocarpine content of the cornea was in the epithelium. This percentage decreased as the epithelium remained in contact with the stroma for longer periods. However, even up to 2 hr, the epithelium retained the major fraction of drug, indicating a reservoir and controlled release of pilocarpine to the underlying layers[9]. It is evident from these corneal studies that the epithelium plays a dual role in the mechanism for the transcorneal flux of pilocarpine, both as a barrier to penetration and as a reservoir for drug in the intact cornea.

Effect of Postinstillation Rinsing on Aqueous Humor Levels of Pilocarpine—The amount of drug ultimately reaching the anterior chamber is determined by the net result of two competitive processes: the rate of drug loss from the precorneal area and the rate of drug uptake by the cornea. The precorneal disposition of pilocarpine was extensively detailed previously (20–22). By manipulating this si-

[9] Preliminary results from this laboratory also show that scraping the endothelium does not remove a significant amount of pilocarpine, indicating no buildup of drug in this single layer of cells.

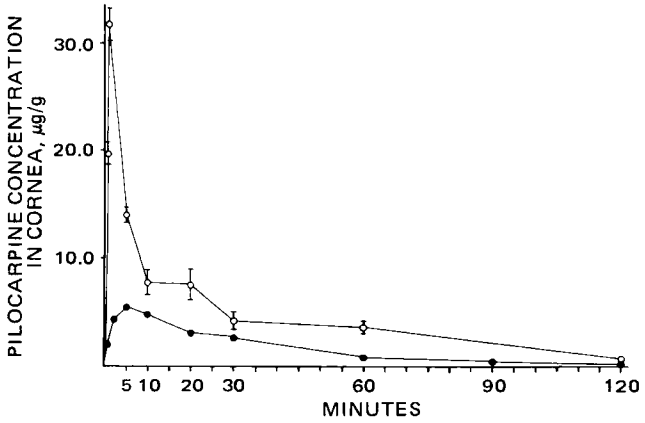

Figure 2—*Corneal drug concentration after topical dosing with pilocarpine solution. Key: ●, corneas with intact epithelium; and ○, corneas with epithelium removed prior to dosing (abraded eyes). Error bars represent the standard error of the mean. Where no error bar is indicated, the standard error of the mean is smaller than the size of the symbol used.*

multaneous process, it is possible to gain insight into the nature of transcorneal flux. Removal of drug from the precorneal area can be accelerated by rinsing the eye with saline. The changes in aqueous humor drug levels produced by varying the rinse time may then be related to the apparent rate of corneal uptake (Fig. 4).

The data in Fig. 4 show that rinsing at various times during the first 5 min caused a reduction in the amount of pilocarpine reaching the anterior chamber. Rinsing beyond 5 min did not alter the aqueous humor drug levels as compared with the nonrinsed data. This result reflects the combined influence of normal drainage, tear turnover, and nonproductive absorption and is not surprising in view of previous drainage studies (20).

The area under the curve for each rinse time was determined by graphical methods and normalized to the nonrinsed data. The percent reduction in area was then calculated and plotted (Fig. 5). The log-linear character is due to the nature of transcorneal flux since the calculated quantities are derived from measured differences between first-order processes. The slope of this line gives the change in aqueous humor pilocarpine bioavailability as a function of instilled solution contact time and, therefore, should be directly related to the apparent rate of corneal uptake. First-order kinetic analysis gave an apparent corneal uptake rate constant of 0.57 min^{-1}.

DISCUSSION

Precorneal Disposition of Pilocarpine—When pilocarpine solution was topically applied to intact eyes, the drug reached a peak concentration in the cornea within 5 min and in the aqueous humor within 20 min (Figs. 1 and 2). At first glance, these results suggest a rapid penetration rate. Similar results with pilocarpine solutions led previous investigators to this conclusion (11–13). However, it is a matter for discussion whether these early peak times are truly a reflection of a large absorption rate constant for pilocarpine.

Normal drainage of an instilled dose of solution is a function of the dosing volume and occurs immediately after instillation (20). This drainage process is essentially completed within 5 min, at which time the volume of fluid present in the precorneal area quickly returns to the normal resident volume of 7.5 μl. The rapid loss of a large volume of the dose, and a large amount of the drug, causes the precorneal drug concentration to become directly susceptible to the dilution effect of incoming tears. Loss of drug through scleral and conjunctival absorption and, to a lesser extent, *via* corneal absorption also has a direct influence (21, 22).

The precorneal drug concentration establishes a representative concentration at the epithelial surface and thus serves as the driving force for drug uptake by the cornea. It can be estimated, allowing for dilution by tears, that the initial concentration of pilocarpine in the precorneal area after instillation of 25 μl of a 10^{-2} *M* solution is about 1.6 mg/ml. The amount of drug required to establish the epithelial concentration is very small and is governed by the surface area of the

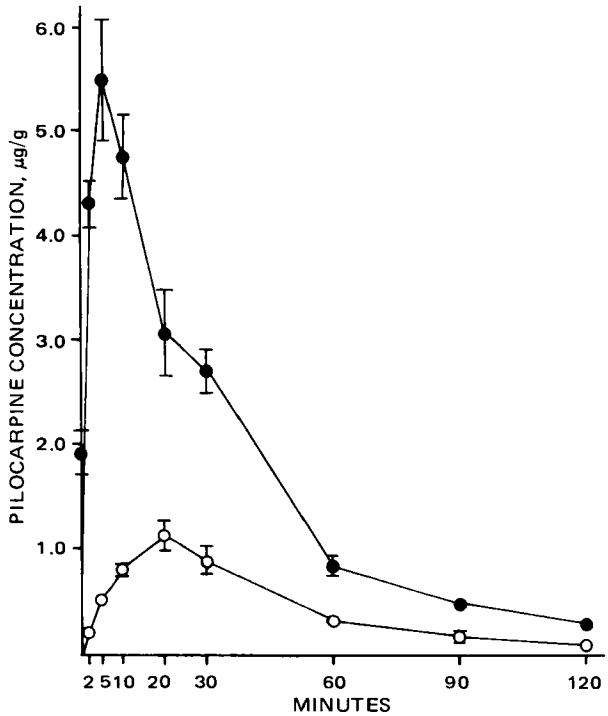

Figure 3—*Corneal drug concentration after topical dosing with pilocarpine solution. Key: ●, normal intact corneas; and ○, corneas with epithelium removed just prior to taking sample (stroma-endothelium concentration). Error bars represent the standard error of the mean. Where no error bar is indicated, the standard error of the mean is smaller than the size of the symbol used.*

epithelium. In addition, localization of drug in the outermost epithelial cells or in the bound fluid layer at short times after dosing means that a high effective concentration is achieved quickly and easily. This concentration would be much higher than the maximum bulk epithelial concentration calculated from the results of the present studies (~35 μg/g) suggests. Flux of drug into the cornea ceases as soon as the precorneal concentration falls below the epithelial surface concentration.

Studies with fluorescein (23) showed that the lacrimal fluid takes some time to equilibrate with the instilled dose; as mixing takes place, the dye concentration quickly drops to a level corresponding to only about one-fourth that of the instilled drop. The concentration in the lacrimal fluid may decrease by half as often as every 3 min. The net result is that only a small fraction of the instilled dose is absorbed and

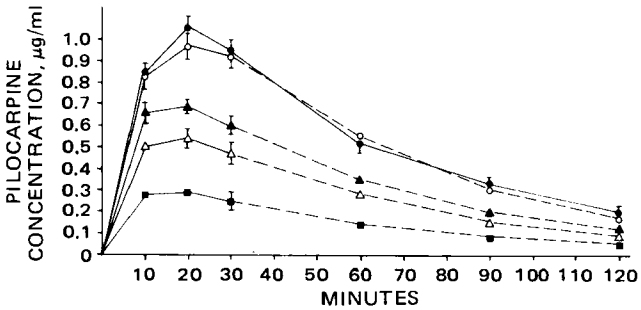

Figure 4—*Aqueous humor pilocarpine levels following rinsing with saline at various times after dosing. The horizontal axis gives the time after dosing at which drug was completely rinsed from the precorneal area. Key: ●, no rinsing; ○, 5-min rinse; ▲, 2-min rinse; △, 1-min rinse; and ■, 30-sec rinse. Solid lines connect actual data points. Dotted lines were calculated using an aqueous humor elimination rate constant of $K_e = 0.017\ min^{-1}$. Error bars represent the standard error of the mean. Where no error bar is indicated, the standard error of the mean is smaller than the size of the symbol used.*

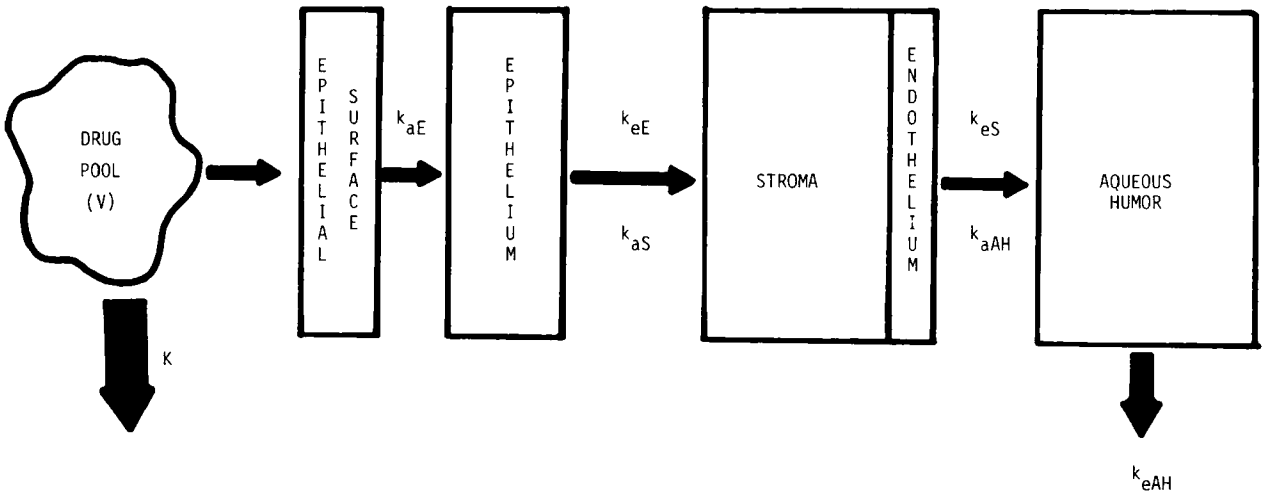

Scheme I—Representation of transcorneal pilocarpine permeation: V = *volume of drug pool after instillation of dose,* K = *composite elimination step,* k_{aE} = *apparent absorption rate constant into epithelium,* k_{eE} = *apparent elimination rate constant from epithelium,* k_{aS} = *apparent absorption rate constant into stroma-endothelium,* k_{eS} = *apparent elimination rate constant from stroma-endothelium,* k_{aAH} = *apparent absorption rate constant into aqueous humor, and* k_{eAH} = *apparent elimination rate constant from aqueous humor.*

the peak time in the cornea appears very early, regardless of the true absorption rate constant of the drug.

The early peak time and small fraction of dose absorbed also cause an overestimate of the apparent absorption rate constant as calculated by usual pharmacokinetic methods (24, 25), and the degree of overestimation increases as the bioavailability of the drug decreases. This process was reported previously for plasma drug concentration–time data (26–28) and was recently discussed as being applicable to the eye (29).

The peak time for any drug in the cornea after topical dosing should be considered to be a false peak, generated by the parallel elimination step rather than by absorption. This will generally be true except in cases involving corneal perfusion studies and sustained-release processes where the precorneal drug concentration remains constant long enough to generate the real pharmacokinetic parameters[10]. Therefore, it can be predicted that topical solutions of most drugs will have early peak times in ocular tissues and relatively large, and somewhat similar, apparent absorption rate constants. This prediction is supported by data from studies with compounds having very low water solubility, such as steroids, where the apparent pharmacokinetic parameters are strikingly similar to those of pilocarpine (18). This aspect of transcorneal drug movement must be recognized in any mechanistic interpretation or clinical evaluation of ocular data.

The data presented in Fig. 5 also suggest an extremely rapid rate of pilocarpine uptake by the cornea. Even when the dose is completely rinsed away after a contact time of only 30 sec, a measurable amount of pilocarpine still penetrates to the anterior chamber. This finding might lead one to postulate a rapid binding mechanism of the drug to the cornea, possibly to the adsorbed mucin layer at the epithelium surface. The binding of drugs to mucosal membranes has been postulated as an alternative to the pH–partition hypothesis (30, 31). However, only about 0.3–1.0% of an instilled dose of pilocarpine is absorbed into the eye (13, 17), and preliminary evidence from this laboratory indicates almost quantitative drug transfer from the cornea to the aqueous humor.

Since the amount of drug absorbed is very small relative to the total amount instilled, it is reasonable to postulate a mechanism with a small initial absorption rate operating in the presence of a large dose. Since a first-order absorption process is a function of both the absorption rate constant and the drug concentration, this mechanism adequately explains how substantial amounts of pilocarpine can penetrate into the eye at very short contact times when the amount and concentration of drug in the precorneal area are high. It also accounts for the relative insensitivity of ocular pilocarpine penetration to increases in contact time of the dosing solution. Previous work with methylcellulose (32) and polyvinyl alcohol (33) vehicles did not show improvements in pilocarpine penetration beyond a factor of two or three. In addition, blocking of the drainage apparatus (21, 22), which reduces the magnitude of the parallel elimination step rate constant, gave similar results. If the initial absorption rate constant is as large as the data indicate, considerable increases in aqueous humor levels would be expected under these conditions. However, a small rate constant would provide only small increases in corneal pilocarpine levels, considering the time factor involved, if the precorneal drug concentration is maintained for longer period. This approach appears to be consistent with observed experimental results.

The observed insensitivity of pilocarpine flux to increases in vehicle contact time can be explained on the basis of the interplay between the precorneal drug concentration and the epithelial concentration. Increasing contact time does not increase the epithelial concentration above its initial maximum value, since this value is fixed by the concentration of the applied dose. Rather, it maintains the epithelial concentration at or near this value for an extended time, causing a shift in the peak time (increase) and a corresponding maintenance of pilocarpine flux. However, since these results are essentially an extension of the normal aqueous humor concentration–time profile (Fig. 1) for a simple solution with the same concentration, dramatic increases are not achieved. Similar reasoning applies to cases where the drainage apparatus is blocked.

The observed linear dose–response relationship for pilocarpine (17) also is easily explained since increasing the concentration of the dosing solution increases, in turn, the epithelial concentration which generates a corresponding increase in pilocarpine flux. Thus, higher levels of pilocarpine in the anterior chamber are quickly and easily achieved by increasing the concentration of the applied dose, whereas only nominal benefits are gained by increasing contact time or by fluctuation of the parallel elimination rate constant.

Mechanism of Transcorneal Pilocarpine Permeation—Scheme I shows the analysis used to determine the disposition of pilocarpine in the cornea and aqueous humor after topical dosing. The tissue scraping technique used to obtain data from the three tissues, the epithelium, stroma-endothelium, and aqueous humor, has the unique advantage that all values are representative of pilocarpine movement through the intact eye. This fact enables separate pharmacokinetic treatment of each tissue and correlation of the various absorption and elimination processes. In this manner, the overall mechanism of pilocarpine flux can be readily constructed.

As previously stated, the data in Fig. 3 show the epithelium acting as a reservoir for pilocarpine in the cornea. Pharmacokinetic analysis of these data shows that elimination of pilocarpine from this tissue was biphasic. The first phase, which occurred from the 5-min peak time until about 20 or 30 min, had an apparent elimination rate constant of 0.06 min^{-1} and an apparent attendant absorption rate constant of 0.50 min^{-1}. The second phase, which carried through the remainder of the 2-hr observation period, had an apparent elimination

[10] Perfusion studies in this laboratory with propanoic, hexanoic, and 1-octanoic acids, where the cornea was bathed with drug solution, yielded corneal uptake constants in the 0.001–0.002-min^{-1} range.

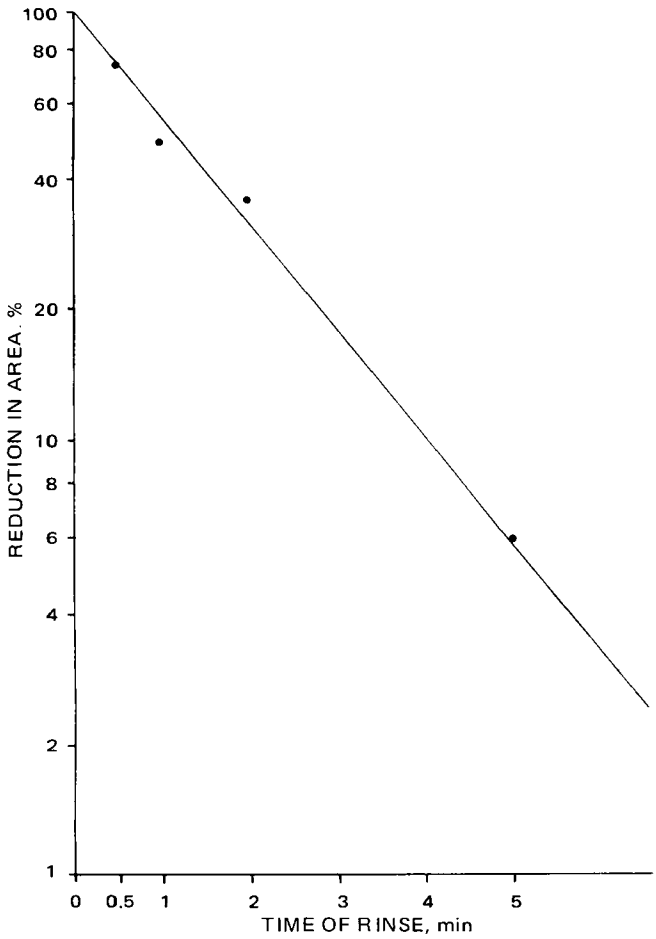

Figure 5—*Effect of rinse time on the area under the curve for pilocarpine in aqueous humor. All values were calculated by graphical methods and normalized to the nonrinsed data.*

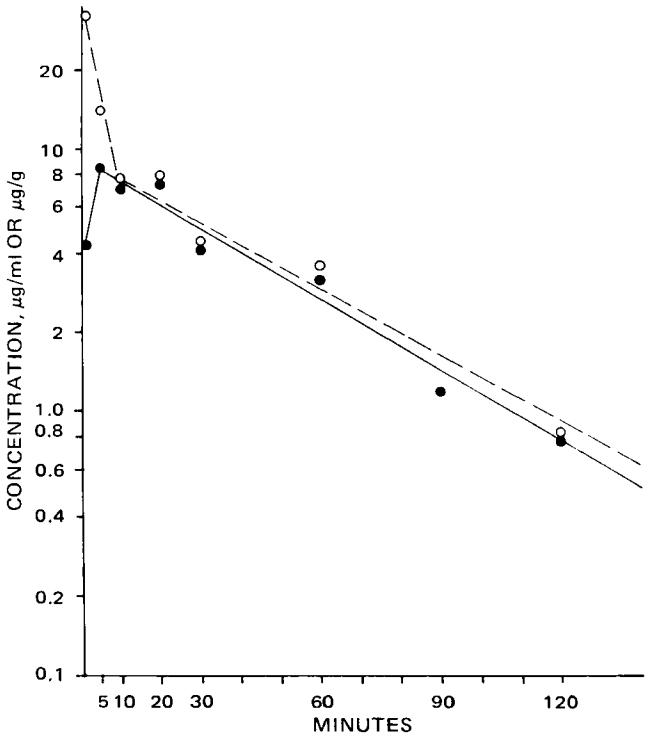

Figure 6—*Concentration of pilocarpine in ocular tissues after topical dosing of abraded eyes. Key:* ●, *aqueous humor; and* ○, *stroma-endothelium.*

rate constant of 0.016 min^{-1}. The data for the stroma-endothelium and aqueous humor were similarly treated, and their tissue concentration–time profiles consisted of a single absorption and elimination phase.

Current studies in this laboratory also showed that elimination of pilocarpine from the aqueous humor after topical dosing was multiphasic at times beyond 2 hr. This finding is in agreement with the results of other recent work (13); presumably this behavior is due to multiple equilibration of pilocarpine with the ocular tissues or possibly is a result of the pharmacological effects of pilocarpine. A summary of the apparent pharmacokinetic parameters obtained for the three tissues is presented in Table III.

The most striking feature of the results is the similarity of the stroma-endothelium and the aqueous humor. Inspection of the tissue concentration–time profiles (Figs. 1 and 3) clearly shows their near identical character. This similarity is also evidenced by the sameness of their pharmacokinetic parameters (Table III). These results indicate almost free diffusion of pilocarpine between these two tissues to the extent that they may be considered to behave as a single phase[11].

Further evidence of this behavior comes from analysis of the stroma-endothelium and aqueous humor profiles obtained for eyes when the epithelium was removed prior to dosing (Fig. 6). Again, the profiles are nearly identical at times beyond 5 or 10 min after dosing. Although early sample times at first seem to be contradictory, they are also consistent. The average wet weight of the stroma-endothelium tissue in this study was approximately 40 mg. It is well established that the corneal stroma contains about 78% water (1). If this amount is combined with an aqueous humor volume of 300 μl, the total volume of distribution of the stroma-endothelium and aqueous humor is about 330 μl. This value is in line with current data from this laboratory concerning intraocular injection of pilocarpine; the 1-min V_d was approximately 300–350 μl (34). Thus, the total initial volume of distribution was about seven to eight times greater than the volume of the stroma-endothelium alone. Since all drug that ultimately distributes in the aqueous humor must come only *via* the stroma, at some point the concentration in the stroma must exceed the aqueous humor by at least a factor of seven. This requirement is reflected well by the data in Fig. 6.

One important consequence of these results is the absence of a measurable endothelial function, at least with respect to the transcorneal mechanism of pilocarpine. It was suggested previously (12) that the endothelium is the controlling factor for movement of pilocarpine through the cornea. The current data are contrary to this premise. Although the endothelium was not separated from the stroma in these experiments, the presence of a significant barrier in the endothelium is not in any way suggested by the results. While some degree of endothelial participation cannot be discounted totally, its role is not sufficiently great to be distinguished by these techniques.

This conclusion is clearly shown by the absence of drug buildup in the stroma-endothelium combination. Also, the increased penetration of pilocarpine through the stroma and endothelium to the anterior

Table III—Pharmacokinetic Parameters for Pilocarpine Distribution in Intact Cornea and Aqueous Humor after Topical Dosing

Tissue	Peak Time, min	k_{abs}, min^{-1}	K_e[a], min^{-1}
Epithelium[b]	4	0.50	0.06, 0.02
Stroma-endothelium	20	0.09	0.021
Aqueous humor	20	0.08	0.017

[a] All pharmacokinetic parameters were calculated by the methods of Wagner and Nelson (24, 25) and are apparent quantities as discussed in the text. [b] Elimination from the epithelium is biphasic.

[11] Preliminary data from this laboratory indicate similar behavior for the iris and ciliary body. Tissue concentration–time profiles for these tissues closely parallel those for the stroma-endothelium and aqueous humor.

chamber in abraded eyes (Fig. 1) shows that there is no barrier function in the absence of the epithelium. Removal of the epithelium also eliminates the reservoir effect in the cornea, since the elimination half-life from the aqueous humor for abraded eyes was 34 min compared to 42 min for intact eyes. The longer half-life for intact eyes was due to the continuing flux of drug into the aqueous humor from the reservoir in the epithelium. This observation agrees well with the findings of other investigators (14, 16, 23) regarding the presence of a depot for pilocarpine in the cornea and is in contradiction with the conclusions of Lazare and Horlington (13).

Another feature of major significance is the consistency of the pharmacokinetic parameters (Table III) with the observed overall movement of pilocarpine through the intact cornea. The apparent absorption rate of pilocarpine into the epithelium (0.50 min^{-1}) agrees well with the apparent uptake rate obtained from the rinsing studies (0.57 min^{-1}). Also, the first-phase elimination rate constant (0.06 min^{-1}) correlates quite well with the apparent absorption rate into the stroma-endothelium (0.09 min^{-1}) and the aqueous humor (0.08 min^{-1}). In addition, the second-phase elimination rate constant equates well with the elimination rate from the stroma-endothelium (0.021 min^{-1}) and almost identically with that from the aqueous humor (0.017 min^{-1}). This overall behavior is to be expected, in fact required, if the epithelium is the controlling factor in transcorneal pilocarpine flux. The results from these experiments clearly demonstrate that the corneal epithelium is the rate-limiting tissue in the mechanism for transcorneal flux of pilocarpine.

The rate constants for the various tissues were generally obtained by graphical methods. Computer fitting of the data using a one-compartment open model also was used in several cases. However, the rate constants obtained with the two methods were comparable so that no advantage was considered to be gained from computer analysis. The rate constants so obtained are estimates only; more time points would be required to obtain precise values of the kinetic constants. The data are sufficient, however, to permit correlation of drug movement between the various tissues in the manner described.

The corneal penetration of pilocarpine can be described as a series of successive first-order absorption and elimination steps. Lateral distribution of drug does not occur in the corneal tissues, since the cornea is not vascularized. Lateral movement of drug occurs only in the precorneal area where a composite parallel first-order elimination process removes most of the instilled dose and in the anterior chamber where multiple tissue equilibrations take place. Deviations from first-order behavior are apparent only at times beyond 2 hr after dosing.

The results of these studies also suggest that the partition coefficient theory of transcorneal permeation should be reexamined in the light of true *versus* apparent pharmacokinetic parameters. Pilocarpine appears to possess optimum solubility character, being soluble in both polar and nonpolar solvents. Yet, the apparent rapid corneal penetration of this molecule, attributed to its solubility by previous investigators (13), is actually an artifact and a consequence of precorneal fluid dynamics. Further investigation of this aspect of corneal penetration of organic molecules is required before a firm relationship between solubility, partition coefficient, and corneal penetration can be established.

SUMMARY

When a topical solution of pilocarpine is instilled into eyes of albino rabbits, there appears to be a rapid uptake and distribution of drug across the cornea to the anterior chamber. This apparent rapid penetration can be attributed to a composite parallel elimination process that occurs in the precorneal area. This elimination step, in combination with a small true absorption rate constant, also accounts for the small fraction of dose absorbed into ocular tissues.

Analysis of the aqueous humor and the various cell layers of the cornea provides pharmacokinetic parameters consistent with the observed overall absorption and elimination rate constants. The corneal epithelium is the rate-limiting tissue and acts as both a barrier to penetration and as a reservoir of pilocarpine in the cornea. The stroma-endothelium and aqueous humor behave as a single aqueous phase for drug distribution, and no significant rate-determining role for the endothelium is evident from the results. The overall mechanism for transcorneal pilocarpine flux can be constructed with the apparent pharmacokinetic parameters obtained for each tissue.

REFERENCES

(1) D. M. Maurice, in "The Eye," vol. 1, 2nd ed., H. Davson, Ed., Academic, New York, N.Y., 1969, p. 489.

(2) H. Benson, *Arch. Ophthalmol.*, **91,** 313(1974).

(3) C. H. Dohlman, *Invest. Ophthalmol.*, **10,** 383(1971).

(4) K. C. Swan and N. G. White, *Am. J. Ophthalmol.*, **25,** 1043(1942).

(5) A. Kupferman, M. V. Pratt, K. Suckewer, and H. M. Leibowitz, *Arch. Ophthalmol.*, **91,** 373(1974).

(6) A. M. Tonjum, *Acta Ophthalmol.*, **52,** 650(1974).

(7) T. Iwata, M. Uyama, and K. Ohkawa, *Jpn. J. Ophthalmol.*, **19,** 139(1975).

(8) A. M. Tonjum, *Acta Ophthalmol.*, **53,** 335(1975).

(9) *Ibid.*, **53,** 348(1975).

(10) *Ibid.*, **53,** 358(1975).

(11) D. L. Krohn and J. M. Breitfeller, *Invest. Ophthalmol.*, **13,** 312(1974).

(12) M. C. Van Hoose and F. E. Leaders, *ibid.*, **13,** 377(1974).

(13) R. Lazare and M. Horlington, *Exp. Eye Res.*, **21,** 281(1975).

(14) R. F. Jones and D. M. Maurice, *ibid.*, **5,** 208(1966).

(15) D. M. Maurice, *Invest. Ophthalmol.*, **6,** 464(1967).

(16) S. Yoshida and S. Mishima, *Jpn. J. Ophthalmol.*, **19,** 121(1975).

(17) S. S. Chrai and J. R. Robinson, *Am. J. Ophthalmol.*, **77,** 735(1974).

(18) J. W. Sieg and J. R. Robinson, *J. Pharm. Sci.*, **64,** 931(1975).

(19) T. F. Patton and J. R. Robinson, *ibid.*, **64,** 267(1975).

(20) S. S. Chrai, T. F. Patton, A. Mehta, and J. R. Robinson, *ibid.*, **62,** 1112(1973).

(21) T. F. Patton and J. R. Robinson, *ibid.*, **65,** 1295(1976).

(22) T. F. Patton, Ph.D. thesis, University of Wisconsin, Madison, Wis., 1975.

(23) D. M. Maurice, *Sight-Saving Rev.*, **42,** 42(1972).

(24) J. G. Wagner and E. Nelson, *J. Pharm. Sci.*, **52,** 610(1963).

(25) *Ibid.*, **53,** 1392(1964).

(26) R. E. Notari, J. L. De Young, and R. H. Reuning, *J. Pharm. Sci.*, **61,** 135(1972).

(27) D. Perrier and M. Gibaldi, *ibid.*, **62,** 225(1973).

(28) L. Leeson and H. Weintraub, *ibid.*, **62,** 1936(1973).

(29) M. C. Makoid, J. W. Sieg, and J. R. Robinson, *ibid.*, **65,** 150(1976).

(30) L. S. Schanker, D. J. Tocco, B. B. Brodie, and C. A. M. Hogben, *J. Pharmacol. Exp. Ther.*, **123,** 81(1958).

(31) C. A. M. Hogben, D. J. Tocco, B. B. Brodie, and L. S. Schanker, *ibid.*, **125,** 275(1959).

(32) S. S. Chrai and J. R. Robinson, *J. Pharm. Sci.*, **63,** 1218(1974).

(33) T. F. Patton and J. R. Robinson, *ibid.*, **64,** 1312(1975).

(34) J. M. Conrad and J. R. Robinson, *ibid.*, in press.

ACKNOWLEDGMENTS AND ADDRESSES

Received December 29, 1975, from the *School of Pharmacy, University of Wisconsin, Madison, WI 53706*

Accepted for publication February 26, 1976.

Supported by Allergan Pharmaceuticals, Irvine, CA 92664, and Grant EY-01332 from the National Institutes of Health.

The authors thank Miss Debra Bahr for technical assistance.

[x] To whom inquiries should be directed.

Correlation of Absorption of Sulfamethazine Boluses with Dissolution Using a New Dissolution Apparatus for Veterinary Tablets

WILLIAM F. FRAZIER * and NOEL O. NUESSLE ˣ

Abstract □ A rotating-basket apparatus for dissolution testing of veterinary bolus tablets was designed and constructed. Sulfamethazine boluses containing different disintegrating agents were evaluated *in vitro* and by blood level data following administration to cattle. The dissolution t_{50} and various pharmacokinetic parameters showed directly compressible starch and carboxymethylstarch to be the most effective disintegrants in the concentrations employed while magnesium aluminum silicate and microcrystalline cellulose were about equal but less effective than the previous disintegrants. A bolus formulation containing no disintegrant gave even less satisfactory results. A correlation was established between the dissolution t_{50} and the time to peak plasma level and also between the t_{50} and the area under the plasma–time curve for the first 36 hr.

Keyphrases □ Sulfamethazine—veterinary bolus tablets, dissolution testing apparatus described, various disintegrating agents evaluated and compared to *in vivo* absorption, cattle □ Dissolution testing apparatus—designed for veterinary bolus tablets, various disintegrating agents evaluated, compared to *in vivo* absorption, cattle □ Disintegrating agents, various—in veterinary bolus tablets, evaluated using dissolution testing apparatus, compared to *in vivo* absorption, cattle □ Absorption—sulfamethazine veterinary bolus tablets, various disintegrating agents evaluated *in vitro*, compared, cattle □ Veterinary bolus tablets—dissolution testing apparatus described, various disintegrating agents evaluated and compared to *in vivo* absorption, cattle □ Tablets, veterinary bolus—dissolution testing apparatus described, various disintegrating agents evaluated and compared to *in vivo* absorption, cattle

Dissolution rate testing has become an increasingly more important part of the pharmaceutical sciences, as evidenced by the volume of research articles reviewed by Wagner (1). These tests may detect potential absorption problems which can be caused by various excipients in the dosage form. Dissolution tests also can become important quality control procedures once the final formulation is established.

Since all apparatus developed for dissolution testing have been designed to accept conventional human dosage forms, the purpose of this work was to develop a larger dissolution apparatus capable of accepting veterinary bolus tablets. The device was used to determine the dissolution of sulfamethazine from bolus tablets containing various disintegrating agents. The boluses also were administered to cattle, and plasma sulfamethazine levels were determined. Various pharmacokinetic parameters were calculated to show an *in vitro–in vivo* correlation.

EXPERIMENTAL

Materials—Sulfamethazine[1] USP, gelatin[2] USP, magnesium stearate[3] USP, reduced iron[4] NF, directly compressible starch[5], carboxymethylstarch[6], magnesium aluminum silicate[7], microcrystalline cellulose[8], and sodium hydroxide USP were used.

Table I—Sulfamethazine Bolus Formulas[a]

Ingredients	Formula A	B	C	D	E
Sulfamethazine USP	67.5	60.75	64.13	65.82	64.13
Reduced iron NF	30.0	27.0	28.5	29.25	28.5
Gelatin USP	2.3	2.07	2.18	2.24	2.18
Magnesium stearate USP	0.2	0.18	0.19	0.19	0.19
Directly compressible starch	—	10.0	—	—	—
Carboxymethyl-starch	—	—	5.0	—	—
Magnesium aluminum silicate	—	—	—	2.5	—
Microcrystalline cellulose	—	—	—	—	5.0
Total	100.0	100.0	100.0	100.0	100.0

[a] Values are in percent (w/w).

Bolus Preparation—A single lot of sulfamethazine granulation containing finely powdered iron was prepared by the wet granulation method, using gelatin solution as the binder. Magnesium stearate was mixed with the dried granulation to serve as the lubricant, and the master lot was divided into five sublots. One sublot was tableted without the addition of a disintegrant. Each disintegrating agent was mixed with one of the four remaining sublots in a tumbler blender[9] for 10 min.

A single-punch tablet press[10] equipped with a bolus-shaped punch and die set, 7.8 cm long × 2.2 cm wide, was used to compress the bolus tablets. Boluses were tableted by manually filling the die with a preweighed portion of granulation and bringing the upper punch to the top of its compression cycle, followed by a power stroke of the machine. Sulfamethazine bolus formulas are given in Table I. The concentration of disintegrant in each formulation was within the concentration range recommended by the manufacturer.

Finely powdered iron was included in all formulations to increase the density of the bolus, since this factor is reported (2) to cause the bolus to remain in the rumeno-reticular sac until disintegration is complete. Since Formulation A contained no disintegrant, it was deemed advisable to include the iron. Bolus tablets were assayed for sulfamethazine content by the Bratton–Marshall (3) method after suitable preparation. Average weight, hardness, and disintegration times also were determined.

Dissolution Basket—The rotating dissolution basket for veterinary boluses (Fig. 1) is an adaptation of the device specified in the official compendia (4, 5). The top plate is a flat Plexiglas disk, 0.6 cm thick, 15 cm in diameter, with four 0.3-cm vent holes. A 25-cm stainless steel shaft is attached at the center. The tube is a Plexiglas pipe, 12.5 cm long, 0.5 cm thick, and 12.5 cm in diameter. Two windows, 8.8 cm high and 17.2 cm long, are cut in the walls of the tube. A 1.9-cm lip remains at each end of the tube, with two 2.5-cm supports between

[1] Napp-Lemke, Lodi, N.J.
[2] Wilson Laboratories, Chicago, Ill.
[3] Mallinckrodt, St. Louis, Mo.
[4] National Pulverized Metals, Chicago, Ill.
[5] STA-Rx 1500, Colorcon, Inc., West Point, Pa.
[6] Primojel, Edward Mendell Co., Yonkers, N.Y.
[7] Veegum WG, Vanderbilt, Inc., New York, N.Y.
[8] Avicel PH-102, FMC Corp., Marcus Hook, Pa.
[9] Twin Shell blender, Patterson Kelly Co., East Stroudsburg, Pa.
[10] Stokes model R, F. J. Stokes Machine Co., Philadelphia, Pa.

Table II—Bolus Properties

	Formula				
	A	B	C	D	E
Sulfamethazine, % (w/w)[a]	66.1	59.8	62.4	64.0	63.2
Weight, g[b]	26.55 (0.047)	29.53 (0.025)	27.95 (0.023)	27.31 (0.028)	27.91 (0.038)
Hardness, kg/cm²[c]	22.6 (0.17)	22.1 (0.62)	20.0 (0.82)	24.1 (0.24)	24.3 (0.37)
Disintegration time[d], min	>90[e]	1.96 (0.08)	1.44 (0.06)	>90[e]	>90[e]

[a] Average of three determinations. [b] USP XVIII, average of 20 tablets ± *SD*. [c] Carver laboratory press, model C, average of five tablets ± *SD*. [d] USP XVIII, average of six tablets ± *SD*. [e] Test stopped at 90 min.

the windows. The bottom plate is a flat Plexiglas disk, 0.6 cm thick, 15 cm in diameter, with a 8.8-cm hole located at the center.

The tube and bottom plate are lined with 40-mesh woven stainless steel cloth. The top and bottom plates are held in place on either end of the tube by four bolts, which pass on the outside of the tube through matching holes in each plate.

***In Vitro* Dissolution Tests**—A 20-liter tank[11] with a tight fitting lid containing a hole for the shaft and sample removal was used. The tank was filled with 18.0 kg of dissolution medium, which was allowed to equilibrate with the room temperature (controlled at 25 ± 1°). When the dissolution medium reached the desired temperature, the weight was rechecked and an addition was made if necessary. Then the bolus tablet to be tested was placed in the basket, and the top plate was attached. The cover was put in place, over the shaft, which was then attached to the constant-speed stirring motor[12].

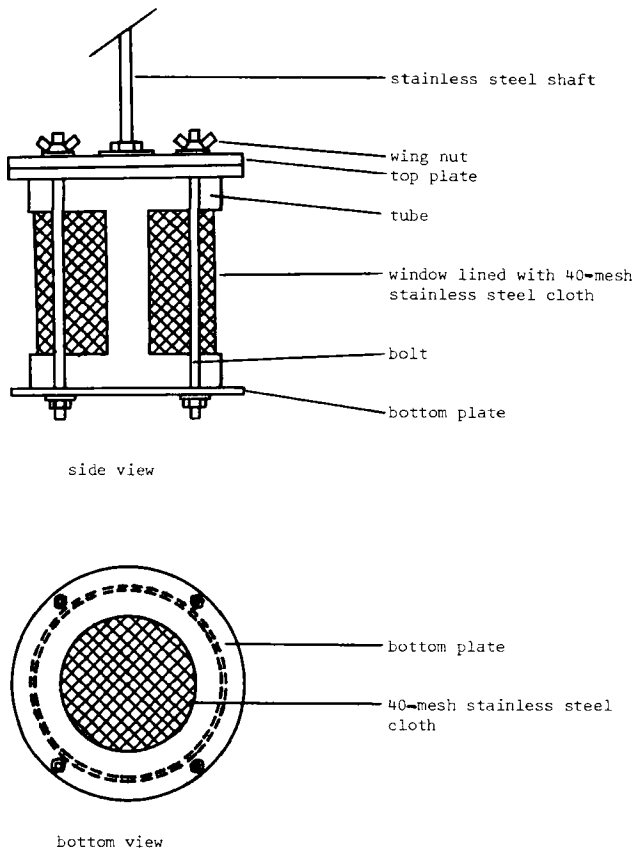

Figure 1—*Veterinary bolus rotating basket.*

[11] United States Plastic Corp., Lima, Ohio.

Table III—Dissolution (Percent) of Sulfamethazine from Bolus Tablets[a]

	Formula				
Minutes	A	B	C	D	E
0	0.0	0.0	0.0	0.0	0.0
5	2.86 (1.28)	58.80 (3.6)	71.25 (7.85)	2.40 (0.51)	2.12 (0.85)
10	4.93 (1.23)	69.75 (1.6)	80.92 (4.72)	5.20 (0.53)	3.86 (0.99)
15	6.22 (0.80)	74.55 (2.06)	84.82 (3.74)	6.79 (0.74)	6.19 (0.94)
30	9.03 (0.94)	80.50 (2.40)	93.07 (4.08)	10.23 (0.87)	8.21 (0.89)
60	12.51 (1.74)	86.15 (2.76)	97.90 (2.80)	16.19 (1.17)	13.47 (2.16)
120	17.83 (1.39)	92.91 (2.83)	99.84 (1.48)	23.12 (1.13)	21.19 (0.73)
180	21.62 (0.84)	95.17 (2.42)	100.18 (0.96)	27.96 (1.14)	27.60 (1.29)
240	25.06 (1.91)	96.66 (1.68)	101.39 (1.06)	32.18 (0.48)	32.76 (0.65)
300	28.61 (1.65)	96.83 (0.67)	101.72 (2.03)	36.16 (1.10)	37.11 (1.04)
360	32.08 (1.56)	97.16 (1.24)	101.98 (1.64)	39.37 (0.70)	39.93 (1.86)

[a] Average of five determinations ± *RSD*.

The basket was lowered into the dissolution medium, a height adjustment was made so that the clearance between the bottom of the tank and the bottom of the basket was 2.5 cm, and rotation was started. Samples were obtained by pipet, followed by replacement of an equal volume of dissolution medium. Sulfamethazine concentration was determined spectrophotometrically at 257 nm. Sodium hydroxide solution, 0.1 *N*, was selected as the dissolution medium to assure sink conditions if complete drug release occurred, and the rotational speed was arbitrarily set at 50 rpm. Five boluses of each formula were tested in the described apparatus.

***In Vivo* Absorption Tests**—Three healthy Black Angus cattle (two heifers and one steer) were kept in an indoor stock pen, 8 × 12 m, allowing for moderate exercise; the building temperature was maintained at approximately 16°. The animals were allowed free access to food[13] and water, except during a 4-hr period on the morning of each dosage administration. All three animals received the same formulation at the same time. Two days after drug could not be detected in their plasma, they were given the next formulation. In this manner, all animals received all five formulations in the order B, C, D, E, and A. The time between the peak blood level and the administration of the next formulation was always in excess of 10 half-lives (elimination), assuring essentially complete "washout" of the drug. It was assumed that no "period" effects occurred.

The dose of sulfamethazine was 21 mg/kg; when necessary, a portion of bolus was cut off to maintain a uniform dose. This procedure avoided different dosages for each animal and kept constant the weight of drug per unit weight of tablet. While there was some increase in surface area of tablet per unit weight of drug, it was minimal since each animal received a minimum of two complete boluses and part of a third bolus and a maximum of three complete boluses and part of a fourth bolus.

Boluses were administered with the aid of a balling gun[14]. Blood samples were taken from the jugular vein with heparinized vacuum tubes[15]. Plasma sulfamethazine was determined by the Bratton–Marshall (3) method after preparation of the samples by hemolysis, deproteinization, and filtration.

RESULTS AND DISCUSSION

The results of the assay for sulfamethazine content of tablets of the different formulations are given in Table II. Also presented are the average weight, hardness, and disintegration times. *In vitro* dissolu-

[12] Hi-Torque stirrer, VWR Scientific, Kansas City, Kans.
[13] Purina Preconditioning Chow V, Ralston-Purina, St. Louis, Mo.
[14] Jensen-Salsbery Laboratories, Kansas City, Mo.
[15] Becton-Dickinson, Rutherford, N.J.

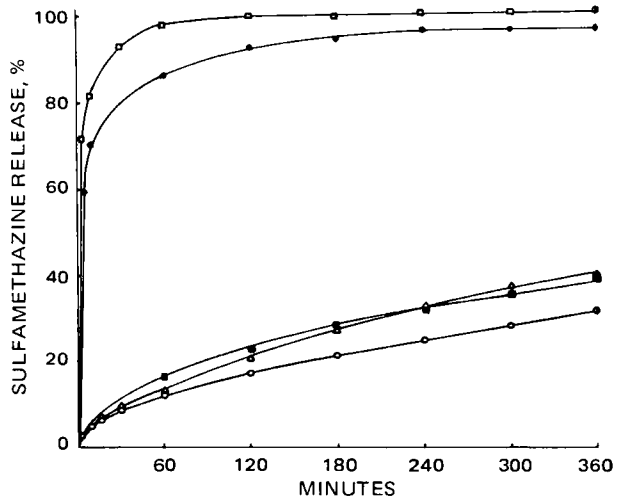

Figure 2—*Dissolution profiles of sulfamethazine from bolus formulations. Key: ○, Formula A; ●, Formula B; □, Formula C; ■, Formula D; and △, Formula E.*

tion tests of five experimental sulfamethazine bolus formulations were conducted in the specially designed rotating-basket apparatus. Concentrations of sulfamethazine in solution are given in Table III, and dissolution profiles are shown in Fig. 2.

Boluses containing directly compressible starch and carboxymethylstarch literally fell apart in the apparatus while those of the other formulas were intact at completion of the test. The time required for 50% of the sulfamethazine to go into solution (t_{50}) was estimated by two different methods. The log of percent drug undissolved plotted against time (6) for the slow dissolving formulations, A, D, and E, was linear, especially for data at 2–6 hr. Calculation of linear regression

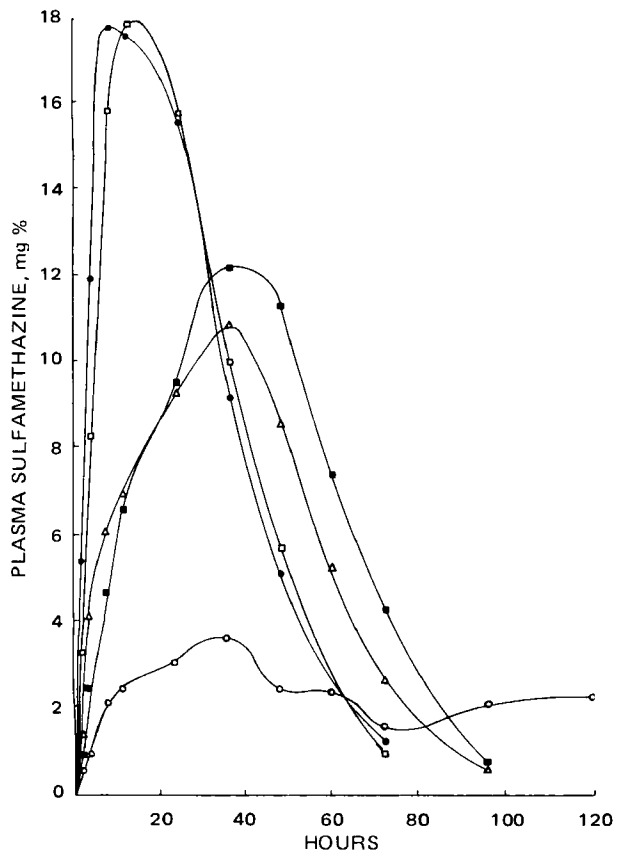

Figure 3—*Plasma levels of sulfamethazine from bolus formulations. Key: ○, Formula A; ●, Formula B; □, Formula C; ■, Formula D; and △, Formula E.*

Table IV—Plasma Sulfamethazine Levels (Milligrams Percent) following Administration of Sulfamethazine Boluses[a]

Hours Post-administration	Formula				
	A	B	C	D	E
0	0.0	0.0	0.0	0.0	0.0
2	0.51 (0.12)	5.46 (0.77)	3.32 (1.55)	0.86 (0.18)	1.46 (0.22)
4	0.87 (0.29)	12.02 (2.35)	8.35 (0.73)	2.46 (1.00)	4.14 (0.86)
8	2.12 (0.51)	17.79 (2.29)	15.91 (0.53)	4.67 (1.47)	6.09 (0.90)
12	2.43 (0.30)	17.57 (0.74)	17.90 (0.59)	6.61 (1.73)	6.97 (1.13)
24	2.97 (0.07)	15.57 (0.89)	15.84 (0.74)	9.46 (1.72)	9.29 (0.39)
36	3.58 (0.21)	9.24 (1.53)	10.10 (0.37)	12.19 (0.44)	10.90 (0.93)
48	2.43 (0.06)	5.19 (1.82)	5.83 (0.48)	11.27 (0.72)	8.57 (1.55)
60	2.35 (0.04)	—	—	7.39 (0.39)	5.32 (1.25)
72	1.57 (0.41)	1.25 (0.92)	1.04 (0.16)	4.31 (0.92)	2.74 (0.72)
96	2.07 (0.42)	—	—	0.78 (0.11)	0.56 (0.20)
120	2.26 (0.79)	—	—	—	—
144	1.44 (0.98)	—	0.0	—	—
168	0.75 (0.90)	0.0	—	0.0	—
192	0.31 (0.44)	—	—	—	0.0
240	0.22 (0.32)	—	—	—	—
288	0.0	—	—	—	—

[a] Average of three cattle ± *SD*.

for the 2–6-hr data for individual tablets was used to predict the t_{50}. The intercepts of linear regressions were consistently close to the theoretical value of 2.0. The fast dissolving formulations, B and C, dissolved so rapidly that the data did not fit either the log percent undissolved–time plot or the probit percent dissolved–log time plot (6). The t_{50} values for individual tablets were thus estimated by proportion from the amount dissolved at 5 min. The mean t_{50} and standard deviations of the five tablet values for each formulation are given in Table V.

Mean plasma sulfamethazine levels determined in the *in vivo* absorption studies are given in Table IV, and plasma sulfamethazine curves are shown in Fig. 3. Various pharmacokinetic parameters determined from these data are given in Table V along with t_{50} dissolution values. The times to reach peak concentrations were estimated from the plasma curves, and absorption half-lives were calculated by the method of residuals (7). Elimination half-lives were calculated from log plasma concentration–time plots. Areas under the plasma

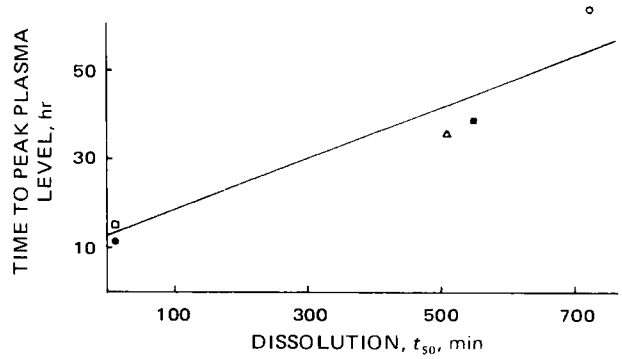

Figure 4—*Correlation of dissolution with peak plasma levels. Key: ○, Formula A; ●, Formula B; □, Formula C; ■, Formula D; and △, Formula E.*

Table V—Pharmacokinetic Parameters

Parameter	Formula A	B	C	D	E
Area under plasma–time curve, mg% × hr	377[a]	680	679	658	571
	(124)[b]	(69.4)	(2.57)	(25.5)	(49.0)
Area under plasma–time curve, 0–36 hr, mg% × hr	88.7	501	490	268	272
	(9.22)	(21.1)	(7.91)	(53.4)	(24.1)
Estimated time to peak plasma concentration, hr	64.0	11.7	15.3	38.7	36.0
	(48.5)	(4.73)	(1.15)	(2.31)	(0.0)
Absorption half-life, hr	19.3	6.6	6.3	9.1	10.7
	(14.6)	(1.07)	(0.52)	(1.71)	(1.76)
Elimination half-life, hr	23.2	10.9	8.6	10.0	12.6
	(20.7)	(3.07)	(1.08)	(1.99)	(1.25)
Estimated t_{50} dissolution, min	722	4.26	3.54	545	509
	(85.7)	(0.285)	(0.425)	(12.2)	(44.4)

[a]Mean of three values. [b]Standard deviation.

curves were calculated for individual animals by the trapezoidal rule and include the area to 288 hr for Formulation A. These areas were subjected to an analysis of variance for single-factor experiments having repeated measures on the same elements, and this analysis showed statistically significant differences among the five formulations at $p = 0.01$. Application of the Tukey t test showed Formulation A to be different from the other four at less than the 0.05 level of confidence; at less than the 0.01 level of confidence, the results showed no significant difference between A and E or between E, D, C, and B.

Two characteristics of the plasma level curve that should be noted are the low concentrations and prolonged time for complete elimination of the drug from Formulation A. An early investigation set a minimum therapeutic blood level at 5 mg% (8). While it is recognized that the minimum therapeutic concentration cannot be set in such broad terms but depends on several factors, one can question whether Formulation A released the drug at a rate to produce an effective antibacterial level. The prolonged blood levels caused by this formulation would result in a longer time between the cessation of treatment and the marketing of the animal for human consumption since tissues of such animals must be free of drug prior to harvesting.

Absorption half-lives were used to evaluate the disintegrating agents. A statistical comparison of absorption half-lives at less than the 0.05 level of confidence revealed that there was no significant difference between half-lives for boluses containing directly compressible starch and carboxymethylstarch but that these values were significantly lower than for the other boluses. There was no significant difference between boluses containing magnesium aluminum silicate and microcrystalline cellulose; the bolus containing no disintegrating agent produced the slowest absorption. Carboxymethylstarch was the most effective disintegrating agent tested since it produced results comparable with directly compressible starch and was used at a lower concentration.

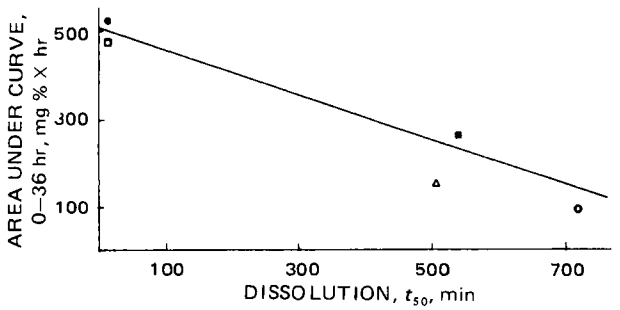

Figure 5—*Correlation of dissolution with area under the plasma level–time curve, 0–36 hr. Key:* ○, *Formula A;* ●, *Formula B;* □, *Formula C;* ■, *Formula D; and* △, *Formula E.*

Comparison of the mean dissolution t_{50} values with the mean pharmacokinetic parameters indicated correlations with the time to peak plasma levels and with the area under the plasma–time curve for the first 36 hr. These correlations are shown in Figs. 4 and 5. Calculations showed Pearson's r to be 0.953 for the t_{50}–time to peak plasma concentration correlation, which was significant at less than the 0.02 level of confidence; $r = -0.980$ for the t_{50}–area under the plasma curve, 0–36 hr, which was significant at less than the 0.01 level of confidence.

In conclusion, the rotating basket gave consistent results and could serve as a useful tool in the development and quality control of veterinary bolus tablets.

REFERENCES

(1) J. G. Wagner, "Biopharmaceutics and Relevant Pharmacokinetics," 1st ed., Drug Intelligence Publications, Hamilton, Ill., 1971, pp. 133–139.

(2) A. B. Rednick and S. J. Tucker, U.S. pat. 3,507,952 (1970).

(3) A. C. Bratton and E. K. Marshall, Jr., *J. Biol. Chem.*, **128**, 537(1939).

(4) "The National Formulary," 13th ed., Mack Publishing Co., Easton, Pa., 1970, p. 802.

(5) "The United State Pharmacopeia," 18th rev., Mack Publishing Co., Easton, Pa., 1970, p. 934.

(6) J. G. Wagner, "Biopharmaceutics and Relevant Pharmacokinetics," 1st ed., Drug Intelligence Publications, Hamilton, Ill., 1971, pp. 115–120.

(7) A. A. Frost and R. G. Pearson, "Kinetics and Mechanism," Wiley, New York, N.Y., 1961, p. 162.

(8) G. H. Schneller, N. E. Foss, and C. F. Sullivan, "Sulfonamides in Veterinary Medicine," Calco Tech. Bull. 723, American Cyanamid Co., Bound Brook, N.J., 1948, p. 47.

ACKNOWLEDGMENTS AND ADDRESSES

Received October 7, 1974, from the *School of Pharmacy, University of Missouri-Kansas City, Kansas City, MO 64110,* and *Jensen-Salsbery Laboratories, Kansas City, MO 64108*

Accepted for publication February 25, 1976.

Abstracted in part from a thesis submitted by W. F. Frazier to the School of Graduate Studies, University of Missouri-Kansas City, in partial fulfillment of the Master of Science degree requirements.

The authors thank Mr. C. H. Moffet, Dr. I. M. Paton, and Dr. J. D. Todd of Jensen-Salsbery Laboratories for their support and encouragement, and Dr. R. C. Lanman, Dr. W. D. Mason, and Dr. H. J. Malinowski for their valuable suggestions.

* Present address: Marion Laboratories, Kansas City, MO 64137

ˣ To whom inquiries should be directed.

GLC Determination of *l*-2-Hydroxy-*N*-cyclopropylmethylmorphinan in Plasma and Urine

ROBERT E. WEINFELD, ALICE HOLAZO, and STANLEY A. KAPLAN ˣ

Abstract □ A specific method was developed for the determination of *l*-2-hydroxy-*N*-cyclopropylmethylmorphinan in plasma and urine by GLC, using flame-ionization detection. The method involves the extraction of the compound into ether from plasma or urine at pH 7.4, followed by back-extraction into 1 *N* HCl. The acid phase is ether washed and made alkaline, and the compound is reextracted into ether. The ether is evaporated to dryness, the residue is dissolved in methanol, and an aliquot is analyzed by GLC. The same method is applicable to plasma and urine samples following deconjugation of the compound with glucuronidase–sulfatase. The overall recovery is 93.1 ± 9.4% (*SD*) in the concentration range of 0.020–2.0 μg/ml. The method was successfully applied to plasma and urine specimens obtained after administering single 25-mg oral doses to humans.

Keyphrases □ *l*-2-Hydroxy-*N*-cyclopropylmethylmorphinan—GLC analysis, human plasma and urine □ GLC—analysis, *l*-2-hydroxy-*N*-cyclopropylmethylmorphinan in human plasma and urine □ Morphinan, substituted—*l*-2-hydroxy-*N*-cyclopropylmethylmorphinan, GLC analysis in human plasma and urine

Studies on the metabolism of the substituted morphinan, *l*-2-hydroxy-*N*-cyclopropylmethylmorphinan (I), in the dog using ^{14}C-labeled compound indicated that, following 50 mg/kg po, the major urinary metabolite identified was a glucuronide conjugate of I. This compound accounted for approximately 35% of the administered dose[1]. Only about 2% of the dose was recovered as unchanged I. Two other isolated urinary metabolites were identified by GLC–mass spectrometry (1) as the *N*-desalkyl (II) and 7-hydroxy (III) analogs, accounting for 0.5 and 4.3% of the dose, respectively. Most carbon-14 in the dog plasma was present as a conjugate of I, which can be enzymatically released by incubation with glucuronidase.

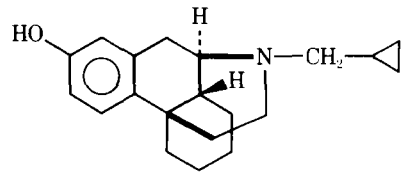

I

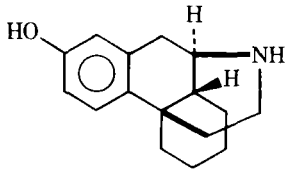

II

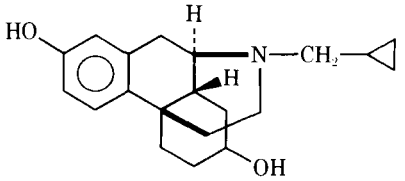

III

The use of flame-ionization detection in the GLC analysis of morphines and morphinans in biological fluids is well documented (2, 3). This report describes a sensitive and specific flame-ionization GLC assay procedure for the determination of I and its glucuronide or sulfate conjugate(s) in human plasma and urine.

EXPERIMENTAL

Reagents—All reagents were analytical reagent grade except where noted. All inorganic reagents were prepared using double-distilled water. These reagents included Dulbecco's sodium phosphate-buffered saline[2], pH 7.4, diluted 1:10 for a working solution; 1 *M* acetate buffer, pH 5, prepared by combining 37 parts of 1 *M* sodium acetate and 13 parts of 1 *M* acetic acid; 1 *N* HCl; and 1 *N* NaOH. Anhydrous ether[3], absolute methanol[4], and glucuronidase–sulfatase diagnostic reagent[5] also were used.

Parameters for GLC Analysis—A gas chromatograph[6] equipped with a flame-ionization detector was used. The column was U-shaped, 1.2 m (4 ft) × 4 mm i.d., borosilicate glass, containing a pretested preparation of 3% OV-17 on 60–80-mesh Gas Chrom Q[7]. The temperature settings were: oven, 230°; injection port, 275°; and detector, 300°. The gas flow rates were: carrier (helium)[8], 50 ml/min; hydrogen[8], 100 ml/min; and air, 400 ml/min. The electrometer sensitivity was 1 × 16 (corresponding to 6.4×10^{-11} amp for full-scale deflection on a 1.0-mv recorder[9]). Under these conditions, the retention time, R_t, of I was 7.5–8.0 min, with 400 ng (0.4 μg) injected giving nearly full-scale response.

Preparation of Standard Solutions of I—Weigh 5.60 mg of the hydrochloride salt of I, equivalent to 5.00 mg of the free base, into a 5-ml volumetric flask and dissolve it in absolute methanol to yield a stock solution equivalent to 1 mg of I/ml. Prepare working standard solutions to contain 0.05, 0.1, 0.2, 0.3, and 0.4 μg/10 μl in methanol.

Aliquots of these working standard solutions are used to establish a GLC calibration curve and for addition to plasma and urine as internal standards for the determination of percent recovery.

Experimental Procedure for "Free" I in Plasma and Urine—*Plasma*—Pipet 2.0 ml of plasma and 2.0 ml of phosphate-buffered saline working solution into a 15-ml centrifuge tube. Mix well and extract twice with 5-ml portions of ether, seal the tube with a tetrafluoroethylene[10] stopper, and shake for 10 min on a reciprocating shaker[11]. Centrifuge for 10 min at 2000 rpm in a refrigerated centrifuge[12] at 10°. Transfer the ether layer after each centrifuge step and

[1] J. J. Kamm, A. Szuna, J. Carbone, J. Cheripko, and C. Coutinho, unpublished data.

[2] Catalog No. 0848, Grand Island Biological Co., Grand Island, N.Y.
[3] Catalog No. A-412, Mallinckrodt Chemical Works, St. Louis, Mo.
[4] Fisher Scientific Co., Fairlawn, N.J.
[5] Glusulase (197,173 units of glucuronidase/ml plus 102,425 units of sulfatase/ml), Endo Laboratories, Garden City, N.Y.
[6] Model 402, Hewlett-Packard Co., Avondale, Pa.
[7] Applied Science Laboratories, State College, Pa.
[8] Matheson.
[9] Model 7127A, Hewlett-Packard, Avondale, Pa.
[10] Chemware, Chemplast, Inc., Wayne, N.J.
[11] Model 6000, Eberbach Corp., Ann Arbor, Mich.
[12] Model PR-J, IEC, Needham Heights, Mass.

Table I—Plasma Levels of Free and Total I following 25-mg Single Oral Dose in Human (Subject 1)

Specimen Time, hr	Micrograms per Milliliter of Plasma		
	Total I[a]	Free I	Conjugated I (by Difference)
0	—	—	—
0.5	0.146	0.028	0.118
1	0.219	0.048	0.171
2	0.183	0.061	0.122
4	0.177	0.068	0.109
6	0.091	0.047	0.044
8	0.061	0.023	0.038
12	n.d.[b]	0.023	—
24	n.d.	(0.009)[c]	—

[a] Analyzed by GLC method following glucuronidase–sulfatase treatment. [b] n.d. = not detectable. [c] Estimated value; trace level by GLC.

combine in a 15-ml centrifuge tube. Add 2 ml of 1.0 *N* HCl to the combined ether extracts, shake for 10 min, and centrifuge for 5 min.

Aspirate the ether phase, taking care not to remove any of the acid phase. Wash the acid extract twice with 10 ml of ether by shaking for 10 min and centrifuging for 5 min. Aspirate and discard the ether layer after each washing. Add sufficient 1.0 *N* NaOH to the acid layer to adjust the pH to 8–9 (about 2 ml). Mix well and extract the pH-adjusted solution twice with 5 ml of ether, shaking for 10 min and centrifuging for 5 min. Combine the ether extracts in a clean 15-ml centrifuge tube and evaporate to dryness in a 40° water bath under a gentle stream of nitrogen. Vacuum desiccate the residue for 15 min (over sodium hydroxide pellets) to remove all traces of moisture. Reconstitute the residue in 100 μl of methanol by vigorous mixing on a mechanical mixer[13]. Inject 10 μl into the gas chromatograph.

Along with the unknown specimens, process internal standards of I corresponding to 0.5, 1.0, 2.0, and 4.0 μg. Prepare these standards by evaporating aliquots of the working standard solutions in 15-ml centrifuge tubes under a nitrogen stream in a 40° water bath. Add to each tube 2 ml of control human plasma taken from each subject prior to drug administration.

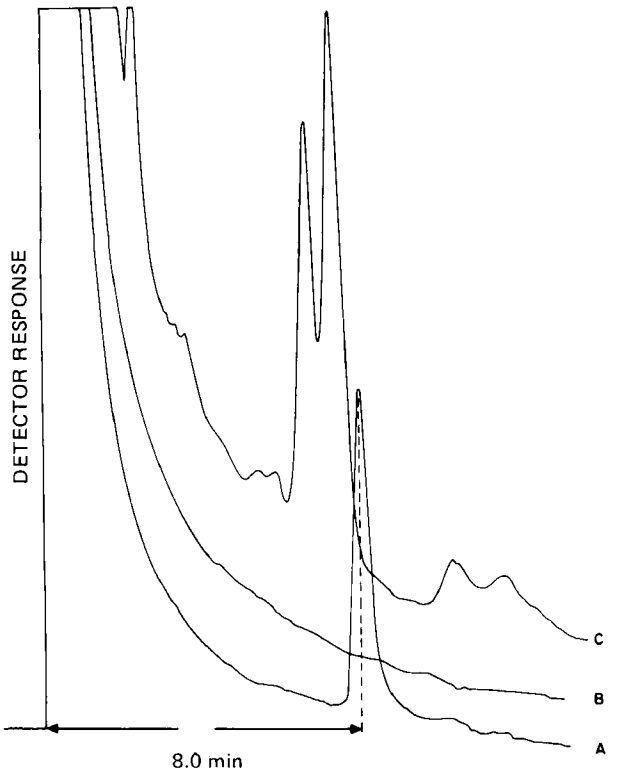

Figure 1—*Chromatograms of: A, authentic standard of I, 200 ng injected; B, control urine following enzymatic hydrolysis and acid cleanup procedure; and C, control urine following enzymatic hydrolysis and no cleanup (10 μl of 100-μl sample injected).*

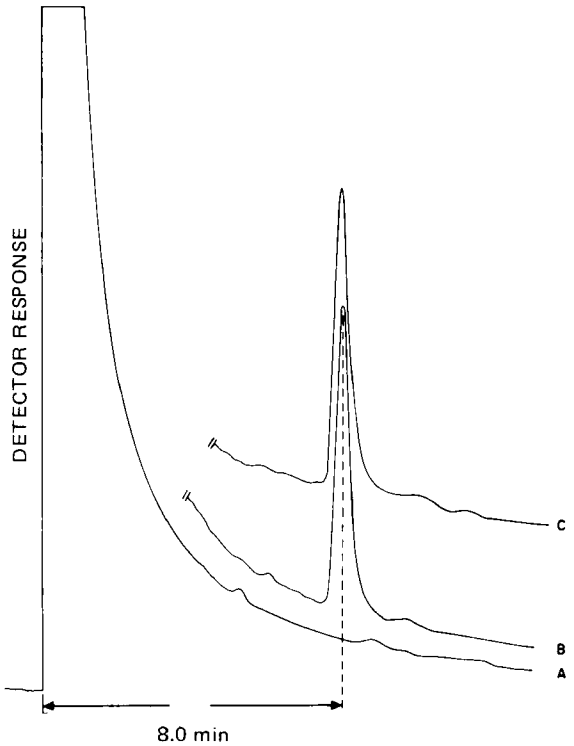

Figure 2—*Chromatograms of: A, control plasma extract; B, internal standard of 2.0 μg of I recovered from control plasma; and C, authentic standard of 200 ng of I injected (10 μl of 100-μl sample injected).*

Urine—Pipet 5 ml of urine into a 50-ml centrifuge tube and adjust to pH 7.4 with 1 *N* NaOH, using a pH meter. Add 5 ml of phosphate-buffered saline working solution, mix well, add 15 ml of ether, and seal the tube with a tetrafluoroethylene stopper. Shake for 10 min and then centrifuge for 5 min at 2000 rpm in a refrigerated centrifuge at 10°. Transfer the ether layer to a fresh 50-ml centrifuge tube and reextract urine with an additional 15 ml of ether. Combine the ether extracts and add 2.0 ml of 1 *N* HCl. Follow the procedure as described for plasma, but wash the acid layer three times with 10 ml of ether. Include a series of internal standards, prepared in the same concentration range as described in the plasma procedure.

Experimental Procedure for "Total" I in Plasma and Urine (I plus Conjugated I)—*Plasma*—Pipet 2.0 ml of plasma into a 25-ml conical centrifuge tube and adjust the pH to 5.0 with 1 *M* acetic acid. Add 0.2 ml of 1 *M* acetate buffer (pH 5), mix, and then add glucuronidase–sulfatase reagent (use 1% of the total aqueous volume after buffer addition). Mix well, stopper loosely with cotton, and incubate overnight (at least 16 hr) at 37° with gentle shaking in a metabolic shaking incubator[14]. Following incubation, adjust the hydrolysate to pH 7.4 with 1 *N* NaOH, add 2 ml of phosphate-buffered saline working solution, mix, and extract twice with 5-ml portions of ether. Then follow the procedure described for I in plasma.

Along with the unknown specimens, process internal standards of I. Prepare these standards by evaporating aliquots of the working standard solutions, corresponding to 0.5, 1.0, 2.0, and 4.0 μg of I, in 25-ml centrifuge tubes under a nitrogen stream in a 40° water bath. Add 2 ml of enzymatically hydrolyzed control (drug-free) plasma to each tube.

Urine—Transfer 1.0 ml of urine into a 25-ml conical centrifuge tube and adjust the pH to 5.0 with 1 *M* acetic acid. Add 0.1 ml of 1 *M* acetate buffer (pH 5), mix, and add glucuronidase–sulfatase reagent (use

[13] Super Mixer, Lab-Line, Melrose Park, Ill.

[14] Precision-Dubnoff, Precision Scientific Co.

Table II—Urinary Concentrations of Free and Total I in Two Subjects following a Single Oral Dose of 25 mg

Subject	Time Period, hr	Percent of Dose, Free	Total I, μg/ml	Total I, mg/hr	Percent of Dose, Total
2	Predrug	—	—	—	—
	0–2		6.5	0.55	4.4
	2–4		25.1	0.29	2.3
	4–6	3.4	23.8	1.01	8.1
	6–8		19.8	0.49	3.9
	8–12		11.0	0.36	5.8
	12–24		1.7	0.18	8.6
	24–48	1.7	3.5	0.11	10.6
(Cumulative)	0–48	5.1	—	—	43.7
3	Predrug	—	—	—	—
	0–2	—	2.1	0.60	4.8
	2–4	—	2.0	0.73	5.8
	4–6	—	9.1	1.04	8.3
	6–8	—	13.3	0.67	5.4
	8–12	—	15.4	0.50	8.0
	12–24	—	3.2	0.24	11.5
	24–48	—	0.9	0.05	4.8
(Cumulative)	0–48	—	—	—	48.6

1% of the total aqueous volume after buffer addition). Mix well, stopper loosely with cotton, and incubate overnight (at least 16 hr) at 37° with gentle shaking in a metabolic shaking incubator. Following incubation, adjust the hydrolysate to pH 7.4 with 1.0 *N* NaOH, add 1 ml of phosphate-buffered saline working solution, mix, and extract twice with 5-ml portions of ether. Then follow the procedure described for free I in urine.

Along with the unknown specimens, process internal standards of I as described in the procedure for total I in plasma; use 1 ml of enzymatically hydrolyzed control urine for each concentration of internal standard used.

Quantitation of I by Flame-Ionization GLC Analysis—The peak height of I in each sample chromatographed is determined by drawing a tangent to the baseline under the peak and measuring the height in centimeters. Peaks that are off scale must be rechromatographed or the electrometer sensitivity must be attenuated to bring the peak on scale for measurement.

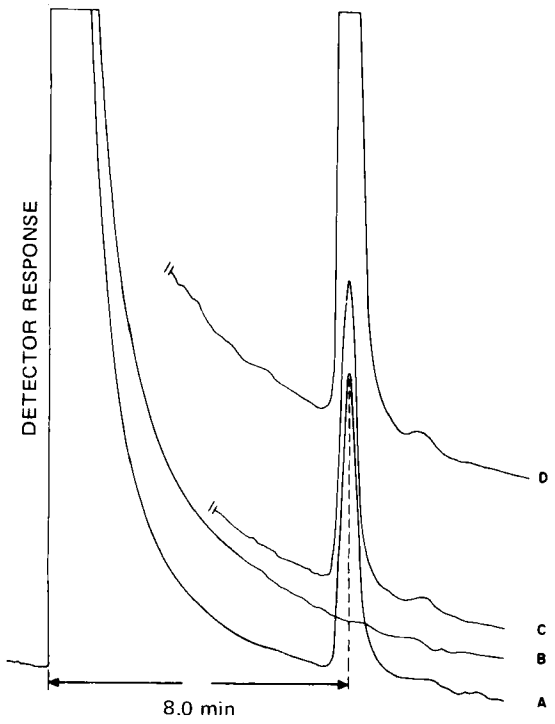

Figure 3—*Chromatograms of: A, authentic standard of 200 ng of I injected; B, control urine extract; C, internal standard of 2.0 μg of I recovered from control urine; and D, patient urine extract following enzymatic deconjugation after 25-mg oral dose of I (10 μl of 100-μl sample injected).*

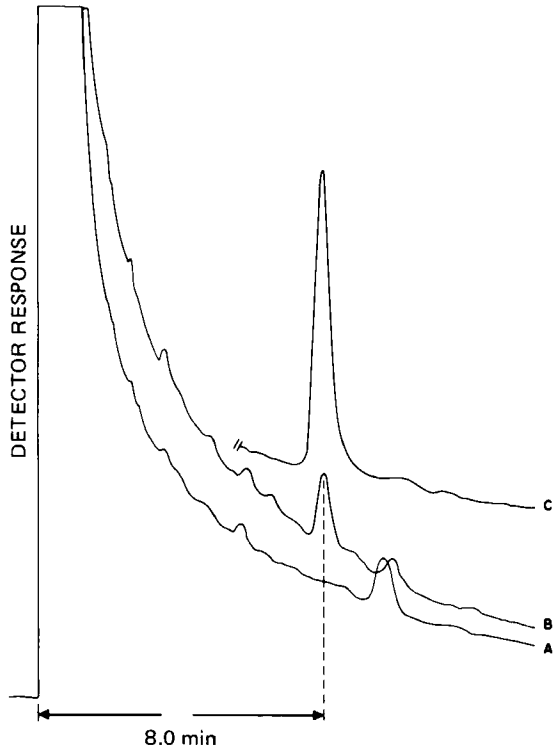

Figure 4—*Chromatograms of: A, control plasma extract injecting 10 of 25 μl; B, patient plasma extract following 25-mg oral dose of I, injecting 10 of 25 μl; and C, authentic standard of 200 ng of I injected.*

A calibration curve of the detector response to I is prepared by plotting peak height *versus* concentration of I injected. The calibration curve of external standards is used to determine the linear response of the detector, the stability of the GLC system, and the percent recovery of added internal standards. The internal standards are used to prepare a calibration curve and for the quantitation of the concentration of I in plasma or urine. Such calibration curves (external and internal) are run with each set of unknowns analyzed. Unknowns are read directly (by interpolation) from the calibration curve to determine the concentration per aliquot injected based on the external standard calibration curve or are read directly from the internal standard calibration curve. The limit of sensitivity is 0.050 μg/ml of biological fluid (using 2 ml for analysis) when injecting 10 μl of the 100 μl of methanol from the reconstituted sample residues for GLC measurement.

If low plasma levels are anticipated, it may be necessary to reconstitute the residue in 25 μl of methanol and inject 10 μl for analysis. The limit of sensitivity is approximately 0.020 μg/ml of biological fluid under these conditions.

The amount of conjugated I per milliliter of plasma or urine is the difference between "total" I and directly extractable I per milliliter measured in each sample. The overall percent recovery of I added to plasma or urine over the range of 0.050–0.400 μg was determined to be 93.1 ± 9.4% (*SD*).

RESULTS AND DISCUSSION

The response of I by flame-ionization detection, using a 1.2-m glass column packed with the phenyl methyl silicone phase (OV-17), was sensitive, reproducible, and linear at levels as low as 20 ng injected. This response to the intact compound was used as the basis for the development of the quantitative determination of I in biological fluids. The extraction of I from plasma and urine at pH 7.4 with ether was quantitative (>93% recovery). Direct GLC analysis could not be performed on the initial ether extract residues without further cleanup, because endogenous impurities extracted from plasma and urine gave interfering peaks.

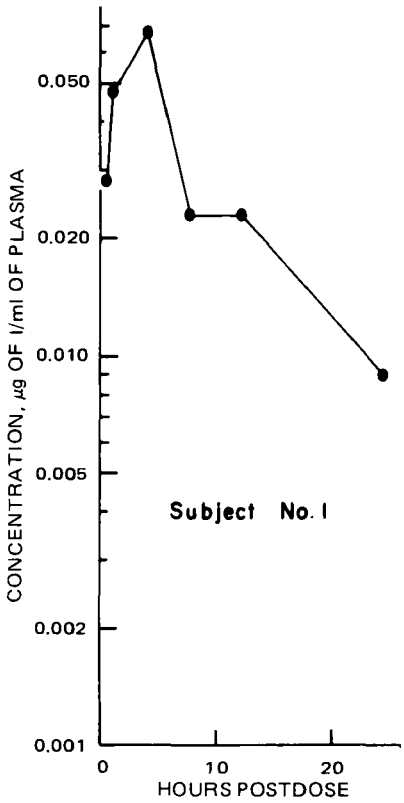

Figure 5—*Plasma levels of free I in a human subject following a single 25-mg oral dose of I, as determined by GLC.*

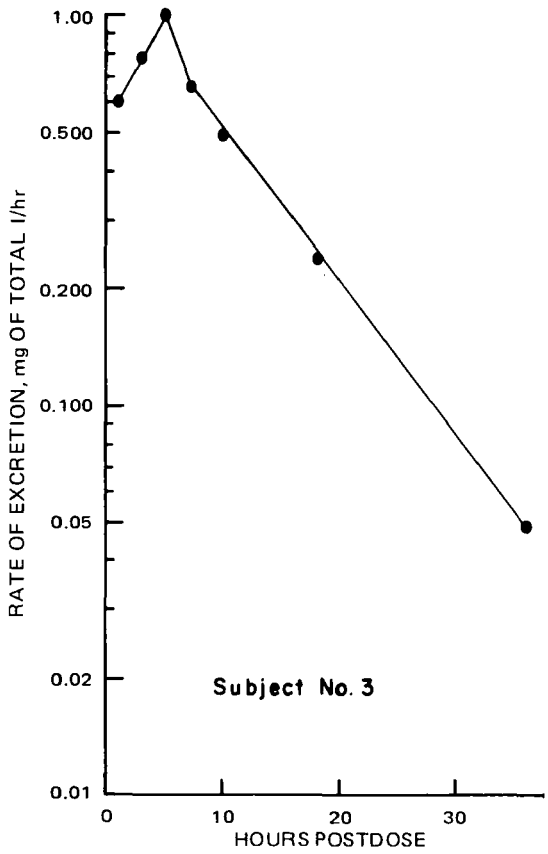

Figure 7—*Urinary excretion rates of total I in a human subject following a single 25-mg oral dose of I.*

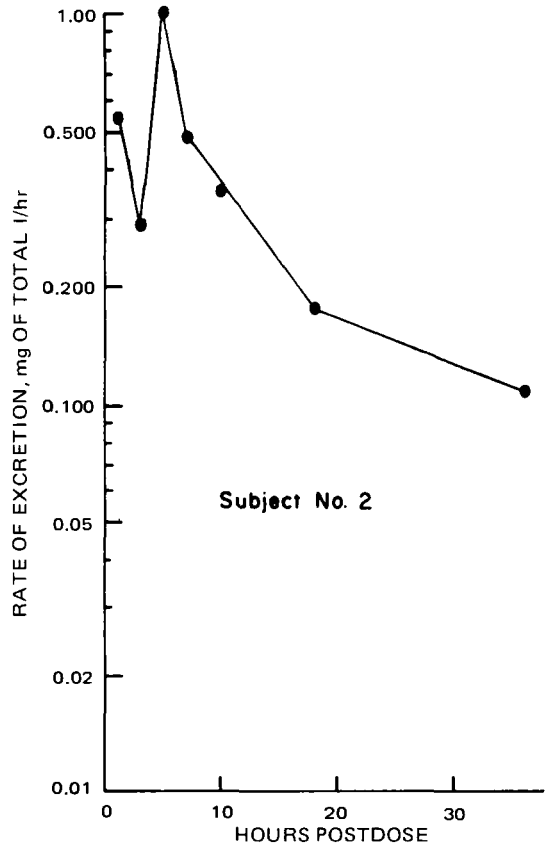

Figure 6—*Urinary excretion rates of total I in a human subject following a single 25-mg oral dose of I.*

This interference was especially evident with urine specimens that were pretreated with glucuronidase–sulfatase, extracted with ether, and analyzed by GLC. The chromatograms showed a major interfering peak eluting near the retention time corresponding to I under the GLC conditions described. These interfering urinary components necessitated additional cleanup of the sample extract, including the acid cleanup step prior to GLC analysis. The resulting chromatograms of control urine (drug free) indicated the absence of the previously interfering peaks (Fig. 1). Plasma samples analyzed by the described method showed no interfering peaks at the retention time, R_t, of I (Fig. 2).

Analysis for total I in urine indicated the excretion of appreciable amounts of I glucuronide or sulfate conjugate(s), determined by the amount of I liberated following glucuronidase–sulfatase incubation, extraction, cleanup, and GLC analysis (Fig. 3).

Adequate sensitivity (0.050 μg of I/ml of plasma) was obtained by injecting 10 μl of the 100 μl of methanol from the reconstituted sample residues, using 2 ml of plasma for analysis. In urine, the analysis of a 5-ml specimen permitted the determination of 0.020 μg of I/ml, using the same aliquot injected for GLC. However, following oral administration of single 25-mg doses of I in humans, the plasma levels fell below 0.050 μg of I/ml (Table I). In these cases, it was necessary to reconstitute the extracts in 25 μl of methanol and to inject 10-μl aliquots (Fig. 4).

Assay Specificity—Specificity of the GLC assay for I was verified by the analysis of authentic standards of two metabolites identified in dog urine. The desalkyl metabolite (II) and the 7-hydroxy metabolite (III) were both chromatographically resolved from I, with retention times of 5.8 and 11.0 min, respectively. These metabolites were not detected in the extracts of human urine following oral administration of I.

Applications to Biological Specimens—Three healthy adult male volunteers[15] received a single 25-mg tablet of I. Plasma speci-

[15] The study was conducted under the supervision of Dr. James Moore, Deer Lodge Research Unit, Deer Lodge, Mont.

mens (Subject 1) were obtained prior to drug administration and at 0.5, 1, 2, 4, 6, 8, 12, 24, and 48 hr postadministration. Urine specimens (Subjects 2 and 3) were collected prior to drug administration from −24 to 0 hr and at the following intervals: 0–2, 2–4, 6–8, 8–12, 12–24, and 24–48 hr after drug administration.

The plasma concentrations for Subject 1 were determined for both free and total I (Table I). The free plasma levels of I are plotted in Fig. 5. The levels of conjugated I (total I − free I) measured were higher than or equal to the corresponding free I levels at each specimen time in this subject.

The urine specimens were pooled for Subject 2 and analyzed for free and total I (Table II). The rate of excretion of total I is plotted in Fig. 6 for this subject. The urine specimens of Subject 3 were analyzed only for total I, because the recovery of the dose as total I in the urines of Subjects 2 and 3 during the 48-hr interval were similar, 43.7 and 48.6%, respectively. The rate of excretion of total I for Subject 3 is plotted in Fig. 7. The levels of free I were only 5% of the dose in Subject 2, and 39% was recovered as conjugated I. The data obtained from these studies indicate that the flame-ionization GLC assay can be successfully used in the pharmacokinetic evaluation of I in humans based on both plasma level and urinary excretion data.

REFERENCES

(1) F. M. Vane, D. H. Ellis, J. Pao, M. J. Petrin, J. F. Blount, E. Mohacsi, and J. J. Kamm, "Differential Metabolism of the Enantiomers of 2-Hydroxy-*N*-Cyclopropylmethylmorphinan in the Dog (Abstract)," Proceedings of the 3rd International Symposium on Mass Spectrometry in Biochemistry and Medicine, Mario Negri Institute, Milan, Italy, June 1975.

(2) S. J. Mulé, *J. Chromatogr. Sci.*, **10**, 275(1972).

(3) A. C. Moffat, *J. Chromatogr.*, **113**, 69(1975).

ACKNOWLEDGMENTS AND ADDRESSES

Received December 18, 1975, from the *Department of Biochemistry and Drug Metabolism, Hoffmann-La Roche Inc., Nutley, NJ 07110*

Accepted for publication March 8, 1976.

[x] To whom inquiries should be directed.

NOTES

Determination of Cyanocobalamin by Thermal Decomposition of the Cyano Group Using an Ion-Selective Electrode

SANDU GOLDSTEIN [x] and ALEXANDRU DUCA

Abstract □ A method for the simultaneous determination of cyanocobalamin, cobinamide (Factor B), and hydroxocobalamin in the solid state is described. The method is based on heating at 120° for cobinamide and at 140–145° for cyanocobalamin (15–20 min). The cyano content in the sample is distilled as hydrocyanic acid, trapped in 0.1 *M* potassium nitrate at pH 12–13, and determined by means of the cyanide ion-selective electrode. The error of this method, statistically established, does not exceed ±3%.

Keyphrases □ Cyanocobalamin—analysis by thermal decomposition of the cyano group, solid pharmaceutical preparations □ Cobinamide—analysis by thermal decomposition of the cyano group, solid pharmaceutical preparations □ Hydroxocobalamin—analysis by thermal decomposition of the cyano group, solid pharmaceutical preparations □ Thermal decomposition—simultaneous analysis of cyanocobalamin, cobinamide, and hydroxocobalamin, solid pharmaceutical preparations □ Vitamins—cyanocobalamin, cobinamide, and hydroxocobalamin, simultaneous analysis by thermal decomposition of the cyano group, solid pharmaceutical preparations

For some time, this laboratory has been investigating methods for extracting and purifying vitamin B_{12} group substances (1–6). In recent years, these studies have been extended to the coordination chemistry of the cobalt corrinoids, the analytical chemistry of cyanocobalamin, and the thermal stability of cyanocobalamin and some of its analogs (7–11). The methods of determining vitamin B_{12} group substances have been reviewed (12–14), but no procedure was found that gives satisfactory results for the cyano group determination of cyanocobalamin in the solid state.

Therefore, it was decided to investigate the decomposition of cyanocobalamin and some analogs [cobi-

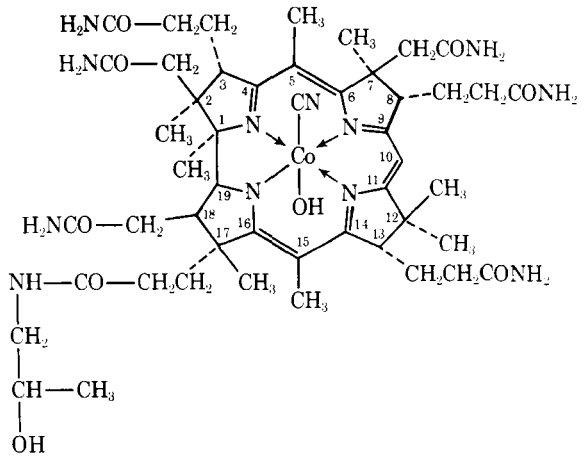

I

mens (Subject 1) were obtained prior to drug administration and at 0.5, 1, 2, 4, 6, 8, 12, 24, and 48 hr postadministration. Urine specimens (Subjects 2 and 3) were collected prior to drug administration from −24 to 0 hr and at the following intervals: 0–2, 2–4, 6–8, 8–12, 12–24, and 24–48 hr after drug administration.

The plasma concentrations for Subject 1 were determined for both free and total I (Table I). The free plasma levels of I are plotted in Fig. 5. The levels of conjugated I (total I − free I) measured were higher than or equal to the corresponding free I levels at each specimen time in this subject.

The urine specimens were pooled for Subject 2 and analyzed for free and total I (Table II). The rate of excretion of total I is plotted in Fig. 6 for this subject. The urine specimens of Subject 3 were analyzed only for total I, because the recovery of the dose as total I in the urines of Subjects 2 and 3 during the 48-hr interval were similar, 43.7 and 48.6%, respectively. The rate of excretion of total I for Subject 3 is plotted in Fig. 7. The levels of free I were only 5% of the dose in Subject 2, and 39% was recovered as conjugated I. The data obtained from these studies indicate that the flame-ionization GLC assay can be successfully used in the pharmacokinetic evaluation of I in humans based on both plasma level and urinary excretion data.

REFERENCES

(1) F. M. Vane, D. H. Ellis, J. Pao, M. J. Petrin, J. F. Blount, E. Mohacsi, and J. J. Kamm, "Differential Metabolism of the Enantiomers of 2-Hydroxy-*N*-Cyclopropylmethylmorphinan in the Dog (Abstract)," Proceedings of the 3rd International Symposium on Mass Spectrometry in Biochemistry and Medicine, Mario Negri Institute, Milan, Italy, June 1975.

(2) S. J. Mulé, *J. Chromatogr. Sci.*, **10**, 275(1972).

(3) A. C. Moffat, *J. Chromatogr.*, **113**, 69(1975).

ACKNOWLEDGMENTS AND ADDRESSES

Received December 18, 1975, from the *Department of Biochemistry and Drug Metabolism, Hoffmann-La Roche Inc., Nutley, NJ 07110*

Accepted for publication March 8, 1976.

[x] To whom inquiries should be directed.

NOTES

Determination of Cyanocobalamin by Thermal Decomposition of the Cyano Group Using an Ion-Selective Electrode

SANDU GOLDSTEIN [x] and ALEXANDRU DUCA

Abstract □ A method for the simultaneous determination of cyanocobalamin, cobinamide (Factor B), and hydroxocobalamin in the solid state is described. The method is based on heating at 120° for cobinamide and at 140–145° for cyanocobalamin (15–20 min). The cyano content in the sample is distilled as hydrocyanic acid, trapped in 0.1 *M* potassium nitrate at pH 12–13, and determined by means of the cyanide ion-selective electrode. The error of this method, statistically established, does not exceed ±3%.

Keyphrases □ Cyanocobalamin—analysis by thermal decomposition of the cyano group, solid pharmaceutical preparations □ Cobinamide—analysis by thermal decomposition of the cyano group, solid pharmaceutical preparations □ Hydroxocobalamin—analysis by thermal decomposition of the cyano group, solid pharmaceutical preparations □ Thermal decomposition—simultaneous analysis of cyanocobalamin, cobinamide, and hydroxocobalamin, solid pharmaceutical preparations □ Vitamins—cyanocobalamin, cobinamide, and hydroxocobalamin, simultaneous analysis by thermal decomposition of the cyano group, solid pharmaceutical preparations

For some time, this laboratory has been investigating methods for extracting and purifying vitamin B_{12} group substances (1–6). In recent years, these studies have been extended to the coordination chemistry of the cobalt corrinoids, the analytical chemistry of cyanocobalamin, and the thermal stability of cyanocobalamin and some of its analogs (7–11). The methods of determining vitamin B_{12} group substances have been reviewed (12–14), but no procedure was found that gives satisfactory results for the cyano group determination of cyanocobalamin in the solid state.

Therefore, it was decided to investigate the decomposition of cyanocobalamin and some analogs [cobi-

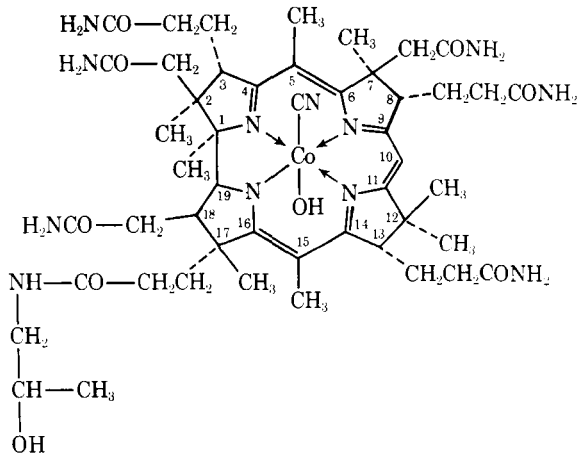

I

Table I—Determination of Cyanocobalamin in Presence of Cobinamide and Hydroxocobalamin

Amount Taken, mg			Amount Found					
			Cyanocobalamin		Cobinamide		Hydroxocobalamin	
Cyano-cobalamin	Cobinamide	Hydroxo-cobalamin	mg	%	mg	%	mg	%
1.35	—	—	1.31	97	—	—	—	—
2.70	—	—	2.75	102	—	—	—	—
6.00	—	—	5.82	92	—	—	—	—
8.50	—	—	8.30	98	—	—	—	—
10.80	—	—	11.20	103	—	—	—	—
—	1.00	—	—	—	0.96	96	—	—
—	3.90	—	—	—	3.80	98	—	—
—	6.50	—	—	—	6.71	102	—	—
6.00	6.20	—	5.79	95	6.00	97	—	—
7.92	4.10	—	8.08	102	3.90	95	—	—
6.00	6.20	2.40	5.76	96	6.30	101	2.31	95
6.00	6.20	4.10	6.06	101	5.83	95	4.07	98

namide (I) and hydroxocobalamin] in a flow of nitrogen at an adequate temperature. This idea was developed into an analytical procedure for the quantitative determination of cyanide in cyanocobalamin, cobinamide, and hydroxocobalamin. By heating at 120° (for cobinamide) or at 140–145° (for cyanocobalamin) in sodium hydroxide solution (pH 12–13) while bubbling nitrogen through the mixture, the cyano group can be converted into cyanide and quantitatively determined by a cyanide ion-selective electrode.

The proposed method has the advantage of permitting a rapid determination of the cyano group in a cyanocobalamin molecule. Moreover, it is selective and accurate. This method is the first that demonstrates the possible direct quantitation of cyanocobalamin together with cobinamide and hydroxocobalamin in the solid state.

EXPERIMENTAL

Apparatus—The apparatus consisted of an electric oven with an iron–constantan thermocouple standardized with a mercury thermometer, a purified nitrogen source, and glass equipment. The glass equipment included a quartz test tube (containing a vial where the sample was introduced) and common test tube (receiver) to receive the hydrocyanic acid from the quartz test tube where it is transformed to cyanide. The two test tubes are connected by a completely leakproof glass tube, and the quartz test tube is connected to the nitrogen system.

A cyanide electrode[1], a saturated calomel electrode[1], an agar–agar bridge, and a scale-expansion pH meter[2] were used for potentiometry. Before measurements were made, the cyanide electrode was kept for 5 hr in a 0.1 *M* potassium nitrate buffer solution at pH 11, adjusted with sodium hydroxide, and then was carefully washed with distilled water and standardized.

Reagents and Standards[3]—All reagents were prepared from analytical grade substances and double-distilled water.

Standard cyanide solutions of known pH and ionic strength were prepared by several dilutions of a 0.1 *M* stock solution in 0.1 *M* potassium nitrate. The pH was adjusted with sodium hydroxide. The stock 0.1 *M* cyanide solution was standardized conductometrically with silver nitrate and potentiometrically with a cyanide ion-selective electrode.

Analytical Procedure—About 1–10 mg of the sample was weighed directly in the vial, avoiding moisture contact, and the vial was carefully introduced into the quartz test tube. Then the quartz test tube was placed in the described installation. After nitrogen was removed from the quartz test tube, the tube was placed in the electric oven. The nitrogen flow was adjusted to 45–50 bubbles/min in the receiving test tube containing 10 ml of 0.1 *M* potassium nitrate (pH adjustment to 12–13 with 0.1 *N* sodium hydroxide). By heating the oven to about 120° for cobinamide or 140–145° for cyanocobalamin (15–20 min), the cyanide content in the sample of the quartz tube was distilled as hydrocyanic acid and trapped in 0.1 *M* potassium nitrate at pH 12–13, where it was determined by means of the ion-selective electrode.

[1] Model OP-CN-7111, Radelkis, Hungary.
[2] Pye model 78.
[3] Cyanocobalamin, cobinamide, and hydroxocobalamin were obtained from the Antibiotics Plant of Jassy, Romania.

RESULTS AND DISCUSSION

For cyanide measurement, a standard curve was prepared in the same manner used for the samples, using known solutions of cyanocobalamin, cobinamide, or potassium cyanide (0.001–0.00001 *M*).

The values for the cyanide solution are in agreement with the results calculated from the Nernst equation, which indicates that the curve should have a slope of −59.2 mv/p(CN) at constant pH and ionic strength. The experimental values for the slope were −59.8 mv/p(CN) for cyanide alone, −59.6 mv/p(cyanocobalamin) for the curve derived from cyanocobalamin solutions, and −59.9 mv/p (cobinamide) for the curve derived from cobinamide solutions, which were evaluated statistically (15).

Results of recovery experiments on cyanide from cyanocobalamin in the presence of cobinamide and hydroxocobalamin are shown in Table I and were satisfactory. By statistical analyses, the relative error was found to be ±3%.

Surprisingly, at higher temperatures than 120° for cobinamide or 140–145° for cyanocobalamin, the potential value of the ion-selective electrode was higher than the value corresponding to the theoretical cyano content of cyanocobalamin or cobinamide. Average values of the potential at different temperatures are shown in Table II. This discrepancy may result because degradation products arising at temperatures higher than 120 or 140–145° interfere with the cyanide ion-selective electrode. Moreover, an undegraded substance possibly could act as a catalyst, facilitating formation of hydrocyanic acid from the carbon and nitrogen atoms of cyanocobalamin, cobinamide, or hydroxocobalamin.

Other aspects of this method are under investigation.

REFERENCES

(1) S. Goldstein and A. Duca, *Rev. Chim. (Bucharest)*, **24**, 871(1973).
(2) *Ibid.*, **25**, 279(1974).
(3) A. Duca, C. Calu, M. Bezdadea, S. Ionescu, S. Goldstein, and

Table II—Potential Values at Different Temperatures by Cyanocobalamin and Cobinamide Determination

Compound	Temperature	Amount Taken, mg	Potential, mv
Cyanocobalamin	140°	6.00	206
Cyanocobalamin	180°	6.00	246
Cyanocobalamin	200°	6.00	260
Cyanocobalamin	260°	6.00	280
Cobinamide	120°	6.00	214
Cobinamide	180°	6.00	230

E. Ursescu, Romania pat. 58023 (1974).
(4) A. Duca, S. Goldstein, S. Ionescu, O. Coman, and G. Ceacoschi, Romania pat. appl. 72401 (1972).
(5) A. Duca and S. Goldstein, Romania pat. appl. 74630 (1973).
(6) A. Duca, S. Goldstein, S. Ionescu, G. Ceacoschi, and O. Coman, Romania pat. appl. 74143 (1973).
(7) A. Duca, C. Calu, and M. Bezdadea, *Chim. Anal. (Bucharest)*, **1**, 169(1971).
(8) S. Goldstein, A. Ciupitoiu, V. Vasilescu, and A. Duca, *Can. J. Pharm. Sci.*, **9**, 96(1974).
(9) S. Goldstein, A. Ciupitoiu, V. Vasilescu, and A. Duca, *Mikrochim. Acta*, **1975 I**, 117.
(10) A. Duca, S. Goldstein, and C. Calu, *ibid.*, **1975 I**, 187.
(11) S. Goldstein, Doctorate thesis, Polytechnic Institute of Jassy, Jassy, Romania, 1975.
(12) W. H. Shaw and C. Bessel, *Analyst*, **85**, 389(1960).
(13) W. J. Mader, in "Pharmaceutical Analysis," T. Higuchi and E. Brochmann-Hanssen, Eds., Interscience, London, England, 1961, p. 671.
(14) M. H. Hashmi, "Assay of Vitamins in Pharmaceutical Preparations," Wiley, London, England, 1973, p. 238.
(15) K. Eckschlager, "Errors, Measurement and Results in Chemical Analysis," Van Nostrand Reinhold, London, England, 1969, p. 142.

ACKNOWLEDGMENTS AND ADDRESSES

Received September 3, 1975, from the *Faculty of Chemistry and Chemical Engineering, Analytical Chemistry Department, Polytechnic Institute of Jassy, Jassy, Romania.*

Accepted for publication February 2, 1976.

The authors express their gratitude to Professor R. Bonnett, Queen Mary College, University of London, and Professor G. N. Schrauzer, University of San Diego, California, for stimulating discussions and encouragement.

[x] To whom inquiries should be directed. Present address: I.C.N. Pharmaceuticals (Canada), 1956 Bourdon Street, Montreal, H4M 1V1, Canada.

Steric Inhibition of Conjugation in Lowest Excited Singlet State of 9-Anthramide by Hydrogen Bond Donor Solvents: Role of Solvent in Chemical Structure

ROY J. STURGEON and STEPHEN G. SCHULMAN [x]

Abstract □ 9-Anthramide has electronic absorption and fluorescence spectra that, in water, are similar to those of anthracene. This result is attributed to steric hindrance of the 9-carboxamido group with the *peri*-hydrogen atoms in the 1- and 8-positions of the anthracene ring. However, in aprotic solvents, although the absorption spectrum of 9-anthramide is anthracene-like, its fluorescence spectrum is red shifted and structureless. This finding is attributed to excited-state rotation of the 9-carboxamido group into coplanarity with the anthracene ring and indicates that, in water, the hydrogen-bonded solvent cage affects the steric inhibition of conjugation in excited 9-anthramide. These findings suggest that studies of structure and reactivity of drugs in nonaqueous or solid matrixes are probably of only limited value, since in the strongly interacting aqueous media the aqueous solvent cage plays a substantial role in determining molecular structure and reactivity.

Keyphrases □ 9-Anthramide—electronic absorption and fluorescence spectral study, effect of solvent on molecular structure □ Solvent—effect on molecular structure of 9-anthramide, electronic absorption and fluorescence spectral study □ Molecular structure—9-anthramide, effect of solvent, electronic absorption and fluorescence spectral study □ Conjugation—steric inhibition in 9-anthramide, effect of solvent, electronic absorption and fluorescence spectral study

9-Anthroic acid and many of its derivatives have absorption spectra that are very similar to those of anthracene in vibrational structure and position in the electromagnetic spectrum. However, in various solvents, these compounds demonstrate a fluorescence band that is unstructured and at considerably longer wavelengths than that of anthracene. This band has been explained in terms of rotation of the carboxyl group from a configuration perpendicular to that of the anthracene ring in the ground state to one coplanar with the anthracene ring in the thermally equilibrated lowest excited singlet state (1).

It has been suggested that the steric hindrance to coplanarity, exerted by the *peri*-hydrogen atoms in the 1- and 8-positions of the anthracene ring in the ground state, is circumvented by reduction of the O—C—O bond angle of the carboxyl group as a result of electronic excitation. In the 9-anthroate anion, however, the greater electron density at the carboxylate group has been suggested to prevent sufficient alteration of the structure of the latter to permit coplanarity, even in the excited state, because both the absorption and fluorescence spectra of the anion are anthracene-like in appearance (2).

Based on spectra of the ethyl esters of 1- and 2-naphthoic acids (3), it was thought that the inability of the 9-anthroate anion to conjugate in the lowest excited singlet state may not be purely a function of structure but may be due to environmental effects such as a tightly bound solvent cage producing the steric interference. This hypothesis is, however, rather difficult to test on the 9-anthroate anion, because the ion-pairs, upon which spectra would be taken in low dielectric media, would include cations; these cations would introduce further complications in the interpretation of the spectra.

The amide of the 9-anthroic acid affords at least a partial solution of this problem. The carboxamido group is intermediate between the carboxyl group and the carboxylate anion in its electronic distribution and, therefore, in its geometrical structure. Moreover, 9-

E. Ursescu, Romania pat. 58023 (1974).
(4) A. Duca, S. Goldstein, S. Ionescu, O. Coman, and G. Ceacoschi, Romania pat. appl. 72401 (1972).
(5) A. Duca and S. Goldstein, Romania pat. appl. 74630 (1973).
(6) A. Duca, S. Goldstein, S. Ionescu, G. Ceacoschi, and O. Coman, Romania pat. appl. 74143 (1973).
(7) A. Duca, C. Calu, and M. Bezdadea, *Chim. Anal. (Bucharest)*, **1**, 169(1971).
(8) S. Goldstein, A. Ciupitoiu, V. Vasilescu, and A. Duca, *Can. J. Pharm. Sci.*, **9**, 96(1974).
(9) S. Goldstein, A. Ciupitoiu, V. Vasilescu, and A. Duca, *Mikrochim. Acta*, **1975 I**, 117.
(10) A. Duca, S. Goldstein, and C. Calu, *ibid.*, **1975 I**, 187.
(11) S. Goldstein, Doctorate thesis, Polytechnic Institute of Jassy, Jassy, Romania, 1975.
(12) W. H. Shaw and C. Bessel, *Analyst*, **85**, 389(1960).
(13) W. J. Mader, in "Pharmaceutical Analysis," T. Higuchi and E. Brochmann-Hanssen, Eds., Interscience, London, England, 1961, p. 671.
(14) M. H. Hashmi, "Assay of Vitamins in Pharmaceutical Preparations," Wiley, London, England, 1973, p. 238.
(15) K. Eckschlager, "Errors, Measurement and Results in Chemical Analysis," Van Nostrand Reinhold, London, England, 1969, p. 142.

ACKNOWLEDGMENTS AND ADDRESSES

Received September 3, 1975, from the *Faculty of Chemistry and Chemical Engineering, Analytical Chemistry Department, Polytechnic Institute of Jassy, Jassy, Romania.*

Accepted for publication February 2, 1976.

The authors express their gratitude to Professor R. Bonnett, Queen Mary College, University of London, and Professor G. N. Schrauzer, University of San Diego, California, for stimulating discussions and encouragement.

[x] To whom inquiries should be directed. Present address: I.C.N. Pharmaceuticals (Canada), 1956 Bourdon Street, Montreal, H4M 1V1, Canada.

Steric Inhibition of Conjugation in Lowest Excited Singlet State of 9-Anthramide by Hydrogen Bond Donor Solvents: Role of Solvent in Chemical Structure

ROY J. STURGEON and STEPHEN G. SCHULMAN [x]

Abstract □ 9-Anthramide has electronic absorption and fluorescence spectra that, in water, are similar to those of anthracene. This result is attributed to steric hindrance of the 9-carboxamido group with the *peri*-hydrogen atoms in the 1- and 8-positions of the anthracene ring. However, in aprotic solvents, although the absorption spectrum of 9-anthramide is anthracene-like, its fluorescence spectrum is red shifted and structureless. This finding is attributed to excited-state rotation of the 9-carboxamido group into coplanarity with the anthracene ring and indicates that, in water, the hydrogen-bonded solvent cage affects the steric inhibition of conjugation in excited 9-anthramide. These findings suggest that studies of structure and reactivity of drugs in nonaqueous or solid matrixes are probably of only limited value, since in the strongly interacting aqueous media the aqueous solvent cage plays a substantial role in determining molecular structure and reactivity.

Keyphrases □ 9-Anthramide—electronic absorption and fluorescence spectral study, effect of solvent on molecular structure □ Solvent—effect on molecular structure of 9-anthramide, electronic absorption and fluorescence spectral study □ Molecular structure—9-anthramide, effect of solvent, electronic absorption and fluorescence spectral study □ Conjugation—steric inhibition in 9-anthramide, effect of solvent, electronic absorption and fluorescence spectral study

9-Anthroic acid and many of its derivatives have absorption spectra that are very similar to those of anthracene in vibrational structure and position in the electromagnetic spectrum. However, in various solvents, these compounds demonstrate a fluorescence band that is unstructured and at considerably longer wavelengths than that of anthracene. This band has been explained in terms of rotation of the carboxyl group from a configuration perpendicular to that of the anthracene ring in the ground state to one coplanar with the anthracene ring in the thermally equilibrated lowest excited singlet state (1).

It has been suggested that the steric hindrance to coplanarity, exerted by the *peri*-hydrogen atoms in the 1- and 8-positions of the anthracene ring in the ground state, is circumvented by reduction of the O—C—O bond angle of the carboxyl group as a result of electronic excitation. In the 9-anthroate anion, however, the greater electron density at the carboxylate group has been suggested to prevent sufficient alteration of the structure of the latter to permit coplanarity, even in the excited state, because both the absorption and fluorescence spectra of the anion are anthracene-like in appearance (2).

Based on spectra of the ethyl esters of 1- and 2-naphthoic acids (3), it was thought that the inability of the 9-anthroate anion to conjugate in the lowest excited singlet state may not be purely a function of structure but may be due to environmental effects such as a tightly bound solvent cage producing the steric interference. This hypothesis is, however, rather difficult to test on the 9-anthroate anion, because the ion-pairs, upon which spectra would be taken in low dielectric media, would include cations; these cations would introduce further complications in the interpretation of the spectra.

The amide of the 9-anthroic acid affords at least a partial solution of this problem. The carboxamido group is intermediate between the carboxyl group and the carboxylate anion in its electronic distribution and, therefore, in its geometrical structure. Moreover, 9-

Table I—Absorption (Abs) and Fluorescence (Fl) of the Neutral and Cationic Species Derived from 9-Anthramide

Cation in	λ, Abs	λ, Fl^{max}	Neutral	λ, Abs	λ, Fl^{max}
Water	383	470	Water	385	407
Ethanol	382	442	Ethanol	385	404
Dioxane	384	440	Dioxane	384	440
Acetonitrile	382	448	Acetonitrile	382	448
Heptane	380	462	Heptane	380	451
Chloroform	384	461	Chloroform	384	461

anthramide is uncharged, so it can be studied in low dielectric media without having to account for ion-pairing phenomena. Consequently, to account for the possibility of solvation phenomena influencing the failure of the carboxamido group of 9-anthramide and, therefore, the carboxylate group of the 9-anthroate anion to achieve coplanarity in the lowest excited singlet state, electronic spectra of 9-anthramide were studied.

EXPERIMENTAL

Reagents—9-Anthroyl chloride[1] was recrystallized several times from absolute ethanol. 9-Anthramide was prepared from 9-anthroyl chloride by the method of Saare (4) and was recrystallized several times from hot water.

Analytical reagent grade sulfuric acid[2] was diluted with distilled, deionized water for the solutions used to study the Hammett acidity region. Solutions in the pH range were citrate and phosphate buffers and sodium hydroxide solutions in distilled, deionized water.

Each sulfuric acid or buffer solution in a 10-ml volumetric flask was injected with 100 μl of a 1.00×10^{-3} *M* stock solution of the appropriate 9-anthramide in absolute ethanol immediately prior to the taking of spectra to minimize decomposition errors. Nonaqueous solvent solutions were prepared by dissolving weighed amounts of the solid in 10.00 ml of the appropriate solvents.

Apparatus — Absorption spectra were taken on a spectrophotometer[3]. Fluorescence spectra were taken on a fluorescence spectrophotometer[4] whose monochromators were calibrated against the xenon line emission spectrum and whose output was corrected for instrumental response by means of a rhodamine-B quantum counter. The pH measurements were made on a pH meter[5] employing a silver–silver chloride–glass combination electrode.

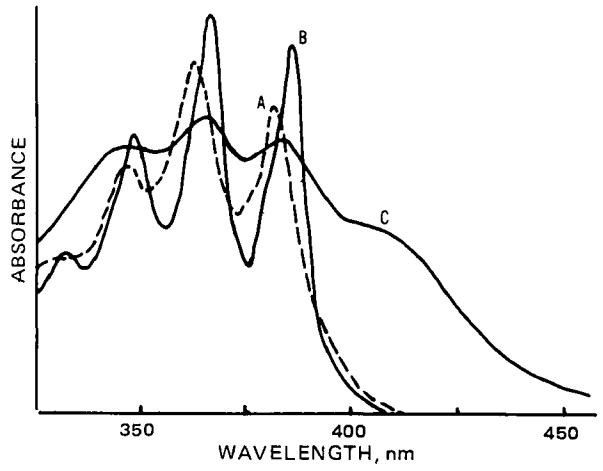

Figure 1—*Electronic absorption spectra of about* 1×10^{-5} M *9-anthramide in hexane (A), water at pH 7.9 (B), and Hammett acidity −4.0 (C).*

[1] Aldrich Chemical Co., Milwaukee, Wis.
[2] Mallinckrodt Chemical Works, St. Louis, Mo.
[3] Beckman DB-GT.
[4] Perkin-Elmer MPF-2A.
[5] Orion model 801.

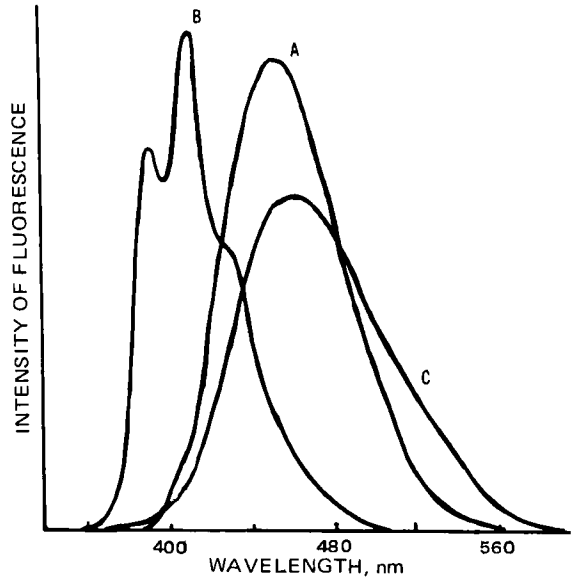

Figure 2—*Fluorescence spectra of about* 1×10^{-5} M *9-anthramide in hexane (A), water at pH 7.9 (B), and Hammett acidity −4.0 (C).*

RESULTS AND DISCUSSION

The principal absorption and fluorescence features of 9-anthramide in various solvents and at various pH's are presented in Table I. The ground-state pKa and excited-state pKa* values were −2.00 (determined absorptiometrically) and 1.50 (determined fluorometrically), respectively.

In anthracenes substituted in the 9-position with strongly interacting substituents, the transversely polarized $^1L_a \leftarrow {}^1A$ transition is more affected by intramolecular charge transfer than the longitudinally polarized $^1L_b \leftarrow {}^1A$ transition. As a result, the ^1L_a band tends to lose vibrational structure and shifts to longer wavelengths relative to its position in anthracene while the ^1L_b band is relatively unaffected (5). In 9-anthramide, steric hindrance in the ground state arising from the interactions between the bulky substituents in the 9-position and the *peri*-hydrogen atoms in the 1- and 8-positions of the anthracene ring prevents the conjugation (coplanarity) of the exocyclic group in the 9-position with the anthracene ring. Since the 9-substituents have little effect on the ^1L_a absorption bands of anthracene in this case, the absorption spectra of the 9-anthramides are almost identical with those of anthracene.

In the ground state of 9-anthramide in various solvents, steric hindrance is observed in the neutral and cationic species, as reflected by the highly structured absorption spectra at only slightly longer wavelengths than those of anthracene (Fig. 1). However, 9-anthramide exhibits an unstructured long wavelength fluorescence band (Fig. 2), indicating that in these solvents, in the lowest excited singlet state, the steric barrier to coplanarity is removed. Rotation of the 9-substituent into coplanarity with the ring occurs in the thermally equilibrated lowest excited singlet state. 9-Anthramide demonstrates this highly diffuse emission band with a maximum at 470 nm.

9-Anthramide, in hydrogen bond donor solvents (water and ethanol), shows no conjugation of the exocyclic group with the ring in the lowest excited singlet state, as reflected by the highly structured emission band with a maximum at 407 nm (Fig. 2). The assumption of the bond angle reduction of the carboxyl group or, in this case, the carboxamido group upon excitation is not sufficient to explain the observation of the structured, anthracene-like spectra of 9-anthramide in hydrogen bond donor solvents.

In the ground state of 9-anthramide in all solvents, the resonance-stabilization due to conjugation of the exocyclic group with the ring system is not large enough to overcome the steric interference from the *peri*-hydrogen atoms in the 1- and 8-positions of the ring. However, in the lowest excited singlet state, the conjugative interaction is much stronger than in the ground state, because of the greater electronic dipole moment of the ^1L_a state, which is stabilized by intramolecular charge transfer from the anthracene ring to the exocyclic group.

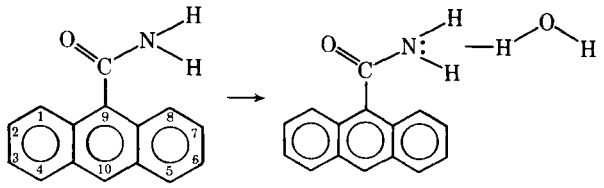

Scheme I

In aprotic solvents, this interaction is strong enough to overcome the steric barrier to it and allows the exocyclic group to attain a coplanar configuration. However, in water and ethanol, the carboxamido group is hydrogen bonded to the solvent (Scheme I), with the result that the group and its solvent cage become more bulky. The resonance interaction even upon excitation is not great enough to overcome the steric interference from the interaction between the *peri*-hydrogen atoms and the solvent cage.

Once 9-anthramide is protonated at the amido nitrogen, the effect of the hydrogen bond donor solvent cage is lost. This loss removes the possibility of hydrogen bonding at the carboxamido group and is observed as a loss of the mirror image relationship between the absorption and fluorescence spectra, with the result that the emission spectrum shifts to much longer wavelengths (Fig. 2).

While the ground-state pKa of 9-anthramide is −2.00, excited-state protonation occurs in this compound, as revealed by variations in the fluorescence spectra with pH or Hammett acidity. 9-Anthramide is more basic in the excited state and exhibits an excited-state pKa* value of 1.50. The decrease in acidity of the protonated amide in the lowest excited singlet state reflects the transfer of electronic charge from the anthracene ring to the exocyclic group upon excitation.

The effect of protonation on the conjugation of the exocyclic group can be observed by following the absorption and fluorescence band shapes and band maxima as they vary with pH or Hammett acidity. In the ground state, in the region below Hammett acidity of −2.0, protonation of the carboxamido group is observed as a slight smearing and red-shift in the absorption spectrum (Fig. 1). In the ground state, protonation apparently causes the resonance interaction to increase enough to allow the exocyclic group to reach a configuration that is nearly coplanar to the ring. The effect of protonation in the excited state is more dramatic, the large red-shift of the emission spectrum, on protonation, suggesting essentially complete conjugation in the excited state.

The solvents used in this study covered a wide range of polarity and hydrogen bond donor capability. It was found that excited-state conjugation in the neutral molecule can occur only in aprotic solvents (regardless of polarity). The hindrance observed in the excited state in hydrogen bond donor solvents is due to the solvent caging effect at the carboxamido group; this effect makes the group too bulky to overcome the steric interference from the *peri*-hydrogen atoms in the 1- and 8-positions of the anthracene ring.

The solvent cage has thus been shown to play an important role in chemical structure. A conclusion that may be drawn from these studies is that the chemical structure (and presumably the reactivity) of a compound may vary substantially from solvent to solvent. As illustrated by the differences in the spectra of 9-anthramide in water and heptane, strongly interacting solvents do affect chemical structure. These findings suggest that studies of structure and reactivity of drugs in nonaqueous solvents and solid matrixes may not always be validly applied to the interpretation of phenomena observed in strongly interacting solvents such as biological fluids because of the solvent caging effect.

REFERENCES

(1) T. C. Werner and D. M. Hercules, *J. Phys. Chem.*, **74**, 1030(1970).

(2) *Ibid.*, **73**, 2005(1969).

(3) P. J. Kovi and S. G. Schulman, *Spectrosc. Lett.*, **5**, 443(1972).

(4) K. Saare, *Kunststoffe*, **30**, 109(1940).

(5) S. G. Schulman, P. J. Kovi, G. Torosian, H. McVeigh, and D. Carter, *J. Pharm. Sci.*, **62**, 1823(1973).

ACKNOWLEDGMENTS AND ADDRESSES

Received December 3, 1975, from the *College of Pharmacy, University of Florida, Gainesville, FL 32610*

Accepted for publication February 12, 1976.

[x] To whom inquiries should be directed.

Effect of Variation in Compaction Force on Properties of Six Direct Compression Tablet Formulations

KARRAR A. KHAN [*] and C. T. RHODES [‡x]

Abstract □ The effect of variation in compaction force on six direct compression tablet matrixes was investigated. An instrumented tablet press allowed direct measurement of applied and ejection forces. Hardness, apparent tablet density, and disintegration times also were determined. The disintegration time of spray-dried lactose tablets was essentially independent of compaction force. However, in the other systems investigated, the properties studied showed varying types of dependence on compaction pressure. A direct compression formula was developed and exhibits a decrease in disintegration time as compaction force is increased.

Keyphrases □ Tablets—six matrixes, effect of various compaction forces on hardness, apparent density, and disintegration time □ Compaction force—effect on tablet hardness, apparent density, and disintegration time, six matrixes □ Hardness, tablet—six matrixes, effect of various compaction forces □ Density, apparent—six tablet matrixes, effect of various compaction forces □ Disintegration time, tablet—six matrixes, effect of various compaction forces □ Dosage forms—tablets, six matrixes, effect of various compaction forces on hardness, apparent density, and disintegration time

The production of pharmaceutical tablets by the direct compression technique has several advantages for many drugs in comparison with wet granulation or other methods. In particular, the relatively small labor content of this technique makes it increasingly attractive to the pharmaceutical industry (1).

Several well-proven materials can be used as tablet matrixes for direct compression, and some investigators

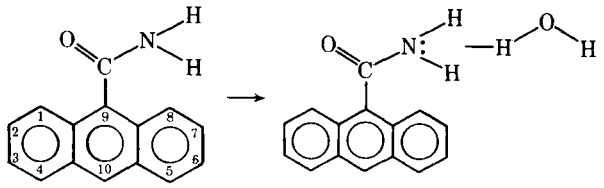

Scheme I

In aprotic solvents, this interaction is strong enough to overcome the steric barrier to it and allows the exocyclic group to attain a coplanar configuration. However, in water and ethanol, the carboxamido group is hydrogen bonded to the solvent (Scheme I), with the result that the group and its solvent cage become more bulky. The resonance interaction even upon excitation is not great enough to overcome the steric interference from the interaction between the *peri*-hydrogen atoms and the solvent cage.

Once 9-anthramide is protonated at the amido nitrogen, the effect of the hydrogen bond donor solvent cage is lost. This loss removes the possibility of hydrogen bonding at the carboxamido group and is observed as a loss of the mirror image relationship between the absorption and fluorescence spectra, with the result that the emission spectrum shifts to much longer wavelengths (Fig. 2).

While the ground-state pKa of 9-anthramide is −2.00, excited-state protonation occurs in this compound, as revealed by variations in the fluorescence spectra with pH or Hammett acidity. 9-Anthramide is more basic in the excited state and exhibits an excited-state pKa* value of 1.50. The decrease in acidity of the protonated amide in the lowest excited singlet state reflects the transfer of electronic charge from the anthracene ring to the exocyclic group upon excitation.

The effect of protonation on the conjugation of the exocyclic group can be observed by following the absorption and fluorescence band shapes and band maxima as they vary with pH or Hammett acidity. In the ground state, in the region below Hammett acidity of −2.0, protonation of the carboxamido group is observed as a slight smearing and red-shift in the absorption spectrum (Fig. 1). In the ground state, protonation apparently causes the resonance interaction to increase enough to allow the exocyclic group to reach a configuration that is nearly coplanar to the ring. The effect of protonation in the excited state is more dramatic, the large red-shift of the emission spectrum, on protonation, suggesting essentially complete conjugation in the excited state.

The solvents used in this study covered a wide range of polarity and hydrogen bond donor capability. It was found that excited-state conjugation in the neutral molecule can occur only in aprotic solvents (regardless of polarity). The hindrance observed in the excited state in hydrogen bond donor solvents is due to the solvent caging effect at the carboxamido group; this effect makes the group too bulky to overcome the steric interference from the *peri*-hydrogen atoms in the 1- and 8-positions of the anthracene ring.

The solvent cage has thus been shown to play an important role in chemical structure. A conclusion that may be drawn from these studies is that the chemical structure (and presumably the reactivity) of a compound may vary substantially from solvent to solvent. As illustrated by the differences in the spectra of 9-anthramide in water and heptane, strongly interacting solvents do affect chemical structure. These findings suggest that studies of structure and reactivity of drugs in nonaqueous solvents and solid matrixes may not always be validly applied to the interpretation of phenomena observed in strongly interacting solvents such as biological fluids because of the solvent caging effect.

REFERENCES

(1) T. C. Werner and D. M. Hercules, *J. Phys. Chem.*, **74**, 1030(1970).

(2) *Ibid.*, **73**, 2005(1969).

(3) P. J. Kovi and S. G. Schulman, *Spectrosc. Lett.*, **5**, 443(1972).

(4) K. Saare, *Kunststoffe*, **30**, 109(1940).

(5) S. G. Schulman, P. J. Kovi, G. Torosian, H. McVeigh, and D. Carter, *J. Pharm. Sci.*, **62**, 1823(1973).

ACKNOWLEDGMENTS AND ADDRESSES

Received December 3, 1975, from the *College of Pharmacy, University of Florida, Gainesville, FL 32610*

Accepted for publication February 12, 1976.

[x] To whom inquiries should be directed.

Effect of Variation in Compaction Force on Properties of Six Direct Compression Tablet Formulations

KARRAR A. KHAN [*] and C. T. RHODES [‡x]

Abstract □ The effect of variation in compaction force on six direct compression tablet matrixes was investigated. An instrumented tablet press allowed direct measurement of applied and ejection forces. Hardness, apparent tablet density, and disintegration times also were determined. The disintegration time of spray-dried lactose tablets was essentially independent of compaction force. However, in the other systems investigated, the properties studied showed varying types of dependence on compaction pressure. A direct compression formula was developed and exhibits a decrease in disintegration time as compaction force is increased.

Keyphrases □ Tablets—six matrixes, effect of various compaction forces on hardness, apparent density, and disintegration time □ Compaction force—effect on tablet hardness, apparent density, and disintegration time, six matrixes □ Hardness, tablet—six matrixes, effect of various compaction forces □ Density, apparent—six tablet matrixes, effect of various compaction forces □ Disintegration time, tablet—six matrixes, effect of various compaction forces □ Dosage forms—tablets, six matrixes, effect of various compaction forces on hardness, apparent density, and disintegration time

The production of pharmaceutical tablets by the direct compression technique has several advantages for many drugs in comparison with wet granulation or other methods. In particular, the relatively small labor content of this technique makes it increasingly attractive to the pharmaceutical industry (1).

Several well-proven materials can be used as tablet matrixes for direct compression, and some investigators

Table I—Properties of Formula I Tablets Prepared at Different Compaction Pressures

Applied Compression Force, kg	Weight, mg	Thickness, mm	Apparent Tablet Density, g/cm³	Hardness, Erweka Units	Ejection Force, kg	Disintegration Time, min
702.7	696.4	5.47	1.30	10.6	69.7	30.3
1241.9	696.8	5.21	1.36	>15	95.4	34.0
2287.0	699.9	5.01	1.42	>15	121.1	34.4
3513.5	701.4	4.91	1.45	>15	146.8	32.3

Table II—Properties of Formula II Tablets Prepared at Different Compaction Pressures

Applied Compression Force, kg	Weight, mg	Thickness, mm	Apparent Tablet Density, g/cm³	Hardness, Erweka Units	Ejection Force, kg	Disintegration Time, min
666.5	429.9	3.92	1.13	0.2	36.7	1.0
1402.5	450.5	3.78	1.24	1.5	36.7	1.4
1575.0	466.1	3.95	1.22	1.7	36.0	3.9
2514.0	455.1	3.66	1.29	3.1	37.0	27.0

Table III—Properties of Formula III Tablets Prepared at Different Compaction Pressures

Applied Compression Force, kg	Weight, mg	Thickness, mm	Apparent Tablet Density, g/cm³	Hardness, Erweka Units	Ejection Force, kg	Disintegration Time, min
242.0	657.3	4.25	1.58	0.28	41.1	7.8
963.0	660.5	3.77	1.80	7.0	37.8	0.6
1950.6	659.5	3.53	1.93	14.5	63.8	0.6
3362.2	658.9	3.43	1.98	>15	91.0	0.6

also proposed blends of various materials for direct compression. Furthermore, a number of direct compression materials are now widely available commercially. However, there is a paucity of comparative quantitative evaluations of direct compression matrixes.

In this study, the effect of variation of compaction force on ejection force, apparent tablet density, hardness, and disintegration time of six direct compression tablet formulations was investigated. Spray-dried lactose, whose properties as a direct compression diluent are well known, was included since it can be regarded, to some extent, as a reference standard.

EXPERIMENTAL

Materials—The six direct compression tablet matrixes had the following percentage (w/w) compositions:

Formula I—spray-dried lactose[1], 99.0; and magnesium stearate[2], 1.0.

Formula II[3]—modified potato starch, 81.0; colloidal silica, 3.0; polyethylene glycol 4000, 3.0; talc, 12.0; and magnesium stearate, 1.0.

Formula III[4]—dicalcium phosphate dihydrate, 89.0; starch, 7.5; microcrystalline cellulose, 2.5; and magnesium stearate, 1.0.

Formula IV—dicalcium phosphate dihydrate[5], 91.5; microcrystalline cellulose[6], 5.0; sodium starch glycolate[7], 2.5; and magnesium stearate, 1.0.

Formula V—microcrystalline cellulose, 24.0; special starch[8], 75.0; and stearic acid,1.0.

Formula VI—dicalcium phosphate dihydrate, 89.3; calcium phosphate–carbonate complex[9], 4.7; cation-exchange resin[10], 5.0; and magnesium stearate, 1.0.

Methods—The components of the various tablet formulations were blended by quartering and shaking vigorously in a plastic bag as described previously (2). A single-punch tablet press[11], used to prepare the tablets [punch size 1.09 cm (0.42 in.), shape flat], was instrumented as described elsewhere (3, 4). Apparent tablet densities were estimated from tablet weight and thickness measurements. Disintegration times were determined using the BP method, without disk.

RESULTS AND DISCUSSION

The data for spray-dried lactose (Table I) demonstrate its good compressibility; hard tablets were produced at low compaction pressures. The disintegration time was not radically modified by an increase in compaction force; indeed, the tablets dissolved rather than disintegrated or broke up into small lumps. The dissolution, which primarily takes place from the external surface, was essentially independent of compaction force. A similar finding was reported in an investigation of sodium chloride tablets (5).

The ejection forces were fairly high and increased with an increase in compaction force, although 1% magnesium stearate was present in the formula. Richman (6), who examined the lubrication of spray-dried lactose, found that lubrication efficiency improved with an increase in lubricant concentration up to 5% instead of reaching an optimum between 1 and 2% as is common for many granulations. Spray-dried lactose tablets were of low friability.

Formula II was a commercially available direct compression tablet matrix. The tablets produced in this study were somewhat disappointing (Table II), being soft and very friable. Disintegration time increased as compaction force was increased. This increase may have been due to some plastic deformation of starch (7), reducing the rate of water penetration into the tablet structure. Ejection forces generated during compaction were low and appeared to be independent of the compaction force. This behavior is similar to that reported for microcrystalline cellulose (8).

Formula III, another well-known commercially available direct compression excipient, was initially marketed as reported in this in-

[1] McKesson and Robbins Ltd., Ramsgate, England.
[2] British Drug Houses, Poole, England.
[3] Nal-Tab, Victor Blagden and Co., London, England.
[4] Emcompress Standard, Kingsley and Keith, Croyden, London, England.
[5] Albright and Wilson Ltd., Oldbury Division, Worcestershire, England.
[6] Honeywell and Stein Ltd., London, England.
[7] Primojel.
[8] Sta-R$_x$ 1500 Starch, Staley Co., London, England.
[9] Calfos 50 mesh, Calfos, London, England.
[10] Amberlite IRP 88, Lennig Chemicals, London, England.
[11] Manesty type F3.

Table IV—Properties of Formula IV Tablets Prepared at Different Compaction Pressures

Applied Compression Force, kg	Weight, mg	Thickness, mm	Apparent Tablet Density, g/cm³	Hardness, Erweka Units	Ejection Force, kg	Disintegration Time, min
227.1	655.0	4.27	1.57	0.4	41.1	2.0
439.3	667.5	3.97	1.72	1.0	44.0	0.7
1774.2	657.1	3.56	1.89	6.4	63.5	0.6
3492.1	663.7	3.44	1.99	>15	91.5	3.3

Table V—Properties of Formula V Tablets Prepared at Different Compaction Pressures

Applied Compression Force, kg	Weight, mg	Thickness, mm	Apparent Tablet Density, g/cm³	Hardness, Erweka Units	Ejection Force, kg	Disintegration Time, min
393.8	382.9	3.49	1.13	3.9	34.1	1.1
1514.4	387.9	3.06	1.32	10.1	36.3	3.9
3210.5	381.3	2.98	1.33	12.6	37.8	4.4
3393.3	383.2	3.04	1.31	11.5	39.6	4.5

Table VI—Properties of Formula VI Tablets Prepared at Different Compaction Pressures

Applied Compression Force, kg	Weight, mg	Thickness, mm	Apparent Tablet Density, g/cm³	Hardness, Erweka Units	Ejection Force, kg	Disintegration Time, min
575.5	686.3	4.25	1.66	2.1	42.2	8.0
1553.8	694.8	3.88	1.85	9.7	60.5	1.2
3634.6	692.8	3.66	1.95	>15	98.3	0.5

vestigation. Recently, the suppliers excluded the other adjuvants and marketed only dicalcium phosphate dihydrate, which was claimed to be in a special physical form. The compression properties of this excipient are shown in Table III. This material had an excellent pressure–hardness profile. The tablets made at the lowest pressure had longer disintegration times than those made at higher pressures. This behavior may have been due to the swelling effect of starch, which is more pronounced in tablets made at higher pressures (low porosity). The effect of pressure on disintegration of tablets containing various disintegrants was described elsewhere (3).

Formulation IV contained an unmilled grade of dicalcium phosphate dihydrate. Its particle-size distribution was reported previously (2). The compression properties of this formulation (Table IV) were similar to those of Formula III (Table III), except that the disintegration time showed a minimum. This minimum may have been caused by the differences in the disintegrant action of corn starch and sodium starch glycolate (3). This study, therefore, appears to indicate that the coarse, unmilled, or graded form of dicalcium phosphate dihydrate is a useful direct compression diluent (9). Also, sodium starch glycolate is an effective disintegrant for insoluble tablet systems (2, 3, 9).

Formulation V was basically similar to that developed by Manudhane (10). Initial experiments with special starch showed that it was not possible to compress this material containing 1% magnesium stearate, which is an indication of a very low compacity of this excipient. The results (Table V) show that the addition of 24% microcrystalline cellulose improved tablet hardness (10); it reached a maximum value of about 12 Erweka units. The disintegration time increased only slightly with increasing compression force, and a further increase in applied force (above 1514 kg) had no effect on tablet disintegration time. It is evident that apparent tablet density, hardness, and disintegration time reached maximum values at the same compression force. The reason that the disintegration time was independent of the compression force may be that no further compaction took place. The results on the ejection force are similar to those obtained with microcrystalline cellulose formulations (8).

Table VI provides useful quantitative data on the formula developed by the present authors, in which the calcium phosphate–carbonate complex was used as a tableting aid instead of microcrystalline cellulose. The selected formula produced hard tablets at moderate and high compaction forces. Ejection forces increased significantly with an increase in compaction force, whereas disintegration time decreased. Formulas III, IV, V, and VI all yielded tablets of low friability.

REFERENCES

(1) K. A. Khan and C. T. Rhodes, *Can. J. Pharm. Sci.*, **8**, 1(1973).

(2) K. A. Khan and C. T. Rhodes, *Manuf. Chem. Aerosol News*, **44**, 48(1973).

(3) K. A. Khan and C. T. Rhodes, *J. Pharm. Sci.*, **64**, 166 (1975).

(4) K. Marshall, Ph.D. thesis, University of Bradford, Yorkshire, England, 1970.

(5) R. F. Haines-Nutt, Ph.D. thesis, University of Wales, Cardiff, Wales, 1971.

(6) M. D. Richman, M.S. thesis, University of Maryland, Baltimore, Md., 1963.

(7) F. Fuchs, *Arch. Pharm.*, **303**, 471(1970).

(8) K. A. Khan and C. T. Rhodes, *Can. J. Pharm. Sci.*, **10**, 62(1975).

(9) *Ibid.*, **8**, 77(1973).

(10) K. S. Manudhane, Ph.D. thesis, University of Maryland, Baltimore, Md., 1967.

ACKNOWLEDGMENTS AND ADDRESSES

Received October 6, 1975, from **Beecham Pharmaceuticals, Worthing, England,* and the *‡Department of Pharmacy, University of Rhode Island, Kingston, RI 02881*

Accepted for publication January 26, 1976.

ˣ To whom inquiries should be directed.

Influence of Steroids and Stress on Toxicity and Disposition of Tetraethylammonium Bromide

PANOS KOUROUNAKIS ˣ and HANS SELYE

Abstract □ In female rats, pretreatment with dexamethasone acetate or triamcinolone reduced the toxicity and plasma concentrations of tetraethylammonium bromide while increasing its level in urine. Pretreatment with corticosterone acetate or pregnenolone-16α-carbonitrile shared none of these effects. Although starvation or restraint neither diminished the tetraethylammonium bromide concentrations in plasma nor accelerated its urinary excretion, its toxicity was diminished by the stress induced with spinal cord lesions, heat, cold, hydrocortisone, or reserpine as well as starvation or restraint. The protection offered against the toxicant by stress and by the potent glucocorticoids seemed to be mediated, at least partly, *via* different mechanisms. Stress-induced resistance to tetraethylammonium bromide could not be attributed to elevated plasma corticosterone levels, whereas glucocorticoid-induced resistance could be partially ascribed to increased urinary excretion of the toxicant.

Keyphrases □ Tetraethylammonium bromide—toxicity and urinary excretion, effect of stress and pretreatment with steroids, rats □ Toxicity—tetraethylammonium bromide, effect of stress and pretreatment with steroids, rats □ Excretion, urinary—tetraethylammonium bromide, effect of stress and pretreatment with steroids, rats □ Stress—effect on toxicity and urinary excretion of tetraethylammonium bromide, rats □ Steroids—pretreatment, effect on toxicity and urinary excretion of tetraethylammonium bromide, rats □ Ganglionic blocking agents—tetraethylammonium bromide, toxicity and urinary excretion, effect of stress and pretreatment with steroids, rats

When systemic adaptation is required, the body can respond *via* the nervous system, the reticuloendothelial–immunological–phagocytic system, and/or the hormonal mechanisms that significantly affect the organism's adaptive reactions, which may vary from nonspecific to highly specific (1, 2). Steroids, which are decisive factors in regulating stress, largely because of their influence upon enzyme-controlled responses (3, 4), can increase the body's resistance to many toxic agents (3, 5, 6). This effect is mediated mainly *via* heightened tissue tolerance for drugs (syntoxic mechanism) and/or enhanced drug disposition (catatoxic mechanism).

Well-documented investigations (7, 8) described the pharmacological and toxicological effects as well as the mechanisms of action of quaternary ammonium ganglionic blocking agents, *e.g.*, tetraethylammonium bromide (I). Earlier (9), stress and some glucocorticoids were shown to reduce the toxicity of some ganglionic blocking agents in rats. Pregnenolone-16α-carbonitrile (II), a potent microsomal enzyme inducer, influences the metabolism and, consequently, the toxicity of several drugs (6). However, sensitization or desensitization of target tissues by various agents (*e.g.*, hormones and stress) is not necessarily dependent upon drug disposition and may alter resistance to drugs. Therefore, it appeared of interest to study the influence of these dissimilar agents on the action of I and to correlate the findings with the *in vivo* protection offered by them.

Table I—Effect of Steroids on Tetraethylammonium Bromide Toxicity in Rats

Pretreatment	Toxicity	
	Dyskinesia (Positive/Total)	Mortality (Dead/Total)
Water plus polysorbate	18/18	4/18
Triamcinolone	3/18[a]	0/18[c]
Dexamethasone acetate	9/18[a]	0/18[c]
Pregnenolone-16α-carbonitrile	13/18[b]	1/18[c]
Corticosterone acetate	12/12[c]	0/12[c]

[a] $p < 0.005$. [b] $p < 0.05$. [c] $p > 0.05$ (not significant).

EXPERIMENTAL

Female Charles River CD rats[1], averaging 120 g and allowed food[2] and tap water *ad libitum*, were used.

First Experiment—The animals were divided into five groups and given either water or 20 μmoles of triamcinolone[3], dexamethasone[4], II[5], or corticosterone[6] orally twice daily for 3 days. Compound I (10 mg/100 g of body weight) was administered intraperitoneally to all animals on the 4th day, 18 hr after the last pretreatment. The effect of the steroids on I[7] toxicity was gauged by dyskinesia (estimated 30 min after I injection) and the mortality rate (measured after 24 hr) (Table I).

Dyskinesia was expressed in terms of an arbitrary scale in which 0 = no change, 1 = just detectable drowsiness or tremor, 2 = severe drowsiness and tremor (the animal did not respond to pinching), and 3 = intense convulsions and/or loss of the righting reflex (3). However, for statistical evaluation, only two grades were recognized: minor and dubious degrees of dyskinesia (0 and 1 in this scale) were rated as negative, and all others were considered positive. These data and the mortality rates were then arranged in a 2 × 2 contingency table, and their statistical significance was determined by the Exact Probability Test of Fisher and Yates (10, 11).

Second Experiment—The rats were divided into eight groups, of which one served as the control. The others were exposed to: (*a*) fasting (Group 2), *i.e.*, food and water deprivation for 48 hr; (*b*) spinal cord transection (Group 3) at the level of the seventh cervical vertebra, using thermocautery under ether anesthesia; (*c*) restraint (Group 4) on a board in a supine position for 47 hr; (*d*) cold (Group 5) at 12°; (*e*) heat (Group 6), *i.e.*, immersion in hot water of 55° for 1 min under light ether anesthesia; (*f*) hydrocortisone (Group 7), 10 mg po twice daily for 2 days; or (*g*) reserpine (Group 8), 50 μg/day sc for 2 days.

In addition, all groups except 1 were deprived of food and water for 48 hr, and all groups received 10 mg sc of I. Dyskinesia and mortality were estimated (Table II) as in the first experiment (Table I).

Third Experiment—The animals were grouped, stressed as in the second experiment, and killed 48 hr after application of the stressors. The thymus, adrenals, and spleen were then excised and weighed. The incidence of gastric ulcers was recorded, and blood was taken by decapitation for the determination of plasma corticosterone (Table II).

Fourth Experiment—Five groups of rats were pretreated as in

[1] Canadian Breeding Farms & Laboratories Ltd., St. Constant, Quebec, Canada.
[2] Purina Lab Chow.
[3] E. R. Squibb & Sons.
[4] Schering Corp. Ltd.
[5] The Upjohn Co.
[6] Merck Sharp & Dohme.
[7] Eastman Organic Chemicals.

Table II—Effect of Various Stressors on Thymus, Adrenal, and Spleen Weight, Gastric Ulcer Formation, Plasma Corticosterone Concentrations, and Tetraethylammonium Bromide Toxicity in Rats

Stressor	Thymus		Adrenals		Spleen		Gastric Ulcers (Positive/Total)	Plasma Corticosterone		Toxicity	
	Weight, mg/100	Decrease, %	Weight, mg	Increase, %	Weight, mg	Decrease, %		mg %	Increase, %	Dyskinesia (Positive/Total)	Mortality (Dead/Total)
Control	430 ± 21	—	14 ± 0.4	—	420 ± 20	—	0/15	7.8 ± 0.4	—	20/20	19/20
Fasting	310 ± 12[a]	28	19 ± 1.0[a]	36	300 ± 20[a]	29	4/20[b]	34.8 ± 6.5[a]	446	4/20[a]	0/20[a]
Restraint	250 ± 24[a]	42	19 ± 0.5[b]	36	160 ± 10[a]	38	13/20[a]	48.8 ± 6.7[a]	530	15/20[a]	9/20[c]
Spinal cord lesions	250 ± 20[a]	42	22 ± 1.0[a]	57	240 ± 10[c]	43	8/20[d]	69.4 ± 12.3[a]	790	9/18[a]	4/18[d]
Heat	230 ± 19[a]	47	25 ± 1.0[a]	79	240 ± 20[d]	43	8/15[a]	46.2 ± 4.0[a]	592	3/19[a]	0/19[a]
Cold	260 ± 13[a]	41	26 ± 1.0[a]	86	240 ± 20[d]	43	4/9[c]	58.8 ± 4.2[a]	620	5/16[a]	3/16[a]
Hydrocortisone	140 ± 8[a]	67	15 ± 0.5[b]	7	220 ± 20[a]	48	8/20[d]	35.0 ± 7.3[d]	449	2/20[a]	2/20[a]
Reserpine	230 ± 13[a]	47	24 ± 0.5[a]	71	280 ± 10[d]	33	9/20[a]	27.4 ± 4.4[a]	250	9/20[a]	2/20[a]

[a] $p < 0.005$. [b] $p > 0.05$ (not significant). [c] $p < 0.05$. [d] $p < 0.01$.

the first experiment. On the 4th day, 8 mg ip of I was administered; blood was collected 15 min later to measure the plasma I level (Table III).

Fifth Experiment—Three groups were used: one for control purposes, another for fasting, and the third for fasting plus restraint, as described in the second experiment. Compound I (8 mg ip) was given, and blood was taken 15 min later to measure the plasma I level (Table III).

Sixth Experiment—The rats were pretreated as in the fourth experiment and then given 6 mg ip of I. Urine was collected during the first 2 hr for I determination (12).

Seventh Experiment—The conditions of the fifth experiment were repeated. Compound I (6 mg ip) was administered, followed by urine collection for 2 hr to measure urinary I levels (12).

RESULTS

The stressor agents applied produced severe stress in all animals, as indicated by increased adrenal weight, decreased thymus and spleen weights, gastric ulcers, and high plasma corticosterone concentrations. These changes were statistically significant when compared with control values (Table II).

The dyskinesia and mortality elicited by I were markedly diminished in the stressed and triamcinolone- or dexamethasone-treated rats, while those given corticosterone or II showed only very moderate amelioration of I intoxication (Tables I and II). The plasma concentrations of I were significantly lower in the triamcinolone- and dexamethasone-treated animals and were relatively higher in the restrained rats; fasted and corticosterone- or II-treated animals exhibited no important alterations in this respect (Table III).

Urine flow was significantly influenced only in rats stressed by fasting or restraint. These two stressors as well as triamcinolone and dexamethasone, unlike II, caused significant body weight reductions. However, whereas II, fasting, and restraint did not increase the percentage of the total I dose excreted, treatment with the two potent glucocorticoids, triamcinolone and dexamethasone, did.

DISCUSSION

The nonspecific response of the body to any demand (stress) made by several agents is estimated by a number of parameters (thymus, spleen, adrenal, and body weight; gastric ulcers; and plasma corticosterone concentration), which can be employed with confidence (1, 4). With the use of these criteria, all applied stressors provoked a severe nonspecific reaction (Table II). The resistance of these animals to I intoxication was increased considerably, as judged by the diminution of dyskinesia and the mortality rate (Table II).

Like most quaternary ammonium salts, I is readily soluble in water. It is not metabolized in the body, and more than 95% of an injected dose is excreted through the kidney *via* glomerular filtration as well as through the proximal tubuli *via* an active transport mechanism (13, 14). Evidently, protection against I is not due to stimulation of its metabolism by stress *via* a regulatory function of the endocrine system, namely rapid induction of hepatic drug-metabolizing enzymes (2). This assumption was confirmed by a lack of any protective activity of II, a potent inducer of drug-metabolizing enzymes that has no other known pharmacological or hormonal properties (6, 15, 16). However, pretreatment with glucocorticoids offered significant protection against I intoxication (Table I). These findings could explain the prophylaxis provided by stress, characterized by high levels of circulating corticoids in the blood. However, triamcinolone and dexamethasone are more potent glucocorticoids than the natural corticosterone liberated during stress in rats (5). The protection offered by the glucocorticoids was well correlated with reduced I concentrations in plasma, whereas there was no such change after II treatment. This result could be partly attributed to a marked increase in I excretion (percentage of eliminated I being significantly greater than in the corresponding controls).

The situation was different in restrained or fasted rats, which exhibited no significant reduction of I concentrations in plasma. On the contrary, the plasma I concentrations were increased significantly in restrained animals. In neither case (restraint or fasting) was there a great alteration in the excretion pattern, although urine flow was diminished, a fact that could be attributed to the "total fasting" (food and water) of the rats. Steroid administration had no influence on

Table III—Effect of Steroid or Stress Conditioning on Tetraethylammonium Bromide Concentrations in Plasma, Its Urinary Excretion, and Urine Flow[a]

Pretreatment	Tetraethylammonium Bromide Concentrations in Plasma		Urinary Excretion of Tetraethylammonium Bromide			
			Urine Flow		Total Excretion	
	μg/ml	Change, %	μl/min	Change, %	% of Administered Dose	Change, %
Triamcinolone	(11) 24.7 ± 1.6[b] (8) [45.1 ± 2.3]	−45	(13) 8.5 ± 1.1[c] (10) [11.2 ± 1.4]	−24	86.6 ± 2.2[d] [74.4 ± 3.5]	16
Dexamethasone acetate	(9) 19.4 ± 0.7[b] (11) [45.1 ± 2.3]	−57	(10) 7.3 ± 1.2[c] (10) [6.2 ± 0.8]	17	85.8 ± 2.6[e] [77.2 ± 2.0]	11
Pregnenolone-16α-carbonitrile	(13) 39.8 ± 2.8[c] (11) [45.1 ± 2.3]	−12	(9) 11.8 ± 1.1[c] (10) [9.5 ± 1.1]	23	62.1 ± 7.2[c] [71.5 ± 7.6]	13
Fasting	(10) 39.0 ± 2.2[c] (7) [46.7 ± 3.8]	−17	(10) 6.2 ± 0.9[d] (3) [10.6 ± 1.0]	−42	89.0 ± 2.0[c] [87.0 ± 5.0]	2
Fasting plus restraint	(10) 96.6 ± 13.6[b] (7) [46.7 ± 3.8]	207	(6) 3.3 ± 0.3[b] (3) [10.6 ± 1.0]	−69	82.0 ± 3.0[c] [87.0 ± 5.0]	−6
Corticosterone acetate	(11) 45.3 ± 3.6[c] (9) [44.4 ± 3.9]	2	—		—	

[a] Figures in parentheses indicate number of animals; figures in square brackets indicate values of the controls. [b] $p < 0.005$. [c] $p > 0.05$ (not significant). [d] $p < 0.01$. [e] $p < 0.05$.

urine flow; therefore, it appears that the protection offered by the glucocorticoids against I is partly due to increased urinary excretion involving an active transport mechanism (17). Glucocorticoid treatment also may help provide readily available sources of energy (carbohydrates and free fatty acids) for I clearance or other adaptive work (2, 6, 16); stressed animals, depending on their state of stress, are handicapped in this respect.

Exhaustion may have been responsible for the high I concentrations in the plasma of restrained rats. However, they became less sensitive to the toxicant, probably through changes *via* unknown mechanisms at the molecular level. In stressful situations, the body's response to drugs apparently is influenced by a constellation of factors including the duration of stress, the time of sacrifice after exposure to stress, the superimposed specific actions of the stressor, the stage of the general adaptation syndrome that the animal has reached at the time of sacrifice for the *in vitro* tests, and the time of administration of the toxicant for the *in vivo* study (2). Thus, although both glucocorticoids and stress increase the organism's resistance to I, this protection probably is mediated, at least partly, *via* different pathways. Exogenous corticosterone did not significantly heighten resistance to I and did not alter the drug concentrations in plasma, which are further indications that the protection offered by stress is not mediated by corticoids produced by the adrenals during stress.

REFERENCES

(1) H. Selye, "Stress in Health and Disease," Butterworths, Reading, Mass., 1976.

(2) P. Kourounakis and H. Selye, *Bull. USSR Acad. Sci.*, in press.

(3) H. Selye, "Hormones and Resistance," Springer-Verlag, Heidelberg, Germany, 1971.

(4) H. Selye, "Stress," Acta Inc., Montreal, Canada, 1951.

(5) H. Selye, S. Szabo, Y. Tache, P. Kourounakis, I. Mecs, and J. Tache, *Steroids Lipids Res.*, **5**, 10(1974).

(6) P. Kourounakis, H. Selye, and Y. Tache, *Adv. Steroid Biochem. Pharmacol.*, in press.

(7) R. L. Volle and G. B. Koelle, in "The Pharmacological Basis of Therapeutics," 4th ed., L. S. Goodman and A. Gilman, Eds., Macmillan, London, England, 1971, pp. 402–441.

(8) G. B. Koelle, in *ibid.*, pp. 585–600.

(9) H. Selye, *Res. Commun. Chem. Pathol. Pharmacol.*, **1**, 572(1970).

(10) D. J. Finney, *Biometrika*, **35**, 145(1948).

(11) S. Siegel, "Nonparametric Statistics for the Behavioral Sciences," McGraw-Hill, New York, N.Y., 1956.

(12) R. Mitchell and B. B. Clark, *Proc. Soc. Exp. Biol. Med.*, **81**, 105(1952).

(13) B. R. Rennick, D. M. Calhoun, H. Gandia, and G. K. Moe, *J. Pharmacol. Exp. Ther.*, **110**, 309(1954).

(14) A. Farrah and B. Rennick, *ibid.*, **117**, 478(1956).

(15) P. Kourounakis, S. Szabo, and H. Selye, *Arzneim.-Forsch.*, **26**, 74(1976).

(16) P. Kourounakis, S. Szabo, and H. Selye, *Biochem. Pharmacol.*, **24**, 1549(1975).

(17) C. W. Driever and W. F. Bousquet, *Life Sci.*, **4**, 1449(1965).

ACKNOWLEDGMENTS AND ADDRESSES

Received December 10, 1975, from the *Institut de médecine et de chirurgie expérimentales, Université de Montréal, Montreal 101, Quebec, Canada.*

Accepted for publication February 23, 1976.

Supported in part by the Medical Research Council of Canada (Block Term Grant MT-1829) and the Ministère des Affaires Sociales, Quebec, Canada.

The authors thank Miss F. Dionne and Mrs. D. Papin for their excellent technical assistance and Mr. O. DaSilva for his editorial remarks.

[x] To whom inquiries should be directed.

Determination of the Nonnutritive Sweetener Sodium Cyclopentylsulfamate and Three of Its Metabolites, Cyclopentylamine, Cyclopentanone, and Cyclopentanol, in Urine of Rats and Rabbits

G. ANTHONY BENSON and WILLIAM J. SPILLANE ˣ

Abstract □ The nonnutritive sweetener sodium cyclopentylsulfamate was fed to Wistar albino rats and New Zealand White rabbits. Urine was collected for 3 days after feeding, combined, and examined for the metabolites cyclopentylamine, cyclopentanone, and cyclopentanol and for sodium cyclopentylsulfamate. A GLC method allowing the simultaneous analysis (with convenient retention times) for the amine, ketone, and alcoholic metabolites was developed. Sodium cyclopentylsulfamate was assayed by hydrolysis in acidified dioxane–water and subsequent measurement of the absorbance of the product formed (λ_{max} = 490 nm) by the liberated amine with *p*-benzoquinone. The average conversion to cyclopentylamine, cyclopentanone, and cyclopentanol was 0.103, 0.171, and 0.054% in the rabbit and 0.057, 0.016, and 0.008% in the rat, respectively.

Keyphrases □ Sodium cyclopentylsulfamate and metabolites—GLC analysis, rat and rabbit urine □ GLC—analysis, sodium cyclopentylsulfamate and metabolites, rat and rabbit urine □ Sweeteners—sodium cyclopentylsulfamate, GLC analysis, rat and rabbit urine □ Sulfamates, substituted—sodium cyclopentylsulfamate, GLC analysis, rat and rabbit urine

Despite the ban (since 1970) on the use of cyclamates, *i.e.*, salts of cyclohexylsulfamic acid, as sweetening additives in foods and soft drinks, considerable interest in these compounds exists. Most recent work has concentrated on the toxicity of cyclamates in humans (1–3) and other species (4–9) and on the metabolic sites of cyclamate breakdown in humans and other animals and the enzymes involved (10–14).

Because of the ban and because no toxicological studies have been reported on other sulfamates, it seemed worthwhile to evaluate some sulfamates that are structurally related to the banned cyclamates. This approach appeared to hold promise because: (*a*) many other sulfamates, especially those retaining the reduced ring, are sweet (15–17); (*b*) certain of these sulfamates, *e.g.*, sodium cyclopentylsulfamate, might be less easily metabolized to primary amines than cyclamates were to cyclohexylamine (18) and would, therefore, lack carcinogenic activity; and (*c*) such compounds might be commercially viable, since routes from the less expensive alcohols or ketones to the amines (which are then sulfamated) can be readily envisaged (16, 17, 19). To determine the level of metabolism to amines and also to check for other metabolites, *in vivo* feeding experiments with sodium cyclopentylsulfamate were conducted.

EXPERIMENTAL

Reagents and Chemicals—Sodium cyclopentylsulfamate was synthesized by reaction of the amine in dry chloroform with chlorosulfonic acid according to the method of Audrieth and Sveda (15) and recrystallized (twice) from ethanol.

Anal.—Calc. for $C_5H_{10}NNaO_3S$: C, 32.1; H, 5.3; N, 7.4. Found: C, 32.2; H, 5.5; N, 7.4.

Cyclopentylamine[1], cyclopentanone[1], cyclopentanol[1], and dichloromethane[2] were redistilled before use. *p*-Benzoquinone was sublimed. *n*-Dodecane[3], sulfosalicylic acid[4], chloroform, ethanol, and dioxane (reagent grade) were used as obtained.

Feeding Experiments—New Zealand White rabbits, female, approximately 2.7 kg, were kept on solid food and water in metabolism cages[5]. Wistar albino rats, female, approximately 300 g, were kept on solid food and water in smaller metabolism cages[6]. Prior to feeding, the urine of both species was collected and monitored using the two detection methods. Sodium cyclopentylsulfamate (370 mg/kg for rabbits, 1330 mg/kg for rats) was administered orally in aqueous solution.

For each species, urine was collected for 3 days after feeding. The urine samples collected from each animal were refrigerated daily. At the end of the 3rd day, the three samples were combined and analyzed as described. The combined samples from each animal were never refrigerated for more than 1 day prior to analysis. The stability of sodium cyclopentylsulfamate in urine was tested by refrigeration of urine containing sodium cyclopentylsulfamate (2.5, 5, and 7.5 mg/ml) for 4–5 days. No amine, ketone, or alcohol could be detected in any solution using the described method.

GLC Analysis and Standardization—Cyclopentylamine, cyclopentanone, and cyclopentanol were determined on a gas chroma-

Table I—Percent Recovery of Cyclopentylamine, Cyclopentanone, and Cyclopentanol from Urine

Amine		Ketone		Alcohol	
μg	%	μg	%	μg	%
860	104.89	940	100.31	940	96.11
860	96.28	940	95.26	940	89.46
1000	104.70	1100	98.43	1100	96.46
1000	107.18	1100	100.86	1100	95.38
1140	96.80	1260	99.85	1260	97.21
1140	99.41	1260	100.86	1260	—
1290	96.27	1420	97.26	1420	88.60
1290	100.93	1420	98.73	1420	91.13
Mean ± *SE*	100.80 ± 3.61		98.94 ± 1.52		93.47 ± 2.78

[1] Aldrich Chemical Co.
[2] May and Baker.
[3] British Drug Houses.
[4] Analar grade, May and Baker.
[5] Bowman Accessories, London, England.
[6] NKP, Kent, England.

Table II—Metabolism of Sodium Cyclopentylsulfamate in Rabbits

Animal Number	Recovered Sulfamate (Visible Spectrophotometry)		Cyclopentanol (GLC)		Cyclopentanone (GLC)		Cyclopentylamine (GLC)		Total Metabolites, %
	mg	%	mg	%	mg	%	mg	%	
1	592.3	59.20	1.096	0.237	0.454	0.100	0.55	0.121	0.458
2	500.8	50.08	0.100	0.022	0.716	0.159	0.62	0.136	0.317
3	778.2	77.82	Trace	—	1.458	0.324	0.48	0.105	0.429
4	439.8	43.98	None	—	0.756	0.168	0.316	0.069	0.237
5	499.8	49.98	0.055	0.012	0.468	0.104	0.394	0.086	0.202
Mean ± *SE*	562.2 ± 98.5	56.2 ± 9.83	0.25 ± 0.24	0.054 ± 0.051	0.77 ± 0.014	0.171 ± 0.061	0.472 ± 0.09	0.103 ± 0.02	0.328 ± 0.091

Table III—Metabolism of Sodium Cyclopentylsulfamate in Rats

Animal Number	Recovered Sulfamate (Visible Spectrophotometry)		Cyclopentanol (GLC)		Cyclopentanone (GLC)		Cyclopentylamine (GLC)		Total Metabolites, %
	mg	%	mg	%	mg	%	mg	%	
1	20.34	5.09	None	—	0.031	0.017	0.083	0.045	0.062
2	199.70	49.96	0.0286	0.015	0.017	0.009	0.173	0.095	0.119
3	26.90	6.72	0.0329	0.017	0.050	0.028	0.243	0.134	0.179
4	60.90	15.20	0.0087	0.004	0.018	0.010	0.020	0.01	0.024
5	22.24	5.60	0.025	0.012	0.027	0.015	0.05	0.02	0.047
6	34.00	8.50	0.0085	0.004	0.040	0.022	0.075	0.04	0.067
Mean ± *SE*	60.68 ± 46.30	15.17 ± 11.59	0.017 ± 0.008	0.008 ± 0.004	0.030 ± 0.009	0.016 ± 0.005	0.107 ± 0.067	0.057 ± 0.037	0.083 ± 0.044

tograph[7] with dual flame-ionization detectors. The column dimensions were 1.5 m × 0.63 cm (5 ft × 0.25 in.) (glass). The packing was 20% Dowfax 9N9 with 2.5% NaOH on 60–80-mesh Diatomite C-AW. The column temperature was 120°, and the gas flow rates were: nitrogen (carrier), 30 ml/min; hydrogen, 30 ml/min; and overall, 500 ml/min. The attenuation was 1×10^2, and the injector sample was 0.5 μl. Under these conditions, the retention times of cyclopentylamine, cyclopentanone, cyclopentanol, and *n*-dodecane were 4.2, 6.2, 9.2, and 12.2 min, respectively (Fig. 1).

A standard curve was prepared by injecting 1-μl portions of amine, ketone, and alcohol into 5-ml samples of urine. Then 5 ml of 20% sulfosalicylic acid (w/v) was added, and the pH was adjusted to 12–13 with 1 ml of 10 *N* NaOH. Then 2-ml samples were taken and extracted with 2 × 3 ml of dichloromethane (containing 0.04 ml of *n*-dodecane/250 ml of dichloromethane). The samples were centrifuged[8], and 2-ml portions were transferred to 5-ml volumetric flasks containing approximately 2–4 mg of anhydrous sodium sulfate. Samples of 0.5 μl were injected onto the column. A plot of peak height ratios (peak height of the amine, ketone, or alcohol/peak height of *n*-dodecane) *versus* concentration was linear over the 10–100-μg/ml range for each compound. Urine samples taken before and after feeding were similarly analyzed.

For purposes of estimating the percent recovery, varying amounts of the amine, ketone, and alcohol were determined by this procedure (Table I).

Visible Spectrophotometry Analysis and Standardization—Quantities from 3 to 33 mg of sodium cyclopentylsulfamate were dissolved in 1-ml samples of urine in 10-ml volumetric flasks. Then 4 ml of dioxane and 0.5 ml of 5 *M* perchloric acid were added. The flasks were placed for 3.5 hr in an oil bath at 95°, after which 2-ml samples were removed and extracted with 2 × 10 ml of chloroform. The extracts were made up to 25 ml with chloroform and transferred to 50-ml volumetric flasks. Then 10 ml of 1% benzoquinone solution was added to each flask.

The solutions were then heated at 60° in a water bath for 1.25 hr, and the absorbances were read[9] at 490 nm. A plot of absorbance *versus* concentration was linear over the 3–33-mg/ml range of sodium cyclopentylsulfamate. Urine samples taken before and after feeding were similarly analyzed. Sometimes emulsions formed during the extraction procedure, but separation of the urine and chloroform layers was achieved by centrifugation at 3000 rpm for 30 min.

RESULTS AND DISCUSSION

In choosing analytical techniques for the determination of sodium cyclopentylsulfamate and its metabolites, established methods for cyclamates and their metabolites should be adaptable with modifications. Accordingly, for the determination of sodium cyclopentylsulfamate in urine, the sulfamate was hydrolyzed to cyclopentylamine and reacted with *p*-benzoquinone and the absorbance of the colored product was determined. This method was mentioned in a survey of the analytical chemistry of cyclamates (20) and was used previously (21–23).

Johnson *et al.* (23) examined the method critically and found that the hydrolysis to the amine, which is carried out with hydrochloric acid in the presence of hydrogen peroxide, does not produce an equivalent amount of amine. They developed a method using hydrochloric acid but involving high temperatures and pressure. Previously, it was found that cyclamates can be hydrolyzed under less forcing conditions by employing an acidified aqueous dioxane medium, and this method has been used for hydrolyzing cyclopentylsulfamate. For the complete analysis of metabolites, the GLC method of Derse and Daun (24) was adapted; the amine, ketone, and alcohol have been determined from a single injection. Previous work with this method involved separate injections and different conditions for the determination of the amine and alcohol or ketone (25).

Results of analyses of the urine of rabbits and rats for unchanged sulfamate and various metabolites are given in Tables II and III, respectively. An average of about 56% of the sulfamate, either as "unchanged" sulfamate or as metabolites, was found for rabbits (Table II), which suggests that a little less than half of the sulfamate fed is excreted in the feces. From feeding studies with ^{14}C-cyclamate sodium

[7] Pye-Unicam 104.
[8] Griffin Christ centrifuge.
[9] Perkin-Elmer 124 double-beam spectrophotometer.

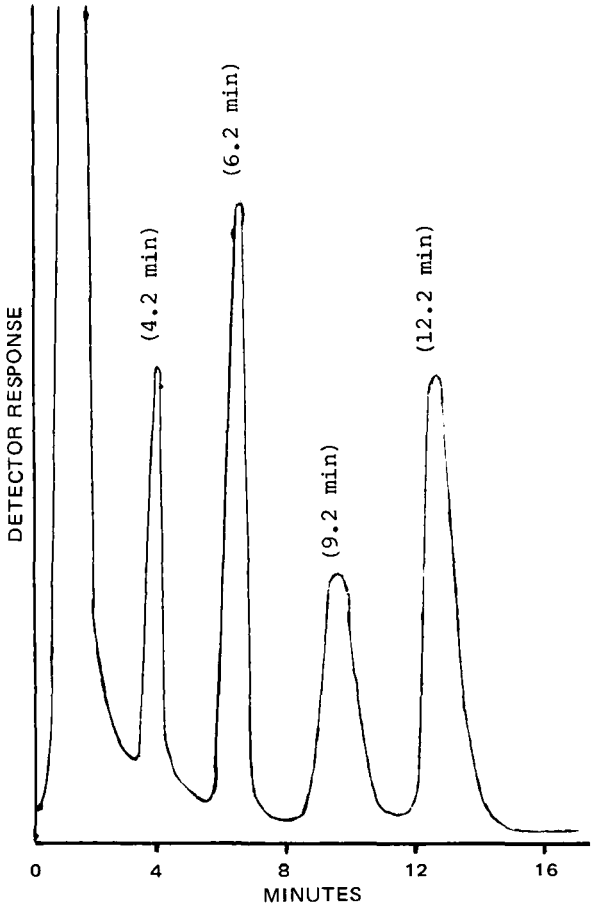

Figure 1—*Gas chromatogram of the urine metabolites of cyclopentylsulfamate: cyclopentylamine (4.2 min), cyclopentanone (6.2 min), and cyclopentanol (9.2 min). The internal standard was n-dodecane (12.2 min).*

in both control and pretreated (with unlabeled cyclamate) rabbits, Renwick and Williams (2) found that the radiolabel was excreted extensively in the urine and only about 6% was found in the feces. For rats, about 15% of the sulfamate was excreted in the urine (Table III); again, Renwick and Williams (2) found that for normal rats the distribution was about 40% in urine and 50% in feces. Derse and Daun (24), however, found that for rats receiving a level of sulfamate feed similar to ours, about 17% of the cyclamate was excreted in the urine and about 70% in the feces.

The conversion of sodium cyclopentylsulfamate to metabolites was calculated on a molar basis. Thus, a rabbit fed 1 g of sulfamate and excreting 0.3 mg of cyclopentylamine converted 0.066% of the sulfamate to cyclopentylamine:

$$(0.0003/85 \div 1/187)100 = 0.066\% \qquad \text{(Eq. 1)}$$

In the rabbit (Table II), the average conversion to metabolites was 0.103% for cyclopentylamine, 0.171% for cyclopentanone, and 0.054% for cyclopentanol. If these percentages are compared with those of previous studies on normal (*i.e.*, nonpretreated) rabbits that had received a single dose of cyclamate, they are found to be somewhat greater than the percentage conversion of cyclamate to cyclohexylamine, cyclohexanone, and cyclohexanol. Thus, the data of Ichibagase *et al.* (11) reveal that the average conversions to these latter three metabolites were 0.003, 0.002, and 0.003%, respectively, after feeding 200 mg/kg of cyclamate sodium. From another report (13) in which 200 mg/kg of cyclamate was also fed, average values of 0.0063, 0.0004, and 0.0004% can be calculated. Renwick and Williams (2) found a 0.04% conversion of cyclamate to cyclohexylamine in rabbits that had received 56 mg/kg. The degree of conversion may be dependent on the amount of cyclamate fed (even where only a single dose is given), since, for example, cyclamate-pretreated species convert a higher percent of fed cyclamate to metabolites than normal species (2, 12).

In the rat (Table III), the average conversions to metabolites were 0.057% for cyclopentylamine, 0.016% for cyclopentanone, and 0.008% for cyclopentanol. Another study (13) reported values of 0.0096, 0.001, and 0.0015% for the conversion of cyclamate to cyclohexylamine, cyclohexanone, and cyclohexanol, respectively, in normal rats receiving a single dose of cyclamate (500 mg/kg).

On the basis of the results presented here, it appears that cyclopentylsulfamate is metabolically cleaved to a somewhat greater extent than cyclamate. However, prolonged feeding experiments with cyclopentyl and other sweet sulfamates are planned to investigate the possibility of using other sulfamates as cyclamate alternatives.

REFERENCES

(1) A. G. Renwick and R. T. Williams, *Biochem. J.*, **129,** 857(1972).

(2) *Ibid.*, **129,** 869(1972).

(3) M. Asahina, T. Yamaha, K. Watanabe, and G. Sarrazin, *Chem. Pharm. Bull.*, **19,** 628(1971), and references cited therein.

(4) *Ibid.*, **20,** 102(1972).

(5) F. J. C. Roe, L. S. Levy, and R. L. Carter, *Food Cosmet. Toxicol.*, **8,** 135(1970).

(6) G. T. Bryan and E. Erturk, *Science*, **167,** 996(1970).

(7) P. G. Brantom, I. F. Gaunt, and P. Grasso, *Food Cosmet. Toxicol.*, **11,** 735(1973).

(8) J. M. Price, C. G. Biava, B. L. Oser, E. E. Vogin, J. Steinfeld, and H. L. Ley, *Science*, **167,** 1131(1970).

(9) C. Parekh, E. K. Goldberg, and L. Golberg, *Toxical. Appl. Pharmacol.*, **17,** 282(1970).

(10) B. S. Drasar, A. G. Renwick, and R. T. Williams, *Biochem. J.*, **129,** 881(1972).

(11) H. Ichibagase, S. Kojima, K. Inoue, and A. Suenaga, *Chem. Pharm. Bull.*, **20,** 175(1972).

(12) *Ibid.*, **20,** 1093(1972).

(13) A. Suenaga, S. Kojima, and H. Ichibagase, *Chem. Pharm. Bull.*, **20,** 1357(1972).

(14) T. Niimura, T. Tokieda, and T. Yamaha, *J. Biochem. (Tokyo)*, **75,** 407(1974).

(15) L. F. Audrieth and M. Sveda, *J. Org. Chem.*, **9,** 89(1944).

(16) B. Unterhalt and L. Boschemeyer, *Z. Lebensm.-Unters.-Forsch.*, **145,** 93(1971).

(17) *Ibid.*, **149,** 227(1972).

(18) W. J. Spillane, *J. Pharm. Sci.*, **62,** 1394(1973).

(19) E. J. Eisenbraun, in "Organic Synthesis," coll. vol. V, H. E. Baumgarten, Ed., Wiley, New York, N.Y., 1973, p. 310.

(20) M. L. Richardson, *Talanta*, **14,** 385(1967).

(21) S. Kojima and H. Ichibagase, *Yakugaku Zasshi*, **83,** 1108(1963); through *Chem. Abstr.*, **60,** 15060(1964).

(22) M. Ichikawa, S. Kojima, and H. Ichibagase, *ibid.*, **84,** 563(1964); through *Chem. Abstr.*, **61,** 10045(1964).

(23) D. E. Johnson, H. E. Nunn, and S. Bruckenstein, *Anal. Chem.*, **40,** 368(1968).

(24) P. H. Derse and R. J. Daun, *J. Assoc. Offic. Anal. Chem.*, **49,** 1090(1966).

(25) S. Kojima and H. Ichibagase, *Chem. Pharm. Bull.*, **17,** 2620(1969).

ACKNOWLEDGMENTS AND ADDRESSES

Received October 17, 1975, from the *Department of Chemistry, University College, Galway, Ireland.*

Accepted for publication February 19, 1976.

The authors thank the Department of Education (Ireland) for a grant to G. A. Benson.

[x] To whom inquiries should be directed.

Relative Aqueous Stabilities of Dinoprostone Free Acid (Prostaglandin E_2) and Its Carbamoylmethyl Ester

Keyphrases □ Dinoprostone—free acid and carbamoylmethyl ester, relative aqueous stabilities, effect of pH □ Stability, aqueous—dinoprostone free acid and carbamoylmethyl ester, effect of pH □ Prostaglandins—dinoprostone free acid and carbamoylmethyl ester, relative aqueous stabilities, effect of pH □ Oxytocic agents—dinoprostone free acid and carbamoylmethyl ester, relative aqueous stabilities, effect of pH

To the Editor:

We wish to report that C_1-esters of dinoprostone (prostaglandin E_2) do not provide an aqueous solution stability advantage over dinoprostone at mildly acidic pH but do provide a measurable improvement at pH > ~5.0. These findings lead to interpretations of the mechanism of dehydration of the E family of prostaglandins.

Recent publications (1, 2) treated the dehydration reaction of such prostaglandins, a degradation that occurs readily because of the labile β-hydroxy keto system in the C-8–C-12 ring. The data of Monkhouse *et al.* (1) revealed that the dehydration rate constant of dinoprostone was greater than that for prostaglandin E_1 in the pH 3–10 region, whereas the two prostaglandins showed equal stability at pH < 3. This difference was considered to be connected with the presence or absence of the C-5–C-6 double bond, which controlled the availability of some component of that side chain to the reaction site. Furthermore, these investigators ruled out the possibility of intramolecular general acid catalysis by the carboxyl group. The rate equation of Thompson *et al.* (2) included terms for specific acid and base catalyses, water catalysis, and general base catalysis.

We performed some kinetic studies comparing the stability of 0.00142 *M* solutions of dinoprostone and its carbamoylmethyl ester[1] (II), mp ~ 84°, under various conditions (Table I). The remaining prostaglandin was assayed in each case by quantitative extraction with ethyl acetate, followed by concentration and quantitative TLC on silica gel[2] with chloroform–methanol–acetic acid (90:5:5) as the developing solvent. Details of this assay procedure were reported previously (3).

It is apparent from Table I that removing the influence of the carboxyl group by esterification has no apparent effect on the rate constant at pH 4.0. The identical rate constants show that the ester has no advantage over the free acid in a mildly acidic medium. At pH 6, where dinoprostone exists mainly as the carboxylate anion, the ester shows a significant increase in stability. This increase is, however, not practical in terms of improving long-term prostaglandin stability in aqueous solution.

The following conclusions can be made from these findings. The pH 4.0 data show that general acid catalysis does not contribute measurably to the dinoprostone dehydration reaction. Because the pH–rate constant profile for dinoprostone "bottoms out" at pH 3–4 (2), water catalysis probably is occurring in the pH 4.0 region. The degradation rate, otherwise dependent only on specific acid catalysis at pH 3–4, would be much lower. The difference between dinoprostone and its carbamoylmethyl ester at pH 6.0 demonstrates intramolecular general base catalysis by the carboxylate anion.

From the comparative data generated by adding acetate anion (Table I) as a similar, but intermolecular, general base catalyst, it may be seen that the intramo-

Table I—Rate Constants for Dinoprostone (I) and Its Carbamoylmethyl Ester (II) in pH 4.0 (0.1 *M* Citrate) and 6.0 (0.1 *M* Phosphate) Buffers under Various Conditions ($C_0 = 1.42 \times 10^{-3}$ *M*)

Compound	pH	Temperature	Rate Constant, hr^{-1}	Comment
I	4.0	70°	0.125 ± 0.0019	—
II	4.0	70°	0.123 ± 0.013	—
I	6.0	70°	0.228 ± 0.0072	$\frac{k_I}{k_{II}} = 1.49$
II	6.0	70°	0.153 ± 0.0031	
I	6.0	60°	0.0817 ± 0.0028[a]	$\frac{k_I}{k_{II}} = 1.49$
II	6.0	60°	0.0547 ± 0.0024	
II	6.0	70°	0.317 ± 0.0045	1.0 *M* acetate anion included in 0.1 *M* phosphate medium
II	6.0	70°	0.213 ± 0.0069	0.4 *M* acetate anion included in 0.1 *M* phosphate medium
I	6.0	60°	0.0829 ± 0.0132[b]	1.0 *M* NaCl included in 0.1 *M* phosphate medium

[a] Two runs. [b] Four runs.

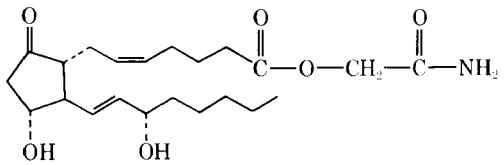

II

[1] Supplied by W. Morozowich, The Upjohn Co.
[2] UNIPLATES, 250-μm Silica Gel GF, Analtech Corp., Newark, DE 19711

lecular carboxylate effect (bulk concentration = 1.4×10^{-3} M) is probably a couple of orders of magnitude more efficient (4) than intermolecular carboxylate (concentration = 0.4–1.0 M). This finding is also consistent with the relative nondependence of the overall degradation rate constant of dinoprostone on concentration.

No attempt was made to equalize the ionic strengths of the media in these experiments, particularly those determining the effect of added acetate. As Table I shows, addition of 1.0 M NaCl makes no significant difference in the observed rate constant at pH 6.0. More detailed findings will be related in a subsequent report.

(1) D. C. Monkhouse, L. VanCampen, and A. J. Aguiar, *J. Pharm. Sci.*, **62**, 576(1973).

(2) G. F. Thompson, J. M. Collins, and L. M. Schmalzried, *ibid.*, **62**, 1738(1973).

(3) T. J. Roseman, B. E. Sims, and R. G. Stehle, *Am. J. Hosp. Pharm.*, **30**, 236(1973).

(4) M. L. Bender and L. J. Brubacher, "Catalysis and Enzyme Action," McGraw-Hill, New York, N.Y., 1973, p. 63ff.

Randall G. Stehle [x]
Russell W. Smith
Pharmacy Research
The Upjohn Company
Kalamazoo, MI 49001

Received April 7, 1976.
Accepted for publication July 21, 1976.
[x] To whom inquiries should be directed.

BOOKS

REVIEWS

Pharmacy and the Law. By CARL T. DeMARCO. Aspen Systems Corp., 20010 Century Blvd., Germantown, MD 20767, 1975. 381 pp. 16 × 24 cm. Price $19.50.

Carl DeMarco has filled a void in pharmacy literature with the publication of this book on pharmacy law. It is a descriptive and interpretive text on the many legal considerations involved with pharmacy practice. An analysis of pharmacy laws and legal issues of current interest is skillfully presented.

The book is divided into four parts. Part I is concerned with the professional practice of pharmacy. Topics of interest to practicing pharmacists as well as students include standards of practice, drug product selection, quality assurance, and the legal aspects of clinical pharmacy. The chapter on standards of practice and a subsequent chapter on negligence contain relevant information on standards with which today's pharmacist is expected to comply. A section on licensure requirements and operating a pharmacy highlights the North Dakota case on pharmacy ownership. Supportive personnel are discussed along with the licensure requirements of a pharmacist.

Drug laws are discussed in Part II. Of interest is a section on the dispensing of a drug for an "unofficial" or "nonapproved" use or dose. Pharmacy applications of the Federal Food, Drug and Cosmetic Act are mentioned. In addition, sections of this act are included in the appendix for those who wish to further examine it.

Part III deals solely with controlled substances. Since failure to comply with the many specific rules of the Controlled Substances Act can result in violation of the law, the author presents an interpretation of the requirements in addition to a copy of a selected section of this act.

Part IV covers professional liability. Various types of liabilities, including malpractice, are presented in a most understandable format. References to specific court cases and to regulations clarify the legal terms and the laws of interest to pharmacists.

A combination of background material, court cases, laws, regulations, and the author's interpretations make this an interesting and informative text. Drug laws and the regulation of drug use control inevitably undergo change. Hence the book will be outdated without periodic supplements or frequent revisions. The author has made a contribution in this well-written text. It should be of interest to practicing pharmacists and students of pharmacy law because it is completely understandable to the nonattorney. It should serve as an excellent reference source book and as a textbook.

Reviewed by Albert I. Wertheimer
University of Minnesota
Minneapolis, MN 55414

Pharmacokinetics. Pharmacy and Related Subjects Series. Vol. 1. By MILO GIBALDI and DONALD PERRIER. Dekker, 270 Madison Ave., New York, NY 10016, 1975. 329 pp. 16 × 24 cm. $19.50.

As a textbook, the choice of topics is excellent and the order of presentation is logical. As a reference source, the reader may find it selectively parsimonious.

There are nine chapters and appendixes in this volume. The subject is introduced through modeling of linear systems of increasing complexity (Chapters 1 and 2). The techniques developed are then applied to study kinetic behavior on multiple dosing and to estimate drug bioavailability (Chapters 3 and 4). The concept of volumes of distribution is discussed in Chapter 5. The remaining chapters may be considered special topics, which include the kinetics of pharmacologic response, nonlinear systems, and the effect of route of administration and of renal impairment on drug disposition. The fact that step-by-step derivations of mathematical expressions are given throughout may be helpful to some but distracting to others.

Even though a glossary of terms is included, duplications remain. For example, the variable t is used to represent real time, time from the last dose, and time after an infusion. The definition of β as the "apparent first-order elimination rate constant for a drug that confers upon the body the characteristics of a multi-compartment model, obtained from the terminal slope . . . " may be less than universally acceptable. While β may be shown to be a constant of proportionality between the disappearance rate and the amount of drug in the body during the log-linear phase, this particular usage is valid only some of the time. For all times, β is a function of drug distribution as well as elimination.

By their recurrence, perhaps greater importance has been ascribed to the assumption concerning the completeness of absorption and to the idea of modeling from radioactivity data of unknown chemical composition than they deserve. In both cases, the practical limitations are formidable in actual usage. On the other hand, the material in Chapter 8 on the route of administration and drug disposition may be difficult for the uninitiated without a fuller discourse of alternative views, at least in reference.

When read in perspective, particularly in the prescribed sequence, this volume is a valuable teaching text in pharmacokinetics. It is the first of its kind in English and fulfills a critical need at an intermediate level between elementary and encyclopedic.

Reviewed by K. C. Kwan
Merck Sharp & Dohme Research Laboratories
West Point, PA 19486

lecular carboxylate effect (bulk concentration = 1.4×10^{-3} M) is probably a couple of orders of magnitude more efficient (4) than intermolecular carboxylate (concentration = 0.4–1.0 M). This finding is also consistent with the relative nondependence of the overall degradation rate constant of dinoprostone on concentration.

No attempt was made to equalize the ionic strengths of the media in these experiments, particularly those determining the effect of added acetate. As Table I shows, addition of 1.0 M NaCl makes no significant difference in the observed rate constant at pH 6.0. More detailed findings will be related in a subsequent report.

(1) D. C. Monkhouse, L. VanCampen, and A. J. Aguiar, *J. Pharm. Sci.*, **62**, 576(1973).

(2) G. F. Thompson, J. M. Collins, and L. M. Schmalzried, *ibid.*, **62**, 1738(1973).

(3) T. J. Roseman, B. E. Sims, and R. G. Stehle, *Am. J. Hosp. Pharm.*, **30**, 236(1973).

(4) M. L. Bender and L. J. Brubacher, "Catalysis and Enzyme Action," McGraw-Hill, New York, N.Y., 1973, p. 63ff.

Randall G. Stehle [x]
Russell W. Smith
Pharmacy Research
The Upjohn Company
Kalamazoo, MI 49001

Received April 7, 1976.
Accepted for publication July 21, 1976.
[x] To whom inquiries should be directed.

BOOKS

REVIEWS

Pharmacy and the Law. By CARL T. DeMARCO. Aspen Systems Corp., 20010 Century Blvd., Germantown, MD 20767, 1975. 381 pp. 16 × 24 cm. Price $19.50.

Carl DeMarco has filled a void in pharmacy literature with the publication of this book on pharmacy law. It is a descriptive and interpretive text on the many legal considerations involved with pharmacy practice. An analysis of pharmacy laws and legal issues of current interest is skillfully presented.

The book is divided into four parts. Part I is concerned with the professional practice of pharmacy. Topics of interest to practicing pharmacists as well as students include standards of practice, drug product selection, quality assurance, and the legal aspects of clinical pharmacy. The chapter on standards of practice and a subsequent chapter on negligence contain relevant information on standards with which today's pharmacist is expected to comply. A section on licensure requirements and operating a pharmacy highlights the North Dakota case on pharmacy ownership. Supportive personnel are discussed along with the licensure requirements of a pharmacist.

Drug laws are discussed in Part II. Of interest is a section on the dispensing of a drug for an "unofficial" or "nonapproved" use or dose. Pharmacy applications of the Federal Food, Drug and Cosmetic Act are mentioned. In addition, sections of this act are included in the appendix for those who wish to further examine it.

Part III deals solely with controlled substances. Since failure to comply with the many specific rules of the Controlled Substances Act can result in violation of the law, the author presents an interpretation of the requirements in addition to a copy of a selected section of this act.

Part IV covers professional liability. Various types of liabilities, including malpractice, are presented in a most understandable format. References to specific court cases and to regulations clarify the legal terms and the laws of interest to pharmacists.

A combination of background material, court cases, laws, regulations, and the author's interpretations make this an interesting and informative text. Drug laws and the regulation of drug use control inevitably undergo change. Hence the book will be outdated without periodic supplements or frequent revisions. The author has made a contribution in this well-written text. It should be of interest to practicing pharmacists and students of pharmacy law because it is completely understandable to the nonattorney. It should serve as an excellent reference source book and as a textbook.

Reviewed by Albert I. Wertheimer
University of Minnesota
Minneapolis, MN 55414

Pharmacokinetics. Pharmacy and Related Subjects Series. Vol. 1. By MILO GIBALDI and DONALD PERRIER. Dekker, 270 Madison Ave., New York, NY 10016, 1975. 329 pp. 16 × 24 cm. $19.50.

As a textbook, the choice of topics is excellent and the order of presentation is logical. As a reference source, the reader may find it selectively parsimonious.

There are nine chapters and appendixes in this volume. The subject is introduced through modeling of linear systems of increasing complexity (Chapters 1 and 2). The techniques developed are then applied to study kinetic behavior on multiple dosing and to estimate drug bioavailability (Chapters 3 and 4). The concept of volumes of distribution is discussed in Chapter 5. The remaining chapters may be considered special topics, which include the kinetics of pharmacologic response, nonlinear systems, and the effect of route of administration and of renal impairment on drug disposition. The fact that step-by-step derivations of mathematical expressions are given throughout may be helpful to some but distracting to others.

Even though a glossary of terms is included, duplications remain. For example, the variable t is used to represent real time, time from the last dose, and time after an infusion. The definition of β as the "apparent first-order elimination rate constant for a drug that confers upon the body the characteristics of a multi-compartment model, obtained from the terminal slope . . . " may be less than universally acceptable. While β may be shown to be a constant of proportionality between the disappearance rate and the amount of drug in the body during the log-linear phase, this particular usage is valid only some of the time. For all times, β is a function of drug distribution as well as elimination.

By their recurrence, perhaps greater importance has been ascribed to the assumption concerning the completeness of absorption and to the idea of modeling from radioactivity data of unknown chemical composition than they deserve. In both cases, the practical limitations are formidable in actual usage. On the other hand, the material in Chapter 8 on the route of administration and drug disposition may be difficult for the uninitiated without a fuller discourse of alternative views, at least in reference.

When read in perspective, particularly in the prescribed sequence, this volume is a valuable teaching text in pharmacokinetics. It is the first of its kind in English and fulfills a critical need at an intermediate level between elementary and encyclopedic.

Reviewed by K. C. Kwan
Merck Sharp & Dohme Research Laboratories
West Point, PA 19486

lecular carboxylate effect (bulk concentration = 1.4×10^{-3} M) is probably a couple of orders of magnitude more efficient (4) than intermolecular carboxylate (concentration = 0.4–1.0 M). This finding is also consistent with the relative nondependence of the overall degradation rate constant of dinoprostone on concentration.

No attempt was made to equalize the ionic strengths of the media in these experiments, particularly those determining the effect of added acetate. As Table I shows, addition of 1.0 M NaCl makes no significant difference in the observed rate constant at pH 6.0. More detailed findings will be related in a subsequent report.

(1) D. C. Monkhouse, L. VanCampen, and A. J. Aguiar, *J. Pharm. Sci.*, **62**, 576(1973).

(2) G. F. Thompson, J. M. Collins, and L. M. Schmalzried, *ibid.*, **62**, 1738(1973).

(3) T. J. Roseman, B. E. Sims, and R. G. Stehle, *Am. J. Hosp. Pharm.*, **30**, 236(1973).

(4) M. L. Bender and L. J. Brubacher, "Catalysis and Enzyme Action," McGraw-Hill, New York, N.Y., 1973, p. 63ff.

Randall G. Stehle [x]
Russell W. Smith
Pharmacy Research
The Upjohn Company
Kalamazoo, MI 49001

Received April 7, 1976.
Accepted for publication July 21, 1976.
[x] To whom inquiries should be directed.

BOOKS

REVIEWS

Pharmacy and the Law. By CARL T. DeMARCO. Aspen Systems Corp., 20010 Century Blvd., Germantown, MD 20767, 1975. 381 pp. 16 × 24 cm. Price $19.50.

Carl DeMarco has filled a void in pharmacy literature with the publication of this book on pharmacy law. It is a descriptive and interpretive text on the many legal considerations involved with pharmacy practice. An analysis of pharmacy laws and legal issues of current interest is skillfully presented.

The book is divided into four parts. Part I is concerned with the professional practice of pharmacy. Topics of interest to practicing pharmacists as well as students include standards of practice, drug product selection, quality assurance, and the legal aspects of clinical pharmacy. The chapter on standards of practice and a subsequent chapter on negligence contain relevant information on standards with which today's pharmacist is expected to comply. A section on licensure requirements and operating a pharmacy highlights the North Dakota case on pharmacy ownership. Supportive personnel are discussed along with the licensure requirements of a pharmacist.

Drug laws are discussed in Part II. Of interest is a section on the dispensing of a drug for an "unofficial" or "nonapproved" use or dose. Pharmacy applications of the Federal Food, Drug and Cosmetic Act are mentioned. In addition, sections of this act are included in the appendix for those who wish to further examine it.

Part III deals solely with controlled substances. Since failure to comply with the many specific rules of the Controlled Substances Act can result in violation of the law, the author presents an interpretation of the requirements in addition to a copy of a selected section of this act.

Part IV covers professional liability. Various types of liabilities, including malpractice, are presented in a most understandable format. References to specific court cases and to regulations clarify the legal terms and the laws of interest to pharmacists.

A combination of background material, court cases, laws, regulations, and the author's interpretations make this an interesting and informative text. Drug laws and the regulation of drug use control inevitably undergo change. Hence the book will be outdated without periodic supplements or frequent revisions. The author has made a contribution in this well-written text. It should be of interest to practicing pharmacists and students of pharmacy law because it is completely understandable to the nonattorney. It should serve as an excellent reference source book and as a textbook.

Reviewed by Albert I. Wertheimer
University of Minnesota
Minneapolis, MN 55414

Pharmacokinetics. Pharmacy and Related Subjects Series. Vol. 1. By MILO GIBALDI and DONALD PERRIER. Dekker, 270 Madison Ave., New York, NY 10016, 1975. 329 pp. 16 × 24 cm. $19.50.

As a textbook, the choice of topics is excellent and the order of presentation is logical. As a reference source, the reader may find it selectively parsimonious.

There are nine chapters and appendixes in this volume. The subject is introduced through modeling of linear systems of increasing complexity (Chapters 1 and 2). The techniques developed are then applied to study kinetic behavior on multiple dosing and to estimate drug bioavailability (Chapters 3 and 4). The concept of volumes of distribution is discussed in Chapter 5. The remaining chapters may be considered special topics, which include the kinetics of pharmacologic response, nonlinear systems, and the effect of route of administration and of renal impairment on drug disposition. The fact that step-by-step derivations of mathematical expressions are given throughout may be helpful to some but distracting to others.

Even though a glossary of terms is included, duplications remain. For example, the variable t is used to represent real time, time from the last dose, and time after an infusion. The definition of β as the "apparent first-order elimination rate constant for a drug that confers upon the body the characteristics of a multi-compartment model, obtained from the terminal slope . . . " may be less than universally acceptable. While β may be shown to be a constant of proportionality between the disappearance rate and the amount of drug in the body during the log-linear phase, this particular usage is valid only some of the time. For all times, β is a function of drug distribution as well as elimination.

By their recurrence, perhaps greater importance has been ascribed to the assumption concerning the completeness of absorption and to the idea of modeling from radioactivity data of unknown chemical composition than they deserve. In both cases, the practical limitations are formidable in actual usage. On the other hand, the material in Chapter 8 on the route of administration and drug disposition may be difficult for the uninitiated without a fuller discourse of alternative views, at least in reference.

When read in perspective, particularly in the prescribed sequence, this volume is a valuable teaching text in pharmacokinetics. It is the first of its kind in English and fulfills a critical need at an intermediate level between elementary and encyclopedic.

Reviewed by K. C. Kwan
Merck Sharp & Dohme Research Laboratories
West Point, PA 19486

Biopharmaceutics and Pharmacokinetics: An Introduction (Second Edition, Revised and Expanded). By ROBERT E. NOTARI. Dekker, 270 Madison Ave., New York, NY 10016, 1975. 285 pp. 15.5 x 23 cm. Price $13.75.

This is the second edition of a book that has already proven valuable to students of biopharmaceutics and to workers in allied biomedical fields who want to teach themselves pharmacokinetics. As the author points out in his preface, the pharmacokinetics portions of the book are organized almost as a programmed learning text. Each new principle is first briefly described, and all working equations are clearly derived. Then an example problem is completely worked out, and at least one practice problem (with answer) is provided. By using this book, it should be possible, even for students with little or no training in calculus, to become competent to handle most one- and two-compartment pharmacokinetic problems.

In the second edition, the chapters titled Rate Processes in Biological Systems (Chapter 2) and Principles of Pharmacokinetics (Chapter 3) have been rewritten, mostly for the purpose of reorganizing the sequence of material. Fortunately, these chapters have not lost any of their original lucidity.

The chapter titled Biopharmaceutics: Clinical Applications of Pharmacokinetic Parameters (Chapter 4) introduces the reader to factors affecting gastrointestinal absorption of drugs, sustained-release dosage forms, and calculation and prediction of drug concentrations in blood during repetitive dosing regimens. A brief discussion of dosage regimen adjustment in patients with compromised renal function has been added to this chapter. This is a welcome addition since so much emphasis is being placed on this aspect of clinical pharmacy practice today. It is hoped that, in future editions, this section will be expanded to include a more thorough discussion of the topic and a broader coverage of the many examples of drugs that are now routinely dosed according to pharmacokinetic principles.

The chapter titled Pharmacokinetic Aspects of Structural Modifications in Drug Design and Therapy (Chapter 5) is a completely new chapter based on a review written by the author for the *Journal of Pharmaceutical Sciences*. Although this chapter covers essentially the same material as the review article, a number of example problems and leading questions have been added, which should be of significant help to the student in understanding the principles discussed.

Significant general improvements over the first edition are that the chapters have been provided with generous lists of references, and several appendices and an author index have been added. These expansions and improvements coupled with retention of the lucid step-by-step approach to pharmacokinetics that characterized the first edition cause this reviewer to rate this book very highly as a beginning text in biopharmaceutics and pharmacokinetics.

Reviewed by Lewis W. Dittert
College of Pharmacy
University of Kentucky
Lexington, KY 40506

Biological Membranes. Their Structure and Function. By ROGER HARRISON and GEORGE G. LUNT. Halsted, 605 Third Ave., New York, NY 10016, 1975. viii + 253 pp. 14.5 × 20.5 cm. Price $9.95.

Membrane biology is a rapidly growing field of research, and there are many texts available on this subject for the expert as well as the student. Harrison and Lunt designed their book for advanced undergraduates in biology and biochemistry. It is also an excellent introduction for those interested in beginning research in this area and a very good review for those with a peripheral interest in the biology and anatomy of membranes. This book is well organized, contains many helpful illustrations, and has an adequate bibliography at the end of each chapter.

The first two chapters provide a historical review of the microscope, a general discussion of cellular organelles, and a brief account of membrane functions, which include transfer systems and the role of membrane-bound enzymes. The next chapter deals with the morphology of membranes and presents many electron micrographs. Included in Chapters 4 and 5 are methods for the preparation of isolated membrane fractions and a detailed account of membrane components. There are considerable illustrations, including space filling models of chemical structures. Chapter 6 is an up-to-date discussion of the structural organization of plasma membranes. It covers the Davson and Danielli model, the current fluid mosaic concept of Singer and Nicholson, and many unanswered questions of membrane structure and biosynthesis.

Chapter 7 contains a general discussion of cell surface specificity, the function of membrane carbohydrates, and the involvement of membrane carbohydrates in histocompatibility antigens and cell recognition and adhesion phenomena. It also includes a cursory look at properties of cancer cells which can be related to alterations in the plasma membrane. Membrane-mediated processes are presented in the next chapter and comprise many cellular activities in which plasma membranes participate.

Chapter 9 is an elementary discussion of transport systems. There are examples and definitions of diffusional processes; however, there are only two mathematical relationships, Fick's law and the Nernst equation. The book ends with a good discussion of ionophoric antibiotics, physical methods used in the study of plasma membranes, and a further reading list categorized by chapter. It is an excellent starting point for students and an enjoyable review for those more familiar with the area.

Reviewed by Joseph S. Turi
Pharmacy Research
The Upjohn Company
Kalamazoo, MI 49001

High-Speed Liquid Chromatography (Chromatographic Science Series Vol. 6). Edited by P. M. RAJCSANYI and E. RAJCSANYI. Dekker, 270 Madison Avenue, New York, NY 10016, 1975. 16 × 23 cm. 203 pp. Price $15.50.

For this concise, well-organized review, the editors divided the high-pressure liquid chromatographic literature into three sections dealing with theory, instrumentation, and applications. In addition to gradient, pump, and injection systems, columns and preparative techniques are discussed in the instrumentation chapter. The section devoted to detectors is particularly detailed. A number of applications of pharmaceutical interest are reported. These are categorized into sections on alkaloids, carbohydrates, drugs, steroids, vitamins, nucleic acid constituents, and compounds in biological fluids.

Since there are only a few references dated later than 1973, this volume is already somewhat dated, as can be expected for any review of a rapidly developing field such as high-pressure liquid chromatography. For instance, the statement that there have been several recent attempts to extend the usefulness of light absorption detectors over the whole UV–visible range could now be amended to state that such detectors are commercially available and in considerable use. Likewise, the column and application sections do not reflect the present literature emphasis on chemically bonded phases and microparticulate supports.

While this volume does represent a partial update to the thorough coverage presented by Snyder and Kirkland in 1974, it is too brief (123 pages of text) to be considered a replacement. Furthermore, this monograph is a review in the strictest sense in that it lacks the generalization and critical commentary that imparts the invaluable element of experience to a book. With its extensive references, however, it would be useful as an index for rapid access to the literature of a specific topic. For this reason, libraries should acquire a copy. While practitioners will be acquainted with much of the information therein, beginners may find this volume useful as a quick introduction to the field. The quality of print and binding are commensurate with price.

Reviewed by Van D. Reif
Drug Research and Testing Laboratory
United States Pharmacopeial Convention, Inc.
Rockville, MD 20852

NEW JOURNALS

Journal of Chromatography, Biomedical Applications. K. MACEK, Editor. American Elsevier, 52 Vanderbilt Ave., New York, NY 10017, January 1977. Price $49.75 annual subscription (six issues).

Biopharmaceutics and Pharmacokinetics: An Introduction (Second Edition, Revised and Expanded). By ROBERT E. NOTARI. Dekker, 270 Madison Ave., New York, NY 10016, 1975. 285 pp. 15.5 x 23 cm. Price $13.75.

This is the second edition of a book that has already proven valuable to students of biopharmaceutics and to workers in allied biomedical fields who want to teach themselves pharmacokinetics. As the author points out in his preface, the pharmacokinetics portions of the book are organized almost as a programmed learning text. Each new principle is first briefly described, and all working equations are clearly derived. Then an example problem is completely worked out, and at least one practice problem (with answer) is provided. By using this book, it should be possible, even for students with little or no training in calculus, to become competent to handle most one- and two-compartment pharmacokinetic problems.

In the second edition, the chapters titled Rate Processes in Biological Systems (Chapter 2) and Principles of Pharmacokinetics (Chapter 3) have been rewritten, mostly for the purpose of reorganizing the sequence of material. Fortunately, these chapters have not lost any of their original lucidity.

The chapter titled Biopharmaceutics: Clinical Applications of Pharmacokinetic Parameters (Chapter 4) introduces the reader to factors affecting gastrointestinal absorption of drugs, sustained-release dosage forms, and calculation and prediction of drug concentrations in blood during repetitive dosing regimens. A brief discussion of dosage regimen adjustment in patients with compromised renal function has been added to this chapter. This is a welcome addition since so much emphasis is being placed on this aspect of clinical pharmacy practice today. It is hoped that, in future editions, this section will be expanded to include a more thorough discussion of the topic and a broader coverage of the many examples of drugs that are now routinely dosed according to pharmacokinetic principles.

The chapter titled Pharmacokinetic Aspects of Structural Modifications in Drug Design and Therapy (Chapter 5) is a completely new chapter based on a review written by the author for the *Journal of Pharmaceutical Sciences*. Although this chapter covers essentially the same material as the review article, a number of example problems and leading questions have been added, which should be of significant help to the student in understanding the principles discussed.

Significant general improvements over the first edition are that the chapters have been provided with generous lists of references, and several appendices and an author index have been added. These expansions and improvements coupled with retention of the lucid step-by-step approach to pharmacokinetics that characterized the first edition cause this reviewer to rate this book very highly as a beginning text in biopharmaceutics and pharmacokinetics.

Reviewed by Lewis W. Dittert
College of Pharmacy
University of Kentucky
Lexington, KY 40506

Biological Membranes. Their Structure and Function. By ROGER HARRISON and GEORGE G. LUNT. Halsted, 605 Third Ave., New York, NY 10016, 1975. viii + 253 pp. 14.5 × 20.5 cm. Price $9.95.

Membrane biology is a rapidly growing field of research, and there are many texts available on this subject for the expert as well as the student. Harrison and Lunt designed their book for advanced undergraduates in biology and biochemistry. It is also an excellent introduction for those interested in beginning research in this area and a very good review for those with a peripheral interest in the biology and anatomy of membranes. This book is well organized, contains many helpful illustrations, and has an adequate bibliography at the end of each chapter.

The first two chapters provide a historical review of the microscope, a general discussion of cellular organelles, and a brief account of membrane functions, which include transfer systems and the role of membrane-bound enzymes. The next chapter deals with the morphology of membranes and presents many electron micrographs. Included in Chapters 4 and 5 are methods for the preparation of isolated membrane fractions and a detailed account of membrane components. There are considerable illustrations, including space filling models of chemical structures. Chapter 6 is an up-to-date discussion of the structural organization of plasma membranes. It covers the Davson and Danielli model, the current fluid mosaic concept of Singer and Nicholson, and many unanswered questions of membrane structure and biosynthesis.

Chapter 7 contains a general discussion of cell surface specificity, the function of membrane carbohydrates, and the involvement of membrane carbohydrates in histocompatibility antigens and cell recognition and adhesion phenomena. It also includes a cursory look at properties of cancer cells which can be related to alterations in the plasma membrane. Membrane-mediated processes are presented in the next chapter and comprise many cellular activities in which plasma membranes participate.

Chapter 9 is an elementary discussion of transport systems. There are examples and definitions of diffusional processes; however, there are only two mathematical relationships, Fick's law and the Nernst equation. The book ends with a good discussion of ionophoric antibiotics, physical methods used in the study of plasma membranes, and a further reading list categorized by chapter. It is an excellent starting point for students and an enjoyable review for those more familiar with the area.

Reviewed by Joseph S. Turi
Pharmacy Research
The Upjohn Company
Kalamazoo, MI 49001

High-Speed Liquid Chromatography (Chromatographic Science Series Vol. 6). Edited by P. M. RAJCSANYI and E. RAJCSANYI. Dekker, 270 Madison Avenue, New York, NY 10016, 1975. 16 × 23 cm. 203 pp. Price $15.50.

For this concise, well-organized review, the editors divided the high-pressure liquid chromatographic literature into three sections dealing with theory, instrumentation, and applications. In addition to gradient, pump, and injection systems, columns and preparative techniques are discussed in the instrumentation chapter. The section devoted to detectors is particularly detailed. A number of applications of pharmaceutical interest are reported. These are categorized into sections on alkaloids, carbohydrates, drugs, steroids, vitamins, nucleic acid constituents, and compounds in biological fluids.

Since there are only a few references dated later than 1973, this volume is already somewhat dated, as can be expected for any review of a rapidly developing field such as high-pressure liquid chromatography. For instance, the statement that there have been several recent attempts to extend the usefulness of light absorption detectors over the whole UV–visible range could now be amended to state that such detectors are commercially available and in considerable use. Likewise, the column and application sections do not reflect the present literature emphasis on chemically bonded phases and microparticulate supports.

While this volume does represent a partial update to the thorough coverage presented by Snyder and Kirkland in 1974, it is too brief (123 pages of text) to be considered a replacement. Furthermore, this monograph is a review in the strictest sense in that it lacks the generalization and critical commentary that imparts the invaluable element of experience to a book. With its extensive references, however, it would be useful as an index for rapid access to the literature of a specific topic. For this reason, libraries should acquire a copy. While practitioners will be acquainted with much of the information therein, beginners may find this volume useful as a quick introduction to the field. The quality of print and binding are commensurate with price.

Reviewed by Van D. Reif
Drug Research and Testing Laboratory
United States Pharmacopeial Convention, Inc.
Rockville, MD 20852

NEW JOURNALS

Journal of Chromatography, Biomedical Applications. K. MACEK, Editor. American Elsevier, 52 Vanderbilt Ave., New York, NY 10017, January 1977. Price $49.75 annual subscription (six issues).

Biopharmaceutics and Pharmacokinetics: An Introduction (Second Edition, Revised and Expanded). By ROBERT E. NOTARI. Dekker, 270 Madison Ave., New York, NY 10016, 1975. 285 pp. 15.5 x 23 cm. Price $13.75.

This is the second edition of a book that has already proven valuable to students of biopharmaceutics and to workers in allied biomedical fields who want to teach themselves pharmacokinetics. As the author points out in his preface, the pharmacokinetics portions of the book are organized almost as a programmed learning text. Each new principle is first briefly described, and all working equations are clearly derived. Then an example problem is completely worked out, and at least one practice problem (with answer) is provided. By using this book, it should be possible, even for students with little or no training in calculus, to become competent to handle most one- and two-compartment pharmacokinetic problems.

In the second edition, the chapters titled Rate Processes in Biological Systems (Chapter 2) and Principles of Pharmacokinetics (Chapter 3) have been rewritten, mostly for the purpose of reorganizing the sequence of material. Fortunately, these chapters have not lost any of their original lucidity.

The chapter titled Biopharmaceutics: Clinical Applications of Pharmacokinetic Parameters (Chapter 4) introduces the reader to factors affecting gastrointestinal absorption of drugs, sustained-release dosage forms, and calculation and prediction of drug concentrations in blood during repetitive dosing regimens. A brief discussion of dosage regimen adjustment in patients with compromised renal function has been added to this chapter. This is a welcome addition since so much emphasis is being placed on this aspect of clinical pharmacy practice today. It is hoped that, in future editions, this section will be expanded to include a more thorough discussion of the topic and a broader coverage of the many examples of drugs that are now routinely dosed according to pharmacokinetic principles.

The chapter titled Pharmacokinetic Aspects of Structural Modifications in Drug Design and Therapy (Chapter 5) is a completely new chapter based on a review written by the author for the *Journal of Pharmaceutical Sciences*. Although this chapter covers essentially the same material as the review article, a number of example problems and leading questions have been added, which should be of significant help to the student in understanding the principles discussed.

Significant general improvements over the first edition are that the chapters have been provided with generous lists of references, and several appendices and an author index have been added. These expansions and improvements coupled with retention of the lucid step-by-step approach to pharmacokinetics that characterized the first edition cause this reviewer to rate this book very highly as a beginning text in biopharmaceutics and pharmacokinetics.

Reviewed by Lewis W. Dittert
College of Pharmacy
University of Kentucky
Lexington, KY 40506

Biological Membranes. Their Structure and Function. By ROGER HARRISON and GEORGE G. LUNT. Halsted, 605 Third Ave., New York, NY 10016, 1975. viii + 253 pp. 14.5 × 20.5 cm. Price $9.95.

Membrane biology is a rapidly growing field of research, and there are many texts available on this subject for the expert as well as the student. Harrison and Lunt designed their book for advanced undergraduates in biology and biochemistry. It is also an excellent introduction for those interested in beginning research in this area and a very good review for those with a peripheral interest in the biology and anatomy of membranes. This book is well organized, contains many helpful illustrations, and has an adequate bibliography at the end of each chapter.

The first two chapters provide a historical review of the microscope, a general discussion of cellular organelles, and a brief account of membrane functions, which include transfer systems and the role of membrane-bound enzymes. The next chapter deals with the morphology of membranes and presents many electron micrographs. Included in Chapters 4 and 5 are methods for the preparation of isolated membrane fractions and a detailed account of membrane components. There are considerable illustrations, including space filling models of chemical structures. Chapter 6 is an up-to-date discussion of the structural organization of plasma membranes. It covers the Davson and Danielli model, the current fluid mosaic concept of Singer and Nicholson, and many unanswered questions of membrane structure and biosynthesis.

Chapter 7 contains a general discussion of cell surface specificity, the function of membrane carbohydrates, and the involvement of membrane carbohydrates in histocompatibility antigens and cell recognition and adhesion phenomena. It also includes a cursory look at properties of cancer cells which can be related to alterations in the plasma membrane. Membrane-mediated processes are presented in the next chapter and comprise many cellular activities in which plasma membranes participate.

Chapter 9 is an elementary discussion of transport systems. There are examples and definitions of diffusional processes; however, there are only two mathematical relationships, Fick's law and the Nernst equation. The book ends with a good discussion of ionophoric antibiotics, physical methods used in the study of plasma membranes, and a further reading list categorized by chapter. It is an excellent starting point for students and an enjoyable review for those more familiar with the area.

Reviewed by Joseph S. Turi
Pharmacy Research
The Upjohn Company
Kalamazoo, MI 49001

High-Speed Liquid Chromatography (Chromatographic Science Series Vol. 6). Edited by P. M. RAJCSANYI and E. RAJCSANYI. Dekker, 270 Madison Avenue, New York, NY 10016, 1975. 16 × 23 cm. 203 pp. Price $15.50.

For this concise, well-organized review, the editors divided the high-pressure liquid chromatographic literature into three sections dealing with theory, instrumentation, and applications. In addition to gradient, pump, and injection systems, columns and preparative techniques are discussed in the instrumentation chapter. The section devoted to detectors is particularly detailed. A number of applications of pharmaceutical interest are reported. These are categorized into sections on alkaloids, carbohydrates, drugs, steroids, vitamins, nucleic acid constituents, and compounds in biological fluids.

Since there are only a few references dated later than 1973, this volume is already somewhat dated, as can be expected for any review of a rapidly developing field such as high-pressure liquid chromatography. For instance, the statement that there have been several recent attempts to extend the usefulness of light absorption detectors over the whole UV–visible range could now be amended to state that such detectors are commercially available and in considerable use. Likewise, the column and application sections do not reflect the present literature emphasis on chemically bonded phases and microparticulate supports.

While this volume does represent a partial update to the thorough coverage presented by Snyder and Kirkland in 1974, it is too brief (123 pages of text) to be considered a replacement. Furthermore, this monograph is a review in the strictest sense in that it lacks the generalization and critical commentary that imparts the invaluable element of experience to a book. With its extensive references, however, it would be useful as an index for rapid access to the literature of a specific topic. For this reason, libraries should acquire a copy. While practitioners will be acquainted with much of the information therein, beginners may find this volume useful as a quick introduction to the field. The quality of print and binding are commensurate with price.

Reviewed by Van D. Reif
Drug Research and Testing Laboratory
United States Pharmacopeial Convention, Inc.
Rockville, MD 20852

NEW JOURNALS

Journal of Chromatography, Biomedical Applications. K. MACEK, Editor. American Elsevier, 52 Vanderbilt Ave., New York, NY 10017, January 1977. Price $49.75 annual subscription (six issues).

Biopharmaceutics and Pharmacokinetics: An Introduction (Second Edition, Revised and Expanded). By ROBERT E. NOTARI. Dekker, 270 Madison Ave., New York, NY 10016, 1975. 285 pp. 15.5 x 23 cm. Price $13.75.

This is the second edition of a book that has already proven valuable to students of biopharmaceutics and to workers in allied biomedical fields who want to teach themselves pharmacokinetics. As the author points out in his preface, the pharmacokinetics portions of the book are organized almost as a programmed learning text. Each new principle is first briefly described, and all working equations are clearly derived. Then an example problem is completely worked out, and at least one practice problem (with answer) is provided. By using this book, it should be possible, even for students with little or no training in calculus, to become competent to handle most one- and two-compartment pharmacokinetic problems.

In the second edition, the chapters titled Rate Processes in Biological Systems (Chapter 2) and Principles of Pharmacokinetics (Chapter 3) have been rewritten, mostly for the purpose of reorganizing the sequence of material. Fortunately, these chapters have not lost any of their original lucidity.

The chapter titled Biopharmaceutics: Clinical Applications of Pharmacokinetic Parameters (Chapter 4) introduces the reader to factors affecting gastrointestinal absorption of drugs, sustained-release dosage forms, and calculation and prediction of drug concentrations in blood during repetitive dosing regimens. A brief discussion of dosage regimen adjustment in patients with compromised renal function has been added to this chapter. This is a welcome addition since so much emphasis is being placed on this aspect of clinical pharmacy practice today. It is hoped that, in future editions, this section will be expanded to include a more thorough discussion of the topic and a broader coverage of the many examples of drugs that are now routinely dosed according to pharmacokinetic principles.

The chapter titled Pharmacokinetic Aspects of Structural Modifications in Drug Design and Therapy (Chapter 5) is a completely new chapter based on a review written by the author for the *Journal of Pharmaceutical Sciences*. Although this chapter covers essentially the same material as the review article, a number of example problems and leading questions have been added, which should be of significant help to the student in understanding the principles discussed.

Significant general improvements over the first edition are that the chapters have been provided with generous lists of references, and several appendices and an author index have been added. These expansions and improvements coupled with retention of the lucid step-by-step approach to pharmacokinetics that characterized the first edition cause this reviewer to rate this book very highly as a beginning text in biopharmaceutics and pharmacokinetics.

Reviewed by Lewis W. Dittert
College of Pharmacy
University of Kentucky
Lexington, KY 40506

Biological Membranes. Their Structure and Function. By ROGER HARRISON and GEORGE G. LUNT. Halsted, 605 Third Ave., New York, NY 10016, 1975. viii + 253 pp. 14.5 × 20.5 cm. Price $9.95.

Membrane biology is a rapidly growing field of research, and there are many texts available on this subject for the expert as well as the student. Harrison and Lunt designed their book for advanced undergraduates in biology and biochemistry. It is also an excellent introduction for those interested in beginning research in this area and a very good review for those with a peripheral interest in the biology and anatomy of membranes. This book is well organized, contains many helpful illustrations, and has an adequate bibliography at the end of each chapter.

The first two chapters provide a historical review of the microscope, a general discussion of cellular organelles, and a brief account of membrane functions, which include transfer systems and the role of membrane-bound enzymes. The next chapter deals with the morphology of membranes and presents many electron micrographs. Included in Chapters 4 and 5 are methods for the preparation of isolated membrane fractions and a detailed account of membrane components. There are considerable illustrations, including space filling models of chemical structures. Chapter 6 is an up-to-date discussion of the structural organization of plasma membranes. It covers the Davson and Danielli model, the current fluid mosaic concept of Singer and Nicholson, and many unanswered questions of membrane structure and biosynthesis.

Chapter 7 contains a general discussion of cell surface specificity, the function of membrane carbohydrates, and the involvement of membrane carbohydrates in histocompatibility antigens and cell recognition and adhesion phenomena. It also includes a cursory look at properties of cancer cells which can be related to alterations in the plasma membrane. Membrane-mediated processes are presented in the next chapter and comprise many cellular activities in which plasma membranes participate.

Chapter 9 is an elementary discussion of transport systems. There are examples and definitions of diffusional processes; however, there are only two mathematical relationships, Fick's law and the Nernst equation. The book ends with a good discussion of ionophoric antibiotics, physical methods used in the study of plasma membranes, and a further reading list categorized by chapter. It is an excellent starting point for students and an enjoyable review for those more familiar with the area.

Reviewed by Joseph S. Turi
Pharmacy Research
The Upjohn Company
Kalamazoo, MI 49001

High-Speed Liquid Chromatography (Chromatographic Science Series Vol. 6). Edited by P. M. RAJCSANYI and E. RAJCSANYI. Dekker, 270 Madison Avenue, New York, NY 10016, 1975. 16 × 23 cm. 203 pp. Price $15.50.

For this concise, well-organized review, the editors divided the high-pressure liquid chromatographic literature into three sections dealing with theory, instrumentation, and applications. In addition to gradient, pump, and injection systems, columns and preparative techniques are discussed in the instrumentation chapter. The section devoted to detectors is particularly detailed. A number of applications of pharmaceutical interest are reported. These are categorized into sections on alkaloids, carbohydrates, drugs, steroids, vitamins, nucleic acid constituents, and compounds in biological fluids.

Since there are only a few references dated later than 1973, this volume is already somewhat dated, as can be expected for any review of a rapidly developing field such as high-pressure liquid chromatography. For instance, the statement that there have been several recent attempts to extend the usefulness of light absorption detectors over the whole UV–visible range could now be amended to state that such detectors are commercially available and in considerable use. Likewise, the column and application sections do not reflect the present literature emphasis on chemically bonded phases and microparticulate supports.

While this volume does represent a partial update to the thorough coverage presented by Snyder and Kirkland in 1974, it is too brief (123 pages of text) to be considered a replacement. Furthermore, this monograph is a review in the strictest sense in that it lacks the generalization and critical commentary that imparts the invaluable element of experience to a book. With its extensive references, however, it would be useful as an index for rapid access to the literature of a specific topic. For this reason, libraries should acquire a copy. While practitioners will be acquainted with much of the information therein, beginners may find this volume useful as a quick introduction to the field. The quality of print and binding are commensurate with price.

Reviewed by Van D. Reif
Drug Research and Testing Laboratory
United States Pharmacopeial Convention, Inc.
Rockville, MD 20852

NEW JOURNALS

Journal of Chromatography, Biomedical Applications. K. MACEK, Editor. American Elsevier, 52 Vanderbilt Ave., New York, NY 10017, January 1977. Price $49.75 annual subscription (six issues).

ERRATA

In the article titled "Field Desorption Mass Spectrometry of Azathioprine and Its Metabolites" (1), the following correction should be made:

On page 1374, column 1, line 15, "*m/e* 261, 57%, $M^{+} - CH_4$" should read "*m/e* 261, 57%, $M^{+} - O$."

(1) D. A. Brent, P. de Miranda, and H.-R. Schulten, *J. Pharm. Sci.*, **63**, 1370(1974).

In the article titled "Application of Trihydroxyindole Reaction to Methanesulfonanilides: Fluorometric Analysis for Soterenol and Mesuprine" (1), the following corrections should be made:

On page 763, in the Abstract, lines 11 and 12 should read "The soterenol counterparts to isoproterenone" instead of "The soterenol counterparts to isoproterenol."

On page 765, column 1, line 7 should read "Prasad *et al.* (2) showed that isoproterenone" instead of "Prasad *et al.* (2) showed that isoproterenol."

(1) T. T. Kensler, D. Brooke, and D. M. Walker, *J. Pharm. Sci.*, **65**, 763(1976).

In the article titled "Fluorometric Determination of Cephradine in Plasma" (1), the following correction should be made:

On page 769, column 1, line 5, "Portions (0.1 ml)" should read "Portions (1.0 ml)."

(1) A. F. Heald, C. E. Ita, and E. C. Schreiber, *J. Pharm. Sci.*, **65**, 768(1976).